

Annual Cumulated Index

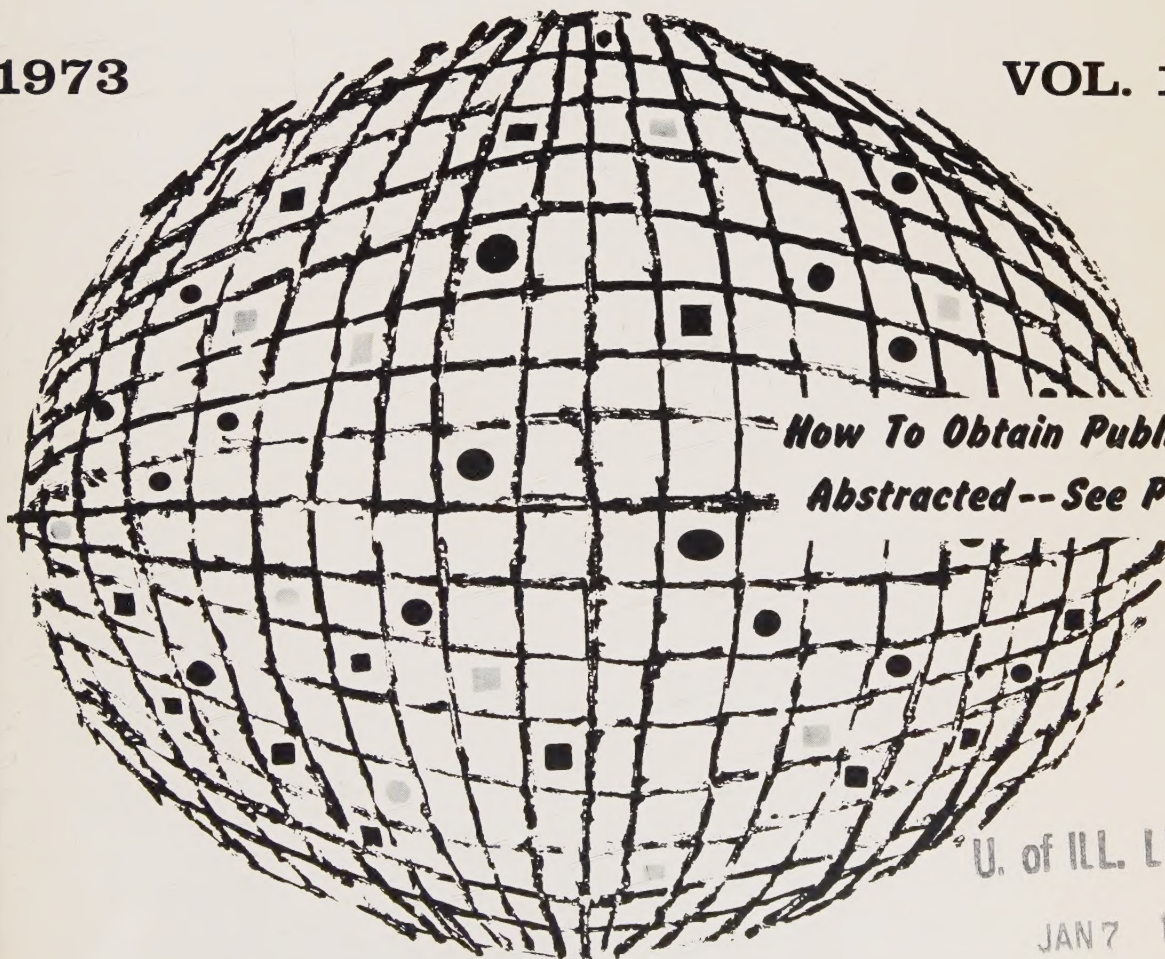
ACCESSION NOS. A73-10001 to A73-45560

INTERNATIONAL AEROSPACE ABSTRACTS

PART 1, PERIODICALS SCANNED, SUBJECT INDEX, A - L

1973

VOL. 13



*How To Obtain Publications
Abstracted -- See Page IV*

U. of ILL. LIBRARY

JAN 7 1974

CHICAGO CIRCLE

PUBLISHED BY THE TECHNICAL INFORMATION SERVICE
AMERICAN INSTITUTE OF AERONAUTICS AND ASTRONAUTICS



Digitized by the Internet Archive
in 2023

INTERNATIONAL AEROSPACE ABSTRACTS

ANNUAL CUMULATED INDEX

PART 1

PERIODICALS SCANNED, SUBJECT INDEX, A – L

VOLUME 13

JANUARY – DECEMBER

1973

ACCESSION NUMBERS A73-10001 to A73-45560

INTERNATIONAL AEROSPACE ABSTRACTS is prepared and published semimonthly (except June and December, which have three issues) by the Technical Information Service, American Institute of Aeronautics and Astronautics, Inc., for the Institute and the National Aeronautics and Space Administration under Contract No. NASW-2532.

SUBSCRIPTION INFORMATION. Semimonthly issues: United States and Possessions, 1 year, \$160 postpaid; all other countries, 1 year, \$175 postpaid. Cumulated index volumes: United States and Possessions, 1 year, \$100 postpaid; all other countries, 1 year, \$115 postpaid. Full service subscription (semimonthly issues and cumulated indexes): United States and Possessions, 1 year, \$240 postpaid; all other countries, 1 year, \$270 postpaid.

EDITORIAL OFFICE: 750 Third Avenue, New York, N.Y. 10017. **SUBSCRIPTION OFFICES:** 750 Third Avenue, New York, N.Y. 10017; Third Avenue and Springtown Road, Alpha, N.J. 08865. Second-class postage paid at New York, N.Y., and at additional mailing offices. Copyright © 1973 by the American Institute of Aeronautics and Astronautics, Inc. (The indexes, however, may be reproduced for any bibliographic purpose.)
TELEPHONE: 212 TN 7-8300

CONTENTS

PART 1

INTRODUCTION	iii
HOW TO OBTAIN PUBLICATIONS ABSTRACTED	iv
CROSS REFERENCES	iv
PERIODICALS SCANNED	v — xxiv
SUBJECT INDEX, A — L	A1 — A988

PART 2

INTRODUCTION	iii
HOW TO OBTAIN PUBLICATIONS ABSTRACTED	iv
CROSS REFERENCES	iv
SUBJECT INDEX, M — Z	A989 — A2008

PART 3

INTRODUCTION	iii
HOW TO OBTAIN PUBLICATIONS ABSTRACTED	iv
PERSONAL AUTHOR INDEX	B1 — B940
CONTRACT NUMBER INDEX	C1 — C35
MEETING PAPER & REPORT NUMBER INDEX	D1 — D13
ACCESSION NUMBER INDEX	E1 — E80

STAFF, TECHNICAL INFORMATION SERVICE

Director, Thomas J. Meskel

Associate Director—Technical, Irene W. Bogolubsky

Abstracts Editor, Nanu Davis

Index Editor, Angelica Mihalakos

Chief Librarian, Patricia M. Marshall

INTRODUCTION

INTERNATIONAL AEROSPACE ABSTRACTS (IAA) is an abstracting and indexing service covering the world's published literature in the field of aeronautics and space science and technology. IAA is issued semimonthly, on the 1st and 15th of each month.

Coverage of Published Literature

The following types of publications are covered in IAA:

- Periodicals (including government-sponsored journals) and books.
- Meeting papers and conference proceedings issued by professional societies and academic organizations.
- Translations of journals and journal articles.

Coverage of Reports ("Unpublished" Literature)

Abstracts and indexes of report literature are issued in SCIENTIFIC AND TECHNICAL AEROSPACE REPORTS (STAR), which is published by the Scientific and Technical Information Office, National Aeronautics and Space Administration.

By special arrangement between NASA and the American Institute of Aeronautics and Astronautics, IAA is issued in coordination with the twice-monthly schedule of STAR, which appears on the 8th and 23rd of each month.

IAA and STAR both utilize identical subject categories and indexes, which are described below.

Thus the two services provide comprehensive access to the national and international unclassified report and published literature of current significance to aerospace science and technology.

Arrangement of the Semimonthly Issues

IAA is arranged in two major sections:

- (1) Abstracts Section. This section contains complete bibliographic citations with informative abstracts as required, arranged by appropriate subject categories to facilitate scanning. The subject categories are numbered from 01 to 34, and the scope of each category is outlined in the Table of Contents and again at the beginning of each category in the Abstracts Section. Each entry is prefixed by the IAA accession number.
- (2) Index Section. Five indexes are contained in this section: Subject, Personal Author, Contract Number, Meeting Paper and Report Number, and Accession Number. Each index is prefaced by explanatory notes.

Cumulated Indexes

The Semiannual Cumulated Index is issued promptly at the end of the first six months and the Annual Cumulated Index is issued promptly at the end of the twelve-month period.

Each cumulated index contains the following sections: A—Subject Index, B—Personal Author Index, C—Contract Number Index, D—Meeting Paper and Report Number Index, and E—Accession Number Index.

Indexing Vocabulary

The Preliminary Edition of the NASA THESAURUS (December 1967) (NASA SP-7030) is the authority for the indexing vocabulary that appears in the subject indexes to STAR and IAA. The NASA Thesaurus should be consulted for a total picture of the current indexing vocabulary and associated cross-reference structure. Copies of the NASA Thesaurus may be obtained from the National Technical Information Service or the U.S. Government Printing Office at a price of \$8.50 for the three-volume set. A one-volume NASA THESAURUS ALPHABETICAL UPDATE (September 1971) of 623 pages is available from the National Technical Information Service (NTIS), Springfield, Va. 22151, for \$6.00.

Information regarding SCIENTIFIC AND TECHNICAL AEROSPACE REPORTS and the availability of INTERNATIONAL AEROSPACE ABSTRACTS to organizations having contractual arrangements with NASA may be obtained from the following address:

National Aeronautics and Space Administration
Scientific and Technical Information Office
Attention: Code KSI
Washington, D. C. 20546

how to obtain publications abstracted

Documents announced are available from the AIAA Technical Information Service as follows:

- Paper copies of accessions announced in IAA and STAR and of other documents in the TIS library are available at \$5.00 per document up to a maximum of 20 pages. The charge for each additional page is \$0.25.
- Microfiche of documents announced in IAA are available at the rate of \$1.00 per microfiche on demand. Documents available in this manner are identified by the symbol # following the accession number in the Abstracts Section and in the Meeting Paper and Report Number and the Accession Number Indexes.
- Minimum air-mail postage to foreign countries is \$1.00.
- A number of publications, because of their special characteristics, are available only for reference in the library.

Address all inquiries and requests to:

Technical Information Service
American Institute of Aeronautics
and Astronautics, Inc.
750 Third Avenue, New York, N. Y. 10017

Telephone: 212 TN 7-8300

**PLEASE REFER TO THE ACCESSION NUMBER
WHEN REQUESTING PUBLICATIONS**

CROSS REFERENCES

The subject index includes two types of cross references to aid the user of the index in locating the material being sought:

1. "USE" references (U) direct the user to alternate headings under which material on the subject will be found, for example

COLUMBIUM
U NIOBIUM

2. "NARROWER TERM" references (NT) refer the user to more specific headings in the same subject area, for example

LUMINESCENCE
NT ELECTROLUMINESCENCE

The periodicals listed in this section were scanned during the preparation of *International Aerospace Abstracts* for 1973. The periodicals were received regularly in all but a few instances. In the case of titles preceded by an asterisk, only the articles announced in *International Aerospace Abstracts* are available. All announced articles can be obtained from the AIAA Technical Information Service.

BM — Bimonthly
BW — Biweekly
Irreg. — Irregular
M — Monthly

Q — Quarterly
SA — Semiannual
SM — Semimonthly
W — Weekly

Abastumanskaia Astrofizicheskaia Observatoriia, Biulleten'. Akademiia Nauk Gruzinskoi SSR, Tiflis. Irreg.

Académie des Sciences (Paris), Comptes Rendus, Série A — Sciences Mathématiques, Série B — Sciences Physiques. Académie des Sciences; Gauthier-Villars, Paris. W

Académie des Sciences (Paris), Comptes Rendus, Série C — Sciences Chimiques. Académie des Sciences; Gauthier-Villars, Paris. W

Académie Polonaise des Sciences, Bulletin, Série des Sciences Mathématiques, Astronomiques et Physiques. Académie Polonaise des Sciences; Państwowe Wydawnictwo Naukowe, Warsaw. M

Académie Polonaise des Sciences, Bulletin, Série des Sciences Techniques. Académie Polonaise des Sciences; Państwowe Wydawnictwo Naukowe, Warsaw. M

Académie Royale de Belgique, Classe des Sciences, Bulletin. Académie Royale de Belgique; Office International de Librairie, Brussels. M

Academy of Sciences, USSR, Bulletin, Physical Series (Akademiia Nauk SSSR, Izvestiia, Serii Fizicheskaiia). Columbia Technical Translations, White Plains, N.Y. M

Academy of Sciences, USSR, Izvestiya, Atmospheric and Oceanic Physics (Akademiia Nauk SSSR, Izvestiia, Fizika Atmosfery i Okeana). American Geophysical Union, Washington, D.C. M

Accademia di Scienze e Lettere, Istituto Lombardo, Rendiconti, Serie della Classe di Scienze Matematiche e Naturali, Sezione A — Scienze Matematiche, Fisiche, Chimiche e Geologiche. Istituto Lombardo di Scienze e Lettere, Milan. Irreg.

Accademia Nazionale dei Lincei, Atti, Memorie — Classe di Scienze Fisiche, Matematiche e Naturali. Accademia Nazionale dei Lincei, Rome.

Acoustical Society of America, Journal. Acoustical Society of America; American Institute of Physics, Inc., New York. M

Acta Astronomica. Polska Akademia Nauk; Państwowe Wydawnictwo Naukowe, Warsaw. Q

Acta Biologica et Medica Germanica. Akademie-Verlag GmbH, Berlin, East Germany. M

Acta Cardiologica. Editions Acta Medica Belgica, Brussels. BM

Acta Cardiologica, Supplementum. Hôtel des Sociétés Scientifiques, Brussels.

**Acta Chemica Scandinavica*. Ed. Karl Myrback, Copenhagen. 10 issues per year

Acta Electronica. Laboratoires d'Electronique et de Physique Appliquée, Limeil-Brévannes (Val-de-Marne), France. Q

Acta Geophysica Polonica. Polska Akademia Nauk; Państwowe Wydawnictwo Naukowe, Warsaw. Q

Acta Mechanica. Springer Verlag, Vienna. 8 issues per year

Acta Metallurgica. Pergamon Press, Inc., Elmsford, N.Y. M

Acta Physica. Akadémiai Kiadó, Budapest. BM

Acta Physica Austriaca. Österreichische Akademie der Wissenschaften; Springer Verlag, Vienna. Q

Acta Physica Polonica, Seria A. Polska Akademia Nauk, Instytut Fizyki and Polskie Towarzystwo Fizyczne, Warsaw.

Acta Physiologica Scandinavica. Scandinavian Physiological Society, Stockholm. 3 vols. per year

Acta Polytechnica Scandinavica, Electrical Engineering Series. Scandinavian Council for Applied Research, Stockholm. Irreg.

Acta Polytechnica Scandinavica, Mechanical Engineering Series. Scandinavian Council for Applied Research, Stockholm. Irreg.

Acta Polytechnica Scandinavica, Physics Including Nucleonics Series. Scandinavian Council for Applied Research, Stockholm. Irreg.

Acta Psychologica. North-Holland Publishing Co., Amsterdam. M

Acta Technica. Akadémiai Kiadó, Budapest. 4 vols. per year

Acta Technica ČSAV. Československá Akademie Věd, Prague. BM

Acustica. S. Hirzel Verlag, KG, Stuttgart, West Germany. Irreg.

Advances in Physics. Taylor & Francis, Ltd., London. BM

AEG-Telefunken, Technische Mitteilungen. AEG-Telefunken, Berlin, West Germany. BM

- Aero-Revue*. Aero-Club der Schweiz and OSTIV; National-Zeitung AG, Basel. M
- Aeronautical Journal*. Royal Aeronautical Society, London. M
- Aeronautical Quarterly*. Royal Aeronautical Society, London. Q
- Aeronautical Society of India, Journal*. Aeronautical Society of India, New Delhi. Q
- L'Aéronautique et l'Astronautique*. Association Française des Ingénieurs et Techniciens de l'Aéronautique et de l'Espace and Société Française de l'Astronautique; Editions Air & Cosmos, Paris. M
- Aerospace Medicine*. Aerospace Medical Association, Washington, D.C. M
- L'Aerotecnica — Missili e Spazio*. Associazione Italiana di Aeronautica e Astronautica; Tamburini Editore S.p.A., Milan. BM
- **Agronomy Journal*. American Society of Agronomy, Madison, Wis. BM
- AIAA Journal*. American Institute of Aeronautics and Astronautics, Inc., New York. M
- AIAA Student Journal*. American Institute of Aeronautics and Astronautics, Inc., New York. Q
- AICHE Journal*. American Institute of Chemical Engineers, New York. BM
- AICHE Symposium Series*. American Institute of Chemical Engineers, New York. Irreg.
- Air et Cosmos*. Paris. W
- Air University Review*. Aerospace Studies Institute, Maxwell Air Force Base, Ala. BM
- Aircraft Engineering*. Bunhill Publications, Ltd., London. M
- Airport Forum*. Bauverlag GmbH, Wiesbaden, West Germany. Q
- Akademiia Nauk Armianskoi SSR, Biurakanskaia Observatoriia, Soobshcheniia*. Akademiia Nauk Armianskoi SSR, Yerevan. Irreg.
- Akademiia Nauk Armianskoi SSR, Doklady*. Akademiia Nauk Armianskoi SSR, Yerevan. 10 issues per year
- Akademiia Nauk Armianskoi SSR, Izvestiia, Fizika*. Akademiia Nauk Armianskoi SSR, Yerevan. BM
- Akademiia Nauk Armianskoi SSR, Izvestiia, Matematika*. Akademiia Nauk Armianskoi SSR, Yerevan. BM
- Akademiia Nauk Armianskoi SSR, Izvestiia, Mekhanika*. Akademiia Nauk Armianskoi SSR, Yerevan. BM
- Akademiia Nauk Armianskoi SSR, Izvestiia, Seriiia Tekhnicheskikh Nauk*. Akademiia Nauk Armianskoi SSR, Yerevan. BM
- Akademiia Nauk Azerbaidzhanskoi SSR, Doklady*. Akademiia Nauk Azerbaidzhanskoi SSR; Izdatel'stvo Elm, Baku. M
- Akademiia Nauk Azerbaidzhanskoi SSR, Izvestiia, Seriiia Fiziko-Tekhnicheskikh i Matematicheskikh Nauk*. Akademiia Nauk Azerbaidzhanskoi SSR; Izdatel'stvo Elm, Baku. BM
- Akademiia Nauk BSSR, Doklady*. Akademiia Nauk Belorusskoi SSR, Minsk. M
- Akademiia Nauk Gruzinskoi SSR, Soobshcheniia*. Akademiia Nauk Gruzinskoi SSR, Tiflis. M
- Akademiia Nauk Kazakhskoi SSR, Izvestiia, Seriiia Fiziko-Matematicheskaiia*. Akademiia Nauk Kazakhskoi SSR, Alma Ata. BM
- Akademiia Nauk Kazakhskoi SSR, Vestnik*. Akademiia Nauk Kazakhskoi SSR; Izdatel'stvo Nauka, Alma Ata. M
- Akademiia Nauk Latvinskoi SSR, Izvestiia, Seriiia Fizicheskikh i Tekhnicheskikh Nauk*. Akademiia Nauk Latvinskoi SSR, Riga. BM
- Akademiia Nauk SSSR, Doklady*. Akademiia Nauk SSSR; Izdatel'stvo Nauka, Moscow. 36 issues per year
- Akademiia Nauk SSSR, Izvestiia, Energetika i Transport*. Akademiia Nauk SSSR; Izdatel'stvo Nauka, Moscow. BM
- Akademiia Nauk SSSR, Izvestiia, Fizika Atmosfery i Okeana*. Akademiia Nauk SSSR; Izdatel'stvo Nauka, Moscow. M
- Akademiia Nauk SSSR, Izvestiia, Mekhanika Tverdogo Tela*. Akademiia Nauk SSSR; Izdatel'stvo Nauka, Moscow. BM
- Akademiia Nauk SSSR, Izvestiia, Mekhanika Zhidkosti i Gaza*. Akademiia Nauk SSSR; Izdatel'stvo Nauka, Moscow. BM
- Akademiia Nauk SSSR, Izvestiia, Metally*. Akademiia Nauk SSSR; Izdatel'stvo Nauka, Moscow. BM
- Akademiia Nauk SSSR, Izvestiia, Neorganicheskie Materialy*. Akademiia Nauk SSSR, Moscow. M
- Akademiia Nauk SSSR, Izvestiia, Seriiia Biologicheskaiia*. Akademiia Nauk SSSR; Izdatel'stvo Nauka, Moscow. BM
- Akademiia Nauk SSSR, Izvestiia, Seriiia Fizicheskaiia*. Akademiia Nauk SSSR; Izdatel'stvo Nauka, Moscow. M
- Akademiia Nauk SSSR, Izvestiia, Tekhnicheskaiia Kibernetika*. Akademiia Nauk SSSR; Izdatel'stvo Nauka, Moscow. BM
- Akademiia Nauk SSSR, Sibirskoe Otdelenie, Izvestiia, Seriiia Tekhnicheskikh Nauk*. Akademiia Nauk SSSR, Sibirskoe Otdelenie; Izdatel'stvo Nauka, Novosibirsk. 3 issues per year
- Akademiia Nauk SSSR, Vestnik*. Akademiia Nauk SSSR; Izdatel'stvo Nauka, Moscow. M
- Akademiia Nauk Tadzhikskoi SSR, Doklady*. Akademiia Nauk Tadzhikskoi SSR; Izdatel'stvo Donish, Dushanbe. M
- Akademiia Nauk Turkmeniskoi SSR, Izvestiia, Seriiia Fiziko-Tekhnicheskikh, Khimicheskikh i Geologicheskikh Nauk*. Akademiia Nauk Turkmeniskoi SSR; Izdatel'stvo Ylym, Ashkhabad. BM
- Akademiia Nauk Ukrain'skoi RSR, Dopovidi, Seriiia A — Fiziko-Tekhnichni i Matematichni Nauki*. Akademiia Nauk Ukrain'skoi RSR; Izdatel'stvo Naukova Dumka, Kiev. M
- Akademiia Nauk Ukrain'skoi RSR, Dopovidi, Seriiia B — Geologiiia, Geofizika, Khimiiia i Biologiiia*. Akademiia Nauk Ukrain'skoi RSR; Izdatel'stvo Naukova Dumka, Kiev. M
- Akademiia Nauk Ukrain'skoi RSR, Visnik*. Akademiia Nauk Ukrain'skoi RSR; Izdatel'stvo Naukova Dumka, Kiev.
- Akademiia Nauk Uzbekskoi SSR, Doklady*. Akademiia Nauk Uzbekskoi SSR, Tashkent. M

- Akademiia Nauk Uzbekskoi SSR, Izvestiia, Serii Fiziko-Matematicheskikh Nauk.* Akademiia Nauk Uzbekskoi SSR, Tashkent. BM
- Akademiia Nauk Uzbekskoi SSR, Izvestiia, Serii Tekhnicheskikh Nauk.* Akademiia Nauk Uzbekskoi SSR, Tashkent. BM
- Akademiia Navuk BSSR, Vestsi, Seryia Fizika-Tekhnichnykh Navuk.* Akademiia Navuk Belaruskai SSR, Minsk. Q
- Akusticheskii Zhurnal.* Akademiia Nauk SSSR; Izdatel'stvo Nauka, Moscow. Q
- Alta Frequenza.* Associazione Elettrotecnica ed Elettronica Italiana, Milan. M
- Alta Frequenza (English Edition).* Associazione Elettrotecnica ed Elettronica Italiana, Milan. M
- **American Alpine Journal.* American Alpine Club, New York. A
- American Ceramic Society Bulletin.* American Ceramic Society, Inc., Columbus, Ohio. M
- American Ceramic Society, Journal.* American Ceramic Society, Inc., Columbus, Ohio. M
- **American Chemical Society, Journal.* American Chemical Society, Washington, D.C. BW
- American Heart Journal.* C. V. Mosby Co., St. Louis, Mo. M
- American Helicopter Society, Journal.* American Helicopter Society, Inc., New York. Q
- American Industrial Hygiene Association Journal.* American Industrial Hygiene Association, Southfield, Mich. BM
- American Journal of Cardiology.* American College of Cardiology; Reuben H. Donnelley Corp., New York. M
- American Journal of Physics.* American Association of Physics Teachers; American Institute of Physics, Inc., New York. M
- American Journal of Physiology.* American Physiological Society, Bethesda, Md. M
- American Journal of Psychology.* University of Illinois Press, Urbana, Ill. Q
- **American Journal of Science.* Yale University, Kline Geology Laboratory, New Haven, Conn. M
- American Meteorological Society, Bulletin.* American Meteorological Society, Boston. M
- **American Mineralogist.* Mineralogical Society of America, Washington, D.C. BM
- **American Nuclear Society, Transactions.* American Nuclear Society, Hinsdale, Ill. SA
- American Society of Civil Engineers, Engineering Mechanics Division, Journal.* American Society of Civil Engineers, New York. BM
- American Society of Civil Engineers, Structural Division, Journal.* American Society of Civil Engineers, New York. M
- **Analytica Chimica Acta.* Elsevier Publishing Co., Amsterdam. M
- **Analytical Biochemistry.* Academic Press, Inc., New York. M
- **Analytical Chemistry.* American Chemical Society, Washington, D.C. M
- Angewandte Informatik.* Friedr. Vieweg & Sohn GmbH, Braunschweig. M
- **Annalen der Meteorologie.* Deutscher Wetterdienst, Offenbach/Main, West Germany. Irreg.
- Annalen der Physik.* Johann Ambrosius Barth Verlag, Leipzig, East Germany. Irreg.
- Annales de Géophysique.* Centre National de la Recherche Scientifique, Paris. Q
- Annales des Télécommunications.* Centre National d'Etudes des Télécommunications, Issy-les-Moulineaux (Hauts-de-Seine), France. BM
- Annali di Geofisica.* Istituto Nazionale di Geofisica, Rome. Q
- Annals of Physics.* Academic Press, Inc., New York. M
- **Annual Review of Physiology.* Annual Reviews, Inc., Palo Alto, Calif. Annual
- Antenny.* Nauchno-Tekhnicheskoe Obshchestvo Radiotekhniki i Elektrosviazi imeni A. S. Popova; Izdatel'stvo Sviaz', Moscow. Irreg.
- APL Technical Digest.* Applied Physics Laboratory, Johns Hopkins University, Silver Spring, Md. BM
- Aplikace Matematiky.* Československá Akademie Věd, Matematický Ústav, Prague. BM
- Applicable Analysis.* Gordon & Breach Science Publishers, Ltd., London. Q
- Applied Microbiology.* American Society for Microbiology, Bethesda, Md. M
- Applied Optics.* Optical Society of America; American Institute of Physics, Inc., New York. M
- Applied Physics.* Springer Verlag, Berlin, West Germany. BM
- Applied Physics Letters.* American Institute of Physics, Inc., New York. SM
- Applied Scientific Research.* Martinus Nijhoff, The Hague. Irreg.
- Applied Spectroscopy.* Society for Applied Spectroscopy, Baltimore, Md. BM
- Archiv für Elektronik und Übertragungstechnik.* S. Hirzel Verlag, KG, Stuttgart, West Germany. Q
- Archiv für Meteorologie, Geophysik und Bioklimatologie, Serie A — Meteorologie und Geophysik.* Springer Verlag, Vienna. Irreg.
- Archiv für technisches Messen/messtechnische Praxis.* Verlag R. Oldenbourg, Munich. M
- Archive for Rational Mechanics and Analysis.* Springer Verlag, Berlin, West Germany. Irreg.
- **Archives of Biochemistry and Biophysics.* Academic Press, Inc., New York. M
- Archives of Environmental Health.* American Medical Association, Chicago. M
- Archiwum Automatyki i Telemekhaniki.* Polska Akademia Nauk; Państwowe Wydawnictwo Naukowe, Warsaw. Q
- Archiwum Budowy Maszyn.* Polska Akademia Nauk, Komitet Budowy Maszyn; Państwowe Wydawnictwo Naukowe, Warsaw. Q
- Archiwum Elektrotechniki.* Polska Akademia Nauk; Państwowe Wydawnictwo Naukowe, Warsaw. Q
- Archiwum Mechaniki Stosowanej.* Polska Akademia Nauk, Instytut Podstawowych Problemów Techniki; Państwowe Wydawnictwo Naukowe, Warsaw. BM
- Archiwum Procesów Spalania.* Polska Akademia Nauk Sekcja Spalania; Państwowe Wydawnictwo Naukowe, Warsaw. Q

- Arizona, University, Lunar and Planetary Laboratory, Communications. University of Arizona, Tucson. Irreg.
- Artificial Satellites. Polish Academy of Sciences, Warsaw. Q
- ASCE, *Transportation Engineering Journal*. American Society of Civil Engineers, New York. Q
- ASLE Transactions. American Society of Lubrication Engineers; Academic Press, Inc., New York. M
- ASME, *Transactions, Series A — Journal of Engineering for Power*. American Society of Mechanical Engineers, New York. Q
- ASME, *Transactions, Series B — Journal of Engineering for Industry*. American Society of Mechanical Engineers, New York. Q
- ASME, *Transactions, Series C — Journal of Heat Transfer*. American Society of Mechanical Engineers, New York. Q
- ASME, *Transactions, Series D — Journal of Basic Engineering* (see *ASME, Transactions, Series I — Journal of Fluids Engineering*).
- ASME, *Transactions, Series E — Journal of Applied Mechanics*. American Society of Mechanical Engineers, New York. Q
- ASME, *Transactions, Series F — Journal of Lubrication Technology*. American Society of Mechanical Engineers, New York. Q
- ASME, *Transactions, Series G — Journal of Dynamic Systems, Measurement, and Control*. American Society of Mechanical Engineers, New York. Q
- ASME, *Transactions, Series H — Journal of Engineering Materials and Technology*. American Society of Mechanical Engineers, New York. Q
- ASME, *Transactions, Series I — Journal of Fluids Engineering* (formerly *ASME, Transactions, Series D — Journal of Basic Engineering*). American Society of Mechanical Engineers, New York. Q
- Association for Computing Machinery, *Journal*. Association for Computing Machinery, Inc., New York. Q
- Association Technique Maritime et Aéronautique, *Bulletin*. Association Technique Maritime et Aéronautique, Paris. Annual
- Astrofizika. Akademiia Nauk Armianskoi SSR, Yerevan. Q
- *Astrometriia i Astrofizika. Akademiia Nauk Ukrainskoi SSR; Izdatel'stvo Naukova Dumka, Kiev. Irreg.
- Astronautica Acta. International Academy of Astronautics; Pergamon Press, Ltd., Oxford. BM
- Astronautics and Aeronautics. American Institute of Aeronautics and Astronautics, Inc., New York. M
- Astronautik. Hermann Oberth-Gesellschaft, e.V., Hannover, West Germany. Q
- Astronomical Institutes of Czechoslovakia, *Bulletin*. Československá Akademie Věd, Prague. BM
- Astronomical Journal. American Astronomical Society; American Institute of Physics, Inc., New York. 10 issues per year
- Astronomical Society of Japan, *Publications*. Astronomical Society of Japan, c/o Tokyo Astronomical Observatory, Mitaka, Tokyo. Q
- Astronomical Society of the Pacific, *Publications*. Astronomical Society of the Pacific, San Francisco. BM
- Astronomicheskii Vestnik. Vsesoiuznoe Astronomo-Geodezicheskoe Obshchestvo; Izdatel'stvo Nauka, Moscow. Q
- Astronomicheskii Zhurnal. Akademiia Nauk SSSR; Izdatel'stvo Nauka, Moscow. BM
- L'Astronomie. Société Astronomique de France, Paris. BM
- Astronomie und Raumfahrt. Deutsche Astronautische Gesellschaft, Berlin, East Germany. BM
- Astronomische Gesellschaft, *Mitteilungen*. Astronomische Gesellschaft, Hamburg; G. Braun GmbH, Karlsruhe, West Germany. Irreg.
- Astronomische Nachrichten. Akademie-Verlag GmbH, Berlin, East Germany. Irreg.
- Astronomy and Astrophysics. Springer Verlag, Berlin, West Germany. M
- Astronomy and Astrophysics Supplement Series. European Southern Observatory; Astronomical Institute Lausanne and Geneva Observatory, Switzerland.
- Astronomy and Space. David & Charles, Newton Abbot, Devon, England. M
- Astrophysical Journal. American Astronomical Society; University of Chicago Press, Chicago. M
- Astrophysical Journal Supplement Series. American Astronomical Society; University of Chicago Press, Chicago. M
- Astrophysical Letters. Gordon & Breach Science Publishers, Ltd., London. M
- Astrophysics and Space Science. D. Reidel Publishing Co., Dordrecht, Netherlands. M
- Atmospheric Technology. National Center for Atmospheric Research, Boulder, Colo. Q
- *Atomkernenergie. Verlag Karl Thieme KG, Munich. Q
- Australian Journal of Physics. Commonwealth Scientific and Industrial Research Organization, Melbourne. BM
- Australian Journal of Physics, *Astrophysical Supplement*. Commonwealth Scientific and Industrial Research Organization, Melbourne. BM
- Automatic Control Theory and Applications. ACTA Press, Calgary, Canada. 3 issues per year
- Automatic Welding (Avtomaticheskaiia Svarka). The Welding Institute, Cambridge. M
- Automatica. Pergamon Press, Ltd., Oxford. BM
- Automation and Remote Control (Avtomatika i Telemechanika). Consultants Bureau, New York. M
- Automatizace. Ministerstvo Průmyslu; Nakladatelství Technické Literatury, Prague. M
- Aviation Review. Smiths Industries, Ltd., Aviation Div., Wembley, Middx., England. Irreg.
- Aviation Week and Space Technology. McGraw-Hill, Inc., New York. W
- Aviatsiia i Kosmonavtika. Voenizdat, Moscow. M
- Aviatsionnaia Tekhnika. Ministerstvo Vysshego i Srednego Spetsial'nogo Obrazovaniia SSSR; Izdanie Kazanskogo Aviatsionnogo Instituta, Kazan. Q
- Aviazione di Linea, Difesa, e Spazio. Rome. M

- Avtomatika. Akademiia Nauk Ukrainskoi SSR; Izdatel'stvo Naukova Dumka, Kiev. BM*
- Avtomatika i Telemekhanika. Akademiia Nauk SSSR; Izdatel'stvo Nauka, Moscow. M*
- Babeş-Bolyai, Universitas, Studia, Series Physica. Babeş-Bolyai, Universitas, Cluj, Rumania. SA*
- Battelle Information (Frankfurt). Battelle-Institut, e.V., Gemeinnützige Laboratorien für Vertragsforschung, Frankfurt am Main, West Germany.*
- Bayerische Akademie der Wissenschaften, mathematisch-naturwissenschaftliche Klasse, Sitzungsberichte. Bayerische Akademie der Wissenschaften, Munich. Irreg.*
- Beiträge aus der Plasmaphysik. Akademie-Verlag GmbH, Berlin, East Germany.*
- Beiträge zur Physik der Atmosphäre. Friedr. Vieweg & Sohn GmbH, Braunschweig. Q*
- Bell System Technical Journal. American Telephone & Telegraph Co., New York. 10 issues per year*
- Bendix Technical Journal. Bendix Corp., Southfield, Mich. 3 issues per year*
- Bildmessung und Luftbildwesen. Deutsche Gesellschaft für Photogrammetrie; Herbert Wichmann Verlag, Karlsruhe, West Germany. Q*
- Biochemical and Biophysical Research Communications. Academic Press, Inc., New York. SM*
- *Biochemistry. American Chemical Society, Washington, D.C. M*
- *Biochimica et Biophysica Acta. Elsevier Publishing Co., Amsterdam. W*
- *Biometrics. North Carolina State University, Institute of Statistics, Raleigh, N.C. Q*
- BioScience. American Institute of Biological Sciences, Washington, D.C. M*
- Biulleten' Eksperimental'noi Biologii i Meditsiny. Akademiia Meditsinskikh Nauk SSSR; Izdatel'stvo Meditsina, Moscow. M*
- B'lgarska Akademiia na Naukite, Fizicheski Institut s ANEB, Izvestiia. B'lgarska Akademiia na Naukite, Otdelenie za Matematicheski i Fizicheski Nauki, Sofia. Irreg.*
- B'lgarska Akademiia na Naukite, Geofizichni Institut, Izvestiia. B'lgarska Akademiia na Naukite, Sofia. Irreg.*
- B'lgarska Akademiia na Naukite, Institut po Khidrologiia i Meteorologiia, Izvestiia. B'lgarska Akademiia na Naukite, Sofia. Irreg.*
- B'lgarska Akademiia na Naukite, Institut po Tekhnicheska Kibernetika, Izvestiia. B'lgarska Akademiia na Naukite, Otdelenie za Tekhnicheski Nauki, Sofia. Irreg.*
- B'lgarska Akademiia na Naukite, Institut po Tekhnicheska Mekhanika, Izvestiia. B'lgarska Akademiia na Naukite, Otdelenie za Tekhnicheski Nauki, Sofia. Irreg.*
- B'lgarska Akademiia na Naukite, Sektsiia po Astronomiia, Izvestiia. B'lgarska Akademiia na Naukite, Sofia. Irreg.*
- B'lgarska Akademiia na Naukite, Tsentralna Laboratoriia po Geodeziia, Izvestiia. B'lgarska Akademiia na Naukite, Otdelenie za Matematicheski i Fizicheski Nauki, Sofia. Irreg.*
- Bolgarskaia Akademiia Nauk, Doklady. B'lgarska Akademiia na Naukite, Sofia. M*
- Bosch Technische Berichte. Robert Bosch GmbH, Stuttgart, West Germany. Irreg.*
- Boundary-Layer Meteorology. D. Reidel Publishing Co., Dordrecht, Netherlands. Q*
- Braunschweigische Wissenschaftliche Gesellschaft, Abhandlungen. Braunschweigische Wissenschaftliche Gesellschaft; Friedr. Vieweg & Sohn GmbH, Braunschweig, West Germany. Irreg.*
- British Acoustical Society, Proceedings. British Acoustical Society, London. M*
- British Astronomical Association, Journal. British Astronomical Association, Hounslow West, Middx., England. BM*
- British Heart Journal. British Medical Association, London. BM*
- British Interplanetary Society, Journal. British Interplanetary Society, London. M*
- *British Journal of Haematology. Blackwell Scientific Publications, Ltd., Oxford. M*
- Bucureşti, Institutul Politehnic Gheorghe Gheorghiu-Dej, Buletinul. Institutul Politehnic Gheorghe Gheorghiu-Dej, Bucharest. BM*
- Bucureşti, Universitatea, Analele, Matematică — Mecanică. Redactia Analele Universitaţii Bucureşti, Bucharest. Irreg.*
- *Building Science. Pergamon Press, Ltd., Oxford. Q*
- *Bulletin of Mathematical Biophysics. MIT Press, Cambridge, Mass. Q*
- Bulletins of American Paleontology. Paleontological Research Institution, Ithaca, N.Y. 2 vols. per year*
- Business and Commercial Aviation. Ziff-Davis Publishing Co., New York. M*
- *Calcutta Mathematical Society, Bulletin. Eds. M. C. Chaki and S. C. Bose, Calcutta. Q*
- Cambridge Philosophical Society, Proceedings. Cambridge University Press, London. BM*
- Canada, National Research Council, Division of Mechanical Engineering and National Aeronautical Establishment, Quarterly Bulletin. National Research Council of Canada, Ottawa. Q*
- Canadian Aeronautics and Space Journal. Canadian Aeronautics and Space Institute, Ottawa. M*
- *Canadian Journal of Chemistry. National Research Council of Canada, Ottawa. SM*
- *Canadian Journal of Microbiology. National Research Council of Canada, Ottawa. M*
- Canadian Journal of Physics. National Research Council of Canada, Ottawa. SM*
- Canadian Journal of Psychology. Canadian Psychological Association; University of Toronto Press, Toronto. Q*
- Canadian Society for Mechanical Engineering, Transactions. Canadian Society for Mechanical Engineering, Montreal. Q*
- *Canadian Spectroscopy. Spectroscopic Society of Canada; Multiscience Publications, Ltd., Montreal. 5 issues per year*
- *Carbohydrate Research. Elsevier Publishing Co., Amsterdam. M*

- Cardiology*. S. Karger AG, Basel. BM
- Cardiovascular Research*. British Cardiac Society; British Medical Association, London. Q
- CASI Transactions*. Canadian Aeronautics and Space Institute, Ottawa. SA
- CATCA Journal*. Canadian Air Traffic Control Association, Inc., Ottawa. SA
- Celestial Mechanics*. D. Reidel Publishing Co., Dordrecht, Netherlands. Q
- Československý Časopis pro Fysiku, Sekce A*. Československá Akademie Věd, Prague. BM
- Chemical and Engineering News*. American Chemical Society, Washington, D.C. W
- **Chemical Communications*. Chemical Society, London. SM
- **Chemical Engineering Science*. Pergamon Press, Ltd., Oxford. M
- Chemical Geology*. Elsevier Publishing Co., Amsterdam. 8 issues per year
- Chemical Physics Letters*. North-Holland Publishing Co., Amsterdam. BW
- **Chemical Society of Japan, Bulletin*. Chemical Society of Japan, Tokyo. M
- **Chemistry Letters*. Chemical Society of Japan, Tokyo.
- Ciel et Terre*. Société Belge d'Astronomie, de Météorologie et de Physique du Globe, Brussels. BM
- Circulation*. American Heart Association, Inc., New York. M
- Circulation Research*. American Heart Association, Inc., New York. M
- **Clinical Biochemistry*. Canadian Society of Clinical Chemists; University of Toronto Press, Toronto. Q
- Cobalt*. Centre d'Information du Cobalt, Brussels. Q
- Combustion and Flame*. Combustion Institute; American Elsevier Publishing Co., Inc., New York. BM
- Combustion Science and Technology*. Gordon & Breach Science Publishers, Ltd., London. BM
- Comments on Modern Physics, Part C — Comments on Astrophysics and Space Physics*. Gordon & Breach Science Publishers, Ltd., London. BM
- Communications in Mathematical Physics*. Springer Verlag, Berlin, West Germany. Irreg.
- Communications on Pure and Applied Mathematics*. New York University, Courant Institute of Mathematical Sciences; Interscience Publishers, New York. BM
- **Comparative Biochemistry and Physiology*. Pergamon Press, Ltd., Oxford. M
- Composites*. Iliffe Science and Technology Publications, Ltd., Guildford, Surrey, England. Q
- Computer Methods in Applied Mechanics and Engineering*. North-Holland Publishing Co., Amsterdam. Q
- Computers and Fluids*. Pergamon Press, Ltd., Oxford. Q
- Computers and Structures*. Pergamon Press, Ltd., Oxford. Q
- Computers in Biology and Medicine*. Pergamon Press, Inc., New York. Q
- Computing*. Springer Verlag, Vienna. Q
- COMSAT Technical Review*. Communications Satellite Corporation, Washington, D.C. SA
- Contamination Control/Biomedical Environments*. Blackwell Publishing Co., Inc., Los Angeles. BM
- Contemporary Physics*. Taylor & Francis, Ltd., London. BM
- **Contributions to Mineralogy and Petrology*. Springer Verlag, Berlin, West Germany. 3 vols. per year
- Corrosion*. National Association of Corrosion Engineers, Inc., Houston, Tex. M
- Cosmic Electrodynamics*. D. Reidel Publishing Co., Dordrecht, Netherlands. Q
- Cosmic Research (Kosmicheskie Issledovaniia)*. Consultants Bureau, New York. BM
- COSPAR Transactions*. COSPAR Secretariat, Paris.
- Cryogenics*. Iliffe Science & Technology Publications, Ltd., London. BM
- **Currents in Modern Biology*. North-Holland Publishing Co., Amsterdam. BM
- Czechoslovak Journal of Physics, Section B*. Československá Akademie Věd, Prague. M
- Czechoslovak Mathematical Journal*. Československá Akademie Věd, Prague. Q
- Defence Science Journal*. Indian Ministry of Defence, New Delhi. Q
- Defense Management Journal*. Directorate for Management Improvement Programs, Office of the Assistant Secretary of Defense; Supt. of Documents, Washington, D.C. Q
- Deutscher Aerokurier*. Deutscher Aero Club, e.V., Frankfurt/Main, West Germany. M
- DEW-Technische Berichte*. Deutsche Edelstahlwerke Aktiengesellschaft, Krefeld, West Germany. Irreg.
- DFVLR-Nachrichten*. Deutsche Forschungs- und Versuchsanstalt für Luft- und Raumfahrt, e.V., Porz-Wahn, West Germany. Irreg.
- DGLR Mitteilungen*. Deutsche Gesellschaft für Luft- und Raumfahrt, e.V., Cologne. Q
- Differentsial'nye Uravneniia*. Izdatel'stvo Nauka i Tekhnika, Minsk. M
- DISA Information*. DISA Elektronik A/S, Herlev, Denmark. M
- Dornier-Post* (English Edition). Dornier AG, Munich. Q
- Earth and Extraterrestrial Sciences*. Gordon & Breach Science Publishers, Ltd., London. Irreg.
- Earth and Planetary Science Letters*. North-Holland Publishing Co., Amsterdam. M
- L'Echo des Recherches*. Centre National d'Etudes des Télécommunications, Issy-les-Moulineaux (Hauts-de-Seine), France. Q
- Eesti NSV Teaduste Akadeemia, Toimetised, Füüsika-Matemaatika*. Izdatel'stvo Periodika, Tallin. Q
- Electrical Communication*. International Telephone and Telegraph Corp., New York. Q
- Electrical Communication Laboratories, Review*. Nippon Telegraph & Telephone Public Corp., Tokyo. BM
- Electro-Optical Systems Design*. Milton S. Kiver Publications, Inc., Madison, Wis. M

- Electrochemical Society, Journal.* Electrochemical Society, Inc., New York. M
- Electroencephalography and Clinical Neurophysiology.* International Federation of Societies for Electroencephalography and Clinical Neurophysiology; Elsevier Publishing Co., Amsterdam. M
- Electron Technology.* Polish Academy of Sciences, Institute of Electron Technology; Państwowe Wydawnictwo Naukowe, Warsaw. Irreg.
- Electronic Applications Bulletin.* N. V. Philips' Gloeilampenfabrieken; N. V. Uitgeversmaatschappij Centrex, Eindhoven. 4 issues per year
- Electronic Design.* Hayden Publishing Co., Inc., New York. BW
- Electronic Progress.* Raytheon Co., Lexington, Mass. Q
- Electronics.* McGraw-Hill, Inc., New York. BW
- Electronics and Communications in Japan (Denshi Tsushin Gakkai Ronbunshi).* Institute of Electronics and Communications Engineers of Japan; Institute of Electrical and Electronics Engineers, Inc., New York. M
- Electronics and Power.* Institution of Electrical Engineers, London. M
- Electronics Letters.* Institution of Electrical Engineers, London. BW
- Elektromekhanika.* Ministerstvo Vysshego i Srednego Spetsial'nogo Obrazovaniia SSSR, Novocherkassk. M
- Elektronik.* Franzis-Verlag, Munich. M
- Elektronika.* Wydawnictwa Czasopism Technicznych NOT, Warsaw. M
- **Endocrinology.* Endocrine Society; J. B. Lippincott Co., Philadelphia, Pa. M
- Energomashinostroenie.* Ministerstvo Tiazhelogo, Energeticheskogo i Transportnogo Mashinostroeniia SSSR and Nauchno-Tekhnicheskoe Obshchestvo Mashinostroitel'noi Promyshlennosti; Izdatel'stvo Mashinostroenie, Leningrad. M
- Energy Conversion.* Pergamon Press, Ltd., Oxford. Q
- Engineering Fracture Mechanics.* Pergamon Press, Ltd., Oxford. Q
- Entropie.* Editions Barthélemy & Cie., Paris. BM
- **Environmental Biology and Medicine.* Gordon & Breach Science Publishers, Ltd., London.
- EOS.* American Geophysical Union, Washington, D.C. M
- Ergonomics.* Ergonomics Research Society, Nederlandse Vereniging voor Ergonomie, International Ergonomics Association; Taylor & Francis, Ltd., London. Q
- Ericsson Technics.* Telefonaktiebolaget LM Ericsson, Stockholm. Q
- ESRO/ELDO Bulletin.* European Space Research Organization and European Space Vehicle Launcher Development Organization, Neuilly-sur-Seine (Hauts-de-Seine), France. Q
- Esso Air World.* ESSO International, Inc., New York. BM
- Eurocontrol.* Eurocontrol, Public Relations Div., Brussels. SA
- Experimental Brain Research.* Springer Verlag, Berlin, West Germany. Irreg.
- Experimental Mechanics.* Society for Experimental Stress Analysis, Westport, Conn. M
- Explosivstoffe.* Erwin Barth Verlag, KG, Mannheim, West Germany. M
- Facilities for Atmospheric Research.* National Center for Atmospheric Research, Boulder, Colo. Q
- **FEBS Letters.* Federation of European Biochemical Societies; North-Holland Publishing Co., Amsterdam. SM
- Finommechanika* (see *Finommechanika — Mikrotechnika*).
- Finommechanika — Mikrotechnika* (formerly *Finommechanika*). Lapkiadó Vállalat, Budapest. M
- Fizicheskaiia Elektronika.* Ministerstvo Vysshego i Srednego Spetsial'nogo Obrazovaniia USSR; Izdatel'stvo L'vovskogo Universiteta, Lvov. Irreg.
- Fizika.* Ministerstvo Vysshego i Srednego Spetsial'nogo Obrazovaniia SSSR; Izdatel'stvo Tomskogo Universiteta, Tomsk. M
- Fizika Aerodispersnykh Sistem.* Izdatel'stvo Kievskogo Universiteta, Kiev. Irreg.
- Fizika Gorenii i Vzryva.* Akademiia Nauk SSSR, Sibirskoe Otdelenie; Izdatel'stvo Nauka, Novosibirsk. Q
- Fizika Metallov i Metallovedenie.* Akademiia Nauk SSSR; Izdatel'stvo Nauka, Sverdlovsk. M
- Fizika Plazmy i Problemy Upravliaemogo Termoiadernogo Sintez.* Akademiia Nauk Ukrainskoi SSR; Izdatel'stvo Naukova Dumka, Kiev. Irreg.
- Fiziko-Khimicheskaiia Mekhanika Materialov.* Akademiia Nauk Ukrainskoi SSR; Izdatel'stvo Naukova Dumka, Kiev. BM
- Fiziologicheskii Zhurnal SSSR.* Akademiia Nauk SSSR; Izdatel'stvo Nauka, Leningrad. M
- Fiziologichnii Zhurnal.* Akademiia Nauk Ukrainskoi SSR, Institut Fiziologii; Izdatel'stvo Naukova Dumka, Kiev. BM
- Flight International.* Royal Aero Club; IPC Business Press, Ltd., London. W
- Flug Revue/Flugwelt International.* Club der Luftfahrt von Deutschland, e.V., Bonn; Vereinigte Motor-Verlage GmbH, Stuttgart, West Germany. M
- Fluid Mechanics — Soviet Research.* Scripta Publishing Corp., Washington, D.C. BM
- Fluidics Quarterly.* Ann Arbor, Mich. Q
- Forschung im Ingenieurwesen.* Verein Deutscher Ingenieure; VDI-Verlag GmbH, Düsseldorf. BM
- Fortune.* Time, Inc., Chicago. M
- Franklin Institute, Journal.* Franklin Institute, Philadelphia, Pa.; Pergamon Press, Ltd., Oxford. M
- Frequenz.* Fachverlag Schiele & Schön, Berlin, West Germany. M
- Fujitsu Scientific and Technical Journal.* Fujitsu, Ltd., Kanagawa, Japan. Q
- GEC Journal of Science and Technology.* General Electric Company, Ltd., London. Q
- Geliotekhnika.* Akademiia Nauk Uzbekskoi SSR, Tashkent. BM

- Genève, Société de Physique et d'Histoire Naturelle, Compte Rendu des Séances.* Société de Physique et d'Histoire Naturelle de Genève, Geneva. 3 issues per year
- Geochimica et Cosmochimica Acta.* Geochemical Society and Meteoritical Society; Pergamon Press, Ltd., Oxford. M
- Geodesy and Aerophotography (Geodeziia i Aerofotos'emka).* American Geophysical Union, Washington, D.C. BM
- Geodeziia, Kartografiia i Aerofotos'emka.* Izdatel'stvo L'vovskogo Universiteta, Lvov. Irreg.
- Geodeziia i Aerofotos'emka.* Ministerstvo Vysshego i Srednego Spetsial'nogo Obrazovaniia SSSR; Izdatel'stvo Moskovskogo Instituta Inzhenerov Geodezii, Aerofotos'emki i Kartografii, Moscow. BM
- Geodeziia i Kartografiia.* Glavnoe Upravlenie Geodezii i Kartografii pri Sovete Ministrov SSSR; Izdatel'stvo Nedra, Moscow. M
- Geodezja i Kartografia.* Polska Akademia Nauk, Komitet Geodezji; Państwowe Wydawnictwo Naukowe, Warsaw. Q
- Geofysikální Sborník.* Československá Akademie Věd, Geofysikální Ústav, Prague.
- Geofysiske Publikasjoner (Geophysica Norvegica).* Norske Videnskaps-Akademi, Oslo. Irreg.
- **Geological Society of America, Memoir.* Geological Society of America, Boulder, Colo. 5 issues per year
- Geological Society of America Bulletin.* Geological Society of America, Boulder, Colo. M
- Geomagnetism and Aeronomy (Geomagnetizm i Aeronomiia).* American Geophysical Union, Washington, D.C. BM
- Geomagnetizm i Aeronomiia.* Akademiia Nauk SSSR; Izdatel'stvo Nauka, Moscow. BM
- Geophysical Fluid Dynamics.* Gordon & Breach Science Publishers, Ltd., London. M
- Geophysical Journal.* Royal Astronomical Society; Blackwell Scientific Publications, Ltd., Oxford. M
- Geophysical Magazine.* Japan Meteorological Agency, Tokyo. SA
- **Geophysics.* Society of Exploration Geophysicists, Tulsa, Okla. BM
- Gerlands Beiträge zur Geophysik.* Akademische Verlagsgesellschaft Geest & Portig, KG, Leipzig, East Germany. BM
- Gidromekhanika.* Akademiia Nauk Ukrainskoi SSR; Izdatel'stvo Naukova Dumka, Kiev. Irreg.
- **Glastechnische Berichte.* Verlag der Deutschen Glas-technischen Gesellschaft, Frankfurt/Main, West Germany. M
- Göttingen, Akademie der Wissenschaften, Nachrichten, mathematisch-physikalische Klasse.* Vandenhoeck & Ruprecht, Göttingen. Irreg.
- Gravitatsiia i Teoriia Otnositel'nosti.* Izdatel'stvo Kazanskogo Universiteta, Kazan. Irreg.
- Heat Transfer — Japanese Research.* Scripta Publishing Corp., Washington, D.C. Q
- Heat Transfer — Soviet Research.* American Society of Mechanical Engineers, New York. BM
- Heidelberger Akademie der Wissenschaften, mathematisch-naturwissenschaftliche Klasse, Sitzungsberichte.* Carl Winter Universitätsverlag, Heidelberg, West Germany.
- High Temperature (Teplofizika Vysokikh Temperatur).* Consultants Bureau, New York. BM
- **High Temperature Science.* Academic Press, Inc., New York. Q
- High Temperatures — High Pressures.* Pion, Ltd., London. BM
- Hiroshima University, Journal of Science, Series A — II.* Hiroshima University, Faculty of Science, Dept. of Chemistry, Hiroshima. 3 issues per year.
- **Histochemie.* Springer Verlag, Berlin, West Germany. SM
- Human Factors.* Human Factors Society, Inc., Santa Monica, Calif.; The Johns Hopkins Press, Baltimore, Md. M
- Hydraulics and Pneumatics.* Industrial Publishing Co., Cleveland, Ohio. M
- I & EC — Industrial and Engineering Chemistry, Fundamentals.* American Chemical Society, Washington, D.C. Q
- I & EC — Industrial and Engineering Chemistry, Product Research and Development.* American Chemical Society, Washington, D.C. Q
- Iași, Institutul Politehnic, Buletinul, Secția I — Matematică, Mecanică Teoretică, Fizică.* Iași, Institutul Politehnic, Iași, Rumania. SA
- Iași, Institutul Politehnic, Buletinul, Secția III — Electrotehnică, Electronică, Automatizări.* Iași, Institutul Politehnic, Iași, Rumania. Irreg.
- Iași, Institutul Politehnic, Buletinul, Secția IV — Mecanică Tehnică.* Iași, Institutul Politehnic, Iași, Rumania. SA
- IBM Journal of Research and Development.* International Business Machines Corp., Armonk, N.Y. BM
- Icarus.* Academic Press, Inc., New York. BM
- IEEE, Proceedings.* Institute of Electrical and Electronics Engineers, Inc., New York. M
- IEEE Journal of Quantum Electronics.* Institute of Electrical and Electronics Engineers, Inc., New York. M
- IEEE Journal of Solid-State Circuits.* Institute of Electrical and Electronics Engineers, Inc., New York. BM
- IEEE Spectrum.* Institute of Electrical and Electronics Engineers, Inc., New York. M
- IEEE Transactions on Aerospace and Electronic Systems.* Institute of Electrical and Electronics Engineers, Inc., New York. BM
- IEEE Transactions on Antennas and Propagation.* Institute of Electrical and Electronics Engineers, Inc., New York. BM
- IEEE Transactions on Automatic Control.* Institute of Electrical and Electronics Engineers, Inc., New York. BM
- IEEE Transactions on Biomedical Engineering.* Institute of Electrical and Electronics Engineers, Inc., New York. M

- IEEE Transactions on Broadcast and Television Receivers.* Institute of Electrical and Electronics Engineers, Inc., New York. Q
- IEEE Transactions on Circuit Theory.* Institute of Electrical and Electronics Engineers, Inc., New York. Q
- IEEE Transactions on Communications.* Institute of Electrical and Electronics Engineers, Inc., New York. BM
- IEEE Transactions on Computers.* Institute of Electrical and Electronics Engineers, Inc., New York. M
- IEEE Transactions on Education.* Institute of Electrical and Electronics Engineers, Inc., New York. Q
- IEEE Transactions on Electromagnetic Compatibility.* Institute of Electrical and Electronics Engineers, Inc., New York. Q
- IEEE Transactions on Electron Devices.* Institute of Electrical and Electronics Engineers, Inc., New York. M
- IEEE Transactions on Engineering Management.* Institute of Electrical and Electronics Engineers, Inc., New York. Q
- IEEE Transactions on Geoscience Electronics.* Institute of Electrical and Electronics Engineers, Inc., New York. Q
- IEEE Transactions on Information Theory.* Institute of Electrical and Electronics Engineers, Inc., New York. BM
- IEEE Transactions on Instrumentation and Measurement.* Institute of Electrical and Electronics Engineers, Inc., New York. Q
- IEEE Transactions on Magnetics.* Institute of Electrical and Electronics Engineers, Inc., New York. Q
- IEEE Transactions on Microwave Theory and Techniques.* Institute of Electrical and Electronics Engineers, Inc., New York. M
- IEEE Transactions on Nuclear Science.* Institute of Electrical and Electronics Engineers, Inc., New York. BM
- IEEE Transactions on Parts, Hybrids, and Packaging.* Institute of Electrical and Electronics Engineers, Inc., New York. Q
- IEEE Transactions on Reliability.* Institute of Electrical and Electronics Engineers, Inc., New York. Q
- IEEE Transactions on Sonics and Ultrasonics.* Institute of Electrical and Electronics Engineers, Inc., New York. Q
- IEEE Transactions on Systems, Man, and Cybernetics.* Institute of Electrical and Electronics Engineers, Inc., New York. Q
- Image Technology.* Society of Photographic Scientists and Engineers; Acolyte Publications Corp., Los Angeles. BM
- Indian Academy of Sciences, Proceedings, Section A.* Indian Academy of Sciences, Bangalore. M
- Indian Institute of Science, Journal.* Indian Institute of Science, Bangalore. Q
- Indian Journal of Pure and Applied Mathematics.* Indian National Science Academy, New Delhi. Q
- Indian Journal of Pure and Applied Physics.* Council of Scientific and Industrial Research, New Delhi. M
- Indian Rocket Society, Journal.* Indian Rocket Society, Trivandrum, India. Q
- Indiana University Mathematics Journal.* Indiana University, Dept. of Mathematics, Bloomington, Ind. M
- Industrial Laboratory (Zavodskaja Laboratorii).* Consultants Bureau, New York. M
- Industries Atomiques et Spatiales.* Sertna, S.A., Geneva. BM
- Information and Control.* Academic Press, Inc., New York. M
- *Information Sciences.* American Elsevier Publishing Co., Inc., New York. Q
- Infrared Physics.* Pergamon Press, Ltd., Oxford. Q
- Ingegneria.* Editore Ulrico Hoepli, Milan. M
- Ingeniería Aeronáutica y Astronáutica.* Asociación de Ingenieros Aeronáuticos, Madrid. BM
- Ingenieur-Archiv.* Springer Verlag, Berlin, West Germany. BM
- *Inorganic Chemistry.* American Chemical Society, Washington, D.C. M
- Institut Henri Poincaré, Annales, Section A — Physique Théorique.* Gauthier-Villars, Paris. BM
- Institut Royal Météorologique de Belgique, Publications, Série A.* Institut Royal Météorologique de Belgique, Brussels. Irreg.
- Institut Royal Météorologique de Belgique, Publications, Série B.* Institut Royal Météorologique de Belgique, Brussels.
- Institut Teoreticheskoi Astronomii, Biulleten'.* Akademiia Nauk SSSR, Institut Teoreticheskoi Astronomii; Izdatel'stvo Nauka, Leningrad. Irreg.
- Institute of Mathematics and Its Applications, Journal.* Academic Press, Inc. (London), Ltd., London. Q
- Institution of Electrical Engineers, Proceedings.* Institution of Electrical Engineers, London. M
- Institution of Engineers (India), Journal, Electronics and Telecommunication Engineering Division.* Institution of Engineers, Calcutta. 3 issues per year
- Institution of Engineers (India), Journal, Mechanical Engineering Division.* Institution of Engineers, Calcutta. BM
- Institution of Mechanical Engineers, Proceedings.* Institution of Mechanical Engineers, London. Irreg.
- Institution of Telecommunication Engineers, Journal.* Institution of Telecommunication Engineers, New Delhi. M
- Instruments and Control Systems.* Chilton Co., Philadelphia, Pa. M
- Instytut Lotnictwa, Biuletyn Informacyjny.* Instytut Lotnictwa, Warsaw. BM
- Instytut Lotnictwa, Prace.* Instytut Lotnictwa Wydawnictwo Naukowo-Techniczne, Warsaw. Irreg.
- Instytut Maszyn Przepływowych, Prace.* Polska Akademia Nauk, Instytut Maszyn Przepływowych, Gdansk; Państwowe Wydawnictwo Naukowe, Warsaw. Irreg.
- Interavia.* Interavia S.A., Geneva. M

- International Journal for Numerical Methods in Engineering.* John Wiley & Sons, Ltd., Chichester, Sussex, England. Q
- International Journal of Control, First Series.* Taylor & Francis, Ltd., London. M
- International Journal of Electronics, First Series.* Taylor & Francis, Ltd., London. M
- International Journal of Engineering Science.* Pergamon Press, Ltd., Oxford. M
- International Journal of Fracture Mechanics.* Wolters-Noordhoff Publishing, Groningen, Netherlands. Q
- International Journal of Heat and Mass Transfer.* Pergamon Press, Ltd., Oxford. M
- International Journal of Man-Machine Studies.* Academic Press, Inc. (London), Ltd., London. Q
- International Journal of Mass Spectroscopy and Ion Physics.* Elsevier Publishing Co., Amsterdam. M
- International Journal of Mechanical Sciences.* Pergamon Press, Ltd., Oxford. M
- **International Journal of Neuroscience.* Gordon & Breach Science Publishers, Inc., New York. M
- International Journal of Non-Linear Mechanics.* Pergamon Press, Ltd., Oxford. Q
- International Journal of Nondestructive Testing.* Gordon & Breach Science Publishers, London.
- International Journal of Powder Metallurgy.* American Powder Metallurgy Institute, New York. Q
- International Journal of Solids and Structures.* Pergamon Press, Ltd., Oxford. M
- International Metallurgical Reviews.* Institute of Metals, London; American Society for Metals, Metals Park, Ohio. Q
- Internationale Elektronische Rundschau.* Verlag für Radio-Foto-Kinotechnik GmbH, Berlin, West Germany. M
- Internationale Zeitschrift für angewandte Physiologie einschliesslich Arbeitsphysiologie.* Springer Verlag, Berlin, West Germany. Q
- Inzhenerno-Fizicheskii Zhurnal.* Akademiia Nauk Belorusskoi SSR; Izdatel'stvo Nauka i Tekhnika, Minsk. M
- Ionosfernye Issledovaniia.* Mezhdudedomstvennyi Geofizicheskii Komitet pri Prezidiume Akademii Nauk SSSR; Izdatel'stvo Nauka, Moscow. Irreg.
- Irish Astronomical Journal.* Observatory, Armagh, Northern Ireland. Q
- ISA Transactions.* Instrument Society of America, Pittsburgh, Pa. Q
- Ishikawajima-Harima Engineering Review.* Ishikawajima-Harima Heavy Industries Co., Ltd., Tokyo. BM
- **Israel Journal of Chemistry.* Weizmann Science Press of Israel, Jerusalem. BM
- Israel Journal of Technology.* Weizmann Science Press of Israel, Jerusalem. BM
- Issledovaniia po Teorii Plastin i Obolochek.* Izdatel'stvo Kazanskogo Universiteta, Kazan. Irreg.
- İstanbul Üniversitesi, Fen Fakültesi Mecmuası, Seri C — Astronomi-Fizik-Kimya.* İstanbul Üniversitesi, İstanbul. Q
- ITU Telecommunication Journal.* International Telecommunication Union, Geneva. M
- Japan Institute of Light Metals, Journal.* Japan Institute of Light Metals, Tokyo. BM
- Japan Institute of Metals, Journal (Nippon Kinzoku Gakkai-si).* Japan Institute of Metals, Sendai. M
- Japan Institute of Metals, Transactions.* Japan Institute of Metals, Sendai. BM
- Japan Society for Aeronautical and Space Sciences, Transactions.* Japan Society for Aeronautical and Space Sciences, Tokyo. Irreg.
- Japan Society of Materials Science, Journal.* Society of Materials Science, Kyoto. M
- Japanese Heart Journal.* Tokyo, University, Faculty of Medicine, Tokyo. BM
- Japanese Journal of Applied Physics.* Physical Society of Japan and Japan Society of Applied Physics, Tokyo. M
- Japanese Journal of Physiology.* Physiological Society of Japan; University of Tokyo Press, Tokyo. BM
- Jemná Mechanika a Optika.* Ministerstvo Průmyslu; Státní Nakladatelství Technické Literatury, Prague. BM
- Jena Review.* VEB Verlag Technik, Berlin, East Germany. BM
- JETP Letters (ZHETF Pis'ma v Redaktsiiu).* American Institute of Physics, Inc., New York. SM
- Journal de Mécanique.* Gauthier-Villars, Paris. Q
- Journal de Physiologie.* Masson & Cie., Paris. BM
- Journal de Physique.* Société Française de Physique, Paris. M
- Journal of Air Law and Commerce.* Southern Methodist University, School of Law, Dallas. Q
- Journal of Air Traffic Control.* Air Traffic Control Association, Inc., Washington, D.C. BM
- Journal of Aircraft.* American Institute of Aeronautics and Astronautics, Inc., New York. BM
- **Journal of Animal Science.* American Society of Animal Science; Ed. V. R. Bohman, Champaign, Ill. M
- Journal of Applied Meteorology.* American Meteorological Society, Boston. BM
- Journal of Applied Physics.* American Institute of Physics, Inc., New York. 13 issues per year
- Journal of Applied Physiology.* American Physiological Society, Washington, D.C. M
- **Journal of Applied Polymer Science.* Interscience Publishers, New York. M
- Journal of Atmospheric and Terrestrial Physics.* Pergamon Press, Ltd., Oxford. M
- Journal of Bacteriology.* American Society for Microbiology, Bethesda, Md. M
- Journal of Biomechanics.* Pergamon Press, Ltd., Oxford. Q
- **Journal of Catalysis.* Academic Press, Inc., New York. BM
- **Journal of Cellular Physiology.* Wistar Institute of Anatomy and Biology, Philadelphia, Pa. BM
- **Journal of Chemical Education.* American Chemical Society, Div. of Chemical Education, New York. M
- Journal of Chemical Physics.* American Institute of Physics, Inc., New York. SM
- **Journal of Chromatography.* Elsevier Publishing Co., Amsterdam. M

- **Journal of Colloid and Interface Science*. Academic Press, Inc., New York. M
- Journal of Composite Materials*. Technomic Publishing Co., Inc., Stamford, Conn. BM
- Journal of Computational Physics*. Academic Press, Inc., New York. Q
- **Journal of Crystal and Molecular Structure*. Plenum Press, New York. BM
- **Journal of Crystal Growth*. North-Holland Publishing Co., Amsterdam. BM
- Journal of Differential Equations*. Academic Press, Inc., New York. BM
- Journal of Elasticity*. Wolters-Noordhoff Publishing, Groningen, Netherlands. Q
- **Journal of Electroanalytical Chemistry and Interfacial Electrochemistry*. Elsevier Sequoia S.A., Lausanne, Switzerland. M
- Journal of Electrocardiology*. Research in Electrocardiology, Inc., Dayton, Ohio. Q
- Journal of Engineering Mathematics*. Wolters-Noordhoff Publishing, Groningen, Netherlands. Q
- Journal of Environmental Sciences*. Institute of Environmental Sciences, Mt. Prospect, Ill. BM
- Journal of Experimental Psychology*. American Psychological Association, Inc., Washington, D.C. M
- Journal of Fire and Flammability*. Technomic Publishing Co., Inc., Stamford, Conn. Q
- Journal of Fluid Mechanics*. Cambridge University Press, London. 20 issues per year
- Journal of Geomagnetism and Geoelectricity*. Society of Terrestrial Magnetism and Electricity, Kyoto, Japan. Q
- Journal of Geophysical Research*. American Geophysical Union, Washington, D.C. 36 issues per year
- **Journal of Heterocyclic Chemistry*. University Station, Provo, Utah. BM
- Journal of Hydronautics*. American Institute of Aeronautics and Astronautics, Inc., New York. Q
- **Journal of Inorganic and Nuclear Chemistry*. Pergamon Press, Ltd., Oxford. M
- Journal of Interdisciplinary Cycle Research*. International Institute for Interdisciplinary Cycle Research, Leiden; Swets & Zeitlinger N.V., Amsterdam. Q
- Journal of Materials* (see *Journal of Testing and Evaluation*).
- Journal of Materials Science*. Chapman & Hall, Ltd., London. M
- Journal of Mathematical Analysis and Applications*. Academic Press, Inc., New York. M
- Journal of Mathematical and Physical Sciences*. Indian Institute of Technology, Madras.
- Journal of Mathematical Physics*. American Institute of Physics, Inc., New York. M
- Journal of Mechanical Engineering Science*. Institution of Mechanical Engineers, London. Q
- Journal of Metals*. American Institute of Mining, Metallurgical and Petroleum Engineers, Inc., New York. M
- Journal of Molecular Evolution*. Springer Verlag, Berlin, West Germany. 4 issues per volume
- **Journal of Molecular Spectroscopy*. Academic Press, Inc., New York. M
- **Journal of Molecular Structure*. Elsevier Publishing Co., Amsterdam. BM
- Journal of Navigation*. Royal Institute of Navigation; John Murray (Publishers), Ltd., London. Q
- **Journal of Non-Crystalline Solids*. North-Holland Publishing Co., Amsterdam.
- Journal of Occupational Medicine*. Industrial Medical Association; Charles B. Slack, Inc., Thorofare, N.J. M
- Journal of Optimization Theory and Applications*. Plenum Publishing Corp., New York. M
- **Journal of Organic Chemistry*. American Chemical Society, Washington, D.C. M
- **Journal of Paint Technology*. Federation of Societies for Paint Technology, Philadelphia, Pa. M
- **Journal of Paleontology*. Society of Economic Paleontologists and Mineralogists; Paleontological Society, Tulsa, Okla. Q
- Journal of Physical Chemistry*. American Chemical Society, Washington, D.C. BW
- Journal of Physical Oceanography*. American Meteorological Society, Boston. Q
- Journal of Physics, Part A — General Physics* (see *Journal of Physics, Part A — Mathematical, Nuclear and General*).
- Journal of Physics, Part A — Mathematical, Nuclear and General* (formerly *Journal of Physics, Part A — General Physics*). Institute of Physics, London. M
- Journal of Physics, Part B — Atomic and Molecular Physics*. Institute of Physics and The Physical Society, London. M
- Journal of Physics, Part C — Solid State Physics*. Institute of Physics and The Physical Society, London. M
- Journal of Physics, Part D — Applied Physics*. Institute of Physics and The Physical Society, London. M
- Journal of Physics, Part E — Scientific Instruments*. Institute of Physics and The Physical Society, London. M
- Journal of Physics, Part F — Metal Physics*. Institute of Physics, London. BM
- **Journal of Physics and Chemistry of Solids*. Pergamon Press, Ltd., Oxford. M
- Journal of Plasma Physics*. Cambridge University Press, London. Q
- **Journal of Polymer Science, Part B — Polymer Letters*. Interscience Publishers, Inc., New York. M
- Journal of Quality Technology*. American Society for Quality Control, Inc., Milwaukee, Wis. Q
- Journal of Quantitative Spectroscopy and Radiative Transfer*. Pergamon Press, Ltd., Oxford. M
- Journal of Research, Section A — Physics and Chemistry*. National Bureau of Standards; Supt. of Documents, Washington, D.C. BM
- Journal of Research, Section C — Engineering and Instrumentation*. National Bureau of Standards; Supt. of Documents, Washington, D.C. Q
- **Journal of Sedimentary Petrology*. Society of Economic Paleontologists and Mineralogists, Tulsa, Okla. Q

- Journal of Sound and Vibration.* British Acoustical Society; Academic Press, Inc., (London), Ltd., London. BM
- Journal of Spacecraft and Rockets.* American Institute of Aeronautics and Astronautics, Inc., New York. M
- Journal of Strain Analysis.* Joint British Committee for Stress Analysis; Institute of Mechanical Engineers, London. Q
- Journal of Structural Mechanics.* Marcel Dekker, Inc., New York. Q
- Journal of Testing and Evaluation* (formerly *Journal of Materials*). American Society for Testing and Materials, Philadelphia. BM
- Journal of the Astronautical Sciences.* American Astronautical Society, Inc., Washington, D.C. BM
- Journal of the Atmospheric Sciences.* American Meteorological Society, Boston. BM
- Journal of the Experimental Analysis of Behavior.* Society for the Experimental Analysis of Behavior, Inc., Indiana University, Bloomington, Ind. BM
- Journal of the Less-Common Metals.* Elsevier Sequoia S.A., Lausanne. M
- Journal of the Mechanics and Physics of Solids.* Pergamon Press, Ltd., Oxford. BM
- **Journal of Theoretical Biology.* Academic Press, Ltd., London. M
- Journal of Vacuum Science and Technology.* American Vacuum Society; American Institute of Physics, Inc., New York. BM
- JSME, Bulletin.* Japan Society of Mechanical Engineers, Tokyo. BM
- Karlsruhe, Universität, Institut für Strömungslehre und Strömungsmaschinen, Mitteilungen.* Verlag G. Braun, Karlsruhe, West Germany. Irreg.
- Kazanskii Aviatsonnyi Institut, Trudy, Seriya Radio-tehnika i Elektronika.* Kazanskii Aviatsonnyi Institut, Kazan. Irreg.
- Khimiia i Tekhnologiia Topliv i Masel.* Ministerstvo Neftpererabatyvaiushchei i Neftekhimicheskoi Promyshlennosti SSSR, Akademiia Nauk SSSR, and Nauchno-Tekhnicheskoe Obshchestvo Nef-tianoi i Gazovoi Promyshlennosti; Izdatel'stvo Khimiia, Moscow. M
- Kibernetika i Vychislitel'naia Tekhnika.* Akademiia Nauk Ukrainskoi SSR; Izdatel'stvo Naukova Dumka, Kiev. Irreg.
- Kleinheubacher Berichte.* Fernmeldetechnischer Zentralamt, Darmstadt, West Germany. Irreg.
- Kontrol'no-Izmeritel'naia Tekhnika.* Izdatel'stvo L'vovskogo Universiteta, Lvov. Irreg.
- Kosmicheskaiia Biologiia i Meditsina.* Ministerstvo Zdravookhraneniia SSSR; Izdatel'stvo Meditsina, Moscow. BM
- Kosmicheskii Issledovaniia.* Akademiia Nauk SSSR; Izdatel'stvo Nauka, Moscow. BM
- Kovové Materiály.* Slovenská Akademia Vied, Bratislava. BM
- Kraevye Zadachi dlia Differentsial'nykh Uravnenii.* Akademiia Nauk Uzbekskoi SSR, Institut Matematiki; Izdatel'stvo FAN, Tashkent. Irreg.
- Krymskaia Astrofizicheskaia Observatoriia, Izvestiia.* Akademiia Nauk SSSR; Izdatel'stvo Nauka, Moscow. BM
- Kvantovaia Elektronika.* Akademiia Nauk Ukrainskoi SSR, Institut Poluprovodnikov; Izdatel'stvo Naukova Dumka, Kiev. Irreg.
- Kybernetika.* Československá Akademie Věd, Prague. BM
- Kyoto University, Faculty of Engineering, Memoirs.* Kyoto University, Kyoto. Q
- Kyushu University, Faculty of Engineering, Memoirs.* Kyushu University, Fukuoka, Japan. Q
- Kyushu University, Research Institute for Applied Mechanics, Reports.* Kyushu University, Fukuoka, Japan. Irreg.
- **Laboratory Animal Science.* American Association for Laboratory Animal Science, Joliet, Ill.
- Laser* (see *Laser/Elektro-Optik*).
- Laser/Elektro-Optik* (formerly *Laser*). Fachschriften-verlag Aargauer Tagblatt AG, Aarau, Switzerland. BM
- Leningradskii Universitet, Vestnik, Matematika, Mekhanika, Astronomiia.* Izdatel'stvo Leningradskogo Universiteta, Leningrad. Q
- Letters in Applied and Engineering Sciences.* Pergamon Press, Ltd., Oxford. BM
- Lietuvos Fizikos Rinkinys.* Akademiia Nauk Litovskoi SSR; Izdatel'stvo Mintis, Vilnius. Q
- Lietuvos Matematikos Rinkinys.* Akademiia Nauk Litovskoi SSR; Izdatel'stvo Mintis, Vilnius. Q
- Life Sciences, Part II — Biochemistry, General and Molecular Biology.* Pergamon Press, Ltd., Oxford. SM
- Logistics Spectrum.* Society of Logistics Engineers, Los Angeles. Q
- Lubrication Engineering.* American Society of Lubrication Engineers, Park Ridge, Ill. M
- Machine Design.* Penton Publishing Co., Cleveland, Ohio. 31 issues per year
- Magnitnaia Gidrodinamika.* Akademiia Nauk Latvinskoi SSR; Izdatel'stvo Zinatne, Riga. Q
- Manufacturing Engineering Transactions.* Society of Manufacturing Engineers, Dearborn, Mich. Irreg.
- Marconi Review.* Marconi Co., Ltd., Chelmsford, Essex, England. Q
- Mashinostroenie.* Ministerstvo Vysshego i Srednego Spetsial'nogo Obrazovaniia SSSR; Izdanie Moskovskogo Tekhnicheskogo Uchilishcha imeni N. E. Baumana, Moscow. M
- Matematicheskaiia Fizika.* Akademiia Nauk Ukrainskoi SSR; Izdatel'stvo Naukova Dumka, Kiev. Irreg.
- Matematicheskii Institut imeni V. A. Steklova, Trudy.* Akademiia Nauk SSSR, Moscow. Irreg.
- Materialprüfung.* VDI-Verlag GmbH, Düsseldorf. M
- Materials Evaluation.* American Society for Non-destructive Testing, Inc., Evanston, Ill. M

- Materials Protection and Performance.* National Association of Corrosion Engineers, Houston, Tex. M
- Materials Research and Standards.* American Society for Testing and Materials, Philadelphia, Pa. M
- Mathematics of Computation.* American Mathematical Society, Providence, R.I. Q
- Mathematika.* University College, Dept. of Mathematics, London. SA
- Meccanica.* Italian Association of Theoretical and Applied Mechanics; Tamburini Editore, Milan. Q
- Mechanika Teoretyczna i Stosowana.* Polskie Towarzystwo Mechaniki Teoretycznej i Stosowanej; Państwowe Wydawnictwo Naukowe, Warsaw. Q
- Medical and Biological Engineering.* International Federation for Medical and Biological Engineering; Pergamon Press, Ltd., Oxford. BM
- Mekhanika Polimerov.* Akademiia Nauk Latvii skoi SSR; Izdatel'stvo Zinatne, Riga. BM
- Mekhanika Tverdogo Tela.* Akademiia Nauk SSSR; Izdatel'stvo Nauka, Moscow. Irreg.
- Mémoires Scientifiques de la Revue de Métallurgie.* Paris. M
- Mérés és Automatika.* Lapkiadó Vállalat, Budapest. M
- Messtechnik.* Friedr. Vieweg & Sohn GmbH, Braunschweig. M
- Metal Construction and British Welding Journal.* The Welding Institute, London. M
- Metal Progress.* American Society for Metals, Metals Park, Ohio. M
- Metal Science and Heat Treatment (Metallovedenie i Termicheskaiia Obrabotka Metallov).* Consultants Bureau, New York. BM
- Metal Science Journal.* Institute of Metals and Institution of Metallurgists, London. BM
- Metallofizika.* Akademiia Nauk Ukrainskoi SSR; Izdatel'stvo Naukova Dumka, Kiev. Irreg.
- Metallovedenie i Termicheskaiia Obrabotka Metallov.* Ministerstvo Stankostroitel'noi i Instrumental'noi Promyshlennosti SSSR and Nauchno-Tekhnicheskoe Obshchestvo Mashinostroitel'noi Promyshlennosti; Izdatel'stvo Mashinostroenie, Moscow. M
- Metallurgia Italiana.* Associazione Italiana di Metallurgia, Milan. M
- Metallurgical Transactions.* Metallurgical Society of the American Institute of Mining, Metallurgical and Petroleum Engineers, Inc., New York; American Society for Metals, Metals Park, Ohio. M
- Metals Engineering Quarterly.* American Society for Metals, Metals Park, Ohio. Q
- Meteoritics.* Meteoritical Society and Arizona State University Bureau of Publications, Tempe, Ariz. Q
- Meteorological Magazine.* Meteorological Office; Her Majesty's Stationery Office, London. M
- Meteorological Society of Japan, Journal.* Meteorological Society of Japan, c/o Japan Meteorological Agency, Tokyo. BM
- Meteorologiia i Gidrologiia.* Glavnoe Upravlenie Gidrometeorologicheskoi Sluzhby SSSR; Gidrometeoizdat, Moscow. M
- Meteorologische Rundschau.* Verband Deutscher Meteorologischer Gesellschaften; Springer Verlag, Berlin, West Germany. BM
- *Microchemical Journal.* Academic Press, Inc., New York. Q
- Microelectronics and Reliability.* Pergamon Press, Ltd., Oxford. BM
- *Micropaleontology.* American Museum of Natural History, New York. Q
- Microwave Journal.* Horizon House, Inc., Dedham, Mass. M
- MicroWaves.* Hayden Microwaves Corp., New York. M
- Middle East Technical University Journal of Pure and Applied Sciences.* Middle East Technical University, Ankara. 3 issues per year
- Mikroelektronika.* Izdatel'stvo Sovetskoe Radio, Moscow.
- Milano, Seminario Matematico e Fisico, Rendiconti.* Milano, Università, Milan. Annual
- Mitsubishi Denki Laboratory Reports.* Mitsubishi Electric Corp., Central Research Laboratory, Amagasaki, Hyogo Prefecture, Japan. Irreg.
- *Modern Geology.* Gordon & Breach Science Publishers, Ltd., London. Q
- *Monatshefte für Chemie.* Springer Verlag, Vienna. 6 issues per year
- Monthly Weather Review.* U. S. Weather Bureau; Supt. of Documents, Washington, D.C. M
- The Moon.* D. Reidel Publishing Co., Dordrecht, Netherlands. Q
- Moskovskii Universitet, Vestnik, Serii I — Matematika, Mekhanika.* Izdatel'stvo Moskovskogo Universiteta, Moscow. BM
- Moskovskii Universitet, Vestnik, Serii III — Fizika, Astronomiia.* Izdatel'stvo Moskovskogo Universiteta, Moscow. BM
- Nachrichtentechnische Zeitschrift.* Nachrichtentechnische Gesellschaft; VDE-Verlag GmbH, Berlin, West Germany. M
- Nagoya University, Faculty of Engineering, Memoirs.* Nagoya University, Nagoya. Irreg.
- National Academy of Sciences, Proceedings.* National Academy of Sciences, Washington, D.C. M
- *National Cancer Institute, Journal.* U.S. Dept. of Health, Education and Welfare; Supt. of Documents, Washington, D.C. M
- Nature.* Macmillan (Journals), Ltd., London. W
- Nature Physical Science.* Macmillan (Journals), Ltd., London. W
- Naturwissenschaftliche Rundschau.* Wissenschaftliche Verlagsgesellschaft mbH, Stuttgart, West Germany. M
- Naval Research Logistics Quarterly.* U.S. Navy, Office of Naval Research; Supt. of Documents, Washington, D.C. Q
- Naval Research Reviews.* U. S. Navy, Office of Naval Research; Supt. of Documents, Washington, D.C. M
- Navigation.* Institute of Navigation, Washington, D.C. Q
- Navigation (Paris).* Institut Français de Navigation, Paris. Q

- Neirofiziologiya.* Akademiia Nauk SSSR; Akademiia Nauk Ukrainkoi SSR; Izdatel'stvo Naukova Dumka, Kiev. BM
- New Mexico State University, Observatory, Contributions.* New Mexico State University, Las Cruces, N.M. Irreg.
- New Scientist.* New Science Publications, London. W
- New York Academy of Sciences, Annals.* New York Academy of Sciences, New York. Irreg.
- New York Academy of Sciences, Transactions, Series 2.* New York Academy of Sciences, New York. 8 issues per year
- Non-Destructive Testing.* IPC Science and Technology Press, Ltd., Guildford, Surrey, England. BM
- Nordrhein-Westfalen, Forschungsberichte.* Westdeutscher Verlag, Cologne, West Germany. Irreg.
- Note, Recensioni e Notizie.* Poste e Telecomunicazioni, Istituto Superiore, Rome. BM
- Nouvelle Revue d'Optique.* Masson & Cie., Editeurs, Paris. BM
- Nouvelle Revue d'Optique Appliquée.* Masson & Cie., Editeurs, Paris. BM
- Nuclear Engineering and Design.* North-Holland Publishing Co., Amsterdam. M
- Nuclear Fusion.* International Atomic Energy Agency, Vienna. Q
- **Nuclear Instruments and Methods.* North-Holland Publishing Co., Amsterdam. BW
- **Nuclear Physics.* North-Holland Publishing Co., Amsterdam. W
- Nuclear Science and Engineering.* American Nuclear Society, Inc., Hinsdale, Ill. M
- Nuclear Technology.* American Nuclear Society, Inc., Hinsdale, Ill. M
- Numerische Mathematik.* Springer Verlag, Berlin, West Germany. Irreg.
- Nuovo Cimento, Lettere.* Società Italiana di Fisica, Bologna. 36 issues per year.
- Nuovo Cimento, Rivista, Serie 2.* Società Italiana di Fisica; Editrice Compositori, Bologna. Q
- Nuovo Cimento, Sezione A.* Società Italiana di Fisica; Editrice Compositori, Bologna. 26 issues per year
- Nuovo Cimento, Sezione B.* Società Italiana di Fisica; Editrice Compositori, Bologna. 26 issues per year.
- The Observatory.* Royal Greenwich Observatory, Hailsham, Sussex, England. M
- L'Onde Electrique.* Société Française des Electroniciens et des Radioélectriciens; Editions Chiron S.A., Paris. M
- ONERA, TP.* Office National d'Etudes et de Recherches Aérospatiales, Châtillon-sous-Bagneux (Hauts-de-Seine), France. Irreg.
- Operations Research.* Operations Research Society of America, Baltimore, Md. BM
- Ophthalmic Research.* S. Karger AG, Basel. BM
- Optica Acta.* Taylor & Francis, Ltd., London. M
- Optical Engineering.* Society of Photo-Optical Instrumentation Engineers, Redondo Beach, Calif. BM
- Optical Sciences Center Newsletter.* University of Arizona, Optical Sciences Center, Tucson, Ariz. Irreg.
- Optical Society of America, Journal.* Optical Society of America, Inc., Washington, D.C.; American Institute of Physics, Inc., New York. M
- Optical Spectra.* Optical Publishing Co., Inc., Pittsfield, Mass. M
- Optics and Laser Technology.* Iliffe Science & Technology Publications, Ltd., Guildford, Surrey, England. Q
- Optics Communications.* North-Holland Publishing Co., Amsterdam. M
- Optika i Spektroskopiia.* Akademiia Nauk SSSR; Izdatel'stvo Nauka, Leningrad. M
- Orion.* Schweizerische Astronomische Gesellschaft, Schaffhausen, Switzerland. BM
- Ortung und Navigation.* Deutsche Gesellschaft für Ortung und Navigation, e.V., Düsseldorf, West Germany. Q
- Osaka Prefecture, University, Bulletin, Series A — Engineering and Natural Sciences.* University of Osaka Prefecture, Osaka, Japan. Irreg.
- Osaka University, Technology Reports.* Osaka University, Osaka, Japan. SA
- Österreichische Akademie der Wissenschaften, mathematisch-naturwissenschaftliche Klasse, Sitzungsberichte, Abteilung 2.* Österreichische Akademie der Wissenschaften; Springer Verlag, Vienna. Irreg.
- Otbor i Peredacha Informatsii.* Akademiia Nauk Ukrainkoi SSR; Izdatel'stvo Naukova Dumka, Kiev. Irreg.
- Oxidation of Metals.* Plenum Publishing Corp., New York. Q
- Papers in Meteorology and Geophysics.* Meteorological Research Institute, Tokyo. Q
- Perception and Psychophysics.* Psychonomic Journals, Inc., Austin, Tex. M
- Perceptual and Motor Skills.* Missoula, Mont. BM
- Periodica Polytechnica, Electrical Engineering.* Budapest, Technical University, Budapest. Q
- Periodica Polytechnica, Mechanical Engineering.* Budapest, Technical University, Budapest. Q
- Pflügers Archiv.* Springer Verlag, Berlin, West Germany.
- Philips Research Reports.* N. V. Philips' Gloeilampenfabrieken, Research Laboratories, Eindhoven. BM
- Philips Research Reports Supplements.* N. V. Philips' Gloeilampenfabrieken, Research Laboratories, Eindhoven. Irreg.
- Philips Technical Review.* N. V. Philips' Gloeilampenfabrieken, Research Laboratories, Eindhoven. M
- Philosophical Magazine, 8th Series.* Taylor & Francis, Ltd., London. M
- Photogrammetria.* International Society of Photogrammetry; Elsevier Publishing Co., Amsterdam. BM
- Photogrammetric Engineering.* American Society of Photogrammetry, Falls Church, Va. M

- Photographic Applications in Science, Technology and Medicine.* Photographic Applications in Science and Technology, Inc., New York. BM
- Physica.* Physica Foundation; North-Holland Publishing Co., Amsterdam. Irreg.
- Physica Scripta.* Royal Swedish Academy of Sciences; Almqvist & Wiksell Periodical Co., Stockholm. M
- Physica Status Solidi (A) — Applied Research.* Akademie-Verlag GmbH, Berlin; Academic Press, Inc., New York. 3 issues per year
- Physical Review A — General Physics, 3rd Series.* American Physical Society; American Institute of Physics, Inc., New York. M
- Physical Review B — Solid State, 3rd Series.* American Physical Society; American Institute of Physics, Inc., New York. SM
- Physical Review C — Nuclear Physics, 3rd Series.* American Physical Society; American Institute of Physics, Inc., New York. M
- Physical Review D — Particles and Fields, 3rd Series.* American Physical Society; American Institute of Physics, Inc., New York. SM
- Physical Review Letters.* American Physical Society, Inc., New York. W
- Physical Society of Japan, Journal.* Physical Society of Japan, Tokyo. M
- Physics in Medicine and Biology.* Hospital Physicists' Association; Taylor & Francis, Ltd., London. Q
- Physics Letters.* North-Holland Publishing Co., Amsterdam. W
- Physics Letters, Section C — Physics Reports.* North-Holland Publishing Co., Amsterdam. 1 vol. per year
- Physics of Fluids.* American Institute of Physics, Inc., New York. M
- Physics of the Earth and Planetary Interiors.* North-Holland Publishing Co., Amsterdam. BM
- Physics Today.* American Institute of Physics, Inc., New York. M
- **Physik in unserer Zeit.* Verlag Chemie GmbH, Weinheim, West Germany. BM
- **Physiologia Plantarum.* Scandinavian Society for Plant Physiology, Copenhagen. 4 vols. per year
- **Phytochemistry.* Pergamon Press, Ltd., Oxford. M
- Pisa, Scuola Normale Superiore, Annali, Scienze Fisiche e Matematiche.* Pisa, Scuola Normale Superiore, Pisa. Q
- Planetary and Space Science.* Pergamon Press, Ltd., Oxford. M
- Planseeberichte für Pulvermetallurgie/Powder Metallurgy Bulletin.* Metallwerk Plansee Aktiengesellschaft, Reutte, Austria. 3 issues per year
- **Plant Physiology.* American Society of Plant Physiologists, Washington, D.C. M
- **Planta.* Springer Verlag, Berlin, West Germany. Q
- Plasma Physics.* Pergamon Press, Ltd., Oxford. M
- PMM — Journal of Applied Mathematics and Mechanics (Prikladnaia Matematika i Mekhanika).* Pergamon Press, Ltd., Oxford. BM
- PMTF — Zhurnal Prikladnoi Mekhaniki i Tekhnicheskoi Fiziki.* Akademiia Nauk SSSR, Sibirskoe Otdelenie; Izdatel'stvo Nauka, Novosibirsk. BM
- Podstawy Sterowania.* Polska Akademia Nauk; Państwowe Wydawnictwo Naukowe, Warsaw. Q
- Point-to-Point Communication.* Marconi Communication Systems, Ltd., Chelmsford, England. 3 issues per year
- Pokroky Matematiky, Fyziky a Astronomie.* Československá Akademie Věd, Prague. BM
- Polish Academy of Sciences, Review.* Polska Akademia Nauk, Warsaw. Q
- Politechnika Czestochowska, Zeszyty Naukowe, Nauki Techniczne — Mechanika.* Wydawnictwa Politechniki Śląskiej, Gliwice. Irreg.
- Politechnika Śląska, Zeszyty Naukowe, Matematyka — Fizyka.* Wydawnictwa Politechniki Śląskiej, Gliwice. Irreg.
- Poluprovodnikovaia Tekhnika i Mikroelektronika.* Akademiia Nauk Ukrainskoi SSR; Izdatel'stvo Naukova Dumka, Kiev. Irreg.
- Poluprovodnikovye Pribory i ikh Primenenie.* Izdatel'stvo Sovetskoe Radio, Moscow. Irreg.
- Poluprovodnikovye Pribory v Tekhnike Elektrosvazi.* Izdatel'stvo Sviaz', Moscow. Irreg.
- Polymer Engineering and Science.* Society of Plastics Engineers, Inc., Greenwich, Conn. BM
- Pomiary, Automatyka, Kontrola.* Naczelna Organizacja Techniczna, Warsaw. M
- Poroshkovaia Metallurgii.* Akademiia Nauk Ukrainskoi SSR; Izdatel'stvo Naukova Dumka, Kiev. M
- Postępy Astronautyki.* Polskie Towarzystwo Astronautyczne, Lodz. Q
- Postępy Astronomii.* Polskie Towarzystwo Astronomiczne; Państwowe Wydawnictwo Naukowe, Warsaw. Q
- Postępy Fizyki.* Polskie Towarzystwo Fizyczne; Państwowe Wydawnictwo Naukowe, Warsaw. BM
- Priboroostroenie.* Ministerstvo Vysshego i Srednego Spetsial'nogo Obrazovaniia SSSR; Izdatel'stvo Leningradskogo Instituta Tochnoi Mekhaniki i Optiki, Leningrad. M
- Pribory i Sistemy Avtomatiki.* Izdatel'stvo Khar'kovskogo Gosudarstvennogo Universiteta, Kharkov. Irreg.
- Pribory i Tekhnika Eksperimenta.* Akademiia Nauk SSSR; Izdatel'stvo Nauka, Moscow. BM
- Prikladnaia Matematika i Mekhanika.* Akademiia Nauk SSSR, Izdatel'stvo Nauka, Moscow. BM
- Prikladnaia Mekhanika.* Akademiia Nauk Ukrainskoi SSR, Otdelenie Matematiki, Mekhaniki i Kibernetiki; Izdatel'stvo Naukova Dumka, Kiev. M
- Problemy Bioniki.* Khar'kovskii Gosudarstvennyi Universitet, Kharkov. Irreg.
- Problemy Difraksii i Rasprostraneniia Voln.* Izdatel'stvo Leningradskogo Universiteta, Leningrad. Irreg.
- Problemy Kosmicheskoi Fiziki.* Izdatel'stvo Kievskogo Universiteta, Kiev. Irreg.
- Problemy Prochnosti.* Akademiia Nauk Ukrainskoi SSR, Institut Problem Prochnosti; Izdatel'stvo Naukova Dumka, Kiev. M
- Problemy Tekhnicheskoi Elektrodinamiki.* Akademiia Nauk Ukrainskoi SSR; Izdatel'stvo Naukova Dumka, Kiev. Irreg.

- Proceedings of Vibration Problems.* Polska Akademia Nauk; Państwowe Wydawnictwo Naukowe, Warsaw. Q
- Progress of Theoretical Physics.* Research Institute for Fundamental Physics and The Physical Society of Japan; Kyoto University, Kyoto. M
- Protective Coatings on Metals (Zashchitnye Pokrytiia na Metallakh).* Consultants Bureau, New York. Irreg.
- **Psychological Review.* American Psychological Association, Inc., Washington, D.C. BM
- Psychonomic Science.* Psychonomic Journals, Inc., Austin, Tex. SM
- Psychonomic Society, Bulletin.* Psychonomic Society, Inc., Austin, Tex. M
- Public Administration Review.* American Society for Public Administration, Washington, D.C. BM
- Pulkovo, Glavnaia Astronomicheskaiia Observatoriia, Izvestiia.* Izdanie Glavnoi Astronomicheskoi Observatorii, Leningrad. Irreg.
- Pulkovo, Glavnaia Astronomicheskaiia Observatoriia, Trudy.* Izdanie Glavnoi Astronomicheskoi Observatorii, Leningrad. Irreg.
- Pure and Applied Chemistry.* International Union of Pure and Applied Chemistry; Butterworth & Co. (Publishers), Ltd., London. Irreg.
- Pure and Applied Geophysics.* Birkhäuser Verlag, Basel. BM
- Quality Progress.* American Society for Quality Control, Inc., Milwaukee, Wis. M
- Quarterly Journal of Mechanics and Applied Mathematics.* Oxford University Press, London. Q
- Quarterly of Applied Mathematics.* Brown University, Providence, R.I. Q
- **Radiation Research.* Academic Press, Inc., New York. 4 vols. per year
- Radio and Electronic Engineer.* Institution of Electronic and Radio Engineers, London. M
- Radio Engineering and Electronic Physics (Radiotekhnika i Elektronika).* Scripta Publishing Corp., Washington, D.C. M
- Radio Research Laboratories, Journal.* Ministry of Posts and Telecommunications, Radio Research Laboratories, Tokyo. BM
- Radio Research Laboratories, Review.* Ministry of Posts and Telecommunications, Radio Research Laboratories, Tokyo. Q
- Radio Science.* American Geophysical Union, Washington, D.C. M
- Radiobiologia — Radiotherapia.* VEB Verlag Volk und Gesundheit, Berlin, East Germany. BM
- Radioelektronika.* Ministerstvo Vysshego i Srednego Spetsial'nogo Obrazovaniia SSSR; Izdatel'stvo Kievskogo Politekhnikheskogo Instituta, Kiev. M
- Radiofizika.* Ministerstvo Vysshego i Srednego Spetsial'nogo Obrazovaniia SSSR; Izdanie Gor'kovskogo Universiteta, Gorki. M
- **Radiology.* Radiological Society of North America, Inc., Syracuse, N.Y. M
- Radiotekhnika.* Nauchno-Tekhnicheskoe Obshchestvo Radiotekhniki i Elektrosviazi; Izdatel'stvo Sviaz', Moscow. M
- Raumfahrtforschung.* Deutsche Gesellschaft für Luft- und Raumfahrt, e.V., Stuttgart, West Germany. BM
- RCA Review.* RCA Research and Engineering, Princeton, N.J. Q
- La Recherche.* Société d'Editions Scientifiques, Paris. M
- La Recherche Aéronautique.* Office National d'Etudes et de Recherches Aéronautiques, Châtillon-sous-Bagneux (Hauts-de-Seine), France. BM
- La Recherche Spatiale.* Centre National d'Etudes Spatiales; Dunod Editeur, Paris. M
- Remote Sensing of Environment.* American Elsevier Publishing Co., Inc., New York. Q
- Report of Ionosphere and Space Research in Japan.* Science Council of Japan, Ionosphere Research Committee, Tokyo. Q
- Research Management.* Industrial Research Institute, Inc.; Interscience Publishers, New York. BM
- Respiration Physiology.* North-Holland Publishing Co., Amsterdam. BM
- Review of Scientific Instruments.* American Institute of Physics, Inc., New York. M
- Reviews of Geophysics and Space Physics.* American Geophysical Union, Washington, D.C. Q
- Reviews of Modern Physics.* American Physical Society; American Institute of Physics, Inc., New York. Q
- Revista Brasileira de Fisica.* Sociedade Brasileira de Fisica, São Paulo, Brazil. 3 issues per year
- Revista de Aeronáutica y Astronáutica.* Ministerio del Aire, Madrid. M
- Revue de Médecine Aéronautique et Spatiale.* Société Française de Physiologie et de Médecine Aéronautique et Cosmonautique; Masson & Cie., Paris. Q
- Revue de Métallurgie.* Paris. M
- Revue de Physique Appliquée.* Société Française de Physique, Paris. M
- Revue des Corps de Santé des Armées.* Centre de Recherches du Service de Santé des Armées, Paris. BM
- **Revue Française d'Automatique, Informatique et de Recherche Opérationnelle.* Dunod Editeur, Paris. M
- Revue Française de Droit Aérien.* Société Française de Droit Aérien et Spatial, Paris. Q
- Revue Française de Mécanique.* Société Française des Mécaniciens, Paris. Q
- Revue Générale de l'Air et de l'Espace.* Editions Internationales, Paris. Q
- Revue Internationale des Hautes Températures et des Réfractaires.* Société Nationale Française des Hautes Températures et des Réfractaires; Masson & Cie., Paris. Q
- Revue Roumaine de Mathématiques Pures et Appliquées.* Académie de la République Socialiste Roumaine, Bucharest. 10 issues per year
- Revue Roumaine de Physique.* Académie de la République Socialiste Roumaine, Bucharest. BM

- Revue Roumaine des Sciences Techniques, Série de Mécanique Appliquée.* Académie de la République Socialiste Roumaine, Bucharest. BM
- Revue Scientifique et Technique CECLES/CERS.* Gauthier-Villars, Paris. Q
- Revue Technique Thomson — CSF.* Thomson — CSF, Service de Documentation Technique; Masson & Cie., Paris. Q
- Ricerche Astronomiche.* Specola Vaticana, Vatican City. Irreg.
- Rivista Aeronautica.* Rome. M
- Rivista di Meteorologia Aeronautica.* Servizio Meteorologico dell'Aeronautica, Rome. Q
- Rivista Italiana di Geofisica.* Associazione Geofisica Italiana, Genoa. 3 issues per year
- Royal Astronomical Society, Memoirs.* Royal Astronomical Society; Blackwell Scientific Publications, Oxford. 4 issues per year
- Royal Astronomical Society, Monthly Notices.* Royal Astronomical Society, London; Blackwell Scientific Publications, Oxford. M
- Royal Astronomical Society, Quarterly Journal.* Royal Astronomical Society, London; Blackwell Scientific Publications, Oxford. Q
- Royal Astronomical Society of Canada, Journal.* Royal Astronomical Society of Canada, Toronto. BM
- Royal Institution of Great Britain, Proceedings.* Royal Institution of Great Britain; Applied Science Publishers, Ltd., London. Annual
- Royal Meteorological Society, Quarterly Journal.* Royal Meteorological Society, London. Q
- Royal Society (Edinburgh), Proceedings, Section A.* Royal Society of Edinburgh, Edinburgh. Irreg.
- Royal Society (London), Philosophical Transactions, Series A.* Royal Society, London. Irreg.
- Royal Society (London), Proceedings, Series A.* Royal Society, London. Irreg.
- Rozprawy Inżynierskie.* Polska Akademia Nauk, Instytut Podstawowych Problemów Techniki; Państwowe Wydawnictwo Naukowe, Warsaw. Q
- SAE Aerospace Information Report.* Society of Automotive Engineers, Inc., New York. Irreg.
- SAE Aerospace Recommended Practice.* Society of Automotive Engineers, Inc., New York. Irreg.
- SAFE Engineering.* Survival and Flight Equipment Association; Value Engineering Publications, Inc., Los Angeles. BM
- Samoletostroenie i Tekhnika Vozdushnogo Flota.* Izdanie Khar'kovskogo Gosudarstvennogo Universiteta, Kharkov. Irreg.
- SAMPE Quarterly.* Society of Aerospace Material and Process Engineers, Azusa, Calif. Q
- Schweizer Archiv.* Schweizer Verband für die Materialprüfungen und Schweizerische Gesellschaft für Vakuumphysik und Technik; Verlag Vogt-Schild AG, Solothurn, Switzerland. M
- Schweizerische Technische Zeitschrift.* Schweizer Technischer Verband, Zurich. M
- Science.* American Association for the Advancement of Science, Washington, D.C. W
- Science Progrès Découverte.* Société des Ingénieurs Civils de France; Dunod Editeur, Paris. M
- Science Progress.* Blackwell Scientific Publications, Ltd., Oxford. Q
- Sciences et Techniques.* Société des Ingénieurs Civils de France, Paris. M
- Sciences et Techniques de l'Armement.* Ministère d'Etat Chargé de la Défense Nationale, Paris. Q
- Scientia Sinica.* Science Press, Peking. Irreg.
- Scientific American.* Scientific American, Inc., New York. M
- Scripta Metallurgica.* Pergamon Press, Inc., New York. M
- Secrétariat Général à l'Aviation Civile, Revue.* Secrétariat Général à l'Aviation Civile, Paris. Irreg.
- Seminar po Kraevym Zadacham, Trudy.* Izdatel'stvo Kazanskogo Universiteta, Kazan. Irreg.
- Shell Aviation News.* Shell Oil Co., London. M
- Shock and Vibration Digest.* The Shock and Vibration Information Center, Naval Research Laboratory, Washington, D.C. M
- SIAM Journal on Applied Mathematics.* Society for Industrial and Applied Mathematics, Philadelphia, Pa. 8 issues per year
- SIAM Journal on Control.* Society for Industrial and Applied Mathematics, Philadelphia, Pa. Q
- SIAM Journal on Mathematical Analysis.* Society for Industrial and Applied Mathematics, Philadelphia, Pa. 8 issues per year
- SIAM Journal on Numerical Analysis.* Society for Industrial and Applied Mathematics, Philadelphia, Pa. Q
- SIAM Review.* Society for Industrial and Applied Mathematics, Philadelphia, Pa. Q
- Siemens Forschungs- und Entwicklungsberichte.* Siemens Aktiengesellschaft; Springer Verlag, Berlin, West Germany. Q
- Siemens-Zeitschrift.* Siemens Aktiengesellschaft, Berlin, West Germany. M
- Signal.* Armed Forces Communications and Electronics Association, Washington, D.C. M
- Simulation.* Simulation Councils, Inc., La Jolla, Calif. M
- Sinteticheskie Almazы.* Gosudarstvennyi Planovyi Komitet Soveta Ministrov Ukrainskoi SSR; Ukrainskii Nauchno-Issledovatel'skii Konstruktor-sko-Tekhnologicheskii Institut Sinteticheskikh Sverkhtrudnykh Materialov i Instrumenta; Ukrainskii Nauchno-Issledovatel'skii Institut Nauchno-Tekhnicheskoi Informatsii i Tekhniko-Ekonomicheskikh Issledovaniy, Kiev. Irreg.
- Sky and Telescope.* Sky Publishing Corp., Cambridge, Mass. M
- Skyline.* North American Rockwell Corp., El Segundo, Calif. Q
- Slaboproudý Obzor.* Státní Nakladatelství Technické Literatury, Prague. M
- SMPTE, Journal.* Society of Motion Picture and Television Engineers, Inc., New York. M
- Società Astronomica Italiana, Memorie.* Gia Società degli Spettroscopisti Italiani, Milan. Q
- Société Royale des Sciences de Liège, Bulletin.* Société Royale des Sciences de Liège: Université de Liège, Liege. Irreg.

- Société Royale des Sciences de Liège, Mémoires.* Société Royale des Sciences de Liège; Université de Liège, Liège. Q
- Society for Experimental Biology and Medicine, Proceedings.* Society for Experimental Biology and Medicine, New York. 11 issues per year
- Society for Information Display, Proceedings.* Society for Information Display; Western Periodicals Co., North Hollywood, Calif. Q
- Society of Environmental Engineers, Journal.* Society of Environmental Engineers, London. Q
- Society of Experimental Test Pilots, Technical Review.* Society of Experimental Test Pilots, Lancaster, Calif. SA
- **Society of Rheology, Transactions.* Interscience Publishers, New York. SA
- **Soil Biology and Biochemistry.* Pergamon Press, Ltd., Oxford. Q
- Solar Energy.* International Solar Energy Society, Victoria, Australia; Pergamon Press, Ltd., Oxford. Q
- Solar Physics.* D. Reidel Publishing Co., Dordrecht, Netherlands. M
- Solar System Research (Astronomicheskii Vestnik).* Consultants Bureau, New York. Q
- Solid-State Electronics.* Pergamon Press, Ltd., Oxford. M
- Soprotivlenie Materialov i Teoriia Sooruzhenii.* Izdatel'stvo Budivelnik, Kiev. Irreg.
- Sound and Vibration.* Acoustical Publications, Inc., Cleveland, Ohio. M
- Soviet Astronomy (Astronomicheskii Zhurnal).* American Institute of Physics, Inc., New York. BM
- Soviet Journal of Nondestructive Testing (Defektoskopiia).* Consultants Bureau, New York. BM
- Soviet Journal of Optical Technology (Optiko-Mekhanicheskaiia Promyshlennost').* Optical Society of America, Inc., Washington, D.C.; American Institute of Physics, Inc., New York. M
- Soviet Journal of Quantum Electronics (Kvantovaiia Elektronika /Moscow/).* American Institute of Physics, Inc., New York. BM
- Soviet Physics — Acoustics (Akusticheskii Zhurnal).* American Institute of Physics, Inc., New York. Q
- Soviet Physics — Doklady (Akademiia Nauk SSSR, Doklady).* American Institute of Physics, Inc., New York. M
- Soviet Physics — JETP (Zhurnal Eksperimental'noi i Teoreticheskoi Fiziki).* American Institute of Physics, Inc., New York. M
- Soviet Physics — Technical Physics (Zhurnal Tekhnicheskoi Fiziki).* American Institute of Physics, Inc., New York. M
- Soviet Physics — Uspekhi (Uspekhi Fizicheskikh Nauk).* American Institute of Physics, Inc., New York. BM
- Soviet Science Review.* IPC Science and Technology Press, Ltd., Guildford, Surrey, England. BM
- Space Life Sciences.* D. Reidel Publishing Co., Dordrecht, Netherlands. Q
- Space Science Reviews.* D. Reidel Publishing Co., Dordrecht, Netherlands. 9 issues per year
- Spaceflight.* British Interplanetary Society, London. M
- SPARMO Bulletin.* Solar Particles and Radiation Monitoring Organization, Meudon (Hauts-de-Seine), France. Irreg.
- Sperry Technology.* Sperry Rand Corp., New York. Q
- Sterne und Weltraum.* Verlag Bibliographisches Institut AG, Mannheim, West Germany. M
- **Strahlentherapie.* Urban & Schwarzenberg, Munich. SA
- Strain.* British Society for Strain Measurement, London. Q
- Strength of Materials (Problemy Prochnosti).* Consultants Bureau, New York. Q
- Studia Geophysica et Geodaetica.* Československá Akademie Věd, Prague. Q
- Studies in Applied Mathematics.* MIT Press, Cambridge, Mass. Q
- Studii și Cercetări de Astronomie.* Academia Republicii Socialiste Române, Bucharest. SA
- Studii și Cercetări de Fizică.* Academia Republicii Socialiste Române, Bucharest. 10 issues per year
- Studii și Cercetări de Mecanică Aplicată.* Academia Republicii Socialiste Române, Bucharest. BM
- Studii și Cercetări Matematice.* Academia Republicii Socialiste Române, Bucharest. 10 issues per year
- Surface Science.* North-Holland Publishing Co., Amsterdam. M
- Systems, Computers, Controls (Denshi Tsushin Gakkai Ronbunshi).* Institute of Electronics and Communication Engineers of Japan; Scripta Publishing Corp., Washington, D.C. BM
- Tech Air.* Society of Licensed Aircraft Engineers and Technologists, Kingston-upon-Thames, England. M
- Technische Rundschau Sulzer.* Gebrüder Sulzer, Aktiengesellschaft, Winterthur, Switzerland. 2 issues per year
- Technika Lotnicza i Astronautyczna.* Stowarzyszenie Inżynierów i Techników Mechaników Polskich, Sekcja Lotnicza; Naczelna Organizacja Techniczna, Warsaw. M
- Technisch-ökonomische Informationen der zivilen Luftfahrt.* Hauptverwaltung der Zivilen Luftfahrt, Zentralflughafen Berlin-Schönefeld, East Germany. M
- Technische Mitteilungen Krupp, Forschungsberichte.* Fried. Krupp GmbH, Essen, West Germany.
- Technische Rundschau Sulzer, Forschungsheft.* Gebrüder Sulzer, Aktiengesellschaft, Winterthur, Switzerland. Annual
- Technological Forecasting and Social Change.* American Elsevier Publishing Co., Inc., New York. Q
- Technology Review.* Massachusetts Institute of Technology, Cambridge, Mass. 9 issues per year
- **Tectonophysics.* Elsevier Publishing Co., Amsterdam. M
- Teknisk Tidskrift.* Svenska Teknologföreningen, Stockholm. W
- Telecommunications and Radio Engineering. Part I — Telecommunications, Part II — Radio Engineering (Elektrosviaz', Radiotekhnika).* Scripta Publishing Corp., Washington, D.C. M

- Telemetry Journal*. International Foundation for Telemetering; Value Engineering Publications, Inc., Los Angeles. BM
- Tellus*. Svenska Geofysiska Föreningen, Stockholm; Almqvist & Wiksells Boktryckeri AB, Uppsala. BM
- Teoreticheskaia i Matematicheskaia Fizika*. Akademiia Nauk SSSR; Izdatel'stvo Nauka, Moscow. M
- Teoriia Sluchainykh Protsesov*. Akademiia Nauk Ukrainskoi SSR; Izdatel'stvo Naukova Dumka, Kiev. Irreg.
- Teoriia Veroiatnostei i ee Primeneniia*. Akademiia Nauk SSSR; Izdatel'stvo Nauka, Moscow. Q
- Teplotfizika i Teplotekhnika*. Akademiia Nauk Ukrainskoi SSR; Izdatel'stvo Naukova Dumka, Kiev. Irreg.
- Teplotfizika Vysokikh Temperatur*. Akademiia Nauk SSSR; Izdatel'stvo Nauka, Moscow. BM
- Teplovye Napriazheniia v Elementakh Konstruktsii*. Akademiia Nauk Ukrainskoi SSR, Institut Mekhaniki; Izdatel'stvo Naukova Dumka, Kiev. Irreg.
- **La Termotecnica*. Associazione Termotecnica Italiana, Milan. M
- Thermochimica Acta*. Elsevier Publishing Co., Amsterdam. BM
- Thin Solid Films*. Elsevier Sequoia S. A., Lausanne. M
- Tohoku University, Institute of High Speed Mechanics, Reports*. Tohoku University, Sendai. Irreg.
- Tohoku University, Research Institute for Strength and Fracture of Materials, Reports*. Tohoku University, Sendai. Irreg.
- Tohoku University, Research Institute of Electrical Communication, Reports*. Tohoku University, Sendai.
- Tokyo, University, Faculty of Engineering, Journal, Series B*. Tokyo, University, Faculty of Engineering, Tokyo. Irreg.
- Tokyo, University, Institute of Space and Aeronautical Science, Bulletin*. Tokyo, University, Institute of Space and Aeronautical Science, Tokyo. Q
- Tokyo, University, Institute of Space and Aeronautical Science, Report*. Tokyo, University, Institute of Space and Aeronautical Science, Tokyo. Irreg.
- Tokyo, University, Tokyo Astronomical Observatory, Annals, Second Series*. Tokyo, University, Tokyo. Irreg.
- Tokyo Astronomical Observatory, Tokyo Astronomical Bulletin, Second Series*. Tokyo Astronomical Observatory, Tokyo. Q
- Tokyo Institute of Technology, Bulletin*. Tokyo Institute of Technology, Tokyo. Irreg.
- Torino, Accademia delle Scienze, Classe di Scienze Fisiche, Matematiche e Naturali, Atti*. Torino, Accademia delle Scienze, Turin. Irreg.
- Toshiba Review*. Tokyo Shibaura Electric Co., Ltd., Tokyo. BM
- Transport Theory and Statistical Physics*. Marcel Dekker, Inc., New York. Q
- Transporturi Auto, Navale și Aeriene*. Ministerul Transporturilor and Consiliul National al Inginerilor și Technicienilor, Bucharest. M
- Trend in Engineering*. Office of Engineering Research, University of Washington, Seattle. Q
- Tsvetnaia Metallurgii*. Ministerstvo Vysshogo i Srednego Spetsial'nogo Obrazovaniia SSSR; Izdanie Severokavkazskogo Gornometallurgicheskogo Instituta, Ordzhonikidze. BM
- Ukrains'kii Fizichnii Zhurnal*. Akademiia Nauk Ukrainskoi SSR, Kiev. M
- Ukrainskii Matematicheskii Zhurnal*. Akademiia Nauk Ukrainskoi SSR; Izdatel'stvo Naukova Dumka, Kiev. BM
- Ultrasonics*. Iliffe Science & Technology Publications, Ltd., Guildford, Surrey, England. Q
- Unione Matematica Italiana, Bollettino*. Nicola Zanichelli Editore, Bologna. BM
- Universitas Comeniana, Acta Facultatis Rerum Naturalium — Mathematica*. Slovenské Pedagogické Nakladateľstvo, Bratislava. Irreg.
- Uprugost' i Neuprugost'*. Izdatel'stvo Moskovskogo Universiteta, Moscow. Irreg.
- Uspekhi Fizicheskikh Nauk*. Akademiia Nauk SSSR; Izdatel'stvo Nauka, Moscow. M
- Uspekhi Fiziologicheskikh Nauk*. Izdatel'stvo Nauka, Moscow. Q
- **Vakuum-Technik*. Rudolf A. Lang, Wiesbaden, West Germany.
- VDI-Forschungsheft*. Verein Deutscher Ingenieure; VDI-Verlag GmbH, Düsseldorf. SM
- VDI-Z*. Verein Deutscher Ingenieure; VDI-Verlag GmbH, Düsseldorf. SM
- VDI-Z Fortschritt-Berichte, Reihe 7 — Strömungstechnik*. Verein Deutscher Ingenieure; VDI-Verlag GmbH, Düsseldorf. Irreg.
- Vertiflite*. American Helicopter Society, Inc., New York. BM
- Le Vide*. Société Française des Ingénieurs et Techniciens du Vide, Paris. BM
- Vilnius, Astronomijos Observatorijos, Biuletėnis*. Vilnius. Irreg.
- Vision Research*. Pergamon Press, Ltd., Oxford. M
- Voenno-Meditsinskii Zhurnal*. Tsentral'noe Voenno-Meditsinskoe Upravlenie Ministerstva Oborony SSSR; Izdatel'stvo Krasnaia Zvezda, Moscow. M
- Voprosy Dinamiki i Prochnosti*. Rizhskii Politehnicheskii Institut; Izdatel'stvo Zinatne, Riga. Irreg.
- Voprosy Teorii Plazmy*. Atomizdat, Moscow. Irreg.
- Vychislitel'naia i Prikladnaia Matematika*. Izdatel'stvo Kievskogo Universiteta, Kiev. Irreg.
- Vychislitel'naia Tekhnika i Voprosy Kibernetiki*. Leningradskii Gosudarstvennyi Universitet, Vychislitel'nyi Tsentr; Izdatel'stvo Moskovskogo Universiteta, Moscow. Irreg.
- Vychislitel'naia Tekhnika v Mashinostroenii*. Akademiia Nauk BSSR, Institut Tekhnicheskoi Kibernetiki, Minsk. Irreg.
- Vychislitel'nye Metody i Programirovanie*. Izdatel'stvo Moskovskogo Universiteta, Moscow. Irreg.

- Wärme- und Stoffübertragung.* Springer Verlag, Berlin, West Germany. Q
- Wear.* Elsevier Sequoia S.A., Lausanne. M
- **Weatherwise.* American Meteorological Society, Boston. BM
- Wehrmedizinische Monatsschrift.* J. F. Lehmanns Verlag, Munich. M
- Welding Journal.* American Welding Society, New York. M
- Welding Production (Svarochnoe Proizvodstvo).* Welding Institute, Cambridge. M
- Welding Research International.* The Welding Institute, Cambridge. Q
- Westinghouse Engineer.* Westinghouse Electric Corp., Pittsburgh, Pa. BM
- Wissenschaftliche Berichte AEG-Telefunken.* AEG-Telefunken, Berlin, West Germany. Q
- Wissenschaftliche Zeitschrift.* Dresden, Technische Universität, Dresden, East Germany. BM
- WRC Bulletin.* Welding Research Council, New York. 10 issues per year
- Zastosowania Matematyki.* Polska Akademia Nauk, Instytut Matematyczny; Państwowe Wydawnictwo Naukowe, Warsaw. 3 issues per year
- **Zeitschrift für Anatomie und Entwicklungsgeschichte.* Springer Verlag, Berlin, West Germany. 8 issues per year
- Zeitschrift für angewandte Mathematik und Mechanik.* Akademie-Verlag GmbH, Berlin, East Germany. M
- Zeitschrift für angewandte Mathematik und Physik.* Birkhäuser Verlag, Basel. BM
- Zeitschrift für elektrische Informations- und Energietechnik.* Akademische Verlagsgesellschaft Geest & Portig, KG, Leipzig, East Germany.
- Zeitschrift für experimentelle und angewandte Psychologie.* Deutsche Gesellschaft für Psychologie; Verlag für Psychologie, Göttingen. Q
- Zeitschrift für Flugwissenschaften.* Deutsche Gesellschaft für Luft- und Raumfahrt, e.V., and Deutsche Forschungs- und Versuchsanstalt für Luft- und Raumfahrt, e.V.; Friedr. Vieweg & Sohn GmbH, Braunschweig. M
- Zeitschrift für Geophysik.* Deutsche geophysikalische Gesellschaft, Hamburg; Physica-Verlag, Würzburg, West Germany. BM
- Zeitschrift für Luftrecht und Weltraumrechtsfragen.* Köln, Universität, Institut für Luftrecht und Weltraumrechtsfragen; Carl Heymanns Verlag, KG, Cologne. Q
- Zeitschrift für Metallkunde.* Deutsche Gesellschaft für Metallkunde, e.V.; Riederer-Verlag GmbH, Stuttgart, West Germany. M
- Zeitschrift für Meteorologie.* Meteorologische Gesellschaft; Akademie-Verlag GmbH, Berlin, East Germany. Irreg.
- Zeitschrift für Naturforschung, Teil a.* Verlag der Zeitschrift für Naturforschung, Tübingen. M
- Zeitschrift für Physik.* Deutsche physikalische Gesellschaft; Springer Verlag, Berlin, West Germany. Irreg.
- Zeitschrift für Werkstofftechnik.* Verlag Chemie GmbH, Weinheim, West Germany. 8 issues per year
- Zemlia i Vselennaiia.* Akademiia Nauk SSSR; Izdatel'stvo Nauka, Moscow. BM
- Zhurnal Eksperimental'noi i Teoreticheskoi Fiziki.* Akademiia Nauk SSSR; Izdatel'stvo Nauka, Moscow. M
- Zhurnal Prikladnoi Spektroskopii.* Izdatel'stvo Nauka i Tekhnika, Minsk. M
- Zhurnal Tekhnicheskoi Fiziki.* Akademiia Nauk SSSR; Izdatel'stvo Nauka, Leningrad. M
- Zhurnal Vychislitel'noi Matematiki i Matematicheskoi Fiziki.* Akademiia Nauk SSSR; Izdatel'stvo Nauka, Moscow. BM
- Zhurnal Vysshei Nervnoi Deiatel'nosti.* Akademiia Nauk SSSR; Izdatel'stvo Nauka, Moscow. BM
- Zpráva VZLÚ.* Výzkumný a Zkušební Letecký Ústav, Prague. Irreg.
- Zpravodaj VZLÚ.* Výzkumný a Zkušební Letecký Ústav, Prague. BM

Either a Notation of Content or the actual title of the publication appears under each subject heading. They are listed under several subject headings which provide multiple access to the subject of each accession. The *IAA* accession number is located under and to the right of the *NOC* or the title. It is preceded by numbers identifying the issue and page of *International Aerospace Abstracts* where the accession is located.

To illustrate:

Issue Number	Page Number	Accession Number
01	p74	A73-10106

A

A STARS

A study of the spectrum-variable silicon Ap star 56 Ari. 01 p0106 A73-11305

The Os-Pt-Hg abundance peak in Ap stars and the problem of very heavy cosmic rays. 02 p0210 A73-12733

Statistical fractions of variable A and F stars, considering main sequence stars, giants, subgiants and open clusters NGC 2548, Praesepe and Coma. 02 p0226 A73-12834

Radial velocity and microturbulence dependence on excitation potential and time in a type supergiants atmosphere, deriving chemical composition. 03 p0371 A73-13215

A-type supergiants - A list of line intensities and radial velocity measurements. 03 p0375 A73-13950

HD 215441 and 53 Camelopardalis - Intrinsic polarization of H-beta and the continuum. 07 p0874 A73-19075

Revised chemical abundances of four population-II A-type stars. 08 p1006 A73-20932

Comparison of telescope magnitudes with model-atmosphere predictions for A, F, and G supergiants. 09 p1142 A73-22030

Spectrophotometric investigation of the star alpha-2 CVn. II. 11 p1416 A73-25232

Electric conductivity in the atmosphere of early-type stars. 11 p1427 A73-26575

Landstreet null line list revision and null lines tabulation to identify spectra of magnetic Ap star atmospheres. 14 p1801 A73-30647

Primordial cosmic ray abundance from rotating magnetic A stars with accelerating ionized interstellar gas particles. 15 p1925 A73-31059

Stellar atmospheric conditions taking into account A5 and early stars, considering spectral characteristics, absorption spectra and spectrum prediction. 15 p1932 A73-31305

Changes of the Balmer-series lines of hydrogen in the spectrum of the spectrally variable silicon Ap star CU Vir. 16 p2057 A73-32711

Nature of the light variation of the peculiar A-star HD 221568. 16 p2058 A73-32836

Studies of beta Coronae Borealis. I - Identification

of the Actinides. 18 p2357 A73-37105

Radial velocity fluctuations of the Ap star HD 224801. 20 p2607 A73-39083

The peculiar A stars and the origin of the heaviest chemical elements. 20 p2611 A73-39623

Analysis of the ultraviolet spectrum of A-type stars observed by the OAO II satellite. 22 p2907 A73-42301

Spectral variabilities of magnetic peculiar A stars associated with atmospheric chemical composition anomalies, using inclined rotator model. 22 p2908 A73-42345

Line identifications, elemental abundances, and equivalent widths for 21 sharp-lined cool peculiar A stars and two comparison standards. 23 p3028 A73-43491

A-11 SATELLITE

U ECHO 1 SATELLITE

A-12 SATELLITE

U ECHO 2 SATELLITE

A-4 AIRCRAFT

Surface effect take-off and landing system for high performance aircraft. 19 p2382 A73-37695

Air cushion landing system twin pod (A/CLS) configuration design and test installation on A-4 Navy fighter. 19 p2383 A73-37702

A-7 AIRCRAFT

Aerospace multiprocessor for A-7D aircraft digital fly by wire flight control, discussing design requirements, software development and reliability. 17 p2107 A73-35223

A-300 AIRCRAFT

Maximum safety hydraulic systems for A300B airbus powered flight for normal flying and auto land operations. 04 p0409 A73-16031

Optimization and design of the rear fuselage of the A 300 B aircraft structure. 10 p1288 A73-23799

A-300 B airbus active and passive operational monitoring systems, considering visual and aural routine functional indicators, emergency warning devices and flight data recorders. 15 p1830 A73-32458

The safety, the reliability, and redundancy in the automatic flight control system of the A300-B Airbus. 15 p1830 A73-32459

ARINC-573 recording system - Application to maintenance. 15 p1883 A73-32462

Minicomputer application to in-flight control of A300-B airbus engines, describing computational procedure for low pressure compressor stage RPM limit /N 1 limit/. 15 p1831 A73-32477

Development of the A300B wide-body twin. [SAE PAPER 730353] 17 p2102 A73-34701

The aerodynamic development of the wing of the A 300B. 21 p2633 A73-41192

ABBREVIATIONS

U SYMBOLS

ABDOMEN

Severe intraabdominal injuries without abdominal protective rigidity after an air crash - Seat belt injury. 20 p2517 A73-39209

ABEL FUNCTION

Conditions for localization of Cesaro's rectangular means and of Abel's method means in the limited summing of a multiple trigonometric Fourier series in the Liouville classes. 01 p0071 A73-11439

Incompressible plane flow subject to infinitely small vibrations, expressing complex potential as Abelian integral [JONERA, TP NO. 1191] 04 p0472 A73-15993

ABERRATION

Schmidt and Maksutov spectrographic cameras, discussing correcting devices for mirror aberrations. 01 p0047 A73-10512

General analysis of aplanatic Cassegrain, Gregorian, and Schwarzschild telescopes. 03 p0309 A73-14426

Design and field tests of astronomical optical theodolite, noting latitude, longitude and azimuth determination and objective aberration. 04 p0447 A73-14849

Thermal defocusing of high intensity continuous Ar laser radiation in absorbing medium with allowance for spherical aberrations. 04 p0458 A73-15562

Evaluation of the wavefront aberration in holography. 08 p0963 A73-21013

Aberrations, astigmatism and coma control for far UV stellar spectrograph design by grating shape and ruling space modification. 08 p0972 A73-21752

Range-azimuth-coupling aberrations in pulse-scanned imaging systems. 10 p1188 A73-23833

The detection and resolution of incoherent objects by an aberrated optical system in the presence of background noise. 10 p1229 A73-24618

Solid ultrasonic cylindrical lens design for off-axis aberration minimization for focusing properties improvement, using method analogous to chromatic aberration correction in optics. 13 p1612 A73-28491

Ray optics model analysis for spherical aberration effects on acoustic hologram resolution in image reconstruction, discussing computer generated correction for quality improvement. 13 p1615 A73-28591

Ultrasonic acoustic holography for wave source and object in relative motion, predicting reconstructed image aberration elimination performance in point-by-point mapping technique. 13 p1616 A73-28597

Eikonal properties for real rays chromatic aberration formulas in terms of path length, image space and lens parameters. 13 p1660 A73-28768

Holographic imaging and aberrations due to an incorrectly repositioned hologram in a system with lenses having aberrations. 15 p1915 A73-31015

Chromatic aberration effects on inelastic image resolution for high voltage electron microscopes. 21 p2702 A73-40789

Main-mirror aberrations in a variable-profile antenna and beam scanning by displacement of the primary radiating element. 21 p2667 A73-41446

The imaging properties and aberrations of thick transmission holograms. 22 p2864 A73-43185

Optical system imaging in partially coherent light, noting Rayleigh criterion insensitivity to aberration as characteristic of two-point resolution criteria. 22 p2889 A73-43187

On separating aberrant effects from random scattering effects in radio telescopes. 23 p2958 A73-43379

ABIOTENESIS

Evolution from amino acids - Lunar occurrence of their precursors. 01 p0008 A73-10249

Chemical evolution under the bion hypothesis. 03 p0265 A73-14316

Concepts related to the origin of the genetic apparatus. 03 p0265 A73-14317

Protobiochemical developments in terms of extraterrestrial life search and roles of nitriles and urea in prebiological chemical evolution. 03 p0265 A73-14319

Book - Molecular evolution: Prebiological and biological. 06 p0651 A73-17926

The origin of life problem - A brief critique. 06 p0651 A73-17927

Atomic, molecular, cellular, genetic, multicellular, neural, mental, social and suprasocial levels of evolution, discussing systems constituents, interactions and selective focus. 06 p0651 A73-17929

Space exploration and the origin of life. 06 p0651 A73-17930

A non-equilibrium thermodynamical analysis of the origin of life.

06 p0651 A73-17931

Thermodynamics of self assembly - An empirical example relating entropy and evolution.

06 p0651 A73-17932

The sources of phosphorus on the primitive earth - An inquiry.

06 p0651 A73-17933

Abiogenic formation of porphyrin, chlorin and bacteriochlorin.

06 p0651 A73-17934

Proteins and nucleic acids in prebiotic evolution.

06 p0652 A73-17937

Model experiments on the prebiological formation of protein.

06 p0652 A73-17938

Myeloperoxidase, the peroxidase of a primitive cell - Its reactivity with Fe and H₂O₂.

06 p0652 A73-17944

Coacervate systems and evolution of matter on the earth.

06 p0652 A73-17951

Conjugation of proteinoid microspheres - A model of primordial recombination.

06 p0652 A73-17952

Search for biogenic structures and viable organisms in lunar samples - A review.

06 p0654 A73-18416

Hydrolysis of aqueous extract of lunar dust samples for identification and quantitation of amino acid precursors in extraterrestrial sources, considering prebiotic evolutionary pathways termination

06 p0655 A73-18421

Organogenic elements in stars, interstellar matter, comets, meteorites and planets, discussing molecular distribution and formation, prebiological chemical evolution, and terrestrial and extraterrestrial biology

06 p0754 A73-18430

Polymerization of amino acids under primitive earth conditions.

07 p0787 A73-19217

Genetic code evolution in terms of abiotic polynucleotide synthesis, suggesting alternating sequences of purines and pyrimidines as polypeptide codes

09 p1044 A73-23469

Laboratory simulation of organic geochemical processes.

11 p1325 A73-25460

Organic inclusions within hydrothermal minerals from S.W. Africa and elsewhere.

11 p1352 A73-25472

Chemical evolution - Recent syntheses of bioorganic molecules.

11 p1319 A73-26477

Criteria for distinguishing biogenic and abiogenic amino acids - Preliminary considerations.

11 p1319 A73-26480

Book - Molecular evolution and the origin of life.

12 p1461 A73-27049

Prebiological synthesis of organic compounds.

14 p1724 A73-30129

Chemical evolution before life from carbonaceous meteorites composition, noting porphyrins, optically active substances and isoprenoid hydrocarbons

14 p1715 A73-30130

Origin of terrestrial polypeptides - A theory based on data from discharge-tube experiments.

20 p2513 A73-39484

Amino acids in the Murchison meteorite.

21 p2771 A73-41010

Life origin hypothesis based on interstellar molecular concentration in gas clouds, examining radical types and molecular Doppler spectra

21 p2638 A73-41080

Gamma irradiation induced abiogenic radiochemical synthesis of deoxynucleosides from dry mixtures of purine bases with deoxyribose and ribose

22 p2803 A73-42166

ABLATION

Meteorite ablation coefficient and brightness dependence on velocity and atmospheric density, considering molecular screen effect

01 p0101 A73-10847

Phenolic resin char-formation during hyperthermal ablation.

01 p0124 A73-11448

Meteor dust motion in the upper atmosphere and in the vicinity of the earth's orbit.

02 p0214 A73-12255

Role of the anelastic behavior of the ablation material on cross-hatching.

03 p0398 A73-14189

Low power pulsed ablation plasma thruster design for satellite attitude control and stationkeeping, describing operating principle and performance measurements

04 p0489 A73-15731

Effects of a fully catalytic wall on a non-equilibrium boundary layer including ablation products.

04 p0519 A73-15826

Effects of nonequilibrium ablation chemistry on Viking radio blackout.

05 p0551 A73-16981

[AIAA PAPER 73-260]

Effect of low heat-shield ablation rates on flight test turbulent base pressure.

07 p0920 A73-19975

Parallel plate electromagnetic shock tube, investigating drive current, gas pressure and electrode material effects on electrode ablation and current sheet velocity

08 p0953 A73-21632

Stagnation region radiative heating with steady-state ablation during Venus entry.

08 p1025 A73-21817

Ablation of large meteor particles

09 p1147 A73-22573

Determination of the electron concentration in the boundary layer of air mixed with ablation products of an asbestos plastic

09 p1128 A73-22622

Temperature gradients and atmospheric ablation rates for the Barwell meteorite.

11 p1419 A73-25779

A mechanism for ablation-induced spin-up.

11 p1431 A73-26402

High pressure plasma torch to heat air for high temperature chemical reactions and hypersonic wind tunnels for reentry vehicle ablation studies

13 p1597 A73-28479

Derivation of shape change equations for asymmetrically heated ablating reentry vehicles.

13 p1706 A73-28750

Meteorite ablation coefficient and brightness dependence on velocity and atmospheric density, considering molecular screen effect

15 p1928 A73-30983

Tektite ablation calculation taking into account transient effects, internal radiation, melting and nonequilibrium vaporization of glass and drag effect of flanges

17 p2233 A73-35272

Fully coupled nongray radiating gas flows with ablation product effects about planetary entry bodies.

18 p2368 A73-36223

Ablation and radiation coupled viscous hypersonic shock layers.

18 p2264 A73-36315

Surface ablation of silica-reinforced composites.

18 p2368 A73-36316

Assessment of chemical nonequilibrium for massively ablating graphite.

18 p2368 A73-36322

Viscous effects in massively-ablating planetary entry body flow fields.

18 p2264 A73-36335

Angle of attack tests for graphite ablation models simulating spacecraft reentry using arc heating, showing temperature and pressure effects, model size and flow field characteristics

18 p2295 A73-36353

Reentry vehicle ablating control surface gap and slot regions flow characteristics prediction based on quasi-one-dimensional compressible flow finite difference solution

18 p2265 A73-36663

Some characteristics of the disintegration of glassy bodies in hot gas flows

18 p2372 A73-37020

Multihundred watt radioactive isotope heat source wind tunnel tests to obtain aerodynamic coefficients, heating rate, stability and ablation for reentry protection design

19 p2456 A73-38425

Multihundred watt radioactive isotope heat source assembly for multiple space missions, discussing aerodynamic heating, shield ablation and thermal stress performance during reentry

19 p2456 A73-38426

Measuring the boundary layer temperature distributions using ablating specimens in an air plasma flow.

21 p2791 A73-41052

Ablation debris and primary micrometeoroids in the stratosphere.

21 p2775 A73-41419

ABLATIVE MATERIALS

Weave geometry effects on pyrolytic infiltration of carbon-carbon /graphite-graphite/ composite structures for nose tip and thermal shield materials

03 p0332 A73-13044

Continuing development of the short-pulsed ablative space propulsion system.

03 p0356 A73-13457

Effect of additives on ablation of phenolic-silica composites.

07 p0842 A73-19486

Method of determining the mass removal from heat-shield materials on the basis of strain measurements in loaded shells

08 p1023 A73-21369

Hypervelocity tactical missile radome materials with noncharring ablator and fiberglass substructure for thermal protection against aerodynamic heating with negligible effects on radio transmission

11 p1336 A73-25307

Missile ablation shields erosion by high velocity dust, considering wind tunnel test data on phenolic cork for various dust materials, particle sizes and velocities

11 p1388 A73-25509

Laser activated, model surface recession compensator system for testing ablative materials.

[AIAA PAPER 73-380] 11 p1343 A73-25510

Investigation of heatproof materials under unsteady operating conditions

11 p1450 A73-25730

Phenolic binder decomposition in silica-phenolic ablator, determining reaction mechanism from Arrhenius rate equations for various temperatures

11 p1452 A73-26376

An experimental method for determining the characteristics of ablative materials

12 p1557 A73-27068

Nonlinear least squares - An aid to thermal property determination.

13 p1706 A73-28806

Surface materials ablation cooling for thermal protection during reentry, discussing chemical reactions, plastics pyrolysis and propulsion chemistry

14 p1724 A73-30133

Low-cost fabrication and installation of ablative heat shields for the space shuttle orbiter.

16 p2072 A73-33060

Reinforced plastics under ablative conditions for thermal insulation and structural applications.

17 p2195 A73-34805

Edgewise tape wound reinforced plastic ablative components for rocket motors to provide balance between optimum char strength, heat flow and insulation characteristics

17 p2195 A73-34809

New thermodynamic functions for the C₃ molecule.

18 p2287 A73-36326

Four Space Shuttle wing leading edge concepts.

18 p2359 A73-36355

Initial development of an ablative leading edge for the Space Shuttle orbiter.

18 p2369 A73-36356

Thermochemical properties of a silicone elastomeric ablator.

18 p2326 A73-36358

Improved technology for multiwatt radioisotope heater units.

18 p2336 A73-36681

ABNORMALITIES

NT MAGNETIC ANOMALIES

NT NEUROSES

NT PSYCHOSES

ABORT APPARATUS

The 600 knot Yankee escape system.

05 p0534 A73-16200

ABORT TRAJECTORIES

Space shuttle abort - Downrange basing and cross-range capability requirements.

02 p0228 A73-12371

Space shuttle orbiter abort guidance for premature or abnormal termination of mission due to system or human failure, discussing predictive algorithm

21 p2735 A73-40045

ABRASION

Certain results of studies of the accuracy in grinding shaped surfaces by the method of nontemplate shaping of the cutting surface of an abrasive ribbon

02 p0172 A73-11798

Early diagnosis of machine damage on the basis of the determination of rubbed-off materials in highly stressed lubricating oils - Employment of spectrographic methods for the analysis of the oil

05 p0582 A73-16998

Metal components wear mechanisms due to adhesion, tribooxidation, abrasion and surface fatigue, discussing prevention by lubrication, suitable mating of materials and surface treatments

11 p1373 A73-25577

ABRASION RESISTANCE

Effect of laser working on the wear of machine parts in an abrasive-lubricant medium

02 p0173 A73-11935

Possibility of reducing the wear of the VD-17 aluminum alloy in a jet of free abrasive particles with the aid of metallic coatings

10 p1226 A73-24796

Wear resistant abrasive and dry lubricant cobalt-chromium carbide composite material coatings obtained by electrolytic codeposition

24 p3094 A73-45073

ABRASIVES

NT CARBORUNDUM [TRADEMARK]

An apparatus for testing components in a high temperature supersonic gas stream containing abrasive particles.

09 p1070 A73-23065

Effect of the characteristics of diamond grinding on the stressed state and strength of hard alloy VK6

24 p3094 A73-44968

ABSOLUTE TEMPERATURE SCALES

U TEMPERATURE SCALES

ABSORBENTS

Effectiveness of the application of tightly bonded sulfo-cation exchange resins in water recycling by the sorption method

06 p0656 A73-17677

Self-mode-locking in an argon ion laser with a nonlinear absorber

09 p1096 A73-22878

ABSORBERS [MATERIALS]

NT SOLAR ENERGY ABSORBERS

Low-sideobe paraboloidal antenna with microwave absorber.

01 p0018 A73-11054
Laser coupling through nonlinear gas filled absorber cell, discussing molecules mean free path
05 p0585 A73-16783
Dependence of characteristics of a gas laser on the parameters of an intracavity absorber.

08 p0974 A73-20953
A mathematical analysis concerning the edge effect of sound absorbing materials.

08 p0987 A73-21124
Equivalence relationships between diffuse radiation fields for finite slabs bounded by a perfect specular reflector and a perfect absorber.

09 p1121 A73-23072
Influence of the spectral characteristics of liquid filters on the thermal regime and efficiency of a neodymium-glass laser

12 p1505 A73-26891
Influence of saturable-absorber transmission and optical pumping on the reproducibility of passive mode locking.

12 p1505 A73-27013
Amplified laser absorption - Detection of nitric oxide.

15 p1885 A73-31844
Laser mode locking using saturable absorbers.

15 p1885 A73-31941
Electromagnetic wave absorbers and anechoic chambers through the years.

17 p2128 A73-35683
Optical pulses interaction with two level atom spins, determining sub-cooperation limit in resonant absorbers

20 p2591 A73-38625
Respirator cartridge filter efficiency under cyclic and steady-flow conditions.

21 p2643 A73-40408
Minimum detectable frequency deviations in output of He-Ne laser stabilized by external methane absorption cell

23 p2989 A73-44366

ABSORPTANCE

Light scattering by cirrus cloud layers.

01 p0038 A73-10376
A biased model for calculating the evolution in solar absorptance.

16 p2060 A73-33128
Theory and technique for surface temperature determinations by measuring the radiance temperatures and the absorptance ratio for two wavelengths.

22 p2853 A73-41986

ABSORPTION

States of absorption, velocities of absorption, of desorption of oxygen on rhenium, and mechanisms of atomization and oxidation at high temperature and low pressure

13 p1580 A73-28451

ABSORPTION BANDS

U ABSORPTION SPECTRA

ABSORPTION COEFFICIENT

U ABSORPTIVITY

ABSORPTION CROSS SECTIONS

Solar neutrino detection methods, capture cross sections, model construction and results

01 p0091 A73-10053
Pressure and temperature effects on carbon dioxide extinction coefficients, tabulating absorption cross sections

02 p0191 A73-11758
The relation between momentum transfer and capture and total scattering cross sections for ion-dipole collisions.

02 p0195 A73-12842
Galactic cosmic radiation He 3 and deuterium abundances interpretation from production cross sections and reaction kinematics

05 p0609 A73-16741
Photoabsorption cross section of argon in the 180-700-A wavelength region.

08 p0990 A73-21050
An effective cross section method of accounting for the selectivity of emission and absorption in a hot gas

09 p1123 A73-22613
Photoabsorption cross sections of H2, D2, N2, O2, Ar, Kr, and Xe at the 584-A line of neutral helium.

12 p1465 A73-26989
Nitrogen and oxygen molecules, photodissociation continuums from absorption and ionization cross sections, calculating upper atmosphere emission rates

12 p1489 A73-26993
Processes altering charge state in collisions of hydrogen atoms with H2 molecules.

14 p1777 A73-30330
Negative oxygen molecular ion formation in low energy electron collision and attachment obtaining capture cross section and resonance width

14 p1777 A73-30775
A general formula for free-free absorption on highly-polarizable neutral atoms.

16 p2039 A73-33740

Kinetic equations for time behavior of solid photochromic film in photocoloration, photobleaching and thermal bleaching, evaluating absorption cross sections and quantum yields

17 p2172 A73-35422
A new technique for Auger analysis of surface species subject to electron-induced desorption.

17 p2175 A73-35757
Treatment of molecular reaction equilibria and opacity calculations for cool circumstellar envelopes

20 p2606 A73-39079
The absorption cross sections of N2, O2, CO, NO, CO2, N2O, CH4, C2H4, C2H6, and C4H10 from 180 to 700 A.

22 p2890 A73-42992
Extinction and scattering cross sections of small planetesimal particles with iron cores and silicate mantles in circumstellar dust of young T Tauri stars

23 p3030 A73-43748

ABSORPTION SPECTRA

NT FRAUNHOFER LINES

NT HERZBERG BANDS

NT TELLURIC LINES

Jovian atmosphere absorption line and spectroscopic data interpretation based on model for structure, composition and radiative properties of visible cloud layers

01 p0097 A73-10359
Synthetic spectra production via solution of radiative transfer equation at frequencies across absorption line for homogeneous and inhomogeneous atmospheres

01 p0097 A73-10362
Atmospheric windows in different spectral bands due to various gases, comparing continuum and line absorption spectra properties

01 p0037 A73-10364
Atmospheric radiative transfer by carbon dioxide.

01 p0037 A73-10366
Transmittance functions for satellite temperature sounding.

01 p0037 A73-10367
Computer programs for realistic calculation of atmospheric absorption spectra, discussing spectroscopic data critical survey, procedures, coefficient generation and data presentation

01 p0037 A73-10368
Theoretical treatment of the translational absorption spectrum induced in mixtures of rare gases

01 p0079 A73-10500

French monograph - Contribution to the experimental study of the integrated intensity of the translational absorption bands induced in pressurized rare-gas mixtures.

01 p0080 A73-10601
Some optical properties of CaMoO4 single crystals

01 p0088 A73-10626
Time variations of the ultraviolet absorption in the continuous spectrum of Jupiter and Saturn

01 p0101 A73-10843
Absorption line profile and equivalent line width derivation for planetary atmosphere with low and high optical thicknesses, assuming arbitrary scattering coefficients

01 p0106 A73-11321
Absorption line shape computerized functional analysis in solar physics, deriving H α /v function from Faddeyeva-Terent'ev probability

01 p0107 A73-11377
Radiant flux densities of Cygnus X-3, observing OH and formaldehyde absorption

02 p0210 A73-11560
Observations of Cygnus X-3 at the Mullard Radio Astronomy Observatory.

02 p0210 A73-11561
Molecular fluorine concentration and pressure change monitor based on UV absorption spectrum during chemical reactants mixing, noting measurement accuracy

02 p0168 A73-11967
The infrared reflection, emission and absorption spectra of regolith from the Sea of Fertility and its scattering coefficient.

02 p0213 A73-12237
Molecular oxygen densities in atmosphere near 100 km from solar hydrogen Lyman alpha absorption measurements by Intercoms 4 satellite and Vertical 1 rocket

02 p0160 A73-12275
Investigation of the radio wave absorption spectrum of atmospheric water vapor in the 1.15 to 1.5-mm range

02 p0142 A73-12487
Long wavelength spectrometry and photometry of M, S and C-stars.

02 p0222 A73-12708
Search for OH-IR stars with emission concentrated in main lines, considering water vapor line emission or absorption band in near IR

02 p0222 A73-12717
The valence states of 3d - Transition elements in Apollo 11 and 12 rocks.

03 p0369 A73-13097

Absorption line width method for stellar population of galaxies NGC 1052, 2655, 2903 and 4569 nuclei

03 p0371 A73-13221
Foreign gas collision broadening effects on 15 micron carbon dioxide bands radiation absorption lines

03 p0345 A73-13697
Gas concentration profiles in combustion gas sampling probes, using IR absorption technique

03 p0399 A73-14397
The interpretation of absorption-line shifts in the solar spectrum.

03 p0377 A73-14407
On the minimum intensity of the Na D2-5890 A line in sunspot umbra /Research note/.

03 p0377 A73-14411

Umbral spectra absorption line feature observation by photoelectric spectroscopy, suggesting Ti abundance in solar atmosphere

03 p0378 A73-14423

Stratospheric nitrogen dioxide from infrared absorption spectra.

04 p0445 A73-15626

Spectroscopic observations of HZ Herculis.

04 p0501 A73-15684

Application possibilities of atomic resonance absorption spectroscopy in vacuum metallurgy.

04 p0455 A73-15754

Study of the dispersion curve of polaritons excited by Raman diffusion in the presence of damping

04 p0476 A73-15997

Influence of a random magnetic field on the properties of stellar absorption lines.

04 p0503 A73-16011

Kappa Cassiopeia H, He and O absorption spectra line widths from spectrophotometric analysis

05 p0613 A73-16207

New laser technique for the identification of molecular transitions.

05 p0585 A73-16597

O stars line spectra from high dispersion photographic spectrograms at 3059-6683 A, tabulating absorption and emission lines identifications, equivalent widths and profiles

05 p0618 A73-16742

Vertical distribution of minor atmospheric constituents as derived from air-borne measurements of atmospheric emission and absorption infrared spectra. [AIAA PAPER 73-103]

05 p0570 A73-16863

Spectral transmittance of cryodeposits on a transmitting substrate.

[AIAA PAPER 73-149]

05 p0598 A73-16897

Solution of the transfer equation for interlocked multiplets by probabilistic method.

05 p0599 A73-17320

Absorption lines in the spectrum of the quasar Ton 1530.

05 p0626 A73-17377

A study of the unidentified interstellar diffuse features.

05 p0626 A73-17379

Temperature-dependent hyperfine interactions in Fe2B.

06 p0734 A73-17833

X ray K absorption spectra shifts /Bergard additivity rule deviations/ in Fe-Cr, Fe-V, Fe-Ni and Fe-Co systems due to lattice characteristics and electron structure changes

06 p0707 A73-18039

Absorption-line profiles in the quasi-stellar object PHL 957.

06 p0751 A73-18125

Observations of the neutral-hydrogen absorption spectrum of Cygnus X-3.

07 p0874 A73-19073

Pressure broadening of magnetically-tuned infrared absorption spectrum of NO using a CO laser.

07 p0833 A73-19145

Violet shift of the H alpha absorption line of the hydrogen-depleted star HD 30353

07 p0877 A73-19598

Crystal field spectra of lunar pyroxenes.

07 p0881 A73-19709

Evidence of lunar surface oxidation processes - Electron spin resonance spectra of lunar materials and simulated lunar materials.

07 p0893 A73-19840

Electronic spectra of pyroxenes and interpretation of telescopic spectral reflectivity curves of the moon.

07 p0897 A73-19885

Reflectance and absorption spectra of Apollo 11 and Apollo 12 samples.

07 p0897 A73-19890

IR absorption spectra of powdered graphite samples during treatment in laminar propane-butane diffusion flame zones

07 p0921 A73-19996

Fine structure in the optical-absorption edge of silicon.

07 p0863 A73-20175

Search for 3C 191 ionization potential-red shift correlations to other quasar absorption lines

07 p0900 A73-20237

H flux density observations for 21 cm absorption spectrum in front of Cyg X-3

07 p0902 A73-20560

The radial amplification profile of the 4880-Å ionic laser line and the distribution of the charge carriers in the wall-stabilized Ar low-pressure arc column

08 p0989 A73-20786

Variations in spectral-energy distributions and absorption-line strengths among elliptical galaxies.

08 p1002 A73-20878

The kinematical distribution of dark clouds surveyed in the 4830 MHz H₂CO line.

08 p1004 A73-20904

Spectroscopic measurement of the source function as a test for deviations from local thermodynamic equilibrium /L.T.E./ in arc plasmas.

08 p0992 A73-21018

Absorption measurements of carbon monoxide laser radiation by water vapor.

08 p0974 A73-21033

Some results of spectrophotometry of the methane absorption band /7250 Å/ on the Jovian disk

08 p1007 A73-21063

Investigation of molecular absorption in the atmospheres of the giant planets

08 p1007 A73-21064

The investigation of the middle infrared absorption spectrum of DyVO₄ at low temperatures.

08 p0994 A73-21219

Studies in molecular dynamics by collision-induced infrared absorption in H₂-rare gas mixtures. I - Profile analysis and the intercollisional interference effect.

08 p0990 A73-21630

327-MHz observations of the galactic center - Possible detection of a deuterium absorption line.

08 p1013 A73-21808

The transfer of radiation from a flame to its fuel.

08 p1025 A73-21822

High-resolution study of anomalous dispersion in the ruby R lines.

09 p1090 A73-21940

A discussion of the new variations observed in the nucleus of the Seyfert galaxy NGC 3516.

09 p1140 A73-22004

H I absorption in the galactic center region and between galactic longitudes 350 deg and 359 deg.

09 p1141 A73-22009

Intensities and half-widths of lines in the A and B bands of the red atmospheric system of O₂ bands

09 p1077 A73-22664

Molecular absorption spectra of S-type stars in the one-micron region.

09 p1123 A73-23130

Opacity probability distribution functions for application to non-grey late-type stars model atmospheres.

09 p1149 A73-23131

Spectroscopic changes in the suspected X-ray source X Persei.

10 p1275 A73-23846

Solar Mn abundance derivation based on center-line absorption line profiles, taking into account hyperfine structure broadening

10 p1278 A73-24130

Quasar characteristics, considering emission or absorption lines, red shift, optical intensity variation, unpolar generator representation and relativistic particle production

10 p1280 A73-24322

Electron absorption spectra of benzochromium-dicarbonyltriphenylphosphine and benzochromium-tricarbonyl and their application to studies of the decomposition kinetics of these compounds

10 p1186 A73-24457

Statistical analysis of multiple absorption spectra in QSO.

10 p1284 A73-24905

Use of the Fabry-Perot etalon to study absorption spectra of the atmosphere

11 p1363 A73-25613

Water vapor lines controlled atmospheric absorption spectrum in 220 GHz window region, discussing approximate calculation for submillimeter lines residual effect

11 p1330 A73-25688

The absorption spectrum of atmospheric water vapor in the vicinity of the He 10830 Å triplet.

11 p1421 A73-25933

Influence of laser field polarization on nonlinear interference effects.

11 p1377 A73-26180

The planet Venus - A new periodic spectrum variable.

11 p1428 A73-26621

A microspectrophotometer that records the first derivative of the absorption spectrum

12 p1496 A73-26957

Amplified laser absorption - Detection of nitric oxide.

12 p1505 A73-27121

Absorption spectrum of Cu I in the vacuum ultraviolet.

12 p1526 A73-27122

Exciton absorption band splitting in the PbI₂ spectrum

12 p1532 A73-27945

Magneto-oscillatory absorption effect in SbI₃

13 p1667 A73-28004

The position of the emission lines of some lasers in the absorption spectrum of the earth's atmosphere.

13 p1626 A73-28174

Formation of spectral lines and study of growth curves in a semiinfinite scattering atmosphere

13 p1680 A73-28458

German monograph - Determination of the OH-concentration distribution in a axisymmetric methane/oxygen flame.

13 p1708 A73-29279

Optical absorption spectrum of excited Cr³⁺ ions in yttrium aluminum garnet.

13 p1629 A73-29432

Black holes and absorption redshifts in quasi-stellar objects.

14 p1797 A73-30006

Gas absorption lines detection based on multiple light passage through absorbing medium during generation process, noting radiation spectra of neodymium glass laser

14 p1757 A73-30331

Absorption spectrum analysis of free Cu, Ca, Na, Zn, Ni and Cr atom concentration in acetylene air flame zones

14 p1817 A73-30458

Interstellar gas abundances from rocket observations of ultraviolet absorption lines.

14 p1801 A73-30734

Interferometric observations of formaldehyde absorption in front of strong galactic sources.

14 p1801 A73-30735

Search for interstellar absorption in 4250 Å line of singly ionized CO in direction of different stars

14 p1801 A73-30736

Spectrophotometric results from the Copernicus satellite. IV - Molecular hydrogen in interstellar space.

14 p1802 A73-30747

Temporal variation of ultraviolet absorption in continuous spectra of Jupiter and Saturn.

15 p1928 A73-30979

Detection of interstellar thioformaldehyde.

15 p1933 A73-31378

Proportional counter energy deposition spectral quality prediction from experimental data, using folding procedure to produce composite energy absorption distributions for biological materials

15 p1839 A73-31549

Reflection-absorption infrared spectrum of alpha- CO chemisorbed on polycrystalline tungsten.

15 p1841 A73-31971

Study of a niobium-aluminum-silicon system. II - Analysis of ternary niobium-aluminum-silicon alloys by atom absorption spectrophotometry

15 p1890 A73-31992

Extinction and scattering by several types of silicate sphere of radius 0.05-1.0 micron, for the wavelength range 0.21-50 microns.

15 p1939 A73-32012

Visible solar disk contrasts in radiation controlled line, noting role of lateral differences in local shapes of line absorption profile

16 p2059 A73-32951

Concentration of OH and NO in YJ93-GE-3 engine exhausts measured in situ by narrow-line UV absorption.

16 p2045 A73-33546

[AIAA PAPER 73-506] Tunable-laser derivative spectroscopy on spectral lines with combined Doppler and collision broadening.

16 p2039 A73-33741

Equivalent widths of the oxygen A-band absorption lines at different pressures

16 p2039 A73-33815

Investigation of molecular absorption features in the spectrum of Jupiter

16 p2070 A73-33839

Results of observations of methane /6190 Å/ and ammonia /6441 and 6478 Å/ absorption bands on the Jovian disk over a period of three years

16 p2070 A73-33840

Spectral characteristics of quasar QO172 with large red shift, considering absorption and emission spectra and Lyman alpha radiation

16 p2070 A73-33925

Spectral intensity of thermal radiation in a medium for frequencies in the neighbourhood of an absorption line.

16 p2038 A73-34028

Nitric oxide detection in stratosphere from characteristic absorption line spectrum via airborne IR spectrometer, obtaining molecular concentration

17 p2159 A73-34552

[ONERA, TP NO. 1256] Solar absorption in the CO fundamental region.

17 p2231 A73-34761

Anisotropy of absorption bands in some lunar, meteoritic, and terrestrial pyroxenes.

17 p2235 A73-35738

Interstellar absorption lines observed with the orbiting spectrophotometer S59.

18 p2349 A73-35993

Spectrophotometry of the 7250-Å methane absorption band over the disk of Jupiter.

18 p2355 A73-36864

Molecular absorption in the atmospheres of the giant planets.

18 p2355 A73-36865

Observation of stratospheric nitric oxide by infrared absorption spectrometry from a balloon

19 p2423 A73-37533

The absorption spectrum of Rb I between 350 and 810 Å.

19 p2462 A73-37623

Optical and near IR absorption line spectra of quasar 1331+170, discussing red shift and line locking process

19 p2487 A73-38508

Solar magnetic field spatial structure in relation to solar activity phenomena, discussing measurements based on Zeeman effect in absorption line spectra formation

20 p2605 A73-39059

A search for high-ionization redshift systems in the absorption spectra of five quasars.

20 p2609 A73-39435

Coude spectroscopy for quasar Markarian 132 absorption lines wavelengths and profiles and red shift systems

20 p2609 A73-39436

A search for 21-centimeter absorption in quasars and other sources near to spiral galaxies.

20 p2609 A73-39437

Balloon-borne measurement of stratospheric methane as function of altitude absorption spectroscopy, obtaining mixing ratios

21 p2680 A73-40076

A photometric system for automatic recording of optical absorption spectra

21 p2700 A73-40561

Absorption line contours in homogeneous plane-parallel semiinfinite aerosol layers and planetary atmosphere overcloud gas layers for nonspherical scattering

21 p2768 A73-40723

Statistical spectral attenuation characteristics of transmittance windows for visible and near IR under various optical weather conditions

21 p2731 A73-40746

Vacuum IR spectrometer measurement of C 12 methane absorption band at 1.1 microns, describing technique for extending standards to photomultiplier region of spectra

21 p2743 A73-40936

Absorption of CO₂ laser radiation by carbonyl fluoride.

21 p2715 A73-40958

Interstellar extinction, relation to spatial dust distribution, light scattering by grains, diffuse absorption lines and polarization

21 p2772 A73-41247

Absorption spectra of lunar sections from different lunar areas.

21 p2774 A73-41406

Carbon, CN, CH, MgH, NH and OH line behavior in solar photospheric spectra

21 p2778 A73-41528

Measurements of neutral-hydrogen absorption in the spectra of eight pulsars.

21 p2779 A73-41538

Aperture synthesis of interstellar neutral hydrogen in absorption. I - The Perseus arm feature of Cassiopeia A.

22 p2904 A73-41756

Short duration temperature measurements by infrared emission-absorption.

22 p2853 A73-41990

Radiation field frequency dependent source function for two level atom, noting different stimulated emission and absorption line profiles

22 p2907 A73-42205

Accurate wavelengths of stellar and telluric absorption lines near lambda 7000 Å.

22 p2907 A73-42208

Optical and electrical properties of doped semiconductors in a strong electromagnetic field.

22 p2896 A73-42252

Mode competition in the 3s sub 2-3p sub 4 transition in a neon laser with a methane absorbing cell.

22 p2869 A73-42256

Observations in linearly polarized light of the intensity of the diffuse 6180 Å absorption band in 49 O, B, and A stars.

22 p2908 A73-42308

Ozone transition detection in earth atmospheric absorption and emission, comparing measured ozone absorption profiles with theoretical computations

22 p2848 A73-42535

A comparison of the sensitivity of atomic-fluorescent and atomic-absorption flame photometry

22 p2862 A73-42720

The temperature dependence of the half widths of some self- and foreign-gas-broadened lines of methane.

22 p2821 A73-42989

Vertical phase variation and mechanical flux in the solar 5-minute oscillation.

22 p2916 A73-43124

- Jupiter HD absorption line measurement for model-independent number ratio D/H 22 p2916 A73-43125
- O, Of, Oe and Wolf-Rayet star comparison in terms of emission and absorption line spectra, noting relationship to evolutionary status on H-R diagram 23 p3026 A73-43197
- Two-phonon absorption in SbSI single crystals 23 p3016 A73-43713
- The shape of the cyclotron absorption line in a weakly ionized plasma 23 p3011 A73-43794
- Multicolor astronomical photography of Jupiter using wideband filters, emphasizing Red Spot, atmospheric bright belts and methane absorption variations above clouds 23 p3032 A73-43941
- High altitude infrared spectroscopic evidence for bound water on Mars. 24 p3127 A73-44395
- Optical characteristics of phononless lines 24 p3109 A73-44427
- On the level of H₂ quadrupole absorption in the Jovian atmosphere. 24 p3129 A73-44443
- Methane absorption in the atmosphere of Saturn - Rotational temperature and abundance from the 3 nu sub 3 band. 24 p3129 A73-44445
- Damping constants and turbulence velocities in the solar photosphere determined by the Voigt method. 24 p3132 A73-44483
- Methane absorption in the Jovian atmosphere. I - The Lorentz half-width in the 3nu/sub 3/ band at 1.1 micron. 24 p3132 A73-44537
- Methane absorption in the Jovian atmosphere. II - Absorption line formation. 24 p3133 A73-44559
- Absorption at about 4.3 microns by /N2-N2/ and /N2-O2/ complexes in the terrestrial atmosphere 24 p3084 A73-44964
- The formation of resonance lines in multidimensional media. II - Radiation operators and their numerical representation. 24 p3113 A73-45041
- Line strength measurements of the 2 nu sub 3 band of methane. 24 p3066 A73-45320
- ABSORPTION SPECTROSCOPY**
- IR radiative energy transfer in gases, applying spectroscopic band absorption information 01 p0120 A73-10291
- An atomic absorption method for cation measurements in Kjeldahl digests of biological materials. 02 p0139 A73-12424
- Activated oxygen ashing of biological specimens for the microdetermination of Na, K, Mg, and Ca by atomic absorption spectrophotometry. 02 p0139 A73-12546
- Microwave rotational spectroscopy - A technique for specific pollutant monitoring. 10 p1221 A73-24891
- Heat pipe oven as instrument for laser absorption and fluorescence spectroscopy of metal vapors, vapor-gas, vapor-vapor mixtures and metal vapor plasmas 11 p1361 A73-25148
- Optical absorption cell with water vapor cross flow instrument designed for wall decontamination and open air meteorological simulation, examining thermodynamic parameters effects 11 p1367 A73-26318
- Reflectance and optical constants of evaporated osmium in the vacuum ultraviolet from 300 to 2000 A. 13 p1660 A73-28936
- Estimates of possible detection limits for combustion intermediates and products with line-center absorption and derivative spectroscopy using tunable lasers. 13 p1618 A73-28996
- Spectroscopic laser methods of automatic gas analysis based on Raman backscattering, resonance fluorescence or absorption measurements for atmospheric pollutant and exhaust gas detection 16 p2023 A73-32876
- Spectral line absorption measurement using optical cavities. 17 p2184 A73-34913
- A comment on the measurement of atmospheric density by absorption of Lyman-alpha. 18 p2309 A73-36054
- Excited state absorption spectroscopy of alkaline earths selectively pumped by tunable dye lasers. I - Barium arc spectra. 21 p2713 A73-40472
- Shock tube kinetics of NO decomposition in mixtures with Ar, measuring ground state atomic oxygen formation rate by resonance absorption spectrophotometry 22 p2818 A73-42766
- Principles and possibilities of a new method of ozone measurements within the Huggins bands. 23 p2982 A73-43854
- High resolution analysis of the sun's radiation received at the ground from 9 to 11.6 microns. 23 p3003 A73-43888
- Multiphotonic absorption spectroscopy without Doppler effect 24 p3096 A73-45327
- ABSORPTIVE INDEX**
- U ABSORPTIVITY**
- ABSORPTIVITY**
- Computer programs for realistic calculation of atmospheric absorption spectra, discussing spectroscopic data critical survey, procedures, coefficient generation and data presentation 01 p0037 A73-10368
- Computed total radiation properties of compressed oxygen between 100 and 1000 K. 01 p0122 A73-10809
- Investigation of the radio wave absorption spectrum of atmospheric water vapor in the 1.15 to 1.5-mm range 02 p0142 A73-12487
- Atmospheric water vapor absorption coefficient in 0.73 mm transmittance window as function of humidity from monochromatic RF radiation measurements 02 p0142 A73-12488
- Some optical properties of solid solutions in the 2GaAs-ZnSiAs2 section 05 p0605 A73-16612
- Radiation transfer in a single-layer spherical planetary atmosphere 05 p0620 A73-17015
- Absorption coefficient due to band-band optical transitions in heavily doped semiconductor, obtaining electron and hole quasi-Fermi levels 06 p0738 A73-18586
- Surface absorption coefficient of electromagnetic wave incident on plasma boundary, considering particle specular reflection and density-frequency relation 06 p0732 A73-18642
- Combustion molecular gases radiative heat transfer, emissivity and absorptivity calculation, presenting high speed computer routine 06 p0770 A73-18832
- White and black paints for satellite thermal control coatings, discussing space environment radiation effects on emissivity and solar absorptance 07 p0841 A73-18909
- Solar radiation absorptivity control by metal film coatings, noting thermal control coatings for heat shielding 07 p0778 A73-19300
- Characteristics of the calculation of radiant transfer in a system of diathermic bodies separated by an absorbing and scattering medium 07 p0921 A73-20080
- Non-grey radiative heat transfer in the picket-fence approximation. 08 p1020 A73-20790
- On the He-H2 thermal opacity in planetary atmospheres. 08 p1003 A73-20890
- Spatial crosscorrelation in anisotropic sound fields. 08 p0987 A73-21125
- Kinetic theory for the reflection of waves obliquely incident on the boundary of a magnetoactive plasma 09 p1052 A73-23078
- Optical constants of water in the 200-nm to 200-micron wavelength region. 11 p1350 A73-25060
- Ionospheric radio wave absorption coefficient correlation with solar activity Wolf number in IGY, IGC and IQSY 11 p1327 A73-25083
- Effect of the May 20, 1966 solar eclipse in the ionosphere on the basis of observations at Rostov on the Don and at Adler 11 p1351 A73-25100
- Coated laser windows characterized by strong surface absorption, calculating absorptivity, transmittance and reflectivity under assumption of insignificant interference effects within substrate 11 p1377 A73-26243
- Simultaneous radiative and conductive heat transfer in non-gray media. 11 p1453 A73-26583
- Radiative transfer in a nongray spherical layer - Simplified rectangular model. 11 p1401 A73-26585
- Sponge rubber absorption coefficient of sound and acoustic impedance measurements to test porous material sound absorption theories 14 p1767 A73-30894
- Ultrasound absorption coefficient measurement in semiconductor crystal lattices based on acoustoelectrical effect 17 p2218 A73-34159
- Ammonia absorption relevant to the albedo of Jupiter. I - Experimental results. 17 p2231 A73-34764
- Transient and steady state sound absorption coefficients of fiberglass and polyurethane foam. 19 p2459 A73-37286
- Determining the absorption coefficients of low-loss bulk glass materials. 20 p2563 A73-38663
- Semiconductor laser beam self focusing action due to combined effects of linear and nonlinear dielectric constant and absorption coefficients, considering n-InSb sample 21 p2711 A73-40226
- GaAs two-photon absorption coefficient obtained from transmission measurements with Q switched Nd-YAG laser, noting thermal self focusing 21 p2713 A73-40459
- Metal oxide absorption coefficients for use in intense laser interaction with solids. 21 p2715 A73-40961
- Light absorption coefficient of disordered semiconductor with random field due to charged impurity centers in presence of constant external electric field 23 p3016 A73-43648
- ABUNDANCE**
- An upper limit on the OH abundance in the intercloud medium. 01 p0096 A73-10314
- Eta Aquilae star molecular abundances of CO, CN, carbon, OH, NH and CH with respect to dissociation equilibrium and light curve correspondence 01 p0103 A73-11022
- Relativistic cosmic rays propagation, calculating abundances of Pt, Pb, actinides and superheavy groups as function of cosmic ray leakage time 01 p0092 A73-11027
- Measurements of the isotopic composition of spherical fluxes carried out on spacecrafts Soyuz, Zond 8 and Luna 16. 02 p0206 A73-12317
- Composition of relativistic cosmic rays near the earth and at the sources. 02 p0207 A73-12327
- The origin of the moon - Theories involving joint formation with the earth. 02 p0217 A73-12386
- Further evidence for a cosmic ray selection mechanism. 02 p0207 A73-12397
- He 4, C 12, O 16, Ne 20, Mg 24, Si 28 and Fe 56 abundance computed as function of time for neutron star atmospheres with strong magnetic fields 02 p0223 A73-12728
- The Os-Pt-Hg abundance peak in Ap stars and the problem of very heavy cosmic rays. 02 p0210 A73-12733
- Surface gravities, Doppler broadening velocities, effective temperatures and metal abundances of K giants from narrow band photometry 03 p0371 A73-13224
- The abundances of solar accelerated nuclei from carbon to iron. 03 p0362 A73-13719
- Umbral spectra absorption line feature observation by photoelectric spectroscopy, suggesting Ti abundance in solar atmosphere 03 p0378 A73-14423
- Changes in thermospheric molecular oxygen abundance inferred from twilight 6300 A airglow. 04 p0440 A73-14963
- The abundances of the elements in the oldest disk stars. 04 p0500 A73-15514
- Interstellar magnesium abundances and electron density in the direction of Orion and Cassiopeia. 04 p0502 A73-15976
- K, Rb, Sr, Ba contents and rare earths in specimens from the Apollonius /lunar mountains/ crater region brought back by the Soviet probe Luna 20 05 p0546 A73-16829
- Coronal abundance of elements and a model of the quiet sun from radio observations. 05 p0621 A73-17034
- On the location of pulsational blue edges and estimates of the luminosity and helium content of RR Lyrae stars. 05 p0625 A73-17335
- Analysis of the extreme-ultraviolet quiet solar spectrum. 05 p0625 A73-17338
- Interstellar elemental abundance table from carbonaceous chondrites and solar abundances, considering solar Fe composition 06 p0752 A73-18232
- Interstellar medium chemical composition, considering emission line spectra, density fluctuations, He/H ratio in different galaxies and H II regions 06 p0752 A73-18233
- Abundance patterns of thirteen trace elements in primitive carbonaceous and unequilibrated ordinary chondrites. 07 p0877 A73-19651
- Bulk, rare earth, and other trace elements in Apollo 14 and 15 and Luna 16 samples. 07 p0885 A73-19754
- Elements abundances in Apollo 14 and 15 soils and breccias and in eucrite Juvinas and howardite Kapoeta, suggesting initial chemical layering of moon. 07 p0886 A73-19758
- Precise determination of rare-earth elements in the Apollo 14 and 15 samples. 07 p0886 A73-19762

Beryllium and chromium abundances in Fra Mauro and Hadley-Apennine lunar samples.

07 p0886 A73-19764

The abundances of components of the lunar soils by a least-squares mixing model and the formation age of KREEP.

07 p0887 A73-19769

Isotopic abundance ratios and concentrations of selected elements in Apollo 14 samples.

07 p0887 A73-19773

Deuterium content of lunar material.

07 p0887 A73-19774

Abundances of primordial and cosmogenic radionuclides in Apollo 14 rocks and fines.

07 p0888 A73-19787

Noble gas studies on regolith materials from Apollo 14 and 15.

07 p0889 A73-19799

Inorganic gas release and thermal analysis study of Apollo 14 and 15 soils.

07 p0890 A73-19814

Total carbon, nitrogen, and sulfur in Apollo 14 lunar samples.

07 p0890 A73-19816

Chemically bound nitrogen abundances in lunar samples, and active gases released by heating at lower temperatures /250 to 500 C/.

07 p0890 A73-19817

Time variation of metal abundance in galaxies - Super-metal-rich stage.

07 p0902 A73-20446

Charge dependence of the energy spectra of cosmic rays.

07 p0873 A73-20561

Energy dependence of primary cosmic ray nuclei abundance ratios.

07 p0873 A73-20564

Chemical fractionations in meteorites. VI - Accretion temperatures of H-, LL-, and E-chondrites, from abundance of volatile trace elements.

07 p0789 A73-20622

Solar nebula Lu 176-Hf 176 pair and Zr abundance determinations, using chondrite fraction and s-process model

08 p1006 A73-20937

On the metal abundance of RR Lyrae stars in the globular cluster M22.

08 p1009 A73-21169

Neutron activation and irradiation analyses of Haverro ureilite elemental abundances

09 p1140 A73-21867

Elemental abundances and chemistry of Haverro carbonaceous ureilite, noting similarity to Allende inclusions pattern

09 p1047 A73-21868

H I absorption in the galactic center region and between galactic longitudes 350 deg and 359 deg.

09 p1141 A73-22009

Tiilaberri /Niger/ stony meteorite elements abundance and radioactivity determination by gamma ray spectrometry

09 p1149 A73-23032

Satellite measurements of the charge composition of solar cosmic rays in the Z = 6 to 26 interval.

10 p1264 A73-23537

Intermediate-coupling line strengths in the iron spectrum and the solar abundance of iron.

10 p1272 A73-23540

Validity of zeta Oph cloud carbon isotope abundance extrapolation to dense dusty regions of Galactic center and Orion Nebula

10 p1275 A73-23824

An abundance analysis of the delta Scuti variable delta Delphini.

10 p1275 A73-23831

Solar cosmic ray heavy nucleus abundances relation to oxygen nuclei in solar corona and photosphere

10 p1265 A73-23898

Noble gas and carbon abundances of the Haverro, Dingo Pup Donga, and North Haig ureilites.

10 p1277 A73-24104

Certain peculiarities in the distribution of mercury in meteorites.

10 p1278 A73-24106

High resolution spectroscopic analysis for photospheric Fe II lines with spectrum synthesis techniques, determining solar isotopic composition and abundance

10 p1278 A73-24129

Solar Mn abundance derivation based on center-line absorption line profiles, taking into account hyperfine structure broadening

10 p1278 A73-24130

Secular stability. V - The perturbation of chemical abundances.

10 p1280 A73-24404

Solar He abundance from neutrino flux, He lines intensity in prominences and chromosphere spectra, solar cosmic rays and solar wind He/H ratio

10 p1284 A73-24780

Molecular abundances in stellar atmospheres. II.

11 p1417 A73-25265

A measurement of cosmic-ray rigidity spectra above 5 GV/c of elements from hydrogen to iron.

11 p1414 A73-26612

Metal content in the atmospheres of red giants which are members of dispersed star clusters and dynamical groups

12 p1537 A73-26853

Indium abundances in cosmos, meteorites, tektites, rock-forming and ore minerals and igneous rocks, considering behavior in magmatogenic processes and rock weathering and alteration

12 p1490 A73-27125

Chemical composition of stars in globular clusters and the morphological characteristics of their horizontal branches

12 p1546 A73-27852

Oxygen and bulk element abundances in Luna 20 fines from instrumental neutron activation analysis, noting comparison with Apollo lunar soil samples

13 p1676 A73-28320

Luna 20 soil - Abundance and composition of phases in the 45-125 micron fraction.

13 p1677 A73-28330

Pb 205 as chronometer for s-process nucleosynthesis mechanism, discussing cosmochronology implications and abundance at solidification

13 p1657 A73-28923

Elemental and isotopic abundances of the volatile elements in the outer planets.

14 p1799 A73-30529

Jupiter He abundance determination methods, considering mean density, spectral line broadening and stellar occultations with emphasis on far IR emission

14 p1799 A73-30533

Low energy galactic cosmic ray exploration via space mission to Jupiter and Saturn, considering nuclear abundances and galactic evolution theories

14 p1787 A73-30542

A photometric study of the integrated light of clusters in the Magellanic Clouds and the Fornax dwarf galaxy.

14 p1801 A73-30726

Interstellar gas abundances from rocket observations of ultraviolet absorption lines.

14 p1801 A73-30734

Spectrophotometric results from the Copernicus satellite. III - Ionization and composition of the intercloud medium.

14 p1801 A73-30746

Spectrophotometric results from the Copernicus satellite. IV - Molecular hydrogen in interstellar space.

14 p1802 A73-30747

Spectrophotometric results from the Copernicus satellite. V - Abundances of molecules in interstellar clouds.

14 p1802 A73-30748

Deuterium in interstellar molecules.

14 p1802 A73-30749

Scanner observations of hot helium-carbon stars.

15 p1932 A73-31269

The fluorine abundance in the galactic cosmic radiation.

15 p1926 A73-31552

Minor and trace elements in some meteoritic minerals.

15 p1941 A73-32387

Cosmic abundance of boron.

15 p1942 A73-32648

Ionization and relative abundance of hydrogen and helium atoms in filaments of the Crab Nebula

16 p2057 A73-32712

Solar system elemental abundance from chondritic meteorites, solar atmosphere and neighborhood stars, considering Galactic and universal compositions

16 p2061 A73-33285

Experiment and observation of isotope and element separation in a plasma with cosmical applications.

17 p2216 A73-34420

A model-atmosphere abundance analysis of the B9 V star nu Capricorni.

17 p2231 A73-34758

Composition of low energy cosmic radiation from silicon to nickel.

17 p2225 A73-35787

Elemental abundance determinations for meteors by spectroscopy.

18 p2352 A73-36287

Studies of beta Coronae Borealis. I - Identification of the Actinides.

18 p2357 A73-37105

The solar abundance of silicon.

19 p2483 A73-37570

On the abundance of secondary nuclei in cosmic rays.

19 p2475 A73-37572

Isotopic composition measurements of cosmic-ray nuclei with Z greater than or equal to 10 made using a new technique.

19 p2475 A73-37628

Solar cosmic ray heavy nucleus abundances relation to oxygen nuclei in solar corona and photosphere

20 p2601 A73-38917

Chemical composition of globular-cluster stars and the form of the horizontal branch.

20 p2608 A73-39226

The peculiar A stars and the origin of the heaviest chemical elements.

20 p2611 A73-39623

Variations in the abundance of chemical elements in the classical Cepheids of the Galaxy

21 p2768 A73-40718

Solar wind alpha particle abundance variations as function of wind velocity from HEOS-1, Vela 3-A and 3-B observations

21 p2763 A73-41500

Absolute oscillator strengths in neutral chromium and the solar chromium abundance.

22 p2905 A73-41764

Observations of silicon monoxide in cool stars at 4.05 microns.

22 p2905 A73-41768

Intermediate-band photometry of RR Lyrae stars. II - Colors of RR Lyrae and ultrashort-period variables.

22 p2906 A73-41962

Doublet ratio method for abundance determination application to interstellar multiple clouds, considering column density error due to velocity distribution simplification

22 p2910 A73-42703

Theory of interstellar abundances of the isotopes of carbon, nitrogen and oxygen.

22 p2914 A73-43006

Cosmic deuterium abundance derived from measured HD/H2 ratio, noting derivation sensitivity to ionizing flux and to oxygen and carbon depletion

22 p2904 A73-43119

Line identifications, elemental abundances, and equivalent widths for 21 sharp-lined cool peculiar A stars and two comparison standards.

23 p3028 A73-43491

Primordial abundance values for heavy nuclei related to content of type 1 and 2 carbonaceous chondrites

23 p2950 A73-43752

Temperature and oxygen abundance determination in the sun from the oxygen lines

23 p3037 A73-44257

Differentiated true abundance Mars air mass calculations for use in spectroscopic observation

24 p3131 A73-44465

Early solar system deuterium abundance based on nebular chemical equilibrium, comparing with Jupiter atmosphere and meteorite data

24 p3131 A73-44468

Rare-earth elements in matrix, inclusions, and chondrules of the Allende meteorite.

24 p3133 A73-44539

Solar system cosmochemistry concerning element abundances, structure and composition of comets, planets, moon, exospheric dust and meteoroids, protosolar magnetic field, nucleosynthesis and cosmic rays

24 p3134 A73-44569

Solar abundance of Th and Pb based on photospheric line spectrum analysis for comparison with chondritic composition data

24 p3135 A73-44627

High rotational velocity correlation with metal abundance interpreted by coronal mass loss rate in metal-poor stars

24 p3140 A73-45184

AC [CURRENT]

U ALTERNATING CURRENT

AC GENERATORS

Use of cycloconverters and variable speed alternators as engine starters.

01 p0006 A73-11511

Feasibility model of airborne ac synchronous generator with rotating superconducting field winding, comparing predicted performance, size and weight with conventional technology

02 p0131 A73-11827

Three-phase-synchronous alternator with a superconducting field winding.

02 p0132 A73-11832

Superconducting magnet ac generators development, emphasizing conversion efficiency, manufacturing, relative costs, machine geometry and interwinding coupling factor effects

02 p0132 A73-11833

Colloid thruster propellants selection for semiconductor liquids with suitable electrochemical properties via cyclic voltametry

04 p0485 A73-15724

Superconducting a.c. machines - An approach to development.

07 p0779 A73-20407

Aircraft power supply alternators with superconductive field windings, calculating specific weights and performance characteristics

07 p0779 A73-20408

Lundell solid rotor brushless alternator windage power losses, measuring aerodynamic drag coefficient over Reynolds number and gap width range

09 p1034 A73-22772

Parallel operation of two Brayton-cycle alternators with parasitic speed controllers.

09 p1035 A73-22773

Three phase alternators with two/four poles superconducting inductors and with outer/inner induction winding, determining magnetic field radial distribution

10 p1177 A73-24411

Brayton cycle solar dynamic turboalternator space electric power system technology developments during 1962m1972, considering power efficiency, components reliability and future missions

11 p1309 A73-25982

Investigation of new elements and equipment configurations in stable-frequency, alternating-current, electrical power supply systems employing primary power plants consisting of engines with varying rotational speed

12 p1460 A73-26785

Features of a high voltage airborne superconducting generator.

17 p2109 A73-35254

AC starter generator featuring variable-to-constant frequency conversion by cycloconverters as switching device for use with aircraft engines

24 p3057 A73-45154

Fixed installation ground electrical power supply system for aircraft service, discussing motor-alternators, plant control cubicles, selector and busbar switchboxes and fault protection devices

24 p3075 A73-45156

ACCELERATED LIFE TESTS

Gas turbine engine hot part equivalent accelerated tests duration determination by analytical method based on Larson-Miller parametric description of long term strength

02 p0236 A73-12216

Accelerated tests for long term stability of CdS solar cells, noting stoichiometry, wavelength, doping and residual atmosphere effects on cell performance

03 p0255 A73-14215

Accelerated life testing of component reliability in aerospace systems, discussing stress tests, Arrhenius model and time transformation method

04 p0453 A73-14854

Accelerated life tests of microelectronic components by operational power dissipation, noting efficiency and profitability

07 p0799 A73-19404

Failure causes probability and accelerated life test conditions for ceramic capacitors, noting product selection by modified quality control procedures

07 p0799 A73-19405

Failure analysis of semiconductor device bonds under on-off operation, noting fatigue testing machine for accelerated life tests

08 p0972 A73-20744

Heat resistant alloys stress-rupture strength tests for operating temperatures based on equivalent high temperatures damageability

09 p1106 A73-23156

Accelerated testing of solid film lubricants.

10 p1225 A73-24635

Accelerated testing of ball bearings.

10 p1225 A73-24636

Experimental evaluation of the single-cell concept for a lightweight, rechargeable hydrogen-oxygen fuel cell.

11 p1309 A73-25987

Hot environment lubrication failures of sleeve bearing diester lubricant system in small electric motors, using reliability-temperature accelerated tests [ASME PAPER 73-DE-13]

14 p1767 A73-30819

Determination of the temperature of a sample undergoing pulsed irradiation by sunlight

15 p1896 A73-30997

Russian book - Accelerated wear-resistance tests for machine components and machinery.

15 p1881 A73-31582

Simplified exfoliation testing of aluminum alloys.

15 p1888 A73-31738

Effect of contamination on fluoric system reliability.

16 p1971 A73-33476

Accelerated testing of air-to-air guided missiles.

16 p2073 A73-33612

The Kolmogorov-Smirnov test modified for censored data.

16 p2033 A73-33619

Failure modes and accelerated life test methods for despun antenna bearings. [ASLE PREPRINT 73AM-1A-4]

17 p2178 A73-34979

Nickel-water heat pipes accelerated life testing, deriving corrosion model based on hydrogen evolution [AIAA PAPER 73-726]

18 p2369 A73-36343

General methods of determining the limiting load in brute-force reliability tests

18 p2321 A73-37023

Prediction of long-term heat-pipe performance from accelerated life tests.

21 p2643 A73-40438

ACCELERATION (PHYSICS)

NT ANGULAR ACCELERATION

NT DECELERATION

NT HIGH ACCELERATION

NT HIGH GRAVITY ENVIRONMENTS

NT IMPACT ACCELERATION

NT LUNAR GRAVITATIONAL EFFECTS

NT PARTICLE ACCELERATION

NT PHYSIOLOGICAL ACCELERATION

NT PLASMA ACCELERATION

NT SPIN REDUCTION

NT TRANSVERSE ACCELERATION

Minimization of spacecraft maximum acceleration in atmosphere after reentry, applying results to reentry trajectory optimization and associated optimal control problems

02 p0219 A73-12457

The secular accelerations of the moon's orbital motion and the earth's rotation.

04 p0497 A73-15176

A numerical study of the influence of advective accelerations in an idealized, low-latitude, planetary boundary layer.

05 p0592 A73-16192

Analytical approach to orbit determination in the presence of model errors. [AIAA PAPER 73-170]

05 p0619 A73-16915

Accuracy of the moon potential computation based on integral formulae

06 p0751 A73-18151

Accelerations of points on a flight vehicle during short-period motion

07 p0777 A73-20095

The propagation and growth of acceleration waves in heat-conducting elastic materials.

07 p0917 A73-20441

The motion of a dynamically unbalanced gyroscopic linear-acceleration integrator

09 p1081 A73-22344

A condition for drift invariance with respect to acting accelerations in a two-degree-of-freedom gyroscope having arbitrary gas lubricated bearings on the main axis

09 p1084 A73-22658

EM induction in a semi-infinite solid, impulsively moving in a uniform magnetic field

11 p1397 A73-25371

High velocity moving body in ideal incompressible fluid flow, determining lift coefficient from acceleration potential algorithm

12 p1486 A73-27239

Regularities in the burning of condensed systems within a field of mass forces at moderate pressures

13 p1706 A73-28975

Heat transfer to a strongly accelerated turbulent boundary layer - Some experimental results, including transpiration.

14 p1818 A73-30615

Zero tangential acceleration points on bodies moving in three dimensional Euclidean space, considering helical-spherical and rotating-spherical motion

14 p1775 A73-30707

Effects of composition on acceleration induced burning-rate augmentation.

15 p1925 A73-31661

Minimization of spacecraft maximum acceleration in atmosphere after reentry, applying results to reentry trajectory optimization and associated optimal control problems

15 p1941 A73-32607

Influence of acceleration on the combustion of solid propellants - Measurement and prediction of the effects

16 p2045 A73-33391

Acceleration waves in simple elastic materials.

16 p2081 A73-33746

Optimization of a vibration generator in the presence of external perturbations

16 p2083 A73-33969

Equations of motion for systems with nonlinear, second-order, nonholonomic connections

17 p2211 A73-34147

Mechanism of burning in condensed systems with solid additions in a field of mass forces

19 p2472 A73-37510

The motion of a brittle crack.

19 p2444 A73-38263

Acceleration waves in ideal fluid mixtures with several temperatures.

22 p2929 A73-41772

ACCELERATION PROTECTION

Inflated air bag head restraints for prevention of brain injuries due to whiplash acceleration during crash landings or ejection

16 p1965 A73-32654

Effects of tilting on pulmonary capillary blood flow in normal man.

20 p2519 A73-39786

Positive-pressure breathing as a protective technique during +Gz acceleration.

20 p2519 A73-39793

Biodynamic applications regarding isolation of humans from shock and vibration.

22 p2816 A73-42926

ACCELERATION STRESSES (PHYSIOLOGY)

NT CENTRIFUGING STRESS

Gravity selection by animals in fields of centrifugal acceleration superimposed on weightlessness during sounding rocket flights.

01 p0009 A73-11209

Aerodynamic pumping-caused spinal fractures in two pilots during high speed flight

02 p0137 A73-12154

DNA catabolism in rat tissues in response to transverse accelerations

06 p0650 A73-17679

Cardiovascular system reactions to alternating transverse accelerations in man

06 p0650 A73-17687

Research on the displacement of blood-plasma proteins and on the nerve conduction velocity in rats subjected to accelerations and hypokinesia

06 p0650 A73-17769

Seat reaction direction in an animal centrifuge.

07 p0780 A73-19478

Disorienting effects of aircraft catapult launchings.

07 p0785 A73-19480

Effect of accelerations on the thiamine-S/35/ distribution in the organism of white mice

08 p0929 A73-20977

Morphological changes in the juxtaglomerular apparatus of rat kidneys exposed to the action of diversely directed accelerations for many hours

08 p0929 A73-20978

The role of vestibulometry in medical evaluation of flight personnel

10 p1183 A73-23821

Positive /+Gz/ acceleration tolerances of the miniature swine - Application as a human analog.

11 p1315 A73-25337

Changes in visual functions after the action of weak vestibular stimuli

12 p1464 A73-27719

Prophylaxis and treatment of the motion sickness syndrome

13 p1580 A73-29410

Features of the influence of hypergravitation on the motor activity of the chicken embryo amnion developing under normal conditions and under conditions of constant rotation

14 p1715 A73-30022

A method of determining spinal alignment and level of vertebral fracture during static evaluation of ejection seats.

16 p1967 A73-32676

Morphological changes in kidneys during exposure to variously oriented accelerations at a level of 4 g for many hours

17 p2111 A73-34226

Impact acceleration effects on rabbit central nervous system, noting changes in nerve tissue elements and cerebral vessels

17 p2111 A73-34227

Physiological effects of acceleration and weightlessness during space flight, discussing cardiovascular system, renal function, respiration, blood volume, metabolism, work capacity, etc [AFOSR-72-2451TR]

17 p2113 A73-35856

Gravitational stress and exercise.

18 p2270 A73-35980

Metabolic responses of monkeys to increased gravitational fields.

18 p2270 A73-35982

Effect of dynamic factors of space flights on green alga *Chlorella vulgaris*.

18 p2270 A73-36098

Cross coupling between effects of linear and angular acceleration on vestibular nystagmus.

18 p2272 A73-36441

On correlation between the changes in cerebellar bioelectric activity and the adaptive reactions under the effect of accelerations.

18 p2279 A73-36915

Inverted posture illusion phenomenon in astronauts during weightless space flight, discussing vestibular organ function, acceleration effects and body gravitation sensing system

20 p2513 A73-39149

Effect of acceleration on distribution of lung perfusion and on respiratory gas exchange.

21 p2643 A73-40274

Chemical protection from genetic damages induced by radiation in the period of aftereffect of acceleration.

21 p2643 A73-40815

Human reactions to whole-body transverse angular vibrations compared to linear vertical vibrations.

23 p2948 A73-43216

ACCELERATION TOLERANCE

Effect of controlled elevation of body temperature on human tolerance to +Gz acceleration.

01 p0007 A73-10159

Direction-specific adaptation effects acquired in a slow rotation room.

03 p0268 A73-14154

Changes in cardiac rhythm during sustained high levels of positive /+Gz/ acceleration. [AD-754146]

03 p0269 A73-14157

Effect of hydrochlorothiazide on +Gz tolerance in normotensives.

03 p0269 A73-14159

Vestibular adaptation in man - Effects of increased acceleration during different phases of adaptation.

04 p0411 A73-15218

Some physiological reactions to acceleration in albino rats in a state of hypothermia

05 p0541 A73-16737

Vestibular reactions to Coriolis accelerations under hypoxia conditions

06 p0650 A73-17691

- Positive $+G_z$ acceleration tolerances of the miniature swine - Application as a human analog. 11 p1315 A73-25337
- Gravitational effects on biological systems in terms of animal body size, age, sex and posture as factors affecting acceleration tolerance 11 p1315 A73-25573
- Vestibular stresses effects on systemic and cerebral hemodynamics, considering human acceleration adaptation and compensation mechanisms 12 p1463 A73-27714
- Some aversive characteristics of centrifugally generated gravity. 13 p1575 A73-28506
- Effect of the Valsalva maneuver on tolerance to $+G_z$ acceleration. 14 p1714 A73-29754
- Cerebellar responses of animals under varied rotation conditions in a centrifuge 15 p1834 A73-31506
- Calculation of a Coriolis acceleration acting on semicircular canal receptors of man in rotating systems 15 p1835 A73-31518
- Certain features of hemodynamics during orthostatic tests with persons of different vestibulo-vegetative tolerance levels 17 p2111 A73-34236
- Normalisation of haemodynamic changes caused by action of prolonged accelerations in rats. 18 p2270 A73-35985
- Changes in whole body force transmission of dogs exposed repeatedly to vibration. 20 p2512 A73-39106
- Positive-pressure breathing as a protective technique during $+G_z$ acceleration. 20 p2519 A73-39793
- Gravitational effects on animal ontogeny from centrifugation studies of acceleration tolerance, considering egg and embryo development, body composition, etc 22 p2804 A73-42174
- Chronic acceleration effects on homeotherm physiological adaptation in terms of body weight, tolerable field intensity, growth and fat deposition inhibition, etc 22 p2804 A73-42177
- Effects of rehydration on $+G_z$ tolerance after 14-days' bed rest. 23 p2946 A73-43524
- ### ACCELEROMETERS
- #### NT STRAIN GAGE ACCELEROMETERS
- Mathematical model and error equations of inertial navigation system with two leveled accelerometers, comparing with three component and pendulum gyroscopic systems 02 p0190 A73-11778
- Performance test of flexible rolled-up solar array /FRUSA/ via telemetered data from accelerometers, strain gages and temperature sensors, noting feasibility for spacecraft power supply 03 p0256 A73-14236
- Development and application of a 0.14 gm piezoelectric accelerometer. 09 p1083 A73-22507
- High resolution accelerometer for sounding rocket, describing calibration methods [ONERA, TP NO. 1215] 10 p1219 A73-24398
- The dependence of piezo-electric accelerometer response on method of attachments. 12 p1496 A73-26974
- Explorer satellite triaxial accelerometer system to determine neutral atmosphere density, monitoring orbit adjust propulsion thrust and measuring spacecraft roll, describing instrument calibration 13 p1688 A73-28631
- Minimax failure detection and identification in redundant gyro and accelerometer systems. 13 p1616 A73-28832
- Vibrating string total field /absolute gravity meter/ accelerometer, discussing calibration at single reference point 13 p1617 A73-28849
- Simultaneous recording of acceleration and brain waves. 14 p1721 A73-29995
- Atmospheric density values from radar-determined low altitude satellite orbit decay and accelerometer data 18 p2302 A73-35942
- Strap-down inertial guidance systems study. 18 p2335 A73-36955
- Single axis analog fluoric accelerometer using mercury as solid proof mass, describing differential gas pressure outputs, porous cylindrical configuration and hydrostatic pressure gradients 19 p2389 A73-38076
- Seismometer compensation for broadband, low-level acceleration measurements. 20 p2563 A73-38773
- Equations for the instrumental errors of a type of inertial navigation system 20 p2590 A73-39045

Fluidic linear nozzle-flapper valve accelerometer for ship motion sensing, describing circuit configuration and performance tests 23 p2981 A73-43428

ACCEPTOR MATERIALS

- Investigation of the emission of donor-acceptor pairs and of their phonon echoes in CdS single crystals 01 p0088 A73-10634
- Quasi-discrete acceptor states in zero forbidden gap n-type semiconductors, showing noncompensation at low temperatures 04 p0484 A73-15567
- Investigation of defects in GaAs on the basis of the photoluminescence 15 p1923 A73-31717
- The Li donor, and binding of excitons at neutral donors and acceptors in crystals 15 p1924 A73-31722
- Luminescence of CdS single crystals doped with various donors and acceptors 19 p2471 A73-37955
- Theory of donor-acceptor radiative and Auger recombination in simple semiconductors. 23 p3016 A73-43796

ACCESS TIME

- Address structure optimization and minimum access time and decoder terminals in nonvolatile core memory array design, noting binary notation for information storage 05 p0554 A73-16991
- Access requirements for offshore airports. 15 p1856 A73-31529
- Cellular dynamic memory array with reduced data-access time. 23 p2956 A73-44116

ACCIDENT INVESTIGATION

- #### NT AIRCRAFT ACCIDENT INVESTIGATION
- Role of static electricity in the incidents recorded during the F11 firing [ONERA, TP NO. 1214] 10 p1285 A73-23750
- Data sample analysis of anomalous in-flight behavior incidents for spacecraft reliability covering incident causes and occurrence time, effects on mission and corrective actions 16 p2073 A73-33625
- Seminar on Accident Analysis and Prevention, Beirut, Lebanon, June 26-28, 1973, Working Documents. 18 p2268 A73-36845
- Engraved foil, photographic and EM flight recorders in aircraft accident investigations, discussing readout, processing and analysis 18 p2317 A73-36848

ACCIDENT PREVENTION

- Pilot incapacitation as cause of aircraft accidents, noting age connected cardiovascular disease as leading cause for loss of pilot license 01 p0013 A73-11238
- Weather condition caused aircraft accident avoidance, considering meteorological factors of air temperature, humidity, cloud formation, fog, haze, precipitation and visibility deterioration 13 p1568 A73-28554
- Aircraft accident prevention problems, considering pilot judgement errors, factory skill degradation, training, lightning and structure factors and air bag use 13 p1570 A73-29349
- Man machine systems for flight safety, studying accidents, human factors in system design and implementation of personnel 17 p2113 A73-34078
- The effects of fatigue on health and flight safety. 17 p2113 A73-34080
- Safety in the accident prone flight phases of take-off, approach and landing. 17 p2098 A73-34085
- Anthropometric dummy design improvements, detailing verisimilitude specifications for harness support in accident tests and design of chest, spine, shoulder and pelvic areas 17 p2114 A73-34617
- General aviation aircraft stall/spin prevention device for limiting tail power near wing stall angle of attack [SAE PAPER 730333] 17 p2102 A73-34686
- Seminar on Accident Analysis and Prevention, Beirut, Lebanon, June 26-28, 1973, Working Documents. 18 p2268 A73-36845
- Aircraft accident statistics for passenger fatalities, worldwide jet hull losses and estimated costs to suggest proposals for approach, landing and takeoff accident reduction 18 p2268 A73-36846
- Objectives of training in relation to accident prevention. 18 p2284 A73-36850
- Annex 13 and the work of the aviation pathologist - Practical problems. 19 p2398 A73-37739
- Corporate aircraft accident analysis to reduce accident rate, examining seasonal and diurnal statistics, aircraft types, runway conditions, crew factors and maintenance defects 20 p2509 A73-39219

Design and analysis of an energy absorbing restraint system for light aircraft crash-inapt. [ASME PAPER 73-DET-111] 22 p2799 A73-42080

Reducing approach and landing accidents. 22 p2799 A73-42523

ACCIDENT PRONENESS

- Personal life changes and health stresses in contrast to accident proneness as factors in pilot error 05 p0545 A73-16732
- Self destructive behavior of aircraft pilot due to stress accumulation, discussing man machine relationship, coping mechanisms, competence and invulnerability myth 17 p2115 A73-34746

ACCIDENTS

- #### NT AIRCRAFT ACCIDENTS
- #### ACCLIMATIZATION
- #### NT ALTITUDE ACCLIMATIZATION
- #### NT COLD ACCLIMATIZATION
- #### NT HEAT ACCLIMATIZATION
- Acclimatization to severe dry heat by brief exposures to humid heat. 03 p0267 A73-13700

ACCOMMODATION

- #### NT VISUAL ACCOMMODATION
- #### ACCOMMODATION COEFFICIENT
- Rarefied gas interaction with spacecraft surface, calculating aerodynamic forces and accommodation coefficient for Proton 2 satellite 03 p0383 A73-14574
- Effect of accommodation coefficient on thermal creep flow of rarefied gas. 04 p0436 A73-15973
- The influence of the accommodation coefficients on the flow variables in the viscous interaction region of a hypersonic slip-flow boundary layer. 07 p0773 A73-19206
- The use of the thermal accommodation coefficients of a rare gas for studying the adsorption of an active gas on a metal, such as in the case of nitrogen and oxygen on tungsten 07 p0839 A73-20150
- Temperature dependence of the accommodation coefficient of liquid-helium film. 10 p1249 A73-24341
- Experimental study of shock-wave reflection from a thermally accommodating wall. 11 p1449 A73-25252
- Lower thermosphere density and composition model from satellite drag and accommodation coefficients 12 p1488 A73-26990
- Reflection of a shock wave from a thermally accommodating wall - Molecular simulation. 22 p2842 A73-42234
- Poiseuille flow at arbitrary Knudsen numbers and tangential momentum accommodation. 24 p3079 A73-45313

ACCRETION

- #### U DEPOSITION
- #### ACCUMLATORS
- #### NT DUST COLLECTORS
- #### NT SOLAR COLLECTORS
- #### ACETALDEHYDE
- Modeling the ignition and cool-flame limits of acetaldehyde oxidation. 13 p1581 A73-28999
- #### ACETANILIDE
- The pharmacology of practolol - A cardioselective beta adrenergic blocking drug. 09 p1044 A73-21850

ACETATES

- Comparative data of investigations of aerial films on lavsan and triacetate bases 04 p0447 A73-14850
- The isolation of a series of acyclic isoprenoid alcohols from an ancient sediment - Approaches to a study of the diagenesis and maturation of phytol. 11 p1326 A73-25465
- Influence of certain hydroxyl- and nitrogen-containing low-molecular-weight substances on the structural viscosity of cellulose acetate solutions 21 p2647 A73-40263
- Influence of a mixture of plasticizers, exhibiting a different mechanism of action, on the deformation of cellulose triacetate over a wide range of temperatures 21 p2647 A73-40264

ACETATION

- #### U ACETYLATION
- #### ACETYL COMPOUNDS
- Gas-liquid chromatography of trifluoroacetyl derivatives of cyclitols. 11 p1325 A73-25150

ACETYLIATION

- Investigation of the possibility of using acetylated oxyethylcellulose as a film forming substance for a moving-picture film base 21 p2647 A73-40262

ACETYLENE

- Radio telescope identification of interstellar isocyanic acid, methylacetylene and hydrogen isocyanide molecules from pure rotational transitions 06 p0751 A73-18229
- Gain measurements on CO P-branch transitions in a C₂H₂-O₂ flame. 07 p0788 A73-19634

- Kinetics of the degassing of oxygen-containing niobium in flowing acetylene to form carbon monoxide
11 p1375 A73-26565
- Methylacetylene and isocyanic acid data from April 1972 and February 1973 observation of interstellar media in direction of Galactic center source Sgr B2
16 p2060 A73-33095
- CW laser action from acetylene oxidation, noting sensitivity to total pressure and helium, oxygen and acetylene partial pressure changes
20 p2573 A73-39676
- Atomic oxygen reaction with acetylene in low pressure fast flow system, measuring free radical formation rate by photoionization mass spectrometer
22 p2818 A73-42768
- ACHONDRITES**
Thallium isotope analysis of terrestrial chondrites and achondrite and lunar soil, noting lunar chronology information from lead isotope extinct radioactivity
03 p0375 A73-14109
- Petrography, mineralogy and composition of plagioclase and pyroxenes of Washougal howardite by density and refraction measurements
09 p1139 A73-21853
- Havero stony ureilite origin modes, composition, textural features, mineralogy and petrology
09 p1139 A73-21860
- Half life and activity of cosmogenic radionuclides in Havero /Finland/ achondrite determined by non-destructive gamma ray spectrometry
09 p1139 A73-21861
- Morphologies of iron crystals from the Havero meteorite.
09 p1140 A73-21862
- Forms of carbon in the new Havero ureilite of Finland.
09 p1140 A73-21863
- Argon-37, argon-39, and tritium radioactivities in the Havero meteorite.
09 p1140 A73-21865
- The highly reflecting and opaque components in the mineral content of the Havero meteorite.
09 p1140 A73-21866
- Neutron activation and irradiation analyses of Havero ureilite elemental abundances
09 p1140 A73-21867
- Elemental abundances and chemistry of Havero carbonaceous ureilite, noting similarity to Allende inclusions pattern
09 p1047 A73-21868
- Havero ureilite - Evidence for recrystallization and partial reduction.
09 p1140 A73-21869
- Noble gas and carbon abundances of the Havero, Dingo Pup Donga, and North Haig ureilites.
10 p1277 A73-24104
- Argon 40-argon 39 chronology of four calcium-rich achondrites.
10 p1278 A73-24110
- Pb isotopic composition measurement in chondrites and achondrite for model ages, noting 50 My variations
17 p2233 A73-35265
- Radiochemical neutron activation analysis for U and Th abundance measurement in achondrites and pallasite olivines
17 p2120 A73-35802
- ACID BASE EQUILIBRIUM**
Control of exercise hyperpnea under varying durations of exposure to moderate hypoxia.
03 p0259 A73-13499
- Pulmonary respiration and acid-base state in hibernating marmots and hamsters.
08 p0932 A73-21613
- Intermittent exercise - Metabolites, oxygen pressure, and acid-base equilibrium in the blood.
09 p1041 A73-22933
- Effect of stepwise adaptation to high-mountain areas on the respiratory function and the acid-alkali equilibrium of blood in subjects with different motor activity stresses
17 p2111 A73-34232
- ACIDITY**
Gas-phase acidities of binary hydrides.
02 p0139 A73-12632
- Accurate relative acidities in the gas phase - Hydrogen sulfide and hydrogen cyanide.
02 p0139 A73-12634
- ACIDOSIS**
Heart muscle viability following hypoxia - Protective effect of acidosis.
17 p2110 A73-34097
- Anaerobic threshold and respiratory gas exchange during exercise.
20 p2519 A73-39785
- ACIDS**
NT AMINO ACIDS
NT ASPARTIC ACID
NT BUTYRIC ACID
NT CARBOXYLIC ACIDS
NT CHROMIC ACID
NT DEOXYRIBONUCLEIC ACID
NT FATTY ACIDS
NT GLUTAMIC ACID
NT HEXOGENES [TRADEMARK]
- NT HYDROCHLORIC ACID
NT HYDROCYANIC ACID
NT HYDROFLUORIC ACID
NT LACTIC ACID
NT LEUCINE
NT LYSINE
NT METHIONINE
NT NITRIC ACID
NT NUCLEIC ACIDS
NT OLEIC ACID
NT OXIDASE
NT PEPTIDES
NT PERCHLORIC ACID
NT PHENYLALANINE
NT PHOSPHORIC ACID
NT PYRIDINE NUCLEOTIDES
NT PYRUVATES
NT RIBONUCLEIC ACIDS
NT SULFURIC ACID
NT THYROXINE
NT TRYPTOPHAN
- Acids obtained by oxidation of kerogens of ancient sediments of different geographic origin.
11 p1326 A73-25467
- ACLINAL VALLEYS**
U VALLEYS
- ACOUSTIC ATTENUATION**
NT SHOCK WAVE ATTENUATION
Dislocation damping in ultrasound-irradiated molybdenum single crystals
01 p0061 A73-10251
- Stability of combustors with partial length acoustic liners.
01 p0090 A73-10641
- Theory of Kapitza's jump in temperature at the interface between a solid body and liquid helium
01 p0079 A73-11281
- The optimisation of sound attenuation in lined ducts containing uniform, axial, subsonic, mean flow.
03 p0291 A73-12987
- On the measurement of the local impedance of acoustical duct liners in the presence of grazing mean air flow.
03 p0342 A73-12989
- Ultrasonic attenuation measurement of a microplastic memory effect in aluminum single crystals.
03 p0323 A73-13331
- Screen and porous absorbing liner design for damping pressure oscillations in ramjet combustors based on acoustic absorption efficiency and combustion instability calculation
[AIAA PAPER 73-226] 06 p0767 A73-17665
- Conservation of energy in random media, with application to the theory of sound absorption by an inhomogeneous flexible plate.
07 p0851 A73-19153
- A mathematical analysis concerning the edge effect of sound absorbing materials.
08 p0987 A73-21124
- Theory of a generalized Helmholtz resonator.
08 p0952 A73-21471
- Experimental verification of the energy dissipation mechanism in acoustic dampers.
08 p1024 A73-21472
- A quality criterion test for tubes intended for measurement of acoustic absorption and impedance coefficients
09 p1121 A73-23105
- Sound absorption in lined rectangular ducts with wall shear layers - Convergence of the numerical procedure to the analytical solution.
13 p1658 A73-28061
- Piezoelectric sound pressure sensor for damping measurement of structural element coatings under intense acoustic loads
13 p1618 A73-29060
- Ultrasonic attenuation measurements in metals at low temperatures.
13 p1662 A73-29639
- Attenuation of an ultrasonic signal in aluminum deformed according to a harmonic law
14 p1764 A73-30857
- Sponge rubber absorption coefficient of sound and acoustic impedance measurements to test porous material sound absorption theories
14 p1767 A73-30894
- The attenuation of ultrasonic waves in cylindrical work pieces with central bore-hole
15 p1882 A73-32053
- The optimization of modal sound attenuation in ducts, in the absence of mean flow.
15 p1865 A73-32152
- Ray models for sound propagation and attenuation in ducts, in the absence of mean flow.
15 p1865 A73-32153
- The propagation and attenuation of sound in lined ducts containing uniform or 'plug' flow.
16 p1970 A73-33944
- Some aspects of 'sound' attenuation in lined ducts containing inviscid mean flows with boundary layers.
16 p2049 A73-33946
- Ultrasound absorption coefficient measurement in semiconductor crystal lattices based on acoustoelectrical effect
17 p2218 A73-34159
- Piezoelectric sound pressure sensor for damping measurement of structural element coatings under intense acoustic loads
18 p2317 A73-36892
- On energy, group velocity and small damping of sound waves in ducts with shear flow.
18 p2302 A73-37031
- Transient and steady state sound absorption coefficients of fiberglass and polyurethane foam.
19 p2459 A73-37286
- Extraneous modes in sound absorbent ducts.
19 p2459 A73-37294
- Noise from turbomachinery.
[AIAA PAPER 73-815] 19 p2473 A73-37469
- The effect of stiffeners on the sound radiation and the transmission loss of metal walls
19 p2460 A73-38181
- A high resolution pulse transmission technique for determining ultrasonic velocities.
20 p2564 A73-38881
- Acoustooptic materials evaluation based on figures of merits and acoustic attenuation for laser beam deflection device design and fabrication
21 p2710 A73-40095
- A rational approach to the synthesis of one-dimensional acoustic filters.
21 p2739 A73-40285
- Attenuation of spiral modes in a circular and annular lined duct.
22 p2839 A73-41714
- Loudness changes resulting from an electrically induced middle-ear reflex.
22 p2811 A73-41815
- Noise reduction by enclosures to block airborne and structure-borne acoustic paths, developing models for insertion loss in different frequency ranges
22 p2888 A73-42924
- Theory of the Kapitza temperature discontinuity at a solid body-liquid helium boundary.
23 p3006 A73-43502
- Further aspects of weak shock theory applied to the solar chromosphere.
24 p3135 A73-44630
- A model for the pressure excitation spectrum and acoustic impedance of sound absorbers in the presence of grazing flow.
[AIAA PAPER 73-995] 24 p3077 A73-44830
- Unsteady aerodynamic loads on slender cones at free-stream Mach numbers from 0 to 22.
[AIAA PAPER 73-998] 24 p3053 A73-44833
- Acoustic propagation in ducts with varying cross sections and sheared mean flow.
[AIAA PAPER 73-1008] 24 p3078 A73-44841
- ACOUSTIC COMBUSTION**
U COMBUSTION STABILITY
ACOUSTIC DELAY LINES
Low cost monolithic range gated radar moving target indicator using bucket brigade delay line circuits
02 p0141 A73-12360
- Acoustic properties of fluid mixtures for ultrasonic delay lines, noting temperature and composition effects on water-glycol mixture parameters
03 p0280 A73-14620
- Convolution and correlation by nonlinear interaction in a diode-coupled tapped delay line.
06 p0678 A73-18746
- Bending waves dispersion properties in rod applied to acoustic LF dispersion delay line design, analyzing signal distortion and attenuation during propagation
10 p1291 A73-24366
- Image processing using acoustic surface waves.
11 p1334 A73-23558
- The design and applications of highly dispersive acoustic surface-wave filters.
12 p1484 A73-27564
- IMCON reflection mode dispersive delay line in large time-bandwidth product pulse compression systems, deriving operational characteristics from transfer function
12 p1480 A73-27565
- Surface acoustic wave multistrip components and their applications.
12 p1484 A73-27567
- Signal processing device with parametric interaction between opposite acoustic waves passing through delay line considering real time convolution and time inversion capabilities
12 p1470 A73-27569
- A programmable surface acoustic wave matched filter for phase-coded spread spectrum waveforms.
12 p1484 A73-27574
- Experimental correlation techniques for the characterisation of vibration transmission paths.
20 p2617 A73-39267
- Octave-bandwidth, acoustic M/W frequency-memory loop.
22 p2834 A73-42873
- ACOUSTIC DUCTS**
Mathematical treatment of long wave sound propagation in curved ducts and junctions, obtaining principal mode from linearized equation of motion solved for eigenvalues
03 p0343 A73-13832
- The transmission of sound in an acoustically treated rectangular duct with boundary layer.
04 p0476 A73-15586

- Attenuation of spiral modes in a circular and annular lined duct. 04 p0487 A73-15591
- Refraction of acoustic duct waveguide modes by exhaust jets. 07 p0812 A73-20338
- Effects of wall admittance changes on duct transmission and absorption of sound. 13 p1658 A73-28060
- Sound absorption in lined rectangular ducts with wall shear layers - Convergence of the numerical procedure to the analytical solution. 13 p1658 A73-28061
- The optimization of modal sound attenuation in ducts, in the absence of mean flow. 15 p1865 A73-32152
- Ray models for sound propagation and attenuation in ducts, in the absence of mean flow. 15 p1865 A73-32153
- Nonlinear acoustics of inviscid fluid in duct with varying cross section, obtaining propagation velocity potential as power series for reduction to Neumann problem. 15 p1865 A73-32154
- Acoustic radiation from the end of a two-dimensional duct - Effects of uniform flow and duct lining. 16 p1999 A73-32914
- The propagation and attenuation of sound in lined ducts containing uniform or 'plug' flow. 16 p1970 A73-33944
- Acoustic energy flow in lined ducts containing uniform or 'plug' flow. 16 p2038 A73-33945
- Some aspects of 'sound' attenuation in lined ducts containing inviscid mean flows with boundary layers. 16 p2049 A73-33946
- Fundamentals of aerodynamic sound theory and flow duct acoustics. 17 p2155 A73-35331
- Wind tunnel acoustic and vibration test facilities, including anechoic chambers, subsonic boundary layer tunnels, acoustic ducts, reverberation rooms, and rotor noise chambers. 17 p2148 A73-35334
- Noise of jets discharging from a duct containing bluff bodies. 19 p2472 A73-37291
- Extraneous modes in sound absorbent ducts. 19 p2459 A73-37294
- Attenuation of spiral modes in a circular and annular lined duct. 22 p2839 A73-41714
- Rolls-Royce RB-211 jet engine noise reduction program, considering fan, compressor, turbine and tail-pipe noise and acoustic linings and powerplant configurations. 22 p2900 A73-41717
- Shear layer effect on acoustic duct wall impedance for sound propagation in uniform flow in terms of parabolic cylinder functions. 22 p2900 A73-41717
- Unsteady aerodynamic loads on slender cones at free-stream Mach numbers from 0 to 22. 24 p3053 A73-44833
- Computational methods for studying acoustic propagation in nonuniform waveguides. 24 p3078 A73-44839
- A difference theory for noise propagation in an acoustically lined duct with mean flow. 24 p3078 A73-44840
- Acoustic propagation in ducts with varying cross sections and sheared mean flow. 24 p3078 A73-44841
- Sound interaction with a helical flow contained in an annular duct with radial gradients of flow, density and temperature. 24 p3078 A73-44842
- Transmission and far field radiation of sound waves in and from lined ducts containing shear flow. 24 p3078 A73-44845
- The influence of aerodynamic flow noise in turbofan engines. 24 p3121 A73-44848
- ACOUSTIC EXCITATION**
- Experimental investigation of stresses in plates acted on by acoustic loads. 02 p0235 A73-12135
- Solid propellant combustion instability suppression devices. 03 p0353 A73-13382
- Holographic correlation offers new possibilities for acoustical NDT. 04 p0446 A73-14675
- Sonic degradation of thermally shocked ceramics. 04 p0448 A73-15124
- Flow induced vibration of cantilever mounted flat plates in an enclosed passage An experimental investigation. 04 p0513 A73-15590
- Two dimensional cascade acoustic resonant frequencies estimation by variational method, presenting results for three cavity modes. 05 p0599 A73-17372
- Experiments on the nonlinear stages of free-shear-layer transition. 06 p0687 A73-18530
- Acoustic amplification during solid propellant combustion. 07 p0865 A73-19390
- Microwave or acoustic holographic synthetic aperture interferometry with pulsed techniques, noting single scan, resolution and fringe number advantages. 07 p0824 A73-20110
- Acoustic radiation from plates excited by flow noise. 08 p0988 A73-21470
- Acoustical holography applications in nondestructive testing. 09 p1083 A73-22514
- Estimation of possible excitation frequencies for shallow rectangular cavities. 09 p1029 A73-23444
- Acoustically induced vibrations of slender rods in a cylindrical duct with parallel flow. 11 p1432 A73-24983
- Acoustical method for determining thermal diffusivity and relative difference in molar heat capacities of tantalum and vanadium. 11 p1448 A73-25127
- Study of excitation conditions for a piezo-semiconductor oscillator by the electron modeling method. 14 p1737 A73-30946
- Observation of stable, high Mach number collisionless electrostatic shocks. 15 p1916 A73-31079
- Flexural wave mechanics - An analytical approach to the vibration of periodic structures forced by convected pressure fields. 16 p2083 A73-33947
- Nonlinear gas oscillations in pipes. I - Theory. 18 p2299 A73-36505
- A real-time software operating system for a computer-controlled acoustic emission flow monitor. 18 p2316 A73-36679
- A closed-loop automatic control system for high-intensity acoustic test systems. 18 p2296 A73-36712
- On the energetics and momentum balance of polequator temperature differences in the sun. 19 p2485 A73-37620
- Sonic wave excitation by optical radiation, considering electrostriction effect and radiation absorption with subsequent intensity inhomogeneity-caused pressure gradients. 22 p2868 A73-41898
- German monograph - Lifetime detection in the case of acoustically loaded structures on the basis of the appropriate form of vibration. 22 p2924 A73-42741
- On aeroacoustic coupling in free-stream turbulence manipulators. 24 p3054 A73-44847
- ACOUSTIC FATIGUE**
- Inlet duct sonic fatigue induced by the multiple pure tones of a high bypass ratio turbofan. 16 p2046 A73-33141
- Acoustic fatigue in ceramic materials, analyzing strength degradation as function of microstructure, structural integrity and properties. 16 p2030 A73-33194
- Procedure for the simulation of sonic fields, particularly for fatigue tests. 16 p1997 A73-33384
- Weldbonding/rivetbonding - Application testing of thin gauge aircraft components. 19 p2433 A73-37464
- Acoustic fatigue resistance of aircraft structures at elevated temperatures. 24 p3056 A73-44829
- ACOUSTIC GENERATORS**
- U SOUND GENERATORS**
- ACOUSTIC IMPEDANCE**
- Study of the acoustic reflex in human beings. I - Dynamic characteristics. 01 p0013 A73-10828
- On the measurement of the local impedance of acoustical duct liners in the presence of grazing mean air flow. 03 p0342 A73-12989
- Dynamic stability of a cylindrical shell in an acoustic medium. 03 p0393 A73-13834
- Piezoelectric transducers for the study of short-duration mechanical loads. 04 p0448 A73-15374
- A quality criterion test for tubes intended for measurement of acoustic absorption and impedance coefficients. 09 p1121 A73-23105
- Effects of wall admittance changes on duct transmission and radiation of sound. 13 p1658 A73-28060
- Dynamic properties of human and animal middle ear in terms of acoustic impedance, transfer function, impulse response, sound diffraction and reflex sensitivity. 14 p1715 A73-30279
- Sponge rubber absorption coefficient of sound and acoustic impedance measurements to test porous material sound absorption theories. 14 p1767 A73-30894
- An impedance tube for precision measurement of acoustic impedance and insertion loss at high sound pressure levels. 16 p2013 A73-32916
- The acoustic impedance of perforates at medium and high sound pressure levels. 18 p2337 A73-37030
- Shear layer effect on acoustic duct wall impedance for sound propagation in uniform flow in terms of parabolic cylinder functions. 22 p2900 A73-43138
- A model for the pressure excitation spectrum and acoustic impedance of sound absorbers in the presence of grazing flow. 24 p3077 A73-44830
- Experimental and theoretical determination of the admittances of a family of nozzles subjected to axial instabilities. 24 p3122 A73-45267
- ACOUSTIC INSTABILITY**
- Evaluation of acoustic cavities for combustion stabilization. 03 p0356 A73-13452
- Acoustic resonance during the vibrations of a plate cascade in subsonic gas flow. 03 p0294 A73-13619
- Spatial plasma echoes of ion acoustic waves in low pressure He and Ne discharges in anode direction. 03 p0348 A73-14622
- Interaction of sound and flow in T-burners - Experiments compared with theory. 06 p0741 A73-17662
- A source of nonlinear distortions in acoustic emission. 11 p1399 A73-26093
- Nonlinear ion sound in a fully ionized current-carrying plasma. 11 p1406 A73-26186
- Acoustic instability of a bounded weakly ionized plasma. 17 p2214 A73-34135
- Absolute instability of the interaction between optical and acoustic waves. 20 p2594 A73-39679
- The ion-sound instability and its associated multimode phenomena. 24 p3115 A73-44874
- ACOUSTIC MEASUREMENTS**
- Helicopter internal and external noise level measurements under various flight conditions, obtaining noise radiation directivity patterns via time measuring trajectoryography equipment. 01 p0004 A73-10241
- The acoustic emission response of mechanically stressed ceramics. 02 p0173 A73-11989
- Russian book on ultrasonic processing in metal crystallization covering design of vibrators and transducers and acoustic power measurement. 02 p0175 A73-12800
- Contribution to the study of noise measured by a microphone placed in a gaseous flow. 03 p0290 A73-12973
- Osaka airport effective continuous perceived noise level measurements, area contour map and noise duration allowance vs aircraft distance diagram. 03 p0249 A73-12977
- Acoustic emission during burst tests of filament wound composite pressure bottles as function of pressure, microscopic damage and winding parameters. 03 p0331 A73-13031
- Atmospheric wind and temperature inhomogeneity induced sound wave refraction effects on acoustic sounder measurements, noting scattering volume displacement and Doppler shift. 03 p0276 A73-13831
- Cross correlations between turbulent jet flow and noise from hot-film and acoustic signal measurement, using Proudman form of Lighthill integral. 03 p0246 A73-13842
- Aerodynamic noise and boundary-layer transition measurements in supersonic test facilities. 03 p0296 A73-14191
- The early detection of fatigue damage by exoelectron emission and acoustic emission. 04 p0453 A73-14858
- Verification of structural integrity of pressure vessels by acoustic emission and periodic proof testing. 04 p0453 A73-14859
- Flap noise measurements for STOL configurations using external upper surface blowing. 04 p0487 A73-14922
- Acoustic emission source location using single and multiple transducer arrays. 04 p0448 A73-15121
- An improved acoustic viscosimeter for studies of the viscosity of simple fluids in the critical region. 04 p0448 A73-15123
- A note on the quantity /effective/ perceived noise and units of perceived noise level. 04 p0406 A73-15587
- Field experience with digital control systems for vibration and acoustic testing. 05 p0554 A73-16637

Evaluation of the noise autocorrelation function of stationary and moving noise sources by a cross correlation method.

[AIAA PAPER 73-186] 05 p0598 A73-16925
Flyover and static tests to investigate external flow effect on jet noise for nonsuppressor and suppressor exhaust nozzles.
[AIAA PAPER 73-190] 05 p0531 A73-16927
Atmospheric attenuation of noise measured in a range of climatic conditions.
[AIAA PAPER 73-242] 05 p0570 A73-16966
Noise characteristics of combustion augmented high speed jets.

[AIAA PAPER 73-189] 06 p0767 A73-17655
Results of an experimental program for the development of sonic inlets for turbofan engines.
[AIAA PAPER 73-222] 06 p0645 A73-17664
Measurements of the acoustical parameters of rock powders and the Gold-Soter lunar model.
07 p0894 A73-19850

Acoustic emission weld monitoring of nuclear components.
07 p0832 A73-20274

Sound pressure level spectra measurements for four- and three-engine jet transport during concrete and grassy surface runup and flyover
[SAE AIR 1216] 08 p0927 A73-20693
Some perspectives on receiver noise performance and its measurement.

08 p0940 A73-21624
Microwave and millimeter wave receiver noise performance state of art and acoustic measurement methods, discussing traveling wave maser, parametric and transistor amplifiers and tunnel diodes.
08 p0940 A73-21625

Multielement scanning system for acoustic holography application in nondestructive testing, combining multiple mechanical sensors with simultaneous electronic commutation
09 p1080 A73-22297

Acoustic emission for monitoring fatigue crack growth.
09 p1083 A73-22511

A quality criterion test for tubes intended for measurement of acoustic absorption and impedance coefficients
09 p1121 A73-23105

Apparatus for recording acoustic signals from cracks initiated in brittle materials.
09 p1086 A73-23165

A single number rating for effective noise reduction.
11 p1397 A73-25000

Ultrasonic measurement of elastic moduli in slender specimens using extensional and torsional wave pulses.
11 p1365 A73-26171

Seismic measurement data from Cornish cottage during Concorde sonic boom flight, using moving coil geophones
11 p1306 A73-26292

Equivalent continuous sound level determination from instantaneous sonic intensity measurement during representative time period, describing electron measuring device and circuitry
11 p1367 A73-26416

Measuring projection weld strength by acoustic emission.
12 p1502 A73-27038

Acoustic and fluid dynamic tests of multilobed discharge silencers scale models, noting optimum jet noise attenuation configuration
12 p1486 A73-27390

Russian book on ultrasonic methods for weld testing covering flaw detection, emitters/receivers, acoustic channels, echo and mirror shadow methods, automatic testing, etc
13 p1624 A73-28949

A potential means of using acoustic emission for crack detection under cyclic-load conditions.
13 p1700 A73-29401

Internal fracture and acoustic emission of fiberglass reinforced plastics.
13 p1647 A73-29544

Acoustic-emission detection techniques for high-cycle-fatigue testing.
14 p1751 A73-29772

Low-frequency noise characteristics of commercial silicon and gallium arsenide IMPATT diodes.
15 p1851 A73-32188

Residual stress measurement and analysis using ultrasonic techniques.
15 p1879 A73-32249

Acoustic generation and propagation in annular ducts of axial flow fans, discussing techniques for in-duct fan noise modal distribution measurement
16 p1999 A73-32846

Standard indoor method of collection and presentation of the bare turboshaft engine noise data for use in helicopter installations.
[SAE ARP 1279] 16 p2046 A73-33020

Prediction and measurement of aircraft noise.
16 p2014 A73-33133

Inlet duct sonic fatigue induced by the multiple pure tones of a high bypass ratio turbofan.
16 p2046 A73-33141

A closed-loop automatic control system for high-intensity acoustic test systems.
16 p1994 A73-33147

Region of existence of frictional noise and experimental verifications
16 p2036 A73-33215

Experimental educational noise surveys of rural, suburban, urban and industrial areas at various times of day, using computerized data processing
16 p2036 A73-33216

Procedure for the simulation of sonic fields, particularly for fatigue tests
16 p1997 A73-33384

Forecasting failures with acoustic emission.
16 p2022 A73-33992

Hydraulic system noise measurements and control, discussing source, vibrating parts isolation, transmission path and acoustic barriers and enclosures
16 p1971 A73-33993

Flaw detection and characterization using acoustic emission.
16 p2022 A73-34013

Acoustic emission coincidence detector for monitoring high residual stress areas in symmetrical pressure vessels.
17 p2166 A73-34620

Continuous monitoring of fatigue crack growth by acoustic emission techniques.
[TR-DE-73-2] 17 p2148 A73-35445

Book - Experimental techniques in fracture mechanics.
17 p2252 A73-35668

Acoustic emission instrumentation and application for plastic deformation, flaw detection monitoring of fatigue crack growth, stress corrosion and hydrogen embrittlement
17 p2175 A73-35670

A survey of nondestructive testing techniques.
18 p2320 A73-36484

Sound measurements within and in the radiated field of an annular duct with flow.
18 p2302 A73-37028

A proposed littoral airport.
19 p2415 A73-37280

Application of the coherence function to acoustic noise measurements.
19 p2458 A73-37284

Correction procedure for outdoor noise measurements.
19 p2458 A73-37285

Fan acoustic measurements by hot-wire anemometers in anechoic chamber, discussing turbulent flow characteristics, noise spectra, wire velocity spectra and blade tip shape
19 p2472 A73-37289

Oblique reflection of a plane acoustic wave from a burning surface
19 p2503 A73-37513

Turbofan suction noise level measurements, discussing octave noise analysis, angular velocity distributions, discharge coefficient, takeoff and landing operations
19 p2473 A73-37816

Jet aircraft noise abatement near airports during takeoff, approach and landing, discussing noise measurement standards and regulatory and noise reduction design efforts
19 p2385 A73-37825

Subsonic jet noise measurements on model jet rig in anechoic chamber, discussing correlation and prediction
19 p2473 A73-38106

Acoustic echo-sounding techniques and their application to gravity-wave, turbulence, and stability studies.
19 p2405 A73-38207

The remote sensing of wind velocity in the lower troposphere using an acoustic sounder.
19 p2427 A73-38208

The design and construction of an anechoic chamber lined with panels and intended for investigation of aerodynamic noise
21 p2674 A73-40942

Sonic bang investigations associated with the Concorde's test flying.
21 p2635 A73-41174

Technical progress on new vibration and acoustic tests for proposed MIL-STD-810C, 'environmental test methods.'
21 p2674 A73-41200

Near-earth micrometeorite flux measurement by rocket-borne acoustic detectors, noting consistency with previous observations
21 p2775 A73-41415

Basic acoustic considerations for model noise experiments in wind-tunnels.
22 p2838 A73-41705

Perceived noise level ratings for helicopter noise, discussing blade slap, tail rotor whine, broadband noise and PNL rating shortcomings
22 p2798 A73-41708

Russian book on electroacoustic and electromechanical devices for sound recording and measurement covering human auditory system,
22 p2800 A73-42945

microphones, loudspeakers, hydrophones, geophones, etc
22 p2832 A73-41882

Acoustic emission measurements during plastic deformation of metals.
22 p2919 A73-41975

Atmospheric absorption considerations in airplane flyover noise at altitudes above sea level.
22 p2799 A73-42943

Helicopter noise experiments in an urban environment.
22 p2800 A73-42944

Runway sideline aircraft noise measurements on takeoff and approach for enforcing community noise levels based on FAA aircraft type certification, noting associated problems
22 p2800 A73-42945

Community noise impact study from military helicopter operations.
22 p2800 A73-42947

Fatigue crack growth detection by acoustic emission monitoring in correlation with stress intensity for high cycle fatigue A1 alloy
23 p2992 A73-43814

Acoustic emission from low-cycle high-stress-intensity fatigue.
23 p2992 A73-43816

Prediction of failure processes in fiberglass-reinforced plastics by a seismoacoustic method. II - Features of damage buildup in woven fiberglass-reinforced plastics in uniaxial tension
24 p3102 A73-44507

Measurements of the distribution of sound source intensities in turbulent jets.
24 p3053 A73-44826

Swirling flow effect on jet noise suppression based on acoustic field and engine thrust measurements with and without stationary swirl vanes in exhaust nozzle
[AIAA PAPER 73-1003] 24 p3077 A73-44836

Noise comparisons from full-scale fan tests at NASA Lewis Research Center.
24 p3121 A73-44849

The effects of modulated blade spacing on static rotor acoustics and performance.
[AIAA PAPER 73-1020] 24 p3121 A73-44852

Acoustic investigation of the engine-over-the-wing concept using a D-shaped nozzle.
[AIAA PAPER 73-1030] 24 p3122 A73-44860

Microphone radiated acoustic power directivity measurement enhancement by integral transform, matrix inversion and relaxation techniques, considering application limits, resolution, noise sensitivity and computation
[AIAA PAPER 73-1040] 24 p3090 A73-44865

A new device for measuring local acoustic power output of subsonic jets.
[AIAA PAPER 73-1042] 24 p3090 A73-44866

Acoustic emission produced during burst tests of filament-wound bottles.
24 p3094 A73-45146

Materials testing by sonic emission analysis (SEA/
24 p3094 A73-45445

ACOUSTIC PROPAGATION

Acoustic feedback phenomena in the case of a subsonic and supersonic free jet which impinges on an obstacle
[DGLR PAPER 72-084] 02 p0127 A73-11683

Russian papers on nonlinear optics and hyperacoustics covering laser use in ultrasound propagation study and thermal and stimulated molecular light scattering effects
02 p0194 A73-11944

Model study of aircraft noise reverberation in a city street.
02 p0130 A73-12199

Aerodynamic noise characteristics, discussing turbulent fluid acoustic propagation equation modification and antinoise legislation
03 p0241 A73-12952

The investigation of the effect of acoustic oscillations on the combustion process of gaseous fuel
03 p0396 A73-12955

Partial optical coherence theory based Greenspon modification for calculation of sound power radiation from statistically vibrating flat surfaces
03 p0384 A73-12991

Perturbation technique for approximation of sound radiation from controlled boundary layer on thin plate, deriving random stationary functions in terms of Fourier integral
03 p0291 A73-12992

Reproduction of sound propagation in the standard atmosphere
03 p0342 A73-12993

Weak normal shock wave interactions with materials, investigating incident pressure ratio, thickness, perforation diameter, close area and flow resistance effects on acoustic reflectance
[AIAA PAPER 73-244] 05 p0598 A73-16968

Character of acoustic dispersion in plasma.
06 p0726 A73-17403

Associated mass of a simple doubly periodic lattice
06 p0643 A73-17465

Use of a paraboloidal layer to study gas-wall interaction 06 p0685 A73-17772

Stress-induced rotation of polarization directions of elastic waves in slightly anisotropic materials. 07 p0908 A73-19083

Analysis of internally generated sound in continuous materials. III - The momentum potential field description of fluctuating fluid motion as a basis for a unified theory of internally generated sound. 07 p0909 A73-19097

A critique of multilayer analyses in application to the propagation of acoustic-gravity waves. 07 p0814 A73-19248

Doppler effect intermodulation distortion derivation by perturbation method for loudspeaker modeled with pulsating sphere, considering boundary condition and nonlinear effect in wave propagation 08 p0987 A73-21123

Spatial crosscorrelation in anisotropic sound fields. 08 p0987 A73-21125

Three-dimensional acoustic-ray tracing in an inhomogeneous anisotropic atmosphere using Hamilton's equations. 08 p0988 A73-21190

Nonlinear acoustics of a radiating gas. I - General analysis of the equations 09 p1119 A73-21920

Self consistent computerized solutions to acoustic wave propagation and shock wave transformation with energy dissipation for solar and stellar chromosphere models 10 p1274 A73-23717

Microsonics /acoustic surface waves/ technology developments covering materials, heteroepitaxial systems, propagation, electron phonon interaction, acoustic amplifiers and waveguides, electromechanical transducers and signal processing 10 p1223 A73-23782

Spectra of short-term fluctuations of line-of-sight signals - Electromagnetic and acoustic. 10 p1190 A73-24893

Acoustic wave propagation, scanning and liquid surface techniques in acoustical holography, noting applications in geophysics, oceanography, medicine and nondestructive testing 11 p1371 A73-26542

Surface acoustic wave multistrip components and their applications. 12 p1484 A73-27567

Anisotropic piezoelectric heterogeneous acoustic surface waveguides of arbitrary cross section computing mode spectrum by efficient and accurate numerical techniques 12 p1480 A73-27568

Signal processing device with parametric interaction between opposite acoustic waves passing through delay line considering real time convolution and time inversion capabilities 12 p1470 A73-27569

Application of acoustic surface-wave technology to spread spectrum communications. 12 p1470 A73-27570

Thermo-acoustical waves in linear thermo-elastic materials. 13 p1691 A73-28088

A two-dimensional mathematical model for an acoustically soft parabolic cylinder reflector. 13 p1597 A73-28493

The influence of acoustic disturbances on the mechanics in shear layer behind a circular cylinder in air flow. 13 p1563 A73-28530

Acoustic field produced in a gas by arbitrary disturbances on a moving plate 14 p1775 A73-30834

Acoustic radiation intensity of a turbulent boundary layer on a plate 14 p1746 A73-30952

Acoustic generation and propagation in annular ducts of axial flow fans, discussing techniques for in-duct fan noise modal distribution measurement 16 p1999 A73-32846

The instability due to acoustic radiation striking a vortex sheet on a supersonic stream, 17 p2151 A73-34824

Book - Acoustic fields and waves in solids. Volumes 1 & 2. 17 p2213 A73-35597

Self consistent computerized solutions to acoustic wave propagation and shock wave transformation with energy dissipation for solar and stellar chromosphere models 18 p2355 A73-36742

Chapman-Jouguet rule for real detonation waves 19 p2419 A73-37516

Verification of sensitivity enhancement factors for CW ultrasonic resonators. 20 p2565 A73-38887

Dispersion curve computation for elastic acoustic waves propagation in /001/-cut cubic free anisotropic plate, noting relationship with slowness curves for bulk waves 20 p2616 A73-39050

Intensity modulated laser with expansion and contraction of absorbing medium for thermoacoustic broadside array with highly directional acoustic propagation 20 p2572 A73-39052

On the nature and origin of the solar five-minute oscillations. 20 p2606 A73-39071

Acoustic surface wave thin film guides for nonlinear signal processing, discussing relative advantages over nonguided arrangements, and application to transverse wave front imaging 20 p2531 A73-39596

Lunar surface fine rock powders seismic measurements in terms of Q factor and acoustic propagation velocity under various temperatures and pressures 20 p2612 A73-39712

Propagation velocities and amplitudes of thermoacoustical waves in thermo-plastic materials. 21 p2789 A73-40088

Vortex sheet model of directional acoustic wave radiation near nozzle exit from supersonic helium jet shear layer instability 21 p2677 A73-40617

Propagation of acoustic waves in a fluid flowing through a cylindrical duct 21 p2677 A73-40944

Finite plasticity theory in acoustic tensor calculation for elastic, viscoplastic and plastic wave propagation 21 p2740 A73-40947

Linear signal processing by acoustic surface-wave transversal filters. 21 p2705 A73-41426

On the derivation of Zone I spectra for a pulsed finite-amplitude source operating in a nonviscous non-dispersive fluid medium. 22 p2885 A73-41819

Acoustic wave fronts in ideal membrane transversely by steady pressure distribution, noting abrupt displacement gradient changes across pressure front 22 p2918 A73-41823

Radiatively driven harmonic acoustic waves in vibrational equilibrium in closed cylindrical tube, deriving pressure response, radiative absorption coefficient and spectral detail 22 p2930 A73-42235

Experiments on radiatively driven harmonic acoustic waves in a confined gas. 22 p2930 A73-42236

The reflexion of an acoustic pulse by a plane vortex sheet. 22 p2842 A73-42348

KRS5 - A new high-performance acousto-optical material 22 p2897 A73-43100

Sound field created in a gas by arbitrary perturbations on a moving plate. 23 p3006 A73-43584

Intensity of sound radiation from a turbulent boundary layer on a plate. 23 p2969 A73-44328

Acoustic wave propagation in axisymmetric swirling subsonic jet flow, obtaining directivity patterns for spinning and nonspinning modes from wave equation numerical integration [AIAA PAPER 73-1004] 24 p3077 A73-44837

Computational methods for studying acoustic propagation in nonuniform waveguides. [AIAA PAPER 73-1006] 24 p3078 A73-44839

Sound interaction with a helical flow contained in an annular duct with radial gradients of flow, density and temperature. [AIAA PAPER 73-1010] 24 p3078 A73-44842

Use of a relaxation technique in nozzle wave propagation problems. [AIAA PAPER 73-1011] 24 p3078 A73-44843

Effect of a slipstream on the acoustic radiation of ultrasonic annular jets 24 p3055 A73-45358

Variation of amplitudes of thermo-acoustical waves of arbitrary form in isotropic linear thermo-elastic materials. 24 p3157 A73-45372

ACOUSTIC PROPERTIES

NT ACOUSTIC IMPEDANCE

NT ACOUSTIC INSTABILITY

NT ACOUSTIC SCATTERING

NT ACOUSTIC VELOCITY

NT REVERBERATION

NT SOUND INTENSITY

Acoustic field of an infinite annular cylindrical transducer partially coated with an acoustically soft material 01 p0077 A73-10927

Aerodynamic sound generation, discussing Lighthill theory, multipole sonic sources, wave equation, power and turbulence models and sound radiating flows 03 p0242 A73-13167

Directional devices for noise reduction of high speed jets 03 p0359 A73-14142

Acoustic properties of fluid mixtures for ultrasonic delay lines, noting temperature and composition effects on water-glycol mixture parameters 03 p0280 A73-14620

Dynamic response of a semi-infinite elastic cylinder containing an acoustic medium. [ASME PAPER 72-WA/APM-3] 04 p0516 A73-15905

Sound field of an infinite circular cylindrical transducer partially coated with an acoustically compliant layer. 10 p1249 A73-24187

Turbulent jet noise generation theory relationship between flow and acoustic characteristics, obtaining intensity expression with velocity space-time derivatives for moving and stationary coordinates 13 p1603 A73-29138

Utilization of hydrostatic compression at high pressures as a means of improving the properties of acoustic nickel ferrite 14 p1765 A73-30890

Insulating houses against aircraft noise. 14 p1743 A73-30913

Design and construction of a reverberation chamber for high-intensity acoustic testing. 16 p1998 A73-33677

A perturbation method for low-frequency fluid-structure interaction problems. [ASME PAPER 72-APM-WWW] 17 p2248 A73-35102

Nonlinear acoustics of a radiating gas. II - Weak shock waves 18 p2337 A73-36989

Acoustical radiation reaction by conservation of energy and Dirac prescription methods and derivation of acoustic index of refraction for system of soft spheres 20 p2592 A73-39049

Turbulent boundary layer noise minimization by acoustic oscillation control, discussing suction and gas injection techniques 23 p2969 A73-43976

Subsonic and supersonic jets and supersonic suppressor characteristics. [AIAA PAPER 73-999] 24 p3077 A73-44834

The problem of natural oscillations of a thin shell containing an elastoacoustic medium 24 p3152 A73-45359

ACOUSTIC RADIATION

U SOUND WAVES

ACOUSTIC SCATTERING

NT REVERBERATION

The fourth annual Fairey lecture - The propagation of sound through moving fluids. 01 p0077 A73-10784

Scattering of sound by an aerofoil of finite span in a compressible stream. 02 p0129 A73-12609

The scattering characteristics of a sonic boom at the passage through a turbulent layer 03 p0290 A73-12967

Acoustic-Doppler-radar scattering equation and general solution. 03 p0276 A73-13830

Atmospheric wind and temperature inhomogeneity induced sound wave refraction effects on acoustic sounder measurements, noting scattering volume displacement and Doppler shift 03 p0276 A73-13831

Acoustic sounding of meteorological phenomena in the planetary boundary layer. 06 p0721 A73-18710

Theory of sound scattering by turbulence applied to scattering cross section calculation for turbulent jet flow and wind, discussing jet noise reduction 11 p1349 A73-26496

LF series expansion for acoustic scattering from soft and hard rotationally symmetric bodies, discussing relevance of magnetic polarizability tensor and electrostatic capacity 13 p1659 A73-28485

Generalisation and application of Rayleigh's theory of sound scattering 14 p1775 A73-30893

Multiple scattering of sound by turbulence and other inhomogeneities. 15 p1865 A73-32151

The interaction between atmospheric microstructure and acoustic and electromagnetic waves. 19 p2406 A73-38242

The comparison of sensitivities of atmospheric echo-sounders. 22 p2862 A73-42727

Lagrangian analysis of multiple scatter in acoustic and electromagnetic reflexion. 24 p3111 A73-45394

ACOUSTIC SIMULATION

Acoustic model of HF damping and microstructure of dispersed aluminum oxide ceramics systems, using Hugoniot elastic limits for Young modulus and fracture determination 04 p0468 A73-15373

Behavioural awakening and subjective reactions to indoor sonic booms. 04 p0412 A73-15592

Radar direction measurements by phase comparison of ultrasonic echo pulses reflected from targets in water tank, using piezoelectric sensors for receiving antennas simulation
10 p1194 A73-23736

Optimal and preferred listening levels for speech in aircraft acoustical environments.
11 p1304 A73-25387

ACOUSTIC STABILITY

U FREQUENCY STABILITY

ACOUSTIC STREAMING

Acoustic streaming and forces generated on circular cylinder in radially oscillatory incompressible fluid, considering steady and unsteady flow
10 p1174 A73-24847

A periodicity phenomenon occurring instantly when a standing ultrasonic wave is switched off
21 p2738 A73-39982

Sound propagation in gases, liquids and solids, discussing effects of nonlinear terms in wave and state equations and boundary conditions on solution
21 p2739 A73-40621

ACOUSTIC VELOCITY

Simulated Brillouin scattering for hypersound speed measurement as function of temperature in polystyrene, observing pulsed laser induced damage
01 p0068 A73-11232

Effect of counterflows of normal and superfluidic fluid on the second-sound velocity in helium II
02 p0154 A73-12543

Computing meteorological effects on aircraft noise.
05 p0536 A73-17121

Velocity measurements of microwave ultrasonic waves in quartz.
06 p0724 A73-18776

Vibrational relaxation times of oxygen in the pressure range 10-110 atm.
07 p0853 A73-19927

Spherical and cylindrical gaseous expansions into a vacuum.
07 p0920 A73-19980

Low speed of sound modeling of a high pressure ratio centrifugal compressor.
13 p1566 A73-29020

Correspondence laws of diabatic and adiabatic gas flows referring to similarity between pressure, temperature, sound velocity and Mach numbers
18 p2299 A73-36488

Ultrasonic pulse techniques based on acoustic velocity for inert gas thermometry, discussing electroacoustic transducer response time, temperature sensitivity and momentary contact coupling technique
22 p2854 A73-41994

Acoustic velocity and sound propagation differences in incompressible and compressible fluids related to Mach cone formation and sonic boom effects
24 p3054 A73-45269

ACOUSTIC VIBRATIONS

U SOUND WAVES

ACUSTICAL HOLOGRAPHY

Optical and acoustical holography; Proceedings of the Advanced Study Institute, Milan, Italy, May 24-June 4, 1971.
11 p1369 A73-26526

Quantitative analysis of sonic fields during their visualization by holographic methods
22 p2852 A73-41899

Ultrasonic holography free from phase turbulence - Construction of the device and experimental results.
23 p2983 A73-44087

ACOUSTICS

NT BIOACOUSTICS

NT MAGNETOACOUSTICS

NT MICROSONICS

NT PSYCHOACOUSTICS

NT UNDERWATER ACOUSTICS

Book - Sound, structures, and their interaction.
02 p0192 A73-11880

International Congress on Acoustics, 7th, Budapest, Hungary, August 18-26, 1971, Proceedings, Volume 1 - General Acoustics, Volume 2 - Technical Acoustics, Volume 4 - Physical Acoustics.
03 p0289 A73-12951

Computer technique for automated acoustical inspection of rotating machines
03 p0311 A73-12958

Ranging and data transmission using digital encoded FM 'chirp' surface acoustic wave filters.
14 p1733 A73-29935

Acoustic matched filters applications for multisubscriber band spread communication in ATC systems
14 p1733 A73-29936

Acoustic model and linguistic, syntactic, lexical and semantic factors in speech perception and production process
14 p1721 A73-30277

Development of data analysis in sound and vibration.
17 p2131 A73-35335

Use of edge-tone resonators as gas temperature sensing devices.
22 p2853 A73-41991

ACOUSTO-OPTICS

Piezoelectric matrices for reception of acoustic images and holograms
01 p0051 A73-10930

Vibrational analysis with the aid of holographic interferometry vibrational analysis of acoustic radiators with the aid of holographic interferometry
03 p0306 A73-12985

Special features of recording 'pure' phase /binary/ acoustic holograms
04 p0450 A73-15619

Electro-optical and acousto-optical methods of laser beam modulation and deflection with emphasis on various modulator and deflector types
05 p0583 A73-16340

Programmable, digital, rapidly frequency-shift-keyed, high-frequency generators for driving acoustooptical light deflectors
05 p0586 A73-17239

Acousto-optical profilometer system with two diffracted laser beams for surface topography holographic measurements
06 p0694 A73-18290

Acoustic-optic modulator design for a high power mode-locked CO₂ laser.
06 p0700 A73-18291

Computer output microfilm system technology assessment, discussing two dimensional acousto-optic laser scanner to write on dry process film
06 p0700 A73-18294

Acousto-optical modulator for carbon dioxide lasers based on Bragg scattering concept, discussing design parameters and application to lidar system
06 p0700 A73-18295

High data rate holographic recorder with six-channel acousto-optical modulator array as input composer and mode locked Ar laser as light source
06 p0694 A73-18311

Experimental results on the application of an x-y acousto-optic deflection system to wide band laser recorders.
06 p0701 A73-18312

Bragg diffraction by standing ultrasonic waves with application to optical demultiplexing.
06 p0701 A73-18364

Angular dispersion of an acoustooptic Bragg cell used in the wavelength tuning of an organic dye laser.
08 p0975 A73-21056

Television rate laser scanner with anisotropic Bragg device of paratellurite as acousto-optic horizontal deflector, noting operation efficiency and limiting resolution
08 p0975 A73-21142

Noise reduction in acousto-optic /Bragg/ imaging systems by holographic recording.
08 p0965 A73-21209

Real time 3-D holographic display, discussing reusable thermoplastic photoconducting recording film and frequency compensation with short laser pulses and acousto-optic modulator
08 p0965 A73-21246

Characteristics of acoustooptic cavity dumping in a mode-locked laser.
09 p1091 A73-22089

Acoustical holography applications in nondestructive testing.
09 p1083 A73-22514

Images and sound rays in the numerical calculation of echograms
09 p1121 A73-23104

Demonstration of the transmission and reception of modulated oscillations with a helium-neon laser beam
09 p1097 A73-23328

Piezoelectric matrices for the reception of acoustic images and holograms.
10 p1218 A73-24190

Nonlinear /binary/ transformation effects on acoustic hologram spatial signal amplitude noting multiple images and reconstructed image distortion
10 p1218 A73-24209

New techniques of acoustic image detection.
11 p1360 A73-25073

Relaxation of the bending vibration of CO₂ in pure CO₂ and in mixtures of CO₂ with noble gases.
13 p1662 A73-28553

International Symposium on Acoustical Holography, 4th, Santa Barbara, Calif., April 10-12, 1972, Proceedings.
13 p1614 A73-28576

A progress report on the laser scanned acoustic camera.
13 p1614 A73-28577

Real-time reconstruction of images from hydroacoustic holograms.
13 p1614 A73-28578

Real time high resolution 100 MHz acoustic image or holograph microscope using optical measurement of boundary displacement by incident angular sound wave
13 p1614 A73-28579

Laser beam scanned 1.1 GHz acoustic microscope based on photoconductive CdS piezoelectric transducer
13 p1614 A73-28580

Multi-information recording and reproduction in the ultrasono-cardio-tomography.
13 p1579 A73-28581

Foil-electret transducer arrays for real-time acoustical holography.
13 p1614 A73-28583

Acoustical hologram recording by electrostatic transducers using rigid backplate electrode insulated with thin dielectric film transparent to ultrasonic radiation
13 p1614 A73-28584

Diffraction theory treatment of long wave holography to demonstrate spiral scan and other circular sampling formats in microwave or acoustic hologram recording
13 p1615 A73-28585

Graphic display for ultrasonic nondestructive testing.
13 p1615 A73-28586

Acoustic hologram irradiation with sound waves to yield image as acoustic intensity pattern, noting parallels in optical holography
13 p1615 A73-28587

Cylindrical scan acoustical holographic transmitter/sensor system for ultrasonic under ocean surveillance and NDT applications
13 p1615 A73-28588

Spatial filtering considerations in Bragg diffraction imaging.
13 p1615 A73-28593

Investigation of rough surfaces by a method based on the scattering of coherent light by the sound reflected from such surfaces
14 p1753 A73-30583

Opto-acoustic signal processors extend radar and communication system capabilities.
14 p1729 A73-30675

Contribution to the theory of single-mode laser modulation. II - Conduction modulation.
14 p1758 A73-30769

Intensity modulated laser with expansion and contraction of absorbing medium for thermoacoustic broadside array with highly directional acoustic propagation
20 p2572 A73-39052

Absolute instability of the interaction between optical and acoustic waves.
20 p2594 A73-39679

Acoustooptic materials evaluation based on figures of merits and acoustic attenuation for laser beam deflection device design and fabrication
21 p2710 A73-40095

Sonic wave excitation by optical radiation, considering electrostriction effect and radiation absorption with subsequent intensity inhomogeneity-caused pressure gradients
22 p2868 A73-41898

KRS5 - A new high-performance acousto-optical material
22 p2897 A73-43100

Distribution of hot phonons generated by laser radiation
23 p2988 A73-44020

Optical modulation of X band microwave transmission by acoustoelectric domains in semiconductor CdS single crystal, noting domain conductivity and permittivity changes
23 p3018 A73-44365

ACQUISITION

NT DATA ACQUISITION

NT TARGET ACQUISITION

ACROBATICS

Analysis of fundamental flight parameters and properties of aerobatic aircraft in a statistical framework
02 p0131 A73-12448

ACRYLIC RESINS

Thin films durability increase of poly(n-alkyl methacrylate)/ polymers with alkyl group length, noting friction coefficient behavior [ASLE PREPRINT 72LC-7C-4]
03 p0317 A73-14373

Oxidation of acrylic fibres for carbon fibre formation.
15 p1898 A73-32049

Heat treated polyacrylonitrile filament produced carbon fiber strengthened after fatigue testing, noting maximum strengthening effect after 1000 load cycles
17 p2194 A73-34635

ACRYLONITRILES

Synthesis of glutamic acid via cyanoethylation of n-acylaminoacetonitriles in liquid ammonia.
06 p0661 A73-17936

Thermal conductivity of carbon fibers
15 p1896 A73-31214

Thermochemical and thermo-oxidative reactions of polyacrylonitrile fibers.
16 p1976 A73-33038

Three dimensional microstructure of carbonized polyacrylonitrile /PAN/ fibers dependence on basal plane alignment and process cycle treatment
16 p2028 A73-33039

Heat treatment effects upon the properties of PAN base carbon fibers.
16 p2028 A73-33040

The development and properties of a polyacrylonitrile (PAN)/ fiber based carbon felt
16 p2028 A73-33041

High modulus graphite fiber preparation from polyacrylonitrile yarn, discussing graphitization, properties and stabilization oxidation treatment
16 p2028 A73-33042

Axial alignment of basal planes in polyacrylonitrile base carbon fibers, increasing axial and radial microstructural textures via heat treatment temperature
17 p2198 A73-35837

A search for interstellar acrylonitrile, pyrimidine, and pyridine.
22 p2821 A73-43004

ACTH
U ADRENOCORTICOTROPIN [ACTH]
ACTINIDE SERIES
NT ACTINIUM
NT CURIUM ISOTOPES
NT CURIUM 244
NT NEPTUNIUM ISOTOPES
NT PLUTONIUM ISOTOPES
NT PLUTONIUM 238
NT THORIUM
NT THORIUM ISOTOPES
NT URANIUM
NT URANIUM ISOTOPES
NT URANIUM 238
Studies of beta Coronae Borealis. I - Identification of the Actinides.
18 p2357 A73-37105

ACTINIDE SERIES COMPOUNDS
NT PLUTONIUM OXIDES
NT THORIUM OXIDES
ACTINIUM
Development of an actinium fueled thermionic converter.
09 p1038 A73-23282

ACTINOGRAPHS
U ACTINOMETERS
ACTINOMETERS
NT DICKE RADIOMETERS
NT INFRARED DETECTORS
NT INFRARED SCANNERS
NT INFRARED SPECTROMETERS
NT INFRARED SPECTROPHOTOMETERS
NT MICROWAVE RADIOMETERS
NT PYRANOMETERS
NT RADIOMETERS
NT SOLAR SPECTROMETERS
NT SPECTROHELIOGRAPHS
NT SPECTROPHOTOMETERS
NT SPECTRORADIOMETERS
NT ULTRAVIOLET SPECTROMETERS
NT ULTRAVIOLET SPECTROPHOTOMETERS
Certain parameters of cumulus clouds as determined from sky photographs and from ground-based actinometric measurements
15 p1905 A73-31793

ACTINOMYCIN
Effect of actinomycin D on aldosterone-mediated changes in electrolyte excretion.
09 p1040 A73-22650

ACTIVATION
Application of activators in contact diffusion saturation processes in metals and powders
18 p2318 A73-35878

ACTIVATION [BIOLOGY]
Action of a serum protein on muscular contraction.
08 p0930 A73-21200

Accelerated coagulation of whole blood and cell-free plasma by bubbling in vitro.
18 p2278 A73-36782

ACTIVATION ANALYSIS
NT NEUTRON ACTIVATION ANALYSIS
Dislocation glide controlled by linear elastic obstacles - A thermodynamic analysis.
08 p1019 A73-21628

Spatial distribution of elements in tektites and comparable materials by charged particle activation analysis.
11 p1418 A73-25584

Russian book - Accelerated wear-resistance tests for machine components and machinery.
15 p1881 A73-31582

Effect of some activators on the molybdenum and niobium siliciding process
15 p1892 A73-32247

ACTIVATION ENERGY
Activation energy volume relation to heat of fusion and lattice characteristics for vacancy diffusion along crystal grains in melting metals
01 p0087 A73-10256

Dry oxidation of nickel by anhydrous carbon dioxide under pressure
01 p0062 A73-10271

Study of creep in copper and aluminum by the differential method of constant-rate temperature change.
01 p0064 A73-10612

Investigation of the interrelation between creep parameters in industrial aluminum during the first and second stages of creep
02 p0179 A73-11567

Relative rate measurements for oxygen atom addition to simple olefins in liquid Ar at 87.5 K, noting activation energies during reactions
02 p0139 A73-12086

Arrhenius rate law for thermally activated processes, deriving master equation based on rates of transition between quantum states
03 p0397 A73-13289

Asymptotic analysis of premixed burning with large activation energy.
03 p0397 A73-13531

Mo addition effect on high temperature creep resistance and diffusion activation energy of Nb alloys tested in torsion and tension at 1100-1500 C in vacuum
03 p0328 A73-14018

Correlation between the diffusion activation energy, the heat of fusion, and the bond energy in metals
06 p0708 A73-18046

Charge carriers concentration growth and decay for semiconductor model with independent capture centers, determining capture level activation energy
07 p0861 A73-19328

Viscous flow behavior of lunar compositions 14259 and 14310.
07 p0895 A73-19857

Dielectric properties of Apollo 14 lunar samples.
07 p0898 A73-19895

An asymptotic analysis of radiant and hypergolic heterogeneous ignition of solid propellants.
07 p0866 A73-20364

The temperature dependence of steady state creep in 20% Cr, 25% Ni, Nb stabilized stainless steel.
08 p0981 A73-21785

Valence-bond study of the H₂, D₂/ exchange reaction mechanism.
09 p1047 A73-22074

Thermoluminescence and activation energies in Al₂O₃, MgO and LiF (TLD-100).
12 p1530 A73-27031

Determination of the basic characteristics of an impurity level by Hall effect measurements
13 p1668 A73-28461

Al alloy rupturing analysis in complex stress state, noting sublimation and self diffusion values of activation energy in torsional to tensile state transition
13 p1643 A73-29624

Activation energy measurement for static strain aging rate controlling process in ferritic chromium steel
14 p1762 A73-30642

Homogeneous turbulent forward and inverted flame front structure during hydrocarbon combustion, investigating gas flow velocity distribution, activation energy levels and burning zone boundaries
14 p1818 A73-30871

Dissociation of carbon dioxide behind reflected shock waves.
17 p2119 A73-35173

Thermodynamic properties and Cr activity measurements in solid Cr-Ni-Fe alloys by solid oxide electrolyte technique
22 p2878 A73-42577

The activation energy for creep of columbium /niobium/.
22 p2879 A73-42580

A single-pulse shock-tube study of the reaction between nitrous oxide and carbon monoxide.
22 p2933 A73-42757

Linear pyrolysis of various polymers under combustion conditions.
22 p2898 A73-42807

ACTIVE GLACIERS
U GLACIERS
ACTIVE SATELLITES
NT SYNCOM SATELLITES
ACTIVITY [BIOLOGY]
Stability criteria in manifestations of the activity of the central nervous system in humans
01 p0006 A73-10152

Activity relation between internal organ receptors and skeletal muscles in terms of laws controlling process coordination
01 p0007 A73-10154

Trypsinogen activation peptides - An example of molecular epigenesis.
06 p0652 A73-17947

Determination of the information-forecasting indices of biometeorological phenomena
13 p1579 A73-28861

Biodegradation from evolution viewpoint as physiological function and fundamental cellular process regulating biological equilibrium, explained by intracellular digestion and phagocytic cells association
21 p2638 A73-41024

Estimate of integrative cerebral activity using an orientation response example
22 p2807 A73-42651

Objective method for classification of multicellular activity patterns of neuron population in the cerebrum of man
22 p2807 A73-42656

ACTIVITY CYCLES [BIOLOGY]
Development of wakefulness-sleep cycles and associated EEG patterns in mammals.
03 p0264 A73-14263

Effect of hypergravity on the circadian rhythms of white rats.
[ASME PAPER 72-WA/BHF-14]
04 p0410 A73-15877

Biological clocks in animal orientation and in other functions.
06 p0651 A73-17825

Drive and performance modification following multiple /light-light/ shifts in the photoperiod.
09 p1039 A73-22528

Circaseptan /7-day/ oviposition rhythm and growth of Spring Tail, *Folsomia candida* /Collembola: Isotomidae/.
15 p1836 A73-32185

Model concept concerning some control principles of the human organism. III - Seasonal adaptation
15 p1836 A73-32357

Serotonin content variations in the fore-brain during hibernation
18 p2276 A73-36567

Control of pineal indole biosynthesis by changes in sympathetic tone caused by factors other than environmental lighting.
19 p2393 A73-37300

Ultradian rhythms in human telemetered gross motor activity.
20 p2512 A73-39102

Variations of heart rate during sleep as a function of the sleep cycle.
20 p2514 A73-39762

Similarities and differences concerning the sleep of two baboons, *Papio hamadryas* and *Papio papio*
20 p2514 A73-39764

Spiral aftereffect durations following awakening from REM sleep and non-REM sleep.
21 p2639 A73-41179

ACTUATOR DISKS
Micromovement servocontrollers in closed loop system, using piezoelectric device, ceramic element actuators and rotary switch derived logic control signal
10 p1199 A73-24027

ACTUATORS
A linear motion generator for physiological research.
01 p0011 A73-10173

Spacecraft control hardware for use with digital processors.
04 p0424 A73-14737

Improvement of the static and dynamic accuracy of a dual-loop control system for an electric actuating element with a proportional velocity controller
09 p1037 A73-22940

A hybrid motor - A high-speed and accuracy final actuator /automatic control element/.
10 p1177 A73-24025

Synchronous motors as speed control system actuators, using static converters for instantaneous voltage or current amplitude and frequency control
10 p1177 A73-24026

Design and evaluation of miniature control surface actuation systems for aeroelastic models.
11 p1305 A73-25553

Hydraulic powered integrated actuator package /IAP/ for V/STOL aircraft flight control, noting advantages in system weight, mechanical complexity and power loss reduction
11 p1313 A73-26271

System for automatic regulation of the constant-absolute-slip mode of an asynchronous electrical actuating element with frequency-modulation control by a thyristor converter
12 p1460 A73-26786

A positional, asynchronous, thyristor-based, electrical servo actuating element with directional shaping of the phase trajectories
12 p1460 A73-26787

The tolerance of fluid machinery to contaminant wear.
13 p1571 A73-29031

High gain hydromechanical servomechanism with multistrip, mass damping and feedback control, deriving transfer function response, with application to aircraft control surface actuator design
13 p1596 A73-29150

Integrated hydraulic flight control actuator packages replacing mechanical linkages for aerodynamic surface control during V/STOL operation
20 p2510 A73-39015

The optimal nonlinear characteristic of the drive element in an stable multivibrator with a tunnel diode
20 p2536 A73-39201

Problems of the theory of multidimensional combined systems with a common output
22 p2836 A73-42611

Pneumatic fluidic operational amplifier application to proportional position servocontrol with hydraulic actuator for high force output, considering working fluid and Reynolds number effects
23 p2941 A73-43397

A hot gas actuator for missile control.
23 p2942 A73-43398

ACYLATION

NT ACETYLATION

ADAPTATION

NT ACCLIMATIZATION
NT ALTITUDE ACCLIMATIZATION
NT COLD ACCLIMATIZATION
NT DARK ADAPTATION
NT DESERT ADAPTATION
NT LIGHT ADAPTATION
NT RETINAL ADAPTATION

Correlations between motor learning and visual and arm adaptation under conditions of computer-simulated visual distortion.

03 p0267 A73-13556

Changes in whole body force transmission of dogs exposed repeatedly to vibration.
[ASME PAPER 72-WA/BHF-11]

04 p0410 A73-15878

Study of the peripheral auditory adaptation in a psycho-acoustic experiment

10 p1179 A73-23807

Adaptation-level and theory of signal detection - An examination and integration of two judgment models for voluntary stimulus generalization.

12 p1464 A73-26749

The gas exchange of hydrogen-adapted algae as followed by mass spectrometry.

17 p2118 A73-34225

ADAPTERS

Helios solar probe structural adapter design for linking to booster rocket end stage, investigating orthotropic cylindrical shell carrying capacity [DGLR PAPER 72-101]

02 p0227 A73-11685

Graphite-epoxy composite missile adapter design, fabrication, tooling, bonded assembly and costs, comparing with boron-aluminum material

03 p0331 A73-13022

ADAPTIVE CONTROL

NT LEARNING MACHINES

NT SELF ADAPTIVE CONTROL SYSTEMS

Multiple correction procedure for motion control ensuring arrival at final state without complete initial state information

01 p0079 A73-11419

Russian book - The designing of quasi-optimal combined-control servosystems.

02 p0149 A73-12867

Lyapunov functions for quadratic differential equations with applications to adaptive control.

03 p0336 A73-13520

An improved design technique for parameter adaptive control systems.

03 p0286 A73-14481

Design of a digital adaptive control system for reentry vehicles.

03 p0286 A73-14482

Comparative analysis of methods of determination of frequency response in searchless adaptive systems.

04 p0430 A73-15206

Adaptive feedback control without complete plant identification, deriving vector cost function and algorithm for performance optimization

04 p0430 A73-15214

Application of stochastic stability theory to model-reference systems.

04 p0430 A73-15215

Analog simulation and design of single- and multiple input/output model reference adaptive systems, using hyperstability concept
[ASME PAPER 72-WA/AUT-13]

04 p0432 A73-15881

Need for within-trial feedback as a function of task similarity in adaptive training of manual control.

05 p0543 A73-16709

Optimization of register length in a control algorithm for a nonstationary plant

05 p0561 A73-17280

Computer adaptive optimization system for problems with nonlinear criteria function and constraints, noting algorithms of deterministic and stochastic categories

05 p0555 A73-17284

On the convergence of random search algorithms in continuous time with applications to adaptive control.

06 p0671 A73-18623

An adaptive bit synchronization algorithm under time-varying environment.

06 p0672 A73-18810

An identification of time varying linear system without a priori information on variation of system parameters.

06 p0681 A73-18812

Adaptive trackers based on continuous learning theory.

06 p0682 A73-18821

Adaptive real time control for defense systems - A minimum risk algorithm.

06 p0682 A73-18823

Adaptive control of linear stochastic systems.

07 p0804 A73-19132

Adaptive algorithms for reducing a random field to a prescribed set of states with constraints on the elements of the approximating sequences

07 p0796 A73-20079

Adaptive reception in a channel with slow total fading.

07 p0794 A73-20132

Human operators and automatic adaptive controllers - A comparative study on a particular control task.

07 p0786 A73-20399

Stability behavior of adapting and untrained random logic nets, enabling intelligent interaction with environment

07 p0786 A73-20400

Conference on Decision and Control and Symposium on Adaptive Processes, 11th, New Orleans, La., December 13-15, 1972, Proceedings.

07 p0805 A73-20576

An analysis of an arbitrary n-element adaptive array.

07 p0795 A73-20583

On stochastic approximation and the hierarchy of adaptive array algorithms.

07 p0846 A73-20585

Current status of models for the human operator as a controller and decision maker in manned aerospace systems.

07 p0787 A73-20587

State of the art and survey of learning control applications.

07 p0806 A73-20590

An actively adaptive control for linear systems with random parameters via the dual control approach.
[AD-751587]

07 p0806 A73-20601

On the adaptive control of linear systems using the open-loop-feedback-optimal approach.

07 p0806 A73-20602

Adaptive control and identification via Liapunov's direct method.

09 p1067 A73-22232

Adaptive algorithm with error control for line by line encoder for image transmission, noting reconstructed image quality improvement

09 p1055 A73-23392

Discrete dynamic adaptive control algorithms for estimation of minimum loss function point trajectory characterizing system quality in nonstationary conditions

10 p1242 A73-24035

On a method of adaptive control under conditions of great uncertainty.

10 p1199 A73-24036

An adaptive convex feedback method for linear control systems with quadratic performance index.

10 p1199 A73-24038

Certain finitely converging algorithms for the solution of infinite systems of inequalities and their application in the theory of adaptive systems

10 p1192 A73-24486

Adaptation algorithms in multilayer pattern-recognition systems

10 p1192 A73-24502

Wide-sense adaptive dual control for nonlinear stochastic systems.

10 p1202 A73-24533

An actively adaptive control for linear systems with random parameters via the dual control approach.

10 p1202 A73-24534

Adaptive control for correction of flexible linear array phase error with resistance strain gages and ferrite phase shifter, noting radiation pattern performance

11 p1332 A73-26283

Single input n-th order linear constant discrete-time adaptive control systems, deriving phase canonical form sensitivity functions by z-transform

11 p1342 A73-26636

The quorum element and its application in the design of adaptive automatic control systems

12 p1482 A73-26758

An adaptive digital compensator for saturating control systems.

12 p1483 A73-27160

Precision low frequency adaptive MOSFET IC electronic oscillators with loose tolerance component timers for cost reduction

12 p1478 A73-27167

Computerized adaptive flight control for helicopter dynamic systems based on identification and optimization methods

13 p1569 A73-28829

Radar system with spatial/antenna pattern/ and temporal/Doppler filter/ responses adaptively controlled for optimum SNR and detection performance

13 p1586 A73-29213

Application of adaptive arrays to suppress strong jammers in the presence of weak signals.

13 p1593 A73-29215

MTI radar filter with adaptively controlled double canceller for frequency shifted clutter spectra effects minimization

13 p1594 A73-29222

Zeros determination in large-scale multivariable systems.

13 p1651 A73-29568

Dynamic scheduling of large digital computer systems using adaptive control and clustering techniques.

14 p1730 A73-30039

An adaptive precision gradient method for optimal control.

14 p1738 A73-30452

Theory and applications of variable structure systems; Proceedings of the Seminar, Sorrento, Italy, April 4-7, 1972.

14 p1739 A73-30776

Some results on the abstract realization theory of multilinear systems.

14 p1740 A73-30781

Suboptimal adaptive control of a class of non-linear systems.

15 p1853 A73-31628

Remarks on the optimum rate of convergence of the on-line identification of non-stationary systems.

17 p2144 A73-34600

Simulation results for a radar multipath angle error reduction method.

17 p2127 A73-35633

Asymptotic methods for the effectiveness computation of a sampling scheme of active sub-channels in an adaptive, multi-channel communication system.

17 p2129 A73-35712

Error maxima for division algorithm adaptiveness evaluation of damaged computer elements with corrective readjustments

19 p2408 A73-38563

Russian book - Optimal and adaptive systems.

20 p2538 A73-38671

Synthesis problems of adaptive systems for processing information and accepting solutions

20 p2531 A73-38684

Multidimensional linear extrapolation in problems of optimal design and control

20 p2539 A73-38687

Methods of adaptation in problems involving non-parametric detection and resolution of signals

20 p2540 A73-38700

Spectral analysis and a synthesis of linear systems with variable and random parameters in finite time intervals

20 p2540 A73-38704

Convergence of learning and adaptation algorithms

20 p2532 A73-38711

An adaptive scheme for PCM transmission.

20 p2523 A73-38728

Adaptive multibeam concepts for traffic management satellite systems.

20 p2525 A73-38746

A 'type one' servo explicit model following adaptive scheme.
[AIAA PAPER 73-862]

20 p2586 A73-38800

An electrical model of the inertial and adaptive properties of vision as a self-regulating system with delayed feedback

20 p2517 A73-39004

A study of systems with time-variable coefficients by the definite-integral method

20 p2542 A73-39037

Papers on adaptive electronic devices, circuits and systems covering logic nets, solid state and ferroelectric devices and memory devices and artificial intelligence

20 p2535 A73-39135

Adaptive control of forced motions in discrete extremal systems with independent search

20 p2542 A73-39346

A nonsearching system of identification with a model, synthesized according to the hyperstability criterion

20 p2532 A73-39347

An adaptive, time-suboptimal position servomechanism

20 p2511 A73-39664

Adaptive multispectral scanner recognition via maximum likelihood classifier for agricultural crops, discussing error sources

20 p2559 A73-39877

Application of the method of slipping modulating functions for identification of plants with time lag

21 p2670 A73-40993

Operator response to sinusoidally varying normal and emergency cycles in dynamic control task, testing anticipatory aversion response ability and error response

22 p2812 A73-41885

Sensitivity, adaptivity and optimality; Proceedings of the Third Symposium, Ischia, Italy, June 18-23, 1973.

23 p2961 A73-43277

A survey of model reference adaptive techniques /Theory and applications/.

23 p2962 A73-43278

Real-time identification using adaptive discrete model.

23 p2962 A73-43286

Design of discrete model reference adaptive systems using the positivity concept.

23 p2962 A73-43287

Design of multivariable adaptive model following control systems.

23 p2962 A73-43288

Adaptive maximum-likelihood receiver for synchronous data signals

23 p2957 A73-43320

Comparative studies of model reference adaptive control systems.

23 p2963 A73-43817

An adaptive observer for single-input single-output linear systems.

23 p2963 A73-43818

On the adaptive control of linear systems using the open-loop-feedback-optimal approach.

23 p2964 A73-43824

Asymptotically stable adaptive observer and identification scheme for linear system, using Liapunov canonical state representation

23 p2954 A73-43825

Model reference adaptive control system design using Kalman-Yacubovich lemma in connection with Lure problem

23 p2964 A73-43827

Adaptive array based on feedback concept for interference rejection, discussing processing of modulated signal with CW reference system

24 p3067 A73-44737

Probability estimate models for reliable function of redundant systems with adaptable and inadaptible neuron-like restoration organs

24 p3063 A73-44904

ADAPTIVE CONTROL SYSTEMS

U ADAPTIVE CONTROL

ADAPTIVE FILTERS

An adaptive Kalman filter using decomposition of the innovations sequence.

04 p0431 A73-15258

Application of adaptive tuning of filters to exoatmospheric target tracking.

04 p0498 A73-15275

Controllable matched filter model for single circuit and twin circuit parametric converters

05 p0558 A73-16786

Adaptive nonlinear filtering for tracking with measurements of uncertain origin.

07 p0805 A73-20584

A comparison of the effectiveness of some adaptive optimal filtering techniques applied to the gyrocompassing problem.

10 p1201 A73-24052

Self adaptive filter algorithm for automatic tracking of high performance maneuvering targets in real time surveillance systems in changing environments

13 p1596 A73-29207

Kalman filter adaptive tracker for ATC applications, modeling aircraft maneuvers by linear system with random noise accelerations based on statistical decision theory

13 p1593 A73-29212

Unsupervised learning of the optimal linear signal estimator in the presence of unknown multiplicative, additive, and message generating noise.

17 p2144 A73-35374

Rapid estimation and detection of impulse inputs under continuity constraints for space vehicles.

17 p2144 A73-35375

Aircraft flight simulator with coordinated adaptive filter derived from continuous steepest descent method

18 p2295 A73-36836

Kalman filter for rapid detection and adaptive estimation of state and covariance, deriving Bayes decision rule and algorithm for spacecraft tracking

19 p2410 A73-38030

A practical filter for noisy dynamic systems with unknown time-varying parameters.

19 p2410 A73-38047

Design and analysis of a practical on-line filter to process gyrocompass data.

[AIAA PAPER 73-841]

20 p2564 A73-38782

Motion cue method featuring coordinated adaptive washout circuitry in flight simulator using nonlinear filter, discussing heave, yaw and six degrees of freedom application

[AIAA PAPER 73-930]

21 p2674 A73-40877

Telephone line echo reduction by adaptive filter compensation, using statistical speech-white noise relations

23 p2952 A73-43318

Adaptive equalization with recursive noncanonical scanning filters

23 p2953 A73-43323

ADDERS [CIRCUITS]

U ADDING CIRCUITS

ADDING CIRCUITS

Full binary adder circuit with p-n-p junction transistor loaded tunnel diode, noting 200 MHz operation rates capability

01 p0026 A73-11480

High speed parallel multiplier design based on threshold logic adder using integrated logic circuits

17 p2139 A73-35238

A study of models of certain digital computer units with the aid of a digital computer

20 p2533 A73-39822

ADDITION

Additions and multiplications number required for fast evaluation of polynomials, investigating savings through preconditioning

01 p0068 A73-10043

ADDITION RESINS

NT ACRYLIC RESINS

Enhancement of polymer adhesion to metals by means of additives with crosslink systems

16 p2030 A73-33941

ADDITIVES

NT ADMIXTURES

NT ANTIKNOCK ADDITIVES

NT ANTIOXIDANTS

NT OIL ADDITIVES

NT PLASTICIZERS

NT PROPELLANT ADDITIVES

NT PROPELLANT BINDERS

NT SOLID ROCKET BINDERS

Formation of carbides in 3% chromium steel after additional alloying

01 p0062 A73-10265

Manganese additive effects on emissions from a model gas turbine combustor.

01 p0121 A73-10644

Activated sintering of ThO₂ and ThO₂-Y₂O₃ with NiO.

01 p0066 A73-11014

Refinement of primary silicon crystals in a hypereutectic Al-20% Si alloy by sulphur addition.

02 p0179 A73-11597

Relative rate measurements for oxygen atom addition to simple olefins in liquid Ar at 87.5 K, noting activation energies during reactions

02 p0139 A73-12086

Impact fracture resistance of Cr-Mn-Si steel, investigating alloying effects on crack initiation and propagation

02 p0181 A73-12211

Effect of rare-earth metals on mechanical characteristics of chromium.

02 p0181 A73-12214

Doping additions dissociation effect on impurities distribution in grown semiconductor crystals of melts, calculating atomic and molecular concentration

02 p0201 A73-12356

Influence of cerium and boron additions on the corrosion properties of Kh18N9TL steel

02 p0181 A73-12538

Effects of alloying elements on the solubility of hydrogen in beta titanium.

03 p0321 A73-12920

Effects of alloying elements on elevated-temperature mechanical strength of high Cr, Ni-base heat resistant alloy.

03 p0321 A73-12921

Performance tests for steel-steel lubrication capability of dimethyl silicone oils and greases modified by soluble, heat-stable extreme pressure and antiwear additives

03 p0329 A73-13011

Incompressible fluid turbulent boundary layer flow stability, considering effect of high polymer additives

03 p0291 A73-13168

High modulus Be-Al alloy strengthening and aging as function of Cu, Mg and Zn additions

03 p0325 A73-13517

Increasing the heat resistance of steel Kh14G14N3T with microadditions of boron.

03 p0327 A73-14006

Progress in the development of radiation-resistant aluminum-doped silicon solar cells.

03 p0258 A73-14248

The additive action of some organic chlorides and sulfides in the four-ball lubricant test.

[ASLE PREPRINT 72LC-3C-2]

03 p0316 A73-14357

Preferential adsorption in the lubrication process of zinc dialkylthiophosphate.

[ASLE PREPRINT 72LC-3C-3]

03 p0274 A73-14358

Electrical properties of electron-irradiated GaAs.

05 p0604 A73-16516

A shocktube study of the combustion of Shell-dyne-H with additives.

[WSCI PAPER 72-29]

05 p0639 A73-16686

Use of ion implantation in the fabrication of semiconductor devices

06 p0672 A73-17449

Diffusion welding of beryllium. II - The role of the microalloying elements.

06 p0704 A73-17597

Resistivity of doped polycrystalline silicon films.

06 p0733 A73-17745

The current-voltage characteristics of boron implanted silicon diodes.

06 p0674 A73-17797

Impurity concentration relationship to electrons and holes density and potential fluctuations in completely compensated crystalline semiconductors with randomly distributed donors and acceptors

06 p0735 A73-17976

Absorption coefficient due to band-band optical transitions in heavily doped semiconductor, obtaining electron and hole quasi-Fermi levels

06 p0738 A73-18586

Doping dependence of photon yield as a function of excitation energy in optically-excited n-type GaAs at 300 K.

06 p0704 A73-18844

Effect of additives on ablation of phenolic-silica composites.

07 p0842 A73-19486

Development and properties of cobalt-base alloys with improved hot-corrosion resistance.

07 p0838 A73-19497

Faraday effect in n-GaAs in the intermediate doping region

07 p0862 A73-20009

Concentration and mobility of electrons in indium-doped zinc oxide crystals

07 p0862 A73-20016

Low-frequency current oscillations in high-resistivity, Au-doped silicon junctions with two Schottky contacts.

07 p0864 A73-20190

Effects of boron density on radiation resistance of copper-contaminated n/p type silicon solar cells.

08 p0928 A73-21114

Numerical calculation of low-frequency capacitance/voltage curves of M.O.S. capacitors with nonconstant doping profiles.

08 p0947 A73-21122

On the mechanism for microwave amplification in 'supercritically' doped n-GaAs.

08 p0947 A73-21212

Spun on arsenosilica films as sources for shallow arsenic diffusions with high surface concentration.

08 p0995 A73-21478

Investigations on 'doping stacking fault' pyramids.

08 p0995 A73-21479

Pulsed and CW water vapor lasers, investigating He addition effects on time-varying gas temperature and power output

[AD-760377]

09 p1091 A73-22082

Additional data on the effect of doping on the lasing characteristics of GaAs-Al_x/Ga_{1-x}/As double-heterostructure lasers.

09 p1091 A73-22373

Effect of addition of Bi on stress-corrosion cracking of Al-Mg alloy.

09 p1102 A73-22421

SiGe alloys thermoelectric properties long term time and temperature dependent behavior, using diffusion limited dopant precipitation model

09 p1136 A73-22762

Performance improvement of cesium thermionic converters by addition of oxygen.

09 p1036 A73-22818

Titanium alloys corrosion resistance modification relative to nonoxidizing acid media by hydrogen reduction conditions or anodic dissociation curve alteration

09 p1104 A73-22965

Electron microscopy study of Nb₃Sn strips

10 p1259 A73-23674

Effects of Ni and Fe addition on various properties in heat-resisting aluminum casting alloys.

10 p1231 A73-23675

Effects of beryllium additions on the microstructure and the type of failure in Al-Mg alloys

10 p1233 A73-24423

Si addition effect on Ni-Cr alloy calorized layer depth, microhardness, phase structure, chemical composition and scaling resistance

10 p1227 A73-24960

Additives alloying with cobalt, discussing allotropic transformation dependence, recrystallization, mobile dislocations, and iron deformation by twinning

11 p1408 A73-25322

The effect of an addition of molybdenum on the quenched and aged structure of a Ti-1 wt % Si alloy.

11 p1384 A73-26048

Effect of polymer additions on some energy balance components in a turbulent flow

11 p1349 A73-26433

Hg vapor laser with He, Ne, Kr, H or N additions, investigating population inversion and lasing properties for optimal performance conditions

12 p1504 A73-26887

The extension of self-registered gate and doped-oxide diffusion technology to the fabrication of complementary MOS transistors.

13 p1595 A73-29576

High temperature tests of microalloying effect on creep and stress rupture characteristics of hot rolled and annealed Mo alloys

13 p1643 A73-29605

German monograph - The effect of germanium additions on the superconductor characteristics and the transition processes in technical titanium-niobium alloys.

14 p1762 A73-30666

Effect of rare earth metal additions on the recrystallization of nickel

14 p1765 A73-30887

Influence of vanadium, niobium, carbon, and silicon on the properties of low-pearlite steel

15 p1889 A73-31810

Properties of low-alloy steels with small niobium additions

15 p1889 A73-31811

Thermal noise behavior of a FET as a function of the doping profile of the gate-channel junction

16 p1988 A73-33274

- Evaluation of additives for prevention of high temperature corrosion of superalloys in gas turbines. [ASME PAPER 73-GT-1] 16 p2047 A73-33479
- Effect of additional alloying and heat treatment on the strength of steels 17 p2187 A73-34336
- Military and civil jet aircraft fuel specifications, discussing additives types, test procedures and quality control complexity 17 p2220 A73-34848
- The electrical properties of phosphorus doped silicon layers obtained by ion implantation through a passivating oxide. 17 p2220 A73-35654
- Effects of small amounts of additional elements on directionality of stress corrosion resistance of the Al-Zn-Mg alloys. 19 p2442 A73-37948
- Gallium phosphide with nitrogen doping from the gas phase 20 p2599 A73-38666
- A neodymium-doped yttrium-aluminum-garnet laser amplifier with an integrated design 20 p2572 A73-38669
- The possibility of crystallization of condensed combustion products in nozzles 21 p2753 A73-40697
- Combustion of a solid fuel in a gaseous oxidizer flow 21 p2754 A73-40701
- Mechanical properties of weldments of AK-3 titanium with an elevated oxygen content. 21 p2720 A73-41036
- Measurement of the doping level distribution in the surface region of a semiconductor 21 p2753 A73-41097
- German monograph - Doping profiles of boron-implanted silicon layers. 22 p2897 A73-42717
- German monograph - The back-scattering method as a procedure for the determination of the radiation damage profile in silicon doped by ion implantation. 22 p2897 A73-42852
- Bipolar transistor emitter efficiency calculation, considering heavy doping induced impurity profiles effects on current gain 23 p2958 A73-43451
- Additive distribution and formation of internal stress in fired magnesia. 23 p2998 A73-44133
- Effects of additions of Al and Ti on electrical resistivities of oxide films of Fe-18 Cr sealing alloy. 23 p2986 A73-44152
- Influence of Co, Ni, Mo, and W on the solubility of Fe16N2 in alpha-iron. 23 p2994 A73-44156
- Si and Ge doping characteristics and energy levels in vapor phase epitaxially grown GaAs from sample photoluminescence spectra 23 p3018 A73-44370
- Effect of vanadium, niobium, and silicon on the properties of low-pearlite steel. 24 p3100 A73-45273
- Properties of low-alloy steels with small niobium additions. 24 p3100 A73-45274
- Influence of nonexplosive liquids on the detonation rate of solid explosives 24 p3157 A73-45380
- Ion-implanted nitrogen in gallium arsenide. 24 p3120 A73-45402
- ADDRESSING**
- Symbol ring as alphabetic element in information processing technique, defining address substitution operation 02 p0143 A73-11642
- Address structure optimization and minimum access time and decoder terminals in nonvolatile core memory array design, noting binary notation for information storage 05 p0554 A73-16991
- Quasi-optimal signal reception in asynchronous addressing communication systems with a time-frequency matrix 17 p2121 A73-34587
- ATS-1 borne Random Access Discrete Address System for multiple access satellite communication, discussing repeater performance concerning CW signal transmission efficiency, intermodulation and SNR 22 p2825 A73-42187
- ADENINES**
- NT RIBONUCLEIC ACIDS**
- ADENOSINE DIPHOSPHATE [ADP]**
- Adenonucleotides, NAD⁺, and NADN in skeletal muscles during intensive work and at rest 07 p0780 A73-19475
- ADENOSINE TRIPHOSPHATE [ATP]**
- Importance of the Lohmann reaction in the response of the heart to anoxic aggression 02 p0133 A73-12152
- Radiation protective effect of a mixture of ATP, AET, and serotonin on yields of 600-R X-ray-induced chromosome aberrations in the rat. 02 p0134 A73-12187
- Myosin ATPase and fiber composition from trained and untrained rat skeletal muscle. 05 p0538 A73-16155
- Effects of physical training on cardiac actomyosin adenosine triphosphatase activity. 05 p0539 A73-16157
- Functional dependence of the ciliary epithelium ATPase activity and intraocular pressure on the autonomic nervous system. 05 p0539 A73-16248
- Adenonucleotides, NAD⁺, and NADN in skeletal muscles during intensive work and at rest 07 p0780 A73-19475
- Embryonic chick heart cell age dependent electrophysiological studies, discussing structure, metabolism, ATPase activity, membrane potential and cell interactions 11 p1315 A73-25589
- Changes caused by illumination in the Na⁺, K⁺ adenosine-triphosphatase and n-nitrophenyl-phosphatase activities of the external segments of the retina 13 p1574 A73-28294
- Glycolytic intermediates and adenosine phosphates in rat liver at high altitude /3,800 m/. 20 p2514 A73-39602
- Influence of electric stimulation of the hypothalamus on catecholamine, phosphorylated compound, and cholesterol levels 21 p2637 A73-40284
- Influence of preliminary adaptation to the main environmental factors on the ATP level and phosphorylation potential in the myocardium during severe heart strain 21 p2640 A73-41278
- Effect of hind-limb immobilization on contractile and histochemical properties of skeletal muscle. 21 p2642 A73-41624
- Glycogen content in the rabbit retina in relation to blood circulation. 22 p2802 A73-41732
- ADENOSINES**
- NT ADENOSINE DIPHOSPHATE [ADP]**
- NT ADENOSINE TRIPHOSPHATE [ATP]**
- High energy phosphate deficit-produced myocardial cell genetic apparatus activation as cardiac hypertrophy mechanism, discussing mitochondrial biogenesis and cardiac hyperfunction roles 02 p0134 A73-12511
- Purification, crystallization, and subunit structure of allosteric adenosine 5'-monophosphate nucleosidase. 03 p0273 A73-13807
- Relationship between cyclic AMP, phosphodiesterase activity, calcium and contraction in intestinal smooth muscle. 21 p2638 A73-41130
- ADHEROMETERS**
- U ADHESION TESTS**
- ADHESION**
- A correlation between static adhesion data and the dynamic friction coefficients for two cobalt alloys and iron under vacuum conditions. [ASLE PREPRINT 72LC-5B-2] 03 p0328 A73-14362
- Metal components wear mechanisms due to adhesion, tribooxidation, abrasion and surface fatigue, discussing prevention by lubrication, suitable mating of materials and surface treatments 11 p1373 A73-25577
- Reinforcing glass fiber preparation effect on fiber wetting by polyethylene melt, analyzing adhesion strength relationship to residual stresses 12 p1516 A73-27178
- Investigation of adhesional and diffusional interaction of instrumental materials with titanium alloys 12 p1502 A73-27466
- Book on fretting corrosion covering contacting surface theory, damage characteristics, wear variables effect, fatigue, adhesion and electrochemical properties, etc 13 p1643 A73-29575
- Detonation propelled metal particle sprayed coatings adhesion strength relation to particle kinetic energy 18 p2318 A73-35884
- Contact problem for infinite elastic isotropic plane weakened by rectilinear cut with free, slipping and adhesive segments and uniformly distributed load at infinity 18 p2363 A73-36415
- Adhesion effect on the tensile properties of fibre reinforced composite materials. 18 p2328 A73-36683
- ADHESION TESTS**
- Carbon fibre adhesion to organic matrices. [ONERA, TP NO. 1173] 01 p0068 A73-11499
- The chemistry of urethane adhesives incorporating silane coupling agents. 03 p0332 A73-13037
- High temperature adhesive shear tests at ambient temperature as function of loading rate and bond overlap length 03 p0332 A73-13040
- Selection process for a structural adhesive system for application of the L-1011 aircraft. 03 p0333 A73-13050
- Detonation gun flame spray coatings, determining adhesive strength as function of coating thickness and process technological parameters 03 p0313 A73-14014
- Experimental studies concerning the adhesion coefficient during slip 04 p0454 A73-15655
- Temperature dependence of the adhesive strength and elasticity of some high-melting coatings 10 p1225 A73-24371
- Solid body contact interaction devices at high temperatures in vacuum, gas and air for evaluation of surface coatings, adhesion, diffusion, mechanical properties, etc 10 p1222 A73-24966
- Temperature, testing rate and substrate choice effects on characteristic energy required to produce separation and failure of adhesively bonded pieces 11 p1443 A73-26203
- Non-destructive testing of adhesive bonding. 11 p1374 A73-26299
- Quantitative measurement of aluminum film adhesion to polymers, noting influence of substrate nature on adhesion strength 14 p1755 A73-30724
- The ultrasonic pulse-echo technique as applied to adhesion testing. 15 p1882 A73-31673
- Mechanical, chemical and physical characteristics of glass and ceramics with respect to adhesion, friction and wear behavior 21 p2707 A73-40633
- Reactive kinetic observations for spraying with Ni-Al powder. 22 p2879 A73-42594
- ADHESIVE BONDING**
- The mechanism of the metallic adhesion bond. 01 p0087 A73-10473
- The influence of adhesive components on the corrosion of aluminum honeycomb. 03 p0321 A73-13038
- A study of environmental degradation of adhesive bonded titanium structures in Army helicopters. 03 p0332 A73-13039
- High temperature adhesive shear tests at ambient temperature as function of loading rate and bond overlap length 03 p0332 A73-13040
- Liquid crystals for nondestructive testing of composite structures. 03 p0349 A73-13041
- Organization and management for adhesive bonding aircraft structures. 03 p0333 A73-13048
- Unmanned spacecraft adhesives and adhesive bonding applications in solar panels, mirrors, circuit boards, antennas, platforms, lunar capsules and reentry heat shields 03 p0333 A73-13049
- Selection process for a structural adhesive system for application of the L-1011 aircraft. 03 p0333 A73-13050
- Stressed state of adhesively bonded plane interfaces in composite systems, applying two dimensional Vocke theory 03 p0311 A73-13129
- Evaluating adhesives for joining aluminum. 03 p0334 A73-13271
- Physicochemical distinction between separating similar and different materials in terms of cohesive or adhesive fracture energy in continuum mechanics 03 p0312 A73-13334
- The application of adhesive bonded structures and composite materials on advanced turbofan engines. 03 p0359 A73-14134
- Russian book - Technology for adhesive bonding of elements in aircraft construction. 04 p0454 A73-15703
- Linear analytical procedure for adhesively bonded flat joints design with minimized shear stress concentration, presenting finite element and automated iterative procedure [ASME PAPER 72-WA/DE-13] 04 p0514 A73-15874
- Adhesively bonded multilayer Al and Ti alloy sheet metals for complex airframe components, discussing design, fabrication, tests and performance comparison with monolithic structures [SME PAPER MF 72-513] 06 p0698 A73-18094
- Extension of an interface flaw under the influence of transient waves. 07 p0908 A73-19080
- Review of recent advances in bonded solid film lubrication at high temperatures. 07 p0842 A73-19552
- Fiber reinforced plastics with adhesive bonded elements, investigating ply number and adhesive pressure effects on shear, bending and impact strengths 07 p0844 A73-20330
- Metallization failures caused by organic adhesives used in hybrid microelectronic devices. 08 p0944 A73-20747

Intermetalbond '72: Conference on the Bonding of Metals, 5th, Boboty, Czechoslovakia, November 21-23, 1972, Proceedings

10 p1224 A73-24088

Bonded joints under long-term dynamic load and their resistance to climatic effects

10 p1224 A73-24089

Technology, strength, and calculation of bonded circular joints

10 p1224 A73-24090

Calculation of the shear strength of an axisymmetric joint constructed out of Locite

10 p1224 A73-24091

Adhesive metal/glass laminate bonding, discussing materials, tests and interlaminar strength effects

10 p1224 A73-24092

Vinyl plastisols with high adhesion to metals

10 p1239 A73-24093

High strength properties and hardening of epoxy resin bonding materials using dicyaninediamides

10 p1239 A73-24094

Layer strength and vulcanization effects on rubber/metal bonding with MEGUM agent

10 p1239 A73-24095

Technology of production of bonded sandwich structures

10 p1224 A73-24096

Fatigue properties of sandwich material with a honeycomb filler

10 p1289 A73-24097

Buckling of partially debonded layered cylindrical shells.

[AIAA PAPER 73-366] 11 p1438 A73-25501

Linear elastic finite element stress analysis of lap and tapered adhesive joint bonding of composite to metal substrate

[AIAA PAPER 73-371] 11 p1438 A73-25505

Environmental stress cracking of epoxy adhesives.

11 p1388 A73-25840

Temperature, testing rate and substrate choice effects on characteristic energy required to produce separation and failure of adhesively bonded pieces

11 p1443 A73-26203

Non-destructive testing of adhesive bonding.

11 p1374 A73-26299

Stresses in bonded joints of circular cylindrical shells and panels

12 p1551 A73-27182

Epoxy adhesive bonding of Concorde light alloy sandwich structure elevons, discussing surface treatment, polymerization and ultrasonic testing

13 p1623 A73-28468

Stresses in adhesive bonds of thin cylindrical shells

13 p1698 A73-29063

German monograph - Investigations regarding the strength characteristics of adhesive bonds involving metals in the case of impact stress.

13 p1625 A73-29277

The relation between tensile bond strength and crystalline properties of the adhesive on the steel-nylon 12-steel system.

13 p1642 A73-29531

Bonding characterization in reinforced composites.

13 p1702 A73-29536

Photoelasticity - An improvement in the sandwich technique.

14 p1765 A73-29703

Stress and fracture analysis of adhesive joints.

[ASME PAPER 73-DE-21] 14 p1755 A73-30822

Effect of lasting high temperatures on the mechanical properties and microstructure of bonded glass mat with an aluminophosphate binder

15 p1896 A73-31213

Effect of Poisson's ratio strains in adherends on stresses of an idealized lap joint.

15 p1948 A73-31620

Techniques and equipment for thermal nondestructive quality control of products and materials.

15 p1882 A73-31692

Bonded structural connections analysis by finite element method, presenting stress distribution in adhesive

15 p1952 A73-32038

Durability of bonded titanium joints increased by new process treatments.

16 p2017 A73-33052

Adhesive viscoelasticity effects on sandwich structure performance, presenting mathematical model for adhesive behavior and time dependent loading

16 p2029 A73-33053

Epoxy resin adhesive for metal-to-metal and honeycomb sandwich bonding, featuring high flow during cure for high structural strength

16 p2029 A73-33054

Factors affecting the survivability of stressed bonds in adverse environments.

16 p2017 A73-33055

Surface morphology after pretreatment in relation with bondability of aluminum alloys.

16 p2018 A73-33056

Epoxy adhesive materials evaluation for microelectronic assemblies of hermetically sealed hybrid circuits with semiconductor chips and thin film substrates

16 p1989 A73-33468

Joining of plastics to plastics and to metals.

16 p2021 A73-33861

Enhancement of polymer adhesion to metals by means of additives with crosslink systems

16 p2030 A73-33941

A solid state bonding and packaging technique for integrated sensor transducers.

17 p2166 A73-34618

Book - Handbook of adhesive bonding.

17 p2180 A73-35337

Protective coating-metal adhesion dependence on chemical bonds, double electric layers at interface and thermoelastic stresses

18 p2319 A73-35893

Stress distribution in a bonded anisotropic lap joint. [ASME PAPER 73-MAT-M]

18 p2365 A73-36618

Stresses in bonded joints of thin cylindrical shells.

18 p2366 A73-36895

A theory of adhesion at a bimetallic interface - Overlap effects.

18 p2287 A73-37032

Temperature dependence of adhesive fracture of epoxy resin.

20 p2580 A73-38642

Probabilistic molecular contact rupture strength at solid-solid adhesive joint interface

24 p3092 A73-44516

Research and development of aerospace adhesive bonded systems and concepts.

24 p3093 A73-44763

The relation of surface condition after pretreatment to bondability of aluminum alloys.

24 p3093 A73-44764

Structural adhesive bonding of titanium - Superior surface preparation techniques.

24 p3093 A73-44765

Spot weld adhesive bonding procedures, examining process and quality control, tooling, curing, surface preparation, adhesive types and corrugated panel application

24 p3093 A73-44766

ADHESIVES

NT GLUES

NT PASTES

Unmanned spacecraft adhesives and adhesive bonding applications in solar panels, mirrors, circuit boards, antennas, platforms, lunar capsules and reentry heat shields

03 p0333 A73-13049

Understanding and applying strain gages. II - Carriers, adhesives, and coatings.

06 p0696 A73-18675

Evaluating structural adhesives under sustained load in a hostile environment.

24 p3093 A73-44767

ADIABATIC CONDITIONS

Adiabatic propagation of cosmic rays in the Galaxy.

03 p0360 A73-12929

Theory of electron cyclotron resonance heating. I - Short time and adiabatic effects.

[AD-759528] 03 p0345 A73-14434

Concerning the accuracy of conservation of the third adiabatic invariant of the motion of a charged particle in axisymmetric fields. I.

05 p0600 A73-16082

Ignition analysis of adiabatic, homogeneous systems including reactant consumption.

[AIAA PAPER 73-215] 05 p0640 A73-16945

Evidence for the existence of adiabatic energy loss in interplanetary space from observations of the decay of the February 25-March 2, 1969 series of solar cosmic ray events.

05 p0611 A73-17048

Two chamber adiabatic test compression system design with controlled throttle for high temperature nitrogen- and nitrous oxide-type gases with exothermal reactions

06 p0683 A73-17413

The behaviour of ULF waves and particles in the magnetosphere.

07 p0792 A73-19666

Heat transfer, adiabatic enthalpy /temperature/ of the wall, and hydrodynamic resistance associated with the turbulent and laminar flow of a compressible fluid in a circular tube.

08 p0954 A73-20858

Small perturbations in flat galaxies. I - Equilibrium models and adiabatic perturbations.

10 p1284 A73-24913

Periodic solutions of the set of equations governing the nonadiabatic convection of dry isolated thermals.

11 p1393 A73-25690

Accuracy of conserving the third adiabatic invariant of the motion of a charged particle in axially symmetrical fields. II.

12 p1535 A73-27634

Anisotropy of gallium elasticity and thermal expansion

12 p1531 A73-27936

Theory of cyclogenesis, taking into account condensation

13 p1653 A73-28744

Collisionless magnetized unstable plasma two dimensional adiabatic compression, calculating gamma from temperature distributions

14 p1779 A73-29984

Contact binary star evolution, discussing adiabatic convection zone entropy, mass flow and relative frequency

15 p1928 A73-31054

The adiabatic stability of stars containing magnetic fields. I.

15 p1933 A73-31395

Exponential distributions of protons according to adiabatic invariants in the outer radiation belt

15 p1926 A73-31898

OH emission band, studying effect of adiabatic infrasonic oscillations on upper atmospheric temperature and intensity

16 p2008 A73-33883

Applicability of an adiabatic compression method to the study of a cesium plasma

17 p2214 A73-34130

Adiabatic following and the self-defocusing of light in rubidium vapor.

20 p2571 A73-38632

Approximate determination of the inverted population and amplification factor of a gas expanding adiabatically in a nozzle

20 p2572 A73-39280

The turbulent boundary layer with stepwise varying boundary conditions at a permeable surface.

20 p2628 A73-39423

Effectiveness of film cooling of an adiabatic wall downstream of the perforated section.

20 p2628 A73-39424

ADIABATIC EQUATIONS

Study of the adiabatic curve of an ionizing shock wave in an inclined magnetic field

06 p0727 A73-17460

Theory of short radio wave propagation over very great distances

15 p1844 A73-31888

Validity of CGL equations in solar wind problems.

18 p2347 A73-36291

Experimental study of the adiabatic invariant of self-oscillating processes

23 p3006 A73-43850

A simple thermodynamic method of estimating the shock compression temperature of a condensed medium

24 p3155 A73-44709

Adiabatic variation. I - Exponential property for the simple oscillator.

24 p3112 A73-45543

ADIABATIC FLOW

A study of the stability of certain self-similar solutions of the theory of explosions in the atmosphere

01 p0035 A73-11429

Study of the stability of some self-similar solutions from the theory of an explosion in the atmosphere.

11 p1348 A73-26051

An approximate method for calculating the interaction between shock wave and turbulent boundary layer.

13 p1602 A73-29018

Determination of the shape of a plane supersonic nozzle

15 p1822 A73-31196

Correspondence laws of diabolic and adiabatic gas flows referring to similarity between pressure, temperature, sound velocity and Mach numbers

18 p2299 A73-36488

Self-similar flows with increasing energy. III - Radiation-driven shock wave.

21 p2793 A73-41673

ADIPOSE TISSUES

Energy requirements of ouabain-sensitive Na-K positive ion membrane pump during norepinephrine induced thermogenesis of brown adipose tissue in cold-exposed hamsters

09 p1040 A73-22649

ADJOINTS

The deficiency indices and spectrum associated with self-adjoint differential expressions having complex coefficients.

02 p0186 A73-11971

Spectrum of the self-adjoint extensions of a minimal operator generated by the Sturm-Liouville equation with an operator potential

04 p0470 A73-14931

On the role of the adjoint problem in dissipative, nonconservative problems of elastic stability.

11 p1434 A73-25214

Asymptotic behavior of the eigenvalues of self-conjugate expansions of the Schroedinger operator in a multidimensional bounded domain

11 p1391 A73-26463

Conditions for convergence of spectral decompositions corresponding to self-adjoint expansions of elliptic operators. IV - Negative-type theorems for arbitrary expansion of a general self-adjoint second-order elliptic operator

12 p1518 A73-27726

Improperly posed initial value problems for self-adjoint hyperbolic and elliptic equations.

13 p1648 A73-28424

Expansion of nonconjugate differential Dirac operators into a series of eigenvalues over the whole axis, and an analytical expression for a spectral matrix-function

14 p1771 A73-30787

Investigation of a weakly generalized solution to the mixed self-conjugate problem of a class of quasi-linear second-order hyperbolic systems with a nonlinear right-hand operator member
14 p1771 A73-30791

Sturm comparison and separation theorems for linear, second order, self-adjoint, ordinary, differential equations and for first order systems.
15 p1902 A73-32377

Generalized Galerkin method for approximate solution of eigenvalue self-adjoint boundary value problems in stability analysis of mechanical distributed parameter systems
19 p2458 A73-37189

Book on oscillation theory covering classical, abstract and complex theories, nonselfadjoint differential equations, hyperbolic and elliptic equations, Sturm-Picone theorem, etc
20 p2582 A73-39141

Boundary value problems for linear generalized differential equations and their adjoints.
20 p2582 A73-39402

Plasticity theory algebraic structure with emphasis on plastic flow laws formulation by adjoint functions and elastoplastic media finite deformations
23 p3044 A73-43972

ADJUSTING
Linearization limits for optimal pulse controller adjustments, using comparison with continuous controller and extrapolation
10 p1198 A73-24000

Adjustment of a variable-profile antenna
21 p2675 A73-41456

ADJUSTMENT
U ADJUSTING

ADMITTANCE
U ELECTRICAL IMPEDANCE

ADMIXTURES
Concentration probability of a passive admixture in turbulent shear flows
03 p0294 A73-13614

Stabilization of superconducting beryllium by addition of aluminum.
05 p0605 A73-16794

ADRENAL GLAND
Effects of endotoxin on monoamine metabolism in the rat.
01 p0009 A73-11100

Cytochemical-luminescence study of adrenal cortex proteins under the influence of ionizing radiation
02 p0134 A73-12354

Circadian rhythms in catecholamines in organs of the golden hamster.
11 p1318 A73-26120

Structural changes in the adrenal nerve apparatus during experimental subtotal pancreatectomy
20 p2513 A73-39400

Participation of the hypophysis and adrenal glands in intra-ocular pressure regulation
22 p2807 A73-42661

ADRENAL METABOLISM
Role of the sympathico-adrenal system during a period of rest and in adaptation to muscular activity
01 p0007 A73-10157

Corticosterone level and the binding capacity of blood plasma proteins under thermal effects
03 p0261 A73-13749

Thyroid and adrenal cortical rhythmicity during bed rest.
03 p0263 A73-14122

Inhibition of the adrenocortical response to hypoxia by dexamethasone.
07 p0780 A73-19476

Human endocrine-metabolic responses to graded oxygen pressures.
07 p0785 A73-19479

Role of adrenal and alpha-receptor deactivation in reactions of hemopoietic organs to stress
07 p0781 A73-19644

Mediator systems and respiratory function during an acute lethal loss of blood
07 p0781 A73-19645

Catecholamine exchange in the hormonal and mediator links of the sympathicoadrenal system under stress
07 p0784 A73-20367

Analysis of some mechanisms of human stability to decompression of the lower portion of the body
08 p0930 A73-20987

Neuroendocrine, cardiorespiratory, and performance reactions of hypoxic men during a monitoring task.
09 p1044 A73-22527

Role of mineralocorticoids in the natriuresis of water immersion in man.
09 p1040 A73-22676

Microchemical urinalysis. VIII - Determination of urinary 17-hydroxycorticosteroids.
11 p1324 A73-25138

Interrelations among the suprarenal gluco-corticoid activity, the cardiovascular systems, and the electrolyte metabolism during prolonged work
11 p1317 A73-26085

Adrenal influence on the supercompensation of cardiac glycogen following exercise.
11 p1318 A73-26121

Hypothalamo-adenohypophysis-adrenal neurosecretory system under hyperthermia
14 p1719 A73-30847

Effect of altitude on renin-aldosterone system and metabolism of water and electrolytes.
22 p2806 A73-42420

Changes in indices of the carbohydrate and fat metabolism, the state of the sympathoadrenal system, and oxidative processes under varying-intensity cold effects
24 p3059 A73-44671

Diurnal variations of plasma cortisol and glucose and of urinary excretion of free cortisol in man at rest
24 p3061 A73-45158

ADRENALINE
U EPINEPHRINE

ADRENERGICS
Time course of pulmonary vascular response to hypoxia in dogs.
07 p0782 A73-20168

Neurochemical aspects of the formation of electrophysiological and behavioral reactions
10 p1184 A73-24327

Drug therapy for treatment of cardiogenic shock syndrome following myocardial infarction, discussing sympathomimetics, alpha-adrenergic blocks and combinations
18 p2276 A73-36546

The nature of chemoreception in posterior hypothalamic structures
21 p2636 A73-40279

ADRENOCORTICOTROPIN [ACTH]
Diurnal rhythm of a corticosteroid reaction to ACTH and physical load
14 p1719 A73-30841

Participation of the hypophysis and adrenal glands in intra-ocular pressure regulation
22 p2807 A73-42661

ADSORPTION
NT CHEMISORPTION
Certain characteristics of the initial phase of the nitriding process
01 p0055 A73-10255

Internal friction study of intercrystalline phosphorus adsorption during temper brittleness development in iron alloys
01 p0064 A73-10608

Adsorption equilibria at high pressures in the helium-nitrogen-activated carbon system.
01 p0014 A73-10725

Preferential adsorption in the lubrication process of zinc dialkylthiophosphate.
[ASLE PREPRINT 72LC-3C-3]
03 p0274 A73-14358

Adsorbed barium films on tungsten and molybdenum /011/ face.
04 p0460 A73-14867

Hydrogen/proton adsorption behavior on fuel cell Pt electrode, considering surface roughness factor, Pt sites number and equilibrium data
04 p0407 A73-15104

Influence of structural perturbations applied to platinum and gold on kinetic processes at the electrode.
04 p0407 A73-15105

Isotherm data for physical adsorption of Ar on pyrex surface at low pressure, noting correlation in terms of Dubinin-Radushkevich equation
04 p0456 A73-15765

Control of the electrical properties of a surface with the aid of adsorption of molecules /Stability of surface parameters and slow relaxation/
06 p0735 A73-18083

Adsorption conditions and vapor molecule balance in wall layer at liquid boiling initiation, noting heat flux dependence on underheating effect, pressure and velocity
06 p0769 A73-18564

Manifestation of the adsorption-induced loss of strength in metals under conditions of selective transfer in boundary friction.
06 p0698 A73-18637

Scale factors of adsorptive reduction in the strength of metals in the presence of melts
06 p0711 A73-18667

Microphysical, microchemical, and adhesive properties of lunar material. III - Gas interaction with lunar material.
07 p0892 A73-19832

The plane-wave method in the study of helium atoms physisorbed on graphite
07 p0843 A73-20000

The use of the thermal accommodation coefficients of a rare gas for studying the adsorption of an active gas on a metal, such as in the case of nitrogen and oxygen on tungsten
07 p0839 A73-20150

Adsorption characteristics of condensed Ar, C2H6, NH3 and CO2 layers with respect to cryopumping.
07 p0922 A73-20413

The adsorption and decomposition of CO on Pt(111).
08 p0937 A73-21617

Cryopumping adsorption-desorption theory and cryosorption and condensation pumps, including bare surface, adsorbents and frozen deposit pumps
08 p0989 A73-21619

Diffusion theory for adsorption and desorption of gas atoms at surfaces.
09 p1047 A73-22073

Relationship between adsorption processes on the cathode surface and processes in the region near the electrode in a high-current plasma discharge
09 p1127 A73-22608

Variation of the work function of W/100/ by adsorption of oxygen, cesium, and coadsorption of oxygen and cesium
10 p1186 A73-23696

Diffraction study of fast electrons of the adsorption layer of oxygen on the surface of a film of epitaxial copper
10 p1259 A73-23767

Coadsorption of oxygen and carbon monoxide on tungsten - Desorption spectra, electron stimulated desorption and field emission microscopy.
11 p1325 A73-25204

Corrosion fatigue due to static and cyclic stress, noting electrochemical adsorption theory
11 p1386 A73-26737

Surface effects on trapping and recombination processes in Bi13 single crystals
12 p1531 A73-27938

A study of the adsorption of oxygen on Ni(111) using Auger electron spectroscopy - Chemical shifts and valence spectra.
15 p1840 A73-31968

Exo-electron emission during heterogeneous catalysis /the effect of external electric potentials/.
15 p1842 A73-32599

Adsorption conditions and vapor molecule balance in wall layer at liquid boiling initiation noting heat flux dependence on underheating effect, pressure and velocity
16 p2086 A73-33589

Characteristics of the electrode-adsorbing potential layer in an alkali metal plasma in the presence of adsorption
17 p2214 A73-34131

Effect of adsorption on the electrical conductivity of thin vanadium films
17 p2220 A73-35557

Adsorption of hydrogen, carbon monoxide, and oxygen on vacuum degassed stainless steel 304 at 20 C.
19 p2402 A73-37194

Adsorption of spacecraft contaminants on Bosch carbon.
[ASME PAPER 73-ENAS-15]
19 p2399 A73-37972

Elements of a model of oxygen interactions under low pressure with transition metals at high temperature
21 p2648 A73-41562

Combined LEED, Auger electron and flash desorption spectroscopy of metals on single crystal surfaces.
21 p2706 A73-41596

Liquid helium cryopump extension to gaseous hydrogen and helium pumping via adsorption on argon cryodeposit, obtaining gases partial pressures evolution
22 p2886 A73-41871

Spacecraft polyurethane foam jacket sterilization by gas method, discussing ethylene oxide and methyl bromide sorption and desorption
22 p2803 A73-42160

Kinetics of the development of structural changes in iron in the presence of adsorption fatigue
23 p2995 A73-44224

On the asymmetric adsorption of phenylalanine enantiomers by kaolin.
24 p3066 A73-44772

ADVANCING GLACIERS
U GLACIERS

ADVECTION
Artificial viscosity truncation error analysis for finite difference analogs of linear advection equations.
01 p0035 A73-11466

A numerical study of the influence of advective accelerations in an idealized, low-latitude, planetary boundary layer.
05 p0592 A73-16192

A numerical study of coupling between the boundary layer and free atmosphere in an accelerated low-latitude flow.
05 p0592 A73-16193

Finite element method for solution of two dimensional flow equations with applications to passive advection and nonlinear gravity wave problems, noting computing time
09 p1113 A73-22955

Application of some numerical techniques in combining satellite and conventional data in the tropics.
09 p1115 A73-23175

Vorticity equation advection, divergence and curl terms effects on vorticity changes over isobaric surfaces and on weather and cyclonic development in synoptic meteorology
13 p1653 A73-28745

AEOLOTROPISM

Formation of optical discontinuities in the atmospheric inversion layer

15 p1903 A73-31424

Some parameters of cyclonic cloud vortices.

18 p2333 A73-37053

AEOLOTROPISM

Yield conditions for plastic deformation of aelotropic bodies, using stress tensor invariants and Tresca form

14 p1811 A73-30480

AERIAL EXPLOSIONS

A study of the stability of certain self-similar solutions of the theory of explosions in the atmosphere

01 p0035 A73-11429

An international review of civil aircraft damaged or destroyed by deliberate detonation of explosives /sabotage/ 1964-1972.

10 p1176 A73-24708

Study of the stability of some self-similar solutions from the theory of an explosion in the atmosphere.

11 p1348 A73-26051

Investigation of some theoretical point-explosion problems by the difference method

24 p3076 A73-44656

AERIAL IMAGERY

U AERIAL PHOTOGRAPHY

AERIAL PHOTOGRAPHY

Multiband and multiemulsion digitized aerial photographs automatic processing by digital computer techniques and statistical pattern recognition algorithms

01 p0044 A73-10140

Simultaneous measurements of solar radiation from aircraft and satellites during BOMEX.

01 p0038 A73-10377

The prediction of resolving power of air and space photographic systems.

02 p0171 A73-12567

The use of stress situations in vegetation for detecting ground conditions on aerial photographs.

03 p0301 A73-13844

Real time linear and nonlinear motion desmearing of imagery telemetered from airborne platform, discussing inverse filter error analysis and analog simulation

03 p0276 A73-13907

Moving vehicle borne automatic sighting device pointing problem mathematical analysis and applications to aircraft and camera aiming for airborne photography

03 p0277 A73-13913

Comparative data of investigations of aerial films on lavalan and triacetate bases

04 p0447 A73-14850

Topographic earth observations using radar techniques with a single flight.

04 p0419 A73-15403

Computerized terrain classification system software features for automatic interpretation of aerial photographic imagery by laser scanning system

04 p0445 A73-15772

Theoretical and experimental automatic exposure control study.

04 p0451 A73-15775

An airborne Ka-band microwave radiometric measurement mapping system.

04 p0451 A73-15783

Optical transfer function /OTF/ measurement standards and specification for high quality aerial photographic mapping lens, discussing error sources

05 p0573 A73-16147

Affine and nonlinear transformations for aerial photography film deformation effects on photogrammetry accuracy

05 p0575 A73-16315

The cost-effectiveness of high altitude systems for regional resource assessment.

05 p0642 A73-17139

Automatic analysis and classification methods based on statistical characteristics of aerial photometric and TV photographs, noting contour related interval distribution

05 p0579 A73-17143

A digital processing and analysis system for multispectral scanner and similar data.

05 p0554 A73-17147

Automatic control for aircraft photographic camera pitch compensation via optical space filters and frequency methods, noting flight velocity to altitude relation

06 p0693 A73-18154

Random optical density fields pertaining to analyses of aerial photo imaging of aerial topographic objects

06 p0693 A73-18155

Aerial photograph distortion due to sealed compartment temperature and pressure effects in terms of internal refraction

06 p0693 A73-18156

Radar imagery and aerial photography for geological remote sensing applications in coastal mapping, landform analysis, engineering and reconnaissance

06 p0667 A73-18282

Radar imagery and supporting aerial photography features for topographic mapping capabilities and metric quality of side-looking stereo radar system

06 p0667 A73-18283

Similarities and differences in the interpretation of air photos and SLAR imagery.

06 p0693 A73-18284

Aerial imagery data statistical processing, discussing probability density and autocorrelation functions and power spectra for automatic pattern recognition

06 p0695 A73-18322

Perception of tone differences from film transparencies.

06 p0695 A73-18388

Measurements regarding the color of aerial photographs in studies of the vegetation

06 p0695 A73-18437

Determination of the true course and instantaneous position of an aircraft from aerial pictures

06 p0721 A73-18467

Drobyshev stereograph corrector operation for aerial photographs processing with transformed beam of stereoprojector

07 p0824 A73-20043

Computer calculation of spectral brightness coefficients on aerial photographs, determining contrast features density gradients

07 p0824 A73-20044

Photography of a lithium vapor trail during the daytime.

07 p0820 A73-20068

Computer aided recognition of objects shapes on aerial photographs, discussing image derivatives and histograms use and flying spot scanner principle

07 p0825 A73-20165

Establishment of a relationship between the frequency and contrast characteristics of objects on aerial photographs and the resolving power

08 p0963 A73-21024

Computation of the minimum bandwidth for aerotriangulation.

08 p0968 A73-21705

Calibration of the aerial photographic system by the method of mixed ranges.

08 p0969 A73-21706

Fine verticality readout accuracy test on film format of each photograph obtained by prime camera, describing aerial photogrammetric data reduction methods

08 p0969 A73-21708

Coordinates correction for atmospheric refraction in aerial photography, noting effects of ground elevation, atmospheric pressure and temperature

08 p0969 A73-21709

The utility of a low flying aircraft or helicopter when collecting ground data for regional resource surveys.

08 p0961 A73-21710

Airborne photogrammetric system with mapping and geodetic surveying data acquisition capability, discussing inertial navigation subsystem, terrain profile recorder and electronic distance measuring equipment

09 p1081 A73-22380

A 35mm aerial photographic system.

09 p1082 A73-22387

Unified time recording for aerial photographic surveys, using exact time synchronized control signal sequences in recording camera shutter release

09 p1084 A73-22672

High-altitude photographs of the Oregon coast.

09 p1078 A73-22719

Redundant area encoding for relieving integration time requirement in airborne reconnaissance photograph transmission, discussing algorithms, display technique, data reduction and pictorial simulation

09 p1054 A73-23386

Damping of an aerial photo camera with the aid of polymeric materials

10 p1219 A73-24478

An analytic expression for the radial photogrammetric distortion of aerial photo cameras

10 p1219 A73-24479

Analytical transformation of photographs for plotting topographic and photographic maps in prescribed projections

10 p1219 A73-24483

Projective properties of an anamorphic bundle of projecting beams

10 p1219 A73-24484

Binary coded aircraft flight data block inclusion in aerial reconnaissance photographs for automated data processing

10 p1222 A73-24948

Nelson Tyler helicopter camera mount for aerial reconnaissance photography providing camera balance and motion stability under combat flight conditions

10 p1222 A73-24949

Photometric error of the NA-MK-25 camera field

11 p1361 A73-25250

Panoramic and frame cameras for aerial phototopographic survey, noting photo quality and high resolution advantages

12 p1497 A73-27423

The application of color and multispectral techniques to the collection of military geographic information.

12 p1500 A73-27952

Piston engine or turboprop aircraft photography, measuring camera vibration components in roll, pitch and yaw by flashing light technique for image quality improvement

12 p1500 A73-27954

Block adjustment for color and multispectral high altitude frame photography in photogrammetry, considering terrain caused sun angle effect as discriminant for automatic photointerpretation

12 p1500 A73-27955

Examination of film deformation for aerial photography

12 p1500 A73-27960

The resolving power and the modulation transfer function of terrestrial and aerial cameras in working conditions.

12 p1501 A73-27963

Aerial camera automatic exposure control design and operation, discussing maxima-minima metering and average brightness measurement techniques

12 p1501 A73-27965

Optimizing sensitometric data for color and black and white aerial film.

12 p1501 A73-27966

Signal color effects on stereoplotters measurements in aerial mapping of built-up areas

12 p1501 A73-27968

Metric calibration of distortion in aerial mapping cameras, using laser, collimator and diffraction grating generated angularly accurate image points matrix

12 p1501 A73-27970

Aerial cameras functional testing and calibration, discussing film plane flatness measurement methods and camera applications to ice surface photography

12 p1502 A73-27971

Aerial radar photograph restitution for photogrammetric application, discussing geometric qualities and methods and instruments for partial removal of distortion

12 p1502 A73-27972

Photomosaic construction high altitude photographs, approximating surface curved areas by planes

13 p1621 A73-29323

Computer program analysis of errors in mutual orientation elements on aerial photographs with different lengthwise overlaps, discussing error minimization

13 p1621 A73-29324

Use of a computer to design surveys made by the stereotopographic method

13 p1621 A73-29416

The problem of the deformation of the photoemulsion layer during artificial marking of points on aerial photos

13 p1621 A73-29417

Experience in constructing analytical planar phototriangulation grids from 1:40,000 and 1:75,000 scale aerial photographs for the preparation of 1:10,000 scale photographic maps

14 p1753 A73-30416

Experiment in stereophotogrammetric processing of aerial photographs with decentrations on an STD-2 stereometer

14 p1753 A73-30417

Remote sensing in a circulatory survey of Boston Harbor.

16 p2003 A73-33356

Airborne remote sensing of Georgia tidal marshes.

16 p2003 A73-33359

Airborne photography with multispectral scanners for remote sensing of large area features, discussing cost and feasibility of computerized pattern recognition and automatic identification

16 p2015 A73-33361

Cartographic applications of high-altitude aircraft photographs.

16 p2016 A73-33362

Slope angle determination with respect to photograph surface from visible horizon line configuration

16 p2017 A73-34049

Correction formulas for aerial photograph distortions due to internal refraction of light rays in separation of gas media by lateral surface of circular cylinder

16 p2038 A73-34050

Airborne remote sensing for forestry and agricultural land imagery and water pollution detection, discussing use of color films and picture processing

17 p2161 A73-34933

Airborne and satellite remote sensing of Anacapa Island for hydrology and aquatic biology.

17 p2161 A73-34944

IR line scanners using stereoscopic techniques for aerial remote sensing of topography, discussing pivoting mechanism, scanner cameras and scan planes

17 p2168 A73-34957

Teledetection experiments using balloons

17 p2176 A73-35815

Optimum parameters of an infrared imaging system for aerial scanning of earth resources.

18 p2317 A73-36874

Photographic processing of aerial imagery for earth resources, discussing photographic developers, film and materials

Remote sensing experiments with balloons

Airborne and spaceborne microwave imaging techniques for earth surface surveys, discussing resolution capabilities and applications for side-looking radar, microwave radiometers and scatterometers [AAS PAPER 73-111]

The use of remote sensing in the USSR for the study of natural resources.

Development of a practical remote sensing water quality monitoring system.

An integrated resource survey using orbital imagery - An example from south-east Spain.

Urban land use from RB-57 photography - Computer graphics of the Boston area.

Remote sensing to detect regional change in land use characteristics, using aerial photo mosaics and high altitude photography

The use of small-scale multi-band photography for detecting land-use change.

Multispectral survey of power plant thermal effluents in Lake Michigan.

The reliability of the interpretation of soils from aerial photographs in highway planning practice.

Automatic terrain mapping by texture recognition.

A new method for evaluating and mapping colours in aerial photographs.

Time sensing and analysis of coastal water dynamic features obtained from aircraft and satellite provided sequential photographic data

Relationship between sea wave parameters and the spectra of aerial photography and radar imagery of sea surface.

Remote sensor geological mapping of Rio Grande rift zone /Colorado/ using aerial color infrared photography for compilation of tectonic and geomorphic histories

Thermal activity of the Uson Caldera based on infrared and photographic aerial survey.

Geological analysis of aerial thermography of the Canary Islands, Spain.

Multispectral scannery imagery in aerial photography of plant communities, discussing reflectance effects, digital processing, vegetation types, classification errors and spectrum analysis

A comparison of four remote sensing media for assessing salt marsh primary productivity.

Detection of small fires and mapping of large forest fires by infrared imagery.

Photodensity and the impact of shifting agriculture on subtropical vegetation - A case study in the Bahamas.

The usefulness of ERTS-I and supporting aircraft data for monitoring plant development in rangeland environments.

Canadian remote sensing programs for ERTS data, describing receiving stations, data acquisition and processing facilities and techniques, digital system and aerial photography

Hailswaths mapping with airborne fixed beam and scanning IR radiometers, noting dimensions, orientation and fine structure

Airborne photographic and visual observation of material from Comet Giacobini-Zinner produced meteor showers due to orbit perturbation and perihelion changes by Jupiter

Aerial-survey aircraft of the new generation

An analysis of the earth's resources satellite /ERTS-I/ data.

Remote sensing of estuarine circulation dynamics.

Radiometric calibration of a multi-spectral aerial camera.

An improved single flight technique for radar stereo.

Book - The surveillant science: Remote sensing of the environment.

Some scale estimates of the three-dimensional structure of cloud fields from aircraft-based aerial photographs

AERIAL RECONNAISSANCE

Side-look radar provides a new tool for topographic and geological surveys.

The measurement of environmental pollution with the aid of aircraft and satellites [DFVLR-SONDDR-247]

IR radiation source shape and size effects on aerial IR surveys at various flight altitudes, noting spectral composition change with height

Diffusion coefficients and current velocities in coastal waters by remote sensing techniques.

Image formation radiometers for blind landing, aerial reconnaissance over land and sea, horizon detection and detection of obstacles at sea

Binary coded aircraft flight data block inclusion in aerial reconnaissance photographs for automated data processing

Nelson Tyler helicopter camera mount for aerial reconnaissance photography providing camera balance and motion stability under combat flight conditions

The application of color and multispectral techniques to the collection of military geographic information.

Evaluation of remote sensor imagery for military geographic information.

Earth resources monitoring from satellites, aircraft and ground stations for fast data acquisition and management

High resolution measurements of snowpack stratigraphy using a short pulse radar.

Two-dimensional statistic analysis of radar imagery of sea ice.

Urban land use from RB-57 photography - Computer graphics of the Boston area.

Land use classification in the southeastern forest region by multispectral scanning and computerized mapping.

A direct comparison of satellite and aircraft infrared /10 to 12 microns/ remote measurements of surface temperature.

Statistical comparison of airborne laser and stereophotogrammetric sea ice profiles.

AEROBEE ROCKET VEHICLE

Open-loop tracking of moving targets with an Aerobee sounding rocket.

AEROBIOLOGY

Reactions of singlet oxygen with pine pollen.

AERODYNAMIC AXIS

U AERODYNAMIC BALANCE

AERODYNAMIC BALANCE

Airships design, constructional and operational characteristics, discussing aerodynamics, flight control, performance and trim

Recovery of sounding rocket payloads by center-of-gravity position control. [AIAA PAPER 73-294]

AERODYNAMIC BRAKES

NT BALLUTES

NT DRAG CHUTES

NT LEADING EDGE SLATS

NT TRAILING-EDGE FLAPS

NT WING FLAPS

Nb refractory alloy sheet mechanical properties for application in space shuttle thermal protection system /TPS/ and space tug aerobraking system

Aerodynamic decelerator dynamics modeling for Viking lander parachute deployment, analyzing unfurling process with attention to longitudinal and rotational dynamics

Viking aerodynamic decelerator for Mars lander mission in 1976, discussing mortared disk-gap-band parachute, qualification flight tests and atmospheric environment effects

Computerized stress analysis of shock load induced circular elastic membrane interaction with fluid stream

AERODYNAMIC CHARACTERISTICS

via method of characteristics related to aerodynamic decelerator design

Viking lander capsule decelerator system candidate materials evaluation, discussing in-situ testing for high density packing and heat sterilization effects on strength

Low altitude flight test phase of Viking decelerator system development, considering low density environment loading condition simulation method

Viking 75 lander deceleration system qualification flight tests at expected Mars conditions, discussing design requirements and full scale vehicle simulation in earth atmosphere

Mortar design for parachute ejection and deployment into airstream to decelerate spacecraft and aircraft pilot escape modules, estimating hardware weight and reaction load

Computerized six degree of freedom parachute deployment model for predicting entry vehicle-decelerator dynamic response to aerodynamic forces and physical property changes

A dynamic and aerodynamic analysis of an articulated autorotor decelerator system.

Drag effectiveness of aerodynamic brakes in series on high speed train-like vehicle, considering fixed and moving model testing techniques

Development and testing of ballute stabilizer/decelerators for aircraft delivery of a 500-lb munition.

Aerodynamic BUZZ

U FLUTTER

AERODYNAMIC CENTER

U AERODYNAMIC BALANCE

AERODYNAMIC CHARACTERISTICS

NT AERODYNAMIC BALANCE

NT AERODYNAMIC DRAG

NT AERODYNAMIC STABILITY

NT INTERFERENCE LIFT

NT LIFT

NT ROTOR LIFT

Aerodynamics of blunted bodies in hypersonic stream at the angle of attack.

High-pressure axial fan for air-cushion vehicles

Design study for long-lived compact 750 kW industrial gas turbine, discussing optimal aerodynamic proportioning and size determination

Computer programs for air cooled gas turbine engine design and performance prediction, noting aerodynamic effect of turbine coolant

Structural and aerodynamic characteristics changes in turbulent propane-butane and air jets interacting with sound

Performance and noise generation studies of supersonic air ejectors.

Problems regarding the use of electronic data processing for the calculation of diagonal cascades in turbomachines

Aerodynamic and temporal parameters of olfactory stimulation - Discussion concerning the lowering of the threshold by prenasal injection in man

Directional devices for noise reduction of high speed jets

Transonic profile theory - Critical comparison of various procedures

Supersonic blowdown wind tunnel modification for transonic airflow profile aerodynamic characteristics measurement, discussing design criteria and operational range

Steady state aerodynamic characteristics of cylinders with spanwise protrusions, presenting wind tunnel drag and lift measurements in Reynolds number transition range

The aerodynamic characteristics of the thin delta wing fitted with a conical body in supersonic flow.

Lifting characteristics and spanwise aerodynamic load distribution of an external flow jet flap.

Study of a series of variable-geometry wings derived from delta wings of different aspect ratios. I - Aerodynamic characteristics of delta wings

Russian book on Il-18 aircraft practical aerodynamics covering aerodynamic characteristics, performance, controllability, stability and flight safety

04 p0406 A73-15968

Wind tunnel experimental verification of flight vehicles aerodynamic characteristics during preliminary design stage, discussing correction procedures for model data extrapolation to full scale parameters [SAE PAPER 720861]

05 p0528 A73-16665

Experimental and theoretical investigations regarding the unsteady aerodynamic derivatives of the longitudinal motion in the case of slender flight bodies at moderate velocity

[DFVLR-SONDDR-206]

05 p0528 A73-16757

B-1 airplane model support and jet plume effects on aerodynamic characteristics.

[AIAA PAPER 73-153]

05 p0563 A73-16901

Experimental aerodynamic studies for intra-urban trains traveling in tunnels.

[AIAA PAPER 73-155]

05 p0566 A73-16903

Reentry vehicle finned roll rate control - Aerodynamic and flight dynamic analysis.

[AIAA PAPER 73-183]

05 p0531 A73-16923

Mach numbers up to 30 obtained in a continuous operating wind tunnel

05 p0533 A73-17194

Aerodynamic technology developments including advanced transonic airfoils, low-drag/high-lift systems and stability augmentation for transport aircraft performance, economics and noise improvements [AIAA PAPER 73-9]

06 p0644 A73-17604

Calculation of the mean parameters of an inhomogeneous flow by the method of sections

06 p0645 A73-17720

The effect of the degree of turbulence on the aerodynamic characteristics of planar decelerating cascades

[DFVLR-SONDDR-275]

07 p0773 A73-19197

Calculation of the aerodynamic characteristics of a rectangular wing with tip plates moving at a low subsonic speed in the proximity of a screen

07 p0775 A73-20094

Aerodynamic characteristics of thin asymmetric wing profiles in supersonic flow

07 p0776 A73-20487

Supersonic-hypersonic motion around a porous circular cone

07 p0776 A73-20615

Aerodynamic experimental investigation of annular cascade of gas turbine nozzle blade in subsonic and supersonic flow.

08 p0925 A73-20939

Theoretical determination of the characteristics of helicopter rotors

09 p1027 A73-22205

Toward simpler prediction of transonic airfoil lift, drag, and moment.

09 p1028 A73-22434

Aerodynamic forces and moments estimation for slender bodies of circular and noncircular cross section without and with lifting surfaces at 0-90 degree angles of attack

09 p1030 A73-23468

Unsteady aerodynamics of separating and reattaching flow on bodies of revolution.

10 p1173 A73-24816

Aeroelastic effects on flying wing aircraft aerodynamic stability characteristics, using elementary beam-rod differential equations and aerodynamic strip theory

[AIAA PAPER 73-397]

11 p1305 A73-25526

An exploratory investigation of the unsteady aerodynamic response of a two-dimensional airfoil at high reduced frequency.

[AIAA PAPER 73-309]

11 p1301 A73-25540

Calculation of unsteady transonic aerodynamics for oscillating wings with thickness.

[AIAA PAPER 73-316]

11 p1301 A73-25547

An investigation of unsteady aerodynamics on an oscillating airfoil.

[AIAA PAPER 73-318]

11 p1301 A73-25549

Analysis of the aerodynamic characteristics of wing-lift augmentation devices. II

11 p1301 A73-25796

Aerodynamic characteristics of torus shaped cascades involved in flame stabilization process of reheat devices for jet engines

11 p1453 A73-26595

Analysis of the aerodynamic characteristics of wing lift augmentation devices

12 p1457 A73-26824

Rogallo variable geometry flexible cambered wing structure and aerodynamic performance for low speed agricultural flight applications

13 p1568 A73-28027

Low speed of sound modeling of a high pressure ratio centrifugal compressor.

13 p1566 A73-29020

A 14.2-ft-Do variable-porosity conical ribbon chute for supersonic application.

[AIAA PAPER 73-472]

15 p1828 A73-31456

Russian book - Practical aerodynamics of the An-24 aircraft /2nd revised and enlarged edition/.

15 p1829 A73-31547

Optimal grid arrangement in vortex lattice method of lifting surface aerodynamic analysis, comparing numerical with kernel function results for simple wing planforms

15 p1824 A73-31746

Calculation of the characteristics of tail fins in the vortical field of a wing

16 p1962 A73-32819

Experimental results in the case of the Nonweiler wave-rider in the subsonic, transonic, and supersonic range

16 p1963 A73-33265

Effect of rotor design tip speed on aerodynamic performance of a model VTOL lift fan under static and crossflow conditions.

[ASME PAPER 73-GT-2]

16 p1963 A73-33480

Investigation of the aerodynamic performance of small axial turbines.

[ASME PAPER 73-GT-3]

16 p1963 A73-33481

Small turbomachinery compressor and fan aerodynamics.

[ASME PAPER 73-GT-6]

16 p2047 A73-33484

Aerodynamic study of a turbine designed for a small low-cost turbofan engine.

[ASME PAPER 73-GT-29]

16 p2048 A73-33500

Heavy lift helicopter rotor blade design including airfoils, fiberglass skin, titanium spar, fail-safety and aerodynamic and structural features

[AHS PREPRINT 710]

17 p2104 A73-35056

An inexpensive technique for the fabrication of two-dimensional wind tunnel models.

17 p2149 A73-35762

Aerodynamic parameters affecting practical gas dynamic laser design.

[AIAA PAPER 73-626]

18 p2321 A73-36173

Experimental developments in V/STOL wind tunnel testing at the National Aeronautical Establishment.

18 p2265 A73-36774

Analysis of the aerodynamic characteristics of devices for increasing wing lift. III - Influence of ground proximity on the aerodynamic characteristics of the flaps

18 p2266 A73-37022

New contributions to the iterative method for aerodynamic calculations of wings in subsonic flows

19 p2376 A73-37545

Space Shuttle Orbiter aerodynamics, discussing wing/body matching, lateral/directional stability, control and reaction systems

19 p2491 A73-37595

On the aerodynamic damping moment in pitch of a rigid helicopter rotor in hovering. I - Experimental phase.

19 p2387 A73-38281

Airfoil profiles aerodynamic characteristics from laminar flow wind tunnel measurements

19 p2377 A73-38361

Jet engine exhaust plume effects on solid bodies, examining nozzle drag effects, nozzle geometry, plume entrainment and shape, wind tunnel tests and pressure effects

20 p2626 A73-38651

Optimal guidance for aerodynamically controlled reentry vehicles.

[AIAA PAPER 73-891]

20 p2588 A73-38827

Neighboring body effects on bluff body tipping moment.

20 p2507 A73-39520

An aerodynamic test facility with free molecular flow and high stagnation temperature

20 p2545 A73-39615

Holographic interferometry applied to aerodynamics

21 p2696 A73-39984

On the aerodynamic damping moment in pitch of a rigid helicopter rotor in hovering. II - Analytical phase.

21 p2631 A73-40087

Investigation of multi-element airfoils with external flow jet flap.

21 p2633 A73-41087

Influence of geometrical parameters on propeller performance at low advance ratios

21 p2635 A73-41582

Aerodynamic and thermal structures of the laminar boundary layer over a flat plate with a diffusion flame.

22 p2933 A73-42774

A simple graphical solution for rocket wake boundaries.

23 p2939 A73-43680

AERODYNAMIC CHORDS

U AIRFOIL PROFILES

U CHORDS [GEOMETRY]

AERODYNAMIC COEFFICIENTS

Simplification of the wing-body interference problem.

01 p0001 A73-10048

An experimental study of the dynamic lift on a cylinder subjected to a high Reynolds number flow perpendicular to its axis.

[ONERA, TP NO. 1073]

01 p0001 A73-10226

Nonlinear characteristics of a slender triangular wing near an interface

02 p0127 A73-11630

Lift of wing-body combination.

03 p0247 A73-14194

Experimental analysis of lift on a fixed cylinder subjected to a flow perpendicular to its axis at high Reynolds numbers

04 p0405 A73-15990

Drag coefficient for particles in rarefied, low Mach-number flows.

05 p0564 A73-16354

Measured axial and normal force coefficients for 9-deg cones in rarefied, hypersonic flow.

[AIAA PAPER 73-154]

05 p0531 A73-16902

Equivalence rule and transonic flows involving lift

[AIAA PAPER 73-88]

06 p0644 A73-17642

Aerodynamic influence coefficient method using singularity splines.

[AIAA PAPER 73-123]

06 p0644 A73-17645

German monograph - The steady and unsteady aerodynamic coefficients for the rolling motion of slender wings.

07 p0774 A73-19578

Multiple element airfoils optimized for maximum lift coefficient.

07 p0775 A73-19956

A four-level technique for estimation of tactical missile aerodynamic parameters.

07 p0777 A73-20592

Fluctuating lift and moment coefficients for cascaded airfoils in a nonuniform compressible flow.

09 p1028 A73-22432

A method of measuring the thrust, the polar, and the performance of an aircraft on the basis of flight tests

10 p1175 A73-24494

Development and applications of supersonic unsteady consistent aerodynamics for interfering parallel wings.

[AIAA PAPER 73-317]

11 p1301 A73-25548

Correction for change in fluid flow curvature about a lift-generating airfoil in a two-dimensional test section with perforated walls

11 p1302 A73-25864

A contribution to the calculation of aerodynamic force and moment coefficients of spacecraft

12 p1457 A73-26819

A method for the calculation of the aerodynamic coefficients of a body of any form.

12 p1457 A73-27067

A note on the lift coefficient of a thin jet-flapped airfoil.

12 p1457 A73-27171

High velocity moving body in ideal incompressible fluid flow, determining lift coefficient from acceleration potential algorithm

12 p1486 A73-27239

Experimental tests on scale models of conical variable geometry propulsion nozzle with short petals for fighter aircraft, discussing aerodynamic and thrust coefficients

12 p1533 A73-27388

Influence of the surface-reradiation law on the calculation of the aerodynamic coefficients in the near free molecular flow transient regime

12 p1487 A73-27391

Experimental drag coefficients for evaporating and burning drops at elevated pressures.

13 p1707 A73-28998

A dynamic and aerodynamic analysis of an articulated autorotor decelerator system.

[AIAA PAPER 73-463]

15 p1827 A73-31449

German monograph - The flow around wings of arbitrary planform in the case of supersonic flow - A computational method.

15 p1824 A73-32581

Aerodynamic coefficients determination for nonlinear equations of motion solution to fit experimental free flight data, obtaining starting solution by noniterative continuation method

18 p2263 A73-36307

A finite-element method for calculating aerodynamic coefficients of a subsonic airplane.

18 p2265 A73-36394

A theoretical note on the lift distribution of a non-planar ground effect wing.

19 p2376 A73-37493

Design method of the axial-flow blade row on modified isolated aerofoil theory with interference coefficient. II - The influence of the aerodynamic parameter on the fan performance at low flow rate.

19 p2377 A73-37671

Surface wind-geostrophic wind relationship at Salisbury Plain, England, deducing geostrophic drag coefficients for open sea

21 p2732 A73-41571

Airfoil theory calculation of bent thin foil lift coefficient and longitudinal moment characteristics at arbitrary flow separation point location

23 p2940 A73-43720

AERODYNAMIC CONFIGURATIONS

Technological and structural design ensuring optimum clearance and aerodynamic coupling of moving units /wing-aileron or aileron-trim tab/

02 p0129 A73-11648

Three dimensional potential flow past arbitrarily shaped aerodynamic configurations, using Hess-Smith numerical method

[DGLR PAPER 72-105]

02 p0127 A73-11657

- Determination of characteristic dimensions in the solution of drag and heat-transfer problems for flows past bodies of arbitrary configuration
07 p0812 A73-20425
- Symmetrical airfoils optimized for small flap deflection.
10 p1174 A73-24915
- Russian book on rockets as control plants covering dynamics equations of motion for different configurations, linearization and matrix description of rockets
11 p1429 A73-25175
- Light weight beaded and tubular structural panels for heat shielded aerodynamic surfaces
[AIAA PAPER 73-370] 11 p1438 A73-25504
- Light motorized glider-type aircraft design, development and flight testing, discussing aerodynamic configuration, structural design and performance characteristics
12 p1459 A73-27732
- Wing-fuselage junctions fairings compromise design, describing rotational eddies formation mechanism for unsteady ducted flow and wing root phenomena
[ONERA, TP NO. 1217] 13 p1564 A73-28836
- Concorde wing and fuselage aerodynamic design modifications for operational efficiency optimization from wind tunnel tests and theoretical computations
14 p1712 A73-30926
- Development of an improved midair-retrieval parachute system for drone/RPV aircraft.
[AIAA PAPER 73-469] 15 p1828 A73-31453
- Aerodynamic rig and wind tunnel developments of compound ejector thrust augmentor for V/STOL aircraft with combined Coanda and center injection flows
[ASME PAPER 73-GT-67] 16 p2048 A73-33519
- Effect of nose geometry on the aerothermodynamic environment of shuttle entry configurations.
[AIAA PAPER 73-638] 18 p2260 A73-36196
- The F-12 series aircraft aerodynamic and thermodynamic design in retrospect.
[AIAA PAPER 73-820] 19 p2380 A73-37472
- Feasibility study of skirt configurations and materials for an ACLS aircraft.
19 p2443 A73-37696
- Integral equation in the theory of lifting surfaces
19 p2377 A73-37846
- Prediction of the lift and moment on a slender cylinder-segment wing-body combination.
19 p2377 A73-38007
- Construction of a minimum-wave-drag profile in inhomogeneous supersonic flow
21 p2631 A73-40184
- The aerodynamic development of the wing of the A 300B.
21 p2633 A73-41192
- Dirigible airship design, operations, payloads, cargo transportation and surveillance applications
23 p2940 A73-44223
- Noise comparisons from full-scale fan tests at NASA Lewis Research Center.
[AIAA PAPER 73-1017] 24 p3121 A73-44849
- Acoustic investigation of the engine-over-the-wing concept using a D-shaped nozzle.
[AIAA PAPER 73-1030] 24 p3122 A73-44860
- AERODYNAMIC DRAG**
- The effects of drag on relativistic spaceflight.
01 p0095 A73-10274
- Missile range dispersions produced by meteorological factors, drag differences and mass changes during passive ballistic flight
02 p0211 A73-11787
- Initially spherical water drops deformation under external flow for wide range of Weber and Bond numbers, investigating drag coefficient and Taylor instability
02 p0153 A73-12037
- Aircraft aftbody/propulsion system integration for low drag.
[AIAA PAPER 72-1101] 03 p0243 A73-13420
- Induced drag of finite wing with antisymmetric incidence distribution due to rolling, deriving relations between wing lift distribution and induced downwash
03 p0248 A73-14472
- Spacecraft optimal control after transfer from hyperbolic trajectory to planetary orbit by atmospheric drag, minimizing engine thrust
03 p0340 A73-14570
- Interplanetary spacecraft transfer maneuver for hyperbolic trajectory change into eccentric orbit, using aerodynamic drag to obtain nearly circular orbit
03 p0379 A73-14571
- Flight and wind tunnel investigation of the effects of Reynolds number on installed boattail drag at subsonic speeds.
[AIAA PAPER 73-139] 05 p0530 A73-16888
- Mean free path of molecules from a surface in rarefied flow with application to correlating drag data.
[AIAA PAPER 73-198] 05 p0531 A73-16933
- Determination of characteristic dimensions in the solution of drag and heat-transfer problems for flows past bodies of arbitrary configuration
07 p0812 A73-20425
- Lundell solid rotor brushless alternator windage power losses, measuring aerodynamic drag coefficient over Reynolds number and gap width range
09 p1034 A73-22772
- Static stability and drag studies for bodies of revolution in supersonic flow.
[AIAA PAPER 73-295] 09 p1156 A73-23214
- Circular cones and cylinder drag in molecular flow, using Schamberg model of molecules/solid surface interaction
09 p1030 A73-23461
- Wind tunnel study of flows generated by slender cones in subcritical Reynolds number regime, examining vortex shedding and drag
10 p1174 A73-24845
- Lift and drag at off-design Mach numbers of conically cambered wings with subsonic leading edges and supersonic trailing edge
12 p1458 A73-27927
- Base drag calculations in supersonic turbulent axisymmetric flows.
13 p1564 A73-28835
- On the motion of small spheres in gases. III - Drag and heat transfer.
13 p1567 A73-29425
- Parachute axisymmetric self excited breathing oscillations dependence on descent velocity, Froude number, canopy/line length ratio, drag and line stiffness
[AIAA PAPER 73-452] 15 p1826 A73-31438
- Drag and stability characteristics of high-speed parachutes in the transonic range.
[AIAA PAPER 73-473] 15 p1828 A73-31457
- Drag effectiveness of aerodynamic brakes in series on high speed train-like vehicle, considering fixed and moving model testing techniques
[AIAA PAPER 73-476] 15 p1828 A73-31460
- A technique for the calculation of the opening-shock forces for several types of solid cloth parachutes.
[AIAA PAPER 73-477] 15 p1829 A73-31461
- Several computerized techniques to aid in the design and optimization of parachute deceleration and aerial-delivery systems.
[AIAA PAPER 73-488] 15 p1829 A73-31470
- Computational program for calculating the Re-number-dependent polar of a glider with arbitrary double trapezoidal wing
16 p1967 A73-33024
- Book - Methods for estimating drag polars of subsonic airplanes.
16 p1963 A73-33422
- Revised calculations of the NACA 6-series of low drag aerofoils.
17 p2094 A73-34536
- An investigation of the flow field and drag of helicopter fuselage configurations.
[AHS PREPRINT 700] 17 p2095 A73-35051
- Tradeoff studies for feasibility of multiblade ring rotor configuration for helicopter design, discussing ring drag
[AHS PREPRINT 714] 17 p2104 A73-35060
- Tektite ablation calculation taking into account transient effects, internal radiation, melting and nonequilibrium vaporization of glass and drag effect of flanges
17 p2233 A73-35272
- The rocket motion in resisting medium on a given trajectory.
18 p2353 A73-36490
- Techniques for studying the aerodynamic characteristics of the bronchial tree of man
18 p2282 A73-36576
- The Dolphin airship with an undulating propulsion system - Surface and width of the fuselage
19 p2387 A73-38122
- Neighboring body effects on bluff body form drag.
20 p2507 A73-39519
- Secular perturbations of the motion of artificial satellites, caused by atmospheric drag
21 p2768 A73-40725
- Problems of the aerodynamics of satellites with uniaxial orientation
21 p2781 A73-40902
- Drag due to regular arrays of roughness elements of varying geometry.
21 p2633 A73-41569
- AERODYNAMIC FORCES**
- NT AERODYNAMIC DRAG
- NT AERODYNAMIC LOADS
- NT BLAST LOADS
- NT GUST LOADS
- NT INTERFERENCE LIFT
- NT LIFT
- NT ROTOR LIFT
- NT WING LOADING
- Flutter analysis method for unsteady aerodynamic forces on wings and rotating blades under harmonic vibrations and uniform flow
[ONERA, TP NO. 1099] 01 p0001 A73-10230
- Calculation and measurement of the aerodynamic forces on an oscillating airfoil profile with and without stall
[ONERA, TP NO. 1132] 01 p0002 A73-10240
- Aerodynamic generalized forces for supersonic shell flutter.
01 p0003 A73-10751
- Secondary jet interaction with emphasis on outflow and jet location.
03 p0243 A73-13496
- Rarefied gas interaction with spacecraft surface, calculating aerodynamic forces and accommodation coefficient for Proton 2 satellite
03 p0383 A73-14574
- Unsteady transonic flow analysis for low aspect ratio, pointed wings.
[AIAA PAPER 73-122] 05 p0530 A73-16878
- Magnus force and moment coefficients for spinning ogive and cone cylinders and conical bodies in laminar compressible flow, including boundary layer and radial pressure gradient effects
[AIAA PAPER 73-124] 05 p0530 A73-16879
- Measured axial and normal force coefficients for 9-deg cones in rarefied, hypersonic flow.
[AIAA PAPER 73-154] 05 p0531 A73-16902
- Leading-edge force features of the aerodynamic finite element method.
05 p0533 A73-17213
- Russian book - Mechanics of optimal spatial motion of flight vehicles in the atmosphere.
07 p0777 A73-20380
- Further results concerning the forces on a flat plate in a Couette flow.
08 p0926 A73-21402
- A linearised theory of parachute opening dynamics.
08 p0928 A73-21692
- Calculation of forces on stores in the vicinity of aircraft.
09 p1028 A73-22433
- Out-of-plane force on a circular cylinder at large angles of inclination to a uniform stream.
09 p1029 A73-23124
- Compressibility effects on unsteady forces generated by jet engine blade rows aerodynamic interference, considering potential flow and viscous wake interactions
09 p1029 A73-23443
- Helicopter main-rotor blade flutter in steady inclined flight
10 p1174 A73-23662
- A precise position and attitude measurement system for free-flying wind-tunnel models
11 p1362 A73-25443
- Study of flow around a rotating circular cylinder.
11 p1302 A73-26337
- Newtonian aerodynamic forces from Poisson's equation.
11 p1303 A73-26382
- A contribution to the calculation of aerodynamic force and moment coefficients of spacecraft
12 p1457 A73-26819
- The effect of aerodynamic moments on the rotational motion of Proton satellites
12 p1548 A73-26820
- Experimental study by resonance method of unsteady aerodynamic forces acting on cascading blades.
13 p1567 A73-29028
- Semiempirical method for flutter prediction of unsteady lift and aerodynamic forces acting on oscillating airfoil in stall regime, using separation function
13 p1566 A73-29029
- Parameter estimation for a specular-diffusion reflection model from the motion of 'Proton' series satellites about their centers of mass
14 p1803 A73-29851
- Characteristics of supercharge devices in gas bearings
15 p1881 A73-31296
- Potential flow induced aerodynamic forces and moments on triaxial ellipsoids, using Lagally theorem based on source, sink and doublet distribution imaging method
15 p1823 A73-31641
- On the unsteady supersonic cascade with a subsonic leading edge - An exact first order theory. II.
[ASME PAPER 73-GT-16] 16 p1964 A73-33493
- Beyond the buffet boundary.
17 p2100 A73-34538
- Book - The aerodynamics of high speed ground transportation.
17 p2097 A73-33854
- Spatial motion of a two body cluster under the action of gravitational and aerodynamic forces
18 p2351 A73-36119
- Wind tunnel and flight tests for Saturn S-2 stage polyurethane spray foam insulation erosion under aerodynamic heating, shear stress and static pressure
[AIAA PAPER 73-740] 18 p2326 A73-36357
- Unsteady aerodynamic forces in transonic turbomachines
18 p2266 A73-37084
- Aerodynamic forces on a triangular cylinder.
21 p2787 A73-40003
- Simplified aerodynamic theory of oscillating thin surfaces in subsonic flow.
21 p2632 A73-40427
- Transverse deflection of guided projectile tail fins during deployment.
22 p2797 A73-42629

The unsteady aerodynamics of a finite supersonic cascade with subsonic axial flow.
[ASME PAPER 73-APMW-6] 22 p2797 A73-42879
Relationships between forces acting on bodies moving in a rarefied gas, in a light flux, and in hypersonic Newtonian flow 24 p3055 A73-45532

AERODYNAMIC HEAT TRANSFER

NT HYPERSONIC HEAT TRANSFER
NT SUPERSONIC HEAT TRANSFER

Investigation of the heat transfer between the gas and casing in the area of the apertures between the nozzle diaphragm blades and guide vanes of turbines 07 p0868 A73-20086
Determination of characteristic dimensions in the solution of drag and heat-transfer problems for flows past bodies of arbitrary configuration 07 p0812 A73-20425

AERODYNAMIC HEATING

NT SHOCK HEATING

A Chebyshev minimax technique oriented to aerospace trajectory optimization problems. 01 p0100 A73-10729
Hypersonic flight vehicles aerodynamic heating, structural design and materials and propulsion problems, discussing research work and facilities 03 p0242 A73-13055
Fluidic ignition system with two-component aerodynamic resonance heating /pneumatic match/ and hand pump for solid propellant sounding rocket engine [AIAA PAPER 72-1197] 03 p0252 A73-13486
Lee-side vortices on delta wings at hypersonic speeds. 03 p0247 A73-14180

The laser heated wind tunnel - A new approach to hypersonic laboratory simulation. [AIAA PAPER 73-211] 05 p0563 A73-16942
Convective heating on delta-wing Space-Shuttle boosters including interference effects. 05 p0533 A73-17202
Temperature of an emitting cone in a supersonic flow of transparent gas 06 p0646 A73-18570

Asbestos-textolite coating required thickness calculation with allowance for aerodynamic heating, discussing softening mechanisms 09 p1110 A73-23057
A method for calculating aerodynamic heating on sounding rocket tangent ogive noses. [AIAA PAPER 73-281] 09 p1167 A73-23202
Ion and electron distributions in the boundary layer of hypersonic vehicles. 11 p1404 A73-25290

Calculation of the temperature distribution within an ogival radome in supersonic flight 11 p1336 A73-25302
Hypervelocity tactical missile radome materials with noncharring ablator and fiberglass substructure for thermal protection against aerodynamic heating with negligible effects on radio transmission 11 p1336 A73-25307
Guidance methods for heat-optimal three-dimensional descent paths of aerodynamic reentry bodies 11 p1430 A73-25350

Determination of the required thickness of thermal insulation casings and evaluation of the weight-based effectiveness of materials 12 p1558 A73-27092
Derivation of shape change equations for asymmetrically heated ablating reentry vehicles. 13 p1706 A73-28750
Convective fluid motion and heat transfer in aircraft wing fuel tanks due to aerodynamic heating, comparing analytical with experimental results 15 p1957 A73-31643

Measured thermal response to the MIL-STD 210B cold atmosphere. 16 p2034 A73-33140
Temperature of a radiating cone in a supersonic flow of transparent gas. 16 p1964 A73-33595
Effect of nose geometry on the aerothermodynamic environment of shuttle entry configurations. [AIAA PAPER 73-638] 18 p2260 A73-36196

Flow field measurements in an asymmetric axial corner at $M = 12.5$. [AIAA PAPER 73-676] 18 p2297 A73-36227
Interference heating due to shock wave impingement on laminar boundary layers. [AIAA PAPER 73-678] 18 p2368 A73-36229
Evaluation of aerodynamic heating uncertainties for Space Shuttle. [AIAA PAPER 73-737] 18 p2359 A73-36354

Wind tunnel and flight tests for Saturn S-2 stage polyurethane spray foam insulation erosion under aerodynamic heating, shear stress and static pressure [AIAA PAPER 73-740] 18 p2326 A73-36357
Transpiration nosetip coolant flow control. [AIAA PAPER 73-767] 18 p2371 A73-36382
Europa III heat shields - Aerothermodynamic analysis and design. 18 p2361 A73-36954

Mach number and Reynolds number effect on orbiter/tank interference heating. 19 p2491 A73-37403
Functional tests with hypersonic flight vehicles, using an infrared heating system to simulate the temperature loads in flight 19 p2419 A73-38269
Multihundred watt radioactive isotope heat source wind tunnel tests to obtain aerodynamic coefficients, heating rate, stability and ablation for reentry protection design 19 p2456 A73-38425

Multihundred watt radioactive isotope heat source assembly for multiple space missions, discussing aerodynamic heating, shield ablation and thermal stress performance during reentry 19 p2456 A73-38426
Development of an infrared scanning system for the empirical evaluation of aerodynamic heating. 22 p2853 A73-41985
Approximation for maximum centerline heating on lifting entry vehicles. 22 p2796 A73-42627

Heat transfer rate and flow field and pressure distribution behind flat plate backward facing step in hypersonic flow 23 p3049 A73-43832
AERODYNAMIC INTERFERENCE
Vortex sheath formalism based on coupled integral equations for rectangular wing-slipstream aerodynamic interference 03 p0244 A73-13562

Correlation of wing-body combination lift data. 09 p1028 A73-22435
Compressibility effects on unsteady forces generated by jet engine blade rows aerodynamic interference, considering potential flow and viscous wake interactions 09 p1029 A73-23443
Lift forces on an oscillating cylinder at low Reynolds number. 10 p1173 A73-24822

Space shuttle aerodynamic interference and elastic response to atmospheric turbulence during ascent flight, including propellant sloshing, gust and automatic control system effects [AIAA PAPER 73-310] 11 p1430 A73-25541
Flutter of pairs of aerodynamically interfering delta wings. [AIAA PAPER 73-314] 11 p1301 A73-25545
Wind tunnel interference on oscillating airfoils in low supersonic flow. 13 p1563 A73-28166

Design method of the axial-flow blade row on modified isolated aerofoil theory with interference coefficient. 13 p1564 A73-28649
V/STOL airframe/propulsion integration problem areas. [ASME PAPER 73-GT-76] 16 p2048 A73-33522
A three-dimensional wing/jet interaction analysis including jet distortion influences. [AIAA PAPER 73-655] 18 p2261 A73-36209

A kernel function method for computing steady and oscillatory supersonic aerodynamics with interference. [AIAA PAPER 73-670] 18 p2262 A73-36221
Numerical solution for the inviscid supersonic flow in the corner formed by two intersecting wedges. [AIAA PAPER 73-675] 18 p2262 A73-36226
Mach number and Reynolds number effect on orbiter/tank interference heating. 19 p2491 A73-37403

Interference between a wing and a surface of velocity discontinuity. 19 p2376 A73-37490
Aerodynamic interference of pitot tubes in a turbulent boundary layer at supersonic speed. 22 p2796 A73-42552
Example of dynamic interference effects between two oscillating vehicles. 22 p2917 A73-42634

An experimental investigation of a jet issuing from a wing in crossflow. 22 p2798 A73-43111
Aerodynamic effects due to configuration of X-wire anemometers. [ASME PAPER 73-APM-P] 23 p2984 A73-44375
AERODYNAMIC LIFT
U LIFT
AERODYNAMIC LOADS
NT BLAST LOADS
NT GUST LOADS

Response of helicopter rotor blades to random loads near hover. 02 p0129 A73-12503
Lifting characteristics and spanwise aerodynamic load distribution of an external flow jet flap. 04 p0404 A73-15513
Dynamic response of a vertical cantilever structure in the natural wind. 07 p0823 A73-19565

Parachute opening dynamic analysis, taking into account risers, shrouds and canopy cloth elastic properties on opening history and loads 10 p1176 A73-24647
Numerical method for predicting unsteady aerodynamic loadings caused by control surface motions in subsonic flow. [AIAA PAPER 73-315] 11 p1301 A73-25546
An improved nonlinear lifting-line theory. 13 p1564 A73-28817

Mortar design for parachute ejection and deployment into airstream to decelerate spacecraft and aircraft pilot escape modules, estimating hardware weight and reaction load [AIAA PAPER 73-459] 15 p1827 A73-31445
A numerical integration method for the determination of flutter speeds. 15 p1955 A73-32163

Flight tests of load factors for multicorder-equipped gliders of various designs during pullout and looping maneuvers 22 p2799 A73-41866
Influence of aerodynamic field on shock-induced combustion of hydrogen and ethylene in supersonic flow. 22 p2934 A73-42786
Critical velocities of the steady motion of a pliable thread in plane homogeneous flow 22 p2928 A73-43061

Calculation of the deformations of a propeller blade in flight 23 p3041 A73-43724
A theoretical and experimental study of sound attenuation in an annular duct. [AIAA PAPER 73-1005] 24 p3077 A73-44838
AERODYNAMIC MOMENTS
U STABILITY DERIVATIVES
AERODYNAMIC NOISE

Effect of streamwise vortices on wake properties associated with sound generation. 01 p0001 A73-10045
Computation of the sound energy radiated from turbulent flows [DGLR PAPER 72-074] 02 p0153 A73-11699
The ordered structure of free-jet turbulence and its significance for the free-jet noise [DGLR PAPER 72-075] 02 p0128 A73-11701

Aerodynamic noise characteristics, discussing turbulent fluid acoustic propagation equation modification and antinoise legislation 03 p0241 A73-12952
Noise from free jets and airfoils in jets. 03 p0290 A73-12969
On the importance of the wake for the noise of an obstacle placed in a flow 03 p0291 A73-12974

Separated flow noise. 03 p0291 A73-12975
An investigation of the near wake properties which lead to the generation of vortex shedding sound from airfoils. 03 p0242 A73-12976
Aerodynamic noise and alternating loads in an idealised turbine stage. 03 p0242 A73-12981

Aerodynamic sound generation, discussing Lighthill theory, multipole sonic sources, wave equation, power and turbulence models and sound radiating flows 03 p0242 A73-13167
Analysis of internally generated sound in continuous materials. II - A critical review of the conceptual adequacy and physical scope of existing theories of aerodynamic noise, with special reference to supersonic jet noise. 03 p0246 A73-13840

Power spectrum due to point source convection at uniform subsonic speed along round jet flow axis 03 p0246 A73-13841
Cross correlations between turbulent jet flow and noise from hot-film and acoustic signal measurement, using Proudman form of Lighthill integral 03 p0246 A73-13842
Acoustic power spectrum of a subsonic jet. 03 p0295 A73-14040

Some experiments on the noise emission of coaxial jets. 03 p0360 A73-14148
Aerodynamic noise and boundary-layer transition measurements in supersonic test facilities. 03 p0296 A73-14191
Application of external aerodynamic diffusion to reduce shrouded propeller noise. 05 p0528 A73-16623

Disturbance of the environment by jet aircraft noise 05 p0535 A73-16760
The effects of leading-edge serrations on reducing flow unsteadiness about airfoils. [AIAA PAPER 73-89] 05 p0529 A73-16853
Evaluation of the noise autocorrelation function of stationary and moving noise sources by a cross correlation method. [AIAA PAPER 73-186] 05 p0598 A73-16925

Analytical and experimental supersonic jet noise research. [AIAA PAPER 73-188] 05 p0531 A73-16926

Thin wing induced undulating viscous wake and far field acoustic wave through interaction with turbulent cylindrical jet, using dipole force field model
[AIAA PAPER 73-223] 05 p0532 A73-16950

Externally blown flap trailing edge noise reduction by slot blowing - A preliminary study.
[AIAA PAPER 73-245] 05 p0532 A73-16969

Phillips aerodynamic noise theory application to directional patterns of high speed hot jets, discussing convection laws and sound field-turbulence correspondence
[AIAA PAPER 73-185] 06 p0684 A73-17654

Noise characteristics of combustion augmented high speed jets.
[AIAA PAPER 73-189] 06 p0767 A73-17655

Analysis of internally generated sound in continuous materials. III - The momentum potential field description of fluctuating fluid motion as a basis for a unified theory of internally generated sound.
07 p0909 A73-19097

Oblique shock-sound interaction at a freestream Mach number of about 20 in helium.
07 p0775 A73-19984

The effect of nozzle inlet shape, lip thickness, and exit shape and size on subsonic jet noise.
[AIAA PAPER 73-187] 07 p0776 A73-20465

Ducts, nacelles, power source components and cabin noise sources identified for aircraft noise control research, considering prerequisites for quiet operations
[SAE AIR 1079] 08 p0928 A73-20698

Noise radiated from a turbulent boundary layer.
11 p1344 A73-24979

Sound directivity pattern radiated from small airfoils.
11 p1345 A73-24980

Aerodynamic noise field associated with pressure distributions generated by local protuberance on launch vehicle during atmospheric flight
11 p1300 A73-25384

Noise intensity in the field of subsonic turbulent jets
11 p1347 A73-25738

Low vs high speed propeller fan noise, discussing pseudosound generation by rotating aerodynamic pressure fields
13 p1603 A73-29030

Two-bladed large rotor mounted on tower in inverted mode to overcome recirculation effects, analyzing broadband noise spectra and directivity pattern
13 p1570 A73-29380

Some noise generation mechanisms in transonic gas jets
14 p1712 A73-30947

Acoustic radiation intensity of a turbulent boundary layer on a plate
14 p1746 A73-30952

Jet noise suppression technology progress review, discussing Lighthill theory of aerodynamic noise, machinery noise and quiet aircraft future
15 p1830 A73-32186

Three bladed model rotor gust induced impulsive discrete noise characteristics prediction by point dipole and rotational noise theories for comparison with measurement
16 p1967 A73-32917

Monograph - Two causality correlation techniques applied to jet noise.
17 p2155 A73-35150

Fundamentals of aerodynamic sound theory and flow duct acoustics.
17 p2155 A73-35331

Jet aircraft noise research, emphasizing pure jet mixing noise, shock wave associated noise, and tail-pipe noise produced in engine or nozzle exit plane
17 p2096 A73-35332

Rotating blades and aerodynamic sound.
17 p2096 A73-35333

Calculated leading-edge bluntness effect on transonic compressor noise.
[AIAA PAPER 73-633] 18 p2260 A73-36192

Velocity decay and acoustic characteristics of various nozzle geometries with forward velocity.
[AIAA PAPER 73-629] 18 p2263 A73-36256

Hot gaseous jet noise emission calculation for dependence on turbulent flow characteristics based on Lighthill theory, using computer program
18 p2343 A73-36997

The ultimate noise barrier - Far field radiated aerodynamic noise.
19 p2375 A73-37278

Fan acoustic measurements by hot-wire anemometers in anechoic chamber, discussing turbulent flow characteristics, noise spectra, wire velocity spectra and blade tip shape
19 p2472 A73-37289

Subsonic jet noise measurements on model jet rig in anechoic chamber, discussing correlation and prediction
19 p2473 A73-38106

Subsonic and supersonic turbulent shear layer aerodynamic noise emission derivation from differential wave equations via Fourier transformation and WKB method
20 p2507 A73-39087

Small-scale suppressor of the aerodynamic noise of a subsonic gas jet
21 p2754 A73-40404

The design and construction of an anechoic chamber lined with panels and intended for investigation of aerodynamic noise
21 p2674 A73-40942

On the radiation from an aerodynamic acoustic dipole source
21 p2633 A73-40943

Noise caused by supersonic jet shock waves as function of jet pressure ratio, determining spectral characteristics
22 p2795 A73-41702

High temperature jet noise dependence on velocity and temperature, discussing Lighthill source term, Reynolds stresses, entropy fluctuations and velocity critical threshold
22 p2795 A73-41703

Boundary layer induced cockpit noise.
22 p2795 A73-41706

Sound generation by open supersonic rotors.
22 p2795 A73-41712

Reduction of fan noise by annulus boundary layer removal.
22 p2795 A73-41713

Turbulent boundary layer noise minimization by acoustic oscillation control, discussing suction and gas injection techniques
23 p2969 A73-43976

Intensity of sound radiation from a turbulent boundary layer on a plate.
23 p2969 A73-44328

Supersonic jet noise generated by large scale disturbances.
[AIAA PAPER 73-992] 24 p3077 A73-44827

Subsonic and supersonic jets and supersonic suppressor characteristics.
[AIAA PAPER 73-999] 24 p3077 A73-44834

A difference theory for noise propagation in an acoustically lined duct with mean flow.
[AIAA PAPER 73-1007] 24 p3078 A73-44840

The influence of aerodynamic flow noise in turbofan engines.
[AIAA PAPER 73-1016] 24 p3121 A73-44848

Progress in source noise suppression of subsonic tip speed fans.
[AIAA PAPER 73-1032] 24 p3122 A73-44861

Comparison of results obtained with various sensors used to measure fluctuating quantities in jets.
[AIAA PAPER 73-1043] 24 p3079 A73-44867

Emission of sound from a rectangular plate vibrating under the action of pressure pulsations in a turbulent boundary layer
24 p3109 A73-44899

AEROELASTICITY

Aerodynamic pumping-caused spinal fractures in two pilots during high speed flight
02 p0137 A73-12154

Stability characteristics of re-entry wing shapes and their measurement.
03 p0244 A73-13567

Three dimensional self oscillating motion study of roll and pitch stabilized vehicle with thrust vector control under resonance, using averaging method
05 p0599 A73-17086

Stabilization concepts for a spherical planetary entry probe configuration.
[AIAA PAPER 73-184] 06 p0756 A73-17653

Sounding rocket vehicles aeroelastic structural analysis, calculating structural flexibility, dynamic pressure and angle of attack effects on aerodynamic stability
[AIAA PAPER 73-284] 09 p1155 A73-23204

Aeroelastic effects on flying wing aircraft aerodynamic stability characteristics, using elementary beam-rod differential equations and aerodynamic strip theory
[AIAA PAPER 73-397] 11 p1305 A73-25526

Stability of symmetric flight vehicles in oblique flow
12 p1548 A73-27076

Drag and stability characteristics of high-speed parachutes in the transonic range.
[AIAA PAPER 73-473] 15 p1828 A73-31457

Development and testing of ballute stabilizer/decelerators for aircraft delivery of a 500-lb munition.
[AIAA PAPER 73-485] 15 p1829 A73-31467

Book - Flight dynamics of rigid and elastic airplanes. Parts I & 2.
17 p2099 A73-34451

Effect of torsion-flap-lag coupling on hingeless rotor stability.
[AHS PREPRINT 731] 17 p2105 A73-35067

Fixed base simulation of variable stability T-33 handling qualities, considering pilot performance in pitch tracking during atmospheric turbulence
19 p2386 A73-38072

Simplified aerodynamic theory of oscillating thin surfaces in subsonic flow.
21 p2632 A73-40427

Control law synthesis and sensor design for active flutter suppression.
[AIAA PAPER 73-832] 21 p2784 A73-40502

Non-linear flap-lag dynamics of hingeless helicopter blades in hover and in dynamic flight.
22 p2800 A73-43134

AERODYNAMIC STALLING

Calculation and measurement of the aerodynamic forces on an oscillating airfoil profile with and without stall
[ONERA, TP NO. 1132] 01 p0002 A73-10240

On the mechanism of dynamic stall.
01 p0003 A73-11015

Inlet produced flow distortion effect on compressor stability and engine stall, presenting unified theoretical analysis technique for compatible inlet/engine design
[AIAA PAPER 72-1115] 03 p0355 A73-13430

Inlet flow distortion induced axial flow compressor stall, converting stagnation pressure and temperature maps into vorticity maps via Crocco theorem
[AIAA PAPER 72-1116] 03 p0243 A73-13431

Analysis of stall flutter of a helicopter rotor blade.
[AIAA PAPER 73-403] 11 p1305 A73-25532

Linear aerodynamic model incorporating torsional oscillations about two dimensional airfoil midchord for stall flutter description
13 p1697 A73-28814

Theoretical investigation on stall flutter of an aerofoil / the case of trailing edge stall.
13 p1566 A73-29027

Semiempirical method for flutter prediction of unsteady lift and aerodynamic forces acting on oscillating airfoil in stall regime, using separation function
13 p1566 A73-29029

Stall/spin studies relating to light general-aviation aircraft.
[SAE PAPER 730320] 17 p2102 A73-34678

General aviation aircraft stall/spin prevention device for limiting tail power near wing stall angle of attack
[SAE PAPER 730333] 17 p2102 A73-34686

A detailed experimental analysis of dynamic stall on an unsteady two-dimensional airfoil.
[AHS PREPRINT 702] 17 p2095 A73-35053

A study of stall-induced flap-lag instability of hingeless rotors.
[AHS PREPRINT 730] 17 p2095 A73-35066

AERODYNAMICS

NT AERODYNAMIC INTERFERENCE

NT AEROTHERMODYNAMICS

NT ROTOR AERODYNAMICS

Russian book on aerodynamic design of axial flow turbomachine blades covering direct and inverse problems for axisymmetric flow in axial turbomachines
04 p0404 A73-15709

German book - Deutsche Gesellschaft fur Luft- und Raumfahrt, 1971 Yearbook.
05 p0528 A73-16755

Birds and aircraft aerodynamics, considering thermal and wind induced updrafts, lift-drag ratio, fuel consumption and maneuverability
06 p0648 A73-18148

Mathematical model of nonstationary linear aeroelasticity
07 p0912 A73-19468

Solution of the plane problem of rarefied-gas aerodynamics on the basis of the Boltzmann kinetic equation
15 p1822 A73-31244

Mathematical model of elastic flight body behavior in continuous medium based on combination solutions to aerodynamics, automatic control and elasticity theory problems
15 p1952 A73-32063

Investigation of a gas flow on an aeroballistic track by holographic methods
15 p1879 A73-32328

Applications of advanced aerodynamic technology to light aircraft.
[SAE PAPER 730318] 17 p2101 A73-34676

Russian book - Aerodynamics and flight dynamics of turbojet aircraft / 2nd revised and enlarged ed./
17 p2104 A73-34900

Book - Experimental methods of hypersonics.
17 p2097 A73-35338

Russian book - Aerohydrodynamic methods for measuring input parameters of automatic systems: Fluidic measuring elements.
21 p2704 A73-41288

Aircraft aerodynamics problems covering slender body theory, atmospheric turbulence and boundary layers, wind tunnel contractions, radiator blocks, vortex induced oscillations, etc
24 p3053 A73-44690

A comparison of the overall and broadband noise characteristics of full-scale and model helicopter rotors.
24 p3057 A73-45264

AEROELASTICITY

NT AEROTHERMOELASTICITY

Flutter analysis method for unsteady aerodynamic forces on wings and rotating blades under harmonic vibrations and uniform flow
[ONERA, TP NO. 1099] 01 p0001 A73-10230

Response of helicopter rotor blades to random loads near hover.
02 p0129 A73-12503

Self-excited and forced vibrations of an aeroelastic system subject to a follower force.

04 p0513 A73-15597
Aeroelastic instabilities of hingeless helicopter blades.
[AIAA PAPER 73-193] 05 p0536 A73-16929
Interpolation methods in aeroelastic analysis, comparing wing structural influence coefficients derived by surface splines and interpolation-in-the-small techniques with static test data

05 p0637 A73-17215
The effects of various parameters on an aeroelastic optimization problem.

06 p0758 A73-17565
Mathematical model of nonstationary linear aeroelasticity

07 p0912 A73-19468
A computerized flutter solution procedure.

07 p0914 A73-20214
A summary of wind tunnel research on tilt-rotors from hover to cruise flight.
[ONERA, TP NO. 1133] 08 p0928 A73-21683
Book - Aircraft structures for engineering students.

08 p1020 A73-21839
Prediction of aeroelastic instabilities in turbines

09 p1135 A73-22204
Sounding rocket vehicles aeroelastic structural analysis, calculating structural flexibility, dynamic pressure and angle of attack effects on aerodynamic stability

09 p1155 A73-23204
[AIAA PAPER 73-284]
Computerized method for designing plate type sounding rocket fins.

09 p1155 A73-23205
[AIAA PAPER 73-285]
The analytical treatment of the nonlinear aeroelastic galloping problem

11 p1432 A73-24997
[DFVLR-SONDDR-289]
The effect of servomechanical control and stability systems on the flutter behavior of aircraft

11 p1304 A73-25349
[DFVLR-SONDDR-272]
Aeroelastic structural weight optimization under strength and flutter constraints, using finite element and displacement methods to describe equations of motion in matrix form

11 p1439 A73-25518
[AIAA PAPER 73-389]
Aeroelastic effects on flying wing aircraft aerodynamic stability characteristics, using elementary beam-rod differential equations and aerodynamic strip theory

11 p1305 A73-25526
[AIAA PAPER 73-397]
Aeroelastic dynamic response to shock induced flow separation, analyzing wing buffet components at high Mach number subsonic flow

11 p1300 A73-25539
[AIAA PAPER 73-308]
Space shuttle aerodynamic interference and elastic response to atmospheric turbulence during ascent flight, including propellant sloshing, gust and automatic control system effects

11 p1430 A73-25541
[AIAA PAPER 73-310]
An investigation of unsteady aerodynamics on an oscillating airfoil.

11 p1301 A73-25549
[AIAA PAPER 73-318]
Design and evaluation of miniature control surface actuation systems for aeroelastic models.

11 p1305 A73-25553
[AIAA PAPER 73-323]
The state of the art in aeroelasticity of aerospace vehicles in Japan.

11 p1305 A73-25560
[AIAA PAPER 73-331]
Influence of structural flexibility on the dynamic stability of rockets.

14 p1803 A73-30043
On the weight minimization of supersonic, axisymmetric circular cylindrical shells of finite length.

14 p1814 A73-30709
Roll coupling moment of deflected wing-body combination.

15 p1823 A73-31573
Normal mode solution to the equations of motion of a flexible airplane.

15 p1950 A73-31747
Mathematical model of elastic flight body behavior in continuous medium based on combination solutions to aerodynamics, automatic control and elasticity theory problems

15 p1952 A73-32063
Book - Flight dynamics of rigid and elastic airplanes. Parts 1 & 2.

17 p2099 A73-34451
On the question of adequate hingeless rotor modeling in flight dynamics.

17 p2105 A73-35068
[AHS PREPRINT 732]
Wind tunnel test technique to establish rotor system aeroelastic characteristics.

17 p2095 A73-35083
[AHS PREPRINT 760]
Critical flow speed divergence in aeroelastic systems stability loss, discussing static analysis using partial differential equation

17 p2250 A73-35119
Turbine engine research activity evolution, considering entry temperature increase, pollution sources nonstationary aerodynamics and aeroelasticity in compressors, and noise problem

18 p2343 A73-36991
Aeroelastic vibrations in labyrinth seals

20 p2569 A73-39373

Linearized characteristics method for supersonic flow past vibrating shells.

21 p2632 A73-40426
An aeroelastic whirl phenomenon in turbomachinery rotors.

22 p2900 A73-42076
[ASME PAPER 73-DET-97]
Vibration and stability of nondivergent elastic systems.

22 p2922 A73-42551
Non-linear flap-lag dynamics of hingeless helicopter blades in hover and in forward flight.

22 p2800 A73-43134
Calculation of the deformations of a propeller blade in flight

23 p3041 A73-43724

AEROEMBOLISM

Pathogenesis of some respiration and circulation reactions to barometric pressure gradients

08 p0929 A73-20980
Changes in the vascular tone of certain organs during experimental embolism of pulmonary circulation

09 p1039 A73-22366
Intravascular changes associated with hyperbaric decompression - Theoretical considerations using ultrasound.

09 p1045 A73-22534

AEROLOGY

Utilization of meteorological data from satellites in studies of the general atmospheric circulation

05 p0593 A73-16245
Spectra of star and planet scintillation and dependence of their characteristics on meteorological conditions

13 p1683 A73-29097
Meteorological lidar for determining aerological data above launching base prior to rocket firing

14 p1771 A73-30115
Aerological investigation of the volcanic beds of Kamchatka by polarizational and spectral methods

16 p1977 A73-33760
Aerological soundings of the atmosphere from NOAA-2 data for operational systems.

18 p2308 A73-36044

AEROMAGNETISM

U GEOMAGNETISM

AEROMAGNETO FLUTTER

U FLUTTER

AERONAUTICAL ENGINEERING

Utilization in aeronautics of composite materials for working structures

03 p0334 A73-13594
Aerodynamic technology developments including advanced transonic airfoils, low-drag/high-lift systems and stability augmentation for transport aircraft performance, economics and noise improvements

06 p0644 A73-17604
[AIAA PAPER 73-9]
Economic performance and cost problems in civil air transport maintenance and engineering quality control related to selling price trends

06 p0647 A73-17888
Wind tunnel facilities in India for subsonic, transonic and supersonic aeronautical R and D, describing design layouts, power requirements, operational functions and instrumentation

07 p0808 A73-20249
Technology advancement effects on military and commercial transport aircraft development and production costs, considering airframes, engines and avionics

07 p0924 A73-20394
Aeronautical turbine blade and vane materials selection, considering Ni alloys with powder metallurgy and oriented solidification, composite materials and eutectics

18 p2326 A73-36993
Russian book on structural mechanics of tapered thin walled conical bodies and wings in aviation and rocket technology

21 p2788 A73-41281
Fabrication techniques for Ti alloys in aerospace applications, discussing hot forming, electron beam and diffusion welding under vacuum and stress relaxation annealing

23 p2985 A73-43911
Management and control of commercial flight test programs.

23 p3050 A73-44057
Management and control of military and commercial flight test programs at Bell Helicopter Company.

23 p3050 A73-44058
Air Force Prototype Program management.

23 p3051 A73-44061
The role of a military flight test engineer in test management.

23 p3051 A73-44062
The capabilities of army test facilities.

23 p2966 A73-44064
Naval test and evaluation capabilities for aircraft, emphasizing organizational relationships

23 p3051 A73-44066

AERONAUTICAL SATELLITES

Operational utilization of an aeronautical satellite system for air traffic control over the North Atlantic.

15 p1911 A73-32487

AERONAUTICS

Radio Technical Commission for Aeronautics, Annual Assembly Meeting, Washington, D.C., November 9, 10, 1972, Proceedings.

12 p1522 A73-27360
Israel Annual Conference on Aviation and Astronautics, 15th, Tel Aviv and Haifa, Israel, March 14, 15, 1973, Proceedings.

15 p1948 A73-31633
NASA in general aviation research: Past - present - future.

17 p2257 A73-34675
[SAE PAPER 730317]
Aeronautics and astronautic history, developments and impact upon civilization, noting Canada role in space age, Apollo program and U.S.S.R. programs

21 p2793 A73-41086
Research Aviation Facility collected aircraft data processing, merging and enhancement problems, software development and future resource requirements

24 p3070 A73-45088

AERONOMY

D and E region aeronomy, discussing ionization sources, ion composition, water cluster ion formation and ratio of molecular oxygen and nitric oxide ions

01 p0040 A73-10877
Aeronomical chemistry of the stratosphere.

02 p0158 A73-11910
Mars oxygen photoelectric spectral and aeronomical study, noting water vapor and carbon dioxide photolytic effects

02 p0224 A73-12787
Chemical kinetics equations of lower ionosphere and D region particle interactions for aeronomical problems

05 p0569 A73-16396
The Federal Republic's AEROS Satellite Programme.

08 p1026 A73-21659
Aeros meteorological research satellite for F region aeronomical parameters and solar UV radiation measurements, discussing performance since launch

11 p1430 A73-25442
Averaged nighttime altitude profile of atmospheric emission at 6300 A

12 p1491 A73-27345
International Symposium on Equatorial Aeronomy, 4th, University of Ibadan, Ibadan, Nigeria, September 4-9, 1972, Proceedings.

15 p1868 A73-31750
Coordinated measurements of atmospheric parameters at stratospheric levels.

16 p2007 A73-33560
[AIAA PAPER 73-526]
Aeronomical consequences of solar flux variations between 2000 and 1325 angstroms.

22 p2902 A73-41931
Average nighttime vertical profile of the 6300 A atmospheric emission.

23 p2970 A73-43242
Ionospheric aeronomy problems with emphasis on photochemical processes of neutral and ionized components, discussing nighttime ionizing agents, ion recombination, water vapor and nitrogen oxide behavior, etc

23 p2978 A73-43977

AEROPHYSICS

U ATMOSPHERIC PHYSICS

AEROS SATELLITE

German-NASA joint Aeros aeronomy satellite project, discussing mission objectives and related instrumentation

01 p0109 A73-10470
The attitude-measuring and attitude-control system of the satellite Aeros and its employment in the acquisition phase

02 p0227 A73-11653
[DGLR PAPER 72-062]
Scientific payload of Aeros German aeronomy satellite for atmospheric upper layers investigation, discussing instruments operation and location and measurement technique

02 p0190 A73-11656
[DGLR PAPER 72-069]
The plasma diagnostics experiments of the Aeros satellite

02 p0166 A73-11669
[DGLR PAPER 72-070]
Development and qualification results of the monergonic propulsion system for the aeronomy satellite Aeros

02 p0228 A73-11696
[DGLR PAPER 72-079]
Contributions to the standardization of control systems for satellites and peak payloads

02 p0228 A73-11705
Aeros satellite component tests for design and manufacturing error detection and failure prevention, using structural, thermal and electrical integration models

03 p0288 A73-13918
Yo-yo system despin mechanism for the Aeros aeronomy satellite.

03 p0382 A73-13919
The attitude measuring system of the AEROS satellite.

05 p0629 A73-16849
German scientific research satellite Aeros, discussing program planning and management, mis-

- sion analysis, attitude control, power supplies, test methods, yo-yo despin and ground operations systems
08 p1014 A73-21658
The Federal Republic's AEROS Satellite Programme.
08 p1026 A73-21659
Attitude control of the AEROS aeronomy satellite during the acquisition phase.
08 p1014 A73-21660
The ground operations system for the AEROS research satellite.
08 p0953 A73-21661
Solar cell generator technology development based on German AEROS satellite project and work on roll-up structure, discussing module concepts and test results
09 p1033 A73-22439
Development of propellant loading systems and checkout systems for the TD-1A and AEROS satellite projects
11 p1430 A73-25354
Aeros meteorological research satellite for F region aeronomic parameters and solar UV radiation measurements, discussing performance since launch
11 p1430 A73-25442
ESRO Aerosol L-band communication techniques experiments with stratospheric balloon-borne transponders relaying ground station signals to aircraft flying over sea
12 p1498 A73-27672
AEROS satellite launching from Western Test Range, describing time sequence of satellite and rocket countdowns and communication system activities coordinated by project management
13 p1689 A73-28781
AEROS research satellite acquisition phase performance, considering injection, attitude determination and control, trajectory measurement and correction, nutation reduction, solar alignment, etc
13 p1689 A73-28782
AEROS aeronomy satellite successfully completes acquisition phase.
13 p1689 A73-28783
Power supply requirements during the AEROS acquisition phase.
13 p1689 A73-28784
The German aeronomy satellite Aeros
15 p1943 A73-32178
Attitude determination-attitude control in the case of the satellite Aeros
15 p1943 A73-32179
Objectives and employment of the integration and system test equipment for Aeros
15 p1943 A73-32180
Aeros satellite simulated environmental testing for thermal behavior under space vacuum, temperature and solar radiation conditions, comparing results with mathematical model calculations
16 p1997 A73-33392
Atomic oxygen profiles determined by EUV absorption analysis.
18 p2308 A73-36049
Attitude measurement and control system of the aeronomy satellite AEROS.
[AIAA PAPER 73-856]
20 p2585 A73-38794
AEROSINUSITIS
Pathophysiological and clinical aspects of aeroinusitis and frontal sinus nematoma formation due to barometric pressure changes from pilot case history studies
09 p1039 A73-22538
AEROSOLS
Optical manifestations of meteoric aerosols. I - The 1970 Orinoids
01 p0096 A73-10332
The effects of aerosols on the outgoing terrestrial radiation.
01 p0072 A73-10357
Radiative calculation models for infrared transfer through cloud, aerosol and the continuum.
01 p0073 A73-10358
IR absorption and refraction index of atmospheric aerosol, using KBr disk transmittance and specular reflection measurements
01 p0038 A73-10373
Measurement of the complex index of refraction of atmospheric aerosols using optical spectral analysis techniques.
01 p0045 A73-10375
Laser radar measurements of atmospheric backscattering turbidity.
01 p0073 A73-10403
Normal flame velocity in aerodisperse systems
01 p0123 A73-11245
Rocket photometric observations of dayglow sky radiation in O green line, noting aerosol scattering coefficient and particle concentration
02 p0161 A73-12277
The spectral characteristics of radiation extinction and the effects of the relative humidity on these characteristics
02 p0189 A73-12368
Atmospheric aerosol Mie scattering calculation as function of polarization parameters based on models for three laser wavelengths and two materials
03 p0341 A73-12900
Degree and direction of polarization of multiple scattered light. II - Earth's atmosphere with aerosols.
03 p0344 A73-14428
Atmospheric windows for HF laser radiation between 2.7 and 3.2 microns.
03 p0319 A73-14431
Meteorological lidar use to obtain backscatter curve produced by aerosols suspended in atmosphere [ONERA, TP NO. 1130]
04 p0432 A73-15091
Continuous flow condensation nucleus counter
04 p0451 A73-15999
Electron density reduction in high temperature air via boron powder aerosol, presenting shock tube data for temperature range 2800-4200 K and pressure range 1-2 atm
[AIAA PAPER 73-261]
05 p0603 A73-16982
Investigation of the scattered-light-flux magnitude dependence on the drop size in the aerosol photoelectric counter
06 p0691 A73-18734
The use of aerosols for the visualization of flow phenomena.
06 p0683 A73-18837
Determination of the concentration and scattering indicatrix of atmospheric dust from primary twilight brightness
07 p0817 A73-19589
Experimental study of water drop evaporation in a heated air flow
07 p0922 A73-20416
Evaporation rate and temperature of liquid drops calculated for low and high temperature aerosols
07 p0922 A73-20417
Phase transition effects at the collecting droplet surface on the capture coefficient magnitude
07 p0922 A73-20418
Stratospheric aerosol measurements with implications for global climate.
[AD-759856]
08 p0984 A73-21041
Short-wave spectral radiant heat influx in the atmosphere
08 p0984 A73-21133
Optical characteristics and structure of the Jovian atmosphere. V - Probable structure of the ammonia aerosol layer.
08 p1012 A73-21577
Electrometric amplifiers for inductive measurement of charges
08 p0949 A73-21713
Effect of the shape and orientation of atmospheric dust particles on the spectral position and form of the attenuation band
09 p1077 A73-22372
Normal flame velocity in aerosol systems.
10 p1295 A73-24185
Optical characteristics of bright day sky in the visual region of the spectrum and the atmospheric aerosol
11 p1353 A73-25606
Sky brightness in solar aureole region relationship to solar radiation single scattering on atmospheric aerosol particles
11 p1353 A73-25607
Daytime cloudless sky glow, atmospheric transmittance, neutral polarization and aerosol optical characteristics in solar almucantar and vertical
11 p1353 A73-25608
Approximation of empirical size distributions of cloud droplets and other aerosol particles
11 p1393 A73-25644
An explicit form of the Mie phase matrix for multiple scattering calculations in the I, Q, U and V representation.
11 p1390 A73-25718
Stratospheric aerosol layer detection.
11 p1355 A73-25773
Stratospheric aerosol properties and their effects on infrared radiation.
11 p1357 A73-26344
Light scattering by atmospheric aerosols.
13 p1653 A73-28517
Attenuation of monochromatic light in bottom layer of atmosphere and some properties of aerosols.
13 p1653 A73-28518
Aerosol particle downward motion in vertical electric field, discussing stability of major axis orientation of ellipsoid of revolution
13 p1654 A73-28881
Observations of aerosol layers in the upper atmosphere by laser radar.
15 p1868 A73-31383
Artificial inducement of drizzling rain in an uncloudy atmosphere at relatively high humidity
16 p2034 A73-33109
Trace gases, aerosols, and solar radiation in the stratosphere - Explored and unexplored problem areas.
[AIAA PAPER 73-509]
16 p2006 A73-33547
Distributions and associations of some of the chemical elements found in the stratosphere.
[AIAA PAPER 73-514]
16 p2006 A73-33551
Lidar measurements of the variability of stratospheric particulates.
[AIAA PAPER 73-520]
16 p2007 A73-33556
Global balloon monitoring program of stratospheric dust, ozone, water vapor, temperature and aerosol determination in northern and southern hemispheres [AIAA PAPER 73-521]
16 p2007 A73-33557
The atmospheric aerosol and its significance for the energy budget of the atmosphere
17 p2159 A73-34749
Forward scattering method for determination of atmospheric aerosols particle size distribution, considering angle-dependent scattering at fixed wave number
17 p2161 A73-34938
Aqueous ammonium sulfate aerosol optical properties via attenuated total reflectance (ATR) spectroscopy
17 p2171 A73-35402
Measurements of aerosol size distributions with a laser Doppler velocimeter (LDV).
[AIAA PAPER 73-705]
18 p2315 A73-36254
Effect of aerosols on the transfer of solar energy through realistic model atmospheres. I - Non-absorbing aerosols.
18 p2333 A73-36704
Investigation of flame expansion inhibition in air-dispersed systems
19 p2503 A73-37506
Respirator cartridge filter efficiency under cyclic and steady-flow conditions.
21 p2643 A73-40408
Absorption line contours in homogeneous plane-parallel semiinfinite aerosol layers and planetary atmosphere overlaid gas layers for nonspherical scattering
21 p2768 A73-40723
Indices of backscattering and attenuation of light by a water aerosol
21 p2731 A73-40747
Tropospheric aerosol - The relative contribution of marine and continental components.
22 p2849 A73-42547
Soot formation by combustion of an atomized liquid fuel.
22 p2936 A73-42800
Aerosol ice nuclei concentration measurements in remote regions of Southern Hemisphere near Australia by shipborne membrane filters, noting land or stratospheric sources
23 p3002 A73-43598
Matrix method evaluating an internal radiation field in a plane-parallel atmosphere.
23 p3030 A73-43754
Aerosols - A limitation on the determination of ozone from UV observations.
23 p2975 A73-43879
Aerosol influence on atmospheric radiative cooling, calculating long wave flux divergence dependence on particle size, relative humidity and refractivity
23 p2978 A73-43984
Influence of the microstructure of water aerosol on the phase function, its asymmetry, and polarization of scattered light
24 p3084 A73-44963
Numerical experiments in laser sounding of aerosol stratification in the atmosphere
24 p3085 A73-44966
Solid fuels combustion stability and shock wave induced detonations propagation stability in aerosols investigation based on one dimensional turbulence, using multistage mathematical models
24 p3157 A73-45383
AEROSPACE ENGINEERING
NT AERONAUTICAL ENGINEERING
Cholesteric liquid crystals thermophysical properties application in aerospace sciences and engineering, noting temperature measurement and nondestructive tests
06 p0733 A73-17767
Clean rooms and contamination-free zones in space technology
07 p0830 A73-19011
Association Technique Maritime et Aeronautique, Session, 72nd, Ecole Nationale Supérieure de Techniques Avancées, Paris, France, May 15-19, 1972, Proceedings.
09 p1031 A73-22201
Study and realization of special parts for aerospace construction by brazing in a fluorided reducing atmosphere
09 p1088 A73-22202
Book on aerospace propulsion covering nozzle, combustors and diffusers flow, space power generation, electrothermal engines, chemical rockets and central force fields
14 p1785 A73-30361
Russian book - Pioneers rocket engineering: Selected works /1929-1945/.
15 p1943 A73-31576
High-temperature low pressure hose assembly, convoluted, tetrafluoroethylene-, for aerospace.
[SAE ARP 1227]
16 p1970 A73-33017
Surface integrity - A new requirement for improving reliability of aerospace hardware.
16 p2018 A73-33067

- Pyrotechnic explosive power devices and systems for aerospace applications. 16 p2045 A73-33106
- Apollo Experience Reports contents and development, detailing engineering, life sciences, flight crew operations, flight control safety and applications 17 p2256 A73-34300
- International Aerospace Instrumentation Symposium, 19th, Las Vegas, Nev., May 21-23, 1973, Proceedings. 17 p2165 A73-34601
- Reinforced plastics for aerospace applications covering history of laminates, use of cellulose, asbestos, boron, glass and oriented carbon fibers, whisker composites and resin matrices 17 p2194 A73-34801
- The processability of unidirectional prepregs in aerospace applications. 17 p2195 A73-34808
- Applications in aerospace construction and fallouts of ONERA thermochemical techniques [ONERA, TP NO. 1246] 18 p2320 A73-36688
- Design-build-fly, an effective method to teach undergraduate aerospace vehicle design. [AIAA PAPER 73-785] 19 p2505 A73-37455
- Design for teaching aerospace engineering at Texas A & M University. [AIAA PAPER 73-786] 19 p2505 A73-37456
- A new approach to aircraft design education. [AIAA PAPER 73-787] 19 p2505 A73-37457
- Computer aided design-drafting /CADD/ - Engineering/manufacturing tool. [AIAA PAPER 73-793] 19 p2407 A73-37460
- Astronautical research 1971; Proceedings of the Twenty-second Congress, Brussels, Belgium, September 20-25, 1971. 19 p2485 A73-37708
- Aerospace applications of heat resistant alloy diffusion welding techniques, describing mechanical properties, metal bonding, surface cleaning, vacuum levels, temperature effects and microstructure 20 p2569 A73-39246
- The capabilities of government test facilities at the Air Force Systems Command. 23 p2966 A73-44065
- ### AEROSPACE ENVIRONMENTS
- #### NT DEEP SPACE
- #### NT INTERPLANETARY SPACE
- #### NT INTERSTELLAR SPACE
- Russian book on physicochemical basis of space research covering near earth and interplanetary environmental factors and effects on spacecraft designs and materials 02 p0211 A73-11886
- Effects of the space flight environment on man's immune system. II - Lymphocyte counts and reactivity. 02 p0135 A73-12565
- Space environment effects on human life and biochemical evolution study in aerospace medicine and biology, noting amino acid molecules synthesis 03 p0265 A73-14589
- Psychological and psychophysiological factors of human performance in manned space missions, considering environmental effects of space flight and man-machine system 06 p0650 A73-17775
- Friction in ultrahigh vacuum, discussing test program definition and testing machine design taking into account space environment effects 07 p0829 A73-18907
- Characteristics, design and performance of power sources in auxiliary systems for spacecraft applications, noting long term standby under environmental conditions [SAE AIR 744 A] 08 p0928 A73-20690
- Aviation medicine assessment of environment effects on pilot responsiveness, task performance and flight safety predictability, considering temperature, oxygen, gravity, acceleration, pressure and stress effects 11 p1321 A73-25039
- #### Aerospace cryogenic static seals.
- 13 p1624 A73-28800
- Space radiation environment effects on Intelsat 4 design, emphasizing trapped electrons and protons influences on solar cell shielding requirements 17 p2108 A73-34864
- Optical stability of coatings exposed to four years space environment on OSO-III. [AIAA PAPER 73-734] 18 p2336 A73-36351
- Russian papers on physical processes in plasma accelerators covering types, diagnostic methods, gas dynamics, control and space studies 19 p2466 A73-37352
- Plasma acceleration techniques in space studies, discussing simulation experiments, solar wind-geomagnetic field interaction and astronomical models 19 p2482 A73-37355
- Large space vehicles - Platforms for second generation in-situ wake observations. 21 p2781 A73-40901
- ### AEROSPACE INDUSTRY
- #### NT AIRCRAFT INDUSTRY
- Packaging in aerospace applications 07 p0830 A73-19010
- Precipitation and dispersion hardened alloys, fiber reinforced metal matrix composites, carbon-carbon composites, and dispersed system, eutectics application in aerospace industry 14 p1759 A73-30067
- Aerospace industry project managers and support personnel authority perceptions based on assessment of situational factors surrounding decision making, tabulating empirical investigation statistics 17 p2257 A73-35214
- Aeronautics and astronautic history, developments and impact upon civilization, noting Canada role in space age, Apollo program and U.S.S.R. programs 21 p2793 A73-41086
- ### AEROSPACE MEDICINE
- Space environment effects on human life and biochemical evolution study in aerospace medicine and biology, noting amino acid molecules synthesis 03 p0265 A73-14589
- Russian book - Biomedical problems of space flights: Index of domestic and foreign literature. 04 p0410 A73-16034
- Developments in space medicine. 06 p0649 A73-17569
- Military contributions to aviation medicine. [AIAA PAPER 73-68] 06 p0656 A73-17636
- Cosmic radiation and research carried out on board the 001 prototype Concorde 07 p0784 A73-19211
- Civil aviation medicine in the coming decade. 07 p0785 A73-19484
- Pathophysiological and clinical aspects of aeroinfluenza and frontal sinus nematoma formation due to barometric pressure changes from pilot case history studies 09 p1039 A73-22538
- Civil aviation medicine functional standardization and expansion, emphasizing preventive medicine, health education and operational safety 10 p1185 A73-24718
- Influence of the packing and of certain conditions of usage on the medications in portable emergency medicine stores 12 p1465 A73-27720
- Russian book - Engineering psychology in aviation and astronautics. 15 p1838 A73-31375
- Injuries induced by high speed ejection - An analysis of USAF noncombat operational experience. 16 p1966 A73-32664
- The application of aerospace technology to patient monitoring. 16 p1975 A73-32804
- Annual Scientific Meeting, Las Vegas, Nev., May 7-10, 1973, Preprints. 16 p1973 A73-33421
- International Congress of Aeronautical and Space Medicine, 20th, Nice, France, September 18-21, 1972, Reports 18 p2284 A73-36901
- Russian papers on populated cosmos covering space exploration impact on human civilization, extraterrestrial life, space medicine and biology, solar system, space law, etc 19 p2393 A73-37398
- Annex 13 and the work of the aviation pathologist - Practical problems. 19 p2398 A73-37739
- SkyLab medical experiments altitude test crew observations. [ASME PAPER 73-ENAS-30] 19 p2400 A73-37985
- SkyLab Medical Experiments Altitude Test /SMEAT/ facility design and operation. [ASME PAPER 73-ENAS-44] 19 p2401 A73-37991
- SkyLab medical experiments altitude test /SMEAT/ chamber atmosphere trace contaminants analysis, describing sample acquisition techniques and instrumentation [ASME PAPER 73-ENAS-45] 19 p2395 A73-37992
- Radiological assessment of the vertebral column from the point of view of aviation medicine 22 p2817 A73-43131
- ### AEROSPACE SCIENCES
- International Symposium on Space Technology and Science, 9th, Tokyo, Japan, May 17-22, 1971, Proceedings. 01 p0110 A73-11101
- German book - Deutsche Forschungs- und Versuchsanstalt für Luft- und Raumfahrt, Annual Report 1971. 02 p0150 A73-11877
- Russian book on physicochemical basis of space research covering near earth and interplanetary environmental factors and effects on spacecraft designs and materials 02 p0211 A73-11886
- Book - Advances in space science and technology. Volume 11. 03 p0376 A73-14166
- Technology transfer from aerospace to public sector, discussing JPL experience, problem definition, funding, user concerns and interpersonal communications 04 p0521 A73-14729
- Book - Progress in aerospace sciences. 05 p0627 A73-16176
- Space technology transfer to community and industry; Proceedings of the Eighteenth Annual Meeting and Tenth Goddard Memorial Symposium, Washington, D.C., March 13, 14, 1972. 06 p0771 A73-17673
- French CNES and Toulouse space center organization and activities, describing installation history 07 p0808 A73-19006
- Papers on chemistry in space research covering planetary atmospheres, organic compounds, carbonaceous meteorites, liquid and solid propellant rockets, and spacecraft sterilization 14 p1723 A73-30126
- High pressure, radiation, high temperature and vacuum chemistries, discussing planetary matter, solar and cosmic radiation effects, plasma temperatures, solar winds and molecular populations 14 p1723 A73-30127
- Processing aerospace textiles into fabric composite reinforcements 'The weaver's viewpoint.' 16 p2018 A73-33065
- Book - Space physics and space astronomy. 17 p2230 A73-34575
- Space science terrestrial applications in biomedical data exchange and telemedicine, propellant technology, life support atmospheres without fire hazard, industrial mixers and nozzle materials [AAS PAPER 73-133] 20 p2629 A73-38589
- Life sciences and space research XI; Proceedings of the Fifteenth Plenary Meeting, Madrid, Spain, May 10-24, 1972. 22 p2803 A73-42158
- ### AEROSPACE SYSTEMS
- A derivation of thermal mathematical model with measured nodal temperatures. 01 p0123 A73-11142
- Flight test of narrow band television system. 01 p0052 A73-11169
- Accelerated life testing of component reliability in aerospace systems, discussing stress tests, Arrhenius model and time transformation method 04 p0453 A73-14854
- Advanced aerospace power distribution and control techniques. 04 p0408 A73-15389
- Book - French space technology. Volumes 1 and 2. 07 p0904 A73-18901
- Spacecraft-borne optical components and systems design and operational requirements, considering thin film filters and mirrors, detectors, diffraction gratings and materials 07 p0821 A73-18978
- The state of the art of system identification of aerospace structures. 07 p0916 A73-20432
- Cryogenic cooling systems technology for spacecraft applications, comparing passive and phase-change coolers and closed cycle refrigerator for capacity and service life 10 p1285 A73-23790
- Aerospace systems evaluation and optimization via systems analysis, discussing capability, dependability and availability and cost 12 p1561 A73-27384
- The use of elastic relaxation for testing aerospace equipment. [AIAA PAPER 73-478] 15 p1948 A73-31462
- Fluidic control modules with temperature sensor and thrust reverser pneumatic actuator for aerospace system applications, investigating reliability test data 16 p1971 A73-33477
- The role of testing in achieving aerospace systems effectiveness. 16 p2020 A73-33605
- Intrasystem electromagnetic compatibility analysis program. 17 p2131 A73-35251
- Microwave equipment reliability design for aerospace environment applications, considering vibration, shock, humidity and temperature effects and frequency stability 18 p2293 A73-36778
- Developments in Canada related to remotely manned systems. 19 p2416 A73-37317
- Book - The role of testing in achieving aerospace systems effectiveness. 21 p2675 A73-41201
- The coupling of high frequency electromagnetic energy into large systems. 22 p2822 A73-41792
- Research and development of aerospace adhesive bonded systems and concepts. 24 p3093 A73-44763
- ### AEROSPACE VEHICLES
- Automating the design process - Progress, problems, prospects, potential. [AIAA PAPER 73-410] 11 p1373 A73-25538
- The state of the art in aeroelasticity of aerospace vehicles in Japan. [AIAA PAPER 73-331] 11 p1305 A73-25560
- Book on aerospace vehicles science covering airfoils, aircrafts, fuel systems, structural weight, instrumentation, taxiing, towing and federal aviation regulations 12 p1458 A73-27054

- Al alloys, steels and superalloys properties improvements for aerospace vehicles structural applications, discussing diffusion bonding and isothermal forging techniques
13 p1633 A73-28180
- Upper atmosphere pollution and near surface climate due to aerospace operations, discussing dynamics and trace gas distribution
[AIAA PAPER 73-492] 16 p2005 A73-33536
- Design-build-fly, an effective method to teach undergraduate aerospace vehicle design.
[AIAA PAPER 73-785] 19 p2505 A73-37455
- Questionnaire survey covering development, qualification, acceptance and flight test roles in achieving aerospace vehicles systems effectiveness/reliability, maintainability and safety/
20 p2544 A73-39248
- Pressure fluctuations underlying attached and separated supersonic turbulent boundary layers and shock waves.
[AIAA PAPER 73-996] 24 p3053 A73-44831
- AEROSTATS**
U AIRSHIPS
- AEROTHERMOCHEMISTRY**
Russian book - Nonequilibrium physicochemical processes in aerodynamics.
09 p1029 A73-23225
- Aerothermochemistry of combustion products in the stratosphere.
[AIAA PAPER 73-540] 16 p1977 A73-33570
- AEROTHERMODYNAMICS**
Aerothermodynamics of the Space Shuttle reaction control system.
[AIAA PAPER 73-93] 05 p0629 A73-16857
- Space shuttle technology, discussing configurational aerothermodynamics, aeroelastic effects on vehicle dynamics and structural design and materials.
[AIAA PAPER 73-31] 06 p0755 A73-17619
- Aerothermodynamics R and D for space shuttle configurational design, discussing program organization and wind tunnel testing to generate design technology base
[AIAA PAPER 73-59] 06 p0755 A73-17632
- A rocket system for hypersonic, high Reynolds number aerothermodynamic research.
[AIAA PAPER 73-304] 09 p1156 A73-23223
- Russian book - Nonequilibrium physicochemical processes in aerodynamics.
09 p1029 A73-23225
- Aerodynamic and thermal problems related to wall deformations
16 p2076 A73-32801
- Development of model atmospheres for aerothermodynamic calculations.
16 p2034 A73-33138
- Space shuttle orbiter and subsystem design, discussing crew cabin, payload accommodations, flight characteristics and aerothermodynamics
[AIAA PAPER 73-604] 18 p2358 A73-36085
- AEROTHERMOELASTICITY**
Aerodynamic and thermal problems related to wall deformations
16 p2076 A73-32801
- AFC [CONTROL]**
U AUTOMATIC FREQUENCY CONTROL
- AFCs [CONTROL SYSTEM]**
U AUTOMATIC FLIGHT CONTROL.
- AFFERENT NERVOUS SYSTEMS**
Comparative physiological characteristics of functional relations among the hypothalamus and the olfactory and limbic systems of the brain
01 p0006 A73-10151
- Changes in ventilatory patterns after ablation of various respiratory feedback mechanisms.
01 p0007 A73-10162
- Topochemical differences in RNA content in spinal cord motoneurons during hypoxia and hypokinesia
02 p0135 A73-12558
- Cardiovascular reflexes evoked by potassium ion stimulation of the heart under conditions of spinal deafferentation and intact innervation
03 p0262 A73-13820
- The dynamic properties of the acoustic middle ear reflex in nonanesthetized rabbits - Quantitative aspects of a polysynaptic reflex system.
05 p0539 A73-16249
- Characteristic of collicular responses to stimulation of various sections of the visual afferent pathway in cats
05 p0539 A73-16332
- Role of visual and articular afferentation in the implementation of motor reactions involving complex coordination and precision
06 p0653 A73-18164
- Synapse localization study by electron microscopy of primary afferent tissues in cochlear nuclei of the brain stem
07 p0781 A73-19650
- Functional organization of the mechanisms of presynaptic inhibition evoked by stimulation of cutaneous afferents
07 p0781 A73-20003
- Changes in the amplitudinal and temporal characteristics of sensorimotor-cortex evoked potentials after deactivation of spino-cervical tracts in cats
07 p0781 A73-20004
- Synaptic activation of thoracic spinal cord interneurons through reticulo-spinal pathways
09 p1039 A73-22576
- Reflex reaction of antagonist muscles during an evoked tendon reflex
10 p1182 A73-24598
- Useful future action models of instrumental reflexes and voluntary actions based on memory role in engram storage of received stimuli
11 p1314 A73-25199
- Dynamics of changes in neuron activity regimes of the ascending auditory pathways
11 p1317 A73-26079
- Hypothalamus, septum and ventrobasal thalamus nuclei single neuron responses to skin thermal stimulation, indicating afferent connections between cerebrum thermoregulation center and peripheral thermoreceptors
11 p1317 A73-26086
- Characteristics of the higher nervous activity of monkeys during a postneurotic period
12 p1462 A73-27108
- Intranuclear organization of the center median nucleus of the thalamus.
13 p1576 A73-29175
- Processing of auditory information by medial superior-olivary neurons.
14 p1715 A73-30281
- Anatomical-functional bases of cerebello-cerebral interrelations
15 p1836 A73-32287
- Variations in the motor potential with force exerted during voluntary arm movements in man.
21 p2638 A73-41013
- Evoked potentials in the hypothalamus and mesencephalic reticular formation upon stimulation of the vagus nerve
21 p2640 A73-41263
- Effect of the electrical stimulation of the sensorimotor cortex on the potentials of dorsal roots and on the depolarization of primary spinal afferents
22 p2807 A73-42652
- Circuit diagram of amplifier-filter for analysis of impulse activity of baroreceptor aortic afferent nerves in rabbits
22 p2816 A73-42681
- AFINITY**
The spray deposition of oxide-free coatings consisting of special metals with a high affinity to oxygen
11 p1372 A73-25411
- Advantage or disadvantage of a decrease of blood oxygen affinity for tissue oxygen supply at hypoxia - A theoretical study comparing man and rat.
21 p2641 A73-41620
- AFRICA**
Trace fossils from the Nama Group, south-west Africa.
12 p1490 A73-27250
- Stable auroral red arc equatorial edge observation with photometer during recovery phase of magnetic storm on 18 December 1971 in Southern Africa
12 p1492 A73-27611
- A study of lineaments from a Zond 5 photograph of northern Africa.
21 p2687 A73-41332
- AFTERBODIES**
Aircraft aftbody/propulsion system integration for low drag.
[AIAA PAPER 72-1101] 03 p0243 A73-13420
- Thrust measurement bench for afterbody and hot and cold jet nozzle simulated tests in Sigma 4 wind tunnel
16 p1993 A73-32820
- Incompressible turbulent boundary layer separation from a curved axisymmetric body.
20 p2548 A73-39525
- AFTERBURNERS**
U AFTERBURNING
- AFTERBURNING**
Control and stability analysis of supersonic aircraft jet engines with afterburner for improved low altitude operation
06 p0741 A73-17722
- Monopropellant and bipropellant thruster systems with afterburning for geostationary satellite orbital control, evaluating performance and reliability based on calculation and test data
07 p0866 A73-18930
- The effect of afterburning on the emission of pollutants by turbojets
18 p2343 A73-36996
- AFTERGLOWS**
NT HELIUM AFTERGLOW
NT OXYGEN AFTERGLOW
- The application of Langmuir probes to the measurement of very low electron temperatures.
02 p0158 A73-11912
- Photoionization of vibrationally excited N₂. II - Quenching by CO₂ and N₂O.
04 p0414 A73-14817
- The mechanism of vacuum ultraviolet emission from the Lewis-Rayleigh nitrogen afterglow.
05 p0600 A73-16560
- Dissociative recombination at elevated temperatures. IV - N₂⁺/+ dominated afterglows.
07 p0853 A73-19149
- Pulsed probe studies on the diffusion coefficient of an afterglow plasma across a magnetic field.
09 p1132 A73-23250
- Recombination of doubly ionized atoms in the afterglow of a helium plasma produced by laser.
15 p1915 A73-31675
- Electron thermal conductivity along the magnetic field in an afterglow.
17 p2215 A73-34310
- Experimental results concerning the time decay of the line emission in luminescent plasmas of medium-pressure inert-gas discharges
20 p2596 A73-39191
- Afterglow studies in helium-cesium mixtures.
21 p2745 A73-40223
- An appraisal of the mass spectrometer diagnostic technique in the study of afterglow plasmas.
21 p2702 A73-40792
- Electron density in a locally ionized plasma afterglow.
21 p2748 A73-40970
- Air afterglow radiative recombination reaction of NO with O yielding nitrogen dioxide, considering pressure dependence in chemiluminescence spectral region
22 p2819 A73-42772
- Measurements of recombination of electrons with HCO⁺ ions.
23 p3007 A73-43530
- AFTERIMAGES**
Some differences among figural aftereffects, apparent motion, and paracontrast.
01 p0011 A73-10435
- Orientation illusion and masking in central and peripheral vision.
03 p0266 A73-12999
- Visual after-images in athletes and coaches as a prestat condition index
06 p0658 A73-18161
- Visibility of an afterimage alone and in the presence of one or two additional afterimages.
09 p1039 A73-21894
- Binaural interaction effects on afterperception of white noise pulse sequences delivered to both ears simultaneously or after various intervals
10 p1180 A73-24333
- Colour selectivity in orientation masking and aftereffect.
11 p1323 A73-26196
- Binocular rivalry and binocular fusion of afterimages.
11 p1318 A73-26200
- The dependence of the negative afterimage on the duration of the stimulus and the stimulus intensity
11 p1321 A73-26550
- After-effects of movement contingent on direction of gaze.
11 p1324 A73-26721
- Monocular fixation tests and prediction model for time course of aftereffect of eye turn on autokinetic illusion direction
13 p1578 A73-28098
- Properties of human visual orientation detectors - A new approach using patterned afterimages.
13 p1579 A73-29124
- Stereoscopic depth aftereffects with random-dot patterns.
17 p2115 A73-34841
- Temporal factors of movements in visual aftereffects
17 p2115 A73-34843
- Investigations of the eye tracking system through stabilized retinal images.
18 p2273 A73-36456
- Spatial determinants of the aftereffect of seen motion.
19 p2394 A73-37415
- Spiral aftereffect durations following awakening from REM sleep and non-REM sleep.
21 p2639 A73-41179
- Effect of eye movements on backward masking and perceived location.
21 p2639 A73-41184
- Stimulus specificity in the human visual system.
22 p2810 A73-42960
- AGC [CONTROL]**
U AUTOMATIC GAIN CONTROL.
- AGE DETERMINATION**
U CHRONOLOGY
- AGE FACTOR**
Pilot incapacitation as cause of aircraft accidents, noting age connected cardiovascular disease as leading cause for loss of pilot license
01 p0013 A73-11238
- Development of wakefulness-sleep cycles and associated EEG patterns in mammals.
03 p0264 A73-14263
- The old open cluster NGC 6819.
05 p0618 A73-16744
- Cardiovascular changes in middle-aged men during two years of training.
08 p0934 A73-21504
- Influence of developmental adaptation on aerobic capacity at high altitude.
09 p1041 A73-22928

- Age-related characteristics of pulmonary edema development during acute hypoxic hypoxia
10 p1180 A73-23939
- Spatial analysis in monkeys of various ages after extirpation of the parietal areas of the cerebral cortex
10 p1180 A73-24329
- Embryonic chick heart cell age dependent electrophysiological studies, discussing structure, metabolism, ATPase activity, membrane potential and cell interactions
11 p1315 A73-25589
- A new age indicator for Galactic clusters.
14 p1799 A73-30449
- Formation of conditioned responses to symbolic stimulations in healthy individuals of different age
15 p1833 A73-31158
- Age peculiarities of whole-blood transketolase activity in healthy persons
15 p1833 A73-31164
- Some statistical techniques useful in system aging studies.
16 p2020 A73-33603
- Sonic booms and sleep - Affect change as a function of age.
18 p2282 A73-36780
- The problem of early presbyopia in aircrew.
18 p2285 A73-36923
- Visual problems among senior flight personnel.
18 p2285 A73-36924
- Glaucoma development in aging flight personnel.
18 p2285 A73-36926
- Binocular vision variation with age in flight crews
18 p2285 A73-36928
- Reinforcement of unconscious traces of stimuli in the human being during ontogenesis
19 p2393 A73-37251
- Corti organ lesion effects on signal perception in patients with noise induced hearing loss, correlating speech discrimination with age and sound level
19 p2396 A73-38182
- Zero-age main sequence stellar model calculations compared to observational data derived for nearby low mass stars
20 p2611 A73-39585
- Human intrapair twin differences, examining age, height, weight, heart volume, metabolism, respiratory rate and monozygous/dizygous differences
20 p2519 A73-39792
- Developments as regards maximum visual acuity with age among cockpit crew members.
21 p2645 A73-41164
- Torsional elasticity of human skin in vivo.
21 p2642 A73-41625
- Prevalence of hyperlipoproteinemias in a random sample of men and in patients with ischaemic heart disease.
22 p2811 A73-42975
- Frequency distribution functions of pulsars, supernovae and sunspot groups relationship to age and lifetime, considering stellar mass and initial luminosity
22 p2915 A73-43033

AGE HARDENING

U PRECIPITATION HARDENING

AGENA ROCKET VEHICLES

- Low altitude orbit feasibility study of integrated SNAP 29/Agena satellite configuration, comparing with solar cell power system
11 p1396 A73-26040

AGGLUTINATION

- Intravascular changes associated with hyperbaric decompression - Theoretical considerations using ultrasound.
09 p1045 A73-22534

AGING [BIOLOGY]

- Ophthalmological assessment of visual functional impairment due to glare, stimulus motion and aging changes
05 p0540 A73-16485
- Photosensitized inhibitor formation in isolated, aging chloroplasts.
07 p0784 A73-20453
- Influence of histamine on cutaneous capillary circulation and on the oxygen tension of subcutaneous cellular tissue in various age periods
10 p1178 A73-23676
- Physiological responses of rats to intermittent high-altitude stress - Effects of age.
10 p1182 A73-24564
- The significance of retinal pathology in ageing aircrew.
18 p2285 A73-36925
- Functional aging - Present status of assessments regarding airline pilot retirement.
21 p2645 A73-41161
- Age-dependent characteristics of myoglobin content and distribution in the heart and skeletal muscles
24 p3059 A73-44669

AGING [MATERIALS]

NT AGING [METALLURGY]

- Age control evaluation of Buna N elastomers by ANA Bulletin 438, using shelf aging and crashed aircraft case studies
03 p0331 A73-13026

- Aging mechanisms in composite-modified double-base propellants.
03 p0351 A73-13410

- Predicting the service life of neoprene launch tube liner pads for the Poseidon missile.
04 p0468 A73-14861

- Aging effects on electrical and radiation characteristics of discrete semiconductors.
05 p0557 A73-16510

- Optimal time calculation for aging complex control system replacement with allowance for downtime losses
05 p0554 A73-16989

- A specific type of carbide phase precipitation during the aging of KhN77TiUa alloy
07 p0841 A73-20640

- Degradation analysis of infrared and visible optoelectronics devices.
08 p0944 A73-20742

- Thermal resistance and aging properties of polybenzimidazoles, polyimides and polyamides-imides used for Mach 3 aircraft radomes
11 p1335 A73-25291

- Hydrolytic stability of electrical insulation materials.
17 p2197 A73-35348

- Austenitic grain structure and strength changes associated with aging in 14Cr-14Ni type steels
18 p2325 A73-36810

- Strain-hardening anisotropy and original anisotropy in creep
20 p2580 A73-39364

- Creep and aging characteristics of glass-fiber-reinforced plastics
24 p3104 A73-44885

AGING [METALLURGY]

- Structure changes during aging in aluminium 4 wt. % copper alloy studied by the channeling technique.
01 p0063 A73-10310

- Microhardness anisotropy of hardened and aged Be single crystal as function of purity
01 p0067 A73-11353

- Sn suppression of Al-Cu-Sn alloy aging at low temperatures, relating to Cu solubility decrease in alpha phase
02 p0179 A73-11599

- Influence of deformations on the mechanical properties of magnesium alloys containing yttrium
03 p0324 A73-13509

- High modulus Be-Al alloy strengthening and aging as function of Cu, Mg and Zn additions
03 p0325 A73-13517

- Physical and chemical aspects of aging of polymer-base composite materials
03 p0273 A73-13590

- Influence of aging on the mechanical properties of polyester glass-resin laminated fabrics
03 p0334 A73-13591

- Hardness-controlling additions in transition metal-beryllium alloys
03 p0328 A73-14655

- Vacancy trapping model inadequacy for aging retardation in Al-Cu-Cd alloys, noting Cd content and Cu solid solubility effects
05 p0587 A73-16576

- Double aging time effects on hardness of solution treated, quenched and heat treated two phase Al-Zn-Mg alloy specimens, obtaining transmission electron micrographs
05 p0587 A73-16577

- Fractographic aspects of the stress corrosion cracking of titanium in a methanol/HCl mixture.
06 p0705 A73-17800

- Aging kinetics of maraging nickel and chromium steels
06 p0705 A73-17877

- Stability of the dislocation structure in cold-deformed Kh18Ni2T and Kh16Ni9M2 steels during high-temperature aging
06 p0707 A73-17905

- Investigation of the temperature dependence of hardening characteristics in an aging nimonic alloy
06 p0707 A73-17908

- Substructure and dispersion hardening in aged, cold worked, and annealed Al-4 wt pct Cu alloy.
06 p0711 A73-18754

- Morphology of gamma prime and gamma double prime precipitates and thermal stability of Inconel 718 type alloys.
06 p0711 A73-18755

- Ferritic chromium steels embrittlement under high temperature aging, using hardness measurements, impact tests and electron metallography
06 p0712 A73-18762

- Contribution to the study of the effect of molybdenum on the aging kinetics of maraging steels.
07 p0838 A73-19499

- High strength and plastic properties of two phase austenitic-martensitic Fe alloys after aging in alpha and gamma states
07 p0841 A73-20522

- The ageing and creep behaviour of a Cr-Ni-Mn austenitic steel.
08 p0981 A73-21791

- Phase separation analysis of ternary Co-W-Ti alloy during high temperature aging by X ray and electron microscopy method
09 p1099 A73-21963

- Austenitic alloys internal friction and strain aging under quenching, cold working and electron irradiation, considering carbon vacancies stress induced reorientation effects
09 p1101 A73-22407

- Ni-Ti alloy aging effects on yield strength explained by internal strain due to lattice modulation and Ti rich region volume fraction
09 p1103 A73-22520

- Plane stress rupture criterion for age hardening materials during plastic deformation, calculating resistance to shear and torsion of solid and hollow round bars
09 p1106 A73-23157

- Temperature range of maximum aging of Mo-Re-C alloys after quenching and tempering, noting carbon solubility effects due to Re content
09 p1106 A73-23187

- Causes of embrittlement in the 11Kh18M steel
09 p1107 A73-23195

- Effects of composition on embrittlement of austenitic stainless steels.
10 p1230 A73-23628

- Short time aging characteristics of inconel X-750.
10 p1230 A73-23631

- Investigation of the morphology and decomposition kinetics of Co-Ni-Ti alloys
10 p1232 A73-24153

- Investigation of the hardening process of alloy D16 in liquid nitrogen.
10 p1226 A73-24929

- The effect of an addition of molybdenum on the quenched and aged structure of a Ti-1 wt % Si alloy.
11 p1384 A73-26048

- Influence of impact deformation on the strengthening and aging kinetics of austenitic steel 4Kh12N8G8MFB
12 p1510 A73-26901

- Variation in the kinetics of the natural aging process for Mg-Li-Al alloys as a function of the presence of impurities and small additions of rare-earth elements
12 p1510 A73-26911

- Laminar precipitation hardening in Al alloy during aging by microscopic, X ray and Widmanstatten structure analyses
12 p1510 A73-26912

- An empirical analysis of titanium stress-strain curves.
13 p1632 A73-28133

- Effect of titanium additions on the aging characteristics of an Al-Zn-Mg alloy.
13 p1632 A73-28134

- Dynamic strain ageing in some titanium-silicon alloys.
13 p1634 A73-28184

- Forged or homogenized aged maraging steels, discussing microstructure, tensile strength and fracture toughness dependence on precipitates morphology
13 p1637 A73-29243

- Serrated flow in quenched duralumin alloy.
14 p1758 A73-29745

- Electron-microscopic investigation of the spatial distribution parameters of second-phase precipitation in aging nickel-base alloys
14 p1764 A73-30862

- Effects of cold plastic deformation and aging temperature on the mechanical properties of dispersively hardening Cr-Ni-Co-Mo steel
17 p2188 A73-34559

- The effect of cobalt on the aging mechanism of maraging steels
18 p2324 A73-36771

- Influence of prolonged aging on the behavior of the microhardness and substructure of El257 austenitic steel
18 p2324 A73-36806

- Principal aspects of thermal treatments of the alloy Ti-11, 5 Mo-6, Zr-4, 5 Sn /Beta III/
19 p2441 A73-37833

- Long period superlattice in an aged beta titanium alloy.
20 p2577 A73-39222

- Influence of coherency strains on precipitate shape in a Fe-Ni-Ta alloy.
20 p2577 A73-39223

- Vacancy precipitation in quenched and aged Zr-Al alloys and Zircaloy 2, obtaining evidence by transmission electron microscopy for detailed dislocation structure examination
20 p2578 A73-39488

- Study of the mechanism of plastic deformation of aging nickel-aluminum alloys with a large volume fraction of gamma prime phase
20 p2579 A73-39740

- Maraging steels with strengths from 110 to 130 kgf/sq-mm
21 p2718 A73-40736

- Effect of explosive impact on hardening and kinetics of aging of austenitic steel 4Kh12N8G8MFB.
21 p2720 A73-41034

Structural transformations in molybdenum-carbon alloys during quenching and aging 22 p2874 A73-42091

Recrystallization and X-ray fine structure studies of the age-hardening characteristics of the metastable titanium alloy Ti-13V-11Cr-3Al 23 p2992 A73-43913

Study of precipitates in an aged Mg-3.6 wt% Zn alloy by an X-ray method. 23 p2993 A73-44124

Influence of dislocation density and aging on the yield point of Al-Cu-Mg-Mn alloys 23 p2995 A73-44285

AGITATION

NT ULTRASONIC AGITATION

AGREEMENTS

Permanent arrangements for the global commercial communications satellite system of INTELSTAT. 04 p0523 A73-15148

AGRICULTURAL AIRCRAFT

U UTILITY AIRCRAFT

AGRICULTURE

Remote sensing for healthier crops. 05 p0569 A73-16745

Rapid processing of multispectral scanner data using linear techniques. 05 p0554 A73-17150

Airborne remote sensing for forestry and agricultural land imagery and water pollution detection, discussing use of color films and picture processing 17 p2161 A73-34933

Remote sensing applications in agriculture and forestry including land inventories, soil classification and water resources detection 17 p2162 A73-34948

Photodensity and the impact of shifting agriculture on subtropical vegetation - A case study in the Bahamas. 20 p2562 A73-39905

AILERONS

Technological and structural design ensuring optimum clearance and aerodynamic coupling of moving units /wing-aileron or aileron-trim tab/ 02 p0129 A73-11648

AIMP-E

U EXPLORER 35 SATELLITE

AIMP-2

U EXPLORER 35 SATELLITE

AIR

NT ALVEOLAR AIR

NT COMPRESSED AIR

NT EXPIRED AIR

NT HIGH TEMPERATURE AIR

Temperatures of aluminum during its combustion in oxygen-argon mixtures, in nitrogen, and in air 01 p0123 A73-11275

Spectral characteristics in visible and UV regions of laser plasma-air interaction, using focused beams on metal targets at atmospheric pressure and vacuum 02 p0176 A73-12351

Experimental investigation of the evaporation rate of water droplets in atmospheres of air and carbon dioxide under conditions of a thermostatic droplet surface 04 p0517 A73-14881

Fuel cell air cathode for high current densities at low polarization and ambient temperature, noting performance improvement with pure oxygen supply 04 p0407 A73-15112

Dwell times of exploding tungsten wires in air. 09 p1119 A73-21929

Electron-optical investigations of discharge of air and carbon dioxide in the nanosecond range 10 p1219 A73-24469

Modeling the effect of air and oil upon the thermal resistance of a sphere-flat contact. [AIAA PAPER 73-746] 18 p2370 A73-36362

Absolute viscosity of air down to cryogenic temperatures and up to high pressures. 19 p2422 A73-38296

AIR BEARINGS

U GAS BEARINGS

AIR BLASTS

U AERIAL EXPLOSIONS

AIR BREATHING ENGINES

NT BRISTOL-SIDDELEY BS 53 ENGINE

NT BRISTOL-SIDDELEY VIPER ENGINE

NT GAS TURBINE ENGINES

NT J-33 ENGINE

NT J-85 ENGINE

NT JET ENGINES

NT PULSEJET ENGINES

NT RAMJET ENGINES

NT SUPERSONIC COMBUSTION RAMJET ENGINES

NT TURBOFAN ENGINES

NT TURBOJET ENGINES

NT TURBOPROP ENGINES

Synerjet composite rocket-air breathing propulsion system for reusable spacecraft mission profile optimization, discussing multimode operation and performance capabilities 01 p0112 A73-11300

The effect of the precooling of the air before compression in the case of air-breathing propulsion systems of boosters for space vehicles [DGLR PAPER 72-060] 02 p0202 A73-11673

The S4-Modane hypersonic wind-tunnel - Its use for air breathing engine tests [ONERA, TP NO. 1103] 03 p0288 A73-14140

Analytical correlation technique for air breathing and rocket engines combustor design and performance prediction based on hydrogen oxygen engines test data [AIAA PAPER 72-1074] 04 p0486 A73-14904

Airbreathing engines for Space Shuttle. [SAE PAPER 720805] 05 p0607 A73-16647

Air breathing hypersonic aircraft technology developments in propulsion systems and structures with emphasis on use of hydrogen fuel [AIAA PAPER 73-58] 06 p0647 A73-17631

Space shuttle air breathing gas turbine engine design, modification, weight and test requirements associated with launch, space residence and reentry 07 p0906 A73-20463

Mixing controlled supersonic combustion for air breathing engine equipped hypersonic aircraft, discussing chemical and fluid dynamic interaction effects 10 p1295 A73-23862

AIR CARGO

Cargo air transport means selection procedure, suggesting methods for economic evaluation of time savings 12 p1560 A73-27066

Air cargo transportation growth since 1945 with comparison to concurrent air passenger evolution, predicting future trends 15 p1859 A73-32555

World air traffic patterns projected to 1988, including present traffic features, supersonic transport utilization, ground transport alternatives, air freight and aircraft types 16 p2088 A73-33180

Large payload aircraft for Alaskan and Canadian gas-oil transportation, examining alternative pipeline economic factors and possible new North Canadian island fuel fields 16 p2088 A73-33183

The possible future of air transport and the airports 17 p2148 A73-35665

Air freight handling equipment, techniques and costs in cargo terminals, including forklifts, pallets, containers, conveyor belts and warehouse configurations 19 p2418 A73-37821

Control requirements for sling-load stabilization in heavy lift helicopters. 20 p2509 A73-39406

Aircraft design for transporting arctic crude oil or liquid natural gas, examining air terminal requirements and handling specifications 21 p2634 A73-41172

Russian book - Economic efficiency and planning of air freight transportation. 21 p2793 A73-41294

Land-air-sea intermodal cargo container movement procedures and equipment design standardization to meet air transportability requirements [ASME PAPER 73-ICT-30] 23 p2965 A73-43493

Dirigible airship design, operations, payloads, cargo transportation and surveillance applications 23 p2940 A73-44223

AIR CONDITIONING

Russian book on passenger aircraft high altitude equipment covering cabin pressurization, air conditioning and temperature and pressure control, human tolerances, reliability factors, etc 14 p1712 A73-30355

Concorde air conditioning, discussing system modifications for production aircraft concerning interconnection of engine air bleeds of adjacent port and starboard groups 14 p1713 A73-30933

Preventing the shut-off punkah louver from jamming. 16 p1970 A73-32925

Study of performances in a warm environment in case of air conditioning breakdown on a supersonic transport 18 p2286 A73-36947

AIR CONDITIONING EQUIPMENT

Pipe array design for thermoelectric air conditioners, noting temperature distribution in half-cell and heat conductor junction 01 p0006 A73-10618

Attenuation of airplane /747/ air-conditioning noise in lined and unlined ducts. 03 p0289 A73-12959

Shell-and-coil condenser for packed air conditioners, testing heat transfer coefficients relationship to Reynolds number, heat flux and condensed refrigerant level 05 p0638 A73-16220

Heat transfer characteristics of air conditioner finned tube heat exchanger surfaces from steady state heat balance, monitoring fluid temperature response at outlet 05 p0638 A73-16223

B-52 aircraft-borne short range attack missile weapon system air conditioner thermal performance fulfillment with Freon refrigerant and air distribution in heat exchangers [AIAA PAPER 73-723] 18 p2269 A73-36340

AIR CONDUCTIVITY

Heat transfer in horizontal annular air gaps at small Grashof numbers 09 p1167 A73-23108

Direct measurements of the electrical conductivity and relaxation time of ionized air in the stratosphere and mesosphere 10 p1211 A73-23890

Experimental determination of the ionization rate behind a strong shock wave in air 11 p1304 A73-26444

Direct measurements of the electrical conductivity and relaxation time of ionized air in the stratosphere and mesosphere. 20 p2551 A73-38909

AIR COOLING

Flow measurement on scale model of air cooling system for various blowing conditions and structure parameters, noting flow resistance of cooling fins 02 p0237 A73-11634

Model tests regarding the characteristics of the boundary layer at effusion-cooled turbine blades [DGLR PAPER 72-059] 02 p0127 A73-11655

Optimum heat transfer characteristics of semi-circular surfaces cooled by air impingement from airjet arrays and row of air jet nozzles. 02 p0237 A73-11692

Computer programs for air cooled gas turbine engine design and performance prediction, noting aerodynamic effect of turbine coolant 02 p0129 A73-12848

Stoichiometric gas turbines - Development problems. 03 p0359 A73-14146

Modeling radial dilution air injection in axial flow combustors. 05 p0639 A73-16689

Heat exchanger for dissipating heat due to energy losses in enclosed dust-proof electronic equipment 07 p0921 A73-20125

Thermal state of a porous plate cooled by intense blowing under conditions of radiative-convective heating 08 p1021 A73-20993

Experiments on a shrouded, parallel disk system with rotation and coolant throughflow. [AD-759594] 08 p1023 A73-21256

Forced air cooling of dual-in-line packages. 10 p1193 A73-23607

On the design of air-cooled radial turbine blades. 11 p1410 A73-25843

Influence of the turbine air cooling system on the characteristics of a turbojet engine during regulation of the latter 12 p1532 A73-27091

Kinetic cooling with CW carbon dioxide laser, observing time constant as function of atmospheric water pressure with three-beam interferometer 13 p1659 A73-28546

Stratospheric cooling and perturbation of the meridional flow during the solar eclipse of 7 March 1970. 14 p1771 A73-30765

Dynamic katathermometer for measuring the cooling effect of an ambient medium 15 p1838 A73-31512

Air/water mist spray coolant for high gas temperature and pressure environment at gas turbine inlet 17 p2221 A73-34388

Experimental heat transfer investigations on modules mounting hybrid packages. 17 p2135 A73-34729

Optimum thermal design of electronic packages cooled by free air convection. 17 p2141 A73-35387

Gas turbine blade effusion cooling by air blowing, determining heat transfer coefficients for laminar and turbulent boundary layer 19 p2504 A73-38156

Effectiveness of film cooling of an adiabatic wall downstream of the perforated section. 20 p2628 A73-39424

Gas turbine nozzle guide vane trailing edge protection by air films cooling, measuring gas temperatures with chromel-alumel thermocouples 20 p2600 A73-39425

Investigation of different air-cooling methods for the first-stage disk of a two-stage gas turbine 21 p2754 A73-40397

Investigation of the influence of the leading-edge configuration on the efficiency of cooled rotor- and guide-vane cascades 21 p2632 A73-40406

Dimensionless pressure method to account for air density variations in gas turbine cooling system design 21 p2677 A73-41051

Effect of deflector geometry on the heat transfer in the coolant passages of deflector blades. 21 p2754 A73-41322

Thermodynamics of an air-cooled gas-turbine stage 23 p3019 A73-43733

The problem of extrapolating test data on the efficiency of turbine-blade cooling to actual conditions
23 p3020 A73-43741

AIR CURRENTS

NT JET STREAMS [METEOROLOGY]

NT MERIDIONAL FLOW

NT VERTICAL AIR CURRENTS

Interaction between long waves and zonal circulation in a baroclinic atmosphere

05 p0592 A73-16230

Strong irradiance fluctuations in turbulent air - Plane waves.

10 p1248 A73-23837

Russian book - Analysis of meteorological conditions for aviation.

17 p2204 A73-34539

Basic characteristics of the temperature distribution and air currents in the free atmosphere of the earth

18 p2332 A73-35915

Long range fluidic acoustic sensors cross air currents and temperature gradient effects on operational characteristics and resolution, and prototype design for industrial applications

20 p2511 A73-39753

AIR CUSHION VEHICLES

U GROUND EFFECT MACHINES

AIR DEFENSE

NT ANTIMISSILE DEFENSE

Command and control for a missile air defense system. I - SAM-D communications.

04 p0417 A73-15377

Command and control for a missile air defense system. II - Implementation of system requirements.

04 p0418 A73-15378

SAM-D system for field army forces to provide air defense against advanced tactical aircraft, discussing equipment, performance, cost reduction and combat readiness

[AIAA PAPER 73-65]

06 p0755 A73-17634

Adaptive real time control for defense systems - A minimum risk algorithm.

06 p0682 A73-18823

German book on national airspace protection against foreign aircraft intrusion in peacetime covering sovereign rights according to international law, conventions and treaties

11 p1454 A73-26257

USAF Airborne Warning and Control System with overland downlook Doppler radar for low-fly aircraft detection in severe clutter environment, discussing design and performance

17 p2121 A73-34371

AIR DUCTS

On the measurement of the local impedance of acoustical duct liners in the presence of grazing mean air flow.

03 p0342 A73-12989

Heat transfer in the thermal entrance region of rectangular channels with a circumference only partially heated

06 p0768 A73-17918

Investigation of the throughput capacity of the longitudinal cooling ducts of gas turbine blades

12 p1532 A73-27093

AIR FLOW

NT AIR CURRENTS

NT JET STREAMS [METEOROLOGY]

NT MERIDIONAL FLOW

NT VERTICAL AIR CURRENTS

Mixed convection over a heated horizontal plane.

01 p0120 A73-10440

Pressure distributions in manifolds with return ducts.

01 p0032 A73-10699

Random stresses effect on dynamic creep properties of Ti alloy in high temperature air flow

02 p0180 A73-11625

Experimental values of turbulence length scales in Lagrange variables in the vicinity of a flat wall

02 p0154 A73-12541

Hot-wire anemometers calibration characteristics for steady channel turbulent air flow measurement, noting linearization error analysis

03 p0306 A73-13166

Breakup and penetration of transverse liquid jets in supersonic air cross flow

[AIAA PAPER 72-1180]

03 p0293 A73-13475

Feasibility of a fluidized powder demand mode gas generator.

[AIAA PAPER 72-1194]

03 p0352 A73-13484

Calculation of the supersonic region of three-dimensional nonequilibrium air flow past bodies

03 p0245 A73-13618

Heat transfer in the turbulent boundary layer of an incompressible fluid flow past a surface when the pressure gradient and temperature on the surface are variable

03 p0295 A73-13622

Equilibrium equation for weightless flexible two dimensional sail in inviscid supersonic airstream, noting centred isentropic compression

03 p0246 A73-13789

Respiratory air flow telemetry during exercise, discussing flowmeter working conditions and equipment testing

03 p0270 A73-14286

Radio telemetric measurements of oxygen consumption during exercise via respiratory air flow and oxygen partial pressure monitors, considering water vapor and temperature

03 p0270 A73-14288

Discharge coefficients for air outflow through a single orifice in the wall of a tube.

03 p0297 A73-14597

Flow induced vibration of cantilever mounted flat plates in an enclosed passage An experimental investigation.

04 p0513 A73-15590

The measurement of a pulsating air flow using a sharp-edged orifice meter.

[ASME PAPER 72-WA/FE-36]

04 p0451 A73-15853

Tangential slot injection of carbon dioxide and helium into a supersonic air stream.

[ASME PAPER 72-WA/FE-37]

04 p0435 A73-15854

An optical system for measurement of mean and fluctuating concentrations in a turbulent air stream.

05 p0576 A73-16437

Study of the steady motion of a ballistic antenna in a plane homogeneous flow

05 p0528 A73-16750

Three dimensional dynamic characteristics of solid particles suspended by polluted air flow in a turbine stage.

[AIAA PAPER 73-140]

05 p0531 A73-16889

Effectiveness of the thermal protection of a plane wall during injection of air through two rows of rectangular holes arranged in a checkered order

06 p0768 A73-18127

Copper resistance thermoanemometer for channel unsteady air flow rate measurement, discussing design, operation principles and maximum error

07 p0823 A73-19623

Multiple-orifice liquid injection into hypersonic air streams.

07 p0775 A73-19976

Pressure gage performance tests for air turbine through flow static pressure measurement

07 p0824 A73-20100

Further results on the stagnation point boundary layer with hydrogen injection.

07 p0921 A73-20358

Experimental study of water drop evaporation in a heated air flow

07 p0922 A73-20416

Inlet air flow distortion in high hub/tip ratio mixed flow turbomachines, using modified actuator disc theory

08 p0925 A73-20784

The mean upper-air flow in Southern Hemisphere temperate latitudes determined from several years of GHOST balloon flights at 200 and 100 mb.

08 p0960 A73-21376

Calculation of the stability of rectangular plates in an air flow by the finite-element method

08 p0108 A73-21512

Swirl injector driven air flow in cylindrical tube, measuring flow velocity and turbulent stress tensor components

08 p0956 A73-21601

Heat transfer for turbulent flow with suction in a porous tube.

08 p1024 A73-21637

Mass spectroscopic investigation of dissociation and ionization in a simulated re-entry plasma.

09 p1130 A73-22843

'Closing volumes' and decreased maximum flow at low lung volumes in young subjects.

09 p1041 A73-22929

Dense air plasma compression and heating by TNT explosive charge, noting shock tube flow patterns

10 p1203 A73-23515

Experimental study of the heat transfer in the separation zones in front of cylindrical projections

10 p1294 A73-23587

An experimental study of combined forced- and free-convective heat transfer from flat plates to air at low Reynolds numbers.

10 p1295 A73-23777

Lift forces on an oscillating cylinder at low Reynolds number.

10 p1173 A73-24822

Heat transfer and friction coefficients for turbulent flow of air in smooth annuli at high temperatures.

10 p1297 A73-24970

Features of the mechanism of vapor condensation from humid air in narrow channels and the hydrodynamics of two-phase flow during droplet condensation

11 p1451 A73-25735

Determination of the convective heat transfer coefficient by 'half-space period' method

11 p1451 A73-25741

Spectra of turbulent pulsations in velocity, temperature, and their correlations for air flow in a circular pipe

11 p1301 A73-25744

Emissions from and within an Allison J-33 combustor. II - The effect of inlet air temperature.

11 p1411 A73-26423

Turbulence intensity and turbulent transfer characteristics behind grids in tubes

11 p1349 A73-26431

Approximate calculation of flow parameters during interaction of supersonic jets

11 p1304 A73-26443

Investigation of the throughput capacity of the longitudinal cooling ducts of gas turbine blades

12 p1532 A73-27093

Hail growth in cold front, discussing relationship to air flow changes

13 p1652 A73-28267

Some remarks on the thermal equilibrium equation of hot-wire probes.

13 p1613 A73-28528

The influence of acoustic disturbances on the mechanics in shear layer behind a circular cylinder in air flow.

13 p1563 A73-28530

Vortex core precession in water or air high swirl flows above critical Reynolds number

13 p1602 A73-29017

Periodic gust and wake induced unsteady air flow, calculating velocity variation with distance from rotor blade for cascade effect

13 p1566 A73-29026

Heat and mass transfer on the surface of a fiberglass-reinforced plastic in a high-temperature air flow

13 p1708 A73-29403

Temperature effects on liquid drop evaporation in an air flow

14 p1816 A73-30015

Boundary layer about a plate assuming an arbitrary gas injection law

14 p1711 A73-30017

Heat transfer to a strongly accelerated turbulent boundary layer - Some experimental results, including transpiration.

14 p1818 A73-30615

Speed control for an air motor using fluidic techniques.

[ASME PAPER 73-DE-35]

14 p1713 A73-30824

Concorde air conditioning, discussing system modifications for production aircraft concerning interconnection of engine air bleeds of adjacent port and starboard groups

14 p1713 A73-30933

Aspects of air flow to the olfactory region of the human nose

15 p1833 A73-31163

Heat transfer in the case of free convection of air between vertical surfaces

15 p1958 A73-31908

Swirl decay in circular pipe air flow in terms of angular and axial momenta, dimensionless parameter and velocity profiles

16 p1999 A73-32825

The significance of the climate factor air velocity in environmental simulation

16 p1997 A73-33381

Hypersonic nozzle flow of air with high initial dissociation levels.

16 p2001 A73-33870

Behavior of a wing panel under transient conditions in a gas flow

17 p2091 A73-34139

Flow of a dust suspension over an ellipsoid of revolution.

17 p2091 A73-34348

Laser anemometer for the measurement of air flow velocities

17 p2167 A73-34775

Stability of the general plane membrane adjacent to a supersonic airstream.

[ASME PAPER 72-APM-UUU]

17 p2248 A73-35103

Dense air plasma compression and heating by TNT explosive charge, noting shock tube flow patterns

17 p2147 A73-35195

Optimum thermal design of electronic packages cooled by free air convection.

17 p2141 A73-35387

Statistical models of turbulent free shear mixing layer structure in incompressible air streams

17 p2156 A73-35507

Experimental study of the stability of differentially heated inclined air layers.

17 p2256 A73-35847

Graphite oxidation at low temperature in subsonic air.

[AIAA PAPER 73-735]

18 p2326 A73-36352

Techniques for studying the aerodynamic characteristics of the bronchial tree of man

18 p2282 A73-36576

The dynamical effects of real Mars orography upon the large-scale air flow and some meteorological phenomena of Mars.

19 p2482 A73-37429

On the correction of anemometric measurements in air flows of slowly varying temperature

19 p2429 A73-37529

A study on opposing jets in air stream and their flame. I - A structure of two dimensional opposing jets in the state without flames.

19 p2377 A73-37945

Experimental investigation of heat transfer and resistance in crimped tubes

19 p2505 A73-38561

Study of turbulent transfer with strong injection, longitudinal pressure gradient and nonisothermicity. 20 p2547 A73-39421

Second-harmonic resonance in the interaction of an air stream with capillary-gravity waves. 20 p2550 A73-39816

Strouhal number and flat plate oscillation in an air stream. 21 p2782 A73-40125

Freon-22 circular and flat jet propagation in air cross flow in wind tunnel, examining air-gas dynamic pressure ratio effects 21 p2676 A73-40405

A method of complex design of the meridional form of the air flow path of a multistage axial-flow compressor 21 p2633 A73-40477

Effect of supersonic gas flows on the structure and heat resistance of metal alloys 21 p2717 A73-40481

Linearized models of two dimensional steady air flow around mountain obstacle for constant temperature gradients and invariant velocity 21 p2731 A73-40741

Investigation of the laminar boundary layer at a permeable surface. 21 p2678 A73-41054

Radiative-convective heat transfer in flows of hot air past a flat plate. 21 p2791 A73-41056

Effect of deflector geometry on the heat transfer in the coolant passages of deflector blades. 21 p2754 A73-41322

The effects of speed and radial flow on the axial force on an enclosed rotating disc. 21 p2754 A73-41685

Experimental investigation of the development of a cavern in the case of unsteady gas-induced cavitation 22 p2841 A73-42128

Flows with and without suspensions in channels with curvilinear segments 22 p2842 A73-42229

The influence of rotation on the heat transfer from a sphere to an air stream. 22 p2938 A73-42955

Emissions from and within an Allison J-33 combustor. II - The effect of inlet air temperature. 23 p3019 A73-43327

Experimental investigation of turbulent flow characteristics in a rotating channel 23 p2968 A73-43443

Variable mass flow rate air injection from porous flat plate into uniform incompressible air flow, obtaining laminar flow velocity profile and pressure measurements 23 p2940 A73-43932

Respiratory work minimization during exercise, using respiratory frequency, functional residual capacity and air flow pattern effects as controlled variables 24 p3060 A73-45066

Air flow in circular convection chamber, investigating transition to turbulence by simultaneous measurements of heat flux and temperature field at low Rayleigh number 24 p3157 A73-45311

Preparation of liquid fuels by evaporation from a hot wall 24 p3158 A73-45389

AIR FREIGHT
U AIR CARGO

AIR INLETS
U AIR INTAKES

AIR INTAKES
NT ENGINE INLETS
NT HYPERSONIC INLETS
NT SUPERSONIC INLETS

F-15 air superiority fighter aircraft flight testing, describing air inlet, flight control, landing gear, flaps, speed brake and cockpit layout 09 p1030 A73-22178

French monograph - Contribution to the experimental study of a boundary layer trap in a supersonic air inlet. 22 p2797 A73-42740

AIR JETS
Combustion chamber pressure calculation for a pulsed air jet engine in the process of filling 02 p0203 A73-11708

A comparison of two prediction methods with experiment for compressible turbulent boundary layers with air injection. 02 p0129 A73-12505

Converging lens effect of air jet for upstream moving waves, describing experimental procedure 03 p0290 A73-12968

Discrete tone radiation arising from a supersonic jet flowing into an unlimited gaseous medium and into a cylindrical ejector. 03 p0290 A73-12970

Structural and aerodynamic characteristics changes in turbulent propane-butane and air jets interacting with sound 03 p0290 A73-12971

Performance and noise generation studies of supersonic air ejectors. 03 p0290 A73-12972

Investigation of air stream from air-entry holes of the high-intensity combustor-liner. 03 p0400 A73-14447

Jet-driven cylindrical cavity oscillators. 04 p0409 A73-15862

[ASME PAPER 72-WA/FLCS-4]

Wing tip vortex modification by tip-mounted upstream and downstream directed air jets, discussing wind tunnel test results 07 p0773 A73-19193

Turbulent intensity induced by wakes near secondary air jet inlet to gas turbine engine flame tube 07 p0867 A73-19625

Motion of a fluid outside a turbulent jet system 07 p0812 A73-20091

Skin friction and heat flux in the impingement region of a low speed air jet upon a normal flat plate. 08 p0925 A73-20941

Incompressible turbulent axisymmetrical impulsive air injection at moderate pressure into stagnant surroundings, measuring flow velocity distribution 10 p1210 A73-24849

Study of the effects of geometrical parameters on the characteristics of air jet flow by some optical methods. 13 p1618 A73-29039

Behavior of a weak turbulent jet in a cross flow 15 p1822 A73-31199

Time evolution of pulsating air jets from schlieren photography and velocity measurements, using motor driven piston 17 p2157 A73-35514

A model for the prediction of the time delay characteristics of turbulence amplifiers. 19 p2389 A73-38075

Visualization of gas flows by means of high-speed holography 21 p2696 A73-39978

Investigation of the mechanism of reverse jet flame stabilization for a heterogeneous mixture. 24 p3158 A73-45388

Influence of a discrete component of acoustic vibration on flow in a supersonic jet with a nondesign ratio of active to passive pressure 24 p3055 A73-45538

AIR LAUNCHING
Stiletto air-launched supersonic aerial target design, development and capabilities, describing configuration, propulsion and control systems and operational envelope 09 p1032 A73-23121

Aircraft-store separation design for angular momentum increase of external weapon with internally mounted spinning flywheel 20 p2508 A73-38652

AIR MASSES
Studies of the atmospheric fine structure with the aid of microwave propagation experiments 10 p1213 A73-24682

Comment on the effect of a vorticity centre on a frontal boundary. 13 p1656 A73-29663

Formation of optical discontinuities in the atmospheric inversion layer 15 p1903 A73-31424

Estimate of the influence of the seasonal redistribution of air masses on the motion of the earth's poles 15 p1939 A73-31967

Electronic developments for performance gliding. III 16 p2014 A73-33023

Long term weather forecasting techniques, criteria and implementation, discussing statistical weather analysis, cloud types, air masses, sunspot activity, precipitation and pressure systems 20 p2584 A73-39628

Nonurban nonmethane low molecular weight hydrocarbon concentrations related to air mass identification. 21 p2680 A73-40084

Differentiated true abundance Mars air mass calculations for use in spectroscopic observation 24 p3131 A73-44465

Estimated seasonal redistribution of air masses affecting motion of earth's poles. 24 p3081 A73-44492

AIR NAVIGATION
NT ALL-WEATHER AIR NAVIGATION
NT AREA NAVIGATION

Summary of navigation aids to civil aviation - Current state and prospects 02 p0190 A73-11851

Comparison of medium-distance navigation systems. II 02 p0191 A73-12014

Determination of the navigational regime for flight over fixed points during the landing maneuver 03 p0339 A73-13071

A system for the precise calibration of air navigational receivers. 03 p0310 A73-14501

Air Force weapon system procurement needs, considering industry technological capabilities, nonlinear estimation in cruise navigation and nonlinear systems design, test and implementation 04 p0430 A73-15252

Automated navigation system design for DC 10 long range version, emphasizing control display unit interface functions with pilot 05 p0594 A73-16050

Modeling of aircraft position errors with independent surveillance. [ALAA PAPER 73-162] 05 p0595 A73-16908

Financing of route installations and services to aircraft in flight, suggesting international rules for rental collection 06 p0771 A73-17862

An all-earth inertial navigation scheme. 06 p0721 A73-18255

Determination of the true course and instantaneous position of an aircraft from aerial pictures 06 p0721 A73-18467

Air traffic control by programmed navigation. 07 p0849 A73-19349

Flight planning and navigation for thermal-IR surveys. 07 p0849 A73-20019

Air navigation development review covering air traffic, civil jet aircraft event, electronics progress and semiconductor revolution 08 p0986 A73-21088

Radio direction finders error compensation in air navigation, considering flight speed, polarization, near field and ground effects and great circle deviation 10 p1246 A73-23686

Determination of the turn start point coordinates for modern commercial aircraft 11 p1307 A73-26723

Inertial air navigation system error minimization, using discrete-sampled position fixing and star sighting data in computerized calculations 12 p1522 A73-26821

A new approach to Doppler-inertial navigation /Doppler Beam Sampling/. 12 p1522 A73-27162

Satellite systems for mobile communications and surveillance; Proceedings of the International Conference, London, England, March 13-15, 1973. 12 p1471 A73-27652

Civil aircraft vertical plane navigation and guidance during climb and descent, discussing atmospheric, performance and passenger comfort constraints on flight path selection 13 p1656 A73-28075

Kalman filter adaptive tracker for ATC applications, modeling aircraft maneuvers by linear system with random noise accelerations based on statistical decision theory 13 p1593 A73-29212

Operation of current navigation aids and future prospects. 14 p1773 A73-29883

Navigation system time dissemination and synchronization, considering timing offset estimation for like events at geographically separated locations and clock characteristics for airborne application 14 p1726 A73-29896

Air navigation evolution and current state of art, discussing MF four axis and nondirectional beacons, VOR, DECCA, DME, TACAN, VOR-Doppler, terminal and landing systems 14 p1773 A73-30445

Russian book - Air navigation: Application of radio navigational aids and automated navigation complexes. 15 p1908 A73-31471

Astronautical coordinate systems definition and applications for flight mechanics problems involving earth curvature and motion effects 15 p1908 A73-32202

A VOR sensor of advanced design - The Bendix RVA-33A. 15 p1909 A73-32454

Doppler VOR area navigation operational principles, emphasizing bearing accuracy improvement compared to conventional VOR systems 15 p1909 A73-32456

MGC 30 inertial navigation system for civil aviation, emphasizing economics and ease of maintenance 15 p1909 A73-32457

Optimal digital modulation techniques for aeronautical communications via satellite, considering air navigational systems for transoceanic flight 15 p1847 A73-32480

Meteorological satellites in the service of aeronautics 15 p1907 A73-32562

Terminal and flight control navigation guidance systems for restricted and short takeoff and landing aircraft air traffic and approach techniques [RAE-TM-AVIONICS-135/BLUEU] 17 p2100 A73-34490

The financing of essential communication, navigation and terminal aids. 17 p2257 A73-34535

Russian book - Analysis of meteorological conditions for aviation.

17 p2204 A73-34539
VLF and Omega signal air navigation at 3 to 30 kHz supplementing VOR-DME and Loran-A navigation frequencies, considering transmission techniques

17 p2209 A73-34614
Aircraft VLF radio navigation, discussing propagation characteristics, Omega and Global Navigation systems and historical development
[SAE PAPER 730313]

17 p2209 A73-34673
VLF navigation development at NAE.
17 p2209 A73-34849
Strapdown air navigation with dry inertial instruments and high speed general purpose digital computer predicting system performance by position error analysis

17 p2210 A73-35211
LN-33 airborne inertial navigation system with low cost precision instruments and miniaturized digital computer, noting built-in calibration and test capability for minimizing maintenance

17 p2210 A73-35212
Digital flight control systems data sampling rate selection effects on intersample ripple, spectral folding and distortion and system bandwidth

17 p2138 A73-35224
Digital V/STOL flight simulation test procedures for aircraft navigation, guidance and control, detailing display device panels, flight path simulation and software configuration

17 p2210 A73-35853
Accurate aircraft trajectory predictions applied to future en-route air traffic control.

18 p2335 A73-37041
On the generation of accurate trajectory predictions for air traffic control purposes.

18 p2336 A73-37042
Plane coordinate transformations for area navigation based on existing VOR/DME network

18 p2336 A73-37043
Radiation pattern of a low-frequency beacon antenna located on a semi-elliptic terrain irregularity.

19 p2409 A73-37716
Transport aircraft external operational environment factors, discussing navigation, ATC, airspace, flight and pilot workload conditions

19 p2450 A73-37727
Simplification of navigation and flight control systems without compromising integrity.

19 p2452 A73-37826
The B.O.A.C. navigation procedures trainer.

19 p2418 A73-37874
Computer program for aircraft navigation error synthesis with evaluation of component error distribution on traffic control system effectiveness to provide cost effective guidance

19 p2452 A73-37875
Strapped down inertial navigation systems.

19 p2452 A73-37876
ASTRO-DABS communication system with hybrid satellite and terrestrial discrete address beacon system for accurate aerial surveillance and navigation with reliable data link

20 p2527 A73-38759
Hybrid-inertial navigation with range updates in a relative grid.

[AIAA PAPER 73-873] 20 p2587 A73-38810
The evaluation of autonomous navigation systems for cruise vehicles.

[AIAA PAPER 73-874] 20 p2587 A73-38811
Digital information management system of navigation and flight data for post-1975 fighter aircraft.

[AIAA PAPER 73-897] 20 p2589 A73-38832
Data compression in recursive estimation with applications to navigation systems.

[AIAA PAPER 73-901] 20 p2589 A73-38835
National Aerospace Meeting, Washington, D.C., March 13, 14, 1973, Proceedings.

21 p2734 A73-40035
Nonlinear trajectory-following and control techniques in the terminal area using the Microwave Landing System Navigation Sensor.

21 p2734 A73-40038
Ground based microwave landing system for aircraft navigation, guidance and control in terminal area, discussing system requirements for flight safety

21 p2735 A73-40047
Relationships between operational flexibility and capacity in contemporary terminal air traffic control operations.

21 p2736 A73-40048
Aircraft and spacecraft radio navigation systems, discussing Doppler, inertial and VHF omnirange techniques, Apollo spacecraft guidance systems, TACAN, Harrier and Swedish SAAB37 aircraft navigation

21 p2736 A73-40514
The development of civil air navigation in the People's Republic of China - Agreements with other states as well as the tasks and the position of the China Civil Aviation Corporation (CAAC)

24 p3159 A73-45346

AIR PIRACY

Illegal seizure of aircraft

01 p0124 A73-10650
Psychological and medical viewpoint for hijacker handling, discussing air crew training program
[AD-757130] 02 p0138 A73-12564
Book - Aviation law: Cases and materials.

06 p0771 A73-17870
Air piracy as grounds for passenger damage claims, discussing legal liability status under Warsaw and Montreal agreements

07 p0923 A73-19203
Civil aircraft commander and crew duties and rights in air piracy cases, discussing international agreements and national legal provisions

10 p1297 A73-23683
Transportation safety - Technology applications: A systems approach to anti-hijacking.

10 p1298 A73-24559
Human threats to air safety; Proceedings of the Twenty-fifth Annual International Air Safety Seminar, Washington, D.C., October 16-18, 1972.

10 p1176 A73-24707
German book - International air traffic conventions: Air piracy - Concept, facts, protective measures.

11 p1454 A73-25570
Aircraft safety engineering for air piracy prevention, discussing cockpit communication isolation from passenger compartment

16 p2087 A73-32662
Air piracy suppression measures adopted 23 September 1971 at Montreal international convention, discussing prevention and punishment provisions

16 p2087 A73-32972
Skyjacking - Its domestic civil and criminal ramifications.

16 p2087 A73-33102
Book - Aircraft hijacking and international law.

20 p2629 A73-39138
'Air piracy' and the latest work of ICAO on this subject

24 p3159 A73-45345

AIR POLLUTION

Nongray atmospheric model to assess radiative effects of water vapor and carbon dioxide layer injected into lower stratosphere by SST and HST exhaust gases

01 p0038 A73-10388
Use of space techniques in the detection and monitoring of climate parameters and air pollutants
[DGLR PAPER 72-081] 02 p0188 A73-11668

The aeroplane as a threat to the environment.

03 p0251 A73-14468
Climatic impact assessment for high-flying aircraft fleets.

04 p0436 A73-14672
The impact of aircraft emissions upon air quality.

04 p0405 A73-14890
Monitoring and modeling of airport air pollution.

04 p0432 A73-14891
Gas turbine engine swirl-can combustor pollution tests of nitrogen oxides, unburned hydrocarbons and carbon monoxide levels for elevated temperature performance

[AIAA PAPER 72-1201] 04 p0485 A73-14921
Principal trends of investigations in the field of theoretical meteorology performed in Hungary

04 p0473 A73-15284
Aircraft turbine engine emissions and the possibilities for control.

[ASME PAPER 72-WA/GT-4] 04 p0490 A73-15868
Assessment of emission control technology for turbine-engine aircraft.

[ASME PAPER 72-WA/GT-8] 04 p0490 A73-15872
The measurement of environmental pollution with the aid of aircraft and satellites

[DFVLR-SONDDR-247] 05 p0570 A73-16767
Turbojet exhaust reactions in stratospheric flight.

[AIAA PAPER 73-99] 05 p0608 A73-16859
Atmospheric dispersion of aircraft exhaust.

[AIAA PAPER 73-100] 05 p0570 A73-16860
Seasonal variations in carbon monoxide content of the atmosphere

05 p0572 A73-17357
Afterburning turbojet engine exhaust emission products measurement under simulated flight conditions, determining Mach number and altitude effects on pollutants formation

[AIAA PAPER 73-98] 06 p0740 A73-17643
Emissions from continuous combustion systems; Proceedings of the Fifteenth Symposium, Warren, Mich., September 27, 28, 1971.

06 p0767 A73-17726
Current kinetic modeling techniques for continuous flow combustors.

06 p0767 A73-17728
Effect of operating variables on pollutant emissions from aircraft turbine engine combustors.

06 p0768 A73-17736
Control and reduction of aircraft turbine engine exhaust emissions.

06 p0768 A73-17737
Global and local scale satellite surveillance of atmospheric pollution.

06 p0691 A73-18305

Exhaust emission reduction through two-stage combustion.

07 p0921 A73-20361
Stratospheric aerosol measurements with implications for global climate.

08 p0984 A73-21041
[AD-759856] Effects of changes in the atmosphere on solar insolation.

08 p0958 A73-21269
A numerical model of thermal radiation in a dusty atmosphere.

08 p0960 A73-21383
Aviation and atmospheric pollution - The real dimension of the problem and its solutions

09 p1136 A73-22216
Symposium on Air Pollution, Turbulence and Diffusion, Las Cruces, N. Mex., December 7-10, 1971, Proceedings.

09 p1114 A73-22326
A differential method for the prediction of the effects of atmospheric boundary layer turbulence using the turbulence kinetic energy equation.

09 p1071 A73-22334
Atmospheric dispersion of air pollutants, analyzing buoyant plumes and wakes

10 p1205 A73-23857
Combustor design effect on jet aircraft engine exhaust pollutants reduction during hydrocarbon fuel burning

10 p1263 A73-24556
Microwave rotational spectroscopy - A technique for specific pollutant monitoring.

10 p1221 A73-24891
Passive and active mode classification of air contamination sources in closed manned spaces, considering mechanical, electrical, chemical, physical and human factors

11 p1321 A73-25037
Laser application for remote analysis of gaseous air pollutants emission based on Raman scattering, resonance fluorescence or absorption measurements

11 p1375 A73-25399
Radiative slip between two adjacent absorbing-emitting gases and its application to air pollution.

11 p1353 A73-25722
Book - The economics of airborne emissions: The case for an air rights market.

12 p1561 A73-27399
Gas turbine engine exhaust pollutants consisting of unburned hydrocarbons, nitric oxide, carbon dioxide, nitrogen dioxide and carbon monoxide

12 p1467 A73-27934
A comparison of time-varying concentrations of air admixtures with those of the corresponding stationary cases

13 p1653 A73-28742
Seasonal variations of the carbon monoxide concentration in the atmosphere.

15 p1865 A73-31007
Mechanism of the formation and control of pollutants due to combustion

15 p1840 A73-31225
Long-path infrared spectra of CO, NO₂, NO, SO₂ and N₂O observed in a simulated atmosphere in trace amounts.

16 p1976 A73-32700
Carbon dioxide laser technological advances and applications including frequency stability systems, remote sensing, air pollution detection, optical heterodyning and pumping

16 p2023 A73-32860
Inverse condemnation of airspace, discussing real property concept relation to aircraft noise, pollution and environment protection

16 p2087 A73-33103
Concorde aircraft design, testing and projected environmental impact, discussing flight tests, sonic booms, atmospheric pollution, ATC problems and fueling

16 p1968 A73-33182
Aircraft produced environmental noise and air pollution, discussing related aircraft power plant technology evolution

16 p2047 A73-33191
Air quality monitoring instruments involving atmospheric pollution chemiluminescent reactions and CO IR, optical absorption and laser detectors

16 p2016 A73-33402
Reduction of nitrogen oxide emissions from a gas turbine by fuel modifications.

[ASME PAPER 73-GT-5] 16 p2045 A73-33483
Upper atmosphere pollution and near surface climate due to aerospace operations, discussing dynamics and trace gas distribution

[AIAA PAPER 73-492] 16 p2005 A73-33536
Correlation interferometric measurement of trace species in the atmosphere.

[AIAA PAPER 73-515] 16 p2006 A73-33552
A three-dimensional stratospheric point-source tracer experiment and its implications for dispersion of effluent from a fleet of supersonic aircraft.

[AIAA PAPER 73-528] 16 p2007 A73-33562
Aircraft exhaust plume dispersion and flight corridor concentration profiles in stratosphere as function of flight frequency and scale dependent diffusion

[AIAA PAPER 73-532] 16 p2046 A73-33565

- Simulated weather records experiment for polluted atmosphere effects on climatic change, using numerical circulation model
[AIAA PAPER 73-537] 16 p2007 A73-33568
- A model for studying the effects of injecting contaminants into the stratosphere and mesosphere.
[AIAA PAPER 73-539] 16 p2008 A73-33569
- An initial estimate of aircraft emissions in the stratosphere in 1990.
[AIAA PAPER 73-508] 16 p2011 A73-34046
- Parameters controlling nitric oxide emissions from gas turbine combustors.
17 p2221 A73-34474
- Profitable transport engines for the environment of the eighties.
[SAE PAPER 730347] 17 p2257 A73-34695
- The atmospheric aerosol and its significance for the energy budget of the atmosphere
17 p2159 A73-34749
- Theoretical analysis of improvements in remote sensing of atmospheric and pollutant gases through high resolution detection of individual infrared emission lines.
[AIAA PAPER 73-703] 18 p2315 A73-36252
- Laser measurement of high-altitude aircraft emissions.
[AIAA PAPER 73-704] 18 p2315 A73-36253
- Spherical harmonics approximation for radiative transfer in polluted atmospheres.
[AIAA PAPER 73-749] 18 p2313 A73-36365
- Civil aviation environmental and economic aspects, discussing noise and air pollution, fuel consumption and airspace and ground space utilization
18 p2267 A73-36685
- SST environment impact aspects in areas of fuel and oxygen consumption, noise, sonic boom, stratospheric pollution and climate modification
18 p2268 A73-36906
- Turbine engine research activity evolution, considering entry temperature increase, pollution sources nonstationary aerodynamics and aeroelasticity in compressors, and noise problem
18 p2343 A73-36991
- The effect of afterburning on the emission of pollutants by turbojets
18 p2343 A73-36996
- Environmental considerations for offshore airports.
19 p2417 A73-37742
- Noise and pollution - The Federal Aviation Administration's views.
19 p2384 A73-37812
- Reactions of singlet oxygen with pine pollen.
19 p2402 A73-38295
- Diffusion and fallout of pollutants emitted by aircraft engines.
19 p2474 A73-38323
- Remote sensing applications in the Metropolitan Washington Council of Governments.
20 p2556 A73-39833
- Anthropogenic CO sources and urban concentrations, considering meteorological factors, nonanthropogenic sources, temporal variations and background levels in remote areas
21 p2729 A73-40080
- Real time nitrogen dioxide and nitric oxide pollution measurement by molecular fluorescence induced by argon laser beam
21 p2671 A73-40135
- Ozone composition and nitric oxide injection upper and lower limits for stratosphere by nuclear bomb tests, comparing to estimated SST contribution
22 p2848 A73-42534
- Electrical control of particulate pollutants from flames.
22 p2935 A73-42799
- Potential of hydrogen fuel for future air transportation systems.
[ASME PAPER 73-ICT-104] 23 p3019 A73-43499
- Use of space techniques for the determination and monitoring of climate parameters and air contaminants
23 p3003 A73-43780
- Optical radar measurements of meteorological parameters and air pollution related to environment protection, using Raman effect and resonance and Mie scattering
24 p3096 A73-44896
- Some characteristics of the global distribution of the trace element concentration in the lower troposphere
24 p3085 A73-44967
- AIR PURIFICATION**
- Nuclear meteorology as branch of atmospheric physics, examining natural and artificial fission products, nuclear explosion effects, atmospheric purification and radioactive tracers for meteorological process investigation
21 p2730 A73-40115
- AIR SAMPLING**
- Southern Hemisphere troposphere atmospheric carbon dioxide monitoring program based on aircraft air sampling, discussing vertical profile data
11 p1358 A73-26472
- Portable respirable dust monitor for continuous concentration measurement by light scattering of gas laser cavity beam
21 p2708 A73-39923
- Nonurban nonmethane low molecular weight hydrocarbon concentrations related to air mass identification.
21 p2680 A73-40084
- Preliminary results from the noctilucent sampling from Kiruna in 1970.
21 p2775 A73-41413
- Noctilucent cloud sampling by a multi-experiment payload.
21 p2775 A73-41414
- Meridional tropospheric ozone distribution north of 50 deg from airplane measurements.
23 p2974 A73-43860
- AIR SEA INTERACTIONS**
- U AIR WATER INTERACTIONS**
- AIR SICKNESS**
- U MOTION SICKNESS**
- AIR TO AIR MISSILES**
- A four-level technique for estimation of tactical missile aerodynamic parameters.
07 p0777 A73-20592
- Calculation of the temperature distribution within an ogival radome in supersonic flight
11 p1336 A73-25302
- TWT for air-to-air missile fire control radar transmitter application, considering high average power, RF gain and PPM focusing requirements
14 p1737 A73-30624
- Accelerated testing of air-to-air guided missiles.
16 p2073 A73-33612
- Airborne air to air and air to ground fire control radar systems for all-weather fighter aircraft, emphasizing cost effectiveness through modularity and commonality
16 p1985 A73-34041
- AIR TO AIR ROCKETS**
- U AIR TO AIR MISSILES**
- AIR TO SURFACE MISSILES**
- Propulsion unit, components, environmental tests and development problems of Swedish air to ground missile rocket engine operating on liquid propellants
[AIAA PAPER 72-1102] 03 p0355 A73-13421
- Safety management of air to surface nuclear short range attack missile /SRAM/ at fabrication, testing and operation levels
16 p2073 A73-33640
- Airborne air to air and air to ground fire control radar systems for all-weather fighter aircraft, emphasizing cost effectiveness through modularity and commonality
16 p1985 A73-34041
- A real-time six-degree-of-freedom hybrid simulation facility for guidance system testing.
[AIAA PAPER 73-876] 20 p2543 A73-38813
- AIR TRAFFIC**
- International convention on damage caused by aircraft concluded 1952 in Rome, proposing revision to include damages before takeoff, after landing and during flight
01 p0124 A73-10566
- Airport requirements for air traffic safety, considering runway drainage and lighting, ILS, rescue and fire services, communications and weather reporting networks
01 p0030 A73-11239
- STOL aircraft technology, operation and markets in view of future European air traffic development, discussing various lift devices, noise aspects and economic factors
[DGLR PAPER 72-054] 02 p0130 A73-11662
- Airport layout planning, considering air traffic, conventional and STOL aircraft, runway requirements, passenger and baggage processing facilities, environmental factors, etc
02 p0150 A73-11704
- Contrail ice budget measurements with optical array particle size spectrometer onboard Sabreliner, noting water abundance reduction at subtrappopause jet traffic levels
02 p0189 A73-12785
- Air traffic volume prediction by 1985, determining passenger growth factors for terminal pairs
07 p0923 A73-19348
- The capacity of a single-runway S.T.O.L./R.T.O.L. airport.
07 p0849 A73-19352
- Air navigation development review covering air traffic, civil jet aircraft event, electronics progress and semiconductor revolution
08 p0986 A73-21088
- Economic-mathematics approaches to prognostic air traffic computations
11 p1455 A73-26724
- Data acquisition process to plan and engineer air traffic system, considering design aspects and piecemeal evolution
12 p1522 A73-27362
- Status of funded improvements to the National Aviation System and planned improvements not yet funded.
12 p1561 A73-27363
- Improvements in the use of FAA resources for system performance assurance.
12 p1561 A73-27364
- Airport planning for 1980s air traffic capacity requirements, considering runways, aprons, air traffic and ground movements control, ground access and terminal facilities
15 p1858 A73-32363
- Roskilde airport for Copenhagen metropolitan area general aviation and domestic air traffic, describing runways, taxiways, drainage, terminal facilities, lighting and navigation aids
15 p1858 A73-32364
- French ATC authority problems generated by north-south air lane crossing of intercontinental east-west routes, considering enroute and terminal airport problems
15 p1960 A73-32558
- World air traffic patterns projected to 1988, including present traffic features, supersonic transport utilization, ground transport alternatives, air freight and aircraft types
16 p2088 A73-33180
- Short haul aircraft design and marketing, examining competing modes, noise factors, airport traffic density patterns and aircraft types dependence on utilization
16 p2088 A73-33184
- STOL aircraft choice for air transportation in low passenger density areas, discussing market characteristics in U.S. and tradeoffs between airline operation and airfield costs
17 p2209 A73-34705
- [SAE PAPER 730357] Simulation of airport traffic flows with interactive graphics.
17 p2147 A73-34821
- Public air transportation service needs for nonurban areas, considering low traffic density problem, operational requirements and future trend
[ASME PAPER 73-ICT-72] 23 p3050 A73-43498
- AIR TRAFFIC CONTROL**
- NT RADAR APPROACH CONTROL**
- A French collision-avoidance system of time-frequency type - Critical analysis of test results
[ONERA, TP NO. 1086] 01 p0074 A73-10227
- Programmed control of a two-level hierarchical system
01 p0027 A73-10665
- Multisatellite systems for transoceanic aircraft communications and ATC, discussing day and night operations, cost-benefit optimization and adaptive techniques for capacity augmentation
01 p0018 A73-11201
- Computerized multichannel alphanumeric TV system for ATC operational information display, describing data acquisition, processor and software peripherals and video display subsystem
02 p0165 A73-11594
- Experimental validation and design refinement program for air-ground-air data link based on automatic time division multiplex transmission of air traffic messages
02 p0190 A73-11852
- ATC simulator, discussing student training routines and exercises, automatic navigation and aircraft piloting
02 p0190 A73-11853
- Assessment and operational implications for ATC capital investment decision making by relative capacity estimating process using analytical models
03 p0280 A73-13801
- Human factors evaluation of labelled radar displays.
03 p0268 A73-14155
- Telemetric transmission of ergonomic and time study data to describe work load of radar controllers.
03 p0272 A73-14308
- The optimal control of merging aircraft-derivation of the hybrid air traffic controller.
03 p0340 A73-14489
- Computer-mediated human communications in an air traffic control environment A preliminary design.
03 p0340 A73-14658
- Computerized ATC automation program, considering system management, hardware, software and test facilities problems
05 p0595 A73-16619
- ATC research - Simulating Arrival/Tower communications.
05 p0595 A73-16620
- The concept of an SST Oceanic Computer Clearance System.
05 p0595 A73-16621
- The employment of a spoken language computer applied to an air traffic control task.
05 p0544 A73-16728
- Modeling of aircraft position errors with independent surveillance.
[AIAA PAPER 73-162] 05 p0595 A73-16908
- Problems related to the measurement and evaluation of ATC/CAS interaction.
06 p0721 A73-17600
- Systems for collision avoidance.
07 p0848 A73-18899
- Ground based and airborne collision avoidance systems comparison, discussing interrogator/transponder concept, pilot warning indicator, and air traffic handling capacity and economics
07 p0848 A73-18900

The Aeronautical Satellite Programme - ATC aspects.

07 p0848 A73-19141

Collection and processing of data for the establishment of route charges.

07 p0796 A73-19182

Two-level computer system with main and display processors as scale working model for semiautomatic digital ATC en route control

07 p0796 A73-19183

Automated radar terminal systems /ARTS/.

07 p0849 A73-19184

Air traffic control by programmed navigation.

07 p0849 A73-19349

A precision position and time service for the air traffic of the future.

07 p0849 A73-19350

Area navigation systems integration with terminal ATC approach procedures, considering computerized data linkage with aircraft navigation system

07 p0849 A73-19351

Distributed ATC with traffic information in cockpit, noting potential for cost and risk reduction and capacity increase based on system performance evaluation

07 p0850 A73-20600

Proposed new test for aptitude screening of air traffic controller applicants.

09 p1045 A73-22535

Russian book on multichannel magnetic tape recorders in civil aviation ATC for speech communication monitoring and preservation covering design and operation principles

09 p1086 A73-23245

Cost effectiveness of planned aviation system improvements, considering ATC automation vs terminal aids, noise control, ground facilities, capacity and en-route situation

10 p1247 A73-24767

Noise abatement two-segment, precision and category I, II and III approaches considerations covering altimetry, cost and safety problems in ATC

10 p1247 A73-24768

Russian book - Network planning and control of air transportation.

10 p1298 A73-24924

Airport computerized departure control for check-in, load control, cargo and catering operations, discussing load optimization and passenger acceptance control /LOPAC/ system

11 p1343 A73-25210

An optimal control approach to terminal area air traffic control.

11 p1394 A73-25786

Signal processing in the Air Traffic Control Radar Beacon System.

12 p1469 A73-27165

National aviation system improvement via cost effectiveness, considering FAA facilities and equipment program, ATC automation and terminal aids

12 p1522 A73-27365

Potential applications of acoustic matched filters to air-traffic control systems.

12 p1522 A73-27572

The use of satellites for aircraft communications and air traffic control.

12 p1472 A73-27666

ATC system requirements for Concorde transoceanic flight operations, considering track allocation, computer system and programming

13 p1656 A73-28178

A flight control simulator - A computer system for the training of flight control personnel

13 p1598 A73-29100

Kalman filter adaptive tracker for ATC applications, modeling aircraft maneuvers by linear system with random noise accelerations based on statistical decision theory

13 p1593 A73-29212

Overview - The role of communication systems in air traffic management.

14 p1725 A73-29876

Historical development of the Air Traffic Control System.

14 p1772 A73-29877

Formulation of the air traffic system as a management problem.

14 p1772 A73-29878

ATC concepts and air/ground data link requirements for U.S. airspace structure in 1980s to support anticipated Los Angeles basin traffic densities in 1995

14 p1772 A73-29879

The development of the ATC radar beacon system - Past, present, and future.

14 p1725 A73-29881

Bit synchronized discrete address radar beacon system with ground based U.S. civil interrogator complex for compatibility with ATC and aircraft operator services

14 p1772 A73-29882

Operation of current navigation aids and future prospects.

14 p1773 A73-29883

Ground communications networks for aeronautical operations.

14 p1740 A73-29885

Computer and digital techniques in ATC automation technology, considering functional organizations, terminal facilities and system capabilities to meet future needs

14 p1730 A73-29886

Improvements in Airport Surface Traffic Control surveillance.

14 p1740 A73-29887

Oceanic ATC by application of aeronautical satellite technology, discussing system design requirements, performance evaluation and international program

14 p1773 A73-29888

Military ATC systems and equipment in U.S. National Aviation System, discussing operations, organizational and facility interfaces, communications, navigation, and surveillance radar requirements

14 p1773 A73-29889

Aeronautical communication technology for civil ATC system development through 1990s, discussing SNR design and need for radio channel models

14 p1725 A73-29890

Multiple access technique for future communication, surveillance and navigation subsystems to meet ATC demands, considering satellite surveillance radar system

14 p1725 A73-29893

The use of specialized antenna technology for air traffic control and communications.

14 p1732 A73-29894

Radar technology applied to air traffic control.

14 p1725 A73-29895

The role of the airborne traffic situation display in future ATC systems.

14 p1773 A73-29897

Acoustic matched filters applications for multisubscriber band spread communication in ATC systems

14 p1733 A73-29936

Automatic runway and aircraft approach path surveillance system /CORAIL/ consisting of Doppler radar, signal extractor and data processing, alarm, display and control equipment

14 p1773 A73-30444

Experimental data processing system for EUROCONTROL scale model semiautomatic digital route control system for operational conditions simulation

15 p1907 A73-31132

Automatic radar terminal system /ARTS/ for high density ATC centers, noting improved target identification and alphanumeric data display

15 p1907 A73-31133

Electronics and civil aviation; International Conference, Paris, France, June 26-30, 1972, Reports. Volumes I & 2

15 p1908 A73-32426

Digital transmission techniques for ATC satellite system, considering technical and economic aspects of various coding systems

15 p1846 A73-32427

Use of associative processors for radar data processing in air traffic control systems.

15 p1849 A73-32434

Radar data digital relay from outlying stations to ATC centers for air traffic image integration, discussing computerized plotting and alphanumeric display techniques

15 p1847 A73-32435

The air traffic control R & D program of the Federal Aviation Administration.

15 p1908 A73-32437

Radiogoniometric vectors superposition on ATC Doppler radar image, noting direction finding display availability and echoes identification

15 p1847 A73-32438

Self-reconfiguring computer complexes for A.T.C. Systems.

15 p1849 A73-32439

ATC radar information processing systems optimization, discussing hard- and software selection criteria

15 p1847 A73-32440

Automation of the print-out of strips of flight plans for air traffic control

15 p1847 A73-32441

Functioning in multiprocessing of two 10020 computers at the Bretigny Eurocontrol Experimental Center

15 p1847 A73-32442

Automated system of mixed /civil and military/ control

15 p1847 A73-32444

ATC system with radar data processing, discussing hardware and software organization, programmed logic integration possibilities and functional flexibility

15 p1909 A73-32445

Some remarks on operational problems associated with the introduction of automatic data processing into air traffic control.

15 p1909 A73-32447

MADAP - Implementation of a large size real time data processing system.

15 p1849 A73-32448

Air traffic control technology progress review and future forecast, noting microelectronics and automation need in civil avionics

15 p1960 A73-32479

Automation of the Yugoslav AFTN network and its future expansion

15 p1855 A73-32482

Real time information processing automated systems for ATC, considering reliability based on redundancy

15 p1910 A73-32483

Application of the visualization of radar information in television

15 p1911 A73-32484

The London Air Traffic Control Centre radar data processing system.

15 p1911 A73-32485

Graphical distribution in colors adapted to traffic control

15 p1911 A73-32486

Operational utilization of an aeronautical satellite system for air traffic control over the North Atlantic.

15 p1911 A73-32487

Procedures and ground methods associated with the exploitation of a system of aeronautical satellites

15 p1911 A73-32488

Area navigation feasibility, discussing computer technology usefulness, time saving and air traffic controller acceptance

15 p1911 A73-32491

STOL operational impact on ATC system support, considering short haul metropolitan and rural transportation modes, landing/takeoff facilities and all-weather operational reliability

15 p1831 A73-32547

Airport or ATC system hourly landing and takeoff capacity concept in terms of hourly demand as function of mean waiting time

15 p1960 A73-32552

French ATC authority problems generated by north-south air lane crossing of intercontinental east-west routes, considering enroute and terminal airport problems

15 p1960 A73-32558

Differential velocity effects on converging target intersection time estimation accuracy, considering plane conditions and air traffic controller experience

16 p1975 A73-32900

FAA air traffic control systems projected improvements, including microwave landing system, aeronautical satellites, electronic voice switching and discrete address radar beacon

16 p2087 A73-33179

Independently targeted short haul individual rotorcraft for air taxi service, considering traffic control system, market possibilities, environmental impact and projected utilization

16 p2088 A73-33186

Nonlinear filter evaluation for estimating vehicle position and velocity using satellites.

16 p1988 A73-33410

Simulation in the design of automated air traffic control functions.

16 p2035 A73-33419

Safety in operation and human error.

17 p2097 A73-34077

Air traffic control, discussing man machine systems, multipath with ILS, target indicator radars and flight progress strip preparation

17 p2206 A73-34086

Automated terminal area ATC operations under FAA ten year plan, investigating analytical model of pilot-aircraft control loop decision making by computer program

17 p2206 A73-34437

Helicopter operations in London area, describing controlled airspace, helicopter routes and heliport approach and takeoff procedures

17 p2206 A73-34446

The functions of regional airports and the resulting requirements for the ground installations

17 p2146 A73-34476

Mixed CTOI-QTOI traffic effects on air traffic controller tasks, microwave landing and radio navigation systems, airport operation and ground equipment [MBB-UH-05-73]

17 p2207 A73-34487

Terminal and flight control navigation guidance systems for restricted and short takeoff and landing aircraft air traffic and approach techniques [RAE-TM-AVIONICS-135/BLUE/]

17 p2100 A73-34490

Electronic landing system satisfying IFR requirements for air traffic, noting simulated ILS and ground controlled approach operations [DGLR PAPER 73-020]

17 p2146 A73-34494

International Aerospace Instrumentation Symposium, 19th, Las Vegas, Nev., May 21-23, 1973, Proceedings.

17 p2165 A73-34601

Aircraft microwave landing system development, including conventional system history and shortcomings, program objectives and implementation schedule for ATC

17 p2208 A73-34611

Automated discrete address radar beacon system and data link for ATC, describing simultaneous message decoding capacity, system specifications and implementation prognosis

17 p2208 A73-34612

Aircraft wake vortex avoidance system for safety management and capacity optimization in airport operations related to ATC, considering various sensors and display subsystem requirements 17 p2166 A73-34613

Encoding altimeter for coding, transmitting and displaying flight altitude information to air traffic controllers [SAE PAPER 733031] 17 p2167 A73-34663

Airtransit - The Canadian demonstration interurban STOL service. [SAE PAPER 730356] 17 p2103 A73-34704

Annual Simulation Symposium, 5th, Tampa, Fla., March 8-10, 1972, Record of Proceedings. 17 p2130 A73-34817

Simulation of a surface traffic control system for John F. Kennedy International Airport. 17 p2147 A73-34818

Prospects of automation of air traffic control systems using satellites for radio navigation 17 p2209 A73-34961

Aeronautical and maritime traffic control by stationary orbit navigation satellites, discussing frequency ranges, aircraft distance control, antenna arrays and multiple data access 17 p2125 A73-35477

The possible future of air transport and the airports 17 p2148 A73-35665

A simulation study for the design of an air terminal building. 17 p2149 A73-35826

Aircraft terminal approach and entry spacing systems supported by automated terminal radar using area navigation techniques 17 p2210 A73-35852

Modeling problems in air traffic control systems. 18 p2335 A73-36427

Offshore airport design, construction and operation on basis of cost/benefit considerations, emphasizing ATC problems generated by ILS localizer and glide path signal reflection 18 p2296 A73-36682

Problems related to the operation of an air-ground data-link system 18 p2289 A73-36686

Computer models for air traffic control system simulation. 18 p2335 A73-36843

Accurate aircraft trajectory predictions applied to future en-route air traffic control. 18 p2335 A73-37041

On the generation of accurate trajectory predictions for air traffic control purposes. 18 p2336 A73-37042

Air traffic control and the prevention of collisions 19 p2450 A73-37386

Operational principles and testing of a digital radar target extractor 19 p2404 A73-37584

Transport aircraft external operational environment factors, discussing navigation, ATC, airspace, flight and pilot workload conditions 19 p2450 A73-37727

STOI pilot functional requirements on air transportation system in terms of airport design, aircraft, ATC, route selection, navigation and communications 19 p2450 A73-37730

New York offshore airport feasibility study. [FAA-RD-73-45] 19 p2418 A73-37750

The Federal Aviation Administration program to improve terminal area traffic control. 19 p2450 A73-37803

Advanced concepts in terminal area control systems - Aircraft tracking and collision alert. 19 p2451 A73-37806

A digital simulation facility for air traffic control experimentation. 19 p2451 A73-37809

United States en route air traffic control systems. 19 p2451 A73-37810

The air traffic controller and control capacity. 19 p2451 A73-37811

United States Microwave Landing System development program. 19 p2451 A73-37815

Area navigation as means for airspace optimal utilization, considering navigation equipment and methods and ATC procedures reorganization 19 p2452 A73-37817

Aircraft wake vortex detection and avoidance systems, examining acoustic sensors, bistatic Doppler sensors, pulsed radar, aircraft spacing techniques and ground wind measurement 19 p2452 A73-37823

Computer program for aircraft navigation error synthesis with evaluation of component error distribution on traffic control system effectiveness to provide cost effective guidance 19 p2452 A73-37875

Optimal aircraft collision avoidance. 19 p2452 A73-38050

Studies on the time-to-go indexing control scheme for an automatic aircraft landing system. 19 p2453 A73-38280

ATC enroute automation program using radar tracking and computer readout system, describing terminal traffic control, wake vortices and aircraft spacing 19 p2453 A73-38439

Air Traffic Control Association, Annual Meeting and Technical Program, 17th, Chicago, Ill., October 9-11, 1972, Proceedings. 19 p2453 A73-38461

Metering and spacing with computerized ARTS III ATC system, discussing display for heading, speed and altitude commands 19 p2453 A73-38462

ARTS II automated air traffic control systems. 19 p2453 A73-38463

NAS enroute automated flight and radar data processing, describing communication facilities, computer complex, software, data entry, display function and ATC personnel interface 19 p2453 A73-38464

Parallel processors and air traffic control automation. 19 p2408 A73-38465

Discrete address beacon system (DABS) data links and digital communication between ground based ATC computer and aircraft for IFR-VFR conflict detection and safety separation 19 p2453 A73-38466

Air based collision avoidance system feasibility appraisal, discussing YG1054 proximity warning indicator, cost analysis and implementation prognosis 19 p2454 A73-38468

SECANT - A solution to the problem of midair collisions. 19 p2454 A73-38469

Ground based aircraft collision avoidance systems, discussing three dimensional tracking, aircraft velocity vector determination, radar systems and tracking errors 19 p2454 A73-38470

Oakland airport oceanic ATC with input-output display device, describing minicomputer, CRT displays and data link system 19 p2454 A73-38471

Air traffic controller responsibilities and performance evaluation criteria development, discussing manager/monitor functions, field evaluation tests and training criteria 19 p2402 A73-38472

Adaptive multibeam concepts for traffic management satellite systems. 20 p2525 A73-38746

The universal data link system for air/ground communications. 20 p2526 A73-38757

Comparison of the job attitudes of personnel in three air traffic control specialties. 20 p2517 A73-39108

Continuous radio telemetric recording of pulse rate in radar controllers while on duty 20 p2517 A73-39208

Digital computer simulation program for North Atlantic hybrid navigation systems configurations, using covariance matrix error analysis for planned increase of commercial air traffic capacity 21 p2733 A73-40028

Operational global navigation system development program with repeater satellites deployed over continental USA to provide radio links for digital communication, surveillance and ATC 21 p2735 A73-40041

Satellite based ATC system with radar range and rate measurements, analyzing errors due to ground station position, transponder delay time and atmospheric refraction uncertainties 21 p2735 A73-40042

Relationships between operational flexibility and capacity in contemporary terminal air traffic control operations. 21 p2736 A73-40048

A survey of satellite-based systems for navigation, position surveillance, traffic control and collision avoidance. 21 p2736 A73-40052

Frequency of anti-collision observing responses by solo pilots as a function of traffic density, ATC traffic warnings, and competing behavior. 21 p2645 A73-41158

A look at Soviet ATC and nav facilities and avionics. 21 p2737 A73-41522

Air traffic control in the EUROCONTROL area. 22 p2884 A73-42321

The MINFAP system - First phase in the automation of the EUROCONTROL Maastricht Centre. 22 p2884 A73-42323

Time, space, and energy management in the airways traffic control medium. 22 p2884 A73-42324

Flow control concepts and airline operations. 22 p2884 A73-42522

Estimation of general aviation air traffic. [ASCE PREPRINT 2041] 22 p2839 A73-42866

GASP simulation of terminal air traffic system. [ASCE PREPRINT 2059] 22 p2839 A73-42868

NAFEC test facilities. 23 p2966 A73-44063

Aviation law development regarding ATC influence on legal liability for aircraft accidents, analyzing controller error influence on liability determination 24 p3159 A73-45444

AIR TRANSPORTATION

Low noise STOL aircraft as solution for short haul transportation, discussing German, British and Swedish industrial development efforts 01 p0004 A73-10468

Monopoly, concentration, and competition in the air transportation industry of the United States 01 p0124 A73-10568

The technical evolution of air transport in the seventies - European contribution to this evolution 02 p0238 A73-11702

Rigid airships as versatile and ecologically clear STOL aircraft, discussing computerized structural analysis, nuclear propulsion and radar guidance systems 02 p0131 A73-12596

Airlines passenger transportation profitability, discussing relationships between service quality, load factor and operating costs 03 p0400 A73-13575

Airship design for short-medium distance heavy payload transport, describing honeycomb skin construction, power plant installation and hovering loading/unloading operations 04 p0405 A73-14825

Air transportation system planning - Progress in noise reduction. 04 p0406 A73-14895

Book - The local service airline experiment. 05 p0534 A73-16360

European regional airports planning for short haul point-to-point air transport and international airports congestion alleviation 05 p0562 A73-16565

Prototype development for Army personnel and equipment airborne mobility, considering various aircraft conceptual designs feasibility relative to logistics requirements [SAE PAPER 720846] 05 p0534 A73-16658

Air transportation systems problems - The airport operators' view. [AIAA PAPER 73-6] 06 p0683 A73-17602

Long range air transportation technical and economic future prospects, discussing passenger and cargo developments, noise reduction and SST technology [AIAA PAPER 73-14] 06 p0646 A73-17607

Supersonic transportation inauguration by Concorde, discussing technological, economic and environmental aspects [AIAA PAPER 73-16] 06 p0646 A73-17609

Review of New York Airways helicopter operations. [AIAA PAPER 73-25] 06 p0647 A73-17614

Economic performance and cost problems in civil air transport maintenance and engineering quality control related to selling price trends 06 p0647 A73-17888

VTOL aircraft and short-haul transportation. 06 p0648 A73-18150

Air-terminal queues under time-dependent conditions. 07 p0850 A73-20375

Russian book on passenger aircraft and air transport design covering technical and economic efficiency, airbus concept, weight and size problems and aft-mounted engine design 07 p0777 A73-20377

Monograph - System analysis of the air-ground transportation interface problem at Bangkok International Airport. 07 p0808 A73-20382

Mass air transportation development in Sweden, discussing flight scheduling, fare structure and quiet STOI aircraft introduction in 1980s 07 p0778 A73-20618

Benefit-cost analysis of delay reduction with STOL. [ASCE PREPRINT 1507] 08 p1025 A73-21000

Co-existence of scheduled and charter services in public air transport. 09 p1168 A73-23123

Short haul air travel with Intermodal Automated Transfer system for integrating ground transportation to allow passenger to stay in seat from origin to destination 10 p1174 A73-23653

Productivity estimates of the strategic airlift system by the use of simulation. 10 p1297 A73-23774

Commercial air transportation projections, discussing mass transportation, international fare structure and exchange of rights, security and technology 10 p1298 A73-24646

Russian book - Network planning and control of air transportation. 10 p1298 A73-24924

Dusseldorf airport passenger terminal facilities project, considering handling capacity, building and wide bodied jet traffic requirements

11 p1343 A73-25206

Malmo-Sturup airport facilities layout, discussing passenger terminal, lounges, baggage and cargo handling, ATC school, etc

11 p1343 A73-25207

Regularization of the legal status of international air charter services.

11 p1454 A73-26349

Cargo air transport means selection procedure, suggesting methods for economic evaluation of time savings

12 p1560 A73-27066

Methodologies for the analysis of transport requirements with particular regard to the aeronautical case

12 p1561 A73-27070

Air transportation direct and indirect costs analysis, considering cruising speed, flight time, aircraft design and manufacture and fuel expenses

13 p1569 A73-28950

Airports: Challenges of the future; Proceedings of the Airports Specialty Conference, Dallas, Tex., March 7-9, 1973.

13 p1598 A73-29101

Projections of the U.S. airline fleet in the early 1980's.

13 p1569 A73-29102

Role of the air line pilot in air transportation.

13 p1570 A73-29105

Status of short haul air transportation.

13 p1570 A73-29108

Central regional airport planning, compatibility and construction/operational costs for freight/passenger transport service in response to future economic growth

13 p1598 A73-29109

Air transport and commercial aviation developments, including revenues, passenger traffic statistics, charter flights and fare levels

13 p1709 A73-29383

Legal consequences resulting from transportation in airline traffic in the case of missing, deficient or not coverage-equivalent contractual basis

14 p1818 A73-30293

Commercial air transportation in France - National administration and aviation enterprises

14 p1818 A73-30294

Book - International bibliography of air law 1900-1971.

14 p1818 A73-30362

Subgrade strengthening of existing airfield runways.

15 p1856 A73-31388

Dallas/Fort Worth airport layout and facilities, describing runway arrangement, passenger, baggage and cargo services, access roads and internal transportation system

15 p1858 A73-32362

STOL operational impact on ATC system support, considering short haul metropolitan and rural transportation modes, landing/takeoff facilities and all-weather operational reliability

15 p1831 A73-32547

Air cargo transportation growth since 1945 with comparison to concurrent air passenger evolution, predicting future trends

15 p1859 A73-32555

International regional rental system for air transportation ground installations and route services, discussing ICAO recommendations

16 p2087 A73-32971

Charters, the new mode - Setting a new course for international air transportation.

16 p2087 A73-33101

Anglo-American Aeronautical Conference, 13th, London, England, June 4-8, 1973, Proceedings.

16 p1968 A73-33176

Canadian air transportation survey, outlining history of other modes, transportation investment trends, modal traffic distribution, STOL applications, airline social services and marketing

16 p2087 A73-33177

Short haul V/STOL air transportation social and economic aspects in comparison with ground transportation modes, emphasizing convenience and frequency of service

16 p2088 A73-33193

City center heliport design and location for scheduled intercity helicopter services, discussing terminal facilities, economic factors, elevated sites, etc

17 p2146 A73-34444

Helicopters for business executive transport between cities or to isolated locations, police use, ambulance service, etc

17 p2256 A73-34445

Ground and air transportation noise propagation and effects, including aircraft engines, airfoils, sonic booms, auto traffic, railroads, subways, seismic noise and vibration

17 p2100 A73-34460

The financing of essential communication, navigation and terminal aids.

17 p2257 A73-34535

Airtransit - The Canadian demonstration interurban STOL service.

[SAE PAPER 730356] 17 p2103 A73-34704

The possible future of air transport and the airports

17 p2148 A73-35665

Air-transport, a main cause of smallpox epidemics today.

18 p2283 A73-36791

Aircraft with air cushion landing system for off airport transport of goods and passengers

19 p2417 A73-37679

ACLS equipped vehicles in inter-city transportation.

19 p2381 A73-37686

Area navigation technology for air transportation in USA, discussing present systems and projections as related to airline and FAA activities

19 p2451 A73-37807

Air transportation economic efficiency as function of fuel consumption, cruising flight speed, altitude range and load factor /payload/

19 p2506 A73-38118

U.S.S.R. laws and regulations regarding civil air transport equipment operations and maintenance, considering personnel training and safety

19 p2435 A73-38119

Calculation of the plan for the transportation performance with the aid of electronic data processing

19 p2506 A73-38121

Aircraft noise consideration for environmental compatibility, airport development, short haul and supersonic air transport and legislation and regulation problems

[AIAA PAPER 73-795] 19 p2387 A73-38368

Maximum air transportation service with minimum community noise.

[AIAA PAPER 73-796] 19 p2388 A73-38369

Rocket vehicle concepts for global transport application, discussing space shuttle technology use, commercial markets, international fleets, single stage feasibility, etc

[AAS PAPER 73-163] 20 p2613 A73-38600

Aircraft ground station site evaluation based on disseminating time synchronization effectiveness, utilizing computer modeling for communication links and airspace population

21 p2734 A73-40033

Russian book - Economic efficiency and planning of air freight transportation.

21 p2793 A73-41294

Europlane QSTOL economical solution to noise and congestion problem in short and medium haul transport

22 p2798 A73-41862

Land-air-sea intermodal cargo container movement procedures and equipment design standardization to meet air transportability requirements

[ASME PAPER 73-ICT-30] 23 p2965 A73-43493

Public air transportation service needs for nonurban areas, considering low traffic density problem, operational requirements and future trend

[ASME PAPER 73-ICT-72] 23 p3050 A73-43498

Short takeoff and landing /STOL/ aircraft technology developments for high density air transport, discussing lift system, handling, airfoil design, acoustics and operating economics

23 p2940 A73-43520

Dirigible airship design, operations, payloads, cargo transportation and surveillance applications

23 p2940 A73-44223

The transatlantic charter policy of the United States.

24 p3158 A73-44575

AIR WATER INTERACTIONS

The spectral density technique for the determination of eddy fluxes.

01 p0072 A73-10145

Numerical simulations of the tropical air-sea planetary boundary layer.

01 p0073 A73-10496

Precipitation detection over the ocean using microwave satellite radiometry.

02 p0188 A73-12268

Some evaluations of drag and bulk transfer coefficients over water bodies of different sizes.

06 p0720 A73-18328

Macroscale interaction between the atmosphere and oceans and the role of the latter in the formation of anomalous circulation in the stratosphere

10 p1246 A73-24374

Oceanographic satellite capabilities, considering sea-air interactions, currents, upwellings, deep sea tides, sea-earth interactions and water mass identification

[AAS PAPER 73-145] 20 p2550 A73-38594

The specific ozone destruction rate of the ocean surface and its dependence on horizontal wind velocity.

23 p2974 A73-43867

AIRBORNE EQUIPMENT

NT AIRBORNE/SPACEBORNE COMPUTERS

An airborne instrument system for atmospheric boundary-layer research.

01 p0073 A73-10498

Compact laser radar for remote atmospheric probing.

01 p0060 A73-11059

Computerized airborne multilateration radar with wide-beam antenna and narrow pulsewidth for high resolution terrain image mapping

01 p0019 A73-11479

Feasibility model of airborne ac synchronous generator with rotating superconducting field winding, comparing predicted performance, size and weight with conventional technology

02 p0131 A73-11827

Airborne radar set for weather surveillance, independent landing monitoring, ground visualization and collision avoidance

02 p0190 A73-11854

Onboard ILS equipment reliability in integrated airborne all-weather landing system

02 p0190 A73-11855

Upward short wave radiation polarization characteristics observation by airborne polarimeter over grey sand desert, dense altocumulus liquid drops and cumulonimbus clouds and seas

02 p0169 A73-12269

Use of airborne radar to evaluate hurricane modification experiments.

03 p0338 A73-14513

An airborne Ka-band microwave radiometric measurement mapping system.

04 p0451 A73-15783

Airborne synthetic aperture /hologram/ radar maximum ambiguity range extension by using additional receive-only antenna ahead of transmit-receive unit

05 p0577 A73-16817

Synthetic aperture SLAR systems and their application for regional resources analysis.

05 p0578 A73-17133

Ground based and airborne collision avoidance systems comparison, discussing interrogator/transponder concept, pilot warning indicator, and air traffic handling capacity and economics

07 p0848 A73-18900

Reliability tests on fire control airborne radars prototypes, measuring MTBF

07 p0800 A73-19416

Compact laser radar probes the upper atmosphere.

07 p0834 A73-19573

Minimum performance standards - Airborne distance measuring equipment /DME/ operating within the radio-frequency range of 960-1215 megahertz.

07 p0849 A73-19575

High resolution spectra of the stratosphere between 30 and 200/cm.

08 p0961 A73-21533

Analysis and interpretation of air-borne multifrequency side-looking radar sea ice imagery.

09 p1080 A73-22150

Airborne photogrammetric system with mapping and geodetic surveying data acquisition capability, discussing inertial navigation subsystem, terrain profile recorder and electronic distance measuring equipment

09 p1081 A73-22380

Airborne visible laser optical communication experiment between high altitude aircraft and ground station, discussing tracker-transmitter equipment and atmospheric effects on performance

09 p1055 A73-23395

Method of calculation of radioelectric performances of airborne radomes

11 p1327 A73-25282

Influence of fabrication inaccuracies on the axis deviation of an airborne radome

11 p1328 A73-25295

Infrared detection techniques for space research; Proceedings of the Fifth ESLAB-ESRIN Symposium, Noordwijk, Netherlands, June 8-11, 1971.

11 p1367 A73-26501

Airborne IR 32 cm observatory, discussing atmospheric transmission and guiding methods to overcome aircraft instability effects

11 p1368 A73-26503

Piston engine or turboprop aircraft photography, measuring camera vibration components in roll, pitch and yaw by flashing light technique for image quality improvement

12 p1500 A73-27954

Airborne fire protection equipment.

13 p1568 A73-28171

Echo signal spectral compression in airborne FM Doppler radar measurement, allowing for flight trajectory and target surface characteristics

13 p1584 A73-28889

VLF/Omega digital airborne area navigation system evaluation tests, discussing transmitting stations and system performance

13 p1656 A73-28904

Michelson shearing interferometer with piezoelectric scanner for atmospheric optical mean transfer function measurements from airborne platform, using laser or white light sources

13 p1621 A73-29332

Megawatt fuel cells for aerospace applications.

13 p1573 A73-29597

The role of the airborne traffic situation display in future ATC systems.

14 p1773 A73-29897

Russian book on aeronautical electric and electronic materials covering physicochemical properties of magnetic, dielectric, conductor, semiconductor, polymer, ferritic, thin film and composite materials

14 p1766 A73-30357
Predicting descent rate for aircraft parachute flares. [AIAA PAPER 73-482] 15 p1829 A73-31464

Development and testing of ballute stabilizer/decelerators for aircraft delivery of a 500-lb munition.

[AIAA PAPER 73-485] 15 p1829 A73-31467
HTS spectrometer for airborne infrared astronomy. 15 p1880 A73-32379

ARINC-573 recording system - Application to maintenance

15 p1883 A73-32462
French civil aviation inexpensive C band landing system with ILS angular coding and simplified onboard equipment for STOL and Alpine airports

15 p1910 A73-32467
Analysis of the reliability of airborne material in an airline company - Objectives and methods

15 p1831 A73-32495
All-weather landing technology and economics, considering ground and airborne equipment and benefits and costs

15 p1859 A73-32553
Airborne mechanical system for sounding rocket experiments.

16 p2072 A73-33119
Vibration and shock qualification testing of an airborne early warning radar.

16 p1987 A73-33137
Avionics systems simplification for cost, weight and space reduction, considering ease of maintenance, failure points reduction and flight director/autopilot computers and couplers elimination

16 p1968 A73-33187
WB-57F aircraft with instrument package for nuclear test detection and upper atmosphere research, discussing range, altitude, speed, payload capacity and onboard equipment

[AIAA PAPER 73-510] 16 p1969 A73-33548
Airborne air to air and air to ground fire control radar systems for all-weather fighter aircraft, emphasizing cost effectiveness through modularity and commonality

16 p1985 A73-34041
Book - Recommended basic characteristics for airborne radar homing and alerting equipment for use with emergency locator transmitters /ELT/.

17 p2207 A73-34475
Digital synchronization of synchronous collision prevention systems in aviation

17 p2207 A73-34480
Nitric oxide detection in stratosphere from characteristic absorption line spectrum via airborne IR spectrometer, obtaining molecular concentration

[ONERA, TP NO. 1256] 17 p2159 A73-34552
Turbo and jet powered general aviation aircraft-borne weather/visibility memory radar system with digital processing technique to eliminate direct view storage tube

[SAE PAPER 730316] 17 p2122 A73-34674
A scheme for estimating aircraft velocity directly from airborne range measurements.

17 p2209 A73-34873
Digitally integrated cockpit simulation facility for display systems and avionics to plan mission/human program and airborne equipment requirements

17 p2139 A73-35236
Features of a high voltage airborne superconducting generator.

17 p2109 A73-35254
Broadband TWT microwave amplifier failure modes in airborne systems related to physical mechanism, fabrication processes and field operator handling

17 p2140 A73-35259
Remote sensing technology - The 24-channel multispectral scanner.

17 p2171 A73-35365
New algae mapping technique by the use of an airborne laser fluorosensor.

17 p2163 A73-35412
Airborne passive IR line scanner, noting spectral resolution and thermal sensitivity for land and water surfaces energy

17 p2174 A73-35577
A flowmeter to measure cloud liquid content.

17 p2174 A73-35578
Testing and calibration of aircraft sensors and systems.

17 p2174 A73-35580
Sabreliner Airborne Data Acquisition and Recording System /ADARS/ for communication with flight observers to evaluate research missions

17 p2174 A73-35582
Oil spills - Measurements of their distributions and volumes by multifrequency microwave radiometry.

17 p2164 A73-35806
Cosmic rays airborne dosimetry from Concorde aircraft, noting passenger and crew radiobiological hazards at supersonic flight altitudes

18 p2348 A73-36908
Airborne IRP alignment using acceleration and angular rate matching.

19 p2386 A73-38048
Airborne multimode radar digital data system using high transfer rate magnetic tape recording, discussing 8 track tape storage capacity, coding and logic circuits

19 p2431 A73-38198
Modular airborne video tape recording systems using wideband frequencies, describing wideband channels, power supply, transport unit, servo module and bit storage rates

19 p2431 A73-38199
The use of remote sensing in the USSR for the study of natural resources.

[AAS PAPER 73-115] 20 p2520 A73-38579
Management looks at the Canadian program of remote sensing, phase I, 1971-1975.

[AAS PAPER 73-129] 20 p2521 A73-38587
Airborne digital data link terminal for commercial airlines' use.

20 p2526 A73-38756
Ground based and airborne microwave radiometer imaging techniques for surface mapping and atmospheric investigations, discussing self calibration, antennas, waveforms and aircraft nose instrumentation

20 p2567 A73-39838
Remote sensing of atmospheric O3 and H2O to 70 km by aircraft measurements of radiation at 1.64 mm wavelength.

20 p2557 A73-39855
Airborne remote sensing of cloud particle size and shapes via IR polarimeter, obtaining polarization vs phase angle curve for thick tropical cirrus clouds

20 p2567 A73-39838
Salinity surveys using an airborne microwave radiometer.

20 p2558 A73-39865
Midair collision avoidance strategies for ATC improvement, discussing relative effectiveness of structural airspace, airborne and ground-based systems based on US statistics

21 p2733 A73-40030
Solar eclipse of 10 July 1972 observed by visual and photographic method from aircraft, taking into account coronal structure

21 p2767 A73-40565
Development programs status report on airborne planar, conforal and distributed aperture phased array antennas for use in radar and communication systems

21 p2662 A73-40646
A goniometer for use with high-frequency circularly disposed aerial arrays.

21 p2703 A73-41207
Microwave radiometric systems.

22 p2859 A73-42059
Airborne IR spectrometer with solar sensor for stratospheric minor molecular constituents vertical distribution, indicating spectral resolution for vibrational-rotational absorption bands

[ONERA, TP NO. 1216] 22 p2847 A73-42221
High power airborne radar CW tube-transmitter interface failures due to design, maintenance, handling and environment effects

22 p2834 A73-42875
Instrumentation for remote sensing solar radiation from light aircraft.

22 p2864 A73-43161
Polarization - A key to an airborne optical system for the detection of oil on water.

23 p2979 A73-43225
Land-air-sea intermodal cargo container movement procedures and equipment design standardization to meet air transportability requirements

[ASME PAPER 73-ICT-30] 23 p2965 A73-43493
AIRBORNE TERRAIN ANALYSIS

U TERRAIN ANALYSIS
AIRBORNE/SPACEBORNE COMPUTERS

Real-time computer for monitoring a rapid-scanning Fourier spectrometer.

01 p0020 A73-11231
Contributions to the standardization of control systems for satellites and peak payloads

02 p0228 A73-11705
Spacecraft digital attitude control.

04 p0504 A73-14736
Airborne associative parallel array digital computer built with MOS LSI technology for size and weight reduction, discussing design and applications

04 p0424 A73-15065
An autonomous navigation technology system.

04 p0474 A73-15274
The Mariner Venus Mercury flight data subsystem.

04 p0425 A73-15423
Problems of the synthesis of spacecraft onboard data computation units

05 p0553 A73-16417
Design of a fault-tolerant, modular computer with dynamic redundancy.

06 p0671 A73-18064
Telemetry data acquisition, transmission lines and delayed time processings onboard spacecraft and at

ground receiving stations and center, discussing multiplexing and computer control

07 p0795 A73-18953
Circuit design, manufacture and testing of static memory for D2 satellite computer, considering test equipment, quality control and fabrication

07 p0796 A73-18958
Design, manufacture and performance of Eole satellite computer core memory, noting circuit reliability and testing

07 p0796 A73-18959
Mechanical and electrical performance of satellite-borne magnetic tape recording system for computer data storage in radio telemetry

07 p0820 A73-18960
Russian book - Dynamics of rocket control systems with onboard digital computers.

07 p0906 A73-20229
Computer-controlled software diagnosis of an airborne computer.

08 p0940 A73-20677
Autonomous power subsystem design for an Outer Planet Spacecraft.

09 p1154 A73-22805
A digital attitude control system for orientation of rocket launched scientific payloads.

[AIAA PAPER 73-292] 09 p1116 A73-23211
The introduction of a digital computer on board ESRO scientific satellites.

09 p1061 A73-23378
Contributions to the design of future on-board data processing systems for scientific space-craft experiments.

09 p1061 A73-23379
Megabit capacity ferrite core memories for scientific satellites, using three dimensional organization with pulse program adapted for buffer application

09 p1087 A73-23426
Role of static electricity in the incidents recorded during the F11 firing

[ONERA, TP NO. 1214] 10 p1285 A73-23750
LSI computer design and fabrication for Space Ultrareliable Modular Computer Demonstration Vehicle, discussing assembly, physical and electrical characteristics and electronic testing procedures

10 p1191 A73-23794
Complementary MOS LSI microprogrammed digital computer design, for Space Ultrareliable Modular Computer Demonstration Vehicle, discussing instruction operation codes, I/O peripherals and software support

10 p1191 A73-23795
Apollo LM guidance computer software for the final lunar descent.

10 p1247 A73-24548
Figure of merit for fault-tolerant space computers.

10 p1192 A73-24870
Explanation of the accident to the Europa II F11 launcher by phenomena of electrostatic origin

11 p1431 A73-25749
Fault-tolerance in the modular spacecraft computer.

12 p1475 A73-27130
Dynamic characteristics, stability and steady state accuracy for orbital gyroscope with digital control, noting bit density requirements of onboard computer

12 p1523 A73-27632
Redundant central processor system for fault tolerant real time operation in space applications, describing systems organization

[AIAA PAPER 73-424] 12 p1476 A73-27821
Optimal aircraft go-around and flare maneuvers.

13 p1657 A73-29217
Design considerations for shuttle information management.

14 p1818 A73-29945
Hardware integration and improved operation of the flight control system.

14 p1713 A73-30932
Area navigation computer TCF-71 A system, discussing central control display and data entry units, inputs/outputs and operating modes

15 p1909 A73-32455
Minicomputer application to in-flight control of A300-B Airbus engines, describing computational procedure for low pressure compressor stage RPM limit /N1 limit/

15 p1831 A73-32477
Operational readiness and maintenance testing of the B-1 strategic bomber.

16 p1969 A73-33631
Development of a low-cost flight director system for general aviation.

[SAE PAPER 730331] 17 p2167 A73-34684
Integrated Propulsion Control System program.

[SAE PAPER 730359] 17 p2222 A73-34707
Military aircraft onboard Digital Avionics Information System for computerized integration of navigation, guidance, weapon delivery, cockpit display, communication, flight control and energy management

17 p2136 A73-35202
Digital avionics systems software development trends, considering compatibility and cost problems in increased use of complex processing hardware, sensors and displays

17 p2137 A73-35203

- Aircraft onboard computerized avionics and electrical systems architecture for information flow and control with maximum efficiency, flexibility, modularity and minimum maintenance
17 p2137 A73-35204
- Unconventional digital avionics black box approach for cost reduction and reliability improvement in terms of packaging, component coding and hardware qualification programs multiplicity
17 p2137 A73-35205
- Strapdown air navigation with dry inertial instruments and high speed general purpose digital computer predicting system performance by position error analysis
17 p2210 A73-35211
- LN-33 airborne inertial navigation system with low cost precision instruments and miniaturized digital computer, noting built-in calibration and test capability for minimizing maintenance
17 p2210 A73-35212
- Low cost data processor and display for ICNI, DME/TACAN, LORAN or range/range difference radio navigation systems in aerospace applications
17 p2210 A73-35213
- Digital fly by wire flight control system with airborne digital processor for increased aircraft survivability, determining redundancy level to satisfy system performance
17 p2138 A73-35222
- Aerospace multiprocessor for A-7D aircraft digital fly by wire flight control, discussing design requirements, software development and reliability
17 p2107 A73-35223
- Modular MOS LSI digital data bus system design for integrated avionics and remote sensors interconnection in aerospace vehicles
17 p2139 A73-35232
- Digital step transform for airborne radar linear FM signal pulse compression, reducing data memory requirements
17 p2123 A73-35237
- B-1 aircraft electrical multiplex system.
17 p2110 A73-35309
- Optical data storage and data processing, and holography in aerospace and electronic instrumentation.
17 p2131 A73-35382
- Word length problems in the on-board computer implementation of digital flight control systems.
17 p2145 A73-35384
- Algorithm construction for the stabilization of a deformable spacecraft using an onboard digital computer
18 p2359 A73-36105
- Strap-down inertial guidance systems study.
18 p2335 A73-36955
- Autonomous satellite navigation - An historical summary and current status.
19 p2452 A73-38056
- System error analysis and algorithms for a strap-down navigation system.
19 p2452 A73-38058
- Failure detection and isolation methods for redundant gimbal inertial measurement units.
20 p2585 A73-38790
- [AIAA PAPER 73-851]
20 p2585 A73-38790
- Synthesis of digital filters for the control of short periodic angular oscillations of aerospace vehicles.
21 p2780 A73-40326
- Mathematical model of spacecraft onboard digital guidance computer under data acquisition conditions, using imbedded Markov chains
23 p2955 A73-43261
- Attitude control for the Netherlands astronomical satellite /ANS/.
24 p3144 A73-45558
- ### AIRCRAFT ACCIDENT INVESTIGATION
- In-flight structural failures involving general aviation aircraft.
02 p0131 A73-12566
- Identifying pilot error potential in the F-4 aircraft.
05 p0545 A73-16731
- Discovery procedures in aircraft accident litigations, considering questions of privileged material, relevancy and attorneys work product
06 p0770 A73-17511
- An international review of civil aircraft damaged or destroyed by deliberate detonation of explosives /sabotage/ 1964-1972.
10 p1176 A73-24708
- Aircraft design and reliability analysis method based on accidents occurrence investigation by Franco-British airworthiness authorities, noting applicability to Concorde aircraft
11 p1306 A73-26589
- Protective helmets performance evaluation for design optimization, considering failure analysis from aircraft accident reports
16 p1973 A73-32655
- Injuries induced by high speed ejection - An analysis of USAF noncombat operational experience.
16 p1966 A73-32664
- Light aircraft vertical gust induced structural failures, analyzing 1960-71 accident reports for injuries biomechanics and environmental conditions
16 p1967 A73-32678
- Dynamic behavior of light aircraft interaction with jet transport vortex on basis of accident records and computer simulation
17 p2094 A73-34660
- [SAE PAPER 730296]
17 p2094 A73-34660
- Pilot error evaluation in aircraft accidents, discussing human failure factors and flight and cockpit voice recorder evidence
17 p2115 A73-34748
- Results of carbon monoxide poisoning checks following aviation accidents or incidents in the French Army
18 p2285 A73-36929
- Symposium on International Aircraft Accidents Investigation, London, England, January 15, 1973, Proceedings.
19 p2505 A73-37736
- International Civil Aviation standards concerning rights and duties of appointed observers at inquiry by state of aircraft accident occurrence
19 p2505 A73-37737
- ICAO meeting reports on international aircraft accident investigation, onboard data recording, inquiry process and low-safety interface
19 p2506 A73-37738
- Annex 13 and the work of the aviation pathologist - Practical problems.
19 p2398 A73-37739
- Annex 13, sabotage and malicious acts against aircraft - Practical problems.
19 p2506 A73-37740
- Systems for collision avoidance - An overview.
19 p2453 A73-38467
- Corporate aircraft accident analysis to reduce accident rate, examining seasonal and diurnal statistics, aircraft types, runway conditions, crew factors and maintenance defects
20 p2509 A73-39219
- Barotrauma in United States Air Force accidents/incidents.
21 p2645 A73-41160
- ### AIRCRAFT ACCIDENTS
- International convention on damage caused by aircraft concluded 1952 in Rome, proposing revision to include damages before takeoff, after landing and during flight
01 p0124 A73-10566
- Pilot incapacitation as cause of aircraft accidents, noting age connected cardiovascular disease as leading cause for loss of pilot license
01 p0013 A73-11238
- Age control evaluation of Buna N elastomers by ANA Bulletin 438, using shelf aging and crashed aircraft case studies
03 p0331 A73-13026
- Personal life changes and health stresses in contrast to accident proneness as factors in pilot error
05 p0545 A73-16732
- Choice of law - Mass disaster cases involving diversity of citizenship.
06 p0770 A73-17510
- Discovery procedures in aircraft accident litigations, considering questions of privileged material, relevancy and attorneys work product
06 p0770 A73-17511
- Counterclaims, cross-claims and impleader in federal aviation litigation.
06 p0770 A73-17512
- Significant elements of an effective search, rescue, and survival system.
10 p1176 A73-24712
- Aircraft and ground equipment damage during ground handling operations, discussing repair costs and out-of-service time
10 p1176 A73-24715
- Weather condition caused aircraft accident avoidance, considering meteorological factors of air temperature, humidity, cloud formation, fog, haze, precipitation and visibility deterioration
13 p1568 A73-28554
- Aircraft accident prevention problems, considering pilot judgement errors, factory skill degradation, training, lightning and structure factors and air bag use
13 p1570 A73-29349
- Behavioral stress response related to passenger briefings and emergency warning systems on commercial airlines.
16 p1965 A73-32660
- Ventilated wet suit for naval aircrews protection against water exposure in aircraft accidents, describing neoprene foam and nylon liner construction with air ventilation
16 p1974 A73-32672
- Airplane accident survival, discussing cabin safety, fire protection, crashworthiness, emergency evacuation and crash landing in water
17 p2097 A73-34079
- The effects of fatigue on health and flight safety.
17 p2113 A73-34080
- Low level wind shear and clear air turbulence effects on flight safety and aircraft accidents
17 p2098 A73-34084
- Digital synchronization of synchronous collision prevention systems in aviation
17 p2207 A73-34480
- Aircraft crash injury reduction through seat and restraint design, discussing dummy size considerations, seat belts, aircraft acceleration and injury types
17 p2114 A73-34655
- [SAE PAPER 730290]
17 p2114 A73-34655
- FAA General Aviation Crashworthiness Program.
17 p2257 A73-34657
- [SAE PAPER 730293]
17 p2257 A73-34657
- A consistent crashworthiness design approach for rotary-wing aircraft.
17 p2106 A73-35094
- [AHS PREPRINT 781]
17 p2106 A73-35094
- Seminar on Accident Analysis and Prevention, Beirut, Lebanon, June 26-28, 1973, Working Documents.
18 p2268 A73-36845
- Aircraft accident statistics for passenger fatalities, worldwide jet hull losses and estimated costs to suggest proposals for approach, landing and takeoff accident reduction
18 p2268 A73-36846
- Engraved foil, photographic and EM flight recorders in aircraft accident investigations, discussing readout, processing and analysis
18 p2317 A73-36848
- Hepatic lesions observed among flight crews following aviation accidents
18 p2279 A73-36933
- Severe intraabdominal injuries without abdominal protective rigidity after an air crash - Seat belt injury
20 p2517 A73-39209
- Crew discipline factors in aircraft accident statistics, linking pilot-related accidents to crew carelessness, flight regulation infractions and unfamiliarity with flight conditions
20 p2509 A73-39216
- Reducing approach and landing accidents.
22 p2799 A73-42523
- Aviation law development regarding ATC influence on legal liability for aircraft accidents, analyzing controller error influence on liability determination
24 p3159 A73-45444
- ### AIRCRAFT ANTENNAS
- Influence of the nonidentity of the antennas of a Doppler speed meter on the accuracy of its operation
10 p1195 A73-24386
- Flush mountable elliptically polarized low silhouette blade antenna for aircraft, describing polarization and radiation characteristics
12 p1478 A73-27043
- Factors relating to the choice of antenna characteristics for the aircraft terminal in an aeronautical satellite communications/surveillance system.
12 p1471 A73-27654
- The disc antenna - A possible L-band aircraft antenna.
12 p1471 A73-27655
- A radiating element giving circularly polarised radiation over a large solid angle.
12 p1471 A73-27656
- An analysis of helicopter rotor modulation interference.
15 p1843 A73-31731
- Light aircraft-borne low cost phased array X band radar and display design requirements for weather detection and ground mapping
15 p1909 A73-32451
- French VOR system with single type equipment for operation on site at performance levels to meet ICAO standards, emphasizing antenna design
15 p1909 A73-32453
- Nonimage glidepath antenna design for ILS system within international civil aviation convention specifications
15 p1909 A73-32463
- Electronic location finder radio antenna homing system for helicopter search and rescue of downed air crewmen
17 p2116 A73-35061
- [AHS PREPRINT 720]
17 p2116 A73-35061
- Radio noise from towns - Measured from an airplane.
19 p2404 A73-37675
- UHF airborne antenna diversity combiner for signal reception using correlation technique for phase variation removal to improve SNR and gain
20 p2523 A73-38725
- A single-plane electronically scanned antenna for airborne radar applications.
21 p2653 A73-40684
- Physical design considerations for airborne electronic-scanning antennas.
21 p2654 A73-40685
- Antenna radiation-pattern measurement using model aircraft.
22 p2831 A73-41841
- ### AIRCRAFT APPROACH INSTRUMENTS
- #### U APPROACH INDICATORS
- #### AIRCRAFT APPROACH SPACING
- Recent advances in aircraft noise reduction.
13 p1570 A73-29104
- Aircraft terminal approach and entry spacing systems supported by automated terminal radar using area navigation techniques
17 p2210 A73-35852
- Metering and spacing with computerized ARTS III ATC system, discussing display for heading, speed and altitude commands
19 p2453 A73-38462

- Discrete address beacon system (DABS) data links and digital communication between ground based ATC computer and aircraft for IFR-VFR conflict detection and safety separation 19 p2453 A73-38466
- AIRCRAFT BRAKES**
- NT LEADING EDGE SLATS
- NT TRAILING-EDGE FLAPS
- NT WING FLAPS
- Speed brake in carbon fibre composite construction. 03 p0393 A73-13920
- Transport aircraft wheels and brakes operational cost minimization, discussing contributory roles of governmental regulations /FAA/, aircraft manufacturer, supplier and user [SAE PAPER 720867] 05 p0534 A73-16650
- Aircraft antiskid system technical history and evolution, presenting frequency response of three-way configuration [SAE PAPER 720868] 05 p0534 A73-16651
- Optimization of commercial transport airplane stopping systems. [SAE PAPER 720872] 05 p0535 A73-16671
- Aircraft brake design and materials, considering thermal, mechanical, friction and wear characteristics of Be, steel, graphite and carbon composites 08 p0928 A73-21688
- Design and simulation of an aircraft brake using a digital computer. 13 p1588 A73-29385
- Russian book - Aircraft wheel and braking system designs. 19 p2384 A73-37768
- Design and development of lightweight wheel braking equipment. [SAE PAPER 995] 19 p2434 A73-37894
- AIRCRAFT BREATHING APPARATUS**
- U BREATHING APPARATUS
- AIRCRAFT CABINS**
- U AIRCRAFT COMPARTMENTS
- AIRCRAFT CARRIERS**
- Suitability of the CL-84 tilting aircraft for the sea control ship system. [SAE PAPER 720852] 05 p0534 A73-16660
- Harrier trial operations onboard Sea Control Ship /SCS/ U.S.S. Guam as model for future V/STOL aircraft-aircraft carrier systems [SAE PAPER 720853] 05 p0534 A73-16661
- Full-scale fire tests on a simulated aircraft carrier flight deck. [WSCI PAPER 72-31] 05 p0639 A73-16684
- V/STOL aircraft testing for the sea control ship environment. [AIAA PAPER 73-810] 19 p2379 A73-37466
- The Navy SETOLS program and its potential applications to Navy aircraft. 19 p2381 A73-37680
- Carrier landing simulation for pilot visual perception, describing Fresnel lens optical landing system, periscopes, cockpit equipment and glide paths. [AIAA PAPER 73-917] 21 p2634 A73-40865
- The transatlantic charter policy of the United States. 24 p3158 A73-44575
- AIRCRAFT COMMUNICATION**
- NT AERONAUTICAL SATELLITES
- Multisatellite systems for transoceanic aircraft communications and ATC, discussing day and night operations, cost-benefit optimization and adaptive techniques for capacity augmentation 01 p0018 A73-11201
- Ground reflection multipath effects on airborne communications. 04 p0422 A73-15439
- Mathematical model for multipath transmission in aircraft and spacecraft communications, presenting Bayes detector for binary PSK 04 p0422 A73-15462
- S-61N helicopter all-weather IFR operation for North Sea oil rigs supply and harbor pilots transportation, describing onboard instrumentation, navigation and communication systems 05 p0535 A73-16847
- AEROSAT - An aeronautical communications satellite for oceanic areas.** [AIAA PAPER 73-46] 06 p0771 A73-17624
- The Aeronautical Satellite Programme - ATC aspects. 07 p0848 A73-19141
- Satellite systems for mobile communications and surveillance; Proceedings of the International Conference, London, England, March 13-15, 1973. 12 p1471 A73-27652
- Factors relating to the choice of antenna characteristics for the aircraft terminal in an aeronautical satellite communications/surveillance system. 12 p1471 A73-27654
- The provision of ground station facilities for an aeronautical satellite system. 12 p1471 A73-27658
- The use of satellites for aircraft communications and air traffic control. 12 p1472 A73-27666
- Factors affecting the frequency chosen for aircraft to satellite communications. 12 p1472 A73-27667
- Message organisation in the ground segment of an aeronautical satellite system. 12 p1472 A73-27668
- Satellite communication channels assignment to ships and aircraft, considering automated digital calling method for ship-to-shore communication 12 p1472 A73-27670
- Satellite communication systems for long haul air transport operations, discussing political, operational/technical and economic problems 12 p1472 A73-27671
- Replacement of a system of aeronautical satellites. 12 p1549 A73-27678
- Balloon-aircraft ranging, data, and voice experiment. 12 p1473 A73-27680
- Overview - The role of communication systems in air traffic management. 14 p1725 A73-29876
- Historical development of the Air Traffic Control System. 14 p1772 A73-29877
- Formulation of the air traffic system as a management problem. 14 p1772 A73-29878
- ATC concepts and air/ground data link requirements for U.S. airspace structure in 1980s to support anticipated Los Angeles basin traffic densities in 1995. 14 p1772 A73-29879
- U.S. civil and military air-ground communications development history and expectations, considering information exchange, radar beacon transponders, digital communication and data links 14 p1725 A73-29880
- The development of the ATC radar beacon system - Past, present, and future. 14 p1725 A73-29881
- Bit synchronized discrete address radar beacon system with ground based U.S. civil interrogator complex for compatibility with ATC and aircraft operator services 14 p1772 A73-29882
- Operation of current navigation aids and future prospects. 14 p1773 A73-29883
- Ground communications networks for aeronautical operations. 14 p1740 A73-29885
- Oceanic ATC by application of aeronautical satellite technology, discussing system design requirements, performance evaluation and international program 14 p1773 A73-29888
- Military ATC systems and equipment in U.S. National Aviation System, discussing operations, organizational and facility interfaces, communications, navigation, and surveillance radar requirements 14 p1773 A73-29889
- Aeronautical communication technology for civil ATC system development through 1990s, discussing SNR design and need for radio channel models 14 p1725 A73-29890
- Aircraft-satellite multipath communication characteristics, considering surface scatter, ionospheric scintillation and refraction and tropospheric refraction and scatter 14 p1725 A73-29891
- Effect of multipath on ranging error for an airplane-satellite link. 14 p1725 A73-29892
- The use of specialized antenna technology for air traffic control and communications. 14 p1732 A73-29894
- Satellite-aircraft multipath and ranging experiment results at L band. 14 p1726 A73-29898
- An efficient multiplexing approach for adaptive aircraft communications via a relay satellite. 14 p1726 A73-29899
- Multibeam satellite Effective Isotropic Radiative Power /EIRP/ for aeronautical communications, discussing carrier-to-noise density increase and communication load per channel decrease 14 p1726 A73-29900
- Multipath propagation in aircraft digital communication with ground terminal, modeling received signal for detection and estimation theories applications 14 p1726 A73-29902
- Aircraft onboard data link and Aerosat equipment integration, considering antenna, duplexer, amplifier and receiver systems 15 p1846 A73-32428
- VOLMET transmission automation with the aid of the 'DECLAM' system using a speech synthesizer 15 p1846 A73-32429
- Optimal digital modulation techniques for aeronautical communications via satellite, considering air navigational systems for transoceanic flight 15 p1847 A73-32480
- Automation of the Yugoslav AFTN network and its future expansion 15 p1855 A73-32482
- Procedures and ground methods associated with the exploitation of a system of aeronautical satellites 15 p1911 A73-32488
- Aircraft safety engineering for air piracy prevention, discussing cockpit communication isolation from passenger compartment 16 p2087 A73-32662
- The financing of essential communication, navigation and terminal aids. 17 p2257 A73-34535
- Processing of aircraft data. 17 p2132 A73-35583
- Problems related to the operation of an air-ground data-link system 18 p2289 A73-36686
- Accurate aircraft trajectory predictions applied to future en-route air traffic control. 18 p2335 A73-37041
- Radiation pattern of a low-frequency beacon antenna located on a semi-elliptic terrain irregularity. 19 p2409 A73-37716
- NAS enroute automated flight and radar data processing, describing communication facilities, computer complex, software, data entry, display function and ATC personnel interface 19 p2453 A73-38464
- Adaptive multibeam concepts for traffic management satellite systems. 20 p2525 A73-38746
- Multipath channel characterization for Aerosat. 20 p2526 A73-38755
- Airborne digital data link terminal for commercial airlines' use. 20 p2526 A73-38756
- The universal data link system for air/ground communications. 20 p2526 A73-38757
- The ARINC plan for implementing air/ground DATALINK. 20 p2527 A73-38758
- ASTRO-DABS communication system with hybrid satellite and terrestrial discrete address beacon system for accurate aerial surveillance and navigation with reliable data link 20 p2527 A73-38759
- The utility of data link to military aircraft communication - An operational view. 20 p2527 A73-38760
- A rational basis for determining the EMC capability of a system. 20 p2528 A73-38770
- Aeronautical/maritime satellite borne two-way L-band transponder weight and power limitation effects on channel capacity 20 p2531 A73-39771
- Symposium on Electromagnetic Interference in Aircraft, London, England, February 15, 1973, Proceedings. 22 p2821 A73-41691
- Electromagnetic interference and compatibility control in aircraft communication, discussing RF current, voltage, impedance and SNR measurement techniques 22 p2821 A73-41692
- The susceptibility of modern aircraft instrument systems to interference in the HF band. 22 p2851 A73-41694
- Aircraft communication and electronic equipment design for interference control to meet electromagnetic compatibility specification requirements 22 p2821 A73-41695
- Electromagnetic compatibility specifications for aircraft communication and electronic equipment, discussing control and test plans, test facilities, cost effectiveness and British standard 22 p2821 A73-41696
- Electromagnetic compatibility program for modern aircraft communication and electronic equipment design, discussing control plan, interference specification, cable separation and final testing 22 p2821 A73-41697
- AIRCRAFT COMPARTMENTS**
- Aerial photograph distortion due to sealed compartment temperature and pressure effects in terms of internal refraction 06 p0693 A73-18156
- A study of Halon 1301 /CBRF3/ toxicity under simulated flight conditions. 09 p1045 A73-22537
- Commercial aircraft passenger cabins interior design, considering seating arrangements, cabin architecture and fittings, materials and color schemes and maintainability 10 p1183 A73-23687
- Optimal and preferred listening levels for speech in aircraft acoustical environments. 11 p1304 A73-25387
- Aircraft cabin altitude hypoxia effects on mother, embryo and fetus during first trimester of pregnancy in air hostesses and women passengers 14 p1718 A73-30519
- High altitude aircraft cabin pressurization for crews and passengers, discussing altitude tolerance, reaction times, decompression and oxygen equipment 14 p1723 A73-30937
- Aircraft safety engineering for air piracy prevention, discussing cockpit communication isolation from passenger compartment 16 p2087 A73-32662

Aircraft cabin noise reduction through composite material insulation, discussing engine noise sources, aircraft fuselage transmission loss characteristics, vibration damping and sandwich structures [SAE PAPER 730339] 17 p2102 A73-34690

Engineering design considerations in the noise control of commercial jet aircraft's vent and drain systems. 19 p2378 A73-37297

Dynamic buckling of an axially compressed cylindrical shell with discrete rings and stringers. 23 p3047 A73-44377

AIRCRAFT CONFIGURATIONS

Optimum configurations for bangless sonic booms. 01 p0031 A73-10302

Control configured vehicle (CCV) technology application for fighter aircraft combat control versatility enhancement, presenting F-4 analytical, simulation and wind tunnel test performance results [AIAA PAPER 73-160] 05 p0535 A73-16907

Research on future short-haul aircraft at the NASA Langley Research Center. 06 p0647 A73-17616

Preliminary design of the man-powered aircraft, Icarus. [AIAA PAPER 73-53] 06 p0647 A73-17629

AH-56A rigid rotor compound helicopter configuration and handling qualities under autorotation conditions, discussing flight test program, piloting descent performance 09 p1030 A73-22179

Dynamics of variable sweep wing aircraft in the course of changing geometry. 10 p1175 A73-24012

Active flutter suppression - B-52 controls configured vehicle. [AIAA PAPER 73-322] 11 p1305 A73-25552

Critique of paper on supersonic aircraft configuration with zero wave drag, discussing tubular outer structure and convergent-divergent inner duct 11 p1305 A73-25798

Swing wing - Modifications in variable geometry configuration concepts. 13 p1568 A73-28157

VFW 614 twin-jet short haul aircraft, discussing layout, auxiliary power supply system for ground handling independence, surface movements maneuverability and low noise characteristics 15 p1830 A73-32365

Automated prediction of light aircraft performance and riding and handling qualities. [SAE PAPER 730305] 17 p2101 A73-34666

Key factors in developing a future wide-bodied twin-jet transport. [SAE PAPER 730354] 17 p2103 A73-34702

The C-401, a STOL transport for many applications 17 p2107 A73-35666

V/STOL hydraulic controls including internal and external blown jet flap and augmentor wing, describing integrated flight control actuator packages and aircraft configuration 17 p2108 A73-35851

Computation of three dimensional flows about aircraft configurations. 18 p2259 A73-36158

Engine-over-the-wing noise research. [AIAA PAPER 73-631] 18 p2267 A73-36190

Review of current sonic boom studies. 18 p2267 A73-36393

Aircraft fuselage structure weight estimation method assuming bending, shear, torque and internal pressurization loading for skin-stringer-shallow frame types [SAE PAPER 981] 19 p2385 A73-37887

A computer-aided design procedure to approximate aircraft area curve shapes. [SAE PAPER 982] 19 p2385 A73-37888

Characteristic overpressure of a supersonic transport of given length in a homogeneous atmosphere. 19 p2377 A73-38006

Europeplane QSTOL economical solution to noise and congestion problem in short and medium haul transport 22 p2798 A73-41862

Airport runway and taxiway surfaces modifications for heavy and supersonic aircraft demonstrated by aircraft static and dynamic landing loads and physical dimensions 24 p3075 A73-45199

AIRCRAFT CONSTRUCTION

U AIRCRAFT STRUCTURES

AIRCRAFT CONTROL

NT HELICOPTER CONTROL

A French collision-avoidance system of time-frequency type - Critical analysis of test results [ONERA, TP NO. 1086] 01 p0074 A73-10227

Optimum position of the center of gravity of a passenger plane in cruising flight 02 p0129 A73-11649

Aircraft performance augmentation through control configured aircraft design based on artificial stabilization instead of inherent aerodynamic static stability [DGLR PAPER 72-094] 02 p0130 A73-11675

Problems of the integration of aircraft and flight control system in the case of new approach procedures [DGLR PAPER 72-096] 02 p0190 A73-11698

Handling characteristics in roll of two light airplanes for steep approach landings. 03 p0250 A73-13701

Application of geometric decoupling theory to synthesis of aircraft lateral control systems. 03 p0250 A73-13703

The optimal control of merging aircraft-derivation of the hybrid air traffic controller. 03 p0340 A73-14489

Russian book on aircraft control systems covering radio communication and navigation, automatic guidance and landing and homing and radar tracking 04 p0474 A73-15964

Russian book on aircraft landing control automation covering radio beacons, communications equipment, instrument landing trajectories, flight control, autopilot, atmospheric disturbances and display systems 04 p0474 A73-15966

Russian book on Il-18 aircraft practical aerodynamics covering aerodynamic characteristics, performance, controllability, stability and flight safety 04 p0406 A73-15968

The problem of human efficiency in automated control systems 05 p0542 A73-16410

Flight vehicle (FV) control optimization taking into account control-function and phase-coordinate constraints 05 p0594 A73-16415

Some structure synthesis problems for systems controlling the three-dimensional motion of orbital-aircraft in the earth's atmosphere 05 p0594 A73-16418

Control configured vehicle (CCV) concept application to fighter aircraft design for combat maneuver capabilities and versatility enhancement, using fly by wire technology [SAE PAPER 720854] 05 p0535 A73-16662

Reorganization of airplane manual flight control dynamics. 05 p0595 A73-16707

Optimal flight control system design for aircraft with large flight envelopes, using optimal control theory with limited measurement feedback [AIAA PAPER 73-159] 05 p0535 A73-16906

Control configured vehicle (CCV) technology application for fighter aircraft combat control versatility enhancement, presenting F-4 analytical, simulation and wind tunnel test performance results [AIAA PAPER 73-160] 05 p0535 A73-16907

Flight control techniques for advanced commercial transports. [AIAA PAPER 73-30] 06 p0647 A73-17618

Observations on perceived changes in aircraft attitude attending head movements made in a 2-g bank and turn. 07 p0785 A73-19485

A flight control system for STOL aircraft. 07 p0777 A73-20171

Russian book - Control of aircraft and helicopter flight. 07 p0850 A73-20381

Recent advances and applications in the prediction of pilot acceptance of aircraft flying qualities. 07 p0777 A73-20586

Nonlinear programming in design of control systems with specified handling qualities. 07 p0777 A73-20588

The effect of servomechanical control and stability systems on the flutter behavior of aircraft [DFVLR-SONDDR-272] 11 p1304 A73-25349

Active flutter suppression - B-52 controls configured vehicle. [AIAA PAPER 73-322] 11 p1305 A73-25552

Iliushin 62 aircraft horizontal stabilizer structural design and control, discussing mounting hardware and electrically driven servomechanism 11 p1305 A73-25795

Advanced flight control systems - Power-by-wire and fly-by-wire. 11 p1306 A73-26272

Practical quadratic optimal control for systems with large parameter variations. 12 p1483 A73-27166

Response-optimum control of the angular and torsional oscillations of an elastic flying wing. 12 p1459 A73-27459

Analytical design of manual control systems for flight bodies 12 p1549 A73-27896

European airbus A300B aircraft flight tests and on-board instrumentation in certification program, illustrating desk layout, control and display panels 13 p1568 A73-28159

Russian book on aircraft, rocket and spacecraft control systems design methods covering ground and on-board systems synthesis, performance estimates, system effectiveness, etc 14 p1773 A73-30353

Hardware integration and improved operation of the flight control system. 14 p1713 A73-30932

Anthropotechnical investigation of an above-ground indication and of an artificial horizon with preindication in connection with the manual control of VTOL aircraft 15 p1839 A73-32044

Russian book - Radio devices for flight vehicle control systems. 15 p1908 A73-32421

Pilot-electronics-control surfaces as feedback loop for aircraft flight control, discussing instruments, pilot training and aircraft flying qualities 15 p1830 A73-32472

Electronic systems as piloting aids in Concorde SST, discussing flight controls, trim computer, autostabilizer, autopilot and automatic engine control 15 p1830 A73-32474

Book - Methods for estimating stability and control derivatives of conventional subsonic airplanes. 16 p1969 A73-33423

Control of turbofan lift engines for VTOL aircraft. [ASME PAPER 73-GT-20] 16 p2047 A73-34496

Book - Flight dynamics of rigid and elastic airplanes. Parts 1 & 2. 17 p2099 A73-34451

Problems concerning the implementation of an integrated flight control system, giving particular attention to curved flight path profiles [DGLR PAPER 73-030] 17 p2208 A73-34498

Control-configured general aviation aircraft. [SAE PAPER 730303] 17 p2101 A73-34664

Application of advanced control system and display technology to general aviation. [SAE PAPER 730321] 17 p2102 A73-34679

Development of a low-cost flight director system for general aviation. [SAE PAPER 730331] 17 p2167 A73-34684

Civil STOL aircraft engine thrust reverser and fast selection control system designs for high performance, low specific weight and acoustic compatibility requirements [SAE PAPER 730358] 17 p2222 A73-34706

Integrated Propulsion Control System program. [SAE PAPER 730359] 17 p2222 A73-34707

V/STOL aircraft pilot-in-loop flight control/display system to overcome pilot limitations with performance and decision making flexibility enhancement [AHS PREPRINT 722] 17 p2105 A73-35063

Flight simulator evaluation of control moment usage and requirements for V/STOL aircraft. [AHS PREPRINT 743] 17 p2147 A73-35076

Flight test and demonstration of digital multiplexing in a fly-by-wire flight control system. 17 p2107 A73-35225

Liquid crystal approach to integrated programmable digital displays and aircraft control, considering flat panel digital-matrix display 17 p2139 A73-35234

Feedback control configured vehicles ride control system design for B-52 aircraft load alleviation and mode stabilization during flight through atmospheric turbulence 17 p2107 A73-35245

Digital V/STOL flight simulation test procedures for aircraft navigation, guidance and control, detailing display device panels, flight path simulation and software configuration 17 p2210 A73-35853

Analytical design of aircraft manual control systems. 18 p2267 A73-36601

Computerized design for moving-base three man aircraft flight simulator servocontrol, considering disturbance torques, damping ratios, natural frequencies, load acceleration and smoothness 18 p2296 A73-36833

Some characteristics of pilot's performance under complicated flight conditions. 18 p2285 A73-36921

Analysis of the aerodynamic characteristics of devices for increasing wing lift. III - Influence of ground proximity on the aerodynamic characteristics of the flaps 18 p2266 A73-37022

B-52 control configured vehicles ride control analysis and flight test. [AIAA PAPER 73-782] 19 p2378 A73-37452

Two man crew cockpit design for commercial 737 jet transport aircraft, discussing pilot vision, control and display panels and avionics disposition 19 p2384 A73-37729

Russian book - Hydraulic ducts of control systems in aviation: The effects of external factors. Shop testing, and reliability. 19 p2389 A73-37766

Decoupling longitudinal motions of an aircraft. 19 p2386 A73-38033

Identification of YT-2B stability and control derivatives via the maximum likelihood method. 19 p2386 A73-38043

A comparative evaluation of the application of several aircraft parameter identification methods to 19 p2386 A73-38043

flight data - with emphasis on the development of rational evaluation criteria.

The sensitivity of optimal flight paths to variations in aircraft and atmospheric parameters.

The effect of ice formation on the stability and maneuverability characteristics of aircraft

Study of control system effectiveness in alleviating vortex wake upsets

An approach to the synthesis of separate surface automatic flight control systems.

A 'type one' servo explicit model following adaptive scheme.

Application of direct side force control to commercial transport.

Direct side-force control for STOL transport aircraft.

Fly-by-wire digital F-8C aircraft control system using Apollo guidance, navigation and control hardware, emphasizing interface design and fault detection

Nonlinear trajectory-following and control techniques in the terminal area using the Microwave Landing System Navigation Sensor.

Ground based microwave landing system for aircraft navigation, guidance and control in terminal area, discussing system requirements for flight safety

Synthesis of digital filters for the control of short periodic angular oscillations of aerospace vehicles.

Influence of the effectiveness of jet vanes on the characteristics of VTOL aircraft

Washout circuit design for multi-degrees-of-freedom moving base simulators.

Visual cues and six degree of freedom motion flight simulation for F-4 aircraft energy maneuvering performance, discussing pilot evaluations

Flight simulation requirement in artificial stabilizer design for VTOL aircraft flight control system, noting agreement with flight tests

A new approach to gust alleviation of a flexible aircraft using an open loop device

Compensation of the longitudinal-trim and altitude control systems of an aircraft

Development of pilot-in-the-loop analysis.

Design of multivariable adaptive model following control systems.

Closed loop linear control system synthesis possibility under condition of incomplete information on state vector with application to aircraft longitudinal motion

Total In-Flight Simulator for X-22A aircraft based on variable stability-and-control system concept for reliability design

AIRCRAFT DESIGN

NT HELICOPTER DESIGN

Multivariate analysis applied to aircraft optimisation - Some effects of research advances on the design of future subsonic transport aircraft.

Aircraft performance augmentation through control configured aircraft design based on artificial stabilization instead of inherent aerodynamic static stability

Aircraft industry design and development costs prediction, using Monte Carlo model to determine effect of poor estimates

Electric generator inside turbojet or turbofan aircraft engine to reduce need for external gearbox, simplifying nacelle assembly and increasing aircraft design flexibility

Aircraft aftbody/propulsion system integration for low drag.

Aft-end design criteria and performance prediction methods applicable to air superiority fighters having twin buried engines and dual nozzles.

Subsonic commercial transport aircraft reduced noise and increased cruise Mach number effects on nacelle design in terms of inlet, fan, cowl and nozzle

Optimum design for air superiority fighter, noting conventional, delta and coupled canard wing configurations and SAAB Viggen aircraft

Light combat aircraft with hover capability.

An advanced concept in electrical power distribution control and management.

Integrated engine-airframe design with fuselage boundary layer ingestion for subsonic-transonic cruise, discussing STOL thrust control via variable pitch fan for landing

Viscous interaction in integrated supersonic intakes.

Rates of change of flutter Mach number and flutter frequency.

SST aircraft wing design for sonic boom avoidance and noise reduction in airport vicinity, describing aerodynamic characteristics from wind tunnel and flying model tests

Airship design for short-medium distance heavy payload transport, describing honeycomb skin construction, power plant installation and hovering loading/unloading operations

Airframe structural testing and safety design for military aircraft, discussing static, dynamic and fatigue tests and environmental effects

Choices for the future - An industry viewpoint on prototyping.

Control configured vehicle /CCV/ concept application to fighter aircraft design for combat maneuver capabilities and versatility enhancement, using fly by wire technology

Aerodynamic technology developments including advanced transonic airfoils, low-drag/high-lift systems and stability augmentation for transport aircraft performance, economics and noise improvements

Aircraft structural engineers prospects in commercial aircraft design, discussing markets, technology escalation and cost effective structural development

Structural design of future commercial transports.

Flight control techniques for advanced commercial transports.

Preliminary design of the man-powered aircraft, Icarus.

Sonic boom reduction through aircraft design and operation.

Technical and economical analysis of various QSTOL concepts

Aircraft radome design mechanical, electrical and aerodynamic requirements, taking into account lightning hazards, electrostatic surface charges and plastic components deformations

Multiple purpose STOL aircraft for passenger or cargo transport, discussing design features, performance and market prospects

Airships design, constructional and operational characteristics, discussing aerodynamics, flight control, performance and trim

Russian book on passenger aircraft and air transport design covering technical and economic efficiency, airbus concept, weight and size problems and aft-mounted engine design

Optimisation in construction of the Jaguar and other military aircraft.

A proposed design for the construction of a VTOL simulator

L-1011 TriStar - Design development.

Formula-one air racing history, aircraft designs and characteristics and low cost amateur constructions

Fighter aircraft survivable flight control system design and flight test philosophy, present status and trends, considering fly-by-wire and power-by-wire systems

Air battle fighter aircraft design, discussing required performance characteristics in terms of lethality, maneuverability, range, visibility, handling qualities, sortie rate, repairability and fire control

F-15 fighter aircraft development, discussing design and functional features of power plant, flight control system, landing gear, flaps, speed brakes and cockpit

Russian book on aircraft natural-climatic environmental factors covering geographic region adverse effects on design, performance and maintenance

Turana drone system design and development for Australian naval guns and guided weapons exercises, describing construction and operational details

Russian book on aviation fundamentals covering aerodynamics and flight theory, designs, components, engines and instrumentation of aircraft, including helicopters, VTOL and STOL

Civil transport aircraft future design trends, discussing subsonic, supersonic, hypersonic and V/STOL aircraft, engine design, fuels and noise reduction

Commercial aircraft passenger cabins interior design, considering seating arrangements, cabin architecture and fittings, materials and color schemes and maintainability

Optimization and design of the rear fuselage of the A 300 B aircraft structure.

Aeritalia-Boeing passenger aircraft design features in short, medium and long haul versions

Breakdown criteria for streamer formation, electrostatic field analysis and laboratory high voltage experiments on aircraft initiation of lightning strikes

Boeing 727 design and development in response to airline market requirements, emphasizing profitability

Varying-temperature test installation for the interior design of the Concorde

Aircraft design philosophies and structural integrity considerations for reliability without major NDT and maintenance, proposing research program for future computerized design

Military aircraft radome design technology developments in Sweden, discussing use of glass fiber reinforced plastics, manufacturing method, computerized optimization and measurement techniques

Taylor series algorithms for computerized structural design and reanalysis of modified structures, applying to aircraft fuselage midsection

Application of computer-aided aircraft design in a multidisciplinary environment.

Preliminary design of aircraft structures to meet structural integrity requirements.

An automated procedure for computing flutter eigenvalues.

Russian book on airplane and helicopter design and stability covering selection of wing /rotor/ configuration and power plant, subsystem design, strength, reliability, lifetime, etc

Hydraulic powered integrated actuator package /IAP/ for V/STOL aircraft flight control, noting advantages in system weight, mechanical complexity and power loss reduction

Optimisation of aircraft structures with multiple stiffness requirements.

Aircraft design and reliability analysis method based on accidents occurrence investigation by Franco-British airworthiness authorities, noting applicability to Concorde aircraft

Transport aircraft maintenance program, discussing safety and reliability correlation with design

Aircraft design parameters optimization based on critical function representing overall deviation for specifications with application to subsonic passenger aircraft

Augmentor wing design and performance tests for multimission XFV-12 V/STOL prototype aircraft

Light motorized glider-type aircraft design, development and flight testing, discussing aerodynamic configuration, structural design and performance characteristics

M-15 agricultural turbojet aircraft design for slow low level flight, tabulating dimensions, weights and performance data

Concorde Olympus 593 axial flow turbojet engine design, detailing variable geometry intake and exhaust nozzles, noise abatement, combustion chamber, gearing and fuel system

13 p1669 A73-28156

Swing wing - Modifications in variable geometry configuration concepts.

13 p1568 A73-28157

Kneeling landing gear - The C5 variable geometry development.

13 p1568 A73-28158

The state of the art in light aircraft design.

13 p1568 A73-28179

Air transportation direct and indirect costs analysis, considering cruising speed, flight time, aircraft design and manufacture and fuel expenses

13 p1569 A73-28950

Critical properties of exterior aircraft finish systems to protect fastener areas.

[NACE PAPER 117]

13 p1638 A73-29317

New inhibited elastomeric finish system designed by corrosion engineers to solve acute corrosion problems on military aircraft.

[NACE PAPER 118]

13 p1638 A73-29318

General aviation aircraft technology developments based on military and transport aircraft design, considering cost, complexity and reliability

13 p1570 A73-29348

Design and simulation of an aircraft brake using a digital computer.

13 p1588 A73-29385

SOKO Galeb 3 cantilever low wing trainer-fighter monoplane with Bristol-Siddeley Viper 20 turbojet engine, describing flight control, loading gear, fuel system and avionics

14 p1712 A73-30240

Concorde wing and fuselage aerodynamic design modifications for operational efficiency optimization from wind tunnel tests and theoretical computations

14 p1712 A73-30926

Concorde cockpit windows design modifications for weight reduction and reliability optimization, discussing transparencies and crew seat movement

14 p1712 A73-30927

Russian book - Practical aerodynamics of the An-24 aircraft (2nd revised and enlarged edition).

15 p1829 A73-31547

Normal mode solution to the equations of motion of a flexible airplane.

15 p1950 A73-31747

Some aerodynamic problems applicable to the light aircraft

16 p1961 A73-32809

Computerized three dimensional calculations of hypersustained aircraft in viscous potential flow in terms of boundary layers and wakes

16 p1962 A73-32816

Lightning protection for boron and graphite reinforced plastic composite aircraft structures, discussing zonal design concept and channel intermittent contact with protrusions on surface

16 p1968 A73-33034

Pressurized fuselage design studies for short haul transport aircraft, discussing sandwich structures and bonding techniques for Al and Ti alloy construction materials

16 p2018 A73-33069

Anglo-American Aeronautical Conference, 13th, London, England, June 4-8, 1973, Proceedings.

16 p1968 A73-33176

World air traffic patterns projected to 1988, including present traffic features, supersonic transport utilization, ground transport alternatives, air freight and aircraft types

16 p2088 A73-33180

Concorde aircraft design, testing and projected environmental impact, discussing flight tests, sonic booms, atmospheric pollution, ATC problems and fueling

16 p1968 A73-33182

Short haul aircraft design and marketing, examining competing modes, noise factors, airport traffic density patterns and aircraft types dependence on utilization

16 p2088 A73-33184

Independently targeted short haul individual rotorcraft for air taxi service, considering traffic control system, market possibilities, environmental impact and projected utilization

16 p2088 A73-33186

Technology developments effect on jet aircraft design, discussing flight controls, engine noise suppression, supercritical aerodynamics and composite structures

16 p1968 A73-33188

Avionics and human factors in flight simulator economics, interrelating aircraft design to simulation system

16 p1995 A73-33206

Book - Methods for estimating drag polars of subsonic airplanes.

16 p1963 A73-33422

Investigation of the aerodynamic performance of small axial turbines.

[ASME PAPER 73-GT-3]

16 p1963 A73-33481

Design considerations for supersonic V/STOL aircraft.

[ASME PAPER 73-GT-65] 16 p1969 A73-33517

Conceptual study of high performance V/STOL fighters.

[ASME PAPER 73-GT-66] 16 p1969 A73-33518

V/STOL airframe/propulsion integration problem

16 p2048 A73-33522

Outlook on safety; Proceedings of the Thirteenth Annual Technical Symposium, London, England, November 14-16, 1972.

17 p2097 A73-34076

Design to detect and avoid failure - One airline's viewpoint.

17 p2097 A73-34081

Aircraft design for operational safety, discussing risk elimination, failure modes, maintenance analysis and fault diagnosis

17 p2098 A73-34083

Effects of new landing approach procedures on cockpit design and possibilities of taking them into account

[MBB-UH-07-73] 17 p2100 A73-34485

L-1011 aircraft hydraulic system layout and installation techniques with modular design and plug-in cartridges for Murphy law error reduction during service

17 p2108 A73-34523

Control-configured general aviation aircraft.

[SAE PAPER 730303] 17 p2101 A73-34664

Stepped aluminum extrusions - Designing for business aircraft.

[SAE PAPER 730308] 17 p2177 A73-34668

Applications of advanced aerodynamic technology to light aircraft.

[SAE PAPER 730318] 17 p2101 A73-34676

Development of airframe design technology for crashworthiness.

[SAE PAPER 730319] 17 p2101 A73-34677

Stall/spin studies relating to light general-aviation aircraft.

[SAE PAPER 730320] 17 p2102 A73-34678

Feasibility and optimization of variable-geometry wing for jet amphibian business aircraft.

[SAE PAPER 730330] 17 p2102 A73-34683

Computer aided parametric analysis for general aviation aircraft.

[SAE PAPER 730332] 17 p2130 A73-34685

General aviation pilot operational profile study, discussing implications for airman certification standards, flight safety regulations and aircraft design

[SAE PAPER 730334] 17 p2115 A73-34687

Aircraft cabin noise reduction through composite material insulation, discussing engine noise sources, aircraft fuselage transmission loss characteristics, vibration damping and sandwich structures

[SAE PAPER 730339] 17 p2102 A73-34690

B-1 technology applications to advanced transport design.

[SAE PAPER 730348] 17 p2102 A73-34696

The Concorde manufacturing consortium - An exercise in international engineering collaboration.

[SAE PAPER 730350] 17 p2257 A73-34698

Transport cargo aircraft design requirements and supporting ground system concepts in view of future market demands with emphasis on economic constraints

[SAE PAPER 730352] 17 p2102 A73-34700

Development of the A300B wide-body twin.

[SAE PAPER 730353] 17 p2102 A73-34701

Key factors in developing a future wide-bodied twin-jet transport.

[SAE PAPER 730354] 17 p2103 A73-34702

Market economic environment change effects on air transport design and use, examining 747 operational requirements in terms of cargo load factor, passenger fares and labor costs

[SAE PAPER 730355] 17 p2103 A73-34703

Integrated Propulsion Control System program.

[SAE PAPER 730359] 17 p2222 A73-34707

The Air Force/Boeing advanced medium STOL transport prototype.

[SAE PAPER 730365] 17 p2103 A73-34710

Technical basis for the STOL characteristics of the McDonnell Douglas/USAF YC-15 prototype airplane.

[SAE PAPER 730366] 17 p2103 A73-34711

Design studies of low-noise propulsive-lift airplanes.

[SAE PAPER 730378] 17 p2103 A73-34717

An airline view of the future of auxiliary power systems.

[SAE PAPER 730379] 17 p2108 A73-34718

The role of the auxiliary power unit in future airplane secondary power systems.

[SAE PAPER 730381] 17 p2108 A73-34720

Application of multiplexing to the B-1 aircraft.

17 p2107 A73-35247

Russian book - The Tu-134 aircraft: Its design and operation.

18 p2266 A73-35870

Influences of international operations on aircraft-transport design /Second William Littlewood Memorial Lecture/.

18 p2373 A73-36165

Symposium on Optimisation in Aircraft Design, London, England, November 15, 1972, Proceedings.

19 p2378 A73-37405

Military aircraft structure computerized design optimization procedures based on local optimum and stiffness requirements

19 p2495 A73-37407

The optimisation of wing design.

19 p2495 A73-37408

A parameter optimisation technique applied to the design of flight control systems.

19 p2378 A73-37409

Whole aircraft and component design optimization, discussing criteria, constraints and performance prediction accuracy during feasibility analysis and project design

19 p2378 A73-37410

Design-build-fly, an effective method to teach undergraduate aerospace vehicle design.

[AIAA PAPER 73-785] 19 p2505 A73-37455

Design for teaching aerospace engineering at Texas A & M University.

[AIAA PAPER 73-786] 19 p2505 A73-37456

A new approach to aircraft design education.

[AIAA PAPER 73-787] 19 p2505 A73-37457

Compatibility of maneuver load control and relaxed static stability.

[AIAA PAPER 73-791] 19 p2379 A73-37458

Managerial implications of computerized aircraft design synthesis.

[AIAA PAPER 73-799] 19 p2379 A73-37462

Aircraft installation requirements and considerations for variable pitch fan engines.

[AIAA PAPER 73-807] 19 p2379 A73-37465

The design or operation of aircraft to minimize their sonic boom.

[AIAA PAPER 73-817] 19 p2380 A73-37470

The F-12 series aircraft aerodynamic and thermodynamic design in retrospect.

[AIAA PAPER 73-820] 19 p2380 A73-37472

ACLS trade study for application to STOL tactical aircraft.

19 p2381 A73-37683

CC-115/Bufalo/ aircraft air cushion landing system design, testing and implementation prognosis, discussing propeller design, power systems, wings and U.S.-Canadian project cooperation

19 p2381 A73-37687

Bufalo aircraft modification for air cushion landing system, considering weight, performance, stability and control, configuration alternatives and ground maneuvering

19 p2382 A73-37688

The aircraft modification phase of the joint U.S./Canadian ACLS program.

19 p2382 A73-37689

Report on an ST6 powered air supply package for air cushion landing systems.

19 p2382 A73-37690

Russian book - Aircraft wheel and braking system designs.

19 p2384 A73-37768

Commercial jet transport aircraft hydraulic fuel distribution tubing systems, discussing maintenance, fabrication problems, fittings, quality control and materials

[SAE SP-378] 19 p2434 A73-37864

Cost estimating techniques for airframe weight-cost interface study for military aircraft design

[SAWE PAPER 969] 19 p2385 A73-37885

A computer-aided design procedure to approximate aircraft area curve shapes.

[SAWE PAPER 982] 19 p2385 A73-37888

DC-10 Twin design, discussing balance characteristics, loading limits and sample forms

[SAWE PAPER 987] 19 p2386 A73-37891

Boron epoxy, polyimide and aluminum composite materials for cost effective high performance aircraft and turbine engine structures, assessing development and application status

[SAWE PAPER 992] 19 p2443 A73-37892

"The hub of the wheel" - A project designer's view of weight.

[SAWE PAPER 996] 19 p2386 A73-37895

VFW-FOKKER VAK-191B VTOL fighter aircraft structural and aerodynamic design, describing airframe construction, power plant arrangement, flight controls, hydraulic and electrical systems

19 p2387 A73-38167

Computerized optimization of interrelated airframe/engine design parameters against variable criteria to satisfy performance constraints in air superiority fighter design

[AIAA PAPER 73-800] 19 p2388 A73-38370

Structural composites on future fighter aircraft.

[AIAA PAPER 73-806] 19 p2388 A73-38371

Boron-stiffened longerons on the B-1.

[SME PAPER EM 73-719] 19 p2436 A73-38499

Dynamic gust, landing, and taxi loads determination in the design of the L-1011.

20 p2508 A73-38647

Aircraft-store separation design for angular momentum increase of external weapon with internally mounted spinning flywheel

20 p2508 A73-38652

A practical load relief control system designed with modern control techniques. [AIAA PAPER 73-863] 20 p2508 A73-38801

Corporate aircraft design and operational problems, including supercritical wing and wasp-waist body design, airport private/airline interfaces, noise criteria, flight simulation and ATC 20 p2509 A73-39218

Cockpit evolution, considering pilot visual problems in approach final stage during poor visibility, instrument number and placement, supersonic aircraft, digital computer-CRT interfaces, etc 20 p2510 A73-39662

Cobra P-530 air superiority fighter adaption to ground attack for international requirements for multipurpose aircraft, discussing avionics for multimission version 21 p2634 A73-40301

Some method of nonlinear programming suitable for solving the task of optimization of a small transport aircraft 21 p2634 A73-40478

Control law synthesis and sensor design for active flutter suppression. [AIAA PAPER 73-832] 21 p2784 A73-40502

Design and application of a part-task trainer to teach formation flying in USAF Undergraduate Pilot Training. [AIAA PAPER 73-935] 21 p2674 A73-40881

Aircraft design for transporting arctic crude oil or liquid natural gas, examining air terminal requirements and handling specifications 21 p2634 A73-41172

Rotorcraft design concepts, considering economics, propulsion, control, trim devices, advancing blade concept, materials and rotor aerodynamics 21 p2635 A73-41189

The aerodynamic development of the wing of the A 300B. 21 p2633 A73-41192

Design and analysis of an energy absorbing restraint system for light aircraft crash-impact. [ASME PAPER 73-DET-111] 22 p2799 A73-42080

Aerial-surveillance aircraft of the new generation 22 p2799 A73-42590

Runway sideline aircraft noise measurements on takeoff and approach for enforcing community noise levels based on FAA aircraft type certification, noting associated problems 22 p2800 A73-42945

On the application of a new version of lifting surface theory to nonslender and kinked wings. 23 p2939 A73-43210

Designing a slender-wing-type cantilever plate under conditions of unsteady creep 23 p3042 A73-43728

On problems of flight over an extended angle-of-attack range. 24 p3056 A73-44692

F-14 replacement for Phantom aircraft for escort missions, fleet defence, interdiction and close support, discussing airborne refuelling capability and composite materials applications 24 p3056 A73-44695

A study to determine the feasibility of a low sonic boom supersonic transport. [AIAA PAPER 73-1035] 24 p3056 A73-44863

AIRCRAFT DETECTION

Modeling of the radar scattering characteristics of aircraft. 04 p0416 A73-15057

Probability of detecting aircraft targets. 11 p1333 A73-26634

Self adaptive filter algorithm for automatic tracking of high performance maneuvering targets in real time surveillance systems in changing environments 13 p1596 A73-29207

A proposal on automatic tracking of an aircraft for the radar. 14 p1728 A73-30471

AIRCRAFT ENGINES

NT HELICOPTER ENGINES

NT TF-30 ENGINE

NT TF-34 ENGINE

Automated test stands for full scale aircraft structure and engine parts fatigue tests, noting equipment for programmed static and dynamic loading 02 p0166 A73-11629

Influence of acceleration on tip clearances in aircraft engine turbines and compressors 02 p0204 A73-12447

Comparison of modern aircraft engines with other power plants used in transportation 03 p0352 A73-13072

Electric generator inside turbojet or turbofan aircraft engine to reduce need for external gearbox, simplifying nacelle assembly and increasing aircraft design flexibility [AIAA PAPER 72-1056] 03 p0252 A73-13387

Portable self contained computerized in-aircraft engine analyzer with cassette tape resident program control and digital display and punched card indicators [AIAA PAPER 72-1080] 03 p0307 A73-13403

Integrated engine diagnostics and displays for Navy aircraft of the 1980's. [AIAA PAPER 72-1084] 03 p0354 A73-13406

Implementing the design of airplane engine exhaust systems. [AIAA PAPER 72-1112] 03 p0355 A73-13427

Oblique shock wave interaction with approach boundary layer at combustor entrance in supersonic scramjet engines, observing wall pressure distribution [AIAA PAPER 72-1181] 03 p0357 A73-13476

Aircraft gas turbine mainshaft ball bearings fatigue life estimation via failure distribution [ASME PAPER 72-LUB-10] 03 p0313 A73-14328

Aircraft engine development in terms of money, manpower, facilities and knowledge, discussing project organization and scheduling 03 p0251 A73-14469

Russian book - VTOL aircraft power plants. 04 p0487 A73-15706

Improved M50 aircraft bearing steel through advanced vacuum melting processes. 04 p0455 A73-15746

Aircraft turbine engine emissions and the possibilities for control. [ASME PAPER 72-WA/GT-4] 04 p0490 A73-15868

A method of early failure detection for gas turbines. 05 p0581 A73-16186

German book - Flight propulsion systems: Principles, systematics, and technology of aeronautical and astronautical propulsion systems. 05 p0606 A73-16355

Small turboshaft aircraft engine historical evolution and current state of art, discussing performance, cost, weight, reliability and maintainability interrelationships [SAE PAPER 720830] 05 p0606 A73-16626

Army 1500 shp advanced technology engine development program, discussing in components design and fabrication, air leakage losses, environmental testing and maintainability oriented design [SAE PAPER 720828] 05 p0606 A73-16627

System monitoring techniques: Practical applications and experience at Eastern - Jet engines. [SAE PAPER 720818] 05 p0606 A73-16639

The evolution and development status of the ALF 502 turbofan engine. [SAE PAPER 720840] 05 p0607 A73-16654

TF34 and F101 turbofan engines for Navy S-3A ASW aircraft and USAF B-1 strategic bomber, respectively, discussing design features, manufacturing techniques and testing procedures [SAE PAPER 720841] 05 p0607 A73-16655

F100/F401 augmented turbofan engines - High thrust-to-weight propulsion systems. [SAE PAPER 720842] 05 p0607 A73-16657

Technology and operation of Olympus engine cycle on Concorde aircraft, discussing chemical and noise pollution and economic factors 05 p0536 A73-17190

Current Pratt & Whitney engine noise reduction programs. [AIAA PAPER 73-8] 06 p0740 A73-17603

Control and stability analysis of supersonic aircraft jet engines with afterburner for improved low altitude operation 06 p0741 A73-17722

Effect of operating variables on pollutant emissions from aircraft turbine engine combustors. 06 p0768 A73-17736

Control and reduction of aircraft turbine engine exhaust emissions. 06 p0768 A73-17737

Development trends in design methods for aircraft engine compressors. II - Centrifugal-flow compressors 06 p0741 A73-17996

Electrochemical machining application to aircraft gas turbine engine components manufacture, discussing removal rate, accuracy and surface finish capability [SME PAPER MR 72-536] 06 p0697 A73-18093

Development trends in aircraft-engine compressor design methods. III 07 p0867 A73-19605

Aircraft and land vehicle electric generators and motors, noting semiconductor application and cooling systems 07 p0779 A73-20124

TF-34 turbofan engines for S-3A and AX aircraft respectively, discussing technological development, and components and characteristic features 07 p0868 A73-20350

Technology and operation of Olympus engine cycle on Concorde aircraft, discussing chemical and noise pollution and economic factors 08 p0996 A73-21687

Russian book on aviation fundamentals covering aerodynamics and flight theory, designs, components, engines and instrumentation of aircraft, including helicopters, VTOL and STOL 09 p1032 A73-23224

Combustor design effect on jet aircraft engine exhaust pollutants reduction during hydrocarbon fuel burning 10 p1263 A73-24556

Twin-engined Anglo-French Lynx helicopter main rotor head, blade and drive train with conformal gearing, discussing design and material features 11 p1374 A73-25790

A modern mechanical laboratory for the support of aircraft engine design 12 p1486 A73-27385

Condition monitoring - A new technology for aircraft engine maintenance 12 p1486 A73-27389

Concorde Olympus 593 axial flow turbojet engine design, detailing variable geometry intake and exhaust nozzles, noise abatement, combustion chamber, gearing and fuel system 13 p1669 A73-28156

Design and evaluation of combustors for reducing aircraft engine pollution. 13 p1670 A73-28932

Protective coating systems for Navy aircraft turbine engines. [NACE PAPER 113] 13 p1637 A73-29313

High bypass fan engines for quiet propulsion and optimal aircraft performance in military and commercial applications 16 p2046 A73-33190

Lift engine bleed flow management for a V/STOL fighter reaction control system. [ASME PAPER 73-GT-70] 16 p2048 A73-33521

An initial estimate of aircraft emissions in the stratosphere in 1990. [AIAA PAPER 73-508] 16 p2011 A73-34046

Effect of 'bulk' heat transfers in aircraft gas turbines on compressor surge margins. 17 p2221 A73-34382

Potential payoffs of variable geometry engines in fighter aircraft. 17 p2099 A73-34436

Market trends and technical progress in small gas turbine engines for general aviation and executive aircraft and helicopters 17 p2225 A73-34447

Book - Gas turbine theory /2nd edition/. 17 p2221 A73-34471

Aircraft engine fuel and oil differential temperature measurement via platinum probes, specifying sensor sensitivity, calibration, circuit operation and data reduction 17 p2165 A73-34607

Pressure measurements for establishing inlet/engine compatibility. 17 p2221 A73-34609

Exhaust emissions analysis system for aircraft gas turbine engines. 17 p2146 A73-34615

New low-pressure-ratio fans for quiet business aircraft propulsion. [SAE PAPER 730288] 17 p2221 A73-34653

The development of reciprocating engine installation data for general aviation aircraft. [SAE PAPER 730325] 17 p2102 A73-34681

Engine cycle considerations for future transport aircraft. [SAE PAPER 730345] 17 p2222 A73-34693

Profitable transport engines for the environment of the eighties. [SAE PAPER 730347] 17 p2257 A73-34695

Civil STOL aircraft engine thrust reverser and fast selection control system designs for high performance, low specific weight and acoustic compatibility requirements [SAE PAPER 730358] 17 p2222 A73-34706

Air Force propulsion maintenance concepts. [SAE PAPER 730373] 17 p2177 A73-34712

The development of a turbine engine maintenance program from a new reliability model. [SAE PAPER 730374] 17 p2177 A73-34713

Advanced aircraft power systems utilizing coupled APU/ECS. [SAE PAPER 730380] 17 p2108 A73-34719

The role of the auxiliary power unit in future airplane secondary power systems. [SAE PAPER 730381] 17 p2108 A73-34720

A simplified fuel control approach for low cost aircraft gas turbines. 17 p2222 A73-34725

Helicopter turboshaft engine vibration reduction through engine-airframe interface compatibility design and torsional stability of drive trains with automatic fuel control [AHS PREPRINT 774] 17 p2106 A73-35092

Aircraft turbine engine exhaust emissions under simulated high altitude, supersonic free-stream flight conditions. [AIAA PAPER 73-507] 17 p2223 A73-35625

Differential temperature measurements in engine fluids. 18 p2315 A73-36071

Reliability of aircraft turbojet bearings 18 p2320 A73-36691

Flight testing of the JT15D in the CF-100. 18 p2268 A73-36775

Aeronautical turbine blade and vane materials selection, considering Ni alloys with powder metallurgy

and oriented solidification, composite materials and eutectics

18 p2326 A73-36993

The effect of afterburning on the emission of pollutants by turbojets

18 p2343 A73-36996

Variable pitch turbofan driven at constant speed through reduction gear to obtain cost-efficiency compromise for future STOL and business aircraft applications

18 p2343 A73-36998

F-12 series aircraft propulsion system performance and development.

[AIAA PAPER 73-821]

19 p2380 A73-37473

The development of propulsion systems in the case of airliners

19 p2473 A73-38120

Diffusion and fallout of pollutants emitted by aircraft engines.

19 p2474 A73-38323

Computerized optimization of interrelated airframe/engine design parameters against variable criteria to satisfy performance constraints in air superiority fighter design

[AIAA PAPER 73-800]

19 p2388 A73-38370

Aircraft economics and its effect on propulsion system design.

[AIAA PAPER 73-808]

19 p2388 A73-38372

Trimming and checking aircraft gas-turbine engines with the aid of the ratio of total pressure behind the turbine to total pressure in front of the compressor

21 p2754 A73-40403

Airframe/propulsion system interactions - An important factor in supersonic aircraft flight control.

[AIAA PAPER 73-831]

21 p2634 A73-40501

Experience with the NRC 10 ft. x 20 ft. V/STOL propulsion tunnel - Some practical aspects of V/STOL engine model testing.

21 p2672 A73-40855

Macrofractographic studies of fatigue fractures in aircraft engine elements

21 p2754 A73-41593

Wind tunnel test for Dolphin airship model static thrust measurements, discussing thrust direction torque moment coefficients and propeller rotation

21 p2635 A73-41648

Application of electron beam welding to aircraft turbine engine parts.

22 p2866 A73-42196

Technological change measurement methodology for cost and production estimates with application to aircraft turbine engine development

23 p3020 A73-44219

Low frequency noise generation within aircraft gas turbine engine core portion, discussing sources prediction, model and full scale engine tests, and future technology

[AIAA PAPER 73-1027]

24 p3122 A73-44858

AC starter generator featuring variable-to-constant frequency conversion by cycloconverters as switching device for use with aircraft engines

24 p3057 A73-45154

Aircraft gas turbine engines with single crystal blades to avoid conventional casting grain boundary weakness and premature damage

24 p3094 A73-45155

Ram air turbine with hydraulic pitch change servo regulated speed as emergency power source for aircraft control in event of main engine failure

24 p3058 A73-45475

AIRCRAFT EQUIPMENT

NT AIRCRAFT HYDRAULIC SYSTEMS

NT AIRCRAFT LIGHTS

NT AIRCRAFT TIRES

NT EJECTION SEATS

Aircraft power supply alternators with superconductive field windings, calculating specific weights and performance characteristics

07 p0779 A73-20408

Ram air turbines for aircraft emergency power supply, discussing design, performance and control

10 p1177 A73-23525

Fabrication and physical, mechanical and electrical properties of inorganic composite material for aircraft radomes

11 p1387 A73-25288

Thermal resistance and aging properties of polybenzimidazoles, polyimides and polyamides-imides used for Mach 3 aircraft radomes

11 p1335 A73-25291

Airliner radomes erosion by atmospheric precipitation, water penetration, icing, bird and stone impact and lightning

11 p1335 A73-25297

Long-life, high energy Ni-Cd aerospace cells.

13 p1572 A73-29585

Sealed aircraft battery with integral power conditioner.

13 p1573 A73-29589

Concorde air conditioning, discussing system modifications for production aircraft concerning interconnection of engine air bleeds of adjacent port and starboard groups

14 p1713 A73-30933

Russian book on civil aviation aircraft and helicopter equipment covering navigation, automatic control, electrical and oxygen systems and aircraft instruments

15 p1829 A73-31548

Onboard electronic equipment optimization and redundancy

15 p1852 A73-32460

Technologies applicable to the development of an onboard L-band transmitter

15 p1852 A73-32481

Selection, application, and inspection of electric overcurrent protective devices.

[SAE ARP 1199]

16 p1987 A73-33016

Performance measurements of aircraft electrical systems having highly distorted voltage and current waveforms.

17 p2135 A73-34604

Restraint systems /lap belts and shoulder harnesses/ for military, transport and general aviation aircraft, with emphasis on pilot and crew systems

[SAE PAPER 730291]

17 p2114 A73-34656

Multiplex data bus techniques for digital avionics, discussing transmission media, modulation methods, remote control and reliability

17 p2138 A73-35231

Expanded built-in-test for advanced electrical systems for aircraft.

17 p2109 A73-35248

Avionics subsystems operational, functional and physical considerations, discussing cost, computer programming, common components, multiplexing and hardware design

17 p2139 A73-35249

Computer analysis of the influence of solid state distribution on aircraft power generation.

17 p2109 A73-35250

150 KVA integrated drive generator for aircraft electrical systems.

17 p2109 A73-35253

Russian book - The Tu-134 aircraft: Its design and operation.

18 p2266 A73-35870

Venturi exhausts for air pumping augmentation in ram air operated aircraft heater or combustor, discussing experimental data on suction variation

18 p2343 A73-36396

Report on an ST6 powered air supply package for air cushion landing systems.

19 p2382 A73-37690

Aircraft radio equipment manufacture, assembling, mounting, installing and testing, discussing hangar installation, bundle elements, castings, printed circuits and welding techniques

19 p2433 A73-37767

On-board navigation and landing systems for local airlines in the USSR

19 p2452 A73-37819

Determination of the proneness of aviation oils to carbon deposition

19 p2472 A73-38491

Electric powered commercial jet aircraft emergency power supplies, discussing attitude gyros, Ni-Cd batteries, voltmeters, equipment running times, static inverters and transmitters

20 p2510 A73-39213

Russian book on aircraft onboard instruments and equipment arrangement and housing for weight reduction covering electric, radar, navigation, control, display and auxiliary devices

21 p2635 A73-41425

Decentralized power processing for large-scale systems.

22 p2801 A73-42905

AIRCRAFT EXHAUST

U EXHAUST GASES

AIRCRAFT FUEL SYSTEMS

Evaluation of the method of characteristics applied to a pressure transient analysis of the B.A.C./S.N.I.A.S. Concorde refuelling system.

02 p0133 A73-12645

Potentials and problems of hydrogen fueled supersonic and hypersonic aircraft.

09 p1032 A73-22830

Book on aerospace vehicles science covering airfoils, aircrafts, fuel systems, structural weight, instrumentation, taxiing, towing and federal aviation regulations

12 p1458 A73-27054

Some causes for the appearance of the 'extraneous noise' defect in transfer pumps of aircraft fuel systems

12 p1460 A73-27094

Up-rating the fuel system flow capacity with high rotational speed.

16 p2046 A73-32922

Concorde aircraft fuel system and component valves design for long term service reliability and ease of maintenance, discussing refueling, fuel jettisoning and feed controls

16 p2046 A73-32923

T700 fuel and control system - A modern system today for tomorrow's helicopters.

[AHS PREPRINT 771]

17 p2109 A73-35089

Corrosiveness of naturally occurring sulfur compounds and organic peroxides in aviation turbine fuels toward Cu and Ag, detailing maximum tolerable ratios

20 p2600 A73-39637

Computerized control system for fuel flow into and out of fuel cells and aircraft gravity center optimization during supersonic cruise and takeoff

21 p2634 A73-40939

VAK 191B.

22 p2798 A73-41752

New developments in aircraft refuelling vehicles.

22 p2838 A73-41861

AIRCRAFT FUELS

Book - ASTM manual for rating motor, diesel, and aviation fuels.

06 p0740 A73-18402

Vapor pressure of supersonic aircraft fuels

07 p0865 A73-20014

Construction of fuel and oil quantity sensors for high-performance aircraft.

13 p1619 A73-29204

Aircraft engine fuel and oil differential temperature measurement via platinum probes, specifying sensor sensitivity, calibration, circuit operation and data reduction

17 p2165 A73-34607

The use of hydrogen for aircraft propulsion in view of the fuel crisis.

17 p2220 A73-35469

Differential temperature measurements in engine fluids.

18 p2315 A73-36071

Russian book - Fuels and lubricants for flight vehicles.

19 p2472 A73-37769

Energy supply and its effect on aircraft of the future. II - Liquid-hydrogen-fueled aircraft: Prospects and design issues.

[AIAA PAPER 73-809]

19 p2388 A73-38373

Potential of hydrogen fuel for future air transportation systems.

[ASME PAPER 73-ICT-104]

23 p3019 A73-43499

AIRCRAFT GUIDANCE

Cockpit device with optical head-up display for visual slope guidance to any runway at any airport

01 p0051 A73-11011

Optimal horizontal guidance law for aircraft in the terminal area.

03 p0340 A73-13518

Extension of a portable tactical instrument approach and landing system.

03 p0340 A73-13574

Trends in helicopter guidance and control systems with bad weather capability.

03 p0340 A73-13921

Russian book on aircraft control systems covering radio communication and navigation, automatic guidance and landing and homing and radar tracking

04 p0474 A73-15964

Aircraft and spacecraft guidance and remote and automatic control of moving objects, using calculus of variations for systems synthesis

05 p0560 A73-16402

Microwave landing system /MLS/ with Doppler scanning technique for aircraft guidance precision improvement over standard VHF/UHF ILS, detailing five-year development plan

10 p1246 A73-23652

Civil aircraft vertical plane navigation and guidance during climb and descent, discussing atmospheric, performance and passenger comfort constraints on flight path selection

13 p1656 A73-28075

Simulated flight tests of a digitally autopiloted STOL-craft on a curved approach with scanning microwave guidance.

[ASME PAPER 73-AUT-1]

13 p1657 A73-29413

Microwave Landing System under U.S. national development plan for replacing ILS, discussing system requirements and design, precision DME and flare-out guidance

14 p1773 A73-29884

Microwave guidance system for aircraft landing, discussing civil and military requirements, position measurement capability, shadowing in propagation, and ground reflection induced signal fading

15 p1910 A73-32468

Guidance of aircraft according to techniques of trajectory plotting with a clock

15 p1911 A73-32489

PB-75 flight guidance system for subsonic commercial transport aircraft operation under Category IIIA conditions, describing cruise and ILS operation

15 p1911 A73-32500

FGS-70 flight guidance system for general aviation, commercial and military transports, discussing ILS and VOR operation modes and autopilot/flight director integration

15 p1912 A73-32501

Doppler scanning landing guidance system based on linear array of equally spaced radiators with RF source commutation

15 p1912 A73-32502

M.A.D.G.E. - Microwave Aircraft Digital Guidance Equipment: Description of the system

15 p1912 A73-32504
 Approach and landing operations and flight guide beam systems, discussing tests, design, improvements and operational requirements
 [DGLR PAPER 73-011] 17 p2208 A73-34491
 Tactical aircraft guidance system for CH-47B helicopter utilizing fly by wire control system, describing design, display devices, flight instruments, computer configuration and crew duties
 [AHS PREPRINT 761] 17 p2210 A73-35084
 Digital V/STOL flight simulation test procedures for aircraft navigation, guidance and control, detailing display device panels, flight path simulation and software configuration

17 p2210 A73-35853
 C band microwave landing system for increased guidance signal accuracy and reliability in azimuth, elevation and range relative to touchdown point

19 p2450 A73-37494
 Guidance, control, and instrumentation progress on the McDonnell Douglas DC-10.

19 p2451 A73-37814
 United States Microwave Landing System development program.

19 p2451 A73-37815
 Airborne IRP alignment using acceleration and angular rate matching.

19 p2386 A73-38048
 Simulated flight tests of a digitally autopiloted STOL-craft on a curved approach with scanning microwave guidance.

19 p2386 A73-38049
 Flight director design for a STOL aircraft.

20 p2508 A73-38649
 Optimal filtering and smoothing simulation results for CIRIS inertial and precision ranging data.

[AIAA PAPER 73-872] 20 p2587 A73-38809
 Nonlinear trajectory following in the terminal area - Guidance, control and flight mechanics concepts using the microwave landing system.

[AIAA PAPER 73-903] 20 p2589 A73-38837
 Microwave landing system elevation data or altitude information for flare-out guidance, considering airport, aircraft autopilot and ground equipment and cost factors

21 p2736 A73-40050
 Low cost airport surveillance and Localized Cable Radar with runway or taxiway vehicle guidance capability for ground traffic control, using solid state equipment

AIRCRAFT HAZARDS

Meteorological parameters conducive to ice formation on aircraft, analyzing data statistics on atmospheric moisture content, temperature and drop size
 [DGLR PAPER 72-109] 02 p0130 A73-11660
 Reducing the smoke hazard in small transformer failures.

03 p0252 A73-13572
 Radiation problems of supersonic flight - The operators' viewpoint.

05 p0542 A73-16624
 Contribution to the protection of flight vehicles against lightning effects

06 p0648 A73-18436
 Aircraft wake vortex avoidance systems with current locus detection and/or prediction capability, discussing design based on hazard assessment and computer simulation for performance

10 p1172 A73-24557
 Pilot incapacitation as cause for aircraft operational risks, discussing flight crews education for emergency situations handling

10 p1185 A73-24717
 Aquaplaning prevention during take-off and landing, discussing friction loss factors, aircraft tires and runway surface treatment by antiskid overlays and grooving

11 p1343 A73-25209
 Study on the limit efficiency of lightning conductors on aircraft radomes.

11 p1336 A73-25303
 Electrostatic charge induction on aircraft due to charged atmosphere and friction effects, noting lightning protection, fuel container shielding and charge removal methods

11 p1307 A73-26722
 Rain erosion of reinforced plastics for aerospace applications in terms of drop size, impact angle and velocity effects and protective coatings

17 p2195 A73-34806

AIRCRAFT HYDRAULIC SYSTEMS

Hydraulic system on de Havilland Twin Otter STOL aircraft for flaps, wheel brakes and nose wheel steering, noting power supply mounting

03 p0252 A73-13350
 Hydrolysis of a disiloxane/ester fluid in a simulated hydraulic system at 275 F.
 [ASLE PREPRINT 72LC-6C-11]

Maximum safety hydraulic systems for A300B Airbus powered flight controls for normal flying and auto land operations

04 p0409 A73-16031
 Aircraft hydraulic system and servocontrol design and performance, noting system reliability and fluid loss prevention

06 p0649 A73-17995
 Hydraulic drive and control systems used for landing gear retraction and extension on Piper Cherokee Arrow and for main wheel braking on F-111

07 p0779 A73-19604
 High gain hydromechanical servomechanism with multispring, mass damping and feedback control, deriving transfer function response, with application to aircraft control surface actuator design

13 p1596 A73-29150
 Quad redundant fly by wire servocontrol system design and tests in F-8C high speed jet aircraft, using fail/safe hydraulic actuators

16 p1970 A73-33080
 L-1011 aircraft hydraulic system layout and installation techniques with modular design and plug-in cartridges for Murphy law error reduction during servicing

17 p2108 A73-34523
 Russian book - Hydraulic ducts of control systems in aviation: The effects of external factors. Shop testing, and reliability.

19 p2389 A73-37766
 Book - Criteria for current and advanced aircraft hydraulic tubing.

[SAE SP-378] 19 p2434 A73-37863
 Commercial jet transport aircraft hydraulic fuel distribution tubing systems, discussing maintenance, fabrication problems, fittings, quality control and materials

[SAE SP-378] 19 p2434 A73-37864
 The application of Armco 21-6-9 steel tubing to the DC-10 hydraulic system.

[SAE SP-378] 19 p2389 A73-37865
 Aircraft hydraulic tubing permissible defects in Cr-Ni-Mn, Al and Ti tubes and return lines, noting wall thickness, chafing, denting, weld seam cracks and impulse tests

[SAE SP-378] 19 p2434 A73-37866
 Defects in high quality aircraft tubing and inspection methods.

[SAE SP-378] 19 p2434 A73-37867
 Integrated hydraulic flight control actuator packages replacing mechanical linkages for aerodynamic surface control during V/STOL operation

20 p2510 A73-39015

AIRCRAFT INDUSTRY

Low noise STOL aircraft as solution for short haul transportation, discussing German, British and Swedish industrial development efforts

01 p0004 A73-10468
 Aircraft industry design and development costs prediction, using Monte Carlo model to determine effect of poor estimates

02 p0238 A73-11860
 Assembling by welding and bonding - Introductory report on assemblies

06 p0698 A73-18692
 Capital equipment marketing, discussing industry-customer-government interface, marketing and sales techniques and functions, products initiation, etc

10 p1298 A73-24650
 The financing of aircraft procurement.

17 p2257 A73-34534
 Russian book - safety measures in aviation industry.

18 p2281 A73-35869

AIRCRAFT INSTRUMENTS

NT ALTIMETERS
 NT ANEMOMETERS
 NT APPROACH INDICATORS
 NT ATTITUDE INDICATORS
 NT AUTOMATIC PILOTS
 NT FLIGHT RECORDERS
 NT GYROCOMPASSES
 NT HOT-WIRE ANEMOMETERS
 NT MAGNETIC COMPASSES
 NT PLAN POSITION INDICATORS
 NT POSITION INDICATORS
 NT RADIO ALTIMETERS
 NT RADIO DIRECTION FINDERS
 NT RATE OF CLIMB INDICATORS
 NT SONIC ANEMOMETERS
 NT SPACECRAFT POSITION INDICATORS
 NT SPEED INDICATORS
 NT TACHOMETERS

Electromechanical and electronic cockpit displays effectiveness in terms of aircraft control and psychological/physiological factors relating to pilot performance and workload

[DGLR PAPER 72-097] 02 p0136 A73-11666
 S-61N helicopter all-weather IFR operation for North Sea oil rigs supply and harbor pilots transportation, describing onboard instrumentation, navigation and communication systems

05 p0535 A73-16847

Aircraft performance augmentation by energy management instruments or systems, considering energy/energy rate meter and algorithm for real time onboard flight path optimization
 [AIAA PAPER 73-228] 05 p0536 A73-16953
 Book - Aircraft Instruments: Principles and applications.

06 p0693 A73-18075
 Basic specification research for the main instruments of light aircraft

07 p0825 A73-20248
 Russian book on onboard distance measuring systems for flight vehicles covering design of cw and pulsed devices, modulators, error analysis, noise, logic elements, etc

07 p0825 A73-20378
 Aeromechanical measurements in free flight on piloted aircraft

09 p1032 A73-22447
 Russian book on aviation fundamentals covering aerodynamics and flight theory, designs, components, engines and instrumentation of aircraft, including helicopters, VTOL and STOL

09 p1032 A73-23224
 Precision hover sensor for heavy-lift helicopter.

10 p1216 A73-23784
 Airborne atmospheric temperature measurements correction for sensor response lag, deriving numerical scheme based on sensing systems wind tunnel calibration

10 p1217 A73-23991
 Design of control and display panels using computer algorithms.

11 p1361 A73-25180
 Utilization of the Doppler effect to measure the drift angle and the ground speed of an aircraft

11 p1305 A73-25797
 A description of the NAE T-33 turbulence research aircraft, instrumentation and data analysis.

11 p1306 A73-26269
 On the estimation of the directional spectrum of surface gravity waves from a programmed aircraft altimeter.

11 p1358 A73-26347
 Human factors aspects in aircraft electronic display systems, discussing cathode ray tubes (CRT) and light emitting diodes (LED) applications and characteristics

11 p1324 A73-26500
 Cockpit instrument display systems visibility and reliability requirements, discussing various illumination methods in terms of power consumption, cost and human factors engineering

12 p1495 A73-26825
 Book on aerospace vehicles science covering airfoils, aircrafts, fuel systems, structural weight, instrumentation, taxiing, towing and federal aviation regulations

12 p1458 A73-27054
 European Airbus A300B aircraft flight tests and on-board instrumentation in certification program, illustrating desk layout, control and display panels

13 p1568 A73-28159
 Aircraft compass design with magnetic needle free turning capability around two orthogonal axes, noting advantage over conventional devices and suitability for glider navigation

13 p1613 A73-28555
 Electronic differentiator for aircraft flight data on-board calculation in performance gliding, discussing compensation method and vertical air velocity measuring instrument advantage

13 p1569 A73-28556
 Construction of fuel and oil quantity sensors for high-performance aircraft.

13 p1619 A73-29204
 Vertical aircraft flight control and navigation instrumentation avionics developments, emphasizing Inertial-lead Vertical Speed Indicator design and command and advisory information displays

13 p1621 A73-29345
 Meteorological radar and the WILM landing aid

14 p1772 A73-29731
 Microwave Landing System under U.S. national development plan for replacing ILS, discussing system requirements and design, precision DME and flare-out guidance

14 p1773 A73-29884
 Russian book on aeronautical electric and electronic materials covering physicochemical properties of magnetic, dielectric, conductor, semiconductor, polymer, ferritic, thin film and composite materials

14 p1766 A73-30357
 Concorde engine monitoring instrumentation, discussing start cycle, temperature sensors and indicators and nozzle position indicators

14 p1754 A73-30931
 Russian book on civil aviation aircraft and helicopter equipment covering navigation, automatic control, electrical and oxygen systems and aircraft instruments

15 p1829 A73-31548
 A-300 B Airbus active and passive operational monitoring systems, considering visual and aural routine

functional indicators, emergency warning devices and flight data recorders

15 p1830 A73-32458

Commercial aircraft flight control instrumentation for safe and efficient flight path management, emphasizing aircrew work load relief under stressful air traffic conditions

15 p1830 A73-32473

FGS-70 flight guidance system for general aviation, commercial and military transports, discussing ILS and VOR operation modes and autopilot/flight director integration

15 p1912 A73-32501

Head-up displays for flight control information on velocity vector, angle of attack, glide path slope and ground reference data, considering VFR and IFR conditions

15 p1831 A73-32507

Aircraft flight control head-up display system design, equipment installation particulars, performance tests and merits evaluation

15 p1831 A73-32508

Instrument-panel electronic display system

15 p1831 A73-32510

Gimbaled electrostatic gyro inertial aircraft navigation system /GEANS/ designs balancing performance against cost of ownership

16 p2034 A73-33086

Avionics systems simplification for cost, weight and space reduction, considering ease of maintenance, failure points reduction and flight director/autopilot computers and couplers elimination

16 p1968 A73-33187

WB-57F aircraft with instrument package for nuclear test detection and upper atmosphere research, discussing range, altitude, speed, payload capacity and onboard equipment

[AIAA PAPER 73-510] 16 p1969 A73-33548

Effects of new landing approach procedures on cockpit design and possibilities of taking them into account

[MBB-UH-07-73] 17 p2100 A73-34485

Airborne flight-test strain gage instrumentation from installation, calibration and data recording and reduction standpoint, discussing ground and airborne minicomputer use

17 p2148 A73-35442

Third generation Aircraft Recording Instrumentation System /ARIS III/, consisting of digitizer and logic, analog interface and hybrid instrumentation recorder

17 p2174 A73-35581

Guidance, control, and instrumentation progress on the McDonnell Douglas DC-10.

19 p2451 A73-37814

Environment effects on tape recorder design for in-flight data collection in military aircraft

19 p2431 A73-38197

Air based collision avoidance system feasibility appraisal, discussing YG1054 proximity warning indicator, cost analysis and implementation prognosis

19 p2454 A73-38468

Annual Corporate Aircraft Safety Seminar, 18th, Arlington, Va., April 1-3, 1973, Proceedings.

20 p2509 A73-39210

Instrument landing monitor /ILM/ evaluation program for potential and actual capability to restore poor and/or missing visibility

20 p2590 A73-39211

Russian book on aircraft onboard instruments and equipment arrangement and housing for weight reduction covering electric, radar, navigation, control, display and auxiliary devices

21 p2635 A73-41425

Russian book on gyroscope theory covering maritime, aircraft, rocket and spacecraft applications, instrument error, differential equations of motion, rotor precession and degrees of freedom

21 p2705 A73-41437

The susceptibility of modern aircraft instrument systems to interference in the HF band.

22 p2851 A73-41694

Eye function and the illumination of instrument dials in aircraft

22 p2817 A73-43133

AIRCRAFT LANDING

NT CRASH LANDING

NT DITCHING [LANDING]

NT SKID LANDINGS

Effect of aircraft reliability regulations on takeoff and landing performance of QSTOL aircraft

[DGLR PAPER 72-056] 02 p0130 A73-11658

Schematic design of an automatic device for correcting aircraft takeoff and landing modes of flight

02 p0190 A73-11801

Determination of the navigational regime for flight over fixed points during the landing maneuver

03 p0339 A73-13071

Handling characteristics in roll of two light airplanes for steep approach landings.

03 p0250 A73-13701

A computer-generated display to isolate essential visual cues in landing.

05 p0595 A73-16704

Perceptual considerations for a wide field of view, helicopter night landing system /HENILAS/.

05 p0543 A73-16705

A statistical analysis of pilot control during a simulation of STOL landing approaches.

[AIAA PAPER 73-182] 05 p0536 A73-16922

Arrested landing studies for STOL aircraft.

[AIAA PAPER 73-51] 06 p0647 A73-17627

Visual systems for indicating approach slope during aircraft landing

09 p1116 A73-22975

Microwave landing system /MLS/ with Doppler scanning technique for aircraft guidance precision improvement over standard VHF/UHF ILS, detailing five-year development plan

10 p1246 A73-23652

All-weather aircraft landing automation, discussing efficient optimal feedback control law selection based on trajectory termination or terminal control requirements

10 p1247 A73-24010

Manned vehicle systems analysis techniques application to manual approach-to-landing phase of aircraft flight, developing analytical control model

10 p1247 A73-24011

Display system for monitoring automatically controlled STOL landing glide paths, discussing computer controlled simulation

11 p1362 A73-25440

An optimal control approach to terminal area air traffic control.

11 p1394 A73-25786

Vibrations of an Euler beam with a system of discrete masses, springs, and dashpots.

11 p1442 A73-25788

Evaluation of glide paths for landing a VTOL airplane using linear regulator theory.

12 p1458 A73-27154

Flight tests of approach path angles and airspeed effects on landing of spoiler equipped light aircraft

13 p1569 A73-28830

Manual vs fully automatic landing concepts, discussing pilots abilities and limitations and primary requirements for displays

13 p1656 A73-28905

Optimal aircraft go-around and flare maneuvers.

13 p1657 A73-29217

Airport runway lights system location and use for aircraft takeoff operations and visual indication of landing approach angle

14 p1743 A73-30242

STOL aircraft flight and landing area considerations.

[ASCE PREPRINT 1726] 15 p1856 A73-31389

An ILS sensor for fail operative autoland systems - The Bendix RIA-32A.

15 p1880 A73-32461

An instrument approach system for Hong-Kong International Airport.

15 p1910 A73-32464

Study of the integrity of an equipment - Application to radio altimeters for category III landing

15 p1880 A73-32493

Microwave holography application to landing without visibility

15 p1911 A73-32497

Independent Landing Monitor for economic Category 3 operation with fail-operational autoland, fog dissipation or fail-passive autoland plus visibility augmentation

15 p1911 A73-32499

Doppler scanning landing guidance system based on linear array of equally spaced radiators with RF source commutation

15 p1912 A73-32502

All-weather landing technology and economics, considering ground and airborne equipment and benefits and costs

15 p1859 A73-32553

Airport lighting systems as visual landing aids, discussing runway disposition, brightness levels, beam orientation, visibility factors and flashing lights

16 p1993 A73-32974

Aircraft performance relationship to safety margins improvement, discussing accelerate stop, approach control, airworthiness, landing and coordination

17 p2097 A73-34082

Safety in the accident prone flight phases of take-off, approach and landing.

17 p2098 A73-34085

Further developments in surface effect takeoff and landing system concepts - Application to high performance aircraft.

17 p2099 A73-34293

Further developments in surface effect takeoff and landing systems concepts - A multicell system.

17 p2099 A73-34294

Monitor display to indicate aircraft position relation to desired flight profile during automatically controlled steep landing approaches with curved segments

17 p2207 A73-34477

Considerations concerning the design of an electronic landing display for STOL aircraft

17 p2146 A73-34478

Possibilities for improving conventional ILS systems

17 p2207 A73-34479

Low visibility/bad weather aircraft landing systems design, discussing developmental stages for all weather landing implementation, automatic landing control and pilot visual discrimination problems

17 p2207 A73-34481

Longitudinal motion of a transport aircraft during steep landing approaches

17 p2100 A73-34482

Digital control of rotary wing aircraft landing approach based on spatially variable preassigned flight path

[MBB-UFE-1021] 17 p2207 A73-34486

Noise reduction of STOL aircraft during landing approach and takeoff via thrust reduction and steepest descent flight paths

[MBB-UH-06-73] 17 p2100 A73-34488

Approach and landing operations and flight guide beam systems, discussing tests, design, improvements and operational requirements

[DGLR PAPER 73-011] 17 p2208 A73-34491

Flight mechanics problems associated with landing approaches using direct lift control, as exemplified by the HFB 320 Hansa aircraft

[DGLR PAPER 73-024] 17 p2100 A73-34496

Russian book - Analysis of meteorological conditions for aviation.

17 p2204 A73-34539

Analysis of visibility conditions during aircraft landing in radiation fog

17 p2204 A73-34540

Inglewood /California/ airport noise abatement monitoring program, discussing landing approach slopes, monitoring equipment and techniques and noise effects on property value

19 p2505 A73-37283

Direct side force control for STOL crosswind landings.

[AIAA PAPER 73-811] 19 p2379 A73-37467

Development of an Air Cushion Landing System.

[AIAA PAPER 73-812] 19 p2379 A73-37468

Air cushion landing systems for aircraft mobility on unprepared surfaces, considering refraction, vertical energy absorption, braking, steering and weight and power reduction

19 p2380 A73-37677

Air cushion landing systems application to tactical airlift aircraft for personnel, and equipment delivery to dispersed sites under diverse climatic, terrain and combat conditions

19 p2380 A73-37678

Aircraft with air cushion landing system for off airport transport of goods and passengers

19 p2417 A73-37679

The Navy SETOLS program and its potential applications to Navy aircraft.

19 p2381 A73-37680

ACLS equipped vehicles in inter-city transportation.

19 p2381 A73-37686

Preliminary results from dynamic model tests of an air cushion landing system.

19 p2382 A73-37694

The Jindivik Drone Program to demonstrate air cushion launch and recovery.

19 p2382 A73-37697

Air cushion landing system /ACLS/ design and drone flight tests for low cost unmanned military aircraft recovery, comparing with mid air retrieval system /MARS/

19 p2383 A73-37699

Simulation of the ACLS during landing roll.

19 p2383 A73-37706

Ground loads analysis for air cushion landing system /ACLS/ equipped aircraft during landing and taxiing, predicting peak trunk pressures via energy considerations

19 p2383 A73-37707

Aircrew workload during the approach and landing.

19 p2401 A73-38005

Studies on the time-to-go indexing control scheme for an automatic aircraft landing system.

19 p2453 A73-38280

Flight director design for a STOL aircraft.

20 p2508 A73-38649

Automatic control of adverse yaw in the landing environment using optimal control theory.

[AIAA PAPER 73-861] 20 p2586 A73-38799

Runway condition effects on landing safety, discussing surface friction, approach control, skidding, directional control, water and ice conditions, tires and brakes

20 p2509 A73-39220

Microwave Landing System with air-derived sample data and scanning narrow beam antennas for signal-in-space generation, discussing design requirements and performance test

21 p2735 A73-40046

Carrier landing simulation for pilot visual perception, describing Fresnel lens optical landing system, periscopes, cockpit equipment and glide paths

[AIAA PAPER 73-917] 21 p2634 A73-40865

Reducing approach and landing accidents.
22 p2799 A73-42523

Evolution of blind landing systems
22 p2885 A73-43032

Optimal landing flare control of aircrafts with sensitivity consideration.
23 p2940 A73-43284

AIRCRAFT LANDING INSTRUMENTS

U LANDING INSTRUMENTS

AIRCRAFT LAUNCHING DEVICES

Further developments in surface effect takeoff and landing system concepts - Application to high performance aircraft.
17 p2099 A73-34293

Further developments in surface effect takeoff and landing systems concepts - A multicell system.
[CASI PAPER 76/11B] 17 p2099 A73-34294

Drone launch and recovery reliability requirements for target, reconnaissance, air-to-air combat, high altitude endurance and defense suppression missions
19 p2381 A73-37681

AIRCRAFT LIGHTS

Aircraft in-flight visibility /conspicuity/ during daytime, discussing exterior paints, tapes and high intensity lighting effectiveness for midair collision avoidance
16 p1965 A73-32661

A new approach to aircraft exterior lighting.
17 p2108 A73-35808

AIRCRAFT MAINTENANCE

Aircraft fault isolation based on pattern of cockpit indications - A human factors approach.
02 p0136 A73-11857

Dual sensitivity liquid penetrants for improving NDT inspection of minute defects in military aircraft structures during rework and repair, noting comparative advantages
02 p0173 A73-11984

Economic performance and cost problems in civil air transport maintenance and engineering quality control related to selling price trends
06 p0647 A73-17888

Business aircraft operational costs, considering maintenance, repair and depreciation
06 p0771 A73-17998

Airlines aircraft, engines and instruments maintenance, overhaul and repair procedures and equipment
06 p0648 A73-18254

Some UK military views on the development and procurement of AIDS, BIT and ATF for avionics.
08 p0962 A73-20679

Russian book on aircraft natural-climatic environmental factors covering geographic region adverse effects on design, performance and maintenance
09 p1031 A73-22349

Russian book - Transport aircraft maintainability.
09 p1032 A73-22375

Charter air fleet maintenance economic management, discussing budget, manpower, time and materials control
09 p1168 A73-23243

Development of maintenance policies in the operation of aircraft
10 p1174 A73-23655

Aircraft maintenance for safety and reliability, considering design requirements, human errors, fault diagnosis, redundancy, failure mode analysis, service data statistics and equipment specifications
10 p1174 A73-23759

Aircraft maintenance manuals optimization for human errors minimization, discussing DC-10 in-flight and ground maintenance fault isolation philosophy and techniques
10 p1226 A73-24716

Transport aircraft maintenance program, discussing safety and reliability correlation with design
11 p1306 A73-26591

Prediction for a park of helicopters of the same type
12 p1561 A73-27077

Condition monitoring - A new technology for aircraft engine maintenance
12 p1486 A73-27389

Tilt-table alignment for inertial-platform maintenance without a surveyed site.
15 p1858 A73-31728

ARINC-573 recording system - Application to maintenance
15 p1883 A73-32462

Maintenance of public transportation aircraft - Evolution of methods
15 p1925 A73-32556

Concorde aircraft fuel system and component valves design for long term service reliability and ease of maintenance, discussing refueling, fuel jettisoning and feed controls
16 p2046 A73-32923

Maintenance of pitot-static systems of transport aircraft.
[SAE AIR 975] 16 p2014 A73-33014

Composite airframe structure effects on jet aircraft maintenance, discussing fire safety, fatigue resistance, environmental durability and quality assurance
16 p1967 A73-33027

Operational readiness and maintenance testing of the B-1 strategic bomber.
16 p1969 A73-33631

Concept and system of the versatile avionics shop test /VAST/ system.
16 p1986 A73-33634

Design to detect and avoid failure - One airline's viewpoint.
17 p2097 A73-34081

Aircraft design for operational safety, discussing risk elimination, failure modes, maintenance analysis and fault diagnosis
17 p2098 A73-34083

L-1011 aircraft hydraulic system layout and installation techniques with modular design and plug-in cartridges for Murphy law error reduction during servicing
17 p2108 A73-34523

Air Force propulsion maintenance concepts.
[SAE PAPER 730373] 17 p2177 A73-34712

The development of a turbine engine maintenance program from a new reliability model.
[SAE PAPER 730374] 17 p2177 A73-34713

Review of engine maintenance concepts applied to wide body jets.
[SAE PAPER 730375] 17 p2178 A73-34714

PLANET scheduling algorithms and their effect on availability.
17 p2130 A73-34822

Westland Sea Lynx naval variant aircraft design and development for multiservice multirole application, emphasizing high reliability and maintenance ease requirements
17 p2104 A73-35057

LN-33 airborne inertial navigation system with low cost precision instruments and miniaturized digital computer, noting built-in calibration and test capability for minimizing maintenance
17 p2210 A73-35212

Expanded built-in-test for advanced electrical systems for aircraft.
17 p2109 A73-35248

Technical and safety aspects of maintenance work on commercial aircraft wing fuel tanks, considering wing deformation effects and sealant materials and reapplications
18 p2286 A73-36932

Commercial jet transport aircraft hydraulic fuel distribution tubing systems, discussing maintenance, fabrication problems, fittings, quality control and materials
19 p2434 A73-37864

U.S.S.R. laws and regulations regarding civil air transport equipment operations and maintenance, considering personnel training and safety
19 p2435 A73-38119

Safe flying, skilled personnel and aircraft maintenance assurance via safety equipment, initial and recurrent training, protective clothing and shelter from inclement weather, maintenance scheduling, etc
20 p2518 A73-39212

Fire hazard reduction in corporate aircraft oxygen system, covering hoses, regulators, manifolds, cylinders, leakage, combustion conditions and servicing procedures
20 p2518 A73-39215

Discourse on comparisons between commercial and military aircraft logistics.
20 p2629 A73-39274

Civil and military aircraft preventive maintenance, discussing on-condition and condition monitoring concepts for equipment reliability enhancement and cost reduction
20 p2544 A73-39275

Helicopter and fixed wing aircraft design consideration comparison, examining maintenance and reliability requirements, rigid, hinged and tilted rotors and load characteristics
21 p2634 A73-40225

The nondestructive tests in the maintenance of commercial aircraft
22 p2799 A73-42186

AIRCRAFT MANEUVERS

Optimal aircraft go-around and flare maneuvers.
13 p1657 A73-29217

Design and application of a part-task trainer to teach formation flying in USAF Undergraduate Pilot Training.
[AIAA PAPER 73-935] 21 p2674 A73-40881

Flight tests of load factors for multirecorder-equipped gliders of various designs during pullout and looping maneuvers
22 p2799 A73-41866

AIRCRAFT MODELS

B-1 airplane model support and jet plume effects on aerodynamic characteristics.
[AIAA PAPER 73-153] 05 p0563 A73-16901

Solid state Digital Slip Sync Strobe/Camera Control System design for powered wind tunnel helicopter models testing
17 p2101 A73-34622

Computer aided parametric analysis for general aviation aircraft.
[SAE PAPER 730332] 17 p2130 A73-34685

Experience with the NRC 10 ft. x 20 ft. V/STOL propulsion tunnel - Some practical aspects of V/STOL engine model testing.
21 p2672 A73-40855

Wind tunnel test for Dolphin airship model static thrust measurements, discussing thrust direction torque moment coefficients and propeller rotation
21 p2635 A73-41648

Antenna radiation-pattern measurement using model aircraft.
22 p2831 A73-41841

AIRCRAFT NOISE

NT JET AIRCRAFT NOISE

NT SONIC BOOMS

Helicopter internal and external noise level measurements under various flight conditions, obtaining noise radiation directivity patterns via time measuring tractography equipment
[ONERA, TP NO. 1136] 01 p0004 A73-10241

Annoyance reactions from aircraft noise exposure.
01 p0005 A73-10781

Remarks on the paper by J. M. Nicholls and B. F. James, 'The location of the ground focus line produced by a transonically accelerating aircraft.'
01 p0005 A73-10786

STOL aircraft technology, operation and markets in view of future European air traffic development, discussing various lift devices, noise aspects and economic factors
[DGLR PAPER 72-054] 02 p0130 A73-11662

Model study of aircraft noise reverberation in a city street.
02 p0130 A73-12199

Statistical analysis of the sound-level distribution of aircraft noise as a function of time. II
02 p0131 A73-12449

NASA Quiet Engine Program review and test results, discussing noise reduction technology application to transport aircraft
02 p0204 A73-12845

On evaluation of aircraft noise around air-bases by factor analysis.
03 p0249 A73-12957

Osaka airport effective continuous perceived noise level measurements, area contour map and noise duration allowance vs aircraft distance diagram
03 p0249 A73-12977

Techniques for determining the noise zones in the vicinity of the central Berlin-Schoenefeld airport, and related problems
03 p0249 A73-12978

The influence of background noise on disturbance due aircraft.
03 p0249 A73-12979

The second noise and social survey around Heathrow, London airport.
03 p0266 A73-12980

Reproduction of sound propagation in the standard atmosphere
03 p0342 A73-12993

Subsonic aircraft noise - A solution by the wider application of today's new engines.
03 p0249 A73-13062

Geared fan engine systems - Their advantages and potential reliability.
[AIAA PAPER 72-1173] 03 p0357 A73-13469

An acceptable exposure level for aircraft noise in residential communities.
03 p0250 A73-13838

The aeroplane as a threat to the environment.
03 p0251 A73-14468

Airlines responsibility and measures for aircraft noise abatement, considering economic and safety aspects
04 p0406 A73-14893

Aircraft noise as a continuing national problem.
04 p0521 A73-14894

Air transportation system planning - Progress in noise reduction.
04 p0406 A73-14895

Flap noise measurements for STOL configurations using external upper surface blowing.
[AIAA PAPER 72-1203] 04 p0487 A73-14922

A note on the quantity /effective/ perceived noisiness and units of perceived noise level.
04 p0406 A73-15587

Atmospheric attenuation of noise measured in a range of climatic conditions.
[AIAA PAPER 73-242] 05 p0570 A73-16966

Computing meteorological effects on aircraft noise.
05 p0536 A73-17121

Recent progress in the field of aircraft noise technology
05 p0537 A73-17272

Aircraft noise reduction problems, noting trained personnel and research laboratories shortage and full scale tests requirements
[AIAA PAPER 73-5] 06 p0646 A73-17601

Book - Aviation law: Cases and materials.
06 p0771 A73-17870

Ducts, nacelles, power source components and cabin noise sources identified for aircraft noise control research, considering prerequisites for quiet operations
[SAE AIR 1079] 08 p0928 A73-20698

Perceived level calculation methods for aircraft flyover noise scaling, rating jets, turboprops, piston aircraft and helicopters with frequency weighting functions, duration and tone corrections
10 p1175 A73-24391

EASCON '72; Electronics and Aerospace Systems Convention, Washington, D.C., October 16-18, 1972, Record.
10 p1298 A73-24551

Aircraft noise reduction technology and certification standards, reviewing federal laws and regulations
10 p1175 A73-24553

Community response to aircraft noise.
10 p1298 A73-24562

Cost effectiveness of planned aviation system improvements, considering ATC automation vs terminal aids, noise control, ground facilities, capacity and en-route situation
10 p1247 A73-24767

A single number rating for effective noise reduction.
11 p1397 A73-25000

A comparative study of augmentor wing, ejector nozzle and power jet flap low noise STOL concepts.
11 p1300 A73-25385

European contribution to structural response to noise.
[AIAA PAPER 73-332] 11 p1305 A73-25561

Airport noise control and minimization for community and airline industry interests by technology application and legal-political approaches
11 p1455 A73-26350

Variations in the sound field of a STOL aircraft as a function of wing-flap deflection
11 p1306 A73-26592

Some causes for the appearance of the 'extraneous noise' defect in transfer pumps of aircraft fuel systems
12 p1460 A73-27094

Book - Human factor aspects of aircraft noise.
12 p1465 A73-27450

Recent advances in aircraft noise reduction.
13 p1570 A73-29104

Airport layout and planning standards, considering dimensions, height restrictions, noise exposure, land use compatibility, and long term community and aeronautical requirements
13 p1598 A73-29347

Helicopter rotor blade passing close to tip vortex, calculating fluctuating lift induced harmonic blade loads and generated cyclic banging noise
13 p1570 A73-29382

Insulating houses against aircraft noise.
14 p1743 A73-30913

Aircraft noise, exposure factor, land use priorities, public environmental concern and jurisdictional considerations impact on offshore airport planning
15 p1959 A73-31530

Book - Aircraft noise: Should the Noise and Number Index be revised.
15 p1830 A73-32414

Book - Aircraft noise: Selection of runway sites for Maplin Airport.
15 p1859 A73-32415

Aircraft noise abatement technological and social aspects, considering aircraft design, airport noise pattern minimization and population removal
15 p1831 A73-32560

Determinants for aircraft noise annoyance - A comparison between French and Scandinavian data.
16 p1967 A73-32915

Aircraft engine noise reduction state of art, discussing FAA requirements, Concorde, DC-9 and Bertin Aladin II aircraft
16 p1967 A73-32970

Definitions and procedures for computing the effective perceived noise level for flyover aircraft noise.
[SAE ARP 1071] 16 p1967 A73-33015

Inverse condemnation of airspace, discussing real property concept relation to aircraft noise, pollution and environment protection
16 p2087 A73-33103

Prediction and measurement of aircraft noise.
16 p2014 A73-33133

Aspects of investigating STOL noise using large-scale wind-tunnel models.
16 p1994 A73-33170

Short haul aircraft design and marketing, examining competing modes, noise factors, airport traffic density patterns and aircraft types dependence on utilization
16 p2088 A73-33184

Aircraft produced environmental noise and air pollution, discussing related aircraft power plant technology evolution
16 p2047 A73-33191

Social acceptability of heliports particularly from the standpoint of noise.
17 p2146 A73-34441

Pilot operation practices for helicopter noise level reduction, with emphasis on flight altitude increase and routing over noise insensitive areas
17 p2099 A73-34442

Noise reduction of STOL aircraft during landing approach and takeoff via thrust reduction and steepest descent flight paths
[MBB-UH-06-73] 17 p2100 A73-34488

Status of international noise certification standards for business aircraft.
[SAE PAPER 730286] 17 p2101 A73-34651

Fundamental aspects of noise reduction from powered-lift devices.
[SAE PAPER 730376] 17 p2103 A73-34715

Status of current development activity related to STOL propulsion noise reduction.
[SAE PAPER 730377] 17 p2222 A73-34716

Design studies of low-noise propulsive-lift airplanes.
[SAE PAPER 730378] 17 p2103 A73-34717

Civil aviation environmental and economic aspects, discussing noise and air pollution, fuel consumption and airspace and ground space utilization
18 p2267 A73-36685

Aircraft noise in airport areas, discussing effects on environment and economics
18 p2373 A73-36949

Laboratory for the automatic treatment of analog signals
18 p2297 A73-37086

Inter-noise 72; International Conference on Noise Control Engineering, Washington, D.C., October 4-6, 1972, Proceedings and Tutorial Papers.
19 p2472 A73-37276

On the role of the radiation directivity in noise reduction for STOL aircraft.
19 p2378 A73-37277

The ultimate noise barrier - Far field radiated aerodynamic noise.
19 p2375 A73-37278

Noise certification of a transport airplane.
19 p2378 A73-37279

A proposed littoral airport.
19 p2415 A73-37280

Aircraft noise disruption in public schools - A definition of an impasse.
19 p2505 A73-37282

Inglewood /California/ airport noise abatement monitoring program, discussing landing approach slopes, monitoring equipment and techniques and noise effects on property value
19 p2505 A73-37283

Correction procedure for outdoor noise measurements.
19 p2458 A73-37285

Engineering design considerations in the noise control of commercial jet aircraft's vent and drain systems.
19 p2378 A73-37297

Effects of noise curfews on airline operations.
[AIAA PAPER 73-798] 19 p2379 A73-37461

Environmental considerations for offshore airports.
19 p2417 A73-37742

Noise and pollution - The Federal Aviation Administration's views.
19 p2384 A73-37812

Transport aircraft noise reduction in airport areas through low noise engine design, traffic control, flight maneuvers and architectural planning
19 p2384 A73-37818

Survey of the civil responsibility for damages caused by aircraft noise in American and French law
19 p2506 A73-37998

Possibilities and problems of achieving community noise acceptance of VTOL.
19 p2386 A73-38010

Contributions of the DFVLR to environmental research and environment protection. II - Noise control, water environment protection, nature and landscape, environmental protection techniques
19 p2506 A73-38266

Aircraft noise consideration for environmental compatibility, airport development, short haul and supersonic air transport and legislation and regulation problems
[AIAA PAPER 73-795] 19 p2387 A73-38368

Basic acoustic considerations for model noise experiments in wind-tunnels.
22 p2838 A73-41705

Boundary layer induced cockpit noise.
22 p2795 A73-41706

Methods for quantifying the effect of noise on people.
22 p2811 A73-41707

Perceived noise level ratings for helicopter noise, discussing blade slap, tail rotor whine, broadband noise and PNL rating shortcomings
22 p2798 A73-41708

The effect of aircraft noise on the countryside.
22 p2798 A73-41709

Europeplane QSTOL economical solution to noise and congestion problem in short and medium haul transport
22 p2798 A73-41862

Atmospheric absorption considerations in airplane flyover noise at altitudes above sea level.
22 p2799 A73-42943

Helicopter noise experiments in an urban environment.
22 p2800 A73-42944

Runway sideline aircraft noise measurements on takeoff and approach for enforcing community noise

levels based on FAA aircraft type certification, noting associated problems
22 p2800 A73-42945

Community noise impact study from military helicopter operations.
22 p2800 A73-42947

Conventional and high frequency hearing of naval aircrewmembers as a function of noise exposure.
23 p2949 A73-43500

Short takeoff and landing /STOL/ aircraft technology developments for high density air transport, discussing lift system, handling, airfoil design, acoustics and operating economics
23 p2940 A73-43520

The effects of modulated blade spacing on static rotor acoustics and performance.
[AIAA PAPER 73-1020] 24 p3121 A73-44852

Multiple pure tone noise generation and control.
[AIAA PAPER 73-1021] 24 p3122 A73-44853

Inlet geometry and axial Mach number effects on fan noise propagation.
[AIAA PAPER 73-1022] 24 p3122 A73-44854

Turbopfan engine core noise prediction and measurement, considering sources from flow passage obstructions, combustion chamber and turbine noise due to interaction with upstream turbulence
[AIAA PAPER 73-1026] 24 p3122 A73-44857

Mechanisms of externally blown flap noise.
[AIAA PAPER 73-1029] 24 p3056 A73-44859

Comparison of aircraft noise measured in flight test and in the NASA Ames 40-by 80-foot wind tunnel.
[AIAA PAPER 73-1047] 24 p3056 A73-44871

A comparison of the overall and broadband noise characteristics of full-scale and model helicopter rotors.
24 p3057 A73-45264

Maplin airport planning history, noise reduction features and government surveys, noting future air traffic trends and planning alternatives
24 p3076 A73-45373

Aircraft noise reduction alternatives for operational aircraft, noting noise generation upstream of final nozzle, reengining, refanning and suppressor techniques
24 p3123 A73-45374

AIRCRAFT PARTS

Aircraft components solid film lubrication problems, discussing surface pretreatment, contamination susceptibility, corrosion prevention and aerosol applicability
07 p0842 A73-19554

Icing testing in the large Modane wind-tunnel on full-scale and reduced scale models
07 p0808 A73-20244

Study and realization of special parts for aerospace construction by brazing in a fluorided reducing atmosphere
09 p1088 A73-22202

Aircraft structural components in-house or subcontracted fabrication, discussing technical performance, economic and manpower aspects
10 p1297 A73-23521

Design and manufacture of structure components made of fiber-reinforced materials
11 p1373 A73-25417

Numerical procedure for determining optimal member sizes of aircraft structural components with weight minimization and flutter speed lower bound
[AIAA PAPER 73-391] 11 p1439 A73-25520

Phenomenological approach to low-cycle fatigue fracture of a typical aircraft full scale component static test.
[AIAA PAPER 73-324] 11 p1305 A73-25554

Aerospace component failure due to corrosion fatigue in aluminum wing attachment spar, helicopter rotor blade, landing gear cylinder and engine bearings
11 p1380 A73-25803

Stress corrosion cracking and corrosion fatigue for hydraulic aluminum pressure cylinders used for landing gear, stabilizers and aircraft systems
11 p1383 A73-25827

Fretting fatigue in titanium helicopter components.
11 p1383 A73-25837

Corrosion performance of new fastener coatings on operational military aircraft.
[NACE PAPER 115] 13 p1637 A73-29315

How to be healthy, wealthy and wise through fastening analysis - The 'how to' of living with fasteners.
[SAE PAPER 730309] 17 p2177 A73-34669

Recognition and control of abusive machining effects on helicopter components.
[AHS PREPRINT 750] 17 p2180 A73-35078

Whole aircraft and component design optimization, discussing criteria, constraints and performance prediction accuracy during feasibility analysis and project design
19 p2378 A73-37410

Weldbonding/rivetbonding - Application testing of thin gauge aircraft components.
[AIAA PAPER 73-805] 19 p2433 A73-37464

The nondestructive tests in the maintenance of commercial aircraft
22 p2799 A73-42186

AIRCRAFT PERFORMANCE NT HELICOPTER PERFORMANCE

Effect of aircraft reliability regulations on takeoff and landing performance of QSTOL aircraft [DGLR PAPER 72-056] 02 p0130 A73-11658

Aircraft performance augmentation through control configured aircraft design based on artificial stabilization instead of inherent aerodynamic static stability [DGLR PAPER 72-094] 02 p0130 A73-11675

Analysis of fundamental flight parameters and properties of aerobatic aircraft in a statistical framework 02 p0131 A73-12448

Flight-mechanical analysis of various flight states of conventional aircraft. VII - Mechanical principles: Rigid-body dynamics 03 p0250 A73-13074

Aft-end design criteria and performance prediction methods applicable to air superiority fighters having twin buried engines and dual nozzles. [AIAA PAPER 72-1111] 03 p0250 A73-13426

Powered model wind tunnel investigation to determine performance trends with nacelle location. [AIAA PAPER 72-1114] 03 p0243 A73-13429

Integrated engine-airframe design with fuselage boundary layer ingestion for subsonic-transonic cruise, discussing STOL thrust control via variable pitch fan for landing 03 p0251 A73-14128

Russian book on Il-18 aircraft practical aerodynamics covering aerodynamic characteristics, performance, controllability, stability and flight safety 04 p0406 A73-13968

Performance and stability of hypervelocity aircraft flying on a minor circle. 05 p0534 A73-16179

Aircraft performance augmentation by energy management instruments or systems, considering energy/energy rate meter and algorithm for real time onboard flight path optimization [AIAA PAPER 73-228] 05 p0536 A73-16953

Airships design, constructional and operational characteristics, discussing aerodynamics, flight control, performance and trim 06 p0648 A73-18510

Aircraft performance calculations in SI units, considering conversion factors for forces, pressures and specific fuel consumption 06 p0648 A73-18511

L-1011 TriStar - Design development. 08 p0928 A73-21574

Formula-one air racing history, aircraft designs and characteristics and low cost amateur constructions 08 p0928 A73-21689

Flight research to develop airworthiness standards for civil aircraft. 09 p1031 A73-22184

Air battle fighter aircraft design, discussing required performance characteristics in terms of lethality, maneuverability, range, visibility, handling qualities, sortie rate, reparability and fire control 09 p1031 A73-22197

Russian book on aircraft natural-climatic environmental factors covering geographic region adverse effects on design, performance and maintenance 09 p1031 A73-22349

Ballistic-tolerant helicopter flight control components from plastic composite materials. 10 p1237 A73-23964

A method of measuring the thrust, the polar, and the performance of an aircraft on the basis of flight tests 10 p1175 A73-24494

A comparative study of augmentor wing, ejector nozzle and power jet flap low noise STOL concepts. 11 p1300 A73-25385

Light motorized glider-type aircraft design, development and flight testing, discussing aerodynamic configuration, structural design and performance characteristics 12 p1459 A73-27732

The state of the art in light aircraft design. 13 p1568 A73-28179

Statistical turbulence model of meteorological and topographical aircraft flight conditions for low altitude critical air turbulence /LO-LOCAT/ environment 13 p1569 A73-28831

Some results of studies of the boundary atmospheric layer and AN-2 aircraft flight conditions in a forest fire area 13 p1655 A73-29192

Concorde wing and fuselage aerodynamic design modifications for operational efficiency optimization from wind tunnel tests and theoretical computations 14 p1712 A73-30926

STOL aircraft flight and landing area considerations. [ASCE PREPRINT 1726] 15 p1856 A73-31389

Some aerodynamic problems applicable to the light aircraft 16 p1961 A73-32809

Wind tunnel gust simulation for STOL aircraft behavior during low velocity flight in turbulent atmosphere near ground 16 p1962 A73-32813

Conceptual study of high performance V/STOL fighters. [ASME PAPER 73-GT-66] 16 p1969 A73-33518

Aircraft performance relationship to safety margins improvement, discussing accelerate stop, approach control, airworthiness, landing and coordination 17 p2097 A73-34082

Automated prediction of light aircraft performance and riding and handling qualities. [SAE PAPER 730305] 17 p2101 A73-34666

Applications of advanced aerodynamic technology to light aircraft. [SAE PAPER 730318] 17 p2101 A73-34676

The development of reciprocating engine installation data for general aviation aircraft. [SAE PAPER 730325] 17 p2102 A73-34681

Technical basis for the STOL characteristics of the McDonnell Douglas/USAF YC-15 prototype airplane. [SAE PAPER 730366] 17 p2103 A73-34711

New constraints of military aviation 18 p2267 A73-36684

Flight testing of the JT15D in the CF-100. 18 p2268 A73-36775

Improved aircraft capability through variable camber. 19 p2378 A73-37275

Flight testing the F-12 series aircraft. [AIAA PAPER 73-823] 19 p2380 A73-37475

The Navy SETOLS program and its potential applications to Navy aircraft. 19 p2381 A73-37680

Air cushion landing system /ACLS/ application to Jindivik target drone aircraft for recovery improvement, considering flight performance degradation 19 p2383 A73-37698

The weight/performance interface - An argument for weight control. [SAWE PAPER 967] 19 p2385 A73-37884

'The hub of the wheel' - A project designer's view of weight. [SAWE PAPER 996] 19 p2386 A73-37895

The prediction of pilot acceptance for a large aircraft. 19 p2453 A73-38073

S-3A aircraft systems, performance and design, discussing flight simulation, wind tunnel tests, weapons systems, flutter tests, avionics, TF-34 engine, stalls and computer programming. [AIAA PAPER 73-778] 19 p2387 A73-38367

Energy supply and its effect on aircraft of the future. II - Liquid-hydrogen-fueled aircraft: Prospects and design issues. [AIAA PAPER 73-809] 19 p2388 A73-38373

Potential of hydrogen fuel for future air transportation systems. [ASME PAPER 73-ICT-104] 23 p3019 A73-43499

AIRCRAFT PILOTS

NT TEST PILOTS

Favorable effect of flight on pilots exhibiting degenerative arteriopathy of the lower limbs 02 p0137 A73-12151

Telemetry of cardiovascular parameters on fighter aircraft flying pilots. 03 p0272 A73-14309

Civil aircraft commander and crew duties and rights in air piracy cases, discussing international agreements and national legal provisions 10 p1297 A73-23683

Airline pilots problems in terms of job security, working conditions, management relations, public relations, flight safety due to noise abatement rules, etc 12 p1562 A73-27599

Role of the air line pilot in air transportation. 13 p1570 A73-29105

Commercial airline operational control, discussing flight plan approval by pilot and ground personnel, preflight duties, weather information assessment and fuel monitoring 15 p1909 A73-32446

Information systems enabling pilots to report incidents involving safety, including human fallibility and system errors in construction, operation and regulation 17 p2256 A73-34087

General aviation pilot operational profile study, discussing implications for airman certification standards, flight safety regulations and aircraft design [SAE PAPER 730334] 17 p2115 A73-34687

Lone woman pilot sleep patterns and sleep disruptions on global flight across time zones 17 p2115 A73-34745

Self destructive behavior of aircraft pilot due to stress accumulation, discussing man machine relationship, coping mechanisms, competence and invulnerability myth 17 p2115 A73-34746

Military aircraft pilot in-flight consciousness loss etiologies, discussing rapid decompression, hypoxia, dysbarism, seizure, improper maneuver, vasovagal syncope, acceleration sensitivity, etc 17 p2115 A73-34747

Further sleep problems in airline pilots on worldwide schedules. 18 p2283 A73-36792

Sudden incapacitation in flight. 18 p2279 A73-36847

Surveillance of the vertebral column in pilots who have undergone an ejection 18 p2284 A73-36914

The problem of early presbyopia in aircrew. 18 p2285 A73-36923

Evaluation of auditory disorders in pilots by examining intratympanic muscles reflexes. 18 p2279 A73-36934

Technique for extemporaneously obtaining an electroencephalogram 18 p2286 A73-36937

STOL pilot functional requirements on air transportation system in terms of airport design, aircraft, ATC, route selection, navigation and communications 19 p2450 A73-37730

Aircrew workload during the approach and landing. 19 p2401 A73-38005

Patterns of diurnal variation in the intraocular pressure of airline pilots. 20 p2512 A73-39107

Aircraft pilot spatial disorientation and illusory perceptual break-off sensations during flight associated with minor vestibular asymmetry 20 p2512 A73-39111

AIRCRAFT POWER SOURCES

U AIRCRAFT ENGINES

AIRCRAFT PRODUCTION

Classification of fitting operations in airframe assembly 02 p0172 A73-11647

Organization and management for adhesive bonding aircraft structures. 03 p0333 A73-13048

Concept and conduct of proof test of F-111 production aircraft. 03 p0317 A73-14467

Russian book - Technology for adhesive bonding of elements in aircraft construction. 04 p0454 A73-15703

Russian book - Organization and planning of production at aircraft-construction plants. 04 p0524 A73-15965

Aircraft structural components in-house or subcontracted fabrication, discussing technical performance, economic and manpower aspects 10 p1297 A73-23521

Russian book - Network planning and control of air transportation. 10 p1298 A73-24924

Reliability and quality control of production engineering computer programs. [AIAA PAPER 73-356] 11 p1373 A73-25493

Aircraft accident prevention problems, considering pilot judgement errors, factory skill degradation, training, lightning and structure factors and air bag use 13 p1570 A73-29349

Some economic aspects of aviation safety. 16 p2089 A73-33648

Helicopter design and production cost target and tradeoff considerations based on past programs, supplier quotations, government documents, estimating practices and functional requirements [AHS PREPRINT 712] 17 p2257 A73-35058

The human side of quality assurance /as viewed from helicopter manufacturing experiences/. [AHS PREPRINT 751] 17 p2180 A73-35079

Interactive computer graphic display and interface system effectiveness for programming numerical control operations for tooling and part machining in aircraft production [AHS PREPRINT 753] 17 p2131 A73-35081

Structural design and technology developments for SST and STOL aircraft, discussing computerized and damage tolerant design, composite materials and cost reducing manufacturing techniques 18 p2362 A73-36167

L-1011 Tristar production, sales and airline service experience, discussing RB-211 turbofan engine and fleet performance 20 p2510 A73-39659

Dynamic model of economically efficient multipurpose plants 21 p2793 A73-40386

AIRCRAFT PROTUBERANCES

U PROTUBERANCES

AIRCRAFT RELIABILITY

Colloquium on Structural Reliability notes on 'Fatigue Lecture.' 04 p0507 A73-14706

Evaluation of a reliability analysis method for fatigue life of aircraft structures. 04 p0452 A73-14715

The corrosion problem in aircraft structures. 07 p0840 A73-20452

Book - Aircraft structures for engineering students. 08 p1020 A73-21839

Flight research to develop airworthiness standards for civil aircraft. 09 p1031 A73-22184

Russian book - Transport aircraft maintainability. 09 p1032 A73-22375

Aircraft maintenance for safety and reliability, considering design requirements, human errors, fault

diagnosis, redundancy, failure mode analysis, service data statistics and equipment specifications

10 p1174 A73-23759

Aircraft design philosophies and structural integrity considerations for reliability without major NDT and maintenance, proposing research program for future computerized design

11 p1433 A73-25128

Aircraft design and reliability analysis method based on accidents occurrence investigation by Franco-British airworthiness authorities, noting applicability to Concorde aircraft

11 p1306 A73-26589

Transport aircraft maintenance program, discussing safety and reliability correlation with design

11 p1306 A73-26591

Prediction for a park of helicopters of the same type

12 p1561 A73-27077

Aerodyne flight vehicle testing for hover flight characteristics during remote control by radio with pilot commands, noting reliability and attitude control

13 p1569 A73-28785

Some aerodynamic problems applicable to the light aircraft

16 p1961 A73-32809

Air Force Increase Reliability of Operational Systems computer program and mathematical models for economic logistic resource allocations and cost effective system modification

16 p2088 A73-33627

Aircraft performance relationship to safety margins improvement, discussing accelerate stop, approach control, airworthiness, landing and coordination

17 p2097 A73-34082

FAA General Aviation Crashworthiness Program. [SAE PAPER 730293]

17 p2257 A73-34657

Electric trim systems - Design and certification considerations under FAR 23.677 [CAM 3.337-2]. [SAE PAPER 730299]

17 p2101 A73-34662

An overview of fatigue and fracture for design and certification of advanced high performance ships.

17 p2246 A73-34881

Westland Sea Lynx naval variant aircraft design and development for multiservice multiple application, emphasizing high reliability and maintenance ease requirements

[AHS PREPRINT 711]

17 p2104 A73-35057

Drone launch and recovery reliability requirements for target, reconnaissance, air-to-air combat, high altitude endurance and defense suppression missions

19 p2381 A73-37681

Civil and military aircraft preventive maintenance, discussing on-condition and condition monitoring concepts for equipment reliability enhancement and cost reduction

20 p2544 A73-39275

Helicopter and fixed wing aircraft design consideration comparison, examining maintenance and reliability requirements, rigid, hinged and tilted rotors and load characteristics

21 p2634 A73-40225

Book - The role of testing in achieving aerospace systems effectiveness.

21 p2675 A73-41201

Fuel tank wall response to hydraulic ram during the shock phase.

22 p2843 A73-43114

Management and control of flight test programs at U.S. Army Aviation Systems Command.

23 p3050 A73-44054

Program plan to develop airworthiness standards for STOL aircraft.

24 p3056 A73-44994

AIRCRAFT SAFETY

Manoeuvre in response to collision warning from airborne devices.

01 p0074 A73-10349

Management system for aviation safety.

01 p0005 A73-10825

Airport requirements for air traffic safety, considering runway drainage and lighting, ILS, rescue and fire services, communications and weather reporting networks

01 p0030 A73-11239

Psychological and medical viewpoint for hijacker handling, discussing air crew training program [AD-757130]

02 p0138 A73-12564

Airlines responsibility and measures for aircraft noise abatement, considering economic and safety aspects

04 p0406 A73-14893

Maximum safety hydraulic systems for A300B airbus powered flight controls for normal flying and auto land operations

04 p0409 A73-16031

Modeling of aircraft position errors with independent surveillance. [AIAA PAPER 73-162]

05 p0595 A73-16908

Systems for collision avoidance.

07 p0848 A73-18899

Distributed ATC with traffic information in cockpit, noting potential for cost and risk reduction and capacity increase based on system performance evaluation

07 p0850 A73-20600

Aircraft maintenance for safety and reliability, considering design requirements, human errors, fault diagnosis, redundancy, failure mode analysis, service data statistics and equipment specifications

10 p1174 A73-23759

Transportation safety - Technology applications: A systems approach to anti-hijacking.

10 p1298 A73-24559

Airport design and management for safe aircraft ground handling, discussing FAA rules on pavement and safety areas, marking and lighting, fire fighting, etc

10 p1204 A73-24714

Noise abatement two-segment, precision and category I, II and III approaches considerations covering altimetry, cost and safety problems in ATC

10 p1247 A73-24768

Aircraft design and reliability analysis method based on accidents occurrence investigation by Franco-British airworthiness authorities, noting applicability to Concorde aircraft

11 p1306 A73-26589

Transport aircraft maintenance program, discussing safety and reliability correlation with design

11 p1306 A73-26591

Airborne fire protection equipment.

13 p1568 A73-28171

Weather condition caused aircraft accident avoidance, considering meteorological factors of air temperature, humidity, cloud formation, fog, haze, precipitation and visibility deterioration

13 p1568 A73-28554

Role of the air line pilot in air transportation.

13 p1570 A73-29105

Conference on General Aviation-Business Flying, University of Tennessee, Tullahoma, Tenn., August 17-19, 1972, Proceedings.

13 p1570 A73-29344

Historical development of the Air Traffic Control System.

14 p1772 A73-29877

Improvements in Airport Surface Traffic Control surveillance.

14 p1740 A73-29887

B-1 bomber crew integrated escape module for safe recovery throughout aircraft operational envelope, discussing capsule configuration and flight tests [AIAA PAPER 73-440]

15 p1825 A73-31426

Experimental investigation and correlation of the ground impact acceleration characteristics of a full scale capsule and a 1/4 scale model aircraft emergency crew escape capsule system.

[AIAA PAPER 73-480]

15 p1829 A73-31463

Multiple occupant flotation devices for commercial transport aircraft survivors sea ditching, discussing slide/raft design improvement for high density loading

16 p1974 A73-32658

Aircraft in-flight visibility /conspicuity/ during daytime, discussing exterior paints, tapes and high intensity lighting effectiveness for midair collision avoidance

16 p1965 A73-32661

Aircraft safety engineering for air piracy prevention, discussing cockpit communication isolation from passenger compartment

16 p2087 A73-32662

Lightning protection for aircraft canopy, discussing simulation tests, safety margins, side puncture, corona streamering and pilot physiological reactions

16 p1968 A73-33036

Lightning simulation testing in aerospace.

16 p1994 A73-33145

Simulation in the design of automated air traffic control functions.

16 p2035 A73-33419

Some economic aspects of aviation safety.

16 p2089 A73-33648

Safety in operation and human error.

17 p2097 A73-34077

Airplane accident survival, discussing cabin safety, fire protection, crashworthiness, emergency evacuation and crash landing in water

17 p2097 A73-34079

Design to detect and avoid failure - One airline's viewpoint.

17 p2097 A73-34081

German book - Fire protection technology in aviation. Volume 1 - Foundations of aviation and fire-protection technology.

17 p2098 A73-34124

Restraint systems /lap belts and shoulder harnesses/ for military, transport and general aviation aircraft, with emphasis on pilot and crew systems [SAE PAPER 730291]

17 p2114 A73-34656

FAA General Aviation Crashworthiness Program.

[SAE PAPER 730293]

17 p2257 A73-34657

Development of airframe design technology for crashworthiness. [SAE PAPER 730319]

17 p2101 A73-34677

A consistent crashworthiness design approach for rotary-wing aircraft. [AHS PREPRINT 781]

17 p2106 A73-35094

Reflection coefficients for wires, cables, ropes and chains from scanning laser radar, discussing wire avoidance system for airplanes and helicopters

17 p2210 A73-35421

Aircraft evacuation and safety procedures during emergencies, discussing negative panic, flight crew training and impact injury minimization

18 p2268 A73-36849

Objectives of training in relation to accident prevention.

18 p2284 A73-36850

ICAO meeting reports on international aircraft accident investigation, onboard data recording, inquiry process and low-safety interface

19 p2506 A73-37738

Annex 13 and the work of the aviation pathologist - Practical problems.

19 p2398 A73-37739

Annex 13, sabotage and malicious acts against aircraft - Practical problems.

19 p2506 A73-37740

Optimal aircraft collision avoidance.

19 p2452 A73-38050

SECANT - A solution to the problem of midair collisions.

19 p2454 A73-38469

Annual Corporate Aircraft Safety Seminar, 18th, Arlington, Va., April 1-3, 1973, Proceedings.

20 p2509 A73-39210

USA government and industry efforts on aircraft midair collision avoidance systems technology advancement, comparing cost effectiveness between airborne and ground based options [ASME PAPER 73-ICT-49]

23 p3005 A73-43495

'Air piracy' and the latest work of ICAO on this subject

24 p3159 A73-45345

Ram air turbine with hydraulic pitch change servo regulated speed as emergency power source for aircraft control in event of main engine failure

24 p3058 A73-45475

AIRCRAFT SPECIFICATIONS

Basic specification research for the main instruments of light aircraft

07 p0825 A73-20248

Formula-one air racing history, aircraft designs and characteristics and low cost amateur constructions

08 p0928 A73-21689

Aircraft design parameters optimization based on critical function representing overall deviation for specifications with application to subsonic passenger aircraft

12 p1458 A73-27095

Projections of the U.S. airline fleet in the early 1980's.

13 p1569 A73-29102

Civil and military aircraft

18 p2268 A73-36889

F-14 replacement for Phantom aircraft for escort missions, fleet defence, interdiction and close support, discussing airborne refuelling capability and composite materials applications

24 p3056 A73-44695

AIRCRAFT STABILITY

NT HOVERING STABILITY

Theory of the motion of a rigid model of an aircraft with a vertical landing-gear strut on a runway

01 p0005 A73-10917

Aircraft performance augmentation through control configured aircraft design based on artificial stabilization instead of inherent aerodynamic static stability [DGLR PAPER 72-094]

02 p0130 A73-11675

Russian book on Il-18 aircraft practical aerodynamics covering aerodynamic characteristics, performance, controllability, stability and flight safety

04 p0406 A73-15968

Performance and stability of hypervelocity aircraft flying on a minor circle.

05 p0534 A73-16179

Aerodynamic technology developments including advanced transonic airfoils, low-drag/high-lift systems and stability augmentation for transport aircraft performance, economics and noise improvements [AIAA PAPER 73-9]

06 p0644 A73-17604

Application of pole-placement theory to helicopter stabilization systems.

06 p0682 A73-18819

Convergent iterative smoothing algorithm for aircraft stability parameter identification from measurement, using variational optimization procedure

09 p1067 A73-22233

Airborne IR 32 cm observatory, discussing atmospheric transmission and guiding methods to overcome aircraft instability effects

11 p1368 A73-26503

Flight-mechanics analysis of various flight conditions of conventional aircraft. VII - Mechanical foundations: Dynamic equations of motion of the translational motion of a rigid body

11 p1307 A73-26725

Solid body on elastic supports as model for helicopter stability and nonlinear oscillations analysis

12 p1459 A73-27791

Book - Methods for estimating stability and control derivatives of conventional subsonic airplanes.
16 p1969 A73-33423

Control-configured general aviation aircraft.
[SAE PAPER 730303] 17 p2101 A73-34664

ABC helicopter stability, control, and vibration evaluation on the Princeton Dynamic Model Track.
[AHS PREPRINT 744] 17 p2105 A73-35077

Feedback control configured vehicles ride control system design for B-52 aircraft load alleviation and mode stabilization during flight through atmospheric turbulence
17 p2107 A73-35245

Response of a rigid aircraft to nonstationary atmospheric turbulence.
18 p2267 A73-36305

Rotorcraft stability augmentation and gust alleviation by collective and cyclical rotor blade pitch angle changes, discussing nonlinear dynamic effects
18 p2267 A73-36397

Surface effect take-off and landing system for high performance aircraft.
19 p2382 A73-37695

The effect of ice formation on the stability and maneuverability characteristics of aircraft
19 p2387 A73-38117

Computerized control system for fuel flow into and out of fuel cells and aircraft gravity center optimization during supersonic cruise and takeoff
21 p2634 A73-40939

Drive logic computation for variable stability aircraft in-flight simulators with six independent controllers providing dynamic motion and ground, crosswind and special effects
[AIAA PAPER 73-933] 22 p2799 A73-41971

Contribution to the rotorcraft ground resonance theory
22 p2800 A73-43056

A study of a fluidic open loop damping flight stability augmentation system.
23 p2941 A73-43396

Total In-Flight Simulator for X-22A aircraft based on variable stability-and-control system concept for reliability design
24 p3057 A73-45153

AIRCRAFT STRUCTURES
NT AIRFRAMES
NT FUSELAGES
NT PLASTIC AIRCRAFT STRUCTURES

Discontinuous or short fiber reinforced composites properties, manufacturing procedures and aircraft structural applications
01 p0057 A73-11240

Automated test stands for full scale aircraft structure and engine parts fatigue tests, noting equipment for programmed static and dynamic loading
02 p0166 A73-11629

Lifetime of Dural structural elements operating in aggressive media
02 p0180 A73-11794

Dual sensitivity liquid penetrants for improving NDT inspection of minute defects in military aircraft structures during rework and repair, noting comparative advantages
02 p0173 A73-11984

Attempts at using fiberglass cloth as skin for aircraft
02 p0185 A73-12450

In-flight structural failures involving general aviation aircraft.
02 p0131 A73-12566

Selection process for a structural adhesive system for application of the L-1011 aircraft.
03 p0333 A73-13050

Utilization in aeronautics of composite materials for working structures
03 p0334 A73-13594

Ni-Cr-Ti steel aircraft structural element fatigue life calculation based on failure mechanism involving crack propagation
03 p0394 A73-14011

Concept and conduct of proof test of F-111 production aircraft.
03 p0317 A73-14467

Reliability analysis methods for metallic structures.
04 p0452 A73-14714

Evaluation of a reliability analysis method for fatigue life of aircraft structures.
04 p0452 A73-14715

The additivity of cumulative damage in the test or use environment.
04 p0507 A73-14716

Metallic materials developments in aircraft construction and gas turbine engine applications, discussing superalloys, refractory metals, composites and directionally solidified alloys
04 p0460 A73-14741

Russian book - Technology for adhesive bonding of elements in aircraft construction.
04 p0454 A73-15703

Composite materials technology for aircraft and spacecraft structures, discussing various fiber-matrix combinations mechanical properties and production volume/price relations
05 p0589 A73-16759

Subsonic jet airframe fatigue cracking as function of load, geometry, material, joint performance and environment
05 p0636 A73-17200

Load-time dependent relaxation of residual stresses.
05 p0636 A73-17214

Interpolation methods in aeroclastic analysis, comparing wing structural influence coefficients derived by surface splines and interpolation-in-the-small techniques with static test data
05 p0637 A73-17215

The USAF aircraft structural integrity program /ASIP/.
[AIAA PAPER 73-18] 06 p0759 A73-17611

Aircraft structural engineers prospects in commercial aircraft design, discussing markets, technology escalation and cost effective structural development
[AIAA PAPER 73-19] 06 p0759 A73-17612

Structural design of future commercial transports.
[AIAA PAPER 73-20] 06 p0759 A73-17613

Air breathing hypersonic aircraft technology developments in propulsion systems and structures with emphasis on use of hydrogen fuel
[AIAA PAPER 73-58] 06 p0647 A73-17631

Fail-safe aircraft composite structures, achieving crack arrestment by integral buffer strips in primary load carrying laminates
06 p0764 A73-18494

The status of engineering knowledge concerning the damping of built-up structures.
07 p0909 A73-19099

Second derivatives of the flutter velocity and the optimization of aircraft structures.
07 p0912 A73-19952

Fatigue life of aircraft structures
07 p0914 A73-20246

Russian book - Methods and equipment for in-flight aircraft strength tests.
07 p0777 A73-20376

The corrosion problem in aircraft structures.
07 p0840 A73-20452

Optimisation in construction of the Jaguar and other military aircraft.
08 p0928 A73-20947

Book - Aircraft structures for engineering students.
08 p1020 A73-21839

Dynamic analysis of helicopter structures
09 p1031 A73-22206

Aircraft surface primers and finishes composition, pretreatment and application, discussing epoxy, acrylic and polyurethane primers mechanical and chemical properties
10 p1237 A73-23522

Test rails possibilities for rain erosion phenomena study on aircraft or missile structures
11 p1335 A73-25296

Design and manufacture of structure components made of fiber-reinforced materials
11 p1373 A73-25417

Preliminary design of aircraft structures to meet structural integrity requirements.
[AIAA PAPER 73-374] 11 p1439 A73-25506

Crippling allowables for elevated temperature and creep environments.
[AIAA PAPER 73-388] 11 p1439 A73-25517

Parametric studies of the wing flutter behavior of a STOL transport.
[AIAA PAPER 73-394] 11 p1304 A73-25523

Optimisation of aircraft structures with multiple stiffness requirements.
11 p1444 A73-26298

In-flight flutter testing methods for determining aircraft structure natural frequencies and vibration damping ratios with air flow
[ONERA, TP NO. 1224] 11 p1306 A73-26593

An-2R aircraft conversion to flying test bed for feasibility studies of jet engine use in agricultural aircraft, describing structural design modifications
12 p1458 A73-26823

Book on aerospace vehicles science covering airfoils, aircrafts, fuel systems, structural weight, instrumentation, taxiing, towing and federal aviation regulations
12 p1458 A73-27054

Certain fatigue phenomena in aeronautical structures with stiffened shells
12 p1553 A73-27394

Al alloys, steels and superalloys properties improvements for aerospace vehicles structural applications, discussing diffusion bonding and isothermal forging techniques
13 p1633 A73-28180

Epoxy adhesive bonding of Concorde light alloy sandwich structure elevons, discussing surface treatment, polymerization and ultrasonic bonding
13 p1623 A73-28468

Russian book on elastic structures vibration in aircraft covering integral equations for beams, damping principles and transcendental equations for flexural and torsional vibrations natural frequencies
14 p1810 A73-30354

Exfoliation corrosion of aluminum alloys.
15 p1888 A73-31737

Mathematical model of elastic flight body behavior in continuous medium based on combination solutions to aerodynamics, automatic control and elasticity theory problems
15 p1952 A73-32063

Wing spar static and fatigue tests and S-N curve for lifetime measurement of root sections of small trainer and passenger aircraft
15 p1955 A73-32190

Lightning protection for boron and graphite fibers in epoxy resins for aircraft composite structures
16 p1967 A73-33032

Pressurized fuselage design studies for short haul transport aircraft, discussing sandwich structures and bonding techniques for Al and Ti alloy construction materials
16 p2018 A73-33069

Titanium casting technology applications to aircraft structures, considering flap tracks, brake torque tubes and arrestor hook mounting brackets
16 p2018 A73-33071

A device for qualifying very low frequency vibration exciters
16 p2083 A73-33970

Boron composites - Status in the USA.
16 p2031 A73-34042

Brazed honeycomb structure design, fabrication and aerospace applications covering brazing methods, filler metal selection, nondestructive testing, sandwich designs, aircraft and spacecraft structures, etc
17 p2177 A73-34100

Use of honeycomb and bonded structures in light aircraft.
[SAE PAPER 730307] 17 p2101 A73-34667

Stepped aluminum extrusions - Designing for business aircraft.
[SAE PAPER 730308] 17 p2177 A73-34668

Filiform corrosion associated with commonly applied aircraft metal pretreatments and finishes.
[SAE PAPER 730311] 17 p2177 A73-34671

A comparison of structural test results with predictions of finite element analysis.
[SAE PAPER 730340] 17 p2102 A73-34691

An inexpensive, full-scale aircraft fatigue test system.
[SAE PAPER 730341] 17 p2102 A73-34692

Aircraft structural applications of filamentary composites, discussing fiberglass, boron-epoxy and graphite-epoxy composites
17 p2103 A73-34814

The successful use of composites in the L-1011 TriStar commercial transport.
17 p2103 A73-34815

High frequency vibration of aircraft structures.
17 p2250 A73-35329

Test on fuselage models at reduced sizes.
17 p2107 A73-35443

Russian book - The Tu-134 aircraft: Its design and operation.
18 p2266 A73-35870

Alteration of a static vibration result by rigidizing some degrees of freedom
18 p2361 A73-36066

Commercial transport aircraft structural design and technology advances, discussing materials and fabrication processes with respect to costs, durability and reliability
18 p2266 A73-36166

Structural design and technology developments for SST and STOL aircraft, discussing computerized and damage tolerant design, composite materials and cost reducing manufacturing techniques
18 p2362 A73-36167

NASA airframe structures program, discussing automated analysis and design, advanced composites, supersonic and hypersonic vehicles technology, active controls, aircraft loads and aeroclasticity prediction methods
18 p2362 A73-36168

USAF aircraft structural integrity requirements, discussing safety and durability concepts for designing, evaluating and substantiating future systems
18 p2267 A73-36169

Military aircraft structure computerized design optimization procedures based on local optimum and stiffness requirements
19 p2495 A73-37407

Automated structural design and analysis of advanced composite wing models.
19 p2497 A73-37486

Air cushion landing system twin pod /ACLS/ configuration design and test installation on A-4 Navy fighter
19 p2383 A73-37702

The weight/performance interface - An argument for weight control.
[SAWE PAPER 967] 19 p2385 A73-37884

Finite element program for flight structure analysis.
22 p2917 A73-41739

German monograph - Lifetime detection in the case of acoustically loaded structures on the basis of the appropriate form of vibration.
22 p2924 A73-42741

- The effect of variable environment temperature on heat transfer in extended surfaces. 23 p3048 A73-43296
- Environmental effects on fracture resistant and biaxial fatigue design of aircraft structures. 23 p3042 A73-43811 [AIAA PAPER 73-994]
- Acoustic fatigue resistance of aircraft structures at elevated temperatures. 24 p3056 A73-44829
- R and D efforts for various aircraft construction materials, considering steels, alloys and fiber-containing laminates 24 p3100 A73-45198
- AIRCRAFT SURVIVABILITY**
- JP8 and JP4 aircraft fuel fire and explosion susceptibility from gunfire hits, discussing combat survivability relative to fuel volatility 16 p2045 A73-32670
- Low cost manufacturing methods for highly reliable ballistic-tolerant composite helicopter flight control components. [AHS PREPRINT 754] 17 p2180 A73-35082
- Digital fly by wire flight control system with airborne digital processor for increased aircraft survivability, determining redundancy level to satisfy system performance 17 p2138 A73-35222
- Fuel tank wall response to hydraulic ram during the shock phase. 22 p2843 A73-43114
- AIRCRAFT TIRES**
- Design of digital force function generator for aircraft tire load testing. 04 p0424 A73-15064
- Transport aircraft wheels and brakes operational cost minimization, discussing contributory roles of governmental regulations /FAA/, aircraft manufacturer, supplier and user [SAE PAPER 720867] 05 p0534 A73-16650
- Cantilever aircraft tires - More than a break for brakes. [SAE PAPER 720870] 05 p0534 A73-16652
- Aircraft tire improvements and possible developments, discussing fibers, rubber compounds, tread, carcass and retreading [SAE PAPER 720869] 05 p0581 A73-16653
- Non-steady-state thermal analysis of a rolling aircraft tire. [SAE PAPER 720871] 05 p0535 A73-16667
- Aquaplaning prevention during take-off and landing, discussing friction loss factors, aircraft tires and runway surface treatment by antiskid overlays and grooving 11 p1343 A73-25209
- Mathematical model for shimmy auto-oscillations of aircraft landing gear nose wheel with pneumatic tire under velocity changes 15 p1825 A73-31044
- AIRCRAFT WAKES**
- NT HELICOPTER WAKES
- NT PROPELLER SLIPSTREAMS
- NT SLIPSTREAMS
- Finite amplitude waves on aircraft trailing vortices. 02 p0129 A73-12506
- Atmospheric dispersion of aircraft exhaust. [AIAA PAPER 73-100] 05 p0570 A73-16860
- Aircraft wake dissipation by sinusoidal instability and vortex breakdown. [AIAA PAPER 73-107] 05 p0529 A73-16867
- Observations of atmospheric effects on the transport and decay of trailing vortex wakes. [AIAA PAPER 73-110] 05 p0529 A73-16869
- The aircraft wake turbulence problem. 06 p0648 A73-18149
- Aircraft wake vortex avoidance systems with current locus detection and/or prediction capability, discussing design based on hazard assessment and computer simulation for performance 10 p1172 A73-24557
- Aerodynamics of wake vortices. 11 p1303 A73-26385
- Computerized three dimensional calculations of hypersustained aircraft in viscous potential flow in terms of boundary layers and wakes 16 p1962 A73-32816
- Aircraft wake vortex avoidance system for safety management and capacity optimization in airport operations related to ATC, considering various sensors and display subsystem requirements 17 p2166 A73-34613
- Aircraft wing tip turbulent wakes producing swirling vortices, discussing wake hazards, wind tunnel research and vortex dissipation procedures [SAE PAPER 730294] 17 p2094 A73-34658
- Flight test studies of the formation and dissipation of trailing vortices. [SAE PAPER 730295] 17 p2094 A73-34659
- Dynamic behavior of light aircraft interaction with jet transport vortex on basis of accident records and computer simulation [SAE PAPER 730296] 17 p2094 A73-34660
- Aircraft wake vortex transport model. [AIAA PAPER 73-679] 18 p2267 A73-36230

- Aircraft wake vortex detection and avoidance systems, examining acoustic sensors, bistatic Doppler sensors, pulsed radar, aircraft spacing techniques and ground wind measurement 19 p2452 A73-37823
- Study of control system effectiveness in alleviating vortex wake upsets. [AIAA PAPER 73-833] 20 p2507 A73-38776
- Sound generation by wake cutting. [AIAA PAPER 73-1019] 24 p3054 A73-44851
- AIRCRAFTS**
- U FLIGHT CREWS**
- AIRFIELD SURFACE MOVEMENTS**
- Analytical elasticity methods for airfield pavement structural stress-strain, failure and reliability performance evaluation 13 p1598 A73-29106
- Improvements in Airport Surface Traffic Control surveillance. 14 p1740 A73-29887
- Automatic runway and aircraft approach path surveillance system /CORAIL/ consisting of Doppler radar, signal extractor and data processing, alarm, display and control equipment 14 p1773 A73-30444
- Airport planning for 1980s air traffic capacity requirements, considering runways, aprons, air traffic and ground movements control, ground access and terminal facilities 15 p1858 A73-32363
- Simulation of a surface traffic control system for John F. Kennedy International Airport. 17 p2147 A73-34818
- Simulation of airport traffic flows with interactive graphics. 17 p2147 A73-34821
- Low cost airport surveillance and Localized Cable Radar with runway or taxiway vehicle guidance capability for ground traffic control, using solid state equipment 21 p2736 A73-40051
- AIRFOIL CHARACTERISTICS**
- U AIRFOILS**
- AIRFOIL PROFILES**
- NT WING PROFILES
- NT WING SPAN
- Calculation and measurement of the aerodynamic forces on an oscillating airfoil profile with and without stall [ONERA, TP NO. 1132] 01 p0002 A73-10240
- The influence of the Mach number on fuselages and profiles with optimized wave resistance in the case of supersonic flow [DGLR PAPER 72-108] 02 p0128 A73-11691
- An investigation of the near wake properties which lead to the generation of vortex shedding sound from airfoils. 03 p0242 A73-12976
- Transonic profile theory - Critical comparison of various procedures 03 p0247 A73-14377
- Supersonic blowdown wind tunnel modification for transonic airfoil profile aerodynamic characteristics measurement, discussing design criteria and operational range [DGLR PAPER 72-133] 03 p0288 A73-14380
- Analog-analytic construction of supercritical flows past profiles [DGLR PAPER 72-129] 03 p0248 A73-14384
- Calculation of supercritical flow past airfoils by the Murman-Krupp difference method [DGLR PAPER 72-128] 03 p0248 A73-14387
- Theoretical low-speed particles collision with symmetrical and cambered aerofoils. [ASME PAPER 72-WA/FE-35] 04 p0404 A73-15852
- The tricuspoid hypocycloid as envelope of the force of lift, calculated in a first compressible approximation, in the case of a symmetrical profile in a flow of variable direction and a given Mach number 05 p0528 A73-16764
- Inverse method of designing two-dimensional transonic airfoil sections. 05 p0533 A73-17104
- Airfoil profile determination in inverse hydrodynamics problem for given flow velocity distribution, discussing univalent solvability conditions 06 p0686 A73-18067
- Conformal mapping of two airfoil profiles symmetric with respect to real axis onto circles, using rational function power series 07 p0812 A73-20200
- Pressure distribution measurement at surface of aerodynamic body by pneumatically activated inductive sensor 08 p0965 A73-21180
- Advances in directional solidification spur usage in turbine airfoil shapes. 09 p1089 A73-23293
- Potential flow past axisymmetric ring wing profiles via singularity method, applying source and vortex distributions to curved thick profiles [DFVLR-SONDDR-271] 11 p1300 A73-25348
- Higher order numerical solution of the integral equation for the two-dimensional Neumann problem. 11 p1300 A73-25348

- Vibration and local edge buckling of thermally stressed, wedge airfoil cantilever wings. [AIAA PAPER 73-327] 11 p1441 A73-25557
- A linearized potential flow theory for airfoils with spoilers. 11 p1301 A73-25853
- The evolution and application of lofting techniques at Hawker Siddeley Aviation. 13 p1623 A73-28054
- Design method of the axial-flow blade row on modified isolated aerofoil theory with interference coefficient. I. 13 p1564 A73-28649
- Discrete vortex method of two-dimensional jet flaps. 17 p2091 A73-34179
- Test techniques for high lift, two-dimensional airfoils with boundary layer and circulation control for application to rotary wing aircraft. 17 p2091 A73-34292
- Revised calculations of the NACA 6-series of low drag aerofoils. 17 p2094 A73-34536
- Experimental and theoretical investigations in two-dimensional transonic flow. [AIAA PAPER 73-659] 18 p2261 A73-36213
- Measurements of surface pressure on an elliptic airfoil oscillating in uniform flow. 19 p2375 A73-37374
- A synthesis of transonic, 2-D airfoil technology. [AIAA PAPER 73-792] 19 p2375 A73-37459
- On the Oseen limited movements around a rectilinear profile placed under a free line 19 p2459 A73-37526
- A computer-aided design procedure to approximate aircraft area curve shapes. [SAWE PAPER 982] 19 p2385 A73-37888
- Airfoil profiles aerodynamic characteristics from laminar flow wind tunnel measurements 19 p2377 A73-38361
- Investigation of multi-element airfoils with external flow jet flap. 21 p2633 A73-41087
- Influence of geometrical parameters on propeller performance at low advance ratios 21 p2635 A73-41582
- Study of flow around an airfoil with a spoiler at Mach numbers ranging from 0.5 to 2.3 21 p2634 A73-41584
- Short takeoff and landing /STOL/ aircraft technology developments for high density air transport, discussing lift system, handling, airfoil design, acoustics and operating economics 23 p2940 A73-43520
- AIRFOIL SECTIONS**
- U AIRFOIL PROFILES**
- AIRFOIL THICKNESS**
- U AIRFOIL PROFILES**
- AIRFOILS**
- NT AILERONS
- NT ARROW WINGS
- NT CAMBERED WINGS
- NT CARET WINGS
- NT DELTA WINGS
- NT ELEVONS
- NT FIXED WINGS
- NT FLAPS [CONTROL SURFACES]
- NT FLEXIBLE WINGS
- NT JET FLAPS
- NT LEADING EDGE SLATS
- NT LIFTING ROTORS
- NT LOW ASPECT RATIO WINGS
- NT PARAWINGS
- NT PROPELLER BLADES
- NT RECTANGULAR WINGS
- NT RIGID ROTORS
- NT RING WINGS
- NT ROTARY WINGS
- NT SLENDER WINGS
- NT SPOILERS
- NT SUPERCritical WINGS
- NT SUPERSONIC AIRFOILS
- NT SWEPT WINGS
- NT SWEPTBACK WINGS
- NT TABS [CONTROL SURFACES]
- NT THIN AIRFOILS
- NT THIN WINGS
- NT TILTING ROTORS
- NT TIP DRIVEN ROTORS
- NT TRAILING-EDGE FLAPS
- NT TRAPEZOIDAL WINGS
- NT UNCAMBERED WINGS
- NT UNSWEPT WINGS
- NT VARIABLE SWEEP WINGS
- NT WING FLAPS
- NT WINGS
- An investigation of particle trajectories in two-phase flow systems. 01 p0002 A73-10439
- On the mechanism of dynamic stall. 01 p0003 A73-11015
- Scattering of sound by an airfoil of finite span in a compressible stream. 02 p0129 A73-12609
- Noise from free jets and airfoils in jets. 03 p0290 A73-12969

The interaction between turbulent wakes and boundary layers. 03 p0244 A73-13561

The prediction of airfoil pressure distributions for subcritical viscous flow and for supercritical inviscid flow. 04 p0404 A73-15858

Some recent work on aspect ratio effects in compressor cascades. [ASME PAPER 72-WA/FE-41] 04 p0404 A73-15858

A class of airfoils designed for high lift in incompressible flow. [AIAA PAPER 73-86] 05 p0528 A73-16851

High subsonic flow past airfoils at 2 deg angle of attack, describing relaxation method for hyperbolic Euler equations conversion to parabolic form. 06 p0645 A73-17738

Conformal mapping for potential flow about airfoils with attached flap. 07 p0773 A73-19192

Flow in the wake of a cascade of oscillating airfoils. 07 p0774 A73-19954

Multiple element airfoils optimized for maximum lift coefficient. 07 p0775 A73-19956

Calculation of the transonic flow around an airfoil, taking account of the exact law of compressibility. 09 p1027 A73-22210

Unsteady nonlinear flow around an airfoil or a blade cascade with emission of turbulent vortices. 09 p1027 A73-22212

Fluctuating lift and moment coefficients for cascaded airfoils in a nonuniform compressible flow. 09 p1028 A73-22432

Toward simpler prediction of transonic airfoil lift, drag, and moment. 09 p1028 A73-22434

Rayleigh-Ritz solution of boundary value problem for plane compressible subsonic flow past airfoil noting convergence. 09 p1028 A73-22954

Transonic airfoils - Recent developments in theory, experiment, and design. 10 p1171 A73-23856

Symmetrical airfoils optimized for small flap deflection. 10 p1174 A73-24915

Sound directivity pattern radiated from small airfoils. 11 p1345 A73-24980

Acoustic dipole source strength on flat plate and simple airfoil surfaces from local surface and far field acoustic pressure cross correlation. 11 p1345 A73-24982

An exploratory investigation of the unsteady aerodynamic response of a two-dimensional airfoil at high reduced frequency. [AIAA PAPER 73-309] 11 p1301 A73-25540

An investigation of unsteady aerodynamics on an oscillating airfoil. [AIAA PAPER 73-318] 11 p1301 A73-25549

Correction for change in fluid flow curvature about a lift-generating airfoil in a two-dimensional test section with perforated walls. 11 p1302 A73-25864

Book on aerospace vehicles science covering airfoils, aircrafts, fuel systems, structural weight, instrumentation, taxiing, towing and federal aviation regulations. 12 p1458 A73-27054

Wind tunnel interference on oscillating airfoils in low supersonic flow. 13 p1563 A73-28166

Semiempirical method for flutter prediction of unsteady lift and aerodynamic forces acting on oscillating airfoil in stall regime, using separation function. 13 p1566 A73-29029

Visualization of unsteady flow over oscillating airfoils. 13 p1620 A73-29270

Pressure distribution on multicomponent airfoils in two dimensional incompressible potential flow, using Martensen-Jacob vorticity distribution method to derive Fredholm type circulation equation. 15 p1823 A73-31637

Subsonic compressible airfoil cascade flow calculations by series, iterative, matrix and streamline curvature methods, discussing transonic and supersonic cases. [ASME PAPER 73-GT-9] 16 p1963 A73-33487

Lift and measurements in an airfoil in unsteady flow. [ASME PAPER 73-GT-41] 16 p1964 A73-33503

Inviscid flow through a cascade of thick, cambered airfoils. I - Incompressible flow. 16 p1964 A73-33527

Inviscid flow through a cascade of thick, cambered airfoils. II - Compressible flow. [ASME PAPER 73-GT-85] 16 p1964 A73-33528

A detailed experimental analysis of dynamic stall on an unsteady two-dimensional airfoil. [AHS PREPRINT 702] 17 p2095 A73-35053

The application of circulation control aerodynamics to a helicopter rotor model. [AHS PREPRINT 704] 17 p2104 A73-35055

Heavy lift helicopter rotor blade design including airfoils, fiberglass skin, titanium spar, fail-safety and aerodynamic and structural features. [AHS PREPRINT 710] 17 p2104 A73-35056

Computational considerations in application of the finite element method for analysis of unsteady flow around airfoils. 17 p2096 A73-35138

Transonic inviscid flows over lifting airfoils with embedded shock wave using method of integral relations. [AIAA PAPER 73-658] 18 p2261 A73-36212

Study of the far wake vortex field generated by a rectangular airfoil in a water tank. [AIAA PAPER 73-682] 18 p2262 A73-36233

On viscous and wind tunnel wall effects in transonic flows over airfoils. [AIAA PAPER 73-660] 18 p2263 A73-36261

Broadband noise generation by aerofoils and axial flow fans. [AIAA PAPER 73-1018] 24 p3054 A73-44850

Sound generation by wake cutting. [AIAA PAPER 73-1019] 24 p3054 A73-44851

Some results from tests in the NAE high Reynolds number two-dimensional test facility on shockless and other airfoils. 24 p3054 A73-44995

AIRFRAME MATERIALS

Test results of fatigue at elevated temperatures on aeronautical materials. [ONERA, TP NO. 1098] 01 p0061 A73-10229

Fabrication of high-strength aluminum products from powder. 01 p0063 A73-10281

Potential titanium airframe applications. 01 p0063 A73-10285

PRD 49 high modulus organic fibre as aluminium replacement. 01 p0068 A73-11510

Hypersonic flight vehicles aerodynamic heating, structural design and materials and propulsion problems, discussing research work and facilities. 03 p0242 A73-13055

Metallic materials developments in aircraft construction and gas turbine engine applications, discussing superalloys, refractory metals, composites and directionally solidified alloys. 04 p0460 A73-14741

Bright future forecast for composites in aerospace. 05 p0589 A73-16185

Subsonic jet airframe fatigue cracking as function of load, geometry, material, joint performance and environment. 05 p0636 A73-17200

Welding airframe structures in titanium alloys using tensile loading as a means of overcoming distortion. 08 p0973 A73-21240

Design and manufacture of structure components made of fiber-reinforced materials. 11 p1373 A73-25417

X2048, a high strength, high toughness alloy for aircraft applications. [AIAA PAPER 73-385] 11 p1380 A73-25514

Al alloys, steels and superalloys properties improvements for aerospace vehicles structural applications, discussing diffusion bonding and isothermal forging techniques. 13 p1633 A73-28180

Composite airframe structure effects on jet aircraft maintenance, discussing fire safety, fatigue resistance, environmental durability and quality assurance. 16 p1967 A73-33027

Boron composites - Status in the USA. 16 p2031 A73-34042

NASA airframe structures program, discussing automated analysis and design, advanced composites, supersonic and hypersonic vehicles technology, active controls, aircraft loads and aeroelasticity prediction methods. 18 p2362 A73-36168

Incremental forging of parts with cross-ribs. [SME PAPER MF 73-164] 19 p2437 A73-38503

AIRFRAMES

Classification of fitting operations in airframe assembly. 02 p0172 A73-11647

Reinforced all-plastic quadrant molded missile airframes design, fabrication and flight testing. 03 p0333 A73-13052

Airframe structural testing and safety design for military aircraft, discussing static, dynamic and fatigue tests and environmental effects. 04 p0454 A73-14865

NASA airframes structures program, discussing automated design, composites, supersonic and hypersonic technologies, control systems, load and aeroelasticity prediction and integrity concepts. [AIAA PAPER 73-17] 06 p0759 A73-17610

Adhesively bonded multilayer Al and Ti alloy sheet metals for complex airframe components, discussing design, fabrication, tests and performance comparison with monolithic structures. [SME PAPER MF 72-513] 06 p0698 A73-18094

V/STOL airframe/propulsion integration problem areas. [ASME PAPER 73-GT-76] 16 p2048 A73-33522

Development of airframe design technology for crashworthiness. [SAE PAPER 730319] 17 p2101 A73-34677

The integration of NASTRAN into helicopter airframe design/analysis. [AHS PREPRINT 780] 17 p2106 A73-35093

DC 10 airframe structure full scale fatigue tests for crack initiation and growth, residual strength and service life. [AIAA PAPER 73-803] 19 p2379 A73-37463

Cost estimating techniques for airframe weight-cost interface study for military aircraft design. [SAWE PAPER 969] 19 p2385 A73-37885

Aircraft fuselage structure weight estimation method assuming bending, shear, torque and internal pressurization loading for skin-stringer-shallow frame types. [SAWE PAPER 981] 19 p2385 A73-37887

Computerized optimization of interrelated airframe/engine design parameters against variable criteria to satisfy performance constraints in air superiority fighter design. [AIAA PAPER 73-800] 19 p2388 A73-38370

Frame of a cylindrical shell under the action of a concentrated radial force. 21 p2783 A73-40388

Airframe/propulsion system interactions - An important factor in supersonic aircraft flight control. [AIAA PAPER 73-831] 21 p2634 A73-40501

Airframe ball, roller and spherical plain bearing designs for flight control, landing gear and wing mechanisms. 21 p2707 A73-41125

AIRGLOW

NT GEOCORONAL EMISSIONS

NT NIGHTGLOW

NT TWILIGHT GLOW

Airglow 6300 A emission predawn enhancement amplitude variation with geomagnetic and solar activity. 01 p0037 A73-10347

Possibility of O III 304-A emissions in the extreme ultraviolet airglow. 02 p0157 A73-11755

Airglow height profiles of forbidden O I 6300 and 5577 A line emissions in morning ionosphere from rocket photometric measurement. 04 p0444 A73-15542

Vertical-ray structure /horizontal inhomogeneity/ of emission from the earth's upper atmosphere on the basis of observations from the Soiuz 3 spacecraft. 05 p0570 A73-16845

Light flash induced by a pulsed X-ray source in the upper atmosphere. 05 p0610 A73-17016

Mariner 9 ultraviolet spectrometer experiment - Mars airglow spectroscopy and variations in Lyman alpha. 06 p0746 A73-17484

Carbon monoxide Cameron bands limb intensity profile in Martian airglow from Mariner 9 UV spectrum observations. 06 p0746 A73-17485

Fraunhofer line depth in daytime airglow. 07 p0817 A73-19471

Photography of the zodiacal light outside the ecliptic in quadrature and in opposition with the sun. 09 p1073 A73-22001

Balloon-borne spectroscopic observation of the infrared hydroxyl airglow. 11 p1350 A73-25061

Spatial and temporal variations of the Lyman-alpha airglow and related atomic hydrogen distributions. 11 p1356 A73-25909

Calibrations of the airglow photometers and spectrometers. 11 p1365 A73-26237

High angular resolution photography of complex OH airglow structures in IR night sky. 11 p1358 A73-26666

Averaged nighttime altitude profile of atmospheric emission at 6300 A. 12 p1491 A73-27345

B system calculation of night airglow stellar component from cataloged photometric scales, obtaining night sky brightness. 12 p1546 A73-27857

Conventional filter photometer onboard Explorer satellite for 3000-7500 A airglow and auroral thermospheric emission features monitoring. 13 p1688 A73-28639

Atmosphere Explorer satellite-borne two channel fixed grating Ebert spectrometer for measurement of airglow at 2150 A, yielding altitude profiles of nitric oxide density. 13 p1689 A73-28640

O I 4368 airglow tropical emission excitation due to conjugate photoelectron escape flux, discussing radiative recombination contribution to intensity. 14 p1749 A73-29981

An observation of polar auroral and airglow from the ISIS-II spacecraft. 15 p1866 A73-31071

A balloon study of the OH airglow emission from evening twilight to sunrise.

15 p1867 A73-31311

Depth of the Fraunhofer lines in the spectrum of the daytime sky.

15 p1873 A73-32061

Airglow green cells diameter, speed and brightness measurements from isophote patterns in diagrams of UT versus distance

16 p2008 A73-33881

Global temperature distributions from OGO VI 6300 A airglow measurements.

18 p2309 A73-36058

Photographic parallax heights of infrared airglow structures.

18 p2313 A73-36510

Interpretation of the H-alpha atmospheric emissions observed by the D-2A Tournesol satellite around the magnetic equator

19 p2423 A73-37538

Evidence for an interstellar or interplanetary source of diffuse He I 584 A radiation.

19 p2475 A73-37629

Asymmetrical global O I airglow emission pattern with respect to magnetic equator from Ogo 4 observations, noting poor correlation with ionospheric electron density

20 p2551 A73-38939

Hydroxyl emission band high resolution spectra in airglow, examining doublet state ratio and rotational temperatures, vibration-rotation levels, temperature sensitivity and Boltzmann equilibrium

20 p2551 A73-38946

B system calculation of night airglow stellar component from cataloged photometric scales, obtaining night sky brightness

20 p2608 A73-39231

Air afterglow radiative recombination reaction of NO with O yielding nitrogen dioxide, considering pressure dependence in chemiluminescence spectral region

22 p2819 A73-42772

Average nighttime vertical profile of the 6300 A atmospheric emission.

23 p2970 A73-43242

Airglow hydroxyl emission IR spectral bands intensity measurements with allowance for atmospheric extinction, deriving vibrational level excitation rates from spontaneous emission transition probabilities

23 p2972 A73-43690

Distribution of atomic oxygen in the upper atmosphere deduced from Ogo 6 airglow observations.

24 p3086 A73-45121

Bandpass filter IR observations of hydroxyl airglow, mapping mean nightly level spatial and temporal fluctuations in brightness

24 p3087 A73-45208

ISIS 2 scanning photometric analysis of E and F region airglow at O 1 5577 A, noting height difference of airglow components at midlatitudes and near equator

24 p3088 A73-45214

AIRLINE OPERATIONS

Meteorological effects on SST operations during various flight phases, considering ATC and communications aspects

01 p0074 A73-10348

Airlines passenger transportation profitability, discussing relationships between service quality, load factor and operating costs

03 p0400 A73-13575

The impact of aircraft emissions upon air quality.

04 p0405 A73-14890

Monitoring and modeling of airport air pollution.

04 p0432 A73-14891

Airlines responsibility and measures for aircraft noise abatement, considering economic and safety aspects

04 p0406 A73-14893

Aircraft noise as a continuing national problem.

04 p0521 A73-14894

Aircraft flight plan data processing in FORTRAN program to predict altitude and time conflicts, noting short CPU time

05 p0595 A73-16618

Radiation problems of supersonic flight - The operators' viewpoint.

05 p0542 A73-16624

System monitoring techniques: Practical applications and experience at Eastern - Jet engines. [SAE PAPER 720818]

05 p0606 A73-16639

Flight simulator development in parallel with aircraft flight test A case study of the American Airlines DC-10 program.

05 p0562 A73-16664

Computerized airlines reservations systems with real time conversational interactive characteristics, discussing initial design, simulation, measurement, stability, reliability and data processing techniques

05 p0551 A73-16806

Air transportation systems problems - The airport operators' view.

06 p0683 A73-17602

Review of New York Airways helicopter operations. [AIAA PAPER 73-25]

06 p0647 A73-17614

Washington Airlines - The short haul /STOL/ experiment.

[AIAA PAPER 73-26] 06 p0771 A73-17615

Sonic boom reduction through aircraft design and operation.

[AIAA PAPER 73-241] 06 p0647 A73-17666

Airlines aircraft, engines and instruments maintenance, overhaul and repair procedures and equipment

06 p0648 A73-18254

Civil aviation medicine in the coming decade.

07 p0785 A73-19484

Mass air transportation development in Sweden, discussing flight scheduling, fare structure and quiet STOL aircraft introduction in 1980s

07 p0778 A73-20618

Benefit-cost analysis of delay reduction with STOL. [ASCE PREPRINT 1507]

08 p1025 A73-21000

Co-existence of scheduled and charter services in public air transport.

09 p1168 A73-23123

Charter air fleet maintenance economic management, discussing budget, manpower, time and materials control

09 p1168 A73-23243

Short haul air travel with Intermodal Automated Transfer system for integrating ground transportation to allow passenger to stay in seat from origin to destination

10 p1174 A73-23653

Development of maintenance policies in the operation of aircraft

10 p1174 A73-23655

Aircraft operations computerized simulation for commercial flight schedules evaluation and optimization, describing operational modeling and programming

10 p1203 A73-23685

Physically or mentally disabled passengers handling on scheduled, charter and group flights, discussing rules for attendants, seating and emergency procedures

10 p1176 A73-24709

Airlines flight safety management, discussing visual systems simulator /VSS/ for Tristar systems environmental and cycling endurance ground tests

10 p1176 A73-24710

Post-crash survival planning and procedures, discussing passenger instructions and control, crew training and rescue signalling devices

10 p1176 A73-24711

Cost effectiveness of planned aviation system improvements, considering ATC automation vs terminal aids, noise control, ground facilities, capacity and en-route situation

10 p1247 A73-24767

Malmö-Sturup airport facilities layout, discussing passenger terminal, lounges, baggage and cargo handling, ATC school, etc

11 p1343 A73-25207

Ireland commercial airports at Dublin, Shannon and Cork, discussing management, terminal facilities and operations

11 p1343 A73-25208

Airport computerized departure control for check-in, load control, cargo and catering operations, discussing load optimization and passenger acceptance control /LOPAC/ system

11 p1343 A73-25210

Regularization of the legal status of international air charter services.

11 p1454 A73-26349

Airport noise control and minimization for community and airline industry interests by technology application and legal-political approaches

11 p1455 A73-26350

Prediction for a park of helicopters of the same type

12 p1561 A73-27077

Satellite communication systems for long haul air transport operations, discussing political, operational/technical and economic problems

12 p1472 A73-27671

ATC system requirements for Concorde transoceanic flight operations, considering track allocation, computer system and programming

13 p1656 A73-28178

Air transportation direct and indirect costs analysis, considering cruising speed, flight time, aircraft design and manufacture and fuel expenses

13 p1569 A73-28950

Projections of the U.S. airline fleet in the early 1980's.

13 p1569 A73-29102

Central regional airport planning, compatibility and construction/operational costs for freight/passenger transport service in response to future economic growth

13 p1598 A73-29109

Conference on General Aviation-Business Flying, University of Tennessee, Tullahoma, Tenn., August 17-19, 1972, Proceedings.

13 p1570 A73-29344

Legal consequences resulting from transportation in airline traffic in the case of missing, deficient or not coverage-equivalent contractual basis

14 p1818 A73-30293

Book - Aircraft noise: Should the Noise and Number Index be revised.

15 p1830 A73-32414

Commercial airline operational control, discussing flight plan approval by pilot and ground personnel, preflight duties, weather information assessment and fuel monitoring

15 p1909 A73-32446

Some remarks on operational problems associated with the introduction of automatic data processing into air traffic control.

15 p1909 A73-32447

Aircraft integrated data systems /AIDS/ utilization for airlines operational flight control and economic exploitation enhancement, discussing aircraft accident investigation, maintenance, navigability, etc

15 p1831 A73-32496

PB-75 flight guidance system for subsonic commercial transport aircraft operation under Category IIIA conditions, describing cruise and ILS operation

15 p1911 A73-32500

STOL operational impact on ATC system support, considering short haul metropolitan and rural transportation modes, landing/takeoff facilities and all-weather operational reliability

15 p1831 A73-32547

Air cargo transportation growth since 1945 with comparison to concurrent air passenger evolution, predicting future trends

15 p1859 A73-32555

Civil aviation research patterns, discussing effects of nonregular carrier competition and Boeing 747 introduction

15 p1859 A73-32557

Radio navigation and landing aid equipment for major airports and airlines, noting simplified equipment for minor airports

15 p1912 A73-32559

Composite airframe structure effects on jet aircraft maintenance, discussing fire safety, fatigue resistance, environmental durability and quality assurance

16 p1967 A73-33027

Canadian air transportation survey, outlining history of other modes, transportation investment trends, modal traffic distribution, STOL applications, airline social services and marketing

16 p2087 A73-33177

World air traffic patterns projected to 1988, including present traffic features, supersonic transport utilization, ground transport alternatives, air freight and aircraft types

16 p2088 A73-33180

Flight Simulation Symposium, 2nd, London, England, May 16, 17, 1973, Proceedings.

16 p1995 A73-33201

Specific Behavior Objective approach to airline flight simulation, featuring duplicate training elimination and education time reduction

16 p1995 A73-33202

Airline flight simulator programs for aircraft type conversion training, outlining flight instructor training, certification and instructional aids

16 p1995 A73-33203

Airline flight simulation program, examining visual system capacity for replacement of in-flight training with pilot learning transfer estimation and simulation effectiveness appraisal

16 p1995 A73-33204

BOAC computer aided flight simulators, detailing simulator systems history, Boeing 747 training adaptation, and simulation types

16 p1996 A73-33212

An initial estimate of aircraft emissions in the stratosphere in 1990.

16 p2011 A73-34046

Hypersonic transports - Economics and environmental effects.

17 p2099 A73-34435

Automated terminal area ATC operations under FAA ten year plan, investigating analytical model of pilot-aircraft control loop decision making by computer program

17 p2206 A73-34437

Helicopter operations in London area, describing controlled airspace, helicopter routes and heliport approach and takeoff procedures

17 p2206 A73-34446

The functions of regional airports and the resulting requirements for the ground installations

17 p2146 A73-34476

Concorde aircraft introduction into airline network, discussing time gain over various routes, operating costs, passenger service, departure and arrival problems, maintenance, etc

[SAE PAPER 730351]

17 p2102 A73-34699

Market economic environment change effects on air transport design and use, examining 747 operational requirements in terms of cargo load factor, passenger fares and labor costs

[SAE PAPER 730355]

17 p2103 A73-34703

STOL aircraft choice for air transportation in low passenger density areas, discussing market characteristics in U.S. and tradeoffs between airline operation and airfield costs
[SAE PAPER 730357] 17 p2209 A73-34705

AIRTRANS - Intra-airport transportation system.
[SAE PAPER 730384] 17 p2146 A73-34721

The possible future of air transport and the airports
17 p2148 A73-35665

Development of methods of forecasting meteorological conditions for aviation
18 p2331 A73-35912

Influences of international operations on aircraft-transport design /Second William Littlewood Memorial Lecture/.
18 p2373 A73-36165

Simulating the introduction of 747 aircraft into airport operations.
18 p2296 A73-36423

Behavioral stress response RE - Passenger briefings and emergency warning systems on commercial airlines.
18 p2285 A73-36922

Management of cataract in commercial flight personnel.
18 p2285 A73-36927

Predicting the reduction in noise exposure around airports.
19 p2378 A73-37281

Effects of noise curfews on airline operations.
[AIAA PAPER 73-798] 19 p2379 A73-37461

The design or operation of aircraft to minimize their sonic boom.
[AIAA PAPER 73-817] 19 p2380 A73-37470

STOL pilot functional requirements on air transportation system in terms of airport design, aircraft, ATC, route selection, navigation and communications
19 p2450 A73-37730

Automation of airline passenger processing.
19 p2506 A73-37804

Area navigation technology for air transportation in USA, discussing present systems and projections as related to airline and FAA activities
19 p2451 A73-37807

On-board navigation and landing systems for local airlines in the USSR
19 p2452 A73-37819

Operational considerations in the design of airports.
19 p2418 A73-37820

Air freight handling equipment, techniques and costs in cargo terminals, including forklifts, pallets, containers, conveyor belts and warehouse configurations
19 p2418 A73-37821

U.S.S.R. laws and regulations regarding civil air transport equipment operations and maintenance, considering personnel training and safety
19 p2435 A73-38119

Operative visibility limits over the airports of Milan Linate and Malpensa in the 1960-1969 decade
19 p2447 A73-38125

Airborne digital data link terminal for commercial airlines' use.
20 p2526 A73-38756

Airline flight crew management and coordination procedures, outlining self-discipline philosophies and criteria, flight training and simulation, and performance records
20 p2509 A73-39217

L-1011 Tristar production, sales and airline service experience, discussing RB-211 turbofan engine and fleet performance
20 p2510 A73-39659

Aircraft ground station site evaluation based on disseminating time synchronization effectiveness, utilizing computer modeling for communication links and airspace population
21 p2734 A73-40033

Relationships between operational flexibility and capacity in contemporary terminal air traffic control operations.
21 p2736 A73-40048

Passenger response to airline service and resultant competition dynamics among air carriers in metropolitan area, indicating satellite airports importance
21 p2671 A73-40210

Functional aging - Present status of assessments regarding airline pilot retirement.
21 p2645 A73-41161

Schiphol as a tourist attraction.
22 p2839 A73-42316

Flow control concepts and airline operations.
22 p2884 A73-42522

Air carrier and general aviation airports system planning with emphasis on economic analysis of operation, ownership and finance
[ASME PAPER 73-ICT-33] 23 p2965 A73-43494

Dual lane runway configuration design and operational characteristics investigation by real time computer simulation for solution to airport capacity problem
[ASME PAPER 73-ICT-61] 23 p2966 A73-43496

Public air transportation service needs for nonurban areas, considering low traffic density problem, operational requirements and future trend
[ASME PAPER 73-ICT-72] 23 p3050 A73-43498

The transatlantic charter policy of the United States.
24 p3158 A73-44575

The development of civil air navigation in the People's Republic of China - Agreements with other states as well as the tasks and the position of the China Civil Aviation Corporation /CAAC/.
24 p3159 A73-45346

Aircraft noise reduction alternatives for operational aircraft, noting noise generation upstream of final nozzle, reengining, refanning and suppressor techniques
24 p3123 A73-45374

Liability and insurance in international air traffic
24 p3159 A73-45443

AIRLINERS
U COMMERCIAL AIRCRAFT
U PASSENGER AIRCRAFT

AIRLOCK MODULES
S Skylab experiments through airlock studying earth atmosphere, particles, background sky light, solar spectra, nebulae, stars and galaxies
13 p1617 A73-28945

Description of the docking module ECS for the Apollo-Soyuz Test Project.
[ASME PAPER 73-ENAS-21] 19 p2493 A73-37977

AIRPLANE PRODUCTION COSTS
Technology advancement effects on military and commercial transport aircraft development and production costs, considering airframes, engines and avionics
07 p0924 A73-20394

Cost estimating techniques for airframe weight-cost interface study for military aircraft design
[SAWE PAPER 969] 19 p2385 A73-37885

AIRPORT LIGHTS
NT RUNWAY LIGHTS
Aircraft-airport system R and D program in terms of efficient planning, lighting and marking, geometric design, safety and pavements
13 p1598 A73-29103

Airport runway lights system location and use for aircraft takeoff operations and visual indication of landing approach angle
14 p1743 A73-30242

Roskilde airport for Copenhagen metropolitan area general aviation and domestic air traffic, describing runways, taxiways, drainage, terminal facilities, lighting and navigation aids
15 p1858 A73-32364

Runway lighting emergency power supplies for low visibility, comparing single supply backed by automatic generator with separate cable and duplicate supplies
22 p2839 A73-42318

AIRPORT MOBILE LOUNGES
U MOBILE LOUNGES

AIRPORT PLANNING
Trends in offshore airports.
[ASCE PREPRINT 1273] 01 p0030 A73-10824

Airport layout planning, considering air traffic, conventional and STOL aircraft, runway requirements, passenger and baggage processing facilities, environmental factors, etc
02 p0150 A73-11704

European regional airports planning for short haul point-to-point air transport and international airports congestion alleviation
05 p0562 A73-16565

Air transportation systems problems - The airport operators' view.
[AIAA PAPER 73-6] 06 p0683 A73-17602

The capacity of a single-runway S.T.O.L./R.T.O.L. airport.
07 p0849 A73-19352

Monograph - System analysis of the air-ground transportation interface problem at Bangkok International Airport.
07 p0808 A73-20382

Community response to aircraft noise.
10 p1298 A73-24562

Airfield requirements for flight safety enhancement, considering approach and takeoff path obstructions, runway conditioning, glide slope information and radio aids
10 p1203 A73-24713

Airport design and management for safe aircraft ground handling, discussing FAA rules on pavement and safety areas, marking and lighting, fire fighting, etc
10 p1204 A73-24714

Cost effectiveness of planned aviation system improvements, considering ATC automation vs terminal aids, noise control, ground facilities, capacity and en-route situation
10 p1247 A73-24767

Dusseldorf airport passenger terminal facilities project, considering handling capacity, building and wide bodied jet traffic requirements
11 p1343 A73-25206

Malmo-Sturup airport facilities layout, discussing passenger terminal, lounges, baggage and cargo handling, ATC school, etc
11 p1343 A73-25207

Ireland commercial airports at Dublin, Shannon and Cork, discussing management, terminal facilities and operations
11 p1343 A73-25208

Regional airport systems study for San Francisco bay area, discussing commercial and general aviation future needs, environmental and economic aspects and alternative options
11 p1454 A73-26125

Airport noise control and minimization for community and airline industry interests by technology application and legal-political approaches
11 p1455 A73-26350

General aviation requirements within National Aviation System, discussing basic services, facilities, federal spending and R and D
12 p1459 A73-27361

An appraisal of the funding provisions of the Airport and Airways Development Act of 1970 to implement system improvements.
12 p1561 A73-27366

Airport and Airway Development Act trust fund surplus, discussing expenditure policy determination and incentive plan provisions to expedite improvements
12 p1561 A73-27367

Airports: Challenges of the future; Proceedings of the Airports Specialty Conference, Dallas, Tex., March 7-9, 1973.
13 p1598 A73-29101

Projections of the U.S. airline fleet in the early 1980's.
13 p1569 A73-29102

Aircraft-airport system R and D program in terms of efficient planning, lighting and marking, geometric design, safety and pavements
13 p1598 A73-29103

Dallas/Fort Worth regional airport land use planning for airport-community compatibility assurance via airspace distribution
13 p1598 A73-29107

Central regional airport planning, compatibility and construction/operational costs for freight/passenger transport service in response to future economic growth
13 p1598 A73-29109

Engineering management for the Dallas/Fort Worth Airport.
13 p1708 A73-29110

Airport planning trends and engineering, discussing systems analysis, pavement design, modular terminal facilities, costs and economic efficiency
13 p1598 A73-29111

Airport layout and planning standards, considering dimensions, height restrictions, noise exposure, land use compatibility, and long term community and aeronautical requirements
13 p1598 A73-29347

Improvements in Airport Surface Traffic Control surveillance.
14 p1740 A73-29887

Parameters of rational airfield pavement design system.
[ASCE PREPRINT 1700] 15 p1855 A73-31386

Effect of openings on stresses in rigid pavements.
15 p1856 A73-31387

Subgrade strengthening of existing airfield runways.
15 p1856 A73-31388

STOL aircraft flight and landing area considerations.
[ASCE PREPRINT 1726] 15 p1856 A73-31389

International Conference on Offshore Airport Technology, 1st, Bethesda, Md., April 29-May 2, 1973, Proceedings. Volume 1.
15 p1856 A73-31526

Design considerations for offshore airports.
15 p1856 A73-31527

Multi-purpose use potential of offshore airports.
15 p1856 A73-31528

Access requirements for offshore airports.
15 p1856 A73-31529

Aircraft noise, exposure factor, land use priorities, public environmental concern and jurisdictional considerations impact on offshore airport planning
15 p1959 A73-31530

Offshore airport planning, discussing selection economics from cost effective alternatives based on usage projection, community benefits and intrinsic and social costs
15 p1856 A73-31531

Operational considerations in the design of offshore airports.
15 p1856 A73-31532

Heavy marine structure engineering in offshore airport planning, discussing construction types and conditions, environmental factors, materials, methods and equipment
15 p1856 A73-31533

A technological development scenario for offshore jetports.
15 p1857 A73-31534

Netherlands international airport planning and site selection, discussing cost/benefit analysis experience from large coastal and offshore projects

15 p1959 A73-31535

Land construction and cost studies for Chicago offshore airport site development in Lake Michigan using rock and landfill dikes for protection against waves

15 p1857 A73-31536

Denmark offshore airport projects progress reports covering historical background, present status, political efforts, legislation, market retention, access problem and technical design considerations

15 p1960 A73-31537

Honolulu International Airport reef runway.

15 p1857 A73-31538

London third airport planning, discussing site selection, large scale urbanization, land use and reclamation, operational aspects and environmental factors

15 p1857 A73-31539

Los Angeles offshore airport planning case study covering design, logistics problems and costs with allowance for airspace and environmental considerations peculiar to Southern California area

15 p1857 A73-31540

Miami offshore airport project rejection reasons, citing commercial and marine ecological considerations

15 p1857 A73-31541

Offshore airport planning in Osaka-Bay, Japan - New Kansai International Airport.

15 p1857 A73-31542

San Diego offshore airport feasibility to meet future air traffic demands, evaluating sites for capacity, environmental impact, access and construction costs

15 p1857 A73-31543

Progress report on Tel Aviv offshore airport project.

15 p1857 A73-31544

Canadian government planning for second land based or offshore jet airport in Toronto area, considering environmental and community factors

15 p1858 A73-31545

Fog frequency and characteristics at the site of the proposed New York offshore airport, as compared with those at J. F. Kennedy International Airport - A preliminary report.

15 p1903 A73-31546

Dallas/Fort Worth airport layout and facilities, describing runway arrangement, passenger, baggage and cargo services, access roads and internal transportation system

15 p1858 A73-32362

Airport planning for 1980s air traffic capacity requirements, considering runways, aprons, air traffic and ground movements control, ground access and terminal facilities

15 p1858 A73-32363

Roskilde airport for Copenhagen metropolitan area general aviation and domestic air traffic, describing runways, taxiways, drainage, terminal facilities, lighting and navigation aids

15 p1858 A73-32364

Book - Aircraft noise: Should the Noise and Number Index be revised.

15 p1830 A73-32414

Book - Aircraft noise: Selection of runway sites for Maplin Airport.

15 p1859 A73-32415

Airport or ATC system hourly landing and takeoff capacity concept in terms of hourly demand as function of mean waiting time

15 p1960 A73-32552

French ATC authority problems generated by north-south air lane crossing of intercontinental east-west routes, considering enroute and terminal airport problems

15 p1960 A73-32558

Radio navigation and landing aid equipment for major airports and airlines, noting simplified equipment for minor airports

15 p1912 A73-32559

Technical studies and research on airport infrastructure

15 p1859 A73-32561

Airports automated meteorological instrumentation, describing cloud base height telemeter and transmissometer for runway visibility measurement

15 p1859 A73-32563

Determinants for aircraft noise annoyance - A comparison between French and Scandinavian data.

16 p1967 A73-32915

Toronto airport relocation project, summarizing provincial government planning and decision making process, site choice and community resistance to airport

16 p1995 A73-33181

STOL short haul system development, discussing airport congestion, operational costs and environmental considerations

16 p1968 A73-33192

Social acceptability of heliports particularly from the standpoint of noise.

17 p2146 A73-34441

Feasibility of downtown heliport facilities in terms of public concerns including fear, noise and economics

17 p2146 A73-34443

City center heliport design and location for scheduled intercity helicopter services, discussing terminal facilities, economic factors, elevated sites, etc

17 p2146 A73-34444

The functions of regional airports and the resulting requirements for the ground installations

17 p2146 A73-34476

Stuttgart airport noise abatement supervisor tasks and experience, describing routing specifications, landing and takeoff procedures and traffic flow [DGLR PAPER 73-022]

17 p2208 A73-34495

STOL aircraft choice for air transportation in low passenger density areas, discussing market characteristics in U.S. and tradeoffs between airline operation and airfield costs

[SAE PAPER 730357]

17 p2209 A73-34705

AIRTRANS - Intra-airport transportation system.

[SAE PAPER 730384]

17 p2146 A73-34721

Simulation of a surface traffic control system for John F. Kennedy International Airport.

17 p2147 A73-34818

The possible future of air transport and the airports

17 p2148 A73-35665

A simulation study for the design of an air terminal building.

17 p2149 A73-35826

Offshore airport design, construction and operation on basis of cost/benefit considerations, emphasizing ATC problems generated by ILS localizer and glide path signal reflection

18 p2296 A73-36682

Airport simulation program describing passenger flow and scheduling considerations, including automobile parking, baggage handling, rapid transit, arrival and departure peaks and passenger decisions

18 p2296 A73-36841

Aircraft noise in airport areas, discussing effects on environment and economics

18 p2373 A73-36949

Inter-noise 72; International Conference on Noise Control Engineering, Washington, D.C., October 4-6, 1972, Proceedings and Tutorial Papers.

19 p2472 A73-37276

A proposed littoral airport.

19 p2415 A73-37280

Predicting the reduction in noise exposure around airports.

19 p2378 A73-37281

Consequences of aircraft noise reduction alternatives on communities around airports.

[AIAA PAPER 73-818]

19 p2380 A73-37471

STOL pilot functional requirements on air transportation system in terms of airport design, aircraft, ATC, route selection, navigation and communications

19 p2450 A73-37730

International Conference on Offshore Airport Technology, 1st, Bethesda, Md., April 29-May 2, 1973, Proceedings. Volume 2.

19 p2417 A73-37741

Environmental considerations for offshore airports.

19 p2417 A73-37742

Urban and regional planning aspects of offshore airport technology.

19 p2417 A73-37743

An offshore airport in Sydney region - Review of a 1972 feasibility study.

19 p2418 A73-37744

Financing the new generation of airports.

19 p2506 A73-37745

Machinery to be developed for an offshore airport constructed by reclamation.

19 p2418 A73-37746

Floating offshore airport in Osaka Bay, Japan - Digest of preliminary engineering study.

19 p2418 A73-37747

Floating superport.

19 p2418 A73-37748

New York offshore airport feasibility study.

[FAA-RD-73-45]

19 p2418 A73-37750

U.S. instrument landing system performance improvements, considering terrain and weather effects, installation requirements, airport limitations, accuracy, reliability and maintainability

19 p2450 A73-37805

Transport aircraft noise reduction in airport areas through low noise engine design, traffic control, flight maneuvers and architectural planning

19 p2384 A73-37818

Operational considerations in the design of airports.

19 p2418 A73-37820

Aircraft noise consideration for environmental compatibility, airport development, short haul and supersonic air transport and legislation and regulation problems

[AIAA PAPER 73-795]

19 p2387 A73-38368

Aircraft ground station site evaluation based on disseminating time synchronization effectiveness, utilizing computer modeling for communication links and airspace population

21 p2734 A73-40033

Low cost airport surveillance and Localized Cable Radar with runway or taxiway vehicle guidance capability for ground traffic control, using solid state equipment

21 p2736 A73-40051

Passenger response to airline service and resultant competition dynamics among air carriers in metropolitan area, indicating satellite airports importance

21 p2671 A73-40210

Russian book on airport cable communication lines, discussing design construction, signal transmission theory and structural and electrical characteristics

21 p2675 A73-41283

Seattle-Tacoma's unconventional concept.

22 p2839 A73-42315

World Bank support for airports.

22 p2938 A73-42317

Runway configuration improvement programming model.

[ASCE PREPRINT 2034]

22 p2839 A73-42864

Use of simulation in airport planning and design.

[ASCE PREPRINT 2038]

22 p2839 A73-42865

Estimation of general aviation air traffic.

[ASCE PREPRINT 2041]

22 p2839 A73-42866

Computer-aided design of airport system plans.

[ASCE PREPRINT 2058]

22 p2839 A73-42867

Air carrier and general aviation airports system planning with emphasis on economic analysis of operation, ownership and finance

[ASME PAPER 73-ICT-33]

23 p2965 A73-43494

Dual lane runway configuration design and operational characteristics investigation by real time computer simulation for solution to airport capacity problem

[ASME PAPER 73-ICT-61]

23 p2966 A73-43496

The role ground transportation can play in the airport site selection process.

[ASME PAPER 73-ICT-70]

23 p2966 A73-43497

Airport runway and taxiway surfaces modifications for heavy and supersonic aircraft demonstrated by aircraft static and dynamic landing loads and physical dimensions

24 p3075 A73-45199

Maplin airport planning history, noise reduction features and government surveys, noting future air traffic trends and planning alternatives

24 p3076 A73-45373

AIRPORT SURFACE DETECTION EQUIPMENT

Airport lighting systems as visual landing aids, discussing runway disposition, brightness levels, beam orientation, visibility factors and flashing lights

16 p1993 A73-32974

AIRPORTS

NT HELIPORTS

Airport internal transportation systems for passengers and baggage, considering time scheduled, continuously moving and individually controlled systems

01 p0029 A73-10306

Trends in offshore airports.

[ASCE PREPRINT 1273]

01 p0030 A73-10824

Airport requirements for air traffic safety, considering runway drainage and lighting, ILS, rescue and fire services, communications and weather reporting networks

01 p0030 A73-11239

Osaka airport effective continuous perceived noise level measurements, area contour map and noise duration allowance vs aircraft distance diagram

03 p0249 A73-12977

Techniques for determining the noise zones in the vicinity of the central Berlin-Schoenefeld airport, and related problems

03 p0249 A73-12978

Monitoring and modeling of airport air pollution.

04 p0432 A73-14891

Advanced transport systems for airports.

05 p0562 A73-16566

Aviation and atmospheric pollution - The real dimension of the problem and its solutions

09 p1136 A73-22216

Digital readout wind measurement and indicator system for data acquisition, processing and display in airports for aircraft wind information service

15 p1874 A73-31318

Aircraft crash fire prevention and fighting in airports, discussing aircraft fuel system fail-safe design concepts and airport fire fighting equipment and procedures

15 p1859 A73-32366

Anglo-American Aeronautical Conference, 13th, London, England, June 4-8, 1973, Proceedings

16 p1968 A73-33176

Air-ground transportation interface at airports, examining baggage handling, ticketing, security procedures, rapid transit access, in-airport time and walking distances

16 p1995 A73-33178

Simulation of airport traffic flows with interactive graphics.

17 p2147 A73-34821

Simulating the introduction of 747 aircraft into airport operations.

18 p2296 A73-36423

Inglewood /California/ airport noise abatement monitoring program, discussing landing approach slopes, monitoring equipment and techniques and noise effects on property value 19 p2505 A73-37283

Very short range local area weather forecasting using measurements from geosynchronous meteorological satellites. 19 p2446 A73-37500

Jet aircraft noise abatement near airports during takeoff, approach and landing, discussing noise measurement standards and regulatory and noise reduction design efforts 19 p2385 A73-37825

Operative visibility limits over the airports of Milan Linate and Malpensa in the 1960-1969 decade 19 p2447 A73-38125

Fire protection and insurance in airport hangars, discussing governmental safety codes, fire prevention systems, aircraft vs building values and legislative proposals 20 p2544 A73-39214

Book - Prestressed pavements of airports and roads. 21 p2675 A73-41287

The effect of aircraft noise on the countryside. 22 p2798 A73-41709

Schiphol as a tourist attraction. 22 p2839 A73-42316

AIRSHIPS

Rigid airships as versatile and ecologically clear STOL aircraft, discussing computerized structural analysis, nuclear propulsion and radar guidance systems 02 p0131 A73-12596

Airship design for short-medium distance heavy payload transport, describing honeycomb skin construction, power plant installation and hovering loading/unloading operations 04 p0405 A73-14825

Stratospheric airship propulsion system using electric engine, hydrogen-air fuel cells and liquid hydrogen 04 p0408 A73-15119

Airships design, constructional and operational characteristics, discussing aerodynamics, flight control, performance and trim 06 p0648 A73-18510

Freighter airships economical and technological feasibility study, discussing performance requirements and design concepts [SAWE PAPER 951] 19 p2385 A73-37879

The Dolphin airship with an undulating propulsion system - Surface and width of the fuselage 19 p2387 A73-38122

Wind tunnel test for Dolphin airship model static thrust measurements, discussing thrust direction torque moment coefficients and propeller rotation 21 p2635 A73-41648

A technology tool for urban applications - The remotely piloted blimp. [AIAA PAPER 73-981] 22 p2799 A73-42533

Dirigible airship design, operations, payloads, cargo transportation and surveillance applications 23 p2940 A73-44223

AIRSPACE

German book on national airspace protection against foreign aircraft intrusion in peacetime covering sovereign rights according to international law, conventions and treaties 11 p1454 A73-26257

Inverse condemnation of airspace, discussing real property concept relation to aircraft noise, pollution and environment protection 16 p2087 A73-33103

Area navigation as means for airspace optimal utilization, considering navigation equipment and methods and ATC procedures reorganization 19 p2452 A73-37817

Midair collision avoidance strategies for ATC improvement, discussing relative effectiveness of structural airspace, airborne and ground-based systems based on US statistics 21 p2733 A73-40030

AIRSPEED

Parachutist biomedical effects during 110-175 knot towing by aircraft, establishing maximum feasible airspeed 16 p1974 A73-32675

A scheme for estimating aircraft velocity directly from airborne range measurements. 17 p2209 A73-34873

Pulsejet engines operational characteristics compared to turbojet engines, noting flight speed limit due to interaction between unsteady gas flow and combustion process 18 p2342 A73-36063

Human physiological responses to high speed aerial tow. 18 p2286 A73-36939

AIRWORTHINESS

U AIRCRAFT RELIABILITY

AIRWORTHINESS REQUIREMENTS

U AIRCRAFT RELIABILITY

AIRY FUNCTION

Elasticity theory contact problem for rectangle under compression loads, using Airy stress function for reduced linear algebraic equations system 01 p0117 A73-11090

Composite approximations to the solutions of the Orr-Sommerfeld equation. 08 p0956 A73-21686

Two dimensional elasticity theory boundary value problem, for inhomogeneous laminar elastic medium, using Airy stress functions and power series expansion of inhomogeneity parameter 12 p1553 A73-27412

Two-dimensional problem in elasticity theory for a rectangle with mixed boundary conditions 19 p2499 A73-37761

Solution of plane problems of elasticity utilizing partitioning concepts. [ASME PAPER 73-APM-C] 23 p3047 A73-44378

ALABAMA

NASA environmental applications demonstrations in southeastern United States. 20 p2557 A73-39848

ALARMS

U WARNING SYSTEMS

ALBEDO

NT COSMIC RAY ALBEDO

NT EARTH ALBEDO

The albedo of snow in relation to the sun position. 01 p0038 A73-10392

Comparison of the linear polarization and albedo of volcanic rocks in the spectral region between 0.75 and 3.0 microns with the values of these parameters for the moon 01 p0101 A73-10841

P, T invariance of electromagnetic interaction and the circular polarization of planetary emission 01 p0092 A73-10940

The spherical albedo of a planetary atmosphere 01 p0102 A73-10942

Radii, albedos, and 20-micron brightness temperatures of Iapetus and Rhea. 01 p0104 A73-11050

Optical measurements of lunar albedo, angular illumination, diffuse and specular reflectance and scattering coefficients on Mare Foecunditatis regolith powder of various sizes 02 p0213 A73-12238

Influence of refractive index on emittance from semi-infinite absorbing scattering media. [AIAA PAPER 73-147] 05 p0598 A73-16895

Mars surface features from Mariner 9 TV photometric observations, discussing albedo variations due to dust storm, topography and craters 06 p0745 A73-17478

Intensity and energy spectrum calculation of albedo electrons recorded in cosmic particle showers by gas discharge counters 07 p0823 A73-19429

Determination of the transfer function for the spectral albedo of the surface-atmosphere system of the planet 07 p0818 A73-19659

Structure of lunar maria from their albedo data 07 p0902 A73-20323

Albedo and illuminance of the surface of a planet with an inhomogeneous, purely scattering atmosphere. 07 p0820 A73-20345

Permanent frost formation on steep north-facing Mars surface slopes above 25 deg north latitude, considering explanation by insolation and surface albedo 09 p1145 A73-22274

P, T invariance of electromagnetic interaction, and circular polarization of planetary radiation. 09 p1138 A73-22735

Spherical albedo of a planetary atmosphere. 09 p1147 A73-22737

Apollo 14 lunar fines thermal radiation properties as function of bulk density, illumination angle and wavelength, calculating solar albedo and total emittance 10 p1277 A73-24080

LiF albedo dosimeter for fast neutron and gamma irradiation measurement on personnel, using Cf-252 source for calibration 11 p1361 A73-25313

The spectral albedo of water clouds in the 1-6 micron band. 11 p1357 A73-26195

Simple model for scanning-angle distribution of planetary albedo gamma-rays. 11 p1414 A73-26475

Multicolor photoelectric photometry of Neptune. 11 p1429 A73-26682

Albedo distribution in lunar maria. 12 p1540 A73-27295

Statistical distribution of albedo over the lunar disk 12 p1546 A73-27863

Comparison of linear polarization and albedo of igneous rocks in the spectral region 0.75-3.0 mu and lunar values of those parameters. 15 p1928 A73-30977

Far ultraviolet reflectivity of lunar dust samples - Apollo 11, 12, and 14. 15 p1932 A73-31270

Monochromatic phase curves and albedos for the lunar disk. 15 p1932 A73-31271

The solar albedo of hard X-ray flares. 16 p2053 A73-32961

Stability levels of the reflectivity of lunar surface details 16 p2063 A73-33761

Infrared radiation of the moon at 3.5 to 3.9 microns 16 p2064 A73-33764

Determination of the lunar albedo at the 6-m wavelength 16 p2064 A73-33772

Monochromatic and radiometric albedo of Mars and Venus 16 p2067 A73-33811

Absorption of centimeter radio waves in the Venusian atmosphere 16 p2068 A73-33821

Continuing activity of Jupiter and comparison of the 1871-1880 and 1961-1965 flare-ups 16 p2057 A73-33842

Ammonia absorption relevant to the albedo of Jupiter. I - Experimental results. 17 p2231 A73-34764

Polar albedo changes and its climatic consequences. 18 p2307 A73-36028

Apparent reflectance from a semi-infinite absorbing-scattering medium. [AIAA PAPER 73-753] 18 p2337 A73-36369

Mars Hellespontus region identification from Mariner 9 photographs as wind produced dunes, considering albedo features 19 p2477 A73-37210

Variable features on Mars. II - Mariner 9 global results. 19 p2478 A73-37212

Martian south polar region albedo map from Mariner 9 photographs, comparing with earth-based telescopic observations 19 p2480 A73-37232

Physical nature of the lunar surface albedo 19 p2480 A73-37234

Spectral albedos of the Galilean satellites. 19 p2483 A73-37578

Statistical distribution of the albedo over the lunar disk. 20 p2608 A73-39237

Possibilities of calculating the spectral albedo of Venus in the near infrared 21 p2770 A73-40914

Illuminance and albedo variations /whiteness constancy/ category judgments for stimuli with unpatterned and patterned surfaces 21 p2639 A73-41183

Low albedo lunar areas, discussing spectral reflectivity, radar backscatter characteristics and Apollo 17 landing site 22 p2909 A73-42495

The wavelength dependence of the albedos of Uranus and Neptune from 0.3 to 1.1 micron. 22 p2914 A73-43014

Combined lidar and radiometric measurements of cirrus clouds for IR emissivity, optical thickness and albedo 23 p3003 A73-43600

Ultraviolet observations of Mars made by the Orbiting Astronomical Observatory. 24 p3128 A73-44397

Asteroid reflectivities from polarization curves - Calibration of the 'slope-albedo' relationship. 24 p3129 A73-44437

Asteroid belt white light polarization curve measurements, indicating surface texturizing and albedo dispersion 24 p3131 A73-44462

Martian surface albedo compared with Mariner-observed topography, noting dark-band correlation with maximum topographic irregularity regions 24 p3133 A73-44551

Posteclipse brightening of Io observed at 3500 and 4000 A suggested as transient partial covering of high-albedo material 24 p3134 A73-44564

Interior radiances in optically deep absorbing media. I - Exact solutions for one-dimensional model. 24 p3111 A73-45318

Radiative transfer through a Compton-scattering atmosphere with continuous energy dependence. 24 p3111 A73-45321

ALBUMINS

An implantable radiotelemetrical measuring device for simultaneous long term measurements of body temperature and turnover of rabbit serum albumin/I-125 in unrestrained rabbits. 03 p0271 A73-14301

IR-spectroscopic investigation of the thermal stability of albumin at different levels of its ionization 10 p1182 A73-24685

Effects of oxygen-augmented atmosphere on the immune response. 17 p2115 A73-34743

ALCOHOLS

NT ETHYL ALCOHOL

NT METHYL ALCOHOLS

NT POLYVINYL ALCOHOL.

The isolation of a series of acyclic isoprenoid alcohols from an ancient sediment - Approaches to a study of the diagenesis and maturation of phytol.
11 p1326 A73-25465

ALDEHYDES

NT ACETALDEHYDE
NT FORMALDEHYDE

Glyoxal cis form as source of microwave spectra from rotational spectrum investigations of B-type transitions
03 p0273 A73-13286

ALDOSTERONE

Renal component of the antigravitation function of the organism
08 p0929 A73-20976

Effects of an hyperoxic hypobaric environment on renin-aldosterone in normal man.
08 p0934 A73-21503

Effect of actinomycin D on aldosterone-mediated changes in electrolyte excretion.
09 p1040 A73-22650

Role of mineralocorticoids in the natriuresis of water immersion in man.
09 p1040 A73-22676

Effects of the hypodynamics and other factors of a spaceflight on the excretion of 17-oxy corticosteroids and aldosterone
17 p2111 A73-34233

Effect of altitude on renin-aldosterone system and metabolism of water and electrolytes.
22 p2806 A73-42420

ALERTNESS

Effects of noise and response complexity upon vigilance performance.
06 p0656 A73-17523

German monograph - Vigilance prognosis with the aid of a computer analysis of the spontaneous electroencephalogram.
07 p0786 A73-20391

Influence of high ambient temperatures on the performance and some physiological parameters in a tracking problem and an optical vigilance problem
08 p0935 A73-21575

ALFVEN WAVES

U MAGNETOHYDRODYNAMIC WAVES

ALGAE

NT BLUE GREEN ALGAE
NT CHLORELLA

Variable photosynthetic units, energy transfer and light-induced evolution of hydrogen in algae and bacteria.
08 p0932 A73-21685

Effect of nitrite and nitrate on chlorophyll fluorescence in green algae.
16 p1973 A73-33226

The gas exchange of hydrogen-adapted algae as followed by mass spectrometry.
17 p2118 A73-34225

New algae mapping technique by the use of an airborne laser fluorosensor.
17 p2163 A73-35412

Application of a pulsed laser for measurements of bathymetry and algal fluorescence.
20 p2574 A73-39863

Theoretical study of primary photosynthesis processes in higher plants and algae
23 p2946 A73-43707

ALGAL BLOOM

U ALGAE

ALGEBRA

NT ADJOINTS
NT AUTOMORPHISMS
NT BANACH SPACE
NT BINOMIALS
NT CANONICAL FORMS
NT DETERMINANTS
NT DUFFING DIFFERENTIAL EQUATION
NT DYADICS
NT EIGENVALUES
NT EIGENVECTORS
NT GROUP THEORY
NT HERMITIAN POLYNOMIAL
NT HILBERT SPACE
NT HOMOMORPHISMS
NT JORDAN FORM
NT LIE GROUPS
NT LINEAR EQUATIONS
NT LINEAR TRANSFORMATIONS
NT MATRICES [MATHEMATICS]
NT NONLINEAR EQUATIONS
NT POLYNOMIALS
NT QUADRATIC EQUATIONS
NT SPINOR GROUPS
NT STATE VECTORS
NT STOKES THEOREM [VECTOR CALCULUS]
NT STRESS TENSORS
NT SUBGROUPS
NT TENSORS
NT VECTOR SPACES
NT VECTORS [MATHEMATICS]
NT VORTICITY

Proof for sigma algebra of asymptotic events represented as sequence of partial sums of series of independent and essentially divergent random variables
01 p0070 A73-10411

Central limiting theorem in the 'noncommutative' probability theory
15 p1899 A73-31215

Statistical models for rounding-off error studies in linear algebraic problems
18 p2292 A73-37144

ALGOL

A program for plate reduction in the case of satellite observations with a satellite observation camera
03 p0274 A73-13254

Automatic optimization of Symbolic Algol programs. I - General principles.
07 p0796 A73-19269

Mathieu function eigenvalue computation based on Algol program, using Fourier series, Bessel functions, wave equations and elliptic domains
23 p2998 A73-43209

ALGORITHMS

Iteration approach for elliptic /nonlinear/ difference operators in divergence form
01 p0069 A73-10075

An improved algorithm for the inversion of limb radiance measurements.
01 p0072 A73-10355

Application of frequency-pulse modulation to adaptive automatic control systems
01 p0027 A73-10597

A digital system for shaping, analysis and control of a random vibration spectrum
01 p0027 A73-10598

Nonlinear method of analyzing electroencephalograms
01 p0012 A73-10661

Algorithms for phase vector coordinates calculation of servomechanism, using measuring instrument data as starting information
01 p0028 A73-10676

Application of the algorithm of a median for accuracy and reliability improvement in data processing
01 p0020 A73-10678

Normality condition derivation for algorithm of first order solution to ideal resonance problem, applying to critical inclination of oblate planet satellite
01 p0077 A73-10686

Numerical solution of one-dimensional non-steady flow with supersonic and subsonic flows and heat transfer.
01 p0003 A73-10765

Trajectory optimization of pursuer vehicle for multitarget rendezvous, noting algorithm for dynamic programming
01 p0105 A73-11124

Discrete control algorithms for spaceborne terminal systems.
01 p0075 A73-11194

Doubly relaxed matrix inverse for linear equations system solution with inadequately conditioned coefficient matrices, noting algorithm for improved conditioning
01 p0071 A73-11279

Error-erasure decoding of product codes.
01 p0020 A73-11296

Investigation of the effectiveness of the variable-step simplex optimization method in a noise environment
01 p0028 A73-11420

Optimal renewal algorithm for control plant with cumulative damage, using failure rate and renewal point spacing model
01 p0058 A73-11421

A fast computational algorithm for optimum digital control systems.
01 p0021 A73-11463

Accelerated convergence of sequences of quadrature approximations.
01 p0072 A73-11471

Space booster control system computerized design algorithm for forward loop compensation filter selection based on minimization of penalty function of stability margin violations
01 p0021 A73-11516

Determination of the theoretical stress-concentration factors in composite systems in bending
02 p0229 A73-11638

A simple method for determining static parameters of large signal semiconductor diode and transistor models.
02 p0147 A73-12044

Method of minimization of description of classes in pattern recognition.
02 p0143 A73-12125

Algorithms for equations of oscillatory motion about moving center, noting disturbing force effect on vibrational frequency
02 p0193 A73-12196

Multistep three-parameter algorithm for spacecraft stabilization on an atmospheric reentry trajectory
02 p0229 A73-12451

Algorithms for spacecraft trajectory optimization programs for orbit perturbations caused by random measurement errors and minimum mathematical expectancy of energy dissipation
02 p0220 A73-12468

Algorithm for automatic optimal control of radio telescope parabolic antenna with extremal characteristics in radiation pattern, noting quasi-steady and steady operation
02 p0147 A73-12497

teristic in radiation pattern, noting quasi-steady and steady operation
02 p0147 A73-12497

Russian book on color recognition methods and devices covering algorithms for radiation color identification and optimal spectra of photosensitive radiation detector
02 p0144 A73-12862

Real time tracking radar for radio guidance system, obtaining algorithm for rocket motor direction and ignition time for satellite orbit optimization
03 p0339 A73-13067

An approximate algorithm for the reanalysis of structures by the finite element method.
03 p0391 A73-13676

Algorithm for stress tensor and stability analysis of glass fiber reinforced plastic shells under hydrostatic pressure
03 p0392 A73-13741

Mathematical algorithm using invariant imbedding method for accurate range and range rate estimates in terms of pulse Doppler radar ambiguity resolution
03 p0276 A73-13902

State augmentation procedure for fixed point smoothing algorithm derivation through known solutions of higher dimensional digital filtering problem
03 p0277 A73-13914

Aircraft reference altitude computation from air data inputs, deriving algorithm for pressure gradient errors correction
03 p0308 A73-13915

A new algorithm for three-dimensional method of characteristics.
03 p0337 A73-14201

Computerized design and algorithm for linear and nonlinear regulators by mathematical programming approach involving vector determination for objective function minimization
03 p0286 A73-14480

Topological analysis of mechanical vibrating linear systems by the method of structural numbers
03 p0396 A73-14598

Certain algorithms and error assessments for the approximate analytical solution of boundary value problems
04 p0470 A73-15090

Adaptive feedback control without complete plant identification, deriving vector cost function and algorithm for performance optimization
04 p0430 A73-15214

A modified conjugate gradient method for optimization problems.
04 p0471 A73-15216

Evaluation of the performance of a variance estimation algorithm using order statistics.
04 p0471 A73-15259

Relaxation algorithms for nonlinear system modal trajectory estimation by approximate step with lower triangular matrix inversions sequence, comparing convergence with Gauss-Newton method
04 p0472 A73-15265

A state covariance matrix computation algorithm for satellite orbit determination sequential filtering.
04 p0431 A73-15267

An error sensitivity analysis for nonlinear second order filters.
04 p0431 A73-15269

Estimation of unmodeled forces on a low-thrust space vehicle.
04 p0504 A73-15272

Optimum quantization and parallel algorithms for nonlinear state estimation.
04 p0472 A73-15276

Real time digital spacecraft TV with data compression/error correction test system, evaluating source encoding algorithm performance from processed picture quality
04 p0449 A73-15409

A study of simple chromatogram - Compression algorithm efficiency.
04 p0449 A73-15445

Image recognition learning algorithm for expanding neural nets composed of active inputs, receptors, associative elements and recognizers
04 p0426 A73-15794

Theoretical foundations for synthesis of learning-type recognition algorithms by the method of R-functions in the complex-plant control problem
05 p0560 A73-16275

Extremal control system efficiency enhancement by information storage, noting algorithms for sequential data storage
05 p0560 A73-16298

Elimination on sparse symmetric systems of a special structure.
05 p0590 A73-16500

A solution of the bilinear matrix equation $AY + YB$ equals $-Q$. [DFVLR-SONDDR-274]
05 p0591 A73-16607

Optimization of register length in a control algorithm for a nonstationary plant
05 p0561 A73-17280

Computer adaptive optimization system for problems with nonlinear criteria function and con-

straints, noting algorithms of deterministic and stochastic categories

05 p0555 A73-17284

A new algorithm for the computation of bending moments and deflections of straight beams.

05 p0637 A73-17325

Summary and comparison of gradient-restoration algorithms for optimal control problems.

06 p0715 A73-17567

Procedural formalization and methodology for automated problem solving in terms of digital program systems for algorithms generation, describing operational procedures

06 p0669 A73-17594

Computer aided shrouded propeller design. [AIAA PAPER 73-54]

06 p0644 A73-17630

A universal method of calculation of the state of a real gas behind primary and reflected shock waves.

06 p0684 A73-17700

Digitalized or sampled data FM demodulator recursive algorithm synthesis and SNR performance comparison with optimum analog and conventional limiter discriminator demodulators

06 p0664 A73-17712

A partitioning algorithm with application in pattern classification and the optimization of decision trees.

06 p0670 A73-17805

Simplex gradientless algorithm for unconstrained static optimization, noting effectiveness for arbitrary goal functions in nonlinear programming

06 p0670 A73-17858

Comparison of the Powell 1, Powell 2, and Zangwill static optimization methods

06 p0670 A73-17859

Synthesis of adaptive systems by Lyapunov's direct method.

06 p0723 A73-17959

Computer control algorithms for transient response optimization in on/off motor control system synthesis

06 p0741 A73-17963

An efficient numerical technique for evaluating large quantities of highly oscillatory integrals.

06 p0716 A73-17982

Quadratic termination properties of minimization algorithms. I - Statement and discussion of results. II - Proofs of theorems.

06 p0716 A73-17983

Computational variants of the Lanczos method for the eigenproblem.

06 p0716 A73-17984

An analysis of optimal control system algorithms.

06 p0670 A73-18059

Mean square error automatic equalizer for synchronous data transmission by gradient projection method for parameter optimization in discrete frequency domain, noting algorithm convergence

06 p0665 A73-18141

A 2-cycle algorithm for source coding with a fidelity criterion.

06 p0671 A73-18142

Complex images application of target isolation algorithms based on brightness distributions, discussing allocation of target classification parameters

06 p0694 A73-18289

Nonsearch algorithms for parametric synthesis of stochastic automatic control systems

06 p0680 A73-18381

A simple interpolation algorithm for improvement of the numerical solution of a differential equation.

06 p0717 A73-18407

A numerical method for solving optimal control problems with unspecified terminal time.

06 p0681 A73-18520

On the convergence of random search algorithms in continuous time with applications to adaptive control.

06 p0671 A73-18623

Computerized optimal control problem formulation in calculus of variations, discussing flexible user-oriented algorithm for terminal point transversality boundary conditions numerical implementation

06 p0672 A73-18806

An adaptive bit synchronization algorithm under time-varying environment.

06 p0672 A73-18810

An algorithm for the assignment of closed-loop poles using output feedback in large linear multivariable systems.

06 p0672 A73-18869

Kron algorithm for complex eigenvalue problems of damped vibrating mechanical systems, using Newton method

07 p0909 A73-19098

The determination of state-space representations for linear multivariable systems.

07 p0804 A73-19131

Acceleration of the convergence in Nesbet's algorithm for eigenvalues and eigenvectors of large matrices.

07 p0844 A73-19271

Control algorithm for digital computer operations organization in real time processing of variable priority assignment tasks, estimating memory storage requirements

07 p0796 A73-20049

Flight vehicle equations of motion with variable information, noting flight control algorithm for random variable with given probability

07 p0849 A73-20077

Adaptive algorithms for reducing a random field to a prescribed set of states with constraints on the elements of the approximating sequences

07 p0796 A73-20079

Algorithm for calculating unsteady heat transfer in liquid-propellant rocket-engine chambers with regenerative cooling

07 p0868 A73-20087

Adaptive nonlinear filtering for tracking with measurements of uncertain origin.

07 p0805 A73-20584

On stochastic approximation and the hierarchy of adaptive array algorithms.

07 p0846 A73-20585

An efficient parallel algorithm for the solution of a tridiagonal linear system of equations.

08 p0983 A73-20960

Scheduling algorithms for multiprogramming in a hard-real-time environment.

08 p0941 A73-20961

Tree-manipulating systems and Church-Rosser theorems.

08 p0941 A73-20962

An algebraic algorithm for the design and analysis of linear dynamical systems.

08 p0984 A73-21468

Nonlinear algorithms for the local solution of an equation with a fixed point in a product of Banach spaces

08 p0984 A73-21489

Parallel algorithms for plotting profiles, projections, and cross sections with the aid of receptor matrices on a digital computer

08 p0941 A73-21588

An algorithmically and physically oriented design approach. I - Problems analysis

09 p1087 A73-21900

Algorithms for calculating disjunctive normal form with minimum number of variables of completely/incompletely determined Boolean functions

09 p1111 A73-22108

Convergent iterative smoothing algorithm for aircraft stability parameter identification from measurement, using variational optimization procedure

09 p1067 A73-22233

Recursive methods in on-line computer photogrammetric data reduction deriving algorithms for fixed and variable parameter numbers cases with matrix partitioning

09 p1059 A73-22381

FORTAN IV program and recursive matrix partitioning algorithm for solution of photogrammetric simultaneous equations, noting computation time

09 p1059 A73-22382

Algorithm for optimal radio signals detection under narrow band anisotropic noise, noting two channel space diversity receiver system

09 p1050 A73-22454

Algorithm for numerical calculation of transmitted and reflected electromagnetic waves, noting multiple reflections for inertial inhomogeneities

09 p1063 A73-22458

An optimal algorithm for measuring the dispersion of a random process in the case of separate allowance for the influence of external and internal additive noise

09 p1051 A73-22462

Operational algorithms for probabilistic digital integrators for Stieltjes integral and nonhypertranscendental functions

09 p1060 A73-22555

Probability characteristics of complex systems with a hierarchical control

09 p1068 A73-22559

Algorithmic construction of optimal controllers on the basis of incomplete information about the state of the plant

09 p1068 A73-22562

Algorithm for spectrum decomposition during continuous man-computer interaction, noting Gaussian distribution of spectral bands and linear approximation for background

09 p1046 A73-22971

Cutpoint cellular switching array synthesis by combined cascade simplification rule, noting algorithm efficiency increase

09 p1065 A73-23101

Redundant area encoding for relieving integration time requirement in airborne reconnaissance photograph transmission, discussing algorithms, display technique, data reduction and pictorial simulation

09 p1054 A73-23386

Multispectral imagery data compression for earth resources satellites, comparing performance of spectral-spatial-delta-interleave and Rice coding algorithms

09 p1055 A73-23391

Adaptive algorithm with error control for line by line encoder for image transmission, noting reconstructed image quality improvement

09 p1055 A73-23392

High data rate hard decision digital IC sequential decoder for earth-orbiting satellite space missions, discussing computational efficiency of modified Fano algorithm

09 p1056 A73-23398

On the solution of linear inequalities with applications to threshold logic.

10 p1191 A73-23746

A mathematical programming approach to identification and optimization of a class of unknown systems.

10 p1242 A73-23773

Radio-guidance algorithms applied to the control of spacecrafts descending in the earth's atmosphere

10 p1247 A73-23880

Optimal entry algorithm and multipulse correction times for spacecraft guidance trajectory of minimum fuel consumption

10 p1247 A73-23881

Alternative algorithmic scheme for spherical harmonics series summation, noting high speed and precision loss at high resolution in comparison with conventional methods

10 p1246 A73-23993

Iterative optimum control function determination without directly solving the system dynamical equations.

10 p1242 A73-24033

Contraction-mapping algorithm with guaranteed convergence.

10 p1242 A73-24034

Discrete dynamic adaptive control algorithms for estimation of minimum loss function point trajectory characterizing system quality in nonstationary conditions

10 p1242 A73-24035

On a method of adaptive control under conditions of great uncertainty.

10 p1199 A73-24036

The algorithms of accuracy research of nonstationary linear systems with continuous and discrete elements.

10 p1200 A73-24048

Estimation theory and system state and parameter identification, developing algorithms for optimum linear sequential and nonlinear filters

10 p1200 A73-24051

Order determination and parameter identification of time-invariant state variable models.

10 p1201 A73-24054

Matrix eigenvalue search algorithms of Rutishauser-Francis type, showing relationship to linear group decompositions

10 p1243 A73-24124

Finite element solution algorithm for viscous incompressible fluid dynamics.

10 p1243 A73-24296

Solution of quadratic matrix equations for free vibration analysis of structures.

10 p1290 A73-24299

Analytical mechanics algorithms based on characteristic equation and canonical equations of system with integral constraints

10 p1249 A73-24312

Certain finitely converging algorithms for the solution of infinite systems of inequalities and their application in the theory of adaptive systems

10 p1192 A73-24486

Adaptation algorithms in multilayer pattern-recognition systems

10 p1192 A73-24502

An actively adaptive control for linear systems with random parameters via the dual control approach.

10 p1202 A73-24534

Discrete-time fixed-lag smoothing algorithms.

10 p1243 A73-24547

A numerical algorithm to design multivariable low-pass equiripple filters.

10 p1202 A73-24600

Real time digital computer algorithm for linear and nonlinear electronic circuit modeling in state variable form for static and dynamic regimes

10 p1196 A73-24607

Algorithmic design methodology, describing functional representation of suitable effect chains

11 p1371 A73-24994

Comparative analysis of algorithms for measurement of correlation functions by the multiplication method /Review/

11 p1360 A73-25018

Field of attraction of a singularity of a nonlinear recurrence of the second order - Method of determination of the boundary

11 p1389 A73-25137

Design of control and display panels using computer algorithms.

11 p1361 A73-25180

Functional analysis and optimal control of linear discrete systems, deriving algorithms for minimum fuel, energy or amplitude from linear equations solution

11 p1390 A73-25188

Irreducible canonical realizations from external data sequences.

11 p1390 A73-25191

Multinput multioutput linear time invariant discrete system optimal approximation, noting algorithms and weighting matrices computational difficulties

11 p1390 A73-25192

Direct time numerical integration of spatially discretized linear elastodynamics integral equations, comparing one-step algorithms for stability and accuracy in terms of frequency spectrum

11 p1435 A73-25439

A method of feasible directions using function approximations, with applications to min max problems.

11 p1390 A73-25474

Automated structural synthesis using a reduced number of design coordinates.

[AIAA PAPER 73-336] 11 p1436 A73-25476

Taylor series algorithms for computerized structural design and reanalysis of modified structures, applying to aircraft fuselage midsection

[AIAA PAPER 73-338] 11 p1436 A73-25478

Linear programming and gradient search algorithms for minimum weight design of finite element structures, applying to bar truss problems

[AIAA PAPER 73-343] 11 p1436 A73-25482

Regularization schemes for solving inverse heat conduction problems

11 p1451 A73-25743

Dynamical system of N degrees of freedom reduced to ideal resonance problem involving Hamiltonian function, presenting algorithm for calculating ignorable coordinates

11 p1423 A73-26071

An analytical iterative algorithm for the prediction of special satellite orbit points with the Brouwer orbit theory.

11 p1423 A73-26075

Algorithm for locating a moving object

11 p1394 A73-26097

Algorithm and convergence behavior of the local variation method for problems with partial derivatives

11 p1400 A73-26326

Algorithm for solution of inverse Stefan problem for flow characteristics determination, stating necessary and sufficient conditions for solution existence and uniqueness

11 p1452 A73-26328

Kramers-Kronig analysis of relative reflectance spectra measured at an oblique angle.

11 p1400 A73-26421

Viterbi algorithm for recursive optimal estimation of state sequence of discrete time finite state Markov process observed in memoryless noise

11 p1333 A73-26690

Automatic control system components optimization for minimal cost, demonstrating algorithm efficiency for servosystem

12 p1482 A73-26775

Computer technology aided machine design automation and structural synthesis by coded information table formulation and conversion, discussing algorithm construction

12 p1502 A73-26784

Supermemory gradient-restoration algorithm in flight-path optimization problems

12 p1548 A73-27082

A numerical algorithm for identifying spread functions of shift-invariant imaging systems

12 p1475 A73-27114

Quadratically convergent algorithms and one-dimensional search schemes.

12 p1517 A73-27118

A self starting predictor corrector algorithm of arbitrary order having exact stability.

12 p1517 A73-27170

Investigation of series pattern-forming circuits for multiple-beam antennas

12 p1479 A73-27231

Algorithm for choosing the optimal disposition of radiating elements in a linear antenna array by the method of coordinate trials

12 p1479 A73-27232

Book - Numerical methods for unconstrained optimization.

12 p1518 A73-27549

An algorithmic procedure for determining discrete transfer matrices of controlled plants

12 p1485 A73-27624

An algorithm for controlling the descent of a spacecraft from an artificial earth satellite orbit.

12 p1543 A73-27631

Applications of vector and parallel computers to radar defense systems.

[AIAA PAPER 73-428] 12 p1476 A73-27822

Methods of quadratic Liapunov vector-function construction for linear systems

12 p1525 A73-27895

Method for synthesizing built-in control circuits of automatic systems with memory

12 p1476 A73-27899

Nonsearch self-adapting identification systems

12 p1485 A73-27900

Application of Liapunov functions for studying the convergence of unconstrained minimization methods

13 p1657 A73-28018

Direct numerical solution of three-dimensional equations containing elliptic operators.

13 p1647 A73-28080

Dynamic structural response analysis with eigenvalue problem solution in terms of stiffness and mass matrices, discussing algorithm selection for efficient computation

13 p1691 A73-28081

Plate theory boundary value problems algorithm from Fourier transformation of ultradistribution functions

13 p1695 A73-28561

An algorithm for the computation of the higher order G-transformation.

13 p1649 A73-28601

A direct method approximation to the linear parabolic regulator problem over multivariate spline bases.

13 p1649 A73-28605

Rate of convergence of a class of methods of feasible directions.

13 p1649 A73-28609

Numerical solution of the problem of transmission of ELF waves through the lower ionosphere.

13 p1582 A73-28651

Theoretical and experimental investigations of a phase-coordinate second-order receiver.

13 p1591 A73-28658

Accelerating search-variable metric algorithm combination for space shuttle atmospheric flight optimization, comparing with cubic fit-golden section method

13 p1650 A73-28825

Minimax failure detection and identification in redundant gyro and accelerometer systems.

13 p1616 A73-28832

Algorithms for finding the coefficients of polynomials of matrix determinants

13 p1587 A73-28864

Russian book on digital computer construction and operation covering data processing and conversion algorithms, memory, arithmetic and control devices, microprogramming, etc

13 p1588 A73-28948

Application of a modified quasilinearization technique to totally singular optimal control problems.

13 p1597 A73-29570

Optimization of turbulence models by means of a logical search algorithm.

14 p1744 A73-29931

Some efficient algorithms for solving systems of nonlinear equations.

14 p1768 A73-29939

Algorithm for statistical error detection in digital control computers

14 p1730 A73-30038

Dynamic scheduling of large digital computer systems using adaptive control and clustering techniques.

14 p1730 A73-30039

An algorithm for numerical integration in triangular domains.

14 p1806 A73-30047

A priori evaluation of the position finding system of the Guiana Space Center /CSG/ by the application of Kalman's algorithm

14 p1727 A73-30092

Comparison between the peak sidelobe of the random array and algorithmically designed aperiodic arrays.

14 p1734 A73-30217

Book - Computational fluid dynamics.

14 p1745 A73-30359

Standard algorithms application to modified matrix and least squares eigenvalues, determining quadratic forms and Gauss-Radau and Gauss-Lobatto quadrature rules coefficients

14 p1769 A73-30409

An historical survey of computational methods in optimal control.

14 p1738 A73-30413

An adaptive precision gradient method for optimal control.

14 p1738 A73-30452

Algebraic decoding algorithms for block codes over q-ary input Q-ary output alphabet channel, presenting examples for Hamming, Lee or burst distance

14 p1730 A73-30501

A minimization algorithm for the design of linear multivariable systems.

14 p1769 A73-30504

An efficient algorithm for calculation of the Luenberger canonical form.

14 p1769 A73-30508

Continuously-discrete method for the construction of control devices

14 p1740 A73-30940

Multistep computer algorithm for Navier-Stokes equations of two dimensional viscous incompressible flow in channel with complex geometry

15 p1860 A73-30965

Linear transformations of variable in system of normal equation in differential correction processes, reducing process to algorithm

15 p1930 A73-31115

A procedure for the minimization of the costs of a project in the case of a given project duration

15 p1959 A73-31224

Unified geometric and analytical treatment of magnetogasdynamics shocks. I - General solutions and theorems.

15 p1917 A73-31339

Arithmetic algorithms for error-coded operands.

15 p1899 A73-31349

An asymptotically optimal rank detection algorithm for a signal in noise of unknown distribution

15 p1842 A73-31490

A modified quasilinearization technique for optimal control problems with unspecified final time.

15 p1853 A73-31627

Suboptimal adaptive control of a class of non-linear systems.

15 p1853 A73-31628

Small digital computer program packet organization for central processor productivity and use coefficient improvement, discussing graph-algorithm language for program splicing

15 p1848 A73-31694

Length minimization in the internal-state code of an asynchronous finite automatic system with a two-step memory

15 p1848 A73-31910

Logic circuit distribution algorithms for asynchronous finite automata synthesis on basis of universal homogeneous medium

15 p1848 A73-31911

Automatic nodal point renumbering algorithm for interconnectivity matrix bandwidth reduction in computer aided structural analysis and design

15 p1848 A73-32029

Optimal algorithms for numerical solutions of singular integral equations

15 p1900 A73-32096

Operations research methods application to meteorological forecasting, discussing optimization algorithm and feedback systems

15 p1907 A73-32354

Papers on digital signal processing covering digital filters, fast Fourier transform, finite word length effects, algorithms, and design and programming considerations

15 p1855 A73-32425

French monograph - Study and preparation of algorithms of coordination in the structures of hierarchized control systems.

15 p1855 A73-32592

Three-parameter multistep algorithms for stabilization of a spacecraft on the descent trajectory through the atmosphere.

15 p1944 A73-32601

Algorithms for spacecraft trajectory optimization programs for orbit perturbations caused by random measurement errors and minimum mathematical expectancy of energy dissipation

15 p1942 A73-32618

The finite element method in shell stability analysis.

16 p2075 A73-32789

Algebraic criteria for positive realness relative to the unit circle.

16 p2032 A73-33162

Matrix theory algorithms for static stresses and elastic deformations in truss structures, deriving equilibrium equations in terms of forces, deformations and node displacements

16 p2080 A73-33258

Computational efficiency comparison for discrete linear filtering Kalman algorithms and information matrix methods, noting Householder square-root implementation identity with Potter technique

16 p2032 A73-33404

An adaptive estimation algorithm for time-varying bit synchronizers.

16 p1988 A73-33411

Numerical experience with algorithms for unconstrained minimization.

16 p2033 A73-33852

The choice of step length, a crucial factor in the performance of variable metric algorithms.

16 p2033 A73-33853

Nonlinear least squares calculations by Gauss-Newton and Levenberg, Marquardt and Morrison methods, discussing algorithm convergence rate and numerical computational scheme

16 p2033 A73-33854

Gradient methods with penalty functions for solution of optimal control with terminal constraints, noting convergence superiority of conjugate gradient algorithm

16 p2034 A73-33998

Computer oriented algorithms for solving systems of simultaneous nonlinear algebraic equations.

17 p2199 A73-34107

An error analysis of a method for solving matrix equations.

17 p2200 A73-34216

Modified quasilinearization method for mathematical programming problems and optimal control problems.

17 p2200 A73-34362

Remarks on the optimum rate of convergence of the on-line identification of non-stationary systems. 17 p2144 A73-34600

PLANET scheduling algorithms and their effect on availability. 17 p2130 A73-34822

Nonphysical self forces removal from electromagnetic plasma models by simulation algorithm, discussing optimization of particle orbit equations integration 17 p2216 A73-34895

Some results obtained in ESRO satellite data compression. 17 p2239 A73-34955

Kantorovich functional analysis algorithms providing rigorous theory for convergence of iterative methods to nonlinear functional equations on Banach spaces, emphasizing Newton method 17 p2163 A73-35268

An optimization technique utilizing the deflected gradient algorithm for dynamic testing of electromechanical equipment. 17 p2202 A73-35386

An integration algorithm for hyperbolic systems having non-zero, non-analytic steady-state solutions. 17 p2203 A73-35610

Sequential analysis algorithm for data channel detection of received signal represented by Poisson sequence of quantum transitions under large SNR 17 p2129 A73-35711

Effectiveness of certain easily realizable rank algorithms for detections of signals against a background of noise. 17 p2130 A73-35720

Algorithm construction for the stabilization of a deformable spacecraft using an onboard digital computer 18 p2359 A73-36105

Methods of constructing quadratic Lyapunov vector functions for linear systems. 18 p2330 A73-36600

Method of synthesizing built-in monitoring arrangements for automata with memory. 18 p2291 A73-36751

Searchless self-adjusting identification systems. 18 p2294 A73-36752

Numerical methods for solving some problems in studies of operations 18 p2331 A73-36985

Probability method and algorithm for analyzing the dynamic precision of pulse generators 18 p2294 A73-37024

Use of weighting functions in conjugate gradient methods 18 p2295 A73-37079

Algorithm for optimal material selection by seeking tradeoff between conflicting multifunctional structural design objectives 19 p2496 A73-37477

Parallel algorithms for optimum nonlinear state estimation. 19 p2413 A73-38041

Stabilization of multivariable systems with constant-gain output feedback. 19 p2413 A73-38046

Sensor concept and algorithms for a completely strapdown autonomous navigation approach. 19 p2452 A73-38057

System error analysis and algorithms for a strapdown navigation system. 19 p2452 A73-38058

A projection operator algorithm for optimal control problems with unspecified initial state values. 19 p2414 A73-38064

An efficient algorithm for calculation of the Luenberger canonical form. 19 p2408 A73-38065

Calculation of the plan for the transportation performance with the aid of electronic data processing 19 p2506 A73-38121

Eigenproblem solution by a combined Sturm sequence and inverse iteration technique. 19 p2408 A73-38188

A continuous-discrete method of design of control devices. 19 p2414 A73-38194

A dual method for optimal control problems with initial and final boundary constraints. 19 p2446 A73-38376

Recursive ideal observer detection of known M-ary signals in multiplicative and additive Gaussian noise. 19 p2407 A73-38385

Error maxima for division algorithm adaptiveness evaluation of damaged computer elements with corrective readjustments 19 p2408 A73-38563

Minimum risk classification algorithms in automatic learning system design, applying to learning pulse signal receiver 20 p2532 A73-38686

Dynamics and stability of the algorithm of a digital adaptive system using a prediction technique 20 p2532 A73-38688

Stochastic process control with a regulated control interval duration 20 p2540 A73-38701

Convergence of learning and adaptation algorithms 20 p2532 A73-38711

Uses of image recognition methods without teaching, in product quality control and lost observation estimations 20 p2568 A73-38712

A practical load relief control system designed with modern control techniques. 20 p2508 A73-38801

[AIAA PAPER 73-863] Attitude determination for a strapdown inertial system using the Euler axis/angle and quaternion parameters. 20 p2589 A73-38834

[AIAA PAPER 73-900] Algorithms for radio guidance with application to control of landing of spacecraft in the earth's atmosphere. 20 p2590 A73-38899

Optimal entry algorithm and multiimpulse correction times for spacecraft guidance trajectory at minimum fuel consumption 20 p2590 A73-38900

Algorithms for calculating Euler angles of moving objects 20 p2590 A73-39044

Statistically optimal sampled data terminal guidance algorithm for complex probabilistic multipurpose control system, using linearized equations 20 p2590 A73-39344

A nonsearching system of identification with a model, synthesized according to the hyperstability criterion 20 p2532 A73-39347

Coefficients of stress intensity near rigid acute-angled inclusions 20 p2619 A73-39370

Development of a program basis for statistical data processing on an analog-digital complex 20 p2532 A73-39392

A comparison of the times of computation required by two approaches for determining a shortest route in a network - A contribution to the economy of programming 20 p2533 A73-39631

Calculation of the radiative characteristics of polydisperse concentric spheres 20 p2531 A73-39728

Environment models and algorithm for obtaining statistically optimal proportions estimates for category mixtures in multispectral sensor data processing 20 p2559 A73-39883

Relationship between sea wave parameters and the spectra of aerial photography and radar imagery of sea surface. 20 p2531 A73-39891

Strapdown inertial navigation with high speed digital computer, discussing attitude propagation algorithms and life cycle system cost advantages 21 p2734 A73-40036

Space shuttle orbiter abort guidance for premature or abnormal termination of mission due to system or human failure, discussing predictive algorithm 21 p2735 A73-40045

A rational approach to the synthesis of one-dimensional acoustic filters. 21 p2739 A73-40285

Suboptimal algorithms for nonlinear smoothing. 21 p2669 A73-40333

A finite algorithm for the minimum l-infinity solution to a system of consistent linear equations. 21 p2725 A73-40376

Nonlinear eigenvalue problem of square matrix of analytic functions of complex number lambda, comparing algorithms convergence by numerical tests 21 p2725 A73-40380

A finite step algorithm for determining the 'strict' Chebyshev solution to $Ax = b$. 21 p2725 A73-40381

A wave propagation method for conversion of grey pictures into line figures. 21 p2654 A73-40688

Russian book - Matrix methods of calculating the strength of low-aspect-ratio wings. 21 p2785 A73-40799

An improved light gun tracking algorithm based on a recursive digital filter. 21 p2654 A73-40834

Linear programming for optimization, discussing definitions, practical examples, simplex algorithm, duality theory, heuristic interpretations and integer solutions 21 p2726 A73-40836

On the uniqueness of search directions in variable-metric algorithms. 21 p2726 A73-40837

A probabilistic algorithm for grouped handling of arguments with sequential discrimination of input features 21 p2658 A73-40994

The variable metric algorithm for non-definite quadratic functions. 21 p2727 A73-40999

Regularization of solutions of inverse problems of heat conduction. 21 p2792 A73-41061

A method of optimization of algorithms for secondary processing of radio signals 21 p2656 A73-41129

Pattern recognition learning machine design heuristics, discussing analysis, synthesis and convergence of algorithms 21 p2659 A73-41290

A recognition learning program based on selecting statistically useful attributes 21 p2659 A73-41291

Algorithm for deriving the equilibrium equations of an electric circuit on the basis of logic rules 21 p2670 A73-41307

An effective algorithm for optimizing electronic circuits 21 p2671 A73-41312

A parallel algorithm for high subsonic compressible flow over a circular cylinder. 21 p2727 A73-41474

A projection method in the problem of the excitation of a dielectric antenna 21 p2667 A73-41512

Higher order accuracy finite difference algorithms for quasi-linear, conservation law hyperbolic systems. 22 p2882 A73-42518

Search properties of some sequential decoding algorithms. 22 p2829 A73-42706

Recursive methods in photogrammetric data reduction. 22 p2862 A73-42825

Orbit osculation control algorithm guaranteeing satellite repeated passage over given point of earth surface, deriving functional for satellite thrust control 23 p3027 A73-43271

Design of discrete model reference adaptive systems using the positivity concept. 23 p2962 A73-43287

Digital filter bank with integrated FFT computer 23 p2956 A73-43326

A simplified minimal-realization algorithm for a symmetric transfer-function matrix. 23 p2999 A73-43382

Extrapolation algorithm for inverse thermal conductivity problem solution of body heat flux and temperature gradients, using successive approximations 23 p3048 A73-43445

Nonlinear methods for evaluating the informative value of meteorological parameters and for classifying meteorological phenomena /Functional methods and algorithms/ 23 p3001 A73-43464

Technically oriented algorithms for unsteady pipe flow. 23 p2968 A73-43800

Numerical stability of various summation schemes in a floating-type R subset 23 p2999 A73-44098

PEARL middle level programming language for process control, discussing algorithms, structure, time behavior and input/output of real time operation 23 p2956 A73-44388

Automatic integration algorithm for computer calculation of definite integral within specified tolerance, discussing computation failures and algorithm reliability 23 p2957 A73-44390

Weak invariance conditions and synthesis algorithms for control systems with discontinuities on hypersurfaces in phase space 24 p3074 A73-44666

Synthesis of a transverse digital filter defined in the complex plane 24 p3072 A73-44973

Algorithmic and computational aspects of the use of optimization methods in engineering design. 24 p3070 A73-45235

A Runge-Kutta Nystrom algorithm. 24 p3142 A73-45290

Certain theorems concerning functions of an incomplete quaternion variable 24 p3107 A73-45512

ALIGNMENT

NT SELF ALIGNMENT

Laser beams for precision alignment and detection using methods based on maximum and minimum principles 05 p0583 A73-16344

Improved mount and alignment procedures for a rapid-scan Fabry-Perot interferometer. 06 p0691 A73-17498

The pre-flight handling of inertial navigation systems. 07 p0849 A73-19347

Laser system output mirrors alignment for beam quality and power performance optimization and external optical component premature degradation prevention, using autocollimator 09 p1094 A73-22445

Preferred a axis orientation parallel to fiber axis in commercial carbon fibers due to lower surface energy of basal plane configuration

11 p1389 A73-25857

Metal matrix composites microstructural alignment by solid state transformation process involving eutectoid decomposition and cellular precipitation

12 p1513 A73-27682

Alignment technique for the Mach-Zehnder interferometer.

17 p2165 A73-34298

Continuous calibration and alignment techniques for an all-attitude inertial platform.

[AIAA PAPER 73-865]

20 p2586 A73-38803

Determination of the centering conditions of two-mirror systems with the aid of Hartmann photographs

20 p2565 A73-39067

Methods for alignment of lasers with unstable resonators.

20 p2573 A73-39686

Field aligned electron anisotropies observed by the ESRO 1 A/Aurora satellite.

21 p2691 A73-41370

Geodetic tasks during the construction and alignment of the RATAN-600 radio telescope

21 p2675 A73-41454

ALIPHATIC COMPOUNDS

NT ACETALDEHYDE
NT ACETYL COMPOUNDS
NT ACETYLENE
NT ACRYLONITRILES
NT ADENOSINE DIPHOSPHATE [ADP]
NT ADENOSINE TRIPHOSPHATE [ATP]
NT ADENOSINES
NT ALKANES
NT ALKENES
NT ALKYL COMPOUNDS
NT ANTHRACENE
NT BUTANES
NT CARBON TETRAFLUORIDE
NT CELLULOSE
NT CHOLINE
NT CYANAMIDES
NT CYANOGEN
NT CYCLIC HYDROCARBONS
NT DEXTRANS
NT DIMETHYLHYDRAZINES
NT ETHANE
NT ETHYL ALCOHOL
NT ETHYLENE
NT GLUCOSE
NT GLUCOSIDES
NT GLUTAMATES
NT GLUTAMIC ACID
NT GLYCEROLS
NT GLYCOGENS
NT HEPTANES
NT HEXOGENES [TRADEMARK]
NT HEXOKINASE
NT HYDRAZINE BORANE
NT HYDRAZINES
NT INOSITOLS
NT KETONES
NT LACTATES
NT LACTIC ACID
NT METHANE
NT METHYL ALCOHOLS
NT METHYL COMPOUNDS
NT NITROAMINES
NT NUCLEASE
NT NUCLEOSIDES
NT OLEIC ACID
NT OXYACETYLENE
NT PENTANES
NT PROPANE
NT PROPYLENE
NT STARCHES
NT STEARATES
NT SUCROSE
NT SUGARS
NT TETRAFLUOROHYDRAZINE
NT URETHANES

ALKALI HALIDES

NT CESIUM HALIDES
NT CESIUM IODIDES
NT POTASSIUM IODIDES
NT SODIUM CHLORIDES
NT SODIUM IODIDES

Thermodynamic functions and molecular parameters of rhombic dimeric molecules of alkali metal halides

01 p0080 A73-10857

Accumulation of the light sum in alkali halide crystals under the action of laser emission

01 p0060 A73-11088

Investigation of laser radiation self-focusing by alkali halide single crystals according to data on the damage-focus displacement effect

01 p0061 A73-11443

Investigation of self-focusing of laser radiation with alkali halide single crystals from data concerning the displacement of the focus of damage.

11 p1376 A73-26065

Confirmation of an electron avalanche causing laser-induced bulk damage at 1.06 micron.

11 p1377 A73-26227

ALKALI METAL COMPOUNDS

On some oxygenated compounds of titanium and alkalis /Li, Na/ - Study of the binaries M2O-TiO2 in the zones rich in alkaline oxide

05 p0547 A73-17219

ALKALI METALS

NT CESIUM
NT CESIUM VAPOR
NT LIQUID POTASSIUM
NT LIQUID SODIUM
NT LITHIUM
NT LITHIUM ISOTOPES
NT POTASSIUM
NT POTASSIUM ISOTOPES
NT RUBIDIUM
NT RUBIDIUM ISOTOPES
NT SODIUM
NT SODIUM ISOTOPES
NT SODIUM VAPOR
NT SODIUM 22
NT SODIUM 24

Mineralogical evidence for subsolidus vapor-phase transport of alkalis in lunar basalts.

07 p0880 A73-19693

Alkali metal intercalates of molybdenum disulfide.

08 p0937 A73-21174

Alkali metal purification and handling for advanced space power systems.

11 p1310 A73-26004

Recent materials compatibility studies in refractory metal-alkali metal systems for space power applications.

11 p1310 A73-26005

High field superconductivity in alkali metal intercalates of MoS2.

11 p1410 A73-26745

Efficiency of the recovery of high thermal energy densities during porous vaporization of alkali metals

15 p1957 A73-31864

Coherent light propagation and scattering in vaporized alkali metal atmosphere as function of refractive index and coherent to incoherent transformation

16 p2086 A73-34002

Characteristics of the electrode-adjointing potential layer in an alkali metal plasma in the presence of adsorption

17 p2214 A73-34131

Investigation of the discharge structure in a noble gas alkali MHD generator plasma. I.

18 p2338 A73-36303

Electric power cell for producing direct/alternating current and shaft horsepower by direct electrochemical reaction of alkali metals with water

19 p2390 A73-38397

Study of induced four-photon parametric scattering of laser light in alkali metal vapor

23 p2988 A73-44009

ALKALIES

NT SODIUM HYDROXIDES
Studies of the anodic oxidation of hydrazine in an alkali electrolyte and of the side reaction of ammonia formation during the decomposition of hydrazine
Investigation of the possibility of obtaining anodesite-based alkali-resistant glass compositions for a continuous glass fiber

04 p0407 A73-15103

23 p2998 A73-44298

ALKALINE BATTERIES

A nickel-hydrogen secondary cell for synchronous orbit application.

09 p1033 A73-22753

Leakable gases and water vapor loss rates and service life predictions for sealed alkaline cells in vacuum or aerospace environments, using mass transfer equations

[ECS PAPER 32]

11 p1307 A73-24973

High energy density silver-hydrogen cells for space and terrestrial applications.

19 p2391 A73-38403

ALKALINE EARTH COMPOUNDS

Genetic significance of chemical, isotopic, and petrographic features of some peralkaline salic rocks from the island of Pantelleria.

05 p0570 A73-16842

German monograph - The tribology of solid lubricants of the type of the alkaline-earth hydroxides in the system Fe-Me/OH2.

22 p2881 A73-42846

ALKALINE EARTH METALS

Selection and preliminary evaluation of three structures as potential solid conductors of alkali ions - Two hollandites, a titanate, and a tungstate.

17 p2219 A73-35325

Excited state absorption spectroscopy of alkaline earths selectively pumped by tunable dye lasers. I - Barium arc spectra.

21 p2713 A73-40472

ALKALINE EARTH OXIDES

NT BARIUM OXIDES
NT BERYLLIUM OXIDES
NT CALCIUM OXIDES

NT MAGNESIUM OXIDES

NT PERICLASE

Effect of alkali-earth oxides on the optical and EPR spectra of irradiated alkali silicate glass

05 p0589 A73-17296

Determination of dissociation energies for some alkaline earth /hydro-/ oxides in CO/N2O flames.

24 p3156 A73-44985

ALKALOIDS

NT HYOSCINE
NT QUINOLINE

ALKANES

NT BUTANES
NT ETHANE
NT HEPTANES
NT METHANE
NT PENTANES
NT PROPANE

The effect of higher alkanes on the ignition of methane-oxygen-argon mixtures in shock waves.

[AD-756982]

07 p0918 A73-19389

Kinetics and convection in the combustion of alkane droplets.

07 p0919 A73-19391

The diagenesis and maturation of phytol - The stereochemistry of 2,6,10,14-tetramethylpentadecane from an ancient sediment.

11 p1326 A73-25466

Proposed stratigraphic controls on the composition of crude oils reservoir in the Green River formation, Uinta Basin, Utah.

11 p1352 A73-25471

Hydroxyl radical mechanism for autoignition inhibition of alkane fuels for antiknock additives at various concentrations

13 p1707 A73-29000

ALKENES

NT ETHYLENE
NT PROPYLENE

Relative rate measurements for oxygen atom addition to simple olefins in liquid Ar at 87.5 K, noting activation energies during reactions

02 p0139 A73-12086

Mineral filler reinforcement value in polyolefins, stressing composite properties at high temperatures

10 p1237 A73-23963

The combustion of the n-pentenes in the cool flame region.

16 p2085 A73-33341

ALKYL COMPOUNDS

Thin films durability increase of poly/n-alkyl methacrylate/ polymers with alkyl group length, noting friction coefficient behavior

[ASLE PREPRINT 72LC-7C-4]

03 p0317 A73-14373

A review of the perfluoroalkyl ether class of greases.

07 p0843 A73-19558

The oxidation of metal alkyls in the presence of isobutane.

13 p1581 A73-29002

Friction induced surface activity of some simple organic chlorides and hydrocarbons with iron.

[ASLE PREPRINT 73AM-8A-1]

17 p2179 A73-34991

ALKYNES

NT ACETYLENE
NT OXYACETYLENE

ALL SKY PHOTOGRAPHY

Differences in auroral intensity at conjugate points.

09 p1074 A73-22059

Universal methods for estimating probabilities of cloud-free lines-of-sight through the atmosphere.

10 p1245 A73-23981

Auroral arcs oval configuration by all-sky photography from Arctica 2, considering difference in dayside and nightside halves from electron precipitation observations

10 p1214 A73-24745

Midday aurora behavior during auroral substorms from all sky photographs at south pole, considering modification of Starkov-Feldstein model

12 p1493 A73-27614

Diffuse auroral belt observation by Isis-2 scanning auroral photometer verified by analysis of ground based all sky photographs

15 p1866 A73-31074

Certain parameters of cumulus clouds as determined from sky photographs and from ground-based actinometric measurements

15 p1905 A73-31793

Observations of the auroral oval and a westward traveling surge from the Isis 2 satellite and the Alaskan meridian all-sky cameras.

16 p2004 A73-33445

North polar aurora oval detection by high frequency sounder radar aided by all sky photography and statistical auroral data, discussing backscatter and auroral echoes

18 p2312 A73-36282

ALL-WEATHER AIR NAVIGATION

Onboard ILS equipment reliability in integrated airborne all-weather landing system

02 p0190 A73-11855

Trends in helicopter guidance and control systems with bad weather capability. 03 p0340 A73-13921

S-61N helicopter all-weather IFR operation for North Sea oil rigs supply and harbor pilot transportation, describing onboard instrumentation, navigation and communication systems 05 p0535 A73-16847

Digital Avionics Information System /DAIS/ development for military supersonic all-weather precision weapon delivery system, emphasizing modular design for different aircraft types 06 p0672 A73-17572

All-weather aircraft landing automation, discussing efficient optimal feedback control law selection based on trajectory termination or terminal control requirements 10 p1247 A73-24010

Meteorological radar and the WILM landing aid 14 p1772 A73-29731

The lowering of minima of third-level and business aircraft 15 p1831 A73-32476

M.A.D.G.E. - Microwave Aircraft Digital Guidance Equipment: Description of the system 15 p1912 A73-32504

STOL operational impact on ATC system support, considering short haul metropolitan and rural transportation modes, landing/takeoff facilities and all-weather operational reliability 15 p1831 A73-32547

All-weather landing technology and economics, considering ground and airborne equipment and benefits and costs 15 p1859 A73-32553

Integrated reliability and safety analysis of the DC-10 all-weather landing system. 16 p1969 A73-33641

Helicopter night and bad weather navigation aids, examining ground-independent navigation, low flight, obstacle warning, terrain detectors, blind landing and optoelectric sensing 17 p2206 A73-34258

Low visibility/bad weather aircraft landing systems design, discussing developmental stages for all weather landing implementation, automatic landing control and pilot visual discrimination problems 17 p2207 A73-34481

ALLOCATIONS

NT RESOURCE ALLOCATION

Continuous analog of dynamic-programming allocation process 09 p1112 A73-22889

A computer method of optimal redundancy allocation in satellite communication system. 10 p1188 A73-23753

ALLOTROPY

Additives alloying with cobalt, discussing allotropic transformation dependence, recrystallization, mobile dislocations, and iron deformation by twinning 11 p1408 A73-25322

The effect of thermomechanical pretreatment on the allotropic transformation in cobalt. 17 p2190 A73-34645

ALLOYS

NT ALUMINUM ALLOYS

NT ANTIMONY ALLOYS

NT AUSTENITIC STAINLESS STEELS

NT BARIUM ALLOYS

NT BEARING ALLOYS

NT BERYLLIUM ALLOYS

NT BINARY ALLOYS

NT BISMUTH ALLOYS

NT BORON ALLOYS

NT BRASSES

NT BRONZES

NT CADMIUM ALLOYS

NT CARBON STEELS

NT CHROMIUM ALLOYS

NT CHROMIUM STEELS

NT COBALT ALLOYS

NT CONSTANTAN

NT COPPER ALLOYS

NT ERBIUM ALLOYS

NT EUTECTIC ALLOYS

NT FERRITIC STAINLESS STEELS

NT GALLIUM ALLOYS

NT GERMANIUM ALLOYS

NT GOLD ALLOYS

NT HAFNIUM ALLOYS

NT HEAT RESISTANT ALLOYS

NT HIGH STRENGTH ALLOYS

NT HIGH STRENGTH STEELS

NT INCONEL [TRADEMARK]

NT INDIUM ALLOYS

NT IRON ALLOYS

NT KAMACITE

NT LANTHANUM ALLOYS

NT LEAD ALLOYS

NT LIGHT ALLOYS

NT LIQUID ALLOYS

NT LITHIUM ALLOYS

NT MAGNESIUM ALLOYS

NT MANGANESE ALLOYS

NT MANGANIN [TRADEMARK]

NT MARAGING STEELS

NT MARTENSITIC STAINLESS STEELS

NT MOLYBDENUM ALLOYS

NT MONEL [TRADEMARK]

NT NEODYMIUM ALLOYS

NT NICHROME [TRADEMARK]

NT NICKEL ALLOYS

NT NICKEL STEELS

NT NIMONIC ALLOYS

NT NIOBIUM ALLOYS

NT NITINOL ALLOYS

NT PALLADIUM ALLOYS

NT PERMALLOYS [TRADEMARK]

NT PLATINUM ALLOYS

NT QUATERNARY ALLOYS

NT RARE EARTH ALLOYS

NT REFRACTORY METAL ALLOYS

NT RENE 41

NT RHENIUM ALLOYS

NT RHODIUM ALLOYS

NT RUTHENIUM ALLOYS

NT SILICON ALLOYS

NT SILVER ALLOYS

NT SOLDER

NT STAINLESS STEELS

NT STEELS

NT TANTALUM ALLOYS

NT TELLURIUM ALLOYS

NT TERNARY ALLOYS

NT TIN ALLOYS

NT TITANIUM ALLOYS

NT TUNGSTEN ALLOYS

NT UDIMET ALLOYS

NT URANIUM ALLOYS

NT VANADIUM ALLOYS

NT WASPALOY

NT WROUGHT ALLOYS

NT YTTRIUM ALLOYS

NT ZINC ALLOYS

NT ZIRCALOY 2 [TRADEMARK]

NT ZIRCALOYS [TRADEMARK]

NT ZIRCONIUM ALLOYS

General analysis and synthesis of alloys and materials with inhomogeneous physical properties, noting thermal physicochemical methods for laminates and metal powders 01 p0066 A73-11340

Metal ions implantation to produce alloy or semiconductor, discussing transmission electron microscopy use for viewing target material defect clusters 03 p0350 A73-13794

Naturally alloyed n-p structures in cadmium telluride 04 p0484 A73-15642

Implosive and explosive welding of mono- and bimetallic duplex cylinders. 08 p0973 A73-21239

Annealing of effects arising during ion-bombardment alloying of metals at energies up to 10 keV 10 p1223 A73-23817

Diffusion processes electron mechanism in metal-metal and metal-nonmetal systems, using configurational model for valence electrons localization 10 p1236 A73-24951

Alloy creep due to temperature and tensile stress in absence of hardening 12 p1513 A73-27479

A high resolution dynamic technique of thermoelectric power measurements. 13 p1612 A73-28370

Mechanical behavior of materials; Proceedings of the First International Conference, Kyoto, Japan, August 15-20, 1971. Volume 1 - Deformation and fracture of metals. Volume 2 - Fatigue of metals. Volume 3 - Temperature effects of metals, environmental effects, polymers. Volume 5 - Composites, testing and evaluation. 13 p1638 A73-29451

Russian book - Superconducting alloys and compounds. 15 p1922 A73-31176

Transition metal alloys solid solutions, discussing thermodynamics, interatomic interactions, Debye temperatures, free energy, entropy, magnetic effects and incomplete d shells 15 p1892 A73-32213

Experimental methods regarding the thermodynamics of metals and alloys. I 16 p2026 A73-33953

Enhanced ductility in metals /Superplasticity/. 17 p2240 A73-34113

Damping properties of turbine blade materials at operational temperatures 17 p2221 A73-34327

Young elastic modulus determination in steel and alloy disks by contact method 17 p2177 A73-34338

Environment-assisted fracture in engineering alloys. I - Monotonic loading. 18 p2365 A73-36613

[ASME PAPER 73-MAT-R]

Second phase particle redistribution in dispersion-hardened alloys by directed particle diffusion via chemical potential control 18 p2325 A73-36807

ALPHA PARTICLES

Friction of hard alloys in vacuum at low temperatures 18 p2320 A73-36861

Application of the 'differential reflectometer' to materials research in corrosion, ordering and alloying. 21 p2719 A73-40897

Two phase alloy internal oxidation kinetics, deriving mathematical model with linear law for penetration velocity fluctuations 21 p2719 A73-40898

Russian papers on metal alloys chemistry covering atomic structure, physicochemical properties, phase diagrams, X ray analysis, laser microanalysis, etc 22 p2873 A73-42083

Russian book - General patterns in the structure of phase diagrams of metal systems. 22 p2877 A73-42451

ALLUVIAL PLAINS

U FLOOD PLAINS

ALLUVIAL TERRACES

U TERRACES [LANDFORMS]

ALMUCANTAR

U ELEVATION ANGLE

ALOUETTE SATELLITES

NT ALOUETTE 2 SATELLITE

ALOUETTE 2 SATELLITE

Conjugate ducted echoes observed on Alouette II ionograms. 05 p0572 A73-17164

Estimation of H+/ fluxes at the polar regions. 18 p2304 A73-35969

The precession of unsymmetric spin-stabilized satellites. 22 p2916 A73-42190

ALPHA DECAY

Alpha spectrometry of a surface exposed lunar rock. 07 p0870 A73-19796

ALPHA PARTICLES

EPR in alpha-particle bombarded silicon single crystals 02 p0201 A73-12171

Internal friction in polycrystalline copper foils after alpha-irradiation at 78 K 03 p0328 A73-14653

Solar electrons and alpha particles during polar-cap absorption events. 04 p0493 A73-15558

Rigidity spectrum of helium nuclei above 17 GV and a search for high energy anti-nuclei in primary cosmic rays. 04 p0493 A73-15980

Dispersion-free X-ray-fluorescent analysis in studies of space and terrestrial objects 05 p0546 A73-17019

Observation of lunar radon emanation with the Apollo 15 alpha particle spectrometer. 07 p0891 A73-19826

Predicting light flashes due to alpha-particle flux on SST planes. 07 p0777 A73-20157

Primary cosmic rays alpha particles and protons energy spectra similarity and intensity difference at .05 to 1.6 TeV, using Proton satellites data 08 p0999 A73-21331

An alpha particle experiment for chemical analysis of the Martian surface and atmosphere. 09 p1048 A73-22190

Possible correlation between the concentration and density of alpha-radioactive fallouts and types of meteorological processes 09 p1115 A73-22995

Solar wind He nuclei kinetic temperature, considering resonant heating and proton temperature 10 p1269 A73-24723

Alpha particles in solar cosmic rays over the last 80,000 years. 11 p1412 A73-25375

Lunar composition from Apollo orbital measurements. 11 p1422 A73-25956

Apollo alpha particle spectrometer design, operation, calibration, packaging and flight results 11 p1363 A73-25957

Preliminary Pioneer-10 intensity gradients of galactic cosmic rays. 11 p1414 A73-26622

Preparation of high-level alpha-particle sources for the Surveyor Alpha Scattering Experiment. 16 p2035 A73-32975

Solar proton, helium, and medium nuclei /Z from 6 to 9/ observed from the IMP-VI satellite. 16 p2054 A73-33280

A new test for solar modulation theory - The 1972 May-July low-energy galactic cosmic-ray proton and helium spectra. 17 p2224 A73-34769

Solar cosmic ray alpha particles and protons flux measurement after events in 1967-1969 for 1-10 MeV particles 18 p2347 A73-36289

Initial observations of geomagnetically trapped alpha particles at the equator. 20 p2552 A73-38950

- A low-background counter telescope for recording alpha particles in n, α -reactions
21 p2699 A73-40173
- Solar wind alpha particle abundance variations as function of wind velocity from HEOS-1, Vela 3-A and 3-B observations
21 p2763 A73-41500
- Inner zone population of trapped 2.14-9.0 MeV alpha particles, noting strong peak in pitch angle and intensity decrease with L value decrease
22 p2901 A73-41910
- The effect of nonstationarity in the chemical composition of plasma flows from the sun.
23 p3027 A73-43252
- Heavy elements in surface materials - Determination by alpha particle scattering.
23 p2981 A73-43529
- ALPHA RADIATION**
U ALPHA PARTICLES
- ALPHABETS**
Symbol ring as alphabetic element in information processing technique, defining address substitution operation
02 p0143 A73-11642
- Amplitude-phase-keying with M-ary alphabets - A technique for bandwidth reduction.
09 p1054 A73-23385
- Algebraic decoding algorithms for block codes over q-ary input Q-ary output alphabet channel, presenting examples for Hamming, Lee or burst distance
14 p1730 A73-30501
- ALPHANUMERIC CHARACTERS**
NT BINARY DIGITS
Computerized multichannel alphanumeric TV system for ATC operational information display, describing data acquisition, processor and software peripherals and video display subsystem
02 p0165 A73-11594
- FORTAN subroutine for X-Y plotting and display of two dimensional alphanumeric finite element mesh on line printer
03 p0280 A73-13340
- Optical Characters Reading and facsimile terminals reduction of message preparation time for electrical transmission in Defense Communications System, considering cost effectiveness and maximum benefit
04 p0418 A73-15380
- The effect of illumination level, stroke width and figure ground on legibility of NAMEL numbers.
05 p0544 A73-16729
- Eye movements during visual search and memory search.
13 p1579 A73-29125
- ASCII code applications to alphanumeric display terminals.
21 p2655 A73-40835
- ALPS MOUNTAINS [EUROPE]**
Mapping of snow cover in the Swiss Alps from ERTS-1 imagery.
18 p2306 A73-36021
- ALSEP**
U APOLLO LUNAR SURFACE EXPERIMENTS PACKAGE
- ALTERNATING CURRENT**
AC studies of a superconducting Nb-52 at. % Ti alloy.
02 p0200 A73-11844
- Push-pull ac modulator design allowing balanced thermal load on plasma electrodes in pulsed high power short arc Xe flash lamps
03 p0282 A73-13933
- Effect of alternating current on the steady-state characteristics of a Josephson junction.
03 p0344 A73-14097
- Alternating current instability produced by the two-stream instability.
07 p0857 A73-19528
- Low-frequency current oscillations in high-resistivity, Au-doped silicon junctions with two Schottky contacts.
07 p0864 A73-20190
- The a.c. losses of non-ideal type II superconductors under parallel configurations of electric currents and magnetic fields.
07 p0864 A73-20403
- Analyses of techniques for measuring DC and AC electric fields in the magnetosphere.
11 p1352 A73-25316
- A group converter of alternating-current signals into a code for control systems
12 p1475 A73-26780
- Effect of the input capacitance of an ac amplifier on the performance of key modulators
13 p1592 A73-28874
- Ion-ion instability induced by ac electric fields.
16 p2042 A73-33336
- Load transfer between AC sources within relay ratings through circuit design.
17 p2133 A73-34094
- The cause and effects of dc offset voltage in solid state ac power controllers.
17 p2109 A73-35255

- Electric power cell for producing direct/alternating current and shaft horsepower by direct electrochemical reaction of alkali metals with water
19 p2390 A73-38397
- AC conductivities of amorphous Ge-As-Te and Ge-As-Se systems.
21 p2753 A73-41119
- The use of operational amplifiers to generate precise current ratios for platinum resistance thermometry.
22 p2832 A73-42028
- Four terminal, optically isolated, zero crossing ac relay.
22 p2834 A73-42913
- ALTERNATING CURRENT GENERATORS**
U AC GENERATORS
- ALTERNATIVES**
Ability of a human operator to estimate the probability characteristics of alternative stimuli
22 p2813 A73-41893
- ALTIMETERS [GENERATORS]**
U AC GENERATORS
- ALTIMETERS**
NT LASER ALTIMETERS
NT RADIO ALTIMETERS
Geopotential /geoid/ representation with spherical harmonics sampling functions for satellite altimeter applications
04 p0438 A73-14792
- Orbiting altimeter system feasibility for global scale geoidal mapping via satellite altimetry
04 p0439 A73-14803
- Encoding altimeter for coding, transmitting and displaying flight altitude information to air traffic controllers
17 p2167 A73-34663
- [SAE PAPER 730301]
Power subsystem for Skylab radiometer/scatterometer/altimeter experiment.
22 p2801 A73-42903
- ALTITUDE**
NT FLIGHT ALTITUDE
NT HIGH ALTITUDE
NT LOW ALTITUDE
NT SIMULATED ALTITUDE
Shimazaki formula corrected for F 2 layer altitude estimation for 2-30 MHz field intensity and transmission losses calculations
12 p1493 A73-27762
- The altitude of the scattering layer near the mesopause over the summer poles.
14 p1750 A73-30768
- Comparison of true and effective altitudes of the sporadic E layer
15 p1872 A73-31899
- Experiments in objectivation of a forecasting method for lower cloud boundary altitudes
17 p2204 A73-34541
- Some results of determining cloud top heights from satellite infrared measurements.
18 p2334 A73-37060
- Comparison of satellite-measured and radar-observed cloud-top heights.
18 p2334 A73-37066
- ALTITUDE ACCLIMATIZATION**
Evolutionary significance of carbohydrate metabolism alterations in animal brains during adaptation to hypoxia
01 p0007 A73-10153
- Arterial oxygen increase by high-carbohydrate diet at altitude.
01 p0007 A73-10164
- Russian papers on human adaptability covering altitude and temperature acclimatization, work capacity and anthropogenetic and medicogenetic factors
02 p0133 A73-11921
- High altitude adaptation in mountain inhabitants of Tian Shan and Pamir, discussing effects on hemodynamic and pulmonary functions
02 p0133 A73-11922
- Hemocoagulation system function in mountain inhabitants and during altitude acclimatization, noting parasympathetic nervous system tonus
02 p0133 A73-11923
- Hydrogen ion concentration in the blood of man under high mountain conditions with physical loads
02 p0133 A73-11924
- Comparative evaluation of the general and specific efficiencies of athletes under normal barometric pressure and in the process of training and acclimatization under highland conditions of Pamir
02 p0136 A73-11925
- Effect of altitude acclimatization and simultaneous acclimatization to altitude and cold on critical flicker frequency at 11,000 ft. altitude in man.
02 p0135 A73-12562
- Control of exercise hyperpnea under varying durations of exposure to moderate hypoxia.
03 p0259 A73-13499
- Dynamic aspects of regulation of ventilation in man during acclimatization to high altitude.
03 p0259 A73-13500
- Cardiocirculatory adaptation to chronic hypoxia. III - Comparative study of cardiac output, pulmonary and systemic circulation between sea level and high altitude residents.
04 p0410 A73-15523

- Adaptation to high altitude hypoxia as a factor preventing development of myocardial ischemic necrosis.
07 p0780 A73-19151
- Mountain inhabitants physiological characteristics due to altitude effects, investigating human tolerance and adaptation to ambient environment
07 p0784 A73-19212
- High altitude acclimatization and mountain climbing effects on human organism, considering oculomotor, cardiovascular and respiratory responses and endurance
08 p0930 A73-20991
- Influence of developmental adaptation on aerobic capacity at high altitude.
09 p1041 A73-22928
- Physiological studies of human organism adaptation to high altitudes in temporary and permanent mountain inhabitants, discussing oxygen uptake, lung ventilation and cardiac ventricle hypertrophy
10 p1181 A73-24514
- Physiological responses of rats to intermittent high-altitude stress - Effects of age.
10 p1182 A73-24564
- Serum creatine phosphokinase activity and urinary excretion of creatine and creatinine in man during acclimatization to high altitude and in high altitude natives.
11 p1315 A73-25333
- Lactate, alpha-GP, and Krebs cycle in sea-level and high-altitude native guinea pigs.
11 p1318 A73-26122
- Role of the arterial chemoreceptors in ventilatory adaptation to hypoxia of awake dogs and rabbits.
11 p1318 A73-26220
- Hemocoagulation and trombocyte state during hypokinesia after highland adaptation
12 p1463 A73-27713
- Myoglobin distribution in the heart of growing rats exposed to a simulated altitude of 3500 m in their youth or born in the low pressure chamber.
14 p1720 A73-30910
- Energy balance during moderate exercise at altitude.
15 p1833 A73-31343
- Effect of protein quality in the diet of rats on their tolerance to severe hypoxia
15 p1835 A73-31511
- Effect of stepwise adaptation to high-mountain areas on the respiratory function and the acid-alkali equilibrium of blood in subjects with different motor activity stresses
17 p2111 A73-34232
- Protein synthesis in the neurons and glial cells of the stellate ganglia of rats during the adaptation to the effects of high altitude hypoxia
19 p2393 A73-37396
- Glycolytic intermediates and adenosine phosphates in rat liver at high altitude /3,800 m/.
20 p2514 A73-39602
- Relationship between organ weight and blood flow in rats adapted to simulated high altitude.
21 p2639 A73-41156
- Influence of preliminary adaptation to the main environmental factors on the ATP level and phosphorylation potential in the myocardium during severe heart strain
21 p2640 A73-41278
- Effect of adaptation to altitude hypoxia on the behavior of animals in a conflict situation
24 p3058 A73-44549
- Regression of altitude-produced cardiac hypertrophy.
24 p3060 A73-45065
- ALTITUDE CONTROL**
Analysis of an altitude control system of a low flying vehicle.
01 p0075 A73-11195
- A procedure for the barometric altitude control in the case of hovering devices and helicopters
03 p0249 A73-12916
- Altitude damping of space-stable inertial navigation systems.
16 p2034 A73-33403
- Compensation of the longitudinal-trim and altitude control systems of an aircraft
22 p2800 A73-42949
- ALTITUDE SICKNESS**
Medical considerations for aircraft passengers.
03 p0267 A73-13802
- Incidence and severity of altitude decompression sickness in Navy hospital corpsmen.
13 p1576 A73-28511
- Effect of certain flight factors on crew efficiency
21 p2643 A73-40350
- Effect of altitude on renin-aldosterone system and metabolism of water and electrolytes.
22 p2806 A73-42420
- ALTITUDE SIMULATION**
Estimation of engine emissions at altitude through ground testing.
04 p0485 A73-14892
- Instrumentation and measurement for determination of emissions from jet engines in altitude test cells. [AIAA PAPER 72-1068]
04 p0432 A73-14902

- Hot particle igniter for end-burning solid propellant rocket motors, noting ignition capability at 219 K and 110,000 ft simulated altitude
[AIAA PAPER 72-1196] 04 p0485 A73-14919
- High altitude chamber effect on thyroid stimulating hormone and thyroxine concentrations, noting shift from extra to intravascular
09 p1041 A73-22926
- Estimation of hypoxia tolerance in a decompression chamber
18 p2280 A73-36945
- Skylab Medical Experiments Altitude Test /SMEAT/ facility design and operation.
[ASME PAPER 73-ENAS-44] 19 p2401 A73-37991
- Skylab medical experiments altitude test /SMEAT/ chamber atmosphere trace contaminants analysis, describing sample acquisition techniques and instrumentation
[ASME PAPER 73-ENAS-45] 19 p2395 A73-37992
- Simulation of the flow past a high-altitude ion-concentration sensor
21 p2633 A73-41223
- The frequency of barotraumas as determined by nasal findings and X-rays of the paranasal sinuses
22 p2817 A73-43132
- Oxygen kinetics for constant work loads at various altitudes.
24 p3060 A73-45062
- ALTITUDE TESTS**
- NT HIGH ALTITUDE TESTS**
- An altitude test facility for large turbofan engines.
[AIAA PAPER 72-1069] 03 p0287 A73-13396
- Skylab medical experiments altitude test crew observations.
[ASME PAPER 73-ENAS-30] 19 p2400 A73-37985
- Atmospheric absorption considerations in airplane flyover noise at altitudes above sea level.
22 p2799 A73-42943
- ALTITUDE TOLERANCE**
- Uncertainties in determining the effective UV radiation at various altitudes.
[AIAA PAPER 73-102] 05 p0570 A73-16862
- Effects of altitude stress on mitochondrial function.
14 p1717 A73-30430
- High altitude aircraft cabin pressurization for crews and passengers, discussing altitude tolerance, reaction times, decompression and oxygen equipment
14 p1723 A73-30937
- Human statokinetic stability as component of non-specific resistance, discussing revolving, altitude, hypoxic and orthostatic stress dependence tests
18 p2279 A73-36904
- Study of performances in a warm environment in case of air conditioning breakdown on a supersonic transport
18 p2286 A73-36947
- Phase IV volume of the single-breath nitrogen washout curve on exposure to altitude.
20 p2518 A73-39783
- ALTOCUMULUS CLOUDS**
- U CUMULUS CLOUDS**
- ALU [COMPUTER COMPONENTS]**
- U ARITHMETIC AND LOGIC UNITS**
- ALUMINA**
- U ALUMINUM OXIDES**
- ALUMINATES**
- Temperature-induced changes of the electron-vibration spectrum of $\text{LaAlO}_3\text{-Cr}^{3+}$ crystals
10 p1260 A73-24578
- ALUMINIZING**
- U ALUMINUM COATINGS**
- ALUMINUM**
- NT ALUMINUM 26**
- NT POWDERED ALUMINUM**
- NT SINTERED ALUMINUM POWDER**
- Effect of visible light on exoelectron emission
01 p0045 A73-10264
- Study of creep in copper and aluminum by the differential method of constant-rate temperature change
01 p0064 A73-10612
- Axisymmetric plastic response of rings to short-duration pressure pulses.
01 p0115 A73-10759
- Temperatures of aluminum during its combustion in oxygen-argon mixtures, in nitrogen, and in air
01 p0123 A73-11275
- Investigation of the interrelation between creep parameters in industrial aluminum during the first and second stages of creep
02 p0179 A73-11567
- Determination of yield locus curves for copper and aluminum crystals with the aid of Knoop hardness measurements
02 p0181 A73-12364
- The influence of texture on the yield loci of copper and aluminium.
02 p0181 A73-12365
- Laser-induced stress-wave and impulse augmentation.
02 p0177 A73-12746
- Mechanical properties of aluminum matrix composites.
02 p0184 A73-12849
- The influence of adhesive components on the corrosion of aluminum honeycomb.
03 p0321 A73-13038
- Evaluating adhesives for joining aluminum.
03 p0334 A73-13271
- Ultrasonic attenuation measurement of a microplastic memory effect in aluminum single crystals.
03 p0323 A73-13331
- Surface properties improvement of Al products by metal coatings, noting corrosion prevention, anodic coatings, enameling and brazing
03 p0312 A73-13580
- Substructural changes during high-temperature creep deformation of aluminum single crystals
03 p0327 A73-13978
- HF transverse resonant vibrations of annular Al plates with polychlorovinyl and polyamide base coatings, noting damping and strain relationship to energy dissipation
03 p0394 A73-14009
- Progress in the development of radiation-resistant aluminum-doped silicon solar cells.
03 p0258 A73-14248
- Visual display of fatigue damage by means of exoelectron emission.
04 p0446 A73-14748
- The spectra of highly ionized aluminum /Al VI-X/ in the extreme-ultraviolet and soft X-ray regions.
04 p0492 A73-15369
- Some experiments on dynamic and quasi-static forging of aluminum at elevated temperatures.
[ASME PAPER 72-WA/MAT-1] 04 p0457 A73-15811
- Internal stress and dislocation structure of aluminum in high-temperature creep.
04 p0467 A73-15930
- High temperature steady state creep determination in Al by dip test technique interpreted in terms of slip and recovery activation energy due to effective and internal stress
04 p0467 A73-15933
- B-Al matrix composites environmental properties, costs and development for aerospace systems, considering corrosion, erosion and thermal cycling effects on tensile strength
04 p0467 A73-15934
- Solidification pressure effect on hydrogen in Al ingots, noting blister formation correlation to pressure
05 p0587 A73-16579
- Stabilization of superconducting beryllium by addition of aluminum.
05 p0605 A73-16794
- Analysis of oxygen in aluminum by activation by means of charged particles and gamma photons
05 p0547 A73-17217
- Dislocation-point defect interactions in fatigued pure aluminum
05 p0588 A73-17231
- A method for performing high precision lattice parameter change measurements on quenched aluminum.
05 p0580 A73-17257
- Effect of recovery on recrystallization of aluminum
99.85 06 p0705 A73-17849
- Intermetallics formation and diffusion of contacting Al-Au thin films dependence on temperature, thickness ratio and contact time
06 p0706 A73-17903
- Influence of annealing at near melting point temperatures on the substructure of aluminum single crystals
06 p0707 A73-18036
- Intensity calculation of X-ray scattering by the atom and ion of aluminum
06 p0725 A73-18216
- Direct observation of tensile and fatigue cracks.
06 p0710 A73-18495
- Influence of the dose of neutron irradiation on the anelastic behavior of an aluminum deformed at 80 K
06 p0710 A73-18542
- The mechanism of surface mass transfer in the thin-film Ge-Al system
06 p0738 A73-18651
- Choosing the parameters for plasma anodizing of aluminum
07 p0830 A73-19293
- The yield point phenomenon in a Be-Al composite.
07 p0839 A73-20115
- Structural fabrication of advanced metal-matrix composites.
[SME PAPER EM 72-108] 07 p0832 A73-20449
- Magnetic field dependence of the surface resistance of pure and impure superconducting aluminum at photon energies near the energy gap.
07 p0864 A73-20573
- An experimental model of the microelectronic ultrasonic wire bonding mechanism.
08 p0972 A73-20734
- Annealing of discontinuities in deformed aluminum
09 p1100 A73-21973
- Substructure formation around fatigue cracks and its role in the propagation of fatigue cracks in aluminum.
09 p1103 A73-22437
- Microstructural observations of arc welded boron-aluminum composites.
10 p1223 A73-23630
- Amplitude-dependent anelasticity in aluminum and copper single crystals
10 p1231 A73-23693
- Contribution to the study of the elasticity of monocrystalline aluminum under very low stresses
10 p1231 A73-23771
- Molybdenum metal by the aluminothermic reduction of calcium molybdate.
10 p1234 A73-24430
- Experimental observations of tensile fracture in unidirectional boron filament reinforced aluminum sheet.
10 p1235 A73-24439
- Influence of the intercrystalline structure on the diffusion of zinc in the symmetrical joints of bending of aluminum
11 p1379 A73-25324
- The photometric determination of aluminum in steel after separation on a cation-exchanger
11 p1380 A73-25447
- Exploratory study of a fluxless aluminum brazing process for beryllium.
11 p1375 A73-26359
- Theoretical and experimental investigation of the nonlinear behavior of anglepiled boron/aluminum composites.
11 p1385 A73-26524
- Low-energy positrons from metallic moderators in a back scattering mode.
11 p1402 A73-26544
- Amplitude-dependent anelasticity in aluminum and copper single crystals. II - Studies in amplitude range III during and after plastic deformation
11 p1385 A73-26567
- Dislocation structure of subgrain boundaries in creep-deformed aluminum.
12 p1511 A73-27028
- Influence of deformation history on the yield locus and stress-strain behavior of aluminum and copper.
13 p1632 A73-28130
- Interpretation of mechanical behavior of pure aluminum in terms of microstructure.
13 p1639 A73-29459
- Pure Al compression tests for strain rate effects on strength in wide temperature range, using split Hopkinson bar apparatus and Instron testing machine
13 p1639 A73-29461
- Aluminum foils crack propagation observation with electron microscope during tensile tests, noting crystal dislocation role in ductile fracture process
13 p1639 A73-29467
- Some observations on grain boundary sliding in aluminum bicrystals deformed at elevated temperatures.
13 p1641 A73-29508
- Radiation-induced strengthening and embrittlement in aluminum.
14 p1761 A73-30628
- Steel reinforcement fiber arrangement and volume content influence on aluminum composites strength and fatigue resistance at room and elevated temperatures
14 p1766 A73-30710
- Attenuation of an ultrasonic signal in aluminum deformed according to a harmonic law
14 p1764 A73-30857
- Aluminum structure effects on thermal activation parameters of plastic deformation, proposing strain rate control mechanism
14 p1764 A73-30867
- Al filament ignition temperature in carbon dioxide flow at various current values, noting relation to surface oxide film melting temperature
14 p1764 A73-30872
- Influence of heating on the intensity and energy of exoelectrons in deformed aluminum
14 p1765 A73-30889
- Two-phase charge-coupled devices with overlapping polysilicon and aluminum gates.
15 p1850 A73-31373
- Yielding in unidirectional composites under external loads and temperature changes.
15 p1949 A73-31679
- Grain boundary dislocations in aluminum bicrystals after high-temperature deformation.
15 p1891 A73-32020
- Behaviour of aluminium during the passage of large-amplitude plastic waves.
15 p1891 A73-32164
- Al addition effect on strength of Ti via short range order, considering strengthening by alpha stabilizing solutes
15 p1893 A73-32273
- Stark broadening and shift of singly ionized aluminum lines.
16 p2040 A73-32845
- Some mechanical properties of carbon fiber reinforced aluminum.
16 p2025 A73-32849
- Thermal cycling effects on void formation in boron-aluminum matrix composites at 70-670 F, considering jet turbine compressor blade applications
16 p2084 A73-33037

Explosive behavior of aluminized ammonium perchlorate.

16 p2045 A73-33346

X-ray investigation of the fine crystalline structure of aluminum with creep

17 p2186 A73-34117

Temperature dependence of low-temperature strength in aluminum single crystals

17 p2189 A73-34581

Room temperature creep of Borsic-aluminum composites.

17 p2189 A73-34644

Stepped aluminum extrusions - Designing for business aircraft.

[SAE PAPER 730308]

17 p2177 A73-34668

Economic and design advantages of aluminum precision forgings.

17 p2177 A73-34672

On the influence of single and multiple peak overloads on fatigue crack propagation in 7075-T6511 aluminum.

17 p2190 A73-34889

A nondestructive measurement of the elastic constants of unidirectional borsic fiber reinforced aluminum composites.

[SC-DC-72-1644]

17 p2182 A73-35439

Continuous monitoring of fatigue crack growth by acoustic emission techniques.

[TK-DE-73-2]

17 p2148 A73-35445

Failure mode multiplicity in Al-stainless steel and Al-W metal matrix composites under various loading conditions

17 p2191 A73-35527

Filament orientation effect on Al and Ti matrix composite tensile properties, using boron, borsic and silicon carbide fibers

17 p2192 A73-35533

Borsic-aluminum composites fracture and flexural behavior from Charpy impact and slow bend tests

17 p2192 A73-35537

Deformation and fracture mechanisms in aluminum reinforced by high strength steel ribbons.

17 p2192 A73-35539

Borsic-Al composites fiber-matrix debonding for toughening mechanism of crack blunting, noting notch insensitivity and delamination

17 p2193 A73-35540

Noncumulative fracture mode of unidirectional boron filament-aluminum matrix composite under axial tension, measuring critical filament stress

17 p2193 A73-35542

Elastic-plastic expansion of 6061-T6 aluminum rings.

18 p2362 A73-36320

Investigation of the kinetics of high-temperature aluminum/oxygen interaction by the ignition method

19 p2503 A73-37504

Effect of rivet spacing on crippling loads of joined aluminum angles.

19 p2499 A73-38009

The effect of elevated temperatures on the mechanical properties of B-Al composites.

19 p2442 A73-38095

The effect of stiffeners on the sound radiation and the transmission loss of metal walls

19 p2460 A73-38181

Anisotropy of the mechanical properties of aluminum hardened by a stainless steel grid

20 p2578 A73-39382

Investigation of the imperfect structure of polycrystalline aluminum after low-temperature rolling and annealing

20 p2579 A73-39747

Thermodynamics of the Al-O and Al-O-C systems

21 p2718 A73-40847

Impulse reaction resulting from the in-air irradiation of aluminum by a pulsed CO₂ laser.

21 p2715 A73-40960

Aluminum and aluminum alloys extrusion processes, discussing form shape, weldability, hardening and metal transformations

21 p2707 A73-41067

Fibre-reinforced metallic and ceramic composites produced by thermal spraying.

22 p2866 A73-42592

Interference filters for the VUV (1200-1900 Å).

22 p2863 A73-43142

Fluxless brazing of aluminum using protective gas.

23 p2985 A73-43997

Soldering technique using reaction flux for metal deposition, obtaining strong joints of Al with other metals

23 p2985 A73-43999

Study of aluminum-oxygen equilibrium in liquid iron at 1600 deg C with the aid of a solid ThO₂-Y₂O₃ electrolyte cell

23 p2995 A73-44178

The Portevin-Le Chatelier effect in compression tests of polycrystalline aluminum

24 p3148 A73-44914

Emission measurement of Surveyor 3 spacecraft aluminum support tubing returned from moon by Apollo 12, noting lunar environment effects from control sample data

24 p3139 A73-45110

ALUMINUM ALLOYS

Test results of fatigue at elevated temperatures on aeronautical materials.

[ONERA, TP NO. 1098]

01 p0061 A73-10229

Fabrication of high-strength aluminum products from powder.

01 p0063 A73-10281

Structure changes during ageing in aluminum 4 wt. % copper alloy studied by the channeling technique.

01 p0063 A73-10310

Temperature dependence of the critical shear stress in single crystals of Al-Mg alloys of various concentration at temperatures between 1.6 and 300 K

01 p0064 A73-10488

Influence of the loading conditions on the propagation of fatigue cracks in D16T-alloy sheet samples

01 p0064 A73-10489

Low-temperature induced changes in the martensite crystalline structure of iron-aluminum-carbon alloys

01 p0064 A73-10607

Mosaic-angle and dislocation-density variations in polycrystalline aluminum alloys under tension

01 p0064 A73-10609

Damping in copper-aluminum-nickel alloys and its causes

01 p0064 A73-10611

Statistical characteristics for duralumin sheets mechanical properties, fatigue life and crack growth

01 p0117 A73-11298

Structured changes and phase transformations of welded joints of Al alloy with Cu addition during welding thermal cycles

01 p0067 A73-11352

Fatigue of duralumin under cyclic loads at ultrasonic frequencies

02 p0179 A73-11566

Fracture characteristics of some aluminum alloy sheets in Charpy impact test at super-low temperatures.

02 p0179 A73-11595

Fracture characteristics of aluminum alloy welds in Charpy impact test at super-low temperatures.

02 p0172 A73-11596

Refinement of primary silicon crystals in a hypereutectic Al-20% Si alloy by sulphur addition.

02 p0179 A73-11597

On the ternary compound G in the Al-Mn-Cr system.

02 p0179 A73-11598

Sn suppression of Al-Cu-Sn alloy aging at low temperatures, relating to Cu solubility decrease in alpha phase

02 p0179 A73-11599

Experimental investigation of the behavior of cylindrical shells under dynamic loads

02 p0229 A73-11626

Conductivity of 2024-T42 aluminum sheet solution heat treated at various temperatures.

02 p0168 A73-11986

Experimental estimation of the deformation criterion of long-term/creep/strength.

02 p0180 A73-12130

The effects of frequency of loading and of nonreactive external media on growth of fatigue cracks.

02 p0235 A73-12132

Experimental investigation of stresses in plates acted on by acoustic loads.

02 p0235 A73-12135

Microstructure and phase relations for Ti-Mo-Al alloys.

02 p0182 A73-12751

Failure mechanisms in transversely loaded boron-aluminum.

02 p0184 A73-12861

Effect of strain-rate and temperature on the resistance to torsional deformation of several aluminum alloys.

03 p0384 A73-13117

Studies of fatigue in smooth AlCuMg specimens

03 p0321 A73-13134

Changes in microhardness as a basis of service life estimates for smooth AlCuMg specimens

03 p0321 A73-13135

Effect of a single plastic deformation on the fatigue behavior of metals

03 p0322 A73-13136

Random fatigue of 2024-T3 aluminum under two spectra with identical peak-probability density functions.

03 p0322 A73-13235

Mechanical properties of Fe, Al, Ti and heat resistant alloys consolidated powders, establishing coupling between fundamental concepts and engineering application

03 p0322 A73-13261

How deformation affects the mechanical properties of aluminum forgings.

03 p0322 A73-13266

Inhomogeneity of the structure and deformability of aluminum and aluminum-magnesium alloys

03 p0324 A73-13506

Hydrogen distribution between the phases in metals

03 p0324 A73-13507

Cast Al-Si alloy strengthening by Mg, Be, Ti, Cu, Cd, Zr and B alloying, refining and modifying techniques

03 p0324 A73-13512

Ways of enhancing the strength characteristics of heat-resistant and high-strength cast aluminum alloys

03 p0324 A73-13514

Elastic damping properties of binary Mg and Al alloy systems with Cd, Mn, Ni, Si, Zr, Nd and Ca alloying

03 p0324 A73-13515

High modulus Be-Al alloy strengthening and aging as function of Cu, Mg and Zn additions

03 p0325 A73-13517

Cumulative fatigue damage tests of Al alloy, evaluating Miner cycle/stress ratio

03 p0325 A73-13571

Reinforcement of aluminum alloys by high strength steel ribbons

03 p0312 A73-13581

Synergistic effects of anions in the corrosion of aluminum alloys.

03 p0325 A73-13729

Loading-rate dependence of the deformation mechanism in a Zn-22% Al superplastic alloy

03 p0326 A73-13970

Influence of the degree of decomposition of a solid solution of zirconium in aluminum on the recrystallization temperature of an aluminum-zinc-magnesium-zirconium system alloy

03 p0327 A73-13972

Hot worked Al alloy machine elements mechanical properties scattering, discussing quality control procedures

03 p0327 A73-14004

Consideration of a number of factors involved in determining the long-term strength of dies used for the extrusion of hollow sections of aluminum alloys

03 p0318 A73-14651

Delay effects in fatigue crack propagation.

04 p0459 A73-14690

Sharp-notch tension testing of thick aluminum alloy plate with cylindrical specimens.

04 p0460 A73-14698

Temperature dependence of impurity resistivity in dilute Al-based Ti, V, Fe, Cu, Zn alloys between 78 and 930 K.

04 p0461 A73-14875

Fatigue crack growth measurement on Al alloy wedge-opening-load specimens under constant amplitude sinusoidal loading, comparing data with existing crack propagation results

04 p0462 A73-15241

Fractographic observations of fatigue crack tip behavior of age hardened Al-Zn-Mg-Cu alloy during static loading

04 p0462 A73-15242

Influence of microstructure on the mechanical properties and stress corrosion susceptibility of 7075 aluminum alloy.

04 p0463 A73-15314

The effect of a hydrogen preheat-treatment on the oxidation behavior of Ni-Cr-Al-ThO₂ alloys.

04 p0463 A73-15319

Influence of the composition and structure on the mechanical properties of ultraplasic alloys of the Al-Zn system

04 p0464 A73-15497

Influence of hydrogen on the technological plasticity of the alloy Ti + 9% Al

04 p0464 A73-15499

Precipitation hardening effect on Co-Ni-Ti-Al alloys stress-strain, grain size and strain resistance behavior in micro- and macrodeformation yield point region

04 p0465 A73-15639

Relationship between cavitation and decontamination during ultrasonic processing of aluminum and its magnesium alloys

04 p0454 A73-15663

Method of repeatedly determining the fracture roughness with one specimen.

04 p0466 A73-15672

Method for fractographic investigation of high-tensile aluminum alloys.

04 p0466 A73-15674

Method of determining the energy of fracture of aluminum alloys during impact-bend tests with sharp notches.

04 p0466 A73-15675

Investigation of the effect of vacuum environment on the fatigue and fracture behavior of 7075-T6.

04 p0466 A73-15764

Compression tests for plastic deformation and fracturing of Al alloy powder at hot working temperatures, noting limiting deformations in forging

[ASME PAPER 72-WA/MAT-5]

04 p0456 A73-15808

Phase transformations in Al-rich Al-W alloys rapidly quenched from the melt.

04 p0468 A73-15983

Boron fiber-aluminum alloy matrix composite structure Charpy impact energy absorbing capacity explained via energy dissipation of matrix by plastic deformation

05 p0588 A73-16111

Creep rupture testing of aluminum alloys to 100,000 hours. 05 p0581 A73-16133

Low cycle fatigue tests of medium strength Al alloys, showing agreement with Manson-Halford fatigue life-strain relation 05 p0586 A73-16135

Vacancy trapping model inadequacy for aging retardation in Al-Cu-Cd alloys, noting Cd content and Cu solid solubility effects 05 p0587 A73-16376

Double aging time effects on hardness of solution treated, quenched and heat treated two phase Al-Zn-Mg alloy specimens, obtaining transmission electron micrographs 05 p0587 A73-16577

Evaluation of fracture toughness in aluminum alloys and welds by the Charpy impact test. 05 p0587 A73-16578

Deep-drawability and some problems after forming by deep-drawing of Al-Mg alloy sheets - Study on Al-Mg alloy sheets for forming use. II. 05 p0581 A73-16580

HF dc straight polarity current pulsations effects on quality and mechanical properties of gas tungsten arc welds in Al alloy [SAE PAPER 720874] 05 p0582 A73-16669

Frame photography for temporary creep in cylindrical Al alloy specimen necks under tensile loads, calculating creep diagrams 05 p0634 A73-16748

Crack growth and failure of aluminum plate under in-plane shear. [AIAA PAPER 73-253] 05 p0635 A73-16975

Material variability as measured by low temperature electrical resistivity. 05 p0588 A73-17287

Book - Advances in corrosion science and technology. Volume 2. 06 p0704 A73-17506

Stress-corrosion cracking of high-strength aluminum alloys. 06 p0704 A73-17509

Heat resistance of alloys of the compound TiAl with niobium at 800 and 1000 C 06 p0708 A73-18049

Adhesively bonded multilayer Al and Ti alloy sheet metals for complex airframe components, discussing design, fabrication, tests and performance comparison with monolithic structures [SME PAPER MF 72-513] 06 p0698 A73-18094

Susceptibility to brittle fracture of simulated weld seams in Ti-Al-V alloys. 06 p0698 A73-18209

Diffusion in the titanium-aluminum system. I - Interdiffusion between solid Al and Ti or Ti-Al alloys. 06 p0709 A73-18332

Diffusion in the titanium-aluminum system. II - Interdiffusion in the composition range between 25 and 100 at.% Ti. 06 p0709 A73-18333

Composition affects tensile strength of welded aluminum-magnesium alloy. 06 p0709 A73-18385

Influence of local variations of yield strength on plastic zones at crack tips. 06 p0709 A73-18480

Fracture due to damage from projectile impact. 06 p0763 A73-18484

Composite Al- and Ni-base alloys strengthened by B and W/Mo fibers respectively for reduced weight wing spars and high temperature applications 06 p0710 A73-18638

X-ray spectral studies of manganese-aluminum binary alloy systems 06 p0710 A73-18644

Substructure and dispersion hardening in aged, cold worked, and annealed Al-4 wt pct Cu alloy. 06 p0711 A73-18754

The orientation dependence of deformation mode and structure in stoichiometric NiAl single crystals deformed by high temperature steady-state creep. 06 p0712 A73-18758

Morphological factors influencing the initial stages of coarsening in the Al-Al3Ni eutectic composite. 06 p0712 A73-18761

Chemical and electrolytic coatings for satellite surface thermal control, discussing surface anodic oxidation treatment of adhesive Au platings on Al alloys 07 p0829 A73-18910

The effect of grain size on the fatigue of an Al-Mg alloy. 07 p0839 A73-20114

Static and dynamic behavior of welded aluminum beams. 07 p0839 A73-20270

Inhibition of corrosion fatigue in 7075 aluminum alloys. 07 p0840 A73-20351

Filler wire welded joints of Al-Zn-Mg and Al-Mg alloys, testing weldability and mechanical properties susceptibility to hot cracking 07 p0840 A73-20372

Fractographic investigation of the resistance to fracture of aluminum and titanium alloys 07 p0840 A73-20505

Estimation of the fatigue characteristics of D16T and AVTT aluminum alloys from the breaking stress 07 p0841 A73-20515

The diffusion coefficient during plastic deformation in AlMg5 08 p0977 A73-21019

On relationship between stress corrosion resistance and grain shape of extruded Al-Zn-Mg alloys with heavy section. 08 p0977 A73-21140

Evaluating the variation in fatigue properties of aluminum alloys due to variable loads by using secondary fatigue curves. 08 p0977 A73-21147

Mechanism by which hot cracks form during welding aluminium and its alloys. 08 p0977 A73-21236

Sliding friction welding of nonferrous Cu, wrought Al alloy and Ti, resting rubbing speed and axial pressure effects on equilibrium condition transition 08 p0973 A73-21238

Influence of nickel on the superconductivity parameters of Nb3Al + Ni 09 p1098 A73-21845

Study of the formation process of corrosion cracks under tension in an aluminum alloy [ONERA, TP NO. 1213] 09 p1098 A73-21925

Electrical conductivity of a directionally crystallized Al-Al3Ni composition 09 p1099 A73-21972

Influence of the frequency of the tension-compression cycle on the fatigue life of D16T alloy 09 p1100 A73-22153

Alloying elements effects on voids nucleation in irradiated Al alloys, tabulating defect concentration 09 p1101 A73-22175

Photoelastic investigation of serrated plastic flow in 6061 Al alloy, considering Luders bands effects relative to type A and B serrations 09 p1101 A73-22408

Influence of inclusion content on fatigue crack propagation in aluminum alloys. 09 p1101 A73-22409

Effect of addition of Bi on stress-corrosion cracking of Al-Mg alloy. 09 p1102 A73-22421

Stress corrosion cracking of commercial Al-Mg alloys and its prevention. 09 p1102 A73-22422

Using fracture mechanics with aluminum alloy structures. 09 p1103 A73-22494

Influence of environment on the appearance of fatigue striations in various alloys 09 p1104 A73-22716

Effects of circular holes on the fatigue resistance of AMg6BM aluminum-alloy sheet in symmetrical bending. 09 p1105 A73-23053

Comparison of the fracture strength KIs of aluminum /AK4-IT1, V95T1, and D16T/ and titanium /VT8 and VT9/ alloys under static and cyclic loads. 09 p1105 A73-23054

Yield and fracture of D16T alloy at low temperatures in the presence of a complex stress pattern. 09 p1105 A73-23055

Investigation of the effect of surface finish and method of surface treatment on the endurance of the steels Kh18N10T and Kh16N6 and of alloy AMG6 at normal and low temperatures. 09 p1106 A73-23163

Mechanisms of stress corrosion cracking of titanium-aluminum alloys in methanol-HCl solutions. 09 p1106 A73-23166

Nonequilibrium crystallization of Al-Ru alloys 09 p1108 A73-23228

Void initiation and growth in Al alloys due to inclusions, presenting dislocation model for ductile fracture strength 09 p1109 A73-23256

Improved fracture resistance of 7075 through thermomechanical processing. 09 p1109 A73-23257

Effect of welding variables on aluminum alloy weldments. 10 p1230 A73-23627

Effect of process variables on partial penetration electron beam welding. 10 p1223 A73-23629

Effects of Ni and Fe addition on various properties in heat-resisting aluminum casting alloys. 10 p1231 A73-23675

The resistance of wrought high strength aluminum alloys to stress corrosion cracking. 10 p1232 A73-23872

Technology of production of bonded sandwich structures 10 p1224 A73-24096

Discrete creep of AMg6 aluminum alloy subjected to repeated static loading 10 p1233 A73-24365

Effects of beryllium additions on the microstructure and the type of failure in Al-Mg alloys 10 p1233 A73-24423

Crystallography and morphology of as-grown and coarsened Al-Al3Ni directionally solidified eutectic. 10 p1234 A73-24432

Interpretation of quench-sensitivity in Al-Zn-Mg-Cu alloys. 10 p1235 A73-24442

Al alloy stress intensity range estimation from surface fatigue striation incidence and modulus of elasticity, noting relationship to crack growth closure in fractography 10 p1235 A73-24447

Possibility of reducing the wear of the VD-17 aluminum alloy in a jet of free abrasive particles with the aid of metallic coatings 10 p1226 A73-24796

Peritectic solid phase transformations in cast homogenized Al-Cu-Li-Mn-Cd alloy, noting Li strengthening effect 10 p1236 A73-24927

Zr additions effect on quenched and aged Al-Mg-Li alloy having phases in equilibrium with solid solution 10 p1236 A73-24928

Investigation of the hardening process of alloy D16 in liquid nitrogen. 10 p1226 A73-24929

Structural transitions and mechanical characteristics in the case of multicomponent aluminum bronze 11 p1378 A73-25106

An investigation into the electron beam welding of five non-ferrous alloys. 11 p1372 A73-25125

Steel wire, boron or carbon filament reinforced Al alloys shaped parts fabrication, discussing sintering, pressure impregnation and filament winding processes 11 p1373 A73-25415

X2048, a high strength, high toughness alloy for aircraft applications. [AIAA PAPER 73-385] 11 p1380 A73-25514

Fatigue crack delay and arrest due to single peak tensile overloads. [AIAA PAPER 73-325] 11 p1441 A73-25555

Corrosion fatigue and stress corrosion crack growth in high strength aluminum alloys, magnesium alloys, and titanium alloys exposed to aqueous solutions. 11 p1381 A73-25815

Frequency and environmental interactions in the fatigue of aluminum alloys. 11 p1382 A73-25824

The effect of environmental relative humidity upon the ultrasonic fatigue endurance of an age hardening aluminum alloy. 11 p1382 A73-25825

Aircraft structures aluminum alloys fatigue crack growth rate relationship to cracking mode, stress ratio, cyclic frequency and corrosive environment severity. 11 p1382 A73-25826

The effect of coatings on the fatigue characteristics of notched aluminum alloy sheet specimens. 11 p1383 A73-25829

An ultrasonic device for the study of fatigue crack initiation in anodized aluminum alloys. [AD-760070] 11 p1363 A73-25830

Stud welding on 5083 aluminum and 9% Ni steel for cryogenic use. 11 p1375 A73-26352

Hot tinning of aluminum bronze. 11 p1375 A73-26353

Constitution and phase relationships in copper-silver-aluminum ternary system. 11 p1385 A73-26566

Coarse grain Al alloys strength characteristics, crack resistance and specific energy of failure due to brittle fracture 11 p1386 A73-26736

Russian papers on nonferrous metals and alloys metallurgy covering phase equilibria, strengthening, deformation and processing of Al, Mg, Cu and Ti alloys 12 p1510 A73-26902

Phase equilibria in the aluminum-chromium-zirconium system 12 p1510 A73-26906

Rhenium solubility determination for deformed and annealed Re-Al alloy at 500 and 600 C by microstructural analysis and hardness and electrical resistance measurements 12 p1510 A73-26907

Laminar precipitation hardening in Al alloy during aging by microscopic, X ray and Widmanstatten structure analyses 12 p1510 A73-26912

Deformation and recrystallization of twin crystals in aluminum and magnesium alloys 12 p1510 A73-26913

The nature of slated cleavage planes in pressed VAD 23 alloy 12 p1511 A73-26915

Crack propagation in some aluminum alloys with tensile stresses 12 p1511 A73-26916

Microstructure, microhardness and mechanical strength of ingots and granules of Al alloys with high refractory metal contents

12 p1511 A73-26917

Optimal electrical conductivity and mechanical properties of Cu-Mg-Fe-Si-Zr and Be-B containing heat resistant Al alloys, comparing to Cu at room and elevated temperatures

12 p1511 A73-26918

On the relationship between grainboundary corrosion and stress corrosion cracking of Al-Zn-Mg alloys.

12 p1511 A73-27059

Yield point phenomenon in Al-Ti alloy.

12 p1511 A73-27060

X-ray structural investigations of Dy-Fe-Al system alloys in the region of 0 to 33 at. % dysprosium

12 p1512 A73-27243

The changes in structural and mechanical properties of construction materials under loads

12 p1513 A73-27500

The pressing of profiles of aluminum casting alloys from granules and the study of their mechanical properties

12 p1503 A73-27560

Stereometric microanalysis of conglomerate, colony and dispersed structures of binary eutectic Fe, Al, Cu and low melting alloys

13 p1631 A73-28109

Use of high cooling rates to obtain aluminum alloys with special properties

13 p1623 A73-28110

Temperature conditions of aluminum alloy crystallization at cooling rates of 10,000 to 1,000,000 deg/sec

13 p1632 A73-28111

Unidirectional solidification formed interdiffusion eutectic composition related to solidification variables, discussing Al-Cu and Al-Cu-Ni systems

13 p1632 A73-28131

Effect of titanium additions on the aging characteristics of an Al-Zn-Mg alloy.

13 p1632 A73-28134

Cast microstructure and fatigue behavior of a high strength aluminum alloy /KO-1/.

13 p1633 A73-28137

Tensile properties of high strength Al-Zn-Mg and Al-Zn-Mg-Cu alloy products processed by T-AHA type final thermomechanical treatments

13 p1633 A73-28141

Transverse creep and stress-rupture of Borsic-aluminum composites and Borsic-aluminum composites containing stainless steel and titanium.

13 p1633 A73-28143

Properties of iron impurity in aluminum matrix studied by Mossbauer spectroscopy.

13 p1634 A73-28220

Crystallographic analysis of hexagonal vacancy type Al-Mg alloy cube plane dislocation loops produced by specimen deformation before quenching

13 p1634 A73-28260

Plastically deformed Fe-Si and Al alloys surface layer crystal dislocation density and plastic flow onset determination as function of depth

13 p1635 A73-28264

Elastic and creep limits of heteroplastic micrograin metallic /duralumin/ materials in terms of stress-strain curve, sliding plane and stress hardening and relaxation

13 p1635 A73-28471

Mechanical properties of 6061 Al-Mg-Si alloy after very rapid heating.

13 p1636 A73-28795

The lattice heat conductivity of aluminum alloys during age-hardening.

13 p1636 A73-29068

Effect of tensile prestrain on fatigue strength of aluminum alloy in high cycle fatigue.

[ASME PAPER 72-MAT-N]

13 p1636 A73-29199

Effect of microstructure and environment on stress corrosion of 7075 aluminum alloy.

[NACE PAPER 97]

13 p1637 A73-29312

Corrosion and corrosion prevention of light metal alloys.

[NACE PAPER 114]

13 p1637 A73-29314

Dynamic and static strain aging in Al-Mg solid solution alloys.

13 p1639 A73-29458

Plasticity and fracture of structural metals in complex stress state at low temperatures.

13 p1639 A73-29462

Fracture toughness-strength relationships in aluminum-zinc-magnesium-copper alloys.

13 p1639 A73-29473

The interaction of material and geometric aspects in the fracture of aluminum alloys.

13 p1640 A73-29475

Thin Al alloy sheet fracture toughness from crack growth resistance curves, discussing failure modes and critical stress intensities

13 p1640 A73-29480

A study of fatigue crack propagation in high strength aluminum alloys at high stresses.

13 p1640 A73-29488

The effect of wave form and cyclic frequency on the fatigue life of aluminum alloys.

13 p1640 A73-29491

A method for the calculation of the fatigue life of unnotched and notched specimens loaded with alternating stresses.

13 p1641 A73-29501

Fatigue analysis considering rotating principal stress axes for aluminum alloy 2024-T351.

13 p1641 A73-29502

Al and Ti alloy corrosion and fretting fatigue in aqueous environment, noting protective oxide surface film effects

13 p1642 A73-29524

Effect of loading frequency and directional anisotropy on the fatigue strength of grade AMg6BM aluminum alloy sheet.

13 p1643 A73-29606

Graphite content effect on vibration damping properties of Al-Sn and Al-Zn alloys

13 p1643 A73-29608

Resonant frequency, fatigue and energy dissipation relations for endurance limit determination in Al alloy specimens under vibrational loads

13 p1643 A73-29618

Al alloy rupturing analysis in complex stress state, noting sublimation and self diffusion values of activation energy in torsional to tensile state transition

13 p1643 A73-29624

Serrated flow in quenched duralumin alloy.

14 p1758 A73-29745

Solidification structure and tensile properties of 2014 aluminum alloy welds.

14 p1755 A73-30149

Nb-Al alloys sigma phase superconductivity characteristics, investigating critical temperature, composition and heat treatment relations

14 p1759 A73-30236

Critical shear stress temperature dependence in Al-Mg single crystal alloys of various concentrations in the range 1.6-300 K.

14 p1759 A73-30313

Effect of loading conditions on the propagation of fatigue cracks in sheet samples of D16T alloy.

14 p1759 A73-30314

Precipitation of iron in rapidly solidified aluminum-iron alloys

14 p1760 A73-30439

Morphology of the structure and the microhardness of Al-Ni, Cu, Be, Fe, Co eutectic compositions

14 p1760 A73-30588

Dislocation structure of Ni3Al intermetallic compound during various stages of deformation

14 p1760 A73-30591

Alpha phase decomposition and precipitation measurement in titanium rich Ti-Al alloys by electrical resistivity and microscopic methods

14 p1761 A73-30638

Solute aluminum strengthening and strain aging in Ti-Al alloys at 78-810 K

14 p1761 A73-30639

Strain ratio data for commercial Al alloys in various temper conditions as drawability criterion for sheet press performance, discussing single tensile test method

14 p1762 A73-30643

German monograph - Elevation of the yield point and pronounced yield range of multicrystalline aluminum-magnesium alloys.

14 p1762 A73-30673

Investigation of crack propagation in small samples under conditions of low-cyclic fatigue

14 p1763 A73-30680

Exfoliation corrosion of aluminum alloys.

15 p1888 A73-31737

Simplified exfoliation testing of aluminum alloys.

15 p1888 A73-31738

Significance of intergranular corrosion in high-strength aluminum alloy products.

15 p1889 A73-31740

Pitting corrosion - A review of recent advances in testing methods and interpretation.

15 p1889 A73-31741

Exfoliation corrosion testing of 7178 and 7075 aluminum alloys.

15 p1889 A73-31742

Hardening and softening of aluminum alloys under an applied load at 135 to 150 C

15 p1889 A73-31808

Crack growth resistance curves /R-curves/ - Literature review.

15 p1950 A73-31983

R-curve determination using a crack-line-wedge-loaded /CLWL/ specimen.

15 p1950 A73-31984

Thin Al alloy sheet plane stress testing with zero K gradient specimen based on tapered double cantilever beam modification, considering fracture toughness and crack propagation

15 p1950 A73-31985

Plane stress fracture testing using center-cracked panels.

15 p1951 A73-31987

Comparison of R-curves determined from different specimen types.

15 p1951 A73-31988

Laser-induced shock effects in Plexiglas and 6061-T6 aluminum.

15 p1956 A73-32259

Investigation of the phase equilibrium of ternary Ti-Al-Nb system alloys

15 p1893 A73-32514

Investigation of the influence of certain elements on the heat resistance of titanium aluminide Ti3Al

15 p1894 A73-32530

Features of the influence of aluminum on the mechanical properties of titanium

15 p1894 A73-32532

Investigation of friction behavior in titanium alloy with 3.8% Al

15 p1894 A73-32535

Corrosion-fatigue crack growth in high-strength aluminum alloys with and without susceptibility to stress-corrosion cracking.

15 p1895 A73-32571

Surface morphology after pretreatment in relation with bondability of aluminum alloys.

16 p2018 A73-33056

Boron fiber coating by chemical vapor deposition of boron carbide for improved mechanical properties and incorporation in Al alloy matrices

16 p2030 A73-33070

Unconventional processes for faster extrusion of aluminum hard alloys

16 p2021 A73-33951

The influence of prior thermal treatment of cast blocks on the coarse grain characteristics in extruded bars and profiles of alloys of the type AlCuSiMn

16 p2021 A73-33952

The precipitation behavior of a commercial aluminum-copper-lithium alloy. I - The microstructure after isothermal heat treatment

16 p2026 A73-33954

The influence of vacancies on the nucleation of incoherent germanium precipitates in aluminum-germanium alloys. III - The effect of germanium nuclei on precipitation at higher temperatures

16 p2026 A73-33959

Relation between grain size and the size of fatigue-striated facets in an aluminum alloy

16 p2027 A73-33972

Inelastic buckling of columns - The effect of imperfections.

16 p2084 A73-33975

Mechanical properties, microstructure and failure characteristics of binary alloys of Al-Mg system determined under different tensile stress rates and temperatures

17 p2187 A73-34339

Composition and temperature effects on hydrogen solubility in Ni-Al liquid alloys

17 p2187 A73-34553

Microstructure and phase composition of oxide scale formation on Ti-Al alloys, noting dependence on Al concentration

17 p2188 A73-34557

Polythermal and isothermal sections of Ti-Al-W phase diagram for Ti corner investigation, determining phase region boundary locations by X ray analysis

17 p2188 A73-34568

A microscopic study of crack initiation mechanisms in 7075 aluminum alloy sheets.

17 p2190 A73-34885

Hydrogen embrittlement and stress corrosion cracking in Ti-Al binary alloys.

17 p2191 A73-35099

Role of stress in the stress corrosion cracking of a Mg-Al alloy.

17 p2191 A73-35100

Dynamic yield strength determination at elevated temperatures after nanosecond pulse heating. [SESA PAPER 2141 A]

17 p2148 A73-35450

Direct observation of the failure of a fibre reinforced composite.

17 p2192 A73-35529

Fatigue and creep behavior of aluminum and titanium matrix composites.

17 p2193 A73-35543

Tension-tension low cycle fatigue failure mechanism in uniaxially and biaxially reinforced boron fiber-aluminum alloy composites, considering matrix plasticity role

17 p2193 A73-35544

Fatigue and corrosion-fatigue crack propagation in intermediate-strength aluminum alloys.

[ASME PAPER 73-MAT-N]

18 p2323 A73-36615

Fatigue strength of materials under a two-frequency load /Review/

18 p2366 A73-36754

Effect of atom ordering on the martensite decomposition mechanism and kinetics in iron-aluminum-carbon alloys

18 p2324 A73-36769

Fractography of stress corrosion in Ti-8Al tested in fatigue.

18 p2326 A73-36972

Special features of the fracture of aluminum and titanium alloys at low temperatures

19 p2439 A73-37267

Strain accumulation and rupture during creep under variable uniaxial tensile loading.

19 p2495 A73-37434

Biaxial cyclic high-strain fatigue of aluminum alloy RR58.

19 p2440 A73-37437

Grain refinement in aluminum-zirconium and aluminum-titanium alloys by metastable phases.
19 p2440 A73-37444

Particle combustion mechanism in aluminum-magnesium alloys
19 p2472 A73-37511

Some studies of the influence of localized and gross plasticity on the monotonic and cyclic concentration factors.
19 p2497 A73-37589

The effect of very short time-at-temperature on the yield stress of 6061-T651 aluminum.
19 p2440 A73-37590

Fractographic investigation of the ductility of fracture in aluminum and titanium alloys.
19 p2440 A73-37780

Evaluation of the fatigue properties of aluminum alloys D16T and AVT1 on the basis of limit stresses.
19 p2440 A73-37790

Investigation of fatigue strength of D1T alloy with due regard to dispersion of results.
19 p2440 A73-37791

Design and development of lightweight wheel braking equipment.
[SAWE PAPER 995] 19 p2434 A73-37894

Effects of small amounts of additional elements on directionality of stress corrosion resistance of the Al-Zn-Mg alloys.
19 p2442 A73-37948

Grain refinement by titanium in the unidirectionally solidified aluminum alloys.
19 p2442 A73-37949

Ultrasonic closure welding of small aluminum tubes.
19 p2435 A73-38003

Yield surfaces of metals at elevated temperatures.
20 p2615 A73-38640

Tensile deformation and fracture in high-strength Al-Zn-Mg alloys.
20 p2575 A73-39019

Partitioning of stress between fiber and matrix during tensile deformation of the Al-Al3Ni eutectic composite.
20 p2576 A73-39024

The influence of heat treatment on the stress-corrosion susceptibility of a ternary Al-5.3 pct Zn-2.5 pct Mg alloy.
20 p2576 A73-39031

Anisotropic nature of strain hardening during unsteady creep of alloy AK-4.1 subject to combined tension and torsion
20 p2577 A73-39288

Properties of boron fibers and of boron-aluminum composites in uniaxial compression
20 p2580 A73-39358

Experimental investigation of changes in the fracture toughness of aluminum alloys
20 p2577 A73-39359

Study of the mechanism of plastic deformation of aging nickel-aluminum alloys with a large volume fraction of gamma prime phase
20 p2579 A73-39740

Changes in the disorientation of the substructure of a nickel-aluminum alloy under ultrasonic treatment and creep
20 p2579 A73-39748

A photographic method for testing the impact strength of metals
21 p2696 A73-39991

The nature of the interaction between scandium and aluminum in the aluminum-rich part of the Al-Sc system
21 p2718 A73-40486

Phase composition of Ni-Al and Ni-Ga alloys hardened from the liquid state
21 p2719 A73-40849

Influence of aluminum on the structure and properties of a Ti + 10% V alloy
21 p2719 A73-40850

The influence of phase size on the creep of lamellar and particulate Al-CuAl2 eutectic composites.
21 p2719 A73-40896

Fractography of stress corrosion cracks in aluminum alloy 7075.
21 p2720 A73-40925

Aluminum and aluminum alloys extrusion processes, discussing form shape, weldability, hardening and metal transformations
21 p2707 A73-41067

Observations of solid/liquid interfaces in dilute binary and ternary Al-rich alloys.
21 p2721 A73-41120

Fabrication of high-reliability sheathed thermocouples.
22 p2865 A73-42041

Investigation of the phase composition of alloys in the Ti-Al-Fe ternary system
22 p2873 A73-42086

Study of the structure and properties of alloys of the V-Al, Cr-Al and V-Cr-Al systems in the region of solid solution bcc ordering
22 p2873 A73-42088

Elastic properties of alloys of the Ti-Al-Mo system as a function of the composition and heat treatment
22 p2874 A73-42095

Effect of the frequency of cyclic tension-compression on the fatigue limit of alloy D16T.
22 p2874 A73-42103

Effect of multiple overloads on fatigue crack propagation in 2024-T3 aluminum alloy.
22 p2875 A73-42139

Influence of stress intensity level during fatigue precracking on results of plane-strain fracture toughness tests.
22 p2876 A73-42149

Influence of sheet thickness upon the fracture resistance of structural aluminum alloys.
22 p2876 A73-42150

Plane-stress fracture toughness and fatigue-crack propagation of aluminum alloy wide panels.
22 p2876 A73-42151

Reactive kinetic observations for spraying with Ni-Al powder.
22 p2879 A73-42594

Transformation temperatures of martensite in beta-phase nickel aluminide.
23 p2989 A73-43275

Al-aluminum nickelide eutectic fiber composite impact strength dependence on crystallization rate, examining crack propagation rate relation to fiber spacing
23 p2996 A73-43437

Improvement of the corrosion-fatigue strength of aluminum alloys by exposure of the medium to a magnetic field
23 p2984 A73-43466

Microstructural characteristics of the plastic deformation and recrystallization of an aluminum alloy of various heterophase structure
23 p2991 A73-43489

The plastic deformation of N1Al single crystals between 300 K and 1050 K. I - Experimental evidence on the role of kinking and uniform deformation in crystals compressed along the 001 direction. II - The mechanism of kinking and uniform deformation.
23 p2991 A73-43773

Fracture behaviour of crystalline Al3Ni intermetallic fibres.
23 p2991 A73-43774

A review of fatigue crack growth in high strength aluminum alloys and the relevant metallurgical factors.
23 p2991 A73-43806

Fracture of thin sections containing surface cracks.
23 p2992 A73-43807

Fatigue crack growth detection by acoustic emission monitoring in correlation with stress intensity for high cycle fatigue Al alloy
23 p2992 A73-43814

Phase transformations in beta-Cu-Al during extremely rapid cooling from the melt
23 p2992 A73-43914

Postannealing isothermal decomposition products of Al-Mn alloys studied by transmission electron microscopy, revealing trigonal and hexagonal lattice diffraction patterns
23 p2993 A73-43916

The effect of composition changes on the fracture toughness of an Al-Zn-Mg-Cu-Mn forging alloy.
23 p2993 A73-44025

The influence of testing temperature and thermal history on the intergranular embrittlement and penetration of aluminium by liquid gallium.
23 p2993 A73-44026

Discontinuous flow in steady-state creep of Al-Mg alloys at high temperatures.
23 p2995 A73-44162

Influence of dislocation density and aging on the yield point of Al-Cu-Mg-Mn alloys
23 p2995 A73-44285

The effect of the intermediate principal stress on triaxial fatigue of 7075-T6 aluminum alloy.
23 p3047 A73-44351

Formation of the overheating structure in cast Al.9 and VAl.5 Silumin alloys
24 p3098 A73-44473

Influence of ultrasonic vibrations on the mechanical properties and fine structure of aluminum and an aluminum-magnesium alloy
24 p3098 A73-44570

Influence of small beryllium, titanium, and zirconium additions on the structure and properties of Al9 alloy
24 p3098 A73-44571

The relation of surface condition after pretreatment to bondability of aluminum alloys.
24 p3093 A73-44764

Vibration characteristics of aluminum plates reinforced with boron-epoxy composite material.
24 p3149 A73-45148

Spatial orientation of phases in the Al-Al3Ni eutectic system
24 p3099 A73-45169

Memory effect on mechanical properties of plastically prestrained Al-Mg alloy sheets
24 p3100 A73-45247

Hardening and softening of aluminum alloys under load at 135-150 C.
24 p3100 A73-45271

Dynamic strain ageing in creep of beta-NiAl
24 p3100 A73-45331

ALUMINUM CARBIDES
Mass spectrometric determination of the dissociation energies of AlC2, Al2C2, and AlAuC2.
09 p1048 A73-23247

ALUMINUM CHLORIDES
Electrode reactions of aromatic amines in solvents containing fused AlCl3.
15 p1841 A73-32224

ALUMINUM COATINGS
Aluminizing process improvement by CaAl and ammonium chloride contents increase in powder
01 p0057 A73-11350

Solid-phase epitaxial growth of Si mesas from Al metallization.
06 p0738 A73-18650

Method of plasticity enhancement in aluminum and nickel-aluminum diffusion coatings on medium-carbon steel
06 p0711 A73-18665

Boundary conditions for diffusion in the pack-aluminizing of nickel.
06 p0713 A73-18774

Diffusion aluminizing of Ni and Ni-base alloys by gas circulation method, investigating gas flow velocity effect relationship to specimen weight gain
10 p1226 A73-24957

Austenitic stainless steels diffusion layer formation and structure by gaseous carburization with Fe-Al-ammonium chloride powder mixture, describing elements redistribution
10 p1226 A73-24958

Cr diffusion into Ni-Cr alloys in presence of aluminized layer, noting increased diffusive mobility
10 p1226 A73-24959

Si addition effect on Ni-Cr alloy carburized layer depth, microhardness, phase structure, chemical composition and scaling resistance
10 p1227 A73-24960

Boridosilicide and boridoaluminide diffusion coatings on iron and steel, investigating formation kinetics structure and properties
10 p1227 A73-24963

Vacuum contactless metallization of carbon steels, stainless steels and nickel alloys, considering Si, Cr and Al coatings
10 p1227 A73-24964

The effect of coatings on the fatigue characteristics of notched aluminum alloy sheet specimens.
11 p1383 A73-25829

Rotating bending fatigue tests on Al coated steels, investigating electroplating, hot dip and spraying production methods effects on fatigue strength
13 p1635 A73-28645

Corrosion performance of new fastener coatings on operational military aircraft.
[NACE PAPER 115] 13 p1637 A73-29315

Comparison of an aluminum-coated phosphor layer and a Channeltron Electron Multiplier Array as extreme ultraviolet-to-visible image converters for use in space applications.
14 p1752 A73-30155

Heating of an oxidizing metal by CO2 laser radiation
17 p2184 A73-34634

Effect of load sequences on crack propagation under random and program loading.
17 p2190 A73-34879

Phase formation investigation in the Mo-Al and W-Al systems when the Mo and W surfaces are saturated with aluminum by diffusion from a vapor phase in a vacuum
18 p2318 A73-35879

Al foil surface properties from electron spectroscopic analysis, determining oxide film thickness, annealing effects and oxidation dependence on surface hydrocarbon deposits
19 p2442 A73-38171

Investigation of the plasticity of coatings on heat-resistant alloys
20 p2566 A73-39367

Optical waveguides in GaAs-AlGaAs epitaxial layers.
21 p2752 A73-40969

Investigation of the effective heat conductivity of plasma-sprayed alumina coatings subject to radiative heating in the temperature range from 100 to 900 C
21 p2792 A73-41220

Investigations into the mechanism of exothermically reacting nickel-aluminum spraying materials.
22 p2879 A73-42595

ALUMINUM COMPOUNDS
NT ALUMINATES
NT ALUMINUM CARBIDES
NT ALUMINUM CHLORIDES
NT ALUMINUM NITRIDES
NT ALUMINUM OXIDES
NT ALUMINUM SILICATES
NT ANDESITE
NT FELDSPARS
NT KAOLINITE
NT LITHIUM ALUMINUM HYDRIDES
NT PYROPHYLLITE
NT SAPPHIRE

- High-efficiency Ga/1-x/Al/x/As-GaAs solar cells.
01 p0005 A73-10132
- Thermal stability of the microstructure in the eutectic composition Al-Al₃Ni
09 p1099 A73-21966
- Intergranular precipitation in the oriented bicrystals of aluminum-copper
09 p1105 A73-23039
- ALUMINUM ISOTOPES**
NT ALUMINUM 26
- ALUMINUM NITRIDES**
Chemical stability and features of the formation of complex nitrides of III-B subgroup elements /Al-B-N system/
24 p3119 A73-44952
- ALUMINUM OXIDES**
NT SAPPHIRE
Effect of various methods of oxide introduction on the properties of dispersion-hardened nickel.
01 p0065 A73-10814
- Characterization of the mixed oxides of lithium and aluminum.
01 p0089 A73-11113
- Effects of alloying on structural stability and cohesion between phases in oxide/metal composites.
03 p0326 A73-13964
- The effect of small magnesium additions on microstructure and high-temperature properties of nickel-2-1/2 vol. % alumina.
03 p0326 A73-13966
- Acoustic model of HF damping and microstructure of dispersed aluminum oxide ceramics systems, using Hugoniot elastic limits for Young modulus and fracture determination
04 p0468 A73-15373
- The reactions of titanium and silicon with Al₂O₃-CaO-CaF₂ slags in the ESR process.
04 p0455 A73-15744
- Effects of electropolishing on the tunneling current in aluminum-aluminum-oxide-aluminum diodes.
06 p0678 A73-18744
- Measurement of high-temperature thermal conductivity of Lucalox /Al₂O₃/ using a heat pipe technique.
06 p0715 A73-18778
- Dispersivity of the combustion products of a mechanical mixture of aluminum and cadmium powders
07 p0923 A73-20421
- The growth of dielectric aluminum and tantalum oxide layers
08 p0977 A73-21023
- Effect of microstructure on measurements of fracture energy of Al₂O₃.
[ACS PAPER 44-BN-71P] 08 p0983 A73-21842
- Effect of surface damage on the strength of Al₂O₃ ceramics with compressive surface stresses.
[ACS PAPER 37-BN-71P] 08 p0983 A73-21843
- Spectroscopic investigation of the interaction of oxides with a metallic surface. III - Systems Al₂O₃-Me/Al, Cu, Ti, Khl8N9T steel, Ni, Co, Mo, W, Si/
09 p1103 A73-22470
- Effectiveness of using the energy of a plasma jet in powder coating deposition
10 p1226 A73-24689
- Electrically stabilized alumina as ceramic material for radome applications, tabulating dielectric, thermal and mechanical properties and firing conditions
11 p1408 A73-25287
- An experiment to correlate the thermal stress failure level to modulus of rupture in ceramic materials.
11 p1387 A73-25304
- Compatibility between material components in metal-ceramics composites
11 p1387 A73-25412
- Investigation of the heat conductivity of aluminum oxide deposited by plasma spraying
11 p1373 A73-25731
- Coherent production of electron-positron pairs and bremsstrahlung on a corundum crystal
11 p1410 A73-26447
- Thermoluminescence and activation energies in Al₂O₃, MgO and LiF /TI.D-100/.
12 p1530 A73-27031
- Deterioration of impermeable alumina tubes in inert atmospheres at elevated temperatures.
12 p1515 A73-27032
- Luna 20 lunar glass particle samples chemical composition, noting aluminum oxide content similarity to Apollo 16 samples
13 p1675 A73-28314
- Al filament ignition temperature in carbon dioxide flow at various current values, noting relation to surface oxide film melting temperature
14 p1764 A73-30872
- Dependence of some physicochemical properties of plasma-deposited aluminum oxide on sputtering conditions
15 p1881 A73-31211
- Enhancement of the electrical strength of deposited aluminum oxide coatings by electrophoretically filling the pores
15 p1881 A73-31212
- High altitude aircraft water vapor measurements using aluminum oxide hygrometer, noting comparison with remote sounders
[AIAA PAPER 73-511] 16 p2006 A73-33549
- Calcium oxide and aluminum oxide constraints removal for lunar interior composition models
17 p2232 A73-35264
- Chemistry of lunar basalts with very high alumina contents.
18 p2354 A73-36598
- Superconductivity of films made from aluminum oxide and niobium mixtures
20 p2579 A73-39744
- Ruby coloring centers and orange coloration dependence in corundum crystals on additive Mg, Cr, V and Ti ions
21 p2752 A73-40560
- Determination of the size and the imaginary part of the refractive index of Al₂O₃ drops in a flame
22 p2932 A73-42724
- German monograph - Investigation of time-variable currents in Al-Al₂O₃-Al thin-film structures.
22 p2897 A73-42855
- Resistance to crack propagation in ceramics subjected to thermal shock.
23 p2997 A73-44031
- Effect of aluminum-containing components on phase alloying in periclase ceramic materials
24 p3104 A73-44953
- ALUMINUM SILICATES**
NT ANDESITE
NT KAOLINITE
NT PYROPHYLLITE
The acoustic emission response of mechanically stressed ceramics.
02 p0173 A73-11989
- ALUMINUM 26**
Aluminum-26 in meteorites. VII - Ureilites, their unique radiation history.
17 p2237 A73-35803
- Al-26 and Na-22 measurements on Luna 16 samples by non-destructive gamma-gamma coincidence spectrometry.
21 p2774 A73-41405
- ALVEOLAR AIR**
Indexes of ventilation distribution before/after airway occlusion in dogs, indicating collateral channel inspired gas distribution reduction
03 p0262 A73-14113
- Regional lung volumes with positive pressure inflation in erect humans.
06 p0653 A73-18334
- Effects of lung volume and disease on the lung nitrogen decay curve.
08 p0934 A73-21501
- Single breath nitrogen washout method for measurement of functional residual capacity.
11 p1315 A73-25332
- Comparison of blood and alveolar gas composition during rebreathing in the dog lung.
11 p1318 A73-26218
- Studies of alveolar-mixed venous CO₂ and O₂ gradients in the rebreathing dog lung.
11 p1318 A73-26219
- Determination of diffusive capacity components in lungs and of alveolar arterial oxygen gradients for the estimation of oxygen transport conditions in lungs
14 p1719 A73-30849
- Transpulmonary pressure gradient and ventilation distribution in excised lungs.
15 p1833 A73-31129
- Breath to breath cyclical variations in functional residual capacity, oxygen uptake, carbon dioxide release, tidal volume, respiratory period, alveolar gas tension and heart rate
15 p1834 A73-31346
- Temperature of exhaled air of healthy subjects
18 p2277 A73-36583
- Gas mixing during breath holding studied by intrapulmonary gas sampling.
18 p2277 A73-36651
- Molecular diffusion model of cardiogenic gas mixing during inspiration at alveolar boundary in dogs
18 p2277 A73-36652
- Pulmonary volume, respiration rate and alveolar air carbon dioxide content measurements in pilots during flight, noting hyperventilation occurrence
19 p2392 A73-37197
- Respiratory nitrogen elimination - A potential source of error in closed-circuit spirometry.
20 p2512 A73-39113
- Transient ventilatory response to hypoxia with and without controlled alveolar PCO₂.
20 p2515 A73-39777
- Gas transport in the human lung.
22 p2806 A73-42421
- A rapid method for determining the CO₂ transport characteristics in man by using a capnograph and a multichannel respirator
22 p2815 A73-42665
- Differences between inspired and expired minute volumes of nitrogen in man.
24 p3060 A73-45069
- ALVEOLI**
Insensitivity of the alveolar septum to local hypoxia.
01 p0006 A73-10134
- Cat and rat lung damage due to hyperbaric oxygen exposure and head injury, discussing alveolar surfactants, sympathetic stimulation and monkey injuries
[AD-759298] 13 p1576 A73-28507
- Blood plasma contamination of the lung alveolar surfactant obtained by various sampling techniques.
21 p2642 A73-41637
- Model experiments on apparent blood viscosity and hematocrit in pulmonary alveoli.
24 p3064 A73-45064
- AMBIENT TEMPERATURE**
Temperature fields and stresses in bodies of simple geometry when the ambient medium temperature is unsteady
01 p0113 A73-10023
- High temperature adhesive shear tests at ambient temperature as function of loading rate and bond overlap length
03 p0332 A73-13040
- A method for evaluating the circuit reliability of electronic equipment
07 p0802 A73-20299
- Dynamic katathermometer for measuring the cooling effect of an ambient medium
15 p1838 A73-31512
- Method of estimating the circuit reliability of electronic devices.
18 p2294 A73-37136
- Temperature measurement, monitoring, and control on a Michelson interferometer for ambient-temperature emission spectroscopy.
22 p2856 A73-42025
- Spinal cord heating effects on frog thermoregulatory behavior in aqueous thermal gradient, noting preference for colder ambient temperature
23 p2947 A73-43994
- AMBIGUITY**
Application of the ambiguity function to seismic signatures.
06 p0690 A73-18009
- Wideband multiphase radio signal processing with given ambiguity function via sequential synthesis
07 p0794 A73-20292
- A new type of PSK anti-ambiguity system for satellite applications.
09 p1156 A73-23431
- Investigation of the mutual ambiguity function of a wideband signal with complex angle modulation
10 p1187 A73-23731
- Wideband multiphase radio signal processing with given ambiguity function via sequential synthesis
18 p2290 A73-37129
- Effect of a subjective ambiguity estimate concerning the duration of work on activity regulation
22 p2812 A73-41892
- AMBIPOLAR DIFFUSION**
Observation and interpretation of ionization drift measurements in the F region at St-Santin-Nancy.
02 p0161 A73-12284
- Diffusion of weak inhomogeneities in a magnetoactive two-ion plasma
06 p0727 A73-17536
- Departure from thermodynamic equilibrium of an ionized cesium vapor - Experimental study and comparison with a statistical model
07 p0854 A73-20607
- Determination of upper atmosphere parameters from measurements of the ambipolar diffusion coefficient by radar observations of meteor trails.
10 p1212 A73-24223
- Ambipolar drift, deformation, and diffusion of a plasma in a magnetic field.
11 p1402 A73-24989
- Ambipolar diffusion in the F1-region of the ionosphere.
11 p1357 A73-25928
- Inhomogeneous plasma density distribution relation to ambipolar diffusion and ionization balance processes of electron cooling, particle recombination and ground state, step wise and Penning ionization
12 p1527 A73-26932
- Analytical model of the unsteady nighttime F2 region of the ionosphere at mid-latitudes
12 p1490 A73-27337
- Diffusion of weak inhomogeneities in a magnetically active plasma consisting of two ions.
16 p2039 A73-32760
- Splitting of an ionospheric layer by ambipolar diffusion.
18 p2313 A73-36388
- A new type of ionizational instability in a plasma with negative ions
20 p2598 A73-39621
- Inhomogeneous plasma density distribution relation to ambipolar diffusion and ionization balance processes of electron cooling, particle recombination and ground state, step wise and Penning ionization
22 p2891 A73-42266
- Anomalous diffusion in a magnetized plasma.
22 p2894 A73-42483
- Ambipolar diffusion generator based on self generated electric fields in premixed ionized methane flame, comparing with opposite electroelectric effects
22 p2895 A73-42773
- Analytical model of the nocturnal nonstationary F2-region of the ionosphere at middle latitudes.
23 p2970 A73-43235

AMIDES

NT ACETANILIDE
NT CYANAMIDES
NT POLYIMIDES
NT THIURONIUM
NT UREAS

Formamide rotational transition microwave emission detection in interstellar medium in Sgr B2 and Sgr A direction

09 p1150 A73-23140

Observations of formamide at 6 cm in Sagittarius B2.

15 p1933 A73-31377

AMINES

NT CATECHOLAMINE
NT DIAMINES
NT DIMETHYLHYDRAZINES
NT HYOSCINE
NT NITROAMINES
NT SEROTONIN
NT TETRAFLUOROXYDRAZINE
NT THIURONIUM
NT TRYPTAMINES

Effect of the administration of free amino acids and metabolic cofactors on the distribution of regional biogenic amine contents in the brain and blood of animals

09 p1040 A73-22864

Organic and species-related differences in the action of certain hydrazine derivatives and of aminoperhydroacridine on the oxidative deamination of serotonin

10 p1183 A73-23679

Life processes in ammonia - Anomalous germination behavior of onion seed in ammonia and amines.

11 p1321 A73-26491

Sterically controlled syntheses of optically active organic compounds. XVI - Temperature dependence of hydrogenolytic asymmetric transamination.

12 p1467 A73-27974

Rapid gas-phase reactions - The reaction of ammonia and the methylamines with boron trifluoride. III - Pressure dependence of rate constant.

14 p1723 A73-30068

Electrode reactions of aromatic amines in solvents containing fused $AlCl_3$.

15 p1841 A73-32224

Amine phosphates as antiwear additives in neopentyl polyol esters.
[ASLE PREPRINT 73AM-9A-1]

17 p2196 A73-34996

AMINO ACIDS

NT ASPARTIC ACID
NT GLUTAMIC ACID
NT LEUCINE
NT LYSINE
NT METHIONINE
NT PEPTIDES
NT PHENYLALANINE
NT PYRIDINE NUCLEOTIDES
NT PYRUVATES
NT THYROXINE
NT TRYPTOPHAN

Evolution from amino acids - Lunar occurrence of their precursors.

01 p0008 A73-10249

Nervous system transmitter biochemistry in terms of excitation and inhibition coordination with emphasis on gamma-aminobutyric acid (GABA) function in cerebellum

03 p0264 A73-14258

Space environment effects on human life and biochemical evolution study in aerospace medicine and biology, noting amino acid molecules synthesis

03 p0265 A73-14589

Biogeochemistry of aragonite mud and oolites.

03 p0266 A73-14662

Oxidation of amino acids by diaphragms from fed and fasted rats.

05 p0538 A73-16153

An investigation of the possible differential radiolysis of amino acid optical isomers by C-14 betas.

06 p0660 A73-17935

On the electrophoretic behavior of thermal polymers of amino acids.

06 p0661 A73-17939

Stereo-enriched poly-alpha-amino acids - Synthesis under postulated prebiotic conditions.

06 p0661 A73-17940

Syntheses and conformational studies of polyacidic amino acids containing optical active side chains.

06 p0661 A73-17942

Quantitative gas-liquid chromatography of non-protein amino acids in the presence of the twenty protein amino acids.

06 p0661 A73-18175

Ion-exchange chromatography in lunar organic analysis.

06 p0662 A73-18414

Hydrolysis of aqueous extract of lunar dust samples for identification and quantitation of amino acid precursors in extraterrestrial sources, considering prebiotic evolutionary pathways termination

06 p0655 A73-18421

Amino acid search in lunar fines, considering terrestrial source contamination, bound and free amino acids, processing and analysis contamination

06 p0754 A73-18422

Apollo 14 fines examination for indigenous amino acids or amino acid convertible materials, optimizing gas-liquid chromatographic systems for separation and flame ionization

06 p0662 A73-18423

Resolution by gas-liquid chromatography of diastereomers of five nonprotein amino acids known to occur in the Murchison meteorite.

06 p0662 A73-18468

Polymerization of amino acids under primitive earth conditions.

07 p0787 A73-19217

Amino acid precursors in lunar fines from Apollo 14 and earlier missions.

07 p0891 A73-19820

Amino acid analyses of Apollo 14 samples.

07 p0891 A73-19821

Optical resolution of aspartic acid by using copper complexes of optically active amino acids.

07 p0789 A73-20457

Gas-liquid chromatographic resolution of several protein amino acid enantiomers on a packed column.

10 p1186 A73-24658

Optical resolution of DL-aspartic acid in the presence of optically active amino acid and copper (III) ion.

11 p1324 A73-25146

Geochemistry of amino acid enantiomers - Gas chromatography of their diastereomeric derivatives.

11 p1326 A73-25469

Amino acid composition significance in sedimentary fossil skeletal protein calcification, discussing diagenetic temperature effects

11 p1326 A73-25470

Carbon compounds in pyrolysates and amino acids in extracts of Apollo 14 lunar samples.

11 p1426 A73-26471

Chemical evolution - Recent syntheses of bioorganic molecules.

11 p1319 A73-26477

Criteria for distinguishing biogenic and abiogenic amino acids - Preliminary considerations.

11 p1319 A73-26480

Effect of lithium on acute oxygen toxicity and associated changes in brain gamma-aminobutyric acid.

13 p1575 A73-28503

Photoinduced fixation of CO₂ by amino acids - Implications for nonbiological reactions on the Martian soil.

16 p1977 A73-33874

Thermal synthesis of amino acids from a simulated primitive atmosphere.

17 p2112 A73-34572

Origin of terrestrial polypeptides - A theory based on data from discharge-tube experiments.

20 p2513 A73-39484

Prebiotic reactions combining amino acids and ribonucleotides into polypeptides and polynucleotides in presence of urea, imidazole and Mg positive ion, suggesting contemporary biosynthesis parallels

21 p2637 A73-40372

Amino acids in the Murchison meteorite.

21 p2771 A73-41010

Gamma-aminobutyric acid antagonism in visual cortex - Different effects on simple, complex, and hypercomplex neurons.

23 p2946 A73-43338

Racemization of amino acids in marine sediments determined by gas chromatography.

23 p2973 A73-43843

AMMONIA

NT LIQUID AMMONIA

The production of nitric oxide in ammonia oxidation flames.

01 p0121 A73-10640

Development of a radioisotope-fueled thruster for satellite propulsion.

[AIAA PAPER 72-1066]

03 p0354 A73-13395

Titan atmosphere composition of methane hydrate with ammonia impurity, discussing hydrogen and hydrocarbon production, liquid water existence and greenhouse effects

04 p0497 A73-14973

Studies of the anodic oxidation of hydrazine in an alkali electrolyte and of the side reaction of ammonia formation during the decomposition of hydrazine

04 p0407 A73-15103

The abundance of NH₃ on Jupiter inferred from UHF radiometry data.

[AIAA PAPER 73-128]

05 p0619 A73-16881

The emission spectrum of the silent electric discharge in ammonia and hydrazine vapor

06 p0723 A73-17916

Heat exchanging and catalytic dissociation of ammonia flowing through tubes - Application to micropropulsion.

07 p0867 A73-18931

Investigation of molecular absorption in the atmospheres of the giant planets

08 p1007 A73-21064

Optical characteristics and structure of the Jovian atmosphere. V - Probable structure of the ammonia aerosol layer.

08 p1012 A73-21577

Spectroscopy of Jupiter - 3200 to 11,200 A.

11 p1418 A73-25720

Life processes in ammonia - Anomalous germination behavior of onion seed in ammonia and amines.

11 p1321 A73-26491

Quantitative analysis of specific gases by means of a microwave cavity spectrometer.

13 p1612 A73-28224

Rapid gas-phase reactions - The reaction of ammonia and the methylamines with boron trifluoride. III - Pressure dependence of rate constant.

14 p1723 A73-30068

The use of nitride intermediates in the preparation of metals - A study of the reduction of Nb₂O₅ with NH₃.

14 p1761 A73-30629

Investigation of the excitation of vibrational levels of the /N-14/H₃ molecule by carbon dioxide laser radiation

14 p1758 A73-30801

Decomposition of hydrazine on Shell 405 catalyst at high pressure.

15 p1841 A73-32174

Mechanism of decay of ammonia in flame gases from an NH₃/O₂ flame.

16 p1976 A73-33345

Investigation of molecular absorption features in the spectrum of Jupiter

16 p2070 A73-33839

Results of observations of methane /6190 A/ and ammonia /6441 and 6478 A/ absorption bands on the Jovian disk over a period of three years

16 p2070 A73-33840

Ammonia absorption relevant to the albedo of Jupiter. I - Experimental results.

17 p2231 A73-34764

Preliminary data on the optical properties of solid ammonia and scattering parameters for ammonia cloud particles.

17 p2211 A73-34858

Molecular absorption in the atmospheres of the giant planets.

18 p2355 A73-36865

The temperature and ammonia profiles in the Jovian atmosphere from inversion of the Jovian emission spectrum.

22 p2915 A73-43017

Ammonia density profiles and photochemical destruction above Jovian tropopause as function of eddy diffusion coefficient, considering background atmosphere scale height

23 p3028 A73-43601

Background concentrations of photochemically active trace constituents in the stratosphere and upper troposphere.

23 p2976 A73-43889

Jovian ammonia photolysis to nitrogen, explaining ammonia observations by deep and hot atmosphere and/or electrical discharge phenomena

24 p3065 A73-44536

Spectral data for the nu sub 2 bands of ammonia with applications to radiative transfer in the atmosphere of Jupiter.

24 p3142 A73-45324

AMMONIUM CHLORIDES

Aluminizing process improvement by CaAl and ammonium chloride contents increase in powder

01 p0057 A73-11350

Effects of inhibitors PB-5 and of dialkyl-dimethyl ammonium chloride on the corrosion resistance and mechanical strength of structural materials during the cleaning of heat exchangers from scale by the hydrochloric acid method

02 p0174 A73-12537

AMMONIUM COMPOUNDS

NT AMMONIUM CHLORIDES

NT AMMONIUM NITRATES

NT AMMONIUM PERCHLORATES

NT AMMONIUM PHOSPHATES

NT AMMONIUM SULFATES

Relative efficiencies of filters and impactors for collecting stratospheric particulate matter.

17 p2167 A73-34863

AMMONIUM NITRATES

Contribution to the phase stabilization of ammonium nitrate

24 p3066 A73-45201

AMMONIUM PERCHLORATES

Catalytic effects of copper chromite and iron oxide on AP-HTPB binder sandwich combustion to 3200 psia by cinephotomicrography

[AIAA PAPER 72-1120]

03 p0352 A73-13434

Ammonium perchlorate/aluminum powder propellant rocket engine feasibility evaluation, considering test firing results on performance and stability characteristics for various injector configurations

[AIAA PAPER 72-1162]

03 p0357 A73-13463

Feasibility of a fluidized powder demand mode gas generator.

[AIAA PAPER 72-1194]

03 p0352 A73-13484

- Combustion mechanisms of fuel rich propellants in flow fields.
[AIAA PAPER 72-1145] 04 p0485 A73-14915
- Combustion catalysis model of a single-component fuel/as applied to ammonium perchlorate/
07 p0865 A73-19991
- An experimental study of ammonium perchlorate-binder sandwich combustion in standard and high acceleration environments.
07 p0866 A73-20363
- Influence of the surface microstructure on the evolution of the combustion velocity of ammonium perchlorate composite solid propellants as a function of pressure
[ONERA, TP NO. 1167] 08 p0995 A73-21678
- Perchlorate degradation of ethyl oleate in solid propellants.
10 p1262 A73-23758
- Vacuum sublimation of ammonium perchlorate.
12 p1466 A73-27127
- Influence of oxidizer dispersy on the efficiency of combustion catalyzers
13 p1669 A73-28973
- The mechanism of catalyzer action on the burning of condensed systems
13 p1669 A73-28974
- Strength and elastic characteristics of ammonium perchlorate whiskers grown with potassium permanganate additions, discussing crystal dislocations and physico-chemical properties
14 p1767 A73-30829
- Explosive behavior of aluminized ammonium perchlorate.
16 p2045 A73-33346
- An experimental study of the low pressure limit for steady deflagration of ammonium perchlorate.
16 p2045 A73-33347
- Specific characteristics of the high-temperature decomposition of ammonium perchlorate and of ammonium perchlorate-based heterogeneous systems
19 p2471 A73-37503
- Kinetics of the catalytic reactions of the thermal decomposition of perchloric acid and ammonium perchlorate
19 p2402 A73-37505
- Effects of additions of metals and metal borides on the burning rates of mixture systems
19 p2503 A73-37509
- Mechanism of burning in condensed systems with solid additions in a field of mass forces
19 p2472 A73-37510
- Particle combustion mechanism in aluminum-magnesium alloys
19 p2472 A73-37511
- Effects of copper chromite and iron oxide catalysts on AP/CTPB sandwiches.
22 p2899 A73-42812
- Effect of composite propellant catalysts on the stabilities of HClO₄ and the HClO₄-NH₃ system.
22 p2899 A73-42814
- Ammonium perchlorate gasification and combustion at high heating rates and low pressures.
22 p2899 A73-42815
- Formation of a pseudoliquefied layer during combustion of condensed systems with solid nonagglomerating additives in a field of mass forces
24 p3121 A73-44705
- Mechanism of erosive burning of solid rocket propellants.
24 p3121 A73-45385
- AMMONIUM PHOSPHATES**
Struvite precipitation from evaporating sea water with added ammonia, considering importance for prebiotic phosphorylation
07 p0787 A73-19168
- AMMONIUM SULFATES**
Aqueous ammonium sulfate aerosol optical properties via attenuated total reflectance (ATR)/ spectroscopy
17 p2171 A73-35402
- AMMUNITION**
Design criteria for inert or consumable polymer cartridge materials.
15 p1925 A73-31919
- AMORPHOUS MATERIALS**
Amorphous magnetism in F.C.C. Vicalloy II.
01 p0087 A73-10242
- Hot-electron concept for Poole-Frenkel conduction in amorphous dielectric solids.
02 p0201 A73-12817
- Viscoelastic properties of amorphous polymers employed in stress investigations by the optical polarization method
03 p0335 A73-13737
- Heat conductivity dependence on temperature for amorphous and crystalline materials, noting integrodifferential equation for conductive heat transfer and Fourier law
06 p0769 A73-18132
- The process of reinforcement of lead shields in electroradiography
07 p0822 A73-19330
- Reflection spectra of lunar dust grains with amorphous coatings.
07 p0876 A73-19583
- Single-phonon contribution to the hopping conductivity of amorphous solids.
08 p0994 A73-20955
- Amorphous thin films of rare earth transition metal alloys for magneto-optic applications, noting SNR in thermomagnetically written film
11 p1409 A73-26325
- Electron-diffraction study of amorphous condensates of barium titanate
12 p1531 A73-27198
- Spectral and boundary effects on coupled conduction-radiation heat transfer through semitransparent solids.
12 p1559 A73-27695
- Low-temperature relaxations in amorphous polymers.
14 p1765 A73-30134
- Cold rolling of polymers. II - Toughness enhancement in amorphous polycarbonates.
17 p2197 A73-35350
- Small angle X ray scattering study of submicroscopic voids in glassy carbon, using two density theory
19 p2444 A73-38091
- Mechanical properties of polymeric solids.
19 p2444 A73-38549
- Amorphous alloy resistance thermometer development.
22 p2856 A73-42015
- AMORPHOUS SEMICONDUCTORS**
Difference of thermal properties between threshold type and memory type chalcogenide glass semiconductors.
01 p0087 A73-10432
- Russian book on spectral composition-dependent photoconductivity in Hg doped amorphous Se films covering effect of quasi-macroscopic centers in semiconductors
02 p0201 A73-12864
- Pre-threshold conductance and polarization effects in amorphous semiconductor switches.
04 p0427 A73-15343
- Macroscopic inhomogeneities in amorphous semiconductors - Contactless conductivity.
05 p0605 A73-16570
- Electron diffraction investigations of the short-range order in GaAs and GaP films
05 p0605 A73-17291
- Magnetic susceptibility of amorphous semiconductors.
06 p0733 A73-17746
- Impurity concentration relationship to electrons and holes density and potential fluctuations in completely compensated crystalline semiconductors with randomly distributed donors and acceptors
06 p0735 A73-17976
- Preservation of threshold on-regime in amorphous semiconductor threshold switch.
06 p0739 A73-18790
- Preswitching and postswitching phenomena in amorphous semiconducting films.
06 p0739 A73-18800
- Amorphous semiconductor devices, materials, operation and technology, noting nonvolatile and optical memories, radiation and noise immune circuits and dry process photographic applications
07 p0861 A73-19150
- Reversible high speed high resolution imaging in amorphous semiconductors.
07 p0862 A73-19609
- Nature of localized states in amorphous semiconductors - A study by electron spin resonance.
07 p0863 A73-20174
- Electron tunnelling into amorphous germanium and silicon.
07 p0864 A73-20454
- Residual conductivity in unannealed amorphous germanium.
07 p0864 A73-20455
- Amorphous semiconductors for switching, memory, and imaging applications.
09 p1132 A73-21984
- Switching and memory effects in amorphous chalcogenide thin films.
09 p1133 A73-21988
- Amorphous chalcogenide Te-As-Si-Ge thin film switch, discussing pressure effect energy accumulation time delay and behavior after voltage removal
09 p1133 A73-21988
- Application circuits for amorphous semiconductor switching devices with thin film active components, discussing electrical characteristics
09 p1061 A73-21990
- Switching in amorphous selenium.
11 p1407 A73-25147
- Light absorption coefficient of disordered semiconductor within external dc field, discussing electron states near band boundaries
11 p1408 A73-25427
- Switching effect in amorphous semiconductors at discontinuous changes in the heat transfer from the sample.
14 p1783 A73-30434
- Field-dependent carrier transport in non-crystalline semiconductors.
15 p1924 A73-32021
- A doped highly compensated crystal semiconductor as a model of amorphous semiconductors.
16 p2044 A73-33196
- A study of the static S-shaped current-voltage characteristics of chalcogenide glass switching devices
18 p2293 A73-36722
- Papers on materials science covering optical and spectroscopic surface analyses, neutron effects, amorphous semiconductors, high temperature superconductivity, etc
19 p2502 A73-38547
- Photoelectric phenomena in amorphous chalcogenide semiconductors.
20 p2599 A73-39133
- Amorphous material conduction, discussing glass transparency relation to electronic properties, semiconducting glasses and switching behavior
21 p2723 A73-40272
- Certain properties of semiconductor glasses from the Ge-As-Se-Te system
21 p2752 A73-40749
- AC conductivities of amorphous Ge-As-Te and Ge-As-Se systems.
21 p2753 A73-41119
- Three layer semiconductor dielectric interface model of structural and electrical properties of silicon-silicon dioxide system involving amorphous regions
23 p3015 A73-43614
- Structural changes caused in glassy arsenic trisulfide and triselenide by penetrating radiation
23 p3017 A73-44042
- Off state I-V characteristics and thermal switching phenomena for tellurium selenium germanide chalcogenide glass semiconductors, assuming internal heat generation
24 p3119 A73-44407
- AMORPHOUSNESS**
U CRYSTALLINITY
U ELECTRIC CURRENT
U ELECTRIC CURRENT
AMPHIBIA
Comparative physiology of movement-detecting neuronal systems in lower vertebrates /anura and urodela/.
18 p2273 A73-36454
- AMPHIBIOUS AIRCRAFT**
Feasibility and optimization of variable-geometry wing for jet amphibian business aircraft.
[SAE PAPER 730330] 17 p2102 A73-34683
- LA-4 aircraft air cushion landing system ACLS development tests covering static and mobile ground tests, flight tests and performance from and to various surfaces
19 p2382 A73-37692
- AMPHIBIOUS VEHICLES**
NT AMPHIBIOUS AIRCRAFT
AMPLIFICATION
NT POWER GAIN
NT WAVE AMPLIFICATION
Influence of satellite antenna gain on a satellite communications system.
03 p0277 A73-14027
- Amplification of turbulence level by a flame and turbulent flame velocity.
03 p0399 A73-14391
- Amplification of the displacement of Goos-Hanchen by interposition of thin films
03 p0320 A73-14605
- Non-ohmic transport and phonon amplification in polar semiconductors.
04 p0484 A73-16035
- Common emitter/common base cascode amplifier overall gain and frequency response dependence on first transistor parameters
07 p0802 A73-20301
- Synchrotron emission amplification by magnetic field in cosmic sources from analysis of relativistic electron system, noting pulsars and UV Ceti stars
10 p1264 A73-23708
- Positioning accuracy with binary selective and fixed gain manual control systems, using finger stick control for operator performance tests
15 p1840 A73-32583
- French monograph - Contribution to the study of systems with periodically variable parameters in time, intended for the continuous amplification of signals of weak amplitude.
15 p1847 A73-32588
- Optical communication channel optimization with binary signals preamplified in optical parametric amplifier, noting amplifier gain and SNR
17 p2123 A73-35155
- Synchrotron radiation stimulated amplification by magnetic field in cosmic sources from analysis of relativistic electron system, noting pulsars and UV Ceti stars
18 p2347 A73-36733
- Common emitter/common base cascode amplifier overall gain and frequency response dependence on first transistor parameters
18 p2294 A73-37138
- The effect of amplifier gain-bandwidth product on the performance of active filters.
24 p3073 A73-45393

Amplification of magnetostatic surface waves in the YIG-Ge hybrid system. 24 p3120 A73-45431

AMPLIFICATION FACTOR

U AMPLIFICATION

AMPLIFIER DESIGN

Selective differential broadband precision amplifier for weak signals of galvanomagnetic sensor of magnetic induction indicator based on Hall effect 01 p0022 A73-10083

Analysis of a dual-signal balanced TWT amplifier 01 p0025 A73-10988
A wideband transistor amplifier at the 4 GHz band for communication satellite use. 01 p0026 A73-11176

Microwave amplifier design based on negative differential mobility in Gunn diodes 02 p0144 A73-11531

Traveling wave tube for satellite applications. 03 p0281 A73-13174

High-power avalanche IMPATT reflection amplifier using the Rucker combining circuit. 03 p0282 A73-13894

Selectivity evaluation for reflection and transmission regenerative amplifiers of complex design 03 p0284 A73-14034

Bandpass amplifier design with differing two-circuit filters, discussing advantages and limitations 03 p0284 A73-14035

Single circuit amplifier design characterized by cascade connections of transistors to resonance network 03 p0284 A73-14036

Computer-aided design of high-frequency transistor amplifiers. 04 p0427 A73-15053

Low-sensitivity, frequency-selective amplifier circuits for hybrid and bipolar fabrication. 04 p0427 A73-15054

An analytical and empirical basis for the design of turbulence amplifiers. I - Analysis and experimental confirmation. [ASME PAPER 72-WA/FLCS-1] 04 p0408 A73-15859

An analytical and empirical basis for the design of turbulence amplifiers. II - Empirical relationships and design procedure. [ASME PAPER 72-WA/FLCS-2] 04 p0408 A73-15860

Stabilization bandwidth reduction in microwave parallel tuned tunnel diode amplifier circuits synthesis 04 p0429 A73-15919

Method for calculating the delay in a time-service photoelectric phase apparatus. 04 p0451 A73-16019

Computerized synthesis of wideband series stabilized tunnel diode amplifier based on distributed constant elements 05 p0555 A73-16061

Nonreciprocal circulator coupled reflection type microwave amplifier gain and stability characteristics, presenting scattering matrix and signal flow diagram 06 p0673 A73-17590

Book - Transistor-circuit design. 06 p0673 A73-17672

The GaAs traveling-wave amplifier as a new kind of microwave transistor. 06 p0673 A73-17788

Design and characteristics of a single pass normal mode ruby oscillator-amplifier laser for hole drilling in metals. 06 p0700 A73-18277

Low noise VHF preamplifier design for backscatter radar, presenting circuit diagram 07 p0801 A73-19536

A charge amplifier for pressure measurements 07 p0827 A73-20543

Design and performance of transferred electron amplifiers using distributed equalizer networks. 07 p0803 A73-20553

X- and Ku-band amplifiers with GaAs Schottky-barriers field-effect transistors. 07 p0803 A73-20555

1-2 GHz high-power linear transistor amplifier. 08 p0947 A73-21146

Measurement of amplifier noise. 08 p0949 A73-21623

Electrometric amplifiers for inductive measurement of charges 08 p0949 A73-21713

Two stage microwave monolithic integrated circuit power amplifier design with matched transistors, calculating distributed matching network 08 p0950 A73-21826

Design a 4 to 8 GHz FET amplifier with a 7 dB NF. 08 p0950 A73-21827

Interference protection of regenerative parametric amplifiers. 09 p1061 A73-22042

Design criteria for high gain, wide band, microwave amplifiers. 09 p1062 A73-22304

Selective amplifier with zero group delay in pass-band phase characteristics for sinusoidal frequency signal measurement 09 p1066 A73-23118

Long life 100 W triode for ATC and telemetry transponders. 09 p1066 A73-23427

VHF preamplifier with FET for resolving crosstalk and overload problems comparing designed and observed specifications 09 p1066 A73-23429

Amplifier design for continuous recording of plasma frequency, using dipolar resonance signal obtained from parallel whip antennas surrounded by plasma sheath 10 p1216 A73-23747

An electrocardiograph amplifier which satisfies the stringent requirements of long-term monitoring of cardiac activity 10 p1184 A73-23849

Spread of transistor parameters as a factor in the design of IF amplifiers with pairs of staggered stages. 10 p1197 A73-24937

Perturbation theory for multistrip acoustoelectric surface-wave amplifier. 11 p1337 A73-25362

Calculation of the y-parameters of an integrated-circuit amplifier by reducing the matrix of an n-terminal network to the matrix of a two terminal pair network 11 p1338 A73-26102

Microwave transistor power amplifier. 11 p1338 A73-26149

High Q bandpass low sensitivity RC amplifier-filter networks, discussing two-step decomposition of denominator polynomial of second order filter transfer function 11 p1338 A73-26417

Design and performance of deflected-beam electron-bombarded semiconductor amplifiers. 12 p1478 A73-27113

Design of sinusoidal and pulsed signal amplification stages with emitter high-frequency compensation. 12 p1480 A73-27273

Errors of the formal theory of amplifiers with a feedback 12 p1481 A73-27594

Pulse amplifier with active gain adjustment for constant bandwidth 13 p1590 A73-28571

A simple method for obtaining a constant input resistance in broadband amplifiers 13 p1590 A73-28572

Use of approximating polynomials in the determination of correction parameters for pulsed amplifiers. 13 p1591 A73-28732

Synthesis of regenerative amplifiers with isothermal approximation of the amplitude-frequency characteristics 13 p1592 A73-28896

A study of switching process and design parameters of supersonic fluidic amplifiers. 13 p1571 A73-29042

Synthesis of a reflection-type broadband Esaki-diode amplifier using rectangular waveguide. 13 p1594 A73-29229

Relationship between the control range and the variation in passband width in a controlled-gain amplifier with nonlinear shunting of the load 14 p1736 A73-30563

Self-stabilizing power amplifiers with combination-type negative feedback 14 p1736 A73-30564

Wide-band power amplifier for studying the high-frequency properties of plasmas 15 p1850 A73-31497

Harmonic enhancement for airborne low voltage lightweight TWT amplifier band edge performance improvement to provide bandwidth in excess of two octaves 16 p1988 A73-33298

Operational amplifier integrator for storage element in track-hold circuit, discussing drift rate reduction with large equal-value resistors from input terminal to ground 16 p1988 A73-33398

Si transistor amplifier design for power gain stability against temperature variations, considering emitter and collector base voltage as stability parameters 16 p1988 A73-33399

Hydraulic jet amplifier design, considering selector static and dynamic characteristics, membrane attached plate, piston with feedback control and self oscillation elimination 16 p1971 A73-33672

A low noise, very low power charge sensitive amplifier for space applications. 17 p2134 A73-34272

Book - Design of modern transistor circuits. 17 p2134 A73-34458

Cryogenic preamplifier with cooled GaAs junction FET in input stage, discussing application to sensor systems using high impedance cryogenically cooled optical detectors 17 p2137 A73-35219

Broadband TWT microwave amplifier failure modes in airborne systems related to physical mechanism, fabrication processes and field operator handling 17 p2140 A73-35259

Two terminal large signal circular coupled wideband TRAPATT diode microwave amplifiers, noting negative resistance characteristics and dc-to-rf conversion efficiency 17 p2140 A73-35321

Microwave amplifier design with discrete variable components, testing power output and efficiency, bandwidth, and temperature, vacuum and vibration effects on performance 17 p2141 A73-35324

Book - Low-noise electronic design. 17 p2143 A73-35825

A new technique for synthesis of broad-band parametric amplifiers. 18 p2292 A73-36604

A distributed amplifier using bipolar transistors in a common-base circuit 19 p2409 A73-37719

High power transistor amplifier thermal design with heat sink convective and radiant cooling for low junction temperature and long service life 19 p2411 A73-38474

Design and application of low noise GaAs FET amplifiers. 20 p2534 A73-38749

Analysis of a resonant amplifier with stagger-tuned circuits at the input and output 20 p2538 A73-39466

Feedback in microminiaturized transistor amplifiers 21 p2659 A73-40010

Design of MOS-transistor integrated-circuit amplifiers. 21 p2660 A73-40021

The Ebers-Moll effect transistor used as a low-value controlled resistor in ACC and other variable-gain applications. 21 p2661 A73-40229

A universal preamplifier for bioelectric signals 21 p2643 A73-40345

Amplifier with distributed gain for use in radiometry 21 p2700 A73-40540

A 50-W VHF amplifier with transistors 21 p2664 A73-41088

Method of calculating the amplitude and phase-amplitude characteristics of high-frequency amplifiers 21 p2666 A73-41314

Russian book on operation and design of bipolar transistor circuits for video amplifiers covering TV, radar, oscilloscope, automatic control and computer applications 22 p2832 A73-41878

High loop gain operational amplifiers voltage changes as slewing rates using nonlinear circuit model, discussing equivalent circuits, frequency characteristics and bandwidth 22 p2832 A73-41896

Pulse push-pull power amplifier 22 p2833 A73-42361

Signal/noise ratio in the recording of human nerve-action potentials. 22 p2814 A73-42372

Circuit diagram of amplifier-filter for analysis of impulse activity of baroreceptor afferent nerves in rabbits 22 p2816 A73-42681

Microwave cross field and traveling wave tube amplifier characteristics for ECM systems, discussing bandwidth, dual mode, modulation and size and weight tradeoffs 22 p2834 A73-42872

System oscillations from negative input resistance at power input port of switching-mode regulator, amplifier, dc/dc converter, or dc/ac inverter. 22 p2802 A73-42911

Oil hydraulic fluidic amplifier mathematical model and computerized design for power consumption optimization at high pressures, testing performance dependence on viscosity 23 p2942 A73-43405

Optimum design of electron beam-semiconductor linear low-pass amplifiers. II - Output capabilities. 23 p2958 A73-43454

Two channel transistor amplifier design with negative capacitance correction for microelectrode applications 23 p3062 A73-44723

The effect of amplifier gain-bandwidth product on the performance of active filters. 24 p3073 A73-45393

AMPLIFIERS

- NT BEAM PLASMA AMPLIFIERS
- NT BROADBAND AMPLIFIERS
- NT CROSSED FIELD AMPLIFIERS
- NT CURRENT AMPLIFIERS
- NT DIFFERENTIAL AMPLIFIERS
- NT DISTRIBUTED AMPLIFIERS
- NT FEEDBACK AMPLIFIERS
- NT FLUID AMPLIFIERS
- NT INTERMEDIATE FREQUENCY AMPLIFIERS
- NT JET AMPLIFIERS

NT LIGHT AMPLIFIERS
NT LIMITER AMPLIFIERS
NT LINEAR AMPLIFIERS
NT MAGNETIC AMPLIFIERS
NT MICROWAVE AMPLIFIERS
NT PARAMETRIC AMPLIFIERS
NT PHOTOMULTIPLIER TUBES
NT POWER AMPLIFIERS
NT PREAMPLIFIERS
NT PUSH-PULL AMPLIFIERS
NT TRANSISTOR AMPLIFIERS
NT TRAVELING WAVE AMPLIFIERS
NT VOLTAGE AMPLIFIERS

Load amplifiers for vibration and shock measurements

Operational amplifier microcircuits intermittent failure due to input offset voltage drift, describing testing and analysis methods

Computer simulations of the large signal characteristics of supercritical GaAs transferred electron amplifiers.

On the stability of amplifiers with amplitude modulation and overall contrareaction

AMPLITRONS [TRADEMARK]

U PLANOTRONS

AMPLITUDE DISTRIBUTION ANALYSIS

Incident plane wave fluctuations effect on diffraction pattern formed by scattering on reflecting sphere, calculating amplitude distribution in Fresnel and Fraunhofer regions

Equipment for determining the amplitude-frequency characteristics of nonlinear elements in the range of low and extra-low frequencies

Diffraction and nonlinearity characteristics of amplitude holograms for reconstructed nonlinear images on photosensitive layer

On quasi-periodic components with periods from 30 to 60 min of amplitude fluctuations of X-band solar radio emission.

Satellite drag data for analysis of semiannual atmospheric density variations, showing latitudinal dependence of amplitude

Estimation of the cumulative amplitude probability distribution function of ionospheric scintillations.

Antenna radiation pattern synthesis, discussing current phase and amplitude distribution determination by iterative and quadratures solutions respectively

Estimation of the cumulative amplitude probability distribution function of ionospheric scintillations.

Diurnal amplitude variations of equatorial electrojet intensity as functions of solar activity, using 1958 South American observatory data

Amplitude-time and polarization characteristics of the subpulses of pulsar CP 1133.

Amplitudes of mth order holographic images recorded on film with power law characteristics.

Axisymmetric lens design for prescribed radiation amplitude patterns

Passage of useful and noise signals through a nonlinear circuit containing a p-n junction capacitance

Rytov method to predict random vibration amplitude and phase fluctuations range and frequency dependence in Mintzer region, noting applicability domain

Non-Gaussian properties of the EEG during sleep.

Intersynchronization processes in Thomson oscillators with constraints of different nature placed on the amplitudes

Linear FM pulses in chirp radar transmitter, calculating and plotting bounds on amplitude, energy and power spectra for electromagnetic compatibility analysis

High power laser light beam stratification with self induced effects in cubic medium, noting amplitude distribution dependence

Amplitude predistortion and deemphasis filters, measuring channel noise immunity enhancement by mean square deviation

Amplitude discriminator with variable effective range design for use with/without digital computer in neuron pulsed activity analysis

Spatial amplitude distribution of vibrating ribbon two dimensional wake mean, periodic and random velocity components measured in uniform flow by hot-wire anemometry

Amplitude analysis of extensive air shower particle fluxes

Investigation of series pattern-forming circuits for multiple-beam antennas

Synthesis of regenerative amplifiers with isothermal approximation of the amplitude-frequency characteristics

Amplitude characteristics of a helium-neon laser at the 0.63-micron wavelength in the region of strong interaction between two modes.

Holographic visualization of large amplitude vibration using reference beam phase modulation.

Daily variations of the characteristics of beating-type Pc3/Bpc3/ pulsations.

Microwave signal source amplitude stabilization, analyzing circuit with doubly balanced electronically regulated attenuator with p-i-n diodes

Scintillations of satellite signals and their observation.

Some properties of the amplitude frequency characteristics of linear automatic control systems and their control quality under random influences

The electrojet field from satellite and surface observations in the Indian equatorial region.

Diurnal amplitude variations of equatorial electrojet intensity as functions of solar activity, using 1958 South American observatory data

Effect of the amplitude-phase distribution of the field in the aperture of an antenna on its directional properties.

Visualization of the amplitude-phase structure of electromagnetic fields in the millimeter and submillimeter ranges

Ionospheric scintillation at 4 and 6 GHz.

Corrugated horn antenna with high efficiency and monotonic amplitude in microwave pattern ranges applicable as calibrating standard

Amplitude stabilization of pulses from a Q-switched ruby laser by means of interaction with a non-linear medium.

Calculation of the current of a nonlinear element with inertia in the presence of a biharmonic input

The effect of valve area gain on the performance of the hydraulic servomechanism.

Frequency distribution of the parameters of the diurnal variation of the cosmic ray intensity

Research of short-period variations in cosmic rays at Moscow's latitude

On the derivation of Zone I spectra for a pulsed finite-amplitude source operating in a nonviscous non-dispersive fluid medium.

Root-mean-square signal amplitude variation measurements of LF radio emission from extensive air showers by whip antenna

Level transgressions and extremal values of continuous stochastic signals

Oscillation amplitude curve determination of negative resistance oscillator connected to LC circuit, obtaining device I-V characteristics

The effect of interaction of array elements with arbitrary amplitude distribution on the radiation pattern.

Measurement of the gain distribution in a helium-neon laser /0.63-micron wavelength/ cell during high-frequency pumping

Variation of amplitudes of thermo-acoustical waves of arbitrary form in isotropic linear thermo-elastic materials.

AMPLITUDE MODULATION

Amplitude modulation of electromagnetic waves by acoustic waves in a dispersive plasma - Modified theory.

Required carrier-to-interference ratios for frequency sharing between frequency-modulation television signal and amplitude-modulation vestigial sideband television signal.

Superconducting time variant filter tracking test for RF signal amplitude modulation, using photodiodelectric perturbation in semiconductor cavity resonant frequency

Variance estimate of random process second order moment by nonlinear correlator in presence of additive amplitude and phase modulated and normal noise processes

Synthesis of an optimal receiver structure for amplitude modulated pseudo-noise signals.

LF spectrum of plasma oscillations from amplitude modulation of plasma SHF radiation, noting Langmuir and magnetoacoustic waves interaction

Quadrature amplitude-shift key satellite communication feasibility based on SNR and transmitter power efficiency comparison with multiphase-shift key system

Pulsed random process energy spectra methods for spectral distribution of signal power in multichannel AM, FM and PM PCM systems with time division multiplexing

Intelligible crosstalk and AM-PM transfer in commercial communication satellites. II

Characteristics of acousto-optic cavity dumping in a mode-locked laser.

Reduction of phase non linearities in Traveling Wave Tubes /TWT/.

Amplitude-phase-keying with M-ary alphabets - A technique for bandwidth reduction.

The effect of carrier phase and timing on a single-sideband data signal.

Influence of signal amplitude changes in systems with phase and frequency modulation

On the stability of amplifiers with amplitude modulation and overall contrareaction

Transient characteristics of simple systems to modulated random noise.

[ASME PAPER 72-APM-FFF] Experimental investigation of the AM-FM distortions of a signal passing through a linear filter

Short term frequency stability and single sideband phase noise measurements on signal generators, considering frequency deviation and amplitude modulation produced by noise

Amplitude modulation effects of the Doppler return at low altitudes.

Intelligibility improvement of analog communication systems using an amplitude control technique.

Signal interference and improvement of signal-to-noise ratios in a half-wave linear detector.

High-frequency oscillation passage through a circuit with modulated damping

Effect of bandlimiting on the noncoherent detection of Amplitude-Shift Keying /ASK/ signals.

A modulation technique for measuring small disturbances in the upstream flow field of a sharp leading edge in a rarefied hypersonic flow.

Electron beams as carriers of optical coherence.

Modulation of gallium arsenide laser diodes

Second harmonic amplitude modulation of an electromagnetic wave by an acoustic wave in a dispersive plasma.

Intrinsic AM noise in singly tuned IMPATT diode oscillators.

Diffraction grating model in terms of amplitude and phase modulation to explain angular spectrum of light reflection from corrugated surface for various incidence angles

Modulation of spectrum and amplitude of VLF signal in the magnetosphere.

Sequence amplitude modulated inverters.

High order nonlinear effects in a gas laser - Saturation anomaly observable on a J equals 1 - J equals 2 transition 22 p2871 A73-43084

Inferior colliculus neuron responses to an amplitude-modulated signal with varying intensity levels 24 p3061 A73-45248

AMPLITUDE PROBABILITY ANALYSIS

U AMPLITUDE DISTRIBUTION ANALYSIS

AMPLITUDES

NT PULSE AMPLITUDE

NT SCATTERING AMPLITUDE

Finite amplitude waves on aircraft trailing vortices. 02 p0129 A73-12506

Characteristics of amplitude discriminators built with transistors operating in the avalanche mode 12 p1479 A73-27209

Method of calculating the amplitude and phase-amplitude characteristics of high-frequency amplifiers 21 p2666 A73-41314

Wave amplitude calculation for propagation in inhomogeneous isotropic media by optical ray tracing consisting of integration of first and second order differential equations 22 p2885 A73-41817

AN-2 AIRCRAFT

An-2R aircraft conversion to flying test bed for feasibility studies of jet engine use in agricultural aircraft, describing structural design modifications 12 p1458 A73-26823

AN-24 AIRCRAFT

Russian book - Practical aerodynamics of the An-24 aircraft /2nd revised and enlarged edition/. 15 p1829 A73-31547

ANACLINAL STREAMS

U STREAMS

ANACLINAL VALLEYS

U VALLEYS

ANAEROBES

The occurrence of nitrate on the early earth and its role in the evolution of the prokaryotes. 11 p1320 A73-26490

ANALOG CIRCUITS

Analog signal to discrete time interval converter /ASDTC/ feedback control for high performance aerospace power supply conditioning [AIAA PAPER 72-1057] 04 p0486 A73-14901

Ligidyn analog components regulator systems for industrial current and speed control, amplifier output voltage control, digital-analog converters, analog storage devices, etc 05 p0556 A73-16075

Dynamic response of digital-analog flow measurement system based on turbine driven pulse generator as sensor element 07 p0828 A73-20545

Subjective comparisons of analog and digital TV transmission system, considering spectral occupancy and picture quality 09 p1055 A73-23387

Jet deviation fluidic analog amplifiers, noting industrial application to pressure, flow rate and dimensional measurements 11 p1308 A73-25379

Effectiveness of analog storage in the detection of signals on a background of noise and strong random pulsed interference 12 p1467 A73-26942

Analog voltage squaring circuits with series-connected resistors shunted by semiconductor diodes or ladder network, discussing design, construction and operation principles 12 p1481 A73-27591

A new zero-beat indicator and its use in frequency measurements 13 p1617 A73-28859

Active analog bandpass RC and LC filters design calculation by wave parameters 13 p1592 A73-28875

Investigation of an analog memory for the computational-measurement complex of an electrodynamic model 13 p1588 A73-29420

Analog transducers based on monocrystalline silicon semiconductors piezoresistivity properties, describing various piezo-FET circuits 14 p1751 A73-29728

Construction principles of a controlled universal functional converter for a hybrid computer 15 p1848 A73-31805

Differential equations modelled on nonalgorithmic digital computers. 19 p2408 A73-38144

COS/MOS phase-locked-loop - A versatile building block for micro-power digital and analog applications. 20 p2534 A73-38657

Extraction of Tscheysheff design data for the low-pass dielectric multilayer. 21 p2665 A73-41135

A study of the physics and non-linear effects in photomultipliers. 22 p2860 A73-42302

Signal transmission in analog fluidic systems mainly with respect to noise influence. 23 p2944 A73-43421

A galvanomagnetic analog device for extracting square roots 24 p3070 A73-45101

Four-quadrant analog multiplier synthesis for IC implementation based on logarithmic addition in all n-p-n bipolar transistor configuration for algebraic product derivation 24 p3074 A73-45260

Design of a controlled general-purpose functional converter for a hybrid computer system. 24 p3071 A73-45349

ANALOG COMPUTERS

Analog computer regression line and correlation ratio determination for random stationary processes with time lag 01 p0028 A73-10928

Solution of navigation problems with a hybrid analog computer 01 p0075 A73-11400

A comparison of analog and digital techniques for pattern recognition. 01 p0021 A73-11478

Improvement of the product accuracy in analog multipliers with the aid of the negative-feedback principle 06 p0672 A73-17400

A hybrid analog computer for schooling in control technology 07 p0796 A73-20302

Realization of digital differential analyser on the basis of multifunction memory units. 10 p1198 A73-24018

Analog computer regression line and correlation ratio determination for random stationary processes with time lag 10 p1201 A73-24188

Hybrid computer systems of high speed and accuracy 10 p1192 A73-24674

Nonalgorithmic design and coding system for digital mathematical machines for accuracy and speed compatible with digital and analog computer, respectively. 11 p1334 A73-25626

Application of nonalgorithmic digital machines in modeling differential equations 11 p1334 A73-25633

Application of analog and digital computers to fatigue testing. 13 p1622 A73-29547

A posteriori estimates of error distribution laws in the solution of linear algebraic equations by analog techniques 14 p1768 A73-30032

Accuracy estimates for analog computer solutions to systems of ordinary linear equations and some algebraic equations 14 p1768 A73-30033

A reflectance analog computer for the determination of thin film optical properties. 17 p2132 A73-35773

Correctness of the solution of signal filtration and reconstruction problems by an analog computer 20 p2522 A73-38702

A simple cardiac contractility computer. 22 p2815 A73-42677

ANALOG DATA

Coherent and non-coherent optical processing of analog signals. 06 p0667 A73-18313

Reconstruction of analog signals and choice of sampling rates in telemetry. 09 p1058 A73-23421

Continuous analog signals optimal discretization involving selected quantization steps and sampling rates 13 p1595 A73-28017

Intelligibility improvement of analog communication systems using an amplitude control technique. 14 p1726 A73-29901

Central digital measuring and data logging systems for electrical and nonelectrical analog signal conversion, display and recording 15 p1849 A73-32204

Laboratory for the automatic treatment of analog signals 18 p2297 A73-37086

Noise immunity of digital methods for the transmission of analog messages with an enhanced information content 20 p2531 A73-39463

Russian book on radio telemetry systems analysis and theory covering analog and digital data, signal processing, algebraic and trigonometric polynomials and discrete representations 22 p2824 A73-41879

Tape recording, off-line digitalization and time series analysis of dynamic field measurement analog data for computerized power spectral density calculation 22 p2859 A73-42197

ANALOG SIMULATION

Design and modeling of periodic magnetic systems for SHF devices. I, II 01 p0025 A73-10981

Comparative simulator studies regarding a contact-analog channel display and conventional instrumentation [DGLR PAPER 72-100] 02 p0150 A73-11680

Analog computer study of the effect of initial conditions on the excitation and sustaining of lower harmonic oscillations in a single-phase electroferromagnetic oscillatory circuit 02 p0147 A73-12352

Simulation of rendezvous of a man in deep space. 03 p0288 A73-13569

Analog simulation for transient and steady state performance of group-triggered cycloconverter supplying controlled slip induction motor, discussing commutation failures 03 p0253 A73-13932

Analog-analytic construction of supercritical flows past profiles [DGLR PAPER 72-129] 03 p0248 A73-14384

Modeling of nonlinear systems for the example of a single-shaft jet turbine engine 03 p0360 A73-14615

Problems in modeling fuel systems for turbine engines 03 p0258 A73-14616

Model studies of an electrohydraulic amplifier 03 p0258 A73-14617

Analog simulation and design of single- and multiple input/output model reference adaptive systems, using hyperstability concept [ASME PAPER 72-WA/AUT-13] 04 p0432 A73-15881

Nonlinear modeling and dynamic simulation of vehicle air cushion suspensions. 04 p0406 A73-15883

Nonlinear analysis for local microwave oscillator voltage waveform across nonlinear junction of Schottky barrier mixer diode, comparing results with analog simulation 06 p0677 A73-18740

Unsteady heat transfer in dispersion media at small values of time 08 p1021 A73-20994

Designing electrical analogs for solving a hyperbolic energy equation 08 p1022 A73-20999

Investigation of the operation of a polarographic sensor under the action of surge-type polarizing voltage, using an electric analog 08 p0965 A73-21107

Analog, digital and hybrid simulation of a planetary boundary layer meteorological forecast model. 09 p1114 A73-22333

Inertialess smoothing of multiplier signals in automatic control system under sinusoidal signal, noting analog simulation of inertialess synchronous detector for self adaptive control 09 p1069 A73-22654

Transfer function model for analog simulation of transient unsteady heat conduction through flat and cylindrical walls, optimizing moving polymer film heating 11 p1451 A73-25732

Differential equations of motion for analog model of M-type TWT performance, proposing block diagram for electron phase and trajectory and field distribution calculations 12 p1478 A73-26950

Control systems synthesis via digital computer techniques, describing numerical optimization procedure and analog simulation method 14 p1730 A73-30921

An analog computer study of a thyristor inverter with opposite-parallel diodes under load switched-on between input throttles 15 p1851 A73-31697

Wideband VHF whip antenna impedance simulation using A1 cylindrical chamber to simplify impedance-controlling network tuning and power testing 17 p2148 A73-35705

Analysis of some functional parameters of rotary hydrostatic engines under dynamic conditions by modeling on a computer 19 p2388 A73-37557

Fine pointing performance characteristics of the Orbiting Astronomical Observatory /OAO-3/. [AIAA PAPER 73-869] 20 p2587 A73-38807

Dynamic stability of a nonlinear beam subjected to both longitudinal and transverse excitation. 20 p2621 A73-39532

Washout circuit design for multi-degrees-of-freedom moving base simulators. [AIAA PAPER 73-929] 21 p2674 A73-40876

Identification and simulation of antenna dynamics. 21 p2667 A73-41525

Russian book on scale selection in modeling for analog and digital computers covering similarity theory, error formation, accuracy optimization, etc 22 p2829 A73-41883

An analogue-computer simulation of the facultative water-reabsorption process in the human kidney - A vascular role for a.d.h. 22 p2815 A73-42668

ANALOG TO DIGITAL CONVERTERS

On the electronic simulation of acceleratory nystagmus.

22 p2816 A73-42683

Dynamic behaviour and z-transform stability analysis of dc/dc regulators with a non linear P.W.M. control loop.

22 p2837 A73-42912

Electronic simulation and analog computer studies of the influence of temperature on the process of nerve impulse shaping

24 p3062 A73-44725

Determination of performance precision and informativeness of electronic models of the sensory system of man

24 p3064 A73-44911

Hemoglobin-oxygen equilibrium and coronary blood flow - An analog model.

24 p3064 A73-45060

ANALOG TO DIGITAL CONVERTERS

Digital apparatus for telemetry of pressure

01 p0044 A73-10034

Periodic motions elimination in servo driven analog to digital converters on phase plane, noting dependence on autoscillations in relay system with time lag

02 p0148 A73-11862

A hybrid broad-band EEG frequency analyzer for use in long-term experiments.

04 p0411 A73-14847

Wideband high-speed high-resolution analog to digital converters technology developments, discussing voltage addressable read-only memory concept and related data sampling

10 p1177 A73-23792

Statistical synthesis of digital parameter-measuring equipment and analysis of its efficiency

11 p1360 A73-25021

An analog-code follow-up converter based on second-harmonic magnetic modulators

12 p1475 A73-26766

Devices for primary processing of information in controller machines, based on the principles of quantum magnetometry

12 p1495 A73-26778

A group converter of alternating-current signals into a code for control systems

12 p1475 A73-26780

Three axis fluxgate magnetometer/analog to digital converter system onboard Explorer D and E for measuring magnetic fields in auroral zone and equatorial electrojet

13 p1689 A73-28643

Problems involving efficient transmission of informative parameters in the adaptive discretization of an analog signal

13 p1583 A73-28852

A method of assigning noise-resistant analog-to-digital converters

15 p1848 A73-31915

HYPHA analog-to-digital converters with phase-locked loops.

16 p1991 A73-32719

Third generation Aircraft Recording Instrumentation System /ARIS III/, consisting of digitizer and logic, analog interface and hybrid instrumentation recorder

17 p2174 A73-35581

Analog to digital converters with logarithmic input-output law, comparing performance and complexity of various realizations

21 p2658 A73-41145

Fluidic circuits application to stochastic computer with analog to digital converter and logic gates for arithmetic operations

23 p2944 A73-43419

Fluidic vortex-type proximity sensor with analog to digital converter, optimizing output nozzle diameter and pressure by steepest ascent method

23 p2981 A73-43431

ANALOGIES

NT HYDRAULIC ANALOGIES

Reasoning by analogy as an aid to heuristic theorem proving.

01 p0020 A73-11453

Energy absorption in cold inhomogeneous plasmas - The Herlofson paradox.

09 p1126 A73-22276

Classical mechanics-quantum mechanics relations and analogies, considering symmetry groups, Casimir invariants, energy levels and quantization

14 p1774 A73-30239

Electrical network analogy application to thermal energy steady diffusion within Knudsen gas filled enclosure, discussing free molecule limit and transition regime

15 p1959 A73-32283

Electric analogy procedure for simulating heat and mass transfer processes

16 p2085 A73-33380

A nonlinear oscillator analog of rigid body dynamics.

18 p2337 A73-36416

Investigation of the distribution of synaptic inputs on an analog model of the motoneurons

19 p2399 A73-37942

ANALYSIS [MATHEMATICS]

NT ABEL FUNCTION

NT AIRY FUNCTION

NT ANALYTIC FUNCTIONS

NT APERIODIC FUNCTIONS

NT ASYMPTOTES

NT ASYMPTOTIC SERIES

NT BANACH SPACE

NT BESSEL FUNCTIONS

NT BIHARMONIC EQUATIONS

NT BINARY INTEGRATION

NT BLASIUS EQUATION

NT BOREL SETS

NT BURGER EQUATION

NT CALCULUS

NT CALCULUS OF VARIATIONS

NT CAUCHY INTEGRAL FORMULA

NT CAUCHY-RIEMANN EQUATIONS

NT CHANDRASEKHAR EQUATION

NT COLLINEARITY

NT COMBINATORIAL ANALYSIS

NT COMPLEX VARIABLES

NT CONFORMAL MAPPING

NT CONJUGATES

NT CONTINUITY [MATHEMATICS]

NT CONVOLUTION INTEGRALS

NT COPLANARITY

NT CURL [VECTORS]

NT DELTA FUNCTION

NT DEPENDENT VARIABLES

NT DIFFERENTIAL CALCULUS

NT DIFFERENTIAL EQUATIONS

NT DUFFING DIFFERENTIAL EQUATION

NT EINSTEIN EQUATIONS

NT ELLIPTIC DIFFERENTIAL EQUATIONS

NT ELLIPTIC FUNCTIONS

NT ENTIRE FUNCTIONS

NT EXISTENCE THEOREMS

NT EXPONENTIAL FUNCTIONS

NT EXTREMUM VALUES

NT FALKNER-SKAN EQUATION

NT FOKKER-PLANCK EQUATION

NT FOURIER ANALYSIS

NT FOURIER SERIES

NT FOURIER TRANSFORMATION

NT FREDHOLM EQUATIONS

NT FUNCTION SPACE

NT FUNCTIONAL ANALYSIS

NT FUNCTIONAL INTEGRATION

NT GAMMA FUNCTION

NT GAUSS EQUATION

NT GREEN FUNCTION

NT HALF PLANES

NT HALF SPACES

NT HANKEL FUNCTIONS

NT HARMONIC ANALYSIS

NT HARMONIC FUNCTIONS

NT HELMHOLTZ VORTICITY EQUATION

NT HILBERT SPACE

NT HILBERT TRANSFORMATION

NT HYPERBOLIC FUNCTIONS

NT HYPERGEOMETRIC FUNCTIONS

NT HYPERPLANES

NT INTEGRAL CALCULUS

NT INTEGRAL EQUATIONS

NT INTEGRAL TRANSFORMATIONS

NT JACOBI INTEGRAL

NT JACOBI MATRIX METHOD

NT KERNEL FUNCTIONS

NT LAGUERRE FUNCTIONS

NT LAME WAVE EQUATIONS

NT LAPLACE TRANSFORMATION

NT LEBESGUE THEOREM

NT LEGENDRE FUNCTIONS

NT LIAPUNOV FUNCTIONS

NT LIMITS [MATHEMATICS]

NT LINEAR EQUATIONS

NT LIOUVILLE EQUATIONS

NT LIOUVILLE THEOREM

NT LIPSCHITZ CONDITION

NT LOGARITHMS

NT MATHIEU FUNCTION

NT MAXIMA

NT MEASURE AND INTEGRATION

NT MEMORPHIC FUNCTIONS

NT NEUMANN PROBLEM

NT NONHOLONOMIC EQUATIONS

NT NONLINEAR EQUATIONS

NT NUMERICAL ANALYSIS

NT NUMERICAL INTEGRATION

NT ORTHOGONAL FUNCTIONS

NT PADE APPROXIMATION

NT PARABOLIC DIFFERENTIAL EQUATIONS

NT PARTIAL DIFFERENTIAL EQUATIONS

NT PERIODIC FUNCTIONS

NT PFAFF EQUATION

NT PHASE-SPACE INTEGRAL

NT POISSON EQUATION

NT POWER SERIES

NT PRONY SERIES

NT QUADRATIC EQUATIONS

NT RATIONAL FUNCTIONS

NT REAL VARIABLES

NT RUNGE-KUTTA METHOD

NT SCHWARZ-CHRISTOFFEL TRANSFORMA-

TION

NT SERIES [MATHEMATICS]

NT SINGULAR INTEGRAL EQUATIONS

NT SINGULARITY [MATHEMATICS]

NT SPHERICAL HARMONICS

NT STIELTJES INTEGRAL

NT STURM-LIOUVILLE THEORY

NT TAYLOR SERIES

NT TESSERAR HARMONICS

NT TRIGONOMETRIC FUNCTIONS

NT VECTOR ANALYSIS

NT VLASOV EQUATIONS

NT VOLTERRA EQUATIONS

NT VORTICITY

NT WEIERSTRASS FUNCTIONS

NT WEIGHTING FUNCTIONS

NT WHITTAKER FUNCTIONS

NT WIENER HOPF EQUATIONS

NT ZONAL HARMONICS

ANALYSIS OF VARIANCE

Radio oscillators short term frequency instability, examining relations between time domain and frequency domain sample variance definitions

07 p0798 A73-19176

Threshold variance analysis of monocular vs binocular visual stimulation in apparent movement perception

07 p0783 A73-20262

Calibration of resistance strain gauges

07 p0828 A73-20538

Computerized trajectory estimation for maneuvering reentry vehicles, obtaining minimum variance trajectory parameters by Kalman filtering of radar, optical and inertial reference measurements [AIAA PAPER 73-902]

20 p2589 A73-38836

Prediction equation validity for response surface methodology analysis of surveillance tracking by human operators, comparing variance and regression procedures

24 p3063 A73-44776

Spectral analysis of frequency noise of oscillators by the Hadamard variance

24 p3073 A73-44974

ANALYTIC FUNCTIONS

NT ENTIRE FUNCTIONS

Theorems on general fluid particle vorticity acquisition by nonanalytic process

03 p0292 A73-13309

A new method of obtaining Q solutions to extremal problems in certain special classes of analytic functions associated with functions whose real part is positive in a circle

04 p0470 A73-15083

Existence of analytic solutions of partial differential equations with constant coefficients in an arbitrary number of variables

05 p0591 A73-17246

Solution stability of autonomous differential equations with holomorphic members under perturbation by time dependent auxiliary functions

06 p0724 A73-18683

On the approximation of the optical modulation transfer function (MTF) by analytical functions.

07 p0786 A73-20264

Certain properties of functions with a non-zero difference quotient

09 p1112 A73-22887

Analytical properties of solutions to linear differential equations and systems

12 p1516 A73-26951

A method for studying the completeness of systems of analytic functions

12 p1516 A73-26960

Inverse problems of a logarithmic potential with analytic closeness

12 p1518 A73-27729

Two dimensional flow of viscous incompressible fluid, discussing formulation in analytic functions with applications to flows past elliptic cylinder and flat plates

13 p1603 A73-29048

Classification theorem for analytical transformations of second order differential equations of motion at arbitrary resonance based on group theory

13 p1661 A73-29081

Unified geometric and analytical treatment of magnetogasdynamics shocks. I - General solutions and theorems.

15 p1917 A73-31339

Solution of certain classes of three-dimensional problems in elasticity theory with the aid of analytic functions

15 p1952 A73-32077

General linear boundary value problem with measurable coefficients for numerous analytical functions of class E sub p

15 p1900 A73-32092

The global aspect of the complex analysis in the theory of the morphic functions

15 p1900 A73-32106

Keraug near-ground wind profiles approximation by Monin-Obuchov universal function, obtaining solutions for turbulent heat flux and shear flow velocity

15 p1906 A73-32343

Singularities of solutions to linear, second order, analytic elliptic equations in two independent variables. II - The piecewise regular boundary.

15 p1901 A73-32374
Dolapchiev-Mangeron-Tsenov analytical mechanics equations extension to potential force systems, applying to electric charge motion in electromagnetic field

16 p2035 A73-32681
Half plane stress boundary value problems in elastodynamics, obtaining similarity solutions in terms of analytic functions via integral transforms

16 p2082 A73-33903
A new fundamental system of modified cylindrical functions for an annular region.

17 p2200 A73-34248
Quaternions equations and hypercomplex potentials in continuous medium mechanics

17 p2201 A73-34793
Computation of the exponential of a matrix. I - Theoretical considerations.

17 p2203 A73-35521
Boundary value problem of the E problem type for mixed equations of the second kind

17 p2203 A73-35588
Classification theorem for analytical transformations of second order differential equations of motion at arbitrary resonance based on group theory

19 p2445 A73-37632
Nonlinear boundary value problem with permissible zeros on the contour

20 p2582 A73-39206
The symmetry method and its application to plane problems of elasticity theory

20 p2618 A73-39325
Fundamental integral representation of x-analytic functions and its application to the solution of some integral equations

20 p2583 A73-39497
Numerical evaluation of integrals around simple closed curves.

21 p2725 A73-40378
Nonlinear eigenvalue problem of square matrix of analytic functions of complex number lambda, comparing algorithms convergence by numerical tests

21 p2725 A73-40380
Geophysical field cartographic isoline recording via least generalized course representation of observation points, discussing analytic functions and least squares method

22 p2850 A73-42734
Continuous dependence of holomorphic functions on partially given boundary values.

23 p3000 A73-44302
Line of symmetry for the classical equation of state.

24 p3110 A73-44987
The Cauchy problem and a general representation of solutions to an elliptic-type fourth-order equation with analytic coefficients

24 p3106 A73-45508
Solution of a mixed axisymmetric problem for an elastic ellipsoid of revolution by the method of p-analytic functions

24 p3153 A73-45509
Certain theorems concerning functions of an incomplete quaternion variable

ANALYTIC GEOMETRY

NT EPICYCLOIDS
NT OBLATE SPHEROIDS
NT PARABOLAS
NT PROLATE SPHEROIDS
NT QUADRANTS
NT SPHEROIDS
NT TORUSES

Elliptical, annular, through, part-through and irregularly shaped crack front curvature effect on stress intensity factor calibration

04 p0506 A73-14682
A geometric solvability characteristic for some boundary value problems of linear elliptic-type equations and strongly elliptic second-order systems

ANALYTICAL CHEMISTRY

Russian book - Spectrophotometry of niobium and tantalum.

ANALYZERS

NT ENGINE ANALYZERS
NT SIGNAL ANALYZERS

Computerized flying spot scanner/analyzer for automatic mensuration analysis of droplets, particles and cell preparations from 35 mm film density distributions

03 p0309 A73-14449
Ion microprobe analyzers for solid surfaces high resolution mass spectrometric chemical analysis, using focused ion beam sputtering technique

07 p0822 A73-19171
Neuron analyzer technique for poststimulus histogram plotting of neuron excitation as function of stimulus onset time

10 p1183 A73-23811
Device for analyzing the electrical activity of nerve fibers in intact nerves

10 p1183 A73-23812

Investigation of a planar analyzing system employing laser illumination for facsimile transmitters

13 p1627 A73-28857

ANATOMY

NT ADRENAL GLAND
NT AORTA
NT ARM [ANATOMY]
NT ARTERIES
NT BARORECEPTORS
NT BLOOD VESSELS
NT BONES
NT BRAIN
NT BRAIN STEM
NT BRONCHI
NT CAPILLARIES [ANATOMY]
NT CARDIAC AURICLES
NT CARDIAC VENTRICLES
NT CARDIOVASCULAR SYSTEM
NT CEREBELLUM
NT CEREBRAL CORTEX
NT CEREBRUM
NT CHEMORECEPTORS
NT CIRCULATORY SYSTEM
NT COCHLEA
NT COLLAGENS
NT CONNECTIVE TISSUE
NT CONSTRICTORS
NT CORNEA
NT CORTI ORGAN
NT CRANIUM
NT DIAPHRAGM [ANATOMY]
NT DIASTOLE
NT EAR
NT EARDRUMS
NT ELBOW [ANATOMY]
NT EOSINOPHILS
NT ERYTHROCYTES
NT ESOPHAGUS
NT EYE [ANATOMY]
NT FINGERS
NT FLEXORS
NT FOREARM
NT FOVEA
NT GENITOURINARY SYSTEM
NT GLANDS [ANATOMY]
NT GLOMERULUS
NT GONADS
NT GRAVIRECEPTORS
NT HAND [ANATOMY]
NT HEAD [ANATOMY]
NT HEART
NT HEMATOPOIESIS
NT HEMATOPOIETIC SYSTEM
NT HIPPOCAMPUS
NT HUMAN BODY
NT INTRACRANIAL CAVITY
NT JOINTS [ANATOMY]
NT KIDNEYS
NT KNEE [ANATOMY]
NT LABYRINTH
NT LEG [ANATOMY]
NT LIMBS [ANATOMY]
NT LIVER
NT LUNGS
NT LYMPHOCYTES
NT MECHANORECEPTORS
NT MIDDLE EAR
NT MUSCULOSKELETAL SYSTEM
NT MYOCARDIUM
NT NECK [ANATOMY]
NT NOSE [ANATOMY]
NT OCULOMOTOR NERVES
NT ORGANS
NT OTOLITH ORGANS
NT PANCREAS
NT PELVIS
NT PHOTORECEPTORS
NT PINEAL GLAND
NT PITUITARY GLAND
NT PUPILS
NT RESPIRATORY SYSTEM
NT RETICULOCYTES
NT RETINA
NT SEMICIRCULAR CANALS
NT SENSE ORGANS
NT SKULL
NT SYSTOLE
NT TESTES
NT THERMORECEPTORS
NT THYROID GLAND
NT TORSO
NT ULNA
NT VASCULAR SYSTEM
NT VEINS
NT VERTEBRAE
NT VERTEBRAL COLUMN
NT VESTIBULES

Book - How man moves: Kinesiological studies and methods.

03 p0268 A73-13993

ANDESITE

Investigation of the possibility of obtaining andesite-based alkali-resistant glass compositions for a continuous glass fiber

23 p2998 A73-44298

ANDROMEDA GALAXIES

Low frequency radio observations of the Andromeda Galaxy.

01 p0096 A73-10313
The spiral arm structure on the southwestern border of M31

02 p0227 A73-12840
Variation of emission-line strengths across M31.

03 p0366 A73-12928
Luminous blue variables in M 31 and 33, discussing light curves, color index and luminosity

09 p1141 A73-22014
Andromeda galaxy absorbing material distribution obtained with population I cepheids in Baade four variable star fields

13 p1671 A73-28031
The dynamics of the Andromeda Nebula.

15 p1941 A73-32400

ANEOCHOIC CHAMBERS

Anechoic funnel and rectangular chambers for antenna measurements

06 p0674 A73-17822
French project of anechoic chamber with wind tunnel for studying jets, turbojets blowers, helicopter rotors and V/STOL aircraft

08 p0953 A73-21529
Wind tunnel acoustic and vibration test facilities, including anechoic chambers, subsonic boundary layer tunnels, acoustic ducts, reverberation rooms, and rotor noise chambers

17 p2148 A73-35334
Electromagnetic wave absorbers and anechoic chambers through the years.

17 p2128 A73-35683
Radio anechoic chamber reflectivity level evaluation, comparing antenna pattern method and free space voltage standing wave ratio technique

17 p2128 A73-35684
Reflection characteristics of quasi-tapered anechoic chamber at VHF and EHF, evaluating broadband response, radar cross sections and field in quiet zone

17 p2129 A73-35701
Subsonic jet noise measurements on model jet rig in anechoic chamber, discussing correlation and prediction

19 p2473 A73-38106
The design and construction of an anechoic chamber lined with panels and intended for investigation of aerodynamic noise

21 p2674 A73-40942

ANELASTICITY

Resonance type facility using dynamic hysteresis loop method to test metal fatigue and anelasticity in torsion at room and high temperatures

03 p0288 A73-14025
Role of the anelastic behavior of the ablation material on cross-hatching.

03 p0398 A73-14189
Influence of the dose of neutron irradiation on the anelastic behavior of an aluminum deformed at 80 K

06 p0710 A73-18542
Amplitude-dependent anelasticity in aluminum and copper single crystals

10 p1231 A73-23693
Prediction of inelastic high temperature materials behavior by strain-rate approach.

11 p1450 A73-25515
[AIAA PAPER 73-386]
Amplitude-dependent anelasticity in aluminum and copper single crystals. II - Studies in amplitude range III during and after plastic deformation

11 p1385 A73-26567
Inelastic buckling of columns - The effect of imperfections.

16 p2084 A73-33975
Anelastic studies of hydrogen diffusion in niobium.

17 p2193 A73-35622
Laws governing the behavior of the electrical resistance during process of inelastic-strain relaxation

23 p3040 A73-43574

ANEMOMETERS

NT HOT-FILM ANEMOMETERS
NT HOT-WIRE ANEMOMETERS
NT SONIC ANEMOMETERS

Instrument requirements for eddy correlation measurements.

01 p0052 A73-11057
Turbulence measurements with a laser anemometer measuring individual realizations.

02 p0168 A73-12057
Laser Doppler anemometer theory and application to radial flow velocity measurement in oscillating boundary layer in front of blunt body

02 p0171 A73-12559
Laser anemometry in an unseeded supersonic wind tunnel by means of photon correlation spectroscopy of backscattered light.

02 p0172 A73-12860
Laser anemometry developments review covering reference-beam, fringe and single-beam modes optical arrangements, signal processing systems and light scattering particles

03 p0308 A73-13535
Optical anemometers applicability to steady atomized fuel sprays, obtaining particle velocity profiles and probability density distributions

05 p0565 A73-16761

- Propeller anemometers as sensors of atmospheric turbulence. 06 p0695 A73-18329
- Broadening of the measured frequency spectrum in a differential laser anemometer due to interference plane gradients. 08 p0967 A73-21596
- Lidar anemometry and atmospheric sounding [ONERA, TP NO. 1151] 08 p0986 A73-21680
- Thermoanemometer errors in turbulent wind velocity pulsations measurement 11 p1367 A73-26436
- A study of systematic errors in measurements with the constant-temperature anemometer in high-turbulence flows with and without hot-wire signal linearization. 13 p1613 A73-28529
- Experimental measurement of ambiguity noise in a laser anemometer. 13 p1622 A73-29641
- Cup anemometer input/output frequency characteristics, determining nonlinear behavior via inertia considerations 15 p1879 A73-32345
- A modified interferometer for vibration amplitude measurement. 16 p2013 A73-32878
- Laser anemometer for the measurement of air flow velocities 17 p2167 A73-34775
- Corrections for response errors in a three-component propeller anemometer. 18 p2316 A73-36710
- Fluidic jet deflection anemometer design and tests of directional wind velocity measurement in rain/sand environments 23 p2981 A73-43429
- Equipment for measuring local plasma flow parameters by a thermoanemometer probe 24 p3089 A73-44761
- ### ANEMOMETRY
- #### U VELOCITY MEASUREMENT
- ### ANESTHESIA
- Effects of anesthesia and muscle paralysis on respiratory mechanics in normal man. 08 p0934 A73-21505
- Accommodation of the eye during sleep and anesthesia. 14 p1716 A73-30391
- ### ANGELS
- Radar angels cross section statistical distribution model based on radar measurement and direct ornithological data on bird populations density 11 p1332 A73-26630
- ### ANGINA PECTORIS
- Pathology of angina pectoris. 05 p0542 A73-17276
- Clinical diagnosis of angina pectoris, implicating obstructive disease of coronary arteries and effects of paroxysmal events on heart rate and blood pressure 05 p0542 A73-17277
- Long-term observations in patients with angina and normal coronary arteriograms. 06 p0655 A73-18871
- Problems in the recognition of angina pectoris. 18 p2275 A73-36541
- Electrocardiographic alterations in the presence of angina pectoris. 18 p2282 A73-36542
- Angina pectoris and ECG abnormalities in relation to prognosis of coronary heart disease in population studies in Finland. 22 p2809 A73-42836
- ### ANGIOGRAPHY
- Q waves and coronary arteriography in cardiomyopathy. 01 p0010 A73-11507
- Left ventricular end-diastolic pressures following selective coronary arteriography. 01 p0010 A73-11508
- Nature of the conduction disturbance in selective coronary arteriography and left heart catheterization. 02 p0134 A73-12443
- Maximal treadmill exercise electrocardiography - Correlations with coronary arteriography and cardiac hemodynamics. 02 p0136 A73-12821
- Correlation of computer-quantitated treadmill exercise electrocardiogram with arteriographic location of coronary artery disease. 03 p0260 A73-13543
- Quantitative radionuclide angiocardiology for determination of chamber to chamber cardiac transit times. 04 p0409 A73-14767
- Elevated ST segments with exercise in ventricular aneurysm. 04 p0410 A73-15643
- Correlation of electrocardiographic studies and arteriographic findings with angina pectoris. 05 p0546 A73-17279
- The reconstruction of three-dimensional objects from two orthogonal projections and its application to cardiac cineangiography. 06 p0657 A73-17801
- Television/computer dimensional analysis interface with special application to left ventricular cineangiograms. 06 p0657 A73-17860
- Long-term observations in patients with angina and normal coronary arteriograms. 06 p0655 A73-18871
- Pattern of blood flow within the heart - A stable system. 08 p0930 A73-21214
- Left ventricular performance after myocardial infarction assessed by radioisotope angiocardiology. 08 p0932 A73-21801
- Inability of the submaximal treadmill stress test to predict the location of coronary disease. 08 p0932 A73-21802
- Ventriculographic patterns and hemodynamics in primary myocardial disease. 08 p0933 A73-21804
- Estimation of left ventricular size by echocardiography. 09 p1046 A73-22999
- Immediate hemodynamic effects of cardiac angiography in man. 10 p1179 A73-23841
- Regional myocardial dynamics from single-plane coronary cineangiograms. 10 p1185 A73-24771
- Comparison of isometric exercise and angiotensin infusion as stress test for evaluation of left ventricular function. 12 p1464 A73-27889
- Assessment of left heart function by noninvasive exercise test in normal subjects. 15 p1834 A73-31345
- Assessment of left ventricular performance in man - Instantaneous tension-velocity-length relations obtained with the aid of an electromagnetic velocity catheter in the ascending aorta. 15 p1836 A73-31996
- Assessment of left ventricular dimensions and function by echocardiography. 16 p1973 A73-34038
- Video instrumentation for radionuclide angiocardiology. 19 p2399 A73-37796
- Use of a video system in the study of ventricular function in man. 19 p2399 A73-37797
- Biplane roentgen videometric system for dynamic, 60/sec, studies of the shape and size of circulatory structures, particularly the left ventricle. 19 p2399 A73-37798
- Detection of left ventricular asynergy by echocardiography. 20 p2512 A73-38869
- The correlation of coronary angiography and the electrocardiographic response to maximal treadmill testing in 76 asymptomatic men. 22 p2806 A73-42342
- The complications of coronary arteriography. 22 p2806 A73-42343
- Indications and value of coronary arteriography. 22 p2808 A73-42830
- The value of different angiographic procedures in coronary heart disease. 22 p2808 A73-42831
- Coronary heart disease; Proceedings of the Second International Symposium, Frankfurt am Main, West Germany, June 1972. 22 p2809 A73-42856
- Fluorescent angiographic technique for fundus oculi 23 p2946 A73-43788
- Measurement of left anterior descending coronary arterial blood flow - Technique, methods of blood flow analysis and correlation with angiography. 24 p3058 A73-44469
- Comparison of ultrasound and cineangiographic measurements of left ventricular performance in patients with and without wall motion abnormalities. 24 p3062 A73-45400
- ### ANGLE OF ATTACK
- #### NT ZERO ANGLE OF ATTACK
- Three-dimensional effects on electron density in a blunt body laminar boundary layer. 01 p0002 A73-10731
- Aerodynamics of blunted bodies in hypersonic stream at the angle of attack. 01 p0003 A73-11133
- Experimental investigation of the supersonic two-dimensional flow past a sail at small angles of attack. 01 p0004 A73-11371
- Indicating instrument for angle of attack and sideslip on subsonic flight vehicles via static pressure sensing, noting wind tunnel tests 02 p0166 A73-11724
- Base resistance of axisymmetric bodies with a variable angle of attack - Analysis and interpretation of the physical phenomenon 03 p0242 A73-13375
- A method of testing full-scale inlet/engine systems at high angles of attack and yaw at transonic velocities. 03 p0287 A73-13417
- [AIAA PAPER 72-1097]
- Thermal stress analysis of reentry vehicle nosetips at angle of attack. 03 p0392 A73-13688
- Finite fringe holographic interferometry applied to a right circular cone at angle of attack. [ASME PAPER 72-APM-PP] 05 p0527 A73-16528
- Viscous shock layer flow in the windward plane of cones at angle of attack. 05 p0530 A73-16886
- [AIAA PAPER 73-134]
- Nose pressure distribution and separation on an inclined axisymmetric body. 05 p0533 A73-17123
- Reentry vehicle dynamic stability mechanism during boundary layer transition, using angle of attack divergence dependence on fluctuating pressure [AIAA PAPER 73-180] 06 p0756 A73-17652
- A flight control system for STOL aircraft. 07 p0777 A73-20171
- Approximate method for calculating heat transfer to yawed cylinders in laminar flow. 08 p1025 A73-21818
- Out-of-plane force on a circular cylinder at large angles of inclination to a uniform stream. 09 p1029 A73-23124
- Aerodynamic forces and moments estimation for slender bodies of circular and noncircular cross section without and with lifting surfaces at 0-90 degree angles of attack 09 p1030 A73-23468
- Experimental determination of the transonic flow on circular cones at angle of attack 10 p1172 A73-24496
- Dynamic stability of cable in incompressible flow at angle of incidence, calculating characteristic lengths and vibration frequencies by singular perturbation theory 11 p1440 A73-25524
- [AIAA PAPER 73-395]
- Correction for change in fluid flow curvature about a lift-generating airfoil in a two-dimensional test section with perforated walls 11 p1302 A73-25864
- Researches on the two-dimensional retarded cascade. III - Cascade performances at high inlet angles. 11 p1302 A73-26338
- Researches on the two-dimensional retarded cascade. IV - Determination of blade elements at retarded blade row. 11 p1302 A73-26339
- Laminar symmetry-plane boundary layer on a sharp spinning body at incidence. 11 p1303 A73-26397
- Lifting-surface theory for a wing oscillating in yaw and sideslip with an angle of attack. 13 p1564 A73-28802
- Theoretical and experimental study of a swept-back wing at low velocity over a wide range of angles of attack 16 p1962 A73-32814
- The use of a finite difference technique to predict cascade, stator, and rotor deviation angles and optimum angles of attack. [ASME PAPER 73-GT-10] 16 p1963 A73-33488
- Behavior of a wing panel under transient conditions in a gas flow 17 p2091 A73-34139
- General aviation aircraft stall/spin prevention device for limiting tail power near wing stall angle of attack [SAE PAPER 730333] 17 p2102 A73-34686
- Calculation of the flow on a cone at high angle of attack. [AIAA PAPER 73-636] 18 p2260 A73-36195
- Engineering analysis of hypersonic lifting body windward surface inviscid and viscous flow fields at high angles of incidence. [AIAA PAPER 73-637] 18 p2263 A73-36257
- Angle of attack tests for graphite ablation models simulating spacecraft reentry using arc heating, showing temperature and pressure effects, model size and flow field characteristics [AIAA PAPER 73-736] 18 p2295 A73-36353
- On the Oseen limiting movements around a rectilinear profile placed under a free line 19 p2459 A73-37526
- Approximation for hypersonic flow past circular cone with angle of attack, discussing matched asymptotic expansion, flow velocity and density distribution 21 p2632 A73-40428
- On problems of flight over an extended angle-of-attack range. 24 p3056 A73-44692
- ### ANGLES (GEOMETRY)
- #### NT ANGLE OF ATTACK
- #### NT BRAGG ANGLE
- #### NT DIHEDRAL ANGLE
- #### NT ELEVATION ANGLE
- On automatic angle measurements and a proposition of their application into zenith distance measurements on the surface of the moon. 03 p0307 A73-13258
- Hall effect gimbal angle transducer /HEGAT/ for relative angular orientation measurement between rotor and stator in low cost inertial platform 04 p0447 A73-15066

- Determination of the angle of incidence of angle probes for ultrasonic testing
05 p0582 A73-17068
- The effect of the rotor pattern on the accuracy of the photoelectric angle-measuring system of a gimbal-less electrostatic gyroscope.
18 p2317 A73-36873
- Algorithms for calculating Euler angles of moving objects
20 p2590 A73-39044

ANGULAR ACCELERATION

- Astronomical evidence concerning non-gravitational forces in the earth-moon system.
02 p0217 A73-12385
- On the influence of acceleration stresses on the yielding of disks of uniform thickness.
03 p0384 A73-13118
- Vestibular adaptation in man - Effects of increased acceleration during different phases of adaptation.
04 p0411 A73-15218
- Equivalence of the action of Coriolis accelerations to that of certain angular accelerations in their effects on the receptors of semicircular canals
12 p1463 A73-27718
- Earth rotational accelerations magnitudes as obtained from astronomical observations, noting semimonthly lunar body tides effects
13 p1679 A73-28395
- Experimental-mathematical analysis of the effects of rotational accelerations on the vestibular apparatus
17 p2110 A73-34120
- Cross coupling between effects of linear and angular acceleration on vestibular nystagmus.
18 p2272 A73-36441
- On the electronic simulation of acceleratory nystagmus.
22 p2816 A73-42683

ANGULAR CORRELATION

- The study of biological macromolecules using perturbed angular correlations of gamma radiation.
02 p0136 A73-12648

ANGULAR DISTRIBUTION

- A note on the angular dispersion of a fluid line element in isotropic turbulence.
01 p0032 A73-10443
- The possibility of a consistent explanation of various phenomena involving cosmic ray muons.
01 p0092 A73-10789
- Study of the angular structure of radio sources from their lunar occultations. II
01 p0102 A73-10951
- Measurement of the angular distribution of light scattered from a glass fiber optical waveguide.
01 p0078 A73-11215
- Angular distributions of auroral electrons in the energy range 0.8 to 16 keV.
02 p0155 A73-11734
- Cosmic ray muon component integral multiplicity calculations with allowance for angular distribution of secondary particles in elementary collision event on atmospheric boundary, using computer
02 p0205 A73-12172
- A preferred orientation of extragalactic double radio sources.
02 p0217 A73-12405
- Secondary cosmic ray shower charged particles angular distribution asymmetry in center-of-mass system and azimuthal plane related to single fireball formation
02 p0208 A73-12657
- High energy muon energy and angular distributions from electron-photon cascades, using emulsion chamber with X ray films
02 p0209 A73-12680
- Auroral precipitating electron angular distributions from polar orbiting satellite OVI-18 measurements, indicating pitch-angle diffusion due to particle-wave interactions
03 p0363 A73-13868
- Angular distribution of radiation reflected from roughened brass - Experiment and analysis.
[AIAA PAPER 73-151] 05 p0598 A73-16899
- Directional measurements of the solar wind by the ESRO HEOS 1 probe, S 58-73
06 p0749 A73-17863
- Nonconventional processes in anomalous cosmic-ray experiments.
06 p0743 A73-17865
- Angular distribution of first Stokes component for stimulated combinational Raman scattering investigated under various excitation conditions
06 p0700 A73-17965
- Effect of molecular shape and flexibility on gamma-ray directional correlations.
06 p0725 A73-18122
- Influence of waveguide properties of heterojunction layers on the principal characteristics of injection lasers.
06 p0702 A73-18585
- Pitch angle distribution of solar flare particles in interplanetary space.
07 p0869 A73-19228
- Axial ratio and position angle of the major axis of the globular cluster M 92
07 p0901 A73-20317

- Holographic method of controlling the spatial-angular characteristics of laser emission
09 p1090 A73-21951
- Ion angular distribution around Explorer 31, discussing observed ion flux relation to ionospheric parameters derived from ambient ion and electron measurements
09 p1075 A73-22136
- Lunar occultations of radio sources as a technique for investigating their angular structure. II.
09 p1148 A73-22745
- Energy and angular correlations of the scattered and ejected electrons in the electron-impact ionization of argon.
10 p1252 A73-24340
- Electron pitch angle distributions throughout the magnetosphere as observed on Ogo 5.
10 p1213 A73-24732
- The circular polarization of sources of synchrotron radiation.
10 p1270 A73-24901
- Angular distribution of induced combinational light scattering in liquid nitrogen
12 p1505 A73-26889
- Improving the angular divergence of the emission from a neodymium-glass laser with a high pulse energy level
12 p1505 A73-26963
- Axial ratio and position angle of the major axis for the globular cluster M92.
12 p1539 A73-27289
- Study of the directional distribution of energetic electrons and protons in the morning sector of the auroral zone during enhanced particle flux
13 p1606 A73-28153
- Low-energy electron experiment for Atmosphere Explorer-C and -D.
13 p1689 A73-28642
- Energy spectra and pitch angle distributions of precipitating incident and backscattered electron fluxes in auroral arcs
14 p1747 A73-29968
- Forward scattering method for determination of atmospheric aerosols particle size distribution, considering angle-dependent scattering at fixed wave number
17 p2161 A73-34938
- Sounding balloon nuclear emulsion chamber recording of energy spectra and angular distribution of incoming and outgoing proton fluxes in atmosphere
18 p2310 A73-36124
- Angular dependence of optically pumped magnetometer - Effects of collisional mixing in the excited states.
19 p2429 A73-37382
- Improving the angular divergence of a neodymium-glass laser beam having a high radiation energy per pulse.
19 p2438 A73-38146
- Angular distribution patterns of thick-film holograms.
20 p2567 A73-39701
- Angular distribution patterns of thick-film holograms obtained by rigorous solution of the diffraction problem.
20 p2567 A73-39702
- Cosmic ray muon zenith angle distribution during horizontal air showers, discussing kaon and pion decay, spectrum characteristics, bremsstrahlung effects and flux upper limits
20 p2603 A73-39708
- Influence of a sudden compression of the magnetosphere on outer zone electron fluxes measured at arbitrary pitch-angle.
21 p2682 A73-40161
- Angular dependence of optical scattering in mixed nematic-cholesteric liquid crystals.
21 p2751 A73-40453
- Field aligned electron anisotropies observed by the ESRO 1 A/Aurorae/satellite.
21 p2691 A73-41370
- Energy spectra and angular distribution measurement for 10-100 MeV earth albedo neutrons by balloon sounding at 116,000 ft
21 p2761 A73-41380
- Angular effects in the propagation of cosmic rays in the atmosphere.
21 p2764 A73-41629
- On the interpretation of the redshift-angular size diagram for quasars.
22 p2907 A73-42211
- Measurements of absolute intensities of cosmic-ray muons in the vertical and greatly inclined directions at geomagnetic latitudes 16 N.
22 p2903 A73-42437
- An operational approach to the energy of gravitational waves.
22 p2888 A73-42929
- The structure of the spatio-angular distribution function of electron-photon shower particles near the axis
23 p3023 A73-43556
- Energy spectrum and angular distribution of outer space muons and the processes of their production in the 1 TeV energy range
23 p3024 A73-43564

- Radiative transfer through a Compton-scattering atmosphere with continuous energy dependence.
24 p3111 A73-45321

ANGULAR MOMENTUM

- Stellar structure and angular momentum evolution of rotating stars, describing interaction in terms of redistribution processes of momentum
01 p0094 A73-10054
- An experimental and analytical investigation of angular momentum exchange in a rotating fluid.
01 p0073 A73-10444
- The mass and angular momentum losses from spinars.
02 p0217 A73-12384
- The dynamical evolution of triple star systems - A numerical study.
02 p0221 A73-12702
- A galactic formation model based on post-big bang fragmentation.
02 p0224 A73-12740
- The transmission of mass and angular momentum from a satellite or planetary system to its primary.
02 p0225 A73-12810
- On the initial distance of the moon forming in the circumterrestrial swarm.
03 p0369 A73-13108
- A mechanism for the exploding granule phenomenon.
05 p0621 A73-17029
- [AD-759887] Inner planets of the solar system - A comparative study.
06 p0749 A73-18007
- Black hole polar flattening and equatorial circumference lengthening as function of angular momentum, considering effects of highly curved space-time.
07 p0899 A73-20176
- The role of the satellite swarm in the origin of the earth's rotation.
08 p1012 A73-21579
- Systematic drift of a gyroscope with variable angular momentum in the gimbal suspension during vibrations of the frame
09 p1084 A73-22657
- Dispersion of the direction of the angular momentum vector of sounding rocket payloads due to atmosphere exit and certain vehicle activities.
[AIAA PAPER 73-293] 09 p1116 A73-23212
- Causes of the rotation of galaxies in terms of the nonlinear theory of gravitational instability
10 p1274 A73-23712
- An exact solution for a collisionless flat galactic model.
10 p1275 A73-23826
- Earth-moon system mass and angular momentum distribution anomaly, considering light gases association with Jupiter, Saturn, Uranus and Neptune satellites
11 p1419 A73-25793
- Primordial random motions and angular momenta of galaxies and galaxy clusters.
11 p1427 A73-26601
- Solar rotation angular velocity variation with heliographic latitude, depth and time, considering superficial circulation as cause of angular momentum transport
14 p1797 A73-30139
- The process of galaxy formation according to the universal turbulence hypothesis.
14 p1798 A73-30142
- Collision induced dissociation - A statistical theory.
15 p1915 A73-31275
- Black holes in binary systems - Observational appearances.
16 p2058 A73-32739
- Mass and angular momentum distribution in primitive solar nebula during rotation and contraction hydrodynamics of collapse
17 p2227 A73-34412
- Revision of initial size, mass and angular momentum of the solar nebula and the problem of its origin.
17 p2229 A73-34431
- Fuel-optimal angular momentum vector control for spinning and dual-spin spacecraft.
17 p2240 A73-35663
- Analysis of nonequilibrium particulate flow.
[AIAA PAPER 73-687] 18 p2298 A73-36238
- Alfvén waves in the solar wind - Wave pressure, Poynting flux, and angular momentum.
18 p2346 A73-36264
- Earth-moon system angular momentum loss from paleontological data and earth rotational moment of inertia effect
18 p2354 A73-36509
- Development of rotation in galaxies in the nonlinear theory of gravitational instability.
18 p2354 A73-36737
- Investigations of the 500mb level in relation to the general circulation. I - Transport of relative angular momentum at the 500mb level, by considering daily and monthly eddies that were obtained by applying Fisher's partitioning.
19 p2446 A73-37499
- Rotational line structure in three-photon scattering by symmetric top molecules.
20 p2574 A73-39723

Angular momentum decrease of slowly rotating Kerr black holes due to stationary distribution of outside matter

21 p2766 A73-40314

The vorticity equation as an angular momentum equation.

22 p2842 A73-42349

The angular momentum of spiral galaxies. I - Methods of rotation-curve analysis. II - Detailed models and correlations for 17 galaxies.

22 p2913 A73-43002

Navier-Stokes equation formulation in parabolic coordinates for flow in trailing vortex, obtaining asymptotic expansions for stream function and angular momentum

23 p2939 A73-43205

ANGULAR MOTION

U ANGULAR VELOCITY

ANGULAR RESOLUTION

Utilization of electro-optical methods in designing angular- and linear-displacement sensors

01 p0052 A73-11074

Solar UV spectra with high angular resolution from rocket observations, obtaining center to limb intensity variations

02 p0207 A73-12325

High angular resolution solar observation from balloon borne instruments.

02 p0169 A73-12334

High angular resolution observations from rockets - Solar XUV observations.

02 p0216 A73-12336

Catalog of angular diameters, absolute magnitudes, spectroscopic parallaxes and linear diameters for 2301 stars, discussing accuracy and frequency distributions of log functions

03 p0375 A73-13948

Observations of maser radio sources with an angular resolution of 0.0002 sec.

04 p0503 A73-16001

Observations of radio sources with an interferometer of 24-km baseline. II - The angular structures at 151 and 408 MHz of 46 unidentified radio sources from the revised 3C catalogue.

07 p0899 A73-19938

Observations of radio sources with an interferometer of 24-km baseline. III - The angular structures at 408 and 1423 MHz of 44 relatively intense radio sources.

07 p0899 A73-19939

Analysis procedure of gamma ray astronomy spark chamber data.

07 p0828 A73-20644

Schmidt telescopes for northern and southern hemispheres, discussing optical design with achromatic corrector to achieve high angular resolution and conversion to Cassegrain configuration

08 p0966 A73-21366

Culgoora-I list of radio source measurements at 80 MHz.

15 p1940 A73-32182

On the angular resolution of a search radar with a mechanically rotated antenna.

17 p2125 A73-35369

Long baseline interferometry with high angular resolution widely separated radio telescopes and video signal magnetic recording tapes, discussing coherence and timing requirements and calibration

23 p2980 A73-43349

Radio spectra and mapping of extragalactic radio sources including radio galaxies and quasars with high angular resolution, noting energy sources and red shift

23 p3029 A73-43625

The accuracy of phase-comparison angle tracking by phased-array antennas

24 p3071 A73-44594

ANGULAR VELOCITY

Energy dissipation and drift angular velocity calculation for horizontal pendulum on vibrating base, using revised differential equation of motion

01 p0079 A73-11417

Investigation of a moving angular-velocity hodograph in the symmetrical solution to the problem of the motion of a body having a fixed point

02 p0191 A73-11762

Time dependence of the basic variables in the symmetric solution to the problem of the motion of a body having a fixed point

02 p0191 A73-11763

Intersection line of axes cone with sphere and locus of angular velocity vectors for uniform gyroscope rotation with different moments of inertia

02 p0191 A73-11764

Average magnetic field strength relationships with angular velocity and stellar activity cycle period, using Leighton solar cycle model with differential rotation and cyclonic turbulence

02 p0224 A73-12741

Optimal speed sharing characteristics of a series-hybrid bearing.

[ASME PAPER 72-LUB-39]

03 p0315 A73-14346

Speed-torque characteristics of a solar cell motor.

04 p0406 A73-15068

Moving visual scenes influence the apparent direction of gravity.

04 p0411 A73-15250

Equations of motion for mathematical models of turbine rotors with elastic shaft in unsteady operation, calculating resonant angular velocity

04 p0514 A73-15654

Angular velocity magnitude conversion into visually perceived apparent velocity, using psychophysical mathematical model based on axisymmetric annular visual field perception

04 p0413 A73-15796

Quasi-static load acting on a rotating shaft in the presence of creep

07 p0830 A73-19309

Determination of the type of motion in spherically symmetric systems of galaxies

07 p0901 A73-20313

A contactless method of measuring the radial deformations of rotating shafts

07 p0827 A73-20533

System for in-flight recording of the rotational speed of the turbine of a jet engine

07 p0828 A73-20546

Fluidic sensing of rotational speed using spur gears.

08 p0928 A73-21829

Errors in measuring the angles of rotation of an object with a triaxial gyro stabilized platform with allowance for its drift

09 p1115 A73-22343

A short periodic irregularity in earth's rotation and the motion of the earth's instantaneous pole

10 p1275 A73-23724

Solar rotation as determined from OSO-4 EUV spectroheliograms.

10 p1278 A73-24127

The free surface on a liquid between cylinders rotating at different speeds. I.

10 p1207 A73-24789

The free surface on a liquid between cylinders rotating at different speeds. II.

10 p1207 A73-24790

Solution of kinematical differential equations for a rigid body.

[ASME PAPER 72-APM-AAA]

11 p1398 A73-25705

Controlling the angular motions of a flight vehicle with the aid of flywheels

12 p1522 A73-27083

Determination of the type of motion in spherically symmetric clusters of galaxies.

12 p1539 A73-27285

Lunar rotation secular acceleration and tidal friction related to earth rotational velocity and creep properties

13 p1677 A73-28378

Earth mantle-core mechanical and electromagnetic interactions influencing rotation rate random variations

13 p1679 A73-28396

Earth polar motion and angular velocity sequential estimation in presence of unmodelled random accelerations, via Gauss-Markov process representation

13 p1679 A73-28397

On some natures of the excitation and damping of the polar motion.

13 p1680 A73-28406

Solar rotation angular velocity variation with heliographic latitude, depth and time, considering superficial circulation as cause of angular momentum transport

14 p1797 A73-30139

Determination of the attitude and angular velocities at the end of a phase of active change in angular velocity

15 p1943 A73-31242

Aided tracking as applied to high accuracy pointing systems.

15 p1854 A73-31726

Anticipated variability of Pulsar NP 0532 emission in the Crab nebula associated with angular velocity jumps

15 p1938 A73-31964

Theory of turbulence with a vortex-type anisotropy

15 p1864 A73-32084

On the vibrations of a rotor with rotating inequality and with variable rotating speed.

15 p1883 A73-32216

Detection and measurement of low-level backscattering of laser radiation

16 p1978 A73-32893

Experimental study of fluctuations of the difference frequency in a ring laser

16 p2024 A73-32895

Comparison of determinations of the rotational velocity of Venus by radar, optical Doppler effect, and spot measurement methods

16 p2067 A73-33809

Critical speeds for cantilever shafts.

18 p2320 A73-36700

A short-period irregularity in the earth's rotation and the motion of the instantaneous pole.

18 p2355 A73-36749

Recording of the angular velocity of meteors by sequential photography

19 p2480 A73-37239

Linear acceleration insensitive balanced rotor seismic angular motion sensor with optical pickoff system, discussing mathematical model and performance tests

[AIAA PAPER 73-829]

20 p2564 A73-38774

Some linear problems in the theory of gyroscopes

20 p2565 A73-38983

Oscillatory motions of an axisymmetric spin-stabilized solid body

20 p2593 A73-39495

Hypervelocity projectile holography for application to bullets and shells, calculating rotational velocity and flight direction from fringe on wave front reconstruction

21 p2694 A73-39957

Use of gyro technology to measure small random angular motion.

[AIAA PAPER 73-839]

21 p2700 A73-40504

Errors of a single-axis gyrostabilizer as an angular velocity integrator

22 p2860 A73-42366

Stability of an indicator gyrostabilizer during the rotation of a three-stage gyroscope

22 p2860 A73-42368

The 4-day rotation of the upper atmosphere of Venus.

22 p2913 A73-42982

Galactic rotation of the centroids of various objects

23 p3035 A73-44239

Expected radiative variability of Crab-Nebula pulsar NP 0532, related to abrupt changes in angular velocity.

24 p3132 A73-44489

High rotational velocity correlation with metal abundance interpreted by coronal mass loss rate in metal-poor stars

24 p3140 A73-45184

The linear spin-up of a strongly stratified fluid of small Prandtl number.

24 p3079 A73-45312

ANHYDRIDES

NT PEROXIDES

Polyimidazopyrrolone model compounds.

15 p1840 A73-31572

ANIMALS

NT AMPHIBIA

NT ARTHROPODS

NT BATS

NT BEES

NT BIRDS

NT CATS

NT CHIMPANZEES

NT CRABS

NT DROSOPHILA

NT FISHES

NT FROGS

NT HOMEOTHERMS

NT INSECTS

NT INVERTEBRATES

NT MAMMALS

NT MICE

NT POIKILOthermia

NT PROTOZOA

NT TRIBOLIA

NT VERTEBRATES

Thermoregulation evolution in various animals, discussing body size and composition effects, body temperature variations, control mechanisms, heat loss and production, behavior and ontogeny

22 p2810 A73-42863

ANIONS

Negative-ion composition measurements in the D and lower E regions.

01 p0042 A73-10896

Rates of clustering of oxygen negative ions with water vapor.

01 p0014 A73-10902

Dinuclear anions of molybdenum VI and tungsten VI with the 'fluoro' and 'oxalato' coordinates

05 p0547 A73-17218

Some anionic tetrahalo/2,4-pentanedionato/stannate/IV complexes.

06 p0661 A73-18271

Multiphoton transitions. III - Rates of multiphotodetachment of negative ions.

07 p0852 A73-19147

Oxygen anions excited electronic states, analyzing energy curves and wave functions via configuration-interaction results obtained by multiconfiguration self consistent field techniques

07 p0853 A73-19333

Measurement of the cross section for photodetachment of O³⁻.

08 p0957 A73-20658

The influence of negative-ion changes in the D-region during sudden ionospheric disturbances.

09 p1075 A73-22126

The negative-ion composition of the daytime D-region.

09 p1048 A73-22127

Use of translational energy measurements in the evaluation of the energetics for dissociative attachment processes.

10 p1251 A73-24244

- Negative oxygen molecular ion formation in low energy electron collision and attachment obtaining capture cross section and resonance width
14 p1777 A73-30775
- Infrared absorption and local symmetry of negative ClO₄ and ReO₄ impurity ions in KCl and CsI crystals
18 p2340 A73-36673
- A new type of ionizational instability in a plasma with negative ions
20 p2598 A73-39621
- High-resolution photodetachment study of Se⁻/ions.
21 p2710 A73-40213

ANISOTROPIC FLUIDS

- Three-dimensional acoustic-ray tracing in an inhomogeneous anisotropic atmosphere using Hamilton's equations.
08 p0988 A73-21190
- Characteristics of waveguides filled with homogeneous lossy anisotropic drifting plasma.
10 p1192 A73-23574
- Semiempirical determination of the anisotropy of turbulent MHD flow in a longitudinal field
10 p1256 A73-24592
- Homogeneous anisotropic to isotropic turbulence convergence based on shear flow component measurements of turbulence energy distribution in axisymmetric flow
20 p2546 A73-39097
- The behavior of nematic liquid crystals in the electric field
23 p3019 A73-44387

ANISOTROPIC MEDIA

NT ANISOTROPIC FLUIDS

- A solution to the auxiliary equation of radiative transfer for a planetary atmosphere with molecular anisotropy.
01 p0097 A73-10352
- Upper bounds to the load for the plane strain working of anisotropic metals.
01 p0057 A73-10696
- Re-interpretation of some simple tension and bulge test data for anisotropic metals.
01 p0065 A73-10764
- Closed form exact solution to quasi-static problem in linear viscoelasticity for homogeneous anisotropic material with time invariant properties
01 p0116 A73-10967
- Rotational perturbations in anisotropic cosmology.
01 p0107 A73-11328
- Acceleration waves in anisotropic thermoelastic materials with internal state variables.
01 p0118 A73-11367
- The velocity of a wave packet in an anisotropic absorbing medium.
01 p0079 A73-11494
- Anisotropic beam elastic deformation under end loads, deriving coefficients for linear relation between cross sectional stresses and elastic deformation curvature
02 p0230 A73-11780
- Radiation from a magnetic line source in a compressible and anisotropic plasma half-space.
03 p0345 A73-12996
- The stability theory of elastic bodies and the theory of thermal stresses of piecewise anisotropic bodies
03 p0386 A73-13156
- Deformation characteristics of plastics reinforced by high-modulus anisotropic fibers
03 p0335 A73-13739
- Strength limits correlation to modulus of elasticity for compact bone material from compression tests, noting anisotropy tensor analysis
03 p0267 A73-13744
- Edge dislocation in an infinite anisotropic elastic medium under consideration of the core conditions.
03 p0392 A73-13774
- The fracture mechanics of slit-like cracks in anisotropic elastic media.
03 p0394 A73-13979
- Anisotropic structures reliability in terms of design safety factor, analyzing composite rocket motor cases under plane stress
04 p0452 A73-14723
- Empirical strength criteria for anisotropic and isotropic composite materials with unequal tensile and compressive strength
04 p0508 A73-14860
- Total reflection of a plane wave by a semi-infinite random medium.
04 p0480 A73-15198
- Characteristics of waveguides containing anisotropic warm plasma in the presence of transverse magnetic field.
04 p0480 A73-15600
- Passage of electric current through an illuminated semiconductor under conditions where the anisotropy parameters, the electrical conductivity, and the relaxation time are nonuniform. I
04 p0484 A73-15641
- Optimal experimental measurements of anisotropic failure tensors.
05 p0631 A73-16113

- Application of the method of least squares to the determination of optical constants of uniaxial isotropic and anisotropic substances, and of the rate of polarization of monochromators in the far UV
05 p0597 A73-16148
- Directional dependence of the thermal conductivity of crystal-oriented pyrolytic graphite at high temperatures.
06 p0713 A73-17405
- Solar wind rotational and tangential velocity discontinuities in anisotropic media, discussing Ivanov, Burlage and Hudson data
06 p0742 A73-17528
- Electrodynamics of anisotropic media with space and time dispersion.
06 p0723 A73-17787
- Wave normal and ray propagation in lossless positive bianisotropic media.
06 p0723 A73-17875
- Diffraction of electromagnetic plane wave by an infinite slit embedded in an anisotropic plasma.
06 p0668 A73-18356
- Normal-mode analysis of anisotropic and gyrotropic thin-film waveguides for integrated optics.
06 p0702 A73-18365
- Nonlinear aspects of cooling of a strongly anisotropic optical element of a laser.
06 p0702 A73-18579
- Stress-induced rotation of polarization directions of elastic waves in slightly anisotropic materials.
07 p0908 A73-19083
- Electrooptic liquid crystal devices - Principles and applications.
07 p0861 A73-19135
- Transient radiation in homogeneous anisotropic cold plasmas.
07 p0856 A73-19381
- Arbitrary source emitted electromagnetic radiation in anisotropic stratified media, evaluating transverse and scattered fields and plane wave response
07 p0791 A73-19382
- Wave pattern of three dimensional hydromagnetic perturbations produced by harmonic magnetic dipole in anisotropic plasma
07 p0816 A73-19461
- Modified negative mass mode stabilization in finite magnetic mirror confined plasmas with highly anisotropic velocity distribution, considering bounce harmonic effects and gyrofrequency
07 p0856 A73-19522
- Computerized simulation for nonlinear evolution of whistler instabilities in anisotropic collisionless plasmas with various Maxwellian electron distributions
07 p0857 A73-19523
- Effect of collision frequency on the characteristics of waveguide filled with homogeneous anisotropic plasma.
07 p0857 A73-19533
- The complete iso-thermalization by collective electromagnetic interactions of strongly anisotropic magnetized collisionless plasmas.
07 p0859 A73-20235
- The behaviour of an edge dislocation in non-homogeneous anisotropic body with cracks.
07 p0915 A73-20285
- Uniaxial magnetic anisotropy of single-crystal permalloy films
09 p1132 A73-21958
- Investigation of the anisotropy of effective masses in the conduction band of semiconductors under uniaxial compression
09 p1132 A73-21959
- Green operator evaluation by Fourier transform method for wave propagation in bianisotropic media, obtaining constitutive equations
09 p1049 A73-22311
- Electromagnetic propagation in bianisotropic stratified media, obtaining Maxwell and constitutive equations in operator form
09 p1049 A73-22312
- Experiment on the mechanical anisotropy of titanium, zirconium, and Zircaloy-2 rolled sheets.
09 p1104 A73-22521
- Propagation through a slab of irregularities in a magneto-ionic medium.
09 p1051 A73-22647
- Solid composite material thermostatics and overall thermoelastic modulus determination, considering arbitrarily anisotropic phases, binary composite and self consistent theory
10 p1295 A73-24099
- Electromagnetic wave reflection at interface between anisotropic Vlasov plasma and vacuum with external magnetic field, deriving electric and magnetic field characteristics
10 p1255 A73-24260
- Yield criteria derivation for laminated media with isotropic and anisotropic layers based on strength constants characterization as tensors
10 p1289 A73-24277
- The propagation of waves from a cylindrical cavity.
10 p1289 A73-24282

- Anisotropies in the interplanetary intensity of solar protons with energies greater than 0.3 MeV.
[AD-759099] 10 p1269 A73-24728
- Kinetic equations describing thermalization of anisotropic solar wind plasma via linear and nonlinear wave-particle interaction
10 p1270 A73-24912
- Rotational discontinuities in an anisotropic plasma.
II. 11 p1405 A73-25922
- Saint Venant principle for plane deformation of anisotropic elastic solid extended to analysis of fiber reinforced transversely isotropic composites
11 p1444 A73-26280
- Displacement boundary value problem of linearized elastodynamics with superimposed small and large deformations in homogeneous anisotropic elastic solid, proving solution uniqueness theorem
11 p1444 A73-26282
- Transient temperature distribution of an anisotropic half space.
11 p1453 A73-26401
- Transversely isotropic /anisotropic/ elastic beam bending and torsion, determining frequency dependent compliances by approximate analytic solution via variational method
11 p1447 A73-26655
- Electromagnetic fields due to dipole antennas over stratified anisotropic media.
[AD-756044] 12 p1523 A73-27146
- Reflection of electromagnetic waves from non-homogeneous anisotropic plasma layers /normal incidence/
12 p1470 A73-27356
- Closed form exact solution to quasi-static problem in linear viscoelasticity for homogeneous anisotropic material with time invariant properties
12 p1554 A73-27543
- Variational treatment of the elastic constants of disordered materials.
13 p1692 A73-28169
- Plane strain slip line theory for anisotropic rigid/plastic materials.
13 p1697 A73-28793
- Analysis of centrifugal stresses in anisotropic viscoelastic cylinder.
13 p1697 A73-28810
- A treatise on the stress-fields produced by moving dislocations Supplementary remarks and applications.
13 p1697 A73-28915
- Scattering by a gyrotropic cylinder coated with another gyrotropic layer.
13 p1586 A73-29232
- Nonlinear heat flow in anisotropic media with property variations and nonlinear heat generation.
14 p1816 A73-29915
- Secondary source method solutions for media interface integral equations of electrostatic fields in piecewise homogeneous anisotropic media
14 p1774 A73-30027
- Thermal stress in an anisotropic elastic half-space.
14 p1810 A73-30407
- An approximate solution of the nonstationary heat conduction problem for laser elements with sharply expressed anisotropy
14 p1758 A73-30467
- Some basic solutions in strain gradient elasticity theory of an arbitrary order.
14 p1812 A73-30546
- Electromagnetic instabilities of finite pressure anisotropic plasma with hot electrons.
15 p1916 A73-31084
- Saint Venant principle investigation for plane problem of linear elastostatics for anisotropic media by energy method, calculating exponential stress decay constant lower bound
15 p1946 A73-31102
- Muskhishvili elastodynamic theorem concerning natural stress-free state extension to three dimensional theory of inhomogeneous anisotropic elastic bodies
15 p1946 A73-31105
- Tensile and compressive strength tensor prediction for anisotropic boron-epoxy composites from off axis tests
15 p1897 A73-31682
- General properties of electromagnetic scattering by inhomogeneous anisotropic composite obstacles of arbitrary shape.
15 p1844 A73-31930
- Discrete element development for anisotropic plates via bicubic Hermite interpolation functions, considering patch generation from boundary geometry data
15 p1951 A73-32033
- Application of the perturbation method in a polarization analysis of anisotropic laser resonators
15 p1886 A73-32334
- Stresses in plastics reinforced by anisotropic fibers in the presence of transversal normal loads
16 p2030 A73-33928
- On the magnetogravitational instability of a plasma which possesses an anisotropic pressure in uniform movement of rotation and under the influence of the Hall current - The equation of dispersion. I
17 p2215 A73-34250

- Theory of disclinations. II - Continuous and discrete disclinations in anisotropic elasticity. 17 p2242 A73-34500
- Book - Applied nonlinear optics. 17 p2212 A73-35274
- Electric potential and current distribution in a rectangular sample of anisotropic material with application to the measurement of the principal resistivities by an extension of van der Pauw's method. 17 p2220 A73-35653
- A method for solving the problem of irradiation in anisotropic plasma. 17 p2217 A73-35724
- Russian book on elastic equilibrium boundary value problems for isotropic and anisotropic bodies under load or temperature field induced plane deformation. 18 p2361 A73-35874
- Stresses in an anisotropic half-space. 18 p2362 A73-36319
- Axisymmetric deformation of soft spherical shells. 18 p2367 A73-37139
- Plastic deformation anisotropy and work-hardening of composite materials. 19 p2444 A73-38261
- Green function and Poynting vector calculation of solid angles of radiation outside and inside anisotropic crystal in laser light scattering experiments. 20 p2591 A73-38617
- Edge dislocation in an anisotropic material with a surface layer. 20 p2593 A73-39342
- Ellipsoidal crack and needle in an anisotropic elastic medium. 21 p2783 A73-40187
- Influence of grain size on effects of thermal expansion anisotropy in MgTiO₅. 21 p2752 A73-40893
- Plane crack problems for ideal fibre-reinforced materials. 21 p2787 A73-41014
- A two-dimensional field induced by travelling sources. 21 p2740 A73-41016
- Dielectric anisotropy of new liquid-crystal mixtures and its effect on dynamic scattering. 21 p2665 A73-41115
- The Bauschinger effect and its role in mechanical anisotropy. 21 p2722 A73-41547
- Electromagnetic field equations in operator form for anisotropic conducting media. 22 p2886 A73-42212
- The use of fundamental Green's functions for the solution of problems of heat conduction in anisotropic media. 22 p2938 A73-42954
- Reflection of electromagnetic waves from inhomogeneous anisotropic plasma sheets /normal incidence/. 23 p2952 A73-43255
- Anisotropic composite material swelling coefficients and elastic compliances data averaging and reduction, using tensor transformation and associated scalar invariants. 23 p3041 A73-43636
- Anisotropic turbulent distributions for waves with a nondecay-type dispersion law. 23 p3012 A73-44018
- Creep rate relationship in terms of stress and strain rate for anisotropic metal based on single crystal theory, applying to pressurized thin cylinder. 23 p3045 A73-44167
- Numerical realization of a possible way of determining the tensor of elastic constants in an anisotropic body. 24 p3144 A73-44506
- Radiation transfer in a multilayer plane-parallel system with nonisotropic scattering. 24 p3154 A73-44659
- Three dimensional elasticity solution for layer interaction and shear coupling and deflection effects of laminated anisotropic composite cylinders under bending. 24 p3149 A73-45152
- ANISOTROPIC PLATES**
- Fourier analysis of laminated anisotropic rectangular plates with strong cross elasticity effects, presenting deflection, bending moments and buckling data. 01 p0115 A73-10735
- Nonlinear axisymmetric flexural vibration equations of a cylindrically anisotropic circular plate. 01 p0115 A73-10756
- Solution to the bending problem and to the plane problem of an anisotropic rectangular plate with arbitrary boundary conditions and the application of the solution to composite structure designs. 02 p0230 A73-11715
- Stressed state of an anisotropic plate with a finite number of curvilinear holes. 02 p0230 A73-11783
- Russian book on temperature and stress distributions in thin plates covering unsteady heat transfer and thermoelasticity of isotropic and anisotropic plates. 02 p0232 A73-11891
- Theoretical and experimental analysis of plane and cylindrical reinforced-plastic structures. 02 p0185 A73-12794
- Some remarks concerning heterogeneous anisotropic plates. 05 p0631 A73-16117
- Stress wave propagation in a laminated plate under impulsive loads. 07 p0908 A73-19089
- Thermal stresses in an anisotropic plate with a circular hole. 07 p0914 A73-20199
- Facility for studying the strength and rigidity of circular plates prepared from an anisotropic material. 07 p0809 A73-20517
- Stress concentration in an anisotropic plate with an insert in pure bending. 11 p1433 A73-25031
- On the vibration of shear deformable curved anisotropic composite plates. 11 p1442 A73-25711
- Bending stresses and strains in anisotropic semi-infinite plates with arbitrary edge and surface loadings. 11 p1445 A73-26404
- Equilibrium of an anisotropic plate reinforced by an isotropic circular ring. 13 p1698 A73-29131
- Convolutional variational principles for stress distribution in anisotropic plates of linear viscoelastic material. 16 p2077 A73-32981
- Equilibrium conditions for multilayer anisotropic viscoelastic plates in a complex stressed state. 16 p2083 A73-33933
- Nonlinear vibration of a rectangular plate arbitrarily laminated of anisotropic material. 17 p2249 A73-35105
- [ASME PAPER 73-APM-F] Anisotropic laminated fiber composite plates under short duration impact line forces, calculating one dimensional transient stress and displacement waves by fast Fourier transform. 17 p2249 A73-35108
- [ASME PAPER 73-APM-L] Thermoelastic state of an anisotropic plate with an elliptic hole and mixed boundary conditions. 18 p2363 A73-36406
- A method for determining the stressed state of anisotropic plates with a nonsymmetrically reinforced edge. 18 p2363 A73-36407
- Device for studying the strength and rigidity of round plates of anisotropic material. 19 p2418 A73-37793
- Dispersion curve computation for elastic acoustic waves propagation in /001/-cut cubic free anisotropic plate, noting relationship with slowness curves for bulk waves. 20 p2616 A73-39050
- On stress-concentration analysis of laminated composite plates. 20 p2622 A73-39551
- An approximate solution for bending of anisotropic laminated plates. 20 p2623 A73-39554
- Antisymmetrical bending of a circular orthotropic plate of variable thickness. 20 p2625 A73-39656
- Sinusoidal response of composite-material plates with material damping. 22 p2919 A73-42082
- [ASME PAPER 73-DET-120] Large deflection theory for viscoelastic anisotropic thin plates, deriving constitutive, plane stress, plate and nonlinear integrodifferential equations. 22 p2923 A73-42638
- Propagation of shock waves in anisotropic composite plates. 24 p3149 A73-45149
- ANISOTROPIC SHELLS**
- Fourier transformation for stress analysis of anisotropic shells under concentrated forces, solving shallow shell equations via MacDonald functions. 01 p0118 A73-11408
- Construction of a general solution for an elastic anisotropic shallow shell with arbitrary boundary conditions, and some of its applications. 02 p0230 A73-11714
- Critical stress in an anisotropic cylindrical shell under nonuniform compression. 02 p0233 A73-11938
- Discussion of the bending theory of cylindrical shells of orthogonally anisotropic structural material, by introducing the displacement function. 02 p0236 A73-12514
- Numerical analysis of anisotropic rotational shells subjected to nonsymmetric loads. 07 p0914 A73-20210
- Plastic analysis of filled, reinforced, circular cylindrical shells. 08 p1015 A73-20672
- Anisotropic membrane shells with, if necessary, uniform strength. 08 p1018 A73-21407
- Stability of a cylindrical anisotropic shell under the action of a ring load with allowance for subcritical deflection. 12 p1553 A73-27373
- Optimum design of composite shells subject to natural frequency constraints. 12 p1554 A73-27734
- Dynamic analysis of viscoelastoplastic anisotropic shells. 16 p2075 A73-32787
- Calculation of joint shells differing in their material and thickness. 20 p2619 A73-39365
- Free vibration and buckling loads of anisotropic pressurized thin walled shells of revolution, considering cylinders, barrels and spherical sections. 20 p2621 A73-39538
- On the problem of flexure of anisotropic cylindrical shells. 24 p3151 A73-45302
- ANISOTROPY**
- NT ELASTIC ANISOTROPY
- NT PLASTIC ANISOTROPY
- Holographic image polarization recording and sum wave simulation on photoanisotropic materials, using Weigert effect. 01 p0052 A73-11086
- Cosmological evolution from initial inhomogeneous and anisotropic universe to present structure, using general relativity for free gravitational field and waves. 01 p0106 A73-11242
- Mechanical properties anisotropy in heat resistant Ni alloys due to strengthening phase nonmetallic inclusions distribution, suggesting purification by vacuum melting. 01 p0066 A73-11346
- Microhardness anisotropy of hardened and aged Be single crystal as function of purity. 01 p0067 A73-11353
- Observed anisotropy in the distribution of radio sources. 04 p0499 A73-15352
- A solar-wind model including proton thermal anisotropy. 04 p0492 A73-15365
- Anisotropy of low-energy solar protons at the boundary of the magnetotail. 04 p0493 A73-15544
- ESRO 1A satellite-borne Langmuir probe measurement for anisotropy in ionospheric thermal electron temperature relative to geomagnetic field. 05 p0571 A73-17053
- Effect of molecular shape and flexibility on gamma-ray directional correlations. 06 p0725 A73-18122
- The influence of anisotropy and crystalline slip on relaxation at a crack tip. 06 p0709 A73-18331
- Anisotropy of piezoelectrical scattering in semiconductors with a wurtzite structure. 06 p0738 A73-18648
- Nature of anisotropy in half-cells made of cold-pressed Bi-Te-Se-Sb alloys. 06 p0738 A73-18653
- Propagation anisotropies of solar flare protons and electrons at low energies in interplanetary space. 07 p0869 A73-19227
- Investigation of the temperature dependence of the anisotropy parameter K in n-Si and n-Ge by using magneto-plasma waves. 07 p0861 A73-19327
- Neutron flux anisotropy from plasma focus measured by gamma spectroscopy of activated Ag target, discussing axial concentration. 07 p0857 A73-19529
- Solar cosmic ray sectorial anisotropy pattern observation, suggesting theoretical propagation model to distinguish between rival candidates for parent flare. 08 p0997 A73-20772
- Spatial crosscorrelation in anisotropic sound fields. 08 p0987 A73-21125
- The anisotropy of carrier lifetime in graphite. 08 p0982 A73-21220
- Three dimensional cosmic ray anisotropy and density distribution at earth orbit and in interplanetary space with allowance for primary particle and nucleon energy spectrum. 08 p1000 A73-21343
- Influence of pressure anisotropy on the fluctuations of the magnetospheric tail. 10 p1276 A73-23884
- Cosmic-ray anisotropy during the disturbed period from Oct. 25 to Nov. 10, 1968. 10 p1267 A73-23919
- Cosmological evolution from initial inhomogeneous and anisotropic universe to present structure, using general relativity for free gravitational field and waves. 10 p1279 A73-24178
- Solar cosmic ray anisotropy 27-day variations during IGY from global network stations neutron component data. 10 p1268 A73-24237
- Anisotropic and isotropic descriptions of physical process speeds in special relativity theory space-time metric. 10 p1250 A73-24944
- Low speed wind tunnel test section anisotropic turbulence decay rates representation by power type

laws, comparing with grid and nearly isotropic turbulence

11 p1348 A73-26390

Magnetic reversal mechanisms of obliquely deposited permalloy films possessing perpendicular anisotropy

12 p1530 A73-26833

Anisotropic contact discontinuities at magnetospheric boundary and tail from MHD space plasma data analysis, suggesting sector boundary identification in interplanetary magnetic field

12 p1528 A73-27329

Theory of turbulence with a vortex-type anisotropy

15 p1864 A73-32084

German monograph - The spontaneous anisotropy of the resistance in nickel - Measurements involving single crystals of nickel and diluted nickel alloys between 4.2 and 358 K.

15 p1896 A73-32582

Torsion of an inhomogeneous body of revolution with variable shear moduli

16 p2074 A73-32682

Radiation transport theory for anisotropic light scattering in planetary atmospheres, formulating transmission and reflection coefficients

16 p2066 A73-33790

Correlation functions of the elastic field of quasi-isotropic composite materials under nonisotropic deformation

17 p2240 A73-34146

Effect of pressure anisotropy on oscillations of magnetotail.

20 p2603 A73-38903

The question of the method of studying cosmic ray anisotropy

21 p2755 A73-40111

Calculation of the power of polarized emission from a laser with an anisotropic resonator

21 p2712 A73-40312

Diurnal, semidiurnal, and the eight-hour components of cosmic-ray anisotropy

21 p2758 A73-40601

Texture and anisotropy of the properties of titanium sheet

21 p2719 A73-40852

Anisotropic contact discontinuities at magnetospheric boundary and tail from MHD space plasma data analysis, suggesting sector boundary identification in interplanetary magnetic field

23 p3008 A73-43227

Higher order Compton-Getting anisotropies in particle population distribution function of low energy solar protons in interplanetary space

23 p3024 A73-43698

Influence of iron ordering on the induced anisotropy in Li-Fe ferrites

23 p3018 A73-44175

Variations of three-dimensional anisotropy of cosmic rays during Forbush decreases.

24 p3125 A73-45102

ANNEALING

NT PULSE HEATING

Structural changes following annealing in a dispersion-strengthened tungsten alloy

01 p0062 A73-10261

Influence of high-temperature annealing on the rupture characteristics of zirconium carbide

02 p0178 A73-11541

Change in critical current of superconducting NbTi by neutron irradiation.

02 p0200 A73-11842

The effect of prior deformation on the strength and annealing of reverted austenite.

02 p0183 A73-12766

Effect of a temperature gradient on bubble growth in tungsten.

04 p0463 A73-15307

Plastic anisotropy of low-carbon, low-manganese steels containing niobium.

04 p0463 A73-15309

Electron microscopic investigation of cold worked and annealed thin V and Mo foils recrystallization characteristics, considering effect of grain boundaries pinning at surface

05 p0588 A73-17245

Influence of annealing at near melting point temperatures on the substructure of aluminum single crystals

06 p0707 A73-18036

Structural changes arising in nickel under the action of ultrasound and subsequent thermal annealings

06 p0708 A73-18053

Surface layer grain boundary corrosion damage of Ti alloys during vacuum annealing, reducing rupture strength, vibration resistance and bending fatigue limit

06 p0698 A73-18205

Structure and properties of nickel-phosphorus coatings in relation to annealing temperature and time.

06 p0698 A73-18214

Viscosity investigation of sintered fiberglass in the region of softening and annealing temperatures

06 p0715 A73-18657

Substructure and dispersion hardening in aged, cold worked, and annealed Al-4 wt pct Cu alloy.

06 p0711 A73-18754

Some further comments on Stage III recovery in Group VA body-centered cubic transition metals.

07 p0839 A73-20113

Effects of heat treatment on the properties of a molybdenum-carbon-nickel alloy and joints in it.

07 p0840 A73-20371

Influence of the substrate and the structure of the metal film on the nature of the annealing treatment of defects formed in the film by proton bombardment

07 p0864 A73-20524

Observation of Bardeen-Herring sources in quenched magnesium

08 p0979 A73-21629

Electric resistance of hydraulically extruded and annealed beryllium

09 p1098 A73-21847

Influence of annealing under load on the structure and properties of a self-ordering Ni3Mn alloy

09 p1099 A73-21957

Annealing of discontinuities in deformed aluminum

09 p1100 A73-21973

Drift of the breakdown voltage in highly doped planar junctions.

09 p1064 A73-23047

Stability of structure and mechanical properties of molybdenum under prolonged influence of temperature and stress.

09 p1106 A73-23160

Electrothermal annealing via electrical heating in vacuum for improved plasticity of thin walled molybdenum alloy elements after cold working

09 p1107 A73-23196

Influence of the degree of deformation and annealing temperature on the recovery of 99.999% pure nickel after plastic deformation at -196 C and 25 C, respectively

10 p1231 A73-23690

Annealing of effects arising during ion-bombardment alloying of metals at energies up to 10 keV

10 p1223 A73-23817

Cu annealability tests for assessing suitability for applications requiring low softening temperature, discussing recrystallization behavior and softness measures

11 p1379 A73-25130

Stability of nickel coated sapphire whiskers.

11 p1389 A73-26044

Pressure sensitization relation to electrical conductivity relaxation during isothermal isobaric annealing of CdTe crystals

12 p1531 A73-27196

The role of annealing twins in the primary recrystallization of nickel 270 work hardened in tension

12 p1514 A73-27988

Optimal conditions for residual stress reduction in a cylindrical shell by local annealing

14 p1814 A73-30721

Influence of annealing temperature on the changes in the chemical and phase compositions of the intercrystalline boundaries of weakly-alloyed molybdenum

14 p1764 A73-30865

Effect of ordering on the properties of oxygen solid solutions in titanium

15 p1893 A73-32516

The influence of prior thermal treatment of cast blocks on the coarse grain characteristics in extruded bars and profiles of alloys of the type AlCuSiMn

16 p2021 A73-33952

Behavior of hafnium dioxide particles in dispersively hardened nickel during isothermal annealing

17 p2188 A73-34560

Some physicochemical and technological aspects of obtaining annealed coatings from melts and semimelts

18 p2318 A73-35887

Threshold voltage stability improvement of p- and n-channel SNOS FET by annealing silicon nitride in oxygen or steam prior to gate deposition

19 p2471 A73-38451

Generation of vacancies in tungsten by rapid-rate deformation at elevated temperature.

20 p2578 A73-39492

Structural changes during plastic deformation and annealing of tungsten single crystals

20 p2579 A73-39738

Electrical resistance variation kinetics in deformed beryllium after annealing

20 p2579 A73-39746

Investigation of the imperfect structure of polycrystalline aluminum after low-temperature rolling and annealing

20 p2579 A73-39747

Influence of relief annealing on the mechanical properties of high-strength hydrogenized steel

21 p2721 A73-41228

The influence of crystal defects in platinum on platinum resistance thermometry.

22 p2855 A73-42009

Investigation of the structure and properties of annealed alloys of the Ti-Mo system

23 p2990 A73-43484

Concentration curves and phase diagram plotted for Nb-Zr system diffusion layers during annealing at 700 to 1700 C

23 p2991 A73-43649

Postannealing isothermal decomposition products of Al-Mn alloys studied by transmission electron microscopy, revealing trigonal and hexagonal lattice diffraction patterns

23 p2993 A73-43916

The metallurgy of Remendur - Effects of processing variations.

23 p2993 A73-43987

ANNIHILATION REACTIONS

NT POSITRON ANNIHILATION

Galaxy formation from annihilation-generated supersonic turbulence in the baryon-symmetric big-bang cosmology and the gamma-ray background spectrum.

04 p0499 A73-15353

Pair annihilation into neutrinos in strong magnetic fields.

11 p1402 A73-26414

Certain quantum-gravitational effects in central classical fields

12 p1538 A73-26970

Generation of magnetic fields in a matter-antimatter universe.

20 p2611 A73-39587

Galactic positronium annihilation gamma ray spectrum with 476 keV photon peak, indicating possible origin in supernova explosive nucleosynthesis of positrons

21 p2770 A73-40941

Ionospheric metastable particle production and annihilation during photochemical reactions, determining neutral and ionized particle abundance profiles

23 p2978 A73-43979

ANNUAL VARIATIONS

A two-component model of the annual line in the spectrum of the geomagnetic field.

01 p0036 A73-10331

Research of the emission at 5577 A in the period of 1958-1967 in Ashkhabad.

01 p0036 A73-10345

Natural variation of the radiation budget of the earth-atmosphere system as measured from satellites.

01 p0038 A73-10390

Winter anomaly in ionospheric absorption of radio waves on 1.725 MHz during sunspot minimum.

01 p0043 A73-10910

Comparative study of monthly and diurnal occurrences of whistlers and gyroelectric echoes in conjugate regions of Europe and South Africa

01 p0043 A73-11274

Annual and sub-annual effects of EUV heating. I - Harmonic analysis. II Comparison with density variations.

02 p0158 A73-11914

The radiation budget of the earth-atmosphere system as measured from the Nimbus 3 satellite 1969-1970/.

02 p0160 A73-12266

Satellite drag data for analysis of semiannual atmospheric density variations, showing latitudinal dependence of amplitude

02 p0161 A73-12281

Effects of vertical mass motions on the composition structure in the thermosphere.

02 p0162 A73-12291

Seasonal and monthly global atmosphere radiative profiles of thermal and solar heating due to ozone and cooling due to carbon dioxide

02 p0165 A73-12780

Lunar axis inclination to ecliptic axis as function of time, tabulating variations during 1971

03 p0367 A73-13078

Simulations of the annual variation of the zonally averaged state of the atmosphere.

03 p0301 A73-13799

Thermospheric parameters seasonal and latitudinal variations calculation based on atmospheric model with components ionization and molecular oxygen dissociation as main heat sources

03 p0304 A73-14563

Equatorial scintillation diurnal and seasonal variations and F region electron density irregularities, noting unusual post sunset behavior of Faraday rotation angle

[AD-757291]

04 p0440 A73-14951

Annual and semi-annual zonal wind components and corresponding temperature and density variations, 60-130 km.

04 p0440 A73-14961

Changes in thermospheric molecular oxygen abundance inferred from twilight 6300 A airglow.

04 p0440 A73-14963

Solar cycle control of the ionospheric E-region.

04 p0441 A73-15291

Theoretical model for the latitude dependence of the thermospheric annual and semiannual variations.

04 p0444 A73-15538

K indices measurements at antipodal earth surface observatories for aa indices, discussing one hundred year series

04 p0444 A73-15547

Altitude variations of the sporadic E layer at geographical mid-latitudes

05 p0568 A73-16217

Diurnal and annual behavior of the radiation balance

05 p0609 A73-16218

Lunisolar tidal effects and motions in the F region
05 p0568 A73-16255

Temperature fluctuations in the ionospheric F region
05 p0568 A73-16256

Equatorial stratosphere quasi-biennial oscillation variations from temperatures and zonal winds measured at Canton Island, Ascension Island and Balboa /Canal Zone/
05 p0594 A73-16573

Diurnal and seasonal variations in conditions for the occurrence of the F1 layer over Middle Asia during the IQSY period
05 p0569 A73-16615

Latitude, longitude and hemisphere effects on Appleton E layer seasonal anomaly from statistical analysis of critical frequency
05 p0571 A73-17059

Upper atmospheric dust particle temperature and related Na atom abundance seasonal variation based on energy budget and Na sublimation rate considerations
05 p0571 A73-17061

Ionospheric electron density profiles model evaluation, considering E region height and thickness seasonal variation
05 p0571 A73-17063

Annual fluctuation in atmospheric transmission of normal incidence solar radiation
05 p0611 A73-17183

Seasonal variations in carbon monoxide content of the atmosphere
05 p0572 A73-17357

Three dimensional summer time sporadic E layer structure and electron concentration during 1966-1969 by ionospheric space diversity sounding
06 p0689 A73-17553

Seasonal variations in the solar and lunar daily geomagnetic variations.
07 p0813 A73-19024

Meteorological rocket observations of amplitudes and phases of zonal wind quasi-biennial oscillations at 25-60 km during 1962-1969
07 p0846 A73-19040

Geomagnetic activity semiannual and diurnal variations due to interplanetary field southward component interaction with magnetosphere based on model ordered in solar equatorial coordinates
07 p0813 A73-19234

Lower ionospheric seasonal anomaly in electron density levels, noting diurnal and latitudinal characteristics at various heights
07 p0816 A73-19453

Scattered twilight light variations at 5500 to 6600-A wavelengths according to spectral observations in 1962 through 1968 at Abastumani
07 p0817 A73-19587

Annual and semi-annual variations in the electron density of the inner magnetosphere deduced from whistler dispersion.
07 p0819 A73-20061

The ground surface of planet Mars
07 p0900 A73-20243

Trigonometric series for earth rotation velocity around solar system center of mass
07 p0902 A73-20325

Zonal and seasonal peculiarities in the influx of diffuse solar radiation
07 p0848 A73-20625

Mariner 9 ultraviolet spectrometer experiment - Seasonal variation of ozone on Mars.
08 p1009 A73-21223

Estimation of the seasonal variation of the gas composition of the atmosphere at the height of the F1 layer from data on the developmental conditions of the layer
08 p0958 A73-21281

Interstellar gas role in cosmic ray yearly variations determined from solar short wave radiation induced gas ionization
08 p0999 A73-21338

Diurnal, sporadic and yearly variations in cosmic ray flux based on neutron component data, noting relation to solar activity cycles
08 p1000 A73-21345

The mean upper-air flow in Southern Hemisphere temperate latitudes determined from several years of GHOST balloon flights at 200 and 100 mb.
08 p0960 A73-21376

Experiments on the seasonal variation of the general circulation in a statistical-dynamical model.
08 p0960 A73-21378

Storms and the seasonal anomaly in the topside ionosphere.
09 p1075 A73-22132

Type variation of solar sudden field anomaly /SFA/ on 164 kHz as an indicator of seasonal structure changes in the D-region.
09 p1076 A73-22141

Exchange of water vapor between the atmosphere and surface of Mars.
09 p1145 A73-22270

Catalog of geomagnetic activity indices for the years 1841-1864 and 1870
09 p1077 A73-22543

Conditions of Leonid meteor shower encounters with the earth in occurrences of the years 1898-2000
09 p1146 A73-22546

Characteristics of the development of the quasi-biennial cycle above the Indian Ocean
09 p1115 A73-22991

Rapid intensification and low-latitude weakening of tropical cyclones of the western North Pacific Ocean.
10 p1245 A73-23986

Signal reflection height seasonal variations effect on radio waves absorption estimation from vertical ionospheric sounding
10 p1188 A73-24242

Investigation of the influence of precession, nutation, and yearly aberration on the average equatorial coordinates, azimuth, and elevation of the North Star
10 p1281 A73-24476

Forecast maps for seasonal variations in the geometrical parameters of the F2 layer
11 p1351 A73-25094

The diurnal and semidiurnal barometric oscillations, global distribution and annual variation.
11 p1351 A73-25167

Seasonal variations in the telluric lines of oxygen and water vapor
11 p1392 A73-25614

Ariel 3 satellite observations of the ionosphere at high southern latitudes.
11 p1353 A73-25754

The nature of seasonal changes in the effects of magnetic storms on mid-latitude F-layer electron concentration.
11 p1358 A73-26708

Diurnal, seasonal and solar cycle changes in southern midlatitude ionosphere electron content from June 1965-August 1971
11 p1359 A73-26712

Seasonal and diurnal variations of forbidden oxygen and sodium lines emission, stressing nightglow zenith intensity fluctuations connection to F layer electric fields
12 p1489 A73-26992

Trigonometric series for earth rotation velocity around solar system center of mass
12 p1540 A73-27297

Annual solar activity changes due to interstellar matter capture by sun, noting uneven sunspots distribution
12 p1535 A73-27770

An analysis of seasonal changes in electron densities at middle latitudes in the lower D-region.
13 p1606 A73-28207

The earth's rotation and atmospheric circulation. I - Seasonal variations.
13 p1606 A73-28282

An interpretation of the ambiguity between annual terms obtained by time and latitude observations.
13 p1678 A73-28384

On the regularity of fluctuations in annual and secular polar motions.
13 p1678 A73-28385

Earth liquid core effect on axis annual nutation, deriving Z term for correction of International Latitude Service latitude variation data
13 p1606 A73-28400

On the relation between the rotation of the earth and solar activity.
13 p1680 A73-28408

Ozone variation in the lower stratosphere and its mechanism.
13 p1611 A73-29664

Seasonal and sunspot cycle variations of F region electron temperatures and protonospheric heat fluxes.
14 p1749 A73-29986

Anisotropy parameters of the ionospheric irregularities at Thumba during high solar activity period.
14 p1750 A73-30905

Seasonal variations of the carbon monoxide concentration in the atmosphere.
15 p1865 A73-31007

Average high latitude magnetic field: Variation with interplanetary sector and with season. I - Disturbed conditions.
15 p1866 A73-31073

Spectral investigations of 6300 A forbidden OI twilight emission at Abastumani
15 p1867 A73-31264

Numerical study of the seasonal variations of the ionosphere.
15 p1867 A73-31381

Short-wave skip distance for various models of the ionosphere
15 p1843 A73-31575

Seasonal movement of the Sq current foci and related effects in the equatorial electrojet.
15 p1869 A73-31754

Semi-annual variation in the true height of the F2-peak in low latitudes /at Puerto Rico/.
15 p1869 A73-31762

Yearly and trimonthly variations in solar activity and cosmic-ray intensity
15 p1926 A73-31879

Electron concentrations increase observed at 60-90 km altitudes during anomalous winter radio wave ab-

sorption, noting association with upward aerosol transport decrease

15 p1844 A73-31889

Comparison of true and effective altitudes of the sporadic E layer
15 p1872 A73-31899

Anomalous winter time absorption of radio waves in the middle latitude ionosphere
15 p1844 A73-31900

Estimate of the influence of the seasonal redistribution of air masses on the motion of the earth's poles
15 p1939 A73-31967

Kinetic energy conversions by horizontal and vertical eddy processes from 5 years of hemispheric data.
15 p1873 A73-32253

Map series for description of annual temperature wave in lower stratosphere in Northern Hemisphere, establishing easterly circulation on south side of Aleutian high
15 p1873 A73-32254

Noctilucent clouds seasonal distribution, altitude and displacement velocity from German observations during 1885-1941
15 p1873 A73-32347

The stability of a time-variable surface wind
15 p1906 A73-32353

Model concept concerning some control principles of the human organism. III - Seasonal adaptation
15 p1836 A73-32357

Three dimensional summer time sporadic E layer structure and electron concentration during 1966-1969 by ionospheric space diversity sounding
16 p2002 A73-32777

On the annual variation of solar faculae.
16 p2053 A73-33073

Geomagnetic effects on cosmic ray cut-off daily, seasonal and secular variations, considering north-south symmetry and magnetospheric models
16 p2055 A73-33297

Role of water vapor in the meteorology of Mars
16 p2069 A73-33831

Primary scattering theory for twilight luminance calculation, considering luminance atmospheric scale height growth in thermosphere and seasonal variation
16 p2009 A73-33889

Atmospheric composition changes and the F2-layer seasonal anomaly.
16 p2010 A73-33915

The inertia tensor of the atmosphere, annual variations in its components, and variations in the earth's rotation
17 p2158 A73-34343

Icing conditions of modern transport aircraft according to cruise flight data
17 p2100 A73-34545

Diurnal, annual and solar cycle variations of hydroxyl and sodium nightglow intensities in the Europe-Africa sector.
17 p2160 A73-34785

Results of simultaneous in-situ-observations in Spain of electron concentration, neutral wind and air pressure in the D-region in different seasons and during an SID-event and their relevance to the winter-anomalous state of the atmosphere.
18 p2305 A73-36001

Air density at heights near 200 km from the orbit of 1970-65D.
18 p2309 A73-36052

Interpretation of short period density changes shown by the drag of satellites.
18 p2310 A73-36133

Differences in circulation of the upper atmosphere in low latitudes of the southern and northern hemispheres.
18 p2310 A73-36138

Semi-annual modulation of earth's magnetic field in the equatorial electrojet region.
18 p2311 A73-36187

Semiannual effect in thermosphere due to solar heat input associated with subsolar point migration and auroral heating by magnetic storms
18 p2312 A73-36300

Mars atmosphere during the Mariner 9 Extended Mission - Television results.
19 p2478 A73-37218

Diurnal and annual temperature variations in the 30-60 km region as indicated by statistical analysis of rocketsonde temperature data.
19 p2424 A73-37662

Estimation of the seasonal variation of the gas composition of the height of the F1-layer from data on the conditions of its development.
19 p2424 A73-37910

Photometric measurements of zenith night sky over Fritz Peak /CO/ for diurnal and seasonal variation of nightglow continuum
19 p2425 A73-38013

Global model of the general circulation of the atmosphere below 75 kilometers with an annual heating cycle.
19 p2449 A73-38287

Effective altitudes of the F region in the IQSY and IQSY periods
20 p2554 A73-39167

Midlatitude ionospheric disturbances
20 p2554 A73-39172

Stratifications in the F region of the ionosphere
20 p2554 A73-39174

Correlational relations between F2 critical frequency deviations and the solar activity cycle according to a number of high-latitude stations
20 p2555 A73-39176

Altitude dependence of F 2 layer electron density annual anomaly, discussing summer-winter density discrepancies and noontime critical frequencies
20 p2555 A73-39177

Variations in the M/3000/F2 coefficient as a function of the solar energy entering the earth's atmosphere
20 p2555 A73-39179

Seasonal and solar cycle dependence of the position of the cusp region of the magnetosphere.
20 p2555 A73-39828

Statistical analysis of daily, monthly, annual and seasonal activity of earth currents field, presenting tables of storms and disturbances
21 p2681 A73-40107

Seasonal variations of the barometric effect of the cosmic ray neutron component intensity
21 p2755 A73-40114

Topside ionospheric winter and summer diurnal electron density variations in Arctic regions as function of universal time, showing Ariel 3 measurements graphically
21 p2682 A73-40171

Atmospheric structure and its variations in the region from 25 to 120 km.
21 p2683 A73-40628

Exospheric and thermospheric structure variations with solar activity, diurnal variation, geomagnetic activity, seasonal-latitudinal variations of He, H and density waves
21 p2683 A73-40630

Thermospheric density diurnal and seasonal variations from cosmos drag data, discussing amplitude, density distribution, coefficients of expansion, summer solstice spherical functions
21 p2689 A73-41351

Ionospheric research by rocket, satellite and ground based methods, discussing ion and neutral chemistry, stratospheric-ionospheric coupling, ionospheric thermal structure, etc
21 p2689 A73-41358

Seasonal variation of atmospheric composition in the F region as a function of solar activity.
21 p2690 A73-41360

Diurnal and seasonal variations of neutral winds and electric fields above 90 km in the vicinity of the auroral electrojet.
21 p2690 A73-41365

Zonal wind semiannual variations at 20-65 km, noting wave maximum amplitude and maximum location.
22 p2883 A73-42550

Polar magnetic storm temporal properties and distribution patterns, discussing solar activity, annual and twenty-seven day variations and sudden commencement
22 p2851 A73-42749

Data reduction for annual, diurnal and satellite observation aberrations via rectangular coordinate method, discussing parallax, refraction, instrument eccentricity and computer applications
22 p2915 A73-43034

Global climatological ozone changes in terms of secular, annual and sunspot cycle-related variability
23 p2974 A73-43858

The average tropospheric ozone content and its variation with season and latitude as a result of the global ozone circulation.
23 p2974 A73-43862

Ozone concentration studies and ozone flux measurements near the ground at Poona.
23 p2974 A73-43868

Six years of regular ozone soundings over Switzerland.
23 p2974 A73-43870

Studies of variations in the vertical ozone profiles over India.
23 p2975 A73-43871

Statistical characteristics of the vertical ozone distribution in mid-latitudes.
23 p2975 A73-43874

Variations of the total amount of ozone and the behaviour of some ionospheric parameters in the winter time upper atmosphere.
23 p2976 A73-43885

Ozone and airglow in the mesosphere region.
23 p2976 A73-43886

Ozone and temperature change in the winter stratosphere.
23 p2977 A73-43901

Atmospheric ozone and the movement of the air in the stratosphere.
23 p2977 A73-43903

Ozone variation in the lower stratosphere and its mechanism.
23 p2977 A73-43908

Mediterranean, south Sahara and northwest India rainfall records analysis, correlating general circulation changes with winter-spring and monsoon rainfall fluctuations
23 p3003 A73-43954

Appleton seasonal anomaly in E region maximum electron density investigated by critical frequency data statistical analysis, showing solar activity effects
23 p2979 A73-44006

Estimated seasonal redistribution of air masses affecting motion of earth's poles.
24 p3081 A73-44492

Mars seasonal effects from observations of contrast changes in blue light, discussing diurnal variations and UV contrast reversal
24 p3134 A73-44567

Vertical and latitudinal development of a seasonal anomaly in the daytime F2 region. I
24 p3083 A73-44791

Short-time fluctuations of the VLF field along polar paths
24 p3067 A73-44809

Some characteristics of satellite-observed bands of persistent cloudiness over the Southern Hemisphere.
24 p3107 A73-45015

Seasonal variations of the south polar cap of Mars according to measurements made on photographs taken near the time of the 1971 opposition.
24 p3143 A73-45439

ANNULAR DRAINAGE PATTERNS
U DRAINAGE PATTERNS
ANNULAR FLOW
Temperature characteristics in the wall of an annular channel heated internally at supercritical pressures
01 p0123 A73-10861

The development of high performance annular combustion chambers at SNECMA
03 p0360 A73-14151

Stability of nonrotationally symmetric disturbances for inviscid flow between rotating cylinders in the presence of an axial magnetic field.
04 p0433 A73-14899

Combustion effectiveness in high speed swirling flow tested in chamber with premixed air-kerosene mixture injected tangentially in annular channel [ONERA, TP NO. 1076]
04 p0517 A73-15098

Turbulence in the annular flow of a conducting-fluid in a magnetic field
05 p0603 A73-16587

Effect of the asymmetry of an external magnetic field on a viscous fluid flow in an annular MHD channel
05 p0603 A73-16589

Application of invariant imbedding techniques to flow instability problems.
05 p0591 A73-16608

Approximate calculations of the hydrodynamic characteristics of a turbulent flow of liquid in annular channels
06 p0688 A73-18562

Mathematical models for critical flow rates of annular two phase mixtures under various discharge conditions
06 p0688 A73-18563

German monograph - Free convection of air in a horizontal circular gap in the case of temperature- and pressure-dependent density.
07 p0920 A73-19579

Spiral flows in finite rotating annular tubes.
07 p0812 A73-20435

Heat transfer and friction coefficients for turbulent flow of air in smooth annuli at high temperatures.
10 p1297 A73-24970

Convection in a rotating annulus uniformly heated from below. II - Nonlinear results.
11 p1449 A73-25159

Movement of viscous incompressible fluids through annular interstices with walls in relative alternating translational motion
12 p1486 A73-26795

Temperature conditions at the wall of an annular channel with internal heating at supercritical pressures.
12 p1560 A73-27910

Supersonic annular blade cascades starting conditions, presenting static pressure and Mach number distributions
13 p1565 A73-28837

Control by pressure drop of the radial distribution of the Mach number behind a subsonic annular cascade [ONERA, TP NO. 1219]
13 p1565 A73-28838

Spiral flows with multiple circulation in channels of simple shape
15 p1861 A73-31284

Laminar stratified flow of a conducting medium in ring channels in the event of great MHD-interaction parameters
15 p1918 A73-31409

Determination, by a wall probe, of the changing regime of the flow between two off-center cylinders with very close radii
15 p1863 A73-31568

by the slow and uniform rotation of walls of a ring-shaped receiver, in the presence of an axial magnetic field, in the case where the mean value of the intensity of the currents induced in a straight section takes a nonzero value
15 p1918 A73-31569

The computation of the flow in the gap between two concentrically rotating spherical surfaces
16 p2000 A73-33255

Stability of a viscous fluid between rotating cylinders with axial flow and pressure gradient round the cylinders.
16 p2000 A73-33312

Approximate calculations of the hydrodynamic characteristics of turbulent fluid flow in annular ducts.
16 p2000 A73-33587

Mathematical models for critical flow rates of annular two phase mixtures under various discharge conditions
16 p2000 A73-33588

Analysis of flow separation in an annular expansion - Contraction with inner cylinder rotating. [ASME PAPER 73-FE-7]
17 p2152 A73-35006

Turbulent viscosities for swirling flow in a stationary annulus. [ASME PAPER 73-FE-16]
17 p2152 A73-35013

Sound measurements within and in the radiated field of an annular duct with flow.
18 p2302 A73-37028

Droplet transfer in two phase annular mist flow. II - Prediction of droplet transfer rate.
19 p2423 A73-38350

MPD annular duct flows in crossed external fields for arbitrary values of the Hall parameter
20 p2599 A73-39675

Reduction of fan noise by annulus boundary layer removal.
22 p2795 A73-41713

Attenuation of spiral modes in a circular and annular lined duct.
22 p2839 A73-41714

Creeping flow of Newtonian fluids in curved rectangular channels.
22 p2840 A73-41745

Thermal convection in a large rotating fluid annulus - Some effects of varying the aspect ratio.
23 p3002 A73-43597

Unsteady aerodynamic loads on slender cones at free-stream Mach numbers from 0 to 22. [AIAA PAPER 73-998]
24 p3053 A73-44833

Effect of a slipstream on the acoustic radiation of ultrasonic annular jets
24 p3055 A73-45358

ANNULAR JETS
U ANNULAR FLOW
U JET FLOW
ANNULAR NOZZLES
Annular truncated plug nozzle flowfield and base pressure characteristics.
05 p0530 A73-16887

[AIAA PAPER 73-137]
Calculation of the potential flow about axisymmetrical fuselages, annular profiles, and propulsion system inlets [DFVLR-SONDDR-265]
07 p0773 A73-19205

Aerodynamic experimental investigation of annular cascade of gas turbine nozzle blade in subsonic and supersonic flow.
08 p0925 A73-20939

ANNULAR PLATES
Axisymmetric buckling and stability of annular sandwich panel under radially varying in-plane stresses
01 p0115 A73-10740

Plane stress analysis of an annular disk with distorted inner hole.
01 p0115 A73-10754

Numerical solution to the problem of the elastoplastic stability of doubly connected plates with curvilinear boundaries
02 p0231 A73-11813

HF transverse resonant vibrations of annular Al plates with polychlorovinyl and polyamide base coatings, noting damping and strain relationship to energy dissipation
03 p0394 A73-14009

Large deflection calculation of circular and annular strain hardenable rigid plastic plates under axisymmetric load, using Kirchhoff-Love hypothesis and Tresca flow condition
03 p0394 A73-14022

Comparison of eigenvalues and characteristic vibration modes of circular ring bars, circular ring disks, and circular ring fibers
06 p0758 A73-17584

Comparison of the characteristic values and characteristic vibration forms of a circular ring beam, a circular ring disk, and a circular ring fiber. II
06 p0759 A73-17586

Muskelishvili boundary value problem of plate bending and point deformation for round and annular plates under uniform loads
09 p1159 A73-22854

Rayleigh-Ritz method for natural frequencies of transversely vibrating polar orthotropic annular per-

forated plates, proposing coordinate transformations for asymmetric mode solutions

11 p1446 A73-26495

On moderately large deflection of multiply connected plates.

12 p1557 A73-27933

Critical load determination for nonsymmetrical stability losses of ring shaped plates clamped against bending

15 p1945 A73-31029

Thin elastic orthotropic annular plate postbuckling behavior under planar edge compression loads, analyzing axisymmetric deformations via nondimensional equations and Keller-Reiss numerical method [ASME PAPER 73-APM-5]

17 p2247 A73-35030

Limiting zero and infinite edge beam stiffness effect on natural vibrational frequencies of reinforced annular plates

20 p2622 A73-39548

Free and forced nonlinear oscillations of anisotropic orthotropic annular plate with free inner boundary and fixed immovable outer boundary

20 p2623 A73-39561

Buckling of continuous circular plates.

21 p2782 A73-40004

Deflection function for the asymmetrical bending of circular plates.

21 p2784 A73-40435

Dynamic stability of rotating disks loaded by a concentrated force

22 p2928 A73-43064

ANNULI

Radiation configuration factors for annular rings and hemispherical sectors.

15 p1959 A73-32281

Stability of parallel flow of a dusty gas in an annulus.

20 p2548 A73-39523

Spaced annular ring shell-to-shell and shell-to-tube view factors for finite difference radiative heat transfer solutions

22 p2923 A73-42564

ANODES

NT CELL ANODES

Characteristics of a vacuum discharge triggered by an electron beam.

06 p0722 A73-17424

Radial anode current density distribution measurement in high current pulsed arcs in air on copper split anode, using Rogowski coils

06 p0723 A73-18357

Coaxial anode for background suppression in X-ray proportional counters.

13 p1612 A73-28367

Self-sustaining Penning avalanche discharge in crossed electric and magnetic fields, discussing anode surface boundary effects and maximum discharge intensity conditions

23 p3015 A73-44345

ANODIC COATINGS

Russian papers on metal corrosion and protection covering additives, annealing, polymer coatings, anodic polarization, electrodeposition, magnetic alloy coatings, etc

02 p0174 A73-12534

Surface properties improvement of Al products by metal coatings, noting corrosion prevention, anodic coatings, enameling and brazing

03 p0312 A73-13580

The growth of dielectric aluminum and tantalum oxide layers

08 p0977 A73-21023

An ultrasonic device for the study of fatigue crack initiation in anodized aluminum alloys.

[AD-760070]

11 p1363 A73-25830

Anodic oxidation and stress corrosion cracking (SCC) of titanium alloys. I - Factors affecting SCC and their influence on the anodic behavior of alloy Ti-6Al-6V-2.5Sn.

17 p2187 A73-34524

Properties of anodic oxide films formed in the anodization of silicon nitride.

[ECS PAPER 81]

21 p2702 A73-40844

The mechanism of electrical erosion in composite materials during electric arc alloying

24 p3093 A73-44743

ANODIZING

Chemical and electrolytic coatings for satellite surface thermal control, discussing surface anodic oxidation treatment of adhesive Au platings on Al alloys

07 p0829 A73-18910

Choosing the parameters for plasma anodizing of aluminum

07 p0830 A73-19293

The electrical properties of anodically grown silicon dioxide films.

09 p1064 A73-23042

ANOLYTES

Composition of anolyte within pit anode of austenitic stainless steels in chloride solution.

07 p0840 A73-20352

ANOMALOUS TEMPERATURE ZONES

Macroscale interaction between the atmosphere and oceans and the role of the latter in the formation of anomalous circulation in the stratosphere

10 p1246 A73-24374

ANORTHOSITE

The composition of the lunar highlands - Evidence from modal and normative plagioclase contents in anorthositic lithic fragments and glasses.

02 p0220 A73-12478

Lunar 'dunite', 'pyroxenite' and 'anorthosite.'

03 p0375 A73-14108

Spinel troctolite and anorthosite in Apollo 16 samples.

05 p0615 A73-16323

Optical and chemical analysis of iron in Luna 20 plagioclase.

13 p1674 A73-28305

Luna 20 - Mineralogy and petrology of fragments less than 125-micron size.

13 p1676 A73-28324

Apollo 17 landing site crystalline rock age determinations for coarse grained basalt and anorthositic gabbro samples via Ar isotope ratios

14 p1788 A73-29720

Natural exoelectron emission from anorthosite rocks supplied by the Luna-20 automatic interplanetary station

14 p1802 A73-30833

Natural exoelectron emission of anorthosite rocks returned by the automatic interplanetary station Luna-20.

23 p3028 A73-43583

ANOXIA

Importance of the Lohmann reaction in the response of the heart to anoxic aggression

02 p0133 A73-12152

ANS

U ASTRONOMICAL NETHERLANDS SATELLITE

ANTARCTIC REGIONS

Geophysical data transmission from automatic stations in the antarctic via earth synchronous satellites.

04 p0421 A73-15430

Solar cosmic ray flare recording in stratosphere in Murmansk and Antarctic regions during February-April 1969

08 p1000 A73-21347

Whistler observations of the depletion of the plasmasphere during a magnetospheric substorm.

09 p1074 A73-22060

ISIS-1 satellite observations of the ionosphere at high southern latitudes.

11 p1353 A73-25753

Ariel 3 satellite observations of the ionosphere at high southern latitudes.

11 p1353 A73-25754

Midday aurora behavior during auroral substorms from all sky photographs at south pole, considering modification of Starkov-Feldstein model

12 p1493 A73-27614

Simultaneous determination of chord length and direction by artificial earth satellite geodetic observations in Arctic and Antarctic regions

13 p1610 A73-29320

French monograph - Interpretation of particle measurements carried out aboard rocket probes during the solar event of Jan. 28 1967.

15 p1927 A73-32586

VLF goniometer observations at Halley Bay, Antarctica. I - The equipment and the measurement of signal bearing. II - Magnetospheric structure deduced from whistler observations.

17 p2159 A73-34777

The cartographic and scientific application of ERTS-1 imagery in polar regions.

18 p2306 A73-36019

Polar albedo changes and its climatic consequences.

18 p2307 A73-36028

Ten years Antarctic region ionosphere investigation during IGY-ISQY period considering ionization maxima, inhomogeneity drifts, electron density and short wave propagation

20 p2554 A73-39171

Arctic-Antarctic geodetic survey program, discussing length and direction determination for lines connecting eight principal locations

21 p2685 A73-40813

Ventifact evolution in Wright Valley, Antarctica.

21 p2687 A73-41211

Observations of electron fluxes and related variations of ionospheric plasma parameters in the south polar cusp.

21 p2690 A73-41369

Soil microbiological tests to evaluate Antarctica as Mars environment model for quarantine standards

22 p2803 A73-42162

ANTARCTICA

U ANTARCTIC REGIONS

ANTENNA ARRAYS

NT LINEAR ARRAYS

NT STEERABLE ANTENNAS

NT TURNSTILE ANTENNAS

NT YAGI ANTENNAS

Aperture matching of wideband phased array radar antennas, using digital ferrite phase shifters and dielectric transformer with magnetic resonance limiting

01 p0022 A73-10178

A decoupling supply network for small antenna arrays

02 p0145 A73-11825

Antenna array synthesis in Chebyshev approximation, calculating array geometry and excitation amplitudes for double secant radiation pattern

02 p0146 A73-12022

X band microstripline slot antenna measurement for input impedance and radiation pattern dependence on slot-to-reflector spacing, applying to array design

02 p0141 A73-12100

Multipole sine-cosine azimuth patterns for wide aperture Adcock direction finders, determining spacing and reradiation errors and array pickup factor

02 p0142 A73-12529

Radiation from a continuous semi-circular arc antenna array.

02 p0148 A73-12852

Theoretical analysis and experimental verification for multielement dipole antenna array of unequal parallel conductors, noting impedance characteristics desirable for broadband use

02 p0148 A73-12853

Far-field simulation of circular antenna arrays on the analog/hybrid computer

03 p0277 A73-13985

Reduction of antenna length via wave channel type antenna design with modulated phase velocity and multiple use of antenna array

03 p0284 A73-14031

Signal relay systems using large space arrays.

04 p0415 A73-14990

Random antenna array design for narrow beam radiation and blind angle avoidance, determining mutual coupling effect on performance

04 p0416 A73-15059

Voltage-controlled variable power divider.

04 p0428 A73-15454

Receiving antenna polarization parameters selection in side-looking synthetic aperture radars

04 p0423 A73-15914

Narrow band linear filter output SNR relationship to orthogonal radiating elements system directional gain and radiation patterns

05 p0555 A73-16056

Requirements for the production of several, mutually independent beams by a transmission-line fed antenna

05 p0559 A73-17238

Array factor of statistically thinned antenna arrays with an increased element-interspace minimum

06 p0674 A73-17810

Low-frequency loop antenna arrays - Ground reaction and mutual interaction.

06 p0665 A73-18176

Two-dimensional optical phased-array beam steering.

06 p0694 A73-18287

Analysis of antenna structures assembled from arbitrarily located straight wires.

06 p0668 A73-18441

An analysis of an arbitrary n-element adaptive array.

07 p0795 A73-20583

On stochastic approximation and the hierarchy of adaptive array algorithms.

07 p0846 A73-20585

Antenna array synthesis for radiation patterns prescribed by continuous function, proposing formulas for current determination

09 p1062 A73-22047

A local point method for problems of diffraction on an array

09 p1051 A73-22860

Computational estimate of applicability of infinite-array theory.

09 p1065 A73-23099

Ring arrays as medium- and long-wave broadcast antennas

11 p1336 A73-25318

Optimization of the loop-coupled log-periodic antenna.

11 p1337 A73-25652

Resonances in circular arrays with dielectric sheet covers.

11 p1337 A73-25654

Synthesis of broad-band arrays with arbitrary frequency-independent elements.

11 p1329 A73-25664

Butler submatrix feed systems for beam forming and scanning networks of linear and circular antenna arrays

11 p1338 A73-25671

Mutual coupling, mainlobe reflected power and radiation patterns of periodic antenna arrays thinned by statistically selected element feeds

11 p1332 A73-26205

Directivities of planar arrays with triangular arrangement of elements. 11 p1333 A73-26699

The significance of the elementary radiator directivity for the determination of the directive gain of linear arrays 12 p1468 A73-27039

Planar dipole antenna arrays directivity evaluation from spatial radiation density distribution, considering arbitrary aperture shape and amplitude loading 12 p1469 A73-27040

The 73.5-cm wavelength radio interferometer of the Burakan Observatory 12 p1479 A73-27226

Arched and spherical antenna arrays synthesis for given vectorial radiation patterns by numerical solution via algorithm using eigenfunctions 12 p1479 A73-27229

Shaping of antenna radiation patterns by passive radiating slots 12 p1479 A73-27230

Precision of amplitude-comparison direction finding by phased array antennas 12 p1470 A73-27579

Diffraction of a plane wave at an array of planar waveguides with projecting dielectric plates. 13 p1582 A73-28655

Space point group theory classification and analysis of antenna array lattices, noting current excitation space symmetries and orthogonal field pattern design 13 p1583 A73-28698

Application of adaptive arrays to suppress strong jammers in the presence of weak signals. 13 p1593 A73-29215

Baseline arrangement of radio interferometer array for tracking artificial satellites. 13 p1586 A73-29233

Radiating waveguide antenna elliptical beam off-axis gain maximization, applying to geostationary satellite 13 p1587 A73-29671

Book - Introduction to defense radar systems engineering. 13 p1587 A73-29677

Mutual coupling effects in semi-infinite arrays. 14 p1734 A73-30202

Comparison between the peak sidelobe of the random array and algorithmically designed aperiodic arrays. 14 p1734 A73-30217

The performance of transistor fed monopoles in active antennas. 14 p1735 A73-30219

Optimal antenna array signal to noise ratio gain comparison with conventional array for narrow band signal environment 14 p1735 A73-30222

E-plane synthesis of dipole array antennas. 14 p1735 A73-30223

Book - Topics in intersystem electromagnetic compatibility. 14 p1729 A73-30596

Experimental investigations of coupling phenomena in a periodic linear antenna array 14 p1729 A73-30697

Self complementary wire element phased array antennas, discussing matching, operating bandwidth, structural design and isolation 15 p1850 A73-31255

Runway VHF localizer antenna array for Norwegian airports II.S, taking into account difficulties due to course bends and snow 15 p1859 A73-32498

Mean value and variance of the directivity of randomly thinned array antennas 16 p1979 A73-33093

Coaxial cable fed dipole antenna array for observation of coherent backscatter radar signal from ionospheric electron density irregularities in electrojet region 16 p1987 A73-33117

Mutual coupling in the signal-to-noise ratio optimization of antenna arrays. 16 p1979 A73-33168

Size-reduced log-periodic dipole array antenna. 16 p1988 A73-33299

Compatible II.S involving pilot signal from microwave oscillator and precision II.S involving linear antenna array of emitter elements 17 p2207 A73-34484

Log-periodic dipole arrays - A numerical analysis. 17 p2141 A73-35367

A concentric ring transverse electromagnetic linear antenna array. 17 p2127 A73-35638

Dependence of sidelobe level on random phase error in a linear array antenna. 17 p2129 A73-35697

Antenna radiation patterns from statistical phase synthesis of antenna arrays, estimating directivity loss for in- and out-of-phase initial current distribution 17 p2129 A73-35708

Contribution to the theory of synthesis of discrete antennas in the case of a uniform approach to a given radiation pattern. 17 p2130 A73-35717

Antenna array facility with small digital computer and multichannel tape recorder for real time simulation of radiation source movement through view field 17 p2149 A73-35755

Tromso /Norway/ Auroral Observatory partial reflection experiment, considering data processing techniques, height resolution, phase detection, antenna arrays and D region drift measurements 18 p2315 A73-36009

Sampled aperture antenna array measurement of RF phase characteristics of diffraction pattern formed on ground by radio waves obliquely reflected from ionosphere 20 p2530 A73-39018

ILS capability improvements on localizer and glide-slope antenna arrays and monitors, considering effects of reflecting objects on or near aerodrome and terrain 21 p2736 A73-40049

Synthesis of impedance-type cylindrical antenna arrays 21 p2661 A73-40197

Application of linear programming in the statistical theory of antennas 21 p2661 A73-40201

Use of the azimuthal equal-area projection to display radiation patterns of complex antennas 21 p2661 A73-40202

Antenna system design for detection of random gravitational waves with separation from effects of antenna random fluctuations 21 p2662 A73-40315

Beam steering system of the north-south array of the DKR-1000 FIAN radio telescope 21 p2662 A73-40542

Phased array antennas; Proceedings of the Symposium, Polytechnic Institute of Brooklyn, Farmingdale, N.Y., June 2-5, 1970. 21 p2651 A73-40643

Phased array antennas in ground based remote sensor system, assessing technologies of AN/FPS-85, HAPDAR and AP/TPN-19 radar systems 21 p2672 A73-40645

Development programs status report on airborne planar, conformal and distributed aperture phased array antennas for use in radar and communication systems 21 p2662 A73-40646

Phased array antennas for applications on spacecraft. 21 p2662 A73-40647

Network analysis of infinite regular antenna arrays, discussing unified approach based on electromagnetic interaction among subarrays as distinguished from boundary value problem solution 21 p2651 A73-40651

Analysis of infinite planar array of rectangular waveguides by generalized scattering matrix approach. 21 p2651 A73-40652

Surface-wave effects and blindness in phased-array antennas. 21 p2651 A73-40653

Time scanned array radar with time delay or phase gradient for electronic beam steering control by signal 21 p2652 A73-40669

Conformal arrays on surfaces with rotational symmetry. 21 p2653 A73-40676

Large phased array antenna pattern measurements for performance, monitoring and maintenance checks 21 p2653 A73-40679

Dual beam antenna - A unique waveguide phased array with independently steered beams. 21 p2653 A73-40683

Advances in the theory and technology of horn antennas and reflector antennas 21 p2664 A73-41073

Polarization characteristics of phased arrays of elliptically polarized elementary radiators 21 p2664 A73-41082

A goniometer for use with high-frequency circularly disposed aerial arrays. 21 p2703 A73-41207

The RATAN-600 radio telescope 21 p2675 A73-41441

A radio-astronomical method of adjusting variable-profile antennas 21 p2667 A73-41458

Synthetic radio direction defining methods with virtual antenna patterns. 21 p2658 A73-41649

Analysis and design of circular antenna arrays by matrix methods. 22 p2830 A73-41828

Broad-band antenna array with application to radio astronomy. 22 p2831 A73-41840

Simple expressions for the electric and magnetic field strengths between the elements of an infinite array. 22 p2831 A73-41849

Yagi type antenna array of vertical monopoles with optimized slot reradiation to modify foreground reflection for performance improvement 22 p2832 A73-42295

Variational and iterative methods for waveguides and arrays. 22 p2834 A73-42843

Stanford radio telescope array with five paraboloid antennas for fast image forming interferometry, using earth rotation synthesis to produce sky continuous radiation brightness map 23 p2957 A73-43359

Radio telescope array of interferometers formed by fixed and movable antennas operating on rotational aperture synthesis for radiation observation, emphasizing electronic system stability 23 p2957 A73-43360

Computer controlled steerable array of multiple conical log spiral antennas for solar and discrete radio source studies 23 p2965 A73-43363

Fixed baseline millimeter wave interferometer with aperture synthesis telescope of antenna array for interstellar and planetary water vapor and radio sources mapping 23 p2980 A73-43364

An aperture-synthesis interferometer at Ooty for operation at 327 MHz. 23 p2980 A73-43366

The accuracy of phase-comparison angle tracking by phased-array antennas 24 p3071 A73-44594

Adaptive array based on feedback concept for interference rejection, discussing processing of modulated signal with CW reference system 24 p3067 A73-44737

ANTENNA COMPONENTS

NT ANTENNA COUPLERS

NT ANTENNA FEEDS

Analysis of the characteristics of radiating elements in antenna arrays on the basis of laws describing cross-coupling variations 21 p2661 A73-40195

Main-mirror aberrations in a variable-profile antenna and beam scanning by displacement of the primary radiating element 21 p2667 A73-41446

Phase errors at the aperture of a curvilinear antenna during displacement of the primary radiating element from the focal point 21 p2667 A73-41447

Adjustment of a variable-profile antenna 21 p2675 A73-41456

ANTENNA COUPLERS

NT COUPLING CIRCUITS

NT DIPLERS

Evaluation of the norm of the wave-impedance distribution function in the synthesis of an inhomogeneous line for wide-band matching 08 p0946 A73-21105

The significance of the elementary radiator directivity for the determination of the directive gain of linear arrays 12 p1468 A73-27039

Optimization and data analysis of the Frascati gravitational-wave detector. 20 p2565 A73-39013

Surface-wave effects and blindness in phased-array antennas. 21 p2651 A73-40653

ANTENNA DESIGN

Ground reflection effects upon radiated and received signals as viewed via image theory. 01 p0015 A73-10181

Transverse resonance solutions for a long slot leaky wave antenna. 01 p0023 A73-10187

Directivity and bandwidth of single-band and double-band Yagi arrays. 01 p0023 A73-10188

Dual frequency antenna design using hollow fin as TE mode waveguide with sidewall radiating elements, calculating attenuation for comparison with experiment 01 p0023 A73-10189

Multifrequency excitation of a wire antenna for an invariant radiation pattern. 01 p0023 A73-10190

Antenna synthesis via inverse electrodynamic problem solution for infinite impedance cylinder excited by traveling wave, noting directional antenna with rotating polarization 01 p0017 A73-10217

Antennas for measurement of microwave electromagnetic field by a light-modulated scattering technique. 01 p0025 A73-11055

A decoupling supply network for small antenna arrays 02 p0145 A73-11825

Antenna array synthesis in Chebyshev approximation, calculating array geometry and excitation amplitudes for double secant radiation pattern 02 p0146 A73-12022

Comparing ECM antennas - Horns vs spirals. 02 p0147 A73-12568

Theoretical analysis and experimental verification for multielement dipole antenna array of unequal parallel conductors, noting impedance characteristics desirable for broadband use

02 p0148 A73-12853

Some aspects of radiation from a circular loop antenna.

02 p0148 A73-12854

Sidelobe reduction for linear arrays with elements sampled from equally spaced arrays, using Fourier coefficients of sampling functions

03 p0274 A73-12998

Reduction of antenna length via wave channel type antenna design with modulated phase velocity and multiple use of antenna array

03 p0284 A73-14031

Antenna radiation pattern synthesis, discussing current phase and amplitude distribution determination by iterative and quadratures solutions respectively

03 p0284 A73-14059

Statistical characteristics of antenna gain threshold as function of link trajectory during radiation pattern shift with respect to fixed orientation

03 p0278 A73-14061

Geometric properties and basic errors of rotating support devices of the gimbal suspension type

04 p0447 A73-14848

Signal relay systems using large space arrays.

04 p0415 A73-14990

Random antenna array design for narrow beam radiation and blind angle avoidance, determining mutual coupling effect on performance

04 p0416 A73-15059

An amplitude-steered, electronically despun antenna for the synchronous meteorological satellite.

04 p0428 A73-15453

A novel VHF turnstile antenna for the SMS satellite.

04 p0428 A73-15456

Input impedance of a thin biconical antenna vertically buried near the air-ground interface.

05 p0548 A73-16162

Radiation from an axial slot antenna coated with a homogeneous material.

06 p0665 A73-18138

On the analysis of scattering and antenna problems using the singularity expansion technique.

06 p0665 A73-18184

Dipole antenna coaxially mounted on a conducting cylinder.

06 p0666 A73-18189

Theory of double parasitic loop counterpoise antenna radiation patterns.

06 p0666 A73-18190

Iterative least-squares synthesis of nonuniformly spaced linear arrays.

06 p0666 A73-18194

Antenna design for Eole satellite radio communications with balloons, noting wave polarization and sea reflection effects

07 p0797 A73-18963

Antenna design for meteorological Meteorostat satellite, noting transmitting and receiving radiation patterns

07 p0797 A73-18964

Optimization of antenna parameters in the presence of random errors.

07 p0801 A73-20128

A relationship between the antenna synthesis for a given radiation pattern and the statistical synthesis of systems for spatial signal processing.

07 p0801 A73-20129

Noise considerations in space communication antennas.

07 p0794 A73-20228

A surface-wave antenna integrated with the excitation device

07 p0802 A73-20294

Antennas have it tough - when forced to ride on spacecraft.

07 p0803 A73-20491

Corrugated horn antenna for constant bandwidth and circularly symmetric radiation pattern free of primary sidelobes, noting VSWR reduction

07 p0803 A73-20492

Axisymmetric lens design for prescribed radiation amplitude patterns

08 p0946 A73-21101

Synthesis of a traveling wave antenna

08 p0946 A73-21103

Probability estimates of the accuracy of a solution to the problem of antenna synthesis in the case of an experimental determination of the direct operator of the problem

08 p0946 A73-21104

Evaluation of the norm of the wave-impedance distribution function in the synthesis of an inhomogeneous line for wide-band matching

08 p0946 A73-21105

A new earth-station antenna for domestic satellite communications.

08 p0947 A73-21144

Antenna array synthesis for radiation patterns prescribed by continuous function, proposing formulas for current determination

09 p1062 A73-22047

Canadian domestic ANIK communication satellite with all-microwave 12-channel repeater, discussing system components, antenna design and performance parameters

09 p1059 A73-23437

Imperfectly conducting circular loop antenna driving-point impedance derivation for uniform resistive loading, comparing differential and integral equation methods for current distribution calculation

10 p1191 A73-24899

Horn antennas dephasing based on quadrupole with circular guides, cones of revolution and air space

11 p1327 A73-25279

Efficiency transition point for inductively loaded monopole.

11 p1337 A73-25364

Computer design of antenna reflectors.

[AIAA PAPER 73-351] 11 p1437 A73-25489

Design of multiple-edge blinders for large horn reflector antennas.

11 p1337 A73-25653

Antenna effective area lower limit based on photon limited localizability and Heisenberg uncertainty principle, deriving directivity dependence on area

11 p1338 A73-25672

Polarization interferometer for 2800 MHz solar noise studies with a 0.5-min fan beam.

11 p1422 A73-25943

Adaptive control for correction of flexible linear array phase error with resistance strain gages and ferrite phase shifter, noting radiation pattern performance

11 p1332 A73-26283

Synthesis of a linear antenna in a class of piecewise-constant current-distribution functions

12 p1479 A73-27228

Shaping of antenna radiation patterns by passive radiating slots

12 p1479 A73-27230

Investigation of series pattern-forming circuits for multiple-beam antennas

12 p1479 A73-27231

Algorithm for choosing the optimal disposition of radiating elements in a linear antenna array by the method of coordinate trials

12 p1479 A73-27232

Circular aperture antenna with quadratic phase distortions, deriving near and far field patterns in terms of linear combinations of Bessel and Lommel functions

12 p1479 A73-27233

Horn-element antenna phase center position calculation for directivity characteristics by power series of radiation patterns

12 p1480 A73-27236

Directional antenna formed by a system of two wires lying along the generatrices of a profiled impedance cylinder.

12 p1480 A73-27269

Factors relating to the choice of antenna characteristics for the aircraft terminal in an aeronautical satellite communications/surveillance system.

12 p1471 A73-27654

The disc antenna - A possible L-band aircraft antenna.

12 p1471 A73-27655

A radiating element giving circularly polarized radiation over a large solid angle.

12 p1471 A73-27656

A shipboard satellite communication experiment.

12 p1473 A73-27675

A broadband antenna and multiplexer system in the decimeter-wave range for solar radio astronomy

12 p1481 A73-27782

A new statistical design method for thinned solid-state phased arrays.

13 p1594 A73-29231

Log periodic triangular dipole antenna design and electrical properties, noting improved frequency transition, gain and axial length reduction

14 p1731 A73-29714

The optimization of the supporting structures of parabolic antennas

14 p1740 A73-29742

The application of Gegenbauer polynomials to antenna array synthesis.

14 p1725 A73-29747

The use of specialized antenna technology for air traffic control and communications.

14 p1732 A73-29894

Spiral top-loaded antenna (STLA) characteristics and design procedure derivation via self consistent field method, noting VLF applications

14 p1734 A73-30204

Log periodic dipole antenna design procedure, discussing gain as function of transmission line characteristic impedance, half length/dipole radius ratio and geometric parameters

14 p1734 A73-30206

Shaping of subreflectors in Cassegrainian antennas for maximum aperture efficiency.

14 p1734 A73-30207

Radiation characteristics of corrugated E-plane sectoral horns.

14 p1734 A73-30209

On the equivalent parabola technique to predict the performance characteristics of a Cassegrainian system with an offset feed.

14 p1734 A73-30211

Fourier decomposition for antenna near field reconstruction from far field pattern data, investigating numerical stability and convergence bounds

14 p1727 A73-30213

Comparison between the peak sidelobe of the random array and algorithmically designed aperiodic arrays.

14 p1734 A73-30217

E-plane synthesis of dipole array antennas.

14 p1735 A73-30223

Matrix analysis of linear antenna arrays of equally spaced elements.

14 p1735 A73-30226

Computer evaluation of large low-frequency antennas.

14 p1735 A73-30227

On the scattering cross section of passive linear arrays.

14 p1735 A73-30229

Depolarisation with Cassegrainian and front-fed reflectors.

14 p1728 A73-30448

A dual-mirror antenna with beam scanning over a ninety-degree sector

14 p1736 A73-30561

Frequency-selective surfaces for multiple-frequency antennas Design data plus experimental results.

14 p1737 A73-30625

Self complementary wire element phased array antennas, discussing matching, operating bandwidth, structural design and isolation

15 p1850 A73-31255

Bringing data processing to projects and tests of large antennas

15 p1846 A73-32430

French VOR system with single type equipment for operation on site at performance levels to meet ICAO standards, emphasizing antenna design

15 p1909 A73-32453

Nonimage glidepath antenna design for ILS system within international civil aviation convention specifications

15 p1909 A73-32463

Runway VHF localizer antenna array for Norwegian airports ILS, taking into account difficulties due to course bends and snow

15 p1859 A73-32498

Design and fabrication of a flight antenna for a planetary spacecraft.

16 p2018 A73-33057

Reliability estimate of a Space Deployable Antenna.

16 p1989 A73-33620

Atmospheric refractivity effects on maximum antenna gain and correlation coefficient in design of microwave line of sight links for high reliability

16 p1981 A73-33704

Italian SIRIO satellite cross polarization signal measurements aided by ground station antenna system using narrow bandwidth

16 p1983 A73-33725

Radio direction finder of increased accuracy with a moving antenna.

16 p1991 A73-33976

Radiation patterns and structural design of two mirror millimeter wave Cassegrain antennas with horn radiator

16 p1991 A73-33985

Failure modes and accelerated life test methods for despun antenna bearings. [ASLE PREPRINT 73AM-1A-4]

17 p2178 A73-34979

Multifield multifrequency broadband constant index lens antenna with high power and variable polarization handling capabilities and low manufacturing cost advantage

17 p2137 A73-35206

General theoretical analysis of impedance loaded rectangular loop antennas.

17 p2141 A73-35368

The Apollo 17 Surface Electrical Properties Experiment antenna performance.

17 p2171 A73-35370

Design techniques for multiple beam reflector antennas.

17 p2142 A73-35366

A concentric ring transverse electromagnetic line antenna array.

17 p2127 A73-35368

Time domain current interaction coefficients for sheet antenna structures.

17 p2142 A73-35647

Planar aperture antenna synthesis for main beam and complex sidelobe patterns by iterative correction with convergence, using computer program

17 p2142 A73-35648

Quadratic antenna systems and noise excited antennas.

17 p2128 A73-35682

Proximity effects for parallel rectangular conductors in nontransmission-line mode.

17 p2129 A73-35703

Contribution to the theory of synthesis of discrete antennas in the case of a uniform approach to a given radiation pattern.

A limited steerable dual reflector antenna.

A surface-wave antenna matched to the exciter.

Impedance and far field characteristics of a linear antenna near a conducting cylinder.

Geometric deformation of spherical dielectric lens antennas

Analysis of two-mirror antennas of a general type.

The effects of multipath on the design of ship board satellite communications antennas.

Small ship antennas for fleet satellite communications.

Implementation of fixed multiple beam spherical antenna systems and measured test results.

Limitation of the axial gain of large antennas under partial coherent illumination.

Design of coincident dual-frequency mirror antennas

Analysis of the characteristics of radiating elements in antenna arrays on the basis of laws describing cross-coupling variations

Frequency dependence of radiation-pattern orientation in phased-array antennas

Synthesis of impedance-type cylindrical antenna arrays

Application of linear programming in the statistical theory of antennas

Antenna system design for detection of random gravitational waves with separation from effects of antenna random fluctuations

Circular synthetic radar with interferometer elements mounted at ends of horizontal boom rotating about vertical mast, predicting echo response to point and multiple targets

Monopulse radar equipment

New multiple-support radially-symmetric design of the parabolic-reflector suspension for a radio telescope

Transverse displacements of the radiating element of the parabolic antenna of a mobile radio telescope

Phased array antennas; Proceedings of the Symposium, Polytechnic Institute of Brooklyn, Farmingdale, N.Y., June 2-5, 1970.

Development programs status report on airborne planar, conforal and distributed aperture phased array antennas for use in radar and communication systems

Phased array antennas for applications on spacecraft.

Design, performance, and cost considerations for solid-state arrays.

Phased array element types comparison, discussing dipole and open-ended waveguide radiator designs with emphasis on driving point impedance accuracy and active element pattern

Network analysis of infinite regular antenna arrays, discussing unified approach based on electromagnetic interaction among subarrays as distinguished from boundary value problem solution

Small arrays - Their analysis and their use for the design of array elements.

A survey of the simulator technique for designing a radiating element in a phased-array antenna.

A new procedure for the design of a waveguide element for a phased-array antenna.

Wide-angle impedance matching of phased-array antennas - A survey of theory and practice.

The design of a wide band wide scan-angle waveguide radiating element.

Multimode phased array element for wide scan angle impedance matching.

Design of a phased array radiating face for prevention of performance degradation in the presence of rain.

Phased array antenna feed systems developments, discussing relative merits, problems and design choices for air surveillance radar applications in microwave region

Diode and ferrite phaser configurations for phased array antenna system, discussing digital and analog versions, driver requirements and design trends

Planar phased array beam steering methods, emphasizing electronic driver and logic circuit sharing between phase shifters for cost reduction

Design guidelines for 180-degree hybrid type multiple beam phased array forming networks with different element numbers and configurations

Bandwidth criteria for phased array antennas.

High resolution beam steering phased array radar antenna design by subarray techniques, using time delay circuit for cost effective driver control simplification

Mutual coupling effects in circular arrays on cylindrical surfaces Aperture design implications and analysis.

Mechanically and electronically switched circular symmetric phased arrays with hybrid matrix phase shifter and lens switch combinations, assessing design and performance characteristics

Basic theoretical aspects of spherical phased arrays.

Limited scan phased array antenna design, featuring electronic beam deflection from few beamwidths to twenty degrees with cost reduction

Dual beam antenna - A unique waveguide phased array with independently steered beams.

A single-plane electronically scanned antenna for airborne radar applications.

Physical design considerations for airborne electronic-scanning antennas.

The RATAN-600 radio telescope

Methods of radio-astronomical utilization of the RATAN-600

Choice of the dimensions of the reflecting elements and calculation of the electrical characteristics of the RATAN-600 radio telescope

Operation of a variable profile antenna with a plane periscopic reflector

Operational features of variable-profile antennas during near-zenith observations

Phase errors at the aperture of a curvilinear antenna during displacement of the primary radiating element from the focal point

Monitoring antenna parameters from radio-astronomical directions

Identification and simulation of antenna dynamics.

An array technique with grating-lobe suppression for limited-scan applications.

Analysis and design of circular antenna arrays by matrix methods.

Scale model development of a high efficiency dual polarized line feed for the Arecibo spherical reflector.

Narrow beam phased array of identical isotropic elements, estimating far field beam width with consideration for element position error effects

Circularly polarized linear waveguide array.

Short axial length broad-band horns.

A cavity-backed dipole antenna with wide-bandwidth characteristics

Yagi type antenna array of vertical monopoles with optimized slot reradiation to modify foreground reflection for performance improvement

Corrugated conical horn antenna feed design, discussing Newton-Raphson iterative solution and computer program for spherical hybrid mode eigenvalues

Numerical solution of wire antenna boundary value problems based on integral equations formulation, considering Yagi-Uda array, antenna design and radiation patterns

Input admittance or impedance and effective height measurement for small metal antennas of prolate and oblate spheroidal and spherical shape, noting transient response

Linear array radio telescope for large aperture synthesis by using earth rotation to change relative orientation to radio source, discussing design and performance

Millimeter wave radio telescope with high resolution for obtaining heliograph, discussing fast rotational synthesis and array redundancy design features

Synthesis and analysis of optimal dual-mirror antennas

Antenna design for intergalactic gravitational wave detection, discussing binary star and pulsar sources, Weber wave receiver and Zeldovich-Braginsky dumb-bell antenna

Synthesis of antennas with minimum mean sidelobe level of the radiation pattern.

German book on HF technology, Volume 1, covering coupling filters, transmission lines, antennas, Lecher waves, waveguides, etc

A fan-beam dual reflector antenna.

Some data for the design of low-crosspolarisation feeds.

Comparative focusing properties of spherical and plane microwave zone plate antennas.

ANTENNA FEEDS

Off-axis polarization characteristics of Cassegrainian and front-fed paraboloidal antennas.

Analysis of an asymmetric dipole antenna with displaced feed points.

A fixed reflector, steerable beam, earth station antenna.

Two channel multimode feed for circular horn tracking antenna applications, discussing channel patterns, coupling, isolation and frequency response

Voltage-controlled variable power divider.

Calculation of input-voltage standing-wave ratio for a reflector antenna.

Requirements for the production of several, mutually independent beams by a transmission-line fed antenna

Threshold value of the input impedance of a propagating-wave fed, long radiator series

The 'Paradisc' antenna - A novel technique to improve the axial ratio of a circularly polarized high gain antenna system.

Radiation patterns of linear equidistant fishbone-type dipole antenna array fed by long symmetrical transmission line

Rectangular horn with dielectric-slab insert.

Radiation characteristics of waveguide-excited dielectric spheres with matched sphere-air boundary.

Feed arrangement for axis definition of paraboloid reflector.

Wideband squintless linear arrays.

Determination of the maximum scan-gain contours of a beam-scanning paraboloid and their relation to the Petzval surface.

Coaxial feeds for high aperture efficiency and low spillover of paraboloidal reflector antennas.

Butler submatrix feed systems for beam forming and scanning networks of linear and circular antenna arrays

Mutual coupling, mainlobe reflected power and radiation patterns of periodic antenna arrays thinned by statistically selected element feeds

Series-fed antennas principal beam direction and grating lobes buildup as function of antenna and feed characteristics, considering frequency dependence

Corrugated circular waveguide horn as monopulse antenna feed for optimal tracking performance, using difference-sum patterns with hybrid modes

14 p1731 A73-29705

Shaping of subreflectors in Cassegrainian antennas for maximum aperture efficiency.

14 p1734 A73-30207

On the equivalent parabola technique to predict the performance characteristics of a Cassegrainian system with an offset feed.

14 p1734 A73-30211

Offset parabolic reflector antennas linearly and circularly polarized excitations, discussing dependence on angle between dual mode feed and axis

14 p1734 A73-30212

The performance of transistor feed monopoles in active antennas.

14 p1735 A73-30219

E-plane synthesis of dipole array antennas.

14 p1735 A73-30223

A simplification in the analysis of four- and five-horn fed Cassegrainian reflectors when the horns have nearly symmetric patterns.

14 p1735 A73-30224

Depolarisation with Cassegrainian and front-fed reflectors.

14 p1728 A73-30448

Radiating slot antenna immittance reactive term due to energy storage in feeding waveguide, discussing resonance characteristics

15 p1849 A73-31097

Coaxial cable fed dipole antenna array for observation of coherent backscatter radar signal from ionospheric electron density irregularities in electrojet region

16 p1987 A73-33117

Multifeed multifrequency broadband constant index lens antenna with high power and variable polarization handling capabilities and low manufacturing cost advantage

17 p2137 A73-35206

Large scanning and multibeam reflector antennas for space communications.

20 p2524 A73-38738

Phased array antenna feed systems developments, discussing relative merits, problems and design choices for air surveillance radar applications in microwave region

21 p2672 A73-40664

Bandwidth criteria for phased array antennas.

21 p2652 A73-40671

Transient frequency response analysis and far field measurement of linear phased array with tandem series feed network, noting instantaneous bandwidth

21 p2653 A73-40673

Operational features of variable-profile antennas during near-zenith observations

21 p2666 A73-41445

Scale model development of a high efficiency dual polarized line feed for the Arecibo spherical reflector.

22 p2831 A73-41830

Experimental verification of the analysis of umbrella parabolic reflectors.

22 p2831 A73-41844

Corrugated conical horn antenna feed design, discussing Newton-Raphson iterative solution and computer program for spherical hybrid mode eigenvalues

22 p2832 A73-42296

Some data for the design of low-crosspolarisation feeds.

24 p3069 A73-45255

ANTENNA FIELDS

U ANTENNA RADIATION PATTERNS

ANTENNA RADIATION PATTERNS

NT SIDELOBES

Off-axis polarization characteristics of Cassegrainian and front-fed paraboloidal antennas.

01 p0022 A73-10177

A comparison of geometrical theory of diffraction and integral equation formulation for analysis of reflector antennas.

01 p0022 A73-10179

Performance of a protruding-dielectric waveguide element in a phased array.

01 p0022 A73-10180

Multifrequency excitation of a wire antenna for an invariant radiation pattern.

01 p0023 A73-10190

Low-sidelobe paraboloidal antenna with microwave absorber.

01 p0018 A73-11054

Omnidirectional satellite antennas with radiation pattern distortion minimization by adjustment of antenna inclination, height above spacecraft structure and angle with metallic objects

01 p0111 A73-11173

VLF-ELF radiation characteristics of a 90 degree-phased crossed-dipole array in a cold multicomponent magnetoplasma.

02 p0140 A73-11739

Optical modeling of antenna radiation patterns by radio holograms of aperture fields

02 p0146 A73-12020

Effects of cross-coupling and of the edge effect on the characteristics of linear phased antenna arrays

02 p0146 A73-12021

Antenna array synthesis in Chebyshev approximation, calculating array geometry and excitation amplitudes for double secant radiation pattern

02 p0146 A73-12022

Target angular characteristics of direction finding antenna in sidelobe region for wideband signals, using single coordinate measurement and amplitude scanning

02 p0146 A73-12023

X band microstripline slot antenna measurement for input impedance and radiation pattern dependence on slot-to-reflector spacing, applying to array design

02 p0141 A73-12100

Tikhonov conditions of field excitation for dipole antenna radiation study in stratified gyrotropic medium

02 p0147 A73-12470

Algorithm for automatic optimal control of radio telescope parabolic antenna with extremal characteristic in radiation pattern, noting quasi-steady and steady operation

02 p0147 A73-12497

Radiation from a continuous semi-circular arc antenna array.

02 p0148 A73-12852

Some aspects of radiation from a circular loop antenna.

02 p0148 A73-12854

Analysis of an asymmetric dipole antenna with displaced feed points.

02 p0148 A73-12856

Analysis of wire antennas in the presence of a conducting half-space. II - The horizontal antenna in free space.

03 p0276 A73-13694

Far-field simulation of circular antenna arrays on the analog/hybrid computer

03 p0277 A73-13985

Influence of satellite antenna gain on a satellite communications system.

03 p0277 A73-14027

Antenna radiation pattern synthesis, discussing current phase and amplitude distribution determination by iterative and quadratures solutions respectively

03 p0284 A73-14059

Linear array antenna radiation pattern synthesis for minimum sidelobe level outside of given intervals, calculating current distribution

03 p0278 A73-14060

Statistical characteristics of antenna gain threshold as function of link trajectory during radiation pattern shift with respect to fixed orientation

03 p0278 A73-14061

Two-channel direction finding with point source emission and spaced antennas reception, investigating cross correlation and background noise interference effects on accuracy

03 p0278 A73-14062

Reciprocity theorem for antenna directivity pattern measurement of optical superheterodyne receiver for carbon dioxide laser radiation

03 p0284 A73-14084

Computation of element patterns of an E plane sectoral-horn planar phased array.

04 p0415 A73-14987

Signal relay systems using large space arrays.

04 p0415 A73-14990

Random antenna array design for narrow beam radiation and blind angle avoidance, determining mutual coupling effect on performance

04 p0416 A73-15059

A fixed reflector, steerable beam, earth station antenna.

04 p0428 A73-15415

A novel VHF turnstile antenna for the SMS satellite.

04 p0428 A73-15456

Radiation pattern of longitudinal magnetic dipole ideally conducting infinite circular cylinder parallel to infinite plane screen

04 p0429 A73-15912

Parabolic, Cassegrain, spherical and horn-parabolic axisymmetric mirror antennas, calculating primary radiating element orientation effects on radiation polarization characteristics

05 p0547 A73-16052

Narrow band linear filter output SNR relationship to orthogonal radiating elements system directional gain and radiation patterns

05 p0555 A73-16056

Use of magnetometers and asymmetric antenna patterns for attitude determination.

05 p0596 A73-17204

Array factor of statistically thinned antenna arrays with an increased element-inter-space minimum

06 p0674 A73-17810

Annular energy vortex in the near field of a directional antenna

06 p0674 A73-17821

Anechoic funnel and rectangular chambers for antenna measurements

06 p0674 A73-17822

Radiation from an axial slot antenna coated with a homogeneous material.

06 p0665 A73-18138

Reflector antenna radiation pattern analysis by equivalent edge currents.

06 p0665 A73-18179

Theory of double parasitic loop counterpoise antenna radiation patterns.

06 p0666 A73-18190

Impedance and radiation pattern of antennas above flat discs.

06 p0676 A73-18191

The 'Paradisc' antenna - A novel technique to improve the axial ratio of a circularly polarized high gain antenna system.

06 p0676 A73-18195

Cross polarization definitions in terms of antenna pattern measurement coordinate system and source current distribution, considering relative merits

06 p0666 A73-18199

Radiation patterns of linear equidistant fishbone-type dipole antenna array fed by long symmetrical transmission line

06 p0677 A73-18392

Antenna-aperture distributions from holographic type of radiation-pattern measurement.

06 p0668 A73-18443

Antenna design for meteorological Meteorstat satellite, noting transmitting and receiving radiation patterns

07 p0797 A73-18964

Propagation and radiation characteristics of corrugated horns.

07 p0798 A73-19156

Influence of horn length on radiation pattern of oblique-flare-angle corrugated horn.

07 p0798 A73-19160

Calculated pattern of a vertical antenna with a finite radial-wave ground system.

[AD-756789]

07 p0792 A73-19384

Corrugated and uniform dielectric rod aerial excited in E sub 0-mode.

07 p0792 A73-19547

German monograph on logarithmic spiral antennas radiation field theory, extending boundary value solution for cylindrical linear antenna to curved structure by segmentwise linearization

07 p0801 A73-19577

A relationship between the antenna synthesis for a given radiation pattern and the statistical synthesis of systems for spatial signal processing.

07 p0801 A73-20129

A statistical estimate of the achievable sidelobe level in phased array antennas with nonlinear initial phase distribution.

07 p0801 A73-20130

A surface-wave antenna integrated with the excitation device

07 p0802 A73-20294

Waves in a hot uniaxial plasma excited by a current source.

07 p0860 A73-20477

Corrugated horn antenna for constant bandwidth and circularly symmetric radiation pattern free of primary sidelobes, noting VSWR reduction

07 p0803 A73-20492

Pattern synthesis for rectangular and hexagonal planar arrays with triangular elements arrangement

08 p0945 A73-20806

Axisymmetric lens design for prescribed radiation amplitude patterns

08 p0946 A73-21101

Synthesis of a traveling wave antenna

08 p0946 A73-21103

Probability estimates of the accuracy of a solution to the problem of antenna synthesis in the case of an experimental determination of the direct operator of the problem

08 p0946 A73-21104

Rectangular horn with dielectric-slab insert.

08 p0946 A73-21117

Radiation characteristics of waveguide-excited dielectric spheres with matched sphere-air boundary.

08 p0947 A73-21121

Some experimental results for a capacitively loaded V antenna.

08 p0939 A73-21431

Antenna array synthesis for radiation patterns prescribed by continuous function, proposing formulas for current determination

09 p1062 A73-22047

Characteristics of the electric field far from and close to a radiating antenna around the lower hybrid resonance in the ionospheric plasma.

09 p1049 A73-22277

Near-field technique for inferring aperture antenna radiation patterns.

09 p1052 A73-22960

Internal equation numerical solution for excitation of multilayer arbitrary shape dielectric body of revolution, considering radome curvature effects on antenna radiation pattern

09 p1052 A73-23084

Study of antenna cross-polarization characteristics by using microwave holography

09 p1065 A73-23087

SUBJECT INDEX

A new log-periodic structure with asymmetric dipole elements. 10 p1194 A73-24172

Computer aided directivity measurements of large antennas in Fresnel zone 10 p1188 A73-24184

Influence of the nonidentity of the antennas of a Doppler speed meter on the accuracy of its operation 10 p1195 A73-24386

Radome precision testing for fire control, missile aiming, Doppler navigation and bombing 11 p1335 A73-25277

Study of the Rayleigh zone of circular radiating apertures 11 p1328 A73-25283

Calculation of the radiation diagram of an antenna in the presence of a radome 11 p1328 A73-25285

Development of loaded resin one-piece radomes 11 p1387 A73-25294

Aircraft and missile radomes technology in France, discussing materials, antenna radiation pattern calculation, computer programming for transmission and angular aberrations, and raindrop erosion tests 11 p1336 A73-25301

Optimization of the loop-coupled log-periodic antenna. 11 p1337 A73-25652

Resonances in circular arrays with dielectric sheet covers. 11 p1337 A73-25654

Coaxial feeds for high aperture efficiency and low spillover of paraboloidal reflector antennas. 11 p1337 A73-25655

Two mode rectangular waveguide longitudinal and transverse narrow half wave slots properties, discussing measurement apparatus and techniques and radiation patterns 11 p1328 A73-25661

Geometrical diffraction theory for radiation pattern of extended vertical monopole antenna over infinitely conducting ground plane, noting back radiation level 11 p1329 A73-25662

Synthesis of broad-band arrays with arbitrary frequency-independent elements. 11 p1329 A73-25664

Field pattern of two identical nonstaggered parallel circular loop antennas. 11 p1337 A73-25667

Approximate log normal distribution of normalized power antenna patterns, relating first sidelobe level and antenna size to 0.5 probability level 11 p1337 A73-25668

Near-field analysis by the plane-wave spectrum approach. 11 p1329 A73-25674

Plane wave expansion approximation for wave field on dielectric wedge representing tapered antenna, considering lateral wave contribution 11 p1329 A73-25681

Polarization interferometer for 2800 MHz solar noise studies with a 0.5-min fan beam. 11 p1422 A73-25943

A brief survey of monopulse techniques. 11 p1331 A73-26148

Influence of phase fluctuations of the received radiation on the performance of a synthetic antenna 11 p1331 A73-26158

Method of measuring the parameters of axisymmetrical mirror antennas on the basis of the emission of a 'black' disk positioned in the Fresnel region 11 p1332 A73-26162

First order effects of terrain on the radiation pattern of a non-directional LF beacon. 11 p1332 A73-26204

Mutual coupling, mainlobe reflected power and radiation patterns of periodic antenna arrays thinned by statistically selected element feeds 11 p1332 A73-26205

Adaptive control for correction of flexible linear array phase error with resistance strain gages and ferrite phase shifter, noting radiation pattern performance 11 p1332 A73-26283

Radiation properties of a composite-dielectric-rod aerial. 11 p1332 A73-26286

Directivities of planar arrays with triangular arrangement of elements. 11 p1333 A73-26699

Series-fed antennas principal beam direction and grating lobes buildup as function of antenna and feed characteristics, considering frequency dependence 12 p1469 A73-27041

Flush mountable elliptically polarized low silhouette blade antenna for aircraft, describing polarization and radiation characteristics 12 p1478 A73-27043

Electromagnetic fields due to dipole antennas over stratified anisotropic media. 12 p1523 A73-27146

[AD-756044] Reconstruction of an antenna radiation pattern from field values available within a limited sector of angles in the Fresnel region 12 p1479 A73-27227

Synthesis of a linear antenna in a class of piecewise-constant current-distribution functions 12 p1479 A73-27228

Arched and spherical antenna arrays synthesis for given vectorial radiation patterns by numerical solution via algorithm using eigenfunctions 12 p1479 A73-27229

Shaping of antenna radiation patterns by passive radiating slots 12 p1479 A73-27230

Investigation of series pattern-forming circuits for multiple-beam antennas 12 p1479 A73-27231

Circular aperture antenna with quadratic phase distortions, deriving near and far field patterns in terms of linear combinations of Bessel and Lommel functions 12 p1479 A73-27233

Characteristics of a dual-mirror antenna producing a sum-difference type of radiation pattern 12 p1480 A73-27234

Horn-element antenna phase center position calculation for directivity characteristics by power series of radiation patterns 12 p1480 A73-27236

Dispersion characteristics of multiloop cylindrical spiral antennas with opposite winding 12 p1480 A73-27237

Directional antenna formed by a system of two wires lying along the generatrices of a profiled impedance cylinder. 12 p1480 A73-27269

Analysis of correlation functions of space-time wideband signals received by linear antennas. 13 p1591 A73-28657

Dipole antenna radiation in homogeneous plasma layer magnetized by normal uniform magnetic field, calculating radiation pattern 13 p1583 A73-28661

Space point group theory classification and analysis of antenna array lattices, noting current excitation space symmetries and orthogonal field pattern design 13 p1583 A73-28698

Radar system with spatial /antenna pattern/ and temporal /Doppler filter/ responses adaptively controlled for optimum SNR and detection performance 13 p1586 A73-29213

A new statistical design method for thinned solid-state phased arrays. 13 p1594 A73-29231

Radiating waveguide antenna elliptical beam off-axis gain maximization, applying to geostationary satellite 13 p1587 A73-29671

Corrugated circular waveguide horn as monopulse antenna feed for optimal tracking performance, using difference-sum patterns with hybrid modes 14 p1731 A73-29705

Radiation from travelling wave circular loop antenna in compressible electron plasma. 14 p1731 A73-29709

Study of two types of turnstile aerial immersed in a warm plasma. 14 p1731 A73-29712

Wave propagation in the ion sheath of an antenna immersed in a plasma 14 p1731 A73-29730

The application of Gegenbauer polynomials to antenna array synthesis. 14 p1725 A73-29747

Approximate near field parameters computation from Kirchhoff boundary values of antenna aperture field intensity 14 p1733 A73-30072

On linear parasitic array of dipoles with reactive loading. 14 p1734 A73-30203

Radial mode analysis of electromagnetic wave propagation on slotted cylindrical structures. 14 p1727 A73-30208

Radiation characteristics of corrugated E-plane sectoral horns. 14 p1734 A73-30209

Finding the approximate angular probability density function of wave arrival by using a directional antenna. 14 p1727 A73-30210

Offset parabolic reflector antennas linearly and circularly polarized excitations, discussing dependence on angle between dual mode feed and axis 14 p1734 A73-30212

Fourier decomposition for antenna near field reconstruction from far field pattern data, investigating numerical stability and convergence bounds 14 p1727 A73-30213

Support scattering effects on low-gain satellite antenna pattern measurements. 14 p1735 A73-30218

The performance of transistor fed monopoles in active antennas. 14 p1735 A73-30219

Radiation patterns of dielectric loaded rectangular horns. 14 p1735 A73-30220

ANTENNA RADIATION PATTERNS

E-plane synthesis of dipole array antennas. 14 p1735 A73-30223

A simplification in the analysis of four- and five-horn fed Cassegrainian reflectors when the horns have nearly symmetric patterns. 14 p1735 A73-30224

Radiation characteristics of a waveguide excited dielectric sphere backed by a metallic hemisphere. 14 p1728 A73-30225

Experimental investigations of coupling phenomena in a periodic linear antenna array 14 p1729 A73-30697

Cross polarization in radomes - A program for its computation. 15 p1851 A73-31730

Radar clutter elimination techniques, considering antenna radiation patterns, resolution cells and Doppler filters 15 p1846 A73-32432

Doppler VOR equipment, economics, blending function and antenna system, discussing ground measurement and monitoring, sideband generation and reference modulation 15 p1859 A73-32452

Tikhonov conditions of field excitation for dipole antenna radiation study in stratified gyrotropic medium 15 p1847 A73-32621

Radiation pattern of a low-frequency beacon antenna in the presence of a semi-elliptic terrain irregularity. 16 p1979 A73-32913

Size-reduced log-periodic dipole array antenna. 16 p1988 A73-33299

Clutter spectra of low PRF AMTI pulse-Doppler radar. 16 p1980 A73-33413

Effect of the amplitude-phase distribution of the field in the aperture of an antenna on its directional properties. 16 p1991 A73-33980

Radiation patterns and structural design of two mirror millimeter wave Cassegrain antennas with horn radiator 16 p1991 A73-33985

Numerical computation of the current distribution and far-field-radiation pattern of the axial-mode helical aerial. 16 p1985 A73-34020

Variation of the antenna radiation pattern during motion of the medium 17 p2122 A73-34924

Log-periodic dipole arrays - A numerical analysis. 17 p2141 A73-35367

Numerical computation of antenna patterns near a conducting elliptic cylinder. 17 p2126 A73-35608

Design techniques for multiple beam reflector antennas. 17 p2142 A73-35636

A concentric ring transverse electromagnetic line antenna array. 17 p2127 A73-35638

Planar aperture antenna synthesis for main beam and complex sidelobe patterns by iterative correction with convergence, using computer program 17 p2142 A73-35648

Probe compensated near-field measurements on a cylinder. 17 p2127 A73-35678

Measurement of near fields of antennas and scatterers. 17 p2142 A73-35679

Radio anechoic chamber reflectivity level evaluation, comparing antenna pattern method and free space voltage standing wave ratio technique 17 p2128 A73-35684

Measurement of the radiation patterns of full-scale HF and VHF antennas. 17 p2128 A73-35689

Corrugated horn antenna with high efficiency and monotonic amplitude in microwave pattern ranges applicable as calibrating standard 17 p2143 A73-35693

Linear phased array antenna focused in Fresnel region, noting radiation pattern indoor measurement simplicity advantage over far field observation in performance monitoring 17 p2128 A73-35694

Large parabolic reflector microwave antenna astigmatism effects on radiation pattern, discussing focusing procedure for phase error reduction 17 p2143 A73-35695

On the relative response and absolute gain toward the zenith of HF field-expedient antennas - measured with an ionospheric sounder. 17 p2129 A73-35698

Antenna radiation pattern recording as functions of two simultaneous parameters, considering measurement time savings 17 p2129 A73-35699

Ground and flight test results for standard VOR and double parasitic loop counterpoise antennas. 17 p2129 A73-35700

A comparison of time- and frequency-domain measurement techniques in antenna theory.

17 p2129 A73-35702

Antenna radiation patterns from statistical phase synthesis of antenna arrays, estimating directivity loss for in- and out-of-phase initial current distribution

17 p2129 A73-35708

Effect of modulating /multiplicative/ interference on signal processing in a system consisting of a phased array antenna and a receiver.

17 p2129 A73-35710

Contribution to the theory of synthesis of discrete antennas in the case of a uniform approach to a given radiation pattern.

17 p2130 A73-35717

A surface-wave antenna matched to the exciter.

18 p2291 A73-37131

Microwave radiation hazards around large microwave antenna.

19 p2397 A73-37274

Radiation pattern of a low-frequency beacon antenna located on a semi-elliptic terrain irregularity.

19 p2409 A73-37716

Large scanning and multibeam reflector antennas for space communications.

20 p2524 A73-38738

Unidirectional small active antenna.

20 p2525 A73-38742

Effect of a statistically uneven underlying surface on the radiation characteristics of a phased antenna array

20 p2537 A73-39453

Lowering of average directive gain caused by cross-polarization radiation in an aperture antenna

20 p2537 A73-39456

Error signal of a scanning antenna with a sum-difference directional pattern

20 p2537 A73-39465

Directional properties of horn-parabolic antennas

21 p2661 A73-40193

Analysis of the characteristics of radiating elements in antenna arrays on the basis of laws describing cross-coupling variations

21 p2661 A73-40195

Frequency dependence of radiation-pattern orientation in phased-array antennas

21 p2661 A73-40196

Radiation patterns of directional end-on antennas, deriving formulas for side lobe levels and main lobe energy distribution

21 p2661 A73-40198

Application of linear programming in the statistical theory of antennas

21 p2661 A73-40201

Use of the azimuthal equal-area projection to display radiation patterns of complex antennas

21 p2661 A73-40202

Surface-wave effects and blindness in phased-array antennas.

21 p2651 A73-40653

Multimode phased array element for wide scan angle impedance matching.

21 p2652 A73-40661

A new flush mounted antenna element for phased array application.

21 p2663 A73-40662

Digitally scanned planar phased arrays, deriving optimum phase perturbation function for quantization and reflection lobe dispersion in terms of aperture distribution amplitude

21 p2652 A73-40667

Design guidelines for 180-degree hybrid type multiple beam phased array forming networks with different element numbers and configurations

21 p2669 A73-40670

Mutual coupling effects in circular arrays on cylindrical surfaces Aperture design implications and analysis.

21 p2653 A73-40674

Conformal arrays on surfaces with rotational symmetry.

21 p2653 A73-40676

Realized gain function for a cylindrical array of open-ended waveguides.

21 p2653 A73-40677

Basic theoretical aspects of spherical phased arrays.

21 p2653 A73-40678

Large phased array antenna pattern measurements for performance, monitoring and maintenance checks

21 p2653 A73-40679

Limited scan phased array antenna design, featuring electronic beam deflection from few beamwidths to twenty degrees with cost reduction

21 p2653 A73-40680

Pattern measurements of phased-arrayed antennas by focusing into the near zone.

21 p2653 A73-40681

Advances in the theory and technology of horn antennas and reflector antennas

21 p2664 A73-41073

Narrow-beam antennas using cylindrical columns of isotropic plasma.

21 p2665 A73-41124

Choice of the dimensions of the reflecting elements and calculation of the electrical characteristics of the RATAN-600 radio telescope

21 p2666 A73-41443

Operation of a variable profile antenna with a plane periscope reflector

21 p2666 A73-41444

Operational features of variable-profile antennas during near-zenith observations

21 p2666 A73-41445

Main-mirror aberrations in a variable-profile antenna and beam scanning by displacement of the primary radiating element

21 p2667 A73-41446

Calculation of the antenna noise temperature in the RATAN-600 radio telescope

21 p2667 A73-41448

Scanning the sky with the aid of the RATAN-600 radio telescope

21 p2776 A73-41464

Measurement of antenna parameters and calibration of the sensitivity of the RATAN-600 radio telescope in the radar mode of operation at the 8-mm wavelength

21 p2667 A73-41467

Experimental verification of the possibility of beam scanning in a variable profile antenna by radial displacement of the primary radiating element

21 p2667 A73-41469

Experimental study of the distribution of irradiation on the variable-profile reflector of the large Pulkovo radio telescope using electronic methods

21 p2667 A73-41470

Accuracy of coordinate measurements with the aid of a variable-profile antenna

21 p2667 A73-41472

A projection method in the problem of the excitation of a dielectric antenna

21 p2667 A73-41512

Synthetic radio direction defining methods with virtual antenna patterns.

21 p2658 A73-41649

Computer program for analysis of radiation pattern distortion and mutual coupling in antenna farms, allowing user specification by types or vertical cylindrical antenna dimensions

22 p2823 A73-41797

Iterative and matrix inversion techniques for antenna electromagnetic radiation and scattering prediction compared for computer storage and execution time

22 p2823 A73-41799

Near fields of wire antennas by matrix methods.

22 p2830 A73-41827

Analysis and design of circular antenna arrays by matrix methods.

22 p2830 A73-41828

A new method for calculating correction factors for near-field gain measurements.

22 p2830 A73-41829

Narrow beam phased array of identical isotropic elements, estimating far field beam width with consideration for element position error effects

22 p2831 A73-41839

Antenna radiation-pattern measurement using model aircraft.

22 p2831 A73-41841

Antenna radiation pattern measurement using time-to-frequency transformation/TFT/ techniques.

22 p2831 A73-41842

Experimental verification of the analysis of umbrella parabolic reflectors.

22 p2831 A73-41844

Short axial length broad-band horns.

22 p2831 A73-41846

Nonlinear optimization reduces the sidelobes of Yagi antenna.

22 p2831 A73-41847

Modification of antenna radiating characteristics with multi-impedance loading.

22 p2831 A73-41848

Simple expressions for the electric and magnetic field strengths between the elements of an infinite array.

22 p2831 A73-41849

The effect of snow on antenna radiation patterns - A presentation of results.

22 p2831 A73-41850

A cavity-backed dipole antenna with wide-bandwidth characteristics.

22 p2831 A73-41851

Calculation of the early time radiated electric field from a linear antenna with a finite source gap.

22 p2832 A73-41856

Experimental determination of the field parameters in a sectorial horn aperture with the aid of a passive probe

22 p2826 A73-42337

Papers on computer techniques for electromagnetic radiation and scattering problems via integral equation formulation covering iterative and variational methods and antenna patterns

22 p2827 A73-42839

Numerical solution of wire antenna boundary value problems based on integral equations formulation,

considering Yagi-Uda array, antenna design and radiation patterns

22 p2827 A73-42840

Computer techniques for scatterer shape from far field data /inverse scattering/ via remote sensing, with application to antenna radiation pattern synthesis and holography

22 p2828 A73-42845

Derivation of diffraction coefficients for a thin wire of finite length.

23 p2955 A73-44106

Beam characteristics of the 300-ft telescope.

24 p3066 A73-44580

Synthesis of antennas with minimum mean sidelobe level of the radiation pattern.

24 p3068 A73-44939

The effect of interaction of array elements with arbitrary amplitude distribution on the radiation pattern.

24 p3068 A73-44942

Radiation characteristics of a corrugated conical horn.

24 p3069 A73-45029

Local form of the radiation condition - Application to curved dielectric structures.

24 p3069 A73-45257

Theory of a corner-driven loop antenna immersed in a warm plasma.

24 p3070 A73-45486

ANTENNAS

NT AIRCRAFT ANTENNAS
NT CASSEGRAIN ANTENNAS
NT CYLINDRICAL ANTENNAS
NT DIPOLE ANTENNAS
NT DIRECTIONAL ANTENNAS
NT FURLABLE ANTENNAS
NT HELICAL ANTENNAS
NT HORN ANTENNAS
NT LENS ANTENNAS
NT LOG PERIODIC ANTENNAS
NT LOG SPIRAL ANTENNAS
NT LOOP ANTENNAS
NT MICROWAVE ANTENNAS
NT MISSILE ANTENNAS
NT MONOPOLE ANTENNAS
NT MONOPULSE ANTENNAS
NT OMNIDIRECTIONAL ANTENNAS
NT PARABOLIC ANTENNAS
NT RADAR ANTENNAS
NT RADIO ANTENNAS
NT SATELLITE ANTENNAS
NT SLOT ANTENNAS
NT SPACECRAFT ANTENNAS
NT SPHERICAL ANTENNAS
NT SPIRAL ANTENNAS
NT STEERABLE ANTENNAS
NT TURNSTILE ANTENNAS
NT TWO REFLECTOR ANTENNAS
NT WAVEGUIDE ANTENNAS
NT WHIP ANTENNAS
NT YAGI ANTENNAS

Impact of solar calibration on telemetry system testing and checkout.

09 p1057 A73-23407

Junction discontinuities in wire antennas and scatterers, obtaining constraint on junction currents via equivalent charge distribution representation

11 p1329 A73-25666

Measurement of the displacement of the electrical axis of an antenna with respect to its geometrical axis by using extraterrestrial radio emission sources

17 p2120 A73-34119

Large antennas and radomes boresight measurement with angular accuracy by laser mirror system incorporated into pattern range for antenna tower alignment

17 p2143 A73-35696

ANTHRACENE

Some characteristics of isopotential curves of photoelectret state formation in compressed polycrystalline anthracene

05 p0605 A73-17176

Drift mobility of holes and electrons in perdeuterated anthracene single crystals.

12 p1531 A73-27688

ANTHROPOMETRY

The use of bivariate distributions in achieving anthropometric compatibility in equipment design. I, II.

05 p0543 A73-16702

The influence of age, sex, body size and lung size on the control and pattern of breathing during CO₂ inhalation in Caucasians.

06 p0654 A73-18337

Redintegrated somatotyping technique for physique measurement and classification based on limb and torso photographic diameter integration with height, using photoelectric cell and electronics

06 p0659 A73-18474

A comparison and analysis of head sizes of Navy aircrew to the standard anthropometric data.

16 p1974 A73-32656

An anthropomorphic master-slave manipulator system.

19 p2397 A73-37316

- Evaluation of the physical conditions of individual
airmen 23 p2949 A73-43790
- ANTIADRENERGICS**
Inhibition of the adrenocortical response to hypoxia
by dexamethasone. 07 p0780 A73-19476
Role of adrenalin and alpha-receptor deactivation in
reactions of hemopoietic organs to stress 07 p0781 A73-19644
Role of the sympathetic nervous system in support-
ing cardiac function in essential arterial hypertension. 08 p0930 A73-21015
The pharmacology of prazosin - A cardioselective
beta adrenergic blocking drug. 09 p1044 A73-21850
Drug therapy for treatment of cardiogenic shock
syndrome following myocardial infarction, discussing
sympathomimetics, alpha-adrenergic blocks and com-
binations 18 p2276 A73-36546
Effects of beta-blocking agents on atrio-ventricular
and intraventricular conduction in man. 21 p2641 A73-41564
Urea content variations in blood and tissues during
muscular activity in relation to the adaptation level of
the organism 22 p2807 A73-42660
- ANTI-AIRCRAFT MISSILES**
Probabilistic Monte Carlo computerized simulation
of surface to air missile systems reaction time from
aircraft attack in non-jamming environment and over
flat terrain 16 p1985 A73-33418
AEGIS Operational Readiness Test System - Design
for system effectiveness. 16 p2073 A73-33609
- ANTIBIOTICS**
NT ACTINOMYCIN
NT PENICILLIN
A study of the secondary structure of ilamycin B1
by 300 MHz proton magnetic resonance. 11 p1326 A73-25572
Effect of iron and salt on prodigiosin synthesis in
Serratia marcescens. 17 p2112 A73-34399
- ANTIBODIES**
Russian book on auto-antibodies of X ray irradiated
animal and human blood and organisms covering cell
formation, isolation, preparations, sickness treatment
and auto-immune reactions 04 p0410 A73-15711
Possible role of antitissular autoantibodies in the
protective mechanism of local shielding during total
radiation exposure 06 p0657 A73-17685
The effects of bilateral destruction of certain medi-
al-hypothalamus structures on the formation of com-
plement-binding antibodies 07 p0781 A73-19647
Effects of chronic irradiation of dogs with Co-60
gamma rays on the level of auto-antibodies 12 p1462 A73-27706
Study of myocardial antigen localization using the
immunofluorescence method 15 p1834 A73-31392
Effects of oxygen-augmented atmosphere on the
immune response. 17 p2115 A73-34743
- ANTICLINAL MOUNTAINS**
U MOUNTAINS
ANTICLINAL VALLEYS
U VALLEYS
ANTICLINES
The tsunami model of the origin of ring structures
concentric with large lunar craters. 11 p1419 A73-25791
- ANTICLINORIA**
U ANTICLINES
ANTICOAGULANTS
Effect of heparin on blood platelet aggregation and
thrombosis under the action of direct electric current 08 p0931 A73-21321
Experimental studies on the production of pulmona-
ry infarction. IV - Effects of UK, heparin, t-AMCHA
or ellagic acid. 22 p2805 A73-42319
- ANTICYCLONES**
Blocking situations lasting less than five days over
the Euro-Atlantic region in the 20-year period from
1951 through 1970 08 p0986 A73-21486
Blocking anticyclones over Siberia in the cold half-
year period and the possibility of forecasting them 12 p1521 A73-27745
Some characteristics of stratiform St-Sc clouds in
various synoptic situations 13 p1654 A73-28885
Relation between the average motion of cyclones
and anticyclones and their shape. 15 p1906 A73-32255
The large-scale displacement of subtropical jet
stream over Western Europe in winter. 19 p2446 A73-37431
- Book - Atmospheric circulation systems and cli-
mates. 21 p2732 A73-41440
- ANTI-DIURETICS**
Renal component of the antigravitation function of
the organism 08 p0929 A73-20976
Role of mineralocorticoids in the natriuresis of
water immersion in man. 09 p1040 A73-22676
- ANTIFERROELECTRICITY**
Phenomenological theory of antiferroelectricity and
ferroelectricity applied to NaNbO₃ and the system
KNbO₃-NaNbO₃. 06 p0737 A73-18354
- ANTIFERROMAGNETISM**
Resonance between spin and magnetohydrodynamic
waves in antiferromagnetic semiconductors and
metals. 11 p1409 A73-26190
Nuclear magnetic resonance thermometry. 22 p2856 A73-42022
- ANTIFRICTION BEARINGS**
NT BALL BEARINGS
NT ROLLER BEARINGS
The role of compressional viscoelasticity in the
lubrication of rolling contacts. 01 p0055 A73-10220
Elastohydrodynamic lubrication in rolling and slid-
ing contacts. 01 p0055 A73-10222
Development of solid lubricant compact bearings
for the supersonic transport. [ASLE PREPRINT 72LC-7C-1] 03 p0316 A73-14370
Antifriction bearing with lubricated rubber and
metal laminations for wear elimination in limited rota-
tion applications, discussing design guidelines and ad-
vantages 03 p0317 A73-14424
A review of thermoelastohydrodynamic lubrication
in rolling and sliding contacts. 07 p0831 A73-20223
Influence of the nonlinear compliance of rolling
contact bearings on the vibrations of a balanced shaft 09 p1088 A73-22479
Character and magnitude determination of residual
stresses in surface layers of rolling bodies 10 p1289 A73-24068
Radial MHD bearing with a floating bush 15 p1881 A73-31412
Effect of nonlinear compliance in rolling motion
bearings on the vibrations of a balanced shaft. 15 p1883 A73-32066
Lubricant testing as an aid to bearing damage analy-
sis. [ASLE PREPRINT 73AM-3B-1] 17 p2178 A73-34983
An analysis and prediction of lubricant film starva-
tion in rolling contact systems. [ASLE PREPRINT 73AM-3B-4] 17 p2179 A73-34985
Turbulent lubrication - Its genesis and role in
modern design. 17 p2181 A73-35398
Contribution to the hydrodynamic lubrication
theory of the bearing with a floating bushing 18 p2319 A73-36411
Lubricating properties of micropolar fluids in com-
posite and step slider bearings, obtaining analytic ex-
pressions for load carrying capacity and skin friction 24 p3092 A73-44409
- ANTIGENS**
Study of myocardial antigen localization using the
immunofluorescence method 15 p1834 A73-31392
Ocular antigens. IV - A comparative study of the lo-
calisation of immunogenic determinants of ocular
structural glycoproteins in connective tissues of vari-
ous organs. 22 p2802 A73-41729
- ANTIGRAVITY**
Renal component of the antigravitation function of
the organism 08 p0929 A73-20976
- ANTIINFECTIVES AND ANTIBACTERIALS**
New formaldehyde base disinfectants. 23 p2948 A73-43276
- ANTI-KNOCK ADDITIVES**
Hydroxyl radical mechanism for autoignition inhibi-
tion of alkane fuels for antiknock additives at various
concentrations 13 p1707 A73-29000
- ANTIMATTER**
NT ANTINEUTRINOS
NT ANTIPARTICLES
NT ANTIPROTONS
NT POSITRONS
Rigidity spectrum of helium nuclei above 17 GV and
a search for high energy anti-nuclei in primary cosmic
rays. 04 p0493 A73-15980
- Faraday rotation of polarized extragalactic radio
sources interpretation as plasmas of mixed matter and
antimatter 07 p0900 A73-20277
Equations for a plasma consisting of matter and an-
timatter. 17 p2216 A73-34508
Generation of magnetic fields in a matter-antimatter
universe. 20 p2611 A73-39587
- ANTIMISSILE DEFENSE**
Optimal evasive tactics against a proportional
navigation missile with time delay. 15 p1908 A73-31918
Optimal SAM defense system - An application of
optimal control concept to operations research. 23 p2964 A73-43823
- ANTIMISSILE MISSILES**
New missile guidance concepts as applied to com-
mand guidance control system. [ATAA PAPER 73-835] 20 p2584 A73-38778
- ANTIMONIDES**
NT CADMIUM ANTIMONIDES
NT INDIUM ANTIMONIDES
Electrophysical parameters of TiSbSe₂ thin films 10 p1260 A73-24471
- ANTIMONY ALLOYS**
Stable or metastable phase crystallization rate of
Cd-Sb liquid alloys as function of time, composition
and temperature above liquidus line 05 p0605 A73-17294
Phase diagram and certain properties of alloys of the
neodymium-antimony system 06 p0707 A73-18041
Certain physical properties of Nd-Sb system alloys
and their correlation with the phase diagram 09 p1134 A73-22679
- ANTIMONY COMPOUNDS**
NT ANTIMONIDES
NT CADMIUM ANTIMONIDES
NT INDIUM ANTIMONIDES
Magneto-oscillatory absorption effect in SbI₃ 13 p1667 A73-28004
Some properties of synthesized stephanite
/Ag₅SbS₄/ specimens 17 p2219 A73-35551
Two-phonon absorption in SbSI single crystals 23 p3016 A73-43713
High temperature electron transfer and Bi and Sb
ion valency pair predictions in ordered perovskite-
type oxides, using lattice constants 23 p3017 A73-44129
- ANTINEUTRINOS**
Thermal conductivity approximation for gasdyna-
mic equations describing stellar gravitational collapse,
calculating neutrino and antineutrino energy and mo-
mentum transport processes 09 p1147 A73-22701
- ANTIOXIDANTS**
Effect of antioxidants on the blood deoxygenation
rate in animals exposed to altered atmospheres 12 p1465 A73-27702
Gas-releasing additives to jet fuels 21 p2754 A73-41070
Selection of phosphate impregnants for graphite ox-
idation inhibition 24 p3104 A73-44954
- ANTIPARTICLES**
NT ANTINEUTRINOS
NT ANTIPROTONS
NT POSITRONS
Upper limit of the antinucleus abundance in primary
cosmic rays 10 p1265 A73-23899
Upper limit of antinuclei content in primary cosmic
rays. 20 p2601 A73-38918
- ANTIPODES**
The influence of chordal paths on signals propagat-
ing to the near antipode of an HF radio transmitter. 01 p0015 A73-10182
K indices measurements at antipodal earth surface
observatories for aa indices, discussing one hundred year
series 04 p0444 A73-15547
- ANTIPROTONS**
Primary cosmic radiation antiproton flux, finding
.005 ratio upper limit to proton flux with balloon-
borne-magnetic spectrometer 08 p0999 A73-21333
Cosmic antiproton production in interstellar pp col-
lisions. 17 p2223 A73-34099
- ANTIRADIATION DRUGS**
Observations concerning the combined radiation-
protective effect of pantothenic acid and
aminoethylisothiuronium 02 p0136 A73-11586
Antiradial properties of DNA and of its denatura-
tion products 06 p0656 A73-18875
Mechanism of the action of radiation protecting
agents - A biochemical shock hypothesis 12 p1465 A73-27499

- Characteristics of the narcotic action of hexenal in combination with aminothyl-series radioprotective drugs in irradiated animals 15 p1838 A73-31391
- Effect of antiradiation drugs on the functional condition of the vestibular analyzer 15 p1838 A73-31509
- Chemical protection from genetic damages induced by radiation in the period of aftereffect of acceleration. 21 p2643 A73-40815

ANTIREFLECTION COATINGS

- Electron beam technique for evaporating titanium and silicon oxides antireflection coatings on solar cells, noting humidity and thermal resistances and UV radiation darkening 03 p0256 A73-14228
- Preparation of transmitting coatings for As₂S₃ glass 05 p0605 A73-17293
- Thin dielectric films as protective coatings for metallic mirrors and antireflective coatings for semiconductors and active laser materials 15 p1884 A73-31416
- Determination of changes in the reflection coefficient of absorbing coatings in the millimeter wavelength band 17 p2120 A73-34156
- Schottky barrier diode solar cells using dielectric antireflection coatings, discussing Nb, Mo and Cr diode metal characteristics, photovoltaic characteristics and conducting properties 19 p2391 A73-38406
- Development of a lightweight body-mounted solar cell array with a high power to weight ratio. 19 p2391 A73-38408
- Threshold, spectral, and output power characteristics of GaAs/Ga_{1-x}Al_x/As single-heterostructure diode lasers. 21 p2713 A73-40462
- ANTISEPTICS**
- Investigation of the disinfecting properties of sorbents which are used in a spacecraft life support system 17 p2114 A73-34240
- New formaldehyde base disinfectants. 23 p2948 A73-43276
- ANTISKID DEVICES**
- Aircraft antiskid system technical history and evolution, presenting frequency response of three-way configuration [SAE PAPER 720868] 05 p0534 A73-16651
- Aquaplaning prevention during take-off and landing, discussing friction loss factors, aircraft tires and runway surface treatment by antiskid overlays and grooving 11 p1343 A73-25209
- ANTISUBMARINE WARFARE**
- Suitability of the CL-84 tilting aircraft for the sea control ship system. [SAE PAPER 720852] 05 p0534 A73-16660
- ANTISUBMARINE WARFARE AIRCRAFT**
- NT CL-84 AIRCRAFT
- NT P-3 AIRCRAFT
- NT S-3 AIRCRAFT
- Navy Transit navigation satellite system, discussing flight test for feasibility of military application to YP-3C Antisubmarine Warfare Weapons System aircraft 21 p2735 A73-40040
- ANTONOV AIRCRAFT**
- NT AN-2 AIRCRAFT
- NT AN-24 AIRCRAFT
- ANTONOV AN-24 AIRCRAFT
- U AN-24 AIRCRAFT
- ANXIETY**
- The effect of anxiety control on the level of information processing 23 p2946 A73-43848
- AORTA**
- Influence of flow and pressure on wave propagation in the canine aorta. 14 p1715 A73-30066
- Assessment of left ventricular performance in man - Instantaneous tension-velocity-length relations obtained with the aid of an electromagnetic velocity catheter in the ascending aorta. 15 p1836 A73-31996
- Assessing the severity of aortic stenosis by phonocardiography and external carotid pulse recordings. 20 p2516 A73-38867
- Echocardiographic evaluation of the hemodynamic effects of chronic aortic insufficiency with observations on left ventricular performance. 20 p2512 A73-38868
- Evaluation of several methods for computing stroke volume from central aortic pressure. 21 p2638 A73-40638
- Nonlinear analysis of aortic flow in living dogs. 21 p2638 A73-40640
- Mechanism of 'readjustment' of aorta baroreceptors during hypertonia 22 p2807 A73-42655
- Velocity distribution in aortic flow. 22 p2811 A73-43104

- Transcutaneous measurement of blood velocity profiles and flow. 22 p2817 A73-43108
- Permanent catheterism of the thoracic aorta - Direct measurement of arterial pressure, injection of substances, and the taking of blood in wake rats 24 p3065 A73-45160
- APATITES**
- U CALCIUM PHOSPHATES
- U MINERALS
- APERIODIC FUNCTIONS**
- The Sorokin damping hypothesis in the case of aperiodic vibrations 17 p2243 A73-34648
- APERTURES**
- NT IRISES [MECHANICAL APERTURES]
- Fresnel diffraction by a circular aperture illuminated with partially coherent light. I. 01 p0078 A73-11004
- Microwave or acoustic holographic synthetic aperture interferometry with pulsed techniques, noting single scan, resolution and fringe number advantages 07 p0824 A73-20110
- Electromagnetic pulse penetration through small apertures. 08 p0940 A73-21664
- Linear aperture distribution synthesis by pattern sampling for arbitrary sampling points location and edge exponent alpha choice, using nonharmonic Fourier series theory 11 p1328 A73-25657
- Near-field analysis by the plane-wave spectrum approach. 11 p1329 A73-25674
- The geometrical factor of large aperture hemispherical electrostatic analyzers. 20 p2564 A73-38877
- Mutual coupling effects in circular arrays on cylindrical surfaces Aperture design implications and analysis. 21 p2653 A73-40674
- Finite aperture waveguide laser resonators with external reflectors by matrices coupling linearly polarized modes, calculating power efficiency, resonant frequencies and radiation patterns 21 p2714 A73-40760
- Large aperture atmospheric pressure excited carbon dioxide laser discharges, using weak volumetric gas preionization to obtain high power for plasma production 21 p2714 A73-40762
- Phase contrast transfer damping functions for various beam apertures in high resolution electron microscopy 21 p2702 A73-40949
- Radiating near-field power density and directivity reduction of tapered circular apertures. 22 p2829 A73-43181
- First-order probability densities of laser speckle patterns observed through finite-size scanning apertures. 22 p2872 A73-43188
- Linear array radio telescope for large aperture synthesis by using earth rotation to change relative orientation to radio source, discussing design and performance 23 p3028 A73-43352
- An aperture-synthesis interferometer at Ooty for operation at 327 MHz. 23 p2980 A73-43366
- APHELIONS**
- Meteorite aphelia calculation from activity levels of accumulated cosmogenic radioisotope due to cosmic ray irradiation 02 p0221 A73-12690
- APNEA**
- U RESPIRATION
- APOGEES**
- Optimization of the apogee impulse during the positioning of a geostationary satellite. [ONERA, TP NO. 1218] 02 p0228 A73-11992
- Analysis of the orbit of Cosmos 316/1969-108 A/. 02 p0225 A73-12824
- Geostationary injection dispersions and thrusting error elimination by apogee motor firing attitude optimization 21 p2780 A73-40614
- Station acquisition fuel minimization for third stage apogee motor impulse compensation of geostationary transfer orbit dispersions 21 p2781 A73-40618
- APOLLO APPLICATIONS PROGRAM**
- SkyLab experience with Apollo docking/latching loads. [AIAA PAPER 73-613] 18 p2358 A73-36091
- APOLLO FLIGHTS**
- NT APOLLO 6 FLIGHT
- NT APOLLO 11 FLIGHT
- NT APOLLO 12 FLIGHT
- NT APOLLO 14 FLIGHT
- NT APOLLO 15 FLIGHT
- NT APOLLO 16 FLIGHT
- NT APOLLO 17 FLIGHT
- Plans and objectives of the remaining Apollo missions. 03 p0368 A73-13086

- Comparative petrology of Apollo 16 sample 68415 and Apollo 14 samples 14276 and 14310. 03 p0375 A73-14103
- Comparison of the analytical results from the Surveyor, Apollo, and Luna missions. 04 p0498 A73-15185
- Resonant coupling of ocean Rayleigh waves to atmospheric shock waves from Apollo rockets. [AD-755609] 05 p0569 A73-16380
- Lunar evolution, age and surface composition data obtained from Apollo missions 05 p0616 A73-16400
- Lunar shape parameter extraction from Apollo 15 and 16 laser altimeter measurements of CSM to surface distance 06 p0751 A73-18223
- Apollo 11, 12 and 14 surface fines analysis by fluorescent technique for porphyrins content 06 p0753 A73-18419
- Porphyrins analysis in Apollo 11, 12 and 14 soils via analytical demetallation followed by recovery and recomplexing with divalent cations 06 p0753 A73-18420
- Terrestrial contamination in Apollo lunar samples. 06 p0754 A73-18425
- Apollo 15 and 16 ground-commanded television assembly. 07 p0823 A73-19375
- Lunar composition and evolution studies results from Apollo and Luna collected soil and rocks radiometric analysis, noting surface materials contamination with solar wind particles 07 p0878 A73-19674
- Mineral-chemical variations in Apollo 14 and Apollo 15 basalts and granitic fractions. 07 p0879 A73-19686
- Petrographic features and petrologic significance of melt inclusions in Apollo 14 and 15 rocks. 07 p0880 A73-19694
- Electron microprobe investigations of the oxidation states of Fe and Ti in ilmenite in Apollo 11, Apollo 12, and Apollo 14 crystalline rocks. 07 p0880 A73-19696
- Electron petrography of Apollo 14 and 15 rocks. 07 p0881 A73-19702
- Clinopyroxenes from Apollo 12 and 14 - Exsolution, domain structure, and cation order. 07 p0881 A73-19708
- Crystal field spectra of lunar pyroxenes. 07 p0881 A73-19709
- Crystal-field effects of iron and titanium in selected grains of Apollo 12, 14, and 15 rocks, glasses, and fine fractions. 07 p0881 A73-19710
- Plagioclase and Ba-K phases from Apollo samples 12063 and 14310. 07 p0881 A73-19714
- Chondrules in Apollo 14 samples and size analyses of Apollo 14 and 15 fines. 07 p0882 A73-19720
- Chemical classification and composition of Apollo 11, 12, 14 and 15 soil samples glasses, describing breccias and chondrules 07 p0882 A73-19723
- Noritic fragments in the Apollo 14 and 12 soils and the origin of Oceanus Procellarum. 07 p0884 A73-19741
- On lunar metallic particles and their contribution to the trace element content of Apollo 14 and 15 soils. 07 p0884 A73-19746
- Bulk, rare earth, and other trace elements in Apollo 14 and 15 and Luna 16 samples. 07 p0885 A73-19754
- Element abundances in Apollo 14 and 15 soils and breccias and in eucrite Juvinas and howardite Kapoeta, suggesting initial chemical layering of moon 07 p0886 A73-19758
- Precise determination of rare-earth elements in the Apollo 14 and 15 samples. 07 p0886 A73-19762
- Major impacts on the moon - Characterization from trace elements in Apollo 12 and 14 samples. 07 p0887 A73-19768
- Apollo 14 and 15 samples - Rb-Sr ages, trace elements, and lunar evolution. 07 p0887 A73-19777
- K-Ar dating of lunar fines - Apollo 12, Apollo 14, and Luna 16. 07 p0888 A73-19781
- Gamma-ray measurements of Apollo 12, 14, and 15 lunar samples. 07 p0888 A73-19789
- Cosmic-ray produced radioisotopes in Apollo 12 and Apollo 14 samples. 07 p0870 A73-19791
- Noble gas studies on regolith materials from Apollo 14 and 15. 07 p0889 A73-19799
- Inert gases from Apollo 12, 14, and 15 fines. 07 p0889 A73-19801
- Volatilized lead from Apollo 12 and 14 soils. 07 p0890 A73-19809
- Inorganic gas release and thermal analysis study of Apollo 14 and 15 soils. 07 p0890 A73-19814

Survey of lunar carbon compounds. II - The carbon chemistry of Apollo 11, 12, 14, and 15 samples.
07 p0890 A73-19818

Analysis of organogenic compounds in Apollo 11, 12, and 14 lunar samples.
07 p0890 A73-19819

Amino acid precursors in lunar fines from Apollo 14 and earlier missions.
07 p0891 A73-19820

Compounds of carbon and other volatile elements in Apollo 14 and 15 samples.
07 p0891 A73-19822

Microphysical, microchemical, and adhesive properties of lunar material. III - Gas interaction with lunar material.
07 p0892 A73-19832

Elastic velocity and Q factor measurements on Apollo 12, 14, and 15 rocks.
07 p0894 A73-19852

Microcrater size frequency distribution and exposure age for Apollo 12 and 14 rocks
07 p0896 A73-19868

Track studies of Apollo 14 rocks, and Apollo 14, Apollo 15, and Luna 16 soils.
07 p0896 A73-19873

Solar flare and galactic cosmic ray studies of Apollo 14 and 15 samples.
07 p0871 A73-19876

Luminescence of Apollo 14 and Apollo 15 lunar samples.
07 p0897 A73-19882

Quantitative size and shape analyses of Apollo 14 and 15 fines by computer evaluation of scanning electron microscope images
07 p0898 A73-19898

Lunar surface radioactivity - Preliminary results of the Apollo 15 and Apollo 16 gamma-ray spectrometer experiments.
08 p1009 A73-21224

Physiological response to exercise after space flight - Apollo 7 to Apollo 11.
11 p1314 A73-25326

Lunar composition from Apollo orbital measurements.
11 p1422 A73-25956

Apollo alpha particle spectrometer design, operation, calibration, packaging and flight results
11 p1363 A73-25957

Far ultraviolet reflectivity of lunar dust samples - Apollo 11, 12, and 14.
15 p1932 A73-31270

Al-Khwarizmi - A new-found basin on the lunar far side.
16 p2060 A73-33125

Urey meteoritic chondrule impact theory confirmation from Apollo sites and Lunar Crater /India/ impact generated silicate spherules
17 p2236 A73-35748

Apollo 15 and 16 subsatellite magnetometer measurements of the lunar magnetic field.
18 p2349 A73-35944

Apollo program contributions to lunar cosmology and composition, discussing core-mantle structure, earth-moon gravitational system, mineral types and cosmological hypotheses
18 p2356 A73-37044

Apollo 14 and Apollo 16 heavy-particle dosimetry experiments.
19 p2396 A73-37150

Russian book on lunar study by telescopes and unmanned and manned spacecraft covering Luna Zond and Lunokhod probes, Apollo flights, topography, structure and magnetic field
19 p2485 A73-37770

Apollo diet evaluation - A comparison of biological and analytical methods including bioisolation of mice and gamma radiation of diet.
20 p2517 A73-39103

Resonant nuclear measurement of hydrogen concentration vs depth in Apollo 11, 15 and 16 lunar soil fragments and platinum foil exposed to solar event
21 p2765 A73-40237

APOLLO LUNAR EXPERIMENT MODULE
Apollo Lunar Module environmental control system - Mission performance and experience.
[ASME PAPER 73-ENAS-28] 19 p2400 A73-37983

APOLLO LUNAR SURFACE EXPERIMENTS PACKAGE
Solar wind observations on the lunar surface with the Apollo-12 ALSEP.
02 p0205 A73-11903

Apollo 16 ultraviolet astronomy observations.
02 p0220 A73-12475

Engineering support activities for the Apollo 17 Surface Electrical Properties Experiment.
04 p0428 A73-15390

Lunar surface SEP transmitter-receiver ground wave experiment, discussing electronic equipment, multifrequency antennas and signal variation
04 p0428 A73-15391

Characteristics of the lunar photoelectron layer in the geomagnetic tail.
04 p0492 A73-15529

Lunar water vapor spectra during Apollo 14 ALSEP suprathermal ion detector experiment /SIDE/ and total ion detector /TID/ observations
07 p0891 A73-19829

Lunar atmosphere gas concentrations from Apollo 14 and 15 ALSEP cold cathode ionization gage measurements, considering solar wind and contamination sources
07 p0891 A73-19830

Surface magnetometer experiments - Internal lunar properties and lunar field interactions with the solar plasma.
07 p0892 A73-19834

Photoelectron layer detection above sunlit lunar surface with ion-electron spectrometer in Apollo 14 charged particle lunar environment experiment, noting energy spectra
07 p0895 A73-19859

SNAP-27/ALSEP power subsystem used in the Apollo program.
11 p1312 A73-26021

Plastic bonded, thermally stable explosive for an Apollo experiment.
18 p2341 A73-36152

Selenographic coordinates determination of ALSEP 12 and 14 telemetry transmitters via differential interferometric signal reception at two tracking stations, discussing instrument error reduction
20 p2603 A73-38894

Apollo 15 measurement of lunar surface brightness temperatures - Thermal conductivity of the upper 1.5 meters of regolith.
21 p2765 A73-40240

Observations of water vapor ions at the lunar surface.
23 p3031 A73-43764

APOLLO PROJECT
Apollo program predictive testing for man machine and environmental capabilities in terms of engineering, qualification, manufacturing, maintenance and training aspects
04 p0453 A73-14863

Apollo project management techniques transfer to socio-economic programs, discussing systems oriented approach to city planning, mass transportation, pollution control, public hygiene, etc
09 p1167 A73-21898

Post-occultation reception of lunar ship America radio transmission.
14 p1725 A73-29733

Apollo, Skylab and shuttle programs, discussing crews, tasks, national economic benefits and earth resources experiments effects
15 p1941 A73-32544

Apollo Experience Reports contents and development, detailing engineering, life sciences, flight crew operations, flight control safety and applications
17 p2256 A73-34300

Apollo program review on resources and technologies utilization, considering budget, radiation and meteoroid hazards, lunar surface, flight design and reliability and Saturn 5 testing
17 p2239 A73-35575

Fly-by-wire digital F-8C aircraft control system using Apollo guidance, navigation and control hardware, emphasizing interface design and fault detection
21 p2733 A73-40027

APOLLO SOYUZ TEST PROJECT
Description of the docking module ECS for the Apollo-Soyuz Test Project.
[ASME PAPER 73-ENAS-21] 19 p2493 A73-37977

Cloud microphysics spaceborne laboratory experimentation under zero-gravity conditions, discussing salt nuclei distribution mechanism due to spray breakup as task for Apollo-Soyuz program
[AAS PAPER 73-135] 20 p2583 A73-38590

APOLLO SPACECRAFT
NT APOLLO LUNAR EXPERIMENT MODULE
Bending and flexing of the Apollo 15 mass spectrometer boom.
05 p0636 A73-17210

Apollo-Soyuz docking project for flight testing systems compatibility for safe and reliable crew transfer, discussing program objectives, technical requirements and solutions
09 p1152 A73-22187

Fuel cell for Apollo command and service module power supply, discussing voltage-power requirements and operating temperature control
09 p1035 A73-22774

Apollo LM guidance computer software for the final lunar descent.
10 p1247 A73-24548

Absolute calibration of Apollo lunar orbital mass spectrometer.
13 p1617 A73-28930

Apollo 15 and 16 lunar orbital X and gamma ray spectrometer for lunar surface composition and radioisotopes surveys, detailing experimental results
16 p2015 A73-33353

Book - Systems concepts: Lectures on contemporary approaches to systems.
17 p2258 A73-35572

Radon emanation from the moon - Spatial and temporal variability.
18 p2349 A73-36033

Hybrid computer technique for desensitized optimal design of system with uncertain plant parameters, with application to Saturn 5 Apollo attitude control system design
18 p2291 A73-36426

APOLLO TELESCOPE MOUNT
Outgassing and contamination properties of prospective Apollo Telescope Mount materials.
03 p0330 A73-13020

Lumped parameter network modeling for spacecraft surface thermal environment analysis, discussing computer program and application to Skylab ATM
07 p0919 A73-19496

Observing programs in solar physics during the 1973 ATM Skylab program.
10 p1278 A73-24126

Nickel-cadmium battery performance prediction models Apollo Telescope Mount application.
19 p2390 A73-38399

Skylab ATM solar array performance characteristics prediction via mathematical model, discussing I-V characteristics, test data computer programming and polynomial curves
19 p2391 A73-38407

Skylab program mission profile, vehicle components, ground station data links, Apollo telescope mount, Saturn V rocket, solar cells and Salyut spacecraft comparison
20 p2615 A73-39150

APOLLO 6 FLIGHT
Geology, hydrology, land use and transportation net of Dallas-Fort Worth area from Apollo 6 photographs, comparing with ground based data
01 p0035 A73-10139

APOLLO 11 FLIGHT
The composition of the lunar highlands - Evidence from modal and normative plagioclase contents in anorthositic lithic fragments and glasses.
02 p0220 A73-12478

X-ray study and Moessbauer spectroscopy on lunar ilmenites /Apollo 11/.
02 p0220 A73-12480

Low molecular weight compounds of organogenic elements on Apollo 11 and 12 fines and breccias obtained by vacuum pyrolysis, acid hydrolysis and crushing
06 p0654 A73-18418

A photometric investigation of the packing state of Apollo 11 lunar regolith samples.
07 p0878 A73-19669

Reflectance and absorption spectra of Apollo 11 and Apollo 12 samples.
07 p0897 A73-19890

Distribution of methane and carbide in Apollo 11 fines.
07 p0900 A73-20188

APOLLO 12 FLIGHT
Erosion, transportation and the nature of the maria.
03 p0368 A73-13083

Low molecular weight compounds of organogenic elements on Apollo 11 and 12 fines and breccias obtained by vacuum pyrolysis, acid hydrolysis and crushing
06 p0654 A73-18418

Lunar crater Copernicus - Search for debris of impacting body at Apollo 12 site.
07 p0877 A73-19653

Some textures in Apollo 12 lunar igneous rocks and in terrestrial analogs.
07 p0879 A73-19688

Chemical characteristics of trace element rich KREEP basaltic rocks from Apollo 12 landing site
07 p0885 A73-19753

Rare-gas analyses on neutron irradiated Apollo 12 samples.
07 p0889 A73-19798

Thermoluminescence of Apollo 12 samples - Implications for lunar temperature and radiation histories.
07 p0897 A73-19880

Reflectance and absorption spectra of Apollo 11 and Apollo 12 samples.
07 p0897 A73-19890

Apollo 12 soil sample strength, compressibility, bulk density, porosity and shear wave velocity
07 p0898 A73-19901

On-surface and laboratory size measurements of fine lunar particles.
07 p0900 A73-20184

Optical properties of Apollo 12 moon samples.
09 p1144 A73-22191

Apollo 12 fines vacuum thermal conductivity as function of temperature for different densities, comparing to terrestrial basalt under vacuum and pressure
11 p1425 A73-26137

APOLLO 14 FLIGHT
Radioactive crystallization ages of Apollo 14 basaltic rocks from Fra Mauro formation, comparing with Apollo 11 samples
02 p0213 A73-12231

Apollo 14 mission, discussing extravehicular activities time and payload increase via enlarged propellant tanks

03 p0368 A73-13085

Visibility of lunar surface features - Apollo 14 orbital observations and lunar landing.

05 p0617 A73-16713

The determination of iron, titanium, and nickel in Apollo 14 samples by cathode ray polarography.

06 p0660 A73-17899

Apollo 14 fines examination for indigenous amino acids or amino acid convertible materials, optimizing gas-liquid chromatographic systems for separation and flame ionization

06 p0662 A73-18423

Geology of the Apollo 14 landing site.

07 p0878 A73-19679

Photogeologic interpretations of Apollo 14 orbital photographs of far side craters and lunar surface formations

07 p0879 A73-19681

Petrology of Apollo 14 high-alumina basalt.

07 p0879 A73-19684

Experimental petrology and petrogenesis of Apollo 14 basalts.

07 p0880 A73-19690

Apollo 14 - Subsolidus reduction and compositional variations of spinels.

07 p0880 A73-19697

Mineralogical and petrographic features of two Apollo 14 rocks.

07 p0880 A73-19699

Analysis of Fra Mauro samples and the origin of the Imbrium Basin.

07 p0880 A73-19701

Pyroxenes from breccia 14303.

07 p0881 A73-19705

Distinct subsolidus cooling histories of Apollo 14 basalts.

07 p0881 A73-19707

Metamorphism of Apollo 14 breccias.

07 p0882 A73-19717

Apollo 14 breccias - General characteristics and classification.

07 p0882 A73-19718

Apollo 14 breccia 14313 - A mineralogical and petrologic report.

07 p0882 A73-19719

Petrology and chemistry of some Apollo 14 lunar samples.

07 p0882 A73-19721

Microstructure and mineral compositions of impact produced lunar chondrules from Apollo 14 breccia by electron microprobe X ray analyzer

07 p0882 A73-19722

Vapor phase crystallization in Apollo 14 breccia.

07 p0882 A73-19724

Apollo 14 regolith and fragmental rocks, their compositions and origin by impacts.

07 p0883 A73-19725

Petrology and origin of lithic fragments in the Apollo 14 regolith.

07 p0883 A73-19730

Chemistry and particle track studies of Apollo 14 glasses.

07 p0884 A73-19736

Apollo 14 soils - Size distribution and particle types.

07 p0884 A73-19740

Chemical and petrographic characterization of Fra Mauro soils.

07 p0884 A73-19742

Chromatographic and mineralogical study of Apollo 14 fines.

07 p0884 A73-19743

Metallic particles in the Apollo 14 lunar soil.

07 p0884 A73-19744

Glassy particles in Apollo 14 soil 14163,88 - Peculiarities and genetic considerations.

07 p0885 A73-19747

A new titanium and zirconium oxide from the Apollo 14 samples.

07 p0885 A73-19749

Distribution of elements between different phases of Apollo 14 rocks and soils.

07 p0885 A73-19751

Oxygen and bulk element composition studies of Apollo 14 and other lunar rocks and soils.

07 p0885 A73-19752

Apollo 14 regolith fractions and soil breccia compositional characteristics by neutron activation analysis

07 p0885 A73-19755

Composition of the lunar uplands - Chemistry of Apollo 14 samples from Fra Mauro.

07 p0886 A73-19757

Rare earths and other trace elements in Apollo 14 samples.

07 p0886 A73-19760

Chondrite normalized major and trace element concentrations of Apollo 14 lunar samples, including basalt, breccia and regolith fines

07 p0886 A73-19761

Chemical analyses of lunar samples 14003, 14311, and 14321.

07 p0886 A73-19765

Isotopic abundance ratios and concentrations of selected elements in Apollo 14 samples.

07 p0887 A73-19773

Apollo 14 mineral ages and the thermal history of the Fra Mauro formation.

07 p0887 A73-19776

Rb-Sr systematics for chemically defined Apollo 14 breccias.

07 p0888 A73-19778

U-Th-Pb and Rb-Sr measurements on some Apollo 14 lunar samples.

07 p0888 A73-19779

Uranium and extinct Pu-244 effects in Apollo 14 materials.

07 p0888 A73-19784

Abundances of primordial and cosmogenic radionuclides in Apollo 14 rocks and fines.

07 p0888 A73-19787

Study on the cosmic ray produced long-lived Mn-53 in Apollo 14 samples.

07 p0870 A73-19795

Isotopic anomalies in lunar rhodium.

07 p0889 A73-19805

Total nitrogen contents of some Apollo 14 lunar samples by neutron activation analysis.

07 p0890 A73-19815

Total carbon, nitrogen, and sulfur in Apollo 14 lunar samples.

07 p0890 A73-19816

Amino acid analyses of Apollo 14 samples.

07 p0891 A73-19821

Spectrofluorometric search for porphyrins in Apollo 14 surface fines.

07 p0891 A73-19823

Lunar water vapor spectra during Apollo 14 ALSEP suprathermal ion detector experiment /SIDE/ and total ion detector /TID/ observations

07 p0891 A73-19829

Some surface characteristics and gas interactions of Apollo 14 fines and rock fragments.

07 p0891 A73-19831

Remanent magnetization of Apollo 14 rocks and fines, discussing iron contribution and early internal magnetic field

07 p0892 A73-19837

Magnetic properties of Apollo 14 breccias and their correlation with metamorphism.

07 p0893 A73-19839

Apollo 14 samples with Fe-bearing minerals examined by Mossbauer spectroscopy, noting parallelism with Apollo 11 and 12 samples

07 p0893 A73-19845

Elastic wave velocities and thermal diffusivities of Apollo 14 rocks.

07 p0894 A73-19851

Apollo 14 returned lunar rock fine thermal conductivity measurement as function of temperature under vacuum conditions, using least squares curve fitting method

07 p0895 A73-19856

Cosmic ray track densities of Apollo 14 breccias, igneous rock and soils from Fra Mauro, indicating surface residence times

07 p0871 A73-19871

Thermoluminescence of Apollo 14 lunar samples following irradiation at -196 C.

07 p0897 A73-19879

Luminescence of lunar material excited by electrons.

07 p0897 A73-19881

Spectral emission of natural and artificially induced thermoluminescence in Apollo 14 lunar sample 14163,147.

07 p0897 A73-19884

Polarimetric properties of the lunar surface and its interpretation. V - Apollo 14 and Luna 16 lunar samples.

07 p0897 A73-19891

Optical properties of lunar glass spherules from Apollo 14 fines.

07 p0898 A73-19893

Dielectric properties of Apollo 14 lunar samples at microwave and millimeter wavelengths.

07 p0898 A73-19894

Dielectric properties of Apollo 14 lunar samples.

07 p0898 A73-19895

Grain size analysis, optical reflectivity measurements, and determination of high-frequency electrical properties for Apollo 14 lunar samples.

07 p0898 A73-19897

Depth relationships for Apollo 14 and 15 core tubes and Apollo 15 drill core, noting sample recovery ratio

07 p0898 A73-19900

Chemical composition of some Apollo 14 lunar samples.

08 p0936 A73-20841

Extinct lunar radio activities - Xenon from Pu-244 and I-129 in Apollo 14 breccias.

08 p0936 A73-20843

Electron microprobe chemical analysis and structural formula of niobian rutile in Apollo 14 microbreccia sample KREEP fragment

09 p1139 A73-21856

Apollo 14 lunar fines thermal radiation properties as function of bulk density, illumination angle and

wavelength, calculating solar albedo and total emittance

10 p1277 A73-24080

Major element chemistry of glasses in Apollo 14 soil 14156.

10 p1278 A73-24111

Carbon compounds in pyrolysates and amino acids in extracts of Apollo 14 lunar samples.

11 p1426 A73-26471

APOLLO 15 FLIGHT

The optical temperature of the Apollo 15 exhaust plume.

[AD-757298] 03 p0358 A73-13497

Hadley Rille geologic and morphologic investigation from Apollo 15 data, supporting collapsed lava tube concept

07 p0878 A73-19677

Apennine Front lineaments origin at Apollo 15 landing site, interpreting topographic irregularities in terms of obliquely incident sunlight illusions

07 p0878 A73-19678

New geological findings in Apollo 15 lunar orbital photography.

07 p0878 A73-19680

Primordial radioelements and cosmogenic radionuclides in lunar samples from Apollo 15.

07 p0888 A73-19788

A first look at the lunar orbital gamma-ray data.

07 p0871 A73-19824

Lunar surface chemical composition mapping with onboard Apollo 15 X ray fluorescence spectrometer, showing Al, Mg and Si ratios

07 p0871 A73-19825

Observation of lunar radon emanation with the Apollo 15 alpha particle spectrometer.

07 p0891 A73-19826

Analysis and interpretation of lunar laser altimetry.

07 p0823 A73-19827

Lunar orbital mass spectrometer experiment.

07 p0891 A73-19828

Lunar magnetic field measurements with Apollo 15 subsatellite, discussing surface remanent magnetization, solar wind interactions and limb shocks

07 p0892 A73-19833

Lunar surface properties as determined from earthshine and near-terminator photography.

07 p0897 A73-19892

Depth relationships for Apollo 14 and 15 core tubes and Apollo 15 drill core, noting sample recovery ratio

07 p0898 A73-19900

Apollo 15 panoramic camera with 24 inch focal length for stereophotography of lunar surface, presenting pictures of lunar craters and landing sites

07 p0824 A73-20021

Rb-Sr ages and initial strontium in basalts from Apollo 15.

08 p0936 A73-20839

Detection of radon emanation from the crater Aristarchus by the Apollo 15 alpha particle spectrometer.

08 p1009 A73-21222

Testing of the Apollo 15 Metric Camera System.

08 p0968 A73-21703

Apollo 15 optical bar panoramic lunar surface photography, considering luminance, exposure time, resolution and camera performance

08 p0970 A73-21735

Depth variation of Apollo 15 deep drill fines trace elements from neutron activation analysis, noting KREEP abundance

10 p1278 A73-24113

Green spherules from Apollo 15 - Inferences about their origin from inert gas measurements.

12 p1541 A73-27490

Apollo 15 soil samples structure and phase equilibrium data noting metal particles of high cobalt content

12 p1466 A73-27544

Apollo 15 mare olivine and quartz basalts major and trace element composition and petrogenesis, deriving model of magma genesis

12 p1466 A73-27545

Apollo 15 soil and rock particle tracks density and stability and uranium content

12 p1542 A73-27547

Apollo 15 photogrammetric measurements of lunar figure, describing system characteristics and analytical triangulation techniques

12 p1501 A73-27967

Particle track record in Apollo 15 deep core from 54 to 80 cm depths.

13 p1686 A73-29566

The cosmic gamma-ray spectrum between 0.3 and 27 MeV measured on Apollo 15.

14 p1788 A73-30731

Significance of a primitive lunar basaltic composition present in Apollo 15 soils and breccias.

17 p2230 A73-34516

Apollo 15 sample 15597 vitrophyric nature, pyroxenes segregation and textural appearance as evidence for arrival on lunar surface in entirely liquid state

17 p2230 A73-34518

Orbital mapping of the lunar magnetic field.

17 p2235 A73-35739

Apollo 15 and 16 results of the integrated geochemical experiment. 17 p2236 A73-35750

Apollo 15 breccia and soils with spheres and fragments of iron-rich green glass originating in Apennine Front materials 19 p2487 A73-38174

Lunar cross hatching lineament patterns at Silver Spur on Apollo 15 landing site, relating to geological, lighting or meteorite impact gas flow effects 23 p3034 A73-43962

APOLLO 16 FLIGHT

Apollo 16 ultraviolet astronomy observations. 02 p0220 A73-12475

Apollo 16 exploration of Descartes - A geologic summary. 05 p0614 A73-16320

Spinel troctolite and anorthosite in Apollo 16 samples. 05 p0615 A73-16323

Luna 20 landing site geologic setting from Apollo 16 panoramic photographs, discussing complexly faulted terrain 05 p0618 A73-16826

Extralunar materials in Apollo 16 soils and the decay rate of the extralunar flux 4.0 Gy ago. 05 p0618 A73-16835

Apollo 16 lunar mission results, discussing lunar geology, spacecraft operational procedures and hardware 09 p1152 A73-22186

Photomicrographic investigation of plutonic and metamorphic equilibration in polished thin sections of Apollo 16 feldspathic microbreccia samples from North Ray crater rim 11 p1326 A73-25863

Zinc, lead, chlorine and FeOOH-bearing assemblages in the Apollo 16 sample 66095 - Origin by impact of a comet or a carbonaceous chondrite. 13 p1686 A73-29565

Volatile elements in Apollo 16 samples - Possible evidence for outgassing of the moon. 15 p1933 A73-31370

Apollo 16 rocks - Petrology and classification. 15 p1937 A73-31850

Detection of a nonuniform distribution of polonium-210 on the moon with the Apollo 16 alpha particle spectrometer. 15 p1941 A73-32266

Apollo 15 and 16 results of the integrated geochemical experiment. 17 p2236 A73-35750

The charge spectrum of heavy cosmic ray nuclei measured on board of Apollo 16 /Biostack/ using plastic detectors. 18 p2344 A73-35987

Apollo 16 flight program for investigating physiological effects of prolonged weightlessness on central nervous system, vestibular, neuromuscular and cardiovascular functions, metabolism, radiation sensitivity and body weight 22 p2814 A73-42176

Apollo 16 Biostack experiment for biological effects of cosmic ray heavy primaries on cell and tissue development and mutations of bacilli, Artemia and plant seeds 22 p2805 A73-42185

Apollo 16 far-ultraviolet camera/spectrograph - Instrument and operations. 22 p2864 A73-43165

APOLLO 17 FLIGHT

Apollo 17 lunar surface experiments for lunar composition, structure and chronology investigation, discussing landing site and instrument selection based on prior Apollo flights 04 p0493 A73-14671

Engineering support activities for the Apollo 17 Surface Electrical Properties Experiment. 04 p0428 A73-15390

The Apollo 17 landing site. 04 p0501 A73-15622

Infrared scanning radiometer for temperature mapping of the lunar surface on the Apollo 17 flight. 06 p0695 A73-18319

Lunar cinder cone deposits in Taurus-Littrow region of Apollo 17 landing site as counterparts of terrestrial pyroclastic eruptions 11 p1426 A73-26375

Far UV scanning spectrometer aboard Apollo 17 CSM to measure lunar atmospheric composition, observing spectral albedo, LEM atmosphere, and galactic and solar system atmospheres 12 p1497 A73-27485

Apollo 17 landing site crystalline rock age determinations for coarse grained basalt and anorthositic gabbro samples via Ar isotope ratios 14 p1788 A73-29720

Apollo 17 basalt ortho- and para-armalcolite, noting differences in optical properties, crystal habit and distribution between coarse and fine grained rocks 14 p1789 A73-29739

Apollo 17 lunar soil magnetic characteristics, covering ilmenite basalts mineralogy and petrology, electrical

cal properties, orange and green glasses origin, and trace elements 16 p2061 A73-33171

The Apollo 17 Surface Electrical Properties Experiment antenna performance. 17 p2171 A73-35370

The Apollo 17 Lunar Sounder. 18 p2288 A73-35959

AgCl detectors in the Biostack II experiment aboard Apollo 17. 18 p2314 A73-35986

APPARATUS

U EQUIPMENT

APPENDAGES

NT ARM [ANATOMY]

NT ELBOW [ANATOMY]

NT FOREARM

NT HAND [ANATOMY]

NT KNEE [ANATOMY]

NT LEG [ANATOMY]

APPLICATIONS OF MATHEMATICS

Book - Introduction to mathematical techniques in pattern recognition. 01 p0019 A73-10050

Mathematical methods in heat transfer analysis, considering perturbation, matched asymptotic expansions, variational, complex variables, matrix and several specialized methods 01 p0119 A73-10288

Combinational noise and interference effects during frequency conversion, noting mathematical methods 10 p1189 A73-24376

Russian book - Problems of applied mathematics. 13 p1650 A73-29126

Some aspects of recent contributions to the mathematical theory of finite elements. 14 p1806 A73-30177

Russian book - Applied mathematics and cybernetics. 20 p2541 A73-38977

Russian book on mathematical theory of optimal control of discrete time systems covering multidimensional geometry, convex sets, Pontryagin maximum principle and dynamic programming 21 p2726 A73-40802

Book - The finite element method: Fundamentals and applications. 22 p2882 A73-42492

APPLICATIONS TECHNOLOGY SATELLITES

NT ATS 1

NT ATS 3

NT ATS 5

NT ATS 6

Design, development, fabrication and qualification load testing of high modulus graphite-epoxy reflector support truss for ATS F and G 03 p0330 A73-13021

Real time programmable data compression system with minicomputers for operation between TV data acquisition ground stations and ATS satellites 04 p0425 A73-15442

Integration of an ion engine on the Communications Technology Satellite. 04 p0487 A73-15448

Applications technology satellite data handling processing and interpretation for future earth survey, communications and meteorological satellite operational programs 08 p1014 A73-21593

Scientific and applications satellite launch site facilities, discussing payload preparation 14 p1742 A73-30109

UN accomplishments in space law, discussing ESRO and ELDO application satellites and international agreements 14 p1819 A73-30898

Thermal control flight experiment onboard ATS-F to evaluate feedback controlled variable conductance heat pipe performance in space environment 18 p2370 A73-36372

[AIAA PAPER 73-757]

System requirements for a free-flying teleoperator to despin the ATS-V. 19 p2490 A73-37304

Communication satellite history and present developments, discussing Intelsat and ATS programs and TDMA techniques 20 p2526 A73-38747

Communications and position fixing experiments using the ATS satellites. 21 p2733 A73-40024

APPROACH

NT INSTRUMENT APPROACH

APPROACH CONTROL

NT RADAR APPROACH CONTROL

Problems of the integration of aircraft and flight control system in the case of new approach procedures [DGLR PAPER 72-096] 02 p0190 A73-11698

Determination of the navigational regime for flight over fixed points during the landing maneuver 03 p0339 A73-13071

A statistical analysis of pilot control during a simulation of STOI. landing approaches. 05 p0536 A73-16922

[AIAA PAPER 73-182]

A precision position and time service for the air traffic of the future. 07 p0849 A73-19350

Area navigation systems integration with terminal ATC approach procedures, considering computerized data linkage with aircraft navigation system 07 p0849 A73-19351

A flight control system for STOL aircraft. 07 p0777 A73-20171

Comparison of conventional flight control systems with a modern integrated flight control system 10 p1175 A73-23762

Manned vehicle systems analysis techniques application to manual approach-to-landing phase of aircraft flight, developing analytical control model 10 p1247 A73-24011

Noise abatement two-segment, precision and category I, II and III approaches considerations covering altimetry, cost and safety problems in ATC 10 p1247 A73-24768

Display system for monitoring automatically controlled STOL landing glide paths, discussing computer controlled simulation 11 p1362 A73-25440

An optimal control approach to terminal area air traffic control. 11 p1394 A73-25786

Evaluation of glide paths for landing a VTOL airplane using linear regulator theory. 12 p1458 A73-27154

Flight tests of approach path angles and airspeed effects on landing of spoiler equipped light aircraft 13 p1569 A73-28830

Curved landing approaches under visual and instrument flight conditions, investigating steep glide slope display configurations and flight control modes 13 p1569 A73-28901

Optimal aircraft go-around and flare maneuvers. 13 p1657 A73-29217

Automatic helicopter approach in poor visibility 15 p1910 A73-32465

AIL-CO-SCAN landing system for STOL and helicopters, combining localizer and glide control functions in 20 by 20 deg approach window 15 p1910 A73-32470

M.A.D.G.E. - Microwave Aircraft Digital Guidance Equipment: Description of the system 15 p1912 A73-32504

Aircraft performance relationship to safety margins improvement, discussing accelerate stop, approach control, airworthiness, landing and coordination 17 p2097 A73-34082

Safety in the accident prone flight phases of take-off, approach and landing. 17 p2098 A73-34085

Monitor display to indicate aircraft position relation to desired flight profile during automatically controlled steep landing approaches with curved segments 17 p2207 A73-34477

Longitudinal motion of a transport aircraft during steep landing approaches 17 p2100 A73-34482

Flight control problems during STOL landing approaches, considering navigation aids, pilot work load and flight safety 17 p2207 A73-34483

Digital control of rotary wing aircraft landing approach based on spatially variable preassigned flight path [MBB-UFEE-1021] 17 p2207 A73-34486

Ground visual aids for civil STOL aircraft steep gradient approach and blind landing, discussing flight trials and simulator experiments [RAE-TM-AVIONICS-136/BLEU/] 17 p2208 A73-34489

Terminal and flight control navigation guidance systems for restricted and short takeoff and landing aircraft air traffic and approach techniques [RAE-TM-AVIONICS-135/BLEU/] 17 p2100 A73-34490

Approach and landing operations and flight guide beam systems, discussing tests, design, improvements and operational requirements [DGLR PAPER 73-011] 17 p2208 A73-34491

Flight-path control device for generating curvilinear flight path profiles using microwave landing systems [DGLR PAPER 73-016] 17 p2208 A73-34492

TACAN based SETAC and L band DME based DLS approach and landing systems for military aircraft, discussing time division multiplexing and antenna array [DGLR PAPER 73-019] 17 p2208 A73-34493

Electronic landing system satisfying IFR requirements for air traffic, noting simulated ILS and ground controlled approach operations [DGLR PAPER 73-020] 17 p2146 A73-34494

Helicopter steep angle approach limits during instrument-guided landing comparison with classical ILS method, describing flight performance results [DGLR PAPER 73-026] 17 p2208 A73-34497

Integrated image and symbolic display hierarchy with increasing horizontal and vertical information content for superposition as helicopter aid in approach and precision hovering [AHS PREPRINT 724] 17 p2168 A73-35065

- Advanced concepts in terminal area control systems - Aircraft tracking and collision alert. 19 p2451 A73-37806
- United States Microwave Landing System development program. 19 p2451 A73-37815
- Aircrew workload during the approach and landing. 19 p2401 A73-38005
- Testing noise-reducing approach techniques with the HFB 320 research aircraft of the DEVLR. 19 p2387 A73-38265
- Flight director design for a STOL aircraft. 20 p2508 A73-38649
- Application of direct side force control to commercial transport. [AIAA PAPER 73-886] 20 p2588 A73-38822
- Runway condition effects on landing safety, discussing surface friction, approach control, skidding, directional control, water and ice conditions, tires and brakes. 20 p2509 A73-39220
- French automatic beam coupler system for V/STOL and helicopter low speed and low altitude instrument approach. 21 p2737 A73-40975
- Flow control concepts and airline operations. 22 p2884 A73-42522
- Reducing approach and landing accidents. 22 p2799 A73-42523

APPROACH INDICATORS

- Cockpit device with optical head-up display for visual slope guidance to any runway at any airport. 01 p0051 A73-11011
- Functional aspects of head-up display operation, discussing data accumulated by pilot during low visibility runway approach in executive jet. 01 p0013 A73-11012
- Visual systems for indicating approach slope during aircraft landing. 09 p1116 A73-22975
- Automotive approach systems certification and short distance takeoff and landing trajectory by cinematheodolites, digital optical, airborne and inertial/radiosonde equipment. 10 p1246 A73-23656
- Simulated flight tests of a digitally autopiloted STOL-craft on a curved approach with scanning microwave guidance. [ASME PAPER 73-AUT-L] 13 p1657 A73-29413
- Aircraft terminal approach and entry spacing systems supported by automated terminal radar using area navigation techniques. 17 p2210 A73-35852

APPROPRIATIONS

- Airport and Airway Development Act trust fund surplus, discussing expenditure policy determination and incentive plan provisions to expedite improvements. 12 p1561 A73-27367

APPROXIMATION

- NT BORN APPROXIMATION
- NT BORN-OPPENHEIMER APPROXIMATION
- NT CHEBYSHEV APPROXIMATION
- NT EDDINGTON APPROXIMATION
- NT FINITE DIFFERENCE THEORY
- NT FINITE ELEMENT METHOD
- NT HARTREE APPROXIMATION
- NT LEAST SQUARES METHOD
- NT NEWTON-RAPHSON METHOD
- NT OSEEN APPROXIMATION
- NT PADE APPROXIMATION
- NT PARTICLE IN CELL TECHNIQUE
- NT RAYLEIGH-RITZ METHOD
- NT RELAXATION METHOD [MATHEMATICS]
- NT RITZ AVERAGING METHOD
- NT SCHWARTZ METHOD
- NT SOMMERFELD APPROXIMATION
- A method of construction and the structure of asymptotic approximations of the solutions of nonlinear mixed boundary value problems in studies of multifrequency oscillation modes. 01 p0076 A73-10097
- Approximate method for solving boundary value problems in the mathematical theory of elasticity of an anisotropic medium. 01 p0113 A73-10098
- Displacements of spatially bounded light beams in a turbulent medium using the approximation of a random Markov process. 01 p0076 A73-10214
- Approximate method to determine collision probabilities, hyperbolas, and direct and retrograde ellipses during single close encounters in three body planetary problem. 01 p0099 A73-10693
- Verification of an approximation method for calculating multiple scattering of sky radiation. 01 p0074 A73-11236
- The role of interpolation and approximation theory in variational and projectional methods for solving partial differential equations. 01 p0071 A73-11458
- Accelerated convergence of sequences of quadrature approximations. 01 p0072 A73-11471

Approximation by functions of fewer variables.

- 02 p0186 A73-11969
- On approximate solutions for rigid-plastic structures subjected to dynamic loading. 02 p0236 A73-12520
- Optimal control approximations for time delay systems. 03 p0286 A73-14195
- System identification using approximate nonlinear filters. 04 p0430 A73-15257
- Transient phenomena in a phase-locked loop with a noisy reference. 04 p0421 A73-15437
- Finite-dimensional approximations of state-constrained continuous optimal control problems. 05 p0561 A73-16490
- Galerkin method for approximate solution of differential equation with boundary conditions, considering applicability to nonself-adjoint and nonlinear systems. 06 p0765 A73-18725
- State estimation of nonlinear system by applying stochastic approximation method. 06 p0681 A73-18813
- An analytical method for certain weakly nonlinear periodic differential systems. 07 p0845 A73-20226
- Nearest neighbor approximation for Kalman-Bucy filtering noisy data generated by multidimensional processes via dimensionality reduction for linear steady state problems. 07 p0805 A73-20579
- On stochastic approximation and the hierarchy of adaptive array algorithms. 07 p0846 A73-20585
- Radiation absorption calculation for nonisothermal gas containing combustion products, noting approximation for water vapor radiation. 08 p1021 A73-20860
- Near-optimal control of high-order systems using low-order models. 08 p0950 A73-21090
- An economical approximation for the coefficients in the development of a function with respect to an orthogonal system. 08 p0984 A73-21413
- Approximate solution of certain optimal-control and discrete-programming problems. 09 p1068 A73-22561
- Numerical computation of forced oscillations in coupled Duffing equations. 09 p1113 A73-23022
- Semivariational approximation for solution of parabolic differential equation with inhomogeneous mixed boundary conditions and abstract equation with operators, noting convergence and stability. 09 p1113 A73-23025
- Continuous best approximation projections in certain Banach spaces. 09 p1113 A73-23027
- Orthotropic material plane crack problem numerical solutions by polynomial approximation and modified mapping-collocation technique involving conformal mapping. 09 p1161 A73-23178
- Conical shell inversion - An approximate energy analysis. [ASME PAPER 72-PVP-4] 09 p1163 A73-23266
- On the instability of leap-frog and Crank-Nicolson approximations of a nonlinear partial differential equation. 10 p1241 A73-23640
- Spline approximation to the solution of the Volterra integral equation of the second kind. 10 p1241 A73-23642
- Asymptotic approximation of an infinitely thin, elastic, nonlinear cylinder by a curvilinear medium. 10 p1288 A73-23765
- An approximate analysis of the diffusing flow in a self-controlled heat pipe. [ASME PAPER 72-HT-M] 10 p1295 A73-23776
- Note on an approximate method for computing consistent conjugate stresses in elastic finite elements. 10 p1290 A73-24293
- Multiinput multioutput linear time invariant discrete system optimal approximation, noting algorithms and weighting matrices computational difficulties. 11 p1390 A73-25192
- An approximate solution to a strongly non-linear, second-order, differential equation. 11 p1390 A73-25195
- Uniform isotropic Brownian motion in a linear-cubic approximation. 11 p1397 A73-25428
- Higher order numerical solution of the integral equation for the two-dimensional Neumann problem. 11 p1300 A73-25434
- A method of feasible directions using function approximations, with applications to min max problems. 11 p1390 A73-25474
- Plane wave expansion approximation for wave field on dielectric wedge representing tapered antenna, considering lateral wave contribution. 11 p1329 A73-25681

Remark on the behavior of an approximated process related to singular integrals near the terminals of an integration segment. 11 p1391 A73-26077

Galerkin method application to approximation functions selection in development of thrust gas bearing with blowing. 11 p1375 A73-26429

Linear system modeling via optimal finite dimensional approximation based on Sard generalized spline, giving error bounds. 11 p1391 A73-26580

Second order approximation to autocorrelation matrix of random variable nonlinear transformation, discussing application to Poisson process and monopulse radar receiver AGC effects. 11 p1333 A73-26695

Synthesis of an approximately optimal control for one class of controlled systems. 12 p1484 A73-27457

Mathematical observations in structural dynamics. 12 p1555 A73-27739

A direct integral equation method for the potential flow about arbitrary bodies. 13 p1563 A73-28083

Methods for the approximate computation of the periodic solutions of systems of nonlinear periodic differential equations. 13 p1647 A73-28193

Method of trigonometric sums in the metric theory of Diophantine approximations of dependent variables. 13 p1648 A73-28343

Best rational approximation and strict quasi-convexity. 13 p1649 A73-28602

A direct method approximation to the linear parabolic regulator problem over multivariate spline bases. 13 p1649 A73-28605

Estimating the eigenvalues of Sturm-Liouville problems by approximating the differential equation. 13 p1649 A73-28606

Nonlinear elements piecewise and continuous approximations for constructing current-voltage characteristic functions. 13 p1596 A73-28871

An approximate solution of the nonstationary heat conduction problem for laser elements with sharply expressed anisotropy. 14 p1758 A73-30467

On the transport of charged particles in turbulent fields - Comparison of an exact solution with the quasilinear approximation. 15 p1916 A73-31083

Approximate solution to the problem of a conducting fluid flow in a weakly curved channel. 15 p1917 A73-31154

The problem of choosing a zero approximation of the angular position of an oriented satellite in the case of a nondipolar approximation of the geomagnetic field. 15 p1942 A73-31238

The Fredholm alternative in the case of linear approximation-regular operators. 15 p1901 A73-32371

Rapidly convergent approximations to Dirichlet's problem for semilinear elliptic equations. 15 p1901 A73-32372

An equivalence theorem on best approximation of continuous functions by algebraic polynomials. 15 p1902 A73-32376

On the generation of rational function approximations for Laplace transform inversion with an application to viscoelasticity. 16 p2032 A73-33307

Earth-flattening approximations in the theory of radio wave propagation near the surface of the earth. 16 p1984 A73-33916

Approximate method of solution for three-dimensional boundary layers. 17 p2150 A73-34188

Iteration methods for finding all zeros of a polynomial simultaneously. 17 p2200 A73-34215

Successive approximations for calculating supersonic flow past wings with subsonic leading edges. 17 p2091 A73-34347

Approximation of the geometric figure of the moon by using spherical functions. 17 p2230 A73-34596

Solution of incorrect problems by methods of successive approximations. 17 p2201 A73-34630

Thin turbulent film analysis with approximation for relationship between flow and wall shear stress and effects of surface roughness and inertia at steps [ASME PAPER 73-LUBS-17] 17 p2181 A73-35396

Computation of the exponential of a matrix. I - Theoretical considerations. 17 p2203 A73-35521

Spline interpolation techniques for approximation of boundary value problem solutions, relating approximation error norm to interpolation error norm from variational formulation. 17 p2203 A73-35607

The numerical derivation of a periodic solution of a second order differential difference equation.
17 p2203 A73-35728

Comparison of three techniques for solving the radiative transport equation.
[AIAA PAPER 73-751] 18 p2337 A73-36367

Approximate solution of second-order nonlinear systems with heredity of a single independent variable
19 p2445 A73-37642

An approximation method for calculating the attenuation characteristic of dielectric-lined circular waveguides.
19 p2404 A73-37723

Derivation of an approximate solution to the equation of geocentric motion of a space vehicle with a solar sail
19 p2492 A73-37849

Some numerical aspects of the solution of functional equations in dynamic programming
19 p2445 A73-38163

A generalization of the concept of equivalent linearization.
19 p2445 A73-38257

On an equilibrium-frozen flow approximation in the analysis of nonequilibrium nozzle flows.
19 p2422 A73-38282

Application of the method of straight lines to the solution of a modified Stefan problem
20 p2626 A73-39253

Successive approximation technique for dynamic-load problems of nonlinear viscoelastic systems
20 p2593 A73-39322

Some aspects of the approximation of functions of many variables, and effective direct methods for solving problems in elasticity theory
20 p2618 A73-39326

Application of a truncation method in the derivation of a multiperiodic solution of a denumerable system of partial differential equations
20 p2582 A73-39473

Zeroth-order approximation by multiple scaling method to analyze nonlinear oscillations with small speed-dependent damping, applying to pendulum problem
20 p2593 A73-39536

Approximation for hypersonic flow past circular cone with angle of attack, discussing matched asymptotic expansion, flow velocity and density distribution
21 p2632 A73-40428

Russian book - Introduction to the statistical dynamics of systems with possible disturbances.
21 p2669 A73-40775

Integration of certain ordinary differential equations based on the approximation of continuous functions by linear functions
21 p2727 A73-41063

Approximate calculation of the optimal suction of a compressible gas on a thermally insulated surface at Prandtl numbers other than unity
22 p2795 A73-42118

Approximate calculation of flows through blade cascades under conditions of partial cavitation
22 p2841 A73-42129

Solving linear boundary value problems by approximating the coefficients.
22 p2882 A73-42519

Approximation for maximum centerline heating on lifting entry vehicles.
22 p2796 A73-42627

Comparison of the Kryloff-Bogoliuboff method and the refined elliptic function method.
22 p2882 A73-43071

Approximation of transfer functions for filters with equalized group-delay characteristics.
23 p2960 A73-43676

Convergence of the method of successive approximations in geometrically nonlinear problems
23 p2999 A73-44197

APPROXIMATION METHODS
U APPROXIMATION
APSIDAL ANGLES
U ANGLES (GEOMETRY)
U APSIDES
APSIDES
NT APHELIONS
NT APOGEES
NT PERIGEEES
NT PERIHELIONS
Determination of the coefficient of displacement of the line connecting the apsides in stellar models and comparison of it with observations
03 p0379 A73-14584

Satellite motion in the equatorial plane of an oblate primary body and apsidal line shift evaluation.
04 p0498 A73-15296

Photometric orbit and apsidal motion of DR Vulpeculae.
07 p0875 A73-19119

Optimal transfer between coplanar elliptic orbits with the aid of tangential impulses applied at the apsidal points
15 p1931 A73-31232

Impulse application for optimal correction of angular position of orbital plane line of apsides, expressing axis angle of rotation as linear function
23 p3027 A73-43269

APT (PICTURE TRANSMISSION)
U AUTOMATIC PICTURE TRANSMISSION
APTITUDE
Proposed new test for aptitude screening of air traffic controller applicants.
09 p1045 A73-22535

AQUARID METEORIODS
The structure of the Eta Aquarid meteor stream.
11 p1426 A73-26573

AQUEOUS SOLUTIONS
Influence of metallurgical factors on the corrosion cracking under tension of TA6V titanium alloy in an aqueous medium at ambient temperature
[ONERA, TP NO. 1100] 01 p0061 A73-10231

Chlorination studies. I - The reaction of aqueous hypochlorous acid with cytosine.
02 p0139 A73-12631

Suppression of evaporation of hydrocarbon liquids and fuels by aqueous films.
05 p0639 A73-16687

[WSCI PAPER 72-27] Optical resolution of aspartic acid by using copper complexes of optically active amino acids.
07 p0789 A73-20457

Thermodynamic properties of gases dissolved in electrolyte solutions.
07 p0789 A73-20642

Kramers-Kronig analysis of relative reflectance spectra measured at an oblique angle.
11 p1400 A73-26421

Stress-corrosion cracking of Ti-8Al-1Mo-1V in aqueous environments. I - The kinetics of subcritical crack propagation. II - Plastic zones, crack morphology, and fractography.
13 p1632 A73-28135

ARAGONITE
Biogeochemistry of aragonite mud and oolites.
03 p0266 A73-14662

Cenozoic coral and aragonitic fossil age determination by He, U, Th and Ru isotope retentivity consistency checks
13 p1609 A73-29178

ARC CHAMBERS
Cone shaped arc discharge driver chamber for high energy shock tube, presenting performance characteristics test data
07 p0808 A73-19969

Biased wall heat transfer in electric arc chamber, noting I-V characteristics and electron current saturation in superimposed axial flow
12 p1560 A73-27700

ARC DISCHARGES
Influence of the parameters of the accelerating circuit of an injector with inductive energy storage on the process of plasma-cluster acceleration
02 p0196 A73-11633

I-V characteristics and luminescence changes in Cs vapor arc discharge at various spark gap widths, noting pressure effect on gas stratification
04 p0481 A73-15613

Electromagnetic thrust from magnetic dc arc discharge plasma accelerators, noting MHD experiments and reentry simulation
04 p0489 A73-15728

Russian book on plasma cutting covering electrophysical and thermophysical principles of arc discharges application for metal cutting, arc I-V characteristics, plasmatrons and operation
04 p0457 A73-15962

Vapour density variations in a pulsed mercury discharge.
05 p0601 A73-16432

Investigation of high-power quasi-steady arcs in strong axial gas flows
05 p0602 A73-16583

Radial anode current density distribution measurement in high current pulsed arcs in air on copper split anode, using Rogowski coils
06 p0723 A73-18357

Characteristics of ionization-recombination processes in a plasma discharge diode
09 p1124 A73-21884

Calculation of the Knudsen-arc ignition potential in a gas-filled diode with cylindrical and spherical electrode geometries
09 p1061 A73-21912

Low temperature plasma electric arc discharge generators, noting electrode interaction, energy losses and high enthalpy efficiencies
10 p1253 A73-23516

I-V characteristics and luminescence changes in Cs vapor arc discharge at various spark gap widths, noting pressure effect on gas stratification
10 p1254 A73-24203

ARC discharge plasma diagnostics for nonuniform nonequilibrium turbulent sources, including automatic methods for control applications
12 p1528 A73-27322

Investigation of a low-pressure arc erosion plasma
14 p1781 A73-30459

Electrical conductivity and total emission coefficient of air plasma.
15 p1918 A73-31657

Quasi-monochromatic measurements of homogeneous arc plasmas.
15 p1841 A73-32393

Ignition potential of a Knudsen arc in a gas-filled diode with cylindrical and spherical electrodes.
15 p1922 A73-32637

Steady state arc discharge physical properties, discussing boundary geometry of plasma column, and stabilities in gas flow and high current and vacuum conditions
16 p2040 A73-32939

Arc discharge properties in ionized gases, discussing interruption and reignition in terms of instabilities, decay processes, and circuit breaker problem
16 p2040 A73-32940

Arc plasmas as radiation standards in the vacuum ultraviolet.
16 p2036 A73-32942

Ionization and recombination in a plasma diode.
17 p2215 A73-34308

Low temperature plasma electric arc discharge generators, noting electrode interaction, energy losses and high enthalpy efficiencies
17 p2217 A73-35196

Transient temperatures in a plate from a Gaussian distribution of normal heat flux and current flow with application to the free arc discharge.
17 p2255 A73-35843

Dynamic characteristics of a plasma diode under conditions of a low-voltage arc discharge. I - Theory of the dynamic characteristics
18 p2339 A73-36557

Stationary high-current plasma accelerators
19 p2466 A73-37359

Analysis and investigation of cathode processes in a high-current arc discharge
19 p2466 A73-37360

Low-frequency flute instabilities of a hollow cathode arc discharge - Theory and experiment.
19 p2468 A73-37858

The breakdown condition of the electrode layer in an ionized gas flow
20 p2597 A73-39278

Determination of work functions near melting points of refractory metals by using a direct-current arc.
21 p2722 A73-41563

Russian book - Physical bases of thermionic energy conversion.
22 p2890 A73-41876

Dynamic characteristics of a plasma diode with a low-voltage arc discharge. II - Experimental study of dynamic characteristics
22 p2833 A73-42386

ARC HEATING
Laser activated, model surface recession compensation system for testing ablative materials.
[AIAA PAPER 73-380] 11 p1343 A73-25510

Computer simulation of arc heaters for production of flow with high enthalpy.
13 p1707 A73-29023

Density measurements in high speed arc heated flows.
13 p1622 A73-29640

Experimental investigations on arc-heated steady plasma flow.
19 p2415 A73-37169

ARC MELTING
Vacuum arc melting for improved heat resistance and mechanical properties of Ni alloy blanks, comparing with electro-beam and plasma arc melting and powder sintering
03 p0323 A73-13502

Liquation-induced microinhomogeneity of heat resistant submerged-arc-smelted steel 4K12N8G8MFB/E1481/
03 p0326 A73-13829

Importance of arc gap control in vacuum consumable arc remelting of superalloys.
04 p0454 A73-15743

Ferrous and nonferrous metal alloys melting and remelting in plasma induction and beam furnaces, noting cost reduction and ingots homogeneity
04 p0455 A73-15748

Titanium nitrides effect on austenite grains formation by high temperature fusion, considering electric arc and vacuum melting of structural steels
06 p0706 A73-17883

The interaction of tungsten and molybdenum melts with gaseous oxygen
15 p1890 A73-31924

ARC SPRAYING
The spray deposition of oxide-free coatings consisting of special metals with a high affinity to oxygen
11 p1372 A73-25411

The technology of plasma arc spraying.
16 p2017 A73-32698

Structure and properties of arc-sprayed titanium coatings.
22 p2879 A73-42597

ARC WELDING
NT GAS TUNGSTEN ARC WELDING

NT PLASMA ARC WELDING

- Impurities effect on Mo plastic properties and toughness, suggesting lower vacuum arc welding rates and increased electron beam zone refining runs 01 p0066 A73-11343
- Thermal-influence region properties in a maraging steel as a function of welding heat cycles 06 p0697 A73-17880
- Possibility of argon-nitrogen gas metal-arc welding of some non-ferrous metals. 08 p0973 A73-21237
- Stud welding on 5083 aluminum and 9% Ni steel for cryogenic use. 11 p1375 A73-26352
- Book - Welding and welding technology. 17 p2177 A73-34454
- Prediction of weld metal hydrogen levels obtained under test conditions. 21 p2708 A73-41252
- Gas metal arc welding of 9% Ni steel using ferritic filler metal. 22 p2866 A73-42226

ARCHES

- The magnetic structure of arch filament systems. 03 p0378 A73-14415
- Transverse oscillations produced by dynamic loads in structural elements of parabolic arc shape 04 p0513 A73-15506
- Finite element analysis of buckling and post-buckling behaviors of arches with geometric imperfections. 07 p0914 A73-20211
- Buckling load of shallow circular vaults, investigating boundary conditions, load intensity and interconnecting beam flexibility and spacing effects 07 p0916 A73-20434
- Large deflexion, geometrically non-linear finite element analysis of circular arches. 08 p1015 A73-20670
- A corrected assessment of the cylindrical shell finite element of Bogner, Fox and Schmit when applied to arches. 11 p1443 A73-26090
- Finite element matrix formulation of post-buckling stability and imperfection sensitivity. 13 p1694 A73-28253
- The behaviour with diminishing curvature of strain-based arch finite elements. 16 p2076 A73-32921
- Free vibration of arches flexible in shear. 21 p2782 A73-40002

ARCHIPELAGOES

- Geological analysis of aerial thermography of the Canary Islands, Spain. 20 p2561 A73-39896

ARCHITECTURE

- Stress analysis of hyperbolic paraboloid membrane shells for applications in architecture 06 p0757 A73-17395

ARCTIC OCEAN

- Aircraft measurements of microwave emission from Arctic Sea ice. 02 p0171 A73-12773
- Sea ice observation by means of satellite. 11 p1358 A73-26346

ARCTIC REGIONS

- Precipitation patterns in the Arctic ionosphere determined from airborne observations. 01 p0036 A73-10341
- Models of extreme arctic and subarctic winter atmospheres between 20 and 90 km. 02 p0160 A73-12274
- Models of the extremal arctic winter atmosphere at heights between 20 and 80 km 09 p1115 A73-22993
- Latitudinal and longitudinal auroral radio wave absorption in Arctic during IQSY, noting comparison with geomagnetic field disturbances 11 p1350 A73-25086
- Simultaneous determination of chord length and direction by artificial earth satellite geodetic observations in Arctic and Antarctic regions 13 p1610 A73-29320
- Large payload aircraft for Alaskan and Canadian gas-oil transportation, examining alternative pipeline economic factors and possible new North Canadian island fuel fields 16 p2088 A73-33183
- The cartographic and scientific application of ERTS-I imagery in polar regions. 18 p2306 A73-36019
- Polar albedo changes and its climatic consequences. 18 p2307 A73-36028
- Atomic hydrogen and water vapour in the lower arctic thermosphere during geomagnetic storm and PCA event. 18 p2310 A73-36141
- Oil spread over Arctic ice, considering spread rate and oil slick size attainment for pollution potential during spills on tundra or pack ice [AIAA PAPER 73-701] 18 p2312 A73-36250
- North polar aurora oval detection by high frequency sounder radar aided by all sky photography and statistical auroral data, discussing backscatter and auroral echoes 18 p2312 A73-36282

Problems related to high-performance flight in the Arctic regions

- 18 p2287 A73-36953
- Topside ionospheric winter and summer diurnal electron density variations in Arctic regions as function of universal time, showing Ariel 3 measurements graphically 21 p2682 A73-40171
- Arctic-Antarctic geodetical survey program, discussing length and direction determination for lines connecting eight principal locations 21 p2685 A73-40813
- Meridional tropospheric ozone distribution north of 50 deg from airplane measurements. 23 p2974 A73-43860
- Surface ozone in the arctic atmosphere. 23 p2974 A73-43866

AREA

- Antenna effective area lower limit based on photon limited localizability and Heisenberg uncertainty principle, deriving directivity dependence on area 11 p1338 A73-25672

AREA NAVIGATION

- A precision position and time service for the air traffic of the future. 07 p0849 A73-19350
- Area navigation systems integration with terminal ATC approach procedures, considering computerized data linkage with aircraft navigation system 07 p0849 A73-19351
- VLF/Omega digital airborne area navigation system evaluation tests, discussing transmitting stations and system performance 13 p1656 A73-28904
- Formulation of the air traffic system as a management problem. 14 p1772 A73-29878
- Area navigation computer TCE-71 A system, discussing central control display and data entry units, inputs/outputs and operating modes 15 p1909 A73-32455
- Doppler VOR area navigation operational principles, emphasizing bearing accuracy improvement compared to conventional VOR systems 15 p1909 A73-32456
- Area navigation feasibility, discussing computer technology usefulness, time saving and air traffic controller acceptance 15 p1911 A73-32491
- Aircraft terminal approach and entry spacing systems supported by automated terminal radar using area navigation techniques 17 p2210 A73-35852
- Plane coordinate transformations for area navigation based on existing VOR/DME network 18 p2336 A73-37043
- Area navigation technology for air transportation in USA, discussing present systems and projections as related to airline and FAA activities 19 p2451 A73-37807
- Area navigation as means for airspace optimal utilization, considering navigation equipment and methods and ATC procedures reorganization 19 p2452 A73-37817
- Automatic flight control and navigation systems on the L-1011 Capabilities and experiences. 19 p2452 A73-37824
- A flight evaluation of pilotage error in area navigation with vertical guidance. 21 p2733 A73-40029

ARGON

NT ARGON ISOTOPES

- Study of the conditions of the breakdown threshold of argon at high pressure under the effect of laser radiation 01 p0058 A73-10175
- Ar and Kr continuous wave ion lasers with electric arc discharge, noting quartz, graphite and beryllium oxide gas discharge tubes 01 p0059 A73-10714
- The rate of vaporization of tungsten in argon. 02 p0183 A73-12767
- Pulse discharge plasma in Ar with gas ionization level near unity, noting plasma cylinder parameters, electron temperature and I-V characteristics 03 p0347 A73-14091
- Investigation of fluctuation and wave phenomena in argon low-current low-pressure discharges, taking place under the influence of a 'brief' axial magnetic field 03 p0348 A73-14623
- Fatigue threshold crack propagation in air and dry argon for a Ti6Al-4V alloy. 04 p0459 A73-14685
- Isotherm data for physical adsorption of Ar on pyrex surface at low pressure, noting correlation in terms of Dubinin-Radushkevich equation 04 p0456 A73-15765
- Study on ionizing shock waves in argon. I - Precursor phenomena. 04 p0436 A73-15974
- Study on ionizing shock waves in argon. II - Ionization relaxation. 04 p0436 A73-15975

Speed distribution measurements of N2 and Ar molecular beams produced by a multichannel source.

- 06 p0726 A73-18261
 - Use of oblique shock waves in high-temperature shock-tube studies. 06 p0683 A73-18793
 - Argon, radon, and tritium radioactivities in the sample return container and the lunar surface. 07 p0870 A73-19792
 - Photoabsorption cross section of argon in the 180-700-A wavelength region. 08 p0990 A73-21050
 - Improved Hanle effect measurement technique for fast ions. 10 p1251 A73-24117
 - Experimental study of shock-wave reflection from a thermally accommodating wall. 11 p1449 A73-25252
 - Nonequilibrium radiative and inelastic collisional transitions structuring of ionizing shock waves in He and Ar 11 p1449 A73-25253
 - Ultra-violet argon dayglow lines in the atmosphere of Mercury. 11 p1421 A73-25916
 - Density measurements in high speed arc heated flows. 13 p1622 A73-29640
 - Thermospheric wind effects on the distribution of helium and argon in the earth's upper atmosphere. 16 p2004 A73-33441
 - New vapour pressure measurements for argon and nitrogen and a new method for establishing rational vapour pressure equations. 19 p2461 A73-38200
 - Experimental investigation of the performance of a porous electrode in an MHD converter during the injection of argon with potassium addition 20 p2511 A73-39619
 - Liquid helium cryopump extension to gaseous hydrogen and helium pumping via adsorption on argon cryodeposit, obtaining gases partial pressures evolution 22 p2886 A73-41871
 - New measurements of the thermal conductivity of argon and nitrogen to 200 C and 1600 atmospheres. 22 p2932 A73-42502
 - Observation of 9.0-micron line emission from Ar III in NGC 7027 and NGC 6572. 22 p2910 A73-42704
 - Exponential projectile charge dependence of Ar K and Ne K X-ray production by fast, highly ionized argon beams in thin neon targets. 22 p2890 A73-42710
- ARGON ISOTOPES
- The ages of lunar material from Fra Mauro, Hadley Rille, and Spur Crater. 07 p0888 A73-19780
 - Lunar rocks age determination by Ar isotopes technique, noting plagioclase gas retention and cosmic ray exposure characteristics 07 p0888 A73-19782
 - Ar-40/Ar-39 ages of Apollo 14 and 15 samples. 07 p0888 A73-19783
 - Solar flare intensity estimation based on measurements for Ar 37 radioactivities and depth dependence of tritium in Apollo 11 and 12 lunar rock samples 07 p0889 A73-19794
 - Atmospheric Ar-40 in lunar fines. 07 p0890 A73-19808
 - Argon-37, argon-39, and tritium radioactivities in the Haverro meteorite. 09 p1140 A73-21865
 - Spallation production of He-3, Ne-21, and Ar-38 from target elements in the Bruderheim chondrite. 10 p1277 A73-24103
 - Argon 40-argon 39 chronology of four calcium-rich achondrites. 10 p1278 A73-24110
 - The age and petrography of two Luna 20 fragments and inferences for widespread lunar metamorphism. 13 p1675 A73-28319
 - The A, B, C's of trapped helium, neon, and argon in meteorites and lunar samples. 17 p2228 A73-34417
 - Laser probe mass spectrometric in situ measurements of stable and radioactive Ar isotopes in lunar breccia 17 p2232 A73-35263
 - He, Ne and Ar in chondritic Ni-Fe as irradiation hardness sensors. 17 p2120 A73-35801
- ARGON LASERS
- Turbulent gas mixing measurements using a laser schlieren technique. 03 p0296 A73-14202
 - CW neutral Ar laser line competition effect observation, establishing correct transition assignment 03 p0320 A73-14461
 - Thermal defocusing of high intensity continuous Ar laser radiation in absorbing medium with allowance for spherical aberrations 04 p0458 A73-15562

Gas velocity measurements within a compressor rotor passage using the laser Doppler velocimeter. [ASME PAPER 72-WA/GT-2] 04 p0451 A73-15866
High data rate holographic recorder with six-channel acousto-optical modulator array as input composer and mode locked Ar laser as light source 06 p0694 A73-18311
Experimental study of argon ion laser discharge at high current. [AD-754727] 06 p0701 A73-18361
The radial amplification profile of the 4880-A ionic laser line and the distribution of the charge carriers in the wall-stabilized Ar low-pressure arc column 08 p0989 A73-20786
Self-mode-locking in an argon ion laser with a non-linear absorbent 09 p1096 A73-22878
Effect of a laser field on the gain line profile of an adjacent transition in an argon laser 09 p1096 A73-22968
Outlet of second harmonic emission for the laser resonant cavity 09 p1097 A73-23011
Output power saturation with a discharge current in powerful continuous argon lasers. 11 p1377 A73-26179
Ar laser output characteristics variation due to mutual influence of 4880 and 5145 A transitions, solving ion density formation rate equations 13 p1628 A73-29184
Theoretical study of the mechanism of the population inversion and of the efficiency in an ionized argon laser operating in the continuous mode 14 p1755 A73-29729
Microwave pulse excited argon ion laser. 14 p1758 A73-30472
Measurement of density and temperature of a hydrogen plasma using an argon laser. 15 p1920 A73-32257
Rotational temperature measurement of gases using laser Raman scattering techniques. 17 p2166 A73-34623
Relative Raman cross section of O3 for four Ar+ laser frequencies. 20 p2595 A73-38893
Argon laser application in a study of velocity in flames 20 p2573 A73-39620
An argon ion laser with a gas-discharge tube of relatively large diameter 21 p2714 A73-40556
Low-noise instrumentation for Raman and luminescence spectrometry with ruby and argon laser excitation. 22 p2868 A73-41783
Performance of a large-bore high-power argon ion laser. 24 p3097 A73-45422
Pulsed argon laser discharge oscillographic electron temperature and time variations measurement, obtaining short and long pulse regime emission characteristics 24 p3097 A73-45516

ARGON PLASMA
Molecular gas presence effect on electron energy balance in atomic gases, noting inelastic collisions loss factor in heated Ar plasma containing nitrogen molecules 03 p0347 A73-14098
Investigation of electronic and gasdynamic parameters of hypersonic wakes behind models moving in argon. 03 p0296 A73-14099
Projectile structure effects on neon K X-ray production by fast, highly ionized argon beams. 04 p0476 A73-14769
Electron-ion density fluctuations in turbulent weakly ionized Ar plasma, comparing experimental results with theory based on quasi-static formulation of Boltzmann equation 04 p0479 A73-15192
Evaluation of an orifice probe for plasma diagnostics. 05 p0601 A73-16431
Characteristics of an argon RF plasma - Active discharge and laminar sonic flow region. 05 p0602 A73-16559
Measurement of continuum radiation from an argon plasma. 05 p0602 A73-16564
Heat removal in a sectioned channel of an electric-arc plasmatron 06 p0731 A73-18572
Argon plasma density and energy distribution development during microwave radiation absorption at upper hybrid resonance 06 p0732 A73-18605
The radial amplification profile of the 4880-A ionic laser line and the distribution of the charge carriers in the wall-stabilized Ar low-pressure arc column 08 p0989 A73-20786
Ar plasma diagnostics from stabilized arc emission spectra, noting thermodynamic equilibrium in central zone of arc channel 08 p0992 A73-20855

Hall current effects in the Lewis magnetohydrodynamic generator. 09 p1130 A73-22823
Plasma excitation by HF field in carbon dioxide-argon flow under low pressure, noting disappearance of striations 10 p1253 A73-24072
X-ray and electron spectra from the double inverse pinch device. 10 p1251 A73-24258
Energy and angular correlations of the scattered and ejected electrons in the electron-impact ionization of argon. 10 p1252 A73-24340
Experimental investigation oscillations in a synthesized plasma jet 10 p1257 A73-24877
Thermal conductivity of the plasma electron component across the magnetic field 10 p1258 A73-24890
Study on ionizing shock waves in argon. III - Thermodynamic properties of the plasma. 12 p1527 A73-27173
Applied electrical potential effect on heat transfer to tube immersed in highly ionized flow of atmospheric pressure Ar plasma 12 p1529 A73-27696
Variation of parameters in a shock-heated argon plasma flow. 13 p1665 A73-28624
Discharge characteristics in cesium-seeded argon. 13 p1665 A73-28807
The radiative properties of high density argon plasma in explosively driven shock waves. 16 p2040 A73-32907
Electric properties of dense plasmas in high current pulsed discharge. 16 p2040 A73-32943
Transport coefficients of ionized argon. 16 p2039 A73-33318
Book - Equilibrium compositions and thermodynamic properties of mixed plasmas. III - Argon-hydrogen plasmas at .01 to 1000 atmospheres between 2,000 and 35,000 K. 16 p2042 A73-33420
Heat removal in the sectionalized channel of an electrode-type plasmatron. 16 p2042 A73-33597
Investigation of plasma inhomogeneities between coaxial electrodes in a magnetic field 17 p2214 A73-34128
Effects of channel size on the ionization instability in MHD generators. 17 p2108 A73-34185
Investigation of the discharge structure in a noble gas alkali MHD generator plasma. I. 18 p2338 A73-36303
Investigation of the discharge structure in a rare gas alkali MHD generator plasma. II. 18 p2339 A73-36304
Laminar boundary layers in low pressure argon plasma. 19 p2464 A73-37163
Theoretical and experimental research on the electromagnetic acceleration of shock-induced flow in argon. 19 p2419 A73-37174
Corner expansion flow of ionized argon, calculating electron density, plasma density and recombination rate constant for comparison with measurements 19 p2465 A73-37177
Coaxial Ar plasma accelerator for spacecraft propulsion, discussing quasi-steady state I-V characteristics and exhaust velocity 19 p2466 A73-37180
Extraction of electrons from a plasma in the presence of a gas in the high-voltage gap 20 p2598 A73-39606
Experimental investigation of the characteristics of a nonequilibrium MHD generator 20 p2511 A73-39618
Wave absorption by a plasma with a nonmonotonic longitudinal distribution of the concentration 21 p2746 A73-40524
Experimental study of conductivity, velocity, and temperature distributions in a submerged jet of low-temperature plasma 21 p2747 A73-40575
Oscillations in a synthesized plasma jet. 21 p2749 A73-41652
Transverse electron thermal conductivity for a plasma in a magnetic field. 21 p2749 A73-41665
Dense argon plasma expansion into vacuum or low density partially ionized hydrogen plasma, examining momentum transfer, electron density and electric field effects 22 p2891 A73-42239
Investigation of the electron concentration behind strong shock waves 22 p2893 A73-42385
Langmuir probe signal analysis of root-mean-square electron density fluctuations in turbulent Ar plasma jet 22 p2893 A73-42394

Measurement of arc radiation for selected spectral regions. 22 p2861 A73-42569
Thermodynamic expansion processes for argon plasma in a convergent-divergent nozzle. 22 p2894 A73-42632
German monograph - Investigation of relaxation effects behind secondary shock fronts in shock-wave heated and partially ionized argon plasmas. 22 p2895 A73-42850
Level populations in plasmas - RF discharges and sonic channel. 22 p2895 A73-42994
UV radiation measurements of Ar-Hg gas discharge plasma as function of temperature and pressure with emphasis on fluorescent light design 23 p3011 A73-43830
Experimental study of shocked-plasma flows with a double search-coil conductivity probe. 24 p3113 A73-44402
Magnetically induced electrothermal instability in unseeded partially ionized shock heated argon plasma 24 p3117 A73-45454

ARGON 36
U ARGON ISOTOPES
ARGON 40
U ARGON ISOTOPES
ARGUMENTS (MATHEMATICS)
U INDEPENDENT VARIABLES
ARIEL SATELLITES
NT ARIEL 4 SATELLITE
Management aspects of the development of the Ariel 4 satellite. 09 p1168 A73-22915
ARIEL 4 SATELLITE
The electron density experiment on-board the Ariel 4 satellite. 09 p1085 A73-22916
ARIP (IMPACT PREDICTION)
U COMPUTERIZED SIMULATION
U IMPACT PREDICTION
ARITHMETIC
NT DOUBLE PRECISION ARITHMETIC
NT FIXED POINT ARITHMETIC
NT FLOATING POINT ARITHMETIC
Modular arithmetic weight and cyclic shifting. 05 p0554 A73-17100
Standard flexible LSI logic cell arrays with uniform interconnections as fourth generation computer components, discussing microprograms and algorithms for arithmetic operations 10 p1198 A73-24017
Arithmetic algorithms for error-coded operands. 15 p1899 A73-31349
ARITHMETIC AND LOGIC UNITS
Error-correcting codes in computer arithmetic. 22 p2830 A73-42713
ARM (ANATOMY)
NT ELBOW (ANATOMY)
NT FOREARM
Functional condition changes of biceps brachii in man under the effect of fatiguing physical stress 07 p0780 A73-19643
ARMATURES
Three-phase-synchronous alternator with a superconducting field winding. 02 p0132 A73-11832
ARMED FORCES
NT ARMED FORCES (FOREIGN)
NT ARMED FORCES (UNITED STATES)
NT NAVY
ARMED FORCES (FOREIGN)
Participation of the Air Force Weather Service in the Fole experiment 17 p2206 A73-34940
Results of carbon monoxide poisoning checks following aviation accidents or incidents in the French Army 18 p2285 A73-36929
ARMED FORCES (UNITED STATES)
Prototype development for Army personnel and equipment airborne mobility, considering various aircraft conceptual designs feasibility relative to logistics requirements [SAE PAPER 720846] 05 p0534 A73-16658
Injuries induced by high speed ejection - An analysis of USAF noncombat operational experience. 16 p1966 A73-32664

AROMATIC COMPOUNDS
Thermogravimetry of thermally stable aromatic and heterocyclic polymers. 01 p0015 A73-11447
Aromatic and heteroatom-containing organic compounds in the lunar samples. 06 p0662 A73-18424
A reliable high efficiency atmospheric pressure CO2 laser. 07 p0836 A73-20194
Low void composites based on NR-150 polyimide binders. 10 p1237 A73-23953
Preparation and thermomechanical properties of pyrrone moldings. 10 p1237 A73-23961

- Photo-induced isomerization of aryl isocyanides into cyanides. 13 p1580 A73-28200
- Electrode reactions of aromatic amines in solvents containing fused AlCl₃. 15 p1841 A73-32224
- Electrical conductivity variations in organic semiconductors in the melting temperature region 16 p2044 A73-34005

ARRAYS

- NT ANTENNA ARRAYS
- NT LINEAR ARRAYS
- NT PHASED ARRAYS
- NT SOLAR ARRAYS
- NT STEERABLE ANTENNAS
- NT SYNTHETIC ARRAYS
- NT TURNSTILE ANTENNAS
- NT YAGI ANTENNAS

ARRESTERS

- A testing procedure for flame arrestors for marine spark ignition engines. [WSCIPAPER 72-34] 05 p0563 A73-16681
- The lightning arrestor-connector concept - Description and data. 19 p2408 A73-37270

ARRESTING GEAR

- Arrested landing studies for STOL aircraft. [AIAA PAPER 73-51] 06 p0647 A73-17627

ARRHYTHMIA

- Exercise testing for detecting changes in cardiac rhythm and conduction. 03 p0260 A73-13542
- Cardiac dysrhythmias associated with exercise stress testing. 03 p0260 A73-13544
- Telemetrical measurements during sport performance on sportsmen with cardiac arrhythmias. 03 p0271 A73-14294
- Use of an on-line computer in a study of cardiac arrhythmia. 04 p0412 A73-15644
- An evaluation of sinus arrhythmia as a measure of mental load. 05 p0543 A73-16718
- Cardiovascular system reactions to alternating transverse accelerations in man 06 p0650 A73-17687
- Pathological cardiac conduction system lesions anatomy associated with arrhythmia, discussing atrioventricular, His bundle and bundle branch blocks 06 p0655 A73-18872
- Ultrastructure of the atrial, ventricular, and Purkinje cell, with special reference to the genesis of arrhythmias. 06 p0655 A73-18873
- Cardiac arrhythmias generation by impulse initiation and conduction abnormalities, considering depressed excitability, reentrant excitation, summation, inhibition and parasystole 06 p0656 A73-18874
- Relation of electrolyte disturbances to cardiac arrhythmias. 08 p0933 A73-21807
- Changes in the cardiac rhythm during a hypoxic functional test 10 p1179 A73-23820
- Cardiac arrhythmias during exercise testing in healthy men. 11 p1315 A73-25336
- Exercise-induced ventricular arrhythmias in patients with coronary artery disease - Their relation to angiographic findings. 12 p1464 A73-27890
- Unreliability of conventional electrocardiographic monitoring for arrhythmia detection in coronary care units. 12 p1465 A73-27891
- Relationship between ventricular premature contractions on routine electrocardiography and subsequent sudden death from coronary heart disease. 14 p1715 A73-30051
- Heart rate variability and the measurement of mental load; Proceedings of the Symposium, London, England, October 1971. 14 p1720 A73-30876
- Psychological factors influencing the relationship between cardiac arrhythmia and mental load. 14 p1720 A73-30877
- Blood pressure and body temperature dynamic control systems and respiration relationship to heart rate variability 14 p1720 A73-30878
- Heart rate variability and work-load measurement. 14 p1720 A73-30879
- Motor, thermal and sensory factors in heart rate variation A methodology for indirect estimation of intermittent muscular work and environmental heat loads. 14 p1720 A73-30880
- Heart rate variability analysis for ergonomics purposes, discussing interpolations, algorithms and physiological effects and spectral analysis methods 14 p1720 A73-30882

- Book on vectorcardiography covering equipment, techniques, lead systems and abnormalities associated with atrial and ventricular hypertrophy, bundle branch blocks, myocardial infarction and arrhythmia 17 p2114 A73-34452
- Digital computer diagnosis of cardiac arrhythmias in a single-lead electrocardiogram. 17 p2114 A73-34533
- Electrocardiographic diagnosis of sinus node rhythm variations and SA block. 18 p2274 A73-36520
- Intra-atrial and esophageal electrography in the diagnosis of complex arrhythmias. 18 p2274 A73-36525
- Mechanisms of cardiac arrhythmias - From hypothesis to physiologic fact. 19 p2394 A73-37582

ARROW WINGS

- Buffet boundaries for arrow wings in transonic flow, presenting methods for pressure distribution and three dimensional turbulent boundary layer calculation [DGLR PAPER 72-123] 03 p0248 A73-14382
- Linear problem for delta and V-shaped wings 15 p1823 A73-31301

ARSENIC

- Spun on arsenosilica films as sources for shallow arsenic diffusions with high surface concentration. 08 p0995 A73-21478

ARSENIC COMPOUNDS

- NT ARSENIDES
- NT GALLIUM ARSENIDES
- NT INDIUM ARSENIDES
- NT PROUSTITE
- Characteristics of the vibrational spectrum of laminar As₂S₃ semiconductors 11 p1408 A73-25244
- Investigation of the molecular composition of the vapors and the structure of the condensate during the evaporation of arsenic chalcogenides by laser radiation 19 p2437 A73-37957
- Structural changes caused in glassy arsenic trisulfide and triselenide by penetrating radiation 23 p3017 A73-44042

ARSENIDES

- NT GALLIUM ARSENIDES
- NT INDIUM ARSENIDES
- NT PROUSTITE
- Electrical properties of semiconductors with non-spherical radiation damage regions. 16 p2044 A73-33198

ARTERIES

- NT AORTA
- A nonlinear analysis of pulsatile flow in arteries. 01 p0011 A73-10449
- Favorable effect of flight on pilots exhibiting degenerative arteriopathy of the lower limbs 02 p0137 A73-12151
- Nature of the conduction disturbance in selective coronary arteriography and left heart catheterization. 02 p0134 A73-12443
- The effect of time of electrical stimulation of the carotid sinus on the amount of reduction in arterial pressure. 03 p0265 A73-14648
- Origin, classification, nomenclature and incidence of the arterial arteries in normal human hearts, with special reference to their clinical importance. 04 p0409 A73-15522
- Application of constant temperature anemometry in measurement of intra-arterial blood flow velocity. 05 p0545 A73-17274
- Long-term observations in patients with angina and normal coronary arteriograms. 06 p0655 A73-18871
- Formalization of an arterial pressure stabilization system 10 p1181 A73-24467
- Role of the arterial chemoreceptors in ventilatory adaptation to hypoxia of awake dogs and rabbits. 11 p1318 A73-26220
- Nonlinear wave propagation processes in elastic tubes 13 p1692 A73-28165
- Factors influencing coronary blood flow in the presence of coronary obstructive disease. 18 p2275 A73-36539
- Angiotensinotography using an air plethysmograph 18 p2282 A73-36575
- Morphometry of the human pulmonary arterial tree. 21 p2638 A73-40639
- Cerebral tolerance to asphyxial hypoxia in the dog. 22 p2805 A73-42202
- A new method of measuring arterial dilation and its application. 22 p2815 A73-42669
- Indications and value of coronary arteriography. 22 p2808 A73-42830
- The value of different angiographic procedures in coronary heart disease. 22 p2808 A73-42831
- Transcutaneous measurement of blood velocity profiles and flow. 22 p2817 A73-43108

- Measurement of left anterior descending coronary arterial blood flow - Technique, methods of blood flow analysis and correlation with angiography. 24 p3058 A73-44469

- Measurements of arterial pressure and of pressure-receptor reactions during prolonged pressure shifts in carotid arteries 24 p3062 A73-44720

ARTERIOSCLEROSIS

- Reactions of the cardiovascular system of pilots with atherosclerosis symptoms under professional activity conditions 06 p0657 A73-17689
- Coronary atherosclerosis development and prevention in children, discussing hyperlipidemia, hypertension, cigarette smoking and high risk identification 14 p1715 A73-30065
- Prevention of the atherosclerotic diseases - Opportunities for military medicine. 14 p1718 A73-30518
- Vein wall changes as the main cause of acute disturbance of blood circulation in the Vena centralis retinae system 15 p1833 A73-31173
- Book - Atherosclerosis and coronary heart disease. 18 p2275 A73-36531
- Hereditary aspects of coronary atherosclerosis. 18 p2275 A73-36532
- Serum cholesterol and plasma lipid elevation separation of hypercholesterolemic patients for atherosclerosis therapy 18 p2275 A73-36533
- Lipids in arteriosclerotic arterial tissues of man. 18 p2275 A73-36534
- Cigarette-smoking and coronary atherosclerosis. 18 p2275 A73-36535
- Localizing factors in experimental atherosclerosis. 18 p2275 A73-36536
- Localizing factors in arteriosclerosis. 18 p2275 A73-36537
- Coronary atherosclerosis and ischemic myocardial damage. 18 p2275 A73-36538
- Electrocardiographic diagnosis of myocardial infarction - Pitfalls of a graphic technique. 18 p2282 A73-36544
- The prognosis of myocardial infarction. 18 p2276 A73-36549
- Detection of atherosclerosis in examinations of flight personnel 18 p2284 A73-36913
- Some metric characteristics of myocardial cells under various conditions of cardiac and cardiovascular pathology 18 p2280 A73-36962
- Information yield of the Annual Medical Examination for Flying. 20 p2517 A73-39110
- Ophthalmodynamography in pilots to test internal carotid insufficiency - Comparison of blood-pressure responses. 21 p2639 A73-41162
- Early diagnosis of coronary heart disease; Proceedings of the Second Paavo Nurmi Symposium, Porvoo, Finland, September 9-11, 1971. 22 p2808 A73-42826
- The early diagnosis of coronary heart disease - Critical review. 22 p2808 A73-42827
- Preventive value of early diagnosis of coronary heart disease, noting importance of screening populations for genetic and environmental risk factors 22 p2808 A73-42828
- Mechanisms of hyperlipidaemias in different clinical conditions. 22 p2809 A73-42832
- Measurement of left anterior descending coronary arterial blood flow - Technique, methods of blood flow analysis and correlation with angiography. 24 p3058 A73-44469

ARTHROPODS

- NT BEES
- NT CRABS
- NT DROSOPHILA
- NT INSECTS
- NT TRIBOLIA
- Dioptric apparatus of arthropod compound eyes, describing optical characteristics of apposition eye 09 p1043 A73-23310
- Circaseptan /7-day/ oviposition rhythm and growth of Spring Tail, Folsomia candida /Collembola: Isotomidae/. 15 p1836 A73-32185

ARTICULATION

- A study of evoked slow activities in man which follow a voluntary movement and articulated speech 20 p2514 A73-39759

ARTIFACTS

- Hazard and interference avoidance in implant telemetry, discussing leakage currents, muscle interference, magnetic influence, high frequency noise, electrode and respiratory artifacts, etc 03 p0271 A73-14295

ARTIFICIAL CLOUDS

Precipitation of auroral and ring current particles by artificial plasma injection.

03 p0301 A73-13711

Results from barium cloud releases in the ionosphere and magnetosphere.

[MPI-PAE-EXTRATERR-67] 03 p0301 A73-13805

Plasma drifts in the auroral ionosphere derived from barium releases.

03 p0303 A73-13876

Magnetospheric electric fields convective motions measurement by Ba ion cloud tracking and symmetric double probe floating potential technique

04 p0442 A73-15333

Numerical integration of equations of Ba cloud motion in ionosphere with end shorting, noting critical electric field for motion stability

04 p0445 A73-15649

Basic formulas for the determination of the altitude of artificial clouds

05 p0572 A73-17160

Molecular beam study on BaO and SrO formation for clarifying interaction of metal-vapors with upper atmosphere oxygen.

07 p0818 A73-19668

A method for the analysis of artificial clouds in the upper atmosphere.

08 p0961 A73-21391

Deformation and striation of plasma clouds in the ionosphere. I, II.

09 p1074 A73-22062

Computer program for extraterrestrial physics barium ion cloud project determining daily release launch window for sky target experiments

[AIAA PAPER 73-297] 09 p1116 A73-23216

Investigation of the motion of artificially ionized clouds in the upper atmosphere.

10 p1212 A73-24225

Wide angle narrow band interference filter for detecting E region barium ion clouds against intense background

11 p1366 A73-26250

Plasma research in space and in the laboratory.

12 p1526 A73-26849

A cylindrical shell model of the NASA-MPE barium ion cloud experiment.

12 p1492 A73-27607

Astrometry applied to artificial clouds

15 p1940 A73-32192

Drift measurement with spectral analysis during period of chemical releases into the ionosphere.

18 p2314 A73-35955

Kinesonde studies of cesium ion clouds in the E-region.

18 p2304 A73-35988

Results of simultaneous wind velocity profile measurements in the lower thermosphere by the meteor radar and rocket methods.

18 p2310 A73-36130

Temperature determination of the upper atmosphere by the low-level detection of artificial luminous cloud radiation.

18 p2311 A73-36149

Results of air temperature, density and pressure measurements obtained with the aid of foil cloud sensors in the height region between 80 and 95 km.

18 p2311 A73-36179

Thermospheric observations combining chemical seeding and ground-based techniques. II - Ionospheric drifts and the Sq current system.

18 p2311 A73-36186

On the Zeeman photometer observing upper atmospheric winds in the daytime.

19 p2429 A73-37377

HF radar observations of cesium plasma cloud released from the rocket K-9 M-39.

19 p2423 A73-37378

The measurement of turbulent spectra and diffusion coefficients in the altitude region 95 to about 110 km.

21 p2688 A73-41341

Lower thermospheric atomic oxygen profile from 18 May 1971 nitric oxide release and mass spectroscopic observation, noting monotonic density increase to 0.8 trillion/cc

21 p2688 A73-41345

Barium cloud release near equatorial plane for investigating interaction with ambient medium and electric and magnetic field properties in outer radiation belt

22 p2852 A73-41932

Geophysical disturbance environment during the NASA-MPE barium release at 5 earth radii on September 21, 1971.

22 p2845 A73-41933

Balloon and VLF whistler measurements of electric fields, equatorial electron density, and precipitating particles during a barium cloud release in the magnetosphere.

22 p2845 A73-41934

Yield and ion distribution for the barium cloud at 31,000 kilometers, September 21, 1971.

22 p2845 A73-41935

High resolution television imaging of barium cloud release in magnetosphere, discussing cloud shape

development, striation patterns, core behavior and diffusion characteristics

22 p2845 A73-41936

Preliminary analysis of NASA optical data obtained in barium ion cloud experiment of September 21, 1971.

22 p2846 A73-41937

Computer model of Ba ion cloud expansion in magnetosphere, taking into account self-consistent electric and magnetic field interactions

22 p2846 A73-41938

Quiet-time nightside magnetic field near geomagnetic equator detected by magnetospheric barium cloud injection, revealing taillike structure from atmospheric models

22 p2846 A73-41939

Diurnal and semidiurnal variations in amplitude and phase of midlatitude ionosphere tidal motions, using sodium cloud drift rate

24 p3082 A73-44732

Probe electric field measurements near a midlatitude ionospheric barium release.

24 p3085 A73-45119

Polar wind measurements by electrically neutral luminous by-product clouds from Ba ion releases, discussing ion drag

24 p3085 A73-45120

Turbulent motions in an artificial plasma inhomogeneity released in the ionosphere.

24 p3088 A73-45238

ARTIFICIAL GRAVITY

Gravity selection by animals in fields of centrifugal acceleration superimposed on weightlessness during sounding rocket flights.

01 p0009 A73-11209

Effect of hypergravity on the circadian rhythms of white rats.

[ASME PAPER 72-WA/BHF-14]

04 p0410 A73-15877

Optimal control of a combined propulsion system of a rotating spacecraft

05 p0630 A73-17003

Seat reaction direction in an animal centrifuge.

07 p0780 A73-19478

Findings on American astronauts bearing on the issue of artificial gravity for future manned space vehicles.

09 p1045 A73-22531

ARTIFICIAL HEART VALVES

Carpentier reconstructive valvuloplasty technique of mitral valve insertion from viewpoint of pilots return to flying duties

02 p0138 A73-12157

ARTIFICIAL INTELLIGENCE

Descriptions and plans in an interactive robot simulation system.

06 p0672 A73-18891

Mars surface exploration by self-guided stereo TV equipped roving vehicle /robot/, describing computerized object and scene ranging and recognition

19 p2429 A73-37321

Technological survey of machine intelligence for real time autonomous manipulation with computer recognition sensory feedback and programmed task control to eliminate human operator

19 p2417 A73-37330

Hierarchical hybrid control of manipulators - Artificial intelligence in LSI.

19 p2407 A73-37334

Adaptive /learning/ intelligent system design and simulation for control with stochastic goal and environment conditions

20 p2532 A73-38685

Papers on adaptive electronic devices, circuits and systems covering logic nets, solid state and ferroelectric devices and memory devices and artificial intelligence

20 p2535 A73-39135

Experiences with an augmented human intellect system - Computer mediated communication.

21 p2654 A73-40833

Monograph on Question-Answerer 4 /QA4/ programming language for artificial intelligence application to problem solving covering pattern matching, built-in functions and robot work tasks

22 p2830 A73-42745

ARTIFICIAL RESPIRATION

U RESUSCITATION

ARTIFICIAL SATELLITES

NT AEROS SATELLITE

NT ALOUETTE 2 SATELLITE

NT APPLICATIONS TECHNOLOGY SATELLITES

NT ARIEL SATELLITES

NT ARIEL 4 SATELLITE

NT ASTRONOMICAL NETHERLANDS SATELLITE

NT ATS 1

NT ATS 3

NT ATS 5

NT ATS 6

NT BEACON SATELLITES

NT COMMUNICATION SATELLITES

NT COSMOS SATELLITES

NT COSMOS 137 SATELLITE

NT COSMOS 381 SATELLITE

NT DIADEME SATELLITES

NT EARTH RESOURCES TECHNOLOGY SATELLITE 1

NT EARTH RESOURCES TECHNOLOGY SATELLITES

NT ECHO 1 SATELLITE

NT ECHO 2 SATELLITE

NT ELEKTRON SATELLITES

NT ENVIRONMENTAL RESEARCH SATELLITES

NT EOLE SATELLITES

NT EROS [SATELLITES]

NT ESRO SATELLITES

NT ESRO 1 SATELLITE

NT ESRO 2 SATELLITE

NT EXPLORER SATELLITES

NT EXPLORER 31 SATELLITE

NT EXPLORER 35 SATELLITE

NT EXPLORER 43 SATELLITE

NT GEODETIC SATELLITES

NT GEOPHYSICAL SATELLITES

NT GEOS SATELLITES [ESRO]

NT GEOS 1 SATELLITE

NT GEOS 2 SATELLITE

NT GEOS-C SATELLITE

NT GOE SATELLITES

NT GRAVITY GRADIENT SATELLITES

NT HELIOS SATELLITES

NT HEOS A SATELLITE

NT HEOS B SATELLITE

NT HEOS SATELLITES

NT INTELSAT SATELLITES

NT INTERCOSMOS SATELLITES

NT ISIS SATELLITES

NT ITOS 1

NT IUE

NT LUNAR ORBITER

NT LUNAR SATELLITES

NT METEOROLOGICAL SATELLITES

NT METEOSAT SATELLITE

NT MOLNIYA SATELLITES

NT NAVIGATION SATELLITES

NT NIMBUS SATELLITES

NT NIMBUS 3 SATELLITE

NT NIMBUS 4 SATELLITE

NT NIMBUS 5 SATELLITE

NT OAO

NT ORBITAL SPACE STATIONS

NT ORBITAL WORKSHOPS

NT OSO

NT OSO-7

NT PAGEOS SATELLITE

NT POGO

NT PROTON SATELLITES

NT PROTON 2 SATELLITE

NT PROTON 3 SATELLITE

NT PROTON 4 SATELLITE

NT RADIO ASTRONOMY EXPLORER SATELLITE

NT RELAY SATELLITES

NT SAN MARCO SATELLITE

NT SIRIO SATELLITE

NT SKYNET SATELLITES

NT SPUTNIK SATELLITES

NT SYMPHONIE SATELLITES

NT SYNCHRONOUS METEOROLOGICAL SATELLITE

NT SYNCHRONOUS SATELLITES

NT SYNCOM SATELLITES

NT TELSTAR 1 SATELLITE

NT TIROS M

NT TIROS SATELLITES

NT TRANSIT SATELLITES

NT UHURU SATELLITE

NT VELA SATELLITES

NT VENERA SATELLITES

NT VENERA 6 SATELLITE

NT VENERA 7 SATELLITE

Geostationary artificial satellite orbital parameters calculation, taking into account lunar, solar and light pressure perturbations

03 p0378 A73-14551

Optimum elliptic orbit characteristics of planetary artificial satellite based on earth-planet-earth flight

03 p0379 A73-14572

A new method for calculating the preliminary orbit of an artificial satellite with the aid of simultaneous observations

03 p0379 A73-14579

Secular inequalities in the motion of earth satellites.

04 p0503 A73-16020

Prediction of the density of the upper atmosphere for the duration of artificial earth satellites.

05 p0567 A73-16091

A possible application of large orbiting space laboratories - An artificial moon

05 p0613 A73-16201

French D2A satellite construction, describing AG5 sheet covering and gold coating fabrication methods

07 p0829 A73-18912

Prospero satellite orbital/operational performance and control, describing ground-station telemetry and data processing operations

07 p0905 A73-19142

- Satellite solar power station for solar energy conversion into electricity and transmission to ground receiving stations via microwave beams
09 p1035 A73-22791
- Investigation of long-term periodic changes of the orbital elements of artificial earth satellites
10 p1283 A73-24699
- On the determination of the long period tidal perturbations in the elements of artificial earth satellites.
11 p1423 A73-26074
- Preliminary orbit determination for lunar satellites.
11 p1426 A73-26396
- Artificial satellites to test general relativity theory
11 p1431 A73-26590
- Earth satellites and the gravitational potential.
12 p1539 A73-27148
- Artificial satellite orbit determination from range measurements, applying to orbits around earth and other planets
12 p1543 A73-27722
- Baseline arrangement of radio interferometer array for tracking artificial satellites.
13 p1586 A73-29233
- Simultaneous determination of chord length and direction by artificial earth satellite geodetic observations in Arctic and Antarctic regions
13 p1610 A73-29320
- Existence of stable relative equilibria of an artificial satellite in a model magnetic field
15 p1872 A73-31956
- Selection of a trajectory for the return to earth from lunar orbit of an artificial satellite
18 p2351 A73-36106
- Artificial earth satellite brightness attenuation and rotation periods from spectral analyses of photometric curves by mathematical simulation
18 p2315 A73-36142
- The global solution of the problem of the critical inclination.
23 p3031 A73-43836
- ARYL COMPOUNDS**
U AROMATIC COMPOUNDS
- ASBESTOS**
Determination of the electron concentration in the boundary layer of air mixed with ablation products of an asbestos plastic
09 p1128 A73-22622
- Asbestos-textolite coating required thickness calculation with allowance for aerodynamic heating, discussing softening mechanisms
09 p1110 A73-23057
- ASCENT**
NT CLIMBING FLIGHT
- ASCENT PROPULSION SYSTEMS**
F/R-101 ejection seat upgrade kit for performance improvement, discussing propulsion, trajectory control, snubber system and rapid recovery parachute opening
16 p1966 A73-32667
- ESCAPAC IE stabilized ejection seat for Navy S-3A and Air Force A-9A aircraft, describing propulsion, stabilization, separation and lateral divergence subsystems
16 p1966 A73-32669
- Design studies of low-noise propulsive-lift air planes.
[SAE PAPER 730378]
17 p2103 A73-34717
- ASCENT TRAJECTORIES**
Asymptotic solution to the problem of optimal low-thrust energy increase.
07 p0899 A73-19962
- Space shuttle ascent-flyback trajectory optimization with in-flight inequality constraints based on accelerated gradient parameters determination including attitude control angles
10 p1276 A73-24002
- Launch vehicle response to inflight winds during ascent, modeling wind velocity as nonstationary random process
[AIAA PAPER 73-398]
11 p1392 A73-25527
- Space shuttle aerodynamic interference and elastic response to atmospheric turbulence during ascent flight, including propellant sloshing, gust and automatic control system effects
[AIAA PAPER 73-310]
11 p1430 A73-25541
- Satellite ascent transfer trajectories equations of motion numerical integration, replacing time parameter by regularizing independent variable for gravitational singularity elimination
[DFVIR-SONDDR-283]
12 p1537 A73-26822
- Space shuttle ascent guidance, using quadratic performance index and reference trajectory kinematics to obtain optimal time-varying feedback control gain
21 p2735 A73-40044
- ASCORBIC ACID METABOLISM**
Vitamin metabolism alteration under increased atmospheric pressure
11 p1321 A73-25036
- Physiological shifts in the human organism under increased neuropsychic stresses
19 p2393 A73-37392
- ASDE**
U AIRPORT SURFACE DETECTION EQUIPMENT

ASHES

- Activated oxygen ashing of biological specimens for the microdetermination of Na, K, Mg, and Ca by atomic absorption spectrophotometry.
02 p0139 A73-12546
- Effects of ash deposition on the fatigue strength of the working blade material in gas turbines
06 p0741 A73-18662
- Sharply defined upper limit existence for lunar ash flow with heat transfer, presenting altitude dependence of pressure, gas density, temperature and velocity distributions
07 p0895 A73-19864
- ASPARTIC ACID**
Non-enzymic beta-decarboxylation of aspartic acid.
04 p0414 A73-16032
- Sterically controlled syntheses of optically active organic compounds. XV - Syntheses of optically active aspartic acid through beta-lactam.
07 p0787 A73-19204
- Optical resolution of aspartic acid by using copper complexes of optically active amino acids.
07 p0789 A73-20457
- Optical resolution of DL-aspartic acid in the presence of optically active amino acid and copper (II) ion.
11 p1324 A73-25146

ASPECT RATIO

- NT HIGH ASPECT RATIO**
NT LOW ASPECT RATIO
Effect of membrane forces on large deflection of simply supported rectangular plates.
03 p0389 A73-13323
- Study of a series of variable-geometry wings derived from delta wings of different aspect ratios. I - Aerodynamic characteristics of delta wings
04 p0404 A73-15651
- Some recent work on aspect ratio effects in compressor cascades.
[ASME PAPER 72-WA/FE-41]
04 p0404 A73-15858
- Experimental investigation of the Magnus effect at a finned body of revolution of large aspect ratio at a Mach number of 4
08 p0927 A73-21604
- Trailing vortex sheet roll-up behind finite aspect ratio wings for different loading conditions, discussing drag penalties for tip vortices strength improvements
09 p1029 A73-23125
- Studies on bounded jets.
13 p1603 A73-29032
- Particle trapping effect on conductivity of toroidal plasma with like-particle collisions taken into account, obtaining results applicable to all aspect ratios
14 p1778 A73-29687
- Surface strip coplanar waveguide characteristic impedance measurement as function of aspect ratio and substrate thickness
20 p2538 A73-39595
- The aerodynamic development of the wing of the A 300B.
21 p2633 A73-41192
- On the application of a new version of lifting surface theory to nonlender and kinked wings.
23 p2939 A73-43210
- Thermal convection in a large rotating fluid annulus - Some effects of varying the aspect ratio.
23 p3002 A73-43597
- ASPHYXIA**
Left ventricular receptors activated by severe asphyxia and by coronary artery occlusion.
01 p0008 A73-10549
- The effects of hypoxia, hypercapnia, and asphyxia on the baroreceptor-cardiac reflex at rest and during exercise in man.
06 p0654 A73-18348
- The influence of change in the functional state of the central nervous system on the course of asphyxia
10 p1179 A73-23937
- Cerebral tolerance to asphyxial hypoxia in the dog.
22 p2805 A73-42202

ASPIRATION**U VACUUM****ASSEMBLIES**

- Mechanical behavior of assemblies welded by fusion on steel
06 p0698 A73-18694
- Microwave electronic packaging with integrated multifunction assemblies, considering stripline choice for transmission line
11 p1338 A73-26113
- High-temperature low pressure hose assembly, convoluted-, tetrafluoroethylene-, for aerospace.
[SAE ARP 1227]
16 p1970 A73-33017
- ASSEMBLING**
NT ORBITAL ASSEMBLY
Classification of fitting operations in airframe assembly
02 p0172 A73-11647
- Assembling by welding and bonding - Introductory report on assemblies
06 p0698 A73-18692
- Joining and assembly by welding.
16 p2021 A73-33860

ASSESSMENTS**NT TECHNOLOGY ASSESSMENT****ASSIGNMENT****U ALLOCATIONS****ASSIMILATION**

- Contrast and assimilation effects analysis based on receptive field models of vertebrate retinal function
08 p0929 A73-20812

ASSOCIATIONS**U ORGANIZATIONS****ASSURANCE**

- Distribution functions with fatigue analysis laws and safety predictions, noting life length and fleet assurance models
04 p0507 A73-14710

ASTEROIDS**NT VESTA ASTEROID**

- Spacecraft-borne IR optical remote sensor for detection, identification and distribution measurement of asteroid and meteoroid particles
01 p0105 A73-11205
- Stability of the solar system - Evidence from the asteroids.
04 p0497 A73-15179
- Resonances and encounters in the inner solar system.
04 p0500 A73-15519
- Computerized Monte Carlo simulation with program flexibility for mass distribution in particle collision processes, applying to accreting and fragmenting systems including asteroid belt
05 p0624 A73-17316
- Exploring the origin of the solar system by space missions to asteroids.
06 p0750 A73-18025
- Structure and evolution of the asteroid ring
07 p0902 A73-20324
- A study of commensurable motion in the asteroid belt.
11 p1417 A73-25264
- Critique of missing planet theory of asteroidal origin, considering mass required, Bode law and disruption forces
11 p1419 A73-25861
- Asteroidal rotational properties interpreted in terms of model with collisional breakup into irregular fragments
11 p1425 A73-26136
- Asteroidal spectral reflectivity measurement with data reduction for various curve types, noting correlations with UVB color, orbital and physical property parameters and albedo
11 p1429 A73-26686
- Positions of minor planets Baumeia 813, Triberga 619, and Jessonda 459.
11 p1429 A73-26687
- Resonances and librations of some Apollo and Amor asteroids with the Earth.
11 p1429 A73-26688
- Structure and evolution of the asteroid belt.
12 p1540 A73-27296
- Observations of the satellites Jupiter VI and VII.
12 p1540 A73-27429
- Astrographic tabulation of southern asteroids astronomical coordinates
12 p1543 A73-27721
- Mineralogical density of sporadic meteoric bodies
13 p1673 A73-28298
- A numerical method of integration by means of Taylor-Steffensen series and its possible use in the study of the motions of comets and minor planets.
14 p1790 A73-29788
- Determination of parabolic orbits on the basis of N observations, by means of an electronic computer
14 p1790 A73-29796
- Determination of the mass of Jupiter from observations of 10 Hygiea during 1932-1969.
14 p1792 A73-29811
- Hidalgo orbit near Saturn, discussing resemblance to extinct comet nucleus, nongravitational forces effects and planetary mass determination
14 p1792 A73-29812
- Saturn mass determination from Hidalgo orbit trajectory and variational equation, obtaining probable error from fitted parabola
14 p1792 A73-29813
- Investigation of the orbital stability of minor planets with cometary eccentricities.
14 p1794 A73-29839
- Evolution of the orbits of selected minor planets during an interval of 1000 years.
14 p1794 A73-29840
- Cometary and asteroidal orbits discrimination using Jacobi integral in three body system with sun and Jupiter
14 p1795 A73-29849
- Determination of the motion and rotation parameters of an asteroid by the measurement of distances to a space station situated on the asteroid surface
14 p1796 A73-29858
- New techniques for determining sizes of satellites and asteroids.
15 p1940 A73-32075
- Pallas evolution on basis of orbital eccentricity and inclination, discussing accumulation in asteroid belt in quiescent solar nebula, collisions and planetary gravitational encounters
17 p2229 A73-34428

- Distribution of satellite bodies according to their mean distances in the systems of the sun, Jupiter, Saturn and Uranus 17 p2231 A73-34598
- Determination of the mass of Saturn from the motion of Trojans. 17 p2234 A73-35615
- Solar electric propulsion comet and asteroid rendezvous missions, examining asteroid perihelion data base, optimum mission length, flight time and exploration vehicle power levels [AIAA PAPER 73-597] 18 p2350 A73-36081
- Pioneer 10 space probe measurement of interplanetary particulates and aggregates via reflected and scattered sunlight, with emphasis on distribution in asteroid belt [AIAA PAPER 73-546] 18 p2350 A73-36095
- Russian book on cosmogenic nuclear reactions in meteorites and asteroid and lunar surface layers covering vertical /depth/ distributions of isotopes and nuclear-active particles 19 p2486 A73-37775
- A study of commensurable motion in the asteroid belt. 20 p2606 A73-39075
- Minor planets and related objects. IX - Photometry and polarimetry of /1685/ Toro. 20 p2607 A73-39119
- Minor planets and related objects. X - Spectrophotometric study of the composition of /1685/ Toro. 20 p2607 A73-39120
- Minor planets and related objects. XI - 0.4-0.8 micron spectrophotometry of /1685/ Toro. 20 p2607 A73-39121
- Minor planets and related objects. XII - Radar observations of /1685/ Toro. 20 p2607 A73-39122
- Minor planets and related objects. XIII - Long-term orbital evolution of /1685/ Toro. 20 p2607 A73-39123
- Apollo asteroid discovery, orbital peculiarities, future earth approaches, Apollo group ephemerides and distribution 21 p2765 A73-40299
- Asteroidal dust population model coinciding with spatial density demonstrating distribution below astrodynamical mass limit and larger time for distribution function extrapolation 21 p2776 A73-41422
- Mineralogical density of sporadic meteoric bodies. 21 p2779 A73-41542
- Cosmogonic prerequisites for the accumulation of volatile substances in the upper mantle of the earth. 22 p2912 A73-42972
- Meteorite production mechanism from asteroid belt via asteroidal collision fragments perihelion changes and orbit perturbation by Jupiter into earth-crossing orbital elements 23 p3027 A73-43336
- Forces acting upon an asteroid moving through a meteoroid stream. 23 p3029 A73-43745
- Asteroid belt observation, spatial distribution and mission planning, considering IR, spectrophotometric, interferometric, polarization and Doppler measurement techniques 23 p3034 A73-43991
- Asteroid reflectivities from polarization curves - Calibration of the 'slope-albedo' relationship. 24 p3129 A73-44437
- Topography on satellite surfaces and the shape of asteroids. 24 p3129 A73-44446
- Determination of radii of satellites and asteroids from radiometry and photometry. 24 p3130 A73-44453
- Asteroid belt white light polarization curve measurements, indicating surface texturizing and albedo dispersion 24 p3131 A73-44462
- Comparisons of meteorite and asteroid spectral reflectivities. 24 p3132 A73-44538
- The asteroid belt and its evolution. 24 p3134 A73-44565
- ASTIGMATISM**
- Meridional amblyopia - Evidence for modification of the human visual system by early visual experience. 08 p0931 A73-21562
- Aberrations, astigmatism and coma control for far UV stellar spectrograph design by grating shape and ruling space modification 08 p0972 A73-21752
- Large parabolic reflector microwave antenna astigmatism effects on radiation pattern, discussing focusing procedure for phase error reduction 17 p2143 A73-35695
- ASTP**
- U APOLLO SOYUZ TEST PROJECT**
- ASTRONICS**
- French Concerto aerospace part procurement program contribution to mass produced electronic component reliability assessment, control and improvement based on tin oxide resistor experience 07 p0829 A73-18923
- High performance three axis attitude control system of TD1/A European scientific satellite, describing control circuits, logic, ancillaries and packaging procedure 07 p0904 A73-18968
- Design considerations for shuttle information management. 14 p1818 A73-29945
- A high-accuracy digital star tracker for advanced planetary missions. 15 p1907 A73-31356
- ASTROBEE ROCKET VEHICLES**
- Astrobe F sounding rocket system design and development, describing advanced propulsion technology test program and results [AIAA PAPER 73-300] 09 p1156 A73-23219
- ASTROBIOLOGY**
- U EXOBIOLOGY**
- ASTRODYNAMICS**
- Second order trajectory optimization tests in terms of Kelley-Contensou extremals and conjugate points, applying to astrodynamical singular arc 02 p0187 A73-11996
- Evidence for elliptical galaxy rotation, considering flattening, orbital statistics and interactions of external and internal forces 05 p0616 A73-16453
- On the third integral of motion in stellar dynamics. I. 08 p1002 A73-20849
- Russian book - Mechanics of controlled motion and problems of cosmic dynamics. 15 p1930 A73-31226
- Russian book - Studies of spacecraft flight dynamics. 23 p3027 A73-43260
- ASTROGRAPHY**
- Jupiter surface maps for 1965-70 from drawings obtained with astrophotograph, noting high activity and eruptive changes after 1961-63 outburst 08 p1012 A73-21583
- Jupiter surface maps from synoptic observations with refracting telescope, considering white cloud formations and atmosphere motions 08 p1012 A73-21584
- Astrographic tabulation of southern asteroids astronomical coordinates 12 p1543 A73-27721
- Automatic coordinate-measuring machine for astrophotography purposes 15 p1878 A73-32144
- ASTROMETRY**
- Book - Astrometry - Theoretical astrophysics instrumentation - Spectroscopy - Galactic structure - Galaxies. 01 p0095 A73-10293
- The mass and figure of Saturn by photographic astrometry of its satellites. 01 p0096 A73-10316
- Accuracy requirements for an objectivized astrolabe 03 p0307 A73-13250
- Determination of systematic errors in time determinations with the passage instrument 03 p0307 A73-13251
- Stellar distances, magnitude and mass measurements methods, noting distance to globular clusters and center of Galaxy 07 p0903 A73-20638
- The beta Scorpii occultation by Jupiter. I - The Jovian diameter. 08 p1006 A73-20934
- Astrometry with Schmidt telescopes, discussing automated computerized plate scanner and measuring machine for star position and relative motion determination 08 p0966 A73-21356
- Computational solution for positions on whole Schmidt-plates - Report on reduction of coordinates measured on 22 plates of the Bergedorf Schmidt telescope. 08 p0966 A73-21357
- Schmidt telescopes application in astrometry, noting image quality uniformity across total field of view 08 p0966 A73-21358
- Comparison of the coordinates of the pole as obtained by classical astrometry /IPMS, BIH/ and as obtained by Doppler measurements on artificial satellites /Dahlgren polar monitoring service/. 13 p1679 A73-28390
- Determination of the astronomical refraction near the horizon at different times of the year 13 p1683 A73-29096
- Determination of the motion and rotation parameters of an asteroid by the measurement of distances to a space station situated on the asteroid surface 14 p1796 A73-29858
- Selection of stars for observations from the lunar surface by the method of equal altitudes 15 p1938 A73-31963
- Astrometry applied to artificial clouds 15 p1940 A73-32192
- Some preliminary conclusions from the available observation results of the International Saturn Patrol of 1966 16 p2070 A73-33847
- Combined determination of the turn value and screw errors of the position micrometer of an astronomical universal instrument 19 p2432 A73-38553
- Application of long-baseline radio interferometers to astrometric tasks 21 p2701 A73-40726
- On the possibility of determining stellar radial velocities to 0.01 km per sec. 22 p2907 A73-42207
- Approximate formula for completeness estimation of radio source distributions in spherical zones in terms of distance to system central source 23 p3037 A73-44358
- Selection of stars for observation from the lunar surface by the method of equal altitudes. 24 p3132 A73-44488
- ASTRON THERMONUCLEAR REACTOR**
- Axial compression of the astron E-layer during neutralization. 16 p2042 A73-33337
- ASTRONAUT LOCOMOTION**
- Dynamics of an astronaut's movement on a tether towards a spacecraft and a spacecraft control concept based on the variable-structure systems theory 05 p0628 A73-16411
- Analysis of the extravehicular activity of an astronaut 18 p2281 A73-36116
- Biomechanics of locomotion via jumping on lunar surface, discussing subgravity effects on energy requirements, body potential and kinetic energy, muscular work, etc 22 p2804 A73-42175
- ASTRONAUT MANEUVERING EQUIPMENT**
- Dynamics of an astronaut's movement on a tether towards a spacecraft and a spacecraft control concept based on the variable-structure systems theory 05 p0628 A73-16411
- An experimental investigation of attitude control systems for astronaut maneuvering units. [AIAA PAPER 73-250] 05 p0563 A73-16973
- Automatic control of the Skylab Astronaut Maneuvering Research Vehicle. [AIAA PAPER 73-857] 20 p2586 A73-38795
- ASTRONAUT PERFORMANCE**
- Quality /probability/ evaluation of human operator ergatic processes controlling spacecraft during rendezvous and docking with orbital station 06 p0657 A73-17686
- Emotional stresses during a space flight 07 p0785 A73-19297
- Findings on American astronauts bearing on the issue of artificial gravity for future manned space vehicles. 09 p1045 A73-22531
- Investigation of the sleep and wakefulness rhythms in the crewmembers of Soiz-3 through Soiz-9 spacecraft prior to, during, and after space flight 10 p1182 A73-24697
- Physiological response to exercise after space flight - Apollo 7 to Apollo 11. 11 p1314 A73-25326
- Work movement performance of the astronaut in flight. 12 p1465 A73-27645
- Asymmetry of otolith responses in fish 15 p1834 A73-31507
- Skylab astronaut vestibular function experiment in orbital flight, discussing motion sickness susceptibility, stimulation thresholds and space perception measurements 17 p2115 A73-34741
- Analysis of the extravehicular activity of an astronaut 18 p2281 A73-36116
- Use of the single-breath method of estimating cardiac output during exercise-stress testing. 18 p2283 A73-36788
- Effect of certain flight factors on crew efficiency 21 p2643 A73-40350
- Skylab I medical experiments concerning astronaut physiological responses and work capability as affected by exposure to space flight environment 21 p2778 A73-41519
- Some psychological and engineering aspects of the extravehicular activity of astronauts. 22 p2814 A73-42167
- Human sensorimotor coordination following space flights. 22 p2814 A73-42170
- Skylab 26 day rescue mission diary, describing docking, communications, extravehicular activity, repair work, medical checkouts, physical exercises, solar array problems, etc 23 p3038 A73-43992
- ASTRONAUT TRAINING**
- Skylab Mission Simulator Facility software, describing electric power systems, solar measurements, display panels, earth resource sensors and spacecraft environmental control 18 p2296 A73-36832
- Some psychological and engineering aspects of the extravehicular activity of astronauts. 22 p2814 A73-42167

ASTRONAUTICS

Israel Annual Conference on Aviation and Astronautics, 15th, Tel Aviv and Haifa, Israel, March 14, 15, 1973, Proceedings.

15 p1948 A73-31633

Astronautical research 1971; Proceedings of the Twenty-second Congress, Brussels, Belgium, September 20-25, 1971.

19 p2485 A73-37708

Aeronautics and astronautic history, developments and impact upon civilization, noting Canada role in space age, Apollo program and U.S.S.R. programs

21 p2793 A73-41086

ASTRONAVIGATION

Astronautical coordinate systems definition and applications for flight mechanics problems involving earth curvature and motion effects

15 p1908 A73-32202

ASTRONOMICAL CATALOGS

Observational data on galaxies with UV continuum, listing objects with emission lines, s-d classification and quasar spectral energy distribution

01 p0099 A73-10701

The classification of intrinsic variable stars. II - The red variables of S and related types.

01 p0104 A73-11038

Determination of the relative orientation of nine selenodetic catalogs in terms of Eulerian angles.

01 p0107 A73-11326

Remarks on the comparison of the Sanduleak and Fehrenbach-Duflo catalogs of stars belonging to the Large Magellanic Cloud

02 p0223 A73-12718

Dollen data reduction method for meridian-observed FK 4 star pairs right ascension and time determination, calculating instrument, personal and catalog errors

03 p0371 A73-13219

Utilization of computers in practical astronomy

03 p0372 A73-13243

Improved positions and some identifications for 108 radio sources between declinations -33 and +27 deg.

03 p0372 A73-13348

Catalog of angular diameters, absolute magnitudes, spectroscopic parallaxes and linear diameters for 2301 stars, discussing accuracy and frequency distributions of log functions

03 p0375 A73-13948

Catalog of selenographic coordinates for libration-zone and far-side points.

04 p0503 A73-16017

Measurements of diameters of galaxies on the Palomar Observatory Sky Survey.

05 p0613 A73-16211

Surface distribution of interacting and normal galaxies near the galactic north pole

05 p0613 A73-16212

Astronomical catalogs for galactic superclusters existence including north galactic pole region, noting distance differentiation for structural singularities isolation

05 p0613 A73-16213

Central portion of the galactic cluster Coma Berenices. III

05 p0617 A73-16458

Zonal spectrophotometric standards - Energy distribution in the spectra of 109 stars in absolute units

05 p0617 A73-16465

The Uhuru catalog of X-ray sources.

05 p0625 A73-17326

The radio continuum of the Large Magellanic Cloud. I - The sources at 6 cm wavelength.

06 p0754 A73-18629

The radio continuum of the Large Magellanic Cloud. III - The sources at 11 cm wavelength.

06 p0754 A73-18631

VV 281-427, variable stars in a Cepheus-Lacerta field of the Milky Way.

07 p0874 A73-19117

Centimeter waves radio sources survey, tabulating position coordinates, 5 GHz flux densities, spectral index and optical identification

07 p0876 A73-19353

Observations of radio sources with an interferometer of 24-km baseline. I - The angular structures at 408 MHz of 106 sources from the Parkes catalogue.

07 p0899 A73-19937

Equatorial coordinates and photographic magnitudes for new carbon stars in Northern Milky Way, noting classification by spectral discontinuity

08 p1005 A73-20916

Frequency of star eliminations in the meridian catalogues constitutive of the Melchior-Dejaiffe ILS stars catalogue.

09 p1141 A73-22011

The Parkes 2700 MHz survey. IV - Catalogue for the south polar cap zone, declinations -75 deg to -90 deg.

10 p1275 A73-23751

Additional observations of supergiants and foreground stars in the direction of the Large Magellanic Cloud.

10 p1279 A73-24167

A first 1415 MHz survey with the Westerbork Synthesis Radio Telescope An attempt to detect radio emission from quasi stellar objects.

10 p1280 A73-24402

Optical identifications of radiosources from the B2 catalogue - Quasi stellar sources.

10 p1280 A73-24403

Near infra-red magnitudes of 248 early-type emission-line stars and related objects.

11 p1415 A73-25172

First results from the Texas interferometer - Positions of 605 discrete sources.

11 p1428 A73-26676

List of clusters of galaxies with published redshifts.

11 p1428 A73-26677

Tables of relative positions of stars in trapezium-type multiple star systems based on photographic observation data

12 p1537 A73-26857

Observations of comets at the Crimean Astrophysical Observatory.

14 p1789 A73-29780

A numerical interpretation of the homogenization of observational material for one-apparition comets.

14 p1790 A73-29792

A list of quasi-stellar radio sources and quasi-stellar radio-source candidates from the 3C and 4C catalogs between declination -7 deg and +40 deg.

14 p1801 A73-30645

A preliminary classification scheme for interstellar absorbing clouds.

15 p1933 A73-31309

Accurate flux densities at 8.87 GHz of 195 radio sources.

15 p1933 A73-31379

Redshifts for 51 galaxies identified with radio sources in the 4C catalog.

15 p1936 A73-31562

Photometric investigation of star magnitude and color index data in Palomar Atlas and Washington Star Catalog, obtaining calibration curves and average error calculations

16 p2063 A73-33659

A catalog of data on optically visible H II regions.

20 p2607 A73-39084

Mars almanac /ephemerides, rotation data, coordinate data, etc/ for Viking lander position definition and stellar and planetary observations from Mars surface

21 p2733 A73-40031

Astronomical constants and cataloging from 1964 International Astronomical Union, discussing inadequacies and different specific reference systems

21 p2780 A73-41612

Energy distribution in stellar spectra of various spectral types and luminosities

22 p2906 A73-41974

Accurate wavelengths of stellar and telluric absorption lines near lambda 7000 A.

22 p2907 A73-42208

German monograph - Polarization measurements in galactic latitudes b less than -45 deg.

22 p2910 A73-42698

The C-classification of the spectra of carbon stars.

24 p3138 A73-44997

An all-sky catalogue of strong radio sources at 408 MHz.

24 p3144 A73-45560

ASTRONOMICAL COORDINATES

Observations at 750, 1400, and 2700 MHz of radio sources in the Vermilion River Observatory survey.

01 p0096 A73-10312

Precise positions of radio sources measured at 2695 MHz.

01 p0098 A73-10580

Literal expressions for the co-ordinates of the moon. I - The first degree terms.

01 p0099 A73-10687

Dollen data reduction method for meridian-observed FK 4 star pairs right ascension and time determination, calculating instrument, personal and catalog errors

03 p0371 A73-13219

Time and latitude observations of star groups with photographic zenith tube, including random, layer distortion and coordinate errors

03 p0307 A73-13249

Positions, periods, period derivatives, dispersion measures and pulse widths of twenty two weak pulsars

03 p0380 A73-14635

Design and field tests of astronomical optical theodolite, noting latitude, longitude and azimuth determination and objective aberration

04 p0447 A73-14849

Rotation of the moon and lunar coordinate systems.

04 p0497 A73-15180

Methods of optimization of a spacecraft angular position control program

05 p0594 A73-16412

Central portion of the galactic cluster Coma Berenices. III

05 p0617 A73-16458

Equatorial coordinates and photographic magnitudes for new carbon stars in Northern Milky Way, noting classification by spectral discontinuity

08 p1005 A73-20916

Investigation of the influence of precession, nutation, and yearly aberration on the average equatorial coordinates, azimuth, and elevation of the North Star

10 p1281 A73-24476

Determination of the relative position of points on the earth surface with the aid of satellite observations

11 p1357 A73-26294

Astrophysical tabulation of southern asteroids astronomical coordinates

12 p1543 A73-27721

Lunar orbit and mapping coordinates, discussing libration effects due to motion and surface features

13 p1681 A73-28947

Automatic coordinate-measuring machine for astrophotography purposes

15 p1878 A73-32144

Precise positions of radio sources. IV - Improved solutions and error analysis for 59 sources.

19 p2488 A73-38510

The application of the method of equal heights to the determination of astronomical azimuth

19 p2490 A73-38557

Conditional equations of astronomical latitudes, longitudes, and azimuths

19 p2490 A73-38559

Mars almanac /ephemerides, rotation data, coordinate data, etc/ for Viking lander position definition and stellar and planetary observations from Mars surface

21 p2733 A73-40031

Application of long-baseline radio interferometers to astrometric tasks

21 p2701 A73-40726

Errors on the dial of cosmic clocks

21 p2701 A73-40728

Results of latitude observations from 1948 to 1954 and analysis of the 1948-1967 latitude series obtained by the ZTF-135 instrument in Pulkovo

21 p2772 A73-41268

Results of the 1959 to 1965 six-year series of latitude observations in Blagoveshchensk

21 p2772 A73-41269

Accuracy of coordinate measurements with the aid of a variable-profile antenna

21 p2667 A73-41472

ASTRONOMICAL MAPS

NT PLANISPHERES

Supernova remnants descriptions, distance and hydrodynamic evolution, considering galactic nonthermal radio sources, radio maps, and X ray and radio polarization

01 p0094 A73-10057

Low frequency radio observations of the Andromeda Galaxy.

01 p0096 A73-10313

21-micron observations of H II regions.

01 p0104 A73-11045

Infrared maps of Jupiter.

01 p0109 A73-11490

Radio observations of Cygnus X-3 and the surrounding region.

02 p0210 A73-11557

Radio telescope for high resolution radio source mapping, discussing system design, computerized control and calibration

02 p0150 A73-11869

The radio emission of NGC 4258 and the possible origin of spiral structure.

02 p0221 A73-12701

Lunar radar mapping at 162.4 MHz from Jodrell Bank observations in January and February 1970, discussing depolarized returns

03 p0368 A73-13084

A radio map of the spiral galaxy Maffei 2 at 1415 MHz.

03 p0370 A73-13210

Properties of the Red Spot of Jupiter in 1971.

03 p0371 A73-13216

New observations of the proton population of the radiation belt between 1.5 and 104 MeV.

03 p0362 A73-13862

Mapping the solar corona in X-ray lines of O VII and Ne IX.

03 p0375 A73-13956

Cartography of the surface markings of Mercury.

06 p0743 A73-17429

Mariner 9 map analysis of Mars geology, covering cratering, circular basins, volcanism, canyons, chaotic terrain, channels and eolian activity

06 p0745 A73-17476

The radio continuum of the Large Magellanic Cloud. II - Continuum observations at 11 cm wavelength.

06 p0754 A73-18630

The radio continuum of the Large Magellanic Cloud. III - The sources at 11 cm wavelength.

06 p0754 A73-18631

High velocity clouds as part of Galactic spiral arms, obtaining spiral structure maps from observations of Galactic plane

08 p1005 A73-20918

Jupiter surface maps for 1965-70 from drawings obtained with astrophot, noting high activity and eruptive changes after 1961-63 outburst

08 p1012 A73-21583

The structure of the Crab Nebula. III - The radio filamentary radiation.

09 p1151 A73-23291

Continuum radio emission from NGC 4656/7 and NGC 891 at 408 MHz.

11 p1415 A73-25170

Preliminary mapping of the lunar magnetic field.
11 p1421 A73-25903

Optical and radio observations of the Orion Nebula.
11 p1425 A73-26265

Infrared and radio observations of the nucleus of NGC 253.
11 p1428 A73-26625

The large-scale distribution of low-velocity hydrogen gas at high galactic latitudes.
13 p1671 A73-28028

A high resolution neutral hydrogen study of the galaxy M 51.
13 p1671 A73-28033

NASA computer generated 136/400-MHz radio sky maps covering whole celestial sphere for earth-based receiver noise temperature determination in satellite communication
13 p1585 A73-29115

Low energy X-ray map of Puppis A supernova remnant.
15 p1933 A73-31353

Determination of the absolute intrinsic motions of stars with respect to galaxies in area 32 of a special Kapteyn map
15 p1938 A73-31961

Photometric relief of the lunar continient cover
16 p2064 A73-33766

Compact radio source associated with the OH source ON-1 /OH69.5-1.0/.
16 p2071 A73-34037

Mars maps based on Mariner 9 pictures and photomosaics, with emphasis on southwest quadrant and south pole topographies
18 p2356 A73-37035

Martian south polar region albedo map from Mariner 9 photographs, comparing with earth-based telescopic observations
19 p2480 A73-37323

Observations of galactic supernova remnants at 1.7 and 2.7 GHz.
19 p2483 A73-37566

Radio maps of sources around spiral galaxies and associated peculiar companion galaxies
19 p2487 A73-38509

Jupiter atmosphere discrete source maps of 5 micron radiation distribution, correlating brightness temperature and photographically recorded colors
19 p2489 A73-38525

Scanning the sky with the aid of the RATAN-600 radio telescope
21 p2776 A73-41464

Galactic spiral arm structure mapping by 21 cm data taken at different latitudes, discussing high velocity hydrogen clouds distribution
21 p2778 A73-41533

Interactive processing of map data produced by the Westerbork supersynthesis radio telescope.
21 p2778 A73-41534

Infrared maps of the galactic nucleus.
22 p2904 A73-41757

Neutral hydrogen spectral line observation for Milky Way Galaxy mapping, discussing role of spiral structure density wave theory in interpretation
23 p3028 A73-43348

An optical Atlas of galactic supernova remnants.
23 p3028 A73-43448

Radio spectra and mapping of extragalactic radio sources including radio galaxies and quasars with high angular resolution, noting energy sources and red shift
23 p3029 A73-43625

Determination of absolute stellar proper motions relative to galaxies in selected area 32 of the special Kapteyn plan.
24 p3132 A73-44486

Optical identifications of radio sources using accurate radio and optical positions.
24 p3135 A73-44579

Solar wind fluctuations mapping procedure applied to Explorer 35 wind data for solar wind structure to Mars orbit
24 p3125 A73-45104

ASTRONOMICAL MODELS

Solar neutrino detection methods, capture cross sections, model construction and results
01 p0091 A73-10053

Heating and cooling mechanisms, ionization processes, time-dependent models and energy requirements of interstellar H I regions
01 p0091 A73-10064

Saturn rings formation explanation by electromagnetic effects, presenting mathematical model
01 p0097 A73-10551

A non-uniform relativistic cosmological model.
01 p0098 A73-10581

Evolutionary models for helium white dwarves with uniformly accreting hydrogen shell, noting thermally unstable laminar energy source formation in shell lower layers
01 p0100 A73-10709

Neptune model calculation from mass, radius and rotation period, comparing with gravitational moment
01 p0101 A73-10844

Hypothetical process of galaxy or quasar formation by material outflow from singularity, discussing ex-

pansion velocity, stellar light concentration, interstellar lines and universe density
01 p0102 A73-10968

Binary stars as X-ray sources.
01 p0102 A73-10969

An approximate form of the third integral in the Galaxy.
01 p0103 A73-11017

Newtonian analysis of cosmological model for galactic accretion from small initial perturbation of central black hole
01 p0104 A73-11048

Single gaseous object and stellar cluster models of quasars and galactic nuclei stability, noting neutron and collapsing star lifetimes
01 p0106 A73-11302

Pregalactic vortex motion decay calculation from kinetic equation of hot expanding universe model
01 p0106 A73-11307

Direction of winding in spiral galaxies.
01 p0106 A73-11317

Gas-liquid hydrogen mixture and helium adiabatic model of Jupiter temperature and pressure distribution, estimating planet center temperature
01 p0107 A73-11324

Rotational perturbations in anisotropic cosmology.
01 p0107 A73-11328

Generation of the large-scale galactic magnetic field.
01 p0107 A73-11329

Gravitational fields of Jupiter and Saturn.
01 p0107 A73-11332

Solar outer layer models of convective zone, photosphere, chromosphere, corona and solar wind, using electron density dependence
01 p0107 A73-11379

Hydrodynamic motions and the vacuum stage in an anisotropic cosmological model
01 p0108 A73-11432

The nature of the first Cygnus X-3 radio outburst.
02 p0204 A73-11551

Observations at 408 MHz of the Cyg X-3 radio outburst.
02 p0204 A73-11552

Time dependence of Cygnus X-3 8 GHz flux density and spectral index during outburst decay, describing source model
02 p0204 A73-11553

Absorbing boundary propagation model for solar cosmic rays energy spectrum kink time behavior, using Gleeson-Ng theory
02 p0205 A73-11753

Gravitational radiation effects on cosmological time scale and models from matter fractional conversion and mass loss rate profile analysis
02 p0205 A73-11873

The structure of the close vicinity of the sun - Investigations concerning star troops, star families, and star streams
02 p0212 A73-12017

Energy distribution of relativistic electrons generated within radio sources with constant magnetic field and diffusion coefficient, discussing simplified model representation for Crab nebula
02 p0207 A73-12379

Biorthogonal function pairs for gravitational field calculations for flat galaxies, deriving algorithms from Hankel-Laguerre functions properties
02 p0216 A73-12380

Self consistent model of closed field lines of pulsar magnetosphere valid for oblique rotators and unipolar inductors
02 p0216 A73-12382

The mass and angular momentum losses from spinars.
02 p0217 A73-12384

Neutrino contribution to relativistic interacting matter-radiation cosmological models, presenting cosmological interpretation of quasars
02 p0218 A73-12410

Theoretical model for tidal evolution induced capture of natural satellite pairs into orbit-orbit resonance, discussing Titan and Hyperion relationship with Saturn
02 p0219 A73-12421

Relativistic electron radio emission models, calculating magnetic bremsstrahlung spectra from galactic electron space-energy distributions
02 p0208 A73-12459

Uniformly rotating stars with hydrogen- and metallic-line blanketed model atmospheres.
02 p0222 A73-12712

Neutron star vibration damping from semirealistic neutron star models with magnetic field, superfluid component, outer crust, normal neutron composition and quantum crystals
02 p0222 A73-12714

Model for meteorite impact generated gas flow on moon as function of mass, velocity and composition, noting wind effects on lunar erosion
02 p0223 A73-12719

Comet nucleus models, discussing classical and icy snowball heads, nongravitational forces, nucleus dimensions and evidence against solid cores
02 p0223 A73-12731

A galactic formation model based on post-big bang fragmentation.
02 p0224 A73-12740

Star formation in the galaxy.
02 p0224 A73-12744

Infrared excesses in early-type stars - Free-free emission.
02 p0225 A73-12826

Theoretical models of photoionized intergalactic hydrogen.
03 p0365 A73-12926

Heavy elements depletion on grains in interstellar medium two phase model, noting gas dynamical analysis of discrete clouds evolution
03 p0366 A73-12931

A search for density and pressure inversions in high-temperature, low-gravity model atmospheres.
03 p0366 A73-12935

Classical hard-sphere gas in spherical box with coupling between local thermodynamics and gravitation, noting stellar core-halo structure from equilibrium state calculations
03 p0366 A73-12936

Thermal instability of the hydrogen-burning shell in nondegenerate stars.
03 p0366 A73-12937

Trapped electrons decay to ground state via nonthermal process in lunar samples during thermoluminescence emission at lunar day temperatures, proposing quantitative model
03 p0369 A73-13101

On the possible differences in the bulk chemical composition of the earth and the moon forming in the circumterrestrial swarm.
03 p0370 A73-13110

On the stationary mass outflow from stars. I - The computational method and the results for a 1 solar mass star.
03 p0370 A73-13195

Blanketed model atmospheres for cool hydrogen-rich white dwarfs.
03 p0371 A73-13225

Giant envelopes structure triple solutions yielding bottom pressure-radius curves, discussing stellar evolution, Cepheid variables and secular instability
03 p0371 A73-13226

A finite expanding universe with matter injection.
03 p0342 A73-13291

Tidal generation of narrow intergalactic filaments from computer simulations, discussing alternative models
03 p0372 A73-13353

Numerical model of transient behavior of radiation dominated shock calculated for neutron star core of imploding supernovae
03 p0372 A73-13354

Near earth electron spectra applied to cosmic ray transport equation numerical solution extension to 1968-1970, providing models for modulation and gradients reproduction
03 p0361 A73-13362

The relative merits of galactic density functions - An orbit computational viewpoint.
03 p0373 A73-13363

Depth profiles of Fe I 5250 A line for three sunspot models, noting line-to-continuum absorption ratio relation to emergent intensity location
03 p0377 A73-14410

The self absorption of gyro-synchrotron emission in a magnetic dipole field - Microwave impulsive burst and hard X-ray burst.
03 p0364 A73-14416

Determination of the coefficient of displacement of the line connecting the apses in stellar models and comparison of it with observations.
03 p0379 A73-14584

Astronomical model for variable RR Lyrae stars pulsation, noting rotation effect on oscillation period
03 p0379 A73-14585

Geomagnetic tail quantitative model with validity to beyond moon orbit, noting adequacy of representation under quiet conditions
03 p0304 A73-14590

A method of solution of Vlasov's equation - Application to a nonlinear overall theory of the galactic rotation and of the galactic spiral structure.
03 p0380 A73-14608

Icy conglomerate cometary nucleus models, discussing clathrates role in comet condensation from solar nebula
04 p0494 A73-14752

Comet nucleus existence in terms of optical effect and particle swarm model of coma
04 p0494 A73-14753

Comet research assessment for 1970-1972, discussing coma and nucleus, icy conglomerate and sandbank models
04 p0495 A73-14765

Geopotential coefficient error model using Geos 2 tracking data and SAO 1969 standard earth
04 p0439 A73-14797

Radio sources in decameter wave range from astronomical model and radio observations, noting spectral characteristics dependence on electron energy spectra
04 p0496 A73-14824

Solar flare development particle acceleration phase model, noting association with white light emission, hard X-rays and PCA
04 p0490 A73-14833

Magnetic models of solar flares.

Time dependent hydrodynamic models of solar wind, considering coronal electron density and temperature distribution and magnetic field
04 p0491 A73-14835

M giant atmospheric molecular evolution, discussing carbon/oxygen ratios, s-process overabundances and relationships between M, S and C stars
04 p0496 A73-14971

Protoplanet cloud model for cosmic OH and water masers in H II regions to account for anomalous hydrogen deficiency, discussing pumping mechanisms and chemical composition
04 p0497 A73-14974

Cooling and evolution of a supernova remnant.

An evolutionary thermal model for the Cygnus Loop.
04 p0499 A73-15361

Electron scattering effect on spectral line profiles from characteristic electron density estimates for astronomical objects with rapid radial matter outflow, using Monte Carlo method
04 p0499 A73-15361

The location and size of the hot spot in cataclysmic variable stars.
04 p0499 A73-15486

Contact binaries - Opacity and rotation.

The mass spectrum of interstellar clouds and the assumption of total coalescence.
04 p0500 A73-15489

A hypothesis, unifying the structure and the entropy of the universe.
04 p0500 A73-15492

Solar core stability via model including plain parallel stratified fluid layer with energy generation, noting ice age correlation with mixing phases during evolution
04 p0501 A73-15623

Secondary component minimum deepening in UV light curve of Beta Lyr eclipsing binary star, suggesting black hole model
04 p0501 A73-15637

The period and light curve of HZ Herculis.

Pulsars and the evolution of supernova remnants.
04 p0501 A73-15686

Cosmological deceleration parameter differences prediction from light evolution correction on diameter-red shift relation of cluster elliptical galaxies
04 p0502 A73-15689

A numerical experiment in the accretion problem.

Stratification of the emission in the envelope of the eclipsing-binary Wolf-Rayet star V444 Cygni.
04 p0503 A73-16009

Differential rotation of polytropic stellar models from structural equations, disproving Porfiriev theory
04 p0504 A73-16025

Disk-shaped diffusion model with inhomogeneous distribution of gas and heavy relativistic nuclei sources for galactic cosmic rays chemical composition
05 p0608 A73-16081

On the equilibrium configuration of the geomagnetic tail.
05 p0568 A73-16140

Stability of a model current sheet with finite transverse field and finite flow velocity.
05 p0568 A73-16141

Nonspherically symmetric polytropic model of azimuthally dependent solar wind in sun equatorial plane, considering coronal temperature, density and radial magnetic component
05 p0609 A73-16143

Lunar thermal model with hot interior and cool lithosphere, considering strength and conductivity profiles, volcanic activity absence and composition and origin implications
05 p0613 A73-16158

X ray background radiation measurement in outer space for proof of Gamow hypothesis on universe chemical composition, indicating improved cosmological models
05 p0613 A73-16210

Cosmological models based on 18th and early 19th century physics for sky darkness resulting from universe expansion, speculating upon Olbers paradox resolution
05 p0614 A73-16308

Integral equations suitability and solution instability of stellar system models, referring to globular cluster densities and mass distribution equations
05 p0616 A73-16452

Stochastic wave model of spiral galaxy rotation based on weak interaction, obtaining frequency spectrum integrals for Milky Way Galaxy
05 p0616 A73-16454

Stability conditions for strongly flattened galaxy model with respect to axisymmetric disturbances of gaseous subsystem in finite isothermal layer
05 p0616 A73-16456

Sphericity distribution function of galaxy-cluster members
05 p0617 A73-16459

Diffuse radiation of a two-layer galaxy with carbon-silicate particles
05 p0617 A73-16460

Solution on a BESM-3M electronic computer of the equation for transfer of diffuse radiation in two-layer plane-parallel models of galaxies
05 p0617 A73-16461

High energy /X ray, gamma ray and cosmic ray/ astronomy research impact on astrophysical and cosmological models
05 p0610 A73-16932

Large-scale photospheric magnetic field - The diffusion of active region fields.
05 p0620 A73-17028

Equator-pole differences in the solar chromosphere from Lyman-continuum data.
05 p0621 A73-17033

Coronal abundance of elements and a model of the quiet sun from radio observations.
05 p0621 A73-17034

Linear series and of stellar models. I - Thermal stability of stars.
05 p0621 A73-17069

A model of the Crab Nebula derived from dual-frequency radio measurements.
05 p0622 A73-17075

Effects of sudden mixing in the solar core on solar neutrinos and ice ages.
05 p0623 A73-17188

A comparative study of Brans-Dicke and general relativistic cosmologies in terms of observationally measurable quantities.
05 p0624 A73-17303

Nonzero radiation pressure inclusion into Einstein cosmological equations, discussing Friedmann models evolution from radiation state epoch to matter domination
05 p0624 A73-17304

Internal models of uniformly rotating synchronous close binary systems via modified double approximation scheme, considering gravity darkening effect on primary position in H-R diagram
05 p0624 A73-17306

Nonsynchronous uniformly rotating binary system polytropic models computed and compared to Roche model
05 p0624 A73-17307

The infrared variability of a dust model for Seyfert galaxies.
05 p0624 A73-17311

Spectroscopic observations of HZ Herculis and a model for Hercules X-1.
05 p0625 A73-17344

Tidal gravity models of interacting pair formation of galactic bridges and tails in terms of orbit geometry, outer shapes and forced spiral waves
05 p0626 A73-17378

Interplanetary cosmic ray low energy electron observation, explaining steep spectrum origin and time variations by model with spectral decomposition
05 p0612 A73-17386

Beta Persei decimetric-centimetric radio emission variations, relating observational data to discontinuous structural adjustment model based on starquakes hypothesis
05 p0627 A73-17392

Ultraviolet clouds on Venus - Observational bias.
06 p0744 A73-17432

High resolution interferometric observations of Venus at three radio wavelengths.
06 p0744 A73-17437

Venus - Measurements of brightness temperatures in the 7-15 cm wavelength range and theoretical radio and radar spectra for a two-layer subsurface model.
06 p0744 A73-17438

Mars microwave spectra computation by improved thermal model with seasonal polar cap effects and accurate aspect geometry, noting lunar-like planetary subsurface nature
06 p0747 A73-17492

Book - Coronal expansion and solar wind.
06 p0742 A73-17671

Pulsar timing techniques for planet discovery, interstellar electron density measurement, braking mechanism and neutron star structure investigation and gravitational red shift verification
06 p0750 A73-18008

Class I OH emission sources structure and variability, considering variable gain maser models
06 p0751 A73-18227

Book - The Titius-Bode Law of planetary distances: Its history and theory.
06 p0753 A73-18403

High-frequency sound waves to eliminate a horizon in the mixmaster universe.
06 p0724 A73-18550

Polarization of radio sources. IV - The compact source PKS 2134+004.
07 p0873 A73-19052

Star formation and evolution in spiral galaxies.
07 p0873 A73-19055

Advanced evolution of massive stars. III - Hydrostatic carbon-burning nucleosynthesis and energy generation.
07 p0874 A73-19062

Scorpius X-1 representation via old-nova model consisting of standing shock and X ray source formed by mass accretion at white dwarf surface
07 p0874 A73-19063

Uranus atmosphere - Structure and composition.
07 p0874 A73-19068

Geomagnetic activity semiannual and diurnal variations due to interplanetary field southward component interaction with magnetosphere based on model ordered in solar equatorial coordinates
07 p0813 A73-19234

A photometric model of the zodiacal light.
07 p0876 A73-19359

On the collisional absorption of radio waves in cosmology.
07 p0877 A73-19602

Star formation from interstellar clouds gravitational collapse, discussing protostars evolution based on model calculations
07 p0878 A73-19675

The abundances of components of the lunar soils by a least-squares mixing model and the formation age of KREEP.
07 p0887 A73-19769

The nature and effect of the volatile cloud produced by volcanic and impact events on the moon as derived from a terrestrial volcanic model.
07 p0890 A73-19812

Measurements of the acoustical parameters of rock powders and the Gold-Soter lunar model.
07 p0894 A73-19850

Applications to lunar geophysical models of the velocity-density properties of lunar rocks, glasses, and artificial lunar glasses.
07 p0894 A73-19854

Gravitational energy conversion into rotational energy in contraction process for pulsars, quasars and galactic radio emission energy sources
07 p0898 A73-19934

The stability of certain model binary stellar systems in galactic gravitational fields.
07 p0898 A73-19935

Observations of radio sources with an interferometer of 24-km baseline. II - The angular structures at 151 and 408 MHz of 46 unidentified radio sources from the revised 3C catalogue.
07 p0899 A73-19938

Observations of radio sources with an interferometer of 24-km baseline. III - The angular structures at 408 and 1423 MHz of 44 relatively intense radio sources.
07 p0899 A73-19939

Terrestrial thermal history from mathematical model of earth formation with low temperature dust and gas accumulation
07 p0818 A73-19997

Black hole polar flattening and equatorial circumference lengthening as function of angular momentum, considering effects of highly curved space-time
07 p0899 A73-20176

Preliminary quasar model based on the Yilmaz exponential metric.
07 p0899 A73-20178

Diffuse cosmic gamma rays - Present status of theory and observations.
07 p0872 A73-20186

Pulsar magnetosphere evolution, discussing electron and positive ion supply at surface, plasma flow and Crab Nebula characteristics
07 p0900 A73-20276

The disc model of gaseous accretion on a relativistic star in a close binary system
07 p0901 A73-20305

Frequency dependent synchrotron emission polarization variation in cosmic radio source models, allowing for cold plasma and relativistic distribution nonuniformities
07 p0872 A73-20307

Finson-Probststein model for dust comets applied to calibrated photographic plates of Comet Bennett, giving dust size distribution, emission rate and initial velocities
07 p0902 A73-20443

He core burning and shell hydrogen burning in horizontal and posthorizontal branch stars
07 p0903 A73-20627

Hydrodynamic calculations for novae origin and mass ejection from luminous red giants, considering planetary nebulae and plausible models
07 p0903 A73-20628

Solar cosmic ray sectorial anisotropy pattern observation, suggesting theoretical propagation model to distinguish between rival candidates for parent flare
08 p0997 A73-20772

Linear series of stellar models. II - Pure carbon stars. 08 p1002 A73-20847

Spiral arm structure as standing wave, of magnetically controlled star creation, considering various hydromagnetic models, dust and H I distributions 08 p1002 A73-20879

Intensity variation across Uranus disk during limb darkening-brightening cycles observations to test cloud absence theory, predicting limb brightening in methane bands 08 p1003 A73-20889

He red giants models with degenerate C-O cores, He burning shell sources and He-rich envelopes, noting stellar luminosity 08 p1004 A73-20903

The distribution of neutral hydrogen and the velocity field of the galaxy NGC 3109. 08 p1004 A73-20905

A neutral hydrogen survey of the galaxy M33. II - Distribution and kinematics of the neutral hydrogen. 08 p1005 A73-20913

Photometric investigations of magnetic stars. 08 p1006 A73-20925

Magnetic field in the plasmasphere of a compact star. 08 p1007 A73-21001

A redshift magnitude relation for radiation universes. 08 p1007 A73-21002

Elemental synthesis during high temperature phase of expansion of big bang universes, obtaining universal baryon density relationship to primordial deuterium abundance 08 p1008 A73-21151

Spectra of the Becklin-Neugebauer point source and the Kleinmann-Low nebula from 2.8 to 13.5 microns. 08 p1008 A73-21157

Stellar evolution at high mass based on the Ledoux criterion for convection. 08 p1008 A73-21159

Neutron-star accretion in a stellar wind - Model for a pulsed X-ray source. 08 p0997 A73-21160

Turbulent heating of colliding streams in the solar wind. 08 p0998 A73-21164

A model for peaking of galactic gravitational radiation. 08 p1009 A73-21201

Papers on cosmology and nuclear fusion covering big bang and expanding universe models, conformal invariance, microwave astronomy, neutrino physics, gravitational constant, cosmic rays, etc 08 p1009 A73-21226

Gamow contributions to cosmology and primeval nucleosynthesis theories, discussing big bang model, residual cosmic black body radiation, stellar energy sources and cosmoneurology 08 p1009 A73-21227

Conformally invariant cosmological and physical models in terms of Einstein, Maxwell and Dirac equations 08 p1009 A73-21228

Friedman expanding universe model based on Gamow theory of weakly interacting black body radiation-filled space at 3 K temperature 08 p1010 A73-21230

Nucleocosmochronology and stellar nucleosynthesis models for Galaxy origin and solar system formation 08 p1010 A73-21231

Mass transfer in close binaries. III - Gaseous rings in algol-like binaries. 08 p1010 A73-21312

Spatial spectroscopic diagnostic of planetary nebulae. III - Numerical investigation of local absolute monochromatic energies and local absolute energies in spherically symmetric models. 08 p1010 A73-21313

Nonstationary and asymmetric cosmic ray modulation theory, discussing moving boundary problem and solar wind model with spherical singularity 08 p0999 A73-21341

Criticism of solar core mixing hypothesis of solar neutrino problem, discussing implications for semiconvection theory 08 p1012 A73-21532

Mass differentiation of X ray sources based on Roche model, identifying pulsating sources with neutron stars and black holes as nonpulsating sources 08 p1013 A73-21810

Monograph on Hamiltonian cosmology, considering cosmological models with Hamiltonian equations of motion, Bianchi universes, superspace concepts and quantum mechanical Hamiltonian construction 08 p0984 A73-21834

Models for extragalactic objects with very high IR and X-ray luminosity. 09 p1141 A73-22007

Cen X-3 and Her X-1 X ray sources emission pulsation explained by model with neutron star accretion of matter from companion via magnetic funnel 09 p1141 A73-22010

Neutrino hindrance of density irregularities growth in expanding radiation dominated cosmological model from numerical integration of perturbation equations 09 p1141 A73-22026

Comparison of telescope magnitudes with model-atmosphere predictions for A, F, and G supergiants. 09 p1142 A73-22030

Electromagnetic field configuration about aligned rotating magnetic star from relativistic model of rotating magnetosphere 09 p1142 A73-22034

Cosmic rays in a random magnetic field - Breakdown of the quasilinear derivation of the kinetic equation. 09 p1137 A73-22036

Forbush predecrease observation by superneutron monitors, interpreting cosmic ray depletion and rigidity dependence by model of interplanetary magnetic field propagating disturbance from sun 09 p1073 A73-22051

The thermal future of the universe. 09 p1143 A73-22109

On the accretion mechanism for the formation of a protoplanetary disc. 09 p1143 A73-22110

A numerical model of the structure and evolution of young supernova remnants. 09 p1143 A73-22111

Tidal, primordial turbulence and spinning core theories for galactic rotation origin, considering rotational waves, gravitational waves and wave excitations 09 p1143 A73-22123

Analytical expressions for the parameters of rotating stars 09 p1145 A73-22292

Two dimensional model of solar wind passage past magnetosphere, assuming hot plasma current sheath in geomagnetic tail 09 p1077 A73-22485

Cosmic gamma ray studies for metagalactic and remote galactic model construction as substitute for radio and X ray emission data 09 p1138 A73-22725

Cosmic maser generator model with resonance scattering feedback for galactic clouds OH molecule radio emission 09 p1147 A73-22729

Isotropic cosmological models of X ray background radiation, presenting observational constraints on source distribution and radiation mechanisms 09 p1138 A73-22869

Anisotropic model of gravitational radiation enhancement from relativistic disk located in Galactic nucleus 09 p1149 A73-22946

Cosmic gamma ray observations for choice between galactic and metagalactic models of cosmic ray origin, discussing proton nuclear component 09 p1138 A73-22952

Opacity probability distribution functions for application to non-grey late-type stars model atmospheres. 09 p1149 A73-23131

The interpretation of continuum and line absorption and radiation by circumstellar dust. 09 p1150 A73-23132

A synchrotron radiation model of the infrared radiation from the nucleus of NGC 1068. 09 p1150 A73-23144

IR galaxy model consisting of low energy cosmic or X rays at center of dust shell, discussing physical dimensions of radiating region 09 p1151 A73-23146

A new cosmological model - Formation of organic molecules, planets, and comets. 09 p1151 A73-23147

The structure of the Crab Nebula. II - The spatial distribution of the relativistic electrons. 09 p1151 A73-23290

Partial differential post-Newtonian equations numerically solved for stellar models with polytropic pressure-density relation for uniform rotation 10 p1271 A73-23490

Universe isotropic state evolution from initial chaotic conditions, considering attractive and repulsive cosmological constants 10 p1271 A73-23526

Galactic background spectrum at 230-2600 kHz from IMP-6 radio astronomy, discussing ambient plasma effects on synchrotron emission in galactic models 10 p1272 A73-23529

The evolution of interstellar clouds. II - Hydrodynamic treatment of the phase change. III - Cloud collisions and statistical theory. 10 p1272 A73-23531

Stellar model chromospheres. I - On the temperature minima of F, G, and K stars. 10 p1272 A73-23533

Luminosity and frequency spectrum of radiation from spherically symmetric steady state accretion of interstellar gas onto nonrotating black hole at rest 10 p1272 A73-23534

Analytic approximation for the saturation behavior of OH emission regions. 10 p1272 A73-23542

New limit on small-scale irregularities of 'blackbody' radiation. 10 p1272 A73-23543

Circumstellar envelope model and shock wave calculations for type II supernovae with radiation transport via diffusion, predicting Rayleigh-Taylor instability 10 p1273 A73-23546

Observation of structure in the X-ray spectrum of Puppis A. 10 p1264 A73-23548

Ejection of supernova shells by magnetic pumping 10 p1273 A73-23701

Interferometric investigations of the A21 nebula /YM29, Medusa/ 10 p1273 A73-23704

Thermal instability caused primary interstellar dust cloud fragmentation and resulting star formation according to Peebles-Dicke hypothesis for cosmological origin of globular clusters 10 p1274 A73-23713

Free particle gravitating cylindrical model for gravitational kinetic instabilities, calculating natural vibration spectrum and parameters for beam instability development 10 p1253 A73-23714

A star-cluster model with axial symmetry and star composition of uniform mass 10 p1274 A73-23715

Self consistent computerized solutions to acoustic wave propagation and shock wave transformation with energy dissipation for solar and stellar chromosphere models 10 p1274 A73-23717

Spectrum of the earth's pole coordinates over the period from 1846 to 1971 10 p1274 A73-23723

Spectroscopic changes in the suspected X-ray source X Persei. 10 p1275 A73-23846

Particle motion diffusion model for cosmic ray propagation in Galaxy, investigating electron component energy spectra and background radio emission 10 p1265 A73-23908

Stress differences in the moon as an evidence for a cold moon. 10 p1277 A73-24084

On the model of the accumulation of the moon compatible with the data on the composition and the age of lunar rocks. 10 p1277 A73-24086

On the small-scale structure of solar magnetic fields. 10 p1279 A73-24135

A model for the polar transition layer and corona for November 1967. 10 p1279 A73-24139

Model solar atmosphere with quiet component involving supergranular velocity field in corona-chromosphere transition layer and vertical magnetic field 10 p1279 A73-24140

Quasar characteristics, considering emission or absorption lines, red shift, optical intensity variation, unipolar generator representation and relativistic particle production 10 p1280 A73-24322

Polarization of synchrotron radiation from relativistic Schwarzschild circular geodesics. 10 p1252 A73-24347

On the relation between optical scale height and density scale height in a stellar atmosphere. 10 p1281 A73-24406

Lyman-alpha radiation in the hydrogen atmospheres of comets - A model with multiple scattering. 10 p1281 A73-24408

20-micron fluxes of bright stellar standards. 10 p1282 A73-24639

Book - Advances in astronomy and astrophysics. Volume 9. 10 p1282 A73-24641

Roche model application to close binary systems, emphasizing geometrical properties of limiting equipotentials for configuration breakup 10 p1282 A73-24642

Stellar magnetospheric model for bounds on surface field strength and trapped particle population 10 p1283 A73-24724

A self-consistent model of a simple magnetic neutral sheet system surrounded by a cold, collisionless plasma. 10 p1257 A73-24725

Directivity of high-energy X-ray emission during flares. 10 p1270 A73-24774

The circular polarization of sources of synchrotron radiation. 10 p1270 A73-24901

The equilibrium, stability and evolution of a rotating magnetized gaseous disk. 10 p1284 A73-24903

Photometric and spectroscopic observations of eclipsing binary object BM Orionis interpreted in terms of thin disk model with collapsed star /black hole/ 10 p1284 A73-24906

On the secondary production of galactic cosmic ray electrons. 10 p1270 A73-24910

Small perturbations in flat galaxies. I - Equilibrium models and adiabatic perturbations. 10 p1284 A73-24913

Generalized electromagnetic torque on a vacuum pulsar model. 10 p1284 A73-24914

Probabilistic fragmentation model for collapsing interstellar cloud, predicting stellar mass spectrum 11 p1415 A73-25171

Kinetic equations for gravitating point rotating system model of stellar systems evolution phases, taking into account dissipation-produced motions 11 p1416 A73-25235

Quasar classes to explain radio, optical and X ray observations, considering models for local quasar intrinsic red shift 11 p1417 A73-25262

A study of commensurable motion in the asteroid belt. 11 p1417 A73-25264

Model universe generalization to minisuperspace with Einstein equation solution and nondiagonal metric replacing wave equation, considering commutation relations for quantization in curved space 11 p1397 A73-25309

Critique of theory on monotonic entropy of black hole as linear function of area, considering gravitational energy and compression to singularity 11 p1418 A73-25650

A model of a Martian Great dust storm. 11 p1418 A73-25715

Friedmann expanding cosmological model with superimposed spherically symmetric inhomogeneity for gravitational lens and point light sources dispersion and motion effects on images 11 p1418 A73-25747

The tsunami model of the origin of ring structures concentric with large lunar craters. 11 p1419 A73-25791

High pressure physics and planetary interiors; Proceedings of the Conference, Houston, Tex., March 1-3, 1972. 11 p1419 A73-25876

High pressure physical model of hydrogen planets Jupiter, Saturn, Uranus and Neptune 11 p1419 A73-25877

Isentropic compression of fused quartz and liquid hydrogen to several Mbar. 11 p1398 A73-25884

Stellar evolutionary calculation for Jupiter, considering gravitational contraction 11 p1420 A73-25892

Deep planetary interior models and internal structure evidence from lunar magnetism, considering planetary magnetic field studies from flyby and orbiting satellite measurements 11 p1420 A73-25893

The elastic energy and character of quakes in solid stars and planets. 11 p1420 A73-25894

Bullen solid core model for earth and Venus vindicated by free earth oscillations records and detection of PKJKP seismic phase, discussing compressibility effects 11 p1421 A73-25897

The present thermal state of the terrestrial planets. 11 p1421 A73-25905

Optical properties of single-component zodiacal light models. 11 p1357 A73-25926

Hydrodynamic motions and the vacuum stage in an anisotropic cosmological model. 11 p1423 A73-26052

Gravitational instability of regular model-universes in a modified theory of general relativity. 11 p1423 A73-26106

Energetic electron production and loss model for Jupiter radiation belt, considering drive mechanisms for electron diffusion from solar wind 11 p1424 A73-26130

Ten-micron eclipse observations of Io, Europa, and Ganymede. 11 p1424 A73-26133

Iapetus UVB light curve minima depths difference explained by two-hemisphere model 11 p1425 A73-26134

Statistical model of meteor streams. III - Stream search among 19303 radio meteors. 11 p1425 A73-26135

Asteroidal rotational properties interpreted in terms of model with collisional breakup into irregular fragments 11 p1425 A73-26136

Saturn disk and ring dimensions, discussing photometric parameters, ice as ring constituent and ring models 11 p1425 A73-26139

Model of a stationary stellar cluster with a high binding energy. 11 p1425 A73-26176

The interaction of weak gravitational waves with a gas. 11 p1400 A73-26177

Observational constraints imposed by Brans-Dicke cosmologies. 11 p1426 A73-26413

Simple model for scanning-angle distribution of planetary albedo gamma-rays. 11 p1414 A73-26475

Evolution of stars with suppressed core convection. 11 p1427 A73-26608

The spectrum and variability of Hercules X-1 observed by OSO-7. 11 p1428 A73-26626

Bode law rationalization based on Dole computer-generated planetary system with constant spacing ratio generated by random number sequence and accretion process closeness constraints 11 p1428 A73-26665

Optical scattering properties of Saturn's ring. 11 p1429 A73-26683

Radiative transfer theory model of isotropic monochromatic scattering of light in plane layer of finite optical thickness 12 p1538 A73-26862

Titan model arising from observations and methane-rich atmosphere thermodynamics, photochemistry and optical properties, considering origins and volatile content of outer planets satellites 12 p1539 A73-27140

Galaxies as local perturbations in homogeneous universe, considering galactic manufacture within Einstein theory context 12 p1539 A73-27141

Criticism of Galactic cosmic ray production model with rotating magnetic white dwarfs, noting contrary evidence in magnetic field observations and decay theories 12 p1539 A73-27149

Disk model of gas accretion on a relativistic star in a close binary system. 12 p1539 A73-27277

Frequency dependent synchrotron emission polarization variation in cosmic radio source models, allowing for cold plasma and relativistic electron distribution nonuniformities 12 p1534 A73-27279

Metal-poor stars. IV - The evolution of red giants. 12 p1540 A73-27328

Modulation of galactic cosmic rays by a solar wind asymmetric with respect to the heliopause 12 p1534 A73-27332

Selection of a propagation model for computing the solar-proton injection spectrum 12 p1534 A73-27333

Model for lateral variations of lunar density minimizing total shear strain energy of moon, noting gravitational potential equal to observed potential at surface 12 p1541 A73-27488

Liquid core model with precessionally driven magnetoturbulence applied to moon, discussing tidal effects in outer solid and liquid shells 12 p1541 A73-27489

Astronomical, geochemical and geophysical data and constraints for lunar evolution, considering remanent magnetization, electrical conductivity and early evolution model 12 p1541 A73-27491

Lunar composition and origin model based on early condensation processes in solar nebula 12 p1542 A73-27546

Universe evolution explanation via interstellar deuterium investigation, discussing galactic gas chemical composition history 12 p1543 A73-27692

Improved three-dimensional mapping of the electron density distribution of the solar corona. 12 p1536 A73-27843

Stability of gravitating systems with a quadratic potential. I - Methods of investigating the stability of systems with a limited phase volume: Vibration spectrum of the Maclaurin stellar disk 12 p1546 A73-27856

Equations of planet figures solved for third order accuracy, covering flattening, density distribution, Jupiter and Saturn models and gravitational moments corrections for radii 12 p1546 A73-27860

Wave model of Galaxy spiral structure, assuming subsystem mass distribution and old star rotating bar mechanism 12 p1547 A73-27879

The large-scale distribution of low-velocity hydrogen gas at high galactic latitudes. 13 p1671 A73-28028

Dependence of the integrated background light on cosmology, galactic spectra, and galactic evolution. 13 p1671 A73-28035

Galactic loops as supernova remnants in the local galactic magnetic field. 13 p1672 A73-28042

Lunar differentiation model based on chemical data from Luna 20 soil and Apollo 16 core samples analysis

by combined semimicro atomic absorption spectrophotometric and colorimetric method 13 p1676 A73-28326

Chandler polar motion due to elastic earth free nutation using models based on historical data 13 p1678 A73-28380

Dynamical contraction of rotating gaseous spheroids. 13 p1680 A73-28774

Stellar structure and evolution models in conformity with observational luminosity, mass and size from H-R diagram 13 p1682 A73-28977

Cepheid variables model characteristics, determining luminosity, radial velocity and radius time dependent variations 13 p1682 A73-28981

White dwarfs model based on zero temperature Fermi gas theory, determining mass-radius relation and limit mass 13 p1682 A73-28982

Close binaries structure and evolution, discussing model computations for H-R diagram and mass-luminosity relations 13 p1682 A73-28983

Neutron stars physical model, deriving mass-density-energy relationships for degenerate electron gas 13 p1682 A73-28985

Stellar magnetism origin via fossil, battery and dynamo theories, discussing two fluid plasma model and turbulence 13 p1683 A73-28992

Theory of the thermal explosion in the hydrogen shell of a white dwarf 13 p1683 A73-29091

Numerical experiments on the stability of spherical stellar systems. 13 p1685 A73-29359

Pulsational instability of a star of 0.5 solar mass during core hydrogen burning. 13 p1685 A73-29362

A forcing mechanism for spiral density waves in galaxies. 13 p1686 A73-29372

Stellar structure deviation from neutron star models, deriving equations for relativistic models with deviation from Einstein principle of equivalence 13 p1686 A73-29655

Lunar magnetic field model with primeval liquid shell dynamo driven by thermal convection or earth tidal motions 14 p1789 A73-29722

Evolution of cometary orbits on a cosmogenic time scale. 14 p1789 A73-29777

A library of standard programmes for constructing numerical theories for studying the motion and evolution of the orbits of the minor bodies of the solar system. 14 p1790 A73-29789

Nongravitational effects on comets - The current status. 14 p1791 A73-29797

Cometary nuclei size determination methods based on model of surface ice regions with mineral crust spots, analyzing brightness decrease 14 p1792 A73-29818

On nongravitational effects in two classes of models for cometary nuclei. 14 p1793 A73-29820

Encke comet icy nucleus core-mantle evolutionary model, investigating mantle sublimation, fading and capture time approximation for nongravitational forces effect in terms of mass output 14 p1793 A73-29822

Astronomical model for Oort comet cloud destruction rate during stellar passage, noting cumulative dispersion mechanism and half life estimates 14 p1793 A73-29826

New estimates of cometary disintegration times and the implications for diffusion theory. 14 p1794 A73-29829

On the rate of ejection of dust by long-period comets. 14 p1795 A73-29841

Monte Carlo technique application to meteor stream formation process modeling, discussing mass ejection from cometary nuclei 14 p1795 A73-29848

Induced lunar magnetosphere and solar wind formed downstream cylindrical cavity for interplanetary magnetic fields arbitrary orientation, assuming lunar core and shell electrical conductivity model 14 p1796 A73-29962

On Compton models of the isotropic X-ray background. 14 p1796 A73-30001

Turbulence dissipation model for galactic origin, accounting for masses and angular momenta of large galaxies 14 p1796 A73-30002

Hypothesis postulating two types of quasars, considering cosmologically distant quasars /type I/ and

type II branch produced by explosions in nearby galaxies

14 p1797 A73-30003

Alfven waves in a two-fluid model of the solar wind.

14 p1787 A73-30005

Societa Astronomica Italiana, Meeting, 15th and Workshop on Rotation as a Phenomenon and Evolutionary Factor in the Universe, Universita degli Studi, Bologna, Italy, October 8, 9, 1971, Proceedings

14 p1797 A73-30138

Solar rotation angular velocity variation with heliographic latitude, depth and time, considering superficial circulation as cause of angular momentum transport

14 p1797 A73-30139

Rotation effects in stellar and quasi-stellar relativistic objects models required for pulsars and quasars explanation, discussing gravitation theories

14 p1798 A73-30141

Rotating neutron star matter and model properties with emphasis on pulsar observations, discussing equations of state, transport processes and relativistic effects

14 p1798 A73-30234

Asymptotic behavior of a kinetic model of the solar wind

14 p1787 A73-30424

Outer planet satellites and atmospheres composition and structure from low temperature condensation accretion models

14 p1724 A73-30530

Major planets gravitational fields models from flyby spacecraft measurements, discussing Red Spot and Jupiter effect on Galilean satellites

14 p1799 A73-30531

The significance of atmospheric measurements for interior models of the major planets.

14 p1799 A73-30532

Pulsar positions, polarization characteristics, intensity and fine structure, considering models explaining rotating neutron stars, galactic magnetic fields and electron densities and temperature

14 p1800 A73-30549

Lunar origin dynamics, discussing earth-moon tidal evolution, capture probability, fragmentary collisions, precession and auxiliary models

14 p1800 A73-30550

Singularity and matter creation in cosmological models.

14 p1800 A73-30599

The particle resonance in spiral galaxies - Nonlinear effects.

14 p1801 A73-30727

Ionization of the intercloud medium and the central disk regions of spiral galaxies.

14 p1801 A73-30729

Hydrostatic, flux constant and LTE stellar atmospheric models at 3800 and 3500 K for Betelgeuse

14 p1801 A73-30737

Time-dependent models of the interstellar gas.

14 p1802 A73-30960

Neptune model calculation from mass, radius and rotation period, comparing computed gravitational moments with observation

15 p1928 A73-30980

Motions of perfect incompressible homogeneous fluid planets surrounded by rigid oscillating rings, noting application to two-satellite planets

15 p1860 A73-31049

Differentially rotating neutron star models calculation for given state equation, examining mass increase relationship to rotational rigidity relaxation via Ostriker-Tassoul instability criterion

15 p1929 A73-31093

Terrestrial planetary core model concerning mantle-core iron oxide composition to avoid phase transition theory difficulties

15 p1867 A73-31100

The adiabatic stability of stars containing magnetic fields. I.

15 p1933 A73-31395

Cosmological information from surveys of radio source spectra.

15 p1933 A73-31396

Solar nearby star velocity field variation model for Oort constants derivation with application to faint stars motion analysis and galactic center distance calculation

15 p1933 A73-31397

Variable X ray sources Cyg X-1, Cen X-3 and Sco X-1 behavioral analysis from Uhuru satellite data, considering pulsating white dwarf model for Cen X-3

15 p1935 A73-31483

Eruptive binary stars evolutionary origin, outburst mechanisms and effects on Galactic evolution

15 p1935 A73-31487

On the origin of SC-storms with respect to forecasting geomagnetic activity.

15 p1868 A73-31520

Pulsar fluctuation spectra and the generalized drifting-subpulse phenomenon.

15 p1936 A73-31558

Lunar interior composition, structure and thermal evolution models to fit surface igneous activity

chronology and lithosphere stress history implied by mascons presence

15 p1937 A73-31778

The direct and inverse problems of cosmic-ray propagation in interplanetary space

15 p1926 A73-31878

Two-component equilibrium model of the HI regions of the interstellar medium satisfying a set of radio observations

15 p1938 A73-31965

Relativistic cosmology of interacting hadronic matter-radiation models, discussing compatibility with Hagedorn equation of state based on statistical mechanics

15 p1939 A73-32002

Genetic relationship between short period comets and meteor streams, considering radial and longitudinal focusing mechanism for particles in meteor streams

15 p1939 A73-32009

Energy losses of galactic cosmic rays in the interplanetary medium.

15 p1927 A73-32010

Bulk viscosity effects in imperfect fluid Friedmann cosmology, considering implications for singularity problem

15 p1939 A73-32011

Temperature dependent nuclear mass and its application to astrophysical problems.

15 p1939 A73-32013

Model for X-ray sources based on magnetic field twisting.

15 p1927 A73-32047

Double structure characterization in ideal model by two extended radio emitting regions near nucleus of optical galaxy or quasar

15 p1940 A73-32073

Relativistic electron radio emission models, calculating magnetic bremsstrahlung spectra from galactic electron space-energy distributions

15 p1927 A73-32609

Crab Nebula pulsar electromagnetic radiation emission model based on high energy electron circular motion around magnetic field lines

15 p1942 A73-32649

Quantitative analysis of the spectrum of beta Lyr. I - Variation of certain hydrogen and helium emission lines

16 p2057 A73-32710

Ionization and relative abundance of hydrogen and helium atoms in filaments of the Crab Nebula

16 p2057 A73-32712

X- and gamma-ray astronomy; Proceedings of the Symposium, Madrid, Spain, May 11-13, 1972.

16 p2049 A73-32727

Compact X ray source models from statistical analysis of Uhuru catalog sources with respect to luminosities, lifetimes and stellar populations

16 p2050 A73-32737

Models for compact pulsing X-ray sources.

16 p2050 A73-32738

X ray background and emission mechanism nature, considering evolutionary effects and unresolved sources

16 p2051 A73-32747

Central gravitational field of stars and evolution to red giants.

16 p2058 A73-32837

Hydrodynamic model calculations of Population I chemical composition massive objects, discussing evolution termination by violent thermonuclear explosions

16 p2059 A73-32840

Thermal and ionization equilibrium in a dense hydrogen cloud.

16 p2059 A73-32841

The prevalence of second harmonic radiation in type III bursts observed at kilometric wavelengths.

16 p2053 A73-32964

Solar wind density model from km-wave type III bursts.

16 p2053 A73-32965

Restrictions on radial magnetic field and flow solutions for the solar wind.

16 p2053 A73-32967

Variable radio emission from the extragalactic supernova 1970g in M101.

16 p2060 A73-33094

A new theory of gravity.

16 p2036 A73-33123

Steady-state solar modulation of cosmic rays.

16 p2055 A73-33296

The velocity of separation of the components of extragalactic radio sources.

16 p2062 A73-33572

Theories of galactic spiral structure comparisons with observations.

16 p2062 A73-33575

Isotropic solution of Einstein gravitational equations for anisotropic homogeneous cosmological models with hydrodynamic energy-momentum tensor

16 p2071 A73-34051

Characteristics of the Bianchi-IX cosmological model from the viewpoint of the qualitative theory of differential equations

16 p2071 A73-34052

Spherically symmetric zero energy Einstein-de Sitter cosmological model validity for world geometry from observational data and invalidity of other models

17 p2225 A73-34110

Magnetic moment generation in pulsars based on baryon model with superconducting proton fluid and normal electron field

17 p2226 A73-34365

Resonance damping of oscillations in a model of a spherical stellar cluster

17 p2226 A73-34367

The origin of the solar system; Symposium, Nice, France, April 3-7, 1972, Proceedings

17 p2226 A73-34401

Solar system origin models in terms of cataclysmic theories, solar nebula concept, planetary accumulation, protoplanets, etc

17 p2226 A73-34402

Magnetohydrodynamics, hydrodynamics and dynamics of solar system model as contracting rotating cloud, discussing effects of turbulence

17 p2226 A73-34403

Presentation of the models.

17 p2227 A73-34404

Numerical model construction for primitive solar nebula and physical accumulation processes within collapsing interstellar gas cloud

17 p2227 A73-34405

Models comparison for heavy elements segregation mechanism from gaseous hydrogen and helium for terrestrial planets formation from primordial granular matter

17 p2228 A73-34422

Chondrule chemical variations in chondrite compared to predictions for different chondrule formation mechanisms

17 p2119 A73-34425

Monte Carlo model of cometary evolution based on hypothetical perturbed orbit calculations, with emphasis on short-period comets

17 p2228 A73-34426

Vaporization theory of cometary nucleus prediction of law of dependence of nongravitational force on heliocentric distance

17 p2228 A73-34427

Mass transport rate in solar nebula model due to turbulence induced by convection

17 p2229 A73-34432

Two fluid models for solar wind heating under boundary conditions, considering enhanced energy transfer between electrons and protons in kinetic theory calculations

17 p2224 A73-34515

Magneto-gravitational and thermal instability in the Galactic disk.

17 p2231 A73-34752

A model-atmosphere abundance analysis of the B9 V star nu Capricorni.

17 p2231 A73-34758

Fundamental data for contact binaries - RZ Comae Berenices, RZ Tauri, and AW Ursae Majoris.

17 p2231 A73-34759

Evaluation of astrophysical hypotheses.

17 p2231 A73-34760

Jupiter atmospheric circulation as manifestation of large scale convective instability generated by internal heat sources, considering Red Spot production

17 p2232 A73-34859

Optical appearance of binary X-ray sources.

17 p2232 A73-35146

Solid state convection role in moon from analysis of models with homogeneous initial distribution of radioactive heat sources

17 p2232 A73-35262

Calcium oxide and aluminum oxide constraints removal for lunar interior composition models

17 p2232 A73-35264

The applications of relativistic kinetic theory to cosmological models - Some observational consequences.

17 p2234 A73-35616

On the origin of short-period comets.

17 p2234 A73-35620

Thermal history and evolution of the moon.

17 p2235 A73-35735

Conjectures about the evolution of the moon.

17 p2235 A73-35737

Properties of the solar nebula and the origin of the moon.

17 p2235 A73-35742

Correlations among the parameters of the spherical model for eclipsing binaries.

17 p2236 A73-35778

Structure and evolutionary history of the solar system. III.

17 p2236 A73-35784

Evolutionary considerations involving the internal density concentration parameter of binary stars.

17 p2237 A73-35786

Book on large scale structure of space-time covering gravity roles, differential geometry, general relativity, gravitational collapse, black holes, spatially homogeneous cosmological models, etc
18 p2336 A73-35901

Photoelectron layer above sunlit lunar surface due to solar photon flux, using models neglecting solar wind electron flux
18 p2351 A73-36267

Cometary composition, structure and atmospheric dynamics, discussing multiconstituent hydrodynamic models in comparison with observation
[AIAA PAPER 73-549]
18 p2353 A73-36495

Extragalactic radio sources modeled as bubbles of relativistic plasma rising through hot gas, producing galactic clusters X ray emission
18 p2353 A73-36508

Jupiter and Saturn interior structure models based on state equations and transport properties of hydrogen and helium at high pressures and temperatures
18 p2354 A73-36644

Ejection of supernova envelopes by magnetic pumping.
18 p2354 A73-36726

Interferometry of the Medusa nebula A21 YM 29/
18 p2354 A73-36729

Thermal instability caused primary interstellar dust cloud fragmentation and resulting star formation according to Peebles-Dicke hypothesis for cosmological origin of globular clusters
18 p2355 A73-36738

Free particle gravitating cylindrical model for gravitational kinetic instabilities, calculating natural vibration spectrum and parameters for beam instability development
18 p2340 A73-36739

Model for axisymmetric clusters of stars with uniform mass.
18 p2355 A73-36740

Self consistent computerized solutions to acoustic wave propagation and shock wave transformation with energy dissipation for solar and stellar chromosphere models
18 p2355 A73-36742

Spectrum of the coordinates of the earth's pole during the period 1846-1971.
18 p2355 A73-36748

A stochastic model of the galactic magnetic field.
18 p2356 A73-36974

On the nature of the infrared point source in the Orion Nebula.
18 p2356 A73-36975

Thermal models of inhomogeneously accreted meteorite parent bodies.
18 p2356 A73-37048

A three-level model for calculating vertical motions generated by planetary orography.
18 p2314 A73-37073

Viscous effects in rapidly rotating stars with application to white-dwarf models. I, II.
18 p2357 A73-37106

Models of the chromospheric-coronal transition layer and lower corona derived from extreme-ultraviolet observations.
18 p2357 A73-37107

Internal structure of the convective shell of the sun
19 p2481 A73-37343

Plasma acceleration techniques in space studies, discussing simulation experiments, solar wind-geomagnetic field interaction and astronomical models
19 p2482 A73-37355

Implications of the statistical bootstrap model for cosmology and galaxy formation.
19 p2482 A73-37559

Structure of helium burning regions in stars - Dependence on molecular weight and burning rates.
19 p2483 A73-37560

The effect of hot white dwarfs on the interstellar medium. II - The changes in its structure with height above the galactic plane and some consequences of the finite lifetimes and velocities of the white dwarfs.
19 p2483 A73-37561

Water masers in a protostellar gas cloud.
19 p2483 A73-37573

Observational nondifferentiability between expanding universe and static world models
19 p2484 A73-37607

Nonuniform model construction for dense intergalactic medium with gravitational binding of all galactic groups and clusters by ionized gas
19 p2484 A73-37608

On the ionization of the intercloud medium by ultraviolet stars.
19 p2484 A73-37611

Synchrotron model limitations for optical pulsars and compact extragalactic objects, considering NP 0532, PKS 2134+004, OQ 208 and NGC 10608
19 p2485 A73-37618

On the energy spectrum of relativistic electrons in the Crab Nebula.
19 p2475 A73-37619

Intense outburst /S/ of radio radiation detected with the Goldstone-Haystack interferometer.
19 p2485 A73-37624

Soft X-ray flux of the Coma cluster of galaxies.
19 p2475 A73-37626

Upper limits to the X-ray emission from Beta Persei during radio flares.
19 p2475 A73-37630

A deduction of the inverse square law from Newtonian cosmology.
19 p2486 A73-38169

Absorber theory of radiation and the future of the universe.
19 p2460 A73-38172

The redshift-distance relation. V - Galaxy colors as functions of galactic latitude and redshift - Observed colors compared with predicted distributions for various world models.
19 p2487 A73-38504

CN red system line opacity codes for late star model atmosphere calculation
19 p2488 A73-38513

Pulsar model magnetosphere for uniformly rotating infinitely conducting magnetized neutron star with aligned magnetic field
19 p2488 A73-38515

The optical polarization of the Crab Nebula pulsar. I - A relativistic vector model.
19 p2489 A73-38517

Optical polarization of the Crab Nebula pulsar. II - Observational results and fits by the relativistic vector model.
19 p2488 A73-38518

Low solar neutrino flux explained by evolution model emphasizing internal rotation effects on solar structure
19 p2488 A73-38519

Interplanetary gas. XVIII - Models and the mean free path of protons at 1 astronomical unit.
19 p2489 A73-38523

Planetary nebula evolution model to explain FG Sagittae luminosity changes due to thermal pulse in He burning shell
19 p2489 A73-38530

Primordial explosion model for universe origin, noting radio astronomy counts of galaxies invalidation of Hoyle steady state cosmology
20 p2604 A73-39008

Massive singlet f-meson gravitational field effects on gravitational collapse in universe model with ten to eightieth power aligned neutrons
20 p2605 A73-39016

A study of commensurable motion in the asteroid belt.
20 p2606 A73-39075

Stability of periodic oscillations of stars.
20 p2606 A73-39081

On the accretion model for X-ray double stars.
20 p2607 A73-39082

Book - Introduction to the physics of stellar interiors.
20 p2607 A73-39144

Stability of gravitating systems with a quadratic potential. I - Systems bounded in phase space - Oscillation spectrum for a Maclaurin stellar disk.
20 p2608 A73-39230

Equations of planet figures solved for third order accuracy, covering flattening, density distribution, Jupiter and Saturn models and gravitational moments corrections for radii
20 p2608 A73-39234

Stability of the sun against spherical thermal perturbations.
20 p2608 A73-39428

Nonspherically symmetric thermal instabilities implied by discrepancy between theory and observation for solar neutrino problem, noting absence in solar numerical model
20 p2608 A73-39429

Meridional flow and the validity of the two-dimensional approximation in stellar-wind modeling.
20 p2602 A73-39430

Universe evolutionary model construction based on observations of high flux gravitational radiation generated within Milky Way Galaxy
20 p2609 A73-39434

A model for compact X-ray sources - Accretion by rotating magnetic stars.
20 p2602 A73-39443

Stimulated linear acceleration radiation - A pulsar radio emission mechanism.
20 p2602 A73-39444

X-ray spectrum of Cassiopeia A - Evidence for iron line emission.
20 p2603 A73-39446

Magnetic fields of the sun and stars
20 p2609 A73-39569

Quasar and galactic nuclei energy source models, considering supermassive rotating magnetoplasma body, black hole and compact star cluster with flares and collisions
20 p2609 A73-39570

Solar brightness temperature measurement relative to lunar brightness temperature, noting agreement with HSRA model
20 p2610 A73-39582

Dynamical models of tailed radio sources in clusters of galaxies.
20 p2610 A73-39584

Zero-age main sequence stellar model calculations compared to observational data derived for nearby low mass stars
20 p2611 A73-39585

Mars internal structure computed via general relativity application to earth-like model
20 p2612 A73-39711

Model for lunar near surface thermal conductivity in terms of contact conductivity, pressure and packing density
20 p2613 A73-39719

Gravitational red shift, Mercury perihelion, light deflection and signal delay tests of Einstein relativity vs Jordan-Brans-Dicke theory
20 p2613 A73-39751

Scalar waves in the mixmaster universe. I - The Helmholtz equation in a fixed background.
21 p2766 A73-40317

Numerical model for cold gaseous planets /Jupiter, Saturn, Uranus, Neptune/ as remnants of star formation attempts, taking into account density fluctuations in collapse region
21 p2766 A73-40374

Permissible hydrodynamic and hydrostatic stellar atmosphere models described by system of equations dependent on initial level conditions
21 p2767 A73-40532

Effects of nuclear reactions with fast protons in a supernova shell and the origin of cosmic rays
21 p2756 A73-40581

Determination and interpretation of solar proton spectra at the earth and in the source
21 p2756 A73-40584

A new estimate of the fluctuation of relic radiation in the universe
21 p2759 A73-40708

Clusters of galaxies - A possible source of background emission in the X-ray band
21 p2759 A73-40709

Evolution of supermassive stars with a strong magnetic field
21 p2767 A73-40711

Stellar masses on the asymptotic branch of red giants in globular clusters
21 p2768 A73-40719

Determination of the temperature behavior in a photospheric facula through the solution of an integral equation by the gradient-random search method
21 p2759 A73-40721

Dissipation of the Venusian atmosphere
21 p2769 A73-40733

Distribution density of small lunar craters - Models and actual distribution
21 p2770 A73-40915

Big Bang model of universe, discussing 3 K background radiation, thermal history of early universe, lepton number conservation and different eras
21 p2772 A73-41242

Cosmological singularity structures, taking into account initial singularity inevitability, uniform models, mixmaster model quantal limitations and physical processes
21 p2772 A73-41249

Terrestrial gravitational models derived from satellite tracking and surface gravimetric data, comparing to 1969 Smithsonian Standard Earth II models
21 p2773 A73-41326

Solar flare forecasting method developed and applied at Crimean observatory, using magnetic instability model for active regions
21 p2762 A73-41391

Optical and mechanical models of interplanetary dust.
21 p2776 A73-41420

Cometary atmospheric dust chemical composition and physical properties estimated from colorimetric, polarimetric and IR data, using models of optically thin polydisperse media
21 p2776 A73-41421

Asteroidal dust population model coinciding with spatial density demonstrating distribution below astrodynamical mass limit and larger time for distribution function extrapolation
21 p2776 A73-41422

The formation of Mg I 4571 A in the solar atmosphere. III - The Holweger solar model /Research note/.
21 p2777 A73-41480

On the possibility of constructing a radiative sunspot model in magnetohydrostatic equilibrium.
21 p2777 A73-41486

Optical solar flare kinematic model, relating chromosphere response to downward propagating supersonic disturbance
21 p2762 A73-41490

On the source of the slowly varying component at centimeter and millimeter wavelengths.
21 p2778 A73-41496

Solar-wind properties at the earth as predicted by the two-fluid model.
21 p2763 A73-41502

Energy losses of solar cosmic rays in interplanetary space.
21 p2763 A73-41503

Model for galactic cluster formation after radiation decoupling from matter in Einstein-De Sitter universe, discussing turbulence in primeval cosmos 21 p2778 A73-41526

Magnetized and nonmagnetized rotating neutron star reactions to applied torques for pulsar slowdown, discussing magnetosphere and wind zone 21 p2778 A73-41529

Model for gas bridge and magnetic field connecting Magellanic Clouds from optical and radio polarization measurements 21 p2779 A73-41535

Solar neutrino fluxes on earth from solar model and analytical approach, discussing neutrino capture rate contributions 21 p2764 A73-41539

Relaxation time in disk galaxy simulations. 22 p2904 A73-41754

Linear convective modes and the energy transport in stellar convection zones. 22 p2905 A73-41761

Uneven illumination of the polar caps by solar protons - Comparison of different particle entry models. 22 p2901 A73-41906

On the infrared emission of H II regions due to dust. 22 p2884 A73-42314

Hydromagnetic stability of a composite plasma in the presence of Hall currents. 22 p2894 A73-42439

Integrals for optimal flight over a spherical earth. 22 p2884 A73-42561

Russian book on eclipsing binary stars covering limb darkening law, photometric eclipsing phases, computer applications and models 22 p2911 A73-42747

On the problem of the initial state in the isotropic scalar-tensor cosmology of Brans-Dicke. 22 p2911 A73-42931

Static stellar envelopes at radiative equilibrium for power law dependence of opacity on temperature and density 22 p2911 A73-42935

Models of force-free magnetic fields in resistive media. 22 p2911 A73-42938

The common convective envelope model for W Ursae Majoris systems and the analysis of their light curves. 22 p2912 A73-42939

Galactic mass distribution models from matter density near sun, discussing halo mass and RR Lyrae effects observation 22 p2912 A73-42940

Atmospheric Uranus and Neptune models with massive atmospheres above solid cores, discussing Uranus solid methane cloud layer 22 p2913 A73-42987

The angular momentum of spiral galaxies. I - Methods of rotation-curve analysis. II - Detailed models and correlations for 17 galaxies. 22 p2913 A73-43002

Theory of interstellar abundances of the isotopes of carbon, nitrogen and oxygen. 22 p2914 A73-43006

Ionised molecules in BCA photospheric model. 22 p2915 A73-43039

Light curve for eclipsing binary systems with an extensive atmosphere. 22 p2916 A73-43044

Cosmic deuterium abundance derived from measured HD/H2 ratio, noting derivation sensitivity to ionizing flux and to oxygen and carbon depletion 22 p2904 A73-43119

Isothermal gas-sphere model with thermal bremsstrahlung for X ray emission from Coma, Perseus and Virgo galactic clusters, noting gas distribution 22 p2904 A73-43120

The Wolf-Rayet stars - The general problems of extended atmospheres and non-classical atmospheric models. 23 p3025 A73-43192

Modulation of galactic cosmic-rays by solar wind which is unsymmetric in solar latitude. 23 p3020 A73-43230

Selection of a propagation model for calculating the injection spectrum of solar protons. 23 p3020 A73-43231

Pulsar properties covering galactic distribution, pulse periodicity computed from arrival time measurements, models, emission mechanisms, total intensity pulse shapes, etc 23 p3028 A73-43351

Structural characteristics of galaxies caused by screening of the Newtonian gravitational potential 23 p3029 A73-43646

Gravitational fields calculation in three dimensional mass distribution galaxies, using biorthogonal functions with ultraspherical polynomials 23 p3030 A73-43749

High concentration of refractory elements in lunar crust explained by melting and differentiation model 23 p3033 A73-43958

The stability of gravitating systems with a quadratic potential. II - The stability of models of spherically symmetric and axisymmetric clusters with elliptic orbits of particles 23 p3035 A73-44236

Chromosphere models for cool stars of various spectral types, calculating temperature-density dependence for sun, giant and dwarf stars 23 p3036 A73-44243

Solar U burst radio source spectrographic and polarization observations, using Waldmeier corona model for particle exciter in magnetic field 23 p3036 A73-44247

Cosmic gamma ray studies for metagalactic and remote galactic model construction as substitute for radio and X ray emission data 23 p3025 A73-44325

Radial and vertical force balance in primitive solar nebula, describing techniques for gravitational potential and gas opacity computation for energy transport 24 p3127 A73-44392

Planetary formation processes in primitive solar nebula analyzed from collapse phase for accumulation time 24 p3127 A73-44393

Topography on satellite surfaces and the shape of asteroids. 24 p3129 A73-44446

Mars precession scheme for prolonged equinoctial habitable spring in terms of Sagan model extension 24 p3131 A73-44464

Many body model for comet nucleus formation from solid materials and interstellar gas consistent with Whipple icy conglomerate model 24 p3131 A73-44466

Orientation-dependent effects in Oort's theory of comet origin. II - Anisotropies in the distribution of long-period comet orbits. 24 p3131 A73-44467

Lunar 25 km discontinuity seismically examined, discussing hypotheses with shock metamorphosis lack and annealing of shock induced microcracks 24 p3131 A73-44470

Two-component equilibrium model of interstellar HI regions that satisfy the overall radio observations. 24 p3132 A73-44490

Refutation of Bagby moonlet theory via analysis of supporting evidence 24 p3133 A73-44542

Mars crustal structure model from analysis of surface markings with Mariner 9 data, showing petrologic distinctions between dark and light regions 24 p3133 A73-44543

Methane absorption in the Jovian atmosphere. II - Absorption line formation. 24 p3133 A73-44559

Radiative damping of trapped gravity waves in the solar atmosphere. 24 p3135 A73-44629

A study of solar radio emission in the light of Sengupta's model of coronal active regions. 24 p3123 A73-44637

On the generation of umbral flashes and running penumbral waves. 24 p3136 A73-44638

W-Ursa-Major stars 24 p3137 A73-44825

Interstellar reddening calculation with respect to U-B/V diagram for hot and main sequence stars as function of luminosity based on model stellar atmospheres 24 p3138 A73-45012

Relativistic gravity in the solar system. III - Experimental disproof of a class of linear theories of gravitation. 24 p3138 A73-45034

Accretion onto black holes - The emergent radiation spectrum. II Magnetic effects. 24 p3138 A73-45036

Gravitational radiation emission by star tidally deformed by black hole, computing energy loss rate 24 p3138 A73-45037

A radially streaming proton model for the broad component of hydrogen emission in Seyfert galaxies. 24 p3138 A73-45039

Heat current and anisotropy-driven instabilities in connection with the solar wind. 24 p3126 A73-45126

Multiple solutions of the equations of stellar structure. II - E model sequences. 24 p3140 A73-45179

Neutral hydrogen rotational motions near galactic center and 3-kpc arm, using dispersion ring model 24 p3140 A73-45180

Single component wind model for stellar rotation dependent mass loss from hot corona with application to T Tauri star observations 24 p3140 A73-45186

Physical conditions in nuclei of spiral galaxies. I - Study of galaxies with a nuclear radio-component. 24 p3141 A73-45192

Thermodynamics of white dwarf matter in crystalline phase. 24 p3143 A73-45435

Magnitude-redshift and count-magnitude relations in presence of an uniform intergalactic absorption. 24 p3143 A73-45436

ASTRONOMICAL NETHERLANDS SATELLITE
The fine solar sensor of the Astronomical Netherlands Satellite. 16 p2012 A73-32852

The fine sun sensor of the astronomical Netherlands satellite. 19 p2431 A73-38100

ASTRONOMICAL OBSERVATORIES
NT HEAO
NT OAO
NT OSO
NT OSO-7
Telescopes for northern and southern hemisphere astronomical observatories, discussing auxiliary instrumentation and construction state on Calar Alto mountain 01 p0046 A73-10507

The lunar regolith as a site for an astronomical observatory. 01 p0105 A73-11204

A description of the lunar ranging station at McDonald Observatory. 02 p0151 A73-12249

Hawaii's Mauna Kea Observatory today. 03 p0287 A73-13549

The Large Space Telescope program. 03 p0382 A73-13550

Culgoora /Australia/ solar radio observatory site, facilities, instrumentation and research activities 10 p1203 A73-24150

The 73.5-cm wavelength radio interferometer of the Biurakan Observatory 12 p1479 A73-27226

Earth rotational accelerations magnitudes as obtained from astronomical observations, noting semimonthly lunar body tides effects 13 p1679 A73-28395

Astronomical telescopes operational efficiency relation to atmospheric optics conditions at various Middle Asian elevated sites 15 p1934 A73-31423

Electrophotometric equipment in the Stara Zagora Observatory 16 p2016 A73-33663

Preliminary progress with digital image-tubes at Cerro Tololo. 17 p2169 A73-35281

Report on the telescope ultraviolet observations from the OAO-2 satellite and associated research at the Smithsonian Astrophysical Observatory. 18 p2349 A73-35996

Tromsø /Norway/ Auroral Observatory partial reflection experiment, considering data processing techniques, height resolution, phase detection, antenna arrays and D region drift measurements 18 p2315 A73-36009

The Lunar and Planetary Laboratory and its telescopes. 19 p2417 A73-37580

Astroclimatic, site, calibration and atmospheric optics conditions for large telescope observations on M. Maidanak 21 p2769 A73-40729

Image tube systems for ground based and spaceborne astronomical observations, considering self scanning diode array, phosphor screen output devices, electronography, etc 21 p2703 A73-41239

National Radio Astronomy Observatory interferometer system with rotating head video tape recording and computerized sampled data processing equipment for use with radio telescope 23 p2980 A73-43358

A supersynthesis radio telescope for neutral hydrogen spectroscopy at the Dominion Radio Astrophysical Observatory. 23 p2958 A73-43362

Spectrum control procedures for the National Radio Astronomy Observatory. 23 p2953 A73-43381

Satellite laser ranging instruments operated at Tokyo Astronomical Observatory. 24 p3068 A73-44998

ASTRONOMICAL PHOTOGRAPHY
Structure and dynamics of barred spiral galaxies, in particular of the Magellanic type. 01 p0096 A73-10298

The mass and figure of Saturn by photographic astrometry of its satellites. 01 p0096 A73-10316

Photographic equipment for astronomical telescopes, considering mechanical devices for plate translation and rotation, guiding microscope and digitally controlled servomotors with incremental feedback 01 p0049 A73-10541

Study of variable stars in two stellar fields in the Lacerta and Lyra constellations 01 p0098 A73-10558

Photographic observations of Mars during the major opposition of 1971 01 p0101 A73-10842

Photographic techniques for earth based planet observation, discussing optical equipment, atmospheric disturbance effects and photointerpretation methods

01 p0051 A73-10991
A near-infrared view of the Uranus system.

01 p0109 A73-11491
Ground based solar astronomy potential for obtaining photographs with factor of two in resolution and time series, discussing optical performance of vacuum solar telescope

02 p0216 A73-12329
Planetary observation by earth based photography, discussing resolution limitation and improvement in terms of modulation transfer function

02 p0216 A73-12330
High resolution limitations and improvement for earth based visual and photographic planetary observation, considering atmospheric boundary layer and use of elevated stations

02 p0169 A73-12331
Preliminary results of the first flight of the Soviet stratospheric solar observatory.

02 p0216 A73-12335
Complex parameter B of Perseids meteors from photographic observations at Dushanbe, giving logarithms

02 p0216 A73-12358
Blue objects in the vicinity of M31. I - Discovery probability of newly found blue objects

02 p0226 A73-12837
Time and latitude observations of star groups with photographic zenith tube, including random, layer distortion and coordinate errors

03 p0307 A73-13249
A program for plate reduction in the case of satellite observations with a satellite observation camera

03 p0274 A73-13254
Photographic observations of Comet Bennett, 1970II.

04 p0495 A73-14766
Search for weak white-light flares by time-wise photographic cancellation.

05 p0610 A73-17042
Schwarzschild effect elimination in stellar color photography via triple black and white photography with film of differing color sensitivities

05 p0578 A73-17096
High-resolution imagery of Uranus obtained by Stratoscope II.

05 p0627 A73-17388
Occultation of the Pleiades by the moon on March 19, 1972

06 p0753 A73-18375
Yale Observatory photographic monitoring program for quasar observation, presenting light curves and magnitudes for 25 objects

07 p0876 A73-19356
Axial ratio and position angle of the major axis of the globular cluster M 92

07 p0901 A73-20317
Radiative transfer theory application to stellar images in photographic emulsions, deriving theoretical relation between star brightness and photographic effective radius

08 p1006 A73-20926
Mariner 9 stellar photography and camera parameters for point source photometric calibration and reference for optical navigation

08 p0964 A73-21043
Polarization of the total coronal emission during the solar eclipse of March 7, 1970

08 p1007 A73-21070
Quasars as events in the nuclei of galaxies - The evidence from direct photographs.

08 p1009 A73-21168
Schmidt telescopes application in astronomy, noting image quality uniformity across total field of view

08 p0966 A73-21358
Image intensifier systems and their applications to astronomy.

08 p0971 A73-21743
Magnetically focused electronographic cameras for far UV imagery and spectrography in astronomical and optical geophysical observations from sounding rockets and space vehicles

08 p0971 A73-21744
New optical measurements of planetary diameters. IV - Size of the North polar cap of Mars.

09 p1145 A73-22273
A new look at the Martian 'violet haze' problem. II - 'Blue clearing' in 1969.

09 p1145 A73-22275
Optical and near-infrared observations of the nearby spiral galaxy Maffei 2.

10 p1272 A73-23528
Long focal length refractor telescopes for high resolution stellar photography, describing follower drive construction and control

10 p1218 A73-24275
Optical system and performance potential of telescopic high-aperture-ratio Schmidt camera designed for photographic studies of faint extended objects

11 p1361 A73-25230
Photographs of comet Bennett 1969 I.

11 p1426 A73-26267

The telescopic radiant areas of the Perseids and the Orionids.

11 p1426 A73-26572

Tables of relative positions of stars in trapezium-type multiple star systems based on photographic observation data

12 p1537 A73-26857

Axial ratio and position angle of the major axis for the globular cluster M92.

12 p1539 A73-27289

Mars photographic observations during opposition, analyzing polar caps, surface reliefs, dust storms and atmospheric optical thickness

12 p1542 A73-27498

Sunspot observations by means of a vidicon camera.

I.

12 p1545 A73-27833

Investigation of the influence of temperature and velocity fields on the quality of an astronomical image

12 p1546 A73-27864

Blue OB stars detection by flicker comparison, astronomical photography and two color diagrams, discussing classification as quasars and white dwarfs

13 p1673 A73-28148

Results of observations of coronal condensation in photographic rays during the solar eclipse of Sept. 22, 1968

13 p1673 A73-28299

Effect of instability of earth's atmosphere on results of solar granulation observations.

13 p1680 A73-28515

Distribution law of light-ray direction fluctuations in telescopes

13 p1618 A73-29098

Photometric analysis of monochromatic photographs of the solar corona taken in the green line (5303 A) and the red line (6374 A).

13 p1685 A73-29363

Observations of comets at the Crimean Astrophysical Observatory.

14 p1789 A73-29780

Photographic observations of Mars during the great opposition of 1971.

15 p1928 A73-30978

Optical study of BL Lacertae. II - Brightness variation from March 1969 to January 1971

15 p1928 A73-31052

Book - Vistas in astronomy. Volume 13.

15 p1932 A73-31302

Calibration of turbulence and visual and photographic scintillation parameters in Pulkovo, Tashkent and Shternberg Institute astroclimate systems for 50 inch reflector

15 p1934 A73-31425

Earth deflections of vertical due to luni-solar gravitation changes determined by astronomical observation with Hermoncourt photographic zenith tube, noting semidiurnal tidal effects

15 p1937 A73-31779

Russian monograph on meteor observation covering telescopic and photographic methods, meteor trail plotting, radiant determination, stream counts and bolide data

15 p1941 A73-32416

Morphological and kinematic study of the fine structures of a sunspot

16 p2052 A73-32956

Photographic measurements of the rotation of Mercury

16 p2066 A73-33797

Identification of certain details on photographs of Mars obtained from Mariner 4 and on the ground

16 p2069 A73-33834

Craters on photographs of the Mars surface taken by the Mariner 4 probe in 1965

16 p2069 A73-33835

Observations of the Saturn rings during the earth's passage through the ring plane in 1966

16 p2070 A73-33846

An experiment in photographic equidensitometry of the moon and planets

16 p2070 A73-33848

Night sky photographic evidence for natural retrograde earth satellites explanation for Vulcan type observations, considering group C orbit anomaly and terrestrial day length errors

16 p2071 A73-34000

Poisson frequency distribution of flare stars in Pleiades, including statistical analysis of photographic amplitudes

17 p2226 A73-34364

Limiting magnitude techniques with the Corralitas 24 inch Cassegrain image orthicon system.

17 p2169 A73-35290

Astronomical optics, including two mirror systems, aspherical plates, lens type field correctors, spectrograph cameras, focal reducers and optical adjustments

17 p2171 A73-35407

The optical design of the 40-in. telescope and of the Irene Dupont telescope at Las Campanas Observatory, Chile.

17 p2171 A73-35408

UV photography of star field by Eridan rocket-borne wide angle camera, noting inertial guidance system pointing errors data reduction problems

18 p2315 A73-35994

Polarization of the resultant emission of the corona during the solar eclipse of March 7, 1970.

18 p2355 A73-36871

Recording of the angular velocity of meteors by sequential photography

19 p2480 A73-37239

Radial velocity measurements of the Cetus Arc nebula around Loop II.

19 p2483 A73-37571

Analysis of a method for obtaining near-diffraction-limited information in the presence of atmospheric turbulence.

19 p2461 A73-38485

The occultation of the star SAO 93826 by Saturn's ring

20 p2606 A73-39076

Effects of temperature and velocity fields on the quality of astronomical images.

20 p2608 A73-39238

A system for the photographic recording of pulsar pulses

21 p2700 A73-40552

Solar eclipse of 10 July 1972 observed by visual and photographic method from aircraft, taking into account coronal structure

21 p2767 A73-40565

A cartographic projection of photographs of celestial bodies obtained from space

21 p2769 A73-40860

Solar photospheric granulation plate statistical properties, establishing two dimensional autocorrelation function and power spectrum as function of wave number

21 p2776 A73-41477

Solar wind interaction with Comet Bennett near earth, examining photographs for momentum flux change-ion tail kink correlations

21 p2763 A73-41501

Observational results on coronal condensation in photographic light during the September 22, 1968 solar eclipse.

21 p2779 A73-41543

Linear polarization in the Orion Nebula.

22 p2908 A73-42313

French eclipse studies.

22 p2911 A73-42870

Airborne studies of the African eclipse.

22 p2911 A73-42871

The International Planetary Patrol Program - An assessment of the first three years.

22 p2912 A73-42978

An optical Atlas of galactic supernova remnants.

23 p3028 A73-43448

Jupiter Red Spot photographic, IR image, spectral, photometric, polarimetric and chemical studies, comparing with earth and Mars atmospheric data

23 p3032 A73-43940

Multicolor astronomical photography of Jupiter using wideband filters, emphasizing Red Spot, atmospheric bright belts and methane absorption variations above clouds

23 p3032 A73-43941

Narrow band IR vidicon Jupiter and Saturn photography, showing limb darkening and surface details

23 p3032 A73-43942

Photographic observations of the occultation of Beta Scorpii by Jupiter.

23 p3033 A73-43944

Initial development of the June 1971 South Equatorial Belt disturbance on Jupiter.

23 p3033 A73-43945

Observations of the South Equatorial Belt disturbance on Jupiter in 1971.

23 p3033 A73-43946

Rotation period for a subsurface source in the NNTEB of Jupiter.

23 p3033 A73-43947

UBV spectral and photographic observations of blue objects around M 92 globular cluster

23 p3037 A73-44355

The Saturn rings in 1969: Morphological and photometric study. I - Photograph acquisition and evaluation

24 p3128 A73-44434

Short-term Jovian rotation profiles, 1970-1972.

24 p3134 A73-44562

Some comments on the photographic subtraction method of determining chromospheric velocities.

24 p3135 A73-44631

Photographic observation of type I supernovae at Asiago Observatory, discussing analysis of B and V light curves and spectra

24 p3143 A73-45437

Seasonal variations of the south polar cap of Mars according to measurements made on photographs taken near the time of the 1971 opposition.

24 p3143 A73-45439

ASTRONOMICAL PHOTOMETRY
NT STELLAR SPECTROPHOTOMETRY

- Spectral classification through seven-colour photometry. 01 p0095 A73-10295
- An investigation of four southern open clusters. 01 p0096 A73-10320
- Electronography application to telescope and auxiliary instrumentation designs for astronomical photometry, considering spectracon and suitable image tubes 01 p0049 A73-10537
- Electronographic photometry of very weak stars of extragalactic origin with shift towards red, discussing accuracy limitation causes 01 p0049 A73-10538
- Electronographic image tubes for stellar field photometry. 01 p0049 A73-10539
- Energy distribution in the near infrared from nuclei of galaxies. I - M31, M32, NGC 3115, NGC 4151, NGC 4406. 01 p0098 A73-10552
- Three color photometric study of open cluster NGC 1647, obtaining distance, B-V and U-B excesses and R_{MC} 01 p0098 A73-10554
- Rocket infrared observations of H II regions. 01 p0103 A73-11026
- Physical reality of apparent carbon star group in Auriga from radial velocity measurements, spectral classification and VR photometry observations 01 p0104 A73-11039
- Thickness of Saturn's rings from observations in 1966. 01 p0107 A73-11325
- The results of coronal investigation at the September 22, 1968 solar eclipse. 01 p0108 A73-11383
- Search for a visible counterpart of the September 2, 1972 radio outburst in Cygnus. 02 p0204 A73-11562
- Narrow band and broadband light curves for Algol eclipsing binary from differential photometry, calculating reflection effect 03 p0366 A73-12940
- Properties of the Red Spot of Jupiter in 1971. 03 p0371 A73-13216
- On the extended van Wijk sequence in the Large Magellanic Cloud. 03 p0371 A73-13217
- Hyades stellar flux parallaxes for cosmic scale photometric distance determinations and calibration 03 p0372 A73-13248
- The light-curve for the minor planet 4/Vesta. 03 p0379 A73-14578
- Comet photometry to explain origin of free radicals discovered in cometary spectra, considering clathrate hydrates and possible parent molecules 04 p0494 A73-14756
- I. alpha photometry of Comet Bennett. 04 p0494 A73-14757
- Jupiter atmosphere density fluctuations as cause of time symmetric light flash occurrence during Beta Scorpis occultation 04 p0496 A73-14926
- Photometry of the lunar surface. 04 p0497 A73-15177
- A photometric and polarimetric study of the moon's surface. 04 p0497 A73-15183
- On surface photometry of the moon. 04 p0448 A73-15188
- UBV photometry of the metal-rich globular cluster NGC 6171. 04 p0500 A73-15487
- The angular diameter of X Cancri. 04 p0500 A73-15518
- The pulse shape of the Crab Nebula pulsar NP 0532 as a function of color. 04 p0501 A73-15685
- Structure of the Cepheid instability strip in the small Magellanic Cloud. 04 p0503 A73-16007
- Certain optical properties of the atmosphere of Venus and the possibilities of interpreting photometric and polarization measurements. 05 p0612 A73-16087
- Mars surface features from Mariner 9 TV photometric observations, discussing albedo variations due to dust storm, topography and craters 06 p0745 A73-17478
- Skylab experiment for measuring color indices of extended sources and of spectral types O, B and A hot stars at various galactic latitudes 07 p0822 A73-18989
- Photometric orbit and apsidal motion of DR Vulpeculae. 07 p0875 A73-19119
- Mutual phenomena of Jupiter's satellites in 1973-74. 07 p0875 A73-19260
- A photometric model of the zodiacal light. 07 p0876 A73-19359
- Methods of studying solar granulation fields in the presence of atmospheric disturbances 07 p0876 A73-19396
- Photometric plane and spherical characteristics of spiral galaxies from statistical analysis of SQ, S and Irr morphological profiles 07 p0901 A73-20314
- On the size of the structure elements in the solar chromosphere. 08 p1001 A73-20754
- Threadlike solar coronal streamer observation at 20 July 1963 eclipse, noting electron density from photometric analysis 08 p1002 A73-20763
- Three-colour photometry of a field in the galactic anticentre section near NGC 1664. 08 p1005 A73-20922
- Three-colour photometry in a field in the direction of the galactic anticentre near M 35. 08 p1005 A73-20923
- Photometric investigations of magnetic stars. 08 p1006 A73-20925
- The spectral classification of the beta Cephei stars and their location in the theoretical Hertzsprung-Russell Diagram. 08 p1006 A73-20927
- Results of contrast measurements of some Martian maria in July-August 1971 08 p1007 A73-21062
- Some results of spectrophotometry of the methane absorption band (7250 Å) on the Jovian disk 08 p1007 A73-21063
- Spectrophotometry of Ton 524a, b. 08 p1009 A73-21170
- Bennett comet head spectrophotometry over 352-612 millimicrons, identifying CN, CH, C2 and Na emission features 08 p1010 A73-21315
- Light distribution in photographic meteors by means of multicolour photometry. 08 p1010 A73-21316
- The role of Schmidt telescopes in the study of galactic structure (Photometric methods). 08 p1011 A73-21355
- Surface colour photometry of galaxies with Schmidt telescopes. 08 p1011 A73-21363
- Galactic structure at high galactic latitudes. 08 p1011 A73-21365
- Ten years of research with the 134 cm Schmidt telescope. 08 p0966 A73-21367
- Photometric characteristics of Jupiter and Saturn in the 0.48-0.33-micron range. 08 p1012 A73-21578
- An automated two-channel scanning spectrophotometer system. 08 p0970 A73-21740
- Theoretical performance figures for low light level TV cameras. 08 p0972 A73-21757
- H beta emitting diffuse nebulae as reflection nebulae illuminated by galactic light, based on photometric observation of H alpha emitting external spiral galaxies 08 p1013 A73-21809
- Photography of the zodiacal light outside the ecliptic in quadrature and in opposition with the sun 09 p1073 A73-22001
- The interstellar reddening law in the ultraviolet deduced from filter photometry obtained by the OAO-2 satellite. 09 p1141 A73-22029
- Infra-red observations of young stars. I - Stars in young clusters. II - T Tauri stars and the Orion population. III - Nebulous emission-line stars. 09 p1143 A73-22112
- Ground based photometric observations of Mars during 1971 opposition, using conventional photography, multichannel spot photometry and dual channel area scanning 09 p1145 A73-22272
- Preliminary data for the optical variability of the eruption from the NGC 4486/M87/ nucleus 09 p1145 A73-22287
- UBV photometry of the irregular galaxies NGC 5363 and NGC 5360 09 p1146 A73-22548
- Precision spectropolarimetry of starlight - Development of a wide-band version of the Dollfus polarization modulator. 09 p1084 A73-22866
- Lunar eclipses in astronomical history, discussing deviations from geometrical theory, earth atmospheric effects, photometric observations, lunar luminescence, etc 10 p1282 A73-24643
- Russian book - Physics of stars and nebulae. 11 p1416 A73-25226
- Photometric characteristics and structure of nebulae NGC 6914a, IC 5076, and Ced 201 11 p1416 A73-25228
- A BESM-3M computer program for processing photographic observations of extended objects 11 p1333 A73-25231
- Two-color electrophotometry of RW in the Northern Crown 11 p1416 A73-25233
- Photometric error of the NA-MK-25 camera field 11 p1361 A73-25250
- Photoelectric observations of the close binary system SZ Camelopardalis. 11 p1425 A73-26266
- UBV photometry of 32 Cygni during the 1971 eclipse. 11 p1426 A73-26268
- Spectral types and UBV photometry of G-K giants at the North Galactic Pole. 11 p1429 A73-26678
- Multicolor photoelectric photometry of Neptune. 11 p1429 A73-26682
- Optical scattering properties of Saturn's ring. 11 p1429 A73-26683
- Photometric characteristics of the star AC Hercules 12 p1537 A73-26851
- Two-color electrophotometric observations of the BD Dra variable 12 p1537 A73-26852
- Optical variability of the nuclei of Seyfert galaxies. 12 p1539 A73-27278
- Photometric plane and spherical characteristics of spiral galaxies from statistical analysis of SQ, S and Irr morphological profiles 12 p1539 A73-27286
- Determination of the characteristics of light-scattering particles in the atmosphere of Venus from photometric measurements. 12 p1543 A73-27640
- Detection of a temporary ozone content decrease in the upper atmosphere at the moment of sunrise 13 p1605 A73-28074
- Photometric investigation of the atmospheric activity of Jupiter during 1962-1969 13 p1673 A73-28297
- Cometary observations and variations in cometary brightness. 14 p1789 A73-29778
- Photometric and spectral observations of Churyumov-Gerasimenko short period comet 1969 IV by fast telescopes, correlating nuclear magnitude with sun-spot area 14 p1789 A73-29781
- Comet nuclei gas liberation, perihelion mass loss and photometric property dependence on water ice evaporation rate and nongravitational effects 14 p1792 A73-29815
- Temperatures of Saturn's rings. 14 p1797 A73-30010
- Surface photometry of galaxies - Comparison of the luminosity profiles and photometric parameters of southern galaxies measured at Cordoba and Mount Stromlo. 14 p1801 A73-30644
- High-speed UBV photometry of Scorpius X-1 flares. 14 p1801 A73-30646
- A photometric study of the integrated light of clusters in the Magellanic Clouds and the Fornax dwarf galaxy. 14 p1801 A73-30726
- Determination of the radius of a cometary nucleus from photometric data 15 p1928 A73-31024
- Monochromatic phase curves and albedos for the lunar disk. 15 p1932 A73-31271
- Photoelectric photometric investigation of brightness behavior of Orion nebula variable stars 15 p1934 A73-31422
- Techniques and results of observations of rapid and ultrarapid variable stars. 15 p1935 A73-31481
- Photometry and some characteristics of spiral Seyfert galaxies beyond the nucleus boundary 15 p1938 A73-31951
- Automatic stellar electrophotometer with photon counting 15 p1878 A73-32136
- High speed photoelectric photometer for night sky scanning 15 p1878 A73-32137
- Equipment for infrared photometric and polarimetric observations 15 p1878 A73-32138
- A three-channel reversible data converter and its possible applications in astronomy 15 p1878 A73-32146
- Multicolor photometry of five SBC galaxies: NGC 925, NGC 1073, NGC 3359, NGC 4088, and NGC 7741 16 p2058 A73-32713
- Optimum astronomical photoelectric photometry - Terrestrial operations in the UV-IR band up to 1 micron wavelength. 16 p2011 A73-32929
- Astronomical educational aids design and application, including photometers for star cluster detection, ocular comparators and projection devices for photograph examination 16 p2014 A73-32950
- Photometric investigation of star magnitude and color index data in Palomar Atlas and Washington Star Catalog, obtaining calibration curves and average error calculations 16 p2063 A73-33659

Structure of the nucleus of the open cluster NGC 1245

16 p2063 A73-33660

Electrophotometric equipment in the Stara Zagora Observatory

16 p2016 A73-33663

New determinations of the diameters of planets and satellites

16 p2066 A73-33792

Spectrophotometry of individual regions of Venus

16 p2068 A73-33814

Statistical brightness distributions for photometric planetary image improvement, considering telescope resolution, diaphragm diffraction and atmospheric turbulence

16 p2069 A73-33832

Photometric studies of the Jovian atmospheric activity

16 p2070 A73-33841

Saturn ring thickness according to 1966 observation data of the Pic-du-Midi Observatory

16 p2070 A73-33845

A portable millisecond-integration-time photoelectric photometer.

17 p2165 A73-34273

The use of television type sensors in astronomy.

17 p2169 A73-35278

The University College London image photon counting system - Performance and observing configuration.

17 p2169 A73-35279

Application of the SIT vidicon to astronomical measurements.

17 p2169 A73-35285

Astronomical observations with an SEC vidicon system.

17 p2233 A73-35289

Preliminary results obtained with astrophotometer installed on Lunokhod II.

18 p2315 A73-35992

A photometric study of the counterglow from space.

18 p2351 A73-36182

Photometric variability of counterglow radiance as evidence for dust cloud presence in earth-moon system region

18 p2351 A73-36183

Contrast measurement data of Martian maria in July-August, 1971.

18 p2355 A73-36863

Spectrophotometry of the 7250-A methane absorption band over the disk of Jupiter.

18 p2355 A73-36864

On the nature of the infrared point source in the Orion Nebula.

18 p2356 A73-36975

Cygnids and Taurids - Two classes of infrared objects.

18 p2357 A73-37111

An adaptation of the Stromgren four-color system to photographic photometry.

19 p2430 A73-37568

Narrow-band photometry of the Galilean satellites.

19 p2483 A73-37577

Application of a photoelectric area scanner to various astronomical problems

19 p2430 A73-37605

The redshift-distance relation. V - Galaxy colors as functions of galactic latitude and redshift - Observed colors compared with predicted distributions for various world models.

19 p2487 A73-38504

The redshift-distance relation. VI - The Hubble diagram from S20 photometry for rich clusters and sparse groups - A study of residuals.

19 p2487 A73-38505

The redshift-distance relation. VII - Absolute magnitudes of the first three ranked cluster galaxies as functions of cluster richness and Bautz-Morgan cluster type - The effect on q sub 0.

19 p2487 A73-38506

Ground based photometry of planets, stars and galactic nebulae at 34 microns

19 p2489 A73-38529

The equipment for photoelectric photometry in the Graz observatory

20 p2565 A73-39068

Minor planets and related objects. IX - Photometry and polarimetry of /1685/ Toro.

20 p2607 A73-39119

Minor planets and related objects. XI - 0.4-0.8 micron spectrophotometry of /1685/ Toro.

20 p2607 A73-39121

Solar eclipse of July 10, 1972 - Comparison of photographic-photometry and K-coronometer measurement data

20 p2611 A73-39589

Narrow-band photoelectric observations of the Wolf-Rayet type eclipsing binary star V444 Cyg in the continuum /4244 - 7512A/

21 p2768 A73-40717

Jupiter satellite Europa polar cap from photoelectric observation of occultations by satellite Io

21 p2687 A73-41077

Photometric studies of atmospheric activity of Jupiter during 1962-1969.

21 p2779 A73-41541

Optical studies of Uhuru sources. VI - Photoelectric photometry of HD 153919 = 2U 1700-37.

22 p2905 A73-41766

Design and test of a photometer with nine wavelength bands for the measurement of astronomical objects

22 p2852 A73-41784

Energy distribution in stellar spectra of various spectral types and luminosities

22 p2906 A73-41974

Luminosity and velocity distribution of high-luminosity stars near the sun. II - The young disk giants.

22 p2909 A73-42585

French monograph - Preliminary photometric study in the far ultraviolet of the zodiacal and galactic emission.

22 p2910 A73-42716

French eclipse studies.

22 p2911 A73-42870

The wavelength dependence of the albedos of Uranus and Neptune from 0.3 to 1.1 micron.

22 p2914 A73-43014

Variation of the colour index along the meteor trail.

22 p2915 A73-43042

Wolf-Rayet stars effective temperature estimation from UVB photometry of surrounding ring nebulae with optically thick H II region excited by stellar Lyman radiation

23 p3025 A73-43195

The problem of the apparent-flattening characteristic of spiral galaxies

23 p3035 A73-44234

Normal galaxy central region dust content /mass/ estimates based on photoelectric measurements

23 p3035 A73-44235

The Saturn rings in 1969: Morphological and photometric study. I - Photograph acquisition and evaluation

24 p3128 A73-44434

The Saturn rings in 1969: Morphological and photometric study. II - Deconvolution of the raw photometric curves

24 p3128 A73-44435

Disk integrated polarization observation for Titan at small phase angles, noting optically thin Rayleigh atmosphere on opaque cloud deck

24 p3130 A73-44451

Area-scanning photometric observations of Galilean satellite surface color variations due to orbital phase and Jupiter environment

24 p3130 A73-44455

Photometry and some features of Seyfert spiral galaxies beyond the nuclear region.

24 p3131 A73-44476

Photoelectric and visual observation of the total eclipse of the moon of August 6, 1971.

24 p3134 A73-44568

ASTRONOMICAL SPECTROSCOPY

Book - Astrometry - Theoretical astrophysics instrumentation - Spectroscopy - Galactic structure - Galaxies.

01 p0095 A73-10293

Spiral structure and kinematics of the galaxy from a study of the H II regions - Fabry-Perot interference methods applied to ionized hydrogen.

01 p0096 A73-10297

Astronomical telescope research programs, emphasizing spectrographic instrumentation to detect and record extragalactic light sources spectra

01 p0046 A73-10502

Luminosity and efficiency of spectrographs with a slit

01 p0046 A73-10508

Echelle spectrographs design, applications and performance, discussing modified Czerny-Turner mounting and Schmidt camera arrangements

01 p0046 A73-10510

Schmidt and Maksutov spectrographic cameras, discussing correcting devices for mirror aberrations

01 p0047 A73-10512

Holographic gratings application to astronomical spectrograph design for IR to extreme UV and X rays, considering characteristics advantage

01 p0047 A73-10519

Stellar spectroscopy with holographic gratings.

01 p0047 A73-10520

The coude spectrograph and echelle scanner of the 2.7 m telescope at McDonald Observatory.

01 p0048 A73-10525

The coude of the 1.2 meter telescope at Victoria.

01 p0048 A73-10527

Secondary electron conduction /SEC/ vidicon television system for space astronomy, discussing data reduction requirements, costs and quasar spectrum observation

01 p0048 A73-10530

High resolution apparatus at the focus of large telescopes

01 p0049 A73-10532

Design features and observational feasibility of high resolution Michelson interferometer for use in visible spectral range at coude focus of astronomical telescope

01 p0049 A73-10533

The image tube nebular spectrograph of the Asiago Observatory.

01 p0050 A73-10543

The spectrum of the compact galaxy III Zw 43.

01 p0098 A73-10557

Preliminary results of the third flight of the Soviet stratospheric solar observatory.

02 p0216 A73-12335

High angular resolution observations from rockets - Solar XUV observations.

02 p0216 A73-12336

The data-handling problem with television recording of spectra.

02 p0170 A73-12340

Earth based and spaceborne stellar interferometer with optical balanced mixer system for coherent detection, discussing principles, construction, SNR and sensitivity

02 p0170 A73-12341

Apollo 16 ultraviolet astronomy observations.

02 p0220 A73-12475

A 1.1 micron spectrogram of the central coma of Comet Bennett /1969 i/.

02 p0226 A73-12832

Measurement of radial velocities with coude spectrograph of the 152-cm telescope of the Haute Provence Observatory

03 p0371 A73-13223

Alpha Lyra and beta Cen spectrograms from Merseisen system telescope aboard Salyut space station, demonstrating viability of space observatories

03 p0375 A73-13953

Spectroscopic techniques in X-ray astronomy.

03 p0375 A73-13961

I Zw 1727 +50 energy distribution relationship to lacertid spectra, noting featureless optical spectrum, flat or inverted radio spectrum and fast irregular variations

03 p0380 A73-14636

Comet spectra and excitation mechanism for spectrum production, discussing structural subdivision into nucleus, coma and tail

04 p0494 A73-14760

The compact central region of the galaxy NGC 1614.

04 p0499 A73-15356

Interstellar molecules detection, sources and destruction observed via visible, UV and radio wave spectra

04 p0501 A73-15627

Spectroscopic observations of HZ Herculis.

04 p0501 A73-15684

NGC 2992 and the blue stellar object Weedman No. 2.

04 p0502 A73-15690

Spectrophotometric survey of diffuse galactic nebulae

05 p0617 A73-16463

Spectroscopic observations of HZ Herculis and a model for Hercules X-1.

05 p0625 A73-17344

Absorption lines in the spectrum of the quasar Ton 1530.

05 p0626 A73-17377

The radio continuum of the Large Magellanic Cloud. IV - Spectra of sources.

06 p0754 A73-18632

Long-term variations of total and polarized fluxes, absolute energy distribution, and line strength of BL Lacertae and four quasi-stellar sources.

07 p0873 A73-19051

Extremely compact galaxy CGCG 1439 + 5344.

07 p0877 A73-19601

Spectroscopic observations of the optical candidate for Cygnus X-1.

08 p1004 A73-20896

Astronomical spectroscopy with prism in front of Schmidt correcting plate, considering spectral resolution and light loss characteristics in plate field

08 p0966 A73-21359

Digicon multichannel image tube photoelectron counter for astronomical spectroscopy, discussing design information density and accuracy, noise and quantum efficiency

08 p0971 A73-21747

Image tube spectra of planetary nebulae for relative line intensities and radial velocities, considering nebulae properties

09 p1141 A73-22015

Ground based radar measurement of Martian topography, surface temperature and thermal properties by microwave and IR radiometry and spectral reflectivity observation

09 p1144 A73-22259

Ground based spectroscopic observation of carbon dioxide distribution on Mars surface, noting Tharsis region pressure anomaly, ridge slope and dust storm activity

09 p1144 A73-22262

Polarization of continuous-spectrum emission in the Larger Orion Nebula

11 p1416 A73-25227

Spectroscopy of Jupiter - 3200 to 11,200 A.

11 p1418 A73-25720

Saturn ring spectral reflectivity at 0.36-1.06 microns, noting maximum at both ends of spectral range for amplitude of opposition effect

11 p1424 A73-26126

Asteroidal spectral reflectivity measurement with data reduction for various curve types, noting correlations with UVB color, orbital and physical property parameters and albedo

11 p1429 A73-26686

Large sunspot high dispersion line spectrum at 6610-6770 Å, noting umbral/photospheric contrast and drift curves across limb from photographic recording

12 p1547 A73-27925

Venus atmospheric model based on spectroscopic evidence of carbon dioxide spectral lines phase variation due to two scattering layers

13 p1680 A73-28459

Photometry of field horizontal-branch stars.

13 p1682 A73-28986

Photometric and spectral observations of Churyumov-Gerasimenko short period comet 1969 IV by fast telescopes, correlating nuclear magnitude with sunspot area

14 p1789 A73-29781

Spectracon camera for astronomical telescope prime focus operation, discussing image tube extended area photocathode and mica window

14 p1751 A73-29906

Device for spectral line interspace measurements

15 p1878 A73-32145

HTS spectrometer for airborne infrared astronomy.

15 p1880 A73-32379

Interstellar microwave radiation measured by spectroscopic analysis of chemical composition, distribution, excitation and emission data

16 p2058 A73-32722

Scanning IR spectrometer combination with optical telescope for 0.8-2.2 microns reflected IR light measurement during full moon phases in lunar surface composition determination

16 p2064 A73-33763

Investigation of molecular absorption features in the spectrum of Jupiter

16 p2070 A73-33839

Astronomical observations with television-type sensors; Proceedings of the Symposium, University of British Columbia, Vancouver, Canada, May 15-17, 1973.

17 p2168 A73-35276

Optical and UV astronomical telescopes and instrumentation for quasar detection, emphasizing observational requirements and emission line red shift problem

17 p2233 A73-35277

Digital pulse counting astronomical spectrograph system with TV camera tube, image intensifier and minicomputer for camera scan control and video data processing

17 p2169 A73-35282

A rapid-scanning image intensifier spectrometer for astronomy.

17 p2169 A73-35286

Experimental use of self-scanned photodiode arrays in astronomy.

17 p2169 A73-35287

Television sensors for ultraviolet space astronomy.

17 p2170 A73-35292

A technique for measuring small displacements in digital spectra.

17 p2170 A73-35297

Elemental abundance determinations for meteors by spectroscopy.

18 p2352 A73-36287

Arizona-NASA Atlas of the Infrared Solar Spectrum. X.

19 p2483 A73-37576

Bragg spectroscopy of Scorpius X-1 in search of the Fe XXV emission lines.

19 p2485 A73-37627

Comet 1969 g emission spectrum observation with 200-inch telescope, obtaining isotope ratio C-12/C-13

20 p2609 A73-39432

Coude spectroscopy for quasar Markarian 132 absorption lines wavelengths and profiles and red shift systems

20 p2609 A73-39436

A mechanically scanned interferometer-echelle spectrometer for the middle ultraviolet.

21 p2692 A73-39924

X-ray studies of the Crab nebula occultations, 1974-75.

21 p2765 A73-40300

Observation of solar submillimeter-band emission at sea level with the aid of a Fourier spectrometer

21 p2760 A73-40731

Mariner Mars 1969 infrared spectrometer - Gas delivery system and Joule-Thomson cryostat.

21 p2702 A73-41101

A 21-cm radio spectrograph

21 p2705 A73-41462

Titan narrow band observations at 8-13 microns, noting temperature inversion and spectroscopically active component

22 p2905 A73-41770

Observation of the Raman effect in the spectrum of Uranus.

22 p2916 A73-43126

Line identifications, elemental abundances, and equivalent widths for 21 sharp-lined cool peculiar A stars and two comparison standards.

23 p3028 A73-43491

Differentiated true abundance Mars air mass calculations for use in spectroscopic observation

24 p3131 A73-44465

ASTRONOMICAL TELESCOPES

NT APOLLO TELESCOPE MOUNT

NT HELIOMETERS

NT PYROHELIOMETERS

NT SPECTROSCOPIC TELESCOPES

NT STRATOSCOPE TELESCOPES

NT X RAY TELESCOPES

Conference on Auxiliary Instrumentation for Large Telescopes, 2nd, Geneva, Switzerland, May 2-5, 1972, Proceedings.

01 p0046 A73-10501

Astronomical telescope research programs, emphasizing spectrographic instrumentation to detect and record extragalactic light sources spectra

01 p0046 A73-10502

Auxiliary instruments for 4-m reflectors related to astronomical telescope focal positions, discussing correlators, cameras, sensitometers, film, rotator-adaptor, guider, echelle spectrograph and photometers

01 p0046 A73-10504

Instrumentation and some principal programs of the McDonald Observatory 2.75-meter /107-inch/ reflector.

01 p0046 A73-10505

Basic instrumentation components for prime, Cassegrain and coude focal positions of Anglo-Australian telescope, discussing acquisition and guiding, photography, photometry and spectrography

01 p0046 A73-10506

Telescopes for northern and southern hemisphere astronomical observatories, discussing auxiliary instrumentation and construction state on Calar Alto mountain

01 p0046 A73-10507

Luminosity and efficiency of spectrographs with a slit

01 p0046 A73-10508

Intermediate dispersion spectrograph instrument design for Cassegrain focus of Anglo-Australian telescope, discussing optical and mechanical layouts and remote control

01 p0046 A73-10509

Prototype design of echelle grating spectrographs for Anglo-Australian 3.8 meter telescope Cassegrain focus, presenting main parameters

01 p0047 A73-10511

A computer-controlled digital spectrum scanner for La Silla.

01 p0047 A73-10515

Some features of the Leiden radial velocity instrument.

01 p0047 A73-10516

Spectrographic equipment of the coude focus of the 3.60-meter telescope - Feasibility study of a universal spectrograph

01 p0048 A73-10522

Design study of the coude spectrographs for the 2.2-m telescopes of the MPI for astronomy.

01 p0048 A73-10524

The coude spectrograph and echelle scanner of the 2.7 m telescope at McDonald Observatory.

01 p0048 A73-10525

Fast spectrograph and image slicers for avoidance of light transmission loss caused by central obscuration in astronomical telescope and image intensifier tubes

01 p0048 A73-10526

The coude of the 1.2 meter telescope at Victoria.

01 p0048 A73-10527

Design features and observational feasibility of high resolution Michelson interferometer for use in visible spectral range at coude focus of astronomical telescope

01 p0049 A73-10533

Long slit spectrographs /Focal reducers - Fabry-Perot spectrographs - Array spectrographs/

01 p0049 A73-10535

Diffraction limited astronomical telescope resolution retrieval by speckle interferometer, noting information extraction via Fourier analysis

01 p0049 A73-10536

Electronography application to telescope and auxiliary instrumentation designs for astronomical photometry, considering spectracon and suitable image tubes

01 p0049 A73-10537

Photographic equipment for astronomical telescopes, considering mechanical devices for plate translation and rotation, guiding microscope and digitally controlled servomotors with incremental feedback

01 p0049 A73-10541

Astronomical position detector with image dissector tube at Cassegrain telescope focus for automatic guiding by illumination distribution analysis

01 p0029 A73-10544

Support method and equipment for observer at Cassegrain focus of large telescopes, emphasizing universal chair structural details and operation principles

01 p0029 A73-10545

A proposed standard mechanical interface for Cassegrain acquisition-guider heads.

01 p0029 A73-10546

Minicomputer based CAMAC modular system for astronomical telescope instrumentation, discussing hardware and software interfaces, squad scaler, photoelectric photometer, Michelson interferometer and multichannel spectrometers

01 p0019 A73-10547

Astronomical seeing and microthermal fluctuations of the atmosphere

01 p0050 A73-10562

The lunar regolith as a site for an astronomical observatory.

01 p0105 A73-11204

Astronomical observatory lunar ranging system with high radiance neodymium-glass laser and transmitting telescope, noting tracking accuracy

02 p0151 A73-12246

The laser telemetry station of the Pic-du-Midi Observatory and the acquisition of the French retroreflectors of Luna 17

02 p0151 A73-12247

Determination of directional corrections and the time required for passage through the meridian on the basis of 'pivot irregularities' obtained with the aid of 'pivot deviations'

03 p0307 A73-13244

The Large Space Telescope program.

03 p0382 A73-13550

General analysis of aplanatic Cassegrain, Gregorian, and Schwarzschild telescopes.

03 p0309 A73-14426

Image quality in telescopes with image motion compensation by secondary mirror control.

03 p0309 A73-14429

Mutual compensation of the unloading-force errors in the axial- and lateral-unloading systems of an astronomical mirror

05 p0575 A73-16317

Stress distribution on astronomical telescope mirror outer surface, calculating deflection and relief load

06 p0693 A73-18157

Cost effectiveness and observation speed of small astronomical telescopes array with TV detection systems

06 p0693 A73-18240

Coupling function for the vertical moon telescope at 60-meters-water-equivalent depth.

07 p0869 A73-19251

Matter heating based IR astronomy, describing liquid helium cooled Ge bolometer and IR telescope

07 p0875 A73-19324

Conference on the Role of Schmidt Telescopes in Astronomy, Hamburg, West Germany, March 21-23, 1972, Proceedings.

08 p0966 A73-21354

The role of Schmidt telescopes in the study of galactic structure [Photometric methods/.

08 p1011 A73-21355

Astrometry with Schmidt telescopes, discussing automated computerized plate scanner and measuring machine for star position and relative motion determination

08 p0966 A73-21356

Computational solution for positions on whole Schmidt-plates - Report on reduction of coordinates measured on 22 plates of the Bergeudorf Schmidt telescope.

08 p0966 A73-21357

Schmidt telescopes application in astrometry, noting image quality uniformity across total field of view

08 p0966 A73-21358

Schmidt telescopes for quasars and blue stars radio astronomy in southern sky survey, considering UV filtering-out for image quality improvement

08 p1011 A73-21362

Surface colour photometry of galaxies with Schmidt telescopes.

08 p1011 A73-21363

Schmidt telescopes in stellar photography of Magellanic clouds, galactic center and Scorpio-Centaurus and globular clusters for southern hemisphere Milky Way structure investigation

08 p1011 A73-21364

Schmidt telescopes for northern and southern hemispheres, discussing optical design with achromatic corrector to achieve high angular resolution and conversion to Cassegrain configuration

08 p0966 A73-21366

Ten years of research with the 134 cm Schmidt telescope.

08 p0966 A73-21367

Considerations about far infrared detectors for astronomical purposes.

08 p0967 A73-21421

Load and support configurations associated with aspherical dioptr of revolution with variable thickness profile generating dioptrers deformed by elasticity

08 p0967 A73-21492

Instrumentation in astronomy; Proceedings of the Seminar-in-Depth, Tucson, Ariz., March 13-15, 1972.

08 p0969 A73-21726

System considerations for a large astronomical space telescope.

08 p0969 A73-21728

Multiple mirror telescope consisting of six Cassegrainian telescopes combined for common focal surface, noting light gathering power equivalent to 180 inch standard telescope

08 p0970 A73-21738

A study of optical image sensors for the large space telescope.

08 p0971 A73-21742

Image integration and display system for guiding on stars beyond the visual detection limit.

08 p0987 A73-21748

Balloon-borne telescope-UV spectrometer for stellar spectrophotometric measurement with high spectral resolution, discussing system design and operation, image motion compensation and data acquisition

08 p0971 A73-21751

Simultaneous design of 24 inch telescope and computer control system, discussing interface and software development

08 p0942 A73-21754

CAMAC - A proposed standard for astronomical instrumentation.

08 p0972 A73-21755

The Coude spectrum scanner at the Lowell Observatory.

11 p1360 A73-25069

Optical system and performance potential of telescopic high-aperture-ratio Schmidt camera designed for photographic studies of faint extended objects

11 p1361 A73-25230

Airborne IR 32 cm observatory, discussing atmospheric transmission and guiding methods to overcome aircraft instability effects

11 p1368 A73-26503

Balloon-borne Newtonian telescope with parabolic pyrex primary mirror for far IR observation of celestial sources

11 p1368 A73-26504

An infrared photometer for the balloon-borne telescope Thisbe.

11 p1368 A73-26505

Problems and design of black-body references.

11 p1401 A73-26514

Radio astronomy telescope all sky survey procedure and data acquisition systems development for use with parametric amplifiers

12 p1544 A73-27781

Scintillation and vibration of stars and structure of a turbulent atmosphere.

13 p1680 A73-28514

Distribution law of light-ray direction fluctuations in telescopes

13 p1618 A73-29098

Effects of polarization on the transmission of coude-spectrometer systems.

13 p1621 A73-29351

The 2.2-m telescope of the Max-Planck Institute for Astronomy

14 p1743 A73-30273

Telescope equipment for future astronomical observatory, favoring array of computerized electronic imaging small telescopes vs single large reflector

14 p1754 A73-30916

Astronomical telescopes operational efficiency relation to atmospheric optics conditions at various Middle Asian elevated sites

15 p1934 A73-31423

Calibration of turbulence and visual and photographic scintillation parameters in Pulkovo, Tashkent and Shternberg Institute astrolimate systems for 50 inch reflector

15 p1934 A73-31425

Electrophotometer control system for the AZT-24 telescope

15 p1877 A73-32131

Angle to digital photoelectric converter for azimuthal telescope, discussing accuracy and temperature effects

15 p1877 A73-32132

Astronomic follow-up systems with mismatch signal buildup

15 p1877 A73-32134

Television in the control system of an optical telescope

15 p1877 A73-32135

Computerized Ritchey-Chretien computation method for telescopic optical system, controlling mirror shape via transparent screen

16 p2011 A73-32715

Atmospheric turbulence vs residual surface inaccuracy refracting and reflecting telescopic image degradation for solar observations

16 p2014 A73-32969

Venus and Jupiter telescopic observation aiming errors using Wanschaff verticle circle, suggesting error sources and correction procedures

17 p2230 A73-34593

Optical and UV astronomical telescopes and instrumentation for quasr detection, emphasizing observational requirements and emission line red shift problem

17 p2233 A73-35277

Astronomical observations with an SEC vidicon system.

17 p2233 A73-35289

The optical design of the 40-in. telescope and of the Irene Dupont telescope at Las Campanas Observatory, Chile.

17 p2171 A73-35408

Geometric factor optimization for a telescope performing charged-particle recording in space

18 p2315 A73-36115

The Lunar and Planetary Laboratory and its telescopes.

19 p2417 A73-37580

Russian book on lunar study by telescopes and unmanned and manned spacecraft covering Luna Zond and Lunokhod probes, Apollo flights, topography, structure and magnetic field

19 p2485 A73-37770

A precision control system for a large astronomical telescope.

19 p2430 A73-38079

Large telescope design, discussing optical telescope efficiency as function of aperture, exposure time auxiliary instrumental parameters

21 p2703 A73-41245

Astrophysical problems to be solved with the RATAN-600 radio telescope

21 p2776 A73-41465

Extragalactic radio sources identification with galaxies and quasars by high sensitivity and resolution astronomical telescopes, obtaining angular structure maps and radio spectra

23 p3028 A73-43347

Television guidance for astronomical telescopes

23 p2984 A73-44362

Beam characteristics of the 300-ft telescope.

24 p3066 A73-44580

A method for accurately compensating for the effects of the error beam of the NRAO 300-ft radio telescope at 21-cm wavelength.

24 p3067 A73-44581

Elastomechanical model measurements conducted with the aid of holographic approaches in the case of a mirror cell

24 p3090 A73-44897

ASTRONOMY

NT INFRARED ASTRONOMY

NT RADAR ASTRONOMY

NT RADIO ASTRONOMY

NT SPACEBORNE ASTRONOMY

NT X RAY ASTRONOMY

Book - Annual review of astronomy and astrophysics.

01 p0094 A73-10051

Gravitational waves astrophysical nature and origin, discussing current theories and possible applications in astronomy

01 p0094 A73-10063

Astronomical determination of pole motions by procedures employed at international latitude stations

02 p0155 A73-11650

Book - The emerging universe: Essays on contemporary astronomy.

05 p0613 A73-16301

Russian book - Problems of galactic and extragalactic astronomy.

05 p0616 A73-16451

Past and future of research methods in problems of the earth's rotation.

13 p1677 A73-28377

The use of the electronic computer for the urgent publication of astronomical material.

14 p1730 A73-29791

Book - Vistas in astronomy. Volume 13.

15 p1932 A73-31302

Akademiia Nauk SSSR, Astronomicheskii Sovet, Meeting of the Commission on Astronomical Instrument Engineering, Sverdlovsk, USSR, July 1-3, 1970, Proceedings

15 p1877 A73-32128

Book - Space physics and space astronomy.

17 p2230 A73-34575

Astronomical optics, including two mirror systems, aspherical plates, lens type field correctors, spectrograph cameras, focal reducers and optical adjustments

17 p2171 A73-35407

ASTROPHYSICS

NT SOLAR PHYSICS

Book - Annual review of astronomy and astrophysics.

01 p0094 A73-10051

Gravitational waves astrophysical nature and origin, discussing current theories and possible applications in astronomy

01 p0094 A73-10063

Book - Astrometry - Theoretical astrophysics instrumentation - Spectroscopy - Galactic structure - Galaxies.

01 p0095 A73-10293

Physical significance of interstellar matter accretion on rotating magnetized star with emphasis on implications for X ray sources

04 p0493 A73-15979

Book - The emerging universe: Essays on contemporary astronomy.

05 p0613 A73-16301

High energy /X ray, gamma ray and cosmic ray/ astronomy research impact on astrophysical and cosmological models

[AIAA PAPER 73-197] 05 p0610 A73-16932

Gravitational contraction and energy dissipation and compensation in stellar nuclear reactions, noting He thermonuclear reactions and nucleosynthesis

06 p0751 A73-18158

Book - Advances in astronomy and astrophysics. Volume 9.

10 p1282 A73-24641

High energy astrophysics research at the Max-Planck-Institut.

11 p1411 A73-25139

Russian book - Physics of stars and nebulae.

11 p1416 A73-25226

Report on the NATO Advanced Study Institute on magnetohydrodynamic phenomena in rotating fluids.

11 p1404 A73-25851

Atoms and molecules in astrophysics; Proceedings of the Twelfth Session of the Scottish Universities Summer School in Physics, University of Stirling, Stirling, Scotland, August 1971.

12 p1538 A73-26920

Book on variable stars, covering high energy astrophysics, low energy outbursts, extensive convection, galaxies, pulsations, white dwarfs, cepheids, flares and gravitational collapse

14 p1796 A73-29950

Cosmological theories historical review, discussing observational background for big bang, steady state and astrophysical theories based on theoretical physics

14 p1797 A73-30059

Kerr metric properties and astrophysical implications, presenting perfect fluid boundaries family in weak field approximation and photon orbits behavior in equatorial plane

14 p1798 A73-30143

Russian book - Plasma astrophysics.

15 p1936 A73-31579

Low cost two-beam multimode nebular/stellar photometer design, construction and use on extended and discrete objects emitting 3700-9000 A radiation

15 p1877 A73-32007

Evaluation of astrophysical hypotheses.

17 p2231 A73-34760

Book - General astrophysics with elements of geophysics.

18 p2356 A73-36968

Book - Atomic physics and astrophysics, Volume 2.

18 p2356 A73-36969

All-Union Conference on the Physics of Cosmic Rays, Apatity, USSR, December 12-15, 1972, Proceedings

21 p2755 A73-40576

Astrophysical problems to be solved with the RATAN-600 radio telescope

21 p2776 A73-41465

ASYMMETRY

Asymmetric principal stress bounds in terms of symmetric part of tensor, considering existence conditions and maximum shear and normal stresses

[ASME PAPER 72-APM-QQ] 05 p0633 A73-16535

Study of the influence of asymmetries on the flight behaviour of a sounding rocket.

[AIAA PAPER 73-283] 09 p1155 A73-23203

Sommerfeld type radiation conditions for asymmetric theory of linear homogeneous and isotropic micropolar elasticity, applying to regular solution to infinite domain field equations

11 p1444 A73-26279

Asymmetric missile subharmonic response to non-linear aerodynamic moments, considering spin and aerodynamic damping effects

15 p1943 A73-31667

ASYMPTOTES

Study of the asymptotic behavior of axial perturbation velocities in the vicinity of singularities

03 p0245 A73-13770

Oscillatory and asymptotic behavior of functional differential equations.

04 p0469 A73-14663

Asymptotic motion stability analysis with respect to part of variables, using Liapunov functions for solution boundedness conditions

07 p0850 A73-19012

Second order differential equations with complex-valued coefficients.

09 p1112 A73-22425

Asymptotic behavior of the eigenvalues of self-conjugate expansions of the Schroedinger operator in a multidimensional bounded domain

11 p1391 A73-26463

- Some aspects of the asymptotic behavior of solutions of nonlinear differential equations with delayed argument
14 p1768 A73-30345
- The asymptotic behavior of the first real eigenvalue of a second order elliptic operator with a small parameter in the highest derivatives.
14 p1769 A73-30457
- Eigenvalues asymptotic behavior in boundary value problems of infinitely expanding region of Euclidean space, applying results to continuous media stability investigation
15 p1860 A73-30964
- Special periodic solutions and asymptotic properties of a class of quasi-linear differential equations with delayed argument
20 p2583 A73-39509
- Quasi-periodic solutions existence, uniqueness and asymptotic behavior to quasi-linear parabolic equations, demonstrating vanishing conditions at boundary
23 p3049 A73-43611
- ### ASYMPTOTIC METHODS
- Application of the asymptotic method to third-order oscillatory systems
01 p0021 A73-10030
- A method of construction and the structure of asymptotic approximations of the solutions of nonlinear mixed boundary value problems in studies of multifrequency oscillation modes
01 p0076 A73-10097
- A comparison of geometrical theory of diffraction and integral equation formulation for analysis of reflector antennas.
01 p0022 A73-10179
- Validity of averaging methods for certain systems with periodic solutions.
01 p0070 A73-10273
- Modified convergence criterion for boundary layers.
01 p0033 A73-10750
- Asymptotic properties of solutions of certain linear systems of differential equations with random coefficients
01 p0070 A73-10913
- Analysis of the problem of the thermal propagation of a flame by the method of joining asymptotic expansions
01 p0123 A73-10958
- Asymptotic method of determining critical buckling loads for strictly convex shallow shells of revolution
01 p0116 A73-10963
- Asymptotic analysis of nonlinearly elastic and plastic thin rectilinear panels under combined bending and tensile stress
01 p0119 A73-11442
- Asymptotic estimates for solutions of linear systems of ordinary differential equations having multiple characteristic roots.
02 p0188 A73-12625
- Asymptotic analysis of premixed burning with large activation energy.
03 p0397 A73-13531
- Time-periodic fluid surface wave radiation and scattering by partially immersed objects in short wave asymptotic limit of nondimensional wavelength approaching zero
03 p0397 A73-13533
- Asymptotic solution for inviscid conducting fluid flow past arbitrary wing profile in magnetic field
03 p0347 A73-14045
- Interpolation theory over curved elements, with applications to finite element methods.
04 p0470 A73-15010
- On the uniformly valid approximate solutions of Laplace equation for an inviscid fluid flow past a three-dimensional thin body.
04 p0433 A73-15094 [ONERA, TP NO. 1145]
- Ellipsoidlike deformations of tubelike balloons - Asymptotic solution with boundary layer.
[ASME PAPER 72-WA/APM-29]
- 04 p0515 A73-15889
- Galerkin stress functions for non-local theories of elasticity.
05 p0631 A73-16123
- Information-loss and risk-increase estimation during observational data reduction in successive estimation problems
05 p0589 A73-16299
- Invariance principle extended to bounded uncertain time-varying systems, deriving asymptotic Liapunov stability criteria with application to guaranteed cost control problems
05 p0590 A73-16492
- Asymptotic analysis of turbulent channel and boundary-layer flow.
06 p0687 A73-18528
- A boundary layer method for the matrix Riccati equation.
06 p0719 A73-18864
- Asymptotic solution to the problem of optimal low-thrust energy increase.
07 p0899 A73-19962
- Matched asymptotic expansions method application to slender cylindrical beams, calculating displacement far field by Navier-Stokes elasticity equation
07 p0913 A73-20075
- Approximations for large deflection of a cantilever beam.
07 p0915 A73-20339
- An asymptotic analysis of radiant and hypergolic heterogeneous ignition of solid propellants.
07 p0866 A73-20364
- Asymptotic theory of the Boltzmann equation at large Knudsen number.
07 p0853 A73-20473
- The asymptotic behavior of solutions of second order systems of partial differential equations.
07 p0845 A73-20495
- A remark on the sloshing frequencies for a half-space.
08 p0953 A73-20788
- Some extremum principles for pipe flow in magneto-hydrodynamics.
08 p0993 A73-21403
- Composite approximations to the solutions of the Orr-Sommerfeld equation.
08 p0956 A73-21686
- The stationary-phase method for a double integral with an arbitrarily located stationary point
09 p1048 A73-21918
- Application of a singular perturbation method to the study of beginning cavitation
09 p1071 A73-22215
- Asymptotic scheme for a class of partial differential equations
09 p1112 A73-22477
- Asymptotic behavior of the distribution of the solution of a stochastic differential equation with coefficients depending on the entire history of the process
09 p1112 A73-22844
- Book - Methods of analysis and solutions of crack problems: Recent developments in fracture mechanics; Theory and methods of solving crack problems.
09 p1161 A73-23176
- Asymptotic approximation to crack problems with emphasis on stress intensity factor, discussing interpolation procedure based on simplified problem form
09 p1162 A73-23180
- 'Farfield' behavior of solutions to partial differential equations asymptotic expansions and maximal rates of decay along a ray.
10 p1241 A73-23700
- Radar filter asymptotic efficiency analysis for pass-band and impulse response duration increase, considering realization of approximate Urkowitz filter with controlled memory
10 p1194 A73-23737
- Asymptotic approximation of an infinitely thin, elastic, nonlinear cylinder by a curvilinear medium
10 p1288 A73-23765
- New criteria for bounded-input-bounded-output and asymptotic stability of nonlinear systems.
10 p1199 A73-24041
- The asymptotic behavior of the supersonic solutions of the two-fluid solar wind equations.
10 p1268 A73-24147
- Equations for nonlinear Benard convection with rotation for fluid layer, investigating asymptotic solution for two dimensional cells at large Rayleigh and Taylor numbers
11 p1448 A73-25052
- Asymptotic analysis of nonlinearly elastic and plastic thin rectilinear panels under combined bending and tensile stress
11 p1443 A73-26060
- Forced convection heat transfer in laminar boundary layer at low Prandtl numbers.
11 p1452 A73-26123
- Optimization problems with large parameters.
11 p1391 A73-26365
- Asymptotic analysis of the equations of oscillations and stability of bodies of revolution in the case of turning points
11 p1445 A73-26459
- Second order closed form asymptotic solution to Donnell type nonlinear equations of elastic homogeneous conical shells for displacement and stress resultants
11 p1447 A73-26650
- A note on the lift coefficient of a thin jet-flapped airfoil.
12 p1457 A73-27171
- Analysis of the problem of thermal flame propagation by the method of matched asymptotic expansions.
12 p1559 A73-27534
- Asymptotic method of determining the critical buckling loads of shallow strictly convex shells of revolution.
12 p1554 A73-27539
- Approximate method for solving dynamic problems in thermoviscoelasticity
13 p1690 A73-27993
- Singular perturbations for a nonlinear differential equation with a small parameter.
13 p1648 A73-28537
- A numerical method for highly accelerated laminar boundary-layer flows.
13 p1600 A73-28608
- Calculation of the low natural frequencies of clamped cylindrical shells by asymptotic methods.
13 p1696 A73-28752
- Transonic flow about lifting configurations.
13 p1564 A73-28828
- Asymptotic behavior of solutions of the Cauchy problem and the first boundary value problem on a half-axis for a linear second-order parabolic equation with the absolute value of x approaching infinity and at large values of the parameter
13 p1651 A73-29680
- Asymptotic solution of initial value problem for weakly nonlinear wave system including dispersive and diffusive effects related to plane Poiseuille flow instability
14 p1744 A73-30171
- Progress in nonlinear finite element analysis using asymptotic solution techniques.
14 p1808 A73-30191
- Boundary value problem of a system of ordinary differential equations with a complex parameter
14 p1768 A73-30346
- Asymptotic solutions for shells with general boundary curves.
14 p1812 A73-30523
- An upper bound for the singular parameter in a stable, singularly perturbed system.
14 p1770 A73-30592
- On asymptotic solutions of nonlinear differential equations with time lag.
14 p1770 A73-30759
- Asymptotic solution of a system of linear differential equations with slowly varying coefficients of the neutral type
15 p1898 A73-31036
- Asymptotic solution of the equations for a multicomponent laminar boundary layer in the case of high injection levels
15 p1822 A73-31292
- An asymptotically optimal rank detection algorithm for a signal in noise of unknown distribution
15 p1842 A73-31490
- An approximate method for the calculation of the velocities induced by a wing oscillating in subsonic flow
15 p1824 A73-31905
- Russian book - Asymptotic theory of diffraction of electromagnetic waves by finite structures.
15 p1845 A73-32294
- Book on perturbation methods covering parameter variation, strained coordinates, averaging, multiple scale and matched and composite asymptotic expansions
15 p1902 A73-32578
- The three-dimensional turbulent boundary layer - Theoretical and experimental analysis
16 p1961 A73-32810
- Analytic and computer solutions for Schwarzschild black hole geometry slicing into asymptotically flat and static maximal spacelike hypersurfaces
16 p2060 A73-33121
- Asymptotic integration method solution for three dimensional equations of geometrically nonlinear theory for thin shells and plates
16 p2080 A73-33243
- The solutions of the boundary layer equations in the case of extremely intensive blowing or suction
16 p1963 A73-33250
- Asymptotic expansions for product integration.
17 p2200 A73-34213
- Asymptotic characteristics of the problem involving intrinsic asymmetrical vibrations of circular conical shells
17 p2241 A73-34267
- Two-variable asymptotic solution to unsteady three dimensional turbulent flow equations describing small scale deformation, determining hot spot or macromolecular size statistical behavior
17 p2201 A73-34800
- Russian book - Asymptotic and qualitative methods in the theory of nonlinear oscillations.
17 p2211 A73-34850
- Asymptotic methods for the effectiveness computation of a sampling scheme of active sub-channels in an adaptive, multi-channel communication system.
17 p2129 A73-35712
- Estimates of unknown parameter from quantized observations given as sequence of evenly distributed random values, noting optimal grouping equations for general distribution function
17 p2130 A73-35722
- The asymptotic dispersion characteristics of the best unbiased linear estimate obtained by the uniform division of the observation interval for the unknown mathematical expectation of a stationary random process
18 p2329 A73-36162
- Book - Theory and design of shells on the basis of asymptotic analysis: A unifying approach to the variety of thick and thin elastic shell theories and problems.
18 p2367 A73-36967
- Approximate methods for analysis and synthesis of nonlinear systems
20 p2592 A73-38692
- Application of the averaging method to the study of oscillatory systems with distributed parameters and time lag
20 p2592 A73-38978

- Asymptotic behaviour of a scalar in an axisymmetric final period turbulent wake. 20 p2507 A73-39086
- Application of G. V. Rozenberg's asymptotic formulas in the interpretation of cloud brightness measurements 20 p2584 A73-39189
- Equilibrium point asymptotic stability for nonlinear generalization of Onsager theory for entropy functions construction with applications to chemical reaction kinetics 20 p2627 A73-39338
- Two-frequency unsteady forced oscillations of a beam 20 p2593 A73-39502
- Multiplicative rule failure in matched asymptotic expansion solutions for velocity distribution in steady incompressible flow of thin elliptic airfoils 20 p2550 A73-39814
- Linear wave motion analysis of viscous incompressible fluid of infinite depth at small and large times by asymptotic quadrature method 21 p2676 A73-40207
- Green function hydrodynamic asymptotic behavior obtained via closed inhomogeneous linear equations, discussing distribution function kinetic equation, correlation function spectral distribution and adiabatic conditions 21 p2677 A73-40636
- Asymptotic unsteady three dimensional flow analysis in axial turbine cascade theory, assuming infinite blade number and unity pitch/chord ratio [ONERA, TP NO. 1249] 22 p2796 A73-42220
- On an asymptotic property of the least-mean-square-error design criterion in pattern recognition. 22 p2835 A73-42274
- The asymptotic analysis of canonical problems in high-frequency scattering theory. I - Stratified media above a plane boundary. II - The circular and parabolic cylinders. 22 p2886 A73-42347
- Semiempirical time dependent climate models formulated for stability of asymptotic steady state equilibrium solutions to perturbations 22 p2883 A73-42540
- Asymptotic method for approximate elastodynamic plate theories derivation from elasticity equations with application to plate free extensional and forced flexural vibration frequency spectrum [ASME PAPER 73-APM-44] 22 p2926 A73-42900
- On an integral equation governing the reflection of electromagnetic waves by a random surface 22 p2888 A73-42948
- Asymptotic forms of solutions to nonrelativistic Compton Fokker-Planck equation for bremsstrahlung X ray spectra changes due to Compton scattering in emitting gas 22 p2904 A73-43018
- Monofrequent oscillations in mechanical systems governed by second order hyperbolic differential equations with small non-linearities. 23 p3044 A73-44077
- Asymptotic mean value method for differential equations solution under given Lipschitz condition generalized via Liapunov procedure elimination 23 p2999 A73-44079
- Asymptotic suction boundary layer profile past porous plane surface, obtaining upper and lower bounds on energy stability limit 23 p2969 A73-44381
- Asymptotic solutions of second-order linear homogeneous differential equations in a Banach space in the case of a higher derivative having a small parameter 24 p3105 A73-44603
- Concentration contours in regions with both normal and enhanced diffusion coefficients. 24 p3120 A73-45404
- Far-field analysis of nonlinear shock waves in a lattice. 24 p3112 A73-45412
- Aggregation scheme solution for uniform asymptotic stability of large dimensionality system, using L-problem moment theory 24 p3112 A73-45505
- ASYMPTOTIC SERIES**
- Proof for sigma algebra of asymptotic events represented as sequence of partial sums of series of independent and essentially divergent random variables 01 p0070 A73-10411
- Singular elliptic perturbations of vanishing first-order differential operators. 02 p0186 A73-11970
- Boundary value problems with a turning point. 03 p0336 A73-13066
- Application of the method of matched asymptotic expansions to calculate the steady-state thermal propagation of an exothermic reaction front in a condensed medium 09 p1167 A73-22616
- Approximate solution of the system of Boltzmann equations for a mixture of reacting gases 10 p1252 A73-24490
- Construction of asymptotic solutions to the Cauchy problem with an initial jump for nonlinear systems of integrodifferential equations containing a small parameter at the higher derivative 12 p1518 A73-27298
- Asymptotic analysis of the steady propagation of a successive two-stage exothermal reaction front in a condensed medium 13 p1707 A73-29166
- Asymptotic solution of a system of linear differential equations with slowly varying coefficients in a complex domain 15 p1898 A73-31028
- Short-wave asymptotics of the Green's function in the problem of diffraction at a plane layer 18 p2290 A73-36987
- Asymptotic expansion of random processes depending on a small parameter 20 p2582 A73-39387
- Asymptotic representation of the fundamental solution of an elliptic equation with a small parameter in the presence of a higher derivative 20 p2582 A73-39474
- Asymptotic properties of solutions to single-point and two-point problems with singular perturbations for systems of ordinary linear differential equations 22 p2882 A73-42473
- Navier-Stokes equation formulation in parabolic coordinates for flow in trailing vortex, obtaining asymptotic expansions for stream function and angular momentum 23 p2939 A73-43205
- ATAXIA**
- Effects of some antionion sickness drugs and secobarbital on postural equilibrium functions at sea level and at 12,000 feet/simulated/. 09 p1045 A73-22529
- ATHEROSCLEROSIS**
- U ARTERIOSCLEROSIS**
- ATHLETES**
- Comparative evaluation of the general and specific efficiencies of athletes under normal barometric pressure and in the process of training and acclimatization under highland conditions of Pamir 02 p0136 A73-11925
- Passive and active warm-up effects on track athletes heart and respiration rates 03 p0266 A73-13123
- Telemetry and ergometry associated to the measure of oxygen consumption during sports events. 03 p0270 A73-14285
- Telemetrical measurements during sport performance on sportsmen with cardiac arrhythmias. 03 p0271 A73-14294
- Visual after-images in athletes and coaches as a prestart condition index 06 p0658 A73-18161
- Effect of physical exercises on the lung rheogram 10 p1182 A73-24524
- ATHODYDS**
- U RAMJET ENGINES**
- ATLANTIC OCEAN**
- Some characteristics of the vertical structure of the humidity field over the North Atlantic. 18 p2334 A73-37076
- Distribution and diagenesis of organic compounds in JOIDES sediment from Gulf of Mexico and western Atlantic. 21 p2683 A73-40562
- Mapping of North Atlantic winds by HF radar sea backscatter interpretation. 22 p2882 A73-41836
- Motion of a tropical hurricane in the field of the North Atlantic trade wind 24 p3107 A73-44428
- ATLAS CENTAUR LAUNCH VEHICLE**
- Launch and orbital injection of Intelsat IV satellites. 09 p1152 A73-22699
- ATLAS LAUNCH VEHICLES**
- NT ATLAS CENTAUR LAUNCH VEHICLE**
- ATMOSPHERIC ABSORPTION**
- U ATMOSPHERIC ATTENUATION**
- ATMOSPHERIC ATTENUATION**
- NT AURORAL ABSORPTION**
- A comparison of precipitation attenuation and radar backscatter along earth-space paths. 01 p0015 A73-10183
- Atmospheric windows in different spectral bands due to various gases, comparing continuum and line absorption spectra properties 01 p0037 A73-10364
- Computer programs for realistic calculation of atmospheric absorption spectra, discussing spectroscopic data critical survey, procedures, coefficient generation and data presentation 01 p0037 A73-10368
- Electromagnetic wave transmission through 8-12 micron atmospheric window, investigating particulate matter effects on radiation energy extinction 01 p0037 A73-10372
- IR absorption and refraction index of atmospheric aerosol, using KBr disk transmittance and specular reflection measurements 01 p0038 A73-10373
- Theoretical calculation of light scattering and measurements with grating UV double monochromator for anomalous atmospheric transparency 01 p0039 A73-10402
- Atmospheric absorption and scattering as radiation extinction mechanisms, discussing attenuation coefficient wavelength and weather dependence 01 p0102 A73-10993
- The spectral characteristics of radiation extinction and the effects of the relative humidity on these characteristics 02 p0189 A73-12368
- Atmospheric water vapor absorption coefficient in 0.73 mm transmittance window as function of humidity from monochromatic RF radiation measurements 02 p0142 A73-12488
- The effects of ions of VLF and ELF propagation in an anisotropically ionized atmosphere. 02 p0143 A73-12851
- ATS-F COMSAT millimeter wave propagation experiment.** 04 p0418 A73-15386
- Absorption in the 220 GHz atmospheric window. 04 p0418 A73-15394
- Rain attenuation of vertically and horizontally polarized signals of 18 GHz communication system 04 p0419 A73-15395
- Equatorial region radio wave enhanced absorption by resonant coupling to electrojet irregularities and damped upper hybrid modes 04 p0423 A73-15548
- Atmospheric attenuation of noise measured in a range of climatic conditions. 05 p0570 A73-16966
- [AIAA PAPER 73-242]
- Propagation characteristics of collimated, pulsed laser beams through an absorbing atmosphere. 07 p0833 A73-19272
- Path diversity for mm-wave earth-to-satellite links. 07 p0791 A73-19376
- Ionospheric attenuation of 3-100 MHz radio waves, interpreting scatter mode propagation mechanism as total reflection from lower ionizational irregularities 07 p0792 A73-19458
- Twilight sounding method for earth upper atmosphere investigation, taking into account earth shadow and effective altitude of solar radiation attenuation/shielding/ zone 07 p0818 A73-19591
- Problem of the influence of absorption on the amplitude fluctuations of submillimeter radio waves in the atmosphere 07 p0793 A73-19922
- Unusually high earth-space path attenuations measured using a 6.4-GHz radiometer. 07 p0793 A73-20111
- Oxygen D line collisional quenching by atmospheric oxygen, nitrogen, carbon monoxide and dioxide, water vapor and ozone, determining absolute rate constants 07 p0788 A73-20239
- Submillimeter radio telescope employing an n-InSb detector 07 p0825 A73-20311
- Reflection and absorption of solar radiant energy by cloud layers. 07 p0820 A73-20344
- Measurements of absorbed short-wave energy in a tropical atmosphere. 08 p0958 A73-21267
- Effect of the shape and orientation of atmospheric dust particles on the spectral position and form of the attenuation band 09 p1077 A73-22372
- Observation of mesospheric ozone at low latitudes. 09 p1079 A73-22841
- Radiometer measurements of atmospheric attenuation at 19 and 37 GHz along sun-earth paths. 09 p1052 A73-22957
- Absorption of laser emission by He-CO₂ mixtures, CO₂ and NH₃ gases, and water vapors 10 p1227 A73-24074
- Broad band solar EUV absorption in the earth's upper atmosphere. 10 p1214 A73-24747
- Russian book - Scattering and absorption of light in the atmosphere. 11 p1392 A73-25602
- Use of the Fabry-Perot etalon to study absorption spectra of the atmosphere 11 p1363 A73-25613
- Investigations of atmospheric extinction using direct solar radiation measurements made with a multiple wavelength radiometer. 12 p1520 A73-26810
- Submillimeter radio telescope with an n-InSb detector. 12 p1497 A73-27283
- Factors affecting the frequency chosen for aircraft to satellite communications. 12 p1472 A73-27667
- Quiet sun millimeter wave emission and brightness temperature, discussing observational difficulties arising from fog, cloud and rain attenuation 12 p1543 A73-27725

Auroras induced attenuation fluctuations of VLF at-mospherics associated with remote tropical thun-derstorms

12 p1522 A73-27786
CO2 laser communication through an urban at-mosphere.

13 p1582 A73-28481
Attenuation of monochromatic light in bottom layer of atmosphere and some properties of aerosols.

13 p1653 A73-28518
Results of optical observations of dust in upper at-mosphere and interplanetary space.

13 p1680 A73-28520
Atmospheric effects in multispectral photographs.

13 p1619 A73-29239
Russian book - Scattering and attenuation of elec-tromagnetic radiation by atmospheric particles.

15 p1843 A73-31586
Integral transmittance function of thermal radiation

15 p1904 A73-31782
Radiation absorption in stellar atmospheres due to photoionization in magnetic field, discussing frequ-ency relation to propagation direction and Larmor frequency

15 p1872 A73-31955
Propagation of radio waves at frequencies above 10 GHz; Proceedings of the Conference, London, En-gland, April 10-13, 1973.

16 p1980 A73-33701
Rain attenuation and fade duration statistics for design of satellite-based communication system, pre-dicting outage for 16 GHz path diversity system

16 p1981 A73-33706
Atmospheric attenuation interrelations at 12 and 35 GHz with meteorological parameters derivation for homogeneous atmosphere, testing dynamic at-mospheric model

16 p1981 A73-33709
The respective influences of multi-path configura-tions and precipitation rates for frequencies lying between 10 GHz and 30 GHz.

16 p1981 A73-33710
The R.S.R.S. ground stations for receiving 11.6 GHz transmission from the SIRIO satellite.

16 p1982 A73-33717
Microwave radiometer measurement at 17 GHz to investigate atmospheric attenuation and radio noise and interference sources for optimal satellite com-munication systems design

16 p1982 A73-33718
Atmospheric attenuation measurement for nine mil-limeter wavelength signal from radio source, discussing solar power, radioisonde, emission tempera-ture and nodding solar methods

16 p1982 A73-33719
Zenith atmospheric emission noise temperature and attenuation measurements including multiple and single frequency statistical observations at 85-118 GHz during 1970-1971

16 p1982 A73-33720
Earth-space slant path radio attenuation measure-ments above 10 GHz over four year period, noting caution in use of long term statistics

16 p1982 A73-33721
Atmospheric attenuation measurements via solar microwave radiometer yielding excess attenuation statistics for communications systems planners

16 p1982 A73-33722
Linear cross-polarisation and attenuation measure-ments at 11 and 36 GHz.

16 p1982 A73-33723
Laboratory measurements of electromagnetic prop-erties of atmospheric gases at millimeter wavelengths.

16 p1983 A73-33731
Absorption of centimeter radio waves in the Venu-sian atmosphere

16 p2068 A73-33821
Analysis of radio-wave propagation in the Venusian atmosphere

16 p1984 A73-33822
Relationship between stratospheric warming and ionospheric absorption.

16 p2009 A73-33887
Atmospheric attenuation anomalies at 2.7 mm from sky noise temperature measurements compared with water vapor and oxygen line strength calculations

17 p2159 A73-34571
The atmospheric aerosol and its significance for the energy budget of the atmosphere

17 p2159 A73-34749
Atmospheric attenuation effects on nitric oxide dis-sociation in mesosphere and stratosphere, noting dis-sociation profile dependence on absorption of discrete oxygen Schumann-Runge bands

17 p2119 A73-34778
CO laser emission lines attenuation measurements in atmosphere, attributing inconsistencies in previous experiments to model

17 p2185 A73-35405
Photo-absorption of the upper atmosphere in the middle ultraviolet region.

18 p2308 A73-36050

Effect of aerosols on the transfer of solar energy through realistic model atmospheres. I - Non-absorb-ing aerosols.

18 p2333 A73-36704
On rainfall and space diversity for millimeter-wave earth-satellite communications systems.

18 p2289 A73-36709
Measurement of the attenuation of 9.303 MHz waves from ISIS-II through the ionosphere.

18 p2289 A73-36876
Correction procedure for outdoor noise measure-ments.

19 p2458 A73-37285
Effect of scattering on radiometer measurements of attenuation in rain.

19 p2403 A73-37426
A method of providing rain margins for 18/30 GHz communications satellites without increasing the solar power requirement.

20 p2524 A73-38731
B-2 installation for radio wave absorption measure-ments in the ionosphere at two frequencies simultane-ously by the /A1/ pulse method

20 p2566 A73-39165
Estimation of the absorptive capacity of atmospher-ic haze from the brightness of clouds

20 p2583 A73-39183
Solar brightness temperature measurement relative to lunar brightness temperature, noting agreement with HSRA model

20 p2610 A73-39582
Indices of backscattering and attenuation of light by a water aerosol

21 p2731 A73-40747
Russian book - The solar constant and the energy distribution in the solar spectrum.

21 p2769 A73-40804
Neutral composition and its variations in the lower thermosphere.

21 p2688 A73-41349
Observations of the ionospheric absorption at oblique incidence during the IASY.

22 p2847 A73-42195
Ozone transition detection in earth atmospheric ab-sorption and emission, comparing measured ozone ab-sorption profiles with theoretical computations

22 p2848 A73-42535
Absorption of vlf and elf waves in whistler mode - Sunrise and sunset effects.

22 p2849 A73-42622
Absorption of whistler waves during night.

22 p2850 A73-42623
Atmospheric absorption considerations in airplane flyover noise at altitudes above sea level.

22 p2799 A73-42943
Role of the outer scale of turbulence in atmospheric degradation of optical images.

23 p3005 A73-43341
Curvature effects in extended stellar atmospheres - Absorption and scattering.

23 p3030 A73-43751
High resolution analysis of the sun's radiation received at the ground from 9 to 11.6 microns.

23 p3003 A73-43888
Radiation absorption in stellar atmospheres due to photoionization in magnetic field, discussing frequ-ency relation to propagation direction and Larmor frequency

24 p3081 A73-44480
Extinction coefficient /point source light loss due to atmospheric scattering/ significance in reduction of night airglow data

24 p3082 A73-44734
Absorption at about 4.3 microns by /N2-N2/ and /N2-O2/ complexes in the terrestrial atmosphere

24 p3084 A73-44964
ATMOSPHERIC BOUNDARY LAYER

Tethered balloon measurements of turbulent wind, temperature and humidity fluctuations up to 200 me-ters over open sea, allowing for wave induced ship motion

01 p0072 A73-10142
Transient variation of martian ground-atmosphere thermal boundary layer structure.

01 p0097 A73-10400
An investigation of high-wavenumber temperature and velocity spectra in air.

01 p0039 A73-10448
Numerical simulations of the tropical air-sea plan-etary boundary layer.

01 p0073 A73-10496
Relations among stability parameters in the surface layer.

01 p0073 A73-10497
An airborne instrument system for atmospheric boundary-layer research.

01 p0073 A73-10498
The Air Force Global Weather Central operational boundary-layer model.

01 p0074 A73-10499
Measurements of microturbulent pulsations of the wind velocity derivative in the ground layer of the at-mosphere

01 p0074 A73-10870

ATMOSPHERIC BOUNDARY LAYER

High resolution limitations and improvement for earth based visual and photographic planetary obser-vation, considering atmospheric boundary layer and use of elevated stations

02 p0169 A73-12331
Energy conversion in the atmospheric boundary layer

04 p0441 A73-15286
The effect of the baroclinicity of the atmosphere on the structure of the wind field in the steady planetary boundary layer

04 p0441 A73-15289
Wind profile models for atmospheric turbulent boundary layers over smooth and rough surfaces, using Heisenberg energy transfer theory and von Kar-man constant

04 p0473 A73-15695
Empirical formulae for the universal functions M sub m/mu/ and N/mu/ in the resistance law for a barotropic and diabatic planetary boundary layer.

04 p0473 A73-15696
Relative importance of terms in the turbulent-ener-gy and momentum equations as applied to the problem of a surface roughness change.

05 p0591 A73-16191
A numerical study of the influence of advective ac-celerations in an idealized, low-latitude, planetary boundary layer.

05 p0592 A73-16192
A numerical study of coupling between the bounda-ry layer and free atmosphere in an accelerated low-latitude flow.

05 p0592 A73-16193
Laser communication lines in atmospheric ground layer, comparing SNR for direct-reception and super-heterodyne video systems

05 p0585 A73-16787
Thermal effects of urbanization and industrializa-tion in the boundary layer A numerical study.

06 p0720 A73-18330
Acoustic sounding of meteorological phenomena in the planetary boundary layer.

06 p0721 A73-18710
Asymptotic formulas for the thickness of the Ekman boundary layer

06 p0691 A73-18730
Time spectra and cross-spectra of kinetic energy in the planetary boundary layer.

07 p0847 A73-19044
The Leipzig wind profile and the boundary layer wind-stress relationship.

07 p0847 A73-19045
Magnetosphere tail internal plasma boundary layer dynamics during substorms based on aurora data

07 p0816 A73-19463
Investigation of the time characteristics of the phase fluctuations of optical waves propagating through the earth atmosphere boundary layer

07 p0792 A73-19914
LF boundary of inertial range in lowest atmospheric layer, comparing turbulence scale and wind velocity components

08 p0954 A73-21185
Second kind conditional instability of resting at-mosphere, noting Ekman boundary layer absence in rain area for given Coriolis parameter

08 p0985 A73-21379
Planetary boundary layer flow of a stable at-mosphere over the globe.

08 p0960 A73-21380
An analytical and numerical study of the Martian planetary boundary layer over slopes.

08 p1011 A73-21381
An investigation of the application of Taylor's hypothesis to atmospheric boundary layer turbulence.

09 p1114 A73-22331
Analog, digital and hybrid simulation of a planetary boundary layer meteorological forecast model.

09 p1114 A73-22333
A differential method for the prediction of the ef-fects of atmospheric boundary layer turbulence using the turbulence kinetic energy equation.

09 p1071 A73-22334
The diurnal wind variation in the lowest 1500 ft in central Oklahoma - June 1966-May 1967.

10 p1245 A73-23987
Statistical laws governing the wind velocity distribu-tion in the atmospheric boundary layer

10 p1246 A73-24373
Measurement of the transparency of the atmospher-ic ground layer at different wavelengths

11 p1363 A73-25612
Light scattering functions in the atmospheric ground layer for a range of large scattering angles

11 p1393 A73-25616
Influence of radiation on the conditions in the at-mospheric boundary layer

11 p1393 A73-25641
An observational study of the vertical profile of the high frequency fluctuations of the wind in the at-mospheric boundary layer.

11 p1393 A73-25691
A study of convective elements in the atmospheric surface layer.

11 p1393 A73-25692

Temperature and humidity spectra in the atmospheric surface layer.

11 p1393 A73-25693

The observed relation between the Kolmogorov and von Karman constants in the surface boundary layer.

11 p1393 A73-25694

Some observations of the influence of geostrophic shear on the cross-isobar angle of the surface wind.

11 p1393 A73-25695

Logarithmic wind profile in neutral barotropic planetary boundary layers, discussing von Karman constant

11 p1394 A73-25717

Some considerations on the atmospheric internal boundary layer over the ground surface.

11 p1394 A73-25725

One method of computing the meteorological variables for mesoscale processes.

11 p1394 A73-26192

Utilization of vacuum ultraviolet radiation for measurement of humidity pulsations

12 p1521 A73-26966

Method for calculating turbulent flows from network data

12 p1521 A73-27744

Momentum and mass transfer in atmospheric boundary layer from surface drag and evaporation data for weather prediction models

13 p1652 A73-28275

Measurements of turbulent microfluctuations of the wind-velocity derivative in the surface layer.

13 p1653 A73-28694

A comparison of time-varying concentrations of air admixtures with those of the corresponding stationary cases

13 p1653 A73-28742

Determination of the astronomical refraction near the horizon at different times of the year

13 p1683 A73-29096

Spatial correlation functions of velocity and temperature components in the atmospheric boundary layer

13 p1654 A73-29153

Some results of studies of the boundary atmospheric layer and AN-2 aircraft flight conditions in a forest fire area

13 p1655 A73-29192

Structure of the lower 300-meter atmospheric layer during the passage of a cold front

13 p1655 A73-29194

Similarity theory of diffusion and the observed vertical spread in the diabatic surface layer.

13 p1655 A73-29339

Turbulent surface layer shear convection analysis, using similarity model based on weak interaction between vertical motion and mechanical turbulence

13 p1655 A73-29340

A comparison of turbulence measurements by different instruments - Tsimlyansk field experiment 1970.

13 p1656 A73-29343

Nonstationarity effects on planetary boundary layer by numerical integration of time dependent boundary layer model

14 p1772 A73-30903

The wind profile very close to the ground.

14 p1772 A73-30904

Closure of the equations for heat influx in the atmospheric boundary layer /according to experimental data/

15 p1905 A73-31789

An aid for the prediction of the nighttime minimum temperature

15 p1906 A73-32352

The regression relations for turbulence parameters in the air layer near the ground in the case of an inhomogeneous base

15 p1907 A73-32359

The simulation of the atmospheric surface layer with volumetric flow control.

16 p1994 A73-33152

The use of subgrid transport equations in a three-dimensional model of atmospheric turbulence.

[ASME PAPER 73-FE-21]

17 p2206 A73-35017

Slant-path scintillation in the planetary boundary layer.

17 p2185 A73-35417

Turbulent flow fields with two dynamically significant scales.

[AIAA PAPER 73-646]

18 p2297 A73-36201

Some laboratory observations on convective plumes.

18 p2333 A73-36711

Utilization of satellite radiation measurements in analyzing the temperature near the ground.

18 p2334 A73-37067

Statistical characteristics of the temperature field near the ground for Europe.

18 p2334 A73-37070

Irreversible processes in the atmosphere. I

18 p2335 A73-37099

Waves and turbulence in stable layers and their effects on EM propagation; Proceedings of the Third Symposium, La Jolla, Calif., June 5-15, 1972. Parts 1 & 2.

19 p2447 A73-38202

The structure of an inversion above a convective boundary layer as observed using high-power pulsed Doppler radar.

19 p2447 A73-38205

Acoustic echo-sounding techniques and their application to gravity-wave, turbulence, and stability studies.

19 p2405 A73-38207

The remote sensing of wind velocity in the lower troposphere using an acoustic sounder.

19 p2427 A73-38208

Earth surface turbulent boundary layer analysis, considering similarity theory limitation, flux profiles, velocity, temperature and humidity spectra, energy budgets, local isotropy, etc

19 p2427 A73-38212

The boundary layer above 30 m. III.

19 p2448 A73-38214

Fine scale structure and mixing within inversion capping convective boundary layer, proposing atmospheric model for sensible downward heat transfer

19 p2448 A73-38215

Turbulence spectra, length scales and structure parameters in the stable surface layer.

19 p2448 A73-38216

Planetary boundary-layer turbulence studies from acoustic echo sounder and in-situ measurements.

19 p2448 A73-38223

Richardson number profiles through shear instability wave regions observed in the lower planetary boundary layer.

19 p2448 A73-38228

Observed generation of an atmospheric gravity wave by shear instability in the mean flow of the planetary boundary layer.

19 p2448 A73-38229

The lower atmosphere in hydrostatically stable conditions.

19 p2449 A73-38245

The radiation balance of the earth's surface and inclinations of isodiptic surfaces

19 p2428 A73-38556

The structure of internal intermittency in turbulent flows at large Reynolds number - Experiments on scale similarity.

20 p2546 A73-39090

Structural characteristic of the temperature field in the boundary layer of the atmosphere

20 p2555 A73-39182

Boundary-layer plasma of a re-entry vehicle - A comparison of prediction models and flight measurements.

21 p2632 A73-40420

Certain parameters of cellular convection according to observations by meteorological earth satellites and from a high mast

21 p2731 A73-40492

Parametrization of orographical effects in the planetary boundary layer.

21 p2732 A73-41570

Use of the numerical method of Estoque and Bhumralkar for the planetary boundary layer.

21 p2732 A73-41572

Diurnal cycles of the refractive index structure function coefficient.

22 p2849 A73-42545

Diurnal harmonic oscillation instability of atmospheric boundary layer as mesoscale internal gravity waves generation mechanism in lower atmosphere, considering unsteady flow equations

23 p3001 A73-43589

Mean Reynolds stress tensor model for analytical prediction of turbulence structure of density-stratified atmospheric boundary layer

23 p3002 A73-43592

An explanation of anomalously large Reynolds stresses within the convective planetary boundary layer.

23 p3002 A73-43593

The structure and dynamics of horizontal roll vortices in the planetary boundary layer.

23 p3002 A73-43594

Mathematical model for temperature inversion rise velocity under penetrative free surface convection based on unstable atmospheric boundary layer environment

23 p3002 A73-43595

Short-term ground ozone fluctuations at Poona.

23 p2974 A73-43865

Eddy heat/momentum diffusivity ratio dependence on Richardson number relationship between Deacon numbers of wind and temperature profiles in Antarctic surface layer

23 p3003 A73-43983

Calculation of a supersonic gas flow about the atmosphere of a spherical body

24 p3053 A73-44658

Aircraft aerodynamics problems covering slender body theory, atmospheric turbulence and boundary layers, wind tunnel contractions, radiator blocks, vortex induced oscillations, etc

24 p3053 A73-44690

The mesoscale structure of the atmospheric boundary layer and its interaction with small-scale turbulence

24 p3107 A73-44960

Superposition technique in numerical integration of generalized Ekman equation for wind profile determination, taking into account eddy diffusivity variation

24 p3108 A73-45019

Parameterization of baroclinicity effects in the planetary boundary layer.

24 p3088 A73-45366

Parametrizing turbulent-friction effects in a planetary boundary layer

24 p3108 A73-45450

ATMOSPHERIC CHEMISTRY

Symposium on D- and E-Region Ion Chemistry, University of Illinois, Urbana, Ill., July 6-8, 1971, Informal Record.

01 p0040 A73-10876

D-region negative-ion chemistry.

01 p0042 A73-10895

SST related ozone photochemical reactions and metastable oxygen system below 100 km, discussing oxygen dissociation and recombination, photolysis, UV absorption, etc

01 p0042 A73-10898

Aeronomical chemistry of the stratosphere.

02 p0158 A73-11910

Turbopause effect on latitudinal diurnal variation of upper atmosphere neutral species, using turbulent diffusion coefficients and photochemical transport theory

02 p0161 A73-12278

Chemical kinetics equations of lower ionosphere and D region particle interactions for aeronomical problems

05 p0569 A73-16396

Effects of nonequilibrium ablation chemistry on Viking radio blackout.

[AIAA PAPER 73-260]

05 p0551 A73-16981

The hydroperoxyl radical in atmospheric chemical dynamics - Reaction with carbon monoxide.

06 p0661 A73-18224

Reaction kinetics of nitric oxide positive ion with ozone yielding nitrogen dioxide positive ion and oxygen, noting impact on ionospheric chemistry

07 p0787 A73-19258

Molecular beam study on BaO and SrO formation for clarifying interaction of metal-vapors with upper atmosphere oxygen.

07 p0818 A73-19668

An alpha particle experiment for chemical analysis of the Martian surface and atmosphere.

09 p1048 A73-22190

Vibrationally-excited nitrogen in the upper atmosphere.

10 p1212 A73-24226

Physics and chemistry of upper atmospheres.

11 p1425 A73-26209

Dynamic model of the interaction between the F region of the ionosphere and the plasmosphere

12 p1490 A73-27335

Photochemistry of minor constituents in the troposphere.

12 p1466 A73-27603

Planetary atmospheres chemistry, discussing physical factors, atomic oxygen reactions, ozone, airglow and mathematical models

14 p1723 A73-30128

The photochemistry of hydrocarbons in the Jovian atmosphere.

14 p1802 A73-30766

Numerical study of the seasonal variations of the ionosphere.

15 p1867 A73-31381

Russian book - Geochemistry and cosmochemistry of inert gas isotopes.

15 p1840 A73-31585

Atmospherical modelling and the chemical data problem.

[AIAA PAPER 73-500]

16 p1977 A73-33542

Recent measurements of stratospheric reactions by flash photolysis resonance fluorescence.

[AIAA PAPER 73-502]

16 p2005 A73-33543

The extinction coefficients of NO₂ between 195 nm and 410 nm.

[AIAA PAPER 73-503]

16 p2005 A73-33544

Distributions and associations of some of the chemical elements found in the stratosphere.

[AIAA PAPER 73-514]

16 p2006 A73-33551

Preliminary estimates of the fate of SST exhaust materials using a coupled diffusion/chemistry model.

[AIAA PAPER 73-535]

16 p2046 A73-33567

Aerothermochemistry of combustion products in the stratosphere.

[AIAA PAPER 73-540]

16 p1977 A73-33570

The production of nitric oxide in the stratosphere by oxidation of nitrous oxide.

16 p2008 A73-33885

Atomic nitrogen ion density measurements for loss rate coefficient of N⁺ reaction with oxygen at 150-220 km

16 p2009 A73-33892

Laboratory methods for study of aeronomical reactions of excited ions.

16 p2009 A73-33894

New rate measurements on the reaction of O(3P), O(3), and OH.

[AIAA PAPER 73-501]

16 p1977 A73-34045

Atomic collision processes applied to earth atmospheric physics and chemistry, Jovian ionospheric composition and terrestrial tropical UV dayglow
17 p2213 A73-34450

Mesospheric and stratospheric nitrogen oxides behavior from model with nitric oxide photodissociation and nitric acid formation
17 p2119 A73-34779

Physics and chemistry of the ionosphere.
17 p2162 A73-35050

Photochemical reactions in the Jovian atmosphere.
17 p2237 A73-35835

Reaction of HO₂ with O₃.
19 p2402 A73-37674

Atmospheric CO production from electron impact on carbon dioxide, considering lightning, radioactivity, discharges, photoelectrons, auroral particles, cosmic rays and solar wind
21 p2680 A73-40079

Tropospheric model for nitrogen-oxygen-carbon-hydrogen atmosphere with time dependent static chemistry, emphasizing methane conversion to CO via OH attack
21 p2646 A73-40081

Photochemical model for homogeneous gas phase radical chain mechanism to remove tropospheric methane, carbon monoxide, molecular hydrogen and formaldehyde
21 p2646 A73-40082

A generalized aeronomical model of the mesosphere and lower thermosphere including ionospheric processes.
21 p2683 A73-40778

Temperature dependence for dissociative recombination of NO⁺ in E- and F-region models.
21 p2684 A73-40787

The optimal number of soundings for a complete investigation of the ionization-neutralization and dynamic characteristics of the middle ionosphere
21 p2686 A73-40911

Variations in density and chemical composition at 120 km from chemical and dynamical processes.
21 p2689 A73-41355

The origin and evolution of the atmospheres of the terrestrial planets.
22 p2912 A73-42976

Dynamic model of interaction of the F-region of the ionosphere with the plasmasphere.
23 p2970 A73-43233

Ammonia density profiles and photochemical destruction above Jovian tropopause as function of eddy diffusion coefficient, considering background atmosphere scale height
23 p3028 A73-43601

A theoretical investigation of tropospheric ozone and stratospheric-tropospheric exchange processes.
23 p2974 A73-43861

Recent developments in photochemistry of atmospheric ozone.
23 p2951 A73-43892

A discussion of the chemistry of some minor constituents in the stratosphere and troposphere.
23 p2951 A73-43893

On the vertical distribution of carbon monoxide and methane in the stratosphere.
23 p2976 A73-43894

OH radical concentration in the stratosphere.
23 p2976 A73-43895

On the behavior of nitrogen oxides in the stratosphere.
23 p2976 A73-43896

The production and distribution of nitrogen oxides in the lower stratosphere.
23 p2977 A73-43897

Nitrogen oxides role in global stratospheric ozone balance demonstrated by observed instantaneous photochemical rates comparison with Chapman ozone formation theory
23 p2952 A73-43900

Ionospheric aeronomy problems with emphasis on photochemical processes of neutral and ionized components, discussing nighttime ionizing agents, ion recombination, water vapor and nitrogen oxide behavior, etc
23 p2978 A73-43977

Ionospheric metastable particle production and annihilation during photochemical reactions, determining neutral and ionized particle abundance profiles
23 p2978 A73-43979

Venus carbon dioxide production kinetics involving quartz reaction with calcite to form wollastonite and carbon dioxide
24 p3133 A73-44540

Layering of the neutral metals of meteoric origin in the lower ionosphere.
24 p3066 A73-44733

Determination of the rate coefficients of ionospheric reactions from experimental data for electron concentration
24 p3083 A73-44787

ATMOSPHERIC CIRCULATION

A general circulation model of the atmosphere suitable for long period integrations.
01 p0072 A73-10143

The estimation of ground-level pressure fields from computer analyses and their application to large-scale atmospheric mass transfer.
01 p0072 A73-10144

Possibilities of measuring the velocity of circulation of the magnetospheric plasma with the help of a quadrupole probe used in the vicinity of the low hybrid frequency
01 p0035 A73-10326

A detailed radiation model for climate studies. Comparisons with a general circulation model radiation subroutine.
01 p0039 A73-10393

The magnitude and character of the radiation induced vertical circulation of the troposphere.
01 p0039 A73-10394

A linear harmonic analysis of atmospheric motion with radiative dissipation.
01 p0039 A73-10399

On the dependence of quietness and sharpness of solar image on local and large scale atmospheric circulation.
01 p0098 A73-10561

Estimation of the global circulation characteristics of planetary atmospheres with various hypotheses concerning the nature of dissipation
01 p0040 A73-10868

Simultaneous measurements of radar reflectivity and refractive index spectra in clear air convection.
01 p0018 A73-11060

On a method of determining the interaction coefficient in convective clouds
01 p0074 A73-11273

Similarity theory of planetary atmosphere circulations applied to solar atmosphere in terms of radius and rotational Mach number
01 p0106 A73-11316

Incoherent scatter observations of meridional winds in the 150-225 km region.
02 p0161 A73-12283

Inaccuracy sources in winds calculation from thermospheric models, considering neutral air motions due to global pressure variations
02 p0189 A73-12293

Momentum deposition by atmospheric waves, and its effects on thermospheric circulation.
02 p0162 A73-12297

On the application of satellite data on cloud brightness to the study of tropical wave disturbances.
02 p0190 A73-12790

Alfven wave induced bulk velocity amplitudes in lower solar atmosphere, discussing relationship between energy flux, bulk velocity, wavelengths and scale height
03 p0360 A73-12944

Synoptic conditions of wave formation above convection streets.
04 p0473 A73-14826

Annual and semi-annual zonal wind components and corresponding temperature and density variations, 60-130 km.
04 p0440 A73-14961

Theoretical model for the latitude dependence of the thermospheric annual and semiannual variations.
04 p0444 A73-15538

Russian book on atmospheric circulation covering temperature distribution, tropospheric and stratospheric winds, jet streams and Southern Hemisphere meteorological features
04 p0474 A73-15961

Numerical solution for the composition of a thermosphere in the presence of a steady subsolar-to-antisolar circulation with application to Venus.
05 p0613 A73-16198

On the damping of high-frequency motions in four-dimensional assimilation of meteorological data.
05 p0592 A73-16199

Russian book - Problems of the general circulation of the atmosphere.
05 p0592 A73-16226

Investigation of the characteristics of atmospheric motion at low latitudes
05 p0592 A73-16227

Application of certain stable methods for numerical solution of forecasting equations
05 p0592 A73-16228

Hemispheric single level model of atmospheric action centers formation due to horizontal baroclinity, including turbulent mixing and circulation index effects
05 p0592 A73-16229

Interaction between long waves and zonal circulation in a baroclinic atmosphere
05 p0592 A73-16230

Physicostatistical investigations of the general atmospheric circulation
05 p0592 A73-16231

Relationship of atmospheric processes in the troposphere and stratosphere
05 p0593 A73-16233

Utilization of radioactive isotopes as tracers in the investigation of general atmospheric circulation
05 p0593 A73-16234

Utilization of the convergence of atmospheric processes during construction of long-range weather forecasts
05 p0593 A73-16236

Certain problems and results of theoretical and experimental research on the energetics of general atmospheric circulation
05 p0593 A73-16237

Typification of circulation processes in the atmosphere over the Northern Hemisphere and the possibility for its objectivization with the aid of numerical characteristics
05 p0593 A73-16238

Investigation of planetary high-altitude frontal zones with the aid of natural orthogonal functions
05 p0568 A73-16239

Application of structural-temporal functions for analysis of periodicities in atmospheric motions
05 p0593 A73-16240

Numerical tests of atmospheric circulation and climate theory and accuracy conditions for atmospheric models, noting temperature dependence on radiative and nonradiative heat transfer
05 p0593 A73-16242

Prospects for the utilization of satellite information in studies of the general atmospheric circulation
05 p0593 A73-16244

Utilization of meteorological data from satellites in studies of the general atmospheric circulation
05 p0593 A73-16245

Utilization of meteorological data from earth satellites in the analysis of global weather maps and in studies of planetary atmospheric circulation
05 p0593 A73-16246

Baroclinic model of zonal atmospheric circulation in the equatorial region
05 p0594 A73-17351

Planet wide circulation in Venus upper atmosphere from UV photographs, noting apparent 4.06 day rotation period
06 p0743 A73-17431

Retrograde rotation of the upper atmosphere of Venus.
06 p0744 A73-17433

Experiments on objectively predicting some atmospheric and oceanic variables for the winter of 1971-72.
[AD-758469] 06 p0720 A73-18702

Theory of inertial atmospheric oscillations in low latitudes
06 p0691 A73-18729

A numerical experiment using a general circulation model of the atmosphere.
07 p0846 A73-19037

Equatorial Kelvin wave oscillations of zonal wind at 100 mb over Eastern Hemisphere
07 p0847 A73-19043

Meridional circulation zonal averaging effects on summer hemisphere Hadley cell in tropical regions
07 p0847 A73-19046

Response of a general circulation model of the atmosphere to removal of the arctic ice-cap.
07 p0848 A73-20122

Nonlinear Boussinesq convective model for large scale solar circulations.
08 p1001 A73-20751

Experiments on the seasonal variation of the general circulation in a statistical-dynamical model.
08 p0960 A73-21378

Integration of the equations of meteorology. III - Integration in time
08 p0986 A73-21495

The vertical thermal structure of the Martian atmosphere - Modification by motions.
09 p1145 A73-22271

Possible correlation between the concentration and density of alpha-radioactive fallouts and types of meteorological processes
09 p1115 A73-22995

Tensor theory of perturbations in atmospheric dynamics
09 p1115 A73-23150

A comparative study of the wind structure in the stratosphere at Sonmiani vis-a-vis CIRA 1965.
10 p1244 A73-23647

Global numerical atmospheric circulation model predictive sensitivity to equator-to-pole temperature gradient changes, applying variance analysis technique to Mintz-Arakawa model
10 p1245 A73-23983

Sierra Nevada mountain lee waves atmospheric structure from lidar, rawinsonde and aircraft observations, delineating atmospheric flow patterns from particulate matter concentrations induced echoes
10 p1245 A73-23988

Macroscale interaction between the atmosphere and oceans and the role of the latter in the formation of anomalous circulation in the stratosphere
10 p1246 A73-24374

Summary of Jovian latitude and rotation period observations from 1898 to 1970.
11 p1415 A73-25134

A model for investigating eddy viscosity effects on mesoscale cellular convection.
11 p1393 A73-25716

Solar magnetic sector structure - Relation to circulation of the earth's atmosphere.

12 p1491 A73-27441

Jupiter atmosphere fluid dynamic models, considering cloud spot markers and wave motions from ground and spacecraft observations

12 p1542 A73-27606

Mass to wind and wind to mass adjustments in dynamic initialization for primitive equation model of atmospheric motion

13 p1652 A73-28270

The earth's rotation and atmospheric circulation. I - Seasonal variations.

13 p1606 A73-28282

On the relation between the rotation of the earth and solar activity.

13 p1680 A73-28408

Estimates of global circulation characteristics of planetary atmospheres.

13 p1607 A73-28692

A 4-year experiment in long-range weather forecasting, using circulation analogues.

13 p1653 A73-28740

The numerical models of general circulation and their employment for medium-term and long-term weather prediction

13 p1653 A73-28741

International polar experiment /POLEX/ program for global circulation research and long range weather forecasting improvement

13 p1654 A73-28933

Terrestrial atmospheric general circulation theoretical and observational research, considering Reynolds or eddy stress distribution across horizontal and vertical surfaces

13 p1610 A73-29333

Barotropic and baroclinic contribution to eddy kinetic energy increase in disturbance amplification using quasi-geostrophic equations of motion and omega equation

13 p1610 A73-29335

Energy and diffusive mass transport relation to thermospheric circulation, composition, temperature and mass density from three dimensional two constituent magnetic storm model

14 p1748 A73-29975

On the atmospheric kinetic energy spectrum and its estimation at some selected stations.

14 p1750 A73-30763

A baroclinic model of the atmospheric zonal circulation in the equatorial region.

15 p1902 A73-31001

Study of the effect of heat influxes on the formation of lower and higher baric fields in the Northern Hemisphere

15 p1903 A73-31602

Vortex conservation mechanism of earth atmosphere jet stream formation in terms of Hadley cell in meridional divergence/convergence velocity region

15 p1903 A73-31603

Some results of ozone observations by satellite on June 17 and 18, 1966

15 p1868 A73-31607

Eole meteorological balloon sounding experiment in Southern Hemisphere, discussing mean circulation, eddy diffusion and data collection and satellite tracking system

15 p1904 A73-31723

Results of the numerical modeling of steady zonal circulation of the atmosphere in the equatorial region

15 p1905 A73-31817

General circulation of the tropical lower stratosphere.

15 p1906 A73-31845

Estimate of the influence of the seasonal redistribution of air masses on the motion of the earth's poles

15 p1939 A73-31967

Map series for description of annual temperature wave in lower stratosphere in Northern Hemisphere, establishing easterly circulation on south side of Aleutian high

15 p1873 A73-32254

Book - The general circulation of the tropical atmosphere and interactions with extratropical latitudes. Volume 1.

15 p1907 A73-32423

Gravity wave magnitudes and horizontal and vertical scales measured and applied to eddy diffusion coefficients in upper stratosphere

[AIAA PAPER 73-495]

16 p2005 A73-33538

Coordinated measurements of atmospheric parameters at stratospheric levels.

[AIAA PAPER 73-526]

16 p2007 A73-33560

A three-dimensional stratospheric point-source tracer experiment and its implications for dispersion of effluent from a fleet of supersonic aircraft.

[AIAA PAPER 73-528]

16 p2007 A73-33562

Numerical atmospheric circulation model of SST effects on stratospheric ozone distribution

[AIAA PAPER 73-529]

16 p2007 A73-33563

Simulated weather records experiment for polluted atmosphere effects on climatic change, using numerical circulation model

[AIAA PAPER 73-537]

16 p2007 A73-33568

Red Spot interaction with small Jupiter dark spots moving along northern edge of south temperate zone

16 p2070 A73-33843

Balloon-borne phosphoric anhydride electrolytic gage measurement of water vapor mixing ratio to 35 km, noting decrease to minimum near tropopause

16 p2008 A73-33844

Finite-difference approximations of the Navier-Stokes equations applied to a geophysical flow. I. II - Three-dimensional approximations on a region homeomorphic to a plane region. III - Three-dimensional approximations over the totality of a spherical region represented by means of a regular polyhedron

16 p2009 A73-33886

Electrical balance in the lower atmosphere.

17 p2158 A73-34359

Book on energy equations for small and large scale atmospheric motion covering laminar and turbulent flow and space-time scales for atmospheric energy balance

17 p2158 A73-34463

The effect of forecast error accumulation on four-dimensional data assimilation.

17 p2205 A73-34853

On the maintenance of the polar front jet stream.

17 p2205 A73-34854

Jupiter atmospheric circulation as manifestation of large scale convective instability generated by internal heat sources, considering Red Spot production

17 p2232 A73-34859

Global circulation numerical modeling problems and numerical weather forecasting status as basis for GARP programs, considering tropical experiment on deep convective cloud systems

17 p2205 A73-34927

Role of the meteorological satellites of the earth atmosphere observation system for the first global experiment of the 'Global Atmospheric Research Programme'

17 p2205 A73-34935

Medium-range forecasting of large-scale atmospheric circulation components on the basis of a nonlinear spectral model

18 p2331 A73-35910

Analysis of atmosphere circulation and climate fluctuations in different portions of the Northern Hemisphere of the earth

18 p2331 A73-35913

Global meridional cross sections and charts for mesospheric circulation and temperature variability via meteorological rocket network

18 p2302 A73-35925

Operational radiance maps of the stratosphere, with preliminary details of a major stratospheric warming.

18 p2303 A73-35950

Dynamic processes as derived from the mean circulation in the upper mesosphere and lower thermosphere.

18 p2307 A73-36036

Midwinter mesospheric cooling during stratospheric warming, discussing circulation, stratosphere-mesosphere interactions and summertime temperature values at midwinter mesopause

18 p2308 A73-36037

The stratospheric-mesospheric circulation over the North Pacific Ocean.

18 p2308 A73-36039

High-level circulation studies based on rawinsonde, rocketsonde and satellite observations.

18 p2350 A73-36040

Atmospheric density, temperature and winds measured during Aladdin II.

18 p2309 A73-36055

Differences in circulation of the upper atmosphere in low latitudes of the southern and northern hemispheres.

18 p2310 A73-36138

The dynamical effects of real Mars orography upon the large-scale air flow and some meteorological phenomena of Mars.

19 p2482 A73-37429

Some effects of surface anomalies in a global general circulation model.

19 p2446 A73-37539

Mechanisms for Mars dust storms.

19 p2485 A73-37656

Numerical models of the circulation of the atmosphere of Venus.

19 p2485 A73-37657

EOLE balloon clusters horizontal trajectories as indicators of southern hemisphere atmospheric circulation, estimating rms divergence as function of scale

19 p2424 A73-37661

Comparison and synthesis of the characteristics of long- and short-duration blocking systems over the Euroatlantic region

19 p2447 A73-38124

Quasi-stationary atmospheric waves and mean monthly vorticity production from development term of two level model

19 p2447 A73-38153

Wave-mean flow interactions in the upper atmosphere.

19 p2427 A73-38217

Capabilities of radar, sodar and lidar for measuring the structure and motion of the stably stratified atmosphere.

19 p2405 A73-38239

Global model of the general circulation of the atmosphere below 75 kilometers with an annual heating cycle.

19 p2449 A73-38287

Dynamics of ionization inhomogeneities in the ionosphere

20 p2553 A73-39152

Neutral air wind influences deduced from solar cycle changes in the F2 region equatorial anomaly.

21 p2679 A73-39932

Satellite techniques for automatic platforms location and data relay.

21 p2737 A73-41335

Use of meteorological rocketsonde and satellite radiation data for constant-pressure analyses at levels between 5 and 0.4 mb.

21 p2732 A73-41336

The establishment of the winter polar vortex in middle latitudes in 1971.

21 p2687 A73-41338

The stratospheric circulation over Middle Atlantic latitudes in the 1966-1971 period.

21 p2687 A73-41339

Diurnal and seasonal variations of neutral winds and electric fields above 90 km in the vicinity of the auroral electrojet.

21 p2690 A73-41365

Book - Atmospheric circulation systems and climates.

21 p2732 A73-41440

Increased influx of stratospheric air into the lower troposphere after solar H alpha and X ray flares.

22 p2848 A73-42538

An exact solution for the rotation of the atmosphere about the spheroidal earth.

22 p2848 A73-42541

The 4-day rotation of the upper atmosphere of Venus.

22 p2913 A73-42982

Upper Venusian atmosphere four-day retrograde zonal circulation, discussing moving flame phenomenon, convective instability to mean shear and tidal forcing

22 p2913 A73-42983

Structure of global geopotential fields in view of the quasi-two-year cyclicity in the equatorial stratosphere

23 p3001 A73-43463

Nonlinear theory of the formation and structure of the intertropical convergence zone.

23 p3001 A73-43586

On the interaction between the zonal mean flow and equatorial waves excited by diabatic heat sources at 20 deg latitude.

23 p3001 A73-43587

An explanation of anomalously large Reynolds stresses within the convective planetary boundary layer.

23 p3002 A73-43593

The structure and dynamics of horizontal roll vortices in the planetary boundary layer.

23 p3002 A73-43594

Venus upper atmosphere retrograde rotation above main cloud cover, investigating equatorial bulge from pressure surfaces at high elevations

23 p3029 A73-43604

Radiosonde ground station ozone concentration measurements as stratospheric motions Lagrangian tracer, noting sonde data inadequacy and alternative measurement possibilities

23 p2975 A73-43873

Remote sensing of the global distribution of total ozone and the inferred upper-tropospheric circulation from Nimbus IRIS experiments.

23 p2975 A73-43876

Influence of the vertical motion field on ozone concentration in the stratosphere.

23 p2977 A73-43904

The effect of dissipation on the vertical propagation of planetary waves in the vicinity of critical levels.

23 p3032 A73-43906

Application of general circulation models to the study of stratospheric ozone.

23 p2978 A73-43909

Rotation period for a subsurface source in the NNTeB of Jupiter.

23 p3033 A73-43947

Recent observations of Jupiter's North North Temperate Belt Current B.

23 p3033 A73-43949

Mediterranean, south Sahara and northwest India rainfall records analysis, correlating general circulation changes with winter-spring and monsoon rainfall fluctuations

23 p3003 A73-43954

Zonally symmetric global general circulation models with and without the hydrologic cycle.

23 p2978 A73-43981

Upper tropospheric disturbances of the equatorial atmosphere and their influence on rainfall near the equator.

23 p3004 A73-44104

A first look at atmospheric dynamics and temperature variations on Titan. 24 p3128 A73-44433

General atmospheric circulation driven by polar and diurnal surface temperature variations. 24 p3131 A73-44463

Estimated seasonal redistribution of air masses affecting motion of earth's poles. 24 p3081 A73-44492

Short-term Jovian rotation profiles, 1970-1972. 24 p3134 A73-44562

The latitudinal motion of sunspots and solar meridional circulations. 24 p3136 A73-44647

Numerical experiments on the steady-state meridional structure and ozone distribution in the stratosphere. 24 p3085 A73-45017

Northern summer tropical upper tropospheric large scale flow dynamics, energy exchange diagram and limited area numerical weather prediction problems 24 p3108 A73-45094

ATMOSPHERIC COMPOSITION

NT ATMOSPHERIC MOISTURE

NT IONOSPHERIC COMPOSITION

Jovian atmosphere absorption line and spectroscopic data interpretation based on model for structure, composition and radiative properties of visible cloud layers 01 p0097 A73-10359

Neutral composition measurements of the mesosphere and lower thermosphere. 01 p0040 A73-10879

The consequences of grains in the atmospheres of late-type stars. I - Intrinsic polarization, infrared excesses, and emission lines. 01 p0103 A73-11035

Nuclear explosions released nitric oxide effect on atmospheric ozone concentration compared with potential effect from SST flights 01 p0043 A73-11068

Observation of upper atmospheric constituents by laser radar systems. 01 p0018 A73-11202

Atmospheric atomic oxygen density vertical distribution measurement by rocket-borne cryocooled mass spectrometer ion source 02 p0157 A73-11756

Daytime laser radar measurements of the atmospheric sodium layer. 02 p0157 A73-11875

The diurnal variations of hydrogen and oxygen constituents in the mesosphere and lower thermosphere. 02 p0158 A73-12026

Nitrogen hydride as a possible stratospheric constituent. 02 p0159 A73-12225

Turbopause effect on latitudinal diurnal variation of upper atmosphere neutral species, using turbulent diffusion coefficients and photochemical transport theory 02 p0161 A73-12278

Restrictions on McElroy theory of Martian chaotic terrain production by permafrost withdrawal, calculating degassed water/carbon dioxide ratios in Mars and earth atmospheres 02 p0218 A73-12418

Mars exploration by spacecraft, discussing erosional processes, atmospheric pressure and composition, heat absorption and radiation and polar caps formation 02 p0221 A73-12575

Distribution of nitric acid vapor in the stratosphere as determined from infrared atmospheric emission data. 02 p0189 A73-12786

Titan atmosphere composition of methane hydrate with ammonia impurity, discussing hydrogen and hydrocarbon production, liquid water existence and greenhouse effects 04 p0497 A73-14973

Tunable dye lidar techniques for measurement of atmospheric constituents. 04 p0423 A73-15769

The influence of atmospheric oxygen on velocity of flame spread along a solid. [ASME PAPER 72-WA/HT-23] 04 p0519 A73-15831

Certain optical properties of the atmosphere of Venus and the possibilities of interpreting photometric and polarization measurements. 05 p0612 A73-16087

Numerical solution for the composition of a thermosphere in the presence of a steady subsolar-to-antisolar circulation with application to Venus. 05 p0613 A73-16198

Utilization of radioactive isotopes as tracers in the investigation of general atmospheric circulation 05 p0593 A73-16234

Vertical distribution of minor atmospheric constituents as derived from air-borne measurements of atmospheric emission and absorption infrared spectra. [AIAA PAPER 73-103] 05 p0570 A73-16863

The abundance of NH3 on Jupiter inferred from UHF radiometry data. [AIAA PAPER 73-128] 05 p0619 A73-16881

Seasonal variations in carbon monoxide content of the atmosphere 05 p0572 A73-17357

Venus high resolution spectra for carbon dioxide abundance variations, discussing CO, HF and HCl composition 06 p0744 A73-17435

Mariner 9 IR spectral features due to carbon dioxide, water vapor and silicate dust suspended in Mars atmosphere before/after planet-wide dust storm 06 p0746 A73-17482

Uranus atmosphere - Structure and composition. 07 p0874 A73-19068

Comment on 'The composition of the Venus cloud tops in light of recent spectroscopic data.' 07 p0874 A73-19076

Potential atmospheric composition of smaller bodies in the solar system and some aspects of planetary evolution. 07 p0875 A73-19249

Atomic hydrogen concentrations in the mesosphere and the hydroxyl emissions. 07 p0815 A73-19257

Determination of the concentration and scattering indicatrix of atmospheric dust from primary twilight brightness 07 p0817 A73-19589

Photoelectric measurement of twilight sky brightness distribution for separation of primary brightness component, noting possibility of secondary component due to dust 07 p0818 A73-19593

Lunar orbital mass spectrometer experiment. 07 p0891 A73-19828

Stability CO2 in the Martian atmosphere and under radiolysis. 07 p0899 A73-20155

Atmospheric dust trace elements levels sampled in United Kingdom, considering natural origin 07 p0820 A73-20279

Distribution of the total ozone content in the atmosphere according to satellite observations. 07 p0820 A73-20346

Photochemical ozone formation in the atmosphere over southern England. 08 p0957 A73-20667

Measurements on the infrared lines of planetary gases at low temperatures. I - Nu-3 fundamental of methane. 08 p1003 A73-20891

Atmospheric abundances in the carbon star HD 156074. 08 p1006 A73-20935

Stratospheric aerosol measurements with implications for global climate. 08 p0984 A73-21041

Mariner 9 Ultraviolet Spectrometer experiment - Observations of ozone on Mars. 09 p1144 A73-22267

Effect of the shape and orientation of atmospheric dust particles on the spectral position and form of the attenuation band 09 p1077 A73-22372

Effect of excited states of atomic oxygen ions on the reaction rates and thermal balance in the F-region. 09 p1078 A73-22832

Ion composition in the E- and lower F-region above Kiruna during sunset and sunrise. 09 p1078 A73-22838

Icelandic geothermal activity and the mercury of the Greenland icecap. 09 p1079 A73-22949

Third elements effect on electrical erosion of steels noting influence of atmospheric composition 09 p1104 A73-22967

Possible correlation between the concentration and density of alpha-radioactive fallouts and types of meteorological processes 09 p1115 A73-22995

Planetary atmospheres 09 p1152 A73-23471

Cosmic ray, solar activity, supernova outbursts and geomagnetic field effects on atmospheric C-14 concentration 10 p1266 A73-23911

High resolution spectroscopic analysis for photospheric Eu II lines with spectrum synthesis techniques, determining solar isotopic composition and abundance 10 p1278 A73-24129

Formation of the density profile of charged particles at heights from 10 to 90 km 11 p1411 A73-25082

Optical characteristics of bright day sky in the visual region of the spectrum and the atmospheric aerosol 11 p1353 A73-25606

Spatial and temporal variations of the Lyman-alpha airglow and related atomic hydrogen distributions. 11 p1356 A73-25909

Stellar occultation measurements of molecular oxygen in the lower thermosphere. 11 p1356 A73-25911

Southern Hemisphere troposphere atmospheric carbon dioxide monitoring program based on aircraft air sampling, discussing vertical profile data 11 p1358 A73-26472

Electric discharge and microbiological experiments in simulated Jovian atmosphere for investigation of Jupiter life prospects 11 p1319 A73-26478

Titan model arising from observations and methane-rich atmosphere thermodynamics, photochemistry and optical properties, considering origins and volatile content of outer planets satellites 12 p1539 A73-27140

Far UV scanning spectrometer aboard Apollo 17 CSM to measure lunar atmospheric composition, observing spectral albedo, LEM atmosphere, and galactic and solar system atmospheres 12 p1497 A73-27485

Preliminary results of the determination of altitudes on Mars from CO2 2-micron wavelength bands aboard the Mars 3 interplanetary automatic station 13 p1673 A73-28288

The open-source neutral-mass spectrometer on Atmosphere Explorer-C, -D, and -E. 13 p1616 A73-28628

A neutral-atmosphere composition experiment for the Atmosphere Explorer-C, -D, and -E. 13 p1687 A73-28629

The magnetic ion-mass spectrometer on Atmosphere Explorer. 13 p1688 A73-28633

Ozone variation in the lower stratosphere and its mechanism. 13 p1611 A73-29664

Cometary head atmospheric gaseous and dust components characteristics in terms of physical processes in comet nucleus vicinity 14 p1792 A73-29814

Solar Lyman alpha radiation scattering analysis to determine neutral hydrogen atom distribution in upper atmosphere 14 p1747 A73-29865

Prebiological synthesis of organic compounds. 14 p1724 A73-30129

Vibrational relaxation effects in weak shock waves in air and the structure of sonic bangs. 14 p1711 A73-30174

Outer planet satellites and atmospheres composition and structure from low temperature condensation accretion models 14 p1724 A73-30530

Seasonal variations of the carbon monoxide concentration in the atmosphere. 15 p1865 A73-31007

Some statistical characteristics of atmospheric ozone measurements 15 p1868 A73-31612

Equatorial ionospheric anomaly related neutral thermospheric composition variation observation fromOGO-6 mass spectroscopic data, noting static diffusion model limitations 15 p1870 A73-31767

Upper stratosphere and lower mesosphere vertical mixing implications of methane observations at 50 km, assuming modelability by eddy transport 15 p1873 A73-32251

Isotope separation factor of carbon dioxide-water system and isotopic composition of atmospheric oxygen. 15 p1873 A73-32252

Long-path infrared spectra of CO, NO2, NO, SO2 and N2O observed in a simulated atmosphere in trace amounts. 16 p1976 A73-32700

A simple technique to estimate large-scale eddy coefficients in the stratosphere. 16 p2005 A73-33541

[AIAA PAPER 73-499] Trace gases, aerosols, and solar radiation in the stratosphere - Explored and unexplored problem areas. [AIAA PAPER 73-509] 16 p2006 A73-33547

Distributions and associations of some of the chemical elements found in the stratosphere. [AIAA PAPER 73-514] 16 p2006 A73-33551

Correlation interferometric measurement of trace species in the atmosphere. [AIAA PAPER 73-515] 16 p2006 A73-33552

Measurement of trace gases in the stratosphere using far infra-red spectroscopy. [AIAA PAPER 73-516] 16 p2006 A73-33553

Measurement of high-altitude air quality using aircraft. [AIAA PAPER 73-517] 16 p2006 A73-33554

Vertical profiles of molecular H2 and CH4 in the stratosphere. [AIAA PAPER 73-518] 16 p2006 A73-33555

Lidar measurements of the variability of stratospheric particulates. [AIAA PAPER 73-520] 16 p2007 A73-33556

Stratospheric contamination experiments with a one-dimensional atmospheric model. [AIAA PAPER 73-531] 16 p2007 A73-33564

Aircraft exhaust plume dispersion and flight corridor concentration profiles in stratosphere as function of flight frequency and scale dependent diffusion [AIAA PAPER 73-532] 16 p2046 A73-33565

Investigation of the chemical composition of the atmosphere of Venus by the automatic station Venus 4 16 p2066 A73-33799

Spectral studies of the atmospheres of Mars and Venus

16 p2067 A73-33812

Venus 4 chemical composition and pressure data for construction of Venus atmospheric model, emphasizing Greenhouse effect

16 p2068 A73-33826

Jupiter and Saturn optical observations, discussing atmospheric composition, cloud layers and temperature distribution

16 p2069 A73-33837

The production of nitric oxide in the stratosphere by oxidation of nitrous oxide.

16 p2008 A73-33885

A comparison of two methods of analysis for the twilight sodium airglow data.

16 p2009 A73-33891

Atmospheric composition changes and the F2-layer seasonal anomaly.

16 p2010 A73-33915

Enhancement of upper atmospheric sodium from sporadic dust influxes.

16 p2010 A73-33917

On the possible effect of NO_x injection in the stratosphere due to past atmospheric nuclear weapons tests.

[AIAA PAPER 73-538]

16 p2011 A73-34047

Noble gas isotope abundances for solar wind and outer convective zone of sun, emphasizing isotopic abundance of deuterium

17 p2228 A73-34416

Carbon isotope abundance ratios in comets and Jupiter atmosphere, discussing hydrogen isotope ratio determination for Saturn and Jupiter atmospheres

17 p2228 A73-34418

Nitric oxide detection in stratosphere from characteristic absorption line spectrum via airborne IR spectrometer, obtaining molecular concentration

[ONERA, TP NO. 1256]

17 p2159 A73-34552

A model-atmosphere abundance analysis of the B9 V star nu Capricorni.

17 p2231 A73-34758

Atomic oxygen profiles determined by EUV absorption analysis.

18 p2308 A73-36049

Sounding balloon nuclear emulsion chamber recording of energy spectra and angular distribution of incoming and outgoing proton fluxes in atmosphere

18 p2310 A73-36124

Theoretical analysis of improvements in remote sensing of atmospheric and pollutant gases through high resolution detection of individual infrared emission lines.

[AIAA PAPER 73-703]

18 p2315 A73-36252

Probing the structure and composition of the Jupiter atmosphere from Pioneer 10/11.

[AIAA PAPER 73-561]

18 p2353 A73-36498

Pioneer spacecraft for atmospheric entry missions to the outer planets.

[AIAA PAPER 73-595]

18 p2360 A73-36500

Composition of the earth's atmosphere by shock-layer radiometry during the PAET entry probe experiment.

18 p2313 A73-36797

Nonequilibrium effects on shock-layer radiometry during earth entry.

18 p2338 A73-36798

Observation of stratospheric nitric oxide by infrared absorption spectrometry from a balloon

19 p2423 A73-37533

Sulfuric acid in the Venus clouds.

19 p2483 A73-37579

Refraction of light beams in an atmosphere with arbitrary parameters

19 p2449 A73-38558

Atmospheric sounding by satellite-borne remote sensors, discussing radiometric measurements of temperature, composition, and reflected and emitted radiance in visible, IR and microwave bands

[AAS PAPER 73-125]

20 p2550 A73-38585

Venus topside ionosphere He content estimated from ionization profiles and discovery of radioactive materials in crust

20 p2604 A73-38942

Remote sensing of stratospheric gases using submillimetre radiation.

20 p2557 A73-39856

Daytime applications of Raman technique of laser backscatter to measure atmospheric composition profiles

21 p2729 A73-40067

Atomic oxygen and helium concentrations variation at 120 km in thermospheric composition models, discussing association with geomagnetic activity

21 p2679 A73-40074

Balloon-borne measurement of stratospheric methane as function of altitude absorption spectroscopy, obtaining mixing ratios

21 p2680 A73-40076

Tropospheric and stratospheric vertical profiles of methane concentration via air sampling and gas chromatography, noting temporal and spatial variations

21 p2680 A73-40077

CO atmospheric vertical distribution from balloon-borne IR grating spectrometer observations, noting concentration decrease with altitude

21 p2680 A73-40078

Atmospheric CO production from electron impact on carbon dioxide, considering lightning, radioactivity, discharges, photoelectrons, auroral particles, cosmic rays and solar wind

21 p2680 A73-40079

Oceanic contribution to atmospheric CO budget estimation from Northern Hemisphere water carbon monoxide content, comparing to anthropogenic production

21 p2680 A73-40083

Nonurban nonmethane low molecular weight hydrocarbon concentrations related to air mass identification.

21 p2680 A73-40084

Theoretical model of vertical distributions of CO and CH₄ in the mesosphere and upper stratosphere.

21 p2680 A73-40085

Geomagnetic field, cosmic rays, and radiocarbon content in the earth's atmosphere

21 p2756 A73-40585

Cosmic ray intensity over the past 100,000 to 1,000,000 years and the Kr-81 isotope content in the atmosphere

21 p2756 A73-40586

Nitrogen oxides, nuclear weapon testing, Concorde and stratospheric ozone.

21 p2686 A73-41076

Study of neutral composition of lower thermosphere at Fort Churchill.

21 p2688 A73-41344

Equatorial thermospheric composition and its variations.

21 p2688 A73-41347

Neutral composition and its variations in the lower thermosphere.

21 p2688 A73-41349

Estimates of thermospheric neutral constituents from ion composition measurements.

21 p2688 A73-41350

Variations in density and chemical composition at 120 km from chemical and dynamical processes.

21 p2689 A73-41355

Seasonal variation of atmospheric composition in the F region as a function of solar activity.

21 p2690 A73-41360

Preliminary results of Martian altitude determinations with CO₂ bands (2 micron wavelength) from the automatic interplanetary space station Mars 3.

22 p2905 A73-41807

Airborne IR spectrometer with solar sensor for stratospheric minor molecular constituents vertical distribution, indicating spectral resolution for vibrational-rotational absorption bands

[ONERA, TP NO. 1216]

22 p2847 A73-42221

The effect of atmospheric and physiological conditions on the homogeneity of observations of noctilucent clouds

22 p2847 A73-42448

Ozone composition and nitric oxide injection upper and lower limits for stratosphere by nuclear bomb tests, comparing to estimated SST contribution

22 p2848 A73-42534

Tropospheric aerosol - The relative contribution of marine and continental components.

22 p2849 A73-42547

The temperature dependence of the half widths of some self- and foreign-gas-broadened lines of methane.

22 p2821 A73-42989

The temperature and ammonia profiles in the Jovian atmosphere from inversion of the Jovian emission spectrum.

22 p2915 A73-43017

Jupiter HD absorption line measurement for model-independent number ratio D/H

22 p2916 A73-43125

Transition effects during the recording of the electron-photon component of extensive air showers

23 p3023 A73-43558

Total ozone measurements in cloudy weather.

23 p2973 A73-43853

Principles and possibilities of a new method of ozone measurements within the Huggins bands.

23 p2982 A73-43854

Total ozone increase over North America during the 1960's.

23 p2973 A73-43857

Global climatological ozone changes in terms of secular, annual and sunspot cycle-related variability

23 p2974 A73-43858

The average tropospheric ozone content and its variation with season and latitude as a result of the global ozone circulation.

23 p2974 A73-43862

A new automatic ozone recorder for near-surface measurements working at 19 stations on a meridional chain between Norway and South Africa.

23 p2982 A73-43863

Problems experienced in continuous recording of surface ozone by the electrochemical method at Poona.

23 p2982 A73-43864

Surface ozone in the arctic atmosphere.

23 p2974 A73-43866

Ozone concentration studies and ozone flux measurements near the ground at Poona.

23 p2974 A73-43868

Fourteen-year series of vertical ozone distribution over Arosa, Switzerland, from Umkehr measurements.

23 p2974 A73-43869

Six years of regular ozone soundings over Switzerland.

23 p2974 A73-43870

Studies of variations in the vertical ozone profiles over India.

23 p2975 A73-43871

Studies of the vertical distribution of atmospheric ozone in association with western disturbances over India.

23 p2975 A73-43872

Statistical characteristics of the vertical ozone distribution in mid-latitudes.

23 p2975 A73-43874

The Nimbus-4 backscatter ultraviolet (BUV) atmospheric ozone experiment Two years' operation.

23 p2975 A73-43877

Aerosols - A limitation on the determination of ozone from BUV observations.

23 p2975 A73-43879

The nighttime distribution of ozone in the low-latitude mesosphere.

23 p2975 A73-43881

Statistical analysis for autocorrelation and cross correlation coefficients of mean annual total atmospheric ozone and relative sunspot number as solar activity indicator

23 p2976 A73-43883

Stratospheric methane and nitrogen dioxide from infrared spectra.

23 p2976 A73-43887

Background concentrations of photochemically active trace constituents in the stratosphere and upper troposphere.

23 p2976 A73-43889

The concentration of molecular H₂ and CH₄ in the stratosphere.

23 p2976 A73-43891

A discussion of the chemistry of some minor constituents in the stratosphere and troposphere.

23 p2951 A73-43893

On the vertical distribution of carbon monoxide and methane in the stratosphere.

23 p2976 A73-43894

OH radical concentration in the stratosphere.

23 p2976 A73-43895

Atmospheric ozone and the movement of the air in the stratosphere.

23 p2977 A73-43903

Influence of the vertical motion field on ozone concentration in the stratosphere.

23 p2977 A73-43904

Ozone variation in the lower stratosphere and its mechanism.

23 p2977 A73-43908

Development of an H₂O atmosphere around Comet Kohoutek /1973/ and its possible detection.

23 p3033 A73-43955

IR absorption spectrometry to determine vertical distribution of nitric oxide abundance in stratosphere

23 p2978 A73-43959

Ultraviolet observations of Mars made by the Orbiting Astronomical Observatory.

24 p3128 A73-44397

Sulfuric acid solution composition to account for Venus cloud temperature, stratosphere dryness and IR spectrum

24 p3129 A73-44441

Analysis of spikes in occultation curves - A critique of Brinkmann's method.

24 p3129 A73-44444

Jovian ammonia photolysis to nitrogen, explaining ammonia observations by deep and hot atmosphere and/or electrical discharge phenomena

24 p3065 A73-44536

Behavior of excited atoms and molecules in the upper atmosphere at heights from 40 to 300 km

24 p3084 A73-44803

Helium in the terrestrial atmosphere.

24 p3107 A73-44948

Interpretation of atmospheric radio emission in the 5-mm spectral region

24 p3068 A73-44961

Some characteristics of the global distribution of the trace element concentration in the lower troposphere.

24 p3085 A73-44967

Atmospheric mixing effects for interpretation of oxygen atom concentration in Mars and Venus upper atmospheres obtained by Mariner and Venera space probes

24 p3139 A73-45134

Line strength measurements of the 2 nu sub 3 band of methane. 24 p0366 A73-45320

ATMOSPHERIC CONDITIONS
U METEOROLOGY
ATMOSPHERIC CONDUCTIVITY
NT IONOSPHERIC CONDUCTIVITY
 Rocket sounding for space charge distribution and electric field strength in stratosphere and mesosphere, noting vertical distribution of atmospheric conductivity 05 p0570 A73-17013
 Magnetospheric and ionospheric potential electric fields, using variational process based on transverse/longitudinal conductivity ratios in plasma 07 p0815 A73-19433
 Direct measurements of the electrical conductivity and relaxation time of ionized air in the stratosphere and mesosphere 10 p1211 A73-23890
 Coefficients of hydromagnetic wave reflection from conjugate ionospheres 10 p1211 A73-23895
 Method for determining the longitudinal conductivity of the magnetosphere from the pulsations of a Pi-2 type magnetic field 13 p1606 A73-28291
 Mesospheric positive ion observation via measurement of polar electrical conductivities by subsonic parachute-borne blunt probe system launched on meteorological rockets 18 p2305 A73-36006
 Direct measurements of the electrical conductivity and relaxation time of ionized air in the stratosphere and mesosphere. 20 p2551 A73-38909
 Reflection coefficients of hydromagnetic waves from conjugate ionospheres. 20 p2551 A73-38914

ATMOSPHERIC DENSITY
 Meteoric ablation coefficient and brightness dependence on velocity and atmospheric density, considering molecular screen effect 01 p0101 A73-10847
 A study of the stability of certain self-similar solutions of the theory of explosions in the atmosphere 01 p0035 A73-11429
 A technique for recovering the vertical number density profile of atmospheric gases from planetary occultation data. 02 p0158 A73-11913
 Annual and sub-annual effects of EUV heating. I - Harmonic analysis. II Comparison with density variations. 02 p0158 A73-11914
 Lunar surface observation with cold cathode ionization gage left by Apollo 14, noting low concentration atmospheric particles and gas clouds 02 p0213 A73-12239
 Molecular oxygen densities in atmosphere near 100 km from solar hydrogen Lyman alpha absorption measurements by Intercosmos 4 satellite and Vertical 1 rocket 02 p0160 A73-12275
 Satellite drag data for analysis of semiannual atmospheric density variations, showing latitudinal dependence of amplitude 02 p0161 A73-12281
 Structure of the thermosphere as inferred from incoherent scatter measurements. 02 p0161 A73-12282
 E region wind and density measurements by VHF radar and atmosphere temperature measurement by radio acoustic sounding technique, describing instrumentation and computerized data reduction 03 p0339 A73-15456
 Jupiter atmosphere density fluctuations as cause of time symmetric light flash occurrence during Beta Scorpil occultation 04 p0496 A73-14926
 Annual and semi-annual zonal wind components and corresponding temperature and density variations, 60-130 km. 04 p0440 A73-14961
 Air density at heights near 200 km from the orbit of 1969-20B. 04 p0440 A73-14965
 Computerized parameter estimation by jump detection scheme for nonlinear atmosphere density and temperature profile tracking 04 p0430 A73-15255
 Complete spectrum of pulsation frequencies for a polytropic atmosphere. 04 p0504 A73-16029
 Prediction of the density of the upper atmosphere for the duration of artificial earth satellites. 05 p0567 A73-16091
 Stellar survey at 2000-4100 A via balloon-borne observations, discussing intensity distributions and earth atmospheric ozone layer density 09 p1140 A73-22006
 Neutral thermosphere temperatures from density scale height measurements. 09 p1074 A73-22063

Low latitude density variations in the earth's neutral atmosphere between 200 and 400 km, from August 1969 to May 1970. 09 p1079 A73-22840
 Exact analytical solutions for orbits of bodies with atmospheric drag. 09 p1152 A73-23454
 Upper atmosphere analytical density model for satellite motion prediction, allowing for diurnal and semiannual density variations and solar activity and geomagnetic disturbances effects 10 p1211 A73-23883
 Variations of the structural parameters of the thermosphere from satellite braking data 11 p1350 A73-25076
 Study of the stability of some self-similar solutions from the theory of an explosion in the atmosphere. 11 p1348 A73-26051
 Lower thermosphere density and composition model from satellite drag and accommodation coefficients 12 p1488 A73-26990
 Magnetic control of near equatorial neutral thermosphere, calculating F region ionization anomaly and molecular nitrogen and atomic oxygen density latitudinal variations 12 p1489 A73-26997
 Photochemistry of minor constituents in the troposphere. 12 p1466 A73-27603
 An investigation of the structure of coronal active regions. 12 p1545 A73-27847
 The open-source neutral-mass spectrometer on Atmosphere Explorer-C, -D, and -E. 13 p1616 A73-28628
 Explorer satellite triaxial accelerometer system to determine neutral atmosphere density, monitoring orbit adjust propulsion thrust and measuring spacecraft roll, describing instrument calibration 13 p1688 A73-28631
 Meteoric ablation coefficient and brightness dependence on velocity and atmospheric density, considering molecular screen effect 15 p1928 A73-30983
 A rocket-borne instrument for the measurement of nighttime atmospheric densities. 17 p2164 A73-34270
 Atmospheric density values from radar-determined low altitude satellite orbit decay and accelerometer data 18 p2302 A73-35942
 Combined temperature, diffusion coefficient and density measurements of photoluminescent A10 releases. 18 p2303 A73-35949
 A study of the time lag of the 27-day variation in the thermospheric density. 18 p2303 A73-35961
 Earth radiation pressure and the determination of density from atmospheric drag. 18 p2308 A73-36051
 Air density at heights near 200 km from the orbit of 1970-65D. 18 p2309 A73-36052
 Drag density data from the Cannon Ball II and Musket Ball satellites. 18 p2309 A73-36053
 A comment on the measurement of atmospheric density by absorption of Lyman-alpha. 18 p2309 A73-36054
 Atmospheric density, temperature and winds measured during Aladdin II. 18 p2309 A73-36055
 Neutral winds in the F-region obtained from new models of density and temperature. 18 p2309 A73-36056
 A study of the diurnal variation in the thermosphere as derived by satellite drag. 18 p2309 A73-36059
 An analysis of the solar-activity effects in the upper atmosphere. 18 p2309 A73-36060
 Interpretation of short period density changes shown by the drag of satellites. 18 p2310 A73-36133
 Density scale height and geopotential coefficients evaluations from analysis of Cosmos 54 rocket orbit perturbations due to drag and odd-zonal harmonics 18 p2351 A73-36176
 Results of air temperature, density and pressure measurements obtained with the aid of foil cloud sensors in the height region between 80 and 95 km. 18 p2311 A73-36179
 Thermospheric density variations associated with auroral electrojet activity. 18 p2312 A73-36280
 Solar wind-Mercury atmosphere interaction - Determination of the planet's atmospheric density. 18 p2352 A73-36294
 Density measurements in the equatorial atmosphere by means of the San Marco 3 satellite 19 p2426 A73-38151

Upper atmosphere analytical density model for satellite motion prediction, allowing for diurnal and semiannual density variations and solar activity and geomagnetic disturbances effects 20 p2550 A73-38902
 Low value atmospheric density extremes evaluation covering ground elevations up to 15,000 feet for engine power calculation in aircraft design 21 p2729 A73-40063
 On the diurnal variations of total mass density, number density and temperature in the upper thermosphere. 21 p2682 A73-40170
 Upper atmospheric models dealing with diurnal variation and latitudinal density dependence to derive time and space dependencies 21 p2683 A73-40631
 Secular perturbations of the motion of artificial satellites, caused by atmospheric drag 21 p2768 A73-40725
 Structure variations in the winter polar atmosphere. 21 p2685 A73-40827
 Diurnal density variations measured by the San Marco III satellite in equatorial orbit. 21 p2685 A73-40830
 Problems of the aerodynamics of satellites with uniaxial orientation 21 p2781 A73-40902
 Thermospheric density diurnal and seasonal variations from cosmos drag data, discussing amplitude, density distribution, coefficients of expansion, summer solstice spherical functions 21 p2689 A73-41351
 Structure of the neutral atmosphere between 150 and 500 km. 21 p2689 A73-41352
 An analysis of the altitude dependence of the geomagnetic effect by means of 'equivalent durations.' 21 p2689 A73-41353
 Global thermospheric wind distribution computed by solving Navier-Stokes equations with models at upper atmospheric densities and ion distribution 21 p2689 A73-41354
 Variations in density and chemical composition at 120 km from chemical and dynamical processes. 21 p2689 A73-41355
 Evaluation of the accuracy of predicting the motion parameters of low-orbit artificial earth satellites 23 p3027 A73-43266
 An atmosphere on Ganymede from its occultation of SAO 186800 on 7 June 1972. 23 p3027 A73-43337
 Densities deduced from perturbations at high altitudes. 23 p2972 A73-43688
 Changes in the distribution of density and radio scattering in the solar corona in 1971. 24 p3138 A73-45049
 Atomic oxygen densities in the lower thermosphere as derived from in situ 5577-A night airglow and mass spectrometer measurements. 24 p3086 A73-45122
 Energetic dissociative recombination oxygen atom production and exospheric redistribution for high/low solar conditions in terms of ballistic trajectories and neutral density models 24 p3086 A73-45131

ATMOSPHERIC DIFFUSION
 Relations among stability parameters in the surface layer. 01 p0073 A73-10497
 Atmospheric diffusion, radio meteor trail radius and electron density distribution effects on radar echoes time position, noting recorder resolution increase 05 p0617 A73-16613
 Approximate analytical solutions of the diffusion equation for Jacchia's statistical models of the upper atmosphere 05 p0570 A73-17014
 Neutron diffusion from a distributed source in a homogeneous atmosphere 06 p0742 A73-17549
 Symposium on Air Pollution, Turbulence and Diffusion, Las Cruces, N. Mex., December 7-10, 1971, Proceedings. 09 p1114 A73-22326
 Atmospheric dispersion of air pollutants, analyzing buoyant plumes and wakes 10 p1205 A73-23857
 Dependence of the diffuse expansion characteristics of a crystallization zone on the vertical stability of the atmosphere 13 p1654 A73-28879
 Energy and diffusive mass transport relation to thermospheric circulation, composition, temperature and mass density from three dimensional two constituent magnetic storm model 14 p1748 A73-29975
 Neutron diffusion from a distributed source in an inhomogeneous atmosphere. 16 p2052 A73-32773
 Preliminary estimates of the fate of SST exhaust materials using a coupled diffusion/chemistry model. [AIAA PAPER 73-535] 16 p2046 A73-33567

The interaction of a transient exhaust plume with a rarefied atmosphere.

16 p2086 A73-33873

Diffusion and fallout of pollutants emitted by aircraft engines.

19 p2474 A73-38323

ATMOSPHERIC ELECTRICITY

NT AURORAL ELECTROJETS

NT ELECTROJETS

NT EQUATORIAL ELECTROJET

NT IONOSPHERIC CURRENTS

Investigation of the electrical parameters and meteorological elements of the atmosphere close to the ground during thunderstorm and thunderstorm-free periods

02 p0189 A73-12589

Electrostatic autopilot using atmosphere electric field lines for stabilization and guidance, applying to remotely piloted vehicles

02 p0191 A73-12595

Plasma convection in the vicinity of the geosynchronous orbit.

03 p0303 A73-13878

Instrument suspended from tethered balloon for oceanic measurement of average lower atmosphere vertical electric field profile

05 p0579 A73-17251

Variation of atmospheric electric field during aurorae.

07 p0820 A73-20216

Measurement of the horizontal component of the electrostatic field intensity in the lower atmosphere

10 p1219 A73-24400

Explanation of the accident to the Europa II F 11 launcher by phenomena of electrostatic origin

11 p1431 A73-25749

Atmospheric convection and its effect on relaxation time and charge distribution.

11 p1394 A73-25759

Measurement of point-discharge current density in the atmosphere.

11 p1354 A73-25767

The orientations of ice crystal models during a fall in an electric field

13 p1654 A73-28882

Stratiform cloud electrical characteristic changes under solid carbon dioxide seeding in aircraft experiments

13 p1654 A73-28884

Electrical breakdown caused by dust motion in low-pressure atmospheres - Considerations for Mars.

15 p1941 A73-32267

Electrical balance in the lower atmosphere.

17 p2158 A73-34359

Statistical analysis of daily, monthly, annual and seasonal activity of earth currents field, presenting tables of storms and disturbances

21 p2681 A73-40107

Point discharge current measurements in trees and metal points during storms, discussing implications for structure of electrified clouds

21 p2684 A73-40779

ATMOSPHERIC EMISSION

U AIRGLOW

ATMOSPHERIC ENTRY

NT HYPERBOLIC REENTRY

NT HYPERSONIC REENTRY

NT MANNED REENTRY

NT SPACECRAFT REENTRY

Radiative and convective heating during Venus entry.

01 p0003 A73-10757

Optimal lift control by Miele's method for the atmospheric entry of a hypersonic glider. I - Simple type problems.

03 p0245 A73-13766

Spacecraft optimal control after transfer from hyperbolic trajectory to planetary orbit by atmospheric drag, minimizing engine thrust

03 p0340 A73-14570

Optimal lift control by Miele's method for the atmospheric entry of a hypersonic glider. II - Isoperimetric type problems.

04 p0404 A73-15168

Prediction in control of re-entry into the atmosphere.

05 p0627 A73-16076

Synthesis of a nonlinear control law for the motion of a space vehicle in the earth's atmosphere.

05 p0627 A73-16077

Problems of realization of optimal trajectories for spacecraft entry into the dense layers of the earth's atmosphere

05 p0616 A73-16409

Effects of nonequilibrium ablation chemistry on Viking radio blackout.

05 p0551 A73-16981

Study of accuracy requirements for autonomous trajectory measurements providing conditions for entering planetary atmospheres

05 p0619 A73-17001

Stabilization concepts for a spherical planetary entry probe configuration.

06 p0756 A73-17653

Aerodynamic entry vehicle autopilots.

06 p0721 A73-18151

Nuclear particle fluxes and radioactive isotopes production rate distribution from cosmic rays data along orbits, calculating iron meteorite dimensions prior to atmosphere entry

08 p1012 A73-21582

Stagnation region radiative heating with steady-state ablation during Venus entry.

08 p1025 A73-21817

Optimal lift control by Miele's method for the atmospheric entry of a hypersonic glider. III.

10 p1285 A73-23616

Some problems of optimal control of space-vehicle trajectories in the Martian atmosphere

10 p1247 A73-23878

Atmospheric braking of a manned spacecraft after interplanetary flight

10 p1286 A73-23879

An analytical estimate of the effect of mobility of a small internal mass on oscillations of a body during deceleration in the atmosphere

10 p1286 A73-24451

Temperature gradients and atmospheric ablation rates for the Barwell meteorite.

11 p1419 A73-25779

Accelerating search-variable metric algorithm combination for space shuttle atmospheric flight optimization, comparing with cubic fit-golden section method

13 p1650 A73-28825

Optimal descent maneuver with a limited-thrust engine for entry at a prescribed angle into the atmosphere of a planet

13 p1689 A73-29139

Development of the Viking parachute configuration by wind tunnel investigation.

[AIAA PAPER 73-454]

15 p1826 A73-31440

Thermodynamic characteristics of the lower atmosphere of Venus on the basis of the results of an experiment conducted with the descent vehicle of the Venus 4 interplanetary probe

16 p2067 A73-33800

Scientific considerations for a common Saturn/Uranus atmospheric entry probe.

[AIAA PAPER 73-594]

18 p2350 A73-36080

Spacecraft microbial burden reduction due to atmospheric entry heating - Jupiter.

18 p2281 A73-36100

Effect of nose geometry on the aerothermodynamic environment of shuttle entry configurations.

[AIAA PAPER 73-638]

18 p2260 A73-36196

Fully coupled nongray radiating gas flows with ablation product effects about planetary entry bodies.

[AIAA PAPER 73-672]

18 p2368 A73-36223

Ablation and radiation coupled viscous hypersonic shock layers.

18 p2264 A73-36315

Heat shielding for Venus entry probes.

[AIAA PAPER 73-712]

18 p2368 A73-36332

Reflecting heat-shield entry analysis computer program for planetary probes.

[AIAA PAPER 73-714]

18 p2368 A73-36333

Planetary atmospheric entry vehicles shock layer energy transport with nongray radiation, using optical thick-thin approximation for radiative transfer in temperature distribution calculation

[AIAA PAPER 73-715]

18 p2369 A73-36334

Viscous effects in massively-ablating planetary entry body flow fields.

[AIAA PAPER 73-716]

18 p2264 A73-36335

Effect of downstream massive blowing on Jovian entry heating.

[AIAA PAPER 73-717]

18 p2264 A73-36336

Thermal control subsystem design of a Saturn/Uranus atmospheric entry probe for descent missions to 20 bars.

[AIAA PAPER 73-770]

18 p2360 A73-36384

Pioneer Venus mission plan for atmospheric probes and an orbiter.

[AIAA PAPER 73-579]

18 p2353 A73-36499

Pioneer spacecraft for atmospheric entry missions to the outer planets.

[AIAA PAPER 73-595]

18 p2360 A73-36500

Nonequilibrium effects on shock-layer radiometry during earth entry.

18 p2338 A73-36798

Analytical estimate of the effect of the motion of a small internal mass on the oscillation of a body decelerating in the atmosphere.

19 p2494 A73-38131

Atmospheric entry and impact behavior of modular disk shaped radioactive isotope heat source for space nuclear power

19 p2454 A73-38387

A new approach to performance optimization of the 1975 Mars Viking lander.

[AIAA PAPER 73-889]

20 p2614 A73-38825

Linear filtering of ballistic-entry-probe data for atmospheric reconstruction.

[AIAA PAPER 73-904]

20 p2589 A73-38838

Some problems in the optimal control of spacecraft trajectories in the Martian atmosphere.

20 p2589 A73-38897

Atmospheric deceleration of a manned spacecraft returning from an interplanetary flight.

20 p2614 A73-38898

Planetary Atmosphere Experiments Test vehicle reentry into earth atmosphere for flight experience, discussing onboard instrumentation

24 p3088 A73-44440

ATMOSPHERIC ENTRY SIMULATION

Molecular beam simulation of planetary atmospheric entry - Some recent results.

03 p0287 A73-13564

The laser heated wind tunnel - A new approach to hypersonic laboratory simulation.

[AIAA PAPER 73-211]

05 p0563 A73-16942

Systems analysis applied to a hybrid computer simulation of a missile reentering the atmosphere.

08 p0941 A73-20825

Measurements of hydrogen-helium radiation at shock-layer temperatures appropriate for Jupiter entry.

22 p2938 A73-42993

ATMOSPHERIC HEAT BUDGET

Condensation trail effects on atmospheric radiation budget from model calculation for ice particle layer near tropopause, using Mie scattering and radiative transfer approximation

01 p0038 A73-10389

Energy balance and field equations of dissipative atmosphere oscillations for zonal semidiurnal Pedersen region, using K-Hermitecity

02 p0158 A73-11907

Upper atmospheric dust particle temperature and related Na atom abundance seasonal variation based on energy budget and Na sublimation rate considerations

05 p0571 A73-17061

Measurements of solar energy reflected by the earth and atmosphere from meteorological satellites.

08 p0958 A73-21268

Some results of investigations programmed according to the complex atmospheric energetics experiment /1970-1972/

09 p1115 A73-22989

The radiation balance of the earth-atmosphere system - Recent results from satellite measurements

10 p1213 A73-24399

Global climatic model based on time and space averaged thermodynamic energy equation for idealized land-water distribution, allowing for continents-oceans seasonal interactions

12 p1519 A73-26801

Diurnal thermospheric heat budget in terms of electron-ion recombination, photodissociation and neutral wind energy transfer and conductive and radiative cooling

12 p1492 A73-27604

Turbulent heat transfer role in atmospheric thermal budget, deriving smoothed local temperature time derivative

15 p1906 A73-32348

The atmospheric aerosol and its significance for the energy budget of the atmosphere

17 p2159 A73-34749

Wave-mean flow interactions in the upper atmosphere.

19 p2427 A73-38217

Lower atmospheric intensity-calibrated thermal emission spectra with digital recording near IR spectrometer, discussing applications to pollutant detection

21 p2692 A73-41574

Relation between the intensity of the stratospheric circumpolar vortex and the accumulation of ozone in the winter hemisphere.

23 p2977 A73-43905

Aerosol influence on atmospheric radiative cooling, calculating long wave flux divergence dependence on particle size, relative humidity and refractivity

23 p2978 A73-43984

Stormy weather vertical air motion velocity calculation for use in synoptic field and atmospheric energy budget evaluations

23 p3003 A73-43996

ATMOSPHERIC HEATING

Book - Emission, absorption, and transfer of radiation in heated atmospheres.

01 p0119 A73-10125

Hemispheric synoptic analysis of upper stratospheric warming for energy transformations in troposphere and lower and middle stratosphere

01 p0072 A73-10141

Global mean radiative equilibrium model for Venusian mesosphere, determining horizontal variation of thermal heating and cooling

01 p0097 A73-10361

Tropical atmosphere radiative heating estimates for BOMEX /Barbados Oceanographic and Meteorological Experiment/ from direct radiation measurements, satellite images and surface and rawinsonde data

01 p0038 A73-10387

Annual and sub-annual effects of EUV heating. I - Harmonic analysis. II Comparison with density variations.

02 p0158 A73-11914

Drag derived density analysis for geomagnetic disturbances effect in thermosphere, noting at-

mospheric reaction time delay and exospheric temperature increment per unit Kp
02 p0161 A73-12280

Corpuscular radiation as an upper atmospheric energy source.
02 p0205 A73-12289

Quiet time magnetosphere-thermosphere couplings, describing global wind system model and convection and auroral Joule heating
02 p0162 A73-12292

Seasonal and monthly global atmosphere radiative profiles of thermal and solar heating due to ozone and cooling due to carbon dioxide
02 p0165 A73-12780

Chromospheric heating of very hot stars by radiation driven sound waves.
03 p0371 A73-13222

Simulations of the annual variation of the zonally averaged state of the atmosphere.
03 p0301 A73-13799

A numerical study of coupling between the boundary layer and free atmosphere in an accelerated low-latitude flow.
05 p0592 A73-16193

Infrared radiative heating and cooling in the Venusian mesosphere. I - Global mean radiative equilibrium.
05 p0613 A73-16197

Calculation of averaged values for short- and long-wave fluxes and influxes in a real atmosphere
05 p0593 A73-16243

Thermal effects experienced by meteoritic particles during atmospheric flight and upon earth surface impact
06 p0749 A73-17839

Heating of the upper atmosphere during aurorae and auroral rays length.
08 p0957 A73-20663

The heating of the solar corona. I - Observation of ion energies in the transition zone.
08 p1005 A73-20919

Short-wave spectral radiant heat influx in the atmosphere
08 p0984 A73-21133

Study of the radiative properties of the atmosphere between cloud layers
09 p1114 A73-22371

Chromospheric heating of very hot stars by radiation driven sound waves. II.
09 p1148 A73-22868

Auroral atmosphere temperature variations relation to nightly auroral streamer length variations, assuming ionospheric current dissipation as heat source
12 p1491 A73-27344

Auroral heating and the composition of the neutral atmosphere.
12 p1492 A73-27602

The heating of the thermosphere by atmospheric gravity waves
12 p1493 A73-27758

Isothermal ionization of the lower ionosphere under the effect of radio waves.
13 p1608 A73-28709

An analytic formula for heating due to ozone absorption.
14 p1750 A73-30767

Relationship between stratospheric warming and ionospheric absorption.
16 p2009 A73-33887

IR laser induced change in atmospheric temperature as function of time, using kinetic model with input molecular energy transfer rates for thermal blooming
17 p2163 A73-35414

Extreme temperature deviations from the climatological mean in the upper stratosphere - observed by rockets, confirmed by satellites.
18 p2304 A73-35962

Meteor radar study of tides in the 80 to 100 km altitude range.
18 p2305 A73-35999

Midwinter mesospheric cooling during stratospheric warming, discussing circulation, stratosphere-mesosphere interactions and summertime temperature values at midwinter mesopause
18 p2308 A73-36037

A prediction of the phenomena that take place during so called 'sudden warmings.'
18 p2308 A73-36038

Spacecraft microbial burden reduction due to atmospheric entry heating - Jupiter.
18 p2281 A73-36100

Semiannual effect in thermosphere due to solar heat input associated with subsolar point migration and auroral heating by magnetic storms
18 p2312 A73-36300

A preliminary study of the transient response of the atmosphere produced by mid-tropospheric heating.
18 p2332 A73-36701

On the energetics and momentum balance of pole-equator temperature differences in the sun.
19 p2485 A73-37620

Global model of the general circulation of the atmosphere below 75 kilometers with an annual heating cycle.
19 p2449 A73-38287

Dynamic coupling of the stratosphere with the troposphere and sudden stratospheric warmings.
19 p2449 A73-38288

New evidence for effects of variable solar corpuscular emission on the weather.
21 p2755 A73-40073

Heating of the low-latitude upper atmosphere caused by the decaying magnetic storm ring current.
21 p2684 A73-40786

The stratospheric circulation over Middle Atlantic latitudes in the 1966-1971 period.
21 p2687 A73-41339

An analysis of the altitude dependence of the geomagnetic effect by means of 'equivalent durations.'
21 p2689 A73-41353

Radio frequency heating effects on electron density in the lower E region.
22 p2845 A73-41930

Measurements of hydrogen-helium radiation at shock-layer temperatures appropriate for Jupiter entry.
22 p2938 A73-42993

Auroral atmosphere temperature variations relation to nightly auroral streamer length variations, assuming ionospheric current dissipation as heat source
23 p2970 A73-43241

Global distribution of thermospheric heat sources - EUV absorption and Joule dissipation.
23 p2971 A73-43681

Model for radiative dynamic instability of cloudy planetary atmosphere from coupling for case of radiative heating rate dependent cloud properties
24 p3132 A73-44534

Further aspects of weak shock theory applied to the solar chromosphere.
24 p3135 A73-44630

The thermospheric heating function. III - The function describing the heating of the thermosphere by short-wave solar radiation during a period of high solar activity
24 p3084 A73-44800

ATMOSPHERIC IMPURITIES

U AIR POLLUTION

ATMOSPHERIC IONIZATION

NT AURORAL IONIZATION

D and E region aeronomy, discussing ionization sources, ion composition, water cluster ion formation and ratio of molecular oxygen and nitric oxide ions
01 p0040 A73-10877

Ionization sources of the ionospheric D and E regions.
01 p0041 A73-10886

Ion composition dependent recombination coefficient loss rate changes in D region during solar flares, using electron density and X ray flux measurements
01 p0042 A73-10903

Synoptic studies of D-region ionization changes and electron densities by the partial reflection differential absorption experiment.
01 p0042 A73-10904

D and E ionospheric regions behavior, emphasizing water cluster ions formation, minor neutral constituents measurement and daytime ionization sources
01 p0043 A73-10912

Upper limits on the lunar atmosphere determined from solar-wind measurements.
02 p0211 A73-11727

Earth atmosphere He isotopes abundance based on calculation of ionization rates and solar wind interaction during geomagnetic dipole reversal
02 p0156 A73-11741

Energetic metastable molecular oxygen as a source of ionization in the D region.
02 p0157 A73-11757

Molecular nitrogen vibrational temperature in E and F regions, using positive ion data and model for ionic reaction rate and continuity equation numerical solution
02 p0161 A73-12279

Observation and interpretation of ionization drift measurements in the F region at St-Santin-Nancy.
02 p0161 A73-12284

Interaction between gravity waves and ionization in the ionospheric F region.
02 p0162 A73-12298

Electron production rates and density profiles in D region during solar flares, presenting ionization vertical distribution model
02 p0206 A73-12304

Electron density fluctuations during periods of scattered reflections at the ionospheric F-region maximum ionization level
02 p0164 A73-12359

Statistical analysis of atmospherics sudden changes in VLF bands, suggesting lower ionosphere ionization increase due to meteors incidence
03 p0299 A73-12948

Possibility of continuous monitoring of celestial X-ray sources through their ionization effects in the nocturnal D-region ionosphere.
03 p0361 A73-13361

Ionospheric total electron content measurements from the Australian zone.
03 p0299 A73-13632

ATMOSPHERIC IONIZATION

Bombardment of the polar-cap ionosphere by solar cosmic rays.
03 p0301 A73-13710

Thermospheric parameters seasonal and latitudinal variations calculation based on atmospheric model with components ionization and molecular oxygen dissociation as main heat sources
03 p0304 A73-14563

Instabilities resulting from gravity wave perturbation of ionization via neutral-charged particle collisions in nighttime E region
03 p0305 A73-14595

Constant height sporadic E velocities and heights at night explained via instabilities generated from recombination and photoionization rate variations induced by gravity wave perturbations
03 p0305 A73-14596

E layer ionization diurnal exponent independence of seasons and station latitude ascertained by statistical tests
05 p0571 A73-17058

Contribution of hard solar X-ray radiation to D-region ionization.
05 p0611 A73-17172

Correlations between X-rays and UV ionizing radiation in the E region from data obtained during the solar eclipse of 25 February 1971
06 p0742 A73-17534

Sporadic E relation to ionized particle redistribution in E layer during solar eclipse
07 p0815 A73-19256

Photoelectron precipitation induced dissociation of atmospheric nitrogen molecules during moderate solar activity
07 p0816 A73-19459

Magnesium and associated ionospheric processes in Es-layer formation.
08 p0957 A73-20655

Impact and bremsstrahlung photoionization due to precipitating electrons in the lower ionosphere.
08 p0957 A73-20657

Collision cross sections for electrons with atmospheric species.
08 p0957 A73-20659

Shock waves and flares by meteors.
08 p1010 A73-21317

Charge separation induced vertical electric field calculated for wind motion periodic with height, latitude and longitude at magnetic equator, noting relationship to electrojet
09 p1074 A73-22067

Nighttime midionosphere dynamical perturbations on ionizations from solutions of time dependent continuity equation with charge transport effects, considering semidiurnal atmospheric tide propagation mode
09 p1075 A73-22130

Investigation of geoactive corpuscular particles and photoelectrons on board the Cosmos 261 satellite. V - Spectra of ionospheric photoelectrons and migration of the latter from the conjugate ionosphere
10 p1211 A73-23887

Nonstationary distribution of the electron-ion gas in the ionosphere.
10 p1212 A73-24239

Upper sporadic E layer downward velocity, considering corkscrew mechanism, ionization following gravity wave particular phase and velocity decrease
10 p1215 A73-24750

Recombination coefficient, heat flux, ionization balance and photoelectron kinetic energy from ionospheric electron temperature and density profiles and solar UV absorption data
11 p1350 A73-25081

Prenoon anomaly of ionization in the F region at the transition latitudes
11 p1350 A73-25090

On the solar Lyman alpha control of the ionospheric absorption at 2775 kHz.
11 p1412 A73-25770

Solar 1.9 A X ray spectral line effects on SOLRAD satellite-borne photometer sensitivity and lower ionospheric ion production rate
11 p1354 A73-25771

Energetic electron precipitation as a source of ionization in the night-time D-region over the mid-latitude rocket range, South Uist.
11 p1358 A73-26701

Magnetic control of near equatorial neutral thermosphere, calculating F region ionization anomaly and molecular nitrogen and atomic oxygen density latitudinal variations
12 p1489 A73-26997

Isothermal ionization of the lower ionosphere under the effect of radio waves.
13 p1608 A73-28709

Effect of Debye shielding on the ionization energy of air plasma components
13 p1667 A73-29164

Rocket-based mass spectrometric measurements of midlatitude and north polar region ionospheric ion composition, discussing ionization of water and heavy water vapors
14 p1747 A73-29864

Ionospheric nitrogen ion density from rocket-borne dayglow spectrometry, considering charge exchange with metastable oxygen ions and solar EUV photoionization as ionizing mechanisms

14 p1723 A73-29953

Jupiter, Saturn, Uranus and Neptune upper atmospheric ionization equilibrium distribution, emphasizing ionosphere

14 p1799 A73-30535

Structure and time variations of the Jovian ionosphere.

15 p1929 A73-31066

Formation of blanketing sporadic E-layers at the magnetic equator due to horizontal wind shears.

15 p1866 A73-31070

Ion and electron diffusion in nonisothermal ionospheric F layer, analyzing ionization balance equations

15 p1871 A73-31882

Ionospheric D region dissociation-recombination reaction constants derived from ion production rate data compiled during polar cap absorption

15 p1872 A73-31887

Ionization of the atmosphere and attenuation of radar waves after a nuclear explosion.

15 p1844 A73-32198

Correlations between X-rays and ionizing ultraviolet radiation in the E-region, according to data from the solar eclipse of February 25, 1971.

16 p2052 A73-32758

F 2 critical frequency and maximum height at high southern latitudes explained via additional ionization provided by energetic particles

16 p2009 A73-33911

Physics and chemistry of the ionosphere.

17 p2162 A73-335050

Construction of D-region electron-density profiles by combined use of ground-based reflection and satellite-based transmission measurements.

18 p2306 A73-36016

Cosmic ray total ionization - 1970-1972.

18 p2347 A73-36293

Investigation of geoeactive corpuscles and photoelectrons with the Cosmos 261 satellite. V - Spectra of ionospheric photoelectrons and their transfer from the conjugate ionosphere.

20 p2550 A73-38906

Venus topside ionosphere He content estimated from ionization profiles and discovery of radioactive materials in crust

20 p2604 A73-38942

Dynamics of ionization inhomogeneities in the ionosphere

20 p2553 A73-39152

Vertical sounding investigation of ionospheric ionization inhomogeneity sizes, orientation, elongation degree and drift rate, determining F region electron density fluctuations

20 p2553 A73-39155

Application of mathematical methods for the description of the planetary distribution of ionosphere parameters

20 p2554 A73-39169

Position of the equatorial boundary of the anomalous ionization occurrence region in relation to the planet's magnetic activity during the solar activity cycle

20 p2554 A73-39175

Functional relation between the F2-layer ionization state in daylight time and the zenith angle of the sun

20 p2555 A73-39178

Laboratory studies of collisions of energetic H⁺ and hydrogen with atmospheric constituents.

21 p2679 A73-40072

Interaction of the lower thermosphere with the solid component of the interplanetary medium.

21 p2682 A73-40158

Jovian ionospheric and magnetospheric ionization and temperature distributions from solutions of momentum and chemical equations for electrons, ions and neutrals, and heat transport equation

21 p2764 A73-40165

Analytical approach to the direct and inverse problems of cosmic ray action on the lower ionosphere

21 p2759 A73-40609

Midlatitude spread F relationship to F region trough formation, considering multiple reflections emanating from steep ionization contours

21 p2684 A73-40784

The optimal number of soundings for a complete investigation of the ionization-neutralization and dynamic characteristics of the middle ionosphere

21 p2686 A73-40911

Rocket measurements of production and ionization during a PCA event.

21 p2760 A73-41371

On the detection of X-rays from celestial sources through their ionization of the terrestrial atmosphere.

21 p2762 A73-41394

Ionospheric aeronomy problems with emphasis on photochemical processes of neutral and ionized components, discussing nighttime ionizing agents, ion recombination, water vapor and nitrogen oxide behavior, etc

23 p2978 A73-43977

Positive nitrogen ions in midlatitude atmosphere, discussing concentration dependence on height, solar zenith angle and activity level

24 p3084 A73-44801

Atomic nitrogen and nitrogen oxide in the perturbed ionosphere at heights ranging from 100 to 200 km

24 p3066 A73-44802

Nighttime sporadic E layer measurements and integrated content measurements at Arecibo Observatory, using Barker coded incoherent scatter radar pulses

24 p3087 A73-45142

E and F layers, discussing formation, collision processes and S and L geomagnetic variations

24 p3087 A73-45204

ATMOSPHERIC MODELS

NT BREADBOARD MODELS

NT DYNAMIC MODELS

NT REFERENCE ATMOSPHERES

A general circulation model of the atmosphere suitable for long period integrations.

01 p0072 A73-10143

Numerical solution for propagation of longitudinal waves along the geomagnetic field using a three-fluid ionosphere model.

01 p0016 A73-10197

An efficient, one-level, primitive-equation spectral model.

01 p0072 A73-10248

Refraction of whistler-mode waves by large-scale gradients in the middle-latitude ionosphere.

01 p0017 A73-10328

A two-component model of the annual line in the spectrum of the geomagnetic field.

01 p0036 A73-10331

Jovian atmosphere absorption line and spectroscopic data interpretation based on model for structure, composition and radiative properties of visible cloud layers

01 p0097 A73-10359

Global mean radiative equilibrium model for Venusian mesosphere, determining horizontal variation of thermal heating and cooling

01 p0097 A73-10361

Synthetic spectra production via solution of radiative transfer equation at frequencies across absorption line for homogeneous and inhomogeneous atmospheres

01 p0097 A73-10362

Transmittance functions for satellite temperature sounding.

01 p0037 A73-10367

Nongray atmospheric model to assess radiative effects of water vapor and carbon dioxide layer injected into lower stratosphere by SST and HST exhaust gases

01 p0038 A73-10388

Condensation trail effects on atmospheric radiation budget from model calculation for ice particle layer near tropopause, using Mie scattering and radiative transfer approximation

01 p0038 A73-10389

A detailed radiation model for climate studies - Comparisons with a general circulation model radiation subroutine.

01 p0039 A73-10393

Nongray theory for temperature wave propagation without turbulent or convective motions, discussing diurnal waves simulation for planetary atmospheres

01 p0039 A73-10396

Model analysis for heat radiation effect on development and evolution of single buoyant thermal rising in neutrally stratified atmosphere, noting radiative relaxation time

[AD-755499]

01 p0039 A73-10398

The Air Force Global Weather Central operational boundary-layer model.

01 p0074 A73-10499

Homogeneous gas sphere model light scattering for different energy source distributions in planetary and stellar atmospheres

01 p0100 A73-10704

The possibility of a consistent explanation of various phenomena involving cosmic ray muons.

01 p0092 A73-10789

Mass spectrometric measurements of minor constituents in the lower thermosphere.

01 p0041 A73-10880

Positive ion composition measurements in disturbed D region, noting positive molecular oxygen ions as major source of water cluster ions

01 p0041 A73-10890

A nighttime ionospheric E-region model.

01 p0042 A73-10893

General solution for polarized radiation in a homogeneous-slab atmosphere.

01 p0078 A73-11033

Backward Monte Carlo calculations of the polarization characteristics of the radiation emerging from spherical-shell atmospheres.

01 p0078 A73-11233

Inner magnetosphere distortions during magnetic storm development phase from Explorer 26 observations, comparing with Williams-Mead, ring current and compression models

02 p0156 A73-11747

E region irregularities investigation via phase path measurements and radio wave ionospheric soundings, using model for undulatory variation of reflection height

02 p0158 A73-12028

Changes of lower ionosphere electron concentrations with solar activity.

02 p0159 A73-12029

Models of extreme arctic and subarctic winter atmospheres between 20 and 90 km.

02 p0160 A73-12274

Global distributions of thermal energy content and losses in thermosphere, discussing energy sources, continuity equations and transport mechanisms for heat balance

02 p0162 A73-12288

Theoretical model of diurnal variations of the equatorial thermosphere at equinox.

02 p0162 A73-12290

Quiet time magnetosphere-thermosphere couplings, describing global wind system model and convection and auroral Joule heating

02 p0162 A73-12292

Inaccuracy sources in winds calculation from thermospheric models, considering neutral air motions due to global pressure variations

02 p0189 A73-12293

Horizontal and vertical drift motions in F 2 region caused by electrostatic and geomagnetic fields

02 p0162 A73-12294

Interaction between gravity waves and ionization in the ionospheric F region.

02 p0162 A73-12298

Electron production rates and density profiles in D region during solar flares, presenting ionization vertical distribution model

02 p0206 A73-12304

Uniformly rotating stars with hydrogen- and metallic-line blanketed model atmospheres.

02 p0222 A73-12712

A method for incorporating nested finite grids in the solution of systems of geophysical equations.

02 p0165 A73-12776

Atmospheric aerosol Mie scattering calculation as function of polarization parameters based on models for three laser wavelengths and two materials

03 p0341 A73-12900

Blanketed model atmospheres for cool hydrogen-rich white dwarfs.

03 p0371 A73-13225

Satellite transmitted impulse response transfer function evaluation by ray tracing technique for ionospheric model with Chapman ionization vertical profile

03 p0299 A73-13630

Computed effects of the ionosphere/protonosphere distribution on VHF signals from ATS-F/G.

03 p0275 A73-13641

Diurnal and latitudinal variations and frequency dependence of scintillation due to ionospheric irregularities, using rms electron density fluctuation and transverse scale size model

03 p0275 A73-13643

Simulations of the annual variation of the zonally averaged state of the atmosphere.

03 p0301 A73-13799

Solar wind interaction with geomagnetic field, discussing magnetosphere polar cusp region and geomagnetic tail neutral sheet structure

03 p0302 A73-13871

Magnetospheric thermal plasma and hydrogen cation density profile characteristics in different local time regions explained by time-varying convection model

03 p0303 A73-13879

High energy proton model for the inner radiation belt.

03 p0363 A73-13880

Atmospheric model for substorm triggering mechanism, plasma sheath behavior and substorm recovery, noting solar wind interaction with magnetosphere

03 p0304 A73-13886

On the meridional form of baroclinic waves in a two-layer quasi-geostrophic model.

03 p0304 A73-14312

Solar atmosphere inhomogeneities from observations, discussing theoretical analysis via two dimensional model atmosphere

03 p0377 A73-14406

Current sheet model for sunspot structure, considering ohmic dissipation as decay mechanism

03 p0377 A73-14408

Observations of the intensity of the penumbra of sunspots.

03 p0377 A73-14409

Degree and direction of polarization of multiple scattered light. I - Homogeneous cloud layers.

03 p0344 A73-14427

Storm cell models from digital radar data.

03 p0338 A73-14510

Thermospheric parameters seasonal and latitudinal variations calculation based on atmospheric model with components ionization and molecular oxygen dissociation as main heat sources

03 p0304 A73-14563

Geomagnetic tail quantitative model with validity to beyond moon orbit, noting adequacy of representation under quiet conditions 03 p0304 A73-14590

Absorption measurements at Calcutta compared with current D region models for atomic oxygen production and loss processes 03 p0305 A73-14594

Solar proton intensity structures in the magnetosphere during interplanetary anisotropies. 04 p0492 A73-14962

M giant atmospheric molecular evolution, discussing carbon/oxygen ratios, s-process overabundances and relationships between M, S and C stars 04 p0496 A73-14971

Helmholtz-Rayleigh instability of nondivergent horizontal flows in a barotropic atmosphere 04 p0441 A73-15287

Magnetosphere configuration models based on open and closed field line hypotheses, discussing solar wind-magnetosphere interactions, magnetotail, sub-storm growth, flux transport, etc 04 p0441 A73-15327

Multipath fading and ionospheric scintillation modes of propagation anomalies measurement to formulate models of propagation media 04 p0422 A73-15440

FM Gaussian electromagnetic pulse distortion during reflection from ionospheric model with linear electron density profile and constant collision frequency 04 p0422 A73-15479

Effects of uncertainties in damping and microturbulence on theoretical deductions from solar equivalent widths. 04 p0500 A73-15491

Theoretical model for the latitude dependence of the thermospheric annual and semiannual variations. 04 p0444 A73-15538

Two layer model for diurnal temperature variations analysis of radiative heat transfer between planetary lower atmosphere and underlying 04 p0473 A73-15574

Steady axisymmetric ring current models computed with energy density distribution parameters variations for effects on magnetic field and particle belt parameters 05 p0609 A73-16144

Ionospheric double layer theory extended to conditions including gravity and expansion effects in diverging geomagnetic flux tubes 05 p0568 A73-16145

Cloudiness as a global climatic feedback mechanism - The effects on the radiation balance and surface temperature of variations in cloudiness. 05 p0591 A73-16187

Adiabatic inviscid quasi-geostrophic planetary scale perturbations forced by stratospheric disturbance, obtaining vertical propagation from layered models representation for zonal wind 05 p0591 A73-16189

Relative importance of terms in the turbulent-energy and momentum equations as applied to the problem of a surface roughness change. 05 p0591 A73-16191

Warm cloud droplet growth analysis based on stochastic coalescence equation model in terms of probability function and time evolution 05 p0592 A73-16194

Convective storm updraft shape calculation based on horizontal momentum changes in rising air, noting effects of mixing and aerodynamic drag 05 p0592 A73-16195

Implications of a quadratic stream definition in radiative transfer theory. 05 p0592 A73-16196

Investigation of the characteristics of atmospheric motion at low latitudes 05 p0592 A73-16227

Application of certain stable methods for numerical solution of forecasting equations 05 p0592 A73-16228

Hemispheric single level model of atmospheric action centers formation due to horizontal baroclinity, including turbulent mixing and circulation index effects 05 p0592 A73-16229

Numerical tests of atmospheric circulation and climate theory and accuracy conditions for atmospheric models, noting temperature dependence on radiative and nonradiative heat transfer 05 p0593 A73-16242

Satellite pictures as aids for the determination of the structure of upper-level cyclones 05 p0593 A73-16347

Passage of medium-frequency radio waves through the ionosphere 05 p0550 A73-16395

The abundance of NH3 on Jupiter inferred from UHF radiometry data. 05 p0619 A73-16881

Engineering models for Jupiter's troposphere and the NH3-H2O cloud systems. 05 p0619 A73-16882

Venus atmosphere engineering models for use in spacecraft design and mission planning from Mariner 5 and Venera spacecraft and earth based measurements [ALAA PAPER 73-130] 05 p0619 A73-16883

Approximate analytical solutions of the diffusion equation for Jacchia's statistical models of the upper atmosphere 05 p0570 A73-17014

Radiation transfer in a single-layer spherical planetary atmosphere 05 p0620 A73-17015

Ionospheric electron density profiles model evaluation, considering E region height and thickness seasonal variation 05 p0571 A73-17063

The effect of photoelectrons on kinetic polar wind models. 05 p0572 A73-17159

Baroclinic model of zonal atmospheric circulation in the equatorial region 05 p0594 A73-17351

Numerical model for calculation of the geopotential field with a new generalized vertical velocity profile incorporating the influence of orography 05 p0572 A73-17352

Jet model of cloud convection - A numerical experiment 05 p0594 A73-17353

Venus atmosphere water vapor content from IR spectra observed by airborne Fourier interferometric spectrometer, discussing different models for abundance 06 p0744 A73-17434

Mariner 9 ultraviolet spectrometer experiment - Mars airglow spectroscopy and variations in Lyman alpha. 06 p0746 A73-17484

The thermal structure within the stratospheres of Venus and Mars. 06 p0747 A73-17493

Earth magnetosphere essential processes, discussing outermost atmosphere, solar wind theory and sector structure, models, plasmopause, polar cusps, tail theory and ionospheric currents 06 p0688 A73-17502

Three component static thermosphere model for oxygen radiative recombination and thermal diffusion dependence on underlying layers and solar UV radiation 06 p0689 A73-17539

Contrast transmittance Monte Carlo computation for atmospheric haze models based on aircraft measurement data from various geographical areas 06 p0694 A73-18302

Extensive air showers and Feynman scaling above 1000 GeV. 06 p0743 A73-18325

A radiative-convective model for the prediction of radiation fog. 06 p0720 A73-18327

Calculation of the transfer coefficients for planetary atmospheres consisting of CO2-N2 mixtures 06 p0754 A73-18568

The use of model output statistics /MOS/ in objective weather forecasting. 06 p0720 A73-18706

A macroscale-mesoscale numerical model of intense baroclinic development. 06 p0720 A73-18708

Parameter value selection in Sasaki's meteorological field coordination method 06 p0721 A73-18731

Optimal conditions for indirect probing of the atmosphere 06 p0721 A73-18732

A numerical experiment using a general circulation model of the atmosphere. 07 p0846 A73-19037

A semiempirical model of large-scale magnetospheric electric fields. 07 p0814 A73-19238

A critique of multilayer analyses in application to the propagation of acoustic-gravity waves. 07 p0814 A73-19248

Comparison of the correlation of incoherent scatter and ionosonde measurements of temperature with calcium plage and 2800-Megahertz intensities. 07 p0815 A73-19250

A modified Monte Carlo model for the ionospheric heating rates. 07 p0815 A73-19380

Three layer atmospheric model for neutral gas motion-produced ionosphere and magnetosphere currents, electromagnetic field and charged particle concentration perturbations 07 p0815 A73-19432

Dipolar coordinate system for geomagnetic field dipole approximation in studies of diffusion and heat conduction in F region and outer ionosphere 07 p0816 A73-19452

Polarization measurement of clear sky light and comparison with theoretical data 07 p0818 A73-19590

Sunlight scattering by dust along lunar horizon at sunset, presenting atmospheric model for dust cloud production 07 p0895 A73-19862

Response of a general circulation model of the atmosphere to removal of the arctic ice-cap. 07 p0848 A73-20122

A direct solution of the radiative transfer equation - Application to Rayleigh and Mie atmospheres. 07 p0852 A73-20220

Pulsar magnetosphere evolution, discussing electron and positive ion supply at surface, plasma flow and Crab Nebula characteristics 07 p0900 A73-20276

Solar two-component atmospheric model for prediction of Ca II emission arches in spectrogram of strong lines near limb from kinetic equilibrium calculation 08 p1001 A73-20753

Revised chemical abundances of four population-II A-type stars. 08 p1006 A73-20932

Equivalent gravity wave mode approximation for main solar diurnal tide in rotating spherical dissipative atmosphere modeled by Newtonian cooling and Rayleigh friction 08 p0958 A73-20959

Some results of spectrophotometry of the methane absorption band /7250 A/ on the Jovian disk 08 p1007 A73-21063

Experiments on the seasonal variation of the general circulation in a statistical-dynamical model. 08 p0960 A73-21378

A numerical model of thermal radiation in a dusty atmosphere. 08 p0960 A73-21383

A note on Eulerian-Lagrangian time scale transformation for large-scale atmospheric turbulence. 08 p0985 A73-21424

Barotropic model of local forecasts of katabatic winds 08 p0985 A73-21451

Optical characteristics and structure of the Jovian atmosphere. V - Probable structure of the ammonia aerosol layer. 08 p1012 A73-21577

Monograph - The quasi-biennial oscillation in the stratosphere. 08 p0986 A73-21841

The metallic-line star 15 UMa and the F 5 V star 5 And. 09 p1141 A73-22013

Comparison of telescope magnitudes with model-atmosphere predictions for A, F, and G supergiants. 09 p1142 A73-22030

Nonadiabatic particle motion in the magnetosphere. 09 p1073 A73-22052

Measurement of auroral Birkeland currents and energetic particle fluxes. 09 p1073 A73-22057

Aurora and the poleward edge of the main ionospheric trough. 09 p1073 A73-22058

Deformation and striation of plasma clouds in the ionosphere. I, II. 09 p1074 A73-22062

Forecasting with a global, three-layer, primitive-equation model. 09 p1114 A73-22124

The influence of negative-ion changes in the D-region during sudden ionospheric disturbances. 09 p1075 A73-22126

The negative-ion composition of the daytime D-region. 09 p1048 A73-22127

Monte Carlo simulation of a model ionosphere. II - Energy flow and energy dissipation. 09 p1075 A73-22129

The gradient instability in Gaussian sporadic E-layers. 09 p1075 A73-22133

Experimental observations of the amplitudes of Es and F-region reflections and their comparison with the thin-layer model for Es. 09 p1076 A73-22138

Exchange of water vapor between the atmosphere and surface of Mars. 09 p1145 A73-22270

Boundary layer wind profile model in a steady state, diabatic, baroclinic atmosphere. 09 p1114 A73-22328

A numerical model for predicting mesoscale winds aloft. 09 p1114 A73-22335

Radiative transfer model for simulation of airborne remote sensing scanner data under flight conditions in hazy atmosphere with scattering and absorption effects 09 p1077 A73-22386

Imaging properties of monostatic and bistatic troposcatter radars. 09 p1050 A73-22426

High-frequency radio-wave propagation through plane-stratified ionospheric models. 09 p1077 A73-22430

Ionospheric and plasma sheet particle densities, fluxes and bulk velocities along auroral magnetic field line for collisionless ion-exosphere model

09 p1079 A73-22842

Solar particle measurements interpretation for closed vs open magnetospheric model determination, considering electron-proton polar cap differences, magnetotail flux asymmetries, etc

09 p1149 A73-22951

Models of the extremal arctic winter atmosphere at heights between 20 and 80 km

09 p1115 A73-22993

Probabilistic model for the resolvent kernel in diffusion problems in spherical-shell media.

09 p1121 A73-23071

Application of some numerical techniques in combining satellite and conventional data in the tropics.

09 p1115 A73-23175

Stellar model chromospheres. I - On the temperature minima of F, G, and K stars.

10 p1272 A73-23533

Ultralong atmospheric waves and a long-range forecasting.

10 p1244 A73-23644

Upper atmosphere analytical density model for satellite motion prediction, allowing for diurnal and semiannual density variations and solar activity and geomagnetic disturbances effects

10 p1211 A73-23883

Development of a global cloud model for simulating earth-viewing space missions.

10 p1244 A73-23979

Global numerical atmospheric circulation model predictive sensitivity to equator-to-pole temperature gradient changes, applying variance analysis technique to Mintz-Arakawa model

10 p1245 A73-23983

On the relation between optical scale height and density scale height in a stellar atmosphere.

10 p1281 A73-24406

Lyman-alpha radiation in the hydrogen atmospheres of comets - A model with multiple scattering.

10 p1281 A73-24408

20-micron fluxes of bright stellar standards.

10 p1282 A73-24639

Saturn magnetospheric model for bounds on surface field strength and trapped particle population

10 p1283 A73-24724

Half-harmonic modes for different frequency ranges and wave vectors from infinite homogeneous plasma model for high frequency electrostatic wave propagation in magnetosphere

10 p1213 A73-24733

Empirical model for F layer electron density irregularities responsible for VHF/UHF amplitude scintillation, considering geomagnetic latitude, local time, season and sunspot effects

10 p1190 A73-24895

On the secondary production of galactic cosmic ray electrons.

10 p1270 A73-24910

Line source functions with variable Doppler width and noncoherent scattering.

11 p1415 A73-25135

Boundary conditions in the problem of short-range weather forecasting on the basis of a baroclinic model of the atmosphere

11 p1393 A73-25639

Periodic solutions of the set of equations governing the nonadiabatic convection of dry isolated thermals.

11 p1393 A73-25690

A study of convective elements in the atmospheric surface layer.

11 p1393 A73-25692

Spectroscopy of Jupiter - 3200 to 11,200 A.

11 p1418 A73-25720

Some considerations on the atmospheric internal boundary layer over the ground surface.

11 p1394 A73-25725

A two-component model of the diurnal variations in the thermospheric composition.

11 p1354 A73-25758

Anomalous diurnal changes of transequatorial VLF radio waves.

11 p1330 A73-25760

On the morphology of auroral-zone X-ray events. II - Events during the early morning hours.

11 p1354 A73-25762

A diffusion model for the electron density distribution along the earth's magnetic field in an F-region plasma cloud.

11 p1354 A73-25768

Thermal radio emission from Jupiter and Saturn.

11 p1420 A73-25883

A possible current system associated with the Sq variation.

11 p1356 A73-25910

On empirical models of the upper atmosphere in the polar regions.

11 p1356 A73-25915

Ionospheric currents induced by solar wind interaction with planetary atmospheres.

11 p1412 A73-25921

The effect of the earth's bow shock and magnetosheath on the interaction of a discontinuity in the solar wind with the magnetosphere.

11 p1357 A73-25924

Magnetotail model for magnetic field strength and particle drift in magnetic equatorial plane earth, using current sheet from satellite observations

11 p1357 A73-25929

Heating effects due to radiative energy loss from acoustic waves in solar atmosphere, estimating temperature difference between radiative equilibrium and empirical model

11 p1421 A73-25931

Stratospheric aerosol properties and their effects on infrared radiation.

11 p1357 A73-26344

Internal atmospheric gravity wave effect on ionospheric columnar electron content on basis of viscous atmosphere model with isothermal layers

11 p1359 A73-26709

Global climatic model based on time and space averaged thermodynamic energy equation for idealized land-water distribution, allowing for continents-oceans seasonal interactions

12 p1519 A73-26801

Titan model arising from observations and methane-rich atmosphere thermodynamics, photochemistry and optical properties, considering origins and volatile content of outer planets satellites

12 p1539 A73-27140

Three-dimensional analytical model of the electron density distribution in a quiet ionosphere

12 p1490 A73-27334

Dynamic model of the interaction between the F region of the ionosphere and the plasmasphere

12 p1490 A73-27335

Influence of a variable ionospheric-protonospheric plasma flow on the nighttime F region of the ionosphere

12 p1490 A73-27336

Analytical model of the unsteady nighttime F2 region of the ionosphere at mid-latitudes

12 p1490 A73-27337

Temperature variations in the upper atmosphere during a period of minimum solar activity from topside ionospheric sounding data

12 p1491 A73-27346

Magnetosphere boundary location relationship to geomagnetic activity level and solar activity cycle during 1963-68 based on theoretical model

12 p1491 A73-27348

Time dependent studies of the aurora. I - Ion density and composition.

12 p1492 A73-27601

Jupiter atmosphere fluid dynamic models, considering cloud spot markers and wave motions from ground and spacecraft observations

12 p1542 A73-27606

Asymmetric eigenmodes in a simple model plasmasphere with non-uniform Alfvén speed.

12 p1529 A73-27613

Middy aurora behavior during auroral substorms from all sky photographs at south pole, considering modification of Starkov-Feldstein model

12 p1493 A73-27614

Applications of methods of geometric optics in the case of tropospheric propagation

12 p1473 A73-27755

Midlatitudinal standard ionospheric profile to construct F-region noon electron density profiles and thermal response to solar activity changes

12 p1493 A73-27761

Hail growth in cold front, discussing relationship to air flow changes

13 p1652 A73-28267

Radiative properties of terrestrial clouds at visible and infra-red thermal window wavelengths.

13 p1652 A73-28274

Venus atmospheric model based on spectroscopic evidence of carbon dioxide spectral lines phase variation due to two scattering layers

13 p1680 A73-28459

Asymmetrical model for F 2 critical frequency variability analysis to determine dimensions and effective number of large scale ionospheric electron density inhomogeneities

13 p1608 A73-28707

Variations of the global values of F2-layer thickness and the parameters of the neutral atmosphere.

13 p1608 A73-28722

A discretization method for atmosphere dynamics equations and for the construction of numerical weather forecast schemes

13 p1654 A73-29151

Terrestrial atmospheric general circulation theoretical and observational research, considering Reynolds or eddy stress distribution across horizontal and vertical surfaces

13 p1610 A73-29333

Stability of a two-layer fluid model to non-geostrophic disturbances.

13 p1610 A73-29334

A rapidly convergent procedure for computing large-scale condensation in a dynamical weather model.

13 p1655 A73-29338

LTE and hydrogen and ionized He lines approximations for model atmosphere computations of hot early stars, discussing UV line blanketing

13 p1686 A73-29367

About the influence of a magnetic field on the model atmosphere of a magnetic star.

13 p1687 A73-29657

Comment on the effect of a vorticity centre on a frontal boundary.

13 p1656 A73-29663

Neutral hydrogen distribution in the upper atmosphere of the earth

14 p1747 A73-29871

Ionospheric model impulse response transfer functions phase and amplitude dependence on profile parameters and TE C, using ray tracing technique

14 p1728 A73-30231

Red arc data from Richland /WA/ and by Ogo 6 satellite observations, discussing thermal conduction formation theory

14 p1749 A73-30500

Outer planet satellites and atmospheres composition and structure from low temperature condensation accretion models

14 p1724 A73-30530

Shock wave propagation in atmospheres with spatially inhomogeneous density and temperature fields, using ideal polytropic gas model

14 p1750 A73-30654

Hydrostatic, flux constant and LTE stellar atmospheric models at 3800 and 3500 K for Betelgeuse

14 p1801 A73-30737

A three-dimensional model of cumulus cloud development.

14 p1771 A73-30764

Nonstationarity effects on planetary boundary layer by numerical integration of time dependent boundary layer model

14 p1772 A73-30903

A baroclinic model of the atmospheric zonal circulation in the equatorial region.

15 p1902 A73-31001

A jet-stream model of cloud convection and a numerical experiment.

15 p1902 A73-31003

IR seeing disks/blurred interference patterns of corrugated wave fronts/ speckles and intensity profiles from atmospheric turbulence models

15 p1929 A73-31061

Structure and time variations of the Jovian ionosphere.

15 p1929 A73-31066

Numerical experiments for the determination of characteristic dimensions and intensities of convection cells

15 p1902 A73-31138

A balloon study of the OH airglow emission from evening twilight to sunrise.

15 p1867 A73-31311

Short-wave skip distance for various models of the ionosphere

15 p1843 A73-31575

Numerical simulation of equatorial electric fields and magnetic variations based on global ionospheric dynamo and equatorial electrojet models

15 p1869 A73-31753

Equatorial electrojet. I - Development of a model including winds and instabilities. II - Use of the model to study the equatorial ionosphere.

15 p1904 A73-31756

Equatorial ionospheric anomaly related neutral thermospheric composition variation observation from OGO-6 mass spectroscopic data, noting static diffusion model limitations

15 p1870 A73-31767

POGO satellite observation of electrojet profiles compared with H variation around measurements, interpreting data by classical band current model

15 p1871 A73-31773

Thermal well representation of cloud layer from radiative cooling and weak dependence on thickness, deriving approximate formulas for radiant fluxes

15 p1904 A73-31784

Comparison of methods for calculating long-wave radiation fields

15 p1904 A73-31785

Cloud cover probability computation models, showing averaged values for direction of sighting and cumulus cloud cover estimations

15 p1905 A73-31797

Results of the numerical modeling of steady zonal circulation of the atmosphere in the equatorial region

15 p1905 A73-31817

Some field characteristics of outgoing thermal radiations in the Venusian and Martian atmospheres

15 p1937 A73-31819

Energy and momentum theorems in magnetospheric processes.

15 p1871 A73-31846

Frequency dependence of radio-wave absorption in a reflecting layer 15 p1844 A73-31884

Gyrotropic flat ionosphere model with elliptical nonuniform conductivity for electrojet generation by magnetosphere current entering and leaving auroral zone 15 p1872 A73-31895

Ionization of the atmosphere and attenuation of radar waves after a nuclear explosion. 15 p1844 A73-32198

Three dimensional ionograms synthesis method, considering quasi-parabolic layer ionospheric model application and ray path parameters 15 p1845 A73-32232

D region partial reflection mechanism model based on multiple reflector concept, presenting electron density vertical distribution 15 p1845 A73-32233

Vorticity advection and geopotential change due to dynamic causes as two-layer problem 15 p1907 A73-32355

Considerations concerning the quasi-geostrophic model equations for an energetically open system 15 p1907 A73-32360

Model of the chromosphere and the transition layer between the chromosphere and solar corona 16 p2057 A73-32703

Three component static thermosphere model for oxygen radiative recombination and thermal diffusion dependence on underlying layers and solar UV radiation 16 p2001 A73-32763

Development of model atmospheres for aerothermodynamic calculations. 16 p2034 A73-33138

Faraday rotation based total ionospheric electron content information for correction of near real time satellite position determination errors, using spherically stratified ionospheric model 16 p2035 A73-33414

The O I 1304- and 1356-A emissions from the atmosphere of Venus. 16 p2062 A73-33431

Model of dayside magnetopause displacement relation to convection currents feeding polar cap ionosphere to estimate electric field and flux return as function of displacement 16 p2003 A73-33432

Satellite studies of magnetospheric substorms on August 15, 1968. IX - Phenomenological model for substorms. 16 p2004 A73-33457

On the extent of the Martian ionosphere. 16 p2062 A73-33462

Atmospherical modelling and the chemical data problem. [AIAA PAPER 73-500] 16 p1977 A73-33542

Radiative transfer considerations for kinetic modeling and sensitivity studies. [AIAA PAPER 73-505] 16 p2005 A73-33545

Photochemical, radiative and dynamic modeling of the stratosphere. [AIAA PAPER 73-527] 16 p2007 A73-33561

A three-dimensional stratospheric point-source tracer experiment and its implications for dispersion of effluent from a fleet of supersonic aircraft. [AIAA PAPER 73-528] 16 p2007 A73-33562

Numerical atmospheric circulation model of SST effects on stratospheric ozone distribution [AIAA PAPER 73-529] 16 p2007 A73-33563

Stratospheric contamination experiments with a one-dimensional atmospheric model. [AIAA PAPER 73-531] 16 p2007 A73-33564

Preliminary estimates of the fate of SST exhaust materials using a coupled diffusion/chemistry model. [AIAA PAPER 73-535] 16 p2046 A73-33567

A model for studying the effects of injecting contaminants into the stratosphere and mesosphere. [AIAA PAPER 73-539] 16 p2008 A73-33569

A two-dimensional theoretical model for stratospheric ozone density distributions in the meridional plane. [AIAA PAPER 73-541] 16 p2008 A73-33571

Calculation of the transfer coefficients of planetary atmospheres formed by mixtures of CO2 and N2. 16 p2039 A73-33593

Atmospheric attenuation interrelations at 12 and 35 GHz with meteorological parameters derivation for homogeneous atmosphere, testing dynamic atmospheric model 16 p1981 A73-33709

Digitized weather radar data models of intense storm cells with 1-2 km resolution and 10 dBZ reflectivity 16 p1983 A73-33727

Study of ultraviolet radiation from the Venera interplanetary probe 16 p2056 A73-33803

Analysis of radio-wave propagation in the Venusian atmosphere 16 p1984 A73-33822

Venus 4 chemical composition and pressure data for construction of Venus atmospheric model, emphasizing Greenhouse effect 16 p2068 A73-33826

Estimates of the intensity of turbulence in the atmospheres of Mars and Venus 16 p2069 A73-33828

Finite-difference approximations of the Navier-Stokes equations applied to a geophysical flow. I. II - Three-dimensional approximations on a region homeomorphic to a plane region. III - Three-dimensional approximations over the totality of a spherical region represented by means of a regular polyhedron 16 p2009 A73-33886

Primary scattering theory for twilight luminance calculation, considering luminance atmospheric scale height growth in thermosphere and seasonal variation 16 p2009 A73-33889

Enhancement of upper atmospheric sodium from sporadic dust influxes. 16 p2010 A73-33917

Pi 2 and geomagnetic bay maximum occurrence dependence on geomagnetic time, discussing computation methods for geomagnetic time 16 p2010 A73-33922

A model of a long-term process of heat and moisture transfer in the atmosphere over the ocean 17 p2158 A73-34344

A self-consistent two-dimensional approach to magnetospheric structures. 17 p2158 A73-34502

Thermal synthesis of amino acids from a simulated primitive atmosphere. 17 p2112 A73-34572

The atmospheric aerosol and its significance for the energy budget of the atmosphere 17 p2159 A73-34749

A model-atmosphere abundance analysis of the B9 V star nu Capricorni. 17 p2231 A73-34758

Mesospheric and stratospheric nitrogen oxides behavior from model with nitric oxide photodissociation and nitric acid formation 17 p2119 A73-34779

The effect of large-scale eddies on climatic change. 17 p2160 A73-34851

Method to apply homogeneous-path transmittance models to inhomogeneous atmospheres. 17 p2205 A73-34856

The effects of water vapor and oxides of nitrogen on the ozone and temperature structure of the stratosphere. 17 p2160 A73-34857

Jupiter atmospheric circulation as manifestation of large scale convective instability generated by internal heat sources, considering Red Spot production 17 p2232 A73-34859

Role of the meteorological satellites of the earth atmosphere observation system for the first global experiment of the 'Global Atmospheric Research Programme' 17 p2205 A73-34935

Application of temperature soundings by the Nimbus 3 satellite to the analysis of the hemispheric-scale stratospheric environment 17 p2206 A73-34937

A synoptic model for evaluation of vertical temperature and geopotential profiles from satellite pictures. 17 p2206 A73-34939

The use of subgrid transport equations in a three-dimensional model of atmospheric turbulence. [ASME PAPER 73-FE-21] 17 p2206 A73-35017

Currents in Florida lightning return strokes. 17 p2163 A73-35465

Numerical weather prediction models based on hydrothermodynamic equations and nonadiabatic factors for short term regional, hemispheric and global forecasting 18 p2331 A73-35909

Three to five day numerical forecasting making use of the complete hydrodynamics equations, and problems of correlating the original fields of meteorological elements 18 p2331 A73-35911

Apollo 17 mass spectrometer indication of rare gases and molecular hydrogen in lunar atmosphere, confirming noncondensable gas model 18 p2349 A73-35973

Velocity of the reflection points reveals structure and motions in the ionosphere. 18 p2305 A73-36000

Trial of existing models of the lower ionosphere by experimental data on Schumann resonances. 18 p2306 A73-36011

Dynamic processes as derived from the mean circulation in the upper mesosphere and lower thermosphere. 18 p2307 A73-36036

Drag density data from the Cannon Ball II and Musket Ball satellites. 18 p2309 A73-36053

Neutral winds in the F-region obtained from new models of density and temperature. 18 p2309 A73-36056

Comparison of the two-dipole and empirical magnetospheric models. 18 p2310 A73-36135

A model of formation of the mean diurnal state of the upper atmosphere and its diurnal variations. 18 p2311 A73-36147

Auroral ion velocity distributions using a relaxation model. 18 p2311 A73-36178

Self consistent geomagnetic tail current sheet model described by exact analytic solution of time independent Vlasov-Maxwell equations 18 p2351 A73-36274

Cometary composition, structure and atmospheric dynamics, discussing multiconstituent hydrodynamic models in comparison with observation [AIAA PAPER 73-549] 18 p2353 A73-36495

Effect of aerosols on the transfer of solar energy through realistic model atmospheres. I - Non-absorbing aerosols. 18 p2333 A73-36704

Some laboratory observations on convective plumes. 18 p2333 A73-36711

Spectrophotometry of the 7250-A methane absorption band over the disk of Jupiter. 18 p2355 A73-36864

Some effects of surface anomalies in a global general circulation model. 19 p2446 A73-37539

Multiple scattering theory of radiative transfer in inhomogeneous atmospheres. 19 p2423 A73-37586

Mechanisms for Mars dust storms. 19 p2485 A73-37656

Numerical models of the circulation of the atmosphere of Venus. 19 p2485 A73-37657

Numerical modeling of the dynamics and microphysics of warm cumulus convection. 19 p2447 A73-37658

A comparison between axisymmetric and slab-symmetric cumulus cloud models. 19 p2447 A73-37659

A phenomenological model of global ionospheric electron density in the E-, F1- and F2-regions. 19 p2425 A73-38014

Skylark rocket magnetometer measurement of sporadic E layer magnetic fields, testing wind shear theory of ionization redistribution at midlatitudes 19 p2426 A73-38022

Quasi-stationary atmospheric waves and mean monthly vorticity production from development term of two level model 19 p2447 A73-38153

Fine scale structure and mixing within inversion capping convective boundary layer, proposing atmospheric model for sensible downward heat transfer 19 p2448 A73-38215

Global model of the general circulation of the atmosphere below 75 kilometers with an annual heating cycle. 19 p2449 A73-38287

Dynamic coupling of the stratosphere with the troposphere and sudden stratospheric warmings. 19 p2449 A73-38288

Matching the geopotential and wind fields with the aim of improving the accuracy of objective analysis 19 p2449 A73-38544

Linear filtering of ballistic-entry-probe data for atmospheric reconstruction. [AIAA PAPER 73-904] 20 p2589 A73-38838

Upper atmosphere analytical density model for satellite motion prediction, allowing for diurnal and semiannual density variations and solar activity and geomagnetic disturbances effects 20 p2550 A73-38902

Propagation of mechanical waves in the solar atmosphere 20 p2606 A73-39078

Solar brightness temperature measurement relative to lunar brightness temperature, noting agreement with HSRA model 20 p2610 A73-39582

Enhancement of Earth Resources Technology Satellite /ERTS/ and aircraft imagery using atmospheric corrections. 20 p2567 A73-39835

Atmospheric radiative transfer model for correction of Apollo photographic remote imagery data degradation due to radiation scattering 20 p2559 A73-39881

Numerical forecasting experiments based on the conservation of potential vorticity on isentropic surfaces. 21 p2728 A73-40053

On the strategy of combining coarse and fine grid meshes in numerical weather prediction. 21 p2728 A73-40055

Cumulus congestus cloud circulation velocity field measurement by balloon, comparing with radar, cameras, satellite and ground based observed meteorological model computations 21 p2728 A73-40060

Atomic oxygen and helium concentrations variation at 120 km in thermospheric composition models, discussing association with geomagnetic activity

21 p2679 A73-40074

Tropospheric model for nitrogen-oxygen-carbon-hydrogen atmosphere with time dependent static chemistry, emphasizing methane conversion to CO via OH attack

21 p2646 A73-40081

Photochemical model for homogeneous gas phase radical chain mechanism to remove tropospheric methane, carbon monoxide, molecular hydrogen and formaldehyde

21 p2646 A73-40082

Theoretical model of vertical distributions of CO and CH₄ in the mesosphere and upper stratosphere.

21 p2680 A73-40085

Photochemical model with vertical transport for CO and hydrocarbons profiles in stratosphere and mesosphere, discussing boundary conditions and water vapor

21 p2681 A73-40086

A mechanism for the growth phase of magnetospheric substorms.

21 p2682 A73-40157

Effects of propagation parallel to the magnetic field on the Type I electrojet irregularity instability.

21 p2682 A73-40160

Jovian ionospheric and magnetospheric ionization and temperature distributions from solutions of momentum and chemical equations for electrons, ions and neutrals, and heat transport equation

21 p2764 A73-40165

A scheme for synoptic-hydrodynamic-statistical weather forecasting for 3 to 10 days

21 p2730 A73-40491

Permissible hydrodynamic and hydrostatic stellar atmosphere models described by system of equations dependent on initial level conditions

21 p2767 A73-40532

Atmospheric structure and its variations in the region from 25 to 120 km.

21 p2683 A73-40628

Atmospheric models for 110-2000 km region, considering composition, temperature profiles, thermosphere and exosphere variations, density and boundary condition computation, etc

21 p2683 A73-40629

Upper atmospheric models dealing with diurnal variation and latitudinal density dependence to derive time and space dependencies

21 p2683 A73-40631

Calculations of the limb radiance of Venus in the 600 to 700 per cm region and their application to spacecraft navigation.

21 p2767 A73-40693

Dissipation of the Venusian atmosphere

21 p2769 A73-40733

Phase integral corrections to radio wave absorption and virtual height for model ionospheric layers.

21 p2654 A73-40777

A generalized aeronomic model of the mesosphere and lower thermosphere including ionospheric processes.

21 p2683 A73-40778

Temperature dependence for dissociative recombination of NO⁺ in E- and F-region models.

21 p2684 A73-40787

Russian book on statistical properties of ionosphere reflected signals covering statistical modeling, random processes, perturbation method and wave reflection problems

21 p2657 A73-41284

An analysis of the altitude dependence of the geomagnetic effect by means of 'equivalent durations.'

21 p2689 A73-41353

Observational comparison with a self-consistent model of the geomagnetic tail.

21 p2691 A73-41377

A numerical diffusion model for continuous releases.

21 p2732 A73-41568

Structure of the solar chromosphere. I - Basic computations and summary of the results.

22 p2905 A73-41762

Quiet-time nighttime magnetic field near geomagnetic equator detected by magnetospheric barium cloud injection, revealing taillike structure from atmospheric models

22 p2846 A73-41939

A nonstationary model of charged-particle diffusion in a gravitational field

22 p2902 A73-41955

Effect of the absorbers upon the thermal structure of a LTE atmosphere, hydrogen and helium.

22 p2908 A73-42309

Resonant oscillations of intermediate frequency in a stratified atmosphere.

22 p2848 A73-42539

Semiempirical time dependent climate models formulated for stability of asymptotic steady state equilibrium solutions to perturbations

22 p2883 A73-42540

An exact solution for the rotation of the atmosphere about the spheroidal earth.

22 p2848 A73-42541

Diurnal thermospheric and ionospheric variations from time dependent continuity equations for O⁺, H⁺, O₂⁺, and NO⁺ ions, motion and heat conduction equations

22 p2849 A73-42572

French monograph - Preparation of a space experiment intended for high resolution study of the far ultraviolet spectrum of the star gamma Gemini.

22 p2910 A73-42714

Atmospheric Uranus and Neptune models with massive atmospheres above solid cores, discussing Uranus solid methane cloud layer

22 p2913 A73-42987

Radiative transfer within the atmospheres of the major planets.

22 p2913 A73-42991

Ionised molecules in BCA photospheric model.

22 p2915 A73-43039

Increase of error in range correction with elapsed time, evaluated by ray tracing through radiosonde-generated atmospheric models.

22 p2828 A73-43176

The Wolf-Rayet stars - The general problems of extended atmospheres and non-classical atmospheric models.

23 p3025 A73-43192

Three-dimensional analytical model of electron density distribution of the quiet ionosphere.

23 p2970 A73-43232

Dynamic model of interaction of the F-region of the ionosphere with the plasmasphere.

23 p2970 A73-43233

Effect of changing ionospheric-protonospheric plasma flow on the nighttime F-region of the ionosphere.

23 p2970 A73-43234

Analytical model of the nocturnal nonstationary F₂-region of the ionosphere at middle latitudes.

23 p2970 A73-43235

Temperature variations in the upper atmosphere during the solar activity minimum based on data of topside sounding of the ionosphere.

23 p2970 A73-43243

Magnetosphere boundary location relationship to geomagnetic activity level and solar activity cycle during 1963-68 based on theoretical model

23 p2970 A73-43245

An exact solution to the system of prognostic equations of a barotropically divergent model of the atmosphere

23 p3001 A73-43461

Nonlinear theory of the formation and structure of the intertropical convergence zone.

23 p3001 A73-43586

Planetary spectrum formation in atmospheric model with lower and upper layers of infinite and small optical thickness respectively

23 p3029 A73-43623

A magnetospheric field model incorporating theOGO 3 and 5 magnetic field observations.

23 p2972 A73-43693

On the theoretical model for vertical ozone density distributions in the mesosphere and upper stratosphere.

23 p2977 A73-43898

The effects of water vapour and oxides of nitrogen on ozone and temperature structure of the stratosphere.

23 p2977 A73-43902

Application of general circulation models to the study of stratospheric ozone.

23 p2978 A73-43909

Zonally symmetric global general circulation models with and without the hydrologic cycle.

23 p2978 A73-43981

A model for estimating joint probabilities of cloud-free lines-of-sight through the atmosphere.

23 p3004 A73-44260

Wind speed variability/standard deviation difference/over 16.25 km distance between observation sites compared to generalized models for varying conditions of cyclonic activity

23 p3004 A73-44267

A first look at atmospheric dynamics and temperature variations on Titan.

24 p3128 A73-44433

Jupiter radiative greenhouse model overestimation of lower cloud level temperature due to convective heat transport neglect, discussing rejection of water cumulus cloud possibility

24 p3129 A73-44439

Formation of spectral lines in planetary atmosphere. IV - Theoretical evidence for structure of the Jovian clouds from spectroscopic observations of methane and hydrogen quadrupole lines.

24 p3129 A73-44449

Disk integrated polarization observation for Titan at small phase angles, noting optically thin Rayleigh atmosphere on opaque cloud deck

24 p3130 A73-44451

A numerical method for determining the temperature structure of planetary atmospheres.

24 p3130 A73-44456

Greenhouse effect for Titanian atmospheric models with different methane, hydrogen, helium and ammonia proportions, deriving brightness temperature spectrum and surface pressure

24 p3130 A73-44457

General atmospheric circulation driven by polar and diurnal surface temperature variations.

24 p3131 A73-44463

Model for radiative dynamic instability of cloudy planetary atmosphere from coupling for case of radiative heating rate dependent cloud properties

24 p3132 A73-44534

Radiative instability model of cloud cover on equatorial beta plane to explain Jupiter bands zonal symmetry and meridional wavelength

24 p3132 A73-44535

The post-eclipse brightening of Io.

24 p3134 A73-44563

Density variation and radiative exchange effects on convective instability of plane-parallel polytropic atmosphere heated from below with application to solar granulation

24 p3135 A73-44628

Radiative damping of trapped gravity waves in the solar atmosphere.

24 p3135 A73-44629

Calculation of a model of the neutral atmosphere of Mars above 140 km from ionospheric data

24 p3137 A73-44785

Numerical experiments in laser sounding of aerosol stratification in the atmosphere

24 p3085 A73-44966

Design criteria for finite-difference models for eddy diffusion with winds that guarantee stability, mass conservation, and nonnegative masses.

24 p3085 A73-45018

H₂ pressure-induced lines in the spectra of the major planets.

24 p3138 A73-45050

On self-consistent models for the pulsar magnetosphere.

24 p3140 A73-45190

The determination of whistler nose-frequency and minimum group delay and its implication for the measurement of the east-west electric field and tube content in the magnetosphere.

24 p3087 A73-45210

ATMOSPHERIC MOISTURE

Atmospheric solid and liquid water particles IR spectral properties, interpreting Nimbus 4 IR spectroscopic cloud observations

01 p0037 A73-10371

Atmospheric moisture and wind field synoptic analysis based on Nimbus 4 temperature-humidity IR radiometer/THIR/measurements

01 p0073 A73-10379

Precipitable water vapor temperature-geopotential height profiles from satellite IR spectrometer/SIRS/measurements, using stepwise regression technique

01 p0073 A73-10380

Radiometric techniques for observing the atmosphere from aircraft.

01 p0073 A73-10404

Meteorological parameters conducive to ice formation on aircraft, analyzing data statistics on atmospheric moisture content, temperature and drop size

[DGLR PAPER 72-109]

Precipitation detection over the ocean using microwave satellite radiometry.

02 p0188 A73-12268

The spectral characteristics of radiation extinction and the effects of the relative humidity on these characteristics

02 p0189 A73-12368

Thermal cycling and frequency tests for lunar soil dielectric constant, loss tangent and dc conductivity, noting moisture effects

02 p0220 A73-12481

Investigation of the radio wave absorption spectrum of atmospheric water vapor in the 1.15 to 1.5-mm range

02 p0142 A73-12487

Atmospheric water vapor absorption coefficient in 0.73 mm transmittance window as function of humidity from monochromatic RF radiation measurements

02 p0142 A73-12488

Moisture effects on the high-temperature strength of fiber-reinforced resin composites.

03 p0328 A73-13002

The friction of boron carbide in controlled atmospheres.

[ASME PAPER 72-LUB-29]

Venus atmosphere water vapor content from IR spectra observed by airborne Fourier interferometric spectrometer, discussing different models for abundance

06 p0744 A73-17434

Effect of humidity on infrared and visual atmospheric transmission.

06 p0694 A73-18304

Numerical model for three dimensional air parcels trajectories computation from operational wind forecasts, deriving atmospheric moisture, dew and temperature distributions predictions

06 p0720 A73-18705

Theoretical possibilities for determining the moisture content of the atmosphere through the thermal radio emission in the submillimeter range.

07 p0848 A73-20347

IC plastic package performance prediction, discussing procedure to estimate degradation rate due to moisture effects

08 p0944 A73-20738

Exchange of water vapor between the atmosphere and surface of Mars.

09 p1145 A73-22270

Venus - New microwave measurements show no atmospheric water vapor.

09 p1151 A73-23171

The absorption spectrum of atmospheric water vapor in the vicinity of the He 10830 A triplet.

11 p1421 A73-25933

Northern Hemisphere climatic trend from monthly atmospheric temperature and water vapor content calculations over five year period, noting humidity decrease and cooling

11 p1358 A73-26663

Application of Nimbus 4 THIR 6.7-micron observations to regional and global moisture and wind field analyses.

12 p1520 A73-26812

Utilization of vacuum ultraviolet radiation for measurement of humidity pulsations

12 p1521 A73-26966

Preliminary measurement data on the H₂O content of the Martian atmosphere from the Mars-3 automatic interplanetary station

12 p1540 A73-27451

Atmospheric moisture effects on hematitic sandstone, pyrite and galena electrical resistivity, noting comparison with semiconductors and insulators

13 p1609 A73-28847

Growth rate calculation for hygroscopic condensation nuclei in the presence and absence of a monolayer of a surface-active substance

13 p1654 A73-28880

Differential difference equations for probability of water droplet electrization in weakly ionized medium during cloud and fog formation

13 p1654 A73-28883

Rotational spectral lines of water vapor dimers in the upper troposphere

13 p1609 A73-29152

Precipitation forecasting by numerical scheme using dew point depression as moisture parameter and gradual onset techniques

13 p1655 A73-29336

Distribution of water vapor in the stratosphere as determined from balloon measurements of atmospheric emission spectra in the 24- to 29-micron region.

14 p1749 A73-30160

Oxidation of powdered germanium, tin and lead tellurides under atmospheric conditions

15 p1887 A73-31594

Integral transmittance function of thermal radiation

15 p1904 A73-31782

Determination of atmospheric water-vapor densities from measurements of the 6943.8-A absorption line strength.

15 p1845 A73-32227

Artificial inducement of drizzling rain in an uncloudy atmosphere at relatively high humidity

16 p2034 A73-33109

Water vapor from a lunar breccia - Implications for evolving planetary atmospheres.

16 p2060 A73-33124

Radiometric observations of atmospheric water vapor injection by thunderstorms.

[AIAA PAPER 73-512]

16 p2006 A73-33550

Microwave transhorizon propagation in atmospheric evaporative duct layer by superdiffraction, using Monin-Obukhov similarity theory for computerized prediction

16 p1981 A73-33712

Correction of electrical path length by passive microwave radiometry.

16 p1983 A73-33729

Estimates of water content in the atmosphere of Venus on the basis of radio-astronomical measurements and space probe data

16 p2068 A73-33823

Balloon-borne phosphoric anhydride electrolytic gage measurement of water vapor mixing ratio to 35 km, noting decrease to minimum near tropopause

16 p2008 A73-33884

A model of a long-term process of heat and moisture transfer in the atmosphere over the ocean

17 p2158 A73-34344

Method to apply homogeneous-path transmittance models to inhomogeneous atmospheres.

17 p2205 A73-34856

Infrared transmittances for indirect soundings of the atmosphere from satellite-based measurements.

18 p2308 A73-36043

Method for analyzing the moisture field by the use of satellite cloud data.

18 p2334 A73-37056

Use of satellite cloud data in moisture field analysis.

18 p2334 A73-37057

Assessment of characteristics of the atmospheric moisture distribution with the aid of satellite measurements.

18 p2334 A73-37064

Interrelationship between developments of synoptic processes and evolution of the integral moisture field according to satellite measurements.

18 p2334 A73-37065

Some characteristics of the vertical structure of the humidity field over the North Atlantic.

18 p2334 A73-37076

Small-scale atmospheric structure deduced from measurements of temperature, humidity and refractive index.

19 p2448 A73-38224

Atmospheric temperature and humidity vertical profiles from satellite-borne IR spectral radiance measurements, using linear extrapolation and statistical regression techniques [AAS PAPER 73-124]

20 p2521 A73-38584

Moisture content determination in rain clouds by simultaneous thermal radiation and radar measurements

20 p2584 A73-39190

Moisture effect on Ni steel fatigue crack propagation under low stresses

20 p2617 A73-39291

Remote sensing of atmospheric O₃ and H₂O to 70 km by aircraft measurements of radiation at 1.64 mm wavelength.

20 p2557 A73-39855

Preliminary results of measurements of the H₂O content of the Martian atmosphere by the unmanned spacecraft Mars 3.

22 p2905 A73-41806

Venus atmosphere water vapor phase transformation possibilities, discussing ice crystal and supercooled water drop formation

22 p2911 A73-42736

Estimation of atmospheric moisture profiles from satellite measurements by a combination of linear and non-linear methods.

23 p3001 A73-43526

Atmospheric water vapor concentration in upper stratosphere above tropopause from balloon observations of solar IR absorption spectra

23 p2976 A73-43890

Nimbus 5 satellite-borne selective chopper radiometer /SCR/ for remote sounding of stratospheric temperature, water vapor and cirrus clouds

23 p2978 A73-43952

Sulfuric acid solution composition to account for Venus cloud temperature, stratosphere dryness and IR spectrum

24 p3129 A73-44441

Clearing of a cloudy atmosphere containing water drops by intense monochromatic radiation

24 p3108 A73-45520

ATMOSPHERIC NEUTRON FLUX DENSITY

U ATMOSPHERIC RADIATION

U NEUTRON FLUX DENSITY

ATMOSPHERIC NOISE

U ATMOSPHERICS

ATMOSPHERIC OPTICS

Optical manifestations of meteoric aerosols. I - The 1970 Orinoids

01 p0096 A73-10332

Influence of haze layers upon remotely-sensed surface properties.

01 p0037 A73-10360

Theoretical calculation of light scattering and measurements with grating UV double monochromator for anomalous atmospheric transparency

01 p0039 A73-10402

Diffraction limited astronomical telescope resolution retrieval by speckle interferometer, noting information extraction via Fourier analysis

01 p0049 A73-10536

Transmittance of the atmosphere and the relationship among optical parameters in the ultraviolet spectral region

01 p0040 A73-10873

General solution for polarized radiation in a homogeneous-slab atmosphere.

01 p0078 A73-11033

Beam spread of laser light propagating through the atmosphere.

01 p0060 A73-11056

Brief history of the Martian 'violet haze' problem.

03 p0373 A73-13707

Degree and direction of polarization of multiple scattered light. I - Homogeneous cloud layers.

03 p0344 A73-14427

Degree and direction of polarization of multiple scattered light. II - Earth's atmosphere with aerosols.

03 p0344 A73-14428

Airborne laser-beam scintillation measurements at high altitudes.

03 p0305 A73-14657

Atmospheric transmittance calculation from 0.76-micron oxygen band fine structure parameters

04 p0473 A73-15571

Two beam optical recording instrument for atmospheric IR transmissivity, discussing spectrophotometers with changeable NaCl, KBr and LiF prisms

04 p0450 A73-15575

Atmospheric optical phenomena, discussing physical origin of rainbows and halos

04 p0445 A73-15629

Certain optical properties of the atmosphere of Venus and the possibilities of interpreting photometric and polarization measurements.

05 p0612 A73-16087

Earth resources remote sensors operation and potential, explaining atmospheric transmission and scattering and radiation polarization

05 p0578 A73-17130

Calculation of light scattering in planetary atmospheres with allowance for refraction

05 p0599 A73-17358

Effect of humidity on infrared and visual atmospheric transmission.

06 p0694 A73-18304

Optimal conditions for indirect probing of the atmosphere

06 p0721 A73-18732

Connection of the linear polarization level of atmosphere-air scattered light with the light reduction in the infrared spectral region

06 p0691 A73-18733

Methods of studying solar granulation fields in the presence of atmospheric disturbances

07 p0876 A73-19396

Optical sounding methods for the upper atmosphere and the earth's dust cloud

07 p0817 A73-19584

Determination of the transfer function for the spectral albedo of the surface-atmosphere system of the planet

07 p0818 A73-19659

Investigation of the time characteristics of the phase fluctuations of optical waves propagating through the earth atmosphere boundary layer

07 p0792 A73-19914

Laser beam spreading, deflection and collimation under atmospheric effects on long high path

08 p0938 A73-21028

Optical characteristics and structure of the Jovian atmosphere. V - Probable structure of the ammonia aerosol layer.

08 p1012 A73-21577

The relation of brightness phase functions to the optical thickness of the atmosphere.

08 p0986 A73-21585

Photography of the zodiacal light outside the ecliptic in quadrature and in opposition with the sun

09 p1073 A73-22001

Influence of atmospheric haze on the color of the underlying surface observed from a manned spacecraft

09 p1077 A73-22484

Measurement of log-irradiance fluctuation of He-Ne laser in the atmosphere.

09 p1096 A73-22750

Strong irradiance fluctuations in turbulent air - Plane waves.

10 p1248 A73-23837

Auroral absorption and magnetospheric plasma dynamics pattern from arctic stations atmospheric opacity data

10 p1212 A73-24220

Venus - Microwave opacity of the minor atmospheric constituents.

11 p1417 A73-25267

Haven View project for atmospheric visibility and radiation measurements, describing airborne and ground based instrumentation and measurement results

11 p1352 A73-25444

Daytime sky brightness from atmospheric transmittance, noting single and multiple scattering calculations

11 p1352 A73-25603

Brightness and polarization of the sky in the solar almucantar in the near infrared region of the spectrum

11 p1353 A73-25604

Correlation between the absolute brightness characteristic of day sky and the optical thickness of the atmosphere

11 p1353 A73-25605

Optical characteristics of bright day sky in the visual region of the spectrum and the atmospheric aerosol

11 p1353 A73-25606

Daytime cloudless sky glow, atmospheric transmittance, neutral polarization and aerosol optical characteristics in solar almucantar and vertical

11 p1353 A73-25608

Possibility of polarimetric monitoring of the optical stability of the atmosphere

11 p1392 A73-25609

Spectroelectrophotometer for atmospheric optical measurements in the near infrared region of the spectrum 11 p1362 A73-25610

Polarization of the cloudless daytime sky in the 1.25- to 2.42-micron range 11 p1353 A73-25645

Focused laser irradiance fluctuations in a turbulent medium. 11 p1376 A73-25874

Density distribution of radiation from a source of limited size in a scattering medium. 11 p1400 A73-26193

The spectral albedo of water clouds in the 1-6 micron band. 11 p1357 A73-26195

Thermally induced nonlinear propagation of a laser beam in an absorbing fluid medium. 11 p1377 A73-26229

Transfer of solar irradiance through cirrus cloud layers. 11 p1357 A73-26345

Airborne IR 32 cm observatory, discussing atmospheric transmission and guiding methods to overcome aircraft instability effects 11 p1368 A73-26503

Investigations of atmospheric extinction using direct solar radiation measurements made with a multiple wavelength radiometer. 12 p1520 A73-26810

Experimental determination of two-dimensional spatiotemporal power spectra of stellar light scintillation - Evidence for a multilayer structure of the air turbulence in the upper troposphere. 12 p1521 A73-27120

Applications of methods of geometric optics in the case of tropospheric propagation 12 p1473 A73-27755

Investigation of the influence of temperature and velocity fields on the quality of an astronomical image 12 p1546 A73-27864

The position of the emission lines of some lasers in the absorption spectrum of the earth's atmosphere. 13 p1626 A73-28174

Book - Atmospheric optics. Volume 2. 13 p1680 A73-28513

Scintillation and vibration of stars and structure of a turbulent atmosphere. 13 p1680 A73-28514

Effect of instability of earth's atmosphere on results of solar granulation observations. 13 p1680 A73-28515

Attenuation of monochromatic light in bottom layer of atmosphere and some properties of aerosols. 13 p1653 A73-28518

Theory of a photometer/actinometer/measuring the brightness of a fixed annular zone of sky around the sun. 13 p1613 A73-28519

Results of optical observations of dust in upper atmosphere and interplanetary space. 13 p1680 A73-28520

Atmospheric transparency and the relationships between optical variables in the ultraviolet. 13 p1607 A73-28697

Atmospheric air characteristics classification as haze, foggy haze, fog and drizzle from light scattering matrix on basis of aerosol condensation 13 p1654 A73-29159

Spatially filtered helium-neon laser link operation parallel to IR radiometer for real time atmospheric propagation monitoring over short path 13 p1661 A73-29328

Michelson shearing interferometer with piezoelectric scanner for atmospheric optical mean transfer function measurements from airborne platform, using laser or white light sources 13 p1621 A73-29332

Influence of atmospheric parameters on the wavelength of single-frequency laser radiation 14 p1756 A73-30023

A nephelometric method for transparency determination in scattering media 14 p1771 A73-30463

Calculation of light scattering in planetary atmospheres with allowance for refraction. 15 p1912 A73-31008

Short-term average optical-beam spread in a turbulent medium. 15 p1913 A73-31016

The effect of the size distribution of the rain drops on the standard visibility 15 p1902 A73-31139

Russian papers on young stellar complexes and astrolimate covering physical nature and activity of nonstationary stars, stellar evolution, T-associations and earth atmosphere optical instability 15 p1934 A73-31418

Astronomical telescopes operational efficiency relation to atmospheric optics conditions at various Middle Asian elevated sites 15 p1934 A73-31423

Formation of optical discontinuities in the atmospheric inversion layer 15 p1903 A73-31424

Calibration of turbulence and visual and photographic scintillation parameters in Pulkovo, Tashkent and Shternberg Institute astrolimate systems for 50 inch reflector 15 p1934 A73-31425

Worldwide variations in atmospheric transmission. I - Baseline results from Smithsonian observations. 15 p1904 A73-31724

Integral transmittance function of thermal radiation 15 p1904 A73-31782

Atmosphere optical thickness determination from satellite and ground measurements of scattered light in solar vertical 15 p1905 A73-31820

Photometric device for an ISP-28 spectrograph in optical atmospheric studies 15 p1875 A73-31822

High-resolution atmospheric-transmission measurement using a laser heterodyne radiometer. 15 p1886 A73-32378

Measuring earth-to-space contrast transmittance from ground stations. 15 p1914 A73-32386

Fully automatic assessment of RVR, and comparison with observers. 15 p1910 A73-32466

Manifestations and causes of atmospheric optical phenomena related to solar light dispersion and diffraction by particles, noting halos, polar auroras and mirages 16 p2002 A73-32949

Correlation measurements on the complex amplitude of stellar plane waves perturbed by atmospheric turbulence. 16 p2037 A73-33684

Radiation transport theory for anisotropic light scattering in planetary atmospheres, formulating transmission and reflection coefficients 16 p2066 A73-33790

Calculation of the diffuse reflection and transmission of light by a semiinfinite atmosphere 16 p2066 A73-33791

Optical properties of the Venus atmosphere 16 p2069 A73-33827

Planet Mars atmospheric physics covering optical parameters, brightness distributions, pressure, aerosol, chemical composition, photometric and surface layer properties and topography 16 p2069 A73-33830

Finite-difference approximations of the Navier-Stokes equations applied to a geophysical flow. I. II - Three-dimensional approximations on a region homeomorphic to a plane region. III - Three-dimensional approximations over the totality of a spherical region represented by means of a regular polyhedron 16 p2009 A73-33886

Analysis of multiwavelength observations of optical scintillation. 17 p2212 A73-35418

Russian book - Optical phenomena in the atmosphere as observed from piloted spacecraft. 18 p2348 A73-35898

Scintillation measurements for large integrated-path turbulence. 19 p2461 A73-38486

Experimental test of optical antenna-gain reciprocity. 19 p2439 A73-38487

Effects of temperature and velocity fields on the quality of astronomical images. 20 p2608 A73-39238

Use of the backscattering method to measure the atmospheric transparency in oblique directions 21 p2731 A73-40495

Considerations about the atmospheric background and the technique of differential modulation in infrared astronomy. 21 p2740 A73-40690

Astrolimate, site, calibration and atmospheric optics conditions for large telescope observations on M. Maidanak 21 p2769 A73-40729

Vector theory of the glory and rainbow 21 p2731 A73-40742

Statistical spectral attenuation characteristics of transmittance windows for visible and near IR under various optical weather conditions 21 p2731 A73-40746

Optical properties of the lower atmosphere of Venus /for interpreting measurements of the Venera 8 planetary probe/ 21 p2686 A73-40913

Results of direct measurements of the illumination in the atmosphere and on the surface of the planet Venus during the flight of the Venera 8 interplanetary probe 21 p2773 A73-41274

Russian book - Scattered daytime sky light. 21 p2691 A73-41439

Russian book - Light scattering in planetary atmospheres. 22 p2906 A73-41877

Remote probing of atmospheric turbulence. 22 p2884 A73-42620

Experiments on light pulse communication and propagation through atmospheric clouds. 22 p2828 A73-43157

Propagation of laser radiation in a turbulent atmosphere. 22 p2828 A73-43159

Role of the outer scale of turbulence in atmospheric degradation of optical images. 23 p3005 A73-43341

Study of laser radiation propagation and the diagnostics of a randomly inhomogeneous troposphere 23 p2954 A73-43572

Total ozone measurements in cloudy weather. 23 p2973 A73-43853

A model for estimating joint probabilities of cloud-free lines-of-sight through the atmosphere. 23 p3004 A73-44260

The optical properties of Venus and the Jovian planets. I - The atmosphere of Jupiter according to polarimetric observations. 24 p3129 A73-44442

Absorption at about 4.3 microns by /N₂-N₂/ and /N₂-O₂/ complexes in the terrestrial atmosphere 24 p3084 A73-44964

The formation of resonance lines in multidimensional media. II - Radiation operators and their numerical representation. 24 p3113 A73-45041

Strengths and air-broadened widths of H₂O lines in the 2950 to 3400 per cm region. 24 p3066 A73-45322

ATMOSPHERIC PHYSICS
NT CLOUD PHYSICS
On a method of determining the interaction coefficient in convective clouds 01 p0074 A73-11273

Scientific payload of Aeros German aeronomy satellite for atmospheric upper layers investigation, discussing instruments operation and location and measurement technique [DGLR PAPER 72-069] 02 p0190 A73-11656

Meteorological and atmospheric physics observations by Soyuz manned spacecraft, analyzing spectrophotometry, photography and visual observation data of twilight, night and day horizons 02 p0160 A73-12265

Theoretical model of diurnal variations of the equatorial thermosphere at equinox. 02 p0162 A73-12290

Investigation of the electrical parameters and meteorological elements of the atmosphere close to the ground during thunderstorm and thunderstorm-free periods 02 p0189 A73-12589

Magnitude estimate for long wave radiative cooling effects for isolated buoyant thermal rising in uniform ambient atmosphere [AD-755500] 02 p0224 A73-12779

Contrail ice budget measurements with optical array particle size spectrometer onboard Sabreliner, noting water abundance reduction at subtropopause jet traffic levels 02 p0189 A73-12785

Direct temperature measurements for rotating annulus experiments, showing symmetric baroclinic instability and Richardson number for baroclinic wave 02 p0189 A73-12788

Magnetospheric structure studies during 1969-1971, discussing bow shock magnetosheath, magnetopause, polar cusps, electric fields and trapped particle composition 03 p0302 A73-13852

Remote sensor for atmospheric physical properties with FM-CW scanning radar, parabolic antennas and waveguide feeds for linear and circular polarization 03 p0339 A73-14544

Mass transport and energy of impulse compression wave traces in atmosphere due to radiation, inner friction, gravity and rotation effects 04 p0440 A73-15285

Magnetopause physical properties, location and shape from continuum gas dynamics analogies, noting agreement with experimental results 04 p0441 A73-15328

Physical phenomena of controlled experiments in earth magnetosphere using test particles, radio emission and electron and ion beams 04 p0443 A73-15342

Tunable dye laser radar observation for Na layer nocturnal vertical distribution, suggesting meteor shower effect on layer content increase 04 p0444 A73-15543

Double layer formation in homogeneous plasma with constant current, considering occurrence in ionosphere and solar atmosphere 05 p0601 A73-16146

Physicostatistical investigations of the general atmospheric circulation 05 p0592 A73-16231

The runaway Greenhouse in the Venus atmosphere. 05 p0622 A73-17124

An earlier generation of long-enduring south temperate ovals on Jupiter. 06 p0745 A73-17441

Mars atmosphere observation from Mariner 9 TV pictures, discussing global and local dust storms, condensate clouds, albedo and polar cover

06 p0745 A73-17479

Upper atmosphere structure from rocket and satellite observations, considering COSPAR International Reference Atmosphere /CIRA 1972/

07 p0813 A73-19221

Upper atmosphere thermodynamic and circulation characteristics for high altitude aircraft flights, including geomagnetic disturbance factors

07 p0847 A73-19298

Nighttime atmosphere emission of atomic oxygen /5577 A/ and its connection with penetrating micrometeorites

07 p0818 A73-19592

Three-dimensional acoustic-ray tracing in an inhomogeneous anisotropic atmosphere using Hamilton's equations.

08 p0988 A73-21190

Second kind conditional instability of resting atmosphere, noting Ekman boundary layer absence in rain area for given Coriolis parameter

08 p0985 A73-21379

Intensities and half-widths of lines in the A and B bands of the red atmospheric system of O₂ bands

09 p1077 A73-22664

Planetary atmospheres

09 p1152 A73-23471

Some considerations on the continuous space-time spectral analysis of atmospheric disturbances.

11 p1394 A73-25723

The variation of temperature with latitude in the lower thermosphere /80-100 km/.

11 p1357 A73-26194

Physics and chemistry of upper atmospheres.

11 p1425 A73-26209

U.S., UK and French research programs on conditions encountered by civil aviation and supersonic transports in stratosphere

11 p1455 A73-26594

The role of convection in stellar atmospheres. I - Observable effects of convection in the solar atmosphere.

11 p1427 A73-26611

The planet Venus - A new periodic spectrum variable.

11 p1428 A73-26621

Ionospheric production and loss processes of atomic sulfur ions, considering dissociative ionization sources

12 p1489 A73-26999

Detection of a temporary ozone content decrease in the upper atmosphere at the moment of sunrise

13 p1605 A73-28074

Photometric investigation of the atmospheric activity of Jupiter during 1962-1969

13 p1673 A73-28297

Role of commercial aircraft in global monitoring systems.

13 p1568 A73-28499

Atmosphere Explorer mission of lower thermosphere and ionospheric physics investigation, discussing orbit selection

13 p1687 A73-28626

Rocket-borne scientific experiment program Sun-Atmosphere 1971, using meteorological rockets for meteor trail, atmospheric and ionospheric observations during geomagnetic disturbances

13 p1609 A73-29188

Cometary head atmospheric gaseous and dust components characteristics in terms of physical processes in comet nucleus vicinity

14 p1792 A73-29814

The dynamics of the atmospheres of the major planets.

14 p1799 A73-30534

On the atmospheric kinetic energy spectrum and its estimation at some selected stations.

14 p1750 A73-30763

Studies on barotropic and baroclinic energy conversions in wave number regime.

14 p1772 A73-30901

Russian papers on heat exchange in atmosphere covering stratus and convective cloud effects, clear sky conditions, turbulent transfer, atmospheric boundary layer, etc

15 p1904 A73-31781

Remote sensing of atmosphere and ocean by lidar, radar, bistatic radio, IR optics, microwave radiometry, crossed-beam correlation, etc

16 p2003 A73-33368

Planet Mars atmospheric physics covering optical parameters, brightness distributions, pressure, aerosol, chemical composition, photometric and surface layer properties and topography

16 p2069 A73-33830

Photometric studies of the Jovian atmospheric activity

16 p2070 A73-33841

Atomic collision processes applied to earth atmospheric physics and chemistry, Jovian ionospheric composition and terrestrial tropical UV dayglow

17 p2213 A73-34450

The effects of the observational system and the method of interpolation on the computation of spectra.

17 p2201 A73-34852

Testing and calibration of aircraft sensors and systems.

17 p2174 A73-35580

Processing of aircraft data.

17 p2132 A73-35583

Book - Progress in high temperature physics and chemistry. Volume 5.

17 p2255 A73-35592

The theory of charged particle temperatures in the upper atmosphere.

17 p2224 A73-35593

Evolution of the hydrodynamic methods for weather forecasting

18 p2331 A73-35906

The atmospheric mixing in the atmospheres of Mars and Venus.

18 p2349 A73-36034

A preliminary study of the transient response of the atmosphere produced by mid-tropospheric heating.

18 p2332 A73-36701

Objective analysis method tested via comparison to known function at radiosonde observation stations, considering description of spectral analyses of wind field kinetic energy

18 p2332 A73-36702

Short-acting repulsive forces between atoms and molecules of atmospheric gases

19 p2462 A73-37350

Numerical solution of hydrothermodynamics equations for atmospheric processes on a flat earth

20 p2584 A73-39471

Russian book - Certain problems concerning solar-terrestrial links and physics of the atmosphere.

21 p2730 A73-40102

Nuclear meteorology as branch of atmospheric physics, examining natural and artificial fission products, nuclear explosion effects, atmospheric purification and radioactive tracers for meteorological process investigation

21 p2730 A73-40115

Space research XIII; Proceedings of the Fifteenth Plenary Meeting, Madrid, Spain, May 10-24, 1972. Volumes 1 & 2.

21 p2687 A73-41325

Russian book - Physics of atmospheric ozone.

21 p2691 A73-41435

Photometric studies of atmospheric activity of Jupiter during 1962-1969.

21 p2779 A73-41541

Parametrization of orographical effects in the planetary boundary layer.

21 p2732 A73-41570

Experimental test to determine the origin of geomagnetically trapped radiation.

22 p2846 A73-41944

Atmospheric gravity wave observations after the solar eclipse of June 30, 1973.

22 p2847 A73-42487

Transition probability matrix method for calculating residence times of moving particles in region of space, determining stratosphere residence time against exit to tropopause

22 p2849 A73-42543

Surface wind stress and threshold friction velocity required to raise dust on Mars, discussing mechanisms for production of strong winds in Ekman layer

22 p2912 A73-42981

Resonance conditions for nonlinear interaction of acoustic gravity waves with viscous damping taken into account

22 p2828 A73-43178

Intensity variations of electron-photon shower particles in the atmosphere

23 p3023 A73-43557

Symposium on Atmospheric Ozone, Arosa, Switzerland, August 21-25, 1972, Proceedings.

23 p2973 A73-43851

Ionosphere dynamic process investigations, describing wind models, E region drift velocity curves and energy distribution chart

23 p2978 A73-43978

ATMOSPHERIC PRESSURE

NT CYCLOGENESIS

The estimation of ground-level pressure fields from computer analyses and their application to large-scale atmospheric mass transfer.

01 p0072 A73-10144

Effect of increased atmospheric pressure on the dynamics of free oxygen content in animal muscle tissues

01 p0007 A73-10156

A study of the stability of certain self-similar solutions of the theory of explosions in the atmosphere

01 p0035 A73-11429

Mars exploration by spacecraft, discussing erosional processes, atmospheric pressure and composition, heat absorption and radiation and polar caps formation

02 p0221 A73-12575

Human thresholds for perceiving sudden changes in atmospheric pressure.

03 p0260 A73-13554

Annual and semi-annual zonal wind components and corresponding temperature and density variations, 60-130 km.

04 p0440 A73-14961

The role of atmospheric pressure variations above the mesopause in the phenomena of winter anomaly and variability of the lower ionosphere.

04 p0441 A73-15290

Planetary-scale fluctuations of pressure in the E-layer, f-min, and pressure in the stratosphere.

05 p0571 A73-17057

Determination of the pass band of a system of measurement of rapidly variable pressures in the air

05 p0579 A73-17228

Barometric coefficients of the nucleon components of cosmic rays of various energies

06 p0742 A73-17550

Long term atmospheric pressure fluctuations in relationship to solar activity over Northern Hemisphere, confirming 22 year cycle

07 p0816 A73-19448

Influence of coherence of sampling on the accuracy of linear statistical forecasting and on the optimal predictor dimension

08 p0985 A73-21452

Thermal diffusivity of lunar rocks under atmospheric and vacuum conditions.

09 p1148 A73-22872

Satellite observed cloud signatures associated with mature and decaying depressions over high and middle southern latitudes, deriving surface pressure and upper geopotential anomaly patterns

10 p1244 A73-23980

Radiosonde soundings for typhoons and hurricanes isobaric surfaces heights, temperatures and humidities, calculating correlation coefficients between sea level pressure and other parameters

10 p1245 A73-23985

Vitamin metabolism alteration under increased atmospheric pressure

11 p1321 A73-25036

The diluter-demand oxygen system used during the international Himalayan expedition to Mount Everest.

11 p1322 A73-25145

The diurnal and semidiurnal barometric oscillations, global distribution and annual variation.

11 p1351 A73-25167

Study of the stability of some self-similar solutions from the theory of an explosion in the atmosphere.

11 p1348 A73-26051

Computerized maritime sea level atmospheric pressure field analysis, using pressure and wind velocity data

12 p1519 A73-26802

A two-satellite microwave occultation system for determining pressure altitude references.

12 p1521 A73-26813

Stratospheric geopotential pressure field numerical prediction based on quasi-geostrophic atmosphere model, considering stratospheric heating period

12 p1521 A73-27742

Relation between the pressure at the center of a tropical cyclone and the dimension of its cloud system

15 p1904 A73-31610

Barometric coefficients of the nucleon component of cosmic rays of different energies.

16 p2052 A73-32774

Relation between turbulence in a clear sky and the evolution of the baric field

17 p2204 A73-34543

Results of simultaneous in-situ-observations in Spain of electron concentration, neutral wind and air pressure in the D-region in different seasons and during an SID-event and their relevance to the winter-anomalous state of the atmosphere.

18 p2305 A73-36001

Influence of longitudinal variations on the structure of temperature, pressure and wind fields in the stratosphere and mesosphere of the Northern Hemisphere.

18 p2310 A73-36139

Results of air temperature, density and pressure measurements obtained with the aid of foil cloud sensors in the height region between 80 and 95 km.

18 p2311 A73-36179

Atmospheric regeneration in closed chambers by potassium superoxide

18 p2287 A73-36951

Analysis of pressure and cloud anomaly fields.

18 p2333 A73-37054

Experiments on incorporating radiative heat influx in numerical forecasting.

18 p2334 A73-37077

CW CO₂ laser at atmospheric pressure.

19 p2438 A73-38277

Influence of the atmosphere on the gravity force and its potential at points on the earth's physical surface

19 p2428 A73-38555

Determination of the wind field from the pressure field and the latitudinal effect of the geomagnetic field in the ionosphere

21 p2681 A73-40105

Seasonal variations of the barometric effect of the cosmic ray neutron component intensity

21 p2755 A73-40114

Oxygen uptake during maximal work at lowered and raised ambient air pressures.

21 p2638 A73-41132

Venera 8 - Measurements of temperature, pressure and wind velocity on the illuminated side of Venus.

23 p3028 A73-43602

Greenhouse effect for Titanian atmospheric models with different methane, hydrogen, helium and ammonia proportions, deriving brightness temperature spectrum and surface pressure

24 p3130 A73-44457

ATMOSPHERIC RADIATION

NT AIRGLOW

NT AURORAL ARCS

NT AURORAS

NT DAWN CHORUS

NT DAYGLOW

NT GEOCORONAL EMISSIONS

NT IONOSPHERIC NOISE

NT NIGHTGLOW

NT RADIO AURORAS

NT RED ARCS

NT SKY RADIATION

NT STRATOSPHERE RADIATION

NT TROPOSPHERIC RADIATION

NT TWILIGHT GLOW

NT WHISTLERS

Conference on Atmospheric Radiation, Fort Collins, Colo., August 7-9, 1972, Preprints.

01 p0037 A73-10351

A solution to the auxiliary equation of radiative transfer for a planetary atmosphere with molecular anisotropy.

01 p0097 A73-10352

Atmospheric radiative transfer by carbon dioxide.

01 p0037 A73-10366

A method for calculating atmospheric thicknesses directly from satellite radiation measurements.

01 p0073 A73-10378

Analysis of a nonisothermal, spherical detector for monitoring the earth's radiative energy budget.

01 p0045 A73-10382

Condensation trail effects on atmospheric radiation budget from model calculation for ice particle layer near tropopause, using Mie scattering and radiative transfer approximation

01 p0038 A73-10389

Natural variation of the radiation budget of the earth-atmosphere system as measured from satellites.

01 p0038 A73-10390

A detailed radiation model for climate studies - Comparisons with a general circulation model radiation subroutine.

01 p0039 A73-10393

A linear harmonic analysis of atmospheric motion with radiative dissipation.

01 p0039 A73-10399

Calculation of the spectral, angular and altitudinal distributions of the thermal radiation field of the atmosphere and the earth's surface

01 p0040 A73-10871

Backward Monte Carlo calculations of the polarization characteristics of the radiation emerging from spherical-shell atmospheres.

01 p0078 A73-11233

Cloud characteristics in problems of radiation energetics in the earth's atmosphere.

02 p0159 A73-12146

The radiation budget of the earth-atmosphere system as measured from the Nimbus 3 satellite (1969-1970).

02 p0160 A73-12266

A measurement of the atmospheric neutron flux in the energy range 50 less than E less than 350 MeV.

03 p0298 A73-12886

Low energy atmospheric gamma rays near geomagnetic equator.

03 p0360 A73-12890

On the altitude dependence of the atmospheric X-rays in the energy range 0.1-1 MeV.

03 p0365 A73-14441

Diurnal and annual behavior of the radiation balance

05 p0609 A73-16218

Prospects for the utilization of satellite information in studies of the general atmospheric circulation

05 p0593 A73-16244

Variational solution to the radiative equation by the use of a step function. II - Extension to nonlinear case by iteration method.

05 p0641 A73-17102

Preliminary results of measurements of UV emissions scattered in the Martian upper atmosphere.

06 p0746 A73-17486

Observations of the He II 304-A radiation in the night sky.

07 p0869 A73-19232

Cross sections for emission of Lyman-alpha radiation in collisions of 1-25 keV protons and hydrogen atoms with constituents of planetary atmospheres.

08 p0957 A73-20660

Atmospheric gamma ray spectra from balloon spectrometer scintillator measured energy loss spectra

08 p0998 A73-21280

On the source of the 3840 A persistent emission by meteors.

08 p1010 A73-21318

Epithermal neutron differential flux spectrum in equilibrium layers of atmosphere at 57 degrees north

08 p1000 A73-21350

Measurement of short- and longwave radiant fluxes from the Kosmos-320 satellite.

08 p0961 A73-21586

Study of the radiative properties of the atmosphere between cloud layers

09 p1114 A73-22371

Spectrophotometric measurements of noctilucent clouds.

09 p1079 A73-23339

Investigation of rigid gamma rays in the atmosphere with the aid of a telescope with an acoustic spark chamber

10 p1267 A73-23923

Studies of the atmospheric fine structure with the aid of microwave propagation experiments

10 p1213 A73-24682

High energy astrophysics research at the Max-Planck-Institut.

11 p1411 A73-25139

Haven View project for atmospheric visibility and radiation measurements, describing airborne and ground based instrumentation and measurement results

11 p1352 A73-25444

Radio Astronomy Explorer /RAE/, I - Observations of terrestrial radio noise.

11 p1356 A73-25920

Measurement of geomagnetic cutoff rigidities and particle fluxes below geomagnetic cutoff near Palestine, Texas.

12 p1533 A73-26978

Measurements and interpretation of the polarization of radiation emerging from the atmosphere at an altitude of 28 km over south-western New Mexico /USA/.

13 p1652 A73-28269

The spectral, angular, and altitudinal distributions of the earth and sky thermal radiation field.

13 p1607 A73-28695

Investigation of cloud cover parameters from measurements on the Cosmos 384 satellite

13 p1654 A73-29155

Magnetospheric dayside cusp - A topside view of its 6300-angstrom atomic oxygen emission.

14 p1750 A73-30620

Time dependent worldwide distribution of atmospheric neutrons and of their products, I, II, III.

16 p2055 A73-33427

The O I 1304- and 1356-A emissions from the atmosphere of Venus.

16 p2062 A73-33431

Observations of the auroral oval and a westward traveling surge from the Isis 2 satellite and the Alaskan meridian all-sky cameras.

16 p2004 A73-33445

Millisecond time scale atmospheric light pulses associated with solar and magnetospheric activity.

16 p2004 A73-33447

The abnormal stratosphere studied with the aid of satellite radiation measurements.

[AIAA PAPER 73-493]

16 p2005 A73-33537

Electrophotometric equipment in the Stara Zagora Observatory

16 p2016 A73-33663

Zenith atmospheric emission noise temperature and attenuation measurements including multiple and single frequency statistical observations at 85-118 GHz during 1970-1971

16 p1982 A73-33720

On relationship between the earth-atmosphere system albedo and the earth's surface albedo.

18 p2308 A73-36042

Density of the radiation of the earth/atmosphere system into space

18 p2309 A73-36112

Satellite observations of strong Balmer alpha atmospheric emissions around the magnetic equator.

18 p2346 A73-36284

Some aspects of the solution of inverse problems of satellite meteorology.

18 p2335 A73-37078

Atmospheric gamma ray spectra from balloon spectrometer scintillator measured energy loss spectra

19 p2476 A73-37909

Atmospheric sounding by satellite-borne remote sensors, discussing radiometric measurements of temperature, composition, and reflected and emitted radiance in visible, IR and microwave bands

[AAS PAPER 73-125]

20 p2550 A73-38585

Mariner 9 ultraviolet spectrometer experiment - Mars atomic oxygen 1304-A emission.

20 p2604 A73-38932

Asymmetrical global O I airglow emission pattern with respect to magnetic equator from Ogo 4 observations, noting poor correlation with ionospheric electron density

20 p2551 A73-38939

Predawn enhancement of 6300-A emission observed near the plasmopause from the Isis-2 spacecraft.

20 p2551 A73-38945

Remote sensing of atmospheric O3 and H2O to 70 km by aircraft measurements of radiation at 1.64 mm wavelength.

20 p2557 A73-39855

Russian book - The stochastic structure of cloud and radiation fields.

21 p2730 A73-40243

Extra-atmospheric photoelectric study of the brightness of the earth's atmosphere

21 p2686 A73-40912

Evidence of features in atmospheric spectra at around 8 per cm of probable solar origin.

21 p2687 A73-41079

Use of meteorological rocketsonde and satellite radiation data for constant-pressure analyses at levels between 5 and 0.4 mb.

21 p2732 A73-41336

Ariel 3 evidence of zones of VLF emission at medium invariant latitudes which co-rotate with the earth.

21 p2691 A73-41382

Enhancements of the photoelectron-excited dayglow during solar flares.

21 p2761 A73-41389

Continuum centimeter wave radiometers circuits, parameters, sensitivity and atmospheric radio emission fluctuations

21 p2705 A73-41460

Lower atmospheric intensity-calibrated thermal emission spectra with digital recording near IR spectrometer, discussing applications to pollutant detection

21 p2692 A73-41574

Angular effects in the propagation of cosmic rays in the atmosphere.

21 p2764 A73-41629

Satellite ultraviolet measurements of nitric oxide fluorescence with a diffusive transport model.

22 p2845 A73-41925

Estimate of extreme ultraviolet dayglow of helium in the Martian atmosphere.

22 p2909 A73-42485

Ozone transition detection in earth atmospheric absorption and emission, comparing measured ozone absorption profiles with theoretical computations

22 p2848 A73-42535

Postsunset oxygen emission observation by radiometer on rocket launched at Natal, Brazil, observing 10-km thick emission layer

22 p2848 A73-42536

French monograph - Contribution to the ultraviolet spectrophotometry of the night sky /1900 to 3400 A/.

22 p2850 A73-42742

Measurements of the energy exchange between earth and space from satellites during the 1960's.

22 p2851 A73-42858

Radiation production and energy deposition by ring current protons precipitated into the mid-latitude upper atmosphere.

23 p3024 A73-43685

Tropospheric vertical energy transfer due to terrestrial and atmospheric water vapor and carbon dioxide radiation calculated for vertical atmospheric temperature and composition distributions

24 p3082 A73-44736

Two types of radio emission from the auroral ionosphere and ionospheric disturbances

24 p3083 A73-44798

Interpretation of atmospheric radio emission in the 5-mm spectral region

24 p3068 A73-44961

Lyman alpha 1216 A intensity behavior for atomic hydrogen density distribution below 200 km on Mars, calculating radiative transfer

24 p3139 A73-45108

ATMOSPHERIC REFRACTION

NT RADIO WAVE REFRACTION

IR absorption and refraction index of atmospheric aerosol, using KBr disk transmittance and specular reflection measurements

01 p0038 A73-10373

Measurement of the complex index of refraction of atmospheric aerosols using optical spectral analysis techniques.

01 p0045 A73-10375

Tropospheric and ionospheric refraction errors in satellite tracking over the Indian sub-continent.

02 p0141 A73-12299

Scintillation phenomenon due to radio wave propagation through ionospheric and tropospheric regions with irregularities in refractive index

02 p0162 A73-12300

Determination of systematic errors in time determinations with the passage instrument

03 p0307 A73-13251

UHF airborne measurement of equatorial ionospheric scintillation fading.

03 p0275 A73-13647

The influence of atmospheric layer structure on space - Earth links.

03 p0275 A73-13653

Atmospheric wind and temperature inhomogeneity induced sound wave refraction effects on acoustic sounder measurements, noting scattering volume displacement and Doppler shift

03 p0276 A73-13831

High power radar for measurement of refractivity inhomogeneities in clear air turbulence from backscattered energy Doppler shift

03 p0338 A73-14530

Radar echo in clear air convection shown due to backscattering from fine refractivity fluctuations caused by turbulent mixing

03 p0280 A73-14543

A study of tropospheric radar propagation characteristics during an unusual spell of persistent dust haze followed by thunderstorm over Delhi during May 1966.

03 p0280 A73-14547

Venus atmospheric parameters below critical refraction and surface refractive index from signal amplitude measurement by radio holographic occultation techniques

03 p0379 A73-14567

Tropospheric refraction effects on satellite range measurements.

04 p0415 A73-14750

Atmospheric correction for the troposphere and stratosphere in radio ranging of satellites.

04 p0439 A73-14808

Ionospheric scale height from the refraction of satellite signals.

04 p0415 A73-14952

Diurnal variation of the effective earth's radius factor k / over India and its influence on microwave propagation.

04 p0423 A73-15599

Diurnal variation of the effective earth's radius factor k / over India and its influence on microwave propagation.

04 p0423 A73-15928

Book - Calculation of wave propagation by nomograms - Frequencies above 30 MHz.

05 p0548 A73-16325

Calculation of light scattering in planetary atmospheres with allowance for refraction

05 p0599 A73-17358

Analysis of light polarization variations in a twilight sky in terms of upper atmosphere effects

07 p0817 A73-19588

Coordinates correction for atmospheric refraction in aerial photography, noting effects of ground elevation, atmospheric pressure and temperature

08 p0969 A73-21709

Preliminary results of studies of the Martian atmosphere with the aid of the Mars-2 satellite

09 p1146 A73-22486

The transition from locked to leaky modes in tropospheric radio propagation.

11 p1327 A73-25122

Integral equation numerical solution by minimum mean-squared estimator for atmospheric electromagnetic refractivity profile from satellite radio tracking data, noting iterative procedure convergence

11 p1330 A73-25686

Comparison of observed and predicted phase-front distortion in line-of-sight microwave signals.

11 p1330 A73-25687

Centimeter wave propagation beyond horizon, considering terrestrial surface curvature and mountain effects on deflection and atmospheric refractivity inhomogeneity caused scattering

12 p1473 A73-27754

Effect of some external factors on accuracy of observations of active satellites.

13 p1680 A73-28516

Determination of the astronomical refraction near the horizon at different times of the year

13 p1683 A73-29096

Near horizon anomalies in astronomical refraction due to ground air layer effects on tropospheric processes

13 p1610 A73-29322

Absorption saturation effects on high-power CO₂ laser beam transmission.

13 p1628 A73-29329

Preliminary results of Martian-atmosphere research with the Mars-2 satellite.

14 p1798 A73-30321

Calculation of light scattering in planetary atmospheres with allowance for refraction.

15 p1912 A73-31008

On the effect of electron-neutral particle collisions upon the refraction of high-frequency radio waves by the lower atmosphere and ionosphere of Mars.

15 p1929 A73-31078

Microwave-propagation studies regarding the isotropy characteristics of the turbulent fine structure of the refractive index in the troposphere

15 p1874 A73-32361

Atmospheric lens effect - Another loss for the radar range equation.

16 p1980 A73-33407

Atmospheric refractivity effects on maximum antenna gain and correlation coefficient in design of microwave line of sight links for high reliability

16 p1981 A73-33704

Atmospheric refractivity fluctuation caused transit time variation effects on propagation noise and frequency stability in microwave radio link signal reception at 36 GHz

16 p1982 A73-33714

Correction of electrical path length by passive microwave radiometry.

16 p1983 A73-33729

Atmospheric refractivity variation, precipitation and wind effects on two orthogonal linearly polarized microwave signals transmission over radio link at 22 and 37 GHz

16 p1983 A73-33733

Correction formulas for aerial photograph distortions due to internal refraction of light rays in separation of gas media by lateral surface of circular cylinder

16 p2038 A73-34050

Propagation of VLF waves in the earth-ionosphere waveguide under nighttime ionospheres.

17 p2126 A73-35629

Correction procedure for outdoor noise measurements.

19 p2458 A73-37285

The structure of an inversion above a convective boundary layer as observed using high-power pulsed Doppler radar.

19 p2447 A73-38205

A note on the FM-CW radar as a remote probe of the Pacific Trade-Wind Inversion.

19 p2448 A73-38211

On the use of forward scatter techniques in the study of turbulent stratified layers in the troposphere.

19 p2427 A73-38219

Optical and millimeter line-of-sight propagation effects in the turbulent atmosphere.

19 p2405 A73-38220

Small-scale atmospheric structure deduced from measurements of temperature, humidity and refractive index.

19 p2448 A73-38224

The radiation balance of the earth's surface and inclinations of isodioptric surfaces

19 p2428 A73-38556

Refraction of light beams in an atmosphere with arbitrary parameters

19 p2449 A73-38558

Refraction of plasma waves in the ionosphere /in connection with topside sounding of the ionosphere/

21 p2691 A73-41507

Diurnal cycles of the refractive index structure function coefficient.

22 p2849 A73-42545

Remote probing of atmospheric turbulence.

22 p2884 A73-42620

Fluctuation characteristics of the electric component of the troposphere.

24 p3084 A73-44940

ATMOSPHERIC SCATTERING

NT TROPOSPHERIC SCATTERING

Radiative calculation models for infrared transfer through cloud, aerosol and the continuum.

01 p0073 A73-10358

Laser radar measurements of atmospheric backscattering turbidity.

01 p0073 A73-10403

The spherical albedo of a planetary atmosphere

01 p0102 A73-10942

Atmospheric absorption and scattering as radiation extinction mechanisms, discussing attenuation coefficient wavelength and weather dependence

01 p0102 A73-10993

Compact laser radar for remote atmospheric probing.

01 p0060 A73-11059

Verification of an approximation method for calculating multiple scattering of sky radiation.

01 p0074 A73-11236

Invariant imbedding and Chandrasekhar's planetary problem of radiative transfer.

02 p0207 A73-12389

Bistatic-radar detection of high-altitude clear-air atmospheric targets.

02 p0142 A73-12526

Atmospheric aerosol Mie scattering calculation as function of polarization parameters based on models for three laser wavelengths and two materials

03 p0341 A73-12900

The University of Oklahoma acoustic radar.

04 p0475 A73-15067

Meteorological lidar use to obtain backscatter curve produced by aerosols suspended in atmosphere

[ONERA, TP NO. 1130]

04 p0432 A73-15091

Optimal processing of the backscatter signal in determining the structure of atmospheric inhomogeneities.

04 p0417 A73-15325

Large ruby laser radar for remote detection and recording of atmospheric scattering data, describing tracking mount, optics, electronic signal processing and display features

04 p0433 A73-15768

Influence of refractive index on emittance from semi-infinite absorbing scattering media.

[AIAA PAPER 73-147]

05 p0598 A73-16895

Study of the scattering properties of the atmosphere by light polarization measurements in a twilight sky

05 p0572 A73-17355

Transmission of a GaAs laser beam through the atmosphere.

06 p0699 A73-17495

Connection of the linear polarization level of atmosphere-air scattered light with the light reduction in the infrared spectral region

06 p0691 A73-18733

Ionospheric attenuation of 3-100 MHz radio waves, interpreting scatter mode propagation mechanism as total reflection from lower ionizational irregularities

07 p0792 A73-19458

Scattered twilight light variations at 5500 to 6600-A wavelengths according to spectral observations in 1962 through 1968 at Abastumani

07 p0817 A73-19587

Determination of the concentration and scattering indicatrix of atmospheric dust from primary twilight brightness

07 p0817 A73-19589

Albedo and illuminance of the surface of a planet with an inhomogeneous, purely scattering atmosphere.

07 p0820 A73-20345

Theorems on symmetries and flux conservation in radiative transfer using the matrix operator theory.

08 p1020 A73-20791

Matrix operator theory of radiative transfer for Rayleigh scattering and radiance calculation of multilayered atmospheres with large optical depths

08 p0958 A73-21040

Effects of changes in the atmosphere on solar insolation.

08 p0958 A73-21269

A numerical model of thermal radiation in a dusty atmosphere.

08 p0960 A73-21383

Influence of the geometrical parameters of a lidar on the applicability of single-scattering approximation

08 p0986 A73-21457

Radiative transfer model for simulation of airborne remote sensing scanner data under flight conditions in hazy atmosphere with scattering and absorption effects

09 p1077 A73-22386

Spherical albedo of a planetary atmosphere.

09 p1147 A73-22737

Light flux vertical distribution in spherical multilayer cloud and gas scattering planetary atmosphere, calculating radiation intensity

10 p1276 A73-23891

Russian book - Scattering and absorption of light in the atmosphere.

11 p1392 A73-25602

Daytime sky brightness from atmospheric transmittance, noting single and multiple scattering calculations

11 p1352 A73-25603

Sky brightness in solar aureole region relationship to solar radiation single scattering on atmospheric aerosol particles

11 p1353 A73-25607

Light scattering functions in the atmospheric ground layer for a range of large scattering angles

11 p1393 A73-25616

Nonlinear hydrodynamic VLF wave scattering in the earth's magnetosphere.

11 p1331 A73-25913

Description of the photoelectron interaction with ambient electrons in the ionosphere.

11 p1357 A73-25927

Density distribution of radiation from a source of limited size in a scattering medium.

11 p1400 A73-26190

Determination of the characteristics of light-scattering particles in the atmosphere of Venus from photometric measurements.

12 p1543 A73-27640

Centimeter wave propagation beyond horizon, considering terrestrial surface curvature and mountain effects on deflection and atmospheric refractivity inhomogeneity caused scattering

12 p1473 A73-27754

Formation of spectral lines and study of growth curves in a semimfinite scattering atmosphere

13 p1680 A73-28458

Venus atmospheric model based on spectroscopic evidence of carbon dioxide spectral lines phase variation due to two scattering layers

13 p1680 A73-28459

Light scattering by atmospheric aerosols.

13 p1653 A73-28517

Radar echo from a 'clear sky' in the decimeter radio wave range

13 p1585 A73-29156

Reflection and transmission of a narrow beam of light in a thick turbid medium layer with isotropic scattering and absorption

13 p1609 A73-29158

Atmospheric effects in multispectral photographs.

13 p1619 A73-29239

Solar Lyman alpha radiation scattering analysis to determine neutral hydrogen atom distribution in upper atmosphere

14 p1747 A73-29865

Investigation of scattered ultraviolet radiation in the upper Martian atmosphere from the Mars-3 automatic interplanetary station

14 p1796 A73-29866

The altitude of the scattering layer near the mesopause over the summer poles.

14 p1750 A73-30768

Derivation of scattering properties of the atmosphere from polarization measurements on the light of the twilight sky.

15 p1865 A73-31005

Russian book - Scattering and attenuation of electromagnetic radiation by atmospheric particles.

15 p1843 A73-31586

Multiple scattering of sound by turbulence and other inhomogeneities.

15 p1865 A73-32151

Turbulent scattering phenomenological model for D region partial coherent reflection experiments with measurement noise, presenting amplitude and phase statistics

15 p1845 A73-32230

The color deficiency of the solar halo of 22 deg radius

15 p1873 A73-32358

Lidar measurements of the variability of stratospheric particulates.

[ATAA PAPER 73-520]

16 p2007 A73-33556

Microwave transhorizon propagation in atmospheric evaporative duct layer by superdiffraction, using Monin-Obukhov similarity theory for computerized prediction

16 p1981 A73-33712

Primary scattering theory for twilight luminance calculation, considering luminance atmospheric scale height growth in thermosphere and seasonal variation

16 p2009 A73-33889

Preliminary data on the optical properties of solid ammonia and scattering parameters for ammonia cloud particles.

17 p2211 A73-34858

Forward scattering method for determination of atmospheric aerosols particle size distribution, considering angle-dependent scattering at fixed wave number

17 p2161 A73-34938

Polarization properties of lidar backscattering from clouds.

17 p2125 A73-35416

Mariner 9 ultraviolet spectrometer experiment - Afternoon terminator observations of Mars.

19 p2479 A73-37220

Multiple scattering theory of radiative transfer in inhomogeneous atmospheres.

19 p2423 A73-37586

FM-CW ground and aircraft radar observations of clear air echo strata, examining turbulence levels, Richardson number, turbulent scattering, radar reflectance and power spectra

19 p2427 A73-38203

The interaction between atmospheric microstructure and acoustic and electromagnetic waves.

19 p2406 A73-38242

Radiative transfer in homogeneous, nongray gases with non-isotropic particle scattering.

[ASME PAPER 73-HT-9]

20 p2625 A73-38566

Light flux vertical distribution in spherical multilayer cloud and gas scattering planetary atmosphere, calculating radiation intensity

20 p2603 A73-38910

Multispectral scanner data analysis by application of spectral radiance signature extension techniques based on preprocessing to reduce atmospheric and scanner look angle effects

20 p2559 A73-39880

Atmospheric radiative transfer model for correction of Apollo photographic remote imagery data degradation due to radiation scattering

20 p2559 A73-39881

Remote measurement of subsurface sea water temperature by airborne Raman scattering with cross polarizer in front of light source and detector, noting precision

20 p2568 A73-39889

Absorption line contours in homogeneous plane-parallel semiinfinite aerosol layers and planetary atmosphere overcloud gas layers for nonspherical scattering

21 p2768 A73-40723

Indices of backscattering and attenuation of light by a water aerosol

21 p2731 A73-40747

Amplification of backscattering by bodies placed in a medium with random inhomogeneities

21 p2657 A73-41513

Russian book - Light scattering in planetary atmospheres.

22 p2906 A73-41877

The comparison of sensitivities of atmospheric echo-sounders.

22 p2862 A73-42727

Certain problems in measuring Cerenkov light on the Yakutsk extensive air shower device

23 p3022 A73-43546

Curvature effects in extended stellar atmospheres - Absorption and scattering.

23 p3030 A73-43751

Matrix method evaluating an internal radiation field in a plane-parallel atmosphere.

23 p3030 A73-43754

Scattering and transmission functions of radiation by finite atmospheres with reflecting surfaces.

23 p3030 A73-43755

Use of cancellation techniques in the measurement of atmospheric crosspolarisation.

23 p2955 A73-44111

Note on the modified two-stream approximation of Sagan and Pollack.

24 p3123 A73-44438

Extinction coefficient / point source light loss due to atmospheric scattering / significance in reduction of night airglow data

24 p3082 A73-44734

Changes in the distribution of density and radio scattering in the solar corona in 1971.

24 p3138 A73-45049

Radiative transfer through a Compton-scattering atmosphere with continuous energy dependence.

24 p3111 A73-45321

ATMOSPHERIC SHELLS

U ATMOSPHERIC STRATIFICATION

ATMOSPHERIC STRATIFICATION

The EM field of a dipole transmitter in the two-layer medium air space-magnetooactive ionosphere

01 p0035 A73-10299

The fourth annual Fairey lecture - The propagation of sound through moving fluids.

01 p0077 A73-10784

Daytime laser radar measurements of the atmospheric sodium layer.

02 p0157 A73-11875

The theory of coupling of characteristic radio waves in the ionosphere.

02 p0141 A73-12030

Atmospheric stratification stability at heights of 30-90 km from grenade test determined wind and temperature data, presenting Richardson number latitudinal and seasonal distribution

02 p0160 A73-12273

The influence of atmospheric layer structure on space - Earth links.

03 p0275 A73-13653

Meteorological structure of thin clear air scatter layers observed by ultra-high resolution radar.

03 p0338 A73-14529

An analysis of coexistent waves and turbulence near clear air echoes.

03 p0339 A73-14535

The influence of planetary vorticity gradient and vertical entropy gradient on the stability of an atmospheric shear layer.

04 p0441 A73-15288

Direct determination of the thickness of stratospheric layers from single-channel satellite radiance measurements.

05 p0569 A73-16574

Critical frequency gradients-geometric parameters equivalence coefficients for ionospheric layer with parabolic vertical ionization distribution for radio wave path determination

06 p0690 A73-17555

The relation between temperature and humidity in the free atmosphere under conditions of stable stratification and strong thermal intermittency - A case study.

07 p0847 A73-19041

A critique of multilayer analyses in application to the propagation of acoustic-gravity waves.

07 p0814 A73-19248

Earth surface and background wind effects on mesoscale and large scale meteorological processes in free stably stratified atmosphere

07 p0848 A73-20343

Fine structure of the temperature stratification in the troposphere and stratosphere.

07 p0848 A73-20348

Planetary boundary layer flow of a stable atmosphere over the globe.

08 p0960 A73-21380

The gradient instability in Gaussian sporadic E-layers.

09 p1075 A73-22133

Experimental observations of the amplitudes of Es and F-region reflections and their comparison with the thin-layer model for Es.

09 p1076 A73-22138

Buoyancy effects in a turbulent boundary layer.

09 p1071 A73-22330

High-frequency radio-wave propagation through plane-stratified ionospheric models.

09 p1077 A73-22430

Study of average and turbulent characteristics of boundary layers stratified in temperature - Comparison with the corresponding characteristics in low layers of the atmosphere

09 p1072 A73-23028

Light flux vertical distribution in spherical multilayer cloud and gas scattering planetary atmosphere, calculating radiation intensity

10 p1276 A73-23891

Internal gravity waves in an atmosphere with wind shear - Validity of the WKB approximation at critical layers in the presence of buoyancy forces.

11 p1394 A73-25721

Stratospheric aerosol layer detection.

11 p1355 A73-25773

Observations of aerosol layers in the upper atmosphere by laser radar.

15 p1868 A73-31383

Critical frequency gradients-geometric parameters equivalence coefficients for ionospheric layer with parabolic vertical ionization distribution for radio wave path determination

16 p2002 A73-32779

Vertical distribution and temperature profile of the night time atmospheric sodium layer obtained by laser backscatter.

16 p2009 A73-33890

Splitting of an ionospheric layer by ambipolar diffusion.

18 p2313 A73-36388

Irreversible processes in the atmosphere. I

18 p2335 A73-37099

Russian book on electromagnetic wave propagation in ionosphere, covering atmospheric structure, electron concentration, waveguides and earth surface effects

19 p2424 A73-37773

FM-CW ground and aircraft radar observations of clear air echo strata, examining turbulence levels, Richardson number, turbulent scattering, radar reflectance and power spectra

19 p2427 A73-38203

Radar and sodar probing of waves and turbulence in statically stable clear-air layers.

19 p2405 A73-38204

On the use of forward scatter techniques in the study of turbulent stratified layers in the troposphere.

19 p2427 A73-38219

Trans-horizon propagation techniques for examining disturbances in stratified tropospheric layers.

19 p2405 A73-38221

Small-scale atmospheric structure deduced from measurements of temperature, humidity and refractive index.

19 p2448 A73-38224

Interactions between internal gravity waves and their traumatic effect on a continuous stratification.

19 p2422 A73-38237

Capabilities of radar, sodar and lidar for measuring the structure and motion of the stably stratified atmosphere.

19 p2405 A73-38239

The formation and breakdown of Kelvin-Helmholtz billows.

19 p2422 A73-38244

Forward scatter propagation measurements /transhorizon and line-of-sight/ applied to specific forms of instabilities in layers.

19 p2406 A73-38247

Refraction of light beams in an atmosphere with arbitrary parameters

19 p2449 A73-38558

Light flux vertical distribution in spherical multilayer cloud and gas scattering planetary atmosphere, calculating radiation intensity

20 p2603 A73-38910

Stratifications in the F region of the ionosphere

20 p2554 A73-39174

Numerical one dimensional cumulus model of stratification and cloud depth-radius relations for convective layer prediction

21 p2729 A73-40068

Permissible hydrodynamic and hydrostatic stellar atmosphere models described by system of equations dependent on initial level conditions

21 p2767 A73-40532

Resonant oscillations of intermediate frequency in a stratified atmosphere.

22 p2848 A73-42539

Wolf-Rayet binary stars detection and use in WR stellar mass, evolutionary status and luminosity estimation, noting atmospheric stratification relationship to temperature

23 p3026 A73-43202

Numerical experiments in laser sounding of aerosol stratification in the atmosphere

24 p3085 A73-44966

E and F layers, discussing formation, collision processes and S and L geomagnetic variations

24 p3087 A73-45204

ATMOSPHERIC TEMPERATURE

NT AUORAL TEMPERATURE

NT IONOSPHERIC TEMPERATURE

Tethered balloon measurements of turbulent wind, temperature and humidity fluctuations up to 200 meters over open sea, allowing for wave induced ship motion

01 p0072 A73-10142

Atmospheric temperature profile determination by limb radiance inversion radiometer, discussing radiative transfer, instrument parameters and inversion process effects on retrievable information content
01 p0072 A73-10354

Inference of stratospheric temperature structure from limb radiance profiles.
01 p0072 A73-10356

The effects of aerosols on the outgoing terrestrial radiation.
01 p0072 A73-10357

Atmospheric radiative transfer by carbon dioxide.
01 p0037 A73-10366

Transmittance functions for satellite temperature sounding.
01 p0037 A73-10367

A method for calculating atmospheric thicknesses directly from satellite radiation measurements.
01 p0073 A73-10378

Numerical simulation of radiative-convective heat transfer in the Martian atmosphere-polar cap utilizing Mariner 9 Iris data.
01 p0097 A73-10401

Radiometric techniques for observing the atmosphere from aircraft.
01 p0073 A73-10404

Estimation of the global circulation characteristics of planetary atmospheres with various hypotheses concerning the nature of dissipation
01 p0040 A73-10868

Atmospheric tidal measurements at 50 km from a constant-altitude balloon.
01 p0043 A73-11061

Meteorological parameters conducive to ice formation on aircraft, analyzing data statistics on atmospheric moisture content, temperature and drop size [DGLR PAPER 72-109]
02 p0130 A73-11660

Results of the Venus atmosphere measurements made by the landing station Venera 7.
02 p0214 A73-12252

Diurnal variation of the exospheric temperatures on Venus and Mars.
02 p0214 A73-12253

Structure of the thermosphere as inferred from incoherent scatter measurements.
02 p0161 A73-12282

Microwave radiometric measurements of atmospheric temperature and water from an aircraft.
02 p0164 A73-12361

Optimization of spectral intervals for remote sensing of atmospheric temperature profiles.
02 p0171 A73-12774

Vertical resolution of temperature profiles obtained from remote radiation measurements.
02 p0165 A73-12778

Rocket sounding and grenade experiments for stratosphere-mesosphere interaction, showing simultaneous winter temperature changes of opposite sign
02 p0165 A73-12789

E region wind and density measurements by VHF radar and atmosphere temperature measurement by radio acoustic sounding technique, describing instrumentation and computerized data reduction
03 p0339 A73-14546

Computerized parameter estimation by jump detection scheme for nonlinear atmosphere density and temperature profile tracking
04 p0430 A73-15255

Two layer model for diurnal temperature variations analysis of radiative heat transfer between planetary lower atmosphere and underlying
04 p0473 A73-15574

Russian book on atmospheric circulation covering temperature distribution, tropospheric and stratospheric winds, jet streams and Southern Hemisphere meteorological features
04 p0474 A73-15961

Attempt at the application of the theory for linear extrapolation of probabilistic processes in long-range temperature forecasts
05 p0593 A73-16235

Diurnal variability of temperature and of isobaric surface heights in the troposphere and lower stratosphere
05 p0593 A73-16241

Numerical tests of atmospheric circulation and climate theory and accuracy conditions for atmospheric models, noting temperature dependence on radiative and nonradiative heat transfer
05 p0593 A73-16242

Radio-wave absorption in the lower ionosphere and stratospheric effects
05 p0569 A73-16265

Equatorial stratosphere quasi-biennial oscillation variations from temperatures and zonal winds measured at Canton Island, Ascension Island and Balboa [Canal Zone]
05 p0594 A73-16573

Computation of upper tropospheric reference heights from winds for use with vertical temperature profile observations.
05 p0569 A73-16575

Jovian atmosphere upper layers high temperature evidenced during star Beta Scorpion occultation by Jupiter
06 p0745 A73-17475

The relation between temperature and humidity in the free atmosphere under conditions of stable stratification and strong thermal intermittency - A case study.
07 p0847 A73-19041

Global mean thermosphere temperature profiles as function of solar EUV flux, considering neutral gas heating and ionospheric electron temperature
07 p0869 A73-19246

Comparison of the correlation of incoherent scatter and ionosonde measurements of temperature with calcium plage and 2800-Megahertz intensities.
07 p0815 A73-19250

Thermosphere kinetic temperature diurnal variation from heat conduction equation periodic solution, determining heat sources from solar radiation atmospheric absorption
07 p0815 A73-19440

Fine structure of the temperature stratification in the troposphere and stratosphere.
07 p0848 A73-20348

Diurnal temperature variations in the thermosphere with solar activity
08 p0959 A73-21288

Measurement of the temperature of an optically thick luminous gas layer in the upper atmosphere by the homodyne detection method
08 p0960 A73-21304

A climatological analysis of oscillations of Kelvin wave period at 50 mb.
08 p0984 A73-21377

An analytical and numerical study of the Martian planetary boundary layer over slopes.
08 p0101 A73-21381

Covariance matrices and means of atmospheric Planck function profiles for application to temperature sounding from satellite measurements.
08 p0967 A73-21385

Neutral thermosphere temperatures from density scale height measurements.
09 p1074 A73-22063

Global time and space changes of satellite radiances received from the stratosphere and lower mesosphere.
09 p1076 A73-22149

Characteristics of the development of the quasi-biennial cycle above the Indian Ocean
09 p1115 A73-22991

Models of the extremal arctic winter atmosphere at heights between 20 and 80 km
09 p1115 A73-22993

An operational upper air analysis using the variational method.
10 p1244 A73-23645

A synoptic investigation of anomalous warmth in the mid and upper troposphere during February 1964.
10 p1244 A73-23978

Airborne atmospheric temperature measurements correction for sensor response lag, deriving numerical scheme based on sensing systems wind tunnel calibration
10 p1217 A73-23991

Variations of the structural parameters of the thermosphere from satellite braking data
11 p1350 A73-25076

Temperature and humidity spectra in the atmospheric surface layer.
11 p1393 A73-25693

Infrared radiative heating and cooling in the Venusian mesosphere. II - Day-to-night variation.
11 p1418 A73-25719

Radiative slip between two adjacent absorbing-emitting gases and its application to air pollution.
11 p1353 A73-25722

On empirical models of the upper atmosphere in the polar regions.
11 p1356 A73-25915

The variation of temperature with latitude in the lower thermosphere /80-100 km/.
11 p1357 A73-26194

Northern Hemisphere climatic trend from monthly atmospheric temperature and water vapor content calculations over five year period, noting humidity decrease and cooling
11 p1358 A73-26663

Lower thermosphere thermal energy and oxygen transport due to photochemical reactions, noting Schumann-Runge band absorption, atomic recombination and collisional deactivation
11 p1358 A73-26706

A two-satellite microwave occultation system for determining pressure altitude references.
12 p1521 A73-26813

Dropsonde for continuous temperature measurement during descent through lower atmospheric level, discussing receiving unit and data conversion unit
12 p1495 A73-26815

Upper atmospheric temperatures from Doppler line widths. V - Auroral electron energy spectra and fluxes deduced from the 5577 and 6300 A atomic oxygen emissions.
12 p1492 A73-27605

Diurnal atomic hydrogen variation at exospheric temperatures as function of thermal ion and proton charge exchange with plasmasphere
12 p1492 A73-27612

Near-satellite neutral gas temperature determination from measurement of molecular nitrogen velocity distribution
13 p1687 A73-28630

Estimates of global circulation characteristics of planetary atmospheres.
13 p1607 A73-28692

Some specific features of the near-ground temperature field mesostructure and air humidity and their influence on convective processes
13 p1654 A73-28886

Spatial correlation functions of velocity and temperature components in the atmospheric boundary layer
13 p1654 A73-29153

Solution of linear equations in remote sensing and picture reconstruction.
14 p1767 A73-29767

Seasonal and sunspot cycle variations of F region electron temperatures and protonospheric heat fluxes.
14 p1749 A73-29986

Thermal convective instability in uniformly rotating magnetized isothermal stellar atmosphere with constant Alfvén speed, discussing heat loss mechanism dependence on temperature
15 p1929 A73-31060

Four dimensional forecast assimilation of temperature data from Nimbus 4 SIRS radiance measurements, using two level model with geostrophic wind adjustment
15 p1902 A73-31314

Formation of optical discontinuities in the atmospheric inversion layer
15 p1903 A73-31424

Estimation of errors arising in calculations of the fluxes and influxes of thermal radiation due to errors in the initial meteorological parameters
15 p1905 A73-31786

Closure of the equations for heat influx in the atmospheric boundary layer /according to experimental data/
15 p1905 A73-31789

Map series for description of annual temperature wave in lower stratosphere in Northern Hemisphere, establishing easterly circulation on south side of Aleutian high
15 p1873 A73-32254

Turbulent heat transfer role in atmospheric thermal budget, deriving smoothed local temperature time derivative
15 p1906 A73-32348

An aid for the prediction of the nighttime minimum temperature
15 p1906 A73-32352

Development of model atmospheres for aerothermodynamic calculations.
16 p2034 A73-33138

Measured thermal response to the MIL-STD 210B cold atmosphere.
16 p2034 A73-33140

The abnormal stratosphere studied with the aid of satellite radiation measurements.
16 p2005 A73-33537

[AIAA PAPER 73-493] Atmospheric temperature measurement with X and K band radiometers, discussing meteorological conditions variation effects on microwave propagation and comparison with spacecraft tracking data
16 p1983 A73-33730

The thermal regime and convective motions in the lower layers of the Venusian atmosphere
16 p2068 A73-33825

OH emission band, studying effect of adiabatic infrasonic oscillations on upper atmospheric temperature and intensity
16 p2008 A73-33883

Experimental determination of small scale transport mechanisms in the stratosphere.
16 p2010 A73-34044

[AIAA PAPER 73-496] The design, construction and calibration of an infrared temperature profile radiometer /ITPR/ for Nimbus E.
17 p2238 A73-34602

The effect of large-scale eddies on climatic change.
17 p2160 A73-34851

The effect of forecast error accumulation on four-dimensional data assimilation.
17 p2205 A73-34853

Method to apply homogeneous-path transmittance models to inhomogeneous atmospheres.
17 p2205 A73-34856

The effects of water vapor and oxides of nitrogen on the ozone and temperature structure of the stratosphere.
17 p2160 A73-34857

On the temperature of the Jovian thermosphere.
17 p2232 A73-34860

Critical analysis of the results obtained by SIRS-A in remote sensing of the temperature field over the Mediterranean
17 p2205 A73-34936

Application of temperature soundings by the Nimbus 3 satellite to the analysis of the hemispheric-scale stratospheric environment

17 p2206 A73-34937

A synoptic model for evaluation of vertical temperature and geopotential profiles from satellite pictures.

17 p2206 A73-34939

Remote measurement of atmospheric temperatures by Raman lidar.

17 p2163 A73-35467

The theory of charged particle temperatures in the upper atmosphere.

17 p2224 A73-35593

Late B6 stars line spectra, atmospheric electron density, microturbulence velocity, excitation temperature, flux envelopes and energy distributions

17 p2233 A73-35612

Basic characteristics of the temperature distribution and air currents in the free atmosphere of the earth

18 p2332 A73-35915

Global meridional cross sections and charts for mesospheric circulation and temperature variability via meteorological rocket network

18 p2302 A73-35925

Combined temperature, diffusion coefficient and density measurements of photoluminescent A10 releases.

18 p2303 A73-35949

Operational radiance maps of the stratosphere, with preliminary details of a major stratospheric warming.

18 p2303 A73-35950

Extreme temperature deviations from the climatological mean in the upper stratosphere - observed by rockets, confirmed by satellites.

18 p2304 A73-35962

Vertical temperature profiles from satellites - Results from second generation instruments aboard Nimbus-5.

18 p2307 A73-36029

Recent stratospheric temperature measurement compatibility tests at Wallops Island.

18 p2307 A73-36035

A prediction of the phenomena that take place during so called 'sudden warmings.'

18 p2308 A73-36038

Infrared transmittances for indirect soundings of the atmosphere from satellite-based measurements.

18 p2308 A73-36043

Aerological soundings of the atmosphere from NOAA-2 data for operational systems.

18 p2308 A73-36044

Atmospheric density, temperature and winds measured during Aladdin II.

18 p2309 A73-36055

Neutral winds in the F-region obtained from new models of density and temperature.

18 p2309 A73-36056

Global temperature distributions from OGO VI 6300 A airglow measurements.

18 p2309 A73-36058

An analysis of the solar-activity effects in the upper atmosphere.

18 p2309 A73-36060

Influence of longitudinal variations on the structure of temperature, pressure and wind fields in the stratosphere and mesosphere of the Northern Hemisphere.

18 p2310 A73-36139

Temperature and wind velocity variations in winter mesosphere of polar regions.

18 p2310 A73-36140

Temperature determination of the upper atmosphere by the low-level detection of artificial luminous cloud radiation.

18 p2311 A73-36149

Neutral wind velocities calculated from temperature measurements during a magnetic storm and the observed ionospheric effects.

18 p2311 A73-36150

Variability of eigenvectors and eigenvalues of correlation matrices for vertical temperature profiles.

18 p2334 A73-37062

Utilization of satellite radiation measurements in analyzing the temperature near the ground.

18 p2334 A73-37067

Statistical characteristics of the temperature field near the ground for Europe.

18 p2334 A73-37070

Calculation of geopotential fields at various atmospheric levels from data on the overall cloudiness and temperature.

18 p2314 A73-37072

Time dependent radiative transfer. III - Development of the formalism.

19 p2503 A73-37565

A comparison of geostrophic and rocket winds at stratospheric levels, measured from a small network of rocket sounding stations.

19 p2424 A73-37604

On the energetics and momentum balance of pole-equator temperature differences in the sun.

19 p2485 A73-37620

Mechanisms for Mars dust storms.

19 p2485 A73-37656

Diurnal and annual temperature variations in the 30-60 km region as indicated by statistical analysis of rocketsonde temperature data.

19 p2424 A73-37662

Evidence for high-frequency synoptic disturbances near the stratopause.

19 p2447 A73-37663

Accuracy and coverage of temperature data derived from the IR radiometer on the NOAA 2 satellite.

19 p2424 A73-37665

Variations in the temperature of the thermosphere in the course of the day and with solar activity.

19 p2424 A73-37917

Measurement of the temperature of an optically dense layer of luminous gas in the upper atmosphere by the homodyne detection method.

19 p2425 A73-37933

The effect of solar activity on temperatures in the equatorial mesosphere.

19 p2426 A73-38015

Vertical profiles of small-scale temperature structure in the atmosphere.

19 p2448 A73-38209

A note on the FM-CW radar as a remote probe of the Pacific Trade-Wind Inversion.

19 p2448 A73-38211

Intermittency of the small-scale structure of atmospheric turbulence. II.

19 p2448 A73-38213

Small-scale atmospheric structure deduced from measurements of temperature, humidity and refractive index.

19 p2448 A73-38224

Numerical investigation of internal waves in jet streams including nonlinear effects.

19 p2449 A73-38233

Atmospheric temperature and humidity vertical profiles from satellite-borne IR spectral radiance measurements, using linear extrapolation and statistical regression techniques

[AAS PAPER 73-124] 20 p2521 A73-38584

Atmospheric sounding by satellite-borne remote sensors, discussing radiometric measurements of temperature, composition, and reflected and emitted radiance in visible, IR and microwave bands

[AAS PAPER 73-125] 20 p2550 A73-38585

Structural characteristic of the temperature field in the boundary layer of the atmosphere

20 p2555 A73-39182

Design and performance characteristics of the Vertical Temperature Profile Radiometer /VTPR/ for atmospheric temperature soundings.

20 p2567 A73-39852

Objective cross-section analyses by Hermite polynomial interpolation on isentropic surfaces.

21 p2728 A73-40054

Stratospheric temperature profiles from limb radiance measurement by Aerobee rocket, comparing with rocket sounding and radiosonde data

21 p2729 A73-40064

Mesospheric temperature response to variations in geomagnetic activity.

21 p2682 A73-40169

On the diurnal variations of total mass density, number density and temperature in the upper thermosphere.

21 p2682 A73-40170

Temperature distribution measurement for air about hot object by double exposure interferometry, using beam from He-Ne laser

21 p2701 A73-40625

Calculations of the limb radiance of Venus in the 600 to 700 per cm region and their application to spacecraft navigation.

21 p2767 A73-40693

Linearized models of two dimensional steady air flow around mountain obstacle for constant temperature gradients and invariant velocity

21 p2731 A73-40741

Internal gravity waves and turbulence in simultaneous upper atmosphere temperature and wind measurements.

21 p2732 A73-41342

Measurements of thermospheric temperatures by incoherent scatter radar.

21 p2688 A73-41346

Remote sounding of atmospheric temperature from satellites. IV - The selective chopper radiometer for Nimbus 5.

21 p2706 A73-41601

Inversion techniques for remote sensing of atmospheric temperature profiles.

22 p2883 A73-42056

Limb scanning as a method for measuring the temperature structure of a planetary atmosphere.

22 p2883 A73-42058

Remote sensing of atmospheric and surface temperatures with microwaves.

22 p2825 A73-42060

Atmospheric temperature measurement using balloons and rockets.

22 p2883 A73-42061

Spectroscopic measurement of upper atmospheric temperature.

22 p2846 A73-42062

The inference of temperature from the infrared spectra of planets.

22 p2906 A73-42065

Measurement of the atmospheric brightness temperature at submillimeter wavelengths

22 p2847 A73-42330

Spectral structure of tropospheric vertical temperature profiles over Cape Kennedy, Florida.

22 p2849 A73-42544

Radiative transfer within the atmospheres of the major planets.

22 p2913 A73-42991

The temperature and ammonia profiles in the Jovian atmosphere from inversion of the Jovian emission spectrum.

22 p2915 A73-43017

Venera 8 - Measurements of temperature, pressure and wind velocity on the illuminated side of Venus.

23 p3028 A73-43602

Short-term ground ozone fluctuations at Poona.

23 p2974 A73-43865

Ozone and temperature change in the winter stratosphere.

23 p2977 A73-43901

Nimbus 5 satellite-borne selective chopper radiometer /SCR/ for remote sounding of stratospheric temperature, water vapor and cirrus clouds

23 p2978 A73-43952

Stratospheric temperature measuring instrument development for Tiros N satellites and ESRO geostationary meteorological satellite development for cloud photography

23 p3004 A73-44103

A first look at atmospheric dynamics and temperature variations on Titan.

24 p3128 A73-44433

Sulfuric acid solution composition to account for Venus cloud temperature, stratosphere dryness and IR spectrum

24 p3129 A73-44441

Titan molecular hydrogen greenhouse effect responsibility for IR temperature disagreement with atmosphereless equilibrium temperature from analysis of nongray radiative and gray convective equilibrium

24 p3129 A73-44450

A numerical method for determining the temperature structure of planetary atmospheres.

24 p3130 A73-44456

Relationship between midstratospheric temperatures and tropospheric synoptic features.

24 p3107 A73-45014

Numerical weather prediction and analysis in isentropic coordinates.

24 p3108 A73-45091

ATMOSPHERIC TIDES

Atmospheric tidal measurements at 50 km from a constant-altitude balloon.

01 p0043 A73-11061

Energy balance and field equations of dissipative atmosphere oscillations for zonal semidiurnal Pedersen region, using K-Hermicity

02 p0158 A73-11907

Upper-atmosphere motion, as determined by observations of radio echoes from meteor trails.

02 p0159 A73-12145

Asymptotic solution for vertical propagation of equatorial planetary waves in shear, noting gravity-Rossby and Kelvin waves and wind effects on diurnal tides

05 p0591 A73-16190

Lunisolar tidal effects and motions in the F region

05 p0568 A73-16255

Equivalent gravity wave mode approximation for main solar diurnal tide in rotating spherical dissipative atmosphere modeled by Newtonian cooling and Rayleigh friction

08 p0958 A73-20959

Nighttime midionosphere dynamical perturbations on ionizations from solutions of time dependent continuity equation with charge transport effects, considering semidiurnal atmospheric tide propagation mode

09 p1075 A73-22130

Ultralong atmospheric waves and a long-range forecasting.

10 p1244 A73-23644

On the determination of the long period tidal perturbations in the elements of artificial earth satellites.

11 p1423 A73-26074

The measurement of winds in the D-region of the ionosphere by the use of partially reflected radio waves.

11 p1358 A73-26707

Thermospheric neutral gas dynamics, discussing acoustic, gravity, tidal and planetary waves disturbance spectrum, propagation characteristics, latitude structure and energy sources

12 p1493 A73-27756

Relation between the tidal-force momentum and atmospheric depressions

13 p1609 A73-28862

Solar and lunar effects on neutral atmospheric tidal winds and induced electrostatic and geomagnetic fields effects on low latitude F2 and sporadic E layers

15 p1868 A73-31751

- Meteor radar study of tides in the 80 to 100 km altitude range. 18 p2305 A73-35999
- Gravity wave nonlinear interactions producing secondary waves of opposite polarization, discussing tide polarization 21 p2688 A73-41343
- Waves and tides and their observation from ground and space. 21 p2689 A73-41356
- Atmospheric oscillations. V - The propagator matrix and the transmission of an electrostatic potential along the geomagnetic field lines. 23 p2971 A73-43686
- Sunspot cycle effects on solar and lunar tide-produced diurnal and seasonal variations in equatorial electrojet 24 p3124 A73-44730
- A numerical study of three-dimensional diurnal variations within the thermosphere. 24 p3082 A73-44731
- Diurnal and semidiurnal variations in amplitude and phase of midlatitude ionosphere tidal motions, using sodium cloud drift rate 24 p3082 A73-44732
- ATMOSPHERIC TURBULENCE**
- NT CLEAR AIR TURBULENCE**
- NT GUSTS**
- NT LOW LEVEL TURBULENCE**
- Tethered balloon measurements of turbulent wind, temperature and humidity fluctuations up to 200 meters over open sea, allowing for wave induced ship motion 01 p0072 A73-10142
- Correlation and structure functions for pulse propagation in a turbulent atmosphere. 01 p0016 A73-10195
- An investigation of high-wavenumber temperature and velocity spectra in air. 01 p0039 A73-10448
- Astronomical seeing and microthermal fluctuations of the atmosphere 01 p0050 A73-10562
- Troposphere turbulence kinetic energy dependence on height and scales of motions, presenting vertical energy profiles 01 p0074 A73-10869
- Measurements of microturbulent pulsations of the wind velocity derivative in the ground layer of the atmosphere 01 p0074 A73-10870
- The fluctuation spectrum of laser radiation in a turbulent atmosphere in the presence of rain 01 p0060 A73-10872
- Lower ionosphere variability due to atmospheric dynamics, considering temperature variations, minor constituent transport and eddy diffusion 01 p0041 A73-10885
- Upper-atmosphere motion, as determined by observations of radio echoes from meteor trails. 02 p0159 A73-12145
- Theory for the propagation of partially coherent light beams in a turbulent atmosphere 02 p0142 A73-12494
- The scattering characteristics of a sonic boom at the passage through a turbulent layer 03 p0290 A73-12967
- Microturbulence in atmospheres of F, G, K, type stars. I - Curve of growth analysis of G, K, type subgiants. 03 p0370 A73-13196
- Radial velocity and microturbulence dependence on excitation potential and time in A type supergiants at atmosphere, deriving chemical composition 03 p0371 A73-13215
- Acoustic-Doppler-radar scattering equation and general solution. 03 p0276 A73-13830
- Application of the spatial spectral power density to the calculation of resolution limits. 03 p0277 A73-13916
- Atmospheric turbulence information in signal backscattered from pulsed radar, discussing Doppler power spectrum variance determination 03 p0279 A73-14528
- Coherent signal from incoherent meteorological radar echoes for atmospheric turbulence intensity measurement, noting autocorrelation function for average frequency 03 p0338 A73-14531
- Measurement of small-scale turbulence and thermal stability in the lower atmosphere by radar. 03 p0279 A73-14536
- Radar measurement of the atmospheric turbulence structure function. 03 p0279 A73-14537
- Inverse problem in the theory of turbulence filtering by the radar pulse volume. 03 p0279 A73-14538
- Doppler turbulence spectrum and intensity measurement in stratocitus region at base of cloud deck cooled by evaporation and destabilized by convection 03 p0339 A73-14539
- The effects of a finite radar pulse volume on turbulence measurements. 03 p0279 A73-14540
- Venera satellite parachute probe method for Doppler measurement of Venus atmosphere wind velocity and turbulence 03 p0379 A73-14566
- Atmospheric microthermal turbulence vertical distribution from balloon flights compared with stellar scintillation data, predicting irradiance spectra from turbulence and wind velocity measurement 03 p0305 A73-14656
- Effects of uncertainties in damping and microturbulence on theoretical deductions from solar equivalent widths. 04 p0500 A73-15491
- Buoyancy forces contribution to heat flux during turbulent mixing in upper atmosphere, noting kinetic turbulence balance components 04 p0473 A73-15573
- The measurement of atmospheric turbulence from a captive balloon. 04 p0473 A73-15698
- Relative importance of terms in the turbulent-energy and momentum equations as applied to the problem of a surface roughness change. 05 p0591 A73-16191
- Hemispheric single level model of atmospheric action centers formation due to horizontal baroclinity, including turbulent mixing and circulation index effects 05 p0592 A73-16229
- Outer-scale effects in turbulence-degraded light-beam spectra. 05 p0597 A73-16498
- Observations of atmospheric effects on the transport and decay of trailing vortex wakes. 05 p0529 A73-16869
- Analysis of flight vehicle response to nonstationary atmospheric turbulence including wing bending flexibility. 05 p0535 A73-16921
- Criterion for the choice of exposure time in atmospheric turbulence investigation with an optical wave. 06 p0691 A73-17497
- Polarization characteristics of partially scattered radio waves for turbulent ionosphere vertical sounding applications 06 p0662 A73-17533
- A new approach to the problem of wave fluctuations in localized smoothly varying turbulence. 06 p0665 A73-18183
- Propeller anemometers as sensors of atmospheric turbulence. 06 p0695 A73-18329
- Time spectra and cross-spectra of kinetic energy in the planetary boundary layer. 07 p0847 A73-19044
- Quasi two dimensional turbulence model of energy spectra and potential enstrophy transfer in synoptic large scale quasi-horizontal atmospheric motions 07 p0820 A73-20342
- Photon counting statistics of the superposition of coherent and chaotic light of arbitrary spectrum passed through the turbulent atmosphere or a Gaussian medium. 08 p0987 A73-20952
- LF boundary of inertial range in lowest atmospheric layer, comparing turbulence scale and wind velocity components 08 p0954 A73-21185
- Turbulence energy spectra in thick convective cumulonimbus cloud zone, using aircraft measurements 08 p0984 A73-21186
- Energy transport over turbulence spectrum of free atmosphere, using aircraft experiments 08 p0984 A73-21187
- Correlation of microthermal turbulence data with meteorological soundings in the troposphere. 08 p0985 A73-21382
- Rossby wave barotropic instability effects on errors leading to large scale atmosphere predictability experiments by numerical simulation of two dimensional turbulence 08 p0985 A73-21386
- Frequency dependence of losses by radio-wave scattering at turbulent discontinuities in the troposphere 08 p0939 A73-21398
- A note on Eulerian-Lagrangian time scale transformation for large-scale atmospheric turbulence. 08 p0985 A73-21424
- Certain feedbacks generated during turbulent cellular convection in the atmosphere 08 p0986 A73-21456
- Turbulence and tropopause evolution in northeast jet stream over Treviso airport, noting Richardson criterion value as diagnostic and short range prognosis tool 08 p0986 A73-21487
- Symposium on Air Pollution, Turbulence and Diffusion, Las Cruces, N. Mex., December 7-10, 1971, Proceedings. 09 p1114 A73-22326
- Atmospheric turbulent fluctuations explained via eddy-wind shear and convective rolls-gravity wave interactions, using wind-temperature data from White Sands 09 p1114 A73-22329
- An investigation of the application of Taylor's hypothesis to atmospheric boundary layer turbulence. 09 p1114 A73-22331
- Measurements and graphs of turbulence autocorrelations in space and time. 09 p1071 A73-22332
- Remote sensing of the turbulence characteristics of a planetary atmosphere by radio occultation of a space probe. 09 p1146 A73-22427
- Number of gust series in turbulent velocity pulsations 09 p1115 A73-22992
- Depolarization of laser radiation in an optical channel 10 p1229 A73-24612
- Space shuttle aerodynamic interference and elastic response to atmospheric turbulence during ascent flight, including propellant sloshing, gust and automatic control system effects [AIAA PAPER 73-310] 11 p1430 A73-25541
- Influence of radiation on the conditions in the atmospheric boundary layer 11 p1393 A73-25641
- An observational study of the vertical profile of the high frequency fluctuations of the wind in the atmospheric boundary layer. 11 p1393 A73-25691
- The observed relation between the Kolmogorov and von Karman constants in the surface boundary layer. 11 p1393 A73-25694
- Focused laser irradiance fluctuations in a turbulent medium. 11 p1376 A73-25874
- Correlation of the shift in the center of gravity of a focused light beam in a turbulent atmosphere 11 p1331 A73-26160
- A description of the NAE T-33 turbulence research aircraft, instrumentation and data analysis. 11 p1306 A73-26269
- Lensless Fourier transform holography with mutual coherent reference source close to object, investigating atmospheric turbulence effects on wavefront reconstructed image quality 11 p1370 A73-26539
- Steady ELF plasmaspheric hiss, studying whistler mode turbulence, band limitation, power spectra and peak intensities 12 p1488 A73-26984
- Russian monograph on turbulence in free atmosphere covering measurement and statistical techniques, tropospheric and stratospheric disturbances, wind pulsations, effects on aircraft flights, etc 12 p1521 A73-27134
- Response-optimum control of the angular and torsional oscillations of an elastic flying wing. 12 p1459 A73-27459
- Turbulence, billows and gravity waves in a high shear region of the upper atmosphere. 12 p1492 A73-27608
- Method for calculating turbulent flows from network data 12 p1521 A73-27744
- Some comparisons between observed wind profiles at Riso and theoretical predictions for flow over inhomogeneous terrain. 13 p1652 A73-28272
- Laboratory simulation of development of superbooms by atmospheric turbulence. 13 p1568 A73-28495
- Scintillation and vibration of stars and structure of a turbulent atmosphere. 13 p1680 A73-28514
- Effect of some external factors on accuracy of observations of active satellites. 13 p1680 A73-28516
- Troposphere turbulence kinetic energy dependence on height and scales of motions, presenting vertical energy profiles 13 p1653 A73-28693
- Measurements of turbulent microfluctuations of the wind-velocity derivative in the surface layer. 13 p1653 A73-28694
- The spectrum of fluctuations of laser radiation in a turbulent atmosphere during rain. 13 p1627 A73-28696
- Solar photosphere turbulent velocity relation to optical depth and deviation from LTE based on Goldberg-Unno method 13 p1683 A73-29093
- Calculation of phase difference power spectrum for slant-path propagation. 13 p1661 A73-29327
- Angle-of-arrival difference spectrum of a simple interferometer in turbulent air. 13 p1621 A73-29330
- A comparison of turbulence measurements by different instruments - Tsimlyansk field experiment 1970. 13 p1656 A73-29343

Unified theory of type I and II irregularities in the equatorial electrojet.

14 p1748 A73-29973

Log-intensity correlations of a laser beam in a turbulent medium.

14 p1757 A73-30162

Statistics of photoelectric sensor readings during propagation of light in a turbulent medium

14 p1753 A73-30270

IR seeing disks /blurred interference patterns of corrugated wave fronts/ speckles and intensity profiles from atmospheric turbulence models

15 p1929 A73-31061

Two descriptions for the photocounting detection of radiation passed through a random medium - A comparison for the turbulent atmosphere.

15 p1914 A73-32291

Turbulent heat transfer role in atmospheric thermal budget, deriving smoothed local temperature time derivative

15 p1906 A73-32348

Stochastic wind field effects on baroclinic wave disturbances vertical propagation through turbulent atmosphere, obtaining stream function and dispersion equation

15 p1907 A73-32356

The regression relations for turbulence parameters in the air layer near the ground in the case of an inhomogeneous base

15 p1907 A73-32359

Microwave-propagation studies regarding the isotropy characteristics of the turbulent fine structure of the refractive index in the troposphere

15 p1874 A73-32361

Polarization characteristics of partially scattered radio waves for turbulent ionosphere vertical sounding applications

16 p1978 A73-32757

On the possibility of turbulent thickening of weak shock waves.

16 p1967 A73-32794

Wind tunnel gust simulation for STOL aircraft behavior during low velocity flight in turbulent atmosphere near ground

16 p1962 A73-32813

Atmospheric turbulence vs residual surface inaccuracy refracting and reflecting telescopic image degradation for solar observations

16 p2014 A73-32969

Monthly mean values of eddy diffusion coefficients in the lower stratosphere.

16 p2005 A73-33540

Angle-of-arrival difference spectrum of a simple interferometer in turbulent air.

16 p2037 A73-33683

Correlation measurements on the complex amplitude of stellar plane waves perturbed by atmospheric turbulence.

16 p2037 A73-33684

Estimates of the intensity of turbulence in the atmospheres of Mars and Venus

16 p2069 A73-33828

Error probability of binary optical communications in turbulent atmosphere - Experimental results.

16 p1984 A73-33995

Application of the ray method to a study of the propagation of large-scale perturbations in a barotropic atmosphere with a mean wind

17 p2204 A73-34345

Russian book - Analysis of meteorological conditions for aviation.

17 p2204 A73-34539

Mountain range effects on tropopause turbulence with mountain waves, examining tropopause layer inversions, vertical wind vectors, temperature distribution and buffeting intensity

17 p2204 A73-34542

Analysis of cases of intense turbulence in the troposphere

17 p2205 A73-34544

Holography of large objects in a turbulent atmosphere with a CW laser.

17 p2167 A73-34896

The use of subgrid transport equations in a three-dimensional model of atmospheric turbulence.

17 p2206 A73-35017

Feedback control configured vehicles ride control system design for B-52 aircraft load alleviation and mode stabilization during flight through atmospheric turbulence

17 p2107 A73-35245

Slant-path scintillation in the planetary boundary layer.

17 p2185 A73-35417

Upper atmospheric turbulence kinetic energy spectrum from radio meteor trails observations, noting relationship to structure function for isotropic turbulence

18 p2312 A73-36288

Response of a rigid aircraft to nonstationary atmospheric turbulence.

18 p2267 A73-36305

Explicit solution for the photocount statistics with application to atmospheric turbulence.

18 p2337 A73-36625

Atmospheric vorticity effects on hexagonal convection cells formation, considering temperature profiles nonlinearity, turbulent viscosity and perturbation scale

18 p2333 A73-37052

Comparison of vertical profile turbulence structure with stellar observations.

19 p2446 A73-37259

Atmospheric turbulence effects on CW carbon dioxide laser propagation, investigating thermal blooming via theoretical diffusion model and experiment

19 p2437 A73-37260

A study of droplet spectra in fogs.

19 p2447 A73-37660

Earth surface turbulent boundary layer analysis, considering similarity theory limitation, flux profiles, velocity, temperature and humidity spectra, energy budgets, local isotropy, etc

19 p2427 A73-38212

Intermittency of the small-scale structure of atmospheric turbulence. II.

19 p2448 A73-38213

Turbulence spectra, length scales and structure parameters in the stable surface layer.

19 p2448 A73-38216

Measurements of the log-irradiance distribution of a laser wave propagated through the turbulent atmosphere.

19 p2405 A73-38222

Turbulence spectra at scales smaller than 1 meter.

19 p2449 A73-38241

The formation and breakdown of Kelvin-Helmholtz billows.

19 p2422 A73-38244

The lower atmosphere in hydrostatically stable conditions.

19 p2449 A73-38245

On the prediction of turbulence in baroclinic zones.

19 p2449 A73-38246

Forward scatter propagation measurements /transhorizon and line-of-sight/ applied to specific forms of instabilities in layers.

19 p2406 A73-38247

Frequency spectra of strong fluctuations of laser radiation in a turbulent atmosphere

19 p2406 A73-38337

Frequency dependence of the loss when radio waves are scattered by turbulent inhomogeneities in the troposphere.

19 p2407 A73-38356

Analysis of a method for obtaining near-diffraction-limited information in the presence of atmospheric turbulence.

19 p2461 A73-38485

Scintillation measurements for large integrated-path turbulence.

19 p2461 A73-38486

Structural characteristic of the temperature field in the boundary layer of the atmosphere

20 p2555 A73-39182

Average intensity of a nonsymmetrical optical radiation beam in a turbulent atmosphere

20 p2555 A73-39187

Diffraction of optical radiation by a reflecting disk in a turbulent atmosphere.

20 p2531 A73-39680

Doppler spectrum turbulence spreading updraft velocity estimation from observation by pulsed radar, noting average value and standard deviation in small thunderstorm

21 p2728 A73-40058

Analysis of airplane response to nonstationary turbulence including wing bending flexibility. II.

21 p2784 A73-40437

The measurement of turbulent spectra and diffusion coefficients in the altitude region 95 to about 110 km.

21 p2688 A73-41341

Microturbulence and the effect of departures from LTE on photospheric iron lines.

21 p2777 A73-41481

Horizontal wind fluctuations coherence at different meteorological sites compared to wind tunnel experiment

21 p2732 A73-41573

Autocorrelation and space-time correlations for probe separations aligned with mean flow to test Pielke-Panofsky hypothesis, comparing laboratory tests to atmospheric turbulence

21 p2733 A73-41575

A new approach to gust alleviation of a flexible aircraft using an open loop device [ONERA, TP NO. 1236]

22 p2799 A73-42219

Remote probing of atmospheric turbulence.

22 p2884 A73-42620

High resolution image formation through the turbulent atmosphere.

22 p2863 A73-43097

Propagation of laser radiation in a turbulent atmosphere.

22 p2828 A73-43159

Role of the outer scale of turbulence in atmospheric degradation of optical images.

23 p3005 A73-43341

Photometric strip blurring and brightness contrast measurements of visual perception in turbulent at-

mosphere as function of distance, turbulence and exposure

23 p3001 A73-43573

Influence of a random transport-velocity component on the space-time correlations of signal fluctuations

23 p2954 A73-43647

Aircraft aerodynamics problems covering slender body theory, atmospheric turbulence and boundary layers, wind tunnel contractions, radiator blocks, vortex induced oscillations, etc

24 p3053 A73-44690

The mesoscale structure of the atmospheric boundary layer and its interaction with small-scale turbulence

24 p3107 A73-44960

Numerical simulation of three dimensional atmospheric turbulence with emphasis on kinetic energy transfer from large to small scales of motion with heat conversion

24 p3108 A73-45092

ATMOSPHERIC WINDOWS

Atmospheric windows for HF laser radiation between 2.7 and 3.2 microns.

03 p0319 A73-14431

Measurement of the vertical transparency of the atmosphere in the infrared using an artificial source.

07 p0848 A73-20349

Equipment and procedures for measurement of atmospheric spectral transmittance in the infrared region of the spectrum

11 p1363 A73-25643

Water vapor lines controlled atmospheric absorption spectrum in 220 GHz window region, discussing approximate calculation for submillimeter lines residual effect

11 p1330 A73-25688

Angular diameter calculation of Ellis atmospheric window via ionospheric wave ray tracing technique

15 p1844 A73-32048

Thermal imaging through hazes and fogs in the middle and far infrared windows - Some experimental results.

16 p2016 A73-33997

Ammonia absorption relevant to the albedo of Jupiter. I - Experimental results.

17 p2231 A73-34764

Spatial frequencies of clear sky radiance in the range 4.5 to 5.2 microns

18 p2314 A73-36899

Statistical spectral attenuation characteristics of transmittance windows for visible and near IR under various optical weather conditions

21 p2731 A73-40746

Observations of far infrared atmospheric windows at 44/cm and 50/cm from Pikes Peak.

21 p2780 A73-41647

The determination of surface temperature from satellite 'window' radiation measurements.

22 p2846 A73-42057

ATMOSPHERICS

NT DAWN CHORUS

NT HISS

NT IONOSPHERICS

NT SUDDEN ENHANCEMENT OF ATMOSPHERICS

NT WHISTLERS

Poisson model of atmospheric noise from lightning discharges as function of thunderstorm distribution and propagation conditions, calculating statistics for narrow band receiver

02 p0142 A73-12528

Statistical analysis of atmospheric sudden changes in VLF bands, suggesting lower ionosphere ionization increase due to meteors incidence

03 p0299 A73-12948

Techniques for short-term predictions of atmospheric noise levels.

08 p0940 A73-21662

Variation of atmospheric radio noise level with sunspot number.

09 p1051 A73-22493

Microwave range-difference measurements on 65-km slanted overwater path, interpreting tropospheric noise power spectra and rms values as function of baseline length

11 p1330 A73-25685

Auroras induced attenuation fluctuations of VLF at atmospherics associated with remote tropical thunderstorms

12 p1522 A73-27786

VLF atmospherics measurement and geophysical analysis, discussing meteorological, geoelectric and propagation aspects

13 p1582 A73-28151

Trial of existing models of the lower ionosphere by experimental data on Schumann resonances.

18 p2306 A73-36011

Distribution of peaks in atmospheric radio noise.

19 p2403 A73-37269

Determination of the root-mean-square and mean intensity of the atmospheric radio noise field

21 p2648 A73-40208

Dispersion characteristics of whistler atmospherics during higher geomagnetic activity.

24 p3088 A73-45365

ATOLL REEFS

U CORAL REEFS

ATOMIC CONCENTRATION

Concentration distribution and effective lifetimes of excited atoms at small optical thicknesses of the plasma

01 p0085 A73-11083

Determination of the dopant concentration profile in epitaxial GaAs by the method of the differential capacitance of a Schottky diode

02 p0145 A73-11548

Atomic oxygen concentration from the forbidden OI 5577 Å line emission at the auroral zone latitude.

02 p0158 A73-11916

Doping additions dissociation effect on impurities distribution in grown semiconductor crystals of melts, calculating atomic and molecular concentration

02 p0201 A73-12356

Study of the effect of cobalt on redistribution of atoms of alloying elements in iron-base alloys by the nuclear gamma resonance method.

02 p0182 A73-12697

Boron segregation at austenite grain boundary and matrix sites in steel by autoradiography

02 p0183 A73-12761

Simultaneous diffusion of photons and particles in a semifinite space. I - Distribution of excited atoms in a semifinite space

09 p1123 A73-23068

Simultaneous diffusion of photons and particles in a semifinite space. II - Concentration of excited atoms before a shock wavefront

09 p1123 A73-23069

Absorption spectrum analysis of free Cu, Ca, Na, Zn, Ni and Cr atom concentration in acetylene air flame zones

14 p1817 A73-30458

Thermodynamic analysis of liquid metal systems by using a cluster model

17 p2188 A73-34555

Effect of zirconium concentration on creep of niobium-zirconium alloys

20 p2579 A73-39739

Measurement of the doping level distribution in the surface region of a semiconductor

21 p2753 A73-41097

A study of the real structure of titanium mononitride in its homogeneity region

21 p2721 A73-41225

Experiment involving the application of the LMA-1 laser microanalyzer to the investigation of metallic materials

22 p2868 A73-42100

Anomalous concentration dependence of thermal expansion coefficients of tungsten-rhenium and tungsten-niobium alloys.

22 p2878 A73-42509

Formation of nitric oxide in fuel-lean and fuel-rich flames.

22 p2820 A73-42794

Transition of a low-pressure plasma into a highly ionized state

23 p3013 A73-44335

Comet Bennett neutral sodium atom and dust particle distribution across head and tail measured by photometry of Na emission radial profile

24 p3133 A73-44560

ATOMIC BATTERIES

U RADIOISOTOPE BATTERIES

ATOMIC BEAMS

Investigation of molybdenum after exposure to single-charge helium atom radiation

06 p0707 A73-17909

A gas cell method for the measurement of secondary electron ejection coefficients for metastable atoms on metal surfaces.

06 p0726 A73-18846

Hafele calculations for jet-borne Cs beam clock difference from ground clock vindicated and generalized to rotating frames of reference

07 p0825 A73-20282

Resonant multiphoton ionization of a cesium atomic beam by a tunable-wavelength Q-switched neodymium-glass laser.

09 p1098 A73-23472

Charge changing processes in hydrogen beams.

14 p1776 A73-30125

A test of Jaynes' neoclassical theory - Incoherent resonance fluorescence from a coherently excited state.

20 p2570 A73-38605

ATOMIC CLOCKS

Application of ultrastable oscillators to aerospace [ONERA, TP NO. 1114]

01 p0045 A73-10235

Geodetic satellite timing accuracies with Loran C, portable atomic clocks and long baseline interferometry

04 p0446 A73-14807

Short term instability of frequency standard using AFC of quartz crystal oscillator by phase locking to optically pumped Rb 87 vapor clock

05 p0583 A73-16071

Accurate time and frequency comparisons based on TV frame pulses

06 p0692 A73-17587

Application of ultrastable oscillators to the aerospace field

07 p0798 A73-19180

Hafele calculations for jet-borne Cs beam clock difference from ground clock vindicated and generalized to rotating frames of reference

07 p0825 A73-20282

Clock synchronization experiments performed via the ATS-1 and ATS-3 satellites.

10 p1217 A73-23996

Frequency generators performance with stability associated with atomic/molecular transition, considering rubidium and hydrogen clocks and He-Ne lasers

10 p1219 A73-24396

Methods for the comparison and the propagation of time scales

12 p1498 A73-27751

VLF navigation development at NAE.

17 p2209 A73-34849

Ultrastable atomic and molecular oscillators and their applications to navigation

19 p2429 A73-37384

Russian book on design and operational principles of monopulse and moving target radar, atomic time and frequency measuring devices, radio navigation and optical processing

21 p2650 A73-40510

Atomic time and frequency standards

21 p2700 A73-40513

Possible scientific utilization of long laser bases

21 p2716 A73-41328

Precision comparison of time and frequency by means of TV signals.

22 p2859 A73-42191

The frequency stability and noise of passive Rb standard.

23 p2965 A73-44137

ATOMIC COLLISIONS

Transfer of electronic excitation by atomic collision between highly excited cesium atoms

01 p0079 A73-10174

Use of the Glauber approximation in atomic collisions - A progress report.

02 p0195 A73-12649

One-electron model for charge exchange in ion-atom collisions.

03 p0344 A73-13283

Intensity calculation of X-ray scattering by the atom and ion of aluminum

06 p0725 A73-18216

Diatomic molecule formation in interstellar medium via two body collision, calculating rate coefficients for radiative association

06 p0752 A73-18231

Collision matrix elements near a pseudocrossing of potential energy curves.

06 p0726 A73-18249

Semiclassical theory of inelastic collisions. II - Momentum-space formulation.

06 p0726 A73-18262

Studies of the potential-curve-crossing problem. II - General theory and a model for close crossings.

06 p0726 A73-18263

Semiclassical theory of inelastic collisions. I - Classical picture and semiclassical formulation.

06 p0726 A73-18264

Electron loss by helium atoms passing through inert gases and molecular hydrogen, nitrogen, and oxygen.

07 p0853 A73-19334

Diatomic molecules dissociation investigation from effective cross section measurement of slow atomic negative ions formation by molecules collisions with fast ions and atoms

08 p0990 A73-21694

On the analysis of glory scattering data for the extraction of information on the interatomic potential well.

09 p1122 A73-22072

The diffusion cross section for scattering of electrons by cesium atoms.

12 p1526 A73-27902

On the motion of small spheres in gases. III - Drag and heat transfer.

13 p1567 A73-29425

Processes altering charge state in collisions of hydrogen atoms with H₂ molecules.

14 p1777 A73-30330

Asymptotic form for the cross section for the Coulomb interacting rearrangement collisions.

14 p1777 A73-30551

Method for measuring the collision-induced broadening of spectral lines

15 p1884 A73-31702

Influence of atom-atom collisions on electron density decay in laser-produced helium plasmas.

16 p2041 A73-32944

Atomic collision processes applied to earth atmospheric physics and chemistry, Jovian ionospheric composition and terrestrial tropical UV daylight

17 p2213 A73-34450

Experimental investigation of collisions of He atoms in the ground state and the 2/3S/ metastable state

19 p2462 A73-37248

ATOMIC ENERGY LEVELS

Dispersion model of a single-vortex function of structural scattering of atoms by surfaces

19 p2462 A73-37842

Polarizability of interacting atoms - Relation to collision-induced light scattering and dielectric models.

21 p2742 A73-40211

Detailed balance as check on impact parameter calculations, discussing proton-hydrogen collisions with small transition amplitudes and interpolation errors

21 p2743 A73-40467

Change in the hyperfine state of the hydrogen atom during its collisions with unsaturated hydrocarbon molecules in the gaseous state.

22 p2889 A73-41719

Catalytic efficiencies of atoms in the vibrational relaxation of HF and DF.

22 p2818 A73-42763

Single s-wave electron-hydrogen scatter below first excitation threshold, computing phase shift in Feshbach operator and static exchange approximation

22 p2890 A73-43127

Stellar radiation Thomson scattering by free electrons compared to atomic processes as mechanism for H II regions continuous emission

23 p3030 A73-43756

Unitary transition probabilities for atom-atom oscillator collisions.

24 p3113 A73-44982

ATOMIC ENERGY

U NUCLEAR ENERGY

ATOMIC ENERGY LEVELS

Second-level population of a hydrogen atom in a plasma medium

01 p0085 A73-10950

UV laser parameters calculation for operation on Lyman transition between H atom resonant excited state and ground state

01 p0061 A73-11334

Distribution function of atomic level populations in a plasma

02 p0196 A73-11603

Neodymium energy level shifts in three oxygen-compensated sites of neodymium oxide-doped calcium fluoride crystals

03 p0349 A73-13288

Projectile structure effects on neon K X-ray production by fast, highly ionized argon beams.

04 p0476 A73-14769

Investigations of a Kr-Hg mixture regarding laser action

04 p0458 A73-14896

P II Zeeman effect spectral line observation for J-value assignments with check on wave functions obtained from energy level least squares fitting

05 p0600 A73-16497

Stimulated collisions in collision processes with transitions between atomic levels and free and bound states, noting population density stabilization

06 p0725 A73-17910

Correlation between the diffusion activation energy, the heat of fusion, and the bond energy in metals

06 p0708 A73-18046

CW He-Cd and He-Se metal vapor lasers, discussing atomic energy states, energy emission and absorption by electrons He storage levels and Penning ionization

07 p0836 A73-19933

Temperature determination of rare gas plasmas seeded with alkali, considering oscillator forces of K excited states in He plasma

08 p0990 A73-20649

Population of the second level of the hydrogen atom in a plasma medium.

09 p1130 A73-22744

Transitions between Zeeman atomic sublevels in a medium

11 p1405 A73-26155

Ionization, recombination, and population of excited levels in hydrogen plasmas.

11 p1407 A73-26584

Atomic L2 and L3 vacancy states absolute width from photoelectron spectroscopy, investigating discontinuities, Auger intensity ratio and Coster-Kronig transition probability

13 p1662 A73-28189

Measurement by double resonance of Lande factors of the 3 s/2/ and 2 p/4/ of neon pumped optically by a laser beam

13 p1627 A73-28568

Investigation by the laser photolysis method of the spectral and time characteristics of tetrapyrrole molecules in a triplet state

13 p1628 A73-29050

Effect of Debye shielding on the ionization energy of air plasma components

13 p1667 A73-29164

Excitation of the Fe XIII spectrum in the solar corona.

13 p1684 A73-29353

Quantum theory of a high energy gas laser

14 p1757 A73-30363

Ionization transitions from the 8/2P(1/2) level of a cesium atom in a low-temperature plasma

14 p1781 A73-30460

- Quasar red shift mechanism based on atomic energy levels and particle rest masses variations in scalar gravitational field 15 p1929 A73-31062
- Upper level populations in optically excited cesium vapor 15 p1914 A73-32337
- Optical pulses interaction with two level atom spins, determining sub-cooperation limit in resonant absorbers 20 p2591 A73-38625
- Radiation field frequency dependent source function for two level atom, noting different stimulated emission and absorption line profiles 22 p2907 A73-42205
- Energy level transitions in Ca XVII and Ti XIX UV spectra, basing identifications on extrapolation method 22 p2914 A73-43016
- Singlet s-wave electron-hydrogen scatter below first excitation threshold, computing phase shift in Feshbach operator and static exchange approximation 22 p2890 A73-43127
- Two level atomic inelastic transitions in plasma with damping for static, Weisskopf, adiabatic, exponential and Purcell/Born particle regions 23 p3008 A73-44014
- Multiphoton absorption spectroscopy without Doppler effect 24 p3096 A73-45327

ATOMIC EXCITATIONS

- Transfer of electronic excitation by atomic collision between highly excited cesium atoms 01 p0079 A73-10174
- Concentration distribution and effective lifetimes of excited atoms at small optical thicknesses of the plasma 01 p0085 A73-11083
- UV laser parameters calculation for operation on Lyman transition between H atom resonant excited state and ground state 01 p0061 A73-11334
- Comet spectra and excitation mechanism for spectrum production, discussing structural subdivision into nucleus, coma and tail 04 p0494 A73-14760
- Application possibilities of atomic resonance absorption spectroscopy in vacuum metallurgy 04 p0455 A73-15754
- Selective reabsorption leading to multiple oscillations in the 8446-A atomic-oxygen laser 07 p0834 A73-19335
- Interactions among multiple lines in the 8446-A atomic-oxygen laser 07 p0834 A73-19336
- Ionospheric electrons and neutral particles temperature and concentration profiles explanation by electron gas cooling due to atomic oxygen excitation, calculating heat flow 07 p0815 A73-19441
- Transfer of Yb(3+/-) excitation energy to TR(3+/-) in CaF2 and BaF2 crystals 07 p0837 A73-20206
- Chaotic photon bunching effect interpretation by theoretical incoherent source model with atomic excitation and emission at stochastically independent times without interaction 07 p0837 A73-20610
- Stark effect and line broadening in three-dimensional stochastic fields 09 p1125 A73-21939
- Experimental investigation of the excitation functions of thallium atoms 09 p1121 A73-21952
- Excitation of autoionization states of the cesium atom by electron impact 09 p1122 A73-21978
- Simultaneous diffusion of photons and particles in a semiinfinite space. I - Distribution of excited atoms in a semiinfinite space 09 p1123 A73-23068
- Simultaneous diffusion of photons and particles in a semiinfinite space. II - Concentration of excited atoms before a shock wavefront 09 p1123 A73-23069
- Inelastic collision of fast charged particles with arbitrary levelled hydrogen-like atoms 10 p1250 A73-23575
- Electron impact excitation rates calculation for He I and II transitions, comparing measured, theoretical and semiempirical impact cross sections 10 p1251 A73-24133
- Experimental study of the relaxation of excited states in a decaying alkaline plasma 10 p1256 A73-24576
- Ultraviolet luminescence and nonlinear extinction in ruby 10 p1260 A73-24579
- Atoms and molecules in astrophysics; Proceedings of the Twelfth Session of the Scottish Universities Summer School in Physics, University of Stirling, Stirling, Scotland, August 1971. 12 p1538 A73-26920
- Reactions of O(1D) with methane and ethane. 12 p1466 A73-27126

- Bounds on mean excitation energies-Lamb shift, stopping power, straggling, and grazing collision of high-energy charged particle. 12 p1526 A73-27128
- Theory for the susceptibility of quantum systems with degenerate levels 13 p1659 A73-28759
- The excitation of atomic oxygen to the Q/I S/ level by energy transfer from N2/A 3 Sigma u+/- molecules in aurora. 15 p1866 A73-31075
- Kinetics of physicochemical processes in a shock wave in mercury vapors. II - The relaxation zone: Region of initial ionization 15 p1916 A73-32314
- Upper level populations in optically excited cesium vapor 15 p1914 A73-32337
- CW metal vapor lasers, discussing discharge conditions, excitation processes, cathaphoretic effect and He-Se and He-Cd lasers output characteristics 16 p2023 A73-32858
- Excitation of atomic nitrogen by electron impact. 16 p2038 A73-33099
- Excitation of highly excited hydrogenic ions and atoms by charged particles. IV. 16 p2039 A73-33865
- Temperature determination of the upper atmosphere by the low-level detection of artificial luminous cloud radiation. 18 p2311 A73-36149
- X radiation arising during collisions between metal bodies 19 p2458 A73-37249
- ISIS-2 red line photometer for global distribution mapping of atomic oxygen 6300 A emission in airglow and auroras, discussing atomic excitation processes in upper atmosphere 19 p2428 A73-37257
- Angular dependence of optically pumped magnetometer - Effects of collisional mixing in the excited states. 19 p2429 A73-37382
- A test of Jaynes' neoclassical theory - Incoherent resonance fluorescence from a coherently excited state. 20 p2570 A73-38605
- Lasing mode generation during normal competition in channels with common upper level, assuming line broadening and atomic diffusion 21 p2712 A73-40307
- Investigation of the radiation properties of a laser without external feedback 22 p2871 A73-42971
- Dipole-quadrupole dispersion coefficient calculation for interactions of atomic pairs formed from hydrogen, alkali and rare gas atoms, using perturbation and variation methods 23 p3007 A73-43522
- Collective spontaneous emission of polyatomic systems 23 p2988 A73-44010
- Energy spectra of localized elementary excitations for dilute solutions of He 3 atoms in superfluid He 4 using Feynman type wave function, considering Raman scattering 23 p3007 A73-44173
- Optical characteristics of phononless lines 24 p3109 A73-44427
- Proton collisional excitation in the ground configuration of Fe(+/12). 24 p3123 A73-44634
- Behavior of excited atoms and molecules in the upper atmosphere at heights from 40 to 300 km 24 p3084 A73-44803
- Excitation mechanisms in He-Cd and He-Zn ion lasers. 24 p3097 A73-45418

ATOMIC EXPLOSIONS

U NUCLEAR EXPLOSIONS

ATOMIC GASES

U MONATOMIC GASES

ATOMIC MOBILITIES

- Effect of atom self-diffusion on evaporation processes and porosity development in solid bodies during electron-beam treatment 18 p2320 A73-36900
- Atomic diffusion mechanisms in multiphase and multicomponent alloys covering relaxation, crystal lattice atom exchange and motion along dislocation lines and to neighboring vacancies 23 p2989 A73-43439

ATOMIC PHYSICS

- Book - Emission, absorption, and transfer of radiation in heated atmospheres. 01 p0119 A73-10125
- Laser photons multiple absorption by atoms, determining transition probabilities from Schroedinger equation solution via space translation operation 14 p1776 A73-29698
- Book - Atomic physics and astrophysics, Volume 2. 18 p2356 A73-36969
- A quantum treatment of spontaneous emission without photons. 20 p2594 A73-38611

ATOMIC RECOMBINATION

NT OXYGEN RECOMBINATION

Atomic recombination rate determination through heat-transfer measurement. 09 p1048 A73-23449

Theory of an infrared high-pressure chemical laser 13 p1627 A73-28762

ATOMIC SPECTRA

- Comet spectra and excitation mechanism for spectrum production, discussing structural subdivision into nucleus, coma and tail 04 p0494 A73-14760
- Cometary heads observations indicating precursor decay lengths from 100-10,000 km, considering visible and UV molecular and atomic emissions 04 p0495 A73-14764
- Need of LS-dependent energy parameters in the second spectra of the fifth-group elements. 05 p0600 A73-16496
- Interstellar Na I, K I, Ca II, and CH+/+ line profiles toward zeta Ophiuchi. 10 p1273 A73-23549
- Simplified Hartree-Fock approximation for complex atom opacity efficient calculation based on homogeneous one-electron orbital equation solution with effective potential optimization 13 p1662 A73-28455
- Diurnal variation of nightglow Na emission, noting linear intensity variation with time, oscillatory and anticovariation characteristics 13 p1610 A73-29337
- Some aspects of the exchange-interaction and dipole-dipole broadening of the individual hyperfine components of the EPR spectrum 14 p1775 A73-30580
- The absorption spectrum of Rb I between 350 and 810 A. 19 p2462 A73-37623
- Nonlinear effects in the emission and absorption spectra of gases in resonant optical fields 21 p2712 A73-40443
- The formation of Mg I 4571 A in the solar atmosphere. III - The Holweger solar model /Research note/. 21 p2777 A73-41480
- An atlas of low-latitude 6300-A forbidden O I night airglow from Ogo 4 observations. 22 p2845 A73-41924
- A comparison of the sensitivity of atomic-fluorescent and atomic-absorption flame photometry 22 p2862 A73-42720
- Pulsed laser saturation spectroscopy - Observation of power broadening by optical nutations. 22 p2871 A73-43082
- Study of induced four-photon parametric scattering of laser light in alkali metal vapor 23 p2988 A73-44009
- Radiation transfer equations for atomic spectra lines in stellar magnetic field, allowing for nonequilibrium population of atomic ground state and excited atom-particle collisions 23 p3036 A73-44242
- Determination of dissociation energies for some alkaline earth /hydro-/ oxides in CO/N2O flames. 24 p3156 A73-44985

ATOMIC STRUCTURE

- Hydrogen atomic structure in magnetic field, using Bohr model, Schroedinger equation and energy eigenvalues 03 p0299 A73-13352
- Phase diagrams and properties of binary alloys of refractory metals, taking into account the electronic structure of the atoms of the components 03 p0328 A73-14652
- Stimulated collisions in collision processes with transitions between atomic levels and free and bound states, noting population density stabilization 06 p0725 A73-17910
- Theory of one-dimensional Mott semiconductors and electronic structure of long molecules with conjugate bonds 06 p0734 A73-17923
- Metal atom migration acceleration under radioactive radiation, showing diffusion coefficient dependence on free and coupling electron interactions 06 p0735 A73-18038
- Mathematical models for yield point dependence on statistical arrangements of ordered precipitated phases, noting crystal dislocations interaction effect 06 p0735 A73-18044
- Thermodynamic stability of ordered phase atomic structure state for antiphase domain formation, noting superstructures in face centered and body centered cubic solutions 06 p0736 A73-18118
- Electronic mechanism of the basic technological processes in the powder metallurgy of high temperature materials. 08 p0982 A73-21825
- Wave functions and energies of the autoionization states of the cesium atom 09 p1122 A73-21976
- Ionization of 6s- and 5p-electrons of the cesium atom by electron impact 09 p1122 A73-21977

Critical evaluation of Zhurkov theory of metallic material fracture by successive rupture of atomic bonds due to atom thermal motion

09 p1100 A73-22160

Electron-spectroscopic investigations of two modifications of the alloy steel Kh18N10T

09 p1104 A73-22690

Investigation of the structure of sodium silicate glass containing oxides of multivalent metals by nuclear spectroscopy methods

09 p1110 A73-22980

Electronic configuration and electrical conductivity in ceramics.

09 p1135 A73-23000

Energetic and structural models of microdefects in germanate glasses

10 p1240 A73-24465

Diffusion processes electron mechanism in metal-metal and metal-nonmetal systems, using configurational model for valence electrons localization

10 p1236 A73-24951

Metal surfaces structure, chemical segregation, electronic properties, space charge and electrode behavior

11 p1381 A73-25809

Influence of deformation and heat treatment on the structural changes of the OKh12N13M alloy

12 p1508 A73-26836

Electron impact excitation of H₂O.

12 p1526 A73-27687

Possibility of atom displacements in solids under the action of laser light pulses

13 p1626 A73-28003

Simplified Hartree-Fock approximation for complex atom opacity efficient calculation based on homogeneous one-electron orbital equation solution with effective potential optimization

13 p1662 A73-28455

The electrical resistivity of transition metals at high temperatures.

14 p1759 A73-29746

ESCA study of fractional monolayer quantities of chemisorbed gases on tungsten.

14 p1724 A73-30421

'Anomalous' alteration of the Moessbauer isomer shift of Te125 in defect diamond-like semiconductors

14 p1784 A73-30809

Superconductivity and electron structures of a solid solution of titanium in niobium

14 p1784 A73-30811

Nuclear gamma resonance spectra of Sn119 and Te125 and the electron structure of ternary diamond-like semiconductors Cu₂SnS₃, Cu₂SnSe₃ and Cu₂SnTe₃

14 p1784 A73-30851

Application of an extended method of calculation to rare-earth atoms and ions in the 4fN configuration

14 p1784 A73-30852

Liquid Ni-Si alloy short range order structure analyzed by X ray scattering, revealing Ni atoms position relation to Si atoms

14 p1764 A73-30870

Metallurgical investigations of atomic ordering and transformation behavior of close packed ordered nine-layered hexagonal structure /kappa phase/ in V-Co-Ni ternary alloys

17 p2190 A73-34646

Effect of atom ordering on the martensite decomposition mechanism and kinetics in iron-aluminum-copper alloys

18 p2324 A73-36769

X ray diffraction analysis of Mo-Ta and Mo-C solid solutions, relating transition and nontransition metal electronic structures and stacking fault energy

18 p2325 A73-36808

Electronic structure of ferric iron octahedrally coordinated to oxygen.

18 p2341 A73-37049

A semiempirical description of the structure of metals

20 p2577 A73-39295

Superconductivity and electronic structure of ultrahigh-purity niobium. I - Synthesis of ultrahigh-purity niobium

20 p2600 A73-39732

Study of the electronic structure of iron, cobalt, and nickel monosilicides by X-ray photoelectron spectroscopy and X-ray spectroscopy

20 p2578 A73-39734

An X-ray spectral study of the electronic structure of nonstoichiometric titanium carbide

21 p2721 A73-41226

Russian papers on metal alloys chemistry covering atomic structure, physicochemical properties, phase diagrams, X ray analysis, laser microanalysis, etc

22 p2873 A73-42083

Critical evaluation of Zhurkov theory of metallic material fracture by successive rupture of atomic bonds due to atom thermal motion

22 p2874 A73-42108

Theory of one-dimensional Mott semiconductors and the electronic structure of long molecules having conjugated bonds.

23 p3018 A73-44323

Metal crystal lattice properties and chemical bond nature in terms of valence concept, analyzing p-electron cloud overlapping

24 p3119 A73-45178

Consideration of lattice translations in computer studies of grain-boundary coincidence.

24 p3120 A73-45405

ATOMIC THEORY

NT HEISENBERG THEORY

Hartree-Fock equation with allowance for the correlation

22 p2889 A73-42647

ATOMIZING

U ATOMIZING

ATOMIZERS

Optical anemometers applicability to steady atomized fuel sprays, obtaining particle velocity profiles and probability density distributions

05 p0565 A73-17671

ATOMIZING

Droplets size and velocity distribution in air-kerosene atomized spray flame as function of fuel-air ratio from double image high speed photographic measurements

[ASME PAPER 72-WA/HT-25] 04 p0519 A73-15829

Application of lateral illumination in holography of small objects

09 p1085 A73-23015

Investigation of the crystallization of metallic powders obtained by liquid-phase atomization

10 p1224 A73-24313

Investigation of metal droplet shaping during atomization

10 p1225 A73-24688

Changes in the optical properties of minerals and their atomization caused by ion bombardment

16 p1977 A73-33756

The effects of imperfect fuel-air mixing in a burner on NO formation from nitrogen in the air and the fuel.

22 p2820 A73-42795

Breakup of liquid drops due to convective flow in shocked sprays.

22 p2937 A73-42819

Some comments to mathematical interpretation of performance characteristics of jet engine combustion chambers.

24 p3123 A73-45381

ATOMS

NT HELIUM ATOMS

NT HYDROGEN ATOMS

NT METASTABLE ATOMS

NT NITROGEN ATOMS

NT OXYGEN ATOMS

ATP

U ADENOSINE TRIPHOSPHATE [ATP]

ATS [SATELLITES]

U APPLICATIONS TECHNOLOGY SATELLITES

ATS 1

Clock synchronization experiments performed via the ATS-1 and ATS-3 satellites.

10 p1217 A73-23996

ATS-1 borne Random Access Discrete Address System for multiple access satellite communication, discussing repeater performance concerning CW signal transmission efficiency, intermodulation and SNR

22 p2825 A73-42187

ATS 3

ATS-3 observed cloud brightness field related to a meso-to-synoptic scale rainfall pattern.

06 p0720 A73-17867

Clock synchronization experiments performed via the ATS-1 and ATS-3 satellites.

10 p1217 A73-23996

Very short range local area weather forecasting using measurements from geosynchronous meteorological satellites.

19 p2446 A73-37500

ATS 5

ATS-5 solar cell experiment after 699 days in synchronous orbit.

03 p0257 A73-14244

Millimeter wave propagation measurement for attenuation probability statistics by ATS-5 satellite, considering impact on space communication system design

04 p0418 A73-15387

Millimeter wave propagation measurements from an orbiting earth satellite.

16 p1982 A73-33716

ATS 6

Future NASA communication satellite technology applications in meeting national education, health care, culture and data transfer needs, considering ATS F and CTS spacecraft

02 p0143 A73-12846

Irradiation of solar cell candidates for the ATS-F solar cell flight experiment.

03 p0257 A73-14245

ATS-F COMSAT millimeter wave propagation experiment.

04 p0418 A73-15386

System design, hardware and software of RF interference measurement experiment regarding microwave frequency optimal sharing between ATS-F satellite and terrestrial relay telecommunication

04 p0422 A73-15460

ATS-F and Nimbus-E satellites use for range and range rate determination, earth gravity anomaly detection and orbital position determination

13 p1656 A73-28391

Mathematical modeling for ATS-F spacecraft louvers and heat pipes thermal control heat rejection capacity, noting correlation with solar environment simulation data

[AIAA PAPER 73-773]

18 p2360 A73-36387

Applications Technology Satellite F aluminum-ammonia heat pipes design, fabrication and life and thermal vacuum testing

[ASME PAPER 73-ENAS-46] 19 p2493 A73-37993

ATTACK AIRCRAFT

NT A-4 AIRCRAFT

NT A-7 AIRCRAFT

NT B-1 AIRCRAFT

NT B-52 AIRCRAFT

NT B-57 AIRCRAFT

NT B-70 AIRCRAFT

NT BOMBER AIRCRAFT

NT F-14 AIRCRAFT

NT F-15 AIRCRAFT

NT F-111 AIRCRAFT

NT FIGHTER AIRCRAFT

NT JAGUAR AIRCRAFT

Light combat aircraft with hover capability.

03 p0251 A73-13923

Volvo RM8 turbopan engine for Viggen fighter and ground attack aircraft, emphasizing low fuel consumption for long range cruise and high thrust/weight ratio

05 p0608 A73-17099

HS 1182 multipurpose ground attack trainer aircraft, describing weapon system, hydraulic flight control, power plant and avionics

14 p1713 A73-30934

V/STOL aircraft testing for the sea control ship environment.

[AIAA PAPER 73-810]

19 p2379 A73-37466

Cobra P-530 air superiority fighter adaption to ground attack for international requirements for multipurpose aircraft, discussing avionics for multimission version

21 p2634 A73-40301

ATTENTION

Attention field and perception probability distribution mechanisms of Muller-Lyer illusion due to angle contour

07 p0783 A73-20255

Self-estimates of distractibility as related to performance decrement on a task requiring sustained attention.

15 p1839 A73-32394

ATTENUATION

NT ACOUSTIC ATTENUATION

NT ATMOSPHERIC ATTENUATION

NT AURORAL ABSORPTION

NT MANDELSTAM REPRESENTATION

NT MICROWAVE ATTENUATION

NT RADAR ATTENUATION

NT RADIO ATTENUATION

NT SHOCK WAVE ATTENUATION

NT SIDELobe REDUCTION

NT WAVE ATTENUATION

Thermal cycling and frequency tests for lunar soil dielectric constant, loss tangent and dc conductivity, noting moisture effects

02 p0220 A73-12481

ATTENUATION COEFFICIENTS

Atmospheric absorption and scattering as radiation extinction mechanisms, discussing attenuation coefficient wavelength and weather dependence

01 p0102 A73-10993

Stratospheric aerosol measurements with implications for global climate.

[AD-759856]

08 p0984 A73-21041

Study of the influence of various parameters on the method used for determining the attenuation lengths through photoelectric yield measurements in the far ultraviolet

15 p1878 A73-32211

Determination of the parameters of particle density and size distribution functions from measurements of attenuation and backscattering coefficients

24 p3112 A73-45519

ATTENUATORS

NT PRINTED RESISTORS

NT RESISTORS

NT THERMISTORS

Reflection and transmission coefficients for stratified media, considering total optical reflection attenuator and metal film reflector

01 p0078 A73-11229

A very accurate X-band rotary attenuator with an absolute digital angular measuring system.

03 p0310 A73-14498

Mathematical description and calculation of the static mode of operation of a microwave power regulator with a semiconductor attenuator.

15 p1849 A73-30993

- Book - Design performance and applications of microwave semiconductor control components.
20 p2535 A73-39136
- ATTITUDE (INCLINATION)**
NT PITCH (INCLINATION)
NT SATELLITE ORIENTATION
NT YAW
Matrix transformations for spacecraft attitude determination.
02 p0228 A73-11905
Natural frequencies, forces and moments for liquid propellant sloshing in tilted cylindrical tank as function of tilt angle and liquid depth
03 p0293 A73-13314
Nonoriented astronomical satellite attitude determination from onboard measurements of geomagnetic field and stellar luminosity
03 p0379 A73-14560
Tilt discrimination and motion aftereffect independence of flicker rate of stroboscopically illuminated contours visual stimuli
06 p0660 A73-18624
Seat reaction direction in an animal centrifuge.
07 p0780 A73-19478
Observations on perceived changes in aircraft attitude attending head movements made in a 2-g bank and turn.
07 p0785 A73-19485
Choice of a zero approximation of the angular position of a satellite on a trajectory segment of oriented motion in the case of a dipolar approximation of the geomagnetic field
15 p1942 A73-31237
Zero order approximation for attitude angle of stabilized satellite at high orbits under solar pressure perturbation, using trigonometric polynomials based on magnetometer data
15 p1943 A73-31241
The application of Kalman filtering to the attitude determination of spinning space vehicles.
15 p1944 A73-32219
Attitude determination for a strapdown inertial system using the Euler axis/angle and quaternion parameters.
[AIAA PAPER 73-900] 20 p2589 A73-38834
Spatial frequency selectivity of a visual tilt illusion.
21 p2642 A73-41642
- ATTITUDE CONTROL**
NT DIRECTIONAL CONTROL
NT LATERAL CONTROL
NT LONGITUDINAL CONTROL
NT SATELLITE ATTITUDE CONTROL
NT THRUST VECTOR CONTROL
Development of pulsed hydrogen/oxygen attitude-control engines
[DGLR PAPER 72-077] 02 p0202 A73-11689
Resistojet and plasma propulsion system technology.
[AIAA PAPER 72-1124] 03 p0355 A73-13436
Hydrogen-oxygen Space Shuttle ACPs thruster technology review.
[AIAA PAPER 72-1158] 03 p0356 A73-13460
Oscillations of spacecraft with on-off attitude control under constant perturbation moment, calculating energy expenditures for desired orientation maintenance
03 p0383 A73-14559
Pulsed motion of gravity gradient vehicle in central gravity field, presenting expressions of optimized attitude control
03 p0383 A73-14573
Spacecraft digital attitude control.
04 p0504 A73-14736
Demonstration of digital three axis spacecraft control.
04 p0432 A73-14738
Spacecraft oscillatory motion as function of attitude control impulse magnitude
05 p0627 A73-16080
Periodic attitude control of a slowly spinning spacecraft.
[AIAA PAPER 73-246] 05 p0596 A73-16970
The effects of trajectory characteristics on scientific objectives for major planetary orbiters.
06 p0757 A73-18376
Aerodynamic entry vehicle autopilots.
06 p0721 A73-18515
Suboptimal guidance for attitude angle constrained flight trajectories.
06 p0721 A73-18825
Cassiopee triaxial gyroscopic aiming device for sounding rocket attitude control, using stellar and inertial sensors and jet micropulsion
07 p0866 A73-18924
Work carried out by Societe Bertin under contract to CNES in the field of fluidic control
07 p0904 A73-18938
Fluidic circuits fabrication and design technology for rocket guidance and attitude control
07 p0778 A73-18939
Astrolabe universal balloon gondola for solar and visible stars targeting, describing acquisition functions and attitude control servos design
07 p0776 A73-18940
Diamant launcher tilting system.
07 p0905 A73-18993

- STRAP IV - High accuracy, low drift attitude control system.
[AIAA PAPER 73-288] 09 p1116 A73-23208
Two concepts for the reduction of payload attitude slewing times.
[AIAA PAPER 73-290] 09 p1155 A73-23209
An attitude control system for a stellar X-ray source mapping payload.
[AIAA PAPER 73-291] 09 p1116 A73-23210
A digital attitude control system for orientation of rocket launched scientific payloads.
[AIAA PAPER 73-292] 09 p1116 A73-23211
Program objectives and propulsive, equipment case, attitude control, interstage, separation skirt and nose cone subassemblies of French Diamant B-P4 launch vehicle
10 p1285 A73-23654
Liapunov stability analysis and attitude response of a passively stabilized space system.
10 p1286 A73-24541
An apparatus for the orientation of stratospheric-balloon payloads
11 p1304 A73-25355
Spacecraft reorientation by successive rotations about nonorthogonal axes, deriving classical Euler angles as special case of general solution
15 p1908 A73-31662
Time and fuel consumption optimal nutation damping and attitude-angular velocity control of spin-stabilized flight vehicles
16 p2072 A73-33234
NASA research commercial VTOL transport propulsion system specifications and components development, discussing lift fan propulsion method for aircraft attitude control
[ASME PAPER 73-GT-24] 16 p2047 A73-33498
Application of advanced control system and display technology to general aviation.
[SAE PAPER 730321] 17 p2102 A73-34679
Attitude control, rotational and positioning mechanisms for orientation of mechanically despun antennas and solar arrays in communication satellites
[DGLR PAPER 73-050] 17 p2126 A73-35486
Some problems of orientation accuracy for a gyroscopic orbit with nonlinear control laws
18 p2335 A73-36118
Hybrid computer technique for desensitized optimal design of system with uncertain plant parameters, with application to Saturn 5 Apollo attitude control system design
18 p2291 A73-36426
Computer simulation for time optimal or energy optimal attitude control of spin-stabilized spacecraft.
18 p2360 A73-36837
Digital control system development for the Delta launch vehicle.
[AIAA PAPER 73-847] 20 p2613 A73-38786
Continuous calibration and alignment techniques for an all-attitude inertial platform.
[AIAA PAPER 73-865] 20 p2586 A73-38803
Attitude control of a large flexible spacecraft using three-axis mass expulsion control.
[AIAA PAPER 73-893] 20 p2588 A73-38829
Design of a digital controller for spinning flexible spacecraft.
[AIAA PAPER 73-894] 20 p2589 A73-38830
2-SPEED, a single-gimbal control moment gyro attitude control system.
[AIAA PAPER 73-895] 20 p2589 A73-38831
Strapdown inertial navigation with high speed digital computer, discussing attitude propagation algorithms and life cycle system cost advantages
21 p2734 A73-40036
Flight vehicle extensive attitude control theory, deriving kinematic relations for optimal control moment selection to ensure required rotation
21 p2780 A73-40385
Gyroscopes as prime attitude references for the large space telescope.
[AIAA PAPER 73-870] 21 p2700 A73-40506
Fluidic bolometer type sensor for reaction wheel control to maintain spacecraft and rocket vehicle attitude relative to sun, discussing design, simulation and tests
23 p3038 A73-43395
A study of a fluidic open loop damping flight stability augmentation system.
23 p2941 A73-43396
- ATTITUDE GYROS**
Non-linear resonant attitude motions in gravity-stabilized gyrostatt satellites.
07 p0905 A73-19162
2-SPEED, a single-gimbal control moment gyro attitude control system.
[AIAA PAPER 73-895] 20 p2589 A73-38831
Spacecraft attitude gyro reference system and readout accuracy, discussing strapdown guidance, electrical suspension, instrument errors, spin and damping coils and degrees of freedom
21 p2733 A73-40026
French paper on satellite attitude stabilization by gyroscopes covering autonomous activator systems, kinetic moment principles and control in roll-yaw for flexible panels
22 p2917 A73-42743

ATTITUDE INDICATORS

- Sun, earth and star attitude sensors for spacecraft, describing design, analysis and hardware aspects in terms of critical parameters
01 p0053 A73-11170
The attitude-measuring and attitude-control system of the satellite Aeros and its employment in the acquisition phase
[DGLR PAPER 72-062] 02 p0227 A73-11653
Measuring rocket attitude by starlight.
05 p0594 A73-16300
The attitude measuring system of the AEROS satellite.
05 p0629 A73-16849
Use of magnetometers and asymmetric antenna patterns for attitude determination.
05 p0596 A73-17204
A simple method for precise attitude determination of a spinning spacecraft.
06 p0722 A73-18827
An instrument panel on an image tube in color
08 p0935 A73-21543
Thin film thermopile for Symphonie geostationary satellite attitude determination based on absorbed energy transformation into heat, discussing design and applications
16 p1988 A73-33275
Selected applications of a biaxial tiltmeter in the ground motion environment.
[AIAA PAPER 73-840] 20 p2564 A73-38781
- ATTITUDE STABILITY**
NT DIRECTIONAL STABILITY
NT GYROSCOPIC STABILITY
NT LONGITUDINAL STABILITY
Analysis of the unbalances in spin-stabilized satellites
03 p0382 A73-13725
The attitude stabilization and control system for the Communications Technology Satellite.
04 p0504 A73-15450
An optimization technique for the transient response of passively stable satellites.
06 p0755 A73-17566
Attitude dynamics of a three-axis stabilized satellite with a large flexible solar array.
06 p0757 A73-18379
Attitude stability of two elastically coupled spinning bodies.
10 p1286 A73-24543
Liapunov stability analysis of spinning flexible spacecraft.
11 p1431 A73-26378
The use of a spinning dissipator for attitude stabilization of earth-orbiting satellites.
13 p1690 A73-29216
Equilibrium configurations and attitude stability criteria for articulated satellite idealized as point-connected rigid two gyrostatt problem
14 p1802 A73-29757
Gravitational stabilization of a two-body satellite.
15 p1943 A73-31916
Gravity-gradient stabilization of synchronous orbiting satellites - Additional considerations of attitude stability.
15 p1944 A73-32218
Precession rate matching for a space station in orbit about an oblate planet.
18 p2351 A73-36153
Dual and triple spin-stabilized deformable spacecraft attitude stability, comparing results based on Sturm theorem with Liapunov analysis
18 p2359 A73-36306
Attitude stability conditions of multiple spin satellites.
18 p2361 A73-36877
The precession of unsymmetric spin-stabilized satellites.
18 p2361 A73-36878
Large scale telescope pointing stability augmentation system, using control moment gyro gimbal servo error signal to command momentum augmentation system
[AIAA PAPER 73-868] 20 p2587 A73-38806
A high-performance test facility for laboratory simulation of the Large Space Telescope orbiting vehicle in a single-degree-of-freedom mode of rotation.
[AIAA PAPER 73-884] 20 p2544 A73-38820
Attitude stability conditions of multiple spin satellites.
22 p2916 A73-42189
The precession of unsymmetric spin-stabilized satellites.
22 p2916 A73-42190
Russian book on satellite attitude stabilization systems design covering gravity gradients, linear and nonlinear control laws, spin stabilization, high torque control moment gyros, etc
23 p3038 A73-43335
- ATTRACTION**
Expansion of the force function of two homogeneous spheroids with noncoincident symmetry planes.
04 p0503 A73-16021

- Field of attraction of a singularity of a nonlinear recurrence of the second order - Method of determination of the boundary 11 p1389 A73-25137
- Stellar system gravitational field structure in terms of system-media attraction /regular force/ and force due to random distribution of stars /irregular force/ 11 p1416 A73-25236
- AUDIO EQUIPMENT**
- NT EARPHONES
- NT LOUDSPEAKERS
- NT MICROPHONES
- AUDIO FREQUENCIES**
- Equipment for determining the amplitude-frequency characteristics of nonlinear elements in the range of low and extra-low frequencies 01 p0023 A73-10679
- Silicon semiconductor resistance strain gage intrinsic thermal noise characteristics at 20 Hz-10 kHz, noting 1/f type as dominant noise component in audio frequency range 13 p1611 A73-28021
- Conventional and high frequency hearing of naval aircrewmembers as a function of noise exposure. 23 p2949 A73-43500
- AUDIO VISUAL EQUIPMENT**
- U TRAINING DEVICES
- U VISUAL AIDS
- AUDIOLOGY**
- Portable electro-phonocardiograph using magnetic tape recorder equipped with patient's voice print. 11 p1323 A73-25475
- AUDIOMETRY**
- Study of the acoustic reflex in human beings. I - Dynamic characteristics. 01 p0013 A73-10828
- German monograph - Investigations regarding auditory depth perception and the problem of in-head localization of acoustic events. 13 p1577 A73-29278
- Current aspects of the cochlear function in members of flight crews 18 p2286 A73-36940
- Voltage controlled attenuator circuit for acoustic signal duration and repetition control in hearing examinations 24 p3064 A73-44910
- AUDITORY DEFECTS**
- Electron-microscopy investigation of Corti's organ after noise trauma 05 p0539 A73-16333
- Book - Human factor aspects of aircraft noise. 12 p1465 A73-27450
- Impairment to hearing from exposure to noise. 16 p1973 A73-33676
- Hearing conservation studies covering impulse noise produced threshold shift, damage risk criteria, ultrasound hazards and hearing protection 17 p2117 A73-35326
- Impulse noise damage risk criteria. 17 p2117 A73-35327
- Evaluation of auditory disorders in pilots by examining intratympanic muscles reflexes. 18 p2279 A73-36934
- Corti organ lesion effects on signal perception in patients with noise induced hearing loss, correlating speech discrimination with age and sound level 19 p2396 A73-38182
- Conventional and high frequency hearing of naval aircrewmembers as a function of noise exposure. 23 p2949 A73-43500
- AUDITORY PERCEPTION**
- Temporary threshold shift caused by combined steady-state and impulse noises. 01 p0077 A73-10785
- Some modeling problems of loudness transformations by the auditory system 04 p0413 A73-15790
- The dynamic properties of the acoustic middle ear reflex in nonanesthetized rabbits - Quantitative aspects of a polysynaptic reflex system. 05 p0539 A73-16249
- Study of the peripheral auditory adaptation in a psycho-acoustic experiment 10 p1179 A73-23807
- Functional model of the frequency channel of the peripheral auditory analyzer 10 p1183 A73-23808
- Binaural interaction effects on afterperception of white noise pulse sequences delivered to both ears simultaneously or after various intervals 10 p1180 A73-24333
- Problem of localization in the median plane - Effect of pinnae cavity occlusion. 11 p1321 A73-24976
- Optimal and preferred listening levels for speech in aircraft acoustical environments. 11 p1304 A73-25387
- Dynamics of changes in neuron activity regimes of the ascending auditory pathways 11 p1317 A73-26079
- German monograph - Investigations regarding auditory depth perception and the problem of in-head localization of acoustic events. 13 p1577 A73-29278
- Book - Foundations of modern auditory theory. Volume 2. 14 p1715 A73-30276
- Acoustic model and linguistic, syntactic, lexical and semantic factors in speech perception and production process 14 p1721 A73-30277
- Psychoacoustic theory of signal detectability based on mathematical input-output mapping model and memory role in human auditory system 14 p1721 A73-30278
- Neuroanatomy of the auditory system. 14 p1715 A73-30280
- Binaural acoustic field sampling, head movement and echo effect in auditory localization of sound sources position, distance and orientation 14 p1715 A73-30282
- Vector correlation theory and neural mechanisms of binaural signal detection in human auditory system 14 p1716 A73-30283
- Damage-risk criteria - The trading relation between intensity and the number of nonreverberant impulses. 16 p1973 A73-33678
- Current aspects of the cochlear function in members of flight crews 18 p2286 A73-36940
- Pure-tone equal-loudness contours for standard tones of different frequencies. 21 p2645 A73-41176
- Loudness changes resulting from an electrically induced middle-ear reflex. 22 p2811 A73-41815
- Mathematical model of human pitch perception based on acoustic stimulus Fourier transformation by sense organ into peripheral neural activity pattern recognition 22 p2811 A73-41816
- Russian book on electroacoustic and electromechanical devices for sound recording and measurement covering human auditory system, microphones, loudspeakers, hydrophones, geophones, etc 22 p2832 A73-41882
- Effect of the stimulation of nonspecific thalamic nuclei on spontaneous and evoked spindles in the auditory cortex 22 p2802 A73-41958
- Experimental substantiation of the optimal method for scaling the duration of acoustic stimuli 22 p2814 A73-42654
- Reaction time to changes in the tempo of acoustic pulse trains. 22 p2816 A73-42705
- Functional state of the auditory analyzer under conditions of prolonged clinostatic hypokinesia 23 p2946 A73-43789
- Asymmetry in perception - Attention versus other determinants. 24 p3065 A73-45338
- AUDITORY SENSATION AREAS**
- Electrophysiological investigation of noise rejection in an auditory system receiving sound from a localized source 09 p1040 A73-22580
- Functional characteristics of different neurons in the auditory cortex 19 p2395 A73-37940
- Functional properties of auditory cortex neurons in a controlled experiment 20 p2516 A73-39802
- Analysis of the changes in glial cell numbers in the auditory cortex during the application of acoustic stimuli of various intensities 22 p2807 A73-42653
- Inferior colliculus neuron responses to an amplitude-modulated signal with varying intensity levels 24 p3061 A73-45248
- AUDITORY SIGNALS**
- Effects of signal duration and masker duration on detectability under diotic and dichotic listening conditions. 01 p0008 A73-10436
- Some modeling problems of loudness transformations by the auditory system 04 p0413 A73-15790
- Electrophysiological investigation of noise rejection in an auditory system receiving sound from a localized source 09 p1040 A73-22580
- The operational control of the alpha component in the electroencephalogram by means of auditory feedback 11 p1324 A73-26549
- Interaural difference thresholds in binaural perception of signals nonexistent in normal acoustic environment, considering beats, memory, learning, and stereophony 14 p1716 A73-30285
- Electrical activity of the external ear muscles in man /at rest and during identification of acoustic signals/ 14 p1719 A73-30843
- Amplitude variations of acoustically evoked potentials as a function of signal information and fatigue due to stress 19 p2396 A73-38161
- Voltage controlled attenuator circuit for acoustic signal duration and repetition control in hearing examinations 24 p3064 A73-44910
- Inferior colliculus neuron responses to an amplitude-modulated signal with varying intensity levels 24 p3061 A73-45248
- AUDITORY STIMULI**
- Loudness enhancement following contralateral stimulation. 01 p0013 A73-10827
- Study of the acoustic reflex in human beings. I - Dynamic characteristics. 01 p0013 A73-10828
- An earphone coupling system for acute physiological studies. 01 p0013 A73-10829
- Auditory rail task for acoustic stimuli effects on human equilibrium under axisymmetric intermittent tone exposure, discussing acoustic energy effect on vestibular receptors 03 p0260 A73-13551
- Effects of intermittent and continuous noise on serial search performance. 03 p0267 A73-13560
- Participation of the hippocampal structures in the formation of external inhibition 06 p0653 A73-18162
- Functional alterations in the auditory and visual analyzer systems of monkeys during experimental neurosis 06 p0653 A73-18163
- The effect of accessory auditory stimulation upon detection of visual signals. 06 p0660 A73-18625
- Cortical potentials evoked by confirming and disconfirming feedback following an auditory discrimination. 09 p1039 A73-21895
- Reaction time method using EEG monitored paroxysm controlled auditory stimuli for responsiveness /consciousness/ evaluation of spike wave burst onset during epileptic seizures 09 p1040 A73-22695
- Polysensory responses and sensory interaction in pulvinar and related postero-lateral thalamic nuclei in cat. 09 p1040 A73-22696
- Sinusoidal stimuli induced electrical activity of hippocampus in waking rhesus monkeys and baboons 10 p1180 A73-24330
- Binaural interaction effects on afterperception of white noise pulse sequences delivered to both ears simultaneously or after various intervals 10 p1180 A73-24333
- Characteristics of the electrical activity of the superior olivary bodies of Vespertilionidae and Rhinolophidae bats in response to ultrasonic stimuli of different frequencies 10 p1182 A73-24596
- Interindividual differences in homomodal and heteromodal scaling of auditory and vibrotactile stimulation intensity and duration, using magnitude estimation method 12 p1464 A73-26750
- Effect of stimulus uncertainty on the pupillary dilation response and the vertex evoked potential. 14 p1714 A73-29991
- Processing of auditory information by medial superior-olivary neurons. 14 p1715 A73-30281
- Binaural signal detection - Equalization and cancellation theory. 14 p1716 A73-30284
- Evoked negative electrical potentials due to auditory zone stimulation by local cooling, mechanical trauma and potential recording, observing reaction regeneration variations 15 p1833 A73-31159
- Functional characteristics of different neurons in the auditory cortex 19 p2395 A73-37940
- Effect of the stimulation of nonspecific thalamic nuclei on spontaneous and evoked spindles in the auditory cortex 22 p2802 A73-41958
- Estimate of integrative cerebral activity using an orientation response example 22 p2807 A73-42651
- Analysis of the changes in glial cell numbers in the auditory cortex during the application of acoustic stimuli of various intensities 22 p2807 A73-42653
- Experimental substantiation of the optimal method for scaling the duration of acoustic stimuli 22 p2814 A73-42654
- Action of stable and pulsed noise on the processes of skeletal muscle excitation 22 p2815 A73-42662
- Reaction time to changes in the tempo of acoustic pulse trains. 22 p2816 A73-42705

AUDITORY TASKS

Auditory rail task for acoustic stimuli effects on human equilibrium under axisymmetric intermittent tone exposure, discussing acoustic energy effect on vestibular receptors

03 p0260 A73-13551

EEG alterations by short time stress due to delayed speech feedback during reading, noting alpha and beta wave changes

03 p0265 A73-14473

Effects of 24-hour sleep deprivation on rate of decrement in a 10-minute auditory reaction time task.

04 p0411 A73-15220

Human performance measures relationship determination across sense modes under visual, auditory and combined stimulus conditions by controlling for task difficulty on individual basis

06 p0658 A73-18244

Comparison of human operator critical tracking task performance with aural and visual displays.

08 p0936 A73-21667

A comparison of visual, auditory, and cutaneous tracking displays when divided attention is required to a cross-adaptive loading task.

15 p1839 A73-32395

Reaction time to changes in the tempo of acoustic pulse trains.

22 p2816 A73-42705

Keeping track of sequential events - Implications for the design of displays.

23 p2948 A73-43215

AUGER EFFECT

Elemental analysis of a friction and wear surface during sliding using Auger spectroscopy.

01 p0057 A73-11277

The adsorption and decomposition of CO on Pt(111).

08 p0937 A73-21617

Atomic L2 and L3 vacancy states absolute width from photoelectron spectroscopy, investigating discontinuities, Auger intensity ratio and Coster-Kronig transition probability

13 p1662 A73-28189

The influence of Auger recombination on the forward characteristic of semiconductor power rectifiers at high current densities.

15 p1850 A73-31130

A study of the adsorption of oxygen on Ni(111) using Auger electron spectroscopy - Chemical shifts and valence spectra.

15 p1840 A73-31968

Auger spectroscopy usefulness demonstration by determination of impurity segregation in localized regions, reviewing grain boundary segregation role in metal properties deterioration

15 p1892 A73-32248

A new technique for Auger analysis of surface species subject to electron-induced desorption.

17 p2175 A73-35757

Oxidation of titanium between 25 C and 400 C.

19 p2442 A73-37950

Combined Auger electron spectroscopy and electron impact desorption studies of silicon surfaces.

20 p2595 A73-39665

Theory of donor-acceptor radiative and Auger recombination in simple semiconductors.

23 p3016 A73-43796

AUGMENTATION

NT THRUST AUGMENTATION

AURORAL ABSORPTION

Observations of simultaneous auroral D and E layers with incoherent scatter radar.

01 p0043 A73-10998

Rapid injection of energetic particles into the gap between the inner and outer radiation belts

08 p0998 A73-21300

Auroral absorption and magnetospheric plasma dynamics pattern from arctic stations atmospheric opacity data

10 p1212 A73-24220

Latitudinal and longitudinal auroral radio wave absorption in Arctic during IQSY, noting comparison with geomagnetic field disturbances

11 p1350 A73-25086

Anomalous absorption of cosmic radio emission in the auroral zone during the IQSY

11 p1411 A73-25087

Occurrence of IPDP events accompanied by cosmic noise absorption in the course of proton aurora substorms.

18 p2312 A73-36298

Fast injection of energetic particles into the gap between the inner and outer radiation belts.

19 p2476 A73-37929

A comparison of the latitudinal variation of auroral absorption at different longitudes.

21 p2684 A73-40785

Short-wave propagation along several paths during auroral storm periods

24 p3067 A73-44796

AURORAL ACTIVITY

U AURORAS

AURORAL ARCS

NT RED ARCS

Electron intensity measurements by sounding rockets over auroral arcs at magnetospheric plasma boundary

03 p0362 A73-13865

Relationship between pi2 geomagnetic pulsations and processes in the auroral zone

06 p0689 A73-17542

Electron intensities over auroral arcs from rocket flight, noting electron phase-space density increase with northward progress

09 p1078 A73-22833

Relationship of southward-drifting auroral arcs to the magnetospheric electric field and substorm activity.

10 p1213 A73-24734

Simultaneous occurrences of hydrogen arcs and mid-latitude stable auroral red arcs.

10 p1214 A73-24740

Auroral arcs oval configuration by all-sky photography from Arctica 2, considering difference in dayside and nightside halves from electron precipitation observations

10 p1214 A73-24745

Energy spectra and pitch angle distributions of precipitating incident and backscattered electron fluxes in auroral arcs

14 p1747 A73-29968

Relationship between the parameters of geomagnetic Pi2 pulsations and processes in the auroral zone.

16 p2001 A73-32766

An example of anticorrelation of auroral particles and electric fields.

18 p2312 A73-36297

Auroral arc mechanism of solar wind intrusion and electron and proton energization and precipitation in magnetosphere from Isis photometric and spectrometric observations

20 p2553 A73-39124

Current flow in auroral loops and surges inferred from ground-based magnetic observations.

22 p2902 A73-41917

Critique of Lukina theory of number of auroral arc orientations related to characteristic precipitation zone

24 p3084 A73-44799

AURORAL ECHOES

Spaced radar observation of auroral scattering cross sections, noting radar backscattering intensity peak and echo detection probability relationship to aspect angles

08 p0957 A73-20661

Radio aurora, storm sudden commencements, and hydromagnetic waves.

18 p2313 A73-36646

VHF radar aurora echo Doppler spectral properties, discussing electron density irregularities, echo power spectra, drift velocity, two stream instability and convection hypothesis

20 p2553 A73-38962

AURORAL ELECTROJETS

On the types of current patterns of weak geomagnetic disturbances at the polar caps.

02 p0158 A73-11915

On the distinction between the auroral electrojet and partial ring current systems.

04 p0444 A73-15550

Relationships between the equatorial electrojet and polar magnetic variations.

07 p0818 A73-19662

Relationship of magnetospheric substorms on the ground and in the distant magnetotail.

08 p0961 A73-21392

Measurement of auroral Birkeland currents and energetic particle fluxes.

09 p1073 A73-22057

Longitudinal magnetospheric currents contribution to auroral electrojet from satellite observation data, noting magnetosphere electric field excitation of meridional Pedersen and Hall currents

12 p1493 A73-27650

Gyrotropic flat ionosphere model with elliptical nonuniform conductivity for electrojet generation by magnetosphere current entering and leaving auroral zone

15 p1872 A73-31895

An instrument for real-time determination of polar electrojet position and current parameters.

17 p2176 A73-35768

X-ray bremsstrahlung at subauroral latitudes

18 p2345 A73-36111

Thermospheric density variations associated with auroral electrojet activity.

18 p2312 A73-36280

Radio auroral measurements near an auroral electrojet.

20 p2550 A73-38862

Diurnal and seasonal variations of neutral winds and electric fields above 90 km in the vicinity of the auroral electrojet.

21 p2690 A73-41365

Bremsstrahlung X ray measurements over subauroral latitudes during substorms, noting e folding energy correlated with local electrojet and anticorrelated with conjugate electrojet

21 p2760 A73-41366

Magnetotail plasma flow observation with Vela 4A oriented perpendicular to ecliptic plane, considering plasma sheet recovery relation to auroral electrojet poleward shift

22 p2844 A73-41907

Response of the polar electrojets in the evening sector to polar magnetic substorms.

22 p2902 A73-41916

Current flow in auroral loops and surges inferred from ground-based magnetic observations.

22 p2902 A73-41917

AURORAL EMISSION

U AURORAS

U LIGHT EMISSION

AURORAL IONIZATION

Auroral sporadic E layer diurnal distribution correlation to charged particle integral flux diurnal variations observed by satellite in winter, noting Kp index effect

07 p0816 A73-19455

Collision cross sections for electrons with atmospheric species.

08 p0957 A73-20659

Auroral He precipitation flux and charge state measurements for auroral ions source location by comparison with ionospheric and solar wind ion abundances

10 p1215 A73-24783

Time dependent studies of the aurora. I - Ion density and composition.

12 p1492 A73-27601

Damping of a discharge in crossed fields - Application to the ionosphere in the auroral zone

13 p1611 A73-29562

Experimental test to determine the origin of geomagnetically trapped radiation.

22 p2846 A73-41944

Auroral electron and proton flux density, energy spectra, acceleration and precipitation mechanisms and turbulent diffusion from rocket and satellite measurements

22 p2850 A73-42748

AURORAL IRRADIATION

Auroral flux enhancements due to solar proton injection at medium energies during flares from ESRO 2 satellite measurements

03 p0362 A73-13859

Auroral He 4 precipitation flux measurements by exposed metal foils recovered from rocket flights

04 p0443 A73-15534

Heating of the upper atmosphere during aurorae and auroral rays length.

08 p0957 A73-20663

AURORAL SPECTROSCOPY

Auroral oval spectral features as basis for particle precipitation and energy deposition determination

10 p1215 A73-24782

Upper atmospheric temperatures from Doppler line widths. V - Auroral electron energy spectra and fluxes deduced from the 5577 and 6300 A atomic oxygen emissions.

12 p1492 A73-27605

Low energy electron fluxes and spectra correlation with auroral forms from weather satellite electrostatic measurements

18 p2304 A73-35964

X-ray bremsstrahlung at subauroral latitudes

18 p2345 A73-36111

Time dependent studies of the aurora. II - Spectroscopic morphology.

18 p2311 A73-36185

VHF radar aurora echo Doppler spectral properties, discussing electron density irregularities, echo power spectra, drift velocity, two stream instability and convection hypothesis

20 p2553 A73-38962

AURORAL TEMPERATURE

Auroral atmosphere temperature variations relation to nightly auroral streamer length variations, assuming ionospheric current dissipation as heat source

12 p1491 A73-27344

Auroral heating and the composition of the neutral atmosphere.

12 p1492 A73-27602

Auroral atmosphere temperature variations relation to nightly auroral streamer length variations, assuming ionospheric current dissipation as heat source

23 p2970 A73-43241

AURORAL ZONES

Angular distributions of auroral electrons in the energy range 0.8 to 16 keV.

02 p0155 A73-11734

Auroral X-ray and conjugate ionospheric absorption observations of an electron precipitation event accompanying a sudden impulse in the geomagnetic field.

02 p0157 A73-11759

A possible method for estimating any indirect process in the production of the O/IS atoms in aurora.

02 p0157 A73-11902

Atomic oxygen concentration from the forbidden OI 5577 A line emission at the auroral zone latitude.

02 p0158 A73-11916

Rocket sounding of ionospheric electron density and temperature profiles during moderate auroral

event, noting field-aligned motion of irregularities in F region
02 p0163 A73-12309

Proton energy spectra from recent rocket measurements in the night and morning time auroral zone.
02 p0206 A73-12315

Low energy auroral electron and proton precipitation patterns from polar orbiting ESRO 1A satellite, noting discontinuities, flux distribution valleys, latitudinal crossover and Kp dependence
03 p0362 A73-13864

Plasma drifts in the auroral ionosphere derived from barium releases.
03 p0303 A73-13876

Geomagnetic tail plasma sheet thinning and auroral zone negative bays development during magnetospheric substorms, suggesting auroral particles acceleration along magnetic field lines
03 p0304 A73-13887

Local time variations of X ray substorm activity observed at auroral zone station, including atmospheric passage and energy spectrum measurements
03 p0363 A73-13889

Auroral-zone X-ray measurements at Kiruna in 1970.
04 p0492 A73-15100

Relationship between pi2 geomagnetic pulsations and processes in the auroral zone
06 p0689 A73-17542

Characteristics of spectra of pi2-type geomagnetic pulsations along the meridional profile
06 p0689 A73-17543

Observed relationships between electric fields and auroral particle precipitation.
07 p0814 A73-19237

Variation of atmospheric electric field during aurora.
07 p0820 A73-20216

Auroral particle influx behavior and electric field aligned electron precipitation observation by Ba release and electrostatic probe in rocket and satellite experiments
08 p0957 A73-20662

Aurora and the poleward edge of the main ionospheric trough.
09 p1073 A73-22058

Balloon observations of auroral-zone X-rays in conjugate regions.
09 p1137 A73-22135

Nighttime electron density in the E region at auroral latitudes in sunspot maximum.
09 p1078 A73-22747

Field-aligned currents between 400 and 3000 km in auroral and polar latitudes.
09 p1078 A73-22834

Ionospheric and plasma sheet particle densities, fluxes and bulk velocities along auroral magnetic field line for collisionless ion-exosphere model
09 p1079 A73-22842

Results of volley flights of radio probes on the Kolsk peninsula during periods of magnetic disturbances in March and April 1971
10 p1267 A73-23929

Effects of interplanetary magnetic sector structure on auroral zone and polar cap magnetic activity.
10 p1213 A73-24730

Auroral arcs oval configuration by all-sky photography from Arctica 2, considering difference in daytime and nighttime halves from electron precipitation observations
10 p1214 A73-24745

Results of an investigation of the ionospheric effect of a sudden commencement of a magnetic storm
11 p1351 A73-25097

On the morphology of auroral-zone X-ray events. II - Events during the early morning hours.
11 p1354 A73-25762

On the morphology of auroral-zone X-ray events. III - Large-scale observations in the midnight-to-morning sector.
11 p1354 A73-25763

Some effects of magnetospheric acceleration mechanisms on variations in ultraviolet intensity height profiles, and on consequent rocket spectrograph sensitivities.
11 p1358 A73-26703

Total electron content measurements during visible auroras.
11 p1359 A73-26714

Enhancements of ionospheric total electron content in the southern auroral zone associated with magnetospheric substorms.
11 p1359 A73-26715

Conjugate asymmetries in sudden commencement absorption and the sudden commencement absorption event of February 28, 1969.
12 p1534 A73-26982

Low energy auroral electron pitch angle diffusion in postbreakup aurora due to injected particle loss in closed magnetic field lines
12 p1488 A73-26987

Distributions and characteristics of high-latitude field-aligned electron precipitation.
12 p1534 A73-26988

Observations of narrow microburst trains in the geomagnetic storm of August 4-6, 1972.
12 p1490 A73-27007

Midday aurora behavior during auroral substorms from all sky photographs at south pole, considering modification of Starkov-Feldstein model
12 p1493 A73-27614

Observation and first evaluation of geomagnetic pulsations near the polar aurora zone in connection with the occurrence of si's and ssc's
12 p1494 A73-27778

Study of the directional distribution of energetic electrons and protons in the morning sector of the auroral zone during enhanced particle flux
13 p1606 A73-28153

Damping of a discharge in crossed fields - Application to the ionosphere in the auroral zone
13 p1611 A73-29562

Electric field and plasma density oscillations due to the high-frequency Hall current two-stream instability in the auroral E region.
14 p1748 A73-29971

Andoya Rocket Range facilities in northern Norway, discussing rocket launching for auroral research
14 p1741 A73-30082

Electron current estimation along auroral zone-plasma neutral sheet field line from steady state one dimensional model
15 p1866 A73-31065

An observation of polar auroral and airglow from the ISIS-II spacecraft.
15 p1866 A73-31071

Diffuse auroral belt observation by Isis-2 scanning auroral photometer verified by analysis of ground based all sky photographs
15 p1866 A73-31074

Relationship between the parameters of geomagnetic Pi2 pulsations and processes in the auroral zone.
16 p2001 A73-32766

Properties of geomagnetic Pi2 pulsation spectra along a meridional profile.
16 p2001 A73-32767

Observations of the auroral oval and a westward traveling surge from the Isis 2 satellite and the Alaskan meridian all-sky cameras.
16 p2004 A73-33445

Radio aurora occurrence data from statistical data on radio echo occurrence, comparing radio zone to optical auroral belts
16 p2009 A73-33893

Photometric investigation of the 4278 A and 5577 A emissions in aurora.
16 p2010 A73-33918

Convection dominated electrons in auroral zone, discussing plasma sheet as magnetospheric electron source, convection electron spatial distribution and convection-precipitation coupling
17 p2223 A73-34358

Balmer-line emission from auroral protons.
17 p2213 A73-34766

Large-scale auroral-zone electron precipitation event, briefly interrupted during a negative magnetic impulse.
18 p2344 A73-35951

Equatorial and auroral zone geomagnetic indices and micropulsations variations relation to 11-18keV protons occurrence in interplanetary space
18 p2345 A73-36120

Auroral ion velocity distributions using a relaxation model.
18 p2311 A73-36178

Thermospheric density variations associated with auroral electrojet activity.
18 p2312 A73-36280

F-layer and 6300-A measurements in the day sector of the auroral oval.
18 p2312 A73-36281

Ionospheric magnetic field measurements at auroral latitudes.
18 p2313 A73-36647

Space-time distribution of Es formations associated with visible auroral forms.
19 p2424 A73-37912

Laboratory studies of collisions of energetic H+ and hydrogen with atmospheric constituents.
21 p2679 A73-40072

The aurora oval in the region of influx of electrons into the earth's atmosphere
21 p2686 A73-40919

Rocket observations of electron precipitation in a westward-traveling surge.
22 p2902 A73-41915

Electron precipitation caused auroral zone bremsstrahlung X rays classification with respect to magnetic storm phases
22 p2851 A73-42750

Two types of radio emission from the auroral ionosphere and ionospheric disturbances
24 p3083 A73-44798

Critique of Lukina theory of number of auroral arc orientations related to characteristic precipitation zone
24 p3084 A73-44799

Influence of the conductivity of the ionosphere on the pulsations of DP1 and DP2 current systems
24 p3084 A73-44806

Ionospheric electric field measurements with a spin stabilized detector.
24 p3090 A73-44818

Energy deposition of protons in molecular nitrogen and applications to proton auroral phenomena.
24 p3126 A73-45116

Electric field observations by incoherent scatter radar in the auroral zone.
24 p3085 A73-45117

Triaxial magnetic measurements of field-aligned currents at 800 kilometers in the auroral region - Initial results.
24 p3087 A73-45140

ESRO 1/Aurora/ satellite observations of aurora, magnetosphere-ionosphere interaction at high latitudes and auroral particle flux density
24 p3087 A73-45207

AURORAS

NT AURORAL ARCS

NT RADIO AURORAS

NT RED ARCS

Oxygen emission volume rate in auroras due to direct electron impact excitation, obtaining integral cross sections and quenching rates
01 p0036 A73-10336

The IR emission spectrum of N2 excited under auroral conditions.
01 p0036 A73-10337

Variations of the auroral electron energy spectra during substorms.
01 p0036 A73-10339

Precipitation patterns in the Arctic ionosphere determined from airborne observations.
01 p0036 A73-10341

Multidiscipline study of perturbations observed on March 8, 1970 in the midnight sector
01 p0036 A73-10343

Rocket measurements of low energy electrons and optical emissions in the dayglow and aurora.
01 p0036 A73-10346

Quiet time magnetosphere-thermosphere couplings, describing global wind system model and convection and auroral Joule heating
02 p0162 A73-12292

Auroral particle precipitation patterns from satellite observations, discussing electron and proton penetration from magnetosheath plasma and magnetotail
02 p0163 A73-12308

Cross spectral analysis for auroral pulsations coherency in spatially separated patches, noting TV image recording of frequency and energy spectra
03 p0298 A73-12879

A dual wavelength ground-based auroral scanner.
03 p0299 A73-12888

A short description of the ESRO-IV satellite.
03 p0381 A73-13274

Precipitation of auroral and ring current particles by artificial plasma injection.
03 p0301 A73-13711

Auroral precipitating electron angular distributions from polar orbiting satellite OV1-18 measurements, indicating pitch-angle diffusion due to particle-wave interactions
03 p0363 A73-13868

Airborne photometric measurements of auroral emissions, indicating soft zone and superimposed energetic electron precipitation
03 p0363 A73-13870

Acceleration of auroral particles by electric double layers.
03 p0303 A73-13877

Ground based goniometric observations of medium and high latitude VLF emissions due to transverse resonance instability and auroral oval Cerenkov radiation from magnetosheath
03 p0276 A73-13884

Electron excitation and auroral emission parameters.
04 p0440 A73-14959

Ion velocity distributions in the auroral ionosphere.
04 p0440 A73-14966

Auroral and magnetospheric phenomena caused by solar wind particles entry and energization via magnetosheath into magnetosphere and upper atmosphere
04 p0492 A73-15331

Two substorm studies of relations between westward electric fields in the outer plasmasphere, auroral activity, and geomagnetic perturbations.
04 p0444 A73-15545

Long term German observations of auroral activity compared to other midlatitude observations
04 p0445 A73-15551

Irregular auroral pulsation commencement and termination times from photometric recordings compared with geomagnetic micropulsations
06 p0690 A73-17557

Dependence of the length of polar rays on the auroral activity level
06 p0690 A73-17558

Auroral electron spectrum space-time dynamics during magnetospheric substorms, using X ray bremsstrahlung balloon data

07 p0815 A73-19437

Magnetosphere tail internal plasma boundary layer dynamics during substorms based on aurora data

07 p0816 A73-19463

Mid-latitude winter anomalies in radio absorption and stratospheric temperature distribution - Observations concerning the influence of auroral and magnetic activity.

07 p0819 A73-20058

Ionograms for slant sporadic E layer under continuous sunlight inside polar cap, noting occurrence probability and auroral activity

07 p0819 A73-20065

Spatial-temporal distribution of E/s formations associated with visible forms of polar aurorae

08 p0958 A73-21283

Modulation of auroral electron fluxes and the geomagnetic pulsations during the storm of March 8, 1970

08 p0959 A73-21291

Differences in auroral intensity at conjugate points.

09 p1074 A73-22059

Bremsstrahlung X-rays in the stratosphere and auroral activity on January 21 and February 3, 1969.

10 p1268 A73-24224

Earth magnetosphere pinch effect related to geomagnetic field pulsations and polar aurora luminosity fluctuations

10 p1212 A73-24228

Auroral He precipitation flux and charge state measurements for auroral ions source location by comparison with ionospheric and solar wind ion abundances

10 p1215 A73-24783

The day-sector polar F-layer during a magnetospheric substorm.

11 p1356 A73-25918

Pi 2 micropulsation period and frequency correlation coefficients for planetary magnetic activity Kp index and magnitude of accompanying auroral bay

11 p1357 A73-25930

Correlation between pulsations in auroral luminosity variations and X-rays.

11 p1359 A73-26710

VHF Doppler spectra of radar echoes associated with a visual auroral form - Observations and implications.

12 p1468 A73-26996

Complex studies of the disturbance of March 8, 1970 from observations in the midnight sector

12 p1490 A73-27342

Dayside polar aurorae during various substorm phases from IGY data, noting time of glow intensity maximum

12 p1490 A73-27343

Auroral atmosphere temperature variations relation to nightly auroral streamer length variations, assuming ionospheric current dissipation as heat source

12 p1491 A73-27344

Auroras induced attenuation fluctuations of VLF atmospherics associated with remote tropical thunderstorms

12 p1522 A73-27786

On the longitudinal extension of electron precipitation during magnetospheric substorms.

13 p1606 A73-28152

Conventional filter photometer onboard Explorer satellite for 3000-7500 A airglow and auroral thermospheric emission features monitoring

13 p1688 A73-28639

Rayed auroral structures and their relation to the drift current instability in a plasma blob.

13 p1607 A73-28705

Nature of auroral emission intensity pulsations associated with geomagnetic pulsations of the Pi2 type.

13 p1607 A73-28706

Auroral electrons of energy less than 1 keV observed at rocket altitudes.

14 p1748 A73-29969

Split Langmuir probe measurements of current density and electric fields in an aurora.

14 p1748 A73-29970

Spatial separation of 3914- and 3160-A emissions of nitrogen in an aurora.

14 p1749 A73-29987

Magnetospheric dayside cusp - A topside view of its 6300-angstrom atomic oxygen emission.

14 p1750 A73-30620

A uniform belt of diffuse auroral emission seen by the ISIS-2 scanning photometer.

15 p1866 A73-31069

The excitation of atomic oxygen to the O(1 S) level by energy transfer from N2/A 3 Sigma u+ molecules in aurora.

15 p1866 A73-31075

ISIS-2 observations of auroral emissions characteristics in polar region during December 1971 magnetic storm recovery phase

15 p1866 A73-31076

Zonal nature of some micropulsation disturbances at the geomagnetic pole

15 p1872 A73-31897

Instabilities in charge sheets and current sheets and their possible occurrence in the aurora.

15 p1873 A73-32235

Irregular auroral pulsation commencement and termination times from photometric recordings compared with geomagnetic micropulsations

16 p2002 A73-32781

Dependence of the length of auroral rays on auroral activity level.

16 p2002 A73-32782

Manifestations and causes of atmospheric optical phenomena related to solar light dispersion and diffraction by particles, noting halos, polar auroras and mirages

16 p2002 A73-32949

Electron precipitation patterns and substorm morphology.

16 p2056 A73-33434

Red auroras in the morning sector.

16 p2004 A73-33446

Russian monograph on polar auroras and magnetospheric geomagnetic disturbances from rocket, balloon and ground station soundings covering magnetic storms, solar wind and geoelectric fields

18 p2302 A73-35873

North polar aurora oval detection by high frequency sounder radar aided by all sky photography and statistical auroral data, discussing backscatter and auroral echoes

18 p2312 A73-36282

Spatially forbidden regions in the aurora.

18 p2313 A73-36648

ISIS-II scanning auroral photometer.

19 p2428 A73-37256

Space-time distribution of Es formations associated with visible auroral forms.

19 p2424 A73-37912

Modulation of auroral electron fluxes and geomagnetic pulsations during the storm of March 8, 1970.

19 p2424 A73-37920

Rocket measurements of electric field and optical aurora during weak PCA event, noting rocket passage through discrete auroral forms

21 p2684 A73-40781

An attempt to explain satellite observations of high latitude VLF hiss in terms of generation by incoherent Cerenkov radiation.

21 p2685 A73-40828

Waves and tides and their observation from ground and space.

21 p2689 A73-41356

Dayside polar aurorae during various substorm phases from IGY data, noting time of glow intensity maximum

23 p2970 A73-43240

Auroral atmosphere temperature variations relation to nightly auroral streamer length variations, assuming ionospheric current dissipation as heat source

23 p2970 A73-43241

Correlation between the excitation of pi 1 and pc 1 geomagnetic pulsations and magnetospheric substorms

24 p3084 A73-44811

Simultaneous observations of auroras from the South Pole Station and of precipitating electrons by Isis I.

24 p3126 A73-45115

Simultaneous growth of high-latitude positive bay and DR-field in the course of proton aurora substorm.

24 p3127 A73-45215

AUSFORMING

Warm forging of steels for increased precision and mechanical properties.

03 p0323 A73-13269

AUSTENITE

The effect of reverted austenite on the mechanical properties and toughness of 12 Ni and 18 Ni/200/ maraging steels.

02 p0183 A73-12758

Boron segregation at austenite grain boundary and matrix sites in steel by autoradiography

02 p0183 A73-12761

Titanium nitrides effect on austenite grains formation by high temperature fusion, considering electric arc and vacuum melting of structural steels

06 p0706 A73-17883

Structural and phase transformations in silicon steels during heat treatment

06 p0707 A73-18035

The distribution of chromium between ferrite and austenite and the thermodynamics of the alpha/gamma equilibrium in the Fe-Cr and Fe-Mn systems.

06 p0712 A73-18759

High strength and plastic properties of two phase austenitic-martensitic Fe alloys after aging in alpha and gamma states

07 p0841 A73-20522

The effect of a dispersed phase on the creep properties of a Cr-Ni steel.

08 p0980 A73-21779

Austenitic alloys internal friction and strain aging under quenching, cold working and electron irradiation, considering carbon vacancies stress induced reorientation effects

09 p1101 A73-22407

Kinetics of transformation of carbon- and nitrogen-enriched austenite by carbonitriding in the gas phase

09 p1105 A73-23038

Correlation of coercive force to microstructure in cyclic martensite/austenite transformations in an Fe-Ni-Co alloy.

10 p1234 A73-24438

Alloy steels supercooled austenite nitriding in ammonia flow, examining diffusion layers by X ray analysis and hardness tests

10 p1236 A73-24956

Stabilization of the austenitic phase of iron-nickel base alloys by cumulative thermal cycling

11 p1379 A73-25323

Strength and ductility of two-phase iron alloy composed of austenite and martensite.

13 p1638 A73-29453

Effect of tensile deformation in the austenite range on transformation kinetics of a high-strength low-alloy /HSLA/ steel.

14 p1762 A73-30641

Austenitic grain structure and strength changes associated with aging in 14Cr-14Ni type steels

18 p2325 A73-36810

Effect of austenizing temperature on the properties of Kh5Ni2M3Ti steel

21 p2718 A73-40738

AUSTENITIC STAINLESS STEELS

Characteristics of the formation of austenite during rapid heating of cold-worked KVK-42 /42Kh2NGSM/ steel

01 p0062 A73-10260

Sinterability of stainless steel powders.

01 p0065 A73-10813

Corrosion behavior of sintered stainless steels.

01 p0065 A73-10815

Nitrided layer effects on austenitic steels mechanical properties at low temperatures, noting improved tensile strength

01 p0067 A73-11347

Austenite deformation effect on thermal stability and hardness of Ni steels at various C and Ni concentrations

01 p0067 A73-11349

The influence of preliminary thermocycling on the high-temperature strength of austenitic steel.

02 p0180 A73-12139

The relation between creep at room temperature and the characteristics of the stress-strain diagram in the case of metallic materials

02 p0181 A73-12366

Performance of an inhibitor-protector of steel against corrosion-fatigue failure at elevated temperatures and pressures.

02 p0182 A73-12700

Microstructure and microsegregation effects in the intergranular corrosion of austenitic stainless steel.

02 p0183 A73-12765

The effect of prior deformation on the strength and annealing of reverted austenite.

02 p0183 A73-12766

The solidification sequence in an 18-8 stainless steel, investigated by directional solidification.

02 p0184 A73-12769

Martensitic transformation kinetics and martensite morphology in the N25KhT2 alloy after aging

03 p0325 A73-13826

Increasing the heat resistance of steel Kh14G14N3T with microadditions of boron.

03 p0327 A73-14006

Flat dendritic carbide effects on crack formation in Ti and Nb stabilized austenitic Cr-Ni corrosion resistant steels after heating to 1250 C

06 p0705 A73-17850

Stability of the dislocation structure in cold-deformed Kh18Ni12T and Kh16Ni9M2 steels during high-temperature aging

06 p0707 A73-17905

Regeneration and recrystallization of austenite in low-carbon stainless steel 18-10 after rolling at room temperature

07 p0837 A73-19113

Behavior of austenitic stainless steels under continuous or repeated strain

07 p0838 A73-19115

Metallographic investigation and notch, tensile and hardness tests for electrosag welding of austenitic stainless steels

07 p0831 A73-19949

Alloy composition and temperature effects on nitrogen solubility in austenitic Cr-Ni steels, noting nitride precipitation effect on impact strength reduction

07 p0839 A73-19950

Calibration procedure for instruments to measure the delta ferrite content of austenitic stainless steel weld metal.

07 p0832 A73-20272

Composition of anolyte within pit anode of austenitic stainless steels in chloride solution.

07 p0840 A73-20352

Temperature dependent pitting corrosion tests of Mo containing austenitic stainless steels

07 p0840 A73-20354

Prediction of the low-temperature stability of type 304 stainless steel from a room temperature deformation test. 07 p0840 A73-20414

Investigation of the structural changes in austenite during martensitic transformation in steels with high stacking-fault energy 07 p0841 A73-20521

Mechanisms of transient and steady state creep in a gamma-prime hardened austenitic steel. 08 p0980 A73-21778

The effect of niobium content on the steady-state creep of stabilized 20/25 austenitic stainless steels. 08 p0981 A73-21786

The effect of creep strain on stacking-fault precipitation in Nb-stabilized 20/25 austenitic stainless steels. 08 p0981 A73-21787

Stress varied creep of 20Cr-25Ni-Nb stabilised austenitic stainless steel. 08 p0981 A73-21788

Low stress creep tests of niobium stabilized austenitic steels. 08 p0981 A73-21789

The effect of niobium carbide on the creep rupture properties of austenitic stainless steels. 08 p0981 A73-21790

The ageing and creep behaviour of a Cr-Ni-Mn austenitic steel. 08 p0981 A73-21791

The creep strength of 17 Cr-11 Ni-2.5 Mo austenitic steel stabilised by titanium. 08 p0982 A73-21792

Irradiation creep in some austenitic stainless steels, nimonic PE16 alloy and nickel. 08 p0982 A73-21794

Influence of hot rolling on the mechanical properties of unstable austenitic chromium-manganese steels. 09 p1098 A73-21848

Transmission electron microscope study on initiation of fatigue crack in 18-8 austenitic steel. 09 p1104 A73-22523

Useful penetration in an austenitic stainless steel, of electrons accelerated under a very high voltage /1500 to 2500 kv/. 09 p1105 A73-23037

An electrochemical testing method for stress corrosion cracking by separating crack anode from cathode. 09 p1106 A73-23168

Austenite stabilization in Kh17N6M3 transition-type steel 09 p1107 A73-23201

Effects of composition on embrittlement of austenitic stainless steels. 10 p1230 A73-23628

Grain-boundary corrosion of type 304 stainless steel by cesium oxides. 10 p1234 A73-24427

Austenitic stainless steels diffusion layer formation and structure by gaseous chlorization with FeAl-ammonium chloride powder mixture, describing elements redistribution 10 p1226 A73-24958

Fatigue-crack growth in Type 304 stainless steel weldments at elevated temperatures. 11 p1379 A73-25131

Dynamic potential method of estimating the susceptibility of corrosion-resistant steels to intercrystalline corrosion 11 p1364 A73-26112

Effect of high dislocation density on stress corrosion cracking and hydrogen embrittlement of type 304L stainless steel. 11 p1385 A73-26174

On the study of the intergranular corrosion of a stainless steel with the help of twin crystals 11 p1385 A73-26297

Crack propagation behavior in type 304 stainless steel weldments at elevated temperature. 11 p1375 A73-26357

Influence of impact deformation on the strengthening and aging kinetics of austenitic steel 4Kh12N8G8MFB 12 p1510 A73-26901

Austenitic steel dislocation density, X ray interference width and hardness changes due to intensified crystal fragmentation from biaxial elongation under tension 12 p1512 A73-27246

Structural evolution of an austenitic-ferritic stainless steel by keeping it between 600 and 1150 C. 12 p1514 A73-27986

Austenite stabilization during inverse transformation in Cr-Co-Mo and Cr-Ni-Co-Mo steels 13 p1630 A73-28012

Substructure alteration in manganese and nickel austenitic alloys under the action of microimpacts 13 p1630 A73-28013

Austenitic stainless steels at cryogenic temperatures. I - Structural stability and magnetic properties. 13 p1636 A73-29070

Fatigue crack initiation and propagation in low stacking fault energy austenite steel related to plastic

deformation induced gamma alpha transformation and martensite failure 13 p1640 A73-29481

Effect of temperature and strain rate on the high temperature, low cycle fatigue behaviour of a 17Cr-10Ni-2Mo stainless steel. 13 p1708 A73-29504

Development of austenitic heat-resistant steel containing a high concentration of nitrogen. 13 p1642 A73-29516

Effects of small amounts of carbide-forming elements on the elevated temperature strength of austenitic stainless steel. 13 p1642 A73-29517

Study on material for investment cast turbine wheel. 13 p1642 A73-29518

Transgranular stress corrosion cracking of austenitic stainless steels - A single crystal study. 13 p1642 A73-29520

An X-ray study of the stress corrosion of austenitic stainless steels. 13 p1625 A73-29521

An X-ray study of hydrogen induced phenomena affecting mechanical behaviours of austenitic stainless steels. 13 p1625 A73-29522

Study on stress corrosion cracking of austenitic stainless steel under pulsating load. 13 p1642 A73-29523

The effect of elevated temperature upon the fatigue-crack propagation behavior of two austenitic stainless steels. 13 p1642 A73-29525

Structure stability of austenitic chromium-nickel steels at the temperature of liquid helium 14 p1760 A73-30420

Stability of the thermomechanical hardening effect in 60N20 nickel steel 14 p1760 A73-30590

Effects of some carbide stabilizing elements on creep-rupture strength and microstructural changes of 18-10 austenitic steel. 14 p1761 A73-30627

Fatigue crack propagation in martensitic and austenitic steels. 14 p1761 A73-30632

Kinetics of gamma-prime phase precipitation in steel N36T21u2 15 p1887 A73-31322

Strengthening of chromium-nickel steels with unstable austenite 15 p1889 A73-31809

Notched austenitic stainless steel stress corrosion cracking tests in boiling magnesium chloride solutions, obtaining relationship between maximum stress and strain rate in graph 15 p1895 A73-32569

Study on stress corrosion cracking of austenitic stainless steel under pulsating load. 15 p1895 A73-32570

Scanning electron microscopic observation of fracture surfaces of austenitic stainless steels in stress corrosion cracking. 16 p2025 A73-33021

Durability of the Kh18N10T steel under the combined influence of creep and thermal cycling 17 p2187 A73-34335

Characteristics of deformation texture development in austenitic steel in a plane stressed state 17 p2188 A73-34564

Ni-Fe-Cr alloy and austenitic stainless steel cyclic stress-strain behavior at 70-1400 F 16 p2323 A73-36586

Investigation of the impact toughness of construction materials at temperatures of 20 and 4.2 K 18 p2324 A73-36767

Influence of prolonged aging on the behavior of the microhardness and substructure of EI257 austenitic steel 18 p2324 A73-36806

Book - Elevated temperature properties as influenced by nitrogen additions to types 304 and 316 austenitic stainless steels. 18 p2325 A73-36971

The application of Armco 21-6-9 steel tubing to the DC-10 hydraulic system. 19 p2389 A73-37865

High-frequency fatigue tests at low temperatures 20 p2619 A73-39363

A photographic method for testing the impact strength of metals 21 p2696 A73-39991

Fine structure of an explosion-hardened chromium-nickel-manganese austenitic steel 21 p2718 A73-40484

Effect of mechanothermal treatment on the heat-resistant properties of 1Kh14N18V2B steel with boron additives 21 p2718 A73-40735

Effect of explosive impact on hardening and kinetics of aging of austenitic steel 4Kh12N8G8MFB. 21 p2720 A73-41034

Overload effects on subcritical crack growth in austenitic manganese steel. 22 p2875 A73-42138

Stress relaxation and mechanical equation of state in austenitic stainless steels. 22 p2878 A73-42578

Intergranular corrosion of iron-nickel-chromium alloys. 23 p2990 A73-43458

Influence of high hydrostatic pressure on the flow stress of 18-8 stainless steel. 23 p2994 A73-44161

Gamma to alpha transformation and notch depth effects on metastable austenitic steel impact strength at cryogenic temperatures 23 p2995 A73-44282

Strengthening of Cr-Ni steels with unstable austenite. 24 p3100 A73-45272

Martensitic transformations in Fe-Cr-Ni austenitic stainless steels - Relation between the parameters of the epsilon phase and the transformation mechanisms 24 p3101 A73-45522

Influence of boron on the precipitation of carbides in Fe-Ni-Cr austenitic matrices 24 p3101 A73-45523

Recrystallization and precipitation induced by high temperature deformation - Case of a weldable construction steel containing niobium 24 p3101 A73-45524

AUSTRIA

NT ALPS MOUNTAINS [EUROPE]

AUTOCATALYSIS

Branched-chain carbohydrate structures resulting from formaldehyde condensation. 15 p1842 A73-32550

Conditions for thermal explosion occurrence during branched-chain reactions 19 p2502 A73-37501

AUTOCCLAIVING

General purpose autoclave processable polyimide laminating resin selection, evaluating molding process techniques 03 p0329 A73-13004

AUTOCOLLIMATORS

U COLLIMATORS

AUTOCORRELATION

Iteration method for statistical treatment of measurements when information on measurement error characteristics is incomplete 02 p0219 A73-12455

Coherent signal from incoherent meteorological radar echoes for atmospheric turbulence intensity measurement, noting autocorrelation function for average frequency 03 p0338 A73-14531

Auto and cross correlation functions of combined binary pseudorandom sequences in digital space communication systems 04 p0423 A73-15916

Indeterminacy functions side maxima for phase manipulated signals with low sidelobe levels in autocorrelation functions, noting Doppler frequency shift effect 04 p0423 A73-15925

Application of structural-temporal functions for analysis of periodicities in atmospheric motions 05 p0593 A73-16240

Pulse and monochromatic short wave signals phase/amplitude autocorrelation functions and probability distributions during oblique incidence reflection from ionosphere 05 p0550 A73-16776

Evaluation of the noise autocorrelation function of stationary and moving noise sources by a cross correlation method. 05 p0598 A73-16925

Anomalous magnetic and gravitational field models autocorrelation function behavior dependence on circular cylindrical sources depth and spacing 07 p0816 A73-19447

Noise immunity of autocorrelated reception of singly phase-shift-keyed signals 07 p0794 A73-20298

Auto- and cross-correlations of diffuse objects for coherent optical data processing, using single lensless Fresnel hologram 08 p0963 A73-21036

Relation between object position and autocorrelation spots in the Vander Lugt filtering process. II - Influence of the volume nature of the photographic emulsion. 08 p0964 A73-21044

Autocorrelation function synthesis from arbitrary function on finite interval for case of random signals 08 p0951 A73-21102

Techniques for short-term predictions of atmospheric noise levels. 08 p0940 A73-21662

Measurements and graphs of turbulence autocorrelations in space and time. 09 p1071 A73-22332

The accuracy of an approximate representation of the correlation functions of complex signals distorted in the linear stages of a radio channel 09 p1051 A73-22461

Autocorrelation function for the 'rapid' light variations of the quasar 3C 273. 09 p1147 A73-22727

- Signal synthesis based on desired autocorrelation function for pulse shaping applications in radar and communications, discussing nonlinear equations solution by decomposition into source polynomials
10 p1187 A73-23730
- Second order approximation to autocorrelation matrix of random variable nonlinear transformation, discussing application to Poisson process and monopulse radar receiver AGC effects
11 p1333 A73-26695
- Log-intensity correlations of a laser beam in a turbulent medium.
14 p1757 A73-30162
- Nonlinear feedback systems and weakly stationary stochastic processes.
14 p1739 A73-30503
- Meteorological time series persistence tendency representation by autocorrelation coefficients, summation, determining independent values effective number by white noise bandpass filtering
15 p1906 A73-32344
- Iterative method for the statistical processing of measurements with incomplete information on the measurement error characteristics.
15 p1902 A73-32605
- Spectral moving frame representation of jet noise by far field acoustic pressure autocorrelation and density function
16 p2000 A73-33681
- Variability of eigenvectors and eigenvalues of correlation matrices for vertical temperature profiles.
18 p2334 A73-37062
- Noise immunity of autocorrelation reception of single PSK signals.
18 p2291 A73-37135
- Noise loading analysis of a memoryless nonlinearity characterized by a Taylor series of finite order.
21 p2656 A73-41147
- Autocorrelation and space-time correlations for probe separations aligned with mean flow to test Pielke-Panofsky hypothesis, comparing laboratory tests to atmospheric turbulence
21 p2733 A73-41575
- The investigation of the periodicity of hydrometeorological phenomena according to the autocorrelation method of Fuhrich
22 p2883 A73-42449
- A meteorological and a geophysical example of the use of the scale autocorrelation coefficient to determine ratios of frequencies present in periodic phenomena.
22 p2883 A73-42542
- Autocorrelation functions for meteorological scatterer velocity measurements in Doppler spectrum from linear, quadratic and logarithmic radar signal detectors
23 p2955 A73-44268
- AUTODYNES**
Sensitivity of optical autodyne quantum receiver in presence of output noise, using photomultiplier signal model
03 p0319 A73-14076
- AUTOGYRO**
Stowable deployable autogyro aircrew vehicle escape rotoseat /SAVER/ conversion to flight vehicle for advanced escape rescue capability (AERCAB/ from hostile areas
16 p1966 A73-32674
- AUTOIONIZATION**
Wave functions and energies of the autoionization states of the cesium atom
09 p1122 A73-21976
- Excitation of autoionization states of the cesium atom by electron impact
09 p1122 A73-21978
- Autoionizing transitions in N2 and H2 produced by electron impact.
14 p1776 A73-29695
- The photoionization cross section of magnesium near threshold.
14 p1776 A73-29699
- AUTOKINESIS**
Autokinetic movement as a function of the implied movement of target shape.
07 p0785 A73-19549
- Random dot pattern luminance and contrast effects on limiting inter-stimulus interval for visual apparent motion masking by bright field
07 p0783 A73-20256
- Threshold variance analysis of monocular vs binocular visual stimulation in apparent movement perception
07 p0783 A73-20262
- Effects of prolonged dark adaptation on autokinetic movement.
11 p1324 A73-26322
- Monocular fixation tests and prediction model for time course of aftereffect of eye turn on autokinetic illusion direction
13 p1578 A73-28098
- AUTOMATA THEORY**
Control efficiency of finite automaton with automatic control, considering system failures and independent and unequally probable transitions
05 p0553 A73-16273
- Automaton synthesis and perceptron learning for controlled objects classification according to unknown features, noting adaptive relationships between retina and associative elements
07 p0786 A73-20047
- Stability behavior of adapting and untrained random logic nets, enabling intelligent interaction with environment
07 p0786 A73-20400
- Certain finitely converging algorithms for the solution of infinite systems of inequalities and their application in the theory of adaptive systems
10 p1192 A73-24486
- Automaton external and internal languages linking by computer programming languages discussing structure and operation relation to language structure and realization
12 p1485 A73-27893
- Application of the describing-function approach to radio engineering problems. II
15 p1853 A73-31254
- Russian book - Problems in the synthesis of finite automata.
15 p1848 A73-31909
- Length minimization in the internal-state code of an asynchronous finite automatic system with a two-step memory
15 p1848 A73-31910
- Logic circuit distribution algorithms for asynchronous finite automata synthesis on basis of universal homogeneous medium
15 p1848 A73-31911
- Construction of a diagnostic sequence of tests of a combination automaton
15 p1848 A73-31913
- Organization of checks of the central control unit in a digital process-control computer operating with fixed word length
16 p1986 A73-33665
- Probabilistic automata minimization for system states reduction by deterministic matrix method
19 p2408 A73-38564
- Adaptive /learning/ intelligent system design and simulation for control with stochastic goal and environment conditions
20 p2532 A73-38685
- Minimum risk classification algorithms in automatic learning system design, applying to learning pulse signal receiver
20 p2532 A73-38686
- Self organizing behavior of multivariable stochastic extremal control systems with environmental or intrinsic positive feedback under perturbation
20 p2539 A73-38689
- Russian book - Automatic control theory.
20 p2539 A73-38690
- Investigation of the nature of biological rhythm sensors by means of automatic networks
22 p2812 A73-41865
- Error detection and synchronization with pseudoternary codes for data transmission.
22 p2827 A73-42464
- Study of the nature of the active tones with the aid of a discrete Wiener-medium analog
22 p2816 A73-42973
- State minimization of incompletely defined deterministic automaton by imbedding one-to-one mapping into homomorphism
24 p3074 A73-44664
- AUTOMATIC CONTROL**
NT ADAPTIVE CONTROL
NT AUTOMATIC FLIGHT CONTROL
NT AUTOMATIC FREQUENCY CONTROL
NT AUTOMATIC GAIN CONTROL
NT AUTOMATIC LANDING CONTROL
NT CASCADE CONTROL
NT DYNAMIC CONTROL
NT FEEDBACK CONTROL
NT FEEDFORWARD CONTROL
NT LEARNING MACHINES
NT NUMERICAL CONTROL
NT OFF-ON CONTROL
NT OPTIMAL CONTROL
NT PROPORTIONAL CONTROL
NT SELF ADAPTIVE CONTROL SYSTEMS
NT SELF ALIGNMENT
NT SEQUENTIAL CONTROL
NT TIME OPTIMAL CONTROL
A method for aiding human operator performance in a noncompensatory tracking task.
01 p0011 A73-10323
- Conditions for the absence of periodic conditions in multivariable pulse-coded systems
01 p0027 A73-10592
- Automatic impulse frequency stabilization of space vehicle rotation angle with respect to inertial coordinates by Liapunov discrete method
01 p0110 A73-10595
- Reliability and failure sequence characteristics of automatic system, using input rarefaction of Markov renewal process
01 p0058 A73-11423
- Signal search networks for enlargement of locking bandwidth of tracking filters in automatic control systems, examining transistorized signal search and acquisition circuits
02 p0145 A73-11793
- Experimental validation and design refinement program for air-ground-air data link based on automatic time division multiplex transmission of air traffic messages
02 p0190 A73-11852
- Discrete systems for automatic control of electronic equipment under conditions of its manufacture
02 p0146 A73-11865
- Zener diodes for overvoltage spark protection circuits in automatic control and measuring equipment operating in explosive environment
02 p0147 A73-12175
- Transient curve construction for analysis and synthesis of automatic control systems with asymmetrical nonlinearities, comparing with harmonic linearization
02 p0149 A73-12342
- Linear characteristics of transistorized Schmitt trigger pulse width regulators in response to sinusoidal and sawtooth signals for automatic control systems
02 p0149 A73-12343
- Thermoanemometer with automatically stabilized temperature of its sensitive element and output signal linearization
02 p0170 A73-12344
- Russian book - Fundamentals of the general theory for the root loci of automatic control systems.
02 p0149 A73-12750
- Method for quantitative estimation of the functional state of the motor apparatus
03 p0268 A73-13822
- Moving vehicle borne automatic sighting device pointing problem mathematical analysis and applications to aircraft and camera aiming for airborne photography
03 p0277 A73-13913
- Single automatic potentiometer based maximum-minimum temperature control unit, noting elimination of dual temperature regulators
03 p0309 A73-14026
- Automated calibration of blood pressure signal conditioners.
04 p0411 A73-14846
- Failure diagnostics in mathematical simulators of automatic control systems.
04 p0430 A73-15209
- Autonomous satellite navigation from strapdown landmark measurements.
04 p0474 A73-15266
- The attitude stabilization and control system for the Communications Technology Satellite.
04 p0504 A73-15450
- Self regulated transistorized voltage and frequency converters for multiple motor drives power supply, discussing circuit design, performance characteristics and overload protection
05 p0556 A73-16074
- Control efficiency of finite automaton with automatic control, considering system failures and independent and unequally probable transitions
05 p0553 A73-16273
- Investigation of the dynamics of nonlinear sampled-data automatic control systems
05 p0560 A73-16296
- Calculation of a photoelectric system for stabilizing the optical axis of an instrument
05 p0575 A73-16316
- Aircraft and spacecraft guidance and remote and automatic control of moving objects, using calculus of variations for systems synthesis
05 p0560 A73-16402
- Application of the control configured vehicle concept to a Space Shuttle configuration.
[AIAA PAPER 73-158]
05 p0629 A73-16905
- Determination of the average duration of a machining process on automatic production lines.
05 p0582 A73-16997
- Study of accuracy requirements for autonomous trajectory measurements providing conditions for entering planetary atmospheres
05 p0619 A73-17001
- Frequency stability criterion for a variable-structure automatic control system.
06 p0680 A73-17958
- The pulse-controlled photoelectric switch as an element in automatic control circuits and in computer equipment
06 p0676 A73-18088
- Automatic control for aircraft photographic camera pitch compensation via optical space filters and frequency methods, noting flight velocity to altitude relation
06 p0693 A73-18154
- Nonsearch algorithms for parametric synthesis of stochastic automatic control systems
06 p0680 A73-18381
- Third generation satellite PCM telemetry data processing with computer control for optimization and supervision, discussing system reliability, automatic control and diagnostic routine
07 p0795 A73-18954

Computer for automatic equipment monitoring, operation control and breakdown diagnosis in telemetry data processing, discussing management routines and reliability

07 p0795 A73-18956

Two-level computer system with main and display processors as scale working model for semiautomatic digital ATC en route control

07 p0796 A73-19183

Automated radar terminal systems [ARTS/]

07 p0849 A73-19184

Mathematical model of nonstationary linear aeroelasticity

07 p0912 A73-19468

Analysis of the stability and periodic motions of nonlinear automatic pulsed systems by the root-locus curve method

07 p0806 A73-20636

Computer-controlled software diagnosis of an airborne computer.

08 p0940 A73-20677

Modal control applied to the real-time figure control of a spaceborne telescope mirror.

08 p0969 A73-21729

An automated two-channel scanning spectrophotometer system.

08 p0970 A73-21740

Simultaneous design of 24 inch telescope and computer control system, discussing interface and software development

08 p0942 A73-21754

Application of a system of orthogonalized windings with automatically regulated current for plasma stabilization in Tokamak systems

09 p1125 A73-21908

French project for high speed hydrofoil marine vehicle with hydrodynamic lifting surfaces, completely submerged wings, gas turbine propulsion and automatic control

09 p1031 A73-22208

Hydrodynamics, hydroelasticity, technology and automatic control of H 890 hydrofoil craft

09 p1031 A73-22209

Construction of quality diagrams for transient processes in nonlinear systems

09 p1068 A73-22558

An approximate continuous representation of discrete control systems

09 p1068 A73-22564

Analysis of the magnetic systems of calculating transducers

09 p1064 A73-22941

Equivalent initial conditions for automatic control systems with variable parameters

09 p1069 A73-22943

Fluidic system design based on miniaturized modular high power fluidic logic elements, discussing applications in production process control

10 p1177 A73-23761

International Federation of Automatic Control, World Congress, 5th, Paris, France, June 12-17, 1972, Proceedings. Part 2 - Transportation, aeronautics and space, ship automation, and control components. Part 3 - Ecology and systems engineering; Large scale, sensitivity, optimization and adaptation theory. Part 4 - Education, feedback, regulators, linear and nonlinear systems; Identification, differential games, discrete and stochastic systems.

10 p1198 A73-24001

Theoretical and practical aspects of an automatic hover control system for an unmanned tethered rotor-platform.

10 p1175 A73-24009

Unified transducers of quantitative and geometrical parameters of different media based on the use of integral properties of electromagnetic fields.

10 p1217 A73-24014

Realization of digital differential analyser on the basis of multifunction memory units.

10 p1198 A73-24018

Analysis and synthesis of automatic control systems with controlled converters.

10 p1198 A73-24019

A hybrid motor - A high-speed and accuracy final actuator/automatic control element/.

10 p1177 A73-24025

Fast and reliable automatic digital control components and transducers for data processing, display and storage, assessing technology development trends and preference over analog devices

10 p1199 A73-24028

Russian book on military application oriented automatic control systems design covering amplifiers, servo elements, stability, performance, optimization, and nonlinear and sampled data systems

10 p1203 A73-24972

Fluidic setup corresponding to automatic control and digital computation circuits, discussing analog elements regulation and applications of logic subassemblies without moving parts

11 p1307 A73-25376

Pneumatic and fluidic automatic controls, investigating peripheral elements and systems feed

11 p1308 A73-25380

Pneumatic sensors without contact

11 p1308 A73-25381

Efficiency estimates of methods for analyzing the precision of nonlinear control systems

11 p1342 A73-26094

Level and density sensors using pneumatic repeaters

11 p1364 A73-26099

French book - Hydraulic and electrohydraulic automatic control. Volume 1 - Theory and technique. Volume 2 - Supplementary techniques and technologies

11 p1313 A73-26253

Digital electrode breakdown potential controller for spark source mass spectrometer automation, using radio frequency pulse amplitude sensing

11 p1367 A73-26315

Asynchronous linear automatic binary control systems, using interpolation theory of Taylor operators for mathematical modeling

11 p1342 A73-26418

Book - Engineering means in automatic control.

12 p1481 A73-26751

A method for substantially improving the reliability of multistable pulse-phase-coded elements

12 p1476 A73-26761

Evaluation of the efficiency of automatic control and observation systems on the basis of mathematical models of potential and real automatic systems

12 p1482 A73-26762

Features of the engineering theory for combined estimates of automatic control system reliability and lifetime

12 p1482 A73-26763

Utilization of thermal phenomena in the construction of signal-energy converters for coupling automatic control devices belonging to different categories of the State Instrument System

12 p1459 A73-26765

Comparative properties, main characteristics, and areas of application of electrochemical transducers

12 p1459 A73-26767

Chemotronic /electrochemical/ transducers of nonelectrical quantities in automatic control

12 p1459 A73-26768

Problems in constructing aerodynamically active elements - Converters of input and output signals in automatic control systems

12 p1459 A73-26769

Automatic control system components optimization for minimal cost, demonstrating algorithm efficiency for servosystem

12 p1482 A73-26775

Devices for primary processing of information in controller machines, based on the principles of quantum magnetometry

12 p1495 A73-26778

High-speed universal digital integrators with multistage increments as elements of automatic control systems

12 p1475 A73-26781

Automation considerations in technological methods for microcircuit fabrication, emphasizing electron-ion technology

12 p1477 A73-26783

System for automatic regulation of the constant-absolute-slip mode of an asynchronous electrical actuating element with frequency-modulation control by a thyristor converter

12 p1460 A73-26786

Opticomechanical system of an automatic stellar electrophotometer

12 p1495 A73-26865

A high-speed automatic strip-chart recorder

12 p1497 A73-27220

National aviation system improvement via cost effectiveness, considering FAA facilities and equipment program, ATC automation and terminal aids

12 p1522 A73-27365

Method for synthesizing built-in control circuits of automatic systems with memory

12 p1476 A73-27899

Aerial camera automatic exposure control design and operation, discussing maxima-minima metering and average brightness measurement techniques

12 p1501 A73-27965

Automatic electronic pendulum astrolabe featuring altitude and azimuth tracking mechanisms, azimuth setter and 180 degree turning mechanism

13 p1612 A73-28394

Computer control of a multifunction radar.

13 p1587 A73-28619

Automation of plotting root-locus curves for automatic control systems

13 p1596 A73-29142

High frequency model U-20P fatigue testing unit with program control of the specimen vibration amplitude.

13 p1599 A73-29637

Pick-up storage tube having an electronic shutter, automatic exposure control, wobbling correction, and slow scanning.

14 p1751 A73-29911

Manufacturing, integration and launching phases of Diamant B launcher inspection, discussing automatic control and testing bench structure and safety

14 p1742 A73-30104

Nonlinear vector matrix differential equations for automatic control systems dynamics, discussing stability, dissipativity and convergence

14 p1768 A73-30344

Continuously-discrete method for the construction of control devices

14 p1740 A73-30940

Russian book on remote guidance control systems covering theory, optimization and constraints for steady, unsteady, linear and nonlinear automatic control systems

15 p1853 A73-31374

Some properties of the amplitude frequency characteristics of linear automatic control systems and their control quality under random influences

15 p1854 A73-31695

Mathematical model of elastic flight body behavior in continuous medium based on combination solutions to aerodynamics, automatic control and elasticity theory problems

15 p1952 A73-32063

Akademia Nauk SSSR, Astronomicheskii Sovet, Meeting of the Commission on Astronomical Instrument Engineering, Sverdlovsk, USSR, July 1-3, 1970, Proceedings

15 p1877 A73-32128

The universal automatic reflector AZT-12

15 p1877 A73-32129

Astronomic follow-up systems with mismatch signal buildup

15 p1877 A73-32134

Automatic stellar electrophotometer with photon counting

15 p1878 A73-32136

Computerized stellar spectrogram processing using semiautomatic diagram-code converters, least squares method and reference spectral lines

15 p1878 A73-32141

Automatic recording method for the moments of exact-time radio signals

15 p1878 A73-32143

Automatic coordinate-measuring machine for astrophotography purposes

15 p1878 A73-32144

Russian book - Radio devices for flight vehicle control systems.

15 p1908 A73-32421

The Corail radar - Automatic equipment for runway surveillance

15 p1846 A73-32431

Automation of the print-out of strips of flight plans for air traffic control

15 p1847 A73-32441

Automated system of mixed /civil and military/ control

15 p1847 A73-32444

Automation of the Yugoslav AFTN network and its future expansion

15 p1855 A73-32482

Real time information processing automated systems for ATC, considering reliability based on redundancy

15 p1910 A73-32483

Airports automated meteorological instrumentation, describing cloud base height telemeter and transmissometer for runway visibility measurement

15 p1859 A73-32563

Magnetic feedback stabilization in a Tokamak.

15 p1922 A73-32633

Automatic detection radar with false alarm rate regulation capability in log-normal and Weibull clutter under severe environments

16 p1980 A73-33412

Simulation in the design of automated air traffic control functions.

16 p2035 A73-33419

Electromagnetic inductive microsystems with synchronization. I Determination of the characteristic functional magnitudes. II - Determination of the magnetic field in a region with linear and nonlinear media

16 p1992 A73-33664

Multipurpose properties and conflict situations in automatic control systems

16 p1992 A73-33666

Synthesis of a universal cell with increased reliability for the realization of an iterative automatic system

16 p1986 A73-33667

Automated discrete address radar beacon system and data link for ATC, describing simultaneous message decoding capacity, system specifications and implementation prognosis

17 p2208 A73-34612

AIRTRANS - Intra-airport transportation system. [SAE PAPER 730384]

17 p2146 A73-34721

Automatic electronic feedback control systems for active wing/external store flutter suppression

17 p2107 A73-35244

Teleoperators - Manual/automatic system requirements.

17 p2180 A73-35315

Method of synthesizing built-in monitoring arrangements for automata with memory.

18 p2291 A73-36751

Some characteristics of pilot's performance under complicated flight conditions.

18 p2285 A73-36921

Design principles for phase-measuring attachments with automatic error corrections

18 p2294 A73-36999

Solving M. A. Aizerman's first problem of absolute stability of nonlinear systems on the basis of the general theory of root trajectories

18 p2337 A73-37025

Free flying teleoperator spacecraft systems for automated satellites retrieval, cargo transfer and orbital operations support

19 p2490 A73-37303

Design and test of a self-controlled heat pipe radiator.

[ASME PAPER 73-ENAS-49] 19 p2435 A73-37996

Joint Automatic Control Conference, 14th, Ohio State University, Columbus, Ohio, June 20-22, 1973, Preprints of Technical Papers.

19 p2412 A73-38028

Autonomous satellite navigation - An historical summary and current status.

19 p2452 A73-38056

A continuous-discrete method of design of control devices.

19 p2414 A73-38194

Parallel processors and air traffic control automation.

19 p2408 A73-38465

Russian book - Automatic control theory.

20 p2539 A73-38690

Approximate methods for analysis and synthesis of nonlinear systems

20 p2592 A73-38692

Conditions, based on the estimation of the sensitivity of a periodic solution, for the application of the harmonic linearization method to higher harmonics and small parameters

20 p2592 A73-38693

The fastest extremum search in sampled-data automatic control systems

20 p2539 A73-38695

Automatic control theory and systems representation in framework of unilateral mechanics, using canonical elastodynamic and elastostatic equations

20 p2540 A73-38703

Methods for calculating and enhancing the efficiency of automatic systems

20 p2540 A73-38705

Synthesis of low-sensitivity automatic control systems

20 p2540 A73-38706

Automatic control of the Skylab Astronaut Maneuvering Research Vehicle.

[AIAA PAPER 73-857] 20 p2586 A73-38795

Root trajectories method for stability analysis of two channel automatic control systems with antisymmetric and symmetric cross couplings

20 p2541 A73-38980

Certain results of the application of the method of sections to typical classes of nonlinear automatic systems

20 p2541 A73-38985

A general quadratic criterion for absolute stability of nonlinear automatic control systems and its application to sampled-data systems with pulse-width modulation

20 p2541 A73-38988

A method of processing a priori information about a controlled plant with the aim of reducing the number of changing parameters of the dynamic characteristics

20 p2541 A73-38993

An electrical model of the inertial and adaptive properties of vision as a self-regulating system with delayed feedback

20 p2517 A73-39004

Transient process quality assessment for dynamic systems with variable parameters

20 p2541 A73-39035

Investigation of the transient process quality of automatic control systems with variable parameters using the method of the biased characteristic equation

20 p2541 A73-39036

Stability and dissipativity of control systems containing unsteady nonlinearities

20 p2542 A73-39041

Flow stabilization by methods of distributed automatic control

20 p2545 A73-39042

Suppression of free convection by a distributed automatic controller

20 p2626 A73-39043

Structure of self-organizing automated design systems and the processes of their functioning

20 p2569 A73-39391

Calculation of processes taking place in digital automatic control systems with finite switch-closing times

20 p2543 A73-39477

Computer controlled automatic TV-microscope system for tracking and measuring nerve cell processes in designated axons and dendrites

20 p2518 A73-39763

A photometric system for automatic recording of optical absorption spectra

21 p2700 A73-40561

An automatic sweep generator for a strobed oscilloscope

21 p2664 A73-41098

Automatic apparatus for the study of conditioned reflexes in a monkey seated in the primateological chair

21 p2644 A73-41140

Russian book on accuracy of automatic systems using digital computers as control devices covering analysis and synthesis, stochastic inputs, system errors and operator methods

21 p2658 A73-41282

Russian book - Aerohydrodynamic methods for measuring input parameters of automatic systems: Fluidic measuring elements.

21 p2704 A73-41288

Russian book on reliability optimization in complex automatic control system information transfer and processing covering performance criteria, noise immunity, error sources and types, etc

21 p2670 A73-41293

Russian book - Psychological problems of activity regulation.

22 p2812 A73-41884

Effect of a subjective ambiguity estimate concerning the duration of work on activity regulation

22 p2812 A73-41892

The MINFAP system - First phase in the automation of the EUROCONTROL Maastricht Centre.

22 p2884 A73-42323

Transfer function root method for synthesis of multiply connected determinate automatic control systems with asymmetrical channels and limited nonautonomous control elements

22 p2836 A73-42614

French paper on satellite attitude stabilization by gyroscopes covering autonomous activator systems, kinetic moment principles and control in roll-yaw for flexible panels

22 p2917 A73-42743

Automatic control theory application to random vibration passive and active isolators synthesis, considering vehicle suspension systems and electrohydraulic damper

22 p2927 A73-42922

Systems engineering approach to pneumatic hybrid automatic/manual control system with fluid logical elements and reduced air consumption

23 p2943 A73-43413

Application of stochastic differential equations in description of automatic control plants

24 p3074 A73-45098

AUTOMATIC CONTROL VALVES

Periodic oscillations of a closed hydraulic throttle servomechanism with inertial and positional loads

23 p2945 A73-43739

AUTOMATIC DATA PROCESSING

U DATA PROCESSING

NT AUTOMATIC FLIGHT CONTROL

Problems of the integration of aircraft and flight control system in the case of new approach procedures

[DGLR PAPER 72-096] 02 p0190 A73-11698

Schematic design of an automatic device for correcting aircraft takeoff and landing modes of flight

02 p0190 A73-11801

ATC simulator, discussing student training routines and exercises, automatic navigation and aircraft piloting

02 p0190 A73-11853

A procedure for the barometric altitude control in the case of hovering devices and helicopters

03 p0249 A73-12916

Variable stability simulation techniques for nonlinear rate-dependent systems.

03 p0285 A73-13521

A universal digital autopilot and integrated avionics system.

04 p0474 A73-14735

Russian book - Control of moving objects.

05 p0628 A73-16401

The problem of human efficiency in automated control systems

05 p0542 A73-16410

Russian book - Control of aircraft and helicopter flight.

07 p0850 A73-20381

Helicopter automatic flight control system design, testing and development, noting stability and control augmentation and attitude retention units

13 p1656 A73-28903

Hardware integration and improved operation of the flight control system.

14 p1713 A73-30932

Night search and rescue techniques over sea in poor visibility by helicopter, discussing automatic flight

control systems, radar, plotting facility and pilot training

15 p1825 A73-31094

Optimal stochastic guidance laws for tactical missiles.

15 p1908 A73-31917

The safety, the reliability, and redundancy in the automatic flight control system of the A300-B Airbus

15 p1830 A73-32459

PB-75 flight guidance system for subsonic commercial transport aircraft operation under Category IIIA conditions, describing cruise and ILS operation

15 p1911 A73-32500

FGS-70 flight guidance system for general aviation, commercial and military transports, discussing ILS and VOR operation modes and autopilot/flight director integration

15 p1912 A73-32501

Experimental autostabilized tethered rotor platform for reconnaissance, communications and ECM, discussing control system effectiveness from flight test results

16 p1969 A73-33736

Separate surfaces for automatic flight controls. [SAE PAPER 730304]

17 p2101 A73-34665

Prospects of automation of air traffic control systems using satellites for radio navigation

17 p2209 A73-34961

A frequency response approach to flying qualities criteria and flight control system design.

[AHS PREPRINT 740] 17 p2105 A73-35073

Word length problems in the on-board computer implementation of digital flight control systems.

17 p2145 A73-35384

The development of the F-12 series aircraft manual and automatic flight control system.

[AIAA PAPER 73-822] 19 p2380 A73-37474

Guidance, control, and instrumentation progress on the McDonnell Douglas DC-10.

19 p2451 A73-37814

Automatic flight control and navigation systems on the L-1011 Capabilities and experiences.

19 p2452 A73-37824

Studies on the time-to-go indexing control scheme for an automatic aircraft landing system.

19 p2453 A73-38280

ARTS II automated air traffic control systems.

19 p2453 A73-38463

Study of control system effectiveness in alleviating vortex wake upsets.

20 p2507 A73-38776

An approach to the synthesis of separate surface automatic flight control systems.

[AIAA PAPER 73-834] 20 p2508 A73-38777

French automatic beam coupler system for V/STOL and helicopter low speed and low altitude instrument approach

21 p2737 A73-40975

AUTOMATIC FREQUENCY CONTROL

Investigation of the dynamics of a pulsed phase-lock automatic frequency control system

02 p0142 A73-12493

Automatic frequency control in the case of manually tuned oscillators

04 p0427 A73-14774

Second order phase lock AFC system transient response duration calculation for rectangular and sawtooth characteristics of phase detector, using averaging method

05 p0547 A73-16059

Sinusoidal signal and stationary quasi-white Gaussian noise mixture effects on stochastic phase locked AFC system operation, noting phase error probability density function

05 p0547 A73-16060

Short term instability of frequency standard using AFC of quartz crystal oscillator by phase locking to optically pumped Rb 87 vapor clock

05 p0583 A73-16071

Probability density characteristics of elapsed time interval to synchronization disruption in phase locked AFC systems

13 p1584 A73-28890

Frequency fluctuations in a gas laser with nonlinear absorption.

13 p1629 A73-29430

Approximate investigation of the dynamics of a digital phase-lock automatic frequency control system /DPAFC/

14 p1728 A73-30269

Possibility of independent control of frequency characteristic and coverage band in a PAFC system.

15 p1842 A73-30987

Fundamental statistical characteristics of a modified phase AFC /PAFC/ system.

15 p1842 A73-30989

Use of computers for calculation of the capture band of nonlinear phase-automatic-frequency-control systems.

15 p1842 A73-30990

Investigation of longitudinal-mode selection and frequency stabilization of the emission from a helium-neon laser with a ring resonator

15 p1886 A73-32335

Two-phase radio-frequency generators employing phase-lock AFC 17 p2135 A73-34590

Bifurcations and certain qualitative characteristics of a phase-locked automatic frequency control system with a second-order filter 20 p2535 A73-38979

Electronically tunable microwave bandpass filters 24 p3071 A73-44606

AUTOMATIC GAIN CONTROL

Reconstitution of signals deformed by a fast AGC application to plasma resonances. 04 p0417 A73-15297

Dynamic AGC correction for angle signal variations in monopulse radar receivers with reference signal, analyzing signal statistics 12 p1469 A73-27163

Some features of the application of controlled-gain transistors. 12 p1480 A73-27271

Relationship between the control range and the variation in passband width in a controlled-gain amplifier with nonlinear shunting of the load 14 p1736 A73-30563

Relation between the N. M. Krylov-N. N. Bogoliubov averaging method and the method of envelopes in studies of a class of control systems 15 p1854 A73-31801

Noise immunity of optical communications links with radio and optical AGC systems. 16 p1984 A73-33977

Theory of optimal AGC system synthesis. 17 p2134 A73-34318

Transient response in a receiving system with AGC under the influence of fluctuating signals 17 p2121 A73-34591

The Ebers-Moll effect transistor used as a low-value controlled resistor in ACC and other variable-gain applications. 21 p2661 A73-40229

Investigation of the gain instability of a semiconductor radiometer 21 p2700 A73-40539

On the connection of the Krylov-Bogolyubov averaging method with the envelop method for investigating one class of control systems. 23 p2965 A73-44330

AUTOMATIC LANDING CONTROL

Problems of the integration of aircraft and flight control system in the case of new approach procedures [DGLR PAPER 72-096] 02 p0190 A73-11698

Russian book on aircraft control systems covering radio communication and navigation, automatic guidance and landing and homing and radar tracking 04 p0474 A73-15964

Russian book on aircraft landing control automation covering radio beacons, communications equipment, instrument landing trajectories, flight control, autopilot, atmospheric disturbances and display systems 04 p0474 A73-15966

Maximum safety hydraulic systems for A300B airbus powered flight controls for normal flying and auto land operations 04 p0409 A73-16031

The role of the test pilot in evaluating auto landing systems. I. 09 p1115 A73-22182

The role of the test pilot in evaluating auto landing systems. II. 09 p1115 A73-22183

Microwave landing system /MLS/ with Doppler scanning technique for aircraft guidance precision improvement over standard VHF/UHF ILS, detailing five-year development plan 10 p1246 A73-23652

All-weather aircraft landing automation, discussing efficient optimal feedback control law selection based on trajectory termination or terminal control requirements 10 p1247 A73-24010

Manual vs fully automatic landing concepts, discussing pilots abilities and limitations and primary requirements for displays 13 p1656 A73-28905

Automatic helicopter approach in poor visibility 15 p1910 A73-32465

Independent Landing Monitor for economic Category 3 operation with fail-operational autoland, fog dissipation or fail-passive autoland plus visibility augmentation 15 p1911 A73-32499

Integrated reliability and safety analysis of the DC-10 all-weather landing system. 16 p1969 A73-33641

Monitor display to indicate aircraft position relation to desired flight profile during automatically controlled steep landing approaches with curved segments 17 p2207 A73-34477

Low visibility/bad weather aircraft landing systems design, discussing developmental stages for all weather landing implementation, automatic landing control and pilot visual discrimination problems 17 p2207 A73-34481

A manual-control approach to development of VTOL automatic landing technology. 17 p2209 A73-35075

[AHS PREPRINT 742] Modular building block microwave landing system for automatic flight in CAT, discussing ICAO and NIAG missions 19 p2450 A73-37495

Results and problems of a theory of final-position control systems with a nonstationary singular feedback 20 p2540 A73-38707

Optimal landing flare control of aircrafts with sensitivity consideration. 23 p2940 A73-43284

AUTOMATIC PATTERN RECOGNITION

U PATTERN RECOGNITION

AUTOMATIC PICTURE TRANSMISSION

Picture information acquisition, storage and transmission characteristics of film and vidicon systems for photographic reconnaissance of planets 06 p0750 A73-18010

Real time quantitative display for visible and IR scanning radiometer in ITOS-D satellite-borne automatic picture transmission system with stations access to computers 12 p1520 A73-26811

AUTOMATIC PILOTS

Electrostatic autopilot using atmosphere electric field lines for stabilization and guidance, applying to remotely piloted vehicles 02 p0191 A73-12595

A universal digital autopilot and integrated avionics system. 04 p0474 A73-14735

Russian book on aircraft landing control automation covering radio beacons, communications equipment, instrument landing trajectories, flight control, autopilot, atmospheric disturbances and display systems 04 p0474 A73-15966

Aerodynamic entry vehicle autopilots. 06 p0721 A73-18515

Accelerations of points on a flight vehicle during short-period motion 07 p0777 A73-20095

Synthesis of nonsearching self-adjusting systems by the root-locus method. II 07 p0807 A73-20637

Simulated flight tests of a digitally autopiloted STOL-craft on a curved approach with scanning microwave guidance. [ASME PAPER 73-AUT-L] 13 p1657 A73-29413

Synthesis of searchless selfadjusting systems on the basis of the root-locus method. II. 15 p1854 A73-31691

PB-75 flight guidance system for subsonic commercial transport aircraft operation under Category IIIA conditions, describing cruise and ILS operation 15 p1911 A73-32500

FGS-70 flight guidance system for general aviation, commercial and military transports, discussing ILS and VOR operation modes and autopilot/flight director integration 15 p1912 A73-32501

Electric trim systems - Design and certification considerations under FAR 23.677/CAM 3.337-2/. [SAE PAPER 730299] 17 p2101 A73-34662

Application of advanced control system and display technology to general aviation. 17 p2102 A73-34679

A high-performance, aerodynamically-controlled, tactical missile hybrid 6-DOF simulation. 18 p2296 A73-36835

Simulated flight tests of a digitally autopiloted STOL-craft on a curved approach with scanning microwave guidance. 19 p2386 A73-38049

An organized approach to the digital autopilot design problem. [AIAA PAPER 73-848] 20 p2585 A73-38787

A nonlinear programming algorithm for the automated design and optimization of flexible space vehicle autopilots. [AIAA PAPER 73-892] 20 p2588 A73-38828

AUTOMATIC ROCKET IMPACT PREDICTORS

U COMPUTERIZED SIMULATION

U IMPACT PREDICTION

AUTOMATIC TEST EQUIPMENT

A digital system for shaping, analysis and control of a random vibration spectrum 01 p0027 A73-10598

Sensitometric instruments for black and white and color photographic material and image measurements, including recording microdensitometer, reflection goniodensitometer, automatic granulometer and projection resolvablemeter 01 p0051 A73-10837

Automated test stands for full scale aircraft structure and engine parts fatigue tests, noting equipment for programmed static and dynamic loading 02 p0166 A73-11629

Discrete systems for automatic control of electronic equipment under conditions of its manufacture 02 p0146 A73-11865

AUTOMATIC TEST EQUIPMENT

Automatic two-coordinate compensator for resistance-measurement studies of steels and special alloys 02 p0167 A73-11867

Automated system with CW signal and feedback to measure delay line group delay and transfer function frequency responses, detailing operation and errors 02 p0146 A73-11952

Computer based data processing system with display for improving ultrasonic pulse echo NDT test equipment resolution and SNR 02 p0173 A73-11983

Automatic magnetic inspection method using magnetoresistive elements and its application. 02 p0173 A73-11988

Two coordinate oscillograph recording device with automatic reversing for stress-strain tests under static and cyclic loads 02 p0168 A73-12144

Portable self contained computerized in-aircraft engine analyzer with cassette tape resident program control and digital display and punched card indicators [AIAA PAPER 72-1080] 03 p0307 A73-13403

An automated jet-engine-blade inspection system. 03 p0312 A73-13524

Pattern classification in scan-type nondestructive tests. 04 p0447 A73-14928

Computerized ground support acceptance checkout systems for space shuttle program, discussing capabilities, future goal and unified test equipment 04 p0432 A73-15458

Russian book on jet engines testing covering tests in research and development, design, production and maintenance, test laboratories and stands and automation 04 p0487 A73-15708

Automatic technique for extending magnetograms and for determining variometer sensitivity 05 p0573 A73-16267

Field experience with digital control systems for vibration and acoustic testing. [SAE PAPER 720821] 05 p0554 A73-16637

Computer-controlled environmental test systems - Criteria for selection, installation, and maintenance. [SAE PAPER 720819] 05 p0562 A73-16638

Enhancing testability of large-scale integrated circuits via test points and additional logic. 06 p0674 A73-17802

The VDTA-3 apparatus for high-temperature differential thermal analysis 06 p0693 A73-18043

Russian book - Methods and equipment for in-flight aircraft strength tests. 07 p0777 A73-20376

Automatic support systems for advanced maintainability; Symposium, Philadelphia, Pa., November 13-15, 1972, Record. 08 p0951 A73-20676

A modular approach to an automated digital test system. 08 p0940 A73-20678

Some UK military views on the development and procurement of AIDS, BIT and ATE for avionics. 08 p0962 A73-20679

AUTOMATE - A self-contained automatic test system. 08 p0951 A73-20680

The use of automatic test equipment for performing screening and production reliability verification testing. 08 p0942 A73-20681

Computer controlled automatic test system for circuits, assemblies and systems performance and test programs on-line generation, editing and validation 08 p0940 A73-20682

Test techniques for advanced avionics displays. 08 p0962 A73-20683

Reversing the trend - Infrared testing is simplicity itself. 08 p0952 A73-20685

Automatic test equipment software configuration management. 08 p0952 A73-20686

Automatic test equipment support software definition and development, describing language, translator and operating system as elements of closed loop ATE system 08 p0952 A73-20687

Test programs design for versatile avionics shop test system /VAST/, discussing compiler problems alleviation by on-station program patching capability 08 p0962 A73-20688

GAELIC - Grumman Aerospace Engineering Language for Instructional Checkout. 08 p0941 A73-20689

Automated vibration shaker calibration data acquisition and analysis system with minicomputer for working transfer standard voltage monitoring and acceleration level determination 09 p1070 A73-22508

The automatic checkout of the Prospero Satellite. 09 p1070 A73-22917

An apparatus for measuring and recording the electrical resistance of metal specimens during mechanical testing.

09 p1070 A73-23066

Data quality assurance in a shipboard computer-controlled telemetry system.

09 p1057 A73-23410

Automatic microscopy for mitotic cell location.

12 p1464 A73-27144

Russian book on ultrasonic methods for weld testing covering flaw detection, emitters/receivers, acoustic channels, echo and mirror shadow methods, automatic testing, etc

13 p1624 A73-28949

Automatic machine test equipment and procedures for hydraulic systems, tractor shafts and automobile wheels

13 p1625 A73-29135

Automatic checkout and monitoring in the AN TPQ-27 radar system.

13 p1585 A73-29210

Machine for investigating the fatigue and inelasticity of metals with programmed load changes both at room and at elevated temperatures.

13 p1599 A73-29636

A high temperature vacuum assembly for precision creep tests

14 p1743 A73-30694

Central digital measuring and data logging systems for electrical and nonelectrical analog signal conversion, display and recording

15 p1849 A73-32204

Spectroscopic laser methods of automatic gas analysis based on Raman backscattering, resonance fluorescence or absorption measurements for atmospheric pollutant and exhaust gas detection

16 p2023 A73-32876

A closed-loop automatic control system for high-intensity acoustic test systems.

16 p1994 A73-33147

AEGLIS Operational Readiness Test System - Design for system effectiveness.

16 p2073 A73-33609

Operational readiness and maintenance testing of the B-1 strategic bomber.

16 p1969 A73-33631

An integrated, modular approach to automatic testing and data monitoring.

16 p1986 A73-33632

Computerized total On-Line Testing System with diagnostic error visibility and preventive and corrective maintenance functions in multiprogramming mode, discussing design features

16 p1986 A73-33633

Concept and system of the versatile avionic shop test (VAST) system.

16 p1986 A73-33634

Assembly for studying oscillation damping in rod elements in the field of centrifugal forces

17 p2145 A73-34340

Computerized automatic microwave testing with pulse measurements of phase and power from Reliable Advanced Solid State Radar phased array modules, discussing system design

17 p2135 A73-34724

Book - Experimental techniques in fracture mechanics.

17 p2252 A73-35668

Fracture mechanics testing systems, discussing closed loop assembly, programming, readout and fail-safe units and fully automated computer-controlled technique

17 p2175 A73-35672

New methods for studying gas solid reaction kinetics using automated resistance monitoring.

17 p2175 A73-35756

A closed-loop automatic control system for high-intensity acoustic test systems.

18 p2296 A73-36712

Self calibrating automatic equipment for pulsed and CW RF testing of phase, amplitude and frequency characteristics of pulsed electronic devices

20 p2535 A73-38870

A system for continuous remote measurements and automatic recording of nonlinear displacements in testing structural materials in the field of reactor emission

20 p2566 A73-39369

Pattern measurements of phased-arrayed antennas by focusing into the near zone.

21 p2653 A73-40681

Malfunction diagnostics in digital integrated-circuit devices

23 p2956 A73-43581

An automated Dobson spectrophotometer.

23 p2982 A73-43855

A new automatic ozone recorder for near-surface measurements working at 19 stations on a meridional chain between Norway and South Africa.

23 p2982 A73-43863

Expanding the capability of a laboratory ultrasonic testing facility.

23 p2966 A73-44168

AUTOMATIC TYPEWRITERS

A flexible automatic typewriting system using three tape readers.

23 p2944 A73-43422

Information dependent frequency control of an automatic typewriter.

23 p2944 A73-43423

AUTOMATION

Synthesis of a multidimensional automatic optimization system with constraints

01 p0028 A73-10674

Theoretical foundations of the development of a system of automated information processing for the problems of manufacturing-process design in the metalworking industry

03 p0400 A73-13240

On automatic angle measurements and a proposition of their application into zenith distance measurements on the surface of the moon.

03 p0307 A73-13258

Computerized flying spot scanner/analyzer for automatic mensuration analysis of droplets, particles and cell preparations from 35 mm film density distributions

03 p0309 A73-14449

Principles of organization and logistical support for systems of automating scientific investigations

04 p0424 A73-14823

Automated navigation system design for DC 10 long range version, emphasizing control display unit interface functions with pilot

05 p0594 A73-16050

Procedural formalization and methodology for automated problem solving in terms of digital program systems for algorithms generation, describing operational procedures

06 p0669 A73-17594

Automated generation and condensation of large mass- and rigidity-matrices

07 p0909 A73-19175

Automation considerations in technological methods for microcircuit fabrication, emphasizing electron-ion technology

12 p1477 A73-26783

Computer technology aided machine design automation and structural synthesis by coded information table formulation and conversion, discussing algorithm construction

12 p1502 A73-26784

Computer and digital techniques in ATC automation technology, considering functional organizations, terminal facilities and system capabilities to meet future needs

14 p1730 A73-29886

Automatic radar terminal system (ARTS) for high density ATC centers, noting improved target identification and alphanumeric data display

15 p1907 A73-31133

Automatic instrument systems for determining cloud amount.

15 p1874 A73-31319

Russian book - Air navigation: Application of radio navigational aids and automated navigation complexes.

15 p1908 A73-31471

VOLMET transmission automation with the aid of the 'DECLAM' system using a speech synthesizer

15 p1846 A73-32429

Airports automated meteorological instrumentation, describing cloud base height telemeter and transmissometer for runway visibility measurement

15 p1859 A73-32563

Development of a data-processing installation for the automatic quality control of spot-welding joints

16 p2019 A73-33222

Surveillance and correction of gas analysis devices and the analysis evaluation with the aid of a process computer

16 p2014 A73-33223

Electronics in the automation of services; International Congress on Electronics, 20th, Rome, Italy, March 28-31, 1973, Proceedings

17 p2122 A73-34960

An automatic system for broadcasting weather data to international civil aviation

17 p2122 A73-34962

Computer aided design-drafting (CADDD) - Engineering/manufacturing tool.

[AIAA PAPER 73-793]

19 p2407 A73-37460

The Federal Aviation Administration program to improve terminal area traffic control.

19 p2450 A73-37803

Automation of airline passenger processing.

19 p2506 A73-37804

The air traffic controller and control capacity.

19 p2451 A73-37811

ATC enroute automation program using radar tracking and computer readout system, describing terminal traffic control, wake vortices and aircraft spacing

19 p2453 A73-38439

Production techniques for advanced composites fabrication by tape machine automation.

[SME PAPER EM 73-718]

19 p2436 A73-38498

Ships inertial navigation system automated degradation detection and isolation, specifying decision error probabilities as function of degradation magnitude and observation time

[AIAA PAPER 73-849]

Discrete reproduction of a random parameter change process in standard automation equipment elements

20 p2585 A73-38788

Electronic moving-target selection systems

20 p2543 A73-39393

Automobile engines

The development of a device for measuring fuel consumption

02 p0165 A73-11521

Mechanism of the formation and control of pollutants due to combustion

15 p1840 A73-31225

Low emissions combustion for the regenerative gas turbine. I - Theoretical and design considerations. [ASME PAPER 73-GT-11]

16 p2086 A73-33489

Low emissions combustion for the regenerative gas turbine. II - Experimental techniques, results, and assessment. [ASME PAPER 73-GT-12]

16 p2086 A73-33490

Automobiles

Experimental studies concerning the adhesion coefficient during slip

04 p0454 A73-15655

Recovery of nonferrous metals from scrap automobiles by magnetic fluid levitation. [AIAA PAPER 73-959]

22 p2878 A73-42531

Automorphisms

Maximal finite groups of $n \times n$ integral matrices and complete groups of integral automorphisms of positive quadratic forms / Bravais types/

13 p1648 A73-28342

Automorphism groups of W algebras operating in Hilbert space with application to noncommutative dynamic systems analysis and ergodic theory

23 p2999 A73-44102

Autonomic nervous system

NT SYMPATHETIC NERVOUS SYSTEM

Activity relation between internal organ receptors and skeletal muscles in terms of laws controlling process coordination

01 p0007 A73-10154

Hemocoagulation system function in mountain inhabitants and during altitude acclimatization, noting parasympathetic nervous system tonus

02 p0133 A73-11923

The role of extrinsic vagal innervation in the motility of the smooth-muscle portion of the esophagus - Electromyographic study in the cat and the baboon

03 p0262 A73-13783

Functional dependence of the ciliary epithelium AT Pace activity and intraocular pressure on the autonomic nervous system.

05 p0539 A73-16248

The role of vestibulometry in medical evaluation of flight personnel

10 p1183 A73-23821

Bioelectric and vegetative components of conditioned reflexes of 'negative-emotional type'

20 p2515 A73-39797

Russian book - Role of the hypothalamus and the limbic system of the brain in regulating vegetative functions.

21 p2636 A73-40276

Changes in respiration accompanying a diencephalic vegetative-vascular syndrome under the action of a hypoxic mixture

21 p2636 A73-40280

Autonomy

Sufficient conditions for the optimal control problem

01 p0071 A73-11269

Behavior of the periodic surface for a periodically perturbed autonomous system and periodic solutions.

04 p0469 A73-14665

Feedback law choice for autonomy properties of controlled object, noting existence and uniqueness theorems

08 p0951 A73-21127

Autonomous second order system model for nonlinear disturbances of multifrequency systems at resonance, using group properties of differential equation

12 p1524 A73-27404

Analytical estimates of the accuracy of spacecraft autonomous navigation based on measurements of flight altitude and zenith-distance inertial-space reference point.

12 p1523 A73-27647

Small perturbation evolutionary motion equations for forced vibrations of quasi-linear two frequency autonomous systems at resonance

13 p1661 A73-29082

Ergatic modeling as dynamic goal-oriented physical process based on heuristic autonomous information-structured organization system with regulated model-human operator interaction

13 p1580 A73-29418

Regulators providing control system autonomy

14 p1740 A73-30938

Decentralized coalition control in data processing systems
15 p1848 A73-31804

Feedback law choice for autonomy properties of controlled object, noting existence and uniqueness theorems
15 p1855 A73-32062

Small perturbation evolutionary motion equations for forced vibrations of quasi-linear two frequency autonomous systems at resonance
19 p2445 A73-37633

Regulators guaranteeing the autonomy of a controlled system.
19 p2414 A73-38192

The evaluation of autonomous navigation systems for cruise vehicles.
[AIAA PAPER 73-874] 20 p2587 A73-38811

An analysis of recent advances in autonomous navigation for near earth applications.
[AIAA PAPER 73-875] 20 p2587 A73-38812

Synthesis of multidimensional automatic optimization systems with allowance for constraints
20 p2542 A73-39040

Normal third-order shapes of nonlinear oscillations
20 p2593 A73-39320

A linear method of autonomous space navigation and guidance
21 p2737 A73-40906

Large-scale systems and operations management decentralized coalitional control in data processing systems.
23 p2956 A73-44333

AUTOPSIES
Mid- and late changes in the QRS complex.
18 p2274 A73-36528

AUTORADIOGRAPHY
An autoradiographic investigation of material transfer and wear during high speed/low load sliding.
01 p0056 A73-10438

Study by autoradiography at high resolution power of the role of hydrogen in the mechanism of cracking of TA6V titanium alloy in salt water
04 p0461 A73-15097

Spatial distribution of elements in tektites and comparable materials by charged particle activation analysis.
11 p1418 A73-25584

AUTOROTATION
AH-56A rigid rotor compound helicopter configuration and handling qualities under autorotation conditions, discussing flight test program, piloting descent performance
09 p1030 A73-22179

A dynamic and aerodynamic analysis of an articulated autorotor decelerator system.
[AIAA PAPER 73-463] 15 p1827 A73-31449

AUTOTROPHS
Properties of phosphoribulokinase from *Thiobacillus neapolitanus*.
03 p0261 A73-13597

Effect of cultural conditions on the fatty acid composition of *Thiobacillus novellus*.
03 p0261 A73-13599

AUXILIARY ELECTRIC POWER UNITS
U AUXILIARY POWER SOURCES
AUXILIARY EQUIPMENT (COMPUTERS)
NT PLOTTERS
AUXILIARY POWER SOURCES
NT CHEMICAL AUXILIARY POWER UNITS
NT NUCLEAR AUXILIARY POWER UNITS
NT SNAP
NT SNAP 19
NT SNAP 27
NT SNAP 29
NT SOLAR AUXILIARY POWER UNITS
NT SPACE POWER REACTORS
NT SPACE POWER UNIT REACTORS
Turbomachinery design for Space Shuttle auxiliary power systems.
[SAE PAPER 720835] 05 p0537 A73-16633

Design and analysis of an APU monopropellant gas generator.
[SAE PAPER 720834] 05 p0537 A73-16635

Characteristics, design and performance of power sources in auxiliary systems for spacecraft applications, noting long term standby under environmental conditions
[SAE ATR 744 A] 08 p0928 A73-20690

Auxiliary power units and their application to the space shuttle.
09 p1153 A73-22778

Open cycle hydrogen-oxygen turbine driven generator system for space shuttle auxiliary power supply, discussing components, control mode and performance potential
09 p1153 A73-22779

Thermionic reactor power systems design for spacecraft auxiliary power supply and electrical propulsion, discussing performance and design guidelines for various applications
09 p1118 A73-22798

Ram air turbines for aircraft emergency power supply, discussing design, performance and control
10 p1177 A73-23525

Liquid or solid fueled gas generators applications to driving rocket fuel turbopumps, ejector pumps, gas turbine engine starters, torpedo propulsion, etc
11 p1307 A73-24991

Performance of an auxiliary power unit on anhydrous hydrazine.
11 p1308 A73-25980

A modular Space Station/Base electrical power system - Requirements and design study.
11 p1311 A73-26015

Sealed aircraft battery with integral power conditioner.
13 p1573 A73-29589

Large area silicon solar array development.
13 p1573 A73-29593

Long-life light weight reliable fuel cell development for long term space missions power supplies, describing system components and construction materials
13 p1573 A73-29596

Megawatt fuel cells for aerospace applications.
13 p1573 A73-29597

Concorde emergency power supply, oxygen and escape systems design and operational features
14 p1713 A73-30929

VFW 614 twin-jet short haul aircraft, discussing layout, auxiliary power supply system for ground handling independence, surface movements maneuverability and low noise characteristics
15 p1830 A73-32365

An airline view of the future of auxiliary power systems.
[SAE PAPER 730379] 17 p2108 A73-34718

Advanced aircraft power systems utilizing coupled APU/ECS.
[SAE PAPER 730380] 17 p2108 A73-34719

The role of the auxiliary power unit in future airplane secondary power systems.
[SAE PAPER 730381] 17 p2108 A73-34720

150 KVA integrated drive generator for aircraft electrical systems.
17 p2109 A73-35253

Application of digital computer APU modeling techniques to control system design.
19 p2392 A73-38416

Electric powered commercial jet aircraft emergency power supplies, discussing attitude gyros, Ni-Cd batteries, voltmeters, equipment running times, static inverters and transmitters
20 p2510 A73-39213

Runway lighting emergency power supplies for low visibility, comparing single supply backed by automatic generator with separate cable and duplicate supplies
22 p2839 A73-42318

Decentralized power processing for large-scale systems.
22 p2801 A73-42905

AUXILIARY PROPULSION
Secondary low thrust propulsion systems technology requirements and parameters, covering electrothermal, radioisotope and ion bombardment thrusters
01 p0090 A73-11109

NASA technology program for auxiliary and primary electric propulsion systems, noting flight tests and solar arrays
[AIAA PAPER 72-1127] 03 p0355 A73-13437

Advanced technology for Space Shuttle Auxiliary Propellant Valves.
[AIAA PAPER 72-1157] 03 p0356 A73-13459

Hydrogen oxygen propulsion component design and hot firing tests for space shuttle auxiliary systems and upper stage applications
[AIAA PAPER 72-1156] 04 p0486 A73-14918

AVAILABILITY
AEGIS AN/SPY-1 radar system - Design for availability.
16 p1980 A73-33607

Testing of spacecraft in long-term storage
16 p2073 A73-33615

Computer program for Equipment Improvement Recommendation (EIR) evaluation relative to reliability, availability, inventory cost and total annual expenditure in Army engineering management decision making
16 p2089 A73-33653

PLANET scheduling algorithms and their effect on availability.
17 p2130 A73-34822

AVALANCHE DIODES
Large-signal calculations on IMPATT oscillators with voltage waveforms giving close-to-optimum efficiency.
01 p0026 A73-11297

50 GHz gallium-arsenide IMPATT oscillator.
02 p0144 A73-11519

An accurate bridge method for impedance measurements of impatt diodes.
03 p0281 A73-13175

High-power avalanche IMPATT reflection amplifier using the Rucker combining circuit.
03 p0282 A73-13894

Permanent and transient radiation effects in BARITT microwave oscillators.
05 p0558 A73-16518

Transient ionizing radiation effects on IMPATT diode oscillators.
05 p0558 A73-16519

Silicon X band oscillation TRAPATT diodes with high power efficiency, presenting electric field variation with distance
05 p0559 A73-16809

Large-signal noise, frequency conversion, and parametric instabilities in IMPATT diode networks.
06 p0677 A73-17789

Measurements of the photomultiplication factor of silicon avalanche photodiodes.
06 p0674 A73-17796

Circuit model for characterizing the nearly linear behavior of avalanche diodes in amplifier circuits.
[AD-757849] 06 p0677 A73-18738

Theoretical and experimental study of GaAs IMPATT oscillator efficiency.
06 p0678 A73-18789

On the theory of the avalanche transit-time diode reflection amplifier.
06 p0678 A73-18838

Mathematical models for failure rates of electronic components, considering tantalum condensers, Zener diodes and n-p-n Si transistors
07 p0830 A73-19413

Regenerative amplifier based on multiple IMPATT diodes
07 p0802 A73-20295

Integrated electrically tuned X-band power amplifier utilizing Gunn and IMPATT diodes.
07 p0803 A73-20551

Direct frequency demodulation with CW Gunn and IMPATT oscillators.
07 p0795 A73-20554

High efficiency microwave avalanche diode capability for digital applications, describing GHz rate 100 V pulse generator circuit
07 p0804 A73-20556

Combined operations with negative resistance and nonlinear characteristics in an avalanche diode.
07 p0804 A73-20569

Solid state microwave electronics technology review covering parametric amplifier, maser, tunnel and avalanche diodes, transistors, and transmission, filtering and passive signal processing techniques
08 p0942 A73-20701

IMPATT diode microwave oscillator performance analysis based on model with ac current and voltage superposition on dc, determining avalanche frequency and negative resistance
08 p0942 A73-20706

IMPATT diode microwave oscillator performance analysis for I-V characteristics, output power, efficiency and starting current from equivalent circuit
08 p0943 A73-20707

IMPATT diode anomalous microwave oscillation mode performance analysis, calculating I-V variation, power and efficiency from equivalent circuit
08 p0943 A73-20708

The use of a diamond heat sink for a high reliability IMPATT diode.
08 p0944 A73-20736

Wideband class-C Trapatt amplifiers.
08 p0947 A73-21145

Computer optimisation of double-drift-region IMPATT diodes.
08 p0947 A73-21433

Microwave oscillation in germanium avalanche diodes. I, II.
08 p0947 A73-21461

Nonlinear properties of microwave avalanche diodes operated in IMPATT mode, discussing current density effect and power efficiency
09 p1063 A73-22489

TRAPATT amplifiers for phased-array radar systems.
09 p1051 A73-22497

The elimination of tuning-induced burnout and bias-circuit oscillations in IMPATT oscillators.
10 p1196 A73-24622

Computerized large signal model of IMPATT diode, calculating output power and admittance as function of frequency and amplitude
11 p1336 A73-25320

Numerical analysis of the properties of an avalanche diode in the avalanche multiplication range
11 p1337 A73-25321

Development of cavities for microwave solid state sources.
11 p1338 A73-26150

Injection-locked IMPATT oscillations applied to F.D.M. microwave transmission.
11 p1338 A73-26285

Pulse avalanche diode oscillators with an injected CW signal.
11 p1339 A73-26698

Thermal limitations of CW and pulsed silicon TRAPATT diodes.
12 p1478 A73-27110

A current-excited large-signal analysis of IMPATT devices and its circuit implications.
12 p1478 A73-27112

Short-pulse modulation of gallium-arsenide lasers with TRAPATT diodes.

13 p1626 A73-28050

Computer simulations of large-signal oscillation behavior of avalanche diodes.

13 p1594 A73-29235

Injection frequency locking of the avalanche transit-time oscillator.

13 p1594 A73-29292

A modified GaAs IMPATT structure for high-efficiency operation.

13 p1595 A73-29577

Efficiencies of Schottky-barrier GaAs and both complementary structures of Si IMPATT diodes.

13 p1595 A73-29579

Noise at large RF amplitudes in IMPATT oscillators.

14 p1731 A73-29713

Circuits for power density reduction in TRAPATT diodes.

14 p1732 A73-29927

Temperature-dependent design parameters of TRAPATT diodes.

14 p1736 A73-30446

High-power high-efficiency operation of Read-type IMPATT-diode oscillators.

14 p1736 A73-30447

A comparison of silicon and gallium arsenide large signal IMPATT diode behaviour between 10 and 100 GHz.

15 p1850 A73-31131

Ge-doped p-type epitaxial GaAs for microwave device application.

15 p1923 A73-31399

A theory of oscillator noise and its application to IMPATT diodes.

15 p1851 A73-31939

X band oscillators for microwave generation based on silicon avalanche diodes, presenting power and efficiency dependence on frequency and bias current

15 p1851 A73-32160

Aftereffects in IMPATT oscillators with transient ionizing radiation.

15 p1851 A73-32187

Low-frequency noise characteristics of commercial silicon and gallium arsenide IMPATT diodes.

15 p1851 A73-32188

Microwave integrated circuit applications at special microwave devices operation.

15 p1851 A73-32274

State of the art of GaAs IMPATT diodes.

16 p1990 A73-33896

Linear theory of an IMPATT diode distributed microwave amplifier.

16 p1991 A73-33983

Inductive relaxation oscillator design using common emitter avalanche transistors with N-shaped I-V characteristics at base input

17 p2133 A73-34154

A study of millimeter-wave GaAs IMPATT oscillator and amplifier noise.

17 p2133 A73-34217

Design considerations of high-efficiency GaAs IMPATT diodes.

17 p2134 A73-34219

State-space analysis of a magnetically tuned IMPATT oscillator lumped model.

17 p2136 A73-34973

Two terminal large signal circular coupled wideband TRAPATT diode microwave amplifiers, noting negative resistance characteristics and dc-to-rf conversion efficiency

17 p2140 A73-35321

Mutual synchronization of oscillators which are coupled by a segment of a long line.

17 p2143 A73-35715

Highly stabilized IMPATT oscillators at millimeter wavelengths.

18 p2293 A73-36607

Main trends of development of avalanche photodiodes as high-speed photodetectors /Review/

18 p2293 A73-36715

Regenerative multidiode IMPATT amplifier.

18 p2294 A73-37132

Ion implanted X-band IMPATT/TRAPATT back-to-back diodes.

19 p2408 A73-37146

Measurement technique for large-signal admittance of IMPATT diodes.

19 p2409 A73-37427

Nonsinusoidal EM waves - State of development

19 p2403 A73-37432

Dynamic thermal properties of IMPATT diodes.

19 p2411 A73-38459

Active electronic devices - Microwave diodes

20 p2535 A73-39054

Intrinsic AM noise in singly tuned IMPATT diode oscillators.

20 p2537 A73-39417

Synchronization of the frequency of tunnel-diode, IMPATT-diode, and Gunn-device oscillators

20 p2537 A73-39460

Analytic theory for silicon double-sided n+/n-p-p+/TRAPATT-diode structures.

20 p2538 A73-39594

Low noise Si multijunction IMPATT diode measurements for large signal FM X band oscillator performance

21 p2668 A73-41588

Power-generation potential of various IMPATT structures from a scaling approximation.

21 p2668 A73-41591

Semiconductor rectifiers and thyristor devices, discussing transistor switching, Zener diode, controlled and light activated p-n-p-n diodes

21 p2668 A73-41619

Voltage-to-frequency converters with an avalanche-recombination discharge diode

22 p2832 A73-42357

Book - Avalanche-diode microwave oscillators.

22 p2833 A73-42490

High power GaAs double-drift IMPATT devices.

22 p2834 A73-42693

IMPATT diode frequency-independent small-signal equivalent circuit incorporated with negative resistance element and white noise source for terminal behavior prediction

23 p2964 A73-44074

Increasing the locking bandwidth of a waveguide-cavity oscillator through the use of a double-tuned circuit.

23 p2965 A73-44109

Silicon Zener diodes used as temperature sensors

24 p3090 A73-44937

Large-signal lumped modelling and characterization of an IMPATT diode.

24 p3073 A73-45478

AVALANCHES

NT ELECTRON AVALANCHE
NT TOWNSEND AVALANCHE

Avalanche mode of motion - Implications from lunar examples.

16 p2059 A73-32901

AVERAGE

NT MEAN

AVIATION

U AERONAUTICS

AVIATORS

U AIRCRAFT PILOTS

AVIONICS

A universal digital autopilot and integrated avionics system.

04 p0474 A73-14735

Digital Avionics Information System (DAIS)/development for military supersonic all-weather precision weapon delivery system, emphasizing modular design for different aircraft types

06 p0672 A73-17572

Avionics systems redundancy and complexity, suggesting component design with guaranteed operational life

06 p0673 A73-17617

Military helicopter avionics for communication, surveillance, navigation, landing approach, flight control, power management, ASW and weapons aiming

06 p0648 A73-18509

Calculation of the reliability of electronic components in an 'aeronautics' environment shaped by the operational service routines of onboard equipment devices used by Air France

07 p0799 A73-19403

Some UK military views on the development and procurement of AIDS, BIT and ATE for avionics.

08 p0962 A73-20679

AUTOMATE - A self-contained automatic test system.

08 p0951 A73-20680

Test techniques for advanced avionics displays.

08 p0962 A73-20683

Test programs design for versatile avionics shop test system (VAST), discussing compiler problems alleviation by on-station program patching capability

08 p0962 A73-20688

Air navigation development review covering air traffic, civil jet aircraft event, electronics progress and semiconductor revolution

08 p0986 A73-21088

An instrument panel on an image tube in color

08 p0935 A73-21543

EASCON '72; Electronics and Aerospace Systems Convention, Washington, D.C., October 16-18, 1972, Record.

10 p1298 A73-24551

Electronic systems for time constant and altitude error compensation of rate of climb indicator used in high performance glider flight

10 p1222 A73-24916

On the improvement in survivability for avionics equipment.

12 p1478 A73-27158

Radio Technical Commission for Aeronautics, Annual Assembly Meeting, Washington, D.C., November 9, 10, 1972, Proceedings.

12 p1522 A73-27360

Microwave transmitter tubes for surface-based and airborne radar applications, considering ATC, output power, stability, spectrum, size, weight, reliability, maintainability and cost requirements

13 p1590 A73-28532

Electronic differentiator for aircraft flight data on-board calculation in performance gliding, discussing compensation method and vertical air velocity measuring instrument advantage

13 p1569 A73-28556

Vertical aircraft flight control and navigation instrumentation avionics developments, emphasizing inertial-lead Vertical Speed Indicator design and command and advisory information displays

13 p1621 A73-29345

Russian book on aeronautical electric and electronic materials covering physicochemical properties of magnetic, dielectric, conductor, semiconductor, polymer, ferritic, thin film and composite materials

14 p1766 A73-30357

Electronics and civil aviation; International Conference, Paris, France, June 26-30, 1972, Reports. Volumes 1 & 2

15 p1908 A73-32426

French VOR system with single type equipment for operation on site at performance levels to meet ICAO standards, emphasizing antenna design

15 p1909 A73-32453

Onboard electronic equipment optimization and redundancy

15 p1852 A73-32460

Pilot-electronics-control surfaces as feedback loop for aircraft flight control, discussing instruments, pilot training and aircraft flying qualities

15 p1830 A73-32472

Electronic systems as piloting aids in Concorde SST, discussing flight controls, trim computer, autostabilizer, autopilot and automatic engine control

15 p1830 A73-32474

Air traffic control technology progress review and future forecast, noting microelectronics and automation need in civil avionics

15 p1960 A73-32479

Limitations in the use of all-electric systems for vital application in civil aircraft.

15 p1852 A73-32492

Study of the integrity of an equipment - Application to radio altimeters for category III landing

15 p1880 A73-32493

System of recording based on partial on-board processing

15 p1880 A73-32494

Analysis of the reliability of airborne material in an airline company - Objectives and methods

15 p1831 A73-32495

Electronic integrated flight data displays for pilot workload reduction at takeoff, approach and landing, considering head-up and head-down and colored displays

15 p1831 A73-32506

Experimental approach for utilization of cathode ray tube piloting instruments

15 p1831 A73-32509

Instrument-panel electronic display system

15 p1831 A73-32510

Avionics systems simplification for cost, weight and space reduction, considering ease of maintenance, failure points reduction and flight director/autopilot computers and couplers elimination

16 p1968 A73-33187

Avionics and human factors in flight simulator economics, interrelating aircraft design to simulation system

16 p1995 A73-33206

Harmonic enhancement for airborne low voltage lightweight TWT amplifier band edge performance improvement to provide bandwidth in excess of two octaves

16 p1988 A73-33298

Concept and system of the versatile avionic shop test (VAST) system.

16 p1986 A73-33634

USAF Airborne Warning and Control System with overlaid downlook Doppler radar for low-fly aircraft detection in severe clutter environment, discussing design and performance

17 p2121 A73-34371

Failure analysis used to vindicate JANTX components.

17 p2135 A73-34731

NAECON '73; Proceedings of the National Aerospace Electronics Conference, Dayton, Ohio, May 14-16, 1973.

17 p2136 A73-35201

Military aircraft onboard Digital Avionics Information System for computerized integration of navigation, guidance, weapon delivery, cockpit display, communication, flight control and energy management

17 p2136 A73-35202

Digital avionics systems software development trends, considering compatibility and cost problems increased use of complex processing hardware, sensors and displays

17 p2137 A73-35203

Aircraft onboard computerized avionics and electrical systems architecture for information flow and control with maximum efficiency, flexibility, modularity and minimum maintenance

17 p2137 A73-35204

- Unconventional digital avionics black box approach for cost reduction and reliability improvement in terms of packaging, component coding and hardware qualification programs multiplicity 17 p2137 A73-35205
- Management approach to integration of B-1 avionics, discussing engineering problems, flight tests, electronic equipment and interface requirements 17 p2137 A73-35218
- Custom LSI technology utilization in low volume avionic systems, discussing handcrafted chip design, wall wafer, array logic and MOS cell approaches and costs 17 p2138 A73-35227
- Information transfer system of digital avionics system, examining signal reduction by baseband time division multiplexing and video distribution systems 17 p2138 A73-35230
- Multiplex data bus techniques for digital avionics, discussing transmission media, modulation methods, remote control and reliability 17 p2138 A73-35231
- Modular MOS LSI digital data bus system design for integrated avionics and remote sensors interconnection in aerospace vehicles 17 p2139 A73-35232
- TDM data bus and interface design for digital avionics system, considering standard remote terminal in terms of system parameters, operation and cost effectiveness 17 p2139 A73-35233
- Thin configuration flat digital CRT display with electron beam control improvement for military avionics applications, discussing performance advantages and ownership cost 17 p2139 A73-35235
- Digitally integrated cockpit simulation facility for display systems and avionics to plan mission/human program and airborne equipment requirements 17 p2139 A73-35236
- Digital time division multiplexing for integrating avionics equipment, discussing electrical power control signal multiplexing 17 p2139 A73-35246
- Avionics subsystems operational, functional and physical considerations, discussing cost, computer programming, common components, multiplexing and hardware design 17 p2139 A73-35249
- B-1 aircraft electrical multiplex system. 17 p2110 A73-35309
- Trends in avionics simplification for light utility aircraft. 19 p2450 A73-37801
- Automatic flight control and navigation systems on the L-1011 Capabilities and experiences. 19 p2452 A73-37824
- S-3A aircraft systems, performance and design, discussing flight simulation, wind tunnel tests, weapons systems, flutter tests, avionics, TF-34 engine, stalls and computer programming [AIAA PAPER 73-778] 19 p2387 A73-38367
- Airborne digital data link terminal for commercial airlines' use. 20 p2526 A73-38756
- A rational basis for determining the EMC capability of a system. 20 p2528 A73-38770
- Digital information management system of navigational and flight data for post-1975 fighter aircraft. [AIAA PAPER 73-897] 20 p2589 A73-38832
- Cobra P-530 air superiority fighter adaption to ground attack for international requirements for multipurpose aircraft, discussing avionics for multimission version 21 p2634 A73-40301
- A look at Soviet ATC and nav facilities and avionics. 21 p2737 A73-41522
- Aircraft communication and electronic equipment design for interference control to meet electromagnetic compatibility specification requirements 22 p2821 A73-41695
- Electromagnetic compatibility specifications for aircraft communication and electronic equipment, discussing control and test plans, test facilities, cost effectiveness and British standard 22 p2821 A73-41696
- Electromagnetic compatibility program for modern aircraft communication and electronic equipment design, discussing control plan, interference specification, cable separation and final testing 22 p2821 A73-41697
- A rational basis for determining the EMC capability of a system. 22 p2823 A73-41802
- NAFEC test facilities. 23 p2966 A73-44063
- Aircraft wake vortex detection and avoidance systems, examining acoustic sensors, bistatic Doppler sensors, pulsed radar, aircraft spacing techniques and ground wind measurement 19 p2452 A73-37823
- AXES [COORDINATES]
U COORDINATES
AXES [REFERENCE LINES]
NT AXES OF ROTATION
NT EARTH AXIS
Feed arrangement for axis definition of paraboloid reflector. 08 p0947 A73-21434
- Preferred a axis orientation parallel to fiber axis in commercial carbon fibers due to lower surface energy of basal plane configuration 11 p1389 A73-25857
- A rapid method for frontal plane axis determination in scalar electrocardiograms. 14 p1721 A73-30063
- Measurement of the displacement of the electrical axis of an antenna with respect to its geometrical axis by using extraterrestrial radio emission sources 17 p2120 A73-34119
- AXES OF ROTATION
NT EARTH AXIS
Intersection line of axes cone with sphere and locus of angular velocity vectors for uniform gyroscope rotation with different moments of inertia 02 p0191 A73-11764
- Equations of motion for Kovalevskiaa gyroscope uniform rotation about axes differing from inertia ellipsoid principal axes, noting sufficient stability conditions 02 p0167 A73-11765
- Drift rate of the rotor axis in the generalized problem of the gyroscope with a Cardan mounting 02 p0167 A73-11768
- Lunar axis inclination to ecliptic axis as function of time, tabulating variations during 1971 03 p0367 A73-13078
- Influence of the rotor weight on the changes in the axial rigidity of gyromotors 13 p1572 A73-29146
- Influence of the orthogonal axes of the suspension of an electrostatic gyroscope at zero rotor potential 13 p1618 A73-29148
- Spacecraft reorientation by successive rotations about nonorthogonal axes, deriving classical Euler angles as special case of general solution 15 p1908 A73-31662
- Motion of a free solid body about its center of mass when the body is stabilized by rotation about a non-principal axis of inertia 18 p2336 A73-36163
- The position of the axis of rotation of a free gyroscope ball rotor 18 p2317 A73-36852
- Effect of the random disturbances in the principal gyro axis on the readings of a ground gyrocompass 18 p2317 A73-36854
- The effect of the rotor pattern on the accuracy of the photoelectric angle-measuring system of a gimbal-less electrostatic gyroscope. 18 p2317 A73-36873
- Impulse application for optimal correction of angular position of orbital plane line of apsides, expressing axis angle of rotation as linear function 23 p3027 A73-43269
- AXIAL COMPRESSION LOADS
Axial compression buckling of single metal fiber embedded in plastic matrix, using photoelastic stress analysis and finite element method 02 p0236 A73-12432
- The effects of matrix and interface modification on local fractures of carbon fibers in epoxy. 03 p0335 A73-13982
- Effect of a circular hole on the buckling of cylindrical shells loaded by axial compression. 03 p0395 A73-14181
- Buckling of a long, axially compressed, thin cylindrical shell with random initial imperfections. [ASME PAPER 72-APM-MMM] 05 p0632 A73-16532
- General instability of cylinders with inclined stiffeners under axial compression. 05 p0633 A73-16541
- Three dimensional static and dynamic stability equations of viscoelastoplastic deformation under axial compression 05 p0635 A73-17078
- Dynamic yield, compressional, and elastic parameters for several lightweight intermetallic compounds. 09 p1099 A73-21926
- Investigation of the anisotropy of effective masses in the conduction band of semiconductors under uniaxial compression 09 p1132 A73-21959
- Stress distortion coefficient of uniaxial tension/compression/ of elastic isotropic medium with flattened ellipsoidal sensor from sensor stress recording 09 p1159 A73-22590
- Stability analysis of axially compressed closed circular cylindrical shells with reinforcement rings 10 p1290 A73-24301
- Stability of transversely isotropic cylindrical shells in nonuniform subcritical states 10 p1290 A73-24311
- Facility for studying the strength and deformability of high-strength brittle materials in biaxial compression 10 p1203 A73-24372
- Limiting deformability of lengthwise-crosswise wound fiberglass-reinforced plastics under conditionally instantaneous and prolonged biaxial compression 11 p1386 A73-25034
- Experimental investigation of the stability of shells with holes 11 p1434 A73-25390
- Stability of cylindrical shells with filler under axial compression and external pressure 11 p1435 A73-25396
- Buckling of partially debonded layered cylindrical shells. [AIAA PAPER 73-366] 11 p1438 A73-25501
- Stability of a reinforced cylindrical shell during axial compression 12 p1553 A73-27463
- Selection of optimal parameters for unidirectionally compressed three-layer plates 12 p1555 A73-27795
- Buckling of unstiffened and ring stiffened cylindrical shells under axial compression. 13 p1696 A73-28758
- Optimal shapes of simply supported vibrating elastic beams for maximum fundamental frequency under axial compressive load 14 p1812 A73-30494
- Buckling of circular cylindrical shells under compression. IV - Solutions based on the modified Flugge equations considering prebuckling edge rotations. 14 p1813 A73-30573
- Conditionally-instantaneous and long term strength of a longitudinally-transversely wound glass-fiber-reinforced plastic under biaxial compression 15 p1896 A73-30975
- Cylindrical panels buckling under nonuniform axial compression with various load distributions, basing analysis on Donnell equations and Galerkin method 15 p1948 A73-31635
- Design of stiffened cylinders to resist axial compression. 15 p1950 A73-31921
- Stability of composite-material cylindrical shells under unsteady heating and axial compression 16 p2083 A73-33934
- Stability of a cylindrical shell under dynamic axial load 17 p2244 A73-34739
- Cylindrical shell postbuckling behavior under axial compression using multiple scale averaging technique, concluding predominance of diamond shaped post-buckling pattern [ASME PAPER 73-APM-7] 17 p2247 A73-35032
- On the buckling of cylinders in axial compression. [ASME PAPER 72-APM-BBB] 17 p2250 A73-35113
- Further experimental studies on buckling of integrally ring-stiffened cylindrical shells under axial compression. 17 p2250 A73-35441
- Properties of boron fibers and of boron-aluminum composites in uniaxial compression 20 p2580 A73-39358
- Effect of porosity on creep in niobium carbide and other powder materials under uniaxial loads 20 p2578 A73-39381
- Buckling analysis of deformation and stress distribution in axially compressed longitudinally stiffened cylindrical shells, considering prebuckling deformation effects 20 p2621 A73-39539
- Effect of the yield point of the material on the stability of cylindrical shells under axial compression 20 p2625 A73-39658
- Nondestructive shell-stability estimation by a combined-loading technique. 21 p2708 A73-41266
- Plastic collapse of steep conical shells under axial compression. 21 p2789 A73-41684
- Dynamic buckling of an axially compressed cylindrical shell with discrete rings and stringers. 23 p3047 A73-44377
- Critical stresses of compressed cylindrical shells consisting of orthotropic layers with various orientations 24 p3145 A73-44529
- AXIAL COMPRESSORS
U TURBOCOMPRESSORS
AXIAL FLOW
Boundary layer formation on hollow circular cylinder walls aligned with axial motion of incompressible rotating fluid as function of Rossby and Reynolds numbers 01 p0032 A73-10451
- Investigation of an axial-flow blower during variation of axial clearance and of blade mounting angles in the stator and rotor sections 02 p0131 A73-11791

- Design and development of a small highly loaded, two-stage, transonic axial compressor. 02 p0203 A73-12009 [SAE PAPER 720712]
- Design and test of a small, high-pressure ratio, axial compressor with tandem and swept stators. 02 p0203 A73-12010 [SAE PAPER 720713]
- An experimental study on noise reduction of axial flow fans. 03 p0241 A73-12961
- The optimisation of sound attenuation in lined ducts containing uniform, axial, subsonic, mean flow. 03 p0291 A73-12987
- Study of the waves configuration in an axial-flow supersonic compressor [ONERA, TP NO. 1104] 03 p0246 A73-14135
- A combined theoretical and empirical method of axial compressor cascade prediction. 04 p0404 A73-15869 [ASME PAPER 72-WA/GT-5]
- Investigation of high-power quasi-steady arcs in strong axial gas flows 05 p0602 A73-16583
- Modeling radial dilution air injection in axial flow combustors. 05 p0639 A73-16689 [WSCI PAPER 72-24]
- Solid particle transport effect on structure and axial speed characteristics of two phase submerged turbulent jet 06 p0684 A73-17455
- Some peculiarities of flames stabilized in pulsating streams. 10 p1294 A73-23551
- Biased wall heat transfer in electric arc chamber, noting I-V characteristics and electron current saturation in superimposed axial flow 12 p1560 A73-27700
- A unified analysis of fan stator noise. 13 p1563 A73-28500
- Design method of the axial-flow blade row on modified isolated aerofoil theory with interference coefficient. I. 13 p1564 A73-28649
- The thick turbulent boundary layers on rotating cylinders in axial flow. 13 p1602 A73-29016
- Unstable operation and rotating stall in axial flow compressors. 13 p1566 A73-29024
- Effect of radial total pressure gradients on the Mach number distribution in turbomachines 13 p1567 A73-29450
- Effect of axial velocity variation on the subsonic flow through a compressor cascade. 17 p2094 A73-34397
- Book - Gas turbine theory /2nd edition/. 17 p2221 A73-34471
- Design method of the axial-flow blade row on modified isolated aerofoil theory with interference coefficient. II - The influence of the aerodynamic parameter on the fan performance at low flow rate. 19 p2377 A73-37671
- The axial flow molecular pump. IV - Performance of a rotor with a single blade row in the transition flow regime. 19 p2433 A73-37673
- Heat transfer in rotating cylindrical enclosures with axial inflow and outflow of coolant. 19 p2504 A73-37877
- Design of axial flow fans by cascade method. 21 p2631 A73-40124
- Dynamics of cylindrical structures subjected to axial flow. 21 p2783 A73-40292
- The unsteady aerodynamics of a finite supersonic cascade with subsonic axial flow. 22 p2797 A73-42879 [ASME PAPER 72-APMW-6]
- ### AXIAL FLOW COMPRESSORS
- #### U TURBOMACHINES
- #### AXIAL FLOW PUMPS
- #### NT TURBINE PUMPS
- Minimum pressure zone determination for pressure field at axial plunger pump inlet during cavitation onset, discussing working fluid temperature and composition 02 p0172 A73-11800
- Visualization study of flow in axial flow inducer. 05 p0565 A73-16547 [ASME PAPER 72-FE-33]
- Possibility of using an axial-flow impeller designed according to the law $c \cdot \text{sub } u/r = \text{const}$ as the primary pump 21 p2754 A73-40394
- ### AXIAL FLOW TURBINES
- Russian book on aerodynamic design of axial flow turbomachine blades covering direct and inverse problems for axisymmetric flow in axial turbomachines 04 p0404 A73-15709
- Predicting method of the change in stage performance of axial flow machinery for the variation of cascade geometry. 07 p0867 A73-19225
- Flow equation for axisymmetric compressible fluid flow in conical turbine stage, calculating radial distribution of flow velocity 07 p0868 A73-20088
- Method of experimental study of cascades of transonic blades with strong deflection 09 p1027 A73-22211
- Concorde Olympus 593 axial flow turbojet engine design, detailing variable geometry intake and exhaust nozzles, noise abatement, combustion chamber, gearing and fuel system 13 p1669 A73-28156
- Effect of trailing edge thickness on the cascade performance of circular-arc blades. 13 p1565 A73-29006
- Influence of the variation of cascade geometry on the performance in axial flow machinery. 13 p1565 A73-29007
- Secondary flow in blade cascades of axial turbomachines and the possibility of reducing its unfavourable effects. 13 p1565 A73-29008
- Fundamental study on compressible transient flow and leakage in partially admitted axial and radial flow turbines. 13 p1566 A73-29025
- Calculation of temperature distribution in multistage axial gas turbine rotor assemblies when blades are uncooled. 16 p2047 A73-33486 [ASME PAPER 73-GT-8]
- Comparative analysis of turbine loss parameters. 16 p1964 A73-33529 [ASME PAPER 73-GT-91]
- The unsteady response of a blade row from measurements of the time-mean total pressure. 16 p1964 A73-33531 [ASME PAPER 73-GT-94]
- Experiments on the design of a small axial turbine. 17 p2092 A73-34379
- Sinusoidal pulse flow through an axial flow gas turbine. 17 p2093 A73-34395
- Some kinematic considerations of tone generation in axial turbomachinery. 22 p2899 A73-41710
- An aeroelastic whirl phenomenon in turbomachinery rotors. 22 p2900 A73-42076 [ASME PAPER 73-DET-97]
- Asymptotic unsteady three dimensional flow analysis in axial turbine cascade theory, assuming infinite blade number and unity pitch/chord ratio 22 p2796 A73-42220 [ONERA, TP NO. 1249]
- Heat release from turbine rotor blades 23 p3020 A73-43744
- Total pressure loss distribution in viscous gas flow through annular cascades of axial flow compressors, examining three dimensional flow effects on boundary layer development 24 p3054 A73-44916
- ### AXIAL LOADS
- #### NT AXIAL COMPRESSION LOADS
- Stress distribution in elastic shell of revolution under axisymmetrical loads, noting thickness distribution for uniform stress in critical edge loading zone 02 p0231 A73-11805
- Rigidly plastic cylindrical shell design for axial-load and lateral-pressure combinations with allowance for large deflections 02 p0231 A73-11808
- Bulging of a circular cylindrical shell under axial compression 02 p0231 A73-11814
- Stability of a cylindrical shell under the action of concentrated axial compression loads 02 p0231 A73-11815
- Fiber strength of S-glass/epoxy composites under biaxial loading. 03 p0330 A73-13017
- The influence of axial load on eigenfrequencies of a vibrating lateral restraint cantilever. 03 p0384 A73-13115
- An accurate approximate formula for assessing the vibration frequency of structures axially loaded. 03 p0384 A73-13116
- Stability of fiberglass-reinforced cylindrical shell under the action of axial dynamic loads 03 p0392 A73-13746
- High frequency fatigue test assembly for glass fiber reinforced plastics specimens under symmetric tension-compression 03 p0288 A73-13747
- Large deflection calculation of circular and annular strain hardenable rigid plastic plates under axisymmetric load, using Kirchhoff-Love hypothesis and Tresca flow condition 03 p0394 A73-14022
- Tubular materials plane stress-strain test facility for combined axial load and internal pressure effects 03 p0288 A73-14024
- Characteristics of inversion tubes under axial loading. 03 p0396 A73-14640
- Size effect in fatigue testing of metals explained, considering implications for bending, torsion and axial loading 03 p0396 A73-14646
- Stress intensity factor for axially stressed thin polymethyl methacrylate plate with cracks, noting fracture angle prediction 04 p0512 A73-15240
- Variable thickness orthotropic shell of revolution with bending suppression. 05 p0633 A73-16537
- Initial postbuckling behavior of optimally designed columns and plates. 07 p0908 A73-19084
- Study on fracture mechanism for composite materials based on the concept of the change in Poisson's ratio. 07 p0915 A73-20328
- Stiffness matrix for a beam with an axial force. 08 p015 A73-20725
- Variable-load endurance criteria for steels under conditions of uniaxial and biaxial static tension 09 p1100 A73-22152
- Optimization of finite element grids based on minimum potential energy. 09 p1163 A73-23268 [ASME PAPER 72-PVP-3]
- High Reynolds number experimental data for forebody axial force. 09 p1030 A73-23453
- Elastic stability of biaxially loaded longitudinally stiffened composite structures. 11 p1438 A73-25502 [AIAA PAPER 73-367]
- Dynamic stiffness matrix method for determining natural frequencies of plane frame with axially loaded Timoshenko members of uniform mass distribution 11 p1446 A73-26494
- Static and dynamic stability of simply supported imperfect beam resting on nonlinear elastic foundation under axial load 12 p1550 A73-27033
- Nonlinear effects of axial load and rigidity changes on ball bearings of gyroscopes with symmetrical gyromotor design 13 p1618 A73-29145
- Deformation mechanism and strength of metals under impulsive loading. 13 p1639 A73-29463
- A study of fatigue crack propagation in high strength aluminum alloys at high stresses. 13 p1640 A73-29488
- Behavior of random micro-structural systems. 13 p1701 A73-29530
- Deformation criteria of failure under simple and composite stresses. 13 p1703 A73-29621
- Variational geometry optimization of thin rotational membrane shells under axisymmetric loading 16 p2079 A73-33011
- Elastic semiinfinite cylindrical shell stress-strain state after axial impact against static rigid plane, obtaining solutions for small time values 17 p2244 A73-34740
- The dynamic response of columns under short duration axial loads. 17 p2248 A73-35040 [ASME PAPER 73-APM-19]
- Stress concentration determination under biaxial tension in a plate weakened by a randomly-shaped hole 18 p2363 A73-36414
- Strain accumulation and rupture during creep under variable uniaxial tensile loading. 19 p2495 A73-37434
- Biaxial cyclic high-strain fatigue of aluminium alloy RR58. 19 p2440 A73-37437
- Nonlinear parametric vibrations of closed cylindrical shells 19 p2499 A73-37764
- Laterally restrained beam columns with uniform biaxial loading. 20 p2616 A73-39117
- Steady-state creep of a thin-walled tube in the general case of applied forces 21 p2787 A73-41194
- The effects of speed and radial flow on the axial force on an enclosed rotating disc. 21 p2754 A73-41685
- Criteria relating to the fatigue life of steels subjected to alternating loads under conditions of uniaxial and biaxial static strain. 22 p2874 A73-42102
- Forced motion of lumped mass systems including the effect of axial force. 22 p2923 A73-42630
- Parametric instability of clamped-clamped and clamped-simply supported columns under periodic axial load. 22 p2929 A73-43137
- Normalized stresses around an elliptic hole in a finite plate of linear material subjected to large uniform in-plane loading. 23 p3039 A73-43386
- Uniaxial pressure effects on diode structures volt-ampere characteristics, examining potential barrier height and photo emf changes 23 p2960 A73-43787
- Strip weakened by array of holes, investigating plastic zone initiation and propagation under uniaxial tension for load bearing capacity estimation 24 p3147 A73-44685
- An elastic-plastic analysis of a bar under repeated axial loading. 24 p3151 A73-45307

Behavior of materials under multiaxial vibrating loads. II - Experimental investigations 24 p3153 A73-45447

AXIAL STRAIN

Axisymmetric buckling and stability of annular sandwich panel under radially varying in-plane stresses 01 p0115 A73-10740

Optimal thickness of a cylindrical shell under external pressure 01 p0116 A73-10964

Finite axisymmetric deformations of elastic membranes. 02 p0234 A73-12089

A time hardening transient creep solution for steadily loaded uniaxial tension panels containing circular and elliptical holes under conditions of plane stress. 06 p0761 A73-17820

Study of the stability of nonshallow spherical shells with finite displacements by applying various equations of the theory of shells 07 p0911 A73-19318

Axisymmetric deformation of a laminar, orthotropic, cylindrical shell 08 p1017 A73-21368

Experimental investigation of the failure mechanism of fiber-reinforced composites subjected to uniaxial tension. 09 p1156 A73-21874

Stability of the axisymmetric form of motion of flexible shallow shells 09 p1164 A73-23344

Small perturbation approximations of plane biaxial tensile deformation of semilinear elastic medium with cavity, using Piola-Kirchhoff stress functions 09 p1164 A73-23347

Combined axial and torsional shear of a tube of incompressible isotropic elastic material. 10 p1291 A73-24336

Axisymmetric buckling of rigidly clamped hemispherical shells. 11 p1447 A73-26648

A comparison of quasi-static uniaxial-strain and Hugoniot tests for quartz-phenolic composite. 12 p1550 A73-27024

On optimal thickness of a cylindrical shell loaded by external pressure. 12 p1554 A73-27540

Strain curves of titanium alloys VT-6S and VT-14 in the temperature range 20-400 C. 13 p1643 A73-29612

Finite difference solution for large deformations of cylindrical shells - A comparison with finite element solutions. 14 p1807 A73-30182

Strains and stress-concentration factors in plates under out-of-phase biaxial cyclic loads. 15 p1948 A73-31614

Axisymmetrical and antisymmetrical stresses and deformations in shells of revolution with a meridional cutout 16 p2074 A73-32683

Geometrically nonlinear axisymmetric deformation of toroidal shells 18 p2362 A73-36403

Theory of hardening applicability to the description of deformation law singleness under various conditions of uniaxial tension 18 p2366 A73-36759

Flexural vibrations of rods with viscoelastic coating subjected to axial force. 19 p2502 A73-38347

Effects of misalignment on the pre-macroyield region of the uniaxial stress-strain curve. 20 p2576 A73-39030

Front-end collision of a partially liquid-filled cylindrical shell with a solid body 20 p2616 A73-39261

Yield criterion in plane stress state for description of second order effect relating to axial strain accumulation in cyclic torsion 20 p2624 A73-39568

Solution of a mixed axisymmetric problem for an elastic ellipsoid of revolution by the method of p-analytic functions 24 p3153 A73-45509

Partial solutions of finite elasticity - Axially symmetric deformations. 24 p3154 A73-45550

AXIAL STRESS

The analysis of nonlinear three dimensional frames. 03 p0391 A73-13684

Electron impulse interactions of heat in semiconductors 04 p0483 A73-15470

Optimal experimental measurements of anisotropic failure tensors. 05 p0631 A73-16113

Bending and rolling methods for tensile testing of metals without local necking, considering fracture under reduced axial stress 05 p0581 A73-16130

Material deformations determined with the aid of X rays in the case of elongations remaining after a uniaxial tensile test involving titanium and TiAl6V4 05 p0588 A73-17243

Multi-axial and reversing stress effects in dislocation creep - A mechanical equation of states. 08 p0980 A73-21781

Behavior of threshold current and polarization of stimulated emission of GaAs injection lasers under uniaxial stress. 09 p1092 A73-22247

Small amplitude surface and plate waves propagation in incompressible biaxially stressed elastic media, obtaining dispersion equation for various phase velocities 11 p1434 A73-25166

Strain gage measurements of elastoplastic deformations under biaxial and triaxial stresses with application to cylindrical steel container 13 p1617 A73-28843

Two dimensional analysis of yielding to fracture process in angle-ply filament wound laminates under biaxial tension and compression 13 p1702 A73-29543

Hot fatigue strength during fluctuating axial tension of PER 7 and IN 100 superalloys 16 p2026 A73-33971

Influence of in-plane displacements at the boundaries of rigid-plastic beams and plates. 16 p2083 A73-33973

Characteristics change of Gunn diodes with uniaxial stress and temperature. 16 p1991 A73-33996

Torsion and extension of a cylinder with an outer annular cut 17 p2240 A73-34143

Limiting equilibrium of reinforced cylindrical shells 18 p2363 A73-36412

Influence of the geometrical configuration of a structure on its carrying capacity 21 p2786 A73-40982

The behavior of materials subjected to multiaxial cyclic stresses. I - Methods of calculation 22 p2917 A73-41781

Experimental determination of the transient uniaxial stress in a bar by dynamic photoplasticity. 22 p2926 A73-42894

Environmental effects on fracture resistant and biaxial fatigue design of aircraft structures. 23 p3042 A73-43811

The strength of orthogonally reinforced plastics during uniaxial tension 24 p3145 A73-44522

'Crack boundaries' in the case of unidirectional glass-fiber-reinforced plastic wound laminates under uniaxial and multiaxial stress 24 p3103 A73-44883

AXISYMMETRIC BODIES

Numerical solution to the axisymmetric thermoplasticity problem of a shell of revolution 01 p0112 A73-10007

Axisymmetric thermoelasticity problem for an infinite body weakened by two parallel circular cracks 01 p0113 A73-10014

Axisymmetrical planet gravitational field potential expression in spherical function series, noting expansion coefficient decrease in power law for smooth density body 01 p0099 A73-10691

Turbulent swirling wake behind spinning axisymmetric body of revolution having axis aligned with free stream direction, obtaining velocity profiles variations 01 p0004 A73-11136

Some exact solutions in the design of technically orthotropic axisymmetric plates. 01 p0118 A73-11365

Calculus of variations and finite difference method for equilibrium equations in axisymmetric plastic shell design 02 p0232 A73-11821

Far field steady inviscid flow behavior of hypersonic blunt axisymmetric slender body, obtaining unsteady two dimensional solution with cylindrical symmetry 03 p0242 A73-13310

Application of a pseudo-viscous method to the calculation of the steady supersonic flow past a waisted body. 03 p0242 A73-13335

Base resistance of axisymmetric bodies with a variable angle of attack - Analysis and interpretation of the physical phenomenon 03 p0242 A73-13375

Investigations on incipient boundary layer separation on axisymmetric compression surfaces. 03 p0246 A73-14127

Periodic axisymmetric waveguide with complex structure, obtaining slow wave dispersion equation solutions 04 p0429 A73-15910

Calculation of the potential flow about axisymmetrical fuscages, annular profiles, and propulsion system inlets [DFVLR-SONDDR-265] 07 p0773 A73-19205

Dynamic analysis of freely supported axisymmetric shells. 08 p1018 A73-21473

Axisymmetric deformation of an elastic layer containing coaxial circular slots 09 p1158 A73-22359

AXISYMMETRIC FLOW

Oscillation of axisymmetric bodies in a stratified fluid. 10 p1205 A73-23625

Base drag reduction on blunt based axisymmetric bodies by base burning, calculating inviscid flow field with heat addition around recirculating bubble 11 p1449 A73-25347

Potential flow past axisymmetric ring wing profiles via singularity method, applying source and vortex distributions to curved thick profiles [DFVLR-SONDDR-271] 11 p1300 A73-25348

Aerodynamical and aeromechanical investigations involving pin-equipped models in hypersonic flow 11 p1300 A73-25441

Solution of kinematical differential equations for a rigid body. [ASME PAPER 72-APM-AAA] 11 p1398 A73-25705

Large particle method for calculation of transonic supercritical vortex flow fields around flat and axisymmetric bodies 11 p1302 A73-26330

LF series expansion for acoustic scattering from soft and hard rotationally symmetric bodies, discussing relevance of magnetic polarizability tensor and electrostatic capacity 13 p1659 A73-28485

Torsion of an axisymmetrical anisotropic body with mixed boundary conditions on the edge surface 13 p1698 A73-29086

The influence of back pressure on the point of instability of axisymmetric shells deformed by fluid pressure. 14 p1813 A73-30662

The thin shock layer in the hypersonic flow problem 15 p1821 A73-31194

Calculation of stress-concentration factors for grooved shafts in bending using the point-matching technique. 15 p1948 A73-31616

Analytic and numerical investigations of boundary layer flows about slender axisymmetrical bodies 16 p1962 A73-33248

Determination of the carrying capacity of axisymmetric shells under piecewise linear plasticity conditions 17 p2244 A73-34738

Incompressible potential flow past axisymmetric bodies in cylindrical pipes. 19 p2376 A73-37489

Torsion of an axisymmetric anisotropic body with mixed boundary conditions on the side surface. 19 p2498 A73-37636

Oscillatory motions of an axisymmetric spin-stabilized solid body 20 p2593 A73-39495

Equations of perturbed motion of a body with a liquid-containing cavity when the normal to the free liquid surface deviates sizably from the axis of the cavity 20 p2547 A73-39510

Incompressible turbulent boundary layer separation from a curved axisymmetric body. 20 p2548 A73-39525

Large deformations of cord-reinforced multilayered axisymmetric shells. 20 p2621 A73-39542

An experimental study of strong injection at axisymmetrical bodies of revolution. 21 p2633 A73-41057

AXISYMMETRIC DEFORMATION

U AXIAL STRAIN

AXISYMMETRIC FLOW

NT ANNULAR FLOW

Shock wave reflections along the axis in a steady axisymmetric flow [ONERA, TP NO. 1128] 01 p0001 A73-10237

Navier-Stokes equations numerical solution for steady state axisymmetric flow of incompressible Newtonian fluid between two parallel infinite rotating disks 01 p0122 A73-10805

Theoretical consideration on the supersonic axisymmetrical nozzle. 01 p0003 A73-11131

Axisymmetric slow viscous flow past an arbitrary convex body of revolution. 02 p0153 A73-12040

Calculation of an axisymmetric supersonic gas jet injected in a supersonic slipstream past a given body with heat supply 02 p0129 A73-12583

Supersonic jet noise suppression using coaxial flow interaction. 03 p0241 A73-12964

German monograph - Axisymmetric free jets and free-jet flames and a numerical procedure for calculating them. 03 p0398 A73-13810

Russian book on aerodynamic design of axial flow turbomachine blades covering direct and inverse problems for axisymmetric flow in axial turbomachines 04 p0404 A73-15709

Eddy-viscosity distribution in thick axisymmetric turbulent boundary layers. [ASME PAPER 72-WA/FE-18] 04 p0435 A73-15845

An explicit numerical method for the solution of jet flows.
[ASME PAPER 72-WA/FE-20] 04 p0435 A73-15846

Optimal profiles of a nozzle for axisymmetric supersonic discharge of a Lighthill dissociating gas
05 p0534 A73-17270

Closed form analytical solution for secondary flow in viscoelastic liquids axisymmetric flow past oblate and prolate ellipsoids
06 p0687 A73-18507

Magnetohydrodynamic laminar source flow between two parallel disks.
07 p0854 A73-19102

Minimum mixing losses of axisymmetric turbulent wakes in profiled wall channels
07 p0811 A73-19611

Flow equation for axisymmetric compressible fluid flow in conical turbine stage, calculating radial distribution of flow velocity
07 p0868 A73-20088

Parameter calculations for a supersonic axisymmetric flow near its expansion center
07 p0775 A73-20093

Simulation of velocity profiles by shaped gauze screens.
08 p0953 A73-20717

Transonic nozzle flow with nonuniform gas properties.
08 p0925 A73-20719

Accuracy studies of the numerical method of characteristics for axisymmetric, steady supersonic flows.
10 p1171 A73-23602

Turbulent viscosity distribution in axisymmetric compressible wake and coaxial mixing flows via Navier-Stokes equations, taking into account pressure gradients
10 p1206 A73-24545

Similarity solutions of unsteady, compressible plane and axisymmetric laminar boundary layer equations.
10 p1208 A73-24807

Lift forces on an oscillating cylinder at low Reynolds number.
10 p1173 A73-24822

Transient Ekman and Stewartson layers in a rotating tank with a spinning cover.
10 p1210 A73-24840

Incompressible turbulent axisymmetrical impulsive air injection at moderate pressure into stagnant surroundings, measuring flow velocity distribution
10 p1210 A73-24849

One parameter family of axisymmetric vortex rings propagating steadily through unbounded ideal fluid at rest at infinity
11 p1345 A73-25051

Axisymmetric flow model of rotating inviscid incompressible fluid into point sink at low Rossby numbers, discussing selective withdrawal and blocking wave
11 p1345 A73-25053

Calculation of nozzle flows using Pade fractions.
11 p1303 A73-26386

Sonic line for a coaxial axisymmetric nozzle.
11 p1303 A73-26403

Influence of the shape of a body on the characteristics of a self-similar axisymmetric wake
12 p1457 A73-26953

Nonvortical axisymmetric flow of inviscid ideal incompressible fluid from partial differential equations solution
12 p1486 A73-27242

Linear axisymmetric self similar solution for blunt nosed rigid cone immersed into ideal compressible fluid at subsonic velocity, computing wetted surface radius increase
12 p1487 A73-27410

Base drag calculations in supersonic turbulent axisymmetric flows.
13 p1564 A73-28835

Axisymmetric inertial oscillations of a fluid in a rotating spherical shell.
13 p1601 A73-28916

Similarity properties of shockless axisymmetric flows with heat addition, considering convergent base and divergent duct flows
13 p1567 A73-29449

Study of a new family of solutions of Navier-Stokes equations
14 p1744 A73-29758

Nonlinear effects in steady supersonic dissipative gasdynamics. II - Three-dimensional axisymmetric flow.
14 p1711 A73-30167

Chandrasekhar equations for axisymmetric MHD flows generalized for steady and unsteady flows
14 p1781 A73-30701

Using the singularity method in studies of potential flow about bulbous streamline bodies
14 p1712 A73-30706

German book - Theoretical gasdynamics. Volume I - Theory of the flows of compressible media.
15 p1863 A73-31474

Analysis of turbulent skin friction in thick axisymmetric boundary layers.
15 p1863 A73-31658

Transonic flow through a turbine stator treated as an axisymmetric problem.
[ASME PAPER 73-GT-51] 16 p1964 A73-33510

Theoretical investigation of the incompressible, turbulent, and axisymmetric internal flow with vanishing wall friction
16 p1964 A73-33749

Axisymmetrical turbulent boundary layer along a slender cylinder.
17 p2150 A73-34400

Relaxation solutions for inviscid axisymmetric transonic flow over blunt or pointed bodies.
17 p2095 A73-35128

A generalized theory for the turbulent mixing of axially symmetric compressible free jets.
17 p2156 A73-35505

Application of turbulence model equations to axisymmetric wakes.
18 p2260 A73-36203

[AIAA PAPER 73-648] 18 p2260 A73-36203

Transonic flow analysis using a streamline coordinate transformation procedure.
18 p2261 A73-36211

[AIAA PAPER 73-657] 18 p2261 A73-36211

Mathematical approximation of turbulent cylindrical jets: Initial core - Velocity distribution
18 p2301 A73-36690

Similarity parameters and approximate relations for the axisymmetric supersonic flow past an ellipsoid
18 p2266 A73-37019

Linearized MPD jet and channel flows in external magnetic fields with the Hall effect.
19 p2465 A73-37175

Calculation of two-dimensional unsteady plasma flows in channels
19 p2467 A73-37369

Influences of the shape of a body on the characteristics of a self-similar axisymmetric wake.
19 p2377 A73-38129

The magnetic channeling of a supersonic axisymmetric plasma jet.
19 p2470 A73-38318

Homogeneous anisotropic to isotropic turbulence convergence based on shear flow component measurements of turbulence energy distribution in axisymmetric flow
20 p2546 A73-39097

Boundary-layer separation at a free streamline. III - Axisymmetric flow and the flow downstream of separation.
20 p2549 A73-39806

Streamline curvature and velocity gradient behind curved shocks.
21 p2632 A73-40441

The integrals of the system of Navier-Stokes equations for axisymmetric motion of an incompressible fluid
22 p2841 A73-42123

Nozzle design for subsonic flow in axisymmetric contractions based on potential flow theory and visual observation, obtaining velocity distribution along wall
22 p2798 A73-43029

On the generalization of the Mangler transformation for axisymmetric boundary layers.
23 p2967 A73-43226

An approximate model of a separated turbulent flow in an abruptly widening channel
23 p2968 A73-43471

Thermal convection in a large rotating fluid annulus - Some effects of varying the aspect ratio.
23 p3002 A73-43597

Classification of methods for solving the direct problem of axisymmetric flow calculation in turbomachines
23 p3020 A73-43736

Acoustic wave propagation in axisymmetric swirling subsonic jet flow, obtaining directivity patterns for spinning and nonspinning modes from wave equation numerical integration
24 p3077 A73-44837

[AIAA PAPER 73-1004] 24 p3077 A73-44837

Spatial and temporal stability of laminar axisymmetric jet and wake shear layers in viscous and inviscid flow
24 p3079 A73-45308

Flows past exponential bodies in the presence of strong compression in the shock layer
24 p3055 A73-45534

The incompressible boundary layer of higher order at the axisymmetrical stagnation point in the case of strong suction or blowing
24 p3056 A73-45545

AXISYMMETRY
U SYMMETRY

AXLES
U SHAFTS [MACHINE ELEMENTS]

AXONS
Structural characteristics of connections between medial efferent systems and spinal cord neurons
09 p1040 A73-22577

Authoradiographic study of protein synthesis in perikaryons and of nitrogen migration into the axons of hypertrophic sympathetic neurons
13 p1574 A73-28296

Circulation of nervous impulses in the cerebral cortex
14 p1718 A73-30569

AXIDES [ORGANIC]
Gas-releasing additives to jet fuels
21 p2754 A73-41070

AZIMUTH
Azimuthal pointing control system for balloon observations of celestial bodies, analyzing suspension rope twisting method
01 p0075 A73-11207

Shadowing of electron azimuthal-drift motions near the noon magnetopause.
02 p0164 A73-12442

Electron and muon density fluctuations, trajectory distribution and azimuthal symmetry in cosmic ray air showers
02 p0209 A73-12673

Fraunhofer zone distribution functions for azimuth and elevation angles of radio waves reflected from inhomogeneous ionospheric scattering layer
03 p0278 A73-14071

Analysis of the accuracy of a determination of the reciprocal azimuths of a geodesic line
04 p0443 A73-15510

Automatic electronic pendulum astrolabe featuring altitude and azimuth tracking mechanisms, azimuth setter and 180 degree turning mechanism
13 p1612 A73-28394

The application of the method of equal heights to the determination of astronomical azimuth
19 p2490 A73-38557

Conditional equations of astronomical latitudes, longitudes, and azimuths
19 p2490 A73-38559

Use of the azimuthal equal-area projection to display radiation patterns of complex antennas
21 p2661 A73-40202

Indoor azimuth reference systems specifications, characteristics and results, discussing optical windows, theodolites, reflectors, bulk monument structure measurements and rocket applications
21 p2671 A73-40505

[AIAA PAPER 73-842] 21 p2671 A73-40505

High precision photoelectric azimuthal polarimeter design, construction and operation for determining angular rotation of polarized light beam
21 p2704 A73-41258

Extremal search method errors in determining azimuthal position of gyro stabilized platform relative to meridian plane, comparing with gyrocompasses
24 p3109 A73-45022

AZINES
Optimization of the rheological properties of s-triazine derivatives.
07 p0787 A73-19561

AZO COMPOUNDS
The effects of Dalmane /flurazepam hydrochloride/ on human EEG characteristics.
08 p0931 A73-21464

Investigation of some electrooptical properties of liquid crystals
14 p1784 A73-30854

AZOLES
NT INDOLES
NT PYRROLES
NT TRYPTOPHAN

AZOTOBACTER
Purification, crystallization, and subunit structure of allosteric adenosine 5'-monophosphate nucleosidase.
03 p0273 A73-13807

A4D AIRCRAFT
U A-4 AIRCRAFT

B
B STARS
Element abundances in O- and early B-stars.
01 p0096 A73-10296

LTE fine analysis of omicron-tw C Ma line profiles, showing chemical composition near iota Her
02 p0221 A73-12705

Continuous near-infrared spectrum of two Be stars - HD 50138 and HD 51585
02 p0224 A73-12735

Spectra of several Be stars between 7000 and 9600 A
02 p0224 A73-12736

Analyses of light-ion spectra in stellar atmospheres. I - Magnesium II in B and O stars.
03 p0366 A73-12934

Two new He I lines in the spectra of B-type supergiants.
03 p0371 A73-13218

A search for He-weak stars in very young clusters.
03 p0372 A73-13227

MWC 349 - A new radio star.
03 p0374 A73-13849

Ultraviolet photometry from the orbiting astronomical observatory. V - The helium-weak stars.
04 p0499 A73-15363

Light variations of high luminosity O and B stars in the Large Magellanic Cloud.
07 p0877 A73-19597

Stellar and interstellar K lines - Gamma Pegasi and iota Herculis.
08 p1003 A73-20882

Cyclic variations of the Be star beta-one Monoceros. 08 p1006 A73-20924

The spectral classification of the beta Cephei stars and their location in the theoretical Hertzsprung-Russell Diagram. 08 p1006 A73-20927

Properties and nature of shell stars. III - Periodic radial-velocity changes of 4 Hercules. 09 p1140 A73-22003

On the nature of X Persei - Evidence from the 1957 outburst. 10 p1275 A73-23845

Spectroscopic changes in the suspected X-ray source X Persei. 10 p1275 A73-23846

The extinction curve for Cygnus OB2 no. 12. 11 p1414 A73-25068

UBV photometry of 32 Cygni during the 1971 eclipse. 11 p1426 A73-26268

Electric conductivity in the atmosphere of early-type stars. 11 p1427 A73-26575

Dust emission nebulae around Orion O and B stars. 11 p1427 A73-26606

On a correlation between the magnitude and the radial velocity of hot stars. 13 p1672 A73-28036

Blue OB stars detection by flicker comparison, astronomical photography and two color diagrams, discussing classification as quasars and white dwarfs. 13 p1673 A73-28148

A problem in distance-determination for Mira variables with an appendix on OB-star distances. 15 p1932 A73-31306

O-B stars in young star clusters associated with nebulae. 15 p1934 A73-31420

Mariner 9 ultraviolet spectrometer experiment - Interstellar absorption at Lyman alpha in OB stars. 15 p1936 A73-31556

Late B6 stars line spectra, atmospheric electron density, microturbulence velocity, excitation temperature, flux envelopes and energy distributions. 17 p2233 A73-35612

The ultraviolet flux envelopes of main-sequence B stars. 17 p2234 A73-35613

The spectrum of eta canis majoris, B5 Ia. 18 p2355 A73-36779

Early type stellar line spectra, discussing LTE, hydrogen and helium lines, stellar element abundance and O and B stars. 18 p2356 A73-36875

Profiles of emission lines in Be stars. II - Interpretation of the long-period V/R variation. 19 p2484 A73-37615

Spectrographic observations of the peculiar Be star with infrared excess HD 45677. 20 p2611 A73-39586

Observation of the star gamma-Cassiopeia of the Be spectral type by Fourier spectrometry from 1 to 2.5 micron. 22 p2908 A73-42354

Study of the kinematics of O and B spectral type stars. 23 p3036 A73-44241

Secular variations in H alpha, H beta and metal line spectra of Be star 88 Hercules from intensity decrease observations, noting envelope hydrogen absorption lines visibility. 24 p3140 A73-45187

B-1 AIRCRAFT

C-5 program developments and alterations in terms of defense requirements and cost problems, discussing objectives and management policies in F-15 and B-1 projects. 01 p0124 A73-11069

B-1 airplane model support and jet plume effects on aerodynamic characteristics. 05 p0563 A73-16901

B-1 bomber crew integrated escape module for safe recovery throughout aircraft operational envelope, discussing capsule configuration and flight tests. 15 p1825 A73-31426

Development of a high-performance ringsail parachute cluster. 15 p1828 A73-31452

Operational readiness and maintenance testing of the B-1 strategic bomber. 16 p1969 A73-33631

B-1 technology applications to advanced transport design. 17 p2102 A73-34696

Management approach to integration of B-1 avionics, discussing engineering problems, flight tests, electronic equipment and interface requirements. 17 p2137 A73-35218

Application of multiplexing to the B-1 aircraft. 17 p2107 A73-35247

B-1 aircraft electrical multiplex system. 17 p2110 A73-35309

Boron-stiffened longerons on the B-1. 19 p2436 A73-38499

Test facilities for B-1 components prior to construction and flight testing, discussing wind tunnel tests for aerodynamic characteristics, stall performance, drag factor and spin. 21 p2675 A73-41431

B-52 AIRCRAFT

Active flutter suppression - B-52 controls configured vehicle. 11 p1305 A73-25552

[AIAA PAPER 73-322] Feedback control configured vehicles ride control system design for B-52 aircraft load alleviation and mode stabilization during flight through atmospheric turbulence. 17 p2107 A73-35245

B-52 aircraft-borne short range attack missile weapon system air conditioner thermal performance fulfillment with Freon refrigerant and air distribution in heat exchangers. 18 p2269 A73-36340

[AIAA PAPER 73-723] B-52 control configured vehicles ride control analysis and flight test. 19 p2378 A73-37452

[AIAA PAPER 73-782]

B-57 AIRCRAFT

WB-57F aircraft with instrument package for nuclear test detection and upper atmosphere research, discussing range, altitude, speed, payload capacity and onboard equipment. 16 p1969 A73-33548

[AIAA PAPER 73-510]

B-70 AIRCRAFT

Mountain waves and CAT encountered by the XB-70 in the stratosphere. 11 p1394 A73-25785

BABBITT METAL

U BEARING ALLOYS

BACILLUS

Properties of phosphoribulokinase from Thiobacillus neapolitanus. 03 p0261 A73-13597

Effect of cultural conditions on the fatty acid composition of Thiobacillus novellus. 03 p0261 A73-13599

Spin-labeling studies on the membrane of a facultative thermophilic bacillus. 07 p0782 A73-20027

Study of intestinal Lactobacillus species composition during a long stay of humans in a closed space. 17 p2112 A73-34239

BACK INJURIES

Aerodynamic pumping-caused spinal fractures in two pilots during high speed flight. 02 p0137 A73-12154

BACKGROUND NOISE

The detection of a point source in the presence of nongaussian background noise. 01 p0017 A73-10832

The influence of background noise on disturbance due aircraft. 03 p0249 A73-12979

Two-channel direction finding with point source emission and spaced antennas reception, investigating cross correlation and background noise interference effects on accuracy. 03 p0278 A73-14062

Modulating /multiplicative/ noise effects on output signal characteristics of receiver designed for optimal reception against background of Gaussian noise. 04 p0423 A73-15915

Optimal optical measurement for two dimensional object position on plane in Gaussian background noise, calculating mean square error for false identification probability determination. 05 p0547 A73-16055

Adaptive algorithms for reducing a random field to a prescribed set of states with constraints on the elements of the approximating sequences. 07 p0796 A73-20079

Detection of a two-frequency signal buried in noise of unknown power. 07 p0794 A73-20144

Noise immunity in the reception of binary radio signals on a correlated-noise background. 08 p0939 A73-21553

Characteristics of the adaptive optimal detection of Gaussian signals on a pulse-noise background in receivers with a logarithmic amplifier. 08 p0940 A73-21554

Measurement of amplifier noise. 08 p0949 A73-21623

Measuring the off-duty factor of chaotic pulsed interference on a Gaussian noise background. 09 p1050 A73-22338

Coherent and noncoherent signal burst detection in background noise of unknown intensity, using maximum likelihood estimates. 09 p1050 A73-22457

Classification of weak signals on a non-Gaussian noise background. 09 p1051 A73-22557

Electrical interference /noise/ effects on measurements of high accuracy low-level differential data signals, discussing noise reduction, capacitive coupling problem and design principles. 10 p1189 A73-24570

The detection and resolution of incoherent objects by an aberrated optical system in the presence of background noise. 10 p1229 A73-24618

Optimal and preferred listening levels for speech in aircraft acoustical environments. 11 p1304 A73-25387

Nonparametric signal detectors in the case of dependent sampled magnitudes. 12 p1467 A73-26868

Effectiveness of analog storage in the detection of signals on a background of noise and strong random pulsed interference. 12 p1467 A73-26942

Long duration radio signals reception on noise background, recording signal/noise mixture on photographic film. 12 p1470 A73-27578

An optimal algorithm for the detection of radar signals on a noise background of unknown power level. 12 p1471 A73-27588

On the existence in Schottky diodes of correlation laws between the parameters of the direct characteristic and the amplitude of low frequency background noise. 13 p1590 A73-28565

Accuracy of target angular coordinate estimates by the maximum likelihood method on a correlated noise background. 14 p1729 A73-30557

Optimal reception of digital signals on an additive noise background. 15 p1843 A73-31493

French monograph - Contribution to the study of background noise in Gunn effect diodes. 15 p1852 A73-32589

Noise properties of a transistor in an integrated circuit. 16 p1987 A73-33089

Fast pulse VHF background noise measurements in site selection for radio detection of cosmic ray air showers. 16 p1984 A73-33924

Generation-recombination noise and the microwave emission from InSb. 17 p2219 A73-34912

Image quality of binary and multigradation microwave holograms, noting HF components and background noise. 17 p2168 A73-35164

Bayes theorem for radio signals parameter estimation on random noise background, using rectangular function of losses. 17 p2123 A73-35167

Small hypervelocity particle in-flight detection against background noise using forward scattering from laser illuminated particle distribution. 17 p2172 A73-35415

Effectiveness of certain easily realizable rank algorithms for detections of signals against a background of noise. 17 p2130 A73-35720

Analysis of optimal recognition of space-time signals. 17 p2130 A73-35721

Optimal Markov sequence signal detection in correlated FM random electronic countermeasure background noise. 20 p2529 A73-38929

Bipolar transistor base region noise current correlation with effective voltage, proposing equivalent circuit. 20 p2538 A73-39597

BACKGROUND RADIATION

The short-wavelength spectrum of the microwave background. 01 p0015 A73-10062

Galactic-latitude dependence of low-energy diffuse X-rays. 01 p0092 A73-11030

[AD-760196] Observations of soft X-rays - Two supernova remnants in the constellation Lupus and the diffuse background. 01 p0103 A73-11031

Observational evidence relating to a recent theory on the origin of the universal X-ray background /Research note/. 02 p0207 A73-12395

Closed time as an explanation of the black body background radiation. 02 p0193 A73-12440

Midlatitude excess radiation energy density relation to primary cosmic ray background from spectrum measurement data. 02 p0208 A73-12460

Spectrum of the cosmic X- and gamma ray background in the energy range 1 keV-1 MeV. 02 p0210 A73-12730

Scor X-1, Crab Nebula, extragalactic, thermal and diffuse background source X ray spectra. 03 p0364 A73-13962

Solar cyclic intensity variation of excess radiation with respect to galactic radiation background at low altitudes from satellite data analysis. 03 p0365 A73-14575

Galaxy formation from amihilation-generated supersonic turbulence in the baryon-symmetric big-bang cosmology and the gamma-ray background spectrum.

04 p0499 A73-15353

X ray background radiation measurement in outer space for proof of Gamow hypothesis on universe chemical composition, indicating improved cosmological models

05 p0613 A73-16210

Rocket-borne measurement of UV background radiation at 1115, 1425 and 1446 Å, setting upper limit to flux from Coma galactic cluster

07 p0868 A73-19057

Composition of radiation excess over primary cosmic ray background recorded by Cosmos satellites below midlatitude belt region

07 p0870 A73-19426

Balloon measurements of the far-infrared background radiation.

[AD-757848]

07 p0825 A73-20177

Night sky background radiation measurement by far IR radiometer carried on rocket launched from Hawaii

07 p0825 A73-20187

Optimum spectral band of an infrared detection system for use against forest background radiation.

08 p0962 A73-20811

Clusters of galaxies and the cosmic light.

08 p1002 A73-20876

Observations of spatial structure in the soft X-ray diffuse flux.

08 p0997 A73-20881

Nonprimordial hypothesis for cosmic microwave background radiation generation by ordinary astronomical processes and subsequent thermalization by interaction with dust grains

08 p1008 A73-21152

Microwave background radiation in terms of isotropy, universe mass density, sky brightness temperature spectra investigations and H distribution in intergalactic space

08 p1010 A73-21229

Hypotheses for excess background radiation at 200-500 km, suggesting single high energy electrons or electron clusters

08 p0999 A73-21336

Solar neutrino flux prediction discrepancies with observation, considering cosmic ray background and flaws in calculation of capture rate

09 p1136 A73-21995

Isotropic cosmological models of X ray background radiation, presenting observational constraints on source distribution and radiation mechanisms

09 p1138 A73-22869

The observation of relic radiation as a test of the nature of X-ray radiation from the clusters of galaxies.

09 p1138 A73-22953

An estimate of the energy spectrum of gamma rays from the central region of the Galaxy and some implications.

10 p1263 A73-23486

X ray background emission and behavior of infalling intergalactic gas into Galaxy resulting from shock wave generation and heating in accretion process

10 p1264 A73-23495

Galactic background spectrum at 230-2600 kHz from IMP-6 radio astronomy, discussing ambient plasma effects on synchrotron emission in galactic models

10 p1272 A73-23529

Investigation of charged-particle fluxes at altitudes of 200 to 300 km with the aid of the Saliut orbital station

10 p1267 A73-23930

Pulsar decametric radiation reception hindrance by SNR deterioration caused by bandwidth decrease and background radiation, discussing signal processing methods

11 p1426 A73-26474

An infrared photometer for the balloon-borne telescope Thisbe.

11 p1368 A73-26505

A balloon-borne helium-cooled interferometer for investigation of the isotropic submillimetre background.

11 p1368 A73-26506

Dependence of the integrated background light on cosmology, galactic spectra, and galactic evolution.

13 p1671 A73-28035

Further measurements of the submillimetre background at balloon altitude.

13 p1606 A73-28188

Universe rest energy density, isotropic background radiation energy and galactic kinetic energy

13 p1686 A73-29654

On Compton models of the isotropic X-ray background.

14 p1796 A73-30001

Extragalactic X ray source data increase from Uhuru catalog publication, discussing relevance to X ray background

14 p1787 A73-30598

The cosmic gamma-ray spectrum between 0.3 and 27 MeV measured on Apollo 15.

14 p1788 A73-30731

Continuum galactic background radio emission, considering rarefied ionized hydrogen gas with filaments due to dense inhomogeneities

15 p1938 A73-31953

Ultrahigh energy photons, electrons, and neutrinos, the microwave background, and the universal cosmic-ray hypothesis.

15 p1927 A73-32004

Measuring earth-to-space contrast transmittance from ground stations.

15 p1914 A73-32386

Midlatitude excess radiation energy density relation to primary cosmic ray background from spectrum measurement data

15 p1927 A73-32610

Extragalactic X-ray sources and their contribution to the diffuse background [Invited paper].

16 p2051 A73-32744

Soft X ray background observations at 0.1-10 keV, considering interstellar absorption effects, galactic radiation and extragalactic components

16 p2051 A73-32745

X ray background and emission mechanism nature, considering evolutionary effects and unresolved sources

16 p2051 A73-32747

Diffuse background X ray origin theories with emphasis on soft flux in galactic plane and at poles

16 p2051 A73-32748

Extragalactic diffuse X ray background above 30 keV, discussing spectral breaks and bumps at various energies

16 p2051 A73-32749

Description of small-scale fluctuations in the diffuse X-ray background.

17 p2224 A73-34753

Search for small-scale anisotropy in the 2.7 K cosmic background radiation at a wavelength of 3.56 centimeters.

17 p2231 A73-34768

Capabilities and limitations of infrared imaging systems.

17 p2167 A73-34902

Explicit solution for the photocount statistics with application to atmospheric turbulence.

18 p2337 A73-36625

Spatially forbidden regions in the aurora.

18 p2337 A73-36648

Solar proton and galactic background radiation measurements project Cold Flare at SST cruising altitudes, using high altitude radiation instrument system /HARIS/

18 p2347 A73-36905

A low-background counter telescope for recording alpha particles in n, α -reactions

21 p2699 A73-40173

Considerations about the atmospheric background and the technique of differential modulation in infrared astronomy.

21 p2740 A73-40690

A new estimate of the fluctuation of relic radiation in the universe

21 p2759 A73-40708

Clusters of galaxies - A possible source of background emission in the X-ray band

21 p2759 A73-40709

X ray background radiation intensity fluctuations from random discrete point sources, indicating extragalactic origin

21 p2759 A73-40710

Big Bang model of universe, discussing 3 K background radiation, thermal history of early universe, lepton number conservation and different eras

21 p2772 A73-41242

Continuum galactic background radio emission, considering rarefied ionized hydrogen gas with filaments due to dense inhomogeneities

24 p3131 A73-44478

BACKSCATTERING

A comparison of precipitation attenuation and radar backscatter along earth-space paths.

01 p0015 A73-10183

Backscatter from snow and ice surfaces at near incident angles.

01 p0016 A73-10191

Discussion of radiative-transfer methods applied to electromagnetic reflection from turbulent plasma.

01 p0081 A73-10196

Laser radar measurements of atmospheric backscattering turbidity.

01 p0073 A73-10403

Compact laser radar for remote atmospheric probing.

01 p0060 A73-11059

Double-reverse-scatter interference in optical fiber communication systems.

01 p0018 A73-11217

Backscatter of solar resonance radiation. II.

02 p0205 A73-11917

A noncoherent model for microwave emissions and backscattering from the sea surface.

02 p0164 A73-12362

Laser anemometry in an unseeded supersonic wind tunnel by means of photon correlation spectroscopy of backscattered light.

02 p0172 A73-12860

A versatile Moessbauer spectrometer and its applications in structural mechanics.

03 p0305 A73-12875

Atmospheric turbulence information in signal backscattered from pulsed radar, discussing Doppler power spectrum variance determination

03 p0279 A73-14528

High power radar for measurement of refractivity inhomogeneities in clear air turbulence from backscattered energy Doppler shift

03 p0338 A73-14530

Radar echo in clear air convection shown due to backscattering from fine refractivity fluctuations caused by turbulent mixing

03 p0280 A73-14543

Moon and Venus relief from backscattering diagrams based on radar echoes, calculating root-mean-square angles of surface inclination

03 p0379 A73-14568

Optimal processing of the backscatter signal in determining the structure of atmospheric inhomogeneities.

04 p0417 A73-15325

A system-synthesis approach to the inverse problem of scattering by smooth, convex-shaped scatterers for the high-frequency case.

04 p0423 A73-15484

Induced enhancement of the plasma line in the backscatter spectrum by ionospheric heating.

04 p0445 A73-15555

Total electron backscatter and backemission yields from metals bombarded at several angles by 0.4 to 1.4 MeV electrons.

05 p0604 A73-16514

Backward elastic proton-deuteron differential cross sections at different energies, describing experimental setup

05 p0601 A73-17322

Backscattering of electromagnetic waves from a rough surface model.

06 p0664 A73-18134

A dual polarization laser backscatter system for water quality studies.

06 p0700 A73-18306

Signal level fluctuations line spectra energy characteristics comparison for oblique and oblique-backscatter sounding, noting changes in harmonics intensity and period

07 p0792 A73-19438

Low noise VHF preamplifier design for backscatter radar, presenting circuit diagram

07 p0801 A73-19536

Remote probing by laser radar.

07 p0793 A73-19947

Spaced radar observation of auroral scattering cross sections, noting radio backscattering intensity peak and echo detection probability relationship to aspect angles

08 p0957 A73-20661

Backscattering of a scalar wave field by an ideally reflecting object situated near the caustic surface

09 p1052 A73-23081

Field-aligned ionospheric E-region irregularities and sporadic E.

10 p1191 A73-24897

Further studies of backscattering from a finite cone.

10 p1191 A73-24898

Geometrical diffraction theory for radiation pattern of extended vertical monopole antenna over infinitely conducting ground plane, noting back radiation level

11 p1329 A73-25662

Low-energy positrons from metallic moderators in a back scattering mode.

11 p1402 A73-26544

Error curve in radiometric beta backscatter measurement of coatings thickness via digital computation

12 p1495 A73-26846

Analogies between substorm phenomena of the visual polar aurora and the radio aurora

12 p1493 A73-27757

Nonlinear behavior of stimulated Brillouin and Raman scattering in laser-irradiated plasmas.

13 p1664 A73-28187

Amplitude modulation effects of the Doppler return at low altitudes.

13 p1586 A73-29223

Energy spectra and pitch angle distributions of precipitating incident and backscattered electron fluxes in auroral arcs

14 p1747 A73-29968

Generalisation and application of Rayleigh's theory of sound scattering

14 p1775 A73-30893

Ionospherically propagated backscatter from Pacific Ocean via swept frequency continuous wave recordings, noting sky wave polarization rotation modulation of received signal

15 p1845 A73-32228

- Ionospheric electron density profiles calculation method based on oblique backscatter ionograms, presenting virtual height vs frequency
15 p1873 A73-32229
- Detection and measurement of low-level backscattering of laser radiation
16 p1978 A73-32893
- Millimeter wave backscatter measurements for snow, ice and sea ice, discussing penetration into snow and ice
16 p1983 A73-33728
- Polarization properties of lidar backscattering from clouds.
17 p2125 A73-35416
- Direct-sampling studies of combustion processes.
19 p2504 A73-38325
- Absolute instability of the interaction between optical and acoustic waves.
20 p2594 A73-39679
- Diffraction of optical radiation by a reflecting disk in a turbulent atmosphere.
20 p2531 A73-39680
- Daytime applications of Raman technique of laser backscatter to measure atmospheric composition profiles
21 p2729 A73-40067
- Use of the backscattering method to measure the atmospheric transparency in oblique directions
21 p2731 A73-40495
- Indices of backscattering and attenuation of light by a water aerosol
21 p2731 A73-40747
- Results of radar experiments performed on automatic stations Luna 16 and Luna 17.
21 p2774 A73-41401
- Amplification of backscattering by bodies placed in a medium with random inhomogeneities
21 p2657 A73-41513
- Mapping of North Atlantic winds by HF radar sea backscatter interpretation.
22 p2882 A73-41836
- Pulse scattering from a sphere coated with an inhomogeneous sheath.
22 p2824 A73-41852
- Low albedo lunar areas, discussing spectral reflectivity, radar backscatter characteristics and Apollo 17 landing site
22 p2909 A73-42495
- German monograph - The back-scattering method as a procedure for the determination of the radiation damage profile in silicon doped by ion implantation.
22 p2897 A73-42852
- Confocal backscatter laser velocimeter with on-axis sensitivity.
22 p2864 A73-43162
- Small angle multiple backscattering from randomly spaced cylindrical plasma cloud striations, obtaining ray density via Fokker-Planck transport equation
22 p2896 A73-43182
- An improved single flight technique for radar stereo.
23 p2953 A73-43449
- On the backscatter of solar He II, 304 A radiation from interplanetary He/+,
23 p3024 A73-43695
- The Nimbus-4 backscatter ultraviolet /BUV/ atmospheric ozone experiment Two years' operation.
23 p2975 A73-43877
- Octave bandwidth microwave spectral response.
24 p3068 A73-44996
- Detection of phosphorus in heavily diffused silicon by He/+ backscattering.
24 p3120 A73-45262
- BACKWARD WAVE TUBES**
NT HELITRONS
Starting conditions for backward-wave tubes with preliminary modulation of the electron beam
09 p1063 A73-22453
- Complete photon conversion in backward-travelling-wave parametric amplification and oscillation.
23 p2955 A73-44108
- BACKWARD WAVES**
Nonlinear computation of a resonant O-type oscillator featuring constant wave amplitude in the presence of losses
01 p0025 A73-10984
- One dimensional periodic slow wave structure interaction with charged particles beam, considering system operation as TWT and backward wave tube
05 p0556 A73-16063
- Resonator polarization parameters effect on backward wave attenuation in three and four mirror TW ring laser, noting colliding waves intensity dependence on polarization angle
06 p0703 A73-18619
- Propagation of backward surface wave along an annular plasma guide with azimuthal electron density variation.
09 p1125 A73-21930
- Electronically-regulated power supplies for microwave backward-wave oscillators.
17 p2142 A73-35643
- Backward ionization waves linear evolution to nonlinear saturated state from gaseous plasma self oscillation instability viewpoint, noting electron temperature and density increase
23 p3011 A73-43829
- BACKWASH**
A numerical method for integrating the unsteady boundary-layer equations when there are regions of backflow.
16 p1998 A73-32799
- Mass flux measurements and correlations in the back flow region of a nozzle plume.
[AIAA PAPER 73-731]
18 p2342 A73-36348
- BACTERIA**
NT AZOTOBACTER
NT BACILLUS
NT NITROBACTER
NT STAPHYLOCOCCUS
Studies of the electron transport chain of extremely halophilic bacteria. VIII - Respiration-dependent detergent dissolution of cell envelopes.
01 p0009 A73-10625
- A salt-inhibited cytochrome c reductase obtained from the moderately halophilic bacterium, *Micrococcus halodenitrificans*.
03 p0261 A73-13598
- Sensitivity to oxygen at high pressure of radioreistant and radiosensitive strains of bacteria.
07 p0780 A73-19483
- Studies on acid production during carbohydrate metabolism by extremely halophilic bacteria.
07 p0780 A73-19500
- Survival of *Arthrobacter crystallopoietes* during prolonged periods of extreme desiccation.
07 p0782 A73-20026
- Variable photosynthetic units, energy transfer and light-induced evolution of hydrogen in algae and bacteria.
08 p0932 A73-21685
- Influence of electron transport on the interaction between membrane lipids and Triton X-100 in *Halobacterium cutirubrum*.
15 p1841 A73-32024
- Survival of common bacteria in liquid culture under carbon dioxide at high temperatures.
15 p1837 A73-32650
- Effect of iron and salt on prodigiosin synthesis in *Serratia marcescens*.
17 p2112 A73-34399
- Structure of the lipid phase in cell envelope vesicles from *Halobacterium cutirubrum*.
17 p2112 A73-34599
- Method allowing biological and biochemical studies of vacuum-exposed bacteria.
20 p2513 A73-39483
- Effect of simulated lunar impact on the survival of bacterial spores.
20 p2513 A73-39485
- On the multiplication of xerophilic micro-organisms under simulated Martian conditions.
22 p2803 A73-42165
- The radiobiological effects of heavy ions on mammalian cells and bacteria.
22 p2805 A73-42182
- Heavy ion irradiation effects on bacteria mutations in balloon flight and accelerator experiments, comparing with cosmic rays
22 p2805 A73-42184
- BACTERICIDES**
Bactericide activity of the integument of man at different times of the day
12 p1463 A73-27716
- BACTERIOLOGY**
Resistance of soil microorganisms to starvation.
02 p0136 A73-12627
- Automatic surface inoculation of agar trays.
09 p1045 A73-22550
- Survival of soil bacteria during prolonged desiccation.
14 p1720 A73-30959
- BAFFLES**
Isothermal wall conical cavity radiant energy streaming, determining annular baffle effects by Monte Carlo method
10 p1295 A73-23835
- Effect of deflector geometry on the heat transfer in the coolant passages of deflector blades.
21 p2754 A73-41322
- BAKELITE [TRADEMARK]**
Bakelite lacquer and epoxy and phenol-formaldehyde solidified resin binders strength at high temperatures
14 p1766 A73-30687
- BAKEOUT**
U DEGASSING
- BALANCE**
Balance threshold of rigid rotors with nonideal bearings
20 p2569 A73-39639
- BALANCED AMPLIFIERS**
U PUSH-PULL AMPLIFIERS
- BALANCING**
Flexible rotor balancing of a high-speed gas turbine engine.
[SAE PAPER 720741]
02 p0203 A73-12007
- Rapid balancing of gyroscopes with TEA CO₂ laser.
15 p1883 A73-30996
- Balancing equipment for jet engine components, compressors, and turbine - Rotating type for measuring unbalance in one or more than one transverse planes.
[SAE ARP 587A]
16 p1993 A73-33013
- Further experiments on balancing of a high-speed flexible rotor.
[ASME PAPER 73-DET-99]
22 p2865 A73-42077
- BALL BEARINGS**
Laboratory experience with long-term bearing lubrication.
01 p0057 A73-11278
- Aircraft gas turbine mainshaft ball bearings fatigue life estimation via failure distribution
[ASME PAPER 72-LUB-10]
03 p0313 A73-14328
- Analysis of an arched outer-race ball bearing considering centrifugal forces.
[ASME PAPER 72-LUB-28]
03 p0314 A73-14339
- A new criterion for predicting rolling-element fatigue lives of through-hardened steels.
[ASME PAPER 72-LUB-32]
03 p0328 A73-14342
- Optimal speed sharing characteristics of a series-hybrid bearing.
[ASME PAPER 72-LUB-39]
03 p0315 A73-14346
- New high performance silicone greases and their applications.
07 p0842 A73-19557
- Metal tongues in trailing edge of surface pits near fracture path end in rolling contact fatigue of failed ball bearings
07 p0831 A73-20158
- An improved method for calculating the spin torque in a fully lubricated ball-race contact.
07 p0833 A73-20485
- Accelerated testing of ball bearings.
10 p1225 A73-24636
- Nonlinear effects of axial load and rigidity changes on ball bearings of gyroscopes with symmetrical gyromotor design
13 p1618 A73-29145
- German monograph - Investigations regarding the elastohydrodynamic lubricant film thickness in the case of elliptical Hertzian contact surfaces.
13 p1625 A73-29287
- Balance threshold of rigid rotors with nonideal bearings
20 p2569 A73-39639
- Airframe ball, roller and spherical plain bearing designs for flight control, landing gear and wing mechanisms
21 p2707 A73-41125
- BALL LIGHTNING**
Optical emission of a ball-lightning
09 p1113 A73-21913
- Optical emission from ball lightning.
15 p1915 A73-32639
- BALLAST [MASS]**
Experimental investigation of a gas-liquid thruster model with a ballasting-reinforced thrust
22 p2841 A73-42127
- BALLISTIC MISSILES**
NT INTERCONTINENTAL BALLISTIC MISSILES
NT MINUTEMAN ICBM
NT POLARIS MISSILES
NT POSEIDON MISSILES
Book - Introduction to defense radar systems engineering.
13 p1587 A73-29677
- External tracking, telemetry and concepts of free flight time, of safety corridor and of destruction time limit for ballistic missile flight tests safety
14 p1804 A73-30095
- PCM multiplexing system for incorporation into telemetry systems of large ballistic missiles or spacecraft launch vehicles
14 p1727 A73-30110
- Russian book - Solid-fuel ballistic rockets.
14 p1804 A73-30356
- Vibration and shock stresses in the case of ballistic rockets. II - Measurement, evaluation, simulation
16 p2072 A73-33388
- Vibration and shock stresses in the case of ballistic rockets. III - Evaluation of the results and comparison with the specifications available
16 p2073 A73-33389
- BMD requirements for phased array radars.
21 p2651 A73-40644
- BALLISTIC RANGES**
A new dimension in front-light laser photography.
03 p0309 A73-14199
- Calorimeter measurement of heat transfer at hypersonic conditions.
[AIAA PAPER 73-760]
18 p2264 A73-36375
- Hyperballistics range erosion tests, describing dust, rain and ice simulation, dust and water fixed grid screens and shadowgraph and laser photography
[AIAA PAPER 73-765]
18 p2295 A73-36380
- Photographic instrumentation in Hyperballistic Range /G/ of the von Karman Gas Dynamics Facility.
22 p2864 A73-43189
- Aeroballistic range facilities development and application to reentry physics, discussing program for turbulent wake properties of hypersonic projectiles
24 p3054 A73-44993

BALLISTIC TRAJECTORIES

Missile range dispersions produced by meteorological factors, drag differences and mass changes during passive ballistic flight

02 p0211 A73-11787

Short term bounds for the effect of oblateness on ballistic trajectories.

03 p0373 A73-13495

Powered-flight trajectory optimization for an inter-arrival guidance ballistic vehicle.

08 p1011 A73-21427

Free flight and re-entry of a missile with a high ballistic coefficient.

09 p1147 A73-22625

Investigation of a gas flow on an aeroballistic track by holographic methods

15 p1879 A73-32328

Differential equations for ballistic motion of meteoric particles in earth atmosphere, noting orbit stability

19 p2480 A73-37237

Critical velocities of the steady motion of a pliable thread in plane homogeneous flow

22 p2928 A73-43061

BALLISTICS

NT INTERIOR BALLISTICS

Investigation of electronic and gasdynamic parameters of hypersonic wakes behind models moving in argon.

03 p0296 A73-14099

Dependence of the base pressure on the ratio of specific heats at supersonic velocities

09 p1027 A73-21917

Solid propellant ballistic properties from pressure changes due to combustion, considering transient effects

13 p1669 A73-28997

Problems related to the development and firing of launchers

14 p1742 A73-30102

Bottom pressure and specific-heat ratio at supersonic velocities.

15 p1825 A73-32643

Optimum shapes of slender axisymmetric missile bodies with minimum ballistic factor, using calculus of variations

16 p2071 A73-32904

BALLISTOCARDIOGRAPHY

Modification of a ballisto-oscillograph for extremities

09 p1046 A73-22865

Clinical evidence of cardiac weakness and incoordination secured by simultaneous records of the force BCG and carotid pulse derivative and interpreted by an electrical analogue.

09 p1046 A73-23174

BALLOON FLIGHT

Azimuthal pointing control system for balloon observations of celestial bodies, analyzing suspension rope twisting method

01 p0075 A73-11207

Prediction of the landing point of a balloon payload.

01 p0005 A73-11208

Atmospheric microthermal turbulence vertical distribution from balloon flights compared with stellar scintillation data, predicting irradiance spectra from turbulence and wind velocity measurement

03 p0305 A73-14656

Long-duration flight performance of medium large unpresurized stratospheric balloons.

04 p0406 A73-15099

Auroral-zone X-ray measurements at Kiruna in 1970.

04 p0492 A73-15100

Design and performance of UHF transmitter and receiver system for two way links between Eole satellite and constant ceiling balloons

07 p0790 A73-18962

Low level wind measurement error as it affects sounding rocket dispersion.

09 p1116 A73-23215

Sco X-1 hard X rays and optical emission time variations from simultaneous observations, using balloon-borne counter telescopes

10 p1263 A73-23493

Eole balloon clusters horizontal trajectories as indicators of southern hemisphere atmospheric circulation, estimating rms divergence as function of scale

19 p2424 A73-37661

Remote sensing experiments with balloons

19 p2431 A73-38180

Eole experiment on dispersion of Lagrangian tracers in quasi-stationary two dimensional turbulent flow, noting rms distance between paired balloons

21 p2687 A73-41337

Tetrahedral Mylar plastic balloon drag coefficient measurement as function of Reynolds numbers from experimental free flight test data

23 p3004 A73-44263

BALLOON SOUNDING

Tethered balloon measurements of turbulent wind, temperature and humidity fluctuations up to 200 meters over open sea, allowing for wave induced ship motion

01 p0072 A73-10142

Atmospheric tidal measurements at 50 km from a constant-altitude balloon.

01 p0043 A73-11061

Simultaneous upper atmospheric measurements of electric field at points differing in altitude via balloon-borne instruments

02 p0156 A73-11736

High angular resolution solar observation from balloon borne instruments.

02 p0169 A73-12334

Low energy atmospheric gamma rays near geomagnetic equator.

03 p0360 A73-12890

A balloon-borne observation of the X-ray source Cygnus XR-1.

03 p0361 A73-13367

Detection of 10-100 MeV gamma-rays from the Crab Nebula pulsar NP 0532.

03 p0362 A73-13847

Dc electric field measurement with rocket-borne double probes and by satellite and balloon observation, noting ionospheric fields, magnetospheric plasma and auroras

03 p0302 A73-13874

Technological evolution of solar generators for terrestrial applications and sounding balloons, discussing environment caused problems and solutions, energy cost estimate and future prospects

03 p0258 A73-14253

12.5-minute periodicity in solar proton fluxes at balloon altitude and in magnetic micropulsations.

04 p0492 A73-15527

The measurement of atmospheric turbulence from a captive balloon.

04 p0473 A73-15698

Instrument suspended from tethered balloon for oceanic measurement of average lower atmosphere vertical electric field profile

05 p0579 A73-17251

Astrolabe universal balloon gondola for solar and visible stars targeting, describing acquisition functions and attitude control servos design

07 p0776 A73-18940

The balloon launch stations of the EOLE program.

07 p0807 A73-18951

Design, production, reliability analysis and testing of Eole satellite decoder for balloon sounding data, noting performance tests

07 p0790 A73-18966

Sounding balloon system SITTEL for upper atmosphere physical parameters measurement, noting PCM telemetry, remote control and vehicle localization

07 p0790 A73-18971

Mobile ground station for sounding balloons remote control, telemetry and localization, noting antenna pointing control, tracking receiver and trajectory recording

07 p0790 A73-18972

Industrial manufacturing of stratospheric balloons.

07 p0829 A73-18998

Balloon measurements of the far-infrared background radiation.

07 p0825 A73-20177

GARP Global Experiment design with satellite and balloon borne systems for meteorological observation and atmospheric research, discussing sounding data numerical simulation

07 p0820 A73-20442

A search for hard X-rays from extragalactic objects.

08 p0997 A73-21153

Atmospheric gamma ray spectra from balloon spectrometer scintillator measured energy loss spectra

08 p0998 A73-21280

Primary cosmic radiation antiproton flux, finding .005 ratio upper limit to proton flux with balloon-borne-magnetic spectrometer

08 p0999 A73-21333

High energy electrons and gamma quantum flux in upper atmospheric layers from high altitude balloon measurements

08 p0999 A73-21337

The mean upper-air flow in Southern Hemisphere temperate latitudes determined from several years of GHOST balloon flights at 200 and 100 mb.

08 p0960 A73-21376

RCW 117 and DR 15 observed in the far infrared.

08 p1012 A73-21531

Balloon-borne UV stellar spectrometer telescope pointing and stabilization, discussing in-house feasibility studies by small scale test payload experiments

08 p0971 A73-21750

Balloon-borne telescope-UV spectrometer for stellar spectrophotometric measurement with high spectral resolution, discussing system design and operation, image motion compensation and data acquisition

08 p0971 A73-21751

Stellar survey at 2000-4100 A via balloon-borne observations, discussing intensity distributions and earth atmospheric ozone layer density

09 p1140 A73-22006

Relations between ionospheric electric fields and energetic trapped and precipitating electrons.

09 p1073 A73-22056

Balloon observations of auroral-zone X-rays in conjugate regions.

09 p1137 A73-22135

Balloon flight observations of Uhuru sources for spectral characteristics, noting hard X ray band sources

09 p1137 A73-22173

Balloon observations of galactic and extragalactic objects at 100 microns.

09 p1150 A73-23134

Diffuse cosmic gamma rays observed at an equatorial balloon altitude.

10 p1263 A73-23491

Balloon-borne spectroscopic observation of the infrared hydroxyl airglow.

11 p1350 A73-25061

An apparatus for the orientation of stratospheric-balloon payloads

11 p1304 A73-25355

On the morphology of auroral-zone X-ray events.

III - Large-scale observations in the midnight-to-morning sector.

11 p1354 A73-25763

Balloon-borne Newtonian telescope with parabolic pyrex primary mirror for far IR observation of celestial sources

11 p1368 A73-26504

An infrared photometer for the balloon-borne telescope Thibbe.

11 p1368 A73-26505

A balloon-borne helium-cooled interferometer for investigation of the isotropic submillimetre background.

11 p1368 A73-26506

Cryostats with and without radiation passage through window into vacuum space in balloon-borne far IR instruments requiring cooling to liquid He temperature

11 p1453 A73-26516

Correlation between pulsations in auroral luminosity variations and X-rays.

11 p1359 A73-26710

Observations of narrow microburst trains in the geomagnetic storm of August 4-6, 1972.

12 p1490 A73-27007

Balloon-aircraft ranging, data, and voice experiment.

12 p1473 A73-27680

The first results of balloon measurements during the solar proton events in the period from August 2 to August 10, 1972

12 p1535 A73-27777

Further measurements of the submillimeter background at balloon altitude.

13 p1606 A73-28188

Distribution of water vapor in the stratosphere as determined from balloon measurements of atmospheric emission spectra in the 24- to 29-micron region.

14 p1749 A73-30160

A balloon study of the OH airglow emission from evening twilight to sunrise.

15 p1867 A73-31311

Eole meteorological balloon sounding experiment in Southern Hemisphere, discussing mean circulation, eddy diffusion and data collection and satellite tracking system

15 p1904 A73-31723

Study of high energy electrons at upper layers of atmosphere during magnetic perturbations.

16 p2054 A73-33282

Global balloon monitoring program of stratospheric dust, ozone, water vapor, temperature and aerosol determination in northern and southern hemispheres [AIAA PAPER 73-521]

16 p2007 A73-33557

Balloon-borne phosphoric anhydride electrolytic gage measurement of water vapor mixing ratio to 35 km, noting decrease to minimum near tropopause

16 p2008 A73-33884

Balloon observations of Sco X-1 in the energy interval 17-106 keV.

17 p2225 A73-35783

Large-scale auroral-zone electron precipitation event, briefly interrupted during a negative magnetic impulse.

18 p2344 A73-35951

Sounding balloon nuclear emulsion chamber recording of energy spectra and angular distribution of incoming and outgoing proton fluxes in atmosphere

18 p2310 A73-36124

Comparison of vertical profile turbulence structure with stellar observations.

19 p2446 A73-37259

Atmospheric gamma ray spectra from balloon spectrometer scintillator measured energy loss spectra

19 p2476 A73-37909

Vertical profiles of small-scale temperature structure in the atmosphere.

19 p2448 A73-38209

Balloon X ray observations of GX 301-2, GX 304-1, GX 1-4, GX 5-1 and GX 3-1 X ray spectra, noting coincidence with Uhuru low energy sources

20 p2602 A73-39441

Cumulus congestus cloud circulation velocity field measurement by balloon, comparing with radar,

cameras, satellite and ground based observed meteorological model computations 21 p2728 A73-40060

Balloon-borne measurement of stratospheric methane as function of altitude absorption spectroscopy, obtaining mixing ratios 21 p2680 A73-40076

CO atmospheric vertical distribution from balloon-borne IR grating spectrometer observations, noting concentration decrease with altitude 21 p2680 A73-40078

Satellite techniques for automatic platforms location and data relay. 21 p2737 A73-41335

Energy spectra and angular distribution measurement for 10-100 MeV earth albedo neutrons by balloon sounding at 116,000 ft 21 p2761 A73-41380

Balloon measurement of angular extent of Coma and Virgo clusters hard X ray emission 21 p2762 A73-41393

Balloon and VLF whistler measurements of electric fields, equatorial electron density, and precipitating particles during a barium cloud release in the magnetosphere. 22 p2845 A73-41934

Atmospheric temperature measurement using balloons and rockets. 22 p2883 A73-42061

French monograph - Contribution to the ultraviolet spectrophotometry of the night sky /1900 to 3400 Å/. 22 p2850 A73-42742

Observation of cosmic-ray particles with Z greater than 35. 23 p3024 A73-43609

Observation of cosmic-ray particles with Z of 50 or greater and interpretation of the charge spectrum. 23 p3024 A73-43610

Description of a photometer suitable for measuring twilight ozone content variations from a stratospheric balloon gondola 23 p2982 A73-43875

Atmospheric water vapor concentration in upper stratosphere above tropopause from balloon observations of solar IR absorption spectra 23 p2976 A73-43890

The concentration of molecular H₂ and CH₄ in the stratosphere. 23 p2976 A73-43891

BALLOONS

NT HIGH ALTITUDE BALLOONS

NT METEOROLOGICAL BALLOONS

NT SKYHOOK BALLOONS

NT TETHERED BALLOONS

Balloon polyethylene film materials orthotropic mechanical properties, considering temperature effects on brittle fracture by transverse tension 01 p0005 A73-11206

Ellipsoidlike deformations of tubelike balloons - Asymptotic solution with boundary layer. [ASME PAPER 72-WA/APM-29] 04 p0515 A73-15889

BALLUTES

Development and testing of ballute stabilizer/decelerators for aircraft delivery of a 500-lb munition. [AIAA PAPER 73-485] 15 p1829 A73-31467

BALMER SERIES

Low-intensity Balmer emissions from the interstellar medium and geocorona. 08 p1009 A73-21167

Spectral energy distribution, photometric gradients and Balmer discontinuities for eclipsing binary RZ Scutum from spectrograms with low dispersion in H gamma line 10 p1273 A73-23707

Changes of the Balmer-series lines of hydrogen in the spectrum of the spectrally variable silicon Ap star CU Vir 16 p2057 A73-32711

Balmer-line emission from auroral protons. 17 p2213 A73-34766

Satellite observations of strong Balmer alpha atmospheric emissions around the magnetic equator. 18 p2346 A73-36284

Spectral energy distribution, spectrophotometric gradients and Balmer discontinuities for eclipsing binary RZ Scuti from spectrograms with low dispersion in H gamma line 18 p2354 A73-36732

Geocorona originated low intensity nighttime H alpha and H beta emission components from high resolution observation, considering Balmer line producing mechanism 20 p2555 A73-39433

A radially streaming proton model for the broad component of hydrogen emission in Seyfert galaxies. 24 p3138 A73-45039

BALTIC SEA

Project VEMNO - North Sea-Baltic measuring network. 13 p1608 A73-28787

BANACH SPACE

Existence theorem for nonlinear parabolic equations of evolution in real Banach space 01 p0071 A73-11270

An optimum settling problem for time lag systems. 06 p0717 A73-18172

Stability of difference approximations to differential equations. 07 p0845 A73-20494

Nonlinear algorithms for the local solution of an equation with a fixed point in a product of Banach spaces 08 p0984 A73-21489

Vector-valued optimization of linear systems 09 p1112 A73-22478

Continuous best approximation projections in certain Banach spaces 09 p1113 A73-23027

Rockafellar duality theorem generalization to integrands over locally convex sublinear topological vector spaces, permitting Banach space transcendence 11 p1390 A73-25866

Some general questions in the theory of probability measures in linear spaces 12 p1517 A73-27187

Fixed point theorems and dissipative processes. 14 p1771 A73-30774

General linear boundary value problem with measurable coefficients for numerous analytical functions of class E sub p 15 p1900 A73-32092

Proof of B-completeness of locally convex spaces in series of quasi-reflective Banach spaces, generalizing Van Dulst theorem 15 p1900 A73-32205

Strong and weak convergence of the sequence of successive approximations for quasi-nonexpansive mappings. 21 p2724 A73-40297

Sufficient optimality conditions for control system described by ordinary differential equations in Banach space with Lebesgue measure of material quantity set. 22 p2882 A73-42604

German monograph on regularization and penalty function methods of numerical analysis in Hilbert or Banach space covering minimax technique and optimal control theory application 22 p2882 A73-42847

On the Stepanov-almost periodic solution of an abstract differential equation. 24 p3105 A73-44420

Asymptotic solutions of second-order linear homogeneous differential equations in a Banach space in the case of a higher derivative having a small parameter 24 p3105 A73-44603

Tensorial norms properties with respect to Hilbert spaces, constructing perfect ideals in Banach space 24 p3105 A73-45010

BAND STRUCTURE OF SOLIDS

Comments on the conduction mechanism in Schottky diodes. 01 p0088 A73-10474

Cadmium sulfide/cuprous sulfide solar cell abrupt heterojunction band model description by two quasi-Fermi levels 03 p0350 A73-14219

Optical band gap energies and stacking sequences of molybdenum tellurides and tungsten selenides derived from dielectric constant measurements 04 p0482 A73-14868

The influence of the electron-phonon scattering on the total energy distribution of field emitted electrons from tungsten. 04 p0477 A73-15000

Gold high temperature thermoelectric properties from electron model based on scattering resulting from d band-Fermi level relative position changes 04 p0463 A73-15313

Electronic transport in insulating films. 05 p0604 A73-16503

Magnetite absolute zero behavior with restriction to three order parameter theory, showing metallic band resultant from interatomic Coulomb energy ratio to bandwidth 06 p0734 A73-17835

Diffusion of hot electrons in n indium phosphide. 07 p0861 A73-19157

Millimeter-wave frequency response of hot electrons in n-type GaAs. 08 p0994 A73-20845

Book - Introduction to quantum electronics. 08 p0994 A73-20951

Surface photovoltage spectroscopy - A new approach to the study of high-gap semiconductor surfaces. 08 p0968 A73-21620

Photoelastic investigation of serrated plastic flow in 6061 Al alloy, considering Luders bands effects relative to type A and B serrations 09 p1101 A73-22408

Frequency multiplication due to nonparabolicity of dispersion law in semiconductor structure subbands, noting electromagnetic signal transformation 09 p1133 A73-22665

A relationship between photoemission-determined valence band gaps in semiconductors and insulators and ionicity parameters. 09 p1134 A73-22903

Electronic configuration and electrical conductivity in ceramics. 09 p1135 A73-23000

Structure diagram, crystal growth, band structure, physical, optical and photoelectric properties of A/IIb/V/ compounds, emphasizing CdSb-ZnSb solid solutions 10 p1258 A73-23566

An observation of vacancy sources during substitutional diffusion in thoriated nickel alloys. 10 p1234 A73-24433

Electronic charge densities in semiconductors. 11 p1408 A73-25374

Light absorption coefficient of disordered semiconductor within external dc field, discussing electron states near band boundaries 11 p1408 A73-25427

Magneto-oscillatory absorption effect in Sb₂ 13 p1667 A73-28004

Band structure, electron energy distribution and emission efficiency of negative electron affinity secondary emitters and cold cathodes 14 p1732 A73-29912

Determination of the main details of the band structure of semiconductors from edge absorption data 14 p1783 A73-30366

Some comments on the importance of third order contributions to the screening of the ionic potential and to the structural energy of metals. 14 p1783 A73-30432

Investigation of the structure of electron bands in In_{1-x}Ga_x/As_{1-y}P_y on the basis of luminescence. 15 p1923 A73-31716

Russian book - Electrons and holes in semiconductors: Energy spectrum and dynamics. 15 p1852 A73-32298

Oscillations of the magnetic susceptibility in n-type semiconductors with a chalcopyrite lattice 16 p2044 A73-34008

Temperature dependent softening effect due to state transition and electronic drag coefficient for dislocations in pure two band superconductors 18 p2341 A73-36768

Effect of impurities on the temperature of the superconducting transition in WSi₂ type compounds 20 p2600 A73-39731

Charge transport bands in the electronic spectra of Fe/III/ complexes with certain oxygen-containing ligands 21 p2751 A73-40310

Theory of the phase transition in group IV-VI compound semiconductors 21 p2751 A73-40369

Pure two band superconductor theory, discussing thermodynamic and electromagnetic properties, London group, mixed state, critical field and weak field penetration 21 p2753 A73-41299

Approximate variational treatment of elastic scattering of electrons from semi-infinite lattices. 21 p2741 A73-41627

Optical and electrical properties of doped semiconductors in a strong electromagnetic field. 22 p2896 A73-42252

X-ray spectral data on the valence and conduction band structures in V3X-type vanadium compounds 23 p3017 A73-44041

Linear external electric field approximation for intervalley scattering effects on nondegenerate semiconductor surface electroconductivity 23 p3017 A73-44045

Evolution of the shape of the current-voltage characteristics of n-p-n and p-n-p three-layer degenerate semiconductor structures 24 p3119 A73-44607

Effects of stress on metal-oxide-semiconductor structures. 24 p3120 A73-45415

BANDPASS FILTERS

NT TRACKING FILTERS

Bandpass amplifier design with differing two-circuit filters, discussing advantages and limitations 03 p0284 A73-14035

The performance of a noncoherent FSK receiver preceded by a bandpass limiter. 04 p0416 A73-14992

Effects of hardlimiting on bandlimited transmissions with conventional and offset QPSK modulation. 04 p0420 A73-15412

The nonlinear analysis and design constraints of a multi-filter phase-lock loop. 04 p0421 A73-15434

The probability density function for the output of a cross-correlator with bandpass inputs. 06 p0665 A73-18139

Bandpass error free wideband PCM communications system response to pulse signal 06 p0668 A73-18391

Transfer matrices determination for two terminal pair network derived from four terminal pair network, considering bandpass filter circuit design 06 p0677 A73-18397

Satellite S-band telemetry evanescent mode waveguide diplexer design with foreshortened bandpass filters to eliminate I junction and connecting flanges

06 p0678 A73-18741

Compact YIG bandpass filter with finite-pole frequencies for applications in microwave integrated circuits.

06 p0678 A73-18742

Report on results of research conducted by the Thin Film Department of SEAVOM, under CNES contract.

07 p0821 A73-18980

Precision design of millimeter-wave band-pass filter.

07 p0799 A73-19371

A wide-band low-shape-factor amplifier module using an acoustic surface-wave bandpass filter.

07 p0804 A73-20557

Improvement of frequency characteristics of digital filters.

08 p0945 A73-20801

The use of solid etalon devices as narrow band interference filters.

08 p0970 A73-21736

Microwave bandpass filters formed by shunt and series stubs with quarter wave matching strip lines, noting advantage of equal lengths

09 p1063 A73-22463

Equivalent resistance, Q factor and winding capacitance of air-core coils with coplanar spiral winding intended for bandpass filters

09 p1065 A73-23073

Microstrip bandpass filters with reduced radiation effects.

09 p1065 A73-23098

The optimization of delay equalized comb-line filters.

10 p1193 A73-23609

Speed active multipole filter design with a flexible computer program that calculates the component values for optimum performance.

10 p1191 A73-23755

Narrow band microwave active bandpass filter with inverted-common-collector transistor circuit, discussing design algorithm, insertion loss, stability, sensitivity and frequency selectivity

10 p1201 A73-24169

Method of designing digital devices for bandpass filtration of signals

11 p1333 A73-25023

Design procedures for matched and broadbanding filters for scanning tests.

11 p1341 A73-25074

High Q bandpass low sensitivity RC amplifier-filter networks, discussing two-step decomposition of denominator polynomial of second order filter transfer function

11 p1338 A73-26417

Frequency characteristics of directional loop-type bandpass filters

12 p1477 A73-26870

Optimal passband of a double-tuned selective amplifier during the simultaneous passage of rectangular radio pulses and white noise

12 p1477 A73-26874

VHF and microwave surface acoustic wave bandpass filter design with impulse model for frequency response and interdigital transducer input admittance calculation

12 p1484 A73-27563

Surface elastic wave microwave bandpass filter for miniaturized frequency synthesizer in satellite communications systems, noting insertion loss and sidelobe reduction

12 p1484 A73-27573

Active analog bandpass RC and LC filters design calculation by wave parameters

13 p1592 A73-28875

Automatic control of positive feedback depth and its application for stabilization of high Q-factor circuit characteristics

15 p1853 A73-31494

Meteorological time series persistence tendency representation by autocorrelation coefficients, summation, determining independent values effective number by white noise bandpass filtering

15 p1906 A73-32344

Approximate procedure for synthesis of interdigital bandpass filters with lumped capacitance loaded bars ends, deriving transmission response from Kirchhoff nodal law

16 p1986 A73-32911

Determination of the geometrical dimensions of a bandpass filter for a microwave hybrid integrated circuit

17 p2134 A73-34584

High performance surface wave bandpass filters for signal processing applications.

17 p2140 A73-35320

Bandpass filter with cooled InSb detector for measurement of far IR radiation and temperature-vs-wavelength characteristics of Hg arc lamp

17 p2176 A73-35774

Parallel resonator with a resistance and a frequency dependent negative resistance realized with a single operational amplifier.

19 p2411 A73-38536

Realization of canonical bandpass filters with frequency-dependent and frequency-independent negative resistances.

19 p2412 A73-38537

FM distortion of a TV signal and subcarriers due to bandpass filtering and additive Gaussian noise.

20 p2523 A73-38722

Optimal matching by using band filters

20 p2537 A73-39452

Probability of error in a bandlimited quadriphase communication system.

21 p2649 A73-40334

Digital LC branch filter transformation with direct element /adapter/ connections, considering gate number and passband attenuation distortion

23 p2957 A73-43314

Adaptive maximum-likelihood receiver for synchronous data signals

23 p2957 A73-43320

Digital filter bank with integrated FFT computer

23 p2956 A73-43326

Theoretical and experimental investigation of fluidic signal and noise filters with application to DC and AC fluidic systems.

23 p2944 A73-43418

Electronically tunable microwave bandpass filters

24 p3071 A73-44606

Bandpass filter IR observations of hydroxyl air-glow, mapping mean nightly level spatial and temporal fluctuations in brightness

24 p3087 A73-45208

BANDWIDTH

NT BROADBAND

NT SPECTRAL LINE WIDTH

The quasi-linear intensity interferometer.

01 p0045 A73-10184

Directivity and bandwidth of single-band and double-band Yagi arrays.

01 p0023 A73-10188

Flight test of narrow band television system.

01 p0052 A73-11169

Output signal-to-noise ratios in frequency measurement system using correlation detector.

01 p0018 A73-11183

Signal search networks for enlargement of locking bandwidth of tracking filters in automatic control systems, examining transistorized signal search and acquisition circuits

02 p0145 A73-11793

Acquisition time evaluation at different input SNR values for pseudonoise signal demodulation, noting common bandwidth detection system advantage

04 p0421 A73-15427

Stabilization bandwidth reduction in microwave parallel tuned tunnel diode amplifier circuits synthesis

04 p0429 A73-15919

Determination of the pass band of a system of measurement of rapidly variable pressures in the air

05 p0579 A73-17228

Dimensional and material effects on microwave waveguide damping and bandwidth characteristics in long distance communications

06 p0663 A73-17583

Modulated laser beam photographic recorder/reproducer system bandwidth and SNR tradeoff alternatives consideration for high dynamic range performance, suggesting FM recording technique superiority

06 p0701 A73-18309

Intrinsic bandwidth of cyclotron resonance in the geomagnetic field.

07 p0792 A73-19532

Wideband class-C Trapatt amplifiers.

08 p0947 A73-21145

Interdigitated power junction transistor technology assessment for power gain, bandwidth and frequency performance, noting packaging effect and thin film module advantage

08 p0949 A73-21648

Computation of the minimum bandwidth for aerotriangulation.

08 p0968 A73-21705

A tunable flashlamp-pumped dye ring laser of extremely narrow bandwidth.

09 p1091 A73-22083

Bandwidth efficiency for digital communication via a hard limiting channel.

09 p1054 A73-23382

L orthogonal signaling scheme transmission bandwidth tradeoff with error probability performance of associated receiver used for data detection

09 p1054 A73-23383

Bandwidth as measure of dimensions added to signal space per unit time in digital transmission power spectral density computation, presenting comparison for telemetry signals

09 p1054 A73-23384

Amplitude-phase-keying with M-ary alphabets - A technique for bandwidth reduction.

09 p1054 A73-23385

Comparing bandwidth requirements for digital baseband signals.

09 p1058 A73-23423

Radar filter asymptotic efficiency analysis for passband and impulse response duration increase, considering realization of approximate Urkowitz filter with controlled memory

10 p1194 A73-23737

Solar chromatograph for monochromatic image production with variable bandwidth and simple shift to visible spectrum, discussing design and applications

11 p1365 A73-26235

A modulator with inherent bandwidth limiting for use with a bi-phase PSK data transmission system.

12 p1472 A73-27663

Representation of real narrowband signals with the use of nonuniformly displaced base functions with positive coefficients.

13 p1583 A73-28668

RF spectrum utilization for optimum communication capacity, considering tradeoff between bandwidth and interference, antenna directivity and wave reflection and scattering effects

13 p1584 A73-29113

On linear parasitic array of dipoles with reactive loading.

14 p1734 A73-30203

Gain-bandwidth limitations of microwave transistor amplifiers.

14 p1735 A73-30247

Relationship between the control range and the variation in passband width in a controlled-gain amplifier with nonlinear shunting of the load

14 p1736 A73-30563

Automatic nodal point renumbering algorithm for interconnectivity matrix bandwidth reduction in computer aided structural analysis and design

15 p1848 A73-32029

Signal bandwidth consideration for electromagnetic compatibility specifications, comparing broad and narrow band measurements performance by computerized simulation

16 p1979 A73-33169

Harmonic enhancement for airborne low voltage lightweight TWT amplifier band edge performance improvement to provide bandwidth in excess of two octaves

16 p1988 A73-33298

Comparing bandwidth requirements for binary baseband signals.

16 p1984 A73-33745

ECM systems with TWT dual moding to provide distinct CW and pulsed microwave power levels, evaluating performance beyond octave in bandwidth

16 p1990 A73-33849

Some results obtained in ESRO satellite data compression.

17 p2239 A73-34955

Digital flight control systems data sampling rate selection effects on intersample ripple, spectral folding and distortion and system bandwidth

17 p2138 A73-35224

Probability of error in binary communication systems with causal band-limiting filters. I - Non-return-to-zero signal. II - Split-phase signal.

19 p2415 A73-38384

PPM pulse waveform synthesis with SNR performance improvement while retaining bandwidth-mean-square error properties inherent in wideband modulation system

20 p2524 A73-38736

Degradation of probability of error due to IF filtering.

21 p2649 A73-40335

Bandwidth criteria for phased array antennas.

21 p2652 A73-40671

Transient frequency response analysis and far field measurement of linear phased array with tandem series feed network, noting instantaneous bandwidth

21 p2653 A73-40673

Frequency response of laser scanners and its optimization through apodization.

21 p2717 A73-41610

High loop gain operational amplifiers voltage changes as slewing rates using nonlinear circuit model, discussing equivalent circuits, frequency characteristics and bandwidth

22 p2832 A73-41896

Continuous information theory and modulation methods.

22 p2826 A73-42463

Applications of digital frequency warping to unequal bandwidth and Vernier spectrum analysis.

23 p2952 A73-43312

Theory of wide-band laser radiation in a spectrally-inhomogeneous medium

23 p2987 A73-43708

Increasing the locking bandwidth of a waveguide-cavity oscillator through the use of a double-tuned circuit.

23 p2965 A73-44109

Rotational line overlap in CO₂ laser transitions.

24 p3096 A73-44872

- The effect of amplifier gain-bandwidth product on the performance of active filters. 24 p3073 A73-45393
- BANG-BANG CONTROL**
U OFF-ON CONTROL
- BANKING FLIGHT**
U TURNING FLIGHT
- BARBED TRIBUTARIES**
U DRAINAGE PATTERNS
- BARDEEN APPROXIMATION**
U BARRIER LAYERS
U ELECTRICAL PROPERTIES
U SURFACE PROPERTIES
- BARDEEN-COOPER-SCHRIEFFER THEORY**
U BCS THEORY
- BARIUM**
Characteristics of a thermionic converter with a cesium-barium filling at a high anodic temperature 01 p0006 A73-10855
Adsorbed barium films on tungsten and molybdenum /011/ face. 04 p0460 A73-14867
Magnetospheric electric fields convective motions measurement by Ba ion cloud tracking and symmetric double probe floating potential technique 04 p0442 A73-15333
Plasma diagnostics in overcompensation operated Knudsen thermionic converter with Cs-Ba filler, noting W cathode surface properties 04 p0481 A73-15614
Photography of a lithium vapor trail during the daytime. 07 p0820 A73-20068
A cylindrical shell model of the NASA-MPE barium ion cloud experiment. 12 p1492 A73-27607
Characteristics of thermionic converter with cesium-barium filling at high anode temperature. 12 p1461 A73-27905
Observations of stimulated anti-Stokes radiation in barium vapour. 14 p1776 A73-29697
Astrometry applied to artificial clouds 15 p1940 A73-32192
Effect of adsorption on the electrical conductivity of thin vanadium films 17 p2220 A73-35557
Excited state absorption spectroscopy of alkaline earths selectively pumped by tunable dye lasers. I - Barium arc spectra. 21 p2713 A73-40472
Geophysical disturbance environment during the NASA/MPE barium release at 5 earth radii on September 21, 1971. 22 p2845 A73-41933
Yield and ion distribution for the barium cloud at 31,000 kilometers, September 21, 1971. 22 p2845 A73-41935
High resolution television imaging of barium cloud release in magnetosphere, discussing cloud shape development, striation patterns, core behavior and diffusion characteristics 22 p2845 A73-41936
Preliminary analysis of NASA optical data obtained in barium ion cloud experiment of September 21, 1971. 22 p2846 A73-41937
Quiet-time nighttime magnetic field near geomagnetic equator detected by magnetospheric barium cloud injection, revealing taillike structure from atmospheric models 22 p2846 A73-41939
Probe electric field measurements near a midlatitude ionospheric barium release. 24 p3085 A73-45119
Turbulent motions in an artificial plasma inhomogeneity released in the ionosphere. 24 p3088 A73-45238
- BARIUM ALLOYS**
Crystallochemical analogy between europium, yttrium, calcium, and barium in their alloys with manganese 09 p1135 A73-23235
- BARIUM COMPOUNDS**
NT BARIUM FLUORIDES
NT BARIUM OXIDES
NT BARIUM TITANATES
High pressure-sintering preparation of barium ferrites, discussing temperature and compression effects on density and magnetic properties 16 p2044 A73-32947
Resistance anomaly in semiconductor barium and strontium niobates 17 p2219 A73-35554
- BARIUM FLUORIDES**
Transfer of Yb3+/ excitation energy to TR3+/ in CaF2 and BaF2 crystals 07 p0837 A73-20206
Sealed off 9.4 micron 15 W output power carbon dioxide laser with barium difluoride windows, noting long service life 09 p1096 A73-23009

BARIUM OXIDES

- Molecular beam study on BaO and SrO formation for clarifying interaction of metal-vapors with upper atmosphere oxygen. 07 p0818 A73-19668
Some physicochemical properties of compounds formed by oxides of rare-earth elements and barium 11 p1410 A73-26673
Microwave optical double resonance spectra of CW dye laser pumped transitions in BaO 24 p3096 A73-44976
- BARIUM TITANATES**
Static electric quadrupole interaction of Ta- and Hf-ions in barium and lead titanate. 07 p0862 A73-20018
Study of the dynamic theory of BaTiO3 in the cubic phase 07 p0864 A73-20612
Influence of a constant electric field on the dielectric properties of polycrystalline BaTiO3 08 p0995 A73-21273
Dielectric dispersion of irradiated BaTiO3 in the phase transition region 09 p1134 A73-22983
Positive thermal coefficient of electrical resistance in BaTiO3 single crystals near the Curie point 10 p1260 A73-24473
Electron-diffraction study of amorphous condensates of barium titanate 12 p1531 A73-27198
Investigation of phase transitions in BaTiO3 15 p1923 A73-31204
Mono- and polycrystalline barium titanate structural and physical properties, discussing thermally induced structural changes effects on polarization, permittivity and loss tangent 15 p1924 A73-31775
Electrooptical modulator employing a barium titanate single crystal. I - Estimates of critical control voltages 23 p2987 A73-43571
Influence of heat treatment on the positron effect of semiconductive BaTiO3-ceramic. 24 p3120 A73-45367

BARKHAUSEN EFFECT

- Development and qualification of a magnetic technique for the nondestructive measurement of residual stress in CH-47 A rotor blade spars. [AHS PREPRINT 752] 17 p2180 A73-35080

BAROCLINIC WAVES

- Direct temperature measurements for rotating annulus experiments, showing symmetric baroclinic instability and Richardson number for baroclinic wave 02 p0189 A73-12788
On the meridional form of baroclinic waves in a two-layer quasi-geostrophic model. 03 p0304 A73-14312
CAT association with Kelvin-Helmholtz wave structures in baroclinic zone, correlating meteorological radar and aircraft observations 03 p0339 A73-14534
Interaction between long waves and zonal circulation in a baroclinic atmosphere 05 p0592 A73-16230
Bounds upon the growth rate of errors in quasi-non-divergent prediction models. 13 p1652 A73-28271
Barotropic and baroclinic contribution to eddy kinetic energy increase in disturbance amplification using quasi-geostrophic equations of motion and omega equation 13 p1610 A73-29335
Studies on barotropic and baroclinic energy conversions in wave number regime. 14 p1772 A73-30901
Stochastic wind field effects on baroclinic wave disturbances vertical propagation through turbulent atmosphere, obtaining stream function and dispersion equation 15 p1907 A73-32356
Large amplitude baroclinic waves generation via instabilities of two layer fluid in rapidly rotating cylinder compared with mathematical model based on quasi-geostrophic equations 23 p3001 A73-43590

BAROCLINITY

- Nonlinear baroclinic instability of a continuous zonal flow of viscous fluid. 02 p0153 A73-12035
The effect of the baroclinicity of the atmosphere on the structure of the wind field in the steady planetary boundary layer 04 p0441 A73-15289
Hemispheric single level model of atmospheric action centers formation due to horizontal baroclinity, including turbulent mixing and circulation index effects 05 p0592 A73-16229
Baroclinic model of zonal atmospheric circulation in the equatorial region 05 p0594 A73-17351
A macroscale-mesoscale numerical model of intense baroclinic development. 06 p0720 A73-18708

On the lateral boundary conditions for the primitive equations. 08 p0985 A73-21387

Boundary layer wind profile model in a steady state, diabatic, baroclinic atmosphere. 09 p1114 A73-22328

Boundary conditions in the problem of short-range weather forecasting on the basis of a baroclinic model of the atmosphere 11 p1393 A73-25639

Mechanisms influencing the distribution of precipitation within baroclinic disturbances. 13 p1652 A73-28266

A baroclinic model of the atmospheric zonal circulation in the equatorial region. 15 p1902 A73-31001

Stratified Taylor column model for topography effect on slow rotating baroclinic flow, considering Jupiter Red Spot and oceanic observations 16 p1998 A73-32797

Three to five day numerical forecasting making use of the complete hydrodynamics equations, and problems of correlating the original fields of meteorological elements 18 p2331 A73-35911

On the prediction of turbulence in baroclinic zones. 19 p2449 A73-38246

Forced convection of a fluid inside an ellipsoidal cavity 21 p2791 A73-40740

Parameterization of baroclinicity effects in the planetary boundary layer. 24 p3088 A73-45366

BAROMETRIC PRESSURE

U ATMOSPHERIC PRESSURE

BARORECEPTORS

- Extent of engagement of various cardiovascular effectors to alterations of carotid sinus pressure. 05 p0539 A73-16250
The effects of hypoxia, hypercapnia, and asphyxia on the baroreceptor-cardiac reflex at rest and during exercise in man. 06 p0654 A73-18348
A mathematical model to assess changes in the baroreceptor reflex. 08 p0934 A73-21475
Sustained human skin and muscle vasoconstriction with reduced baroreceptor activity. 15 p1833 A73-31344
Circulatory reflexes from mechanoreceptors in the cardio-aortic area. 21 p2638 A73-40637
Mechanism of 'readjustment' of aorta baroreceptors during hypertension 22 p2807 A73-42655
Circuit diagram of amplifier-filter for analysis of impulse activity of baroreceptor aortic afferent nerves in rabbits 22 p2816 A73-42681

BAROTRAUMA

- Pathophysiological and clinical aspects of aeroinjury and frontal sinus nematoma formation due to barometric pressure changes from pilot case history studies 09 p1039 A73-22538
Evaluation of auditory disorders in pilots by examining intratympanic muscles reflexes. 18 p2279 A73-36934
Barotrauma in United States Air Force accidents/incidents. 21 p2645 A73-41160
The frequency of barotraumas as determined by nasal findings and X-rays of the paranasal sinuses 22 p2817 A73-43132

BAROTROPIC FLOW

- Ponderable barotropic fluid irrotational flow in horizontal cylindrical channel, noting solitary depression waves possibility 03 p0289 A73-12911
Helmholtz-Rayleigh instability of nondivergent horizontal flows in a barotropic atmosphere 04 p0441 A73-15287
Empirical formulae for the universal functions M sub m/mu and N/mu in the resistance law for a barotropic and diabatic planetary boundary layer. 04 p0473 A73-15696
A numerical study of the influence of advective accelerations in an idealized, low-latitude, planetary boundary layer. 05 p0592 A73-16192
On the damping of high-frequency motions in four-dimensional assimilation of meteorological data. 05 p0592 A73-16199
Rossby wave barotropic instability effects on errors leading to large scale atmosphere predictability experiments by numerical simulation of two dimensional turbulence 08 p0985 A73-21386
On the lateral boundary conditions for the primitive equations. 08 p0985 A73-21387
On the simplest example of the barotropic instability of Rossby wave motion. 08 p0985 A73-21388

Barotropic model of local forecasts of katabatic winds
08 p0985 A73-21451

Logarithmic wind profile in neutral barotropic planetary boundary layers, discussing von Karman constant
11 p1394 A73-25717

Bounds upon the growth rate of errors in quasi-non-divergent prediction models.
13 p1652 A73-28271

Barotropic and baroclinic contribution to eddy kinetic energy increase in disturbance amplification using quasi-geostrophic equations of motion and omega equation
13 p1610 A73-29335

An exact solution to the system of prognostic equations of a barotropically divergent model of the atmosphere
23 p3001 A73-43461

Numerical study of the unstable modes of a hyperbolic-tangent barotropic shear flow.
23 p3002 A73-43591

Laminar flow of a viscous barotropic gas through a circular pipe
23 p2968 A73-43721

Spectral analysis of traveling planetary scale waves - Vertical structure in middle latitudes of Northern Hemisphere.
23 p2978 A73-43982

BAROTROPISM

Studies on barotropic and baroclinic energy conversions in wave number regime.
14 p1772 A73-30901

Application of the ray method to a study of the propagation of large-scale perturbations in a barotropic atmosphere with a mean wind
17 p2204 A73-34345

Speed variation in the earth's rotation and the baric field of the earth's Northern Hemisphere
17 p2159 A73-34637

BARRICADES

U BARRIERS

BARRIER ISLANDS

U ISLANDS

BARRIER LAKES

U LAKES

BARRIER LAYERS

Determination of the complete set of physical parameters of Schottky-barrier diodes
01 p0022 A73-10041

Spatial distribution of charge carriers and radiant energy in single and double heterostructure semiconductor lasers, noting technology of potential barriers formation
01 p0059 A73-10715

Alloying profile measurer for epitaxial films
01 p0050 A73-10799

Further exact and approximate considerations of the barrier problem.
06 p0716 A73-17981

Photoconductor-metal contact at higher densities.
11 p1407 A73-24985

Schottky barrier diode solar cells using dielectric antireflection coatings, discussing Nb, Mo and Cr diode metal characteristics, photovoltaic characteristics and conducting properties
19 p2391 A73-38406

The rectifying barrier in gallium arsenide Schottky diodes
23 p2959 A73-43618

Diffusionless theory of the current-voltage characteristics of a metal/monopolar semiconductor contact in the case of current limiting by an arbitrary space charge
23 p3015 A73-43621

Influence of the image force and tunnel effect on shot noise in diodes with a Schottky barrier
23 p2960 A73-43715

Two-loop frequency multipliers employing the barrier capacitance of a p-n junction and exhibiting maximum energetic indices
24 p3071 A73-44592

BARRIER REEFS

U REEFS

BARRIERS

Unbounded nondiffusive high Reynolds number stratified flow with lee waves over vertical barrier investigated for Froude number range on basis of Oseen-Boussinesq approximation
15 p1863 A73-31341

BARRIERS (LANDFORMS)

NT REEFS

BARS

NT ELASTIC BARS

NT PRISMATIC BARS

Propagation of elastic waves in a cylindrical bar subject to a moving load on its lateral surface.
03 p0343 A73-13833

The modal density for flexural vibration of thick plates and bars.
03 p0393 A73-13839

Material resistance analogies, relating shear, force and strain factors for bar deformation in tension, compression, torsion and bending
09 p1157 A73-22162

Elastic and elastoviscoplastic unloading waves propagation in semiinfinite bar under axial impact stress, considering bilinear stress-strain curve
11 p1447 A73-26646

Elastic deformation of thin walled U-bars lateral stiffeners under torsion, eccentric tension and bending loads, determining vaulting stiffness by finite element method
15 p1950 A73-31906

Torsional vibrations of a bar of variable cross-section.
16 p2079 A73-33075

A biaxial split Hopkinson bar for simultaneous torsion and compression.
17 p2149 A73-35754

Torsional rigidities for bars under fully plastic torsion.
18 p2365 A73-36695

Round bars of an anisotropically hardening material in torsion
20 p2619 A73-39356

State-change equations relating generalized load increment to response of constraint connected bars, deriving compatibility and equilibrium equations and matrix coefficients
21 p2788 A73-41604

Material resistance analogies, relating shear, force and strain factors for bar deformation in tension, compression, torsion and bending
22 p2919 A73-42110

Experimental determination of the transient uniaxial stress in a bar by dynamic photoplasticity. [ASME PAPER 73-APMW-37]
22 p2926 A73-42894

An elastic-plastic analysis of a bar under repeated axial loading.
24 p3151 A73-45307

BARYCENTER

U CENTER OF GRAVITY

BARYONS

Nuclear energy sources in superdense celestial bodies.
01 p0106 A73-11311

CP-noninvariance model of baryon asymmetry of universe, postulating kappa particle /neutral massive fermion/
02 p0221 A73-12669

A hypothesis, unifying the structure and the entropy of the universe.
04 p0500 A73-15492

Determination of properties of cold stars in general relativity by a variational method.
07 p0874 A73-19065

Elemental synthesis during high temperature phase of expansion of big bang universes, obtaining universal baryon density relationship to primordial deuterium abundance
08 p1008 A73-21151

Evolution of universe filled with cold baryons at cosmological singularity from Friedmann solution and equation of state for cold baryons
10 p1284 A73-24753

Equation of state of matter at supernuclear densities deduced from particle interactions nature and effective baryon mass spectrum
14 p1777 A73-30739

Neutron matter solidification in neutron star cores, discussing energy minimization through strongly interacting baryon system via arrangement into lattice structure
16 p2061 A73-33220

Magnetic moment generation in pulsars based on baryon model with superconducting proton fluid and normal electron field
17 p2226 A73-34365

Relativistic baryon effective masses and thresholds for strongly interacting superdense matter.
21 p2766 A73-40318

BASALT

Radioactive crystallization ages of Apollo 14 basaltic rocks from Fra Mauro formation, comparing with Apollo 11 samples
02 p0213 A73-12231

Major element composition of Luna 20 glasses.
05 p0546 A73-16827

Petrology of Apollo 14 high-alumina basalt.
07 p0879 A73-19684

Petrography and crystallization history of basalts 14310 and 14072.
07 p0879 A73-19685

Mineral-chemical variations in Apollo 14 and Apollo 15 basalts and granitic fractions.
07 p0879 A73-19686

Petrology of Fra Mauro basalt 14310.
07 p0879 A73-19687

Experimental petrology and petrogenesis of Apollo 14 basalts.
07 p0880 A73-19690

Mineralogical evidence for subsolidus vapor-phase transport of alkalis in lunar basalts.
07 p0880 A73-19693

Mineralogical and petrographic features of two Apollo 14 rocks.
07 p0880 A73-19699

Pyroxenes as recorders of lunar basalt petrogenesis - Chemical trends due to crystal-liquid interaction.
07 p0881 A73-19704

Distinct subsolidus cooling histories of Apollo 14 basalts.
07 p0881 A73-19707

Clinopyroxenes from Apollo 12 and 14 - Exsolution, domain structure, and cation order.
07 p0881 A73-19708

Petrology and origin of lithic fragments in the Apollo 14 regolith.
07 p0883 A73-19730

Noritic fragments in the Apollo 14 and 12 soils and the origin of Oceanus Procellarum.
07 p0884 A73-19741

Chemical characteristics of trace element rich KREEP basaltic rocks from Apollo 12 landing site
07 p0885 A73-19753

Apollo 12 lunar KREEP samples possible origin, considering mixture of ejecta from Copernicus, Reinhold and local highlands and Fra Mauro deposits
07 p0886 A73-19763

Apollo 14 mineral ages and the thermal history of the Fra Mauro formation.
07 p0887 A73-19776

Ar-40/Ar-39 ages of Apollo 14 and 15 samples.
07 p0888 A73-19783

Primordial radioelements and cosmogenic radionuclides in lunar samples from Apollo 15.
07 p0888 A73-19788

Thermal volatilization studies on lunar samples.
07 p0890 A73-19811

Rb-Sr ages and initial strontium in basalts from Apollo 15.
08 p0936 A73-20839

Analytical approach to estimating the source rock of basaltic magmas - Major elements.
09 p1076 A73-22147

Volatilization studies on a terrestrial basalt and their applicability to volatilization from the lunar surface.
10 p1275 A73-23738

Major element chemistry of glasses in Apollo 14 soil 14156.
10 p1278 A73-24111

Apollo 12 fines vacuum thermal conductivity as function of temperature for different densities, comparing to terrestrial basalt under vacuum and pressure.
11 p1425 A73-26137

Apollo 15 mare olivine and quartz basalts major and trace element composition and petrogenesis, deriving model of magma genesis
12 p1466 A73-27545

An unusual basalt fragment in Luna 20 sample L2010.
13 p1675 A73-28309

Petrology of Luna 20 regolith from the lunar highlands.
13 p1675 A73-28311

Apollo 17 landing site crystalline rock age determinations for coarse grained basalt and anorthositic gabbro samples via Ar isotope ratios
14 p1788 A73-29720

Apollo 17 basalt ortho- and para-armalcolite, noting differences in optical properties, crystal habit and distribution between coarse and fine grained rocks
14 p1789 A73-29739

Rare-earth elements, Co, Sc and Hf in the Steens Mountain basalts.
15 p1874 A73-32389

Apollo 17 lunar soil magnetic characteristics, covering ilmenite basalts mineralogy and petrology, electrical properties, orange and green glasses origin, and trace elements
16 p2061 A73-33171

Changes in the optical properties of minerals and their atomization caused by ion bombardment
16 p1977 A73-33756

Surface diffusion and migration on dispersed silicon and basalt during weak heating in a vacuum
16 p1977 A73-33757

Certain problems of the internal structure of the moon /Pyrolyte models of the moon/
16 p2066 A73-33789

Petrology of the 2-4 mm soil fraction from the Hadley-Apennine region of the moon.
17 p2230 A73-34517

Apollo 15 sample 15597 vitrophilic nature, pyroxenes segregation and textural appearance as evidence for arrival on lunar surface in entirely liquid state
17 p2230 A73-34518

A response to a comment on U-Pb systematics in lunar basalts.
18 p2354 A73-36512

Chemistry of lunar basalts with very high alumina contents.
18 p2354 A73-36598

Experimental data on the investigation of lunar surface chemical composition.
21 p2774 A73-41403

Russian book - Chemistry of terrestrial and lunar basaltic rocks.
21 p2648 A73-41436

BASE FLOW

Measurements on separated supersonic boundary layer flows after an expansion corner.
01 p0003 A73-11135

Basic flow characteristics of a linear aerospike nozzle segment.
[ASME PAPER 72-WA/AERO-2]

- Wind tunnel study of flow structure and turbulent wakes on base surfaces of sharp or blunt edged flat bodies at various Mach and Reynolds numbers
04 p0405 A73-15908
- Exhaust plume prediction model for a low-altitude supersonic missile.
[AIAA PAPER 72-1170] 06 p0741 A73-18399
- Base drag reduction on blunt based axisymmetric bodies by base burning, calculating inviscid flow field with heat addition around recirculating bubble
11 p1449 A73-25347
- Structure of the base flow in a four-nozzle cluster rocket engine
21 p2754 A73-40392
- Some investigation on base flow behind cylindrical bodies in incompressible flow.
22 p2797 A73-42997
- BASE HEATING**
Radiation base heating from solid propellant launch vehicle exhaust plumes.
[AIAA PAPER 72-1168] 03 p0397 A73-13466
- Titan III convective base heating from solid rocket motor exhaust plumes.
[AIAA PAPER 72-1169] 03 p0382 A73-13467
- Finite-amplitude convection occurring in a modulated gravitational field
06 p0767 A73-17463
- Base drag reduction on blunt based axisymmetric bodies by base burning, calculating inviscid flow field with heat addition around recirculating bubble
11 p1449 A73-25347
- Flight test correlation technique for turbulent base heat transfer with low ablation.
11 p1453 A73-26671
- Rearward-facing steps in laminar supersonic flows with and without suction.
[AIAA PAPER 73-667] 18 p2261 A73-36218
- BASE PRESSURE**
Base resistance of axisymmetric bodies with a variable angle of attack - Analysis and interpretation of the physical phenomenon
03 p0242 A73-13375
- Annular truncated plug nozzle flowfield and base pressure characteristics.
[AIAA PAPER 73-137] 05 p0530 A73-16887
- Measurements of base pressure upon a plate and a wedge in the 2.8 to 6.8 Mach number range
[DFVLR-SONDDR-256] 06 p0645 A73-17740
- Effect of low heat-shield ablation rates on flight test turbulent base pressure.
07 p0920 A73-19975
- Dependence of the base pressure on the ratio of specific heats at supersonic velocities
09 p1027 A73-21917
- Base pressures in flow expansions by hydraulic analogy.
13 p1564 A73-28811
- Detection of flight vehicle transition from base measurements.
13 p1706 A73-28834
- Base drag calculations in supersonic turbulent axisymmetric flows.
13 p1564 A73-28835
- Bottom pressure and specific-heat ratio at supersonic velocities.
15 p1825 A73-32643
- The effect of the wedge angle on the similarity parameter of the turbulent mixing region in the case of an incompressible flow
20 p2547 A73-39408
- Vortex shedding from and base pressure distribution on bluff body measured in shear or uniform flow, calculating Strouhal number
23 p2940 A73-43939
- A theoretical and experimental study of sound attenuation in an annular duct.
[AIAA PAPER 73-1005] 24 p3077 A73-44838
- Supersonic laminar flow over wedge or backward-facing step for large Reynolds number and small base or step height, predicting pressure distribution at reattachment
24 p3055 A73-45314
- BASES [FOUNDATIONS]**
U FOUNDATIONS
- BASINS**
U STRUCTURAL BASINS
- BATCH PROCESSING**
Traffic analysis by statistical tests for batch mode operated digital computer network design, considering user habits, and interarrival, waiting and partition times
12 p1475 A73-27159
- Unit batch size optimization in mass production, discussing labor efficiency, operational cycle length, unfinished volume and total cost
12 p1562 A73-27477
- Data compression in recursive estimation with applications to navigation systems.
[AIAA PAPER 73-901] 20 p2589 A73-38835
- BATHS**
NT SALT BATHS
- BATHYMETERS**
Application of a pulsed laser for measurements of bathymetry and algal fluorescence.
20 p2574 A73-39863
- A statistical-temporal image merging technique for automatic bathymetry applied to southern California coastal waters.
20 p2560 A73-39887
- BATHYMETRY**
U BATHYMETERS
- BATS**
Characteristics of the electrical activity of the superior olivary bodies of Vespertilionidae and Rhinolophidae bats in response to ultrasonic stimuli of different frequencies
10 p1182 A73-24596
- BATTERIES**
U ELECTRIC BATTERIES
- BATTERY CHARGERS**
The reflex principle of charging nickel-cadmium and other batteries.
03 p0253 A73-13938
- High-efficiency converter and battery charger for an RTG power source.
22 p2801 A73-42906
- Bilateral power conditioner with common filters and transistor control circuits for battery charge and discharge functions onboard near earth orbit spacecraft
22 p2802 A73-42916
- BATTERY SEPARATORS**
U SEPARATORS
- BAUSCHINGER EFFECT**
The Bauschinger effect in annealed and irradiated titanium
01 p0064 A73-10495
- A numerical method considering the Bauschinger effect for large deflection analysis of elastic-plastic circular plates.
02 p0236 A73-12522
- Mechanical properties and stress analysis of elastoplastic body, noting yield conditions and Bauschinger effect
03 p0386 A73-13155
- A new relationship between pre-strain and yield stress drop due to Bauschinger effect.
06 p0713 A73-18772
- Bauschinger effect in annealed and irradiated titanium.
14 p1759 A73-30320
- Work hardened plastic material mechanical properties changes manifested by Bauschinger effect defined as acquired anisotropy, examining plastic deformation conditions
15 p1952 A73-32079
- The Bauschinger effect and its role in mechanical anisotropy.
21 p2722 A73-41547
- Influence of the offset on the experimental yield surfaces of metals - A theoretical evaluation.
24 p3147 A73-44747
- BAYES THEOREM**
Conjoint-measurement framework for the study of probabilistic information processing.
02 p0138 A73-12545
- A Bayes analysis of availability for a system consisting of several independent subsystems.
03 p0336 A73-13732
- An application of Bayes-law estimation to nonlinear phase demodulation.
04 p0471 A73-12523
- Bayes criteria and previous test data for industrial equipment test optimization, using linear and quadratic programming
07 p0831 A73-20076
- Bayesian MFR life test sampling plans.
08 p0973 A73-20950
- Bayesian prior distributions for multi-component systems.
09 p1111 A73-22374
- Asymptotic behavior of some statistical estimates. II - Limit theorems for a-posteriori density and Bayesian estimates
12 p1517 A73-27188
- An empirical Bayes approach for the Poisson life distribution.
15 p1901 A73-32262
- Quasi-optimal signal reception in asynchronous addressing communication systems with a time-frequency matrix
17 p2121 A73-34587
- Bayes theorem for radio signals parameter estimation on random noise background, using rectangular function of losses
17 p2123 A73-35167
- A projection model for Bayesian estimation of distributed functions.
17 p2202 A73-35373
- Bayesian estimation of life parameters in the Weibull distribution.
17 p2204 A73-35810
- Kalman filter for rapid detection and adaptive estimation of state and covariance, deriving Bayes decision rule and algorithm for spacecraft tracking
19 p2410 A73-38030
- Selection of analogs to composite kinematic charts of natural synoptic periods
19 p2449 A73-38545
- A probabilistic algorithm for grouped handling of arguments with sequential discrimination of input features
21 p2658 A73-40994
- The estimate feedback equalizer - A suboptimum nonlinear receiver.
21 p2656 A73-41165
- Bayes theorem for probabilistic analysis of logic circuits applied to reliability estimation of switching circuits
23 p2965 A73-44107
- An empirical Bayes estimator for the scale parameter of the two-parameter Weibull distribution.
24 p3105 A73-44577
- BAYESIAN STATISTICS**
U BAYES THEOREM
- BBGKY HIERARCHY**
Isotropic system development of gravitating point particles in galactic clusters and superclusters in expanding universe from Liouville theorem and BBGKY hierarchy
03 p0365 A73-12927
- Kinetic theory of a two-dimensional magnetized plasma. III - Limit of very large magnetic field.
09 p1127 A73-22283
- BCC LATTICES**
U BODY CENTERED CUBIC LATTICES
- BCH CODES**
Sphere packings constructed from BCH and Justesen codes.
13 p1584 A73-28919
- Logic and computational complexity of decoders for BCH codes, discussing channel capacity, error correction and information theory
13 p1587 A73-29672
- BCS THEORY**
The superconductor maser - A calculation of the gain from the two-level model and the BCS theory, and some new experimental results.
02 p0175 A73-11848
- BEACON SATELLITES**
Application of satellite radio beacons for measurement of small-scale ionospheric irregularities.
03 p0300 A73-13642
- Some results about the satellite scintillation on 150/400 MHz and the horizontal gradient of the total electron content in the polar ionosphere.
03 p0300 A73-13648
- Characteristics of large scale ionospheric irregularities.
03 p0300 A73-13652
- BEACONS**
NT RADAR BEACONS
NT RADIO BEACONS
NT RADIO DIRECTION FINDERS
- BEADS**
Light weight beaded and tubular structural panels for heat shielded aerodynamic surfaces
[AIAA PAPER 73-370] 11 p1438 A73-25504
- BEAM COLUMNS**
U BEAMS [SUPPORTS]
U COLUMNS [SUPPORTS]
- BEAM CURRENTS**
A target design for irradiation of NaI at high beam current.
07 p0853 A73-20469
- Features of the flow of a nonisothermal plasma, obtained in a beam-plasma discharge, through a magnetic nozzle
09 p1124 A73-21890
- Flow of nonisothermal plasma through a magnetic nozzle.
17 p2215 A73-34313
- Low cost beam current integrator for use with decelerators in ion implantation experiments
17 p2175 A73-35759
- Electron beam current fluctuation reduction by placing hot filament into Wheatstone bridge arm for temperature regulation in power supply for electron gun
17 p2176 A73-35776
- Investigation of conditions for the formation of a beam-plasma discharge without a magnetic field
21 p2748 A73-41516
- Correlation of ion and beam current densities in Kaufman thrusters.
22 p2900 A73-42636
- BEAM PLASMA AMPLIFIERS**
Difference frequency generation using non-linear interaction between a modulated electron beam and a collisionless plasma.
06 p0733 A73-18839
- BEAM SPLITTERS**
Optical birefringent multichannel splitting and combining wideband FDM communications filters, considering crosstalk, pulse response, extinction ratio and detuning
08 p0939 A73-21046
- Interference patterns and operation of four unit interferometer consisting of beam splitter, mirrors and analyzer
21 p2704 A73-41261
- Nonlinear transmission loss in Ge beam splitter in pulsed HF and DF lasers operating at 2.5 to 4 microns
22 p2897 A73-43145

BEAM SWITCHING

Experimental investigation of a test-model two-beam TWT /electron-wave TWT/

- 01 p0025 A73-10986
TWT power gain, efficiency and output variations compensation methods during electron beam switching between pulsed and CW modes
- 02 p0148 A73-12570
Series diode SP4T switch for satellite applications.
- 04 p0428 A73-15455
High-frequency electro-optic prism deflector with application to optical demultiplexing and multiplexing.
- 06 p0701 A73-18363
Change of vibrational temperature due to laser action in CO₂ lasers.
- 09 p1089 A73-21933
Self-switching in single-heterojunction injection lasers.
- 20 p2574 A73-39690

BEAM WAVEGUIDES

- Dispersion equation of parametric longitudinal LF instability of electromagnetic wave propagation in bounded electron beam in metallic waveguide
- 10 p1257 A73-24876
Study of the effect of a plasma on the microwave radiation of a helical beam in a waveguide
- 12 p1527 A73-26935
Contribution to the theory of the natural vibration spectra of a nonequilibrium resonant cavity
- 13 p1589 A73-28290
Feasibility experiments for high capacity Hertzian cables to distribute and collect data within urban areas, using cylindrical mirrors
- 16 p1982 A73-33715
Dispersion equation of parametric longitudinal LF instability of electromagnetic wave propagation in bounded electron beam in metallic waveguide
- 21 p2744 A73-41651
Theory of eigenmode spectra of a nonequilibrium resonator.
- 22 p2830 A73-41814
Effect of a plasma on the microwave radiation from a helical beam in a waveguide.
- 22 p2892 A73-42269

BEAMS (RADIATION)

- NT ATOMIC BEAMS
- NT ELECTRON BEAMS
- NT ION BEAMS
- NT LIGHT BEAMS
- NT MICROBEAMS
- NT MOLECULAR BEAMS
- NT NEUTRAL BEAMS
- NT NEUTRON BEAMS
- NT PARTICLE BEAMS
- NT PHONON BEAMS
- NT PHOTON BEAMS
- NT PION BEAMS
- NT PROTON BEAMS
- NT RADAR BEAMS
- Requirements for the production of several, mutually independent beams by a transmission-line fed antenna
- 05 p0559 A73-17238
A new method of local X-ray structural analysis - The method of an X-ray beam converging in a solid angle
- 08 p0965 A73-21131
Projective properties of an anamorphic bundle of projecting beams
- 10 p1219 A73-24484
Possibility of correlating the field of a wide wave beam in a smoothly nonhomogeneous medium with the field of a beam in vacuum
- 11 p1331 A73-26161
A dual-mirror antenna with beam scanning over a ninety-degree sector
- 14 p1736 A73-30561
Approach and landing operations and flight guide beam systems, discussing tests, design, improvements and operational requirements [DGLR PAPER 73-011]
- 17 p2208 A73-34491
The beaming of radiation from an accreting magnetic neutron star and the X-ray pulsars.
- 17 p2225 A73-35618
Linear scan receiver for electronic beam steering of the north-south array of the DKR-1000 radio telescope
- 21 p2662 A73-40543
Evanescent fields produced by totally reflected beams.
- 22 p2824 A73-41853
Beam characteristics of the 300-ft telescope.
- 24 p3066 A73-44580

BEAMS (SUPPORTS)

- NT BOX BEAMS
- NT CANTILEVER BEAMS
- NT CURVED BEAMS
- NT I BEAMS
- NT RECTANGULAR BEAMS
- Steady creep bending in a beam with random material parameters.
- 01 p0113 A73-10198
Photoelastic model analysis of sandwich beams.
- 01 p0050 A73-10737
Bending stresses propagating from the clamped support of an impulsively loaded beam.
- 01 p0115 A73-10753

Grillages of maximum strength and maximum stiffness.

- 01 p0115 A73-10767
Anisotropic beam elastic deformation under end loads, deriving coefficients for linear relation between cross sectional stresses and elastic deformation curvature
- 02 p0230 A73-11780
Scheme for calculating the process of elastic wave propagation in a composite beam
- 02 p0233 A73-11943
The post-buckled behaviour of a thin-walled box beam in pure bending.
- 03 p0384 A73-13114
Rotatory inertia and hub radius effects on transverse vibrational characteristics of clamped Rayleigh beam, using Galerkin method
- 03 p0388 A73-13316
Beam vibration frequencies tables handbook preparation technique
- 03 p0388 A73-13317
On the unbonded contact between a beam and a semi-infinite plate.
- 03 p0389 A73-13324
Convergence of consistently derived Timoshenko beam finite elements.
- 03 p0390 A73-13342
Beams subjected to follower force within the span.
- 04 p0508 A73-14938
Beam transverse vibration with nonlinear-spring supported free end and concentrated mass, determining free vibration frequencies
- 04 p0508 A73-14940
Static analysis of beams with random material or environmental characteristics, deriving probability functions for beam descriptors
- 04 p0509 A73-14945
Extended validity of single segment stepwise integration schemes for solution of two-point boundary value problems.
- 04 p0510 A73-15015
Minimum-weight plastic design of continuous beams subjected to one single moveable load.
- 04 p0510 A73-15030
Symmetrical bending for the general case of oscillating beams under transverse loads
- 04 p0511 A73-15174
Buckling of continuously supported beams. [ASME PAPER 72-WA/APM-34]
- 04 p0515 A73-15886
Governing equations for vibrating constrained-layer damping sandwich plates and beams. [ASME PAPER 72-WA/APM-24]
- 04 p0515 A73-15892
Dynamic stability of monosymmetrical thin-walled structures. [ASME PAPER 72-APM-SS]
- 05 p0632 A73-16530
Free vibration of a beam with one end spring-hinged and the other free.
- 05 p0633 A73-16542
Finite element analysis of nonlinear vibration of beam columns.
- 05 p0636 A73-17118
A new algorithm for the computation of bending moments and deflections of straight beams.
- 05 p0637 A73-17325
Sandwich beams of unsymmetrical structure.
- 06 p0759 A73-17699
On the torsional static stability and response of open section tubes subjected to thermal radiation loading.
- 07 p0908 A73-19086
The status of engineering knowledge concerning the damping of built-up structures.
- 07 p0909 A73-19099
Thin walled beam composed indeterminate elastic framed structures minimum weight design, obtaining solutions by nonlinear programming algorithm
- 07 p0912 A73-19951
Matched asymptotic expansions method application to slender cylindrical beams, calculating displacement far field by Navier-Stokes elasticity equation
- 07 p0913 A73-20075
Piecewise linear approximation of thin walled rib and diaphragm reinforced conical beams under thermal field and axial loads, using limit stress-strain diagrams
- 07 p0913 A73-20096
Finite element displacement method for large amplitude free flexural vibrations of beams and plates.
- 07 p0914 A73-20212
Static and dynamic behavior of welded aluminum beams.
- 07 p0839 A73-20270
Response of nonlinear beam to random excitation.
- 07 p0916 A73-20436
Stiffness matrix for a beam with an axial force.
- 08 p1015 A73-20725
Effect of transverse shear deformation on vibrations of planar structures composed of beam-type elements.
- 08 p1017 A73-21192
On one-dimensional finite-strain beam theory - The plane problem.
- 08 p1018 A73-21405

Beams and membranes nonlinear vibrations via modified perturbation method based on Linstedt-Poincare technique

- 08 p1018 A73-21406
Improved finite elements for vibration analysis of tapered beams.
- 08 p1018 A73-21439
Bending of an orthotropic prismatic beam by a transverse force in a geometrically nonlinear formulation
- 08 p1020 A73-21769
Book - Vibration of solids and structures under moving loads.
- 09 p1159 A73-22526
Optimal beam frequencies by the finite element displacement method.
- 09 p1160 A73-22898
Orthotropic almost cylindrical beams - Bending by a transverse load.
- 09 p1160 A73-23023
Buckling of a simply-supported beam between two unattached elastic foundations.
- 09 p1166 A73-23466
Computation of the deflections of straight beams with any variation of the moment of inertia by the method of the three unknowns.
- 10 p1287 A73-23617
Application of the finite element method to the study of the stability of plane structures
- 10 p1287 A73-23618
Flange-to-web connection requirements on beams with corrugated webs.
- 10 p1223 A73-23632
Impact strength and fracture of carbon fiber composite beams.
- 10 p1238 A73-23972
Bending and vibration of multilayer sandwich beams and plates.
- 10 p1289 A73-24290
Stresses in a partly yielded notched bar - An assessment of three alternative programs.
- 10 p1290 A73-24294
Beam and plate flexural vibration damping by free or uncompressed rigid viscoelastic coatings applied on sides
- 10 p1293 A73-24794
Torsion of a sectorially composite hollow circular cylindrical beam.
- 11 p1432 A73-24996
Elastic impact against a beam with allowance for internal energy absorption
- 11 p1433 A73-25032
Dynamic characteristics of space thin beams.
- 11 p1433 A73-25126
Application of general variational methods with discontinuous fields to bending, buckling, and vibration of beams.
- 11 p1435 A73-25436
Vibrations of an Euler beam with a system of discrete masses, springs, and dashpots.
- 11 p1442 A73-25788
Transversely isotropic /anisotropic/ elastic beam bending and torsion, determining frequency dependent compliances by approximate analytic solution via variational method
- 11 p1447 A73-26655
Static and dynamic stability of simply supported imperfect beam resting on nonlinear elastic foundation under axial load
- 12 p1550 A73-27033
Book - Introductory structural analysis with matrix methods.
- 12 p1554 A73-27548
Compressive buckling analysis and design of stiffened flat plates with multilayered composite reinforcement.
- 12 p1554 A73-27736
Design of an infinite beam with an elastic base in a nonclassical formulation
- 12 p1555 A73-27796
Flexural response of tapered beam on elastic-plastic foundation, solving in closed form to evaluate efficiency of numerical methods
- 12 p1557 A73-27932
Free vibrations of a laminated beam by a microstructure theory.
- 13 p1691 A73-28063
Natural frequencies of a beam considering support characteristics.
- 13 p1691 A73-28065
Initial-boundary value problems of nonlinear extensible beam equation as mathematical model for transverse deflections of beam with hinged or clamped ends
- 13 p1695 A73-28438
Nonlinear transverse vibrations of beams with properties that vary along the length.
- 13 p1695 A73-28488
Elastic structures nonlinear free vibrations theory based on Hamilton principle and perturbation method, applying to beams and rectangular plates
- 13 p1696 A73-28751
Ultraharmonic motion of a viscously damped nonlinear beam.
- 13 p1697 A73-28809

Multiphase composite material models for elastoplastic beam bending under loading and unloading, using stress-strain diagram in tension and compression

13 p1698 A73-29052

The employment of special methods of the matrix-eigenvalue theory in the calculation of the resistance to buckling according to Vianello

14 p1805 A73-29740

Vibration analysis of sandwich beam with constrained viscoelastic layers on both sides.

14 p1806 A73-30046

Optimal shapes of simply supported vibrating elastic beams for maximum fundamental frequency under axial compressive load

14 p1812 A73-30494

The transient response of non-uniform, non-homogeneous beams.

14 p1813 A73-30664

Oblique bending of a homogeneous orthotropic prismatic beam by a force couple in the quadratic theory of elasticity

14 p1815 A73-30785

A method for studying the stressed state during torsion of hollow prismatic beams

14 p1815 A73-30790

A test machine for fatigue under pulsed moving loads

15 p1855 A73-31144

Optimal forms of the thin-walled closed cross-section of a beam subjected to bending

15 p1947 A73-31365

Computation of upper and lower bounds to the frequencies of elastic systems by the method of Lehmann and Machly.

15 p1951 A73-32027

Considerations on the centres of shear and of twist in the theory of beams.

15 p1954 A73-32111

Small parameter series convergence evaluation in geometrically nonlinear problems by Cauchy majorants, applying to flat curvilinear beam deflection

16 p2074 A73-32689

Stress calculation for plates and beams via finite element method, improving accuracy by smoothing stress and strain distributions at element boundaries

16 p2080 A73-33262

Lateral instability of thin-walled beams - Considerations regarding methods of experimental investigation

16 p2081 A73-33372

Damped lateral vibration in an axially creeping beam with random material parameters.

16 p2082 A73-33902

Influence of in-plane displacements at the boundaries of rigid-plastic beams and plates.

16 p2083 A73-33973

Contraction of an elastic layer by girder slabs

17 p2240 A73-34148

Coupled thermally induced vibrations of beams.

17 p2241 A73-34190

Buckling of beams supported by Pasternak foundation.

17 p2243 A73-34531

Welded steel beam fatigue behavior evaluation via stable crack growth concepts, developing fracture mechanics model for cracks originating from pores

17 p2246 A73-34887

Performance, structural reliability and fatigue life of glass fiber-epoxy twin beam helicopter rotor blades [AHS PREPRINT 782]

17 p2106 A73-35095

Hopscotch method for one-space dimensional bending beam elliptic differential equation solution, noting mesh ratio stability range

17 p2251 A73-35518

Dirac's distribution in the study of statically indeterminate beams.

18 p2364 A73-36491

Multiphase composite material models for elastoplastic beam bending under loading and unloading, using stress-strain diagram in tension and compression

18 p2366 A73-36884

Nonlinear bending problem for a beam of variable rigidity

18 p2366 A73-36959

On the flexural vibration frequencies of statically loaded beams.

18 p2367 A73-37091

Natural transverse vibrations of sandwich beams of unsymmetrical structure.

18 p2367 A73-37141

Calculation of a system of two infinite beams on an elastic base

19 p2495 A73-37190

Post-buckling behavior of cold-formed thin-walled stainless steel beams.

19 p2496 A73-37481

Flexural wave fields in infinite beam-reinforced plates under point excitation.

19 p2498 A73-37725

Non-linear vibration of beams with time-dependent boundary conditions.

19 p2501 A73-38253

Localized creep of a nonhomogeneous beam subjected to loads exceeding the true elastic limit

19 p2501 A73-38306

Monograph on optimal structure design by linear programming and calculus of variations covering pin jointed frameworks, beams, circular sandwich plates, Michell continua, etc

19 p2502 A73-38364

Calculation of bending vibrations in beams with the aid of a discrete model

20 p2615 A73-38982

Laterally restrained beam columns with uniform biaxial loading.

20 p2616 A73-39117

Motion of a rigid-plastic beam in a resistant medium under the action of a local load

20 p2620 A73-39470

Two-frequency unsteady forced oscillations of a beam

20 p2593 A73-39502

Transverse oscillations of a beam lying on an elastic base under the action of a perturbation force which has several harmonics with frequencies close to the first natural frequency

20 p2620 A73-39512

Approximate solutions for heat conduction and thermal stresses in thermoelasticity of solids and beam and ring structures, considering dynamic, coupling, melting and solidification effects

20 p2620 A73-39514

Dynamic stability of a nonlinear beam subjected to both longitudinal and transverse excitation.

20 p2621 A73-39532

Rotary inertia and energy dissipation effects on dynamic response of three layered symmetrical laminate beam with viscoelastic core vibrating in flexural mode, using variational calculus

20 p2623 A73-39555

Dynamics of cylindrical structures subjected to axial flow.

21 p2783 A73-40292

Parametric study of multiple-layer damping treatments on beams.

21 p2785 A73-40752

Critical load analysis of strip /beam/ with arched crack under compressive stress and bending moments

21 p2786 A73-40985

Effect of support flexibility on the fundamental frequency of vibrating beams.

22 p2918 A73-41966

A numerical study of damping in viscoelastic sandwich beams.

[ASME PAPER 73-DET-73]

The theory of elasticity of flexural-stiffness exhibiting, planar particle systems with a rectangular net

22 p2922 A73-42526

Vibration of beams with overhangs.

22 p2923 A73-42563

Probability displacement and modal cross spectral density parameters of two span beam random vibrations under white noise

23 p3039 A73-43304

A general conclusion regarding the large amplitude flexural vibration of beams and plates.

23 p3039 A73-43305

Effects of specimen geometry on the strength of composite materials.

23 p2996 A73-43633

The mechanism of fracture of reinforced beams during bending. I

24 p3146 A73-44531

Bellman dynamic programming principle for elastic-perfectly plastic beam structure design optimization with respect to cross-sections, span lengths and weight

24 p3148 A73-45003

BEAMSHAPING

U COLLIMATION

BEARING ALLOYS

Improved M50 aircraft bearing steel through advanced vacuum melting processes.

04 p0455 A73-15746

BEARINGS

NT ANTIFRICTION BEARINGS

NT BALL BEARINGS

NT GAS BEARINGS

NT JOURNAL BEARINGS

NT LIQUID BEARINGS

NT ROLLER BEARINGS

NT THRUST BEARINGS

Effect of friction in suspension bearings on the motion of a gyroscope with a forced rotation of its base

01 p0054 A73-11415

Externally pressurized bearings; Proceedings of the Conference, London, England, November 17, 18, 1971.

03 p0311 A73-13201

The performance of a four-pocket conical hydrostatic bearing.

03 p0311 A73-13206

Linearized Kalman filtering for turbopump rotating assembly inertial and bearing parameter identification and state estimation, noting state-space model feasibility

03 p0313 A73-13904

Development and application of magnetic bearings.

03 p0313 A73-13924

Investigation of the friction and wear behavior of polytetrafluoro-ethylene composite materials as compared to synthetic carbon and sintered metal. I

06 p0714 A73-18449

Low peak temperatures and hydrodynamic bearings - Key to long life organic Rankine cycle systems.

09 p1034 A73-22770

Fluid film lubrication fluid mechanical theory, considering non-Newtonian fluids, turbulence, inertia and elastohydrodynamic effects in various bearing types

10 p1223 A73-23858

Gear and bearing designs with lubricated and reinforced thermoplastics.

10 p1223 A73-23957

Bearing materials from graphite fiber composites.

10 p1238 A73-23974

Motion of a magnetizable fluid in the lubrication film of a cylindrical bearing

10 p1225 A73-24586

Hot environment lubrication failures of sleeve bearing diester lubricant system in small electric motors, using reliability-temperature accelerated tests

[ASME PAPER 73-DE-13]

Self excited whirl stability limits and frequencies of continuous rotors under gyroscopic, damping and hydrodynamic bearing film forces

16 p2022 A73-34035

Investigations of the Intelsat IV bearing and power transfer assembly.

17 p2238 A73-34867

Static, dynamic and fatigue load influence on solid lubricant compact bearings.

[ASLE PREPRINT 73AM-1A-1]

17 p2178 A73-34976

Sikorsky CH-53D helicopter main rotor head design, considering spherical elastomeric bearing, microstructural analysis, flight and ground fatigue tests and forging techniques

[AHS PREPRINT 713]

Turbulent lubrication theory - Application to designs.

[ASME PAPER 73-LUBS-10]

Reliability of aircraft turbojet bearings

18 p2320 A73-36691

Hydrodynamic bearing damping in infinitely broad gap between oppositely oscillating parallel boundary surfaces, discussing inertia, Reynolds number and coefficient of friction

20 p2547 A73-39409

Airframe ball, roller and spherical plain bearing designs for flight control, landing gear and wing mechanisms

21 p2707 A73-41125

Transient response simulation model for stability analysis of flexible high speed rotor-bearing system dynamics, examining nonlinear effects

[ASME PAPER 73-DET-102]

Study and calculation of the vibrations of a rotating rotor with allowance for clearances in the bearings

23 p3041 A73-43725

BEAT

U SYNCHRONISM

BEAT FREQUENCIES

Ionospheric resonance signal envelope and waveform observation by rocket-borne RF sounder, noting electron gyrofrequency third harmonic due to beating waves

02 p0140 A73-11750

Amplitude-frequency and stability characteristics of parametric amplification by triple-frequency interaction in nonlinear nonautonomous system

02 p0147 A73-12491

Beat conditions during synchronization of an oscillator by an external sinusoidal force

02 p0147 A73-12492

Laser frequency fluctuations due to mechanical vibrations.

03 p0319 A73-14451

Characteristics of acoustooptic cavity dumping in a mode-locked laser.

09 p1091 A73-22089

A new zero-beat indicator and its use in frequency measurements

13 p1617 A73-28859

Effect of an external magnetic field on the beat frequency of opposite waves in a ring laser with a noninterfering phase-shifting device

13 p1627 A73-28965

Daily variations of the characteristics of beating-type Pc3/Bpc3/pulsations.

13 p1611 A73-29661

Evidence for non-linear response processes in the human visual system from measurements on the thresholds of spatial beat frequencies.

17 p2112 A73-34839

General method for the calculation of the frequency of beats in a single-mode ring laser.

20 p2573 A73-39678

Laser mode locking effect on conversion efficiency of beat frequency excitation in multimode emission, using two photon fluorescence method

21 p2712 A73-40308

- Lamb-dip-stabilized carbon dioxide laser line frequency separations, discussing beat frequencies, C 12 and O 16 molecular rotation constants and vibration level reduction
21 p2712 A73-40324
- Nonstationarity of the three-mode regime in a gas laser in the case of mode-frequency symmetry
22 p2870 A73-42388
- Implementation problems of a multichannel digital filter in the case of beat frequencies in the MHz range
23 p2957 A73-43316
- Effect of external magnetic field on the beat frequency in a ring laser with nonreciprocal phase shifter.
23 p2989 A73-44317
- BED REST**
Circadian rhythm asynchrony in man during hypokinesia.
03 p0263 A73-14121
- Thyroid and adrenal cortical rhythmicity during bed rest.
03 p0263 A73-14122
- Vertical posture control after Soiuz 6, 7 and 8 flights and 120-day hypokinesia
08 p0933 A73-20985
- Effect of passive 70-deg head-up tilt on peripheral visual response time.
10 p1185 A73-24566
- Circadian rhythm of urinary calcium excretion during immobilization.
14 p1717 A73-30512
- Study of nitrogen balance and creatine and creatinine excretion during recumbency and ambulation of five young adult human males.
18 p2278 A73-36786
- Effects of rehydration on +Gz tolerance after 14-days' bed rest.
23 p2946 A73-43524
- BEDS (PROCESS ENGINEERING)**
Heat transfer in static packed beds - Effects of radiation on temperature distribution.
05 p0638 A73-16219
- BEES**
Bee image detection by ommatidium based on physical model using electromagnetic analysis of light absorption in photoreceptor
23 p2946 A73-43344
- BEEETLES**
NT TRIBOLIA
- BEHAVIOR**
NT HUMAN BEHAVIOR
Inhibitive mechanisms activity in behavior control by neostriatum, discussing suppressive reactions, evoked sleep, conditioned and instrumental reflexes and neurophysiological aspects
01 p0009 A73-11025
- Hypothalamic norepinephrine - Circadian rhythms and the control of feeding behavior.
02 p0134 A73-12417
- Self-imposed timeouts under increasing response requirements.
10 p1185 A73-24625
- The role of analyzers of conditional and unconditional stimuli in the functional system of the behavioral conditioned-reflex action
12 p1461 A73-27105
- Frontal eye-field lesions in monkeys.
18 p2272 A73-36446
- Changes in some behavioral reactions and in the bioelectric activity of the brain in cats during the development of sleep under polarization of individual brain structures
19 p2393 A73-37393
- Physiological study of dynamics and evolution of chimpanzee complex behavior, considering motor reactions, group behavior and nerve mechanisms of voluntary acts
23 p2947 A73-43928
- Effect of adaptation to altitude hypoxia on the behavior of animals in a conflict situation
24 p3058 A73-44549
- BELL AIRCRAFT**
NT UH-1 HELICOPTER
NT X-22 AIRCRAFT
Management and control of military and commercial flight test programs at Bell Helicopter Company.
23 p3050 A73-44058
- BELL MILITARY AIRCRAFT**
U MILITARY AIRCRAFT
- BELLMAN THEORY**
Optimization of control and observation processes in dynamic systems under random perturbations.
02 p0149 A73-12118
- Approximate method for the synthesis of the optimal control of a dynamic system subjected to random disturbances
06 p0725 A73-18879
- Investigation of the smoothness characteristics of the Bellman function on the basis of the equation of motion of the system in time-optimal problems. I Linear case
07 p0806 A73-20633

- Group properties and invariant solutions of the Bellman equation in the problem of optimal control synthesis for second-order systems
12 p1483 A73-27079
- Use of the dynamic programming method for optimization of relay systems
13 p1596 A73-28853
- Study of the smoothness properties of the Bellman function in time-optimal problems, based on the equation of motion of the system. I - The linear case.
15 p1854 A73-31687
- Approximate synthesis method for optimal control of a system subjected to random perturbations.
15 p1915 A73-32404
- Some problems in the analysis and synthesis of statistically optimal constrained control
20 p2539 A73-38681
- Approximate solution of Bellman's equation for a class of problems involving optimal terminal control
21 p2668 A73-40179
- Bellman dynamic programming principle for elastic-perfectly plastic beam structure design optimization with respect to cross-sections, span lengths and weight
24 p3148 A73-45003
- BELTRAMI FLOW**
A note on Beltrami and complex-lamellar flows behind a three-dimensional curved gasdynamic shock wave.
19 p2420 A73-37753
- BELTS**
The thermal analysis of a belt type radiator by the method of matched asymptotic expansions.
14 p1817 A73-30609
- BENARD CELLS**
A note on a minimum principle in Benard convection.
04 p0520 A73-15940
- Longitudinal rolls and Benard cells in water layer natural convection, predicting wavelength-depth relations and Rayleigh numbers for comparison with experiments [AIAA PAPER 73-42]
06 p0684 A73-17623
- Certain feedbacks generated during turbulent cellular convection in the atmosphere
08 p0986 A73-21456
- Intensive probing of a clear air convective field by radar and instrumental drone aircraft.
10 p1245 A73-23989
- Equations for nonlinear Benard convection with rotation for fluid layer, investigating asymptotic solution for two dimensional cells at large Rayleigh and Taylor numbers
11 p1448 A73-25052
- Numerical experiments for the determination of characteristic dimensions and intensities of convection cells
15 p1902 A73-31138
- Wavelength and cell size determination of steady supercritical Taylor vortex flow for long rotating cylinders with radius, viscosity and end boundary variations
16 p1998 A73-32798
- Thermal stability of radiating fluids - The Benard problem.
16 p2085 A73-33313
- Thermal stability of radiating fluids - Asymmetric slot problem.
16 p2085 A73-33314
- A numerical study in three space dimensions of Benard convection in a rotating fluid.
17 p1251 A73-34855
- Temperature field and motion oscillations in water-methanol and water-isopropanol Benard cells, taking into account thermal diffusion
23 p3049 A73-43936
- BENCHES**
U SEATS
- BENDING**
NT ELASTIC BENDING
Glass laminates and high strength oriented fiberglass reinforced plastics failure mechanism in tension and bending, noting equalizing effect through proper cohesion characteristics between layers
02 p0185 A73-12134
- Bending rigidity of an inflated circular cylindrical membrane of rubbery materials.
03 p0395 A73-14183
- Stress intensity factor for an elliptical crack approaching the surface of a plate in bending.
04 p0505 A73-14677
- Effect of the cross sectional shape of specimens on their strength under transverse-bending impact loads
05 p0632 A73-16327
- On the elastoplastic problem of cantilever subject to combined bending and twisting.
09 p1164 A73-23320
- Carbon-carbon composites and bulk graphite fracture toughness and failure modes determination from single-edge-notched specimen responses under three-point bending
10 p1239 A73-24276
- Special features of the fracture of aluminum and titanium alloys at low temperatures
19 p2439 A73-37267

- Antisymmetrical bending of a circular orthotropic plate of variable thickness
20 p2625 A73-39656
- BENDING DIAGRAMS**
Analysis of the elastoplastic bending of profiles whose cross sections are asymmetric with respect to the bending plane
07 p0913 A73-20090
- Low-temperature impact bending with recording of the stress-strain diagrams
09 p1100 A73-22157
- Recording strain diagrams in low-temperature impact bending tests.
22 p2874 A73-42105
- BENDING FATIGUE**
Observations of failure modes in carbon composite materials.
03 p0332 A73-13042
- Size effect in fatigue testing of metals explained, considering implications for bending, torsion and axial loading
03 p0396 A73-14646
- Consideration of a number of factors involved in determining the long-term strength of dies used for the extrusion of hollow sections of aluminum alloys
03 p0318 A73-14651
- On the production of fatigue cracks for determining the work of rupture in bending tests.
04 p0450 A73-15670
- Borated steel fracture characteristics in the case of cyclic plane bending
06 p0711 A73-18663
- Flat laminated FRP-FRTP and carbon FRP-FRTP composites, testing lamination effects on bending and impact strengths
07 p0844 A73-20331
- A new method of measurement to determine the stress-strain relation in a bending fatigue specimen.
07 p0917 A73-20488
- Device for endurance testing of materials at low temperatures
09 p1070 A73-22168
- Transmission electron microscope study on initiation of fatigue crack in 18-8 austenitic steel.
09 p1104 A73-22523
- Effects of circular holes on the fatigue resistance of AMg6BM aluminum-alloy sheet in symmetrical bending.
09 p1105 A73-23053
- Resistance to brittle fracture of high-strength steel.
09 p1106 A73-23161
- Atmospheric corrosion fatigue tests for environmental conditions and superimposed stress wave effects on Cr-Mo steel fatigue life under rotating bending
10 p1235 A73-24917
- Bending-produced cracks, stresses and fracture of rectangular cross section beam from brittle body homogeneous model
12 p1552 A73-27255
- A hypothesis of non-propagating fatigue crack.
13 p1635 A73-28644
- Rotating bending fatigue tests on Al coated steels, investigating electroplating, hot dip and spraying production methods effects on fatigue strength
13 p1635 A73-28645
- Effect of tensile prestrain on fatigue strength of aluminum alloy in high cycle fatigue.
13 p1636 A73-29199
- Residual surface stress changes dependence on fatigue life and steel specimen size during rotating bending fatigue tests from X ray diffraction study
13 p1625 A73-29485
- Correlation between notch sensitivity of a material and its non-propagating crack, under rotating bending stress.
13 p1641 A73-29493
- Effect of cooling to -269 C/ on failure in Kh18N10T and Kh16N6 steels under impact bending
14 p1763 A73-30692
- A unit for fatigue testing of materials at low temperatures.
22 p2838 A73-42116
- Transverse deflection of guided projectile tail fins during deployment.
22 p2797 A73-42629
- Evaluation of the sensitivity of materials to stress concentrations in cyclic loading
23 p3047 A73-44279
- BENDING MOMENTS**
The post-buckled behaviour of a thin-walled box beam in pure bending.
03 p0384 A73-13114
- Thermal stresses in circular plates including the influence of transverse shear.
05 p0633 A73-16539
- A new algorithm for the computation of bending moments and deflections of straight beams.
05 p0637 A73-17325
- Interaction curves for bending and axial forces of perfectly plastic curved I-beams.
06 p0762 A73-18339

Analysis of the elastoplastic bending of profiles whose cross sections are asymmetric with respect to the bending plane

07 p0913 A73-20090

Pure moment loading of axisymmetric finite element models.

09 p1158 A73-22391

Elasto-plastic stress analysis of prismatic bar under combined bending and torsion.

10 p1289 A73-24160

A modification of the moire fringes technique for the analysis of moments and deflections in a laterally loaded plate.

10 p1220 A73-24573

Singular nonaxisymmetric shallow shell equation solutions for concentrated normal and tangential forces and bending and twisting moments

12 p1550 A73-27034

Improvement of damping characteristics of structural members with high damping elastic inserts.

13 p1690 A73-28056

Shape function generation for high order conforming rectangular plate element in bending theory, noting rapid convergence of deflection and bending moments

13 p1691 A73-28087

Relative magnitudes of stresses caused by static and dynamic launch vehicle loads.

13 p1697 A73-28833

Finite element analysis with improved accuracy for rectangular plate bending element.

14 p1810 A73-30456

Three-dimensional stress-strain state of turbine blades

14 p1813 A73-30677

Use of the surface of influence of the clamping couple on a circular plate for design calculation under an asymmetrical load

15 p1944 A73-30974

Rectangular cross section isotropic elastoplastic material behavior under combined compressive and bending stresses with allowance for work hardening

16 p2076 A73-32931

Effect of torsion-flap-lag coupling on hingeless rotor stability.

[AHS PREPRINT 731]

17 p2105 A73-35067

Inextensional approximations in cylindrical shells.

18 p2362 A73-36329

Dirac's distribution in the study of statically indeterminate beams.

18 p2364 A73-36491

Photoelastic study of rectangular plates under bending.

19 p2498 A73-37667

The vibrations of a circular plate with uniformly distributed load around the outer periphery.

19 p2502 A73-38348

In-plane and lateral displacements triangular elements represented by cubic and quintic polynomials for folded plate structural analysis

20 p2622 A73-39545

An approximate solution for bending of anisotropic laminated plates.

20 p2623 A73-39554

Critical load analysis of strip /beam/ with arched crack under compressive stress and bending moments

21 p2786 A73-40985

Experimental investigation of a cylindrical shell loaded by a concentrated tangential force and a bending moment

21 p2787 A73-41193

Analytic treatment of minimum weight design of cantilevers.

[ASME PAPER 73-APMW-29]

22 p2925 A73-42889

Mixed boundary value problem of thin isotropic plate under edge loading, examining bending moment applied to plate with intermittent edge clamping

22 p2928 A73-43065

Determination of the deflections and stresses in a small-aspect-ratio wing by the displacement method

23 p3041 A73-43723

In-plane vibration of continuous curved beams.

23 p3045 A73-44165

The mechanism of fracture of reinforced beams during bending. I

24 p3146 A73-44531

BENDING THEORY

Iterative solution of thermal bending problem for nonuniformly heated thin rectangular plate with discrete boundary conditions

01 p0113 A73-10020

Steady creep bending in a beam with random material parameters.

01 p0113 A73-10198

Rectangular plates with unidirectionally variable rigidity

01 p0114 A73-10572

Thermal bending of moderately thick rectangular plate.

01 p0115 A73-10739

Mesh subdivision type influence on convergence properties of mixed triangular elements in plate bending analysis

01 p0115 A73-10745

Bending stresses propagating from the clamped support of an impulsively loaded beam.

01 p0115 A73-10753

Bending of a uniformly loaded clamped sector plate.

01 p0116 A73-11006

Determination of the theoretical stress-concentration factors in composite systems in bending

02 p0229 A73-11638

Possibility of using the method of time characteristics for solving applied problems concerning the bending of sandwich plates with allowance for creep of the materials

02 p0230 A73-11641

Solution to the bending problem and to the plane problem of an anisotropic rectangular plate with arbitrary boundary conditions and the application of the solution to composite structure designs

02 p0230 A73-11715

Anisotropic beam elastic deformation under end loads, deriving coefficients for linear relation between cross sectional stresses and elastic deformation curvature

02 p0230 A73-11780

Crack initiation and propagation in glass fiber reinforced plastic materials, noting rod bending

02 p0231 A73-11810

Integration of a differential equation describing the bending of a physically nonlinear plate of variable thickness

02 p0231 A73-11811

Discussion of the bending theory of cylindrical shells of orthogonally anisotropic structural material, by introducing the displacement function.

02 p0236 A73-12514

General non-linear plate theory applied to a circular plate with large deflections.

02 p0236 A73-12517

Non-linear oscillations of a nonuniform fixed circular plate.

02 p0236 A73-12519

Bending of a physically nonlinear viscoelastic rectangular plate under the action of a transversely distributed load

02 p0237 A73-12587

Application of the Dirac delta function in the calculation of the bending of a rectangular beam with shear strain

03 p0384 A73-13130

Effect of residual or characteristic stresses on the deformation of plates

03 p0385 A73-13143

Stress-strain diagrams for stability of structures under plastic bending, noting differential equations for rigidity characteristics

03 p0386 A73-13144

On bending and vibration of reinforced and bireinforced elastic and viscoelastic shells.

03 p0387 A73-13160

Effect of membrane forces on large deflection of simply supported rectangular plates.

03 p0389 A73-13323

A simple finite element model for elastic-plastic plate bending.

03 p0391 A73-13680

On the conforming cubic triangular element for plate bending.

03 p0391 A73-13682

Influence of the bending radius on the strength, volume deformation, and bending rigidity of high-pressure hoses

03 p0318 A73-14599

Large elasto-plastic deflection of a circular plate of mild steel under cyclic loading.

03 p0396 A73-14626

A study of local stresses near surface flaws in bending fields.

04 p0505 A73-14678

Stress intensity factors for surface cracks in bending.

04 p0505 A73-14679

Plate bending analysis using 12 degrees of freedom isoparametric and assumed-stress hybrid plate element theory

04 p0508 A73-14943

A method for including the effects of transverse shear and rotatory inertia on flexural motion of elastic plates.

04 p0510 A73-15074

Electric and thermal conductivity, elastic properties, and resistance to bending of porous tungsten throughout the porosity range

04 p0464 A73-15371

Bending and rolling methods for tensile testing of metals without local necking, considering fracture under reduced axial stress

05 p0581 A73-16130

Convergence and error estimation of Svirskii approximation method for determining circular plate deflections

05 p0635 A73-17081

Bending and flexing of the Apollo 15 mass spectrometer boom.

05 p0636 A73-17210

Some finite element solutions for plate bending problems by simplified hybrid displacement method.

06 p0758 A73-17444

Monograph - Grid analysis of orthotropic plates.

06 p0761 A73-17873

Bending theory of rectangular plates loaded along curve, obtaining solutions by Fourier single and double series

06 p0763 A73-18451

Plate stretching and plane strain and plate bending.

06 p0765 A73-18723

The quadratic programming approach to the finite element method.

07 p0907 A73-19030

A creep bending analysis of plates by the finite element method.

07 p0908 A73-19093

Bending stress in an impulsively loaded cylindrical shell of exponentially varying thickness.

07 p0913 A73-19973

Approximations for large deflection of a cantilever beam.

07 p0915 A73-20339

Bending of nonuniform plates with asymmetric thickness variation inclusion of shear deformation.

08 p1015 A73-20716

Corner supported equilateral triangular plates.

08 p1016 A73-20827

Non-linear bending of beams of variable cross-section.

08 p1016 A73-20831

Thermoelastic bending theory based on structural analysis of multilayer reinforced shells and plates

08 p1017 A73-21373

The application of nodal stress concepts to the bending of plates and shells.

08 p1019 A73-21691

Bending of an orthotropic prismatic beam by a transverse force in a geometrically nonlinear formulation

08 p1020 A73-21769

Determination of stresses during pure elastoplastic bending and torsion

09 p1157 A73-22163

Muskelishvili boundary value problem of plate bending and point deformation for round and annular plates under uniform loads

09 p1159 A73-22854

A triangular plate bending element for contact problems.

09 p1160 A73-22899

Orthotropic almost cylindrical beams - Bending by a transverse load.

09 p1160 A73-23023

Mathematical analogy between the bending of a plate and the circulating motion of a liquid in a geometrically similar region

10 p1205 A73-23598

Bending and vibration of multilayer sandwich beams and plates.

10 p1289 A73-24290

Stresses in a partly yielded notched bar - An assessment of three alternative programs.

10 p1290 A73-24294

Reissner's edge effect in three-layer plates with filler

11 p1433 A73-25030

Stress concentration in an anisotropic plate with an insert in pure bending

11 p1433 A73-25031

Finite element method for structural analysis, discussing theory for isoparametric stress quadrilateral plate bending elements with curved boundaries

11 p1435 A73-25437

Bending stresses and strains in anisotropic semi-finite plates with arbitrary edge and surface loadings.

11 p1445 A73-26404

Differential equations for asymmetric bending of circular sandwich plates.

11 p1445 A73-26406

Flexural/torsional deformations of material line in continuous body in terms of curvature and bending vectors, using Frenet-Serret equations

11 p1445 A73-26408

Influence of a small bending stiffness on the lateral vibrations of a clamped rectangular membrane

11 p1445 A73-26425

Bending problem for shell of revolution with finite displacements, axisymmetric loading and nonlinear strain functions

11 p1445 A73-26460

Eigenfunction analysis for bending of clamped rectangular, orthotropic plates.

11 p1447 A73-26653

Infinitesimal deflections of finned surfaces of revolution fixed along the edge with respect to points in space

12 p1552 A73-27299

Thin piezoelectric plate bending deformation and polarization theory in terms of piezoelectricity, electrostatics and elasticity equations for anisotropic body

12 p1552 A73-27371

Study of the rigidity of rectangular plates during bending by the finite-element method

12 p1553 A73-27461

Elastoplastic bending of a cylindrical shell according to the Prandtl-Reuss theory 12 p1554 A73-27472

Bending of a circular nonlinearly-elastic plate by a concentrated force 12 p1555 A73-27794

Branched solution of integro-power equation for nonlinear bending of shallow spherical shells with clamped edge under uniform radial compression load 12 p1556 A73-27816

Discrete flexural analyses of rectangular plates of abruptly varying stiffnesses. 12 p1556 A73-27926

Flexural response of tapered beam on elastic-plastic foundation, solving in closed form to evaluate efficiency of numerical methods 12 p1557 A73-27932

On the unity of the constant strain/constant moment finite element methods. 13 p1691 A73-28079

Shape function generation for high order conforming rectangular plate element in bending theory, noting rapid convergence of deflection and bending moments 13 p1691 A73-28087

Triangular finite elements for plate bending with constant and linearly varying bending moments. 13 p1692 A73-28230

The local solution approach in the finite element method. 13 p1692 A73-28232

Finite element method analysis of thin shells, discussing reference surface geometry and membrane and bending theory 13 p1693 A73-28234

The application of a curved, mixed-type shell element. 13 p1693 A73-28237

Glass fiber reinforced plastics optimum glass volume fraction for maximum flexural rigidity and strength 13 p1645 A73-28777

Equivalent finite element model derivation from plate bending triangular element, assumed stress hybrid method and elements with polynomial deflection function 14 p1807 A73-30184

Note on the application of the Tresca criterion to the problem of circular bending of an elastoplastic cylinder 14 p1811 A73-30485

Finite bending of incompressible hyperelastic plastic strip, analyzing stress and stored energy function 14 p1812 A73-30496

Oblique bending of a homogeneous orthotropic prismatic beam by a force couple in the quadratic theory of elasticity 14 p1815 A73-30785

Bending of rectangular plates of variable thickness with edges reinforced by elastic ribs 14 p1815 A73-30796

Coupled twist-bending waves and natural frequencies of multispan curved beams. 14 p1815 A73-30914

Optimal forms of the thin-walled closed cross-section of a beam subjected to bending 15 p1947 A73-31365

Calculation of stress-concentration factors for grooved shafts in bending using the point-matching technique. 15 p1948 A73-31616

Program for triangular bending elements with derivative smoothing. 15 p1848 A73-32028

Theorem concerning possible bendings in zero-moment shell theory 15 p1953 A73-32090

Saint Venant problem for a continuously inhomogeneous anisotropic beam 15 p1953 A73-32103

Considerations on the centres of shear and of twist in the theory of beams. 15 p1954 A73-32111

Antiplane elasticity boundary value problem solution for isotropic bars under tangential loads, considering twisting and bending 15 p1955 A73-32127

Russian book - Plane bending and tension of curvilinear thin-walled beams. 15 p1956 A73-32296

Small parameter series convergence evaluation in geometrically nonlinear problems by Cauchy majorants, applying to flat curvilinear beam deflection 16 p2074 A73-32689

Design for bending of a clamped infinite strip with a prestressed stiffness rib along the edge 16 p2075 A73-32695

Variational principles for plate bending - A unified approach. 16 p2077 A73-32983

Solution of equations of Reissner's theory of plates by application of Hajdin's method. 16 p2078 A73-33004

Theory for the flexural vibrations of a rotating viscoelastic cantilever 16 p2083 A73-33936

Book - Stresses in shells /2nd edition/. 17 p2242 A73-34469

The supporting effect of bending specimens under static load in the temperature range from 400 to 500 C 17 p2187 A73-34521

Strongly curved finite element for shell analysis. 17 p2242 A73-34529

Variational methods for vibratory bending equations of asymmetrical sandwich plates with mode families in terms of displacement ratios, taking into account inertia effects 17 p2243 A73-34548

A note on bending-shear interaction in the limit analysis of cylindrical shells 17 p2243 A73-34650

A necessary condition for the nonoccurrence of von Mises yielding in impulsively loaded plates. 17 p2250 A73-35118

Hopscotch method for one-space dimensional bending beam elliptic differential equation solution, noting mesh ratio stability range 17 p2251 A73-35518

Stiffness matrix displacement analysis via curved elements for plane stress and thin plate bending problems 17 p2252 A73-35606

Mechanical properties of weld, base metal and coated columbium FS85. 17 p2182 A73-35842

Book - Stress analysis of polymers. 17 p2253 A73-35861

Determination of stiffness and critical loads of a circular plate from a simple bending test. 18 p2362 A73-36327

The plastic bending of beams and their failure by low cycle fatigue. 18 p2365 A73-36617

Nonlinear bending problem for a beam of variable rigidity 18 p2366 A73-36959

Transverse bending of an annular slab with supporting ribs 18 p2367 A73-36960

On a formulation of the bending of elastic plates. 19 p2500 A73-38112

Localized creep of a nonhomogeneous beam subjected to loads exceeding the true elastic limit 19 p2501 A73-38306

Creep relaxation approximations and exact solutions, discussing rectangular beam pure bending, spherical shell internal pressure loading and thin circular tube bending 20 p2616 A73-39115

Theory of shallow shells with allowance for couple stresses without applying the Kirchhoff-Love hypothesis 20 p2618 A73-39309

Axisymmetrical bending of circular plates and shallow spherical cupulas with allowance for physical and geometrical nonlinearities 20 p2618 A73-39310

Certain approximations in the solution of shell and plate bending problems with allowance for physical and geometrical nonlinearity 20 p2618 A73-39311

Large deflections and stability of a long shallow orthotropic cylindrical panel under the action of a local load 20 p2618 A73-39312

Moderate-thickness plate equilibrium equations and boundary value problems, discussing successive approximation method, static bending and potential energy 20 p2618 A73-39317

Motion of a rigid-plastic beam in a resistant medium under the action of a local load 20 p2620 A73-39470

Application of the Peaceman-Rochford method to the solution of the deflection problem for a plate strengthened by a square grid 20 p2620 A73-39496

Finite-element formulations for elastic plates by general variational statements with discontinuous fields. 20 p2623 A73-39558

Sandwich plates minimum volume design for elliptic, triangular and annular structures, discussing Mises criterion and bending coordinates 20 p2623 A73-39559

Stability of the bending equilibrium of shells beyond the elastic limit 20 p2625 A73-39657

The boundary theory of strength and nonlinear programming of boundary value problems of plate bending 20 p2625 A73-39821

Russian book on elasticity theory for multilayer media covering plate compression and bending under boundary contact conditions, Algol programming, tensile stress, functional equations, etc 21 p2782 A73-40175

Deflection function for the asymmetrical bending of circular plates. 21 p2784 A73-40435

Russian book on R-function method for solving boundary value problems of bending and vibration of thin plates with complex configurations 21 p2787 A73-41250

Discretized solution of junction problems in shells. 22 p2917 A73-41740

Determination of the stresses for pure elastic-plastic flexure and torsion. 22 p2919 A73-42111

Local stresses near deep surface flaws under cylindrical bending fields. 22 p2880 A73-42135

Complementary variational principles and error bounds for biharmonic boundary value problems. 22 p2921 A73-42433

Book - Elasticity. 23 p3039 A73-43434

Bending of a rectangular piezoelectric plate clamped over its edge 23 p3043 A73-43923

Solution of physically nonlinear quasi-static problems of viscoelasticity 24 p3145 A73-44519

Dynamical bending resistance of circular piecewise nonhomogeneous rigid-plastic plates in terms of Tresca yield condition for pressure pulse loads 24 p3146 A73-44679

Plastic plate bending under concentrated forces, defining stress and strain principles at yield limit 24 p3148 A73-44919

Three dimensional elasticity solution for layer interaction and shear coupling and deflection effects of laminated anisotropic composite cylinders under bending 24 p3149 A73-45152

Bending of transversely isotropic plates with a reinforced edge 24 p3149 A73-45174

Stress concentration in infinite strip with periodically spaced circular holes under uniformly distributed bending loads 24 p3149 A73-45176

Influence of initial deflections on the work of a rectangular plate subject to bending in its plane 24 p3150 A73-45244

On the problem of flexure of anisotropic cylindrical shells. 24 p3151 A73-45302

BENDING VIBRATION

Nonlinear axisymmetric flexural vibration equations of a cylindrically anisotropic circular plate. 01 p0115 A73-10756

Dynamics of a rotating free system of bodies with an oriented axis of rotation 02 p0192 A73-11774

The modal density for flexural vibration of thick plates and bars. 03 p0393 A73-13839

Frequency dependence of the damping of mechanical vibrations in some commercially pure metals 03 p0327 A73-13976

Symmetrical bending for the general case of oscillating beams under transverse loads 04 p0511 A73-15174

Study of the dynamics of the preliminary-damping system of a gravitationally stable satellite with allowance for constraints on its sensors and on the flexural vibrations of the stabilizer 05 p0628 A73-16406

Dynamic stability of monosymmetrical thin-walled structures. [ASME PAPER 72-APM-SS] 05 p0632 A73-16530

Calculation of the deflections of fast-rotating rotors on elastic-damping supports with allowance for unilateral electromagnetic attraction forces 07 p0779 A73-20084

Finite element displacement method for large amplitude free flexural vibrations of beams and plates. 07 p0914 A73-20212

Optimized design - Characteristic vibration shapes and resonators. 08 p1017 A73-21191

Measurement of the flexural damping capacity and dynamic Young's modulus of metals and reinforced plastics. 08 p0967 A73-21594

High temperature mechanical properties measurements verifying metal polycrystal internal friction background origin in diffusion of vacancies formed under grain boundary loading 09 p1105 A73-23060

Experimental study of the damping of bending vibrations in supported square plates with coatings. 09 p1161 A73-23153

Determination of the modulus of elasticity of metallic and nonmetallic fibers based on bending oscillations 10 p1231 A73-23691

Flexural vibrations of a cantilever strut mounted on a rotating disk 10 p1290 A73-24308

Bending waves dispersion properties in rod applied to acoustic LF dispersion delay line design, analyzing signal distortion and attenuation during propagation 10 p1291 A73-24366

Beam and plate flexural vibration damping by free or uncompressed rigid viscoelastic coatings applied on sides 10 p1293 A73-24794

Acoustically induced vibrations of slender rods in a cylindrical duct with parallel flow. 11 p1432 A73-24983

Application of general variational methods with discontinuous fields to bending, buckling, and vibration of beams. 11 p1435 A73-25436

On the vibration of shear deformable curved anisotropic composite plates. 11 p1442 A73-25711

Thin uniform circular rings axial and radial bending vibrations under perturbing effect of circumferentially attached small cylinder, comparing theoretical with experimental results 11 p1444 A73-26290

A quantum model for bending vibrations and thermodynamic properties of C3. 12 p1526 A73-27019

Dynamic moire methods for the bending of plates. 12 p1550 A73-27023

Mathematical observations in structural dynamics. 12 p1555 A73-27739

Nonlinear transverse vibrations of beams with properties that vary along the length. 13 p1695 A73-28488

Relaxation of the bending vibration of CO2 in pure CO2 and in mixtures of CO2 with noble gases. 13 p1662 A73-28553

A finite element study of the vibration of trapezoidal plates. 13 p1700 A73-29378

Bending vibration test of glass-textolites, noting temperature effect on vibration damping properties 13 p1647 A73-29607

Large amplitude vibrations of certain deformable bodies. II Plates and shells. 14 p1806 A73-30041

Vibration analysis of sandwich beam with constrained viscoelastic layers on both sides. 14 p1806 A73-30046

Simultaneous flexural and torsional vibrations of multidisk rotors 16 p2075 A73-32691

Forced extensional vibrations of isotropic elastic plates with time dependent body forces, surface tractions and nonhomogeneous boundary conditions, using Kane-Mindlin theory 16 p2076 A73-32920

Finite element analysis of coupled vibration of tapered twisted blades. 16 p2078 A73-33005

Flexural vibrations of clamped orthotropic plates. 16 p2081 A73-33680

Theory for the flexural vibrations of a rotating viscoelastic cantilever 16 p2083 A73-33936

Flexural wave mechanics - An analytical approach to the vibration of periodic structures forced by connected pressure fields. 16 p2083 A73-33947

Coupled thermally induced vibrations of beams. 17 p2241 A73-34190

The influence of pitch and twist on blade vibrations. 17 p2099 A73-34440

Variational methods for vibratory bending equations of asymmetrical sandwich plates with mode families in terms of displacement ratios, taking into account inertia effects 17 p2243 A73-34548

Effect of a connecting plane link on the excitation and propagation of flexural oscillations in parallel plates 17 p2244 A73-34737

Lateral bending-torsion vibrations of a thin beam under parametric excitation. [ASME PAPER 73-APM-13] 17 p2247 A73-35037

Nonlinear vibration of a rectangular plate arbitrarily laminated of anisotropic material. [ASME PAPER 73-APM-F] 17 p2249 A73-35105

Flexural vibration frequencies of right circular cylindrical tensor gravitational wave detectors in regime with sound wavelength comparable to diameter 17 p2176 A73-35763

Approximate method for determining the natural frequencies of flexible rectangular plates 18 p2363 A73-36408

On the flexural vibration frequencies of statically loaded beams. 18 p2367 A73-37091

Flexural wave fields in infinite beam-reinforced plates under point excitation. 19 p2498 A73-37725

Free harmonic vibrations of thin pretwisted rectangular plates analyzed in terms of torsional and bending vibration coupling based on shell theory 19 p2500 A73-38115

Flexural vibrations of rods with viscoelastic coating subjected to axial force. 19 p2502 A73-38347

Calculation of bending vibrations in beams with the aid of a discrete model 20 p2615 A73-38982

Aeroelastic vibrations in labyrinth seals 20 p2569 A73-39373

Rotary inertia and energy dissipation effects on dynamic response of three layered symmetrical laminate beam with viscoelastic core vibrating in flexural mode, using variational calculus 20 p2623 A73-39555

Effect of ultrasound on the dislocation structure and mechanical properties of molybdenum 20 p2579 A73-39745

Square plate symmetrically supported at four diagonal points, evaluating fundamental vibration frequency with accuracy by finite element method 21 p2783 A73-40293

Large amplitude flexural vibration of simply supported skew plates. 21 p2784 A73-40423

Coupled bending-twisting vibrations of a single boom flexible solar array and spacecraft. 21 p2781 A73-40619

Optimum tapering design of vibrating cantilever beams, considering geometrically similar and rectangular cross sections and degenerated end mass case 21 p2785 A73-40839

Free flexural vibrations of elliptical thin plate with free edge, calculating mode shapes and frequencies by use of Mathieu function 22 p2918 A73-41822

German monograph - A contribution to the investigation of the stability of pipelines with flowing liquids according to the method of finite elements. 22 p2924 A73-42737

Newton method relationship to Floquet theory for nonlinear vibration problems, considering Van der Pol equation periodic solutions for breathing and bending modes [ASME PAPER 73-APMW-20] 22 p2924 A73-42883

Stress amplification in a ring caused by dynamic instability. [ASME PAPER 73-APMW-35] 22 p2925 A73-42893

An exact method for the study of the dynamic stability of supporting structures acted upon by periodic impulses. 22 p2927 A73-43031

A general conclusion regarding the large amplitude flexural vibration of beams and plates. 23 p3039 A73-43305

Manufacture and properties of compressor blades made of plastics reinforced with carbon filaments 24 p3122 A73-44880

Bending potential of an H2O molecule. 24 p3113 A73-44977

Natural, flexural and torsional vibration frequencies and modes for helicopter tail rotor blades 24 p3057 A73-45245

Small transverse vibrations of a flexible rod under the action of a variable axial force 24 p3153 A73-45504

BENDS (PHYSIOLOGY)
U DECOMPRESSION SICKNESS

BERGMAN OPERATOR
Coherent state systems for groups of motions of Hermitian bounded homogeneous regions in terms of Bergman kernels 10 p1249 A73-24463

BERNOULLI EQUATION
U BERNOULLI THEOREM

BERNOULLI THEOREM
An action principle in general relativistic magnetohydrodynamics. 01 p0079 A73-11258

Thin shells stability equations based on Bernoulli normal hypothesis, investigating stresses and deformations for equilibrium state under arbitrary load conditions 06 p0759 A73-17743

BERNSTEIN ENERGY PRINCIPLE
Nonlinear parametric electron plasma instability due to cyclotron harmonic Bernstein wave interaction in strong electric field 21 p2747 A73-40791

BERYLLIUM
Plastic strain anisotropy changes in single crystals of beryllium following programmed load application 01 p0064 A73-10610

Microhardness anisotropy of hardened and aged Be single crystal as function of purity 01 p0067 A73-11353

Diffusion welding of beryllium. I - Basic studies. 04 p0451 A73-14669

Charge density distribution in Be single crystals from X ray structure amplitudes for lowest angle Bragg reflections, comparing with Hartree-Fock and free electron plane wave models 04 p0467 A73-15932

Beryllium parts machining and surface finishing techniques for maximum fracture strength and fatigue life 05 p0587 A73-16754

Stabilization of superconducting beryllium by addition of aluminum. 05 p0605 A73-16794

Diffusion welding of beryllium. II - The role of the microalloying elements. 06 p0704 A73-17597

Saturation of 1Kh18N9T steel with beryllium and corrosion resistance of the coating in a lithium melt 06 p0711 A73-18669

Beryllium for nonstructural and structural applications in aerospace systems, considering high dimensional stability, mechanical and thermodynamic properties, and metal sintering techniques for production 07 p0828 A73-18904

Beryllium and chromium abundances in Fra Mauro and Hadley-Apennine lunar samples. 07 p0886 A73-19764

The yield point phenomenon in a Be-Al composite. 07 p0839 A73-20115

Electric resistance of hydraulically extruded and annealed beryllium 09 p1098 A73-21847

Fine grained ingot source Be ductility at 700 C as function of strain rate, noting superplastic behavior with grain boundary sliding at low strain rates 09 p1102 A73-22413

Effects of beryllium additions on the microstructure and the type of failure in Al-Mg alloys 10 p1233 A73-24423

High modulus composites versus beryllium for achieving stiffness in spacecraft structural applications. [AIAA PAPER 73-384] 11 p1430 A73-25513

The fracture toughness of beryllium. 11 p1384 A73-26168

Crack toughness evaluation of hot pressed and forged beryllium. 11 p1384 A73-26169

S-200 grade beryllium fracture toughness properties. 11 p1384 A73-26170

Exploratory study of a fluxless aluminum brazing process for beryllium. 11 p1375 A73-26359

Precipitation in EB welded beryllium ingot sheet. 14 p1759 A73-30146

The application of strip strain gages for measuring residual surface stresses in beryllium. [UCRL-74078] 17 p2191 A73-35438

Temperature dependence of the yield point in grain-oriented beryllium 18 p2324 A73-36773

Electrical resistance variation kinetics in deformed beryllium after annealing 20 p2579 A73-39746

Fabrication methods for beryllium spacecraft components. 20 p2615 A73-39775

BERYLLIUM ALLOYS
High modulus Be-Al alloy strengthening and aging as function of Cu, Mg and Zn additions 03 p0325 A73-13517

Hardness-controlling additions in transition metal-beryllium alloys 03 p0328 A73-14655

Critical transition temperatures and magnetic moment measurements of superconducting state of binary Be alloys 11 p1409 A73-25630

Crystallostructural investigation of the eutectoid decomposition of copper-beryllium alloys - Ordering accompanied by formation of Cu2Be metastable solid solution 14 p1760 A73-30587

Diffusion creep by dislocation climb in beryllium and Be-Cu single crystals. 14 p1761 A73-30633

BERYLLIUM BOROHYDRIDES
Structure of beryllium boron hydrides BeBH5 and BeB2H8. 12 p1466 A73-27045

BERYLLIUM COMPOUNDS
NT BERYLLIUM BOROHYDRIDES
NT BERYLLIUM OXIDES
Superconductivity of beryllides of some transition metals 18 p2340 A73-36678

BERYLLIUM OXIDES
Small nuclear light bulb engines with cold beryllium reflectors. [AIAA PAPER 72-1093] 04 p0475 A73-14907

Reliable starting technique for an ion laser tube with internal gas return bores. [AD-758556] 05 p0586 A73-17263

Studies of the performance of W-Re type thermocouples. 22 p2858 A73-42039

BESSEL FUNCTIONS
NT HANKEL FUNCTIONS
Solutions of some Fredholm integral equations using fractional integration, with an application to a forced convection problem. 13 p1704 A73-28413

A new fundamental system of modified cylindrical functions for an annular region. 17 p2200 A73-34248

Thermoelasticity problems and related particular solutions of a nonhomogeneous Bessel equation 21 p2787 A73-41273

The Dirichlet and Neumann problems for parabolic equations with a Bessel operator in Dini spaces 24 p3106 A73-45510

BETA PARTICLES

Neutrino archaeology - The simulation of double beta-decay by solar neutrinos.

03 p0344 A73-13293

Beta irradiation of silicon junction devices - Effects on diffusion length.

05 p0537 A73-16522

Re-187, recycling r-process elements through stars, and the age of the Galaxy.

15 p1939 A73-32014

BETATRONS

Investigation of low-frequency instabilities in a linear plasma betatron

14 p1782 A73-30805

BIAS

Breakdown phenomena in reverse biased silicon solar cells.

03 p0256 A73-14234

Recurrent orbit estimation biases by filtering, using method representing motion by finite difference equations

09 p1143 A73-22098

Parallel-redundant flight control systems, discussing sensor bias and combined control computer input effects on controllability and steady state model response

11 p1342 A73-25783

A high performance 4500 volt electron multiplier bias supply for satellite use.

11 p1363 A73-25959

Biased wall heat transfer in electric arc chamber, noting I-V characteristics and electron current saturation in superimposed axial flow

12 p1560 A73-27700

Measurement of semiconductor junction parameters using lock-in amplifiers.

13 p1595 A73-29578

The dynamic-bias in radiation interrogation of two-phase flow.

17 p2256 A73-35846

Suboptimal filter design for dynamic measurement systems, deriving bias and Kalman covariance formulae for error analysis and model sensitivity

19 p2410 A73-38031

Aspects of field-effect transistor applications in amplifier stages with feedback

24 p3072 A73-44936

BIBLIOGRAPHIES

Bibliography on Resistance Welding, 1950-1971.

01 p0058 A73-11374

Book - Holography: State of the art review 1971-72.

03 p0309 A73-14440

Russian book - Biomedical problems of space flights: Index of domestic and foreign literature.

04 p0410 A73-16034

Chemical laser device bibliography.

07 p0836 A73-19642

Chemical lasers - A comprehensive literature survey.

08 p0974 A73-21026

Chemical laser research survey covering device performance, reaction kinetics, theoretical modeling for population inversion and bibliography

13 p1628 A73-29112

Bibliography on the measurement of electrical parameters of layered lunar/earth surfaces.

13 p1619 A73-29221

Book - International bibliography of air law 1900-1971.

14 p1818 A73-30362

Axial and radial turbocompressor analysis and design, presenting literature survey on cascade aerodynamics, iterative and hodograph computational methods, etc

14 p1712 A73-30429

Geomagnetic pulsations and micropulsation research bibliography covering January 1969 through July 1972 with theoretical and observational groupings and Pc and Pi classifications

15 p1869 A73-31759

Literature survey on high speed photography and cinematography, discussing gas discharge tube and open spark equipment, Kerr cells, image dissection and holographic interferometry

21 p2693 A73-39934

Liquid-vapour equilibria research on systems of interest in cryogenics - A survey.

24 p3155 A73-44821

BICARBONATES

U CARBONATES

BICRYSTALS

Pseudo-subgrain-boundaries in stainless steel.

04 p0461 A73-14872

Intergranular precipitation in the oriented bicrystals of aluminum-copper

09 p1105 A73-23039

Influence of the intercrystalline structure on the diffusion of zinc in the symmetrical joints of bending of aluminum

11 p1379 A73-25324

On the study of the intergranular corrosion of a stainless steel with the help of twin crystals

11 p1385 A73-26297

Some observations on grain boundary sliding in aluminum bicrystals deformed at elevated temperatures.

13 p1641 A73-29508

Grain boundary dislocations in aluminum bicrystals after high-temperature deformation.

15 p1891 A73-32020

Molybdenum bicrystals mechanical properties dependence on mismatch angle under bending with torsion and brittle cleavage under critical stresses

17 p2189 A73-34636

BIG BANG COSMOLOGY

Universe evolution model, considering quasar number density, radio source counts and big-bang cosmologies

05 p0614 A73-16309

Thermonuclear reactions and nucleosynthesis in stellar interiors, initial big bang, supermassive objects and supernovae explosions

13 p1663 A73-28989

Relativistic cosmology of interacting hadronic matter-radiation models, discussing compatibility with Hagedorn equation of state based on statistical mechanics

15 p1939 A73-32002

Implications of the statistical bootstrap model for cosmology and galaxy formation.

19 p2482 A73-37559

Primordial explosion model for universe origin, noting radio astronomy counts of galaxies invalidation of Hoyle steady state cosmology

20 p2604 A73-39008

Big Bang model of universe, discussing 3 K background radiation, thermal history of early universe, lepton number conservation and different eras

21 p2772 A73-41242

BIHARMONIC EQUATIONS

Bending of a uniformly loaded clamped sector plate.

01 p0116 A73-11006

Grid model to derive biharmonic difference operators with computer programming application, assessing errors in boundary conditions

02 p0236 A73-12512

Differential solutions of the biharmonic Poisson and first order Stokes equations.

08 p0983 A73-21203

Biharmonic coupling solutions of Saint Venant equation for elastoplastic plane under unequal loads, using Kolosov-Muskhelishvili functions and conformal mapping

09 p1165 A73-23350

Biharmonic solutions of problems for elastoplastic bodies in the presence of nonuniformity of the stress field

11 p1446 A73-26598

Construction of upper and lower functions during approximate integration of a nonlinear system containing a biharmonic operator

13 p1651 A73-29678

Monte Carlo method for biharmonic boundary value problems solution, using isotropic random walk and mean value relation

20 p2581 A73-39094

Calculation of the current of a nonlinear element with inertia in the presence of a biharmonic input

20 p2537 A73-39454

Complementary variational principles and error bounds for biharmonic boundary value problems.

22 p2921 A73-42433

BILLETS

Hot extrusion and filled billet techniques to process superalloy powder metallurgy products into complex shapes, bars or wire

01 p0056 A73-10284

BILLOW CLOUDS

U CLOUDS (METEOROLOGY)

Structural changes in Kh18N9T steel during explosion welding

01 p0055 A73-10262

The mechanism of the metallic adhesion bond.

01 p0087 A73-10473

Use of ultrasonic emission in nondestructive inspection.

02 p0169 A73-12148

The orientation dependence of deformation mode and structure in stoichiometric NiAl single crystals deformed by high temperature steady-state creep.

06 p0712 A73-18758

Implosive and explosive welding of mono- and bimetallic duplex cylinders.

08 p0973 A73-21239

Production of a niobium-stainless steel bimetal by explosion welding

14 p1755 A73-30386

A theory of adhesion at a bimetallic interface - Overlap effects.

18 p2287 A73-37032

Determination of the temperature fields and thermal stresses in a bimetallic layer subjected to induction heating

23 p3046 A73-44194

BINARY ALLOYS

Alloy hardening and softening in binary molybdenum alloys as related to electron concentration.

03 p0323 A73-13300

Elastic damping properties of binary Mg and Al alloy systems with Cd, Mn, Ni, Si, Zr, Nd and Ca alloying

03 p0324 A73-13515

Phase diagrams and properties of binary alloys of refractory metals, taking into account the electronic structure of the atoms of the components

03 p0328 A73-14652

Alloying effects on Ta binary alloy tensile strength brittleness and yield point at low temperatures

04 p0466 A73-15669

Phase equilibrium diagram of the lanthanum-germanium system

04 p0484 A73-15692

Vacuum deposition of alloys - Theoretical and practical considerations.

04 p0456 A73-15756

Mo disilicide-Ti disilicide system phase diagram based on metallographic, X ray structural and high temperature differential thermal analyses

05 p0587 A73-16846

High temperature and metallographic investigation of Nd-Y alloys, measuring heat and electrical conductivity, thermal expansion and emf, magnetic susceptibility and Hall coefficient

06 p0735 A73-18050

X-ray spectral studies of manganese-aluminum binary alloy systems

06 p0710 A73-18644

Internal oxidation of silver-beryllium and silver-lithium alloys.

08 p0977 A73-21022

A review of the diffusion path concept and its application to the high-temperature oxidation of binary alloys.

08 p0978 A73-21414

Grain size effects on strength and ductility of two phase Ni-Cr and Ni-Mo alloys at high and low deformation temperatures

09 p1101 A73-22164

Electron microscopic determination of orientation relationship and habit plane for Ti-Cu martensite.

09 p1101 A73-22406

Ultrafine grained two-phase alloys fatigue properties as function of phase volume fractions and grain size, noting Coffin law type behavior from low cycle fatigue tests

09 p1102 A73-22411

Concentrational dependence of resistivity in solid disordered binary alloys of nontransition metals

09 p1104 A73-22687

Phase equilibria and crystal structure of intermediate phases in Er-Rh binary alloys

10 p1260 A73-24435

Formation of continuous solid solutions of intermetallic compounds

10 p1260 A73-24512

Critical transition temperatures and magnetic moment measurements of superconducting state of binary Be alloys

11 p1409 A73-25630

New mechanism of slowing down screw dislocations in ordered alloys with a bcc lattice

12 p1508 A73-26837

Crack propagation in some aluminum alloys with tensile stresses

12 p1511 A73-26916

Investigation of the sintering of binary alloys with limited solubility in the solid state. I - Concentration dependence of shrinkage during sintering of two-component systems with a eutectic type of phase diagram

12 p1503 A73-27558

Strengthening and fracture of Ta, Nb, Mo and W binary solid solutions with short range order.

13 p1638 A73-29452

Solid solution strengthening of high purity niobium alloys.

14 p1761 A73-30631

Phase diagram of the niobium-gallium system

15 p1922 A73-31182

Influence of heat treatment on the critical currents in binary alloys of niobium with zirconium and titanium

15 p1887 A73-31185

Application of a cluster component technique in the interpretation of concentration dependences of the properties of binary metal alloys and anion-substituted spinel solid solutions

15 p1923 A73-31205

Investigation of titanium alloys containing refractory elements

15 p1889 A73-31813

Mechanical properties, microstructure and failure characteristics of binary alloys of Al-Mg system determined under different tensile stress rates and temperatures

17 p2187 A73-34339

The oxidation of binary alloys of chromium with metals of the first long period.

19 p2442 A73-38098

Binary and ternary Laves phases in systems composed of zirconium and transition metals of the V through VII groups of the periodic system

21 p2718 A73-40848

Observations of solid/liquid interfaces in dilute binary and ternary Al-rich alloys. 21 p2721 A73-41120

Grain size effects on strength and ductility of two phase Ni-Cr and Ni-Mo alloys at high and low deformation temperatures 22 p2875 A73-42112

Specific structural features of the binary phase diagrams of some transition metals in a region containing Laves phases 22 p2877 A73-42453

Application of a computer image recognition technique to the determination of phase diagram types for binary metal systems 22 p2877 A73-42457

Role of electron processes in the vaporization mechanism and in the formation of binary semiconductor alloy compositions with ion bonds 23 p3016 A73-43711

Deformation characteristics and ductility of two-phase titanium alloys of laminated structure 24 p3099 A73-44573

Alloys of titanium with refractory elements. 24 p3100 A73-45276

BINARY CODES

Error-erasure decoding of product codes. 01 p0020 A73-11296

Synchronous multiplexing of digital signals using a combination of time- and code-division multiplexing /t.d.m. and c.d.m./ 02 p0140 A73-11588

Standard format for reporting electron content data using magnetic tape. 03 p0308 A73-13655

Multidimensional coding for telemetric transmission of work load factors in ergonomics research. 03 p0272 A73-14307

Modular arithmetic weight and cyclic shifting. 05 p0554 A73-17100

Code correcting nonsymmetrical bursts of errors during data exchange between computers. 06 p0670 A73-17962

Polynomial weights and code constructions. 06 p0671 A73-18143

Compact digital coding of electrocardiographic data. 06 p0660 A73-18815

GAELIC - Grumman Aerospace Engineering Language for Instructional Checkout. 08 p0941 A73-20689

Hadamard transform spectrometer designed for airborne IR astronomical observations of Mars, using binary orthogonal pseudonoise codes in multiplexing scheme 08 p0972 A73-21753

Optimal binary quantum signal detection in two dimensional Hilbert space by a priori probability vector projection method, using randomized decision strategy 09 p1049 A73-22230

Theory of incoherent-scatter measurements using compressed pulses. 09 p1050 A73-22429

Recording of paraphase-coded binary information on phase holograms 09 p1085 A73-22881

Cyclic binary coding and decoding circuits for high reliability data and command transmission, discussing analytical relations and design aspects 09 p1060 A73-22923

Analysis of the mechanical and energetic characteristics in pulse-coded regulation of an asynchronous motor 09 p1037 A73-22939

Concatenated coding for deep space interplanetary communication with low data rate and SNR, comparing performance of three binary codes 09 p1058 A73-23424

Binary cyclic code detection capability, polynomial description, coder-decoder circuits and error correction application 10 p1197 A73-23848

Quantization circuit for radio astronomical signals conversion into binary code and bit blocks recording on magnetic tape via Razdan-3 computer 10 p1220 A73-24698

Binary coded aircraft flight data block inclusion in aerial reconnaissance photographs for automated data processing 10 p1222 A73-24948

Nonalgorithmic design and coding system for digital mathematical machines for accuracy and speed compatible with digital and analog computer, respectively. 11 p1334 A73-25626

Cyclic binary codes circuit technology, discussing error types and decoding circuits for error detection and correction 11 p1332 A73-26254

An analog-code follow-up converter based on second-harmonic magnetic modulators 12 p1475 A73-26766

A simple method for converting a pulse code into a phase code by using parametrons 12 p1481 A73-27590

Information transmission reliability enhancement via digital code group symbol transmission by wide-band linear FM radio signals 12 p1471 A73-27593

Sphere packings constructed from BCH and Justesen codes. 13 p1584 A73-28919

Detection of informational constraints related to multi-variate visual displays. 13 p1580 A73-29185

Extraterrestrial messenger probe recognition from inhabited planet via message involving home constellation binary coded signals 14 p1796 A73-29946

Code division multiplexing system for multiple signal binary transmission in branched glass fiber optical communication network 14 p1729 A73-30696

Probabilistic properties and spectral characteristics of the duobinary code in the baseband 14 p1729 A73-30897

Length minimization in the internal-state code of an asynchronous finite automatic system with a two-step memory 15 p1848 A73-31910

Analysis of the correlation properties of certain PSK signal systems 17 p2121 A73-34586

Huffman binary codes for pulse compression radar, evaluating ambiguity or cross correlation by computer program for replicas formation performance 17 p2131 A73-35221

Holographic coding plate - A new application of holographic memory. 17 p2173 A73-35431

ASCII code applications to alphanumeric display terminals. 21 p2655 A73-40835

Probabilistic analysis of random and deterministic phase coding for lowering Fourier transform spectrum dynamic range in digitally generated hologram and kinoform memories 22 p2864 A73-43149

A digital system for receiving binary phase-coded signals 23 p2952 A73-43319

BINARY DATA

Full binary adder circuit with p-n-p junction transistor loaded tunnel diode, noting 200 MHz operation rates capability 01 p0026 A73-11480

Binary noncoherent FSK communication under influence of bandpass Gaussian noise and linear FM jamming waveform, deriving error probability 03 p0276 A73-13905

Partially coherent detection of binary FSK system with adaptive receiver, determining optimum and sub-optimum estimators of channel parameters for phase and bit synchronization 03 p0277 A73-13909

Effects of a finite-width decision threshold on binary CPSK and FSK communication systems. 03 p0277 A73-13911

Comparison of coherent and noncoherent detection of phase continuous binary FM signals. 04 p0420 A73-15410

Auto and cross correlation functions of combined binary pseudorandom sequences in digital space communication systems 04 p0423 A73-15916

Address structure optimization and minimum access time and decoder terminals in nonvolatile core memory array design, noting binary notation for information storage 05 p0554 A73-16991

Flawless operation probability for information transmission reliability of electronic logic circuits with binary data inputs 07 p0801 A73-20040

Noise immunity in the reception of binary radio signals on a correlated-noise background 08 p0939 A73-21553

Application of lens-raster optics for recording holograms with discrete information 09 p1079 A73-21916

Effect of flutter on theoretical bit error rates for digital recording systems. 09 p1087 A73-23369

Magnetic tape recorder parameters effect on PCM telemetry bit error rate, discussing contribution factors and test methods 09 p1087 A73-23370

Hybrid coding/decoding scheme for deep space probes data transmission, estimating bit error probability for given SNR 09 p1054 A73-23376

Comparing bandwidth requirements for digital baseband signals. 09 p1058 A73-23423

Intersymbol interference in binary communication systems with single-pole band-limiting filters. 10 p1186 A73-23498

Binary coded aircraft flight data block inclusion in aerial reconnaissance photographs for automated data processing 10 p1222 A73-24948

Binary counters design based on TTL, DTL and ECL integrated circuits, giving circuit diagrams for 70 MHz 24 stage and 20 MHz dual 16 stage counters 12 p1497 A73-27208

Correlated clutter and resultant properties of binary signals. 13 p1585 A73-29208

Decision-directed detector for overlapping PCM/NRZ signals. 15 p1843 A73-31732

Lens raster optics for holograms with digital information. 15 p1880 A73-32642

Comparing bandwidth requirements for binary baseband signals. 16 p1984 A73-33745

Optimal detection of binary signals with an arbitrary distribution of state durations at the output of a binary symmetrical Markov channel 20 p2541 A73-38992

Binary error estimation in real time for channel quality monitoring, comparing upper and lower bounds with number of errors for bit sequence 21 p2656 A73-41170

Digital fluidic systems application to binary signal transmission via system with fluid transmission lines and switching element-based transmitters and receivers 23 p2944 A73-43417

BINARY DIGITS

Angle to digital photoelectric converter for azimuthal telescope, discussing accuracy and temperature effects 15 p1877 A73-32132

BINARY FLUIDS

Interferometric and thermoanemometric methods of studying binary boundary layers 15 p1876 A73-31859

State variables and transport coefficients of binary gaseous mixtures. I - A simple method for the accurate determination of the second virial coefficient of binary gaseous mixtures [DFVLR-SONDDR-273] 22 p2931 A73-42373

State variables and transport coefficients of binary gaseous mixtures. II - The binary interaction between identical and nonidentical molecules [DFVLR-SONDDR-279] 22 p2931 A73-42374

State variables and transport coefficients of binary gaseous mixtures. III - The calculation of transport coefficients with the aid of consistent potential parameters [DFVLR-SONDDR-280] 22 p2931 A73-42375

Effect of an electric field on the ignition of a reacting binary gas mixture 23 p3009 A73-43441

Temperature field and motion oscillations in water-methanol and water-isopropanol Benard cells, taking into account thermal diffusion 23 p3049 A73-43936

Transfer phenomena in nonreactive binary fluid mixtures analyzed by nonlinear continuum thermodynamics of irreversible processes 24 p3156 A73-45081

BINARY INTEGRATION

Equivalence of systems that follow a stochastic principle of computation 09 p1059 A73-22554

BINARY MIXTURES

NT BINARY FLUIDS

NT EUTECTIC ALLOYS

NT EUTECTICS

Effects of forced flow, noncondensables, and variable properties on film condensation of pure and binary vapors at the forward stagnation point of a horizontal cylinder. 01 p0122 A73-10806

Velocity, temperature and component concentration distributions in laminar boundary layer at blown surface for binary mixture flow 01 p0034 A73-10957

Acoustic properties of fluid mixtures for ultrasonic delay lines, noting temperature and composition effects on water-glycol mixture parameters 03 p0280 A73-14620

On some oxygenated compounds of titanium and alkalis /Li, Na/ - Study of the binaries M2O-TiO2 in the zones rich in alkaline oxide 05 p0547 A73-17219

The stability of a layer of binary gas mixture heated below. 11 p1449 A73-25222

Velocity, temperature and component concentration distributions in laminar boundary layer at blown surface for binary mixture flow 12 p1487 A73-27533

A method for ingredient composition control in binary and quasi-binary systems 15 p1881 A73-31222

- Experimental investigation of longitudinal flow over a flat plate during strong blowing of a foreign gas under isothermal conditions 15 p1957 A73-31856
- Thermodynamic analysis of liquid metal systems by using a cluster model 17 p2188 A73-34555
- Influence of heat conducting elements on the burning rate of mixture system models 18 p2342 A73-37120
- Lattice constants vs compositions of body centered tetragonal solid solutions of mixed rare earth dicarbides according to Vegard law 21 p2751 A73-40322
- Papkovitch-Neiber solution for stress-strain state of initially isotropic mixture of two elastic bodies 23 p3007 A73-44183
- BINARY STARS**
- NT COMPANION STARS**
- NT ECLIPSING BINARY STARS**
- Binary stars as X-ray sources. 01 p0102 A73-10969
- Mass-luminosity relation for eclipsing and visual binary stars, analyzing observational data by least squares method 02 p0218 A73-12409
- Binary stars tidal evolution theory, deriving energy and momentum equations for arbitrary internal structures 02 p0218 A73-12411
- Statistical studies in stellar rotation. II - A method of analyzing rotational coupling in double stars and an introduction to its applications. 03 p0366 A73-12938
- Rapid changes in the new shell star HR 6000. 03 p0366 A73-12941
- On the Napier method for the photometric reflection effect in close binary stars. 03 p0379 A73-14583
- The location and size of the hot spot in cataclysmic variable stars. 04 p0499 A73-15486
- Contact binaries - Opacity and rotation. 04 p0500 A73-15488
- Spectroscopic study of the nebula NGC 7635 and the star BD +60.2522 deg. 04 p0503 A73-16005
- Internal models of uniformly rotating synchronous close binary systems via modified double approximation scheme, considering gravity darkening effect on primary position in H-R diagram 05 p0624 A73-17306
- Nonsynchronous uniformly rotating binary system polytropic models computed and compared to Roche model 05 p0624 A73-17307
- Small Magellanic Cloud X-1 X ray source binary nature, occultation, energy spectrum and intensity from Uhuru satellite observation 05 p0626 A73-17345
- Multiple and intrinsic variable stars, considering pulsars, binary systems, Cepheids, stellar structure and evolution 06 p0750 A73-18014
- Mass transfer during evolution of close binaries within zero velocity surfaces related to nova outbursts and Wolf-Rayet star composition 06 p0753 A73-18246
- The disc model of gaseous accretion on a relativistic star in a close binary system 07 p0901 A73-20305
- Energy distribution in the spectra of some binaries in a wide spectral range /3300-7300 A and 0.88-1.53 microns/ 07 p0901 A73-20318
- Possible explanation for nonthermal radio noise from binary stars. 08 p1003 A73-20883
- Spectroscopic observations of the optical candidate for Cygnus X-1. 08 p1004 A73-20896
- Neutron-star accretion in a stellar wind - Model for a pulsed X-ray source. 08 p0997 A73-21160
- Mass transfer in close binaries. III - Gaseous rings in algol-like binaries. 08 p1010 A73-21312
- Dwarf binary component convective shell behavior under gravitational field periodic tidal action, noting conditions for thermal instability 08 p1012 A73-21548
- Elongated shells around novae and concentration near orbital planes resulting from perpetual matter losses, considering close dwarf binaries and recurrent novae 09 p1145 A73-22288
- Supernova explosions in close binary systems 09 p1145 A73-22289
- Close binaries and their significance in the theory of evolution of stars 09 p1151 A73-23332
- Close binary systems orbital elements perturbations due to stellar material viscosity effects on dynamical tide lag 10 p1271 A73-23478

- Roche model application to close binary systems, emphasizing geometrical properties of limiting equipotentials for configuration breakup 10 p1282 A73-24642
- Disk model of gas accretion on a relativistic star in a close binary system. 12 p1539 A73-27277
- Spectral energy distribution in several binaries at 3300-7300 A and 0.88-1.53 micron wavelengths. 12 p1540 A73-27290
- Massive X ray binaries consisting of early type star with neutron stars or black holes as companions 12 p1535 A73-27597
- Radiation pressure effects on close binary mass loss and luminosity in terms of Roche potential, using contact surface model 12 p1537 A73-27881
- RY Sct detection from search for binary systems with early type star and mass exchange for radio source candidacy 14 p1789 A73-29736
- SMC X-1 binary source observation via UCSD OSO-7 X ray telescope, discussing luminosity and optical identification with variable star SK 160 14 p1786 A73-29738
- Black holes in binary systems, discussing radiation spectrum, disk formation, optical luminosity, X rays, UV regions and temperature distribution 15 p1928 A73-31051
- Contact binary star evolution, discussing adiabatic convection zone entropy, mass flow and relative frequency 15 p1928 A73-31054
- Recent advances of celestial mechanics in the Soviet Union. 15 p1932 A73-31303
- Duplicity and its consequences among variable stars in general. 15 p1935 A73-31484
- The effect of binary motion on period changes in RR Lyrae stars. 15 p1935 A73-31486
- Eruptive binary stars evolutionary origin, outburst mechanisms and effects on Galactic evolution 15 p1935 A73-31487
- Model for X-ray sources based on magnetic field twisting. 15 p1927 A73-32047
- X ray power derivation from gravitational energy release during matter accretion onto surface of component of mass transfer binary star 16 p2049 A73-32730
- Radio counterparts of X-ray sources and X-ray counterparts of radio stars. 16 p2050 A73-32734
- Black holes in binary systems - Observational appearances. 16 p2058 A73-32739
- HZ Hercules periodically pulsating variable extra in binary system detected by Uhuru satellite, detailing X ray emission, rotation pattern and mass exchange mechanism 16 p2059 A73-32948
- Shock waves in gas flows in close binary dwarf star systems 17 p2226 A73-34366
- Optical appearance of binary X-ray sources. 17 p2232 A73-35146
- Evolutionary considerations involving the internal density concentration parameter of binary stars. 17 p2237 A73-35786
- Light curves of the gravitational lens-like action for binaries with degenerate stars. 19 p2483 A73-37563
- Radio binaries observation, noting black hole, large magnetic field or thermal bremsstrahlung as possible origin of strong X-ray radiation 21 p2770 A73-40940
- The common convective envelope model for W Ursae Majoris systems and the analysis of their light curves. 22 p2912 A73-42939
- Wolf-Rayet binary stars detection and use in WR stellar mass, evolutionary status and luminosity estimation, noting atmospheric stratification relationship to temperature 23 p3026 A73-43202
- WC and WR binary stars spectra differences attributed to variations in effects of companion on principal star atmosphere 23 p3026 A73-43203
- Interaction of the X-ray source radiation with the atmosphere of the normal star in close binary systems. 23 p3030 A73-43750

- BINARY SUMMATORS**
- U ADDING CIRCUITS**
- BINARY SYSTEMS [DIGITAL]**
- U DIGITAL SYSTEMS**
- BINARY SYSTEMS [MATERIALS]**
- NT BINARY ALLOYS**
- NT BINARY FLUIDS**
- NT BINARY MIXTURES**
- NT EUTECTIC ALLOYS**
- NT EUTECTICS**

- Phase diagrams, microstructure and interface composition of two phase metallic particles from lunar soils and rocks, determining equilibrium temperature and equilibration time 03 p0376 A73-14110
- Influence of the composition and structure on the mechanical properties of ultraplasic alloys of the Al-Zn system 04 p0464 A73-15497
- Phase equilibrium in the TeO₂-V₂O₅ system 05 p0589 A73-17173
- Structure of the borated layer after diffusion saturation with other elements 06 p0707 A73-18040
- Interaction between the ZrCr₂ intermetallic compound and some zirconium compounds with iron, cobalt, and nickel 06 p0708 A73-18056
- Solid composite material thermostatics and overall thermoelastic modulus determination, considering arbitrarily anisotropic phases, binary composite and self consistent theory 10 p1295 A73-24099
- The behavior of vapors of soluble binary systems during expansion in supersonic nozzles - Droplet coalescence in a potential vortex flow 10 p1205 A73-24162
- Diffusion processes electron mechanism in metal-metal and metal-nonmetal systems, using configurational model for valence electrons localization 10 p1236 A73-24951
- Phase diagrams, microstructure and superconducting properties of thermally diffused Nb-Sn system 12 p1508 A73-26835
- Phase transformations in the bismuth ferrites BiFeO₃ and Bi₂Fe₄O₉ 12 p1531 A73-27199
- High Reynolds number fluid dynamics and heat and mass transfer in real concentrated particulate two-phase systems. 13 p1704 A73-28427
- Calculation of the binary phase diagrams of iron, chromium, nickel and cobalt. 14 p1760 A73-30440
- Weak solutions existence and uniqueness for boundary value problem in linearized theory for mixtures of two isotropic incompressible elastic solids, obtaining differentiability conditions 15 p1947 A73-31336
- Thermionic properties of zirconium carbide/rhenium composites 21 p2751 A73-40530
- Anomalous behaviour during interdiffusion in the system Nb-Mo. 22 p2876 A73-42340
- Time variation in the reaction-zone structure of two-phase spray detonations. 22 p2936 A73-42811
- BINAURAL HEARING**
- Effects of signal duration and masker duration on detectability under diotic and dichotic listening conditions. 01 p0008 A73-10436
- Loudness enhancement following contralateral stimulation. 01 p0013 A73-10827
- Binaural interaction effects on afterperception of white noise pulse sequences delivered to both ears simultaneously or after various intervals 10 p1180 A73-24333
- Problem of localization in the median plane - Effect of pinnae cavity occlusion. 11 p1321 A73-24976
- Binaural acoustic field sampling, head movement and echo effect in auditory localization of sound sources position, distance and orientation 14 p1715 A73-30282
- Vector correlation theory and neural mechanisms of binaural signal detection in human auditory system 14 p1716 A73-30283
- Binaural signal detection - Equalization and cancellation theory. 14 p1716 A73-30284
- Interaural difference thresholds in binaural perception of signals nonexistent in normal acoustic environment, considering beats, memory, learning, and stereophony 14 p1716 A73-30285
- BINDERS [ADHESIVES]**
- U ADHESIVES**
- BINDERS [MATERIALS]**
- NT PROPELLANT BINDERS**
- NT SOLID ROCKET BINDERS**
- Carbonyl terminated polybutadiene polymer binder development for solid propellant, describing properties, manufacturing processes and performance reproducibility 01 p0089 A73-11111
- Lubricating characteristics of polyimide bonded graphite fluoride and polyimide thin films. [ASLE PREPRINT 72LC-7C-3] 03 p0317 A73-14372

- An experimental study of ammonium perchlorate-binder sandwich combustion in standard and high acceleration environments. 07 p0866 A73-20363
- Rheological equation for expansion rate effects on stress-strain relation of polyester binders hardened thermochemically and by gamma radiation 08 p1019 A73-21764
- Influence of thermally stabilizing alloying additions on the antifriction properties of lamellar graphites with a organic silicon binders 09 p1110 A73-22978
- Low void composites based on NR-150 polyimide binders. 10 p1237 A73-23953
- Organic coating technology review, discussing binders, pigments and various processing techniques 11 p1388 A73-25848
- Phenolic binder decomposition in silica-phenolic ablator, determining reaction mechanism from Arrhenius rate equations for various temperatures 11 p1452 A73-26376
- Epoxy-thiocol binder viscoelastic deformation under short and long term loads, noting stress-strain linearity limit 13 p1647 A73-29610
- Bakelite lacquer and epoxy and phenol-formaldehyde solidified resin binders strength at high temperatures 14 p1766 A73-30687
- Processing and properties of composites based on NR-150 polyimide binders. 16 p2029 A73-33047
- Heat and mass transfer processes during thermal decomposition of resin binders in fiberglass reinforced plastics 18 p2328 A73-36814
- Investigation of the dross molding process for titanium carbide 23 p2991 A73-43490
- BINOCLAR VISION**
- The colour vision characteristics of an observer with unilateral defective colour vision - Results and analysis. 02 p0137 A73-12077
- Tests for binocular rivalry of light contours for detection of randomness in disappearance patterns 03 p0261 A73-13557
- Stereoscopic depth magnitude in viewing background-contrasted superimposed half-fields, noting relation to binocular disparity detection 03 p0261 A73-13762
- Study of variations of retinal disparities around the fixation point by the binocular vernier method in the foveal region 03 p0261 A73-13763
- Cortical area of neural loci involved in monoptic and dichoptic metacontrast occurring for target and masking stimuli imaged on different retinal regions 03 p0261 A73-13764
- Monocular and binocular clues interaction in depth perception and spatial orientation, discussing stereopsis testing 05 p0542 A73-16483
- Threshold variance analysis of monocular vs binocular visual stimulation in apparent movement perception 07 p0783 A73-20262
- Eye dominance measurement relationship to image sharpness or visual acuity from binocular and monocular tests, obtaining dominance normal distribution 09 p1039 A73-21893
- Corpus callosum role in monocular system transcommisural interactions from binocular interaction studies of stimulus-evoked potentials in rat visual cortex 10 p1180 A73-24332
- Binocular rivalry and binocular fusion of after-images. 11 p1318 A73-26200
- Scalar perceptions with binocular cues of distance. 13 p1578 A73-28176
- Monocular contribution to binocular vision in normals and amblyopes. 13 p1575 A73-28359
- The Mach-Dvorak phenomenon and binocular fusion of moving stimuli. 14 p1717 A73-30392
- Binocular color resolution capability of the eyes as a function of the characteristics of vision during anisometropia 15 p1832 A73-30999
- Stereoscopic depth aftereffects with random-dot patterns. 17 p2115 A73-34841
- Extended border enhancement during intermittent illumination - Binocular effects. 17 p2112 A73-34842
- Amplitude of visual suppression during the control of binocular rivalry. 17 p2117 A73-35491
- Supranuclear structures regulating binocular eye and head movements. 18 p2272 A73-36451
- Binocular vision variation with age in flight crews 18 p2285 A73-36928
- Non-linearity of visual signals in relation to shape-sensitive adaptation responses. 19 p2394 A73-37418
- Disparity detectors in human depth perception - Evidence for directional selectivity. 21 p2637 A73-40413
- The psychophysical inquiry into binocular summation. 21 p2640 A73-41187
- BINOCLAR**
- Gyroscopic device for compensating external moments of sextants or binoculars optical axis due to spontaneous hand movements 09 p1084 A73-22673
- BINOCLAR**
- Integral transform theory for derivation of compound binomial beta, uniform, and gamma distributions with applications to series-parallel systems reliability determination in manufacturing 16 p2020 A73-33604
- BINOCLAR**
- Dynamic properties of human and animal middle ear in terms of acoustic impedance, transfer function, impulse response, sound diffraction and reflex sensitivity 14 p1715 A73-30279
- Binaural signal detection - Equalization and cancellation theory. 14 p1716 A73-30284
- Action of stable and pulsed noise on the processes of skeletal muscle excitation 22 p2815 A73-42662
- Orbit and superior orbital fissure acoustic window for cranium posterior structures imaging by echoencephalographic techniques 22 p2815 A73-42667
- Simple simulated human head for checking echoencephalographic equipment. 22 p2815 A73-42672
- Signal processing in medical technology 23 p2948 A73-43317
- BINOCLAR**
- An atomic absorption method for cation measurements in Kjeldahl digests of biological materials. 02 p0139 A73-12424
- The study of biological macromolecules using perturbed angular correlations of gamma radiation. 02 p0136 A73-12648
- Accelerated chromatographic method for determination of hydroxyproline. 03 p0273 A73-13600
- Twin spectrograph measurements at 2520-3375 A of metal trace elements in biological sample solutions 06 p0657 A73-17692
- Determination of oxidized and reduced pyridine nucleotides in human and rabbit blood with the aid of the polarographic cycling technique 09 p1044 A73-21871
- Study of myocardial antigen localization using the immunofluorescence method 15 p1834 A73-31392
- Bioassay method for thermal protective clothing fabrics evaluation, measuring skin damage with various fabric combinations under exposure to calibrated flame source 16 p1974 A73-32671
- Apollo diet evaluation - A comparison of biological and analytical methods including bioisolation of mice and gamma radiation of diet. 20 p2517 A73-39103
- Effect of training with eccentric muscle contractions on skeletal muscle metabolites. 21 p2641 A73-41523
- Blood plasma contamination of the lung alveolar surfactant obtained by various sampling techniques. 21 p2642 A73-41637
- BINOCLAR**
- Space environment effects on human life and biochemical evolution study in aerospace medicine and biology, noting amino acid molecules synthesis 03 p0265 A73-14589
- Russian book - Biomedical problems of space flights: Index of domestic and foreign literature. 04 p0410 A73-16034
- Microflora of a sealed cabin with human subjects in a 3-day experiment with reduced temperature and high relative humidity 06 p0657 A73-17697
- Astronauts diurnal life cycle inversion during space flight missions, considering social factors and work-rest cycle effects 12 p1463 A73-27715
- BINOCLAR**
- NT BACTERIOLOGY**
- NT BIOGEOCHEMISTRY**
- Atomic and molecular interactions investigation by computer aided mass spectrometry, considering applications in bio-organic chemistry, isotope analysis, geochemistry and cosmochemistry 02 p0139 A73-12425
- Biochemical processes during the maturation of erythrocytes - Further results with regard to the action site of the respiratory inhibitor F from reticulocytes in the respiratory chain 02 p0134 A73-12510
- Nervous system transmitter biochemistry in terms of excitation and inhibition coordination with emphasis on gamma-aminobutyric acid (GABA) function in cerebellum 03 p0264 A73-14258
- Developmental changes in neurochemistry during the maturation of sleep behavior. 03 p0264 A73-14261
- Maturation of neurobiochemical systems related to the ontogeny of sleep behavior. 03 p0264 A73-14262
- Chemical evolution under the bion hypothesis. 03 p0265 A73-14316
- Protobiochemical developments in terms of extraterrestrial life search and roles of nitriles and urea in prebiological chemical evolution 03 p0265 A73-14319
- Biological, chemical and cytological methods of microorganism detection integrated into single instrument 03 p0272 A73-14320
- Circadian rhythms - Subcellular and biochemical aspects. 06 p0651 A73-17824
- Book - Molecular evolution: Prebiological and biological. 06 p0651 A73-17926
- Life origin on earth, considering hydrocarbon molecules and macromolecular synthesis under earth atmospheric evolutionary conditions 06 p0651 A73-17928
- Synthesis of glutamic acid via cyanoethylation of n-acylaminoacetoneitriles in liquid ammonia. 06 p0661 A73-17936
- Model experiments on the prebiological formation of protein. 06 p0652 A73-17938
- Modified rhodopsin in the pigment epithelium. 07 p0783 A73-20263
- Liquid ammonia life existence in universe, considering halogen and silicon life chemistry 11 p1326 A73-26662
- Mechanism of the action of radiation protecting agents - A biochemical shock hypothesis 12 p1465 A73-27499
- Study of the relations between various mechanical properties and biochemical composition of bone tissues in man 13 p1577 A73-27996
- Histochemical investigation of some energy metabolism characteristics in a rat heart after acute fatigue 15 p1834 A73-31393
- Total lipid and sterol components of Rhizopus arrhizus - Identification and metabolism. 16 p1973 A73-33900
- Extraterrestrial life existence evidence, discussing biochemical properties, evolution and mental and moral characteristics of extraterrestrial life 17 p2113 A73-35657
- Method allowing biological and biochemical studies of vacuum-exposed bacteria. 20 p2513 A73-39483
- Continual mechanochemical model of muscular tissue 21 p2643 A73-40182
- Abnormal biochemistry in myocardial failure. 22 p2808 A73-42686
- BINOCLAR**
- Thermal protective garment using independent regional control of coolant temperature. 07 p0785 A73-19481
- Determination of the information-forecasting indices of biometeorological phenomena 13 p1579 A73-28861
- The combined influence of microwave radiation and an adverse climate on the organism 15 p1837 A73-31170
- BINOCLAR**
- Activity relation between internal organ receptors and skeletal muscles in terms of laws controlling process coordination 01 p0007 A73-10154
- Functional models adequacy for brain activity simulation, discussing transfer, forward and feedback loops, hierarchy, reciprocity and self organizing aspects 01 p0011 A73-10651
- Neuron networks modeling from viewpoint of intracellular and cell-medium interaction, discussing coding properties and nonsingular self adjusting system response 01 p0012 A73-10652
- Investigation of the recovery dynamics of the mimic muscle function and choice of an optimal bioelectric stimulation program with the aid of an electronic digital computer 01 p0012 A73-10656
- Certain aspects of the bionic analysis and control of dynamic systems 01 p0012 A73-10658

Inhibitive mechanisms activity in behavior control by neostriatum, discussing suppressive reactions, evoked sleep, conditioned and instrumental reflexes and neurophysiological aspects

01 p0009 A73-11025

Muscular activity control mechanism interactions in vertical posture maintenance from stabilogram, mechanogram and electromyogram data

02 p0137 A73-12119

Hypothalamic norepinephrine - Circadian rhythms and the control of feeding behavior.

02 p0134 A73-12417

Dynamic aspects of regulation of ventilation in man during acclimatization to high altitude.

03 p0259 A73-13500

Circadian rhythm asynchrony in man during hypokinesia.

03 p0263 A73-14121

Human body mathematical model described by kinematic and dynamic equations of joined rigid bodies for investigation of self-controlled movements in specified goal attainment

04 p0411 A73-15207

Biological role of atmospheric oxygen in the mechanism of blood coagulation

06 p0650 A73-17678

Prolonged control of cardiac bioelectrical activity in man in ground experiments and during spaceflight

06 p0657 A73-17694

Biological clocks in animal orientation and in other functions.

06 p0651 A73-17825

Muscle control models of joint angle spatial motions, including circle, ellipse and straight line trajectories and orientations in space

06 p0680 A73-17960

The influence of age, sex, body size and lung size on the control and pattern of breathing during CO₂ inhalation in Caucasians.

06 p0654 A73-18337

The control of sensitivity in the retina.

06 p0655 A73-18673

Ergatic organism defined as multipurpose nonautonomous control system with homeostasis with respect to functional operations conservation

07 p0786 A73-20048

Human operators and automatic adaptive controllers - A comparative study on a particular control task.

07 p0786 A73-20399

Digital computer studies of respiratory control.

07 p0787 A73-20577

Renal component of the antigravitation function of the organism

08 p0929 A73-20976

Mathematical analysis of the responses of the human respiratory system to hypoxia and hypercapnia

08 p0931 A73-21322

Order and disorder in the rhythm of the heart (Fifth Annual George C. Griffith Lecture).

08 p0933 A73-21806

A frequency response analysis of fusimotor-driven muscle spindles.

09 p1041 A73-22934

Organism-machine interactions in hybrid control systems for cardiac stimulation, artificial breathing apparatus and intelligence assignments

09 p1047 A73-23298

Features of supraspinal control of the reflex paths of the spinal cord during walking

10 p1178 A73-23677

Formalization of an arterial pressure stabilization system

10 p1181 A73-24467

Voluntary activation of individual motor units in man

10 p1181 A73-24519

Controlled tachycardia through voluntary change in exercise regime, investigating relation between heart rate and blood circulation

10 p1185 A73-24521

The operational control of the alpha component in the electroencephalogram by means of auditory feedback

11 p1324 A73-26549

Motor functions and control of sensorial messages of somatic origin

13 p1576 A73-29174

Anatomical and neurophysiological investigations of centrifugal control of retinal activity via efferent optic nerve fibers

14 p1714 A73-29875

Periodic conditions in artificial-muscle autotranslators

14 p1721 A73-30289

Saccadic eye movement control system, investigating response characteristics to variously timed pulse stimuli

14 p1716 A73-30389

Accuracy of saccadic eye movements and maintenance of eccentric eye positions in the dark.

14 p1716 A73-30390

Voluntary small saccadic eye movements in presence of stationary visible target, considering scanning function of fixation saccades

14 p1717 A73-30394

Blood pressure and body temperature dynamic control systems and respiration relationship to heart rate variability

14 p1720 A73-30878

The role of carotid sinuses in the regulation of hemodynamics during motor activity

15 p1833 A73-31161

Intervention of cerebello-cortical and cortico-cerebellar paths in the organization and regulation of movement

15 p1836 A73-32288

Model concept concerning some control principles of the human organism. III - Seasonal adaptation

15 p1836 A73-32357

Book - Principles of biological regulation: An introduction to feedback systems.

15 p1840 A73-32576

The explanation and investigation of biological rhythms.

16 p1972 A73-33155

Amplitude of visual suppression during the control of binocular rivalry.

17 p2117 A73-35491

Cerebral control of eye movements and motion perception; Proceedings of the Symposium, Freiburg im Breisgau, West Germany, July 20-22, 1971.

18 p2271 A73-36432

Vestibular and cerebellar control of oculomotor functions.

18 p2271 A73-36438

Optomotor integration in the colliculus superior of the cat.

18 p2272 A73-36443

Central programming and peripheral feedback during eye-head coordination in monkeys.

18 p2273 A73-36452

The control of eye movements in the saccadic system.

18 p2273 A73-36453

Rabbit optokinetic reactions and retinal direction-selective cells / A preliminary model/.

18 p2273 A73-36455

Investigations of the eye tracking system through stabilized retinal images.

18 p2273 A73-36456

Teleoperator system incorporating touch feedback and sequenced automatic control for experimental investigation of human touch sensing relation to manipulative skills

19 p2397 A73-37328

The control of a manipulator by a computer model of the cerebellum.

19 p2398 A73-37333

Model of evaporation responses to heat load increases

19 p2395 A73-38150

An electrical model of the inertial and adaptive properties of vision as a self-regulating system with delayed feedback

20 p2517 A73-39004

Mathematical analysis of the operation of regulatory mechanisms of the spinal cord

20 p2517 A73-39005

Russian book - Role of the hypothalamus and the limbic system of the brain in regulating vegetative functions.

21 p2636 A73-40276

The role of the amygdaloid nuclei in the regulation of water intake

21 p2636 A73-40278

The nature of chemoreception in posterior hypothalamic structures

21 p2636 A73-40279

Control of the duration of expiration.

21 p2642 A73-41635

Effect of chronic pyramid insufficiency on the function of spinal centers of shin and foot muscles in man

22 p2807 A73-42658

On the electronic simulation of acceleratory nystagmus.

22 p2816 A73-42683

The effect of anxiety control on the level of information processing

23 p2946 A73-43848

Neurogenic and local regulation of resistance and capacitance blood vessels, noting sympathetic nervous system influence on musculocutaneous and splanchnic regions

23 p2947 A73-43927

BIODYNAMICS

Some biomechanical properties of the pelvic girdle of man

03 p0267 A73-13743

German monograph - Experimental investigation of the structure of joint movements in the range of motions of the arms and of the entire body, giving attention to a presentation in a man-related basic system.

03 p0267 A73-13812

Book - How man moves: Kinesiological studies and methods.

03 p0268 A73-13993

Telemetry methods for maximum static muscle strength measurements, considering dynamic force measurement possibilities

03 p0271 A73-14296

Finite element displacement analysis of a lung.

03 p0273 A73-14661

Human body mathematical model described by kinematic and dynamic equations of joined rigid bodies for investigation of self-controlled movements in specified goal attainment

04 p0411 A73-15207

The dynamic properties of the acoustic middle ear reflex in nonanesthetized rabbits - Quantitative aspects of a polysynaptic reflex system.

05 p0539 A73-16249

Muscle control models of joint angle spatial motions, including circle, ellipse and straight line trajectories and orientations in space

06 p0680 A73-17960

The biodynamic aspects of low altitude, high speed flight.

06 p0659 A73-18471

Human tendon stress recovery after load removal as function of time, sex, age and side differences

07 p0782 A73-20033

A method for chronocyclographical motion analysis with the aid of an on-line computer

07 p0785 A73-20036

A model for the elastic properties of the lung and their effect on expiratory flow.

08 p0934 A73-21502

Regional myocardial dynamics from single-plane coronary cineangiograms.

10 p1185 A73-24771

Analysis of swimming motions.

11 p1322 A73-25184

Mechanics of breathing in high altitude and sea level subjects.

11 p1318 A73-26217

Myocardial contraction velocity and acceleration in man measured by ultrasound echocardiography differentiation.

12 p1461 A73-27026

Study of the relations between various mechanical properties and biochemical composition of bone tissues in man

13 p1577 A73-27996

Transpulmonary pressure gradient and ventilation distribution in excised lungs.

15 p1833 A73-31129

Book - Principles of biological regulation: An introduction to feedback systems.

15 p1840 A73-32576

Dynamic analyses of hybrid bio/mechanical networks with feedback characterization.

16 p1975 A73-33161

Adequate vestibular stimulants on earth and in space

17 p2110 A73-34122

Analysis of the extravehicular activity of an astronaut

18 p2281 A73-36116

Properties of biological fluids and solids: Mechanics of tissues and organs; Proceedings of the Biomechanics Symposium, Georgia Institute of Technology, Atlanta, Ga., June 20-22, 1973.

18 p2281 A73-36428

Endolymph fluid mechanics in semicircular canals approximated by rigid torus filled with incompressible Newtonian fluid

18 p2281 A73-36430

Three models of the vibrating ulna.

19 p2398 A73-37543

Changes in whole body force transmission of dogs exposed repeatedly to vibration.

20 p2512 A73-39106

Volume-pressure characteristics of rib cage-diaphragm interaction in standing subjects during voluntary relaxation

20 p2518 A73-39778

A model to predict the mechanical impedance of the sitting primate during sinusoidal vibration.

[ASME PAPER 73-DET-78] 22 p2813 A73-42073

Some psychological and engineering aspects of the extravehicular activity of astronauts.

22 p2814 A73-42167

Biomechanics of locomotion via jumping on lunar surface, discussing subgravity effects on energy requirements, body potential and kinetic energy, muscular work, etc

22 p2804 A73-42175

Climbing and cycling with additional weights on the extremities.

22 p2806 A73-42418

Reflex arch lability in rabbits at synchronous maximum frequency of electromyographic and muscle stretching vibration measurement

22 p2807 A73-42659

Biodynamic applications regarding isolation of humans from shock and vibration.

22 p2816 A73-42926

Vertical arm reaching movements for various gravitational levels, measuring reach time and angular and lower arm velocities

23 p2948 A73-43218

Evaluation of the physical conditions of individual airmen

23 p2949 A73-43790

- Physiological study of dynamics and evolution of chimpanzee complex behavior, considering motor reactions, group behavior and nerve mechanisms of voluntary acts
23 p2947 A73-43928
- Sentography - Dynamic forms of communication of emotion and qualities.
23 p2949 A73-44180
- Physical model selection for the balance preservation system in man
24 p3063 A73-44903
- Dynamics of the balance preservation system of man
24 p3064 A73-44909
- BIOELECTRIC POTENTIAL**
- Numerical analysis of spontaneous electric activity of the brain - Study of the statistical properties of the power density spectra
02 p0138 A73-12160
- ERG late photoreceptor potential components time course in macaque monkey cones and rods, noting pure cone foveal response
03 p0261 A73-13761
- Variations of evoked potentials during various mental stress situations
03 p0268 A73-13825
- Source locations of pattern-specific components of human visual evoked potentials. I - Component of striate cortical origin. II - Component of extrastriate cortical origin.
04 p0409 A73-15024
- A new method to measure non-uniformity in the intact heart.
04 p0412 A73-15645
- Mathematical analysis of body surface potentials.
04 p0412 A73-15646
- Genesis mechanism of slow cortical after-discharges during brain injury by radiation
05 p0539 A73-16331
- Correlation between the impulse activity of bulbar respiratory neurons, the electrical activity of respiratory muscles, and pulmonary respiration volume during obstructed respiration
06 p0650 A73-17683
- Miniature four-channel radiotelemetry system for the transmission of cerebral biopotentials
06 p0658 A73-18167
- Visual evoked responses elicited by rapid stimulation.
06 p0654 A73-18350
- Functional organization of the mechanisms of presynaptic inhibition evoked by stimulation of cutaneous afferents
07 p0781 A73-20003
- Changes in the amplitudinal and temporal characteristics of sensorimotor-cortex evoked potentials after deactivation of spinocervical tracts in cats
07 p0781 A73-20004
- Physiological mechanisms of evoked-potential habituation in the visual analyzer
07 p0782 A73-20006
- German monograph - The objectivization of the effect of load and stress on an information-reception process of man with the aid of acoustically evoked potentials.
07 p0786 A73-20389
- Evoked potential correlates of expected stimulus intensity.
08 p0930 A73-21225
- Relation between the frequency-amplitude characteristics of cerebral electrical activity and gonadotropic hormone excretion levels at various stages of ontogenesis
08 p0930 A73-21319
- Relation of electrolyte disturbances to cardiac arrhythmias.
08 p0933 A73-21807
- Cortical potentials evoked by confirming and disconfirming feedback following an auditory discrimination.
09 p1039 A73-21895
- Investigation of evoked activity in the ventral horn of lumbar segments during the interaction of efferent extrapyramidal and cortical stimuli
09 p1040 A73-22579
- Biopotential alpha and theta rhythms of neocortex and hippocampus of milk drinking cats after food and water deprivation
09 p1040 A73-22862
- Light evoked changes in potential difference between inside and outside of cells in *Limulus* ommatidia, describing multistage model of generator potential
09 p1043 A73-23309
- Light-induced potential and resistance changes in vertebrate photoreceptors.
09 p1043 A73-23313
- Retinal S-potential receptive field relationship to light energy and wavelength, considering cone and rod potentials, ganglion cells and vision
09 p1043 A73-23314
- Correlation analysis of the bioelectrical activity of the brain during mental work
10 p1178 A73-23678
- Examination of responses evoked in the sensory cortex by thalamic stimulation.
10 p1178 A73-23772
- Sinusoidal stimuli induced electrical activity of hippocampus in waking rhesus monkeys and baboons
10 p1180 A73-24330
- Corpus callosum role in monocular system transcommissural interactions from binocular interaction studies of stimulus-evoked potentials in rat visual cortex
10 p1180 A73-24332
- Cardiac potential measuring and recording instrument with 240 probes, presenting circuit and block diagrams
10 p1184 A73-24422
- Electrophysiological study of the topographic organization of Deiters' lateral vestibular nucleus
10 p1181 A73-24515
- Amplitude discriminator with variable effective range design for use with/without digital computer in neuron pulsed activity analysis
10 p1184 A73-24516
- Features of the spontaneous and evoked neuronal activity of deep brain structures in man during voluntary movements
10 p1181 A73-24517
- Short-term latent reactions of the lateral geniculate body neurons in the rat to electrical stimulation of the optical tract
10 p1182 A73-24595
- Memory process in terms of cortex-subcortex interaction, brain lability level and biopotential trace processes
11 p1314 A73-25198
- Cell membrane molecular structure and lipid composition, discussing phospholipid role in membrane potential maintenance in myocardial cells
11 p1315 A73-25591
- Neurogenic and myogenic mechanisms of myocardium cell electrical activity and excitation in vertebrate and invertebrate neural and muscle tissues
11 p1316 A73-25599
- Single unit and evoked potential responses in cat optic tract to paired light flashes.
11 p1317 A73-25647
- Single unit reactions in the visual cortex of the unanesthetized rabbit to the light flashes of different intensities.
11 p1321 A73-26719
- Comparative analysis of the electrical activity of the cortex and of cerebral subcortical formations in the process of the alteration of conditioned reactions
12 p1461 A73-27104
- The role of analyzers of conditional and unconditional stimuli in the functional system of the behavioral conditioned-reflex action
12 p1461 A73-27105
- Heart function mechanism explanation by activation potential stimulation of muscular contraction via calcium ions
12 p1462 A73-27690
- Dynamics of certain characteristics of the evoked potential of the optic cortex in rabbits under conditions of increasing hypoxia
12 p1463 A73-27709
- Light adaptation of the late receptor potential in the cat retina.
13 p1574 A73-28352
- Theoretical models of the generation of steady-state evoked potentials, their relation to neuroanatomy and their relevance to certain clinical problems.
13 p1574 A73-28354
- Evoked potentials to changes in the chromatic contrast and luminance contrast of checkerboard stimulus patterns.
13 p1575 A73-28355
- Scotopic visibility curve in man obtained by the VER.
13 p1575 A73-28356
- A clinical method for obtaining pattern visual evoked responses.
13 p1575 A73-28357
- Motor functions and control of sensorial messages of somatic origin
13 p1576 A73-29174
- Behavioral and electrophysiological correlates during flash-frequency discrimination learning in monkeys.
14 p1714 A73-29989
- Human average evoked potential distribution over scalp to associate cortical electrical activity with voluntary movement, reacting to EMG activity
14 p1714 A73-29990
- Effect of stimulus uncertainty on the pupillary dilation response and the vertex evoked potential.
14 p1714 A73-29991
- German monograph - Comparative investigations regarding the phenomenon of force potentiation in the case of the heart muscle of cold-blooded and warm-blooded animals.
14 p1719 A73-30669
- Loss of information during central summation of local postsynaptic potentials
14 p1719 A73-30825
- Subjective brightness contrast lack of correlation with steady state evoked potential amplitude in suprathreshold stimuli range
15 p1837 A73-31017
- Evoked negative electrical potentials due to auditory zone stimulation by local cooling, mechanical trauma and potential recording, observing reaction regeneration variations
15 p1833 A73-31159
- Electrophysiological evidence that abnormal early visual experience can modify the human brain.
15 p1838 A73-31371
- Technique for recording muscle biopotentials by means of implanted electrodes
15 p1839 A73-31799
- Opponent-colors responses in the visually evoked potential in man.
17 p2112 A73-34844
- Frequency analysis of spatio-temporal visually evoked cortical potentials during binocular rivalry.
17 p2118 A73-35645
- Saccade correlated events in the lateral geniculate body.
18 p2272 A73-36449
- Intracellular-extracellular action potentials - Considerations for the formation of wavefronts and their detection on the body surface.
18 p2282 A73-36518
- Physiologic correlates and clinical comparisons of isopotential surface maps with other electrocardiographic methods.
18 p2282 A73-36519
- Effect of sonic boom on hearing and vestibular equilibrium
18 p2284 A73-36910
- The value of data processing in the analysis of visual evoked potentials
18 p2279 A73-36911
- Monkey rod receptor potential suppression at photopic stimulus intensities by neurophysiological inhibitory mechanism for clearing cone initiated visual pathway
19 p2393 A73-37412
- Slowed decay of the monkey's cone receptor potential by intense stimuli, and protection from this effect by light adaptation.
19 p2394 A73-37413
- The effect of social-emotional environmental stress on the functional state of the neocortical structures of rhesus monkeys
19 p2394 A73-37755
- Quantitative evoked-potential analyses for the neurophysiological characterization of faulty learning processes in the experimental arterial hypertension-pathogenesis
19 p2394 A73-37756
- Functional characteristics of different neurons in the auditory cortex
19 p2395 A73-37940
- Evoked potentials in the hypothalamus in response to stimulation of the vagus and sciatic nerves
19 p2395 A73-37941
- Motor unit reactions of man to spinal and supraspinal inhibitory stimuli
19 p2395 A73-37943
- Amplitude variations of acoustically evoked potentials as a function of signal information and fatigue due to stress
19 p2396 A73-38161
- Visually evoked cortical potentials to patterned stimuli in monkey and man.
20 p2514 A73-39760
- Role of associations in the formation of evoked potentials from the human cerebral cortex
20 p2515 A73-39798
- A universal preamplifier for bioelectric signals
21 p2643 A73-40345
- Symmetry of the visual evoked potential in normal subjects.
21 p2638 A73-41012
- Variations in the motor potential with force exerted during voluntary arm movements in man.
21 p2638 A73-41013
- Evoked potentials in the hypothalamus and mesencephalic reticular formation upon stimulation of the vagus nerve
21 p2640 A73-41263
- Performance decrement, under prolonged testing, across the visual field.
22 p2802 A73-41730
- Individual physiological differences in evoked potential reactions to light sources, discussing latent periods, potential amplitude distribution and EEG measurement techniques
22 p2812 A73-41888
- Operator reaction functional readiness manifestation in evoked potential characteristics of stimulus-response situations, obtaining response amplitude distribution
22 p2812 A73-41891
- Effect of the stimulation of nonspecific thalamic nuclei on spontaneous and evoked spindles in the auditory cortex
22 p2802 A73-41958

Examination of a multiple dipole inverse cardiac generator, based on accurately determined model data.

22 p2813 A73-41961

Signal/noise ratio in the recording of human nerve-action potentials.

22 p2814 A73-42372

Russian book - Integral topograms of heart potentials.

22 p2807 A73-42489

Effect of the electrical stimulation of the sensorimotor cortex on the potentials of dorsal roots and on the depolarization of primary spinal afferents

22 p2807 A73-42652

Statistical treatment of evoked electrical potentials during experiments on a Dnepr-1 computer

22 p2814 A73-42657

Relation between vibratory sensibility and electric signal of living body.

22 p2816 A73-42680

Rectifier-like color dependent phase shifts in electrophysiological responses to different colored stimuli at evoked potential and single neuron levels

22 p2810 A73-42961

Recovery of cone receptor activity in the frog's isolated retina.

22 p2810 A73-42962

Frog red rod dark adaptation from recorded receptor potentials of isolated retina, examining permanent sensitivity loss due to pigment bleaching

22 p2810 A73-42963

Structurally functional properties of the dendrites of central neurons

23 p2947 A73-43926

Electrical field distribution in the human body.

23 p2950 A73-44216

Intracellular measurements in a closed hyperbaric chamber.

24 p3065 A73-45072

Cortical and intracortical study of the frontal visual evoked potential in photosensitive Papio papio

24 p3061 A73-45159

Visual evoked potentials to changes in the motion of a patterned field.

24 p3061 A73-45167

Comparison of visual evoked potentials to stationary and to moving patterns.

24 p3061 A73-45168

Local resistance variations caused by membrane potential shifts in the interior of the horizontal retina cell

24 p3061 A73-45250

BIOELECTRICITY

Stability criteria in manifestations of the activity of the central nervous system in humans

01 p0006 A73-10152

Left ventricular receptors activated by severe asphyxia and by coronary artery occlusion.

01 p0008 A73-10549

Computerized correlation analysis of single and multiple neuron pulse activity, considering temporal, sequential and entropy characteristics

01 p0012 A73-10653

Complex processing of discrete biological information

01 p0012 A73-10662

Stable frequency and synchronicity alterations in the discharges of cortical neuron populations in feedback experiments

01 p0010 A73-11445

Induced retinal image blurring effects on rabbit mid-brain single cell trigger features and response efficiencies, noting receptive field responsive area

01 p0010 A73-11503

Analysis of the response characteristics of optic tract and geniculate units and their mutual relationship.

02 p0134 A73-12162

Mathematical model for spectral distribution function of brain waves, noting analogy with RC oscillator

02 p0135 A73-12557

Phasic discharge activity and localization of sheep medullary neurons in relation to swallowing reflex after superior laryngeal nerve stimulation

03 p0262 A73-13786

Response of single units of the posterior hypothalamus to thermal stimulation.

03 p0262 A73-14111

Telemetered EEG and neuronal spike activity in olfactory bulb and amygdala in free moving rabbits.

03 p0271 A73-14299

Derivation of a function of nerve-fiber distribution according to fiber diameters on the basis of electrophysiological measurements

04 p0413 A73-15787

Characteristic of collicular responses to stimulation of various sections of the visual afferent pathway in cats

05 p0539 A73-16332

Space-time dynamics of the impulse activity in human-brain neuron populations

05 p0540 A73-16692

Intercortical functional connections in lower monkeys, *Macacus rhesus*, exhibited by evoked responses

05 p0540 A73-16693

Utilization extent of the muscle apparatus capabilities during maximum voluntary force exertion

05 p0541 A73-16696

Responses of bulbar respiratory neurons to apparatus-aided artificial respiration

05 p0541 A73-16699

Effect of hypercapnia on the electrical discharges of the bulbar respiratory neurons and motor neuron ganglia of respiratory muscles

05 p0541 A73-16735

Functional state of various portions of the cerebrum under the action of extremal stimulation

05 p0541 A73-16736

Rabbit hippocampal neuron activity relation to theta-wave phases from cell potential and extracellular recording analyses

07 p0782 A73-20005

Influence of a low-intensity ultrahigh-frequency electromagnetic field on the bioelectrical activity of the brain in rabbits

09 p1044 A73-22367

Electrophysiological investigation of noise rejection in an auditory system receiving sound from a localized source

09 p1040 A73-22580

Modification and updating of the bioelectric DS2C amplifier for a FET input.

09 p1046 A73-22936

Statistical investigation of the impulse activity of neurons in various hypothalamic regions

10 p1179 A73-23802

Role of the medial area of the medulla oblongata in the rhythmical activity of respiratory-center neurons

10 p1179 A73-23804

Neuron analyzer technique for poststimulus histogram plotting of neuron excitation as function of stimulus onset time

10 p1183 A73-23811

Device for analyzing the electrical activity of nerve fibers in intact nerves

10 p1183 A73-23812

Alternative mechanisms of apparent supernormal atrioventricular conduction.

10 p1184 A73-23843

The influence of change in the functional state of the central nervous system on the course of asphyxia

10 p1179 A73-23937

Origin of the external electric field detected near animals and men

10 p1184 A73-23942

Role of nerve structures in the action of low-frequency sinusoidally modulated currents on synovial membrane permeability in the knee joint

10 p1180 A73-23943

Functional state of the cerebral cortex and of the mesencephalic reticular formation during prolonged action of impulsive and stable noise

10 p1181 A73-24334

Characteristics of the electrical activity of the superior olivary bodies of *Vespertilionidae* and *Rhinolophidae* bats in response to ultrasonic stimuli of different frequencies

10 p1182 A73-24596

Effect of whole-body vibration on peripheral nerve conduction time in the Rhesus monkey.

11 p1315 A73-25335

Dynamics of changes in neuron activity regimes of the ascending auditory pathways

11 p1317 A73-26079

Nature and significance of periodic electrical activity variations in the neocortex and the hippocampus during the paradoxical phase of sleep

11 p1317 A73-26083

Hypothalamus, septum and ventrobasal thalamus nuclei single neuron responses to skin thermal stimulation, indicating afferent connections between cerebrum thermoregulation center and peripheral thermoreceptors

11 p1317 A73-26086

Influence of synchronized sleep upon spontaneous and induced discharges of single units in visual system.

11 p1319 A73-26223

On the functional significance of subcortical single unit activity during sleep.

14 p1714 A73-29993

Oscillatory waves in intraretinally recorded electroretinograms in primates, considering electrode depth, stimulus duration and intensity and background illumination, anesthesia and tetrodotoxin effects

14 p1717 A73-30393

Circulation of nervous impulses in the cerebral cortex

14 p1718 A73-30569

Neurophysiological characteristics of isolated structures of the cerebral cortex

14 p1718 A73-30570

Effects of vagotomy on the impulse activity of respiratory neurons

15 p1833 A73-31160

Transmission of nerve pulses at the switching locations of the brain

16 p1973 A73-33424

The neuronal mechanism of nystagmus.

18 p2271 A73-36437

Limitations of the dipole concept in electrocardiographic interpretation.

18 p2281 A73-36517

Changes in the electrical activity of the brain and in some thermoregulation indices of nonanesthetized male cats during cooling

18 p2276 A73-36569

On correlation between the changes in cerebellar bioelectric activity and the adaptive reactions under the effect of accelerations.

18 p2279 A73-36915

Reinforcement of unconscious traces of stimuli in the human being during ontogenesis

19 p2393 A73-37251

Changes in some behavioral reactions and in the bioelectric activity of the brain in cats during the development of sleep under polarization of individual brain structures

19 p2393 A73-37393

Probabilistic statistical methods for analysis of impulse flows in nerves

20 p2516 A73-39002

A mathematical model of the peripheral pain signalization mechanism

20 p2516 A73-39003

Effects of round window stimulation on unit discharges in the visual cortex and superior colliculus.

20 p2513 A73-39146

A study of evoked slow activities in man which follow a voluntary movement and articulated speech

20 p2514 A73-39759

Bioelectric and vegetative components of conditioned reflexes of 'negative-emotional type'

20 p2515 A73-39797

Functional properties of auditory cortex neurons in a controlled experiment

20 p2516 A73-39802

Diminution of uncertainty in the firing of hippocampal units in response to a stimulus

20 p2516 A73-39803

Hybrid biological power cells for cardiac pacemakers - Materials evaluation.

20 p2520 A73-39823

High-frequency synchronized activity of the amygdaloid complex as an EEG indicator of certain psychophysiological states

21 p2636 A73-40277

Correlative function formalism for neuron networks with limited communication channels and active-refractive-storing signal action

21 p2645 A73-41277

Russian book - Electrical activity of the human brain in the process of motor action.

21 p2640 A73-41289

Influence of small electromagnetic-field fluctuations on the bioelectric activity of the human brain

22 p2813 A73-41964

Objective method for classification of multicellular activity patterns of neuron population in the cerebrum of man

22 p2807 A73-42656

Shaping device for frequency analysis of electrical processes in peripheral neural stems and ganglia

22 p2815 A73-42664

Computer acquisition of multiunit nerve-spike signals.

22 p2815 A73-42671

Circuit diagram of amplifier-filter for analysis of impulse activity of baroreceptor aortic afferent nerves in rabbits

22 p2816 A73-42681

The nature and significance of the dynamics of electrical activity in the neocortex and hippocampus during the paradoxical phase of sleep

24 p3059 A73-44718

Electronic simulation and analog computer studies of the influence of temperature on the process of nerve impulse shaping

24 p3062 A73-44725

BIOENGINEERING

NT ANTHROPOMETRY

NT BALLISTOCARDIOGRAPHY

NT BIOINSTRUMENTATION

NT BIOMETRICS

NT BIOTELEMETRY

NT BODY MEASUREMENT (BIOLOGY)

NT CARDIOGRAPHY

NT ELECTROCARDIOGRAPHY

NT ELECTROENCEPHALOGRAPHY

NT ELECTROMYOGRAPHY

NT ELECTROPLETHYSMOGRAPHY

NT ELECTRORETINOGRAPHY

NT PLETHYSMOGRAPHY

Periodic conditions in artificial-muscle autopsaltors

14 p1721 A73-30289

Automatic apparatus for the study of conditioned reflexes in a monkey seated in the primatological chair

21 p2644 A73-41140

BIOGENESIS

U BIOLOGICAL EVOLUTION

BIOGENY

The role of biogenic amines in sleep.

03 p0264 A73-14260

Silk fibroin, collagen, glycoproteins, keratin and protamines formation in single evolutionary event by de novo synthesis of DNA 07 p0780 A73-19219

Geochemical significance of perylene occurrence in marine sediments, discussing land organism biogenic pigment precursors and polycyclic aromatic hydrocarbon conversion 10 p1211 A73-24105

Lifes possible origin on earth from extraterrestrial organisms, discussing galactic intelligent life and intelligent signals from extrasolar planets 21 p2639 A73-41175

BIOGEOCHEMISTRY

Biogeochemistry of aragonite mud and oolites. 03 p0266 A73-14662

Biogenic elemental distribution and isotopic abundance in lunar samples, discussing heavy isotopes enrichment by solar wind irradiation, meteorite impacts and hydrogen stripping 06 p0654 A73-18417

Carboxylic acids derived from Tasmanian tasmantane by extractions and kerogen oxidations. 10 p1211 A73-24108

A technique for extracting Radiolaria from radiolarian cherts. 11 p1324 A73-25141

Laboratory simulation of organic geochemical processes. 11 p1325 A73-25460

Deep sea drilling core sample analysis methods and results relation to sediment age and fossil fauna and flora 11 p1325 A73-25462

Amino acid composition significance in sedimentary fossil skeletal protein calcification, discussing diagenetic temperature effects 11 p1326 A73-25470

Organic inclusions within hydrothermal minerals from S.W. Africa and elsewhere. 11 p1352 A73-25472

Chemical evolution - Recent syntheses of bioorganic molecules. 11 p1319 A73-26477

A search for porphyrin biomarkers in Nonesuch Shale and extraterrestrial samples. 11 p1319 A73-26481

BIOINSTRUMENTATION

NT BIOTELEMETRY

A linear motion generator for physiological research. 01 p0011 A73-10173

Automated calibration of blood pressure signal conditioners. 04 p0411 A73-14846

A hybrid broad-band EEG frequency analyzer for use in long-term experiments. 04 p0411 A73-14847

Application of frequency discrimination technique to the analysis of electroencephalographic signals. 04 p0411 A73-15052

External field electromagnetic measurement of blood flow - An alternative approach to the solution of the baseline problem. 04 p0414 A73-15992

Three channel transistorized pulse generator for electric stimuli used in electrophysiological studies 05 p0545 A73-16739

Redintegrated somatotyping technique for physique measurement and classification based on limb and torso photographic diameter integration with height, using photoelectric cell and electronics 06 p0659 A73-18474

Linearity of the horizontal component of the electro-oculogram. 07 p0784 A73-19125

Modulated light transmission for electrical isolation in a multichannel physiological monitoring system. 07 p0785 A73-19482

A respirometer for the continuous measurement of respiration volume with remote transmission 07 p0785 A73-20035

A method for chronocyclographical motion analysis with the aid of an on-line computer 07 p0785 A73-20036

Method for measuring the contractions of small hearts in organ culture. 08 p0933 A73-21218

A method for electrocardiogram recording in Rhesus monkeys 08 p0934 A73-21324

Heated Fleisch pneumotachometer - A calibration procedure. 08 p0935 A73-21509

An implantable glass electrode used for pH measurement in working skeletal muscle. 08 p0935 A73-21510

Technique for the implantation of long-term diagnostic electrodes in the amygdaloid complex of the human brain 09 p1046 A73-22857

Modification of a ballisto-oscillograph for extremities 09 p1046 A73-22865

Electrical operational and pneumatic /variometer/ differentiation recording of displaced volume derivative from pneumotachograph in spontaneous breathing 09 p1046 A73-22937

The electroretinogram, as analyzed by microelectrode studies. 09 p1047 A73-23318

Electromagnetic 60 Hz interference in ECG recordings, discussing sources, identifying tests, elimination and ECG amplifier design 10 p1183 A73-23648

An IC piezoresistive pressure sensor for biomedical instrumentation. 10 p1183 A73-23649

An electrocardiograph amplifier which satisfies the stringent requirements of long-term monitoring of cardiac activity 10 p1184 A73-23849

Cardiac potential measuring and recording instrument with 240 probes, presenting circuit and block diagrams 10 p1184 A73-24422

Development of neurosurgical instrumentation and procedures for emergency use in null and low-gravity environments - A speculative approach. 11 p1323 A73-25342

Implantable transducer for in vivo measurement of bone strain. 12 p1464 A73-27443

Bragg-diffraction imaging - A potential technique for medical diagnosis and material inspection. 13 p1614 A73-28582

Analysis of various ultrasonic holographic imaging methods for medical diagnosis. 13 p1615 A73-28589

Decatron indicator for a micromanipulator controlled by a stepping motor 14 p1722 A73-30850

Procedure for recording the rate of pressure changes in heart cavities 15 p1837 A73-31167

Technique for measuring the vessel blood pressure in long continued experiments 15 p1838 A73-31394

The application of aerospace technology to patient monitoring. 16 p1975 A73-32804

Book - Biomedical instrumentation and measurements. 17 p2118 A73-35860

Techniques for microinjection of biologically active substances into subcortical structures of the brain 18 p2282 A73-36574

Measurement of cardiac output with and organ trapping of radioactive microspheres. 18 p2282 A73-36661

Hybrid biological power cells for cardiac pacemakers - Materials evaluation. 20 p2520 A73-39823

Evaluation of effects of the microwave oven /915 and 2450 MHz/ and radar /2810 and 3050 MHz/ electromagnetic radiation on noncompetitive cardiac pacemakers. 20 p2520 A73-39824

Thin film temperature sensor with polymer coating for medical research providing good sensitivity and stability for rapid temperature changes in biochemical reactions 22 p2813 A73-42055

An assembly for electrophysiological and thermometric studies 22 p2815 A73-42663

Measuring characteristics of the displacement cardiograph. 22 p2815 A73-42676

A simple cardiac contractility computer. 22 p2815 A73-42677

Influence of nonideal flow conditions in haemodialysers on mass-transfer theories. 22 p2816 A73-42678

Circuit diagram of amplifier-filter for analysis of impulse activity of baroreceptor aortic afferent nerves in rabbits 22 p2816 A73-42681

BIOLOGICAL ACTIVITY

U ACTIVITY [BIOLOGY]

BIOLOGICAL ANALYSIS

U BIOASSAY

BIOLOGICAL CELLS

U CELLS [BIOLOGY]

BIOLOGICAL CLOCKS

U RHYTHM [BIOLOGY]

BIOLOGICAL EFFECTS

NT RELATIVE BIOLOGICAL EFFECTIVENESS [RBE]

Russian monograph on radioactive isotopes effects on organisms covering metabolism, elimination acceleration methods, pathogenesis and treatment of damage, toxicity, biological action, etc 02 p0138 A73-12865

Pathomorphological and histochemical analysis of Luna 16 fine lunar soil fraction biological effect on mice 03 p0272 A73-14569

Russian book on radiation genetics of microorganisms covering lethal and mutagenic action of radiation on fungi, microscopic algae, bacteria and viruses 04 p0410 A73-15701

Effect of lunar soil on radiation injuries in mice. 05 p0538 A73-16090

Solar activity effects on tree growth, farm crop yield, fish availability and human sickness trends, discussing indirect effects via meteorological factors 05 p0622 A73-17171

Effect of a 30-day stay in a medium with increased oxygen content on the discharge of some gaseous bioactivity products in rats 06 p0650 A73-17676

Biological role of atmospheric oxygen in the mechanism of blood coagulation 06 p0650 A73-17678

The null magnetic field as reference for the study of geomagnetic directional effects in animals and man. 06 p0658 A73-18033

Morphological changes in the testicles of dogs exposed to chronic and combined gamma-radiation 08 p0929 A73-20981

Biological effects of lasting hypodynamia on young albino rats in 62 day confinement, considering weight, growth and sexual behavior 08 p0929 A73-20983

A method for studying the action of high-intensity electric fields on microorganisms 10 p1184 A73-24419

Proposed stratigraphic controls on the composition of crude oils reservoir in the Green River formation, Uinta Basin, Utah. 11 p1352 A73-25471

Gravitational effects on biological systems in terms of animal body size, age, sex and posture as factors affecting acceleration tolerance 11 p1315 A73-25573

Biochemical and morphological studies of lunar material effects on plant tissue culture cells, noting nonpathological increased cellular activity and chloroplast and cytoplasm changes 11 p1320 A73-26482

Response of tobacco tissue cultures growing in contact with lunar fines. 11 p1320 A73-26483

Mammalian tissue response to subcutaneous and intraperitoneal injection of aqueous suspensions of lunar fine material, noting insolubility in tissue and irritant action 11 p1320 A73-26484

Plant growth response to low temperature and UV treatment, discussing chlorophyll synthesis, carbohydrate levels, ion balance and enzyme characteristics 11 p1320 A73-26486

Results and prospects of microbiological studies in outer space. 11 p1320 A73-26487

Life processes in ammonia - Anomalous germination behavior of onion seed in ammonia and amines. 11 p1321 A73-26491

Book - An introduction to radiation protection. 12 p1464 A73-27048

The effects of mercury compounds on the growth and orientation of cucumber seedlings. 12 p1462 A73-27274

Mechanism of the action of radiation protecting agents - A biochemical shock hypothesis 12 p1465 A73-27499

Overview of the biological effects of electromagnetic radiation. 13 p1580 A73-29211

Investigation of the influence of biologically active substances on the permeability of the skin 15 p1838 A73-31174

Retinal vessel reactions and intraocular tension in humans staying in a horizontal position for 120 days 15 p1835 A73-31514

Survival of common bacteria in liquid culture under carbon dioxide at high temperatures. 15 p1837 A73-32650

Parachutist biomedical effects during 110-175 knot towing by aircraft, establishing maximum feasible airspeed 16 p1974 A73-32675

Biophysical hazards of microwave radiation. 16 p1974 A73-32723

Biological indicators and the effectiveness of sterilization procedures. 16 p1976 A73-33692

Formaldehyde gas as a sterilant. 16 p1976 A73-33694

Russian book - Primary and initial processes of the biological action of radiation. 18 p2269 A73-35896

Experimental methods of correlation between the trajectories of cosmic heavy ions and biological objects: Dosimetric results - Experiment Biostack on Apollo XVI and XVII. 18 p2270 A73-35946

Ten years of development of the Planetary Quarantine Program of the United States. 18 p2281 A73-35966

Influence of simulated weightlessness on the mutational rate of *Tribolium confusum*.
18 p2270 A73-35984

The charge spectrum of heavy cosmic ray nuclei measured on board of Apollo 16 /Biostack/ using plastic detectors.
18 p2344 A73-35987

Survival and mutability of *Chlorella* under various orientation in the earth's gravitational field.
18 p2270 A73-35997

Effect of dynamic factors of space flights on green alga *Chlorella vulgaris*.
18 p2270 A73-36098

Cytogenetic analysis of diploid and autotetraploid *Crepis capillaris* seeds following space travel on the 'Cosmos-368' artificial earth satellite
18 p2271 A73-36117

Preliminary results of the action of cosmic heavy ions on development of eggs of *Artemia salina*.
18 p2271 A73-36129

Method allowing biological and biochemical studies of vacuum-exposed bacteria.
20 p2513 A73-39483

The effect of immobilization on body fluid volume in the rat.
20 p2513 A73-39487

Protection of mineral oils from microbiological damage by compounds of the quinone group
21 p2723 A73-41069

Changes in the peripheral blood of the rat exposed to microwave radiation /2400 MHz/ in conditions of chronic exposure.
21 p2645 A73-41159

RF fields as new ecological factor in environment pollution, considering radiation interaction with biological systems and increased use of electromagnetic spectrum
22 p2811 A73-41787

Life sciences and space research XI: Proceedings of the Fifteenth Plenary Meeting, Madrid, Spain, May 10-24, 1972.
22 p2803 A73-42158

Free fall effects on differential growth and radiation sensitivity of higher plants in space flight and ground based clinostat experiments
22 p2804 A73-42172

Estimation of the biological danger of the very high energy component of space radiation.
22 p2805 A73-42180

Biological effects due to single accelerated heavy particles and the problems of nervous system exposure in space.
22 p2814 A73-42181

The radiobiological effects of heavy ions on mammalian cells and bacteria.
22 p2805 A73-42182

Apollo 16 Biostack experiment for biological effects of cosmic ray heavy primaries on cell and tissue development and mutations of bacilli, *Artemia* and plant seeds
22 p2805 A73-42185

Compartmental analysis of biological system with a digital computer.
22 p2829 A73-42228

Reactions of living organisms to the action of electromagnetic waves in the millimeter range
23 p2949 A73-44094

Effects of electromagnetic waves of the millimeter range on a cell and on some structural elements of a cell
23 p2949 A73-44095

Prospects for studying mechanisms responsible for the nonthermal effects of millimeter- and submillimeter-band electromagnetic radiation on biologically active compounds
23 p2949 A73-44096

Solar activity cycles effects on physical and biological processes in helioterrestrial domain, discussing crops, tree growth, diseases and fishing
24 p3088 A73-45364

BIOLOGICAL EVOLUTION

NT ABIOTIC GENESIS

Comparative physiological characteristics of functional relations among the hypothalamus and the olfactory and limbic systems of the brain
01 p0006 A73-10151

Evolutionary significance of carbohydrate metabolism alterations in animal brains during adaptation to hypoxia
01 p0007 A73-10153

The evolution of ferredoxins from primitive life to higher organisms.
03 p0265 A73-14318

A note on the hypothesis - Protein polymorphism as a phase of molecular evolution.
04 p0410 A73-16033

Book - Molecular evolution: Prebiological and biological.
06 p0651 A73-17926

The origin of life problem - A brief critique.
06 p0651 A73-17927

Atomic, molecular, cellular, genetic, multicellular, neural, mental, social and suprasocial levels of evolu-

tion, discussing systems constituents, interactions and selective focus
06 p0651 A73-17929

Informational biopolymer structure in early living forms.
06 p0652 A73-17946

Trypsinogen activation peptides - An example of molecular epigenesis.
06 p0652 A73-17947

Modelling of structure and functional unity on coacervate systems.
06 p0652 A73-17950

Coacervate systems and evolution of matter on the earth.
06 p0652 A73-17951

In-depth exploration of the solar system and its utilization for the benefit of Earth.
06 p0751 A73-18029

Stochastic model application to divergence of horse-pig lineage from common ancestor in terms of hemoglobin and fibrinopeptides alpha and beta chains
07 p0780 A73-19218

Ribosomal RNA base composition and molecular evolution in plants and animals of various taxonomic groups
07 p0780 A73-19220

Electrophysiological investigation of suprasegmental motor control systems evolution through Cyclostoma-Primate series, noting preservation of reticulomotor neuron projection characteristics
07 p0781 A73-20001

Chemical volatilization as a technique for the detection of extraterrestrial biopolymers and possible metabolic products.
11 p1319 A73-26479

Criteria for distinguishing biogenic and abiogenic amino acids - Preliminary considerations.
11 p1319 A73-26480

The occurrence of nitrate on the early earth and its role in the evolution of the prokaryotes.
11 p1320 A73-26490

Liquid ammonia life existence in universe, considering halogen and silicon life chemistry
11 p1326 A73-26662

The evolution of lignin - Experiments and observations.
13 p1577 A73-29649

Late Precambrian microfossils - A new stromatolitic biota from Boorthanna, South Australia.
14 p1713 A73-29723

Relationship of theoretical physics to molecular biology, considering synthesis, ontogenesis, phylogenesis, evolution models, thermodynamic applications and Eugen prebiological evolution theory
15 p1835 A73-31823

Self organized biological systems analysis, including deterministic and phenomenological selection theories, molecular level cell instructive properties and self reproducing hypercycles
15 p1835 A73-31825

Extraterrestrial life existence evidence, discussing biochemical properties, evolution and mental and moral characteristics of extraterrestrial life
17 p2113 A73-35657

Gravity, weightlessness and organismic genetic structures.
18 p2269 A73-35923

Biodegradation from evolution viewpoint as physiological function and fundamental cellular process regulating biological equilibrium, explained by intracellular digestion and phagocytic cells association
21 p2638 A73-41024

Life origin hypothesis based on interstellar molecular concentration in gas clouds, examining radical types and molecular Doppler spectra
21 p2638 A73-41080

Book on comparative physiology of thermoregulation covering primitive and aquatic mammals, torpidity aspects, evolution and newborns
22 p2809 A73-42859

Primitive mammals phylogeny relationship to homeothermic abilities, discussing body temperature, thermoregulation, basal metabolism rates, hibernation, nycthemeral rhythms and responses to heat and cold
22 p2809 A73-42860

Thermoregulation evolution in various animals, discussing body size and composition effects, body temperature variations, control mechanisms, heat loss and production, behavior and ontogeny
22 p2810 A73-42863

Directed Panspermia theory of terrestrial bioevolution, suggesting microorganism transmission to earth by intelligent technologically advanced civilization via spacecraft
24 p3058 A73-44553

BIOLOGICAL MODELS

U BIONICS

BIOLOGICAL RHYTHM

U RHYTHM [BIOLOGY]

BIOOLUMINESCENCE

Measurements of the ultraweak bioluminescence phenomena as a new biotelemetric method.
03 p0272 A73-14304

BIOMECHANICS

U BIODYNAMICS

BIOMEDICAL DATA

Automated system of storing and processing vector-cardiograms
01 p0012 A73-10660

Complex processing of discrete biological information
01 p0012 A73-10662

Computation of solutions to the inverse problem of electrocardiography.
01 p0013 A73-11465

Vector summation dial for analysis of time-nonstationary cyclic biological data, applying to peak time change detection and random walks
03 p0263 A73-14120

A programmable four channel system for long-time radio telemetry of biomedical parameters.
03 p0270 A73-14280

Surgically implanted single and multichannel telemetry systems for monitoring single and multiple physiological parameters, discussing size and power requirements
03 p0271 A73-14302

Miniature biotelemeter giving 10 channels of wide-band biomedical data.
04 p0412 A73-15388

The transmission of low frequency medical data using delta modulation techniques.
04 p0412 A73-15408

Emotional stresses during a space flight
07 p0785 A73-19297

USAF WAVR file of epidemiologic data on medically waived flying personnel, describing computerized updating system
09 p1039 A73-22539

The use of sampling quantiles for the compression of telemetric transmission and the statistical handling of medical information.
12 p1465 A73-27646

Automatic methods for smoothing and separation of characteristic points in an electrocardiographic signal
14 p1721 A73-30387

Waveform vector analysis of orthogonal electrocardiograms - Quantification and data reduction.
16 p1975 A73-33115

Pilot workload immediate, duty day and long term period evaluation from heart rate, subjective, psychological, biochemical stress and sleep pattern measurements
19 p2398 A73-37734

BIOMETEOROLOGY

U BIOCLIMATOLOGY

BIOMETRICS

NT ANTHROPOMETRY

NT BALLISTOCARDIOGRAPHY

NT BODY MEASUREMENT [BIOLOGY]

NT CARDIOGRAPHY

NT ELECTROCARDIOGRAPHY

NT ELECTROENCEPHALOGRAPHY

NT ELECTROMYOGRAPHY

NT ELECTROPLETHYSMOGRAPHY

NT ELECTRORETINOGRAPHY

NT PHONOCARDIOGRAPHY

NT PLETHYSMOGRAPHY

A system for continuous measurement of gas exchange and respiratory functions.
01 p0011 A73-10172

Non-invasive technique for diagnosing atrial septal defect and assessing shunt volume using directional Doppler ultrasound - Correlations with phasic flow velocity patterns of the shunt.
01 p0014 A73-11505

Recording and discrimination of pulsed neuron activity responses to stimulus application and removal
03 p0268 A73-13823

A quick and inexpensive method of monitoring on tape the heart rate during exposure of the human head to pulsed magnetic fields.
03 p0270 A73-14289

Methodical studies concerning the polarographic measurement of respiration and 'critical oxygen pressure' in mitochondria and isolated cells with the aid of the membrane-covered platinum electrode
03 p0272 A73-14647

A new method for simultaneous measurement of total respiratory resistance and compliance.
05 p0545 A73-16799

Apparatus note - A system for detecting and recording movements of the head.
06 p0656 A73-17522

Examples for signal-noise improvement with the aid of polarity correlation analysis in the biological sector
06 p0656 A73-17593

Television/computer dimensional analysis interface with special application to left ventricular cineangiograms.
06 p0657 A73-17860

Devices for dynamic recording of volumetric blood flow rates lower than 1 ml per minute
08 p0934 A73-21325

On-line computer analysis and breath-by-breath graphical display of exercise function tests.
08 p0935 A73-21511

A frequency response analysis of fusimotor-driven muscle spindles. 09 p1041 A73-22934

Modification and updating of the bioelectric DS2C amplifier for a FET input. 09 p1046 A73-22936

Neuron analyzer technique for poststimulus histogram plotting of neuron excitation as function of stimulus onset time 10 p1183 A73-23811

Device for analyzing the electrical activity of nerve fibers in intact nerves 10 p1183 A73-23812

Procedures for polarocochleography and for pressure measurement in the inner ear perilymph in acute experiments on animals 11 p1314 A73-25043

Clinical applications of averaging techniques in studies of vestibulo-oculomotor function. I - Basic techniques and illustrative cases. [AD-758545] 11 p1315 A73-25339

A simplified method for the in vitro calibration of electromagnetic flowmeters. 12 p1464 A73-27027

Work-rest cycle effects on airline pilots performance, considering central nervous system changes measurement techniques 15 p1839 A73-32059

Book - Biomedical instrumentation and measurements. 17 p2118 A73-35860

A monkey metabolism pod for space-flight weightlessness studies. 18 p2270 A73-35963

Angiotensinonography using an air plethysmograph 18 p2282 A73-36575

Ejection time by ear densitogram and its derivative - Clinical and physiologic applications. 20 p2511 A73-38866

Computer controlled automatic TV-microscope system for tracking and measuring nerve cell processes in designated axons and dendrites 20 p2518 A73-39763

A system for automatic end-tidal gas sampling at rest and during exercise. 20 p2519 A73-39794

Nonlinear analysis of aortic flow in living dogs. 21 p2638 A73-40640

Design considerations and applications of gradient layer calorimeters for use in biological heat production measurement. 22 p2813 A73-42054

Sentography - Dynamic forms of communication of emotion and qualities. 23 p2949 A73-44180

Oxygen consumption measurements during continual centrifugation of mice. 24 p3065 A73-45071

Intracellular measurements in a closed hyperbaric chamber. 24 p3065 A73-45072

BIONICS

Isovolumic contraction dynamics in man according to two different muscle models. 01 p0007 A73-10158

A continuum analysis of a two-dimensional mechanical model of the lung parenchyma. 01 p0010 A73-10168

Bronchial tree model simulation of pressure-flow-volume relationships during expiration, using gas physics and lung physiology and anatomy data 01 p0011 A73-10169

Functional models adequacy for brain activity simulation, discussing transfer, forward and feedback loops, hierarchy, reciprocity and self organizing aspects 01 p0011 A73-10651

Neuron networks modeling from viewpoint of intracellular and cell-medium interaction, discussing coding properties and nonsingular self adjusting system response 01 p0012 A73-10652

Computerized correlation analysis of single and multiple neuron pulse activity, considering temporal, sequential and entropy characteristics 01 p0012 A73-10653

Certain aspects of the bionic analysis and control of dynamic systems 01 p0012 A73-10658

Mathematical description of certain properties of human sensitivity to vibration 01 p0012 A73-10659

Reduced dimensionality for minimization of degrees of freedom of skeletal activity models for anthropomorphic locomotion system synthesis 01 p0013 A73-11052

Computation of solutions to the inverse problem of electrocardiography. 01 p0013 A73-11465

Mathematical model for spectral distribution function of brain waves, noting analogy with RC oscillator 02 p0135 A73-12557

Perspiration secretion distribution over human body based on extended Kerslake cylinder model, comparing with predicted 4 hr sweat rate 03 p0259 A73-13122

Micropolar model of blood steady flow through rigid circular tubes, presenting equations solutions and velocity profiles 03 p0266 A73-13302

Electrooptical model of the first retina layers of a visual analyzer 03 p0267 A73-13657

Method for quantitative estimation of the functional state of the motor apparatus 03 p0268 A73-13822

Prediction tests for pulmonary elasticity model of expansion stresses in lung region restricted by obstructed airways 03 p0262 A73-14114

Finite element displacement analysis of a lung. 03 p0273 A73-14661

Human body mathematical model described by kinematic and dynamic equations of joined rigid bodies for investigation of self-controlled movements in specified goal attainment 04 p0411 A73-15207

Information theory mathematical models applied to different visual function activity phases, covering Shannon and Fisher probability models, Shreider semantic theory and Kolmogorov algorithm 04 p0412 A73-15784

Mathematical models for distance perception of earth surface features observed from ascending vehicle, considering convergence, accommodation and monocular parallax mechanisms 04 p0413 A73-15785

Mathematical description of some visual inertia effects 04 p0413 A73-15786

Axiomatic mathematical model for human visual edge contrast based on additivity, one-dimensionality and contrast continuity parameters 04 p0413 A73-15788

Visual field image analysis via investigation of receptor-furnished signal analysis by network of neuron-like structures 04 p0413 A73-15789

A model of a memory device based on neuron-like elements which realizes the holographic principles of data recording and readout 04 p0413 A73-15792

Mathematical and physical models of human long and short term memory, considering information processing and memorization at lower visual perception levels 04 p0413 A73-15793

Image recognition learning algorithm for expanding neural nets composed of active inputs, receptors, associative elements and recognizers 04 p0426 A73-15794

An optical model of a detector of oriented segments of the visual analyzer in animals 04 p0413 A73-15795

Angular velocity magnitude conversion into visually perceived apparent velocity, using psychophysical mathematical model based on axisymmetric annular visual field perception 04 p0413 A73-15796

Human memory model with associative linkage between neuronal network information elements 04 p0413 A73-15797

Muscle control models of joint angle spatial motions, including circle, ellipse and straight line trajectories and orientations in space 06 p0680 A73-17960

A robot conditioned reflex system modeled after the cerebellum. 06 p0658 A73-18065

A model of image-shape analysis based on fiber-optics elements and on the principle of photoelectric conversion 06 p0671 A73-18084

Mechanical modeling of eye muscle dynamics. 06 p0660 A73-18816

Structural models of simple sensory motor co-ordination. 06 p0660 A73-18890

Predictions of the dynamic response of the lung. 07 p0785 A73-19477

Search of optimal biological conservation conditions for a heart, using methods of mathematical experiment planning 07 p0781 A73-19648

Ergatic organism defined as multipurpose nonautonomous control system with homeostasis with respect to functional operations conservation 07 p0786 A73-20048

Human operators and automatic adaptive controllers - A comparative study on a particular control task. 07 p0786 A73-20399

Stability behavior of adapting and untrained random logic nets, enabling intelligent interaction with environment 07 p0786 A73-20400

Digital computer studies of respiratory control. 07 p0787 A73-20577

A model to predict respiration from VCG measurements. 07 p0787 A73-20578

Current status of models for the human operator as a controller and decision maker in manned aerospace systems. 07 p0787 A73-20587

Contrast and assimilation effects analysis based on receptive field models of vertebrate retinal function 08 p0929 A73-20812

Blood vessels simulation by muscle pump represented by elastically deformable pipe with valves, solving Navier-Stokes equation for viscous fluid flow 08 p0934 A73-21375

Application of the numerical study of random time series to the analysis of the electroencephalogram of the normal infant 08 p0935 A73-21540

Human retina-patterned ideal perceiving machine to calculate visual acuities for spatial arrangement in line figures 08 p0932 A73-21564

Russian book on mathematical models of biological systems covering biogeocenosis, optimal crop, chemostat cultivation, predator-victim society, trophic control, and life support systems 09 p1044 A73-22347

Theoretical trans-respiratory pressure during rapid decompression. I Model experiment. II - Animal experiments. 09 p1045 A73-22530

Assessment of temperature rise suppression by edge losses during irradiation. 09 p1045 A73-22533

Clinical evidence of cardiac weakness and incoordination secured by simultaneous records of the force BCG and carotid pulse derivative and interpreted by an electrical analogue. 09 p1046 A73-23174

Light evoked changes in potential difference between inside and outside of cells in Limulus ommatidia, describing multistage model of generator potential 09 p1043 A73-23309

Functional model of the frequency channel of the peripheral auditory analyzer 10 p1183 A73-23808

Possibility of modeling the relationship between the intracellular potential of individual muscle fibers and the overall electromyogram for tonic muscles 10 p1179 A73-23810

Water-salt homeostasis mathematical model, solving equations with analog and digital computers 10 p1184 A73-23941

Formalization of an arterial pressure stabilization system 10 p1181 A73-24467

Impact on a simple physical model of the head. 10 p1185 A73-24770

The nature of the optimum muscular performance achieved in the execution of fast eye rotations. 10 p1185 A73-24772

Brain tissue functional organization based on models for cell pseudorandom behavior, information processing, learning and memory, considering spontaneous wave and unit firing 11 p1314 A73-25143

Analysis of swimming motions. 11 p1322 A73-25184

Useful future action models of instrumental reflexes and voluntary actions based on memory role in engraving storage of received stimuli 11 p1314 A73-25199

Calcium movements and excitation-contraction coupling in cardiac cells. 11 p1316 A73-25601

Probability summation model for heterochromatic luminance additivity failure at absolute visual threshold. 13 p1578 A73-28099

Acoustic model and linguistic, syntactic, lexical and semantic factors in speech perception and production process 14 p1721 A73-30277

Periodic conditions in artificial-muscle autotransistors 14 p1721 A73-30289

Photoelectric servo simulator for pupil, using Wheatstone bridge with CdS light dependent resistor 14 p1722 A73-30399

Heart rate variability and work-load measurement. 14 p1720 A73-30879

Simulation of a steady-state integrated human thermal system. 15 p1839 A73-32225

A standard psychophysiological preparation for the study of environmental stress. 16 p1975 A73-33130

Dynamic analyses of hybrid bio/mechanical networks with feedback characterization. 16 p1975 A73-33161

Adequate vestibular stimulants on earth and in space 17 p2110 A73-34122

Analysis of vestibular effects in experiments on swings

17 p2111 A73-34235

Human visual system model based on neurological connectivity data from anatomical dissection, in vivo physiological measurements and psychological experimentation

17 p2116 A73-35239

Pattern recognition techniques suggested from psychological correlates of a model of the human visual system.

17 p2116 A73-35241

Applications of a model of the human visual system to pattern recognition problems.

17 p2116 A73-35242

Modeling, instrumentation and data evaluation in clinical electroretinography, discussing Fourier analysis of sinusoidal light stimulation response in normal and abnormal humans

17 p2117 A73-35359

A distributed parameter model of the inertially loaded human spine.

18 p2281 A73-36429

Endolymph fluid mechanics in semicircular canals approximated by rigid torus filled with incompressible Newtonian fluid

18 p2281 A73-36430

A non-Newtonian model for fluid flow in the semicircular canals.

18 p2281 A73-36431

Limitations of the dipole concept in electrocardiographic interpretation.

18 p2281 A73-36517

Power failure of the heart in acute myocardial infarction.

18 p2276 A73-36547

The role of the elastic properties of brain and spine cavities in hyperemia compensation

18 p2276 A73-36572

The control of a manipulator by a computer model of the cerebellum.

19 p2398 A73-37333

Three models of the vibrating ulna.

19 p2398 A73-37543

Investigation of the distribution of synaptic inputs on an analog model of the motoneurons

19 p2399 A73-37942

Some aspects of the inverted pendulum problem for modelling of locomotion systems.

19 p2460 A73-38035

Modeling the human in a time-varying anti-aircraft tracking loop.

19 p2401 A73-38071

A diagnostic program - Problems of predicting myocardial infarction on a digital computer

20 p2516 A73-38998

Probabilistic statistical methods for analysis of impulse flows in nerves

20 p2516 A73-39002

A mathematical model of the peripheral pain signalization mechanism

20 p2516 A73-39003

An electrical model of the inertial and adaptive properties of vision as a self-regulating system with delayed feedback

20 p2517 A73-39004

Mathematical analysis of the operation of regulatory mechanisms of the spinal cord

20 p2517 A73-39005

A Lie algebra of visual piloting

20 p2590 A73-39038

Management of the treatment of illnesses as a problem of modern control theory

20 p2518 A73-39348

Continual mechanochemical model of muscular tissue

21 p2643 A73-40182

Automatic identification of cardiac rhythm and conductivity disturbances with the aid of digital computers

21 p2643 A73-40751

Response delays and the timing of discrete motor responses.

21 p2645 A73-41177

Correlative function formalism for neuron networks with limited communication channels and active-refractive-storing signal action

21 p2645 A73-41277

A model of diffusion in the respiratory unit.

21 p2645 A73-41638

Rebreathing and steady state pulmonary diffusing capacity for O₂ in the dog and in inhomogeneous lung models.

21 p2645 A73-41639

Mathematical model of human pitch perception based on acoustic stimulus Fourier transformation by sense organ into peripheral neural activity pattern recognition

22 p2811 A73-41816

Investigation of the nature of biological rhythm sensors by means of automatic networks

22 p2812 A73-41865

Examination of a multiple dipole inverse cardiac generator, based on accurately determined model data.

22 p2813 A73-41961

A comparison of predicted skin temperatures with thermographic measurements.

22 p2813 A73-42053

A model to predict the mechanical impedance of the sitting primate during sinusoidal vibration.

[ASME PAPER 73-DET-78] 22 p2813 A73-42073

A model of the human in a cognitive prediction task.

22 p2814 A73-42223

Compartmental analysis of biological system with a digital computer.

22 p2829 A73-42228

An analogue-computer simulation of the facultative water-reabsorption process in the human kidney - A vascular role for a.d.h.

22 p2815 A73-42668

Simple simulated human head for checking echoencephalographic equipment.

22 p2815 A73-42672

On the electronic simulation of acceleratory nystagmus.

22 p2816 A73-42683

Study of the nature of the active tonus with the aid of a discrete Wiener-medium analog

22 p2816 A73-42973

Flow patterns and velocity and shear stress distribution downstream of steady and pulsatile flow models for fluid dynamics of blood vessel branches

22 p2816 A73-43103

Mathematical model of collateral blood vessels caliber changes due to hydrodynamic drag /shear stress/ effects on vascular endothelium

22 p2817 A73-43105

A model of heat transfer in a biological tissue perfused by blood of arbitrary temperature.

23 p2948 A73-43292

Bee image detection by ommatidium based on physical model using electromagnetic analysis of light absorption in photoreceptor

23 p2946 A73-43344

Electrical field distribution in the human body.

23 p2950 A73-44216

A method for the approximation of processes in homogeneous biological structures

24 p3062 A73-44663

Electronic simulation and analog computer studies of the influence of temperature on the process of nerve impulse shaping

24 p3062 A73-44725

Physical model selection for the balance preservation system in man

24 p3063 A73-44903

Probability estimate models for reliable function of redundant systems with adaptable and inadaptably neuron-like restoration organs

24 p3063 A73-44904

Algebraic nature of thought formation structures

24 p3063 A73-44905

Dynamics of the balance preservation system of man

24 p3064 A73-44909

Determination of performance precision and informativeness of electronic models of the sensory system of man

24 p3064 A73-44911

Optical electronic model of local detectors of the visual analyser

24 p3064 A73-44912

Fundamental frequency analysis of pulmonary mechanical resistance and compliance.

24 p3060 A73-45067

BIOPHYSICS

NT HEALTH PHYSICS

On the decomposition of a dynamical system into non-interacting subsystems.

05 p0591 A73-16824

Biophysical properties of vibration energy transfer to human body structure, noting harmful effects dependence on frequency range

06 p0657 A73-17748

Theory of cooperative defect formation in a biopolymer molecule under the action of radiation

11 p1323 A73-25637

The visual system: Neurophysiology, biophysics, and their clinical applications; Proceedings of the Ninth Symposium, Brighton, England, July 1971.

13 p1574 A73-28351

Relationship of theoretical physics to molecular biology, considering synthesis, ontogenesis, phylogenesis, evolution models, thermodynamic applications and Eugen prebiological evolution theory

15 p1835 A73-31823

Biological order, structure and instabilities in terms of irreversible thermodynamic processes, entropy, dissipative structures, randomness, abiogenesis, hierarchic organization, chemical reactions and molecular biology

15 p1835 A73-31824

Biophysical considerations concerning gravity receptors and effectors including experimental studies on *Phycomyces blakesleeana*.

22 p2804 A73-42171

BIOREGENERATION

U REGENERATION (PHYSIOLOGY) BIOREGENERATIVE LIFE SUPPORT SYSTEMS U CLOSED ECOLOGICAL SYSTEMS

BIOSENSORS

U BIOINSTRUMENTATION

BIOSIMULATION

U BIONICS

BIOSPHERE

U EARTH HYDROSPHERE

U LOWER ATMOSPHERE

BIOSYNTHESIS

Brain serotonin content - Physiological regulation by plasma neutral amino acids.

01 p0008 A73-10408

Triparanol inhibition of sterol biosynthesis in *Chlorella emersonii*.

02 p0139 A73-12547

Hydroxyindole-O-methyl transferases in rat pineal, retina and Harderian gland.

02 p0136 A73-12644

Hepatic lipogenesis in fasted, re-fed rats and mice - Response to dietary fats of differing fatty acid composition.

03 p0258 A73-13054

Effect of cultural conditions on the fatty acid composition of *Thiobacillus novellus*.

03 p0261 A73-13599

Carbon-13 nuclear magnetic resonance in biosynthetic studies of lipids.

03 p0274 A73-14550

Conditioned reflex learning and phenamine-stimulated functional activation of cerebral synaptic, protein synthesizing and energy generating apparatus

05 p0541 A73-17177

Abiogenic formation of porphyrin, chlorin and bacteriochlorin.

06 p0651 A73-17934

A mechanism for polypeptide synthesis on a protein template.

06 p0652 A73-17943

Dependence of poly U-directed cell-free system on ratios of divalent and monovalent cations.

06 p0652 A73-17945

Genetic code evolution in terms of abiotic polynucleotide synthesis, suggesting alternating sequences of purines and pyrimidines as polypeptide codes

09 p1044 A73-23469

Criteria for distinguishing biogenic and abiogenic amino acids - Preliminary considerations.

11 p1319 A73-26480

An experimental basis for carcinogenic effects of ultraviolet radiation.

11 p1320 A73-26485

Autoradiographic study of protein synthesis in perikaryons and of nitrogen migration into the axons of hypertrophic sympathetic neurons

13 p1574 A73-28296

The evolution of lignin - Experiments and observations.

13 p1577 A73-29649

Effect of iron and salt on prodigiosin synthesis in *Serratia marcescens*.

17 p2112 A73-34399

Protein synthesis in lung - Recovery from exposure to hypoxia.

18 p2277 A73-36653

Control of pineal indole biosynthesis by changes in sympathetic tone caused by factors other than environmental lighting.

19 p2393 A73-37300

Protein synthesis in the neurons and glial cells of the stellate ganglia of rats during the adaptation to the effects of high altitude hypoxia

19 p2393 A73-37396

Prebiotic reactions combining amino acids and ribonucleotides into polypeptides and polynucleotides in presence of urea, imidazole and Mg positive ion, suggesting contemporary biosynthesis parallels

21 p2637 A73-40372

Effect of convulsions on certain aspects of the biosynthesis of proteins in the brain cortex

21 p2638 A73-40750

Biosynthesis of RNA in the brain cortex during various functional states

21 p2640 A73-41262

Influence of preliminary adaptation to the main environmental factors on the ATP level and phosphorylation potential in the myocardium during severe heart strain

21 p2640 A73-41278

Ribonucleic acid (RNA) polymerase and adenyl cyclase in cardiac hypertrophy and cardiomyopathy.

22 p2808 A73-42687

Sterols of the fungi - Distribution and biosynthesis.

24 p3059 A73-44699

BIOT METHOD

Critical analysis of the method of M. A. Biot for determining natural torsional frequencies

22 p2867 A73-43047

BIOTECHNOLOGY

Search of optimal biological conservation conditions for a heart, using methods of mathematical experiment planning

07 p0781 A73-19648

Two dimensional eye movement recording using a photo-electric matrix method. 07 p0786 A73-20259

Automatic surface inoculation of agar trays. 09 p1045 A73-22550

Organism-machine interactions in hybrid control systems for cardiac stimulation, artificial breathing apparatus and intelligence assignments 09 p1047 A73-23298

Proportional counter energy deposition spectral quality prediction from experimental data, using folding procedure to produce composite energy absorption distributions for biological materials 15 p1839 A73-31549

Applications of liquid crystals to information display, fault detection, and medical thermography. 22 p2897 A73-42524

BIOTELEMETRY

Fatigue in flight personnel during long flights 02 p0137 A73-12153

Biotelemetry; Proceedings of the International Symposium, Nijmegen, Netherlands, May 5-8, 1971. 03 p0269 A73-14276

A three channel telemetry system, compatible with the British medical and biological telemetry regulations. 03 p0269 A73-14277

A time-division multiplexed telemetry system using delta-modulation. 03 p0270 A73-14279

A programmable four channel system for long-time radio telemetry of biomedical parameters. 03 p0270 A73-14280

Pulse duration-frequency modulation multichannel biotelemetry system for physiological parameter assessment during exercise, noting circuit diagrams of radio transmitter and receiver 03 p0270 A73-14281

Telemetric measurement of local blood flow by heat conduction probes. 03 p0270 A73-14282

Development and adjustment of a multi-channel miniaturized FM/AM telemetering system adapted to the primates. 03 p0270 A73-14284

Respiratory air flow telemetry during exercise, discussing flowmeter working conditions and equipment testing 03 p0270 A73-14286

Telemetry of venous blood pressure at rest and at muscle activity during running. 03 p0271 A73-14290

Radiotelemetry of direct bloodpressure measurements in aorta, pulmonary artery and heart. 03 p0271 A73-14291

Electro-rheocardiotelemetric device for complex monitoring of the dynamics and efficiency of cardiac contraction. 03 p0271 A73-14292

Voltage controlled subcarrier oscillator design and performance for FM/FM multiplex telemetry system for ECG recording during exercise 03 p0271 A73-14293

Telemetrical measurements during sport performance on sportsmen with cardiac arrhythmias. 03 p0271 A73-14294

Hazard and interference avoidance in implant telemetry, discussing leakage currents, muscle interference, magnetic influence, high frequency noise, electrode and respiratory artifacts, etc 03 p0271 A73-14295

Telemetry methods for maximum static muscle strength measurements, considering dynamic force measurement possibilities 03 p0271 A73-14296

EMG from smooth musculature /uterus, ureter, gut/ in unrestrained animals monitored by telemetry. 03 p0271 A73-14297

Three channel FM telemetry system for long term EEG monitoring, discussing routine clinical operation results 03 p0271 A73-14298

Telemetered EEG and neuronal spike activity in olfactory bulb and amygdala in free moving rabbits. 03 p0271 A73-14299

The use of telemetry to study the physiological and clinical variations of intracranial pressure in man. 03 p0271 A73-14300

An implantable radiotelemetrical measuring device for simultaneous long term measurements of body temperature and turnover of rabbit serum albumin/I-125 in unrestrained rabbits. 03 p0271 A73-14301

Surgically implanted single and multichannel telemetry systems for monitoring single and multiple physiological parameters, discussing size and power requirements 03 p0271 A73-14302

A remotely operated ECG telemeter for chronic implantation in rats. 03 p0272 A73-14303

Measurements of the ultraweak bioluminescence phenomena as a new biotelemetric method. 03 p0272 A73-14304

Multichannel telemetry of physiological parameters /body temperature ecg, eeg/ in the rat. I - Design and methods. 03 p0272 A73-14305

Multichannel telemetry of physiological parameters /body temperature, EKG, EEG/ in the rat. II - Applications in neuropharmacology. 03 p0272 A73-14306

Multidimensional coding for telemetric transmission of work load factors in ergonomics research. 03 p0272 A73-14307

Telemetric transmission of ergonomic and time study data to describe work load of radar controllers. 03 p0272 A73-14308

Telemetry of cardiovascular parameters on fighter aircraft flying pilots. 03 p0272 A73-14309

An implantable blood pressure and flow transmitter. 04 p0447 A73-14845

Miniature biotelemeter giving 10 channels of wide-band biomedical data. 04 p0412 A73-15388

The transmission of low frequency medical data using delta modulation techniques. 04 p0412 A73-15408

Use of an on-line computer in a study of cardiac arrhythmia. 04 p0412 A73-15644

Computer-aided ECG analysis and research in a clinical setting. 04 p0412 A73-15648

The potential application of space technology to the radio tracking and biotelemetry of unrestrained animals. 05 p0545 A73-17134

The design of electronic equipment for biotelemetry using microcircuit techniques. 06 p0673 A73-17674

Miniature four-channel radiotelemetric system for the transmission of cerebral biopotentials 06 p0658 A73-18167

A respirometer for the continuous measurement of respiration volume with remote transmission 07 p0785 A73-20035

Miniature single channel narrow-band differential pulse width modulation-FM crystal controlled transmitter for biomedical telemetry system 09 p1047 A73-23381

The use of sampling quantiles for the compression of telemetric transmission and the statistical handling of medical information. 12 p1465 A73-27646

Circuit technology of a temperature-measurement transmitter for biotelemetric applications 13 p1579 A73-28575

The application of aerospace technology to patient monitoring. 16 p1975 A73-32804

Space science terrestrial applications in biomedical data exchange and telediagnosis, propellant technology, life support atmospheres without fire hazard, industrial mixers and nozzle materials [AAS PAPER 73-133] 20 p2629 A73-38589

Ultradian rhythms in human telemetered gross motor activity. 20 p2512 A73-39102

Statistical treatment of evoked cerebral potentials during experiments on a Dnepr-1 computer 22 p2814 A73-42657

Ultrasonic transducer instrument with broad beam dispersal for blood vessel displacement recording in chronic animal experimentation 22 p2817 A73-43109

Transient S-T elevation detected by 24-hour ECG monitoring during normal daily activity. 23 p2946 A73-43492

Oxygen consumption measurements during continual centrifugation of mice. 24 p3065 A73-45071

BIOTIN

Observations concerning the combined radiation-protective effect of pantothenic acid and aminoethyliothiuronium 02 p0136 A73-11586

BIPLANES

Contribution to the theory of biplane wing sections. 17 p2091 A73-34325

BIPOLAR TRANSISTORS

Microwave small signal bipolar transistor evolution, design and applications, noting cost effectiveness and surface geometry control 09 p1064 A73-22499

Ion-implanted bipolar transistor carrier concentration profiles. 10 p1194 A73-24155

Microwave characteristics of ion-implanted bipolar transistors. 10 p1194 A73-24156

Effect of compressive stress on silicon bipolar devices. 11 p1410 A73-26422

Book - Introduction to semiconductor devices: Diodes, bipolar transistors, JFETs, IGFETs, SCRs and integrated circuits. 12 p1478 A73-27050

BIREFRINGENCE

A bipolar transistor model for high frequencies 13 p1589 A73-28124

The insulated-gate field-effect transistor - A bipolar transistor in disguise. 15 p1850 A73-31372

Book - The physics and circuit properties of transistors. 15 p1850 A73-31574

Integrated semiconductor storage devices, discussing bipolar transistor, Schottky diode and MOS memories and RAM, ROM and PROM types with circuit compatibility considerations 16 p1991 A73-33960

Transistor design and thermal stability. 17 p2133 A73-34218

A distributed amplifier using bipolar transistors in a common-base circuit 19 p2409 A73-37719

Computer-aided two-dimensional analysis of bipolar transistors. 20 p2536 A73-39410

Bipolar transistor base region noise current correlation with effective voltage, proposing equivalent circuit 20 p2538 A73-39597

Present state and future prospects of the design of large-scale integrated circuits using MIS transistors 21 p2660 A73-40018

Reduction of power requirements in dynamic elements based on bipolar transistor 21 p2660 A73-40022

Noise characteristics in bipolar transistor differential amplifiers, discussing current sources, circuit configurations, feedback amplifiers and equivalent circuits 22 p2832 A73-41897

New device techniques for microwave bipolar power transistors. 22 p2833 A73-42692

Bipolar transistor emitter efficiency calculation, considering heavy doping induced impurity profiles effects on current gain 23 p2958 A73-43451

Fall-off of base component of fT/ at low currents in a bipolar transistor. 23 p2961 A73-44148

Four-quadrant analog multiplier synthesis for IC implementation based on logarithmic addition in all n-p-n bipolar transistor configuration for algebraic product derivation 24 p3074 A73-45260

BIPROPELLANTS

U LIQUID ROCKET PROPELLANTS

BIRDS

NRN HOMOTHERMS

Birds and aircraft aerodynamics, considering thermal and wind induced updrafts, lift-drag ratio, fuel consumption and maneuverability 06 p0648 A73-18148

Radar angels cross section statistical distribution model based on radar measurement and direct ornithological data on bird populations density 11 p1332 A73-26630

BIREFRINGENCE

Solar flares recognition from H-alpha centered birefringent filtered photographs, determining statistical pattern of filament movements 04 p0491 A73-14842

Differential interference contrast microscope with continuously variable wavefront shear and pupil compensation. 05 p0573 A73-16150

Methods of birefringence-parameter determination in tension studies by photoelasticity techniques 05 p0635 A73-17077

Optical constitutive equation derivation for Tresca type plastic dielectrics, calculating birefringence and extinction angle in simple shear 06 p0723 A73-18458

Dioptric powers of transparent plates in a plane state of tension 06 p0765 A73-18697

Linear and nonlinear dielectric properties of tetrahedral structure crystals. III - Theory of dielectric properties of tetrahedral structure compounds 08 p0990 A73-20965

Optical birefringent multichannel splitting and combining wideband FDM communications filters, considering crosstalk, pulse response, extinction ratio and detuning 08 p0939 A73-21046

New techniques of acoustic image detection. 11 p1360 A73-25073

Tresca-type plastic materials in the theory of hypoelasticity. II Optical constitutive equations and birefringence in simple shear. 11 p1447 A73-26649

Experimental studies on the scattering pattern from a ruby laser rod. 16 p2023 A73-32875

Polycarbonate as a model material for three-dimensional photoplasticity. 17 p2247 A73-35029

Kerr response of nematic liquids. 18 p2340 A73-36620

- Isochromatic and isoclinic parameters for fiber reinforced birefringent composite materials, discussing mechanical and optical characterization
19 p2495 A73-37195
- Thermal lensing of laser beams in optically transmitting materials. I.
19 p2438 A73-38023
- Incident-light double-refracting interference microscope with variable wavefront shear.
21 p2703 A73-41134
- Lyot birefringent filter contrast element thickness effects on SNR performance and transmission loss.
21 p2706 A73-41505
- Propagation velocity of picosecond pulse from mode locked Nd-glass laser investigated by optically induced birefringence, self phase modulation and self focused light
23 p2988 A73-44120

BIREFRINGENT COATINGS

- A dynamic polariscope for stress wave analysis.
08 p0962 A73-20668
- BISMUTH**
Improved responsivity and sensitivity characteristics of the thin-film bismuth bolometer.
09 p1080 A73-22087
- Effect of addition of Bi on stress-corrosion cracking of Al-Mg alloy.
09 p1102 A73-22421

- Electrical and structural properties of low-temperature bismuth films
09 p1133 A73-22603
- Incident radio wave resonance effect on stationary electric and magnetic fields and standing magnetoplasma wave excitation in Bi plates
09 p1127 A73-22604
- Bi implant CdS studies, discussing sputtering, surface concentration, p-type behavior and light emission characteristics
21 p2752 A73-40951

BISMUTH ALLOYS

- Nature of anisotropy in half-cells made of cold-pressed Bi-Te-Se-Sb alloys
06 p0738 A73-18653
- Effect of oxygen on the structure and properties of Bi₂Te₃-based alloys
15 p1923 A73-31209
- Propagation of microwaves in a solid-state plasma
21 p2753 A73-41292

BISMUTH COMPOUNDS

- NT BISMUTH OXIDES**
NT BISMUTH TELLURIDES
Galvanomagnetic effects measured in p-type bismuth selenide single crystal within magnetic field for Hall and conductivity mobilities, determining temperature dependences
06 p0733 A73-17741

- Bismuth germanate and silicate single crystals refractive index and electro-optic coefficient measurement
06 p0737 A73-18367
- Electro-optic contrast observations in single-domain epitaxial films of bismuth titanate.
06 p0739 A73-18748
- Surface effects on trapping and recombination processes in Bi₁₃ single crystals
12 p1531 A73-27938
- Bi₂Se₃ Hall effect magnetometer for reliable low temperature use.
13 p1612 A73-28368

- High temperature electron transfer and Bi and Sb ion valency pair predictions in ordered perovskite-type oxides, using lattice constants
23 p3017 A73-44129

BISMUTH OXIDES

- Phase transformations in the bismuth ferrites BiFeO₃ and Bi₂Fe₄O₉
12 p1531 A73-27199
- Spatial resolution of an incoherent-to-coherent converter using bismuth germanium oxide.
22 p2863 A73-43098

BISMUTH TELLURIDES

- Electrophysical properties of BiTe thin films
10 p1259 A73-24154
- Fabrication procedures, structure, and mechanical properties of BiTe thin films
10 p1260 A73-24470
- Thermoelectric nuclear batteries fabrication in milliwatt power range combining bismuth telluride thermopiles with plutonia fuel capsules
19 p2455 A73-38410
- Compressive strength and plastic deformation of monocrystal bismuth telluride, polycrystal lead telluride, Cu-Te compounds and Pb-Sn-Te solid solution
23 p3015 A73-43480

BISTABLE AMPLIFIERS

- U FLIP-FLOPS**
BISTABLE CIRCUITS
Low-dissipation memories by p-channel MOS technology with special processes and by complementary-channel MOS technology
08 p0945 A73-21073

BISTATIC REFLECTIVITY

- Bistatic-radar detection of high-altitude clear-air atmospheric targets.
02 p0142 A73-12526

- Dual frequency bistatic radar lunar investigations from Apollo 14 and 15 echo spectra
20 p2612 A73-39714

BIT SYNCHRONIZATION

- Partially coherent detection of binary FSK system with adaptive receiver, determining optimum and sub-optimum estimators of channel parameters for phase and bit synchronization
03 p0277 A73-13909
- Source encoding with fixed ward length and synchronous bit rate.
04 p0425 A73-15420

- Analysis of a dual mode digital synchronization system employing digital rate-locked loops.
05 p0549 A73-16369

- Data link control procedures for error-free transmission channels, discussing serialization and synchronization techniques and reverse interrupt facilities in sequential machine model
05 p0551 A73-16802

- An adaptive bit synchronization algorithm under time-varying environment.
06 p0672 A73-18810

- Common-bandwidth transmission of data signals and wide-band pseudonoise synchronization waveforms.
07 p0790 A73-19200

- German monograph - Synchronization of digital telephone networks by means of phase averaging with parameter transfer.
07 p0794 A73-20386

- A new analysis of the digital data transition tracking loop.
09 p1062 A73-22302

- Phase locked bit synchronization design tradeoffs between acquisition and noise performance, considering frequency tolerance of decision-directed loop with nonreturn-to-zero input
09 p1056 A73-23403

- Clock synchronization experiments performed via the ATS-1 and ATS-3 satellites.
10 p1217 A73-23996

- Study of carrier and bit-timing recovery of ultrahigh speed PSK-TDMA systems
13 p1584 A73-28909

- Bit synchronized discrete address radar beacon system with ground based U.S. civil interrogator complex for compatibility with ATC and aircraft operator services
14 p1772 A73-29882

- Navigation system time dissemination and synchronization, considering timing offset estimation for like events at geographically separated locations and clock characteristics for airborne application
14 p1726 A73-29896

- Noise immunity of the optimal noncoherent reception of an FM signal in the presence of fluctuations in the synchronization channel
14 p1729 A73-30558

- An adaptive estimation algorithm for time-varying bit synchronizers.
16 p1988 A73-33411

- Digital synchronization of synchronous collision prevention systems in aviation
17 p2207 A73-34480

- VLF navigation development at NAE.
17 p2209 A73-34849

- Prototype TDMA system design for Intelsat 4 satellite, discussing separate synchronization and data bursts transmission feature for service quality and reliability improvement
17 p2122 A73-34967

- High speed bit synchronizer for mode-locked laser communications.
17 p2138 A73-35220

- Maximum likelihood synchronizer for binary overlapping PCM/NRZ signals.
17 p2127 A73-35641

- A digital optimization device for directional charged particle measurements in space research.
19 p2428 A73-37148

- Binary error estimation in real time for channel quality monitoring, comparing upper and lower bounds with number of errors for bit sequence
21 p2656 A73-41170

- Noise immunity of quasi-optimal noncoherent reception during resynchronization with respect to time and frequency
24 p3067 A73-44590

- Choice of the duration of an elementary signal in the presence of fluctuations in the synchronization channel
24 p3067 A73-44605

BITERNARY CODE

- Probabilistic properties and spectral characteristics of the duobinary code in the baseband
14 p1729 A73-30897

BITUMENS

- 17alpha/H/ hopane identified in oil shale of the Green River formation/Eocene/ by carbon-13 NMR.
14 p1746 A73-29734

BIVARIATE ANALYSIS

- The use of bivariate distributions in achieving anthropometric compatibility in equipment design. I, II.
05 p0543 A73-16702

- A probabilistic evaluation of helicopter lift capability.
10 p1175 A73-23775

- A statistical investigation of the properties of quasars.
10 p1280 A73-24401

BLACK AND WHITE PHOTOGRAPHY

- Schwarzschild effect elimination in stellar color photography via triple black and white photography with film of differing color sensitivities
05 p0578 A73-17096

- Run length code for redundancy encoding of black-white facsimile picture data transmission to allow channel or storage capacity reduction and hardware simplification
10 p1188 A73-23741

- The application of color and multispectral techniques to the collection of military geographic information.
12 p1500 A73-27952

- Optimizing sensitometric data for color and black and white aerial film.
12 p1501 A73-27966

- Remote sensing and photointerpretation, discussing black and white, color and IR photography, microwave imagery, atmospheric attenuation, reflectance and potential application for ERTS satellites
16 p2014 A73-33100

BLACK ARROW LAUNCH VEHICLE

U BLACK KNIGHT ROCKET VEHICLE

BLACK BODY RADIATION

- An approximation to radiative transfer in a nongray gas.
01 p0121 A73-10733

- Closed time as an explanation of the black body background radiation.
02 p0193 A73-12440

- Properties of photons determined by interferometric spectroscopy.
04 p0475 A73-15046

- Apparatus for measuring spectral emissivity of metals.
08 p0962 A73-20868

- Friedman expanding universe model based on Gamow theory of weakly interacting black body radiation-filled space at 3 K temperature
08 p1010 A73-21230

- Energy release mechanism during early universe expansion leading to distortion of relic black body spectrum, noting Comptonization effects
08 p1013 A73-21693

- Electron beam refined niobium melting temperature determination from black body brightness change
10 p1230 A73-23508

- New limit on small-scale irregularities of 'blackbody' radiation.
10 p1272 A73-23543

- Problems and design of black-body references.
11 p1401 A73-26514

- Models for compact pulsing X-ray sources.
16 p2050 A73-32738

- Spectral intensity of thermal radiation in a medium for frequencies in the neighbourhood of an absorption line.
16 p2038 A73-34028

- Passive microwave radiometry and its potential applications to earth resources surveys.
17 p2162 A73-34958

- Electron beam refined niobium melting temperature determination from black body brightness change
17 p2191 A73-35188

- VUV radiometry with hydrogen arcs. I - Principle of the method and comparisons with blackbody calibrations from 1650 A to 3600 A.
17 p2212 A73-35425

- A comparison between Compton-synchrotron and Compton black-body emission in radio sources.
17 p2237 A73-35785

- Book - Physics of stellar interiors.
18 p2356 A73-36965

- Basic method for realization of temperature scale at 10,000 K by photometric comparison between vacuum-UV-blackbody radiation of a plasma and synchrotron radiation.
22 p2852 A73-41978

- Calorimetric measurement of thermodynamic temperatures above 0 C using total blackbody radiation.
22 p2853 A73-41980

- The emittance of blackbody cavities.
22 p2930 A73-41981

BLACK HOLES [ASTRONOMY]

- Autocorrelation function of the 'rapid' brightness variations of the 3C 273 quasar
01 p0101 A73-10932

- Newtonian analysis of cosmological model for galactic accretion from small initial perturbation of central black hole
01 p0104 A73-11048

- Equations of motion for steady state spherically symmetric flow of polytropic gases into or out of neutron stars, black holes or Schwarzschild singularities
02 p0223 A73-12729

Gaseous star as first limit to nebular matter gravitational collapse, considering equilibrium, neutron stars, black holes, forbidden lines and ionized hydrogen clouds
03 p0365 A73-12913

Astronomical applications of general relativity, considering energy and matter outbursts, black holes and Kerr and Schwarzschild metrics
03 p0374 A73-13895

The universe as a black hole.
04 p0501 A73-15624

Secondary component minimum deepening in UV light curve of Beta Lyr eclipsing binary star, suggesting black hole model
04 p0501 A73-15637

Maxwell equations in a spherically symmetric black-hole background and radiation by a radially moving charge.
05 p0597 A73-16470

Rotating black holes - Locally nonrotating frames, energy extraction, and scalar synchrotron radiation.
05 p0625 A73-17331

Mass formula for Kerr black holes.
06 p0747 A73-17521

Spinning test bodies motion in metric fields, applying to spinning stars in orbit around black holes
06 p0749 A73-17869

Newtonian and relativistic gravitational theories, discussing gravitational waves generating mechanism and black holes formation
06 p0753 A73-18274

Limits on gravitational radiation from two gravitationally bound black holes.
07 p0876 A73-19346

Black hole polar flattening and equatorial circumference lengthening as function of angular momentum, considering effects of highly curved space-time
07 p0899 A73-20176

Black hole creation via partial gravitational collapse of matter ejected by explosion within asymptotically Friedmannian space-time
07 p0900 A73-20182

Spectroscopic observations of the optical candidate for Cygnus X-1.
08 p1004 A73-20896

A model for peaking of galactic gravitational radiation.
08 p1009 A73-21201

Mass differentiation of X ray sources based on Roche model, identifying pulsating sources with neutron stars and black holes as nonpulsating sources
08 p1013 A73-21810

Emission spectrum of a source moving along a stable circular orbit near a rotating 'black hole'
09 p1145 A73-22295

Autocorrelation function for the 'rapid' light variations of the quasar 3C 273.
09 p1147 A73-22272

Luminosity and frequency spectrum of radiation from spherically symmetric steady state accretion of interstellar gas onto nonrotating black hole at rest
10 p1272 A73-23534

Quasi-periodic variations in X ray emission from black holes for accretion-formed disk with surface bright spots
10 p1273 A73-23703

Extraction of energy and charge from a black hole.
10 p1280 A73-24342

Gravitational radiation from a mass projected into a Schwarzschild black hole.
10 p1280 A73-24343

Vector and tensor radiation from Schwarzschild relativistic circular geodesics.
10 p1249 A73-24346

Polarization of synchrotron radiation from relativistic Schwarzschild circular geodesics.
10 p1252 A73-24347

Black holes existence and tentative configuration, discussing galaxies great group missing mass mystery and X ray source investigation
10 p1282 A73-24653

Wave amplification during the reflection from a rotating 'black hole'
10 p1283 A73-24752

Photometric and spectroscopic observations of eclipsing binary object BM Orionis interpreted in terms of thin disk model with collapsed star /black hole/
10 p1284 A73-24906

Rotating galaxies gravothermal catastrophe via violent relaxation leading to black hole core and halo system
10 p1284 A73-24911

Critique of theory on monotonic entropy of black hole as linear function of area, considering gravitational energy and compression to singularity
11 p1418 A73-25650

Massive X ray binaries consisting of early type star with neutron stars or black holes as companions
12 p1535 A73-27597

Relativistic astrophysics. III - Gravitational collapse, singularities, and black holes
12 p1543 A73-27749

Black holes and absorption redshifts in quasi-stellar objects.
14 p1797 A73-30006

White dwarfs, neutron stars and black hole identification by satellite X ray astronomy, discussing gas temperature and mass relation to cluster parameters
14 p1797 A73-30075

Black holes in binary systems, discussing radiation spectrum, disk formation, optical luminosity, X rays, UV regions and temperature distribution
15 p1928 A73-31051

Phenomena of scattering of electromagnetic and gravitational wave packets in the gravitational field of a black hole
15 p1932 A73-31245

Black holes in binary systems - Observational appearances.
16 p2058 A73-32739

Scattering of electromagnetic radiation from a black hole.
16 p2060 A73-33120

Analytic and computer solutions for Schwarzschild black hole geometry slicing into asymptotically flat and static maximal spacelike hypersurfaces
16 p2060 A73-33121

Quasi-periodic variations in X ray emission from black holes for accretion-formed disk with surface bright spots
18 p2354 A73-36728

Light curves of the gravitational lens-like action for binaries with degenerate stars.
19 p2483 A73-37563

Quasar and galactic nuclei energy source models, considering supermassive rotating magnetoplasma body, black hole and compact star cluster with flares and collisions
20 p2609 A73-39570

Black hole formation conditions in terms of critical masses, spherical symmetry and asymmetrical star collapse
21 p2765 A73-40233

Angular momentum decrease of slowly rotating Kerr black holes due to stationary distribution of outside matter
21 p2766 A73-40314

Radio binaries observation, noting black hole, large magnetic field or thermal bremsstrahlung as possible origin of strong X-ray radiation
21 p2770 A73-40940

Charged black hole collisions as gravitational radiation sources in terms of conservation of mass and surface area
22 p2908 A73-42428

Tungusk meteorite event with thermal radiation and severe blast wave attributed to black hole of substellar mass
22 p2909 A73-42488

Amplification of electromagnetic and gravitational waves during scattering on a rotating black hole
23 p3034 A73-44008

The relativistic Roche problem. I - Equilibrium theory for a body in equatorial, circular orbit around a Kerr black hole.
24 p3138 A73-45035

Accretion onto black holes - The emergent radiation spectrum. II Magnetic effects.
24 p3138 A73-45036

Gravitational radiation emission by star tidally deformed by black hole, computing energy loss rate
24 p3138 A73-45037

Ergosphere concept extended to classical mechanics from relativistic black hole mechanics
24 p3142 A73-45341

BLACK KNIGHT ROCKET VEHICLE
A description of the design, testing and application of the 'Waxwing' apogee boost motor for the 'Black Arrow' satellite launcher, with particular reference to development problems.
03 p0355 A73-13441

BLACKOUT [PHYSIOLOGY]
Effect of controlled elevation of body temperature on human tolerance to +G acceleration.
01 p0007 A73-10159

BLACKOUT [PROPAGATION]
NT ATMOSPHERICS
NT COSMIC NOISE
NT DAWN CHORUS
NT ELECTROMAGNETIC NOISE
NT HISS
NT IONOSPHERIC NOISE
NT IONOSPHERICS
NT SHOT NOISE
NT SUDDEN ENHANCEMENT OF ATMOSPHERICS
NT THERMAL NOISE
NT WHISTLERS
Effects of nonequilibrium ablation chemistry on Viking radio blackout.
05 p0551 A73-16981

BLADDERS [MECHANICS]
U DIAPHRAGMS [MECHANICS]

BLADE TIPS
Influence of acceleration on tip clearances in aircraft engine turbines and compressors
02 p0204 A73-12447

BLIND LANDING
Synthesis of helicopter rotor tips for less noise.
11 p1299 A73-24981

Flow at the trailing edges of a blade cascade at variable M and Re numbers
12 p1457 A73-27096

Experimental investigation of model variable-geometry and ogee tip rotors.
17 p2104 A73-35054

[AHS PREPRINT 703]
An investigation of the vibratory and acoustic benefits obtainable by the elimination of the blade tip vortex.
17 p2105 A73-35071

[AHS PREPRINT 735]
Fan acoustic measurements by hot-wire anemometers in anechoic chamber, discussing turbulent flow characteristics, noise spectra, wire velocity spectra and blade tip shape
19 p2472 A73-37289

Blade tip clearance loss between centrifugal impellers and shrouds during two dimensional viscous laminar flow, discussing energy dissipation and pressure and temperature distribution
19 p2474 A73-38417

Heat release from turbine rotor blades
23 p3020 A73-43744

BLADES
Finite element analysis of coupled vibration of tapered twisted blades.
16 p2078 A73-33005

BLANKS
Vacuum arc melting for improved heat resistance and mechanical properties of Ni alloy blanks, comparing with electro-beam and plasma arc melting and powder sintering
03 p0323 A73-13502

BLASIUS EQUATION
Analysis of unsteady laminar boundary layer flow by an integral method.
[ASME PAPER 72-WA/FE-2]
04 p0434 A73-15839

Perturbation solutions to laminar boundary layer flow over flat plate with small hump downstream of leading edge, using Blasius equation
11 p1302 A73-25855

On Blasius's equation governing flow in the boundary layer on a flat plate.
19 p2421 A73-38101

BLASIUS FLOW
Vectored injection into isobaric laminar boundary layer flows.
06 p0685 A73-17917

Linear stability of nearly parallel flows. II - The Blasius boundary layer
14 p1744 A73-29759

Non-parallel flow corrections for the stability of shear flows.
20 p2546 A73-39092

BLAST LOADS
Response of a cylindrical fiberglass-reinforced plastic shell to the action of an explosive load
05 p0635 A73-17079

Experiments on the non-linear dynamic response of shells under blast waves.
11 p1446 A73-26492

Calibration of Sandia Laboratories' 19-foot diameter explosively driven blast simulator.
16 p1994 A73-33136

BLASTOFF
U ROCKET LAUNCHING

BLEACHING
The effect of pH on photobleaching of organic laser dyes.
03 p0320 A73-14462

Time characteristics of a ring laser with a bleachable filter.
12 p1507 A73-27509

The recording of three-dimensional holograms on photochromic glass with the use of an optical bleaching process. I
13 p1616 A73-28765

Three-dimensional hologram recordings on photochrome glass with the application of an optical discoloration process. II
15 p1879 A73-32340

Kinetics of bleaching in polymethine cyanine dyes.
17 p2186 A73-35793

BLEED-OFF
U PRESSURE REDUCTION

BLEEDING
Boundary layer bleed system design for supersonic inlets, discussing bleed hole geometry effects on boundary layer velocity profile and inlet efficiency
[AIAA PAPER 72-1138]
03 p0243 A73-13445

BLENDS
U MIXTURES

BLIGHT
Corn blight epiphytotic remote sensing, data acquisition and crop identification by photointerpretation and computer aided multispectral band scanner data analysis
20 p2556 A73-39836

BLIND LANDING
Image formation radiometers for blind landing, aerial reconnaissance over land and sea, horizon detection and detection of obstacles at sea
08 p0986 A73-21087

- Microwave holography application to landing without visibility 15 p1911 A73-32497
- Ground visual aids for civil STOL aircraft steep gradient approach and blind landing, discussing flight trials and simulator experiments [RAE-TM-AVIONICS-136/BLEU/] 17 p2208 A73-34489
- Evolution of blind landing systems 22 p2885 A73-40302

BLINDNESS

NT FLASH BLINDNESS

- Residual visual function after brain wounds involving the central visual pathways in man. 16 p1975 A73-33218

BLISTERS [PROTUBERANCES]

U PROTUBERANCES

BLOCK DIAGRAMS

- Differential equations of motion for analog model of M-type TWT performance, proposing block diagram for electron phase and trajectory and field distribution calculations 12 p1478 A73-26950

BLOCKING

- Pyrometric obturation devices effect on sample temperature level during high temperature tests with radiant heating 03 p0306 A73-13189

- Blocking anticyclones over Siberia in the cold half-year period and the possibility of forecasting them 12 p1521 A73-27745

- Effects of wall boundary layers in wind tunnels on blocking phenomena 16 p1962 A73-32815

BLOOD

NT EOSINOPHILS

NT ERYTHROCYTES

NT LYMPHOCYTES

NT RETICULOCYTES

NT WHITE BLOOD CELLS

- Hydrogen ion concentration in the blood of man under high mountain conditions with physical loads 02 p0133 A73-11924

- Perceived exertion, heart rate, oxygen uptake and blood lactate in different work operations. 03 p0267 A73-13698

- Determination of the value of blood oxygen capacity and of the oxyhemoglobin dissociation curves by polarographic coulombometry 03 p0267 A73-13750

- Gas-blood CO₂ equilibration in dog lungs during rebreathing. 03 p0263 A73-14115

- Mechanisms of certain functional shifts during change in the blood of the content level of external pancreatic-gland secretion components 05 p0541 A73-16700

- Daily rhythm of biogenic amine/histamine and serotonin/ contents in human blood during usual and shifted work schedules 06 p0650 A73-17688

- Effect of accelerations on the thiamine-S/35/ distribution in the organism of white mice 08 p0929 A73-20977

- Determination of oxidized and reduced pyridine nucleotides in human and rabbit blood with the aid of the polarographic cycling technique 09 p1044 A73-21871

- Influence of certain brain structures on the sulphydryl-group, diphosphopyridine-nucleotide, and serotonin contents of the blood 09 p1040 A73-22856

- Effect of the administration of free amino acids and metabolic cofactors on the distribution of regional biogenic amine contents in the brain and blood of animals 09 p1040 A73-22864

- Intermittent exercise - Metabolites, oxygen pressure, and acid-base equilibrium in the blood. 09 p1041 A73-22933

- Investigation of the exchange between the blood and the intraocular fluid with the aid of radioactive phosphorus 10 p1185 A73-24520

- Effect of antioxidants on the blood deoxygenation rate in animals exposed to altered atmospheres 12 p1465 A73-27702

- Water and salt metabolism in hypokinesia-subjected animals 12 p1462 A73-27704

- Changes in the gas content of blood in man during exposure to high ambient temperatures 12 p1463 A73-27711

- Carbon monoxide content in the exhaled air and carboxyhemoglobin in the blood of subjects equipped with an isolating protective garment 12 p1463 A73-27712

- Reactivity and certain metabolic indices during prolonged sustenance of animals in artificial nutrient conditions 15 p1833 A73-31162

- Age peculiarities of whole-blood transketolase activity in healthy persons 15 p1833 A73-31164

- Changes in the quantity of overall sulfhydryl groups in the blood of persons coming in contact with microwave radiation sources 15 p1837 A73-31169

- Temperature conditions and blood supply of the brain in animals 17 p2111 A73-34229

- Effect of stepwise adaptation to high-mountain areas on the respiratory function and the acid-alkali equilibrium of blood in subjects with different motor activity stresses 17 p2111 A73-34232

- Urea content variations in blood and tissues during muscular activity in relation to the adaptation level of the organism 22 p2807 A73-42660

- A rapid method for determining the CO₂ transport characteristics in man by using a capnograph and a multichannel respirator 22 p2815 A73-42665

- The specific resistance of blood at body temperature. 22 p2807 A73-42670

- An equation for the oxygen hemoglobin dissociation curve. 24 p3064 A73-45070

BLOOD CIRCULATION

NT BRAIN CIRCULATION

NT CARBOXYHEMOGLOBIN

NT CORONARY CIRCULATION

NT INTERCRANIAL CIRCULATION

NT INTRAVASCULAR SYSTEM

NT ISCHEMIA

NT OCULAR CIRCULATION

NT PULMONARY CIRCULATION

- A criterion for oxygen supply optimality in tissues and the capillary circulation rate 03 p0268 A73-13821

- Biological role of atmospheric oxygen in the mechanism of blood coagulation 06 p0650 A73-17678

- Mixed-venous oxygen tension by nitrogen rebreathing - A critical, theoretical analysis. 06 p0654 A73-18336

- Central, femoral, and brachial circulation during exercise in hypoxia. 08 p0934 A73-21506

- Clinical evidence of cardiac weakness and incoordination secured by simultaneous records of the force BCG and carotid pulse derivative and interpreted by an electrical analogue. 09 p1046 A73-23174

- Controlled tachycardia through voluntary change in exercise regime, investigating relation between heart rate and blood circulation 10 p1185 A73-24521

- Human forearm-muscle blood supply regimes after 'static' exercise with increasing stress 10 p1181 A73-24522

- Changes in microvascular diameter and oxygen tension induced by carbon dioxide. 11 p1317 A73-26116

- A new phenomenon of an active intraorgan pumping function of skeletal muscles 12 p1462 A73-27446

- Nonlinear wave propagation processes in elastic tubes 13 p1692 A73-28165

- Changes in blood-flow distribution during acute emotional stress in dogs. 13 p1576 A73-28533

- Influence of flow and pressure on wave propagation in the canine aorta. 14 p1715 A73-30066

- Vein wall changes as the main cause of acute disturbance of blood circulation in the Vena centralis retinae system 15 p1833 A73-31173

- Some compensatory adjustment reactions of the blood circulation system in pulmonary pathology 15 p1835 A73-31623

- Mechanism of working hyperemia condition alteration in the forearm muscles of man under increased loads 18 p2276 A73-36570

- Specific features in the activity of the oxygen transport system of the organism during hand-performed working cycles of submaximum intensity 18 p2277 A73-36579

- The effects of training on some parameters of hemodynamics and of the oxygen transportation function of the blood during static strains 18 p2277 A73-36581

- Measurement of cardiac output with and organ trapping of radioactive microspheres. 18 p2282 A73-36661

- Neurogenic and local regulation of resistance and capacitance blood vessels, noting sympathetic nervous system influence on musculocutaneous and splanchnic regions 23 p2947 A73-43927

BLOOD COAGULATION

- Hemocoagulation system function in mountain inhabitants and during altitude acclimatization, noting parasympathetic nervous system tonus 02 p0133 A73-11923

- Biological role of atmospheric oxygen in the mechanism of blood coagulation 06 p0650 A73-17678

- Effect of heparin on blood platelet aggregation and thrombosis under the action of direct electric current 08 p0931 A73-21321

- Intravascular platelet aggregation in the heart induced by stress. 08 p0933 A73-21805

- Hemocoagulation and trombocyte state during hypokinesia after highland adaptation 12 p1463 A73-27713

- Emotional overstress effects on the indices of the blood coagulation system in monkeys 14 p1719 A73-30846

- Accelerated coagulation of whole blood and cell-free plasma by bubbling in vitro. 18 p2278 A73-36782

- Hemotherapy of coagulation system disturbances of hepatolienal origin 23 p2947 A73-44299

BLOOD FLOW

- A nonlinear analysis of pulsatile flow in arteries. 01 p0011 A73-10449

- The statistical evaluation of the measurement of viscosity of a non-Newtonian liquid. 03 p0306 A73-12899

- Normal pulmonary pressure-flow relationship during exercise in the sitting position. 03 p0266 A73-13302

- Micropolar model of blood steady flow through rigid circular tubes, presenting equations solutions and velocity profiles 03 p0266 A73-13302

- Telemetric measurement of local blood flow by heat conduction probes. 03 p0270 A73-14282

- Blood flow and pressure and ECG data acquisition and transmission via radio telemetry system with electromagnetic flowmeter 03 p0270 A73-14283

- An implantable blood pressure and flow transmitter. 04 p0447 A73-14845

- External field electromagnetic measurement of blood flow - An alternative approach to the solution of the baseline problem. 04 p0414 A73-15992

- Application of constant temperature anemometry in measurement of intra-arterial blood flow velocity. 05 p0545 A73-17274

- Effect of ultrafiltration and plasma osmolality upon the flow properties of blood - A possible mechanism for control of blood flow in the renal medullary Vasa recta. 08 p0930 A73-21199

- Pattern of blood flow within the heart - A stable system. 08 p0930 A73-21214

- Devices for dynamic recording of volumetric blood flow rates lower than 1 ml per minute 08 p0934 A73-21325

- Intravascular changes associated with hyperbaric decompression - Theoretical considerations using ultrasound. 09 p1045 A73-22534

- Red cell flexibility and pressure-flow relations in isolated lungs. 09 p1041 A73-22927

- Distribution of systemic blood flow during cardiopulmonary bypass. 09 p1041 A73-22930

- Left ventricular blood flow velocity in man studied with the Doppler ultrasonic flowmeter. 09 p1042 A73-23173

- Coronary flow and left ventricular function during environmental stress. 09 p1047 A73-23380

- A simplified method for the in vitro calibration of electromagnetic flowmeters. 12 p1464 A73-27027

- Oxygen consumption alteration effects on human endurance capacity as function of relative work, muscle blood flow and anaerobic metabolism 14 p1714 A73-29753

- Sustained human skin and muscle vasoconstriction with reduced baroreceptor activity. 15 p1833 A73-31344

- Factors influencing coronary blood flow in the presence of coronary obstructive disease. 18 p2275 A73-36539

- Control of forearm skin blood flow during periods of steadily increasing skin temperature. 18 p2278 A73-36657

- Influence of carbon monoxide and of hemodilution on cerebral blood flow and blood gases in man. 18 p2278 A73-36659

- Experimental studies on the mechanisms of closure of cardiac valves with use of roentgen videodensitometry. 19 p2395 A73-37795

Nonlinear analysis of aortic flow in living dogs. 21 p2638 A73-40640

Relationship between organ weight and blood flow in rats adapted to simulated high altitude. 21 p2639 A73-41156

Mathematics of interaction between blood and electromagnetic fields. 22 p2802 A73-41788

Absorption of gas bubbles in flowing blood. 22 p2806 A73-42414

Influence of nonideal flow conditions in haemodialysers on mass-transfer theories. 22 p2816 A73-42678

Measurement of coronary blood flow by radiocardiography - Study of 116 cases. 22 p2809 A73-42838

Flow patterns and velocity and shear stress distribution downstream of steady and pulsatile flow models for fluid dynamics of blood vessel branches 22 p2816 A73-43103

Velocity distribution in aortic flow. 22 p2811 A73-43104

Transcutaneous measurement of blood velocity profiles and flow. 22 p2817 A73-43108

A model of heat transfer in a biological tissue perfused by blood of arbitrary temperature. 23 p2948 A73-43292

Comparison of plethysmographic and electromagnetic flow measurements. 23 p2950 A73-44215

Measurement of left anterior descending coronary arterial blood flow - Technique, methods of blood flow analysis and correlation with angiography. 24 p3058 A73-44469

Doppler echocardiography - The localization of cardiac murmurs. 24 p3064 A73-44947

Hemoglobin-oxygen equilibrium and coronary blood flow - An analog model. 24 p3064 A73-45060

BLOOD GROUPS

Blood groups and plasma cholesterol esterification. 22 p2811 A73-43106

Blood group A sub-groups and serum cholesterol. 22 p2811 A73-43107

BLOOD PLASMA

Corticosterone level and the binding capacity of blood plasma proteins under thermal effects 03 p0261 A73-13749

Multiple hormonal responses to graded exercise in relation to physical training. 03 p0263 A73-14116

Multiple hormonal responses to prolonged exercise in relation to physical training. 03 p0263 A73-14117

An implantable radiotelemetric measuring device for simultaneous long term measurements of body temperature and turnover of rabbit serum albumin/I-125 in unrestrained rabbits. 03 p0271 A73-14301

Body temperature effect on protein conformation stability in healthy and diseased organisms, noting blood plasma albumin fractions 04 p0409 A73-14822

Research on the displacement of blood-plasma proteins and on the nerve conduction velocity in rats subjected to accelerations and hypokinesia 06 p0650 A73-17769

The effect of temperature on the mitotic activity of human peripheral blood lymphocytes in a culture 07 p0781 A73-19649

Effect of ultrafiltration and plasma osmolality upon the flow properties of blood - A possible mechanism for control of blood flow in the renal medullary Vasa recta. 08 p0930 A73-21199

Changes in total plasma content of electrolytes and proteins with maximal exercise. 08 p0934 A73-21507

Determination of iodo amino acids in plasma by gel chromatography 10 p1178 A73-23760

Binding of Melatonin to human and rat plasma proteins. 10 p1182 A73-24657

An automated gas chromatographic analysis of phenylalanine in serum. 11 p1326 A73-25571

Quaternary structure /subunit composition/ of human ceruloplasmin 11 p1316 A73-25638

Serum tryptophan level after carbohydrate ingestion - Selective decline in non-albumin-bound tryptophan coincident with reduction in serum free fatty acids. 12 p1464 A73-27975

Human hematologic responses to 4 hr of isobaric hyperoxic exposure /100% oxygen at 760 mm Hg/. 14 p1714 A73-29751

Plasma electrolytes, pH, and ECG during and after exhaustive exercise. 15 p1834 A73-31347

Investigation of some blood characteristics in albino rats subjected to 60-day hypokinesia 15 p1834 A73-31502

Serum cholesterol and plasma lipid elevation separation of hypercholesterolemic patients for atherosclerosis therapy 18 p2275 A73-36533

Red cell volume with changes in plasma osmolality during maximal exercise. 18 p2277 A73-36654

Accelerated coagulation of whole blood and cell-free plasma by bubbling in vitro. 18 p2278 A73-36782

Blood electrolytes and exercise in relation to temperature regulation in man. 18 p2280 A73-36983

The nature of chemoreception in posterior hypothalamic structures 21 p2636 A73-40279

Serum tryptophan level after carbohydrate ingestion - Selective decline in non-albumin-bound tryptophan coincident with reduction in serum free fatty acids. 21 p2640 A73-41218

Plasma insulin and carbohydrate metabolism after sucrose ingestion during rest and prolonged aerobic exercise. 21 p2641 A73-41622

Blood plasma contamination of the lung alveolar surfactant obtained by various sampling techniques. 21 p2642 A73-41637

Effect of altitude on renin-aldosterone system and metabolism of water and electrolytes. 22 p2806 A73-42420

Mechanisms of hyperlipidaemias in different clinical conditions. 22 p2809 A73-42832

Blood groups and plasma cholesterol esterification. 22 p2811 A73-43106

Apparatus for measuring the colloid osmotic pressure in blood serum 23 p2949 A73-43792

Oxygen affinity and electrolyte distribution of human blood - Changes induced by propranolol. 24 p3062 A73-44689

Model experiments on apparent blood viscosity and hematocrit in pulmonary alveoli. 24 p3064 A73-45064

Lactate origins and renewal in blood plasma, considering metabolism, enzymatic resynthesis and final excretion in urine 24 p3061 A73-45157

BLOOD PRESSURE

NT DIASTOLIC PRESSURE

NT HYPERTENSION

NT HYPOTENSION

NT SYSTOLIC PRESSURE

Isovolumic contraction dynamics in man according to two different muscle models. 01 p0007 A73-10158

Normal pulmonary pressure-flow relationship during exercise in the sitting position. 03 p0266 A73-13124

Blood flow and pressure and ECG data acquisition and transmission via radio telemetry system with electromagnetic flowmeter 03 p0270 A73-14283

Telemetry of venous blood pressure at rest and at muscle activity during running. 03 p0271 A73-14290

Radiotelemetry of direct bloodpressure measurements in aorta, pulmonary artery and heart. 03 p0271 A73-14291

Telemetry of cardiovascular parameters on fighter aircraft flying pilots. 03 p0272 A73-14309

The effect of time of electrical stimulation of the carotid sinus on the amount of reduction in arterial pressure. 03 p0265 A73-14648

An implantable blood pressure and flow transmitter. 04 p0447 A73-14845

Automated calibration of blood pressure signal conditions. 04 p0411 A73-14846

A mathematical model to assess changes in the baroreceptor reflex. 08 p0934 A73-21475

Significance of the Bohr and Haldane effects in the pulmonary capillary. 08 p0935 A73-21614

Red cell flexibility and pressure-flow relations in isolated lungs. 09 p1041 A73-22927

Clinical evidence of cardiac weakness and incoordination secured by simultaneous records of the force BCG and carotid pulse derivative and interpreted by an electrical analogue. 09 p1046 A73-23174

Isometric effects on treadmill exercise response in healthy young men. 10 p1179 A73-23842

The influence of change in the functional state of the central nervous system on the course of asphyxia 10 p1179 A73-23937

Effect of respiration stabilization on hemodynamic reactions during acute hypoxic hypoxia 10 p1180 A73-23938

BLOOD VESSELS

Formalization of an arterial pressure stabilization system 10 p1181 A73-24467

Positive /+Gz/ acceleration tolerances of the miniature swine - Application as a human analog. 11 p1315 A73-25337

A new phenomenon of an active intraorgan pumping function of skeletal muscles 12 p1462 A73-27446

High-fidelity left ventricular pressure measurements for the assessment of cardiac contractility in man. 12 p1464 A73-27888

Blood pressure and body temperature dynamic control systems and respiration relationship to heart rate variability 14 p1720 A73-30878

Procedure for recording the rate of pressure changes in heart cavities 15 p1837 A73-31167

Technique for measuring the vessel blood pressure in long continued experiments 15 p1838 A73-31394

Cardiovascular responses to sudden strenuous exercise - Heart rate, blood pressure, and ECG. 17 p2112 A73-35461

Current status of correlations between vectorcardiogram and hemodynamic data. 18 p2274 A73-36526

The use of simple indicators for detecting potential coronary heart disease susceptibility in the third-class airman population. 18 p2284 A73-36912

A new technique for the study of left ventricular pressure-volume relations in man. 19 p2401 A73-38259

Assessing the severity of aortic stenosis by phonocardiography and external carotid pulse recordings. 20 p2516 A73-38867

Effect of prior adaptation to cold on the development of experimental hypertonia 21 p2636 A73-40209

Effect of stimulation of certain hypothalamic structures on systemic and pulmonary circulation 21 p2637 A73-40282

Evaluation of several methods for computing stroke volume from central aortic pressure. 21 p2638 A73-40638

Nonlinear analysis of aortic flow in living dogs. 21 p2638 A73-40640

Ophthalmodynamography in pilots to test internal carotid insufficiency - Comparison of blood-pressure responses. 21 p2639 A73-41162

Mathematics of interaction between blood and electromagnetic fields. 22 p2802 A73-41788

Mechanism of 'readjustment' of aorta baroreceptors during hypertonia 22 p2807 A73-42655

A new method of measuring arterial dilation and its application. 22 p2815 A73-42669

Myocardial oxygen consumption in experimental hypertrophy and congestive heart failure due to pressure overload. 22 p2808 A73-42688

Measurements of arterial pressure and of pressure-receptor reactions during prolonged pressure shifts in carotid arteries 24 p3062 A73-44720

Permanent catheterism of the thoracic aorta - Direct measurement of arterial pressure, injection of substances, and the taking of blood in wake rats 24 p3065 A73-45160

BLOOD VESSELS

NT AORTA

NT ARTERIES

NT CAPILLARIES [ANATOMY]

NT GLOMERULUS

NT VEINS

Cerebral circulation alteration during hypothermia 05 p0541 A73-16698

Ultrasonic Doppler locators for peripheral vessel blood circulation and myocardium and valvular motor activity measurements 06 p0656 A73-17682

Blood vessels simulation by muscle pump represented by elastically deformable pipe with valves, solving Navier-Stokes equation for viscous fluid flow 08 p0934 A73-21375

Changes in the vascular tone of certain organs during experimental embolism of pulmonary circulation 09 p1039 A73-22366

Modification of the electroencephalograph EEG-I for polygraphy 09 p1044 A73-22370

Book - The physiology of the cerebral circulation. 10 p1180 A73-23945

Changes in microvascular diameter and oxygen tension induced by carbon dioxide. 11 p1317 A73-26116

- Technique for measuring the vessel blood pressure in long continued experiments 15 p1838 A73-31394
- Retinal vessel reactions and intracocular tension in humans staying in a horizontal position for 120 days 15 p1835 A73-31514
- Impact acceleration effects on rabbit central nervous system, noting changes in nerve tissue elements and cerebral vessels 17 p2111 A73-34227
- Role of arterial and venous vessels of limbs in the process of cardiovascular reflex responses 18 p2277 A73-36578
- Analysis of pressure waves as a mean of diagnosing vascular obstructions. 19 p2398 A73-37524
- Effect of stimulation of the hypothalamus on the pH of arterial and venous blood 21 p2637 A73-40281
- Flow patterns and velocity and shear stress distribution downstream of steady and pulsatile flow models for fluid dynamics of blood vessel branches 22 p2816 A73-43103
- Mathematical model of collateral blood vessels caliber changes due to hydrodynamic drag /shear stress/ effects on vascular endothelium 22 p2817 A73-43105
- Ultrasonic transducer instrument with broad beam dispersal for blood vessel displacement recording in chronic animal experimentation 22 p2817 A73-43109
- Neurogenic and local regulation of resistance and capacitance blood vessels, noting sympathetic nervous system influence on musculocutaneous and splanchnic regions 23 p2947 A73-43927
- BLOOD VOLUME**
- Mediator systems and respiratory function during an acute lethal loss of blood 07 p0781 A73-19645
- Devices for dynamic recording of volumetric blood flow rates lower than 1 ml per minute 08 p0934 A73-21325
- Estimation of left ventricular size by echocardiography. 09 p1046 A73-22999
- Immediate hemodynamic effects of cardiac angiography in man. 10 p1179 A73-23841
- Effect of electrostimulation on hemodynamic shifts during prolonged hypokinesia 10 p1180 A73-23940
- Apparent paradoxical patterns of anaerobic glycolysis and hexokinase activity in the red blood cells of acutely bled rats, with evidence that the responses were in part hormone-dependent. 11 p1315 A73-25568
- Xenon 133 measurement of cerebral volumetric circulation rates during papaverin and intensin vasodilation of canine and feline intracranial vessels, showing vessel resistance reduction 13 p1576 A73-29074
- A simplified method of calculating thermolimation curves 15 p1837 A73-31168
- Investigation of some blood characteristics in albino rats subjected to 60-day hypokinesia 15 p1834 A73-31502
- Power failure of the heart in acute myocardial infarction. 18 p2276 A73-36547
- Mechanism of working hyperemia condition alteration in the forearm muscles of man under increased loads 18 p2276 A73-36570
- The role of the elastic properties of brain and spine cavities in hyperemia compensation 18 p2276 A73-36572
- Angiotensinography using an air plethysmograph 18 p2282 A73-36575
- Respiratory changes in the stroke volume of the left ventricle in healthy humans 19 p2393 A73-37397
- Ejection time by ear densitogram and its derivative - Clinical and physiologic applications. 20 p2511 A73-38866
- Correlation between arterial carbon dioxide tension and regional cerebral blood volume by X-ray fluorescence. 20 p2519 A73-39790
- Evaluation of several methods for computing stroke volume from central aortic pressure. 21 p2638 A73-40638
- The relationship between left ventricular ejection time and stroke volume during passive cardiovascular stress. 21 p2641 A73-41565
- Structural conditions in the hypertrophied and failing heart. 22 p2807 A73-42685
- Stroke volume measurement from an integral rheogram of human body 24 p3062 A73-44719
- Comparison of ultrasound and cineangiographic measurements of left ventricular performance in patients with and without wall motion abnormalities. 24 p3062 A73-45400
- BLOWDOWN WIND TUNNELS**
- Some development of hypersonic flow experiment by the gun tunnel. 01 p0003 A73-11129
- Supersonic blowdown wind tunnel modification for transonic airfoil profile aerodynamic characteristics measurement, discussing design criteria and operational range [DGLR PAPER 72-133] 03 p0288 A73-14380
- Diagnostic simulation of a pneumatically controlled blowdown wind tunnel. 11 p1344 A73-26546
- Discharge characteristics in cesium-seeded argon. 13 p1665 A73-28807
- BLOWERS**
- Flow twisting in front of rotor for centrifugal blower operation control, predicting efficiency criteria 10 p1173 A73-24671
- BLOWING**
- Skin friction on porous surfaces calculated by a simple integral method. 01 p0057 A73-10726
- Velocity, temperature and component concentration distributions in laminar boundary layer at blown surface for binary mixture flow 01 p0034 A73-10957
- STOL aircraft with mechanical high-lift systems in comparison to STOL aircraft with wings having blown flaps [DGLR PAPER 72-057] 02 p0130 A73-11665
- Flow characteristics in air injection through porous surface of blunt bodies, noting blowing parameter effect on boundary layer flow 07 p0774 A73-19622
- Acoustic results obtained with upper-surface-blowing lift-augmentation systems. 07 p0776 A73-20458
- Kochin hydrodynamic equation solutions for gas injection through plate for intense blowing at constant and changing rates 08 p0927 A73-21772
- Solution of the Cauchy problem for a nonlinear equation describing a gas flow in the presence of strong blowing 09 p1029 A73-23352
- Calculation of the gas parameters in the injection region for the flow at an angle of incidence past a porous cone 10 p1172 A73-24505
- Velocity and concentration profiles of isothermal laminar boundary layer flow of incompressible multicomponent gas under strong blowing 11 p1347 A73-25728
- Asymptotic solution of shock-layer equations in the vicinity of the stagnation point of a sphere in the case of strong blowing 11 p1304 A73-26442
- Velocity, temperature and component concentration distributions in laminar boundary layer at blown surface for binary mixture flow 12 p1487 A73-27533
- Approximate method for solving a boundary value problem describing gas flow during strong blowing 12 p1458 A73-27811
- Use of blowing during tests of blade cascades 13 p1623 A73-28469
- On the flow between two independently rotating disks of variable distance with blowing. 13 p1605 A73-29295
- Experimental investigation of the convection inversion process in the viscous sublayer of a turbulent boundary layer during blowing of carbon dioxide through a vertical porous heated surface under conditions of natural convection 13 p1708 A73-29407
- The solutions of the boundary layer equations in the case of extremely intensive blowing or suction 16 p1963 A73-33250
- Numerical stability of boundary layers with massive blowing. 18 p2298 A73-36321
- Effect of downstream massive blowing on Jovian entry heating. 18 p2264 A73-36336
- IAIA PAPER 73-717] Burnout of a graphite surface during the blowing of an inert gas through it 21 p2790 A73-40698
- Investigation of the flow pattern in the wall region of a turbulent boundary layer during injection with a positive pressure gradient 24 p3079 A73-45080
- BLUE GREEN ALGAE**
- Circadian rhythms - Subcellular and biochemical aspects. 06 p0651 A73-17824
- Carbon dioxide concentration, pH and nutrient concentration effects on blue-green algae relative abundance to green algae in lakes 06 p0655 A73-18577
- Purification of *Synechococcus lividus* by equilibrium centrifugation and its synchronization by differential centrifugation. 18 p2274 A73-36503
- BLUFF BODIES**
- A free-streamline theory for bluff bodies attached to a plane wall. 04 p0403 A73-15160
- Unsteady wakes of bluff and streamlined bodies with screens behind them. 10 p1173 A73-24823
- Two dimensional inviscid flow model of shear layer motion and vortex shedding in near wake of bluff-based body, using Schwarz-Christoffel transformation 11 p1300 A73-25155
- Using the singularity method in studies of potential flow about bulbous streamline bodies 14 p1712 A73-30706
- Noise of jets discharging from a duct containing bluff bodies. 19 p2472 A73-37291
- Neighboring body effects on bluff body form drag. 20 p2507 A73-39519
- Neighboring body effects on bluff body tipping moment. 20 p2507 A73-39520
- Vortex shedding from and base pressure distribution on bluff body measured in shear or uniform flow, calculating Strouhal number 23 p2940 A73-43939
- BLUNT BODIES**
- Three-dimensional effects on electron density in a blunt body laminar boundary layer. 01 p0002 A73-10731
- Correlation function for prediction of surface roughness induced supersonic boundary layer transition on blunt bodies, taking into account compressibility and centrifugal force effects 01 p0002 A73-10742
- Hypersonic, viscous shock layer with chemical nonequilibrium for spherically blunted cones. 01 p0002 A73-10746
- Convective heat transfer coefficients at stagnation point of blunt body immersed in flames of fuel gases combustion with pure oxygen 01 p0122 A73-10807
- Numerical calculation of supersonic opposing jet directed upstream against supersonic main stream by the use of time-dependent finite-difference method. 01 p0003 A73-11130
- Aerodynamics of blunted bodies in hypersonic stream at the angle of attack. 01 p0003 A73-11133
- Least-squares solution for the blunt body hypersonic flow problem. 01 p0004 A73-11473
- Far field steady inviscid flow behavior of hypersonic blunt axisymmetric slender body, obtaining unsteady two dimensional solution with cylindrical symmetry 03 p0242 A73-13310
- Radiative and convective heat transfer occurring in the hypersonic flow past a blunted body 03 p0244 A73-13617
- Calculation of supersonic viscous gas flow past blunt bodies at large Reynolds numbers 05 p0527 A73-16448
- Numerical solution of viscous reacting blunt body flows of a multicomponent mixture. 05 p0532 A73-16936
- IAIA PAPER 73-202] A study of fin-induced laminar interactions on sharp and spherically blunted cones. 05 p0532 A73-16960
- IAIA PAPER 73-235] Shock impingement caused by boundary layer separation ahead of blunt fins. 05 p0532 A73-16961
- IAIA PAPER 73-236] Experimental investigation of hypersonic helium flow around sharp and blunted cones in the presence of strong injection 06 p0643 A73-17466
- Investigation of convective and radiative heating of blunted bodies in hypersonic flow 06 p0644 A73-17469
- Flow characteristics in air injection through porous surface of blunt bodies, noting blowing parameter effect on boundary layer flow 07 p0774 A73-19622
- Band position predictions in schlieren visualization of hypersonic entropy wake behind blunt bodies, assuming bow shock geometry 07 p0775 A73-19970
- Effect of ionization nonequilibrium on the shock wave in the stagnation region 07 p0776 A73-20616
- Supersonic flow of a viscous gas about a spherically blunt cooled object 09 p1028 A73-22620
- Numerical analysis of the viscous, hypersonic, MHD blunt-body problem. 09 p1132 A73-23455
- Flow of a supersonic nitrogen jet and of a low-density nitrogen-hydrogen mixture around a blunted body 10 p1171 A73-23582

Electron temperature profile in stagnation region flow of blunt bodies with consideration of ionization recombination in shock layer
10 p1296 A73-24256

Some characteristics of the flow downstream of a blunt trailing edge in the presence of a neighbouring wall.
10 p1173 A73-24818

Numerical computation for entropy layer on blunt nosed cone in terms of shock layer fraction for given free stream and Mach number
11 p1299 A73-25113

Base drag reduction on blunt based axisymmetric bodies by base burning, calculating inviscid flow field with heat addition around recirculating bubble
11 p1449 A73-25347

Radar cross section measurements for right circular cones with spherically blunted noses, presenting as functions of diameter/wavelength ratio and aspect angle
11 p1330 A73-25682

Linear axisymmetric self similar solution for blunt nosed rigid cone immersed into ideal compressible fluid at subsonic velocity, computing wetted surface radius increase
12 p1487 A73-27410

Three-dimensional motion of a reacting gas mixture around a blunt body
15 p1822 A73-31290

Flows past thin blunt bodies with shock layer separation
15 p1822 A73-31291

Unsteady shock wave interaction with plane hypersonic flow about a blunt body investigated by second order difference method
15 p1862 A73-31326

A numerical solution for the transonic flow around blunt wedges
15 p1823 A73-31330

Experimental evaluation of the effects of a blunt leading edge on the performance of a transonic rotor. [ASME PAPER 73-GT-60]
16 p1964 A73-33515

Correlation of the mass flow rate in the laminar boundary layer on a sphere-cone.
17 p2091 A73-34195

Relaxation solutions for inviscid axisymmetric transonic flow over blunt or pointed bodies.
17 p2095 A73-35128

Supersonic flow around concave and convex blunt bodies.
17 p2097 A73-35865

Finite-difference solution of the incompressible three-dimensional boundary layer equations for a blunt body.
18 p2259 A73-36156

Hypersonic merged stagnation shock layers. [AIAA PAPER 73-639]
18 p2260 A73-36197

Investigation of multiple slot film cooling to a blunt nose cone. [AIAA PAPER 73-698]
18 p2368 A73-36247

Viscous effects in massively-ablating planetary entry body flow fields. [AIAA PAPER 73-716]
18 p2264 A73-36335

Effect of downstream massive blowing on Jovian entry heating. [AIAA PAPER 73-717]
18 p2264 A73-36336

Supersonic gas flow pattern at blunt body of revolution with attached shock wave
21 p2632 A73-40400

Streamline curvature and velocity gradient behind curved shocks.
21 p2632 A73-40441

Interaction of a shock wave with blunt bodies in supersonic flow
21 p2633 A73-41222

Flowing gas mixture ignition at heated blunt body stagnation point, examining Van't Hoff criterion
23 p3048 A73-43328

Calculation of supersonic flow around blunt bodies using complete and simplified Navier-Stokes equations
24 p3053 A73-44657

BLUNTNESS
U ELLIPTICITY
BLURRING
A study of basilar membrane vibrations. I - Fuzziness-detection: A new method for the analysis of microvibrations with laser light.
01 p0013 A73-10973

Induced retinal image blurring effects on rabbit mid-brain single cell trigger features and response efficiencies, noting receptive field responsive area
01 p0010 A73-11503

Single step detection of blurred images in a coherent optical processor.
17 p2173 A73-35436

Space-variant system analysis of image motion.
21 p2706 A73-41609

High resolution image formation through the turbulent atmosphere.
22 p2863 A73-43097

Photometric strip blurring and brightness contrast measurements of visual perception in turbulent at-

mosphere as function of distance, turbulence and exposure
23 p3001 A73-43573

BOATTAILS
Flight and wind tunnel investigation of the effects of Reynolds number on installed boattail drag at subsonic speeds. [AIAA PAPER 73-139]
05 p0530 A73-16888

BODIES
Influence of structural flexibility on attitude control of spacecraft
17 p2162 A73-34950

BODIES OF REVOLUTION
NT CELESTIAL SPHERE
NT CONICAL BODIES
NT CYLINDRICAL BODIES
NT PARABOLIC BODIES
NT POINCARÉ SPHERES
NT ROTATING CYLINDERS
NT ROTATING SPHERES
NT SLENDER CONES
NT SPHERES
NT TORUSES

Numerical solution to the axisymmetric thermoplasticity problem of a shell of revolution
01 p0112 A73-10007

The extended boundary condition solution of the dipole antenna of revolution.
01 p0016 A73-10186

Application of shell equations to an unsymmetrically loaded corrugated shell of revolution.
01 p0115 A73-10769

Turbulent swirling wake behind spinning axisymmetric body of revolution having axis aligned with free stream direction, obtaining velocity profiles variations
01 p0004 A73-11136

Buoyancy distribution of slender axisymmetric bodies of higher order in the case of compressible subsonic flow
02 p0127 A73-11681

[DGLR PAPER 72-067]
The influence of the Mach number on fuselages and profiles with optimized wave resistance in the case of supersonic flow
02 p0128 A73-11691

Stress distribution in elastic shell of revolution under axisymmetrical loads, noting thickness distribution for uniform stress in critical edge loading zone
02 p0231 A73-11805

Elastic deformation of a single-cavity hyperboloid of revolution under given forces at the boundary
02 p0233 A73-11939

Axisymmetric slow viscous flow past an arbitrary convex body of revolution.
02 p0153 A73-12040

Finite plastic deformation of pressurized membranes of revolution.
03 p0384 A73-13120

Stockings, extensible plane structures and three dimensional textile fiber blocks reinforced materials, noting application to structures of revolution under external pressure
03 p0334 A73-13585

Experimental investigation of a turbulent boundary layer on a highly elongated body of revolution in a supersonic flow
03 p0245 A73-13669

A finite element analysis of an axisymmetrically loaded orthotropic shell of revolution.
03 p0391 A73-13677

Transient response of inelastic shells of revolution.
03 p0392 A73-13686

Finite difference theory for bending stress concentration in shells of revolution, noting constitutive equation for thermal stress analysis
03 p0393 A73-13793

Vibrational frequency density analysis of thin spherical and cylindrical shells of revolution, using asymptotic integration method
03 p0394 A73-14051

Natural vibration frequency spectra of circular cylindrical and spherical shells of revolution, using Bessel function
03 p0395 A73-14052

Calculus of variations for functional conditional extremum, determining minimum drag shape for body of revolution in hypersonic flow
04 p0403 A73-14886

Electromagnetic wave diffraction by ideally conducting homogeneous bodies of revolution with arbitrary complex permittivity and permeability, using separation of variables method
05 p0547 A73-16054

Nonlinear shell theory with finite rotation and stress-function vectors. [ASME PAPER 72-APM-CC]
05 p0633 A73-16533

On finite symmetrical strain in thin shells of revolution.
05 p0633 A73-16536

Variable thickness orthotropic shell of revolution with bending suppressed.
05 p0633 A73-16537

Calculation of subsonic and transonic flow at the stern of bodies of revolution
06 p0643 A73-17468

The thermal shock on the shell of revolution-coupled and uncoupled theory.
06 p0763 A73-18452

Transversal vibrations of the thin shell of revolution produced by the thermal shock.
06 p0763 A73-18453

Finite-element analysis of shells of revolution by two doubly curved quadrilateral elements.
07 p0912 A73-19368

Numerical analysis of anisotropic rotational shells subjected to nonsymmetric loads.
07 p0914 A73-20210

Experimental investigation of the Magnus effect at a finned body of revolution of large aspect ratio at a Mach number of 4
08 p0927 A73-21604

Internal equation numerical solution for excitation of multilayer arbitrary shape dielectric body of revolution, considering radome curvature effects on antenna radiation pattern
09 p1052 A73-23084

Static stability and drag studies for bodies of revolution in supersonic flow.
09 p1156 A73-23214

Deformation of shells of revolution with attached rings under different local loads, deriving approximate expressions for stressed state
10 p1287 A73-23592

Electromagnetic field of rotating charged oblate ellipsoid of revolution with infinite conductivity and vacuum or infinite magnetic susceptibility
10 p1252 A73-24344

Application of a variational difference method to the calculation of forced vibrations of shells of revolution
10 p1292 A73-24487

Iterative method for solving some boundary value problems for the equations of an orthotropic shell of revolution
10 p1292 A73-24503

Unsteady aerodynamics of separating and reattaching flow on bodies of revolution.
10 p1173 A73-24816

Application of the extended Newton method to the creep analysis of shells of revolution.
11 p1432 A73-24998

Horn antennas dephasing based on quadrupole with circular guides, cones of revolution and air space
11 p1327 A73-25279

Nonlinear transient analysis of shells and solids of revolution by convected elements.
11 p1437 A73-25495

[AIAA PAPER 73-359]
Stress, stability, and vibration of complex, branched shells of revolution.
11 p1437 A73-25496

[AIAA PAPER 73-360]
A finite element method for nonaxisymmetric vibrations of pressurized shells of revolution partially filled with liquid.
11 p1440 A73-25528

[AIAA PAPER 73-399]
Earliest classic result for the turbulent hydraulic wake behind body of revolution.
11 p1348 A73-25781

A numerical method for solving the stationary diffraction problem of electromagnetic waves on bodies of revolution
11 p1332 A73-26332

Transient creep of shells of revolution.
11 p1444 A73-26336

Variational method for a generalized class of functionals and its application to aeromechanics problems
11 p1304 A73-26438

Asymptotic analysis of the equations of oscillations and stability of bodies of revolution in the case of turning points
11 p1445 A73-26459

Bending problem for shell of revolution with finite displacements, axisymmetric loading and nonlinear strain functions
11 p1445 A73-26460

Oscillations of a shell partially filled with a liquid and containing sources of the liquid
11 p1446 A73-26462

Influence of the shape of a body on the characteristics of a self-similar axisymmetric wake
12 p1457 A73-26953

Infinitesimal deflections of finned surfaces of revolution fixed along the edge with respect to points in space
12 p1552 A73-27299

Book - Mathematical problems in wave propagation theory.
12 p1524 A73-27625

Solvability of the boundary value problem in the theory of shallow shells of revolution and estimation of errors in the approximate solution
12 p1556 A73-27813

Criteria for finite element discretization of shells of revolution.
13 p1691 A73-28084

Computer programs for analysis of shells of revolution based on numerical integration and finite difference procedures
13 p1693 A73-28236

Geometrically nonlinear static and dynamic analysis of shells of revolution.

13 p1693 A73-28239

A contribution to Hertz's theory of elastic impact.

13 p1696 A73-28748

Aerosol particle downward motion in vertical electric field, discussing stability of major axis orientation of ellipsoid of revolution

13 p1654 A73-28881

Free vibrations of shells of revolution with variable thickness.

14 p1805 A73-29768

Formulation of local stability problems of shells of revolution.

14 p1810 A73-30326

Fredholm integral equation singularity method solution for calculating stresses and elastic displacements in bodies of revolution of arbitrary shape under torsional loads

15 p1947 A73-31327

Analysis of turbulent skin friction in thick axisymmetric boundary layers.

15 p1863 A73-31658

Solution of certain classes of three-dimensional problems in elasticity theory with the aid of analytic functions

15 p1952 A73-32077

Torsion of an inhomogeneous body of revolution with variable shear moduli

16 p2074 A73-32682

Axisymmetrical and antisymmetrical stresses and deformations in shells of revolution with a meridional cutout

16 p2074 A73-32683

Deformation of a multilayer shell of revolution under nonisothermal loading

16 p2074 A73-32684

Natural vibrations of variable-thickness shells of revolution with apparent additional masses

16 p2074 A73-32685

Resolvent equations, in complex form, of the theory of transversely isotropic shells of revolution

16 p2074 A73-32686

Forced vibrations of elastic shells of revolution filled with liquid

16 p2074 A73-32687

Nonlinear behavior of shells of revolution under cyclic loading.

16 p2075 A73-32791

Curved rotational shell elements by the constraint method.

16 p2078 A73-33002

Analytic and numerical investigations of boundary layer flows about slender axisymmetrical bodies

16 p1962 A73-33248

Torsional vibrations of shells of revolution of variable thickness.

16 p2081 A73-33682

Chernin type second order equation for complex stress function for elastic shells of revolution under lateral load and tilting moment

16 p2084 A73-34034

Flow of a dust suspension over an ellipsoid of revolution.

17 p2091 A73-34348

Book - Stresses in shells /2nd edition/.

17 p2242 A73-34469

Jet boundary and a free surface behind a body of revolution in the presence of a longitudinal pressure gradient

17 p2094 A73-34774

A new finite element method for analysing symmetrically loaded thin shells of revolution.

17 p2252 A73-35601

On the higher approximations of the supersonic projectile theory.

[AIAA PAPER 73-669] Shells of revolution belonging to a spherical class subjected to local loads at the pole

18 p2362 A73-36402

Experimental investigation of the velocities in the turbulent wake behind bodies of revolution

18 p2266 A73-37017

Diffraction of waves at finite bodies of revolution

19 p2458 A73-37182

Influences of the shape of a body on the characteristics of a self-similar axisymmetric wake.

19 p2377 A73-38129

Free vibration and buckling loads of anisotropic pressurized thin walled shells of revolution, considering cylinders, barrels and spherical sections

20 p2621 A73-39538

Method for calculation of natural and induced oscillations in elastic shells of revolution which are filled with an ideal incompressible liquid

20 p2624 A73-39647

Some mathematically equivalent problems in the statics of shells of revolution

20 p2624 A73-39649

Natural oscillations of shells of revolution with an open profile and concentrated inclusions

20 p2625 A73-39654

Supersonic gas flow pattern at blunt body of revolution with attached shock wave

21 p2632 A73-40400

An experimental study of strong injection at axisymmetrical bodies of revolution.

21 p2633 A73-41057

Canonical differential equations from equilibrium and compatibility conditions for boundary loaded, shell of revolution, simplifying and transforming by canonical transformations

21 p2788 A73-41616

Geometrical characteristics of flat-faced bodies of revolution.

22 p2842 A73-42425

Numerical integration of shell equations using the field method.

[ASME PAPER 73-APMW-27] Saint Venant continuity equation for identical formulation of Lamé equations and elasticity theory problem of stress-strain state in bodies of revolution

22 p2925 A73-42888

Thermal stresses in rotationally symmetric semi-infinite elastic body with heat input along hole boundary and on plane bounding surface, reducing to solution of Fredholm equation

23 p3045 A73-44185

Universal equations for the laminar boundary layer on a body of revolution in oblique flow

24 p3147 A73-44745

Determination of the impulses and moments imparted by shock waves to bodies of revolution

24 p3055 A73-45529

On the ternary compound G in the Al-Mn-Cr system.

24 p3055 A73-45542

BODY CENTERED CUBIC LATTICES

Characteristics of the process of plastic deformation of bcc metals in the microyield zone

02 p0179 A73-11598

Effects of alloying elements on the solubility of hydrogen in beta titanium.

02 p0179 A73-11622

Stresses governing the high-temperature creep rate in single crystals with a bcc lattice

03 p0321 A73-12920

Investigation of dislocation locking by interstitial impurities in bcc-lattice metals

03 p0326 A73-13971

Thermodynamic stability of ordered phase atomic structure state for antiphase domain formation, noting superstructures in face centered and body centered cubic solutions

06 p0708 A73-18055

The mechanical properties of titanium alloys with isomorphous beta-stabilizing elements.

06 p0736 A73-18118

The martensitic transformation during deformation of titanium alloys with metastable beta phase.

06 p0708 A73-18206

Environmental hydrogen embrittlement of an alpha-beta titanium alloy - Effect of hydrogen pressure.

06 p0708 A73-18207

Mechanical properties of interstitial alloys of niobium.

06 p0713 A73-18769

Body centered cubic transition metal stage 3 electrical resistivity recovery mechanism from experiment on recrystallized and stress-relieved plastically deformed Nb wire

07 p0838 A73-19123

Some further comments on Stage III recovery in Group VA body-centered cubic transition metals.

07 p0839 A73-20112

The effect of shear stress on the screw dislocation core structure in body-centred cubic lattices.

07 p0839 A73-20113

Mixed viscous-brittle fracture model of plastic crack distribution and propagation pattern in bcc polycrystal by electron raster microscope analysis

08 p0978 A73-21525

Recrystallization in Ti-15 Mo base beta titanium alloys.

09 p1157 A73-21961

Ti based beta alloy strain hardening and failure characteristics, emphasizing initial deformation phase and microdefect onset and development

09 p1103 A73-22423

Recrystallization of the IVT-1 beta titanium alloy

09 p1105 A73-23064

Application of the Moessbauer effect to the study of the mechanism of iron diffusion in beta-titanium

09 p1107 A73-23192

Mechanical behavior of solid solutions of centered cubic symmetry obtained by limited addition of titanium to the iron

09 p1108 A73-23240

Importance of slip mode for dispersion-hardened beta-titanium alloys.

10 p1231 A73-23770

Relaxation processes in metastable beta titanium alloys.

10 p1235 A73-24441

New mechanism of slowing down screw dislocations in ordered alloys with a bcc lattice

11 p1385 A73-26498

Fracture characteristics of thermally strengthened titanium beta-alloys

12 p1508 A73-26837

Dynamic strain ageing in creep of beta-NiAl.

24 p3100 A73-45331

Effect of accelerations on the thiamine-S/35 distribution in the organism of white mice

03 p0259 A73-13370

Effect of chronic centrifugation on body composition in the rat.

08 p0929 A73-20977

Body centered cubic lattice transition metals favored cleavage plane prediction for crack propagation

13 p1635 A73-28261

Apollo lunar fines ferromagnetic resonance spectral line shape anomaly and anisotropy energy attributed to Fe particles with body centered cubic structure

13 p1684 A73-29177

The effect of neutron irradiation damage on the low temperature deformation characteristics of b.c.c. metals and their alloys.

13 p1638 A73-29454

Mechanical behavior of high-strength beta-titanium alloys.

13 p1638 A73-29456

Influence of alpha- and beta-stabilizers on the plastic deformation mechanism of titanium

14 p1765 A73-30888

Enhanced strain aging of niobium by cyclic deformation.

15 p1890 A73-31990

Structure and decay characteristics of unstable beta-solid solutions of the Ti-V system

15 p1893 A73-32519

Diffusional and nondiffusional metastable-phase transformations in titanium alpha + beta alloys

15 p1893 A73-32520

Influence of plastic deformation and of alloying with small additions of oxygen on the decomposition of the metastable beta phase in the TS6 alloy

15 p1894 A73-32526

Properties of titanium-niobium based stable beta alloys

15 p1894 A73-32534

Investigation of the structure and corrosion behavior of alloys of the Ti-Ta-Cr system

15 p1895 A73-32542

Low temperature deformation of commercial Ti alloys.

16 p2024 A73-32848

An X-ray examination of deformation in beta Ti-V alloys.

17 p2189 A73-34642

Solid cadmium cracking of titanium alloys.

17 p2191 A73-35123

Thermodynamics of b.c.c. solid solutions of hydrogen in niobium, vanadium and tantalum.

17 p2193 A73-35623

Certain law controlling the temperature dependence of the microdeformation of Fe-Cu-Ti, W, and W-Re bcc alloys

18 p2324 A73-36803

Some electron structure characteristics of W-Re solid solutions

18 p2325 A73-36809

Grain growth in commercial alpha and /alpha + beta/ Ti alloys.

18 p2326 A73-37143

Principal aspects of thermal treatments of the alloy Ti-11, 5 Mo-6, Zr-4, 5 Sn /Beta III/

19 p2441 A73-37833

Long period superlattice in an aged beta titanium alloy.

20 p2577 A73-39222

Study of the structure and properties of alloys of the V-Al, Cr-Al and V-Cr-Al systems in the region of solid solution bcc ordering

22 p2873 A73-42088

Decay of the solid beta-solution in beta alloys of titanium and zirconium during tempering

22 p2874 A73-42092

Nature of the strain-hardening of titanium beta solid solutions

22 p2874 A73-42096

Calculation of the physicochemical constants of metals associated with the strength of interatomic bonds

22 p2874 A73-42097

Bcc and fcc metal crystal growth, determining thermodynamic and kinetic conditions, surface texture and favored crystal types

23 p2990 A73-43487

Phase transformations in beta-Cu-Al during extremely rapid cooling from the melt

23 p2992 A73-43914

On the age-hardening of Fe-Pt-Mn ternary alloys.

23 p2994 A73-44139

Morphology and crystallography of beta prime martensite in TiNi alloys.

23 p2994 A73-44160

Influence of titanium on the beta and beta-two phase properties and brittleness of InNDK35T5-type annealed alloys

24 p3098 A73-44472

Dynamic strain ageing in creep of beta-NiAl.

24 p3100 A73-45331

BODY COMPOSITION [BIOLOGY]

Effect of chronic centrifugation on body composition in the rat.

03 p0259 A73-13370

Effect of accelerations on the thiamine-S/35 distribution in the organism of white mice

08 p0929 A73-20977

Effect of training on enzyme activity and fiber composition of human skeletal muscle.

08 p0935 A73-21508

Study of the relations between various mechanical properties and biochemical composition of bone tissues in man

13 p1577 A73-27996

Circadian rhythms of free radical state concentrations in the organs of mice.

20 p2512 A73-39104

BODY FLUIDS

NT BLOOD

NT ENDOLYMPH

NT EOSINOPHILS

NT ERYTHROCYTES

NT LYMPHOCYTES

NT RETICULOCYTES

NT SWEAT

NT URINE

NT WHITE BLOOD CELLS

Cardiovascular and temperature regulatory changes during progressive dehydration and euhydration.

01 p0008 A73-10165

Unusual diastolic heart beat in pericardial effusion.

03 p0259 A73-13059

Symposium on Capillary Exchange and the Interstitial Space, Bad Duerkheim, West Germany, May 3-6, 1972, Proceedings.

03 p0265 A73-14649

Investigation of the exchange between the blood and the intracellular fluid with the aid of radioactive phosphorus

10 p1185 A73-24520

Procedures for polarocochleography and for pressure measurement in the inner ear perilymph in acute experiments on animals

11 p1314 A73-25043

Properties of biological fluids and solids: Mechanics of tissues and organs; Proceedings of the Biomechanics Symposium, Georgia Institute of Technology, Atlanta, Ga., June 20-22, 1973.

18 p2281 A73-36428

The role of the elastic properties of brain and spine cavities in hyperemia compensation

18 p2276 A73-36572

Body fluid volume changes during a 14-day continuous exposure to 5.2% O₂ in N₂ at pressure equivalent to 100 FSW /4 ata/.

18 p2279 A73-36796

The effect of immobilization on body fluid volume in the rat.

20 p2513 A73-39487

Blood plasma contamination of the lung alveolar surfactant obtained by various sampling techniques.

21 p2642 A73-41637

Energy balance and change in body weight and body water in man during a 2-day cold exposure.

24 p3060 A73-45059

BODY KINEMATICS

Dynamics of gravitating systems against the neutrino background of the universe

01 p0100 A73-10712

Angular measurements of foot motion for application to the design of foot-pedals.

01 p0013 A73-10773

Uniqueness and continuous dependence for the equations of elastodynamics without strain energy function.

01 p0115 A73-10777

Certain problems of dynamics and accuracy of gyroscopes in gimbals.

01 p0053 A73-11197

A theory of perturbations in angle-action variables: Application to the motion of a solid about a fixed point - Precession-nutation

01 p0107 A73-11362

Three linear invariant relations in the problem of motion of a heavy solid body with a liquid filler

02 p0153 A73-11773

Dynamics of flexible satellites with active attitude control.

02 p0228 A73-11994

Three-degree-of-freedom motions of a slender asymmetric cone in a hypersonic wind tunnel.

03 p0287 A73-13494

Air-space analogies - The velocity limits in aeronautics and astronautics

03 p0374 A73-13765

Discretized body mechanics equilibrium, constitutive and motion equations application to elastic lattice type shell structures

03 p0393 A73-13779

German monograph - Experimental investigation of the structure of joint movements in the range of motions of the arms and of the entire body, giving attention to a presentation in a man-related basic system.

03 p0267 A73-13812

Book - How man-moves: Kinesiological studies and methods.

03 p0268 A73-13993

The motion of a plate in a rotating fluid at an arbitrary angle of attack.

04 p0404 A73-15161

Human body mathematical model described by kinematic and dynamic equations of joined rigid bodies for investigation of self-controlled movements in specified goal attainment

04 p0411 A73-15207

Structural comparison of articulated plane kinematic chains (PKC) with the aid of graph theory

04 p0476 A73-15656

Numerical integration of rotating body dynamic and kinematic equations, noting orthogonalization, normalization and error minimization methods

05 p0595 A73-16423

Motional effects in retardation plates and mode locking in ring lasers.

06 p0699 A73-17496

Discretized body defined as special system with finite degrees of freedom, describing mechanics in terms of constitutive and motion equations

06 p0723 A73-17894

Space-time transformation for equation of relative motion of two bodies on gravitating matter background of Einstein-de Sitter universe

06 p0724 A73-18689

Approximate calculation of flutter regions for collision body systems in phase space, noting fluttering duration as function of post-impact velocity recovery factor

06 p0725 A73-18880

Resonances and certain cases of integrability of the motion of a heavy solid about a fixed point

07 p0851 A73-19469

On the demonstration and interpretation of the Coriolis effect.

09 p1120 A73-22475

Phase double plane as a method to study the dynamics of a spacecraft with limited constructional rigidity.

10 p1286 A73-24006

Variational determination of electric field induced by charge separation in near wake of negatively charged body moving at mesothermal speeds in collisionless plasma

10 p1254 A73-24116

An analytical estimate of the effect of mobility of a small internal mass on oscillations of a body during deceleration in the atmosphere

10 p1286 A73-24451

Analysis of swimming motions.

11 p1322 A73-25184

The dynamical effect of inertial waves on the gyroscopic motion of a body containing several eccentrically located liquid-filled cylinders.

11 p1346 A73-25224

Solution of kinematical differential equations for a rigid body.

[ASME PAPER 72-APM-AAA]

11 p1398 A73-25705

Errors associated with Rodrigues-Hamilton parameters /vector space basis quaternions/ calculation by numerical integration of kinematic equations of moving body orientation

11 p1400 A73-26454

Flight-mechanics analysis of various flight conditions of conventional aircraft. VII - Mechanical foundations: Dynamic equations of motion of the translational motion of a rigid body

11 p1307 A73-26725

Planck relativistic equations of moving body heat and absolute temperature transformation /1907/ and alternative equations by Ott /1963/, comparing validity

12 p1557 A73-26973

High velocity moving body in ideal incompressible fluid flow, determining lift coefficient from acceleration potential algorithm

12 p1486 A73-27239

Three body system successive states classified as triple approach, simple interplay, ejection without escape and escape /final state/ during course of motion

13 p1683 A73-29140

Correlation and statistical characteristics of turbulence fronts in the wakes of hypervelocity bodies.

13 p1567 A73-29269

Zero tangential acceleration points on bodies moving in three dimensional Euclidean space, considering helical-spherical and rotating-spherical motion

14 p1775 A73-30707

Slow motions of bodies in gas mixtures

15 p1861 A73-31198

Plasma and fields in the vicinity of a rapidly moving body in the presence of an external magnetic field

15 p1919 A73-31880

Resonances and some cases of integrability of the motion of a heavy rigid body about a fixed point.

15 p1914 A73-32068

Approximate calculation of flutter regions for collision body systems in phase space, noting fluttering duration as function of post-impact velocity recovery factor

15 p1915 A73-32405

Continuum mechanics - A brief review.

17 p2244 A73-34827

Analysis of the extravehicular activity of an astronaut

18 p2281 A73-36116

Spatial motion of a two body cluster under the action of gravitational and aerodynamic forces

18 p2351 A73-36119

A nonlinear oscillator analog of rigid body dynamics.

18 p2337 A73-36416

Forces acting on a small body in an arbitrary incompressible fluid flow and equations of motion of a two-phase medium

18 p2302 A73-37008

Analytical estimate of the effect of the motion of a small internal mass on the oscillation of a body decelerating in the atmosphere.

19 p2494 A73-38131

Motion of a solid body having a cavity completely filled with two immiscible liquids

20 p2547 A73-39507

Small oscillations of a heavy solid body about a stationary point and certain cases of the existence of 'linear integrals'

21 p2738 A73-40188

Flight vehicle extensive attitude control theory, deriving kinematic relations for optimal control moment selection to ensure required rotation

21 p2780 A73-40385

Errors of a single-axis gyro stabilizer as an angular velocity integrator

22 p2860 A73-42366

Vertical arm reaching movements for various gravitational levels, measuring reach time and angular and lower arm velocities

23 p2948 A73-43218

Dynamics of the rotary motions with respect to the center of mass of a system of solids with a variable geometry of the masses

23 p3007 A73-44187

Analysis of the perturbed motion of a solid with cavities partially filled with liquid

23 p2969 A73-44198

Motion of a solid with a nonholonomic constraint at a fixed point

23 p3007 A73-44200

Physical model selection for the balance preservation system in man

24 p3063 A73-44903

Decomposition and determination of the parameters of a system for angular motion stabilization in an asymmetric solid body

24 p3074 A73-45099

Kustaanheimo-Stiefel transformation in Kepler motion perturbation theory derived from general solution of two body problem, noting application to collision orbits and Lagrange solutions

24 p3142 A73-45298

Continuous body kinematics and thermodynamics covering frame and motion, differential calculus in Euclidean spaces, deformations, interactions, force equilibrium, entropy and dissipation principle

24 p3112 A73-45472

The motion of a body containing a liquid-filled cavity with elastic radial ribs and exhibiting perturbations relative to the longitudinal axis

24 p3112 A73-45513

Relationships between forces acting on bodies moving in a rarefied gas, in a light flux, and in hypersonic Newtonian flow

24 p3055 A73-45532

BODY MEASUREMENT [BIOLOGY]

NT ANTHROPOMETRY

NT ELECTROPLETHYSMOGRAPHY

Mathematical analysis of body surface potentials.

04 p0412 A73-15646

A method for chronocyclographical motion analysis with the aid of an on-line computer

07 p0785 A73-20036

Estimation of left ventricular size by echocardiography.

09 p1046 A73-22999

Some metric characteristics of myocardial cells under various conditions of cardiac and cardiovascular pathology

18 p2280 A73-36962

Biplane roentgen videometric system for dynamic, 60/sec, studies of the shape and size of circulatory structures, particularly the left ventricle.

19 p2399 A73-37798

BODY SIZE [BIOLOGY]

Redintegrated somatotyping technique for physique measurement and classification based on limb and torso photographic diameter integration with height, using photoelectric cell and electronics

06 p0659 A73-18474

Changes in functional construction of bone in rats under conditions of simulated increased gravity.

17 p2113 A73-35863

Regression of altitude-produced cardiac hypertrophy.

24 p3060 A73-45065

BODY SWAY TEST

Effect of forward head inclination on visual orientation during lateral body tilt.

03 p0266 A73-13000

BODY TEMPERATURE

Effect of controlled elevation of body temperature on human tolerance to +Gz acceleration.

01 p0007 A73-10159

Utility of heat stress indices and effect of humidity and temperature on single physiologic strains. [AD-751735]

01 p0007 A73-10163

Unacclimatized male Caucasians lower critical temperature determination for subsequent investigation of ethnic variability in acute cold exposure responses
01 p0008 A73-10166

Effects of endotoxin on monoamine metabolism in the rat.
01 p0009 A73-11100

Muscle, skin and esophageal temperature measurement during transient and steady state phases of negative work exercise on bicycle ergometer
03 p0262 A73-14112

Heat flow meter and calorimeter measurements of heat transfer between human body and environment under various climatic conditions for temperature regulation studies
03 p0268 A73-14123

Telemetric measurement of local blood flow by heat conduction probes.
03 p0270 A73-14282

An implantable radiotelemetric measuring device for simultaneous long term measurements of body temperature and turnover of rabbit serum albumin/I-125 in unrestrained rabbits.
03 p0271 A73-14301

Multichannel telemetry of physiological parameters /body temperature, eeg/ in the rat. I - Design and methods.
03 p0272 A73-14305

Multichannel telemetry of physiological parameters /body temperature, EKG, EEG/ in the rat. II - Applications in neuropharmacology.
03 p0272 A73-14306

Body temperature effect on protein conformation stability in healthy and diseased organisms, noting blood plasma albumin fractions
04 p0409 A73-14822

Low body temperature effects on learned behavior retention under hibernation conditions in squirrels
05 p0539 A73-16324

Body thermotopography and some metabolic process characteristics in scuba divers under various underwater exposure conditions
05 p0545 A73-16734

Thermoregulatory reactions of animals in a helium-oxygen medium
06 p0650 A73-17695

Predicting heart rate response to work, environment, and clothing.
09 p1046 A73-22931

Thermoregulatory behavior of man during rest and exercise.
10 p1178 A73-23572

Thermosensitive interoceptors and their interaction with thermosensitive structures of the hypothalamus
10 p1179 A73-23803

Cerebral temperature oscillations and vascular responses in man
10 p1179 A73-23805

Portable electronic thermometer for temperature measurement during exercise elevation of body temperature in heat acclimatization experiment
10 p1185 A73-24567

Quantitative influence of CO2 inhalation on thermal sweating in man.
11 p1314 A73-25331

Digital temperature-measuring device for medical applications
13 p1578 A73-28338

Some effects of cooling and heating areas of the head and neck on body temperature measurement at the ear.
13 p1575 A73-28504

Step-wise changes in thermoregulatory responses to slowly changing thermal stimuli.
13 p1576 A73-28535

Blood pressure and body temperature dynamic control systems and respiration relationship to heart rate variability
14 p1720 A73-30878

Effect of body temperature on ventilatory transients at start and end of exercise in man.
15 p1832 A73-31127

Energy balance during moderate exercise at altitude.
15 p1833 A73-31343

Calculation of temperature distribution in the human body.
15 p1839 A73-31999

The effects of core temperature elevation and thermal sensation on performance.
15 p1839 A73-32396

Temperature conditions and blood supply of the brain in animals
17 p2111 A73-34229

Investigation of the possibility of human adaptation to a 16-hour day
17 p2114 A73-34238

Temperature of exhaled air of healthy subjects
18 p2277 A73-36583

Tolerance to heat following cold stress.
18 p2283 A73-36784

Human performance at elevated environmental temperatures.
18 p2283 A73-36787

Blood electrolytes and exercise in relation to temperature regulation in man.
18 p2280 A73-36983

Inversion of lighting regimen alters acrophase relations of circadian rhythms in body temperature, heart rate and movement of pocket mice.
20 p2513 A73-39480

Design considerations and applications of gradient layer calorimeters for use in biological heat production measurement.
22 p2813 A73-42054

The specific resistance of blood at body temperature.
22 p2807 A73-42670

Book on comparative physiology of thermoregulation covering primitive and aquatic mammals, torpidity aspects, evolution and newborns
22 p2809 A73-42859

Primitive mammals phylogeny relationship to homeothermic abilities, discussing body temperature, thermoregulation, basal metabolism rates, hibernation, nycthemeral rhythms and responses to heat and cold
22 p2809 A73-42860

Aquatic and diving mammals in fresh water and marine environments, discussing aquatic thermal conditions, body temperature distribution, thermoregulation, metabolic heat production, etc
22 p2809 A73-42861

Torpor and hibernation physiology in mammals covering evolution, hypothermia, energy conservation, cell and organ adaptations, nervous and cardiovascular system changes, etc
22 p2809 A73-42862

Thermoregulation evolution in various animals, discussing body size and composition effects, body temperature variations, control mechanisms, heat loss and production, behavior and ontogeny
22 p2810 A73-42863

Spinal cord heating effects on frog thermoregulatory behavior in aqueous thermal gradient, noting preference for colder ambient temperature
23 p2947 A73-43994

Spectral emissivity of skin and pericardium.
23 p2950 A73-44213

Cardiovascular adjustments to progressive dehydration.
24 p3060 A73-45063

BODY TEMPERATURE REGULATION
U THERMOREGULATION

BODY WEIGHT
Effect of chronic centrifugation on body composition in the rat.
03 p0259 A73-13370

Organ and body mass changes in restrained and fasted domestic fowl.
04 p0409 A73-14975

Statistical correlations of maximum oxygen consumption, body weight and endurance /work/ performance in exercise-oxygen studies
06 p0659 A73-18472

Biological effects of lasting hypodynamic on young albino rats in 62 day confinement, considering weight, growth and sexual behavior
08 p0929 A73-20983

Physiological responses of rats to intermittent high-altitude stress - Effects of age.
10 p1182 A73-24564

Helium-cold induced hypothermia in the white rat.
12 p1461 A73-26975

Some aversive characteristics of centrifugally generated gravity.
13 p1575 A73-28506

Changes in functional construction of bone in rats under conditions of simulated increased gravity.
17 p2113 A73-35863

Responses of men and women to two-hour walks in desert heat.
20 p2518 A73-39784

Relationship between organ weight and blood flow in rats adapted to simulated high altitude.
21 p2639 A73-41156

Chronic acceleration effects on homeotherm physiological adaptation in terms of body weight, tolerable field intensity, growth and fat deposition inhibition, etc
22 p2804 A73-42177

Climbing and cycling with additional weights on the extremities.
22 p2806 A73-42418

Energy balance and change in body weight and body water in man during a 2-day cold exposure.
24 p3060 A73-45059

BODY-WING AND TAIL CONFIGURATIONS
Aerodynamic interference between jet propulsion system and airframe for supersonic transport with wing-mounted nacelles, noting wing performance role in lift effectiveness
03 p0243 A73-13428

[AIAA PAPER 72-1113]
BODY-WING CONFIGURATIONS
Simplification of the wing-body interference problem.
01 p0001 A73-10048

Slowly oscillating lifting surfaces at subsonic and supersonic speeds.
03 p0245 A73-13704

Study of the asymptotic behavior of axial perturbation velocities in the vicinity of singularities
03 p0245 A73-13770

Lift of wing-body combination.
03 p0247 A73-14194

Correlation of wing-body combination lift data.
09 p1028 A73-22435

Aerodynamic studies of spacecraft in the freestream Mach number range of 3 to 10 at high Reynolds numbers [DFVLR-SONDDR-286]
13 p1567 A73-29447

Roll coupling moment of deflected wing-body combination.
15 p1823 A73-31573

Lifting body configurations for sustained hypersonic flight.
19 p2377 A73-37710

Prediction of the lift and moment on a slender cylinder-segment wing-body combination.
19 p2377 A73-38007

Pressure fields over hypersonic wing-bodies at moderate incidence.
20 p2508 A73-39808

The panel method for the calculation of the pressure distribution on missiles in the subsonic range
22 p2797 A73-43028

BOEING AIRCRAFT

NT B-52 AIRCRAFT
NT BOEING 727 AIRCRAFT
NT BOEING 737 AIRCRAFT
NT BOEING 747 AIRCRAFT
NT CH-46 HELICOPTER
NT CH-47 HELICOPTER

The Air Force/Boeing advanced medium STOL transport prototype.
[SAE PAPER 730365]
17 p2103 A73-34710

BOEING MILITARY AIRCRAFT
U MILITARY AIRCRAFT

BOEING 727 AIRCRAFT
Boeing 727 design and development in response to airline market requirements, emphasizing profitability
10 p1176 A73-24875

BOEING 737 AIRCRAFT
Two man crew cockpit design for commercial 737 jet transport aircraft, discussing pilot vision, control and display panels and avionics disposition
19 p2384 A73-37729

BOEING 747 AIRCRAFT
Attenuation of airplane /747/ air-conditioning noise in lined and unlined ducts.
03 p0289 A73-12959

BOAC computer aided flight simulators, detailing simulator systems history, Boeing 747 training adaptation, and simulation types
16 p1996 A73-33212

Market economic environment change effects on air transport design and use, examining 747 operational requirements in terms of cargo load factor, passenger fares and labor costs
17 p2103 A73-34703

[SAE PAPER 730355]
Simulating the introduction of 747 aircraft into airport operations.
18 p2296 A73-36423

The universal data link system for air/ground communications.
20 p2526 A73-38757

BOGOLIOBOV THEORY

Application of the asymptotic method to third-order oscillatory systems
01 p0021 A73-10030

Integral of collisions for a rarefied plasma /Quantum theory/
01 p0086 A73-11287

Relation between the N. M. Krylov-N. N. Bogoliubov averaging method and the method of envelopes in studies of a class of control systems
15 p1854 A73-31801

Collision integral for a low-density plasma /quantum theory/.
23 p3009 A73-43508

On the connection of the Krylov-Bogolyubov averaging method with the envelop method for investigating one class of control systems.
23 p2965 A73-44330

BOGS
U MARSHLANDS

BOILERS

The design of components for an advanced Rankine cycle test facility.
11 p1344 A73-25995

Guide to a quality control system for Code vessels.
14 p1755 A73-30144

High-temperature corrosion in gas turbines and steam boilers by fuel impurities. II - The sodium sulfate-magnesium sulfate-vanadium pentoxide system.
15 p1841 A73-32175

BOILING

NT FILM BOILING
NT LEIDENFROST PHENOMENON
NT NUCLEATE BOILING

Experimental study of heat transfer in the boiling of nitrogen tetroxide.

03 p0397 A73-13188

Peak pool boiling heat flux from finite heater configurations, improving Zuber hydrodynamic theory by combining vapor escape path thickness empirical values with velocity matching hypothesis

[ASME PAPER 72-WA/HT-10] 04 p0519 A73-15835

Adsorption conditions and vapor molecule balance in wall layer at liquid boiling initiation, noting heat flux dependence on underheating effect, pressure and velocity

06 p0769 A73-18564

Determination of the statistical characteristics of temperature fluctuation in pool boiling.

08 p1022 A73-21252

A graphical method for analyzing pool-boiling systems.

08 p1023 A73-21262

Inert-gas transport in liquid metals during boiling experiments.

08 p1023 A73-21263

Stability of heat transfer during boiling at a nonisothermal surface

12 p1558 A73-27314

Adsorption conditions and vapor molecule balance in wall layer at liquid boiling initiation noting heat flux dependence on underheating effect, pressure and velocity

16 p2086 A73-33589

BOLIDES

Russian monograph on meteor observation covering telescopic and photographic methods, meteor trail plotting, radiant determination, stream counts and bolide data

15 p1941 A73-32416

BOLOGRAMS

U BOLOGRAMS

BOLOMETERS

Practical and precise means of microwave power meter calibration transfer.

03 p0310 A73-14499

Newly developed bolometer mounts for the short millimeter wave region.

03 p0310 A73-14500

Matter heating based IR astronomy, describing liquid helium cooled Ge bolometer and IR telescope

07 p0875 A73-19324

Comparative studies of noise limitations in superconducting thin-film radiation detectors.

07 p0863 A73-20105

Improved responsivity and sensitivity characteristics of the thin-film bismuth bolometer.

09 p1080 A73-22087

Infrared detectors - Survey of the present state of the art.

11 p1368 A73-26509

High responsivity large surface liquid helium cooled IR bolometers based on carbon resistors and Ge and Si elements

11 p1368 A73-26510

A new type of helium-cooled bolometer.

11 p1368 A73-26511

InSb and Ga-doped Ge bolometers performance tests, discussing detector circuitry and dc, noise and responsivity measurements

11 p1368 A73-26512

Worldwide variations in atmospheric transmission. I - Baseline results from Smithsonian observations.

15 p1904 A73-31724

A low temperature bolometer heterodyne receiver for millimeter wave astronomy.

20 p2564 A73-38878

Fluidic bolometer type sensor for reaction wheel control to maintain spacecraft and rocket vehicle attitude relative to sun, discussing design, simulation and tests

23 p3038 A73-43395

BOLTS

Criteria for self loosening of fasteners under vibration.

01 p0058 A73-11512

Stress corrosion crack protection from coatings on high strength H-11 steel aerospace bolts.

10 p1232 A73-23874

Mechanical properties of AFC77 stainless steel bolts.

21 p2721 A73-41085

Investigation on the optimum tightening force of bolted joint in torque control method.

23 p2986 A73-44140

BOLTZMANN DISTRIBUTION

Solution of the Boltzmann equation for a fully ionized plasma in an oscillatory electric field and a steady magnetic field. VI - The first velocity moments of distribution function for a homogeneous plasma in a high-frequency electric field.

03 p0349 A73-14650

Consideration on the 'equilibrium' electrons distribution function for a homogeneous, high-frequency, fully ionized plasma.

14 p1779 A73-29998

BOLTZMANN TRANSPORT EQUATION

Hypersonic spherical source flow expansion into rarefied atmosphere of same gas, using kinetic model and asymptotic solution of Boltzmann equation

02 p0154 A73-12054

Local transport equations for turbulent shear flow.

02 p0154 A73-12825

Boltzmann equation model approach for prediction of velocity profiles and gas flow rates through trapezoidal microgaps

[ASME PAPER 72-LUB-15] 03 p0297 A73-14331

Boltzmann transport equation for plasma probe detector characteristics for Maxwellian and non-Maxwellian distribution functions of electrons in dc and ac electric fields

04 p0480 A73-15602

Zero and first velocity moments of Boltzmann equation with complications placed on Ohm Law in plasmas, considering momentum exchange

06 p0730 A73-18462

Asymptotic theory of the Boltzmann equation at large Knudsen number.

07 p0853 A73-20473

Computer simulation of semiconductor devices.

08 p0948 A73-21534

Application of the method of Boltzmann-Krook-Morse to the Knudsen layer of a polyatomic gas which is solidified or in equilibrium - Expression of discontinuities of wall temperatures

09 p1072 A73-23033

Boltzmann transport equation for plasma probe detector characteristics for Maxwellian and non-Maxwellian distribution functions of electrons in dc and ac electric fields

10 p1254 A73-24192

Approximate solution of the system of Boltzmann equations for a mixture of reacting gases

10 p1252 A73-24490

Boltzmann equation integral form derived tensorial formulation of monoenergetic neutron diffusion theory, evaluating components of diffusion coefficient tensor

11 p1401 A73-25211

Uniform isotropic Brownian motion in a linear-cubic approximation

11 p1397 A73-25428

Boltzmann kinetic equation for nonideal plasma with allowance for polarization effects, noting collision integral convergence

11 p1406 A73-26187

Boltzmann transport equation solution for electron mobility in ellipsoidal valleys of n-type GaAs and GaP, taking into account arbitrary magnetic fields and scattering mechanisms

13 p1668 A73-28217

A transport equation treatment of tunnelling in semiconductors.

13 p1668 A73-28218

Fundamental equations of a mixture of gas and small spherical solid particles from simple kinetic theory.

13 p1600 A73-28616

Transport effects in a turbulent flowing plasma - The moment relations.

15 p1916 A73-31082

Solution of the plane problem of rarefied-gas aerodynamics on the basis of the Boltzmann kinetic equation

15 p1822 A73-31244

The use of subgrid transport equations in a three-dimensional model of atmospheric turbulence.

[ASME PAPER 73-FE-21] 17 p2206 A73-35017

Unique solution of boundary value problem of Boltzmann equation for unsteady rarefied gas flow of formless particles past arbitrary surface

19 p2462 A73-37843

Modification of the Chapman-Enskog method for a mixture of reactive gases with allowance for fast and slow processes

19 p2462 A73-37845

Integral transport equations for component distribution function of gas mixture with internal degrees of freedom and chemical reactions

19 p2463 A73-37847

Boltzmann equation with Gross-Krook type model for investigation of steady plane shock wave structure in fully ionized gas

20 p2596 A73-38968

Chapman-Enskog-Hilbert expansion for a Markovian model of the Boltzmann equation.

20 p2549 A73-39627

Directional plasma transport equations derived from Boltzmann equation by averaging of velocity space subset, applying to plasma confinement by external time dependent electromagnetic fields

21 p2748 A73-41127

Kinetic models and the problem of shock-wave structure

24 p3081 A73-45537

BOLZA PROBLEMS

Variational optimization problems for hyperbolic-type equations

01 p0077 A73-10952

A proof of the Pontryagin maximum principle for initial-value problems.

12 p1517 A73-27117

Variational optimization problems for equations of hyperbolic type.

12 p1518 A73-27528

Second-order optimality conditions for the Bolza problem with variable endpoints and separated end conditions.

19 p2445 A73-38039

BOMBER AIRCRAFT

NT A-4 AIRCRAFT

NT B-1 AIRCRAFT

NT B-52 AIRCRAFT

NT B-57 AIRCRAFT

NT B-70 AIRCRAFT

Advanced aircraft power systems utilizing coupled APU/ECS.

[SAE PAPER 730380] 17 p2108 A73-34719

Compatibility of maneuver load control and relaxed static stability.

[AIAA PAPER 73-791] 19 p2379 A73-37458

BOMBS [PRESSURE GAGES]

U PRESSURE GAGES

BOMBS [SAMPLERS]

U SAMPLERS

BONDING

NT ADHESIVE BONDING

NT AGGLUTINATION

NT CERAMIC BONDING

NT EXPLOSIVE WELDING

NT METAL BONDING

NT METAL-METAL BONDING

NT RESIN BONDING

High temperature solid lubrication technology developments, discussing bonded films, plastic and metal bonded composites and temperature ranges

03 p0330 A73-13013

Shock wave generation for industrial applications in graphite to diamond conversion and incompatible materials bonding

07 p0850 A73-19048

Investigation of the bond strength between layers of textile materials

17 p2194 A73-34333

BONE MARROW

Radiation protective effect of a mixture of ATP, AET, and serotonin on yields of 600-R X-ray-induced chromosome aberrations in the rat.

02 p0134 A73-12187

Differentiations and maturations in red and white blood cells construction in red bone marrow, noting hematopoietic system formation from single source cell

06 p0649 A73-17473

Proliferative activity of bone marrow cells in dogs exposed to chronic and repeated acute gamma irradiation

12 p1463 A73-27708

BONES

NT CEREBRUM

NT CRANIUM

NT INTRACRANIAL CAVITY

NT PELVIS

NT SKULL

NT ULNA

NT VERTEBRAE

Experimental determination of shear moduli in a compact bone tissue

03 p0267 A73-13742

Strength limits correlation to modulus of elasticity for compact bone material from compression tests, noting anisotropy tensor analysis

03 p0267 A73-13744

Implantable transducer for in vivo measurement of bone strain.

12 p1464 A73-27443

Study of the relations between various mechanical properties and biochemical composition of bone tissues in man

13 p1577 A73-27996

Changes in functional construction of bone in rats under conditions of simulated increased gravity.

17 p2113 A73-35863

Low calcium diet produced chronic decalcification effect on osseous repair of experimentally induced cortical bone defect in chickens

18 p2270 A73-35981

BOOLEAN ALGEBRA

NT BOOLEAN FUNCTIONS

Continuum thermodynamics-based formulation of mixture theory using Boolean algebra with emphasis on partial stress tensors, considering force, moment and energy balance equations

22 p2885 A73-41771

Algebraic nature of thought formation structures

24 p3063 A73-44905

BOOLEAN FUNCTIONS

Application of the device of linear programming to solve certain optimal problems of reliability theory.

02 p0187 A73-12121

Method of minimization of description of classes in pattern recognition.

02 p0143 A73-12125

- Algorithms for calculating disjunctive normal form with minimum number of variables of completely/incompletely determined Boolean functions
09 p1111 A73-22108
- Sequential systems fault detection methods based on topological description and Boolean analysis of internal variables, obtaining fanout free equivalent network by tree expansion
10 p1201 A73-24055
- Formal treatment and optimization of Boolean expressions.
18 p2292 A73-36956
- Synthesis of combination circuits in a universal basis and its use in estimating the complexity of digital structures containing integrated circuits
21 p2668 A73-40017
- BOOMS [EQUIPMENT]**
- Bending and flexing of the Apollo 15 mass spectrometer boom.
05 p0636 A73-17210
- Near field of scattering by a hollow semi-infinite cylinder and its application to sensor booms.
11 p1328 A73-25658
- Buffalo aircraft fiberglass laminated polyester nose boom for mounting horizontal and vertical wind sensing probes, describing instruments and measurement procedures
17 p2174 A73-35576
- BOOST**
- U ACCELERATION [PHYSICS]**
- BOOSTER RECOVERY**
- Cost effective space shuttle solid rocket booster recovery parachute system planning, discussing model drop and structural load testings
[AIAA PAPER 73-441] 15 p1825 A73-31427
- An airdrop system for testing large parachutes for recovery of loads in excess of 50,000 lb.
[AIAA PAPER 73-471] 15 p1828 A73-31455
- Space shuttle solid rocket boosters ocean recovery, discussing mission requirements, parachute configurations, tradeoff studies and model testing
[AIAA PAPER 73-602] 18 p2358 A73-36084
- BOOSTER ROCKET ENGINES**
- Space booster control system computerized design algorithm for forward loop compensation filter selection based on minimization of penalty function of stability margin violations
01 p0021 A73-11516
- A description of the design, testing and application of the 'Waxwing' apogee boost motor for the 'Black Arrow' satellite launcher, with particular reference to development problems.
[AIAA PAPER 72-1134] 03 p0355 A73-13441
- L 17 satellite booster development from Emeraude stage, discussing gas generator, Valois thruster engine and assembly tests, combustion instability and launching results
07 p0905 A73-18990
- Reinforced plastics role in construction and shielding of Diamant B satellite booster main components
07 p0905 A73-18995
- EUROPA III - Description of the work performed during the preparatory phase and characteristics of the booster**
12 p1548 A73-27377
- Europa 3 booster heat shields configuration selection factors and design, considering mechanical and electrical interfaces with vehicle equipment
12 p1548 A73-27378
- Strain measurements in the solid propellant of a large booster structural test vehicle.
13 p1669 A73-29304
- Space shuttle solid rocket boosters mission and systems requirements, considering thrust vector control and staging/separation, electrical and recovery systems
[AIAA PAPER 73-606] 18 p2358 A73-36086
- BOOSTER ROCKETS**
- Evolution of the Space Shuttle. I.
16 p2074 A73-34024
- Example of dynamic interference effects between two oscillating vehicles.
22 p2917 A73-42634
- BOOSTERS**
- The effect of the precooling of the air before compression in the case of air-breathing propulsion systems of boosters for space vehicles
[DGLR PAPER 72-060] 02 p0202 A73-11673
- BOOTS [FOOTWEAR]**
- Mercury, Gemini and Apollo space suits, discussing glove development, boot design, portable life support equipment and extravehicular mobility
16 p1976 A73-34025
- BORANES**
- NT HYDRAZINE BORANE**
- BORATES**
- Borating kinetics and coating phase composition and thickness on cobalt and cobalt base alloys by metallographic, microhardness and X ray analyses
09 p1103 A73-22467
- BORREL SETS**
- Arithmetic of probability laws defined on a separable Hilbert space
07 p0845 A73-20148

- Probability series weak uniform convergence based on Billingsley-Topsoe uniformity theorem, using Borel set theory for separable metric space
16 p2031 A73-33107
- A topology on a group of measurements of probability defined on a Borelian tribe with an enumerable base, and an associated Glivenko-Cantelli theorem
19 p2444 A73-37534
- Concentration functions of finite-dimensional and infinite-dimensional random vectors
22 p2882 A73-42649
- BORES**
- U CAVITIES**
- BORESIGHTS**
- Large antennas and radomes boresight measurement with angular accuracy by laser mirror system incorporated into pattern range for antenna tower alignment
17 p2143 A73-35696
- BORIDES**
- NT TITANIUM BORIDES**
- Temperature-dependent hyperfine interactions in Fe₂B.
06 p0734 A73-17833
- Structure of the borated layer after diffusion saturation with other elements
06 p0707 A73-18040
- Borated steel fracture characteristics in the case of cyclic plane bending
06 p0711 A73-18663
- Stability of reactive and refractory metal borides in ternary chromium-base alloys.
07 p0838 A73-19122
- Interaction between zirconium diboride and molybdenum
09 p1105 A73-22981
- Temperature dependent thermal conductivity coefficient and electron and phonon components for group IV-VI transition metal diborides at 2300 K, using Wiedemann-Frantz law
10 p1236 A73-23518
- Temperature dependent heat conductivity, Lorentz number and electrical resistivity of high melting Ti, Zr, Nb, Cr, Mo and W carbides and borides at 300-1200 K
10 p1230 A73-23519
- Development of a production technology for high-density metal-ceramic materials by the method of impregnating porous preforms with low-melting iron boride alloys
10 p1224 A73-24316
- Thermal oscillations of hexaboride atoms of some metals
10 p1261 A73-24777
- Boridosilicide and boridoaluminide diffusion coatings on iron and steel, investigating formation kinetics structure and properties
10 p1227 A73-24963
- Transition metal borides ESCA spectra observation for metal-boron bonding energy based on spectral sensitivity to surface oxidation, discussing relevant features
11 p1325 A73-25202
- Effect of carbon on the growth of boride layers
11 p1374 A73-26109
- Crystalline structure of the TaCoB and NbCoB₂ compounds
12 p1512 A73-27244
- Thermionic emission properties of refractory metal borides
13 p1634 A73-28201
- High-temperature oxidation of tungsten boride in oxygen and the effect of scale evaporation.
16 p1976 A73-33076
- Temperature dependent thermal conductivity coefficient and electron and phonon components for group IV-VI transition metal diborides at 2300 K, using Wiedemann-Frantz law
17 p2196 A73-35198
- Temperature dependent heat conductivity, Lorentz number and electrical resistivity of high melting Ti, Zr, Nb, Cr, Mo and W carbides and borides at 300-1200 K
17 p2191 A73-35199
- Protection of certain borides from oxidation in air at 1200 C
18 p2318 A73-35888
- Possibility of predicting the residual stress pattern in boronized steels
21 p2721 A73-41229
- Intensity of charged particle recombination on the surface of certain borides of high-melting-point metals in a weakly ionized hydrogen plasma
24 p3098 A73-44418
- BORING MACHINES**
- Machining precision in deep-hole boring by a feed-division technique
02 p0174 A73-12578
- BORN APPROXIMATION**
- Excitation of highly excited hydrogenic ions and atoms by charged particles. IV.
16 p2039 A73-33865
- BORN-MAYER EQUATION**
- U BORN APPROXIMATION**

- BORN-OPPENHEIMER APPROXIMATION**
- Electron scattering from diatomic molecules in the first Born approximation.
22 p2889 A73-42446
- BOROXYDRIDES**
- NT BERYLLIUM BOROXYDRIDES**
- BORON**
- Boron combustion, covering thermochemistry application to chemical propulsion systems, temperature effects on oxidation, single particle ignition and powder burning
01 p0089 A73-11112
- Influence of cerium and boron additions on the corrosion properties of Kh18N9TL steel
02 p0181 A73-12538
- Failure mechanisms in transversely loaded boron-aluminum.
02 p0184 A73-12861
- Development and evaluation of graphite and boron polyimide composites.
03 p0329 A73-13003
- Filament wound boron/epoxy rocket motor chamber fabrication and hydroproof, burst and firing tests, including failure and deformation evaluation
03 p0331 A73-13024
- Response of boron/epoxy composite materials to simulated lightning current.
03 p0331 A73-13025
- Preparations and properties of boron and silicon carbide filaments
03 p0334 A73-13588
- Increasing the heat resistance of steel Kh14G14N3T with microadditions of boron.
03 p0327 A73-14006
- The effect of boron concentration on radiation damage in silicon solar cells.
03 p0258 A73-14249
- Threshold voltage shift for low voltage operation of transistor circuits with boron ion implanted MOS
04 p0427 A73-15322
- B-Al matrix composites environmental properties, costs and development for aerospace systems, considering corrosion, erosion and thermal cycling effects on tensile strength
04 p0467 A73-15934
- Boron fiber-aluminum alloy matrix composite structure Charpy impact energy absorbing capacity explained via energy dissipation of matrix by plastic deformation
05 p0588 A73-16111
- Effect of specimen geometry on fatigue strength of boron and glass epoxy composites.
05 p0588 A73-16139
- Electron density reduction in high temperature air via boron powder aerosol, presenting shock tube data for temperature range 2800-4200 K and pressure range 1-2 atm
[AIAA PAPER 73-261] 05 p0603 A73-16982
- On the establishment of a diffusion barrier between a boron fiber and its tungsten substrate
05 p0589 A73-17049
- The current-voltage characteristics of boron implanted silicon diodes.
06 p0674 A73-17797
- Direct mixing and combustion measurements in ducted, particle-laden jets.
[AIAA PAPER 72-1177] 06 p0769 A73-18400
- Polyimide composites development for aircraft structures.
06 p0715 A73-18720
- Structural fabrication of advanced metal-matrix composites.
[SME PAPER EM 72-108] 07 p0832 A73-20449
- Effects of boron density on radiation resistance of copper-contaminated n/p type silicon solar cells.
08 p0928 A73-21114
- Phase transformational kinetics and hardenability of low-carbon, boron-treated steels.
09 p1102 A73-22416
- Investigation of the compatibility of boron fibers with tungsten substrates and titanium matrices
09 p1103 A73-22469
- Properties of silicon implanted with boron ions through thermal silicon dioxide.
09 p1064 A73-23040
- Microstructural observations of arc welded boron-aluminum composites.
10 p1223 A73-23630
- Boron filament reinforced Al and Ti matrices manufactured by pressure-sintering method, investigating filament external silicon carbide effects on mechanical properties
11 p1379 A73-25402
- Plasma sprayed boron fiber reinforced titanium oxide and Al matrix composites, discussing temperature control for particle size and SiC coating effects on strength
11 p1388 A73-25413
- Effects of prestressing boron/epoxy prepreg on composite strength properties.
[AIAA PAPER 73-382] 11 p1388 A73-25512
- The impact toughness of discontinuous boron-reinforced epoxy composites.
11 p1389 A73-26046

Theoretical and experimental investigation of the nonlinear behavior of angleplied boron/aluminum composites.

11 p1385 A73-26524

Transverse creep and stress-rupture of Borsic-aluminum composites and Borsic-aluminum composites containing stainless steel and titanium.

13 p1633 A73-28143

Vapor-phase deposition of elementary boron at substrate temperatures in the range from 1100 to 1400 C

13 p1645 A73-28181

Low-temperature internal friction in boron fibers

14 p1766 A73-30380

Technical note on some mechanical properties of a magnesium-25 vol% boron particulate composite.

14 p1765 A73-30935

Transformations in crystalline boron during mechanical dispersion

15 p1897 A73-31600

Theoretical post-yielding behavior of composite laminates. I - Inelastic micromechanics.

15 p1897 A73-31678

Yielding in unidirectional composites under external loads and temperature changes.

15 p1949 A73-31679

Tensile and compressive strength tensor prediction for anisotropic boron-epoxy composites from off axis tests

15 p1897 A73-31682

Cosmic abundance of boron.

15 p1942 A73-32648

Thermal cycling effects on void formation in boron-aluminum matrix composites at 70-670 F, considering jet turbine compressor blade applications

16 p2084 A73-33037

Boron composites - Status in the USA.

16 p2031 A73-34042

Study of gas-phase reactions in particle-laden, ducted flows.

17 p2150 A73-34194

Room temperature creep of Borsic-aluminum composites.

17 p2189 A73-34644

Development of advanced composite rocket motor chambers using boron and graphite fibers.

17 p2194 A73-34803

Aircraft structural applications of filamentary composites, discussing fiberglass, boron-epoxy and graphite-epoxy composites

17 p2103 A73-34814

Carbon, boron and glass fiber-epoxy resin composites fracture processes, predicting fracture strength of aligned fibrous composites via linear elastic fracture mechanics concepts

17 p2198 A73-35530

Tensile fracture of boron-epoxy composites with ordered filament packing geometry.

17 p2198 A73-35535

Borsic-aluminum composites fracture and flexural behavior from Charpy impact and slow bend tests

17 p2192 A73-35537

Borsic-Al composites fiber-matrix debonding for toughening mechanism of crack blunting, noting notch insensitivity and delamination

17 p2193 A73-35540

Noncumulative fracture mode of unidirectional boron filament-aluminum matrix composite under axial tension, measuring critical filament stress

17 p2193 A73-35542

Boron epoxy, polyimide and aluminum composite materials for cost effective high performance aircraft and turbine engine structures, assessing development and application status

19 p2443 A73-37892

The effect of elevated temperatures on the mechanical properties of B-Al composites.

19 p2442 A73-38095

Production techniques for advanced composites fabrication by tape machine automation.

[SME PAPER EM 73-118] 19 p2436 A73-38498

Boron-stiffened longerons on the B-1.

[SME PAPER EM 73-719] 19 p2436 A73-38499

Properties of boron fibers and of boron-aluminum composites in uniaxial compression

20 p2580 A73-39358

Heat resistance of chromium-nickel and chromium-nickel-molybdenum steels with additions of boron

21 p2718 A73-40734

Effect of mechanothermal treatment on the heat-resistant properties of 1KH14N18V2B steel with boron additives

21 p2718 A73-40735

High-temperature internal friction in boron fibers

22 p2880 A73-41957

Fibre-reinforced metallic and ceramic composites produced by thermal spraying.

22 p2866 A73-42592

German monograph - Doping profiles of boron-implanted silicon layers.

22 p2897 A73-42717

Combustion of boron particles - Experiment and theory.

22 p2899 A73-42821

Deformation and failure of boron-epoxy plate with circular hole.

23 p3040 A73-43631

Mechanical properties of boron fibers

24 p3102 A73-44524

Boron particle ignition limit dependence on particle size and oxygen content, taking into account kinetic and diffusion resistance

24 p3155 A73-44708

Theoretical post-yielding behavior of composite laminates. II - Inelastic macromechanics.

24 p3104 A73-45145

BORON ALLOYS

High-temperature thermal analysis of high boron alloys using automatic optical pyrometry.

01 p0015 A73-11450

Quadrilateral packet structure and lattice atom positions in single crystal ternary Re-Co-B alloy by X ray analysis

02 p0181 A73-12198

Boron segregation at austenite grain boundary and matrix sites in steel by autoradiography

02 p0183 A73-12761

Thermal fatigue resistance of borided alloy KhN70VMYuT.

06 p0709 A73-18215

Mo-W-B alloy phase equilibria, isothermal cross sections, liquidus, solubility and mechanical properties by thermal, X ray and microstructural analyses

12 p1510 A73-26904

The vanadium-iron-boron, vanadium-cobalt-boron, and vanadium-nickel-boron systems

15 p1887 A73-31202

Phase diagram thermal sections and concentration corner of Mo-Zr-B system by microstructure, X ray and electron microscope analysis

21 p2718 A73-40490

The copper-boron eutectic - Unidirectionally solidified.

23 p2993 A73-44035

Influence of boron on the precipitation of carbides in Fe-Ni-Cr austenitic matrices

24 p3101 A73-45523

BORON CARBIDES

Diffusive boronizing of molybdenum and niobium in boron carbide powder

02 p0178 A73-11544

The friction of boron carbide in controlled atmospheres.

[ASME PAPER 72-LUB-29] 03 p0315 A73-14340

Enthalpy and heat capacity of boron carbide in the temperature range 273-2600 K.

06 p0714 A73-17415

Thermophysical and electrical properties of powdered boron carbonitride as high temperature insulating and refractory material at 1800-2020 C

10 p1241 A73-24687

Effect of carbon on the growth of boride layers

11 p1374 A73-26109

Indenter materials for use in high-temperature hardness measurements

12 p1513 A73-27561

Preparation of a rhombohedral boron carbide of the composition of B13C2

13 p1645 A73-28185

Characterization of boron carbide with an electronic microprobe

13 p1645 A73-28346

Boron fiber coating by chemical vapor deposition of boron carbide for improved mechanical properties and incorporation in Al alloy matrices

16 p2030 A73-33070

BORON COMPOUNDS

NT BERYLLIUM BOROHYDRIDES

NT BORATES

NT BORIDES

NT BORON CARBIDES

NT BORON FLUORIDES

NT BORON NITRIDES

NT HYDRAZINE BORANE

NT TITANIUM BORIDES

Creep and long-term strength of molybdenum with a boron silicide coating in vacuum at temperatures from 1000 to 1400 C

12 p1512 A73-27257

Detonation of explosives containing boron and its organic derivatives

13 p1669 A73-28971

BORON FLUORIDES

Rapid gas-phase reactions - The reaction of ammonia and the methylamines with boron trifluoride. III - Pressure dependence of rate constant.

14 p1723 A73-30068

BORON HYDRIDES

NT BERYLLIUM BOROHYDRIDES

NT HYDRAZINE BORANE

BORON NITRIDES

Thermophysical and electrical properties of powdered boron carbonitride as high temperature insulating and refractory material at 1800-2020 C

10 p1241 A73-24687

Borazon compact cutting tools.

[SME PAPER MR 73-143] 19 p2436 A73-38500

Turning high-temperature alloys with Borazon tools. [SME PAPER MR 73-145] 19 p2437 A73-38501

Chemical stability and features of the formation of complex nitrides of III-B subgroup elements /Al-B-N system/

24 p3119 A73-44952

BORON OXIDES

Direct mixing and combustion measurements in ducted, particle-laden jets. [AIAA PAPER 72-1177] 06 p0769 A73-18400

BORON TRIFLUORIDE

U BORON FLUORIDES

BOROSILICATE GLASS

Isotherm data for physical adsorption of Ar on pyrex surface at low pressure, noting correlation in terms of Dubinin-Radushkevich equation

04 p0456 A73-15765

Thin In film sealing techniques at temperatures below 300 C for binding Pyrex to various materials, using Au layer as alloy flux

09 p1085 A73-22950

BOSE-CHAUDHURI-HOCQUENGHEM CODES

U BCH CODES

BOSE-EINSTEIN STATISTICS

U QUANTUM STATISTICS

BOSONS

NT ALPHA PARTICLES

NT LIGHT BEAMS

NT MESONS

NT PHOTONS

NT PIONS

BOTTLES

Acoustic emission produced during burst tests of filament-wound bottles.

24 p3094 A73-45146

BOUGUER LAW

Propagation laws of a spatially bounded radiation flow in a scattering medium

15 p1903 A73-31324

BOULES

Microwave method of investigating the quality of ruby boules.

06 p0734 A73-17813

BOUNDARIES

NT FLUID BOUNDARIES

NT FREE BOUNDARIES

NT GAS-SOLID INTERFACES

NT GRAIN BOUNDARIES

NT JET BOUNDARIES

NT LIQUID-LIQUID INTERFACES

NT LIQUID-SOLID INTERFACES

NT LIQUID-VAPOR INTERFACES

Magnetospheric trapped particle populations boundaries properties, discussing dynamic boundaries during magnetic disturbances and substorm effect on night magnetosphere configuration

04 p0442 A73-15332

Equatorward shift of the polar F layer irregularity zone as a function of the Kp index.

04 p0445 A73-15557

BOUNDARY LAYER COMBUSTION

An analysis of the chemically reacting boundary layer during hybrid combustion.

[AIAA PAPER 72-1144] 03 p0273 A73-13450

Heat and mass transfer at the surfaces of glass-graphite materials in a high-temperature gas flow

06 p0766 A73-17457

Estimate of the influence of thermal diffusion on the surface burnout rate in a nonhomogeneous turbulent boundary layer

09 p1167 A73-22618

Determination of the electron concentration in the boundary layer of air mixed with ablation products of an asbestos plastic

09 p1128 A73-22622

Analytical investigation of heat transfer in bodies with moving boundaries

11 p1450 A73-25622

Experimental study of heat exchange in a chemically reacting laminar boundary layer

15 p1958 A73-31874

Direct-sampling studies of combustion processes.

19 p2504 A73-38325

Ignition and flame spreading over a solid fuel - Non-similar theory for a hot oxidizing boundary layer.

22 p2936 A73-42809

BOUNDARY LAYER CONTROL

NT POROUS BOUNDARY LAYER CONTROL

Boundary-layer separation - Effect of low-speed wall jets.

01 p0030 A73-10047

Model tests regarding the characteristics of the boundary layer at effusion-cooled turbine blades [DGLR PAPER 72-059] 02 p0127 A73-11655

Perturbation technique for approximation of sound radiation from controlled boundary layer on thin plate, deriving random stationary functions in terms of Fourier integral

03 p0291 A73-12992

Boundary layer bleed system design for supersonic inlets, discussing bleed hole geometry effects on boundary layer velocity profile and inlet efficiency [AIAA PAPER 72-1138] 03 p0243 A73-13445

Integrated engine-airframe design with fuselage boundary layer ingestion for subsonic-transonic cruise, discussing STOL thrust control via variable pitch fan for landing

03 p0251 A73-14128

Application of external aerodynamic diffusion to reduce shrouded propeller noise.

05 p0528 A73-16623

A boundary layer method for the matrix Riccati equation.

06 p0719 A73-18864

A subsonic diffuser with moving walls for boundary-layer control.

08 p0953 A73-20723

A radial diffuser with a rotating boundary layer at the throat.

08 p0953 A73-20795

Oblique shock wave generation and quenching in curved supersonic diffusers at Mach 1.6, noting dependence on boundary layer properties

13 p1566 A73-29021

Magnetohydrodynamic boundary layer control with suction or injection.

15 p1864 A73-31931

Test techniques for high lift, two-dimensional airfoils with boundary layer and circulation control for application to rotary wing aircraft.

17 p2091 A73-34292

STOL light aircraft wing with circulation control through blowing around trailing edge, boundary layer control through suction, leading edge modification and increase in chord length

17 p2094 A73-34682

Investigation of nozzles with cryogenic suction of the boundary layer

21 p2678 A73-41221

French monograph - Contribution to the experimental study of a boundary layer trap in a supersonic air inlet.

22 p2797 A73-42740

Turbulent boundary layer noise minimization by acoustic oscillation control, discussing suction and gas injection techniques

23 p2969 A73-43976

BOUNDARY LAYER EQUATIONS

The universalization of unsteady boundary layer equations

10 p1207 A73-24805

Prandtl boundary layer equations for unsteady three dimensional axisymmetrical and two dimensional symmetrical incompressible flows about solid bodies, considering approximate solution convergence

10 p1208 A73-24808

German monograph on compressible turbulent boundary layer equations solution for heat transfer in divergent nozzle flow based on modified Patankar-Spalding difference method

13 p1605 A73-29276

Construction of solutions for the equations of a compressible laminar boundary layer on a plate with abruptly changing boundary conditions

13 p1567 A73-29408

A simple integration method for the momentum and energy theorem of boundary layer theory

14 p1745 A73-30300

The theory of fluctuating flow fields near walls.

14 p1746 A73-30704

Internal stress-strain boundary layer theory of shells and orthotropic plates with zero stress conditions at upper and lower planes and edge distance dependent attenuation

14 p1815 A73-30815

Nonstationarity effects on planetary boundary layer by numerical integration of time dependent boundary layer model

14 p1772 A73-30903

The wind profile very close to the ground.

14 p1772 A73-30904

The turbulent boundary layer on a long thin filament

15 p1822 A73-31197

Application of the energy equation for turbulence in the theory of jet flows

15 p1862 A73-31288

Asymptotic solution of the equations for a multicomponent laminar boundary layer in the case of high injection levels

15 p1822 A73-31292

Application of the method of characteristics in solving the universal equation of the plane boundary layer of a conducting fluid

15 p1918 A73-31407

On the propagation of disturbances in a laminar boundary layer. I, II.

15 p1863 A73-31725

Plane boundary layer equations of asymmetric MHD incompressible fluid motion for case of high and low electroconductivity

15 p1919 A73-31829

A numerical method for integrating the unsteady boundary-layer equations when there are regions of backflow.

16 p1998 A73-32799

The principle of spatial variations - Application to the boundary layer theory.

16 p1999 A73-32978

The solutions of the boundary layer equations in the case of extremely intensive blowing or suction

16 p1963 A73-33250

Integration of an extended Orr-Sommerfeld equation in connection with a stability investigation of laminar boundary-layer flows

16 p1963 A73-33252

A finite difference solution of the two and three-dimensional incompressible turbulent boundary layer equations.

[ASME PAPER 73-FE-20] 17 p2153 A73-35016

An approximate method for the solution of a class nonlinear equations in fluid mechanics and magnetohydrodynamics.

[ASME PAPER 73-FE-22] 17 p2216 A73-35018

Boundary-layer separation from downstream moving boundaries.

[ASME PAPER 73-APM-11] 17 p2153 A73-35036

Stress analysis of composite materials with strong fibers in weak matrix, obtaining tensile stress boundary layer equations via elasticity theory and perturbation methods

[ASME PAPER 72-APM-TTT] 17 p2249 A73-35110

Finite difference solution of Prandtl boundary layer equations for steady incompressible laminar and turbulent boundary layer flows

17 p2154 A73-35136

Finite-difference solution of the incompressible three-dimensional boundary layer equations for a blunt body.

18 p2259 A73-36156

Prediction of turbulent separated boundary layers.

[AIAA PAPER 73-663] 18 p2261 A73-36214

Computation of hypersonic turbulent boundary layers with heat transfer.

18 p2263 A73-36248

An integral procedure for estimating boundary layer parameters and heat transfer in arbitrary pressure gradients.

[AIAA PAPER 73-700] 18 p2298 A73-36249

Two field continuum model of magnetic sheath adjacent to absorbing solid surfaces, using Bohm criterion and MHD boundary layer equation approximation

19 p2464 A73-37162

Numerical solution existence for three dimensional boundary layer equations governing corner flow in symmetry plane with critical pressure gradients

19 p2419 A73-37492

Three dimensional boundary layer flow with streamwise vorticity decay, deriving solutions as expansions in terms of eigenfunctions

19 p2420 A73-37851

Numerical investigation of unsteady boundary-layer separation.

19 p2420 A73-37852

MHD boundary layers on a segmented electrode-wall of a nonequilibrium generator.

19 p2470 A73-38314

A method for calculating three-dimensional turbulent boundary layer by using streamline co-ordinates.

20 p2546 A73-39225

Second-approximation boundary layer equations in Prandtl-Mises variables

20 p2549 A73-39610

Branching solutions for supersonic interacting boundary layers.

21 p2632 A73-40440

Asymptotic behavior of the solutions to the Navier-Stokes equations near ribs

21 p2678 A73-41275

Nonisothermal surface cooling for arbitrary temperature distribution and Prandtl number approaching zero, solving thermal boundary layer equations by series expansion

21 p2792 A73-41323

Use of the numerical method of Estoque and Bhattacharya for the planetary boundary layer.

21 p2732 A73-41572

On the generalization of the Mangler transformation for axisymmetric boundary layers.

23 p2967 A73-43226

Plane boundary layer equations for viscous incompressible fluid with asymmetric stress tensor produced by moment stresses and mass moments

23 p2968 A73-43922

Approximate calculation of dividing streamline of heterogeneous coaxial supersonic jets.

23 p2940 A73-44127

A numerical study of separating supersonic laminar boundary layers.

[ASME PAPER 73-APM-H] 23 p2969 A73-44376

Boundary layer equations of magnetohydrodynamics with moment stresses

23 p3015 A73-44385

Superposition technique in numerical integration of generalized Ekman equation for wind profile determination, taking into account eddy diffusivity variation

24 p3108 A73-45019

Numerical methods of boundary layer type for stiff systems of differential equations.

24 p3106 A73-45333

On the existence, uniqueness, and stability of solutions of a new boundary layer problem concerning cer-

tain nonlinear integral-differential polyvibratory systems. I

24 p3106 A73-45395

Compressible laminar boundary layer differential equations solution for incident viscous gas flow on flat plate at high flow velocity

24 p3080 A73-45471

Dynamic and temperature boundary layers of a submerged jet of viscous fluid spreading over the bottom

24 p3080 A73-45503

Universal equations for the laminar boundary layer on a body of revolution in oblique flow

24 p3055 A73-45529

BOUNDARY LAYER FLOW

NT BOUNDARY LAYER SEPARATION

NT REATTACHED FLOW

NT SECONDARY FLOW

NT SEPARATED FLOW

Behaviour of boundary layers on plane or annular fixed or mobile supersonic blade cascades

[ONERA, TP NO. 1110] 01 p0001 A73-10232

Natural convective heat transfer in cavities and horizontal circular tubes, considering boundary layer and core flow interaction effects

01 p0120 A73-10290

Boundary layer formation on hollow circular cylinder walls aligned with axial motion of incompressible rotating fluid as function of Rossby and Reynolds numbers

01 p0032 A73-10451

Skin friction on porous surfaces calculated by a simple integral method.

01 p0057 A73-10726

An experimental investigation of the downstream effects of upstream boundary-layer injection.

01 p0002 A73-10732

Modified convergence criterion for boundary layers.

01 p0033 A73-10750

Representation of a 1/N power law boundary layer in the sheared flow acoustic transmission problem.

01 p0033 A73-10783

Variational analysis of high mass transfer rates from spherical particles - Boundary-layer injection suction considerations at low particle Reynolds numbers and high Peclet numbers.

01 p0122 A73-10802

Developing laminar free convection between vertical flat plates with asymmetric heating.

01 p0122 A73-10811

Boundary layer equation complete solution from first order differential equation graphic solution by Poincare method

01 p0034 A73-11360

A boundary value problem for a system of temperature boundary layer equations

01 p0123 A73-11433

Finite difference method for boundary layer flow, noting truncation errors due to nonuniform grid

01 p0035 A73-11468

Hydromagnetic flow about a curved neutral sheet.

01 p0086 A73-11495

Investigation of a laminar boundary layer on a continuously moving smooth surface with allowance for heat transfer

02 p0153 A73-11786

Boundary layer growth of a micropolar fluid.

02 p0154 A73-12093

A numerical analysis for chemical non-equilibrium boundary layer of dissociated gases over a flat plate with arbitrary catalyticity.

03 p0291 A73-13068

Consideration of wall friction in the streamline procedure with the aid of a modified boundary layer calculation for laminar flows according to the momentum method

03 p0291 A73-13126

Incompressible fluid turbulent boundary layer flow stability, considering effect of high polymer additives

03 p0291 A73-13168

Hypersonic turbulent boundary layer flow parameters and heat transfer during blowing of coolant air and He through slot

03 p0242 A73-13186

Similarity solution of boundary layer flow due to uniform streaming past infinite flat plate with uniform suction at plate surface

03 p0292 A73-13306

Some effects of normal shock boundary layer interaction on the performance of straight walled conical diffusers.

[AIAA PAPER 72-1140] 03 p0243 A73-13446

An analysis of the chemically reacting boundary layer during hybrid combustion.

[AIAA PAPER 72-1144] 03 p0273 A73-13450

Boundary-layer development at a two-dimensional rear stagnation point.

03 p0294 A73-13536

The interaction between turbulent wakes and boundary layers.

03 p0244 A73-13561

Study of the boundary layers of a completely ionized two-temperature plasma on the nonconducting wall of an MHD channel

03 p0346 A73-13610

Practical application of boundary layer theory to flow and heat transfer problems in turbomachines.

03 p0398 A73-14145

Role of the anelastic behavior of the ablation material on cross-hatching.

03 p0398 A73-14189

Effect of nozzle boundary layers on rocket exhaust plumes.

03 p0247 A73-14193

Russian book - Heat transfer in liquid films.

04 p0517 A73-15710

Analysis of unsteady laminar boundary layer flow by an integral method.

[ASME PAPER 72-WA/FE-2] 04 p0434 A73-15839

Free convection along the downward-facing surface of a heated horizontal plate.

04 p0520 A73-15943

A momentum integral solution of a three-dimensional turbulent boundary layer.

[ASME PAPER 72-FE-1] 05 p0565 A73-16548

A non-similar solution of heat transfer in external non-Newtonian flow with thermal radiation.

[AIAA PAPER 73-116] 05 p0640 A73-16873

Calculations of turbulent shear stress in supersonic turbulent boundary layer zero and adverse pressure gradient flow.

[AIAA PAPER 73-166] 05 p0566 A73-16911

Nonsimilar flows between the solution branches of the Falkner-Skan equation.

05 p0567 A73-17116

On unsteady forced flow against a rotating disk.

06 p0643 A73-17394

A method for measuring the sublayer velocity profile of a liquid with polymer additive.

[AIAA PAPER 73-39] 06 p0692 A73-17621

Measurements in a transitional/turbulent Mach 10 boundary layer at high-Reynolds numbers.

[AIAA PAPER 73-165] 06 p0645 A73-17649

High Reynolds number steady separated flow past a wedge of negative angle.

06 p0685 A73-17710

Vectored injection into isobaric laminar boundary layer flows.

06 p0685 A73-17917

On the series solution to the laminar boundary layer with stationary origin on a continuous, moving porous surface.

06 p0687 A73-18505

Asymptotic analysis of turbulent channel and boundary-layer flow.

06 p0687 A73-18528

Time-periodic solution of the system of boundary layer equations.

07 p0809 A73-19019

On the plane-parallel symmetric boundary layer generated by sudden motion.

07 p0809 A73-19020

Diffusion on a particle in the shear flow of a viscous fluid - Approximation of the diffusion boundary layer.

07 p0809 A73-19021

The effect of the degree of turbulence on the aerodynamic characteristics of planar decelerating cascades

[DFVLR-SONDDR-275] 07 p0773 A73-19197

Spatial stability of stagnation water boundary layer with heat transfer.

07 p0919 A73-19503

Visualization of boundary layer flow patterns around protuberances using an optical-surface indicator technique.

07 p0808 A73-19530

Two dimensional semibounded jets in laminar and turbulent flows, discussing boundary layers skin and stream regions, step flow velocities, temperatures and self similar problems

07 p0811 A73-19612

Flow characteristics in air injection through porous surface of blunt bodies, noting blowing parameter effect on boundary layer flow

07 p0774 A73-19622

On unsteady magnetohydrodynamic boundary layers in a rotating flow.

07 p0859 A73-20290

Further results on the stagnation point boundary layer with hydrogen injection.

07 p0921 A73-20358

Unsteady boundary layer flows at general three-dimensional stagnation points.

08 p0954 A73-21008

Numerical calculation of the laminar inlet flow. I.

08 p0954 A73-21011

Planetary boundary layer flow of a stable atmosphere over the globe.

08 p0960 A73-21380

Self-similar hypersonic flows of an inviscid gas

08 p0927 A73-21545

Boundary layer theory approximation for hydrodynamic parameters of unsteady laminar boundary layer on body moving in incompressible fluid

08 p0956 A73-21546

Influence of various surface roughness on the natural convection.

08 p1024 A73-21639

Calculation of the boundary layers of a fully ionized two-temperature plasma for given temperatures of components at the electrodes

09 p1127 A73-22605

Viscous energy transfer from elliptical orifice originated laminar three dimensional jet, using boundary layer assumptions in jet mixing region

09 p1072 A73-22827

Boundary layer efficiency as working fluid in ram-jets for high aircraft speeds, obtaining external efficiency as function of boundary layer parameters and flow rate

09 p1073 A73-23360

The Knudsen layer in a flow with two-temperature relaxation

10 p1250 A73-23580

Free boundary flow invariant solutions of Navier-Stokes equations for optimal S/H subgroup systems, using continuous transformation group operators

10 p1204 A73-23583

Effect of jet turbulence on the flow in a wall boundary layer

10 p1205 A73-23586

Book - Annual review of fluid mechanics. Volume 5.

10 p1205 A73-23851

Statistical properties of intermittency in large scale turbulent flows, considering boundary layer, shear and convective flows

10 p1205 A73-23855

Prandtl's boundary-layer theory from the viewpoint of a mathematician.

10 p1172 A73-23866

The initial flow past an impulsively started circular cylinder.

10 p1172 A73-24338

Free convection from a semi-infinite flat plate inclined at a small angle to the horizontal.

10 p1296 A73-24339

Weakly rarefied gas flow described by simplified Barnett equations, analyzing boundary layer structure

10 p1172 A73-24491

Calculation of a three-dimensional boundary layer in revolving channels of centrifugal rotors

10 p1173 A73-24672

Recent research on unsteady boundary layers; Symposium, Universite du Quebec, Quebec, Canada, May 24-28, 1971, Proceedings. Volumes 1 & 2

10 p1207 A73-24801

Unsteady boundary layer flow, considering Stokes, Rayleigh and Heisenberg-Tollmien theories application to oscillatory, fluctuating, impulsive and rotational effects

10 p1207 A73-24802

Prandtl boundary layer equations for unsteady three dimensional axisymmetrical and two dimensional symmetrical incompressible flows about solid bodies, considering approximate solution convergence

10 p1208 A73-24808

Incompressible boundary layer flow over semi-infinite plate with impulsive heat transfer, obtaining numerical solution for time dependent boundary layer growth

10 p1296 A73-24812

Universal equations of the three-dimensional laminar boundary layer in the unsteady state and their treatment

10 p1209 A73-24820

Unsteady boundary layer and wake near the trailing edge of a flat plate.

10 p1173 A73-24826

Unsteady boundary layer over a flat plate started from rest.

10 p1209 A73-24829

Recent studies in the field of unsteady boundary layers

10 p1173 A73-24833

Unsteady turbulent boundary layer flow past infinite flat plates with free stream acceleration or deceleration, computing characteristics by finite difference method

10 p1209 A73-24834

Some solutions of the unsteady two-dimensional turbulent boundary layer equations.

10 p1209 A73-24835

Prominent vertical shear layers and zonal currents in axisymmetric fluid filled spherical/conical rotating container due to nonlinear interactions in boundary layers

10 p1210 A73-24839

On unsteady magnetohydrodynamic boundary layers in a rotating flow.

10 p1257 A73-24841

Hydrodynamic visualization technique application to unsteady flow patterns around models and analysis of boundary layers, separation and wakes

10 p1174 A73-24842

Velocity field determination for limitless steady boundary layer on circular cylinder and swirling flow produced by generalized vortex

10 p1210 A73-24843

Unsteady viscous jet flow into stationary surroundings.

11 p1345 A73-25117

Unsteady boundary layer flow of homogeneous viscous fluid in nonrotating environment or bounded by oscillating flat plates, determining velocity field by exact solutions

11 p1346 A73-25165

A higher order theory for compressible turbulent boundary layers at moderately large Reynolds number.

11 p1346 A73-25218

Velocity and concentration profiles of isothermal laminar boundary layer flow of incompressible multicomponent gas under strong blowing

11 p1347 A73-25728

Nonlinear resistive boundary layer in rotating hydromagnetic flow related to earth dynamo theory, discussing steady solution uniqueness and numerical temporal stability

11 p1355 A73-25794

Perturbation solutions to laminar boundary layer flow over flat plate with small hump downstream of leading edge, using Blasius equation

11 p1302 A73-25855

Boundary-value problem for a system of equations with a temperature boundary layer.

11 p1452 A73-26055

Nonlinear problem of a shock-tube interaction-region boundary layer.

11 p1348 A73-26391

Shock attenuation in a shock tube due to boundary layer.

12 p1486 A73-27174

Compressible boundary layer flow at a three-dimensional stagnation point with intensive suction or injection

12 p1458 A73-27699

Potential flow of an inviscid incompressible liquid around a profile in the presence of solid rectilinear boundaries

12 p1487 A73-27797

Application of small perturbation method in calculations of turbulent boundary layers on a curvilinear surface with suction

13 p1600 A73-28447

A numerical method for highly accelerated laminar boundary-layer flows.

13 p1600 A73-28608

Rectangular channel mixed boundary layer flow patterns dependence on inlet edge configurations, channel geometry and hydrodynamic flow core parameters

13 p1601 A73-28737

Increase of boundary-layer heat transfer by mass injection.

13 p1706 A73-28816

Turbulent velocity and pressure fields in boundary-layer flows over rough surfaces.

13 p1604 A73-29264

Investigation of the influence of compressibility and the pressure gradient on the value of the permissible Reynolds number of roughness

13 p1567 A73-29406

Three dimensional turbulent boundary layers prediction methods and flow measurements, considering swept and slender wings

14 p1744 A73-30173

Two dimensional incompressible turbulent boundary layer flow theory, considering Bradshaw turbulence field and Felsch integral methods

14 p1745 A73-30298

Book - A course in continuum mechanics. Volume 3 - Fluids, gases and the generation of thrust.

14 p1745 A73-30594

Natural convection boundary layer flow over horizontal and slightly inclined surfaces.

14 p1817 A73-30607

On the stability of natural convection boundary layer flow over horizontal and slightly inclined surfaces.

14 p1817 A73-30608

Natural convection in a sound field giving large streaming Reynolds numbers.

14 p1817 A73-30613

Gas flow properties in curvilinear turbine ducts, considering pressure gradient, outer flow shear and Coriolis force on boundary layer

14 p1712 A73-30649

Velocity profile determination in a turbulent boundary layer

14 p1746 A73-30795

Effective-viscosity model for turbulent wall boundary layers.

15 p1860 A73-31119

Reynolds stresses in plane-parallel flows disturbed by Tollmein-Schlichting waves

15 p1861 A73-31193

Experimental investigation of longitudinal flow over a flat plate during strong blowing of a foreign gas under isothermal conditions

15 p1957 A73-31856

Determination of the thickness of a wall layer by an approximate method in the presence of intense injection

15 p1876 A73-31861

Investigation of boundary layer flow on a flat porous plate with a regulated pressure gradient in the outer flow

15 p1864 A73-31873

Forced convective heat transfer of a gas with condensing vapor around a flat plate.

15 p1958 A73-32058

The simulation of the atmospheric surface layer with volumetric flow control.

16 p1994 A73-33152

Analytic and numerical investigations of boundary layer flows about slender axisymmetric bodies

16 p1962 A73-33248

The numerical integration of the Navier-Stokes equations for the two-dimensional incompressible flow along a planar plate

16 p2000 A73-33261

Approximation for thin boundary layers in the sheared flow duct transmission problem.

16 p2000 A73-33679

Theoretical investigation of the incompressible, turbulent, and axisymmetric internal flow with vanishing wall friction

16 p1964 A73-33749

Bifurcated small parameter perturbation solutions in boundary layer theory, applying to Falkner-Skan equation and instability in stratified shear flow

16 p2001 A73-33871

Some aspects of 'sound' attenuation in lined ducts containing inviscid mean flows with boundary layers.

16 p2049 A73-33946

Nonlinear algebraic equations in continuum mechanics.

17 p2199 A73-34102

Heat-transfer regimes during mixed convection in vertical pipes

17 p2253 A73-34133

Generalized random forces in time domain for rectangular panels under subsonic and supersonic boundary layer turbulence, investigating probabilistic nature by Monte Carlo method

17 p2241 A73-34182

Continuum gas plasma boundary layer flow over flat plate, obtaining ion sheath characteristics and downstream solutions by asymptotic and characteristics methods

17 p2149 A73-34186

Correlation of the mass flow rate in the laminar boundary layer on a sphere-cone.

17 p2091 A73-34195

Natural convection flow equations and stability of laminar and transition flows, external and free boundary flows and boundary layer regimes

17 p2254 A73-34354

Secondary loss measurements in a cascade of turbine blades.

17 p2092 A73-34380

Effect of axial velocity variation on deviation for compressor cascades.

17 p2092 A73-34383

Two dimensional diffuser flow measurement and model calculation for curvature effects on wall pressure and boundary layer velocity distributions

[ASME PAPER 73-FE-2] 17 p2152 A73-35002

An investigation of the flow field and drag of helicopter fuselage configurations.

[AHS PREPRINT 700] 17 p2095 A73-35051

Finite difference solution of Prandtl boundary layer equations for steady incompressible laminar and turbulent boundary layer flows

17 p2154 A73-35136

Book - Radiative transfer and interactions with conduction and convection.

17 p2256 A73-35864

Observation and calculation of a steady, laminar separated flow.

17 p2157 A73-35866

Three-dimensional compressible boundary layer flow over a yawed cone.

[AIAA PAPER 73-634] 18 p2260 A73-36193

Theory of supersonic laminar non-adiabatic boundary layer flow past small rearward-facing steps including viscous-inviscid interaction.

[AIAA PAPER 73-668] 18 p2261 A73-36219

Supersonic turbulent boundary-layer flows with tangential slot injection.

[AIAA PAPER 73-696] 18 p2262 A73-36245

Engineering analysis of hypersonic lifting body windward surface inviscid and viscous flow fields at high angles of incidence.

[AIAA PAPER 73-637] 18 p2263 A73-36257

Recombination effects in chemical laser nozzles.

[AIAA PAPER 73-643] 18 p2287 A73-36258

Turbulent boundary-layer flow from stationary to moving surfaces.

18 p2298 A73-36313

Calculation of turbulent boundary layers over flat plates with different phenomenological theories of turbulence and variable turbulent Prandtl number.

18 p2301 A73-36699

Pulsation-energy balance equation in turbulent boundary layer theory

18 p2301 A73-37002

Recent progress in boundary layer research.

[AIAA PAPER 73-780] 19 p2419 A73-37451

Three dimensional boundary layer flow with stream-wise vorticity decay, deriving solutions as expansions in terms of eigenfunctions

19 p2420 A73-37851

A variational principle for the laminar boundary layer theory.

19 p2421 A73-38026

On Blasius's equation governing flow in the boundary layer on a flat plate.

19 p2421 A73-38101

Non-reacting and equilibrium chemically reacting turbulent boundary-layer flows.

19 p2421 A73-38187

Instabilities in buoyancy-driven boundary-layer flows in a stably stratified medium.

19 p2422 A73-38231

Non-parallel flow corrections for the stability of shear flows.

20 p2546 A73-39092

Hankel transforms and boundary layer solutions for pulsating laminar flow in curved circular tube under sinusoidal pressure gradients

20 p2549 A73-39809

A three-dimensional MHD boundary layer in an incompressible fluid

21 p2747 A73-40882

Magnetohydrodynamic wake behind a body placed in a homogeneous flow in the presence of a longitudinal magnetic field

21 p2747 A73-40890

Complex flow in vapour columns over boiling cryogenic liquids.

21 p2740 A73-41102

Application of a general finite-difference method to boundary layer flows.

21 p2678 A73-41686

High Reynolds number flow in a moving corner.

22 p2840 A73-41746

Calculation of the two-dimensional turbulent wake behind a thin obstacle

[ONERA, TP NO. 1253] 22 p2796 A73-42222

Solution of nonlinear problems in magnetofluid-dynamics and non-Newtonian fluid mechanics through parametric differentiation.

22 p2843 A73-42556

Heat transfer in liquids due to second order boundary layer flows with dissipation.

22 p2938 A73-42996

Calculation of a supersonic gas flow about the atmosphere of a spherical body

24 p3053 A73-44658

A model for the pressure excitation spectrum and acoustic impedance of sound absorbers in the presence of grazing flow.

[AIAA PAPER 73-995] 24 p3077 A73-44830

A biparametric method for laminar boundary layer calculations

24 p3079 A73-45173

The flow of a viscous liquid down a variable incline.

24 p3080 A73-45368

Boundary layer on flat plate in shear flow, calculating induced pressure gradients near leading edge and far downstream

24 p3080 A73-45369

New kind of boundary layer over a convex solid boundary in a rarefied gas.

24 p3080 A73-45453

BOUNDARY LAYER NOISE

U AERODYNAMIC NOISE

U BOUNDARY LAYERS

BOUNDARY LAYER SEPARATION

Boundary-layer separation - Effect of low-speed wall jets.

01 p0030 A73-10047

On the mechanism of dynamic stall.

01 p0003 A73-11015

Nonlinear boundary-value problem for a conducting source flow in an inhomogeneous magnetic field.

01 p0085 A73-11064

Measurements on separated supersonic boundary layer flows after an expansion corner.

01 p0003 A73-11135

Separation of turbulent boundary layer - Wall pressure distribution near separation.

02 p0154 A73-12523

Investigations on incipient boundary layer separation on axisymmetric compression surfaces.

03 p0246 A73-14127

Viscous interaction in integrated supersonic intakes.

03 p0246 A73-14149

Optimization of drag minimums including effects of flow separation.

[ASME PAPER 72-WA/AERO-1]

04 p0405 A73-15909

The transpired turbulent boundary layer in an adverse pressure gradient.

04 p0520 A73-15936

The Joukowski condition in three-dimensional flow

04 p0405 A73-15988

Boundary layer characteristics with radiant energy transfer under adverse pressure gradient.

[AIAA PAPER 73-117] 05 p0530 A73-16874

Shock wave-turbulent boundary layer interactions in rectangular channels. II - The influence of sidewall

boundary layers on incipient separation and scale of the interaction.

[AIAA PAPER 73-234] 05 p0566 A73-16959

Shock impingement caused by boundary layer separation ahead of blunt fins.

[AIAA PAPER 73-236] 05 p0532 A73-16961

Dimension-theory determination of the separation parameter for an incompressible magnetohydrodynamic boundary layer.

06 p0726 A73-17406

Perturbation about one dimensional parabolic flow field in three dimensional boundary layer separation, obtaining skin friction from linear equation eigensolutions

[AD-755557] 07 p0774 A73-19502

Boundary-layer separation on rotating blades in forward flight.

07 p0774 A73-19955

Experimental and theoretical study of supersonic viscous flow over a yawed circular cone.

07 p0775 A73-19957

Turbulent boundary layer separation in supersonic air flow around flat rectangular plate, calculating flow geometry and pressure distribution

07 p0775 A73-20082

A subsonic diffuser with moving walls for boundary-layer control.

08 p0953 A73-20723

Linearized solutions to supersonic laminar boundary layer structure near flat plate with slot injection, using triple deck separation theory

08 p0956 A73-21524

Experimental study of the heat transfer in the separation zones in front of cylindrical projections

10 p1294 A73-23587

Two dimensional laminar boundary layer separation for unsteady flow or flow past moving walls, considering singularity due to bifurcating wake bubble

10 p1208 A73-24813

Kaplan perturbation method for incipient flow separation, considering three dimensional, compressible and unsteady boundary layers

10 p1208 A73-24815

Analysis of stall flutter of a helicopter rotor blade.

[AIAA PAPER 73-403] 11 p1305 A73-25532

Low velocity wind tunnel design with adjustable pressure gradient, determining contraction section wall contour to avoid boundary layer separation via velocity distribution improvement

11 p1347 A73-25714

Incompressible laminar boundary layer separation, displacing separation point by adjusting flow surface velocity

13 p1600 A73-28445

Incipient separation pressure rise for a Mach 3.8 turbulent boundary layer.

13 p1601 A73-28827

Theoretical investigation on stall flutter of an aerofoil (the case of trailing edge stall).

13 p1566 A73-29027

Visualization of unsteady flow over oscillating airfoils.

13 p1620 A73-29270

Generalized relations for the parameters at the flow separation boundary in compressor cascades

13 p1567 A73-29551

Plate-injection into a separated supersonic boundary layer.

14 p1711 A73-30172

Boundary layer separation in a steady plane-parallel incompressible fluid flow

15 p1864 A73-32110

A wake and an eddy in a rotating, radial-flow passage. I - Experimental observations.

[ASME PAPER 73-GT-57] 16 p1964 A73-33512

Rotating stall in an isolated rotor row and a single-stage compressor.

17 p2093 A73-34386

The prevention of separation and flow reversal in the corners of compressor blade cascades.

17 p2094 A73-34448

Beyond the buffet boundary.

17 p2100 A73-34538

An initial value method for the study of shock-induced laminar compressible boundary layers.

[ASME PAPER 73-FE-4] 17 p2152 A73-35004

Analysis of flow separation in an annular expansion - Contraction with inner cylinder rotating.

[ASME PAPER 73-FE-7] 17 p2152 A73-35006

Boundary-layer separation from downstream moving boundaries.

[ASME PAPER 73-APM-11] 17 p2153 A73-35036

Prediction of turbulent separated boundary layers.

[AIAA PAPER 73-663] 18 p2261 A73-36214

Turbulent boundary layer flow separation measurements using holographic interferometry.

[AIAA PAPER 73-664] 18 p2261 A73-36215

Supersonic, turbulent boundary layer separation measurements at Reynolds number of 10,000,000 to 100,000,000.

[AIAA PAPER 73-665] 18 p2261 A73-36216

Separation of a supersonic turbulent boundary layer at moderate to high Reynolds numbers.

[AIAA PAPER 73-666] 18 p2261 A73-36217

The response of unsteady boundary-layer separation to impulsive changes of outer flow.
[AIAA PAPER 73-684] 18 p2298 A73-36235

Convective heating in dust-laden hypersonic flows.
[AIAA PAPER 73-761] 18 p2371 A73-36376

The singularity at boundary layer separation due to mass injection.
18 p2301 A73-36696

Investigation of the flow in regions of turbulent boundary layer separation in front of a subsonic jet blown from a circular nozzle
18 p2265 A73-37003

Numerical investigation of unsteady boundary-layer separation.
19 p2420 A73-37852

Calculation and measurement of MHD generator boundary layer velocity profiles.
19 p2470 A73-38315

Incompressible turbulent boundary layer separation from a curved axisymmetric body.
20 p2548 A73-39525

Numerical experiment in a study of the separation of a laminar boundary layer in an MHD channel
20 p2598 A73-39611

Boundary-layer separation at a free streamline. III - Axisymmetric flow and the flow downstream of separation.
20 p2549 A73-39806

Aerodynamic forces on a triangular cylinder.
21 p2782 A73-40003

Flow measurements over compression corner in supersonic separated laminar boundary layers with hot-wire probes
21 p2631 A73-40247

Pressure distribution and boundary layer separation measurement on circular cylinder at critical subsonic velocities for various Reynolds and Mach numbers
21 p2632 A73-40476

Reattachment of a separated boundary layer to a convex surface.
22 p2843 A73-42554

A numerical study of separating supersonic laminar boundary layers.
[ASME PAPER 73-APM-H] 23 p2969 A73-44376

A method for solving problems involving viscous flows past bodies at large Reynolds numbers
24 p3081 A73-45530

BOUNDARY LAYER STABILITY

Relations among stability parameters in the surface layer.
01 p0073 A73-10497

Hydrodynamic stability of boundary layers with surface suction.
01 p0033 A73-10749

Existence in the laminar boundary layer of a natural instability not predicted by theory and connected to a wall deformation
03 p0294 A73-13576

Unsteady compressible boundary layers with arbitrary pressure gradients.
[AIAA PAPER 73-132] 05 p0565 A73-16885

A force field theory. I - Laminar flow instability.
05 p0567 A73-17103

Small perturbation stability of two dimensional incompressible viscous fluid flow with periodic velocity function, reduced to undulating surface boundary layer problem
06 p0684 A73-17452

Experiments on the nonlinear stages of free-shear-layer transition.
06 p0687 A73-18530

On the plane-parallel symmetric boundary layer generated by sudden motion.
07 p0809 A73-19020

Stability of an electrical discharge surrounded by a free vortex.
07 p0848 A73-19514

Unsteady laminar boundary layers calculation for arbitrary velocity distributions at inner boundary in presence of suction/blowing through porous surface
08 p0954 A73-21176

Numerical study of the stability of a supersonic laminar boundary layer
09 p1028 A73-22624

On the response of laminar boundary layers to periodic changes in free-stream speed.
10 p1207 A73-24803

The universalization of unsteady boundary layer equations
10 p1207 A73-24805

On some aspects of unsteady boundary layers induced by shock waves.
10 p1209 A73-24832

Parametric excitation of Tollmein-Schlichting waves in a boundary layer
11 p1347 A73-25430

Flow near the stagnation point of a body which undergoes a sudden change in a steady stream.
[ASME PAPER 72-APM-UU] 11 p1347 A73-25701

Experimental investigation of hydrodynamic stability at rigid and elastic-damping surfaces
11 p1349 A73-26440

On thermal convection between non-uniformly heated planes.
13 p1705 A73-28430

Experimental investigation of the convection inversion process in the viscous sublayer of a turbulent boundary layer during blowing of carbon dioxide through a vertical porous heated surface under conditions of natural convection
13 p1708 A73-29407

Linear stability of nearly parallel flows. II - The Blasius boundary layer
14 p1744 A73-29759

Free stream vorticity effect on incompressible boundary layer stability via Orr-Sommerfeld equation, considering self-similar flows with pressure gradients
14 p1712 A73-30651

On the propagation of disturbances in a laminar boundary layer. I, II.
15 p1863 A73-31725

Leading edge effects on displacement thickness and skin friction variations of unsteady boundary layer on flat plate under impulsive motion in viscous fluid
16 p1962 A73-32927

Laminar-turbulent transition in incompressible boundary layer flow from stability theoretical viewpoint, considering pressure gradient, free stream turbulence and wall roughness effects
16 p1999 A73-33229

Experimental investigation of secondary instabilities in the unstable laminar boundary layer of a concave wall in parallel flow
16 p1999 A73-33247

Integration of an extended Orr-Sommerfeld equation in connection with a stability investigation of laminar boundary-layer flows
16 p1963 A73-33252

On unsteady Stokes, Ekman and Rayleigh layers in a rotating fluid.
17 p2150 A73-34322

The effect of heat transfer on boundary layer stability in axial flow compressors.
17 p2093 A73-34394

A method for calculating unsteady turbulent boundary layers in two- and three-dimensional flows.
17 p2154 A73-35135

Numerical stability of boundary layers with massive blowing.
18 p2298 A73-36321

Unsteady thermal boundary-layer on an infinite yawed wedge whose temperature gradient is prescribed.
19 p2377 A73-37575

The lower atmosphere in hydrostatically stable conditions.
19 p2449 A73-38245

Stability of a compressible boundary layer with regard to a localized disturbance
20 p2547 A73-39285

On the coexistence of laminar and turbulent flow in a narrow triangular duct.
20 p2549 A73-39813

Vortex sheet model of directional acoustic wave radiation near nozzle exit from supersonic helium jet shear layer instability
21 p2677 A73-40617

Investigation of the laminar boundary layer at a permeable surface.
21 p2678 A73-41054

Stability of a plane boundary layer with allowance for nonparallelism
23 p2968 A73-43472

Mathematical model for temperature inversion rise velocity under penetrative free surface convection based on unstable atmospheric boundary layer environment
23 p3002 A73-43595

Asymptotic suction boundary layer profile past porous plane surface, obtaining upper and lower bounds on energy stability limit
23 p2969 A73-44381

On the existence, uniqueness, and stability of solutions of a new boundary layer problem concerning certain nonlinear integral-differential polyvibratory systems. I
24 p3106 A73-45395

Linearized theory of two and three dimensional incompressible viscous flows based on locally unstable velocity profiles related to boundary layer instability mechanism
24 p3081 A73-45546

BOUNDARY LAYER TRANSITION

Correlation function for prediction of surface roughness induced supersonic boundary layer transition on blunt bodies, taking into account compressibility and centrifugal force effects
01 p0002 A73-10742

Boundary layer transition on cones in hypersonic He wind tunnel tests, obtaining turbulent spot geometry and propagation velocity by spark schlieren photography
01 p0003 A73-10762

Nonlinear baroclinic instability of a continuous zonal flow of viscous fluid.
02 p0153 A73-12035

Aerodynamic noise and boundary-layer transition measurements in supersonic test facilities.
03 p0296 A73-14191

Theoretical investigation of transition phenomena in the boundary layer on an infinite swept wing
[DGLR PAPER 72-124] 03 p0248 A73-14379

Study of the effect of surface roughness on the laminar boundary layer transition in a turbulent boundary layer
04 p0404 A73-15653

The oscillatory boundary layer growth over the top and bottom plates of a rotating channel.
[ASME PAPER 72-WA/FE-5] 04 p0434 A73-15842

An engineering approach to the design of laminarizing nozzle flows.
[ASME PAPER 72-FE-19] 05 p0565 A73-16549

Shockwave-boundary layer interference heating analysis.
[AIAA PAPER 73-237] 05 p0532 A73-16962

Experimental results on the intermittent properties of the boundary layer pressure field during transition.
[AIAA PAPER 73-243] 05 p0566 A73-16967

Transition effects on slender vehicle stability and trim characteristics.
[AIAA PAPER 73-126] 06 p0756 A73-17646

Reentry vehicle dynamic stability mechanism during boundary layer transition, using angle of attack divergence dependence on fluctuating pressure
[AIAA PAPER 73-180] 06 p0756 A73-17652

On the determination of the height of the Ekman boundary layer.
06 p0720 A73-18326

Experiments on the nonlinear stages of free-shear-layer transition.
06 p0687 A73-18530

Critical conditions for steady/unsteady laminar shear flow breakdown into HF oscillations, using kinematic wave theory
[AD-758579] 06 p0687 A73-18533

Transition of the boundary layer on a cone in a supersonic flow
06 p0646 A73-18540

Asymptotic formulas for the thickness of the Ekman boundary layer
06 p0691 A73-18730

Steady nonlinear Ekman-Hartmann boundary layer on flat surface, evaluating pumping and electric current as functions of Rossby number and magnetic interaction parameter
07 p0856 A73-19512

Oblique shock-sound interaction at a freestream Mach number of about 20 in helium.
07 p0775 A73-19984

Second kind conditional instability of resting atmosphere, noting Ekman boundary layer absence in rain area for given Coriolis parameter
08 p0985 A73-21379

Calculation of one-dimensional hydrodynamic in Eulerian coordinates
09 p1070 A73-21922

Hydrodynamic wind tunnel investigation of drag reduction and propulsion effect by flexible walls, observing boundary layer transition and turbulence
09 p1071 A73-22207

Experimental study of the laminar-turbulent transition on a concave wall in a parallel flow
09 p1071 A73-22450

Turbulent interface structure from eddy viscosity models, discussing equations of motion and Nee-Kovaszny and Prandtl models
10 p1205 A73-24253

Evaluation of the characteristics of the boundary layer in transitional flow on a flat plate
10 p1296 A73-24497

On the response of laminar boundary layers to periodic changes in free-stream speed.
10 p1207 A73-24803

Transient Ekman and Stewartson layers in a rotating tank with a spinning cover.
10 p1210 A73-24840

Nonlinear hydrodynamic and hydromagnetic spin-up driven by Ekman-Hartmann boundary layers.
11 p1403 A73-25156

Investigation of the transition of a turbulent boundary layer into a laminar boundary layer in the presence of deep negative pressure gradients
11 p1347 A73-25737

Calculation of transitional boundary-layer flows.
11 p1348 A73-26394

Influence of total temperature on transition in supersonic flow.
11 p1303 A73-26400

Detection of flight vehicle transition from base measurements.
13 p1706 A73-28834

Free stream turbulence and transition in a circular duct.
13 p1602 A73-29014

Effects of sweepback angle and unit Reynolds number on boundary layer transition at supersonic velocities
13 p1567 A73-29172

Effects of buoyancy and of acceleration owing to thermal expansion on forced turbulent convection in vertical circular tubes - Criteria of the effects, velocity and temperature profiles, and reverse transition from turbulent to laminar flow.
14 p1818 A73-30614

Laminar-turbulent transition in incompressible boundary layer flow from stability theoretical viewpoint, considering pressure gradient, free stream turbulence and wall roughness effects

16 p1999 A73-33229

Criteria regarding the predetermination of the laminar-turbulent boundary layer transition in the case of flows about body contours

16 p1965 A73-33750

On unsteady Stokes, Ekman and Rayleigh layers in a rotating fluid.

17 p2150 A73-34322

Three-dimensional hypersonic transitional/turbulent mean flow profiles.

18 p2260 A73-36194

Practical calculations of transitional boundary layers.

19 p2423 A73-38479

Influence of the shape of the leading edge on the transition process in the boundary layer on a plate in longitudinal flow

21 p2676 A73-40399

Surface wind stress and threshold friction velocity required to raise dust on Mars, discussing mechanisms for production of strong winds in Ekman layer

22 p2912 A73-42981

Superposition technique in numerical integration of generalized Ekman equation for wind profile determination, taking into account eddy diffusivity variation

24 p3108 A73-45019

Radiating optically thick gas boundary layer based on approximation of gray gas in LTE, noting similarity to Knudsen layer

24 p3158 A73-45535

BOUNDARY LAYERS

NT ATMOSPHERIC BOUNDARY LAYER

NT COMPRESSIBLE BOUNDARY LAYER

NT HYPERSONIC BOUNDARY LAYER

NT INCOMPRESSIBLE BOUNDARY LAYER

NT LAMINAR BOUNDARY LAYER

NT SUPERSONIC BOUNDARY LAYERS

NT THERMAL BOUNDARY LAYER

NT THREE DIMENSIONAL BOUNDARY LAYER

NT TURBULENT BOUNDARY LAYER

NT TWO DIMENSIONAL BOUNDARY LAYER

Approximate solutions of laminar flow between two rotating coaxial disks.

02 p0151 A73-11527

Thrust nozzle optimization including boundary-layer effects.

02 p0129 A73-12508

Experimental investigation of the pressure and velocity fluctuations in a sound-affected free jet

03 p0290 A73-12965

Temperature, velocity, and stress distribution in thermo-viscoplastic boundary layers

03 p0386 A73-13145

Unsteady laminar natural and forced convection at transparent medium boundary layer radiating surface, noting turbulence effects on heat exchange

03 p0397 A73-13187

Boundary-layer methods in microstructure theories of elasticity.

03 p0390 A73-13330

Boundary conditions for temperature perturbations in stability problems of compressible gas flows

03 p0245 A73-13672

Closed form linearized solutions of plane laminar jets boundary layer equations based on Legendre functions

03 p0297 A73-14628

Axial flow turbomachines annulus wall boundary layer growth calculation methods, deriving momentum integral equations from passage averaged equations of motion through cascaded blades

03 p0249 A73-14645

The transmission of sound in an acoustically treated rectangular duct with boundary layer.

04 p0476 A73-15586

Ellipsoidal deformations of tubelike balloons - Asymptotic solution with boundary layer.

[ASME PAPER 72-WA/APM-29]

04 p0515 A73-15889

CO₂ laser radiation absorption in SF₆-air boundary layers.

05 p0585 A73-16983

Longitudinal rolls and Benard cells in water layer natural convection, predicting wavelength-depth relations and Rayleigh numbers for comparison with experiments

06 p0684 A73-17623

Unsteady heat transfer in dispersion media at small values of time

08 p1021 A73-20994

Boundary layers calculation for nonporous surface extended to porous with suction by replacing velocity distribution with longitudinal pressure gradient

08 p0954 A73-21179

Boundary layer wind profile model in a steady state, diabatic, baroclinic atmosphere.

09 p1114 A73-22328

Thermal instability in a viscoelastic fluid layer in hydromagnetics.

09 p1166 A73-22418

Dynamic viscous pressure interaction on a cone.

10 p1173 A73-24821

Porous layer strongly nonlinear heat transfer curve bounds numerical computation by variational method, using boundary layer analysis

11 p1448 A73-25055

Boundary layer due to sphere rotation in a medium at rest

13 p1599 A73-28068

Reference wave elimination in acoustic holographic experiments via boundary surface of medium having sound wave propagation used as hologram

13 p1616 A73-28687

German monograph - Investigations regarding the structure of planar boundary layers between magnetic field and plasma.

15 p1921 A73-32584

Computerized three dimensional calculations of hypersustained aircraft in viscous potential flow in terms of boundary layers and wakes

16 p1962 A73-32816

A survey and comparison of methods for predicting the profile loss of turbine blades.

17 p2093 A73-34391

On the free shear layer downstream of a backstep in supersonic flow.

[ASME PAPER 73-FE-3]

17 p2095 A73-35003

Two dimensional half-jet mixing of dissociated air, investigating chemical rate and diffusion processes interaction effects on mixing layer thermodynamics

17 p2156 A73-35503

Boundary layer concept /attenuating stress-strain state with homogeneous boundary conditions/ incorporation into internal stress-strain state theory for orthotropic rectangular elastic plates

19 p2499 A73-37763

Influence of non-singular stress terms and specimen geometry on small-scale yielding at crack tips in elastic-plastic materials.

19 p2501 A73-38264

Study of heat transfer in boundary layer taking into account the radiation at the surface.

20 p2507 A73-39420

Microarc current flow and potential drop through cold boundary layer near plasma electrodes in MHD generators

20 p2598 A73-39604

Radiative and convective heat transfer in a magnetic field

20 p2628 A73-39608

Plume boundary jump of an underexpanded jet exhausting counter to a freestream.

21 p2790 A73-40433

Measuring the boundary layer temperature distributions using ablating specimens in an air plasma flow.

21 p2791 A73-41052

Reduction of fan noise by annulus boundary layer removal.

22 p2795 A73-41713

Interactions of plasmas with magnetic field boundaries.

22 p2851 A73-42977

BOUNDARY LUBRICATION

Boundary lubrication and wear of slow moving sliding concentrated hardened steel contacts as function of geometry, load, speed, lubricant and oxygen content

05 p0580 A73-16104

Manifestation of the adsorption-induced loss of strength in metals under conditions of selective transfer in boundary friction.

06 p0698 A73-18637

Investigation of fatigue effects in thinnest surface layers of metals with boundary friction

14 p1815 A73-30838

BOUNDARY VALUE PROBLEMS

NT NEUMANN PROBLEM

Solution of the thermoelasticity problem for half-spaces with boundary conditions divided by circular lines

01 p1113 A73-10013

Iterative solution of thermal bending problem for nonuniformly heated thin rectangular plate with discrete boundary conditions

01 p1113 A73-10020

Existence of solutions of certain nonlinear elliptic boundary-value problems

01 p0069 A73-10067

Application of the boundary-value method to the solution of weakly nonlinear parabolic differential equations

01 p0069 A73-10070

Some numerical experiments with Dafermos's method for nonlinear hyperbolic equations.

01 p0069 A73-10071

Difference procedures of monotonic type for nonlinear parabolic boundary value problems

01 p0069 A73-10072

Solution to certain boundary value problems of a generalized axisymmetric theory of potential

01 p0070 A73-10092

Determination of the dynamic characteristics of a fluid in a moving vessel in the presence of a weak gravitational field by the eigenfunction expansion method

01 p0030 A73-10095

A method of construction and the structure of asymptotic approximations of the solutions of nonlinear mixed boundary value problems in studies of multifrequency oscillation modes

01 p0076 A73-10097

Approximate method for solving boundary value problems in the mathematical theory of elasticity of an anisotropic medium

01 p0113 A73-10098

A variant of the solution of problems of fluid oscillations in cylindrical cavities by the Bubnov-Galerkin method

01 p0031 A73-10101

The extended boundary condition solution of the dipole antenna of revolution.

01 p0016 A73-10186

Generation and stability of subharmonic and modulated subharmonic oscillations in nonlinear systems.

01 p0076 A73-10303

Rigid and free boundaries effects on radiative heat transfer stabilization of fluid layer against Benard thermal convection

01 p0120 A73-10397

Structural members optimal shaping in terms of stress concentration, analyzing plane elasticity boundary value problem

01 p0114 A73-10600

Method for deriving normal solutions to kinetic equations by using boundary conditions

01 p0076 A73-10623

Free vibration of prestressed cylindrical shells having arbitrary homogeneous boundary conditions.

01 p0114 A73-10730

Solution of stresses and strains for laminated monoclinic cylinders.

01 p0115 A73-10748

Modified convergence criterion for boundary layers.

01 p0033 A73-10750

Nonlinear axisymmetric flexural vibration equations of a cylindrically anisotropic circular plate.

01 p0115 A73-10756

Explicit alternating-direction methods of solving the boundary value problem for a fourth-order self-conjugate elliptical differential equation with variable coefficients

01 p0070 A73-10915

Unsteady thermal stress in an infinite strip with mixed boundary conditions

01 p0115 A73-10916

Study of a mixed problem for a third-order nonlinear differential equation with degeneration or singularity

01 p0070 A73-10920

Effect of gas-surface interaction on the transmission of sound through a collisionless gas.

01 p0077 A73-10972

Nonlinear boundary-value problem for a conducting source flow in an inhomogeneous magnetic field.

01 p0085 A73-11064

Effective solutions to the third and fourth boundary value problems of a sphere in the theory of elasticity

01 p0116 A73-11077

Conical solutions for diffraction of plane pulse wave by three dimensional trihedron corner via boundary conditions reduction to eigenvalue problem, presenting sonic boom example

01 p0019 A73-11424

A boundary value problem for a system of temperature boundary layer equations

01 p0123 A73-11433

Uniqueness of a solution to an inverse problem in the case of a second order equation with continuous boundary conditions: Regularized sums of a portion of eigenvalues - Factorization of the characteristic determinant

01 p0071 A73-11440

The role of interpolation and approximation theory in variational and projectional methods for solving partial differential equations.

01 p0071 A73-11458

Numerical solutions for MHD equations, considering initial values, time independence and mathematical models including hyperbolic, parabolic and elliptic differential equations

01 p0086 A73-11459

A discrete numerical approach to fluid dynamics.

01 p0071 A73-11461

Continuous methods based on particular solutions for free boundary problems in partial differential equations, considering heat equation Stefan problem and Laplace equation interface

01 p0071 A73-11462

Solution of Troesch's two-point boundary value problem by a combination of techniques.

01 p0035 A73-11470

Rectangular plate stability under compression by uniformly distributed loads applied to two opposite simply supported edges with mixed boundary conditions at other edges

02 p0230 A73-11640

Construction of a general solution for an elastic anisotropic shallow shell with arbitrary boundary conditions, and some of its applications

02 p0230 A73-11714

Solution to the bending problem and to the plane problem of an anisotropic rectangular plate with arbitrary boundary conditions and the application of the solution to composite structure designs
02 p0230 A73-11715

Stressed state of an isotropic half-plane with a finite number of circular holes situated along the boundary
02 p0230 A73-11782

Equilibrium equations in theory of anisotropic shells and plates with arbitrary boundary conditions under external loads, noting thin walled reinforced shells
02 p0231 A73-11807

Elastic deformation of a single-cavity hyperboloid of revolution under given forces at the boundary
02 p0233 A73-11939

Boundary value problems of thermoelastic wave diffraction in elasticity theory of multiply connected domains bounded by circular cylindrical surfaces
02 p0233 A73-11940

Oscillations of open cylindrical shells of variable curvature
02 p0233 A73-11941

Singular elliptic perturbations of vanishing first-order differential operators.
02 p0186 A73-11970

Linearly elastic materials theory covering kinematics, momentum balance, constitutive relation, boundary value problems and field equations
02 p0233 A73-11977

Three dimensional linear theory of thermoelasticity covering homogeneous and isotropic bodies, work, free energy, boundary value problems and variational principles
02 p0233 A73-11978

Existence theorems for boundary value problems of elasticity defined by unilateral constraints, developing abstract theory of functional inequalities
02 p0233 A73-11979

Boundary value problems of elasticity with unilateral constraints.
02 p0234 A73-11980

Rods theory covering constitutive equations, boundary value problems, variational formulation of equilibrium problems and uniqueness theorems
02 p0234 A73-11982

Homogeneous linear partial differential equation for optimal control with boundary condition formed by terminal component, noting weighting functions for linear plant
02 p0149 A73-12116

The method of variable directions for solving a boundary-value problem for a self-conjugate elliptic fourth-order differential equation with variable coefficients
02 p0187 A73-12190

Three parameter boundary value problem for trajectory optimization of maximum weight station injection from earth orbit into interplanetary flight trajectory
02 p0219 A73-12454

Nonlinear initial and boundary value problems of thermoviscoplasticity, discussing uses of Vainberg theorem and functional convolution in variational principle formulation
02 p0236 A73-12516
[AD-758580]

Non-linear oscillations of a nonuniform fixed circular plate.
02 p0236 A73-12519

Boundary value problem of Lamé equation in elasticity theory of two dimensional region with angular points, solving by Fredholm integral equation
02 p0237 A73-12591

Difference approximations for boundary and eigenvalue problems for ordinary differential equations.
02 p0188 A73-12613

Semidiscrete-least squares methods for a parabolic boundary value problem.
02 p0188 A73-12615

Stability theory of difference approximations for mixed initial boundary value problems. II.
02 p0188 A73-12616

Exact cosmological solutions in Brans and Dicke's scalar-tensor theory. II.
02 p0224 A73-12743

On some solutions of the Falkner-Skan equation.
02 p0154 A73-12797

Reverse flow solutions of the Falkner-Skan equation for a lambda greater than one.
02 p0154 A73-12799

Calculation of the potential created and the velocity induced by a uniform source distribution on a polygon and on a periodic distribution of polygons for the solution of two-dimensional Poisson fields
03 p0241 A73-12910

Existence and uniqueness of heat equation two phase free boundary problem classical solutions
03 p0336 A73-12922

Numerical simulation of initial value problem of axisymmetric equatorially trapped oscillation modes of constant density viscous fluid in rotating spherical shell
03 p0384 A73-13064

Boundary value problems with a turning point.
03 p0336 A73-13066

Analytical representation of boundary conditions in the technical theory of shells
03 p0384 A73-13127

Boundary value problem for flow equation of multiphase viscous fluid with given velocity distribution, noting equations of motion for incompressible micropolar fluid flow
03 p0291 A73-13164

Electric field in a segmented MHD generator for a finite conductivity of the walls at the channel inlet
03 p0346 A73-13621

Boundary conditions for temperature perturbations in stability problems of compressible gas flows
03 p0245 A73-13672

Static boundary value problem of asymmetric elasticity for elastic isotropic media with small energy contribution to potential due to moment effects
03 p0394 A73-14050

Boundary value problems with variable boundaries for a special differential equation
03 p0337 A73-14630

A class of neutral functional differential equations.
04 p0469 A73-14666

Boundary value problems of the Laplace equation in a circle
04 p0470 A73-14933

Solution of an inhomogeneous boundary value problem with continuous discrete parameters in the presence of discrete disturbances
04 p0470 A73-14934

Cauchy problem and mixed boundary value problems for parabolic and hyperbolic wave equations of heat conductivity for boundary operators given on hyperplane
04 p0517 A73-14935

Extended validity of single segment stepwise integration schemes for solution of two-point boundary value problems.
04 p0510 A73-15015

On the application of the SHEBA shell element.
04 p0510 A73-15016

Partial differential equations with random coefficients and boundary conditions for stochastic processes in plasma, using parabolic equations for distribution function
04 p0479 A73-15037

The solvability of integral equations of shell theory
04 p0511 A73-15082

Certain algorithms and error assessments for the approximate analytical solution of boundary value problems
04 p0470 A73-15090

On the semi-discrete Galerkin method for hyperbolic problems and its application to problems in elastodynamics.
04 p0471 A73-15222

On the uniqueness of singular solutions to boundary-initial value problems in linear elastodynamics.
04 p0512 A73-15226

Boundary techniques for the multistep formulation of the optimized Lax-Wendroff method for non-linear hyperbolic systems in two space dimensions.
04 p0471 A73-15227

The integral equation and boundary conditions for a cylindrical antenna in a warm plasma.
04 p0429 A73-15482
[AD-760102]

Proof of the eigenvalues 0 and -1 in the spectra of integral operators of two-dimensional elasticity theory
04 p0514 A73-15677

A multi-step method for the numerical integration of ordinary differential equations.
05 p0589 A73-16100

Variational-difference method for solving the third boundary value problem of an elliptic equation in a three-dimensional region with a smooth boundary
05 p0590 A73-16445

The Green's function of the linearized viscous transonic equation
05 p0527 A73-16446

Numerical solution of a boundary value problem for the Navier-Stokes equations
05 p0564 A73-16449

Necessary conditions for optimal controls of elliptic or parabolic problems.
05 p0590 A73-16487

Initial and boundary value problems for melting propagation from solid cylinder axis and sphere center, assuming pure conductive heat transfer
05 p0638 A73-16595

Coupled thermoelasticity with a finite heat propagation rate
05 p0634 A73-16770

Solution of some boundary-value problems in the theory of potential flows of a gas and the propagation of weak shock waves.
05 p0565 A73-16790

Effect of boundary conditions on the radiative reflectance of dielectric coatings.
05 p0598 A73-16896
[AIAA PAPER 73-148]

Boundary value problems of elastic wave diffraction by spherical cavities, using vector equation of motion solutions
05 p0636 A73-17091

Vibration of thermally stressed plates with various boundary conditions.
05 p0636 A73-17101

Transformation of the hypersonic compressible Navier-Stokes equations.
05 p0567 A73-17120

On the evolution toward equilibrium in the kinetic theory of gases
05 p0599 A73-17229

Boundary conditions for penetration of an electromagnetic wave into a plasma.
06 p0727 A73-17418

Boundary-value problem for a Langmuir probe in a dense plasma.
06 p0727 A73-17420

Finite element model for discontinuous potential flow field analysis leading to Dirichlet, Neumann and mixed boundary value problems solution
06 p0644 A73-17514

Summary and comparison of gradient-restoration algorithms for optimal control problems.
06 p0715 A73-17567

Numerical simulation of a plasma. I - General description of the model
06 p0727 A73-17574

Matrix transformation in hyperplanes method for successive solution of boundary value problems of multidimensional differential equations, using space-time functions
06 p0715 A73-17718

Solvability in the large of the first boundary value problem for a certain class of quasi-linear one-dimensional parabolic equations
06 p0716 A73-17719

Parameter identification using the Galerkin procedure in nonlinear boundary-value problems.
[ASME PAPER 73-AUT-C] 06 p0716 A73-17724

A method for solving moving boundary problems in heat flow using cubic splines or polynomials.
06 p0768 A73-17979

A note on a general linear initial-boundary value problem.
06 p0716 A73-17980

On forced vibrations in the linear theory of micropolar elasticity.
06 p0762 A73-17987

Edge crack in a strip of an elastic solid.
06 p0762 A73-17991

The correspondence principle of linear viscoelasticity for problems that involve time-dependent regions.
06 p0762 A73-17992

Riemann-method solution of the Cauchy problem for a system of first-order equations with a degeneracy at the boundary
06 p0717 A73-18068

Boundary value problem for subsonic gas flow, proving existence theorem for gas dynamics problem solution
06 p0645 A73-18069

Approximate analytical solution of an asymmetrical problem of unsteady heat conduction with nonlinear boundary conditions
06 p0768 A73-18128

On a set of continuous wave electromagnetic inverse scattering boundary conditions.
06 p0664 A73-18136

Convergent finite difference schemes for nonlinear parabolic equations.
06 p0717 A73-18405

Comparing numerical methods for ordinary differential equations.
06 p0717 A73-18406

Galerkin methods for vibration problems in two space variables.
06 p0717 A73-18408

Multistep methods with variable matrix coefficients.
06 p0718 A73-18409

Low Reynolds number flow past a porous spherical shell.
06 p0687 A73-18506

Dynamic system optimal control problems with higher order state variable inequality constraints, obtaining solutions with boundary arcs and isolated points
06 p0680 A73-18519

A numerical method for solving optimal control problems with unspecified terminal time.
06 p0681 A73-18520

Boundary value problems of viscous fluid dynamic system generated by Navier-Stokes equations, using Hopf theory
06 p0724 A73-18634

The direct and inverse boundary value problems for the heat-conduction equation
06 p0770 A73-18682

Classical solvability of a problem of conjugation of two equations with the third boundary condition
06 p0718 A73-18684

Multipoint boundary problem for differential equations with a deviating argument
06 p0718 A73-18685

Solution of a boundary problem for a second-order delayed-argument differential equation by the spline-function method
06 p0719 A73-18688

Boundary value problems for non-elliptic first-order systems of pseudo-differential operators.

06 p0719 A73-18699

Uniqueness of non-linear elastic equilibrium for prescribed boundary displacements and sufficiently small strains.

06 p0719 A73-18700

The calculus of variations and various direct methods in engineering analysis.

06 p0719 A73-18722

Galerkin method for approximate solution of differential equation with boundary conditions, considering applicability to nonself-adjoint and nonlinear systems

06 p0765 A73-18725

Boundary conditions for diffusion in the pack-aluminizing of nickel.

06 p0713 A73-18774

Matrix exponential series approach to distributed parameter systems.

06 p0719 A73-18803

Invariant imbedding and a transformation procedure for reducing classes of boundary value problems into equivalent initial value systems.

06 p0719 A73-18804

Computerized optimal control problem formulation in calculus of variations, discussing flexible user-oriented algorithm for terminal point transversality boundary conditions numerical implementation

06 p0672 A73-18806

Calculus of variations for mathematical model of elastic shell with internal degrees of freedom, noting boundary and discontinuity conditions

06 p0766 A73-18877

Method of solution of certain boundary value problems for nonlinear hyperbolic equations and propagation of weak shock waves.

07 p0809 A73-19015

Estimate of the time of occurrence of discontinuities in the solution of a boundary value problem for a second order quasilinear hyperbolic system.

07 p0844 A73-19023

The finite element method in domains with curved boundaries.

07 p0907 A73-19029

The quadratic programming approach to the finite element method.

07 p0907 A73-19030

The treatment of natural boundary conditions in the finite element and finite difference methods.

07 p0907 A73-19033

Laplace equation and elasticity theory problems solution via Fredholm integral equation, noting boundary value problems for discrete points of given curve

07 p0909 A73-19127

The finite element method with Lagrangian multipliers.

07 p0844 A73-19137

Galerkin methods for parabolic equations with nonlinear boundary conditions.

07 p0844 A73-19138

Extremal boundary value problems of plasticity theory

07 p0910 A73-19304

Numerical solution of the Navier-Stokes equations by the finite element method.

07 p0810 A73-19501

A general scheme for solving ordinary differential equations under two-point boundary conditions.

07 p0845 A73-19546

Lower bound estimates of solutions to a second boundary-value problem for a second-order parabolic equation in regions with unrestricted spatial variables

07 p0845 A73-19655

Electromagnetic wave propagation in a circular waveguide with spirally conducting inserts

07 p0793 A73-19920

The existence and the numerical evaluation of generalized solutions of semilinear initial value problems

07 p0845 A73-20288

Boundary value problem solution method for hyperbolic partial differential equations based on theory of retarded potentials

07 p0845 A73-20440

Kinetic theory of suction flow, discussing slip coefficient determination for perturbation boundary conditions in Chapman-Enskog-Hilbert method and pressure gradient effects

07 p0812 A73-20474

A proposal for the calculation of characteristic functions for certain differential and integral operators via initial-value methods.

07 p0845 A73-20490

A unified boundary controllability theory for hyperbolic and parabolic distributed parameter systems.

07 p0846 A73-20591

The method of internal force parameters in elastokinetics

08 p0106 A73-20782

Treatment of harmonic mixed boundary problems by conformal transformation methods.

08 p0983 A73-20785

Vibration of four point-supported plates by a finite element method.

08 p0107 A73-20945

Application of the regularization principle to the construction of approximate solutions to inverse heat-conduction problems

08 p1022 A73-21097

Contact problem with one governing parameter in elasticity theory

08 p1017 A73-21099

Axiymmetric Stefan problem with boundary conditions of the third kind

08 p1022 A73-21100

Solvability of mixed boundary value problems for second-order parabolic equations with degeneration

08 p0983 A73-21126

Boundary value problems for the Maxwell equations

08 p0988 A73-21130

Nonstationary and asymmetric cosmic ray modulation theory, discussing moving boundary problem and solar wind model with spherical singularity

08 p0999 A73-21341

On the lateral boundary conditions for the primitive equations.

08 p0985 A73-21387

On the solution of the nonlinear heat conduction equations by numerical methods.

08 p1024 A73-21636

Hemispherical reflectivity and transmissivity of an absorbing, isotropically scattering slab with a reflecting boundary.

08 p1025 A73-21643

Convergence of difference methods for certain degenerating quasi-linear parabolic equations

09 p1111 A73-21919

On degenerate elliptic-parabolic operators of second order and their associated diffusions.

09 p1111 A73-21996

Numerical solution of mixed boundary value problems using numerical Green's functions.

09 p1112 A73-22394

On the generalization of stress function procedure for dynamic analysis of plates.

09 p1158 A73-22395

Finite difference programs with grid self adjustment for steady or unsteady problems with arbitrary boundaries and without coordinate hierarchy, noting computer time saving

09 p1071 A73-22400

An iteration procedure for the solution of special nonlinear boundary-value problems

09 p1112 A73-22448

Difference iterative solution for two dimensional boundary value problem for rectangular elastic plate with rectangular cutout

09 p1159 A73-22584

Computerized two dimensional boundary value problem solutions for bounded multiply connected structural regions with periodic inclusions, using three step R-functions and Rvachev method

09 p1120 A73-22586

Muskelishvili boundary value problem of plate bending and point deformation for round and annular plates under uniform loads

09 p1159 A73-22854

Equivalent initial conditions for automatic control systems with variable parameters

09 p1069 A73-22943

Rayleigh-Ritz solution of boundary value problem for plane compressible subsonic flow past aerofoil noting convergence

09 p1028 A73-22954

The numerical solution of boundary value problems for second order functional differential equations by finite differences.

09 p1113 A73-23021

Semivariational approximation for solution of parabolic differential equation with inhomogeneous mixed boundary conditions and abstract equation with operators, noting convergence and stability

09 p1113 A73-23025

Kinetic theory for the reflection of waves obliquely incident on the boundary of a magnetoactive plasma

09 p1052 A73-23078

Fundamental and parasitic modes of a shielded microstrip transmission line

09 p1052 A73-23085

Integral transform solution of mixed boundary value problem for Griffith cracks with complicated geometries and external, star-shaped, cruciform-shaped and circular cracks

09 p1162 A73-23183

Mixed boundary value problems in solid contact and crack mechanics, discussing numerical solution of singular integral equations with simple and generalized Cauchy kernels

09 p1162 A73-23184

Book on boundary value problems in physics and engineering covering Fourier series and integrals, heat, wave and potential equations, Laplace transforms and numerical methods

09 p1113 A73-23300

Periodic method of characteristics for solution of hyperbolic partial differential equations of physical system specified by two boundary conditions at single spatial location

10 p1241 A73-23604

Local extrapolation in the solution of ordinary differential equations.

10 p1241 A73-23641

Boundary value problems for a nonlinear differential equation with a deviating argument of neutral type

10 p1241 A73-23742

Finite-element method applied to heat conduction in solids with nonlinear boundary conditions.

10 p1295 A73-23778

Numerical solution of some boundary value problems for an isotropic cylindrical shell

10 p1288 A73-24060

Potential energy method for boundary value problem of axisymmetric elastic contact of solid and hollow cylinders compressed by plane walls

10 p1289 A73-24064

Nonlinear singular multipoint boundary value problems.

10 p1243 A73-24161

A finite element method for non-self-adjoint problems.

10 p1243 A73-24292

Thermoelastic boundary value problem for heat conduction in elastic bodies with linear and three dimensional inserts

10 p1290 A73-24305

Determination of eigenvalues in a class of waveguides of doubly connected cross section.

10 p1249 A73-24392

Calculation of the steady thermal and stress boundary conditions in the Phoebus 2 reactor

10 p1248 A73-24495

Iterative method for solving some boundary value problems for the equations of an orthotropic shell of revolution

10 p1292 A73-24503

Application of the averaging method to the solution of the mixed boundary value problem for a class of nonlinear partial differential equations

10 p1243 A73-24504

Construction of the solution to a nonlinear boundary value problem for a heat-radiating body of complex shape

10 p1296 A73-24510

Boundary conditions model calculations for thermoelastic deformations of continuum body with surface tractions on interface, discussing energy balance laws derivation for loading devices

10 p1292 A73-24659

Studies in the application of recurrence relations to special perturbation methods. II - Comparison of the Encke and Cowell methods of integration in the restricted three-body problem.

10 p1283 A73-24668

Two dimensional statics for isotropic elastic body with inhomogeneous mechanical properties, discussing two-step solutions for differential equilibrium equation and boundary value problem

10 p1293 A73-24676

Initial conditioned solutions of a second-order nonlinear conservative differential equation with a periodically varying coefficient.

10 p1244 A73-24706

The initial value problem for the free-space Schroedinger equation.

10 p1244 A73-24787

Unsteady creep in a symmetrical cylindrical shell

10 p1293 A73-24793

On the Kutta-condition at the trailing edge of a nozzle in a weakly nonstationary jet flow.

10 p1209 A73-24827

Some solutions of the unsteady two-dimensional turbulent boundary layer equations.

10 p1209 A73-24835

Some finite extremum principles in piecewise linear elasto-plasticity.

11 p1434 A73-25215

Maximum principle and uniform convergence for the finite element method.

11 p1390 A73-25435

Buckling analysis of elastically constrained conical shells under hydrostatic pressure by the collocation method.

11 p1438 A73-25499

Heat conduction nonlinear boundary value problems approximate solution via Westphal similarity theorem, considering inhomogeneous media with temperature dependent heat transfer coefficients

11 p1451 A73-25742

Boundary-value problem for a system of equations with a temperature boundary layer.

11 p1452 A73-26055

Static method for fiber-reinforced plate design optimization for important boundary conditions, noting topographies associated with piecewise linear specific cost functions

11 p1443 A73-26092

Displacement boundary value problem of linearized elastodynamics with superimposed small and large deformations in homogeneous anisotropic elastic solid, proving solution uniqueness theorem

11 p1444 A73-26282

Calculation of functionals of the eigenfunctions in the boundary value problem of a system of linear ordinary differential equations

11 p1391 A73-26331

Entropy minimum principle applied to boundary value problem of non-linear heat conduction.

11 p1452 A73-26342

Differential equations for asymmetric bending of circular sandwich plates.

11 p1445 A73-26406

Method of initial functions for the plane problem of a linearly orthotropic body in the theory of elasticity

11 p1445 A73-26457

Optimal inputs and sensitivities for parameter estimation.

11 p1391 A73-26579

Solvability of the mixed boundary value problem for higher-order parabolic quasi-linear equations with discontinuous and rapidly growing coefficients in the Orlich classes

11 p1392 A73-26599

Thermodynamic methods applied to self gravitating n-body systems for different boundary conditions, considering energy transfer

11 p1427 A73-26604

Admissible step sizes for Adams-Bashforth, Adams-Moulton, Nystrom and Milne-Simpson difference methods for initial value problems solution

11 p1392 A73-26729

A boundary value problem for higher-order hyperbolic equations

12 p1516 A73-26961

Necessary and sufficient condition for stability of a class of difference-type boundary value problems

12 p1517 A73-26962

On the formulation of the traction problem for the flow theory of plasticity.

12 p1551 A73-27046

A proof of the Pontryagin maximum principle for initial-value problems.

12 p1517 A73-27117

The asymptotic behavior of Green's function for a heat-conduction equation with a small parameter

12 p1558 A73-27248

Stability of heat transfer during boiling at a nonisothermal surface

12 p1558 A73-27314

Temperature calculation for heat emitting surface in transparent gas flow, using linearizing function method for heat transfer problems with nonlinear boundary conditions

12 p1558 A73-27316

Constant cross section composite circular rod, deriving torsional stress behavior near division line intersection with rod contour from closed solution

12 p1552 A73-27368

Boundary value problems in elastoplastic plate theory, obtaining solution through reduction to operator equations

12 p1552 A73-27370

Stability of rectangular plates under mixed boundary conditions

12 p1552 A73-27372

Two dimensional elasticity theory boundary value problem, for inhomogeneous laminar elastic medium, using Airy stress functions and power series expansion of inhomogeneity parameter

12 p1553 A73-27412

Classical solutions to the second boundary value problem for the unsteady free convection equations

12 p1559 A73-27421

A uniqueness theorem for the solution of the inverse problem of spectral analysis in the case of a differential equation with periodic boundary conditions

12 p1518 A73-27727

Behavior of eigenfunctions and values in elliptical boundary value problems in a variable region

12 p1518 A73-27728

Equivalence of one type of a Riemann boundary value problem for a system of n pairs of functions relative to a complete singular integral equation with a Cauchy kernel

12 p1518 A73-27730

Ritz method extension to mechanics problems by introducing artificial spring parameters at boundary and using Legendre functions as coordinate functions

12 p1555 A73-27740

Boundary value problem solution uniqueness in dynamic linear theory of hereditary-elastic rheologically composite media

12 p1555 A73-27793

Russian papers on mathematical physics boundary value problems covering electrodynamics, electromagnetic fields in conducting channels and ferromagnetic cylinders, heat transfer, shell theory, etc

12 p1525 A73-27803

Nonlinear integral equations for the electrodynamics of conducting media

12 p1525 A73-27805

Approximate method for solving a boundary value problem describing gas flow during strong blowing

12 p1458 A73-27811

Solvability of the boundary value problem in the theory of shallow shells of revolution and estimation of errors in the approximate solution

12 p1556 A73-27813

Linear systems with aftereffects of delayed feedback described by differential equations, obtaining optimal control solution in terms of parameters and boundary value problem

12 p1486 A73-27950

Point matching /collocation/ computation of transverse resonances by complex valued solutions of Helmholtz equation with Neumann or Dirichlet problems, applying to electromagnetic waveguides

13 p1581 A73-28076

A characteristic initial value problem in general relativity in the case of a perfect fluid with axial symmetry.

13 p1658 A73-28199

Two-sided difference methods of solving linear boundary value problems for ordinary differential equations

13 p1647 A73-28341

On the eigenvalue problem for fluid sloshing in a half-space.

13 p1599 A73-28410

The numerical treatment of natural eigenvalue problems of the 4th order according to the collocation method with a Lagrange polynomial approach

13 p1695 A73-28411

Singular perturbation analysis of a certain Volterra integral equation.

13 p1648 A73-28412

Extended Mellin transforms for boundary value problems, discussing inversion integral, operational properties convolution formulas, and application to circular sector steady state heat problem

13 p1648 A73-28422

The Rayleigh-Faber-Krahn theorem for the characteristic values associated with a class of nonlinear boundary value problems.

13 p1648 A73-28423

Improperly posed initial value problems for self-adjoint hyperbolic and elliptic equations.

13 p1648 A73-28424

Composite materials transient thermal boundary conditions analytical derivation from initial and time dependent internal temperature distribution or gradient

13 p1705 A73-28436

Initial-boundary value problems of nonlinear extensible beam equation as mathematical model for transverse deflections of beam with hinged or clamped ends

13 p1695 A73-28438

Generalization of the integral balance method in problems of correlated heat and mass transfer

13 p1705 A73-28464

A two-dimensional mathematical model for an acoustically soft parabolic cylinder reflector.

13 p1597 A73-28493

Characteristic initial value problem for class of differential equations, proving solution existence and uniqueness as generic properties

13 p1648 A73-28536

Singular perturbations for a nonlinear differential equation with a small parameter.

13 p1648 A73-28537

Generalized Green function for infinite plate strip with free edges, noting application to elastic boundary value problems

13 p1695 A73-28560

Plate theory boundary value problems algorithm from Fourier transformation of ultradistribution functions

13 p1695 A73-28561

On an Euler-like method with exponential correction for initial-value problems.

13 p1650 A73-28799

Russian book - Problems of applied mathematics.

13 p1650 A73-29126

Automation of variational methods of solving boundary value problems

13 p1650 A73-29127

Computer realization of a method of scaling the gravity force

13 p1609 A73-29128

Automation of a solution to the general boundary value problem of a plane self-conjugate elliptic equation

13 p1650 A73-29129

Computational algorithm for three dimensional mixed boundary value problem for perturbing potential in earth figure theory

13 p1609 A73-29130

The static-geometric duality and a staggered mesh scheme in the numerical solution of some shell problems.

13 p1699 A73-29373

Application of a variational method to dissipative, non-conservative problems of elastic stability.

13 p1700 A73-29376

Analysis of self-excited and forced vibrations of a rectangular plate on many supports in supersonic flow.

13 p1700 A73-29392

On the stability of numerical integration routines for ordinary differential equations.

13 p1650 A73-29397

Rayleigh-Ritz method for approximate solutions to nonlinear ordinary differential equations with nonlinear boundary conditions

13 p1650 A73-29399

Effects of specimen geometry and loading conditions on the crack tip plastic zone.

13 p1701 A73-29474

Application of a modified quasilinearization technique to totally singular optimal control problems.

13 p1597 A73-29570

State space approach to mixed boundary value problems.

13 p1651 A73-29571

Asymptotic behavior of solutions of the Cauchy problem and the first boundary value problem on a half-axis for a linear second-order parabolic equation with the absolute value of x approaching infinity and at large values of the parameter

13 p1651 A73-29680

Solution of a boundary value problem for the oblique incidence of a plane E-polarized wave on a metallic strip array with an optically active medium

13 p1623 A73-29682

Uniqueness theorems for the Dirichlet boundary value problem in the case of elliptic-parabolic differential equations and lower bounds for the smallest eigenvalue

14 p1767 A73-29765

Thermal diffusivity measuring technique for hazardous materials.

14 p1752 A73-29914

Numerical implementation of the Schwarz alternating procedure for elliptic partial differential equations.

14 p1768 A73-29938

Bubnov-Galerkin method for mixed boundary value problem solution via sequence of coordinate functions, illustrated by steady state conductive heat transfer problem

14 p1768 A73-30019

Asymptotic solution of initial value problem for weakly nonlinear wave system including dispersive and diffusive effects related to plane Poiseuille flow instability

14 p1744 A73-30171

Implicit predictor-corrector difference scheme for boundary value problem solution in propagation of spherical and cylindrical N waves /asymptotic pulse forms/

14 p1745 A73-30175

Stability and convergence of finite element methods for elastic structures vibration analysis, stressing application to mixed boundary value problems

14 p1807 A73-30185

Finite element method investigation of branch and secondary crack formation and multiple fracture, solving sequences of boundary value problems and strain energy release rates

14 p1808 A73-30195

Integral equation formulation for electromagnetic scattering by conducting cylinders, investigating coupling between complementary boundary value problem and nonuniqueness consequences on numerical resolution

14 p1727 A73-30215

A uniqueness theorem for a system of stress equations of motion in linear elasticity.

14 p1809 A73-30255

Boundary value problem of a system of ordinary differential equations with a complex parameter

14 p1768 A73-30346

Solution of certain nonlinear boundary value problems for regions of complex shape by a structural method

14 p1769 A73-30349

Book - Computational fluid dynamics.

14 p1745 A73-30359

Solution of the first boundary value problem of statics in the moments theory of elasticity

14 p1810 A73-30382

Third basic boundary value problem of dynamics for a three-dimensional elastic body

14 p1810 A73-30383

Boundary value problem solutions for parallelogram and elliptical thin plates vibration frequencies and mode shapes based on eigenvalues domain dependence and parameter differentiation technique

14 p1810 A73-30408

Convergence of a difference procedure for quasi-linear parabolic initial boundary-value problems in cylinder symmetry

14 p1769 A73-30422

Numerical solutions by the continuation method.

14 p1769 A73-30454

Asymptotic solutions for shells with general boundary curves.

14 p1812 A73-30523

An existence theorem for linear boundary value problems.

14 p1770 A73-30524

Hyperbolic equation initial-boundary problem in finite cylinder solved via elliptic boundary problem with parameter

14 p1770 A73-30545

Control of functional differential equations with function space boundary conditions.

14 p1770 A73-30754

Numerical methods for functional differential equations.

14 p1770 A73-30755

Dynamic singular boundary value problem of elastic body with propagating crack under concentrated force

14 p1814 A73-30784

Solution of three-dimensional contact problems in elasticity theory

14 p1775 A73-30831

Estimated solutions for the second and third boundary value problems of a second-order parabolic equation in regions with unbounded spatial variables

14 p1771 A73-30836

Boundary conditions in primitive equation weather prediction models with special emphasis on the control of gravity wave propagation.

14 p1772 A73-30902

Eigenvalues asymptotic behavior in boundary value problems of infinitely expanding region of Euclidean space, applying results to continuous media stability investigation

15 p1860 A73-30964

Solution of the fundamental boundary value problems for a closed semifinite cylindrical shell

15 p1945 A73-31023

Static problem of elastic body with stresses at boundary, solving incompatible difference equations by explicit iteration methods

15 p1945 A73-31026

Derivation of a normal displacement function for the triangular finite element of plates and shells

15 p1945 A73-31032

A new method for the Lebedev-Ufliand integral equation for contact problems of elasticity.

15 p1946 A73-31103

Application of inverse boundary value problems in the theory of dimensional electrochemical working

15 p1881 A73-31153

Boundary value problems for a first-order differential equation with operator coefficients and for the expansion of this equation in a series of its eigenvalues

15 p1899 A73-31216

A numerical solution for the transonic flow around blunt wedges

15 p1823 A73-31330

Weak solutions existence and uniqueness for boundary value problem in linearized theory for mixtures of two isotropic incompressible elastic solids, obtaining differentiability conditions

15 p1947 A73-31336

An explicit second order method of characteristics for the initial value problem in the case of quasi-linear hyperbolic differential-equations systems of the first order with two independent variables

15 p1899 A73-31361

Uniqueness and existence estimates of third order differential equation solutions for nonlinear boundary value problem in fluid mechanics

15 p1863 A73-31363

Error investigations regarding the solution of the inhomogeneous natural boundary value problem by means of a Ritz approach with standardized coordinate functions

15 p1899 A73-31364

Effect of openings on stresses in rigid pavements.

15 p1856 A73-31387

Calculation of stress-concentration factors for grooved shafts in bending using the point-matching technique.

15 p1948 A73-31616

A modified quasilinearization technique for optimal control problems with unspecified final time.

15 p1853 A73-31627

Riccati transformation for optimal control linear two-point boundary value problems formulated from first order numerical integration methods

15 p1908 A73-31666

Integral equations for piecewise-homogeneous media in the solution of boundary value problems of electrodynamics

15 p1913 A73-31693

Nature of stresses in the internal vicinity of the edge of the joint surface in a compound body loaded under conditions of the plane problem of the theory of elasticity

15 p1950 A73-31827

Method for boundary condition selection in the heat transfer problem with phase transition

15 p1958 A73-31872

The solution of heat conduction problems with the aid of the Laplace transformation. II - Numerical evaluation and graphical representation of two specific boundary value problems

15 p1958 A73-31907

Single point solutions of Dirichlet boundary value problems by Monte Carlo and successive over-relaxation.

15 p1899 A73-32037

Numerical solution of the integral equations for optimal sequential filtering.

15 p1844 A73-32039

Solutions of boundary value problems of multilayer analogs of geoelectrics and hydrology.

15 p1872 A73-32040

Boundary-value problems for Maxwell's equations.

15 p1900 A73-32065

Book - Continuum mechanics and related problems of analysis.

15 p1952 A73-32076

Contribution to the theory of mixed-type equations whose order degenerates along the line describing the changes in the type

15 p1900 A73-32080

Hilbert boundary value problem solution for piecewise holomorphic vector in singly connected region with Liapunov contour bound

15 p1900 A73-32086

Mixed boundary value problem solution for strip under elastic deformation due to external loads based on reduction to system of integrodifferential equations

15 p1952 A73-32088

Theorem concerning possible bendings in zero-moment shell theory

15 p1953 A73-32090

General linear boundary value problem with measurable coefficients for numerous analytical functions of class E sub p

15 p1900 A73-32092

Stress distribution near holes

15 p1953 A73-32097

Boundary value properties of weighting space functions and applications of the functions in boundary value problems

15 p1900 A73-32101

Solution to a three-dimensional mixed boundary value problem in the theory of elasticity

15 p1953 A73-32102

Boundary value problem of linear conjugation with a piecewise-continuous matrix coefficient

15 p1900 A73-32104

Structural components shape optimization for stress concentration reduction, solving complex boundary value problem via conformal transformation to curvilinear coordinates

15 p1954 A73-32108

An approach to the analysis of boundary value problems in the theory of functions and two-dimensional problems in the theory of elasticity

15 p1954 A73-32124

Antiplane elasticity boundary value problem solution for isotropic bars under tangential loads, considering twisting and bending

15 p1955 A73-32127

Existence and uniqueness of positive eigenfunctions for a class of quasilinear elliptic boundary value problems of sublinear type.

15 p1900 A73-32181

Book - Two-point boundary value problems: Shooting methods.

15 p1901 A73-32299

The Dirichlet boundary and initial value problem for hyperbolic differential equations

15 p1901 A73-32369

A criterion for global existence in case of ordinary differential equations.

15 p1901 A73-32370

Singularities of solutions to linear, second order, analytic elliptic equations in two independent variables. II - The piecewise regular boundary.

15 p1901 A73-32374

Existence and uniqueness of solutions of boundary value problems for third order differential equations.

15 p1902 A73-32398

Integral operators and the first initial boundary value problem for pseudoparabolic equations with analytic coefficients.

15 p1902 A73-32399

Calculus of variations for mathematical model of elastic shell with internal degrees of freedom, noting boundary and discontinuity conditions

15 p1956 A73-32402

Three parameter boundary value problem for trajectory optimization of maximum weight station injection from earth orbit into interplanetary flight trajectory

15 p1941 A73-32604

Solution on a digital computer of boundary value problems for three-dimensional rod systems with branchings

16 p2075 A73-32692

Numerical method for mixed elliptical-hyperbolic nonlinear Cauchy problem with boundary conditions, applying to sonic flow around wing sections

16 p1961 A73-32807

Forced extensional vibrations of isotropic elastic plates with time dependent body forces, surface tractions and nonhomogeneous boundary conditions, using Kane-Mindlin theory

16 p2076 A73-32920

The iterative solution of two-point linear differential eigenvalue problems.

16 p2031 A73-32930

Extension of the Caratheodory theory to multivalued differential systems with nonlinear boundary conditions

16 p2031 A73-32932

Steady solutions of a nonlinear problem for the Navier-Stokes equations

16 p2031 A73-32933

The principle of minimum entropy applied to boundary value problem of non-linear heat conduction.

16 p2084 A73-32984

Nonlinear shell theory, obtaining differential equilibrium equations and boundary conditions from three dimensional variational energy expression by kinematic hypothesis and Ritz method

16 p2078 A73-32996

The analysis of three dimensional problems of elasticity by integral representation of displacement.

16 p2078 A73-33003

Solution of equations of Reissner's theory of plates by application of Hajdin's method.

16 p2078 A73-33004

The analytical aspects of the reduction of boundary errors in the case of numerical weather predictions

16 p2034 A73-33074

New problems pertaining to nonlinear integro-differential equations with several independent variables. I - Search for solutions in the case of initial integral boundary conditions

16 p2032 A73-33172

Viscoelastic body stress-strain state under quasi-static loads, obtaining boundary value problem solution via finite element method

16 p2080 A73-33244

Principle of virtual work and Piola theorem for motion and constitutive equations and boundary conditions of oriented elastic media, using point continuum mechanics assumptions

16 p2080 A73-33245

Weak disturbances upstream propagation in supersonic boundary layer, deriving homogeneous boundary value problem for complex amplitude function

16 p2000 A73-33263

Initial-value problems in potential theory.

16 p2032 A73-33304

An integral representation of the Dirac delta function for axisymmetric boundary value problems.

16 p2032 A73-33309

Numerical representation of inlet and exit boundary conditions in transient cascade flow.

[ASME PAPER 73-GT-55] 16 p2048 A73-33511

The mixed boundary value problem for the elastic half space.

16 p2081 A73-33901

Half plane stress boundary value problems in elastodynamics, obtaining similarity solutions in terms of analytic functions via integral transforms

16 p2082 A73-33903

Influence of in-plane displacements at the boundaries of rigid-plastic beams and plates.

16 p2083 A73-33973

A difference method of solving boundary value problem for a parabolic-type quasi-linear integro-differential equation

16 p2034 A73-34070

Interaction of an air-cushioned vehicle with an elastic guideway.

17 p2098 A73-34181

Formulation of stable difference schemes for systems of initial-value partial differential equations.

17 p2200 A73-34284

Solution of the plane problem in elasticity theory for an incompressible material by the fractional step method

17 p2211 A73-34299

On an initial value problem for a nonlinear system of Vlasov-Maxwell equations.

17 p2200 A73-34320

Book - Non-homogeneous boundary value problems and applications. Volume 3.

17 p2200 A73-34464

Riemannian homogeneous boundary-value problem with an infinite index and a coefficient having a denumerable set of discontinuities of the first kind

17 p2200 A73-34629

Russian book - Linear and nonlinear boundary value problems.

17 p2201 A73-34640

On the distribution of the eigenvalues and the order of the eigenfunctions of a fourth-order singular boundary value problem.

17 p2201 A73-34823

Finite element formulation of nonlinear boundary-value problems.

17 p2201 A73-34831

An initial value method for the study of shock-induced laminar compressible boundary layers.

[ASME PAPER 73-FE-4] 17 p2152 A73-35004

Continuum theory for elastic laminates in terms of effective stiffness, deriving displacement and stress interface boundary conditions with illustrative wave propagation examples

[ASME PAPER 72-WA/APM-13]

- 17 p2249 A73-35112
A necessary condition for the nonoccurrence of von Mises yielding in impulsively loaded plates.
- 17 p2250 A73-35118
Boundary condition calculation procedures for inviscid supersonic flow fields.
- 17 p2155 A73-35143
Current distribution of a dipole antenna of revolution in dissipative media.
- 17 p2141 A73-35366
Quasi-Newton methods for discretized non-linear boundary problems.
- 17 p2202 A73-35520
Boundary value problems with a normal derivative for a mixed-type equation with discontinuous coefficients
- 17 p2203 A73-35584
Boundary value problem of the E problem type for mixed equations of the second kind
- 17 p2203 A73-35588
Book - Variational analysis: Critical extremals and sturmian extensions.
- 17 p2203 A73-35598
Spline interpolation techniques for approximation of boundary value problem solutions, relating approximation error norm to interpolation error norm from variational formulation
- 17 p2203 A73-35607
Two dimensional static, dynamic and three dimensional photoelasticity measurement techniques for stress intensity, factors determination in boundary value problems of fracture mechanics
- 17 p2252 A73-35673
Estimate of error in the solution of interior problems of microwave electrodynamics.
- 17 p2143 A73-35706
Nonlinear boundary value problems and several Lyapunov functions.
- 17 p2203 A73-35730
Russian book on elastic equilibrium boundary value problems for isotropic and anisotropic bodies under load or temperature field induced plane deformation
- 18 p2361 A73-35874
Sensitivity of the numerical analysis of the three-fluid plasma mixed initial-boundary value problem.
- 18 p2338 A73-36160
Effects of the boundary conditions and of the deformation of a region on the spectrum of operators which are generated by boundary value problems with a spectral parameter contained in the boundary conditions on a boundary section
- 18 p2329 A73-36161
Theorems concerning isomorphisms for elliptic boundary value problems with nonnormal boundary conditions
- 18 p2329 A73-36164
Shock wave generation by moving distributed non-diffusive force, solving initial value problem for single fluid model to obtain supersonic force field velocity
- 18 p2299 A73-36323
Thermoelastic state of an anisotropic plate with an elliptic hole and mixed boundary conditions
- 18 p2363 A73-36406
Nonlinear gas oscillations in pipes. I - Theory.
- 18 p2299 A73-36505
An iterative solution to the second order eigenvalue equation with periodic boundary conditions.
- 18 p2330 A73-36609
A perturbation treatment for optimal slightly nonlinear systems with linear control and quadratic criteria.
- 18 p2294 A73-36637
Wazewski retract method application to boundary value problems for second order generalized differential equations, proving solutions existence
- 18 p2330 A73-36693
Homogeneous isotropic body thermoelasticity boundary value problems solved by quadrature series using Green function of Laplace equation, determining circular cylinder stress concentration
- 18 p2366 A73-36753
Coordinate function construction in solving the boundary value problems of heat conductivity by direct methods
- 18 p2372 A73-36818
Numerical methods based on very accurate approximation of partial derivatives.
- 18 p2330 A73-36828
Approximate method for solving a boundary value problem in the theory of zero-moment elastic spherical shells
- 18 p2367 A73-36988
Diffraction of an acoustic wave at a moving plate
- 18 p2265 A73-37012
Natural transverse vibrations of sandwich beams of unsymmetrical structure.
- 18 p2367 A73-37141
Generalized Galerkin method for approximate solution of eigenvalue self-adjoint boundary value problems in stability analysis of mechanical distributed parameter systems
- 19 p2458 A73-37189
A new form of the integral equations of a boundary value problem in the theory of simply supported shallow spherical shells
- 19 p2495 A73-37198
Membrane statics of parachute-like shells.
- 19 p2496 A73-37480
A procedure for solving problems of elasto-plastic flow.
- 19 p2496 A73-37484
Boundary value problem of steady MHD flow in rotating cylindrical pipe under uniform magnetic field
- 19 p2468 A73-37647
Boundary conditions and stability of inviscid plane-parallel flows.
- 19 p2420 A73-37751
Two-dimensional problem in elasticity theory for a rectangle with mixed boundary conditions
- 19 p2499 A73-37761
Unique solution of boundary value problem of Boltzmann equation for unsteady rarefied gas flow of formless particles past arbitrary surface
- 19 p2462 A73-37843
Stability criteria for explicit finite difference solutions of the parabolic diffusion equation with nonlinear boundary conditions.
- 19 p2445 A73-38189
An indirect trajectory optimization algorithm based on the continuation method for solution of nonlinear equations.
- 20 p2588 A73-38826
[AIAA PAPER 73-890]
An initial value method for the eigenvalue problem for systems of ordinary differential equations.
- 20 p2581 A73-38970
Calculation of bending vibrations in beams with the aid of a discrete model
- 20 p2615 A73-38982
An integral-equation approach to dispersion relations for guided elastic surface waves.
- 20 p2592 A73-39048
Monte Carlo method for biharmonic boundary value problems solution, using isotropic random walk and mean value relation
- 20 p2581 A73-39094
Flow theoretical model for nonstationary creep in metals, using Galerkin method for approximate solution of boundary value problem
- 20 p2616 A73-39099
Convergence of Huber's method for heat conduction problems with change of phase.
- 20 p2626 A73-39100
Book - An analysis of the finite element method.
- 20 p2581 A73-39139
Book - Hyperbolic systems of conservation laws and the mathematical theory of shock waves.
- 20 p2581 A73-39140
Nonlinear boundary value problem with permissible zeros on the contour
- 20 p2582 A73-39206
The Cauchy problem and some basic problems of mathematical physics about parabolic systems with discontinuous coefficients
- 20 p2582 A73-39252
Moderate-thickness plate equilibrium equations and boundary value problems, discussing successive approximation method, static bending and potential energy
- 20 p2618 A73-39317
Fredholm integral equation for solving boundary value problem of heat transfer across contact of two regions bounded by simple closed Jordan curves
- 20 p2628 A73-39399
Boundary value problems for linear generalized differential equations and their adjoints.
- 20 p2582 A73-39402
Solution of a boundary-value problem for a second-order differential equation with a lagging argument by the method of spline functions - A scheme of increased accuracy
- 20 p2582 A73-39472
A geometric solvability characteristic for some boundary value problems of linear elliptic-type equations and strongly elliptic second-order systems
- 20 p2583 A73-39498
Some three-dimensional boundary value problems for an elastic medium bounded by cylindrical surfaces
- 20 p2620 A73-39508
Mixed finite-difference scheme for a class of linear and nonlinear structural mechanics problems.
- 20 p2621 A73-39544
A unified method for determination of fundamental natural frequency of orthotropic plate with arbitrary boundary.
- 20 p2622 A73-39546
Series analysis of cylindrical shells - New look at an old problem.
- 20 p2622 A73-39550
The local role of the limit line in the well-posing of steady state problems in gas dynamics. II - Two dimensional plane flow.
- 20 p2549 A73-39562
Corrugated circular waveguide boundary value problem solution to predict lower attenuation for HE sub 11 mode
- 20 p2538 A73-39598
Overheat instability in a flow of electrically conducting incompressible medium under conditions of an internal boundary value problem
- 20 p2598 A73-39605
The role of Korteweg-de Vries equation in plasma physics.
- 20 p2599 A73-39625
Gevrey hypoelliptic differential operators for subelliptic boundary value problems, considering relationship to size of derivative fractional loss in subelliptic estimate
- 20 p2583 A73-39626
Van der Waals energy calculation from electromagnetic mode quantum energy in spheres and cylinders, considering finite boundary conditions, Green function techniques, and periodic lattices
- 20 p2538 A73-39706
No-slip boundary condition origin for viscous incompressible Newtonian fluid flow over family of models for rough wall
- 20 p2549 A73-39810
A singular boundary value problem for a system of ordinary differential equations
- 20 p2583 A73-39817
The boundary theory of strength and nonlinear programming of boundary value problems of plate bending
- 20 p2625 A73-39821
Diffuse parasitics gain thresholds of laser modes for rectangular geometries, discussing radiation field and boundary conditions
- 21 p2710 A73-40145
Uniqueness of solutions and some approximate methods of solving problems in linear viscoelasticity
- 21 p2782 A73-40186
The numerical solution of nonlinear parabolic problems by variational methods.
- 21 p2725 A73-40382
A class of heat conduction problems with a time-variable heat transfer coefficient
- 21 p2790 A73-40396
Boundary residual methods limitation on elasticity problem solution accuracy, considering torsional stress analysis of square and hexagonal cylinders with circular hollow cores
- 21 p2784 A73-40431
Phased array analysis by circuit and field theory approaches, discussing boundary value problems formulation and solutions for systems with current carrying and aperture elements
- 21 p2651 A73-40650
Initial-value problems for pseudo-parabolic partial differential equations.
- 21 p2726 A73-40694
Solution of the mixed boundary value problem of plane elasticity theory with the aid of singular integral equations
- 21 p2785 A73-40931
Free boundary problem involving elliptic differential equation, discussing iterative method instabilities inhibition of convergence
- 21 p2727 A73-40998
Integral representations for solution of mixed boundary value problems for generalized axisymmetric Helmholtz equation, considering Sommerfeld half plane and transonic flow problems
- 21 p2727 A73-41017
Relation between the fundamental solutions in cylindrical and spherical coordinates /with identical coordinate origins/ for certain equations of mathematical physics
- 21 p2753 A73-41025
Reflection and transmission of plane waves at a boundary between two conducting media.
- 21 p2655 A73-41047
Integration of a nonlinear partial differential mixed boundary value problem
- 21 p2792 A73-41065
Necessary and sufficient conditions for solvability of certain boundary value problems for a second-order ordinary differential equation
- 21 p2727 A73-41272
A parallel algorithm for high subsonic compressible flow over a circular cylinder.
- 21 p2727 A73-41474
Plane strain and generalized plane stress problems for fibre-reinforced materials.
- 21 p2788 A73-41546
Canonical differential equations from equilibrium and compatibility conditions for boundary loaded, shell of revolution, simplifying and transforming by canonical transformations
- 21 p2788 A73-41616
Thermoelastic wave propagation in a random medium and some related problems.
- 21 p2789 A73-41667
Micropolar elasticity solution for static plane boundary value problems in circular ring shaped region, considering Volterra dislocation example
- 21 p2789 A73-41670
Russian book - Qualitative theory of boundary value problems for quasi-linear second-order parabolic equations.
- 22 p2881 A73-41701
Electromagnetic inverse boundary conditions determination of profile and material surface characteristics of conducting circular cylindrical shape scatterer
- 22 p2824 A73-41834

Study of self-excitation conditions in an acoustic oscillator in relation to the type of boundary conditions

22 p2886 A73-41900

Proof for the existence of a solution to the fundamental quadrantal problem of dynamics for a three-dimensional elastic body, and approximate computation of the solution

22 p2918 A73-41951

Mixed boundary value problem solution for dynamic thermoelasticity, using Laplace transforms in cylindrical coordinates

22 p2918 A73-41952

Light weight shaft design using minimum principle for nonlinear multipoint boundary value problem

[ASME PAPER 73-DET-10] 22 p2919 A73-42068

Gradient methods for extremum solutions of two-point boundary value problems of dynamics.

[ASME PAPER 73-DET-44] 22 p2916 A73-42069

Approximate calculation of flows through blade cascades under conditions of partial cavitation

22 p2841 A73-42129

A method of solving a slightly disturbed mixed problem for a hyperbolic equation with a small delay of the argument

22 p2881 A73-42277

Equations of an elastic medium with a large number of absolutely solid inclusions

22 p2921 A73-42278

Maxwell integral equations in problems of wave scattering by moving media

22 p2826 A73-42376

Complementary variational principles and error bounds for biharmonic boundary value problems.

22 p2921 A73-42433

Asymptotic properties of solutions to single-point and two-point problems with singular perturbations for systems of ordinary linear differential equations

22 p2882 A73-42473

Solving linear boundary value problems by approximating the coefficients.

22 p2882 A73-42519

Monograph - Quasi homogeneous approximations for the calculation of wings with curved subsonic leading edges flying at supersonic speeds.

22 p2797 A73-42675

On the integral equations of three-dimensional multiple inclusion problems.

22 p2924 A73-42682

Stress distribution around an elliptic hole in an infinite micropolar elastic plate.

22 p2924 A73-42684

Monograph - Singular perturbation problems for partial differential equations.

22 p2882 A73-42715

Numerical solution of wire antenna boundary value problems based on integral equations formulation, considering Yagi-Uda array, antenna design and radiation patterns

22 p2827 A73-42840

Integral equation solutions of three-dimensional scattering problems.

22 p2827 A73-42842

The Morley-Koiter equations for thin-walled circular cylindrical shells. I - General solution for symmetrical shells of uniform thickness.

[ASME PAPER 73-APMW-22] 22 p2924 A73-42884

Numerical integration of shell equations using the field method.

[ASME PAPER 73-APMW-27] 22 p2925 A73-42888

Phase plane analysis of the commensurable restricted three-body problem.

22 p2912 A73-42942

Amplification of short pulses in CO₂ laser amplifiers.

22 p2871 A73-43025

Resolvent boundary solutions for Vlasov shallow shell equations in terms of force and deflection functions over entire contour

22 p2928 A73-43055

Mixed boundary value problem of thin isotropic plate under edge loading, examining bending moment applied to plate with intermittent edge clamping

22 p2928 A73-43065

On the construction of accurate difference schemes for hyperbolic partial differential equations.

23 p3000 A73-43208

Solution of spatial contact problems of the theory of elasticity.

23 p3040 A73-43585

Quasi-periodic solutions existence, uniqueness and asymptotic behavior to quasi-linear parabolic equations, demonstrating vanishing conditions at boundary

23 p3049 A73-43611

Boundary value problems for elliptic equations in domains with an unlimited boundary

23 p2999 A73-43622

Helical wound composite cylindrical tube under pure bending, determining elastic response from boundary value problem solution

23 p3041 A73-43637

Sandwich shells nonlinear theory with stress-strain relations in tensor notation, using Hamilton principle for equations of motion and boundary conditions

23 p3044 A73-44078

Complex elastoplastic torsion of cylindrical shafts

23 p3045 A73-44184

Practical implementation of the perturbation method in an inhomogeneous boundary value problem of thermoviscoelasticity

23 p3046 A73-44189

Perturbation method applications to elasticity theory three-dimensional problems, discussing differential operator construction via recursion relations

23 p3046 A73-44190

Solution of boundary value problems in thermoviscoelasticity with allowance for mass forces exhibiting a potential

23 p3046 A73-44196

Boundary value problem solutions uniqueness and existence for ordinary differential equations under Cauchy condition

23 p3000 A73-44209

Continuous dependence of holomorphic functions on partly given boundary values.

23 p3000 A73-44302

An unsteady heat-conduction problem in a system of diathermally separated bodies

23 p3154 A73-44422

Computation of plane-meridional fields of non-homogeneous coaxial cables

24 p3067 A73-44598

The axisymmetric Dirichlet problem of the static theory of elasticity in displacements for a region bounded by cylindrical and spherical surfaces

24 p3146 A73-44604

Mixed boundary value problem solution for stress-strain state of anisotropic elastic cylinder and layer under joint torsion, using Fourier and Hankel transforms

24 p3146 A73-44676

Static theory of plane micropolar strain for homogeneous orthotropic elastic solids, deriving existence and uniqueness theorems and reducing boundary value problems to Fredholm equations

24 p3147 A73-44684

Deformation history approach compared to internal variables introduced by solution of initial value problem for materials, obtaining constitutive equation

24 p3109 A73-44749

Function space approach to prestressed nonlinear orthotropic shallow shell theory boundary value problems

24 p3149 A73-45006

Numerical convective schemes based on accurate computation of space derivatives.

24 p3105 A73-45026

Temperature field boundary value problem with variable heat transfer coefficients and specific heat, using Laplace transformation and variation methods

24 p3156 A73-45083

Free vibration of square plates under different boundary conditions, determining opening geometry effects on fundamental frequencies by grid framework model with finite difference operators

24 p3151 A73-45266

Vibration of rectangular plates with mixed boundary conditions.

24 p3151 A73-45268

A Runge-Kutta Nystrom algorithm.

24 p3142 A73-45290

Optimal force transmission by flexure-clamped boundaries.

24 p3152 A73-45317

Numerical methods of boundary layer type for stiff systems of differential equations.

24 p3106 A73-45333

Extremum principles and error bound for a nonlinear boundary value problem in the theory of laminar boundary layers.

24 p3080 A73-45340

Solutions of boundary value problems with integral conditions for linear ordinary differential equations by the method of decomposition

24 p3106 A73-45351

Integral representations of solutions for general parabolic boundary value problems and the correct solution in spaces of increasing functions

24 p3106 A73-45352

Transient ion neutralization by electrons.

24 p3111 A73-45411

Solution of the Riemann problem for a class of hyperbolic systems of conservation laws by the viscosity method.

24 p3112 A73-45469

A method for solving problems involving viscous flows past bodies at large Reynolds numbers

24 p3081 A73-45530

A numerical conformal transformation method for harmonic mixed boundary value problems in polygonal domains.

24 p3107 A73-45544

BOUSSINESQ APPROXIMATION

Dynamic and thermodynamic effects addition to basic Boussinesq convection for convection in stars, discussing rotation, magnetic fields, radiative transfer and state equation

01 p0094 A73-10061

French monograph - A method of calculating the turbulent boundary layer using an equation for the behavior of the Boussinesq coefficient.

01 p0032 A73-10602

Nonlinear baroclinic instability of a continuous zonal flow of viscous fluid.

02 p0153 A73-12035

Computer methods for simulation of multidimensional, nonlinear, subsonic, incompressible flow.

[ASME PAPER 72-HT-61] 03 p0294 A73-13546

Application of general Boussinesq-Galerkin forms of the Navier equation solution to a plane problem

05 p0632 A73-16328

The axisymmetric Boussinesq problem in the micropolar theory of elasticity.

06 p0760 A73-17763

Nonlinear Boussinesq convective model for large scale solar circulations.

08 p1001 A73-20751

Finite amplitude Kelvin-Helmholtz billows, describing periodic solutions of nonlinear Boussinesq equation

19 p2448 A73-38230

The effect of rotation on nonlinear thermal convection.

24 p3158 A73-45559

BOW SHOCK WAVES

U BOW WAVES

O SHOCK WAVES

BOW WAVES

Numerical model and computational results for earth bow shock structure, discussing linear dispersion relation for magnetized plasma with counterstreaming ion beams

02 p0155 A73-11728

Pioneer 6 crossing of earth bow shock on 16 December 1965 reexamined and interpreted by magnetic field measurement combination with plasma data

02 p0155 A73-11729

Atmospheric gravity waves to be expected from the solar eclipse of June 30, 1973.

02 p0159 A73-12223

Hypersonic and supersonic flow over caret wings at off-design conditions with attached bow shock at leading edges

02 p0128 A73-12502

Magnetospheric structure studies during 1969-1971, discussing bow shock magnetosheath, magnetopause, polar cusps, electric fields and trapped particle composition

03 p0302 A73-13852

Hypersonic solar wind flow interactions with comet emitted gas forming tails, discussing contact surface with stagnation point and bow shock front

04 p0494 A73-14758

Detachment of the outer shock from underexpanded rocket plumes.

07 p0920 A73-19977

Proton scattering in the region near the earth's bow shock.

09 p1137 A73-22054

Aerodynamical and aeromechanical investigations involving pin-equipped models in hypersonic flow

11 p1300 A73-25441

The effect of the earth's bow shock and magnetosheath on the interaction of a discontinuity in the solar wind with the magnetosphere.

11 p1357 A73-25924

Plasma radiation from collisionless MHD shock waves and the high-frequency waves in the upstream solar wind.

14 p1786 A73-29978

Greenstadt binary index criterion for laminar and pulsating bow shock crossings separation in terms of angle, solar wind velocity and Galilean invariance

14 p1748 A73-29979

Earth nonuniform bow shock oblique structure and pulsation, obtaining statistical occurrences from three dimensional distribution of interplanetary field directions for solar wind sector

14 p1749 A73-29983

Bow shock waves and flow field preceding pointed slender bodies subject to supersonic flow, analyzing wave distance from body and frozen flow characteristics

16 p1962 A73-33249

Directional diffusion coefficients of solar protons inside and outside the bow shock.

17 p2224 A73-34781

Solar wind heat transport in the vicinity of the earth's bow shock.

18 p2346 A73-36269

Solar wind interaction with the earth's magnetic field. I - Magnetosheath.

18 p2346 A73-36270

Solar wind interaction with the earth's magnetic field. II - Magnetohydrodynamic bow shock.

18 p2346 A73-36271

Solar wind interaction with the earth's magnetic field. III - On the earth's bow shock structure.

18 p2346 A73-36272

Predicted acoustic gravity wave enhancement during the solar eclipse of June 30, 1973.

18 p2352 A73-36301

- Composition of the earth's atmosphere by shock-layer radiometry during the PAET entry probe experiment. 18 p2313 A73-36797
- Pioneer 10 flyby trajectory relationship to analogy between earth and Jupiter bow shocks with emphasis on oblique shock structure 22 p2906 A73-41942
- Heos 1 plasma and magnetic field experiments during bow shock crossings for turbulent bow structure, discussing proton velocity distribution 24 p3125 A73-45111
- Solar wind and magnetosheath electron temperature measurements by triaxial electron analyzer onboard Ogo-5, presenting data for bow shock 24 p3125 A73-45112
- Bow shock position from OGO-5, Explorer 35 and Heos satellites observation, emphasizing shock in tail for low Mach numbers 24 p3086 A73-45136
- BOX BEAMS**
- Impact response of curved box beam-columns with large global and local deformations. [AIAA PAPER 73-401] 11 p1440 A73-25530
- Ritz method application to structural eigenvalue problems, considering plate buckling in box beams 14 p1805 A73-29741
- BOXES [CONTAINERS]**
- Computer based analyses of the response of box type structures to random pressures. 19 p2497 A73-37485
- BRADYCARDIA**
- Reflex bradycardia elicited from left ventricular receptors during acute severe hypoxia in cats. 09 p1042 A73-23244
- BRAGG ANGLE**
- Charge density distribution in Be single crystals from X ray structure amplitudes for lowest angle Bragg reflections, comparing with Hartree-Fock and free electron plane wave models 04 p0467 A73-15932
- Bragg diffraction by standing ultrasonic waves with application to optical demultiplexing. 06 p0701 A73-18364
- Noise reduction in acousto-optic /Bragg/ imaging systems by holographic recording. 08 p0965 A73-21209
- Bragg-diffraction imaging - A potential technique for medical diagnosis and material inspection. 13 p1614 A73-28582
- Spatial filtering considerations in Bragg diffraction imaging. 13 p1615 A73-28593
- Acoustic imaging by Bragg diffraction using point sources and spherical optics 13 p1616 A73-28594
- Bragg diffraction of light by two orthogonal ultrasonic waves in water. 15 p1914 A73-32256
- Radiation emitted by a charge in a stack of plates at frequencies approaching the Bragg frequencies 17 p2120 A73-34114
- Angular selectivity of lithium niobate volume holograms. 24 p3092 A73-45424
- BRAIDED STREAMS**
- U STREAMS**
- BRAIN**
- NT BRAIN STEM
- NT CEREBELLUM
- NT CEREBRAL CORTEX
- NT CEREBRUM
- NT HIPPOCAMPUS
- Evolutionary significance of carbohydrate metabolism alterations in animal brains during adaptation to hypoxia 01 p0007 A73-10153
- Brain serotonin content - Physiological regulation by plasma neutral amino acids. 01 p0008 A73-10408
- Functional models adequacy for brain activity simulation, discussing transfer, forward and feedback loops, hierarchy, reciprocity and self organizing aspects 01 p0011 A73-10651
- Effects of endotoxin on monoamine metabolism in the rat. 01 p0009 A73-11100
- Induced retinal image blurring effects on rabbit mid-brain single cell trigger features and response efficiencies, noting receptive field responsive area 01 p0010 A73-11503
- Numerical analysis of spontaneous electric activity of the brain - Study of the statistical properties of the power density spectra 02 p0138 A73-12160
- Analysis of the response characteristics of optic tract and geniculate units and their mutual relationship. 02 p0134 A73-12162
- Mathematical model for spectral distribution function of brain waves, noting analogy with RC oscillator 02 p0135 A73-12557
- Differential housing /isolation vs aggregation/ as factor in postnatal development of mouse brain cell specificity and metabolism, noting relation to sleep behavior 03 p0264 A73-14259
- Developmental changes in neurochemistry during the maturation of sleep behavior. 03 p0264 A73-14261
- Maturation of neurobiochemical systems related to the ontogeny of sleep behavior. 03 p0264 A73-14262
- Space-time dynamics of the impulse activity in human-brain neuron populations 05 p0540 A73-16692
- The superior colliculus of the brain. 06 p0654 A73-18347
- Russian book - Tissue, oxygen in the presence of extremal flight factors. 07 p0780 A73-19425
- Electrophysiological investigation of suprasegmental motor control systems evolution through Cyclostomata-Primate series, noting preservation of reticulomotor neuron projection characteristics 07 p0781 A73-20001
- Inter-hemispheric transfer of meaningful visual information in normal human subjects. 07 p0782 A73-20123
- Single cell analysis of saturation discrimination in the macaque. 08 p0932 A73-21568
- Influence of a low-intensity ultrahigh-frequency electromagnetic field on the bioelectrical activity of the brain in rabbits 09 p1044 A73-22367
- Influence of certain brain structures on the sulphydryl-group, diphosphopyridine-nucleotide, and serotonin contents of the blood 09 p1040 A73-22856
- Technique for the implantation of long-term diagnostic electrodes in the amygdaloid complex of the human brain 09 p1046 A73-22857
- Effect of the administration of free amino acids and metabolic cofactors on the distribution of regional biogenic amine contents in the brain and blood of animals 09 p1040 A73-22864
- Correlation analysis of the bioelectrical activity of the brain during mental work 10 p1178 A73-23678
- Role of the medial area of the medulla oblongata in the rhythmic activity of respiratory-center neurons 10 p1179 A73-23804
- Cerebral temperature oscillations and vascular responses in man 10 p1179 A73-23805
- Corpus callosum role in monocular system transcommissural interactions from binocular interaction studies of stimulus-evoked potentials in rat visual cortex 10 p1180 A73-24332
- Features of the spontaneous and evoked neuronal activity of deep brain structures in man during voluntary movements 10 p1181 A73-24517
- Short-term latent reactions of the lateral geniculate body neurons in the rat to electrical stimulation of the optical tract 10 p1182 A73-24595
- Brain tissue functional organization based on models for cell pseudorandom behavior, information processing, learning and memory, considering spontaneous wave and unit firing 11 p1314 A73-25143
- Nitrogen metabolite dynamics in the brain during repeated hypothermia and subsequent spontaneous warming 12 p1462 A73-27703
- On the functional significance of subcortical single unit activity during sleep. 14 p1714 A73-29993
- Simultaneous recording of acceleration and brain waves. 14 p1721 A73-29995
- Effect of stimulation of the mesencephalic reticular formation on the convulsive electrical activity of the brain 14 p1716 A73-30381
- Characteristics of spontaneous oxygen tension variations in human brain structures 14 p1719 A73-30844
- Decatron indicator for a micromanipulator controlled by a stepping motor 14 p1722 A73-30850
- Electrophysiological evidence that abnormal early visual experience can modify the human brain. 15 p1838 A73-31371
- Serotonin content in various parts of the brain during hibernation and awakening 15 p1834 A73-31390
- Histochemical correlates of changes in the primate brain associated with varying environmental light conditions. 15 p1837 A73-32600
- Brain alpha rhythm activity relationship to perceptual and motor performance, correlating with reaction time and computer cycle time analogy 16 p1972 A73-33159
- Transmission of nerve pulses at the switching locations of the brain 16 p1973 A73-33424
- Cerebral control of eye movements and motion perception; Proceedings of the Symposium, Freiburg im Breisgau, West Germany, July 20-22, 1971. 18 p2271 A73-36432
- Some functional characteristics of the superior colliculus of the Rhesus monkey. 18 p2272 A73-36442
- Optomotor integration in the colliculus superior of the cat. 18 p2272 A73-36443
- The role of the superior colliculus in visually-evoked eye movements. 18 p2272 A73-36445
- Saccade correlated events in the lateral geniculate body. 18 p2272 A73-36449
- Changes in the electrical activity of the brain and in some thermoregulation indices of nonanesthetized male cats during cooling 18 p2276 A73-36569
- Techniques for microinjection of biologically active substances into subcortical structures of the brain 18 p2282 A73-36574
- The inhibiting action of 5-oxytryptophan on thermal regulation during the awakening from hibernation 19 p2393 A73-37252
- Changes in some behavioral reactions and in the bioelectric activity of the brain in cats during the development of sleep under polarization of individual brain structures 19 p2393 A73-37393
- Regional serotonin content variations in the brain of cats during a prolonged absence of sleep 19 p2393 A73-37394
- Quantitative evoked-potential analyses for the neurophysiological characterization of faulty learning processes in the experimental arterial hypertension-pathogenesis 19 p2394 A73-37756
- Evoked potentials in the hypothalamus in response to stimulation of the vagus and sciatic nerves 19 p2395 A73-37941
- Brain calcium - Role in temperature regulation. 19 p2396 A73-38294
- Formation of various functional states in the symmetrical structures of the brain as a function of the intensity of unconditioned excitation 20 p2516 A73-39801
- Russian book - Role of the hypothalamus and the limbic system of the brain in regulating vegetative functions. 21 p2636 A73-40276
- High-frequency synchronized activity of the amygdaloid complex as an EEG indicator of certain psychophysiological states 21 p2636 A73-40277
- The role of the amygdaloid nuclei in the regulation of water intake 21 p2636 A73-40278
- Symmetry of the visual evoked potential in normal subjects. 21 p2638 A73-41012
- Evoked potentials in the hypothalamus and mesencephalic reticular formation upon stimulation of the vagus nerve 21 p2640 A73-41263
- Russian book - Electrical activity of the human brain in the process of motor action. 21 p2640 A73-41289
- Influence of small electromagnetic-field fluctuations on the bioelectric activity of the human brain 22 p2813 A73-41964
- Estimate of integrative cerebral activity using an orientation response example 22 p2807 A73-42651
- Orbit and superior orbital fissure acoustic window for cranium posterior structures imaging by echoencephalographic techniques 22 p2815 A73-42667
- Simple simulated human head for checking echoencephalographic equipment. 22 p2815 A73-42672
- On the electronic simulation of acceleratory nystagmus. 22 p2816 A73-42683
- Anatomic and functional organization of the ventral anterior and reticular nuclei of the thalamus 24 p3059 A73-44675
- Some physiological mechanisms of alpha-rhythm frequency fluctuations in man under conditions of relative rest 24 p3059 A73-44717
- Inferior colliculus neuron responses to an amplitude-modulated signal with varying intensity levels 24 p3061 A73-45248
- Visual and verbal coding in the interhemispheric transfer of information. 24 p3065 A73-45337

BRAIN CIRCULATION

- Studies of blood gas analysis at abnormal environment. 01 p0013 A73-11210
- Airline flight and ground personnel fatigue and orthostatic hypotension syndrome manifested by variations in retinal arterial pressure and brain circulation 02 p0134 A73-12156
- Modification of the electroencephalograph EEG-1 for polygraphy 09 p1044 A73-22370
- Oxygen consumption and its "critical" tension for the cerebral cortex in situ 10 p1179 A73-23801
- Book - The physiology of the cerebral circulation. 10 p1180 A73-23945
- Characteristics of vasomotor alterations during brief arbitrary hyperventilation according to data from rheographic and plethysmographic studies 11 p1314 A73-25041
- Vestibular stresses effects on systemic and cerebral hemodynamics, considering human acceleration adaptation and compensation mechanisms 12 p1463 A73-27714
- Xenon 133 measurement of cerebral volumetric circulation rates during papaverin and intensin vasodilation of canine and feline intracranial vessels, showing vessel resistance reduction 13 p1576 A73-29074
- Temperature conditions and blood supply of the brain in animals 17 p2111 A73-34229
- Influence of carbon monoxide and of hemodilution on cerebral blood flow and blood gases in man. 18 p2278 A73-36659
- Intracranial hemodynamic changes in pilots to tilting. 18 p2279 A73-36916
- Correlation between arterial carbon dioxide tension and regional cerebral blood volume by X-ray fluorescence. 20 p2519 A73-39790
- Cerebral tolerance to asphyxial hypoxia in the dog. 22 p2805 A73-42202
- BRAIN DAMAGE**
- Stability criteria in manifestations of the activity of the central nervous system in humans 01 p0006 A73-10152
- Functional state of various portions of the cerebrum under the action of extremal stimulation 05 p0541 A73-16736
- The effects of bilateral destruction of certain medial-hypothalamus structures on the formation of complement-binding antibodies 07 p0781 A73-19647
- Spatial analysis in monkeys of various ages after extirpation of the parietal areas of the cerebral cortex 10 p1180 A73-24329
- Sensitivity of the brain to repeated exposures of hyperbaric oxygen. 11 p1314 A73-25328
- Results of electron microscopic studies in the rat brain under oxygen at high pressure. 11 p1314 A73-25330
- Photostimulation significance in electroencephalographic examinations of pilots and aviation school applicants 12 p1465 A73-27717
- Effect of lithium on acute oxygen toxicity and associated changes in brain gamma-aminobutyric acid. 13 p1575 A73-28503
- Residual visual function after brain wounds involving the central visual pathways in man. 16 p1975 A73-33218
- Pontine reticular formation as origin of neural mechanism generating saccades and nystagmus quick phases in horizontal plane, investigating effects of various brain lesions 18 p2271 A73-36436
- Cerebellar ablations and spontaneous eye movements in monkey. 18 p2272 A73-36447
- Participation of cholinergic mechanisms in negative human emotions 20 p2515 A73-39799
- Visual field defects after missile injuries to the geniculostriate pathway in man. 21 p2641 A73-41600
- Prefrontal lobe functions and the neocortical commissures in monkeys. 24 p3061 A73-45166
- BRAIN STEM**
- Phasic discharge activity and localization of sheep medullary neurons in relation to swallowing reflex after superior laryngeal nerve stimulation 03 p0262 A73-13786
- Patterns of reflex excitability during the ontogenesis of sleep and wakefulness. 03 p0264 A73-14264
- Synapse localization study by electron microscopy of primary afferent tissues in cochlear nuclei of the brain stem 07 p0781 A73-19650

- Physiological mechanisms of evoked-potential habituation in the visual analyzer 07 p0782 A73-20006
- Unit activity in the brainstem related to eye movement - Possible inputs to the motor nuclei. 18 p2271 A73-36434
- Pontine reticular formation as origin of neural mechanism generating saccades and nystagmus quick phases in horizontal plane, investigating effects of various brain lesions 18 p2271 A73-36436
- Brain stem reticular formation influence on lateral geniculate body neurons during eye movements, suggesting cortical oculomotor impulse influence mediation by perigeniculate nucleus 18 p2272 A73-36448
- BRAKES [FOR ARRESTING MOTION]**
- NT AERODYNAMIC BRAKES 20 p2614 A73-38898
- NT AIRCRAFT BRAKES 20 p2614 A73-38898
- NT BALLUTES 20 p2614 A73-38898
- NT DRAG CHUTES 20 p2614 A73-38898
- NT LEADING EDGE SLATS 20 p2614 A73-38898
- NT TRAILING-EDGE FLAPS 20 p2614 A73-38898
- NT WHEEL BRAKES 20 p2614 A73-38898
- NT WING FLAPS 20 p2614 A73-38898
- Factors affecting coefficient of friction and wear of friction materials for brakes, discussing fillers use as reinforcements and friction modifiers 05 p0580 A73-16106
- BRAKING**
- Atmospheric braking of a manned spacecraft after interplanetary flight 10 p1286 A73-23879
- Atmospheric deceleration of a manned spacecraft returning from an interplanetary flight. 20 p2614 A73-38898
- Use of two-stage condenser braking of the single-motor drive for the mirror sections of the RATAN-600 radio telescope 21 p2675 A73-41450
- Synthesis of optimal control with allowance for the real characteristics of the executive mechanism 22 p2835 A73-42363
- BRANCHING [MATHEMATICS]**
- Perturbed bifurcation and buckling of circular plates. 02 p0186 A73-11973
- Existence theorems for Navier-Stokes equations periodic solution bifurcation in convection between two horizontal plates at different time periodical temperature [ONERA, TP NO. 1179] 03 p0343 A73-13602
- Method of branches and bounds as a regular method for the solution of irregular mathematical programming problems. I. 06 p0716 A73-17961
- Generalized m series in tree enumeration. 06 p0717 A73-18000
- Allowable set construction of noncrossing branched paths over prescribed length in unidirectional finite multinetworks 10 p1201 A73-24062
- A priori bounds for some bifurcation problems in fluid dynamics. 10 p1207 A73-24786
- Steady doubly periodic convection regimes in horizontal fluid layer heated at lower surface, considering branching from state of rest 12 p1559 A73-27420
- Branched solution of integro-power equation for nonlinear bending of shallow spherical shells with clamped edge under uniform radial compression load 12 p1556 A73-27816
- Construction of doubly branched fundamental solutions of the Cauchy problem for homogeneous rotationally invariant hyperbolic operators with constant coefficients 12 p1518 A73-27817
- Perturbed bifurcations problems due to initial imperfections caused by small deviations from ideal configuration in nonlinear theory 14 p1767 A73-29764
- Bifurcations and certain qualitative characteristics of a phase-locked automatic frequency control system with a second-order filter 20 p2535 A73-38979
- BRANCHING [PHYSICS]**
- Liapunov-Schmidt analysis of convection bifurcation scheme in internally heated viscous fluid layers of infinite horizontal extent 02 p0238 A73-12053
- Bifurcation of rings under concentrated centrally directed loads. [ASME PAPER 72-WA/APM-37] 04 p0515 A73-15885
- Molecular branching-ratio method for intensity calibration of optical systems in the vacuum ultraviolet. 05 p0597 A73-16495
- Determination of limits bounding the bifurcational relationship between parameters of two-stage nonlinear servo mechanisms 09 p1033 A73-22653

- Bifurcation of the equilibrium of a randomly inhomogeneous nonlinearly elastic plate 09 p1165 A73-23356
- Neutron emission after muon capture in Ce, Ba and Sn, analyzing delayed gamma ray energies and branching ratios to excited nuclear states 13 p1662 A73-28650
- Symmetrical crack branching in polymethyl methacrylate plates, using method of caustics for stress intensity factor evaluation 13 p1645 A73-28842
- Solution on a digital computer of boundary value problems for three-dimensional rod systems with branchings 16 p2075 A73-32692
- Kirchhoff mode theory application to electrical network analysis with arbitrary branch couplings including ideal transformers and controlled sources 16 p1992 A73-32909
- Conditions for thermal explosion occurrence during branched-chain reactions 19 p2502 A73-37501
- Branching solutions for supersonic interacting boundary layers. 21 p2632 A73-40440
- BRASSES**
- Angular distribution of radiation reflected from roughened brass - Experiment and analysis. [AIAA PAPER 73-151] 05 p0598 A73-16899
- Effect of thermomechanical processing on fatigue crack propagation. 09 p1102 A73-22415
- A method of measuring thermal conductivity in the presence of extraneous heat currents and the thermal conductivity of brass at low temperatures. 11 p1367 A73-26307
- The influence of the thermal properties of the heating-surface on the heat-transfer of bubble boiling 12 p1559 A73-27698
- Cu content comparison of Eaton meteorite to true extraterrestrial meteorites, determining dendritic structure and terrestrial origin from similarity to brass 13 p1684 A73-29179
- Brass matrix composites tensile strain characteristics and fracture mode dependence on fiber volume fraction and properties 17 p2192 A73-35531
- BRAVAIS CRYSTALS**
- Maximal finite groups of $n \times n$ integral matrices and complete groups of integral automorphisms of positive quadratic forms / Bravais types/ 13 p1648 A73-28342
- BRAYTON CYCLE**
- Design point characteristics of a 500 - 2500 watt isotope-Brayton power system. [AIAA PAPER 72-1059] 03 p0252 A73-13388
- Isotope Brayton space power systems and their technology. 07 p0850 A73-20467
- Parallel operation of two Brayton-cycle alternators with parasitic speed controllers. 09 p1035 A73-22773
- Isotope Brayton electric power system for the 500 to 2500 watt range. 09 p1118 A73-22793
- Concepts for application of 500- to 2500-Watt Brayton power systems for shuttle-launched missions. 09 p1154 A73-22794
- Recent technology advances in the NASA-Lewis Research Center Brayton program. 09 p1037 A73-23249
- Brayton cycle solar dynamic turboalternator space electric power system technology developments during 1962-1972, considering power efficiency, components reliability and future missions 11 p1309 A73-25982
- Evaluation testing of a closed Brayton-cycle electrical-power-conversion system. 11 p1309 A73-25983
- A power and load priority control concept as applied to a Brayton cycle turbo-electric generator. 11 p1309 A73-25984
- Low temperature-reactor Brayton cycle for Space Station/Base application. 11 p1311 A73-26013
- An isotope heat source integrated with a 7 kW/e/ to 25 kW/e/ Brayton cycle space power supply. 11 p1312 A73-26019
- Standardized space shuttle launched multipurpose spacecraft design using nuclear electric power systems with radioisotope thermoelectric generators or Brayton cycle alternators 19 p2455 A73-38393
- Feasibility analysis of satellite solar/thermal power generation and transmission to earth, describing Brayton cycle heat engine for initial energy conversion 19 p2391 A73-38404
- Design of a nuclear isotope heat source assembly for a spaceborne mini-Brayton power module. 19 p2457 A73-38431
- Nuclear safety considerations for the design of a shuttle launched 500 to 2000 watt isotope Brayton power system. 19 p2457 A73-38432

BRAZIL

Two probable astrobleses in Brazil, considering meteorite impact origin by discovery of diagnostic shock-metamorphic effects in rocks from ERTS-1 satellite and aerial photographs

21 p2771 A73-41078

BRAZING

Surface properties improvement of Al products by metal coatings, noting corrosion prevention, anodic coatings, enameling and brazing

03 p0312 A73-13580

Nondestructive eddy current tests of Al braze alloy fillet size and flatwise distribution in Ti honeycomb sandwich panels

05 p0581 A73-16131

Surface preparation and heating and control processes in diffusion brazing and welding, illustrating with turboreactor construction

06 p0698 A73-18695

Joining copper and copper alloys.

07 p0831 A73-20269

Study and realization of special parts for aerospace construction by brazing in a fluorided reducing atmosphere

09 p1088 A73-22202

Exploratory study of a fluxless aluminum brazing process for beryllium.

11 p1375 A73-26359

Selection of brazing solders according to technical requirements and economy

16 p2026 A73-33350

Competitive processes in joining; Proceedings of the Twenty-sixth Autumn Review Course, Eastbourne, England, October 27-29, 1972.

16 p2021 A73-33859

Brazed honeycomb structure design, fabrication and aerospace applications covering brazing methods, filler metal selection, nondestructive testing, sandwich designs, aircraft and spacecraft structures, etc

17 p2177 A73-34100

Brazing of nickel base alloys.

[SME PAPER AD 73-222]

19 p2436 A73-38494

Fluxless brazing of aluminum using protective gas.

23 p2985 A73-43997

Technique for resistance brazing of thin copper conductors.

23 p2985 A73-43998

Aluminum brazed titanium honeycomb sandwich structure - A new system.

23 p2985 A73-44000

Procedure development for brazing Inconel 718 honeycomb sandwich structures.

23 p2985 A73-44001

Soldering and brazing of advanced metal-matrix structures.

23 p2986 A73-44003

Development of corrosion resistant filler metals for brazing molybdenum.

23 p2986 A73-44004

Brazeability of Ni-Cr heat resistant cermets on stainless steel.

23 p2986 A73-44005

BREADBOARD MODELS

System design, breadboard construction and tests of slope reversal video processor based on tapped delay line estimation with timing discriminator

02 p0167 A73-11957

Information management system breadboard data acquisition and control system.

04 p0425 A73-15461

Design and manufacture of delay equalized comb-line filters.

10 p1193 A73-23608

Wide view field laser target designation seeker system with photodetector for multiple returns discrimination, discussing sensor breadboard model, signal processing and design feasibility

10 p1216 A73-23788

A power and load priority control concept as applied to a Brayton cycle turbo-electric generator.

11 p1309 A73-25984

BREAKAWAY

U BOUNDARY LAYER SEPARATION

BREAKDOWN

Optical breakdown of compressed gases by carbon dioxide laser emission

09 p1094 A73-22594

BREAKERS [ELECTRIC]

U CIRCUIT BREAKERS

BREATHING

NT HIGH ALTITUDE BREATHING

NT OXYGEN BREATHING

Formalization of certain functional aspects of the external respiration system

01 p0012 A73-10657

Effect of body temperature on ventilatory transients at start and end of exercise in man.

15 p1832 A73-31127

Effects of hyperinflation of the thorax on the mechanics of breathing.

22 p2806 A73-42415

BREATHING APPARATUS

Organism-machine interactions in hybrid control systems for cardiac stimulation, artificial breathing apparatus and intelligence assignments

09 p1047 A73-23298

Space technology utilization for firefighters breathing equipment development, discussing design and field testing program

[ASME PAPER 73-ENAS-24]

19 p2400 A73-37980

Respirator cartridge filter efficiency under cyclic and steady-flow conditions.

21 p2643 A73-40408

BREATHING MODE

U BREATHING VIBRATION

Dynamic stability of a cylindrical shell in an acoustic medium.

03 p0393 A73-13834

Parachute axisymmetric self excited breathing oscillations dependence on descent velocity, Froude number, canopy/line length ratio, drag and line stiffness

[AIAA PAPER 73-452]

15 p1826 A73-31438

Newton method relationship to Floquet theory for nonlinear vibration problems, considering Van der Pol equation periodic solutions for breathing and bending modes

[ASME PAPER 73-APMW-20]

22 p2924 A73-42883

Stress amplification in a ring caused by dynamic instability.

[ASME PAPER 73-APMW-35]

22 p2925 A73-42893

BRECCIA

Lunar breccias lithification and metamorphism model construction from experimental and analytical data, discussing scale of lunar metamorphic temperatures

02 p0220 A73-12476

Low energy solar nuclear particle irradiation of lunar and meteoritic breccias.

03 p0361 A73-13100

Breccias from the lunar highlands - Preliminary petrographic report on Apollo 16 samples 60017 and 63335.

05 p0615 A73-16322

Mineralogical and petrographic features of two Apollo 14 rocks.

07 p0880 A73-19699

Electron petrography of Apollo 14 and 15 rocks.

07 p0881 A73-19702

Pyroxenes from breccia 14303.

07 p0881 A73-19705

Metamorphism of Apollo 14 breccias.

07 p0882 A73-19717

Apollo 14 breccias - General characteristics and classification.

07 p0882 A73-19718

Apollo 14 breccia 14313 - A mineralogical and petrologic report.

07 p0882 A73-19719

Chondrules in Apollo 14 samples and size analyses of Apollo 14 and 15 fines.

07 p0882 A73-19720

Petrology and chemistry of some Apollo 14 lunar samples.

07 p0882 A73-19721

Microstructure and mineral compositions of impact produced lunar chondrules from Apollo 14 breccia by electron microprobe X ray analyzer

07 p0882 A73-19722

Vapor phase crystallization in Apollo 14 breccia.

07 p0882 A73-19724

Mineralogy and origin of Fra Mauro fines and breccias.

07 p0883 A73-19726

Thermal and mechanical history of breccias 14306, 14063, 14270, and 14321.

07 p0883 A73-19729

Petrology and origin of lithic fragments in the Apollo 14 regolith.

07 p0883 A73-19730

Inclusions and interface relationships between glass and breccia in lunar sample 14306.50.

07 p0883 A73-19731

Rock 14068 - An unusual lunar breccia.

07 p0883 A73-19732

The magnesian spinel-bearing rocks from the Fra Mauro formation.

07 p0883 A73-19733

Deformation of silicates in some Fra Mauro breccias.

07 p0883 A73-19734

Noritic fragments in the Apollo 14 and 12 soils and the origin of Oceanus Procellarum.

07 p0884 A73-19741

Apollo 14 regolith fractions and soil breccia compositional characteristics by neutron activation analysis

07 p0885 A73-19755

Compositional data for twenty-one Fra Mauro lunar materials.

07 p0885 A73-19756

Elements abundances in Apollo 14 and 15 soils and breccias and in eucrite Juvinas and howardite Kapoeta, suggesting initial chemical layering of moon.

07 p0886 A73-19758

The extralunar component in lunar soils and breccias.

07 p0887 A73-19767

Isotopic abundance ratios and concentrations of selected elements in Apollo 14 samples.

07 p0887 A73-19773

Rb-Sr systematics for chemically defined Apollo 14 breccias.

07 p0888 A73-19778

Ar-40/Ar-39 ages of Apollo 14 and 15 samples.

07 p0888 A73-19783

Primordial radioelements and cosmogenic radionuclides in lunar samples from Apollo 15.

07 p0888 A73-19788

Gamma-ray measurements of Apollo 12, 14, and 15 lunar samples.

07 p0888 A73-19789

Noble gas studies on regolith materials from Apollo 14 and 15.

07 p0889 A73-19799

Trapped solar wind noble gases in Apollo 12 lunar fines 12001 and Apollo 11 breccia 10046.

07 p0871 A73-19800

Volatilized lead from Apollo 12 and 14 soils.

07 p0890 A73-19809

Thermal volatilization studies on lunar samples.

07 p0890 A73-19811

Survey of lunar carbon compounds. II - The carbon chemistry of Apollo 11, 12, 14, and 15 samples.

07 p0890 A73-19818

Magnetic properties of Apollo 14 breccias and their correlation with metamorphism.

07 p0893 A73-19839

Lunar breccia 14321 natural remanent magnetization characteristics from alternating field and thermal demagnetization tests, describing magnetic measurement procedures

07 p0893 A73-19841

Apollo 14 and 15 igneous rock, fines and breccia intrinsic and structure-sensitive magnetic parameters

07 p0893 A73-19842

Ultrasonic P and S waves velocity of Apollo 14 and 15 lunar igneous and breccia rocks for elastic properties determination, noting cracks distribution function

07 p0894 A73-19853

Cosmic ray track densities of Apollo 14 breccias, igneous rock and soils from Fra Mauro, indicating surface residence times

07 p0871 A73-19871

Radiation and shock effects on Apollo 14 and 15 breccias substructure history, reporting optical microscope observations of solar flares and cosmic ray tracks

07 p0896 A73-19872

Temperature scaling of heat metamorphism evolved during lunar and meteoritic brecciation, evaluating dust sintering degree

07 p0896 A73-19874

Luminescence of Apollo 14 and Apollo 15 lunar samples.

07 p0897 A73-19882

Extinct lunar radio activities - Xenon from Pu-244 and I-129 in Apollo 14 breccias.

08 p0936 A73-20843

Electron microprobe chemical analysis and structural formula of niobian rutile in Apollo 14 microbreccia sample KREEP fragment

09 p1139 A73-21856

Photomicrographic investigation of plutonic and metamorphic equilibration in polished thin sections of Apollo 16 feldspathic microbreccia samples from North Ray crater rim

11 p1326 A73-25863

Lunar highland soils and breccias chemistry representation by model for mixing during intense cratering period, discussing chemical composition

12 p1466 A73-27493

A determination of the intensity of the ancient lunar magnetic field.

12 p1542 A73-27494

Petrology of fine-grained rock fragments and petrologic implications of single crystal from the Luna 20 soil.

13 p1674 A73-28307

Petrology of Luna 20 regolith from the lunar highlands.

13 p1675 A73-28311

Luna 20 metaigneous rocks, breccia and soil and Apollo 16 soils chemical composition by neutron activation analysis, tabulating major, minor and trace elements

13 p1676 A73-28323

Siderophile and volatile elements in Luna 20 fine soil and breccia samples from radiochemical neutron activation analysis, noting comparing with Apollo 16 results

13 p1676 A73-28325

Volatile elements in Apollo 16 samples - Possible evidence for outgassing of the moon.

15 p1933 A73-31370

Apollo 16 rocks - Petrology and classification.

15 p1937 A73-31850

Water vapor from a lunar breccia - Implications for evolving planetary atmospheres.

16 p2060 A73-33124

- Sintering and hot pressing of Fra Mauro composition glass and the lithification of lunar breccias.
16 p2070 A73-33875
- Significance of a primitive lunar basaltic composition present in Apollo 15 soils and breccias.
17 p2230 A73-34516
- Petrology of the 2-4 mm soil fraction from the Hadley-Apennine region of the moon.
17 p2230 A73-34517
- Laser probe mass spectrometric *in situ* measurements of stable and radioactive Ar isotopes in lunar breccia
17 p2232 A73-35263
- Apollo 15 breccia and soils with spheres and fragments of iron-rich green glass originating in Apennine Front materials
19 p2487 A73-38174
- Track density gradient and light noble gas isotope analysis of lunar breccia, postulating higher solar flux densities during early brecciation history
23 p2950 A73-43766

BREECHES

U CLOSURES

BREMSSTRAHLUNG

- Interaction between intense optical radiation and free electrons [Nonrelativistic case]
01 p0061 A73-11248
- Relativistic electron radio emission models, calculating magnetic bremsstrahlung spectra from galactic electron space-energy distributions
02 p0208 A73-12459
- The directivity and polarisation of thick target X-ray bremsstrahlung from solar flares.
05 p0610 A73-17045
- Soft X-ray spectra of the Cygnus Loop and Cygnus X-2 in the energy range of 0.16-6.7 keV.
05 p0612 A73-17332
- Steady state dense arc plasma heating by inverse bremsstrahlung process with IR carbon dioxide laser, calculating maximum attainable temperature
07 p0857 A73-19531
- Evaluation of gamma-ray shielding calculations and determination of shielding parameters with bremsstrahlung radiation.
07 p0850 A73-20232
- Impact and bremsstrahlung photoionization due to precipitating electrons in the lower ionosphere.
08 p0957 A73-20657
- White dwarf flares UVB energy spectra, assuming mechanism of nonthermal bremsstrahlung due to fast electrons
09 p1146 A73-22296
- Relativistic electron bremsstrahlung suppression in isotropic plasma, noting analogy to synchrotron radiation
10 p1252 A73-23476
- Bremsstrahlung X-rays in the stratosphere and auroral activity on January 21 and February 3, 1969.
10 p1268 A73-24224
- On the morphology of auroral-zone X-ray events. III - Large-scale observations in the midnight-to-morning sector.
11 p1354 A73-25763
- Thick target X-ray bremsstrahlung from partially ionised targets in solar flares.
11 p1412 A73-25945
- Coherent production of electron-positron pairs and bremsstrahlung on a corundum crystal
11 p1410 A73-26447
- Correlation between pulsations in auroral luminosity variations and X-rays.
11 p1359 A73-26710
- Midlatitude bremsstrahlung X rays, VLF propagation disturbances and electron precipitation during magnetospheric substorm
12 p1468 A73-26983
- Complex studies of the disturbance of March 8, 1970 from observations in the midnight sector
12 p1490 A73-27342
- Magnetopause plasma oscillations excitation and transformation into electromagnetic waves, estimating magnetic bremsstrahlung and X ray emission intensities
15 p1926 A73-31892
- Relativistic electron radio emission models, calculating magnetic bremsstrahlung spectra from galactic electron space-energy distributions
15 p1927 A73-32609
- Extragalactic X ray source physical properties, discussing thermal bremsstrahlung X ray generation by synchrotron mechanism or by Compton scattering
16 p2051 A73-32743
- Cylindrical X ray source with Al K-alpha radiation production for spherical photoelectron spectrometer, discussing radiation intensity with minimum bremsstrahlung
17 p2176 A73-35765
- X-ray bremsstrahlung at subauroral latitudes
18 p2345 A73-36111
- Procedure for measuring plasma electron energies from the bremsstrahlung with the aid of Cerenkov detectors
18 p2339 A73-36566

Radiative corrections and soft-photon emission in magnetic bremsstrahlung.
20 p2602 A73-39445

Quantized magnetic bremsstrahlung from white dwarfs surface layer as possible source of Galactic center infrared radiation
20 p2611 A73-39709

New tubes and techniques for flash X-ray diffraction and high contrast radiography.
21 p2696 A73-39974

Radio binaries observation, noting black hole, large magnetic field or thermal bremsstrahlung as possible origin of strong X-ray radiation
21 p2770 A73-40940

Bremsstrahlung X ray measurements over subauroral latitudes during substorms, noting e folding energy correlated with local electrojet and anticorrelated with conjugate electrojet
21 p2760 A73-41366

Laser-induced gas breakdown in superhigh pressure region.
22 p2869 A73-42227

Interaction of intense optical radiation with free electrons /nonrelativistic case/.
22 p2892 A73-42346

Electron precipitation caused auroral zone bremsstrahlung X rays classification with respect to magnetic storm phases
22 p2851 A73-42750

Asymptotic forms of solutions to nonrelativistic Compton Fokker-Planck equation for bremsstrahlung X ray spectra changes due to Compton scattering in emitting gas
22 p2904 A73-43018

Isothermal gas-sphere model with thermal bremsstrahlung for X ray emission from Coma, Perseus and Virgo galactic clusters, noting gas distribution
22 p2904 A73-43120

Are the recently observed soft gamma-ray bursts from stellar superflares.
24 p3124 A73-44989

BRIDGES

An optical bridge for the assessment of mode-locked CO₂ lasers.
01 p0058 A73-10471

BRIDGES (STRUCTURES)

Functional reliability of structures.
19 p2501 A73-38279

BRIGHTNESS

Two stage mathematical model of brightness perception operation for stimuli having luminance field with asymmetric discontinuity
02 p0137 A73-12078

Influence of border and background on perception of straightness.
02 p0137 A73-12081

Correlation between the brightness of comets and solar wind fluctuations
02 p0208 A73-12471

A photometric and polarimetric study of the moon's surface.
04 p0497 A73-15183

On surface photometry of the moon.
04 p0448 A73-15188

Solutions of the light curves of eclipsing binaries by the generalized method of least squares.
04 p0503 A73-16010

Computer calculation of spectral brightness coefficients on aerial photographs, determining contrast features density gradients
07 p0824 A73-20044

Periodic comet disintegration considerations, discussing comet Tempel 2 absolute magnitude from visual brightness estimates and Meisel statements on secular decrease
09 p1146 A73-22544

A BESM-3M computer program for processing photographic observations of extended objects
11 p1333 A73-25231

Superthermal plasma nodules and their relation to solar flares.
11 p1413 A73-25949

Iapetus UVB light curve minima depths difference explained by two-hemisphere model
11 p1425 A73-26134

Radio-brightness distribution over the Crab Nebula at 3.55 and 1.28 cm.
12 p1539 A73-27281

Temporal intensity fluctuation measurements in K line wing near solar disk center, noting power spectrum peaks and brightness relationship to Fe I line displacement
12 p1544 A73-27830

Further evidence for a complex limb structure in the solar radial brightness distribution at mm wavelengths.
12 p1545 A73-27841

Cometary nucleus evolution dependence on secular brightness decrease relationship to dust particle size distribution, nuclear radius and screened surface area
14 p1792 A73-29817

Foveal threshold additivity measurements for monochromatic and mixed light, using grating resolution as brightness criterion
14 p1717 A73-30398

Probability distribution function of cloud spectral brightness for IR range based on 1966-1969 observations
15 p1905 A73-31821

Correlation between the brightness of comets and fluctuations of the solar wind.
15 p1927 A73-32622

The large-scale velocity field, the magnetic fields, and the brightness of the solar atmosphere
16 p2057 A73-32701

CRT designs for high-sensitivity high speed broadband oscilloscopes, discussing brightness characteristics enhancement
16 p1987 A73-33167

Statistical brightness distributions for photometric planetary image improvement, considering telescope resolution, diaphragm diffraction and atmospheric turbulence
16 p2069 A73-33832

Airglow green cells diameter, speed and brightness measurements from isophote patterns in diagrams of UT versus distance
16 p2008 A73-33881

Outermost low surface brightness regions of interacting galaxies in Stephan Quintet from interference filter, hydrogen spectra and long exposure direct photograph observations
19 p2484 A73-37609

The possibility of using information theory in optics
21 p2740 A73-41100

Observations of zodiacal light from the Pioneer 10 Asteroid-Jupiter probe - Preliminary results.
21 p2776 A73-41423

Comet Kohoutek development predictions for various orbital locations, discussing brightness changes, tail production, nucleus ice melting by solar heating at perihelion, etc
23 p3033 A73-43956

On the variation with height of the top brightness of precipitating convective clouds.
23 p3005 A73-44270

BRIGHTNESS DISCRIMINATION

Investigation of the edge vision contrast phenomenon using the null method
01 p0009 A73-10654

Axiomatic formulation of a mathematical model for visual adaptation
01 p0012 A73-10655

Visual performance with high-contrast cathode-ray tubes at high levels of ambient illumination.
06 p0658 A73-18243

Complex images application of target isolation algorithms based on brightness distributions, discussing allocation of target classification parameters
06 p0694 A73-18289

Intrinsic light brightness and intensity estimation tests for foveal and peripheral retina under photopic and scotopic stimuli
07 p0783 A73-20257

Evoked potential correlates of expected stimulus intensity.
08 p0930 A73-21225

The brightness of coloured flashes on backgrounds of various colours and luminances.
08 p0935 A73-21565

Analysis of transient visual sensations above the flicker fusion frequency.
08 p0932 A73-21566

Numerical computation of photosphere temperature-associated equatorial brightening in red and green bands used in solar oblateness measurements [AD-758969]
09 p1142 A73-22040

Brightness functions for a complex field with changing illumination and background.
13 p1578 A73-28100

Manipulating the response criterion in visual monitoring.
14 p1722 A73-30499

On the rate of acquisition of visual information about space, time, and intensity.
17 p2118 A73-35496

Illuminance and albedo variations /whiteness constancy/ category judgments for stimuli with unpatterned and patterned surfaces
21 p2639 A73-41183

Photometric strip blurring and brightness contrast measurements of visual perception in turbulent atmosphere as function of distance, turbulence and exposure
23 p3001 A73-43573

BRIGHTNESS TEMPERATURE

Low frequency radio observations of the Andromeda Galaxy.
01 p0096 A73-10313

Brightness temperature measurement of Callisto satellite thermal radio emission, using ice layer model
01 p0101 A73-10845

Meteorite ablation coefficient and brightness dependence on velocity and atmospheric density, considering molecular screen effect
01 p0101 A73-10847

Autocorrelation function of the 'rapid' brightness variations of the 3C 273 quasar
01 p0101 A73-10932

Radii, albedos, and 20-micron brightness temperatures of Iapetus and Rhea.

01 p0104 A73-11050

Measurement of Jupiter's radio emission at 2.94 m.

01 p0107 A73-11330

Observations of precipitation zones from satellites using microwave radiometers.

02 p0160 A73-12267

Jovian spectrum at 8-13 microns from 60 inch IR telescope, discussing surface brightness of central disk and brightness temperature spectrum

03 p0374 A73-13850

Equator-pole differences in the solar chromosphere from Lyman-continuum data.

05 p0621 A73-17033

Far IR brightness temperature, opacity and emissivity of Jupiter, Venus, Mars and Saturn

05 p0626 A73-17348

Venus - Measurements of brightness temperatures in the 7-15 cm wavelength range and theoretical radio and radar spectra for a two-layer subsurface model.

06 p0744 A73-17438

Brightness temperature of Mars thermal emission in two orthogonal polarizations by microwave radiometry from Mars 2 and 3 orbiters

06 p0747 A73-17490

Interferometric observations of Mars at 21-cm wavelength.

06 p0747 A73-17491

Temperatures of Uranus and Neptune at 24 microns.

07 p0874 A73-19067

Brightness temperatures in the southern sky at 408 MHz.

07 p0876 A73-19357

Brightness distribution of the sun at 8.6 mm wavelength.

07 p0877 A73-19596

2.8 cm radio emission from alpha Orionis, HBV 475 and MWC 349.

07 p0899 A73-20120

Brightness balancing spectrograph method for flame temperature measurement of liquid fuel drop

07 p0826 A73-20423

On the radio optical depth of the layer where the temperature equals the brightness temperature.

08 p1002 A73-20761

Jupiter upper atmosphere temperature inversion to explain brightness temperature variation in 7.9 micron methane band, observing limb brightening

08 p1004 A73-20900

The observation of relic radiation as a test of the nature of X-ray radiation from the clusters of galaxies.

09 p1138 A73-22953

Electron beam refined niobium melting temperature determination from black body brightness change

10 p1230 A73-23508

Stellar model chromospheres. I - On the temperature minima of F, G, and K stars.

10 p1272 A73-23533

Ultraviolet ion chamber measurements of the solar minimum brightness temperature.

10 p1279 A73-24136

Saturn 49.5 and 94.3 cm brightness temperature, considering magnetic field effects, synchrotron emission and atmosphere

11 p1424 A73-26127

The moon as a proposed radiometric standard for microwave and infrared observations of extended sources.

11 p1426 A73-26545

Quiet sun millimeter wave emission and brightness temperature, discussing observational difficulties arising from fog, cloud and rain attenuation

12 p1543 A73-27725

A recalibration of the quiet sun millimeter spectrum based on the moon as an absolute radiometric standard.

12 p1545 A73-27840

Radiation temperatures of the earth's blankets in the microwave and infrared ranges according to experiment data on the Cosmos-384 artificial satellite

13 p1609 A73-29154

Investigation of cloud cover parameters from measurements on the Cosmos 384 satellite

13 p1654 A73-29155

Temperatures of Saturn's rings.

14 p1797 A73-30010

Long wave measurements of brightness temperature for thermal structure of major planet atmospheres at great depths, discussing Jupiter and Saturn microwave spectra

14 p1800 A73-30537

Brightness temperature measurement of Callisto thermal radio emission, using ice layer model

15 p1928 A73-30981

High-resolution survey of thermal sources of radio emission at the 8.2-mm wavelength

15 p1938 A73-31952

Solar limb brightening at the 8-mm wavelength

16 p2057 A73-32705

Studies of the solar chromosphere from millimeter and sub-millimeter observations. I - Isophotometric mapping.

16 p2060 A73-32953

Distribution of radio brightness across the disk of Venus at the 8-mm wavelength

16 p2068 A73-33816

Electron beam refined niobium melting temperature determination from black body brightness change

17 p2191 A73-35188

Some aspects of the solution of inverse problems of satellite meteorology.

18 p2335 A73-37078

Preliminary report on infrared radiometric measurements from the Mariner 9 spacecraft.

19 p2479 A73-37221

Radio noise from towns - Measured from an airplane.

19 p2404 A73-37675

Jupiter atmosphere discrete source maps of 5 micron radiation distribution, correlating brightness temperature and photographically recorded colors

19 p2489 A73-38525

The brightness temperature of Venus at 70 centimeters.

19 p2489 A73-38526

The brightness temperature of Venus and the absolute flux-density scale at 608 MHz.

19 p2489 A73-38527

Cold gas cloud embeddings in interstellar hot gas, determining radiation temperature from absorption line profiles and kinetic temperature from thermal and turbulent energy components

20 p2606 A73-39066

Solar brightness temperature measurement relative to lunar brightness temperature, noting agreement with HSRA model

20 p2610 A73-39582

Satellite measurements of microwave and infrared radiobrightness temperature of the earth's cover and clouds.

20 p2556 A73-39844

Apollo 15 measurement of lunar surface brightness temperatures - Thermal conductivity of the upper 1.5 meters of regolith.

21 p2765 A73-40240

First observations of the granulation at 1.65 microns, center to limb variation of the contrast.

21 p2776 A73-41476

The emissivities of liquid metals at their fusion temperatures.

22 p2930 A73-41983

Measurement of the atmospheric brightness temperature at submillimeter wavelengths

22 p2847 A73-42330

Absolute measurements and computed values for Martian irradiance between 10.5 and 12.5 microns.

24 p3127 A73-44394

Greenhouse effect for Titanian atmospheric models with different methane, hydrogen, helium and ammonia proportions, deriving brightness temperature spectrum and surface pressure

24 p3130 A73-44457

Planetary brightness temperature measurements at 8.6 mm and 3.1 mm wavelengths.

24 p3130 A73-44458

High-resolution survey of thermal radio sources at 8.2 mm.

24 p3131 A73-44477

A method for accurately compensating for the effects of the error beam of the NRAO 300-ft radio telescope at 21-cm wavelength.

24 p3067 A73-44581

Interpretation of atmospheric radio emission in the 5-mm spectral region

24 p3068 A73-44961

BRILLOUIN EFFECT

Optical power handling capacity of low loss optical fibers as determined by stimulated Raman and Brillouin scattering.

01 p0078 A73-11216

Stimulated Brillouin scattering for hypersound speed measurement as function of temperature in polystyrene, observing pulsed laser induced damage

01 p0068 A73-11232

Stimulated molecular light scattering in gases

02 p0195 A73-11946

Rayleigh and Brillouin scattering from fluids in thermal equilibrium and light scattering from macromolecules in solution, discussing light and medium properties interrelationship

05 p0583 A73-16345

Mandelstam-Brillouin laser light scattering theory and application to atmospheric parameters remote sensing

09 p1094 A73-22327

Frequency selective coupler with thin film waveguides in periodic medium, discussing bandwidth and coupling factor from Brillouin diagram

12 p1504 A73-26827

Nonlinear behavior of stimulated Brillouin and Raman scattering in laser-irradiated plasmas.

13 p1664 A73-28187

Memory effects associated with bulk viscosity on the spectrum of stimulated Brillouin scattering.

13 p1626 A73-28372

Theory of resonant light scattering processes in solids.

20 p2570 A73-38612

Absolute instability of the interaction between optical and acoustic waves.

20 p2594 A73-39679

Switching of the resonator Q factor by stimulated Mandel'shtam-Brillouin scattering.

20 p2574 A73-39703

The mechanism responsible for shortening of the stimulated Mandelstam-Brillouin scattering light-pulse duration and for generation of nanosecond-duration pulses

21 p2739 A73-40355

Effect of saturation on light amplification in stimulated Mandelstam-Brillouin scattering

21 p2739 A73-40359

Stimulated entropy /temperature/ scattering and its effect on stimulated Mandel'shtam-Brillouin scattering.

22 p2868 A73-41720

Velocity of hypersonic waves in liquid oxygen.

24 p3110 A73-44984

BRILLOUIN ZONES

Numerical integration over Brillouin zone for solids spectral properties calculation, considering crystal optical spectra, phonon effects, IR absorption, electron emission and magnetic susceptibilities

07 p0861 A73-19266

Study of the dynamic theory of BaTiO₃ in the cubic phase

07 p0864 A73-20612

Symmetry properties of energy zones in rhombohedral-system crystals

09 p1134 A73-22682

Data acquisition technique for Fabry-Perot spectroscopy, noting application to Brillouin spectra recording of solid Ne

17 p2171 A73-35403

Theory of the phase transition in group IV-VI compound semiconductors

21 p2751 A73-40369

BRISTOL-SIDDELEY BS 53 ENGINE

Pegasus vectored thrust turbofan engine for Harrier class VISTOL aircraft, describing design and operational details

01 p0090 A73-10200

BRISTOL-SIDDELEY VIPER ENGINE

SOKO Galeb 3 cantilever low wing trainer-fighter monoplane with Bristol-Siddeley Viper 20 turbojet engine, describing flight control, loading gear, fuel system and avionics

14 p1712 A73-30240

BRITTLE MATERIALS

Statistical evaluation of strength of metals at brittle fracture.

02 p0235 A73-12133

Thermal shock produced edge effect in thermoelastic heated cylinder analyzing brittle material heat resistance and failure

03 p0394 A73-14019

Relationships between failure modes and fatigue scatter.

04 p0460 A73-14721

Recent studies towards the development of procedures for design of brittle materials.

04 p0508 A73-14725

Weibull flaw distribution models for fracture strength and failure analysis of brittle materials and fiber reinforced composites

04 p0468 A73-14726

The significance of impact data for brittle non-metallic materials.

04 p0469 A73-15985

Susceptibility to brittle fracture of simulated weld seams in Ti-Al-V alloys.

06 p0698 A73-18209

Creep tests and fracture mechanics for high temperature properties of steels and alloys under static load, noting discrepancies for brittle materials

07 p0840 A73-20510

Static and kinetic strength estimation of ionic and metal single crystals, discussing microcracks in brittle materials and surface quality and pore distribution effects

09 p1160 A73-22900

Apparatus for recording acoustic signals from cracks initiated in brittle materials.

09 p1086 A73-23165

Facility for studying the strength and deformability of high-strength brittle materials in biaxial compression

10 p1203 A73-24372

Investigation of the durability of metals under conditions of transition from brittle to plastic failure

10 p1235 A73-24456

A statistical theory for failure of brittle materials under combined stresses.

11 p1439 A73-25511

Coarse grain Al alloys strength characteristics, crack resistance and specific energy of failure due to brittle fracture

11 p1386 A73-26736

Statistical criteria of ultimate strength and plasticity of materials in the complex stress state.

13 p1703 A73-29620

Investigation of the strength of construction materials for different ratios of the main stresses.

13 p1703 A73-29622

Test equipment for thermal stability determination of brittle refractory material, noting data processing procedure and formulas for temperature distribution and thermal stress

13 p1599 A73-29629

Failure under thermal loads of cylindrical bodies consisting of brittle materials

14 p1813 A73-30683

Application of cylindrical specimens with a ring crack for determining the brittle strength in materials

14 p1814 A73-30719

Brittle fracture of a body with a crack under variable shear load

15 p1945 A73-31040

Time required for the destruction of a nonuniformly heated wall

15 p1953 A73-32098

Allowance for the influence of temperature in statistical estimates of the strength of metals in the brittle condition

17 p2186 A73-34328

Effect of group VIII elements on the temperature of plastic-to-brittle transition of states in molybdenum-carbon alloys

17 p2189 A73-34576

Brittle fracture mechanics models of structural materials in terms of elastic continuum with crack

18 p2366 A73-36823

Creep tests and fracture mechanics for high temperature properties of steels and alloys under static load, noting discrepancies for brittle materials

19 p2440 A73-37785

Fracture toughness and absorbed energy measurements in impact tests on brittle materials.

19 p2500 A73-38094

Investigation of the durability of metals under conditions of a transition from brittle fracture to plastic flow.

19 p2442 A73-38138

Determination of the limiting equilibrium of a brittle body weakened by a system of cracks whose form on a plane approaches a circular form

22 p2921 A73-42284

The stress pulses propagated as a result of the rapid growth of brittle fracture.

23 p3042 A73-43805

Opening time of brittle shock-tube diaphragms for dense fluids.

24 p3075 A73-44820

Ultrasonic treatment of nonmetallic materials with a diamond instrument

24 p3094 A73-44969

BRITTLENESS

Intergrain boundary shape effects on the impact strength and character of brittle fracture

01 p0064 A73-10606

Internal friction study of intercrystalline phosphorus adsorption during temper brittleness development in iron alloys

01 p0064 A73-10608

Cold shortness of W and related refractory metals, noting oxide phases and impurities effects on mechanical properties temperature dependence

01 p0066 A73-11341

C and Re effects on brittleness threshold temperature and plasticity of Mo-Re alloy

01 p0066 A73-11342

Simultaneous manifestation of temper brittleness and hydrogen embrittlement during low-cycle fatigue of high-strength structural steel

02 p0180 A73-11927

Limiting crack propagation rates during a quasi-brittle failure

02 p0236 A73-12582

Brittle crack initiation at the elastic-plastic interface.

02 p0182 A73-12752

Fracture toughness of duplex structures. I - Tough fibers in a brittle matrix.

04 p0460 A73-14700

Fracture mechanism theories based on discrete and continuous models of solids, explaining Griffith brittle crack dynamics

06 p0760 A73-17776

Premature and delayed fractures of high strength martensitic steels with graduated carbon contents, including brittle and ductile intercrystalline and transcrystalline cleavage fractures

06 p0705 A73-17848

The effect of carbon and oxygen on the brittleness characteristics of molybdenum

08 p0978 A73-21417

Mixed viscous-brittle fracture model of plastic crack distribution and propagation pattern in bcc polycrystal by electron raster microscope analysis

09 p1157 A73-21961

Resistance to brittle fracture of high-strength steel.

09 p1106 A73-23161

Brittle fracture tests of Ti-Cr steels with/without nitrogen hardened layer under shock impact loads

09 p1107 A73-23199

Molybdenum and nickel alloying effect on time and temperature range of reversible temper brittleness of chromium steels

09 p1107 A73-23200

Fracture mechanics of brittle matrix ductile fiber composites.

09 p1111 A73-23251

Plastic strain rates within discrete crack tip zones at running brittle cracks in mild steel plates, identifying twinning as main deformation mode

09 p1163 A73-23258

Brittle fracture of orthogonally reinforced glass-fiber plastics during tension

09 p1111 A73-23349

Effect of prestraining on the brittleness of molybdenum.

12 p1511 A73-27058

Brittle failure of infinite plate with circular hole and radial cracks under two perpendicular uniformly distributed tensile loads

12 p1556 A73-27802

Propagation of a brittle crack at constant and accelerating speeds.

13 p1635 A73-28755

The effect of brittle interfacial compounds on deformation and fracture of molybdenum-aluminum fiber composites.

13 p1636 A73-28794

Brittle fracture strength and non-crack propagation.

13 p1639 A73-29470

Solid fracture theories based on brittle region toughness parameter and absorbed specific fracture work factor above ductile-brittle transition respectively

13 p1640 A73-29479

Stress gradient as one of the causes of the scale effect on the brittle fracture of materials.

13 p1703 A73-29614

Investigation of fatigue and brittle failure patterns in 15G2AFDps steel at low temperatures

14 p1762 A73-30678

Influence of air pressure on the brittle fracture of graphite

14 p1766 A73-30715

Mechanism of plastic deformation and low-temperature brittleness of a Cr alloy containing 45 at.% Fe

14 p1764 A73-30866

Brittle fracture and crack propagation prediction in unidirectionally fiber reinforced composites via Sc theory, comparing with stress intensity factor Kc concept

15 p1949 A73-31681

High strength Ti alloy cracking and brittle fracture prevention during aging by high heat rate treatment at 250-500 C

15 p1889 A73-31814

Relation between the brittle-viscous transition temperature and structural characteristics in certain low-alloyed chromium alloys

17 p2189 A73-34579

Brittleness of coated tungsten wire

20 p2577 A73-39361

Effect of structural and mechanical factors on the nature of cold shortness curves for steels

20 p2578 A73-39378

Determination of the resistance of VT-14 alloy to brittle fracture

21 p2722 A73-41232

Method of determining the susceptibility of metals to brittle fracture under shock loads

23 p2965 A73-43470

Influence of titanium on the beta and beta-two phase properties and brittleness of InNDK35T5-type annealed alloys

24 p3098 A73-44472

High strength Ti alloy cracking and brittle fracture prevention during aging by high heat rate treatment at 250-500 C

24 p3100 A73-45277

BROADBAND

Aperture matching of wideband phased array radar antennas, using digital ferrite phase shifters and dielectric transformer with magnetic resonance limiting

01 p0022 A73-10178

Spectral behaviour and proton effects of the type IV broad-band continua.

01 p0093 A73-11394

Theoretical analysis and experimental verification for multielement dipole antenna array of unequal parallel conductors, noting impedance characteristics desirable for broadband use

02 p0148 A73-12853

Wideband varactor-tuned Gunn effect oscillators.

04 p0426 A73-14732

Some theoretical and practical considerations in the design of wideband varactor tuned Gunn oscillators.

04 p0426 A73-14733

High speed wideband laser scanning technology for extremely small focal points

06 p0701 A73-18307

Broad-band laser emission from optically pumped PbS(1-x)Se(x).

09 p1092 A73-22249

Ultrawideband longitudinal magnetic tape recording of 120 MHz biased LF/HF signal frequencies, describing high velocity tape transport and recording heads design

09 p1087 A73-23366

Design procedures for matched and broadbanding filters for scanning tests.

11 p1341 A73-25074

Thick walled multilayer wideband radomes for supporting high hydrostatic pressures and protecting weakly directional submarine antennas with circular polarization

11 p1336 A73-25305

Analysis of correlation functions of space-time wideband signals received by linear antennas.

13 p1591 A73-28657

Broad-band impedance matching of rectangular waveguide phased arrays.

14 p1734 A73-30205

Broadband ultraviolet reflectance filters for space applications.

15 p1914 A73-32381

CRT designs for high-sensitivity high speed broadband oscilloscopes, discussing brightness characteristics enhancement

16 p1987 A73-33167

Wideband varactor-tuned solid-state sources to 20 GHz.

16 p1991 A73-33898

Q band /38 GHz/ varactor-tuned Gunn oscillators.

16 p1991 A73-34018

Broad-band antenna array with application to radio astronomy.

22 p2831 A73-41840

Short axial length broad-band horns.

22 p2831 A73-41846

A cavity-backed dipole antenna with wide-bandwidth characteristics.

22 p2831 A73-41851

Russian book on wideband microwave oscillatory systems covering stepwise and smoothly irregular stripline and coaxial line resonators for radio receivers, multipliers, etc

22 p2832 A73-41881

Octave bandwidth microwave spectral response.

24 p3068 A73-44996

A comparison of the overall and broadband noise characteristics of full-scale and model helicopter rotors.

24 p3057 A73-45264

BROADBAND AMPLIFIERS

Selective differential broadband precision amplifier for weak signals of galvanomagnetic sensor of magnetic induction indicator based on Hall effect

01 p0022 A73-10083

A wideband transistor amplifier at the 4 GHz band for communication satellite use.

01 p0026 A73-11176

Computerized synthesis of wideband series stabilized tunnel diode amplifier based on distributed constant elements

05 p0555 A73-16061

On the theory of the avalanche transit-time diode reflection amplifier.

06 p0678 A73-18838

Design and performance of transferred electron amplifiers using distributed equalizer networks.

07 p0803 A73-20553

A wide-band low-shape-factor amplifier module using an acoustic surface-wave bandpass filter.

07 p0804 A73-20557

Characteristics of a gallium-arsenide travelling-wave amplifier with Schottky-barrier contacts.

08 p0946 A73-21118

Wideband class-C Trapatt amplifiers.

08 p0947 A73-21145

1-2 GHz high-power linear transistor amplifier.

08 p0947 A73-21146

Design criteria for high gain, wide band, microwave amplifiers.

09 p1062 A73-22304

Pulse amplifier with active gain adjustment for constant bandwidth

13 p1590 A73-28571

A simple method for obtaining a constant input resistance in broadband amplifiers

13 p1590 A73-28572

Use of approximating polynomials in the determination of correction parameters for pulsed amplifiers.

13 p1591 A73-28732

Optimization of the operating conditions of planar transistors in stages with inductive correction.

13 p1591 A73-28733

A wideband transistor amplifier at the 4-GHz band for communication satellite use.

13 p1594 A73-29228

Synthesis of a reflection-type broadband Esaki-diode amplifier using rectangular waveguide.

13 p1594 A73-29229

Gain-bandwidth limitations of microwave transistor amplifiers.

14 p1735 A73-30247

Computation of nonlinear distortions of a wideband amplifier in the vicinity of the overload point

14 p1737 A73-30896

- Wide-band power amplifier for studying the high-frequency properties of plasmas
15 p1850 A73-31497
- Wideband monopulse radio direction finding measurement improvement, using receiver with log video IF amplifier, multiplexing filters and detectors to provide signal normalization
16 p1990 A73-33850
- Broadband TWT microwave amplifier failure modes in airborne systems related to physical mechanism, fabrication processes and field operator handling
17 p2140 A73-35259
- Two terminal large signal circular coupled wideband TRAPATT diode microwave amplifiers, noting negative resistance characteristics and dc-to-rf conversion efficiency
17 p2140 A73-35321
- The transversely adjusted gap laser for optical communication systems.
17 p2186 A73-35795
- A new technique for synthesis of broad-band parametric amplifiers.
18 p2292 A73-36604
- A distributed amplifier using bipolar transistors in a common-base circuit
19 p2409 A73-37719
- Self-pulsing in laser amplification of broadband noise.
20 p2571 A73-38635
- BROADCASTING**
- A study of frequency sharing between satellite and terrestrial broadcasting systems.
01 p0018 A73-11179
- Optimization study of the satellite broadcasting system for television.
01 p0018 A73-11180
- Required carrier-to-interference ratios for frequency sharing between frequency-modulation television signal and amplitude-modulation vestigial sideband television signal.
01 p0018 A73-11181
- Communications technology satellite /CTS/ with transponder and TWT operating into steerable antenna, discussing experiments on TV broadcast, data transmission, FM and transportable terminals
04 p0422 A73-15446
- Computerized short- and long term ionospheric propagation forecasting for HF communications, frequency scheduling and broadcasting circuits
09 p1048 A73-21983
- Ring arrays as medium- and long-wave broadcast antennas
11 p1336 A73-25318
- A transmission and receiving system for a direct broadcasting television satellite - Telecommunications, satellite, broadcasting, experimentation, microwaves
12 p1469 A73-27074
- Communications aspects of broadcast TV satellites.
14 p1725 A73-29716
- A study of frequency sharing between satellite and terrestrial broadcasting systems.
14 p1725 A73-29748
- Efficient utilization of orbit/frequency for satellite broadcasting.
16 p1979 A73-33401
- Book - Satellite broadcasting.
17 p2121 A73-34473
- An automatic system for broadcasting weather data to international civil aviation
17 p2122 A73-34962
- Two-way wideband microwave communication system oriented toward PCM-TDM digital technique for covering telephone, videophone and radio broadcasting services
17 p2123 A73-34968
- International law aspects of direct broadcasting communication satellites, discussing United Nations, UNESCO and International Telecommunications Union contributions
18 p2373 A73-36392
- Some developments in semi-direct broadcast satellites and community receiving systems.
20 p2521 A73-38599
- Multiple-beam satellite repeater tradeoffs applied to a multifunctional system.
20 p2524 A73-38732
- Optimization in the design of a 12 GHz low cost ground receiving system for broadcast satellites.
20 p2527 A73-38762
- BROKEN CLOUDS**
- U CLOUDS [METEOROLOGY]**
- BROMIDES**
- NT SILVER BROMIDES**
- Inhibition of the first limit of the hydrogen-oxygen reaction by ethyl bromide.
22 p2898 A73-42777
- BROMINE**
- Shock tube investigation of bromine dissociation rates in the presence of carbon dioxide.
06 p0661 A73-18123
- BROMINE COMPOUNDS**
- NT BROMIDES**
- NT SILVER BROMIDES**
- Flame suppression technique using halogen compounds with hydrogen and carbon, considering bromotrifluoromethane application in propane spray cloud seeding
12 p1521 A73-26818
- BRONCHI**
- Bronchial tree model simulation of pressure-flow-volume relationships during expiration, using gas physics and lung physiology and anatomy data
01 p0011 A73-10169
- Techniques for studying the aerodynamic characteristics of the bronchial tree of man
18 p2282 A73-36576
- Morphometry of the human pulmonary arterial tree.
21 p2638 A73-40639
- A model of diffusion in the respiratory unit.
21 p2645 A73-41638
- Gas transport in the human lung.
22 p2806 A73-42421
- BRONZES**
- Investigation of the sintering process and physicomachanical properties of products prepared from spherical bronze pellets
10 p1225 A73-24319
- Structural transitions and mechanical characteristics in the case of multicomponent aluminum bronze
11 p1378 A73-25106
- Hot tinning of aluminum bronze.
11 p1375 A73-26353
- BROWNIAN MOVEMENTS**
- Cinematicographic study of the development of sub-surface colonies of Staphylococcus aureus in soft agar.
08 p0933 A73-21828
- Brownian motion of electrons in time-dependent magnetic fields.
11 p1403 A73-25124
- Uniform isotropic Brownian motion in a linear-cubic approximation
11 p1397 A73-25428
- Stochastic integrals of cylindrical Brownian movements on Hilbert space
15 p1900 A73-32207
- Application of the Kubo-Mori theory to the line shape of plasma oscillations.
16 p2041 A73-33332
- Acceleration of the convergence of functions related to the orientation of a Brownian particle in a laminar flow
19 p2419 A73-37536
- Representation of functions of Markov processes as solutions of stochastic equations.
23 p3000 A73-44207
- BRUDERHEIM METEORITE**
- Spallation production of He-3, Ne-21, and Ar-38 from target elements in the Bruderheim chondrite.
10 p1277 A73-24103
- BRUSHES**
- Friction, wear, and noise of slip ring and brush contacts for synchronous satellite use.
11 p1374 A73-26211
- BUBBLE CHAMBERS**
- Influence of an ultrasonic field on the behavior of a vapor bubble in liquid hydrogen
01 p0077 A73-10929
- Effect of an ultrasonic field on the behavior of a vapor bubble in liquid hydrogen.
10 p1249 A73-24189
- BUBBLES**
- Effect of a temperature gradient on bubble growth in tungsten.
04 p0463 A73-15307
- Bubbles and operating voltage effects in electrochemical machining of tungsten carbide and discharge machining of glass
[ASME PAPER 72-WA/PROD-21]
04 p0456 A73-15804
- Limited cavitation and the related scale effects problem.
06 p0686 A73-18435
- Temperature field structure in strongly heated buoyant thermals.
07 p0919 A73-19504
- Equation of motion and bubble size distribution function for nucleate boiling, noting balance equation for two phase fluid
08 p1022 A73-21096
- Interaction of pulsating bubbles in a viscous fluid
08 p0955 A73-21446
- Flow characteristics of spherically capped gas bubbles buoyancy induced motion in liquids, discussing Reynolds and Froude number effects
10 p1205 A73-23854
- Optical method for studying the heat transfer mechanism in bubble boiling
13 p1708 A73-29173
- Two-dimensional bubbles in slow viscous flows. II.
14 p1744 A73-30170
- Bubble domain memory materials production, processing and testing, discussing crystal growth, propagation margins, interaction effects and stroboscopic observations
16 p2044 A73-32864
- The dynamic behavior and compliance of a stream of cavitating bubbles.
[ASME PAPER 73-FE-34]
17 p2153 A73-35025
- Gas occlusions in arterial heat pipes.
[AIAA PAPER 73-724]
18 p2369 A73-36341
- Development of a high capacity variable conductance heat pipe.
[AIAA PAPER 73-728]
18 p2369 A73-36345
- Flow of a mixture consisting of a fluid and gas bubbles past a corner
18 p2301 A73-37007
- Cavitation and boiling bubble growth, collapse and damage effects, discussing liquid jet formation temperature effects, glycerol, ethanol and water solutions and bubble geometry
20 p2548 A73-39516
- High-speed photography of laser-induced cavities in liquids
21 p2709 A73-39968
- Photographic investigation of hailstone form, size and structure, determining layer growth from air bubble shape and spectrum
21 p2730 A73-40116
- The Lagrange function for a gas bubble in an inhomogeneous flow
21 p2676 A73-40206
- Law of micro-liquid-layer formation between a growing bubble and a solid surface with a special reference to nucleate boiling.
21 p2792 A73-41144
- Rayleigh-Taylor instability in octyl alcohol-water interface, observing bubble and spike formation with flattening and curling of spike due to Kelvin-Helmholtz instability
22 p2842 A73-42232
- Absorption of gas bubbles in flowing blood.
22 p2806 A73-42414
- Helium bubble survey of an opening parachute flowfield.
22 p2798 A73-43112
- Experimental investigation of the viscosity of lubricating oil containing air
24 p3094 A73-45548
- BUCKETS**
- Determination of the shape of jets flowing off the walls of an asymmetrically positioned bucket
07 p0776 A73-20098
- BUCKLING**
- NT CREEP BUCKLING**
- NT ELASTIC BUCKLING**
- NT EULER BUCKLING**
- NT THERMAL BUCKLING**
- Axiallysymmetric buckling and stability of annular sandwich panel under radially varying in-plane stresses
01 p0115 A73-10740
- Initial postbuckling of circular rings under pressure loads.
01 p0115 A73-10744
- Buckling of laterally loaded plates having initial curvature.
01 p0115 A73-10768
- Phase plane analysis of free vibration of rectangular plate loaded by in-plane compressive load, calculating critical load and amplitude in postbuckling region
01 p0115 A73-10770
- Asymptotic method of determining critical buckling loads for strictly convex shallow shells of revolution
01 p0116 A73-10963
- Perturbed bifurcation and buckling of circular plates.
02 p0186 A73-11973
- Stability characteristics of thin elastic plate with time varying temperature under transversal magnetic field, calculating buckling probability
02 p0234 A73-12016
- Axial compression buckling of single metal fiber embedded in plastic matrix, using photoelastic stress analysis and finite element method
02 p0236 A73-12432
- The post-buckled behaviour of a thin-walled box beam in pure bending.
03 p0384 A73-13114
- An accurate approximate formula for assessing the vibration frequency of structures axially loaded.
03 p0384 A73-13116
- A computational method for optimal structural design. I - Piecewise uniform structures.
03 p0390 A73-13337
- Vibration and buckling of a rectangular plate with an internal support.
03 p0391 A73-13372
- Stability of an idealized circular three-layer plate beyond the elastic limit
03 p0393 A73-13777
- Effect of a circular hole on the buckling of cylindrical shells loaded by axial compression.
03 p0395 A73-14181
- Inelastic spherical shells elastic-plastic buckling, presenting numerical procedure for critical loads and stresses
04 p0508 A73-14942
- Modified shear-flexible orthotropic plate theory application to simply supported rectangular sandwich

plates buckling problem, comparing results with Reissner theory and experimental data 04 p0509 A73-14946

Constrained optimal design of columns against buckling. 04 p0510 A73-15029

Buckling of continuously supported beams. [ASME PAPER 72-WA/APM-34] 04 p0515 A73-15886

Classical and nonlinear buckling analyses of spherical sandwich shells. 05 p0631 A73-16121

Buckling of a long, axially compressed, thin cylindrical shell with random initial imperfections. [ASME PAPER 72-APM-MMM] 05 p0632 A73-16532

Buckling of columns with variable moment of inertia. 05 p0633 A73-16538

Truncated conical shell buckling and stability beyond elastic limit, deriving lower critical loads by orthogonalization method 06 p0760 A73-17781

Buckling of a circular sandwich plate beyond the elastic limit 06 p0760 A73-17784

Constrained optimal design of circular plates against buckling. 06 p0762 A73-18338

On the buckling of thin tensioned sheets with cracks and slots. 06 p0764 A73-18497

Initial postbuckling behavior of optimally designed columns and plates. 07 p0908 A73-19084

Imperfection-sensitivity of a wide integrally stiffened panel under compression. 07 p0908 A73-19087

The concept of snap-buckling illustrated by a simple model. 07 p0909 A73-19163

Fracture mechanics application to initial notch extension under tension in quasi-isotropic fiberglass reinforced laminates, noting transplanar buckling effects on fracture toughness 07 p0841 A73-19186

A theoretical and experimental investigation of torsional-flexural buckling in thin-walled prismatic members. 07 p0912 A73-19366

Axissymmetric buckling of uniformly loaded spherical caps undergoing plastic deformation. 07 p0913 A73-19971

Buckling load of shallow circular vaults, investigating boundary conditions, load intensity and interconnecting beam flexibility and spacing effects 07 p0916 A73-20434

Postbuckling analysis of rectangular orthotropic plates. 08 p1015 A73-20673

Lateral buckling of cantilevered I beam columns. 08 p1017 A73-20942

Use of chromoplastic models for the study of the behaviour of rectangular plates after buckling. 08 p1017 A73-20946

Inelastic buckling of shallow spherical shells under external pressure. [ASME PAPER 72-PVP-6] 09 p1164 A73-23270

Vertical circular cylindrical shells buckling under axisymmetric compressive stress due to own structural weight, using Timoshenko elastic stability theory 09 p1166 A73-23459

Buckling of a simply-supported beam between two unattached elastic foundations. 09 p1166 A73-23466

Post-buckling behaviour of rectangular orthotropic plates. 10 p1288 A73-23699

A yield-surface corner lowers the buckling stress of an elastic-plastic plate under compression. 10 p1289 A73-24100

Isogrid as integral stiffened waffle with triangular pattern to allow simple graphical solution for optimizing spherical caps or cylinders under various buckling loads [AIAA PAPER 73-365] 11 p1438 A73-25500

Buckling of partially debonded layered cylindrical shells. [AIAA PAPER 73-366] 11 p1438 A73-25501

Elastic stability of biaxially loaded longitudinally stiffened composite structures. [AIAA PAPER 73-367] 11 p1438 A73-25502

Buckling and vibration of unsymmetrically laminated cross-ply rectangular plates. [AIAA PAPER 73-368] 11 p1438 A73-25503

Vibration and local edge buckling of thermally stressed, wedge airfoil cantilever wings. [AIAA PAPER 73-327] 11 p1441 A73-25557

Edge buckling of cylindrical shells with low in-plane shear moduli. 11 p1445 A73-26392

Axissymmetric buckling of rigidly clamped hemispherical shells. 11 p1447 A73-26648

On the buckling and postbuckling behavior of thin-walled circular cylinders. [DFVLR-SONDDR-261] 12 p1550 A73-26843

Stability of rectangular plates under mixed boundary conditions 12 p1552 A73-27372

Certain fatigue phenomena in aeronautical structures with stiffened shells 12 p1553 A73-27394

Asymptotic method of determining the critical buckling loads of shallow strictly convex shells of revolution. 12 p1554 A73-27539

Compressive buckling analysis and design of stiffened flat plates with multilayered composite reinforcement. 12 p1554 A73-27736

Static, vibration and buckling analysis of axisymmetric circular plates using finite elements. 12 p1555 A73-27738

Ferritic stainless steel transverse tension ridging mechanism in terms of CF and CC mixed texture bands, contradicting plastic buckling theory 13 p1633 A73-28147

Effective use of the incremental stiffness matrices in nonlinear geometric analysis. 13 p1694 A73-28252

Finite element matrix formulation of post-buckling stability and imperfection sensitivity. 13 p1694 A73-28253

Buckling of unstiffened and ring stiffened cylindrical shells under axial compression. 13 p1696 A73-28758

Postbuckling behavior of orthotropic skew plates. 13 p1697 A73-28813

Inelastic column buckling of internally pressurized tubes. [SESA PAPER 2049] 13 p1699 A73-29305

Graphite- and boron-epoxy composite curved panels, determining shear buckling stress and post-buckling strength by visual and photographic observations [SESA PAPER 2030A] 13 p1699 A73-29308

The optimum distribution of diagonal stiffeners reinforcing a clamped infinitely long plate buckling under shear. 13 p1700 A73-29386

Ritz method application to structural eigenvalue problems, considering plate buckling in box beams 14 p1805 A73-29741

Progress in nonlinear finite element analysis using asymptotic solution techniques. 14 p1808 A73-30191

Perturbation method in the analysis of geometrically nonlinear and stability problems. 14 p1808 A73-30196

Buckling of viscoplastic cylindrical shells loaded by radial pressure impulse. 14 p1811 A73-30481

Buckling of circular cylindrical shells under compression. IV - Solutions based on the modified Flugge equations considering prebuckling edge rotations. 14 p1813 A73-30573

The large deflection and post-buckling behaviour of some laminated plates. 15 p1946 A73-31117

Cylindrical panels buckling under nonuniform axial compression with various load distributions, basing analysis on Donnell equations and Galerkin method 15 p1948 A73-31635

Buckling analysis of elastically constrained stiffened conical shells under hydrostatic pressure by the collocation method. 15 p1948 A73-31642

Nonlinear tension and buckling stress behavior of angle ply unidirectional laminated composites 15 p1949 A73-31683

Buckling of eccentrically stiffened rectangular plates subjected to linearly varying longitudinal compression. 15 p1952 A73-32043

Thin plates and shells post-buckling behavior analysis by discrete element method, noting computer program capabilities 16 p2078 A73-32997

Incremental variational method for the large displacement analysis of shells with geometric imperfections. 16 p2078 A73-32999

Stability analysis of shell-like structures by complementary energy. 16 p2078 A73-33000

Application of an irregular mesh finite difference approximation to the plate buckling problem. 16 p2079 A73-33008

Iterative finite element method for minimum weight structural design with respect to buckling constraints applied to beam and orthogonal frame design 16 p2082 A73-33908

Inelastic buckling of columns - The effect of imperfections. 16 p2084 A73-33975

Inelastic buckling of eccentrically loaded columns. 17 p2240 A73-34180

Buckling of beams supported by Pasternak foundation. 17 p2243 A73-34531

Instability analysis using the incremental stiffness matrices. 17 p2245 A73-34838

Cylindrical shell postbuckling behavior under axial compression using multiple scale averaging technique, concluding predominance of diamond shaped post-buckling pattern [ASME PAPER 73-APM-7] 17 p2247 A73-35032

Buckling of rectangular plates with general variation in thickness. [ASME PAPER 73-APM-10] 17 p2247 A73-35035

Dynamic buckling of shallow spherical shells. [ASME PAPER 73-APM-A] 17 p2249 A73-35104

On the buckling of cylinders in axial compression. [ASME PAPER 72-APM-BBB] 17 p2250 A73-35113

Further experimental studies on buckling of integrally ring-stiffened cylindrical shells under axial compression. 17 p2250 A73-35441

Post-buckling behavior of cold-formed thin-walled stainless steel beams. 19 p2496 A73-37481

Postbuckling behavior of circular rings with two or four concentrated loads. 19 p2501 A73-38251

Supercritical strains in nonlinear elastic shells 20 p2616 A73-39259

Stability and postbuckling behavior of hyperelastic bodies at finite strain by the finite element method. 20 p2620 A73-39529

Free vibration and buckling loads of anisotropic pressurized thin walled shells of revolution, considering cylinders, barrels and spherical sections 20 p2621 A73-39538

Buckling analysis of deformation and stress distribution in axially compressed longitudinally stiffened cylindrical shells, considering prebuckling deformation effects 20 p2621 A73-39539

Buckling of continuous circular plates. 21 p2782 A73-40004

Evaluation of various analytical models for buckling and vibration of stiffened shells. 21 p2784 A73-40424

Nonsymmetric buckling of cylinders with axisymmetric thermal discontinuities. 21 p2784 A73-40425

Buckling of segments of toroidal shells. 22 p2923 A73-42553

Buckling of toroidal shells under hydrostatic pressure. 22 p2923 A73-42560

Critical velocity for collapse of a shell of circular cross section without buckling. [ASME PAPER 73-APMW-31] 22 p2925 A73-42891

Compressive strength and failure modes of unidirectional composites. 23 p3041 A73-43634

Buckling of short viscoplastic cylindrical shells subjected to radial impulse. 23 p3045 A73-44080

Surface buckling of a laminated medium 24 p3145 A73-44525

BUDGETING

NT FEDERAL BUDGETS

Budgeting role in development and implementation of five year plan of operations at French space research center 01 p0124 A73-11253

A method for re-allocating funds to meet a reduced budget. 02 p0239 A73-12348

Status of funded improvements to the National Aviation System and planned improvements not yet funded. 12 p1561 A73-27363

Book - Zero-base budgeting: A practical management tool for evaluating expenses. 17 p2258 A73-35674

BUFFALO AIRCRAFT

U DHC 5 AIRCRAFT

BUFFERS (CHEMISTRY)

Rb87 vapor maser with optical pumping, measuring nitrogen or nitrogen argon mixture buffer gas partial pressure effect on power output 04 p0459 A73-15920

BUFFETING

Buffet boundaries for arrow wings in transonic flow, presenting methods for pressure distribution and three dimensional turbulent boundary layer calculation [DGLR PAPER 72-123] 03 p0248 A73-14382

Aeroelastic dynamic response to shock induced flow separation, analyzing wing buffet components at high Mach number subsonic flow [AIAA PAPER 73-308] 11 p1300 A73-25539

Buffeting pressures on a swept wing in transonic flight - Comparison of model and full scale measurements. [AIAA PAPER 73-311] 11 p1305 A73-25542

Beyond the buffet boundary. 17 p2100 A73-34538

BUILDING MATERIALS U CONSTRUCTION MATERIALS BUILDING STRUCTURES U BUILDINGS BUILDINGS

- Computer method for analysis of multistory structures. 03 p0391 A73-13683
- Reduction of ILS errors caused by building reflections. 11 p1330 A73-25784
- Disturbances of directional radio due to echoes caused by high buildings 12 p1473 A73-27753
- Tall buildings induced microwave scattering coefficient measurement with helicopter-borne bistatic pulse radar, explaining coefficient dependence on azimuth, elevation and range 20 p2530 A73-39127

- BULGING**
Re-interpretation of some simple tension and bulge test data for anisotropic metals. 01 p0065 A73-10764

- BULK MODULUS**
Theoretical calculation of the compressibility of porous media. 09 p1157 A73-22144
- Bulk compressibility of carbon fibre reinforced plastics. 10 p1240 A73-24288
- The thermal expansion of composites based on polymers. 12 p1515 A73-27030
- An equation for thermal expansion coefficient at high pressures. 13 p1673 A73-28206
- Bulk viscosity effects in imperfect fluid Friedmann cosmology, considering implications for singularity problem 15 p1939 A73-32011

- BUNA [TRADEMARK]**
Age control evaluation of Buna N elastomers by ANA Bulletin 438, using shelf aging and crashed aircraft case studies 03 p0331 A73-13026

- BUNCHING**
NT ELECTRON BUNCHING
Chaotic photon bunching effect interpretation by theoretical incoherent source model with atomic excitation and emission at stochastically independent times without interaction 07 p0837 A73-20610

- BUNDLES**
Graphite fiber tensile property evaluation, discussing single filament method and improved dry bundle test including electrical resistivity measurement and stress-strain curve analysis 23 p2996 A73-43644
- High strength filaments for cables and lines, discussing bundle theory and comparing dielectric and tensile properties for glass, graphite and organic fibers 23 p2997 A73-43645

- BUOYANCY**
Model analysis for heat radiation effect on development and evolution of single buoyant thermal rising in neutrally stratified atmosphere, noting radiative relaxation time [AD-754599] 01 p0039 A73-10398
- Free and forced convection from fine hot wires. 01 p0120 A73-10447
- A comparison of neutral buoyancy and free fall for liquid propellant system zero-G simulations. [AIAA PAPER 72-1041] 03 p0287 A73-13376
- Buoyancy forces contribution to heat flux during turbulent mixing in upper atmosphere, noting kinetic turbulence balance components 04 p0473 A73-15573
- Temperature field structure in strongly heated buoyant thermals. [AD-754728] 07 p0919 A73-19504
- Buoyancy effects in a turbulent boundary layer. 09 p1071 A73-22330
- Flow characteristics of spherically capped gas bubbles buoyancy induced motion in liquids, discussing Reynolds and Froude number effects 10 p1205 A73-23854
- Instability, transition, and turbulence in buoyancy-induced flows. 10 p1205 A73-23859
- Transient flows, effects of unsteady surface conditions on stability, and flow separation in buoyancy induced flows. 10 p1208 A73-24817
- An investigation of internal gravity waves generated by a buoyantly rising fluid in a stratified medium. 11 p1351 A73-25152
- Natural convection in a sound field giving large streaming Reynolds numbers. 14 p1817 A73-30613
- Effects of buoyancy and of acceleration owing to thermal expansion on forced turbulent convection in vertical circular tubes - Criteria of the effects, velocity and temperature profiles, and reverse transition from turbulent to laminar flow. 14 p1818 A73-30614

- Exhaust cloud rise and growth for Apollo Saturn engines. 15 p1906 A73-31920
- Thermal stability of radiating fluids - Asymmetric slot problem. 16 p2085 A73-33314
- Book - Buoyancy effects in fluids. 17 p2155 A73-35336
- Laminar mixed convection from a horizontal rotating disc. 17 p2256 A73-35848
- Instabilities in buoyancy-driven boundary-layer flows in a stably stratified medium. 19 p2422 A73-38231

- BUOYS**
Moored radio telemetering buoy relay stations for North Pacific climatological data acquisition, noting optimum channel frequency for data transmission error rate reduction 04 p0421 A73-15429
- Environmental data transmission from arctic data buoys via polar orbiting satellite. 04 p0421 A73-15431
- Ocean currents observation by ship and satellite tracking of free-drifting Lagrangian platforms [AAS PAPER 73-144] 20 p2550 A73-38593
- BURGER EQUATION**
An evaluation of cell type finite difference methods for solving viscous flow problems. 11 p1345 A73-25112
- Liapunov direct method extended to stability of nonlinear parabolic systems, noting application to Burgers equation 17 p2200 A73-34398
- On Burgers' model equations for turbulence. 18 p2299 A73-36507
- Numerical methods based on very accurate approximation of partial derivatives. 18 p2330 A73-36828

- BURNERS**
Recent developments in testing unstable burning characteristics of solid propellants. 01 p0089 A73-11115
- The T-burner test method for determining the combustion response of solid propellants. 03 p0353 A73-13384
- A novel high area ratio T-burner for characterizing metalized propellants. 05 p0563 A73-16949
- Interaction of sound and flow in T-burners - Experiments compared with theory. 06 p0741 A73-17662
- Fuel-air turbulent mixing process in double concentric jet type burner, measuring average velocity, pressure distribution, turbulence intensity and shear stress 13 p1601 A73-28648

- BURNING RATE**
The role of impurity particles in the combustion of double-base propellants. 01 p0089 A73-10639
- Erosive burning rate perturbation in colloidal propellant slab combustor channel as function of lateral velocity gradient and chamber pressure [AIAA PAPER 72-1108] 03 p0351 A73-13423
- Pressure exponent of controllable solid rocket propellants. 03 p0352 A73-13442
- Supersonic mixing and combustion of a hydrogen jet in a coaxial high-temperature test gas. [AIAA PAPER 72-1179] 03 p0397 A73-13474
- Physical and chemical properties of solid propellant igniter materials, determining averaged heat of reaction and burning rate values [AIAA PAPER 72-1195] 03 p0352 A73-13485
- Methane-air mixtures burning velocity as function of equivalence ratio at atmospheric pressure, using bomb/hot-wire and corrected density ratio techniques 03 p0399 A73-14398
- Propellants and combustion. I - Role of binder in solid propellant combustion. 04 p0485 A73-14910
- Thermal analysis of combustion of fabric in oxygen-enriched atmospheres. [ASME PAPER 72-WA/HT-22] 04 p0519 A73-15832
- Characterization and suppression of aircraft and fuel fires. [WSCIP PAPER 72-26] 05 p0639 A73-16688
- Role of condensed phase details in the oscillatory combustion of composite propellants. 05 p0641 A73-16948
- Theory of steady-state burning of porous propellants by means of a gas-penetrative mechanism. [AIAA PAPER 73-221] 06 p0767 A73-17663
- Kinetics and convection in the combustion of alkane droplets. 07 p0919 A73-19391
- Convective combustion of porous explosives 07 p0920 A73-19990
- Fire retardance of mixtures of inert gases and oxygen. 09 p1045 A73-22532
- Application of the method of matched asymptotic expansions to calculate the steady-state thermal

- propagation of an exothermic reaction front in a condensed medium 09 p1167 A73-22616
- Determination of burning velocity by double ignition in a closed vessel. 10 p1294 A73-23559
- The influence of diameter on the burning velocity of strands of solid propellant. 10 p1261 A73-23560
- Ballistic burning rate in sonic gas flow in super-sonic conical nozzles as function of flow velocity and combustion chamber pressure 13 p1706 A73-28972
- The mechanism of catalyzer action on the burning of condensed systems 13 p1669 A73-28974
- Regularities in the burning of condensed systems within a field of mass forces at moderate pressures 13 p1706 A73-28975
- Surface temperature measurement of regressing polymethyl methacrylate slabs burning in oxygen-nitrogen mixtures, discussing chemical mechanism for condensed phase depolymerization 13 p1707 A73-28994
- Experimental drag coefficients for evaporating and burning drops at elevated pressures. 13 p1707 A73-28998
- Research on ignition and combustion in oxygen systems. 13 p1708 A73-29402
- Effects of composition on acceleration induced burning-rate augmentation. 15 p1925 A73-31661
- Russian book - Transition of burning of compacted systems to detonation. 15 p1959 A73-32420
- Shock-tube measurements of soot oxidation rates. 16 p2085 A73-33344
- Deflagration in the combustion of hydrogen-fluorine mixtures. 16 p2045 A73-33349
- Solid propellant rocket burning rate optimization at constant thrust by imbedded inert heat conducting fibers, analyzing flight performance 18 p2342 A73-36064
- Influence of heat conducting elements on the burning rate of mixture system models 18 p2342 A73-37120
- Stepwise burning of non-volatile readily dispersible substances 19 p2503 A73-37502
- Effects of additions of metals and metal borides on the burning rates of mixture systems 19 p2503 A73-37509
- Mechanism of burning in condensed systems with solid additions in a field of mass forces 19 p2472 A73-37510
- Oxygen index flammability test relationship to flame spread model for polystyrene film burning rate as function of gas velocity and film thickness 19 p2504 A73-38274
- Quasi-steady gas-phase flame theory in unsteady burning of a homogeneous solid propellant. 21 p2790 A73-40430
- Comparative study of the combustion of 6-, 5-, 4-, and 3-amines of nitrate of cobalt (III)/ 21 p2647 A73-40703
- Some reactions and hydroperoxyl and hydroxyl radicals at high temperatures. 22 p2898 A73-42754
- High-temperature fast-flow reactor studies of metal-atom oxidation kinetics. 22 p2898 A73-42761
- Reaction of H atoms with CH₂Cl₂ - Application to the inhibition of flames. 22 p2819 A73-42779
- Pressure waves generated by constant velocity deflagration flame in explosive hydrocarbon-air mixture for self-similar flow field 22 p2936 A73-42808
- Experimental studies on the flame structure in the wake of a burning droplet. 22 p2937 A73-42816
- High pressure burning rates of liquid alcohol and hydrocarbon fuels with droplet simulation by porous spheres, deriving surface temperature, pressure distribution and critical burning conditions 22 p2937 A73-42817
- Liquid fuel spray burning characteristics in stabilizer disk wake of luminous hollow cone pressure jet flame, using spark photographic technique 22 p2937 A73-42818
- Combustion of boron particles - Experiment and theory. 22 p2899 A73-42821
- A method for calculating the burning rates of solid fuels in a turbulent gaseous oxidizer flow at Le unequal to unity 23 p3049 A73-43729
- Formation of a pseudoliquidified layer during combustion of condensed systems with solid nonagglomerating additives in a field of mass forces 24 p3121 A73-44705

- Transient process due to pressure increase during combustion of condensed material, using fractional-differentiation operator method to determine unsteady burning velocity
24 p3155 A73-44715
- Burning rate studies of fuel air mixtures at high pressures.
24 p3156 A73-45162
- Solid propellants with a pulsating burning rate
24 p3121 A73-45200
- Fuel combustion rate and turbulent diffusion induced self ignition in pulsejet engine combustion chamber from schlieren photography and pressure distribution measurements
24 p3123 A73-45377
- Influence of nonexplosive liquids on the detonation rate of solid explosives
24 p3157 A73-45380
- Mechanism of erosive burning of solid rocket propellants.
24 p3121 A73-45385

BURNOUT

Point contact and Schottky barrier microwave mixer diodes reliability under X band RF pulse operating conditions, considering burnout alleviating fabrication techniques

- 08 p0943 A73-20735
- Estimate of the influence of thermal diffusion on the surface burnout rate in a nonhomogeneous turbulent boundary layer
09 p1167 A73-22618
- Ignition temperature of conglomerates which form by burnout of the binder in a suspension of aluminum powder in kerosene
18 p2372 A73-37118
- Pulse burnout of microwave mixer diodes.
22 p2835 A73-42965

BURNS (INJURIES)

Time-temperature safety thresholds for human epidermal injury related to materials thermal properties
05 p0637 A73-16138

BURSTS

- NT RADIO BURSTS
NT SOLAR RADIO BURSTS
NT TYPE 2 BURSTS
NT TYPE 3 BURSTS
NT TYPE 4 BURSTS
NT TYPE 5 BURSTS
- Digital communication channel with noisy errors, discussing statistical analysis of binary burst sequences for coding design
21 p2655 A73-41090
- Gilbert burst noise model for statistical analysis of nonindependent errors in digital data transmission systems, noting performance and utility in communication theory
23 p2954 A73-43986

BUS CONDUCTORS
A sequenced PWM controlled power conditioning unit for a regulated bus satellite power system.
03 p0252 A73-13930

Optimal sizing of modular bus bars for rectangular solar cell arrays as function of power/weight ratio
03 p0255 A73-14225

BUSHINGS

- Radial MHD bearing with a floating bush
15 p1881 A73-31412
- Contribution to the hydrodynamic lubrication theory of the bearing with a floating bushing
18 p2319 A73-36411

BUTANES

The oxidation of metal alkyls in the presence of isobutane.
13 p1581 A73-29002

BUTT JOINTS

- Determination of the extent of ultrasonically detected defects - Application to welded butt joint quality control
07 p0831 A73-19904
- Investigation of the low-cycle fatigue of light-alloy welds
07 p0833 A73-20506
- Estimation of fatigue-crack propagation life in butt welds.
14 p1755 A73-30147
- Fatigue crack propagation in butt welds containing joint penetration defects.
14 p1755 A73-30148
- Determination of fatigue strength of welded joints with artificial flaws by radiographic examination
15 p1882 A73-32051
- Investigation of low-cycle fatigue of welded joints in light alloys.
19 p2433 A73-37781
- Calculation of joint shells differing in their material and thickness
20 p2619 A73-39365

BUTTONS

Oil hydraulic button vortex valve optimization experiment for power consumption reduction, noting Reynolds number effects on turn down and pressure ratios
23 p2942 A73-43404

BUTYRIC ACID

- Nervous system transmitter biochemistry in terms of excitation and inhibition coordination with emphasis on gamma-aminobutyric acid /GABA/ function in cerebellum
03 p0264 A73-14258
- Effect of lithium on acute oxygen toxicity and associated changes in brain gamma-aminobutyric acid.
13 p1575 A73-28503
- Gas-releasing additives to jet fuels
21 p2754 A73-41070
- Gamma-aminobutyric acid antagonism in visual cortex - Different effects on simple, complex, and hypercomplex neurons.
23 p2946 A73-43338

BY-PASSES

Electrical model for calculation of resistance strain gage errors due to grid-grid and grid-body shunt currents
13 p1622 A73-29617

C

C BAND

- C band low noise IC microwave amplifier for phased array module in multiple access communication links, discussing photofabrication for low cost batch processing
17 p2135 A73-34727
- C band microwave landing system for increased guidance signal accuracy and reliability in azimuth, elevation and range relative to touchdown point
19 p2450 A73-37494

C-5 AIRCRAFT

C-5 program developments and alterations in terms of defense requirements and cost problems, discussing objectives and management policies in F-15 and B-1 projects
01 p0124 A73-11069

Kneeling landing gear - The C5 variable geometry development.
13 p1568 A73-28158

C-130 AIRCRAFT

The STAN /R/ 'S' Integral Weight and Balance System for the C-130 aircraft.
[SAWE PAPER 985] 19 p2385 A73-37889

C-141 AIRCRAFT

Evaluation of a reliability analysis method for fatigue life of aircraft structures.
04 p0452 A73-14715

CABIN ATMOSPHERES

NT SPACECRAFT CABIN ATMOSPHERES
Habitat atmospheres which do not support combustion.
10 p1183 A73-23562

High altitude aircraft cabin pressurization for crews and passengers, discussing altitude tolerance, reaction times, decompression and oxygen equipment
14 p1723 A73-30937

Skylab Medical Experiments Altitude Test /SMEAT/ facility design and operation.
[ASME PAPER 73-ENAS-44] 19 p2401 A73-37991

Skylab medical experiments altitude test /SMEAT/ chamber atmosphere trace contaminants analysis, describing sample acquisition techniques and instrumentation
[ASME PAPER 73-ENAS-45] 19 p2395 A73-37992

CABLES (ROPES)

- Equations of motion for flexible cables.
03 p0343 A73-13706
- Geometric nonlinearity effects on rigid joint deformation of three dimensional skeletal structures, including roofing, cable and shallow dome systems
06 p0762 A73-18342
- Dynamic stability of cable in incompressible flow at angle of incidence, calculating characteristic lengths and vibration frequencies by singular perturbation theory
[AIAA PAPER 73-395] 11 p1440 A73-25524
- Force-strain characteristics of dacron parachute suspension-line cord under dynamic loading conditions.
[AIAA PAPER 73-446] 15 p1825 A73-31432
- High strength filaments for cables and lines, discussing bundle theory and comparing dielectric and tensile properties for glass, graphite and organic fibers
23 p2997 A73-43645
- Static and dynamic finite deformations of cables using rate equations.
23 p3042 A73-43804

CADMIUM

- Morphology and capacity of a cadmium electrode - Studies on a simulated pore.
[ECS PAPER 68] 06 p0649 A73-17744
- Dispersivity of the combustion products of a mechanical mixture of aluminum and cadmium powders
07 p0923 A73-20421
- Solid cadmium cracking of titanium alloys.
17 p2191 A73-35123
- Cadmium embrittlement of high strength, low alloy steels at elevated temperatures.
22 p2873 A73-41968

CADMIUM ALLOYS

Vacancy trapping model inadequacy for aging retardation in Al-Cu-Cd alloys, noting Cd content and Cu solid solubility effects
05 p0587 A73-16576

Stable or metastable phase crystallization rate of Cd-Sb liquid alloys as function of time, composition and temperature above liquidus line
05 p0605 A73-17294

Temperature and concentration dependence of the electrical resistivity of solid alloys in the magnesium-cadmium system
11 p1386 A73-26570

Superconductivity of cadmium-magnesium alloys.
13 p1668 A73-28223

CADMIUM ANTIMONIDES

Doped CdSb single crystal production and physical properties for IR detectors and thermocouple use
01 p0087 A73-10040

Characteristics of recombination centers defining the high sensitivity of n-CdSb photoresistors
06 p0675 A73-18082

CADMIUM COMPOUNDS

- NT CADMIUM ANTIMONIDES
NT CADMIUM FLUORIDES
NT CADMIUM SELENIDES
NT CADMIUM SULFIDES
NT CADMIUM TELLURIDES
- Certain resonance properties of nickel-cadmium ferrites
08 p0995 A73-21513

Optical and luminescent properties of CdBr₂-Sn and CdCl₂-Sn single crystals
17 p2219 A73-35553

CADMIUM FLUORIDES

Cooperative luminescence in trivalent ytterbium and erbium ions in cadmium fluoride crystals
06 p0738 A73-18543

CADMIUM NICKEL BATTERIES

U NICKEL CADMIUM BATTERIES

- CADMIUM SELENIDES
Effect of surface states on surface-wave amplification in a composite structure of CdSe film on LiNbO₃.
05 p0559 A73-17073
- Infrared detection by reconfiguration of high field domains in CdS:Ag, Al.
06 p0733 A73-17500

Characteristics of the reflection spectra of CdS/x/Se/1-x/ mixed crystals in their exciton absorption region
14 p1783 A73-30578

Structure, composition and photoelectrical properties of cadmium sulfide and selenide epitaxial layers subjected to heat treatment
14 p1784 A73-30856

Influence of electric field strength on effective carrier mobility in polycrystalline CdSe thin films
20 p2536 A73-39200

Two-photon absorption in cadmium sulfide selenide single crystals employing pulsed ruby laser, discussing optical pumping, absorption anisotropy, ray refraction and luminous intensity
20 p2573 A73-39682

Temperature dependence of dc electroconductivity of CdSe single crystals and compressed micron particle size powders, noting pressure and annealing effects on powder conductivity
23 p3018 A73-44372

CADMIUM SULFIDES

- Electron beam pumped super radiant light source.
01 p0058 A73-10311
- Investigation of the emission of donor-acceptor pairs and of their phonon echoes in CdS single crystals
01 p0088 A73-10634
- Accelerated tests for long term stability of CdS solar cells, noting stoichiometry, wavelength, doping and residual atmosphere effects on cell performance
03 p0255 A73-14215
- High efficiency Cu₂S-CdS-solar cells with improved thermal stability.
03 p0255 A73-14216
- Diffusion and conduction processes in CdS-Cu/x/S thin film photocells.
03 p0350 A73-14217

Optical degradation and thermal restoration - New inputs to the mechanism of the photovoltaic effects in Cu₂S-CdS heterojunctions.
03 p0350 A73-14218

Cadmium sulfide/cuprous sulfide solar cell abrupt heterojunction band model description by two quasi-Fermi levels
03 p0350 A73-14219

New results on the development of a thin-film p-CdTe-n-CdS heterojunction solar cell.
03 p0255 A73-14220

Thin film CdS solar cell stability improvement by etching, noting cuprous sulfide oxidation effects on degradation from short term tests at high temperature
03 p0255 A73-14221

Investigations of the inhomogeneity of polycrystalline Cu/x/S-CdS solar cells.
03 p0255 A73-14222

Saturation and acoustoelectric oscillations of a photocurrent in CdS and CdSe
06 p0737 A73-18218

- IR and thermal extinction spectra of luminescence and photoconductivity of zinc cadmium sulfide solid solution films doped with Cu and Cl
06 p0738 A73-18643
- CdS-metal contact at higher current densities.
11 p1407 A73-24984
- Photoconductor-metal contact at higher densities.
11 p1407 A73-24985
- Investigation of the relationship between 'edge' and exciton emission in CdS single crystals
11 p1408 A73-25246
- KGP-2 - An electron-beam pumped cadmium sulfide laser.
12 p1507 A73-27520
- Laser beam scanned 1.1 GHz acoustic microscope based on photoconductive CdS piezoelectric transducer
13 p1614 A73-28580
- Historical development of solar cells.
13 p1573 A73-29590
- Characteristics of the reflection spectra of CdS/x/Se/1-x/ mixed crystals in their exciton absorption region
14 p1783 A73-30578
- Structure, composition and photoelectrical properties of cadmium sulfide and selenide epitaxial films subjected to heat treatment
14 p1784 A73-30856
- Preparation of CdS single crystals with a radiation-stable sensitivity to ionizing emissions
15 p1923 A73-31208
- Interaction of nearly monochromatic LA phonons with excitons in CdS crystals
15 p1924 A73-31718
- Electrical properties and photoconductivity of CdS thin films obtained in a hydrogen atmosphere
17 p2219 A73-34281
- Determination of ultramicro-impurities in CdS-type semiconductor materials - Determination of copper
17 p2220 A73-35558
- Parameters of fast recombination centers in CdS single crystals and the effect of the parameters on photosensitivity
18 p2340 A73-36669
- High temperature investigations of the steady and nonequilibrium electrical conductivity of cadmium sulfide crystals
18 p2340 A73-36670
- Investigation of 'external' self-focusing of ruby laser emission in CdS crystals
18 p2322 A73-36674
- A study of electrical conductivity inhomogeneities in CdS single crystals
18 p2341 A73-36963
- Luminescence of CdS single crystals doped with various donors and acceptors
19 p2471 A73-37955
- Effect of the surface condition on the reflection and luminescence spectra of CdS crystals
19 p2471 A73-37961
- Two-photon absorption in cadmium sulfide selenide single crystals employing pulsed ruby laser, discussing optical pumping, absorption anisotropy, ray refraction and luminous intensity
20 p2573 A73-39682
- Bi implant CdS studies, discussing sputtering, surface concentration, p-type behavior and light emission characteristics
21 p2752 A73-40951
- Influence of mechanical treatment of the resonator on the parameters of an electron-beam-pumped cadmium sulfide laser.
22 p2869 A73-42259
- Whisker junctions between growth structures on CdS layers.
23 p2997 A73-44027
- Transverse elastic wave propagation in CdS crystal wafer coated on both sides with AgBr, titanium oxide, Si or polystyrene
23 p3017 A73-44038
- Optical modulation of X band microwave transmission by acoustoelectric domains in semiconducting CdS single crystal, noting domain conductivity and permittivity changes
23 p3018 A73-44365
- Development and properties of CdP2S4
24 p3119 A73-44951
- Diffusion treatment of CdS and ZnO crystals and their applications in microwave acoustics.
24 p3120 A73-45433
- CADMIUM TELLURIDES**
Spontaneous luminescence of ZnTe single crystals and mixed zinc cadmium telluride crystals at low temperatures, describing spectral lines
01 p0088 A73-10628
- New results on the development of a thin-film p-CdTe-n-CdS heterojunction solar cell.
03 p0255 A73-14220
- Naturally alloyed n-p structures in cadmium telluride
04 p0484 A73-15642
- Exciton-phonon interaction in recrystallized CdTe layers
06 p0737 A73-18219
- Low-resistance CdTe films exhibiting a constant emf under the action of an ac field
06 p0737 A73-18222
- Monte Carlo simulation for electron diffusion in Cd Te, noting effects of applied electric field near threshold value for negative differential mobility
06 p0739 A73-18799
- Manifestation of the defect structure of cadmium telluride through high-temperature electrical conductivity
10 p1261 A73-24776
- Pressure sensitization relation to electrical conductivity relaxation during isothermal isobaric annealing of CdTe crystals
12 p1531 A73-27196
- CdTe thin film fabrication by direct synthesis of vacuum evaporated Cd and Te, noting solar cell efficiency increase after storage in room temperature exsiccator
14 p1713 A73-30475
- Cd doped CdTe microwave film detectors sensitivity, frequency response, thermal characteristics and stability
14 p1737 A73-30855
- High-temperature electrical conductivity relaxations induced in CdTe crystals by variations in cadmium vapor pressure
15 p1923 A73-31201
- Cadmium mercury telluride thin film coatings preparation by HgTe layers deposition onto previously vapor deposited CdTe layers under isothermal conditions
15 p1924 A73-32158
- Effect of an electric field on the negative photoconductivity of high-resistance ZnTe-CdTe crystals
17 p2219 A73-35552
- Principal component determination in mercury and cadmium tellurides and in solid solutions of them
17 p2220 A73-35559
- CALCIFICATION**
Amino acid composition significance in sedimentary fossil skeletal protein calcification, discussing diagenetic temperature effects
11 p1326 A73-25470
- CALCITE**
Venus carbon dioxide production kinetics involving quartz reaction with calcite to form wollastonite and carbon dioxide
24 p3133 A73-44540
- CALCIUM**
Physical properties of solar chromospheric plages. I - Line profiles of the CaII H, K, and infrared triplet lines.
01 p0108 A73-11385
- Interstellar molecular hydrogen cloud size and optical extinction by interstellar Na D and Ca lines, estimating molecular lifetime within dark cloud
06 p0752 A73-18230
- Charge assignment to cosmic ray heavy ion tracks in lunar pyroxenes.
07 p0872 A73-19877
- The spectra of near-vertical structures on the solar disk.
08 p1001 A73-20752
- Solar two-component atmospheric model for prediction of Ca II emission arches in spectrogram of strong lines near limb from kinetic equilibrium calculation
08 p1001 A73-20753
- Study of the galactic structure from observations of interstellar calcium. I - Analysis of radial velocities
08 p1004 A73-20909
- Shock waves and flares by meteors.
08 p1010 A73-21317
- Crystallochemical analogy between europium, yttrium, calcium, and barium in their alloys with manganese
09 p1135 A73-23235
- Heart function mechanism explanation by activation potential stimulation of muscular contraction via calcium ions
12 p1462 A73-27690
- Solar limb Ca I Fraunhofer line polarization rate computation, considering radiation field anisotropy effects and depolarizing collisions in wings
12 p1544 A73-27826
- Emission core widths of K Ca II line in umbra and penumbra of sunspots near solar disk center, noting relationship to stellar luminosity
12 p1545 A73-27835
- Cavity-like instability observed in quiescent prominence from H alpha slit-yaw pictures shown with Ca ion 8542 A spectra
13 p1670 A73-29371
- Violet and UV laser transitions in Ca II and Sr II resulting from impact radiation recombination of doubly charged metal ions
21 p2712 A73-40358
- CALCIUM CARBONATES**
NT ARAGONITE
NT CALCITE
- CALCIUM CHLORIDES**
Nutritional circulation in the heart. IV - Effect of calcium chloride and potassium chloride on myocardial hemodynamics and clearance of rubidium-86.
16 p1973 A73-33990
- CALCIUM COMPOUNDS**
NT ARAGONITE
NT CALCITE
NT CALCIUM CHLORIDES
NT CALCIUM FLUORIDES
NT CALCIUM OXIDES
NT CALCIUM PHOSPHATES
NT FLUORITE
NT PEROVSKITES
Some optical properties of CaMoO4 single crystals
01 p0088 A73-10626
- Aluminizing process improvement by CaAl and ammonium chloride contents increase in powder
01 p0057 A73-11350
- Confirmation of electronic paramagnetic resonance of the existence of an ordered phase in the zirconium-calcium system
09 p1135 A73-23031
- Molybdenum metal by the aluminothermic reduction of calcium molybdate.
10 p1234 A73-24430
- CALCIUM FLUORIDES**
Neodymium energy level shifts in three oxygen-compensated sites of neodymium oxide-doped calcium fluoride crystals
03 p0349 A73-13288
- Metallic additions effect on wear and friction behavior of lead monoxide, lead silicate and calcium fluoride solid lubricants coatings for high temperature operations
[ASLE PREPRINT 72LC-7C-5]
- Spectroscopy of optical centers of Nd3+/ in CaF2 and SrF2 crystals
07 p0836 A73-20203
- Transfer of Yb3+/ excitation energy to TR3+/ in CaF2 and BaF2 crystals
07 p0837 A73-20206
- Electron-hole processes in CaF2 crystals doped with rare-earth ions
07 p0837 A73-20208
- Two-photon excitation of luminescence in CaF2:Er3+/ crystals by a frequency-scanning laser employing organic dye solutions
10 p1227 A73-24075
- Investigation of the delay of stimulated emission from a CaF2:Dy2+/ laser relative to pumping pulses.
13 p1629 A73-29431
- Concentration dependence of the lasing parameters of a laser based on CaF2:Dy2+ crystals
15 p1884 A73-31221
- Stimulation of two-valent rare earth ion luminescence in CaF2 crystals by ruby and neodymium lasers
22 p2870 A73-42725
- CALCIUM METABOLISM**
Deep hypothermia induced in the golden hamster by altering cerebral calcium levels.
05 p0538 A73-16151
- Calcium movements and excitation-contraction coupling in cardiac cells.
11 p1316 A73-25601
- Circadian rhythm of urinary calcium excretion during immobilization.
14 p1717 A73-30512
- Low calcium diet produced chronic decalcification effect on osseous repair of experimentally induced cortical bone defect in chickens
18 p2270 A73-35981
- Brain calcium - Role in temperature regulation.
19 p2396 A73-38294
- Relationship between cyclic AMP, phosphodiesterase activity, calcium and contraction in intestinal smooth muscle.
21 p2638 A73-41130
- Abnormal biochemistry in myocardial failure.
22 p2808 A73-42686
- CALCIUM OXIDES**
Thermogravimetry system designed for use in dispersion strengthening studies.
01 p0015 A73-11449
- Calcia stabilized zirconia electrolyte with appreciable oxygen ionic diffusivity used as permeation membrane for oxygen leak source
02 p0167 A73-11955
- Calcium oxide and aluminum oxide constraints removal for lunar interior composition models
17 p2232 A73-35264
- CALCIUM PHOSPHATES**
Optical centers of Nd3+/ in calcium and strontium fluorophosphate crystals
07 p0836 A73-20204
- CALCULATION**
U COMPUTATION
- CALCULATORS**
Microcomputer programs for data reduction and quality control chart work, using Olivetti P-101, HP 9100-B and Wang 700-A calculators
16 p1986 A73-33642
- CALCULUS**
NT ASYMPTOTIC SERIES
NT COLLINEARITY
NT CONTINUITY [MATHEMATICS]
NT COPLANARITY
NT CURL [VECTORS]
NT DIFFERENTIAL CALCULUS

NT FOURIER SERIES
 NT INTEGRAL CALCULUS
 NT LIMITS [MATHEMATICS]
 NT PADE APPROXIMATION
 NT POWER SERIES
 NT PRONY SERIES
 NT SERIES [MATHEMATICS]
 NT TAYLOR SERIES
 NT VECTOR ANALYSIS
 NT VORTICITY
 Russian book on tensor calculus fundamentals covering tensor algebra and analysis and applications to mechanics of discrete and continuous systems 02 p0192 A73-11888

CALCULUS OF VARIATIONS
 On the regularity of solutions of two-dimensional variational problems with obstructions. 01 p0069 A73-10044
 Variational methods for linear numerical filtering with operator and transfer function spreads compromise, presenting graphical data [ONERA, TP NO. 1127] 01 p0070 A73-10236
 Variational formulation for hydromagnetic stability 01 p0084 A73-10550
 Certain generalizations of load-limit theorems for a Cosserat medium 01 p0114 A73-10573
 Variational analysis of high mass transfer rates from spherical particles - Boundary-layer injection suction considerations at low particle Reynolds numbers and high Peclet numbers. 01 p0122 A73-10802
 Variational optimization problems for hyperbolic-type equations 01 p0077 A73-10952
 Application of the variational method in the analysis of a limiter based on a symmetrical strip line 01 p0026 A73-11264
 The role of interpolation and approximation theory in variational and projectional methods for solving partial differential equations. 01 p0071 A73-11458
 Least-squares solution for the blunt body hypersonic flow problem. 01 p0004 A73-11473
 On a semi-variational method for parabolic equations. I. 02 p0186 A73-11589
 Study of the oscillations of plates, shells and combined systems by the basis vector method with difference discretization 02 p0232 A73-11817
 Calculus of variations and finite difference method for equilibrium equations in axisymmetric plastic shell design 02 p0232 A73-11821
 On certain parabolic differential equations and an equivalent variational problem. 02 p0186 A73-11972
 Rods theory covering constitutive equations, boundary value problems, variational formulation of equilibrium problems and uniqueness theorems 02 p0234 A73-11982
 Variational method in the invariance problem for controlled systems. 02 p0149 A73-12117
 Functions of a generalized restricted variation and the convergence of their Fourier series and conjugate trigonometric series 02 p0188 A73-12551
 Variational aspects of oscillation phenomena for higher order differential equations. 02 p0188 A73-12823
 Hilbert space and calculus of variations for eigenvalue bounds of integral equations of elasticity and potential theories 03 p0387 A73-13162
 Supersonic nozzle design for prescribed flight trajectory and variable gas flow parameters, solving variational problem of optimal contour for given Mach number 03 p0244 A73-13616
 A variational solution of the Rayleigh problem for a power law non-Newtonian conducting fluid. 03 p0347 A73-13790
 Discontinuous variational problems in time optimal control of systems describable by ordinary differential equations, deriving Weierstrass optimality conditions 03 p0286 A73-14055
 Calculus of variations for functional conditional extremum, determining minimum drag shape for body of revolution in hypersonic flow 04 p0403 A73-14886
 Calculus of variations for minimum energy method in elasticity theory of incompressible elastic body, calculating elastic deformations 04 p0509 A73-14980
 Calculus of variations for maximum payload of partitioned variable mass system, considering optimal weight control effect on motion 04 p0475 A73-15084
 On the prediction of the expansion coefficients in a variational calculation. 04 p0471 A73-15228

Experimental studies concerning the adhesion coefficient during slip 04 p0454 A73-15655
 Russian book - Variational method and the method of monotonic operators in the theory of nonlinear equations. 04 p0472 A73-15963
 Variational method of moments and some iteration procedures for determining the characteristics of VLF wave propagation in the earth-anisotropic ionosphere waveguide channel. I 05 p0549 A73-16387
 Aircraft and spacecraft guidance and remote and automatic control of moving objects, using calculus of variations for systems synthesis 05 p0560 A73-16402
 Pontryagin principle for variational problem of controllability region in three dimensional pursuit tracking, noting rendezvous optimal control system 05 p0560 A73-16403
 Variational-difference method for solving the third boundary value problem of an elliptic equation in a three-dimensional region with a smooth boundary 05 p0590 A73-16445
 Analysis of optimal conditions for energy conversion in an MHD-generator channel 05 p0602 A73-16586
 Variational solution to the radiative equation by the use of a step function. II - Extension to nonlinear case by iteration method. 05 p0641 A73-17102
 Two dimensional cascade acoustic resonant frequencies estimation by variational method, presenting results for three cavity modes 05 p0599 A73-17372
 Numerical solution of elastoplastic problems by the method of local variations 06 p0760 A73-17777
 Discretized elastic multipolar bodies equations of motion and conservation laws from variational formulation, considering virtual work, Betti principle and Somigliana formulae 06 p0761 A73-17892
 Book on nonlinear optimization covering search, iteration, gradient, algorithmic and computer techniques, mathematical and dynamic programming, calculus of variations, Pontryagin maximum principle, etc 06 p0717 A73-18401
 The variational derivative of degenerate Lagrange densities. 06 p0718 A73-18504
 Workshop on the Application of Variational Methods to the Calculation of Structures, Senlis, Oise, France, June 19-21, 1972, Proceedings. Numbers 1, 2, 3, 4 & 5 06 p0765 A73-18721
 The calculus of variations and various direct methods in engineering analysis. 06 p0719 A73-18722
 Computerized optimal control problem formulation in calculus of variations, discussing flexible user-oriented algorithm for terminal point transversality boundary conditions numerical implementation 06 p0672 A73-18806
 Calculus of variations for mathematical model of elastic shell with internal degrees of freedom, noting boundary and discontinuity conditions 06 p0766 A73-18877
 Equations of motion for mechanical system with imposed servo couplings, discussing Gauss variational principle applicability for system analysis 07 p0851 A73-19128
 Methods of reducing continual nonlinear mechanics problems for deformable solids to discrete problems 07 p0910 A73-19303
 Magnetospheric and ionospheric potential electric fields, using variational process based on transverse/longitudinal conductivity ratios in plasma 07 p0815 A73-19433
 Application of a variational technique to wedge flow with variable properties. 07 p0775 A73-19963
 Two dimensional steady nonrotational flow of perfect compressible fluid around symmetric convex profile, reducing to variational inequality in hodograph plane 07 p0776 A73-20147
 Variational determination of electric field induced by charge separation in near wake of negatively charged body moving at mesothermal speeds in collisionless plasma 10 p1254 A73-24116
 Russian book on analytical theory of optimization in gravitational fields covering orbital transfer trajectories, variational optimization problems, Lagrange multiplier properties, etc 10 p1284 A73-24800
 Algorithm and convergence behavior of the local variation method for problems with partial derivatives 11 p1400 A73-26326
 Variational method for a generalized class of functionals and its application to aeromechanics problems 11 p1304 A73-26438

Variational equations of unsteady near-similar perfect gas flow at strong shock front in terms of mass, energy and momentum in perturbed region 12 p1487 A73-27408
 Variational optimization problems for equations of hyperbolic type. 12 p1518 A73-27528
 Finite element incremental solutions for geometrically nonlinear problems based on second variations of variational functionals, discussing numerical integration and variational principles 13 p1692 A73-28228
 The transient temperature distribution in a slab subjected to radiative and convective heating calculated by variational method. 13 p1704 A73-28429
 Automation of variational methods of solving boundary value problems 13 p1650 A73-29127
 An historical survey of computational methods in optimal control. 14 p1738 A73-30413
 Duality of limit theorems for a structure of a standard rigid-plastic material 14 p1812 A73-30491
 On the connection between the elliptic equations of the Navier-Stokes type and the theory of harmonic functionals. 14 p1769 A73-30521
 Some questions of approximation in the variational difference method 14 p1771 A73-30830
 Convergence of the upper relaxation method for solving variational-difference equations for elliptic equations in an arbitrary plane 15 p1898 A73-30967
 Gaussian variational equations for osculating elements of an arbitrary separable reference orbit. 15 p1930 A73-31113
 Calculus of variations for mathematical model of elastic shell with internal degrees of freedom, noting boundary and discontinuity conditions 15 p1956 A73-32402
 Galerkin variational method combination with least squares error distribution technique for application in plate and shell theory 16 p2077 A73-32992
 A variational approach to grid optimization in the finite element method. 16 p2079 A73-33010
 Electromagnetic induction microsystems with synchronization. III - Distribution of magnetic characteristics in complex linear and nonlinear regions. IV - Modeling of nonstationary electromechanical processes 16 p1992 A73-33668
 Book - Variational analysis: Critical extremals and sturmian extensions. 17 p2203 A73-35598
 Spline interpolation techniques for approximation of boundary value problem solutions, relating approximation error norm to interpolation error norm from variational formulation 17 p2203 A73-35607
 Duality relationships for a nonlinear version of the generalized Neyman-Pearson problem. 18 p2330 A73-36636
 Fractured solutions in the calculus of variations. 18 p2330 A73-36640
 Bounding flow existence for turbulent convection in fluid and porous layers analysis between parallel plates based on calculus of variations in Banach spaces 20 p2626 A73-39012
 Construction of a minimum-wave-drag profile in inhomogeneous supersonic flow 21 p2631 A73-40184
 Approximate variational treatment of elastic scattering of electrons from semi-infinite lattices. 21 p2741 A73-41627
 The existence of a minimal surface with a free boundary of a given length 22 p2885 A73-41774
 On some further applications of the variational formulation based on local potential to the solution of diffusion equation. I - Temperature distribution in a transpiration cooled half-space with variable thermal properties. II - Heat conduction in an ablating solid with variable thermal properties. 22 p2931 A73-42468
 Book - The finite element method: Fundamentals and applications. 22 p2882 A73-42492
 A minimum principle in dynamics of elastic-plastic continua at finite deformation. 24 p3146 A73-44678
 Elliptic restricted three body problem equations derived from linear variational equations with periodic coefficients describing motion near libration centers 24 p3141 A73-45284

CALIBRATING
 NT WIND TUNNEL CALIBRATION

- Intermediate resistance standards for low resistivity resistance thermometer calibration, discussing accuracy requirements and error analysis 02 p0167 A73-11866
- Radio telescope for high resolution radio source mapping, discussing system design, computerized control and calibration 02 p0150 A73-11869
- The analysis of particulate contaminants in hydraulic fluids. 02 p0132 A73-12004
- On the calibration system of the amplifying tract of spherical ion trappers. 02 p0169 A73-12186
- Spark calorimeter calibration by particle accelerator induced high energy pions, noting neutral and charged particles track detectors high geometric resolution 02 p0171 A73-12686
- UV light intensities calibration in astrophysics and high temperature metrology with thermal arc plasma as radiation sources, discussing intensity standard establishment 02 p0199 A73-12715
- Thermal radio source DR 21 centimeter flux density measurements for antenna aperture calibration, comparing with standard sources 03 p0366 A73-12932
- Hot-wire anemometers calibration characteristics for steady channel turbulent air flow measurement, noting linearization error analysis 03 p0306 A73-13166
- ATS-F satellite borne radio beacon transmitter experiment for obtaining ionospheric electron content, discussing design, in-orbit performance, calibration information dissemination and propagation measurement 03 p0275 A73-13639
- A calorimeter for high-power CW lasers. 03 p0310 A73-14495
- Practical and precise means of microwave power meter calibration transfer. 03 p0310 A73-14499
- A system for the precise calibration of air navigational receivers. 03 p0310 A73-14501
- Computerized weather radar data central processor design, implementation and programs for data reduction and calibration 03 p0281 A73-14548
- Elliptical, annular, through, part-through and irregularly shaped crack front curvature effect on stress intensity factor calibration 04 p0506 A73-14682
- Camera calibration technique treating inner cone parameters as variables subject to adjustment or recovery in simultaneous analytical stereotriangulation solution 04 p0446 A73-14768
- Survey improvement and calibration analysis for the Air Force Eastern Test Range with Geos C. 04 p0437 A73-14786
- Automated calibration of blood pressure signal conditioners. 04 p0411 A73-14846
- Molecular branching-ratio method for intensity calibration of optical systems in the vacuum ultraviolet. 05 p0597 A73-16495
- A solar radio spectrograph with high time resolution. 05 p0621 A73-17039
- Spectrophotofluorometers for returned lunar samples and geological materials organic analyses, discussing optical component performance and calibration to avoid instrumental artifacts effect on spectra 06 p0662 A73-18415
- Macroscopic systems response to gravitational radiation for detector design and calibration, noting accessibility to people unfamiliar with general relativity 06 p0724 A73-18549
- Transverse sensitivity effect on measurement errors and rig calibrating of strain gages 07 p0823 A73-19568
- Calibration procedure for instruments to measure the delta ferrite content of austenitic stainless steel weld metal. 07 p0832 A73-20272
- Calibration of resistance strain gauges 07 p0827 A73-20538
- A thermal calibrator for radiometers used in radioastronomy. 08 p0963 A73-20873
- Pyranometer calibration by substandard and working instrument comparison on X-Y recorder, using computerized statistical analysis 08 p0966 A73-21264
- Vacuum system for an infrared calibration facility. 08 p0968 A73-21622
- Calibration of the aerial photographic system by the method of mixed ranges. 08 p0969 A73-21706
- Laser interferometric alignment sensor for the large space telescope /LST/. 08 p0970 A73-21732
- The calibration of electrostatic analyzers and channel electron multipliers using laboratory simulated omnidirectional electron beams. 09 p1080 A73-22104
- Automated vibration shaker calibration data acquisition and analysis system with minicomputer for working transfer standard voltage monitoring and acceleration level determination 09 p1070 A73-22508
- Impact of solar calibration on telemetry system testing and checkout. 09 p1057 A73-23407
- On the calibration of flux densities and the determination of spectra at radio frequencies. 10 p1272 A73-23527
- Calibration of a hot-wire anemometer for velocity perturbation measurement. 10 p1218 A73-24121
- High resolution accelerometer for sounding rocket, describing calibration methods [ONERA, TP NO. 1215] 10 p1219 A73-24398
- Equipment for highly accurate and repeatable strain gauge factor determination. 10 p1220 A73-24574
- Calibrations of the airflow photometers and spectrometers. 11 p1365 A73-26237
- Total irradiance calibrations using electrically calibrated radiometer, discussing lamp detector alignment procedures 11 p1366 A73-26252
- Problems and design of black-body references. 11 p1401 A73-26514
- A simplified method for the in vitro calibration of electromagnetic flowmeters. 12 p1464 A73-27027
- A recalibration of the quiet sun millimeter spectrum based on the moon as an absolute radiometric standard. 12 p1545 A73-27840
- Mariner Mars 1971 photogrammetry, discussing spacecraft scan platform mounted TV camera calibration procedure for interior orientation parameters and opto-mechanical orthogonality 12 p1500 A73-27953
- Metric calibration of distortion in aerial mapping cameras, using laser, collimator and diffraction grating generated angularly accurate image points matrix 12 p1501 A73-27970
- Aerial cameras functional testing and calibration, discussing film plane flatness measurement methods and camera applications to ice surface photography 12 p1502 A73-27971
- An automatic reflectometer for the upper shortwave range 13 p1590 A73-28569
- Adjustment of thick-film resistors by laser and new pastes for the thick-film technology 13 p1627 A73-28574
- Long term temperature control and calibration system for creep testing facility temperature drift monitoring and correction 13 p1597 A73-28841
- Vibrating string total field/absolute gravity meter/accelerometer, discussing calibration at single reference point 13 p1617 A73-28849
- Absolute calibration of Apollo lunar orbital mass spectrometer. 13 p1617 A73-28930
- An electronically gated gamma and X-ray calibration scheme. 15 p1879 A73-32222
- A method for the determination of the multiplicative constants of thermoelectric pyranometers 15 p1879 A73-32350
- Extra-atmospheric observations of the luminosity of the sky from the Cosmos 51 and Cosmos 213 satellites. I - Method and calibration of the measurements 16 p2011 A73-32706
- Arc plasmas as radiation standards in the vacuum ultraviolet. 16 p2036 A73-32942
- Absolute calibration of solar radio flux density in the microwave region. 16 p1993 A73-32968
- Calibration of Sandia Laboratories' 19-foot diameter explosively driven blast simulator. 16 p1994 A73-33136
- In-flight frequency calibration of IR sensor systems using LEDs. 17 p2165 A73-34275
- Alignment technique for the Mach-Zehnder interferometer. 17 p2165 A73-34298
- The design, construction and calibration of an infrared temperature profile radiometer /ITPR/ for Nimbus E. 17 p2238 A73-34602
- Accuracy of type K thermocouple wire below 500 F - A statistical analysis. 17 p2167 A73-34624
- Strapdown electrostatic gyroscope spin axis precession drift rate calibration, using virtual work technique for modeling bearing torques on rotor 17 p2137 A73-35210
- A rapid-scanning image intensifier spectrometer for astronomy. 17 p2169 A73-35286
- VUV radiometry with hydrogen arcs. I - Principle of the method and comparisons with blackbody calibrations from 1650 A to 3600 A. 17 p2212 A73-35425
- Testing and calibration of aircraft sensors and systems. 17 p2174 A73-35580
- Absolute calibration of antennas at extremely low frequencies. 17 p2128 A73-35686
- Antenna gain calibration on a ground reflection range. 17 p2128 A73-35688
- Analysis of solar flare X-ray radiation with Bragg spectrometers. 18 p2344 A73-36014
- Electron calibration on a high-energy cosmic ray detector. 18 p2317 A73-36979
- System for calibrating on-board instruments and for laboratory simulation of low-density plasma flows past models 19 p2417 A73-37351
- Method of measuring the size of defects without using calibrating standards and adjusting the sensitivity of ultrasonic defectoscopes. 19 p2432 A73-38358
- Continuous calibration and alignment techniques for an all-altitude inertial platform. [AIAA PAPER 73-865] 20 p2586 A73-38803
- Self calibrating automatic equipment for pulsed and CW RF testing of phase, amplitude and frequency characteristics of pulsed electronic devices 20 p2535 A73-38870
- Mobile IC coherent radar with computerized display and calibration, incorporating cold cathode crossed field amplifier tube in transmitter amplifier stage 20 p2528 A73-38871
- A universal static calibration procedure for yawed hot wires. 21 p2693 A73-39926
- Why exact metrology in an ultrahigh-speed cinematographic system - An application example: Calibration of image converters with a view to photometric measurements 21 p2694 A73-39951
- Ultrashort laser pulse generators for dynamic marking of 'chronodiode' and 'chronolas' slit cameras 21 p2709 A73-39953
- A method for the calibration of a quantitative high-speed schlieren procedure involving photographic recording 21 p2694 A73-39955
- Rainfall estimation from satellite visible and IR imagery, discussing calibration and accuracy requirements 21 p2730 A73-40093
- Electron calibration of a high-energy cosmic ray detector. 21 p2703 A73-41150
- NBS radiometric calibration services extended to far UV spectrum with dc high power hydrogen wall stabilized arc as primary standard of spectral radiance 21 p2703 A73-41256
- Reference indication and setting devices for circular mirror sections of the RATAN-600 radio telescope 21 p2675 A73-41452
- A radio-astronomical method of adjusting variable-profile antennas 21 p2667 A73-41458
- Measurement of antenna parameters and calibration of the sensitivity of the RATAN-600 radio telescope in the radar mode of operation at the 8-mm wavelength 21 p2667 A73-41467
- A survey of thermometric characteristics of recently produced Allen-Bradley/Ohmite resistors. 22 p2854 A73-41996
- Platinum resistance thermometry below 13.81 K. 22 p2854 A73-42002
- Intercomparison of standard platinum thermometers calibrated on IPTS-68 between 13.81 and 273.15 K. 22 p2854 A73-42003
- Calibration of platinum resistance thermometers. 22 p2855 A73-42011
- A fixed point calibration procedure for precision platinum resistance thermometers. 22 p2857 A73-42026
- Calibration of capsule platinum resistance thermometers at the triple point of water. 22 p2857 A73-42027
- Tungsten-rhenium thermocouple, describing alloys behavior, fabrication, insulation sheaths, calibration, stability and applications 22 p2857 A73-42037
- Fabrication of high precision strain gauge dynamometers and balances at the O.N.E.R.A. Modane Centre. [ONERA, TP NO. 1196] 22 p2839 A73-42217

- Cerenkov-effect based standard radiation source designed for the calibration of space experiments - Spectral energy distribution measurement 22 p2860 A73-42307
- Radiometric calibration of a multi-spectral aerial camera. 22 p2862 A73-42824
- Low-noise microwave receiving systems in a world-wide network of large antennas. 23 p2958 A73-43376
- Use of a fluidic distributor for the calibration of unsteady flow probes. 23 p2945 A73-43430
- The behavior of hot-film anemometers in gas mixtures. 24 p3091 A73-45325

CALORIC STIMULI

- Response of single units of the posterior hypothalamus to thermal stimulation. 03 p0262 A73-14111
- Caloric vestibular stimulation via UHF-microwave irradiation. 10 p1178 A73-23650
- Some effects of cooling and heating areas of the head and neck on body temperature measurement at the ear. 13 p1575 A73-28504
- Nystagmic response persistence to Fitzgerald-Hallpike caloric tests as function of directional cupular deflections due to head movement 13 p1576 A73-28510
- Step-wise changes in thermoregulatory responses to slowly changing thermal stimuli. 13 p1576 A73-28535
- Differential thermal sensitivity in the human skin. 14 p1720 A73-30912

CALORIMETERS

- NT FLAME CALORIMETERS
- Solid-solid phase transitions determined by differential scanning calorimetry. 01 p0014 A73-11062
- Multilayer X ray film chamber for gamma quanta energy spectrum determination by primary photon impact and absorber calorimetric methods 02 p0208 A73-12660
- Spark calorimeter calibration by particle accelerator induced high energy pions, noting neutral and charged particles track detectors high geometric resolution 02 p0171 A73-12686
- Heat flow meter and calorimeter measurements of heat transfer between human body and environment under various climatic conditions for temperature regulation studies 03 p0268 A73-14123
- Calorimetric measurement of optical power from pulsed lasers. 03 p0310 A73-14494
- A calorimeter for high-power CW lasers. 03 p0310 A73-14495
- Balanced heat transfer type calorimeter designed and tested for spark energy measurement, comparing performance to conventional calorimeters of transient heat transfer type 07 p0922 A73-20365
- Dynamic method for measuring thermal conductivity of liquids and gases at high pressures. 08 p1021 A73-20861
- Calorimetric measurements of laser energy and power. 08 p0963 A73-20872
- Measurement of plasmoid energy in a time-variable magnetic field 10 p1258 A73-24881
- Modified X band microwave calorimeter design for precision power and attenuation measurements in GHz and MHz ranges 12 p1498 A73-27752
- An absolute method of measuring energy outputs from CO₂ lasers. 13 p1626 A73-28369
- Electronic specific heat of nickel-base alloys containing small amounts of transition metals [ONERA, TP NO. 1250] 15 p1924 A73-32210
- Experimental methods regarding the thermodynamics of metals and alloys. I 16 p2026 A73-33953
- Differential calorimetry technique with heat link placement between samples for maintaining near equilibrium state to achieve accuracy in specific heat ratio measurement 17 p2175 A73-35753
- Small surface plate calorimeter for convection and radiation heat transfer measurements from heated body in air 21 p2692 A73-39920
- Measurement of plasmoid energy in a time-varying magnetic field. 21 p2749 A73-41656
- Calorimetric measurement of thermodynamic temperatures above 0°C using total blackbody radiation. 22 p2853 A73-41980
- Precision measurements of temperature differences with thermistors by a simple technique. 22 p2855 A73-42014

Design considerations and applications of gradient layer calorimeters for use in biological heat production measurement. 22 p2813 A73-42054

Calorimeter for picosecond laser pulses. 22 p2872 A73-43153

A method for studying the radiant flux distribution in the circumfocal area of a concentrator with the aid of an asymptotic calorimeter 24 p3058 A73-45253

CALORIMETRY
U HEAT MEASUREMENT

- CAMBER
- NT CONICAL CAMBER
- NT WING CAMBER
- Inviscid flow through a cascade of thick, cambered airfoils. I - Incompressible flow. 16 p1964 A73-33527
- [ASME PAPER 73-GT-84]
- Inviscid flow through a cascade of thick, cambered airfoils. II - Compressible flow. 16 p1964 A73-33528
- [ASME PAPER 73-GT-85]
- CAMBERED WINGS
- High-frequency vibrations of a circular wing in the flow of an ideal fluid 05 p0636 A73-17089
- Conically cambered triangular wings with reflex spanwise curvature. 08 p0925 A73-20938
- Lift and drag at off-design Mach numbers of conically cambered wings with subsonic leading edges and supersonic trailing edge 12 p1458 A73-27927
- Rogallo variable geometry flexible cambered wing structure and aerodynamic performance for low speed agricultural flight applications 13 p1568 A73-28027
- Revised calculations of the NACA 6-series of low drag aerofoils. 17 p2094 A73-34536
- Improved aircraft capability through variable camber. 19 p2378 A73-37275

CAMERA SHUTTERS

- Flight test of narrow band television system. 01 p0052 A73-11169
- Photoelectric measurement of satellite camera shutter opening time delay and photographic plate motion synchronization, calculating root-mean-square error in observation time 03 p0307 A73-13253
- A diode-type shutter tube for ultrahigh-speed photography 06 p0679 A73-18854
- Some applications of a tube with proximity focusing in ultrahigh-speed motion-picture photography 06 p0696 A73-18858
- Microchannel image intensifiers - Applications to ultrahigh-speed photography 06 p0697 A73-18860
- Unified time recording for aerial photographic surveys, using exact time synchronized control signal sequences in recording camera shutter release 09 p1084 A73-22672
- Ultrahigh-speed high-frequency motion picture camera type W.K.2 21 p2693 A73-39939
- Characteristics and limitation of microchannel plates used in shutters for ultrahigh-speed photography 21 p2694 A73-39943
- Automatic accurate full-range synchronization of light strobe with shutter opening of fast-framing camera. 21 p2697 A73-39997
- Radiometric calibration of a multi-spectral aerial camera. 22 p2862 A73-42824

CAMERA TUBES

- NT IMAGE DISSECTOR TUBES
- NT IMAGE ORTHICONS
- NT RETURN BEAM VIDICONS
- NT VIDICONS
- The microchannel Picoscope - A tube with high-temporal-resolution scanning for studying luminous phenomena in the subnanosecond range 06 p0679 A73-18862
- Development of a new kind of Lallemand camera. 14 p1751 A73-29905
- Spectracon camera for astronomical telescope prime focus operation, discussing image tube extended area photocathode and mica window 14 p1751 A73-29906
- A proximity focused ultraviolet-sensitive SEC camera tube. 14 p1732 A73-29910
- The detector system of the International Ultraviolet Explorer satellite. 17 p2170 A73-35295
- The oblique electron lens. 18 p2316 A73-36597
- CAMERAS
- NT DIFFRACTION LIMITED CAMERAS
- NT FRAMING CAMERAS
- NT HIGH SPEED CAMERAS
- NT LALLEMAND CAMERAS

NT PANORAMIC CAMERAS

NT SCHMIDT CAMERAS

NT TELEVISION CAMERAS

Blank pupil arrangement of coude spectrograph with echelette for 1.52 meter reflector, describing dispersions obtained, receivers used and electronic camera adaptation 01 p0048 A73-10523

Adaptation of the electronic camera to the coronagraph 02 p0170 A73-12544

The prediction of resolving power of air and space photographic systems. 02 p0171 A73-12567

Photographic satellite tracking instrument technology and data reduction methods, describing various camera types and for photogrammetric and astrometric position determination 03 p0274 A73-13252

Camera calibration technique treating inner cone parameters as variables subject to adjustment or recovery in simultaneous analytical stereotriangulation solution 04 p0446 A73-14768

Electro-optical multiband cameras for spaceborne remote sensing, discussing optical multiplexing, return beam vidicon, intensifier vidicon storage tube, image spectrophotometer and dissector 04 p0450 A73-15770

Lunar Surface Ultraviolet Spectrographic Camera for location and extent determination of gaseous material, describing capability for acquisition of direct imagery and spectroscopy 05 p0576 A73-16746

Lunar metric camera used during Apollo landings, discussing lenses and test and calibration work for inner orientation 07 p0824 A73-20020

Magnetically focused electronographic cameras for far UV imagery and spectroscopy in astronomical and optical geophysical observations from sounding rockets and space vehicles 08 p0971 A73-21744

Damping of an aerial photo camera with the aid of polymeric materials 10 p1219 A73-24478

An analytic expression for the radial photogrammetric distortion of aerial photo cameras 10 p1219 A73-24479

Photometric error of the NA-MK-25 camera field 11 p1361 A73-25250

Holographic motion picture camera allows front surface detail to be recorded in real time using a continuous wave laser. 11 p1366 A73-26249

The facsimile camera - Its potential as a planetary lander imaging system. 12 p1495 A73-26875

Piston engine or turboprop aircraft photography, measuring camera vibration components in roll, pitch and yaw by flashing light technique for image quality improvement 12 p1500 A73-27954

Skylab earth terrain camera for high resolution photography of areas covered by other Earth Resources Experiment Package sensors to aid in data interpretation 12 p1500 A73-27958

The resolving power and the modulation transfer function of terrestrial and aerial cameras in working conditions. 12 p1501 A73-27963

Aerial camera automatic exposure control design and operation, discussing maxima-minima metering and average brightness measurement techniques 12 p1501 A73-27965

Metric calibration of distortion in aerial mapping cameras, using laser, collimator and diffraction grating generated angularly accurate image points matrix 12 p1501 A73-27970

Aerial cameras functional testing and calibration, discussing film plane flatness measurement methods and camera applications to ice surface photography 12 p1502 A73-27971

Photographic satellite observations with the Automatic Camera for Astrogeodesy. 13 p1611 A73-28150

A progress report on the laser scanned acoustic camera. 13 p1614 A73-28577

Camera design with deep-cooled photographic emulsion for low intensity light photography, discussing gas filling and vacuum techniques for water condensation avoidance 14 p1753 A73-30275

IR line scanners using stereoscopic techniques for aerial remote sensing of topography, discussing pivoting mechanism, scanner cameras and scan planes 17 p2168 A73-34957

CANADAIR AIRCRAFT

- NT CL-84 AIRCRAFT
- CANADAIR CL-84 AIRCRAFT
- U CL-84 AIRCRAFT

CANALS

Martian canals interpretation based on thermodynamic subsurface cells with time-limited cellular convection and densification of dust masses along cell boundaries

04 p0501 A73-15628

CANARD CONFIGURATIONS

B-52 control configured vehicles ride control analysis and flight test.

[AIAA PAPER 73-782] 19 p2378 A73-37452

CANBERRA BOMBER

U B-57 AIRCRAFT

CANCER

Influence of rare-earth metal dust containing radioactive components on the development of reticulosarcoma of the lungs

10 p1183 A73-23680

Incidence of Lucke renal adenocarcinoma in Rana pipiens as determined by histological examination.

11 p1314 A73-25136

CANONICAL FORMS

Canonical expansions of random processes, discussing discrete and continuous set transformations for spectral representation and shaping filters in time domain

01 p0068 A73-10027

Newtonian dynamics canonical formulation in Galilean relativity framework, representing motions of bodies as integral manifolds of 2-form characteristic distribution

01 p0079 A73-11256

Matrix method for canonical transformations in many body problem of celestial mechanics

03 p0379 A73-14587

Representation of oscillations in piecewise-linear systems by the phase-shift-averaging method.

06 p0717 A73-18146

Monofrequent resonance oscillations with external excitation.

07 p0851 A73-19544

On the analytical study of Saturn's satellites, Enceladus-Dione

08 p1005 A73-20921

Distributed parameter system a priori stochastic optimal control, deriving canonical differential equations from dynamic programming formulation for insight into feedback control problem

08 p0950 A73-21093

Analysis of load distribution in multiple-row bolt joints

10 p1222 A73-23595

Analytical mechanics algorithms based on characteristic equation and canonical equations of system with integral constraints

10 p1249 A73-24312

Canonical form of hybrid matrix for linear multipole network circuit, discussing synthesis and analysis

10 p1195 A73-24378

Canonical perturbation theory solution for nonconservative dynamic systems equations of motion, considering Duffing and van der Pol equations

10 p1283 A73-24665

Irreducible canonical realizations from external data sequences.

11 p1390 A73-25191

Canonical representations of random processes with multiplicities of one and two

12 p1518 A73-27193

Rigorous resolution of the hierarchy of grand-canonical-ensemble Green functions.

13 p1662 A73-28552

An efficient algorithm for calculation of the Luenberger canonical form.

14 p1769 A73-30508

Book on perturbation methods for nonlinear differential equations covering canonical transformation theory, Hamiltonian and integrable systems, area preserve mapping and resonance problem

15 p1899 A73-31472

Basic trends in the development of modern analytic mechanics

15 p1913 A73-31622

Infinitesimal canonical transformation for obtaining the thermal conductivity coefficient under the theory of linear response

17 p2253 A73-34126

Satellite vibration-rotation motions studied via canonical transformations.

18 p2352 A73-36422

On the equivalence between Hori and Lacina perturbations theories.

19 p2483 A73-37564

An efficient algorithm for calculation of the Luenberger canonical form.

19 p2408 A73-38065

Symmetry transformations of the classical Kepler problem.

19 p2446 A73-38382

Automatic control theory and systems representation in framework of unilateral mechanics, using canonical elastodynamic and elastostatic equations

20 p2540 A73-38703

Method of analyzing electronic circuits on the basis of a hybrid-parameter matrix in a canonical system of coordinates

21 p2670 A73-41306

Canonical differential equations from equilibrium and compatibility conditions for boundary loaded, shell of revolution, simplifying and transforming by canonical transformations

21 p2788 A73-41616

The asymptotic analysis of canonical problems in high-frequency scattering theory. I - Stratified media above a plane boundary. II - The circular and parabolic cylinders.

22 p2886 A73-42347

Canonical elements based on polar coordinates in Kustanheimo-Stiefel space and applications to satellite motion perturbation from oblate bodies

24 p3111 A73-45293

The governing equations and extremum principles of elasticity and plasticity generated from a single functional. I.

24 p3152 A73-45315

Adiabatic variation. I - Exponential property for the simple oscillator.

24 p3112 A73-45543

CANOPES

Theory of light deviation by sheets of circular cone geometry

11 p1397 A73-25565

A model and calculation procedure for predicting parachute inflation.

[AIAA PAPER 73-453] 15 p1826 A73-31439

Lightning protection for aircraft canopy, discussing simulation tests, safety margins, side puncture, corona streamer and pilot physiological reactions

16 p1968 A73-33036

Plant canopy models for simulating composite scene spectroradiance in the 0.4 to 1.05 micrometer region.

20 p2562 A73-39906

Helium bubble survey of an opening parachute flowfield.

22 p2798 A73-43112

CANTILEVER BEAMS

Heating of a viscoelastic beam subjected to transverse vibrations

01 p0112 A73-10003

Dynamic programming and a max-min problem in the theory of structures.

01 p0019 A73-10199

Transverse vibrations generated in a bracket bar by the reciprocating linear displacements of its seal which are damped in the course of time.

02 p0235 A73-12127

The influence of axial load on eigenfrequencies of a vibrating lateral restraint cantilever.

03 p0384 A73-13115

Numerical integration of nonlinear integrodifferential equations of thin viscoelastic beams deflection, considering cantilever beam under uniformly distributed loads

03 p0390 A73-13343

A theoretical and numerical comparison of elastic nonlinear finite element methods.

03 p0392 A73-13689

The vibration of cantilever beams of fiber reinforced material.

05 p0631 A73-16115

On the determination of the centers of twist and of shear for cylindrical shell beams.

[ASME PAPER 72-APM-XX] 05 p0633 A73-16534

Approximations for large deflection of a cantilever beam.

07 p0915 A73-20339

Effect of major axis curvature on l-beam stability.

07 p0916 A73-20437

The minimum weight structural configuration of pin-jointed truss cantilevers of given external shape.

08 p1015 A73-20671

Diffraction moire technique illustrated by determination of beam deflections.

08 p1016 A73-20797

Non-linear bending of beams of variable cross-section.

08 p1016 A73-20831

Lateral buckling of cantilevered l beam columns.

08 p1017 A73-20942

Cantilever beam dynamic stability under follower force, investigating divergence, flutter and autoparametric resonance relations

09 p1161 A73-23088

On the elastoplastic problem of cantilever subject to combined bending and twisting.

09 p1164 A73-23320

Free vibration of cantilever beam with/without tip mass and with nonlinear material properties, using perturbation and finite element techniques

12 p1556 A73-27928

Thin Al alloy sheet plane stress testing with zero K gradient specimen based on tapered double cantilever beam modification, considering fracture toughness and crack propagation

15 p1950 A73-31985

Saint Venant problem for a continuously inhomogeneous anisotropic beam

15 p1953 A73-32103

Dual extremum principles relating to optimum beam design.

16 p2081 A73-33748

Matrix displacement solution to elastica problems of beams and frames.

16 p2082 A73-33906

Lateral bending-torsion vibrations of a thin beam under parametric excitation.

[ASME PAPER 73-APM-13] 17 p2247 A73-35037

Differential equations for the vibrations of twisted rods with allowance for energy dissipation

20 p2619 A73-39372

Optimum tapering design of vibrating cantilever beams, considering geometrically similar and rectangular cross sections and degenerated end mass case

21 p2785 A73-40839

Improvement of damping capacity of structural members by introduced stress concentration.

[ASME PAPER 73-DET-76] 22 p2919 A73-42072

Analytic treatment of minimum weight design of cantilevers.

[ASME PAPER 73-APMW-29] 22 p2925 A73-42889

Beck cantilever problem solution for quasi- and purely dynamic case by Euler or energy method under internal constraint

24 p3147 A73-44892

An examination of the edge effect in a cantilever beam.

24 p3152 A73-45371

CANTILEVER MEMBERS

NT CANTILEVER BEAMS

NT CANTILEVER PLATES

Stress analysis of cantilever thin walled cylindrical shell with concentrated force on free reinforcement ring, noting members rigidity relationship to internal stress concentration

02 p0230 A73-11718

Free vibration of cantilever circular cylindrical shells - A comparative study.

04 p0513 A73-15589

Cantilever aircraft tires - More than a break for brakes.

[SAE PAPER 720870] 05 p0534 A73-16652

Dynamic response of a vertical cantilever structure in the natural wind.

07 p0823 A73-19565

Influence coefficients for end-loaded conical frustums.

07 p0913 A73-19983

Cantilever cylindrical shells of rigid-plastic material, determining collapse loads under external pressure combined with end moment by numerical solution to limit analysis

[ASME PAPER 72-PVP-B] 09 p1164 A73-23271

Flexural vibrations of a cantilever strut mounted on a rotating disk

10 p1290 A73-24308

Plane strain plastic yielding due to bending of end-loaded cantilevers containing circular, triangular or diamond-shaped holes.

11 p1443 A73-26091

Theory for the flexural vibrations of a rotating viscoelastic cantilever

16 p2083 A73-33936

Critical speeds for cantilever shafts.

18 p2320 A73-36700

Flutter-divergence transition criteria in certain viscoelastic polygenic systems.

20 p2623 A73-39556

CANTILEVER PLATES

Non-linear vibration of rotating cantilever blades treated by the Ritz averaging process.

02 p0232 A73-11859

Flow induced vibration of cantilever mounted flat plates in an enclosed passage An experimental investigation.

04 p0513 A73-15590

Self-excited and forced vibrations of an aeroelastic system subject to a follower force.

04 p0513 A73-15597

Vibration of thermally stressed plates with various boundary conditions.

05 p0636 A73-17101

Influence of an intermediate stiffener on the vibration frequency spectrum of a cantilever plate

10 p1291 A73-24357

Stability of elastic bending and torsion of uniform cantilevered rotor blades in hover.

[AIAA PAPER 73-405] 11 p1440 A73-25534

Photoelastic study of rectangular plates under bending.

19 p2498 A73-37667

Aeroelastic vibrations in labyrinth seals

20 p2569 A73-39373

Reduction of the degrees of freedom in solving dynamic problems by the finite element method.

22 p2922 A73-42479

Designing a slender-wing-type cantilever plate under conditions of unsteady creep

23 p3042 A73-43728

Vibration characteristics of aluminum plates reinforced with boron-epoxy composite material.

24 p3149 A73-45148

CANTILEVER WINGS

U WINGS

CAPACITANCE

- Determination of the dopant concentration profile in epitaxial GaAs by the method of the differential capacitance of a Schottky diode 02 p0145 A73-11548
- Multilayer thin film microcircuit and printed circuit conductors partial capacitance and potential coefficients, using matrix method for approximate calculation 03 p0284 A73-14070
- Theory of dynamic charge and capacitance characteristics in MIS systems containing discrete surface traps. 04 p0427 A73-15344
- Theory of dynamic charge current and capacitance characteristics in MIS systems containing distributed surface traps. 04 p0427 A73-15345
- MIS and Schottky barrier microstrip devices consisting of microstrip transmission line fabricated on semiconductor substrate, causing capacitance dependence on electric field 05 p0559 A73-16818
- Instrument circuitry, calibration and errors in p-n junction capacitance measurement 06 p0691 A73-17399
- Microwave oscillator subharmonic phase locking, discussing nonlinear capacitance and linear frequency-dependent parameter and broadband tuning characteristics comparison with fundamental injection locking 06 p0677 A73-18739
- Plasma sheath capacitance and resistance in double inverse pinch device from I-V measurements with Langmuir probe, noting relationship to plasma temperature and density 06 p0696 A73-18784
- Investigation of the influence of the emitter current on the collector junction capacitance of transistors 07 p0799 A73-19399
- Some experimental results for a capacitively loaded V antenna. 08 p0939 A73-21431
- Interference protection of regenerative parametric amplifiers. 09 p1061 A73-22042
- Threshold voltage of nonuniformly doped MOS structures. 09 p1064 A73-23046
- Analysis of parametron oscillation characteristics based on the collector-junction capacitance of the transistor. 10 p1193 A73-23666
- Active RC filter synthesis with decoupling stage and third order element for minimizing impedance mismatching and overall capacitance 10 p1193 A73-23734
- Effect of the nonlinearity of the junction capacitance on the spectral characteristics of the current of a tunnel diode. 10 p1197 A73-24939
- Cardiac membrane capacitance physiological properties and measurements in Purkinje fibers, ventricular and atrial muscles and heart tissues 11 p1316 A73-25596
- Analysis of commutator inverters with allowance for capacitive coupling to an ac amplifier 13 p1591 A73-28854
- Influence of the parasitic capacitance of a field effect transistor and of the input capacitance of the amplifier on the null shift of a modulator 13 p1591 A73-28856
- Effect of the input capacitance of an ac amplifier on the performance of key modulators 13 p1592 A73-28874
- Approximate procedure for synthesis of interdigital bandpass filters with lumped capacitance loaded bar ends, deriving transmission response from Kirchhoff nodal law 16 p1986 A73-32911
- Convergence of periodic solutions of differential equations for resonance circuits with nonlinear semiconductor capacitance 17 p2144 A73-34585
- Absolute calibration of antennas at extremely low frequencies. 17 p2128 A73-35686
- Method for plotting frequency cutoff measurements for GaAs varactor diodes. 18 p2292 A73-36596
- Capacitance of a field-effect MOS transistor gate 18 p2293 A73-36721
- A study of the effect of the emitter current on the barrier capacitance of a transistor collector junction. II 20 p2536 A73-39395
- Theory of successive electron transfer steps in cyclic voltammetry Application to oxygen pseudocapacitance on platinum. 21 p2636 A73-40843
- Ion-implanted varicaps with a steep capacitance-voltage characteristic 21 p2664 A73-41096

Diffusion profile measurements in the base of a microwave transistor. 21 p2668 A73-41560

A low-temperature, glass-ceramic capacitance thermometer. 22 p2856 A73-42020

The design of digital fluidic components and systems - A review. 23 p2945 A73-43433

Two-loop frequency multipliers employing the barrier capacitance of a p-n junction and exhibiting maximum energetic indices 24 p3071 A73-44592

Experimental study of the dynamic parameters of varactor diodes 24 p3072 A73-44929

Analysis of a frequency-modulated tunnel-diode oscillator. 24 p3072 A73-44941

Experimental investigation of the low-frequency capacitive response of a plasma sheath. 24 p3117 A73-45408

Effects of stress on metal-oxide-semiconductor structures. 24 p3120 A73-45415

CAPACITANCE SWITCHES

Coaxial gas discharge tubes for pulsed lasers 01 p0059 A73-10796

CAPACITORS

Low pass Butterworth and Chebyshev filters design with Sallen-Key network for fabrication of microelectronic circuits 01 p0024 A73-10682

Nonlinear radio-frequency response of a non-uniform plasma slab-condenser system with realistic density and velocity profiles. 04 p0479 A73-15189

Inductance and magnetic reversal losses in pulse operated communication, describing bridge circuit for comparing test sample current with capacitor voltage/time characteristics 05 p0559 A73-17241

Reliability tests on miniature ceramic capacitors encapsulated by epoxy-novolac block polymer compounds 06 p0677 A73-18398

Failure causes probability and accelerated life test conditions for ceramic capacitors, noting product selection by modified quality control procedures 07 p0799 A73-19405

Tantalum thin film capacitors fabrication procedure for hybrid ICs, presenting temperature and frequency responses and I-V characteristics of test samples 07 p0801 A73-19535

Fabrication, electrical properties and reliability of thin film capacitors, noting surface irregularity and impurity effects on reliability 08 p0946 A73-21082

Numerical calculation of low-frequency capacitance/voltage curves of M.O.S. capacitors with nonconstant doping profiles. 08 p0947 A73-21122

Bulk lifetime determination from current and capacitance transient response of MOS capacitors. 09 p1062 A73-22307

Electrical properties of MOS capacitors with oxide grown in the presence of HCl. 09 p1062 A73-22308

Dynamic operating regime of multistage diode-capacitor storage networks 09 p1063 A73-22459

High voltage phase meter with electrostatic logometer for loss angle measurements in capacitors and power cables during operation 12 p1495 A73-26790

Influence of gate metal on gamma-ray induced defects in MOS structures. 13 p1589 A73-28421

Thermal IR radiation receiver with ferroelectric capacitor for amplification and transformation of signals from RF oscillator 13 p1618 A73-29133

Thermal expansion compatibility of ceramic chip capacitors mounted on alumina substrates. 16 p1989 A73-33472

Binary capacitors made with p-channel MOS Si gate technology, discussing threshold voltage effects, structural characteristics, bootstrapping and artificial voltage enhancement 16 p1991 A73-33962

Precise and rapid measurements of small currents from high impedance sources. 17 p2143 A73-35775

Solid tantalum capacitor failure modes, discussing slug impurities, dielectric imperfections, short circuits, scintillation shorts, anodizing, soldering, screening methods and cost reduction 19 p2410 A73-38443

Powder geometry and structural design of the high volumetric efficiency tantalum electrolytic capacitor. 21 p2663 A73-40770

Thin film capacitor with anodic tantalum oxide overlaid with silicon dioxide deposited by RF sputter-

ing, noting reliability under various voltage, temperature and humidity conditions 21 p2663 A73-40771

Electrical design requirements for electrolytic capacitors used in regulated low voltage DC power supplies. 21 p2663 A73-40772

A bilevel thin film hybrid circuit containing cross-overs, resistors, capacitors, and integrated circuits. 21 p2669 A73-40773

Use of two-stage condenser braking of the single-motor drive for the mirror sections of the RATAN-600 radio telescope 21 p2675 A73-41450

A new type of charge trapping in MOS systems. 22 p2896 A73-42275

Dipole antenna with variable capacitance diodes for wideband tuning, calculating and measuring input impedance frequency response 23 p2960 A73-44110

CAPACITY

Airport or ATC system hourly landing and takeoff capacity concept in terms of hourly demand as function of mean waiting time 15 p1960 A73-32552

CAPE KENNEDY LAUNCH COMPLEX

Electric field intensity of the lightning return stroke. 17 p2163 A73-35464

Kennedy Space Center Space Shuttle facilities. 19 p2417 A73-37601

CAPILLARIES [ANATOMY]

A criterion for oxygen supply optimality in tissues and the capillary circulation rate 03 p0268 A73-13821

Symposium on Capillary Exchange and the Interstitial Space, Bad Duerkheim, West Germany, May 3-6, 1972, Proceedings. 03 p0265 A73-14649

Intravascular platelet aggregation in the heart induced by stress. 08 p0933 A73-21805

Influence of histamine on cutaneous capillary circulation and on the oxygen tension of subcutaneous cellular tissue in various age periods 10 p1178 A73-23676

Morphometry of the human pulmonary arterial tree. 21 p2638 A73-40639

Model experiments on apparent blood viscosity and hematocrit in pulmonary alveoli. 24 p3064 A73-45064

CAPILLARY CIRCULATION

U CAPILLARY FLOW

CAPILLARY FLOW

Radiation and conductivity of a high current constricted discharge plasma. 01 p0081 A73-10119

Heat and mass transfer theory and applications in aerothermooptics, thermoconvective and ferromagnetic fluid studies, chemical engineering, capillary transport and heat pipes 01 p0029 A73-10624

Discharge of a capillary fluid from under a rectilinear shield 06 p0686 A73-18070

Significance of the Bohr and Haldane effects in the pulmonary capillary. 08 p0935 A73-21614

Navier-Stokes equation solution for steady state, tandem and Rankine capillary viscometer precision measurements, including compressibility correction 11 p1361 A73-25367

Analysis of external mass transfer and choice of its parameters for convective removal of reaction-product vapors in a hydrogen-oxygen fuel cell with a capillary membrane 11 p1308 A73-25727

Nonlinear behavior of capillary liquid jets ejected from nonsymmetric nozzles, showing effect on flow stability 11 p1349 A73-26432

Effects of tilting on pulmonary capillary blood flow in normal man. 20 p2519 A73-39786

Concerning the stability of the triple-phase boundary in gas-diffusion electrodes of fuel cells. 21 p2636 A73-41320

Capillary breakup length and stability of Newtonian and viscoelastic cylindrical liquid jets in terms of dimensionless viscosity and relaxation time 23 p2967 A73-43307

Determination of the equilibrium state of a capillary liquid in a vessel 24 p3080 A73-45526

CAPILLARY TUBES

Arterial wick heat pipes self filling capability theoretical and experimental investigation, deriving expressions for mesh size, artery radius and stem height relationships 04 p0518 A73-15819

Properties of electrocapillary transducers and possibilities of their application in vibration measurements 07 p0826 A73-20530

Laminar steady state flow resistor design featuring temperature independence achieved with flattened core capillary tube 20 p2511 A73-39754

Deformation of molten glass in the zone where a hollow glass fiber is formed 24 p3102 A73-44520

CAPILLARY WAVES

NT BAROCLINIC WAVES

NT GRAVITY WAVES

An existence proof for permanent capillary gravity waves with general vortex distributions 11 p1349 A73-26747

Steady induced capillary-gravitational finite-amplitude waves on the surface of a finite-depth liquid 15 p1865 A73-32116

Optical wave measurement technique and experimental comparison with conventional wave height probes. 19 p2458 A73-37263

Capillarity induced stresses effects on dislocations generation during early stage sintering, predicting plastic flow via modified Hirth method of surface nucleation 20 p2576 A73-39221

Second-harmonic resonance in the interaction of an air stream with capillary-gravity waves. 20 p2550 A73-39816

CAPSULES

Steady flow of neutrally buoyant flat-faced rigid cylindrical capsules along pipeline under hydraulic pressure gradient effect, noting toroidal vortices 03 p0293 A73-13528

CAPTIVE TESTS

NT STATIC FIRING

NT STATIC TESTS

CAPTURE CROSS SECTIONS

U ABSORPTION CROSS SECTIONS

CAPTURE EFFECT

Solar neutrino detection methods, capture cross sections, model construction and results 01 p0091 A73-10053

Changes in the gravitational energy of galaxies during collisions. 02 p0217 A73-12392

Charge carriers concentration growth and decay for semiconductor model with independent capture centers, determining capture level activation energy 07 p0861 A73-19328

Cosmic ray exposure ages from Apollo 14 lunar rocks isotopic anomalies due to neutron capture effect in Gd, Br and Ba 07 p0871 A73-19803

Capture of primary cosmic rays in the upper atmosphere as a source of excess radiation 10 p1268 A73-23931

Nuclear laser realizability for gamma quanta production from population inversion during radiative capture of neutrons, considering constraints imposed on heating of active medium 10 p1229 A73-24754

Ring laser output calculation in the region of capture 12 p1504 A73-26885

Calculation of the nonlinear polarizability of a gas at a lasing transition with allowance for capture of resonance emission 14 p1757 A73-30367

Lunar origin dynamics, discussing earth-moon tidal evolution, capture probability, fragmentary collisions, precession and auxiliary models 14 p1800 A73-30550

Recent advances of celestial mechanics in the Soviet Union. 15 p1932 A73-31303

Evidence for objects of lunar mass in the early solar system and for capture as a general process for the origin of satellites. 17 p2228 A73-34415

On the origin of short-period comets. 17 p2234 A73-35620

MIS structures with reversible charge capture capability, discussing I-V characteristics and applications similar to FET, image storage and charge coupled devices 20 p2534 A73-38853

Low energy gamma ray spectrum following muon capture by oxygen 16 leading to bound states of nitrogen 16 21 p2743 A73-40475

CARBAMATES [TRADENAME]

NT URETHANES

CARBIDES

NT ALUMINUM CARBIDES

NT BORON CARBIDES

NT CEMENTITE

NT CHROMIUM CARBIDES

NT HAFNIUM CARBIDES

NT MOLYBDENUM CARBIDES

NT NIOBIUM CARBIDES

NT SILICON CARBIDES

NT TANTALUM CARBIDES

NT TITANIUM CARBIDES

NT TUNGSTEN CARBIDES

NT VANADIUM CARBIDES

NT ZIRCONIUM CARBIDES

Formation of carbides in 3% chromium steel after additional alloying 01 p0062 A73-10265

Cast Nb alloys ductility enhancement by heat treatment, discussing solid solution decay kinetics and carbides composition of Nb-Mo-Zr-C system 01 p0066 A73-11344

Cr, Ti, Ce, V and Nb carbide-forming additives effects on crystal dislocations growth and movement during strain hardening of Mn rich steel 01 p0066 A73-11345

Carbide hardening of chromium-molybdenum-vanadium steel. 03 p0327 A73-14005

A new criterion for predicting rolling-element fatigue lives of through-hardened steels. [ASME PAPER 72-LUB-32] 03 p0328 A73-14342

Concentration dependence of the hardness of non-stoichiometric group IV and V transition metal carbides 06 p0710 A73-18658

Distribution of methane and carbide in Apollo 11 fines. 07 p0900 A73-20188

Investigation of partially dissolved secondary-phase precipitates in a molybdenum-based alloy 09 p1098 A73-21849

Phase composition of Nb-1% Zr-C and Nb-2% Hf-C alloys 09 p1108 A73-23237

Temperature dependent heat conductivity, Lorentz number and electrical resistivity of high melting Ti, Zr, Nb, Cr, Mo and W carbides and borides at 300-1200 K 10 p1230 A73-23519

Carbon content relationship to rhénium microhardness, determining cast specimens phase composition by X ray analysis and microstructure observations 10 p1234 A73-24424

Obtaining of carbide and nitride dispersions in iron 13 p1633 A73-28182

Effects of some carbide stabilizing elements on creep-rupture strength and microstructural changes of 18-10 austenitic steel. 14 p1761 A73-30627

The wetting of carbon and carbides by copper alloys. 15 p1897 A73-31837

Variation with temperature of free enthalpy of formation of certain carbides 15 p1898 A73-32644

Temperature dependent heat conductivity, Lorentz number and electrical resistivity of high melting Ti, Zr, Nb, Cr, Mo and W carbides and borides at 300-1200 K 17 p2191 A73-35199

Formation of carbides during tempering of complexly alloyed chromium steel 18 p2324 A73-36770

Observations on the directional solidification of cobalt-base alloys strengthened by carbide fibres. 19 p2443 A73-38249

Lattice constants vs compositions of body centered tetragonal solid solutions of mixed rare earth dicarbides according to Vegard law 21 p2751 A73-40322

Formation of lunar carbide from lunar iron silicates. 21 p2780 A73-41643

Structure of the phase diagrams of the ternary systems /Mo, W/ - /Ti, Zr, Hf, V, Nb, Ta/ - C 22 p2877 A73-42455

Interaction of molybdenum with cobalt and carbon 22 p2877 A73-42460

The mechanism of electrical erosion in composite materials during electric arc alloying 24 p3093 A73-44743

Influence of boron on the precipitation of carbides in Fe-Ni-Cr austenitic matrices 24 p3101 A73-45523

CARBOHYDRATE METABOLISM

NT HYPOGLYCEMIA

Evolutionary significance of carbohydrate metabolism alterations in animal brains during adaptation to hypoxia 01 p0007 A73-10153

Diet, exercise, and glycogen changes in human muscle fibers. 01 p0007 A73-10160

Arterial oxygen increase by high-carbohydrate diet at altitude. 01 p0007 A73-10164

Brain serotonin content - Physiological regulation by plasma neutral amino acids. 01 p0008 A73-10408

Effects of hypoxemia and acute coronary occlusion on myocardial metabolism in dogs. 05 p0538 A73-16154

Studies on acid production during carbohydrate metabolism by extremely halophilic bacteria. 07 p0780 A73-19500

Effect of low temperature on metabolism of rat liver slices and epididymal fat pads. 07 p0782 A73-20170

Effect of excessive glucose administration on the lipid level, glycolysis rates, and oxygen uptake in the tissues of the liver, heart, cerebrum and aorta 11 p1314 A73-25042

Apparent paradoxical patterns of anaerobic glycolysis and hexokinase activity in the red blood cells of acutely bled rats, with evidence that the responses were in part hormone-dependent. 11 p1315 A73-25568

Adrenal influence on the supercompensation of cardiac glycogen following exercise. 11 p1318 A73-26121

Serum tryptophan level after carbohydrate ingestion - Selective decline in non-albumin-bound tryptophan coincident with reduction in serum free fatty acids. 12 p1464 A73-27975

Energy supply in acute cold-exposed dogs. 18 p2278 A73-36655

Glycolytic intermediates and adenosine phosphates in rat liver at high altitude /3,800 m/. 20 p2514 A73-39602

Studies on the metabolism of glucose-1,6-diphosphate in human erythrocytes. 21 p2639 A73-41139

Serum tryptophan level after carbohydrate ingestion - Selective decline in non-albumin-bound tryptophan coincident with reduction in serum free fatty acids. 21 p2640 A73-41218

The significance of an increased RQ after sucrose ingestion during prolonged aerobic exercise. 21 p2641 A73-41621

Plasma insulin and carbohydrate metabolism after sucrose ingestion during rest and prolonged aerobic exercise. 21 p2641 A73-41622

Changes in indices of the carbohydrate and fat metabolism, the state of the sympathoadrenal system, and oxidative processes under varying-intensity cold effects 24 p3059 A73-44671

Lactate origins and renewal in blood plasma, considering metabolism, enzymatic resynthesis and final excretion in urine 24 p3061 A73-45157

Diurnal variations of plasma cortisol and glucose and of urinary excretion of free cortisol in man at rest 24 p3061 A73-45158

CARBOHYDRATES

NT ADENOSINE DIPHOSPHATE [ADP]

NT ADENOSINE TRIPHOSPHATE [ATP]

NT ADENOSINES

NT CELLULOSE

NT CHOLINE

NT DEXTRANS

NT GLUCOSE

NT GLUCOSIDES

NT GLYCOGENS

NT HEXOKINASE

NT INOSITOLS

NT NUCLEOSIDES

NT STARCHES

NT SUCROSE

NT SUGARS

Gas-liquid chromatography of trifluoroacetyl derivatives of cyclitols. 11 p1325 A73-25150

Homogeneously catalyzed formaldehyde condensation to carbohydrates. II - Instabilities and Cannizzaro effects. 15 p1841 A73-32200

CARBON

NT CARBON ISOTOPES

NT CARBON 12

NT CARBON 13

NT CARBON 14

Adsorption equilibria at high pressures in the helium-nitrogen-activated carbon system. 01 p0014 A73-10725

C and Re effects on brittleness threshold temperature and plasticity of Mo-Re alloy 01 p0066 A73-11342

The effect of crystallite size on the strength of carbon-graphite materials. 02 p0185 A73-12142

Carbon and pyrolytic graphite isothermal chemical vapor deposited /CVD/ composite coated and free standing products fluid bed manufacturing and applications 03 p0333 A73-13053

Nitrogen-containing active carbon as the cathode catalyst in acid fuel cells. 04 p0407 A73-15107

Study of the diffusion of carbon in structural steel plates clad with stainless steels 04 p0467 A73-15951

Pyrolysis of kerosene and mechanism of formation of carbon deposits 04 p0485 A73-15989

[ONERA, TP NO. 1157] Carbon replicas for fracture failure electron fractography by two stage Lucite technique 05 p0586 A73-16134

Enrichment of heavy nuclei in the 17 April 1972 solar flare. 05 p0609 A73-16571

Carbon and graphite sublimation in inert gas flow at 2800-3000 K, determining rate dependence on temperature under kinetic and diffusive conditions 06 p0713 A73-17411

Solar wind, meteoritic, and cometary carbon sources for moon, discussing lunar atmospheric steady state carbon component sustained by meteoritic and cometary carbon vaporization

06 p0754 A73-18427

Lunar carbon chemistry - Relations to and implications for terrestrial organic geochemistry.

06 p0662 A73-18429

The effect of carbon on the hot corrosion of cobalt-base alloys.

07 p0838 A73-19498

Successive diffusion in a ternary system of the iron-metal-carbon type

07 p0841 A73-20520

Linear series of stellar models. II - Pure carbon stars.

08 p1002 A73-20847

Equatorial coordinates and photographic magnitudes for new carbon stars in Northern Milky Way, noting classification by spectral discontinuity

08 p1005 A73-20916

The effect of carbon and oxygen on the brittleness characteristics of molybdenum

08 p0978 A73-21417

Problem of the selective mechanism for the excitation of the C III 5696-A line in the spectra of certain stars. I

08 p1012 A73-21549

UHV outgassing measurements on various carbons.

08 p0937 A73-21621

Investigation of carbon- and manganese-diffusion processes in the metal-ceramic steel G13M

09 p1103 A73-22466

Temperature range of maximum aging of Mo-Re-C alloys after quenching and tempering, noting carbon solubility effects due to Re content

09 p1106 A73-23187

Effect of carbon on the fine structure of cast molybdenum

09 p1108 A73-23232

Influence of the combined effect of plastic deformation and high temperatures on the diffusion mobility of carbon

09 p1108 A73-23241

Electron microscopy study of Nb3Sn strips

10 p1259 A73-23674

Noble gas and carbon abundances of the Haverro, Dingo Pup Donga, and North Haig ureilites.

10 p1277 A73-24104

The effect of carbon and titanium on the hot workability of 25Cr-6Ni stainless steels.

10 p1235 A73-24440

Temperature dependence of the activity and solubility of carbon in pure nickel

11 p1384 A73-26110

Interaction of molybdenum with elements of the iron group and carbon

12 p1510 A73-26903

A quantum model for bending vibrations and thermodynamic properties of C3.

12 p1526 A73-27019

Nuclear reactions in carbon stars.

13 p1672 A73-28038

Radiative transfer through carbon ablation layers.

13 p1705 A73-28457

An empirical function between the resistance and the temperature of a carbon thermometer for 0.3 to 4.2 K.

13 p1618 A73-29071

Diffraction spectra and electron density distributions of interatomic graphitizing carbon molecule bonds as polymer combinations, using diffractometer and scintillation counter recording

14 p1767 A73-30839

Scanner observations of hot helium-carbon stars.

15 p1932 A73-31269

Mo-W-C phase equilibria study at 1000 C, obtaining isothermal cross sections for various carbon contents from X ray and microstructural analysis

15 p1888 A73-31598

Dynamic mechanical properties of graphite-epoxy and carbon-epoxy composites.

15 p1897 A73-31677

The wetting of carbon and carbides by copper alloys.

15 p1897 A73-31837

Calculation of the composition of 79% N2 + 21% O2 and 50% N2 + 50% O2 mixtures containing carbon at high temperatures

15 p1840 A73-31853

The interaction of gases and carbon with refractory metals

15 p1890 A73-31925

A proposed correction to the solar abundances of carbon and oxygen utilizing new and accurate theoretical forbidden transition probabilities.

16 p2060 A73-32952

Synthetic foam from Pyrrone prepolymer and hollow carbon microsphere mixtures, discussing low curing shrinkage and high thermal stability

16 p2029 A73-33051

Investigation of molybdenum-rich Mo-Ni-C, Mo-Ni-Zr, and Mo-Zr-Ni-C alloys

17 p2188 A73-34569

Effect of group VIII elements on the temperature of plastic-to-brittle transition of states in molybdenum-carbon alloys

17 p2189 A73-34576

Effect of carbon on the structure and properties of molybdenum

17 p2189 A73-34582

High temperature thermal cavity system with vitreous carbon tube and end plugs for material and thermochemical environment investigations, discussing mass spectroscopic measurement

17 p2149 A73-35752

Assessment of chemical nonequilibrium for massively ablating graphite.

18 p2368 A73-36322

New thermodynamic functions for the C3 molecule.

18 p2287 A73-36326

Investigation of failure of a fiberglass plastic due to differential carbon burnup

18 p2328 A73-36813

Small angle X ray scattering study of submicroscopic voids in glassy carbon, using two density theory

19 p2444 A73-38091

The effect of carbon on the sulphidation of Co-Cr alloys.

19 p2443 A73-38250

Determination of the proneness of aviation oils to carbon deposition

19 p2472 A73-38491

Carbon deposition and the role of reducing agents in hot-corrosion processes.

20 p2576 A73-39027

Influence of alloying with elements of group VIII on the mechanical properties of a molybdenum alloy containing carbon in the cast and recrystallized states

20 p2577 A73-39366

A study of the extraction of oxygen from molybdenum by dissolving it in metallic carbon-containing melts in a vacuum

21 p2717 A73-40479

Thermodynamics of the Al-O and Al-O-C systems

21 p2718 A73-40847

Mixed particle sizes in fast carbon thermometry.

22 p2854 A73-41997

Thermal conductivity of low density carbon.

[ECTP PAPER C-5]

22 p2881 A73-42404

Phase diagrams of ruthenium and rhodium systems with carbon

22 p2878 A73-42461

The influence of carbon on the interdiffusion of Mo and Ni.

22 p2878 A73-42579

Electrical control of particulate pollutants from flames.

22 p2935 A73-42799

Carbon particles size distribution and charged fraction in acetylene-oxygen flame using molecular beam system and electron microscopy, noting particle interaction formation mechanism

22 p2936 A73-42801

Measurement of the effective cross section of inelastic interaction between protons and carbon nuclei in the energy range 0.1 TeV to 1.0 TeV, on the Proton-4 space station

23 p3021 A73-43539

Electron temperature of regions of the formation of recombinational continua on the sun - Temperature of the carbon emission regions

23 p3036 A73-44246

Influence of temperature on the behavior of the rheological properties of plastic carbon-black systems

24 p3101 A73-44471

CARBON COMPOUNDS

NT ALUMINUM CARBIDES

NT ARAGONITE

NT BORON CARBIDES

NT CALCITE

NT CARBIDES

NT CARBONATES

NT CEMENTITE

NT CHROMIUM CARBIDES

NT HAFNIUM CARBIDES

NT MOLYBDENUM CARBIDES

NT NIOBIUM CARBIDES

NT POLYCARBONATES

NT SIDERITES

NT SILICON CARBIDES

NT SODIUM CARBONATES

NT TANTALUM CARBIDES

NT TITANIUM CARBIDES

NT TUNGSTEN CARBIDES

NT VANADIUM CARBIDES

NT ZIRCONIUM CARBIDES

Survey of lunar carbon compounds. II - The carbon chemistry of Apollo 11, 12, 14, and 15 samples.

07 p0890 A73-19818

Compounds of carbon and other volatile elements in Apollo 14 and 15 samples.

07 p0891 A73-19822

Laboratory simulation of organic geochemical processes.

11 p1325 A73-25460

Luna 16 and 20 sample carbon chemistry analysis for volatilizable species by vacuum pyrolysis and mass spectrometry

13 p1580 A73-28333

Far infrared and Raman spectra of gaseous carbon suboxide and the potential function for the low frequency bending mode.

21 p2740 A73-40935

CARBON DIOXIDE

Dry oxidation of nickel by anhydrous carbon dioxide under pressure

01 p0062 A73-10271

Line-by-line computations of transmittance for non-homogeneous paths in designing application-oriented representations for water vapor and carbon dioxide channels IR spectral responses

01 p0037 A73-10365

Atmospheric radiative transfer by carbon dioxide.

01 p0037 A73-10366

Ionization cross sections for H2, N2, and CO2 clusters by electron impact.

01 p0080 A73-10563

Vibrational relaxation in CO2 with selected collision partners. I - H2O and D2O.

01 p0080 A73-10775

Analytical model potential function application to Ar, Kr, Xe, nitrogen, methane and carbon dioxide, applying to different properties

01 p0122 A73-10850

CO2 plasma emissivity at temperatures from 7000 to 9000 K in the spectral range of 2100 to 10,000 Å

01 p0085 A73-10854

Relation of the equation of state of compressed gases with the optical complex and the specific refraction - Virial coefficients of carbon dioxide

01 p0080 A73-10856

Pressure and temperature effects on carbon dioxide extinction coefficients, tabulating absorption cross sections

02 p0191 A73-11758

Carbon dioxide turbulent flow heat transfer in single phase near-critical region under forced and free convection

03 p0396 A73-13185

Molecular beam simulation of planetary atmospheric entry - Some recent results.

03 p0287 A73-13564

Foreign gas collision broadening effects on 15 micron carbon dioxide bands radiation absorption lines

03 p0345 A73-13697

Shock-tube study of vibrational energy transfers in the CO2-N2 and the CO2-CO systems.

03 p0345 A73-14442

Experimental investigation of the evaporation rate of water droplets in atmospheres of air and carbon dioxide under conditions of a thermostatic droplet surface

04 p0517 A73-14881

Tangential slot injection of carbon dioxide and helium into a supersonic air stream.

[ASME PAPER 72-WA/FE-37]

04 p0435 A73-15854

Martian topography from radar observations and the Mariner 6 and 7 and ground-based CO2 measurements.

04 p0503 A73-16016

Oxygen 1S production efficiency of photons at 812-1216 Å measured by O I 577 Å green line detection during carbon dioxide photodissociation

05 p0546 A73-16049

The runaway Greenhouse in the Venus atmosphere.

05 p0622 A73-17124

Experimental investigation of worsened heat-transfer conditions with the turbulent flow of carbon dioxide at supercritical pressure.

06 p0766 A73-17410

Venus high resolution spectra for carbon dioxide abundance variations, discussing CO, HF and HCl composition

06 p0744 A73-17435

Shock tube investigation of bromine dissociation rates in the presence of carbon dioxide.

06 p0661 A73-18123

Stability CO2 in the Martian atmosphere and under radiolysis.

07 p0899 A73-20155

On calculating the radiation from two plane isothermal layers of carbon dioxide and/or water vapor.

08 p1021 A73-20859

Reaction of graphite with carbon dioxide at temperatures from 1200 to 2400 C

08 p0982 A73-21095

Ground based spectroscopic observation of carbon dioxide distribution on Mars surface, noting Tharsis region pressure anomaly, ridge slope and dust storm activity

09 p1144 A73-22262

Plasma excitation by HF field in carbon dioxide-argon flow under low pressure, noting disappearance of striations

10 p1253 A73-24072

Doppler broadening of OI 1304 Å multiplet in dissociative excitation of CO2 and O2.

10 p1251 A73-24243

Electron-optical investigations of discharge in air and carbon dioxide in the nanosecond range
10 p1219 A73-24469

Venus - Microwave opacity of the minor atmospheric constituents.
11 p1417 A73-25267

Southern Hemisphere troposphere atmospheric carbon dioxide monitoring program based on aircraft air sampling, discussing vertical profile data
11 p1358 A73-26472

The planet Venus - A new periodic spectrum variable.
11 p1428 A73-26621

Carbon dioxide thermodynamic and transport characteristics calculation, treating gas as multicomponent ideal mixture including carbon monoxide and oxygen and carbon atoms and ions
12 p1526 A73-27308

The radiative capacity of a CO₂ plasma at temperatures 7000-9000 K in the spectral interval 2100-10,000 Å.
12 p1529 A73-27904

Connection between the equation of state of compressed gases with an optical complex and the specific refraction - The virial coefficients of carbon dioxide.
12 p1526 A73-27906

Preliminary results of the determination of altitudes on Mars from CO₂-micron wavelength bands aboard the Mars 3 interplanetary automatic station
13 p1673 A73-28288

Venus atmospheric model based on spectroscopic evidence of carbon dioxide spectral lines phase variation due to two scattering layers
13 p1680 A73-28459

Relaxation of the bending vibration of CO₂ in pure CO₂ and in mixtures of CO₂ with noble gases.
13 p1662 A73-28553

Al filament ignition temperature in carbon dioxide flow at various current values, noting relation to surface oxide film melting temperature
14 p1764 A73-30872

Empirical intermolecular potentials for N₂ and CO₂ from crystal data.
15 p1915 A73-31272

Fluorescent cross sections and yields of CO₂+/ from threshold to 185 Å.
15 p1915 A73-31274

Isotope separation factor of carbon dioxide-water system and isotopic composition of atmospheric oxygen.
15 p1873 A73-32252

Optical study of charge exchange collisions between He⁺ and CO₂.
16 p2039 A73-33675

Photoinduced fixation of CO₂ by amino acids - Implications for nonbiological reactions on the Martian soil.
16 p1977 A73-33874

Investigation of the dynamic modulus of polymethyl methacrylate saturated by carbon dioxide
16 p2031 A73-33943

Dissociation of carbon dioxide behind reflected shock waves.
17 p2119 A73-35173

Results of an experimental investigation of local heat transfer at supercritical pressure in a rectangular channel heated from one side.
17 p2255 A73-35190

Fluorescence excitation and photoelectron spectra of CO₂ induced by vacuum ultraviolet radiation between 185 and 716 angstroms.
18 p2346 A73-36266

Martian polar stacked laminae interpreted in terms of conditions for carbon dioxide liquefaction, considering atmospheric history
19 p2478 A73-37217

Theoretical assignments of the low-lying electronic states of carbon dioxide.
19 p2462 A73-37583

Adsorption of spacecraft contaminants on Bosch carbon.
[ASME PAPER 73-ENAS-15] 19 p2399 A73-37972

Heat release by free convection from horizontal cylinders to CO₂ under near-critical conditions
20 p2628 A73-39613

Drift tube and mass spectrometric measurement of molecular positive ion drift velocities in carbon dioxide
21 p2742 A73-40221

Condensation in CO₂ free jet expansions. I - Dimer formation.
21 p2743 A73-40937

Condensation in CO₂ free jet expansions. II - Growth of small clusters.
21 p2743 A73-40938

Preliminary results of Martian altitude determinations with CO₂ bands /2 micron wavelength/ from the automatic interplanetary space station Mars 3.
22 p2905 A73-41807

Excitation of the CO fourth positive system by the dissociative recombination of CO₂⁺/ions.
22 p2843 A73-41904

A new determination of the second virial coefficient of carbon dioxide at temperatures between 0 and 150 C, and an evaluation of its reliability.
22 p2932 A73-42507

Line intensities of CO₂ in the 2.0 micron region.
22 p2890 A73-42708

Venus carbon dioxide production kinetics involving quartz reaction with calcite to form wollastonite and carbon dioxide
24 p3133 A73-44540

Vibrational relaxation of CO₂/nu sub 3/ by ozone.
24 p3066 A73-44988

An expanded theoretical interpretation of the Venus 1.05-micron CO₂ line and the Venus 0.8226-micron H₂O line.
24 p3139 A73-45052

Air-hydrogen-carbon fuel mixtures chemical composition determination by measuring carbon dioxide and moisture content of combustion products, presenting nomogram
24 p3157 A73-45378

CARBON DIOXIDE CONCENTRATION
The role of the vagus nerves in the respiratory response to CO₂ under hyperoxic conditions.
01 p0010 A73-11501

The investigation of the effect of acoustic oscillations on the combustion process of gaseous fuel
03 p0396 A73-12955

Quantitative estimation of the gas metabolism of continuous higher plant cultures as a life support system component
06 p0656 A73-17680

The influence of age, sex, body size and lung size on the control and pattern of breathing during CO₂ inhalation in Caucasians.
06 p0654 A73-18337

Carbon dioxide concentration, pH and nutrient concentration effects on blue-green algae relative abundance to green algae in lakes
06 p0655 A73-18577

Changes in microvascular diameter and oxygen tension induced by carbon dioxide.
11 p1317 A73-26116

Effect of acute exposure to CO₂ on lung mechanics in normal man.
11 p1318 A73-26216

Comparison of blood and alveolar gas composition during rebreathing in the dog lung.
11 p1318 A73-26218

Studies of alveolar-mixed venous CO₂ and O₂ gradients in the rebreathing dog lung.
11 p1318 A73-26219

Changes in the gas content of blood in man during exposure to high ambient temperatures
12 p1463 A73-27711

Use of fluidic and pneumatic elements to determine the composition of a gas mixture
16 p1970 A73-33025

Pulmonary volume, respiration rate and alveolar air carbon dioxide content measurements in pilots during flight, noting hyperventilation occurrence
19 p2392 A73-37197

Ultraviolet observations of Mars made by the Orbiting Astronomical Observatory.
24 p3128 A73-44397

Rebreathing equilibration of CO₂ during exercise.
24 p3060 A73-45068

CARBON DIOXIDE LASERS
An optical bridge for the assessment of mode-locked CO₂ lasers.
01 p0058 A73-10471

Q-switching of a CO₂ laser with the aid of an active gas cell
02 p0175 A73-11617

Double discharge TEA carbon dioxide laser trigger circuit, using plastic materials with selected dielectric constant and resistivity for trigger current increase
02 p0175 A73-11958

Gain distribution in a CO₂ TEA laser.
02 p0177 A73-12434

Dynamics of the CO₂ atmospheric pressure laser with transverse pulse excitation.
[AD-760231] 02 p0177 A73-12435

Space discharge instability in carbon dioxide laser pumping by ionization source and electric field for time difference in heat removal and gas heating
02 p0177 A73-12553

Performance characteristics of a helical TEA CO₂ laser.
02 p0177 A73-12745

Mode-locked high-pressure waveguide CO₂ laser.
02 p0178 A73-12748

High power carbon dioxide electric discharge convection laser operation in closed cycle mode with combined dc and RF excitation and aerodynamic stabilization techniques
02 p0178 A73-12749

Cutting thin metal sheets with the CW CO₂ laser.
02 p0175 A73-12819

Relaxation of excess populations in the lower laser level CO₂/100/.
03 p0318 A73-13278

Carbon dioxide laser output signature calculation as function of cavity length based on homogeneously broadened line with dispersion
03 p0320 A73-14455

An experimental study of unstable confocal CO₂ resonators.
03 p0320 A73-14456

Chemical lasers population inversion mechanism and excitation energy comparison with other molecular gas lasers including carbon dioxide systems, considering efficiency
04 p0458 A73-14749

Proton beam effect on carbon dioxide laser discharge I-V characteristics and emission power
04 p0458 A73-15559

The role of CO in CO₂ lasers.
04 p0459 A73-16039

Q switched carbon dioxide laser based on PM by rotating mirror in one arm of Michelson interferometer, establishing phase relationships
05 p0583 A73-16062

Operational characteristics of a volume excited TEA CO₂ laser.
05 p0584 A73-16436

Atmospheric pressure CO₂ pulsed laser with semiconducting plastic electrodes.
05 p0585 A73-16567

CO₂ laser radiation absorption in SF₆-air boundary layers.
[AIAA PAPER 73-262] 05 p0585 A73-16983

High intensity CO₂ laser-plasma interaction.
05 p0603 A73-17224

Cutting and welding using a CO₂ laser.
05 p0582 A73-17264

Effects of contaminants in CO₂ lasers.
[AIAA PAPER 73-52] 06 p0699 A73-17628

Gain correlation with sidelight and plasma impedance properties of a CO₂ laser discharge.
06 p0700 A73-18137

Acoustic-optic modulator design for a high power mode-locked CO₂ laser.
06 p0700 A73-18291

Acousto-optical modulator for carbon dioxide lasers based on Bragg scattering concept, discussing design parameters and application to lidar system
06 p0700 A73-18295

CO₂ laser-induced gas breakdown in hydrogen.
06 p0701 A73-18355

Five temperature model of pumping and output power pulse shape predictions for carbon dioxide-nitrogen-helium TEA lasers
06 p0701 A73-18362

Observation of laser oscillation in a 1-atm CO₂-N₂-He laser pumped by an electrically heated plasma generated via photoionization.
[AD-759094] 06 p0703 A73-18649

Unstable resonators for CO₂ electric-discharge convection lasers.
06 p0703 A73-18747

An efficient electrical CO₂ laser using preionization by ultraviolet radiation.
06 p0704 A73-18797

Steady state dense arc plasma heating by inverse bremsstrahlung process with IR carbon dioxide laser, calculating maximum attainable temperature
07 p0857 A73-19531

Exothermic deuterium-fluorine chain reaction pumping of high pressure pulsed carbon dioxide chemical transfer laser
07 p0835 A73-19631

A kinetic model and computer simulation for a pulsed DF-CO₂ chemical transfer laser.
07 p0835 A73-19632

Comparison of theory and experiment for a transversely excited high-pressure CO₂ laser.
[AD-756053] 07 p0835 A73-19637

Intracavity breakdown in CO and CO₂ lasers.
07 p0835 A73-19638

Electron-beam-controlled CO₂ laser amplifiers.
07 p0835 A73-19639

Chemical laser device bibliography.
07 p0836 A73-19642

Comparative study of reflectivity measurements performed in the visible and infrared wavelengths.
07 p0824 A73-19945

A possible mechanism for the change in the discharge current in CO₂ through the action of laser radiation.
07 p0836 A73-20137

A reliable high efficiency atmospheric pressure CO₂ laser.
07 p0836 A73-20194

Interaction of TEA-CO₂-laser pulses with metals enhanced by liquid layers.
07 p0836 A73-20195

Severe self-induced beam distortion in laboratory simulated laser propagation at 10.6 microns.
08 p0974 A73-21031

Relaxation and pumping processes in thermally excited carbon dioxide lasers.
08 p0975 A73-21194

Photoinitiated transversely sustained CO₂ laser.
08 p0975 A73-21208

Frequency stabilization of a CO₂ or N₂O power laser by a fast sampling method 08 p0976 A73-21444

Submillimeter-band gas laser pumped by a CO₂ laser. 08 p0976 A73-21654

Change of vibrational temperature due to laser action in CO₂ lasers. 09 p1089 A73-21933

CO₂ laser induced Compton effect in underdense hydrogen plasma. 09 p1125 A73-22025

High energy and power carbon dioxide laser with nitrogen and He mixtures, transverse electric discharge excitation and modular construction, noting efficiency and gain 09 p1090 A73-22081

Directly excited subsonically flowing CW gas laser with carbon monoxide and dioxide generation as reaction products formed by organic molecule electrochemical oxidation 09 p1091 A73-22084

Optical breakdown of compressed gases by carbon dioxide laser emission 09 p1094 A73-22594

Luminescence of a molecular gas under the action of a carbon dioxide laser pulse 09 p1094 A73-22595

Lasing characteristics of flat resonator carbon dioxide-nitrogen-helium gasdynamic laser in terms of mirror reflection index, resonator length and gas pressure and composition 09 p1095 A73-22609

A high pressure gas-dynamic laser powered by a slow compression heater [ONERA, TP NO. 1184] 09 p1096 A73-22712

Sealed off 9.4 micron 15 W output power carbon dioxide laser with barium difluoride windows, noting long service life 09 p1096 A73-23009

Nanosecond pulse amplification in electron-beam-pumped CO₂ amplifiers. 09 p1097 A73-23336

Pulse amplitude modulation of a CO₂ laser in an electro-optic thin-film waveguide. 09 p1098 A73-23337

Performance of an unstable repetitive pulsed CO₂ laser oscillator. 09 p1098 A73-23338

Powerful nanosecond pulses by stable passive mode-locking of TEA CO₂ lasers. 09 p1098 A73-23340

Plasma self radiation and absorption, schlieren signals and lasing levels recording methods based on dioxide lasers, using Mach-Zehnder IR interferometer 10 p1253 A73-23517

Population inversion and radiation density in a Q-switched CO₂ laser 10 p1227 A73-23578

Transverse discharge pulsed CO₂ chemical transfer laser. 10 p1227 A73-23840

Space discharge instability in carbon dioxide laser pumping by ionization source and electric field for time difference in heat removal and gas heating 10 p1228 A73-24182

Heating of theta-pinch plasmas by pulsed CO₂ lasers. 10 p1256 A73-24527

Research and technology assessment of high power short wavelength molecular lasers, emphasizing carbon dioxide laser efficiency 10 p1229 A73-24654

Carbon dioxide laser active medium excitation by ionizing radiation from external source during electric current passage, discussing gain dependence on pressure and mixture 10 p1229 A73-24756

Optical waveguide structures for CO₂ lasers. 11 p1375 A73-25058

High speed welding of sheet steel with a CO₂ laser. 11 p1375 A73-26351

Performance characteristics of a TEA double-discharge grid amplifier. 12 p1505 A73-27015

Properties of a radial mode CO₂ laser. 12 p1505 A73-27016

Gain and saturation intensity measurements in a waveguide CO₂ laser. 12 p1505 A73-27017

Electron-beam ionized pulsed CO₂ laser 12 p1506 A73-27216

Ring cavity for analyzing the spectral composition of CO₂-laser radiation 12 p1506 A73-27217

Gasdynamic laser with a high water vapor content. 12 p1507 A73-27510

Separation of rotational lines of a CO₂ laser with a film selector in the resonator. 12 p1508 A73-27527

Quantum oscillations and pump depletion effects in an efficient high-power tunable spin-flip laser. 13 p1626 A73-28216

An absolute method of measuring energy outputs from CO₂ lasers. 13 p1626 A73-28369

CO₂ laser communication through an urban atmosphere. 13 p1582 A73-28481

Relaxation rates of lower laser levels in CO₂. 13 p1626 A73-28544

Kinetic cooling with CW carbon dioxide laser, observing time constant as function of atmospheric water pressure with three-beam interferometer 13 p1659 A73-28546

Characteristics of a high-pressure carbon dioxide laser with a transverse discharge 13 p1627 A73-28966

Relaxation processes in electrically excited discharge pumped gasdynamic lasers with supersonic gas mixture flow 13 p1627 A73-28967

Investigation of the inversion medium of a quasi-stationary CO₂ laser with 'pulsed' excitation 13 p1628 A73-29162

Heterodyne detection of frequency sweeping in the output of transverse-excitation CO₂ lasers. 13 p1628 A73-29186

Parametric studies on CO₂ TEA lasers with extracavity and intracavity electrodes. 13 p1628 A73-29187

Absorption saturation effects on high-power CO₂ laser beam transmission. 13 p1628 A73-29329

Measurement of the radius of curvature of a laser beam by an interferometric method. 13 p1629 A73-29442

Performance comparison of pulsed discharge and E-beam controlled CO₂ lasers. 14 p1756 A73-29918

Influence of CO on the population inversion in CO₂ lasers. 14 p1756 A73-29921

Focused high power CW carbon dioxide laser sustained Xe, Kr and Ar continuous plasmas, investigating plasma radiative properties by calorimetric techniques 14 p1779 A73-29922

Experiments on CO₂-laser heating of magnetically confined underdense plasmas. 14 p1780 A73-30123

High-pressure CO₂-N₂ laser excited by electric discharge controlled by means of electron beam. 14 p1757 A73-30260

Measurement of the temperature coefficient of the refractive index of infrared materials with the aid of a carbon dioxide laser 14 p1757 A73-30371

Investigation of the excitation of vibrational levels of the /N-14/H₃ molecule by carbon dioxide laser radiation 14 p1758 A73-30801

Rapid balancing of gyroscopes with TEA CO₂ laser. 15 p1883 A73-30996

The laser - A unique tool for /for the time being/ unique applications 15 p1884 A73-31325

Ignition and maintenance of a CW plasma in atmospheric-pressure air with CO₂ laser radiation. 15 p1884 A73-31398

Pulsed holographic interferometry at 10.6 microns. 15 p1875 A73-31400

Time-resolved gain of a volume-excited TEA CO₂ laser amplifier. 15 p1885 A73-31945

Triggering characteristics of TEA CO₂ laser. 15 p1885 A73-32019

Ionization instability in CO₂ laser discharges. 15 p1885 A73-32258

Gas dynamic lasers - A state-of-the-art survey. 16 p2022 A73-32726

Carbon dioxide laser technological advances and applications including frequency stability systems, remote sensing, air pollution detection, optical heterodyning and pumping 16 p2023 A73-32860

Vibrational relaxation measurements in CO₂ employing an incremental TEA laser gain technique. 16 p2024 A73-33083

Detection of short CO₂ laser pulses using the optical Kerr effect. 16 p2024 A73-34027

Visual observation of the picture of a CO₂-laser radiation field 17 p1882 A73-34166

Carbon dioxide laser active element design features for service life extension through regenerating working mixture composition while preserving discharge tube seal tightness 17 p1882 A73-34167

Supersonic mixing nozzle for gas-dynamic lasers. 17 p1883 A73-34205

Continuous uniform excitation of medium-pressure CO₂ laser plasmas by means of controlled avalanche ionization. 17 p1883 A73-34207

Measurement of the spectrum of a helical TEA CO₂ laser. 17 p2183 A73-34208

Effect of temperature and composition of gas mixture on population inversion in pulsed CO₂ laser. 17 p2183 A73-34295

High-energy pulsed CO₂-laser-target interactions in air. 17 p2184 A73-34914

Laser power and vibrational energy transfer in CO₂ lasers. 17 p2185 A73-35177

Plasma self radiation and absorption, schlieren signals and lasing levels recording methods based on carbon dioxide lasers, using Mach-Zehnder IR interferometer 17 p2217 A73-35197

Effect of rotational level coupling on pulse sharpening in CO₂ amplifiers. 17 p2143 A73-35791

CW IR laser action in slowly flowing premixed He-air-CO mixture with simultaneous molecular excitation and carbon dioxide generation by discharge-initiated CO oxidation 17 p2186 A73-35799

Self-focusing of CO₂ laser radiation in resonantly absorbing gases. 17 p2186 A73-35811

Two dimensional Mach 5 supersonic nozzle configurations with hot nitrogen expansion for mixing carbon dioxide gasdynamic laser, calculating and measuring gain distribution [AIAA PAPER 73-622] 18 p2321 A73-36170

Propulsion by absorption of laser radiation. [AIAA PAPER 73-624] 18 p2342 A73-36172

Perturbation of a plasma by a focused CO₂ laser beam. 18 p2339 A73-36623

Problems connected with an employment of carbon dioxide lasers in space communications systems 18 p2290 A73-37087

A search for laser-amplified cosmic ray tracks. 19 p2437 A73-37254

Atmospheric turbulence effects on CW carbon dioxide laser propagation, investigating thermal blooming via theoretical diffusion model and experiment 19 p2437 A73-37260

Plasma characteristics with TEA-CO₂ laser and wavelength scaling law. 19 p2468 A73-37520

Parametric measurements on a CO₂ TEA laser with electrodes which have a Rogowsky profile 19 p2438 A73-37999

Shock and compression by TEA-CO₂-laser pulses drastically enhanced by liquid layers spread on surfaces of solids. 19 p2438 A73-38024

Formation of a periodic wave structure on the dry surface of a solid by TEA-CO₂-laser pulses. 19 p2438 A73-38025

CW CO₂ laser at atmospheric pressure. 19 p2438 A73-38277

Laser cutting of aerospace materials. [SME PAPER EM 73-214] 19 p2436 A73-38496

Technique for gain determinations in pulsed CO₂ TEA lasers. 20 p2572 A73-38885

Output-power-characteristics of a CW-gasdynamic-laser. 20 p2572 A73-39224

Effect of water vapor on output power of CO₂ gasdynamic laser. 20 p2573 A73-39303

Carbon dioxide jet laser cutting technology and rate calculations for metals and dielectrics as function of laser power and material thermal properties 20 p2569 A73-39677

Schlieren-optic and interferometric methods using TEA-CO₂ lasers and thermal liquid crystal IR image converters in the diagnostics of fast processes 21 p2744 A73-39998

High power carbon dioxide-nitrogen gasdynamic laser vibration kinetics model, suggesting closed cycle photon generator engine for energy conversion to work 21 p2710 A73-40094

Absorption saturation effects on high-power CO₂ laser beam transmission. 21 p2710 A73-40152

Lamb-dip-stabilized carbon dioxide laser line frequency separations, discussing beat frequencies, C 12 and O 16 molecular rotation constants and vibration level reduction 21 p2712 A73-40324

Carbon dioxide laser pumped dielectric and metallic far IR waveguide, discussing size, mirror coupling and gas medium 21 p2713 A73-40461

Q switched carbon dioxide laser pulse forms and spectrum, covering mirror and prism configurations, sodium chloride plate irradiation, laser wavelengths and pressure effects 21 p2714 A73-40572

Large aperture atmospheric pressure excited carbon dioxide laser discharges, using weak volumetric gas preionization to obtain high power for plasma production

21 p2714 A73-40762

Sealed-off waveguide carbon dioxide laser, investigating gas mixture and pressure effects on power gain and output and optical properties effects on losses

21 p2715 A73-40763

Absorption of CO₂ laser radiation by carbonyl fluoride.

21 p2715 A73-40958

Impulse reaction resulting from the in-air irradiation of aluminum by a pulsed CO₂ laser.

21 p2715 A73-40960

Laser gain characterization of near-atmospheric CO₂:N₂:He glows in a planar electrode geometry.

21 p2715 A73-40965

Variable pulse-length electron beam CO₂ laser.

21 p2716 A73-40973

Kinetic effects in drilling with the CO₂ laser.

21 p2707 A73-40974

Charge collection measurements on a plasma induced by the CO₂ laser.

21 p2748 A73-41021

Parametric study of a helical TEA CO₂ laser.

21 p2716 A73-41050

A parametric study of the performance of a TEA CO₂ laser.

22 p2868 A73-41700

Dependence of the output power of CO₂ gasdynamic laser on the distance from nozzle throat.

22 p2869 A73-42225

Rotational relaxation effects in short-pulse CO₂ amplifiers.

22 p2870 A73-42520

Comparison of theory and experiment for nanosecond-pulse amplification in high-gain CO₂ amplifier systems.

22 p2870 A73-42521

Amplification of short pulses in CO₂ laser amplifiers.

22 p2871 A73-43025

Sealed carbon dioxide laser design for transverse mode output power in terms of beam, transmission loss, Fresnel number and cavity parameters

22 p2872 A73-43155

A method for the study of the gain and the oscillating modes of a CO₂ laser.

23 p2989 A73-44176

High-pressure CO₂ laser with a transverse discharge.

23 p2989 A73-44318

Relaxation processes in electrically excited discharge pumped gasdynamic lasers with supersonic gas mixture flow

23 p2989 A73-44319

Sealed carbon dioxide laser output anomalous transient pulsed behavior attributed to gas dissociation and recombination from electron density and temperature measurements

24 p3095 A73-44408

Optically pumped 33-atm CO₂ laser.

24 p3095 A73-44587

Low-pressure gas breakdown with CO₂ laser radiation.

24 p3095 A73-44589

Study of the processes in a gasdynamic laser in a large-diameter shock tube

24 p3095 A73-44701

Rotational line overlap in CO₂ laser transitions.

24 p3096 A73-44872

Fast linear detection system for TE CO₂ lasers.

24 p3096 A73-44922

Utilization of the impedance variation of the plasma of a CO₂ laser for frequency stabilization on the 'Lamb dip'

24 p3096 A73-45223

Predicted electron transport coefficients and operating characteristics of CO₂-N₂-He laser mixtures.

24 p3097 A73-45420

Pulsed high output double discharge TEA carbon dioxide laser with multiple electrodes and gas preionization in cavity, noting energy conversion efficiency

24 p3098 A73-45551

CARBON DIOXIDE REMOVAL

Atmospheric regeneration in closed chambers by potassium superoxide

18 p2287 A73-36951

CARBON DIOXIDE TENSION

NT HYPERCAPNIA

Gas-blood CO₂ equilibration in dog lungs during rebreathing.

03 p0263 A73-14115

Gas dynamic theory of gas exchange in organisms based on oxygen and carbon dioxide permanent partial pressure gradients in tissues, blood and lungs

10 p1181 A73-24523

Independent effects of changes in H⁺ and CO₂ concentrations on hypoxic pulmonary vasoconstriction.

10 p1182 A73-24565

Quantitative influence of CO₂ inhalation on thermal sweating in man.

11 p1314 A73-25331

Threshold Pco₂ as a chemical stimulus for ventilation during acute hypoxia in dogs.

13 p1576 A73-28534

Method of PaCO₂ determination in men with functional disorders of external respiration

13 p1579 A73-29075

Hypoxic pulmonary steady-state diffusing capacity for CO and cardiac output in rats born at a simulated altitude of 3500 m.

14 p1720 A73-30911

Survival of common bacteria in liquid culture under carbon dioxide at high temperatures.

15 p1837 A73-32650

Correlation of ventilatory responses to hypoxia and hypercapnia.

20 p2514 A73-39776

Transient ventilatory response to hypoxia with and without controlled alveolar PCO₂.

20 p2515 A73-39777

Correlation between arterial carbon dioxide tension and regional cerebral blood volume by X-ray fluorescence.

20 p2519 A73-39790

External airway resistance effects on ventilation and carbon dioxide response during human steady state exercise

22 p2806 A73-42417

A rapid method for determining the CO₂ transport characteristics in man by using a capnograph and a multichannel respirator

22 p2815 A73-42665

CARBON DISULFIDE

Kinetics of a pulsed chemical CO laser with photostimulation based on the carbon disulfide oxidation reaction

06 p0700 A73-18103

Reaction mechanisms of the CS₂-O₂ chemical laser.

06 p0702 A73-18370

Characteristics of a CS₂/O₂ chemical laser with flow transverse to the optical axis.

22 p2870 A73-42764

CARBON FIBER REINFORCED PLASTICS

The effect of processing on the microstructure of CFRP.

13 p1645 A73-28779

Linear elastic fracture mechanics applicability to graphite-epoxy laminated fracture specimens configuration from fractographic studies

15 p1897 A73-31684

High modulus filament wound vessels for cryogenic containers in spacecraft.

17 p2238 A73-34807

The processability of unidirectional prepreps in aerospace applications.

17 p2195 A73-34808

High strength continuous filament wound carbon fiber reinforced plastic performance evaluation for use in light weight rocket motors

17 p2195 A73-34810

The potential application of carbon fibres to spacecraft.

17 p2238 A73-34811

An appreciation of the design of carbon fibre rigid solar panels for spacecraft.

17 p2238 A73-34812

Carbon, boron and glass fiber-epoxy resin composites fracture processes, predicting fracture strength of aligned fibrous composites via linear elastic fracture mechanics concepts

17 p2198 A73-35530

Failure mechanisms in impact loaded carbon and glass fiber reinforced plastics, discussing specimen geometry, notch presence, fiber type, fiber orientation and hybridization effects

17 p2198 A73-35538

Graphite fiber optimization and evaluation efforts for utilization as fiber-epoxy composites reinforcement in tensile-critical applications

17 p2198 A73-35838

High modulus graphite fabrics production processes for applications in composite aerospace materials reinforcement, discussing winding, creeling, sizing, drawing, reeling and weaving

17 p2182 A73-35840

An improved method of production for high strength fibre-reinforced thermoplastics.

18 p2329 A73-37092

The tensile strength of pultruded carbon fibre/epoxy resin composite.

21 p2723 A73-40923

Materials testing via ultrasonic spectroscopy developed from pulse-echo technique, discussing application to metal grain size determination and carbon fiber composite quality control

21 p2707 A73-41136

Polyquinazolines, thermostable polymers with thermoplastic properties

22 p2881 A73-42218

[ONERA, TP NO. 1228] Some important aspects in testing high-modulus fiber composite tubes in axial tension.

23 p2996 A73-43639

High modulus carbon fiber reinforced epoxy composite elastic constant determination by ultrasonic wave propagation velocity measurement in immersion tank, discussing data error sources

23 p2985 A73-43642

Influence of fiber property variation on composite failure mechanisms.

23 p2996 A73-43643

Shear strength of whiskered-fiber reinforced composites

24 p3102 A73-44513

Load capacity of rings formed by winding of composites reinforced with high-modulus anisotropic fibres

24 p3093 A73-44528

Arbeitsgemeinschaft Verstaerkte Kunststoffe, Open Meeting, 10th, Freudenstadt, West Germany, October 3-6, 1972, Reports

24 p3103 A73-44876

Manufacture and properties of compressor blades made of plastics reinforced with carbon filaments

24 p3122 A73-44880

Improved mechanical properties of composites reinforced with neutron-irradiated carbon fibres.

24 p3104 A73-45143

CARBON FIBERS

Investigation of structural changes during the heat treatment of carbonized fibers with the aid of a scanning electron microscope

01 p0068 A73-11246

Spiral wrap - A technique for fabricating thick-wall carbon composites.

01 p0057 A73-11294

Mechanical properties of glassy carbon fibres derived from phenolic resin.

01 p0068 A73-11498

Carbon fiber adhesion to organic matrices.

[ONERA, TP NO. 1173] 01 p0068 A73-11499

The fracture energy of carbon-fibre reinforced glass.

01 p0068 A73-11500

Scanning electron microscope investigation of interaction between pyrolytic carbon fibers and oxidizer, noting periodic variations of carbon chemical activity in radial direction

02 p0185 A73-12556

Preparation and high-temperature properties of carbon fiber-Ni composites.

03 p0321 A73-12919

Development and evaluation of graphite and boron polyimide composites.

03 p0329 A73-13003

Observations of failure modes in carbon composite materials.

03 p0332 A73-13042

Effect of heat treatment on filament wound carbon composites.

03 p0332 A73-13043

Weave geometry effects on pyrolytic infiltration of carbon-carbon /graphite-graphite/ composite structures for nose tip and thermal shield materials

03 p0332 A73-13044

Deformation characteristics of plastics reinforced by high-modulus anisotropic fibres

03 p0335 A73-13739

Effects of process and test variables on the properties of carbon-fibre/epoxide-resin composites.

03 p0335 A73-13800

Speed brake in carbon fibre composite construction.

03 p0393 A73-13920

The effects of matrix and interface modification on local fractures of carbon fibers in epoxy.

03 p0335 A73-13982

The application of adhesive bonded structures and composite materials on advanced turbofan engines.

03 p0359 A73-14134

The influence of temperature on the wear of carbon fiber reinforced resins.

[ASLE PREPRINT 72LC-5B-3] 03 p0335 A73-14363

The energy of crack propagation in carbon fibre-reinforced resin systems.

04 p0469 A73-15981

The mechanical properties of thermoplastics strengthened by short discontinuous fibres

05 p0589 A73-16434

High strength and low density graphite fiber yarn for reinforcement in structural composite components on heavily loaded flight vehicles

06 p0715 A73-18716

Relationship between structure and strength for CVD carbon infiltrated substrates. II - Three dimensional woven, tufted and needled substrates.

06 p0715 A73-18718

The Kaiser effect in stress wave emission testing of carbon fiber composites.

07 p0843 A73-20185

The erosion of carbon fiber reinforced plastic by repeated liquid impact.

07 p0843 A73-20224

Hybrid composite of carbon and glass fiber reinforced epoxy resin, testing mechanical properties and optimal fibrous modulus ratios and volume fraction

07 p0844 A73-20327

Flat laminated FRP-FRTP and carbon FRP-FRTP composites, testing lamination effects on bending and impact strengths

Graphite fiber reinforced polyimide resin composites for structural applications in long duration high temperature environments, discussing fabrication with match-metal die
[SME PAPER EM 72-107]

Friction and wear of graphite fiber composites.

Thermal expansion at elevated temperatures. IV - Carbon-fibre composites.

Izod impact properties of carbon-fibre/glass-fibre sandwich structures.

Analysis, test, and comparison of composite material laminates configured for isotropic low thermal expansion.

Fatigue and creep testing of unidirectional carbon fibre reinforced plastics.

Impact strength and fracture of carbon fiber composite beams.

Izod impact tests of carbon fiber composites strength, measuring residual compressive strength

Bearing materials from graphite fiber composites.

The influence of interfacial bonding on the properties of carbon fiber composites.

High modulus graphite fiber-epoxy composite shear strength and structural observation by X ray and electron diffraction and surface dark field electron microscopy

Effects of shear damage on the torsional behaviour of carbon fibre reinforced plastics.

The effect of specimen and testing variables on the fracture of some fibre reinforced epoxy resins.

Graphitization of carbon fibre/glassy carbon composites.

Interlaminar shear strength of a carbon fibre reinforced composite material under impact conditions.

Bulk compressibility of carbon fibre reinforced plastics.

High modulus composites versus beryllium for achieving stiffness in spacecraft structural applications.

[AIAA PAPER 73-384]

Dynamic properties of graphite fiber honeycomb panels.

Preferred a axis orientation parallel to fiber axis in commercial carbon fibres due to lower surface energy of basal plane configuration

Stability of micromorphology of carbon fibres and their interstitial compounds.

The elastic constants of carbon-fibre composites.

Elevated temperature stability of carbon-fibre, nickel-matrix composites Morphological and mechanical property degradation.

Carbon fiber reinforced epoxy resins mechanical properties, correlating test parameters with observed failure mechanism

Fiber strength, fracture types and material elastic properties relationship to impact resistance in carbon fiber reinforced plastics

The effect of fibre-matrix interface strength on the impact and fracture properties of carbon-fibre-reinforced epoxy resin composites.

Temperature sensitivity of cfrr honey-comb structures under holographic ndt.

Deformation and strength characteristics of carbon-fiber strengthened plastics in compression

Carbon fibre reinforced ceramics.

Thermal conductivity of carbon fibers

Theoretical post-yielding behavior of composite laminates. I - Inelastic micromechanics.

Oxidation of acrylic fibres for carbon fibre formation.

Some mechanical properties of carbon fiber reinforced aluminum.

Three dimensional microstructure of carbonized polyacrylonitrile /PAN/ fibers dependence on basal plane alignment and process cycle treatment

Heat treatment effects upon the properties of PAN base carbon fibers.

The development and properties of a polyacrylonitrile /PAN/ fiber based carbon felt

High modulus graphite fiber preparation from polyacrylonitrile yarn, discussing graphitization, properties and stabilization oxidation treatment

Polyphenylquinoxaline/graphite composite laminates tests for flexure, shear and tensile strength at 316 C

High strength low density Hyfil carbon fiber prepreg sheet properties and production for aircraft applications

The effect of cure cycle on the mechanical properties of carbon-fibre/epoxide resin.

Heat treated polyacrylonitrile filament produced carbon fiber strengthened after fatigue testing, noting maximum strengthening effect after 1000 load cycles

Development of advanced composite rocket motor chambers using boron and graphite fibers.

Aircraft structural applications of filamentary composites, discussing fiberglass, boron-epoxy and graphite-epoxy composites

Axial alignment of basal planes in polyacrylonitrile base carbon fibers, increasing axial and radial microstructural textures via heat treatment temperature

Graphite fiber optimization and evaluation efforts for utilization as fiber-epoxy composites reinforcement in tensile-critical applications

High modulus graphite fabrics production processes for applications in composite aerospace materials reinforcement, discussing winding, creeling, sizing, drawing, reeling and weaving

Surface properties of carbon and graphite fibers

The elastic properties of carbon fibres and their composites.

Fracture mechanics of carbon fibres at high temperatures due to fine structure, discussing effects of ribbon unbending during extension

Production techniques for advanced composites fabrication by tape machine automation.

Special features of the structure and growth of pyrocarbon whiskers

Graphite fiber tensile property evaluation, discussing single filament method and improved dry bundle test including electrical resistivity measurement and stress-strain curve analysis

High strength filaments for cables and lines, discussing bundle theory and comparing dielectric and tensile properties for glass, graphite and organic fibers

NT CARBON 12

NT CARBON 13

NT CARBON 14

Astrophysical CO isotopic constituents from H II regions line emissions, determining relative abundances

Absolute cross section for producing C-11 from carbon by 270-MeV/nucleon N-14 ions.

Validity of zeta Oph cloud carbon isotope abundance extrapolation to dense dusty regions of Galactic center and Orion Nebula

The isotopic composition of 'graphitic' carbon from iron meteorites and some remarks on the troilite sulfur of iron meteorites.

Carbon isotope abundance ratios in comets and Jupiter atmosphere, discussing hydrogen isotope ratio determination for Saturn and Jupiter atmospheres

Theory of interstellar abundances of the isotopes of carbon, nitrogen and oxygen.

CARBON MONOXIDE

Electron scattering by molecules with and without vibrational excitation. VI - Elastic scattering by CO at 6-80 eV.

Observations of carbon monoxide in cool stars at 4.7 microns.

Fuel-rich and stoichiometric carbon monoxide-nitrous oxide premixed laminar flames with varying water contents, determining flame temperature by line reversal method

Shock-tube study of vibrational energy transfers in the CO₂-N₂ and the CO₂-CO systems.

Vibrational excitation in CO by electron impact in the energy range 10-90 eV.

Molecular clouds in the galactic center region - Carbon monoxide observations at 2.6 millimeters.

Astrophysical CO isotopic constituents from H II regions line emissions, determining relative abundances

Behavior of carbon monoxide in the upper photosphere.

The role of CO in CO₂ lasers.

Seasonal variations in carbon monoxide content of the atmosphere

Carbon monoxide Cameron bands limb intensity profile in Martian airglow from Mariner 9 UV spectrum observations

Gas turbine combustion rig simulation of pollutant carbon and nitrogen oxide emissions as function of air-fuel mixing, metallic additions and chamber design

Laser-induced fast thermal desorption from solid surfaces

The hydroperoxyl radical in atmospheric chemical dynamics - Reaction with carbon monoxide.

The role of mixing in burner-generated carbon monoxide and nitric oxide.

Laser-excited vibrational energy transfer studies of HF, CO, and NO.

The adsorption and decomposition of CO on Pt(111).

Carbon monoxide rotational transitions as dark cloud cooling mechanism during protostar formation

Cooling effects of CO IR opacity in stellar atmospheres of dwarfs and supergiants, considering application to sun and grain formation in cooler stars

Measurement of vibrational temperature of CO and N₂ using the He/2 3S/ Penning ionization technique.

Decomposition of carbon monoxide on a /110/ nickel surface.

Coadsorption of oxygen and carbon monoxide on tungsten - Desorption spectra, electron stimulated desorption and field emission microscopy.

Kinetics of the degassing of oxygen-containing niobium in flowing acetylene to form carbon monoxide

Photo-decarbonylation of beta-styryl isocyanates.

Carbon monoxide content in the exhaled air and carboxyhemoglobin in the blood of subjects equipped with an isolating protective garment

Equator-pole temperature difference and the solar oblateness /Research note/.

Influence of CO on the population inversion in CO₂ lasers.

Reactions of HO₂ with carbon monoxide and nitric oxide and of O/I D/ with water.

Search for interstellar absorption in 4250 A line of singly ionized CO in direction of different stars

Spectrophotometric results from the Copernicus satellite. V - Abundances of molecules in interstellar clouds.

Seasonal variations of the carbon monoxide concentration in the atmosphere.

Study of gas-solid chemical interactions by the molecular beam technique. V - Reactions of oxygen and carbon monoxide with polycrystalline tantalum strips

15 p1841 A73-31970

Reflection-absorption infrared spectrum of alpha-CO chemisorbed on polycrystalline tungsten.

15 p1841 A73-31971

Solar absorption in the CO fundamental region.

17 p2231 A73-34761

Vibrational relaxation of CO by O atoms.

17 p2119 A73-35174

Self consistent field calculations of CO positive ion dipole moment in ground state

17 p2119 A73-35180

Influence of carbon monoxide and of hemodilution on cerebral blood flow and blood gases in man.

18 p2278 A73-36659

Chemisorption of CO on tungsten /100/- Combined flash desorption and electron stimulated desorption study. II.

18 p2287 A73-37033

Observations of carbon monoxide at 4.7 microns in IRC + 10216, VY Canis Majoris, and NML Cygni.

19 p2484 A73-37612

Laser absorption study of carbon monoxide vibrational relaxation behind incident shock waves, discussing vibration-rotation levels, shock tubes, oscilloscope traces and Boltzmann distributions

19 p2437 A73-37900

Compact carbon monoxide sensor utilizing a confocal optical cavity.

[ASME PAPER 73-ENAS-20] 19 p2400 A73-37976

The cosmological significance of molecular band strengths in the infrared spectra of elliptical galaxies.

20 p2609 A73-39447

CO atmospheric vertical distribution from balloon-borne IR grating spectrometer observations, noting concentration decrease with altitude

21 p2680 A73-40078

Atmospheric CO production from electron impact on carbon dioxide, considering lightning, radioactivity, discharges, photoelectrons, auroral particles, cosmic rays and solar wind

21 p2680 A73-40079

Anthropogenic CO sources and urban concentrations, considering meteorological factors, nonanthropogenic sources, temporal variations and background levels in remote areas

21 p2729 A73-40080

Oceanic contribution to atmospheric CO budget estimation from Northern Hemisphere water carbon monoxide content, comparing to anthropogenic production

21 p2680 A73-40083

Theoretical model of vertical distributions of CO and CH₄ in the mesosphere and upper stratosphere.

21 p2680 A73-40085

Photochemical model with vertical transport for CO and hydrocarbons profiles in stratosphere and mesosphere, discussing boundary conditions and water vapor

21 p2681 A73-40086

Excitation of the CO fourth positive system by the dissociative recombination of CO₂⁺/ions.

22 p2843 A73-41904

A single-pulse shock-tube study of the reaction between nitrous oxide and carbon monoxide.

22 p2933 A73-42757

Kinetics of carbon monoxide oxidation in postflame gases.

22 p2820 A73-42803

Turbulent flow reactor for oxidation of moist CO and postinduction phase oxidation of methane, using chemical sampling and gas chromatographic analysis

22 p2820 A73-42804

On the vertical distribution of carbon monoxide and methane in the stratosphere.

23 p2976 A73-43894

OH radical concentration in the stratosphere.

23 p2976 A73-43895

Determination of dissociation energies for some alkaline earth /hydro-/ oxides in CO/N₂O flames.

24 p3156 A73-44985

CARBON MONOXIDE LASERS

Time dependence of carbon monoxide TEA laser emission at 77 K, presenting time resolved transitions spectral data

01 p0058 A73-10128

Electric discharge CO mixing gas dynamic laser, noting nitrogen molecules vibrational excitation and mixing with cold CO in supersonic expansion with population inversion

02 p0175 A73-12050

Numerical model of energy transfer in carbon monoxide-nitrogen laser, considering electron-molecule excitation and vibration-vibration exchange

02 p0178 A73-12816

Nitric oxide detection by use of Zeeman-effect and CO laser.

03 p0318 A73-12871

Kinetics of a pulsed chemical CO laser with photostimulation based on the carbon disulfide oxidation reaction

06 p0700 A73-18103

Dissociation of carbon monoxide in a pumped CO laser.

06 p0703 A73-18613

Electrical characteristics of the plasma in a CO laser.

06 p0703 A73-18614

CW operation in some CO lines below 5.0 microns.

06 p0704 A73-18892

Pressure broadening of magnetically-tuned infrared absorption spectrum of NO using a CO laser.

07 p0833 A73-19145

Carbon dioxide-nitrogen gasdynamic lasers, predicting population inversion from numerical model of vibrational relaxation of anharmonic diatomic oscillators in supersonic expansions

07 p0834 A73-19511

A CW-CO chemical laser from the reaction of active nitrogen with O₂ + CS₂.

07 p0835 A73-19633

Pulsed CO laser vibrational distribution function time dependent evolution, considering V-V and V-T processes, spontaneous and stimulated emission, electron impact excitation and kinetic heating

07 p0835 A73-19635

Intracavity breakdown in CO and CO₂ lasers.

07 p0835 A73-19638

Chemical laser device bibliography.

07 p0836 A73-19642

Chemical lasers - A comprehensive literature survey.

08 p0974 A73-21026

Absorption measurements of carbon monoxide laser radiation by water vapor.

08 p0974 A73-21033

Electron energy distribution function in CO laser discharge for elastic collisions, noting kinetic equation solution

09 p1089 A73-21914

Lamb dip measurements on low pressure CO laser vibrational-rotational lines, determining line widths, velocity-changing collision rate and saturation intensities with curve fitting

09 p1090 A73-22078

Directly excited subsonically flowing CW gas laser with carbon monoxide and dioxide generation as reaction products formed by organic molecule electrochemical oxidation

09 p1091 A73-22084

IR spectrum line reversal for measurement of CO and gas mixture laser plasma vibrational temperatures as function of discharge current and gas pressure

10 p1230 A73-24884

Amplified laser absorption - Detection of nitric oxide.

12 p1505 A73-27121

Gas discharge CW and pulsed CO laser population inversion mechanism, noting high output and efficiency in CW and Q switched modes

13 p1629 A73-29428

Evolution of the CO vibrational energy distribution in a transverse flow laser.

15 p1884 A73-31313

Amplified laser absorption - Detection of nitric oxide.

15 p1885 A73-31844

Electron energy distribution function in CO laser discharge for elastic collisions, noting kinetic equation solution

15 p1886 A73-32640

Transient oscillator analysis of a high-pressure electrically excited CO laser.

16 p2024 A73-33082

CO laser emission lines attenuation measurements in atmosphere, attributing inconsistencies in previous experiments to model

17 p2185 A73-35405

CW IR laser action in slowly flowing premixed He-air-CO mixture with simultaneous molecular excitation and carbon dioxide generation by discharge-initiated CO oxidation

17 p2186 A73-35799

Theoretical investigation of the CO supersonic electric discharge laser.

[AIAA PAPER 73-623] 18 p2321 A73-36171

Cryogenically cooled CO-He TEA laser.

19 p2437 A73-37253

Single-line operation of a 2-W longitudinal cw CO chemical laser with no frequency-selective element in the optical cavity.

19 p2439 A73-38475

The carbon monoxide laser - Mechanism of formation of population inversion

21 p2712 A73-40444

IR spectrum line reversal for measurement of CO and gas mixture laser plasma vibrational temperatures as function of discharge current and gas pressure

21 p2717 A73-41659

A kinetic model of population inversion generation in a gas-discharge carbon monoxide laser

23 p2988 A73-44012

CARBON MONOXIDE POISONING

Myocardial metabolism during exposure to carbon monoxide in the conscious dog.

09 p1042 A73-22935

Influence of restricted motor activity on the resistance of animals to acute action of carbon monoxide

15 p1835 A73-31519

Results of carbon monoxide poisoning checks following aviation accidents or incidents in the French Army

18 p2285 A73-36929

Erythropoietin production in dogs exposed to high altitude and carbon monoxide.

20 p2513 A73-39599

Effect of carbon monoxide on time perception.

21 p2642 A73-40000

Effects of single exposures of carbon monoxide on sensory and psychomotor response.

21 p2637 A73-40409

CARBON STEELS

Physical fatigue limit of hardened steels

01 p0063 A73-10485

Diffusive thermal bonding of cermet elements on steel and iron substrates in vacuum

02 p0172 A73-11537

The effect of a preliminary plastic strain on the form of a mechanical hysteresis loop.

02 p0235 A73-12208

The tempering of low carbon steels containing tungsten.

02 p0183 A73-12760

Significance of the sequence of treatment for the notch impact strength of cold-worked steel samples

02 p0175 A73-12850

Experimental analysis of the low-temperature strength of notched bars

06 p0705 A73-17779

Effect of gamma irradiation on carbon redistribution processes in the martensite lattice

06 p0706 A73-17902

Study of fatigue crack propagation by X-ray diffraction approach.

06 p0698 A73-18496

Method of plasticity enhancement in aluminum and nickel-aluminum diffusion coatings on medium-carbon steel

06 p0711 A73-18665

Temperature and loading rate effects on yield stress and specific fracture work in tempered carbon steel from notch tests, correlating with linear fracture mechanics

07 p0838 A73-19215

Cr-Ni carbon steel testing for stress and temperature dependencies of secondary creep rate, noting grain boundary diffusion controlled mechanism

08 p0980 A73-21674

Some problems in the assessment of high temperature properties for engineering purposes.

08 p0981 A73-21782

The creep strength of 17 Cr-11 Ni-25 Mo austenitic steel stabilised by titanium.

08 p0982 A73-21792

Phase transformational kinetics and hardenability of low-carbon, boron-treated steels.

09 p1102 A73-22416

Thermophysical effects of solidification on dendritic structure and mechanical properties of cast stainless and low alloy carbon steels for different crystallization rates

09 p1107 A73-23198

Tensile, fracture toughness and crack growth properties of a roll-extruded HP 9Ni-4Co-25C steel alloy.

09 p1109 A73-23260

Investigation of stress state at fatigue crack tip by means of X-ray microbeam.

10 p1293 A73-24918

Carbon and stainless steels chemical composition effects on diffusion layer structure and fatigue strength after diffusive boring

10 p1236 A73-24954

Vacuum contactless metallization of carbon steels, stainless steels and nickel alloys, considering Si, Cr and Al coatings

10 p1227 A73-24964

Effect of carbon on the growth of boride layers

11 p1374 A73-26109

Characteristics of martensite decomposition during the tempering of rhenium steels

12 p1509 A73-26894

Studies on fatigue damage caused by stresses below the endurance limit - The effect of program period and fatigue failure by stresses below the endurance limit.

13 p1692 A73-28197

Fatigue damage by a stress below the endurance limit.

13 p1641 A73-29498

Influence of temperature on the initial yield of notch strength.

13 p1641 A73-29511

Low carbon steel S-N diagram for stresses ranging to fatigue limit, noting cyclic creep, macroplastic cyclic stress and fatigue failure

13 p1703 A73-29603

Fatigue crack propagation in butt welds containing joint penetration defects.

14 p1755 A73-30148

Physical fatigue limit of hardened steels.

14 p1759 A73-30310

- Properties of low-alloy steels with small niobium additions
15 p1889 A73-31811
- Strength of joints produced by melting high-carbon chromium alloys on low-carbon steel
17 p2188 A73-34566
- Yield surfaces of metals at elevated temperatures.
20 p2615 A73-38640
- Effect of structural and mechanical factors on the nature of cold shortness curves for steels
20 p2578 A73-39378
- Decomposition of martensite during tempering of rhodium steels.
21 p2720 A73-41027
- Residual-stress measurement using surface displacements around an indentation.
21 p2704 A73-41265
- Properties of low-alloy steels with small niobium additions.
24 p3100 A73-45274
- CARBON TETRAFLUORIDE**
- Habitable atmospheres which do not support combustion.
10 p1183 A73-23562
- CARBON 12**
- URCA process and the evolution of carbon stellar core.
13 p1673 A73-28173
- Comet 1969 g emission spectrum observation with 200-inch telescope, obtaining isotope ratio C-12/C-13
20 p2609 A73-39432
- Proton beam measurement of absolute cross section for neutron knockout reaction on C 12 at pion-nucleon resonance, correcting for muon and electron contamination
21 p2743 A73-40686
- Vacuum IR spectrometer measurement of C 12 methane absorption band at 1.1 microns, describing technique for extending standards to photomultiplier region of spectra
21 p2743 A73-40936
- CARBON 13**
- Carbon-13 nuclear magnetic resonance in biosynthetic studies of lipids.
03 p0274 A73-14550
- C-13 nuclear magnetic resonance in organic geochemistry.
11 p1325 A73-25461
- Comet 1969 g emission spectrum observation with 200-inch telescope, obtaining isotope ratio C-12/C-13
20 p2609 A73-39432
- CARBON 14**
- Lunar rock C 14 production rate as function of depth, discussing solar and galactic cosmic radiation induced nuclear reactions
02 p0220 A73-12479
- Cosmic ray, solar activity, supernova outbursts and geomagnetic field effects on atmospheric C-14 concentration
10 p1266 A73-23911
- Geomagnetic field, cosmic rays, and radiocarbon content in the earth's atmosphere
21 p2756 A73-40585
- CARBON-CARBON COMPOSITES**
- Carbon-carbon composites and bulk graphite fracture toughness and failure modes determination from single-edge-notched specimen responses under three-point bending
10 p1239 A73-24276
- Carbon-felt, carbon-matrix composites - Dependence of thermal and mechanical properties on fiber volume percent.
10 p1240 A73-24278
- Relationship between structure and strength for CVD carbon infiltrated substrates. III - Fabric lay-up substrates.
13 p1645 A73-29272
- Precipitation and dispersion hardened alloys, fiber reinforced metal matrix composites, carbon-carbon composites, and dispersed system, eutectics application in aerospace industry
14 p1759 A73-30067
- Oxidation resistant carbon-carbon composite for Space Shuttle application.
16 p2028 A73-33043
- The relationship between thermal history, X-ray crystallographic structure and thermal properties of Pyco-bond rayon precursor carbon-carbon composites.
16 p2028 A73-33044
- The relationship between thermal history, X-ray crystallographic structure and thermal properties of rayon precursor carbon-carbon composites A literature review.
16 p2028 A73-33045
- Design and development of lightweight wheel braking equipment.
19 p2434 A73-37894
- Microstructure and its related properties on carbon fiber composites.
23 p2998 A73-44134
- The dynamic fracture toughness of carbon-carbon composites.
24 p3105 A73-45147
- CARBONACEOUS METEORITES**
- NT ORGUEIL METEORITE

- Relation between solar and planetary neon in carbonaceous chondrites.
02 p0211 A73-11744
- Xenon in carbonaceous chondrites.
04 p0501 A73-15631
- Natural remanent magnetizations of carbonaceous chondrites and the magnetic field in the early solar system.
05 p0619 A73-16839
- Natural remanent magnetization and thermomagnetic properties of the Allende meteorite.
05 p0619 A73-16840
- Double spiral DNA-like nucleotide analog in carbonaceous chondrite, indicating organic compound synthesis at low temperature
05 p0619 A73-16843
- Abundance patterns of thirteen trace elements in primitive carbonaceous and unequilibrated ordinary chondrites.
07 p0877 A73-19651
- Allende meteorite carbonaceous phase - Intractable nature and scanning electron morphology.
07 p0900 A73-20283
- Inter-element relationships between trace elements in primitive carbonaceous and unequilibrated ordinary chondrites.
07 p0903 A73-20619
- Morphologies of iron crystals from the Haverro meteorite.
09 p1140 A73-21862
- Forms of carbon in the new Haverro ureilite of Finland.
09 p1140 A73-21863
- Elemental abundances and chemistry of Haverro carbonaceous ureilite, noting similarity to Allende inclusions pattern
09 p1047 A73-21868
- Historical treatment and inconclusiveness of evidence of extraterrestrial life traces and organic matter in carbonaceous and other meteorites
09 p1146 A73-22545
- Heterocyclic compounds extraction and identification from carbonaceous meteorites by gas chromatography and mass spectrometry, noting pyrimidine distribution and absence of biological heterocycles
10 p1277 A73-24101
- Volatile organic compounds from Murchison, carbonaceous chondrite by vaporization-pyrolysis at different temperatures, comparing with Allende meteorite and terrestrial rocks
10 p1277 A73-24102
- High-temperature condensates in chondrites and the environment in which they formed.
10 p1278 A73-24109
- Double spiral DNA-like polynucleotide analog in carbonaceous chondrite, indicating organic compound synthesis at low temperature
11 p1423 A73-26053
- Allende carbonaceous chondrite Ca-Al rich inclusion refractory trace metals condensation temperature calculation, indicating high temperature primitive solar nebula condensates
13 p1684 A73-29176
- Carbonaceous chondrite neutron activation analysis for trace elements, revealing compositional homogeneity
13 p1684 A73-29181
- Composition of metal in type III carbonaceous chondrites and its relevance to the source-assignment of lunar metal.
13 p1686 A73-29564
- Zinc, lead, chlorine and FeOOH-bearing assemblages in the Apollo 16 sample 66095 - Origin by impact of a comet or a carbonaceous chondrite.
13 p1686 A73-29565
- Chemical evolution before life from carbonaceous meteorites composition, noting porphyrins, optically active substances and isoprenoid hydrocarbons
14 p1715 A73-30130
- Memory of early magnetic fields in carbonaceous chondrites.
17 p2228 A73-34421
- Isotopic composition of solar wind xenon in carbonaceous chondrites, discussing evolution of meteoritic matter
17 p2233 A73-35266
- Lead isotopic composition ages of carbonaceous chondritic meteorites with correction for terrestrial lead contamination
21 p2765 A73-40239
- Chromium and phosphorus enrichment in the metal of type II/C2 carbonaceous chondrites.
21 p2771 A73-41007
- Amino acids in the Murchison meteorite.
21 p2771 A73-41010
- Primordial abundance values for heavy nuclei related to content of type 1 and 2 carbonaceous chondrites
23 p2950 A73-43752
- Rare-earth elements in matrix, inclusions, and chondrules of the Allende meteorite.
24 p3133 A73-44539
- The Mighei meteorite.
24 p3137 A73-44950
- Curium-248 in the early solar system.
24 p3143 A73-45348

CARBONACEOUS ROCKS

- NT COAL
- Carboxylic acids derived from Tasmanian tasmanite by extractions and kerogen oxidations.
10 p1211 A73-24108
- CARBONATES**
- NT ARAGONITE
- NT CALCITE
- NT POLYCARBONATES
- NT SIDERITES
- NT SODIUM CARBONATES
- Cell assemblies for a molten carbonate fuel battery. I - The construction of cell assemblies. II - Electrolyte paste discs for molten carbonate fuel cells.
04 p0406 A73-14985
- CARBONIZATION**
- Comment on the nature of the disaccommodation in HCP Co-C alloys.
01 p0066 A73-10999
- Interaction of graphite with titanium and zirconium
09 p1105 A73-22977
- Influence of gas carburizing on the structure and properties of electrolytically deposited chromium
11 p1375 A73-26734
- CARBONYL COMPOUNDS**
- Carbonyl terminated polybutadiene polymer binder development for solid propellant, describing properties, manufacturing processes and performance reproducibility
01 p0089 A73-11111
- New infrared laser line in OCS and new method for C atom lasing.
03 p0320 A73-14465
- Electron absorption spectra of benzochromium-dicarbonyltriphenylphosphine and benzochromium-tricarbonyl and their application to studies of the decomposition kinetics of these compounds
10 p1186 A73-24457
- Carbonyl nickel recrystallization characteristics from hardness-temperature graphs and X ray analyses
14 p1765 A73-30891
- Stresses in molybdenum coatings obtained by thermal decomposition of Mo/CO/6
18 p2319 A73-35892
- Absorption of CO₂ laser radiation by carbonyl fluoride.
21 p2715 A73-40958
- CARBORUNDUM [TRADEMARK]**
- Study of the deformation structure in alpha-SiC single crystals
24 p3099 A73-44741
- CARBOXYHEMOGLOBIN**
- Myocardial metabolism during exposure to carbon monoxide in the conscious dog.
09 p1042 A73-22935
- Carbon monoxide content in the exhaled air and carboxyhemoglobin in the blood of subjects equipped with an isolating protective garment
12 p1463 A73-27712
- Influence of carbon monoxide and of hemodilution on cerebral blood flow and blood gases in man.
18 p2278 A73-36659
- CARBOXYHEMOGLOBIN TEST**
- Significance of the Bohr and Haldane effects in the pulmonary capillary.
08 p0935 A73-21614
- Effects of single exposures of carbon monoxide on sensory and psychomotor response.
21 p2637 A73-40409
- CARBOXYL GROUP**
- Zirconium sorption by and release from carboxyl cationates in nitric and sulfuric acids, discussing pH dependence
14 p1765 A73-30884
- CARBOXYLIC ACIDS**
- NT ASPARTIC ACID
- NT HEXOGENES [TRADEMARK]
- NT LACTIC ACID
- NT LYSINE
- NT OLEIC ACID
- NT TRYPTOPHAN
- Accelerated chromatographic method for determination of hydroxyproline.
03 p0273 A73-13600
- Carboxylic acids derived from Tasmanian tasmanite by extractions and kerogen oxidations.
10 p1211 A73-24108
- CARBURIZING**
- Phenomena of precipitation observed in carburized tantalum in the vapor phase
15 p1896 A73-32645
- CARCINOGENS**
- An experimental basis for carcinogenic effects of ultraviolet radiation.
11 p1320 A73-26485
- CARCINOMA**
- U CANCER
- CARDIAC AURICLES**
- Quantitative radionuclide angiocardiology for determination of chamber to chamber cardiac transit times.
04 p0409 A73-14767
- Ultrastructure of the atrial, ventricular, and Purkinje cell, with special reference to the genesis of arrhythmias.
06 p0655 A73-18873

- Morphometric and histochemical investigation on human right atrial and mitral papillary muscle.
08 p0930 A73-21215
- Cardiac activity potentials, P-R interval and impulse propagation across atrioventricular node, ventricular conduction and Purkinje fiber-muscle junctions
11 p1316 A73-25598
- Stethoscope- or phonocardiograph-detectable systole-associated left atrial sound in terms of activity recording, sound genesis, hemodynamic correlations and clinical applications
11 p1317 A73-25696
- Temporal sequence of right and left atrial contractions during spontaneous sinus rhythm and paced left atrial rhythm.
11 p1317 A73-25699
- Electrocardiographic evidence of left atrial hyper-tension in acute myocardial infarction.
11 p1319 A73-26287
- Electrocardiographic diagnosis of sinus node rhythm variations and SA block.
18 p2274 A73-36520
- Intra-atrial and esophageal electrography in the diagnosis of complex arrhythmias.
18 p2274 A73-36525
- Experimental studies on the mechanisms of closure of cardiac valves with use of roentgen videoden-sitometry.
19 p2395 A73-37795
- P wave analysis in 2464 orthogonal electrocardio-graphs from normal subjects and patients with atrial overload.
22 p2806 A73-42341
- CARDIAC VENTRICLES**
- Left ventricular receptors activated by severe asphyxia and by coronary artery occlusion.
01 p0008 A73-10549
- On the causes of the changes of the second heart sound in left bundle branch block.
01 p0009 A73-11008
- Atrioventricular block response to exercise and in-traventricular conduction at rest.
01 p0010 A73-11506
- Left ventricular end-diastolic pressures following selective coronary arteriography.
01 p0010 A73-11508
- Nature of the conduction disturbance in selective coronary arteriography and left heart catheterization.
02 p0134 A73-12443
- Echocardiographic findings in experimental myocardial infarction of the posterior left ventricular wall.
02 p0138 A73-12446
- Maximal treadmill exercise electrocardiography - Correlations with coronary arteriography and cardiac hemodynamics.
02 p0136 A73-12821
- Quantitative radionuclide angiocardiology for determination of chamber to chamber cardiac transit times.
04 p0409 A73-14767
- Elevated ST segments with exercise in ventricular aneurysm.
04 p0410 A73-15643
- A new method to measure non-uniformity in the in-tact heart.
04 p0412 A73-15645
- Systolic time intervals in constrictive pericarditis and severe primary myocardial disease.
06 p0649 A73-17596
- Television/computer dimensional analysis interface with special application to left ventricular cineangi-grams.
06 p0657 A73-17860
- Geometry of left ventricular contraction in the systolic click syndrome - Characterization of a seg-mental myocardial abnormality.
06 p0655 A73-18870
- Pathological cardiac conduction system lesions anatomy associated with arrhythmia, discussing atrioventricular, His bundle and bundle branch blocks
06 p0655 A73-18872
- Ultrastructure of the atrial, ventricular, and Pur-kinje cell, with special reference to the genesis of ar-rhythmias.
06 p0655 A73-18873
- Left ventricular performance after myocardial in-farction assessed by radioisotope angiocardiology.
08 p0932 A73-21801
- Ventriculographic patterns and hemodynamics in primary myocardial disease.
08 p0933 A73-21804
- Estimation of left ventricular size by echocardiog-raphy.
09 p1046 A73-22999
- Left ventricular blood flow velocity in man studied with the Doppler ultrasonic flowmeter.
09 p1042 A73-23173
- Reflex bradycardia elicited from left ventricular receptors during acute severe hypoxia in cats.
09 p1042 A73-23244
- Coronary flow and left ventricular function during environmental stress.
09 p1047 A73-23380
- Immediate hemodynamic effects of cardiac angio-graphy in man.
10 p1179 A73-23841
- Alternative mechanisms of apparent supernormal atrioventricular conduction.
10 p1184 A73-23843
- Physiological studies of human organism adaptation to high altitudes in temporary and permanent moun-tain inhabitants, discussing oxygen uptake, lung ven-tilation and cardiac ventricle hypertrophy
10 p1181 A73-24514
- Physiological responses of rats to intermittent high-altitude stress - Effects of age.
10 p1182 A73-24564
- Depolarization phase of the spatial velocity elec-trocardiogram in normal and ventricular overloading.
10 p1185 A73-24900
- Cardiac activity potentials, P-R interval and impulse propagation across atrioventricular node, ventricular conduction and Purkinje fiber-muscle junctions
11 p1316 A73-25598
- Temporal sequence of right and left atrial contractions during spontaneous sinus rhythm and paced left atrial rhythm.
11 p1317 A73-25699
- Slow and fast heart rates and syncope and dizzy at-tacks as manifestations of sick sinus syndrome, discussing ventricular artificial pacemaker as therapy
11 p1319 A73-26289
- Myocardial contraction velocity and acceleration in man measured by ultrasound echocardiography dif-ferentiation.
12 p1461 A73-27026
- High-fidelity left ventricular pressure measure-ments for the assessment of cardiac contractility in man.
12 p1464 A73-27888
- Comparison of isometric exercise and angiotensin infusion as stress test for evaluation of left ventricular function.
12 p1464 A73-27889
- Exercise-induced ventricular arrhythmias in pa-tients with coronary artery disease - Their relation to angiographic findings.
12 p1464 A73-27890
- Relationship between ventricular premature con-tractions on routine electrocardiography and sub-sequent sudden death from coronary heart disease.
14 p1715 A73-30051
- Echocardiography status, potentialities and require-ments in congenital heart disease diagnosis, consider-ing feasibility in left ventricular performance evalua-tion
14 p1721 A73-30053
- Book on echocardiography covering examination of mitral, aortic, tricuspid and pulmonic valves, ventri-cles, atrium, pericardial effusion, coronary artery dis-ease and tumors
14 p1721 A73-30358
- Myoglobin distribution in the heart of growing rats exposed to a simulated altitude of 3500 m in their youth or born in the low pressure chamber.
14 p1720 A73-30910
- Procedure for recording the rate of pressure changes in heart cavities
15 p1837 A73-31167
- Assessment of left heart function by noninvasive exercise test in normal subjects.
15 p1834 A73-31345
- Assessment of left ventricular performance in man - Instantaneous tension-velocity-length relations ob-tained with the aid of an electromagnetic velocity catheter in the ascending aorta.
15 p1836 A73-31996
- Echocardiographic detection of regional myocardial infarction - An experimental study.
15 p1839 A73-31997
- Intracardiac heart murmurs and sounds influenced by respiration.
15 p1836 A73-32546
- Assessment of left ventricular dimensions and func-tion by echocardiography.
16 p1973 A73-34038
- Book on vectorcardiography covering equipment, techniques, lead systems and abnormalities associated with atrial and ventricular hypertrophy, bundle branch blocks, myocardial infarction and arrhythmia
17 p2114 A73-34452
- QRS abnormalities in AV block - Variations and their significance.
18 p2274 A73-36521
- Identification of the sites of atrioventricular con-duction defects by means of His bundle electrography and atrial pacing.
18 p2282 A73-36522
- The clinical causes and mechanisms of intraven-tricular conduction disturbances.
18 p2274 A73-36524
- Current status of correlations between vectorcar-diogram and hemodynamic data.
18 p2274 A73-36526
- Respiratory changes in the stroke volume of the left ventricle in healthy humans
19 p2393 A73-37397
- Experimental studies on the mechanisms of closure of cardiac valves with use of roentgen videoden-sitometry.
19 p2395 A73-37795
- Use of a video system in the study of ventricular function in man.
19 p2399 A73-37797
- Biplane roentgen videometric system for dynamic, 60/sec, studies of the shape and size of circulatory structures, particularly the left ventricle.
19 p2399 A73-37798
- A new technique for the study of left ventricular pressure-volume relations in man.
19 p2401 A73-38259
- Ejection time by ear densitogram and its derivative - Clinical and physiologic applications.
20 p2511 A73-38866
- Echocardiographic evaluation of the hemodynamic effects of chronic aortic insufficiency with observa-tions on left ventricular performance.
20 p2512 A73-38868
- Detection of left ventricular asynergy by echocar-diography.
20 p2512 A73-38869
- Contraction kinetics of ventricular muscle from hibernating and nonhibernating mammals.
20 p2514 A73-39603
- Effects of beta-blocking agents on atrio-ventricular and intraventricular conduction in man.
21 p2641 A73-41564
- The relationship between left ventricular ejection time and stroke volume during passive cardiovascular stress.
21 p2641 A73-41565
- Examination of a multiple dipole inverse cardiac generator, based on accurately determined model data.
22 p2813 A73-41961
- A simple cardiac contractility computer.
22 p2815 A73-42677
- Structural conditions in the hypertrophied and fail-ing heart.
22 p2807 A73-42685
- Nature and significance of alterations in myocardial compliance.
22 p2808 A73-42689
- Polyparametric information of the electrocardio-gram in injured tissue.
22 p2809 A73-42834
- Coronary heart disease; Proceedings of the Second International Symposium, Frankfurt am Main, West Germany, June 1972.
22 p2809 A73-42856
- Transient S-T elevation detected by 24-hour ECG monitoring during normal daily activity.
23 p2946 A73-43492
- Stroke volume measurement from an integral rheo-graph of human body
24 p3062 A73-44719
- Comparison of ultrasound and cineangiographic measurements of left ventricular performance in pa-tients with and without wall motion abnormalities.
24 p3062 A73-45400
- CARDIOGRAMS**
- Mechanisms of cardiac arrhythmias - From hypothesis to physiologic fact.
19 p2394 A73-37582
- Russian book - Integral topograms of heart poten-tials.
22 p2807 A73-42489
- CARDIOGRAPHY**
- NT BALLISTOCARDIOGRAPHY
- NT ECHOCARDIOGRAPHY
- NT ELECTROCARDIOGRAPHY
- NT PHONOCARDIOGRAPHY
- Left ventricular end-diastolic pressures following selective coronary arteriography.
01 p0010 A73-11508
- The value of the ultrasonic Doppler method and apexcardiography as reference tracings in phonocar-diography.
01 p0014 A73-11509
- Echocardiographic analysis of mitral valve motion in atrial septal defect.
02 p0138 A73-12444
- Echocardiographic findings in experimental myocardial infarction of the posterior left ventricular wall.
02 p0138 A73-12446
- A quick and inexpensive method of monitoring on tape the heart rate during exposure of the human head to pulsed magnetic fields.
03 p0270 A73-14289
- Quantitative radionuclide angiocardiology for determination of chamber to chamber cardiac transit times.
04 p0409 A73-14767
- Evaluation of the state of the cardiovascular system from polycardiographic test data
06 p0650 A73-17749
- The use of a compartmental hypothesis for the esti-mation of cardiac output from dye-dilution curves and the analysis of radiocardiograms.
07 p0784 A73-19124

The influence of recording speed on apexcardiographic timing - A multi-observer study of precision and performance utilizing randomized tracings in multiple subjects.

07 p0785 A73-19932

Pattern of blood flow within the heart - A stable system.

08 p0930 A73-21214

Left ventricular performance after myocardial infarction assessed by radioisotope angiography.

08 p0932 A73-21801

Ventriculographic patterns and hemodynamics in primary myocardial disease.

08 p0933 A73-21804

Video instrumentation for radionuclide angiography.

19 p2399 A73-37796

Measuring characteristics of the displacement cardiograph.

22 p2815 A73-42676

Early diagnosis of coronary heart disease; Proceedings of the Second Paavo Nurmi Symposium, Porvoo, Finland, September 9-11, 1971.

22 p2808 A73-42826

Indications and value of coronary arteriography.

22 p2808 A73-42830

The value of different angiographic procedures in coronary heart disease.

22 p2808 A73-42831

Ischemic polarcardiographic changes induced by exercise - A new criterion.

24 p3060 A73-44946

CARDIOLOGY

Fingerprint patterns incidence relation in congenital vitium cordis patients, using Henry dactyloscopic classification

01 p0009 A73-11080

Effect of a 5-day space flight on cardiodynamics during physical work of moderate intensity

02 p0138 A73-12467

Unusual diastolic heart beat in pericardial effusion.

03 p0259 A73-13059

Evaluation of cardiac performance in exercise.

03 p0259 A73-13539

Computerized ECG interpretation system for heart and circulatory disorder detection and diagnosis and health screening

03 p0272 A73-14660

Intermittent trifascicular block - Different mechanisms of conduction disturbances in the bundle branches.

07 p0780 A73-19152

The contractile function of the myocardium in two types of cardiac adaptation to a chronic load.

07 p0781 A73-19931

A comparison between the effects of dynamic and isometric exercise as evaluated by the systolic time intervals in normal man.

07 p0784 A73-20369

Papers on cardiac electrophysiology covering heart cells, membrane mechanism, molecular structure, excitation-contraction coupling, muscular ion transport, synaptic and atrioventricular transmissions, healing, etc

11 p1315 A73-25588

Effect of a 5-day space flight on the cardiac dynamics during moderately severe physical work.

15 p1840 A73-32617

The differential electrocardiographic manifestations of hemiblocks, bilateral bundle branch block, and trifascicular blocks.

18 p2274 A73-36523

Book - Atherosclerosis and coronary heart disease.

18 p2275 A73-36531

Localizing factors in experimental atherosclerosis.

18 p2275 A73-36536

Problems in the recognition of angina pectoris.

18 p2275 A73-36541

CARDIOVASCULAR SYSTEM

NT AORTA
NT ARTERIES
NT BLOOD VESSELS
NT CAPILLARIES [ANATOMY]
NT CARDIAC AURICLES
NT CARDIAC VENTRICLES
NT DIASTOLE
NT EOSINOPHILS
NT ERYTHROCYTES
NT GLOMERULUS
NT HEART
NT HEMATOPOIESIS
NT HEMATOPOIETIC SYSTEM
NT LYMPHOCYTES
NT MYOCARDIUM
NT RETICULOCYTES
NT SYSTOLE
NT VEINS

Cardiovascular and temperature regulatory changes during progressive dehydration and euhydration.

01 p0008 A73-10165

Automated system of storing and processing vectorcardiograms

01 p0012 A73-10660

Pilot incapacitation as cause of aircraft accidents, noting age connected cardiovascular disease as leading cause for loss of pilot license

01 p0013 A73-11238

Cardiovascular reflexes evoked by potassium ion stimulation of the heart under conditions of spinal deafferentation and intact innervation

03 p0262 A73-13820

Absence of appreciable cardiovascular and respiratory responses to muscle vibration.

03 p0263 A73-14119

Telemetry of cardiovascular parameters on fighter aircraft flying pilots.

03 p0272 A73-14309

Extent of engagement of various cardiovascular effectors to alterations of carotid sinus pressure.

05 p0539 A73-16250

Cardiovascular system reactions to alternating transverse accelerations in man

06 p0650 A73-17687

Reactions of the cardiovascular system of pilots with atherosclerosis symptoms under professional activity conditions

06 p0657 A73-17689

Application of multichannel rheography to physiological studies on a centrifuge

06 p0657 A73-17693

Evaluation of the state of the cardiovascular system from polycardiographic test data

06 p0650 A73-17749

The effects of hypoxia, hypercapnia, and asphyxia on the baroreceptor-cardiac reflex at rest and during exercise in man.

06 p0654 A73-18348

The use of a compartmental hypothesis for the estimation of cardiac output from dye-dilution curves and the analysis of radiocardiograms.

07 p0784 A73-19124

Sinus venosus atrial septal defect - Analysis of fifty cases.

07 p0784 A73-20368

Analysis of some mechanisms of human stability to decompression of the lower portion of the body

08 p0930 A73-20987

High altitude acclimatization and mountain climbing effects on human organism, considering oculomotor, cardiovascular and respiratory responses and endurance

08 p0930 A73-20991

Cardiovascular changes in middle-aged men during two years of training.

08 p0934 A73-21504

Central, femoral, and brachial circulation during exercise in hypoxia.

08 p0934 A73-21506

Changes in hemodynamics and efferent sympathetic pulsation during pressor cardiovascular reflexes under conditions of acute hypoxic hypoxia

09 p1039 A73-22365

Distribution of systemic blood flow during cardiopulmonary bypass.

09 p1041 A73-22930

Clinical evidence of cardiac weakness and incoordination secured by simultaneous records of the force BCG and carotid pulse derivative and interpreted by an electrical analogue.

09 p1046 A73-23174

Changes in the cardiac rhythm during a hypoxic functional test

10 p1179 A73-23820

The role of vestibulometry in medical evaluation of flight personnel

10 p1183 A73-23821

Effect of electrostimulation on hemodynamic shifts during prolonged hypokinesia

10 p1180 A73-23940

Interrelations among the supranal glucocorticoid activity, the cardiovascular systems, and the electrolyte metabolism during prolonged work

11 p1317 A73-26085

Hemodynamics alteration caused by acute hypoxia in animals with denervated carotid sinuses

13 p1574 A73-28350

Changes in cardiac activity and in the latter's phase structure during decompression of the lower half of the body

15 p1835 A73-31513

Influence of lower-body decompression on the state of the human cardiovascular system /according to roentgenokymographic data/

17 p2111 A73-34234

Cardiovascular responses to sudden strenuous exercise - Heart rate, blood pressure, and ECG.

17 p2112 A73-35461

Lipids in arteriosclerotic arterial tissues of man.

18 p2275 A73-36534

Localizing factors in experimental atherosclerosis.

18 p2275 A73-36536

Localizing factors in arteriosclerosis.

18 p2275 A73-36537

Experimental myocardial infarction - Hemodynamic evaluation.

18 p2275 A73-36540

Role of arterial and venous vessels of limbs in the process of cardiovascular reflex responses

18 p2277 A73-36578

Cardiovascular reactions of a healthy man exposed to sonic booms

18 p2284 A73-36909

On correlation between the changes in cerebellar bioelectric activity and the adaptive reactions under the effect of accelerations.

18 p2279 A73-36915

A study of Halon 1301 /CBrF3/ toxicity under simulated flight conditions.

18 p2285 A73-36930

Physiological shifts in the human organism under increased neuropsychic stresses

19 p2393 A73-37392

Evaluation of positive end-expiratory pressure in hypoxic dogs.

20 p2515 A73-39781

Oxygen delivery and oxygen return to the lungs at onset of exercise in man.

20 p2519 A73-39788

Effect of stimulation of certain hypothalamic structures on systemic and pulmonary circulation

21 p2637 A73-40282

Circulatory reflexes from mechanoreceptors in the cardio-aortic area.

21 p2638 A73-40637

The relationship between left ventricular ejection time and stroke volume during passive cardiovascular stress.

21 p2641 A73-41565

The energetic metabolism and some reactions of the cardiovascular system during multichannel electrical stimulation and voluntary stressing of muscles

24 p3059 A73-44670

Cardiopulmonary responses of male and female swine to simulated high altitude.

24 p3060 A73-45058

CARDS

NT PUNCHED CARDS

CARET WINGS

The pressure on flat and anhedra delta wings with attached shock waves.

02 p0128 A73-12501

Hypersonic and supersonic flow over caret wings at off-design conditions with attached bow shock at leading edges

02 p0128 A73-12502

Stability characteristics of re-entry wing shapes and their measurement.

03 p0244 A73-13567

Experimental results in the case of the Nonweiler wave-rider in the subsonic, transonic, and supersonic range

16 p1963 A73-33265

CARGO

NT AIR CARGO

CARGO AIRCRAFT

NT C-5 AIRCRAFT

NT C-130 AIRCRAFT

NT C-141 AIRCRAFT

Technical and economic analysis of nuclear power reactors application for international cargo ship and air transportation, noting feasibility study of airborne power plants

[AIAA PAPER 72-1061] 03 p0340 A73-13390

Transport cargo aircraft design requirements and supporting ground system concepts in view of future market demands with emphasis on economic constraints

[SAE PAPER 730352] 17 p2102 A73-34700

The C-401, a STOI. transport for many applications

17 p2107 A73-35666

The potential influence of the ACLS on the development of logistical cargo aircraft.

19 p2383 A73-37701

Freighter airships economical and technological feasibility study, discussing performance requirements and design concepts

[SAE PAPER 951] 19 p2385 A73-37879

CARGO SHIPS

NT TANKER SHIPS

Technical and economic analysis of nuclear power reactors application for international cargo ship and air transportation, noting feasibility study of airborne power plants

[AIAA PAPER 72-1061] 03 p0340 A73-13390

CARGO SPACECRAFT

Free flying teleoperator spacecraft systems for automated satellites retrieval, cargo transfer and orbital operations support

19 p2490 A73-37303

CARIBBEAN SEA

A synoptic investigation of anomalous warmth in the mid and upper troposphere during February 1964.

10 p1244 A73-23978

North American microtektites from the Caribbean Sea and their fission track age.

18 p2354 A73-36511

CARNOT CYCLE

The cooling of a sunspot. I - A Carnot cycle and the hydromagnetic interactions. II - Convection zone models and the magnetic power supply.

10 p1279 A73-24137

CAROTID SINUS REFLEX

The effect of time of electrical stimulation of the carotid sinus on the amount of reduction in arterial pressure.

Extent of engagement of various cardiovascular effectors to alterations of carotid sinus pressure.

A mathematical model to assess changes in the baroreceptor reflex.

Hemodynamics alteration caused by acute hypoxia in animals with denervated carotid sinuses

Posthyperventilation breathing - Different effects of active and passive hyperventilation.

The role of carotid sinuses in the regulation of hemodynamics during motor activity

Circulatory reflexes from mechanoreceptors in the cardio-aortic area.

Ophthalmodynamography in pilots to test internal carotid insufficiency - Comparison of blood-pressure responses.

Measurements of arterial pressure and of pressure-receptor reactions during prolonged pressure shifts in carotid arteries

24 p3062 A73-44720

CARRIER FREQUENCIES

Maximum likelihood estimate of carrier frequency and arrival direction of radio signals in background noise for large aperture antennas

OMECA time transmissions and receiver design.

Moored radio telemetering buoy relay stations for North Pacific climatological data acquisition, noting optimum channel frequency for data transmission error rate reduction

Undistorted short sounding pulse reception at exit from ionosphere obtained by signal carrier frequency modulation

Separate generation of odd and even harmonics of a fundamental frequency, with the aid of pulse circuits

Intelligible crosstalk and AM/PM transfer in commercial communications satellites. I

Carrier-frequency photography - Principle and application of lattice-coded image tracing

Effects of tape flutter on notch noise loading test performance of predetection recording of a frequency modulated carrier.

Circular carrier-frequency photography for observing phase objects.

Increasing the capacity of a discrete communications channel by additional modulation of a carrier parameter

Shaping circuit for complex RF pulse consisting of simultaneous equal-length square pulses with different frequencies, discussing carrier frequencies selection

Multipaths by diffusion on the ground and application to the transmission of digital messages affected by jumps of the carrier frequency

Utilization of optical-frequency carriers for low- and moderate-bandwidth channels.

A study of integral pulse frequency modulation of a random carrier.

Relation between the N. M. Krylov-N. N. Bogolyubov averaging method and the method of envelopes in studies of a class of control systems

Undistorted short sounding pulse reception at exit from ionosphere obtained by signal carrier frequency modulation

Ground stations in Intelsat 4 communication satellite radio relay system, discussing all-solid-state equipment design, carrier frequency assignment and antenna installation

Television sound subcarrier transmission in space communication.

Adjacent-channel interference between unfiltered and filtered QPSK signals.

Carrier-frequency distance dependence of a pulse propagating in a two-level system.

21 p2649 A73-40224

On the connection of the Krylov-Bogolyubov averaging method with the envelop method for investigating one class of control systems.

Noise immunity of quasi-optimal noncoherent reception during resynchronization with respect to time and frequency

Electrohydrodynamic stability of insulating fluids subjected to a unipolar injection

Transit mode operation of thermionic injection diodes

Instabilities and small-signal response of double injection structures with deep traps.

Calculation of the complex conductivity of a monopolar semiconductor with a finite-injection contact

Oscillations of injected carriers in p-type indium antimonide.

Impurity centers effect on I-V characteristics of double injection level semiconductors, noting negative resistance region

CW microwave oscillations of reach-through p-n-p barrier injection transit time /BARITT/ diodes, calculating small signal impedance and noise measure for comparison with experiment

P-n-p-n junction thyristor turnoff process under reverse anode voltage at high injection level, examining current voltage curve and switching time constant

Third side of the Lampert triangle - Evidence of traps-filled-limit single-carrier injection.

Forward biased P-N junction photoelectric current shown resulting from photovoltaic, photoresistive and electric injection currents superposition

Thermal free electron constant approximation in space charge current theory, considering I-V characteristics and ionized donor concentrations at injection levels

Characteristics of infrared photodetectors produced by radiation doping.

Additional data on the effect of doping on the lasing characteristics of GaAs-Al_xGa_{1-x}As double-heterostructure lasers.

The effect of an interfacial layer on minority carrier injection in forward-biased silicon Schottky diodes.

A unified approach to the theory of double injection in solids with traps uniformly and non-uniformly distributed in the energy band gap.

The measurement of the lifetime in psn diodes at high injection levels

Small-signal analysis of punch-through injection microwave devices.

Injection and field processes in thin semiconductor films in the current jump region

Injection currents in semiconductors with deep polarizable impurity centers

Injection-modulation devices as elements of integrated circuits

Observation of turn-on action in a gate-triggered thyristor using a new microwave technique.

Measurements of refractive index step and of carrier confinement at AlGaAs-GaAs heterojunctions.

Heterojunction injection lasers /Review/.

Theory and operation of space-charge-limited transistors with transverse injection.

Eigenfunction calculation of injected carrier density in doped semiconductor filaments, relating negative eigenvalues to Suhl effect and lifetime dependence to bulk and surface recombination

Fall-off of base component of I_T/I at low currents in a bipolar transistor.

Trap-assisted charge injection in MNOS structures.

Stationary charge transport in metal-semiconductor-metal/MSM/ structures.

CARRIER MOBILITY

NT ELECTRON MOBILITY

NT HOLE MOBILITY

Laser beam self focusing possibility in GaAs, considering nonlinearity mechanism of intervalley carrier transfer due to applied dc field

Influence of carrier drift on the propagation of electromagnetic wave in a solid-state plasma.

Electronic transport in insulating films.

Galvanomagnetic effects measured in p-type bismuth selenide single crystal within magnetic field for Hall and conductivity mobilities, determining temperature dependences

Kinetics of electrostatic image formation during exposure of electrophotographic layers

On the form and stability of electric-field profiles within a negative differential mobility semiconductor.

Transconductance and distortion of a thin-film transistor

The bus-probe and multiprobe methods of measuring Hall mobility in semiconductor layers of nonuniform depth

Ion-implanted bipolar transistor carrier concentration profiles.

Temperature dependence of kinetic properties of photoconductivity produced by carrier redistribution across attachment centers, discussing results with Ag and Al doped ZnS single crystals

Some operational aspects of an indirectly loaded transistorized pulse amplifier at short time intervals

Field-dependent carrier transport in non-crystalline semiconductors.

Studies of galvanomagnetic and thermomagnetic phenomena in selenium and tellurium doped InSb.

Theory of the oscillations and stability of a semiconductor plasma with a small number of carriers in a strong electric field

Charge carrier mobility distribution along the channel of an MDS field transistor

Semiconductor carrier mobility measurements with Hall generator, calculating sample geometry and finite dimension electrical contact effects on error

On the validity of the gradual channel approximation for junction field effect transistors with drift velocity saturation.

Influence of electric field strength on effective carrier mobility in polycrystalline CdSe thin films

The relation between the diffusivity-mobility ratio and the linewidth of spontaneous emission in degenerate semiconductors at relatively high temperatures.

CARRIER MODULATION

U MODULATION

CARRIER ROCKETS

U LAUNCH VEHICLES

CARRIER WAVES

Nonlinear wave modulation in cold magnetized plasmas.

The effect of carrier phase and timing on a single-sideband data signal.

Transmission characteristics of PSK wave in nonlinear system - Application to INTELSAT IV satellite systems.

Electron beams as carriers of optical coherence.

FM distortion of a TV signal and subcarriers due to bandpass filtering and additive Gaussian noise.

Communication system with self limiting multiple access repeaters, calculating critical intermodulation power levels resulting from N equal amplitude carriers for comparison with measurements

The effect of carrier recovery and bit timing errors in the coherent reception of 2 and 4 phase PSK signals.

CARTESIAN COORDINATES

Literat expressions for the co-ordinates of the moon. I - The first degree terms.

Cartesian coordinates for panoramic perspective position of point on conical map, noting relationship to semipolar coordinates of object point

- Linear regression filtering and prediction for tracking maneuvering aircraft targets.
11 p1333 A73-26640
- CARTRIDGE ACTUATED DEVICES**
U ACTUATORS
U EXPLOSIVE DEVICES
CARTRIDGES
Design criteria for inert or consumable polymer cartridge materials.
15 p1925 A73-31919
- L-1011 aircraft hydraulic system layout and installation techniques with modular design and plug-in cartridges for Murphy law error reduction during servicing
17 p2108 A73-34523
- CASCADE CONTROL**
Cascade phase-lock loops for the generation of harmonic and subharmonic components.
04 p0421 A73-15433
- Synthesis of statistically optimal multiloop control systems containing essentially nonlinear elements.
06 p0679 A73-17955
- Determination of limits bounding the bifurcational relationship between parameters of two-stage nonlinear servo mechanisms
09 p1033 A73-22653
- Synthesis of gyrator RC filters from the cascaded model
10 p1193 A73-23729
- Some features of the application of controlled-gain transistors.
12 p1480 A73-27271
- Design of sinusoidal and pulsed signal amplification stages with emitter high-frequency compensation.
12 p1480 A73-27273
- Optimization of the operating conditions of planar transistors in stages with inductive correction.
13 p1591 A73-28733
- Circuit variants and applications of series regulated transistor amplifiers, considering trigger circuit, bistable switch, power amplifier, tape recorder monitoring amplifier, etc
21 p2659 A73-40011
- Possibilities of improving the characteristics of operational amplifiers by using thermostated input cascades
21 p2660 A73-40023
- Cascade n-phase transistorized astable multivibrator circuit design for digital and tool control clock applications
23 p2983 A73-44142
- Synthesis of cascaded multiple-loop feedback systems with large plant parameter ignorance.
24 p3073 A73-44584
- CASCADE FLOW**
Behaviour of boundary layers on plane or annular fixed or mobile supersonic blade cascades
[ONERA, TP NO. 1110] 01 p0001 A73-10232
- Simulation of the flow past turbomachine blades in the study of plane-cascade vibrations
01 p0029 A73-10494
- Method of calculating vortex-free flow around hydrodynamic cascades composed of arbitrary profiles
02 p0128 A73-11788
- Subsonic centrifugal compressor efficient operating range extension by collector and diffuser blade cascades separation, presenting performance test results
02 p0204 A73-12792
- Aerodynamic noise and alternating loads in an idealized turbine stage.
03 p0242 A73-12981
- Problems regarding the use of electronic data processing for the calculation of diagonal cascades in turbomachines
03 p0242 A73-13169
- Acoustic resonance during the vibrations of a plate cascade in subsonic gas flow
03 p0294 A73-13619
- Small disturbance theory of rotating subsonic and transonic cascades.
03 p0246 A73-14136
- Flow conditions at inlet and exit of a flat plate cascade at supersonic velocities.
03 p0246 A73-14139
- Supersonic compressor performance for gas turbine engines, discussing cascade, single stage compressor rigs and experimental engine test results
03 p0360 A73-14152
- Axial flow turbomachines annulus wall boundary layer growth calculation methods, deriving momentum integral equations from passage averaged equations of motion through cascaded blades
03 p0249 A73-14645
- Some recent work on aspect ratio effects in compressor cascades.
[ASME PAPER 72-WA/FE-41] 04 p0404 A73-15858
- A combined theoretical and empirical method of axial compressor cascade prediction.
[ASME PAPER 72-WA/GT-5] 04 p0404 A73-15869
- Two dimensional cascade acoustic resonant frequencies estimation by variational method, presenting results for three cavity modes
05 p0599 A73-17372

- Associated mass of a simple doubly periodic lattice
06 p0643 A73-17465
- Calculation of the mean parameters of an inhomogeneous flow by the method of sections
06 p0645 A73-17720
- The effect of the degree of turbulence on the aerodynamic characteristics of planar decelerating cascades
[DFVLR-SONDDR-275] 07 p0773 A73-19197
- Predicting method of the change in stage performance of axial flow machinery for the variation of cascade geometry.
07 p0867 A73-19225
- Flow in the wake of a cascade of oscillating airfoils.
07 p0774 A73-19954
- Repeated cascade structure and kinetic description for homogeneous turbulence spectrum, considering coupled hierarchies origin from transfer function and eddy viscosity development
07 p0812 A73-20472
- Aerodynamic experimental investigation of annular cascade of gas turbine nozzle blade in subsonic and supersonic flow.
08 p0925 A73-20939
- Method of experimental study of cascades of transonic blades with strong deflection
09 p1027 A73-22211
- Unsteady nonlinear flow around an airfoil or a blade cascade with emission of turbulent vortices
09 p1027 A73-22212
- Fluctuating lift and moment coefficients for cascaded airfoils in a nonuniform compressible flow.
09 p1028 A73-22432
- Static tests of the working-channel cascade of a tangential turbine
09 p1028 A73-22571
- Flow through moving cascades of lifting lines with fluctuating lift.
10 p1171 A73-23697
- Secondary flows - Theory, experiment, and application in turbomachinery aerodynamics.
10 p1171 A73-23860
- Transonic gas flow in rotating turbomachine cascade channels, reducing flow equations to second order differential equation
10 p1172 A73-24507
- Researches on the two-dimensional retarded cascade. III - Cascade performances at high inlet angles.
11 p1302 A73-26338
- Researches on the two-dimensional retarded cascade. IV - Determination of blade elements at retarded blade row.
11 p1302 A73-26339
- Theoretical, quasi-static analysis of cavitation compliance in turbopumps.
11 p1349 A73-26667
- Flow at the trailing edges of a blade cascade at variable M and Re numbers
12 p1457 A73-27096
- Graphic-interactive analysis of the velocity field around blade cascades for turbomachines
12 p1458 A73-27387
- Use of blowing during tests of blade cascades
13 p1623 A73-28469
- Design method of the axial-flow blade row on modified isolated aerofoil theory with interference coefficient. I.
13 p1564 A73-28649
- Supersonic annular blade cascades starting conditions, presenting static pressure and Mach number distributions
[ONERA, TP NO. 1219] 13 p1565 A73-28837
- Control by pressure drop of the radial distribution of the Mach number behind a subsonic annular cascade
[ONERA, TP NO. 1220] 13 p1565 A73-28838
- Calculation of the unsteady subsonic aerodynamic pressures on compressor blades
[ONERA, TP NO. 1221] 13 p1565 A73-28839
- Two dimensional steady subsonic flow through airfoil cascades, predicting turbomachine performance from boundary layer calculation for comparison with experiments
13 p1565 A73-29005
- Effect of trailing edge thickness on the cascade performance of circular-arc blades.
13 p1565 A73-29006
- Influence of the variation of cascade geometry on the performance in axial flow machinery.
13 p1565 A73-29007
- Secondary flow in blade cascades of axial turbomachines and the possibility of reducing its unfavourable effects.
13 p1565 A73-29008
- Potential flow about arbitrary thick blades of large camber in cascade.
13 p1565 A73-29009
- A comparison between potential flow studies through blade cascade by theoretical and rheo-electric analogy methods.
13 p1565 A73-29010
- Experimental studies on high speed performance of two-dimensional turbine cascades.
13 p1566 A73-29019

- Periodic gust and wake induced unsteady air flow, calculating velocity variation with distance from rotor blade for cascade effect
13 p1566 A73-29026
- Experimental study by resonance method of unsteady aerodynamic forces acting on cascading blades.
13 p1566 A73-29028
- Optimization of energy transfer in cascaded fluid jet deflection amplifiers.
13 p1571 A73-29045
- Generalized relations for the parameters at the flow separation boundary in compressor cascades
13 p1567 A73-29551
- Providing a model of flow round a turbine blade when investigating the vibration of flat blading.
14 p1743 A73-30319
- Axial and radial turbocompressor analysis and design, presenting literature survey on cascade aerodynamics, iterative and hodograph computational methods, etc
14 p1712 A73-30429
- Velocity hodograph solvability and univalence problems in hydromechanics for profiles in duct, bounded flow and cascades
15 p1861 A73-31151
- Subcritical and supercritical compressible shock-free flows in blade cascades
16 p1962 A73-32812
- Subsonic compressible airfoil cascade flow calculations by series, iterative, matrix and streamline curvature methods, discussing transonic and supersonic cases
[ASME PAPER 73-GT-9] 16 p1963 A73-33487
- The use of a finite difference technique to predict cascade, stator, and rotor deviation angles and optimum angles of attack.
[ASME PAPER 73-GT-10] 16 p1963 A73-33488
- On the unsteady supersonic cascade with a subsonic leading edge - An exact first order theory.
[ASME PAPER 73-GT-15] 16 p1963 A73-33492
- On the unsteady supersonic cascade with a subsonic leading edge - An exact first order theory. II.
[ASME PAPER 73-GT-16] 16 p1964 A73-33493
- A contribution to the theoretical and experimental examination of the flow through plane supersonic deceleration cascades and supersonic compressor rotors.
[ASME PAPER 73-GT-17] 16 p2047 A73-33494
- Interface effects between a moving supersonic blade cascade and a downstream diffuser cascade.
[ASME PAPER 73-GT-23] 16 p1964 A73-33497
- Numerical representation of inlet and exit boundary conditions in transient cascade flow.
[ASME PAPER 73-GT-55] 16 p2048 A73-33511
- Calculation of compressible subsonic flow in cascades with varying blade height.
[ASME PAPER 73-GT-59] 16 p1964 A73-33514
- Turbulence downstream of stationary and rotating cascades.
[ASME PAPER 73-GT-80] 16 p1964 A73-33525
- Inviscid flow through a cascade of thick, cambered airfoils. I - Incompressible flow.
[ASME PAPER 73-GT-84] 16 p1964 A73-33527
- Inviscid flow through a cascade of thick, cambered airfoils. II - Compressible flow.
[ASME PAPER 73-GT-85] 16 p1964 A73-33528
- The unsteady response of a blade row from measurements of the time-mean total pressure.
[ASME PAPER 73-GT-94] 16 p1964 A73-33531
- Theoretical and experimental work on losses in 2-D turbine cascades with supersonic outlet flow.
17 p2092 A73-34377
- Secondary loss measurements in a cascade of turbine blades.
17 p2092 A73-34380
- Effect of axial velocity variation on deviation for compressor cascades.
17 p2092 A73-34383
- Method for calculating the steady irrotational isentropic flow in a two-dimensional supercritical turbine cascade.
17 p2093 A73-34390
- Low-speed performance of a compressor cascade designed for prescribed velocity distribution and tested with variable axial velocity ratio.
17 p2093 A73-34393
- Effect of axial velocity variation on the subsonic flow through a compressor cascade.
17 p2094 A73-34397
- The prevention of separation and flow reversal in the corners of compressor blade cascades.
17 p2094 A73-34448
- Simple universal equilibrium spectrum.
18 p2300 A73-36634
- Calculation of plane blade cascades in isentropic flow
18 p2266 A73-37085
- Effect of spanwise circulation on compressor noise generation.
19 p2473 A73-37292
- Stability and convergence of streamline curvature flow analysis procedures.
19 p2421 A73-38190
- Design of axial flow fans by cascade method.
21 p2631 A73-40124

Approximate calculation of flows through blade cascades under conditions of partial cavitation
22 p2841 A73-42129

Asymptotic unsteady three dimensional flow analysis in axial turbine cascade theory, assuming infinite blade number and unity pitch/chord ratio
[ONERA, TP NO. 1249] 22 p2796 A73-42220

Calculation of the maximum attainable efficiency of a moving compressor blade cascade
22 p2797 A73-42646

The unsteady aerodynamics of a finite supersonic cascade with subsonic axial flow.
[ASME PAPER 73-APMW-6] 22 p2797 A73-42879

Total pressure loss distribution in viscous gas flow through annular cascades of axial flow compressors, examining three dimensional flow effects on boundary layer development
24 p3054 A73-44916

Transonic equation for flow in apertures between compressor and turbine blades, examining gas dynamic and geometric parameter influence on near-sonic flow
24 p3054 A73-45024

CASCADE WIND TUNNELS
Application of certain generalized data from wind-tunnel tests with plane subsonic compressor cascades to the calculation of the characteristic flow regimes in supersonic cascades
12 p1458 A73-27480

Development of experimental turbine facilities for testing scaled models in air or freon.
17 p2145 A73-34381

CASCADES
Aerodynamic characteristics of torus shaped cascades involved in flame stabilization process of re-heat devices for jet engines
11 p1453 A73-26595

CASCADES [FLUID DYNAMICS]
U FLUID DYNAMICS
CASCADE MOSFET
U FIELD EFFECT TRANSISTORS
CASE BONDED PROPELLANTS
A description of the design, testing and application of the 'Waxwing' apogee boost motor for the 'Black Arrow' satellite launcher, with particular reference to development problems.
[AIAA PAPER 72-1134] 03 p0355 A73-13441

German book - Solid rocket propulsion systems II: Theory and technology.
06 p0740 A73-18074

CASE HISTORIES
Class action rule application in damage liability litigation, considering various case histories
06 p0771 A73-17513

Case histories of valvular cardiopathies in military pilots, determining tolerance to flight
07 p0784 A73-19209

Application of the numerical study of random time series to the analysis of the electroencephalogram of the normal infant
08 p0935 A73-21540

Project analysis - An evaluation tool for positive development direction.
10 p1298 A73-24634

CASES [CONTAINERS]
NT ROCKET ENGINE CASES
CASING
Feasibility evaluation of graphite/epoxy composite materials to helicopter transmission housing.
10 p1238 A73-23969

CASPIAN SEA
Remote sounding of water surface conditions from aboard artificial satellites.
21 p2657 A73-41333

CASSEGRAIN ANTENNAS
Off-axis polarization characteristics of Cassegrainian and front-fed paraboloidal antennas.
01 p0022 A73-10177

Parabolic, Cassegrain, spherical and horn-parabolic axisymmetric mirror antennas, calculating primary radiating element orientation effects on radiation polarization characteristics
05 p0547 A73-16052

A new earth-station antenna for domestic satellite communications.
08 p0947 A73-21144

Approximate calculation of the small-reflector surface from the deformations of the large reflector of a Cassegrainian antenna
12 p1480 A73-27235

Shaping of subreflectors in Cassegrainian antennas for maximum aperture efficiency.
14 p1734 A73-30207

On the equivalent parabola technique to predict the performance characteristics of a Cassegrainian system with an offset feed.
14 p1734 A73-30211

A simplification in the analysis of four- and five-horn fed Cassegrainian reflectors when the horns have nearly symmetric patterns.
14 p1735 A73-30224

Depolarisation with Cassegrainian and front-fed reflectors.
14 p1728 A73-30448

Radiation patterns and structural design of two mirror millimeter wave Cassegrain antennas with horn radiator
16 p1991 A73-33985

Large scanning and multibeam reflector antennas for space communications.
20 p2524 A73-38738

Multiple-beam spherical-reflector antenna systems for satellite communications.
20 p2525 A73-38739

Implementation of fixed multiple beam spherical antenna systems and measured test results.
20 p2525 A73-38740

Synthesis and analysis of optimal dual-mirror antennas
23 p2959 A73-43516

Radiation characteristics of a corrugated conical horn.
24 p3069 A73-45029

A fan-beam dual reflector antenna.
24 p3069 A73-45030

CASSEGRAIN OPTICS
Basic instrumentation components for prime, Cassegrain and coude focal positions of Anglo-Australian telescope, discussing acquisition and guiding, photography, photometry and spectrography
01 p0046 A73-10506

Intermediate dispersion spectrograph instrument design for Cassegrain focus of Anglo-Australian telescope, discussing optical and mechanical layouts and remote control
01 p0046 A73-10509

Prototype design of echelle grating spectrographs for Anglo-Australian 3.8 meter telescope Cassegrain focus, presenting main parameters
01 p0047 A73-10511

A new Cassegrain grating spectrograph. I - Optical design.
01 p0047 A73-10513

A new Cassegrain grating spectrograph. II - Mechanical design and operation.
01 p0047 A73-10514

Astronomical position detector with image dissector tube at Cassegrain telescope focus for automatic guiding by illumination distribution analysis
01 p0029 A73-10544

Support method and equipment for observer at Cassegrain focus of large telescopes, emphasizing universal chair structural details and operation principles
01 p0029 A73-10545

A proposed standard mechanical interface for Cassegrain acquisition-guider heads.
01 p0029 A73-10546

Lunar laser observatory equipment modifications, noting change of Cassegrain primary mirror from spherical metal alloy to hyperboloidal glass construction
02 p0176 A73-12244

General analysis of aplanatic Cassegrain, Gregorian, and Schwarzschild telescopes.
03 p0309 A73-14426

Image quality in telescopes with image motion compensation by secondary mirror control.
03 p0309 A73-14429

Schmidt telescopes for northern and southern hemispheres, discussing optical design with achromatic corrector to achieve high angular resolution and conversion to Cassegrain configuration
08 p0966 A73-21366

Multiple mirror telescope consisting of six Cassegrainian telescopes combined for common focal surface, noting light gathering power equivalent to 180 inch standard telescope
08 p0970 A73-21738

The universal automatic reflector AZT-12
15 p1877 A73-32129

The automatic telescope AZT-11
15 p1877 A73-32130

The fine solar sensor of the Astronomical Netherlands Satellite.
16 p2012 A73-32852

Limiting magnitude techniques with the Corralitas 24 inch Cassegrain image orthicon system.
17 p2169 A73-35290

The fine sun sensor of the astronomical Netherlands satellite.
19 p2431 A73-38100

Lidar measurements for the exploration of the atmosphere
22 p2823 A73-41825

CASSIOPEIA A
An interferometric survey of the areas surrounding four intense radio sources.
03 p0380 A73-14637

Aperture synthesis of interstellar neutral hydrogen in absorption. I - The Perseus arm feature of Cassiopeia A.
22 p2904 A73-41756

CASTIGLIANO VARIATIONAL THEOREM
The Castigliano variational equation in the theory of nonlinearly hereditary creep
07 p0912 A73-19322

The Castigliano variational equation and strain continuity relations for a thin shell
12 p1555 A73-27788

Method of orthogonal projections for three-dimensional problems of elasticity theory
18 p2362 A73-36401

Uniqueness theorems and variational principles derivation for free viscoplastic flow and constrained plastic deformation, obtaining Castigliano theorem from boundary value problem solution
23 p3044 A73-43974

CASTING
NT INVESTMENT CASTING
Improved melting and casting procedures for a cobalt-base magnetic alloy.
04 p0455 A73-15750

Liquid rubber formulation for cold and hot urethane casting of photoelastic models, including membranes and thin walled structures
07 p0843 A73-19566

The partitioning of refractory metal elements in hafnium-modified cast nickel-base superalloys.
13 p1633 A73-28138

Titanium casting technology applications to aircraft structures, considering flap tracks, brake torque tubes and arrestor hook mounting brackets
16 p2018 A73-33071

Effect of small group-VIII metal additions on the structure and properties of cast molybdenum
17 p2189 A73-34578

Investigation of the dross molding process for titanium carbide
23 p2991 A73-43490

CASTING SOLVENTS
U PLASTICIZERS
CASTINGS
Mechanical properties and applications of reinforced plastics for cast alloy elements, machine parts and noncorrosive light structures production, emphasizing glass fiber reinforcement
03 p0334 A73-13593

Fine precipitate within coarse gamma-prime particles in cast Ni-base superalloy during elevated temperature exposure
10 p1235 A73-24446

Mechanical and corrosion resistant properties of titanium castings.
19 p2442 A73-37947

Influence of alloying with elements of group VIII on the mechanical properties of a molybdenum alloy containing carbon in the cast and recrystallized states
20 p2577 A73-39366

Interaction of interstitial impurities with iron-subgroup metals in as-cast molybdenum-based dilute solid solutions
22 p2873 A73-42090

CATABOLISM
Role of the sympathico-adrenal system during a period of rest and in adaptation to muscular activity
01 p0007 A73-10157

Thermal factor and dehydration influences on protidic and lipidic catabolisms of young men with partial food deprivation in hot climate, discussing metabolic balances
08 p0934 A73-21248

CATALOGS [PUBLICATIONS]
NT ASTRONOMICAL CATALOGS
CATALYSIS
NT AUTOCATALYSIS
Chemisorption and catalysis of hydrogen on polycrystalline wires of tungsten and nickel.
06 p0661 A73-18253

Propulsion system for space applications, based on the catalytic decomposition of hydrazine
07 p0866 A73-18929

Heat exchanging and catalytic dissociation of ammonia flowing through tubes - Application to micropropulsion.
07 p0867 A73-18931

Combustion catalysis model of a single-component fuel/as applied to ammonium perchlorate/
07 p0865 A73-19991

Decomposition of hydrazine on Shell 405 catalyst at high pressure.
15 p1841 A73-32174

Exo-electron emission during heterogeneous catalysis /the effect of external electric potentials/.
15 p1842 A73-32599

The effects of catalysis in measuring the temperature of incompletely-burned gases with noble-metal thermocouples.
22 p2857 A73-42035

CATALYSTS
NT ELECTROCATALYSTS
Depressurization extinguishment of composite solid propellants - Influence of composition and catalysts.
[AIAA PAPER 72-1136] 03 p0352 A73-13443

Kinetics of the sulphur dioxide catalyzed recombination of radicals in hydrogen flames.
03 p0352 A73-14393

Red fuming nitric acid suitability for nonhypergolic rocket fuel ignition in presence of chromate and dichromate catalysts
07 p0865 A73-19986

A technique for measuring relative threshold nucleation temperatures for active nucleation catalysts.
12 p1521 A73-26816

Influence of oxidizer dispersity on the efficiency of combustion catalyzers

13 p1669 A73-28973

Ignition of nonhypergolic bipropellants in presence of suitable catalysts.

14 p1784 A73-30044

Investigation of cobalt molybdate polymorphism

15 p1887 A73-31207

Effects of copper chromite and iron oxide catalysts on AP/CTPB sandwiches.

22 p2899 A73-42812

CATALYTIC ACTIVITY

Long-life firings of a catalytic reactor for monopropellant hydrazine.

03 p0350 A73-13378

Catalytic effects of copper chromite and iron oxide on AP-HTPB binder sandwich combustion to 3200 psia by cinephotomicrography

03 p0352 A73-13434

Chemical evolution under the bion hypothesis.

03 p0265 A73-14316

Organic compounds catalytic activity comparison for use in fuel cell, noting superiority of dihydro-dibenzo-tetraazaannulene cobalt complex

04 p0407 A73-15109

Effects of a fully catalytic wall on a non-equilibrium boundary layer including ablation products.

04 p0519 A73-15826

Solvent effects on enzymes - Implications for extraterrestrial life.

06 p0652 A73-17948

Ir catalysts for high performance hydrazine decomposition, discussing preparation by coprecipitation of active metallic element with support in chloroiridic acid solution

07 p0865 A73-18928

Effects of experimental conditions on parameter estimated when using the Hill model

09 p1044 A73-21872

Effect of surface catalytic activity on stagnation heat-transfer rates.

13 p1706 A73-28804

The mechanism of catalyzer action on the burning of condensed systems

13 p1669 A73-28974

Catalytic effects in corrosion processes with hydrogen depolarization of multiphase magnesium alloys

14 p1764 A73-30827

Reduction of oxygen compounds of cobalt by methane

14 p1724 A73-30828

Homogeneously catalyzed formaldehyde condensation to carbohydrates. II - Instabilities and Cannizzaro effects.

15 p1841 A73-32200

Kinetics of the catalytic reactions of the thermal decomposition of perchloric acid and ammonium perchlorate

19 p2402 A73-37505

Studies of a homogeneous copper catalyst for fuel cell air cathodes in acid media.

19 p2390 A73-38400

Molybdenum-oxygen-sulfur fuel cell anode catalysts capable of oxidizing low cost fuels in acid electrolytes

19 p2390 A73-38401

Prebiotic reactions combining amino acids and ribonucleotides into polypeptides and polynucleotides in presence of urea, imidazole and Mg positive ion, suggesting contemporary biosynthesis parallels

21 p2637 A73-40372

Catalytic activity in platinum group temperature sensors, discussing elimination by noncatalytic coatings

22 p2857 A73-42034

Catalytic efficiencies of atoms in the vibrational relaxation of HF and DF.

22 p2818 A73-42763

Effect of composite propellant catalysts on the stabilities of HClO₄ and the HClO₄-NH₃ system.

22 p2899 A73-42814

CATAPULTS

NT ROCKET CATAPULTS

Disorienting effects of aircraft catapult launchings.

07 p0785 A73-19480

CATARACTS

Management of cataract in commercial flight personnel.

18 p2285 A73-36927

CATECHOLAMINE

NT EPINEPHRINE

Effects of endotoxin on monoamine metabolism in the rat.

01 p0009 A73-11100

Intensity of exercise and heart tissue catecholamine content.

03 p0259 A73-13498

The role of biogenic amines in sleep.

03 p0264 A73-14260

Catecholamine exchange in the hormonal and mediator links of the sympathoadrenal system under stress

07 p0784 A73-20367

Circadian rhythms in catecholamines in organs of the golden hamster.

11 p1318 A73-26120

Relative rates of arterial lactate and oxygen-deficit accumulation in hypoxic dogs.

15 p1836 A73-31922

Influence of electric stimulation of the hypothalamus on catecholamine, phosphorylated compound, and cholesterol levels

21 p2637 A73-40284

Emotionally induced increases in heart rate and plasma catecholamine and free fatty acids, noting relation to coronary heart disease

22 p2809 A73-42837

CATHETERIZATION

On the causes of the changes of the second heart sound in left bundle branch block.

01 p0009 A73-11008

Nature of the conduction disturbance in selective coronary arteriography and left heart catheterization.

02 p0134 A73-12443

Comparison of isometric exercise and angiotensin infusion as stress test for evaluation of left ventricular function.

12 p1464 A73-27889

Assessment of left ventricular performance in man - Instantaneous tension-velocity-length relations obtained with the aid of an electromagnetic velocity catheter in the ascending aorta.

15 p1836 A73-31996

Permanent catheterism of the thoracic aorta - Direct measurement of arterial pressure, injection of substances, and the taking of blood in wake rats

24 p3065 A73-45160

CATHODE RAY TUBES

NT PICTURE TUBES

Coding technique to record computer generated binary hologram on numerically controlled CRT with resolution cell of two beam spots

01 p0019 A73-11235

Traveling wave tube for satellite applications.

03 p0281 A73-13174

Visual performance with high-contrast cathode-ray tubes at high levels of ambient illumination.

06 p0658 A73-18243

Electron-beam tube with semiconducting laser screen.

06 p0677 A73-18636

Accelerated generation of deflecting voltages by the functional beam-control method

08 p0967 A73-21589

Human factors aspects in aircraft electronic display systems, discussing cathode ray tubes (CRT) and light emitting diodes (LED) applications and characteristics

11 p1324 A73-26500

A visual stimulator employing a T.V. raster display.

14 p1722 A73-30400

Experimental approach for utilization of cathode ray tube piloting instruments

15 p1831 A73-32509

A moderately-priced modern cathode-ray tube without intensifier electrode

16 p1987 A73-33166

CRT designs for high-sensitivity high speed broadband oscilloscopes, discussing brightness characteristics enhancement

16 p1987 A73-33167

Thin configuration flat digital CRT display with electron beam control improvement for military avionics applications, discussing performance advantages and ownership cost

17 p2139 A73-35235

Storage tube with silicon target captures very fast transients.

21 p2661 A73-40228

Some problems associated with the construction of scanner employing a cathode-ray tube and programmed control

21 p2665 A73-41270

A multiplex cathode-ray-tube display with digital readout for a body plethysmograph.

22 p2815 A73-42666

CATHODES

NT CELL CATHODES

NT COLD CATHODES

NT HOLLOW CATHODES

NT HOT CATHODES

NT PHOTOCATHODES

NT PHOTOMULTIPLIER TUBES

NT THERMIONIC CATHODES

NT TUBE CATHODES

Phase diagrams of ternary Ni-Re alloys with La, Y, Sc, Hf, Si and Mo for cathode applications in electronic vacuum devices

03 p0325 A73-13516

Pressed cathodes made from barium scandate and refractory metals mixture, investigating operation in plasma discharge of He-Ne lasers

06 p0703 A73-18601

Relationship between adsorption processes on the cathode surface and processes in the region near the electrode in a high-current plasma discharge

09 p1127 A73-22608

Investigation of the steady-state temperature field in a composite cathode of a plasmatron

15 p1917 A73-31192

The signal-to-noise ratio of a photodetector with a virtual cathode.

17 p2168 A73-35172

Titanium cathode blanks in electrolytic production of metals, noting titanium oxide nonstick properties, electron transmission and corrosion resistance

19 p2442 A73-37841

Studies of a homogeneous copper catalyst for fuel cell air cathodes in acid media.

19 p2390 A73-38400

Cathodoluminescence of ruby /0.05 wt %/ at high temperatures

21 p2752 A73-40797

Ions bombarding the cathode of a pulsed plasma accelerator and their participation in the development of thermal fluxes

23 p3014 A73-44343

CATIONS

NT FERRIC IONS

NT MANGANESE IONS

NT METAL IONS

Positive ion composition measurements in disturbed D region, noting positive molecular oxygen ions as major source of water cluster ions

01 p0041 A73-10890

Probe measurements of positive ions and electron temperatures in high latitude rocket flights.

02 p0159 A73-12032

E and F regions ion composition measurement with rockets, noting nitric oxide variation with molecular/atomic oxygen cations ratios at different solar activity phases

02 p0206 A73-12305

An atomic absorption method for cation measurements in Kjeldahl digests of biological materials.

02 p0139 A73-12424

Activated oxygen ashing of biological specimens for the microdetermination of Na, K, Mg, and Ca by atomic absorption spectrophotometry.

02 p0139 A73-12546

Cation determinative curves for Mg-Fe-Mn olivines from vibrational spectra.

02 p0139 A73-12636

Effectiveness of the application of tightly bonded sulfo-cation exchange resins in water recycling by the sorption method

06 p0656 A73-17677

A comparative experimental study of electron and positive-ion current collection by a cylindrical Langmuir probe under orbital-limited conditions.

08 p0967 A73-21598

Titanium monoxide system cation self-diffusion coefficients, and quenched-in vacancy concentrations as function of stoichiometry, tabulating Arrhenius parameters

13 p1633 A73-28145

Diffusion spreading of weak plasma inhomogeneities in the presence of two kinds of positive ions.

13 p1608 A73-28710

Zirconium sorption by and release from carboxyl cationates in nitric and sulfuric acids, discussing pH dependence

14 p1765 A73-30884

Self consistent field calculations of CO positive ion dipole moment in ground state

17 p2119 A73-35180

Dissociative recombination rate for CH positive ions in interstellar clouds

19 p2490 A73-38531

CATS

Roentgenographic study of relative heart motion during vibration in water-immersed cats.

16 p1973 A73-34039

CAUCHY INTEGRAL FORMULA

Mixed boundary value problems in solid contact and crack mechanics, discussing numerical solution of singular integral equations with simple and generalized Cauchy kernels

09 p1162 A73-23184

A new method for the Lebedev-Ufliand integral equation for contact problems of elasticity.

15 p1946 A73-31103

Boundary value problem of linear conjugation with a piecewise-continuous matrix coefficient

15 p1900 A73-32104

Certain theorems concerning functions of an incomplete quaternion variable

24 p3107 A73-45512

CAUCHY PROBLEM

Asymptotic properties of solutions of certain linear systems of differential equations with random coefficients

01 p0070 A73-10913

A priori estimate of the solution to a Cauchy problem with data prescribed on a time-like surface for a 2-nd order parabolic equation and the uniqueness theorems associated with it

01 p0071 A73-11426

Second-order abstract and Schrodinger linear differential equations in Beurling spaces

02 p0186 A73-11570

Complex variable analysis for exact solution to Kepler equation for elliptical and hyperbolic orbits based on canonical solutions to Riemann problem

03 p0376 A73-14269

Cauchy problem and mixed boundary value problems for parabolic and hyperbolic wave equations of heat conductivity for boundary operators given on hyperplane

04 p0517 A73-14935

Approximate solution of the Cauchy problem by the method of polynomial operators

04 p0470 A73-14936

Certain analytical solutions of the Cauchy problem for a disturbed loaded linear integrodifferential equation

04 p0470 A73-15080

Hyperbolic equations and systems with multiple characteristics.

04 p0471 A73-15224

Asymptotic waves and Cauchy problem with singular data for a system of linear equations with a double characteristic

04 p0471 A73-15245

Riemann-method solution of the Cauchy problem for a system of first-order equations with a degeneracy at the boundary

06 p0717 A73-18068

Invariant imbedding and a transformation procedure for reducing classes of boundary value problems into equivalent initial value systems.

06 p0719 A73-18804

Method of solution of certain boundary value problems for nonlinear hyperbolic equations and propagation of weak shock waves.

07 p0809 A73-19015

Electromagnetic wave propagation in a circular waveguide with spirally conducting inserts

07 p0793 A73-19920

Electrodynamical mathematical model for electroconductivity of nonuniform plasma with Hall effect, calculating current distribution from Riemann problem solution

08 p0992 A73-20863

Solution of the Cauchy problem for a nonlinear equation describing a gas flow in the presence of strong blowing

09 p1029 A73-23352

'Farfield' behavior of solutions to partial differential equations asymptotic expansions and maximal rates of decay along a ray.

10 p1241 A73-23700

Heat conductivity equation solution stabilization for Cauchy problem with oblique derivative and arbitrary number of geometrical variables

10 p1295 A73-24061

Approximate solution of the system of Boltzmann equations for a mixture of reacting gases

10 p1252 A73-24490

Method for successively increasing the step of numerical integration for systems of ordinary differential equations

12 p1516 A73-26952

Construction of asymptotic solutions to the Cauchy problem with an initial jump for nonlinear systems of integrodifferential equations containing a small parameter at the higher derivative

12 p1518 A73-27298

Equivalence of one type of a Riemann boundary value problem for a system of n pairs of functions relative to a complete singular integral equation with a Cauchy kernel

12 p1518 A73-27730

Cauchy problem solution stability for non-homogeneous heat conduction equation with two space variables, allowing specular reflection on rectilinear boundary

12 p1560 A73-27809

Construction of doubly branched fundamental solutions of the Cauchy problem for homogeneous rotationally invariant hyperbolic operators with constant coefficients

12 p1518 A73-27817

Global solutions to a class of nonlinear hyperbolic systems of equations.

13 p1647 A73-28024

Improperly posed initial value problems for self-adjoint hyperbolic and elliptic equations.

13 p1648 A73-28424

Asymptotic behavior of solutions of the Cauchy problem and the first boundary value problem on a half-axis for a linear second-order parabolic equation with the absolute value of x approaching infinity and at large values of the parameter

13 p1651 A73-29680

The Cauchy problem in classes of increasing functions for some second-order quasi-linear degenerate parabolic equations

14 p1769 A73-30347

Cauchy problem solution for motion of plasma generating shock wave after fast impact under influence of one dimensional gas flow

15 p1822 A73-31289

Numerical method for mixed elliptical-hyperbolic nonlinear Cauchy problem with boundary conditions, applying to sonic flow around wing sections

16 p1961 A73-32807

Initial-value problems in potential theory.

16 p2032 A73-33304

Regularity theorems for the solution of a second-order abstract linear differential equation

16 p2032 A73-33373

The mixed boundary value problem for the elastic half space.

16 p2081 A73-33901

Overall existence of a solution of the Cauchy problem for the system of equations with Liouville-Newton partial derivatives

17 p2201 A73-35045

Linearization of Cauchy's problem for quadratic semilinear partial differential equations.

20 p2581 A73-38865

Improvable estimates in some non-well-posed problems for a system of elliptic equations.

20 p2581 A73-38975

The Cauchy problem and some basic problems of mathematical physics about parabolic systems with discontinuous coefficients

20 p2582 A73-39252

Asymptotic properties of solutions to single-point and two-point problems with singular perturbations for systems of ordinary linear differential equations

22 p2882 A73-42473

Second order cross stress study of elastic shear deformation, considering rotation invariant Cauchy tensor and Poynting effect

23 p3039 A73-43306

A Riemann-Hilbert problem for a heat conduction in a finned surface.

23 p3049 A73-44051

Boundary value problem solutions uniqueness and existence for ordinary differential equations under Cauchy condition

23 p3000 A73-44209

Solution of the Riemann problem for a class of hyperbolic systems of conservation laws by the viscosity method.

24 p3112 A73-45469

The Cauchy problem and a general representation of solutions to an elliptic-type fourth-order equation with analytic coefficients

24 p3106 A73-45508

CAUCHY-RIEMANN EQUATIONS

Riemannian homogeneous boundary-value problem with an infinite index and a coefficient having a denumerable set of discontinuities of the first kind

17 p2200 A73-34629

CAUSTICS

U AI.KALIES

CAVITATION

U CAVITATION FLOW

CAVITATION CORROSION

Investigation of the corrosion-erosion resistance of niobium alloys

06 p0711 A73-18668

Possibility of improving the erosive activity of a cavitation bubble by the combined effect of continuous and pulsed sound

08 p0955 A73-21448

Cavitation erosion in geometrically similar nozzles with lead and plastic liners, presenting expressions for erosion rates dependence on scale

10 p1206 A73-24669

CAVITATION FLOW

Ideal fluid flow past a body with an upstream jet

01 p0035 A73-11427

Minimum pressure zone determination for pressure field at axial plunger pump inlet during cavitation onset, discussing working fluid temperature and composition

02 p0172 A73-11800

Impulsive loading of liquid squeeze film plane circular bounding surfaces, showing fluid inertia effect on bonding strength and cavitation relationship to viscosity

03 p0292 A73-13305

Eddy cavitation flow past a wedge

06 p0686 A73-18071

Limited cavitation and the related scale effects problem.

06 p0686 A73-18435

Interaction of pulsating bubbles in a viscous fluid

08 p0955 A73-21446

Application of a singular perturbation method to the study of beginning cavitation

09 p1071 A73-22215

A numerical-analytical method of calculating stream flow of a heavy liquid around curvilinear obstacles

10 p1205 A73-23585

Flow of an ideal fluid past a body with a reverse-stream.

11 p1348 A73-26056

Nonlinear plane cavity flow past flexible barrier, deriving uniqueness theorem by variational operator formulation in terms of potentialness conditions

11 p1391 A73-26547

Theoretical, quasi-static analysis of cavitation compliance in turbopumps.

11 p1349 A73-26667

On the numerical treatment of the Navier-Stokes equations for an incompressible fluid.

13 p1599 A73-28090

Perforated water tunnel to decrease wall effect on deflected cavitation flow, studying suction coefficient, pressure losses and blowing parameters

13 p1597 A73-28450

Possibility of enhancing the erosive activity of a cavitation void under the simultaneous action of continuous and pulsed sound.

15 p1860 A73-31012

Experimental study of cavitation oscillations in a centrifugal screw pump

15 p1832 A73-31499

The dynamic behavior and compliance of a stream of cavitating bubbles.

[ASME PAPER 73-FF-34] 17 p2153 A73-35025

Cavitation and boiling bubble growth, collapse and damage effects, discussing liquid jet formation temperature effects, glycerol, ethanol and water solutions and bubble geometry

20 p2548 A73-39516

High-speed photography of laser-induced cavities in liquids

21 p2709 A73-39968

Heat resistant materials cracking and fracturing caused by ductility loss at high temperatures, discussing cavitation mechanisms, microcracks, creep tests and time dependence

21 p2722 A73-41576

Equations of the boundary perturbations of a cavity moving near a solid wall

22 p2841 A73-42124

Influence of suction on the supercavitation flow behind a body in a porous tube

22 p2841 A73-42125

Experimental investigation of the development of a cavern in the case of unsteady gas-induced cavitation

22 p2841 A73-42128

Approximate calculation of flows through blade cascades under conditions of partial cavitation

22 p2841 A73-42129

Approximate calculation of the cavitation flow past low-aspect-ratio wings

24 p3055 A73-45540

CAVITIES

Natural convective heat transfer in cavities and horizontal circular tubes, considering boundary layer and core flow interaction effects

01 p0120 A73-10290

Creep life and strain estimation for Nimonic alloy by monitoring cavity density under optical microscope

03 p0326 A73-13965

Radially symmetrical thermoelastic disturbances in generalised dynamical theory of thermoelasticity.

03 p0395 A73-14311

The effect of polarity on the diffraction of plane elastic waves by a cylindrical cavity.

03 p0396 A73-14627

Relationship between cavitation and decontamination during ultrasonic processing of aluminum and its magnesium alloys

04 p0454 A73-15663

The propagation of waves from a cylindrical cavity.

10 p1289 A73-24282

The effect of couple-stresses on the stress concentration around an elliptic hole.

15 p1947 A73-31335

Qualitative study of flow deviation by a wall cavity

16 p1962 A73-32811

Numerical solution for the flow of a fluid in a heated closed cavity.

16 p2084 A73-32929

High temperature thermal cavity system with vitreous carbon tube and end plugs for material and thermochemical environment investigations, discussing mass spectroscopic measurement

17 p2149 A73-35752

Investigation of two-dimensional cavity diffusers.

[AIAA PAPER 73-685] 18 p2262 A73-36236

Numerical study of viscous flow in a cavity.

20 p2545 A73-38971

Equations of perturbed motion of a body with a liquid-containing cavity when the normal to the free liquid surface deviates sizably from the axis of the cavity

20 p2547 A73-39510

The emittance of blackbody cavities.

22 p2930 A73-41981

Free surface profile of wedge-shaped cavity in metal during collapse due to incident shock wave with decreasing pressure behind shock front

24 p3093 A73-44711

Nonlinear transient effects of separated unstable flow on vortex generated acoustic waves in cavities

[AIAA PAPER 73-1014] 24 p3078 A73-44846

CAVITY RESONATORS

Book - Handbook of microwave techniques and equipment.

01 p0021 A73-10025

Series-connected operation of Gunn diodes in a coaxial resonator

01 p0025 A73-10980

Nonlinear computation of a resonant O-type oscillator featuring constant wave amplitude in the presence of losses

01 p0025 A73-10984

Experimental investigation of the coupling impedance in resonator chains with a positive mutual inductance coefficient

01 p0025 A73-10987

Variable reflectivity unstable laser resonator mode selectivity solution by perturbation analysis for mirror misalignment effects, obtaining Fresnel number and output coupling conditions

01 p0060 A73-11223

Coupling losses in hollow waveguide laser resonators.

02 p0177 A73-12573

Evaluation of acoustic cavities for combustion stabilization.

[AIAA PAPER 72-1147]

03 p0356 A73-13452

Diffraction losses and corrections for lower order transverse modes and resonance conditions in optical resonators with cylindrical mirrors

03 p0319 A73-14079

Carbon dioxide laser output signature calculation as function of cavity length based on homogeneously broadened line with dispersion

03 p0320 A73-14455

An experimental study of unstable confocal CO₂ resonators.

03 p0320 A73-14456

Pulse pumped Q switched Nd-YAG and ruby lasers single longitudinal mode selection by providing intracavity resonator with active medium

03 p0320 A73-14464

Mode losses in hollow-waveguide lasers.

04 p0457 A73-14747

Jet-driven cylindrical cavity oscillators.

[ASME PAPER 72-WA/FLCS-4]

04 p0409 A73-15862

Density changes in a laser cavity including wall reflections and kinetics of energy release.

[AIAA PAPER 73-141]

05 p0585 A73-16890

Nonlinearity of Helmholtz resonators

05 p0599 A73-17269

Determination of the spatial distribution of a plasma with a microwave resonator.

06 p0727 A73-17423

Zero-g propellant gauging

06 p0755 A73-17573

Design and characteristics of a single pass normal mode ruby oscillator-amplifier laser for hole drilling in metals.

06 p0700 A73-18277

Laser diodes cavity radiative efficiency loss due to sidewall induced internally circulating modes, considering cavity length, width and reflectivity relations

06 p0701 A73-18358

Unstable resonators for CO₂ electric-discharge convection lasers.

06 p0703 A73-18747

Cylindrical laser resonators with partial radial radiation and strong axial energy focusing, relating low-loss cavity modes to Gaussian beam modes

07 p0833 A73-19273

Attainment of a low-noise high-power and highly stable Gunn oscillator by coupling to a superconducting cavity.

07 p0801 A73-20109

High-Q toroidal cavities for high frequency klystrons.

07 p0803 A73-20550

Waveguide cavity multistage Gunn reflection amplifiers for FM-CW systems, discussing stabilization techniques, bandwidth, noise, power variation with temperature and group delay distortion

07 p0803 A73-20552

A three-cavity ring type filter.

07 p0804 A73-20572

Dependence of characteristics of a gas laser on the parameters of an intracavity absorber.

08 p0974 A73-20953

Plasma diagnostics with open microwave cavities

08 p0963 A73-21014

Study of the geometrical resonances of superconducting tunnel junctions.

08 p0994 A73-21207

Energy and threshold characteristics of chemical lasers.

08 p0975 A73-21213

Theory of a generalized Helmholtz resonator.

08 p0952 A73-21471

Electron admittance and efficiency of the output cavity of a klystron

08 p0948 A73-21557

Cavity dimension effect on single mode generation spectrum of GaAs epitaxial CW injection laser at 77 K

08 p0976 A73-21655

Emission from a bunch of charged particles in multiple transit through a cylindrical resonant cavity

09 p1061 A73-21885

An antiresonant ring interferometer for coupled laser cavities, laser output coupling, mode locking, and cavity dumping.

09 p1091 A73-22085

Characteristics of acoustooptic cavity dumping in a mode-locked laser.

09 p1091 A73-22089

The design, analysis, and performance of resonant and nonresonant microwave transmission devices with theoretically infinite rejection.

09 p1080 A73-22103

The effect of an external signal on a ruby laser in the free-emission mode

09 p1095 A73-22667

Generation spectra of a ruby laser with frequency scanning

09 p1095 A73-22680

Effects of plasma temperature on the frequency shift in resonant cavities.

09 p1131 A73-22907

Outlet of second harmonic emission for the laser resonant cavity

09 p1097 A73-23011

Open resonator operating at 337-micron wavelength.

09 p1097 A73-23094

Estimation of possible excitation frequencies for shallow rectangular cavities.

09 p1029 A73-23444

Density homogeneity in a laser cavity due to energy release.

09 p1098 A73-23450

Tunnel and Gunn diode oscillators coupled to superconducting cavity as S and X band frequency standards

10 p1195 A73-24397

Microwave cavity measurements of electron densities in a shock tube.

10 p1220 A73-24620

A quick accurate method to measure the dielectric constant of microwave integrated-circuit substrates.

10 p1197 A73-24866

Development of cavities for microwave solid state sources.

11 p1338 A73-26150

Mechanism of passive negative feedback in the cavity of a solid-state laser

12 p1504 A73-26884

Laddertron oscillator /klystron/ cavity dispersion characteristics via electrodynamic analysis of dispersion equation for surface wave operation and coupled modes

12 p1477 A73-26948

An analysis of pulsation in coupled-cavity structure semiconductor lasers.

12 p1505 A73-27014

Ring cavity for analyzing the spectral composition of CO₂-laser radiation

12 p1506 A73-27217

Cavity-backed panel resonance.

13 p1690 A73-28062

Contribution to the theory of the natural vibration spectra of a nonequilibrium resonant cavity

13 p1589 A73-28290

Method of experimental study of fields in electromagnetic resonators - Application to helicoidal resonators

13 p1589 A73-28472

Noise in cavity-stabilized microwave oscillators.

13 p1595 A73-29294

High frequency discharges sustained either on a cavity resonance or on a plasma resonance

14 p1779 A73-29923

Iterative diffraction calculations of transverse mode distributions in confocal unstable laser resonators.

14 p1756 A73-30156

Optimal electron grouping arrangements in multi-resonator klystrons

14 p1736 A73-30565

A dual-resonator quantum amplifier operating at a wavelength of 1.35 cm for radio-astronomical observations

15 p1851 A73-31832

Spectral line absorption measurement using optical cavities.

17 p2184 A73-34913

Properties of a superconducting point contact connected to a resonator.

17 p2220 A73-35725

Properties of microwave cavities containing magnetic resonant samples.

17 p2130 A73-35758

Unstable cavities with a central coupling hole in lasers and amplifiers

18 p2322 A73-36559

Reproducibility of the frequency of a stabilized laser employing a ring cavity

19 p2437 A73-37246

Cavity perturbation technique for determining the presence of molecular ions of helium in a dc discharge plasma.

19 p2469 A73-37901

Verification of sensitivity enhancement factors for CW ultrasonic resonators.

20 p2565 A73-38887

Characteristics of a laser using a grid as the resonator output mirror

21 p2713 A73-40528

Hole-type confocal active optical cavity resonator loss distribution, discussing Fresnel zone oscillation type intensity within resonator and diffraction at cavity

21 p2714 A73-40559

Theory of eigenmode spectra of a nonequilibrium resonator.

22 p2830 A73-41814

A cavity-backed dipole antenna with wide-bandwidth characteristics.

22 p2831 A73-41851

Self-resonant LSA oscillator diode of rectangular cross-section.

22 p2832 A73-41895

Boost klystron efficiency with three-cavity design.

22 p2833 A73-42400

German monograph on microwave filters for communication channels separation at millimeter wavelengths covering coupling circuits design and resonant frequencies of coaxial resonator

22 p2827 A73-42701

An analog investigation of the gas jet resonance tube.

23 p2967 A73-43401

Real laser cavity with nonideal reflecting mirrors, showing Q factor increase relation to mode order for plane monochromatic linearly polarized waves

23 p2987 A73-43650

A possible Q-factor modulation mechanism in a ruby laser with a misaligned resonator

23 p2988 A73-44047

Increasing the locking bandwidth of a waveguide-cavity oscillator through the use of a double-tuned circuit.

23 p2965 A73-44109

Short-term frequency stability of an L band oscillator with a superconducting cavity.

23 p2961 A73-44117

A method for the study of the gain and the oscillating modes of a CO₂ laser.

23 p2989 A73-44176

Calculation of the mode structure in the Fabry-Perot cavity of a laser with a high flow rate

24 p3095 A73-44752

Determination of the transmittance of an optically not dense plasma by an intracavity method

24 p3115 A73-44762

A model for the pressure excitation spectrum and acoustic impedance of sound absorbers in the presence of grazing flow.

24 p3077 A73-44830

CEILINGS [METEOROLOGY]
Climatic presentations for short-range forecasting based on event occurrence and reoccurrence profiles.

06 p0720 A73-18707

Use of model output statistics for predicting ceiling height.

09 p1114 A73-22125

CEILOMETERS
U CLOUD HEIGHT INDICATORS

CELESCOPES
Ultraviolet photometry of the moon with the telescope experiment on the OAO-II.

01 p0096 A73-10317

Intrinsic ultraviolet colors from OAO-2 Telescope observations for stars on the main sequence.

17 p2225 A73-34290

Report on the telescope ultraviolet observations from the OAO-2 satellite and associated research at the Smithsonian Astrophysical Observatory.

18 p2349 A73-35996

CELESTIAL BODIES

NT A STARS

NT ACHONDrites

NT ANDROMEDA GALAXIES

NT AQUARIUS METEORIDS

NT ASTEROIDS

NT B STARS

NT BINARY STARS

NT BOLIDES

NT BRUDERHEIM METEORITE

NT CARBONACEOUS METEORITES

NT CASSIOPEIA A

NT CEPHEID VARIABLES

NT CHONDRITES

NT COMET TAILS

NT COMETS

NT CRAB NEBULA

NT DEIMOS

NT DRACONID METEORIDS

NT DWARF STARS

NT EARLY STARS

NT EARTH [PLANET]

NT ECLIPSING BINARY STARS

NT EUROPA

NT EXTARS

NT EXTRASOLAR PLANETS

NT GALAXIES

NT GEMINID METEORIDS

NT GIACOBINI-ZINNER COMET

NT GIANT STARS

NT GLOBULAR CLUSTERS

NT GUM NEBULA
 NT HERCULES NOVA
 NT HOT STARS
 NT IAPETUS
 NT INFRARED STARS
 NT IO
 NT IRON METEORITES
 NT JUPITER [PLANET]
 NT LATE STARS
 NT LEONID METEORIDS
 NT M STARS
 NT MAGNETIC STARS
 NT MAIN SEQUENCE STARS
 NT MARS [PLANET]
 NT MERCURY [PLANET]
 NT METEORITES
 NT METEOROID DUST CLOUDS
 NT METEOROID SHOWERS
 NT METEORIDS
 NT MICROMETEORITES
 NT MICROMETEORIDS
 NT MILKY WAY GALAXY
 NT MOON
 NT NATURAL SATELLITES
 NT NEBULAE
 NT NEPTUNE [PLANET]
 NT NEUTRON STARS
 NT NOVAE
 NT O STARS
 NT ORGUEIL METEORITE
 NT ORIONID METEORIDS
 NT PERSEID METEORIDS
 NT PHOBOS
 NT PLANETARY NEBULAE
 NT PLANETS
 NT PLUTO [PLANET]
 NT PRAESEPE STAR CLUSTERS
 NT PROTOSTARS
 NT PULSARS
 NT QUADRANTID METEORIDS
 NT QUASARS
 NT RADIO GALAXIES
 NT RADIO METEORS
 NT RADIO SOURCES [ASTRONOMY]
 NT RADIO STARS
 NT REFERENCE STARS
 NT SATURN [PLANET]
 NT SIKHOTE-LIN METEORITE
 NT SOLAR SYSTEM
 NT SPIRAL GALAXIES
 NT SPORADIC METEORIDS
 NT STAR CLUSTERS
 NT STARS
 NT STONY METEORITES
 NT SUBDWARF STARS
 NT SUN
 NT SUPERGIANT STARS
 NT SUPERNOVAE
 NT T TAURI STARS
 NT TAURID METEORIDS
 NT TEKTTITES
 NT TITAN
 NT TUNGUSK METEORITE
 NT URANUS [PLANET]
 NT VARIABLE STARS
 NT VENUS [PLANET]
 NT VESTA ASTEROID
 NT VIRGO STAR CLUSTER
 NT WHITE DWARF STARS
 NT ZODIACAL DUST
 The n-body problem with variable gravitational constant, and some dynamical consequences for large-scale cosmic systems. 01 p0107 A73-11327
 The effects of viscous friction on the precession and nutation of celestial bodies. 02 p0217 A73-12396
 Space exploration and celestial bodies natural resources exploitation legislation proposals evaluation 04 p0523 A73-15152
 UN space treaty proposals relating to moon and other celestial bodies natural resources utilization 04 p0524 A73-15158
 Russian monograph on relativistic celestial mechanics covering celestial and solar system bodies motion, Riemann geometry, tensor analysis, N body problem and cosmology 04 p0502 A73-15969
 Redshifts of a BSO and galaxies in the vicinity of the radio source RN 8. 08 p1009 A73-21171
 Circular polarization of the emission of cosmic objects 09 p1151 A73-23329
 Calculation of higher-order perturbations in the motion of celestial bodies 10 p1282 A73-24482
 A BESM-3M computer program for processing photographic observations of extended objects 11 p1333 A73-25231
 Influence of the thrust interruption during passage through the shadow cone of a celestial body on the trajectory of a space vehicle using solar electric propulsion - First-approximation calculation 12 p1540 A73-27393

Painleve metric replacement for Schwarzschild metric in tests of general relativity, considering problem of supermassive celestial body gravitational collapse 15 p1937 A73-31650
 On the use of a dual spin vehicle for scanning a celestial body. [AIAA PAPER 73-910] 20 p2614 A73-38844
 Celestial bodies gravitational potential mathematical representation by Lamé functions via series expansion of Laplace differential equation in ellipsoidal coordinates 20 p2606 A73-39080
 Tidal generation of magnetic fields in binary celestial systems, calculating growth times 24 p3134 A73-44578
CELESTIAL GEODESY
 Space geodetic techniques since 1957 covering photography, radar and laser uses in satellite observations with geodetic applications 13 p1671 A73-28006
 Determination of equations of conditions between harmonics of resonance of the order of 14 starting with observations from the Eole satellite 21 p2781 A73-41327
CELESTIAL MECHANICS
 Satellite orbit inclination function computation as representative problem in symbolic programming applied to celestial mechanics 01 p0099 A73-10688
 Dynamics of gravitating systems against the neutrino background of the universe 01 p0100 A73-10712
 Universal dimensionless formulas for physical property and trajectory computation in cosmic spherical media, applying to Kepler orbits, particle motions and radio wave paths 01 p0103 A73-11019
 A solution to the problem of the third integral of motion. I. 01 p0106 A73-11318
 Brady trans-Plutonian planet existence rejection from dynamical considerations, noting disruption of coplanar configuration in outer solar system 02 p0226 A73-12833
 Solar-planetary system mechanical parameters determination based on astronomical unit, discussing conversion into terrestrial units via radar distance measurements 03 p0376 A73-14174
 Sufficient conditions for return in the three-body problem. 03 p0377 A73-14274
 Epicyclic motion of stars at different regions of the galaxy. 03 p0379 A73-14586
 Matrix method for canonical transformations in many body problem of celestial mechanics 03 p0379 A73-14587
 Hubble law correspondence in invariant mechanical theory of universe expansion to direct consequence of impulse conservation in inertially moving many body system 03 p0380 A73-14603
 Some consequences of the Mach-Einstein doctrine for celestial mechanics and geophysics 04 p0498 A73-15280
 Russian monograph on relativistic celestial mechanics covering celestial and solar system bodies motion, Riemann geometry, tensor analysis, N body problem and cosmology 04 p0502 A73-15969
 Interaction of stars with local dust formations. 04 p0503 A73-16008
 Investigation of the process of the explosive disintegration and simultaneous collision of n gravitating material points 05 p0619 A73-16844
 Accelerated numerical integration of the equations of motion of celestial mechanics 05 p0619 A73-17002
 Book - The Titius-Bode Law of planetary distances: Its history and theory. 06 p0753 A73-18403
 Analytical theory of the motion of the fifth Jupiter satellite 07 p0876 A73-19395
 Russian book on celestial and space flight mechanics covering trajectory and orbit evolution problems, resonance effects, relative motion dynamics and mathematical treatment 09 p1146 A73-22350
 Geometrical dynamics method for orbit geometry in configuration space of dynamical system, using polar coordinates as generalized coordinates for circular restricted three body problem 09 p1148 A73-22911
 Satellite orientation relative to force center, considering condition for maximum lock strength of resonance rotation 09 p1149 A73-22912
 Studies in the application of recurrence relations to special perturbation methods. 09 p1149 A73-22914

Close binaries and their significance in the theory of evolution of stars 09 p1151 A73-23332
 Smithsonian Package for Algebraic and Symbolic Manipulation /SPASM/ computer program with generality and efficiency for Poisson series processing in celestial mechanics 10 p1283 A73-24667
 Dense stellar systems dynamics, considering gravitation relaxation, star evaporation, antiequidistribution, growth of dense galactic cores, stellar coalescence, disruption and formation 11 p1414 A73-25065
 Explosive disintegration and simultaneous collision of n material gravitating points. 11 p1423 A73-26054
 Past and future of research methods in problems of the earth's rotation. 13 p1677 A73-28377
 A numerical method of integration by means of Taylor-Steffensen series and its possible use in the study of the motions of comets and minor planets. 14 p1790 A73-29788
 A library of standard programmes for constructing numerical theories for studying the motion and evolution of the orbits of the minor bodies of the solar system. 14 p1790 A73-29789
 Determination of the form of the Oort cometary cloud as the Hill surface in the galactic field. 14 p1793 A73-29827
 Periodic solutions of the restricted three-body problem encompassing a large number of revolutions about the smaller body 15 p1931 A73-31240
 Book - Vistas in astronomy. Volume 13. 15 p1932 A73-31302
 Recent advances of celestial mechanics in the Soviet Union. 15 p1932 A73-31303
 Genetic relationship between short period comets and meteor streams, considering radial and longitudinal focusing mechanism for particles in meteor streams 15 p1939 A73-32009
 Book on Cartesian vortex theory of planetary motions covering celestial mechanics theories of Galileo, Kepler, Descartes, Leibniz and Newton 15 p1960 A73-32422
 Small grain aggregates created by equalized grain orbits on Kepler trajectories, with low collisional frequency in early state of solar system planetary evolution 17 p2227 A73-34407
 Mariner 9 celestial mechanics experiment - A status report. 19 p2479 A73-37223
 On the equivalence between Hori and Lacina perturbations theories. 19 p2483 A73-37564
 A stable manifold theorem for degenerate fixed points with applications to celestial mechanics. 19 p2486 A73-37799
 Computerized simultaneous numerical integration of motion equations for solar system, star cluster and galaxies, considering radar observations of moon, Mercury, Venus, Mars and Icarus 21 p2772 A73-41241
 Properties of galactic orbits and motion integrals of high-velocity stars. II - Periodic and nonperiodic orbits in the 2nd Schmidt potential 22 p2907 A73-42303
 Phase plane analysis of the commensurable restricted three-body problem. 22 p2912 A73-42942
 On global existence and uniqueness theorems for gravitational systems. 24 p3141 A73-45280
 Three body problem triple close approaches within escape mechanism, discussing method to control numerical integrations accuracy 24 p3141 A73-45281
 Periodic symmetric solution properties of restricted three body problem for case with lunar mass parameter tending to zero, discussing bifurcation orbit dynamics 24 p3141 A73-45286
CELESTIAL NAVIGATION
NT ASTRONAVIGATION
 Position locus by measurement of the ascension speed of a real or fictitious star 02 p0190 A73-12011
 Statistical data processing method for accuracy evaluation of satellite orbit parameters obtained from onboard measurements of two stars angular positions 03 p0379 A73-14554
CELESTIAL OBSERVATION
U ASTRONOMY
CELESTIAL REFERENCE SYSTEMS
 On space-time, reference frames and the structure of relativity groups. 01 p0079 A73-11255
 Dollen data reduction method for meridian-observed FK 4 star pairs right ascension and time deter-

mination, calculating instrument, personal and catalog errors

03 p0371 A73-13219

Rotation of the moon and lunar coordinate systems.

04 p0497 A73-15180

Methods of optimization of a spacecraft angular position control program

05 p0594 A73-16412

Conservation laws and preferred frames in relativistic gravity. I Preferred-frame theories and an extended PPN formalism. II - Experimental evidence to rule out preferred-frame theories of gravity.

12 p1540 A73-27326

Earth rotation measurements relative to reference frames and changes and mechanisms of axis orientation and spin rate

20 p2553 A73-39125

CELESTIAL SPHERE

New statistical laws governing the system of long-period comets

19 p2480 A73-37235

CELL ANODES

Electrode kinetic studies on the anodic oxidation of methanol.

04 p0406 A73-15102

Molybdenum-oxygen-sulfur fuel cell anode catalysts capable of oxidizing low cost fuels in acid electrolytes

19 p2390 A73-38401

CELL CATHODES

Nitrogen-containing active carbon as the cathode catalyst in acid fuel cells.

04 p0407 A73-15107

Electronically conducting oxides as cathodes or interconnection materials in high-temperature fuel cell batteries.

04 p0407 A73-15111

Fuel cell air cathode for high current densities at low polarization and ambient temperature, noting performance improvement with pure oxygen supply

04 p0407 A73-15112

CELL DIVISION

Effects of the space flight environment on man's immune system. II - Lymphocyte counts and reactivity.

02 p0135 A73-12565

Mitotic activity in dorsal epidermis of *Rana pipiens*.

07 p0784 A73-20456

CELLS

Martian canals interpretation based on thermodynamic subsurface cells with time-limited cellular convection and densification of dust masses along cell boundaries

04 p0501 A73-15628

Cellular or filamentary structure of galactic magnetic fields, noting correlations between rotations of radio sources and angular separation

08 p1002 A73-20880

CELLS (BIOLOGY)

NT AXONS

NT CARBOXYHEMOGLOBIN

NT CHROMOSOMES

NT COLLAGENS

NT EOSINOPHILS

NT ERYTHROCYTES

NT GAMETOCYTES

NT HEMATOPOIESIS

NT HEMOGLOBIN

NT LYMPHOCYTES

NT MITOCHONDRIA

NT NEURONS

NT OXYHEMOGLOBIN

NT RETICULOCYTES

Studies of the electron transport chain of extremely halophilic bacteria. VIII - Respiration-dependent detergent dissolution of cell envelopes.

01 p0009 A73-10625

Neuron networks modeling from viewpoint of intracellular and cell-medium interaction, discussing coding properties and nonsingular self adjusting system response

01 p0012 A73-10652

Induced retinal image blurring effects on rabbit mid-brain single cell trigger features and response efficiencies, noting receptive field responsive area

01 p0010 A73-11503

Triparanol inhibition of sterol biosynthesis in *Chlorella emersonii*.

02 p0139 A73-12547

Cation exchange binding of rubidium and cesium by rat liver cell microsomes.

02 p0135 A73-12549

Resistance of soil microorganisms to starvation.

02 p0136 A73-12627

Electron-microscopic investigations regarding the protective effect of hyperthermia on cell organelles in the case of whole-body X-irradiation

03 p0262 A73-13824

Methodical studies concerning the polarographic measurement of respiration and 'critical oxygen pressure' in mitochondria and isolated cells with the aid of the membrane-covered platinum electrode

03 p0272 A73-14647

Circadian rhythms - Subcellular and biochemical aspects.

06 p0651 A73-17824

Atomic, molecular, cellular, genetic, multicellular, neural, mental, social and suprasocial levels of evolution, discussing systems constituents, interactions and selective focus

06 p0651 A73-17929

Myeloperoxidase, the peroxidase of a primitive cell - Its reaction with Fe and H₂O₂.

06 p0652 A73-17944

Dependence of poly U-directed cell-free system on ratios of divalent and monovalent cations.

06 p0652 A73-17945

Comparative anatomy of the vestibular nuclear complex in submammalian vertebrates.

06 p0655 A73-18575

Ultrastructure of the atrial, ventricular, and Purkinje cell, with special reference to the genesis of arrhythmias.

06 p0655 A73-18873

Rabbit hippocampal neuron activity relation to theta-wave phases from cell potential and extracellular recording analyses

07 p0782 A73-20005

Single cell analysis of saturation discrimination in the macaque.

08 p0932 A73-21568

Order and disorder in the rhythm of the heart /Fifth Annual George C. Griffith Lecture/.

08 p0933 A73-21806

Vertebrate photoreceptor cell /rods and cones/ development and structure, discussing light pathway, ciliary connective and microtubules, outer and inner segments, etc.

09 p1042 A73-23303

Light evoked responses in invertebrate photoreceptor cells, considering cell organization, microvilli, lateral eye of *Limulus*, generator potentials, visual responses, etc

09 p1042 A73-23307

Light evoked changes in potential difference between inside and outside of cells in *Limulus* ommatidia, describing multistage model of generator potential

09 p1043 A73-23309

Receptive fields of retinal ganglion cells.

09 p1043 A73-23315

Effect of light deprivation on the metabolic reaction development in retinal ganglion cells

10 p1178 A73-23681

Possibility of modeling the relationship between the intracellular potential of individual muscle fibers and the overall electromyogram for tonic muscles

10 p1179 A73-23810

Incidence of Lucke renal adenocarcinoma in *Rana pipiens* as determined by histological examination.

11 p1314 A73-25136

Brain tissue functional organization based on models for cell pseudorandom behavior, information processing, learning and memory, considering spontaneous wave and unit firing

11 p1314 A73-25143

Embryonic chick heart cell age dependent electrophysiological studies, discussing structure, metabolism, ATPase activity, membrane potential and cell interactions

11 p1315 A73-25589

Morphological and experimental excitation models of cardiac muscle ultrastructure, transmission activity and intercellular contact relationships

11 p1315 A73-25590

Cardiac action potential rising phase and generation mechanism, discussing pacemaker potential and slow depolarization initiating upstroke in spontaneously active cardiac cells

11 p1316 A73-25592

Ionic current mechanisms for cardiac muscle repolarization time course of Purkinje fibers and other heart cells, relating charge transfer data to earlier studies

11 p1316 A73-25593

Electrogenic potassium inward transport involvement in mechanism of enhanced repolarization, correlating cardiac excitation with Na, K and Ca ions transfer and active ion transport

11 p1316 A73-25594

Calcium movements and excitation-contraction coupling in cardiac cells.

11 p1316 A73-25601

Biochemical and morphological studies of lunar material effects on plant tissue culture cells, noting nonpathological increased cellular activity and chloroplast and cytoplasm changes

11 p1320 A73-26482

Automatic microscopy for mitotic cell location.

12 p1464 A73-27144

Proliferative activity of bone marrow cells in dogs exposed to chronic and repeated acute gamma irradiation

12 p1463 A73-27708

Responses of indigenous microorganisms to soil incubation as viewed by transmission electron microscopy of cell thin sections.

14 p1714 A73-29724

The effect of iontophoretically applied acetylcholine upon the cat's retinal ganglion cells.

14 p1715 A73-30061

Structure of the lipid phase in cell envelope vesicles from *Halobacterium cutirubrum*.

17 p2112 A73-34599

Russian book - Primary and initial processes of the biological action of radiation.

18 p2269 A73-35896

Rabbit optokinetic reactions and retinal direction-selective cells /A preliminary model/.

18 p2273 A73-36455

Cell viability in acute myocardial infarction, discussing pathogenesis, histological, histochemical and biochemical responses to ischemia, homeostasis maintenance and treatment methods

18 p2276 A73-36545

Some metric characteristics of myocardial cells under various conditions of cardiac and cardiovascular pathology

18 p2280 A73-36962

Biodegradation from evolution viewpoint as physiological function and fundamental cellular process regulating biological equilibrium, explained by intracellular digestion and phagocytic cells association

21 p2638 A73-41024

The radiobiological effects of heavy ions on mammalian cells and bacteria.

22 p2805 A73-42182

Probability cross sections of heavy ion single hit inactivation paths for human cells using nitrogen ion accelerator experiments

22 p2805 A73-42183

Analysis of the changes in glial cell numbers in the auditory cortex during the application of acoustic stimuli of various intensities

22 p2807 A73-42653

Abnormal biochemistry in myocardial failure.

22 p2808 A73-42686

Study of the nature of the active tonus with the aid of a discrete Wiener-medium analog

22 p2816 A73-42973

Effects of electromagnetic waves of the millimeter range on a cell and on some structural elements of a cell

23 p2949 A73-44095

Local resistance variations caused by membrane potential shifts in the interior of the horizontal retina cell

24 p3061 A73-45250

CELLULOSE

Use of cellulose crystallite structures with solid state strain gages for humidity and moisture measurement.

17 p2166 A73-34621

Investigation of the possibility of using acetylated oxyethylcellulose as a film forming substance for a moving-picture film base

21 p2647 A73-40262

Influence of certain hydroxyl- and nitrogen-containing low-molecular-weight substances on the structural viscosity of cellulose acetate solutions

21 p2647 A73-40263

Influence of a mixture of plasticizers, exhibiting a different mechanism of action, on the deformation of cellulose triacetate over a wide range of temperatures

21 p2647 A73-40264

CELLULOSE NITRATE

Simulation of the compounder in a single base propellant /SBP/ process.

17 p2220 A73-34819

Stepwise burning of non-volatile readily dispersible substances

19 p2503 A73-37502

Dye laser tuning with pellicles.

22 p2870 A73-42707

CELSIUS TEMPERATURE SCALE

U TEMPERATURE SCALES

CEMENTATION

Niobium and tungsten cementation in a glow-discharge plasma

09 p1089 A73-23197

CEMENTITE

The tempering of low carbon steels containing tungsten.

02 p0183 A73-12760

Investigation of the kinetics of the redistribution of alloying elements between the alpha solid solution and cementite in cobalt and nickel steels

24 p3100 A73-45362

CEMS SYSTEM

U CENTRAL. ELECTRONIC MANAGEMENT SYSTEM

CENSORED DATA [MATHEMATICS]

The Kolmogorov-Smirnov test modified for censored data.

16 p2033 A73-33619

CENTAUR LAUNCH VEHICLE

NT ATLAS CENTAUR LAUNCH VEHICLE

Titan/Centaur launch vehicle for high payload escape missions and large synchronous orbit spacecraft, describing propulsion, control/guidance and telemetry systems

18 p2359 A73-36094

CENTAUR VEHICLE

U CENTAUR LAUNCH VEHICLE

CENTER OF GRAVITY

A method of determining the center of mass of the moon from ground observations 01 p0100 A73-10840

Optimum position of the center of gravity of a passenger plane in cruising flight 02 p0129 A73-11649

A method of a determination of earth's motions around its mass center from simultaneous laser and photographic observations of artificial earth satellites made by two stations. 02 p0159 A73-12168

Some differences between geometrical and dynamical figures of the moon. 03 p0367 A73-13080

'Barycentric' averaging of the hydro-dynamical equations with respect to coordinate systems with arbitrary vertical coordinate 04 p0473 A73-15697

Electric forces in electrostatic gyroscope for rotor gravity center displacement, taking into account mutual effects of electrode pairs 05 p0577 A73-16994

Fourier analysis of Mars radar topographic data for magnitude and direction of center of mass/center of figure offset, comparing to earth and moon 11 p1419 A73-25862

Correlation of the shift in the center of gravity of a focused light beam in a turbulent atmosphere 11 p1331 A73-26160

Evidence for convection in planetary interiors from first-order topography. 12 p1542 A73-27492

Earth axis displacement and continental drift related to lack of coincidence of core and mantle-crust centers of mass 13 p1679 A73-28399

A method for determining the position of the moon's center of mass from earth-based observations. 15 p1927 A73-30976

Center of forces existence and related configurations for given law of force, rejecting Wintner conjecture 15 p1913 A73-31109

Two dimensional nonlinear oscillations around center of mass of vehicle moving along circular orbit with magnetic damping under gravitational field and external perturbation 15 p1942 A73-31233

Application of methods of mathematical statistics to study the motion of an artificial earth satellite about its center of mass 15 p1931 A73-31234

Null correlation method for estimation of the primary energies of cosmic ray jets. 15 p1927 A73-32149

Optimal motions of a spacecraft relative to its center of mass 21 p2781 A73-40903

Computerized control system for fuel flow into and out of fuel cells and aircraft gravity center optimization during supersonic cruise and takeoff 21 p2634 A73-40939

Dynamics of the rotary motions with respect to the center of mass of a system of solids with a variable geometry of the masses 23 p3007 A73-44187

Rectilinear trajectories of the three-body problem when the constant of line forces is zero 24 p3141 A73-45282

CENTER OF PRESSURE

The tricuspid hypocycloid as envelope of the force of lift, calculated in a first compressible approximation, in the case of a symmetrical profile in a flow of variable direction and a given Mach number 05 p0528 A73-16764

CENTIGRADE TEMPERATURE SCALE

U TEMPERATURE SCALES

CENTRAL ELECTRONIC MANAGEMENT SYSTEM

Principles of spacecraft telemetry data management. 11 p1333 A73-25351

MADAP - Implementation of a large size real time data processing system. 15 p1849 A73-32448

Evolution of the satellite telemetry data processing facility at the Goddard Space Flight Center. 17 p2123 A73-35300

Station Data Acquisition and Control System. 17 p2147 A73-35301

CENTRAL NERVOUS SYSTEM

NT BRAIN

NT BRAIN STEM

NT CEREBELLUM

NT CEREBRAL CORTEX

NT CEREBRUM

NT HIPPOCAMPUS

NT SPINAL CORD

NT SPINE

NT THALAMUS

Stability criteria in manifestations of the activity of the central nervous system in humans 01 p0006 A73-10152

CNS epinephrine tone, a possible etiology for the threshold in susceptibility to oxygen toxicity seizures. 03 p0263 A73-14156

The role of biogenic amines in sleep. 03 p0264 A73-14260

Influence of different motor regimes on the convulsive reactivity of the central nervous system. 05 p0542 A73-17178

Information processing in the visual system. 07 p0786 A73-20374

Central nervous system stresses effects estimation, discussing ocular positioning movements functional significance and psychological processes 08 p0935 A73-21542

The influence of change in the functional state of the central nervous system on the course of asphyxia 10 p1179 A73-23937

Role of nerve structures in the action of low-frequency sinusoidally modulated currents on synovial membrane permeability in the knee joint 10 p1180 A73-23943

Dynamics of changes in neuron activity regimes of the ascending auditory pathways 11 p1317 A73-26079

Conditioned reflex switching effects in higher nervous system reactions as function of experimental stimuli background conditions /arousal, diurnal rhythms, test conditions, physiological condition/ 14 p1718 A73-30567

Physical and psychological effects of electromagnetic fields on human and animal central nervous system 14 p1718 A73-30571

RNA and DNA of internal organs during a remote postreanimation period in animals with complete and incomplete functional recovery of the central nervous system 14 p1719 A73-30842

Ventilatory responses to transient hypoxia and hypercapnia in man. 15 p1832 A73-31126

Impact acceleration effects on rabbit central nervous system, noting changes in nerve tissue elements and cerebral vessels 17 p2111 A73-34227

Cholinergic activation of vestibular neurones leading to rapid eye movements in the mesencephalic cat. 18 p2272 A73-36439

Central nervous system influence upon electrocardiographic waveforms. 18 p2275 A73-36530

A study of Halon 1301 /CBF3/ toxicity under simulated flight conditions. 18 p2285 A73-36930

The problem of spiritual requirements and the theory of human higher nervous activity 20 p2515 A73-39796

Formation of various functional states in the symmetrical structures of the brain as a function of the intensity of unconditioned excitation 20 p2516 A73-39801

Structurally functional properties of the dendrites of central neurons 23 p2947 A73-43926

The effect of low X-ray doses on the central nervous system 23 p2947 A73-44179

Influence of histotoxic hypoxia on the activity of lactic dehydrogenase isoenzymes in neurons and neuroglia of various sections of the central nervous system 24 p3058 A73-44429

CENTRAL NERVOUS SYSTEM STIMULANTS

Conditioned reflex learning and phenamine-stimulated functional activation of cerebral synaptic, protein synthesizing and energy generating apparatus 05 p0541 A73-17177

CENTRAL PROCESSING UNITS

NT ARITHMETIC AND LOGIC UNITS

Computerized weather radar data central processor design, implementation and programs for data reduction and calibration 03 p0281 A73-14548

Apparatus replicating and extending development work on real-time time-compressed radar observation processor and display system 05 p0576 A73-16714

Two-level computer system with main and display processors as scale working model for semiautomatic digital ATC en route control 07 p0796 A73-19183

Redundant central processor system for fault tolerant real time operation in space applications, describing systems organization [AIAA PAPER 73-424] 12 p1476 A73-27821

Organization of checks of the central control unit in a digital process-control computer operating with fixed word length 16 p1986 A73-33665

Future trends in computer hardware. 17 p2131 A73-35127

CPU design for command and control system with programmable read-only control memory, discussing self microdiagnostics for control store error detection 17 p2144 A73-35258

Parallel processors and air traffic control automation. 19 p2408 A73-38465

CENTRIFUGAL COMPRESSORS

Unsteady modes of operation of a centrifugal compressor with a vaneless diffuser 02 p0203 A73-11790

Subsonic centrifugal compressor efficient operating range extension by collector and diffuser blade cascades separation, presenting performance test results 02 p0204 A73-12792

Development trends in design methods for aircraft engine compressors. II - Centrifugal-flow compressors 06 p0741 A73-17996

Development trends in aircraft-engine compressor design methods. III 07 p0867 A73-19605

Theory on blades of axial, mixed, and radial turbomachines by inverse method. 11 p1303 A73-26340

A new approach to the problem of predicting the performance of centrifugal compressors. 13 p1565 A73-29012

Low speed of sound modeling of a high pressure ratio centrifugal compressor. 13 p1566 A73-29020

Features of flow-parameter measurement by a cylindrical probe in the vaneless diffuser of a small centrifugal compressor 13 p1568 A73-29552

Small turbomachinery compressor and fan aerodynamics. [ASME PAPER 73-GT-6] 16 p2047 A73-33484

Book - Gas turbine theory /2nd edition/. 17 p2221 A73-34471

High performance supersonic axial and centrifugal compressors theoretical and experimental research, assessing and forecasting technological developments 18 p2343 A73-36992

Blade tip clearance loss between centrifugal impellers and shrouds during two dimensional viscous laminar flow, discussing energy dissipation and pressure and temperature distribution 19 p2474 A73-38417

The use of analytic surfaces for the design of centrifugal impellers by computer graphics. 22 p2900 A73-42477

Evaluation of slip factor of centrifugal impellers. 22 p2796 A73-42625

CENTRIFUGAL FORCE

Stress separation in the photoelastic study of centrifugal stresses. 01 p0116 A73-11013

Equilibrium equations for rotating conical shells under centrifugal forces and compression loads, calculating revolutions number and stability limits 02 p0232 A73-11819

Swirling jet of gases mixture into vacuum. 03 p0289 A73-12908

Analysis of an arched outer-race ball bearing considering centrifugal forces. [ASME PAPER 72-LUB-28] 03 p0314 A73-14339

Analysis of the shrouded Rayleigh step pad for an incompressible fluid film with the centrifugal inertia effect included. 09 p1089 A73-23103

Subharmonic resonance of order 1/2 with an asymmetrical restoring force. 10 p1292 A73-24649

On the design of air-cooled radial turbine blades. 11 p1410 A73-25843

Deformation equations of a propeller blade and the orthogonality characteristics of its normal mode shapes of vibration 12 p1458 A73-27085

Analysis of centrifugal stresses in anisotropic viscoelastic cylinder. 13 p1697 A73-28810

Critical rpm of conical shells incorporated in turbine rotors 14 p1814 A73-30686

Assembly for studying oscillation damping in rod elements in the field of centrifugal forces 17 p2145 A73-34340

An exact solution for the rotation of the atmosphere about the spheroidal earth. 22 p2848 A73-42541

Centrifugal force effects on flame spread and extinction limits of fuel-air mixture combustion with laminar, turbulent and buoyant bubble transport 22 p2993 A73-42776

CENTRIFUGAL PUMPS

Supercavitating pumps for cryogenic liquids. 05 p0582 A73-17286

Improvement of the calculation of the guide vanes of centrifugal pumps 09 p1028 A73-22569

Flow twisting in front of rotor for centrifugal blower operation control, predicting efficiency criteria 10 p1173 A73-24671

Calculation of a three-dimensional boundary layer in revolving channels of centrifugal rotors 10 p1173 A73-24672

Calculation of forced vibrations in damped centrifugal pumps with a given level of rotor imbalance 10 p1263 A73-24673

- Experimental study of cavitation oscillations in a centrifugal screw pump
15 p1832 A73-31499
- Relationship between the hydraulic losses of a centrifugal wheel and the energy imparted by the wheel to the fluid by circulation in the relative motion
21 p2676 A73-40407
- The vapour core pump vortex inlet valve.
23 p2941 A73-43393
- Synchronized operation of a positive-displacement gear pump and a vane pump within the lubricant oil delivery system of a jet engine
23 p3020 A73-43742

CENTRIFUGES

NT HUMAN CENTRIFUGES

- Seat reaction direction in an animal centrifuge.
07 p0780 A73-19478
- Low threshold unstable nonpotential oscillations of weakly ionized rotating plasma in crossed field centrifuge, noting MHD generator and ionospheric implications
09 p1124 A73-21891
- Low threshold unstable nonpotential oscillations of weakly ionized rotating plasma in crossed field centrifuge, noting MHD generator and ionospheric implications
17 p2215 A73-34314

CENTRIFUGING

- Purification of *Synechococcus lividus* by equilibrium centrifugation and its synchronization by differential centrifugation.
18 p2274 A73-36503

CENTRIFUGING STRESS

- Effect of chronic centrifugation on body composition in the rat.
03 p0259 A73-13370
- Application of multichannel rheography to physiological studies on a centrifuge
06 p0657 A73-17693
- Observations on perceived changes in aircraft attitude attending head movements made in a 2-g bank and turn.
07 p0785 A73-19485
- Comparison of the metabolic effects of centrifugation and heat stress in man.
11 p1315 A73-25338
- Some aversive characteristics of centrifugally generated gravity.
13 p1575 A73-28506
- Effect of the Valsalva maneuver on tolerance to +Gz acceleration.
14 p1714 A73-29754
- Cerebellar responses of animals under varied rotation conditions in a centrifuge
15 p1834 A73-31506
- Changes in functional construction of bone in rats under conditions of simulated increased gravity.
17 p2113 A73-35863
- Normalisation of haemodynamic changes caused by action of prolonged accelerations in rats.
18 p2270 A73-35985
- Human static kinetic stability as component of non-specific resistance, discussing revolving, altitude, hypoxic and orthostatic stress dependence tests
18 p2279 A73-36904
- Gravitational effects on animal ontogeny from centrifugation studies of acceleration tolerance, considering egg and embryo development, body composition, etc
22 p2804 A73-42174
- Effects of rehydration on +Gz tolerance after 14-days' bed rest.
23 p2946 A73-43524
- Oxygen consumption measurements during continual centrifugation of mice.
24 p3065 A73-45071

CENTROIDS

- Instability of rotation about a centroidal axis of maximum moment of inertia.
01 p0077 A73-10743
- Radar scatterer ensemble cross section centroid tracking by raster scan observation technique, estimating mean-squared dimensions
11 p1333 A73-26644
- The variation of the electronic transition moment, Re, in the intensity theory of diatomic molecules.
15 p1916 A73-32392
- Galactic rotation of the centroids of various objects
23 p3035 A73-44239

CEPHEID VARIABLES

- Eta Aquilae star molecular abundances of CO, CN, carbon, OH, NH and CH with respect to dissociation equilibrium and light curve correspondence
01 p1003 A73-11022
- RR Lyrae star mean absolute magnitude determination via maximum likelihood method after elimination of stars with high velocity or errors in proper motion
02 p0222 A73-12707
- Giant envelopes structure triple solutions yielding bottom pressure-radius curves, discussing stellar evolution, Cepheid variables and secular instability
03 p0371 A73-13226
- Astronomical model for variable RR Lyrae stars pulsation, noting rotation effect on oscillation period
03 p0379 A73-14585

- Small Magellanic cloud large depth along line of sight shown from supergiant stars and cepheids observation
03 p0380 A73-14610

- Bright red giants in the globular clusters M3, M5, and M13.
04 p0503 A73-16006

- Structure of the Cepheid instability strip in the small Magellanic Cloud.
04 p0503 A73-16007

- Some relations between the photometric characteristics of the brightness curves and color indexes of Cepheid variables in the system U,B,V,II
05 p0613 A73-16209

- Comments on a PLC relationship for Cepheids and on the comparison between pulsation and evolution masses for Cepheids.
05 p0625 A73-17334

- On the location of pulsational blue edges and estimates of the luminosity and helium content of RR Lyrae stars.
05 p0625 A73-17335

- Observational aspects of RR Lyrae and W Virginis stars - Some conundrums of stellar populations and galactic distribution.
07 p0903 A73-20629

- RR Lyrae, W Virginis and RV Tauri population II variables, considering pulsation problem, instability mechanisms and He ionization
07 p0903 A73-20630

- On the metal abundance of RR Lyrae stars in the globular cluster M22.
08 p1009 A73-21169

- Chemical composition of classical Cepheids in the Galaxy and Magellanic Clouds
10 p1273 A73-23705

- Velocity gradients and microturbulence in Cepheids.
11 p1427 A73-26607

- Andromeda galaxy absorbing material distribution obtained with population I cepheids in Baade four variable star fields
13 p1671 A73-28031

- Cepheid variables model characteristics, determining luminosity, radial velocity and radius time dependent variations
13 p1682 A73-28981

- Absolute magnitude of stars of the RR Lyrae type
13 p1686 A73-29370

- On the stability of the light-variations of RR Lyrae stars.
15 p1933 A73-31308

- The effect of binary motion on period changes in RR Lyrae stars.
15 p1935 A73-31486

- Radial velocity, light and colour curves of RZ Cep, an RR Lyrae star.
15 p1937 A73-31700

- Chemical composition of the classical Cepheids in the Galaxy and the Magellanic Clouds.
18 p2354 A73-36730

- Variations in the abundance of chemical elements in the classical Cepheids of the Galaxy
21 p2768 A73-40718

- Intermediate-band photometry of RR Lyrae stars. II - Colors of RR Lyrae and ultrashort-period variables.
22 p2906 A73-41962

- Galactic mass distribution models from matter density near sun, discussing halo mass and RR Lyrae effects observation
22 p2912 A73-42940

CERAMAL PROTECTIVE COATINGS

U CERMETS

U PROTECTIVE COATINGS

CERAMALS

U CERMETS

CERAMIC BONDING

- Ceramic-to-metal sealing and joining technology assessment, discussing noble filler metal properties, ceramic surface preparation and thermal tests for performance evaluation
09 p1088 A73-22444

- Study of electromechanical coupling in a non-piezoelectric dielectric with a high dielectric constant
11 p1408 A73-25249

CERAMIC COATINGS

- Cermet-oxide plasma jet spray coating of metal surfaces, determining thermal performance characteristics by calorimetric measurements
06 p0714 A73-18448

- Investigation of high-temperature evaporation of heat-resistant ceramic coatings on metals
06 p0714 A73-18656

- Thermal conductivity of mixed-composition plasma-sprayed coatings.
09 p1111 A73-23464

- Elastomeric and ceramic coatings for aircraft and missile radomes protection in subsonic and supersonic rain erosion environments
16 p2027 A73-33031

- Ceramic waveguide microwave integrated circuits.
16 p1989 A73-33470

- Plasma sprayed coatings
18 p2318 A73-35882

- Effect of oxides on certain properties of glass-ceramic coatings for titanium
18 p2319 A73-35889

- Synthesis of metal-ceramic and other heat-resistant coatings by the electrochemical method
18 p2319 A73-35890

- Application of a microanalyzer to the investigation of the interaction between titanium and coatings
18 p2323 A73-35894

- Nonstandard thermocouple materials, discussing metal and nonmetal thermoelements and ceramic insulating materials
22 p2857 A73-42036

CERAMICS

NT PORCELAIN

- Load carrying capacity of ceramic spherical shells under external pressure
01 p0114 A73-10481

- Ceramic film indicator for determining and recording of temperatures on space vehicle heat shield.
01 p0052 A73-11168

- The acoustic emission response of mechanically stressed ceramics.
02 p0173 A73-11989

- Evaluation of materials for sliding at 600F-1800F in air.
[ASLE PREPRINT 72LC-7C-2]

- Frequency spectra of acoustic emissions generated by deforming metals and ceramics.
04 p0448 A73-15122

- Sonic degradation of thermally shocked ceramics.
04 p0448 A73-15124

- Acoustic model of HF damping and microstructure of dispersed aluminum oxide ceramics systems, using Hugoniot elastic limits for Young modulus and fracture determination
04 p0468 A73-15373

- Certain electrophysical properties of zinc oxide base semiconductor ceramics with admixtures of transition-metal oxides
06 p0735 A73-18079

- Reliability tests on miniature ceramic capacitors encapsulated by epoxy-novolac block polymer compounds
06 p0677 A73-18398

- Elastic behavior of polymer-impregnated porous ceramics.
07 p0842 A73-19198

- Influence of a constant electric field on the dielectric properties of polycrystalline BaTiO₃
08 p0995 A73-21273

- Effect of microstructure on measurements of fracture energy of Al₂O₃.
[ACS PAPER 44-BN-71P]

- Effect of surface damage on the strength of Al₂O₃ ceramics with compressive surface stresses.
[ACS PAPER 37-BN-71P]

- Electronic configuration and electrical conductivity in ceramics.
09 p1135 A73-23006

- Weibull distribution government of dispersion of destructive temperature gradients characteristic of fireproof ceramic materials heat resistance
09 p1110 A73-23061

- Facility for studying the strength and deformability of high-strength brittle materials in biaxial compression
10 p1203 A73-24372

- Russian book on thermal stability of refractory ceramics covering strength and thermophysical characteristics, high temperature thermal fracture and facilities for normal and cyclic load tests
11 p1386 A73-25174

- The state of technology of ceramic radomes, their use and possibilities for the future.
11 p1335 A73-25286

- Electrically stabilized alumina as ceramic material for radome applications, tabulating dielectric, thermal and mechanical properties and firing conditions
11 p1408 A73-25287

- Contribution to the study and perfecting of materials for radomes in the field of refractory ceramics
11 p1387 A73-25289

- Mechanical, thermal and electrical properties of machinable glass ceramics, discussing application as electromagnetic window materials
11 p1387 A73-25293

- An experiment to correlate the thermal stress failure level to modulus of rupture in ceramic materials.
11 p1387 A73-25304

- Raindrop impact erosion damage on ceramic radome materials, discussing Rayleigh wave mathematical model comparison with sled test data, and laboratory simulation
11 p1336 A73-25306

- Compatibility between material components in metal-ceramics composites
11 p1387 A73-25412

- Structural testing of ceramic nose cap and leading edge components for a reusable entry vehicle.
[AIAA PAPER 73-376]

- Temperature field calculation for certain elements located in microwave channels
12 p1558 A73-27247

- Copper deposition on ceramic plate, studying interdigital slow wave structure and thin film meander-line coupling impedance and dispersion characteristics
12 p1480 A73-27581
- Carbon fibre reinforced ceramics.
13 p1646 A73-29541
- Load-bearing capacity of ceramic spherical shells under external pressure.
14 p1810 A73-30306
- The features of disk shape piezoelectric ceramic transducer equivalent circuit.
14 p1754 A73-30892
- Ceramics replacement for Ni-Cr superalloys to improve automotive gas turbine performance by increasing inlet temperature, considering material selection
15 p1897 A73-31250
- Coating development of Martin Marietta's reusable surface insulation /MAR-SI/ for Space Shuttle applications.
16 p2071 A73-33059
- Acoustic fatigue in ceramic materials, analyzing strength degradation as function of microstructure, structural integrity and properties
16 p2030 A73-33194
- Thermal expansion compatibility of ceramic chip capacitors mounted on alumina substrates.
16 p1989 A73-33472
- Transient analysis of ceramic vanes for heavy duty gas turbines.
[ASME PAPER 73-GT-46] 16 p2048 A73-33507
- Silicon nitride materials for gas turbine components.
[ASME PAPER 73-GT-47] 16 p2048 A73-33508
- Work function and surface ionization currents in steatite ceramics from nickel electrode and thermocouple measurements, plotting temperature dependent Paschen curves
16 p2031 A73-34011
- Monograph - Fibre reinforcement.
17 p2240 A73-34125
- Investigation of the effect of pressed-powder grain composition on the physico-mechanical properties of magnesia refractory materials
17 p2187 A73-34337
- Russian book on radiation effects on ferroelectric crystals and ceramic materials covering changes in dielectric, piezoelectric and optical properties, structure and phase transitions
20 p2600 A73-39757
- Spectral determination of rare-earth components in Seignette-ceramic and piezoceramic materials
21 p2752 A73-40555
- Mechanical, chemical and physical characteristics of glass and ceramics with respect to adhesion, friction and wear behavior
21 p2707 A73-40633
- Ceramic component strength degradation by projectile impacts in terms of momentum and elasticity relation
21 p2723 A73-40892
- Influence of grain size on effects of thermal expansion anisotropy in MgTi2O5.
21 p2752 A73-40893
- Hot-pressed eutectics of oxides and metal fibers.
21 p2723 A73-40895
- A low-temperature, glass-ceramic capacitance thermometer.
22 p2856 A73-42020
- Material preparation and fabrication techniques for the production of high reliability thermocouple devices.
22 p2858 A73-42040
- Fibre-reinforced metallic and ceramic composites produced by thermal spraying.
22 p2866 A73-42592
- Effective application of double exposure holographic interferometry to the study of deformations of ceramics due to the impact of a projectile
22 p2863 A73-43096
- High temperature creep of lithium zinc silicate glass-ceramics. I - General behaviour and creep mechanisms. II - Compression creep and recovery.
23 p2997 A73-44030
- Resistance to crack propagation in ceramics subjected to thermal shock.
23 p2997 A73-44031
- Effect of aluminum-containing components on phase alloying in periclase ceramic materials
24 p3104 A73-44953
- Influence of heat treatment on the posistor effect of semiconductive BaTiO3-ceramic.
24 p3120 A73-45367
- Nd-doped Yttralox ceramic lasing performance and interrelationship between ceramic processing, microstructure and optical quality of sintered product
24 p3097 A73-45414
- CEREBELLUM**
- Morphological, physiological and pharmacological investigations of rat cerebellar cortex synaptic structure and function maturation and neurotransmitter receptivity development
03 p0264 A73-14256
- Nervous system transmitter biochemistry in terms of excitation and inhibition coordination with emphasis on gamma-aminobutyric acid /GABA/ function in cerebellum
03 p0264 A73-14258
- Telemetered EEG and neuronal spike activity in olfactory bulb and amygdala in free moving rabbits.
03 p0271 A73-14299
- A robot conditioned reflex system modeled after the cerebellum.
06 p0658 A73-18065
- Cerebellar responses of animals under varied rotation conditions in a centrifuge
15 p1834 A73-31506
- Anatomo-functional bases of cerebello-cerebral interrelations
15 p1836 A73-32287
- Intervention of cerebello-cortical and cortico-cerebellar paths in the organization and regulation of movement
15 p1836 A73-32288
- Vestibular and cerebellar control of oculomotor functions.
18 p2271 A73-36438
- Cerebellar ablations and spontaneous eye movements in monkey.
18 p2272 A73-36447
- On correlation between the changes in cerebellar bioelectric activity and the adaptive reactions under the effect of accelerations.
18 p2279 A73-36915
- The control of a manipulator by a computer model of the cerebellum.
19 p2398 A73-37333
- Cerebral tolerance to asphyxial hypoxia in the dog.
22 p2805 A73-42202
- CEREBRAL CORTEX**
- Changes of the free radical concentration in the cerebral cortex depending on the functional state of the cerebrum
01 p0009 A73-11082
- Y-chromosome localization in the interphase nuclei of cerebral neurons in man
01 p0010 A73-11444
- Stable frequency and synchronicity alterations in the discharges of cortical neuron populations in feedback experiments
01 p0010 A73-11445
- Asymmetries related to cerebral dominance in returning the eyes to specified target positions in the dark.
03 p0261 A73-13760
- Cortical area of neural loci involved in monoptic and dichoptic metacortical occurring for target and masking stimuli imaged on different retinal regions
03 p0261 A73-13764
- Source locations of pattern-specific components of human visual evoked potentials. I - Component of striate cortical origin. II - Component of extrastriate cortical origin.
04 p0409 A73-15024
- Visual receptive fields sensitive to absolute and relative motion during tracking.
04 p0409 A73-15072
- Genesis mechanism of slow cortical afterdischarges during brain injury by radiation
05 p0539 A73-16331
- Intercortical functional connections in lower monkeys, Macacus rhesus, exhibited by evoked responses
05 p0540 A73-16693
- Cerebral circulation alteration during hypothermia
05 p0541 A73-16698
- Functional state of various portions of the cerebrum under the action of extremal stimulation
05 p0541 A73-16736
- Role of the visual cortex in the organization of nystagmic reactions evoked by optokinetic stimulation
06 p0653 A73-18165
- Miniature four-channel radiotelemetry system for the transmission of cerebral biopotentials
06 p0658 A73-18167
- Cortico- and rubrofugal activation of interneurons forming propriospinal paths in the dorsolateral funiculi of the cat spinal cord
07 p0781 A73-20002
- Changes in the amplitudinal and temporal characteristics of sensorimotor-cortex evoked potentials after deactivation of spinocervical tracts in cats
07 p0781 A73-20004
- Cerebral localization of speech, discussing cortical lesions, aphasia and mental activity correlation theories
08 p0931 A73-21425
- Cortical potentials evoked by confirming and disconfirming feedback following an auditory discrimination.
09 p1039 A73-21895
- Cortico-pyramidal and cortico-extrapyramidal synaptic effects on lumbar motor neurons in monkeys
09 p1040 A73-22578
- Investigation of evoked activity in the ventral horn of lumbar segments during the interaction of efferent extrapyramidal and cortical stimuli
09 p1040 A73-22579
- Biopotential alpha and theta rhythms of neocortex and hippocampus of milk drinking cats after food and water deprivation
09 p1040 A73-22862
- Examination of responses evoked in the sensory cortex by thalamic stimulation.
10 p1178 A73-23772
- Oxygen consumption and its 'critical' tension for the cerebral cortex in situ
10 p1179 A73-23801
- Neurochemical aspects of the formation of electrophysiological and behavioral reactions
10 p1184 A73-24327
- Spatial analysis in monkeys of various ages after extirpation of the parietal areas of the cerebral cortex
10 p1180 A73-24329
- Functional state of the cerebral cortex and of the mesencephalic reticular formation during prolonged action of impulsive and stable noise
10 p1181 A73-24334
- Acetylcholinesterase activity of hypothalamic and cortical structures under pharmacological effects
10 p1182 A73-24597
- Memory process in terms of cortex-subcortex interrelation, brain lability level and biopotential trace processes
11 p1314 A73-25198
- Nature and significance of periodic electrical activity variations in the neocortex and the hippocampus during the paradoxical phase of sleep
11 p1317 A73-26083
- Single unit reactions in the visual cortex of the unanesthetized rabbit to the light flashes of different intensities.
11 p1321 A73-26719
- Comparative analysis of the electrical activity of the cortex and of cerebral subcortical formations in the process of the alteration of conditioned reactions
12 p1461 A73-27104
- Dynamics of certain characteristics of the evoked potential of the optic cortex in rabbits under conditions of increasing hypoxia
12 p1463 A73-27709
- Late visual cortical region reactions during the convergence of light stimulation and electrocutaneous stimulation
13 p1576 A73-29073
- Human average evoked potential distribution over scalp to associate cortical electrical activity with voluntary movement, reacting to EMG activity
14 p1714 A73-29990
- Circulation of nervous impulses in the cerebral cortex
14 p1718 A73-30569
- Neurophysiological characteristics of isolated structures of the cerebral cortex
14 p1718 A73-30570
- Anatomo-functional bases of cerebello-cerebral interrelations
15 p1836 A73-32287
- Intervention of cerebello-cortical and cortico-cerebellar paths in the organization and regulation of movement
15 p1836 A73-32288
- The visual cortex as a spatial frequency analyser.
17 p2112 A73-34840
- Opponent-colors responses in the visually evoked potential in man.
17 p2112 A73-34844
- Frequency analysis of spatio-temporal visually evoked cortical potentials during binocular rivalry.
17 p2118 A73-35645
- Stereoscopic vision - Cortical limitations and a disparity scaling effect.
18 p2269 A73-35922
- Brain stem reticular formation influence on lateral geniculate body neurons during eye movements, suggesting cortical oculomotor impulse influence mediation by perigeniculate nucleus
18 p2272 A73-36448
- Neurophysiological correlates of eye movements in the visual cortex.
18 p2272 A73-36450
- Orientation specificity and response variability of cells in the striate cortex.
19 p2394 A73-37421
- The effect of social-emotional environmental stress on the functional state of the neocortical structures of rhesus monkeys
19 p2394 A73-37755
- Role of specific and nonspecific thalamic nuclei in the genesis of certain slow rhythms on the human electrocorticogram
19 p2395 A73-37939
- Functional characteristics of different neurons in the auditory cortex
19 p2395 A73-37940
- Effects of round window stimulation on unit discharges in the visual cortex and superior colliculus.
20 p2513 A73-39146
- Visually evoked cortical potentials to patterned stimuli in monkey and man.
20 p2514 A73-39760
- Role of associations in the formation of evoked potentials from the human cerebral cortex
20 p2513 A73-39798
- Functional properties of auditory cortex neurons in a controlled experiment
20 p2516 A73-39802
- Effect of convulsions on certain aspects of the biosynthesis of proteins in the brain cortex
21 p2638 A73-40750

- Biosynthesis of RNA in the brain cortex during various functional states
21 p2640 A73-41262
- Russian book - Electrical activity of the human brain in the process of motor action.
21 p2640 A73-41289
- Effect of the stimulation of nonspecific thalamic nuclei on spontaneous and evoked spindles in the auditory cortex
22 p2802 A73-41958
- Effect of the electrical stimulation of the sensorimotor cortex on the potentials of dorsal roots and on the depolarization of primary spinal afferents
22 p2807 A73-42652
- Analysis of the changes in glial cell numbers in the auditory cortex during the application of acoustic stimuli of various intensities
22 p2807 A73-42653
- Investigation of complex and hypercomplex receptive fields of visual cortex of the cat as spatial frequency filters.
22 p2810 A73-42958
- Gamma-aminobutyric acid antagonism in visual cortex - Different effects on simple, complex, and hypercomplex neurons.
23 p2946 A73-43338
- Neuronal activity of the sensorimotor and visual cortex in rabbits during development of a summation focus in the reticular formation
24 p3058 A73-44550
- The nature and significance of the dynamics of electrical activity in the neocortex and hippocampus during the paradoxical phase of sleep
24 p3059 A73-44718
- Application of factor analysis to the encephalographic characterization of sleep
24 p3062 A73-44722
- Cortical and intracortical study of the frontal visual evoked potential in photosensitive Papio papio
24 p3061 A73-45159
- ### CEREBRUM
- Inhibitory mechanisms activity in behavior control by neostriatum, discussing suppressive reactions, evoked sleep, conditioned and instrumental reflexes and neurophysiological aspects
01 p0009 A73-11025
- Deep hypothermia induced in the golden hamster by altering cerebral calcium levels.
05 p0538 A73-16151
- Functional state of various portions of the cerebrum under the action of extremal stimulation
05 p0541 A73-16736
- Some physiological reactions to acceleration in albino rats in a state of hypothermia
05 p0541 A73-16737
- Conditioned reflex learning and phenamine-stimulated functional activation of cerebral synaptic, protein synthesizing and energy generating apparatus
05 p0541 A73-17177
- Ontogenic cerebrospinal reflex activity studies, covering spinal cord morphology, reflex arches, inhibition, intracranial responses and post-tetanic potentiation
07 p0784 A73-20366
- Fatigue levels of cerebral hemispheres in response to visual task and test stimuli, noting left handed reduced performance capacity
09 p1040 A73-22925
- Book - The physiology of the cerebral circulation.
10 p1180 A73-23945
- Functional and morphological structures of motor activity events, noting central integration ensemble of cerebrum transmitter sequences
11 p1314 A73-25200
- Hypothalamus, septum and ventrobasal thalamus nuclei single neuron responses to skin thermal stimulation, indicating afferent connections between cerebrum thermoregulation center and peripheral thermoreceptors
11 p1317 A73-26086
- Correlation between arterial carbon dioxide tension and regional cerebral blood volume by X-ray fluorescence.
20 p2519 A73-39790
- Objective method for classification of multicellular activity patterns of neuron population in the cerebrum of man
22 p2807 A73-42656
- ### CERENKOV COUNTERS
- Scintillation and anticoincidence Cerenkov counters for recording heavy nonrelativistic single charge particles in cosmic rays at sea level
02 p0209 A73-12670
- Russian book on elementary particle counters covering gas discharge /Geiger-Muller/, scintillation, Cerenkov and semiconductor counters and matter-radiation interactions
15 p1880 A73-32418
- Procedure for measuring plasma electron energies from the bremsstrahlung with the aid of Cerenkov detectors
18 p2339 A73-36566
- Monte-Carlo-method based calculation of the linearity and resolving power of a Cerenkov spectrometer for purposes of gamma astronomy
21 p2701 A73-40613
- Certain problems in measuring Cerenkov light on the lakutsk extensive air shower device
23 p3022 A73-43546
- A device for recording the energy spectrum and fluxes of electrons with energies greater than 100 MeV in cosmic rays
24 p3124 A73-44782
- ### CERENKOV EFFECT
- #### U CERENKOV RADIATION
- #### CERENKOV RADIATION
- Dispersion relation for Cerenkov radiation of moving test particles in a magnetoplasma.
01 p0083 A73-10453
- Cherenkov and transient radiation of uniformly moving charge in random inhomogeneous medium.
02 p0193 A73-12381
- Amplification of signal by Cerenkov resonance interaction.
04 p0415 A73-14958
- Plasma instability in terms of electron oscillations due to parametric interaction with UHF electric field, noting inverse Cerenkov effect for electrons
06 p0729 A73-18111
- Incoherent Cerenkov radiation in the magnetosphere and the ground observations of VLF hiss.
07 p0814 A73-19240
- Cerenkov shower spectrometer with a conical radiator made of TF-5 glass
09 p1085 A73-23002
- Spontaneous Cerenkov emission of longitudinal waves produced by single particle and cylindrical electron beam moving inside magnetosphere along magnetic field
10 p1269 A73-24722
- Radiation source motion at superluminal speed in vacuum, defining conditions for Vavilov-Cerenkov and Doppler effects
10 p1250 A73-24943
- Influence of the shape of radiators on the energy resolution of Cerenkov shower spectrometers
12 p1496 A73-27205
- Theory of transient radiation in a waveguide with a piecewise-homogeneous dielectric filler
16 p1978 A73-32898
- The Compton effect in a medium near a Cerenkov cone
17 p2120 A73-34115
- Space probe observed VLF hiss powers disparity with theoretical prediction for incoherent Cerenkov radiation, considering Landau instability generated wave amplification
17 p2160 A73-34788
- Photon lateral distribution sensitivity to longitudinal development of electron cascade via computer simulations of optical Cerenkov emission from cosmic ray showers
20 p2603 A73-39704
- An attempt to explain satellite observations of high latitude VLF hiss in terms of generation by incoherent Cerenkov radiation.
21 p2685 A73-40828
- Cerenkov-effect based standard radiation source designed for the calibration of space experiments - Spectral energy distribution measurement
22 p2860 A73-42307
- Calculation of the fluctuations of the Cerenkov radiation of an electron-photon shower in the atmosphere
23 p3022 A73-43554
- Plasma instability in terms of electron oscillations due to parametric interaction with UHF electric field, noting inverse Cerenkov effect for electrons
24 p3114 A73-44500
- ### CERIUM
- Influence of cerium and boron additions on the corrosion properties of K18N9TiL steel
02 p0181 A73-12538
- Evaluation of cerium stabilised microsheet coverslips for higher solar cell outputs.
03 p0256 A73-14229
- Theoretical consideration of soft X-ray absorption by the metallic films of lanthanum and cerium
06 p0737 A73-18220
- On the process of precipitation in Mg-Ce alloy.
23 p2994 A73-44155
- ### CERIUM COMPOUNDS
- Cerium-germanium system state diagram based on microstructural, differential thermal, dilatometric and X ray phase analyses, emphasizing intermetallics observation
10 p1260 A73-24684
- ### CERMETS
- Test results of fatigue at elevated temperatures on aeronautical materials.
[ONERA, TP NO. 1098]
01 p0061 A73-10229
- Diffusive thermal bonding of cermet elements on steel and iron substrates in vacuum
02 p0172 A73-11537
- Properties and fabrication of cermet fibers from refractory compounds and of porous materials based on these fibers
02 p0178 A73-11538
- Evaluation of materials for sliding at 600F-1800F in air.
[ASLE PREPRINT 72LC-7C-2]
03 p0317 A73-14371
- Synthesis and fabrication of high purity hafnium nitride and hafnium carbide.
04 p0455 A73-15752
- Tantalum-glass cermet thin-film resistors.
08 p0945 A73-20809
- Investigation of carbon- and manganese-diffusion processes in the metal-ceramic steel G13M
09 p1103 A73-22466
- Heat conductivity of cermets with titanium carbide as function of temperature and metal content
09 p1103 A73-22471
- Interaction between zirconium diboride and molybdenum
09 p1105 A73-22981
- Compressibility of heterogeneous powder mixtures during rolling
10 p1224 A73-24314
- Development of a production technology for high-density metal-ceramic materials by the method of impregnating porous preforms with low-melting iron boride alloys
10 p1224 A73-24316
- Development and investigation of fine-grain metal ceramic contacts of silver/graphite and silver/nickel/graphite composition for low-voltage device applications
10 p1225 A73-24320
- Hot deformation of metal ceramic titanium preforms
10 p1225 A73-24321
- Effect of solid lubricants on the physicomechanical and friction properties of materials
10 p1225 A73-24686
- Field-ion microscopic study of the high-speed deformation of tungsten
12 p1509 A73-26838
- Conditions for powder compaction over the deformation zone width during rolling
12 p1503 A73-27554
- Cermet cathode materials for electric vacuum equipment
12 p1503 A73-27562
- Compatibility of components in metal-ceramics composites
14 p1766 A73-30442
- Effect of dispersity on spectral analysis data for alloyed powders
15 p1888 A73-31597
- Investigation of friction and wear mechanisms in a friction coupling with a small overlapping coefficient.
15 p1882 A73-31599
- Some laws of chromium oxide-chromium cermet sintering
15 p1892 A73-32240
- Electrophysical properties of TiC-Nb, TiC-Ta, TiC-Mo, and TiC-W cermets
15 p1892 A73-32242
- Electrical resistance of tungsten-rhenium cermet alloys
15 p1892 A73-32243
- Synthesis of metal-ceramic and other heat-resistant coatings by the electrochemical method
18 p2319 A73-35890
- Brazeability of Ni-Cr heat resistant cermets on stainless steel.
23 p2986 A73-44005
- ### CERTIFICATION
- Automotive approach systems certification and short distance takeoff and landing trajectory by cinetheodolites, digital optical, airborne and inertial/radiosonde equipment
10 p1246 A73-23656
- Aircraft noise reduction technology and certification standards, reviewing federal laws and regulations.
10 p1175 A73-24553
- European airbus A300B aircraft flight tests and on-board instrumentation in certification program, illustrating desk layout, control and display panels
13 p1568 A73-28159
- Status of international noise certification standards for business aircraft.
[SAE PAPER 730286]
17 p2101 A73-34651
- Electric trim systems - Design and certification considerations under FAR 23.677/CAM 3.337-2.
[SAE PAPER 730299]
17 p2101 A73-34662
- An overview of fatigue and fracture for design and certification of advanced high performance ships.
17 p2246 A73-34881
- Management and control of flight test programs of the Western Region FAA.
23 p3050 A73-44053
- Management and control of flight test programs at U.S. Army Aviation Systems Command.
23 p3050 A73-44054
- ### CESIUM
- #### NT CESIUM VAPOR

Transfer of electronic excitation by atomic collision between highly excited cesium atoms 01 p0079 A73-10174

Plasma diagnostics in overcompensation operated Knudsen thermionic converter with Cs-Ba filler, noting W cathode surface properties 04 p0481 A73-15614

Hafele calculations for jet-borne Cs beam clock difference from ground clock vindicated and generalized to rotating frames of reference 07 p0825 A73-20282

Resonant multiphoton ionization of a cesium atomic beam by a tunable-wavelength Q-switched neodymium-glass laser. 09 p1098 A73-23472

Oscillator strength and photoionization cross section computation for Cs ground state during photoabsorption, using semiempirical model potential with adjustable parameters 10 p1250 A73-23672

Variation of the work function of W(100) by adsorption of oxygen, cesium, and coadsorption of oxygen and cesium 10 p1186 A73-23696

Certain results of flight tests of a model ion thruster employing contact ionization of cesium on tungsten 10 p1262 A73-23892

Review of liquid-metal magnetohydrodynamic spacecraft energy conversion cycles. 11 p1308 A73-25977

Discharge characteristics in cesium-seeded argon. 13 p1665 A73-28807

CESIUM COMPOUNDS

NT CESIUM HALIDES

NT CESIUM IODIDES

NT CESIUM OXIDES

CESIUM DIODES

Performances of the better metallic electrodes in cesium thermionic converters. 09 p1036 A73-22817

Ionization transitions from the 8/2/P(1/2) level of a cesium atom in a low-temperature plasma 14 p1781 A73-30460

Dynamic characteristics of a plasma diode under conditions of a low-voltage arc discharge. I - Theory of the dynamic characteristics 18 p2339 A73-36557

CESIUM ENGINES

Research at O.N.E.R.A. on ion thrusters suitable for satellite station-keeping 04 p0505 A73-15719

Long life contact-ionized cesium low thrust engine design, considering ionizer working temperatures and neutralizer ion current densities 04 p0488 A73-15720

Ion thrusters with cesium contact ionization - Study of the main elements. 07 p0867 A73-18933

CESIUM HALIDES

NT CESIUM IODIDES

Equations of state and dissociation equilibrium for CsCl plasma, noting thermodynamic model for phase transitions of liquid metal into nonideal ion plasma 01 p0084 A73-10851

Equations of state and dissociation equilibrium for CsCe plasma, noting thermodynamic model for phase transitions of liquid metal into nonideal ion plasma 12 p1529 A73-27901

CESIUM IODIDES

CsI thin film photoemission spectra resolution maximization, rejecting localized ionic state transitions model 11 p1407 A73-24986

CsI optical and photoemission spectra computed from first order allowed transitions between Bloch-wave states, using energy band data 11 p1407 A73-24987

Infrared absorption and local symmetry of negative ClO4 and ReO4 impurity ions in KI and CsI crystals 18 p2340 A73-36673

CESIUM ION

Cation exchange binding of rubidium and cesium by rat liver cell microsomes. 02 p0135 A73-12549

Cs ion bombardment and contact ionization engines in French space program for communication and geostationary satellites electric propulsion 04 p0488 A73-15715

Cs ion bombardment engines for communication satellites stationkeeping and attitude control, noting mission life and test facilities 04 p0488 A73-15718

Production of porous tungsten thin walls intended for cesium ionization by contact 04 p0454 A73-15721

Conformal mapping for Cs ion engine beam optical system with laminar flux, calculating design parameters for current limitation by Cs flow 04 p0488 A73-15722

High voltage fuel supplies intended for ion thrusters 04 p0489 A73-15734

Energy spectra of Cs+ ions scattered from the surface of a tungsten single crystal. 06 p0726 A73-18615

French research on cesium contact ion sources. [AIAA PAPER 72-495] 08 p0996 A73-21815

Wave functions and energies of the autoionization states of the cesium atom 09 p1122 A73-21976

Ionization of 6s- and 5p-electrons of the cesium atom by electron impact 09 p1122 A73-21977

Excitation of autoionization states of the cesium atom by electron impact 09 p1122 A73-21978

Ionization transitions from the 8/2/P(1/2) level of a cesium atom in a low-temperature plasma 14 p1781 A73-30460

Kinesonde studies of cesium ion clouds in the E-region. 18 p2304 A73-35988

Molecular beam study of the desorption of cesium ions from tungsten crystals. 18 p2338 A73-36976

Some results of flight tests of an ion-engine model using surface ionization of cesium on tungsten. 20 p2600 A73-38911

CESIUM OXIDES

Photoemission from cesium-oxide-activated In-GaAsP. 10 p1259 A73-23839

Grain-boundary corrosion of type 304 stainless steel by cesium oxides. 10 p1234 A73-24427

Plasma chemical synthesis of higher oxides of cesium and rubidium. 13 p1581 A73-29599

CESIUM PLASMA

The electron diffusion scattering cross section of cesium atoms 01 p0080 A73-10852

Resonances of an antenna associated with the excitation of ion Bernstein modes. 02 p0198 A73-12071

Measurement of electron distribution function in a cesium plasma. 02 p0199 A73-12815

Damping of an ion acoustic wave in a weakly ionized plasma 06 p0730 A73-18460

Characteristics of ionization-recombination processes in a plasma discharge diode 09 p1124 A73-21884

Dynamic viscosity and current distribution model of inhomogeneous Cs plasma flow in coaxial plasma gun with thermionic cathode 10 p1258 A73-24886

Microwave oscillations and the visible radiation spectrum of a cesium plasma diode 12 p1527 A73-26938

The diffusion cross section for scattering of electrons by cesium atoms. 12 p1526 A73-27902

Experiments on the containment of an alkali plasma in a corrugated magnetic field. 13 p1664 A73-28612

Relaxation to Maxwellian distribution of electrons near low voltage Cs arc plasma discharge cathode 13 p1666 A73-28962

Observations of two-stream ion wave instability. 16 p2041 A73-33335

Investigation of plasma inhomogeneities between coaxial electrodes in a magnetic field 17 p2214 A73-34128

Applicability of an adiabatic compression method to the study of a cesium plasma 17 p2214 A73-34130

Ionization and recombination in a plasma diode. 17 p2215 A73-34308

Electron energy distribution function validity for nonequilibrium plasma in presence of electric field verified for ionized cesium vapor positive column 17 p2216 A73-34551

Measurement of electron-ion recombination rate of a dense high-temperature cesium plasma. 18 p2339 A73-36622

HF radar observations of cesium plasma cloud released from the rocket K-9M-39. 19 p2423 A73-37378

Cooling and heating of electrons during the decay and development of a cesium discharge plasma 19 p2469 A73-37962

Local thermodynamic equilibrium validity limits in short spaced cesium plasmas, discussing electron density and temperature, Maxwell and Boltzmann distributions and total pressure 20 p2599 A73-39673

Afterglow studies in helium-cesium mixtures. 21 p2745 A73-40223

Calculations of state functions behind ionizing shock-waves in potassium and caesium vapour. 21 p2745 A73-40474

Mass-spectrometric investigation of the ion composition of potassium and cesium discharge plasmas 21 p2746 A73-40526

Dynamic viscosity and current distribution model of inhomogeneous Cs plasma flow in coaxial plasma gun with thermionic cathode 21 p2749 A73-41661

Microwave oscillations and visible emission in a cesium diode. 22 p2892 A73-42272

Relaxation to Maxwellian distribution of electrons near low voltage Cs arc plasma discharge cathode 23 p3013 A73-44314

CESIUM VAPOR

Fabrication of porous tungsten foils for contact ionization of cesium [ONERA, TP NO. 1113] 01 p0055 A73-10234

Characteristics of a thermionic converter with a cesium-barium filling at a high anodic temperature 01 p0006 A73-10855

Experimental study of the saturated-vapor pressure of rubidium and cesium 01 p0080 A73-10858

Cs vapors thermal conductivity at various temperatures and pressures, using low emissivity Ni cylinders 03 p0396 A73-13181

I-V characteristics and luminescence changes in Cs vapor arc discharge at various spark gap widths, noting pressure effect on gas stratification 04 p0481 A73-15613

Investigation of the vapor pressure of cesium by the boiling-point method. 06 p0722 A73-17404

Pulsed X-ray photography of a shock wave in cesium vapor using two X-ray tubes 06 p0731 A73-18554

Departure from thermodynamic equilibrium of an ionized cesium vapor - Experimental study and comparison with a statistical model 07 p0854 A73-20607

Efficient parametric conversion in cesium vapor irradiated by 3470-A mode-locked pulses. 09 p1090 A73-22079

Performance improvement of cesium thermionic converters by addition of oxygen. 09 p1036 A73-22818

Experimental investigation of the viscosity of cesium vapors 10 p1253 A73-23506

I-V characteristics and luminescence changes in Cs vapor arc discharge at various spark gap widths, noting pressure effect on gas stratification 10 p1254 A73-24203

Investigation of a liquid-metal magnetohydrodynamic power system. 11 p1308 A73-25978

Condensation of cesium from an incident shock wave in cesium vapors 12 p1528 A73-27323

Characteristics of thermionic converter with cesium-barium filling at high anode temperature. 12 p1461 A73-27905

Experimental investigation of the pressure of the saturated vapor of rubidium and cesium. 12 p1526 A73-27907

Sources of spurious background in the Spectracon. 14 p1732 A73-29907

Upper level populations in optically excited cesium vapor 15 p1914 A73-32337

Potential distribution in a two-gas thermionic converter at current saturation. 15 p1832 A73-32638

Pulse X-ray photography of a shock wave in cesium vapor using two X-ray tubes. 16 p2042 A73-33579

Experimental investigation of the viscosity of cesium vapor. 17 p2217 A73-35186

Angular dependence of optically pumped magnetometer - Effects of collisional mixing in the excited states. 19 p2429 A73-37382

Revision of high temperature and critical properties of cesium. 22 p2932 A73-42513

CESSNA AIRCRAFT

NT CESSNA 172 AIRCRAFT

CESSNA MILITARY AIRCRAFT

U MILITARY AIRCRAFT

CESSNA 172 AIRCRAFT

An approach to the synthesis of separate surface automatic flight control systems. [AIAA PAPER 73-834] 20 p2508 A73-38777

CFRP

U CARBON FIBER REINFORCED PLASTICS

CH-53 HELICOPTER

U H-53 HELICOPTER

CH-113 HELICOPTER

U CH-46 HELICOPTER

CH-46 HELICOPTER

Application of pole-placement theory to helicopter stabilization systems. 06 p0682 A73-18819

CH-47 HELICOPTER

Redundant system design and flight test evaluation for the TAGS digital control system. [AHS PREPRINT 721] 17 p2131 A73-35062

Development and qualification of a magnetic technique for the nondestructive measurement of residual stress in CH-47 A rotor blade spars. [AHS PREPRINT 752] 17 p2180 A73-35080

- Tactical aircraft guidance system for CH-47B helicopter utilizing fly by wire control system, describing design, display devices, flight instruments, computer configuration and crew duties
[AHS PREPRINT 761] 17 p2210 A73-35084
- A dynamics approach to helicopter transmission noise reduction and improved reliability.
[AHS PREPRINT 772] 17 p2106 A73-35090
- CHAFF**
Forward scatter chaff system for air-ground long haul communications.
04 p0418 A73-15393

CHAINS

U SEATS

CHALCOGENIDES

- NT ALKALINE EARTH OXIDES
NT ALUMINUM OXIDES
NT BARIUM OXIDES
NT BERYLLIUM OXIDES
NT BISMUTH OXIDES
NT BISMUTH TELLURIDES
NT BORON OXIDES
NT CADMIUM SELENIDES
NT CADMIUM SULFIDES
NT CADMIUM TELLURIDES
NT CALCIUM OXIDES
NT CARBON DIOXIDE
NT CARBON DISULFIDE
NT CARBON MONOXIDE
NT CESIUM OXIDES
NT CHROMITES
NT CHROMIUM OXIDES
NT COBALT OXIDES
NT COPPER SULFIDES
NT DISULFIDES
NT ENSTATITE
NT GALLIUM SELENIDES
NT GERMANIUM OXIDES
NT HAFNIUM OXIDES
NT HEAVY WATER
NT HEMATITE
NT HYDROGEN SULFIDE
NT ILMENITE
NT INDIUM SULFIDES
NT INDIUM TELLURIDES
NT INORGANIC PEROXIDES
NT INORGANIC SULFIDES
NT IRON OXIDES
NT LANTHANUM OXIDES
NT LEAD OXIDES
NT LEAD SELENIDES
NT LEAD SULFIDES
NT LEAD TELLURIDES
NT LITHIUM OXIDES
NT MAGNESIUM OXIDES
NT MAGNETITE
NT MERCURY TELLURIDES
NT METAL OXIDES
NT MOLYBDENUM DISULFIDES
NT MOLYBDENUM OXIDES
NT MOLYBDENUM SULFIDES
NT NICKEL OXIDES
NT NIOBIUM OXIDES
NT NITRIC OXIDE
NT NITROGEN DIOXIDE
NT NITROGEN OXIDES
NT NITROGEN TETROXIDE
NT NITROUS OXIDES
NT OXIDES
NT PERCLASE
NT PEROXIDES
NT PLUTONIUM OXIDES
NT POLYSULFIDES
NT POTASSIUM OXIDES
NT PYRITES
NT PYROXENES
NT QUARTZ
NT RUTILE
NT SAPPHIRE
NT SCANDIUM OXIDES
NT SELENIDES
NT SILICON DIOXIDE
NT SILICON OXIDES
NT SULFIDES
NT SULFUR OXIDES
NT TANTALUM OXIDES
NT TELLURIDES
NT THORIUM OXIDES
NT TIN TELLURIDES
NT TITANIUM OXIDES
NT TROILITE
NT TUNGSTEN OXIDES
NT VANADIUM OXIDES
NT WURTZITE
NT YTTRIUM OXIDES
NT ZINC OXIDES
NT ZINC SELENIDES
NT ZINC SULFIDES
NT ZINC TELLURIDES
NT ZINCBLENDE
NT ZIRCONIUM OXIDES
- Difference of thermal properties between threshold type and memory type chalcogenide glass semiconductors.
01 p0087 A73-10432

Electronic conduction and switching in chalcogenide glasses.
09 p1133 A73-21985

Reversible thermal breakdown as a switching mechanism in chalcogenide glasses.
09 p1133 A73-21986

Switching and memory effects in amorphous chalcogenide thin films.
09 p1133 A73-21987

Amorphous chalcogenide Te-As-Si-Ge thin film switch, discussing pressure effect energy accumulation time delay and behavior after voltage removal
09 p1133 A73-21988

Subnanosecond pulse-front shaping with the aid of switches based on chalcogenide glass
10 p1196 A73-24614

Reversible recording of holograms on chalcogenide glass films
12 p1495 A73-26940

Chalcogenide glass threshold switch conceptual model based on electronic origin of firing, discussing applications to contactless switches, bistable relays decoupling and display triggering
12 p1478 A73-27042

Stimulated emission of light from solid solutions of tin and lead chalcogenides in the region of 10 microns.
12 p1507 A73-27519

A study of the static S-shaped current-voltage characteristics of chalcogenide glass switching devices
18 p2293 A73-36722

Investigation of the molecular composition of the vapors and the structure of the condensate during the evaporation of arsenic chalcogenides by laser radiation
19 p2437 A73-37957

Photoelectric phenomena in amorphous chalcogenide semiconductors.
20 p2599 A73-39133

Study of the properties of thick-film chalcogenide glass holograms
21 p2701 A73-40571

Certain properties of semiconductor glasses from the Ge-As-Se-Te system
21 p2752 A73-40749

Properties of thin-film holograms on chalcogenide glasses
22 p2860 A73-42409

Off state I-V characteristics and thermal switching phenomena for tellurium selenium germanide chalcogenide glass semiconductors, assuming internal heat generation
24 p3119 A73-44407

CHANCE-VOUGHT MILITARY AIRCRAFT

U MILITARY AIRCRAFT

CHANDRASEKHAR EQUATION

Invariant imbedding and Chandrasekhar's planetary problem of radiative transfer.
02 p0207 A73-12389

Considerations concerning the solution of Chandrasekhar's system of equations in the case of MHD turbulence
11 p1404 A73-25700

Chandrasekhar equations for axisymmetric MHD flows generalized for steady and unsteady flows
14 p1781 A73-30701

Comparison of three techniques for solving the radiative transport equation.
[AIAA PAPER 73-751] 18 p2337 A73-36367

Reflection function for an isotropically scattering finite medium.
22 p2887 A73-42565

CHANNEL CAPACITY

Multisatellite systems for transoceanic aircraft communications and ATC, discussing day and night operations, cost-benefit optimization and adaptive techniques for capacity augmentation
01 p0018 A73-11201

Effects of a finite-width decision threshold on binary CPSK and FSK communication systems.
03 p0277 A73-13911

Noise characteristics, channel capacities, power requirements and transmission efficiencies of various semiconductor transmitter designs for FM directional radio systems
03 p0284 A73-14125

Data return maximization for unpredictable channel capacity, considering planetary entry probe to Venus or Jupiter with unknown atmospheric transmission characteristics
04 p0420 A73-15425

Datran TDM switching system with stored program controller and IC components providing reliability, flexibility and high channel capacity in data transmission
05 p0551 A73-16804

Increasing the traffic-capacity utilization factor of a telemetry channel
07 p0794 A73-20297

IR laser terrestrial communication system with 5 Mbit/sec digital data capacity, using intracavity optical frequency modulation or frequency shift keying modulation
09 p1055 A73-23394

Optical fiber waveguide operational principles, discussing information transfer rate capability, channel characteristics and input and output devices
09 p1055 A73-23396

Multichannel wideband FM communication systems, discussing method for channel density increase with reduced linearity requirement and enhanced noise immunity
10 p1187 A73-23732

Run length code for redundancy encoding of black-white facsimile picture data transmission to allow channel or storage capacity reduction and hardware simplification
10 p1188 A73-23741

Information in the time of arrival of a photon packet - Capacity of PPM channels.
10 p1188 A73-23836

Commercial communications satellite technology trends, stressing wideband capabilities, flexibility, multiple access and channel capacity increase
10 p1189 A73-24561

Increasing the capacity of a discrete communication channel by additional modulation of a carrier parameter
12 p1467 A73-26941

Calculation of the average usage time of a channel in an adaptive multichannel communications system
12 p1471 A73-27585

L-band satellite systems for mobile applications.
12 p1472 A73-27664

The operational requirements for a maritime satellite communication service.
12 p1473 A73-27676

Maritime Satellite System with broadband and multibeam dish antennas, assessing FDM communication capability as function of channel quality and ship terminal antenna gain
12 p1473 A73-27679

RF spectrum utilization for optimum communication capacity, considering tradeoff between bandwidth and interference, antenna directivity and wave reflection and scattering effects
13 p1584 A73-29113

Logic and computational complexity of decoders for BCH codes, discussing channel capacity, error correction and information theory
13 p1587 A73-29672

Utilization of optical-frequency carriers for low- and moderate-bandwidth channels.
14 p1728 A73-30418

Direct modulation of a double heterostructure laser at a rate of 2.3 Gbit/s
14 p1758 A73-30700

Comparing bandwidth requirements for binary baseband signals.
16 p1984 A73-33745

Application of data compression techniques to spacecraft imaging systems.
17 p2122 A73-34910

VM 256 - Experimental system of a 3-D radar installation
18 p2335 A73-37040

Increasing the utilization factor of the carrying capacity of a telemetry channel.
18 p2291 A73-37134

Theory of two-channel laser action in spectrally inhomogeneous media. I - Noncorrelated frequencies
19 p2437 A73-37958

A proposed time division multiple access (TDMA) satellite system for Anik I.
20 p2523 A73-38719

Multiple-beam satellite repeater tradeoffs applied to a multifunctional system.
20 p2524 A73-38732

Aeronautical/maritime satellite borne two-way L-band transponder weight and power limitation effects on channel capacity
20 p2531 A73-39771

Risk of estimation by data obtained via communication channel.
21 p2654 A73-40689

A semiconductor-laser communication system using differential pulse position modulation.
21 p2656 A73-41094

Binary error estimation in real time for channel quality monitoring, comparing upper and lower bounds with number of errors for bit sequence
21 p2656 A73-41170

Continuous information theory and modulation methods.
22 p2826 A73-42463

Level transgressions and extremal values of continuous stochastic signals
23 p2952 A73-43310

CHANNEL FLOW

Analytical method of gasdynamic semibounded-space parameter computation allowing for velocity profile inhomogeneity and turbulent combustion of condensed systems
01 p0121 A73-10619

Viscous steady Couette flow between two parallel flat walls with particle injection, obtaining velocity and temperature distribution
01 p0033 A73-10808

Developing laminar free convection between vertical flat plates with asymmetric heating.
01 p0122 A73-10811

Temperature characteristics in the wall of an annular channel heated internally at supercritical pressures
01 p0123 A73-10861

Vibrational instability of plane-parallel convective motion in a vertical duct
01 p0034 A73-10966

Confined laminar jet mixing in a circular channel with arbitrary entrance velocity distribution.
[AD-758758] 01 p0034 A73-11363

Nonlinear baroclinic instability of a continuous zonal flow of viscous fluid.
02 p0153 A73-12035

Local transport equations for turbulent shear flow.
02 p0154 A73-12825

Ponderable barotropic fluid irrotational flow in horizontal cylindrical channel, noting solitary depression waves possibility
03 p0289 A73-12911

Hot-wire anemometers calibration characteristics for steady channel turbulent air flow measurement, noting linearization error analysis
03 p0306 A73-13166

Applying quasilinearization to the steady laminar flow between two parallel porous plates.
03 p0292 A73-13307

Existence theorems for Navier-Stokes equations periodic solution bifurcation in convection between two horizontal plates at different time periodical temperature
[ONERA, TP NO. 1179] 03 p0343 A73-13602

Hydrodynamics in weak gravitational fields - Plane oscillations of an ideal fluid in a rectangular channel
03 p0294 A73-13606

Electric field in a segmented MHD generator for a finite conductivity of the walls at the channel inlet
03 p0346 A73-13621

Acoustic and shock waves interaction in axisymmetric gas flow through variable section channel, calculating flow characteristics variations via isentropic theory of steady flow
03 p0295 A73-13673

A theoretical analysis of non-isentropic flow of a compressible, viscous gas in narrow passages.
[ASLE PREPRINT 72LC-3A-1] 03 p0297 A73-14355

Stability of nonrotationally symmetric disturbances for inviscid flow between rotating cylinders in the presence of an axial magnetic field.
04 p0433 A73-14899

The oscillatory boundary layer growth over the top and bottom plates of a rotating channel.
[ASME PAPER 72-WA/FE-5] 04 p0434 A73-15842

Heat and mass transfer laws for fully turbulent wall flows.
04 p0520 A73-15935

Empirical equations for calculating the heat and mass transfer for the special case of separated flow
04 p0520 A73-15941

Temperature distribution in non-Newtonian MHD channel flow by shear stress integral evaluation, investigating power law and Prandtl-Eyring fluids
04 p0520 A73-15947

Heat transfer in fully developed laminar flow between flat parallel boundary walls, deriving approximations to higher eigenvalues
05 p0563 A73-16101

Numerical solutions of the Navier-Stokes equations in inlet regions.
[ASME PAPER 72-APM-DD] 05 p0564 A73-16526

Two-dimensional viscid MHD flows in coaxial channels
05 p0603 A73-16588

Effect of the asymmetry of an external magnetic field on a viscous fluid flow in an annular MHD channel
05 p0603 A73-16589

The applicability of Stokes expansions to reversed flow.
05 p0565 A73-16606

Application of invariant imbedding techniques to flow instability problems.
[AD-75824] 05 p0591 A73-16608

Fluid undercutting in the successive channel flow of two gases.
[AIAA PAPER 73-214] 05 p0566 A73-16944

Shock wave-turbulent boundary layer interactions in rectangular channels. II - The influence of sidewall boundary layers on incipient separation and scale of the interaction.
[AIAA PAPER 73-234] 05 p0566 A73-16959

Flow of a gas in a flat channel at a diminishing flow rate
05 p0533 A73-17090

Effects of spanwise rotation on the structure of two-dimensional fully developed turbulent channel flow.
06 p0685 A73-17708

Flow visualization of the near-wall region in a drag-reducing channel flow.
06 p0685 A73-17709

Temperature of a duct flow under conditions of unsteady-state heat transfer
06 p0769 A73-18131

Asymptotic analysis of turbulent channel and boundary-layer flow.
06 p0687 A73-18528

Numerical prediction of the phenomenon of transition for a flow between two parallel planes
06 p0687 A73-18537

Approximate calculations of the hydrodynamic characteristics of a turbulent flow of liquid in annular channels
06 p0688 A73-18562

Magnetohydrodynamic laminar source flow between two parallel disks.
07 p0854 A73-19102

Minimum mixing losses of axisymmetric turbulent wakes in profiled wall channels
07 p0811 A73-19611

Velocity and resistance profiles for unsteady turbulent flow in rough pressure channels, using Prandtl hypothesis
07 p0811 A73-19614

Viscous incompressible gas turbulent flow in axisymmetric channel under preliminary twist conditions at inlet, using computer numerical solution
07 p0774 A73-19621

Copper resistance thermoanemometer for channel unsteady air flow rate measurement, discussing design, operation principles and maximum error
07 p0823 A73-19623

The study of film boiling crises and transient boiling of cryogenic liquids.
07 p0922 A73-20410

Velocity distribution of the turbulent motion of a fluid between two plane-parallel walls
08 p0954 A73-21175

Dynamic model of flow separation of plane fluid past body in channel with eddy wake formation
08 p0954 A73-21183

Pressure changes produced by sudden expansion of a two-phase flow
08 p0955 A73-21197

Variable properties laminar gas flow heat transfer in the entry region of parallel porous plates.
[AD-759455] 08 p1024 A73-21640

Two phase channel flow behavior from three dimensional phase diagram for one dimensional steady flow of ideal gas carrying solid particles
09 p1072 A73-22621

Certain results of an experimental study of local heat transfer under supercritical pressure in a unilaterally heated rectangular channel
10 p1293 A73-23510

Book - Turbulence transport modeling.
10 p1206 A73-24350

Transonic gas flow in rotating turbomachine cascade channels, reducing flow equations to second order differential equation
10 p1172 A73-24507

Unsteady viscoplastic electrically conducting MHD flow in moving-wall channel, assuming time-variable pressure gradient and uniform transverse magnetic field
10 p1256 A73-24588

Electrically conducting unsteady viscoplastic plane channel Hartmann and Couette MHD flows in presence of uniform transverse magnetic field and time variable electric field
10 p1256 A73-24589

Unsteady motion of a viscoplastic medium in a plane MHD channel at a constant flow rate
10 p1256 A73-24590

Inertia effects in laminar radial flow of power law fluids.
10 p1206 A73-24660

Hydrodynamic theory of heat transfer between a stabilized gas suspension flow and channel walls.
10 p1297 A73-24968

Viscous incompressible Jeffery-Hamel fluid flow in divergent channel, discussing secondary supercritical flow, winding and vortex formation
11 p1346 A73-25223

Steady plane flow of viscous fluid in symmetrical channels with curved walls, considering approximate series for stream function
11 p1347 A73-25646

Second-order solutions for steady magnetohydrodynamic channel flow with anisotropic conductivity.
11 p1404 A73-25746

Investigation of heat and mass transfer for plasma flows in channels of various shape under conditions of intense condensation
12 p1558 A73-27318

Qualitative analysis of MHD energy conversion efficiency
12 p1460 A73-27321

Electrohydrodynamic equation solutions for non-collinear current density and velocity vectors of unipolarly charged fluid flow in channel with wall-type electrodes
12 p1528 A73-27406

On oscillatory instability of plane-parallel convective motion in a vertical channel.
12 p1559 A73-27542

Temperature conditions at the wall of an annular channel with internal heating at supercritical pressures.
12 p1560 A73-27910

The channel flow of an electrically conducting Prandtl-Eyring fluid in a magnetic and an electric field
13 p1663 A73-28161

MHD free convective flow in a vertical channel.
13 p1663 A73-28164

Integral properties of viscous channel or pipe flow satisfying mixed no-slip and no-shear conditions from total momentum flux considerations
13 p1599 A73-28417

Influence of wall proximity on hot-wire velocity measurements.
13 p1613 A73-28527

Air injection from wall slot into turbulent boundary layer of high temperature gas channel flow, calculating film cooling effectiveness in flat plate
13 p1706 A73-28675

Rectangular channel mixed boundary layer flow patterns dependence on inlet edge configurations, channel geometry and hydrodynamic flow core parameters
13 p1601 A73-28737

Equilibrium three-dimensional turbulent boundary layer on the end wall of a curved channel.
13 p1602 A73-29015

Turbulence in liquids; Proceedings of the Symposium, University of Missouri, Rolla, Mo., October 4-6, 1971.
13 p1604 A73-29251

Effect of randomly fluctuating pressure gradients, with arbitrarily specified power spectrum and probability density, on flow in channels.
13 p1604 A73-29263

On the flow between two independently rotating disks of variable distance with blowing.
13 p1605 A73-29295

Solution of the problem of unsteady heat transfer for a body and the liquid flow around it
14 p1744 A73-30018

Multistep computer algorithm for Navier-Stokes equations of two dimensional viscous incompressible flow in channel with complex geometry
15 p1860 A73-30965

Calculation of a subsonic radiating gas flow by an adjustment method
15 p1821 A73-30969

A theory for rectangular wings with small tip clearance in a channel.
15 p1821 A73-31120

Approximate solution to the problem of a conducting fluid flow in a weakly curved channel
15 p1917 A73-31154

Reynolds stresses in plane-parallel flows disturbed by Tollmein-Schlichting waves
15 p1861 A73-31193

Spiral flows with multiple circulation in channels of simple shape
15 p1861 A73-31284

Nonlinear development of disturbances in a plane-parallel Poiseuille flow
15 p1861 A73-31285

Experimental investigation of the velocity structure and of hydraulic resistances in unsteady forced turbulent flows
15 p1862 A73-31287

Supersonic flow along a wavy wall in a channel
15 p1823 A73-31332

Experimental investigation of the pressure distribution in constrained MHD flows past cylinders
15 p1917 A73-31401

Uses of the equation of pulsation energy balance in the theory of MHD flows in channels and tubes
15 p1917 A73-31404

Nonlinear MHD equations solution for conducting fluid plane periodic channel flow in traveling magnetic field by net point method
15 p1917 A73-31406

Motion of a magnetized fluid between parallel plates
15 p1918 A73-31408

Laminar stratified flow of a conducting medium in ring channels in the event of great MHD-interaction parameters
15 p1918 A73-31409

Poiseuille flow and thermal creep of a rarefied gas between parallel plates.
16 p2085 A73-33315

A wake and an eddy in a rotating, radial-flow passage. I - Experimental observations.
[ASME PAPER 73-GT-57] 16 p1964 A73-33512

Approximate calculations of the hydrodynamic characteristics of turbulent fluid flow in annular ducts.
16 p2000 A73-33587

Acoustic instability of a bounded weakly ionized plasma
17 p2214 A73-34135

Viscous flow in radial turbomachine blade passages.
17 p2093 A73-34389

Method for calculating the steady irrotational isentropic flow in a two-dimensional supercritical turbine cascade.
17 p2093 A73-34390

Results of an experimental investigation of local heat transfer at supercritical pressure in a rectangular channel heated from one side.

17 p2255 A73-35190

Calculation of viscous gas flows in flat channels

18 p2265 A73-36990

Pulsation-energy balance equation in turbulent boundary layer theory

18 p2301 A73-37002

Plasma channel flow theoretical and experimental review, considering heat transfer studies, turbulent nonequilibrium plasma boundary layers and plasma sheaths

19 p2464 A73-37161

Linearized MPD jet and channel flows in external magnetic fields with the Hall effect.

19 p2465 A73-37175

Calculation of two-dimensional unsteady plasma flows in channels

19 p2467 A73-37369

Turbulent flow development characteristics in channel inlets.

19 p2421 A73-38184

Stability and convergence of streamline curvature flow analysis procedures.

19 p2421 A73-38190

Development of a turbulent boundary layer in MHD channel.

19 p2470 A73-38316

Heat transfer in an absorbing, emitting and scattering slug flow between parallel plates.

[ASME PAPER 73-HT-13] 20 p2625 A73-38568

Combined forced convection and radiation heat transfer in the thermal entrance region of a non-isothermal parallel plate channel - Optical thin gases.

[ASME PAPER 73-HT-14] 20 p2625 A73-38569

Flow film boiling heat transfer correlations - Parametric study with data comparisons.

[ASME PAPER 73-HT-50] 20 p2626 A73-38574

Bounding flow existence for turbulent convection in fluid and porous layers analysis between parallel plates based on calculus of variations in Banach spaces

20 p2626 A73-39012

Flow stabilization by methods of distributed automatic control

20 p2545 A73-39042

Variational analysis of the flow development in the entrance region of circular tubes and parallel-plate channels.

20 p2548 A73-39527

Numerical experiment in a study of the separation of a laminar boundary layer in an MHD channel

20 p2598 A73-39611

Electric field in an MHD channel of rectangular cross section in the presence of the Hall effect

21 p2744 A73-40183

Asymmetric heat transfer in turbulent flow through a plane slot

21 p2790 A73-40398

Formation of a plasma focus in erosion-type plasma accelerators. I

21 p2746 A73-40525

A numerical study of three-dimensional problems of MHD flow

21 p2747 A73-40887

Some integral characteristics of an MHD channel at finite magnetic Reynolds numbers

21 p2747 A73-40889

Convective heat transfer with allowance for three-dimensional heat sources in the fluid for turbulent flow in a plane slit

21 p2792 A73-41196

Effect of deflector geometry on the heat transfer in the coolant passages of deflector blades.

21 p2754 A73-41322

Creeping flow of Newtonian fluids in curved rectangular channels.

22 p2840 A73-41745

Flows with and without suspensions in channels with curvilinear segments

22 p2842 A73-42229

Flow stability of viscous homogeneous incompressible electrically conducting fluid between nonconducting walls at large magnetic Reynolds numbers

22 p2894 A73-42639

Heat transfer in plane Couette flow of rarefied gas between parallel plates, determining temperature jumps at plates from transfer equations

23 p3048 A73-43206

Viscous laminar Hartmann flow of electrically conducting liquid between parallel walls in transverse magnetic field, assessing thermal radiation effects and temperature distribution

23 p3008 A73-43207

An experimental investigation of the induced turbulence in laminar channel flow due to a transverse ion current and its applications to fluidic turbulence amplifiers.

23 p2942 A73-43402

Effectiveness of film cooling in a curvilinear channel formed by guide vanes

23 p3048 A73-43442

Experimental investigation of turbulent flow characteristics in a rotating channel

23 p2968 A73-43443

An approximate model of a separated turbulent flow in an abruptly widening channel

23 p2968 A73-43471

A study of the interaction between two compressible fluid flows in a flat channel at low Mach numbers

23 p2968 A73-43731

Unsteady transonic flows with shock waves in two-dimensional channels.

23 p2969 A73-43938

Piecewise-one-dimensional models of supersonic combustion and pseudoshock in a channel

24 p3154 A73-44702

Effects of thermal conductivity in radiative magnetohydrodynamic channel flow.

24 p3117 A73-45370

CHANNEL MULTIPLIERS

Visual display of fatigue damage by means of exoelectron emission.

04 p0446 A73-14748

The HR 300 ultrafast photomultiplier with a microchannel plate

06 p0678 A73-18852

Microchannel electron multipliers application to X ray cinematography of laser generated plasma

06 p0697 A73-18861

The microchannel Picoscope - A tube with high-temporal-resolution scanning for studying luminous phenomena in the subnanosecond range

06 p0679 A73-18862

A light and compact X-ray image read-out system for space applications.

11 p1364 A73-26050

Some aspects of the design and performance of a small high-contrast channel image intensifier.

14 p1751 A73-29909

Comparison of an aluminum-coated phosphor layer and a Channeltron Electron Multiplier Array as extreme ultraviolet-to-visible image converters for use in space applications.

14 p1752 A73-30155

Effect of longitudinal magnetic field on the performance of a channel electron multiplier.

20 p2565 A73-38884

Microchannel image intensifiers for detection at low light levels

23 p2979 A73-43222

Multichannel secondary electron image intensifier design, using dynode and separate channel transmission

23 p2961 A73-44386

CHANNELS [DATA TRANSMISSION]

Theory of multistep coding and its application to multipulse-modulation communication systems.

01 p0018 A73-11053

Optimum detection and signal design for channels with non- but near-Gaussian additive noise.

04 p0415 A73-14988

Gaussian channel model for long tropospheric scatter link verification by time varying bandpass impulse response measurements, using Kolmogoroff-Smirnoff tests

04 p0418 A73-15392

Information transfer satellite system (ITSS) design for earth resource and meteorological data collection and relay from remote sensing platforms

04 p0419 A73-15404

State and integral equations formulations for signal design problem of channels with known time dispersion and additive white Gaussian noise

04 p0419 A73-15405

Optimal equalization of discrete signals passed through a random channel.

04 p0420 A73-15418

Channel equalization in presence of intersymbol interference, comparing sequential statistical, dynamic programming, delay line and minimum mean square error techniques

04 p0425 A73-15419

Data link control procedures for error-free transmission channels, discussing serialization and synchronization techniques and reverse interrupt facilities in sequential machine model

05 p0551 A73-16802

Digital transmission performance on fading dispersive diversity channels.

06 p0664 A73-17711

Code correcting nonsymmetrical bursts of errors during data exchange between computers.

06 p0670 A73-17962

Adaptive maximum-likelihood sequence estimation for digital signaling in the presence of intersymbol interference.

06 p0665 A73-18144

Adaptive reception in a channel with slow total fading.

07 p0794 A73-20132

Internal additive noise generated by a random pulse process

08 p0939 A73-21395

Periodic regime stability of two channel relay system as function of main channels identicalness and cross coupling symmetry, using Tsypkin method

09 p1063 A73-22340

A five-channel time-scale converter

09 p1064 A73-23007

Satellite-borne programmable communications distribution subsystem, controlling microwave switch matrix by ground command via onboard memory for traffic flow data

09 p1053 A73-23364

Bandwidth efficiency for digital communication via a hard limiting channel.

09 p1054 A73-23382

Optical communication theory application to free space, turbulent and scatter channels, discussing background noise, detector statistical model and quantum receivers

10 p1188 A73-23757

Amplitude predistortion and deemphasis filters, measuring channel noise immunity enhancement by mean square deviation

10 p1195 A73-24379

Linear codes and transverse equalization for limiting the effects of intersymbolic interference in the transmission of digital signals

10 p1189 A73-24416

Unified approach to the performance analysis of linear modulation systems with coherent detection.

12 p1469 A73-27072

Message organisation in the ground segment of an aeronautical satellite system.

12 p1472 A73-27668

Optimal data sampling in communication channels system, discussing algorithms for data transmission and control

13 p1587 A73-28870

Modified Kalman filter for digital communication channel equalization with tap gains and initial state variable estimated by decision feedback and prediction process respectively

13 p1593 A73-29118

Multibeam satellite Effective Isotropic Radiative Power (EIRP) for aeronautical communications, discussing carrier-to-noise density increase and communication load per channel decrease

14 p1726 A73-29900

Intelligibility improvement of analog communication systems using an amplitude control technique.

14 p1726 A73-29901

Noise immunity of the optimal noncoherent reception of an FM signal in the presence of fluctuations in the synchronization channel

14 p1729 A73-30558

A three-channel reversible data converter and its possible applications in astronomy

15 p1878 A73-32146

Procedures and ground methods associated with the exploitation of a system of aeronautical satellites

15 p1911 A73-32488

Error probability of binary optical communications in turbulent atmosphere - Experimental results.

16 p1984 A73-33995

Pseudo random modulation - An effective means of enhancing PSK signal transmission in a diffuse multipath environment.

17 p2125 A73-35376

Sequential analysis algorithm for data channel detection of received signal represented by Poisson sequence of quantum transitions under large SNR

17 p2129 A73-35711

Internal additive interference produced by a pulsed random process.

19 p2407 A73-38353

Sampling, quantization and channel errors in differential pulse code modulation systems, discussing SNR, quantizer levels, standard PCM systems, reconstruction filters and bit errors

19 p2407 A73-38383

Error rate of a 4-phase coherent PSK satellite channel with non-Gaussian interference.

20 p2523 A73-38721

An adaptive scheme for PCM transmission.

20 p2523 A73-38728

Effect of nonlinear channel characteristics on QPSK system performance.

20 p2526 A73-38752

High-bit-rate transmissions through a channelized repeater.

20 p2526 A73-38753

Adjacent-channel interference between unfiltered and filtered QPSK signals.

20 p2526 A73-38754

Optimal detection of binary signals with an arbitrary distribution of state durations at the output of a binary symmetrical Markov channel

20 p2541 A73-38992

Transmission strategy and optimal block size in high-speed data communication.

20 p2530 A73-39128

Performance degradation plots for comparison of signal fading and intersymbol interference effects in two-component specular multipath digital microwave communication channel

21 p2649 A73-40336

Digital codings of multi-dimensional information sources and applications to image coding.
21 p2655 A73-41043

Digital communication channel with noisy errors, discussing statistical analysis of binary burst sequences for coding design
21 p2655 A73-41090

A few error detection codes for decision feedback system and error characteristics of channels.
22 p2835 A73-42192

Triple Modular Redundancy Single Single voter-switch with majority voting of three parallel data channels or converters, estimating reliability for short and long missions
22 p2825 A73-42294

Russian monograph on signal transmission channel identification systems in statistical communication theory covering mathematical models, design principles, radio electronic systems, etc
22 p2827 A73-42600

Structural methods of multichannel systems synthesis with the aid of the graph theory
22 p2836 A73-42602

Multicircuit structural analysis of linear multiple link control systems with dynamic interchannel cross couplings
22 p2836 A73-42608

German monograph on microwave filters for communication channels separation at millimeter wavelengths covering coupling circuits design and resonant frequencies of coaxial resonator
22 p2827 A73-42701

Adaptive maximum-likelihood receiver for synchronous data signals
23 p2957 A73-43320

Adaptive equalization with recursive noncanonical scanning filters
23 p2953 A73-43323

Suppression of equichannel interference in the case of binary phase shift keying employing a limiter
23 p2953 A73-43324

Optimum mean-square decision feedback equalization.
23 p2964 A73-43988

Calculation of the spectrum of a sinusoidal signal modulated by phase displacement with one, two, or three states for any values of phase jumps
24 p3068 A73-44972

Digital communication system with known channel characteristics, discussing intersymbol interference dependence on signalling rate based on Nyquist criteria consideration
24 p3070 A73-45482

CHANNELTRONS
U CHANNEL MULTIPLIERS
CHAOTIC CLOUD PATTERNS
U CLOUDS [METEOROLOGY]
CHAPARRAL MISSILE
Packaged servosystem drives mobile missile launcher.
08 p0929 A73-21844

CHAPLYGIN EQUATION
Ultraelliptic integrals degeneration to elliptic integrals in Goriachev-Chaplygin equation of rotating body, noting asymptotic approach to limiting motion
02 p0191 A73-11761

Application of the Chaplygin method to the solution of Volterra-type nonlinear integro-differential equations
11 p1391 A73-26521

Conjugating a Chaplygin operator with a differential operator in gasdynamics
13 p1563 A73-28443

CHAPMAN SHEAR LAYER
U SHEAR LAYERS
CHAPMAN-ENSKOG THEORY
Book - Kinetic theory. Volume 3 - The Chapman-Enskog solution of the transport equation for moderately dense gases.
03 p0345 A73-13991

Kinetic theory of suction flow, discussing slip coefficient determination for perturbation boundary conditions in Chapman-Enskog-Hilbert method and pressure gradient effects
07 p0812 A73-20474

Transport equations for dilute plasma in a magnetic field.
07 p0860 A73-20479

Correlation and prediction of gaseous diffusion coefficients.
15 p1958 A73-31998

Modification of the Chapman-Enskog method for a mixture of reactive gases with allowance for fast and slow processes
19 p2462 A73-37845

Chapman-Enskog-Hilbert expansion for a Markovian model of the Boltzmann equation.
20 p2549 A73-39627

CHAPMAN-FERRARO PROBLEM
Energy and momentum theorems in magnetospheric processes.
15 p1871 A73-31846

CHAPMAN-LOUET FLAME
U CHEMICAL EQUILIBRIUM
U DETONATION
U FLAME PROPAGATION

CHARACTER RECOGNITION

Optical Characters Reading and facsimile terminals reduction of message preparation time for electrical transmission in Defense Communications System, considering cost effectiveness and maximum benefit
04 p0418 A73-15380

Double cross-validation of video cartographic symbol location performance.
05 p0543 A73-16719

Visual pattern matching - An investigation of some effects of decision task, auditory codability, and spatial correspondence.
13 p1579 A73-29123

Factors affecting processing mode in visual search.
17 p2117 A73-35493

Searching for many targets - An analysis of speed and accuracy.
17 p2118 A73-35498

Visual search, complex backgrounds, mental counters, and eye movements.
21 p2639 A73-41185

Effect of exercise on the response time in an identification problem
22 p2813 A73-41894

CHARACTERISTIC EQUATIONS

U EIGENVALUES
U EIGENVECTORS
CHARACTERISTIC FUNCTIONS
U EIGENVALUES
U EIGENVECTORS
CHARACTERISTIC METHOD
U METHOD OF CHARACTERISTICS
CHARACTERS
U SYMBOLS
CHARGE CARRIERS

NT FREE ELECTRONS
NT HOLES [ELECTRON DEFICIENCIES]
NT MAJORITY CARRIERS
NT MINORITY CARRIERS
Excitation of space charge waves in a one-carrier semiconductor with variable doping.
01 p0088 A73-10680

Spatial distribution of charge carriers and radiant energy in single and double heterostructure semiconductor lasers, noting technology of potential barriers formation
01 p0059 A73-10715

Third harmonic generation in Ge induced by conduction nonlinearity during bulk heating of charge carriers by microwave fields
03 p0350 A73-14077

Shubnikov-de Haas oscillations in graphite selective scattering by charged impurities.
04 p0468 A73-14871

Theory of dynamic charge and capacitance characteristics in MIS systems containing discrete surface traps.
04 p0427 A73-15344

Theory of dynamic charge current and capacitance characteristics in MIS systems containing distributed surface traps.
04 p0427 A73-15345

Charge carrier cooling in nonhomogeneous semiconductors by static electric field, plotting average electron temperature as function of current.
04 p0484 A73-15569

Space-time distribution of excess carriers and their space charge in doped semiconductors.
06 p0734 A73-17814

Shot noise in diodes with a Schottky barrier in the case of a disturbed carrier distribution function
06 p0676 A73-18090

Effect of carrier multiplication in the collector junction of an alloyed transistor on the behavior of the transistor at high current densities
07 p0798 A73-19292

Diffusion equation for current carriers in solar cell with inhomogeneous internal electric field, determining photoelectric current in p-n junction
07 p0778 A73-19299

Charge carriers concentration growth and decay for semiconductor model with independent capture centers, determining capture level activation energy
07 p0861 A73-19328

Kinetics of electrostatic image formation during exposure of electrophotographic layers
07 p0823 A73-19331

The anisotropy of carrier lifetime in graphite.
08 p0982 A73-21220

Concentrations of carriers and electric field along an insulating or semiconducting sample: Developments of steady solutions up to the second order Case of weak potentials
08 p0995 A73-21443

Ion-implanted bipolar transistor carrier concentration profiles.
10 p1194 A73-24155

Temperature dependence of kinetic properties of photoconductivity produced by carrier redistribution across attachment centers, discussing results with Ag and Al doped ZnS single crystals
10 p1260 A73-24468

Determination of attachment center parameters in semiconductors from the temperature dependence of the photocurrent
11 p1408 A73-25248

CHARGE DISTRIBUTION

Thermal noise calculation of single-carrier space-charge-limited current in a non-insulating solid.
12 p1530 A73-27029

The connection between the thermodynamics of chemisorption on semiconductor surfaces and surface scattering of carriers.
13 p1668 A73-28454

Determination of the diffusion length of excess carriers in semiconductors under a polyethylene film
13 p1668 A73-28462

Phenomenological analysis of thermostimulated depolarization effects
13 p1668 A73-28463

Carrier heating or cooling in semiconductor devices.
13 p1590 A73-28540

Polarization charge capture dependence of two layer dielectric metal-silicon nitride-silica-silicon semiconductor structures on pulse duration and temperature
16 p1991 A73-34003

Gamma detectors using mercuric iodide and other heavy metal compounds as semiconductors with charge carriers for current surge in quantum energy resolution
17 p2134 A73-34247

Charge carrier mobility distribution along the channel of an MDS field transistor
18 p2293 A73-36720

Injection currents in semiconductors with deep polarizable impurity centers
18 p2341 A73-37046

Influence of intervalley scattering on the size effect in the electrical conductivity of semiconductors
19 p2471 A73-37956

Current carriers and electron impurity centers in ferrimagnetic semiconductors - The case of weak interaction
19 p2471 A73-37959

Dynamic scattering of oscillating charged centers in semiconductors
19 p2471 A73-38541

Unpaired electrons and charge carriers in oxide semiconductor glasses based on the oxides of titanium, vanadium, and phosphorus
20 p2599 A73-39394

Determination of the bulk carrier lifetime in the low-doped region of a silicon power diode, by the method of open circuit voltage decay.
21 p2665 A73-41123

A new type of charge trapping in MOS systems.
22 p2896 A73-42275

Trap-assisted charge injection in MNOS structures.
24 p3120 A73-45419

CHARGE DISTRIBUTION
Charge density distribution in Be single crystals from X ray structure amplitudes for lowest angle Bragg reflections, comparing with Hartree-Fock and free electron plane wave models
04 p0467 A73-15932

Theory of scattering of electrons in a non-degenerate-semiconductor-surface inversion layer by surface-oxide charges.
06 p0733 A73-17747

Electromagnetic interactions of cosmic ray muons in iron. I - Search for a charge asymmetry.
06 p0743 A73-18386

Charge carriers concentration growth and decay for semiconductor model with independent capture centers, determining capture level activation energy
07 p0861 A73-19328

Satellite measurements of the charge composition of solar cosmic rays in the Z = 6 to 26 interval.
10 p1264 A73-23537

Tangential electric field near base driven cylindrical antenna surrounded by free space or by homogeneous isotropic dissipative medium from charge distribution measurement
11 p1329 A73-25665

Junction discontinuities in wire antennas and scatterers, obtaining constraint on junction currents via equivalent charge distribution representation
11 p1329 A73-25666

Atmospheric convection and its effect on relaxation time and charge distribution.
11 p1394 A73-25759

Development of spark chambers for use in measurements of the charge spectrum of high energy cosmic rays.
11 p1363 A73-25961

A modified GaAs IMPATT structure for high-efficiency operation.
13 p1595 A73-29577

Static electromagnetic field structure in elastic homogeneous medium for sources distributed by simple and double layers in terms of scalar and vector potentials
14 p1774 A73-30030

Charge changing processes in hydrogen beams.
14 p1776 A73-30125

Measurement of cosmic-ray muon charge ratio at sea level between energies of 10 and 1500 GeV.
14 p1787 A73-30455

Study on the charge and isotope composition of medium cosmic ray particles.
16 p2054 A73-33278

- Charge and energy spectra of cosmic rays with Z equal to or greater than 30. 16 p2054 A73-33279
- Charge and energy spectra of particles with E from 0.2 to 30 MeV/nuc in the January 25, 1971 solar flare. 16 p2054 A73-33281
- Interpretation of the charge ratio of cosmic ray muons. 17 p2223 A73-34242
- Measurement techniques for antennas in dissipative media. 17 p2143 A73-35685
- Composition of low energy cosmic radiation from silicon to nickel. 17 p2225 A73-35787
- Fluctuations in plasma and nonlinear susceptibilities. 17 p2143 A73-35817
- Process control stress test of MOS IC circuit susceptibility to charge spreading with channel formation. 19 p2436 A73-38452
- A technique for the investigation of deep-level states in diffused p-n junction devices - Application to GaAs electroluminescent diodes. 20 p2536 A73-39412
- Exponential projectile charge dependence of Ar K and Ne K X-ray production by fast, highly ionized argon beams in thin neon targets. 22 p2890 A73-42710
- Insulated electrically thin dipole antenna with surrounding large wave number isotropic medium, discussing transmission line properties and current and charge distribution. 22 p2829 A73-43183
- Thunderstorm electrification by the inductive charging mechanism. I - Particle charges and electric fields. II - Possible effects of updraft on the charge separation process. 23 p3002 A73-43599
- Observation of cosmic-ray particles with Z of 50 or greater and interpretation of the charge spectrum. 23 p3024 A73-43610
- Light absorption coefficient of disordered semiconductor with random field due to charged impurity centers in presence of constant external electric field. 23 p3016 A73-43648
- Redistribution of charged particles and self-distortion of high-amplitude electromagnetic waves in a plasma. 24 p3117 A73-45413
- CHARGE EXCHANGE**
- NT RESONANCE CHARGE EXCHANGE**
- Energetic protons detection below radiation belt at equatorial latitudes from Azur satellite measurements, hypothesizing exospheric and upper atmospheric charge exchange processes. 01 p0043 A73-11514
- Ion density and electron temperature calculations for metallic plasma population inversion possibility by near resonant charge exchange with inert gas ions. 02 p0194 A73-12847
- One-electron model for charge exchange in ion-atom collisions. 03 p0344 A73-13283
- Diurnal atomic hydrogen variation at exospheric temperatures as function of thermal ion and proton charge exchange with plasmasphere. 12 p1492 A73-27612
- Population inversion calculations using near-resonant charge exchange as a pumping mechanism. 13 p1627 A73-28549
- Distribution of flux of charge-exchange atoms from a plasma over the cross section of the plasma filament in the Tokamak-4 apparatus. 13 p1664 A73-28611
- Optical study of charge exchange collisions between He⁺ and CO₂. 16 p2039 A73-33675
- Decay of the magnetic storm ring current by the charge-exchange mechanism. 17 p2159 A73-34782
- Heating of the low-latitude upper atmosphere caused by the decaying magnetic storm ring current. 21 p2684 A73-40786
- Energy deposition of protons in molecular nitrogen and applications to proton auroral phenomena. 24 p3126 A73-45116
- CHARGE SEPARATION**
- U POLARIZATION [CHARGE SEPARATION]**
- CHARGE TRANSFER**
- Effects of transverse diffusion and transverse stored charge in alloy transistor base. 01 p0023 A73-10681
- Thermal energy charge transfer reactions of rare-gas ions to methane, ethane, propane, and silane - The importance of Franck-Condon factors. 02 p0195 A73-12084
- Polycrystalline organic compounds effect on second harmonic generation of neodymium laser, noting relation between nonlinear susceptibility and intramolecular charge transport. 02 p0176 A73-12097

- Rate coefficient calculation for near resonant charge transfer reaction between oxygen cations and hydrogen atoms as function of temperature at thermal energies. 02 p0217 A73-12391
- Gas-phase acidities of binary hydrides. 02 p0139 A73-12632
- Laser beam self focusing possibility in GaAs, considering nonlinearity mechanism of intervalley carrier transfer due to applied dc field. 04 p0458 A73-14874
- Influence of structural perturbations applied to platinum and gold on kinetic processes at the electrode. 04 p0407 A73-15105
- De Gaston decharger with ionizing radiation for temporary jet fuel conductivity increase and charge density reduction, discussing theory, design and tests [SAE PAPER 720864]. 05 p0537 A73-16673
- Buried channel MOS, double junction and Schottky barrier charge coupled devices, noting higher speeds, charge transfer efficiencies and radiation resistance. 05 p0559 A73-16810
- The charge transfer spectrum of LiNa^+ . 06 p0726 A73-18250
- Charged coupled IC image sensors based on MOS capacitors for low light level TV, considering operation, performance and production technologies. 06 p0676 A73-18301
- Double charge transfer spectroscopy of diatomic molecules. 09 p1122 A73-22118
- Extraction of energy and charge from a black hole. 10 p1280 A73-24342
- Differential mode of operation for bucket-bridge circuits. 11 p1341 A73-25360
- Differential difference equations for probability of water droplet electrization in weakly ionized medium during cloud and fog formation. 13 p1654 A73-28883
- Charge transfer semiconductor devices operational principles and possible structures with two or three phases, discussing efficiency, regeneration circuitry and noise and dissipation problems. 14 p1731 A73-29727
- Instabilities in charge sheets and current sheets and their possible occurrence in the aurora. 15 p1873 A73-32235
- Charge transfer in overlapping gate charge-coupled devices. 16 p1988 A73-33396
- MIS structures with reversible charge capture capability, discussing I-V characteristics and applications similar to FET, image storage and charge coupled devices. 20 p2534 A73-38853
- A study of the characteristics of surface charge transfer devices. 20 p2534 A73-38854
- Charge transport bands in the electronic spectra of Fe(III) complexes with certain oxygen-containing ligands. 21 p2751 A73-40310
- N_2^+/N and O_2^+/O second negative bands laser theory. 22 p2871 A73-43144
- Charge transfer from a highly electrically stressed water surface during drop impact. 24 p3108 A73-45206
- Excitation mechanisms in He-Cd and He-Zn ion lasers. 24 p3097 A73-45418
- Stationary charge transport in metal-semiconductor-metal/MSM/ structures. 24 p3120 A73-45421
- CHARGED PARTICLES**
- NT ALPHA PARTICLES**
- NT ANIONS**
- NT ANTIPROTONS**
- NT ARGON PLASMA**
- NT BETA PARTICLES**
- NT CATIONS**
- NT CESIUM PLASMA**
- NT COLD PLASMAS**
- NT COLLISIONLESS PLASMAS**
- NT CONDUCTION ELECTRONS**
- NT COSMIC PLASMA**
- NT DEUTERIUM PLASMA**
- NT DEUTERONS**
- NT ELECTRON PLASMA**
- NT ELECTRONS**
- NT FERRIC IONS**
- NT FREE ELECTRONS**
- NT HELIUM PLASMA**
- NT HIGH ENERGY ELECTRONS**
- NT HIGH TEMPERATURE PLASMAS**
- NT HOT ELECTRONS**
- NT HYDROGEN PLASMA**
- NT INNER RADIATION BELT**
- NT MAGNETICALLY TRAPPED PARTICLES**
- NT MANGANESE IONS**
- NT METAL IONS**
- NT METALLIC PLASMAS**
- NT NONEQUILIBRIUM PLASMAS**

- NT NONUNIFORM PLASMAS**
- NT NUCLEI [NUCLEAR PHYSICS]**
- NT OUTER RADIATION BELT**
- NT PHOTOELECTRONS**
- NT PI-ELECTRONS**
- NT PLASMA CLOUDS**
- NT PLASMA LAYERS**
- NT PLASMA SHEATHS**
- NT PLASMA SLABS**
- NT PLASMAS [PHYSICS]**
- NT POLARONS**
- NT POSITRONS**
- NT PROTON BELTS**
- NT PROTONS**
- NT RADIATION BELTS**
- NT RAREFIED PLASMAS**
- NT RECOIL PROTONS**
- NT RELATIVISTIC PLASMAS**
- NT ROTATING PLASMAS**
- NT SOLAR ELECTRONS**
- NT SOLAR PROTONS**
- NT SOLAR WIND**
- NT STELLAR WINDS**
- NT THERMAL PLASMAS**
- NT TOROIDAL PLASMAS**
- Transition radiation from a plasma boundary. 01 p0085 A73-11063
- Electric potential and particle concentration of a plasma in the proximity of a projectile moving rapidly toward the plasma. 01 p0086 A73-11289
- Corpuscular radiation as an upper atmospheric energy source. 02 p0205 A73-12289
- Cherenkov and transient radiation of uniformly moving charge in random inhomogeneous medium. 02 p0193 A73-12381
- Secondary cosmic ray shower charged particles angular distribution asymmetry in center-of-mass system and azimuthal plane related to single fireball formation. 02 p0208 A73-12657
- Scintillation and anticoincidence Cerenkov counters for recording heavy nonrelativistic single charge particles in cosmic rays at sea level. 02 p0209 A73-12670
- Circular polarization of synchrotron radiation in the presence of hydromagnetic waves. 02 p0224 A73-12739
- Magnetospheric charged particle populations in magnetosheath, plasma sheet, extraterrestrial ring current, electron trough and trapping regions. 03 p0302 A73-13856
- The effect of an electric field induced by a time-dependent ring current on the particle drift motion. 04 p0440 A73-14954
- On the potential difference between two immiscible media. 04 p0483 A73-15106
- One dimensional periodic slow wave structure interaction with charged particles beam, considering system operation as TWT and backward wave tube. 05 p0556 A73-16063
- Charged particle beams focusing in combined dual spiral system with uniform magnetic field along axis, applying to imaging of flat object. 05 p0556 A73-16067
- Concerning the accuracy of conservation of the third adiabatic invariant of the motion of a charged particle in axisymmetric fields. I. 05 p0600 A73-16082
- Investigations of high-energy charged particles and VLF radiation with the Interkosmos 3 satellite. 05 p0608 A73-16085
- Green's function of the Maxwell equations in laminar media. 05 p0598 A73-16819
- Analysis of oxygen in aluminum by activation by means of charged particles and gamma photons. 05 p0547 A73-17217
- On the transport properties of charged particles in one dimension in random electric fields. 05 p0612 A73-17384
- Diffusion time of charged particles in a plasma with volume ionization. 06 p0726 A73-17417
- On a quadratic first integral for the charged particle orbits in the charged Kerr solution. 06 p0725 A73-17889
- Steady-state charged and neutral particle densities in a bounded turbulent high-temperature plasma. 06 p0732 A73-18607
- Conversion of trapped charged particles into untrapped particles in a high-frequency electric field. 06 p0732 A73-18608
- Charged-particle lifetime measurements in a helium plasma. 07 p0855 A73-19284
- Auroral sporadic E layer diurnal distribution correlation to charged particle integral flux diurnal variations observed by satellite in winter, noting Kp index effect. 07 p0816 A73-19455
- Charge dependence of the energy spectra of cosmic rays. 07 p0873 A73-20561

- Possibilities of using a quadrupole probe in the 0 to 1000-Hz range to measure the collision frequencies of charged particles in the ionosphere 08 p0957 A73-20654
- Energy loss of charged particles in Maxwellian plasmas. 08 p0992 A73-20823
- Influence of radiation damping on the motion of a charge in a uniform magnetic field and in the field of a plane electromagnetic wave 08 p0989 A73-21516
- Emission from a bunch of charged particles in multiple transit through a cylindrical resonant cavity 09 p1061 A73-21885
- Plasma effects and the acceleration of charged particles in pulsar fields. 09 p1141 A73-22016
- Diffusion of charged particles in a random magnetic field. 09 p1137 A73-22035
- Relaxation in a two-temperature plasma with directed motion of electrons 09 p1127 A73-22601
- Visual display of the spatial distribution of colloidal particle beams. 09 p1136 A73-23448
- Charged particle thermonuclear reactions in nucleosynthesis. 10 p1271 A73-23479
- Compton effect in charged particle under intense circularly polarized electromagnetic wave, noting application to Crab pulsar 10 p1271 A73-23485
- Inelastic collision of fast charged particles with arbitrary levelled hydrogen-like atoms. 10 p1250 A73-23575
- Theory of cosmic ray transport with anisotropic particle scattering and convection 10 p1265 A73-23903
- Methods for determining the charges of heavy primary nuclei Z greater than 26/ in photonuclear emulsions of different sensitivities 10 p1267 A73-23922
- Investigation of charged-particle fluxes at altitudes of 200 to 300 km with the aid of the Saliut orbital station 10 p1267 A73-23930
- Formation of the density profile of charged particles at heights from 10 to 90 km 11 p1411 A73-25082
- Energetic solar particles and their relation to optical flares. 11 p1413 A73-25952
- A charged-particle scintillation spectrometer with large geometric factor. 11 p1364 A73-25965
- Emission from a point charge during motion along the plane boundary of a dielectric with periodically varying density 11 p1402 A73-26448
- Charged particle production and plasma electron/ion current discharges from W targets under laser beam, noting dependence on electric field strength, pressure and operation mode 11 p1378 A73-26522
- Bounds on mean excitation energies-Lamb shift, stopping power, straggling, and grazing collision of high-energy charged particle. 12 p1526 A73-27128
- Electrostatic toroidal analyzer for studying charged particle fluxes in outer space 12 p1496 A73-27203
- Propagation of unipolarly charged jets in hydrodynamic flows 12 p1528 A73-27407
- Accuracy of conserving the third adiabatic invariant of the motion of a charged particle in axially symmetrical fields. II. 12 p1535 A73-27634
- Lifetime of charged particles in a helium plasma. 13 p1665 A73-28684
- Charged stopping pions from nuclear-electromagnetic cascades in rock, calculating number and energy spectra by Monte Carlo method 13 p1671 A73-29667
- Effect of radial profile of a charged particle pulse on the electromagnetic wake in a plasma 14 p1779 A73-29710
- Measurement of cosmic-ray muon charge ratio at sea level between energies of 10 and 1500 GeV. 14 p1787 A73-30455
- German book on physical foundations of electronics covering charged particle motions in electric and magnetic fields, relativistic effects, electron and ion optics, etc 14 p1736 A73-30597
- On the transport of charged particles in turbulent fields - Comparison of an exact solution with the quasilinear approximation. 15 p1916 A73-31083
- Calculation of the electron density in heterogeneous mixtures with allowance for the tunneling effect and for super-barrier reflection 15 p1915 A73-31854
- Reliability testing of high-perveance three-electrode guns 15 p1851 A73-32215
- The electric field and structure of a weakly ionized plasma in the vicinity of a small charged body 15 p1921 A73-32322
- Dolapchiev-Mangeron-Tsenov analytical mechanics equations extension to potential force systems, applying to electric charge motion in electromagnetic field 16 p2035 A73-32681
- Klein-Gordon equation for a charged particle interacting with an electromagnetic wave. 16 p1979 A73-33164
- Superconducting magnetic spectrometer technique application to charged primary cosmic rays, discussing calibration, experiments and electron-positron and isotopic separation 16 p2014 A73-33277
- Study on the charge and isotope composition of medium cosmic ray particles. 16 p2054 A73-33278
- Evidence for the possible existence of a charged particle with large mass. 16 p2016 A73-33700
- Excitation of highly excited hydrogenic ions and atoms by charged particles. IV. 16 p2039 A73-33865
- Radiation emitted by a charge in a stack of plates at frequencies approaching the Bragg frequencies 17 p2120 A73-34114
- The Compton effect in a medium near a Cerenkov cone 17 p2120 A73-34115
- Transient radiation in a shortened waveguide 17 p2120 A73-34116
- A magnetic spectrometer for recording particles in a range up to 4 GeV/c 17 p2164 A73-34151
- A generalization of the equations governing the evolution of a particle distribution in a random force field. 17 p2213 A73-34449
- The theory of charged particle temperatures in the upper atmosphere. 17 p2224 A73-35593
- Some characteristics of charged particle flux studies using traps and analyzers. II - Modulation trap utilization for investigating the solar wind 18 p2345 A73-36113
- Geometric factor optimization for a telescope performing charged-particle recording in space 18 p2315 A73-36115
- A digital optimization device for directional charged particle measurements in space research. 19 p2428 A73-37148
- Transport of charged particles in the earth's magnetosphere 19 p2474 A73-37348
- Use of charged particle beams for low temperature plasma measurement in magnetosphere and interplanetary space. 19 p2429 A73-37381
- Constitutive equations of a plasma with bound charges. 19 p2468 A73-37521
- Continuum theory of a slightly ionized plasma, diamagnetic effects. 19 p2468 A73-37522
- Medium-velocity and electric-current concepts in restricted relativity 19 p2459 A73-37535
- Kinetic equation for one particle cosmic ray distribution function in static random magnetic field on basis of diffusion theory 19 p2476 A73-38291
- Emission of longitudinal waves from a charge in an external high-frequency electric field in a magnetoactive plasma 19 p2470 A73-38331
- Explorer 45 mission objectives discussing magnetospheric ring current, magnetic storm detection, particle energy and interactions, electric and magnetic fields measurements, etc 20 p2614 A73-38949
- Charged particle acceleration in strong dipole fields. 20 p2595 A73-39077
- Preferential acceleration of heavy nuclei on the sun 21 p2756 A73-40582
- A nonstationary model of charged-particle diffusion in a gravitational field 22 p2902 A73-41955
- Containment stability of charged particles captured by a plane electromagnetic wave propagating at a slowly varying velocity 22 p2826 A73-42377
- Computer simulation of the acceleration of charged particles captured by plane electromagnetic waves 22 p2826 A73-42378
- Nonsingular unified field model for charged particle described by interrelation of gravitational mass, global energy and effective charge, considering comparison with Reissner metric 22 p2887 A73-42432
- Carbon particles size distribution and charged fraction in acetylene-oxygen flame using molecular beam system and electron microscopy, noting particle interaction formation mechanism 22 p2936 A73-42801
- The parallel diffusion of cosmic rays in a random magnetic field. 22 p2904 A73-43011
- On Kraichnan's direct interaction approximation applied to charged-particle transport in turbulent magnetic fields. 22 p2904 A73-43013
- Electric potential and particle concentration of a plasma in the vicinity of a rapidly moving charge. 23 p3009 A73-43510
- Fluctuations of the total path of charged particles in electron-photon showers caused by gamma-quanta with energies of 40, 60 and 200 m/c-squared/ 23 p3023 A73-43555
- Accretion and electrostatic interaction of interstellar dust grains - Interstellar grit. 23 p3030 A73-43757
- Scientific equipment for studying cosmic rays on Prognoz satellites. I 24 p3144 A73-44783
- Drift of radiation-belt particles during substorms 24 p3124 A73-44804
- Breakdown potential of potassium-seeded combustion products. 24 p3121 A73-45164
- CHARGING**
The reflex principle of charging nickel-cadmium and other batteries. 03 p0253 A73-13938
- CHARPY IMPACT TEST**
Fracture characteristics of some aluminum alloy sheets in Charpy impact test at super-low temperatures. 02 p0179 A73-11595
- Fracture characteristics of aluminum alloy welds in Charpy impact test at super-low temperatures. 02 p0172 A73-11596
- Postirradiation notch ductility and fracture strength of pressure vessel steel plate by Charpy V tests 04 p0460 A73-14702
- Relationship between material fracture toughness using fracture mechanics and transition temperature tests. 04 p0506 A73-14703
- Boron fiber-aluminum alloy matrix composite structure Charpy impact energy absorbing capacity explained via energy dissipation of matrix by plastic deformation 05 p0588 A73-16111
- Evaluation of fracture toughness in aluminum alloys and welds by the Charpy impact test. 05 p0587 A73-16578
- Borsic-aluminum composites fracture and flexural behavior from Charpy impact and slow bend tests 17 p2192 A73-35537
- Fracture toughness and absorbed energy measurements in impact tests on brittle materials. 19 p2500 A73-38094
- Procedure and device for the study of the behavior of metals subjected to dynamic torsional stresses 22 p2868 A73-43171
- CHARRING**
Phenolic resin char-formation during hyperthermal ablation. 01 p0124 A73-11448
- CHARTS**
NT FLOW CHARTS
NT GRAPHS [CHARTS]
NT METEOROLOGICAL CHARTS
- CHASSIS**
Lunokhod 1 vehicle chassis design and mobility characteristics in Mare Imbrium, discussing wheels, suspension, movement control, traction, cohesion and lunar surface maneuverability 02 p0151 A73-12235
- Calculation of the temperature field of the heated zone of a complex shape consisting of a chassis with parts mounted on it. 06 p0766 A73-17412
- CHEBYSHEV APPROXIMATION**
Low pass Butterworth and Chebyshev filters design with Sallen-Key network for fabrication of microelectronic circuits 01 p0024 A73-10682
- Antenna array synthesis in Chebyshev approximation, calculating array geometry and excitation amplitudes for double scan radiation pattern 02 p0146 A73-12022
- Approximate perturbation solution in Chebyshev polynomials for partial differential equation of heat conduction with cylindrical, spherical or hyperspherical symmetry 06 p0769 A73-18503
- Use of Olver's algorithm to evaluate certain definite integrals of plasma physics involving Chebyshev polynomials. 07 p0854 A73-19270

Computerized normal loci plotting by orthogonal Chebyshev approximation, using minimum variance principle and Fisher test for regression curve selection
09 p1143 A73-22094

Extremum criteria for Gato differentiable mappings in hypercomplex domains derived for nonlinear Chebyshev problems, extending results to partially ordered sets of operators
09 p1112 A73-22581

Chebyshev projections properties, determining method for minimum linear distortion in class of conformal mappings of given region
10 p1212 A73-24300

Quasi-conformal mapping theory of two- and multidimensional regions, considering superposition, hyperbolic and mixed systems and Chebyshev problem
13 p1647 A73-28339

The numerical solution of parabolic partial differential equations using the method of Lanczos.
13 p1650 A73-29398

Uniqueness of Chebyshev approximation representation by ratios of exponential functions with restricted number of zeros
13 p1651 A73-29400

Chebyshev polynomial series solution method for highly eccentric perturbed orbits of comets, using modified Hansen method of partial anomalies
14 p1790 A73-29783

Implementation of simultaneous iteration for vibration analysis.
16 p2075 A73-32788

Chebyshev minimax functional solution for optimal control system design, noting flexible rocket and nuclear reactor control applications
20 p2592 A73-38683

A finite step algorithm for determining the 'strict' Chebyshev solution to $Ax = b$.
21 p2725 A73-40381

German monograph on display unit nonlinear interpolation approach based on higher order curve for reduced computer storage requirements covering Chebyshev approximation and coordinate transformations
22 p2830 A73-42738

Chebyshev solution to elliptical equilibrium equations of elastic reticular cylindrical and toroidal shells under distributed loads, applying to extensible fiber structures /tires/
24 p3146 A73-44652

CHECKOUT

Analytical method for diagnostic and checkout testing of logic element faults in complex combinational circuits
01 p0026 A73-10035

Multilayer debugging process /A new method of screening/.
03 p0336 A73-13734

Solar cell dark I-V characteristics and their applications.
11 p1310 A73-26003

CHECKOUT EQUIPMENT

U TEST EQUIPMENT

CHEMICAL ANALYSIS

NT ELECTROPHOTOMETRY

NT GAS ANALYSIS

NT GAS SPECTROSCOPY

NT KJELDAHL METHOD

NT MICROANALYSIS

NT NEUTRON ACTIVATION ANALYSIS

NT OZONOMETRY

NT POTENTIOMETRIC ANALYSIS

NT QUALITATIVE ANALYSIS

NT QUANTITATIVE ANALYSIS

NT SPECTROSCOPIC ANALYSIS

NT URINALYSIS

NT VOLUMETRIC ANALYSIS

Determination of chromatographic resolution for peaks of vast concentration differences.
01 p0014 A73-10225

Design of an extremely sensitive flame-photometer for analyses in the picogram range using a lock-in amplifier
01 p0051 A73-10925

Elemental analysis of a friction and wear surface during sliding using Auger spectroscopy.
01 p0057 A73-11277

Chemical fractionation in iron meteorites and its interpretation.
01 p0108 A73-11474

Analysis of electrolytes for electrochemical polishing of steel with cationite application
02 p0174 A73-12536

Hornblendes from calc-alkaline volcanic rocks of island arcs and continental margins.
02 p0165 A73-12635

Petrochemistry and chemical features of lunar glassy spherules.
03 p0273 A73-13089

K, Rb, Sr, Ba contents and rare earths in specimens from the Apollonius /lunar mountains/ crater region brought back by the Soviet probe Luna 20
05 p0546 A73-16829

Lunar highlands soil analysis from Luna 20 and Apollo 16 samples, estimating lunar crust differentiation process age from Rb-Sr concentrations
05 p0618 A73-16833

Dispersion-free X-ray-fluorescent analysis in studies of space and terrestrial objects
05 p0546 A73-17019

Analysis of oxygen in aluminum by activation by means of charged particles and gamma photons
05 p0547 A73-17217

The determination of iron, titanium, and nickel in Apollo 14 samples by cathode ray polarography.
06 p0660 A73-17899

The organic analysis and carbon chemistry of lunar samples: Their significance for exobiology; Proceedings of the Conference, University of Maryland, College Park, Md., October 26-28, 1971.
06 p0753 A73-18410

An evaluation of pyrolytic techniques with regard to the Apollo 11, 12 and 14 lunar samples analyses.
06 p0753 A73-18411

Review of methods used in lunar organic analysis - Extraction and hydrolysis techniques.
06 p0661 A73-18412

Nanogram level lunar organic compound separation and detection by gas-liquid chromatography
06 p0661 A73-18413

Ion-exchange chromatography in lunar organic analysis.
06 p0662 A73-18414

Porphyrins analysis in Apollo 11, 12 and 14 soils via analytical demetallation followed by recovery and recomplexing with divalent cations
06 p0753 A73-18420

Amino acid search in lunar fines, considering terrestrial source contamination, bound and free amino acids, processing and analysis contamination
06 p0754 A73-18422

Lunar samples organic analysis avoiding organic molecules synthesis from indigenous constituents, considering pyrosynthetic and ionic reactions in solution
06 p0662 A73-18426

Electrical measurements, metallographic microscopy and chemical analysis for failure analysis
07 p0800 A73-19409

Crystallography and chemical trends of orthopyroxene-pigeonite from rock 14310 and coarse fine 12033.
07 p0881 A73-19703

Chondrite normalized major and trace element concentrations of Apollo 14 lunar samples, including basalt, breccia and regolith fines
07 p0886 A73-19761

Chemical analyses of lunar samples 14003, 14311, and 14321.
07 p0886 A73-19765

Analysis of lunar samples 14163, 14259, and 14321 with isotopic data for Li-7/Li-6.
07 p0887 A73-19766

O-18/O-16, Si-30/Si-28, C-13/C-12, and D/H studies of Apollo 14 and 15 samples.
07 p0887 A73-19771

Analysis of single particles of lunar dust for dissolved gases.
07 p0890 A73-19813

Total carbon, nitrogen, and sulfur in Apollo 14 lunar samples.
07 p0890 A73-19816

Survey of lunar carbon compounds. II - The carbon chemistry of Apollo 11, 12, 14, and 15 samples.
07 p0890 A73-19818

Amino acid analyses of Apollo 14 samples.
07 p0891 A73-19821

Comparative investigations regarding the determination of nitrogen in tantalum
08 p0978 A73-21418

The Gosnells iron - A fragment of the Mount Dooling octahedrite.
09 p1139 A73-21855

An alpha particle experiment for chemical analysis of the Martian surface and atmosphere.
09 p1048 A73-22190

Deep sea drilling core sample analysis methods and results relation to sediment age and fossil fauna and flora
11 p1325 A73-25462

Optical and chemical analysis of iron in Luna 20 plagioclase.
13 p1674 A73-28305

Luna 16 and 20 sample carbon chemistry analysis for volatilizable species by vacuum pyrolysis and mass spectrometry
13 p1580 A73-28333

AC polarographic determination of sulfur in molybdenum-rhenium alloy.
17 p2118 A73-34276

Physical and chemical analysis of germanium tunnel diodes.
17 p2219 A73-34865

Principal component determination in mercury and cadmium tellurides and in solid solutions of them
17 p2220 A73-35559

Organic compounds chemical analysis with cold trap to allow materials evaporation according to vapor

pressure characteristics for replacing gas chromatograph
17 p2175 A73-35760

High resolution nondispersive electron energy analyzer for electron spectroscopy for chemical analysis, using spherical mirror and grid retarding potential field as filters
17 p2176 A73-35770

Russian book - Spectrophotometry of niobium and tantalum.
21 p2648 A73-40803

Synthesis and characterization of isomeric cis- and trans-pyrone model compounds.
21 p2648 A73-41215

Ionospheric research by rocket, satellite and ground based methods, discussing ion and neutral chemistry, stratospheric-ionospheric coupling, ionospheric thermal structure, etc
21 p2689 A73-41358

Chemical analysis of surfaces by mass spectrography with secondary ion emission
21 p2648 A73-41595

Organic geochemical analysis of lunar samples with emphasis on detecting biologically significant organogenic elements, projecting techniques to Mars soil analysis
22 p2803 A73-42163

CHEMICAL ATTACK

NT INTERGRANULAR CORROSION

Inter- and transcrystallite breakdown of steels and alloys under the action of various media /A review/
01 p0062 A73-10258

Polyamide compounds stress corrosion properties and chemical resistance in different test fluids, discussing fluid effect on flaw development rate
02 p0184 A73-11583

Chemical stability of tantalum germanide powders in air and aggressive media, including acids, fluorine ions and perhydrol
09 p1133 A73-22465

Stress corrosion cracking behavior of nickel and nickel alloys.
10 p1232 A73-23870

Corrosion fatigue and stress corrosion crack growth in high strength aluminum alloys, magnesium alloys, and titanium alloys exposed to aqueous solutions.
11 p1381 A73-25815

Factors affecting the impact strength of glass-fiber reinforced polyester composites.
16 p2031 A73-33987

The relationship between relative oxide ion content of Na₂SO₄, the presence of liquid metal oxides and sulfidation attack.
20 p2575 A73-39023

Carbon deposition and the role of reducing agents in hot-corrosion processes.
20 p2576 A73-39027

Ventifact evolution in Wright Valley, Antarctica.
21 p2687 A73-41211

Pitting of titanium. I - Titanium-foil experiments. II - One-dimensional pit experiments.
23 p2991 A73-43521

CHEMICAL AUXILIARY POWER UNITS

H2-O2 auxiliary power unit for Space Shuttle vehicles - A progress report.
19 p2392 A73-38436

CHEMICAL BONDS

NT COVALENT BONDS

NT HYDROGEN BONDS

Reaction mechanisms and bonding energies for ion-hydrates /ion-water clusters/ of ionospheric interest.
01 p0014 A73-10896

The chemistry of urethane adhesives incorporating silane coupling agents.
03 p0332 A73-13037

Theory of one-dimensional Mott semiconductors and electronic structure of long molecules with conjugate bonds
06 p0734 A73-17923

A mechanism for polypeptide synthesis on a protein template.
06 p0652 A73-17943

Nature of chemical bonds in metal-like compounds based on transition metals
07 p0841 A73-20519

Effects of experimental conditions on parameter estimated when using the Hill model
09 p1044 A73-21872

Valence-bond study of the /H2, D2/ exchange reaction mechanism.
09 p1047 A73-22074

Critical evaluation of Zhurkov theory of metallic material fracture by successive rupture of atomic bonds due to atom thermal motion
09 p1100 A73-22160

Photochemical reactions in condensed phase relevant to biology, discussing molecular energy states, isomerization reactions and bond making/breaking processes
09 p1121 A73-23305

Interpretation of K X-ray emission spectra and chemical bonding in oxides of Mg, Al and Si using quantitative molecular orbital theory.
10 p1211 A73-24107

Study of the possibilities of histone-RNA complex formation in experiments in vitro 10 p1181 A73-24513

Deformable body with reticular structure, studying microstructural transitions using physical model with isolated-valence bond coupling 13 p1690 A73-27992

Interaction of haemoglobin with ions - Binding of inorganic phosphate to human oxyhaemoglobin. 14 p1714 A73-29850

Natural and synthetic thermally stable polymers, discussing pyrolysis, structure-property relationships and bond strengths 14 p1724 A73-30132

Diffraction spectra and electron density distributions of interatomic graphitizing carbon molecule bonds as polymer combinations, using diffractometer and scintillation counter recording 14 p1767 A73-30839

Protective coating-metal adhesion dependence on chemical bonds, double electric layers at interface and thermoelastic stresses 18 p2319 A73-35893

A theory of adhesion at a bimetallic interface - Overlap effects. 18 p2287 A73-37032

Photoelectron energy spectra for atomic and molecular binding energies, examining spectrum signatures, angular distribution, autoionization, rare gases, carbon monoxide and cyanocobalamin 20 p2520 A73-39634

Ti-V alloys elastic modulus and paramagnetic susceptibility, considering composition vs property curve salient point indications of changes in interatomic bonding energy and electron structure 21 p2718 A73-40487

Critical evaluation of Zhurkov theory of metallic material fracture by successive rupture of atomic bonds due to atom thermal motion 22 p2874 A73-42108

Theory of one-dimensional Mott semiconductors and the electronic structure of long molecules having conjugated bonds. 23 p3018 A73-44323

Metal crystal lattice properties and chemical bond nature in terms of valence concept, analyzing p-electron cloud overlapping 24 p3119 A73-45178

CHEMICAL CLEANING

Effects of inhibitors PB-5 and of dialkyl-dimethyl ammonium chloride on the corrosion resistance and mechanical strength of structural materials during the cleaning of heat exchangers from scale by the hydrochloric acid method 02 p0174 A73-12537

Removal of hydrocarbon contaminant film from spacecraft optical surfaces using a radiofrequency-excited oxygen plasma. [AIAA PAPER 72-263] 08 p0989 A73-21835

Surface morphology after pretreatment in relation with bondability of aluminium alloys. 16 p2018 A73-33056

The relation of surface condition after pretreatment to bondability of aluminium alloys. 24 p3093 A73-44764

CHEMICAL COMPOSITION

NT CARBON DIOXIDE CONCENTRATION

Element abundances in O- and early B-stars. 01 p0096 A73-10296

Petrographic and electron microprobe study of the Monturaqui impactite. 01 p0040 A73-10575

Chemical fractionation in iron meteorites and its interpretation. 01 p0108 A73-11474

Major, minor and trace elements, specific gravities and refraction indices of Ivory Coast tektites, comparing composition to Bosumtwi crater glasses and Apollo lunar materials 01 p0109 A73-11475

Investigation of the chemical composition of lunar surface along the route of Lunokhod 1. 02 p0212 A73-12228

Luna 16 rock composition, gamma radiation and natural radioactive element content determination by neutron activation and radiometric analysis 02 p0213 A73-12230

The composition and crystalline structure of the minerals of regolith from the Sea of Fertility. 02 p0214 A73-12243

Cosmic black glassy spherules composition, mineralogy and physical properties compared to lunar fines, considering possible common origin 02 p0214 A73-12254

Apollo 14 lunar rock ultrabasic fragments chemical analysis, noting pyroxene and olivine compositions 02 p0219 A73-12441

Cation determinative curves for Mg-Fe-Mn olivines from vibrational spectra. 02 p0139 A73-12636

Study of the composition of inclusions in synthetic diamond crystals by microanalysis. 02 p0185 A73-12691

Chlorine, bromine, iodine, and uranium in tektites, obsidians, and impact glasses. 02 p0223 A73-12720

Studies of the chemical composition of cosmic rays with $Z = 3-30$ at high and low energies. 02 p0210 A73-12737

On the possible differences in the bulk chemical composition of the earth and the moon forming in the circumterrestrial swarm. 03 p0370 A73-13110

Observations of carbon monoxide in cool stars at 4.7 microns. 03 p0374 A73-13717

The Angra dos Reis /stone/ mineral assemblage and the Genesis of stony meteorites. 03 p0374 A73-13797

Disk-shaped diffusion model with inhomogeneous distribution of gas and heavy relativistic nuclei sources for galactic cosmic rays chemical composition 05 p0608 A73-16081

X ray background radiation measurement in outer space for proof of Gamow hypothesis on universe chemical composition, indicating improved cosmological models 05 p0613 A73-16210

Radio spectroscopy superiority for interstellar cloud chemical composition studies, detecting formaldehyde, X-ogen, HNC and other exotic molecular species 05 p0546 A73-16305

The Apollo 16 lunar samples - Petrographic and chemical description. 05 p0614 A73-16319

Major element composition of Luna 20 glasses. 05 p0546 A73-16827

Luna 20 and Apollo 16 core fines - Large-ion lithophile trace-element abundances. 05 p0546 A73-16828

The chemical composition of soil from the Apollo 16 and Luna 20 sites. 05 p0546 A73-16831

Double spiral DNA-like nucleotide analog in carbonaceous chondrite, indicating organic compound synthesis at low temperature 05 p0619 A73-16843

A search for the solar Sr-87 content and the solar Rb/Sr ratio. 05 p0620 A73-17027

Coronal abundance of elements and a model of the quiet sun from radio observations. 05 p0621 A73-17034

On the location of pulsational blue edges and estimates of the luminosity and helium content of RR Lyrae stars. 05 p0625 A73-17335

Analysis of the extreme-ultraviolet quiet solar spectrum. 05 p0625 A73-17338

Interstellar medium chemical composition, considering emission line spectra, density fluctuations, He/H ratio in different galaxies and H II regions 06 p0752 A73-18233

Global and local scale satellite surveillance of atmospheric pollution. 06 p0691 A73-18305

Mineral-chemical variations in Apollo 14 and Apollo 15 basalts and granitic fractions. 07 p0879 A73-19686

The major element compositions of lunar rocks as inferred from glass compositions in the lunar soils. 07 p0880 A73-19700

Twin laws, optic orientation, and composition of plagioclases from rocks 12051, 14053, and 14310. 07 p0881 A73-19713

Chemical classification and composition of Apollo 11, 12, 14 and 15 soil samples glasses, describing breccias and chondrules 07 p0882 A73-19723

Apollo 14 regolith and fragmental rocks, their compositions and origin by impacts. 07 p0883 A73-19725

Mineralogy, petrology, and chemical composition of lunar samples 15085, 15256, 15271, 15471, 15475, 15476, 15535, 15555, and 15556. 07 p0883 A73-19727

Apollo 14 glasses of impact origin and their parent rock types. 07 p0883 A73-19735

Structure of lunar glasses by Raman and soft X-ray spectroscopy. 07 p0788 A73-19737

Metallic particles in the Apollo 14 lunar soil. 07 p0884 A73-19744

Distribution of elements between different phases of Apollo 14 rocks and soils. 07 p0885 A73-19751

Oxygen and bulk element composition studies of Apollo 14 and other lunar rocks and soils. 07 p0885 A73-19752

Chemical characteristics of trace element rich KREEP basaltic rocks from Apollo 12 landing site 07 p0885 A73-19753

CHEMICAL COMPOSITION

Apollo 14 regolith fractions and soil breccia compositional characteristics by neutron activation analysis 07 p0885 A73-19755

Compositional data for twenty-one Fra Mauro lunar materials. 07 p0885 A73-19756

Composition of the lunar uplands - Chemistry of Apollo 14 samples from Fra Mauro. 07 p0886 A73-19757

Major, minor, and trace element data for some Apollo 11, 12, 14, and 15 samples. 07 p0886 A73-19759

Rb-Sr systematics for chemically defined Apollo 14 breccias. 07 p0888 A73-19778

Trace element relations between Apollo 14 and 15 and other lunar samples, and the implications of a moon-wide Cl-KREEP coherence and Pt-metal non-coherence. 07 p0890 A73-19810

Characterization of passivation films formed at the surface of stainless steels in magnesium chloride solutions 08 p0976 A73-20650

Chemical composition of some Apollo 14 lunar samples. 08 p0936 A73-20841

Evolution from the main sequence to the helium flash for population II stars. 08 p1005 A73-20915

On the metal abundance of RR Lyrae stars in the globular cluster M22. 08 p1009 A73-21169

Cosmic ray source composition calculated from diffusion-produced path length spreads 08 p0998 A73-21232

Effects of composition and structure on the creep strength of molybdenum bearing ferritic steels. 08 p0982 A73-21796

Petrography, mineralogy and composition of plagioclase and pyroxenes of Washougal howardite by density and refraction measurements 09 p1139 A73-21853

Electron microprobe chemical analysis and structural formula of niobian rutile in Apollo 14 microbreccia sample KREEP fragment 09 p1139 A73-21856

The Oro Grande, New Mexico, chondrite and its lithic inclusion. 09 p1139 A73-21858

Elemental abundances and chemistry of Haverro carbonaceous ureilite, noting similarity to Allende inclusions pattern 09 p1047 A73-21868

Processes determining the composition of a two-dimensional oxide film on a molybdenum surface 09 p1098 A73-21886

Analytical approach to estimating the source rock of basaltic magmas - Major elements 09 p1076 A73-22147

Conductivity and solubility measurements and potentiometry for composition of yttrium nitrate-potassium metaniobate/potassium niobate-water system 09 p1134 A73-22979

Magnetic permeability dependence on temperature and composition of hexaferrites with various Sc ion contents 09 p1134 A73-22982

Ultraviolet effects on the chemical composition and optical properties of interstellar grains. 09 p1150 A73-23138

Phase composition of Nb-1% Zr-C and Nb-2% Hf-C alloys 09 p1108 A73-23237

Determination of the composition of Ni-NiMo eutectic by the zone recrystallization method 09 p1108 A73-23239

Chemical composition of the interstellar gas - X-ray determinations. 10 p1263 A73-23480

Effects of composition on embrittlement of austenitic stainless steels. 10 p1230 A73-23628

Chemical composition of classical Cepheids in the Galaxy and Magellanic Clouds 10 p1273 A73-23705

High-temperature condensates in chondrites and the environment in which they formed. 10 p1278 A73-24109

Secular stability. V - The perturbation of chemical abundances. 10 p1280 A73-24404

Effect of chemical composition on the heat resistance of steel Kh25N16G7AR. 10 p1236 A73-24932

Elements distribution in ternary alloy system during simultaneous saturation and burning-out of two components and successive diffusion into third 10 p1236 A73-24953

Carbon and stainless steels chemical composition effects on diffusion layer structure and fatigue strength after diffusive boring 10 p1236 A73-24954

Proposed stratigraphic controls on the composition of crude oils reservoir in the Green River formation, Uinta Basin, Utah.

11 p1352 A73-25471

Spatial distribution of elements in tektites and comparable materials by charged particle activation analysis.

11 p1418 A73-25584

Depth variation of cosmogenic noble gases in the approximately 120-kg Keyes chondrite.

11 p1418 A73-25587

Applications of activation analysis to geochemical, meteorite and lunar studies.

11 p1326 A73-25800

The origin and chemical composition of the earth's core.

11 p1355 A73-25896

Double spiral DNA-like polynucleotide analog in carbonaceous chondrite, indicating organic compound synthesis at low temperature

11 p1423 A73-26053

Temperature and concentration dependence of the electrical resistivity of solid alloys in the magnesium-cadmium system

11 p1386 A73-26570

Alpha phase lattice constant curves and composition effects of Cr-Ni-Co-Mo steels on microstress rate reduction during age hardening

12 p1509 A73-26840

X ray and microanalysis of Luna 16 recovered Fe-Ni fragment structure and composition, showing alpha solid solution octahedrite

12 p1538 A73-26893

Lunar highland soils and breccias chemistry representation by model for mixing during intense cratering period, discussing chemical composition

12 p1466 A73-27493

Apollo 15 mare olivine and quartz basalts major and trace element composition and petrogenesis, deriving model of magma genesis

12 p1466 A73-27545

Sintering of refractory titanium carbide with varied bound nitrogen content, discussing crystal dislocation effects on initial stage compaction intensification in nonstoichiometric specimens

12 p1503 A73-27556

Study of the relations between various mechanical properties and biochemical composition of bone tissues in man

13 p1577 A73-27996

Luna 20: A study of samples from the lunar highlands returned by the unmanned Luna 20 spacecraft.

13 p1674 A73-28301

Preliminary data on lunar soil collected by the Luna 20 unmanned spacecraft.

13 p1674 A73-28302

Chemistry and surface morphology of soil particles from Luna 20 LRI sample 22003.

13 p1674 A73-28308

An unusual basalt fragment in Luna 20 sample L2010.

13 p1675 A73-28309

Luna 20 lunar glass particle samples chemical composition, noting aluminum oxide content similarity to Apollo 16 samples

13 p1675 A73-28314

Luna 20 soil and rock fragments chemical composition from neutron activation analysis, noting low rare earth content and contamination with W and Mo

13 p1676 A73-28321

Luna 20 highland soil samples mineralogical and petrological analysis, comparing chemical composition with Apollo 16 soil samples

13 p1676 A73-28322

Lunar differentiation model based on chemical data from Luna 20 soil and Apollo 16 core samples analysis by combined semimicro atomic absorption spectrophotometric and colorimetric method

13 p1676 A73-28326

Surface solid solutions and chemical compounds formation due to gas sorption by titanium and barium

13 p1663 A73-28968

Cometary nuclei chemical composition and molecular structure, suggesting radial-forming organic molecules synthesis by solar and galactic cosmic radiation

14 p1723 A73-29816

A photometric study of the integrated light of clusters in the Magellanic Clouds and the Fornax dwarf galaxy.

14 p1801 A73-30726

Influence of annealing temperature on the changes in the chemical and phase compositions of the intercrystalline boundaries of weakly-alloyed molybdenum

14 p1764 A73-30865

Composition of galactic cosmic rays with energy ranging between 10 and 30 MeV/nucleon.

15 p1926 A73-31355

Effect of dispersity on spectral analysis data for alloyed powders

15 p1888 A73-31597

High strength steel developments, discussing chemical compositions, mechanical properties, production technology and applications

15 p1888 A73-31624

Calculation of the composition of 79% N₂ + 21% O₂ and 50% N₂ + 50% O₂ mixtures containing carbon at high temperatures

15 p1840 A73-31853

Variation of chemical composition on the surface of cobalt-base alloys by oxidation in air.

15 p1891 A73-32016

Fatty acids of *Pinus elliottii* tissues.

15 p1841 A73-32199

Fluorine in lunar samples - Implications concerning lunar fluorapatite.

15 p1941 A73-32388

Rare-earth elements, Co, Sc and Hf in the Steens Mountain basalts.

15 p1874 A73-32389

Interstellar microwave radiation measured by spectroscopic analysis of chemical composition, distribution, excitation and emission data

16 p2058 A73-32722

Hydrodynamic model calculations of Population I chemical composition massive objects, discussing evolution termination by violent thermonuclear explosions

16 p2059 A73-32840

Solar system elemental abundance from chondritic meteorites, solar atmosphere and neighborhood stars, considering Galactic and universal compositions

16 p2061 A73-33285

Cosmic ray trapping region and characteristic exit time from Galaxy, discussing electronic component and chemical composition

16 p2054 A73-33286

Investigation of the dielectric properties of terrestrial rocks at super-high frequencies for the purpose of improving accuracy for the composition of lunar material

16 p2064 A73-33771

Internal structure and chemical composition of Mercury

16 p2066 A73-33796

Composition of a two-dimensional oxide film on a molybdenum surface.

17 p2186 A73-34309

Accretion processes to account for chemical differences among chondrites formed in cooling solar nebula

17 p2227 A73-34414

Whole rock Th-Pb age for the Masuke and Dembe-Divula complexes, Rhodesia.

17 p2159 A73-34519

Thermodynamic analysis of the distribution of silver in the Cu-Cu₂S system in the presence of Ni₃S₂ and FeS

17 p2188 A73-34556

Cometary composition, structure and atmospheric dynamics, discussing multiconstituent hydrodynamic models in comparison with observation [AIAA PAPER 73-549]

18 p2353 A73-36495

Chemistry of lunar basalts with very high alumina contents.

18 p2354 A73-36598

Chemical composition of the classical Cepheids in the Galaxy and the Magellanic Clouds.

18 p2354 A73-36730

The combustibility of aluminum-nickel powders

18 p2325 A73-36862

The solar abundance of silicon.

19 p2483 A73-37570

Some considerations about the upper and the lower limits of the planetary dimensions.

19 p2486 A73-38152

Minor planets and related objects. X - Spectrophotometric study of the composition of /1685/ Toro.

20 p2607 A73-39120

Mass-luminosity relations for unevolved stars in high mass eclipsing binaries and low mass visual binary systems for hydrogen and metal abundances of Population I stars

20 p2609 A73-39439

The peculiar A stars and the origin of the heaviest chemical elements.

20 p2611 A73-39623

Effect of iron on the phase composition and mechanism of plastic deformation of titanium

20 p2579 A73-39737

Influence of chemical composition on the structure and mechanical properties of polycarbonate films and the possibility of using them as a substrate for moving-picture films

21 p2646 A73-40259

Spectral determination of rare-earth components in Seignette-ceramic and piezoceramic materials

21 p2752 A73-40555

The chemical classification of iron meteorites. VII - A reinvestigation of irons with Ge concentrations between 25 and 80 ppm.

21 p2647 A73-40564

Sample preparation, irradiation, and counting and data reduction scheme for trace element analysis of coal using neutron activation

21 p2737 A73-40632

X ray and microanalysis of Luna 16 recovered Fe-Ni fragment structure and composition, showing alpha solid solution octahedrite

21 p2771 A73-41026

Ti, Al, W and Mo concentrations effect on heat resistance of precipitation hardened Ni-based alloys

21 p2720 A73-41035

Variations in density and chemical composition at 120 km from chemical and dynamical processes.

21 p2689 A73-41355

Experimental data on the investigation of lunar surface chemical composition.

21 p2774 A73-41403

Cometary atmospheric dust chemical composition and physical properties estimated from colorimetric, polarimetric and IR data, using models of optically thin polydisperse media

21 p2776 A73-41421

Russian book - Chemistry of terrestrial and lunar basaltic rocks.

21 p2648 A73-41436

Elastic properties of alloys of the Ti-Al-Mo system as a function of the composition and heat treatment

22 p2874 A73-42095

Structure of the phase diagrams of the ternary systems /Mo, W/ - /Ti, Zr, Hf, V, Nb, Ta/ - C

22 p2877 A73-42455

Expected gamma ray emission spectra from the lunar surface as a function of chemical composition.

22 p2903 A73-42494

Tropospheric aerosol - The relative contribution of marine and continental components.

22 p2849 A73-42547

The abundances of galactic cosmic-ray carbon, nitrogen, and oxygen and their astrophysical implications.

22 p2914 A73-43012

Galactic nuclei, pulsars and supernovae as sources of primary cosmic rays from ground based and satellite observations, relating chemical composition to origin

22 p2904 A73-43116

The effect of nonstationarity in the chemical composition of plasma flows from the sun.

23 p3027 A73-43252

Phase composition of Cu-Ni-O alloys with Ir additions, examining oxygen content influence on Ir distribution and solid solution formation

23 p2990 A73-43483

Transition effects during the recording of the electron-photon component of extensive air showers

23 p3023 A73-43558

Lunar surface meteoritic material composition, distribution and amounts from trace element studies, discussing micrometeorites, ancient planetesimal debris and recent crater-forming projectiles

23 p3030 A73-43758

Crater Copernicus age determination using mass spectrometric Ar isotope ratio dating of KREEP glasses from lunar soil

23 p3031 A73-43763

Major and trace elements in igneous rocks from Apollo 15.

23 p2950 A73-43765

A survey of the selenochemistry of major, minor and trace elements.

23 p2951 A73-43768

Rare gas diffusion studies in individual lunar soil particles and in artificially implanted glasses.

23 p3031 A73-43769

Problems experienced in continuous recording of surface ozone by the electrochemical method at Poona.

23 p2982 A73-43864

High concentration of refractory elements in lunar crust explained by melting and differentiation model

23 p3033 A73-43958

The effect of composition changes on the fracture toughness of an Al-Zn-Mg-Cu-Mn forging alloy.

23 p2993 A73-44025

Preparation of lanthanum sulfides using carbon disulfide as a sulfurizing agent and the change of these sulfides on heating in air.

23 p3018 A73-44130

Surface solid solutions and chemical compounds formation due to gas sorption by titanium and barium

23 p3008 A73-44320

Ac electroconductivity of polycrystalline Co-Fe ferrite as function of temperature, composition and frequency at 1 kHz-200 MHz

24 p3119 A73-44403

Solar system cosmochemistry concerning element abundances, structure and composition of comets, planets, moon, exospheric dust and meteorites, protosolar magnetic field, nucleosynthesis and cosmic rays

24 p3134 A73-44569

Air-hydrogen-carbon fuel mixtures chemical composition determination by measuring carbon dioxide

and moisture content of combustion products, presenting nomogram 24 p3157 A73-45378

CHEMICAL EFFECTS
Effects of chemical impurities, oxygen and dopant, on the gamma and neutron damage of silicon solar cells. 01 p0006 A73-11163
Ultrasonic measurements of cold-work percentages in Type 316 stainless steel. 02 p0173 A73-11987
The additive action of some organic chlorides and sulfides in the four-ball lubricant test. [ASLE PREPRINT 72LC-3-2] 03 p0316 A73-14357
Effects of small amounts of additional elements on directionality of stress corrosion resistance of the Al-Zn-Mg alloys. 19 p2442 A73-37948
Mechanical face seal between rotating shaft and surrounding member using stationary and rotating ultraflat radial sealing faces, discussing temperature and chemical considerations 22 p2865 A73-41775

CHEMICAL ELEMENTS
NT ACTINIDE SERIES
NT ACTINIUM
NT ALKALI METALS
NT ALKALINE EARTH METALS
NT ALUMINUM
NT ALUMINUM 26
NT ARGON
NT ARGON ISOTOPES
NT ARSENIC
NT BARIUM
NT BERYLLIUM
NT BISMUTH
NT BORON
NT BROMINE
NT CADMIUM
NT CALCIUM
NT CARBON
NT CARBON ISOTOPES
NT CARBON 12
NT CARBON 13
NT CARBON 14
NT CERIUM
NT CESIUM
NT CESIUM VAPOR
NT CHROMIUM
NT COBALT
NT COBALT ISOTOPES
NT COBALT 60
NT COPPER
NT CURIUM ISOTOPES
NT CURIUM 244
NT DEUTERIUM
NT DEUTERIUM PLASMA
NT DYSPROSIUM
NT ERBIUM
NT EUROPIUM
NT FLUORINE
NT GADOLINIUM
NT GALLIUM
NT GERMANIUM
NT GOLD
NT HAFNIUM
NT HALOGENS
NT HELIUM
NT HELIUM ATOMS
NT HELIUM FILM
NT HELIUM ISOTOPES
NT HOLMIUM
NT HYDROGEN
NT HYDROGEN ATOMS
NT HYDROGEN IONS
NT HYDROGEN ISOTOPES
NT HYDROGEN PLASMA
NT INDIUM
NT IODINE
NT IODINE ISOTOPES
NT IRIIDIUM
NT IRON
NT IRON 57
NT ISOTOPES
NT KRYPTON ISOTOPES
NT LANTHANUM
NT LEAD [METAL]
NT LEAD ISOTOPES
NT LIGHT ELEMENTS
NT LIQUID HELIUM
NT LIQUID HELIUM 2
NT LIQUID HYDROGEN
NT LIQUID NITROGEN
NT LIQUID POTASSIUM
NT LIQUID SODIUM
NT LITHIUM
NT LITHIUM ISOTOPES
NT MAGNESIUM
NT MANGANESE
NT MANGANESE ISOTOPES
NT MERCURY [METAL]
NT MERCURY ISOTOPES
NT MERCURY VAPOR
NT METALLIC HYDROGEN

NT METALLOIDS
NT MOLYBDENUM
NT NEODYMIUM
NT NEON
NT NEON ISOTOPES
NT NEPTUNIUM ISOTOPES
NT NICKEL
NT NIOBIUM
NT NITROGEN
NT NITROGEN ATOMS
NT NITROGEN IONS
NT NITROGEN ISOTOPES
NT NUCLIDES
NT ORTHO HYDROGEN
NT OSMIUM
NT OXYGEN ISOTOPES
NT OXYGEN PLASMA
NT OXYGEN 18
NT PALLADIUM
NT PARA HYDROGEN
NT PLATINUM
NT PLUTONIUM ISOTOPES
NT PLUTONIUM 238
NT POLONIUM 210
NT POTASSIUM
NT POTASSIUM ISOTOPES
NT POWDERED ALUMINUM
NT PROMETHIUM
NT RADIOACTIVE ISOTOPES
NT RADON
NT RADON ISOTOPES
NT RARE EARTH ELEMENTS
NT RARE GASES
NT REFRACTORY METALS
NT RUBIDIUM
NT RUBIDIUM ISOTOPES
NT SAMARIUM
NT SAMARIUM ISOTOPES
NT SCANDIUM
NT SELENIUM
NT SILICON
NT SILICON ISOTOPES
NT SILVER
NT SINTERED ALUMINUM POWDER
NT SODIUM
NT SODIUM ISOTOPES
NT SODIUM VAPOR
NT SODIUM 22
NT SODIUM 24
NT SOLID NITROGEN
NT STRONTIUM
NT STRONTIUM ISOTOPES
NT STRONTIUM 90
NT SULFUR
NT TANTALUM
NT TELLURIUM
NT TELLURIUM ISOTOPES
NT THALLIUM
NT THALLIUM ISOTOPES
NT THORIUM
NT THORIUM ISOTOPES
NT TIN
NT TITANIUM
NT TRACE ELEMENTS
NT TRITIUM
NT TUNGSTEN
NT URANIUM
NT URANIUM ISOTOPES
NT URANIUM 238
NT VANADIUM
NT XENON
NT XENON ISOTOPES
NT XENON 129
NT YTTERBIUM
NT YTTRIUM
NT ZINC
NT ZIRCONIUM
The abundances of the elements in the oldest disk stars. 04 p0500 A73-15514
Elements distribution in ternary alloy system during simultaneous saturation and burning-out of two components and successive diffusion into third 10 p1236 A73-24953
Distributions and associations of some of the chemical elements found in the stratosphere. [AIAA PAPER 73-514] 16 p2006 A73-33551
Experiment and observation of isotope and element separation in a plasma with cosmical applications. 17 p2216 A73-34420
Elemental abundance determinations for meteors by spectroscopy. 18 p2352 A73-36287
Thermal conductivities of the elements - Results of a critical evaluation. 21 p2792 A73-41300
Solar system cosmochemistry concerning element abundances, structure and composition of comets, planets, moon, exospheric dust and meteorites, protosolar magnetic field, nucleosynthesis and cosmic rays 24 p3134 A73-44569

CHEMICAL ENERGY
Square well fluid liquid-vapor interface density profiles from perturbation expansion in chemical

potential, comparing to BGYB and excess free energy minimization approaches 03 p0342 A73-13277
Chemical lasers and chemical reactions induced by lasers. 17 p2182 A73-34112
Second phase particle redistribution in dispersion-hardened alloys by directed particle diffusion via chemical potential control 18 p2325 A73-36807

CHEMICAL EQUILIBRIUM
NT ACID BASE EQUILIBRIUM
On self-similar blast waves headed by the Chapman-Jouguet detonation. 01 p0120 A73-10441
Adsorption equilibria at high pressures in the helium-nitrogen-activated carbon system. 01 p0014 A73-10725
Vibrational and chemical nonequilibrium in a stoichiometric turbojet engine using kerosene-type fuel. 03 p0273 A73-13491
Hydrogen/proton adsorption behavior on fuel cell Pt electrode, considering surface roughness factor, Pt sites number and equilibrium data 04 p0407 A73-15104
F-19 chemical shift tensor in group II difluorides. 05 p0546 A73-16046
Constitution and phase relationships in copper-silver-aluminum ternary system. 11 p1385 A73-26566
Thermodynamics of heterogeneous gas equilibria. VII - Gas phase composition and chemical transport reactions in the tungsten-oxygen-hydrogen system 11 p1386 A73-26568
Assessment of chemical nonequilibrium for massively ablating graphite. 18 p2368 A73-36322
Chapman-Jouguet rule for real detonation waves 19 p2419 A73-37516
Molybdenum sintering and the molybdenum-oxygen-carbon system. 21 p2722 A73-41585
Theory of nonequilibrium phenomena in chemically reacting gas mixtures 23 p2950 A73-43703
Early solar system deuterium abundance based on nebular chemical equilibrium, comparing with Jupiter atmosphere and meteorite data 24 p3131 A73-44468
Chemical stability and features of the formation of complex nitrides of III-B subgroup elements /Al-B-N system/ 24 p3119 A73-44952
A method of calculating a chemically nonequilibrium flow of gas in a heated tube under conditions close to the equilibrium or frozen state 24 p3081 A73-45527

CHEMICAL EXPLOSIONS
NT GAS EXPLOSIONS
Critical mass of cryogenic rocket propellants. 07 p0866 A73-20415
Conditions for thermal explosion occurrence during branched-chain reactions 19 p2502 A73-37501
Time variation in the reaction-zone structure of two-phase spray detonations. 22 p2936 A73-42811

CHEMICAL EXTINGUISHERS
U FIRE EXTINGUISHERS
CHEMICAL FUELS
NT AIRCRAFT FUELS
NT HIGH ENERGY FUELS
NT HYDROCARBON FUELS
NT HYDROGEN FUELS
NT JET ENGINE FUELS
NT JP-5 JET FUEL

CHEMICAL INDICATORS
Analysis of indicator distribution in the determination of cardiac output by thermal dilution. 08 p0933 A73-21216
Solubilization and accumulation of copper from elementary surfaces by Penicillium notatum. 21 p2648 A73-41217

CHEMICAL KINETICS
U REACTION KINETICS
CHEMICAL LASERS
Flame-sheet analysis of C.W. diffusion-type chemical lasers. II - Coupled radiation. 01 p0059 A73-10727
Chemical lasers population inversion mechanism and excitation energy comparison with other molecular gas lasers including carbon dioxide systems, considering efficiency 04 p0458 A73-14749
Molecular iodine photolysis in photodissociative laser due to selective pumping, noting recombination-like storage mechanism 04 p0458 A73-15561
Effect of H2 pressure on pulsed H2 + F2 laser - Experiment and theory. 05 p0583 A73-16043
Book - Advances in electronics and electron physics. Volume 31. 05 p0558 A73-16601

Chemical lasers with molecular gas excitation and population inversion by chemical reactions, discussing lasing conditions, vibrational transition and pumping mechanism

05 p0585 A73-16602

Kinetics of a pulsed chemical CO laser with photostimulation based on the carbon disulfide oxidation reaction

06 p0700 A73-18103

Reaction mechanisms of the CS₂-O₂ chemical laser.

06 p0702 A73-18370

Conference on Chemical and Molecular Lasers, 3rd, St. Louis, Mo., May 1-3, 1972, Proceedings.

07 p0834 A73-19626

Measurement of the temperature dependence of the vibrational relaxation rate of HF and the effect of SF₆, N₂, and F₂ as diluents.

07 p0853 A73-19628

Chemical laser studies of vibrational energy distributions - The equal-gain and zero-gain temperature techniques.

07 p0834 A73-19629

CW and pulsed deuterium fluoride-carbon dioxide transfer chemical laser with molecular vibrational energy transfer for population inversion to obtain high power output

07 p0834 A73-19630

Exothermic deuterium-fluorine chain reaction pumping of high pressure pulsed carbon dioxide chemical transfer laser

07 p0835 A73-19631

A kinetic model and computer simulation for a pulsed DF-CO₂ chemical transfer laser.

07 p0835 A73-19632

A CW-CO chemical laser from the reaction of active nitrogen with O₂ + CS₂.

07 p0835 A73-19633

Gain measurements on CO P-branch transitions in a C₂H₂-O₂ flame.

07 p0788 A73-19634

Vibration-rotation state populations and laser output spectra of CW chemical hydrogen halide lasers under subsonic transverse flow

07 p0835 A73-19640

Parametric studies of pulsed HF lasers using transverse excitation.

[AD-760268]

07 p0835 A73-19641

Chemical laser device bibliography.

07 p0836 A73-19642

Numerical study of a diffusion-type chemical laser.

07 p0836 A73-19959

Chemical lasers - A comprehensive literature survey.

08 p0974 A73-21026

Low cost nitrogen laser design for dye laser pumping.

08 p0974 A73-21027

Energy and threshold characteristics of chemical lasers.

08 p0975 A73-21213

Numerical formulation for constant-gain chemical laser calculations.

08 p0975 A73-21411

HF chemical lasers kinetics, radiative interactions and gas dynamics, deriving closed form solutions for excited states populations

08 p0976 A73-21671

Transverse discharge pulsed CO₂ chemical transfer laser.

10 p1227 A73-23840

Hydrogen fluoride chemical laser with high voltage pulse initiation in simple transverse discharge geometry, measuring maximum energy output and corresponding efficiency

11 p1378 A73-26323

Theory of an infrared high-pressure chemical laser

13 p1627 A73-28762

Chemical laser research survey covering device performance, reaction kinetics, theoretical modeling for population inversion and bibliography

13 p1628 A73-29112

Pulsed laser utilizing a fluorine and hydrogen mixture.

13 p1629 A73-29434

Chlorine trifluoride chemical laser emission, discussing output power dependence on partial pressures and chemical reaction kinetics

13 p1630 A73-29444

Kinetics of high-pressure chemical lasers

14 p1758 A73-30577

HF laser flow visualization with an infrared television system.

15 p1874 A73-31357

Design and performance characteristics of a small subsonic flow HF chemical laser.

15 p1885 A73-31978

High power chemical laser technology.

16 p2022 A73-32724

Trends in physics; General Conference, 2nd, Wiesbaden, West Germany, October 3-6, 1972, Lectures.

17 p2256 A73-34109

Chemical lasers and chemical reactions induced by lasers.

17 p2182 A73-34112

Chemical laser power output prediction by laminar analysis modification with conventional gross mixing concept of turbulent flow in population inversion

17 p2183 A73-34193

Gain and energy measurements on an HF/DF electrically pulsed chemical laser.

17 p2183 A73-34203

Perfectly stirred reactor - New concept for a CW chemical laser.

17 p2184 A73-34911

Vibrational relaxation in the HF-HCl, HF-HBr, HF-HI, and HF-DF systems.

17 p2119 A73-35176

Laser energy absorption by plasma for controlled thermonuclear fusion, comparing uses of electrically pumped gas, chemical and solid state lasers

17 p2185 A73-35379

Pressure dependency of the NF₃-H₂ transverse-discharge pulse-initiated HF chemical laser.

17 p2186 A73-35790

New improved laser dye for the blue-green spectral region.

17 p2186 A73-35800

Chemical laser and molecular amplifiers characteristics covering population inversion and vibrational energy generation, storage, distribution and transfer

18 p2321 A73-35902

Experimental studies of chemically reactive F + H₂/flow in supersonic free jet mixing layers.

[AIAA PAPER 73-640]

18 p2321 A73-36198

An investigation of velocity fields in chemical laser nozzles.

[AIAA PAPER 73-641]

18 p2322 A73-36199

Specie number density, pitot pressure, and flow visualization in the near field of two supersonic nozzle banks used for chemical laser systems.

[AIAA PAPER 73-642]

18 p2322 A73-36200

Recombination effects in chemical laser nozzles.

[AIAA PAPER 73-643]

18 p2287 A73-36258

Electron-beam irradiated discharges for initiating high-pressure pulsed chemical lasers.

[AIAA PAPER 73-645]

18 p2322 A73-36259

Measurements of F₂, NO, and ONF Raman cross sections and depolarization ratios for diagnostics in chemical lasers.

18 p2322 A73-36978

Single-line operation of a 2-W longitudinal cw CO chemical laser with no frequency-selective element in the optical cavity.

19 p2439 A73-38475

CW laser action from acetylene oxidation, noting sensitivity to total pressure and helium, oxygen and acetylene partial pressure changes

20 p2573 A73-39676

Relative performance of a variety of NF₃+/-hydrogen-donor transverse-discharge HF chemical-laser systems.

21 p2714 A73-40757

Kinetics of the generation spectrum of a photodissociation iodine laser.

22 p2868 A73-41722

Characteristics of a CS₂/O₂ chemical laser with flow transverse to the optical axis.

22 p2870 A73-42764

Kinetics of chemical high-pressure lasers

23 p2987 A73-43716

CHEMICAL MACHINING

NT ELECTROCHEMICAL MACHINING

CHEMICAL PROPERTIES

NT ACIDITY

NT HEAT OF COMBUSTION

NT HEAT OF FORMATION

NT SALINITY

NT THERMOCHEMICAL PROPERTIES

Russian book on titanium chemistry covering physicochemical and electrochemical properties, hydrolysis and production of metal-organic and complex titanium compounds

02 p0139 A73-11890

Moon and solar system origin in view of chemical evidence and Apollo lunar rock RB-87/SR-87 ages and remelting conditions

03 p0370 A73-13111

Physical and chemical properties of solid propellant igniter materials, determining averaged heat of reaction and burning rate values

[AIAA PAPER 72-1195]

03 p0352 A73-13485

Bottle green microtektites from Australasian and Ivory Coast deep sea sediments, discussing physical and chemical properties, age and origin

05 p0615 A73-16383

Physicochemical parameters associated with surfactants, investigating effects on hydrocarbon fuels coalescence

[SAE PAPER 720863]

05 p0582 A73-16674

Alkali metal intercalates of molybdenum disulfide.

08 p0937 A73-21174

Chemical stability of tantalum germanide powders in air and aggressive media, including acids, fluorine ions and perhydrol

09 p1133 A73-22465

Preparation and thermomechanical properties of pyrrone moldings.

10 p1237 A73-23961

Some physicochemical properties of compounds formed by oxides of rare-earth elements and barium

11 p1410 A73-26673

The physics and chemistry of high pressures.

12 p1523 A73-26923

Physicochemical properties of metal silicides under vacuum at high temperatures, assessing suitability as antiemission materials on Mo grids in high power vacuum electron tubes

15 p1898 A73-31842

Chemo-rheology of two high temperature epoxy resins.

17 p2197 A73-35347

Silver halogenide bichromatic gelatin chemical and photographic properties, noting decelerating development effect

21 p2647 A73-40266

Russian papers on metal alloys chemistry covering atomic structure, physicochemical properties, phase diagrams, X ray analysis, laser microanalysis, etc

22 p2873 A73-42083

On the dimensions of intramolecularly crosslinked polymer molecules. I - The synthesis and chemical characterization of intramolecularly crosslinked polystyrene molecules having a narrow distribution of molecular weight. II - The theoretical prediction of the dimensions in solution of intramolecularly crosslinked polystyrene molecules. III - The measurement of the dimensions of intramolecularly crosslinked polystyrene.

23 p3008 A73-43795

Line of symmetry for the classical equation of state.

24 p3110 A73-4987

CHEMICAL PROPULSION

Unmanned planetary spacecraft chemical rocket propulsion.

01 p0090 A73-10102

Boron combustion, covering thermochemistry application to chemical propulsion systems, temperature effects on oxidation, single particle ignition and powder burning

01 p0089 A73-11112

Chemical and nuclear space tugs in the earth orbital shuttle mission.

02 p0216 A73-12372

German book - Flight propulsion systems: Principles, systematics, and technology of aeronautical and astronautical propulsion systems.

05 p0606 A73-16355

German book - Hybrid rocket propulsion systems: An introduction to theoretical and technical problems.

06 p0741 A73-17669

Book on aerospace propulsion covering nozzle, combustors and diffusers flow, space power generation, electrothermal engines, chemical rockets and central force fields

14 p1785 A73-30361

High pressure dual fuel chemical LOX/hydrocarbon rocket vehicle concepts for reusable one stage to orbit shuttles

16 p2072 A73-33085

CHEMICAL REACTION CONTROL

Multi balance measurement of flow systems.

16 p2016 A73-33656

High-temperature gas-solid reactions.

19 p2403 A73-38552

CHEMICAL REACTIONS

NT ACETYLATION

NT ATOMIC RECOMBINATION

NT CARBONIZATION

NT CHLORINATION

NT COPOLYMERIZATION

NT DECARBONATION

NT DECARBOXYLATION

NT DENITROGENATION

NT DEOXIDIZING

NT DEPOLYMERIZATION

NT ELECTROCHEMICAL OXIDATION

NT EXOTHERMIC REACTIONS

NT GLYCOLYSIS

NT HYDROGENATION

NT HYDROGENOLYSIS

NT HYDROLYSIS

NT ION RECOMBINATION

NT METAL-WATER REACTIONS

NT NITRATION

NT NITRIDING

NT OXIDATION

NT OXYGEN RECOMBINATION

NT OXYGENATION

NT PHOSPHORYLATION

NT PHOTOCHEMICAL REACTIONS

NT PHOTOCROMISM

NT PHOTODECOMPOSITION

NT PHOTOLYSIS

NT PHOTOOXIDATION

NT PHOTOSYNTHESIS

NT PYROHYDROLYSIS

NT PYROLYSIS

NT RADIOLYSIS

NT REDUCTION [CHEMISTRY]

NT RUSTING

NT THERMAL DISSOCIATION

NT TITRATION

On turbulent flows with fast chemical reactions. I - The closure problem.

01 p0032 A73-10637

On turbulent flows with fast chemical reactions. II - The distribution of reactants and products near a reacting surface.

[AD-753565] 01 p0032 A73-10638

Radiation in the reacting boundary layer.

01 p0121 A73-10642

Temperature changes in hydrogen-oxygen explosions.

01 p0121 A73-10646

D-region negative-ion chemistry.

01 p0042 A73-10895

Scanning electron microscope investigation of interaction between pyrolytic carbon fibers and oxidizer, noting periodic variations of carbon chemical activity in radial direction

02 p0185 A73-12556

Experimental study of heat transfer in the boiling of nitrogen tetroxide.

03 p0397 A73-13188

Light scattering from systems with chemical oscillations and dissipative structures.

03 p0273 A73-13285

Effect of reagent vibrational excitation on reaction rate and product energy distribution in $F + HCl$ yields $HF + Cl$.

03 p0273 A73-13290

An analysis of the chemically reacting boundary layer during hybrid combustion.

[AIAA PAPER 72-1144] 03 p0273 A73-13450

Energy distribution among reaction products. VII - $H + F_2$.

04 p0414 A73-14820

The reactions of titanium and silicon with Al_2O_3 - CaO - CaF_2 slags in the ESR process.

04 p0455 A73-15744

Enthalpy driving forces for gas cooling data correlation in convective heat transfer in reacting turbulent boundary layers with mass injection

[ASME PAPER 72-WA/HT-31] 04 p0519 A73-15824

Molecular beam study of the $K + CH_3I$ reaction - Energy dependence of the detailed differential reactive cross section.

05 p0546 A73-16047

Pollutant formation in reacting turbulent jet flow field with recirculation, presenting methane-air system pointwise properties determination by numerical analysis

[WSCI PAPER 72-21] 05 p0638 A73-16676

Turbojet exhaust reactions in stratospheric flight.

[AIAA PAPER 73-99] 05 p0608 A73-16859

Interstellar molecules and cosmochemistry; Proceedings of the Conference, New York, N.Y., June 16-18, 1971.

06 p0751 A73-18226

Polymerization of amino acids under primitive earth conditions.

07 p0787 A73-19217

Reaction kinetics of nitric oxide positive ion with ozone yielding nitrogen dioxide positive ion and oxygen, noting impact on ionospheric chemistry

07 p0787 A73-19258

Energetically and financially economical hydrazine synthesis method based on ammonia oxidation by water solution of hydrogen peroxide

07 p0787 A73-19325

The gas-phase reaction of perchloric acid with hydrogen.

07 p0787 A73-19387

Explosive systems with reactant fuel consumption, deriving asymptotic stability, with application to self heating chemical reaction via Liapunov functions

07 p0919 A73-19393

Distribution of reaction products /theory/. VIII - $Cl + HI$, $Cl + DI$.

07 p0788 A73-19926

Equation of state of a mixture of nonideal, chemically reacting gases.

08 p0936 A73-20856

Quasi isothermal, transonic flow of radiating gases

08 p1024 A73-21497

Analytical predictions of emissions from and within an Allison J-33 combustor.

08 p1025 A73-21670

Prohibited autodetachment in OD- formed by collisions of O- with D2.

09 p1048 A73-22075

A mass spectrometric investigation of reactions involving tungsten and molybdenum with potassium-seeded H_2/O_2 flames.

10 p1186 A73-23554

A mass spectrometric investigation of reactions involving vanadium and chromium with potassium-seeded H_2/O_2 flames.

10 p1186 A73-23555

The gas-phase reaction of perchloric acid with ethylene.

10 p1186 A73-23556

Criteria for oscillations in closed isothermal reacting systems.

10 p1294 A73-23561

Explosion gas dynamics experimental investigation, noting fast chemical reactions induced exothermic processes and detonation wave structure

10 p1295 A73-23853

Approximate solution of the system of Boltzmann equations for a mixture of reacting gases

10 p1252 A73-24490

Mathematical description of the turbulent isobaric flow of a chemically reacting gas in a heated pipe

11 p1453 A73-26428

Chemical evolution - Recent syntheses of biorganic molecules.

11 p1319 A73-26477

Liquid ammonia life existence in universe, considering halogen and silicon life chemistry

11 p1326 A73-26662

Ionospheric production and loss processes of atomic sulfur ions, considering dissociative ionization sources

12 p1489 A73-26999

Molecule formation. I - In normal H I clouds. II - In interstellar shock waves.

12 p1547 A73-27973

Chemical reaction stimulation by laser radiation

12 p1467 A73-27978

The addition of tert-butyl hypochlorite to isocyanates.

13 p1580 A73-28022

Stationary composition of a nonisothermal plasma in chemically active media

13 p1664 A73-28420

Reaction $H + C_2H_4$ - Investigation into the effects of pressure, stoichiometry, and the nature of the third body species.

13 p1581 A73-29426

Classical dynamical investigations of reaction mechanism in three-body hydrogen-halogen systems.

13 p1581 A73-29427

Reactions of HO_2 with carbon monoxide and nitric oxide and of O/I D/ with water.

14 p1723 A73-30069

Planetary atmospheres chemistry, discussing physical factors, atomic oxygen reactions, ozone, airglow and mathematical models

14 p1723 A73-30128

Calculation of the parameters of a chemically reacting gas behind an incident and reflected shock wave

15 p1840 A73-31855

Study of gas-solid chemical interactions by the molecular beam technique. V - Reactions of oxygen and carbon monoxide with polycrystalline tantalum strips

15 p1841 A73-31970

Homogeneously catalyzed formaldehyde condensation to carbohydrates. II - Instabilities and Cannizzaro effects.

15 p1841 A73-32200

Electrode reactions of aromatic amines in solvents containing fused $AlCl_3$.

15 p1841 A73-32224

Critical behaviour in chemically reacting systems. I - Difficulties with the Semenov theory. II - An exactly soluble model.

16 p1976 A73-33342

Atmospherical modelling and the chemical data problem.

[AIAA PAPER 73-500] 16 p1977 A73-33542

Recent measurements of stratospheric reactions by flash photolysis resonance fluorescence.

[AIAA PAPER 73-502] 16 p2005 A73-33543

Chemical lasers and chemical reactions induced by lasers.

17 p2182 A73-34112

Study of gas-phase reactions in particle-laden, ducted flows.

17 p2150 A73-34194

Book - Gasdynamic theory of detonation.

17 p2253 A73-34297

The analysis of nonequilibrium, chemically reacting, supersonic flow in three dimensions using a bicharacteristics method.

17 p2151 A73-34891

Chemically reacting gas flow numerical calculations from stiff nonlinear ordinary differential equations solution in finite difference form

17 p2119 A73-35609

Application of a microanalyzer to the investigation of the interaction between titanium and coatings

18 p2323 A73-35894

On the solution of the unsteady Navier-Stokes equations including multicomponent finite rate chemistry.

18 p2259 A73-36157

Linear theory for chemically reacting flows.

[AIAA PAPER 73-688] 18 p2298 A73-36239

Corrosion wear mechanism with emphasis on chemical and mechano-chemical reaction products formation and removal from friction surface /tribo-mechanical processes/

18 p2320 A73-36494

Ignition temperature of liquid fuel-fuel droplets

18 p2342 A73-37115

Stepwise burning of non-volatile readily dispersible substances

19 p2503 A73-37502

Integral transport equations for component distribution function of gas mixture with internal degrees of freedom and chemical reactions

19 p2463 A73-37847

Electric power cell for producing direct/alternating current and shaft horsepower by direct electrochemical reaction of alkali metals with water

19 p2390 A73-38397

Dynamics of step heat waves in gases and plasmas.

20 p2592 A73-38863

Numerical and analytical prediction methods for time dependent reactions in homogeneous gas mixtures, considering accuracy and computing times

20 p2626 A73-39095

Equilibrium point asymptotic stability for nonlinear generalization of Onsager theory for entropy functions construction with applications to chemical reaction kinetics

20 p2627 A73-39338

Cross-linking ambient curing mechanisms for air-drying oxidizable coatings, involving chemical film-forming reactions

20 p2580 A73-39636

Photographic nuclear emulsions with total replacement of gelatin by synthetic polymers

21 p2647 A73-40269

Prebiotic reactions combining amino acids and ribonucleotides into polypeptides and polynucleotides in presence of urea, imidazole and Mg positive ion, suggesting contemporary biosynthesis parallels

21 p2637 A73-40372

Burning gunpowder interaction with an acoustic field in the presence of balanced chemical reactions behind the flame

21 p2791 A73-40699

Experimental study of heat and mass transfer in chemically reacting laminar boundary layers.

21 p2791 A73-41058

A single-pulse shock-tube study of the reaction between nitrous oxide and carbon monoxide.

22 p2933 A73-42757

Reaction rate constants for carbon monoxide-hydrogen-oxygen and hydrogen-nitrogen-oxygen systems at high temperatures, modeling hydrocarbon combustion for product distribution

22 p2933 A73-42758

Atomic oxygen reaction with acetylene in low pressure fast flow system, measuring free radical formation rate by photoionization mass spectrometer

22 p2818 A73-42768

Nitrogen dioxide and ozone photolysis as oxygen atom sources for high pressure addition reaction rate studies, discussing quantum yields and photolysis dependence on pressure

22 p2819 A73-42769

Regularities in the behavior of semiconductors and dielectrics in connection with deviation from stoichiometry

23 p2959 A73-43479

Theory of nonequilibrium phenomena in chemically reacting gas mixtures

23 p2950 A73-43703

Curve crossing theory for N molecule-O atom reactions in terms of spin-orbit coupling, considering nitrous oxide unimolecular decomposition and molecular N vibrational relaxation

24 p3113 A73-44979

CHEMICAL REACTORS

Long-life firings of a catalytic reactor for monopropellant hydrazine.

[AIAA PAPER 72-1045] 03 p0350 A73-13378

Perfectly stirred reactor - New concept for a CW chemical laser.

17 p2184 A73-34911

High-temperature fast-flow reactor studies of metal-atom oxidation kinetics.

22 p2898 A73-42761

Effects of turbulent mixing and chemical kinetics on nitric oxide production in a jet-stirred reactor.

22 p2820 A73-42796

Turbulent flow reactor for oxidation of moist CO and postinduction phase oxidation of methane, using chemical sampling and gas chromatographic analysis

22 p2820 A73-42804

CHEMICAL RELAXATION

U MOLECULAR RELAXATION

CHEMICAL SHIFT

U CHEMICAL EQUILIBRIUM

CHEMICAL STERILIZATION

Formaldehyde gas as a sterilant.

16 p1976 A73-33694

Spacecraft polyurethane foam jacket sterilization by gas method, discussing ethylene oxide and methyl bromide sorption and desorption

22 p2803 A73-42160

CHEMICAL TESTS

NT CHEMICAL ANALYSIS

NT ELECTROPHOTOMETRY

NT GAS ANALYSIS

NT GAS SPECTROSCOPY

NT KJELDAHL METHOD

NT MICROANALYSIS

NT NEUTRON ACTIVATION ANALYSIS

NT OZONOMETRY

NT POTENTIOMETRIC ANALYSIS

NT QUALITATIVE ANALYSIS
 NT QUANTITATIVE ANALYSIS
 NT SALT SPRAY TESTS
 NT SPECTROSCOPIC ANALYSIS
 NT URINALYSIS
 NT VOLUMETRIC ANALYSIS
 The testing of varnishing products used in aeronautics

21 p2724 A73-41557

CHEMILUMINESCENCE

Intensity variation of CN bands with temperature in active nitrogen methylene chloride chemiluminescent reaction.

01 p0014 A73-10333

Cytochemical-luminescence study of adrenal cortex proteins under the influence of ionizing radiation

02 p0134 A73-12354

Air quality monitoring instruments involving atmospheric pollution chemiluminescent reactions and CO IR, optical absorption and laser detectors

16 p2016 A73-33402

Chemiluminescence spectra from cool and blue flames - Electronically excited formaldehyde.

24 p3066 A73-45163

CHEMISORPTION

Chemisorption and catalysis of hydrogen on polycrystalline wires of tungsten and nickel.

06 p0661 A73-18253

Temperature dependent chemisorption effects on hydrogen embrittlement of steel, showing strength-ductility correlation

09 p1100 A73-22158

Decomposition of carbon monoxide on a α /110/nickel surface.

11 p1325 A73-25203

The interaction between two hydrogen atoms adsorbed on α /100/tungsten.

13 p1580 A73-28215

The connection between the thermodynamics of chemisorption on semiconductor surfaces and surface scattering of carriers.

13 p1668 A73-28454

The chemical stage in the mechanism of metal oxide reduction

13 p1581 A73-28937

ESCA study of fractional monolayer quantities of chemisorbed gases on tungsten.

14 p1724 A73-30421

Zirconium sorption by and release from carboxyl cationic in nitric and sulfuric acids, discussing pH dependence

14 p1765 A73-30884

Reflection-absorption infrared spectrum of α -CO chemisorbed on polycrystalline tungsten.

15 p1841 A73-31971

The passivation behaviour of the Ti-6Al-4V alloy.

15 p1895 A73-32567

The kinetics of the dissolution of oxygen in niobium at low oxygen pressures and high temperatures

16 p2026 A73-33955

Chemisorption of CO on tungsten α /100 - Combined flash desorption and electron stimulated desorption study. II.

18 p2287 A73-37033

Temperature dependent chemisorption effects on hydrogen embrittlement of steel, showing strength-ductility correlation

22 p2874 A73-42106

Chemisorption of H₂ on W(111).

22 p2817 A73-42444

Microplasticizing mechanism of hydrogen embrittlement due to stress activated chemisorption, noting association with temperature dependent hydrogen-metal atomic interaction

23 p3039 A73-43465

CHEMISTRY

Papers on chemistry in space research covering planetary atmospheres, organic compounds, carbonaceous meteorites, liquid and solid propellant rockets, and spacecraft sterilization

14 p1723 A73-30126

High pressure, radiation, high temperature and vacuum chemistries, discussing planetary matter, solar and cosmic radiation effects, plasma temperatures, solar winds and molecular populations

14 p1723 A73-30127

CHEMONUCLEAR PROPULSION

U CHEMICAL PROPULSION

U NUCLEAR PROPULSION

CHEMORECEPTORS

The role of the vagus nerves in the respiratory response to CO₂ under hyperoxic conditions.

01 p0010 A73-11501

The role of the carotid chemoreceptors in the CO₂-hyperpnea under hyperoxia.

01 p0010 A73-11502

Augmentation of chemosensitivity during mild exercise in normal man.

05 p0540 A73-16610

Role of adrenalin and alpha-receptor deactivation in reactions of hemopoietic organs to stress

07 p0781 A73-19644

Role of the arterial chemoreceptors in ventilatory adaptation to hypoxia of awake dogs and rabbits.

11 p1318 A73-26220

Threshold Pco₂ as a chemical stimulus for ventilation during acute hypoxia in dogs.

13 p1576 A73-28534

Role of peripheral chemoreceptors in reactions of rats to short and lasting hypoxia

14 p1719 A73-30840

Ventilatory responses to transient hypoxia and hypercapnia in man.

15 p1832 A73-31126

The nature of chemoreception in posterior hypothalamic structures

21 p2636 A73-40279

Effects of beta-blocking agents on atrio-ventricular and intraventricular conduction in man.

21 p2641 A73-41564

CHEMOTHERAPY

Effect of ethimazol on short term memory and mental working capacity

06 p0653 A73-18160

Long-term observations in patients with angina and normal coronary arteriograms.

06 p0655 A73-18871

Effect of some pharmacological preparations on the fall-out nystagmus and Bechterew nystagmus

08 p0929 A73-20982

Use of sodium hydrocarbonate for medication and prophylaxis of motion sickness

08 p0933 A73-20990

The effects of Dalmene/flurazepam hydrochloride/ on human EEG characteristics.

08 p0931 A73-21464

Antidiabetic medications and aircrew

08 p0935 A73-21541

Hydrazine derivative poisoning in industry and clinical medicine treatments, noting causes of vitamin B6 deficiency

10 p1183 A73-23819

Acetylcholinesterase activity of hypothalamic and cortical structures under pharmacological effects

10 p1182 A73-24597

High temperature tolerance enhancement in rats by thermal training and medicinal preparations

12 p1462 A73-27705

Prophylaxis and treatment of the motion sickness syndrome

13 p1580 A73-29410

Investigation of the influence of biologically active substances on the permeability of the skin

15 p1838 A73-31174

Effect of antiradiation drugs on the functional condition of the vestibular analyzer

15 p1838 A73-31509

Cobalt compound administration effects on hypoxic stress control, testing polycythemic response and cobalt retention in rats

17 p2115 A73-34744

Drug therapy for treatment of cardiogenic shock syndrome following myocardial infarction, discussing sympathomimetics, alpha-adrenergic blocks and combinations

18 p2276 A73-36546

Power failure of the heart in acute myocardial infarction.

18 p2276 A73-36547

Effects of beta-blocking agents on atrio-ventricular and intraventricular conduction in man.

21 p2641 A73-41564

Coronary heart disease; Proceedings of the Second International Symposium, Frankfurt am Main, West Germany, June 1972.

22 p2809 A73-42856

Functional state of the auditory analyzer under conditions of prolonged clinostatic hypokinesia

23 p2946 A73-43789

Oxygen affinity and electrolyte distribution of human blood - Changes induced by propranolol.

24 p3062 A73-44689

CHILDREN

Coronary atherosclerosis development and prevention in children, discussing hyperlipidemia, hypertension, cigarette smoking and high risk identification

14 p1715 A73-30065

CHILLING

U COOLING

CHIMES

U AUDITORY SIGNALS

CHIMPANZEES

Physiological study of dynamics and evolution of chimpanzee complex behavior, considering motor reactions, group behavior and nerve mechanisms of voluntary acts

23 p2947 A73-43928

CHINOOK HELICOPTER

U CH-47 HELICOPTER

CHIPS

Cooling of IC chips by heat conduction.

13 p1590 A73-28480

Description of the measurement design and the measurement principle in the measurement of the chip impedance of coaxially mounted semiconductor diodes in the microwave range

14 p1733 A73-30058

Investigation of mounting discrete chip components for hybrid microelectronic applications.

16 p1989 A73-33467

Thermal expansion compatibility of ceramic chip capacitors mounted on alumina substrates.

16 p1989 A73-33472

Detection of random chip defects in monolithic microcircuits.

17 p2135 A73-34732

An elusive open-circuit failure mode in thin-film chip resistors.

19 p2410 A73-38444

A design approach for LSI using chip selection and circuit modification techniques.

21 p2670 A73-41049

Eye movements of trained inspectors recorded during visual inspection of colored slides of IC chips, determining performance with emphasis on speed

23 p2947 A73-43212

Large-signal lumped modelling and characterization of an IMPATT diode.

24 p3073 A73-45478

CHIRP

NT CHIRP SIGNALS

CHIRP SIGNALS

Detection of multichannel FSK signals using chirp dispersion method.

04 p0419 A73-15407

Linear FM pulses in chirp radar transmitter, calculating and plotting bounds on amplitude, energy and power spectra for electromagnetic compatibility analysis

08 p0949 A73-21665

Ionospheric and pulse compression induced distortions in chirped Gaussian electromagnetic pulses

14 p1728 A73-30323

Measurement of the spectrum of a helical TEA CO₂ laser.

17 p2183 A73-34208

First order theory of steady state single optical pulses/solitons/ phase modulation during propagation in nonlinear absorbers, predicting nonchirped and chirped pulse trains

20 p2591 A73-38626

CHLORELLA

Triparanol inhibition of sterol biosynthesis in Chlorella emersonii.

02 p0139 A73-12547

Study of the effect of increased oxygen concentration on the metabolism of Chlorella

15 p1838 A73-31508

Survival and mutability of Chlorella under various orientation in the earth's gravitational field.

18 p2270 A73-35997

Effect of dynamic factors of space flights on green alga Chlorella vulgaris.

18 p2270 A73-36098

CHLORIDES

NT ALUMINUM CHLORIDES

NT AMMONIUM CHLORIDES

NT CALCIUM CHLORIDES

NT COPPER CHLORIDES

NT HYDROCHLORIC ACID

NT HYDROGEN CHLORIDES

NT MAGNESIUM CHLORIDES

NT POTASSIUM CHLORIDES

NT SILVER CHLORIDES

NT SODIUM CHLORIDES

NT SULFUR CHLORIDES

The additive action of some organic chlorides and sulfides in the four-ball lubricant test.

[ASLE PREPRINT 72LC-3C-2]

03 p0316 A73-14357

Effect of chloride ions on the dissolution behavior of Fe-Ni alloys.

15 p1895 A73-32565

Friction induced surface activity of some simple organic chlorides and hydrocarbons with iron.

[ASLE PREPRINT 73AM-8A-1]

17 p2179 A73-34991

Kinetics of formation of chloride ions in atmospheric pressure flames by way of the reversible reaction $HCl + e^- \rightarrow H + Cl^-$.

24 p3085 A73-44991

CHLORINATION

Chlorination studies. I - The reaction of aqueous hypochlorous acid with cytosine.

02 p0139 A73-12631

Chlorination studies. IV - The reaction of aqueous hypochlorous acid with pyrimidine and purine bases.

23 p2950 A73-43274

CHLORINE COMPOUNDS

NT ALUMINUM CHLORIDES

NT AMMONIUM CHLORIDES

NT AMMONIUM PERCHLORATES

NT CALCIUM CHLORIDES

NT CHLORIDES

NT CHLORINE FLUORIDES

NT COPPER CHLORIDES

NT HYDROCHLORIC ACID

NT MAGNESIUM CHLORIDES

NT POTASSIUM CHLORIDES

NT SILVER CHLORIDES

NT SODIUM CHLORIDES

NT SULFUR CHLORIDES

Chlorination studies. I - The reaction of aqueous hypochlorous acid with cytosine.

02 p0139 A73-12631

The addition of tert-butyl hypochlorite to isocyanates. 13 p1580 A73-28022

CHLORINE FLUORIDES
Chlorine trifluoride chemical laser emission, discussing output power dependence on partial pressures and chemical reaction kinetics 13 p1630 A73-29444
The acute inhalation toxicology of chlorine pentafluoride. 15 p1839 A73-32173

CHLOROPHYLLS
Effects of leaf age for four growth stages of cotton and corn plants on leaf reflectance, structure, thickness, water and chlorophyll concentrations and selection of wavelengths for crop discrimination. 05 p0571 A73-17128
Effect of nitrite and nitrate on chlorophyll fluorescence in green algae. 16 p1973 A73-33226
Remote sensing of chlorophyll and temperature in marine and fresh waters. 17 p2164 A73-35664
Eutrophication assessment using remote sensing techniques. 20 p2558 A73-39861

CHLOROPLASTS
Photosensitized inhibitor formation in isolated, aging chloroplasts. 07 p0784 A73-20453

CHLOROPRENE RESINS
Predicting the service life of neoprene launch tube liner pads for the Poseidon missile. 04 p0468 A73-14861

CHOKES [RESTRICTIONS]
Determination of the hydraulic resistance of throats by short unsteady blowing 07 p0779 A73-20083

CHOLESTEROL
Dielectric properties of cholesteric liquid crystals. 02 p0199 A73-11577
An epidemiological survey of risk factors for ischemic heart disease in 42,804 men. I - Serum cholesterol value. 04 p0409 A73-15521
Cholesteric liquid crystals thermophysical properties application in aerospace sciences and engineering, noting temperature measurement and nondestructive tests 06 p0733 A73-17767
An experimental basis for carcinogenic effects of ultraviolet radiation. 11 p1320 A73-26485
Prevention of the atherosclerotic diseases - Opportunities for military medicine. 14 p1718 A73-30518
Emotional overstress effects on the indices of the blood coagulation system in monkeys 14 p1719 A73-30846
Investigation of some electrooptical properties of liquid crystals 14 p1784 A73-30854
Serum cholesterol and plasma lipid elevation separation of hypercholesterolemic patients for atherosclerosis therapy 18 p2275 A73-36533
Influence of electric stimulation of the hypothalamus on catecholamine, phosphorylated compound, and cholesterol levels 21 p2637 A73-40284
Mechanisms of hyperlipidaemias in different clinical conditions. 22 p2809 A73-42832
Blood groups and plasma cholesterol esterification. 22 p2811 A73-43106
Blood group A sub-groups and serum cholesterol. 22 p2811 A73-43107

CHOLINE
Acetylcholinesterase activity of hypothalamic and cortical structures under pharmacological effects 10 p1182 A73-24597
The effect of iontophoretically applied acetylcholine upon the cat's retinal ganglion cells. 14 p1715 A73-30061

CHOLINERGICS
Mediator systems and respiratory function during an acute lethal loss of blood 07 p0781 A73-19645
Neurochemical aspects of the formation of electrographical and behavioral reactions 10 p1184 A73-24327
Cholinergic activation of vestibular neurones leading to rapid eye movements in the mesencephalic cat. 18 p2272 A73-36439
Participation of cholinergic mechanisms in negative human emotions 20 p2515 A73-39799

CHONDRITES
NT BRUDERHEIM METEORITE
NT CARBONACEOUS METEORITES
NT ORGUEIL METEORITE
Cosmogenic rare gas production rates in chondritic meteorites. 03 p0375 A73-14107

Thallium isotope analysis of terrestrial chondrites and achondrite and lunar soil, noting lunar chronology information from lead isotope extinct radioactivity 03 p0375 A73-14109
Natural remanent magnetizations of carbonaceous chondrites and the magnetic field in the early solar system. 05 p0619 A73-16839
Natural remanent magnetization and thermomagnetic properties of the Allende meteorite. 05 p0619 A73-16840
Siberian iron meteorites and chondrites characteristics and histories during 1965-1971 06 p0753 A73-18247
Vanadium isotopic composition and the concentrations of it and ferromagnesian elements in lunar material. 07 p0889 A73-19797
Inter-element relationships between trace elements in primitive carbonaceous and unequilibrated ordinary chondrites. 07 p0903 A73-20619
Fine structures of mutually normalized rare-earth patterns of chondrites. 07 p0789 A73-20620
Gallium and germanium in the metal and silicates of L- and LL-chondrites. 07 p0789 A73-20621
Chemical fractionations in meteorites. VI - Accretion temperatures of H-, LL-, and E-chondrites, from abundance of volatile trace elements. 07 p0789 A73-20622
Noble gas measurement in powdered aliquots of eleven H-chondrites, using Reynolds type mass spectrometer 07 p0789 A73-20623
Solar nebula Lu 176-Hf 176 pair and Zr abundance determinations, using chondrite fraction and s-process model 08 p1006 A73-20937
Mineralogy and petrology of the Yilmia enstatite chondrite. 09 p1139 A73-21852
Seminole meteorite external form chondrite composition and structure, noting brecciation and chondrules 09 p1139 A73-21854
The Oro Grande, New Mexico, chondrite and its lithic inclusion. 09 p1139 A73-21858
Ransom /Kansas/ stony meteorites discovery location map, describing megascopic appearance, petrology and chemical group 09 p1139 A73-21859
Depth variation of cosmogenic noble gases in the approximately 120-kg Keyes chondrite. 11 p1418 A73-25587
Mineralogical characteristics of the Reckhi meteorite 13 p1677 A73-28349
Hammond Downs, a new chondrite from the Tenham area, Queensland, Australia. 13 p1680 A73-28618
Accretion processes to account for chemical differences among chondrites formed in cooling solar nebula 17 p2227 A73-34414
Chondrule chemical variations in chondrite compared to predictions for different chondrule formation mechanisms 17 p2119 A73-34425
Pb isotopic composition measurement in chondrites and achondrite for model ages, noting 50 My variations 17 p2233 A73-35265
He, Ne and Ar in chondritic Ni-Fe as irradiation hardness sensors. 17 p2120 A73-35801
Lead isotopic composition ages of carbonaceous chondritic meteorites with correction for terrestrial lead contamination 21 p2765 A73-40239
Sequential nondestructive neutron activation analysis for bulk abundance of Fe, Al, Na, Mn, Cr, Sc, Co and Ir in chondrules from chondrites 21 p2647 A73-40563
Variability of the He-3 and Ne-21 production rates in ordinary chondrites. 21 p2771 A73-41008
Distribution of Ni, Ga, Ge and Ir between metal and silicate portions of H-group chondrites. 21 p2771 A73-41009
Photometric and polarimetric properties of the Bruderheim chondritic meteorite. 24 p3133 A73-44557
Chondrites - Initial strontium-87/strontium-86 ratios and the early history of the solar system. 24 p3137 A73-44688
Curium-248 in the early solar system. 24 p3143 A73-45348

CHONDRULE
Chondrules in Apollo 14 samples and size analyses of Apollo 14 and 15 fines. 07 p0882 A73-19720

Microstructure and mineral compositions of impact produced lunar chondrules from Apollo 14 breccia by electron microprobe X ray analyzer 07 p0882 A73-19722
Chemical classification and composition of Apollo 11, 12, 14 and 15 soil samples glasses, describing breccias and chondrules 07 p0882 A73-19723
Chondrule chemical variations in chondrite compared to predictions for different chondrule formation mechanisms 17 p2119 A73-34425
Urey meteoritic chondrule impact theory confirmation from Apollo sites and Lomar Crater /India/ impact generated silicate spherules 17 p2236 A73-35748
Sequential nondestructive neutron activation analysis for bulk abundance of Fe, Al, Na, Mn, Cr, Sc, Co and Ir in chondrules from chondrites 21 p2647 A73-40563
Study of a chondrule extracted from Lot 118-111 of the lunar soil of Mare Fecunditatis 21 p2770 A73-41006
Rare-earth elements in matrix, inclusions, and chondrules of the Allende meteorite. 24 p3133 A73-44539

CHOPPERS [ELECTRIC]
U ELECTRIC CHOPPERS

CHORDS [GEOMETRY]
Finite chord effects on vortex induced large aspect ratio wing loads, noting rolling moment magnitude overestimate from lifting line solution 15 p1823 A73-31670

CHORUS [DAWN PHENOMENON]
U DAWN CHORUS

CHORUS PHENOMENON
U DAWN CHORUS

CHROMATES
NT POTASSIUM CHROMATES
Red fuming nitric acid suitability for nonhypergolic rocket fuel ignition in presence of chromate and dichromate catalysts 07 p0865 A73-19986
Silver halogenide bichromatic gelatin chemical and photographic properties, noting decelerating development effect 21 p2647 A73-40266

CHROMATOGRAPHY
Determination of chromatographic resolution for peaks of vast concentration differences. 01 p0014 A73-10225
Accelerated chromatographic method for determination of hydroxyproline. 03 p0273 A73-13600
A study of simple chromatogram - Compression algorithm efficiency. 04 p0449 A73-15445
Ion-exchange chromatography in lunar organic analysis. 06 p0662 A73-18414
Chromatographic and mineralogical study of Apollo 14 fines. 07 p0884 A73-19743
A new approach to the isolation of milligram amounts of significant geochemical compounds. 11 p1325 A73-25463
Solar chromatograph for monochromatic image production with variable bandwidth and simple shift to visible spectrum, discussing design and applications 11 p1365 A73-26235
Chromatographic separation of niobium from titanium, tungsten, molybdenum, and vanadium on the fluoroform of the AV-16 anion exchanger 20 p2520 A73-39820
Multidirectional scanning of active regions with a slit-jaw spectrograph and a solar chromatograph. I - Description of the method and some preliminary results for the flare event of August 4th 1972. 21 p2777 A73-41491

CHROME
U CHROMIUM

CHROMIC ACID
The relation of surface condition after pretreatment to bondability of aluminum alloys. 24 p3093 A73-44764

CHROMITES
Electrical evaluation of doped and undoped cobalt chromite as the interconnection material for high-temperature, zirconia-electrolyte, fuel-cell batteries. [ECS PAPER 16] 01 p0006 A73-10724
Interaction between the CrZr2 intermetallic compound and some zirconium compounds with iron, cobalt, and nickel 06 p0708 A73-18056
Iron-titanium-chromite, a possible new carrier of remanent magnetization in lunar rocks. 07 p0892 A73-19836
Luna 20 - Mineral chemistry of spinel, pleonaste, chromite, ulvöspinel, ilmenite and rutile. 13 p1675 A73-28316
Effects of copper chromite and iron oxide catalysts on AP/CTPB sandwiches. 22 p2899 A73-42812

CHROMIUM

Effect of the quality of electrolytic chromium plating on the endurance of steel

02 p0173 A73-11926

Effect of rare-earth metals on mechanical characteristics of chromium.

02 p0181 A73-12214

Cr heat vacuum decarburization equipment for stainless steel vacuum melting, noting cost analysis, vacuum pumping curve and desulfurization

04 p0455 A73-15745

The concentration-dependent diffusion of chromium in nickel oxide.

06 p0712 A73-18760

Thoria stability in TD-NiCr at high temperatures in the presence of chromium in solution.

06 p0713 A73-18771

Beryllium and chromium abundances in Fra Mauro and Hadley-Apennine lunar samples.

07 p0886 A73-19764

Study of the wear resistance of nitrated electrolytic chromium coatings on certain alloy steels

10 p1223 A73-24065

Diffusion layer structure and phase composition during quenched and annealed steel saturation by Cr at high heating rates

10 p1236 A73-24962

V and Cr thin film lattice parameter decrease with thickness, discussing vacuum effects and surface energies estimation

12 p1531 A73-27935

UV radiation effects on gamma irradiated Cr ions spin lattice relaxation rate in ruby and on resonant phonon scattering

13 p1668 A73-28219

Conditions of Cr IX and Fe XI luminescence in the corona

13 p1683 A73-29094

Optical absorption spectrum of excited Cr³⁺/ions in yttrium aluminum garnet.

13 p1629 A73-29432

Influence of interstitial impurities on the formation of a cellular structure and on the properties of chromium

14 p1764 A73-30858

Quantum losses during excitation of ruby luminescence

15 p1924 A73-31721

Heating of an oxidizing metal by CO₂ laser radiation

17 p2184 A73-34634

Comparative evaluation of the wear resistance of electrolytic and plasma chromium coatings

18 p2318 A73-35883

Nd laser radiation thermochemical effects on oxide formation on thin Cr films, noting resistance and etching rates

19 p2438 A73-38148

Bonding degradation in the tantalum nitride-chromium-gold metallization system.

19 p2435 A73-38440

Chromium-rare-earth energy transfer in YAlO₃.

21 p2752 A73-40957

Chromium-ytterbium energy transfer in silicate glass.

21 p2752 A73-40963

Chromium and phosphorous enrichment in the metal of type II/C₂/carbonaceous chondrites.

21 p2771 A73-41007

Absolute oscillator strengths in neutral chromium and the solar chromium abundance.

22 p2905 A73-41764

Thermodynamics of transition metal-hydrogen solid solutions.

22 p2880 A73-43076

CHROMIUM ALLOYS

NT CHROMIUM STEELS

NT RENE 41

Properties and uses of UMoCo-50 and related Co-Cr-Fe alloys.

01 p0066 A73-11051

Influence of repeated loads on the resistance to relaxation of a heat-resistant nickel-chromium alloy

02 p0180 A73-11624

Metallographic investigation of electrodeposited iron-nickel-chromium alloys

02 p0174 A73-12535

The growth process of oxide layers during the initial oxidation of a 80Ni-20Cr alloy.

03 p0321 A73-12917

Changes in the fine structure of heat-resistant nickel-chromium alloys during the creep process

03 p0324 A73-13505

Oxidation and nitridation of Cr-W alloy.

03 p0325 A73-13803

Sn alloying effect on heat resistant Ni-Cr alloys plastic strain resistance and strength at room and high temperatures

03 p0327 A73-14003

A correlation between static adhesion data and the dynamic friction coefficients for two cobalt alloys and iron under vacuum conditions.

[ASLE PREPRINT 72LC-5B-2]

03 p0328 A73-14362

The high-temperature oxidation of nickel-20 wt. % chromium alloys containing dispersed oxide phases.

04 p0461 A73-14923

The functional form of rate curves for the high-temperature oxidation of dispersion-containing alloys forming Cr₂O₃ scales.

04 p0461 A73-14924

The high-temperature oxidation of cobalt-21 wt % chromium-3 vol. % Y₂O₃ alloys.

04 p0461 A73-14925

Heat resistant Ni and Cr alloys powder metallurgy, discussing inert and solute gas atomization, rotating electrode and gatorizing processes for powder fabrication

04 p0461 A73-15023

Chromium diffusion in Ni-20 wt pct Cr-3 vol pct Y₂O₃ and Co-21 wt pct Cr-3 vol pct Y₂O₃.

04 p0463 A73-15317

The effect of a hydrogen preheat-treatment on the oxidation behavior of Ni-Cr-Al-ThO₂ alloys.

04 p0463 A73-15319

Oxygen and nonmetallic inclusions in chromium and aluminothermic ferrochrome

04 p0465 A73-15662

Preparation of alloy deposits by continuous electron beam evaporation from a single rod-fed source.

04 p0456 A73-15761

Cyclic loads for decrease in relaxation softening of heat resistant Ni-Cr alloys, noting working temperature effects

06 p0706 A73-17885

Zone refining of chromium alloys with rare-earth metals

06 p0707 A73-18042

Cr effect on N solubility increase during Fe alloy nitriding, noting temperature effect on nitrides precipitation

06 p0697 A73-18054

Mechanical properties of heat and corrosion resistant nonmagnetic Ni-Cr-Nr spring alloys with W addition tested in aggressive and nitric acid base media

06 p0709 A73-18211

The distribution of chromium between ferrite and austenite and the thermodynamics of the alpha/gamma equilibrium in the Fe-Cr and Fe-Mn systems.

06 p0712 A73-18759

Stability of reactive and refractory metal borides in ternary chromium-base alloys.

07 p0838 A73-19122

A specific type of carbide phase precipitation during the aging of KhN77TiU alloy

07 p0841 A73-20640

Shock deformation of K-state in Ni-Cr alloys.

08 p0979 A73-21626

The influence of some structural factors on the creep strength of wrought precipitation-hardened Ni-Cr alloys.

08 p0982 A73-21793

Concentration profiles through thin oxide scales by ion-probe microanalysis.

09 p1101 A73-22402

Protecting metals in corrosive high-temperature environments.

09 p1089 A73-23296

Cr diffusion into Ni-Cr alloys in presence of aluminized layer, noting increased diffusive mobility

10 p1226 A73-24959

Si addition effect on Ni-Cr alloy calorized layer depth, microhardness, phase structure, chemical composition and scaling resistance

10 p1227 A73-24960

Phase structure and composition during the crystallization of eutectic-type alloys of the Ni-Cr system

12 p1509 A73-26897

Phase equilibria in the aluminum-chromium-zirconium system

12 p1510 A73-26906

Cast and annealed chromium-yttrium and chromium-lanthanum alloys peak solubility from metallographic, durometric and differential thermal analyses

12 p1512 A73-27245

X-ray spectral study of the K state in a nickel-chromium alloy

12 p1514 A73-27943

Influence of the chrome content and the interstitial impurities content /carbon and nitrogen/ on the volumetric and intergranular diffusion of iron 59⁺ in iron-chrome alloys with from 0 to 15 per cent chrome - Relations with alpha to alpha plus gamma reversible transformations

12 p1514 A73-27985

Dislocation structure and low-temperature plasticity of chromium alloys with rare earth metals

13 p1630 A73-28011

Study of precipitates formed by internal oxidation in cobalt-nickel-chromium alloys with a cobalt base. I - Precipitates formed by oxidation in air

14 p1759 A73-29750

Effects of deformation on diffusion in iron-nickel and iron-chrome systems

14 p1760 A73-30379

Calculation of the binary phase diagrams of iron, chromium, nickel and cobalt.

14 p1760 A73-30440

Mechanism of plastic deformation and low-temperature brittleness of a Cr alloy containing 45 at. % Fe

14 p1764 A73-30866

A scanning electron microscope study of the surface morphology of TD-NiCr oxidized at 800 C to 1200 C.

15 p1892 A73-32270

Mach 1 oxidation of thoriated nickel chromium at 1204 C /2200 F/.

15 p1892 A73-32271

Deformation and fracture behaviours of composites of copper and copper-chromium alloys reinforced with tungsten or molybdenum fibres.

16 p2025 A73-33022

Diffusional creep and creep-degradation in dispersion-strengthened Ni-Cr base alloys.

16 p2025 A73-33111

Phase constitution of the Ni-Cr-S alloy system between 600 and 850 C.

16 p2025 A73-33112

Strength of joints produced by melting high-carbon chromium alloys on low-carbon steel

17 p2188 A73-34566

Relation between the brittle-viscous transition temperature and structural characteristics in certain low-alloyed chromium alloys

17 p2189 A73-34579

Tracer diffusion of Ni-63 in Fe-17 wt pct Cr-12 wt pct Ni.

17 p2189 A73-34641

Superconducting properties of alloys of the vanadium-niobium-chromium system

18 p2325 A73-36898

The oxidation of binary alloys of chromium with metals of the first long period.

19 p2442 A73-38098

The effect of carbon on the sulphidation of Co-Cr alloys.

19 p2443 A73-38250

Dislocation structure of Ni₃Fe and Ni₃FeCr alloys in various stages of strain hardening

20 p2579 A73-39742

Preparation and properties of materials containing titanium carbide

21 p2719 A73-40851

Structure and composition of phases during solidification of Ni-Cr alloys of the eutectic type.

21 p2720 A73-41030

Microstructure of recrystallized alloy Kh20N80.

21 p2721 A73-41042

Electrical conductivity and superconductivity of vanadium, niobium, and chromium solid solutions

22 p2873 A73-41963

Fabrication of high-reliability sheathed thermocouples.

22 p2865 A73-42041

Specific structural features of the phase diagrams of the Ti-Cr-V, Ti-Cr-Nb and Ti-Cr-Ta ternary systems

22 p2873 A73-42087

Study of the structure and properties of alloys of the V-Al, Cr-Al and V-Cr-Al systems in the region of solid solution bcc ordering

22 p2873 A73-42088

Thermodynamic properties and Cr activity measurements in solid Cr-Ni-Fe alloys by solid oxide electrolyte technique

22 p2878 A73-42577

A thermodynamic calculation of the iron-chromium-vanadium equilibrium diagram.

23 p2993 A73-43918

Brazability of Ni-Cr heat resistant cermets on stainless steel.

23 p2986 A73-44005

Effects of additions of Al and Ti on electrical resistivities of oxide films of Fe-18 Cr sealing alloy.

23 p2986 A73-44152

Influence of deformation on the strength and ductility of low-alloy chromium

23 p2996 A73-44290

Static and fatigue strength of the KhN40MDTiU /EP 543/ alloy after various hardening treatments

24 p3098 A73-44475

CHROMIUM CARBIDES

Interaction of chromium carbide with copper-nickel melts

02 p0178 A73-11539

Activity of carbon and solubility of carbides in the fcc Fe-Mo-C, Fe-Cr-C, and Fe-V-C alloys.

02 p0183 A73-12755

A specific type of carbide phase precipitation during the aging of KhN77TiU alloy

07 p0841 A73-20640

Characteristics of the microstructural wear pattern of carbided chromium coatings

09 p1088 A73-22592

Carbide separation and carbide equilibrium in the Co-Cr-C system

12 p1509 A73-26895

Carbide precipitation and carbide equilibrium in the Co-Cr-C system.

21 p2720 A73-41028

Wear resistant abrasive and dry lubricant cobalt-chromium carbide composite material coatings obtained by electrolytic codeposition

24 p3094 A73-45073

CHROMIUM COMPOUNDS

- NT CHROMATES
- NT CHROMIC ACID
- NT CHROMITES
- NT CHROMIUM CARBIDES
- NT CHROMIUM OXIDES
- NT POTASSIUM CHROMATES
- Crystalline structure of the Cr₃AlB₄ compound

10 p1259 A73-24066

CHROMIUM OXIDES

- NT CHROMITES
- Some laws of chromium oxide-chromium cermet sintering

15 p1892 A73-32240

CHROMIUM STEELS

- Formation of carbides in 3% chromium steel after additional alloying
- Physical fatigue limit of hardened steels
- Strength and ductility of chromium-nickel-manganese steel as a function of the carbon and nitrogen content in the range from 20 to 253 C
- Sinterability of stainless steel powders.
- Corrosion behavior of sintered stainless steels.
- Sintered chromium-nickel steel of high tungsten content.
- Internal friction and heat release in engineering and tool steels in the presence of intense ultrasonic oscillations
- New morphological element of the microsurface of ductile fracture of hypoeutectoid steel.
- Certain regularities in the influence of preliminary loading by alternating tensile stress on the long-term strength of Kh18N10T steel
- Impact fracture resistance of Cr-Mn-Si steel, investigating alloying effects on crack initiation and propagation
- Influence of cerium and boron additions on the corrosion properties of Kh18N9TL steel
- Temper embrittlement response and toughness of a rare earth treated Ni-Cr-Mo steel.
- Dependence of the deformability of the Kh17 high-chromium steel on texture
- Delta-ferrite alteration in steel 1Kh16N4B during homogenization
- Liquation-induced microinhomogeneity of heat resistant submerged-arc-smelted steel 4Kh12N8G8MFB/EI481/
- Ni, Si and Mn alloying effect on structural transformations, phase composition and mechanical properties of cast Cr-Ni steels
- Carbide hardening of chromium-molybdenum-vanadium steel.
- Transitions in the friction coefficients, the wear rates, and the compositions of the wear debris produced in the unlubricated sliding of chromium steels.
- [ASLE PREPRINT 72LC-7B-2]
- Parametric-graphical method of cumulative creep damage evaluation for Cr-Mo-V steel in terms of postexposure rupture and hardness measurements
- The effect of alloying elements on creep rupture strength and microstructure of 12 percent chromium heat resisting steel.
- Phase transformations and mechanical properties of highly alloyed Cr-Mn-Ni steels
- Composition and structure of rust layers and corrosion rate of chromium steels exposed to a marine atmosphere.
- A stochastic model of creep in the heat-resistant low-alloy CrMoV steel
- Aging kinetics of maraging nickel and chromium steels
- Ferritic chromium steels embrittlement under high temperature aging, using hardness measurements, impact tests and electron metallography
- Passivation of chrome steels under isothermal oxidation at 1020 deg C

07 p0839 A73-19660

Alloy composition and temperature effects on nitrogen solubility in austenitic Cr-Ni steels, noting nitride precipitation effect on impact strength reduction

07 p0839 A73-19950

Damping properties of 1Kh13 and 2Kh13 high-chromium steels in a uniform stress-strain state in tension and compression at room and high temperatures

07 p0841 A73-20513

The influence of prior fatigue deformation on creep behaviour.

08 p0979 A73-21672

Cr-Ni carbon steel testing for stress and temperature dependencies of secondary creep rate, noting grain boundary diffusion controlled mechanism

08 p0980 A73-21674

The influence of microstructure on creep properties of low alloy ferritic chromium-molybdenum-vanadium steel.

08 p0980 A73-21675

A recovery creep model based on dislocation distributions.

08 p0980 A73-21777

The effect of a dispersed phase on the creep properties of a Cr-Ni steel.

08 p0980 A73-21779

Dislocation distributions during creep and recovery of a 20% Cr-35% Ni steel at 700 deg C.

08 p0981 A73-21784

The influence of nickel content on the structure and high temperature properties of a 12% Cr Mo V Nb steel.

08 p0982 A73-21799

Influence of hot rolling on the mechanical properties of unstable austenitic chromium-manganese steels

09 p1098 A73-21848

Structure and properties of electron-beam-melted 1Kh12N3M3B steel

09 p1107 A73-23194

Causes of embrittlement in the 1Kh18M steel

09 p1107 A73-23195

Brittle fracture tests of Ti-Cr steels with/without nitrogen hardened layer under shock impact loads

09 p1107 A73-23199

Molybdenum and nickel alloying effect on time and temperature range of reversible temper brittleness of chromium steels

09 p1107 A73-23200

Atmospheric corrosion fatigue tests for environmental conditions and superimposed stress wave effects on Cr-Mo steel fatigue life under rotating bending

10 p1235 A73-24917

Corrosion and electrochemical characteristics of oxidized steels Kh15N5D2T and Kh15N4AM3.

10 p1236 A73-24926

Effect of chemical composition on the heat resistance of steel Kh25Ni16G7AR.

10 p1236 A73-24932

On the nature of films over corrosion pits in stainless steel.

11 p1378 A73-24975

Consideration of creep probability in a low-alloyed heat-resistant CrMoV steel

11 p1384 A73-26111

Dynamic potential method of estimating the susceptibility of corrosion-resistant steels to intercrystalline corrosion

11 p1364 A73-26112

Embrittlement of 2-1/4Cr-1Mo steel weld metal by postweld heat treatment.

11 p1375 A73-26354

Alpha phase lattice constant curves and composition effects of Cr-Ni-Co-Mo steels on microstress rate reduction during age hardening

12 p1509 A73-26840

Tensile behaviors of high Cr-low Ni two-phase stainless steels at room and low temperatures.

12 p1511 A73-27056

German monograph - Effect of creep strains at 700 C on the hardening characteristics of the steel X 8 Cr-NiMoNb 16 16 at room temperature.

13 p1637 A73-29281

Random and program fatigue tests of Cr-Mo steel specimen with V-grooved notch.

13 p1641 A73-29494

Investigation of the thermal fatigue of type Kh18N10T steel under complex stress distributions.

13 p1643 A73-29623

Redistribution of nickel and chromium during alpha to gamma transformation in stainless nickel-chromium steels

13 p1644 A73-29646

Mo and W alloying effects on low carbon chromium nickel steels intergranular corrosion resistance

13 p1644 A73-29648

Delta ferrite and martensite formation in stainless steels.

14 p1759 A73-30145

Physical fatigue limit of hardened steels.

14 p1759 A73-30310

Strength and ductility of chromium-nickel-manganese steel as a function of carbon and nitrogen contents over the range 20-253 C.

14 p1759 A73-30315

Structure stability of austenitic chromium-nickel steels at the temperature of liquid helium

14 p1760 A73-30420

Activation energy measurement for static strain aging rate controlling process in ferritic chromium steel

14 p1762 A73-30642

Thermal expansion, Young's modulus, and magnetostriction of a stainless iron-chromium-nickel alloy in the temperature range between 80 and 280 K

14 p1764 A73-30868

Stacking fault energy in iron-nickel and iron-nickel-chromium alloys

14 p1764 A73-30869

Strengthening of chromium-nickel steels with unstable austenite

15 p1889 A73-31809

Nonisothermal creep of chrome-nickel steel

15 p1890 A73-31830

Effect of additional alloying and heat treatment on the strength of steels

17 p2187 A73-34336

Effects of cold plastic deformation and aging temperature on the mechanical properties of dispersively hardening Cr-Ni-Co-Mo steel

17 p2188 A73-34559

High strength Ni-Cr-Mo steel plane-strain fracture toughness measured with circumferentially cracked-notched round bars, discussing heat treatment and test temperature effects

17 p2190 A73-34890

Formation of carbides during tempering of complexly alloyed chromium steel

18 p2324 A73-36770

Austenitic grain structure and strength changes associated with aging in 14Cr-14Ni type steels

18 p2325 A73-36810

The damping properties of high-chrome steels 1Kh13 and 2Kh13 in a homogeneous stress state of tension-compression under the conditions of normal and elevated temperatures.

19 p2440 A73-37788

Heat resistance of chromium-nickel and chromium-nickel-molybdenum steels with additions of boron

21 p2718 A73-40734

Redistribution of nickel and chromium during the alpha to gamma transformation in Cr-Ni stainless steels.

21 p2720 A73-41039

Mo and W alloying effects on low carbon chromium nickel steels intergranular corrosion resistance

21 p2721 A73-41041

How composition affects properties of a ferritic stainless steel.

21 p2721 A73-41084

The creep characteristics of the heat-resistant ferritic steels X 20 CrMoV 12 1 and X 18 CrMoNi V Nb 12 1 and their welded connections

22 p2872 A73-41780

Influence of heat treatment and surface quality on the endurance of EI961 steel

23 p2995 A73-44288

Ten years' experience of UMCo-type alloys in a special steel foundry.

24 p3099 A73-45074

Microstructural features of Cr12NiWMoV Ti /T60/ steel after electroslag remelting

24 p3100 A73-45170

Strengthening of Cr-Ni steels with unstable austenite.

24 p3100 A73-45272

CHROMOSOMES

Y-chromosome localization in the interphase nuclei of cerebral neurons in man

01 p0010 A73-11444

Radiation protective effect of a mixture of ATP, AET, and serotonin on yields of 600-R X-ray-induced chromosome aberrations in the rat.

02 p0134 A73-12187

Study of lymphocyte chromosome aberrations in human peripheral blood under in vitro exposures to 645-MeV protons and X-rays

15 p1835 A73-31517

Cytogenetic analysis of diploid and autotetraploid Crepis capillaris seeds following space travel on the 'Cosmos-368' artificial earth satellite

18 p2271 A73-36117

CHROMOSPHERE

The empirical determination of line source functions, beta-L-values, and the microturbulent and convective velocity components as functions of depth in the photosphere-chromosphere transition region.

01 p0107 A73-11378

Solar outer layer models of convective zone, photosphere, chromosphere, corona and solar wind, using electron density dependence

01 p0107 A73-11379

Temperature structure and conductive flux in the chromosphere-corona transition region.

01 p0107 A73-11380

Tunnel-effect and propagation of 5-min oscillations in the solar atmosphere.

01 p0107 A73-11381

Physical properties of solar chromospheric plages. I - Line profiles of the CaII H, K, and infrared triplet lines.

Chromospheric heating of very hot stars by radiation driven sound waves.

Differential rotation in the solar atmosphere inferred from optical, radio, and interplanetary data.

Moustaches in solar H alpha filtergrams and spectra, studying relations to photospheric and chromospheric phenomena

Analysis of some aspects of 25 chromospheric events. I - Reduction of the optical data. II - Discussion on the optical data.

Investigation of the chromosphere in the D3 helium line at the eclipse of September 22, 1968.

Equator-pole differences in the solar chromosphere from Lyman-continuum data.

The absence of flares in 3835 A and the heating of the chromosphere.

Brightness distribution of the sun at 8.6 mm wavelength.

The spectra of near-vertical structures on the solar disk.

On the size of the structure elements in the solar chromosphere.

Magnesium II doublet profiles of chromospheric inhomogeneities at the center of the solar disk.

Chromospheric flares and shock waves in interplanetary space

Chromospheric heating of very hot stars by radiation driven sound waves. II.

Stellar model chromospheres. I - On the temperature minima of F, G, and K stars.

Self consistent computerized solutions to acoustic wave propagation and shock wave transformation with energy dissipation for solar and stellar chromosphere models

Solar rotation as determined from OSO-4 EUV spectroheliograms.

Energy balance in the chromosphere-corona transition region.

A model for the polar transition layer and corona for November 1967.

Simultaneous determination of the electron temperature and density in the chromospheric-coronal transition region of the sun.

Time dependent geophysical effects associated with chromospheric and coronal flares, tabulating for 1957-1961

The absorption spectrum of atmospheric water vapor in the vicinity of the He 10830 A triplet.

Intensive chromospheric flares and rotational discontinuities in the solar wind

Solar surface photospheric oscillation spatiotemporal power spectrum observation, considering long-period oscillation correlation with chromospheric flare

Spectral investigation of the chromosphere. II.

EUV and radio observation of energy flux from corona into chromosphere, considering coronal holes as source of high energy streams of solar wind

Dynamics and localization of surges in the chromosphere.

The configuration of interplanetary shock waves produced by strong chromospheric flares [according to space sonde measurements]

Rocket flight observations of solar UV chromosphere at 1190-1320A, considering spectral and angular resolutions

The correlation between 10.7-cm/2800 MHz/ solar radio emission and chromospheric flares

Metallic lines in the solar flare of July 12, 1961 and properties of the corresponding emission regions

Model of the chromosphere and the transition layer between the chromosphere and solar corona

Studies of the solar chromosphere from millimetre and sub-millimetre observations. I - Isophotometric mapping.

On some transient H-alpha features associated with metric type III bursts.

Solar convective motions and associated magnetic fields, discussing photospheric cellular and chromospheric vertical motions, fibril structures, sunspot magnetic properties and faculae

Self consistent computerized solutions to acoustic wave propagation and shock wave transformation with energy dissipation for solar and stellar chromosphere models

Models of the chromospheric-coronal transition layer and lower corona derived from extreme-ultraviolet observations.

Search for solar recombination lines in the frequency range 110-115 GHz.

H alpha line contrast profiles evaluation from solar chromosphere supergranulation observations, obtaining chromospheric fine structure characteristics

Line widths of CaII K2 and H-alpha and the chromospheres of late stars

Configuration of interplanetary shock waves from powerful chromospheric flares /from space probe measurements/.

High flux cosmic ray variations following solar chromospheric flares in August 1972 from stratospheric balloon measurements

Solar proton measurements during August 1972 cosmic ray and magnetic field events caused by chromospheric flares associated with sunspots on east limb

Investigation of shock waves responsible for Forbush decreases

Solar spicule morphology, observing diameter, height, expansion and threshold intensity with H alpha filtergrams

Spectroscopic investigation of the chromosphere. III - H-alpha line profile from the interior of supergranular cells.

Optical solar flare kinematic model, relating chromosphere response to downward propagating supergranular disturbance

Stellar chromospheric velocity fields and the width luminosity relations.

Structure of the solar chromosphere. I - Basic computations and summary of the results.

Chromospheric hydrogen and helium spectral lines investigation in solar flares determining plasma and ionization temperatures, energy spectra and electron density

Coupling between thermal conduction and radiative transfer in a moving atmosphere.

Some statistical characteristics of sudden ionospheric disturbances, and the distribution of geoeffective chromospheric flares over the solar disk

Resistive diffusion of force-free magnetic fields in a passive medium. II - A nonlinear analysis of the one-dimensional case.

Saha's equation under deviation from thermodynamic equilibrium.

Vertical phase variation and mechanical flux in the solar 5-minute oscillation.

Powerful chromospheric flares and rotational discontinuities in the solar wind.

Chromosphere models for cool stars of various spectral types, calculating temperature-density dependence for sun, giant and dwarf stars

Metal lines in the solar flare of July 12, 1961, and the properties of the emission region.

Further aspects of weak shock theory applied to the solar chromosphere.

Some comments on the photographic subtraction method of determining chromospheric velocities.

Statistical analysis of transient brightenings in solar chromosphere /Elerman bombs/ from H alpha filtergrams, obtaining histograms for durations near disk center and limb

CHRONIC CONDITIONS

Effect of chronic centrifugation on body composition in the rat.

Morphological and electron-microscopic alterations of the myocardium in dogs subjected to lasting chronic gamma irradiation

Low calcium diet produced chronic decalcification effect on osseous repair of experimentally induced cortical bone defect in chickens

Management of the treatment of illnesses as a problem of modern control theory

Chronic acceleration effects on homeotherm physiological adaptation in terms of body weight, tolerable field intensity, growth and fat deposition inhibition, etc

Effect of chronic pyramid insufficiency on the function of spinal centers of shin and foot muscles in man

CHRONOGRAPHS

U CHRONOMETERS

CHRONOLOGY

NT GEOCHRONOLOGY

Lunar surface cratering history from Apollo rock age data, implying earth-moon and solar system evolution mechanism

The geomorphic evolution of the lunar surface.

The abundances of the elements in the oldest disk stars.

Crater frequency age determinations for the proposed Apollo 17 site at Taurus-Littrow.

A new age indicator for Galactic clusters.

Cosmic ray bombardment of meteorites allowing solar system age estimation from spallation product concentration and subatomic particle track distribution

Martian cratering. IV - Mariner 9 initial analysis of cratering chronology.

CHRONOMETERS

Ultrashort laser pulse generators for dynamic marking of 'chronodiode' and 'chronolas' slit cameras

CHRONOPHOTOGRAPHY

A method for chronocyclographical motion analysis with the aid of an on-line computer

Cinemicographic study of the development of sub-surface colonies of *Staphylococcus aureus* in soft agar.

CHRONOTRONS

U PULSE RATE

U TIME LAG

CHUGGING

U COMBUSTION STABILITY

CHUTES

DC-10 aircraft slide/raft system for emergency personnel evacuation, discussing certification test program for performance, reliability, seaworthiness and compliance with regulations

Certification program for the DC-10 slide/raft.

CINEFLUOROGRAPHY

U MOTION PICTURES

U RADIOGRAPHY

CINEMATOGRAPHY

The reconstruction of three-dimensional objects from two orthogonal projections and its application to cardiac cineangiography.

Ultrahigh-speed electronic camera - CELER 2-500

Contribution of 1- and 5-nsec frame-type motion-picture photography to the study of dense plasmas

Some applications of a tube with proximity focusing in ultrahigh-speed motion-picture photography

Microchannel electron multipliers application to X ray cinematography of laser generated plasma

Advances in high-speed photography 1957-1972.

Space flight exercise regimen proposals, exploring moving picture/electric muscle stimuli program as earth gravity simulator in weightlessness

15 p1838 A73-31515

International Conference on Ultrahigh-Speed Cinematography, 10th, Nice, France, September 25-30, 1972, Transactions

21 p2693 A73-39933

Literature survey on high speed photography and cinematography, discussing gas discharge tube and open spark equipment, Kerr cells, image dissection and holographic interferometry

21 p2693 A73-39934

Mechano-optical camera giving ten million images per second

21 p2693 A73-39935

Ultrahigh speed cinematography with rotating Ti drums bound by monocrystalline boron fibers, noting prototype performance

21 p2693 A73-39937

High-speed SFKF photographic camera of the continuous type.

21 p2693 A73-39938

Ultrahigh-speed high-frequency motion picture camera type W.K.2

21 p2693 A73-39939

Slit electronic camera with scanned memory used in high speed cineradiography

21 p2694 A73-39942

Image-converter camera with subpicosecond temporal resolution.

21 p2694 A73-39947

The microchannel picroscope - A high temporal resolution scanning tube for study of luminous phenomena in the subnanosecond range

21 p2694 A73-39949

Subpicosecond time-resolution image converter - The picochron.

21 p2694 A73-39950

Why exact metrology in an ultrahigh-speed cinematographic system - An application example: Calibration of image converters with a view to photometric measurements

21 p2694 A73-39951

Resetting in time of recordings in ultrahigh-speed cinematography

21 p2694 A73-39952

Utilization for high speed cinematography of phased-locked CW lasers

21 p2709 A73-39954

The use of holographic techniques for recording high-speed events.

21 p2695 A73-39962

Flash photography using laser excited fluorescent tracers.

21 p2709 A73-39969

Utilization of the laser as a source in ultrahigh-speed cinematography

21 p2709 A73-39972

A streak technique for measuring the initial movement of a rocket with four unknown and two known degrees of motion.

21 p2696 A73-39986

Visualization of the shape and symmetry of detonation waves by a slit camera - Application to hollow charges

21 p2697 A73-39992

High-speed cine-photography and oscillography in a boiling simulation.

21 p2697 A73-39994

Technique of an ultrahigh-speed sampling camera based on the use of a unique photomultiplier

21 p2697 A73-39995

Investigation of the possibility of using acetylated oxyethylcellulose as a film forming substance for a moving-picture film base

21 p2647 A73-40262

Physico-mechanical properties and damage mechanism of moving-picture photographic materials as film systems

21 p2699 A73-40270

Photographic laboratory studies of explosions.

21 p2706 A73-41553

CINERADIOGRAPHY

U MOTION PICTURES

U RADIOGRAPHY

CINETHEODOLITES

High speed cinetheodolite for missile tracking incorporating LED /light emitting diode/ system for metric data recording

10 p1222 A73-24950

CIRCADIAN RHYTHMS

Hypothalamic norepinephrine - Circadian rhythms and the control of feeding behavior.

02 p0134 A73-12417

Regulation of testis function in golden hamsters - A circadian clock measures photoperiodic time.

02 p0134 A73-12422

Effect of sleep-wake reversal and sleep deprivation on the circadian rhythm of oxygen toxicity seizure susceptibility.

02 p0135 A73-12561

Circadian rhythm asynchrony in man during hypokinesis.

03 p0263 A73-14121

Thyroid and adrenal cortical rhythmicity during bed rest.

03 p0263 A73-14122

CNS epinephrine tone, a possible etiology for the threshold in susceptibility to oxygen toxicity seizures.

03 p0263 A73-14156

Effect of hypergravity on the circadian rhythms of white rats.

[ASME PAPER 72-WA/BHF-14]

04 p0410 A73-15877

Daily rhythm of biogenetic amine /histamine and serotonin/ contents in human blood during usual and shifted work schedules

06 p0650 A73-17688

Circadian rhythms - Subcellular and biochemical aspects.

06 p0651 A73-17824

Biological clocks in animal orientation and in other functions.

06 p0651 A73-17825

Diurnal rhythm oscillations of fat metabolism indices in healthy young men

07 p0781 A73-19646

Mitotic activity in dorsal epidermis of Rana pipiens.

07 p0784 A73-20456

Diurnal psychic working capacity dynamics under conditions of continuous 72-hr wakefulness

08 p0930 A73-20989

Drive and performance modification following multiple /light-light/ shifts in the photoperiod.

09 p1039 A73-22528

Circadian rhythms in catecholamines in organs of the golden hamster.

11 p1318 A73-26120

Characteristics of the higher nervous activity of monkeys during a postneurotic period

12 p1462 A73-27108

Astronauts diurnal life cycle inversion during space flight missions, considering social factors and work-rest cycle effects

12 p1463 A73-27715

German monograph - Investigation concerning a consideration of the human circadian rhythm by means of a variable working time.

13 p1580 A73-29283

Circadian rhythm of urinary calcium excretion during immobilization.

14 p1717 A73-30512

Diurnal rhythm of a corticosteroid reaction to ACTH and physical load

14 p1719 A73-30841

Model concept concerning some control principles of the human organism. III - Seasonal adaptation

15 p1856 A73-32357

Histochemical correlates of changes in the primate brain associated with varying environmental light conditions.

15 p1837 A73-32600

Circadian rhythms in human mental performance from waking day, round of clock and simulated shift-work studies

16 p1972 A73-33156

Daytime human performance and temperament rhythms as function of individual introversion-extroversion rating

16 p1972 A73-33157

Sleep behaviour as a biorhythm.

16 p1972 A73-33158

Investigation of the possibility of human adaptation to a 16-hour day

17 p2114 A73-34238

Control of pineal indole biosynthesis by changes in sympathetic tone caused by factors other than environmental lighting.

19 p2393 A73-37300

Ultradian rhythms in human telemetered gross motor activity.

20 p2512 A73-39102

Circadian rhythms of free radical state concentrations in the organs of mice.

20 p2512 A73-39104

Patterns of diurnal variation in the intraocular pressure of airline pilots.

20 p2512 A73-39107

Inversion of lighting regimen alters acrophase relations of circadian rhythms in body temperature, heart rate and movement of pocket mice.

20 p2513 A73-39480

Effects of a synchronizer phase-shift on circadian rhythms in response of mice to ethanol or ouabain.

20 p2513 A73-39481

Circadian variations in presumably healthy men under conditions of peace-time army reserve unit training.

20 p2513 A73-39482

Spiral aftereffect durations following awakening from REM sleep and non-REM sleep.

21 p2639 A73-41179

Diurnal variations of plasma cortisol and glucose and of urinary excretion of free cortisol in man at rest

24 p3061 A73-45158

CIRCLES [GEOMETRY]

Boundary value problems of the Laplace equation in a circle

04 p0470 A73-14933

Algebraic algorithm for positive realness of real rational functions and matrices relative to unit circle in complex plane, determining real polynomial zeros distribution

19 p2446 A73-38488

CIRCUIT BOARDS

An advanced printed circuit board system having outstanding resistance to humid environments.

03 p0281 A73-13047

Forced air cooling of dual-in-line packages.

10 p1193 A73-23607

The role of temperature in the environmental acceptance testing of electronic equipment.

16 p1989 A73-33606

Fault ambiguity repair optimization /FARO/ computer program for electronic circuit card group replacement strategy, using FORTRAN IV for SPEC-TRA 70/55 batch processing

16 p1990 A73-33626

An improved epoxy resin formulation for multi-layer circuit boards.

17 p2196 A73-35341

Some considerations on solder flow-up into plated-through holes.

23 p2986 A73-44002

CIRCUIT BREAKERS

Arc discharge properties in ionized gases, discussing interruption and reignition in terms of instabilities, decay processes, and circuit breaker problem

16 p2040 A73-32940

Selection, application, and inspection of electric overcurrent protective devices.

[SAE ARP 1199]

16 p1987 A73-33016

Logic-controlled solid-state switchgear for 270 volt dc.

22 p2802 A73-42915

CIRCUIT DIAGRAMS

A new uncomplicated method for the simultaneous determination of various parameters in explosive welding

06 p0698 A73-18446

Facility for roller bearing parameters testing during high speed rotation in ultrahigh vacuum, discussing circuitry and principal elements

07 p0807 A73-18908

Circuit diagrams, electronic modules and design of PCM telemetry encoder for Eole satellite, noting data multiplexing and processing

07 p0789 A73-18957

Circuit diagram and electrical characteristics of semiconductor memory cell consisting of thyristor and n-p-n transistors, noting parameters stability

09 p1063 A73-22460

Temperature measuring devices based on operational amplifier circuits, considering design and applications

09 p1085 A73-22924

Amplitude selector for linear transistorized devices

09 p1064 A73-23006

Block diagram of transistorized phase instability meter for statistical analysis of one dimensional density distributions, noting two series connected identical delay lines

09 p1064 A73-23008

Feedback loop and forward path electronic circuits, discussing two port network representation

10 p1201 A73-24384

Real time digital computer algorithm for linear and nonlinear electronic circuit modeling in state variable form for static and dynamic regimes

10 p1196 A73-24607

Multivibrator with p-n-p and n-p-n transistors, noting circuit diagram, operation and power dissipation

10 p1197 A73-24940

Differential mode of operation for bucket-bridge circuits.

11 p1341 A73-25360

Equivalent continuous sound level determination from instantaneous sonic intensity measurement during representative time period, describing electron measuring device and circuitry

11 p1367 A73-26416

Constant-Q pulsed feedback electronics for strapped-down gyro systems.

11 p1342 A73-26635

Direct conversion s.s.b. receivers - A comparison of possible circuit configurations for speech communication.

12 p1467 A73-26800

Inductive flow meter sensor design for optimal electrode diameter to ensure signal quality and impedance matching, proposing circuit diagram

13 p1611 A73-28019

Standard Hydraulic Impulse Machine design for testing hose assemblies, tubing, coils and fittings, including circuit diagrams and component identifications

16 p1970 A73-33018

Performance measurements of aircraft electrical systems having highly distorted voltage and current waveforms.

17 p2135 A73-34604

An accelerated electron beam position and shape meter

21 p2699 A73-40172

- A computer for modeling and calculating technological dimensional circuits
22 p2829 A73-42365
- Requirements of switching devices in dc-to-dc converters.
22 p2801 A73-42908
- Linearized stability analysis and design of a flyback dc-dc boost regulator.
22 p2801 A73-42910
- Semiconductor rectifiers analysis, considering triac and thyristor tetrode circuits, trigger devices and circuit diagrams
22 p2835 A73-43128

CIRCUIT PROTECTION

- Zener diodes for overvoltage spark protection circuits in automatic control and measuring equipment operating in explosive environment
02 p0147 A73-12175
- Overload tolerance formulas for differential voltage null measuring system with amplifier for trigger circuit drive
02 p0170 A73-12345
- The IHTS - A new building block for power conditioners.
03 p0282 A73-13934
- Circuitry for battery cell control and protection from overcharge and over-discharge for long service life operation
03 p0253 A73-13937
- Self healing fuse for fast acting current overload protection of electric circuits, discussing design and performance
03 p0283 A73-13942
- Pulse width amplitude converter design and performance for ion engine high voltage power supply, noting oscillator, modulator and circuit protection
04 p0489 A73-15733
- Adaptation of the P-N junction burnout model to circuit analysis codes.
05 p0557 A73-16506
- Study on the limit efficiency of lightning conductors on aircraft radomes.
11 p1336 A73-25303
- Selection, application, and inspection of electric overcurrent protective devices.
16 p1987 A73-33016
- Protecting a quantum amplifier from saturation by pulsed modulation of the pumping.
17 p2184 A73-35157
- The lightning arrestor-connector concept - Description and data.
19 p2408 A73-37270
- Prediction of RS01 design requirements for MIL-STD-461A.
22 p2823 A73-41803
- Electromagnetic shielding techniques and testing for environment and instrument protection from radio emission and noise
22 p2823 A73-41804
- Fixed installation ground electrical power supply system for aircraft service, discussing motor-alternators, plant control cubicles, selector and busbar switchboxes and fault protection devices
24 p3075 A73-45156

CIRCUIT RELIABILITY

- Analytical method for diagnostic and checkout testing of logic element faults in complex combinational circuits
01 p0026 A73-10035
- Reliable uninterrupted controlled transient voltage dc power supplies with active energy storage element, comparing three system configurations, design features and applications
03 p0253 A73-13946
- A reliable all-silver front contact for silicon solar cells.
03 p0256 A73-14230
- Datran TDM switching system with stored program controller and IC components providing reliability, flexibility and high channel capacity in data transmission
05 p0551 A73-16804
- Reliable starting technique for an ion laser tube with internal gas return bores.
05 p0586 A73-17263
- Design, manufacture and performance of Eole satellite computer core memory, noting circuit reliability and testing
07 p0796 A73-18959
- Reliability of thin nickel-chromium resistance layers deposited by sublimation under vacuum on a glass substrate
07 p0862 A73-19424
- Flawless operation probability for information transmission reliability of electronic logic circuits with binary data inputs
07 p0801 A73-20040
- A method for evaluating the circuit reliability of electronic equipment
07 p0802 A73-20299
- Design and fabrication of MOS/LSI circuits for reliability, discussing layout rules and protective circuitry
08 p0943 A73-20733

IC reliability enhancement by molded dual in-line packaging /DIP/ technique, considering mold shrinkage effects on failure rates during temperature cycling tests
08 p0944 A73-20737

Operational amplifier microcircuits intermittent failure due to input offset voltage drift, describing testing and analysis methods
08 p0944 A73-20740

Book - MOS/LSI design and application.
08 p0950 A73-21840

Cyclic binary coding and decoding circuits for high reliability data and command transmission, discussing analytical relations and design aspects
09 p1060 A73-22923

A method for the assessment of the electrical stability of TTL gates
10 p1194 A73-23995

The application of integrated magnetic devices for circuit checking and error correcting.
10 p1198 A73-24021

The quorum element and its application in the design of adaptive automatic control systems
12 p1482 A73-26758

A method for substantially improving the reliability of multistable pulse-phase-coded elements
12 p1476 A73-26761

Reliability considerations in hybrid microcircuits.
13 p1588 A73-28045

Avalanche transistor circuit with controlled S shaped I-V characteristics, discussing equivalent circuits and operating points stability
13 p1591 A73-28731

Taking into account correlation when forecasting the parameters of failure-free operation of radio equipment.
15 p1849 A73-30994

Fluidic component performance and circuit reliability.
16 p1971 A73-33475

Effect of contamination on fluoric system reliability.
16 p1971 A73-33476

The hazards of transferring loads between phases, sources and ground.
17 p2133 A73-34092

Computerized automatic microwave testing with pulse measurements of phase and power from Reliable Advanced Solid State Radar phased array modules, discussing system design
17 p2135 A73-34724

Detection of random chip defects in monolithic microcircuits.
17 p2135 A73-34732

Thin film hybrid microwave integrated circuit.
17 p2141 A73-35323

Method of estimating the circuit reliability of electronic devices.
18 p2294 A73-37136

Reliability physics 1973; Proceedings of the Eleventh Annual Symposium, Las Vegas, Nev., April 3-5, 1973.
19 p2410 A73-38438

An elusive open-circuit failure mode in thin-film chip resistors.
19 p2410 A73-38444

Torque and thermal cycling as methods of testing reliability of reflow-soldered chip-to-substrate joints.
19 p2436 A73-38445

Improve reliability of electron devices through optimized coverage of surface topography.
19 p2411 A73-38453

High-reliability plastic package for integrated circuits.
19 p2411 A73-38455

High reliability manufacturing technology for COS/MOS IC devices, discussing failure mechanisms and MIL-STD-883 and MIL-M-38510 tests for quality control
20 p2534 A73-38656

The selection of test frequencies for system fault diagnosis.
20 p2586 A73-38802

Morphological indices of digital microelectronic structures
21 p2660 A73-40016

Computerized synthesis of optimal fault-diagnosable logical circuits capable of detecting and repairing faulty modules for circuit reliability and availability improvements
21 p2669 A73-40687

Circumvention design of active circuitry and passive shielding for electromagnetic pulse environment with application to Minuteman ICBM system
22 p2822 A73-41786

Microelectronic circuitry for monitoring stray electromagnetic energy coupled into electroexplosive device, using fiber optic transmission with photovoltaic energy conversion to eliminate wiring caused interference
22 p2822 A73-41794

Triple Modular Redundancy Single Single voter-switch with majority voting of three parallel data chan-

nels or converters, estimating reliability for short and long missions
22 p2825 A73-42294

Pulse burnout of microwave mixer diodes.
22 p2835 A73-42965

Bayes theorem for probabilistic analysis of logic circuits applied to reliability estimation of switching circuits
23 p2965 A73-44107

CIRCUITS

- NT ADDING CIRCUITS
- NT ANALOG CIRCUITS
- NT AUTODYNES
- NT BISTABLE CIRCUITS
- NT CIRCUITORS [PHASE SHIFT CIRCUITS]
- NT CLIPPER CIRCUITS
- NT COINCIDENCE CIRCUITS
- NT COMPARATOR CIRCUITS
- NT COUNTING CIRCUITS
- NT COUPLING CIRCUITS
- NT DELAY CIRCUITS
- NT DIGITAL INTEGRATORS
- NT DIPLEXERS
- NT DISCRIMINATORS
- NT ECHO SUPPRESSORS
- NT ELECTRIC BRIDGES
- NT EQUIVALENT CIRCUITS
- NT FEEDBACK CIRCUITS
- NT FIRE CONTROL CIRCUITS
- NT FLIP-FLOPS
- NT FLUID SWITCHING ELEMENTS
- NT FLUIDIC CIRCUITS
- NT GATES [CIRCUITS]
- NT INTEGRATED CIRCUITS
- NT LC CIRCUITS
- NT LIMITER CIRCUITS
- NT LINEAR CIRCUITS
- NT LOGIC CIRCUITS
- NT MAGNETIC CIRCUITS
- NT MATRICES [CIRCUITS]
- NT MICROWAVE CIRCUITS
- NT MIXING CIRCUITS
- NT MULTIVIBRATORS
- NT NEGATIVE RESISTANCE CIRCUITS
- NT OHMS LAW
- NT PHASE DETECTORS
- NT PHASE SHIFT CIRCUITS
- NT PNEUMATIC CIRCUITS
- NT POWER SUPPLY CIRCUITS
- NT PRINTED CIRCUITS
- NT RC CIRCUITS
- NT RL CIRCUITS
- NT RLC CIRCUITS
- NT SWEEP CIRCUITS
- NT SWITCHING CIRCUITS
- NT THRESHOLD GATES
- NT TRANSISTOR CIRCUITS
- NT TRIGGER CIRCUITS
- NT VARACTOR DIODE CIRCUITS
- NT WHEATSTONE BRIDGES
- NT WIRE BRIDGE CIRCUITS

Annual Allerton Conference on Circuit and System Theory, 9th, Monticello, Ill., October 6-8, 1971, Proceedings.
03 p0286 A73-14476

Constitutive equation for electronic circuits without topologically dependent variables, noting numerical analysis of equations of state for nonlinear circuits
08 p0951 A73-21551

Annual Allerton Conference on Circuit and System Theory, 10th, Monticello, Ill., October 4-6, 1972, Proceedings.
09 p1067 A73-22226

CIRCULAR CONES

Finite fringe holographic interferometry applied to a right circular cone at angle of attack.
05 p0527 A73-16528

Temperature of an emitting cone in a supersonic flow of transparent gas
06 p0646 A73-18570

Experimental and theoretical study of supersonic viscous flow over a yawed circular cone.
07 p0775 A73-19957

Supersonic-hypersonic motion around a porous circular cone
07 p0776 A73-20615

Locally similar solutions of equations of a turbulent boundary layer on a circular cone
08 p0925 A73-20646

Circular cones and cylinder drag in molecular flow, using Schamberg model of molecules/solid surface interaction
09 p1030 A73-23461

Experimental determination of the transonic flow on circular cones at angle of attack
10 p1172 A73-24496

Further studies of backscattering from a finite cone.
10 p1191 A73-24898

Radar cross section measurements for right circular cones with spherically blunted noses, presenting as functions of diameter/wavelength ratio and aspect angle
11 p1330 A73-25682

- Temperature of a radiating cone in a supersonic flow of transparent gas. 16 p1964 A73-33595
- Current distribution of a dipole antenna of revolution in dissipative media. 17 p2141 A73-35366
- CIRCULAR CYLINDERS**
- A variant of the solution of problems of fluid oscillations in cylindrical cavities by the Bubnov-Galerkin method 01 p0031 A73-10101
- An investigation of particle trajectories in two-phase flow systems. 01 p0002 A73-10439
- Boundary layer formation on hollow circular cylinder walls aligned with axial motion of incompressible rotating fluid as function of Rossby and Reynolds numbers 01 p0032 A73-10451
- Skin friction on porous surfaces calculated by a simple integral method. 01 p0057 A73-10726
- Low Reynolds number flow past a transverse cylinder at Mach two. 01 p0003 A73-10758
- Heat transfer from a circular cylinder in a rarefied gas stream. 01 p0122 A73-10761
- Stability of orthotropic circular cylindrical shells reinforced by annular ribs under external pressure 01 p0118 A73-11409
- Axisymmetric problem of the equilibrium of a cylindrical film under hydrostatic pressure 01 p0035 A73-11412
- Incompressible elastic circular cylinders quasi-equilibrated motions analysis, obtaining free and forced oscillations periods 02 p0191 A73-11573
- Bulging of a circular cylindrical shell under axial compression 02 p0231 A73-11814
- Circular cylindrical shell stability for thermal shock on end face, calculating critical thermal flux 02 p0232 A73-11818
- Linear equations for steady wave diffraction and propagation in deformable bodies in multiply connected regions, considering circular cylinders, spherical cavities and fibrous media 02 p0232 A73-11889
- Boundary value problems of thermoelastic wave diffraction in elasticity theory of multiply connected domains bounded by circular cylindrical surfaces 02 p0233 A73-11940
- Relation between plasticity characteristics and geometrical dimensions of cylindrical specimens under tension. 02 p0235 A73-12140
- Vibrations of circular cylindrical shells subjected to nonuniform initial stress. 03 p0384 A73-12984
- Thermomechanical dissipation analysis of thermoviscoelastic solids by finite elements. 03 p0389 A73-13326
- Lagrange equations of motion for ideal incompressible fluid flow under asymmetric deformation of expanding circular cylinders and spheres, calculating resistance forces 03 p0294 A73-13613
- Determination of the flow past a cylinder and a sphere in the presence of an incident shock wave 03 p0294 A73-13615
- Experimental investigation of the base pressure on slender circular cylinders 03 p0245 A73-13674
- Stress analysis of thick walled hollow viscoelastic circular cylinder enclosed in elastic shell and subjected to nonlinear creep conditions, noting temperature effects 03 p0394 A73-14021
- Natural vibration frequency spectra of circular cylindrical and spherical shells of revolution, using Bessel function 03 p0395 A73-14052
- Determination of the natural oscillation frequencies of three-layer circular cylindrical shells by a numerical method 04 p0510 A73-15081
- Numerical determination of the sound field and the characteristic frequencies in a circular enclosure by the discretization method 04 p0476 A73-15375
- A system-synthesis approach to the inverse problem of scattering by smooth, convex-shaped scatterers for the high-frequency case. 04 p0423 A73-15484
- Thermoelastic wave propagation in a transversally isotropic circular cylinder 04 p0512 A73-15501
- Elastic waves in an infinite cylinder with micropolar structure 04 p0513 A73-15502
- Elastic wave propagation in a circular cylinder subjected to finite deformation Compressible material 04 p0513 A73-15503
- Law governing the oscillations of a circular cylindrical shell of finite length containing a liquid with a variable level 04 p0434 A73-15505
- Free vibration of cantilever circular cylindrical shells - A comparative study. 04 p0513 A73-15589
- Effect of an oscillating free stream on the unsteady pressure on a circular cylinder. [ASME PAPER 72-WA/FE-12] 04 p0434 A73-15843
- Vortex induced vibration of circular cylindrical structures. [ASME PAPER 72-WA/FE-39] 04 p0404 A73-15856
- Radiation pattern of longitudinal magnetic dipole ideally conducting infinite circular cylinder parallel to infinite plane screen 04 p0429 A73-15912
- Experimental analysis of lift on a fixed cylinder subjected to a flow perpendicular to its axis at high Reynolds numbers 04 p0405 A73-15990
- Experiments on flow about a yawed circular cylinder. [ASME PAPER 72-FE-2] 05 p0527 A73-16546
- Evaluation of numerical viscosity effects in transonic flow calculations. [AIAA PAPER 73-131] 05 p0530 A73-16884
- Vibrations of circular cylinders of a perfectly conducting elastic material. 05 p0637 A73-17298
- The correspondence principle of linear viscoelasticity for problems that involve time-dependent regions. 06 p0762 A73-17992
- Scattering by nonconcentric circular plasma cylinders with axial magnetic fields. 06 p0729 A73-18204
- Small amplitude viscous similarity solution for vertical two dimensional internal wave production by circular cylindrical resonant oscillation in incompressible stratified fluid 06 p0646 A73-18527
- Cut-off frequency calculation for TE and TM modes in doubly ridged circular and elliptical microwave waveguides, using Mathieu function and eigenfunctions 06 p0669 A73-18736
- Surface wave characteristics of circular cylindrical corrugated and uniform dielectric rod excited in E sub 0-mode. 07 p0792 A73-19545
- German monograph - An iteration procedure for the calculation of planar compressible flows around circular profiles. 07 p0774 A73-19580
- Diffraction of a plane electromagnetic wave at an array of circular cylinders with a spiral slot 07 p0793 A73-19917
- Nonlinear multiple-scale solution of a cylindrical shell. 07 p0915 A73-20337
- Plastic analysis of filled, reinforced, circular cylindrical shells. 08 p01015 A73-20672
- The secondary flow about circular cylinders mounted normal to a flat plate. 08 p0926 A73-21440
- Flow parameters and cylinder elongation effects on turbulent boundary layer characteristics for compressible fluid flow, calculating velocity distribution 08 p0956 A73-21602
- Influence of various surface roughness on the natural convection. 08 p1024 A73-21639
- Axisymmetric hydroelastic sloshing in a circular cylindrical container. 08 p0956 A73-21690
- Resonant excitation of a circular cylinder with a longitudinal slit by a plane wave 09 p1048 A73-21905
- Out-of-plane force on a circular cylinder at large angles of inclination to a uniform stream. 09 p1029 A73-23124
- Circular cones and cylinder drag in molecular flow, using Schamberg model of molecules/solid surface interaction 09 p1030 A73-23461
- Numerical study of the flow of a viscous incompressible fluid around a circular cylinder 10 p1171 A73-23766
- Sound field of an infinite circular cylindrical transducer partially coated with an acoustically compliant layer. 10 p1249 A73-24187
- The initial flow past an impulsively started circular cylinder. 10 p1172 A73-24338
- Torsion of a circular-section bar weakened by two longitudinal circular-cylindrical cavities 10 p1293 A73-24702
- Visualization experiments on unsteady viscous flows around cylinders and plates. 10 p1174 A73-24836
- Unsteady two dimensional flow within circular cavity with arbitrary velocity distribution on cylinder wall, investigating recirculating flow initiation 10 p1210 A73-24838
- Velocity field determination for limitless steady boundary layer on circular cylinder and swirling flow produced by generalized vortex 10 p1210 A73-24843
- Interaction between a sound field and natural convection on a horizontal cylinder. 10 p1296 A73-24846
- Acoustic streaming and forces generated on circular cylinder in radially oscillatory incompressible fluid, considering steady and unsteady flow 10 p1174 A73-24847
- Torsion of a sectorially composite hollow circular cylindrical beam. 11 p1432 A73-24996
- Karman vortex street characteristics of single circular cylinders and heat exchanger tube bundles, presenting drag, lift and Strouhal number as function of Reynolds number 11 p1299 A73-25108
- Newton method for calculation of viscous flow around circular cylinder with Fourier series truncation for stream function and vorticity, evaluating numerical error 11 p1345 A73-25115
- Pressure distributions on circular cylinders at critical Reynolds numbers. 11 p1300 A73-25151
- Thermoelastic response of a cylinder in the generalised dynamical theory of thermoelasticity. 11 p1433 A73-25161
- The free vibrations of a thin circular finite rotating cylinder. 11 p1443 A73-26088
- Study of flow around a rotating cylindrical cylinder. 11 p1302 A73-26337
- Waves produced by a source of harmonic oscillations located in a cylindrical layer of liquid 11 p1349 A73-26468
- Axially symmetric transient wave propagation in elastic rods with nonuniform section. 11 p1447 A73-26652
- On the buckling and postbuckling behavior of thin-walled circular cylinders. [DFVLR-SONDDR-261] 12 p1550 A73-26843
- Determination of the stressed state of a circular cylindrical shell with stepwise variation in wall thickness along the generatrix under the action of a local load 12 p1552 A73-27261
- Constant cross section composite circular rod, deriving torsional stress behavior near division line intersection with rod contour from closed solution 12 p1552 A73-27368
- Effect of shroud eccentricity on suppression of flow induced vibrations. 13 p1690 A73-28059
- Transient cooling of a solid cylinder by combined convection and radiation at its surface. 13 p1704 A73-28086
- Plane electromagnetic wave diffraction by ideally conducting circular cylinder in far and bright spot zones, using Green theorem for field calculation 13 p1583 A73-28851
- Asymptotic pressure calculation of plane acoustic wave diffraction by infinitely long isotropic solid elastic circular cylinder in viscous liquid medium 13 p1583 A73-28863
- Flow visualization of two and three dimensional wall jets on circular cylinder, observing flow characteristics sensitivity to curved boundary 13 p1603 A73-29038
- German monograph on calculation of thermal and transformation stresses in long circular cylinders covering austenite-martensite transformation, thermal expansion and viscous bodies 13 p1699 A73-29284
- Refined method of determining tangential stresses and testing the strength of cylinders subjected to transverse flexure. 13 p1703 A73-29635
- Buckling of circular cylindrical shells under compression. IV - Solutions based on the modified Fluegge equations considering prebuckling edge rotations. 14 p1813 A73-30573
- The turbulent boundary layer on a long thin filament 15 p1822 A73-31197
- The effects of couple-stresses on thermal stress distributions in multiply-connected domains. 15 p1947 A73-31362
- Noncirculative MHD inviscid conducting fluid flow past circular cylinder and plane profile in magnetic field, using Fredholm equation 15 p1918 A73-31414
- Resonant excitation of a circular cylinder with a longitudinal slot by a plane wave. 15 p1847 A73-32630
- Torsion and extension of a cylinder with an outer annular cut 17 p2240 A73-34143

Axissymmetrical turbulent boundary layer along a slender cylinder.

17 p2150 A73-34400

Large amplitude forced vibrations of simply supported thin cylindrical shells.

[ASME PAPER 73-APM-Q] 17 p2249 A73-35107

On the buckling of cylinders in axial compression.

[ASME PAPER 72-APM-BBB] 17 p2250 A73-35113

On an accurate theory for circular cylindrical shells.

[ASME PAPER 73-APM-E] 17 p2250 A73-35114

Turbulent mixing of cylindrical jet with parallel stream in terms of mixing length concepts and velocity profiles

17 p2157 A73-35515

Probe compensated near-field measurements on a cylinder.

17 p2127 A73-35678

Flexural vibration frequencies of right circular cylindrical tensor gravitational wave detectors in regime with sound wavelength comparable to diameter

17 p2176 A73-35763

Numerical solutions of time-dependent incompressible Navier-Stokes equations using an integro-differential formulation.

18 p2297 A73-36159

Certain vortical flows with variable vorticity past a circular cylinder

18 p2302 A73-37009

Thermal stresses in axially connected circular cylinders.

19 p2495 A73-37435

Incompressible potential flow past axisymmetric bodies in cylindrical pipes.

19 p2376 A73-37489

Inhomogeneous yield limit effect on elastic-plastic boundary of circular cylinder in torsion, considering radial and angular dependencies

19 p2498 A73-37651

A variational principle for the laminar boundary layer theory.

19 p2421 A73-38026

Some new results for the vibrations of circular cylinders.

19 p2500 A73-38107

Heat transfer from a vibrating circular cylinder.

19 p2505 A73-38478

Using the new fundamental system of modified cylindrical functions for designing optical core fiber waveguides with cladding of finite thickness.

20 p2522 A73-38661

Design study of a glass meridian circle.

20 p2565 A73-39064

The two-dimensional slow flow of a conducting fluid.

20 p2598 A73-39340

Dynamic response of laminated composite circular cylindrical shells with freely supported or clamped edges.

20 p2621 A73-39543

The elastic layer with a cylindrical hole subjected to a nonuniform axisymmetric radial displacement.

20 p2624 A73-39566

Numerical integration method for Navier-Stokes equation of time dependent flow past impulsively started circular cylinder, calculating length of separated wake and pressure distribution

21 p2631 A73-40248

Pressure distribution and boundary layer separation measurement on circular cylinder at critical subsonic velocities for various Reynolds and Mach numbers

21 p2632 A73-40476

Mutual coupling effects in circular arrays on cylindrical surfaces Aperture design implications and analysis.

21 p2653 A73-40674

Vibration analysis of circular cylinders by holographic interferometry.

21 p2701 A73-40756

Hot-wire investigation of the steady laminar wake behind a circular cylinder.

21 p2703 A73-41117

A parallel algorithm for high subsonic compressible flow over a circular cylinder.

21 p2727 A73-41474

Electromagnetic inverse boundary conditions determination of profile and material surface characteristics of conducting circular cylindrical shape scatterer

22 p2824 A73-41834

Knudsen free molecular flow explanation of thermomagnetic torque on circular cylinder suspended in axial molecular field, noting apparatus tilt effect

22 p2842 A73-42233

E-polarized electromagnetic scattering by conducting circular cylinder coated with plasma sheath during spacecraft reentry flight under plane wave incidence

22 p2827 A73-42466

The cyclic elastoplastic torsion of the circular cylinder in the case of finite deformations

22 p2922 A73-42527

The calculation of open circular cylindrical shells with the aid of partial discretization

22 p2922 A73-42528

The Morley-Koiter equations for thin-walled circular cylindrical shells. I - General solution for symmetrical shells of uniform thickness.

[ASME PAPER 73-APMW-22] 22 p2924 A73-42884

The Morley-Koiter equations for thin-walled circular cylindrical shells. II - Solution for a line loaded cylinder with close-spaced circumferential grooves.

[ASME PAPER 73-APMW-23] 22 p2925 A73-42885

Contact pressure problem solution for circular cylindrical shell resting on circular Winklerian bases under external load in terms of Fourier expansion

22 p2928 A73-43053

Study of the steady flow of an incompressible viscous fluid around a cylinder in rotation

24 p3079 A73-45219

Study of the field of fluctuating pressures at the surface of a circular cylinder

24 p3079 A73-45220

New kind of boundary layer over a convex solid boundary in a rarefied gas.

24 p3080 A73-45453

Partial solutions of finite elasticity - Axially symmetric deformations.

24 p3154 A73-45550

CIRCULAR ORBITS

NT STATIONARY ORBITS

Circular orbit stability in restricted two body problem with secular variations, giving disturbing function secular terms to eighth order

02 p0222 A73-12710

Fabrication of a lightweight circular orbit passive radiative cooler.

03 p0329 A73-13010

Equilibrium motions of rigid spinning satellite in circular orbit around central body subject to gravitational torque

03 p0376 A73-14268

Interplanetary spacecraft transfer maneuver for hyperbolic trajectory change into eccentric orbit, using aerodynamic drag to obtain nearly circular orbit

03 p0379 A73-14571

Subsatellite point coordinates calculation for artificial earth satellites with nearly circular orbits, noting ephemeris application

05 p0613 A73-16203

Control of a maneuver involving rotation of the plane of a circular satellite orbit while ensuring passage through a prescribed point

05 p0595 A73-16426

Orbital parameters optimization of circular orbit earth satellites network for continuous earth observation, using group theory

05 p0620 A73-17004

Acoustic emission of a body moving along a circle near a sphere

08 p0988 A73-21445

Emission spectrum of a source moving along a stable circular orbit near a rotating 'black hole'

09 p1145 A73-22295

Periodic solutions of the third sort for restricted problem of three bodies and their stability.

11 p1423 A73-26068

Investigation of star orbits in stellar clusters with allowance for the disturbing force of the galaxy

12 p1538 A73-26863

Hohmann trajectories efficiency for interplanetary transfers of spacecraft between circular coplanar orbits, considering earth-Mars-earth flight and transition to parabolic trajectory

12 p1538 A73-27065

Determination of the circular orbit of an artificial earth satellite from optical observations at undetermined moments of time

12 p1547 A73-27867

Stabilization of steady motions of mechanical systems with respect to some of the variables

13 p1660 A73-29076

Energy optimal four impulse transfer maneuver with return between two moving points in circular coplanar orbits under transit time and stay duration constraints

15 p1931 A73-31230

Two dimensional nonlinear oscillations around center of mass of vehicle moving along circular orbit with magnetic damping under gravitational field and external perturbation

15 p1942 A73-31233

Asymmetrical spun satellite rotation prediction in circular orbit at 700 km in terms of perturbing moment vector function

15 p1931 A73-31235

Application of the theory of Markov processes in state estimation of dynamic systems and in control of flight-vehicle oscillations

15 p1942 A73-31239

Spatial motion of a two body cluster under the action of gravitational and aerodynamic forces

18 p2351 A73-36119

On stabilization of steady-state motions of mechanical systems with respect to a part of the variables.

19 p2459 A73-37631

The fastest transfer from one circular orbit to another under the action of a small thrust

20 p2604 A73-38990

Determination of a circular orbit for an earth satellite from optical observations at unknown times.

20 p2608 A73-39241

Utilization of tangential trajectories for lowering high-altitude elliptic orbits of artificial satellites of planets

23 p3027 A73-43265

Some useful results on initial node locations for near-equatorial circular satellite orbits.

23 p3031 A73-43837

The relativistic Roche problem. I - Equilibrium theory for a body in equatorial, circular orbit around a Kerr black hole.

24 p3138 A73-45035

Construction of particular solutions of the restricted plane circular three-body problem

24 p3112 A73-45506

CIRCULAR PLATES

Stress function for estimating mutual effects of strain and temperature fields in dynamic coupled thermoelasticity problem for thin circular plates

01 p0113 A73-10094

Nonlinear axisymmetric flexural vibration equations of a cylindrically anisotropic circular plate.

01 p0115 A73-10756

Two dimensional elasticity theory for radial crack effects on tensile stress concentration in circular elastic isotropic plate

01 p0117 A73-11092

Perturbed bifurcation and buckling of circular plates.

02 p0186 A73-11973

Experimental investigation of stresses in plates acted on by acoustic loads.

02 p0235 A73-12135

General non-linear plate theory applied to a circular plate with large deflections.

02 p0236 A73-12517

Non-linear oscillations of a nonuniform fixed circular plate.

02 p0236 A73-12519

A numerical method considering the Bauschinger effect for large deflection analysis of elastic-plastic circular plates.

02 p0236 A73-12522

Nonlinear responses for a circular plate subjected to a dynamic ring load.

03 p0388 A73-13319

Thermal stresses due to a moving heat source in a circular disk.

03 p0389 A73-13328

Stability of an idealized circular three-layer plate beyond the elastic limit

03 p0393 A73-13777

Large deflection calculation of circular and annular strain hardenable rigid plastic plates under axisymmetric load, using Kirchhoff-Love hypothesis and Tresca flow condition

03 p0394 A73-14022

Large elasto-plastic deflection of a circular plate of mild steel under cyclic loading.

03 p0396 A73-14626

Stability of thick circular plates subjected to compressive loads and finite strains

04 p0513 A73-15504

Thermal stresses in circular plates including the influence of transverse shear.

05 p0633 A73-16539

Stationary temperature field of a disk under conditions of convective heat transfer on its surface

05 p0640 A73-16775

Optimal and stiffened simply supported circular plates comparison under uniform pressure and uniform compression loads

05 p0635 A73-16976

Convergence and error estimation of Svirskii approximation method for determining circular plate deflections

05 p0635 A73-17081

High-frequency vibrations of a circular wing in the flow of an ideal fluid

05 p0636 A73-17089

Diffraction of the emission field of a horizontal dipole on a circular hole in a plane screen in the presence of a circular disk coaxial with the hole

06 p0664 A73-17716

Surface tractions, heat fluxes and body forces required for deformation of flat perforated thermoelastic circular plate into pierced spherical cap

06 p0759 A73-17757

Stress analysis for homogeneous elastic disk under continuous and concentrated load distribution

06 p0760 A73-17783

Buckling of a circular sandwich plate beyond the elastic limit

06 p0760 A73-17784

Constrained optimal design of circular plates against buckling.

06 p0762 A73-18338

Initial postbuckling behavior of optimally designed columns and plates.

07 p0908 A73-19084

Weight minimization of axisymmetric clamped plates subject to constraints.

07 p0908 A73-19092

Lateral vibration and stability relationship of elastically restrained circular plates.

07 p0913 A73-19967

Vibration of cylindrically orthotropic circular plates.

07 p0913 A73-19968

Calculation of the natural and forced vibrations of circular plates with allowance for energy dissipation in the material

07 p0917 A73-20501

Facility for studying the strength and rigidity of circular plates prepared from an anisotropic material

07 p0809 A73-20517

The stress intensity factors of a radial crack in a point loaded disc.

07 p0918 A73-20567

A theoretical study of natural convection heat transfer from downward-facing horizontal surfaces with uniform heat flux.

08 p1024 A73-21638

Axisymmetric vibrations of circular plates with stepped thickness.

10 p1291 A73-24394

Three-dimensional problem of the vibrations of a circular plate with initial stresses

10 p1292 A73-24506

Differential equations for asymmetric bending of circular sandwich plates.

11 p1445 A73-26406

Solution of the dynamic problem of thermoelasticity for a circular plate with allowance for the finite velocity of heat propagation

12 p1552 A73-27263

Stability of a nonuniformly heated circular shell

12 p1554 A73-27471

Static, vibration and buckling analysis of axisymmetric circular plates using finite elements.

12 p1555 A73-27738

Bending of a circular nonlinearly-elastic plate by a concentrated force

12 p1555 A73-27794

Stressed state of multilayer spherical vessels, cylindrical tubes and circular disks consisting of a linear viscoelastic material

13 p1690 A73-27994

Incremental solution of axisymmetric plate and shell finite deformation.

13 p1694 A73-28250

Axisymmetric vibrations of circular plates of linearly varying thickness.

13 p1695 A73-28415

Application of Pontryagin's maximum principle for minimum weight design of rigid-plastic circular plates.

13 p1696 A73-28754

Mode factor and stress concentration parameter for sudden heating of solid cylinders and disks, noting thermal stability criterion with allowance for statistical strength

13 p1703 A73-29611

Unsymmetric wrinkling of circular plates.

14 p1812 A73-30522

Stress concentration determination near a small hole on a plate in three-dimensional representation

14 p1813 A73-30682

Use of the surface of influence of the clamping couple on a circular plate for design calculation under an asymmetrical load

15 p1944 A73-30974

Poisson's Ratio and the deflection of a viscoelastic plate.

15 p1956 A73-32342

Shear waves in infinitely extended double walls with coupling rods of circular cross section. I - Shear waves in the infinitely extended disk

17 p2241 A73-34246

Transient thermal stresses in a disc of linearly strain-hardening material.

17 p2243 A73-34547

Determination of stiffness and critical loads of a circular plate from a simple bending test.

18 p2362 A73-36327

Limiting equilibrium of a circular plate with allowance for the shearing stress

18 p2363 A73-36405

Transverse bending of an annular slab with supporting ribs

18 p2367 A73-36960

Calculation of forced and free oscillations of round plates taking into account the dissipation of energy in the material.

19 p2499 A73-37776

Device for studying the strength and rigidity of round plates of anisotropic material.

19 p2418 A73-37793

The vibrations of a circular plate with uniformly distributed load around the outer periphery.

19 p2502 A73-38348

Axisymmetrical bending of circular plates and shallow spherical cupolas with allowance for physical and geometrical nonlinearities

20 p2618 A73-39310

Investigation of the free vibrations of sectorial plates and conical panels by a theoretical-experimental method

20 p2618 A73-39314

Rigid viscoplastic thin circular plate under uniformly distributed transverse pressure, deriving Mises and Tresca yield surface conditions

20 p2624 A73-39567

Antisymmetrical bending of a circular orthotropic plate of variable thickness

20 p2625 A73-39656

Buckling of continuous circular plates.

21 p2782 A73-40004

Deflection function for the asymmetrical bending of circular plates.

21 p2784 A73-40435

Stress distribution in thin circular plate with equiarmed cruciform crack, obtaining stress intensity factor and crack energy by numerical solution of Fredholm equation

21 p2785 A73-40932

Evaluation of error bounds in an optimization problem using the finite-element method.

[ASME PAPER 73-APMW-15] 22 p2924 A73-42882

Normal modes of elastically connected circular plates.

22 p2929 A73-43140

Limit loads of circular plates under combined loading.

[ASME PAPER 73-APM-G] 23 p3047 A73-44379

Dynamic bending resistance of circular piecewise nonhomogeneous rigid-plastic plates in terms of Tresca yield condition for pressure pulse loads

24 p3146 A73-44679

Transverse coupled thermoelastic vibrations of elastically supported rectangular and circular plates under nonstationary harmonic temperature field

24 p3147 A73-44682

Generalized shear stress and shearing strain rate variables for thick circular plate, using von Mises yield criterion for limit load analysis

24 p3148 A73-44895

Semicircular plate uniformly loaded over diameter and with concentrated force at arc top, determining stress distribution by complex variable and conformal mapping

24 p3148 A73-45001

Three-dimensional axisymmetric problem of a normal load concentrated on an elastic free-underface plate of constant thickness - Expression for the stresses in the vicinity of the load

24 p3149 A73-45218

CIRCULAR POLARIZATION

P, T invariance of electromagnetic interaction and the circular polarization of planetary emission

01 p0092 A73-10940

Nonlinear inverse Compton radiation and the circular polarization of diffuse radiation from the Crab nebula.

01 p0092 A73-11032

Experimental study of the inverse Faraday effect in plasmas

02 p0196 A73-11587

Circular polarization of synchrotron radiation in the presence of hydromagnetic waves.

02 p0224 A73-12739

Polarimeter search for optical circular polarization in eclipsing binaries, magnetic Ap stars, planetary nebula, Hubble and Orion nebulae, M87 and Sirius

03 p0366 A73-12939

Circular polarization of Saturn.

04 p0499 A73-15368

On the circular polarization of Sco X-1 and the adjacent sky.

04 p0501 A73-15634

Discovery of circular polarization in the red degenerate star G99-47.

04 p0502 A73-15687

Nonlinear interaction between circular coherent light and modulating electromagnetic waves in presence of quadratic electrooptical effect, noting frequency shift

04 p0459 A73-15921

The 'Paradisc' antenna - A novel technique to improve the axial ratio of a circularly polarized high gain antenna system.

06 p0676 A73-18195

Measurements of the integrated Stokes parameters of compact radio sources.

07 p0876 A73-19354

Parametric excitation of circularly polarized and Langmuir waves in a magnetized plasma.

07 p0859 A73-20197

On the long-term behaviour of the circular polarization from coronal condensation radio emission at 4.3 cm wavelength.

08 p0997 A73-20769

Radio sources with variable circular polarization, noting synchrotron radiation theory applicability

08 p1006 A73-20936

Infrared circular polarization of NML Cygni and VY Canis Majoris.

08 p1009 A73-21172

Observations of circumstellar circular polarization in four more infrared stars.

08 p1013 A73-21813

On the definitions of parameters in ferrite-electromagnetic wave interactions.

09 p1062 A73-22323

Electrically controlled microwave polarization transformer

09 p1064 A73-22675

P, T invariance of electromagnetic interaction, and circular polarization of planetary radiation.

09 p1138 A73-22735

Parametric excitation of circularly polarized and ion waves in a magnetized plasma.

09 p1131 A73-22905

Circular polarization of the emission of cosmic objects

09 p1151 A73-23329

Compton effect in charged particle under intense circularly polarized electromagnetic wave, noting application to Crab pulsar

10 p1271 A73-23485

Faraday pulsations and circular polarization of optical radiation from cosmic sources in terms of angle between interstellar dust orientation vector and galactic plane

10 p1273 A73-23709

Polarization of synchrotron radiation from relativistic Schwarzschild circular geodesics.

10 p1252 A73-24347

The circular polarization of sources of synchrotron radiation.

10 p1270 A73-24901

Kirchhoff and small perturbation methods identify in composite model calculation for rough surface electromagnetic scattering of circularly polarized wave by perfectly conducting body

11 p1329 A73-25678

Frequency dependence of circular polarization in three compact radio sources.

11 p1419 A73-25777

Jupiter radio observations at 13 cm during 1969 and 1971 oppositions for circular polarization and flux density

11 p1424 A73-26128

Twilight circular polarization due to Mie scattering, analyzing polarimeter measurements in IR and UV spectral bands

12 p1490 A73-27150

Competition between longitudinal modes in a ring laser with an anisotropic resonator.

12 p1507 A73-27508

A radiating element giving circularly polarized radiation over a large solid angle.

12 p1471 A73-27656

Offset parabolic reflector antennas linearly and circularly polarized excitations, discussing dependence on angle between dual mode feed and axis

14 p1734 A73-30212

Printed circuit meander line polarizer for converting microwaves in 1-20 GHz range from linear to circular polarization, describing construction and performance

14 p1735 A73-30221

A wide-band square-waveguide array polarizer.

14 p1735 A73-30228

Longitudinal force exerted by circularly polarized high-powered laser radiation in a dense electron plasma.

15 p1917 A73-31091

A circular waveguide 'hybrid-T' and its applications.

18 p2292 A73-36606

Faraday pulsations and circular polarization of optical radiation from cosmic sources in terms of angle between interstellar dust orientation vector and galactic plane

18 p2354 A73-36734

Circular polarized emission from solar active regions at millimeter wavelengths.

20 p2601 A73-39070

Circular polarization of light reflected from the planets

21 p2769 A73-40732

Polarization characteristics of phased arrays of elliptically polarized elementary radiators

21 p2664 A73-41082

Polarization inversions in the radio emission at 237 MHz of McMath zone 11482/Research note/.

21 p2657 A73-41495

Circularly polarized linear waveguide array.

22 p2831 A73-41843

On the observation of linear polarization of solar microwave bursts.

24 p3136 A73-44644

Parametric instability of strong circularly polarized electromagnetic wave in plasma producing relativistic electrons and backscattered light

24 p3117 A73-45459

CIRCULAR SHELLS

Prediction of the response of a cylindrical shell to arbitrary or boundary-layer-induced random pressure fields.

02 p0237 A73-12601

Bending rigidity of an inflated circular cylindrical membrane of rubbery materials.

03 p0395 A73-14183

Propagation of harmonic waves in orthotropic circular cylindrical shells.

[ASME PAPER 72-WA/APM-23] 04 p0515 A73-15893

- Roots of the circular cylindrical shell characteristic equation. 05 p0632 A73-16499
- Thin-walled pipe designs with a curvilinear axis 09 p1158 A73-22362
- Vertical circular cylindrical shells buckling under axisymmetric compressive stress due to own structural weight, using Timoshenko elastic stability theory 09 p1166 A73-23459
- Iterative method for solving some boundary value problems for the equations of an orthotropic shell of revolution 10 p1292 A73-24503
- Stresses in bonded joints of circular cylindrical shells and panels 12 p1551 A73-27182
- Large amplitude vibrations of certain deformable bodies. I - Discs, membranes and rings. 12 p1556 A73-27929
- Calculation of the low natural frequencies of clamped cylindrical shells by asymptotic methods. 13 p1696 A73-28752
- Buckling of unstiffened and ring stiffened cylindrical shells under axial compression. 13 p1696 A73-28758
- Formulation of local stability problems of shells of revolution. 14 p1810 A73-30326
- On the weight minimization of supersonic, axisymmetric circular cylindrical shells of finite length. 14 p1814 A73-30709
- Hydraulic impact in a circular cylindrical shell 15 p1860 A73-31047
- Asymptotic characteristics of the problem involving intrinsic asymmetrical vibrations of circular conical shells 17 p2241 A73-34267
- Numerical solution of problems of stability of three-layer cylindrical shells 20 p2620 A73-39503
- Optimum design of three-layer shells 20 p2625 A73-39655
- Deformation of shells with a circular axis and variable cross-section parameters 21 p2786 A73-40978
- Cylindrical circular shell vibrational frequencies, examining free surface or solid plane influence on shell natural vibrations in incompressible fluids 22 p2920 A73-42130
- Dynamic stability of transverse axisymmetric waves in circular/cylindrical shells. [ASME PAPER 73-APMW-26] 22 p2925 A73-42887
- Critical velocity for collapse of a shell of circular cross section without buckling. [ASME PAPER 73-APMW-31] 22 p2925 A73-42891
- ### CIRCULAR TUBES
- The influence of preliminary thermocycling on the high-temperature strength of austenitic steel. 02 p0180 A73-12139
- Characteristics of inversion tubes under axial loading. 03 p0396 A73-14640
- Inflation-extension and eversion of a tube of incompressible isotropic elastic material. 04 p0512 A73-15234
- Three-roll flow turning. 06 p0697 A73-17827
- Unsteady laminar flow in a pipe with arbitrarily changing flow rate. 08 p0954 A73-20867
- Velocity distribution in tubes of circular cross section 09 p1072 A73-22846
- Experimental investigation of turbulent flow structure in a circular pipe with delivery through a porous wall 10 p1204 A73-23512
- Combined axial and torsional shear of a tube of incompressible isotropic elastic material. 10 p1291 A73-24336
- Circular cylindrical tube lap joints elastic strain relations based on plane contact problem reduction to Prandtl type equation in finite-span wing theory 10 p1225 A73-24363
- Errors in the velocity-area method of measuring asymmetric flows in circular pipes. 10 p1221 A73-24861
- Karman vortex street characteristics of single circular cylinders and heat exchanger tube bundles, presenting drag, lift and Strouhal number as function of Reynolds number 11 p1299 A73-25108
- Laminar incompressible fluid steady secondary flow in circular cross section curved tube at various Reynolds numbers 11 p1346 A73-25225
- Turbulence intensity and turbulent transfer characteristics behind grids in tubes 11 p1349 A73-26431
- Rotating flow evolution in long circular tubes, deriving mathematical formulation for laminar and turbulent flow 14 p1745 A73-30296
- Hydraulic impact in coaxial cylindrical tubes 15 p1860 A73-31046
- Emission characteristics of a tube-shaped laser oscillator. 15 p1885 A73-31940
- Swirl decay in circular pipe air flow in terms of angular and axial momenta, dimensionless parameter and velocity profiles 16 p1999 A73-32825
- Thermal creep of rarefied gas in a circular tube. 16 p2039 A73-33328
- Experimental investigation of turbulent flow structure in a circular tube with expansion through a porous wall. 17 p2155 A73-35192
- On the convective diffusion in tubes of circular section 18 p2299 A73-36489
- Cylindrical Poiseuille flow and thermal creep of a rarefied gas. 18 p2300 A73-36635
- Evaluating the performance of shell-and-tube heat-exchangers. 23 p3048 A73-43299
- Helical wound composite cylindrical tube under pure bending, determining elastic response from boundary value problem solution 23 p3041 A73-43637
- Some important aspects in testing high-modulus fiber composite tubes in axial tension. 23 p2996 A73-43639
- Post-yielding behavior of torsionally loaded composite tubes. 23 p3041 A73-43640
- Laminar flow of a viscous barotropic gas through a circular pipe 23 p2968 A73-43721
- ### CIRCULATION
- NT ATMOSPHERIC CIRCULATION
- NT BLOOD CIRCULATION
- NT BRAIN CIRCULATION
- NT CARBOXYHEMOGLOBIN
- NT CONGESTION
- NT CORONARY CIRCULATION
- NT INTRACRANIAL CIRCULATION
- NT INTRAVASCULAR SYSTEM
- NT ISCHEMIA
- NT OCULAR CIRCULATION
- NT PERIPHERAL CIRCULATION
- NT PULMONARY CIRCULATION
- Experimental determination of the structure of plants with recycling 07 p0805 A73-20045
- Experimental method for structure identification in nonlinear objects with recycling processes 11 p1342 A73-26082
- The application of circulation control aerodynamics to a helicopter rotor model. 17 p2104 A73-35055
- [AHS PREPRINT 704]
- Ideal resonance problem for dynamic system of N degrees of freedom, obtaining global solution covering libration and circulation regimes under normality condition 24 p3141 A73-45287
- ### CIRCULATORS [PHASE SHIFT CIRCUITS]
- Nonreciprocal circulator coupled reflection type microwave amplifier gain and stability characteristics, presenting scattering matrix and signal flow diagram 06 p0673 A73-17590
- On the theory of the avalanche transit-time diode reflection amplifier. 06 p0678 A73-18838
- Design and manufacture of delay equalized comb-line filters. 10 p1193 A73-23608
- Microwave integrated circuit applications at special microwave devices operation. 15 p1851 A73-32274
- Microstrip junction circulators with fixed ferrite disks, achieving broadband impedance matching between center conductor and transmission line by transformer on alumina substrate 20 p2538 A73-39668
- ### CIRCULATORY SYSTEM
- NT AORTA
- NT ARTERIES
- NT BLOOD VESSELS
- NT CAPILLARIES [ANATOMY]
- NT GLOMERULUS
- NT VASCULAR SYSTEM
- NT VEINS
- Computerized ECG interpretation system for heart and circulatory disorder detection and diagnosis and health screening 03 p0272 A73-14660
- Effect of stimulation of certain hypothalamic structures on systemic and pulmonary circulation 21 p2637 A73-40282
- Morphometry of the human pulmonary arterial tree. 21 p2638 A73-40639
- ### CIRCUMPOLAR WESTERLIES
- Relation between the intensity of the stratospheric circumpolar vortex and the accumulation of ozone in the winter hemisphere. 23 p2977 A73-43905
- ### CIRCUMSTELLAR MATTER
- U STELLAR ENVELOPES
- ### CIRRUS CLOUDS
- Light scattering by cirrus cloud layers. 01 p0038 A73-10376
- Particle size spectra measurement in cirrus generating cells, deriving particle concentration, crystal length, ice water content, reflectivity and precipitation rate 02 p0189 A73-12784
- Transfer of solar irradiance through cirrus cloud layers. 11 p1357 A73-26345
- Cirrus-contrail cloud spectra studies with the Sabreliner. 17 p2206 A73-35579
- Airborne remote sensing of cloud particle size and shapes via IR polarimeter, obtaining polarization vs phase angle curve for thick tropical cirrus clouds 20 p2567 A73-39859
- Combined lidar and radiometric measurements of cirrus clouds for IR emissivity, optical thickness and albedo 23 p3003 A73-43600
- Nimbus 5 satellite-borne selective chopper radiometer (SCR) for remote sounding of stratospheric temperature, water vapor and cirrus clouds 23 p2978 A73-43952
- ### CIVIL AVIATION
- NT A-300 AIRCRAFT
- Illegal seizure of aircraft 01 p0124 A73-10650
- Summary of navigation aids to civil aviation - Current state and prospects 02 p0190 A73-11851
- Review of radio navigation of civil aircraft - Current and future outlook 02 p0191 A73-12015
- Realistic pilot training and aircraft handling qualities in pilot error risk minimization for military, commercial and general aviation 05 p0545 A73-16733
- Supersonic transportation inauguration by Concorde, discussing technological, economic and environmental aspects [AIAA PAPER 73-16] 06 p0646 A73-17609
- Military contributions to civil aviation. [AIAA PAPER 73-67] 06 p0647 A73-17635
- Book - Aviation law: Cases and materials. 06 p0771 A73-17870
- Civil aviation medicine in the coming decade. 07 p0785 A73-19484
- Renal lithiasis among civil operating aircrew 08 p0931 A73-21536
- Proteinuria and civil aviation aircrew 08 p0931 A73-21538
- Formula-one air racing history, aircraft designs and characteristics and low cost amateur constructions 08 p0928 A73-21689
- Book - Civil aviation development - A policy and operations analysis. 08 p1026 A73-21837
- Flight research to develop airworthiness standards for civil aircraft. 09 p1031 A73-22184
- Russian book on multichannel magnetic tape recorders in civil aviation ATC for speech communication monitoring and preservation covering design and operation principles 09 p1086 A73-23245
- Civil transport aircraft future design trends, discussing subsonic, supersonic, hypersonic and V/STOL aircraft, engine design, fuels and noise reduction 10 p1174 A73-23682
- The DOT/NASA Civil Aviation Research and Development Policy Study. 10 p1298 A73-24552
- Transportation safety - Technology applications: A systems approach to anti-hijacking. 10 p1298 A73-24559
- Commercial air transportation projections, discussing mass transportation, international fare structure and exchange of rights, security and technology 10 p1298 A73-24646
- An international review of civil aircraft damaged or destroyed by deliberate detonation of explosives /sabotage/ 1964-1972. 10 p1176 A73-24708
- Civil aviation medicine functional standardization and expansion, emphasizing preventive medicine, health education and operational safety 10 p1185 A73-24718
- Russian book - Network planning and control of air transportation. 10 p1298 A73-24924
- Regional airport systems study for San Francisco bay area, discussing commercial and general aviation future needs, environmental and economic aspects and alternative options 11 p1454 A73-26125
- Regularization of the legal status of international air charter services. 11 p1454 A73-26349

U.S., UK and French research programs on conditions encountered by civil aviation and supersonic transports in stratosphere

11 p1455 A73-26594

General aviation requirements within National Aviation System, discussing basic services, facilities, federal spending and R and D

12 p1459 A73-27361

An appraisal of the funding provisions of the Airport and Airways Development Act of 1970 to implement system improvements.

12 p1561 A73-27366

Airport and Airway Development Act trust fund surplus, discussing expenditure policy determination and incentive plan provisions to expedite improvements

12 p1561 A73-27367

Airline pilots problems in terms of job security, working conditions, management relations, public relations, flight safety due to noise abatement rules, etc

12 p1562 A73-27599

The provision of ground station facilities for an aeronautical satellite system.

12 p1471 A73-27658

Civil aircraft vertical plane navigation and guidance during climb and descent, discussing atmospheric, performance and passenger comfort constraints on flight path selection

13 p1656 A73-28075

Projections of the U.S. airline fleet in the early 1980's.

13 p1569 A73-29102

Conference on General Aviation-Business Flying, University of Tennessee, Tullahoma, Tenn., August 17-19, 1972, Proceedings.

13 p1570 A73-29344

General aviation aircraft technology developments based on military and transport aircraft design, considering cost, complexity and reliability

13 p1570 A73-29348

Air transport and commercial aviation developments, including revenues, passenger traffic statistics, charter flights and fare levels

13 p1709 A73-29383

Commercial air transportation in France - National administration and aviation enterprises

14 p1818 A73-30294

Progress report on Tel Aviv offshore airport project.

15 p1857 A73-31544

Electronics and civil aviation; International Conference, Paris, France, June 26-30, 1972, Reports. Volumes 1 & 2

15 p1908 A73-32426

Automated system of mixed /civil and military/ control

15 p1847 A73-32444

Commercial airline operational control, discussing flight plan approval by pilot and ground personnel, preflight duties, weather information assessment and fuel monitoring

15 p1909 A73-32446

French civil aviation inexpensive C band landing system with ILS angular coding and simplified on-board equipment for STOL and Alpine airports

15 p1910 A73-32467

Pulse coded scanning beam microwave landing system technology assessment for civil aviation application, describing ground equipment and procedures

15 p1910 A73-32469

Air traffic control technology progress review and future forecast, noting microelectronics and automation need in civil avionics

15 p1960 A73-32479

Limitations in the use of all-electric systems for vital application in civil aircraft.

15 p1852 A73-32492

Training simulator for civil aviation schools

15 p1859 A73-32511

Role of the Juridical Committee of the International Civil Aviation Organization in the elaboration of air law

15 p1960 A73-32551

History, evolution, and role of the Civil Aviation Secretariat General

15 p1960 A73-32554

Civil aviation research patterns, discussing effects of nonregular carrier competition and Boeing 747 introduction

15 p1859 A73-32557

International regional rental system for air transportation ground installations and route services, discussing ICAO recommendations

16 p2087 A73-32971

Air piracy suppression measures adopted 23 September 1971 at Montreal international convention, discussing prevention and punishment provisions

16 p2087 A73-32972

Charters, the new mode - Setting a new course for international air transportation.

16 p2087 A73-33101

Skyjacking - Its domestic civil and criminal ramifications.

16 p2087 A73-33102

Future technology and economy of the VTOL aircraft; International Helicopter Forum, 10th, Bueckeburg, West Germany, June 5-7, 1973, Proceedings

17 p2098 A73-34251

Turboshaft engine for 5-8 passenger single and twin engine commercial helicopter, discussing cost reduction design emphasis, gearbox module and particle separator

17 p2220 A73-34253

Ground visual aids for civil STOL aircraft steep gradient approach and blind landing, discussing flight trials and simulator experiments

[RAE-TM-AVIONICS-136/BLEU/]

17 p2208 A73-34489

Separate surfaces for automatic flight controls.

[SAE PAPER 730304]

17 p2101 A73-34665

An airline view of the future of auxiliary power systems.

[SAE PAPER 730379]

17 p2108 A73-34718

An automatic system for broadcasting weather data to international civil aviation

17 p2122 A73-34962

Civil aviation environmental and economic aspects, discussing noise and air pollution, fuel consumption and airspace and ground space utilization

18 p2267 A73-36685

International Civil Aviation standards concerning rights and duties of appointed observers at inquiry by state of aircraft accident occurrence

19 p2505 A73-37737

ICAO meeting reports on international aircraft accident investigation, onboard data recording, inquiry process and low-safety interface

19 p2506 A73-37738

Noise and pollution - The Federal Aviation Administration's views.

19 p2384 A73-37812

VTOL applications in civil aviation, discussing safety, noise reduction, fatigue life, industrial applications, economic factors, short haul utilization and wind tunnel tests

19 p2384 A73-37813

U.S.S.R. laws and regulations regarding civil air transport equipment operations and maintenance, considering personnel training and safety

19 p2435 A73-38119

Aerosat program for civil aviation needs established by Seventh Air Navigation Conference of ICAO, discussing airborne equipments specification development

[AAS PAPER 73-120]

20 p2520 A73-38581

Book - Aircraft hijacking and international law.

20 p2629 A73-39138

Discourse on comparisons between commercial and military aircraft logistics.

20 p2629 A73-39274

Public air transportation service needs for nonurban areas, considering low traffic density problem, operational requirements and future trend

[ASME PAPER 73-ICT-72]

23 p3050 A73-43498

The development of civil air navigation in the People's Republic of China - Agreements with other states as well as the tasks and the position of the China Civil Aviation Corporation /CAAC/

24 p3159 A73-45346

CL-84 AIRCRAFT

Suitability of the CL-84 tiltwing aircraft for the sea control ship system.

[SAE PAPER 720852]

05 p0534 A73-16660

CLADDING

Stress varied creep of 20Cr-25Ni-Nb stabilised austenitic stainless steel.

08 p0981 A73-21788

Small-scale explosion seam welding.

10 p1223 A73-23626

Metal cladding lubricants tests with powdered lead, copper, zinc, iron, silver and bearing alloys fillers for friction and wear reduction

10 p1239 A73-24249

Using the new fundamental system of modified cylindrical functions for designing optical core fiber waveguides with cladding of finite thickness.

20 p2522 A73-38661

CLAMPS

Use of the surface of influence of the clamping couple on a circular plate for design calculation under an asymmetrical load

15 p1944 A73-30974

CLARK Y AIRFOIL

U AIRFOIL PROFILES

CLASSIC AIRCRAFT

U IL-62 AIRCRAFT

CLASSICAL MECHANICS

NT ASTRODYNAMICS

NT CELESTIAL MECHANICS

NT KEPLER LAWS

NT ORBITAL MECHANICS

Classical mechanics and field theory derivation based on material points motion in space, discussing space-time metric, electromagnetic and gravitational fields and quantum mechanics

01 p0076 A73-10599

Entropy supply for classical and relativistic heat conducting fluids, assuming linearity for momentum and energy supplies

13 p1704 A73-28286

Spontaneous-emission feedback in a three-level quantum system - A case of conflict between semi-classical and quantum theories of radiation.

13 p1659 A73-28375

Deformable solid as discretized body in classical continuum mechanics, deriving motion and constitutive equations

13 p1659 A73-28558

Classical mechanics-quantum mechanics relations and analogies, considering symmetry groups, Casimir invariants, energy levels and quantization

14 p1774 A73-30239

Dolapchiev-Mangeron-Tsenov analytical mechanics equations extension to potential force systems, applying to electric charge motion in electromagnetic field

16 p2035 A73-32681

Automatic control theory and systems representation in framework of unilateral mechanics, using canonical elastodynamic and elastostatic equations

20 p2540 A73-38703

Ehrenfest equations for thermostatic equilibrium in classical body second order phase changes using caloric equations of state, relating specific heat discontinuities and equilibrium manifold

22 p2885 A73-41737

Dynamical symmetries of the Kepler problem and of the harmonic oscillator in classical mechanics revisited.

22 p2887 A73-42429

Differential and integral formulations of variational principles in mechanics, discussing Hoelder-Voss, d'Alembert-Lagrange, Gauss and Jourdain principles

24 p3110 A73-45246

Ergosphere concept extended to classical mechanics from relativistic black hole mechanics

24 p3142 A73-45341

CLASSIFICATIONS

NT HIERARCHIES

NT INDEXES [DOCUMENTATION]

Interactive pattern analysis and classification systems - A survey and commentary.

01 p0021 A73-11477

Pattern classification in scan-type nondestructive tests.

04 p0447 A73-14928

Origin, classification, nomenclature and incidence of the atrial arteries in normal human hearts, with special reference to their clinical importance.

04 p0409 A73-15522

Numerical classification and coding of electrocardiograms.

04 p0412 A73-15647

Extragalactic objects state of knowledge including galaxy definition and classification systems and quasar characteristics

05 p0614 A73-16307

Mean vector and covariance matrix estimation for training class sample statistics updating in pattern recognition, applying to crops or any category of objects

08 p0984 A73-21668

Automatic classification of G5-K5 stars by means of 166 A/mm objective prism spectra /4000-4550 A/.

12 p1538 A73-26858

A preliminary classification scheme for interstellar absorbing clouds.

15 p1933 A73-31309

Multivalued solutions and the classification principle for nonlinear differential equations

17 p2200 A73-34628

Automatic analysis and classification of electroencephalograms

17 p2116 A73-34966

Analysis of methods for selecting significant attributes in the classification of patterns

20 p2532 A73-38999

The problem of structural analysis of a wave gear

21 p2708 A73-41198

MK spectral classification system validity, discussing standards for O4-G2 spectral range and limits in visual spectral classification

21 p2771 A73-41236

Carbon star classification problems in effective temperatures, luminosities and radii, considering mass measurement, surface gravity, chemical composition, model atmospheres, stellar evolution, etc

21 p2772 A73-41240

The east-west asymmetry in the number of spot-groups in relation to their classification.

21 p2777 A73-41488

CLASSIFIERS

Hybrid techniques for automatic imagery interpretation.

16 p2016 A73-33367

Adaptive multispectral scanner recognition via maximum likelihood classifier for agricultural crops, discussing error sources

20 p2559 A73-39877

CLASSIFYING

A model for the automatic classification of signals with applications for the automatic language recognition

06 p0663 A73-17591

The problem of elaboration and classification of observational material for one-apparition comets.

14 p1790 A73-29793

Orbital classification for short period comets based on minimum approach distances to respective planets

14 p1794 A73-29833

Automatic cataloging of electrocardiographic patterns

17 p2116 A73-34965

Unsupervised maximum likelihood classification technique multispectral remote sensing data, using two-part statistical clustering technique of sequential variance analysis

20 p2559 A73-39879

Remotely sensed multispectral scanner data collection over agricultural area, discussing spatial resolution modification for crops and unresolved objects classification

20 p2559 A73-39882

CLATHRATES

Icy conglomerate cometary nucleus models, discussing clathrates role in comet condensation from solar nebula

04 p0494 A73-14752

CLAYS

NT KAOLINITE

Ultrafiltration by a compacted clay membrane. I - Oxygen and hydrogen isotopic fractionation. II - Sodium ion exclusion at various ionic strengths.

23 p2973 A73-43845

CLEAN ROOMS

Clean rooms and contamination-free zones in space technology

07 p0830 A73-19011

CLEANING

Oxygen plasma for cleaning polymerized organic material contaminated oil-pumped channel electron multiplier arrays used as vacuum UV to visible radiation converters

01 p0054 A73-11237

Cleaning and activation of beryllium-copper electron multiplier dynodes.

02 p0146 A73-11966

Laundrying in space - A summary of recent developments.

19 p2401 A73-37990

CLEAR AIR TURBULENCE

Bistatic-radar detection of high-altitude clear-air atmospheric targets.

02 p0142 A73-12526

Meteorological structure of thin clear air scatter layers observed by ultra-high resolution radar.

03 p0338 A73-14529

High power radar for measurement of refractivity inhomogeneities in clear air turbulence from backscattered energy Doppler shift

03 p0338 A73-14530

Doppler radar measurements of the velocity field associated with a turbulent clear air layer.

03 p0338 A73-14532

Life cycle of brief CAT episodes determined by mesoscale analysis.

03 p0338 A73-14533

CAT association with Kelvin-Helmholtz wave structures in baroclinic zone, correlating meteorological radar and aircraft observations

03 p0339 A73-14534

An analysis of coexistent waves and turbulence near clear air echoes.

03 p0339 A73-14535

Intensive probing of clear air convective fields by radar and instrumented drone aircraft.

03 p0339 A73-14542

Radar echo in clear air convection shown due to backscattering from fine refractivity fluctuations caused by turbulent mixing

03 p0380 A73-14543

Internal gravity wave-atmospheric wind interaction - A cause of clear air turbulence.

04 p0473 A73-15071

Remote CAT detection by IR scanning of atmospheric temperature profiles, discussing flight tests design and results

04 p0450 A73-15767

Turbulence variations during the high altitude clear air turbulence/HICAT/program.

07 p0847 A73-19190

Intensive probing of a clear air convective field by radar and instrumented drone aircraft.

10 p1245 A73-23989

Mountain waves and CAT encountered by the XB-70 in the stratosphere.

11 p1394 A73-25785

Experimental determination of two-dimensional spatiotemporal power spectra of stellar light scintillation - Evidence for a multilayer structure of the air turbulence in the upper troposphere.

12 p1521 A73-27120

Observation of Kelvin-Helmholtz billows and their mesoscale environment by radar, instrumented aircraft, and a dense radiosonde network.

13 p1652 A73-28268

Radar echo from a 'clear sky' in the decimeter radio wave range

13 p1585 A73-29156

Stratospheric mixing estimated from high altitude turbulence measurements.

[AIAA PAPER 73-497] 16 p2005 A73-33539

Low level wind shear and clear air turbulence effects on flight safety and aircraft accidents

17 p2098 A73-34084

Relation between turbulence in a clear sky and the evolution of the baric field

17 p2204 A73-34543

Determination of statistics of turbulence in clear air

18 p2332 A73-36687

Modular building block microwave landing system for automatic flight in CAT, discussing ICAO and NIAG missions

19 p2450 A73-37495

Survey of clear air turbulence detection methods.

19 p2430 A73-37822

Radar and sodar probing of waves and turbulence in statically stable clear-air layers.

19 p2405 A73-38204

Satellite radiances and clear air turbulence probabilities.

19 p2448 A73-38218

Optical and millimeter line-of-sight propagation effects in the turbulent atmosphere.

19 p2405 A73-38220

Clear air turbulence mesoscale history from sequential analysis of rawinsonde stations network observed data

21 p2728 A73-40057

Internal gravity wave-mean wind interaction.

23 p3000 A73-43339

CLEARANCES

Technological and structural design ensuring optimum clearance and aerodynamic coupling of moving units /wing-aileron or aileron-trim tab/

02 p0129 A73-11648

Inspection of fir-tree roots of gas-turbine rotor blades

05 p0578 A73-17025

A theory for rectangular wings with small tip clearance in a channel.

15 p1821 A73-31120

Leakage and frictional characteristics of turbulent helical flow in fine clearance.

17 p2152 A73-35001

[ASME PAPER 73-FE-1] Influence of clearances on the behavior of a gyroscope on a vibrating base

19 p2428 A73-37188

Blade tip clearance loss between centrifugal impellers and shrouds during two dimensional viscous laminar flow, discussing energy dissipation and pressure and temperature distribution

19 p2474 A73-38417

CLEAVAGE

Premature and delayed fractures of high strength martensitic steels with graduated carbon contents, including brittle and ductile intercrystalline and transcrystalline cleavage fractures

06 p0705 A73-17848

Determining the technical cohesive strength of polycrystalline metals from the internal energy.

09 p1106 A73-23158

Brittle cleavage crack propagation in crystals in terms of bonds acting between pairs of atoms, considering stress distribution around crack tip

11 p1409 A73-25812

The nature of slated cleavage planes in pressed VAD 23 alloy

12 p1511 A73-26915

Body centered cubic lattice transition metals favored cleavage plane prediction for crack propagation

13 p1635 A73-28261

Cleaved Si and Ge surfaces roughness investigation by low energy electron diffraction, electron microscopy and optical reflection technique

13 p1668 A73-28452

Molybdenum bicrystals mechanical properties dependence on mismatch angle under bending with torsion and brittle cleavage under critical stresses

17 p2189 A73-34636

Fracture toughness, ductility and cleavage mechanisms of crack extension in structural materials

19 p2502 A73-38550

Anisotropy of low-temperature plasticity and the tendency of deformed molybdenum toward exfoliation

20 p2578 A73-39377

Cleavage fracture in alpha phase Ti, considering embrittling species effects on electronic band structure

20 p2578 A73-39490

CLIMATE

Russian book on aircraft natural-climatic environmental factors covering geographic region adverse effects on design, performance and maintenance

09 p1031 A73-22349

Astroclimatic, site, calibration and atmospheric optics conditions for large telescope observations on M. Maidanak

21 p2769 A73-40729

Climatic change on Mars.

21 p2773 A73-41301

Semiempirical time dependent climate models formulated for stability of asymptotic steady state equilibrium solutions to perturbations

22 p2883 A73-42540

CLIMATOLOGY

NT BIOCLIMATOLOGY

NT MICROCLIMATOLOGY

A detailed radiation model for climate studies - Comparisons with a general circulation model radiation subroutine.

01 p0039 A73-10393

Use of space techniques in the detection and monitoring of climate parameters and air pollutants

[DGLR PAPER 72-081] 02 p0188 A73-11668

Climatic impact assessment for high-flying aircraft fleets.

04 p0436 A73-14672

Cloudiness as a global climatic feedback mechanism - The effects on the radiation balance and surface temperature of variations in cloudiness.

05 p0591 A73-16187

Numerical tests of atmospheric circulation and climate theory and accuracy conditions for atmospheric models, noting temperature dependence on radiative and nonradiative heat transfer

05 p0593 A73-16242

Climatic presentations for short-range forecasting based on event occurrence and recurrence profiles.

06 p0720 A73-18707

Stratospheric aerosol measurements with implications for global climate.

[AD-759856] 08 p0984 A73-21041

A climatological analysis of oscillations of Kelvin wave period at 50 mb.

08 p0984 A73-21377

Blocking situations lasting less than five days over the Euro-Atlantic region in the 20-year period from 1951 through 1970

08 p0986 A73-21486

Cometary collision energy triggering of catastrophic changes in climate, geological period terminations and lava flow initiation, noting tektite-geologic period ages correlation

10 p1275 A73-23823

Solar radiation climate correlation with long term sunshine records, comparing radiation measurements with predictions based on regression equations for Brisbane area

10 p1269 A73-24450

U.S., UK and French research programs on conditions encountered by civil aviation and supersonic transports in stratosphere

11 p1455 A73-26594

Northern Hemisphere climatic trend from monthly atmospheric temperature and water vapor content calculations over five year period, noting humidity decrease and cooling

11 p1358 A73-26663

Global climatic model based on time and space averaged thermodynamic energy equation for idealized land-water distribution, allowing for continents-oceans seasonal interactions

12 p1519 A73-26801

A 4-year experiment in long-range weather forecasting, using circulation analogues.

13 p1653 A73-28740

Problems and methods of simulating the environment; Annual Meeting, Karlsruhe, West Germany, September 27-29, 1972, Reports

16 p1997 A73-33376

Environmental damage avoidance via climatic and mechanical factors simulation tests for vibration, humidity, temperature, sunlight, rain, salt spray, shock and altitude

16 p1997 A73-33377

Climate simulation via environmental test chambers examining mechanical, thermal and pressure effects to determine functional component suitability

16 p1997 A73-33382

Simulated weather records experiment for polluted atmosphere effects on climatic change, using numerical circulation model

[AIAA PAPER 73-537] 16 p2007 A73-33568

Dynamic climatology in the light of satellite information /1973 Harry Wexler Memorial Lecture/.

17 p2204 A73-34375

The effect of large-scale eddies on climatic change.

17 p2160 A73-34851

Satellite monitoring of climate parameters, discussing energy transfer in atmosphere, energy distribution, radiation balance, climatic models

17 p2205 A73-34928

All-Union Meteorological Conference, 5th, Leningrad, USSR, June 21-25, 1971, Transactions. Volume 1 - General information, resolutions and plenary reports. Volume 2 - Weather prediction section. Volume 3 Climate section. Volume 4 - Section on seeding effects on atmospheric processes

18 p2331 A73-35905

- Analysis of atmosphere circulation and climate fluctuations in different portions of the Northern Hemisphere of the earth
18 p2331 A73-35913
- Climatological studies based on satellite data, including cloud, snow and ice cover, wind measurement, convection currents, temperature fields and earth thermal balance
18 p2331 A73-35914
- Problems associated with automation of the checking and processing of meteorological and climatological data
18 p2332 A73-35916
- Polar albedo changes and its climatic consequences.
18 p2307 A73-36028
- New evidence for effects of variable solar corpuscular emission on the weather.
21 p2755 A73-40073
- Book - Atmospheric circulation systems and climates.
21 p2732 A73-41440
- Use of space techniques for the determination and monitoring of climate parameters and air contaminants
23 p3003 A73-43780
- Global climatological ozone changes in terms of secular, annual and sunspot cycle-related variability
23 p2974 A73-38588
- Provisional climatology of most probable wind for application to low latitude operational weather analysis and forecasting, based on ATS-3 observed low level winds
23 p3004 A73-44262
- Climatic means finite time average estimation standard error calculation by stochastic model with application to long range forecasting
23 p3004 A73-44264
- CLIMBING FLIGHT**
Glider soaring flight energy budget analysis, discussing rate of climb indicator error compensation
08 p0968 A73-21656
- Maximum range flight path during climb with specified fuel supply and variable lift coefficient, solving differential equations system by conjugate gradient procedure
10 p1175 A73-24542
- Civil aircraft vertical plane navigation and guidance during climb and descent, discussing atmospheric, performance and passenger comfort constraints on flight path selection
13 p1656 A73-28075
- Recent advances in aircraft noise reduction.
13 p1570 A73-29104
- CLINICAL MEDICINE**
Three channel FM telemetry system for long term EEG monitoring, discussing routine clinical operation results
03 p0271 A73-14298
- Clinical electrocardiographic and vectorcardiographic diagnosis of left posterior subdivision block, isolated or associated with BBBB.
04 p0409 A73-15200
- Origin, classification, nomenclature and incidence of the atrial arteries in normal human hearts, with special reference to their clinical importance.
04 p0409 A73-15522
- Computer-aided ECG analysis and research in a clinical setting.
04 p0412 A73-15648
- Clinical diagnosis of angina pectoris, implicating obstructive disease of coronary arteries and effects of paroxysmal events on heart rate and blood pressure
05 p0542 A73-17277
- The visual system: Neurophysiology, biophysics, and their clinical applications: Proceedings of the Ninth Symposium, Brighton, England, July 1971.
13 p1574 A73-28351
- Theoretical models of the generation of steady-state evoked potentials, their relation to neuroanatomy and their relevance to certain clinical problems.
13 p1574 A73-28354
- A clinical method for obtaining pattern visual evoked responses.
13 p1575 A73-28357
- A rapid method for frontal plane axis determination in scalar electrocardiograms.
14 p1721 A73-30063
- The application of aerospace technology to patient monitoring.
16 p1975 A73-32804
- Modeling, instrumentation and data evaluation in clinical electroretinography, discussing Fourier analysis of sinusoidal light stimulation response in normal and abnormal humans
17 p2117 A73-35359
- The clinical causes and mechanisms of intraventricular conduction disturbances.
18 p2274 A73-36524
- Mid- and late changes in the QRS complex.
18 p2274 A73-36528
- The pathogenesis and clinical significance of primary T-wave abnormalities.
18 p2274 A73-36529
- Clinical manifestations of acute myocardial infarction.
18 p2275 A73-36543
- Evaluation, diagnosis and treatment of common structural complications of acute myocardial infarction.
18 p2276 A73-36548
- Clinical applications of spectral analysis and extraction of features from electroencephalograms with slow waves in adult patients.
21 p2638 A73-41011
- Early diagnosis of coronary heart disease; Proceedings of the Second Paavo Nurmi Symposium, Porvoo, Finland, September 9-11, 1971.
22 p2808 A73-42826
- Mechanisms of hyperlipidaemias in different clinical conditions.
22 p2809 A73-42832
- Clinical psychology diagnostic methods in military aviation medicine, considering neurotic symptoms and psychosomatic disorders in flight fitness examinations
22 p2817 A73-43129
- CLIPPER CIRCUITS**
Signal extraction from channel with noise- and signal-like interferences, analyzing clipping effect on SNR in time averaging processor
21 p2650 A73-40452
- CLOCK PARADOX**
Hafele calculations for jet-borne Cs beam clock difference from ground clock indicated and generalized to rotating frames of reference
07 p0825 A73-20282
- Sagnac effect on clock synchronization of two clocks moving under equal equatorial westward and eastward velocities
11 p1398 A73-25860
- Airborne clock change from synchronized stationary clock after circumnavigation of earth, discussing directional dependence
13 p1660 A73-28922
- The rod contraction-clock retardation ether theory and the special theory of relativity.
21 p2739 A73-40622
- Experiments to determine satellite orbit geometry in spherically symmetric gravitational field, discussing aging asymmetry in clock paradox
21 p2739 A73-40623
- Unaccelerated-returning-twin paradox in flat space-time.
23 p3006 A73-43608
- CLOCKS**
NT ATOMIC CLOCKS
NT CHRONOMETERS
Clock comparisons by short wave, ULF and VLF signals, Loran C and Omega methods, onboard aircraft atomic clocks and TV synchronizing pulses
03 p0307 A73-13246
- Navigation system time dissemination and synchronization, considering timing offset estimation for like events at geographically separated locations and clock characteristics for airborne application
14 p1726 A73-29896
- Guidance of aircraft according to techniques of trajectory plotting with a clock
15 p1911 A73-32489
- COS-MOS applications to clock and watch, automotive, aerospace and military, industrial and consumer markets
20 p2533 A73-38654
- Errors on the dial of cosmic clocks
21 p2701 A73-40728
- Techniques for decreasing power and increasing legibility of electronic watches.
22 p2863 A73-43101
- CLOSE PACKED LATTICES**
Sn suppression of Al-Cu-Sn alloy aging at low temperatures, relating to Cu solubility decrease in alpha phase
02 p0179 A73-11599
- Stacking faults in alpha titanium alloys
03 p0327 A73-13977
- Environmental hydrogen embrittlement of an alpha-beta titanium alloy - Effect of hydrogen pressure.
06 p0713 A73-18769
- Thermal-activation parameters of plastic deformation in alpha-titanium single crystals
09 p1099 A73-21964
- Determination of hydrogen permeation parameters in alpha titanium using the mass spectrometer.
09 p1102 A73-22412
- Importance of slip mode for dispersion-hardened beta-titanium alloys.
10 p1235 A73-24441
- Alpha phase lattice constant curves and composition effects of Cr-Ni-Co-Mo steels on microstress rate reduction during age hardening
12 p1509 A73-26840
- The nature of the nonuniformity of the structure and properties of semiproducts pressed from titanium and its alpha-alloys
12 p1502 A73-26909
- Solubility of vanadium and tungsten in alpha and gamma phases in the Fe-V and Fe-W binary systems
12 p1513 A73-27683
- Monotonic and cyclic prestrain influence on alpha-Ti fatigue life, suggesting twin/grain boundary dislocation interactions
13 p1640 A73-29486
- Influence of alloying on the phase composition and properties of maraging stainless steels
13 p1644 A73-29647
- Anomalous creep behavior of crystal bar alpha-Zr during dynamic strain aging at 723-823 K as function of temperature, stress and oxygen content
14 p1760 A73-30626
- Alpha phase decomposition and precipitation measurement in titanium rich Ti-Al alloys by electrical resistivity and microscopic methods
14 p1761 A73-30638
- Influence of alpha- and beta-stabilizers on the plastic deformation mechanism of titanium
14 p1765 A73-30888
- Al addition effect on strength of Ti via short range order, considering strengthening by alpha stabilizing solutes
15 p1893 A73-32273
- Diffusional and nondiffusional metastable-phase transformations in titanium alpha + beta alloys
15 p1893 A73-32520
- Failure retardation mechanism in plastic titanium alloys
15 p1894 A73-32529
- Characteristics of failure in alpha-titanium alloys at high temperatures
15 p1894 A73-32536
- Certain systematic errors in determining parameters of oxygen diffusion in alpha titanium
15 p1894 A73-32540
- Passive alpha structure Ti base alloys with Al, Mn, Sn, Nb, Cr or Mo, investigating dissolution characteristics by chronoamperometric measurement using sulfuric acid
15 p1895 A73-32568
- Low temperature deformation of commercial Ti alloys.
16 p0204 A73-32848
- Metallurgical investigations of atomic ordering and transformation behavior of close packed ordered nine-layered hexagonal structure /kappa phase/ in V-Co-Ni ternary alloys
17 p1910 A73-34646
- Grain growth in commercial alpha and /alpha + beta/ Ti alloys.
18 p2326 A73-37143
- Cleavage fracture in alpha phase Ti, considering embrittling species effects on electronic band structure
20 p2578 A73-39490
- Effect of alloying and phase composition on the properties of maraging stainless steels.
21 p2720 A73-41040
- Influence of Co, Ni, Mo, and W on the solubility of Fe16N2 in alpha-iron.
23 p2994 A73-44156
- Study of the deformation structure in alpha-SiC single crystals
24 p3099 A73-44741
- Investigation of the kinetics of the redistribution of alloying elements between the alpha solid solution and cementite in cobalt and nickel steels
24 p3100 A73-45362
- CLOSED BASINS**
U STRUCTURAL BASINS
CLOSED CIRCUIT TELEVISION
Flight simulation visual image innovations, including closed circuit television, motion pictures and computer generated imagery with wide angle presentation and day/night realizations
16 p1995 A73-33205
- A compound wide angle color visual display system and a high resolution, high sensitivity close circuit color television camera developed for wide angle color visual systems.
21 p2702 A73-40872
- CLOSED CYCLES**
High power carbon dioxide electric discharge convection laser operation in closed cycle mode with combined dc and RF excitation and aerodynamic stabilization techniques
02 p0178 A73-12749
- Evaluation testing of a closed Brayton-cycle electrical-power-conversion system.
11 p1309 A73-25983
- CLOSED ECOLOGICAL SYSTEMS**
Quantitative estimation of the gas metabolism of continuous higher plant cultures as a life support system component
06 p0656 A73-17680
- Passive and active mode classification of air contamination sources in closed manned spaces, considering mechanical, electrical, chemical, physical and human factors
11 p1321 A73-25037
- CLOSED FAULTS**
U GEOLOGICAL FAULTS
CLOSED LOOP SYSTEMS
U FEEDBACK CONTROL.
CLOSURES
Ultrasonic closure welding of small aluminum tubes.
19 p2435 A73-38003
- CLOTH**
U FABRICS
CLOTHING
NT BOOTS [FOOTWEAR]
NT FLIGHT CLOTHING

- NT GLOVES
NT HELMETS
NT PRESSURE SUITS
NT PROTECTIVE CLOTHING
NT SPACE SUITS
Predicting heart rate response to work, environment, and clothing.
09 p1046 A73-22931
Thermal comfort - New directions and standards.
18 p2283 A73-36785
- CLOUD CHAMBERS**
A search for the quark in extensive air showers, using a counter-controlled cloud chamber.
01 p0093 A73-11249
Particle multiplicity and momentum spectra for high energy inelastic nuclear interactions in Wilson chamber with polyethylene target
02 p0208 A73-12655
Muon track curvatures in Wilson chamber magnetic field for calibrating ionization levels of logarithmic increase
02 p0171 A73-12687
Search for quarks using a flash-tube chamber.
13 p1670 A73-28210
Evidence for the possible existence of a charged particle with large mass.
16 p2016 A73-33700
Vertical plate steady flow thermal diffusion chamber for cloud condensation nucleus counter, featuring long available growth time for operation below 0.2 percent supersaturation
21 p2697 A73-40059
Experimental investigation of transient supersaturations in a thermal diffusion chamber.
23 p3004 A73-44259
- CLOUD COVER**
Light scattering by cirrus cloud layers.
01 p0038 A73-10376
Atmospheric ozone distribution from remote sensing with spaceborne IR interferometer spectrometer, estimating error due to cloud cover
01 p0038 A73-10384
Cloud characteristics in problems of radiation energetics in the earth's atmosphere.
02 p0159 A73-12146
On the application of satellite data on cloud brightness to the study of tropical wave disturbances.
02 p0190 A73-12790
Doppler turbulence spectrum and intensity measurement in stalactites region at base of cloud deck cooled by evaporation and destabilized by convection
03 p0339 A73-14539
Spectroscopic sounding of cloud; snow and ice covers from below /earth surface/ and above /space or planet/
04 p0473 A73-15570
Cloudiness as a global climatic feedback mechanism - The effects on the radiation balance and surface temperature of variations in cloudiness.
05 p0591 A73-16187
Utilization of meteorological data from satellites in studies of the general atmospheric circulation
05 p0593 A73-16245
Satellite pictures as aids for the determination of the structure of upper-level cyclones
05 p0593 A73-16347
Data on dynamics of the subcloud Venus atmosphere from Venera spaceprobe measurements.
06 p0744 A73-17436
ATS-3 observed cloud brightness field related to a meso-to-synoptic scale rainfall pattern.
06 p0720 A73-17867
Uranus atmosphere - Structure and composition.
07 p0874 A73-19068
U.S. and U.S.S.R. Venus probes data on Venus atmosphere, discussing atmospheric heat transfer mechanism and cloud structure
07 p0874 A73-19110
Reflection and absorption of solar radiant energy by cloud layers.
07 p0820 A73-20344
Intensity variation across Uranus disk during limb darkening-brightening cycles observations to test cloud absence theory, predicting limb brightening in methane bands
08 p1003 A73-20889
Jupiter surface maps from synoptic observations with refracting telescope, considering white cloud formations and atmosphere motions
08 p1012 A73-21584
Universal methods for estimating probabilities of cloud-free lines-of-sight through the atmosphere.
10 p1245 A73-23981
Large scale surface structure of Mars.
11 p1417 A73-25268
Estimate of the mean size of cloud layer particles in the Jovian atmosphere
11 p1423 A73-26080
Transfer of solar irradiance through cirrus cloud layers.
11 p1357 A73-26345
Baseline survey of cloud cover with the aid of two mirrors
12 p1521 A73-26968
Jupiter atmosphere fluid dynamic models, considering cloud spot markers and wave motions from ground and spacecraft observations
12 p1542 A73-27606
Investigation of cloud cover parameters from measurements on the Cosmos 384 satellite
13 p1654 A73-29155
Atmospheric effects on ocean surface temperature sensing from the NOAA satellite scanning radiometer.
13 p1610 A73-29195
Definition and radar measurement of the parameters characterizing the cloud environment of a launch base
14 p1743 A73-30114
The dynamics of the atmospheres of the major planets.
14 p1799 A73-30534
Cloud-free line-of-sight calculations.
15 p1903 A73-31317
Automatic instrument systems for determining cloud amount.
15 p1874 A73-31319
Russian papers on heat exchange in atmosphere covering stratus and convective cloud effects, clear sky conditions, turbulent transfer, atmospheric boundary layer, etc
15 p1904 A73-31781
Integral transmittance function of thermal radiation
15 p1904 A73-31782
Features of the long-wave radiant influx in the presence of stratified cloudiness /A numerical experiment/
15 p1904 A73-31783
Thermal well representation of cloud layer from radiative cooling and weak dependence on thickness, deriving approximate formulas for radiant fluxes
15 p1904 A73-31784
Short wave radiation flux calculation method for cloudless and cloudy atmospheres, computing geographic distribution of daily absorbed solar radiation
15 p1905 A73-31787
Accuracy of averaging total-radiation fluxes
15 p1905 A73-31791
A procedure for studying the statistical structure of solar radiation fluxes at the ground under clouded conditions
15 p1905 A73-31792
Cloud cover probability computation models, showing averaged values for direction of sighting and cumulus cloud cover estimations
15 p1905 A73-31797
Mars blue haze, earth noctilucent clouds and Venus blue clouds, considering mechanism and condensate chemical composition for formation
16 p2069 A73-33833
Jupiter and Saturn optical observations, discussing atmospheric composition, cloud layers and temperature distribution
16 p2069 A73-33837
Experiments in objectivization of a forecasting method for lower cloud boundary altitudes
17 p2204 A73-34541
Evidence of active and ancient volcanism on Mars - A review.
17 p2233 A73-35482
Development of methods of forecasting meteorological conditions for aviation
18 p2331 A73-35912
Climatological studies based on satellite data, including cloud, snow and ice cover, wind measurement, convection currents, temperature fields and earth thermal balance
18 p2331 A73-35914
Analysis of pressure and cloud anomaly fields.
18 p2333 A73-37054
Possibility of computing the cloud field on the basis of vertical velocities.
18 p2334 A73-37055
Method for analyzing the moisture field by the use of satellite cloud data.
18 p2334 A73-37056
Use of satellite cloud data in moisture field analysis.
18 p2334 A73-37057
Some results of determining cloud top heights from satellite infrared measurements.
18 p2334 A73-37060
Features of the evolution of depressions and their cloud systems over the Pacific Ocean.
18 p2334 A73-37061
Comparison of satellite-measured and radar-observed cloud-top heights.
18 p2334 A73-37066
Automatic analysis of cloud cover by infrared photography of the earth from meteor satellites.
18 p2334 A73-37068
Effect of cloud cover on the variability of outgoing radiation.
18 p2314 A73-37069
Effectiveness of utilizing cloudiness data obtained from satellites in objective analysis of the wind field.
18 p2334 A73-37071
Calculation of geopotential fields at various atmospheric levels from data on the overall cloudiness and temperature.
18 p2314 A73-37072
Meteorological satellite TV cloud cover photographs of cyclogenesis over Mediterranean Sea and cyclone arrival to European U.S.S.R. and Scandinavian Peninsula
18 p2334 A73-37074
An upper limit on the 4.9-micron flux from Titan.
18 p2357 A73-37112
Mars atmosphere during the Mariner 9 Extended Mission - Television results.
19 p2478 A73-37218
Aircraft measurements of effective photon paths in cloud-reflected and transmitted light in the 0.76-micron oxygen band
20 p2583 A73-39184
Satellite measurements of microwave and infrared radiobrightness temperature of the earth's cover and clouds.
20 p2556 A73-39844
An experimental model for the automated detection, measurement, and quality control of low-level cloud motion vectors from geosynchronous satellite data.
20 p2533 A73-39853
Numerical one dimensional cumulus model of stratification and cloud depth-radius relations for convective layer prediction
21 p2729 A73-40068
Russian book - The stochastic structure of cloud and radiation fields.
21 p2730 A73-40243
The International Planetary Patrol Program - An assessment of the first three years.
22 p2912 A73-42978
Atmospheric Uranus and Neptune models with massive atmospheres above solid cores, discussing Uranus solid methane cloud layer
22 p2913 A73-42987
Computer simulation of light pulse propagation for communication through thick clouds.
22 p2828 A73-43156
Experiments on light pulse communication and propagation through atmospheric clouds.
22 p2828 A73-43157
Total ozone measurements in cloudy weather.
23 p2973 A73-43853
A model for estimating joint probabilities of cloud-free lines-of-sight through the atmosphere.
23 p3004 A73-44260
Jupiter radiative greenhouse model overestimation of lower cloud level temperature due to convective heat transport neglect, discussing rejection of water cumulus cloud possibility
24 p3129 A73-44439
Formation of spectral lines in planetary atmosphere. IV - Theoretical evidence for structure of the Jovian clouds from spectroscopic observations of methane and hydrogen quadrupole lines.
24 p3129 A73-44449
Radiative instability model of cloud cover on equatorial beta plane to explain Jupiter bands zonal symmetry and meridional wavelength
24 p3132 A73-44535
A procedure for estimating cloud amount and height from satellite infrared radiation data.
24 p3084 A73-44925
Some characteristics of satellite-observed bands of persistent cloudiness over the Southern Hemisphere.
24 p3107 A73-45015
- CLOUD GLACIATION**
Terminal velocity equations for ice crystal growth forms and precipitation rates calculation in clouds, using drag coefficients, aspect ratios and densities
02 p0189 A73-12783
Particle size spectra measurement in cirrus generating cells, deriving particle concentration, crystal length, ice water content, reflectivity and precipitation rate
02 p0189 A73-12784
Calculation of the growth and melting of ice particles and the radar signal reflection profiles in cumulonimbus clouds
13 p1653 A73-28878
- CLOUD HEIGHT INDICATORS**
Echo top height characteristics based on convection cloud reflectivity structures measured by radar
03 p0338 A73-14516
Experience with the cross-beam photometer system.
05 p0579 A73-17156
Use of model output statistics for predicting ceiling height.
09 p1114 A73-22125
Baseline survey of cloud cover with the aid of two mirrors
12 p1521 A73-26968
Automatic instrument systems for determining cloud amount.
15 p1874 A73-31319
A comparison of radar-determined cloud height and reflected solar radiance measured from the geosynchronous satellite ATS-3.
23 p3005 A73-44269
A procedure for estimating cloud amount and height from satellite infrared radiation data.
24 p3084 A73-44925

CLOUD PHOTOGRAPHS

Certain parameters of cumulus clouds as determined from sky photographs and from ground-based actinometric measurements 15 p1905 A73-31793

Rapid motions of ultraviolet clouds on Venus 16 p2067 A73-33810

Computer processing and analysis of TV cloud photographs. 18 p2334 A73-37058

Yield and ion distribution for the barium cloud at 31,000 kilometers, September 21, 1971. 22 p2845 A73-41935

A correlation between colors of Jovian clouds and their 5-micron temperatures. 23 p3033 A73-43948

Some characteristics of satellite-observed bands of persistent cloudiness over the Southern Hemisphere. 24 p3107 A73-45015

CLOUD PHOTOGRAPHY

Simultaneous measurements of solar radiation from aircraft and satellites during BOMEX. 01 p0038 A73-10377

Satellite data and estimates of precipitation for hydrologic applications. 04 p0473 A73-15774

Time lapse stereo photogrammetry of ring vortex type circulation in cumulonimbus cloud tops of hail bearing storms 07 p0847 A73-19042

Baseline survey of cloud cover with the aid of two mirrors 12 p1521 A73-26968

Dynamic climatology in the light of satellite information /1973 Harry Wexler Memorial Lecture/. 17 p2204 A73-34375

Automatic analysis of cloud cover by infrared photography of the earth from meteor satellites. 18 p2334 A73-37068

Techniques for deriving winds from cloud movement. [AAS PAPER 73-126] 20 p2583 A73-38586

Influence of the resolution of television cameras and radiometers on the accuracy of determining the quantity of clouds from satellites 21 p2731 A73-40493

Statistical analysis of satellite-observed trade wind cloud clusters in the western North Pacific. 23 p3003 A73-43980

Stratospheric temperature measuring instrument development for Tiros N satellites and ESRO geostationary meteorological satellite development for cloud photography 23 p3004 A73-44103

Martian W cloud diurnal brightening observation by Mariners 6 and 7 flyby missions, considering probable water ice formation 24 p3128 A73-44398

Some scale estimates of the three-dimensional structure of cloud fields from aircraft-based aerial photographs 24 p3107 A73-44962

CLOUD PHYSICS

The infrared spectrum of Jupiter - Structure and radiative properties of the clouds. 01 p0097 A73-10370

Atmospheric solid and liquid water particles IR spectral properties, interpreting Nimbus 4 IR spectroscopic cloud observations 01 p0037 A73-10371

Thermal effect of optical radiation on water drops of small size 01 p0074 A73-11244

Two dimensional deep convection rimitive model of pressure perturbation in cumulus cloud with precipitation 02 p0189 A73-12781

A new Monte-Carlo simulation model for the temporal development of cloud droplet spectra. 02 p0144 A73-12782

Heavy elements depletion on grains in interstellar medium two phase model, noting gas dynamical analysis of discrete clouds evolution 03 p0366 A73-12931

Results from barium cloud releases in the ionosphere and magnetosphere. [MPI-PAE-EXTRATERR-67] 03 p0301 A73-13805

Sporadic F cloud focusing of radio waves as interpretation of observed short duration bursts accompanied by rapid phase variation 03 p0280 A73-14592

Principal trends of investigations in the field of theoretical meteorology performed in Hungary 04 p0473 A73-15284

Warm cloud droplet growth analysis based on stochastic coalescence equation model in terms of probability function and time evolution 05 p0592 A73-16194

Numerical simulation of precipitation development in supercooled cumuli. I, II. 05 p0594 A73-16572

Engineering models for Jupiter's troposphere and the NH3-H2O cloud systems. [AIAA PAPER 73-129] 05 p0619 A73-16882

Basic formulas for the determination of the altitude of artificial clouds 05 p0572 A73-17160

A synoptic climatology of satellite observed cloud vortices over the Southern Hemisphere. 07 p0846 A73-19039

On the differing molecular line widths in dense interstellar clouds. 07 p0874 A73-19072

The nature and effect of the volatile cloud produced by volcanic and impact events on the moon as derived from a terrestrial volcanic model. 07 p0890 A73-19812

The kinematical distribution of dark clouds surveyed in the 4830 MHz H2CO line. 08 p1004 A73-20904

Turbulence energy spectra in thick convective cumulonimbus cloud zone, using aircraft measurements 08 p0984 A73-21186

Effects of multiple scattering on laser pulses transmitted through clouds. 08 p0976 A73-21423

Influence of the geometrical parameters of a lidar on the applicability of single-scattering approximation 08 p0986 A73-21457

Lidar anemometry and atmospheric sounding [ONERA, TP NO. 1151] 08 p0986 A73-21680

Galactic dust region molecular cloud effects on cloud chemical evolution, star and planetary formation and life development on planets 09 p1140 A73-21975

Cloud-cloud collision destruction of interstellar clouds in inter-spiral arm regions, discussing observational tests 09 p1141 A73-22028

Study of the radiative properties of the atmosphere between cloud layers 09 p1114 A73-22371

The evolution of interstellar clouds. II - Hydrodynamic treatment of the phase change. III - Cloud collisions and statistical theory. 10 p1272 A73-23531

Continuously recording cloud nuclei counter, describing diffusion chamber with separate functions of sample supersaturation and photoelectric droplets recording 10 p1217 A73-23990

Effect of heating water droplets by optical radiation. 10 p1246 A73-24181

Isotopic combination identification in interstellar clouds through radio spectral line observations, discussing millimeter wave astronomy, molecular clouds, excitation mechanisms, galactic structure, etc 10 p1280 A73-24323

Particle injection in the Cygnus X-3 radio outburst. 11 p1419 A73-25859

The spectral albedo of water clouds in the 1-6 micron band. 11 p1357 A73-26195

An experimental investigation of the nature of changes in the intensity of precipitations from stratiform and cumuliform clouds 12 p1522 A73-27747

Radiative properties of terrestrial clouds at visible and infra-red thermal window wavelengths. 13 p1652 A73-28274

Russian book - Physics of clouds and seeding effects. 13 p1653 A73-28876

Study of droplet size distribution in a two-phase stratiform cloud - A numerical experiment 13 p1653 A73-28877

The orientations of ice crystal models during a fall in an electric field 13 p1654 A73-28882

Differential difference equations for probability of water droplet electrization in weakly ionized medium during cloud and fog formation 13 p1654 A73-28883

Stratiform cloud electrical characteristic changes under solid carbon dioxide seeding in aircraft experiments 13 p1654 A73-28884

Some characteristics of stratiform St-Sc clouds in various synoptic situations 13 p1654 A73-28885

Heavy precipitation from mixed phase composition cloud systems vs light precipitation from droplet and crystal containing clouds 13 p1654 A73-28887

Mesoscale cloud systems analysis from meteorological observations and weather satellite data nephanalysis, applying to weather forecasting 13 p1655 A73-29191

Spectrophotometric results from the Copernicus satellite. V - Abundances of molecules in interstellar clouds. 14 p1802 A73-30748

A three-dimensional model of cumulus cloud development. 14 p1771 A73-30764

Russian monograph on convective cumulus and cumulonimbus cloud physics covering atmospheric con-

vection, meteorological field structure and dynamic-kinematic schemes 15 p1903 A73-31584

Relation between the pressure at the center of a tropical cyclone and the dimension of its cloud system 15 p1904 A73-31610

Cloud research by radar, describing tracking, imaging and Doppler techniques 15 p1904 A73-31748

Features of the long-wave radiant influx in the presence of stratified cloudiness /A numerical experiment/ 15 p1904 A73-31783

Thermal well representation of cloud layer from radiative cooling and weak dependence on thickness, deriving approximate formulas for radiant fluxes 15 p1904 A73-31784

Experimental investigations of solar radiation fluxes in the lower troposphere in the presence of St and Sc clouds 15 p1905 A73-31788

Transmission of solar radiation by stratified cloudiness as a function of the statistical characteristics of its structure 15 p1905 A73-31796

Probability distribution function of cloud spectral brightness for IR range based on 1966-1969 observations 15 p1905 A73-31821

The interaction of a transient exhaust plume with a rarefied atmosphere. 16 p2086 A73-33873

The geometry and physical properties of exhaust clouds generated during the static firing of large rocket engines. 17 p2253 A73-34349

Electrical balance in the lower atmosphere. 17 p2158 A73-34359

Disk formation by collapsing rotating gas cloud, considering free turbulence and intermittency effects on gravitational instability 17 p2227 A73-34413

Diffusive motion of initially ellipsoidal plasma irregularities or ion clouds in upper atmosphere, considering space charge electric field effects 17 p2160 A73-34787

A flowmeter to measure cloud liquid content. 17 p2174 A73-35578

Cirrus-contrail cloud spectra studies with the Sabreliner. 17 p2206 A73-35579

Cumuli structure at various stages of development. 18 p2333 A73-36705

Some parameters of cyclonic cloud vortices. 18 p2333 A73-37053

Cloud eddy formation in wakes of single mountain islands similar to Karman vortex streets, noting application to wind field forecasting 18 p2334 A73-37075

A survey of interstellar formaldehyde in dust clouds. 19 p2475 A73-37610

Numerical modeling of the dynamics and microphysics of warm cumulus convection. 19 p2447 A73-37658

A comparison between axisymmetric and slab-symmetric cumulus cloud models. 19 p2447 A73-37659

Laboratory vortices in rotating, sheared flow. 19 p2420 A73-37664

Radiative transfer in homogeneous, nongray gases with non-isotropic particle scattering. [ASME PAPER 73-HT-9] 20 p2625 A73-38566

Cloud microphysics spaceborne laboratory experimentation under zero-gravity conditions, discussing salt nuclei distribution mechanism due to spray breakup as task for Apollo-Soyuz program [AAS PAPER 73-135] 20 p2583 A73-38590

Estimation of the absorptive capacity of atmospheric haze from the brightness of clouds 20 p2583 A73-39183

Structure of cumulus clouds during various development phases 20 p2583 A73-39186

Application of G. V. Rozenberg's asymptotic formulas in the interpretation of cloud brightness measurements 20 p2584 A73-39189

Integral moisture content determination in rain clouds by simultaneous thermal radiation and radar measurements 20 p2584 A73-39190

Liquid droplet and ice particle distribution in spatially homogeneous mixed clouds, solving kinetic coagulation equations via distribution function moments 21 p2730 A73-40119

Effect of coagulation and spatial redistribution of cloud particles on the precipitation spectrum 21 p2730 A73-40120

Long wave radiation flux, water content and temperature measurements in stratus and cumulostratus clouds by aircraft radiometry 21 p2731 A73-40496

- Condensation of drops in motion through a gravitational field
21 p2731 A73-40743
- Point discharge current measurements in trees and metal points during storms, discussing implications for structure of electrified clouds
21 p2684 A73-40779
- Dense cloud formation and gravitational collapse onset, discussing thermal properties and magnetic field presence
21 p2772 A73-41244
- Dynamical evolution of an expanding gas cloud.
22 p2840 A73-41758
- Numerical simulation of maritime warm cumulus by one dimensional cylindrical cloud model incorporating nucleation and raindrop breakup processes
22 p2883 A73-42546
- Water condensation coefficient for 3-micron radius droplets, noting expected error confirmation with standard deviation in experiment
22 p2883 A73-42548
- Doublet ratio method for abundance determination application to interstellar multiple clouds, considering column density error due to velocity distribution simplification
22 p2910 A73-42703
- Experimental investigation of transient supersaturations in a thermal diffusion chamber.
23 p3004 A73-44259
- Model for radiative dynamic instability of cloudy planetary atmosphere from coupling for case of radiative heating rate dependent cloud properties
24 p3132 A73-44534
- Numerical solution of linearized kinetic equations for coagulation of cloud particles by the Monte-Carlo method
24 p3107 A73-44965
- Cloud destabilization due to long wave radiative cooling resulting from IR radiative heat transfer in cloudy atmosphere, considering temperature inversion effects and cyclogenesis mechanism
24 p3108 A73-45016
- Clearing of a cloudy atmosphere containing water drops by intense monochromatic radiation
24 p3108 A73-45520
- CLOUD SEEDING**
- Project Cloud Catcher weather radar data system revisions in radar set, echo pulse integrator, data logging and analysis and graphic displays
03 p0289 A73-14523
- Flame suppression technique using halogen compounds with hydrogen and carbon, considering bromotrifluoromethane application in propane spray cloud seeding
12 p1521 A73-26818
- Russian book - Physics of clouds and seeding effects.
13 p1653 A73-28876
- Dependence of the diffuse expansion characteristics of a crystallization zone on the vertical stability of the atmosphere
13 p1654 A73-28879
- Stratiform cloud electrical characteristic changes under solid carbon dioxide seeding in aircraft experiments
13 p1654 A73-28884
- All-Union Meteorological Conference, 5th, Leningrad, USSR, June 21-25, 1971, Transactions. Volume 1 - General information, resolutions and plenary reports. Volume 2 - Weather prediction section. Volume 3 Climate section. Volume 4 - Section on seeding effects on atmospheric processes
18 p2331 A73-35905
- A numerical analysis of some practical aspects of airborne urea seeding for warm fog dispersal at airports.
21 p2728 A73-40056
- Certain results of radar studies of the evolution of convective clouds
21 p2731 A73-40494
- CLOUD STREETS**
- U CLOUDS [METEOROLOGY]**
- CLOUDS**
- NT ARTIFICIAL CLOUDS
- NT CIRRUS CLOUDS
- NT CLOUDS [METEOROLOGY]
- NT CONVECTION CLOUDS
- NT CUMULONIMBUS CLOUDS
- NT CUMULUS CLOUDS
- NT HYDROGEN CLOUDS
- NT MAGELLANIC CLOUDS
- NT NOCTILUCENT CLOUDS
- NT PLASMA CLOUDS
- NT STRATOCUMULUS CLOUDS
- NT STRATUS CLOUDS
- NT VENUS CLOUDS
- Planetary cosmogony theory review emphasizing cold evolution through dust-gas protoplanetary cloud nucleosynthesis, discussing iron fractionation, organic compounds and planetary thermal history
16 p2066 A73-33793
- CLOUDS [METEOROLOGY]**
- NT ARTIFICIAL CLOUDS
- NT CIRRUS CLOUDS
- NT CONVECTION CLOUDS

- NT CUMULONIMBUS CLOUDS
- NT CUMULUS CLOUDS
- NT NOCTILUCENT CLOUDS
- NT STRATOCUMULUS CLOUDS
- NT STRATUS CLOUDS
- Radiative calculation models for infrared transfer through cloud, aerosol and the continuum.
01 p0073 A73-10358
- Polarization of near-infrared sunlight reflected by terrestrial clouds.
01 p0073 A73-10363
- Multispectral cloud type identification based on Nimbus 3 medium resolution IR radiometer measurements, using radiative transfer theory
01 p0073 A73-10381
- An electrostatic cloud droplet probe.
01 p0052 A73-11058
- Radar observations of intense undulance in an evaporating cloud layer.
03 p0339 A73-14541
- Significant vortex structures occurrences from ESSA 3 and 5 global cloud observations, discussing source and formation patterns over Northern and Southern Hemisphere regions
05 p0593 A73-16346
- Possibility of affecting the coagulation of droplets in warm clouds and fog by electrical methods
06 p0719 A73-17840
- Light flux vertical distribution in spherical multilayer cloud and gas scattering planetary atmosphere, calculating radiation intensity
10 p1276 A73-23891
- Development of a global cloud model for simulating earth-viewing space missions.
10 p1244 A73-23979
- Satellite observed cloud signatures associated with mature and decaying depressions over high and middle southern latitudes, deriving surface pressure and upper geopotential anomaly patterns
10 p1244 A73-23980
- Universal methods for estimating probabilities of cloud-free lines-of-sight through the atmosphere.
10 p1245 A73-23981
- Approximation of empirical size distributions of cloud droplets and other aerosol particles
11 p1393 A73-25644
- Hail growth in cold front, discussing relationship to air flow changes
13 p1652 A73-28267
- The cloud bright spot.
13 p1619 A73-29238
- Certain methodological aspects of measurements of the average short-wave radiation fluxes in the presence of cloudiness
15 p1905 A73-31790
- Role of water vapor in the meteorology of Mars
16 p2069 A73-33831
- Analysis of cases of intense turbulence in the troposphere
17 p2205 A73-34544
- Preliminary data on the optical properties of solid ammonia and scattering parameters for ammonia cloud particles.
17 p2211 A73-34858
- Polarization properties of lidar backscattering from clouds.
17 p2125 A73-35416
- Experimental and theoretical investigation of the process of artificial crystallization and dissipation of supercooled clouds
18 p2332 A73-35919
- Spectrum analysis of tropical cloudiness. II.
19 p2446 A73-37430
- Light flux vertical distribution in spherical multilayer cloud and gas scattering planetary atmosphere, calculating radiation intensity
20 p2603 A73-38910
- Long term weather forecasting techniques, criteria and implementation, discussing statistical weather analysis, cloud types, air masses, sunspot activity, precipitation and pressure systems
20 p2584 A73-39628
- Russian book on UHF meteorological radar techniques and applications covering precipitation and cloud monitoring radiolocation stations, lidar, sonar, echo signals and meteorological satellites
20 p2584 A73-39758
- Nonlinear methods for evaluating the informative value of meteorological parameters and for classifying meteorological phenomena /Functional methods and algorithms/
23 p3001 A73-43464
- CLUTCHES**
- Experimental investigation of undulatory multiplication gear systems
10 p1222 A73-23597
- A method for selecting a nonlinear clutch in a system undergoing vibration forced by polyharmonic excitation
21 p2708 A73-41583
- CLUTTER**
- Backscatter from snow and ice surfaces at near incident angles.
01 p0016 A73-10191

- Optimal nonlinear estimator algorithms for tracking in face of incorrect sensor returns in multitarget environments, using posteriori probability selective measurements
04 p0431 A73-15260
- Recursive MTI radar filter design for sharp spectrum rolloff and flat pass band, investigating clutter rejection performance vs spectral spread
05 p0558 A73-16808
- Ground and angel clutter in radar systems - The two-beam antenna solution.
07 p0794 A73-20250
- Use of a surface-acoustic-wave delay line to provide pseudocoherence in a clutter-reference pulse doppler radar.
08 p0939 A73-21113
- Complex target resolution with the random signal radar.
10 p1189 A73-24560
- Signal accumulation efficiency for single-site coherent pulse radar moving over earth surface, using Tarasikin approximation of signal/ground clutter ratio for monopulse radars
12 p1467 A73-26944
- Correlated clutter and resultant properties of binary signals.
13 p1585 A73-29208
- MTI radar filter with adaptively controlled double canceller for frequency shifted clutter spectra effects minimization
13 p1594 A73-29222
- The effect of limiting upon the mean cross section of log-normal radar clutter.
13 p1586 A73-29224
- Radar clutter elimination techniques, considering antenna radiation patterns, resolution cells and Doppler filters
15 p1846 A73-32432
- Automatic detection radar with false alarm rate regulation capability in log-normal and Weibull clutter under severe environments
16 p1980 A73-33412
- Clutter spectra of low PRF AMTI pulse-Doppler radar.
16 p1980 A73-33413
- USAF Airborne Warning and Control System with overland downlook Doppler radar for low-fly aircraft detection in severe clutter environment, discussing design and performance
17 p2121 A73-34371
- Incoherent radar target extraction in clutter of unknown level by recursive integration for signal and threshold.
18 p2290 A73-37089
- Signal filtering using hard-limited digital processing. II - Performance with a single target in a coloured-noise background.
20 p2530 A73-39126
- Limitation of m.t.i. improvement factor due to oscillator instability.
24 p3069 A73-45259
- COAGULATION**
- NT BLOOD COAGULATION**
- Possibility of affecting the coagulation of droplets in warm clouds and fog by electrical methods
06 p0719 A73-17840
- Liquid droplet and ice particle distribution in spatially homogeneous mixed clouds, solving kinetic coagulation equations via distribution function moments
21 p2730 A73-40119
- Effect of coagulation and spatial redistribution of cloud particles on the precipitation spectrum
21 p2730 A73-40120
- Numerical solution of linearized kinetic equations for coagulation of cloud particles by the Monte-Carlo method
24 p3107 A73-44965
- COAL**
- Investigation of the friction and wear behavior of polytetrafluoroethylene composite materials as compared with that of artificial coal and sintered metal. II.
13 p1647 A73-29652
- Sample preparation, irradiation, and counting and data reduction scheme for trace element analysis of coal using neutron activation
21 p2737 A73-40632
- COALESCENCE**
- U COALESCING**
- COALESCING**
- Warm cloud droplet growth analysis based on stochastic coalescence equation model in terms of probability function and time evolution
05 p0592 A73-16194
- Effects of fuel corrosion inhibitors on filter-separator coalescence.
05 p0582 A73-16666
- Physicochemical parameters associated with surfactants, investigating effects on hydrocarbon fuels coalescence
05 p0582 A73-16674
- Elastic-plastic fracture by homogeneous microvoid coalescence tearing along alternating shear planes.
13 p1633 A73-28142

COANDA EFFECT

Theoretical analysis of the flow through a particular wall-attachment fluidic component.

- 03 p0295 A73-13767
- Contactless switch for three stage gas flow using symmetric jet booster based on Coanda effect
- 09 p1037 A73-22848
- Coanda effect physical explanation and applications to free jet and partially bounded jet, analyzing surface shutter characteristics
- 13 p1601 A73-28913

Measurement of Coanda flow in fluidic elements by a laser Doppler velocimeter method and a quantitative tracer method.

- 13 p1618 A73-29040
- Aerodynamic rig and wind tunnel developments of compound ejector thrust augments for V/STOL aircraft with combined Coanda and center injection flows
- [ASME PAPER 73-GT-67] 16 p2048 A73-33519
- The application of circulation control aerodynamics to a helicopter rotor model.
- [AHS PREPRINT 704] 17 p2104 A73-35055
- Rumanian contributions regarding the application of the Coanda effect
- 19 p2387 A73-38303

COARSENESS

The effect of molybdenum on gamma prime coarsening and on elevated-temperature hardness in some experimental nickel-base superalloys.

- 20 p2576 A73-39029

COASTAL CURRENTS

- Suspended sediment observations from ERTS-1.
- 22 p2850 A73-42726

COASTAL DUNES

U DUNES

COASTAL ECOLOGY

- Remote sensing application to the fisheries environment.
- [AIAA PAPER 73-12] 06 p0690 A73-17606
- Orbit analysis for coastal zone oceanography observations.
- [AIAA PAPER 73-207] 06 p0748 A73-17659
- Wetlands mapping in New Jersey.
- 13 p1619 A73-29237
- Simulated ERTS data for coastal management.
- 17 p2157 A73-34285
- Airborne and satellite remote sensing of Anacapa Island for hydrology and aquatic biology.
- 17 p2161 A73-34944

COASTAL MARSHES

U MARSHLANDS

COASTAL WATER

- High-altitude photographs of the Oregon coast.
- 09 p1078 A73-22719
- Applications of high-altitude remote sensing to coastal zone ecological studies.
- 16 p2003 A73-33364
- Remote sensing techniques for support of coastal zone resource management.
- 18 p2306 A73-36020
- Time sensing and analysis of coastal water dynamic features obtained from aircraft and satellite provided sequential photographic data
- 20 p2560 A73-39885
- Southern California coastal processes as analyzed from multi-sensor data.
- 20 p2560 A73-39886
- A statistical-temporal image merging technique for automatic bathymetry applied to southern California coastal waters.
- 20 p2560 A73-39887
- Isothermal mapping of temperature patterns from thermal discharges in Italian coastal waters.
- 20 p2560 A73-39888
- NOAA environmental satellites with IR remote sensors for detection of upwelling off Mexican Pacific Coast and cold water eddies in Sargasso Sea
- 20 p2560 A73-39890
- Suspended sediment observations from ERTS-1.
- 22 p2850 A73-42726
- Remote sensing of estuarine circulation dynamics.
- 22 p2851 A73-42823

COATING

- NT ANODIZING
- NT ELECTROPLATING
- NT ENCAPSULATING
- NT METALLIZING
- Utilization of the detonation phenomenon for the deposition of coatings [Survey/]
- 09 p1088 A73-22468
- High-temperature protective coatings; All-Union Conference on Heat Resistant Coatings, 5th, Kharkov, Ukrainian SSR, May 12-16, 1970, Transactions
- 18 p2318 A73-35876

COATINGS

- NT ALUMINUM COATINGS
- NT ANODIC COATINGS
- NT ANTIREFLECTION COATINGS
- NT BIREFRINGENT COATINGS
- NT CERAMIC COATINGS
- NT ELECTROPLATING
- NT ENAMELS
- NT ENCAPSULATING
- NT GLASS COATINGS

- NT GOLD COATINGS
- NT INORGANIC COATINGS
- NT LACQUERS
- NT MAGNETIC FILMS
- NT METAL COATINGS
- NT METALLIZING
- NT NICKEL COATINGS
- NT PAINTS
- NT PLASTIC COATINGS
- NT PRIMERS [COATINGS]
- NT PROTECTIVE COATINGS
- NT SPRAYED COATINGS
- NT THERMAL CONTROL COATINGS

Detonation gun flame spray coatings, determining adhesive strength as function of coating thickness and process technological parameters

- 03 p0313 A73-14014
- Radiation from an axial slot antenna coated with a homogeneous material.
- 06 p0665 A73-18138

Understanding and applying strain gages. II - Carriers, adhesives, and coatings.

- 06 p0696 A73-18675
- Thin reinforcing coatings effect on mechanical behavior of homogeneous isotropic prismatic bars under torsion, obtaining stress-strain expressions
- 09 p1165 A73-23358
- Moisture absorption characteristics of solid lubricant coatings
- 10 p1239 A73-24247

Creep and long-term strength of molybdenum with a boron silicide coating in vacuum at temperatures from 1000 to 1400 C

- 12 p1512 A73-27257
- Use of interferential filters for optical control during deposition of reflecting coatings
- 17 p2183 A73-34171

COAXIAL CABLES

Calculation of the asymptotic behaviour of the TDR step response related to the asymptotic behaviour of dielectrics in the frequency domain.

- 07 p0797 A73-19107
- On near-field distributions along the leaky coaxial cable.
- 08 p0937 A73-20804

High vacuum coaxial and coaxial push-pull rotary motion feedthroughs with continuous well shielded low noise cable mounted on vacuum flange

- 11 p1344 A73-26314
- Propagation constant and wave resistance in the case of coaxial and hollow conductors with lossy dielectric and magnetic materials
- 14 p1730 A73-30920

Coaxial cable fed dipole antenna array for observation of coherent backscatter radar signal from ionospheric electron density irregularities in electrojet region

- 16 p1987 A73-33117
- Ceramic waveguide microwave integrated circuits.
- 16 p1989 A73-33470

Load currents in missile circuits excited by a plane polarized field.

- 19 p2409 A73-37272
- Note regarding the propagation of electromagnetic fields through slots in cylinders.
- 19 p2403 A73-37273

Use of magnetic materials for improvement of screening properties of different types of cables.

- 22 p2830 A73-41805
- Russian book on wideband microwave oscillatory systems covering stepwise and smoothly irregular stripline and coaxial line resonators for radio receivers, multipliers, etc
- 22 p2832 A73-41881

Computation of plane-meridional fields of non-homogeneous coaxial cables

- 24 p3067 A73-44598

COAXIAL FLOW

Supersonic jet noise suppression using coaxial flow interaction.

- 03 p0241 A73-12964
- Optimum design of space storable gas/liquid coaxial injectors.
- [AIAA PAPER 72-1076] 03 p0354 A73-13400
- Two-dimensional viscid MHD flows in coaxial channels
- 05 p0603 A73-16588

Supersonic flow past notch in lateral body surface or in two closely lying coaxial bodies, applying turbulent jet theory to separation zone

- 07 p0774 A73-19618
- Prandtl eddy viscosity model for incompressible coaxial jet far field velocity decay prediction with non-dimensional term inclusion
- [AD-758488] 07 p0811 A73-19965

Sonic line for a coaxial axisymmetric nozzle.

- 11 p1303 A73-26403
- Turbulent mixing in the developing region of coaxial jets.
- [ASME PAPER 73-FE-19] 17 p2153 A73-35015

Coaxial jet mixing in confined tube simulating combustion chamber, considering Reynolds number, stream functions, recirculation, lip condition, vorticity and inlet conditions

- 20 p2548 A73-39518

Investigation of secondary flows between coaxial rotating cylinders

- 21 p2676 A73-40574
- A model of the dynamic behavior of the coaxial-flow gaseous-core nuclear reactor.
- 23 p3005 A73-43387

Approximate calculation of dividing streamline of heterogeneous coaxial supersonic jets.

- 23 p2940 A73-44127

COAXIAL PLASMA ACCELERATORS

X-ray fine structure of dense plasma in a co-axial accelerator.

- 01 p0086 A73-11493
- Experimental study of the luminous front produced by a coaxial plasma accelerator.
- 02 p0197 A73-12060

Electron density measurement in a pulsed ablation accelerator plasma.

- 02 p0198 A73-12110
- Potential drops near the electrodes in a pulsed plasma accelerator.
- 03 p0347 A73-14096

Investigation of a coaxial plasma accelerator with a uniform gas pressure distribution in the electrode gap

- 04 p0481 A73-15616
- Investigation of the operation of a coaxial plasma injector employing preionization of the gas
- 09 p1124 A73-21880

Dynamics of the current sheath in a pulsed electrodynamic plasma accelerator

- 09 p1125 A73-21910
- Investigation of the azimuthal symmetry of the discharge in a coaxial plasma injector
- 09 p1125 A73-21911

Coaxial plasma accelerator with uniform pressure distribution.

- 10 p1254 A73-24206
- Dependence of the parameters of a plasma cluster obtained from a coaxial source on the polarity of the central electrode
- 10 p1257 A73-24878

Dynamic viscosity and current distribution model of inhomogeneous Cs plasma flow in coaxial plasma gun with thermionic cathode

- 10 p1258 A73-24886
- Influence of initial gas conditions in a coaxial accelerator on plasma parameters
- 13 p1666 A73-28956

Magnetogasdynamic compression of a coaxial plasma accelerator flow for micrometeoroid simulation.

- 15 p1919 A73-31932
- Current-shell dynamics in a pulsed electrodynamic plasma accelerator.
- 15 p1922 A73-32635

Azimuthal symmetry in a coaxial plasma injector.

- 15 p1922 A73-32636
- Operational aspects of coaxial plasma accelerator with gas preionization by induction electric field introduced into interelectrode gap via longitudinal slits in external electrode
- 17 p2215 A73-34304

Formation and decay of vortex filaments in a plasma current sheath.

- 19 p2465 A73-37173
- Coaxial Ar plasma accelerator for spacecraft propulsion, discussing quasi-steady state I-V characteristics and exhaust velocity
- 19 p2466 A73-37180

Coaxial hydrogen and erosion pulsed plasma accelerators in vacuum, discussing experiment design, discharge characteristics and practical applications

- 19 p2466 A73-37361
- Investigation of the high-frequency oscillations in the flow of a pulsed coaxial plasma accelerator - One mechanism of inhomogeneity
- 19 p2467 A73-37364

Investigation of the performance of a coaxial accelerator in the production of a dense high-energy plasma

- 19 p2467 A73-37367
- Methods of corpuscular plasma diagnostics in a pulsed coaxial accelerator
- 19 p2467 A73-37371

Dependence of the parameters of a plasmoid obtained from a coaxial source on the polarity of the central electrode.

- 21 p2749 A73-41653
- Dynamic viscosity and current distribution model of inhomogeneous Cs plasma flow in coaxial plasma gun with thermionic cathode
- 21 p2749 A73-41661

A magnetogasdynamic accelerometer for the simulation of micrometeoroids

- 23 p2966 A73-43781
- Effect of initial gas conditions in a coaxial accelerator on the plasma parameters.
- 23 p3013 A73-44308

COAXIAL TRANSMISSION

U COAXIAL CABLES

COBALT

NT COBALT ISOTOPES

NT COBALT 60

- Influence of cobalt on the maraging of Fe-Ni-Mo alloys 06 p0705 A73-17876
- Site preferences of Ni²⁺ and Co²⁺ in clinopyroxene and olivine - Limitations of the statistical approach. 06 p0690 A73-18268
- Features of the domain structure of cobalt-doped lithium ferrite when changing the direction of easy magnetization 10 p1260 A73-24508
- Apollo 15 soil samples structure and phase equilibrium data noting metal particles of high cobalt content 12 p1466 A73-27544
- Composition of metal in type III carbonaceous chondrites and its relevance to the source-assignment of lunar metal. 13 p1686 A73-29564
- Rare-earth elements, Co, Sc and Hf in the Steens Mountain basalts. 15 p1874 A73-32389
- The effect of thermomechanical pretreatment on the allotropic transformation in cobalt. 17 p2190 A73-34645
- Phase equilibrium technique to measure oxygen solubility in liquid Co at 1510 to 1700 C, determining thermodynamic characteristics and deoxidation curves 23 p2990 A73-43482
- Wear resistant abrasive and dry lubricant cobalt-chromium carbide composite material coatings obtained by electrolytic codeposition 24 p3094 A73-45073
- COBALT ALLOYS**
NT RENE 41
 Comment on the nature of the disaccommodation in HCP Co-C alloys. 01 p0066 A73-10999
- Properties and uses of UMCo-50 and related Co-Cr-Fe alloys. 01 p0066 A73-11051
- Quadrilateral packet structure and lattice atom positions in single crystal ternary Re-Co-B alloy by X ray analysis 02 p0181 A73-12198
- Study of the effect of cobalt on redistribution of atoms of alloying elements in iron-base alloys by the nuclear gamma resonance method. 02 p0182 A73-12697
- Electron-vacancy prediction methods for sigma phase precipitation in residual matrix compositions of austenitic Niand Co-base superalloys 02 p0183 A73-12757
- Interdendritic structures of a directionally solidified cobalt-base alloy. 02 p0184 A73-12770
- A correlation between static adhesion data and the dynamic friction coefficients for two cobalt alloys and iron under vacuum conditions. [ASLE PREPRINT 72LC-5B-2] 03 p0328 A73-14362
- The high-temperature oxidation of cobalt-21 wt % chromium-3 vol. % Y2O3 alloys. 04 p0461 A73-14925
- Chromium diffusion in Ni-20 wt pct Cr-3 vol pct Y2O3 and Co-21 wt pct Cr-3 vol pct Y2O3. 04 p0463 A73-15317
- Characterization of age-hardenability and stress-rupture properties of some cobalt-base alloys. 04 p0465 A73-15579
- Precipitation hardening effect on Co-Ni-Ti-Al alloys stress-strain, grain size and strain resistance behavior in micro- and macrodeformation yield point region 04 p0465 A73-15639
- Temperature dependence of the elastic micro- and macro-stiffness of dispersion hardenable Co-Ni-Ti and Co-Ni-Ti-Al alloys. II 04 p0465 A73-15640
- Improved melting and casting procedures for a cobalt-base magnetic alloy. 04 p0455 A73-15750
- Properties of a cobalt superalloy resistant to hot corrosion 05 p0588 A73-17247
- X ray analysis of high coercivity Ticonal alloy single crystal microstructure after isothermal thermomagnetic treatment 06 p0709 A73-18210
- The application of magnetic after-effects in research on the real structure and migrational properties of metals and alloys 07 p0837 A73-19049
- Development and properties of cobalt-base alloys with improved hot-corrosion resistance. 07 p0838 A73-19497
- The effect of carbon on the hot corrosion of cobalt-base alloys. 07 p0838 A73-19498
- Phase separation analysis of ternary Co-W-Ti alloy during high temperature aging by X ray and electron microscopy method 09 p1099 A73-21963
- Borating kinetics and coating phase composition and thickness on cobalt and cobalt base alloys by metallographic, microhardness and X ray analyses 09 p1103 A73-22467
- Dependence on the cobalt content of the strength of a WC-Co cutting alloy in tension 09 p1159 A73-22473
- Grain growth inhibition by carbide additives in hard metal alloys of the ISO-K 10 type 10 p1231 A73-23688
- Investigation of the morphology and decomposition kinetics of Co-Ni-Ti alloys 10 p1232 A73-24153
- Additives alloying with cobalt, discussing allotropic transformation dependence, recrystallization, mobile dislocations, and iron deformation by twinning 11 p1408 A73-25322
- Directionally solidified eutectic high temperature alloys. 11 p1379 A73-25404
- Order-disorder alpha and gamma phase transformations as function of temperature in Co-Fe-V alloy by dilatometric, magnetostuctural, neutron diffraction and X ray analyses 12 p1508 A73-26834
- Temperature dependence of the Moessbauer spectra of iron-cobalt-vanadium alloys 12 p1509 A73-26839
- Carbide separation and carbide equilibrium in the Co-Cr-C system 12 p1509 A73-26895
- Influence of niobium on the magnetic properties of high-titanium Al-Ni-Co alloys - Second communication. 13 p1637 A73-29244
- Solubility of nitrogen and hydrogen in cobalt and cobalt alloys - A review. 13 p1637 A73-29245
- Mechanical behavior of WC-Co composite alloys. 13 p1643 A73-29545
- Study of precipitates formed by internal oxidation in cobalt-nickel-chromium alloys with a cobalt base. I - Precipitates formed by oxidation in air 14 p1759 A73-29750
- Calculation of the binary phase diagrams of iron, chromium, nickel and cobalt. 14 p1760 A73-30440
- The effect of stacking-fault energy on the stress-strain curve of dispersion-hardened Ni-Co alloys. 15 p1887 A73-31351
- Grain-boundary sliding and recrystallization of Nimonic 108 during creep. 15 p1887 A73-31352
- Hard WC-Co alloys as dispersion strengthened materials 15 p1887 A73-31591
- Temperature dependence of the single-crystal elastic constants of Co-rich Co-Fe alloys. 15 p1890 A73-31926
- Variation of chemical composition on the surface of cobalt-base alloys by oxidation in air. 15 p1891 A73-32016
- Structure, strength, and fracture of electrodeposited nickel and Ni-Co alloys. 16 p2025 A73-33113
- Hall effect and electrical resistance in Ni, Co and Ni-Co alloys 16 p2027 A73-34009
- Study of fretting wear in titanium, Monel-400, and cobalt-25 percent molybdenum using scanning electron microscopy. [ASLE PREPRINT 73AM-8A-3] 17 p2190 A73-34993
- The effect of cobalt on the aging mechanism of maraging steels 18 p2324 A73-36771
- High temperature cyclic oxidation resistance tests on Ni-, Co- and Fe-base alloys for aircraft gas turbine engines 19 p2440 A73-37496
- Effect of autoclave heat treatments on the mechanical properties of the prealloyed-powder cobalt-base alloy HS-31. 19 p2443 A73-38248
- Observations on the directional solidification of cobalt-base alloys strengthened by carbide fibres. 19 p2443 A73-38249
- The effect of carbon on the sulphidation of Co-Cr alloys. 19 p2443 A73-38250
- Structures and properties of cobalt base-TaC eutectic alloys. 20 p2575 A73-39020
- Carbide precipitation and carbide equilibrium in the Co-Cr-C system. 21 p2720 A73-41028
- Interaction of molybdenum with cobalt and carbon 22 p2877 A73-42460
- The effect of stacking fault energy on the plastic deformation of polycrystalline Ni-Co alloys. 22 p2879 A73-43074
- Substitution of molybdenum for tungsten in heat resistant cobalt-base alloys 23 p2989 A73-43436
- Precipitation and magnetic hardening in sintered WC-Co composite materials. 23 p2997 A73-43776
- Influence of titanium on the beta and beta-two phase properties and brittleness of InNDK3ST5-type annealed alloys 24 p3098 A73-44472
- Ten years' experience of UMCo-type alloys in a special steel foundry. 24 p3099 A73-45074
- Stability of the gamma-prime Co3Ti compound in simple and complex cobalt alloys. 24 p3099 A73-45075
- Investigation of the kinetics of the redistribution of alloying elements between the alpha solid solution and cementite in cobalt and nickel steels 24 p3100 A73-45362
- Plastic deformation of Co-Ni-Cr and Co-Ni-Cr-Mo alloys 24 p3101 A73-45525
- COBALT COMPOUNDS**
NT COBALT OXIDES
 Electrical evaluation of doped and undoped cobalt chromite as the interconnection material for high-temperature, zirconia-electrolyte, fuel-cell batteries. [ECS PAPER 16] 01 p0006 A73-10724
- Cobalt phosphide CoP3 as a catalyst for electrochemical H2 oxidation in acid fuel cells. 04 p0407 A73-15108
- Application of gamma-resonance emission spectroscopy to the study of the structure of laminar compounds of graphite with Co-57-labeled cobalt and cobalt chloride 10 p1186 A73-24466
- Crystalline structure of the TaCoB and NbCoB2 compounds 12 p1512 A73-27244
- Investigation of cobalt molybdate polymorphism 15 p1887 A73-31207
- Cobalt compound administration effects on hypoxic stress control, testing polycythemic response and cobalt retention in rats 17 p2115 A73-34744
- Study of the electronic structure of iron, cobalt, and nickel monosilicides by X-ray photoelectron spectroscopy and X-ray spectroscopy 20 p2578 A73-39734
- Comparative study of the combustion of 6-, 5-, 4-, and 3-amines of nitrate of cobalt (III) 21 p2647 A73-40703
- Ac electroconductivity of polycrystalline Co-Fe ferrite as function of temperature, composition and frequency at 1 kHz-200 MHz 24 p3119 A73-44403
- COBALT ISOTOPES**
NT COBALT 60
 Application of gamma-resonance emission spectroscopy to the study of the structure of laminar compounds of graphite with Co-57-labeled cobalt and cobalt chloride 10 p1186 A73-24466
- COBALT OXIDES**
 On the electrical properties of nonstoichiometric oxides alpha-Nb2O5, MnO, and CoO at high temperature 13 p1634 A73-28202
- Contribution to the study of the behavior of liquid cobaltous oxide in an oxidizing atmosphere 13 p1634 A73-28204
- NiO-CoO solid solutions defect structure from high temperature measurements of integrated Bragg peak intensities 13 p1645 A73-28934
- Reduction of oxygen compounds of cobalt by methane 14 p1724 A73-30828
- NiO and CoO single crystal thermal conductivities, reporting specific heat and electrical resistivity near magnetic transition 20 p2600 A73-39826
- COBALT 60**
 Saturation of stimulated ruby laser radiation under the action of CO-60 gamma rays 02 p0176 A73-12353
- Spectroscopic properties of ruby and neodymium lasers under the action of a Co-60 gamma ray 02 p0176 A73-12355
- Co-60 fueled tubular radioisotope thermoelectric generator, correlating long term test data with performance prediction model results 09 p1117 A73-22764
- The Gicodyne 400 power generator using a radioisotopic source with thermodynamic conversion 09 p1038 A73-23283
- Co-60 kernel modular power and reentry system design for space station and base, noting fuel and launch cost savings over Pu-238 systems 11 p1310 A73-25998
- Co-60 concentration measurement for lunar soil and rock samples, determining lunar neutron production rate 21 p2765 A73-40238

COCHLEA

Synapse localization study by electron microscopy of primary afferent tissues in cochlear nuclei of the brain stem

07 p0781 A73-19650

Procedures for polarocochleography and for pressure measurement in the inner ear perilymph in acute experiments on animals

11 p1314 A73-25043

Neuroanatomy of the auditory system.

14 p1715 A73-30280

Processing of auditory information by medial superior-olivary neurons.

14 p1715 A73-30281

Effect of sonic boom on hearing and vestibular equilibrium

18 p2284 A73-36910

Current aspects of the cochlear function in members of flight crews

18 p2286 A73-36940

COCKPIT SIMULATORS

Digitally integrated cockpit simulation facility for display systems and avionics to plan mission/human program and airborne equipment requirements

17 p2139 A73-35236

Cockpit mock-ups and simulator design for pilot workload assessment for Concorde program and V/STOL research

19 p2384 A73-37735

The Large Amplitude Multi-Mode Aerospace Research/LAMAR/Simulator.
[AIAA PAPER 73-922]

21 p2673 A73-40870

COCKPITS

Cockpit device with optical head-up display for visual slope guidance to any runway at any airport

01 p0051 A73-11011

Electromechanical and electronic cockpit displays effectiveness in terms of aircraft control and psychological/physiological factors relating to pilot performance and workload

[DGLR PAPER 72-097] 02 p0136 A73-11666

Cockpit instrument display systems visibility and reliability requirements, discussing various illumination methods in terms of power consumption, cost and human factors engineering

12 p1495 A73-26825

Concorde cockpit windows design modifications for weight reduction and reliability optimization, discussing transparencies and crew seat movement

14 p1712 A73-30927

Effects of new landing approach procedures on cockpit design and possibilities of taking them into account

[MBB-UH-07-73] 17 p2100 A73-34485

Mathematical method for calculating the optical characteristics of cone-shaped cockpit windscreens.

18 p2266 A73-36069

Symposium on Flight Deck Environment and Pilot Workload, London, England, March 15, 1973, Proceedings.

19 p2383 A73-37726

Internal operational environment effects on pilot errors in commercial aircraft flights in terms of man machine interface and flight deck design

19 p2384 A73-37728

Two man crew cockpit design for commercial 737 jet transport aircraft, discussing pilot vision, control and display panels and avionics disposition

19 p2384 A73-37729

Flight deck management and pilot operation priorities in high pressure and emergency situations, using integrated aircraft-environment mental model

19 p2384 A73-37731

Pilot workload and performance measures in terms of physiological activity in flight deck environment for reduced aircraft accidents due to human error

19 p2398 A73-37732

Cockpit layout effects on pilot and flight crew activities, using in-flight observation, photography and pilot eye movement evaluation

19 p2384 A73-37733

Cockpit evolution, considering pilot visual problems in approach final stage during poor visibility, instrument number and placement, supersonic aircraft, digital computer-CRT interfaces, etc

20 p2510 A73-39662

Boundary layer induced cockpit noise.

22 p2795 A73-41706

CODERS

Circuit diagrams, electronic modules and design of PCM telemetry encoder for Eole satellite, noting data multiplexing and processing

07 p0789 A73-18957

GAELIC - Grumman Aerospace Engineering Language for Instructional Checkout.

08 p0941 A73-20689

Constant factor delta modulator with adaptive voltage feedback to error point in coder for SNR improvement and hunting characteristic removal

09 p1065 A73-23100

Video signals differential pulse code modulation, improving SNR by quantizing characteristics modification via nonlinear coder

09 p1054 A73-23375

Binary cyclic code detection capability, polynomial description, coder-decoder circuits and error correction application

10 p1197 A73-23848

The optimality of variable sampling schemes for a digital encoder.

11 p1327 A73-25194

CODES

Linear codes and transverse equalization for limiting the effects of intersymbolic interference in the transmission of digital signals

10 p1189 A73-24416

Secondary Surveillance Radar application to aircraft identification in upper airspace of Eurocontrol member states, emphasizing code assignment

22 p2884 A73-42322

CODING

NT DECODING

NT REDUNDANCY ENCODING

NT SIGNAL ENCODING

Synchronous multiplexing of digital signals using a combination of time- and code-division multiplexing /t.d.m. and c.d.m./.

02 p0140 A73-11588

Numerical classification and coding of electrocardiograms.

04 p0412 A73-15647

Polynomial weights and code constructions.

06 p0671 A73-18143

Neural channel mechanism for real light and equivalent background coding, using test flashes under bleaching and field adaptation

07 p0783 A73-20258

Hybrid coding/decoding scheme for deep space probes data transmission, estimating bit error probability for given SNR

09 p1054 A73-23376

Quantization circuit for radio astronomical signals conversion into binary code and bit blocks recording on magnetic tape via Razdan-3 computer

10 p2220 A73-24698

Nonalgorithmic design and coding system for digital mathematical machines for accuracy and speed compatible with digital and analog computer, respectively

11 p1334 A73-25626

Book - Sensory coding in the mammalian nervous system.

11 p1317 A73-25799

Computer generated binary synthetic holograms, discussing information coding and processing, detour phase effect and kinoforms

11 p1370 A73-26534

The interpretation of signals from space.

11 p1428 A73-26661

Computer technology aided machine design automation and structural synthesis by coded information table formulation and conversion, discussing algorithm construction

12 p1502 A73-26784

Length minimization in the internal-state code of an asynchronous finite automatic system with a two-step memory

15 p1848 A73-31910

Digital transmission techniques for ATC satellite system, considering technical and economic aspects of various coding systems

15 p1846 A73-32427

Encoding altimeter for coding, transmitting and displaying flight altitude information to air traffic controllers

[SAE PAPER 730301] 17 p2167 A73-34663

Automatic cataloging of electrocardiographic patterns

17 p2116 A73-34965

Spatial information coding in the human visual system - Psychophysical data.

17 p2116 A73-35240

Visual and verbal coding in the interhemispheric transfer of information.

24 p3065 A73-45337

COEFFICIENT OF FRICTION

The friction of boron carbide in controlled atmospheres.

[ASME PAPER 72-LUB-29] 03 p0315 A73-14340

A correlation between static adhesion data and the dynamic friction coefficients for two cobalt alloys and iron under vacuum conditions.

[ASLE PREPRINT 72LC-5B-2] 03 p0328 A73-14362

The relative validity of the concepts of coefficient of friction and interface friction shear factor for use in metal deformation studies.

[ASLE PREPRINT 72LC-7A-3] 03 p0316 A73-14368

Transitions in the friction coefficients, the wear rates, and the compositions of the wear debris produced in the unlubricated sliding of chromium steels.

[ASLE PREPRINT 72LC-7B-2] 03 p0316 A73-14369

Thin films durability increase of poly(n-alkyl methacrylate)/ polymers with alkyl group length, noting friction coefficient behavior

[ASLE PREPRINT 72LC-7C-4] 03 p0317 A73-14373

Optimal efficiency of satellite passive nutation damper, noting system moment of inertia and flywheel axis relationship and viscous friction coefficient

03 p0383 A73-14558

Frictional behaviour of molybdenum disulphide in high vacuum.

04 p0454 A73-14997

Surface effects during fretting fatigue of Ti-6Al-4V.

04 p0461 A73-14998

Factors affecting coefficient of friction and wear of friction materials for brakes, discussing fillers use as reinforcements and friction modifiers

05 p0580 A73-16106

Low temperature tests for magnetic field and temperature effects on differential resistance of lead alloy superconductors, calculating viscous friction coefficient

06 p0736 A73-18116

Two dimensional indentation of elastic half space by rigid punch under slowly applied normal load for case with finite friction between surfaces

06 p0765 A73-18508

Reference temperature method for predicting turbulent compressible skin-friction coefficient.

08 p0925 A73-20722

Heat transfer and friction in the turbulent boundary layer of a compressible gas on a permeable surface

08 p0926 A73-20992

Cylinder surface roughness and transverse curvature effects on turbulent boundary layer in incompressible and compressible flows, deriving formula for skin friction coefficient

08 p0956 A73-21603

Features of the influence of the ambient medium on the friction of plastics against metal during intermittent travel

09 p1089 A73-22855

Dependence of the coefficient of external friction on a normal load during elastic saturated contact

10 p1222 A73-23596

Effect of solid lubricants on the physicochemical and friction properties of materials

10 p1225 A73-24686

Heat transfer and friction coefficients for turbulent flow of air in smooth annuli at high temperatures.

10 p1297 A73-24970

The reason for noncorrespondence of the values of the static and kinematic coefficients of sliding friction

12 p1502 A73-27445

Unbalance vibration of a rotor-bearing system supported by floating-ring journal bearings.

13 p1623 A73-28647

Mechanism of the lubricating action of sulfides and selenides of refractory metals

14 p1755 A73-30717

Investigation of friction and wear mechanisms in a friction coupling with a small overlapping coefficient

15 p1882 A73-31599

Analysis of turbulent skin friction in thick axisymmetric boundary layers.

15 p1863 A73-31658

Friction of hard alloys in vacuum at low temperatures

18 p2320 A73-36861

Hydrodynamic bearing damping in infinitely broad gap between oppositely oscillating parallel boundary surfaces, discussing inertia, Reynolds number and coefficient of friction

20 p2547 A73-39409

Mechanical, chemical and physical characteristics of glass and ceramics with respect to adhesion, friction and wear behavior

21 p2707 A73-40633

Experimental investigation of the antifriction properties of Teflon-base materials at low temperatures

21 p2724 A73-41197

COEFFICIENTS

NT ACCOMMODATION COEFFICIENT

NT AERODYNAMIC COEFFICIENTS

NT ATTENUATION COEFFICIENTS

NT COEFFICIENT OF FRICTION

NT COHERENCE COEFFICIENT

NT CORRELATION COEFFICIENTS

NT COUPLING COEFFICIENTS

NT DIFFUSION COEFFICIENT

NT DISCHARGE COEFFICIENT

NT FLOW COEFFICIENTS

NT HEAT TRANSFER COEFFICIENTS

NT INFLUENCE COEFFICIENT

NT IONIZATION COEFFICIENTS

NT NOZZLE THRUST COEFFICIENTS

NT RECOMBINATION COEFFICIENT

NT REGRESSION COEFFICIENTS

NT SCATTERING COEFFICIENTS

NT STRUCTURAL INFLUENCE COEFFICIENTS

NT WIGNER COEFFICIENT

Conversion coefficients of optical heterodyne receiver mixer for various amplitude-phase distributions of interfering signal

03 p0319 A73-14067

COERCIVITY

X ray analysis of high coercivity Ticonal alloy single crystal microstructure after isothermal thermomagnetic treatment

06 p0709 A73-18210

- Low-frequency creep in CoNiFe films.
[IEEE PAPER 7,1] 07 p0861 A73-19362
Correlation of coercive force to microstructure in cyclic martensite/austenite transformations in an Fe-Ni-Co alloy. 10 p1234 A73-24438
Effect of austenitization temperature on the properties of K₅Ni₂M₃Ti steel 21 p2718 A73-40738

COGNITION

- A model of the human in a cognitive prediction task. 22 p2814 A73-42223

COHERENCE

- Coherent signal from incoherent meteorological radar echoes for atmospheric turbulence intensity measurement, noting autocorrelation function for average frequency 03 p0338 A73-14531
Coherent state systems for groups of motions of Hermitian bounded homogeneous regions in terms of Bergman kernels 10 p1249 A73-24463
Investigation of coherence with the aid of the diffraction shearing interferometer. 12 p1507 A73-27515
Limitation of the axial gain of large antennas under partial coherent illumination. 21 p2660 A73-40098
Degree of coherence mapping of single ruby laser pulses using holographic interferometry, discussing self-coherence, length and photographic recording 21 p2710 A73-40146
Horizontal wind fluctuations coherence at different meteorological sites compared to wind tunnel experiment 21 p2732 A73-41573
Successively forward-scattered wave propagating through a random medium. 24 p3110 A73-45028
Flare triggering by coherent oscillations. 24 p3124 A73-45048
Coherence of an electromagnetic field propagating in a weakly guiding fiber. 24 p3097 A73-45416

COHERENCE COEFFICIENT

- Diffuser box for holography spatial and temporal coherence requirements relaxation, explaining speckling and SNR reduction by time and frequency domain analysis 08 p0963 A73-21035
Application of the coherence function to acoustic noise measurements. 19 p2458 A73-37284

COHERENT ACOUSTIC RADIATION

- Partial optical coherence theory based Greenspon modification for calculation of sound power radiation from statistically vibrating flat surfaces 03 p0384 A73-12991

COHERENT ELECTROMAGNETIC RADIATION

- NT COHERENT LIGHT
Application of longitudinal multimode laser coherence properties to increase the holographic depth of field. 12 p1504 A73-26830
An optimal electrooptical method of signal processing in coherent pulse reception 12 p1468 A73-26947
Investigation of the signal-to-noise ratio of ionospheric reflection by the method of coherent reception 15 p1844 A73-31890
Radio astronomy millimeter wave receiver techniques and atmospheric restrictions for coherent (radio) detection 21 p2771 A73-41237

COHERENT LIGHT

- New mechanism for generating coherent emission from ionized oxygen and nitrogen in the visible region of the spectrum 01 p0059 A73-10630
Fresnel diffraction by a circular aperture illuminated with partially coherent light. I. 01 p0078 A73-11004
Holo-diagram coherent optics device for studying interference patterns of object near focal points representing illumination and/or observation points. 01 p0053 A73-11220
Higher conservation laws for coherent optical pulse propagation in an inhomogeneously broadened medium. 01 p0078 A73-11221
Second harmonic generation in an inhomogeneous laser plasma 01 p0086 A73-11288
Earth based and spaceborne stellar interferometer with optical balanced mixer system for coherent detection, discussing principles, construction, SNR and sensitivity 02 p0170 A73-12341
Theory for the propagation of partially coherent light beams in a turbulent atmosphere 02 p0142 A73-12494
German monograph - Effect of spatial partial coherence on the measurement of optical transfer functions. 03 p0343 A73-13813

- German monograph - Spatial oscillations of light in the refraction and image field of rough objects. 03 p0319 A73-13817

- Granularity produced by a diffuser illuminated in partially coherent light 03 p0320 A73-14606

- Nonlinear interaction between circular coherent light and modulating electromagnetic waves in presence of quadratic electrooptical effect, noting frequency shift 04 p0459 A73-15921

- Some applications of interferometry in coherent light 05 p0586 A73-17321

- Three dimensional models images information content increase in coherent light by interference shadow marking, noting automatic systems for distant objects recognition 07 p0824 A73-20140

- Photon counting statistics of the superposition of coherent and chaotic light of arbitrary spectrum passed through the turbulent atmosphere or a Gaussian medium. 08 p0987 A73-20952

- Speckle reduction by simulation of partially coherent object illumination in holography. 08 p0964 A73-21037

- Coherent optical processing with spatial frequency diversity speckle and reflection noise reduction, discussing coding by illuminating input transparency through square screen mesh 08 p0964 A73-21045

- Optimization of detection systems for quasi-classical optical signals 08 p0940 A73-21558

- Characteristics of interference pattern formation during a self-reproduction process 09 p1096 A73-22858

- Method of increasing the noise immunity of optical communications lines 10 p1190 A73-24615

- Coherent light optical filtering, holographically produced complex filters, imaging systems and pattern recognition multiplex arrangement for optical data processing, discussing image reconstruction 11 p1370 A73-26533

- Semiconductor injection lasers discussing optical transitions threshold effects, radiative recombination, coherent emission, etc 12 p1506 A73-27136

- Optical interferometry for ultrasonic surface wave detection, using two coherent light beams focusing for recording standing wave ratio, attenuation, transmission and harmonic content 13 p1613 A73-28497

- Coherent optical signal superregenerative amplification in Q switched gas laser, calculating sensitivity of He-Ne laser light amplifier 13 p1627 A73-28663

- Light scattering in coherent systems for Stokes and anti-Stokes impurity centers in terms of classical and quantum mechanical theories 13 p1660 A73-28770

- Theory of image conversion in nonlinear optical systems 13 p1660 A73-28772

- Optical fibre guide measurements with short coherent light pulses. 14 p1756 A73-30056

- Holographic method for measuring spatial coherence functions 15 p1879 A73-32339

- Coherent light propagation and scattering in vaporized alkali metal atmosphere as function of refractive index and coherent to incoherent transformation 16 p2086 A73-34002

- Properties and fabrication of micro Fresnel zone plates. 17 p2173 A73-35434

- Single step detection of blurred images in a coherent optical processor. 17 p2173 A73-35436

- Coherence and quantum optics; Proceedings of the Third Rochester Conference, University of Rochester, Rochester, N.Y., June 21-23, 1972. 20 p2569 A73-38601

- Higher conservation laws and coherent pulse propagation. 20 p2570 A73-38603

- Photodetection volume of coherence for thermal optical source with given intensity and spectral density, defining photon phase space cell concept 20 p2570 A73-38610

- Electron beams as carriers of optical coherence. 20 p2570 A73-38621

- Unified thermodynamics of dissipative structures and coherence in nonlinear optics. 20 p2571 A73-38633

- Spatially locked laser mode formation of coherent wave fields with improved angular divergence by degenerate oscillation superposition in laser resonator 20 p2573 A73-39681

- Coherent oscillation modes of optical waveguide resonators, noting selectivity and thermo-optic insensitivity to pumping and active medium deformation 20 p2574 A73-39692

- Relaxation of coherence requirements in holography. 21 p2695 A73-39961

- Mutual coherence function of a finite optical beam and application to coherent detection. 21 p2710 A73-40147

- Coherent imaging system suppression of noise (extraneous non-image light) through multiple-wave illumination, periodic phase modulation and diffuse wave illumination 21 p2698 A73-40148

- A study of the effect of the number of axial modes of a laser on its degree of coherence 21 p2714 A73-40748

- Thermal lensing of laser beams in optically transmitting materials. II - Numerical computations. 22 p2870 A73-42515

- Self diffraction of coherent wave radiation by absorption from excited levels of Nd laser light induced phase diffraction gratings in thin layer rhodamine 22 p2870 A73-42723

- Spatial resolution of an incoherent-to-coherent converter using bismuth germanium oxide. 22 p2863 A73-43098

- Optical system imaging in partially coherent light, noting Rayleigh criterion insensitivity to aberration as characteristic of two-point resolution criteria 22 p2889 A73-43187

- Second-harmonic generation in an inhomogeneous laser plasma. 23 p3009 A73-43509

- Laser interferometer for displaying small rapid motions 24 p3092 A73-45468

COHERENT RADAR

- Radar techniques for planetary mapping with orbiting vehicle. 06 p0664 A73-18011

- Signal accumulation efficiency for single-site coherent pulse radar moving over earth surface, using Taraskin approximation of signal/ground clutter ratio for monopulse radars 12 p1467 A73-26944

- A semicoherent detection and Doppler estimation statistic. 13 p1585 A73-29202

- Mapping with coherent-radiation focused synthetic-aperture side-looking radar. 16 p2015 A73-33357

- The Apollo 17 Lunar Sounder. 18 p2288 A73-35959

- Mobile IC coherent radar with computerized display and calibration, incorporating cold cathode crossed field amplifier tube in transmitter amplifier stage 20 p2528 A73-38871

- Optical processing of radar signals 21 p2651 A73-40515

COHERENT RADIATION

- NT COHERENT ACOUSTIC RADIATION

- NT COHERENT ELECTROMAGNETIC RADIATION

- NT COHERENT LIGHT

- Coherence of the radiation of a pulsed single-mode injection semiconductor laser. 01 p0061 A73-11335

- Coherent laser radiation and holography in an optically inhomogeneous medium. 02 p0176 A73-12111

- Cross spectral analysis for auroral pulsations coherency in spatially separated patches, noting TV image recording of frequency and energy spectra 03 p0298 A73-12879

- Receiving characteristics of antennas in the case of coherent and incoherent radiation. 04 p0427 A73-14775

- The macroscopic high-frequency quantum generator and detector of the gravitational radiation. 08 p0987 A73-21017

- Production of a coherent submillimetric radiation by a heterodyne method 09 p1097 A73-23030

- The generation of tunable coherent radiation in the wavelength range 2300-3000 Å using lithium formate monohydrate. 12 p1504 A73-26826

- High-power broadly tunable difference-frequency generation in prosthite. 13 p1626 A73-28548

- Group theory generalization of Dicke quantum theory for spontaneous coherent radiation of multilevel molecules, noting angular distribution of photon echo effects 14 p1757 A73-30332

- Spatial correlation functions of the field and intensity of laser radiation 16 p2024 A73-34053

- Spatial coherence characteristics of noise emission in active waveguide channel, considering Raman scattering of focused beam 19 p2437 A73-37247

Master equations in the theory of incoherent and coherent spontaneous emission. 20 p2570 A73-38608

Coupled superradiance master equations - Application to fluctuations in coherent pulse propagation in resonant media. 20 p2571 A73-38627

Average intensity of a nonsymmetric optical radiation beam in a turbulent atmosphere 20 p2555 A73-39187

Coherent X ray emission from plasma generated by laser irradiation of copper sulfate doped thin gelatin layer 21 p2710 A73-40126

Amplification of backscattering by bodies placed in a medium with random inhomogeneities 21 p2657 A73-41513

Investigation of the radiation properties of a laser without external feedback 22 p2871 A73-42971

The nature of quasi-axial reconstructed pictures generated by 'nonreferenced' focused-image holograms 23 p2982 A73-43705

COHERENT SCATTERING

Secondary particles in pion-nucleon and coherent interactions, measuring momentum from multiple Coulomb scattering 02 p0209 A73-12666

Forward and specular scattering from a rough surface - Theory and experiment. 13 p1659 A73-28490

Spatial coherence characteristics of noise emission in active waveguide channel, considering Raman scattering of focused beam 19 p2437 A73-37247

Multiple scattering theory of radiative transfer in inhomogeneous atmospheres. 19 p2423 A73-37586

On the possibility of measuring gas concentrations by stimulated anti-Stokes scattering. 21 p2699 A73-40458

COHERENT SOUND

U COHERENT ACOUSTIC RADIATION

U SOUND WAVES

COHERENT SOURCES

U COHERENT RADIATION

U RADIATION SOURCES

COHERENT TRANSMISSION

U COHERENT RADIATION

COHESION

Physicochemical distinction between separating similar and different materials in terms of cohesive or adhesive fracture energy in continuum mechanics 03 p0312 A73-13334

Decohesive load carrying capacity of elastoplastic bodies based on permissible discontinuities due to strain increase, relating to structural strength determination 07 p0908 A73-19082

Determining the technical cohesive strength of polycrystalline metals from the internal energy. 09 p1106 A73-23158

Non-destructive testing of adhesive bonding. 11 p1374 A73-26299

COINCIDENCE CIRCUITS

Multichannel differential coincidence circuit in the nanosecond range 01 p0024 A73-10792

Study of the time correlation of multifrequency-laser emission by the photon coincidence method 09 p1096 A73-22877

COKE AIRCRAFT

U AN-24 AIRCRAFT

COLD ACCLIMATIZATION

Russian papers on human adaptability covering altitude and temperature acclimatization, work capacity and anthropogenetic and medicogenetic factors 02 p0133 A73-11921

Effect of altitude acclimatization and simultaneous acclimatization to altitude and cold on critical flicker frequency at 11,000 ft. altitude in man. 02 p0135 A73-12562

Contributions of quick and slow muscle fibers to changes in the electrical activity of skeletal muscles in rats under acute and chronic effects of cold 08 p0931 A73-21323

Circadian rhythms in catecholamines in organs of the golden hamster. 11 p1318 A73-26120

Effect of adaptation to cold on the energy characteristics of muscular activity 13 p1574 A73-28295

Changes in the electrical activity of the brain and in some thermoregulation indices of nonanesthetized male cats during cooling 18 p2276 A73-36569

Effect of prior adaptation to cold on the development of experimental hypertension 21 p2636 A73-40209

Changes in indices of the carbohydrate and fat metabolism, the state of the sympathoadrenal system, and oxidative processes under varying-intensity cold effects 24 p3059 A73-44671

Metabolic and myoelectric reactions under chemical thermoregulation in rats after accelerated cold adaptation 24 p3059 A73-44721

Energy balance and change in body weight and body water in man during a 2-day cold exposure. 24 p3060 A73-45059

COLD CATHODE TUBES

NT PHOTOMULTIPLIER TUBES

COLD CATHODES

Oscillation modes and cathode potential drop in plasma generated by continuous electric discharge at low pressure between anode and cold cathode 03 p0346 A73-13603

High-current gas lasers with a mercury cathode 08 p0976 A73-21717

Band structure, electron energy distribution and emission efficiency of negative electron affinity secondary emitters and cold cathodes 14 p1732 A73-29912

Analysis and investigation of cathode processes in a high-current arc discharge 19 p2466 A73-37360

Low temperature thermionic cathode. 22 p2834 A73-42695

COLD FLOW TESTS

Hypergol rocket engines restart difficulties investigation via cold flow and hot firing tests, simulating worst case environmental conditions [AIAA PAPER 72-1160] 03 p0357 A73-13461

Investigation of damping methods for low frequency augmentor combustion instability. [AIAA PAPER 72-1207] 03 p0358 A73-13490

COLD FORMING

U COLD WORKING

COLD FRONTS

Note on the extratropical transformation of a typhoon in relation with cold outbreaks. 05 p0594 A73-16349

Structure of the lower 300-meter atmospheric layer during the passage of a cold front 13 p1655 A73-29194

COLD GAS

Stability of a plasma with an axial current surrounded by a cold gas with a pressure gradient. 02 p0198 A73-12108

Space-flight qualification of solid-propellant units in the example of the cold-gas generator for the booster rocket Europa I/II 16 p2047 A73-33394

Cold gas cloud embeddings in interstellar hot gas, determining radiation temperature from absorption line profiles and kinetic temperature from thermal and turbulent energy components 20 p2606 A73-39066

Cold gas noncentral point explosion generated shock wave propagation in interplanetary medium, discussing shock front geometry, earth orbit parameters and gas dynamics 24 p3137 A73-44781

COLD MOLDING

U COLD PRESSING

COLD PLASMAS

Radiation resistance of small electric and magnetic antennas in a cold uniaxial plasma. 01 p0081 A73-10194

Excitation of electromagnetic waves in a plasma by a flux of phased oscillators 01 p0082 A73-10207

Reductive perturbation theory application to nonlinear Schroedinger equation for plasma of cold ions and isothermal electrons, investigating ion oscillation mode automodulation 01 p0082 A73-10420

Electron-ion recombination in cryogenic helium plasmas. 01 p0084 A73-10565

Ergodic behaviour of nonlinear hydromagnetic waves in a cold collisionless plasma. 01 p0087 A73-11496

On the stability of nonlinear cold plasma waves. 01 p0087 A73-11497

VLF-ELF radiation characteristics of a 90 degree-phased crossed-dipole array in a cold multicomponent magnetoplasma. 02 p0140 A73-11739

Nonlinear waves in a multicomponent plasma with weak dissipation. 02 p0198 A73-12103

Uniform low temperature gas discharge plasma diagnostics in shielded volume, noting application of stable plasma generation effect for isotope analysis 02 p0199 A73-12693

Incoherent excitation of plasma oscillations by an almost-monoenergetic relativistic beam. 03 p0347 A73-14102

Turbulent wave field growth rate and saturation amplitude for nonresonant instability in weak cold beam plasma system, using Dupree plasma turbulence theory 04 p0479 A73-15193

Net-field polarization in a magnetically biased plasma. 04 p0422 A73-15481

Use of an electron beam for low-temperature plasma measurement in the magnetosphere and interplanetary space. 04 p0450 A73-15553

Parametric excitation of high-frequency potential oscillations in a cold magnetoactive plasma by the field of an electromagnetic wave 04 p0481 A73-15612

Magnetically coupled transport of a cold plasma in the outer ionosphere at low latitudes. 05 p0567 A73-16094

Electron energy distribution in a low-temperature plasma. 06 p0727 A73-17419

Stream instabilities in a cold plasma in the presence of a magnetic field. 06 p0728 A73-17793

Thin walled open ended cylindrical antenna in cold magnetoplasma, calculating current distribution by approximations based on Wiener-Hopf procedure 06 p0729 A73-18193

Self trapping modulational instability of electron cyclotron wave whistler in cold and hot dense plasmas, discussing relevance to phenomena in magnetosphere 07 p0814 A73-19239

Nonlinear wave modulation in cold magnetized plasmas. 07 p0855 A73-19338

Transient radiation in homogeneous anisotropic cold plasmas. 07 p0856 A73-19381

Thermonuclear reactor model with core surrounded by dense cold plasma, noting temperature profile effects on fusion and energy release locations 08 p0991 A73-20818

Cold collisionless plasma equations for electromagnetic waves absorption near lower hybrid resonance in inhomogeneous magnetized plasma contained in ideally conducting cylinder 09 p1125 A73-21906

Energy absorption in cold inhomogeneous plasmas - The Herlofson paradox. 09 p1126 A73-22276

Steady state Lie group solutions to nonlinear partial differential equations of low temperature plasma ionization instability in strong magnetic field 09 p1127 A73-22591

Cyclotron heating of plasmas with finite amplitude waves. 09 p1128 A73-22630

Electron-beam excitation of finite-sized plasma near the lower-hybrid frequency. 09 p1129 A73-22638

Low temperature plasma electric arc discharge generators, noting electrode interaction, energy losses and high enthalpy efficiencies 10 p1253 A73-23516

The energy-momentum tensor for an electromagnetic wave in plasma. 10 p1254 A73-24115

Parametric excitation of high-frequency electrostatic oscillations in a cold magnetoactive plasma by an electromagnetic wave. 10 p1254 A73-24202

Electromagnetic wave instability characteristics during propagation oblique to electron stream in cold electron-ion plasma 10 p1255 A73-24268

A self-consistent model of a simple magnetic neutral sheet system surrounded by a cold, collisionless plasma. 10 p1257 A73-24725

The ion cyclotron drift loss-cone instability with a coexisting cold plasma. 11 p1404 A73-25271

Coupling coefficients for resonant interaction between three waves with well-defined phases in cold magnetized plasma, applying to solar corona 11 p1405 A73-25917

Ionization transitions from the 8/2P1/2 level of a cesium atom in a low-temperature plasma 14 p1781 A73-30460

Magnetic neutralization and discharge neutralization of an electron beam injected into a magnetoactive plasma 14 p1782 A73-30807

Current distribution on an infinite tubular antenna immersed in a cold collisional magnetoplasma. 15 p1920 A73-32236

Cold collisionless plasma equations for electromagnetic waves absorption near lower hybrid resonance in inhomogeneous magnetized plasma contained in ideally conducting cylinder 15 p1922 A73-32631

Nonlinear frequency shift and damping stabilization mechanisms of unstable plasma waves in hot beam-cold plasma system 16 p2043 A73-34058

Low temperature plasma electric arc discharge generators, noting electrode interaction, energy losses and high enthalpy efficiencies 17 p2217 A73-35196

- Normal Doppler shifted cyclotron radiation from a cold plasma. 18 p2338 A73-36189
- Interaction between a tubular electron beam and a plasma 18 p2339 A73-36555
- Cold collisionless plasma flow along magnetic field, deriving quasi-shock wave characteristics from Vlasov-Maxwell equations 19 p2463 A73-37152
- Study of plasma systems with a closed electron drift and a distributed electric field 19 p2466 A73-37357
- Electromagnetic load propagation for an oblique incidence in a nonhomogeneous magnetized plasma 19 p2468 A73-37447
- Theory of electromagnetic wave in a nonuniformly moving magnetoactive plasma 19 p2406 A73-38328
- Excitation of electromagnetic waves propagating along a magnetic field in a cold plasma by a beam of phased oscillators 19 p2406 A73-38330
- Non-turbulent electric fields in soliton and shock-like structures in magnetized plasmas. 20 p2596 A73-38967
- Russian book on low temperature plasmatron-generated plasmas covering physical and transport properties, optical, thermophysical and gasdynamic analytic methods, etc 21 p2746 A73-40516
- Experimental study of conductivity, velocity, and temperature distributions in a submerged jet of low-temperature plasma 21 p2747 A73-40575
- Growth rates of the ion cyclotron instability in the earth's magnetosphere. 21 p2685 A73-40824
- Plasma instability in a collisional and thermal magnetoplasma. 21 p2748 A73-40928
- On the reflection of transverse waves from a cold plasma. 21 p2748 A73-40930
- On input impedance of an arbitrarily oriented small loop antenna in a cold collisionless magnetoplasma. 22 p2824 A73-41858
- Cyclotron resonance in a weakly ionized hydrogen plasma with nitrogen, oxygen and air impurities 22 p2890 A73-41864
- Kinetics of impact-radiation ionization and recombination. 22 p2892 A73-42344
- Possible emission of transverse electromagnetic waves in an isotropic plasma 22 p2893 A73-42390
- Propagation mode with fine structure interpreted as quasi-cylindrical electrostatic wave interference with cold plasma field from potential measurements near point source antenna 22 p2895 A73-43021
- Reflection and transmission of electromagnetic waves at a moving magnetoplasma half-space. 22 p2896 A73-43179
- Volt-ampere characteristics of double electrical plasma probe measuring ionization level in low temperature dense plasma under interelectrode gap near-breakdown conditions 23 p2983 A73-44344
- COLD PRESSING**
- Nature of anisotropy in half-cells made of cold-pressed Bi-Te-Se-Sb alloys 06 p0738 A73-18653
- COLD ROLLING**
- Cold rolling of dispersion-strengthened nickel. 01 p0063 A73-10282
- Cracking of Zircaloy as a result of unusual localized texturing. 02 p0183 A73-12756
- Dependence of the deformability of the Kh17 high-chromium steel on texture 03 p0326 A73-13827
- Plastic anisotropy of low-carbon, low-manganese steels containing niobium. 04 p0463 A73-15309
- Cold rolling of polymers. II - Toughness enhancement in amorphous polycarbonates. 17 p2197 A73-35350
- Cold rolling of polymers. III - Properties of rolled crystallized polycarbonates. 17 p2197 A73-35351
- Investigation of the imperfect structure of polycrystalline aluminum after low-temperature rolling and annealing 20 p2579 A73-39747
- Texture and anisotropy of the properties of titanium sheet 21 p2719 A73-40852
- How composition affects properties of a ferritic stainless steel. 21 p2721 A73-41084
- The effect of cold and hot rolling on the microstructure and fracture characteristics of titanium-to-steel explosion welds. 23 p2985 A73-43912
- Deformation behaviour and deviation from the simple rule of mixture for the ultimate tensile strength in the cold rolled fibre-reinforced composites. 23 p2998 A73-44151
- COLD STRENGTH**
- Cold shortness of W and related refractory metals, noting oxide phases and impurities effects on mechanical properties temperature dependence 01 p0066 A73-11341
- Effect of structural and mechanical factors on the nature of cold shortness curves for steels 20 p2578 A73-39378
- Gamma to alpha transformation and notch depth effects on metastable austenitic steel impact strength at cryogenic temperatures 23 p2995 A73-44282
- Influence of deformation on the strength and ductility of low-alloy chromium 23 p2996 A73-44290
- COLD TOLERANCE**
- Unacclimatized male Caucasians lower critical temperature determination for subsequent investigation of ethnic variability in acute cold exposure responses 01 p0008 A73-10166
- Effect of high-fat diet on thermal acclimation with special reference to thyroid activity. 05 p0541 A73-16800
- Physiological effect of air nitrogen replacement by inert gases under high and low temperature conditions 12 p1465 A73-27701
- Energy supply in acute cold-exposed dogs. 18 p2278 A73-36655
- Thermographic evaluation of relative heat loss areas of man during cold water immersion. 18 p2283 A73-36781
- Tolerance to immersion in cold water 18 p2280 A73-36943
- Effect of skin wetting on finger cooling and freezing. 20 p2518 A73-39779
- FFA metabolism in thyroidectomized and normal dogs during rest and acute cold exposure. 20 p2515 A73-39787
- COLD TRAPS**
- Organic compounds chemical analysis with cold trap to allow materials evaporation according to vapor pressure characteristics for replacing gas chromatograph 17 p2175 A73-35760
- COLD WALLS**
- U WALLS**
- COLD WATER**
- Tolerance to immersion in cold water 18 p2280 A73-36943
- NOAA environmental satellites with IR remote sensors for detection of upwelling off Mexican Pacific Coast and cold water eddies in Sargasso Sea 20 p2560 A73-39890
- COLD WEATHER**
- Operative visibility limits over the airports of Milan Linate and Malpensa in the 1960-1969 decade 19 p2447 A73-38125
- COLD WORKING**
- NT COLD ROLLING**
- NT ELECTROHYDRAULIC FORMING**
- NT EXPLOSIVE FORMING**
- Characteristics of the formation of austenite during rapid heating of cold-worked KVK-42 /42Kh2NGSM/ steel 01 p0062 A73-10260
- Processing and properties of powder forgings. 01 p0056 A73-10279
- Ultrasonic measurements of cold-work percentages in Type 316 stainless steel. 02 p0173 A73-11987
- Significance of the sequence of treatment for the notch impact strength of cold-worked steel samples 02 p0175 A73-12850
- How deformation affects the mechanical properties of aluminum forgings. 03 p0322 A73-13266
- Warm forging of steels for increased precision and mechanical properties. 03 p0323 A73-13269
- Influence of cold deformation and subsequent heating on the structure and properties of dispersion-strengthened nickel 04 p0466 A73-15666
- Electron microscopic investigation of cold worked and annealed thin V and Mo foils recrystallization characteristics, considering effect of grain boundaries pinning at surface 05 p0588 A73-17245
- The martensitic transformation during deformation of titanium alloys with metastable beta phase. 06 p0708 A73-18207
- Substructure and dispersion hardening in aged, cold worked, and annealed Al-4 wt pct Cu alloy. 06 p0711 A73-18754
- The creep strength of 17 Cr-11 Ni-2.5 Mo austenitic steel stabilised by titanium. 08 p0982 A73-21792
- Surface work hardening as a means of increasing the resistance of machine parts to low cycle fatigue. 09 p1089 A73-23162
- Electrothermal annealing via electrical heating in vacuum for improved plasticity of thin walled molybdenum alloy elements after cold working 09 p1107 A73-23196
- Improved fracture resistance of 7075 through thermomechanical processing. 09 p1109 A73-23257
- Cold forming stainless steels and other specialty grades. 15 p1883 A73-32168
- Transage 129 Ti-Al-V-Sn-Zr alloy fabrication cost reduction through good cold formability and weldability with weight saving due to high strength and fatigue resistance 15 p1891 A73-32172
- Effects of cold plastic deformation and aging temperature on the mechanical properties of dispersively hardening Cr-Ni-Co-Mo steel 17 p2188 A73-34559
- Effects of cold deformation and heat treatment on the elastic properties of niobium 17 p2188 A73-34562
- Influence of cold work on the stress corrosion susceptibility of Ti-13V-11Cr-3Al. 17 p2194 A73-35675
- Quality requirements for Ti-3Al-2.5V annealed and cold worked hydraulic tubing. 19 p2434 A73-37868
- Plastic deformation of Co-Ni-Cr and Co-Ni-Cr-Mo alloys 24 p3101 A73-45525
- COLLAGENS**
- Accelerated chromatographic method for determination of hydroxyproline. 03 p0273 A73-13600
- Physical nature of gelatin as polymer material, emphasizing low temperature restoration of collagen structure, supermolecular structure formation capability and glassy-elastic state transition temperature. 21 p2647 A73-40265
- Microchemical urinalysis. IX - Determination of hydroxyproline in urine. 21 p2648 A73-41213
- COLLAPSE**
- Plastic collapse of steep conical shells under axial compression. 21 p2789 A73-41684
- Critical velocity for collapse of a shell of circular cross section without buckling. [ASME PAPER 73-APMW-31] 22 p2925 A73-42891
- COLLIMATION**
- Beam diverging lens system for high power laser transmitters. 03 p0319 A73-14432
- Determination of the collimation error of a radio telescope 15 p1849 A73-31021
- Emission characteristics of a tube-shaped laser oscillator. 15 p1885 A73-31940
- Methods for alignment of lasers with unstable resonators. 20 p2573 A73-39686
- COLLIMATORS**
- Laser system output mirrors alignment for beam quality and power performance optimization and external optical component premature degradation prevention, using autocollimator 09 p1094 A73-22445
- Collimator corrections to the measured diffuse X-ray background. 12 p1537 A73-27885
- Design study of a glass meridian circle. 20 p2565 A73-39064
- Experimental study of an autocollimation method for alignment of a variable-profile antenna 21 p2675 A73-41457
- Crystal spectrometry of active regions on the sun. 21 p2706 A73-41602
- COLLINEARITY**
- Collinear theory of photogrammetry developed from projective equations in three dimensional space through singular transformation with 11 independent parameters 09 p1082 A73-22383
- COLLISION AVOIDANCE**
- A French collision-avoidance system of time-frequency type - Critical analysis of test results [ONERA, TP NO. 1086] 01 p0074 A73-10227
- Application of ultrastable oscillators to aerospace [ONERA, TP NO. 1114] 01 p0045 A73-10235
- Manoeuvre in response to collision warning from airborne devices. 01 p0074 A73-10349
- Some considerations on utilization control of the near earth space in future. 01 p0074 A73-11125
- Airborne radar set for weather surveillance, independent landing monitoring, ground visualization and collision avoidance 02 p0190 A73-11854
- Problems related to the measurement and evaluation of ATC/CAS interaction. 06 p0721 A73-17600

- Systems for collision avoidance. 07 p0848 A73-18899
- Ground based and airborne collision avoidance systems comparison, discussing interrogator/transponder concept, pilot warning indicator, and air traffic handling capacity and economics 07 p0848 A73-18900
- Game problem of the rigid collision of two points with impulsive thrust in a linear central field 13 p1660 A73-29080
- Historical development of the Air Traffic Control System. 14 p1772 A73-29877
- Guidance of aircraft according to techniques of trajectory plotting with a clock 15 p1911 A73-32489
- Aircraft in-flight visibility /conspicuity/ during daytime, discussing exterior paints, tapes and high intensity lighting effectiveness for midair collision avoidance 16 p1965 A73-32661
- Differential velocity effects on converging target intersection time estimation accuracy, considering plane conditions and air traffic controller experience 16 p1975 A73-32900
- Digital synchronization of synchronous collision prevention systems in aviation 17 p2207 A73-34480
- A new approach to aircraft exterior lighting. 17 p2108 A73-35808
- Air traffic control and the prevention of collisions 19 p2450 A73-37386
- Advanced concepts in terminal area control systems - Aircraft tracking and collision alert. 19 p2451 A73-37806
- Optimal aircraft collision avoidance. 19 p2452 A73-38050
- Discrete address beacon system /DABS/ data links and digital communication between ground based ATC computer and aircraft for IFR-VFR conflict detection and safety separation 19 p2453 A73-38466
- Systems for collision avoidance - An overview. 19 p2453 A73-38467
- Air based collision avoidance system feasibility appraisal, discussing YG1054 proximity warning indicator, cost analysis and implementation prognosis 19 p2454 A73-38468
- SECANT - A solution to the problem of midair collisions. 19 p2454 A73-38469
- Ground based aircraft collision avoidance systems, discussing three dimensional tracking, aircraft velocity vector determination, radar systems and tracking errors 19 p2454 A73-38470
- Midair collision avoidance strategies for ATC improvement, discussing relative effectiveness of structural airspace, airborne and ground-based systems based on US statistics 21 p2733 A73-40030
- Horizontal aircraft maneuver strategy for maximum miss distance and minimum course deviation, examining filtering techniques, collision avoidance system and signal error analysis 21 p2734 A73-40032
- A survey of satellite-based systems for navigation, position surveillance, traffic control and collision avoidance. 21 p2736 A73-40052
- Frequency of anti-collision observing responses by solo pilots as a function of traffic density, ATC traffic warnings, and competing behavior. 21 p2645 A73-41158
- USA government and industry efforts on aircraft midair collision avoidance systems technology advancement, comparing cost effectiveness between airborne and ground based options [ASME PAPER 73-ICT-49] 23 p3005 A73-43495
- COLLISION PARAMETERS**
- NT COLLISION RATES**
- Approximate method to determine collision probabilities, hyperbolas, and direct and retrograde ellipses during single close encounters in three body planetary problem 01 p0099 A73-10693
- Collisional-radiative coefficients and population coefficients of hydrogen plasma. 02 p0198 A73-12347
- A general study of the effect of collision parameters on the cosmic-ray fluxes in the atmosphere. 06 p0743 A73-17831
- Collision matrix elements near a pseudocrossing of potential energy curves. 06 p0726 A73-18249
- Radiative and collisional effects in a cylindrically confined plasma. I - Optically thin considerations. II - Absorption effects. 08 p1021 A73-20793
- Asteroidal rotational properties interpreted in terms of model with collisional breakup into irregular fragments 11 p1425 A73-26136
- Book - Low energy electron collisions in gases: Swarm and plasma methods applied to their study. 17 p2213 A73-34461
- A tensor surface harmonic expansion of the collision integral for a weakly ionized plasma. I 20 p2596 A73-39193
- Relaxation time in disk galaxy simulations 22 p2904 A73-41754
- The asteroid belt and its evolution. 24 p3134 A73-44565
- COLLISION RATES**
- Vertical profiles of the effective collision number in the E and F regions of the ionosphere 06 p0689 A73-17552
- Scattering of microwaves by a stratified overdense plasma at high collision frequencies. [AD-756733] 06 p0732 A73-18780
- Effect of collision frequency on the characteristics of waveguide filled with homogeneous anisotropic plasma. 07 p0857 A73-19533
- Possibilities of using a quadrupole probe in the 0 to 1000-Hz range to measure the collision frequencies of charged particles in the ionosphere 08 p0957 A73-20654
- Measurement of effective collision frequency in RF heating through parametric instabilities. [TTU-SR-2] 09 p1128 A73-22634
- Consideration of the different wave paths of the ordinary and extraordinary component in the calculation of electron density and collision frequency with the aid of the Faraday experiment 12 p1494 A73-27773
- Temporal development of longitudinal plasma current radial profile, obtaining effective collision frequency estimation for electron heating, hot plasma production conditions and stability restoration force 14 p1777 A73-29685
- Vertical profiles of the effective collision frequency in the E- and F-regions of the ionosphere. 16 p2002 A73-32776
- Ionospheric electron thermal conductivity obtained for power law dependence of electron-neutral collision frequency dependence on velocity 16 p2010 A73-33923
- Small grain aggregates created by equalized grain orbits on Kepler trajectories, with low collisional frequency in early state of solar system planetary evolution 17 p2227 A73-34407
- Effect of collisions on the random electron density fluctuations in a plasma. 19 p2468 A73-37519
- Electromagnetic absorption in magnetized cold plasma, discussing definition and use of velocity dependent collision frequencies with Legendre polynomials as weighting functions 21 p2654 A73-40818
- Determination of electron density and electron collision frequency in a plasma by an RF nonimmersive probe. 21 p2748 A73-40953
- Parametric instabilities of weakly turbulent plasma, determining collision frequencies characterizing high frequency electric field energy absorption 21 p2750 A73-41681
- Electron-molecule collision frequencies in a crossed electric and magnetic field. 24 p3118 A73-45476
- COLLISION WARNING DEVICES**
- U COLLISION AVOIDANCE**
- U WARNING SYSTEMS**
- COLLISIONAL PLASMAS**
- Conductivity tensor and dispersion equation for collisional magnetoactive plasma. 09 p1131 A73-22922
- Electron-neutral particle collisions effect on potential of test charge moving at velocity lower than plasma electrons, using BGK model and Lorentz collision operator 11 p1404 A73-25260
- Consideration on the 'equilibrium' electrons distribution function for a homogeneous, high-frequency, fully ionized plasma. 14 p1779 A73-29998
- Quantum correction to the electrical conductivity of a Coulomb plasma 14 p1781 A73-30584
- The effect of temperature perturbations on ion-acoustic and drift waves in a weakly collisional plasma. 15 p1916 A73-31087
- Current distribution on an infinite tubular antenna immersed in a cold collisional magnetoplasma. 15 p1920 A73-32236
- Transient current overshoot to electrostatic probes in continuum, slightly ionized plasmas. 16 p2041 A73-33331
- The kinetic characteristics of the electrons of the anisothermal homogeneous steady neon plasma in the ionization level range from 10 to the minus 9th power to 0.01 16 p2043 A73-34022
- Edge instability of transverse electromagnetic waves in a weakly ionized plasma 17 p2214 A73-34249
- Book - Low energy electron collisions in gases: Swarm and plasma methods applied to their study. 17 p2213 A73-34461
- Experiments of shock waves in a fully ionized plasma flow. 19 p2464 A73-37159
- Current driven ion wave instability in a weakly ionized collisional magnetoplasma. 20 p2599 A73-39725
- Electromagnetic absorption in magnetized cold plasma, discussing definition and use of velocity dependent collision frequencies with Legendre polynomials as weighting functions 21 p2654 A73-40818
- Plasma instability in a collisional and thermal magnetoplasma. 21 p2748 A73-40928
- Comparison of the plane, cylindrical and spherical one-dimensional models of the free expansion of a collisionless plasma. 21 p2748 A73-40929
- Kinetic theory of a collision-dominated plasma. 21 p2749 A73-41618
- Conductivity tensor of a collisional plasma in a magnetic field. 21 p2749 A73-41628
- Parametric instabilities of weakly turbulent plasma, determining collision frequencies characterizing high frequency electric field energy absorption 21 p2750 A73-41681
- COLLISIONLESS PLASMAS**
- Slightly oblique shock waves in a collisionless magnetized plasma. 01 p0082 A73-10421
- Stimulated Raman scattering of microwaves in a layer of collisionless plasma. 01 p0082 A73-10423
- Collisionless magnetoactive plasma nonlinear responses tensors symmetry properties, stressing Onsager relations generalization 01 p0083 A73-10454
- Ergodic behaviour of nonlinear hydromagnetic waves in a cold collisionless plasma. 01 p0087 A73-11496
- Magnetization currents effect on linear hydromagnetic instabilities development in collisionless anisotropic plasmas 02 p0196 A73-11899
- Collisionless plasma flow over a conducting sphere. 02 p0158 A73-11919
- Third order collisionless electron plasma echo signal wavelength and rise and fall rate about central position, comparing experiment with Vlasov equation theory 02 p0197 A73-12064
- Resonance, particle trapping, and Landau damping in finite amplitude obliquely propagating waves. 02 p0197 A73-12068
- Nonrelativistic collisionless plasma ion acoustic waves modulation by hf electromagnetic oscillation, calculating wave complex frequency [AD-753362] 02 p0197 A73-12069
- Nonlinear waves in a multicomponent plasma with weak dissipation. 02 p0198 A73-12103
- Wave coupling at a collisionless plasma discontinuity. 02 p0198 A73-12408
- Collisionless plasma compression shock waves thermodynamics, noting entropy variations along shock adiabat under plasma heating in magnetic field 02 p0198 A73-12552
- Wave scattering in collisionless magnetoactive plasma, taking into account magnetic field effects, spiral motion of scattering particle and shielding fields 03 p0346 A73-13357
- Kinetic and dispersion equations for collisionless plasma interaction with HF magnetic and electric fields, noting conical, drift and cyclotron instabilities prevention 04 p0478 A73-15019
- The thickness of perpendicular collisionless shocks in a hot plasma. 04 p0479 A73-15191
- Plasma heating and acceleration due to Landau damping of hydromagnetic waves. 04 p0480 A73-15197
- Helicon /whistler/ turbulence spectra in collisionless plasma, noting ion scattering relation to self trapping and concentration along magnetic field with Landau absorption decay 04 p0480 A73-15564
- Non-linear damping of longitudinal ion oscillations in a collisionless non-isothermal plasma. 04 p0482 A73-16042
- Numerical simulation of high Mach number supercritical magnetosonic collisionless shock wave propagation perpendicular to magnetic field, considering cause of anomalous ion heating 05 p0604 A73-17365

Evolutionary aspects of shock waves in the Chew, Goldberg, and Low approximation

06 p0727 A73-17471

Numerical simulation of a plasma. I - General description of the model

06 p0727 A73-17574

Current-induced nonlinear ion oscillations in a plasma

06 p0729 A73-18112

Effects of non-Maxwellian electron energy distributions on the orbital limited current-voltage characteristics of cylindrical and spherical Langmuir probes under collisionless conditions.

06 p0730 A73-18463

Two dimensional simulation of nonlinear ion-sound instability in current carrying collisionless plasma due to modification of electron distribution function

06 p0730 A73-18464

Difference frequency generation using non-linear interaction between a modulated electron beam and a collisionless plasma.

06 p0733 A73-18839

Stochastic ion heating by ion-acoustic turbulence.

06 p0733 A73-18850

Variational algorithms for numerical simulation of collisionless plasma with point particles including electromagnetic interactions.

07 p0854 A73-19264

Kelvin-Helmholtz instability in a high-beta collisionless plasma.

07 p0856 A73-19520

Computerized simulation for nonlinear evolution of whistler instabilities in anisotropic collisionless plasmas with various Maxwellian electron distributions

07 p0857 A73-19523

Nonlinear small amplitude behavior of collisionless plasma at mirror flute instability threshold, using modified constant gravity model and magnetic moment variation

07 p0857 A73-19525

Turbulence spectra of collisionless magnetized plasma produced in high voltage theta pinch, considering initial magnetic field orientation and instability theories tests

07 p0857 A73-19527

Intrinsic bandwidth of cyclotron resonance in the geomagnetic field.

07 p0792 A73-19532

The complete iso-thermalization by collective electromagnetic interactions of strongly anisotropic magnetized collisionless plasmas.

07 p0859 A73-20235

German monograph on collective dissipation processes in collisionless shock waves in high ion temperature plasma, using laser beam scattering technique

07 p0837 A73-20387

Privileged equilibria of a collisionless homogeneous or inhomogeneous plasma.

07 p0860 A73-20480

Cold collisionless plasma equations for electromagnetic waves absorption near lower hybrid resonance in inhomogeneous magnetized plasma contained in ideally conducting cylinder

09 p1125 A73-21906

Dissipation of hydromagnetic waves with application to the outer solar corona. I - Collisionless protons and collisional electrons. II - Transition from collisional to collisionless electrons.

09 p1142 A73-22038

Propagation of electronic longitudinal modes in a non-Maxwellian plasma.

09 p1126 A73-22278

Structure of a collisionless boundary layer and the turbulent braking of ions

09 p1127 A73-22607

Radio-frequency heating of a collisionless plasma. [TTU-SR-2]

09 p1128 A73-22627

Drift-like instability in density modulated plasmas in a static magnetic field.

09 p1131 A73-22904

The energy-momentum tensor for an electromagnetic wave in plasma.

10 p1254 A73-24115

Variational determination of electric field induced by charge separation in near wake of negatively charged body moving at mesothermal speeds in collisionless plasma

10 p1254 A73-24116

Collisionless plasma compression shock waves thermodynamics, noting entropy variations along shock adiabat under plasma heating in magnetic field

10 p1254 A73-24179

First order approximation of collisionless protons expansion in quiet solar wind

10 p1269 A73-24651

A self-consistent model of a simple magnetic neutral sheet system surrounded by a cold, collisionless plasma.

10 p1257 A73-24725

Strong plasma turbulence at helicon frequencies

10 p1257 A73-24757

Unstable Langmuir or ion acoustic wave saturation in collisionless plasma due to electron trapping, esti-

imating amplitude via adiabatic and sudden approximation

11 p1404 A73-25258

The ion cyclotron drift loss-cone instability with a coexisting cold plasma.

11 p1404 A73-25271

Dissipation of hydromagnetic waves with application to the outer solar corona. III - Transition from collisional to collisionless protons.

11 p1428 A73-26619

Cosmic dilute collisionless plasma physical properties, discussing plasma wave turbulence characteristics, particle acceleration, relativistic plasmas, synchrotron emission, pulsars and galactic nuclei

12 p1537 A73-26850

Application of the collisionless absorption of an extraordinary wave to the determination of plasma electron temperatures

12 p1528 A73-27302

Nonlinear propagation of electromagnetic waves in a weakly ionized plasma.

13 p1665 A73-28677

Wave periodic structure solution instability and unstable oscillation growth rates for nonlinear drift waves and solitons in collisionless plasma

14 p1778 A73-29692

Plasma radiation from collisionless MHD shock waves and the high-frequency waves in the upstream solar wind.

14 p1786 A73-29978

Collisionless magnetized unstable plasma two dimensional adiabatic compression, calculating gamma from temperature distributions

14 p1779 A73-29984

Investigation of the heating of a plasma ion component by a collisionless shock wave.

14 p1780 A73-30336

Magnetospheric collisionless drift waves from ATS-5 electron and proton velocity distribution measurements, comparing with predicted perturbation distribution function

14 p1750 A73-30659

Observation of stable, high Mach number collisionless electrostatic shocks.

15 p1916 A73-31079

Wake past an obstacle in a magnetized plasma flow.

15 p1916 A73-31089

Kinetic models of the solar and polar winds.

15 p1926 A73-31847

Cold collisionless plasma equations for electromagnetic waves absorption near lower hybrid resonance in inhomogeneous magnetized plasma contained in ideally conducting cylinder

15 p1922 A73-32631

Lagrangian description of phase space flow - Turbulent heating.

16 p2041 A73-33322

Magnetic multipole containment of large uniform collisionless quiescent plasmas.

17 p2215 A73-34271

Cold collisionless plasma flow along magnetic field, deriving quasi-shock wave characteristics from Vlasov-Maxwell equations

19 p2463 A73-37152

Rarefied collisionless plasma turbulence and dissipation process due to instability, examining magnetic field effects on shock wave front nature

19 p2464 A73-37154

Structure of almost collisionless shocks in a magnetoplasma and the ion-acoustic instability.

19 p2464 A73-37158

A review of electrostatic probe response in a flowing, low density plasma.

19 p2465 A73-37165

Solar wind-geomagnetic field interaction simulation by plasma flow and magnetic dipole, proving collisionless dissipation presence

19 p2481 A73-37339

Application of cylindrical Langmuir probes to streaming plasma diagnostics.

19 p2469 A73-37862

Magnetically induced collisionless coupling between counterstreaming laser-produced plasmas.

19 p2469 A73-38290

Low-frequency flute instabilities of a bounded plasma column.

20 p2595 A73-38889

Hydrogen plasma compression producing collisionless shock waves, measuring turbulence intensity as function of cut-off angle and anisotropy

20 p2596 A73-38966

Unsteady shock waves in a rarefied plasma

20 p2597 A73-39277

Electron plasma wave shocks in a collisionless plasma.

20 p2598 A73-39301

The role of Korteweg-de Vries equation in plasma physics.

20 p2599 A73-39625

Shielding of a moving test charge in a turbulent plasma.

20 p2599 A73-39722

On input impedance of an arbitrarily oriented small loop antenna in a cold collisionless magnetoplasma.

22 p2824 A73-41858

Interference structure of oscillating point charge near resonance cone in warm magnetized collisionless plasma, relating structure location to cyclotron frequency and plasma parameters

22 p2891 A73-42242

Instabilities of drift magnetosonic waves due to the magnetic drift resonance.

22 p2894 A73-42395

German monograph - Model of a parallel shock wave with turbulent dissipation in a hot plasma.

22 p2895 A73-42718

Collisionless shock wave propagation parallel to magnetic field for large plasma/magnetic pressure ratio, discussing shock structure in developing turbulence

22 p2851 A73-42932

Interactions of plasmas with magnetic field boundaries.

22 p2851 A73-42977

Nonlinear interaction of high-amplitude Langmuir waves in a collisionless plasma

23 p3012 A73-44015

Langmuir wave attenuation in collisionless plasma of variable density due to field generated by resonant particle currents moving toward lower density region

23 p3015 A73-44349

Nonlinear plasma ion oscillations excited by a current.

24 p3114 A73-44501

Collisionless magnetospheric-solar wind plasmas interactions, noting boundary stability and tail instability

24 p3127 A73-45213

Stability of two-dimensional collision-free plasmas.

24 p3116 A73-45237

Neutron emission from laser produced plasmas and collisionless electrostatic shock waves.

24 p3116 A73-45242

Determination of the voltage distribution in the interelectrode space of a grid probe immersed in a Maxwellian plasma

24 p3116 A73-45328

Experimental investigation of the low-frequency capacitive response of a plasma sheath.

24 p3117 A73-45408

COLLISIONS

NT ATOMIC COLLISIONS

NT COULOMB COLLISIONS

NT INELASTIC COLLISIONS

NT IONIC COLLISIONS

NT METEORITE COLLISIONS

NT MIDAIR COLLISIONS

NT MOLECULAR COLLISIONS

NT PARTICLE COLLISIONS

Planar three body problem singularities due to binary collisions, regularizing equations of motion by Levi-Civita coordinate transformation

01 p0099 A73-10692

Changes in the gravitational energy of galaxies during collisions.

02 p0217 A73-12392

A numerical hydrodynamic study of coalescence in head-on collisions of identical stars.

02 p0223 A73-12727

Approximative calculation of flutter regions for collision body systems in phase space, noting fluttering duration as function of post-impact velocity recovery factor

06 p0725 A73-18880

Approximative calculation of flutter regions for collision body systems in phase space, noting fluttering duration as function of post-impact velocity recovery factor

15 p1915 A73-32405

Charged black hole collisions as gravitational radiation sources in terms of conservation of mass and surface area

22 p2908 A73-42428

Isosceles case of rectilinear restricted three body problem with two equal mass primaries in rectilinear ellipses, deriving escape and collision conditions

24 p3141 A73-45285

COLLOCATION

A finite element collocation method for quasilinear parabolic equations.

10 p1241 A73-23638

Buckling analysis of elastically constrained conical shells under hydrostatic pressure by the collocation method.

11 p1438 A73-25499

Point matching /collocation/ computation of transverse resonances by complex valued solutions of Helmholtz equation with Neumann or Dirichlet problems, applying to electromagnetic waveguides

13 p1581 A73-28076

The numerical treatment of natural eigenvalue problems of the 4th order according to the collocation method with a Lagrange polynomial approach

13 p1695 A73-28411

COLLOIDAL GENERATORS

Emitter efficiency increase in annular colloid microthrusters with single sharp tips for high specific charge of conducting liquid droplets under low potential

04 p0488 A73-15723

Electric propulsion systems for satellite station-keeping, discussing developments in colloid thrusters and diagnostic equipment for performance measurement 07 p0867 A73-19222

COLLOIDAL PROPELLANTS
Erosive burning rate perturbation in colloidal propellant slab combusting channel as function of lateral velocity gradient and chamber pressure [AIAA PAPER 72-1108] 03 p0351 A73-13423
One-millipound colloid thruster system development. [AIAA PAPER 72-1153] 03 p0356 A73-13456
Colloid thruster propellants selection for semiconductor liquids with suitable electrochemical properties via cyclic voltametry 04 p0485 A73-15724
Linear slit colloid electrostatic thruster development and testing, discussing emitter geometry, gap design, exhaust velocity, operating voltage and power efficiency relationships 04 p0488 A73-15725
Direct measurement of colloid microthruster thrust and propellant mass flow rate, using microbalance 04 p0433 A73-15727
Investigation of a single spraying site of a colloid thruster. 08 p0996 A73-21599

COLLOIDS
NT AEROSOLS
NT COLLOIDAL PROPELLANTS
NT FOG
An analysis of the operating characteristics of the Colloid Core Reactor. [AIAA PAPER 72-1094] 03 p0341 A73-13414
Modelling of structure and functional unity on coacervate systems. 06 p0652 A73-17950
Coacervate systems and evolution of matter on the earth. 06 p0652 A73-17951
Visual display of the spatial distribution of colloidal particle beams. 09 p1136 A73-23448
Flow regimes for a magnetic suspension under a rotating magnetic field. 14 p1774 A73-29924
Apparatus for measuring the colloid osmotic pressure in blood serum 23 p2949 A73-43792

COLOR
NT WATER COLOR
Color image quantization error assessment from noninferior bit assignment determination for several coordinate systems by color shift comparison, using computer simulation 04 p0449 A73-15444
Comments on a PLC relationship for Cepheids and on the comparison between pulsation and evolution masses for Cepheids. 05 p0625 A73-17334

COLOR BLINDNESS
U COLOR VISION
COLOR CENTERS
Color centers in gamma-irradiated ruby with vanadium additions 10 p1259 A73-24069
Three-dimensional hologram recordings on photochrome glass with the application of an optical discoloration process. II 15 p1879 A73-32340
Ruby coloring centers and orange coloration dependence in corundum crystals on additive Mg, Cr, V and Ti ions 21 p2752 A73-40560

COLOR PERCEPTION
U COLOR VISION
COLOR PHOTOGRAPHY
Colour separation and electronic analysis of Gemini V and Apollo spacecraft photography. 01 p0045 A73-10275
Three color photometric study of open cluster NGC 1647, obtaining distance, B-V and U-B excesses and age 01 p0098 A73-10554
Ocean color measurements utilizing a noon orbit for earth resources satellite applications. 04 p0445 A73-15778
Schwarzschild effect elimination in stellar color photography via triple black and white photography with film of differing color sensitivities 05 p0578 A73-17096
Investigation of color detail, color analysis and false-color representation in satellite photographs. 05 p0578 A73-17136
Multispectral additive color viewer for ERTS satellite photography, discussing colorimetric measurement usefulness and photo processing and image density control effects on color characteristics 05 p0579 A73-17145
Source limited gray scale and color selection capabilities for direct and reflected light scanners. 06 p0701 A73-18308

Measurements regarding the color of aerial photographs in studies of the vegetation 06 p0695 A73-18437
Light distribution in photographic meteors by means of multicolour photometry. 08 p1010 A73-21316
The role of Schmidt telescopes in the study of galactic structure /Photometric methods/. 08 p1011 A73-21355
Surface colour photometry of galaxies with Schmidt telescopes. 08 p1011 A73-21363
Remote sensing of lunar color differences using sololuminous enhancement techniques. 09 p1082 A73-22384
Color encoded multispectral image recording on black-and-white photographic film with synthetically generated diffraction gratings, noting color recognition, resolution and contrast ratio 10 p1216 A73-23786
Multicolor documentation type information holographic storage, recording, indexing, registration and reconstruction technology assessment and application, emphasizing displays and automatic test equipment systems 10 p1216 A73-23797
Multicolor photoelectric photometry of Neptune. 11 p1429 A73-26682
The application of color and multispectral techniques to the collection of military geographic information. 12 p1500 A73-27952
Block adjustment for color and multispectral high altitude frame photography in photogrammetry, considering terrain caused sun angle effect as discriminant for automatic photointerpretation 12 p1500 A73-27955
Optimizing sensitometric data for color and black and white aerial film. 12 p1501 A73-27966
Signal color effects on stereoplotters measurements in aerial mapping of built-up areas 12 p1501 A73-27968
Remote sensing and photointerpretation, discussing black and white, color and IR photography, microwave imagery, atmospheric attenuation, reflectance and potential application for ERTS satellites 16 p2014 A73-33100
Cartographic applications of high-altitude aircraft photographs. 16 p2016 A73-33362
Airborne remote sensing for forestry and agricultural land imagery and water pollution detection, discussing use of color films and picture processing 17 p2161 A73-34933
On-axis computer generated hologram with multiemulsion color film for retaining kinoform advantages and effective control over amplitude and phase transmittance 17 p2171 A73-35401
An adaptation of the Stromgren four-color system to photographic photometry. 19 p2430 A73-37568
A new method for evaluating and mapping colours in aerial photographs. 20 p2568 A73-39884
Color holographic technique through wave front coding of colored object, discussing He-Ne, He-Cd and argon laser irradiation, coding masks and image reconstruction 21 p2697 A73-40128
Variation of the colour index along the meteor trail. 22 p2915 A73-43042
Multicolor astronomical photography of Jupiter using wideband filters, emphasizing Red Spot, atmospheric bright belts and methane absorption variations above clouds 23 p3032 A73-43941
A correlation between colors of Jovian clouds and their 5-micron temperatures. 23 p3033 A73-43948

COLOR TELEVISION
Recent advances in low light level field sequential color television. 06 p0694 A73-18298
Graphical distribution in colors adapted to traffic control 15 p1911 A73-32486
A compound wide angle color visual display system and a high resolution, high sensitivity close circuit color television camera developed for wide angle color visual systems. [AIAA PAPER 73-925] 21 p2702 A73-40872

COLOR VISION
The colour vision characteristics of an observer with unilateral defective colour vision - Results and analysis. 02 p0137 A73-12077
Color effects in visual discrimination, measuring response times in letter matching task 02 p0135 A73-12525
Reaction time as a measure of the temporal response properties of individual colour mechanisms. 03 p0267 A73-13757

Reduced illumination effects on visual acuity, color vision, dark adaptation, accommodation, visual fields and glare 05 p0540 A73-16480
Color vision in terms of spectral sensitivity, color appearance and discrimination, chromatic stimuli production, pigments spectral response, etc 05 p0540 A73-16481
Congenital and acquired color vision defects, discussing color blindness incidence, defect nomenclature and eye tests 05 p0540 A73-16482
Color structure in Jupiter observations, discussing use of binoculars and graphical representation methods 05 p0578 A73-17097
Color naming and hue discrimination in congenital tritanopia and tritanomaly. 07 p0782 A73-20251
Stimulus effect on spatial summation of color receptive pathways and discrimination thresholds as function of color, gradient, retinal illumination and field size 07 p0783 A73-20254
Photochemical receptor mechanism of chromatic vision and scotopic contrast hue sensation due to cone and rod activity interaction 07 p0783 A73-20261
The role of colour perception and 'pattern' recognition in stereopsis. 07 p0783 A73-20266
The brightness of coloured flashes on backgrounds of various colours and luminances. 08 p0935 A73-21565
Single cell analysis of saturation discrimination in the macaque. 08 p0932 A73-21568
Simultaneous motor and verbal processing of visual information in a modified Stroop test. 09 p1044 A73-21896
Retinal mechanisms of colour vision. 09 p1043 A73-23316
Colour selectivity in orientation masking and aftereffect. 11 p1323 A73-26196
The influence of wavelength on visual adaptation to spatially periodic stimuli. 11 p1318 A73-26199
Spectral sensitivities of colour mechanisms isolated by the human visual evoked response. 12 p1461 A73-26919
Probability summation model for heterochromatic luminance additivity failure at absolute visual threshold. 13 p1578 A73-28099
Evoked potentials to changes in the chromatic contrast and luminance contrast of checkerboard stimulus patterns. 13 p1575 A73-28355
Cone spectral sensitivity studied with an ERG method. 13 p1575 A73-28358
The macular and paramacular local electroretinograms of the human retina and their clinical application. 13 p1575 A73-28364
Binocular color resolution capability of the eyes as a function of the characteristics of vision during anisometropia 15 p1832 A73-30999
Threshold and suprathreshold perceptual color differences. 15 p1837 A73-31019
Opponent-colors responses in the visually evoked potential in man. 17 p2112 A73-34844
The effect of colour on time delays in the human oculomotor system. 17 p2112 A73-34847
Book - The psychology of visual perception. 17 p2117 A73-35474
Contrast sensitivity, Westheimer function and Stiles-Crawford effect in a blue cone monochromat. 19 p2394 A73-37414
Spatial characteristics of chromatic induction - The segregation of lateral effects from straylight artefacts. 19 p2394 A73-37419
Dichromatic convergence points obtained by subtractive colour matching. 19 p2398 A73-37420
Reaction times for focal and nonfocal /peripheral/ processing of simultaneously presented color and form stimuli 21 p2639 A73-41182
Colored aftereffects after prolonged inspection of convex lines of one color and concave lines of another color 21 p2640 A73-41303
Rectifier-like color dependent phase shifts in electrophysiological responses to different colored stimuli at evoked potential and single neuron levels 22 p2810 A73-42961
Bezold-Bruecke effect and visual nonlinearity. 23 p2946 A73-43342

Prefrontal lobe functions and the neocortical commissures in monkeys. 24 p3061 A73-45166

COLORADO

A crustal-upper-mantle model for the Colorado plateau based on observations of crystalline rock fragments in the Moses Rock dike. 05 p0569 A73-16381

Photometric measurements of zenith night sky over Fritz Peak /CO/ for diurnal and seasonal variation of nightglow continuum 19 p2425 A73-38013

COLORATION

U COLOR

COLORIMETRY

Russian book on color recognition methods and devices covering algorithms for radiation color identification and optimal spectra of photosensitive radiation detector 02 p0144 A73-12862

Multispectral additive color viewer for ERTS satellite photography, discussing colorimetric measurement usefulness and photo processing and image density control effects on color characteristics 05 p0579 A73-17145

Skylab experiment for measuring color indices of extended sources and of spectral types O, B and A hot stars at various galactic latitudes 07 p0822 A73-18989

Numerical computation of photosphere temperature-associated equatorial brightening in red and green bands used in solar oblateness measurements [AD-758969] 09 p1142 A73-22040

Dichromatic convergence points obtained by subtractive colour matching. 19 p2398 A73-37420

COLUMNS [SUPPORTS]

Matrix analysis of local instability in plates, stiffened panels and columns. 03 p0390 A73-13339

Constrained optimal design of columns against buckling. 04 p0510 A73-15029

Buckling of columns with variable moment of inertia. 05 p0633 A73-16538

Finite element analysis of nonlinear vibration of beam columns. 05 p0636 A73-17118

Initial postbuckling behavior of optimally designed columns and plates. 07 p0908 A73-19084

Impact response of curved box beam-columns with large global and local deformations. [AIAA PAPER 73-401] 11 p1440 A73-25530

Inelastic buckling of columns - The effect of imperfections. 16 p2084 A73-33975

Inelastic buckling of eccentrically loaded columns. 17 p2240 A73-34180

The dynamic response of columns under short duration axial loads. [ASME PAPER 73-APM-19] 17 p2248 A73-35040

Effect of rivet spacing on crippling loads of joined aluminum angles. 19 p2499 A73-38009

Column instability under nonconservative forces, with internal and external damping - Finite element using adjoint variational principles. 20 p2621 A73-39540

Parametric instability of clamped-clamped and clamped-simply supported columns under periodic axial load. 22 p2929 A73-43137

Non-linear creep buckling with random temperature variations. 23 p3045 A73-44166

COMA

Comet nucleus models, discussing classical and icy snowball heads, nongravitational forces, nucleus dimensions and evidence against solid cores 02 p0223 A73-12731

A 1.1 micron spectrogram of the central coma of Comet Bennett /1969 i/. 02 p0226 A73-12832

Comet research assessment for 1970-1972, discussing coma and nucleus, icy conglomerate and sandbank models 04 p0495 A73-14765

COMBAT

Control configured vehicle /CCV/ concept application to fighter aircraft design for combat maneuver capabilities and versatility enhancement, using fly by wire technology [SAE PAPER 720854] 05 p0535 A73-16662

Control configured vehicle /CCV/ technology application for fighter aircraft combat control versatility enhancement, presenting F-4 analytical, simulation and wind tunnel test performance results [AIAA PAPER 73-160] 05 p0535 A73-16907

Air combat roles identification by reachable sets technique, evaluating aircraft/weapon systems potential performance vs given threat [AIAA PAPER 73-232] 05 p0536 A73-16957

Decomposition strategies for one on one aerial dog-fight game models with reinforcement learning [AIAA PAPER 73-233] 05 p0536 A73-16958

JP8 and JP4 aircraft fuel fire and explosion susceptibility from gunfire hits, discussing combat survivability relative to fuel volatility 16 p2045 A73-32670

Remotely piloted vehicle /RPV/ for reconnaissance, electronic warfare systems, target acquisition, weapon delivery, air-air combat and different combinations 24 p3057 A73-45399

COMBINATIONS [MATHEMATICS]

Synthesis of combination circuits in a universal basis and its use in estimating the complexity of digital structures containing integrated circuits 21 p2668 A73-40017

COMBINATORIAL ANALYSIS

NT COMBINATIONS [MATHEMATICS]

NT PARTITIONS [MATHEMATICS]

A combinatorial method to compute a global solution of certain non-convex optimization problems. 16 p2033 A73-33855

Umbral /finite operator/ calculus in combinatorial theory of special polynomial sequences as technique for expressing one polynomial set in terms of another 17 p2204 A73-35732

COMBINED STRESS

Asymptotic analysis of nonlinearly elastic and plastic thin rectilinear panels under combined bending and tensile stress 01 p0119 A73-11442

Isotropy postulate verification for strain vectors measurement in annealed steel tubular specimens, showing coincidence of tension-internal pressure and tension-torsion test values 02 p0235 A73-12206

Singular solutions of the plane distortion problem of micropolar elasticity. 03 p0392 A73-13776

Dimensionless results for plane stress creep behavior of thin disks with central rigid inserts under combined loading 03 p0396 A73-14644

Interaction curves for bending and axial forces of perfectly plastic curved I-beams. 06 p0762 A73-18339

Changes in the durability and lifetime of polymer films under simultaneous exposures to an electric field and mechanical loading 07 p0842 A73-19394

The application of nodal stress concepts to the bending of plates and shells. 08 p1019 A73-21691

Device for investigating the mechanical characteristics of materials in a complex stressed state 09 p1070 A73-22167

On the elastoplastic problem of cantilever subject to combined bending and twisting. 09 p1164 A73-23320

Elasto-plastic stress analysis of prismatic bar under combined bending and torsion. 10 p1289 A73-24160

Combined axial and torsional shear of a tube of incompressible isotropic elastic material. 10 p1291 A73-24336

Investigation of the fracture of carbon-graphite materials in a complex stress-strain state 10 p1240 A73-24360

A note on the arrangement of strain gauges and the sensitivity of strain measurement. 10 p1219 A73-24572

Structural design for weight or volume minimization in deformable body under combined loads, comparing structures with different boundary configurations 10 p1226 A73-24791

A statistical theory for failure of brittle materials under combined stresses. 11 p1439 A73-25511

Asymptotic analysis of nonlinearly elastic and plastic thin rectilinear panels under combined bending and tensile stress 11 p1443 A73-26060

An examination of dynamic fracture under biaxial-strain conditions. 12 p1550 A73-27022

Damping properties of soft viscoelastic materials for certain plane stress combinations 12 p1515 A73-27176

Procedure for studying fatigue failure features in metals under harmonic and complex loading at low temperatures 12 p1486 A73-27254

Couple-stresses effects in vicinity of interface for infinite elastic plane with a rigid inclusion. 13 p1702 A73-29533

The effects of out-of-phase biaxial-strain cycling on low-cycle fatigue. 14 p1806 A73-29774

Service life determination in heat-resistant alloys under unsteady working conditions with allowance for brief overloading 14 p1763 A73-30690

Thermal stresses and couple-stresses in square cylinder with a circular hole. 14 p1815 A73-30919

Combined tension-torsion creep of polyethylene with abrupt changes of stress. 15 p1897 A73-31613

Rectangular cross section isotropic elastoplastic material behavior under combined compressive and bending stresses with allowance for work hardening 16 p2076 A73-32931

Nonlinear creep in glassfiber-reinforced plastics in the presence of some types of complex stress conditions 16 p2030 A73-33926

Experimental investigation of the effect of vibrations on the creep of glassfiber-reinforced plastics in the presence of complex stress conditions 16 p2030 A73-33939

Meridional geometries for orthotropic shells with bending suppressed for different loading conditions, deriving shell configurations for combined loading via equilibrium equations 17 p2243 A73-34530

A biaxial split Hopkinson bar for simultaneous torsion and compression. 17 p2149 A73-35754

Anisotropic nature of strain hardening during unsteady creep of alloy AK4-1 subject to combined tension and torsion 20 p2577 A73-39288

Stability of cylindrical shells beyond the elastic limit 21 p2786 A73-40979

Experimental investigation of a cylindrical shell loaded by a concentrated tangential force and a bending moment 21 p2787 A73-41193

Steady-state creep of a thin-walled tube in the general case of applied forces 21 p2787 A73-41194

Polish book - Theory of coupled stresses. 21 p2787 A73-41219

The interaction of creep and fatigue for a rotor steel /The William M. Murray Lecture, 1972/. 21 p2722 A73-41264

Nondestructive shell-stability estimation by a combined-loading technique. 21 p2708 A73-41266

The behavior of materials subjected to multiaxial cyclic stresses. I - Methods of calculation 22 p2917 A73-41781

A device for the investigation of the mechanical characteristics of materials under a complex stress system. 22 p2838 A73-42115

Some observations on fracture under combined loading. 22 p2920 A73-42133

Post-yielding behavior of torsionally loaded composite tubes. 23 p3041 A73-43640

A device for durability and creep testing of fiberglass-reinforced plastic pipes and shells in a complex stressed state 23 p2967 A73-44293

Limit loads of circular plates under combined loading. [ASME PAPER 73-APM-G] 23 p3047 A73-44379

Nonlinear parametric vibrations of cylindrical shells prepared from composite materials 23 p3145 A73-44517

Transverse coupled thermoelastic vibrations of elastically supported rectangular and circular plates under nonstationary harmonic temperature field 24 p3147 A73-44682

Mechanical properties of unidirectionally reinforced polyester and epoxy resin laminates under combined stresses perpendicular or parallel to glass fiber direction 24 p3104 A73-44886

COMBUSTIBILITY

U FLAMMABILITY

COMBUSTIBLE FLOW

On turbulent flows with fast chemical reactions. I - The closure problem. 01 p0032 A73-10637

Transport phenomena of reactive fluid flow in heterogeneous combustion processes. [ASME PAPER 72-WA/HT-30] 04 p0519 A73-15825

Computerized mathematical models of two- and three-dimensional turbulent flow combustion, considering temperature and concentration fluctuations, particle size, NO formation and radiative transfer 06 p0767 A73-17727

Comparison of four simple models of steady flow combustion of pyrolyzed methane and air. 07 p0865 A73-20360

Theoretical investigation on laminar boundary layer with combustion on a flat plate. 14 p1817 A73-30611

Spectroscopic studies of supersonic heterogeneous flows with a combustible condensed phase 21 p2754 A73-40702

Russian book - Solid-propellant rocket engines. 22 p2900 A73-41880

Effect of combustion upon precessing vortex cores generated by swirl combustors. 22 p2934 A73-42781

Combustion in high speed swirling flow in gas turbine combustion chamber, discussing flame stability, pressure measurements and chamber configuration
22 p2935 A73-42790

Flowing gas mixture ignition at heated blunt body stagnation point, examining Van't Hoff criterion
23 p3048 A73-43328

Piecewise-one-dimensional models of supersonic combustion and pseudoshock in a channel
24 p3154 A73-44702

Influence of velocity pulsations on the range of stable combustion of homogeneous mixtures
24 p3157 A73-45382

Mechanism of erosive burning of solid rocket propellants.
24 p3121 A73-45385

Vortex model for flames and free jets characteristic velocities based on three dimensional turbulent combustible flow
24 p3158 A73-45387

COMBUSTION

NT AFTERBURNING
NT BOUNDARY LAYER COMBUSTION
NT DEFLAGRATION
NT FUEL COMBUSTION
NT HYDROCARBON COMBUSTION
NT HYPERSONIC COMBUSTION
NT METAL COMBUSTION
NT PROPELLANT COMBUSTION
NT SOLID PROPELLANT IGNITION
NT SPONTANEOUS COMBUSTION
NT SUPERSONIC COMBUSTION

COMBUSTION CHAMBERS

Stability of combustors with partial length acoustic liners.
01 p0090 A73-10641

Manganese additive effects on emissions from a model gas turbine combustor.
01 p0121 A73-10644

Application of basic research to the study of combustion in turbine combustion chambers
[DGLR PAPER 72-058] 02 p0237 A73-11693

Combustion chamber pressure calculation for a pulsed air jet engine in the process of filling
02 p0203 A73-11708

Sound propagation in a combustion can with axial temperature and density gradients.
02 p0238 A73-12608

Scaling of performance and thermal environment in fuel-vortex cooled rocket engines.
[AIAA PAPER 72-1075] 03 p0354 A73-13399

Effect of injection velocity ratio and combustion chamber pressure on experimental performance of throttleable LO2/GH2-rocket engines with coaxial injectors.
[AIAA PAPER 72-1079] 03 p0354 A73-13402

Optimal stabilization conditions of turboreactor combustor initial recirculation zone determined by hydraulic analogy technique, describing vorticity generation and mass flow rates
[ONERA, TP NO. 1105] 03 p0359 A73-14126

The development of high performance annular combustion chambers at SNECMA
03 p0360 A73-14151

Inlet-combustor interface problems in scramjet engines.
03 p0360 A73-14153

Investigation of air stream from air-entry holes of the high-intensity combustor-liner.
03 p0400 A73-14447

Analytical correlation technique for air breathing and rocket engines combustor design and performance prediction based on hydrogen oxygen engines test data
[AIAA PAPER 72-1074] 04 p0486 A73-14904

Combustion effectiveness in high speed swirling flow tested in chamber with premixed air-kerosene mixture injected tangentially in annular channel
[ONERA, TP NO. 1076] 04 p0517 A73-15098

Heat transfer to film-cooled combustion chamber liners.
[ASME PAPER 72-WA/HT-32] 04 p0518 A73-15823

The influence of fuel preparation and operating conditions on flame radiation in a gas turbine combustor.
[ASME PAPER 72-WA/HT-26] 04 p0519 A73-15828

A proposed method for calculating film-cooled wall temperatures in gas turbine combustion chambers.
[ASME PAPER 72-WA/HT-24] 04 p0519 A73-15830

Modelling of gas turbine combustors - Considerations of combustion efficiency and stability.
[ASME PAPER 72-WA/GT-1] 04 p0489 A73-15865

Modeling radial dilution air injection in axial flow combustors.
[WSCI PAPER 72-24] 05 p0639 A73-16689

Gas temperature, carbon monoxide and nitric oxide axial and radial distribution in J-33 combustor, presenting combustion process model based on measurements
[WSCI PAPER 72-22] 05 p0639 A73-16690

The influence of combustor parameters on the combustion of particle-laden fuels in ducted flows.
[AIAA PAPER 73-177] 05 p0640 A73-16919

Screen and porous absorbing liner design for damping pressure oscillations in ramjet combustors based on

acoustic absorption efficiency and combustion instability calculation
[AIAA PAPER 73-226] 06 p0767 A73-17665

Algorithm for calculating unsteady heat transfer in liquid-propellant rocket-engine chambers with regenerative cooling
07 p0868 A73-20087

Emissions from and within an Allison J-33 combustor.
07 p0868 A73-20359

Analytical predictions of emissions from and within an Allison J-33 combustor.
08 p1025 A73-21670

Gas turbine combustor optimization dependence on combustion length and efficiency, cutoff pressure fall, wall cooling and pollution
09 p1135 A73-22213

Necessary conditions of stable combustion of powder in a semiclosed chamber
10 p1294 A73-23588

Loading configurations with large combustion surface and reduced thickness for solid propellant rocket ignition
[ONERA, TP NO. 1211] 10 p1262 A73-23658

Russian book - Fundamentals of the theory of operational processes in solid-propellant rocket systems.
10 p1262 A73-23948

Combustor design effect on jet aircraft engine exhaust pollutants reduction during hydrocarbon fuel burning
10 p1263 A73-24556

Emissions from and within an Allison J-33 combustor. II - The effect of inlet air temperature.
11 p1411 A73-26423

Effects of prevaporized fuel on exhaust emissions of an experimental gas turbine combustor.
11 p1411 A73-26424

Design and evaluation of combustors for reducing aircraft engine pollution.
13 p1670 A73-28932

Ballistite burning rate in sonic gas flow in supersonic conical nozzles as function of flow velocity and combustion chamber pressure
13 p1706 A73-28972

Condition of the medium before the flame front during the initial phase of a combustion process
15 p1957 A73-31867

Permeable elastic piston models of shock wave formation before flame front during inflammable gas mixture combustion in channels
15 p1957 A73-31868

Low emissions combustion for the regenerative gas turbine. II - Experimental techniques, results, and assessment.
[ASME PAPER 73-GT-12] 16 p2086 A73-33490

Development of advanced composite rocket motor chambers using boron and graphite fibers.
17 p2194 A73-34803

Reinforced plastics under ablative conditions for thermal insulation and structural applications.
17 p2195 A73-34805

Parametric test results of a swirl-can combustor.
17 p2222 A73-35471

Venturi exhausts for air pumping augmentation in ram air operated aircraft heater or combustor, discussing experimental data on suction variation
18 p2343 A73-36396

Combustion noise prediction techniques for small gas turbine engines.
19 p2473 A73-37296

Film effectiveness and heat transfer coefficient downstream of a metered injection slot.
[ASME PAPER 73-HT-31] 20 p2625 A73-38570

Coaxial jet mixing in confined tube simulating combustion chamber, considering Reynolds number, stream functions, recirculation, lip condition, vorticity and inlet conditions
20 p2548 A73-39518

Influence of combustion phenomena on the Pogo effect
21 p2754 A73-41551

Analytical modeling of a spherical combustor including recirculation.
22 p2934 A73-42783

Stirring factors in combustion chambers - A finite-element model of mixing along an 'information flow path.'
22 p2934 A73-42784

Mathematical modeling of combustors based on turbulent mixing, droplet evaporation and chemical kinetics, considering stirred reactor heat balance and combustor performance prediction
22 p2935 A73-42789

Emissions from and within an Allison J-33 combustor. II - The effect of inlet air temperature.
23 p3019 A73-43327

Burner dimension and flame size effects on relative contributions of luminous soot and nonluminous molecular band radiations from combustion fires
23 p3048 A73-43329

Turbofan engine core noise prediction and measurement, considering sources from flow passage obstruc-

tions, combustion chamber and turbine noise due to interaction with upstream turbulence
[AIAA PAPER 73-1026] 24 p3122 A73-44857

Some comments to mathematical interpretation of performance characteristics of jet engine combustion chambers.
24 p3123 A73-45381

COMBUSTION CONTROL

Pressure exponent of controllable solid rocket propellants.
[AIAA PAPER 72-1135] 03 p0352 A73-13442

Investigation of damping methods for low frequency augmentor combustion instability.
[AIAA PAPER 72-1207] 03 p0358 A73-13490

Photochemical ignition and combustion enhancement in high speed flows of fuel-air mixtures.
[AIAA PAPER 73-216] 05 p0641 A73-16946

Fire retardance of mixtures of inert gases and oxygen.
09 p1045 A73-22532

Mathematical model for extinguishing gunpowder combustion via pressure variations, assuming gunpowder surface dependence on combustion rates
09 p1167 A73-22617

Unsteady combustion of a confined spray.
[AICHE PREPRINT 23] 20 p2626 A73-39250

Stability of a conical burning surface during solid fuel combustion in a semiclosed volume
20 p2627 A73-39290

COMBUSTION EFFICIENCY

Investigations in connection with the preliminary development of a FLOX-polyethylene hybrid propulsion system
[DGLR PAPER 72-086] 02 p0202 A73-11676

Studies leading to the realization of supersonic combustion in propulsion applications.
03 p0398 A73-14141

Combustion effectiveness in high speed swirling flow tested in chamber with premixed air-kerosene mixture injected tangentially in annular channel
[ONERA, TP NO. 1076] 04 p0517 A73-15098

Modelling of gas turbine combustors - Considerations of combustion efficiency and stability.
[ASME PAPER 72-WA/GT-1] 04 p0489 A73-15865

The influence of combustor parameters on the combustion of particle-laden fuels in ducted flows.
[AIAA PAPER 73-177] 05 p0640 A73-16919

Direct mixing and combustion measurements in ducted, particle-laden jets.
[AIAA PAPER 72-1177] 06 p0769 A73-18400

One dimensional model for spark ignition Wankel engine combustion, presenting unsteady turbulent flame propagation equations
09 p1136 A73-22824

Thermodynamic cycle processes in liquid propellant rocket engines, taking into account combustion products chemical dissociation, wall and nozzle heat losses, friction effects, etc
10 p1263 A73-24700

Determination of the combustion efficiency by continuous analysis of the combustion products
12 p1558 A73-27386

Influence of oxidizer dispersity on the efficiency of combustion catalyzers
13 p1669 A73-28973

Combustion of fuel vapor-drops air systems. I - Open burner flames. II - Spherical flames in a vessel.
16 p2085 A73-33343

Study of gas-phase reactions in particle-laden, ducted flows.
17 p2150 A73-34194

Effect of secondary oxidizer supply through a porous solid fuel on the hybrid combustion process
23 p3019 A73-43783

Some comments to mathematical interpretation of performance characteristics of jet engine combustion chambers.
24 p3123 A73-45381

COMBUSTION HEAT

U HEAT OF COMBUSTION

COMBUSTION INSTABILITY

U COMBUSTION STABILITY

COMBUSTION PHYSICS

Analytical method of gasdynamic semibounded-space parameter computation allowing for velocity profile inhomogeneity and turbulent combustion of condensed systems
01 p0121 A73-10619

A critical discussion of theories of flame spread across solid and liquid fuels.
01 p0121 A73-10643

Boron combustion, covering thermochemistry application to chemical propulsion systems, temperature effects on oxidation, single particle ignition and powder burning
01 p0089 A73-11112

Combustion theory of hybrid rocket propellant-oxidizer combinations based on heat transfer limited model, discussing chemical kinetics and temperature effects on regression rate
[AIAA PAPER 72-1143] 03 p0397 A73-13449

An analysis of the chemically reacting boundary layer during hybrid combustion.
[AIAA PAPER 72-1144] 03 p0273 A73-13450

Steady state spray combustion model, using Nukiyama-Ianasawa drop distribution function, Stokes drag and modified Priem-Heidmann or Spalding vaporization rate equations
[WSCI PAPER 72-36] 05 p0639 A73-16680

Study of exothermic processes in shock ignited gases by the use of laser shear interferometry.
[AIAA PAPER 73-178] 05 p0640 A73-16920

Emissions from continuous combustion systems; Proceedings of the Fifteenth Symposium, Warren, Mich., September 27, 28, 1971. 06 p0767 A73-17726

Current kinetic modeling techniques for continuous flow combustors. 06 p0767 A73-17728

Some observations on flows described by coupled mixing and kinetics. 06 p0767 A73-17729

Flame structure and flame reaction kinetics. VIII - Structure, properties and mechanism of a rich hydrogen + nitrogen + oxygen flame at low pressure. 07 p0918 A73-19154

Convective combustion of porous explosives 07 p0920 A73-19990

Combustion catalysis model of a single-component fuel/as applied to ammonium perchlorate/ 07 p0865 A73-19991

Some studies on opposed-jet diffusion flame considering general Lewis numbers. 07 p0921 A73-20357

An experimental study of ammonium perchlorate-binder sandwich combustion in standard and high acceleration environments. 07 p0866 A73-20363

Investigation of the burnup process structure under spin conditions 07 p0923 A73-20424

Experimental study of influence of an electric field on a laminar flame. 08 p1021 A73-20864

Application of the method of matched asymptotic expansions to calculate the steady-state thermal propagation of an exothermic reaction front in a condensed medium 09 p1167 A73-22616

Reduced scale experimental study of propogol propulsion system ignition phases, defining pressure buildup curve shape and ignition limits [ONERA, TP NO. 1182] 09 p1135 A73-22711

Two zone model of multizone condensed system combustion, showing front velocity dependence on leading heat zone and dispersion depth 10 p1294 A73-23589

German handbook of functions and numerical values in physics, chemistry, astronomy, geophysics and engineering covering thermodynamics, combustion physics and heat transfer 11 p1450 A73-25473

Soot oxidation kinetics at combustion temperatures. 12 p1557 A73-26844

Chain interaction and heat release near the lower limit for self-ignition of hydrogen with oxygen 12 p1465 A73-26967

New phenomena during the burning of condensed systems 12 p1559 A73-27454

A probe system for spectrometric determination of temperature and concentration distributions in combustion gases. 13 p1612 A73-28432

Investigation of the detonation characteristics of hexogen-filler systems 13 p1706 A73-28970

Regularities in the burning of condensed systems within a field of mass forces at moderate pressures 13 p1706 A73-28975

Laminar flame propagation in hydrogen, oxygen, nitrogen mixtures. 13 p1707 A73-29001

Russian book - Transition of burning of compacted systems to detonation. 15 p1959 A73-32420

Combustion of droplets of liquid fuels - A review. 18 p2372 A73-37096

Quasi-stationary theory of hydrocarbon droplet ignition. II - Ignition limits of cold and hot droplets 18 p2372 A73-37117

Experimental investigation of premixed swirling jet flames - Combustion characteristics. 19 p2504 A73-37946

Calculation of the generation of inversion and the laser output power for expanding combustion gases /CO₂-N₂-He/ 19 p2504 A73-38157

Direct-sampling studies of combustion processes. 19 p2504 A73-38325

Russian book - Burning of metal powders in active media. 21 p2753 A73-40418

International Symposium on Combustion, 14th, Pennsylvania State University, University Park, Pa., August 20-25, 1972, Proceedings. 22 p2933 A73-42751

Some reactions and hydroperoxyl and hydroxyl radicals at high temperatures. 22 p2898 A73-42754

Elementary reaction rates from post-induction-period profiles in shock-initiated combustion. 22 p2933 A73-42755

Estimation of rate constants of elementary processes - A review of the state of the art. 22 p2933 A73-42759

Spectroscopic studies of low-pressure hydrogen-fluorine flames. 22 p2898 A73-42760

High temperature ionic and charged species reactions in hydrocarbon and cyanogen flames and additive combustion systems 22 p2819 A73-42770

Aerodynamic and thermal structures of the laminar boundary layer over a flat plate with a diffusion flame. 22 p2933 A73-42774

An analytical and experimental investigation of gravity effects upon laminar gas jet-diffusion flames. 22 p2933 A73-42775

Centrifugal force effects on flame spread and extinction limits of fuel-air mixture combustion with laminar, turbulent and buoyant bubble transport 22 p2933 A73-42776

Refraction, convection, and diffusion flame effects in combustion-generated noise. 22 p2934 A73-42780

Nitric oxide formation kinetics in combustion processes, discussing formation from nitrogen-containing compounds 22 p2819 A73-42791

Nitric oxide generation in turbulent diffusion flames, discussing limits for constant pressure turbulent reacting mixing zone between parallel flowing streams of fuel and oxidizer 22 p2935 A73-42798

Two modes of interaction of NaOH and SO₂ in gases from fuel-lean H₂-air flames. 22 p2820 A73-42802

Laminar combustion of polymethylmethacrylate in O₂/N₂ mixtures. 22 p2898 A73-42805

Combustion of thermoplastic polymer particles in various oxygen atmospheres - Comparison of theory and experiment. 22 p2937 A73-42822

German monograph - A method for the calculation of mixing and combustion processes in a rocket propulsion system with air-augmentation. 22 p2900 A73-42851

Formation of a pseudoliquidified layer during combustion of condensed systems with solid nonagglomerating additives in a field of mass forces 24 p3121 A73-44705

A self-similar regime of powder combustion with variable optical constants 24 p3154 A73-44706

Experimental study of the critical conditions of powder ignition and combustion 24 p3155 A73-44707

The theory of free ambient fires - The convectively mixed combustion of fuel reservoirs. 24 p3156 A73-45161

Thermokinetics and combustion phenomena in non-flowing gaseous systems - An invited review. 24 p3157 A73-45165

Study of the spatial development of oxidation and combustion reactions by means of image photoelectric receivers, and of a thermometric method 24 p3091 A73-45398

COMBUSTION PRODUCTS

The production of nitric oxide in ammonia oxidation flames. 01 p0121 A73-10640

Manganese additive effects on emissions from a model gas turbine combustor. 01 p0121 A73-10644

Analysis of NO formation in single droplet combustion. 01 p0014 A73-10645

Convective heat transfer coefficients at stagnation point of blunt body immersed in flames of fuel gases combustion with pure oxygen 01 p0122 A73-10807

Analysis of volatile combustion products and a study of their toxicological effects. 02 p0138 A73-12429

Solid propellant rocket motors exhaust smoke minimization, discussing smoke formation mechanism and optical properties relationship to propellant characteristics [AIAA PAPER 72-1192] 03 p0352 A73-13482

Gas concentration profiles in combustion gas sampling probes, using IR absorption technique 03 p0399 A73-14397

Gas turbine engine swirl-can combustor pollution tests of nitrogen oxides, unburned hydrocarbons and carbon monoxide levels for elevated temperature performance [AIAA PAPER 72-1201] 04 p0485 A73-14921

Pollutants from methane fueled gas turbine combustion. [ASME PAPER 72-WA/GT-3] 04 p0485 A73-15867

Gas temperature, carbon monoxide and nitric oxide axial and radial distribution in J-33 combustor, presenting combustion process model based on measurements [WSCI PAPER 72-22] 05 p0639 A73-16690

Afterburning turbojet engine exhaust emission products measurement under simulated flight conditions, determining Mach number and altitude effects on pollutants formation [AIAA PAPER 73-98] 06 p0740 A73-17643

Radial concentration profiles of NO and combustion products formation in laminar diffusion flames, using vertical coaxial burner and quartz microprobe 06 p0740 A73-17730

Investigation of NO formation kinetics in combustion processes - The methane-oxygen-nitrogen reaction. 06 p0767 A73-17731

Gas turbine combustion rig simulation of pollutant carbon and nitrogen oxide emissions as function of air-fuel mixing, metallic additions and chamber design 06 p0767 A73-17732

Effect of fuel composition on particulate emissions from gas turbine engines. 06 p0740 A73-17733

Measurement of nitric oxide formation within a multi-fueled turbine combustor. 06 p0740 A73-17734

Effects of fuel injection method on gas turbine combustor emissions. 06 p0768 A73-17735

Effect of operating variables on pollutant emissions from aircraft turbine engine combustors. 06 p0768 A73-17736

Control and reduction of aircraft turbine engine exhaust emissions. 06 p0768 A73-17737

Pressure, temperature, current density and potential difference fluctuations in subsonic flow of combustion products plasma, noting steadiness, ergodicity and distribution functions 06 p0732 A73-18616

Combustion molecular gases radiative heat transfer, emissivity and absorptivity calculation, presenting high speed computer routine 06 p0770 A73-18832

The role of mixing in burner-generated carbon monoxide and nitric oxide. 07 p0919 A73-19392

Ignition of systems having refractory reaction products 07 p0920 A73-19988

Slow combustion of n-pentane in single pulse chemical shock tube, discussing yields of oxygenated products 07 p0788 A73-20356

Emissions from and within an Allison J-33 combustor. 07 p0868 A73-20359

Dispersy of the combustion products of a mechanical mixture of aluminum and cadmium powders 07 p0923 A73-20421

Radiation absorption calculation for nonisothermal gas containing combustion products, noting approximation for water vapor radiation 08 p1021 A73-20860

Analytical predictions of emissions from and within an Allison J-33 combustor. 08 p1025 A73-21670

Combustion products of polymeric materials containing nitrogen in their chemical structure. 08 p0983 A73-21821

Effect of plasma inhomogeneity on the spectral-line profile and the reversal temperature 09 p1129 A73-22662

Thermodynamic cycle processes in liquid propellant rocket engines, taking into account combustion products chemical dissociation, wall and nozzle heat losses, friction effects, etc 10 p1263 A73-24700

Approximate nomograms for the characteristics of chemical-fuel combustion products 12 p1532 A73-27087

Determination of the combustion efficiency by continuous analysis of the combustion products 12 p1558 A73-27386

Mechanism and kinetics of the formation of intermediate products in an auxiliary mixture and the effect of such products on the combustion of the working mixture 13 p1704 A73-28293

Nitric oxide formation in gas turbine combustors. 13 p1670 A73-28805

Estimates of possible detection limits for combustion intermediates and products with line-center absorption and derivative spectroscopy using tunable lasers. 13 p1618 A73-28996

Test data obtained with an experimental gas turbine operated with kerosene combustion products artificially contaminated by dust 14 p1785 A73-30650

Mechanism of decay of ammonia in flame gases from an NH₃/O₂ flame. 16 p1976 A73-33345

- Sampling nitric oxide from combustion gases.
16 p2085 A73-33438
- Reduction of nitrogen oxide emissions from a gas turbine by fuel modifications.
[ASME PAPER 73-GT-5] 16 p2045 A73-33483
- Aerothermochemistry of combustion products in the stratosphere.
[AIAA PAPER 73-540] 16 p1977 A73-33570
- Experimental study of the condensed phase in the combustion products of metallized solid propellants
16 p2086 A73-33965
- Parameters controlling nitric oxide emissions from gas turbine combustors.
17 p2221 A73-34474
- Profitable transport engines for the environment of the eighties.
[SAE PAPER 730347] 17 p2257 A73-34695
- Nitric oxide emissions from tube combustor burning premixed gaseous propane-air mixture, considering inlet conditions for equivalence ratios
17 p2222 A73-35468
- Spectroscopic investigations of the combustion zone of flame jets of compacted systems
19 p2402 A73-37508
- Method of selecting particles formed during the burning of metallized compacted systems in a constant-pressure chamber
19 p2503 A73-37518
- The possibility of crystallization of condensed combustion products in nozzles
21 p2753 A73-40697
- Burning gunpowder interaction with an acoustic field in the presence of balanced chemical reactions behind the flame
21 p2791 A73-40699
- Comparative study of the combustion of 6-, 5-, 4-, and 3-amines of nitrate of cobalt /III/
21 p2647 A73-40703
- Reaction rate constants for carbon monoxide-hydrogen-oxygen and hydrogen-nitrogen-oxygen systems at high temperatures, modeling hydrocarbon combustion for product distribution
22 p2933 A73-42758
- Kinetics of nitric oxide formation in premixed laminar flames.
22 p2820 A73-42792
- Experimental and theoretical studies of NO/x/ formation in a jet-stirred combustor.
22 p2820 A73-42793
- Formation of nitric oxide in fuel-lean and fuel-rich flames.
22 p2820 A73-42794
- The effects of imperfect fuel-air mixing in a burner on NO formation from nitrogen in the air and the fuel.
22 p2820 A73-42795
- Nitric oxide formation weightless in diffusion flame ethanol drop combustion as function of air temperature and diffusion and spray characteristics
22 p2935 A73-42797
- Soot formation by combustion of an atomized liquid fuel.
22 p2936 A73-42800
- Kinetics of carbon monoxide oxidation in postflame gases.
22 p2820 A73-42803
- Study of light amplification in a pulsed gas-dynamic laser with burning acetylene-air mixtures
23 p2988 A73-44011
- A laser Doppler velocimeter for studying fast gas-dynamic flows
24 p3089 A73-44714
- Burn-up of the high temperature products of incomplete combustion in a supersonic flow by a second injection of oxidizer
24 p3156 A73-45076
- Breakdown potential of potassium-seeded combustion products.
24 p3121 A73-45164
- Air-hydrogen-carbon fuel mixtures chemical composition determination by measuring carbon dioxide and moisture content of combustion products, presenting nomogram
24 p3157 A73-45378
- Propane-air flame stabilization via combustion product recirculation due to transverse gas jet injection, increasing fuel-air ratio
24 p3123 A73-45379
- COMBUSTION STABILITY**
NT FLAME STABILITY
Stability of combustors with partial length acoustic liners.
01 p0090 A73-10641
- Recent developments in testing unstable burning characteristics of solid propellants.
01 p0089 A73-11115
- Stability boundaries of solid rocket motors.
01 p0091 A73-11116
- Research on combustion instability and application to solid propellant rocket motors. II.
[AIAA PAPER 72-1049] 03 p0353 A73-13380
- Review of nozzle damping in solid rocket instabilities.
[AIAA PAPER 72-1050] 03 p0353 A73-13381
- Solid propellant combustion instability suppression devices.
[AIAA PAPER 72-1051] 03 p0353 A73-13382
- Survey of ONERA and SNPE work on combustion instability in solid propellant rockets.
[AIAA PAPER 72-1052] 03 p0353 A73-13383
- The T-burner test method for determining the combustion response of solid propellants.
[AIAA PAPER 72-1053] 03 p0353 A73-13384
- Erosive burning rate perturbation in colloidal propellant slab combustor channel as function of lateral velocity gradient and chamber pressure
[AIAA PAPER 72-1108] 03 p0351 A73-13423
- A nonlinear model of combustion instability in liquid propellant rocket engines.
[AIAA PAPER 72-1146] 03 p0356 A73-13451
- Evaluation of acoustic cavities for combustion stabilization.
[AIAA PAPER 72-1147] 03 p0356 A73-13452
- TF-30-P1 engine mixed flow augmentor test for combustion instability under operation with abnormal fuel zone combination, comparing with predicted pressure oscillations from model
[AIAA PAPER 72-1206] 03 p0358 A73-13489
- Investigation of damping methods for low frequency augmentor combustion instability.
[AIAA PAPER 72-1207] 03 p0358 A73-13490
- Combustion of stabilized ethylene within a supersonic flow by a Mach configuration
03 p0352 A73-13578
- Performance optimization for supersonic ramjet - Theoretical and experimental studies
[ONERA, TP NO. 1106] 03 p0359 A73-14144
- Modelling of gas turbine combustors - Considerations of combustion efficiency and stability.
[ASME PAPER 72-WA/GT-1] 04 p0489 A73-15865
- Nonlinear longitudinal combustion instability in rocket motors.
[AIAA PAPER 73-217] 05 p0641 A73-16947
- Role of condensed phase details in the oscillatory combustion of composite propellants.
[AIAA PAPER 73-218] 05 p0641 A73-16948
- Interaction of sound and flow in T-burners - Experiments compared with theory.
[AIAA PAPER 73-220] 06 p0741 A73-17662
- L 17 satellite booster development from Emeraude stage, discussing gas generator, Valois thruster engine and assembly tests, combustion instability and launching results
07 p0905 A73-18990
- Acoustic amplification during solid propellant combustion.
07 p0865 A73-19390
- Explosive systems with reactant fuel consumption, deriving asymptotic stability, with application to self heating chemical reaction via Liapunov functions
07 p0919 A73-19393
- Liapunov method for LF and HF instability of liquid propellant rocket engines
07 p0867 A73-20078
- A study of the stability of slow combustion of gas mixtures subjected to the action of a magnetic field
09 p1167 A73-23351
- Experimental determination of three-dimensional liquid rocket nozzle admittances.
09 p1167 A73-23438
- Necessary conditions of stable combustion of powder in a semiclosed chamber
10 p1294 A73-23588
- Heterogeneity effect on L instability of solid rocket propellant combustion, using sideways sandwich model
11 p1450 A73-25373
- Linear nonstationary effects - A source of information on the kinetics of reactions on the surface of a solid fuel
14 p1818 A73-30873
- An experimental study of the low pressure limit for steady deflagration of ammonium perchlorate.
16 p2045 A73-33347
- Oblique reflection of a plane acoustic wave from a burning surface
19 p2503 A73-37513
- Stability of a conical burning surface during solid fuel combustion in a semiclosed volume
20 p2627 A73-39290
- Contribution to the theory of high-frequency pulsations caused by instability of the combustion process in a solid-propellant rocket engine
21 p2753 A73-40391
- Quasi-steady gas-phase flame theory in unsteady burning of a homogeneous solid propellant.
21 p2790 A73-40430
- Similarity relations derived for unsteady powder burning with light irradiation or occurrence in semiclosed volume
21 p2791 A73-40700
- Effect of combustion upon precessing vortex cores generated by swirl combustors.
22 p2934 A73-42781
- Mathematical modeling of combustors based on turbulent mixing, droplet evaporation and chemical kinetics, considering stirred reactor heat balance and combustor performance prediction
22 p2935 A73-42789
- Experimental study of the critical conditions of powder ignition and combustion
24 p3155 A73-44707
- Transient process due to pressure increase during combustion of condensed material, using fractional-differentiation operator method to determine unsteady burning velocity
24 p3155 A73-44715
- Solid propellants with a pulsating burning rate
24 p3121 A73-45200
- Experimental and theoretical determination of the admittances of a family of nozzles subjected to axial instabilities.
24 p3122 A73-45267
- Influence of velocity pulsations on the range of stable combustion of homogeneous mixtures
24 p3157 A73-45382
- Solid fuels combustion stability and shock wave induced detonations propagation stability in aerosols investigation based on one dimensional turbulence, using multistage mathematical models
24 p3157 A73-45383
- COMBUSTION TEMPERATURE**
Temperature changes in hydrogen-oxygen explosions.
01 p0121 A73-10646
- Temperatures of aluminum during its combustion in oxygen-argon mixtures, in nitrogen, and in air
01 p0123 A73-11275
- Combustion chamber temperature profiles analytical derivation from simultaneous radiative and turbulent diffusion heat transfer of turbulent flame front
[ASME PAPER 72-WA/HT-27] 04 p0519 A73-15827
- Predicting the critical boundary temperature of multidimensional explosives.
07 p0918 A73-19386
- Spectroscopic investigations of the combustion zone of flame jets of compacted systems
19 p2402 A73-37508
- Comparative study of the combustion of 6-, 5-, 4-, and 3-amines of nitrate of cobalt /III/
21 p2647 A73-40703
- The effects of catalysis in measuring the temperature of incompletely-burned gases with noble-metal thermocouples.
22 p2857 A73-42035
- COMBUSTION VIBRATION**
Contribution to the theory of high-frequency pulsations caused by instability of the combustion process in a solid-propellant rocket engine
21 p2753 A73-40391
- Forced vibrations of a cylindrical shell in the presence of gas pressure fluctuations
22 p2928 A73-43057
- Noise generation by turbulent combustion, discussing sound power, spectral content, enclosure effect, and importance in turbopropulsion system core engine noise
[AIAA PAPER 73-1023] 24 p3155 A73-44855
- Combustion noise radiation by open turbulent flames.
[AIAA PAPER 73-1025] 24 p3156 A73-44856
- COMBUSTION WAVES**
U FLAME PROPAGATION
COMBUSTORS
U COMBUSTION CHAMBERS
COMET HEADS
Type II comet model for head and tail regions release of dust particles having wide size distribution
04 p0494 A73-14759
- Bennett comet head spectrophotometry over 352-612 millimicrons, identifying CN, CH, C2 and Na emission features
08 p1010 A73-21315
- The motion of dust and gas in the heads of comets with type II tails.
10 p1271 A73-23494
- Cometary head atmospheric gaseous and dust components characteristics in terms of physical processes in comet nucleus vicinity
14 p1792 A73-29814
- Weakly-shocked flows of the solar wind plasma through atmospheres of comets and planets.
23 p3024 A73-43682
- Comet Bennett neutral sodium atom and dust particle distribution across head and tail measured by photometry of Na emission radial profile
24 p3133 A73-44560
- COMET NUCLEI**
Icy conglomerate cometary nucleus models, discussing clathrates role in comet condensation from solar nebula
04 p0494 A73-14752
- Photometric and spectral observations of Churyum-Gerasimenko short period comet 1969 IV by fast telescopes, correlating nuclear magnitude with sun-spot area
14 p1789 A73-29781
- Hidalgo orbit near Saturn, discussing resemblance to extinct comet nucleus, nongravitational forces effects and planetary mass determination
14 p1792 A73-29812
- Cometary head atmospheric gaseous and dust components characteristics in terms of physical processes in comet nucleus vicinity
14 p1792 A73-29814

Comet nuclei gas liberation, perihelion mass loss and photometric property dependence on water ice evaporation rate and nongravitational effects

14 p1792 A73-29815

Cometary nuclei chemical composition and molecular structure, suggesting radial-forming organic molecules synthesis by solar and galactic cosmic radiation

14 p1723 A73-29816

Cometary nucleus evolution dependence on secular brightness decrease relationship to dust particle size distribution, nuclear radius and screened surface area

14 p1792 A73-29817

Cometary nuclei size determination methods based on model of surface ice regions with mineral crust spots, analyzing brightness decrease

14 p1792 A73-29818

Splitting and sudden outbursts of comets as indicators of nongravitational effects.

14 p1793 A73-29819

On nongravitational effects in two classes of models for cometary nuclei.

14 p1793 A73-29820

Rotation effects in the nongravitational parameters of comets.

14 p1793 A73-29821

Encke comet icy nucleus core-mantle evolutionary model, investigating mantle sublimation, fading and capture time approximation for nongravitational forces effect in terms of mass output

14 p1793 A73-29822

Icy cometary nuclei laboratory simulation by sublimation of dust particle containing ice and frozen electrolyte mixtures in high vacuum at low temperature

14 p1793 A73-29823

New estimates of cometary disintegration times and the implications for diffusion theory.

14 p1794 A73-29829

Theoretical cometary radiants and the structure of meteor streams.

14 p1795 A73-29845

Monte Carlo technique application to meteor stream formation process modeling, discussing mass ejection from cometary nuclei

14 p1795 A73-29848

Determination of the radius of a cometary nucleus from photometric data

15 p1928 A73-31024

Cometary Science Working Group, Meeting, Williams Bay, Wis., June 9-11, 1971, Proceedings.

15 p1941 A73-32413

Vaporization theory of cometary nucleus prediction of law of dependence of nongravitational force on heliocentric distance

17 p2228 A73-34427

Stationary target identification with radar beam for comet nucleus within coma, noting echo spatial extent and Doppler bandwidth effects on data processing

17 p2174 A73-35634

Urey hypothesis for tektites origin via earth-comet collisions dependence on cometary structure, considering solid nucleus vs meteoric particle swarms

23 p3033 A73-43953

Development of an H₂O atmosphere around Comet Kohoutek /1973I/ and its possible detection.

23 p3033 A73-43955

Many body model for comet nucleus formation from solid materials and interstellar gas consistent with Whipple icy conglomerate model

24 p3131 A73-44466

COMET TAILS

The Kelvin-Helmholtz instability in type-I cometary tails

01 p0102 A73-10946

Natural oscillations of type-I comet tails.

01 p0107 A73-11331

The kinematical behaviour of the plasma tail of Comet Tago-Sato-Kosaka 1969 IX.

02 p0221 A73-12704

Interplanetary gas. XVII - An astrometric determination of solar-wind velocities from orientations of ionic comet tails.

03 p0361 A73-12947

Hypersonic solar wind flow interactions with comet emitted gas forming tails, discussing contact surface with stagnation point and bow shock front

04 p0494 A73-14758

Type II comet model for head and tail regions release of dust particles having wide size distribution

04 p0494 A73-14759

Photographic observations of Comet Bennett, 1970II.

04 p0495 A73-14766

Kelvin-Helmholtz instability in type I comet tails.

09 p1148 A73-22741

Contributions to the kinematics of type I tails of comets.

10 p1271 A73-23477

The motion of dust and gas in the heads of comets with type II tails.

10 p1271 A73-23494

Nonlinear helical waves formation due to Kelvin-Helmholtz instability in type I comet tail modeled as plasma cylinder immersed in solar wind

12 p1542 A73-27609

Solar wind flow in interplanetary space, discussing comets, cometary tail, interplanetary magnetic field and Alfvén waves characteristics

15 p1940 A73-32183

Solar wind interaction with Comet Bennett near earth, examining photographs for momentum flux change-ion tail kink correlations

21 p2763 A73-41501

Comet Kohoutek development predictions for various orbital locations, discussing brightness changes, tail production, nucleus ice melting by solar heating at perihelion, etc

23 p3033 A73-43956

Comet Bennett neutral sodium atom and dust particle distribution across head and tail measured by photometry of Na emission radial profile

24 p3133 A73-44560

COMETS

NT COMET HEADS

NT COMET NUCLEI

NT COMET TAILS

NT GLACOBINI-ZINNER COMET

Correlation between the brightness of comets and solar wind fluctuations

02 p0208 A73-12471

Lyman-alpha emission of comet Bennett 1969I and the determination of the solar wind flux

02 p0208 A73-12472

Comet nucleus models, discussing classical and icy snowball heads, nongravitational forces, nucleus dimensions and evidence against solid cores

02 p0223 A73-12731

Tago-Sato-Kosaka and Bennett comets Lyman alpha radiation explanation via resonant scattering on neutral hydrogen formed by water vaporized from ice core

02 p0224 A73-12742

A 1.1 micron spectrogram of the central coma of Comet Bennett /1969 i/.

02 p0226 A73-12832

Improved orbit and ephemeris of the periodic Comet Reinmuth 1 for its apparition in 1972-73.

03 p0370 A73-13197

Trans-Plutonian planet calculations by Brady, discussing Halley, Olbert and Pons-Brook comet trajectories and perturbations and planet parameters

03 p0370 A73-13199

Comets: Scientific data and missions; Proceedings of the Tucson Comet Conference, University of Arizona, Tucson, Ariz., April 8, 9, 1970.

04 p0494 A73-14751

Comet nucleus existence in terms of optical effect and particle swarm model of coma

04 p0494 A73-14753

IR observations of comets Bennett and Tago-Sato-Kosaka, noting thermal origin of flux, source structure and material temperature, emissivity and composition

04 p0494 A73-14754

Infrared observations of Comets Ikeya-Seki /1965f/ and Bennett /1969i/.

04 p0494 A73-14755

Comet photometry to explain origin of free radicals discovered in cometary spectra, considering clathrate hydrates and possible parent molecules

04 p0494 A73-14756

L alpha photometry of Comet Bennett.

04 p0494 A73-14757

Comet spectra and excitation mechanism for spectrum production, discussing structural subdivision into nucleus, coma and tail

04 p0494 A73-14760

Comets Tago-Sato-Kosaka and Bennett spectra twilight observation by 200 inch reflector, considering Comet d'Arrest for in situ study by instrumented space probe

04 p0495 A73-14761

Comet orbit calculation in terms of nongravitational force effects, emphasizing periodic comet return predictions

04 p0495 A73-14762

Cometary structure from ground based observations of meteor showers, noting fireball characteristics difference

04 p0495 A73-14763

Cometary heads observations indicating precursor decay lengths from 100-10,000 km, considering visible and UV molecular and atomic emissions

04 p0495 A73-14764

Comet research assessment for 1970-1972, discussing coma and nucleus, icy conglomerate and sandbank models

04 p0495 A73-14765

Photographic observations of Comet Bennett, 1970II.

04 p0495 A73-14766

Volatile-rich lunar soil - Evidence of possible cometary impact.

05 p0615 A73-16321

Earth-based orbit determination for solar electric spacecraft with application to a Comet Encke rendezvous.

[AIAA PAPER 73-174]

06 p0748 A73-17651

Increase of Na twilight emission after the earth's crossing of the orbital planes of Comets Halley and Encke.

07 p0899 A73-20063

Finson-Probstein model for dust comets applied to calibrated photographic plates of Comet Bennett, giving dust size distribution, emission rate and initial velocities

07 p0902 A73-20443

Definitive orbit of the comet 1937 V Finser.

08 p1012 A73-21580

Periodic comet disintegration considerations, discussing comet Tempel 2 absolute magnitude from visual brightness estimates and Meisel statements on secular decrease

09 p1146 A73-22544

A new cosmological model - Formation of organic molecules, planets, and comets.

09 p1151 A73-23147

Cometary collision energy triggering of catastrophic changes in climate, geological period terminations and lava flow initiation, noting tektite-geologic period ages correlation

10 p1275 A73-23823

Note on Brady's hypothetical trans-Plutonian planet.

10 p1275 A73-23847

Lyman-alpha radiation in the hydrogen atmospheres of comets - A model with multiple scattering.

10 p1281 A73-24408

Photographs of comet Bennett 1969 i.

11 p1426 A73-26267

The structure of the Eta Aquarid meteor stream.

11 p1426 A73-26573

Nongravitational force variation with heliocentric distances computed for long and short period comets, deriving force law from water snow vaporization rate

12 p1540 A73-27428

The origin of Jupiter's family of comets.

13 p1672 A73-28037

Zinc, lead, chlorine and FeOOH-bearing assemblages in the Apollo 16 sample 66095 - Origin by impact of a comet or a carbonaceous chondrite.

13 p1686 A73-29565

The motion, evolution of orbits, and origin of comets; Proceedings of the Symposium, Leningrad, USSR, August 4-11, 1970.

14 p1789 A73-29776

Evolution of cometary orbits on a cosmogonic time scale.

14 p1789 A73-29777

Cometary observations and variations in cometary brightness.

14 p1789 A73-29778

Cometary brightness variations and conditions in interplanetary space.

14 p1789 A73-29779

Observations of comets at the Crimean Astrophysical Observatory.

14 p1789 A73-29780

Comet orbit and ephemeris calculations with reference to position and magnitude to facilitate reobservation with long focus telescopes

14 p1789 A73-29782

Chebyshev polynomial series solution method for highly eccentric perturbed orbits of comets, using modified Hansen method of partial anomalies

14 p1790 A73-29783

On the application of Hansen's method of partial anomalies to the calculation of perturbations in cometary motions.

14 p1790 A73-29784

Orbital characteristics of comets passing through the 1:1 commensurability with Jupiter.

14 p1790 A73-29785

On the motion of short-period comets in the neighbourhood of Jupiter.

14 p1790 A73-29786

Disturbing functions application to secular perturbation calculation for periodic comets with validity for any eccentricity and inclination

14 p1790 A73-29787

A numerical method of integration by means of Taylor-Steffensen series and its possible use in the study of the motions of comets and minor planets.

14 p1790 A73-29788

A method of integrating the equations of motion in special coordinates and the elimination of a discontinuity in the theory of the motion of periodic comet Wolf.

14 p1790 A73-29790

A numerical interpretation of the homogenization of observational material for one-apparition comets.

14 p1790 A73-29792

The problem of elaboration and classification of observational material for one-apparition comets.

14 p1790 A73-29793

The influence of properties of a set of observations on the weights of determination of the orbital elements of a one-apparition comet.

14 p1790 A73-29794

Standardization of the calculation of nearly parabolic cometary orbits.

14 p1790 A73-29795

Determination of parabolic orbits on the basis of N observations, by means of an electronic computer
14 p1790 A73-29796

Nongravitational effects on comets - The current status.
14 p1791 A73-29797

On the determination of nongravitational forces acting on comets.
14 p1791 A73-29798

A search for Encke's comet in ancient Chinese records - A progress report.
14 p1791 A73-29799

Numerical analysis of the motion of periodic comet Brooks 2.
14 p1791 A73-29800

Linkage of seven apparitions of periodic comet Faye 1925-1970 and investigation of the orbital evolution during 1660-2060.
14 p1791 A73-29801

Osculating orbital elements and nongravitational parameters for non-Newtonian orbit of periodic comet Borrelly
14 p1791 A73-29804

Borrelly periodic comet motion, including secular acceleration due to nongravitational forces and orbital elements perturbations by planets from Venus to Pluto
14 p1791 A73-29805

Pons-Brooks comet orbit calculation based on observations in 1812, 1883-1884 and 1953-1954, noting impossibility of single orbit fitting
14 p1791 A73-29806

Periodic comet Tempel-Tuttle orbital elements relation to Leonid meteor shower, using computer program for numerical integration
14 p1791 A73-29807

Periodic comet Stephan-Oterma orbit, taking into account perturbations by major planets
14 p1792 A73-29808

Determination of planetary masses from the motions of comets.
14 p1792 A73-29809

The determination of Jupiter's mass from large perturbations on cometary orbits in Jupiter's sphere of action.
14 p1792 A73-29810

A nongravitational effect in the simulation of cometary phenomena.
14 p1793 A73-29824

Ejection of bodies from the solar system in the course of the accumulation of the giant planets and the formation of the cometary cloud.
14 p1793 A73-29825

Astronomical model for Oort comet cloud destruction rate during stellar passage, noting cumulative dispersion mechanism and half life estimates
14 p1793 A73-29826

Determination of the form of the Oort cometary cloud as the Hill surface in the galactic field.
14 p1793 A73-29827

Diffusion of comets from parabolic into nearly parabolic orbits.
14 p1793 A73-29828

Comet motion and hyperbolic orbital statistics, discussing secular accelerations, decelerations and nongravitational effects
14 p1794 A73-29830

The effect of the ellipticity of Jupiter's orbit on the capture of comets to short-period orbits.
14 p1794 A73-29831

Evolution of short-period cometary orbits due to close approaches to Jupiter.
14 p1794 A73-29832

Orbital classification for short period comets based on minimum approach distances to respective planets
14 p1794 A73-29833

The major planets as powerful transformers of cometary orbits.
14 p1794 A73-29834

Comets and cometsimals formation from icy material during solar system evolution from collapsing dust and gas cloud
14 p1794 A73-29835

On the origin of comets and their importance for the cosmogony of the solar system.
14 p1794 A73-29836

The origin and evolution of the comets and other small bodies in the solar system.
14 p1794 A73-29837

Comets origin in interstellar space or solar system evaluated with reference to comet streaming from perihelions statistical analysis, assuming Oort cloud accretion
14 p1794 A73-29838

On the rate of ejection of dust by long-period comets.
14 p1795 A73-29841

Focusing effect of planetary perturbations on meteor stream particles for comet formation
14 p1795 A73-29846

Meteor streams and comet orbital statistics from radar observations during 1967-1968
14 p1795 A73-29847

Cometary and asteroidal orbits discrimination using Jacobi integral in three body system with sun and Jupiter
14 p1795 A73-29849

Book - Vistas in astronomy. Volume 13.
15 p1932 A73-31302

Numerical experiments by Monte Carlo method to examine comet orbits evolution within solar system, noting Trojan, horseshoe and Jupiter-Saturn midrange orbits
15 p1938 A73-31949

Genetic relationship between short period comets and meteor streams, considering radial and longitudinal focusing mechanism for particles in meteor streams
15 p1939 A73-32009

Correlation between the brightness of comets and fluctuations of the solar wind.
15 p1927 A73-32622

Lyman-alpha radiation from comet Bennet 1969i.
15 p1927 A73-32623

The effect of multiple encounters on short-period comet orbits.
17 p2226 A73-34291

Carbon isotope abundance ratios in comets and Jupiter atmosphere, discussing hydrogen isotope ratio determination for Saturn and Jupiter atmospheres
17 p2228 A73-34418

Monte Carlo model of cometary evolution based on hypothetical perturbed orbit calculations, with emphasis on short-period comets
17 p2228 A73-34426

Characteristics of the future orbital evolution of the comet Churumov-Gerasimenko, 1969h
17 p2230 A73-34597

On the origin of short-period comets.
17 p2234 A73-35620

Solar electric propulsion comet and asteroid rendezvous missions, examining asteroid perihelion data base, optimum mission length, flight time and exploration vehicle power levels
18 p2350 A73-36081

Cometary composition, structure and atmospheric dynamics, discussing multiconstituent hydrodynamic models in comparison with observation
18 p2353 A73-36495

Comet exploration - Scientific objectives and mission strategy for a rendezvous with comet Encke.
18 p2353 A73-36496

Cometary exploration - A case for Encke.
18 p2353 A73-36501

New statistical laws governing the system of long-period comets
19 p2480 A73-37235

Comet 1969 g emission spectrum observation with 200-inch telescope, obtaining isotope ratio C-12/C-13
20 p2609 A73-39432

Cometary atmospheric dust chemical composition and physical properties estimated from colorimetric, polarimetric and IR data, using models of optically thin polydisperse media
21 p2776 A73-41421

Hydrogen production rates of comet Bennett /1969i/ in the first half of April 1970.
21 p2778 A73-41530

The cause of the residuals in the motion of Halley's comet.
22 p2907 A73-42210

Airborne photographic and visual observation of material from Comet Giacobini-Zinner produced meteor showers due to orbit perturbation and perihelion changes by Jupiter
22 p2909 A73-42588

Russian book - Accuracy of comet and satellite orbits.
22 p2910 A73-42640

Determination of nongravitational forces in the motion of comets. I - Analysis of observation errors
22 p2910 A73-42643

Comet Kohoutek development predictions for various orbital locations, discussing brightness changes, tail production, nucleus ice melting by solar heating at perihelion, etc
23 p3033 A73-43956

Comet Kohoutek earth orbit properties and rocket and satellite observations, including parent molecule and inner solar system measurements
23 p3034 A73-44222

On the process of accretion in the formation of the planets and comets.
24 p3128 A73-44400

Orientation-dependent effects in Oort's theory of comet origin. II - Anisotropies in the distribution of long-period comet orbits.
24 p3131 A73-44467

The next return of the comet of the Perseid meteors.
24 p3135 A73-44583

COMFORT
The effects of various seat surface inclinations on posture and subjective feeling of comfort
03 p0266 A73-13121

COMMAND AND CONTROL
Synthesis of a multidimensional automatic optimization system with constraints
01 p0028 A73-10674

Command and control for a missile air defense system. I - SAM-D communications.
04 p0417 A73-15377

Command and control for a missile air defense system. II - Implementation of system requirements.
04 p0418 A73-15378

Real-time analysis and ground command control to achieve accurate vehicle and payload event functions.
09 p1117 A73-23217

Synthesis and analysis of tracking systems with optimal acquisition.
15 p1854 A73-31727

Commercial airline operational control, discussing flight plan approval by pilot and ground personnel, preflight duties, weather information assessment and fuel monitoring
15 p1909 A73-32446

Simulation of a multiple element test environment.
16 p1985 A73-33417

Remote viewing system with TV cameras to duplicate human visual field and acuity functions, featuring operator command and data link bandwidth minimization
19 p2416 A73-37319

Command language for supervisory control of remote manipulation.
19 p2403 A73-37329

Development of pilot-in-the-loop analysis.
22 p2817 A73-43110

COMMAND GUIDANCE
The German telecommand ground station for HELIOS - A new concept.
09 p1070 A73-23418

Apollo LM guidance computer software for the final lunar descent.
10 p1247 A73-24548

New missile guidance concepts as applied to command guidance control system.
20 p2584 A73-38778

COMMAND MODULES
Apollo command and service module environmental control system - Mission performance and experience.
19 p2493 A73-37984

COMMAND SERVICE MODULES
Far UV scanning spectrometer aboard Apollo 17 CSM to measure lunar atmospheric composition, observing spectral albedo, LEM atmosphere, and galactic and solar system atmospheres
12 p1497 A73-27485

Skylab flight schedule emphasizing Command Service, Module, discussing meteoroid shield deployment difficulties and rescue team development of solar heat shield
21 p2767 A73-40415

COMMAND SYSTEMS
U COMMAND GUIDANCE
COMMAND-CONTROL
U COMMAND AND CONTROL

COMMERCE
Capital equipment marketing, discussing industry-customer-government interaction, marketing and sales techniques and functions, products initiation, etc
10 p1298 A73-24650

COMMERCIAL AIRCRAFT
NT A-300 AIRCRAFT
NT BOEING 727 AIRCRAFT
NT BOEING 737 AIRCRAFT
NT BOEING 747 AIRCRAFT
NT DC 9 AIRCRAFT
NT DC 10 AIRCRAFT
NT EUROPEAN AIRBUS
NT IL-62 AIRCRAFT
NT L-1011 AIRCRAFT
NT SUPERSONIC COMMERCIAL AIR TRANSPORT
NT TU-134 AIRCRAFT

Review of radio navigation of civil aircraft - Current and future outlook
02 p0191 A73-12015

Comparison of propulsion system concepts for V/STOL commercial transports.
03 p0250 A73-13472

[AIAA PAPER 72-1176]
Subsonic commercial transport aircraft reduced noise and increased cruise Mach number effects on nacelle design in terms of inlet, fan, cowl and nozzle
03 p0358 A73-13488

[AIAA PAPER 72-1204]
Jet noise suppression for commercial CTOL, STOL and SST aircraft, discussing various devices effective-
03 p0251 A73-14130

Optimization of commercial transport airplane stopping systems.
05 p0535 A73-16671

[SAE PAPER 720872]
Aircraft structural engineers prospects in commercial aircraft design, discussing markets, technology escalation and cost effective structural development
06 p0759 A73-17612

[AIAA PAPER 73-19]
Flight control techniques for advanced commercial transports.
06 p0647 A73-17618

[AIAA PAPER 73-30]
Crew station lighting - Commercial aircraft.
08 p0925 A73-20692

[SAE ARP 1161]
1972 report to the aerospace profession; Proceedings of the Sixteenth Symposium, Beverly Hills, Calif., September 28-30, 1972.
09 p1030 A73-22176

- Commercial aircraft passenger cabins interior design, considering seating arrangements, cabin architecture and fittings, materials and color schemes and maintainability 10 p1183 A73-23687
- Ireland commercial airports at Dublin, Shannon and Cork, discussing management, terminal facilities and operations 11 p1343 A73-25208
- Determination of the turn start point coordinates for modern commercial aircraft 11 p1307 A73-26723
- Role of commercial aircraft in global monitoring systems. 13 p1568 A73-28499
- Air transport and commercial aviation developments, including revenues, passenger traffic statistics, charter flights and fare levels 13 p1709 A73-29383
- Commercial air transportation in France - National administration and aviation enterprises 14 p1818 A73-30294
- Behavioral stress response related to passenger briefings and emergency warning systems on commercial airlines. 16 p1965 A73-32660
- Charters, the new mode - Setting a new course for international air transportation. 16 p2087 A73-33101
- Skyjacking - Its domestic civil and criminal ramifications. 16 p2087 A73-33102
- NASA research commercial VTOL transport propulsion system specifications and components development, discussing lift fan propulsion method for aircraft attitude control [ASME PAPER 73-GT-24] 16 p2047 A73-33498
- An airline view of the future of auxiliary power systems. [SAE PAPER 730379] 17 p2108 A73-34718
- Civil and military aircraft 18 p2268 A73-36689
- Engineering design considerations in the noise control of commercial jet aircraft's vent and drain systems. 19 p2378 A73-37297
- On the cost benefits of air cushion landing gear to civil aviation. 19 p2381 A73-37685
- Commercial jet transport aircraft hydraulic fuel distribution tubing systems, discussing maintenance, fabrication problems, fittings, quality control and materials [SAE SP-378] 19 p2434 A73-37864
- The development of propulsion systems in the case of airliners 19 p2473 A73-38120
- Optimum propulsion system design for advanced technology commercial transport, emphasizing low noise and emission, performance, reliability, maintainability and economics [AIAA PAPER 72-760] 20 p2600 A73-38648
- Commercial aircraft system effectiveness survey questionnaire response data concerning various tests in manufacturing and operational environments 21 p2635 A73-41205
- The nondestructive tests in the maintenance of commercial aircraft 22 p2799 A73-42186
- Management and control of commercial flight test programs. 23 p3050 A73-44057
- COMMERCIAL AVIATION**
U CIVIL AVIATION
U COMMERCIAL AIRCRAFT
COMMITTEE ON SPACE RESEARCH
 Highlights of the COSPAR Symposium on the solar eclipse of 7 March 1970. 01 p0101 A73-10911
- National reports on earth resources surveys at 1971 COSPAR meeting, including remote sensing techniques application in agriculture, forestry, geology and oceanography 02 p0160 A73-12264
- CIRA 1972: COSPAR international reference atmosphere 1972. 21 p2683 A73-40626
- COSPAR mean international reference atmosphere for 25-500 km region, considering 25-75, 75-120 and regions above 120 km 21 p2683 A73-40627
- COMMUNICATING**
NT AIRCRAFT COMMUNICATION
NT GROUND-AIR-GROUND COMMUNICATIONS
NT INFORMATION DISSEMINATION
NT INTERSTELLAR COMMUNICATION
NT POINT TO POINT COMMUNICATIONS
NT VERBAL COMMUNICATION
 Thermodynamics and morphological orders - A generalized concept of information transfer. 06 p0749 A73-18003
- German monograph on human information transmission by multidimensional tactile stimuli investigation using method of learned signals identification 07 p0786 A73-20393

COMMUNICATION

- NT INFORMATION DISSEMINATION**
NT UNDERWATER COMMUNICATION
NT VERBAL COMMUNICATION
COMMUNICATION CABLES
NT BEAM WAVEGUIDES
NT COAXIAL CABLES
NT PLASMA GUIDES
NT WAVEGUIDES
 Russian book on airport cable communication lines, discussing design construction, signal transmission theory and structural and electrical characteristics 21 p2675 A73-41283
- COMMUNICATION EQUIPMENT**
NT CLOSED CIRCUIT TELEVISION
NT DIGITAL SPACECRAFT TELEVISION
NT DIPLEXERS
NT RADIO RECEIVERS
NT SATELLITE TELEVISION
NT SPACECRAFT TELEVISION
NT STEREOTELEVISION
NT SUPERHETERODYNE RECEIVERS
NT TRANSMITTER RECEIVERS
 Computer-mediated human communications in an air traffic control environment A preliminary design. 03 p0340 A73-14658
- Noise immunity of diversity reception with threshold switching of antennas 07 p0802 A73-20291
- Symphonic satellite communication equipment payload, discussing mission requirements, receiving and transmitting antennas, transponder and ground testing methods and arrangements 11 p1417 A73-25356
- Acoustic matched filters applications for multisubscriber band spread communication in ATC systems 14 p1733 A73-29936
- Portable radio communication system for guided tours in industrial plants, construction sites and museums, discussing transmitter, receiver, earphones and rechargeable battery power supply 16 p1987 A73-33165
- Noise immunity of diversity reception with antenna threshold switching. 18 p2290 A73-37128
- Experiences with an augmented human intellect system - Computer mediated communication. 21 p2654 A73-40833
- COMMUNICATION SATELLITES**
NT AERONAUTICAL SATELLITES
NT COMMUNICATIONS TECHNOLOGY SATELLITE
NT INTELSAT SATELLITES
NT MOLNIYA SATELLITES
NT RELAY SATELLITES
NT SYMPHONIE SATELLITES
NT SYNCOM SATELLITES
 A wideband transistor amplifier at the 4 GHz band for communication satellite use. 01 p0026 A73-11176
- Microwave varactor upconverter in radio repeater for domestic wideband communication satellite, emphasizing transmission characteristics design 01 p0006 A73-11177
- A study of frequency sharing between satellite and terrestrial broadcasting systems. 01 p0018 A73-11179
- Optimization study of the satellite broadcasting system for television. 01 p0018 A73-11180
- Application of random time and frequency multiplexing to a data collection satellite. 01 p0018 A73-11182
- The telecommunication payload of the satellite Symphonie [DGLR PAPER 72-089] 02 p0140 A73-11678
- Orientation accuracy of the Symphonie communication antennas [DGLR PAPER 72-063] 02 p0140 A73-11684
- Radio sensors for the three-axis attitude fine measurement of geostationary communication satellites 02 p0228 A73-11822
- Future NASA communication satellite technology applications in meeting national education, health care, culture and data transfer needs, considering ATS F and CTS spacecraft 02 p0143 A73-12846
- Optimization of ion propulsion for north-south stationkeeping of communications satellites. [AIAA PAPER 72-1150] 03 p0356 A73-13454
- Satellite charges for a mixed pre-demand-assigned system. 03 p0276 A73-13901
- Influence of satellite antenna gain on a satellite communications system. 03 p0277 A73-14027
- Satellite digital communications over domestic and international networks for data, voice and video signal transmission 04 p0415 A73-14739
- International telecommunication law with respect to space laboratories /space vehicles, orbital stations or lunar bases/, discussing protection for communication satellites 04 p0521 A73-15128

- Juridical problems connected with European network of telecommunication satellites, discussing satellite direct transmission 04 p0497 A73-15146
- CERS/ESRO role, nonmember states participation and experimental systems in European telecommunication satellites program 04 p0523 A73-15147
- Some international legal issues on the direct television broadcast satellites. 04 p0523 A73-15149
- European space conference, discussing space program priorities relative to applications or research satellites, communication satellites, launch vehicles and facilities and participation in post-Apollo program 04 p0523 A73-15151
- Effects of hardlimiting on bandlimited transmissions with conventional and offset QPSK modulation. 04 p0420 A73-15412
- Spin and three-axis stabilized geosynchronous tracking and data relay satellite system for telecommunication service to user spacecraft in low earth orbit 04 p0420 A73-15422
- Digital link for bidirectional communication between manned spacecraft and ground terminal by synchronous communication relay satellite, noting coding parameters effects on error rate 04 p0421 A73-15426
- Communications technology satellite /CTS/ with transponder and TWT operating into steerable antenna, discussing experiments on TV broadcast, data transmission, FM and transportable terminals 04 p0422 A73-15446
- Integration of an ion engine on the Communications Technology Satellite. 04 p0487 A73-15448
- The attitude stabilization and control system for the Communications Technology Satellite. 04 p0504 A73-15450
- Cs ion bombardment and contact ionization engines in French space program for communication and geostationary satellites electric propulsion 04 p0488 A73-15715
- Cs ion bombardment engines for communication satellites stationkeeping and attitude control, noting mission life and test facilities 04 p0488 A73-15718
- Contribution to the analysis and conception of satellite stabilization systems based on ion propulsion 04 p0505 A73-15737
- Orbit transfer, -corrections, and attitude control of a lightweight direct broadcasting satellite for Europe. 04 p0505 A73-15738
- Hydrogen resistojets for primary propulsion of communications satellites. 04 p0489 A73-15741
- NASA space program value to humanity, discussing Skylab solar and earth observations and communications satellites 05 p0613 A73-16181
- Some problems of the optimal angular stabilization of an artificial earth satellite 05 p0628 A73-16413
- Book - Advances in electronics and electron physics. Volume 31. 05 p0558 A73-16601
- Communication satellite technology development, discussing INTELSAT and Russian Orbita systems, spectrum and orbit utilization, modulation, multiplexing, electron devices, radiation environment and power generation 05 p0550 A73-16604
- Intermodulation noise and system analysis in SSB-PM multiple access system. 05 p0552 A73-17169
- Transoceanic telephony via communication satellites, discussing satellite reliability and placement in synchronous orbit 06 p0663 A73-17577
- Intelligible crosstalk and AM/PM transfer in commercial communications satellites. I 06 p0663 A73-17589
- AEROSAT - An aeronautical communications satellite for oceanic areas. [AIAA PAPER 73-46] 06 p0771 A73-17624
- Communication satellite application to shipping company operations for cost benefits and alleviation of distress alerting, search and rescue, and heavy weather damage problems [AIAA PAPER 73-47] 06 p0755 A73-17625
- Attitude dynamics of a three-axis stabilized satellite with a large flexible solar array. 06 p0757 A73-18379
- Canadian Anik I synchronous domestic communication satellite for color TV broadcasting or telephony, considering northerners reaction and community beneficiaries 06 p0668 A73-18432
- On the reduction of rainfall outages by space diversity for millimeter-wave earth-satellite communications systems. 06 p0668 A73-18712
- Communications Satellites and the international communications industry. 07 p0923 A73-19139

The experimental telecommunication satellite Project Symphonie.

07 p0905 A73-19140

The Aeronautical Satellite Programme - ATC aspects.

07 p0848 A73-19141

Intelligible crosstalk and AM-PM transfer in commercial communication satellites. II

08 p0937 A73-20773

A new earth-station antenna for domestic satellite communications.

08 p0947 A73-21144

TDMA satellite telephonic communication network with preassigned channeled radio carrier, describing four phase demodulator and channel units regrouping

09 p1050 A73-22320

Lunar and solar perturbation effects on communication satellite orbits, considering Kozai luni-solar theories

09 p1149 A73-22913

International Telemetry Conference, Los Angeles, Calif., October 10-12, 1972, Proceedings.

09 p1053 A73-23361

Satellite frequency division multiple access communication net, examining channel monitoring and self regulating downlink power output for performance improvement

09 p1053 A73-23363

Satellite-borne programmable communications distribution subsystem, controlling microwave switch matrix by ground command via onboard memory for traffic flow data

09 p1053 A73-23364

Convolutional coding for multiple-access satellite communication.

09 p1056 A73-23399

Canadian domestic ANIK communication satellite with all-microwave 12-channel repeater, discussing system components, antenna design and performance parameters

09 p1059 A73-23437

Commercial communications satellite technology trends, stressing wideband capabilities, flexibility, multiple access and channel capacity increase

10 p1189 A73-24561

Symphonic satellite communication equipment payload, discussing mission requirements, receiving and transmitting antennas, transponder and ground testing methods and arrangements

11 p1417 A73-25356

Design and performance of the TACSAT power subsystem.

11 p1312 A73-26020

Project management and installation of the Arvi satellite communication earth station.

11 p1344 A73-26147

Canadian telecommunications satellite system for TV, voice and analog or digital data transmission, describing space segment, satellite control and ground station network

11 p1431 A73-26259

Problems and possibilities related to transmissions by satellites covering large zones in Africa

11 p1454 A73-26274

The satellite system as an integrated telecommunication switching center.

12 p1468 A73-27011

Satellite systems for mobile communications and surveillance; Proceedings of the International Conference, London, England, March 13-15, 1973.

12 p1471 A73-27652

Mobile satellite communication systems constraints imposed by international institution disagreements on management, procurement and operation, considering US and European conflicts on Aerosat project

12 p1471 A73-27653

Factors relating to the choice of antenna characteristics for the aircraft terminal in an aeronautical satellite communications/surveillance system.

12 p1471 A73-27654

A planning study for a multi-purpose communications satellite serving northern Canada.

12 p1471 A73-27657

Satellite design considerations.

12 p1549 A73-27659

Skyнет satellite communication service for small dish antenna equipped mobile ground stations, emphasizing necessity of rapid central control response to configuration and propagation condition changes

12 p1471 A73-27660

Naval satellite communications terminal design for shipboard use to meet low cost, small size, light weight and printed circuit module replacement demands

12 p1471 A73-27661

Modulation and speech processing techniques for a maritime-satellite service.

12 p1472 A73-27662

L-band satellite systems for mobile applications.

12 p1472 A73-27664

A maritime communications concept using spaceborne phased arrays.

12 p1472 A73-27665

The use of satellites for aircraft communications and air traffic control.

12 p1472 A73-27666

Factors affecting the frequency chosen for aircraft to satellite communications.

12 p1472 A73-27667

Message organisation in the ground segment of an aeronautical satellite system.

12 p1472 A73-27668

ESRO Aerosat L-band communication techniques experiments with stratospheric balloon-borne transponders relaying ground station signals to aircraft flying over sea

12 p1498 A73-27672

Technical factors determining the choice of frequency bands for the links between satellite and coast stations of a maritime communications satellite service.

12 p1473 A73-27674

The operational requirements for a maritime satellite communication service.

12 p1473 A73-27676

Engineering economic considerations for a maritime-satellite service.

12 p1473 A73-27677

Replacement of a system of aeronautical satellites.

12 p1549 A73-27678

Maritime Satellite System with broadband and multibeam dish antennas, assessing FDM communication capability as function of channel quality and ship terminal antenna gain

12 p1473 A73-27679

Multiple access system by time division with synchronization in the S2 TDMA satellite

13 p1584 A73-28908

A wideband transistor amplifier at the 4-GHz band for communication satellite use.

13 p1594 A73-29228

European telephony traffic and Eurovision TV program exchanges via three-axis stabilized communications satellite with fold out solar panel arrays

14 p1724 A73-29715

Communications aspects of broadcast TV satellites.

14 p1725 A73-29716

A study of frequency sharing between satellite and terrestrial broadcasting systems.

14 p1725 A73-29748

Book - The politics and technology of satellite communications.

14 p1818 A73-29949

European geostationary communication satellite system for telephone and TV transmission, discussing stabilization, command and power subsystems, modulation methods, power budgets, satellite configurations, etc

14 p1728 A73-30431

The impact of satellites on military communications.

14 p1729 A73-30874

European telecommunication satellite program implementation and preoperational phase regulation, stressing international constraints

14 p1819 A73-30900

Statistical computation of compatibility of tropospheric and satellite communication lines.

15 p1842 A73-30986

Effects of flexibility on a momentum-stabilised communication-satellite attitude-control system.

15 p1942 A73-31099

Requirements regarding the position and the attitude of future application satellites

15 p1907 A73-31134

Book on earth satellites covering transmission technology, cost effectiveness and materials development for communication, meteorological, earth resources, navigational, research and military applications

15 p1944 A73-32292

Digital transmission techniques for ATC satellite system, considering technical and economic aspects of various coding systems

15 p1846 A73-32427

Aircraft onboard data link and Aerosat equipment integration, considering antenna, duplexer, amplifier and receiver systems

15 p1846 A73-32428

Optimal digital modulation techniques for aeronautical communications via satellite, considering air navigational systems for transoceanic flight

15 p1847 A73-32480

Synchronous communication satellite crosslink antenna design and tracking and acquisition procedures for Ka band frequencies, describing reflectors, paraboloids, and five horn feed system

16 p1977 A73-32721

Microwave radiometer measurement at 17 GHz to investigate atmospheric attenuation and radio noise and interference sources for optimal satellite communication systems design

16 p1982 A73-33718

German national geostationary TV satellite project, discussing thermal and attitude control, launch and guidance problems, solar power supply and antenna systems

16 p2074 A73-33737

Interference into angle-modulated systems carrying multichannel telephony signals.

16 p1983 A73-33742

Book - Satellite broadcasting.

17 p2121 A73-34473

Monitoring interruptions at the satellite earth station.

17 p2122 A73-34870

Demand-assignment multiple-access control techniques.

17 p2144 A73-35304

Multiple access techniques for the Canadian domestic satellite communications systems.

17 p2124 A73-35305

Time Division Multiple Access for the defense satellite communications system.

17 p2124 A73-35307

Canadian domestic satellite system applications.

17 p2124 A73-35311

Communication satellites attitude control methods, considering conventional attitude gyros, control moment gyroscopes, reaction wheels and optimal solar cell utilization

17 p2239 A73-35476

Regional and international communication satellite systems, discussing frequencies assignment, power supplies, three axis stabilization trends and military, navigation and TV developments

[DGLR PAPER 73-039] 17 p2125 A73-35478

Mission, project profile, and description of the Symphonie satellite

[DGLR PAPER 73-043] 17 p2126 A73-35480

The orbital test satellite for the European Communications Satellites Programme - Performance and growth capability.

[DGLR PAPER 73-044] 17 p2126 A73-35481

Utilization of electric propulsion systems in communications satellites

[DGLR PAPER 73-048] 17 p2126 A73-35484

Attitude control, rotational and positioning mechanisms for orientation of mechanically despun antennas and solar arrays in communication satellites

[DGLR PAPER 73-050] 17 p2126 A73-35486

Communications systems of television-radio satellites

[DGLR PAPER 73-053] 17 p2126 A73-35487

Radio-TV satellite ground support systems, discussing frequency ranges, satellite orbit, transponder signal amplification and ground reception systems

[DGLR PAPER 73-055] 17 p2126 A73-35488

Communications system of the Symphonie satellite and special transmission parameters

[DGLR PAPER 73-056] 17 p2126 A73-35489

Transponder for European communications satellite systems/ECS and OTS program/

[DGLR PAPER 73-057] 17 p2126 A73-35490

Range and range-rate measuring equipments for communication satellites.

17 p2130 A73-35813

A reliability, cost and risk analysis of establishing and maintaining a space communications satellite network.

[AIAA PAPER 73-582] 18 p2288 A73-36074

International law aspects of direct broadcasting communication satellites, discussing United Nations, UNESCO and International Telecommunications Union contributions

18 p2373 A73-36392

Soviet communications satellite systems

18 p2289 A73-36400

The application of simulation to mission planning for communications and data relay satellites.

18 p2291 A73-36424

Raindrops in satellite communications.

18 p2289 A73-36515

Domestic communication satellite systems with microwave transmission links and coast-to-coast earth stations and receivers, detailing design and interference problems

18 p2289 A73-36776

Technological trends in commercial satellite communications.

18 p2290 A73-37034

Solar arrays for the next generation of communication satellites.

18 p2269 A73-37036

Satellite telecommunications systems

18 p2290 A73-37050

Problems connected with an employment of carbon dioxide lasers in space communications systems

18 p2290 A73-37087

Satellites for maritime applications.

19 p2494 A73-38099

Small earth terminal applications for satellite communications.

[AAS PAPER 73-121] 20 p2543 A73-38582

Communication satellites future use in Europe, considering mission requirements, data transmission, specialized TV distribution, cost effectiveness and shuttle/tug launch system

[AAS PAPER 73-148] 20 p2521 A73-38596

Some developments in semi-direct broadcast satellites and community receiving systems.

[AAS PAPER 73-155] 20 p2521 A73-38599

Concepts of high-capacity communications satellites.

20 p2613 A73-38714

Future communication satellite technology improvement, market expansion and cost effectiveness.

COMMUNICATION SYSTEMS

considering foreign domestic, and international light-to-medium and high density systems

20 p2522 A73-38715

A proposed time division multiple access (TDMA)/satellite system for Anik I.

20 p2523 A73-38719

System aspects of the initial Telesat Thin Route satellite communication system.

20 p2523 A73-38720

Small ship antennas for fleet satellite communications.

20 p2523 A73-38727

Adaptive ground implemented phased arrays.

20 p2523 A73-38729

A method of providing rain margins for 18/30 GHz communications satellites without increasing the solar power requirement.

20 p2524 A73-38731

Implementation of fixed multiple beam spherical antenna systems and measured test results.

20 p2525 A73-38740

Design of the 14/11 GHz repeater for the European Orbital Test Satellite.

20 p2525 A73-38745

Adaptive multibeam concepts for traffic management satellite systems.

20 p2525 A73-38746

Communication satellite history and present developments, discussing Intelsat and ATS programs and TDMA techniques

20 p2526 A73-38747

Effect of nonlinear channel characteristics on QPSK system performance.

20 p2526 A73-38752

Multipath channel characterization for Aerosat.

20 p2526 A73-38755

ASTRO-DABS communication system with hybrid satellite and terrestrial discrete address beacon system for accurate aerial surveillance and navigation with reliable data link

20 p2527 A73-38759

Orbital design strategy for domestic communication satellite systems.

20 p2527 A73-38761

Optimization in the design of a 12 GHz low cost ground receiving system for broadcast satellites.

20 p2527 A73-38762

TDMA system design for small satellite terminals.

20 p2528 A73-38767

Availability, maintenance and cost of communication satellite systems.

20 p2613 A73-38768

Calculation of structurally compressed satellite radio lines

20 p2531 A73-39469

Aeronautical/maritime satellite borne two-way L-band transponder weight and power limitation effects on channel capacity

20 p2531 A73-39771

Maritime communications via satellites employing phased arrays.

21 p2649 A73-40330

Satellite techniques for automatic platforms location and data relay.

21 p2737 A73-41335

Telesat Canada-Anik - Canada's domestic satellite communications system

24 p3069 A73-45392

COMMUNICATION SYSTEMS

U TELECOMMUNICATION

COMMUNICATION THEORY

NT WORDS [LANGUAGE]

Signal interpolation errors in adaptive-discretization systems

01 p0015 A73-10029

Theory of multistep coding and its application to multiphase-modulation communication systems.

01 p0018 A73-11053

Some results on zero crossing distribution of non-stationary random noise.

02 p0143 A73-12857

The average duration of the failed state in the interval between adjacent tests of a periodically verified standby radio system with z-multiple redundancy

09 p1051 A73-22464

Wiener and Kalman filters theory for stochastic processes in communication, demonstrating optimum demodulator derivation by Kalman-Bucy theory application to double sideband amplitude modulation

09 p1065 A73-23112

International Telemetry Conference, Los Angeles, Calif., October 10-12, 1972, Proceedings.

09 p1053 A73-23361

Optical communication theory application to free space, turbulent and scatter channels, discussing background noise, detector statistical model and quantum receivers

10 p1188 A73-23757

Calculation of the average usage time of a channel in an adaptive multichannel communications system

12 p1471 A73-27585

Numerical solution of the integral equations for optimal sequential filtering.

15 p1844 A73-32039

Atmospheric attenuation measurements via solar microwave radiometer yielding excess attenuation statistics for communications systems planners

16 p1982 A73-33722

French book - Theory of communication: Signals, noises, and modulations.

17 p2123 A73-35149

Annual Southwestern Conference and Exhibition, 25th, Houston, Tex., April 4-6, 1973, Record.

17 p2124 A73-35357

The scope for electron-optical devices for the optimal processing of composite signals in communications systems.

18 p2290 A73-37127

Russian monograph on signal transmission channel identification systems in statistical communication theory covering mathematical models, design principles, radio electronic systems, etc

22 p2827 A73-42600

Digital communication system with known channel characteristics, discussing intersymbol interference dependence on signalling rate based on Nyquist criteria consideration

24 p3070 A73-45482

COMMUNICATIONS TECHNOLOGY SATELLITE

High power SHF transmitter experiment using TWT depressed collector beam microwave amplifier for flight testing on communications technology satellite (CTS/)

04 p0428 A73-15447

The liquid metal slip ring experiment for the Communications Technology Satellite.

04 p0408 A73-15449

The Canadian/U.S. High-Power Communications Technology Satellite.

12 p1472 A73-27669

Television satellite transmission systems capabilities and technology, discussing Communications Technology Satellite [DGLR PAPER 73-040]

17 p2125 A73-35479

COMMUNITIES

NT MOUNTAIN INHABITANTS

COMMUTATION

Measurement of phase fluctuation dispersion for narrow-band signals

01 p0015 A73-10077

Investigation of residual resistance in semiconductor switches used to commutate the measuring circuits of alternating-current bridge networks

01 p0022 A73-10080

Analog simulation for transient and steady state performance of group-triggered cycloconverter supplying controlled slip induction motor, discussing commutation failures

03 p0253 A73-13932

Analysis of primary currents in a three-phase/single-phase frequency converter with direct coupling and artificial commutation

13 p1592 A73-28940

Harmonic analysis of voltages and currents at the output of a frequency converter with direct coupling and artificial commutation

13 p1593 A73-28941

COMMUTATORS

High power inverter with commutator of single LC network and steering SCR capable of multiple high voltage dc bridge operation

03 p0253 A73-13936

Electric arc motion during initiation by plasma injection between static electrodes in dc circuit, applying to pulsed arc commutator design

09 p1131 A73-22938

Ferrite component for waveguide commutator used as microwave switching element and modulator, noting application in navigation instruments and avionics

15 p1849 A73-30995

COMPACTING

The role of plastic deformation in metal powder compaction.

11 p1374 A73-26270

Conditions for powder compaction over the deformation zone width during rolling

12 p1503 A73-27554

Preparation of porous electrodes from titanium nitrides

15 p1881 A73-31592

Compacting of metallic powders by plane explosive charges. I

24 p3092 A73-44414

Kinetics of shrinkage during the sintering of porous glass/metal composites

24 p3092 A73-44415

Shrinkage of reinforced sandwich-type materials during hot pressing

24 p3092 A73-44416

COMPACTNESS

U VOID RATIO

COMPANION STARS

Photometric search for H alpha optical emission in Sco X-1 nebulousity region for linking companion radio sources to X ray source

03 p0373 A73-13374

MWC 349 - A new radio star.

03 p0374 A73-13849

Cen X-3 and Her X-1 X ray sources emission pulsation explained by model with neutron star accretion of matter from companion via magnetic funnel

09 p1141 A73-22010

Massive X ray binaries consisting of early type star with neutron stars or black holes as companions

12 p1535 A73-27597

The effect of binary motion on period changes in RR Lyrae stars.

15 p1935 A73-31486

WC and WR binary stars spectra differences attributed to variations in effects of companion on principal star atmosphere

23 p3026 A73-43203

COMPARATOR CIRCUITS

Punched card controlled program units including readers, comparator circuits, pneumomechanical counters and fluidic feedback oscillators

23 p2944 A73-43424

COMPARATORS

An electromagnetic comparator system with improved possibilities in regard of sorting and recording of absolute test parameters

01 p0056 A73-10588

Displacement comparator based on laser interferometer with photoelectric counter for monitoring inside and outside dimensions of cylinder bores, shafts, spheres, etc

11 p1364 A73-26103

Instrument providing dc voltage corresponding to amplitude of uniform pulse train, using differential comparator as sensing element and closed loop control scheme

11 p1313 A73-26316

Performance and possibilities of application of an electromagnetic comparator

15 p1883 A73-32056

Astronomical educational aids design and application, including photometers for star cluster detection, ocular comparators and projection devices for photograph examination

16 p2014 A73-32950

A non-contacting length comparator with 10 nanometer precision.

21 p2704 A73-41257

COMPARTMENTATION

U COMPARTMENTS

COMPARTMENTS

NT AIRCRAFT COMPARTMENTS

NT ANECHOIC CHAMBERS

NT COMMAND MODULES

NT PRESSURE CHAMBERS

NT PRESSURIZED CABINS

NT SPACECRAFT CABINS

NT TEST CHAMBERS

NT VACUUM CHAMBERS

Smoke and fire propagation in compartment spaces.

[WSCIPAPER 72-32] 05 p0639 A73-16683

COMPASSES

NT GYROCOMPASSES

NT MAGNETIC COMPASSES

COMPATIBILITY

Elastomer compatibility considerations relative to O-ring and sealant selection.

[SAE AIR 786 A] 08 p0982 A73-20691

Compatibility between material components in metal-ceramics composites

11 p1387 A73-25412

Compatibility of components in metal-ceramics composites

14 p1766 A73-30442

Compatibility and satisfactory performance of individual Space Shuttle elements, discussing development/flight cost tradeoff, booster thrust vector and optimal control

19 p2492 A73-37600

Multihundred watt radioisotope thermoelectric generator heat source materials compatibility with thermochemical environment, considering maximum operational and reentry temperatures

19 p2457 A73-38427

Canonical differential equations from equilibrium and compatibility conditions for boundary loaded, shell of revolution, simplifying and transforming by canonical transformations

21 p2788 A73-41616

COMPENSATION

Loss compensation in the case of filters with additional resistors

03 p0284 A73-14124

Compensating for distortion in viewing pictures obliquely.

21 p2639 A73-41178

COMPENSATORS

Space booster control system computerized design algorithm for forward loop compensation filter selection based on minimization of penalty function of stability margin violations

01 p0021 A73-11516

Automatic two-coordinate compensator for resistance-measurement studies of steels and special alloys

02 p0167 A73-11867

An adaptive digital compensator for saturating control systems. 12 p1483 A73-27160

Adaptive equalization with recursive noncanonical scanning filters 23 p2953 A73-43323

Compensation of an underdamped fluidic position control system by a digital pulse compensator. 23 p2944 A73-43420

Compensation method for non-linear systems having jump and hysteresis properties. 24 p3075 A73-45555

COMPENSATORY TRACKING

Noise effects on the critical tracking performance of the human operator. 01 p0010 A73-10107

Operator remnant power spectral density measurement during compensatory tracking task by serial segments method, noting Fourier coefficient processing 01 p0011 A73-10324

Central tracking task performance simultaneously with response to peripheral stimulus under high heat stress environments 06 p0659 A73-18473

Type L linear multivariable systems with state integral feedback control, deriving optimal conditions for zero steady state error compensatory tracking by frequency domain techniques 07 p0805 A73-19133

Nonadjunct rating scales in human response experiments. 17 p2117 A73-35400

A deterministic model of a well trained human operator performing compensatory tracking. 18 p2283 A73-36844

On the stabilization of aided track pointing systems. 19 p2404 A73-38070

Time domain analysis of human operator manual control function for second order oscillatory divergent system with error signals for compensatory tracking. 21 p2634 A73-40090

Optimal work-rest schedules under prolonged vibration. 23 p2948 A73-43217

Decrements in tracking and visual performance during vibration. 24 p3063 A73-44777

COMPETITION

Formula-one air racing history, aircraft designs and characteristics and low cost amateur constructions 08 p0928 A73-21689

COMPILATION [COMPUTERS]

U COMPILERS

COMPILER PROGRAMS

U COMPILERS

COMPILERS

GALIC - Grumman Aerospace Engineering Language for Instructional Checkout. 08 p0941 A73-20689

COMPLETENESS

A method for studying the completeness of systems of analytic functions 12 p1516 A73-26960

COMPLEX NUMBERS

The deficiency indices and spectrum associated with self-adjoint differential expressions having complex coefficients. 02 p0186 A73-11971

Stability in the critical case of purely imaginary roots for neutral functional differential equations. 14 p1771 A73-30773

Complex roots onset in secular stellar spectrum extended to case with shell sources present, determining eigenvalues for different intensity and position parameters 16 p2058 A73-32830

Nonlinear eigenvalue problem of square matrix of analytic functions of complex number lambda, comparing algorithms convergence by numerical tests 21 p2725 A73-40380

COMPLEX SYSTEMS

Stability of large-scale systems under structural perturbations. 01 p0070 A73-10322

Stochastic behaviour of a complex system with standby redundancy. 01 p0023 A73-10649

Liapunov function for complex system motion stability analysis, noting stability criteria for subsystems satisfying Routh-Hurwitz conditions 01 p0076 A73-10668

Mathematical models, systems analysis and synthesis in control theory of large scale systems, illustrating on agriculture center planning 01 p0078 A73-11070

Survival probability of a system with a Poisson flow of losses in life-sustaining elements 01 p0028 A73-11422

The system approach to the design of engineering systems from the standpoint of reliability and efficiency 02 p0145 A73-11547

A method for computing complex system reliability. 03 p0336 A73-13733

A digital simulation method for interconnected continuous systems. 03 p0281 A73-14479

Large scale systems with linear and nonlinear subsystems and coupling connections, investigating connective stability under perturbations due to subsystem on-off participation 03 p0337 A73-14484

Dynamic structural analysis large eigenvalue problems, presenting subspace iteration algorithm for arbitrary system size and bandwidth 04 p0509 A73-14944

Theoretical foundations for synthesis of learning-type recognition algorithms by the method of R-functions in the complex-plant control problem 05 p0560 A73-16275

Interactive aspects of man/learning system control teams. 05 p0543 A73-16708

Optimal time calculation for aging complex control system replacement with allowance for downtime losses 05 p0554 A73-16989

Numerical difficulties and accuracy losses avoidance methods for ill conditioned stiffness matrices encountered in complex structural analyses 05 p0636 A73-17113

Outline of a new approach to the analysis of complex systems and decision processes. 06 p0671 A73-18622

Application of pole-placement theory to helicopter stabilization systems. 06 p0682 A73-18819

Kron algorithm for complex eigenvalue problems of damped vibrating mechanical systems, using Newton method 07 p0909 A73-19098

Fault isolation in complex systems via Bode diagram technique. 08 p0941 A73-20684

Near-optimal control of high-order systems using low-order models. 08 p0950 A73-21090

Some delinearization problems in the dynamics of complex vibrational systems 08 p0989 A73-21768

Global asymptotic stability estimation for large scale systems of interconnected exponentially stable subsystems, using aggregated comparison and Liapunov function description 09 p1120 A73-22227

Optimal sequence for introducing elements of large system into operation, using resource allocation cost criterion 09 p1068 A73-22551

Maintenance and repair planning and control of complex series-parallel and hierarchical branched systems with discrete sampling of operational status 09 p1064 A73-22553

Probability characteristics of complex systems with a hierarchical control 09 p1068 A73-22559

Applications of symbolic computing methods to the dynamic analysis of large systems. 10 p1192 A73-24029

Stability theory of dynamic large scale system under structural perturbations based on comparison principle and vector Liapunov functions 10 p1248 A73-24039

The algorithms of accuracy research of nonstationary linear systems with continuous and discrete elements. 10 p1200 A73-24048

Conditions for termination of tracking in electronic servo systems 10 p1202 A73-24610

Optimal control methods for combined signal processing, using complex filtration-compensation system principles and mean square measurement error criteria 11 p1340 A73-25003

A dynamic transformation method for modal synthesis. 11 p1440 A73-25525

[AIAA PAPER 73-396] Method of Liapunov vector functions in the analysis of complex systems with distributed parameters /Survey/ 11 p1398 A73-25617

The principle of complexity and the method of regularization in stochastic problems of optimal automatic control system synthesis 11 p1341 A73-25634

The limiting advantage derived from the compounding of information-extracting devices in the presence of wideband Gaussian noise 12 p1482 A73-26867

Zeros determination in large-scale multivariable systems. 13 p1651 A73-29568

Russian papers on cybernetic systems reliability and accuracy covering analog, hybrid and digital computers, electronic modeling, nonlinear control systems, computer and complex system design, etc 14 p1730 A73-30031

Calculation of redundant equipment recovery time when only failures of entire systems are detected by inspection 14 p1754 A73-30036

Prediction of failures and efficiency characteristics of a system 14 p1740 A73-30799

Book - Interorganizational decision making. 15 p1960 A73-31577

Operational behaviour of a complex system with two out of M failed components. 16 p2022 A73-34030

Complex system reliability with general repair time distributions under preemptive repeat repair discipline. 16 p2022 A73-34031

Vibration analysis of finite element systems. 17 p2245 A73-34837

Book - Systems concepts: Lectures on contemporary approaches to systems. 17 p2258 A73-35572

The engineering of large-scale systems. 17 p2258 A73-35573

On stability of large-scale systems under structural perturbations. 17 p2213 A73-35827

Synthesis of optimal automatic control systems by use of the complexity principle and of the regularization method. 19 p2414 A73-38145

Influence of low-frequency periodic interference on the operation of a complex system with variable structure 20 p2539 A73-38694

Correctness, regularization, and the maximum complexity principle in the statistical dynamics of automatic control systems 20 p2540 A73-38699

Synthesis of low-sensitivity automatic control systems 20 p2540 A73-38706

Complex stochastic control system identification by distribution and moments characteristics in form of Gaussian densities, perturbation polynomials and sedastic functions 20 p2540 A73-38708

A method of processing a priori information about a controlled plant with the aim of reducing the number of changing parameters of the dynamic characteristics 20 p2541 A73-38993

Problems in the theory and practice of the self-tuning of compensating signals in complex control systems 20 p2541 A73-38994

Russian book - Complex control systems 20 p2541 A73-39033

A programmed control task in a two-level hierarchical system under conditions of uncertainty 20 p2541 A73-39034

Statistically optimal sampled data terminal guidance algorithm for complex probabilistic multipurpose control system, using linearized equations 20 p2590 A73-39344

Bifurcation and stability of steady motions of complex mechanical systems 21 p2738 A73-40176

Russian book on reliability optimization in complex automatic control system information transfer and processing covering performance criteria, noise immunity, error sources and types, etc 21 p2670 A73-41293

Russian book - Theory and methods for constructing multiple-link control systems. 22 p2835 A73-42601

Gradient control laws in stabilization problems of multidimensional control systems 22 p2887 A73-42605

Liapunov vector functions for solving stability problems of complex multidimensional dynamic control systems with nonlinear interactions and delay 22 p2887 A73-42606

Decomposition of the solution to optimal synthesis problems of multiple-link control systems 22 p2887 A73-42610

Problems of the theory of multidimensional combined systems with a common output 22 p2836 A73-42611

Structural sensitivity transfer matrix for dynamic multiple link control system response minimization with corrections within frequency range 22 p2836 A73-42613

Transfer function root method for synthesis of multiply connected determinate automatic control systems with asymmetrical channels and limited nonautonomous control elements 22 p2836 A73-42614

Quasi-autonomous dynamic control subsystem interrelation and location for nonlinear multiple link automatic control synthesis with iterative integration of motion equations 22 p2836 A73-42616

Optimal dynamic accuracy measurement complexing for combined data processing in multidimensional automatic control systems with various sensors 22 p2836 A73-42618

On stability of large-scale systems under structural perturbations.

23 p2963 A73-43290

Performance criteria selection for complex system parameter optimization based on minimum deviation from extremal values

23 p2963 A73-43737

Linear time variant multivariable decentralized system stabilization by feedback control laws with dynamic compensation

23 p2964 A73-43821

Discrete time composite system stability with non-periodic sampling in terms of vector Liapunov functions and real symmetric matrix test

23 p2964 A73-43826

Synthesis of cascaded multiple-loop feedback systems with large plant parameter ignorance.

24 p3073 A73-44584

Frequency methods for simulation, analysis and identification of multiply-connected dynamic systems with delay

24 p3074 A73-45097

Aggregation scheme solution for uniform asymptotic stability of large dimensionality system, using L-problem moment theory

24 p3112 A73-45505

COMPLEX VARIABLES

NT AIRY FUNCTION

NT ANALYTIC FUNCTIONS

NT BESSEL FUNCTIONS

NT CAUCHY INTEGRAL FORMULA

NT CONFORMAL MAPPING

NT CONJUGATES

NT ELLIPTIC FUNCTIONS

NT ENTIRE FUNCTIONS

NT EXPONENTIAL FUNCTIONS

NT GAMMA FUNCTION

NT HANKEL FUNCTIONS

NT HARMONIC FUNCTIONS

NT HYPERBOLIC FUNCTIONS

NT HYPERGEOMETRIC FUNCTIONS

NT LAGUERRE FUNCTIONS

NT LEGENDRE FUNCTIONS

NT LIOUVILLE THEOREM

NT LOGARITHMS

NT MATHIEU FUNCTION

NT MEROMORPHIC FUNCTIONS

NT NONHOLONOMIC EQUATIONS

NT ORTHOGONAL FUNCTIONS

NT RATIONAL FUNCTIONS

NT SCHWARZ-CHRISTOFFEL TRANSFORMATION

NT SINGULARITY [MATHEMATICS]

NT SPHERICAL HARMONICS

Complex variable analysis for exact solution to Kepler equation for elliptical and hyperbolic orbits based on canonical solutions to Riemann problem

03 p0376 A73-14269

Complex wave existence in some two-layer isotropic structures

07 p0793 A73-19921

Second order differential equations with complex-valued coefficients.

09 p1112 A73-22425

Sturm-Liouville problem monotone proper function zeros lower and upper bounds evaluation using Barta inequality and Schwartz iteration

09 p1113 A73-23026

Isotropic homogeneous elastic medium internal crack analysis based on Laurent series expansions of complex potentials consistent with displacements and stress-strain single valuedness

09 p1162 A73-23179

Exact analytical solutions basic to a class of two-body orbits.

11 p1423 A73-26072

On the mapping associated with the complex representation of functions and processes.

11 p1333 A73-26645

Elastic circular inclusion in an infinite plane containing two cracks.

13 p1696 A73-28749

Convergence of the arithmetic-geometric mean procedure for the complex variables and the calculation of the complete elliptic integrals with complex modulus.

14 p1769 A73-30423

Asymptotic solution of a system of linear differential equations with slowly varying coefficients in a complex domain

15 p1898 A73-31028

Calculation of the resultant moment of the hydrodynamic forces on jet profiles

15 p1824 A73-32000

The global aspect of the complex analysis in the theory of the morphic functions

15 p1900 A73-32106

The median problem of the theory of elastic mobility with polar effects of spectral type.

18 p2364 A73-36492

Algebraic algorithm for positive realness of real rational functions and matrices relative to unit circle in complex plane, determining real polynomial zeros distribution

19 p2446 A73-38488

Semicircular plate uniformly loaded over diameter and with concentrated force at arc top, determining stress distribution by complex variable and conformal mapping

24 p3148 A73-45001

COMPLEXITY

NT TASK COMPLEXITY

COMPLIANCE [ELASTICITY]

U MODULUS OF ELASTICITY

COMPONENT RELIABILITY

Mathematical formulation for classification, realization and evaluation of electronic components and systems reliability tests

01 p0023 A73-10647

The generalized gamma distribution and the power distribution as element lifetime distributions

02 p0145 A73-11584

Generalized gamma distribution with a negative shape parameter as a model of the lifetime distribution of electrical elements with a single-maximum failure rate

02 p0145 A73-11585

Onboard ILS equipment reliability in integrated airborne all-weather landing system

02 p0190 A73-11855

Study of the nonstationary characteristics of a doubled system with an unreliable servicing device

02 p0188 A73-12588

Analyzing failures of metal components.

03 p0323 A73-13270

Multilayer debugging process /A new method of screening/.

03 p0336 A73-13734

Extreme value methods for design, production, testing and maintenance of components and system with low failure probability

04 p0507 A73-14709

Kinetic model considering cumulative fatigue damage interaction with chance overload on component or structure under probabilistic service load, discussing crack growth in composites

04 p0508 A73-14717

Accelerated life testing of component reliability in aerospace systems, discussing stress tests, Arrhenius model and time transformation method

04 p0453 A73-14854

Probability model and causal approach to failure mechanisms and reliability of control system elements applied to IC

04 p0424 A73-15208

Estimates of reliability functions for systems with redundancy.

04 p0471 A73-15210

Information criterion for optimal planning of reliability control tests, maximizing average effect

04 p0430 A73-15211

Survey of heat transfer techniques applied to electronic equipment.

[ASME PAPER 72-WA/HT-39]

04 p0518 A73-15816

Avionics systems redundancy and complexity, suggesting component design with guaranteed operational life

06 p0673 A73-17617

Aircraft hydraulic system and servocontrol design and performance, noting system reliability and fluid loss prevention

06 p0649 A73-17995

Optimal currents, voltages and frequencies for noise measurement in HF transistors for reliability prediction and failure analysis, noting diffusion alloyed and planar transistors

06 p0675 A73-18078

French spacecraft electronic components reliability program, considering failure characteristics, operating limits, environmental conditions and confidence level

07 p0797 A73-18915

High reliability semiconductors development, discussing research in Si single crystals growth, epitaxial films, photoengraving, oxidation/passivation and large-scale integration techniques

07 p0829 A73-18919

Quality control in Concerto reliable space components procurement program for multilayer ceramic capacitors and thermistors manufacture

07 p0829 A73-18920

High reliability technology assessment for metal film resistors production, discussing qualification tests

07 p0829 A73-18921

Scanning electron microscope operation and application to technology research and electronic components and circuits failure and reliability analysis

07 p0797 A73-18922

French Concerto aerospace part procurement program contribution to mass produced electronic component reliability assessment, control and improvement based on tin oxide resistor experience

07 p0829 A73-18923

French Concerto program for component reliability and quality assurance in manufacturing and procurement controls for Symphonic satellite

07 p0790 A73-18975

Some effects of temperature on material properties and device reliability.

07 p0797 A73-19134

Calculation of the reliability of electronic components in an 'aeronautics' environment shaped by the operational service routines of onboard equipment devices used by Air France

07 p0799 A73-19403

Accelerated life tests of microelectronic components by operational power dissipation, noting efficiency and profitability

07 p0799 A73-19404

Analysis of a defect of electromagnetic relays used in an electronic assembly

07 p0799 A73-19406

Service life estimation of electro-optic devices and degradation kinetics, noting reliability of light transmitters and receivers

07 p0800 A73-19407

Application of the analysis of correspondences to the study of the reliability of electronic components

07 p0800 A73-19412

Influence of repeated voltage applications on the reliability of a system

07 p0800 A73-19417

Reliability design of type 2N 3966 field effect elements

07 p0801 A73-19421

Quality control of semiconductor elements manufactured in low-run series production - Ultrahigh frequency components

07 p0801 A73-19422

Reliability of sealed reed switches /SRS/

07 p0801 A73-19423

Contamination damage avoidance concepts for propulsion feed system components.

07 p0868 A73-20470

Point contact and Schottky barrier microwave mixer diodes reliability under X band RF pulse operating conditions, considering burnout alleviating fabrication techniques

08 p0943 A73-20735

The use of a diamond heat sink for a high reliability IMPATT diode.

08 p0944 A73-20736

Reliability aspects of plastic encapsulated integrated circuits.

08 p0944 A73-20739

Degradation of MNOS memory transistor characteristics and failure mechanism model.

08 p0944 A73-20741

Fabrication, electrical properties and reliability of thin film capacitors, noting surface irregularity and impurity effects on reliability

08 p0946 A73-21082

Amorphous semiconductors for switching, memory, and imaging applications.

09 p1132 A73-21984

Bayesian prior distributions for multi-component systems.

09 p1111 A73-22374

Hydrogen-oxygen fuel cell as reliable electric power supply for space shuttle mission requirements, assessing technological developments

09 p1035 A73-22777

Electronic system reliability improvement by partitioning into functional parallel redundant blocks

10 p1193 A73-23651

Method of calculating yield for LSI arrays considering radial distribution of defects on wafers.

10 p1193 A73-23668

A computer method of optimal redundancy allocation in satellite communication system.

10 p1188 A73-23753

Ballistic-tolerant helicopter flight control components from plastic composite materials.

10 p1237 A73-23964

Fast and reliable automatic digital control components and transducers for data processing, display and storage, assessing technology development trends and preference over analog devices

10 p1199 A73-24028

Reliability analysis of helicopter mechanical transmission components and reduction gearboxes

11 p1306 A73-26596

Two component system reliability model, taking into account stress effects under failure normal distribution assumption

11 p1448 A73-26730

Diagnostic tests and failure checkout for interconnected combinational micrologic circuit components in manufacturing process, tabulating individual failure functions

12 p1474 A73-26755

Book - Reliability concepts in engineering manufacture.

12 p1502 A73-27398

A confidence estimate of the reliability of a system from the results of tests of its components

12 p1503 A73-27618

Thermal/electrical design of spaceborne microelectronic components.

13 p1588 A73-28046

Taking into account correlation when forecasting the parameters of failure-free operation of radio equipment.

15 p1849 A73-30994

Reliability analysis of time to failure distribution of redundant system with failing elements number as periodic function of time

15 p1880 A73-30998

Concorde aircraft fuel system and component valves design for long term service reliability and ease of maintenance, discussing refueling, fuel jettisoning and feed controls

16 p2046 A73-32923

Utilization of realization to optimize the choices of reliability from the economic point of view

16 p2088 A73-33270

The analysis of defects and the possibilities brought by the scanning electron microscope

16 p2019 A73-33272

Hydrofluidic component and system reliability.

16 p1971 A73-33478

Computerized analysis of reliability or failure rate function data from electronic component and equipment operation and testing, using hazard plotting technique

16 p1989 A73-33613

Tactical weapon system final test for random failures, discussing electronic component defects effects and semiconductor device screening for system reliability improvement

16 p1990 A73-33624

Lower confidence bounds determination for component or system reliability by sampling with and without replacement, censored, truncated and mixed sampling test programs

16 p2033 A73-33629

A statistical analysis of product reliability due to random vibration.

16 p2020 A73-33637

DC9-30 refrigeration system diagnosis by computer.

16 p1969 A73-33654

Reliability of diversity reception by antennas with different polarizations.

16 p1991 A73-33984

Operational behaviour of a complex system with two out of M failed components.

16 p2022 A73-34030

Military specifications provisions regarding load transfer.

17 p2133 A73-34093

Fatigue life of structural components under random loading

17 p2242 A73-34520

Book - Compatibility and testing of electronic components.

17 p2134 A73-34573

Failure analysis used to vindicate JANTX components.

17 p2135 A73-34731

Computerized approach for aerospace electronic components standardization for procurement cost, logistics and warehousing problems reduction and reliability improvement

17 p2140 A73-35260

Reliability of aircraft turbojet bearings

18 p2320 A73-36691

Reliability estimation for integral logical elements from intermittent failures under noise effects

18 p2292 A73-37045

Russian book - Hydraulic ducts of control systems in aviation: The effects of external factors. Shop testing, and reliability.

19 p2389 A73-37766

Long term life tests for thermal shock cycles effects on plastic encapsulated semiconductor device reliability, presenting salt atmosphere testing data for silicone package

19 p2471 A73-38454

Dual spin gas bearing reaction wheel for spacecraft fine pointing applications requiring long component life, describing manufacturing methods, safety factors and testing

[AIAA PAPER 73-907] 20 p2568 A73-38841

Discrete reproduction of a random parameter change process in standard automation equipment elements

20 p2543 A73-39393

Computer program using successive system reduction on basis of calculation of reliability of pure parallel and series arrangements

20 p2533 A73-39632

Thin film capacitor with anodic tantalum oxide overlaid with silicon dioxide deposited by RF sputtering, noting reliability under various voltage, temperature and humidity conditions

21 p2663 A73-40771

Electric connector reliability assessment model based on operating conditions and failure modes analysis without using MTBF

21 p2665 A73-41208

Test facilities for B-I components prior to construction and flight testing, discussing wind tunnel tests for aerodynamic characteristics, stall performance, drag factor and spin

21 p2675 A73-41431

Macrofractographic studies of fatigue fractures in aircraft engine elements

21 p2754 A73-41593

The accuracy and operational stability of a transistorized time-delay relay with an RC network

21 p2668 A73-41640

Fabrication of high-reliability sheathed thermocouples.

22 p2865 A73-42041

Failure diagnosis using quadratic programming.

22 p2867 A73-42966

The robustness of reliability predictions for series systems of identical components.

22 p2867 A73-42967

Product reliability management, providing MTBF charts for relationships between part count, laboratory test results and operational performance

22 p2867 A73-42969

Use of fluidics in explosive component fabrication.

23 p2941 A73-43391

Probability estimate models for reliable function of redundant systems with adaptable and inadaptable neuron-like restoration organs

24 p3063 A73-44904

COMPONENTS

Microwave lumped passive and active circuit components properties assessment, considering inductor, capacitor, resistor, gyrator, tunnel diode amplifier, varactor Gunn oscillator, and parametric amplifier

08 p0942 A73-20703

COMPOSITE MATERIALS

NT CARBON FIBER REINFORCED PLASTICS

NT CARBON-CARBON COMPOSITES

NT CERMETS

NT COMPOSITE PROPELLANTS

NT GLASS FIBER REINFORCED PLASTICS

NT LAMINATES

NT METAL MATRIX COMPOSITES

NT PLYWOOD

NT REINFORCED PLASTICS

NT THREE DIMENSIONAL COMPOSITES

NT WHISKER COMPOSITES

Book - Deformations of fibre-reinforced materials.

01 p0113 A73-10148

Discontinuous or short fiber reinforced composites properties, manufacturing procedures and aircraft structural applications

01 p0057 A73-11240

Spiral wrap - A technique for fabricating thick-wall carbon composites.

01 p0057 A73-11294

The fracture energy of carbon-fibre reinforced glass.

01 p0068 A73-11500

PRD 49 high modulus organic fibre as aluminium replacement.

01 p0068 A73-11510

Plane electromagnetic wave diffraction by periodic grid of dielectric cylindrical filaments, determining reflection and transmission coefficients of radome composite materials

02 p0141 A73-12024

The effect of crystallite size on the strength of carbon-graphite materials.

02 p0185 A73-12142

Glass bead reinforced epoxy and polyester resins mechanical properties as function of volume fraction and interfacial bond strength, discussing beads chemical surface treatment effects

02 p0185 A73-12428

Applications of dynamic photoelasticity in flaw detection analysis. I.

02 p0175 A73-12868

High temperature solid lubrication technology developments, discussing bonded films, plastic and metal bonded composites and temperature ranges

03 p0330 A73-13013

Observations of failure modes in carbon composite materials.

03 p0332 A73-13042

Carbon and pyrolytic graphite isothermal chemical vapor deposited /CVD/ composite coated and free standing products fluid bed manufacturing and applications

03 p0333 A73-13053

Composite materials of today and tomorrow: New materials and conventional industries; International Conference, 1st, Lyons, France, September 22-24, 1971, Proceedings

03 p0334 A73-13579

Structure-property relationships for composites.

03 p0334 A73-13587

Utilization in aeronautics of composite materials for working structures

03 p0334 A73-13594

Utilization of composite materials for the fabrication of fuel cells

03 p0334 A73-13595

Tutorial lecture notes for experimental modelling in testing.

04 p0452 A73-14711

Kinetic model considering cumulative fatigue damage interaction with chance overload on component or structure under probabilistic service load, discussing crack growth in composites

04 p0508 A73-14717

Statistical stress concentration effects in composites.

04 p0468 A73-14718

Fiberglass reinforced composite material application to light weight ballistic damage tolerant military helicopter flight control components previously vulnerable to small arms fire

04 p0452 A73-14722

Weibull flaw distribution models for fracture strength and failure analysis of brittle materials and fiber reinforced composites

04 p0468 A73-14726

Discussion of the Colloquium on Structural Reliability.

04 p0468 A73-14727

Empirical strength criteria for anisotropic and isotropic composite materials with unequal tensile and compressive strength

04 p0508 A73-14860

Cu and Cu-Sn base self lubricating composites, testing solid lubricants effects on friction coefficient, wear, electrical resistance, hardness, porosity and structure

04 p0454 A73-14996

Upper bound tensile strength analysis of reinforced composite materials in terms of matrix/particle bond strength, void formation and geometrical factors [ASME PAPER 72-WA/PROD-7]

04 p0469 A73-15805

Upper bound predictions of composite tensile strength as function of transitions from homogeneous to nonhomogeneous deformation [ASME PAPER 72-WA/PROD-8]

04 p0469 A73-15806

Mean field equations for dynamic response of homogeneous linearly elastic solids, obtaining formulation for ensemble averaged displacement and stress fields of composite [ASME PAPER 72-WA/APM-28]

04 p0515 A73-15890

Plane time-harmonic wave propagation through periodically arranged composite material, determining displacement mode shapes and dispersion relations by variational method [ASME PAPER 72-WA/APM-10]

04 p0516 A73-15902

On the effective moduli of composite materials - Slender rigid inclusions at dilute concentrations.

05 p0630 A73-16099

Geometric dispersion of acoustic waves by a fibrous composite.

05 p0597 A73-16114

Effective stiffness of randomly oriented fibre composites.

05 p0631 A73-16116

Elastic wave propagation in filamentary composite materials.

05 p0631 A73-16122

Bright future forecast for composites in aerospace.

05 p0589 A73-16185

Far field solution for stress wave attenuation and dispersion in composite materials, noting pulse shape

05 p0633 A73-16540

Composite materials technology for aircraft and spacecraft structures, discussing various fiber-matrix combinations mechanical properties and production volume/price relations

05 p0589 A73-16759

Analytical and experimental methods in composite mechanics. [ASCE PREPRINT 1655]

06 p0758 A73-17448

Heat and mass transfer at the surfaces of glass-graphite materials in a high-temperature gas flow

06 p0766 A73-17457

Book - Electronic properties of composite materials.

06 p0714 A73-17872

Investigation of the friction and wear behavior of polytetrafluoro-ethylene composite materials as compared to synthetic carbon and sintered metal. I

06 p0714 A73-18449

Stress intensity factors and singularity power and strain energy release rate near localized cracks and inclusions in composite materials

06 p0764 A73-18489

High strength and low density graphite fiber yarn for reinforcement in structural composite components on heavily loaded flight vehicles

06 p0715 A73-18716

On the reflection of harmonic waves in fiber-reinforced materials.

07 p0909 A73-19096

Study on fracture mechanism for composite materials based on the concept of the change in Poisson's ratio.

07 p0915 A73-20328

On the torsional strength of composite materials reinforced with glass fabric laminates and the effect of the voids in matrix.

07 p0915 A73-20332

On the compressive strength of composite materials reinforced with glass fabric laminates.

07 p0844 A73-20333

A new method of measurement to determine the stress-strain relation in a bending fatigue specimen.

07 p0917 A73-20488

Impact-deflection by oblique fibers in sparsely reinforced composites.

08 p1018 A73-21408

Mechanical behaviour of unidirectionally solidified composites.

08 p0983 A73-21676

[ONERA, TP NO. 1147]
Experimental investigation of the failure mechanism of fiber-reinforced composites subjected to uniaxial tension.

09 p1156 A73-21874

Variational bounds of unidirectional fiber-reinforced composites.

09 p1157 A73-21931

Thermal expansion at elevated temperatures. IV - Carbon-fibre composites.

09 p1110 A73-22121

Investigation of the strength and deformability of thin composite materials used as magnetic recording media. II - Strength and deformability at low temperatures

09 p1110 A73-22156

Application of simultaneous DTA/TGA and DTA/MS analysis for predicting the flammability of composite textile fabrics and polymers.

09 p1110 A73-22515

Elastic stiffness properties and structural designs of fiber composite materials, including laminate and plate problems

09 p1110 A73-22516

High modulus organic fiber/epoxide properties for reinforced composites, including strands, rings and filament wound vessels

09 p1110 A73-22518

A continuum mixture theory of wave propagation in laminated and fiber reinforced composites.

09 p1160 A73-22897

Effective use of composite materials directionally reinforced with hollow fibers.

09 p1111 A73-23151

Fracture mechanics of brittle matrix ductile fiber composites.

09 p1111 A73-23251

Fiber reinforced composite design and application within performance and cost parameters, considering composite structure cost reduction and functional redesign increase

10 p1238 A73-23968

The effect of long-time thermal exposure on the mechanical properties of graphite/polyimide composites.

10 p1238 A73-23970

Izod impact tests of carbon fiber composites strength, measuring residual compressive strength

10 p1238 A73-23973

Solid composite material thermodynamics and overall thermoelastic modulus determination, considering arbitrarily anisotropic phases, binary composite and self consistent theory

10 p1295 A73-24099

The propagation of waves from a cylindrical cavity.

10 p1289 A73-24282

Graphitization of carbon fibre/glassy carbon composites.

10 p1240 A73-24284

In-plane shear stress-strain response of unidirectional composite materials.

10 p1240 A73-24285

Moire fringe method for stationary and running cracks length and crack opening displacement measurements in composite materials

10 p1240 A73-24287

Elastic properties of materials strengthened by short unidirectional fibers

10 p1240 A73-24306

Investigation of the fracture of carbon-graphite materials in a complex stress-strain state

10 p1240 A73-24360

Direct nondestructive prediction of engineering properties.

11 p1372 A73-25129

Fabrication and physical, mechanical and electrical properties of inorganic composite material for aircraft radomes

11 p1387 A73-25288

Composite material production by grinding Ni-Al-Ti alloy powder with other mixed powders, noting alloying elements effects on corrosion resistance and ductility

11 p1372 A73-25406

The joining of fiber-reinforced composite-material components with similar or different components

11 p1373 A73-25418

Possibilities regarding the development and the employment of fiber-reinforced composites in comparison with conventional materials

11 p1454 A73-25419

Synthesis of compression panels having non-uniform stiffener sections.

[AIAA PAPER 73-347] 11 p1437 A73-25485

A synthesis procedure for mechanically fastened joints in advanced composite materials.

[AIAA PAPER 73-348] 11 p1437 A73-25486

High modulus composites versus beryllium for achieving stiffness in spacecraft structural applications.

[AIAA PAPER 73-384] 11 p1430 A73-25513

Composite solid with two contacting or bonded half planes of different elastic moduli, considering inter-plane force transmission from stress distribution calculation

11 p1443 A73-26277

Saint Venant principle for plane deformation of anisotropic elastic solid extended to analysis of fiber reinforced transversely isotropic composites

11 p1444 A73-26280

Universal solutions for fiber-reinforced incompressible isotropic elastic materials.

11 p1447 A73-26656

Influence of the shape of inclusions on the initial stage of failure of two-component composite materials

11 p1389 A73-26738

Fracture mechanism transitions in laminate composites.

12 p1550 A73-26921

A comparison of quasi-static uniaxial-strain and Hugoniot tests for quartz-phenolic composite.

12 p1550 A73-27024

The thermal expansion of composites based on polymers.

12 p1515 A73-27030

Damping properties of a composite material with monodirectional continual fibers

12 p1516 A73-27258

Elastic and viscoelastic zero moment reinforced and weakened shells of composite materials, calculating deformation mode characteristics

12 p1553 A73-27375

Composite materials transient thermal boundary conditions analytical derivation from initial and time dependent internal temperature distribution or gradient

13 p1705 A73-28436

Friction and wear of self-lubricating composite materials.

13 p1624 A73-28776

Graphite- and boron-epoxy composite curved panels, determining shear buckling stress and post-buckling strength by visual and photographic observations [SESA PAPER 2030A]

13 p1699 A73-29308

Fiber composite materials properties, technological assessment and future development and application for aerospace flight structures, considering manufacturing cost, tailorability and stiffness requirements

13 p1699 A73-29346

Mechanical behavior of materials; Proceedings of the First International Conference, Kyoto, Japan, August 15-20, 1971. Volume 1 - Deformation and fracture of metals. Volume 2 - Fatigue of metals. Volume 3 - Temperature effects of metals, environmental effects, polymers. Volume 5 - Composites, testing and evaluation.

13 p1638 A73-29451

The relation between tensile bond strength and crystalline properties of the adhesive on the steel-nylon 12-steel system.

13 p1642 A73-29531

A variational method for micromechanics of composite materials.

13 p1702 A73-29534

Mathematical theory of elasticity for stress concentration in homogeneous isotropic perfectly elastic composites with spherical inclusions, noting grain boundary stresses

13 p1702 A73-29535

Bonding characterization in reinforced composites.

13 p1702 A73-29536

Metal-filament-reinforced materials and their mechanical behaviour.

13 p1642 A73-29537

Theory and experiments of compressive strength of unidirectionally fiber-reinforced composite materials.

13 p1702 A73-29539

Conditions for rational arrangement of reinforcing fibres in materials and structures.

13 p1702 A73-29540

Carbon fibre reinforced ceramics.

13 p1646 A73-29541

Fracture strength of helically wound composite cylinders.

13 p1702 A73-29542

Investigation of the friction and wear behavior of polytetrafluoroethylene composite materials as compared with that of artificial coal and sintered metal. II

13 p1647 A73-29652

Lubricant film and self lubricating composite materials optimum selection in solid lubricant design, considering performance and cost criteria

[ASME PAPER 73-DE-8] 14 p1766 A73-30817

Stresses in a fiber-reinforced elastic sheet containing a circular hole.

15 p1949 A73-31655

Brittle fracture and crack propagation prediction in unidirectionally fiber reinforced composites via Sc theory, comparing with stress intensity factor K_{IC} concept

15 p1949 A73-31681

Interacting continuum theory concerning steady shock wave in composite materials, discussing energy interaction terms error correction effects on Hugoniot relations

15 p1949 A73-31685

Macroscopic elastic constant determination for randomly reinforced composite materials by equilibrium method

15 p1954 A73-32115

An invariant treatment of interfacial discontinuities in elastic composites.

15 p1954 A73-32121

Evaluation of composite failures through fracture signal analysis.

15 p1879 A73-32250

Strain analysis of composites by moire methods.

15 p1956 A73-32269

New horizons in materials and processing; Proceedings of the Eighteenth National Symposium and Exhibition, Los Angeles, Calif., April 3-5, 1973.

16 p2027 A73-33026

Composite material design criteria, discussing fatigue, stress concentration, safety factors, scaling effects and load characteristics

16 p1967 A73-33028

Processing and properties of composites based on NR-150 polyimide binders.

16 p2029 A73-33047

Processing aerospace textiles into fabric composite reinforcements 'The weaver's viewpoint.'

16 p2018 A73-33065

On the observability and stability of the temperature distribution in a composite heat conductor.

16 p2034 A73-33311

Investigation of the thermophysical and antifriction characteristics of polyethylene composites. III - The effect of fillers on the heat conductivity of polyethylene

16 p2030 A73-33930

Correlation functions of the elastic field of quasi-isotropic composite materials under nonisotropic deformation

17 p2240 A73-34146

Influence of the structure of a composite material on its elastic properties

17 p2194 A73-34269

Fatigue and fracture of advanced composite materials.

[SAE PAPER 730337] 17 p2194 A73-34688

Aircraft cabin noise reduction through composite material insulation, discussing engine noise sources, aircraft fuselage transmission loss characteristics, vibration damping and sandwich structures [SAE PAPER 730339]

17 p2102 A73-34690

Polyimide resin dielectric and mechanical properties, discussing syntactic foam composite with aluminum filler for radome construction

17 p2195 A73-34804

Applications and concepts for the incorporation of composites in large military transport aircraft.

17 p2104 A73-34816

Composite materials structure, describing component interactions, major constituents, determinants of mechanical properties, particulate composites, materials applications and fiber types

17 p2195 A73-34974

High speed oscillating tests of lubricating composites.

[ASLE PREPRINT 73AM-3C-2] 17 p2179 A73-34987

Propagation of stress gradient through an inclusion. I.

[ASME PAPER 73-APM-15] 17 p2247 A73-35038

Propagation of stress gradient through an inclusion. II.

[ASME PAPER 73-APM-16] 17 p2247 A73-35039

Stress analysis of composite materials with strong fibers in weak matrix, obtaining tensile stress boundary layer equations via elasticity theory and perturbation methods

[ASME PAPER 72-APM-TTT] 17 p2249 A73-35110

On the transverse strength of fiber-reinforced materials.

[ASME PAPER 72-APM-EEE] 17 p2249 A73-35111

Failure modes in composites; Proceedings of the Symposium, Boston, Mass., May 8-11, 1972.

17 p2191 A73-35526

Stress distribution in a bonded anisotropic lap joint.

[ASME PAPER 73-MAT-M] 18 p2365 A73-36618

Radiative heat transfer through composite materials.

18 p2371 A73-36621

Isochromatic and isoclinic parameters for fiber reinforced birefringent composite materials, discussing mechanical and optical characterization

19 p2495 A73-37195

A study on graphite-base high-temperature composite materials. II Graphite-tantalum composite materials.

19 p2443 A73-37375

A parametric weights study of a composite material prop/rotor blade.

[SAWE PAPER 950] 19 p2385 A73-37878

Boron epoxy, polyimide and aluminum composite materials for cost effective high performance aircraft and turbine engine structures, assessing development and application status

[SAWE PAPER 992] 19 p2443 A73-37892

Fibrous composite materials orthogonal shear properties related to laminate construction, discussing

shear load tests, fiber orientation, boron, graphite, aluminum and titanium properties
[SAWE PAPER 993] 19 p2443 A73-37893

Plastic deformation anisotropy and work-hardening of composite materials.
19 p2444 A73-38261

Structural composites on future fighter aircraft.
[AIAA PAPER 73-806] 19 p2388 A73-38371

Production techniques for advanced composites fabrication by tape machine automation.
[SME PAPER EM 73-718] 19 p2436 A73-38498

Strength of fibrous composite materials.
19 p2502 A73-38551

Japan Congress on Materials Research, 16th, Osaka, Japan, August 1972, Proceedings.
20 p2575 A73-38636

Stress singularities associated with a crack inclined to a bi-material interface.
20 p2620 A73-39531

Impact generated elastic strain low amplitude pulses propagating in filamentary composite rods, using Fourier transform technique and viscoelastic relation
20 p2623 A73-39557

Three-dimensional problem of the stability of fibers in a matrix in the presence of highly elastic strains
20 p2581 A73-39642

High-speed photographic study of failure processes in composite materials.
21 p2723 A73-39988

An improved test for interfacial shear strength.
21 p2719 A73-40922

Nonlinear elasticity of random inhomogeneous materials reinforced by grains or oriented fibers, using Kauderer stress relation
21 p2787 A73-40987

Pure torsion of prismatic rods composed of different materials
21 p2787 A73-40990

Plane crack problems for ideal fibre-reinforced materials.
21 p2787 A73-41014

Plane strain and generalized plane stress problems for fibre-reinforced materials.
21 p2788 A73-41546

Aircraft windshield stretched acrylic plastic, chemically strengthened glass, and clad polycarbonate curved composite materials
22 p2799 A73-41863

High-temperature internal friction in boron fibers
22 p2880 A73-41957

Interaction of cracks with rigid inclusions in longitudinal shear deformation. II - Further results.
22 p2920 A73-42134

An application of topographical analysis to the wear of polymers.
22 p2881 A73-42355

Alloy or metal coated composite powder thermal spraying applications, discussing bonding properties, wear resistance, low friction applications and abrasability
22 p2866 A73-42593

On the integral equations of three-dimensional multiple inclusion problems.
22 p2924 A73-42682

The effect of plasticity and crack blunting on the stress distribution in orthotropic composite materials.
[ASME PAPER 73-APMW-2] 22 p2924 A73-42876

Experimental verification of dispersion relations for layered composites.
[ASME PAPER 73-APMW-14] 22 p2924 A73-42881

Finite difference scheme for wave equation solution for wave propagation in layered composite materials, obtaining matrix eigenvalues with Floquet condition for various methods
[ASME PAPER 73-APMW-40] 22 p2926 A73-42897

Comment on 'Film reinforced multifastened mechanical joints in fibrous composites.'
22 p2928 A73-43115

Statistical theory of solid heterogeneous materials, discussing constant elastic bounds, fiber reinforced cell model, thermal expansion and stress-strain relations
23 p3038 A73-43303

Analysis of the test methods for high modulus fibers and composites; Proceedings of the Symposium, San Antonio, Tex., April 12, 13, 1972.
23 p2996 A73-43626

Characterization of composites for the purpose of reliability evaluation.
23 p3040 A73-43627

Fracture mechanics and composite materials - A critical analysis.
23 p3040 A73-43628

Fiber reinforced composite crack model performance prediction and tests, noting fiber volume fraction for maximum fracture toughness
23 p3040 A73-43629

Method for estimating fracture strength of specially orthotropic composite laminates.
23 p3040 A73-43630

Deformation and failure of boron-epoxy plate with circular hole.
23 p3040 A73-43631

Free-edge effects in the characterization of composite materials.
23 p3040 A73-43632

Effects of specimen geometry on the strength of composite materials.
23 p2996 A73-43633

Compressive strength and failure modes of unidirectional composites.
23 p3041 A73-43634

Anisotropic composite material swelling coefficients and elastic compliances data averaging and reduction, using tensor transformation and associated scalar invariants
23 p3041 A73-43636

Helical wound composite cylindrical tube under pure bending, determining elastic response from boundary value problem solution
23 p3041 A73-43637

Prediction and control of macroscopic fabrication stresses in hoop wound, fiberglass rings.
23 p3041 A73-43638

Post-yielding behavior of torsionally loaded composite tubes.
23 p3041 A73-43640

Ultrasonic spectroscopy for NDT of composite material tube, noting role of frequency signature and pulse spreading in flaw detection
23 p2984 A73-43641

Singular approximation in the calculation of the elastic properties of reinforced systems
24 p3145 A73-44514

F-14 replacement for Phantom aircraft for escort missions, fleet defence, interdiction and close support, discussing airborne refuelling capability and composite materials applications
24 p3056 A73-44695

The mechanism of electrical erosion in composite materials during electric arc alloying
24 p3093 A73-44743

Wear resistant abrasive and dry lubricant cobalt-chromium carbide composite material coatings obtained by electrolytic codeposition
24 p3094 A73-45073

Toward reliable composites - An examination of design methodology.
24 p3094 A73-45144

Vibration characteristics of aluminum plates reinforced with boron-epoxy composite material.
24 p3149 A73-45148

A note on determination of the shear stress-strain response of unidirectional composites.
24 p3149 A73-45150

Optimization of fiber reinforced composite structures.
24 p3151 A73-45304

COMPOSITE PROPELLANTS

Development of a small end-burning type motor by using pellet impregnated propellant.
01 p0090 A73-11108

On some relation between the mechanical properties and the bond strength of elastomer to solid inclusion in solid propellant.
01 p0090 A73-11117

Failure criterion for a propellant of a spherical solid rocket motor.
[AIAA PAPER 72-1088] 03 p0351 A73-13409

Aging mechanisms in composite-modified double-base propellants.
[AIAA PAPER 72-1089] 03 p0351 A73-13410

Prediction of the critical diameter of composite propellants.
[AIAA PAPER 72-1117] 03 p0351 A73-13432

Catalytic effects of copper chromite and iron oxide on AP-HTPB binder sandwich combustion to 3200 psia by cinephotomicrography
[AIAA PAPER 72-1120] 03 p0352 A73-13434

Pressure exponent of controllable solid rocket propellants.
[AIAA PAPER 72-1135] 03 p0352 A73-13442

Depressurization extinguishment of composite solid propellants - Influence of composition and catalysts.
[AIAA PAPER 72-1136] 03 p0352 A73-13443

Propellants and combustion. I - Role of binder in solid propellant combustion.
[AIAA PAPER 72-1121] 04 p0485 A73-14910

The thermal decomposition of nitroglycerin and its relation to the stability of CMDB propellants.
[WSCI PAPER 72-30] 05 p0605 A73-16685

Extinguishment of composite propellants at low pressures.
[AIAA PAPER 73-175] 05 p0640 A73-16918

Role of condensed phase details in the oscillatory combustion of composite propellants.
[AIAA PAPER 73-218] 05 p0641 A73-16948

German book - Solid rocket propulsion systems II: Theory and technology.
06 p0740 A73-18074

Influence of the surface microstructure on the evolution of the combustion velocity of ammonium perchlorate composite solid propellants as a function of pressure
[ONERA, TP NO. 1167] 08 p0995 A73-21678

Heterogeneity effect on L instability of solid rocket propellant combustion, using sideways sandwich model
11 p1450 A73-25373

Homogeneous and composite solid propellants, discussing rocket motor performance, energetics, smokeless exhaust, energy-weight relations and cost
14 p1784 A73-30135

Effects of composition on acceleration induced burning-rate augmentation.
15 p1925 A73-31661

Explosive behavior of aluminized ammonium perchlorate.
16 p2045 A73-33346

Influence of acceleration on the combustion of solid propellants - Measurement and prediction of the effects
16 p2045 A73-33391

Effects of additions of metals and metal borides on the burning rates of mixture systems
19 p2503 A73-37509

Effects of copper chromite and iron oxide catalysts on AP/CTPB sandwiches.
22 p2899 A73-42812

Effect of composite propellant catalysts on the stabilities of HClO₄ and the HClO₄-NH₃ system.
22 p2899 A73-42814

COMPOSITE STRUCTURES

NT LAMINATES

NT PLYWOOD

Fracture strength of helical-wound composite cylinders.
01 p0117 A73-11121

Determination of the theoretical stress-concentration factors in composite systems in bending
02 p0229 A73-11638

Solution to the bending problem and to the plane problem of an anisotropic rectangular plate with arbitrary boundary conditions and the application of the solution to composite structure designs
02 p0230 A73-11715

Scheme for calculating the process of elastic wave propagation in a composite beam
02 p0233 A73-11943

Graphite-epoxy composite properties, fabrication and tests for light weight low distortion spacecraft antenna reflector applications
03 p0331 A73-13023

Recent advances in automated manufacture of composite structures, e.g., tape laying and pultrusion.
03 p0332 A73-13033

Liquid crystals for nondestructive testing of composite structures.
03 p0349 A73-13041

Weave geometry effects on pyrolytic infiltration of carbon-carbon/graphite-graphite/ composite structures for nose tip and thermal shield materials
03 p0332 A73-13044

Stressed state of adhesively bonded plane interfaces in composite systems, applying two dimensional Vocke theory
03 p0311 A73-13129

Stockings, extensible plane structures and three dimensional textile fiber blocks reinforced materials, noting application to structures of revolution under external pressure
03 p0334 A73-13585

Structure-property relationships for composites.
03 p0334 A73-13587

Three-dimensional finite-element analysis of laminated composites.
[AD-759453] 03 p0392 A73-13687

Strength analyses for design with composite materials using metals technology.
04 p0507 A73-14713

Toward reliable composites - An examination of design methodology.
04 p0508 A73-14720

Anisotropic structures reliability in terms of design safety factor, analyzing composite rocket motor cases under plane stress
04 p0452 A73-14723

Torsion of prismatic bars made of various materials
04 p0510 A73-15077

Monograph on structural element and structures reliability covering structural design, failure analysis and reinforced element collapse under moment and force loads
04 p0472 A73-15694

Study of modeling of substructure damping matrices.
[SAE PAPER 720813] 05 p0634 A73-16645

NASA airframes structures program, discussing automated design, composites, supersonic and hypersonic technologies, control systems, load and aeroelasticity prediction and integrity concepts
[AIAA PAPER 73-17] 06 p0759 A73-17610

Fail-safe aircraft composite structures, achieving crack arrestment by integral buffer strips in primary load carrying laminates
06 p0764 A73-18494

Reinforced plastics role in construction and shielding of Diamant B satellite booster main components
07 p0905 A73-18995

Graphite fiber reinforced polyimide resin composites for structural applications in long duration high temperature environments, discussing fabrication with match-metal die

[SME PAPER EM 72-107] 07 p0832 A73-20448
High modulus organic fibre composites in aircraft applications.

09 p1110 A73-22519
Design of rotating discs of irregular outline.

09 p1161 A73-23051
Post-buckling behaviour of rectangular orthotropic plates.

10 p1288 A73-23699
Acoustic emission studies of large advanced composite rocket motor cases.

10 p1288 A73-23967
Torsion of a sectorially composite hollow circular cylindrical beam.

11 p1432 A73-24996
Elastic stability of biaxially loaded longitudinally stiffened composite structures.

[AIAA PAPER 73-367] 11 p1438 A73-25502
Linear elastic finite element stress analysis of lap and tapered adhesive joint bonding of composite to metal substrate

[AIAA PAPER 73-371] 11 p1438 A73-25505
Radiation properties of a composite-dielectric-rod aerial.

11 p1332 A73-26286
Constant cross section composite circular rod, deriving torsional stress behavior near division line intersection with rod contour from closed solution

12 p1552 A73-27368
Optimum design of composite shells subject to natural frequency constraints.

12 p1554 A73-27734
Free vibrations of a laminated beam by a microstructure theory.

13 p1691 A73-28063
Natural vibrations of thin, prismatic flat-walled structures.

13 p1694 A73-28247
Light-weight Al isogrid panel design with triangular reinforcement elements for aerospace structural applications, discussing load response characteristics, fabrication and cost reduction

13 p1624 A73-28906
Multiphase composite material models for elastoplastic beam bending under loading and unloading, using stress-strain diagram in tension and compression

13 p1698 A73-29052
Crack formation in orthogonally reinforced glass-fiber ware.

14 p1765 A73-30307
Statistical displacement characteristics of random multiphase composite elastic structures in terms of stochastic Green functions and Neumann series

14 p1811 A73-30482
General properties of electromagnetic scattering by inhomogeneous anisotropic composite obstacles of arbitrary shape.

15 p1844 A73-31930
Composite airframe structure effects on jet aircraft maintenance, discussing fire safety, fatigue resistance, environmental durability and quality assurance

16 p1967 A73-33027
Lightning protection for boron and graphite fibers in epoxy resins for aircraft composite structures

16 p1967 A73-33032
Lightning protection for boron and graphite reinforced plastic composite aircraft structures, discussing zonal design concept and channel intermittent contact with protrusions on surface

16 p1968 A73-33034
Graphite-epoxy composite door landing gear assembly for space shuttle orbiter, discussing design, analysis, fabrication and structural testing

16 p2029 A73-33058
Technology developments effect on jet aircraft design, discussing flight controls, engine noise suppression, supercritical aerodynamics and composite structures

16 p1968 A73-33188
Stability of composite-material cylindrical shells under unsteady heating and axial compression

16 p2083 A73-33934
Natural frequencies and normal modes of a four plate structure.

16 p2083 A73-33948
Boron composites - Status in the USA.

16 p2031 A73-34042
Applications and concepts for the incorporation of composites in large military transport aircraft.

17 p2104 A73-34816
An advanced composite tailboom for the AH-1G helicopter.

[AHS PREPRINT 785] 17 p2107 A73-35098
Layered composite plate theory with interlaminar transverse shear stress as unknown variables, demonstrating agreement with elasticity solutions

17 p2250 A73-35116
Ultimate tensile properties and composite structure of flow-molded short fiber composites.

17 p2197 A73-35352
Effects of material and stacking sequence on behavior of composite plates with holes.

[SESA PAPER 2157A] 17 p2198 A73-35452
Residual stresses and mechanical properties of circumferentially wrapped metal-metal composite cylinders fabricated from plasma sprayed Al reinforced with steel filaments

17 p2251 A73-35534
Rational winding of vessels with nonlinear winding programs

18 p2319 A73-36470
Multiphase composite material models for elastoplastic beam bending under loading and unloading, using stress-strain diagram in tension and compression

18 p2366 A73-36884
Studies on the impact resistance of composite plates.

18 p2367 A73-37093
Applications of a symbolic algebra manipulation language for composite structures analysis.

19 p2496 A73-37482
Automated structural design and analysis of advanced composite wing models.

19 p2497 A73-37486
Longitudinal shear waves in a fiber-reinforced composite.

19 p2500 A73-38113
Composite fabrication and structural design for commercial aircraft, discussing graphite post installation and testing and pultrusion and autoclave molding processes

[SME PAPER EM 73-717] 19 p2436 A73-38497
Coefficients of stress intensity near rigid acute-angled inclusions

20 p2619 A73-39370
Vibration and noise damping of steel structures by prebonded laminates or viscoelastic layer additions, discussing steel sheets

21 p2717 A73-40236
The plane elastostatic solution for a symmetrically loaded crack in a strip composite.

21 p2789 A73-41669
A higher order theory for extensional motion of laminated composites.

22 p2929 A73-43139
Normal modes of elastically connected circular plates.

22 p2929 A73-43140
Upper bounds to in-plane shear strength of unidirectional fiber-reinforced composites.

23 p3048 A73-44383
Nonlinear parametric vibrations of cylindrical shells prepared from composite materials

24 p3145 A73-44517
The theory of distribution of elastic deformations in two-component composites

24 p3102 A73-44521
Analytical relations of physicomechanical, strength and geometrical factors in formation of high strength monolithic glass fiber reinforced structures

24 p3103 A73-44533
Calculation of the thermal field of an inhomogeneous plate of complex composition with energy sources

24 p3157 A73-45361
COMPOSITE WRAPPING

Acoustic emission during burst tests of filament wound composite pressure bottles as function of pressure, microscopic damage and winding parameters

03 p0331 A73-13031
Recent advances in automated manufacture of composite structures, e.g., tape laying and pultrusion.

03 p0332 A73-13033
Effect of heat treatment on filament wound carbon composites.

03 p0332 A73-13043
COMPOSITES

U COMPOSITE MATERIALS

COMPOSITION (PROPERTY)

NT ATMOSPHERIC COMPOSITION

NT ATMOSPHERIC MOISTURE

NT ATOM CONCENTRATION

NT BODY COMPOSITION [BIOLOGY]

NT CARBON DIOXIDE CONCENTRATION

NT CHEMICAL COMPOSITION

NT CONCENTRATION [COMPOSITION]

NT GAS COMPOSITION

NT IONOSPHERIC COMPOSITION

NT LUNAR COMPOSITION

NT METEORITIC COMPOSITION

NT METEOROID CONCENTRATION

NT MOISTURE CONTENT

NT PLANETARY COMPOSITION

NT PLASMA COMPOSITION

Superplasticity in two phase compositions based on refractory compounds, noting creep rate dependence on concentration and electroconductivity

01 p0066 A73-11339
A method for ingredient composition control in binary and quasi-binary systems

15 p1881 A73-31222
COMPOUND HELICOPTERS

AH-56A rigid rotor compound helicopter configuration and handling qualities under autorotation conditions, discussing flight test program, piloting descent performance

09 p1030 A73-22179
Development program of medium range winged design helicopter, describing wing-fuselage structure, propulsion and power transmission systems and combustion, electrical and hydraulic plants

COMPOUND HELICOPTERS

AH-56A rigid rotor compound helicopter configuration and handling qualities under autorotation conditions, discussing flight test program, piloting descent performance

09 p1030 A73-22179
Development program of medium range winged design helicopter, describing wing-fuselage structure, propulsion and power transmission systems and combustion, electrical and hydraulic plants

12 p1459 A73-27383
Handling qualities comparison of two hingeless rotor control system designs.

[AHS PREPRINT 741] 17 p2105 A73-35074
Analysis of the use of an auxiliary wing on a helicopter

18 p2268 A73-37021
COMPOUNDING

Simulation of the compounder in a single base propellant/SBP process.

17 p2220 A73-34819
COMPOUNDS

The relationship of certain mechanical and thermophysical properties of polymer composites with the reduced filler concentration

24 p3102 A73-44512
COMPRESSED AIR

Dense air plasma compression and heating by TNT explosive charge, noting shock tube flow patterns

10 p1203 A73-23515
Dense air plasma compression and heating by TNT explosive charge, noting shock tube flow patterns

17 p2147 A73-35195
High performance vibration isolated tables.

20 p2544 A73-39266
COMPRESSED GAS

NT HIGH PRESSURE OXYGEN

Relation of the equation of state of compressed gases with the optical complex and the specific refraction - Virial coefficients of carbon dioxide

01 p0080 A73-10856
Stimulated molecular light scattering in gases

02 p0195 A73-11946
Nonadiabatic temperature change in rapidly expanded or compressed gas, discussing shearing and volume viscosity effects

05 p0597 A73-16350
Two chamber adiabatic test compression system design with controlled throttle for high temperature nitrogen- and nitrous oxide-type gases with exothermal reactions

06 p0683 A73-17413
Dielectric constant and molar polarizability of compressed gaseous and liquid fluorine.

06 p0661 A73-18124
High temperature compressed gas heat conductivity calculation by least squares and basis isotherm methods

06 p0770 A73-18569
Theoretical study of a flow-resistance gas heater.

08 p1023 A73-21436
Optical breakdown of compressed gases by carbon dioxide laser emission

09 p1094 A73-22594
Electric current in pressurized N₂, CO₂, and their mixtures under conditions of strong ionization by an electron beam

10 p1230 A73-24883
Pneumosomatic data transmission and processing based on pressurized gases and dynamic body interactions

12 p1460 A73-26771
Connection between the equation of state of compressed gases with an optical complex and the specific refraction - The virial coefficients of carbon dioxide.

12 p1526 A73-27906
Experimental study by resonance method of unsteady aerodynamic forces acting on cascading blades.

13 p1566 A73-29028
High temperature compressed gas heat conductivity calculation by least squares and isotherm methods

16 p2086 A73-33594
System of experimentally verified equations for calculating the thermodynamic characteristics of some technologically important gases at temperatures ranging from the normal boiling point to 1300 K at pressures up to 1000 bar

20 p2627 A73-39297
Exact steady-state analogy of transient gas compression by coalescing waves.

21 p2790 A73-40439
Design of a piston-driven shock tube

21 p2675 A73-41552
Electrical current in electron-beam ionized N₂ and CO₂.

21 p2749 A73-41658
Acoustic turbulence generation of shock waves in compressed gas or plasma excited by random potential forces based on energy transfer along spectrum

22 p2840 A73-41809
Branched-chain mechanism of propane-oxygen-fluorine explosions.

22 p2819 A73-42778

Flows past exponential bodies in the presence of strong compression in the shock layer

24 p3055 A73-45534

COMPRESSIBILITY

Statistical mechanics and virial functions for equation of state of dense gas with spherical nonpolar molecules, calculating compressibility factor for methane and Ar

06 p0726 A73-18555

The compressional modulus of a material permeated by a random distribution of circular cracks.

07 p0915 A73-20335

Theoretical calculation of the compressibility of porous media.

09 p1157 A73-22144

Bulk compressibility of carbon fibre reinforced plastics.

10 p1240 A73-24288

Compressibility of heterogeneous powder mixtures during rolling

10 p1224 A73-24314

Tensorial expansions for the plastic flow of partially compressible media.

10 p1290 A73-24325

Thin flexible inextensible fiber reinforced compressible isotropic elastic materials under large elastic deformations, obtaining solutions to equilibrium and constitutive equations

15 p1946 A73-31101

Statistical mechanics and virial functions for equation of state of dense gas with spherical nonpolar molecules, calculating compressibility factor for methane and Ar

16 p2039 A73-33580

COMPRESSIBILITY EFFECTS

Shell designs by the theory of small elastoplastic deformations with allowance for the compressibility of material

01 p0112 A73-10005

Effect of high isostatic pressures on the compressibility and sinterability of tungsten powders.

01 p0665 A73-10819

A linear approach to the analysis of a force control system incorporating a hydraulic pressure-ratio valve.

02 p0132 A73-12002

A method of analysing the effect of inertia and compressibility in an externally pressurized gas lubricated thrust bearing.

03 p0312 A73-13209

The effects of compressibility in multi-element hydraulic lines.

[ASME PAPER 72-WA/FE-43]

04 p0435 A73-15857

The tricuspid hypocycloid as envelope of the force of lift, calculated in a first compressible approximation, in the case of a symmetrical profile in a flow of variable direction and a given Mach number

05 p0528 A73-16764

Experimental investigation of two-dimensional, supersonic flow impingement on a normal surface.

08 p0925 A73-20720

Calculation of the transonic flow around an airfoil, taking account of the exact law of compressibility

09 p1027 A73-22210

Fluctuating lift and moment coefficients for cascaded airfoils in a nonuniform compressible flow.

09 p1028 A73-22432

Compressibility effects on unsteady forces generated by jet engine blade rows aerodynamic interference, considering potential flow and viscous wake interactions

09 p1029 A73-23443

Bullen solid core model for earth and Venus vindicated by free earth oscillations records and detection of PKJKP seismic phase, discussing compressibility effects

11 p1421 A73-25897

On the Aller's admixture radiation effect during the compression process in the solar corona and generation of coronal formations.

12 p1536 A73-27844

Hysteresis loop equation for calculation of elastoplastic deformations caused by forced vibrations, taking into account medium compressibility and inertial forces

13 p1703 A73-29609

Collisionless magnetized unstable plasma two dimensional adiabatic compression, calculating gamma from temperature distributions

14 p1779 A73-29984

Analytical investigation of compressibility and three-dimensionality on the unsteady response of an airfoil in a fluctuating flow field.

[AIAA PAPER 73-683]

18 p2262 A73-36234

Application of compressibility correction to calculation of flow in inlets.

18 p2265 A73-36395

A note on the finite elastic inflation of a thin spherical shell.

21 p2789 A73-41688

Vela 3 proton data analysis for compressions and rarefactions effects on solar wind density, temperature and velocity behavior

24 p3125 A73-45106

Optimization of compression constants for cumulated plane shock waves in a closed tube.

24 p3117 A73-45428

Transformation of shock compression into isentropic compression in a nonhomogeneous body.

24 p3117 A73-45429

COMPRESSIBLE BOUNDARY LAYER

A solution of the three-dimensional unsteady compressible boundary layer equations.

01 p0004 A73-11356

A comparison of two prediction methods with experiment for compressible turbulent boundary layers with air injection.

02 p0129 A73-12505

Compressible boundary layer formation on shock tube walls after bursting of diaphragm separating gases at different pressures

03 p0293 A73-13527

Turbulent properties of a compressible boundary layer.

03 p0296 A73-14177

Calculation of compressible turbulent boundary layers with roughness and heat transfer.

03 p0296 A73-14179

Theoretical investigation of transition phenomena in the boundary layer on an infinite swept wing

[DGLR PAPER 72-124]

03 p0248 A73-14379

Unsteady compressible boundary layers with arbitrary pressure gradients.

[AIAA PAPER 73-132]

05 p0565 A73-16885

Turbulence measurements in a compressible boundary layer subjected to a shock-wave-induced adverse pressure gradient.

[AIAA PAPER 73-167]

05 p0566 A73-16912

Reference temperature method for predicting turbulent compressible skin-friction coefficient.

08 p0925 A73-20722

A two-layer model of high speed two- and three dimensional turbulent boundary layers with pressure gradient, surface mass injection and entropy layer swallowing.

[AIAA PAPER 73-135]

08 p0956 A73-21800

Some heat transfer measurements in compressible turbulent boundary layers.

10 p1296 A73-24648

Similarity solutions of unsteady, compressible plane and axisymmetric laminar boundary layer equations.

10 p1208 A73-24807

Kaplan perturbation method for incipient flow separation, considering three dimensional, compressible and unsteady boundary layers

10 p1208 A73-24815

Recent studies in the field of unsteady boundary layers

10 p1173 A73-24833

A higher order theory for compressible turbulent boundary layers at moderately large Reynolds number.

11 p1346 A73-25218

Compressible boundary layer flow at a three-dimensional stagnation point with intensive suction or injection

12 p1458 A73-27699

Increase of boundary-layer heat transfer by mass injection.

13 p1706 A73-28816

German monograph on compressible turbulent boundary layer equations solution for heat transfer in divergent nozzle flow based on modified Patankar-Spalding difference method

13 p1605 A73-29276

Construction of solutions for the equations of a compressible laminar boundary layer on a plate with abruptly changing boundary conditions

13 p1567 A73-29408

Effects of wall boundary layers in wind tunnels on blocking phenomena

16 p1962 A73-32815

A modified wall wake velocity profile for turbulent compressible boundary layers.

17 p2150 A73-34439

An initial value method for the study of shock-induced laminar compressible boundary layers.

[ASME PAPER 73-FE-4]

17 p2152 A73-35004

Study of the similarity solution in three dimensional compressible laminar boundary layer.

17 p2157 A73-35862

Practical calculations of transitional boundary layers.

19 p2423 A73-38479

Stability of a compressible boundary layer with regard to a localized disturbance

20 p2547 A73-39285

Flow measurements over compression corner in supersonic separated laminar boundary layers with hot-wire probes

21 p2631 A73-40247

Compressible laminar boundary layer differential equations solution for incident viscous gas flow on flat plate at high flow velocity

24 p3080 A73-45471

**COMPRESSIBLE FLOW
NT TRANSONIC FLOW**

An extremum principle for three-dimensional compressible inviscid flows.

01 p0031 A73-10427

Numerical method for describing turbulent, compressible, subsonic separated jet flows.

01 p0035 A73-11467

Buoyancy distribution of slender axisymmetric bodies of higher order in the case of compressible subsonic flow

[DGLR PAPER 72-067]

02 p0127 A73-11681

Boundary conditions for temperature perturbations in stability problems of compressible gas flows

03 p0245 A73-13672

Extension of the Miles-Howard theorem to the circular flows of a compressible fluid.

03 p0297 A73-14443

Unsteady one-dimensional compressible frictional flow with heat transfer.

03 p0298 A73-14639

Performance of truncated conical diffusers with compressible flow.

03 p0249 A73-14641

Compressible flow characteristic generalizations, considering flow with/without heat transfer and losses in terms of empirical loss coefficient or heat transfer coefficient

[ASME PAPER 72-WA/PWR-1]

04 p0434 A73-15803

An explicit numerical method for the solution of jet flows.

[ASME PAPER 72-WA/FE-20]

04 p0435 A73-15846

Unsteady-state conjugated heat transfer between a semi-infinite surface and incoming flow of a compressible fluid. I - Reduction to the integral relation. II - Determination of a temperature field and analysis of results.

04 p0520 A73-15944

On the numerical solution of two-dimensional, laminar compressible flows with imbedded shock waves.

[ASME PAPER 72-FE-7]

05 p0564 A73-16545

The tricuspid hypocycloid as envelope of the force of lift, calculated in a first compressible approximation, in the case of a symmetrical profile in a flow of variable direction and a given Mach number

05 p0528 A73-16764

Isentropic compressible flow equations for pressure and velocity distributions across vortex in axial core mass flow, noting atmospheric circulation and pressure effects

[AIAA PAPER 73-106]

05 p0529 A73-16866

Magnus force and moment coefficients for spinning ogive and cone cylinders and conical bodies in laminar compressible flow, including boundary layer and radial pressure gradient effects

[AIAA PAPER 73-124]

05 p0530 A73-16879

Evaluation of numerical viscosity effects in transonic flow calculations.

[AIAA PAPER 73-131]

05 p0530 A73-16884

Unsteady compressible potential flow around lifting bodies - General theory.

[AIAA PAPER 73-196]

05 p0531 A73-16931

Inverse method of designing two-dimensional transonic airfoil sections.

05 p0533 A73-17104

Transformation of the hypersonic compressible Navier-Stokes equations.

05 p0567 A73-17120

Viscous compressible flow near right angle corner of two flat plates, presenting streamwise and secondary flow velocities and skin friction coefficient distribution

06 p0687 A73-18532

A computational method for low Mach number unsteady compressible free convective flows.

07 p0918 A73-19268

German monograph - An iteration procedure for the calculation of planar compressible flows around circular profiles.

07 p0774 A73-19580

Analysis of flow of viscous fluids by the finite-element method.

07 p0811 A73-19953

Cylinder surface roughness and transverse curvature effects on turbulent boundary layer in incompressible and compressible flows, deriving formula for skin friction coefficient

08 p0956 A73-21603

Periodic nozzle flow with heat addition.

[AD-758555]

08 p1025 A73-21669

Remarks on variational principle for an inviscid, perfect, magnetized plasma.

09 p1126 A73-22122

Estimation of possible excitation frequencies for shallow rectangular cavities.

09 p1029 A73-23444

Turbulent viscosity distribution in axisymmetric compressible wake and coaxial mixing flows via Navier-Stokes equations, taking into account pressure gradients

10 p1206 A73-24545

Compressible magnetorelativistic flow character in subsonic, supersonic and transonic regions, obtaining pressure coefficient, free stream Mach number and Alfvén speed interrelationships

10 p1210 A73-24921

- An evaluation of cell type finite difference methods for solving viscous flow problems. [AD-757443] 11 p1345 A73-25112
- Unsteady subsonic compressible flow around finite thickness wings. [AIAA PAPER 73-313] 11 p1301 A73-25544
- Turbulent transport coefficients for compressible heterogeneous mixing. 13 p1705 A73-28435
- Variational formalism of a quasi-linear compressible fluid flow with heat exchange. 13 p1602 A73-29022
- Fundamental study on compressible transient flow and leakage in partially admitted axial and radial flow turbines. 13 p1566 A73-29025
- Linear stability to axisymmetric perturbations of compressible nondissipative swirling flow, noting Richardson number role 13 p1605 A73-29374
- Investigation of the influence of compressibility and the pressure gradient on the value of the permissible Reynolds number of roughness 13 p1567 A73-29406
- Compressor or fan location at intake or outflow side of compressible flow plant, considering power and size requirements with and without heat exchange 14 p1711 A73-30297
- The local role of the limit line in the well-posed of steady state problems in gas dynamics. I - Problems involving one space dimension. 15 p1862 A73-31328
- German book - Theoretical gasdynamics. Volume I - Theory of the flows of compressible media. 15 p1863 A73-31474
- Magnetogasdynamic compression of a coaxial plasma accelerator flow for micrometeoroid simulation. 15 p1919 A73-31932
- Subcritical and supercritical compressible shock-free flows in blade cascades 16 p1962 A73-32812
- Subsonic compressible airfoil cascade flow calculations by series, iterative, matrix and streamline curvature methods, discussing transonic and supersonic cases [ASME PAPER 73-GT-9] 16 p1963 A73-33487
- Calculation of compressible subsonic flow in cascades with varying blade height. [ASME PAPER 73-GT-59] 16 p1964 A73-33514
- Inviscid flow through a cascade of thick, cambered airfoils. II - Compressible flow. [ASME PAPER 73-GT-85] 16 p1964 A73-33528
- Book - Physical fluid dynamics. 17 p2151 A73-34472
- Numerical solution method for Navier-Stokes equations of a compressible gas over a wide range of Reynolds numbers 17 p2151 A73-34632
- The finite element method in fluid mechanics. 17 p2151 A73-34830
- Discontinuity of the vortex on a shock in thermodynamic variables 17 p2154 A73-35047
- A note on compressible flow through a vortex swirl cup. 17 p2154 A73-35120
- A generalized theory for the turbulent mixing of axially symmetric compressible free jets. 17 p2156 A73-35505
- Three-dimensional compressible boundary layer flow over a yawed cone. [AIAA PAPER 73-634] 18 p2260 A73-36193
- Reentry vehicle ablating control surface gap and slot regions flow characteristics prediction based on quasi-one-dimensional compressible flow finite difference solution [AIAA PAPER 73-742] 18 p2265 A73-36663
- Compressible fluid dynamic theory, using stress tensors to derive constitutive equations for plane homogeneous and shear flows 19 p2420 A73-37644
- Book - Hyperbolic systems of conservation laws and the mathematical theory of shock waves. 20 p2581 A73-39140
- Friction, heat transfer and material removal in a turbulent boundary layer of a compressible high-enthalpy gas under conditions of marked nonisothermicity, injection and negative pressure gradient. 20 p2628 A73-39422
- A parallel algorithm for high subsonic compressible flow over a circular cylinder. 21 p2727 A73-41474
- Laminar and turbulent mixing of compressible jets at low Reynolds numbers. 23 p2967 A73-43403
- A study of the interaction between two compressible fluid flows in a flat channel at low Mach numbers 23 p2968 A73-43731
- Modal analysis of turbulent correlations in compressible flow. 23 p2970 A73-44382
- Shear waves and perturbations in linearized steady plane flows of a thermally nonconducting compressible ideal fluid [ONERA, TP NO. 1169] 01 p0034 A73-11359
- Scattering of sound by an aerofoil of finite span in a compressible stream. 02 p0129 A73-12609
- Flow stability of ideal compressible and incompressible fluids, solving Navier-Stokes equation for rotating liquid with free boundary in gravitational field 02 p0154 A73-12692
- A variational principle for the nonrotational flow of a perfect compressible liquid in a flexible tank [ONERA, TP NO. 1178] 03 p0294 A73-13601
- A theoretical analysis of non-isentropic flow of a compressible, viscous gas in narrow passages. [ASLE PREPRINT 72LC-3A-1] 03 p0297 A73-14355
- Hydrodynamic phenomena during high-speed collision between liquid droplet and rigid plane. [ASME PAPER 72-WA/FE-30] 04 p0435 A73-15850
- Impact of a cylindrical shell against the surface of a compressible fluid 06 p0758 A73-17451
- Flow equation for axisymmetric compressible fluid flow in conical turbine stage, calculating radial distribution of flow velocity 07 p0868 A73-20088
- Two dimensional steady nonrotational flow of perfect compressible fluid around symmetric convex profile, reducing to variational inequality in hodograph plane 07 p0776 A73-20147
- Heat transfer, adiabatic enthalpy /temperature/ of the wall, and hydrodynamic resistance associated with the turbulent and laminar flow of a compressible fluid in a circular tube. 08 p0954 A73-20858
- Heat transfer and friction in the turbulent boundary layer of a compressible gas on a permeable surface 08 p0926 A73-20992
- Steady turbulent boundary layer of compressible perfect gas on heat insulated surface with suction and longitudinal pressure gradient 08 p0954 A73-21177
- Flow parameters and cylinder elongation effects on turbulent boundary layer characteristics for compressible fluid flow, calculating velocity distribution 08 p0956 A73-21602
- Penetration of a solid into a half-space of compressible liquid in the presence of a magnetic field 08 p0994 A73-21724
- Steady nonviscous nonheat-conducting plane flow of compressible fluid, calculating entropy, speed and pressure under assumption of variable pressure along streamlines 09 p1071 A73-22419
- Nonstationary flow downwash behind a delta wing during supersonic motion 11 p1299 A73-25046
- Internal gravity waves in an atmosphere with wind shear - Validity of the WKB approximation at critical layers in the presence of buoyancy forces. 11 p1394 A73-25721
- Resistive diffusion of force-free magnetic fields in a passive medium. 11 p1428 A73-26620
- The wave patterns produced by a moving body in a compressible, density-stratified fluid. 13 p1606 A73-28273
- Acoustic field produced in a gas by arbitrary disturbances on a moving plate 14 p1775 A73-30834
- Hydraulic impact in a circular cylindrical shell 15 p1860 A73-31047
- Stability analysis procedure for shock wave in steady compressible fluid flow, obtaining equations of motion 15 p1864 A73-32113
- Transonic flow through a turbine stator treated as an axisymmetric problem. [ASME PAPER 73-GT-51] 16 p1964 A73-33510
- Numerical solution procedure for calculating the unsteady, one-dimensional flow of compressible fluid /with allowance for the effects of heat transfer and friction/. [ASME PAPER 73-FE-30] 17 p2153 A73-35022
- On the mass transfer produced by oscillations in a compressible, dissipative, and inhomogeneous medium 19 p2503 A73-37528
- Decay of the kinetic energy of compressible micropolar fluids. 20 p2547 A73-39341
- Study of heat transfer in boundary layer taking into account the radiation at the surface. 20 p2507 A73-39420
- Russian book on turbomachinery using compressible and incompressible working fluids covering gas and fluid flow equations, energy losses in axial and radial flow stages, etc 21 p2633 A73-40807
- Thermodynamic conditions of conservation of irrotational or oligotropic motions across a shock wave 21 p2677 A73-40948
- Approximate calculation of the optimal suction of a compressible gas on a thermally insulated surface at Prandtl numbers other than unity 22 p2795 A73-42118
- Sound field created in a gas by arbitrary perturbations on a moving plate. 23 p3006 A73-43584
- Compacting of metallic powders by plane high-explosive charges. I 24 p3092 A73-44414
- Acoustic velocity and sound propagation differences in incompressible and compressible fluids related to Mach cone formation and sonic boom effects. 24 p3054 A73-45269
- COMPRESSING**
Applicability of an adiabatic compression method to the study of a cesium plasma 17 p2214 A73-34130
- COMPRESSION BUCKLING**
U BUCKLING
COMPRESSION LOADS
NT AXIAL COMPRESSION LOADS
NT IMPACT LOADS
Initial postbuckling of circular rings under pressure loads. 01 p0115 A73-10744
- Phase plane analysis of free vibration of rectangular plate loaded by in-plane compressive load, calculating critical load and amplitude in postbuckling region 01 p0115 A73-10770
- Elasticity theory contact problem for rectangle under compression loads, using Airy stress function for reduced linear algebraic equations system 01 p0117 A73-11090
- Rectangular plate stability under compression by uniformly distributed loads applied to two opposite simply supported edges with mixed boundary conditions at other edges 02 p0230 A73-11640
- Bulging of a circular cylindrical shell under axial compression 02 p0231 A73-11814
- Stability of a cylindrical shell under the action of concentrated axial compression loads 02 p0231 A73-11815
- Effect of the length on the stability of cylindrical shells compressed by longitudinal local forces 02 p0231 A73-11816
- Equilibrium equations for rotating conical shells under centrifugal forces and compression loads, calculating revolutions number and stability limits 02 p0232 A73-11819
- Critical stress in an anisotropic cylindrical shell under nonuniform compression 02 p0233 A73-11938
- Three-dimensional problem of the deformation instability of incompressible layered materials in the case of highly elastic strains 02 p0235 A73-12191
- Determination of critical stresses for elements of cylindrical shells in the plastic state 03 p0396 A73-14619
- Characteristics of inversion tubes under axial loading. 03 p0396 A73-14640
- Stability of thick circular plates subjected to compressive loads and finite strains 04 p0513 A73-15504
- Optimal and stiffened simply supported circular plates comparison under uniform pressure and uniform compression loads [AIAA PAPER 73-254] 05 p0635 A73-16976
- Tensile and compressive prestressing effects on notched steel cantilever beam specimens low cycle fatigue life 06 p0764 A73-18490
- Coupled thermoelastic stability effect on critical thermal buckling of strip under compression in temperature field 06 p0765 A73-18686
- Imperfection-sensitivity of a wide integrally stiffened panel under compression. 07 p0908 A73-19087
- Application of the fourth-order anharmonic theory to the prediction of equations of state at high compressions and temperatures. 07 p0851 A73-19925
- The influence of orthotropy on the stability of some multi-plate structures in compression. 08 p1018 A73-21435
- Influence of the frequency of the tension-compression cycle on the fatigue life of D16T alloy 09 p1100 A73-22153
- A special theory of crack propagation. 09 p1161 A73-23177
- Cantilever cylindrical shells of rigid-plastic material, determining collapse loads under external pressure combined with end moment by numerical solution to limit analysis [ASME PAPER 72-PVP-B] 09 p1164 A73-23271
- Post-buckling behaviour of rectangular orthotropic plates. 10 p1288 A73-23699

Potential energy method for boundary value problem of axisymmetric elastic contact of solid and hollow cylinders compressed by plane walls
10 p1289 A73-24064

A yield-surface corner lowers the buckling stress of an elastic-plastic plate under compression.
10 p1289 A73-24100

Investigation of the strong anisotropy and resistance of fiber-strengthened plastics to interlayer shearing and compression normal to the fibers
10 p1240 A73-24353

An upper bound solution for rectangular plate in plane stress compression.
10 p1292 A73-24640

Stability of a shell in the form of a hyperbolic paraboloid subjected to compression along straight generating lines
11 p1435 A73-25397

Effect of compressive stress on silicon bipolar devices.
11 p1410 A73-26422

Damping properties of a composite material with monodirectional continual fibers
12 p1516 A73-27258

Ideal plasticity theory for solid bodies of isotropic materials with different yield points in extension and compression
12 p1553 A73-27374

Branched solution of integro-power equation for nonlinear bending of shallow spherical shells with clamped edge under uniform radial compression load
12 p1556 A73-27816

Nonlinear axisymmetric subcritical deformation effect on elastic stability of locally loaded thin circular cylindrical shells under free end compressive load
13 p1698 A73-29089

Parametric vibrations of elastically connected two mass system with two degrees of freedom, considering dynamic response to excitation by external compression loads
13 p1700 A73-29391

Forced vibration solution and wind tunnel investigation of shallow cylindrical shells under moving pulsating pressure discontinuities, noting compression shock effects
13 p1703 A73-29602

Deformation and transformation of rock-forming minerals by natural and experimental shock processes. I - Behavior of minerals under shock compression.
14 p1750 A73-30958

Interpretation of tensile and compressive creep behaviour of two nickel alloys.
15 p1888 A73-31618

Stability of a spherical shell containing an elastic filler
15 p1950 A73-31828

Buckling of eccentrically stiffened rectangular plates subjected to linearly varying longitudinal compression.
15 p1952 A73-32043

Rectangular cross section isotropic elastoplastic material behavior under combined compressive and bending stresses with allowance for work hardening
16 p2076 A73-32931

Contraction of an elastic layer by girder slabs
17 p2240 A73-34148

Shell stability effects of holes from review of published studies, emphasizing cylindrical shells under uniformly distributed compression loads
17 p2244 A73-34789

Thin elastic orthotropic annular plate postbuckling behavior under planar edge compression loads, analyzing axisymmetric deformations via nondimensional equations and Keller-Reiss numerical method [ASME PAPER 73-APM-5]
17 p2247 A73-35030

Nonlinear axisymmetric subcritical deformation effect on elastic stability of locally loaded thin circular cylindrical shells under free end compressive load
19 p2498 A73-37639

Changes in the microhardness of lithium fluoride crystals subjected to cyclic elastic compression
19 p2470 A73-37954

Degradation studies of diffused GaAs electroluminescent diodes subjected to mechanical stress.
19 p2439 A73-38458

Rigid-plastic collapse of compression-bent shallow shells.
20 p2616 A73-39114

Determination of the critical load for a compressed plate weakened by a circular hole and by cracks propagating toward the hole contour
20 p2617 A73-39263

Three-dimensional problem of the stability of fibers in a matrix in the presence of highly elastic strains
20 p2581 A73-39642

Russian book on elasticity theory for multilayer media covering plate compression and bending under boundary contact conditions, Algol programming, tensile stress, functional equations, etc
21 p2782 A73-40175

Work hardening of copper, nickel, and alloy H31 by compression and explosion
21 p2707 A73-40705

Effect of the frequency of cyclic tension-compression on the fatigue limit of alloy D16T.
22 p2874 A73-42103

The yield stress of Ni3/Al, W/L.
22 p2880 A73-43075

Investigation of the substructure in molybdenum single crystals deformed by compression
23 p2991 A73-43712

Transformation of meteorite material in experiments on explosively produced shock compression at pressures of 500 and 1000 kbar
24 p3137 A73-44710

COMPRESSION TESTERS
U COMPRESSION TESTS
COMPRESSION TESTS
Application of the VEDS-200A electrodynamic vibrator to fatigue tests in symmetric tension and compression
01 p0029 A73-10492

Tensile, compressive and shear strength and absolute modulus of PRD fibers from reinforced plastic honeycomb and filament wound strand tests
03 p0330 A73-13015

The relative validity of the concepts of coefficient of friction and interface friction shear factor for use in metal deformation studies.
[ASLE PREPRINT 72/LC-7A-3]
03 p0316 A73-14368

Compression tests for plastic deformation and fracturing of Al alloy powder at hot working temperatures, noting limiting deformations in forging
04 p0456 A73-15808

Finite element model use for deducing errors magnitude in stress-strain properties obtained from laboratory compression test results
05 p0631 A73-16175

Determination of the mechanical characteristics of fiberglass-strengthened plastics in the winding state
13 p1644 A73-27998

Pure Al compression tests for strain rate effects on strength in wide temperature range, using split Hopkinson bar apparatus and Instron testing machine
13 p1639 A73-29461

Mechanical behavior of WC-Co composite alloys.
13 p1643 A73-29545

The use of a type VEDS-200A vibrostand for fatigue tests under conditions of symmetrical tension-compression.
14 p1743 A73-30317

Determination of displacements during compression of an oval seal ring
16 p2021 A73-33942

Creep and recovery of polycarbonate.
17 p2194 A73-34525

The compression yield behaviour of polymethyl methacrylate over a wide range of temperatures and strain-rates.
19 p2444 A73-38097

Microstrain gage for plastic deformation measurements of crystalline solids in compression, obtaining stress-strain diagrams for Ta single crystals
23 p2986 A73-44036

Investigation of the initial stage of crack development during compression and tension of polymethylmethacrylate samples
23 p2998 A73-44278

The Portevin-Le Chatelier effect in compression tests of polycrystalline aluminum
24 p3148 A73-44914

COMPRESSION WAVES
Long-wave approximation in problems of stability loss by impact
01 p0118 A73-11410

Collisionless plasma compression shock waves thermodynamics, noting entropy variations along shock adiabat under plasma heating in magnetic field
02 p0198 A73-12552

Equilibrium equation for weightless flexible two dimensional sail in inviscid supersonic airstream, noting centred isentropic compression
03 p0246 A73-13789

Compression shock formation in arbitrary medium described by first order quasi-linear partial differential equations, considering strongly radiating and emission dominated gases
03 p0400 A73-14629

Mass transport and energy of impulse compression wave traces in atmosphere due to radiation, inner friction, gravity and rotation effects
04 p0440 A73-15285

Elastic wave velocities and thermal diffusivities of Apollo 14 rocks.
07 p0894 A73-19851

Effect of diffusion on the growth and decay of acceleration waves in gases.
08 p0955 A73-21189

Compression wave interaction induced shock wave formation in shock tube, studying unsteady gas flow near opening diaphragm
08 p0955 A73-21520

Collisionless plasma compression shock waves thermodynamics, noting entropy variations along shock adiabat under plasma heating in magnetic field
10 p1254 A73-24179

Transient compressional wave propagation in a two-layered circular rod with imperfect bonding.
10 p1291 A73-24390

Compressional wave velocity profile of lunar near-surface and crust derived from seismic refraction data at Apollo 14 and 16 sites
12 p1541 A73-27486

Transition of a shock wave into a sound wave.
15 p1912 A73-31010

Behaviour of aluminium during the passage of large-amplitude plastic waves.
15 p1891 A73-32164

Power law recompression of fully developed centered gas expansion, obtaining flow distribution via closed form integral solution based on similarity theory
16 p2000 A73-33317

Elasticity of water-saturated rocks as a function of temperature and pressure.
17 p2163 A73-35271

A biaxial split Hopkinson bar for simultaneous torsion and compression.
17 p2149 A73-35754

Exact steady-state analogy of transient gas compression by coalescing waves.
21 p2790 A73-40439

COMPRESSIVE STRENGTH
Compression and elastic moduli of heterogeneous viscoelastic materials consisting of mechanical mixture of homogeneous phases, using elastic-viscoelastic analogy
03 p0385 A73-13139

Effect of the glass fiber diameter on the compressive strength of glass fiber reinforced plastics
03 p0335 A73-13738

Strength limits correlation to modulus of elasticity for compact bone material from compression tests, noting anisotropy tensor analysis
03 p0267 A73-13744

Empirical strength criteria for anisotropic and isotropic composite materials with unequal tensile and compressive strength
04 p0508 A73-14860

Observations on the deformation properties of sandwich materials.
06 p0761 A73-17819

On the compressive strength of composite materials reinforced with glass fabric laminates.
07 p0844 A73-20333

Damping properties of 1Kh13 and 2Kh13 high-chromium steels in a uniform stress-strain state in tension and compression at room and high temperatures
07 p0841 A73-20513

Effect of surface damage on the strength of Al2O3 ceramics with compressive surface stresses.
08 p0983 A73-21843

Stress-strain relations for materials with different tension, compression yield strengths.
09 p1166 A73-23452

Criteria for selecting resin matrices for improved composite strength.
10 p1238 A73-23966

Large elastic flexural and elongation strains in a portion of tube prepared from a material with different resistance to tensile and compressive strains
12 p1552 A73-27369

Deformation and strength characteristics of carbon-fiber strengthened plastics in compression
13 p1644 A73-27991

Pure Al compression tests for strain rate effects on strength in wide temperature range, using split Hopkinson bar apparatus and Instron testing machine
13 p1639 A73-29461

Theory and experiments of compressive strength of unidirectionally fiber-reinforced composite materials.
13 p1702 A73-29539

Investigation of the strength of construction materials for different ratios of the main stresses.
13 p1703 A73-29622

Conditionally-instantaneous and long term strength of a longitudinally-transversely wound glass-fiber-reinforced plastic under biaxial compression
15 p1896 A73-30975

Tensile and compressive strength tensor prediction for anisotropic boron-epoxy composites from off axis tests
15 p1897 A73-31682

Buckling of beams supported by Pasternak foundation.
17 p2243 A73-34531

Effects of material and stacking sequence on behavior of composite plates with holes.
[SESA PAPER 2157A]
17 p2198 A73-35452

The damping properties of high-chrome steels 1Kh13 and 2Kh13 in a homogeneous stress state of tension-compression under the conditions of normal and elevated temperatures.
19 p2440 A73-37788

Compressive strength and plastic deformation of monocrysal bismuth telluride, polycrystal lead telluride, Cu-Te compounds and Pb-Sn-Te solid solution
23 p3015 A73-43480

Compressive strength and failure modes of unidirectional composites.
23 p3041 A73-43634

Conditions of production of high-compressive-strength, orthogonally reinforced fiberglass plastics
24 p3102 A73-44526

COMPRESSOR BLADES

Preparation of information for programming machining operations during grinding of a blade profile by the continuous-shaping method
02 p0172 A73-11799

Fatigue strength of constructional materials and components of GTD-type compressors under conditions of fretting corrosion.
02 p0181 A73-12217

Some recent work on aspect ratio effects in compressor cascades.
[ASME PAPER 72-WA/FE-41] 04 p0404 A73-15858
Influence of regulated unequal guide-vane spacing on the alternating stress level in the working blades of a compressor
09 p1157 A73-22165

Experimental method for analyzing the unsteady flow in a transonic aircraft compressor
09 p1028 A73-22715

Researches on the two-dimensional retarded cascade. III - Cascade performances at high inlet angles.
11 p1302 A73-26338

Researches on the two-dimensional retarded cascade. IV - Determination of blade elements at retarded blade row.
11 p1302 A73-26339

Calculation of the unsteady subsonic aerodynamic pressures on compressor blades
[ONERA, TP NO. 1221] 13 p1565 A73-28839
A method for complex design of axial-flow compressor stages at the mean streamline
15 p1925 A73-32203

Sand erosion tests and protective coatings for aircraft jet and turbojet engines and helicopter compressor airfoils
16 p2046 A73-33029

Interface effects between a moving supersonic blade cascade and a downstream diffuser cascade.
[ASME PAPER 73-GT-23] 16 p1964 A73-33497

Calculation of compressible subsonic flow in cascades with varying blade height.
16 p1964 A73-33514

Pressure measurements on the rotating blades of an axial-flow compressor.
[ASME PAPER 73-GT-79] 16 p2049 A73-33524
Conditions of rotating stall suppression in axial compressors
16 p2049 A73-33964

Effect of axial velocity variation on deviation for compressor cascades.
17 p2092 A73-34383

Effect of axial velocity variation on the subsonic flow through a compressor cascade.
17 p2094 A73-34397

The prevention of separation and flow reversal in the corners of compressor blade cascades.
17 p2094 A73-34448

Calculated leading-edge bluntness effect on transonic compressor noise.
[AIAA PAPER 73-633] 18 p2260 A73-36192

Effect of spanwise circulation on compressor noise generation.
19 p2473 A73-37292

A method of complex design of the meridional form of the air flow path of a multistage axial-flow compressor
21 p2633 A73-40477

Effect of an adjustable nonuniform pitch in the distributor on the alternating stresses in compressor rotor blades.
22 p2919 A73-42113

Calculation of the maximum attainable efficiency of a moving compressor blade cascade
22 p2797 A73-42646

Manufacture and properties of compressor blades made of plastics reinforced with carbon filaments
24 p3122 A73-44880

COMPRESSOR EFFICIENCY

Subsonic centrifugal compressor efficient operating range extension by collector and diffuser blade cascades separation, presenting performance test results
02 p0204 A73-12792

Supersonic compressor performance for gas turbine engines, discussing cascade, single stage compressor rigs and experimental engine test results
03 p0360 A73-14152

Generalized relations for the parameters at the flow separation boundary in compressor cascades
13 p1567 A73-29551

Small turbomachinery compressor and fan aerodynamics.
[ASME PAPER 73-GT-6] 16 p2047 A73-33484

Calculation of the maximum attainable efficiency of a moving compressor blade cascade
22 p2797 A73-42646

COMPRESSOR ROTORS

A method for complex design of axial-flow compressor stages at the mean streamline
15 p1925 A73-32203

A contribution to the theoretical and experimental examination of the flow through plane supersonic deceleration cascades and supersonic compressor rotors.
[ASME PAPER 73-GT-17] 16 p2047 A73-33494

Upstream attenuation and quasi-steady rotor lift fluctuations in asymmetric flows in axial compressors.
[ASME PAPER 73-GT-30] 16 p2048 A73-33501

Experimental evaluation of the effects of a blunt leading edge on the performance of a transonic rotor.
[ASME PAPER 73-GT-60] 16 p1964 A73-33515

Blade synchronous rotation about pitch axis in single stage axial compressor at front of gas turbine engine during fan rotation
20 p2601 A73-39663

COMPRESSORS

NT CENTRIFUGAL COMPRESSORS

NT SUPERCHARGERS

NT TRANSONIC COMPRESSORS

NT TRANSONIC COMPRESSORS

NT TURBOCOMPRESSORS

High-pressure axial fan for air-cushion vehicles
02 p0203 A73-11713

Compressor or fan location at intake or outflow side of compressible flow plant, considering power and size requirements with and without heat exchange
14 p1711 A73-30297

Rotating stall in an isolated rotor row and a single-stage compressor.
17 p2093 A73-34386

COMPTON EFFECT

Polarization of relativistic-electron emission in the case of Compton scattering at turbulent plasma oscillations
01 p0085 A73-10949

Nonlinear inverse Compton radiation and the circular polarization of diffuse radiation from the Crab nebula.
01 p0092 A73-11032

Interaction between intense optical radiation and free electrons /Nonrelativistic case/
01 p0061 A73-11248

High intensity CO₂ laser-plasma interaction.
05 p0603 A73-17224

Stimulated Compton scattering of laser radiation by electron plasma, determining electrons diffusion coefficient and velocity distribution function
06 p0700 A73-17970

Plasma heating, emission spectrum distortion and light pressure effects under stimulated Compton scattering, noting upper bound of cosmic maser brightness temperature
06 p0729 A73-18110

The interpretation of the X-ray emission detected from some nearby radio galaxies.
07 p0872 A73-19940

Effects of Compton scattering in a moving gas
07 p0853 A73-20308

CO₂ laser induced Compton effect in underdense hydrogen plasma.
09 p1125 A73-22025

Polarized radiation of relativistic electrons scattered by plasma turbulence.
09 p1130 A73-22743

Compton effect in charged particle under intense circularly polarized electromagnetic wave, noting application to Crab pulsar
10 p1271 A73-23485

The dependence of Compton X-ray emission from clusters of galaxies on the velocity dispersion of the cluster.
10 p1264 A73-23544

Means of measuring the linear polarization of cosmic gamma quanta by means of the Compton effect
12 p1496 A73-27204

Compton-scattering effects in a moving gas.
12 p1526 A73-27280

A telescope for soft gamma ray astronomy.
12 p1499 A73-27892

Role of stimulated Compton scattering in the interaction of laser radiation with a superdense plasma.
13 p1664 A73-28615

On Compton models of the isotropic X-ray background.
14 p1796 A73-30001

The solar albedo of hard X-ray flares.
16 p2053 A73-32961

Luminosity of thermal X-ray sources with a strong magnetic field.
16 p2062 A73-33574

The Compton effect in a medium near a Cerenkov cone
17 p2120 A73-34115

A comparison between Compton-synchrotron and Compton black-body emission in radio sources.
17 p2237 A73-35785

Statistical acceleration of ultrarelativistic electrons by random electromagnetic waves.
19 p2462 A73-37558

Gravitational Compton effect and graviton photoproduction by electrons
21 p2742 A73-40351

Interaction of intense optical radiation with free electrons /nonrelativistic case/.
22 p2892 A73-42346

Asymptotic forms of solutions to nonrelativistic Compton Fokker-Planck equation for bremsstrahlung X ray spectra changes due to Compton scattering in emitting gas
22 p2904 A73-43018

Higher order Compton-Getting anisotropies in particle population distribution function of low energy solar protons in interplanetary space
23 p3024 A73-43698

Plasma heating, emission spectrum distortion and light pressure effects under stimulated Compton scattering, noting upper bound of cosmic maser brightness temperature
24 p3114 A73-44499

Radiative transfer through a Compton-scattering atmosphere with continuous energy dependence.
24 p3111 A73-45321

COMPUTATION

NT ORBIT CALCULATION

An efficient algorithm for calculation of the Luenberger canonical form.
19 p2408 A73-38065

COMPUTER COMPONENTS

The pulse-controlled photoelectric switch as an element in automatic control circuits and in computer equipment
06 p0676 A73-18088

Design of a search memory using elements with reluctance modulation
08 p0941 A73-21108

Standard flexible LSI logic cell arrays with uniform interconnections as fourth generation computer components, discussing microprograms and algorithms for arithmetic operations
10 p1198 A73-24017

Russian book on digital computer construction and operation covering data processing and conversion algorithms, memory, arithmetic and control devices, microprogramming, etc
13 p1588 A73-28948

Electromagnetic core storage and switching elements design for Setun threshold ternary logic computer
19 p2408 A73-38562

Error maxima for division algorithm adaptiveness evaluation of damaged computer elements with corrective readjustments
19 p2408 A73-38563

Multivalued models of computer electronic circuits
20 p2532 A73-39001

A study of models of certain digital computer units with the aid of a digital computer
20 p2533 A73-39822

Ultrahigh-speed unsaturated diode-transistor logic elements with a small logic differential
21 p2660 A73-40013

Gunn effect digital functional device.
22 p2829 A73-42204

Error-correcting codes in computer arithmetic.
22 p2830 A73-42713

COMPUTER DESIGN

Electronic computer design and programming for solving high order linear equations, using matrix determinants and graph trees in letter symbols
01 p0019 A73-10033

Computerized weather radar data central processor design, implementation and programs for data reduction and calibration
03 p0281 A73-14548

Airborne associative parallel array digital computer built with MOS LSI technology for size and weight reduction, discussing design and applications
04 p0424 A73-15065

Optical computer technology based on Fourier transform optics and holography, discussing speed and parallel processing capabilities, image deblurring, and applications
04 p0426 A73-15957

Fall Joint Computer Conference, Anaheim, Calif., December 5-7, 1972, Proceedings. Parts 1 & 2.
06 p0670 A73-18057

A cellular processor for task assignments in polymorphic, multiprocessor computers.
06 p0671 A73-18061

Design of a fault-tolerant, modular computer with dynamic redundancy.
06 p0671 A73-18064

Josephson tunneling devices - A new technology with potential for high-performance computers.
06 p0735 A73-18066

A general model for the study of fault tolerance and diagnosis.
06 p0672 A73-18808

A special purpose computer for the study of fading signals.
08 p0939 A73-21139

Computer protection mechanisms design principles for operating system and hardware architecture implementation, considering access matrix storage, efficiency and subject and object selection
09 p1059 A73-22223

- Book - RCA advanced technology.
10 p1216 A73-23781
 - Digital simulation methodology for LSI computer design and technology assessment to assure competitive cost, schedule and implementation cycles in manufacturing
10 p1191 A73-23793
 - LSI computer design and fabrication for Space Ultra-reliable Modular Computer Demonstration Vehicle, discussing assembly, physical and electrical characteristics and electronic testing procedures
10 p1191 A73-23794
 - Complementary MOS LSI microprogrammed digital computer design, for Space Ultra-reliable Modular Computer Demonstration Vehicle, discussing instruction operation codes, I/O peripherals and software support
10 p1191 A73-23795
 - Figure of merit for fault-tolerant space computers.
10 p1192 A73-24870
 - Nonalgorithmic design and coding system for digital mathematical machines for accuracy and speed compatible with digital and analog computer, respectively
11 p1334 A73-25626
 - Fault-tolerance in the modular spacecraft computer.
12 p1475 A73-27130
 - A simulation model for a memory organization for a multiprocessor.
12 p1475 A73-27155
 - Russian book on digital computer construction and operation covering data processing and conversion algorithms, memory, arithmetic and control devices, microprogramming, etc
13 p1588 A73-28948
 - Algorithms of formal selection for optimal control systems of digital computers
14 p1730 A73-30034
 - Design principles for control systems of digital computers
14 p1730 A73-30035
 - Prediction of failures and efficiency characteristics of a system
14 p1740 A73-30799
 - Arithmetic algorithms for error-coded operands.
15 p1899 A73-31349
 - Decentralized coalition control in data processing systems
15 p1848 A73-31804
 - Construction principles of a controlled universal functional converter for a hybrid computer
15 p1848 A73-31805
 - Russian book - Problems in the synthesis of finite automata.
15 p1848 A73-31909
 - French monograph on numerical data processing organs for real time process control, describing modular computer design project
15 p1849 A73-32590
 - Future trends in computer hardware.
17 p12131 A73-35127
 - Technological forecasting for microcomputer architecture and fabrication on LSI chip, considering cost effectiveness, pins number, packing density, power and speed factors
17 p12131 A73-35226
 - Mathematical functional modular building block implementation in LSI microelectronics for signal and data processing, discussing primitive functions and 8-bit family design example
17 p12138 A73-35229
 - CPU design for command and control system with programmable read-only control memory, discussing self microdiagnostics for control store error detection
17 p12144 A73-35258
 - Multivalued models of computer electronic circuits
20 p2532 A73-39001
 - A study of models of certain digital computer units with the aid of a digital computer
20 p2533 A73-39822
 - Russian book on probabilistic computer simulation and statistical processing techniques covering linear algebra and partial differential equations, Markov chains, random numbers, automata, and analog modeling
21 p2659 A73-41432
 - A computer for modeling and calculating technological dimensional circuits
22 p2829 A73-42365
 - A simple cardiac contractility computer.
22 p2815 A73-42677
 - Theory and design of pipelined fast Fourier transform processors.
23 p2956 A73-43325
 - Fluidic circuits application to stochastic computer with analog to digital converter and logic gates for arithmetic operations
23 p2944 A73-43419
 - Large-scale systems and operations management decentralized coalitional control in data processing systems.
23 p2956 A73-44333
 - Parallel and string array processor hardware design and computer programs for computing speed increase over conventional series computers
24 p3070 A73-45086
 - Design of a controlled general-purpose functional converter for a hybrid computer system.
24 p3071 A73-45349
- COMPUTER GRAPHICS**
- Interactive pattern analysis and classification systems - A survey and commentary.
01 p0021 A73-11477
 - Digital storage of graphs and curves and their representation on visual displays
01 p0021 A73-11484
 - FORTTRAN subroutine for X-Y plotting and display of two dimensional alphanumeric finite element mesh on line printer
03 p0280 A73-13340
 - Computer-aided design and graphics applied to the study of inductor-energy-storage dc-to-dc electronic power converters.
03 p0252 A73-13931
 - Project Cloud Catcher weather radar data system revisions in radar set, echo pulse integrator, data logging and analysis and graphic displays
03 p0289 A73-14523
 - Computer development of holographic mass memory plans
05 p0553 A73-16168
 - Application of graphic display to ultrasonic testing.
05 p0574 A73-16282
 - A computer-generated display to isolate essential visual cues in landing.
05 p0595 A73-16704
 - Computer and interactive graphics as applied to mission analysis.
05 p0554 A73-16870
 - Application of the graphic flight path design program /FPDP/ for fast interactive trajectory design.
05 p0619 A73-16871
 - Universal data system for image processing of earth resources observations, discussing input/output film, tape and multispectral data, interactive control and video color displays
05 p0555 A73-17155
 - Electronic creation of still and animated complex images, discussing techniques for supplying computer with object description
06 p0669 A73-17474
 - The reconstruction of three-dimensional objects from two orthogonal projections and its application to cardiac cineangiography.
06 p0657 A73-17801
 - Syntax specification system for computerized hand-drawn pattern grammar generation with user style description for concurrent inputting and analysis at high recognition speed
06 p0671 A73-18535
 - Spline function interpolation in interactive hemodynamic simulation.
06 p0660 A73-18889
 - Numerically controlled plotters THD 605.
07 p0795 A73-18944
 - On-line computer analysis and breath-by-breath graphical display of exercise function tests.
08 p0935 A73-21511
 - Parallel algorithms for plotting profiles, projections, and cross sections with the aid of receptor matrices on a digital computer
08 p0941 A73-21588
 - Computer systems configurations for design and engineering, considering graphic and conversational capability and cost and time reduction
09 p1168 A73-21949
 - PRADIS - An advanced programming system for 3-D-display.
09 p1059 A73-22225
 - Computerized interactive graphic display systems for three dimensional shape design
10 p1222 A73-23523
 - Computer generated displays of structures in vibration.
11 p1334 A73-25498
 - Eigenvalue problem and stiffness optimization procedure for incremental flutter analysis, describing method use in computer graphics mode
11 p1439 A73-25521
 - Digital computer graphic data feeder with electric pulsed-voltage coordinate matrix and readout probe sensor for input data code coordinate selection
12 p1475 A73-26779
 - The growth and decay of the main phase of the September 21-23, 1963 magnetic storm.
12 p1490 A73-27275
 - Graphic-interactive analysis of the velocity field around blade cascades for turbomachines
12 p1458 A73-27387
 - RAPID - A system for online radar data reduction and performance analysis.
12 p1476 A73-27825
 - Temporal and spatial features in detecting one- and two-dimensional constraints in complementary visual displays.
13 p1578 A73-28095
 - Response time in the application of interactive graphics in structural analysis.
13 p1693 A73-28244
 - Computer graphics applied to production structural analysis.
13 p1693 A73-28245
 - Graphic display for ultrasonic nondestructive testing.
13 p1615 A73-28586
 - Computer aided design with finite element method for two and three dimensional curved line and surface approximation and representation on interactive graphic console
13 p1587 A73-28850
 - Detection of informational constraints related to multi-variate visual displays.
13 p1580 A73-29185
 - Book - Optimum structural design: Theory and applications.
17 p2242 A73-34350
 - Simulation of airport traffic flows with interactive graphics.
17 p2147 A73-34821
 - Interactive computer graphic display and interface system effectiveness for programming numerical control operations for tooling and part machining in aircraft production
17 p2131 A73-35081
 - [AHS PREPRINT 753] The application of interactive graphics to the numerical methods used in structural analysis.
17 p2250 A73-35314
 - Sorcerer Apprentice head mounted display with wand for interaction with computer generated synthetic objects, describing creation of illusory three dimensional environment
19 p2397 A73-37323
 - Computer aided design-drafting /CADD/ - Engineering/manufacturing tool.
19 p2407 A73-37460
 - A computer-aided design procedure to approximate aircraft area curve shapes.
19 p2385 A73-37888
 - Urban land use from RB-57 photography - Computer graphics of the Boston area.
20 p2556 A73-39845
 - Use of the azimuthal equal-area projection to display radiation patterns of complex antennas
21 p2661 A73-40202
 - Computer-aided design and graphics applied to the study of inductor-energy-storage dc-to-dc electronic power converters.
21 p2635 A73-40340
 - An improved light gun tracking algorithm based on a recursive digital filter.
21 p2654 A73-40834
 - Touchdown performance with a computer graphics night visual attachment.
21 p2673 A73-40874
 - An approach to computer image generator for visual simulation.
21 p2673 A73-40875
 - The use of analytic surfaces for the design of centrifugal impellers by computer graphics.
22 p2900 A73-42477
 - Study of the nature of the active tonus with the aid of a discrete Wiener-medium analog
22 p2816 A73-42973
 - Numerical method for computer generated kinoform image reconstruction error minimization, comparing with random phase method
22 p2863 A73-43148
 - National Center for Atmospheric Research utility plotting programs for computer graphics, two and three dimensional fields display and movie generation
24 p3070 A73-45089
 - Three dimensional computer plots of zero velocity contours for restricted three and four body problems, discussing motion stability near equilibrium points
24 p3142 A73-45297
- COMPUTER METHODS**
- U COMPUTER PROGRAMS**
- COMPUTER PROGRAMMING**
- NT LANGUAGE PROGRAMMING
- NT MICROPROGRAMMING
- NT MULTIPROGRAMMING
- NT ON-LINE PROGRAMMING
- NT PARALLEL PROGRAMMING
- NT SYMBOLIC PROGRAMMING
- Computation of solutions to the inverse problem of electrocardiography.
01 p0013 A73-11465
- Grid model to derive biharmonic difference operators with computer programming application, assessing errors in boundary conditions
02 p0236 A73-12512
- On the number of operations simultaneously executable in Fortran-like programs and their resulting speedup.
05 p0553 A73-16450
- Computer adaptive optimization system for problems with nonlinear criteria function and constraints, noting algorithms of deterministic and stochastic categories
05 p0555 A73-17284
- Procedural formalization and methodology for automated problem solving in terms of digital program systems for algorithms generation, describing operational procedures
06 p0669 A73-17594

One dimensional elastoplastic system optimal design by stochastic programming, determining limiting stresses and random load distribution

07 p0914 A73-20151

Spring Joint Computer Conference, Atlantic City, N.J., May 16-18, 1972, Proceedings.

09 p1059 A73-22221

Computer assisted instruction for commercial programmer and systems analyst education and training, discussing government use, pretest importance and future developments

09 p1168 A73-22222

PRADIS - An advanced programming system for 3-D-display.

09 p1059 A73-22225

Computerized optimal tube heat exchanger design, discussing programming for heat transfer surface area and operating point determination

11 p1448 A73-25102

Applications of vector and parallel computers to radar defense systems.

[AIAA PAPER 73-428]

12 p1476 A73-27822

Automaton external and internal languages linking by computer programming languages discussing structure and operation relation to language structure and realization

12 p1485 A73-27893

Application of mathematical programming methods to determine the optimal control for systems described by heat conduction equations

13 p1704 A73-28016

Small digital computer program packet organization for central processor productivity and use coefficient improvement, discussing graph-algorithm language for program splicing

15 p1848 A73-31694

Papers on digital signal processing covering digital filters, fast Fourier transform, finite word length effects, algorithms, and design and programming considerations

15 p1855 A73-32425

Interactive computer graphic display and interface system effectiveness for programming numerical control operations for tooling and part machining in aircraft production

[AHS PREPRINT 753]

17 p2131 A73-35081

A procedure for solving problems of elasto-plastic flow.

19 p2496 A73-37484

Development of a program basis for statistical data processing on an analog-digital complex

20 p2532 A73-39392

Mathieu function eigenvalue computation based on Algol program, using Fourier series, Bessel functions, wave equations and elliptic domains

23 p2998 A73-43209

COMPUTER PROGRAMS

NT COMPILERS

NT COMPUTER SYSTEMS PROGRAMS

NT INPUT/OUTPUT ROUTINES

NT OPERATING SYSTEMS [COMPUTERS]

NT SUBROUTINES

Computer programs for realistic calculation of atmospheric absorption spectra, discussing spectroscopic data critical survey, procedures, coefficient generation and data presentation

01 p0037 A73-10368

Minicomputer based CAMAC modular system for astronomical telescope instrumentation, discussing hardware and software interfaces, squad scaler, photoelectric photometer, Michelson interferometer and multichannel spectrometers

01 p0019 A73-10547

A new program for the dc one-dimensional analysis of semiconductor devices.

01 p0023 A73-10576

Complex processing of discrete biological information

01 p0012 A73-10662

Computer programs for radiative heat transfer and thermal equilibrium equations, noting transient temperature distribution measurement of two stage radiant cooler

01 p0111 A73-11151

PLANEX 1 plan executor program for robot system, creating plan for sequence of actions via problem solving program STRIPS

01 p0020 A73-11452

Reasoning by analogy as an aid to heuristic theorem proving.

01 p0020 A73-11453

Roundoff and uncertain data error analysis, discussing hasty judgements, double precision, trajectory problems, ill-posed problems, computer software and hardware flaws, etc

01 p0021 A73-11460

A computer program for molecular dynamics of dilute gases.

01 p0081 A73-11472

Determination of the theoretical stress-concentration factors in composite systems in bending

02 p0229 A73-11638

Determination of geometrical characteristics in computer solutions of strength problems for shells of complex configuration

02 p0231 A73-11809

Calculation of the stress distribution in rotating disks in the case of unsteady creep with the aid of a digital computer

03 p0385 A73-13140

Problems regarding the use of electronic data processing for the calculation of diagonal cascades in turbomachines

03 p0242 A73-13169

The performance of a four-pocket conical hydrostatic bearing.

03 p0311 A73-13206

From earth to Mars orbit - Mariner 9 propulsion flight performance with analytical correlations.

[AIAA PAPER 72-1185]

03 p0382 A73-13478

A finite element analysis of an axisymmetrically loaded orthotropic shell of revolution.

03 p0391 A73-13677

Thermal stress analysis of reentry vehicle nosetips at angle of attack.

03 p0392 A73-13688

Computerized multiple level substructuring analysis.

03 p0392 A73-13690

Effective development, documentation, and distribution of computer programs.

03 p0392 A73-13691

A new algorithm for three-dimensional method of characteristics.

03 p0337 A73-14201

Computerized weather radar data central processor design, implementation and programs for data reduction and calibration

03 p0281 A73-14548

Computer application for management of Skylab launch operations.

[AIAA PAPER 72-1083]

04 p0424 A73-14905

The solution of linear, constant-coefficient, ordinary differential equations with APL.

04 p0470 A73-15008

A numerical computer method for computing the electrostatic field and electron paths of focusing optoelectronic systems

04 p0448 A73-15078

System time domain simulation computer aided analysis program for communication systems, presenting mathematical and functional models

04 p0425 A73-15459

Computerized terrain classification system software features for automatic interpretation of aerial photographic imagery by laser scanning system

04 p0445 A73-15772

Transport phenomena of reactive fluid flow in heterogeneous combustion processes.

[ASME PAPER 72-WA/HT-30]

04 p0519 A73-15825

Terminal modeling and photocompensation of complex microcircuits.

05 p0557 A73-16508

Classical minimization procedure without iteration for digital computation of generalized inverse of rectangular matrix with real or complex coefficients

05 p0590 A73-16581

Smoke and fire propagation in compartment spaces.

[WSCI PAPER 72-32]

05 p0639 A73-16683

Computer programs for operator performance time prediction and workspace design

05 p0544 A73-16721

Teleprocessing systems communication software functions and construction, considering network control, message preprocessing, queuing and error recovery in multiprogramming and multiprocessing environment

05 p0551 A73-16803

Analysing vibration and shock data. II - Processing and presentation of results.

05 p0637 A73-17234

Automation of reliability evaluation procedures through CARE - The computer-aided reliability estimation program.

06 p0670 A73-18058

An analysis of optimal control system algorithms.

06 p0670 A73-18059

Intrinsic models for computer storage allocation program locality concept, comparing performance in terms of working set size and missing page probability by experiments

06 p0670 A73-18060

A program for the analysis and design of general dynamic mechanical systems.

[AD-754496]

06 p0671 A73-18063

Fasp - A student developed application program.

06 p0671 A73-18265

Contrast transmittance Monte Carlo computation for atmospheric haze models based on aircraft measurement data from various geographical areas

06 p0694 A73-18302

Source limited gray scale and color selection capabilities for direct and reflected light scanners.

06 p0701 A73-18308

Computerized optimal control problem formulation in calculus of variations, discussing flexible user-

oriented algorithm for terminal point transversality boundary conditions numerical implementation

06 p0672 A73-18806

Computer for automatic equipment monitoring, operation control and breakdown diagnosis in telemetry data processing, discussing management routines and reliability

07 p0795 A73-18956

Free vibration analysis of spinning structural systems.

07 p0907 A73-19032

Air traffic control by programmed navigation.

07 p0849 A73-19349

Effect of suspension-line viscous damping on parachute opening load amplification.

07 p0777 A73-19495

Lumped parameter network modeling for spacecraft surface thermal environment analysis, discussing computer program and application to Skylab ATM

07 p0919 A73-19496

Computerized static and dynamic structural analysis, discussing modeling, programs, input preparation, solution algorithms, numerical errors, output interpretation and applications

07 p0914 A73-20209

Recent advances and applications in the prediction of pilot acceptance of aircraft flying qualities.

07 p0777 A73-20586

Automatic test equipment software configuration management.

08 p0952 A73-20686

Automatic test equipment support software definition and development, describing language, translator and operating system as elements of closed loop ATE system

08 p0952 A73-20687

Test programs design for versatile avionics shop test system (VAST), discussing compiler problems alleviation by on-station program patching capability

08 p0962 A73-20688

Gas turbine engine transient performance presentation for digital computer programs.

[SAE ARP 1257]

08 p0996 A73-20696

Thermal analysis-mass spectrometer computer system and its application to the evolved gas analysis of Green River shale and lunar soil samples.

08 p0936 A73-20824

Computation of the minimum bandwidth for aerotriangulation.

08 p0968 A73-21705

Computerized precession and nutation matrix calculations of rectangular equatorial coordinates with longitude and inclination allowance for radar data processing

09 p1142 A73-22092

Computerized normal loci plotting by orthogonal Chebyshev approximation, using minimum variance principle and Fisher test for regression curve selection

09 p1143 A73-22094

RC planar distributed networks one and two dimensional analysis techniques and frequency response characterization, noting FORTRAN program use

09 p1067 A73-22309

FORTRAN IV program and recursive matrix partitioning algorithm for solution of photogrammetric simultaneous equations, noting computation time

09 p1059 A73-22382

Large deflection analysis of plates and shallow shells using the finite element method.

09 p1158 A73-22396

Finite difference programs with grid self adjustment for steady or unsteady problems with arbitrary boundaries and without coordinate hierarchy, noting computer time saving

09 p1071 A73-22400

Computer program for the transient analysis of radioisotope thermoelectric generators.

09 p1060 A73-22768

Viking Orbiter power subsystem performance prediction computer program simulating solar array, battery charge controls, zener diodes and power conditioning equipment characteristics and interactions

09 p1060 A73-22802

Shuttle Orbiter fuel cell power system simulation, describing data management, programming and computational control

09 p1060 A73-22804

Computational estimate of applicability of infinitesimal theory.

09 p1065 A73-23099

Analysis of the shrouded Rayleigh step pad for an incompressible fluid film with the centrifugal inertia effect included.

09 p1089 A73-23103

Computer program for extraterrestrial physics barium ion cloud project determining daily release launch window for sky target experiments

[AIAA PAPER 73-297]

09 p1116 A73-23216

Communication system for digital image processing services over Advanced Research Project Agency computer network, describing hardware facilities and software capacity

09 p1061 A73-23390

Magnetic field intensity and invariant shell parameters computer programs, assessing error in expansion coefficients
10 p1276 A73-23888

Apollo LM guidance computer software for the final lunar descent.
10 p1247 A73-24548

Application of a digital computer in the processing and presentation of tensile test results.
10 p1192 A73-24569

Smithsonian Package for Algebraic and Symbolic Manipulation / SPASM/ computer program with generality and efficiency for Poisson series processing in celestial mechanics
10 p1283 A73-24667

A BESM-3M computer program for processing photographic observations of extended objects
11 p1333 A73-25231

Computer programs for structural design optimization, discussing automated structural optimization program /ASOP/, component display analysis and stiffened panel programs
[AIAA PAPER 73-345] 11 p1436 A73-25484

Computerized design of an outer planets spacecraft structure to survive the meteoroid environment.
[AIAA PAPER 73-349] 11 p1430 A73-25487

Application of computer-aided aircraft design in a multidisciplinary environment.
[AIAA PAPER 73-353] 11 p1304 A73-25490

Interdisciplinary computer analyses of three-dimensional solids defined by polyhedral surfaces.
[AIAA PAPER 73-354] 11 p1437 A73-25491

Reliability and quality control of production engineering computer programs.
[AIAA PAPER 73-356] 11 p1373 A73-25493

Stress, stability, and vibration of complex, branched shells of revolution.
[AIAA PAPER 73-360] 11 p1437 A73-25496

Simulation capability for dynamics of rotating counterweight space stations.
[AIAA PAPER 73-320] 11 p1343 A73-25551

Compact gas transpiration cooling system for thermal protection of hypersonic flight leading edges, discussing computer program
11 p1452 A73-26212

Algorithm and convergence behavior of the local variation method for problems with partial derivatives
11 p1400 A73-26326

Diagnostic simulation of a pneumatically controlled blowdown wind tunnel.
11 p1344 A73-26546

Electronic equipment computerized radiation hardness assurance program for retaliatory or deterrent missile system, discussing supplier data monitoring, verification test and radiation shield assurance
11 p1342 A73-26637

An analytical model for the prediction of liquid rocket plume contamination effects on sensitive surfaces.
[AIAA PAPER 72-1172] 12 p1532 A73-27099

The evolution of a computer program for obtaining optimum computer simulation solutions.
12 p1475 A73-27133

RAPID - A system for online radar data reduction and performance analysis.
[AIAA PAPER 73-438] 12 p1476 A73-27825

Numerical Master Geometry computer programs for smooth surface shape mathematical representation, manipulation, definition and interrogation in design and production
13 p1623 A73-28053

A computer program for filter design having arbitrary magnitude specifications in the frequency domain.
13 p1587 A73-28085

Analysis of finite deformations of elastic solids by the finite element method.
13 p1692 A73-28229

Computer programs for analysis of shells of revolution based on numerical integration and finite difference procedures
13 p1693 A73-28236

Automatic system for kinematic analysis /ASKA/ computer programs for structural finite element solution, discussing design concepts, element types, user interface and computation time
13 p1693 A73-28243

Natural vibrations of thin, prismatic flat-walled structures.
13 p1694 A73-28247

Effect of out-of-planeness of membrane quadrilateral finite elements.
13 p1697 A73-28818

NASA computer generated 136/400-MHz radio sky maps covering whole celestial sphere for earth-based receiver noise temperature determination in satellite communication
13 p1585 A73-29115

Kalman filter design considerations for space-stable inertial navigation systems.
13 p1657 A73-29220

A computer program for plotting exponentially smoothed average control charts.
13 p1588 A73-29299

Computer program analysis of errors in mutual orientation elements on aerial photographs with different lengthwise overlaps, discussing error minimization
13 p1621 A73-29324

Creep analysis of transversely isotropic bodies subjected to time-dependent loading.
14 p1805 A73-29769

A library of standard programmes for constructing numerical theories for studying the motion and evolution of the orbits of the minor bodies of the solar system.
14 p1790 A73-29789

Standardization of the calculation of nearly parabolic cometary orbits.
14 p1790 A73-29795

Algorithm for statistical error detection in digital control computers
14 p1730 A73-30038

PCM mobile ground station design covering telemetry receivers, digital data magnetic recording and computer interface circuitry and software
14 p1742 A73-30112

Finite element models for continuum structural analysis, considering variational principles, element base functions and general purpose computer program
14 p1807 A73-30183

Finite element analysis programs for general applications, considering state of art
14 p1808 A73-30197

NASTRAN digital computer program for static and dynamic structural analysis by finite element method, including nonlinear static and dynamic response
14 p1808 A73-30198

High speed pyrometer for high temperature measurement of thermophysical properties, presenting experiment computer program outline
[ECTP PAPER I2-3] 14 p1753 A73-30438

Use of computers for calculation of the capture band of nonlinear phase-automatic-frequency-control systems.
15 p1842 A73-30990

Basic theory for PROD, a program for computing the development of satellite orbits.
15 p1930 A73-31108

Artificial satellites photographic observations reduction by Turner and colineation methods, considering IBM 360 FORTRAN program application
15 p1843 A73-31648

Cross polarization in radomes - A program for its computation.
15 p1851 A73-31730

Program for triangular bending elements with derivative smoothing.
15 p1848 A73-32028

Software design and implementation for real time power spectral analysis on IBM-1130 8K-core computer, discussing coherence and cross spectra estimation and arithmetic errors
15 p1848 A73-32032

A spectrometric setup for magnetic-tape recording of spectra
15 p1878 A73-32140

Computerized stellar spectrogram processing using semiautomatic diagram-code converters, least squares method and reference spectral lines
15 p1878 A73-32141

A punched tape recorder for observation data
15 p1878 A73-32142

Solution of the three-parameter Weibull equations by constrained modified quasilinearization /progressively censored samples/.
15 p1901 A73-32263

ATC radar information processing systems optimization, discussing hard- and software selection criteria
15 p1847 A73-32440

Blocking procedure for large scale structural analysis in conjunction with plane truss using stiffness matrix method, considering computer subroutines in finite element method
16 p1985 A73-32793

Thin plates and shells post-buckling behavior analysis by discrete element method, noting computer program capabilities
16 p2078 A73-32997

Digital simulation of physical systems using CSMP.
16 p1985 A73-33129

Testing of spacecraft in long-term storage.
16 p2073 A73-33615

Fault ambiguity repair optimization /FARO/ computer program for electronic circuit card group replacement strategy, using FORTRAN IV for SPEC-TRA 70/55 batch processing
16 p1990 A73-33626

Air Force Increase Reliability of Operational Systems computer program and mathematical models for economic logistic resource allocations and cost effective system modification
16 p2088 A73-33627

Microcomputer programs for data reduction and quality control chart work, using Olivetti P-101, HP 9100-B and Wang 700-A calculators
16 p1986 A73-33642

A synergistic reliability and maintainability prediction package.
16 p1986 A73-33652

Computer program for Equipment Improvement Recommendation /EIR/ evaluation relative to reliability, availability, inventory cost and total annual expenditure in Army engineering management decision making
16 p2089 A73-33653

Computer oriented algorithms for solving systems of simultaneous nonlinear algebraic equations.
17 p2199 A73-34107

Book - Minicomputers for engineers and scientists.
17 p2130 A73-34455

Digital computer diagnosis of cardiac arrhythmias in a single-lead electrocardiogram.
17 p2114 A73-34533

Dynamic buckling of shallow spherical shells.
[ASME PAPER 73-APM-A] 17 p2249 A73-35104

Viscous fluid dynamic problem solution method implementation in Eulerian code AZTEC within continuum mechanics-kinetic theory union, preserving conservation properties throughout time integration
17 p2155 A73-35142

Digital avionics systems software development trends, considering compatibility and cost problems in increased use of complex processing hardware, sensors and displays
17 p2137 A73-35203

Huffman binary codes for pulse compression radar, evaluating ambiguity or cross correlation by computer program for replicas formation performance
17 p2131 A73-35221

Intrasystem electromagnetic compatibility analysis program.
17 p2131 A73-35251

An optimization technique utilizing the deflected gradient algorithm for dynamic testing of electromechanical equipment.
17 p2202 A73-35386

Computer program for solution of large, sparse, unsymmetric systems of linear equations.
17 p2132 A73-35603

A computer program to find analytical solutions of second order linear differential equations.
17 p2132 A73-35611

Planar aperture antenna synthesis for main beam and complex sidelobe patterns by iterative correction with convergence, using computer program
17 p2142 A73-35648

Spatial statistics of instrument-limited angular measurement errors in phased array radars.
17 p2128 A73-35687

Easing international language difficulties via an accommodating software design.
[AIAA PAPER 73-614] 18 p2288 A73-36092

Reflecting heat-shield entry analysis computer program for planetary probes.
[AIAA PAPER 73-714] 18 p2368 A73-36333

Skylab Mission Simulator Facility software, describing electric power systems, solar measurements, display panels, earth resource sensors and spacecraft environmental control
18 p2296 A73-36832

Formal treatment and optimization of Boolean expressions.
18 p2292 A73-36956

Hot gaseous jet noise emission calculation for dependence on turbulent flow characteristics based on Lighthill theory, using computer program
18 p2343 A73-36997

Managerial implications of computerized aircraft design synthesis.
[AIAA PAPER 73-799] 19 p2379 A73-37462

Computer program for aircraft navigation error synthesis with evaluation of component error distribution on traffic control system effectiveness to provide cost effective guidance
19 p2452 A73-37875

Non-reacting and equilibrium chemically reacting turbulent boundary-layer flows.
19 p2421 A73-38187

Eigenproblem solution by a combined Sturm sequence and inverse iteration technique.
19 p2408 A73-38188

Calculation and measurement of MHD generator boundary layer velocity profiles.
19 p2470 A73-38315

Metering and spacing with computerized ARTS III ATC system, discussing display for heading, speed and altitude commands
19 p2453 A73-38462

Availability, maintenance and cost of communication satellite systems.
20 p2613 A73-38768

Intrasystem electromagnetic compatibility analysis program.
20 p2528 A73-38771

Linear filtering of ballistic-entry-probe data for atmospheric reconstruction.
[AIAA PAPER 73-904] 20 p2589 A73-38838

Magnetic field intensity and invariant shell parameters computer programs, assessing errors in expansion coefficients
20 p2603 A73-38907

- A diagnostic program - Problems of predicting myocardial infarction on a digital computer
20 p2516 A73-38998
- Study of methods of computing transition matrices /Computer-program description/.
20 p2532 A73-39129
- New initiatives in engineering computer software sharing.
20 p2533 A73-39515
- A unified method for determination of fundamental natural frequency of orthotropic plate with arbitrary boundary.
20 p2622 A73-39546
- Computer program using successive system reduction on basis of calculation of reliability of pure parallel and series arrangements
20 p2533 A73-39632
- Russian book on elasticity theory for multilayer media covering plate compression and bending under boundary contact conditions, Algol programming, tensile stress, functional equations, etc
21 p2782 A73-40175
- Computer program for determining system resonance frequencies and damping via numerical analysis of vector modal response loci plots
21 p2783 A73-40290
- A finite algorithm for the minimum 1-infinity solution to a system of consistent linear equations.
21 p2725 A73-40376
- SAFE - Six axis frequency evaluation of a motion simulator.
[AIAA PAPER 73-932] 21 p2674 A73-40879
- Computer checking of rotational line intensity factors for diatomic transitions.
21 p2744 A73-41212
- Automated systems for designing electronic circuits
21 p2665 A73-41304
- Finite element program for flight structure analysis.
22 p2917 A73-41739
- Computer program for analysis of radiation pattern distortion and mutual coupling in antenna farms, allowing user specification by types or vertical cylindrical antenna dimensions
22 p2823 A73-41797
- Further experiments on balancing of a high-speed flexible rotor.
[ASME PAPER 73-DET-99] 22 p2865 A73-42077
- A method for numerically solving second-order non-homogeneous linear differential equations with variable coefficients.
22 p2882 A73-42482
- A computer model for three-dimensional flow in furnaces.
22 p2934 A73-42787
- Numerical solution of electromagnetic scattering problems.
22 p2827 A73-42841
- FORTH computer program for National Radio Astronomy Observatory telescope observed millimeter wave spectral line data reduction, summarizing language capabilities
23 p2956 A73-43380
- Technically oriented algorithms for unsteady pipe flow.
23 p2968 A73-43800
- A computer program SNR-2 for solving an optimal control problem with state constraints.
23 p2956 A73-44126
- Count of radio sources at a frequency of 86 MHz. I - Method of processing observations in the radio source survey by the East-West arm of the DKR-1000
23 p3035 A73-44230
- An equation for the oxygen hemoglobin dissociation curve.
24 p3064 A73-45070
- Parallel and string array processor hardware design and computer programs for computing speed increase over conventional series computers
24 p3070 A73-45086
- Research Aviation Facility collected aircraft data processing, merging and enhancement problems, software development and future resource requirements
24 p3070 A73-45088
- National Center for Atmospheric Research utility plotting programs for computer graphics, two and three dimensional fields display and movie generation
24 p3070 A73-45089
- Stress wave calculations in composite plates using the fast Fourier transform.
24 p3150 A73-45232
- Skylab complex stiffened structure shell instability analysis by computer program, discussing convergence of finite difference formulation and eigenvalue calculation
24 p3144 A73-45234
- Attitude control for the Netherlands astronomical satellite /ANS/.
24 p3144 A73-45558
- NT MAGNETIC TAPES
NT RANDOM ACCESS MEMORY
NT REGISTERS [COMPUTERS]
Computer development of holographic mass memory plans
05 p0553 A73-16168
- High density coupled flat thin film magnetic memories for large capacity storage, using point density/signal amplitude simulation model
05 p0553 A73-16169
- Semiconductor photodetection matrices for holographic memory reading
05 p0553 A73-16170
- Description and utilization of the TMS 4062 dynamic memory
05 p0553 A73-16171
- Address structure optimization and minimum access time and decoder terminals in nonvolatile core memory array design, noting binary notation for information storage
05 p0554 A73-16991
- Intrinsic models for computer storage allocation program locality concept, comparing performance in terms of working set size and missing page probability by experiments
06 p0670 A73-18060
- Satellite data concentration, memorization, transmission and processing, discussing central computer control unit, ground stations peripheral links, magnetic tapes and system reliability
07 p0793 A73-18952
- Circuit design, manufacture and testing of static memory for D2 satellite computer, considering test equipment, quality control and fabrication
07 p0796 A73-18958
- INTERMAG Conference, 10th, Kyoto, Japan, April 10-13, 1972, Proceedings.
07 p0861 A73-19360
- A procedure for the evaluation and failure analysis of M.O.S. memory circuits using the scanning electron microscope in potential contrast mode.
08 p0943 A73-20730
- Degradation of MNOS memory transistor characteristics and failure mechanism model.
08 p0944 A73-20741
- Low-dissipation memories by p-channel MOS technology with special processes and by complementary-channel MOS technology
08 p0945 A73-21073
- Low-field tunnelling current in thin-oxide M.N.O.S. memory transistors.
08 p0946 A73-21115
- Switching and memory effects in amorphous chalcogenide thin films.
09 p1133 A73-21987
- Circuit diagram and electrical characteristics of semiconductor memory cell consisting of thyristor and n-p-n transistors, noting parameters stability
09 p1063 A73-22460
- Processing the spectra of semiconductor detectors in a semiautomatic system containing data storage elements and a computer
09 p1085 A73-23005
- Photodetector matrix circuit for holographic memory converting optical bits into electrical signals
09 p1086 A73-23074
- Megabit capacity ferrite core memories for scientific satellites, using three dimensional organization with pulse program adapted for buffer application
09 p1087 A73-23426
- Wideband high-speed high-resolution analog to digital converters technology developments, discussing voltage addressable read-only memory concept and related data sampling
10 p1177 A73-23792
- Holographic read-only memory with high speed and density optical storage on low-cost changeable media, discussing feasibility model design, construction and test
10 p1216 A73-23796
- Realization of digital differential analyser on the basis of multifunction memory units.
10 p1198 A73-24018
- Some principles of domain device designing for data processing and means of control.
10 p1198 A73-24022
- Modeling of a bubble-memory organization with self-checking translators to achieve high reliability.
10 p1192 A73-24872
- Computer executive system for design automation file network creation and monitoring to permit input/output operations, storage information updating and display
[AIAA PAPER 73-355] 11 p1334 A73-25492
- Memory included linear stochastic system optimum control over finite time, using Liapunov-Krasovskii functionals
11 p1398 A73-25618
- On a 'memory' effect in N-type silicon Schottky diodes in the presence of metallic impurities
11 p1338 A73-25872
- Wave front reconstruction principle application to side-looking radar, diffused holograms, holographic interferometry and computer storage
11 p1369 A73-26527
- Photochromic glass as reversible optical recording storage medium, discussing image resolution, configuration improvements, merits and applications in holography, random access memory and displays
11 p1370 A73-26537
- Holographic optical memory superiority over conventional localized computer storage devices, considering capacity, access time, immunity to local imperfections, and crosstalk problem
11 p1370 A73-26538
- A method for substantially improving the reliability of multistable pulse-phase-coded elements
12 p1476 A73-26761
- External static and dynamic characteristics of input-output sequences of logic elements
12 p1475 A73-26764
- Digital computers with multistage storage in control systems, determining algorithms for data exchange between operative, superoperative and external memory devices
12 p1475 A73-26782
- A simulation model for a memory organization for a multiprocessor.
12 p1475 A73-27155
- An advanced computer communication network.
[AIAA PAPER 73-414] 12 p1474 A73-27820
- VIEW - A distributed system for graphical analysis of large data bases.
[AIAA PAPER 73-431] 12 p1476 A73-27824
- Study of a read-only optical memory addressed by an array of electroluminescent diodes
14 p1755 A73-29726
- German monograph - The design of digital filters with minimal storage word length for coefficients and state parameters.
14 p1737 A73-30667
- Electronic control units, discussing automanual transfer, integral desaturation, proportional and compensatory action, position regulation with incorporated memory and computer applications
14 p1737 A73-30923
- Reliability testing functions for memory elements
15 p1848 A73-31914
- Bubble domain memory materials production, processing and testing, discussing crystal growth, propagation margins, interaction effects and stroboscopic observations
16 p2044 A73-32864
- A fast access holographic memory.
16 p2012 A73-32868
- Holographic document data recording and storage for single- and multiterminal information processing system, emphasizing Fourier and carrier frequency photography techniques
16 p2013 A73-32873
- A doped highly compensated crystal semiconductor as a model of amorphous semiconductors.
16 p2044 A73-33196
- Integrated semiconductor storage devices, discussing bipolar transistor, Schottky diode and MOS memories and RAM, ROM and PROM types with circuit compatibility considerations
16 p1991 A73-33960
- Light sensitive MNOS /metal-nitride-oxide-silicon/ memory transistor space charge layers current-field relationships and steady state I-V measurements
17 p2134 A73-34221
- CPU design for command and control system with programmable read-only control memory, discussing self microdiagnostics for control store error detection
17 p2144 A73-35258
- Digital hardware and computer system for a digital image recorder.
17 p2131 A73-35280
- Optical data storage and data processing, and holography in aerospace and electronic instrumentation.
17 p2131 A73-35382
- Block oriented random access and read-only archival holographic memories design, considering relationships between lens geometric parameters, laser power and packing density requirements
17 p2173 A73-35432
- Data compression techniques as a means of reducing the storage requirements for satellite data - A quantitative comparison.
19 p2405 A73-38196
- Papers on adaptive electronic devices, circuits and systems covering logic nets, solid state and ferroelectric devices and memory devices and artificial intelligence
20 p2535 A73-39135
- Reduction of power requirements in dynamic elements based on bipolar transistor
21 p2660 A73-40022
- German monograph on display unit nonlinear interpolation approach based on higher order curve for reduced computer storage requirements covering Chebyshev approximation and coordinate transformations
22 p2830 A73-42738
- Cellular dynamic memory array with reduced data-access time.
23 p2956 A73-44116

COMPUTER SYSTEMS DESIGN

Digital computers with multistage storage in control systems, determining algorithms for data exchange between operative, superoperative and external memory devices

12 p1475 A73-26782

Traffic analysis by statistical tests for batch mode operated digital computer network design, considering user habits, and interarrival, waiting and partition times

12 p1475 A73-27159

Response time in the application of interactive graphics in structural analysis.

13 p1693 A73-28244

A unified method for analyzing mission reliability for fault tolerant computer systems.

15 p1901 A73-32261

Self-reconfiguring computer complexes for A.T.C. Systems.

15 p1849 A73-32439

Area navigation computer TCE-71 A system, discussing central control display and data entry units, inputs/outputs and operating modes

15 p1909 A73-32455

Aircraft onboard computerized avionics and electrical systems architecture for information flow and control with maximum efficiency, flexibility, modularity and minimum maintenance

17 p2137 A73-35204

DONAR - A computer processing system to extend ultrasonic pulse-echo testing.

19 p2407 A73-37448

United States en route air traffic control systems.

19 p2451 A73-37810

The use of logic simulation in the design of a large computer system.

21 p2658 A73-41210

Interconnecting computer network theory and system types, discussing data coordination and transformation, host computer links with system participants and network applications

23 p2957 A73-44389

COMPUTER SYSTEMS PROGRAMS

NT INPUT/OUTPUT ROUTINES

NT OPERATING SYSTEMS [COMPUTERS]

Simulation aids for designing integrated information systems - The ECSS language.

02 p0144 A73-12600

Computer-controlled software diagnosis of an airborne computer.

08 p0940 A73-20677

Automatic test equipment software configuration management.

08 p0952 A73-20686

Automatic test equipment support software definition and development, describing language, translator and operating system as elements of closed loop ATE system

08 p0952 A73-20687

Test programs design for versatile avionics shop test system [VAST], discussing compiler problems alleviation by on-station program patching capability

08 p0962 A73-20688

GALIC - Grumman Aerospace Engineering Language for Instructional Checkout.

08 p0941 A73-20689

Simultaneous design of 24 inch telescope and computer control system, discussing interface and software development

08 p0942 A73-21754

CAMAC - A proposed standard for astronomical instrumentation.

08 p0972 A73-21755

The introduction of a digital computer on board ERSO scientific satellites.

09 p1061 A73-23378

ATC system requirements for Concorde transoceanic flight operations, considering track allocation, computer system and programming

13 p1656 A73-28178

New initiatives in engineering computer software sharing.

20 p2533 A73-39515

COMPUTER TECHNIQUES

The estimation of ground-level pressure fields from computer analyses and their application to large-scale atmospheric mass transfer.

01 p0072 A73-10144

A system for continuous measurement of gas exchange and respiratory functions.

01 p0011 A73-10172

A high-precision computer-controlled dual-channel polarizing radiometer.

01 p0045 A73-10383

Ionospheric propagation indexes prediction based on computer filtered values obtained during solar activity cycles ascending and descending parts

01 p0017 A73-10416

A computer-controlled digital spectrum scanner for La Silla.

01 p0047 A73-10515

The coude spectrograph and echelle scanner of the 2.7 m telescope at McDonald Observatory.

01 p0048 A73-10525

Computerized correlation analysis of single and multiple neuron pulse activity, considering temporal, sequential and entropy characteristics

01 p0012 A73-10653

Investigation of the recovery dynamics of the mimic muscle function and choice of an optimal bioelectric stimulation program with the aid of an electronic digital computer

01 p0012 A73-10656

Analog computer regression line and correlation ratio determination for random stationary processes with time lag

01 p0028 A73-10928

Thermal analysis and its verification test of a small probe for space use.

01 p0052 A73-11147

Minicomputer for real time sequential decoding of convolutional code transmission in space communication, discussing system design, performance and metric bias effect

01 p0020 A73-11185

Interferometric testing of large optical components with circular computer holograms.

01 p0053 A73-11225

Coding technique to record computer generated binary hologram on numerically controlled CRT with resolution cell of two beam spots

01 p0019 A73-11235

Absorption line shape computerized functional analysis in solar physics, deriving H/α_v function from Faddeyeva-Terentev probability

01 p0107 A73-11377

Solution of navigation problems with a hybrid analog computer

01 p0075 A73-11400

Optimal fixed message block size for computer communications.

01 p0019 A73-11454

Data processing for radioastronomy and cosmic ray air shower arrays.

01 p0020 A73-11455

Digital image processing for the earth resources technology satellite data.

01 p0020 A73-11457

A discrete numerical approach to fluid dynamics.

01 p0071 A73-11461

Digital filters applicable to electroencephalographic pattern recognition.

01 p0013 A73-11464

A comparison of analog and digital techniques for pattern recognition.

01 p0021 A73-11478

Computerized airborne multilateration radar with wide-beam antenna and narrow pulsewidth for high resolution terrain image mapping

01 p0019 A73-11479

Symbol ring as alphabetic element in information processing technique, defining address substitution operation

02 p0143 A73-11642

Radio telescope for high resolution radio source mapping, discussing system design, computerized control and calibration

02 p0150 A73-11869

Computer based data processing system with display for improving ultrasonic pulse echo NDT test equipment resolution and SNR

02 p0173 A73-11983

Computer analyses of gravitational radiation detector coincidences.

02 p0144 A73-12222

Russian book on machine-based determination of random process characteristics covering correlation, moment functions, spectral features, probability functions, etc

02 p0149 A73-12866

Computer technique for automated acoustical inspection of rotating machines

03 p0311 A73-12958

Utilization of computers in practical astronomy

03 p0372 A73-13243

Portable self contained computerized in-aircraft engine analyzer with cassette tape resident program control and digital display and punched card indicators

[AIAA PAPER 72-1080] 03 p0307 A73-13403

Integrated engine diagnostics and displays for Navy aircraft of the 1980's.

[AIAA PAPER 72-1084] 03 p0354 A73-13406

Optimal horizontal guidance law for aircraft in the terminal area.

03 p0340 A73-13518

An automated jet-engine-blade inspection system.

03 p0312 A73-13524

Computer methods for simulation of multidimensional, nonlinear, subsonic, incompressible flow.

[ASME PAPER 72-HT-61] 03 p0294 A73-13546

Computerized radial turbine blades thickness identification, considering temperature distribution and effects and mathematical model parameters for constraints

03 p0312 A73-13565

Recording and data processing equipment proposed for scintillation measurements.

03 p0308 A73-13646

Computers and the analysis of pressure vessels.

03 p0391 A73-13678

Computer method for analysis of multistory structures.

03 p0391 A73-13683

Computation and solution procedures for nonlinear analysis by combined finite element-finite difference methods.

03 p0391 A73-13685

Pulsar associated with the supernova remnant IC 443.

03 p0374 A73-13848

An advanced concept in electrical power distribution control and management.

03 p0253 A73-13945

Computerized analyses of radar photographs.

03 p0281 A73-14524

Computer-mediated human communications in an air traffic control environment A preliminary design.

03 p0340 A73-14658

Computerized ECG interpretation system for heart and circulatory disorder detection and diagnosis and health screening

03 p0272 A73-14660

A universal digital autopilot and integrated avionics system.

04 p0474 A73-14735

Considerations for an earth physics information-management service.

04 p0439 A73-14814

Principles of organization and logistical support for systems of automating scientific investigations

04 p0424 A73-14823

Stabilization of constraints and integrals of motion in dynamical systems.

04 p0470 A73-15002

Hypermatrix solution of large sets of symmetric positive-definite linear equations.

04 p0470 A73-15009

Certain algorithms and error assessments for the approximate analytical solution of boundary value problems

04 p0470 A73-15090

An application of Bayes-law estimation to nonlinear phase demodulation.

04 p0471 A73-15253

Computerized parameter estimation by jump detection scheme for nonlinear atmosphere density and temperature profile tracking

04 p0430 A73-15255

New developments in EEG signal processing.

04 p0411 A73-15279

Message switching for multiplexing data of computer users with interactive access onto common facilities, evaluating traffic induced time delay performance

04 p0425 A73-15428

Computerized ground support acceptance checkout systems for space shuttle program, discussing capabilities, future goal and unified test equipment

04 p0432 A73-15458

Use of an on-line computer in a study of cardiac arrhythmia.

04 p0412 A73-15644

Computer-aided ECG analysis and research in a clinical setting.

04 p0412 A73-15648

Metal-dielectric-semiconductor junction transistor HF response analysis by digital computer, deriving switching time as function of impurity concentration and electrode voltage

05 p0556 A73-16069

Quantitative materials evaluation and inspection with the image analysing computer.

05 p0575 A73-16288

Applications of the discriminant function in automatic pattern recognition of side-looking radar imagery.

05 p0553 A73-16289

Computerized ATC automation program, considering system management, hardware, software and test facilities problems

05 p0595 A73-16619

The concept of an SST Oceanic Computer Clearance System.

05 p0595 A73-16621

Field experience with digital control systems for vibration and acoustic testing.

05 p0554 A73-16637

Computer-controlled environmental test systems - Criteria for selection, installation, and maintenance.

[SAE PAPER 720819] 05 p0562 A73-16638

Interactive aspects of man/learning system control teams.

05 p0543 A73-16708

Computer-assisted instruction in pilot training and certification.

05 p0544 A73-16724

Computer-controlled differential review-time payoff as a training aid.

05 p0544 A73-16725

The employment of a spoken language computer applied to an air traffic control task.

05 p0544 A73-16728

Data processing remote terminals for real time on-line computer communication systems, discussing design, characteristics and applications
05 p0551 A73-16801

Datran TDM switching system with stored program controller and IC components providing reliability, flexibility and high channel capacity in data transmission
05 p0551 A73-16804

Computer communication networks with programmable concentrators for combining multiple terminals, discussing structure, message handling and transmission, routing and reliability
05 p0551 A73-16805

Computerized airlines reservations systems with real time conversational interactive characteristics, discussing initial design, simulation, measurement, stability, reliability and data processing techniques
05 p0551 A73-16806

Two dimensional digital Fourier transform applications to picture processing, noting economy in computer storage
05 p0554 A73-17146

An integrated feature selection and supervised learning scheme for fast computer classification of multi-spectral data.
05 p0555 A73-17153

Digital control mounts on jet engine.
05 p0608 A73-17249

Analysis of noncircular cylindrical shells.
06 p0758 A73-17446

Electronic creation of still and animated complex images, discussing techniques for supplying computer with object description
06 p0669 A73-17474

Computer-aided solution of nonlinear differential equations in electrical engineering, using an extension of Wolinkin's procedure
06 p0669 A73-17595

A universal method of calculation of the state of a real gas behind primary and reflected shock waves.
06 p0684 A73-17700

Parameter identification using the Galerkin procedure in nonlinear boundary-value problems.
[ASME PAPER 73-AUT-C] 06 p0716 A73-17724

Enhancing testability of large-scale integrated circuits via test points and additional logic.
06 p0674 A73-17802

The representation and matching of pictorial structures.
06 p0692 A73-17804

Television/computer dimensional analysis interface with special application to left ventricular cineangiograms.
06 p0657 A73-17860

Code correcting nonsymmetrical bursts of errors during data exchange between computers.
06 p0670 A73-17962

An efficient numerical technique for evaluating large quantities of highly oscillatory integrals.
06 p0716 A73-17982

Computational variants of the Lanczos method for the eigenproblem.
06 p0716 A73-17984

A robot conditioned reflex system modeled after the cerebellum.
06 p0658 A73-18065

Computer output microfilm system technology assessment, discussing two dimensional acousto-optic laser scanner to write on dry process film
06 p0700 A73-18294

The selection and design of electro-optical instruments for outer planet exploration.
06 p0695 A73-18320

Book on nonlinear optimization covering search, iteration, gradient, algorithmic and computer techniques, mathematical and dynamic programming, calculus of variations, Pontryagin maximum principle, etc
06 p0717 A73-18401

Identification of multivalued nonlinearities in a class of noisy time invariant dynamic systems.
06 p0681 A73-18811

Compact digital coding of electrocardiographic data.
06 p0660 A73-18815

Space/rocket/ launch vehicle computer guidance and targeting equations, discussing Q, Delta, explicit, linear tangent, optimal, numerical integration and parameter optimization techniques
06 p0721 A73-18824

Digital-computer analysis of linear electronic circuits by the method of structural numbers
07 p0804 A73-18894

Third generation satellite PCM telemetry data processing with computer control for optimization and supervision, discussing system reliability, automatic control and diagnostic routine
07 p0795 A73-18954

Reliable, high performance magnetic tape recorder/reproducer for third generation telemetry data computer processing lines, noting human error possibility reduction
07 p0795 A73-18955

FORTRAN sequence with economical computer storage requirement for matrix method application to rigid plastic collapse analysis of frame, considering bounded variable problem
07 p0907 A73-19034

Two-level computer system with main and display processors as scale working model for semiautomatic digital ATC en route control
07 p0796 A73-19183

Automated radar terminal systems (ARTS).
07 p0849 A73-19184

Area navigation systems integration with terminal ATC approach procedures, considering computerized data linkage with aircraft navigation system
07 p0849 A73-19351

A method for chronocyclographical motion analysis with the aid of an on-line computer
07 p0785 A73-20036

Computer calculation of spectral brightness coefficients on aerial photographs, determining contrast features density gradients
07 p0824 A73-20044

Control algorithm for digital computer operations organization in real time processing of variable priority assignment tasks, estimating memory storage requirements
07 p0796 A73-20049

Calculation of temperature fields in cooled gas-turbine blades on a digital computer
07 p0868 A73-20099

Analog-computer studies on microwave mixing in superconducting weak links.
07 p0863 A73-20103

Computer aided recognition of objects shapes on aerial photographs, discussing image derivatives and histograms use and flying spot scanner principle
07 p0825 A73-20165

A computerized flutter solution procedure.
07 p0914 A73-20214

German monograph - Vigilance prognosis with the aid of a computer analysis of the spontaneous electroencephalogram.
07 p0786 A73-20391

State of the art and survey of learning control applications.
07 p0806 A73-20590

AUTOMATE - A self-contained automatic test system.
08 p0951 A73-20680

Scheduling algorithms for multiprogramming in a hard-real-time environment.
08 p0941 A73-20961

Pyranometer calibration by substandard and working instrument comparison on X-Y recorder, using computerized statistical analysis
08 p0966 A73-21264

The third international comparisons of pyrheliometers and a comparison of radiometric scales.
08 p0966 A73-21266

Astrometry with Schmidt telescopes, discussing automated computerized plate scanner and measuring machine for star position and relative motion determination
08 p0966 A73-21356

Natural resources information system.
08 p0961 A73-21707

Simultaneous design of 24 inch telescope and computer control system, discussing interface and software development
08 p0942 A73-21754

An evaluation of the heat pulse anemometer for velocity measurement in inhomogeneous turbulent flow.
[AD-758460] 09 p1071 A73-22102

Real time display, processing and image-data products production system for supporting Mariner 9 TV experiment, discussing computer algorithms
09 p1080 A73-22266

Recursive methods in on-line computer photogrammetric data reduction deriving algorithms for fixed and variable parameter numbers cases with matrix partitioning
09 p1059 A73-22381

USAF WAVR file of epidemiologic data on medically waived flying personnel, describing computerized updating system
09 p1039 A73-22539

Computer calculation of the characteristics of multistage gas turbines
09 p1136 A73-22567

Autonomous power subsystem design for an Outer Planet Spacecraft.
09 p1154 A73-22805

TV vidicon image converter with arbitrary scanning format and computer-compatible output signals, using power spectrum redistribution functions
09 p1060 A73-22945

Processing the spectra of semiconductor detectors in a semiautomatic system containing data storage elements and a computer
09 p1085 A73-23005

Contributions to the design of future on-board data processing systems for scientific space-craft experiments.
09 p1061 A73-23379

A mobile tone range/RDF system for telemetry tracking of sounding rockets.
09 p1057 A73-23412

Orthogonal polynomials for computerized construction of equations of state for substances under thermodynamic restrictions
10 p1293 A73-23505

A computer method of optimal redundancy allocation in satellite communication system.
10 p1188 A73-23753

Applications of symbolic computing methods to the dynamic analysis of large systems.
10 p1192 A73-24029

The evaluation of the domain of attraction of nonlinear control systems with hybrid computing systems.
10 p1192 A73-24040

The algorithms of accuracy research of nonstationary linear systems with continuous and discrete elements.
10 p1200 A73-24048

Determination of changes in the properties and recognition of random processes with a complicated structure.
10 p1201 A73-24057

Computer aided directivity measurements of large antennas in Fresnel zone
10 p1188 A73-24184

Analog computer regression line and correlation ratio determination for random stationary processes with time lag
10 p1201 A73-24188

A finite element method for block adjustment problems of photogrammetry.
10 p1218 A73-24291

Solution of quadratic matrix equations for free vibration analysis of structures.
10 p1290 A73-24299

Prospects of developing an automated hydrometeorological system
10 p1203 A73-24375

Methods of representation and machine analysis of random fields and processes; All-Union Symposium, 5th, Vilnius, Lithuanian SSR, May 1972, Transactions. Sections 1, 2, 3 & 4
11 p1339 A73-25001

The Coude spectrum scanner at the Lowell Observatory.
11 p1360 A73-25069

Airport computerized departure control for check-in, load control, cargo and catering operations, discussing load optimization and passenger acceptance control (LOPAC) system
11 p1343 A73-25210

Pattern recognition based on visual perception relation to transformations and identification by coded sentences
11 p1334 A73-25621

Application of nonalgorithmic digital machines in modeling differential equations
11 p1334 A73-25633

Parallel-redundant flight control systems, discussing sensor bias and combined control computer input effects on controllability and steady state modal response
11 p1342 A73-25783

Steady state mathematical theory for the insulated gate field effect transistor.
11 p1338 A73-25789

Partitioning techniques for solving large systems of equations in structural analysis.
11 p1442 A73-25844

Sea ice observation by means of satellite.
11 p1358 A73-26346

Computer analysis of the orthogonal electrocardiogram and vectorcardiogram in 939 cases with hypertensive cardiovascular disease.
11 p1324 A73-26361

Hologram interferometry and laser speckle methods - Further applications.
11 p1370 A73-26532

Computer generated binary synthetic holograms, discussing information coding and processing, detour phase effect and kinoforms
11 p1370 A73-26534

Boole law rationalization based on Dole computer-generated planetary system with constant spacing ratio generated by random number sequence and accretion process closeness constraints
11 p1428 A73-26665

Digitally scanned spectral convolution by computerized filtering for noise spectra quality improvement with instrument signature removal
11 p1334 A73-26679

Weather forecasts in tabulated and worded form by computer interpretation of forecast charts.
12 p1520 A73-26806

Automatic classification of G5-K5 stars by means of 166 A/mm objective prism spectra /4000-4550 A/.
12 p1538 A73-26858

Differential equations of motion for analog model of M-type TWT performance, proposing block diagram for electron phase and trajectory and field distribution calculations
12 p1478 A73-26950

A numerical algorithm for identifying spread functions of shift-invariant imaging systems. 12 p1475 A73-27114

Quadratically convergent algorithms and one-dimensional search schemes. 12 p1517 A73-27118

Techniques for simulation of radar displays. 12 p1475 A73-27132

Selection of optimal rigidities for elastic regions of a mechanical system with resonance oscillations. 12 p1524 A73-27473

A programmable surface acoustic wave matched filter for phase-coded spread spectrum waveforms. 12 p1484 A73-27574

An algorithmic procedure for determining discrete transfer matrices of controlled plants. 12 p1485 A73-27624

Calculation of the stress-strain state of a toroidal shell with holes. 12 p1555 A73-27787

Image analysis techniques associated with automatic data base generation. 12 p1499 A73-27823 [AIAA PAPER 73-430]

Electronic image enhancement in remote sensing by information content reduction before computer read-in, discussing electronic image transformations. 12 p1501 A73-27961

Three dimensional elastic stress analysis by finite element method within reasonable computer costs, noting problem simplification. 13 p1693 A73-28240

Automatic mesh generation in two and three dimensional inter-connected domains. 13 p1693 A73-28242

The splitting-up method and its application to elasticity problems. 13 p1694 A73-28254

Harmonic spectral analysis of nystagmus waveform frequency content for clinical vestibular examination via digital computer. 13 p1579 A73-28502

A two-dimensional mathematical model of the insulated-gate field-effect transistor. 13 p1590 A73-28543

Ray optics model analysis for spherical aberration effects on acoustic hologram resolution in image reconstruction, discussing computer generated correction for quality improvement. 13 p1615 A73-28591

Computer control of a multifunction radar. 13 p1587 A73-28619

A 4-year experiment in long-range weather forecasting, using circulation analogues. 13 p1653 A73-28740

Computerized adaptive flight control for helicopter dynamic systems based on identification and optimization methods. 13 p1569 A73-28829

The hyperelliptical and other new pseudo cylindrical equal area map projections. 13 p1608 A73-28845

Algorithms for finding the coefficients of polynomials of matrix determinants. 13 p1587 A73-28864

Method of studying the fatigue damage of metals with automatic data processing on a computer. 13 p1597 A73-29053

Russian book - Problems of applied mathematics. 13 p1650 A73-29126

Automation of variational methods of solving boundary value problems. 13 p1650 A73-29127

Computer realization of a method of scaling the gravity force. 13 p1609 A73-29128

A first experiment in constructing a weather forecast for a month by the synoptic method on a computer. 13 p1655 A73-29193

Application of analog and digital computers to fatigue testing. 13 p1622 A73-29547

Zeros determination in large-scale multivariable systems. 13 p1651 A73-29568

Application of a modified quasilinearization technique to totally singular optimal control problems. 13 p1597 A73-29570

Book - Computer fluid dynamics: Recent advances. 14 p1744 A73-29743

The use of the electronic computer for the urgent publication of astronomical material. 14 p1730 A73-29791

Determination of parabolic orbits on the basis of N observations, by means of an electronic computer. 14 p1790 A73-29796

Computer and digital techniques in ATC automation technology, considering functional organizations, terminal facilities and system capabilities to meet future needs. 14 p1730 A73-29886

Russian book - Methods for calculating electromagnetic fields by electronic digital computers. 14 p1774 A73-30026

Russian papers on cybernetic systems reliability and accuracy covering analog, hybrid and digital computers, electronic modeling, nonlinear control systems, computer and complex system design, etc. 14 p1730 A73-30031

A posteriori estimates of error distribution laws in the solution of linear algebraic equations by analog techniques. 14 p1768 A73-30032

Accuracy estimates for analog computer solutions to systems of ordinary linear equations and some algebraic equations. 14 p1768 A73-30033

Telescope equipment for future astronomical observatory, favoring array of computerized electronic imaging small telescopes vs single large reflector. 14 p1754 A73-30916

Multistep computer algorithm for Navier-Stokes equations of two dimensional viscous incompressible flow in channel with complex geometry. 15 p1860 A73-30965

Projection method in the shell theory and its realization on a computer. 15 p1944 A73-30971

Use of computers for calculation of the capture band of nonlinear phase-automatic-frequency-control systems. 15 p1842 A73-30990

Technological weather forecasting advances, including use of satellites, global meteorological network, computer techniques and mechanical recorders. 15 p1902 A73-31149

Attempted prediction of the superconducting transition temperature for some metallic compounds with the aid of a computer. 15 p1922 A73-31177

Computerized stress analysis of shock load induced circular elastic membrane interaction with fluid stream via method of characteristics related to aerodynamic decelerator design. 15 p1948 A73-31429 [AIAA PAPER 73-443]

Viking 75 Mars lander parachute high altitude qualification flight tests for camera, telemetry and radar performance, using ground based computer-radar monitoring system. 15 p1826 A73-31442 [AIAA PAPER 73-456]

Computer experiments in selective distribution of hydrometeorological bibliographic information. 15 p1904 A73-31611

Digital image processing for information extraction. 15 p1875 A73-31800

Equipment for recording and computer input of solar magnetograph data. 15 p1878 A73-32139

Radiation configuration factors for annular rings and hemispherical sectors. 15 p1959 A73-32281

Bringing data processing to projects and tests of large antennas. 15 p1846 A73-32430

Functioning in multiprocessing of two 10020 computers at the Bretigny Eurocontrol Experimental Center. 15 p1847 A73-32442

Some remarks on operational problems associated with the introduction of automatic data processing into air traffic control. 15 p1909 A73-32447

Area navigation feasibility, discussing computer technology usefulness, time saving and air traffic controller acceptance. 15 p1911 A73-32491

Variation with temperature of free enthalpy of formation of certain carbides. 15 p1898 A73-32644

Solution on a digital computer of boundary value problems for three-dimensional rod systems with branchings. 16 p2075 A73-32692

Book - Techniques involving extreme environment, nondestructive techniques, computer methods in metals research, and data analysis. Part 1. 16 p2017 A73-32696

Computerized Ritchey-Chretien computation method for telescopic optical system, controlling mirror shape via transparent screen. 16 p2011 A73-32715

Implementation of a frog's eye type discriminator, responsive only to pattern changes, as a pre-processor for visual data. 16 p2014 A73-33127

BOAC computer aided flight simulators, detailing simulator systems history, Boeing 747 training adaptation, and simulation types. 16 p1996 A73-33212

A new method for diagnosing myocardial damage in patients with normal electrocardiograms and vector cardiograms. 16 p1973 A73-33375

Computational efficiency comparison for discrete linear filtering Kalman algorithms and information matrix methods, noting Householder square-root implementation identity with Potter technique. 16 p2032 A73-33404

AEGIS Operational Readiness Test System - Design for system effectiveness. 16 p2073 A73-33609

Computerized analysis of reliability or failure rate function data from electronic component and equipment operation and testing, using hazard plotting technique. 16 p1989 A73-33613

Operational readiness and maintenance testing of the B-1 strategic bomber. 16 p1969 A73-33631

An integrated, modular approach to automatic testing and data monitoring. 16 p1986 A73-33632

Computerized total On-Line Testing System with diagnostic error visibility and preventive and corrective maintenance functions in multiprogramming mode, discussing design features. 16 p1986 A73-33633

Concept and system of the versatile avionics shop test/VAST/ system. 16 p1986 A73-33634

DC9-30 refrigeration system diagnosis by computer. 16 p1969 A73-33654

Computer analysis of reflected signals obtained during radar sounding of Venus. 16 p2067 A73-33807

Some computational techniques for the nonlinear least squares problem. 17 p2199 A73-34105

A survey and comparison of methods for predicting the profile loss of turbine blades. 17 p2093 A73-34391

Book - Minicomputers for engineers and scientists. 17 p2130 A73-34455

A performance data acquisition and analysis system for turbine engine component testing. 17 p2146 A73-34610

Computerized automatic microwave testing with pulse measurements of phase and power from Reliable Advanced Solid State Radar phased array modules, discussing system design. 17 p2135 A73-34724

Monitoring interruptions at the satellite earth station. 17 p2122 A73-34870

Prospects of automation of air traffic control systems using satellites for radio navigation. 17 p2209 A73-34961

Automatic recognition of electrocardiographic patterns. 17 p2116 A73-34964

Automatic cataloging of electrocardiographic patterns. 17 p2116 A73-34965

Alternating direction implicit finite difference computational method for solving two dimensional Navier-Stokes equations for high and low speed flows. 17 p2202 A73-35140

Orthogonal polynomials for computerized construction of equations of state for substances under thermodynamic restrictions. 17 p2255 A73-35185

Computer data base use by industrial management for product design, development, manufacturing, testing and documentation coordination to achieve system communication and control improvement. 17 p2257 A73-35215

Avionics subsystems operational, functional and physical considerations, discussing cost, computer programming, common components, multiplexing and hardware design. 17 p2139 A73-35249

Computer analysis of the influence of solid state distribution on aircraft power generation. 17 p2109 A73-35250

Computerized approach for aerospace electronic components standardization for procurement cost, logistics and warehousing problems reduction and reliability improvement. 17 p2140 A73-35260

Preliminary progress with digital image-tubes at Cerro Tololo. 17 p2169 A73-35281

Experimental use of self-scanned photodiode arrays in astronomy. 17 p2169 A73-35287

Astronomical observations with an SEC vidicon system. 17 p2233 A73-35289

A multi-channel coronal spectrophotometer. 17 p2170 A73-35291

Institute of Electrical and Electronics Engineers, International Convention and Exposition, New York, N.Y., March 26-30, 1973, Technical Papers. 17 p2140 A73-35299

Control of multiplexed communications channels. 17 p2144 A73-35310

Annual Southwestern Conference and Exhibition, 25th, Houston, Tex., April 4-6, 1973, Record. 17 p2124 A73-35357

Word length problems in the on-board computer implementation of digital flight control systems. 17 p2145 A73-35384

On-axis computer generated hologram with multieulusion color film for retaining kinoform advantages and effective control over amplitude and phase transmittance

17 p2171 A73-35401

Airborne flight-test strain gage instrumentation from installation, calibration and data recording and reduction standpoint, discussing ground and airborne minicomputer use

17 p2148 A73-35442

Book - Computer methods in structural analysis.

17 p2251 A73-35473

Computer program for solution of large, sparse, unsymmetric systems of linear equations.

17 p2132 A73-35603

Book - Experimental techniques in fracture mechanics.

17 p2252 A73-35668

Fracture mechanics testing systems, discussing closed loop assembly, programming, readout and fail-safe units and fully automated computer-controlled technique

17 p2175 A73-35672

The generalized multiprobe reflectometer and its application to automated transmission line measurements.

17 p2143 A73-35691

A reflectance analog computer for the determination of thin film optical properties.

17 p2132 A73-35773

Computerized finite difference method with reduced core storage requirements for solving boundary value problem of forced random vibration of rotating beam

17 p2204 A73-35830

Hydrometeorological data processing and dissemination techniques and equipment, with emphasis on computerized regional centers and space-based systems

18 p2295 A73-35907

Problems associated with automation of the checking and processing of meteorological and climatological data

18 p2332 A73-35916

Computerized flight test data processing, emphasizing speed in turnaround and data analysis efficiency

18 p2266 A73-36070

Computerized processing system with real time control, data analysis and display capabilities for space shuttle checkout, servicing, launching and landing to reduce cost

[AIAA PAPER 73-601]

18 p2295 A73-36083

Vehicle management and mission planning in support of shuttle operations.

[AIAA PAPER 73-612]

18 p2358 A73-36090

Finite element and finite difference energy techniques for the numerical solution of partial differential equations.

18 p2330 A73-36827

Hidden-line removal at 20 pictures/second through hybrid techniques.

18 p2291 A73-36830

Method of investigating fatigue damage of metals with automatic information processing by computer.

18 p2297 A73-36885

Computer processing and analysis of TV cloud photographs.

18 p2334 A73-37058

Automatic analysis of cloud cover by infrared photography of the earth from meteor satellites.

18 p2334 A73-37068

Statistical models for rounding-off error studies in linear algebraic problems

18 p2292 A73-37144

Method of detecting meteor streams and associations

19 p2480 A73-37236

Technological survey of machine intelligence for real time autonomous manipulation with computer recognition sensory feedback and programmed task control to eliminate human operator

19 p2417 A73-37330

Performance improvement in remote manipulation with time delay by means of a learning system.

19 p2417 A73-37331

The control of a manipulator by a computer model of the cerebellum.

19 p2398 A73-37333

Computer based analyses of the response of box type structures to random pressures.

19 p2497 A73-37485

Space shuttle payload definition, design and planning, using computers for scheduling and costing

19 p2491 A73-37593

Automation of airline passenger processing.

19 p2506 A73-37804

Advanced concepts in terminal area control systems - Aircraft tracking and collision alert.

19 p2451 A73-37806

The B.O.A.C. navigation procedures trainer.

19 p2418 A73-37874

Differential equations modelled on nonalgorithmic digital computers.

19 p2408 A73-38144

Determination of dynamic loads on elastic structures caused by external excitations

19 p2500 A73-38155

Computer processing of earth resources data from mono- and multispectral band scanners and IR photography

19 p2431 A73-38178

A computational technique for the efficient handling of large matrices.

19 p2445 A73-38191

Schlieren and computer studies of the interaction of ultrasound with defects.

19 p2461 A73-38201

Method of holography in nondestructive testing.

19 p2432 A73-38359

Metal oxide semiconductor/large scale integration circuit failure analysis and diagnosis, discussing short circuits, cholesteric liquid crystal coloring and aluminum anodization

19 p2411 A73-38448

Oakland airport oceanic ATC with input-output display device, describing minicomputer, CRT displays and data link system

19 p2454 A73-38471

Design concepts for an earth resources data management system.

[AAS PAPER 73-151]

20 p2521 A73-38597

Computerized analytical methods for optimal control synthesis of linear and nonlinear systems with constraints, using integral quadratic weighing function estimates

20 p2539 A73-38679

Gradient method of nonsmooth function minimization on an analog computer

20 p2531 A73-38682

Correctness of the solution of signal filtration and reconstruction problems by an analog computer

20 p2522 A73-38702

The application of digital filters using observers to the design of an ICBM flight control system.

[AIAA PAPER 73-845]

20 p2541 A73-38784

Computerized trajectory estimation for maneuvering reentry vehicles, obtaining minimum variance trajectory parameters by Kalman filtering of radar, optical and inertial reference measurements

[AIAA PAPER 73-902]

20 p2589 A73-38836

An initial value method for the eigenvalue problem for systems of ordinary differential equations.

20 p2581 A73-38970

The suitability of the microdensitometer PDS 1000 for the measurement of radial velocities

20 p2565 A73-39065

A numerical realization of the Bubnov-Galerkin method using a computer for the solution of nonlinear problems in the theory of shallow shells

20 p2617 A73-39307

The application of constrained least squares estimation to image restoration by digital computer.

20 p2533 A73-39401

Computer-aided two-dimensional analysis of bipolar transistors.

20 p2536 A73-39410

IR scanner for aerial stereoscopic photography, discussing use of computer controlled orthophoto printer for image distortion reduction by rectification

20 p2566 A73-39671

Computer controlled automatic TV-microscope system for tracking and measuring nerve cell processes in designated axons and dendrites

20 p2518 A73-39763

IR test data evaluation for printed circuits using computer techniques, discussing testing time reduction and efficiency optimization, programming language and error analysis

20 p2567 A73-39769

Strapdown inertial navigation with high speed digital computer, discussing attitude propagation algorithms and life cycle system cost advantages

21 p2734 A73-40036

A fast IR spectral transform imager.

21 p2699 A73-40273

Some results of fuselage calculations on a digital computer by the finite-element method

21 p2783 A73-40387

Hurricane prediction - Progress and problem areas.

21 p2731 A73-40641

Automatic identification of cardiac rhythm and conductivity disturbances with the aid of digital computers

21 p2643 A73-40751

Experiences with an augmented human intellect system - Computer mediated communication.

21 p2654 A73-40833

Computerized simultaneous numerical integration of motion equations for solar system, star cluster and galaxies, considering radar observations of moon, Mercury, Venus, Mars and Icarus

21 p2772 A73-41241

Computer analysis of mixed coordinate base transistor circuits determining matrix numbers without main path or generalized node delineation

21 p2670 A73-41308

Computer processing of RF neutral-hydrogen line observations carried out with a fixed antenna

21 p2659 A73-41468

Identification and simulation of antenna dynamics.

21 p2667 A73-41525

Interactive processing of map data produced by the Westerbork supersynthesis radio telescope.

21 p2778 A73-41534

Conditional computer analysis of the onset-to-onset duration of spikes from the electromyographic interference pattern of extraocular muscles.

22 p2802 A73-41731

Gravitational radiation detection via computerized delay-dependent coincidence comparisons of squared time derivatives of output powers of Argonne and Maryland cylindrical antenna detectors

22 p2885 A73-41734

The coupling of high frequency electromagnetic energy into large systems.

22 p2822 A73-41792

Straight wire monopole and dipole antenna near field coupling characteristics prediction, deriving mathematical model by method of moments for computerized analysis

22 p2823 A73-41798

Improved point-matching method with application to scattering from a periodic surface.

22 p2824 A73-41833

Simulator performance validation and improvement through recorded data.

[AIAA PAPER 73-938]

22 p2838 A73-41972

Development of an infrared scanning system for the empirical evaluation of aerodynamic heating.

22 p2853 A73-41985

A fixed point calibration procedure for precision platinum resistance thermometers.

22 p2857 A73-42026

Tape recording, off-line digitalization and time series analysis of dynamic field measurement analog data for computerized power spectral density calculation

22 p2859 A73-42197

Application of a computer image recognition technique to the determination of phase diagram types for binary metal systems

22 p2877 A73-42457

Computerized analysis using sparse matrices/matrices with large number of zero elements/describing sorting, reordering and inverse computing techniques and linear equations solution methods

22 p2922 A73-42480

Approximation for maximum centerline heating on lifting entry vehicles.

22 p2796 A73-42627

Objective method for classification of multicellular activity patterns of neuron population in the cerebrum of man

22 p2807 A73-42656

Statistical treatment of evoked cerebral potentials during experiments on a Dnepri-1 computer

22 p2814 A73-42657

Computer acquisition of multiunit nerve-spike signals.

22 p2815 A73-42671

Russian book on eclipsing binary stars covering limb darkening law, photometric eclipsing phases, computer applications and models

22 p2911 A73-42747

Papers on computer techniques for electromagnetic radiation and scattering problems via integral equation formulation covering iterative and variational methods and antenna patterns

22 p2827 A73-42839

Computer techniques for scatterer shape from far field data/inverse scattering/ via remote sensing, with application to antenna radiation pattern synthesis and holography

22 p2828 A73-42845

Computer analysis of clamped-clamped and clamped-supported cylindrical shells.

22 p2927 A73-42995

Digital filter bank with integrated FFT computer

23 p2956 A73-43326

National Radio Astronomy Observatory interferometer system with rotating head video tape recording and computerized sampled data processing equipment for use with radio telescope

23 p2980 A73-43358

Computer controlled steerable array of multiple conical log spiral antennas for solar and discrete radio source studies

23 p2965 A73-43363

Multifrequency meter wave Culgoora radioheliograph design, picture format and operation, using automatic switching and track-scan computer

23 p2958 A73-43372

Multidimensional scaling methods and data visualization [Review/]

23 p2949 A73-43578

Improvement of the electron optics of X-ray image-intensifiers.

23 p2982 A73-43678

Hybrid computer laboratory construction, organization and operation principles, including computer selection and personnel requirements

23 p2956 A73-43950

The 'multiplexing' CTDS method of solving certain second-order partial differential equations on a hybrid computer system 23 p2956 A73-43951

Expanding the capability of a laboratory ultrasonic testing facility. 23 p2966 A73-44168

Automatic integration algorithm for computer calculation of definite integral within specified tolerance, discussing computation failures and algorithm reliability 23 p2957 A73-44390

Numerical realization of a possible way of determining the tensor of elastic constants in an anisotropic body 24 p3144 A73-44506

The role of computers in the development of numerical weather prediction. 24 p3108 A73-45085

National Center for Atmospheric Research collected synoptic meteorological data from earth surface, upper air and satellite observations for handling on computers 24 p3075 A73-45087

Computerized structural analysis by finite element method, discussing round-off and truncation errors with emphasis on inherited error effects minimization 24 p3150 A73-45233

COMPUTERIZED CONTROL

U NUMERICAL CONTROL

COMPUTERIZED DESIGN

The radiation efficiency of a dipole antenna located above an imperfectly conducting ground. 01 p0015 A73-10185

Space booster control system computerized design algorithm for forward loop compensation filter selection based on minimization of penalty function of stability margin violations 01 p0021 A73-11516

Multivariate analysis applied to aircraft optimization - Some effects of research advances on the design of future subsonic transport aircraft. [DGLR PAPER 72-093] 02 p0130 A73-11661

Computer programs for air cooled gas turbine engine design and performance prediction, noting aerodynamic effect of turbine coolant 02 p0129 A73-12848

Computer-aided design of externally pressurized bearings. 03 p0311 A73-13202

Possibilities of rationalizing the design of flow-through turbomachine components 03 p0353 A73-13239

A procedure for optimum rocket engine system/turbopump integration. [AIAA PAPER 72-1183] 03 p0357 A73-13477

An approximate algorithm for the reanalysis of structures by the finite element method. 03 p0391 A73-13676

Computerized multiple level substructuring analysis. 03 p0392 A73-13690

Computer-aided design and graphics applied to the study of inductor-energy-storage dc-to-dc electronic power converters. 03 p0252 A73-13931

Computerized design and algorithm for linear and nonlinear regulators by mathematical programming approach involving vector determination for objective function minimization 03 p0286 A73-14480

Computer-aided design of high-frequency transistor amplifiers. 04 p0427 A73-15053

Computerized synthesis of wideband series stabilized tunnel diode amplifier based on distributed constant elements 05 p0555 A73-16061

Book - Non-linear structures: Matrix methods of analysis and design by computers. 05 p0632 A73-16358

Computer programs for operator performance time prediction and workspace design 05 p0544 A73-16721

Application of the graphic flight path design program /FPDP/ for fast interactive trajectory design. [AIAA PAPER 73-113] 05 p0619 A73-16871

Computer aided shrouded propeller design. [AIAA PAPER 73-54] 06 p0644 A73-17630

An automated method for determining the flutter velocity and the matched point. [AIAA PAPER 73-195] 06 p0645 A73-17656

Fault insertion techniques and models for digital logic simulation. 06 p0671 A73-18062

A program for the analysis and design of general dynamic mechanical systems. 06 p0671 A73-18063

The selection and design of electro-optical instruments for outer planet exploration. 06 p0695 A73-18320

Analysis of antenna structures assembled from arbitrarily located straight wires. 06 p0668 A73-18441

Design of dynamic programming feedback controllers for multivariable time-invariant linear systems. 06 p0680 A73-18517

Computer analysis of latching phase shifters in rectangular waveguide. 06 p0678 A73-18743

A computer-aided design procedure for flyback step-up dc-to-dc converters. [IEEE PAPER 4,4] 07 p0779 A73-19361

Precision design of millimeter-wave band-pass filter. 07 p0799 A73-19371

High-Q toroidal cavities for high frequency klystrons. 07 p0803 A73-20550

Nonlinear programming in design of control systems with specified handling qualities. 07 p0777 A73-20588

Computer optimisation of double-drift-region IM-PATT diodes. 08 p0947 A73-21433

Construction of analytical formulas for functions of linear circuits by means of engineering-application digital computers 08 p0941 A73-21552

Parallel algorithms for plotting profiles, projections, and cross sections with the aid of receptor matrices on a digital computer 08 p0941 A73-21588

Computer systems configurations for design and engineering, considering graphic and conversational capability and cost and time reduction 09 p1168 A73-21949

Realization of two-dimensional state space digital filters. 09 p1068 A73-22398

Optimization of system reliability using a parametric approach. 09 p1112 A73-22646

Topological design of thin-film resistors with the aid of a digital computer 09 p1066 A73-23119

Computerized method for designing plate type sounding rocket fins. [AIAA PAPER 73-285] 09 p1155 A73-23205

Computerized interactive graphic display systems for three dimensional shape design 10 p1222 A73-23523

The optimization of delay equalized comb-line filters. 10 p1193 A73-23609

Speed active multipole filter design with a flexible computer program that calculates the component values for optimum performance. 10 p1191 A73-23755

Digital simulation methodology for LSI computer design and technology assessment to assure competitive cost, schedule and implementation cycles in manufacturing 10 p1191 A73-23793

Optimization and design of the rear fuselage of the A 300 B aircraft structure. 10 p1288 A73-23799

A numerical algorithm to design multivariable low-pass equiripple filters. 10 p1202 A73-24600

Real time digital computer algorithm for linear and nonlinear electronic circuit modeling in state variable form for static and dynamic regimes 10 p1196 A73-24607

A photoelastic and finite-element investigation of a nonsymmetrical plug-hatch configuration. 10 p1293 A73-24721

Algorithmic design methodology, describing functional representation of suitable effect chains 11 p1371 A73-24994

Computerized optimal tube heat exchanger design, discussing programming for heat transfer surface area and operating point determination 11 p1448 A73-25102

Aircraft design philosophies and structural integrity considerations for reliability without major NDT and maintenance, proposing research program for future computerized design 11 p1433 A73-25128

Design of control and display panels using computer algorithms. 11 p1361 A73-25180

Iterative computer-aided design of optimum cascaded digital recursive filter, using unconstrained Fletcher-Powell algorithm for frequency domain synthesis 11 p1327 A73-25189

Military aircraft radome design technology developments in Sweden, discussing use of glass fiber reinforced plastics, manufacturing method, computerized optimization and measurement techniques 11 p1335 A73-25300

Automated structural synthesis using a reduced number of design coordinates. [AIAA PAPER 73-336] 11 p1436 A73-25476

A unified approach to the problem of optimization in the design of structures. [AIAA PAPER 73-337] 11 p1436 A73-25477

Taylor series algorithms for computerized structural design and reanalysis of modified structures, applying to aircraft fuselage midsection 11 p1436 A73-25478

Mathematical programming techniques of dimensionless index solutions for optimal structural design by iterative search on computer, applying to beam column steel structures 11 p1436 A73-25483

Computer programs for structural design optimization, discussing automated structural optimization program /ASOP/, component display analysis and stiffened panel programs [AIAA PAPER 73-345] 11 p1436 A73-25484

Synthesis of compression panels having non-uniform stiffener sections. [AIAA PAPER 73-347] 11 p1437 A73-25485

A synthesis procedure for mechanically fastened joints in advanced composite materials. [AIAA PAPER 73-348] 11 p1437 A73-25486

Computerized design of an outer planets spacecraft structure to survive the meteoroid environment. [AIAA PAPER 73-349] 11 p1430 A73-25487

Computer design of antenna reflectors. [AIAA PAPER 73-351] 11 p1437 A73-25489

Application of computer-aided aircraft design in a multidisciplinary environment. [AIAA PAPER 73-353] 11 p1304 A73-25490

Computer executive system for design automation file network creation and monitoring to permit input/output operations, storage information updating and display [AIAA PAPER 73-355] 11 p1334 A73-25492

An automated procedure for computing flutter eigenvalues. [AIAA PAPER 73-393] 11 p1440 A73-25522

Automating the design process - Progress, problems, prospects, potential. [AIAA PAPER 73-410] 11 p1373 A73-25538

An electrochemical cell equivalent circuit for storage battery/power system calculations by digital computer. 11 p1309 A73-25985

Vapor chamber fin radiator study for the potassium Rankine cycle. 11 p1451 A73-25991

An integrated radiation physics computer code system. 11 p1334 A73-25997

Computerized design of electromagnetic systems in electric power conversion and electromechanical devices, noting mathematical models for electromagnetic field calculations 11 p1313 A73-26114

Automation of thermal design calculations for electrical machines 11 p1313 A73-26115

Computer technology aided machine design automation and structural synthesis by coded information table formulation and conversion, discussing algorithm construction 12 p1502 A73-26784

Arched and spherical antenna arrays synthesis for given vectorial radiation patterns by numerical solution via algorithm using eigenfunctions 12 p1479 A73-27229

Design optimization of prestressed concrete spans for high speed ground transportation. 12 p1554 A73-27735

Compressive buckling analysis and design of stiffened flat plates with multilayered composite reinforcement. 12 p1554 A73-27736

Digital computer aided control systems design, discussing components dynamic behavior mathematical modeling and control processes simulation 12 p1476 A73-27872

Russian book - Design of structural elements with the use of electronic digital computers. 12 p1556 A73-27923

Numerical Master Geometry computer programs for smooth surface shape mathematical representation, manipulation, definition and interrogation in design and production 13 p1623 A73-28053

The evolution and application of lofting techniques at Hawker Siddeley Aviation. 13 p1623 A73-28054

A computer program for filter design having arbitrary magnitude specifications in the frequency domain. 13 p1587 A73-28085

Computer graphics applied to production structural analysis. 13 p1693 A73-28245

Use of approximating polynomials in the determination of correction parameters for pulsed amplifiers. 13 p1591 A73-28732

Computer aided design with finite element method for two and three dimensional curved line and surface approximation and representation on interactive graphic console 13 p1587 A73-28850

Design and simulation of an aircraft brake using a digital computer. 13 p1588 A73-29385

Use of a computer to design surveys made by the stereotopographic method

13 p1621 A73-29416

On numerical convergence of moment solutions of moderately thick wire antennas using sinusoidal basis functions.

14 p1734 A73-30216

Comparison between the peak sidelobe of the random array and algorithmically designed aperiodic arrays.

14 p1734 A73-30217

Computer evaluation of large low-frequency antennas.

14 p1735 A73-30227

Gain-bandwidth limitations of microwave transistor amplifiers.

14 p1735 A73-30247

Parachutes computer aided design and performance analysis system development and operation, presenting information storage and retrieval tasks mechanics [AIAA PAPER 73-484]

15 p1829 A73-31466

Several computerized techniques to aid in the design and optimization of parachute deceleration and aerial-delivery systems.

[AIAA PAPER 73-488]

15 p1829 A73-31470

Automatic nodal point renumbering algorithm for interconnectivity matrix bandwidth reduction in computer aided structural analysis and design

15 p1848 A73-32029

Iterative finite element method for minimum weight structural design with respect to buckling constraints applied to beam and orthogonal frame design

16 p2082 A73-33908

Revised calculations of the NACA 6-series of low drag aerofoils.

17 p2094 A73-34536

Computer aided parametric analysis for general aviation aircraft.

[SAE PAPER 730332]

17 p2130 A73-34685

A comparison of structural test results with predictions of finite element analysis.

[SAE PAPER 730340]

17 p2102 A73-34691

On the optimum design of tapered waveguide transitions.

17 p2136 A73-34970

The integration of NASTRAN into helicopter airframe design/analysis.

[AHS PREPRINT 780]

17 p2106 A73-35093

Intrasystem electromagnetic compatibility analysis program.

17 p2131 A73-35251

Log-periodic dipole arrays - A numerical analysis.

17 p2141 A73-35367

Book - Graph theory in modern engineering: Computer aided design, control, optimization, reliability analysis.

17 p2132 A73-35600

Planar aperture antenna synthesis for main beam and complex sidelobe patterns by iterative correction with convergence, using computer program

17 p2142 A73-35648

A simulation study for the design of an air terminal building.

17 p2149 A73-35826

A finite-element method for calculating aerodynamic coefficients of a subsonic airplane.

18 p2265 A73-36394

Hybrid computer technique for desensitized optimal design of system with uncertain plant parameters, with application to Saturn 5 Apollo attitude control system design

18 p2291 A73-36426

Computerized design for moving-base three man aircraft flight simulator servocontrol, considering disturbance torques, damping ratios, natural frequencies, load acceleration and smoothness

18 p2296 A73-36833

Symposium on Optimisation in Aircraft Design, London, England, November 15, 1972, Proceedings.

19 p2378 A73-37405

Simplex method for linear programming for computerized design global optimization problems involving large numbers of equations and variables

19 p2407 A73-37406

Military aircraft structure computerized design optimization procedures based on local optimum and stiffness requirements

19 p2495 A73-37407

The optimisation of wing design.

19 p2495 A73-37408

A parameter optimisation technique applied to the design of flight control systems.

19 p2378 A73-37409

Design-build-fly, an effective method to teach undergraduate aerospace vehicle design.

[AIAA PAPER 73-785]

19 p2505 A73-37455

Computer aided design-drafting/CADD/ - Engineering/manufacturing tool.

[AIAA PAPER 73-793]

19 p2407 A73-37460

Managerial implications of computerized aircraft design synthesis.

[AIAA PAPER 73-799]

19 p2379 A73-37462

National Symposium on Computerized Structural Analysis and Design, George Washington University, Washington, D.C., March 27-29, 1972, Proceedings.

19 p2496 A73-37476

Algorithm for optimal material selection by seeking tradeoff between conflicting multifunctional structural design objectives

19 p2496 A73-37477

Structural optimization by methods of feasible directions.

19 p2496 A73-37478

Applications of a symbolic algebra manipulation language for composite structures analysis.

19 p2496 A73-37482

Automated structural design and analysis of advanced composite wing models.

19 p2497 A73-37486

A computer-aided design procedure to approximate aircraft area curve shapes.

[SAE PAPER 982]

19 p2385 A73-37888

Computerized optimization of interrelated airframe/engine design parameters against variable criteria to satisfy performance constraints in air superiority fighter design

[AIAA PAPER 73-800]

19 p2388 A73-38370

A computer study of the design and operating performance of a photovoltaic cell for thermophotovoltaic energy conversion applications.

19 p2391 A73-38405

International Symposium on Circuit Theory, Toronto, Canada, April 9-11, 1973, Proceedings.

19 p2411 A73-38532

Book - RCA COS/MOS technology.

20 p2533 A73-38653

Design of the 14/11 GHz repeater for the European Orbital Test Satellite.

20 p2525 A73-38745

An organized approach to the digital autopilot design problem.

[AIAA PAPER 73-848]

20 p2585 A73-38787

A nonlinear programming algorithm for the automated design and optimization of flexible space vehicle autopilots.

[AIAA PAPER 73-892]

20 p2588 A73-38828

A method of computer design of microelectronic equipment

20 p2534 A73-38852

Mathematical equipment of a system of automatic designing of components of logic-type semiconductor integrated circuits

21 p2660 A73-40015

Computer-aided design and graphics applied to the study of inductor-energy-storage dc-to-dc electronic power converters.

21 p2635 A73-40340

Linear Kalman filter triangular square root formulation guaranteeing positive covariance matrix, computation and time savings and core storage requirement standardization

21 p2736 A73-40422

Computerized synthesis of optimal fault-diagnosable logical circuits capable of detecting and repairing faulty modules for circuit reliability and availability improvements

21 p2669 A73-40687

A photoneutron antimony-124-beryllium system for fissile materials assay.

21 p2738 A73-40769

Russian book - Matrix methods of calculating the strength of low-aspect-ratio wings.

21 p2785 A73-40799

CAD for realization of an impurity distribution in a semiconductor.

21 p2753 A73-41095

The use of logic simulation in the design of a large computer system.

21 p2658 A73-41210

Automated systems for designing electronic circuits

21 p2665 A73-41304

An automated system for designing integrated circuits

21 p2666 A73-41305

Algorithm for deriving the equilibrium equations of an electric circuit on the basis of logic rules

21 p2670 A73-41307

Computer simulation of complex electronic circuit equations derived from subcircuit equations combined with coupling equations, noting topological modification ease and run time savings

21 p2671 A73-41309

Means of improving the effectiveness of designing nonlinear electronic circuits on a digital computer by the method of nodal potentials

21 p2666 A73-41310

An effective algorithm for optimizing electronic circuits

21 p2671 A73-41312

Tapered corrugated waveguide low-pass filters.

21 p2666 A73-41427

Journal bearings computerized design optimization by geometric programming with volume, dimensions, torque and horsepower absorption, shaft strength, speed, load, pressure and Sommerfeld number as constraints

21 p2708 A73-41668

The use of analytic surfaces for the design of centrifugal impellers by computer graphics.

22 p2900 A73-42477

Computer-aided design of airport system plans.

[ASCE PREPRINT 2058]

22 p2839 A73-42867

Oil hydraulic fluidic amplifier mathematical model and computerized design for power consumption optimization at high pressures, testing performance dependence on viscosity

23 p2942 A73-43405

Theoretical and experimental investigation of fluidic signal and noise filters with application to DC and AC fluidic systems.

23 p2944 A73-43418

Digital-computer aided analysis and synthesis of specialized functional diode converter circuits

23 p2959 A73-43579

Small signal duality theory of linear optoelectronic circuits with optical coupling for equivalent circuit computerized design and analysis

23 p2963 A73-43615

A new approach to optimal design of elastic structures.

23 p3042 A73-43798

Designing with microprocessors instead of wired logic asks more of designers.

23 p2956 A73-44122

Finite element analysis on L-L type vibration energy concentrator/divider considering its design.

23 p2961 A73-44138

Representation of the computer-aided design process by a network of decision tables.

24 p3070 A73-45230

Algorithmic and computational aspects of the use of optimization methods in engineering design.

24 p3070 A73-45235

Optimization of fiber reinforced composite structures.

24 p3151 A73-45304

COMPUTERIZED SIMULATION

NT ANALOG SIMULATION

NT DIGITAL SIMULATION

Automation of solutions to mathematical physics problems described by partial differential equations

01 p0019 A73-10100

An efficient, one-level, primitive-equation spectral model.

01 p0072 A73-10248

A detailed radiation model for climate studies - Comparisons with a general circulation model radiation subroutine.

01 p0039 A73-10393

Simulation program for satellite operation status prediction in space environment.

01 p0110 A73-11146

Comparison of Kalman filter and stepwise methods for real time orbit determination.

01 p0105 A73-11187

Rocket payload designs simulated by Monte Carlo method for aerodynamic properties during D region composition measurements

02 p0156 A73-11740

Multistep three-parameter algorithm for spacecraft stabilization on an atmospheric reentry trajectory

02 p0229 A73-12451

The dynamical evolution of a stellar cluster with initial subclustering.

02 p0222 A73-12709

Computerized operational simulation for space shuttle program in terms of flight units, launch rate, success probabilities and costs

03 p0381 A73-13298

Numerical model of transient behavior of radiation dominated shock calculated for neutron star core of imploding supernovae

03 p0372 A73-13354

Three-degree-of-freedom motions of a slender asymmetric cone in a hypersonic wind tunnel.

03 p0287 A73-13494

Computer methods for simulation of multidimensional, nonlinear, subsonic, incompressible flow.

[ASME PAPER 72-HT-61]

03 p0294 A73-13546

Far-field simulation of circular antenna arrays on the analog/hybrid computer

03 p0277 A73-13985

Evaluation and reduction on the electromagnetic fields associated with a solar array.

03 p0256 A73-14233

Static and dynamic behavior of spherical hydrostatic bearings - Theory and experiments.

[ASME PAPER 72-LUB-35]

03 p0315 A73-14344

Transient analysis of an electronically tunable dye laser. I - Simulation study.

03 p0320 A73-14457

Monitoring and modeling of airport air pollution.

04 p0432 A73-14891

Failure diagnostics in mathematical simulators of automatic control systems.

04 p0430 A73-15209

Low error rate transmission by iterative probabilistic threshold decoding, noting performance improvement over sequential and low density parity check code techniques from simulation

04 p0425 A73-15399

Effects of hardlimiting on bandlimited transmissions with conventional and offset QPSK modulation.

04 p0420 A73-15412

A model of signal detection for the instrument landing system.

04 p0474 A73-15441

Color image quantization error assessment from noninfrared bit assignment determination for several coordinate systems by color shift comparison, using computer simulation

04 p0449 A73-15444

System time domain simulation computer aided analysis program for communication systems, presenting mathematical and functional models

04 p0425 A73-15459

Effect of H2 pressure on pulsed H2 + F2 laser - Experiment and theory.

05 p0583 A73-16043

Implications of a quadratic stream definition in radiative transfer theory.

05 p0592 A73-16196

ATC research - Simulating Arrival/Tower communications.

05 p0595 A73-16620

Smoke and fire propagation in compartment spaces. [WSCI PAPER 72-32]

05 p0639 A73-16683

The employment of a spoken language computer applied to an air traffic control task.

05 p0544 A73-16728

A computerized technique for mission profile design analysis.

05 p0629 A73-16872

Interactive real time simulation for scheduling and monitoring of STOL aircraft in the terminal area.

05 p0535 A73-16909

The determination of free-body responses of a structure from constrained test data.

05 p0635 A73-16928

The use of a simulator in a synthetic aperture radar data processing tradeoff study.

05 p0554 A73-17149

Assessment of ISS topside sounder system by computer simulation.

05 p0579 A73-17168

Computerized Monte Carlo simulation with program flexibility for mass distribution in particle collision processes, applying to accreting and fragmenting systems including asteroid belt

05 p0624 A73-17316

Problems related to the measurement and evaluation of ATC/CAS interaction.

06 p0721 A73-17600

Arrested landing studies for STOL aircraft.

06 p0647 A73-17627

Solar electric space mission risk analysis, describing computerized multistage failure process simulation procedure with application to Encke comet rendezvous mission

06 p0748 A73-17660

Computerized mathematical models of two- and three-dimensional turbulent flow combustion, considering temperature and concentration fluctuations, particle size, NO formation and radiative transfer

06 p0767 A73-17727

Digital and hybrid computational aspects of the discrete representation theorem of nonlinear estimation.

06 p0670 A73-17803

Fall Joint Computer Conference, Anaheim, Calif., December 5-7, 1972, Proceedings. Parts 1 & 2.

06 p0670 A73-18057

Adaptive maximum-likelihood sequence estimation for digital signaling in the presence of intersymbol interference.

06 p0665 A73-18144

Monte Carlo computer technique for one-dimensional random media.

06 p0665 A73-18188

Low power thermoelectric cascade for cooling substrates to 145 K, discussing materials electrical and thermal properties, design optimization, computerized performance simulation, fabrication and testing

06 p0683 A73-18316

Computer simulation model of field independent trapping effects on slow Gunn domains in gallium arsenide, noting double symmetry electron-ion density distributions

06 p0737 A73-18368

Monte Carlo simulation for electron diffusion in Cd Te, noting effects of applied electric field near threshold value for negative differential mobility

06 p0739 A73-18799

Spline function interpolation in interactive hemodynamic simulation.

06 p0660 A73-18889

Descriptions and plans in an interactive robot simulation system.

06 p0672 A73-18891

A mathematical model of the opposed-jet diffusion flame - Effect of an electric field on concentration and temperature profiles.

07 p0918 A73-19388

Electron cyclotron off-resonance heating rate in hot electron plasmas, comparing numerical calculation in terms of harmonic resonance with computerized simulation

07 p0856 A73-19519

Computerized simulation for nonlinear evolution of whistler instabilities in anisotropic collisionless plasmas with various Maxwellian electron distributions

07 p0857 A73-19523

Theory and simulation of turbulent heating by the modified two-stream instability.

07 p0857 A73-19526

A kinetic model and computer simulation for a pulsed DF-CO2 chemical transfer laser.

07 p0835 A73-19632

The performance of a satellite-borne infrared target acquisition system.

07 p0824 A73-19946

Simulation of sequential decoding with phase-locked demodulation.

07 p0794 A73-20498

Digital computer studies of respiratory control.

07 p0787 A73-20577

System modeling and optimal design of a Mars-roving vehicle.

07 p0906 A73-20593

Majority logic detection scheme of differentially phase-modulated waves.

08 p0937 A73-20802

Systems analysis applied to a hybrid computer simulation of a missile reentering the atmosphere.

08 p0941 A73-20825

Computer simulation of semiconductor devices.

08 p0948 A73-21534

Performance comparison of suboptimal Kalman filters modeled for a continuous nonlinear system.

09 p1067 A73-22228

Computer simulations of the large signal characteristics of supercritical GaAs transferred electron amplifiers.

09 p1063 A73-22492

Analytical and computer simulation of two ion species RF heated magnetoplasmas response to driving electric fields near lower hybrid frequency, observing parametric instabilities

09 p1129 A73-22640

Computer simulation of ion heating by pulsed microwaves.

09 p1129 A73-22642

Computer simulation concept for a large solar array/battery power system.

09 p1060 A73-22803

Shuttle Orbiter fuel cell power system simulation, describing data management, programming and computational control

09 p1060 A73-22804

First order phase locked loop statistical transient behavior in presence of noise from differential equation numerical solution, noting correlation with computer simulation

09 p1036 A73-23404

The complex digital filter and its applications in digital signal processing.

09 p1058 A73-23425

Weaver modulator with digital filter for single sideband transmission in radio communication and telemetry, discussing FORTRAN simulation for cost, computation time and accuracy

09 p1186 A73-23499

Aircraft operations computerized simulation for commercial flight schedules evaluation and optimization, describing operational modeling and programming

10 p1203 A73-23685

Productivity estimates of the strategic airlift system by the use of simulation.

10 p1297 A73-23774

Statistical analysis and computer simulation of laser Doppler velocimeter systems.

10 p1217 A73-23997

On a method of adaptive control under conditions of great uncertainty.

10 p1199 A73-24036

Low-frequency parametric instabilities of magnetized plasmas with two ion species.

10 p1255 A73-24261

Computer simulation of two dimensional plasma diffusion via wave interactions descriptions by nonlinear differential equations, considering electric field and particle velocity correlations

10 p1255 A73-24266

On the normality and accuracy of simulated random processes.

10 p1292 A73-24395

Cylindrical metal projectile impact induced elastoplastic deformation, determining dynamic yield point by computer simulation of Taylor stress wave propagation model

10 p1292 A73-24529

Aircraft wake vortex avoidance systems with current locus detection and/or prediction capability, discussing design based on hazard assessment and computer simulation for performance

10 p1172 A73-24557

Computer simulation of HF frequency-selective fading and performance of the mode-averaging diversity combiner.

10 p1190 A73-24894

Simulation of random processes with the aid of piecewise linear transformations of unit interval

11 p1340 A73-25012

Numerical simulation and theory of plasma diffusion across magnetic field at thermal equilibrium, noting collective mode domination at moderate and high fields

11 p1403 A73-25257

Computerized large signal model of IMPATT diode, calculating output power and admittance as function of frequency and amplitude

11 p1336 A73-25320

Solar cell battery operational performance test equipment and computerized simulation programs for post-1975 satellite and space station systems integration and design

11 p1309 A73-25986

Code law rationalization based on Dole computer-generated planetary system with constant spacing ratio generated by random number sequence and accretion process closeness constraints

11 p1428 A73-26665

Computerized maritime sea level atmospheric pressure field analysis, using pressure and wind velocity data

12 p1519 A73-26802

The evolution of a computer program for obtaining optimum computer simulation solutions.

12 p1475 A73-27133

Book - Reliability concepts in engineering manufacture.

12 p1502 A73-27398

A cylindrical shell model of the NASA-MPE barium ion cloud experiment.

12 p1492 A73-27607

Formation and solution of the equations of state of electronic circuits

12 p1485 A73-27623

Formulation of time variant stiffness matrices due to changing joint properties.

12 p1555 A73-27737

VIEW - A distributed system for graphical analysis of large data bases.

12 p1476 A73-27824

Improved three-dimensional mapping of the electron density distribution of the solar corona.

12 p1536 A73-27843

Digital computer aided control systems design, discussing components dynamic behavior mathematical modeling and control processes simulation

12 p1476 A73-27872

Improvements in surface-acoustic-wave pulse-compression filters.

13 p1595 A73-28048

A comparison of holographic versus lens type acoustic image systems by computer simulation.

13 p1616 A73-28595

A flight control simulator - A computer system for the training of flight control personnel

13 p1598 A73-29100

Computer simulations of large-signal oscillation behavior of avalanche diodes.

13 p1594 A73-29235

Experimental data processing system for EUROCONTROL scale model semiautomatic digital route control system for operational conditions simulation

15 p1907 A73-31132

Automatic instrument systems for determining cloud amount.

15 p1874 A73-31319

Computer simulation of gas exchange in human lungs.

15 p1838 A73-31348

A simulative study of correlated error propagation in various finite-precision arithmetics.

15 p1899 A73-31350

Computerized six degree of freedom parachute deployment model for predicting entry vehicle-decelerator dynamic response to aerodynamic forces and physical property changes

15 p1827 A73-31446

Parachute-payload system performance prediction for cause and effect relationships by parametric sensitivity and regression analysis for optimal design with computer simulation

15 p1829 A73-31469

Digital correlator-computer-pattern recognition system for VLF phenomena investigation, discussing electromagnetic waves structure and spectrum analysis

15 p1845 A73-32234

Three-parameter multistep algorithms for stabilization of a spacecraft on the descent trajectory through the atmosphere.

15 p1944 A73-32601

Signal bandwidth consideration for electromagnetic compatibility specifications, comparing broad and narrow band measurements performance by computerized simulation

16 p1979 A73-33169

Flight simulation visual image innovations, including closed circuit television, motion pictures and computer generated imagery with wide angle presentation and day/night realizations

16 p1995 A73-33205

Bucket-brigade shift-register operation-exact correlation between experimental data and a computer model.

16 p1988 A73-33397

An adaptive estimation algorithm for time-varying bit synchronizers.

16 p1988 A73-33411

Winter simulation conference, San Francisco, Calif., January 17-19, 1973, Proceedings.

16 p1985 A73-33416

Probabilistic Monte Carlo computerized simulation of surface to air missile systems reaction time from aircraft attack in non-jamming environment and over flat terrain

16 p1985 A73-33418

Simulation in the design of automated air traffic control functions.

16 p2035 A73-33419

Theory and computer simulation of whistler turbulence and velocity space diffusion in the magnetospheric plasma.

16 p2003 A73-33439

The use of a hybrid computer in the optimization of gas turbine control parameters.

[ASME PAPER 73-GT-13]

16 p2047 A73-33491

Equipment life cycle costs dependence on acquisition decision making, discussing stochastic computer simulation of failure times, repairs, inventory replacement and personnel availability

16 p2089 A73-33655

Automated terminal area ATC operations under FAA ten year plan, investigating analytical model of pilot-aircraft control loop decision making by computer program

17 p2206 A73-34437

Dynamic behavior of light aircraft interaction with jet transport vortex on basis of accident records and computer simulation

[SAE PAPER 730296]

17 p2094 A73-34660

Transient temperature response of semiconductor devices under pulsed power operation.

17 p2135 A73-34728

Annual Simulation Symposium, 5th, Tampa, Fla., March 8-10, 1972, Record of Proceedings.

17 p2130 A73-34817

Simulation of a surface traffic control system for John F. Kennedy International Airport.

17 p2147 A73-34818

Visual scene simulation with computer generated images.

17 p2147 A73-34820

PLANET scheduling algorithms and their effect on availability.

17 p2130 A73-34822

A real-time simulator for image data systems.

17 p2147 A73-34903

Laser guided weapon system optical countermeasures /OCM/ vulnerability evaluation, discussing use of LED laser in computerized simulation at low cost

17 p2147 A73-35208

Solid state null tracking Doppler radar ground velocity sensor for supersonic weapon delivery aircraft precision bombing, discussing design and test with computer simulation

17 p2137 A73-35209

Applications of a model of the human visual system to pattern recognition problems.

17 p2116 A73-35242

Institute of Electrical and Electronics Engineers, International Convention and Exposition, New York, N.Y., March 26-30, 1973, Technical Papers.

17 p2140 A73-35299

Techniques for digital-microwave hybrid real-time radar simulation.

17 p2131 A73-35303

Review of some mathematical models of non-linear domain dynamics in bulk-effect semiconductors.

17 p2129 A73-35516

The engineering of large-scale systems.

17 p2258 A73-35573

Antenna array facility with small digital computer and multichannel tape recorder for real time simulation of radiation source movement through view field

17 p2149 A73-35755

Bayesian estimation of life parameters in the Weibull distribution.

17 p2204 A73-35810

The impact of launch vehicle reliability on the financial risks associated with multiple payload space functions.

[AIAA PAPER 73-591]

18 p2358 A73-36079

Simulation of gyroresonant electron-whistler interactions in the outer radiation belts.

18 p2347 A73-36296

Simulating the introduction of 747 aircraft into airport operations.

18 p2296 A73-36423

The application of simulation to mission planning for communications and data relay satellites.

18 p2291 A73-36424

A serial CSDT predictor-corrector technique for the hybrid computer solution of partial differential equations.

18 p2291 A73-36425

Modeling problems in air traffic control systems.

18 p2335 A73-36427

Summer Computer Simulation Conference, Montreal, Canada, July 17-19, 1973, Proceedings. Volumes 1 & 2.

18 p2291 A73-36826

Numerical methods based on very accurate approximation of partial derivatives.

18 p2330 A73-36828

Real-time, three-dimensional, visual scene generation with computer generated images.

18 p2291 A73-36831

Real-time hybrid hardware-in-the-loop simulation of a terminal homing missile.

18 p2291 A73-36834

A high-performance, aerodynamically-controlled, tactical missile hybrid 6-DOF simulation.

18 p2296 A73-36835

Computer simulation for time optimal or energy optimal attitude control of spin-stabilized spacecraft.

18 p2360 A73-36837

Computation of launch vehicle system requirements using hybrid computer.

18 p2360 A73-36838

Optimal feedback control and Kalman filter design via an interactive computing and visual display system.

18 p2295 A73-36839

A deterministic model of a well trained human operator performing compensatory tracking.

18 p2283 A73-36844

Hologram matrix and its application to a novel radar.

19 p2428 A73-37145

Numerical models of the circulation of the atmosphere of Venus.

19 p2485 A73-37657

A digital computer flight simulation of an ACLS vehicle.

19 p2383 A73-37705

Simulation of the ACLS during landing roll.

19 p2383 A73-37706

Numerical simulation of counterstreaming high Mach number plasma laminar interactions, using one dimensional model based on Vlasov equation

19 p2469 A73-37861

The prediction of pilot acceptance for a large aircraft.

19 p2453 A73-38073

Exploratory study of several advanced nuclear-MHD power plant systems.

19 p2454 A73-38313

Multihundred watt power supply with Si-Ge thermoelectric couples for Pu-238 source heat energy conversion into electric power, discussing computer model for performance projection

19 p2456 A73-38422

Adjacent-channel interference between unfiltered and filtered QPSK signals.

20 p2526 A73-38754

Orbital design strategy for domestic communication satellite systems.

20 p2527 A73-38761

Design and analysis of a practical on-line filter to process gyrocompass data.

[AIAA PAPER 73-841]

20 p2564 A73-38782

Assessment of fine stabilization problems for the LST.

[AIAA PAPER 73-881]

20 p2587 A73-38817

Magnetospheric implications of the nonlinear whistler instability obtained in a computer experiment.

20 p2553 A73-38961

Photon lateral distribution sensitivity to longitudinal development of electron cascade via computer simulations of optical Cerenkov emission from cosmic ray showers

20 p2603 A73-39704

A study of models of certain digital computer units with the aid of a digital computer

20 p2533 A73-39822

Aircraft ground station site evaluation based on disseminating time synchronization effectiveness, utilizing computer modeling for communication links and airspace population

21 p2734 A73-40033

A numerical analysis of some practical aspects of airborne urea seeding for warm fog dispersal at airports.

21 p2728 A73-40056

Probability distribution of electric fields in thermal and nonthermal plasmas.

21 p2744 A73-40216

Computerized simulation of radio telescope control for minimum rms error and system parameter optimization

21 p2672 A73-40551

Thermal response of microwave transistors under pulsed power operation.

21 p2663 A73-40774

One dimensional computer simulation model of spaced-receiver drift experiment with radio fading produced by reflections from perfectly reflecting ionosphere

21 p2684 A73-40783

Russian book on probabilistic computer simulation and statistical processing techniques covering linear algebra and partial differential equations, Markov chains, random numbers, automata, and analog modeling

21 p2659 A73-41432

Investigation of the nature of biological rhythm sensors by means of automatic networks

22 p2812 A73-41865

A computer for modeling and calculating technological dimensional circuits

22 p2829 A73-42365

Computer simulation of the acceleration of charged particles captured by plane electromagnetic waves

22 p2826 A73-42378

Nonlinear development and Fourier analysis of the whistler mode instability.

22 p2893 A73-42391

Analytical modeling of a spherical combustor including recirculation.

22 p2934 A73-42783

A computer model for three-dimensional flow in furnaces.

22 p2934 A73-42787

Use of simulation in airport planning and design.

[ASCE PREPRINT 2038]

22 p2839 A73-42865

GASP simulation of terminal air traffic system.

[ASCE PREPRINT 2059]

22 p2839 A73-42868

Computer simulation of light pulse propagation for communication through thick clouds.

22 p2828 A73-43156

Use of a digital computer for studying velocity judgements of radar targets.

23 p2948 A73-43213

Carrier-phase tracking-loop computer simulation and performance evaluation in high-speed SSB data transmission.

23 p2953 A73-43322

Dual lane runway configuration design and operational characteristics investigation by real time computer simulation for solution to airport capacity problem

[ASME PAPER 73-ICT-61]

23 p2966 A73-43496

Computerized simulation of isotropic three dimensional turbulence velocity field growth and energy decay based on Navier-Stokes equation numerical integration

23 p3001 A73-43588

Comparative studies of model reference adaptive control systems.

23 p2963 A73-43817

Absolute measurements and computed values for Martian irradiance between 10.5 and 12.5 microns.

24 p3127 A73-44394

Monte Carlo computer simulation of lunar regolith evolution, considering buffering regolith effect via computation for debris produced by crater

24 p3130 A73-44460

A variant of the Monte-Carlo method for solving the linear dynamics problems of a rarefied gas

24 p3076 A73-44660

Computerized simulation of plasma particle collisions, using electric dipole expansion method for grid charge density and electrostatic force determination with Fourier transformation

24 p3116 A73-45027

Numerical weather prediction and analysis in isentropic coordinates.

24 p3108 A73-45091

Consideration of lattice translations in computer studies of grain-boundary coincidence.

24 p3120 A73-45405

Current driven ion acoustic plasma instability based on ion orbit perturbation by turbulent waves, calculating angular spectrum for comparison with computerized simulation

24 p3118 A73-45463

Computerized simulation of electrostatic instabilities development in underdense plasmas during heating by high output lasers with frequencies above electron plasma frequency

24 p3118 A73-45466

Large-signal lumped modelling and characterization of an IMPATT diode.

24 p3073 A73-45478

COMPUTERS

NT AIRBORNE/SPACEBORNE COMPUTERS

NT ANALOG COMPUTERS

NT DIGITAL COMPUTERS

NT HYBRID COMPUTERS

NT IBM 1130 COMPUTER

NT MINICOMPUTERS

NT PARALLEL COMPUTERS

NT SEQUENTIAL COMPUTERS

Apparatus replicating and extending development work on real-time time-compressed radar observation processor and display system

05 p0576 A73-16714

Parallel processors and air traffic control automation.

19 p2408 A73-38465

COMSAT PROGRAM

Progress in commercial satellite communications.

03 p0381 A73-13200

High capacity, dual antenna earth station.

04 p0432 A73-15416

CONCAVITY

On quasi-concave and strictly quasi-concave functions on a convex set relative to one of its nonvacant subsets

21 p2727 A73-41023

CONCENTRATION [COMPOSITION]

NT ATMOSPHERIC MOISTURE
NT ATOM CONCENTRATION
NT CARBON DIOXIDE CONCENTRATION
NT MASCONS
NT METEOROID CONCENTRATION
NT MOISTURE CONTENT

Determination of chromatographic resolution for peaks of vast concentration differences.

01 p0014 A73-10225
Alloying profile measurer for epitaxial films

01 p0050 A73-10799
Gas concentration profiles in combustion gas sampling probes, using IR absorption technique

03 p0399 A73-14397
Continuous flow condensation nucleus counter

04 p0451 A73-15999
Temperature and concentration effects on heterodiffusion coefficient of diffusion welded Mo-W alloy rods

06 p0707 A73-17907
Effect of hydrostatic extrusion on the composition and properties of Nb3Sn compounds.

06 p0736 A73-18213
Difference between the principal element concentrations on the surface and in the volume of lunar regolith particles

07 p0876 A73-19474
Distribution coefficients and solubility curves of certain rare-earth elements in GaAs

12 p1531 A73-27194
Investigation of interdiffusion in the nickel-tungsten and palladium-tungsten systems

14 p1764 A73-30864
Application of a cluster component technique in the interpretation of concentration dependences of the properties of binary metal alloys and anion-substituted spinel solid solutions

15 p1923 A73-31205
Young modulus of elasticity measurement in alloys of Fe with Cr, W and Mo, examining concentration dependence at 20 to 500 C

17 p2187 A73-34334
Mo-W alloys mechanical characteristics dependence on temperature and W content

19 p2439 A73-37265
On the possibility of measuring gas concentrations by stimulated anti-Stokes scattering.

21 p2699 A73-40458
Opto-thermal gas concentration detector operation by measuring temperature variations caused by chopped laser beam in sample cell, using pyroelectric material as temperature sensor

21 p2701 A73-40691
Ti, Al, W and Mo concentrations effect on heat resistance of precipitation hardened Ni-based alloys

21 p2720 A73-41035
Solubilization and accumulation of copper from elementary surfaces by Penicillium notatum.

21 p2648 A73-41217
Concentration curves and phase diagram plotted for Nb-Zr system diffusion layers during annealing at 700 to 1700 C

23 p2991 A73-43649

CONCENTRATORS

Computer communication networks with programmable concentrators for combining multiple terminals, discussing structure, message handling and transmission, routing and reliability

05 p0551 A73-16805
Finite element analysis on L-L type vibration energy concentrator/divider considering its design.

23 p2961 A73-44138
A method for studying the radiant flux distribution in the circumfocal area of a concentrator with the aid of an asymptotic calorimeter

24 p3058 A73-45253

CONCENTRIC CYLINDERS

Dipole antenna coaxially mounted on a conducting cylinder.

06 p0666 A73-18189
Acoustic radiation from two concentric cylindrical shells.

07 p0851 A73-19958
Natural convection in annular horizontal space

08 p1024 A73-21498
Heat transfer in horizontal annular air gaps at small Grashof numbers

09 p1167 A73-23108
A note on the unsteady motion of a viscous conducting liquid between two porous concentric circular cylinders acted on by a radial magnetic field.

11 p1404 A73-25368
Heat transfer law for free convection in cylindrical and spherical interlayers

11 p1450 A73-25726
Experimental determination of the integral radiative capacity of nickel

11 p1398 A73-25739
Motion of a conducting gas with variable properties between rotating cylinders

12 p1487 A73-27798
Instability of density-stratified incompressible inviscid rotary Couette flow between corotating coaxial vertical cylinders due to gravitational effects

13 p1600 A73-28439

The contact problem of two coaxial cylindrical shells.

14 p1813 A73-30663
Hydraulic impact in coaxial cylindrical tubes

15 p1860 A73-31046
Stability of a viscous fluid between rotating cylinders with axial flow and pressure gradient round the cylinders.

16 p2000 A73-33312
Experimental evidence of a couple-stress effect.

17 p2241 A73-34200
Leakage and frictional characteristics of turbulent helical flow in fine clearance.

17 p2152 A73-35001
The Taylor vortex regime in the flow between eccentric rotating cylinders.

17 p2181 A73-35391
Note regarding the propagation of electromagnetic fields through slots in cylinders.

19 p2403 A73-37273
Experimental study of rotational MHD Couette flow in a coplanar field

21 p2747 A73-40886

CONCORDE AIRCRAFT

Evaluation of the method of characteristics applied to a pressure transient analysis of the B.A.C./S.N.I.A.S. Concorde refueling system.

02 p0133 A73-12645
Development of the Olympus turbojet to meet supersonic civil transport requirements.

03 p0359 A73-14131
Radiation problems of supersonic flight - The operators' viewpoint.

05 p0542 A73-16624
Technology and operation of Olympus engine cycle on Concorde aircraft, discussing chemical and noise pollution and economic factors

05 p0536 A73-17190
Supersonic transportation inauguration by Concorde, discussing technological, economic and environmental aspects

06 p0646 A73-17609
Solar flare frequency and associated physical phenomena diversity, discussing earth atmosphere protective effects and impact on Concorde flights

07 p0784 A73-19210
Cosmic radiation and research carried out on board the 001 prototype Concorde

07 p0784 A73-19211
Technology and operation of Olympus engine cycle on Concorde aircraft, discussing chemical and noise pollution and economic factors

08 p0996 A73-21687
Varying-temperature test installation for the interior design of the Concorde

11 p1342 A73-25103
Seismic measurement data from Cornish cottage during Concorde sonic boom flight, using moving coil geophones

11 p1306 A73-26292
Geomagnetic latitude variation of cosmic radiation rates measured on board Concorde SST prototypes, investigating solar flares

11 p1324 A73-26588
Aircraft design and reliability analysis method based on accidents occurrence investigation by Franco-British airworthiness authorities, noting applicability to Concorde aircraft

11 p1306 A73-26589
Concorde Olympus 593 axial flow turbojet engine design, detailing variable geometry intake and exhaust nozzles, noise abatement, combustion chamber, gearing and fuel system

13 p1669 A73-28156
ATC system requirements for Concorde transoceanic flight operations, considering track allocation, computer system and programming

13 p1656 A73-28178
Epoxy adhesive bonding of Concorde light alloy sandwich structure elevons, discussing surface treatment, polymerization and ultrasonic testing

13 p1623 A73-28468
Concorde wing and fuselage aerodynamic design modifications for operational efficiency optimization from wind tunnel tests and theoretical computations

14 p1712 A73-30926
Concorde cockpit windows design modifications for weight reduction and reliability optimization, discussing transparencies and crew seat movement

14 p1712 A73-30928
Electronic safety test replaces radioactive test source.

14 p1712 A73-30928
Concorde emergency power supply, oxygen and escape systems design and operational features

14 p1713 A73-30929
Concorde engine noise reduction at takeoff, initial climb and landing, discussing noise sources research and exhaust system nozzle modifications

14 p1785 A73-30930
Concorde engine monitoring instrumentation, discussing start cycle, temperature sensors and indicators and nozzle position indicators

14 p1754 A73-30931

Hardware integration and improved operation of the flight control system.

14 p1713 A73-30932
Concorde air conditioning, discussing system modifications for production aircraft concerning interconnection of engine air bleeds of adjacent port and starboard groups

14 p1713 A73-30933
Electronic systems as piloting aids in Concorde SST, discussing flight controls, trim computer, autostabilizer, autopilot and automatic engine control

15 p1830 A73-32474
System of electric control of surveillance of the control surfaces of the Concorde

15 p1830 A73-32475
Up-rating the fuel system flow capacity with high rotational speed.

16 p2046 A73-32922
Concorde aircraft fuel system and component valves design for long term service reliability and ease of maintenance, discussing refueling, fuel jettisoning and feed controls

16 p2046 A73-32923
Preventing the shut-off punkah louvre from jamming.

16 p1970 A73-32925
Concorde aircraft design, testing and projected environmental impact, discussing flight tests, sonic booms, atmospheric pollution, ATC problems and fueling

16 p1968 A73-33182
The Concorde manufacturing consortium - An exercise in international engineering collaboration.

17 p2257 A73-34698
Concorde aircraft introduction into airline network, discussing time gain over various routes, operating costs, passenger service, departure and arrival problems, maintenance, etc

17 p2102 A73-34699
Cosmic rays airborne dosimetry from Concorde aircraft, noting passenger and crew radiobiological hazards at supersonic flight altitudes

18 p2348 A73-36908
Geophysical effects of Concorde sonic boom.

20 p2509 A73-39624
Nitrogen oxides, nuclear weapon testing, Concorde and stratospheric ozone.

21 p2686 A73-41076
Sonic bang investigations associated with the Concorde's test flying.

21 p2635 A73-41174

CONCRETES

Calculations of the transport of neutrons and secondary gamma rays through concrete for incident neutrons in the energy range 15 to 75 MeV.

08 p0987 A73-21528
Design optimization of prestressed concrete spans for high speed ground transportation.

12 p1554 A73-27735

CONDENSATES

Analytical method of gasdynamic semibounded-space parameter computation allowing for velocity profile inhomogeneity and turbulent combustion of condensed systems

01 p0121 A73-10619
Condensate droplets heat conductivity as function of drop geometry and vapor mass transport interaction with interior heat conduction, using finite difference method

06 p0768 A73-17920
Adsorption characteristics of condensed Ar, C2H6, NH3 and CO2 layers with respect to cryopumping.

07 p0922 A73-20413
Application of the method of matched asymptotic expansions to calculate the steady-state thermal propagation of an exothermic reaction front in a condensed medium

09 p1167 A73-22616
High-temperature condensates in chondrites and the environment in which they formed.

10 p1278 A73-24109
The mechanism of catalyzer action on the burning of condensed systems

13 p1669 A73-28974
Regularities in the burning of condensed systems within a field of mass forces at moderate pressures

13 p1706 A73-28975
Asymptotic analysis of the steady propagation of a successive two-stage exothermal reaction front in a condensed medium

13 p1707 A73-29166
Allende carbonaceous chondrite Ca-Al rich inclusion refractory trace metals condensation temperature calculation, indicating high temperature primitive solar nebula condensates

13 p1684 A73-29176
Investigation of the molecular composition of the vapors and the structure of the condensate during the evaporation of arsenic chalcogenides by laser radiation

19 p2437 A73-37957
Formation of a pseudoliquidified layer during combustion of condensed systems with solid nonagglomerating additives in a field of mass forces

24 p3121 A73-44705

CONDENSATION

One-dimensional electrohydrodynamic flows with a variable mobility coefficient - Evaporation and condensation discontinuities

01 p0077 A73-10954

Periodic nozzle flow with heat addition.

[AD-758555] 08 p1025 A73-21669

One-dimensional electrohydrodynamic flows with variable mobility coefficient, evaporation and condensation jumps.

12 p1524 A73-27530

Lunar composition and origin model based on early condensation processes in solar nebula

12 p1542 A73-27546

Laboratory modeling of 'vaporization-condensation and spilling' type processes taking place on the lunar surface

13 p1672 A73-28118

Growth rate calculation for hygroscopic condensation nuclei in the presence and absence of a monolayer of a surface-active substance

13 p1654 A73-28880

A shock tube study on condensation kinetics.

21 p2792 A73-41143

Water condensation coefficient for 3-micron radius droplets, noting expected error confirmation with standard deviation in experiment

22 p2883 A73-42548

CONDENSATION PUMPS

The VAK-2 unit with heated condenser pumps for obtaining a vacuum better than 0.1 mm Hg

23 p2966 A73-43672

CONDENSATION TRAILS

U CONTRAILS

CONDENSER RADIATORS

U CONDENSERS [LIQUIFIERS]

U HEAT RADIATORS

CONDENSERS [LIQUIFIERS]

Shell-and-coil condenser for packed air conditioners, testing heat transfer coefficients relationship to Reynolds number, heat flux and condensed refrigerant level

05 p0638 A73-16220

The design of components for an advanced Rankine cycle test facility.

11 p1344 A73-25995

Development of a direct condensing radiator for use in a spacecraft vapor compression refrigeration system.

[ASME PAPER 73-ENAS-5] 19 p2493 A73-37967

CONDENSING

NT FILM CONDENSATION

Ethanol condensation by homogeneous nucleation and growth of liquid droplets in steady state supersonic nozzle flow of ethanol-air and ethanol-nitrogen mixtures

02 p0153 A73-12051

Phase transition effects at the collecting droplet surface on the capture coefficient magnitude

07 p0922 A73-20418

Two zone model of multizone condensed system combustion, showing front velocity dependence on leading heat zone and dispersion depth

10 p1294 A73-23589

Critique of Anderson hypothesis of moon origin by condensation of material off median plane of initial solar nebula

11 p1428 A73-26664

Experimental investigation of heat and mass transfer in the condensation of vapor from gas-vapor mixtures under viscous and viscous-gravitational flow conditions

12 p1558 A73-27315

Theory of cyclogenesis, taking into account condensation

13 p1653 A73-28744

Chemical fractionations in meteorites. VII - Cosmethermometry and cosmochemistry.

15 p1841 A73-32390

Study of the conditions defining the passivating action of surface-active substances on hygroscopic condensation nuclei

18 p2332 A73-35918

Condensation of drops in motion through a gravitational field

21 p2731 A73-40743

Condensation in CO₂ free jet expansions. I - Dimer formation.

21 p2743 A73-40937

Condensation in CO₂ free jet expansions. II - Growth of small clusters.

21 p2743 A73-40938

Lunar and planetary chemical composition dependence on condensation temperature in solar nebula

23 p3030 A73-43760

CONDITIONED RESPONSES

U CONDITIONING [LEARNING]

CONDITIONING [LEARNING]

Conditioned reflex learning and phenamine-stimulated functional activation of cerebral synaptic, protein synthesizing and energy generating apparatus

05 p0541 A73-17177

A robot conditioned reflex system modeled after the cerebellum.

06 p0658 A73-18065

Participation of the hippocampal structures in the formation of external inhibition

06 p0653 A73-18162

Functional alterations in the auditory and visual analyzer systems of monkeys during experimental neurosis

06 p0653 A73-18163

Statistical distribution methods for analyzing formation of reflexes conditioned to time intervals between periodic unconditioned stimuli

06 p0653 A73-18166

Learning ability of rats to regulate hypoxic ambient atmosphere by instrumental response, discussing motivation and reinforcement factors

06 p0655 A73-18439

German monograph on human information transmission by multidimensional tactile stimuli investigation using method of learned signals identification

07 p0786 A73-20393

Hippocampus contribution to conditioned reflexes, memory, voluntary motions, orientation and emotional reactions, noting theta rhythm in stimuli response

10 p1180 A73-24326

Self-imposed timeouts under increasing response requirements.

10 p1185 A73-24625

The operational control of the alpha component in the electroencephalogram by means of auditory feedback

11 p1324 A73-26549

Comparative analysis of the electrical activity of the cortex and of cerebral subcortical formations in the process of the alteration of conditioned reactions

12 p1461 A73-27104

The role of analyzers of conditional and unconditional stimuli in the functional system of the behavioral conditioned-reflex action

12 p1461 A73-27105

Physiological nature of the electroencephalographic and vegetative components of human conditioned reactions

12 p1462 A73-27107

Characteristics of the higher nervous activity of monkeys during a postneurotic period

12 p1462 A73-27108

Behavioral and electrophysiological correlates during flash-frequency discrimination learning in monkeys.

14 p1714 A73-29989

Alpha wave peak amplitude dependence on blocking pattern after stimulation during habituation-pseudoconditioning, conditioning and extinction

14 p1714 A73-29992

Conditioned reflex switching effects in higher nervous system reactions as function of experimental stimuli background conditions /arousal, diurnal rhythms, test conditions, physiological condition/

14 p1718 A73-30567

Forward and backward conditional link formation as physiological mechanism for reinforcement conditioning connection

14 p1718 A73-30568

Formation of conditioned responses to symbolic stimulations in healthy individuals of different age

15 p1833 A73-31158

Acquisition of signal concepts under conditions of aversion activation. I - Theoretical part and form interpretation test

16 p1972 A73-33091

Quantitative evoked-potential analyses for the neurophysiological characterization of faulty learning processes in the experimental arterial hypertension-pathogenesis

19 p2394 A73-37756

Bioelectric and vegetative components of conditioned reflexes of 'negative-emotional type'

20 p2515 A73-39797

Formation of various functional states in the symmetrical structures of the brain as a function of the intensity of unconditioned excitation

20 p2516 A73-39801

Successive differentiation of visual stimuli in monkeys under various conditions of presentation

20 p2516 A73-39805

Automatic apparatus for the study of conditioned reflexes in a monkey seated in the primatological chair

21 p2644 A73-41140

Use of the conditioned reflex method to study the motor analyzer during hygienic evaluation of working conditions in the presence of vibrations

24 p3062 A73-44673

Prefrontal lobe functions and the neocortical commissures in monkeys.

24 p3061 A73-45166

CONDITIONS

NT ADIABATIC CONDITIONS

NT CHRONIC CONDITIONS

NT FLIGHT CONDITIONS

NT KUTTA-JOUKOWSKI CONDITION

NT LIPSCHITZ CONDITION

NT NONEQUILIBRIUM CONDITIONS

NT RUNWAY CONDITIONS

CONDUCTING FLUIDS

Streaming two dimensional Oseen MHD flow of conducting fluid past semiinfinite needle within aligned field

01 p0031 A73-10305

Nonlinear boundary-value problem for a conducting source flow in an inhomogeneous magnetic field.

01 p0085 A73-11064

Temperature field and heat transfer equation of unsteady conducting fluid motion on porous plate within magnetic field, allowing for Joule dissipation

01 p0085 A73-11079

Magnetohydrodynamic flow around a hollow sphere

01 p0085 A73-11259

MHD equations for velocity distribution of magnetic field motion in conducting fluid, noting evolution equations of geomagnetic field

02 p0164 A73-12555

The propagation of small disturbances in radiative magnetogasdynamics.

03 p0345 A73-12923

Magnetic field effect on friction shear stress in turbulent slipstreams of conducting fluids, calculating mixing zone width

03 p0346 A73-13609

Magnetogasdynamic characteristics, transonic and compression regions and pressure losses of conducting gas flow in circular tube within axisymmetric magnetic field

03 p0346 A73-13620

Electric field in a segmented MHD generator for a finite conductivity of the walls at the channel inlet

03 p0346 A73-13621

A variational solution of the Rayleigh problem for a power law non-Newtonian conducting fluid.

03 p0347 A73-13790

Asymptotic solution for inviscid conducting fluid flow past arbitrary wing profile in magnetic field

03 p0347 A73-14045

Emitter efficiency increase in annular colloid microthrusters with single sharp tips for high specific charge of conducting liquid droplets under low potential

04 p0488 A73-15723

Hydromagnetic stability of a laminary boundary layer in a flow past a planar plate

05 p0601 A73-16096

Rotating paraboloid of revolution in viscous conducting fluid, calculating flow velocity and magnetic field from MHD equations

05 p0601 A73-16172

Equations of motion for two dimensional steady conducting gas flow in transverse magnetic field deriving flow equations for transcritical region via small perturbation theory

05 p0602 A73-16586

Turbulence in the annular flow of a conducting fluid in a magnetic field

05 p0603 A73-16587

Two-dimensional viscous MHD flows in coaxial channels

05 p0603 A73-16588

MHD-rotation of a conducting fluid in a rotationally symmetric electromagnetic field

05 p0603 A73-16590

Relativistic thermodynamics of simple heat conducting fluids.

05 p0641 A73-17235

Dimension-theory determination of the separation parameter for an incompressible magnetohydrodynamic boundary layer.

06 p0726 A73-17406

Hartmann flow stability of conducting incompressible viscous fluid between parallel plates at arbitrary Reynolds numbers under transverse magnetic field

06 p0727 A73-17453

Motion of a magnetized conducting liquid between two plane electrodes in a transverse magnetic field

06 p0727 A73-17472

The development of magnetohydrodynamic flow due to the passage of an electric current past a sphere immersed in a fluid.

06 p0728 A73-17705

Magnetohydrodynamic viscous flow induced by an oscillating disk.

06 p0728 A73-17792

Magnetohydrodynamic laminar source flow between two parallel disks.

07 p0854 A73-19102

Hall current effects on waves in an electrically conducting rotating fluid.

07 p0854 A73-19104

Transverse hydromagnetic plane waves in the presence of a temperature gradient.

07 p0856 A73-19339

Nonlinear thermal convection in electrically conducting Boussinesq fluid subject to temperature gradient and magnetic field, calculating flow stability limit by energy method

07 p0920 A73-19513

Unsteady motion of a viscous electrically conducting fluid around a flat plate in the case of orthogonal fields

07 p0858 A73-19999

The laws of reflection and refraction of incompressible magnetohydrodynamic waves at a fluid-solid interface.

07 p0858 A73-20028

Flow of a conductive fluid through a cylindrical duct with periodic deformations in the presence of an azimuthal magnetic field

07 p0858 A73-20073

Some problems in the theory of an electrochemical velocity sensor for current-conducting fluids

08 p0965 A73-21106

Penetration of a solid into a half-space of compressible liquid in the presence of a magnetic field

08 p0994 A73-21724

Remarks on variational principle for an inviscid, perfect, magnetized plasma.

09 p1126 A73-22122

Equations of motion of ideally conducting medium in MHD approximation, solving under constant magnetic field and magnetic-hydrodynamic pressure equilibrium

09 p1126 A73-22280

Putting an electrically conducting fluid in rotation by a rotating magnetic field

10 p1254 A73-24125

Conducting medium flow in cylinder with nonconducting walls, solving nonlinear elliptic equation/Dirichlet problem/ by projective-iterative method

10 p1256 A73-24509

Flow near an accelerated plate in the presence of a magnetic field.

10 p1206 A73-24528

Unsteady flow of a conducting viscous fluid between parallel porous walls with heat transfer

10 p1256 A73-24587

Uniform variable transverse magnetic field effects on convective instability of plane electrically conducting layer, reducing perturbed equilibrium equations to linear ordinary differential equations

10 p1256 A73-24593

Parallel magnetic field effect upon plane interface stability between two conducting viscous fluids in uniform relative motion, obtaining neutral shear flow stability curves

11 p1402 A73-25054

On hydromagnetic Rossby waves excited by travelling forcing effects.

11 p1403 A73-25154

Nonlinear hydrodynamic and hydromagnetic spin-up driven by Ekman-Hartmann boundary layers.

11 p1403 A73-25156

Pressure shocks in thermally and electrically conducting viscous gas, discussing growth equation and radiation effects

11 p1403 A73-25164

A note on the unsteady motion of a viscous conducting liquid between two porous concentric circular cylinders acted on by a radial magnetic field.

11 p1404 A73-25368

On MHD flow along an infinite flat wall with constant suction.

11 p1405 A73-25975

Laminar free convection flow of an electrically conducting fluid from an inclined isothermal plate.

11 p1452 A73-26369

Thermodynamic theory of heat conducting fluids with constitutive quantities dependence on rate of density, gradient, velocity and temperature

11 p1453 A73-26746

Hydromagnetic stability of plane heterogeneous shear flow.

12 p1527 A73-27129

Electrohydrodynamic equation solutions for non-collinear current density and velocity vectors of unipolarly charged fluid flow in channel with wall-type electrodes

12 p1528 A73-27406

Propagation of unipolarly charged jets in hydrodynamic flows

12 p1528 A73-27407

Motion of a conducting gas with variable properties between rotating cylinders

12 p1487 A73-27798

Propagation of electrohydrodynamic surface waves in a conducting fluid.

13 p1663 A73-28160

The channel flow of an electrically conducting Prandtl-Eyring fluid in a magnetic and an electric field

13 p1663 A73-28161

Entropy supply for classical and relativistic heat conducting fluids, assuming linearity for momentum and energy supplies

13 p1704 A73-28286

Instability of hydromagnetic perpendicular shocks in inhomogeneous fluids.

13 p1601 A73-28775

Low Hartmann number MHD flow of weakly conducting viscous fluid past nonconducting sphere within aligned uniform magnetic field

14 p1781 A73-30655

Approximate solution to the problem of a conducting fluid flow in a weakly curved channel

15 p1917 A73-31154

Linearized theory of finite conductivity steady ideal MGD flow past thin wedge in aligned magnetic field, using Fourier integral transform

15 p1917 A73-31338

Motion of a sphere in a conducting fluid under the action of crossed electric and magnetic fields

15 p1917 A73-31405

Nonlinear MHD equations solution for conducting fluid plane periodic channel flow in traveling magnetic field by net point method

15 p1917 A73-31406

Application of the method of characteristics in solving the universal equation of the plane boundary layer of a conducting fluid

15 p1918 A73-31407

Laminar stratified flow of a conducting medium in ring channels in the event of great MHD-interaction parameters

15 p1918 A73-31409

Noncirculative MHD inviscid conducting fluid flow past circular cylinder and plane profile in magnetic field, using Fredholm equation

15 p1918 A73-31414

On the establishment and solution of equations of motion of an electrically conducting fluid set in motion by the slow and uniform rotation of walls of a ring-shaped receiver, in the presence of an axial magnetic field, in the case where the mean value of the intensity of the currents induced in a straight section takes a nonzero value

15 p1918 A73-31569

Plane boundary layer equations of asymmetric MHD incompressible fluid motion for case of high and low electroconductivity

15 p1919 A73-31829

Hydromagnetic stability of parallel flow of an ideal heterogeneous fluid.

16 p2043 A73-33872

Unsteady Couette flow in hydromagnetics.

17 p2154 A73-35121

Impulsively started viscous flow past a finite flat plate with and without an applied magnetic field.

17 p2217 A73-35604

Re-connexion of magnetic lines of force - Evolution in incompressible MHD fluids.

18 p2338 A73-36181

Incompressible conducting fluid flows in an arbitrary region in the presence of a strong magnetic field

18 p2340 A73-37015

Theoretical and experimental study, for different electrical conditions, of the laminar motion of an incompressible and electrically conducting fluid drawn along in a confined medium, and in the presence of an axial magnetic field, by the uniform rotation of a disk

19 p2468 A73-37531

Numerical solutions of the kinematic dynamo problem.

19 p2460 A73-38102

On the effects of uniform high suction on the rotationally symmetric flow of a conducting liquid near a stationary disc in the presence of a transverse magnetic field.

19 p2469 A73-38186

The two-dimensional slow flow of a conducting fluid.

20 p2598 A73-39340

Overheat instability in a flow of electrically conducting incompressible medium under conditions of an internal boundary value problem

20 p2598 A73-39605

Solar atmosphere and ionosphere phenomena in terms of conducting gas motion at magnetic field neutral points

21 p2681 A73-40106

Regular reflection of an oblique shock in a plane flow of ideally dissociating gas in the presence of a transverse magnetic field

21 p2744 A73-40189

The decay of perturbations in an electrically conducting and thermally radiating gas.

21 p2789 A73-40246

Rotation of a cylinder in a conducting fluid in an axial magnetic field

21 p2747 A73-40883

Study of MHD effects in a viscous conducting fluid flow in a traveling magnetic field

21 p2747 A73-40884

Rotation of an electrically conducting fluid with a free surface in a rotating field

21 p2747 A73-40885

Experimental study of rotational MHD Couette flow in a coplanar field

21 p2747 A73-40886

Conducting fluid jets in a transverse magnetic field

21 p2747 A73-40888

Electrohydrodynamic Rayleigh-Taylor instabilities of a plane circular interface.

21 p2749 A73-41626

Magnetogasdynamic shock polar - Exact solution in aligned fields.

22 p2893 A73-42393

Numerical analysis of magnetic field lines of force reconnection along transition layers or at flow stagnation point of incompressible conducting viscous fluid

22 p2894 A73-42396

Study of hydromagnetic stability of a hot rotating layer of fluid by Liapunov method.

22 p2894 A73-42474

A note on the drag due to steady flow of a conducting fluid past a disk at high Hartmann number.

22 p2894 A73-42475

Solution of nonlinear problems in magnetofluid-dynamics and non-Newtonian fluid mechanics through parametric differentiation.

22 p2843 A73-42556

Flow stability of viscous homogeneous incompressible electrically conducting fluid between nonconducting walls at large magnetic Reynolds numbers

22 p2894 A73-42639

Turbulent mean emf in presence of nonvanishing mean conducting fluid flow, modifying Green tensor of induction equation for constant strain rate velocity fields

23 p2969 A73-44050

On laminar two-phase flows in magnetohydrodynamics.

23 p3013 A73-44228

CONDUCTING MEDIA U CONDUCTORS CONDUCTION BANDS

Multiphonon transition theory for electron transitions probability between conduction and forbidden bands, noting semiconductor surface states with long relaxation time

01 p0089 A73-11438

Hot-electron concept for Poole-Frenkel conduction in amorphous dielectric solids.

02 p0201 A73-12817

Investigation of the anisotropy of effective masses in the conduction band of semiconductors under uniaxial compression

09 p1132 A73-21959

X-ray spectral data on the valence and conduction band structures in V3X-type vanadium compounds

23 p3017 A73-44041

A simple theory of the anomalous Hall effect in semiconductors.

24 p3120 A73-45329

CONDUCTION ELECTRONS

Comments on the conduction mechanism in Schottky diodes.

01 p0088 A73-10474

Indirect interaction of nuclear spins through valence band electrons in semiconductors

03 p0350 A73-13754

Conduction electrons collective wave properties in metals, discussing energy structure, ground state, Fermi surface and quasi-particle concept for crystal conductivity

06 p0739 A73-18674

Electron and X ray transitions between conduction band and bound level and between two bound levels in transition metals, investigating edge singularity and spectrum shape

07 p0864 A73-20614

Experimental study of the diffusion of electrons of conduction by superficial defects of thin gold films

13 p1668 A73-28453

Dependence of the variation of the electronic dislocation drag force in a superconducting transition on the stress, temperature, and velocity.

14 p1783 A73-30341

Electron characteristics of sprayed vanadium-gallium alloys

15 p1922 A73-31178

Reflection of conductivity electrons from an atomically pure 110/ face of a tungsten crystal

21 p2751 A73-40367

Effective interchange effects between the ions in metals

21 p2721 A73-41141

Heterojunction injection lasers /Review/.

22 p2869 A73-42244

CONDUCTIVE HEAT TRANSFER

Orthogonal function approximation of uniform thickness plate temperature distribution, using reduced two dimensional unsteady heat conduction equations

01 p0119 A73-10010

Application of the Meier-Fok complex conversion formulas in the solution of certain problems of heat conductivity

01 p0119 A73-10011

Application of the averaging method to the problem of plane wave propagation in a dissipative heat conducting medium

01 p0075 A73-10086

Numerical simulation of radiative-conductive heat transfer in the Martian atmosphere-polar cap utilizing Mariner 9 Iris data.

01 p0097 A73-10401

Comparison of solutions to the inverse unsteady heat conduction problem by the successive interval method and by the Sparrow, Hadji Sheikh and Lundgren method

01 p0123 A73-10862

Some variational principles pertaining to non-stationary heat conduction and coupled thermoelasticity.

01 p0118 A73-11369

On certain parabolic differential equations and an equivalent variational problem.

02 p0186 A73-11972

Transformation group theory for Poisson equation solutions to boundary value problem of steady heat conduction with generation

03 p0400 A73-14631

One-dimensional shock waves in heat conducting materials with memory. II.

04 p0511 A73-15225

A note on a minimum principle in Benard convection.

04 p0520 A73-15940

Initial and boundary value problems for melting propagation from solid cylinder axis and sphere center, assuming pure conductive heat transfer

05 p0638 A73-16395

Nonsteady heat conduction of multilayer cylindrical and conical shells in periodic radiation flux, calculating temperature distribution

05 p0640 A73-16798

The linear thermoelastic problem of uniform heat flow disturbed by a two-dimensional crack in a strip.

06 p0762 A73-17985

Heat conductivity dependence on temperature for amorphous and crystalline materials, noting integrodifferential equation for conductive heat transfer and Fourier law

06 p0769 A73-18132

Approximate perturbation solution in Chebyshev polynomials for partial differential equation of heat conduction with cylindrical, spherical or hyperspherical symmetry

06 p0769 A73-18503

Integral equations for temperature distribution in radiative and conductive heat transfer in semitransparent medium, noting temperature oscillation propagation

06 p0769 A73-18565

High temperature compressed gas heat conductivity calculation by least squares and basis isotherm methods

06 p0770 A73-18569

Thermal processes in metals exposed to high power laser pulses

06 p0702 A73-18571

The direct and inverse boundary value problems for the heat-conduction equation

06 p0770 A73-18682

Classical solvability of a problem of conjugation of two equations with the third boundary condition

06 p0718 A73-18684

Thermosphere kinetic temperature diurnal variation from heat conduction equation periodic solution, determining heat sources from solar radiation atmospheric absorption

07 p0815 A73-19440

Radiating-conducting thick-transparent normal shock solution.

07 p0919 A73-19507

Turbulent mixing at homogeneous wakes boundary, using heat conduction equivalence

07 p0810 A73-19610

Algorithm for calculating unsteady heat transfer in liquid-propellant rocket-engine chambers with regenerative cooling

07 p0868 A73-20087

Numerical method of transient heat conduction with temperature dependent thermal properties.

07 p0921 A73-20118

Steady-state heat conduction in slabs, cylindrical and spherical shells with non-uniform heat generation.

07 p0921 A73-20181

Application of the solution to an inverse heat conduction problem to the calculation of the heat transfer coefficient from experimentally measured temperatures at internal point of the body

08 p1021 A73-20996

Cyclically symmetrical heat conduction problems for perforated plates and shells in the presence of heat transfer

08 p1021 A73-20997

Application of the regularization principle to the construction of approximate solutions to inverse heat-conduction problems

08 p1022 A73-21097

Temperature distribution in a wedge-shaped prism

08 p1022 A73-21098

Laminar flow heat transfer from wedge-shaped bodies with limited heat conductivity.

08 p1023 A73-21257

On the solution of the nonlinear heat conduction equations by numerical methods.

08 p1024 A73-21636

Solution of the three-dimensional thermoelasticity problem for a long cylinder with mixed heating conditions

08 p1019 A73-21758

Electron heat conductivity along a magnetic field in a decaying plasma

09 p1124 A73-21887

An axisymmetrical nonstationary heat-conduction problem for a system of two cylinders contacting at the end faces

09 p1166 A73-22363

Stability of certain finite-difference schemes for solving heat conduction equations with a nonself-conjugate elliptic operator

09 p1167 A73-22582

Finite-element method applied to heat conduction in solids with nonlinear boundary conditions.

10 p1295 A73-23778

Heat conductivity equation solution stabilization for Cauchy problem with oblique derivative and arbitrary number of geometrical variables

10 p1295 A73-24061

Optimal conductive heating of hollow cylinder inner surface with temperature dependent thermal stress limits for internal/external surfaces

10 p1289 A73-24063

Energy balance in the chromosphere-corona transition region.

10 p1279 A73-24138

Thermoelastic boundary value problem for heat conduction in elastic bodies with linear and three dimensional inserts

10 p1290 A73-24305

Temperature at the surface of a heat-conducting liquid behind a shock wave in the presence of mass transfer and chemical reactions in the boundary layer

10 p1296 A73-24679

Integral transform and heat conduction in a hollow cone with radiation.

10 p1297 A73-24920

Principles of evacuated cryogenic insulations.

11 p1450 A73-25581

Method of solving heat conduction problems with nonideal thermal contact

11 p1450 A73-25624

Transfer function model for analog simulation of transient unsteady heat conduction through flat and cylindrical walls, optimizing moving polymer film heating

11 p1451 A73-25732

Heat conduction nonlinear boundary value problems approximate solution via Westphal similarity theorem, considering inhomogeneous media with temperature dependent heat transfer coefficients

11 p1451 A73-25742

Regularization schemes for solving inverse heat conduction problems

11 p1451 A73-25743

Accuracy and convergence of absolutely stable finite difference procedures for solution of multidimensional heat conductivity equation with discontinuous coefficients

11 p1452 A73-26327

Steady conditions of a radiating self-constricted high-current discharge in a plasma

11 p1406 A73-26333

Entropy minimum principle applied to boundary value problem of non-linear heat conduction.

11 p1452 A73-26342

Transient temperature distribution of an anisotropic half space.

11 p1453 A73-26401

Thermal cumulation equations for concentric conductive laser heating of two temperature D-T plasma with nuclear fusion energy recovery

11 p1406 A73-26411

Laser concentric conduction heating of two-temperature D-T plasma.

11 p1406 A73-26412

The asymptotic behavior of Green's function for a heat-conduction equation with a small parameter

12 p1558 A73-27248

Simplification of one-dimensional heat-conduction problems in the case of impulsive radiative heating of flat bodies

12 p1558 A73-27317

Application of the finite-element method to the study of heat problems

12 p1558 A73-27397

Mathematical model of heat conduction medium thermophysical properties based on one dimensional nonlinear thermal conductivity equation solution

12 p1559 A73-27444

Spectral and boundary effects on coupled conduction-radiation heat transfer through semitransparent solids.

12 p1559 A73-27695

Power series solution of quasi-linear parabolic heat conduction equation for temperature wave propagation in soil

12 p1560 A73-27807

Cauchy problem solution stability for non-homogeneous heat conduction equation with two space variables, allowing specular reflection on rectangular boundary

12 p1560 A73-27809

Nonlinear problems for a system of two heat-radiating gray bodies separated by a diathermic medium

12 p1560 A73-27810

Comparison of the solutions found for the inverse transient heat-conduction problem by the method of successive intervals and the method of Sparrow, Haji-Sheikh, and Lundgren.

12 p1560 A73-27911

Application of mathematical programming methods to determine the optimal control for systems described by heat conduction equations

13 p1704 A73-28016

Thermo-acoustical waves in linear thermo-elastic materials.

13 p1691 A73-28088

Wave propagation aspects of the generalized theory of heat conduction.

13 p1704 A73-28414

Unsteady temperature condition of a conductor with a nonlinear source of heat

13 p1705 A73-28466

Cooling of IC chips by heat conduction.

13 p1590 A73-28480

Modified separable kernel method for heat conduction with a nonlinear boundary condition.

13 p1706 A73-28819

Human thermoregulatory system examination under thermodynamic equilibrium based on conductive and convective metastable heat transfer from skin to environment

[ASME PAPER 73-AUT-J] 13 p1577 A73-29414

On the concepts of viscous fluids, of elastic solids, and of heat conduction in relativity

13 p1661 A73-29555

Temperature fields in a hollow cylinder in presence of heat source under the boundary conditions of the second kind.

13 p1708 A73-29666

On nongravitational effects in two classes of models for cometary nuclei.

14 p1793 A73-29820

Nonlinear heat flow in anisotropic media with property variations and nonlinear heat generation.

14 p1816 A73-29915

Solution of the problem of unsteady heat transfer for a body and the liquid flow around it

14 p1744 A73-30018

Bubnov-Galerkin method for mixed boundary value problem solution via sequence of coordinate functions, illustrated by steady state conductive heat transfer problem

14 p1768 A73-30019

Convergence of the net-point method for multidimensional quasi-linear heat-conduction problems

14 p1816 A73-30020

Determining unknown coefficients in a nonlinear heat conduction problem.

14 p1817 A73-30406

An approximate solution of the nonstationary heat conduction problem for laser elements with sharply expressed anisotropy

14 p1758 A73-30467

The thermal analysis of a belt type radiator by the method of matched asymptotic expansions.

14 p1817 A73-30609

The conservative method of flows and the calculation of a viscous heat conducting gas flow past a body of finite size

15 p1821 A73-30962

Viscosity coefficients and heat conductivity of dense gases with rotational degrees of freedom

15 p1915 A73-31022

The solution of heat conduction problems with the aid of the Laplace transformation. II - Numerical evaluation and graphical representation of two specific boundary value problems

15 p1958 A73-31907

Stability and oscillation characteristics of finite-element, finite-difference, and weighted-residuals methods for transient two-dimensional heat conduction in solids.

[ASME PAPER 73-HT-E] 15 p1958 A73-32277

The principle of minimum entropy applied to boundary value problem of non-linear heat conduction.

16 p2084 A73-32984

On the observability and stability of the temperature distribution in a composite heat conductor.

16 p2034 A73-33311

On the role of fluctuations in the interplanetary magnetic field on heat conduction in the solar wind.

16 p2056 A73-33461

The drilling of a metal plate by a laser beam.

[ASME PAPER 73-PROD-6] 16 p2019 A73-33535

Integral equations for temperature distribution in radiative and conductive heat transfer in semitransparent medium, noting temperature oscillation propagation

16 p2086 A73-33590

High temperature compressed gas heat conductivity calculation by least squares and isotherm methods

16 p2086 A73-33594

Thermal processes in metals irradiated by powerful laser pulses.

16 p2086 A73-33596

Coupled thermally induced vibrations of beams.

17 p2241 A73-34190

Electron thermal conductivity along the magnetic field in an afterglow.

17 p2215 A73-34310

Finite element approximations in nonlinear thermoviscoelasticity.

17 p2245 A73-34829

The finite element method in fluid mechanics.
17 p2151 A73-34830

Russian book on radiative and complex heat transfer covering electromagnetic energy-matter interaction, modeling, convective and conductive transfer and thermodynamic equilibrium radiation
17 p2254 A73-34899

Solution for the pressure and temperature in thrust bearings operating in the thermohydrodynamic turbulent regime.
[ASME PAPER 73-LUBS-14] 17 p2181 A73-35394

Experimental study of the stability of differentially heated inclined air layers.
17 p2256 A73-35847

Book - Radiative transfer and interactions with conduction and convection.
17 p2256 A73-35864

Development of a high capacity variable conductance heat pipe.
[AIAA PAPER 73-728] 18 p2369 A73-36345

A note on uniqueness in the linear theory of heat conduction with finite wave speeds.
18 p2371 A73-36692

Coordinate function construction in solving the boundary value problems of heat conductivity by direct methods
18 p2372 A73-36818

Influence of heat conducting elements on the burning rate of mixture system models
18 p2342 A73-37120

Application of heat pipes and their thermal transport capability.
19 p2502 A73-37445

On the stability of the conduction regime of natural convection in a vertical slot.
19 p2505 A73-38476

Shape of porous cooled region for surface heat flux and temperature both specified.
19 p2505 A73-38482

Heat transfer in an absorbing, emitting and scattering slug flow between parallel plates.
[ASME PAPER 73-HT-13] 20 p2625 A73-38568

Unified thermodynamics of dissipative structures and coherence in nonlinear optics.
20 p2571 A73-38633

Convergence of Huber's method for heat conduction problems with change of phase.
20 p2626 A73-39100

Solution of a nonlinear problem of heat conductivity concerning a multilayer cylindrical wall with a nonideal thermal contact
20 p2627 A73-39257

A method of obtaining approximate solutions to unsteady-state heat conduction problems
20 p2627 A73-39258

Approximate solutions for heat conduction and thermal stresses in thermoelasticity of solids and beam and ring structures, considering dynamic, coupling, melting and solidification effects
20 p2620 A73-39514

The incremental theory of three dimensional transient thermoelastoplasticity - Formulation and solution.
20 p2622 A73-39552

Method for determining the heat conductivity coefficient of high-temperature materials during unsteady heating
20 p2629 A73-39616

Heat conduction in blackened skin accompanying pulsatile heating with a xenon flash lamp.
20 p2519 A73-39791

A class of heat conduction problems with a time-variable heat transfer coefficient
21 p2790 A73-40396

Regularization of solutions of inverse problems of heat conduction.
21 p2792 A73-41061

Fiber glass reinforced plastics measurement for ratio of elastic modulus to mean thermal conduction for use in cryostat to resist large forces
21 p2723 A73-41106

Hybrid finite methods for linear and nonlinear unsteady heat conduction problems
21 p2793 A73-41617

Transient heat conduction in laminated composites.
[ASME PAPER 73-HT-R] 22 p2930 A73-42286

Unsteady, combined radiation and conduction in an absorbing, scattering, and emitting medium.
[ASME PAPER 73-HT-J] 22 p2930 A73-42288

The use of fundamental Green's functions for the solution of problems of heat conduction in anisotropic media.
22 p2938 A73-42954

The relation between the internal thermal resistance of transistors and the method of alloying
23 p2960 A73-43677

Effect of wall conduction on convective heat transfer with laminar boundary layer.
23 p3049 A73-43833

A Riemann-Hilbert problem for a heat conduction in a finned surface.
23 p3049 A73-44051

Thermal stresses in heated orthotropic plates with variable heat-transfer coefficients
23 p3046 A73-44195

A two-layer slab method for measuring thermal diffusivity of polymer by irradiated light heat-wave. I. II - Transient response of temperature sensor attached on a polymer substrate. III - Quantitative evaluation of the effect of edge losses in a parallelepiped.
23 p3049 A73-44363

An unsteady heat-conduction problem in a system of diathermally separated bodies
24 p3154 A73-44422

Radiant-conductive heat transfer in a plane layer of an absorbing and scattering medium
24 p3155 A73-44754

Numerical solution of a nonlinear inverse heat-conduction problem
24 p3156 A73-45084

Quasi-steady Stefan problem solutions for nonlinear heat conduction in two phase /liquid-solid/ state crystallizer
24 p3158 A73-45501

CONDUCTIVITY
Equivalent conductivity of a longitudinal slot on the broad wall of a uniformly curved rectangular waveguide
21 p2648 A73-40199

CONDUCTORS
NT AIRCRAFT ANTENNAS
NT ANOLYTES
NT BUS CONDUCTORS
NT CASSEGRAIN ANTENNAS
NT DIPOLE ANTENNAS
NT DIRECTIONAL ANTENNAS
NT ELECTRIC CONDUCTORS
NT ELECTRIC WIRE
NT ELECTROLYTES
NT EXPLODING WIRES
NT HELICAL ANTENNAS
NT HORN ANTENNAS
NT ION EXCHANGE MEMBRANE ELECTROLYTES
NT LENS ANTENNAS
NT LOG PERIODIC ANTENNAS
NT LOG SPIRAL ANTENNAS
NT LOOP ANTENNAS
NT MICROWAVE ANTENNAS
NT MISSILE ANTENNAS
NT MOLTEN SALT ELECTROLYTES
NT MONOPOLE ANTENNAS
NT MONOPULSE ANTENNAS
NT OMNIDIRECTIONAL ANTENNAS
NT PARABOLIC ANTENNAS
NT PHOTOCONDUCTORS
NT RADAR ANTENNAS
NT RADIO ANTENNAS
NT SLOT ANTENNAS
NT SPIRAL ANTENNAS
NT STEERABLE ANTENNAS
NT SUPERCONDUCTORS
NT THERMAL CONDUCTORS
NT TURNSTILE ANTENNAS
NT TWO REFLECTOR ANTENNAS
NT WAVEGUIDE ANTENNAS
NT YAGI ANTENNAS

Average monostatic scattering cross section for plane electromagnetic wave incident on ideally conducting convex body, considering wavelength relation to body dimensions
03 p0278 A73-14072

CONES
NT CIRCULAR CONES
NT CONICAL BODIES
NT NOSE CONES
NT ROCKET NOSE CONES
NT SLENDER CONES

Boundary layer transition on cones in hypersonic He wind tunnel tests, obtaining turbulent spot geometry and propagation velocity by spark schlieren photography
01 p0003 A73-10762

Viscous shock layer flow in the windward plane of cones at angle of attack.
[AIAA PAPER 73-134] 05 p0530 A73-16886

A study of fin-induced laminar interactions on sharp and spherically blunted cones.
[AIAA PAPER 73-235] 05 p0532 A73-16960

An investigation of shock strengthening in a conical convergent channel.
06 p0684 A73-17706

Transition of the boundary layer on a cone in a supersonic flow
06 p0646 A73-18540

Circular conical diffuser inlet velocity profile effect on efficiency, presenting experimental results for different cone angles and expansion ratios
07 p0774 A73-19616

Approximate method for calculating heat transfer to yawed cylinders in laminar flow.
08 p1025 A73-21818

Vertebrate photoreceptor cell /rods and cones/ development and structure, discussing light pathway, ciliary connective and microtubules, outer and inner segments, etc.
09 p1042 A73-23303

Laminar boundary layer on a cone near a plane of symmetry.
09 p1029 A73-23442

Calculation of the gas parameters in the injection region for the flow at an angle of incidence past a porous cone
10 p1172 A73-24505

Study of the fluctuations of wall pressures in transonic flow on a cone-cylinder group presenting a constriction
10 p1173 A73-24825

Three-dimensional compressible boundary layer flow over a yawed cone.
[AIAA PAPER 73-634] 18 p2260 A73-36193

Supersonic-hypersonic motion past a permeable cone at zero angle of attack
19 p2376 A73-37544

CONFERENCES
International Conference on Gas Discharges, 2nd, London, England, September 11-15, 1972, Proceedings.
01 p0081 A73-10111

Conference on Atmospheric Radiation, Fort Collins, Colo., August 7-9, 1972, Preprints.
01 p0037 A73-10351

Conference on Auxiliary Instrumentation for Large Telescopes, 2nd, Geneva, Switzerland, May 2-5, 1972, Proceedings.
01 p0046 A73-10501

Symposium on D- and E-Region Ion Chemistry, University of Illinois, Urbana, Ill., July 6-8, 1971, Informal Record.
01 p0040 A73-10876

International Symposium on Space Technology and Science, 9th, Tokyo, Japan, May 17-22, 1971, Proceedings.
01 p1100 A73-11101

International Conference on Cosmic Rays, 12th, University of Tasmania, Hobart, Tasmania, Australia, August 16-25, 1971, Papers. Volume 1, 2, 3, 4, 5 & 6.
01 p0093 A73-11375

North American Thermal Analysis Society, Annual Meeting, 3rd, Waco, Tex., February 7, 8, 1972, Proceedings.
01 p0015 A73-11446

Information processing 71; Proceedings of the Congress, Ljubljana, Yugoslavia, August 23-28, 1971. Volume 1 - Foundation and Systems. Volume 2 Applications.
01 p0020 A73-11451

Applied Superconductivity Conference, 5th, Annapolis, Md., May 1-3, 1972, Proceedings.
02 p0200 A73-11826

Conference on the Theory of Ordinary and Partial Differential Equations, Dundee, Scotland, March 28-31, 1972, Proceedings.
02 p0186 A73-11968

Space research XII; Proceedings of the Fourteenth Plenary Meeting, Seattle, Wash., June 18-July 2, 1971. Volumes 1 & 2.
02 p0212 A73-12226

All-Union Conference on the Physics of Cosmic Rays, Moscow, USSR, October 26-November 2, 1970, Transactions.
02 p0208 A73-12651

International Symposium on Metrology, Bratislava, Czechoslovakia, September 5-8, 1972, Proceedings.
03 p0305 A73-12893

International Congress on Acoustics, 7th, Budapest, Hungary, August 18-26, 1971, Proceedings. Volume 1 - General Acoustics. Volume 2 - Technical Acoustics. Volume 4 - Physical Acoustics.
03 p0289 A73-12951

Non-metallic materials selection, processing and environmental behavior; Proceedings of the Fourth National Technical Conference and Exhibition, Palo Alto, Calif., October 17-19, 1972.
03 p0328 A73-13001

The moon; Proceedings of the Second Symposium, University of Newcastle-upon-Tyne, Newcastle-upon-Tyne, England, March 22-26, 1971.
03 p0367 A73-13076

Conference on Mechanics, Berlin, East Germany, October 13-15, 1971, Reports
03 p0386 A73-13151

Externally pressurized bearings; Proceedings of the Conference, London, England, November 17, 18, 1971.
03 p0311 A73-13201

Probabilistic aspects of fatigue; Proceedings of the Symposium, Atlantic City, N.J., June 27-July 2, 1971.
03 p0387 A73-13228

National Powder Metallurgy Conference, Chicago, Ill., April 17-19, 1972, Proceedings.
03 p0322 A73-13259

Southeastern Conference on Theoretical and Applied Mechanics, 6th, University of South Florida, Tampa, Fla., March 23, 24, 1972, Proceedings.
03 p0388 A73-13301

Composite materials of today and tomorrow: New materials and conventional industries; International Conference, 1st, Lyons, France, September 22-24, 1971, Proceedings
03 p0334 A73-13579

Symposium on the Future Application of Satellite Beacon Measurements, Graz, Austria, May 29-June 2, 1972, Proceedings.
03 p0299 A73-13626

Earth's magnetospheric processes; Proceedings of the Symposium, Cortina, Italy, August 30-September 10, 1971.

03 p0302 A73-13851

Power Processing and Electronics Specialists Conference, Atlantic City, N.J., May 22, 23, 1972, Record.

03 p0252 A73-13926

Ultraviolet and X-ray spectroscopy of astrophysical and laboratory plasmas; Proceedings of the Third Symposium, Utrecht, Netherlands, August 24-26, 1971.

03 p0363 A73-13951

Photovoltaic Specialists Conference, 9th, Silver Spring, Md., May 2-4, 1972, Record.

03 p0254 A73-14203

Sleep and the maturing nervous system; Proceedings of the Symposium on the Maturation of Brain Mechanisms Related to Sleep Behavior, Boiling Springs, Pa., June 21-24, 1970.

03 p0263 A73-14255

Biotelemetry; Proceedings of the International Symposium, Nijmegen, Netherlands, May 5-8, 1971.

03 p0269 A73-14276

Annual Allerton Conference on Circuit and System Theory, 9th, Monticello, Ill., October 6-8, 1971, Proceedings.

03 p0286 A73-14476

Conference on Precision Electromagnetic Measurements, 13th, Boulder, Colo., June 26-29, 1972, Proceedings.

03 p0309 A73-14490

Radar Meteorology Conference, 15th, Urbana, Ill., October 10-12, 1972, Preprints.

03 p0337 A73-14504

Symposium on Capillary Exchange and the Interstitial Space, Bad Duerkheim, West Germany, May 3-6, 1972, Proceedings.

03 p0265 A73-14649

National Symposium on Fracture Mechanics, 5th, University of Illinois, Urbana, Ill., August 31-September 2, 1971, Proceedings. Part 1 - Stress analysis and growth of cracks.

04 p0505 A73-14676

National Symposium on Fracture Mechanics, 5th, University of Illinois, Urbana, Ill., August 31-September 2, 1971, Proceedings. Part 2 - Fracture toughness.

04 p0506 A73-14693

Colloquium on Structural Reliability: The Impact of Advanced Materials on Engineering Design, Carnegie-Mellon University, Pittsburgh, Pa., October 9-12, 1972, Proceedings.

04 p0507 A73-14704

Western Electronic Show and Convention, Los Angeles, Calif., September 19-22, 1972, Proceedings.

04 p0426 A73-14728

Opportunities in materials; Proceedings of the Fourth Buhl International Conference, Pittsburgh, Pa., November 16-18, 1971.

04 p0460 A73-14740

Comets: Scientific data and missions; Proceedings of the Tucson Comet Conference, University of Arizona, Tucson, Ariz., April 8, 9, 1970.

04 p0494 A73-14751

The use of artificial satellites for geodesy; Proceedings of the Third International Symposium, Washington, D.C., April 15-17, 1971.

04 p0436 A73-14776

Solar activity observations and predictions, Proceedings of the Conference, Huntsville, Ala., November 16-18, 1970.

04 p0490 A73-14827

Testing for prediction of material performance in structures and components, Proceedings of the Symposium, Anaheim, Calif., April 21-23, 1971 and Atlantic City, N.J., June 29-July 1, 1971.

04 p0452 A73-14851

International Conference on Transportation and the Environment, Washington, D.C., May 31-June 2, 1972, Proceedings. Part 1.

04 p0405 A73-14889

National Electronics Conference, 28th, Chicago, Ill., October 9-11, 1972, Proceedings. Volume 27.

04 p0416 A73-15051

International Symposium on Fuel Cells, 4th, Antwerp, Belgium, October 2, 3, 1972, Proceedings. Volume 1.

04 p0406 A73-15101

Ultrasonics Symposium, Boston, Mass., October 4-7, 1972, Proceedings.

04 p0448 A73-15120

Colloquium on the Law of Outer Space, 14th, Brussels, Belgium, September 20-25, 1971, Proceedings.

04 p0521 A73-15126

Symposium on Nonlinear Estimation Theory and its Applications, 3rd, San Diego, Calif., September 11-13, 1972, Proceedings.

04 p0430 A73-15251

Critical problems of magnetospheric physics; Proceedings of the Symposium, Madrid, Spain, May 11-13, 1972.

04 p0441 A73-15326

NTC '72: National Telecommunications Conference, Houston, Tex., December 4-6, 1972, Record.

04 p0417 A73-15376

International conference of the CNRS on the physics of very high frequency phonons, Sainte-Maxime, Var, France, June 27-30, 1972, Proceedings

04 p0483 A73-15464

Japan-U.S. Seminar on the Physical Metallurgy of Heat Resisting Alloys, Diamond Point, N.Y., September 13-15, 1972, Proceedings.

04 p0464 A73-15576

Electric propulsion and its space applications; Workshop, 2nd, Toulouse, France, June 21-23, 1972, Proceedings

04 p0487 A73-15712

Remote sensing of earth resources and the environment; Proceedings of the Seminar-in-Depth, Palo Alto, Calif., November 8, 9, 1971.

04 p0450 A73-15766

Imaging techniques for testing and inspection; Proceedings of the Seminar-in-Depth, Los Angeles, Calif., February 14, 15, 1972.

05 p0573 A73-16276

Course on Physical and Technical Measurements with Lasers, Erice, Italy, May 8-21, 1971, Proceedings.

05 p0583 A73-16336

Annual Conference on Nuclear and Space Radiation Effects, 9th, University of Washington, Seattle, Wash., July 24-27, 1972, Proceedings.

05 p0557 A73-16501

Technology for man 72; Proceedings of the Sixteenth Annual Meeting, Los Angeles, Calif., October 17-19, 1972.

05 p0542 A73-16701

Remote sensing of earth resources; Proceedings of the Conference on Earth Resources Observation and Information Analysis Systems, Tullahoma, Tenn., March 13, 14, 1972. Volume 1.

05 p0571 A73-17126

Symposium on Planetary Atmospheres and Surfaces, Madrid, Spain, May 10-13, 1972, Proceedings.

06 p0743 A73-17427

Emissions from continuous combustion systems; Proceedings of the Fifteenth Symposium, Warren, Mich., September 27, 28, 1971.

06 p0767 A73-17726

Conference on Planetology and Space Mission Planning, 3rd, New York, N.Y., October 28-30, 1970, Proceedings.

06 p0749 A73-18001

Orientation: Sensory basis; Proceedings of the Conference, New York, N.Y., February 8-10, 1971.

06 p0653 A73-18030

Fall Joint Computer Conference, Anaheim, Calif., December 5-7, 1972, Proceedings. Parts 1 & 2.

06 p0670 A73-18057

Interstellar molecules and cosmochemistry; Proceedings of the Conference, New York, N.Y., June 16-18, 1971.

06 p0751 A73-18226

Annual Electro-Optical Systems Design Conference, 4th, New York, N.Y., September 12-14, 1972, Proceedings of the Technical Program.

06 p0693 A73-18276

The organic analysis and carbon chemistry of lunar samples: Their significance for exobiology; Proceedings of the Conference, University of Maryland, College Park, Md., October 26-28, 1971.

06 p0753 A73-18410

Workshop on the Application of Variational Methods to the Calculation of Structures, Senlis, Oise, France, June 19-21, 1972, Proceedings. Numbers 1, 2, 3, 4 & 5

06 p0765 A73-18721

Hawaii International Conference on System Sciences, 6th, University of Hawaii, Honolulu, Hawaii, January 9-11, 1973, Proceedings.

06 p0681 A73-18801

INTERMAG Conference, 10th, Kyoto, Japan, April 10-13, 1972, Proceedings.

07 p0861 A73-19360

National Congress on Reliability, Perros-Guirec, Cotes-du-Nord, France, September 20-22, 1972, Text of the Lectures

07 p0799 A73-19401

Assessment of lubricant technology; Proceedings of the Annual Spring Lubrication Symposium, Boston, Mass., June 6-8, 1972.

07 p0842 A73-19551

Conference on Chemical and Molecular Lasers, 3rd, St. Louis, Mo., May 1-3, 1972, Proceedings.

07 p0834 A73-19626

Lunar Science Conference, 3rd, Houston, Tex., January 10-13, 1972, Proceedings. Volume 1 - Mineralogy and petrology. Volume 2 - Chemical and isotope analyses, organic chemistry. Volume 3 - Physical properties.

07 p0878 A73-19676

International Cryogenic Engineering Conference, 4th, Eindhoven, Netherlands, May 24-26, 1972, Proceedings.

07 p0922 A73-20401

System identification of vibrating structures: Mathematical models from test data; Proceedings of the Winter Annual Meeting, New York, N.Y., November 26-30, 1972.

07 p0915 A73-20426

Measurement of dynamic mechanical quantities; Scientific-Engineering Conference, 3rd, Warsaw, Poland, October 26-28, 1972, Summaries

07 p0826 A73-20526

Conference on Decision and Control and Symposium on Adaptive Processes, 11th, New Orleans, La., December 13-15, 1972, Proceedings.

07 p0805 A73-20576

The evolution of population II stars; Proceedings of the Conference, State University of New York, Stony Brook, N.Y., December 3, 4, 1970.

07 p0903 A73-20626

Automatic support systems for advanced maintainability; Symposium, Philadelphia, Pa., November 13-15, 1972, Record.

08 p0951 A73-20676

Reliability physics; Proceedings of the Tenth Annual Symposium, Las Vegas, Nev., April 5-7, 1972.

08 p0943 A73-20729

Welding and fabrication of non-ferrous metals; Proceedings of the International Conference, Eastbourne, Sussex, England, May 2, 3, 1972. Volume 1.

08 p0973 A73-21235

Conference on Display Devices, New York, N.Y., October 11, 12, 1972, Conference Record.

08 p0965 A73-21244

Conference on the Role of Schmidt Telescopes in Astronomy, Hamburg, West Germany, March 21-23, 1972, Proceedings.

08 p0966 A73-21354

American Society of Photogrammetry and American Congress of Surveying and Mapping, Fall Convention, Columbus, Ohio, October 11-14, 1972, Proceedings.

08 p0968 A73-21701

Instrumentation in astronomy; Proceedings of the Seminar-in-Depth, Tucson, Ariz., March 13-15, 1972.

08 p0969 A73-21726

Creep strength in steel and high temperature alloys; Meeting, Sheffield, England, September 20-22, 1972, Preprints.

08 p0980 A73-21776

1972 report to the aerospace profession; Proceedings of the Sixteenth Symposium, Beverly Hills, Calif., September 28-30, 1972.

09 p1030 A73-22176

Association Technique Maritime et Aeronautique, Session, 72nd, Ecole Nationale Supérieure de Techniques Avancées, Paris, France, May 15-19, 1972, Proceedings.

09 p1031 A73-22201

Spring Joint Computer Conference, Atlantic City, N.J., May 16-18, 1972, Proceedings.

09 p1059 A73-22221

Annual Allerton Conference on Circuit and System Theory, 10th, Monticello, Ill., October 4-6, 1972, Proceedings.

09 p1067 A73-22226

Semiconductor Laser Conference, Boston, Mass., May 15-17, 1972, Proceedings.

09 p1091 A73-22235

Symposium on Air Pollution, Turbulence and Diffusion, Las Cruces, N. Mex., December 7-10, 1971, Proceedings.

09 p1114 A73-22326

American Society of Photogrammetry, Annual Meeting, 38th, Washington, D.C., March 12-17, 1972, Proceedings.

09 p1081 A73-22376

Instrument Society of America, Annual Conference, 27th, New York, N.Y., October 9-12, 1972, Proceedings. Part 2.

09 p1082 A73-22501

STOL Seminar, St. Louis, Mo., March 24, 1972, Record.

09 p1032 A73-22524

Topical Conference on RF Plasma Heating, 1st, Texas Tech University, Lubbock, Tex., July 6-8, 1972, Proceedings.

09 p1128 A73-22626

Intersociety Energy Conversion Engineering Conference, 7th, San Diego, Calif., September 25-29, 1972, Proceedings.

09 p1033 A73-22751

The infrared and microwave spectra of stars; International Colloquium on Astrophysics, 17th, Université de Liege, Liege, Belgium, June 28-30, 1971, Proceedings

09 p1149 A73-23126

Power from radioisotopes; International Symposium, 2nd, Madrid, Spain, May 29-June 1, 1972, Proceedings

09 p1037 A73-23276

International Telemetering Conference, Los Angeles, Calif., October 10-12, 1972, Proceedings.

09 p1053 A73-23361

Stress corrosion cracking of metals - A state of the art; Proceedings of the Symposium, Detroit, Mich., October 18, 1971.

10 p1231 A73-23867

All-Union Conference on the Physics of Cosmic Rays, Tiflis, Georgian SSR, October 18-21, 1971, Proceedings

10 p1265 A73-23901

Reinforced plastics - Ever new; Proceedings of the Twenty-eighth Annual Conference, Washington, D.C., February 6-9, 1973.

10 p1237 A73-23951
International Federation of Automatic Control, World Congress, 5th, Paris, France, June 12-17, 1972, Proceedings. Part 2 - Transportation, aeronautics and space, ship automation, and control components. Part 3 - Ecology and systems engineering; Large scale, sensitivity, optimization and adaptation theory. Part 4 - Education, feedback, regulators, linear and nonlinear systems; Identification, differential games, discrete and stochastic systems.

10 p1198 A73-24001
Intermetalbond '72; Conference on the Bonding of Metals, 5th, Boboty, Czechoslovakia, November 21-23, 1972, Proceedings

10 p1224 A73-24088
EASCON '72; Electronics and Aerospace Systems Convention, Washington, D.C., October 16-18, 1972, Record.

10 p1298 A73-24551
Human threats to air safety; Proceedings of the Twenty-fifth Annual International Air Safety Seminar, Washington, D.C., October 16-18, 1972.

10 p1176 A73-24707
Recent research on unsteady boundary layers; Symposium, Universite du Quebec, Quebec, Canada, May 24-28, 1971, Proceedings. Volumes 1 & 2

10 p1207 A73-24801
Modern developments in flow measurement; Proceedings of the International Conference, Harwell, Berks., England, September 21-23, 1971.

10 p1220 A73-24852
Methods of representation and machine analysis of random fields and processes; All-Union Symposium, 5th, Vilnius, Lithuanian SSR, May 1972, Transactions. Sections 1, 2, 3 & 4

11 p1339 A73-25001
The solid-vacuum interface; Proceedings of the Second International Symposium on Surface Physics, Technische Hogeschool Twente, Enschede, Netherlands, June 21-23, 1972.

11 p1325 A73-25201
International Conference on Electromagnetic Windows, 2nd, Ecole Nationale Supérieure de Techniques Avancées, Paris, France, September 8-10, 1971, Proceedings. Volume 1, 2 & 3

11 p1334 A73-25276
Radiation protection at the work site: Scientific, technical and organizational aspects; Annual Scientific Conference, 6th, Karlsruhe, West Germany, May 17-19, 1972, Reports

11 p1322 A73-25310
Composite materials; Meeting, 2nd, Konstanz, West Germany, March 15, 16, 1972, Technical Reports

11 p1372 A73-25401
Vacuum technology at low temperatures; Proceedings of the Symposium, Denver, Colo., August 31, 1970.

11 p1398 A73-25578
Corrosion fatigue: Chemistry, mechanics and microstructure; Proceedings of the International Conference, University of Connecticut, Storrs, Conn., June 14-18, 1971.

11 p1380 A73-25801
Applications of solid mechanics; Proceedings of the Symposium, University of Waterloo, Waterloo, Ontario, Canada, June 26, 27, 1972.

11 p1442 A73-25842
High pressure physics and planetary interiors; Proceedings of the Conference, Houston, Tex., March 1-3, 1972.

11 p1419 A73-25876
Nuclear Science Symposium, 19th, and Nuclear Power Systems Symposium, 4th, Miami, Fla., December 6-8, 1972, Proceedings.

11 p1363 A73-25955
Energy 70; Proceedings of the Fifth Intersociety Energy Conversion Engineering Conference, Las Vegas, Nev., September 21-25, 1970, Volumes 1 & 2.

11 p1308 A73-25976
Infrared detection techniques for space research; Proceedings of the Fifth ESLAB-ESRIN Symposium, Noordwijk, Netherlands, June 8-11, 1971.

11 p1367 A73-26501
Optical and acoustical holography; Proceedings of the Advanced Study Institute, Milan, Italy, May 24-June 4, 1971.

11 p1369 A73-26526
Atoms and molecules in astrophysics; Proceedings of the Twelfth Session of the Scottish Universities Summer School in Physics, University of Stirling, Stirling, Scotland, August 1971.

12 p1538 A73-26920
Asilomar Conference on Circuits and Systems, 6th, Pacific Grove, Calif., November 15-17, 1972, Conference Record.

12 p1483 A73-27151
Radio Technical Commission for Aeronautics, Annual Assembly Meeting, Washington, D.C., November 9, 10, 1972, Proceedings.

12 p1522 A73-27360

Italian contributions to present aerospace activities; Conference, 2nd, Turin, Italy, June 9, 10, 1972, Proceedings

12 p1548 A73-27376
Czechoslovak Seminar on Plasma Physics, 6th, Liblice, Czechoslovakia, May 10-12, 1972, Research Report.

12 p1528 A73-27430
Satellite systems for mobile communications and surveillance; Proceedings of the International Conference, London, England, March 13-15, 1973.

12 p1471 A73-27652
Arbeitsgemeinschaft Ionosphäre, URSI, and Nachrichtentechnische Gesellschaft, General Session, Kleinheubach, West Germany, October 9-14, 1972, Reports

12 p1493 A73-27750
Study of crystalline transformations at high temperature above 2000 K; International Colloquium, Odeillo, Pyrenées-Orientales, France, September 27-30, 1971, Proceedings

12 p1514 A73-27918
Symposium on Ordinary Differential Equations, University of Minnesota, Minneapolis, Minn., May 29, 30, 1972, Proceedings.

12 p1519 A73-27919
Stability of stochastic dynamical systems; Proceedings of the International Symposium, University of Warwick, Coventry, England, July 10-14, 1972.

12 p1519 A73-27920
The mathematical foundations of the finite element method with applications to partial differential equations; Proceedings of the Symposium, University of Maryland, Baltimore, Md., June 26-30, 1972.

12 p1519 A73-27921
Laser interaction and related plasma phenomena; Proceedings of the Second Workshop, Rensselaer Polytechnic Institute of Connecticut, Hartford, Conn., August 30-September 3, 1971, Volume 2.

12 p1508 A73-27922
Metallic crystal growth and defects; All-Union Conference on Metallic Crystal Growth and Imperfections, 2nd, Kiev, Ukrainian SSR, June 15-18, 1970, Proceedings

13 p1631 A73-28101
High speed computing of elastic structures; Proceedings of the Symposium, Université de Liege, Liege, Belgium, August 23-28, 1970, Volumes 1 & 2.

13 p1692 A73-28226
The visual system: Neurophysiology, biophysics, and their clinical applications; Proceedings of the Ninth Symposium, Brighton, England, July 1971.

13 p1574 A73-28351
Rotation of the earth; Proceedings of the Symposium, Morioka, Japan, May 9-15, 1971.

13 p1677 A73-28376
International Symposium on Acoustical Holography, 4th, Santa Barbara, Calif., April 10-12, 1972, Proceedings.

13 p1614 A73-28576
Fluid machinery and fluidics; Proceedings of the Second International Symposium, Tokyo, Japan, September 4-9, 1972, Volumes 1 & 2 - Fluid machinery. Volume 3 - Fluidics. Volume 4 - General lectures, discussions, events.

13 p1602 A73-29004
Airports: Challenges of the future; Proceedings of the Airports Specialty Conference, Dallas, Tex., March 7-9, 1973.

13 p1598 A73-29101
Turbulence in liquids; Proceedings of the Symposium, University of Missouri, Rolla, Mo., October 4-6, 1971.

13 p1604 A73-29251
Conference on General Aviation-Business Flying, University of Tennessee, Tullahoma, Tenn., August 17-19, 1972, Proceedings.

13 p1570 A73-29344
Mechanical behavior of materials; Proceedings of the First International Conference, Kyoto, Japan, August 15-20, 1971. Volume 1 - Deformation and fracture of metals. Volume 2 - Fatigue of metals. Volume 3 - Temperature effects of metals, environmental effects, polymers. Volume 5 - Composites, testing and evaluation.

13 p1638 A73-29451
Power Sources Symposium, 25th, Atlantic City, N.J., May 23-25, 1972, Proceedings.

13 p1572 A73-29581
The motion, evolution of orbits, and origin of comets; Proceedings of the Symposium, Leningrad, USSR, August 4-11, 1970.

14 p1789 A73-29776
Photo-electronic image devices; Proceedings of the Fifth Symposium, Imperial College of Science and Technology, London, England, September 13-17, 1971.

14 p1751 A73-29903
IMEKO Symposium on Microwave Measurement, Budapest, Hungary, May 10-13, 1972, Proceedings.

14 p1733 A73-30054
Launching bases; International Conference, Kourou, French Guiana, November 22-28, 1972, Proceedings

14 p1741 A73-30076

Symposium on Plasma Heating and Injection, Varenna, Italy, September 21-October 4, 1972, Lectures and Seminars.

14 p1779 A73-30117
Societa Astronomica Italiana, Meeting, 15th and Workshop on Rotation as a Phenomenon and Evolutionary Factor in the Universe, Università degli Studi, Bologna, Italy, October 8, 9, 1971, Proceedings

14 p1797 A73-30138
International Conference on the Physics of Semiconductors, 11th, Warsaw, Poland, July 25-29, 1972, Proceedings. Volumes 1 & 2.

14 p1783 A73-30572
Delay and functional differential equations and their applications; Proceedings of the Conference, Park City, Utah, March 6-11, 1972.

14 p1770 A73-30753
Theory and applications of variable structure systems; Proceedings of the Seminar, Sorrento, Italy, April 4-7, 1972.

14 p1739 A73-30776
Heart rate variability and the measurement of mental load; Proceedings of the Symposium, London, England, October 1971.

14 p1720 A73-30876
New directions and new frontiers in variable star research; Colloquium on Variable Stars, 5th, Bamberg, West Germany, August 31-September 3, 1971, Proceedings.

15 p1934 A73-31476
International Conference on Offshore Airport Technology, 1st, Bethesda, Md., April 29-May 2, 1973, Proceedings. Volume 1.

15 p1856 A73-31526
Israel Annual Conference on Aviation and Astronautics, 15th, Tel Aviv and Haifa, Israel, March 14, 15, 1973, Proceedings.

15 p1948 A73-31633
International Conference on Luminescence, Leningrad, USSR, August 17-22, 1972, Proceedings

15 p1884 A73-31711
Localized corrosion - Cause of metal failure; Proceedings of the Symposium, Atlantic City, N.J., June 27-July 2, 1971.

15 p1888 A73-31736
International Symposium on Equatorial Aeronomy, 4th, University of Ibadan, Ibadan, Nigeria, September 4-9, 1972, Proceedings.

15 p1868 A73-31750
Fracture toughness evaluation by R-curve methods; Proceedings of the Symposium, Hawthorne, Calif., September 29-October 1, 1971.

15 p1950 A73-31982
Akademii Nauk SSSR, Astronomicheskii Sovet, Meeting of the Commission on Astronomical Instrument Engineering, Sverdlovsk, USSR, July 1-3, 1970, Proceedings

15 p1877 A73-32128
Cometary Science Working Group, Meeting, Williams Bay, Wis., June 9-11, 1971, Proceedings.

15 p1941 A73-32413
Electronics and civil aviation; International Conference, Paris, France, June 26-30, 1972, Reports. Volumes 1 & 2

15 p1908 A73-32426
International Congress on Metallic Corrosion, 5th, Tokyo, Japan, May 21-27, 1972, Proceedings.

15 p1895 A73-32564
Survival and Flight Equipment Association, Annual Symposium, 10th, Phoenix, Ariz., October 2-5, 1972, Proceedings.

16 p1965 A73-32653
NEREM 72; Northeast Electronics Research and Engineering Meeting, Boston, Mass., October 30-November 3, 1972, Record. Part 1 - Technical Papers.

16 p1986 A73-32717
X- and gamma-ray astronomy; Proceedings of the Symposium, Madrid, Spain, May 11-13, 1972.

16 p2049 A73-32727
European Electro-Optics Markets and Technology Conference, 1st, Geneva, Switzerland, September 13-15, 1972, Proceedings.

16 p2022 A73-32851
Physics of ionized gases 1972; Proceedings of the Sixth Yugoslav Symposium and Summer School, Miljevac, Yugoslavia, July 16-21, 1972.

16 p2040 A73-32938
International Conference on Variational Methods in Engineering, University of Southampton, Southampton, England, September 25-29, 1972, Proceedings. Sessions 1-4, 6-12.

16 p2076 A73-32976
Realism in environmental testing and control; Proceedings of the Nineteenth Annual Technical Meeting, Anaheim, Calif., April 2-5, 1973.

16 p1993 A73-33126
Anglo-American Aeronautical Conference, 13th, London, England, June 4-8, 1973, Proceedings.

16 p1968 A73-33176
Flight Simulation Symposium, 2nd, London, England, May 16, 17, 1973, Proceedings.

16 p1995 A73-33201
International Conference on Cosmic Rays, 12th, University of Tasmania, Hobart, Tasmania, Australia,

August 16-25, 1971, Papers. Volume 7 & Invited and Rapporteur Papers.

16 p2054 A73-33276
Operational remote sensing; Proceedings of the Seminar, Houston, Tex., February 1-4, 1972.

16 p2002 A73-33351
Problems and methods of simulating the environment; Annual Meeting, Karlsruhe, West Germany, September 27-29, 1972, Reports

16 p1997 A73-33376
Winter simulation conference, San Francisco, Calif., January 17-19, 1973, Proceedings.

16 p1985 A73-33416
Annual Scientific Meeting, Las Vegas, Nev., May 7-10, 1973, Preprints.

16 p1973 A73-33421
International Microelectronic Symposium, Washington, D.C., October 30-November 1, 1972, Proceedings.

16 p1989 A73-33466
Annual Reliability and Maintainability Symposium, Philadelphia, Pa., January 23-25, 1973, Proceedings.

16 p2020 A73-33601
Industrial sterilization; Proceedings of the International Symposium, Amsterdam, Netherlands, September 1972.

16 p1975 A73-33691
Propagation of radio waves at frequencies above 10 GHz; Proceedings of the Conference, London, England, April 10-13, 1973.

16 p1980 A73-33701
Numerical methods for non-linear optimization; Proceedings of the Conference, University of Dundee, Dundee, Scotland, June 28-July 1, 1971.

16 p2033 A73-33851
Competitive processes in joining; Proceedings of the Twenty-sixth Autumn Review Course, Eastbourne, England, October 27-29, 1972.

16 p2021 A73-33859
Outlook on safety; Proceedings of the Thirteenth Annual Technical Symposium, London, England, November 14-16, 1972.

17 p2097 A73-34076
Annual National Relay Conference, 21st, Oklahoma State University, Stillwater, Okla., May 1, 2, 1973, Proceedings.

17 p2132 A73-34088
Numerical solution of systems of nonlinear algebraic equations; Proceedings of the Regional Conference, University of Pittsburgh, Pittsburgh, Pa., July 10-14, 1972.

17 p2199 A73-34101
Trends in physics; General Conference, 2nd, Wiesbaden, West Germany, October 3-6, 1972, Lectures.

17 p2256 A73-34109
Conference on Heat and Fluid Flow in Steam and Gas Turbine Plant, University of Warwick, Coventry, England, April 3-5, 1973, Proceedings.

17 p2092 A73-34376
The origin of the solar system; Symposium, Nice, France, April 3-7, 1972, Proceedings

17 p2226 A73-34401
International Aerospace Instrumentation Symposium, 19th, Las Vegas, Nev., May 21-23, 1973, Proceedings.

17 p2165 A73-34601
Electronic Components Conference, 23rd, Washington, D.C., May 14-16, 1973, Proceedings.

17 p2135 A73-34726
Annual Simulation Symposium, 5th, Tampa, Fla., March 8-10, 1972, Record of Proceedings.

17 p2130 A73-34817
Finite element methods in continuum mechanics; Advanced Study Institute, Lisbon, Portugal, September 7-17, 1971, Lectures.

17 p2244 A73-34826
Developments in electronic imaging techniques; Proceedings of the Seminar-in-Depth, San Mateo, Calif., October 16, 17, 1972.

17 p2167 A73-34901
The control of the terrestrial environment from space: International collaboration, methods and technologies; International Conference on Space, 13th, Rome, Italy, March 22-24, 1973, Proceedings.

17 p2160 A73-34926
Electronics in the automation of services; International Congress on Electronics, 20th, Rome, Italy, March 28-31, 1973, Proceedings

17 p2122 A73-34960
Computational Fluid Dynamics Conference, Palm Springs, Calif., July 19, 20, 1973, Proceedings.

17 p2095 A73-35126
NAECON 73; Proceedings of the National Aerospace Electronics Conference, Dayton, Ohio, May 14-16, 1973.

17 p2136 A73-35201
Astronomical observations with television-type sensors; Proceedings of the Symposium, University of British Columbia, Vancouver, Canada, May 15-17, 1973.

17 p2168 A73-35276

Institute of Electrical and Electronics Engineers, International Convention and Exposition, New York, N.Y., March 26-30, 1973, Technical Papers.

17 p2140 A73-35299
Society of Plastics Engineers, Annual Technical Conference, 31st, Montreal, Canada, May 7-10, 1973, Proceedings.

17 p2196 A73-35339
Annual Southwestern Conference and Exhibition, 25th, Houston, Tex., April 4-6, 1973, Record.

17 p2124 A73-35357
Fluid mechanics of mixing; Proceedings of the Joint Meeting, Georgia Institute of Technology, Atlanta, Ga., June 20-22, 1973.

17 p2156 A73-35501
Failure modes in composites; Proceedings of the Symposium, Boston, Mass., May 8-11, 1972.

17 p2191 A73-35526
Electrical engineering - Service to mankind; Proceedings of the Southeast Region 3 Conference, Louisville, Ky., April 30-May 2, 1973.

17 p2142 A73-35626
High-temperature protective coatings; All-Union Conference on Heat Resistant Coatings, 5th, Kharkov, Ukrainian SSR, May 12-16, 1970, Transactions

18 p2318 A73-35876
All-Union Meteorological Conference, 5th, Leningrad, USSR, June 21-25, 1971, Transactions. Volume 1 - General information, resolutions and plenary reports. Volume 2 - Weather prediction section. Volume 3 Climate section. Volume 4 - Section on seeding effects on atmospheric processes

18 p2331 A73-35905
Properties of biological fluids and solids: Mechanics of tissues and organs; Proceedings of the Biomechanics Symposium, Georgia Institute of Technology, Atlanta, Ga., June 20-22, 1973.

18 p2281 A73-36428
Cerebral control of eye movements and motion perception; Proceedings of the Symposium, Freiburg im Breisgau, West Germany, July 20-22, 1971.

18 p2271 A73-36432
Reinforced plastics; Conference, Karlovy Vary, Czechoslovakia, May 15-17, 1973, Lectures

18 p2326 A73-36464
Fracture and flaws; Proceedings of the Thirteenth Annual Symposium, Albuquerque, N. Mex., March 1, 2, 1973.

18 p2363 A73-36482
Advances in electrocardiography; Proceedings of the Symposium, Emory University, Atlanta, Ga., May 10-13, 1971.

18 p2274 A73-36516
Cyclic stress-strain behavior - Analysis, experimentation, and failure prediction; Proceedings of the Symposium, Bal Harbour, Fla., December 7, 8, 1971.

18 p2364 A73-36584
Summer Computer Simulation Conference, Montreal, Canada, July 17-19, 1973, Proceedings. Volumes 1 & 2.

18 p2291 A73-36826
Seminar on Accident Analysis and Prevention, Beirut, Lebanon, June 26-28, 1973, Working Documents.

18 p2268 A73-36845
International Congress of Aeronautical and Space Medicine, 20th, Nice, France, September 18-21, 1972, Reports

18 p2284 A73-36901
Dynamics of ionized gases; Proceedings of the International Symposium, Tokyo, Japan, September 13-17, 1971.

19 p2463 A73-37151
Inter-noise 72; International Conference on Noise Control Engineering, Washington, D.C., October 4-6, 1972, Proceedings and Tutorial Papers.

19 p2472 A73-37276
Remotely manned systems: Exploration and operation in space; Proceedings of the First National Conference, California Institute of Technology, Pasadena, Calif., September 13-15, 1972.

19 p2415 A73-37301
Symposium on Optimisation in Aircraft Design, London, England, November 15, 1972, Proceedings.

19 p2378 A73-37405
National Symposium on Computerized Structural Analysis and Design, George Washington University, Washington, D.C., March 27-29, 1972, Proceedings.

19 p2496 A73-37476
Space Shuttle Program; Proceedings of the Short Course, Boulder, Colo., October 6, 7, 1972.

19 p2491 A73-37591
Air cushion landing systems; Proceedings of the First Conference, Miami Beach, Fla., December 12-14, 1972.

19 p2380 A73-37676
Astronautical research 1971; Proceedings of the Twenty-second Congress, Brussels, Belgium, September 20-25, 1971.

19 p2485 A73-37708
Symposium on Flight Deck Environment and Pilot Workload, London, England, March 15, 1973, Proceedings.

19 p2383 A73-37726

Symposium on International Aircraft Accidents Investigation, London, England, January 15, 1973, Proceedings.

19 p2505 A73-37736
International Conference on Offshore Airport Technology, 1st, Bethesda, Md., April 29-May 2, 1973, Proceedings. Volume 2.

19 p2417 A73-37741
Workshop on Titanium and its Alloys, 3rd, Nantes, France, May 17, 18, 1973, Proceedings

19 p2440 A73-37827
Joint Automatic Control Conference, 14th, Ohio State University, Columbus, Ohio, June 20-22, 1973, Preprints of Technical Papers.

19 p2412 A73-38028
Conference on Video and Data Recording, University of Birmingham, Birmingham, England, July 10-12, 1973, Proceedings.

19 p2431 A73-38195
Waves and turbulence in stable layers and their effects on EM propagation; Proceedings of the Third Symposium, La Jolla, Calif., June 5-15, 1972. Parts 1 & 2.

19 p2447 A73-38202
Engineering aspects of magnetohydrodynamics; Proceedings of the Thirteenth Symposium, Stanford University, Stanford, Calif., March 26-28, 1973.

19 p2469 A73-38310
Intersociety Energy Conversion Engineering Conference, 8th, University of Pennsylvania, Philadelphia, Pa., August 13-16, 1973, Proceedings and Addendum.

19 p2390 A73-38386
Reliability physics 1973; Proceedings of the Eleventh Annual Symposium, Las Vegas, Nev., April 3-5, 1973.

19 p2410 A73-38438
Air Traffic Control Association, Annual Meeting and Technical Program, 17th, Chicago, Ill., October 9-11, 1972, Proceedings.

19 p2453 A73-38461
International Symposium on Circuit Theory, Toronto, Canada, April 9-11, 1973, Proceedings.

19 p2411 A73-38532
Coherence and quantum optics; Proceedings of the Third Rochester Conference, University of Rochester, Rochester, N.Y., June 21-23, 1972.

20 p2569 A73-38601
Japan Congress on Materials Research, 16th, Osaka, Japan, August 1972, Proceedings.

20 p2575 A73-38636
International Conference on Communications, Seattle, Wash., June 11-13, 1973, Conference Record. Volumes 1 & 2.

20 p2522 A73-38713
Astronomische Gesellschaft, Scientific Meeting, Vienna, Austria, September 18-23, 1972, Reports

20 p2605 A73-39056
Annual Corporate Aircraft Safety Seminar, 18th, Arlington, Va., April 1-3, 1973, Proceedings.

20 p2509 A73-39210
Vibrations in environmental engineering; Proceedings of the Symposium, Imperial College of Science and Technology, London, England, July 4, 5, 1973.

20 p2544 A73-39265
Midwestern Mechanics Conference, 13th, University of Pittsburgh, Pittsburgh, Pa., August 13-15, 1973, Proceedings.

20 p2620 A73-39513
International Symposium on Remote Sensing of Environment, 8th, University of Michigan, Ann Arbor, Mich., October 2-6, 1972, Proceedings. Volumes 1 & 2.

20 p2556 A73-39829
International Conference on Ultrahigh-Speed Cinematography, 10th, Nice, France, September 25-30, 1972, Transactions

21 p2693 A73-39933
National Aerospace Meeting, Washington, D.C., March 13, 14, 1973, Proceedings.

21 p2734 A73-40035
All-Union Conference on the Physics of Cosmic Rays, Apatity, USSR, December 12-15, 1972, Proceedings

21 p2755 A73-40576
CIRA 1972: COSPAR international reference atmosphere 1972.

21 p2683 A73-40626
Phased array antennas; Proceedings of the Symposium, Polytechnic Institute of Brooklyn, Farmingdale, N.Y., June 2-5, 1970.

21 p2651 A73-40643
Symposium on Electromagnetic Interference in Aircraft, London, England, February 15, 1973, Proceedings.

22 p2821 A73-41691
International Electromagnetic Compatibility Symposium, New York, N.Y., June 20-22, 1973, Record.

22 p2822 A73-41785
Vacuum Technology Workshop, Versailles, France, May 30-June 3, 1972, Proceedings

22 p2886 A73-41867
Symposium on Temperature, 5th, Washington, D.C., June 21-24, 1971, Proceedings. Part 1 - Basic

methods. Scales and fixed points. Radiation. Part 2 - Resistance, electronic and magnetic thermometry. Controls and calibration. Bridges. Part 3 - Thermocouples. Biology and medicine. Geophysics and space.

22 p2852 A73-41976

Progress in flaw growth and fracture toughness testing; Proceedings of the Sixth National Symposium on Fracture Mechanics, Philadelphia, Pa., August 28-30, 1972.

22 p2920 A73-42131

Life sciences and space research XI; Proceedings of the Fifteenth Plenary Meeting, Madrid, Spain, May 10-24, 1972.

22 p2803 A73-42158

European Conference on Thermophysical Properties, 3rd, Turin, Italy, June 20-23, 1972, Proceedings.

22 p2876 A73-42401

Symposium on Thermophysical Properties, 6th, Atlanta, Ga., August 6-8, 1973, Proceedings.

22 p2932 A73-42501

International Metal Spraying Conference, 7th, London, England, September 10-14, 1973, Proceedings.

22 p2879 A73-42591

Conference on Electron Device Techniques, New York, N.Y., May 1, 2, 1973, Record.

22 p2833 A73-42691

International Symposium on Combustion, 14th, Pennsylvania State University, University Park, Pa., August 20-25, 1972, Proceedings.

22 p2933 A73-42751

Early diagnosis of coronary heart disease; Proceedings of the Second Paavo Nurmi Symposium, Porvoo, Finland, September 9-11, 1971.

22 p2808 A73-42826

Coronary heart disease; Proceedings of the Second International Symposium, Frankfurt am Main, West Germany, June 1972.

22 p2809 A73-42856

Power Electronics Specialists Conference, California Institute of Technology, Pasadena, Calif., June 11-13, 1973, Record.

22 p2801 A73-42901

Isolation of mechanical vibration, impact, and noise; Proceedings of the Colloquium, Cincinnati, Ohio, September 9-12, 1973.

22 p2926 A73-42920

Wolf-Rayet and high temperature stars; Proceedings of the Symposium, Buenos Aires, Argentina, August 9-14, 1971.

23 p3025 A73-43191

Sensitivity, adaptivity and optimality; Proceedings of the Third Symposium, Ischia, Italy, June 18-23, 1973.

23 p2961 A73-43277

Israel Conference on Mechanical Engineering, 7th, Haifa, Israel, June 27, 28, 1973, Proceedings.

23 p2967 A73-43291

Israel Conference on Theoretical and Applied Mechanics, 20th, Tel Aviv, Israel, April 18, 1973, Proceedings.

23 p3038 A73-43302

Signal processing; Specialists' Conference, Erlangen, West Germany, April 4-6, 1973, Reports

23 p2952 A73-43308

Cranfield Fluidics Conference, 5th, University of Uppsala, Uppsala, Sweden, June 13-16, 1972, Proceedings. Volumes I & 2.

23 p2941 A73-43390

Analysis of the test methods for high modulus fibers and composites; Proceedings of the Symposium, San Antonio, Tex., April 12, 13, 1972.

23 p2996 A73-43626

Symposium on Atmospheric Ozone, Arosa, Switzerland, August 21-25, 1972, Proceedings.

23 p2973 A73-43851

Society of Flight Test Engineers, National Symposium, 3rd, Arlington, Tex., September 11-14, 1972, Proceedings.

23 p3050 A73-44052

Arbeitsgemeinschaft Verstaerkte Kunststoffe, Open Meeting, 10th, Freudenstadt, West Germany, October 3-6, 1972, Reports

24 p3103 A73-44876

CONFIDENCE LIMITS

A Bayes analysis of availability for a system consisting of several independent subsystems.

03 p0336 A73-13732

Random coding bound of information theory providing upper bound to decoding error probability for best code of given rate and block length

09 p1111 A73-22117

Gamma-ray emission from the region of the Galactic center.

10 p1264 A73-23530

[AD-759042]

Effect of process variables on partial penetration electron beam welding.

10 p1223 A73-23629

Approximate log normal distribution of normalized power antenna patterns, relating first sidelobe level and antenna size to 0.5 probability level

11 p1337 A73-25668

A confidence estimate of the reliability of a system from the results of tests of its components

12 p1503 A73-27618

Automatic evaluation of strain gage data reliability by comparison with a preset parameter and determination of a statistical yield strength.

13 p1622 A73-29549

Interpretation of the results of simulation tests, taking into account scatter effects

16 p2019 A73-33378

Magnetic-tape qualification and acceptance testing.

16 p2016 A73-33616

Lower confidence bounds determination for component or system reliability by sampling with and without replacement, censored, truncated and mixed sampling test programs

16 p2033 A73-33629

Probability of reception of discrete information with a specified reliability under conditions of random radio interference.

17 p2129 A73-35713

CONFIGURATION MANAGEMENT

Automatic test equipment software configuration management.

08 p0952 A73-20686

CONFINEMENT

Biological effects of lasting hypodynamia on young albino rats in 62 day confinement, considering weight, growth and sexual behavior

08 p0929 A73-20983

CONFORMAL MAPPING

Conformal transformation of semiordeered linear space via inclusion statement, considering second order differential operators

01 p0069 A73-10068

Integral transformations and conformal mapping for velocity distribution of steady two dimensional potential flow along given profile curve

03 p0241 A73-12904

Solution of the wedge entry problem by numerical conformal mapping.

03 p0244 A73-13537

Conformal mapping for Cs ion engine beam optical system with laminar flux, calculating design parameters for current limitation by Cs flow

04 p0488 A73-15722

Applications of conformal mappings to the diffraction of electromagnetic waves by a grating.

06 p0665 A73-18182

Conformal mapping for potential flow about airfoils with attached flap.

07 p0773 A73-19192

Conformal mapping of two airfoil profiles symmetric with respect to real axis onto circles, using rational function power series

07 p0812 A73-20200

Treatment of harmonic mixed boundary problems by conformal transformation methods.

08 p0983 A73-20785

Conformally invariant cosmological and physical models in terms of Einstein, Maxwell and Dirac equations

08 p1009 A73-21228

Orthotropic material plane crack problem numerical solutions by polynomial approximation and modified mapping-collocation technique involving conformal mapping

09 p1161 A73-23178

Conformal invariance of the equations of motion in curved spaces.

10 p1241 A73-23637

Chebyshev projections properties, determining method for minimum linear distortion in class of conformal mappings of given region

10 p1212 A73-24300

Conformal mapping method application to unsteady motion of arbitrary deformable contour in potential flow of ideal incompressible fluid

11 p1348 A73-26426

Quasi-conformal mapping theory of two- and multidimensional regions, considering superposition, hyperbolic and mixed systems and Chebyshev problem

13 p1647 A73-28339

Conformal mapping technique for stress concentration around elliptical hole in shallow spherical shell under internal pressure

14 p1806 A73-30045

Stellar resonant motion in axisymmetric galactic potential, deriving invariant energy mappings from Hamiltonian system of differential equations

14 p1770 A73-30772

Structural components shape optimization for stress concentration reduction, solving complex boundary value problem via conformal transformation to curvilinear coordinates

15 p1954 A73-32108

Inviscid flow through a cascade of thick, cambered airfoils. I - Incompressible flow.

16 p1964 A73-33527

[ASME PAPER 73-GT-84]

Discrete vortex method of two-dimensional jet flaps.

17 p2091 A73-34179

Contribution to the theory of biplane wing sections.

17 p2091 A73-34325

Einstein-Maxwell fields in conformal space, studying field equations, reducible electromagnetic field in

space-time and constraints on metric tensor by Rainich conditions

17 p2212 A73-35560

Almost projective mapping of gravitational fields - Degenerate case

17 p2212 A73-35564

Nonconformally plane relativistic recurrent-curvature spaces

17 p2212 A73-35567

The symmetry method and its application to plane problems of elasticity theory

20 p2618 A73-39325

Russian book on conformal mapping of plane multiply connected singly periodic regions covering Laurent series, lattice regions, trigonometric interpolation and boundary differential characteristics

21 p2726 A73-40806

Finite-boundary corrections to the coplanar waveguide analysis.

23 p2954 A73-44075

Determination of heat flow shape factors for hollow, regular polygonal prisms.

23 p3049 A73-44164

Solution of plane problems of elasticity utilizing partitioning concepts.

23 p3047 A73-44378

[ASME PAPER 73-APM-C]

Semicircular plate uniformly loaded over diameter and with concentrated force at arc top, determining stress distribution by complex variable and conformal mapping

24 p3148 A73-45001

A numerical conformal transformation method for harmonic mixed boundary value problems in polygonal domains.

24 p3107 A73-45544

CONFORMAL TRANSFORMATIONS

U CONFORMAL MAPPING

CONGENITAL ANOMALIES

Fingerprint patterns incidence relation in congenital vitium cordis patients, using Henry dactyloscopic classification

01 p0009 A73-11080

Congenital and acquired color vision defects, discussing color blindness incidence, defect nomenclature and eye tests

05 p0540 A73-16482

Color naming and hue discrimination in congenital tritanopia and tritanomaly.

07 p0782 A73-20251

An automated gas chromatographic analysis of phenylalanine in serum.

11 p1326 A73-25571

Echocardiography status, potentialities and requirements in congenital heart disease diagnosis, considering feasibility in left ventricular performance evaluation

14 p1721 A73-30053

Influence of simulated weightlessness on the mutational rate of Tribolium confusum.

18 p2270 A73-35984

CONGENITAL CONDITIONS

U CONGENITAL ANOMALIES

CONGESTION

Human forearm-muscle blood supply regimes after 'static' exercise with increasing stress

10 p1181 A73-24522

CONICAL BODIES

NT SLENDER CONES

Radially conducting cone wave spectrum calculation for noncophasal excitation, noting circularly polarized TEM and elliptically polarized TM wave amplitudes

03 p0278 A73-14058

The aerodynamic characteristics of the thin delta wing fitted with a conical body in supersonic flow.

04 p0404 A73-15167

The Green's function of the linearized viscous transonic equation

05 p0527 A73-16446

Experimental investigation of hypersonic helium flow around sharp and blunted cones in the presence of strong injection

06 p0643 A73-17466

Three-roll flow turning.

06 p0697 A73-17827

Supersonic flow past large-angle pointed cones.

07 p0775 A73-19981

Application of equiangular conical antennas with thick leads

08 p0938 A73-20963

Further studies of backscattering from a finite cone.

10 p1191 A73-24898

Turbulence in a conical diffuser with fully developed flow at entry.

11 p1345 A73-25057

Supersonic gas flow past the leeward side of a conical wing

11 p1304 A73-26439

Flight test correlation technique for turbulent base heat transfer with low ablation.

11 p1453 A73-26671

Linear axisymmetric self similar solution for blunt nosed rigid cone immersed into ideal compressible

- fluid at subsonic velocity, computing wetted surface radius increase 12 p1487 A73-27410
- Stability of sheet metal drawn by a rigid stamp to cylindrical and conical shapes 12 p1503 A73-27476
- Derivation of shape change equations for asymmetrically heated ablating reentry vehicles. 13 p1706 A73-28750
- Normal impact of a cone against an elastoplastic membrane 14 p1815 A73-30789
- Viscous flow over spinning cones at angle of attack. 17 p2096 A73-35132
- Mathematical method for calculating the optical characteristics of cone-shaped cockpit windscreens. 18 p2266 A73-36069
- Three-dimensional hypersonic transitional/turbulent mean flow profiles. 18 p2260 A73-36194
- [AIAA PAPER 73-635] 18 p2260 A73-36194
- Inviscid supersonic far wake flow past pointed bodies using the method of integral relations. 18 p2262 A73-36222
- [AIAA PAPER 73-671] 18 p2262 A73-36222
- Approximate configuration factors for a gray nonisothermal gas-filled conical enclosure. 18 p2370 A73-36368
- [AIAA PAPER 73-752] 18 p2370 A73-36368
- Study of turbulent wakes behind cones in hypersonic flight using Schlieren photograph correlation 21 p2696 A73-39985
- 21 p2696 A73-39985
- Ultrahigh frequency radar scattering by perfectly conducting conical pyramidal noded bodies, deriving polarized radar cross sections via wedge diffracted field integration 22 p2824 A73-41854
- Some effects of pipe flow generated entry conditions on the performance of straight walled conical diffusers with high sub-sonic entry Mach number. 23 p2939 A73-43294
- CONICAL CAMBER**
- Conically cambered triangular wings with reflex spanwise curvature. 08 p0925 A73-20938
- Lift and drag at off-design Mach numbers of conically cambered wings with subsonic leading edges and supersonic trailing edge 12 p1458 A73-27927
- CONICAL FLARE**
- U CONES**
- CONICAL FLOW**
- A series of evolved shadowgraphs of shock waves induced by secondary injection in a conical supersonic flow. 01 p0003 A73-11128
- Some effects of normal shock boundary layer interaction on the performance of straight walled conical diffusers. 03 p0243 A73-13446
- [AIAA PAPER 72-1140] 03 p0243 A73-13446
- Turbulent shear flow structure parameters in conical diffuser, investigating Reynolds number and turbulent kinetic energy effects 03 p0247 A73-14176
- Performance of truncated conical diffusers with compressible flow. 03 p0249 A73-14641
- Finite fringe holographic interferometry applied to a right circular cone at angle of attack. 05 p0527 A73-16528
- [ASME PAPER 72-APM-PP] 05 p0527 A73-16528
- Experimental and theoretical study of supersonic viscous flow over a yawed circular cone. 07 p0775 A73-19957
- An extension of the vector potential concept to the case of a three-dimensional unsteady boundary layer. 07 p0776 A73-20287
- Perturbation method for linearizing equations of supersonic flow over conical bodies, obtaining potential velocity and entropy solutions 10 p1171 A73-23615
- Study of a new family of solutions of Navier-Stokes equations 14 p1744 A73-29758
- Steady solutions of a nonlinear problem for the Navier-Stokes equations 16 p2031 A73-32933
- Prediction of flow outlet angle in blade rows with conical stream surfaces. 16 p2048 A73-33502
- [ASME PAPER 73-GT-32] 16 p2048 A73-33502
- Flow deflection characteristics of short pyramid wire gauze conical diffuser with high expansion ratio, showing satisfactory uniformity, pressure loss and flow steadiness 16 p2001 A73-34032
- Calculation of the flow on a cone at high angle of attack. 18 p2260 A73-36195
- [AIAA PAPER 73-636] 18 p2260 A73-36195
- A kernel function method for computing steady and oscillatory supersonic aerodynamics with interference. 18 p2262 A73-36221
- [AIAA PAPER 73-670] 18 p2262 A73-36221
- Supersonic conical flow past delta and tapered structures, considering angle of attack, leading edges, flow separation, negative slope concept and pressure distribution 19 p2376 A73-37546
- Determination of a combustion wave in a conical supersonic flow 19 p2503 A73-37551
- Viscous flow over a cone at moderate incidence. II - Supersonic boundary layer. 20 p2507 A73-39093
- Approximation for hypersonic flow past circular cone with angle of attack, discussing matched asymptotic expansion, flow velocity and density distribution 21 p2632 A73-40428
- Methods for calculating nonlinear flows with attached shock waves over conical wings. 22 p2796 A73-42562
- Finite difference and truncation method comparison for supersonic conical flow equations solution, obtaining flow field and shock wave shape 22 p2796 A73-42574
- French monograph - Study of the behavior of the laminar boundary layer in the presence of a positive or negative pressure gradient in hypersonic flow around obstacles. 22 p2797 A73-42744
- CONICAL NOZZLES**
- Numerical calculations of the flow field of low Reynolds number viscous flow with or without real-gas-effects in slender-channel-nozzles. 02 p0152 A73-11674
- [DGLR PAPER 72-110] 02 p0152 A73-11674
- Investigation of the effect of the nozzle cone angle on the parameters of a rarefied gas flow 03 p0245 A73-13624
- Investigation of flow characteristics behind diffusers with large cone angles 03 p0245 A73-13671
- Highly uniform inlet velocity profile influence on conical diffuser characteristics 07 p0774 A73-19615
- Experimental tests on scale models of conical variable geometry propulsion nozzle with short petals for fighter aircraft, discussing aerodynamic and thrust coefficients 12 p1533 A73-27388
- Forces acting on conical diffusers and their relation to integral performance parameters. 18 p2262 A73-36237
- [AIAA PAPER 73-686] 18 p2262 A73-36237
- CONICAL SCANNING**
- A brief survey of monopulse techniques. 11 p1331 A73-26148
- CONICAL SHELLS**
- Bubnov-Galerkin method for natural vibration frequencies of thin elastic circular conical shell under thermal loading 01 p0113 A73-10015
- Designing of shells with a zero Gaussian curvature under an edge load applied to a portion of the shell contour 02 p0230 A73-11717
- Equilibrium equations for rotating conical shells under centrifugal forces and compression loads, calculating revolutions number and stability limits 02 p0232 A73-11819
- Experimental investigation of the influence of initial flexures on the stability of smooth conical shells loaded by external pressure 02 p0236 A73-12576
- Transient axisymmetric response of a conical shell frustum. 04 p0513 A73-15585
- Nonsteady heat conduction of multilayer cylindrical and conical shells in periodic radiation flux, calculating temperature distribution 05 p0640 A73-16798
- Truncated conical shell buckling and stability beyond elastic limit, deriving lower critical loads by orthogonalization method 06 p0760 A73-17781
- Influence coefficients for end-loaded conical frustums. 07 p0913 A73-19983
- Dynamic analysis of freely supported axisymmetric shells. 08 p1018 A73-21473
- Conical shell inversion - An approximate energy analysis. 09 p1163 A73-23266
- [ASME PAPER 72-PVP-4] 09 p1163 A73-23266
- Stress state around an elliptic hole in a conical shell under tension. 09 p1163 A73-23269
- [ASME PAPER 72-PVP-11] 09 p1163 A73-23269
- Isothermal wall conical cavity radiant energy streaming, determining annular baffle effects by Monte Carlo method 10 p1295 A73-23835
- Vibrations of segmented shells. 10 p1293 A73-24720
- Integral transform and heat conduction in a hollow cone with radiation. 10 p1297 A73-24920
- Nonlinear transient stress-waves in cylindrical and conical shells. 11 p1432 A73-24978
- Experimental investigation of the stability of shells with holes 11 p1434 A73-25390
- Nonlinear transient analysis of shells and solids of revolution by convected elements. 11 p1437 A73-25495
- [AIAA PAPER 73-359] 11 p1437 A73-25495
- Buckling analysis of elastically constrained conical shells under hydrostatic pressure by the collocation method. 11 p1438 A73-25499
- [AIAA PAPER 73-364] 11 p1438 A73-25499
- Second order closed form asymptotic solution to Donnell type nonlinear equations of elastic homogeneous conical shells for displacement and stress resultants 11 p1447 A73-26650
- Shallow conical closed shell stability under axisymmetric loads, using variational difference method 12 p1556 A73-27799
- Large amplitude vibrations of certain deformable bodies. I - Discs, membranes and rings. 12 p1556 A73-27929
- Critical rpm of conical shells incorporated in turbine rotors 14 p1814 A73-30686
- Supersonic flutter of truncated multilayered orthotropic conical thin shells. 14 p1814 A73-30702
- Note on forced vibration of a non-homogeneous cone with spherical caps. 14 p1814 A73-30708
- Construction of refined applied theories for a truncated hollow cone of variable thickness 14 p1815 A73-30786
- Stability and free oscillations of conjugate conical shells 15 p1944 A73-30972
- Limit equilibrium of thin-walled containers composed of joined conical sections 15 p1944 A73-30973
- Buckling analysis of elastically constrained stiffened conical shells under hydrostatic pressure by the collocation method. 15 p1948 A73-31642
- Deformation of a multilayer shell of revolution under nonisothermal loading 16 p2074 A73-32684
- Torsional vibrations of shells of revolution of variable thickness. 16 p2081 A73-33682
- Asymptotic characteristics of the problem involving intrinsic asymmetrical vibrations of circular conical shells 17 p2241 A73-34267
- Dynamically-induced large deformations of multilayer, variable thickness shells. 18 p2362 A73-36317
- Stability of truncated conical shells under dynamic external pressure 18 p2363 A73-36413
- Experimental investigation of the stability of oblique conical panels under the action of uniform external pressure 20 p2617 A73-39308
- Investigation of the free vibrations of sectorial plates and conical panels by a theoretical-experimental method 20 p2618 A73-39314
- Russian book on structural mechanics of tapered thin walled conical bodies and wings in aviation and rocket technology 21 p2788 A73-41281
- Plastic collapse of steep conical shells under axial compression. 21 p2789 A73-41684
- CONICS**
- NT PARABOLAS**
- CONJUGATE POINTS**
- Comparative study of monthly and diurnal occurrences of whistlers and gyroelectric echoes in conjugate regions of Europe and South Africa 01 p0043 A73-11274
- Second order trajectory optimization tests in terms of Kelley-Contensou extremals and conjugate points, applying to astrodynamical singular arc 02 p0187 A73-11996
- Conjugate ducted echoes observed on Alouette II ionograms. 02 p0143 A73-12624
- Cosmos 381 onboard ionospheric station signals received from magnetically conjugate region by ground wideband antennas 03 p0280 A73-14576
- Observations of ionospheric electron content at medium latitude geomagnetically conjugate stations. 04 p0440 A73-14955
- Morphology and interpretation of magnetospheric plasma waves at conjugate points during December solstice. 04 p0443 A73-15535
- Magnetically coupled transport of a cold plasma in the outer ionosphere at low latitudes. 05 p0567 A73-16094
- Differences in auroral intensity at conjugate points. 09 p1074 A73-22059
- Balloon observations of auroral-zone X-rays in conjugate regions. 09 p1137 A73-22135
- A study of ionospheric absorption in conjugate regions produced by storm sudden commencements and sudden impulses in the geomagnetic field. 12 p1489 A73-26994

Determination of the effect of electric fields on the ionosphere, based on the behavior of the F2-layer above geomagnetically conjugate points
12 p1493 A73-27760

Nonoscillation and disconjugacy of systems of linear differential equations.
13 p1648 A73-28441

Polar cap E layer conductivity difference effects on ring currents associated with vertical current along lines of force at conjugate points
13 p1608 A73-28717

Theory of conjugate projections in finite element analysis.
17 p2201 A73-34828

ULF geomagnetic power near L = 4. I - Quiet day power spectra at conjugate points during December solstice.
18 p2352 A73-36278

ULF geomagnetic power near L = 4. II - Temporal variation of the radial diffusion coefficient for relativistic electrons.
20 p2551 A73-38936

Bremsstrahlung X ray measurements over subauroral latitudes during substorms, noting e folding energy correlated with local electrojet and anticorrelated with conjugate electrojet
21 p2760 A73-41366

Effect of neutral winds on ionospheric F-region at a pair of conjugate stations in low latitude.
24 p3082 A73-44729

CONJUGATES

NT CONJUGATE POINTS

The conjugate gradient method and its application to aerospace vehicle guidance and control. I - Basic results in the conjugate gradient method.
08 p0951 A73-21428

The conjugate gradient method and its application to aerospace vehicle guidance and control. II - Mars entry guidance and control.
08 p0986 A73-21429

Note on an approximate method for computing consistent conjugate stresses in elastic finite elements.
10 p1290 A73-24293

Immittance functions realizability by passive normal bipoles based on poles and zeros dislocations
10 p1202 A73-24415

Multistep conjugate gradient search methods with memory, describing convergence of iterative procedure for functional minimization
12 p1485 A73-27617

Automation of a solution to the general boundary value problem of a plane self-conjugate elliptic equation
13 p1650 A73-29129

An approach to nonlinear programming.
16 p2032 A73-33301

CONJUGATION

Conjugation of proteinoid microspheres - A model of primordial recombination.
06 p0652 A73-17952

Classical solvability of a problem of conjugation of two equations with the third boundary condition
06 p0718 A73-18684

Boundary value problem of linear conjugation with a piecewise-continuous matrix coefficient
15 p1900 A73-32104

CONNECTIONS

U JOINTS (JUNCTIONS)

CONNECTIVE TISSUE

NT COLLAGENS

Ocular antigens. IV - A comparative study of the localization of immunogenic determinants of ocular structural glycoproteins in connective tissues of various organs.
22 p2802 A73-41729

CONNECTORS

NT ELECTRIC CONNECTORS

Detachable liquid filled capillary waveguide connector for glass fiber multimode optical transmission lines, discussing propagation efficiency as function of dimensional tolerances
20 p2522 A73-38662

CONNECTORS (ELECTRIC)

U ELECTRIC CONNECTORS

CONOIDS

U CONICAL BODIES

CONSCIOUSNESS

Clairvoyant perception of target material in three states of consciousness.
03 p0260 A73-13555

Reaction time method using EEG monitored paroxysm controlled auditory stimuli for responsiveness /consciousness/ evaluation of spike wave burst onset during epileptic seizures
09 p1040 A73-22695

CONSECUTIVE EVENTS

Electronic programming timer with crystal oscillator, IC counters and memory core matrix for event sequence radio control during spacecraft or rocket launchings
01 p0020 A73-11167

Estimation of the passing of four consecutive hours.
06 p0656 A73-17524

CONSEQUENT LAKES

U LAKES

CONSEQUENT STREAMS

U STREAMS

CONSEQUENT VALLEYS

U VALLEYS

CONSERVATION EQUATIONS

A mechanism for the exploding granule phenomenon.
[AD-759887]
05 p0621 A73-17029

Conservation of quasiparticles in weakly turbulent plasmas.
06 p0730 A73-18273

The movement of Volterra disclinations and the associated mechanical forces.
08 p0995 A73-21627

Quantum mechanical formalism for unitary transformations of wave functions, gauge transformations and current conservation, discussing use of gauge invariant atomic orbitals
10 p1251 A73-24245

Initial conditioned solutions of a second-order nonlinear conservative differential equation with a periodically varying coefficient.
10 p1244 A73-24706

Potential operator theory in Hilbert spaces applied to rigorous definition of conservative loading, examining pressure loading case
11 p1434 A73-25212

Asymmetric mechanics of turbulent flows - Energy and entropy
12 p1487 A73-27411

Accuracy of conserving the third adiabatic invariant of the motion of a charged particle in axially symmetrical fields. II.
12 p1535 A73-27634

Periodic rectilinear solutions close to normal mode shapes of vibration of nonlinear conservative system described by differential equations generated by homogeneous potential systems
13 p1661 A73-29083

Periodic solutions close to rectilinear normal mode shapes of vibration of nonlinear conservative system described by differential equations generated by homogeneous potential systems
19 p2459 A73-37634

CONSERVATION LAWS

Higher conservation laws for coherent optical pulse propagation in an inhomogeneously broadened medium.
01 p0078 A73-11221

Gravitational equations derivation identical to electromagnetic Maxwell equations, noting nonviolation of energy conservation
03 p0373 A73-13358

Hubble law correspondence in invariant mechanical theory of universe expansion to direct consequence of impulse conservation in inertially moving many body system
03 p0380 A73-14603

Concerning the accuracy of conservation of the third adiabatic invariant of the motion of a charged particle in axisymmetric fields. I.
05 p0600 A73-16082

Discretized elastic multipolar bodies equations of motion and conservation laws from variational formulation, considering virtual work, Betti principle and Somigliana formulae
06 p0761 A73-17892

Conservation of energy in random media, with application to the theory of sound absorption by an inhomogeneous flexible plate.
07 p0851 A73-19153

Theorems on symmetries and flux conservation in radiative transfer using the matrix operator theory.
08 p1020 A73-20791

Resonant oscillations of conservative system with nonlinear component, obtaining differential equations of motion solution
11 p1448 A73-26731

Conservation laws and preferred frames in relativistic gravity. I Preferred-frame theories and an extended PPN formalism. II - Experimental evidence to rule out preferred-frame theories of gravity.
12 p1540 A73-27326

Elastic unipolar discretized linear bodies, considering motion and constitutive equations, conservation laws, virtual work principle and uniqueness and reciprocity theorems
13 p1659 A73-28559

The conservative method of flows and the calculation of a viscous heat conducting gas flow past a body of finite size
15 p1821 A73-30962

A generalized flux-vorticity theorem. I.
15 p1916 A73-31088

Shock waves, jump relations, and structure.
15 p1864 A73-31974

Viscous fluid dynamic problem solution method implementation in Eulerian code AZTEC within continuum mechanics-kinetic theory union, preserving conservation properties throughout time integration
17 p2155 A73-35142

Higher conservation laws and coherent pulse propagation.
20 p2570 A73-38603

CONSTITUTIVE EQUATIONS

Book - Hyperbolic systems of conservation laws and the mathematical theory of shock waves.
20 p2581 A73-39140

The laws of conservation of energy and momentum during emission of electromagnetic waves /photons/ in a medium and the energy-momentum tensor in macroscopic electrodynamics
21 p2739 A73-40447

Charged black hole collisions as gravitational radiation sources in terms of conservation of mass and surface area
22 p2908 A73-42428

Higher order accuracy finite difference algorithms for quasi-linear, conservation law hyperbolic systems.
22 p2882 A73-42518

The entropy rate admissibility criterion for solutions of hyperbolic conservation laws.
23 p3000 A73-44203

Numerical stabilization of all laws of conservation in the many body problem.
24 p3142 A73-45289

Solution of the Riemann problem for a class of hyperbolic systems of conservation laws by the viscosity method.
24 p3112 A73-45469

CONSOLES

NT REMOTE CONSOLES

CONSTANT SPEED PROPELLERS

U VARIABLE PITCH PROPELLERS

CONSTANTAN

Thermal characteristics of constantan, Ni-Cr-Fe, Ni-Mo, Ce-Al-Fe and Ni-Cr alloy filaments for high temperature strain gages
11 p1362 A73-25456

Theory and performance of plated thermocouples.
22 p2859 A73-42051

CONSTANTS

NT GRAVITATIONAL CONSTANT

NT PERCEPTUAL TIME CONSTANT

NT PLANCKS CONSTANT

NT SOLAR CONSTANT

NT TIME CONSTANT

Astronomical constants and cataloging from 1964 International Astronomical Union, discussing inadequacies and different specific reference systems
21 p2780 A73-41612

CONSTELLATIONS

NT CORONA BOREALIS CONSTELLATION

NT CYGNUS CONSTELLATION

NT ORION CONSTELLATION

NT TAURUS CONSTELLATION

CONSTITUTIONAL DIAGRAMS

U PHASE DIAGRAMS

CONSTITUTIVE EQUATIONS

An action principle in general relativistic magnetohydrodynamics.
01 p0079 A73-11258

Linearly elastic materials theory covering kinematics, momentum balance, constitutive relation, boundary value problems and field equations
02 p0233 A73-11977

Shell and plate theory covering constitutive and equilibrium equations, Cosserat surfaces and uniqueness theorem
02 p0234 A73-11981

Rods theory covering constitutive equations, boundary value problems, variational formulation of equilibrium problems and uniqueness theorems
02 p0234 A73-11982

International system of units applicability to constitutive equations of four dimensional relativistic electrodynamics
03 p0341 A73-12896

Constitutive equation for shock waves under dynamic load in prismatic bar axially prestressed to plastic range
03 p0383 A73-12903

Discretized body mechanics equilibrium, constitutive and motion equations application to elastic lattice type shell structures
03 p0393 A73-13779

Finite difference theory for bending stress concentration in shells of revolution, noting constitutive equation for thermal stress analysis
03 p0393 A73-13793

Constitutive analysis of elastic-plastic crystals at arbitrary strain.
03 p0394 A73-13983

Energy balance, motion and constitutive equations of polar fluids, considering entropy inequality, viscosity and dissipation rate
04 p0434 A73-15679

Motion, constitutive and energy balance equations for materials with microstructure, considering elastic bodies
04 p0514 A73-15680

Discretized body defined as special system with finite degrees of freedom, describing mechanics in terms of constitutive and motion equations
06 p0723 A73-17894

French monograph - Determination and utilization of the laws of viscoelastic fluid behavior.
06 p0686 A73-18098

Optical constitutive equation derivation for Tresca type plastic dielectrics, calculating birefringence and extinction angle in simple shear

06 p0723 A73-18458

Homogeneous flat elastic plate theory in Cosserat surface context, considering application of general constitutive equations and extension to right circular cylindrical shells

07 p0908 A73-19085

Tresca-type plastic materials in the theory of hypoelasticity. I Mechanical constitutive equations and simple shear deformation.

07 p0909 A73-19161

Thermal hereditary constitutive law for linear viscoelastic materials time response in transient temperature environment

08 p1018 A73-21409

Constitutive equation for electronic circuits without topologically dependent variables, noting numerical analysis of equations of state for nonlinear circuits

08 p0951 A73-21551

On dynamic plasticity. I

08 p1020 A73-21823

Green operator evaluation by Fourier transform method for wave propagation in bianisotropic media, obtaining constitutive equations

09 p1049 A73-22311

Electromagnetic propagation in bianisotropic stratified media, obtaining Maxwell and constitutive equations in operator form

09 p1049 A73-22312

A comparison of solutions in first approximation shell theory.

10 p1291 A73-24337

Optically active materials light reflection polarization characteristics, comparing theories based on wave vector and permittivity tensor and on polarization/magnetization current constitutive equations

10 p1261 A73-24693

Rigorous analogies between elastic and electromagnetic systems.

10 p1250 A73-24873

Gradient decomposition and kinematic constitutive equations for elastoplastic material behavior under large strains

11 p1445 A73-26410

Tresca-type plastic materials in the theory of hypoelasticity. II Optical constitutive equations and birefringence in simple shear.

11 p1447 A73-26649

Deformation bounds for a creeping structure approaching rupture.

11 p1447 A73-26654

Thermodynamic theory of heat conducting fluids with constitutive quantities dependence on rate of density, gradient, velocity and temperature

11 p1453 A73-26746

On a finite strain theory of elastic-inelastic materials.

13 p1692 A73-28167

The general form of constitutive equations in relativistic physics.

13 p1658 A73-28374

Deformable solid as discretized body in classical continuum mechanics, deriving motion and constitutive equations

13 p1659 A73-28558

Elastic unipolar discretized linear bodies, considering motion and constitutive equations, conservation laws, virtual work principle and uniqueness and reciprocity theorems

13 p1659 A73-28559

Boltzmann-Volterra constitutive law for viscoelastic linear materials, investigating criteria for relaxation properties

13 p1659 A73-28562

A theoretical study of fracture and yield conditions derived from hypo-elasticity.

13 p1639 A73-29464

Incremental formulation for problems with geometric and material nonlinearities.

14 p1808 A73-30190

Linearized constitutive equations for thin viscoplastic shell deflection under dynamic loads

14 p1811 A73-30488

Rate-type constitutive equations for plateau predictions in dynamic plasticity for stress, strain and particle velocity functions

14 p1812 A73-30492

Constitutive equations and directors in plastic and viscoplastic media

15 p1947 A73-31368

Finite amplitude dynamic motion of viscoelastic materials.

15 p1956 A73-32223

Three-dimensional turbulent boundary layer - Calculations and experiments

16 p1961 A73-32806

Constraints theory for Cosserat surfaces with applications in thermomechanics and shell theory, investigating equilibrium laws transformation properties and constitutive equations restrictions

16 p2076 A73-32936

Principle of virtual work and Piola theorem for motion and constitutive equations and boundary conditions of oriented elastic media, using point continuum mechanics assumptions

16 p2080 A73-33245

One dimensional shock waves in heat conducting materials with memory. III - Evolutionary behaviour.

16 p2081 A73-33747

Book - Nonlinear viscoelastic solids.

17 p2243 A73-34574

Continuum mechanics - A brief review.

17 p2244 A73-34827

On one-dimensional large-displacement finite-strain beam theory.

17 p2252 A73-35828

Constitutive equations of a plasma with bound charges.

19 p2468 A73-37521

Compressible fluid dynamic theory, using stress tensors to derive constitutive equations for plane homogeneous and shear flows

19 p2420 A73-37644

Constitutive equations for isotropic and anisotropic perfectly plastic materials derived from Clausius-Duhem inequality, considering thermal influences, plastic flow, entropy and elastic deformation

19 p2501 A73-38283

Propagation of stress wave with plastic deformation in metal obeying the constitutive equation of the Johnston-Gilman type.

20 p2615 A73-38888

Material indifference - A principle or a convenience.

20 p2619 A73-39337

Statistical continuum mechanics and constitutive theories governing microfluid behavior, noting relations with aid of tables

20 p2547 A73-39343

Stability of waves and shock structure in generalised thermoelasticity at low temperatures.

20 p2624 A73-39564

Response function class for constitutive equations in nonlinear isothermal theory of elastic-plastic metals, discussing free energy and stress response as measure of deformation

[ASME PAPER 73-APMW-30] Finite amplitude dynamic motion of viscoelastic materials.

23 p3038 A73-43273

Prediction of stability of viscoelastic Couette flow based on network rupture hypothesis.

23 p2967 A73-43300

Constitutive equations of elastoplastic and elastoviscoplastic bodies based on thermodynamic state, considering deformation velocity and stress relaxation

23 p3043 A73-43967

Mandel viscoplasticity theory constitutive equations satisfying causality principle, considering finite deformations tensor representation by partial differentials

23 p3044 A73-43970

Buckling of short viscoplastic cylindrical shells subjected to radial impulse.

23 p3045 A73-44080

Dislocation plasticity theory for slip system in terms of constitutive equations for dislocation speeds and densities, extending to rigid viscoplastic body

23 p3046 A73-44226

On the description of cyclic deformation processes using a more general elasto-plastic constitutive law.

24 p3147 A73-44683

Constitutive equations, creep laws, stress functions, variational principles and differential operators in dynamic and static linear viscoelasticity theory

24 p3153 A73-45496

CONSTRAINTS

NT METEOROLOGICAL PARAMETERS

Infinite groups with constraints on subgroups, discussing Chernikov theorems, minimality requirements, laminarly finite groups and Abelian subgroups

01 p0070 A73-11075

Existence theorems for boundary value problems of elasticity defined by unilateral constraints, developing abstract theory of functional inequalities

02 p0233 A73-11979

Boundary value problems of elasticity with unilateral constraints.

02 p0234 A73-11980

Multidimensional judgments in design of ideal organisms with integral number of resource units allocated among characteristics such as memory, vision, resourcefulness, etc

03 p0261 A73-13559

Momentum constraints as integrability conditions for the Hamiltonian constraint in general relativity.

05 p0599 A73-17350

Absolute minima determination for homogeneous polynomial real valued goal function under equality constraints, solving nonlinear programming problem by penalty function method

06 p0716 A73-17851

Relations between the first integrals of a non-holonomic mechanical system and of the corresponding system freed of constraints.

07 p0850 A73-19013

Optimization of system reliability using a parametric approach.

09 p1112 A73-22646

Anholonomic constraints imposed on mechanical systems which have rigid solid bodies as constituent elements. II - Anholonomic constraints realized by nonsliding roller bearings

12 p1523 A73-26794

Kron's method - A consequence of the minimization of the primitive Lagrangian in the presence of displacement constraints.

13 p1700 A73-29381

A survey of methods for solving constrained minimization problems via unconstrained minimization.

16 p2033 A73-33857

Generalization of an exact method for solving equality constrained problems to deal with inequality constraints.

16 p2033 A73-33858

Equations of motion for systems with nonlinear, second-order, nonholonomic connections

17 p2211 A73-34147

Constrained continuous media mechanics, discussing basic assumptions, integrable and nonintegrable constraints and motion

17 p2241 A73-34321

A comparison of the complex method of optimization with the penalty function approach using Zangwill's method for constrained optimization problems.

17 p2202 A73-35385

A dual method for optimal control problems with initial and final boundary constraints.

19 p2446 A73-38376

Determination of an optimal dynamic system according to complex statistical criteria in the presence of constraints

20 p2539 A73-38680

Constrained optimization using a nondifferentiable penalty function.

21 p2725 A73-40384

Motion of a solid with a nonholonomic constraint at a fixed point

23 p3007 A73-44200

CONSTRICTIONS

A new explanation for the creep of domain boundaries with transverse constrictions

09 p1098 A73-21846

CONSTRUCTORS

Numerical calculations for the turbulent arc constrictor.

07 p0858 A73-19960

CONSTRUCTION MATERIALS

Construction materials selection for thermal dimensional stability in critically sensitive precision instruments and mechanical components, considering economic factors

01 p0066 A73-11293

Rocket nozzles fabrication technology, discussing construction materials and manufacturing processes [AIAA PAPER 72-1191]

03 p0358 A73-13481

Experience with the application parametric diagrams to the calculation of the heat resistance of construction materials

04 p0466 A73-15665

Welding airframe structures in titanium alloys using tensile loading as a means of overcoming distortion.

08 p0973 A73-21240

Russian book on extra light engineering alloys covering Mg-Li alloys structure and mechanical properties, aging and strain hardening characteristics, corrosion resistance, etc

08 p0979 A73-21600

Influence of notch and thread rolling on the fatigue strength of samples prepared from VT3-1 and VT16 alloys

10 p1233 A73-24370

Design of lowest-cost prestressed combined metallic systems

11 p1371 A73-25035

Gaseous environments compatibility with structural alloys under fatigue loading, presenting crack growth rate data

11 p1381 A73-25816

Aircraft structures aluminum alloys fatigue crack growth rate relationship to cracking mode, stress ratio, cyclic frequency and corrosive environment severity

11 p1382 A73-25826

The effect of vacuum on the high temperature, low cycle fatigue behavior of structural metals.

11 p1383 A73-25834

Cumulative creep formulas for construction steels at stepwise increasing temperatures

12 p1510 A73-26900

A new method for the study of the phenomenon of dynamic instability of thin-walled bars used in the construction of aeroplanes, ships and bridges.

12 p1551 A73-27063

The changes in structural and mechanical properties of construction materials under loads

12 p1513 A73-27500

Al alloys, steels and superalloys properties improvements for aerospace vehicles structural applications,

discussing diffusion bonding and isothermal forging techniques 13 p1633 A73-28180

Choice of materials on the basis of random vibration and structural fatigue. 13 p1641 A73-29495

Minimum creep lives of structural metallic materials at elevated temperatures. 13 p1701 A73-29514

Investigation of the strength of construction materials for different radii of the main stresses. 13 p1703 A73-29622

Test assembly for structural component members under different climatic conditions 14 p1743 A73-30689

Russian book - Titanium - The new structural material. 15 p1893 A73-32512

Brittle fracture mechanics models of structural materials in terms of elastic continuum with crack 18 p2366 A73-36823

Aeronautical turbine blade and vane materials selection, considering Ni alloys with powder metallurgy and oriented solidification, composite materials and eutectics 18 p2326 A73-36993

Solid refractory metal and nonmetal alloys for machine structural components under dynamic and steady cumulative stresses 18 p2326 A73-37000

Algorithm for optimal material selection by seeking tradeoff between conflicting multifunctional structural design objectives 19 p2496 A73-37477

Large floating ocean platforms for US Navy bases, discussing concrete construction techniques and costs for different configurations 19 p2418 A73-37749

Method of studying the resistivity to external effects in fiberglass plastic structural elements with highly dispersed initial-state properties 20 p2580 A73-39380

Cumulative creep formulas for construction steels at stepwise increasing temperatures 21 p2720 A73-41033

Aircraft windshield stretched acrylic plastic, chemically strengthened glass, and clad polycarbonate curved composite materials 22 p2799 A73-41863

Low-pressure prepreps as structural material for light-construction designs 24 p3104 A73-44887

R and D efforts for various aircraft construction materials, considering steels, alloys and fiber-containing laminates 24 p3100 A73-45198

CONSUMPTION

NT FUEL CONSUMPTION

NT OXYGEN CONSUMPTION

NT WATER CONSUMPTION

CONTACT LENSES

Management of cataract in commercial flight personnel. 18 p2285 A73-36927

CONTACT POTENTIALS

Influence of changes in the contact region on the basic characteristics of a semiconductor in the illuminated mode 09 p1134 A73-22685

Potential energy method for boundary value problem of axisymmetric elastic contact of solid and hollow cylinders compressed by plane walls 10 p1289 A73-24064

Pressure effects on contact potential in diode p-n junction, discussing potential barrier height variation, minority carrier concentration changes and relative position of energy bands 11 p1338 A73-26520

CONTACT RESISTANCE

Design and practical aspects of maximum efficiency silicon solar cells for satellite applications. 03 p0254 A73-14205

Metallic contact resistance and friction behavior under microdisplacement for lead/gold surfaces with lubricant or oxide film, noting consistency with Greenwood theory [ASLE PREPRINT 72LC-6B-1] 03 p0316 A73-13464

Frictional behaviour of molybdenum disulphide in high vacuum. 04 p0454 A73-14997

Surface effects during fretting fatigue of Ti-6Al-4V. 04 p0461 A73-14998

Electrical contacts to ion cleaned n-type gallium arsenide. 07 p0797 A73-19136

Bielayev's point in poroelastic bodies in contact. 08 p1016 A73-20829

Electric relay contacts physical characteristics and state changes during dry circuit, low level, intermediate and power switchings 17 p2132 A73-34090

Electric relay operating envelope definition and test plan for contact contamination and deterioration and

resistance determination through controlled environmental changes 17 p2132 A73-34091

Modeling the effect of air and oil upon the thermal resistance of a sphere-flat contact. 18 p2370 A73-36362

[AIAA PAPER 73-746]

Determination of thermal contact resistance using a pulse technique. 22 p2878 A73-42511

CONTACTS [ELECTRIC]

U ELECTRIC CONTACTS

CONTAINERS

Evaluation of materials for underground exposure in extreme environments. 03 p0329 A73-13006

Land-air-sea intermodal cargo container movement procedures and equipment design standardization to meet air transportability requirements [ASME PAPER 73-ICT-30] 23 p2965 A73-43493

CONTAINMENT

Post impact behavior of mobile reactor core containment systems. 07 p0850 A73-20468

CONTAMINANTS

NT RADIOACTIVE CONTAMINANTS

NT TRACE CONTAMINANTS

The analysis of particulate contaminants in hydraulic fluids. 02 p0132 A73-12004

The removal of impurities from hydrazine for control of contamination caused by rocket engine exhaust. [AIAA PAPER 72-1046] 03 p0351 A73-13379

Pollutants from methane fueled gas turbine combustion. 04 p0485 A73-15867

Effects of contaminants in CO2 lasers. 06 p0699 A73-17628

[AIAA PAPER 73-52]

Quantitative evaluation of superficial organic contaminants, soluble in halogenated solvents, discussing sampled surface solvent extraction method and subsequent IR absorption spectrographic analysis 06 p0660 A73-18547

An analytical model for the prediction of liquid rocket plume contamination effects on sensitive surfaces. [AIAA PAPER 72-1172] 12 p1532 A73-27099

The tolerance of fluid machinery to contaminant wear. 13 p1571 A73-29031

Stratospheric contamination experiments with a one-dimensional atmospheric model. [AIAA PAPER 73-531] 16 p2007 A73-33564

A model for studying the effects of injecting contaminants into the stratosphere and mesosphere. [AIAA PAPER 73-539] 16 p2008 A73-33569

Static-kinetic dichotomy in friction theory, examining atmospheric contaminants effects on surfaces, theoretical basis of static friction postulation and sliding velocity effect on theory [ASLE PREPRINT 73AM-8A-2] 17 p2179 A73-34992

Evaluation of 165 deg F reverse osmosis modules for wastewater purification. [ASME PAPER 73-ENAS-2] 19 p2399 A73-37964

Nuclear submarine atmospheric constituent monitoring, covering mass spectrometers, IR carbon monoxide sensors, system development, requirements testing and spacecraft applications [ASME PAPER 73-ENAS-9] 19 p2399 A73-37970

Solid tantalum capacitor failure modes, discussing slug impurities, dielectric imperfections, short circuits, scintillation shorts, anodizing, soldering, screening methods and cost reduction 19 p2410 A73-38443

Electrical control of particulate pollutants from flames. 22 p2935 A73-42799

CONTAMINATION

NT FUEL CONTAMINATION

NT SPACECRAFT CONTAMINATION

A fundamental method for evaluating the contaminant tolerance of fluid power control valves. 02 p0132 A73-12003

Propellant grain surface contamination effect on ignition transient characteristics of solid rocket motor [AIAA PAPER 72-1198] 04 p0487 A73-14920

Development and evaluation of materials for vacuum power interrupters. 04 p0456 A73-15763

Spectral transmittance of cryodeposits on a transmitting substrate. [AIAA PAPER 73-149] 05 p0598 A73-16897

Prevention of pollution in hydraulic circuits. 06 p0649 A73-17845

Terrestrial contamination in Apollo lunar samples. 06 p0754 A73-18425

Passive and active mode classification of air contamination sources in closed manned spaces, considering mechanical, electrical, chemical, physical and human factors 11 p1321 A73-25037

Effect of contamination on flueric system reliability. 16 p1971 A73-33476

Electric relay operating envelope definition and test plan for contact contamination and deterioration and resistance determination through controlled environmental changes 17 p2132 A73-34091

An evaluation of ionospheric probe performance. I - Evidence of contamination and clean-up of probe surfaces. II - The influence of vehicle wake effects on electron density and temperature measurements. 17 p2160 A73-34786

Satellite retarding potential trap contamination relationship to electron and ion temperatures evaluation, discussing Langmuir probes, sweep frequency and plasma density 19 p2429 A73-37373

Blood plasma contamination of the lung alveolar surfactant obtained by various sampling techniques. 21 p2642 A73-41637

CONTINENTAL DRIFT

Seismicity as a guide to global tectonics and earthquake prediction. 11 p1352 A73-25563

Secular pole motion vs continental drift effects from geodetic, astronomical and time base observations 13 p1678 A73-28386

Earth pole secular motion analyzed by latitude observations, suggesting northward drift of major continents 13 p1679 A73-28389

Earth axis displacement and continental drift related to lack of coincidence of core and mantle-crust centers of mass 13 p1679 A73-28399

Polar wandering and the earth's dynamical evolution cycle. 13 p1679 A73-28403

The implications for geophysics of modern cosmologies in which G is variable. 14 p1799 A73-30525

Worldwide sea level pulsations and interpolations relation to elevation and subsidence of oceanic ridge systems, discussing sea floor spreading hypotheses 17 p2164 A73-35858

CONTINENTS

NT AFRICA

NT EUROPE

NT NORTH AMERICA

NT SOUTH AMERICA

CONTINUITY [MATHEMATICS]

Approximation by functions of fewer variables. 02 p0186 A73-11969

A digital simulation method for interconnected continuous systems. 03 p0281 A73-14479

Gravitation finite range evidence presentation of major theoretical problem for general relativity, discussing continuity and invariance 06 p0724 A73-18548

Vectorial topological continuous function spaces bounded parts, constructing tunneled, quasi-tunneled and nontunneled spaces 11 p1390 A73-25865

Absolute continuity of estimates corresponding to uniform Gaussian fields 12 p1523 A73-27185

Nonlinear elements piecewise and continuous approximations for constructing current-voltage characteristic functions 13 p1596 A73-28871

First derivative discontinuities of space-time metric tensor in Einstein equations solution for nonisotropic and isotropic hypersurfaces, proving coordinate system existence for continuity 14 p1774 A73-30328

Nonlocal continuance of solutions to vibration-stable differential equations 15 p1899 A73-31219

Liapunov functions and boundedness and global existence of solutions. 15 p1901 A73-32375

An equivalence theorem on best approximation of continuous functions by algebraic polynomials. 15 p1902 A73-32376

Isoparametric element forms in finite element analysis. 17 p2245 A73-34834

Optimal control of linear systems in the case of continuous and discrete controls 18 p2337 A73-36410

Discontinuous solutions of hyperbolic optimum problems 20 p2581 A73-38675

Russian book on topological spaces and groups with continuous operations covering rings, Lie group, compact groups, homomorphism, automorphism, isomorphism, etc 21 p2726 A73-40801

CONTINUITY EQUATION

Global distributions of thermal energy content and losses in thermosphere, discussing energy sources, continuity equations and transport mechanisms for heat balance 02 p0162 A73-12288

- Coupling between the F-region and protonosphere - Numerical solution of the time-dependent equations. 07 p0818 A73-19665
- Nighttime midionosphere dynamical perturbations on ionizations from solutions of time dependent continuity equation with charge transport effects, considering semidiurnal atmospheric tide propagation mode. 09 p1075 A73-22130
- The continuity and Poisson's equations for semiconductors with many coexisting kinds of multiple energy-level defects. 09 p1133 A73-22306
- A theoretical study of lunar variations in foF2 at low latitude. 11 p1354 A73-25764
- The Castiglione variational equation and strain continuity relations for a thin shell. 12 p1555 A73-27788
- A dynamic modeling method of unsteady flows in long fluid lines with turbulent bulk velocities. [ASME PAPER 73-FE-18] 17 p2153 A73-35014
- A method for calculating unsteady turbulent boundary layers in two- and three-dimensional flows. 17 p2154 A73-35135
- Flux-corrected transport - A minimum-error finite-difference technique designed for vector solution of fluid equations. 17 p2202 A73-35145
- Diffusion of a vertical jet into a fluid medium of arbitrary density. 19 p2420 A73-37547
- Diurnal thermospheric and ionospheric variations from time dependent continuity equations for O⁺, H⁺, O₂⁺, and NO⁺ ions, motion and heat conduction equations. 22 p2849 A73-42572
- Continuity equation and equations of motion for ideal plastic body based on von Mises yield condition, considering stress discontinuity and boundary value problems. 24 p3153 A73-45499
- ### CONTINUOUS NOISE
- Effects of signal duration and masker duration on detectability under diotic and dichotic listening conditions. 01 p0008 A73-10436
- ### CONTINUOUS RADIATION
- #### NT MODULATED CONTINUOUS RADIATION
- Passive mode locking of the cw dye laser. 01 p0058 A73-10129
- Subsonic plasma motion in continuous laser light. 01 p0084 A73-10472
- Organic dye lasers tuning by diffraction gratings and prisms, noting CW, pulsed and mode locking operations. 01 p0059 A73-10716
- Flame-sheet analysis of C.W. diffusion-type chemical lasers. II - Coupled radiation. 01 p0059 A73-10727
- Phase switched FM-CW radio altimeter, noting error reduction by controlled switching of phase difference between emitted and echo signals. 02 p0165 A73-11526
- Mobile FM-CW radar sounder with scanning capability for high resolution remote sensing in lower troposphere, discussing design and performance. 02 p0140 A73-11959
- Gain and frequency characteristics of a 20 mW C.W. water vapour laser oscillating at 118.6 microns. 02 p0177 A73-12724
- Cutting thin metal sheets with the CW CO₂ laser. 02 p0175 A73-12819
- 4830 MHz observations of the formaldehyde molecule in the direction of discrete radio sources. 03 p0371 A73-13214
- CW dye laser with dye solution pumped through simple nozzles to provide unconfined flowing thin streams with optical quality and long term stability. 03 p0320 A73-14460
- CW neutral Ar laser line competition effect observation, establishing correct transition assignment. 03 p0320 A73-14461
- A calorimeter for high-power CW lasers. 03 p0310 A73-14495
- Low current mercury vapor discharge positive column plasma continuous radiation measurements as function of pressure, current density and temperature at 2300-14,000 Å. 03 p0348 A73-14624
- Thermal defocusing of high intensity continuous Ar laser radiation in absorbing medium with allowance for spherical aberrations. 04 p0458 A73-15562
- Correlation analysis of the continuum radio emission of noise storms. 04 p0504 A73-16028
- Continuum radiation from nonisothermal hydrogen plasmas. 05 p0602 A73-16558
- Measurement of continuum radiation from an argon plasma. 05 p0602 A73-16564
- Picosecond pulses from a passively mode-locked cw dye laser. 05 p0585 A73-17222
- On a set of continuous wave electromagnetic inverse scattering boundary conditions. 06 p0664 A73-18136
- CW Q band Gunn diode microwave oscillator fabricated by integral heat sink technique for high power output and efficiency. 06 p0677 A73-18345
- Output power dependence on mode geometry in CW gas dynamic laser resonator within kinetic theory of interaction between radiation field and optically active medium stream. 06 p0702 A73-18459
- Efficient pumping of a CW garnet laser by water-cooled metal-halide lamps. 06 p0703 A73-18600
- Properties of the radio continuum emission from interacting galaxies. 07 p0900 A73-20280
- Propagational mode deducted from signal strengths in the VHF band on the trans-equatorial path. 09 p1051 A73-22749
- Thermal limitation for CW output power of a Gunn diode. 09 p1064 A73-23043
- The generation of tunable coherent radiation in the wavelength range 2300-3000 Å using lithium formate monohydrate. 12 p1504 A73-26826
- Thermal limitations of CW and pulsed silicon TRAPATT diodes. 12 p1478 A73-27110
- An electrooptical method for storage of weak linear-FM signals. 12 p1470 A73-27577
- The concept of an installation for measuring partial reflections with the aid of the FM-CW procedure and the principle of measurement involved. 12 p1486 A73-27764
- HF CW ultrasonics, discussing elimination of electromagnetic leakage or crosstalk between transmitter and receiver by sampling technique. 13 p1612 A73-28483
- CW NMR millidegree thermometer using oscillator to detect resonance, noting Curie law, magnetogyric ratio, spin-lattice relaxation time and low electrical conductivity. 13 p1618 A73-29072
- Continuum galactic background radio emission, considering rerefied ionized hydrogen gas with filaments due to dense inhomogeneities. 15 p1938 A73-31953
- Microwave capabilities of transferred-electron devices. 16 p1986 A73-32720
- Biophysical hazards of microwave radiation. 16 p1974 A73-32723
- Time dependent diffusion equation for solar flare cosmic ray propagation through interplanetary space, specifying continuous emission curve shape and period. 16 p2053 A73-32966
- FM-CW method application to partial reflection measurements of ionospheric electron density to avoid man-made interference and interpretation difficulties from frequency spectrum broadening. 18 p2305 A73-36008
- Continuum emission from recombining oxygen and nitrogen plasmas. 18 p2338 A73-36799
- Non-Gaussian statistics of superradiant radiation from saturated xenon 3.5-micron laser amplifier. 20 p2570 A73-38620
- Self calibrating automatic equipment for pulsed and CW RF testing of phase, amplitude and frequency characteristics of pulsed electronic devices. 20 p2535 A73-38870
- Verification of sensitivity enhancement factors for CW ultrasonic resonators. 20 p2565 A73-38887
- Analysis of the solar X-ray spectrum of 20 August 1971. 21 p2760 A73-40826
- Continuum centimeter wave radiometers circuits, parameters, sensitivity and atmospheric radio emission fluctuations. 21 p2705 A73-41460
- Vacuum-UV radiation of laser-produced plasmas. 23 p3008 A73-43340
- Stellar radiation Thomson scattering by free electrons compared to atomic processes as mechanism for H II regions continuous emission. 23 p3030 A73-43756
- Continuum galactic background radio emission, considering rarefied ionized hydrogen gas with filaments due to dense inhomogeneities. 24 p3131 A73-44478
- Wolf-Rayet stars continuous and line spectral features interpretation by model involving wide emission lines due to Doppler effect in rapidly expanding envelope. 23 p3026 A73-43201
- ### Kinetics of chemical high-pressure lasers
- 23 p2987 A73-43716
- Spectrophotometric gradients, temperatures and continuous spectra energy distribution of star SS Cyg, showing dependence on flare development. 23 p3036 A73-44245
- ### CONTINUOUS WAVE LASERS
- CW laser beams steady state thermal self focusing stability, deriving nonlinear absorbing medium geometrical optics ray equation and aberration pattern. 06 p0702 A73-18583
- High-power Y3AlO12:Nd3+/ laser with an explosion-type lamp. 06 p0703 A73-18597
- Optimization of the parameters of a quasi-CW YAG:Nd3+/ laser with a nonlinear element in the resonator. 06 p0703 A73-18599
- CW operation in some CO lines below 5.0 microns. 06 p0704 A73-18892
- CW and pulsed deuterium fluoride-carbon dioxide transfer chemical laser with molecular vibrational energy transfer for population inversion to obtain high power output. 07 p0834 A73-19630
- A CW-CO chemical laser from the reaction of active nitrogen with O₂ + CS₂. 07 p0835 A73-19633
- Vibration-rotation state populations and laser output spectra of CW chemical hydrogen halide lasers under subsonic transverse flow. 07 p0835 A73-19640
- CW He-Cd and He-Se metal vapor lasers, discussing atomic energy states, energy emission and absorption by electrons He storage levels and Penning ionization. 07 p0836 A73-19933
- A laser optical lever system for measuring the pitch and yaw of a ground-launched rocket. 08 p0974 A73-20669
- ### Chemical lasers - A comprehensive literature survey.
- 08 p0974 A73-21026
- Submillimeter-band gas laser pumped by a CO₂ laser. 08 p0976 A73-21654
- Cavity dimension effect on single mode generation spectrum of GaAs epitaxial CW injection laser at 77 K. 08 p0976 A73-21655
- HF chemical lasers kinetics, radiative interactions and gas dynamics, deriving closed form solutions for excited states populations. 08 p0976 A73-21671
- Loss analysis and design improvement for a continuous dye laser. 09 p1090 A73-22080
- Directly excited subsonically flowing CW gas laser with carbon monoxide and dioxide generation as reaction products formed by organic molecule electrochemical oxidation. 09 p1091 A73-22084
- Variation of spontaneous emission with current in GaAs homostructure and double-heterostructure injection lasers. 09 p1091 A73-22236
- Mesa-stripe-geometry double-heterostructure injection lasers. 09 p1093 A73-22251
- Dielectric modulation of single mode CW gas laser by acoustic wave, solving equations for creation and annihilation operators to obtain quantum number. 09 p1096 A73-22973
- A hollow cathode device for CW helium-metal vapour laser systems. 10 p1229 A73-24617
- Holographic contour mapping using a dye laser. 10 p1221 A73-24874
- Design of an R.F. excited helium-neon visible gas laser and study of the optimal conditions for gas mixtures and pressures. 10 p1230 A73-24923
- Laser beam welding technology review, discussing technical and economic aspects of pulse and CW techniques. 11 p1374 A73-25850
- Output power saturation with a discharge current in powerful continuous argon lasers. 11 p1377 A73-26179
- Holographic motion picture camera allows front surface detail to be recorded in real time using a continuous wave laser. 11 p1366 A73-26249
- Continuous-wave laser with a vortex-stabilized lamp. 12 p1506 A73-27503
- Studies of noble-gas lasers for continuous operation. 13 p1627 A73-28790

Theoretical study of the mechanism of the population inversion and of the efficiency in an ionized argon laser operating in the continuous mode

14 p1755 A73-29729
Focused high power CW carbon dioxide laser sustained Xe, Kr and Ar continuous plasmas, investigating plasma radiative properties by calorimetric techniques

14 p1779 A73-29922
Heterojunction laser diode fabrication procedures operation and details, considering peak power levels, wavelengths and operating temperatures for CW and pulsed operations

14 p1736 A73-30575
Ignition and maintenance of a CW plasma in atmospheric-pressure air with CO₂ laser radiation.

15 p1884 A73-31398
Design and performance characteristics of a small subsonic flow HF chemical laser.

15 p1885 A73-31978
CW metal vapor lasers, discussing discharge conditions, excitation processes, cathaporetic effect and He-Se and He-Cd lasers output characteristics

16 p2023 A73-32858
Chemical lasers and chemical reactions induced by lasers.

17 p2182 A73-34112
Holography of large objects in a turbulent atmosphere with a CW laser.

17 p2167 A73-34896
Perfectly stirred reactor - New concept for a CW chemical laser.

17 p2184 A73-34911
Electron temperature and density in the He-Cd²⁺ positive column used for an I/+ laser.

17 p2186 A73-35798
CW IR laser action in slowly flowing premixed He-air-CO mixture with simultaneous molecular excitation and carbon dioxide generation by discharge-initiated CO oxidation

17 p2186 A73-35799
Theoretical investigation of the CO supersonic electric discharge laser.

[AIAA PAPER 73-623] 18 p2321 A73-36171
Atmospheric turbulence effects on CW carbon dioxide laser propagation, investigating thermal blooming via theoretical diffusion model and experiment

19 p2437 A73-37260
A frequency-tunable mode-locked CW Nd:glass laser.

19 p2438 A73-38276
CW CO₂ laser at atmospheric pressure.

19 p2438 A73-38277
A study of the CW 28-micron water-vapor laser.

19 p2438 A73-38278
Single-line operation of a 2-W longitudinal cw CO chemical laser with no frequency-selective element in the optical cavity.

19 p2439 A73-38475
Non-Gaussian statistics of superradiant radiation from saturated xenon 3.5-micron laser amplifier.

20 p2570 A73-38620
Tuning and bandwidth control of laser pumped continuous dye lasers for obtaining stable single axial mode operation

20 p2571 A73-38624
Output-power-characteristics of a CW-gasdynamic-laser.

20 p2572 A73-39224
CW laser action from acetylene oxidation, noting sensitivity to total pressure and helium, oxygen and acetylene partial pressure changes

20 p2573 A73-39676
Utilization for high speed cinematography of phased-locked CW lasers

21 p2709 A73-39954
Laser induced red-blue energy transfer upon conversion in Pr³⁺/doped lanthanum fluorides via excitation annihilation involving pairs of ions

21 p2715 A73-40934
CW degradation at 300 K of GaAs double-heterostructure junction lasers. I - Emission spectra. II - Electronic gain.

21 p2715 A73-40964
Tunable Pb-Sn-Te junction laser characteristics and fabrication by impurity diffusion for IR CW operation at liquid helium temperatures

21 p2716 A73-40967
Red-light-emitting Al_xGa_{1-x}As heterojunction laser diodes.

21 p2716 A73-40971
Characteristics of a CS₂/O₂ chemical laser with flow transverse to the optical axis.

22 p2870 A73-42764
Ultrashort pulses from mode-locked cw dye lasers.

22 p2871 A73-43079
On the thermomdiffusion effect in the CW He-Ne lasers.

22 p2871 A73-43080
CW single mode He-Ne laser intensity fine structure fluctuations correlation measurement near threshold by digital correlator, obtaining higher order relaxation rates

22 p2871 A73-43085

CONTINUOUS WAVE RADAR

FM-CW radar range measurement at 10-micron wavelength.

03 p0278 A73-14459
Remote sensor for atmospheric physical properties with FM-CW scanning radar, parabolic antennas and waveguide feeds for linear and circular polarization

03 p0339 A73-14544
Simultaneous FM-CW radar and lidar observations of climatological regions, convective activity, cloud echoes, layered structures, insects and breaking Kelvin-Helmholtz waves

03 p0280 A73-14545
Lunar maps from CW radar imagery by aperture synthesis method at long wavelengths, noting depolarized return from highland regions

04 p0417 A73-15178
Interferometric CW radar for group delay difference measurement of reflected signal components in ionospheric sounding

05 p0548 A73-16253
Multiple target CW FM Doppler radar with solid state devices and CRT indicator, noting range resolution advantage over pulse radar

12 p1469 A73-27164
New developments in FM-CW radar sounding.

19 p2405 A73-38210
A note on the FM-CW radar as a remote probe of the Pacific Trade-Wind Inversion.

19 p2448 A73-38211
High power airborne radar CW tube-transmitter interface failures due to design, maintenance, handling and environment effects

22 p2834 A73-42875
Forward scatter CW radar effectiveness for cross path wind velocity profile measurements compared with radiosonde and pilot balloon observations

23 p3004 A73-44261

CONTINUOUS WAVES

U CONTINUOUS RADIATION

CONTINUUM FLOW
Application of the moire effect for studying flows of a continuous medium

02 p0230 A73-11721
Three dimensional boundary layer theory, applying Navier-Stokes equations to Newtonian fluids continuous flow over solid bodies or through finite ducts

10 p1171 A73-23863
Solar wind-lunar limb interaction from viscous MHD approach including continuum fluids, kinetic plasma and magnetic boundary layer

12 p1534 A73-27003
Interplanetary gas dynamics, discussing solar atmospheric structure, plasma kinetics, continuous flows, collective particle behavior, hydrodynamic coronal and free expansions

15 p1939 A73-31975

CONTINUUM MECHANICS

Book - Deformations of fibre-reinforced materials.

01 p0113 A73-10148
A continuum analysis of a two-dimensional mechanical model of the lung parenchyma.

01 p0010 A73-10168
Wave propagation in elastic laminates using a multi-continuum theory.

01 p0117 A73-11364
Deformation and stress analysis in continuum mechanics problems of solid bodies near singular points, noting applicability of linear theory of elasticity

01 p0118 A73-11404
The relation between three-dimensional and two-dimensional problems in the mechanics of continuous media

01 p0119 A73-11430
Investigation of the first forming phase of transverse corrugations

02 p0172 A73-11722
Nonclassical flow theory for continuum mechanics with asymmetrical stress concentration, noting rheological problems in laminar high polymers flow, hydrodynamic instability and turbulent flow

03 p0291 A73-13152
The application of electrical analogy to the solution of problems of continuum mechanics

03 p0342 A73-13161
Physicochemical distinction between separating similar and different materials in terms of cohesive or adhesive fracture energy in continuum mechanics

03 p0312 A73-13334
Dynamic singularity in the continuum theory of dislocations

03 p0343 A73-13775
The effect of polarity on the diffraction of plane elastic waves by a cylindrical cavity.

03 p0396 A73-14627
A new mathematical theory of simple materials.

04 p0511 A73-15221
Relativistic equations of balance in continuum mechanics.

04 p0476 A73-15223
A finite element based procedure for simulating the transient response and failure of a two-dimensional material with nonlinear material characteristics.

[ASME PAPER 72-WA/DE-4] 04 p0515 A73-15875

Buckling of continuously supported beams.

[ASME PAPER 72-WA/APM-34]

04 p0515 A73-15886
A continuum theory for wave propagation in laminated composites. I - Propagation normal to the laminates.

[ASME PAPER 72-WA/APM-20] 04 p0516 A73-15896

Minimum principles in the dynamics of isotropic rigid-plastic and rigid-viscoplastic continuous media.

06 p0757 A73-17396
Analytical and experimental methods in composite mechanics.

[ASCE PREPRINT 1655] 06 p0758 A73-17448

Application of linear feedback control theory techniques to continuum dominated by electrostatic and gravitational fields.

06 p0680 A73-18004
Book - On elastic stability under nonconservative loads.

06 p0762 A73-18275
Investigation of auto-oscillations of a continuous medium, occurring at loss of stability of a stationary mode.

07 p0809 A73-19018
Systems with internal parameters obeying the orthogonality condition.

08 p0987 A73-20777
A continuum mixture theory of wave propagation in laminated and fiber reinforced composites.

09 p1160 A73-22897
Hybrid stress finite element models for elastic continuum, discussing variational principle and macroscopic equilibrium

09 p1166 A73-23457
Continuum theory of wave propagation in laminated composites.

10 p1287 A73-23565
Nonlinear problem for a plane continuous medium in Euler coordinates

10 p1292 A73-24489
Boundary conditions model calculations for thermoelastic deformations of continuum body with surface tractions on interface, discussing energy balance laws derivation for loading devices

10 p1292 A73-24659
Applications of solid mechanics; Proceedings of the Symposium, University of Waterloo, Waterloo, Ontario, Canada, June 26, 27, 1972.

11 p1442 A73-25842
The present thermal state of the terrestrial planets.

11 p1421 A73-25905
Relationship of spatial and planar problems in the mechanics of continuous media.

11 p1443 A73-26059
Flexural/torsional deformations of material line in continuous body in terms of curvature and bending vectors, using Frenet-Serret equations

11 p1445 A73-26408
Nitrogen and oxygen molecules, photodissociation continua from absorption and ionization cross sections, calculating upper atmosphere emission rates

12 p1489 A73-26993
Continuum mechanics analysis of local rupture and plastic strains near cracks and fractures, noting elastoplastic applications

12 p1551 A73-27251
The elastic dielectric as oriented elastic continuum

13 p1658 A73-28163
Dual analysis principle application to accuracy verification of finite element solutions of problems in continuum mechanics

13 p1693 A73-28233
Continuous-discrete and probability-deterministic theory of space-time and matter, considering resolution of antagonism between relativity and quantum theories

13 p1658 A73-28373
Deformable solid as discretized body in classical continuum mechanics, deriving motion and constitutive equations

13 p1659 A73-28558
A variant of the moment theory of elasticity for a one-dimensional continuous medium with a non-homogeneous periodic structure

13 p1698 A73-29085
Book - Illustrated experiments in fluid mechanics - The NCFMF book of film notes.

14 p1743 A73-29725
Stress convexity domains for rigid perfectly plastic continuum, using directional derivative and distance function

14 p1811 A73-30483
Some thermodynamic considerations of phenomenological theory of non-isothermal elastoplastic deformations.

14 p1811 A73-30490
Basic concepts of the mechanics of discretized bodies with an introduction to discrete element calculus.

14 p1775 A73-30548
Book - A course in continuum mechanics. Volume 3 - Fluids, gases and the generation of thrust.

14 p1745 A73-30594

CONTOURS

Book - A course in continuum mechanics. Volume 4 - Elastic and plastic solids and the formation of cracks. 14 p1813 A73-30595

Eigenvalues asymptotic behavior in boundary value problems of infinitely expanding region of Euclidean space, applying results to continuous media stability investigation 15 p1860 A73-30964

Metric tensor properties of physical space with deformable continuum in terms of kinetic stress function, approximating Einstein constant 15 p1945 A73-31041

Basic trends in the development of modern analytic mechanics 15 p1913 A73-31622

Macromechanic model of notch size effects on tensile fracture strength in angle ply laminated composites 15 p1897 A73-31680

Interacting continuum theory concerning steady shock wave in composite materials, discussing energy interaction terms error correction effects on Hugoniot relations 15 p1949 A73-31685

Book - Advances in applied mechanics. Volume 12. 15 p1950 A73-31972

Finite element methods in continuum mechanics. 15 p1950 A73-31973

Book - Continuum mechanics and related problems of analysis. 15 p1952 A73-32076

Problems of reliability theory in the mechanics of deformable solids 15 p1914 A73-32082

Rigid motion of relativistic surfaces 15 p1914 A73-32095

Kinetic stress functions and the geometry of space in a deformed continuum 15 p1953 A73-32099

Lie group theory of differential equations in continuum mechanics, gas dynamics, heat conduction, biharmonic and second order quasi-linear equations 15 p1914 A73-32109

A consistent finite-difference model for the two-dimensional continuum. 15 p1954 A73-32122

Symmetric vector-type tensor functions of elastic bodies related to strain measure invariants, formulating limited hardness principle in terms of Poisson ratio 15 p1954 A73-32123

A stress-strain relation for homogeneous and isotropic continua 16 p2035 A73-32934

Variational principles in nonlinear continuum mechanics. 16 p2036 A73-32979

Finite element methods by variational principles with relaxed continuity requirement. 16 p2031 A73-32985

A survey of finite element methods in continuum mechanics. 16 p2036 A73-32988

Discrete approximations of elastic-plastic bodies by variational methods. 16 p2078 A73-32994

Variational methods applied to nonconservative stability problems of elastic continua. 16 p2078 A73-32995

The derivation of the mechanical balance equations of the Cosserat continuum on the basis of the energy equation and its behavior at the transition to rotating systems 16 p2080 A73-33240

Principle of virtual work and Piola theorem for motion and constitutive equations and boundary conditions of oriented elastic media, using point continuum mechanics assumptions 16 p2080 A73-33245

Nonlinear algebraic equations in continuum mechanics. 17 p2199 A73-34102

Book on wave propagation in continuous media covering Hamilton principle, energy theorems, elastic waves, electromagnetic and hydromagnetic waves, Green function and nonlinear effects 17 p2211 A73-34280

Constrained continuous media mechanics, discussing basic assumptions, integrable and nonintegrable constraints and motion 17 p2241 A73-34321

Quaternion equations and hypercomplex potentials in continuous medium mechanics 17 p2201 A73-34793

Finite element methods in continuum mechanics; Advanced Study Institute, Lisbon, Portugal, September 7-17, 1971, Lectures. 17 p2244 A73-34826

Continuum mechanics - A brief review. 17 p2244 A73-34827

Linear structure theory from analysis of structural mechanical models, proposing three dimensional model for behavior of granular materials 17 p2245 A73-34832

Continuum theory for elastic laminates in terms of effective stiffness, deriving displacement and stress interface boundary conditions with illustrative wave propagation examples [ASME PAPER 72-WA/APM-13] 17 p2249 A73-35112

Viscous fluid dynamic problem solution method implementation in Eulerian code AZTEC within continuum mechanics-kinetic theory union, preserving conservation properties throughout time integration 17 p2155 A73-35142

Continuum mechanics analysis of solid particle suspension flow of viscous gas, noting demixed region near wall 17 p2156 A73-35508

Book - Stress analysis of polymers. 17 p2253 A73-35861

The method of virtual powers in mechanics of continuous media. I - Theory of the second gradient 19 p2495 A73-37424

Continuum theory of a slightly ionized plasma, diamagnetic effects. 19 p2468 A73-37522

A version of the couple stress theory of elasticity for a one-dimensional continuous medium with inhomogeneous periodic structure. 19 p2498 A73-37635

General theory of constrained continuous media and plastic materials, deriving Huber-Mises yield condition by finite element method 19 p2501 A73-38304

Mathematical theory of nonlinear viscoelasticity 20 p2618 A73-39330

Material indifference - A principle or a convenience. 20 p2619 A73-39337

Statistical continuum mechanics and constitutive theories governing microfluid behavior, noting relations with aid of tables 20 p2547 A73-39343

Midwestern Mechanics Conference, 13th, University of Pittsburgh, Pittsburgh, Pa., August 13-15, 1973, Proceedings. 20 p2620 A73-39513

Bifurcation and stability of steady motions of complex mechanical systems 21 p2738 A73-40176

Continual mechanochemical model of muscular tissue 21 p2643 A73-40182

Continuum thermodynamics-based formulation of mixture theory using Boolean algebra with emphasis on partial stress tensors, considering force, moment and energy balance equations 22 p2885 A73-41771

Book - Elasticity. 23 p3039 A73-43434

Mixed finite element models for nonlinear thermomechanical responses of continuous dissipative media based on Oden variational principle and theory of thermoplastically simple materials 23 p3044 A73-44049

Geometry, kinematics and dynamics of dislocations in non-linear continuum mechanics. 23 p3045 A73-44082

A minimum principle in dynamics of elastic-plastic continua at finite deformation. 24 p3146 A73-44678

Fundamentals of the theory of plastic flow in discretized bodies 24 p3110 A73-44917

Transfer phenomena in nonreactive binary fluid mixtures analyzed by nonlinear continuum thermodynamics of irreversible processes 24 p3156 A73-45081

Continuous body kinematics and thermodynamics covering frame and motion, differential calculus in Euclidean spaces, deformations, interactions, force equilibrium, entropy and dissipation principle 24 p3112 A73-45472

CONTOURS

Curvilinear holes bi-periodic array in isotropic plane, determining hole shape for constant shear stress around contours 02 p0235 A73-12193

The stationary-phase method for a double integral with an arbitrarily located stationary point 09 p1048 A73-21918

Holographic contour mapping using a dye laser. 10 p1221 A73-24874

Conformal mapping method application to unsteady motion of arbitrary deformable contour in potential flow of ideal incompressible fluid 11 p1348 A73-26426

Nonlinear boundary value problem with permissible zeros on the contour 20 p2582 A73-39206

Numerical evaluation of integrals around simple closed curves. 21 p2725 A73-40378

The precision of contour lines and contour intervals of large- and medium-scale maps. 23 p2979 A73-44123

CONTRACT MANAGEMENT

Statistical expectation application to risk density functions and fee/incentive-element relationships for contract incentive structuring, considering C-5A procurement 08 p1025 A73-20958

Government request to industry to propose product or service for buyer, discussing procurement role and centralized vs decentralized control 09 p1168 A73-21946

USAF experience in lightweight fighter aircraft acquisition as illustration of requests for industrial proposals simplification and source selection process streamlining 09 p1168 A73-21947

Government request to industry to propose product or service to buyer, discussing communications effectiveness, technical and management requirements and procurement 09 p1168 A73-21948

Management and control of flight test programs at U.S. Army Aviation Systems Command. 23 p3050 A73-44054

Management and control of flight test programs of the Naval Air Systems Command. 23 p3050 A73-44056

Management and control of military flight test programs at McDonnell Douglas St. Louis, Missouri. 23 p3050 A73-44059

Flight test programs management and control, considering weapon systems performance tests relative to contractual requirements, personnel allocation and supporting facilities 23 p3051 A73-44060

CONTRACTION

Numerical solution of the Navier-Stokes equations by the finite element method. 07 p0810 A73-19501

CONTRACTS

NT SUBCONTRACTS

Legal consequences resulting from transportation in airline traffic in the case of missing, deficient or not coverage-equivalent contractual basis 14 p1818 A73-30293

CONTRAILS

Condensation trail effects on atmospheric radiation budget from model calculation for ice particle layer near tropopause, using Mie scattering and radiative transfer approximation 01 p0038 A73-10389

Contrail ice budget measurements with optical array particle size spectrometer onboard Sabreliner, noting wave abundance reduction at sub-tropopause jet traffic levels 02 p0189 A73-12785

Multiple contrail streamers observed by radar. 03 p0279 A73-14519

Photography of a lithium vapor trail during the daytime. 07 p0820 A73-20068

Cirrus-contrail cloud spectra studies with the Sabreliner. 17 p2206 A73-35579

CONTRALATERAL FUNCTIONS

Loudness enhancement following contralateral stimulation. 01 p0013 A73-10827

CONTRAST

NT IMAGE CONTRAST

NT PHASE CONTRAST

CONTROL BOARDS

Analysis of dynamic-excitation conditions for electrotropical-coupling switches in control circuits of electroluminescent panels 03 p0282 A73-13658

Design of control and display panels using computer algorithms. 11 p1361 A73-25180

The automatic telescope AZT-11 15 p1877 A73-32130

Two man crew cockpit design for commercial 737 jet transport aircraft, discussing pilot vision, control and display panels and avionics disposition 19 p2384 A73-37729

Effect of the information panel structure on operator activity 22 p2812 A73-41889

CONTROL DEVICES

U CONTROL EQUIPMENT

CONTROL EQUIPMENT

NT CONTROL STICKS

NT CRYOSTATS

NT SPEED REGULATORS

NT TELEOPERATORS

NT THERMOSTATS

Basic instrumentation components for prime, Cassegrain and coude focal positions of Anglo-Australian telescope, discussing acquisition and guiding, photography, photometry and spectrography 01 p0046 A73-10506

Synthesis of a magnetoelastic control medium for stabilization of hydrodynamic flows 01 p0084 A73-10669

Logidyn analog components regulator systems for industrial current and speed control, amplifier output voltage control, digital-analog converters, analog storage devices, etc
05 p0556 A73-16075

Digital vibration control systems for structural design dynamic testing and evaluation, discussing state of art and trends toward multichannel and multi-axis control
[SAE PAPER 720820] 05 p0553 A73-16628

Optimal time calculation for aging complex control system replacement with allowance for downtime losses
05 p0554 A73-16989

European space operations control center subsystems for PCM telemetry data acquisition and processing
07 p0790 A73-18973

Vibration test facilities and control techniques for application to industrial products, discussing shakers, signal generation and amplification, and data recording and reduction
07 p0809 A73-20575

Sensitivity of variable-amplifier circuits to variation of the controlled parameters
09 p1069 A73-22651

Analysis of the magnetic systems of calculating transducers
09 p1064 A73-22941

Fast and reliable automatic digital control components and transducers for data processing, display and storage, assessing technology development trends and preference over analog devices
10 p1199 A73-24028

Advanced flight control systems - Power-by-wire and fly-by-wire.
11 p1306 A73-26272

The quorum element and its application in the design of adaptive automatic control systems
12 p1482 A73-26758

Influence of control periodicity on the reliability of repairable devices
12 p1502 A73-26760

SkyNet satellite communication service for small dish antenna equipped mobile ground stations, emphasizing necessity of rapid central control response to configuration and propagation condition changes
12 p1471 A73-27660

Iris photometer electronic control system, presenting NGC 1778 cluster stars photoelectric UVB magnitudes
12 p1498 A73-27723

The effectiveness of flow control devices and circuits.
16 p1970 A73-33473

Experimental evaluation of remote manipulator systems.
19 p2416 A73-37305

Automatic flight control and navigation systems on the L-1011 Capabilities and experiences.
19 p2452 A73-37824

Book - Design performance and applications of microwave semiconductor control components.
20 p2535 A73-39136

Indicator and setting devices for circular-mirror sections of the RATAN-600 radio telescope
21 p2675 A73-41451

Reference indication and setting devices for circular mirror sections of the RATAN-600 radio telescope
21 p2675 A73-41452

CONTROL MOMENT GYROSCOPES
Demonstration of digital three axis spacecraft control.
04 p0432 A73-14738

An experimental investigation of attitude control systems for astronaut maneuvering units.
[AIAA PAPER 73-250] 05 p0563 A73-16973

Quasi time-optimal spacecraft reorientation maneuvers using single gimbal control moment gyros /SG CMG's/.
12 p1548 A73-27153

Communication satellites attitude control methods, considering conventional attitude gyros, control moment gyroscopes, reaction wheels and optimal solar cell utilization
17 p2239 A73-35476

Large scale telescope pointing stability augmentation system, using control moment gyro gimbal servo error signal to command momentum augmentation system
[AIAA PAPER 73-868] 20 p2587 A73-38806

Precision gimbal rate control for single gimbal control moment gyro /CMG/ pointing control systems, designing for high frequency response, bandwidth and output torque dynamic range
[AIAA PAPER 73-871] 20 p2587 A73-38808

Achieving ultrahigh accuracy with a body pointing CMG/RW control system.
[AIAA PAPER 73-883] 20 p2588 A73-38819

2-SPED, a single-gimbal control moment gyro attitude control system.
[AIAA PAPER 73-895] 20 p2589 A73-38831

Russian book on satellite attitude stabilization systems design covering gravity gradients, linear and nonlinear control laws, spin stabilization, high torque control moment gyros, etc
23 p0308 A73-43335

CONTROL PANELS
U CONTROL BOARDS
CONTROL SIMULATION
A universal three-angle basis for rotational kinematic analysis, simulation and control.
01 p0109 A73-10108

Comparative simulator studies regarding a contact-analog channel display and conventional instrumentations
[DGLR PAPER 72-100] 02 p0150 A73-11680

Demonstration of digital three axis spacecraft control.
04 p0432 A73-14738

An actively adaptive control for linear systems with random parameters via the dual control approach.
[AD-751587] 07 p0806 A73-20601

Digital computer aided control systems design, discussing components dynamic behavior mathematical modeling and control processes simulation
12 p1476 A73-27872

The role of the airborne traffic situation display in future ATC systems.
14 p1773 A73-29897

Modeling problems in air traffic control systems.
18 p2335 A73-36427

Summer Computer Simulation Conference, Montreal, Canada, July 17-19, 1973, Proceedings. Volumes 1 & 2.
18 p2291 A73-36826

Computerized design for moving-base three man aircraft flight simulator servocontrol, considering disturbance torques, damping ratios, natural frequencies, load acceleration and smoothness
18 p2296 A73-36833

A digital simulation facility for air traffic control experimentation.
19 p2451 A73-37809

Adaptive /learning/ intelligent system design and simulation for control with stochastic goal and environment conditions
20 p2532 A73-38685

Three-axis attitude control system air-bearing tests with flexible dynamics.
[AIAA PAPER 73-866] 20 p2543 A73-38804

A real-time six-degree-of-freedom hybrid simulation facility for guidance system testing.
[AIAA PAPER 73-876] 20 p2543 A73-38813

SAM-D guidance system simulator for design verification, preflight checkout and performance demonstration based on real time digital communication between missile computer and simulator hybrid computer
[AIAA PAPER 73-877] 20 p2587 A73-38814

Closed loop preflight qualification testing of a reentry vehicle roll rate control system.
[AIAA PAPER 73-878] 20 p2587 A73-38815

Computerized simulation of radio telescope control for minimum rms error and system parameter optimization
21 p2672 A73-40551

Washout circuit design for multi-degrees-of-freedom moving base simulators.
[AIAA PAPER 73-929] 21 p2674 A73-40876

Comparative studies of model reference adaptive control systems.
23 p2963 A73-43817

CONTROL STABILITY
Almost sure exponential bounds for stochastic operator systems, with applications to randomly sampled control.
01 p0027 A73-10426

Iteration accuracy effect on optimal discrete control system synthesis and stability, applying to Zubov damping problem
01 p0027 A73-10591

Conditions for the absence of periodic conditions in multivariable pulse-coded systems
01 p0027 A73-10592

Investigation of the dissipativity of a pulse-frequency modulated system of stabilizing an unsteady plant
01 p0027 A73-10596

Application of frequency-pulse modulation to adaptive automatic control systems
01 p0027 A73-10597

Liapunov vector functions in stability analysis of nonlinear dynamic distributed parameter, interconnected and multivariable systems
01 p0078 A73-11073

Space booster control system computerized design algorithm for forward loop compensation filter selection based on minimization of penalty function of stability margin violations
01 p0021 A73-11516

Effects of controller dynamics on the stability of a class of optimal control systems.
01 p0028 A73-11518

Periodic motions elimination in servo driven analog to digital converters on phase plane, noting dependence on autooscillations in relay system with time lag
02 p0148 A73-11862

A new circle criterion for the stability of nonlinear control system.
02 p0149 A73-12346

Lyapunov functions for quadratic differential equations with applications to adaptive control.
03 p0336 A73-13520

Variable stability simulation techniques for nonlinear rate-dependent systems.
03 p0285 A73-13521

Application of stochastic stability theory to model-reference systems.
04 p0430 A73-15215

Analog simulation and design of single- and multiple input/output model reference adaptive systems, using hyperstability concept
[ASME PAPER 72-WA/AUT-13] 04 p0432 A73-15881

Automatic control system synthesis for optimal correction, maximum accuracy and stability of linear unsteady final action systems under deterministic and random actions
05 p0561 A73-16420

A stability theory for perturbed difference equations.
05 p0590 A73-16491

Critical lag of the driving element in a parametric system
05 p0561 A73-16990

Control and stability analysis of supersonic aircraft jet engines with afterburner for improved low altitude operation
06 p0741 A73-17722

The method of Lyapunov functions in control problems for distributed-parameter systems /A survey/.
06 p0723 A73-17953

Error incidence probability for system control reliability determination, assuming error function as Markov process
06 p0680 A73-17956

Disturbance accommodation in linear systems with chattering controllers.
06 p0681 A73-18818

Modeling of linear time-varying systems by linear time-invariant systems of lower order.
06 p0682 A73-18867

Determination of limits bounding the bifurcational relationship between parameters of two-stage nonlinear servo mechanisms
09 p1033 A73-22653

Liapunov vector functions in stability analysis of nonlinear dynamic distributed parameter, interconnected and multivariable systems
09 p1121 A73-22998

The evaluation of the domain of attraction of nonlinear control systems with hybrid computing systems.
10 p1192 A73-24040

Rational methods for controlling multistable elements on the basis of an analysis of the preferential domains of steady states
12 p1482 A73-26774

Autonomous second order system model for nonlinear disturbances of multifrequency systems at resonance, using group properties of differential equation
12 p1524 A73-27404

Stability of a multivariable discrete system for controlling a fatigue testing process with random loading
12 p1557 A73-27949

Controllability and stabilizability of decentralized dynamic systems.
19 p2413 A73-38045

Optimal stabilization of moving control plants during multichannel measurement of their coordinates
20 p2542 A73-39039

Stability and dissipativity of control systems containing unsteady nonlinearities
20 p2542 A73-39041

Approximate methods for the mathematical description and analysis of processes controlling the spectral characteristics of random vector signals
20 p2542 A73-39047

On-off control of an unstable plant with time lag
20 p2542 A73-39345

Adaptive control of forced motions in discrete extremal systems with independent search
20 p2542 A73-39346

A nonsearching system of identification with a model, synthesized according to the hyperstability criterion
20 p2532 A73-39347

Multidimensional cross control stabilization of multiple link feedback control systems, applying 70 dc 70 ac power converter
22 p2836 A73-42603

Gradient control laws in stabilization problems of multidimensional control systems
22 p2887 A73-42605

Liapunov vector functions for solving stability problems of complex multidimensional dynamic control systems with nonlinear interactions and delay
22 p2887 A73-42606

Dynamic behaviour and z-transform stability analysis of loop/dc regulators with a non linear P.W.M. control loop.
22 p2837 A73-42912

- Analysis of transient oscillations in nonlinear control systems. 22 p2837 A73-43019
- Liapunov-like theorems of quantitative stability information on trajectory bounds in state space subset form 22 p2888 A73-43020
- Compensation of an underdamped fluidic position control system by a digital pulse compensator. 23 p2944 A73-43420
- Linear time variant multivariable decentralized system stabilization by feedback control laws with dynamic compensation 23 p2964 A73-43821
- Stabilization of unstable plants through automatic search 24 p3074 A73-44662
- CONTROL STICKS**
A short description of the NAE airborne simulator feel system. 21 p2672 A73-40854
- CONTROL SURFACES**
NT AILERONS
NT ELEVONS
NT FLAPS [CONTROL SURFACES]
NT GUIDE VANES
NT JET FLAPS
NT JET VANES
NT LEADING EDGE SLATS
NT RUDDERS
NT SPOILERS
NT TABS [CONTROL SURFACES]
NT TRAILING-EDGE FLAPS
NT WING FLAPS
On the importance of the wake for the noise of an obstacle placed in a flow 03 p0291 A73-12974
- Experimental investigation of hypersonic buzz on a high cross-range shuttle configuration. [AIAA PAPER 73-157] 05 p0531 A73-16904
- An automated method for determining the flutter velocity and the matched point. 06 p0645 A73-17656
- Numerical method for predicting unsteady aerodynamic loadings caused by control surface motions in subsonic flow. [AIAA PAPER 73-315] 11 p1301 A73-25546
- Active flutter suppression - B-52 controls configured vehicle. [AIAA PAPER 73-322] 11 p1305 A73-25552
- Design and evaluation of miniature control surface actuation systems for aeroelastic models. [AIAA PAPER 73-323] 11 p1305 A73-25553
- The theoretical and experimental methods used in France for flutter prediction. [AIAA PAPER 73-329] 11 p1305 A73-25558
- System of electric control of surveillance of the control surfaces of the Concorde 15 p1830 A73-32475
- Alteration of a static vibration result by rigidizing some degrees of freedom 18 p2361 A73-36066
- Reentry vehicle ablating control surface gap and slot regions flow characteristics prediction based on quasi-one-dimensional compressible flow finite difference solution [AIAA PAPER 73-742] 18 p2265 A73-36663
- Integrated hydraulic flight control actuator packages replacing mechanical linkages for aerodynamic surface control during V/STOL operation 20 p2510 A73-39015
- Control law synthesis and sensor design for active flutter suppression. [AIAA PAPER 73-832] 21 p2784 A73-40502
- CONTROL THEORY**
R-function numerical analysis method for motion stability criteria, developing algorithms for Liapunov function construction and controller design for conservative control system stability 01 p0076 A73-10096
- A universal three-angle basis for rotational kinematic analysis, simulation and control. 01 p0109 A73-10108
- Investigation of a class of nonsearching extremal-control systems with pulse frequency modulation 01 p0027 A73-10594
- Abstract theory of systems - Current state and development trends 01 p0027 A73-10664
- Programmed control of a two-level hierarchical system 01 p0027 A73-10665
- Programming and correcting control effects for prescribed interrelationship between variable states of dynamic control, noting system synthesis for programmed motion 01 p0027 A73-10667
- Method of structural synthesis of multivariable systems for automatic control of plants with incomplete information 01 p0028 A73-10672
- A complex approach to flight vehicle control system designs 01 p0074 A73-10673

- Synthesis of active controllers for vibratory systems. 01 p0057 A73-10697
- Mathematical models, systems analysis and synthesis in control theory of large scale systems, illustrating on agriculture center planning 01 p0078 A73-11070
- Optimal processes theory, discussing Pontryagin principle, special controls, dynamic programming, discrete systems, algorithms, identification and controllability 01 p0028 A73-11072
- Sufficient conditions for the optimal control problem 01 p0071 A73-11269
- Control theory analysis of equilibrium state asymptotic stability of system with dry friction, applying to power driven gyrostabilizer 01 p0054 A73-11402
- Multiple correction procedure for motion control ensuring arrival at final state without complete initial state information 01 p0079 A73-11419
- Non-interacting control of non-linear multivariable systems. 01 p0028 A73-11517
- Homogeneous linear partial differential equation for optimal control with boundary condition formed by terminal component, noting weighting functions for linear plant 02 p0149 A73-12116
- Variational method in the invariance problem for controlled systems. 02 p0149 A73-12117
- Optimization of control and observation processes in dynamic systems under random perturbations. 02 p0149 A73-12118
- Construction of Lyapunov functions for nonstationary systems containing memoryless nonlinearities. 02 p0193 A73-12123
- Linear dynamic control system synthesis methods based on aggregation and suboptimal control by decomposition, minimizing quadratic performance criterion 02 p0149 A73-12124
- Transient curve construction for analysis and synthesis of automatic control systems with asymmetrical nonlinearities, comparing with harmonic linearization 02 p0149 A73-12342
- Synthesis of optimal control over the motion of a material point in a thin spherical layer of a central gravitational field with noncollinear vectors of the final gross error in the radius vector and velocity vector 02 p0193 A73-12452
- Application of relaxed solutions to minimum sensitivity optimal control. 02 p0149 A73-12509
- Russian book - Fundamentals of the general theory for the root loci of automatic control systems. 02 p0149 A73-12750
- Russian book - The designing of quasi-optimal combined-control servosystems. 02 p0149 A73-12867
- A graphical test for checking the stability of a linear time-invariant feedback system. 03 p0285 A73-13519
- Application of geometric decoupling theory to synthesis of aircraft lateral control systems. 03 p0250 A73-13703
- German monograph - Application of estimation procedures for the characteristic parameters of controlled systems on the basis of measurements on the closed control loop. 03 p0285 A73-13811
- On the almost-sure sample stability of systems with randomly time-varying delays. 03 p0285 A73-13898
- Optimal control of nonlinear time-lag systems. 03 p0285 A73-13899
- Moving vehicle borne automatic sighting device pointing problem mathematical analysis and applications to aircraft and camera aiming for airborne photography 03 p0277 A73-13913
- Book on control engineering covering dynamic system state representation, finite and infinite dimensional optimization, dynamic programming, stochastic estimation, applications, etc 03 p0285 A73-13987
- Book on modal control theory and applications covering continuous and discrete time lumped parameter linear dynamic systems controllability and observability characteristics 03 p0285 A73-13989
- Book on linear optimal control theory covering systems analysis, state reconstruction, stochastic nature and feedback control 03 p0286 A73-13992
- Optimal control of observation processes, formulating solvability conditions in terms of ordinary differential equations 03 p0286 A73-14043

- Discontinuous variational problems in time optimal control of systems describable by ordinary differential equations, deriving Weierstrass optimality conditions 03 p0286 A73-14055
- Annual Allerton Conference on Circuit and System Theory, 9th, Monticello, Ill., October 6-8, 1971, Proceedings. 03 p0286 A73-14476
- Nonlinear stochastic optimal control theory application to guidance policies determination of nonmaneuvering target interception or rendezvous and goal-tending game 03 p0286 A73-14478
- An improved design technique for parameter adaptive control systems. 03 p0286 A73-14481
- Optimal trajectory control system synthesis via Pontryagin maximum principle, taking into account system dynamics, control constraints and boundary conditions 04 p0429 A73-15201
- Choice of a rational control law for control systems for delayed objects subjected to random load disturbances. 04 p0429 A73-15202
- Optimal risk equation and solution existence and uniqueness of dual control problems with unknown parameter and additive noise 04 p0429 A73-15203
- Absolute instability of nonlinear pulse-amplitude control systems - Frequency criteria. 04 p0430 A73-15204
- Probability model and causal approach to failure mechanisms and reliability of control system elements applied to IC 04 p0424 A73-15208
- The time optimal control of a class of distributed systems. 04 p0517 A73-15230
- Solution structure duality between nonlinear filtering with finite dimensional sensor orbit and nonlinear control with involutory actuator orbit 04 p0431 A73-15264
- Switch transistor control using an intensity transformer 04 p0489 A73-15736
- The selection of performance indices for optimal control problems. [ASME PAPER 72-WA/AUT-15] 04 p0432 A73-15880
- Control efficiency of finite automaton with automatic control, considering system failures and independent and unequally probable transitions 05 p0553 A73-16273
- Theoretical foundations for synthesis of learning-type recognition algorithms by the method of R-functions in the complex-plant control problem 05 p0560 A73-16275
- Search stability and steady motion region characteristics of self oscillatory extremal automatic control system under additive disturbances on controlled object input 05 p0560 A73-16293
- Synthesis of an optimal discrete control system in the presence of control delay 05 p0560 A73-16295
- Extremal control system efficiency enhancement by information storage, noting algorithms for sequential data storage 05 p0560 A73-16298
- Some structure synthesis problems for systems controlling the three-dimensional motion of orbital-aircraft in the earth's atmosphere 05 p0594 A73-16418
- Statistical synthesis of optimal pulsed control systems for spacecraft while taking into account system structural constraints 05 p0595 A73-16419
- Optimal control of extraatmospheric spacecraft motion stability by variable structure system with logic circuits 05 p0628 A73-16421
- Spacecraft motion control as stochastic dynamic problem formulated according to single criterion for deterministic programmed and stochastic perturbed motions 05 p0629 A73-16425
- Fredholm operator theory application to linear feedback system input-output stability in terms of origin encirclement counting in complex plane 05 p0561 A73-16488
- Finite-dimensional approximations of state-constrained continuous optimal control problems. 05 p0561 A73-16490
- Invariance principle extended to bounded uncertain time-varying systems, deriving asymptotic Liapunov stability criteria with application to guaranteed cost control problems 05 p0590 A73-16492
- Control of the motion of a solid body with servo couplings 05 p0597 A73-16611
- Controllable matched filter model for single circuit and twin circuit parametric converters 05 p0558 A73-16786

Optimal flight control system design for aircraft with large flight envelopes, using optimal control theory with limited measurement feedback [AIAA PAPER 73-159] 05 p0535 A73-16906
Summary and comparison of gradient-restoration algorithms for optimal control problems. 06 p0715 A73-17567
High-order necessary conditions of optimality for singular controls of discrete systems 06 p0679 A73-17717
Decoupling in a class of nonlinear systems by state variable feedback. [ASME PAPER 72-AUT-V] 06 p0679 A73-17725
On the controllability conditions for systems with distributed delays in state and control. 06 p0716 A73-17852
Nonlinear dynamic systems controllability theorem formulation and proof using matrix theory 06 p0716 A73-17853
On an application of Lie group theory to the optimal control problem for linear dynamic systems with time-varying parameters. 06 p0679 A73-17954
Global asymptotic stability of two classes of control systems with pulse duration and pulse frequency modulations. 06 p0680 A73-17957
Synthesis of adaptive systems by Lyapunov's direct method. 06 p0723 A73-17959
Application of linear feedback control theory techniques to continuum dominated by electrostatic and gravitational fields. 06 p0680 A73-18004
A new method of calculating controller constants according to an optimal modulus criterion 06 p0680 A73-18169
Relationship between conventional-control-theory figures of merit and quadratic performance index in optimal control theory for a single-input/single-output system. 06 p0680 A73-18445
Dynamic system optimal control problems with higher order state variable inequality constraints, obtaining solutions with boundary arcs and isolated points 06 p0680 A73-18519
Possibilities of control of radiation emitted by lasers with telescopic resonators. 06 p0702 A73-18588
Discrete maximum principle (local cross sections)/method applications to optimal control and mathematical programming 06 p0718 A73-18676
Nonlinear time-varying control systems transformation, deriving conditions for existence of observable system representation and corresponding scalar differential equation 06 p0719 A73-18802
Noisy data filtering of linear steady state control problems based on nearest neighbor interaction, discussing dimensionality reduction model for saving computer time 06 p0682 A73-18868
On parameter identification for distributed systems using Galerkin's criterion. 07 p0804 A73-19130
Necessary condition of optimality for some problems of optimal control theory 07 p0844 A73-19296
Stochastic linear system observer eigenvalue optimal placement with respect to quadratic error criterion for adaptation to digital computation and applicability to higher order system 07 p0849 A73-19966
Experimental determination of the structure of plants with recycling 07 p0805 A73-20045
Ergatic organism defined as multipurpose nonautonomous control system with homeostasis with respect to functional operations conservation 07 p0786 A73-20048
Thin elastic plate stability characteristic values control through elemental boundary forces variation, applying von Karman nonlinear differential equations system eigenvalue problem 07 p0915 A73-20289
A hybrid analog computer for schooling in control technology 07 p0796 A73-20302
Conference on Decision and Control and Symposium on Adaptive Processes, 11th, New Orleans, La., December 13-15, 1972, Proceedings. 07 p0805 A73-20576
A unified boundary controllability theory for hyperbolic and parabolic distributed parameter systems. 07 p0846 A73-20591
An approximate method for the synthesis of optimal control of distributed systems. 07 p0806 A73-20596
Feedback regulators for jump parameter systems with state and control dependent transition rates. 07 p0806 A73-20597
Dual characterizations of optimal control systems governed by linear and nonlinear differential equations

with dynamic constraints, using complementary variational principle in Hilbert space 07 p0846 A73-20598
Evolution equations of motion for program manifold of continuous control system with given transient response 07 p0852 A73-20632
Investigation of the smoothness characteristics of the Bellman function on the basis of the equation of motion of the system in time-optimal problems. I Linear case 07 p0806 A73-20633
Analysis of the stability and periodic motions of nonlinear automatic pulsed systems by the root-locus curve method 07 p0806 A73-20636
Mathematical description of nonlinear systems with distributed parameter 08 p0938 A73-20964
Scalar and block decoupling of time varying and invariant linear multivariable control systems, discussing sufficiency conditions, state estimation and order reduction possibility 08 p0950 A73-21089
Near-optimal control of high-order systems using low-order models. 08 p0950 A73-21090
Feedback law choice for autonomy properties of controlled object, noting existence and uniqueness theorems 08 p0951 A73-21127
Frequency criteria for the absolute stability and instability of pulse-width modulated control systems 08 p0951 A73-21544
Adaptive control and identification via Liapunov's direct method. 09 p1067 A73-22232
Feedback control theory as general network analysis tool based on circuit decomposition 09 p1067 A73-22303
Vector-valued optimization of linear systems 09 p1112 A73-22478
Calculation of the reliability of hierarchical systems with quorum redundancy 09 p1088 A73-22552
Maintenance and repair planning and control of complex series-parallel and hierarchical branched systems with discrete sampling of operational status 09 p1064 A73-22553
Probability characteristics of complex systems with a hierarchical control 09 p1068 A73-22559
Algorithmic construction of optimal controllers on the basis of incomplete information about the state of the plant 09 p1068 A73-22562
An approximate continuous representation of discrete control systems 09 p1068 A73-22564
Optimal observation laws for certain controlled motions 09 p1069 A73-22565
Optimal control problems under conditions of a priori indeterminateness 09 p1069 A73-22566
Application of the principle of invariant imbedding in the solution of optimal control problems 09 p1069 A73-22722
Continuous analog of dynamic-programming allocation process 09 p1112 A73-22889
Equivalent initial conditions for automatic control systems with variable parameters 09 p1069 A73-22943
Optimal control of n-order system with transport delay by variational calculation, comparing with proportional integrator /PI/ controller 09 p1069 A73-22974
Optimal processes theory, discussing Pontryagin principle, special controls, dynamic programming, discrete systems, algorithms, identification and controllability 09 p1069 A73-22997
Method of variation of parameters starting with linear damped vibration solution as its generating solution. 09 p1121 A73-23324
Optimal lift control by Miele's method for the atmospheric entry of a hypersonic glider. III. 10 p1285 A73-23616
A first-approximation theory of discrete nonautonomous stabilization systems 10 p1248 A73-23745
Numerical solution of the optimal control problem by the direct method 10 p1197 A73-23999
International Federation of Automatic Control, World Congress, 5th, Paris, France, June 12-17, 1972, Proceedings. Part 2 - Transportation, aeronautics and space, ship automation, and control components. Part 3 - Ecology and systems engineering; Large scale, sensitivity, optimization and adaptation theory. Part 4 - Education, feedback, regulators, linear and nonlinear

systems; Identification, differential games, discrete and stochastic systems. 10 p1198 A73-24001
Vehicle coordinate-parametric control problems and some solution methods. 10 p1198 A73-24007
Configuration control of dual satellite systems in earth orbit, obtaining equations of motion, deployment paths and force functions 10 p1276 A73-24008
Manned vehicle systems analysis techniques application to manual approach-to-landing phase of aircraft flight, developing analytical control model 10 p1247 A73-24011
Applications of symbolic computing methods to the dynamic analysis of large systems. 10 p1192 A73-24029
The design of optimally parameter insensitive control systems. 10 p1199 A73-24030
Iterative optimum control function determination without directly solving the system dynamical equations. 10 p1242 A73-24033
Contraction-mapping algorithm with guaranteed convergence. 10 p1242 A73-24034
Discrete dynamic adaptive control algorithms for estimation of minimum loss function point trajectory characterizing system quality in nonstationary conditions 10 p1242 A73-24035
On a method of adaptive control under conditions of great uncertainty. 10 p1199 A73-24036
Study of recurrence relationships and their applications by the Laboratoire d'Automatique et de ses Applications Spatiales. 10 p1200 A73-24042
Linear stochastic, multivariable, optimal control, realization and time-varying systems theory developments covering external and internal representations and variance computation problems 10 p1200 A73-24045
Order determination and parameter identification of time-invariant state variable models. 10 p1201 A73-24054
On optimization of control systems according to vector-valued performance criteria. 10 p1201 A73-24056
Certain finitely converging algorithms for the solution of infinite systems of inequalities and their application in the theory of adaptive systems 10 p1192 A73-24486
Wide-sense adaptive dual control for nonlinear stochastic systems. 10 p1202 A73-24533
Necessary and sufficient conditions for differentiable nonscalar-valued functions to attain extrema. 10 p1243 A73-24537
An optimal control problem for a class of distributed parameter systems. 10 p1202 A73-24549
Russian book on military application oriented automatic control systems design covering amplifiers, servo elements, stability, performance, optimization, and nonlinear and sampled data systems 10 p1203 A73-24972
Methods of representation and machine analysis of random fields and processes; All-Union Symposium, 5th, Vilnius, Lithuanian SSR, May 1972, Transactions. Sections 1, 2, 3 & 4 11 p1339 A73-25001
Determination of the statistical characteristics of signals parametrically affecting a dynamic plant 11 p1340 A73-25006
Russian book on rockets as control plants covering dynamics equations of motion for different configurations, linearization and matrix description of rockets 11 p1429 A73-25175
Converse theorems for Liapunov stability and boundedness of nonlinear discrete-time systems described by difference equations 11 p1389 A73-25186
Nonlinear delay-differential control systems described by periodic functional differential equations with small real parameter, investigating asymptotic stability in Liapunov sense 11 p1390 A73-25190
Irreducible canonical realizations from external data sequences. 11 p1390 A73-25191
Two quadratic cost functionals equivalence conditions derivation in terms of system parameters and weighting matrices for optimal control law generation 11 p1341 A73-25196
Suboptimal input signal synthesis for linear control system identification based on output SNR maximization, bandwidth matching and pseudorandom binary noise nature 11 p1327 A73-25197
Sequential pneumatic distribution system/Biselector/ with logic control by leakage obstruction, describing industrial pressure perforated card programmer 11 p1307 A73-25377

Extension of the principle of variable structure systems to the case where the slip hypersurface is nonlinear - Application to suboptimal control

11 p1341 A73-25574

Method of Liapunov vector functions in the analysis of complex systems with distributed parameters /Survey/

11 p1398 A73-25617

Synthesis, with the aid of Liapunov functions, of optimal and suboptimal discrete systems for controlling determinate and stochastic plants

11 p1341 A73-25619

Essentially incomplete model construction by non-search method in linear plant parametric control

11 p1341 A73-25620

The principle of complexity and the method of regularization in stochastic problems of optimal automatic control system synthesis

11 p1341 A73-25634

Control improving variation for optimum speed of response, describing differential equations and vector functions

11 p1342 A73-26078

Experimental method for structure identification in nonlinear objects with recycling processes

11 p1342 A73-26082

Efficiency estimates of methods for analyzing the precision of nonlinear control systems

11 p1342 A73-26094

On a solution of an optimization problem in linear control systems with quadratic performance index.

11 p1342 A73-26224

Synthesis of time-optimal control for linear systems and the minimal-time Lyapunoff function.

11 p1342 A73-26225

French book - Hydraulic and electrohydraulic automatic control. Volume 1 - Theory and technique. Volume 2 - Supplementary techniques and technologies

11 p1313 A73-26253

Book on fluid power control covering servovalve orifices discharge characteristics, flow forces, hydraulic and pneumatic servomechanisms, fluid logic and sequential circuits

11 p1313 A73-26258

Time-related behavior of causal, anticausal, memoryless and crosscausal nonlinear control systems modeled as operator on group-valued function space

11 p1391 A73-26366

Asynchronous linear automatic binary control systems, using interpolation theory of Taylor operators for mathematical modeling

11 p1342 A73-26418

Single input n-th order linear constant discrete-time adaptive control systems, deriving phase canonical form sensitivity functions by z-transform

11 p1342 A73-26636

Optimal control theory for constant gain radar filter design with weighted variance average minimization comparable with Kalman filter performance

11 p1339 A73-26643

Evaluation of the efficiency of automatic control and observation systems on the basis of mathematical models of potential and real automatic systems

12 p1482 A73-26762

Pneumostatic data transmission and processing based on pressurized gases and dynamic body interactions

12 p1460 A73-26771

Oscillatory operational amplifiers for control systems and computer technology

12 p1477 A73-26773

Rational methods for controlling multistable elements on the basis of an analysis of the preferential domains of steady states

12 p1482 A73-26774

Devices for primary processing of information in controller machines, based on the principles of quantum magnetometry

12 p1495 A73-26778

A group converter of alternating-current signals into a code for control systems

12 p1475 A73-26780

Nonsingular control, determining optimum shape of straight bar under stress and inertial moment restrictions

12 p1482 A73-26793

Group properties and invariant solutions of the Bellman equation in the problem of optimal control synthesis for second-order systems

12 p1483 A73-27079

Quasi time-optimal spacecraft reorientation maneuvers using single gimbal control moment gyros /SG CMG's/.

12 p1548 A73-27153

Practical quadratic optimal control for systems with large parameter variations.

12 p1483 A73-27166

Fourth order linear differential equations solution for time optimal control synthesis with phase limitations

12 p1483 A73-27403

Control system equations of motion construction based on program manifold, determining multidimen-

sional piecewise continuous controller vectors under assigned inequalities

12 p1484 A73-27455

Optimization of the parameters of heterogeneous multipurpose controlled systems using standard elements.

12 p1484 A73-27456

Synthesis of an approximately optimal control for one class of controlled systems.

12 p1484 A73-27457

Synthesis of searchless self-adjusting systems based on the root locus method. I.

12 p1484 A73-27460

Mean time of the failure-free operation of a redundant system with allowance for monitoring of operational efficiency

12 p1504 A73-27619

Analysis of the stochastic stability of pulsed control systems in the frequency domain

12 p1485 A73-27622

An algorithmic procedure for determining discrete transfer matrices of controlled plants

12 p1485 A73-27624

An algorithm for controlling the descent of a spacecraft from an artificial earth satellite orbit.

12 p1543 A73-27631

Optimal control with probabilistic quadratic performance criterion and constraints, using stochastic principle for reduction to time derivative maximization problem

12 p1485 A73-27897

Stability of stochastic dynamical systems; Proceedings of the International Symposium, University of Warwick, Coventry, England, July 10-14, 1972.

12 p1519 A73-27920

Verification of the 'potential' work capacity of dynamic systems by a frequency-time technique

12 p1485 A73-27946

A direct method approximation to the linear parabolic regulator problem over multivariate spline bases.

13 p1649 A73-28605

The Ritz-Galerkin procedure for nonlinear control problems.

13 p1649 A73-28607

Computer control of a multifunction radar.

13 p1587 A73-28619

Linear distributed parameter system minimum time control, considering Hilbert space final value and Banach space inequality solutions

13 p1596 A73-28700

Ergatic modeling as dynamic goal-oriented physical process based on heuristic autonomous information-structured organization system with regulated model-human operator interaction

13 p1580 A73-29418

Routh-Hurwitz method for optimal algebraic stability of ordinary differential equations of fourth order systems with linear control law

13 p1597 A73-29419

Book - Optimal control of differential and functional equations.

13 p1651 A73-29550

The sensitivity of nominally time-optimal control systems to parameter variation.

13 p1597 A73-29567

Russian papers on cybernetic systems reliability and accuracy covering analog, hybrid and digital computers, electronic modeling, nonlinear control systems, computer and complex system design, etc

14 p1730 A73-30031

Synthesis of a control coupling in a nonlinear servosystem

14 p1738 A73-30287

Optimal control of discrete systems

14 p1738 A73-30348

Solution of a dual problem in optimal control theory.

14 p1738 A73-30405

Cone-bounded nonlinearities and mean-square bounds - Estimation upper bound.

14 p1769 A73-30505

Frequency-domain criteria for stability of a class of nonlinear stochastic systems.

14 p1739 A73-30506

Controllability of discrete bilinear systems with bounded control.

14 p1739 A73-30510

The infinite time quadratic cost problem for certain classes of infinite dimensional control systems.

14 p1770 A73-30758

Theory and applications of variable structure systems; Proceedings of the Seminar, Sorrento, Italy, April 4-7, 1972.

14 p1739 A73-30776

Modelling and identification theory - A flight control application.

14 p1739 A73-30777

Near optimal control laws and controller realization for multilevel feedback and time optimal control design and simulation

14 p1739 A73-30780

Some results on the abstract realization theory of multilinear systems.

14 p1740 A73-30781

Algebraic Lie structure theory of bilinear systems in terms of controllability, observability and equivalent realization

14 p1771 A73-30783

Regulators providing control system autonomy

14 p1740 A73-30938

Continuously-discrete method for the construction of control devices

14 p1740 A73-30940

Use of the principle of invariant imbedding in solving an optimal control problem.

14 p1740 A73-30955

Minimum time response control problem of moving point in state space, determining piecewise-continuous vector function for optimal system transfer to coordinate reference point

15 p1931 A73-31231

Russian book on remote guidance control systems covering theory, optimization and constraints for steady, unsteady, linear and nonlinear automatic control systems

15 p1853 A73-31374

A computational scheme used with the epsilon-technique in synthesizing optimal controls.

15 p1853 A73-31625

Optimal and linear sub-optimal control of second-order saturating control systems.

15 p1853 A73-31626

Construction of equations of motion for program manifold of continuous control system with given transient response

15 p1913 A73-31686

Study of the smoothness properties of the Bellman function in time-optimal problems, based on the equation of motion of the system. I - The linear case.

15 p1854 A73-31687

Analysis of stability and periodic motions in nonlinear sampled-data systems by the root locus method.

15 p1854 A73-31690

Some properties of the amplitude frequency characteristics of linear automatic control systems and their control quality under random influences

15 p1854 A73-31695

Relation between the N. M. Krylov-N. N. Bogoliubov averaging method and the method of envelopes in studies of a class of control systems

15 p1854 A73-31801

Optimal control in a finite time interval for discrete systems in the minimization problem of an inhomogeneous quadratic functional /a case of fixed terminals/

15 p1854 A73-31802

Synthesis of optimal discrete control systems with persisting perturbations

15 p1854 A73-31803

Feedback law choice for autonomy properties of controlled object, noting existence and uniqueness theorems

15 p1855 A73-32062

The method of penalty functions and necessary conditions of optimality for generalized solutions of the optimal control problem

15 p1901 A73-32367

Simultaneous control of temperature and humidity in a confined space. III Feedback control synthesis via optimal control theory.

15 p1855 A73-32549

Book - Principles of biological regulation: An introduction to feedback systems.

15 p1840 A73-32576

Optimal control theory for systems with inequality restrictions on control and state variables and time delay, using maximum principle and variational techniques

15 p1855 A73-32580

French monograph - Study and preparation of algorithms of coordination in the structures of hierarchized control systems.

15 p1855 A73-32592

Simultaneous control of temperature and humidity in a confined space. II - Feedback control synthesis via classical control theory.

15 p1855 A73-32598

Contribution to the synthesis of optimum control of motion of a point mass in a spherical lamella of a central gravitational field with finite miss vectors noncollinear with respect to radius vector and velocity vector.

15 p1915 A73-32602

Differential equations with free boundaries in stochastic control problems

16 p2031 A73-32822

Minimum-norm control of linear systems with partially known initial conditions.

16 p1992 A73-33163

Optimal control solution existence for relaxed linear systems with strictly convex Hamiltonian

16 p1992 A73-33303

Gradient methods with penalty functions for solution of optimal control with terminal constraints, noting convergence superiority of conjugate gradient algorithm

16 p2034 A73-33998

Minimization of quadratic functionals in the presence of quadratic constraints and the necessity of a frequency condition in the quadratic criterion of absolute stability for nonlinear control systems
16 p2034 A73-34071

Papers on optimal control and dynamic systems theory covering linear discrete systems observers, quasi-linearization, national economic policy, decision theory and closed loop formulation
17 p2143 A73-34360

Optimal observer techniques for linear discrete time systems.
17 p2144 A73-34361

Closed loop formulations of optimal control problems for minimum sensitivity.
17 p2144 A73-34363

State space attitude control synthesis for a satellite with flexible appendages.
17 p2239 A73-34951

Control of multiplexed communications channels.
17 p2144 A73-35310

Annual Southwestern Conference and Exhibition, 25th, Houston, Tex., April 4-6, 1973, Record.
17 p2124 A73-35357

Solution of coupled and singular perturbation methods using duality theory.
17 p2202 A73-35358

Limit cycle stability determination for nonlinear system with single loop feedback, using describing function method and z transform
17 p2202 A73-35517

Nonlinear optimal control synthesis for oscillating second-order systems with a convex control region
17 p2213 A73-35589

Electrical engineering - Service to mankind; Proceedings of the Southeast Region 3 Conference, Louisville, Ky., April 30-May 2, 1973.
17 p2142 A73-35626

Magnitude error bounds for sampled-data frequency response obtained from the truncation of an infinite series.
17 p2145 A73-35640

Limit cycles resulting from quantization in digital control systems.
17 p2145 A73-35642

Control laws of magnetic attitude stabilization systems of earth satellites
18 p2359 A73-36103

Application of the dynamic filtration method to spacecraft orientation control problems
18 p2359 A73-36104

Some problems of orientation accuracy for a gyroscopic orbit with nonlinear control laws
18 p2335 A73-36118

Neighboring extremals for optimal control problems.
18 p2294 A73-36308

Optimal control of linear systems in the case of continuous and discrete controls
18 p2337 A73-36410

Optimal control with probabilistic quadratic performance criterion and constraints, using stochastic principle for reduction to time derivative maximization problem
18 p2294 A73-36602

Chattering arcs and chattering controls.
18 p2294 A73-36639

On the existence of an optimal solution of the epsilon variational problem.
18 p2330 A73-36641

Existence of optimal controls for processes described by a system of hyperbolic equations
18 p2331 A73-36986

Solving M. A. Aizerman's first problem of absolute stability of nonlinear systems on the basis of the general theory of root trajectories
18 p2337 A73-37025

Hierarchical hybrid control of manipulators - Artificial intelligence in LSI.
19 p2407 A73-37334

Joint Automatic Control Conference, 14th, Ohio State University, Columbus, Ohio, June 20-22, 1973, Preprints of Technical Papers.
19 p2412 A73-38028

Design of decoupled multivariable control systems.
19 p2412 A73-38032

A sensitivity approach to the decoupling of linear systems with parameter disturbances.
19 p2412 A73-38034

A constraining hyperplane technique for state variable constrained optimal control techniques.
19 p2413 A73-38036

On the use of singular perturbation methods in the solution of variational problems.
19 p2386 A73-38038

Second-order optimality conditions for the Bolza problem with variable endpoints and separated end conditions.
19 p2445 A73-38039

An application of truncated power series controllers for optimization of dynamic systems.
19 p2413 A73-38040

An optimal feedback control law for regulator problems with linear state inequality constraints.
19 p2413 A73-38060

Performance of LQG control systems using optimal k-step-ahead control laws.
19 p2413 A73-38062

A new approach to the 'inverse problem of optimal control theory' by use of a generalized performance index /GPI/.
19 p2414 A73-38063

A projection operator algorithm for optimal control problems with unspecified initial state values.
19 p2414 A73-38064

Controllability of discrete bilinear systems with bounded control.
19 p2414 A73-38067

Suboptimal design of a class of nonlinear controllers.
19 p2414 A73-38068

Synthesis of optimal automatic control systems by use of the complexity principle and of the regularization method.
19 p2414 A73-38145

Regulators guaranteeing the autonomy of a controlled system.
19 p2414 A73-38192

A continuous-discrete method of design of control devices.
19 p2414 A73-38194

The Ritz-Galerkin procedure for parabolic control problems.
19 p2446 A73-38375

A dual method for optimal control problems with initial and final boundary constraints.
19 p2446 A73-38376

Necessary conditions for Chebyshev-Bolza optimal control problems.
19 p2415 A73-38489

Russian book - Optimal and adaptive systems.
20 p2538 A73-38671

Controllability conditions and optimization solution to finite control problem during prescribed time for lumped parameter system
20 p2591 A73-38673

Approximate synthesis theory in problems of optimization of automatic control systems
20 p2591 A73-38674

Discontinuous solutions of hyperbolic optimum problems
20 p2581 A73-38675

Construction of improving variations during the optimization of determinate and stochastic systems
20 p2539 A73-38677

Multidimensional linear extrapolation in problems of optimal design and control
20 p2539 A73-38687

Self organizing behavior of multivariable stochastic extremal control systems with environmental or intrinsic positive feedback under perturbation
20 p2539 A73-38689

Russian book - Automatic control theory.
20 p2539 A73-38690

Nonlinear control systems analysis, discussing phase space method, Taylor-Cauchy transform, Volterra functions, Liapunov stability, Popov-Kalman-Yakubovich theorems and limit cycle oscillations
20 p2592 A73-38691

Conditions, based on the estimation of the sensitivity of a periodic solution, for the application of the harmonic linearization method to higher harmonics and small parameters
20 p2592 A73-38693

Influence of low-frequency periodic interference on the operation of a complex system with variable structure
20 p2539 A73-38694

Fundamentals of the theory of nonlinear control systems with pulsed frequency and width modulation
20 p2539 A73-38696

Information processes in control systems, discussing stability, state reproduction, invariance, entropy balance and statistical physics analogies
20 p2539 A73-38698

Stochastic process control with a regulated control interval duration
20 p2540 A73-38701

Automatic control theory and systems representation in framework of unilateral mechanics, using canonical elastodynamic and elastostatic equations
20 p2540 A73-38703

Spectral analysis and a synthesis of linear systems with variable and random parameters in finite time intervals
20 p2540 A73-38704

Synthesis of low-sensitivity automatic control systems
20 p2540 A73-38706

Complex stochastic control system identification by distribution and moments characteristics in form of Gaussian densities, perturbation polynomials and sedastic functions
20 p2540 A73-38708

Determination of the structural features of nonlinear dynamic systems
20 p2540 A73-38709

Certain methods of determining the dynamic characteristics of stochastic objects
20 p2540 A73-38710

Direct statistical evaluation of nonlinear guidance systems.
20 p2584 A73-38779

[AIAA PAPER 73-836]
Automatic control of adverse yaw in the landing environment using optimal control theory.
20 p2586 A73-38799

[AIAA PAPER 73-861]
Certain results of the application of the method of sections to typical classes of nonlinear automatic systems
20 p2541 A73-38985

Choice of optimal parameters for flight-vehicle control systems in the presence of random disturbances
20 p2590 A73-38991

A method of processing a priori information about a controlled plant with the aim of reducing the number of changing parameters of the dynamic characteristics
20 p2541 A73-38993

Problems in the theory and practice of the self-tuning of compensating signals in complex control systems
20 p2541 A73-38994

Some nonlinear problems in optimal control
20 p2541 A73-38995

Optimal statistical solution methods in recognition, data processing, and control problems
20 p2532 A73-38997

Russian book - Complex control systems.
20 p2541 A73-39033

A programmed control task in a two-level hierarchical system under conditions of uncertainty
20 p2541 A73-39034

Transient process quality assessment for dynamic systems with variable parameters
20 p2541 A73-39035

Synthesis of multidimensional automatic optimization systems with allowance for constraints
20 p2542 A73-39040

The maximum principle in problems of optimal control of systems having a nonsmooth right side
20 p2593 A73-39323

Management of the treatment of illnesses as a problem of modern control theory
20 p2518 A73-39348

Parametric sensitivity in the problem of control with reference to an incomplete model of the plant
20 p2542 A73-39350

Reproduction of a useful signal by linear feedback systems
20 p2543 A73-39506

An adaptive, time-suboptimal position servomechanism
20 p2511 A73-39664

Flight vehicle extensive attitude control theory, deriving kinematic relations for optimal control moment selection to ensure required rotation
21 p2780 A73-40385

Passive stochastic feedback stability. I - A general theory. II - Applications.
21 p2669 A73-40450

Use of piecewise linearization for suboptimal control of nonlinear systems.
21 p2669 A73-40451

Control law synthesis and sensor design for active flutter suppression.
21 p2784 A73-40502

[AIAA PAPER 73-832]
Russian book on mathematical theory of optimal control of discrete time systems covering multidimensional geometry, convex sets, Pontryagin maximum principle and dynamic programming
21 p2726 A73-40802

Certain problems in the use of the maximum principle to determine optimal controls in the case of special controls and sliding regimes
21 p2670 A73-40858

Application of the method of slipping modulating functions for identification of plants with time lag
21 p2670 A73-40993

Selection of an optimal structure for a tabular model of a control plant
21 p2670 A73-40995

Convex approximation of the control process and a method for constructing generalized optimum regimes
21 p2727 A73-41064

Russian book on accuracy of automatic systems using digital computers as control devices covering analysis and synthesis, stochastic inputs, system errors and operator methods
21 p2658 A73-41282

Possibilities of suboptimal control in a linear-quadratic problem
21 p2671 A73-41606

Russian book - Theory and methods for constructing multiple-link control systems.
22 p2835 A73-42601

Structural methods of multichannel systems synthesis with the aid of the graph theory
22 p2836 A73-42602

Gradient control laws in stabilization problems of multidimensional control systems
22 p2887 A73-42605

Optimal control of multiple-link plants with bounded phase coordinates
22 p2887 A73-42607

Optimal closed automatic control systems synthesis in terms of minimum integral square error of phase coordinates during transient response time

22 p2836 A73-42609

Decomposition of the solution to optimal synthesis problems of multiple-link control systems

22 p2887 A73-42610

Problems of the theory of multidimensional combined systems with a common output

22 p2836 A73-42611

Application of stochastic programming methods for solving certain optimization problems of multiple-link plants without memory

22 p2836 A73-42612

Transfer function root method for synthesis of multiply connected determinate automatic control systems with asymmetrical channels and limited nonautonomous control elements

22 p2836 A73-42614

Linearization technique for synthesis of nonlinear two dimensional automatic control systems with cross disturbances, imposing constraints on motion coordinate deviations

22 p2836 A73-42615

Quasi-autonomous dynamic control subsystem interrelation and location for nonlinear multiple link automatic control synthesis with iterative integration of motion equations

22 p2836 A73-42616

Iteration methods for identification of multiple-link controlled plants for self-adaptation purposes

22 p2836 A73-42617

Synthesis of optimal discrete controls for a continuous plant over a fixed time interval

22 p2837 A73-42619

German monograph on regularization and penalty function methods of numerical analysis in Hilbert or Banach space covering minimax technique and optimal control theory application

22 p2882 A73-42847

German monograph - Principles concerning proofs regarding optimality conditions in the case of time-dependent processes.

22 p2888 A73-42853

Automatic control theory application to random vibration passive and active isolators synthesis, considering vehicle suspension systems and electrohydraulic damper

22 p2927 A73-42922

Dynamic programming application to extremal fields topological singularity in optimal control theory for flight vehicle with state variables satisfying initial conditions and ordinary differential equations

22 p2917 A73-43030

Sensitivity of optimal control systems with bang-bang control.

22 p2837 A73-43068

On the Volterra series functional evaluation of the response of non-linear discrete-time systems.

22 p2837 A73-43069

Optimal discrete-time feedback control of mixed distributed and lumped parameter systems.

22 p2837 A73-43072

Classical mechanics Noether theorem and variational calculus for optimal control, noting Pontryagin maximum principle equations first integral solution existence condition

22 p2837 A73-43073

Sensitivity, adaptivity and optimality; Proceedings of the Third Symposium, Ischia, Italy, June 18-23, 1973.

23 p2961 A73-43277

A survey of model reference adaptive techniques /Theory and applications/.

23 p2962 A73-43278

The state space and transfer function approaches in practical linear multivariable systems design.

23 p2962 A73-43281

Synthesis of feedback systems with large plant ignorance for prescribed time domain tolerances.

23 p2962 A73-43282

Synthesis of parameter and state insensitive feedback systems with constraints based on piecewise constant linear control laws.

23 p2962 A73-43283

Reduction of the sensitivity of optimal control systems by using two degrees of freedom.

23 p2962 A73-43285

Synthesis of two-level controller for a class of linear plants in an unknown environment.

23 p2963 A73-43289

On stability of large-scale systems under structural perturbations.

23 p2963 A73-43290

Application of finite integral transformations to optimal control problems

23 p2963 A73-43576

Problem of synthesizing a control system in the case of a plant involving random jerky forces

23 p2963 A73-43577

An adaptive observer for single-input single-output linear systems.

23 p2963 A73-43818

Nonlinear regulator theory and an inverse optimal control problem.

23 p2963 A73-43820

Model reference adaptive control system design using Kalman-Yacubovich lemma in connection with Lure problem

23 p2964 A73-43827

Closed loop linear control system synthesis possibility under condition of incomplete information on state vector with application to aircraft longitudinal motion

23 p2965 A73-44329

On the connection of the Krylov-Bogolyubov averaging method with the envelop method for investigating one class of control systems.

23 p2965 A73-44330

Optimal control over a finite time-interval for discrete systems in the problem of minimizing an inhomogeneous quadratic functional /The case of fixed end-points/.

23 p2965 A73-44331

Synthesis of optimal sampled-data control systems in the presence of continuous disturbances.

23 p2965 A73-44332

Synthesis of cascaded multiple-loop feedback systems with large plant parameter ignorance.

24 p3073 A73-44584

Discrete time invariant bilinear systems analysis for controllability, using decomposition by multiplicative feedback and linear compensation loops

24 p3073 A73-44585

Optimality condition based on maximum principle-derived convex reference function for control plants with continuous and discrete times

24 p3105 A73-44601

Certain problems of the correctness of the minimum-impulse linear optimal control problem. I - Dependence of the optimal control on the initial state and parameters

24 p3105 A73-44602

Stabilization of unstable plants through automatic search

24 p3074 A73-44662

Weak invariance conditions and synthesis algorithms for control systems with discontinuities on hypersurfaces in phase space

24 p3074 A73-44666

Application of the sensitivity theory to an analysis of the high-frequency components of motion

24 p3074 A73-45096

Application of stochastic differential equations in description of automatic control plants

24 p3074 A73-45098

A criterion for a free choice of decisions involving continuous control systems

24 p3074 A73-45100

Compensation method for non-linear systems having jump and hysteresis properties.

24 p3075 A73-45555

CONTROL UNITS [COMPUTERS]

Information management system breadboard data acquisition and control system.

04 p0425 A73-15461

Satellite data concentration, memorization, transmission and processing, discussing central computer control unit, ground stations peripheral links, magnetic tapes and system reliability

07 p0795 A73-18952

Digital computers with multistage storage in control systems, determining algorithms for data exchange between operative, superoperative and external memory devices

12 p1475 A73-26782

Algorithms of formal selection for optimal control systems of digital computers

14 p1730 A73-30034

Design principles for control systems of digital computers

14 p1730 A73-30035

Organization of checks of the central control unit in a digital process-control computer operating with fixed word length

16 p1986 A73-33665

CONTROL VALVES

A linear approach to the analysis of a force control system incorporating a hydraulic pressure-ratio valve.

02 p0132 A73-12002

A fundamental method for evaluating the contaminant tolerance of fluid power control valves.

02 p0132 A73-12003

Optimum operational flow characteristics derivation for control valves based on frequency distribution of relative pressure drop occurring in practical applications

10 p1223 A73-24015

The tolerance of fluid machinery to contaminant wear.

13 p1571 A73-29031

Concorde aircraft fuel system and component valves design for long term service reliability and ease of maintenance, discussing refueling, fuel jettisoning and feed controls

16 p2046 A73-32923

Electro-mechano-hydraulic servovalve system, calculating dynamic frequency response in vibrating accelerated field under external disturbance

19 p2388 A73-37670

The effect of valve area gain on the performance of the hydraulic servomechanism.

20 p2511 A73-39755

Axial vortex and Coanda vortex flow controllers.

23 p2941 A73-43392

A hot gas actuator for missile control.

23 p2942 A73-43398

Oil hydraulic button vortex valve optimization experiment for power consumption reduction, noting Reynolds number effects on turn down and pressure ratios

23 p2943 A73-43404

Pneumatic sequential circuits assembly method involving modules with switching elements and shift register, considering control valves and operation modes

23 p2943 A73-43416

CONTROLLABILITY

Handling characteristics in roll of two light airplanes for steep approach landings.

03 p0250 A73-13701

Algebraic and transfer-function criteria of fixed-time controllability of delay-differential systems.

04 p0430 A73-15212

Realistic pilot training and aircraft handling qualities in pilot error risk minimization for military, commercial and general aviation

05 p0545 A73-16733

On the controllability conditions for systems with distributed delays in state and control.

06 p0716 A73-17852

Nonlinear dynamic systems controllability theorem formulation and proof using matrix theory

06 p0716 A73-17853

An optimum settling problem for time lag systems.

06 p0717 A73-18172

Matrices, polynomials, and linear time-invariant systems.

06 p0719 A73-18863

Properties of linear time-invariant multivariable systems subject to arbitrary output and state feedback.

06 p0682 A73-18865

Nonlinear programming in design of control systems with specified handling qualities.

07 p0777 A73-20588

A unified boundary controllability theory for hyperbolic and parabolic distributed parameter systems.

07 p0846 A73-20591

Necessary condition for complete controllability with respect to arbitrary function for linear time-invariant differential equation system with time lag

08 p0950 A73-21092

Parallel-redundant flight control systems, discussing sensor bias and combined control computer input effects on controllability and steady state modal response

11 p1342 A73-25783

Minimum fuel problem link to Kalman controllability theorem, deriving solution based on state transition and controllability matrices

12 p1517 A73-27152

Controllability of discrete bilinear systems with bounded control.

14 p1739 A73-30510

Control of functional differential equations with function space boundary conditions.

14 p1770 A73-30754

The infinite time quadratic cost problem for certain classes of infinite dimensional control systems.

14 p1770 A73-30758

Algebraic Lie structure theory of bilinear systems in terms of controllability, observability and equivalent realization

14 p1771 A73-30783

VTOL and STOL projects flight simulation trials for autostabilization, head-up displays and flight controls effectiveness in handling qualities improvement and pilot workload reduction

16 p1996 A73-33209

Royal Aircraft Establishment Aerodynamics Flight Division flight simulators for V/STOL and helicopters, emphasizing handling, aircraft mathematical models and cockpit simulation

16 p1996 A73-33211

Automated prediction of light aircraft performance and riding and handling qualities.

[SAE PAPER 730305]

Technical basis for the STOL characteristics of the McDonnell Douglas/USAF YC-15 prototype airplane.

[SAE PAPER 730366]

Controllability and stabilizability of decentralized dynamic systems.

19 p2413 A73-38045

Controllability of discrete bilinear systems with bounded control.

19 p2414 A73-38067

Control configuration optimization of linear engineering systems.

19 p2414 A73-38082

- The effect of ice formation on the stability and maneuverability characteristics of aircraft
19 p2387 A73-38117
- Controllability and synthesis of optimal dynamic systems
20 p2591 A73-38672
- Controllability conditions and optimization solution to finite control problem during prescribed time for lumped parameter system
20 p2591 A73-38673
- Conditions of existence of steady representations for discrete linear systems given in terms of unsteady representations
21 p2669 A73-40497
- Discrete time invariant bilinear systems analysis for controllability, using decomposition by multiplicative feedback and linear compensation loops
24 p3073 A73-44585

CONTROLLED ATMOSPHERES

- NT CABIN ATMOSPHERES
- NT INERT ATMOSPHERE
- NT SPACECRAFT CABIN ATMOSPHERES
- The friction of boron carbide in controlled atmospheres.
[ASME PAPER 72-LUB-29] 03 p0315 A73-14340
- Thermal analysis of combustion of fabric in oxygen-enriched atmospheres.
[ASME PAPER 72-WA/HT-22] 04 p0519 A73-15832
- Solid-state sliding friction and wear in the case of iron, cobalt, copper, silver, magnesium, and aluminum, kept in an oxygen-nitrogen mixture at pressures from 760 torr to 0.2 microtorr
05 p0581 A73-16107
- Thermoregulatory reactions of animals in a helium-oxygen medium
06 p0650 A73-17695
- Clean rooms and contamination-free zones in space technology
07 p0830 A73-19011
- Thermoregulatory reactions of rats in a nitrogen and helium-diluted hypoxic atmosphere
08 p0929 A73-20979
- Study and realization of special parts for aerospace construction by brazing in a fluorided reducing atmosphere
09 p1088 A73-22202
- Applications in aerospace construction and fallout of ONERA thermochemical techniques
[ONERA, TP NO. 1246] 18 p2320 A73-36688
- Nuclear submarine atmospheric constituent monitoring, covering mass spectrometers, IR carbon monoxide sensors, system development, requirements testing and spacecraft applications
[ASME PAPER 73-ENAS-9] 19 p2399 A73-37970
- Fluxless brazing of aluminum using protective gas.
23 p2985 A73-43997

CONTROLLED FUSION

- Engineering problems in the design of controlled thermonuclear reactors.
[AIAA PAPER 73-259] 05 p0596 A73-16980
- Review of controlled fusion research using laser heating.
[AIAA PAPER 73-258] 06 p0728 A73-17667
- Controlled nuclear fusion process based on laser heating of deuterium-tritium pellets, considering laser energy reduction by pulse induced plasma compression
06 p0699 A73-17752
- Nuclear Science Symposium, 19th, and Nuclear Power Systems Symposium, 4th, Miami, Fla., December 6-8, 1972, Proceedings.
11 p1363 A73-25955
- Role of stimulated Compton scattering in the interaction of laser radiation with a superdense plasma.
13 p1664 A73-28615
- Laser energy absorption by plasma for controlled thermonuclear fusion, comparing uses of electrically pumped gas, chemical and solid state lasers
17 p2185 A73-35379
- Application of cybernetic means and methods in studies of plasma physics and controlled thermonuclear synthesis
23 p3011 A73-43671

CONTROLLED STABILITY

U STABILITY

CONTROLLERS

- NT SERVOMECHANISMS
- NT SERVOMOTORS
- Synthesis of active controllers for vibratory systems.
01 p0057 A73-10697
- The optimal control of merging aircraft-derivation of the hybrid air traffic controller.
03 p0340 A73-14489
- Improvement of the static and dynamic accuracy of a dual-loop control system for an electric actuating element with a proportional velocity controller
09 p1037 A73-22940
- Linearization limits for optimal pulse controller adjustments, using comparison with continuous controller and extrapolation
10 p1198 A73-24000
- Stabilization of linear dynamical systems with output feedback.
10 p1199 A73-24037

Control system equations of motion construction based on program manifold, determining multidimensional piecewise continuous controller vectors under assigned inequalities
12 p1484 A73-27455

Structural requirements for decoupling, disturbance insensitivity and parametric insensitivity, considering synthesis procedures for multivariable dynamic regulators
14 p1739 A73-30779

Near optimal control laws and controller realization for multilevel feedback and time optimal control design and simulation
14 p1739 A73-30780

Group properties and invariant solutions in the problem of the analytic design of controllers for a process with distributed parameters
24 p3074 A73-44661

CONVAIR MILITARY AIRCRAFT

U MILITARY AIRCRAFT

CONVECTION

NT FORCED CONVECTION

NT FREE CONVECTION

Ring current effect on plasma convection in magnetosphere, assuming pressure due to proton population
03 p0302 A73-13854

Doppler turbulence spectrum and intensity measurement in stactacties region at base of cloud deck cooled by evaporation and destabilized by convection
03 p0339 A73-14539

Intensive probing of clear air convective fields by radar and instrumented drone aircraft.
03 p0339 A73-14542

Radar echo in clear air convection shown due to backscattering from fine refractivity fluctuations caused by turbulent mixing
03 p0280 A73-14543

Progressive waves analysis, considering nonlinear convective, dissipative and dispersive effects
05 p0528 A73-16756

On the dynamo action of the global convection in the solar convection zone.
05 p0627 A73-17387

Direct measurements of plasma convection in the upper ionosphere
10 p1211 A73-23885

Theory of cosmic ray transport with anisotropic particle scattering and convection
10 p1265 A73-23903

Solar cosmic ray diffusion, convection, accumulation and acceleration as function of interplanetary medium perturbation and flare coordinates
10 p1266 A73-23909

Uniform variable transverse magnetic field effects on convective instability of plane electrically conducting layer, reducing perturbed equilibrium equations to linear ordinary differential equations
10 p1256 A73-24593

Some specific features of the near-ground temperature field mesostructure and air humidity and their influence on convective processes
13 p1654 A73-28886

A three-dimensional model of cumulus cloud development.
14 p1771 A73-30764

Morphological characteristics of the moon and convection in its mantle
16 p2065 A73-33784

Internal structure of the convective shell of the sun
19 p2481 A73-37343

Direct measurements of plasma convection in the upper ionosphere.
20 p2550 A73-38904

Numerical one dimensional cumulus model of stratification and cloud depth-radius relations for convective layer prediction
21 p2729 A73-40068

Certain results of radar studies of the evolution of convective clouds
21 p2731 A73-40494

A physical-numerical model for the determination of the meteorological environmental effects produced by cooling towers
23 p3003 A73-43995

CONVECTION CLOUDS

NT CIRRUS CLOUDS

NT CUMULONIMBUS CLOUDS

NT STRATOCUMULUS CLOUDS

NT STRATUS CLOUDS

On a method of determining the interaction coefficient in convective clouds
01 p0074 A73-11273

Two dimensional deep convection rimitive model of pressure perturbation in cumulus cloud with precipitation
02 p0189 A73-12781

Echo top height characteristics based on convection cloud reflectivity structures measured by radar
03 p0338 A73-14516

Jet model of cloud convection - A numerical experiment
05 p0594 A73-17353

Influence of vertical wind shear on the development of convective cloudiness
11 p1393 A73-25640

A jet-stream model of cloud convection and a numerical experiment.
15 p1902 A73-31003

Russian monograph on convective cumulus and cumulonimbus cloud physics covering atmospheric convection, meteorological field structure and dynamic-kinematic schemes
15 p1903 A73-31584

Global circulation numerical modeling problems and numerical weather forecasting status as basis for GARP programs, considering tropical experiment on deep convective cloud systems
17 p2205 A73-34927

Scheme for evaluating the influence of convective-cloud modifications aimed at controlling precipitations artificially, and the results of cumulus cloud structure investigations from aircraft
18 p2332 A73-35917

Influence of the vertical structure of the wind field on the development of cumulus and cumulonimbus clouds
18 p2332 A73-35920

Experimental investigation of the velocities of vertical motions in convective clouds
21 p2730 A73-40121

On the variation with height of the top brightness of precipitating convective clouds.
23 p3005 A73-44270

CONVECTION CURRENTS

Injun 5 observations of magnetospheric electric fields and plasma convection.
03 p0303 A73-13875

Synoptic conditions of wave formation above convection streets.
04 p0473 A73-14826

Magnetospheric convection, discussing ionospheric twin vortex pattern, reconnection model for solar wind induced generation, plasmasphere response and magnetotail dynamics
04 p0442 A73-15337

Isotropic conducting plasma dynamic behavior near rotating magnetized sphere, showing electric field-produced meridional convective currents
07 p0856 A73-19430

Turbulence energy spectra in thick convective cumulonimbus cloud zone, using aircraft measurements
08 p0984 A73-21186

Certain feedbacks generated during turbulent cellular convection in the atmosphere
08 p0986 A73-21456

Dwarf binary component convective shell behavior under gravitational field periodic tidal action, noting conditions for thermal instability
08 p1012 A73-21548

Mode of thickening of a low morning convective layer in clear sky
09 p1115 A73-23036

Martian spin axis wandering resulting from equatorial volcanic convections and gravity field non-hydrostatic low order components
09 p1151 A73-23172

Intensive probing of a clear air convective field by radar and instrumental drone aircraft.
10 p1245 A73-23989

Convection in a rotating annulus uniformly heated from below. II - Nonlinear results.
11 p1449 A73-25159

Periodic solutions of the set of equations governing the nonadiabatic convection of dry isolated thermals.
11 p1393 A73-25690

A study of convective elements in the atmospheric surface layer.
11 p1393 A73-25692

Convection near critical Rayleigh numbers in the case of an almost vertical temperature gradient
11 p1453 A73-26435

Turbulent surface layer shear convection analysis, using similarity model based on weak interaction between vertical motion and mechanical turbulence
13 p1655 A73-29340

Optimal electron grouping arrangements in multi-resonator klystrons
14 p1736 A73-30565

Numerical experiments for the determination of characteristic dimensions and intensities of convection cells
15 p1902 A73-31138

Convective fluid motion and heat transfer in aircraft wing fuel tanks due to aerodynamic heating, comparing analytical with experimental results
15 p1957 A73-31643

Development of convection in horizontal layers of a non-Newtonian fluid
16 p2084 A73-32679

Model of dayside magnetopause displacement relation to convection currents feeding polar cap ionosphere to estimate electric field and flux return as function of displacement
16 p2003 A73-33432

A numerical study in three space dimensions of Benard convection in a rotating fluid.
17 p2151 A73-34855

Climatological studies based on satellite data, including cloud, snow and ice cover, wind measure-

ment, convection currents, temperature fields and earth thermal balance

18 p2331 A73-35914

Atmospheric vorticity effects on hexagonal convection cells formation, considering temperature profiles nonlinearity, turbulent viscosity and perturbation scale

18 p2333 A73-37052

Thermal instabilities and energy relations in convective shells of slowly rotating stars

19 p2481 A73-37346

Horizontal electric fields and currents caused by depths-to-surface oceanic water exchange in geomagnetic field, discussing electric field distribution and magnetic field distortion

19 p2426 A73-38175

The structure of an inversion above a convective boundary layer as observed using high-power pulsed Doppler radar.

19 p2447 A73-38205

Fine scale structure and mixing within inversion capping convective boundary layer, proposing atmospheric model for sensible downward heat transfer

19 p2448 A73-38215

Structure of cumulus clouds during various development phases

20 p2583 A73-39186

Convection in a liquid heated from below in a closed cavity with temperature-dependent viscosity

20 p2628 A73-39612

Certain parameters of cellular convection according to observations by meteorological earth satellites and from a high mast

21 p2731 A73-40492

Linear convective modes and the energy transport in stellar convection zones.

22 p2905 A73-41761

Strong magnetic fields occurrence in sunspot penumbra dark filaments related to hypothesis of penumbral convection rolls existence

23 p3026 A73-43224

Nonlinear theory of the formation and structure of the intertropical convergence zone.

23 p3001 A73-43586

The mesoscale structure of the atmospheric boundary layer and its interaction with small-scale turbulence

24 p3107 A73-44960

CONVECTIVE FLOW

Book - Lectures in mathematical models of turbulence.

01 p0031 A73-10123

Rigid and free boundaries effects on radiative heat transfer stabilization of fluid layer against Benard thermal convection

01 p0120 A73-10397

Floating potential and diffusion coefficients of viscosity damping of convective cells in stellarator for confined He, Ar and Xe plasmas

01 p0083 A73-10462

Nonequilibrium thermodynamics description of convective motion, using internal energy and absolute mass flows as generalized convective flow

01 p0123 A73-10867

Vibrational instability of plane-parallel convective motion in a vertical duct

01 p0034 A73-10966

Simultaneous measurements of radar reflectivity and refractive index spectra in clear air convection.

01 p0018 A73-11060

The empirical determination of line source functions, beta-L-values, and the microturbulent and convective velocity components as functions of depth in the photosphere-chromosphere transition region.

01 p0107 A73-11378

Liapunov-Schmidt analysis of convection bifurcation scheme in internally heated viscous fluid layers of infinite horizontal extent

02 p0238 A73-12053

Characteristics of quiet as well as enhanced diurnal anisotropy of cosmic radiation.

03 p0360 A73-12876

Existence theorems for Navier-Stokes equations periodic solution bifurcation in convection between two horizontal plates at different time periodical temperature

[ONERA, TP NO. 1179]

03 p0343 A73-13602

Convective transport terms effect on laminar flow-field of Newtonian fluid between rotating cylinders, using adapted finite difference solution technique

03 p0298 A73-14643

Remarks on the steady and time dependent mathematical convection models.

04 p0443 A73-15341

Convective storm updraft shape calculation based on horizontal momentum changes in rising air, noting effects of mixing and aerodynamic drag

05 p0592 A73-16195

Finite-amplitude convection occurring in a modulated gravitational field

06 p0767 A73-17463

Unstable resonators for CO₂ electric-discharge convection lasers.

06 p0703 A73-18747

Diffusion on a particle in the shear flow of a viscous fluid - Approximation of the diffusion boundary layer.

07 p0809 A73-19021

A computational method for low Mach number unsteady compressible free convective flows.

07 p0918 A73-19268

Nonlinear thermal convection in electrically conducting Boussinesq fluid subject to temperature gradient and magnetic field, calculating flow stability limit by energy method

07 p0920 A73-19513

Numerical solutions to flow and heat transfer characteristics of free convection micropolar flow with Newtonian solvent substructure

08 p1023 A73-21260

Mars surface ellipticity discrepancy with dynamic value obtained from satellite orbital precession explained by solid state convection in deep interior and Martian evolution

09 p1144 A73-22268

Periodic semi-integral solutions of secondary unsteady convective flows in external force field for critical Rayleigh numbers by Liapunov-Schmidt method

10 p1204 A73-23584

Statistical properties of intermittency in large scale turbulent flows, considering boundary layer, shear and convective flows

10 p1205 A73-23855

Transient flows, effects of unsteady surface conditions on stability, and flow separation in buoyancy induced flows.

10 p1208 A73-24817

A numerical study of unsteady laminar combined convective flow over vertical plates.

10 p1296 A73-24848

Equations for nonlinear Benard convection with rotation for fluid layer, investigating asymptotic solution for two dimensional cells at large Rayleigh and Taylor numbers

11 p1448 A73-25052

Analysis of external mass transfer and choice of its parameters for convective removal of reaction-product vapors in a hydrogen-oxygen fuel cell with a capillary membrane

11 p1308 A73-25727

Atmospheric convection and its effect on relaxation time and charge distribution.

11 p1394 A73-25759

Vertical distribution of viscosity and convection conditions in earth mantle, discussing shallow convection model and geophysical evidence for validity

11 p1356 A73-25906

Photospheric convective network as a determining factor in sunspot and group development and stabilization.

11 p1426 A73-26574

On the relationship between the growth and expansion phases of substorms and magnetospheric convection.

12 p1489 A73-27005

On oscillatory instability of plane-parallel convective motion in a vertical channel.

12 p1559 A73-27542

The role of the Coriolis force on the stability of rotating magnetic stars and the origin of convective motions.

12 p1547 A73-27883

Nonequilibrium thermodynamics description of convective motion, using internal energy and absolute mass flows as generalized convective flow

12 p1560 A73-27917

The pressure and velocity fields of convected vortices.

13 p1599 A73-28067

MHD free convective flow in a vertical channel.

13 p1663 A73-28164

Earth mantle convection theory, calculating polar secular wandering from inertia product change due to mass transfer

13 p1607 A73-28404

Flame quenching, extinction, propagation, convection and ignition limits in premixed gas mixtures

13 p1707 A73-29003

Book on variable stars, covering high energy astrophysics, low energy outbursts, extensive convection, galaxies, pulsations, white dwarfs, cepheids, flares and gravitational collapse

14 p1796 A73-29950

Contact binary star evolution, discussing adiabatic convection zone entropy, mass flow and relative frequency

15 p1928 A73-31054

Planar free convection flow over horizontal cylinders with a small Grashof number under the influence of a planar wall

16 p2085 A73-33254

Satellite studies of magnetospheric substorms on August 15, 1968. III - Some features of magnetospheric convection.

16 p2004 A73-33451

On the extent of the Martian ionosphere.

16 p2062 A73-33462

The magnetohydrodynamic stability of white dwarfs and neutron stars.

16 p2062 A73-33573

Natural convection flow equations and balloons of laminar and transition flows, external and free boundary flows and boundary layer regimes

17 p2254 A73-34354

Mass transport rate in solar nebula model due to turbulence induced by convection

17 p2229 A73-34432

Jupiter atmospheric circulation as manifestation of large scale convective instability generated by internal heat sources, considering Red Spot production

17 p2232 A73-34859

An analytical and experimental investigation of turbulent flow in bearing films including convective fluid inertia forces.

[ASME PAPER 73-LUBS-1]

17 p2181 A73-35388

Application of energy model of turbulence to calculation of lubricant flows.

[ASME PAPER 73-LUBS-18]

17 p2181 A73-35397

Book - Radiative transfer and interactions with conduction and convection.

17 p2256 A73-35864

On the convective diffusion in tubes of circular section

18 p2299 A73-36489

Generation of time-periodic secondary convective flows

18 p2301 A73-37006

Laboratory vortices in rotating, sheared flow.

19 p2420 A73-37664

The photolytic stability of the Martian atmosphere.

21 p2764 A73-40159

Two types of instability of steady convective motion caused by internal heat sources

21 p2789 A73-40192

Russian book - Convective stability of an incompressible fluid.

21 p2790 A73-40417

Forced convection of a fluid inside an ellipsoidal cavity

21 p2791 A73-40740

On the possibility of constructing a radiative sunspot model in magnetohydrostatic equilibrium.

21 p2777 A73-41486

Breakup of liquid drops due to convective flow in shocked sprays.

22 p2937 A73-42819

Nonstationary mass transfer during the longitudinal flow of a nonlinearly viscous fluid past a flat plate and the forward stagnation point

23 p2967 A73-43440

An explanation of anomalously large Reynolds stresses within the convective planetary boundary layer.

23 p3002 A73-43593

Some further studies on the transition to turbulent convection.

23 p3003 A73-43935

Density variation and radiative exchange effects on convective instability of plane-parallel polytropic atmosphere heated from below with application to solar granulation

24 p3135 A73-44628

On the generation of umbral flashes and running penumbral waves.

24 p3136 A73-44638

Meteorological Doppler radar for measurements of particle velocity and horizontal winds inside convective storms, discussing signal processing and multiple radar method

24 p3107 A73-44687

Numerical convective schemes based on accurate computation of space derivatives.

24 p3105 A73-45026

Polar cap electric field measurements by balloons indicating ionospheric convection control by interplanetary magnetic field

24 p3086 A73-45135

Measurements of the structure of the Reynolds stress in a turbulent boundary layer.

24 p3079 A73-45310

Air flow in circular convection chamber, investigating transition to turbulence by simultaneous measurements of heat flux and temperature field at low Rayleigh number

24 p3157 A73-45311

CONVECTIVE HEAT TRANSFER

Unsteady temperature and stress distribution in variable thickness disk under convective heat transfer with ambient medium, using approximation method

01 p0113 A73-10021

Dynamic and thermodynamic effects addition to basic Boussinesq convection for convection in stars, discussing rotation, magnetic fields, radiative transfer and state equation

01 p0094 A73-10061

Natural convective heat transfer in cavities and horizontal circular tubes, considering boundary layer and core flow interaction effects

01 p0120 A73-10290

Mixed convection over a heated horizontal plane.

01 p0120 A73-10440

Free and forced convection from fine hot wires.
01 p0120 A73-10447

Radiative and convective heating during Venus entry.
01 p0003 A73-10757

Heat transfer from a circular cylinder in a rarefied gas stream.
01 p0122 A73-10761

Convective heat transfer coefficients at stagnation point of blunt body immersed in flames of fuel gases combustion with pure oxygen
01 p0122 A73-10807

Developing laminar free convection between vertical flat plates with asymmetric heating.
01 p0122 A73-10811

Evolutionary sequences for massive stars with various initial chemical compositions, studying semiconvection effects on core helium burning star distribution in H-R diagram
01 p0104 A73-11037

Heat transfer from a sphere with injection in a slow moving flow
02 p0152 A73-11611

Combined forced and free-convection heat transfer from vertical thin needles in a uniform stream.
02 p0238 A73-12052

Lunar thermal convection via solid state creep processes, discussing departure from hydrostatic equilibrium figure
03 p0369 A73-13105

Infinite Prandtl number fluids with constraint characterized by Taylor number heated from below, choosing boundary conditions for laminar convection
03 p0293 A73-13329

Convection heat transfer in a contained fluid subjected to vibration.
03 p0398 A73-13547

Hydrodynamics of the convective zone of the sun
03 p0373 A73-13608

Radiative and convective heat transfer occurring in the hypersonic flow past a blunted body
03 p0244 A73-13617

Resultant value of the inertial emf during thermal convection in a rotating plasma
04 p0481 A73-15604

Study of the laminar free convection wake above an isothermal vertical plate.
[ASME PAPER 72-WA/HT-41] 04 p0518 A73-15815

Enthalpy driving forces for gas cooling data correlation in convective heat transfer in reacting turbulent boundary layers with mass injection
[ASME PAPER 72-WA/HT-31] 04 p0519 A73-15824

A note on a minimum principle in Benard convection.
04 p0520 A73-15940

Empirical equations for calculating the heat and mass transfer for the special case of separated flow
04 p0520 A73-15941

Free convection along the downward-facing surface of a heated horizontal plate.
04 p0520 A73-15943

Unsteady-state conjugated heat transfer between a semi-infinite surface and incoming flow of a compressible fluid. I - Reduction to the integral relation. II - Determination of a temperature field and analysis of results.
04 p0520 A73-15944

Forced convective heat transfer to supercritical water flowing in tubes.
04 p0520 A73-15945

Insulating materials fireproofing effectiveness prediction by finite element method for combined time dependent convective-radiative boundary conditions
05 p0637 A73-16132

Combined free and forced laminar convection in inclined tubes.
05 p0564 A73-16173

Free convective heat transfer between vertical parallel plates One plate isothermally heated and the other thermally insulated.
05 p0638 A73-16221

Influence of thermal nonstationarity on convective heat-transfer intensity
05 p0640 A73-16773

Stationary temperature field of a disk under conditions of convective heat transfer on its surface
05 p0640 A73-16775

Boundary layer characteristics with radiant energy transfer under adverse pressure gradient.
[AIAA PAPER 73-117] 05 p0530 A73-16874

Analysis of sublimation-cooled coated mirrors in convective and radiative environments.
05 p0641 A73-17108

Heat transfer downstream of attachment of a turbulent supersonic shear layer.
05 p0533 A73-17112

Convective heating on delta-wing Space-Shuttle boosters including interference effects.
05 p0533 A73-17202

Investigation of convective and radiative heating of blunted bodies in hypersonic flow
06 p0644 A73-17469

Approximate analytical solution of an asymmetrical problem of unsteady heat conduction with nonlinear boundary conditions
06 p0768 A73-18128

Temperature of a duct flow under conditions of unsteady-state heat transfer
06 p0769 A73-18131

Possibilities of changing the microstructure of turbulent flow in investigations of convective heat transfer
06 p0686 A73-18133

Description of the transfer of heat by natural convection in a horizontal porous layer with the help of a solid-fluid transfer coefficient
06 p0769 A73-18538

On laminar free convection stagnation heat transfer from an isothermal cylinder with internal sources-sinks.
07 p0918 A73-19101

Temperature field structure in strongly heated buoyant thermals.
[AD-754728] 07 p0919 A73-19504

German monograph - Free convection of air in a horizontal circular gap in the case of temperature- and pressure-dependent density.
07 p0920 A73-19579

Convective combustion of porous explosives
07 p0920 A73-19990

Time optimal heating of thin plates with constraints placed on the thermal stresses
07 p0923 A73-20634

Thermal state of a porous plate cooled by intense blowing under conditions of radiative-convective heating
08 p1021 A73-20993

Axisymmetric Stefan problem with boundary conditions of the third kind
08 p1022 A73-21100

Thermo-acoustic oscillations in forced convection heat transfer to supercritical pressure water.
08 p1022 A73-21253

Natural convection in annular horizontal space
08 p1024 A73-21498

Study of thermal phenomena in a Hartmann-Sprenger tube
08 p1024 A73-21634

A theoretical study of natural convection heat transfer from downward-facing horizontal surfaces with uniform heat flux.
08 p1024 A73-21638

Destabilization of vapor film boiling around spheres.
08 p1024 A73-21641

Scanning electron microscope for heat transfer surfaces characterization, noting Inconel surface roughness change in convective heat transfer experiment
08 p1025 A73-21642

Heat transfer in horizontal annular air gaps at small Grashof numbers
09 p1167 A73-23108

Influence of the Reynolds number on nonstationary convective heat transfer in a pipe during a change in the thermal load
10 p1204 A73-23511

An experimental study of combined forced- and free-convective heat transfer from flat plates to air at low Reynolds numbers.
10 p1295 A73-23777

The cooling of a sunspot. I - A Carnot cycle and the hydromagnetic interactions. II - Convection zone models and the magnetic power supply.
10 p1279 A73-24137

Inertial emf due to thermal convection in a rotating plasma.
10 p1254 A73-24194

Temperature fluctuations in the turbulent wake behind an optically heated sphere.
10 p1296 A73-24251

Free convection from a semi-infinite flat plate inclined at a small angle to the horizontal.
10 p1296 A73-24339

Interaction between a sound field and natural convection on a horizontal cylinder.
10 p1296 A73-24846

A note on the structure of thermal convection in a slightly slanted slot.
10 p1297 A73-24969

Convection in a rotating annulus uniformly heated from below. II - Nonlinear results.
11 p1449 A73-25159

Transpiration and natural convection - The vertical-flat-plate problem.
11 p1449 A73-25219

Natural convection in a sloping porous layer.
11 p1449 A73-25220

Unsteady laminar convection in uniformly heated vertical pipes.
11 p1449 A73-25221

Approximate calculation of thermoelastic stresses in an arbitrarily heated slab
11 p1434 A73-25393

Heat transfer law for free convection in cylindrical and spherical interlayers
11 p1450 A73-25726

Determination of the convective heat transfer coefficient by 'half-space period' method
11 p1451 A73-25741

Forced convection heat transfer in laminar boundary layer at low Prandtl numbers.
11 p1452 A73-26123

Laminar free convection flow of an electrically conducting fluid from an inclined isothermal plate.
11 p1452 A73-26369

Simultaneous radiative and conductive heat transfer in non-gray media.
11 p1453 A73-26583

The role of convection in stellar atmospheres. I - Observable effects of convection in the solar atmosphere.
11 p1427 A73-26611

Determination of the coefficient alpha real in convection in air with allowance for the Jacq effect
12 p1557 A73-26797

Photon conductivity analysis for homogeneous isotropic solid body based on convective-radiant transfer equations, determining molten quartz thermal conductivity and diffusivity
12 p1516 A73-27311

Convective heat transfer in the region of interaction between a supersonic overexpanded jet and an oblique obstacle
12 p1458 A73-27324

Steady doubly periodic convection regimes in horizontal fluid layer heated at lower surface, considering branching from state of rest
12 p1559 A73-27420

Evidence for convection in planetary interiors from first-order topography.
12 p1542 A73-27492

Transient cooling of a solid cylinder by combined convection and radiation at its surface.
13 p1704 A73-28086

High Reynolds number fluid dynamics and heat and mass transfer in real concentrated particulate two-phase systems.
13 p1704 A73-28427

The transient temperature distribution in a slab subjected to radiative and convective heating calculated by variational method.
13 p1704 A73-28429

On thermal convection between non-uniformly heated planes.
13 p1705 A73-28430

Massive main sequence stars structure and evolution within core hydrogen burning models, giving mathematical relation and conditions for convective instability
13 p1682 A73-28979

Experiments in magneto-fluid-mechanic natural and forced heat transfer from horizontal hot-film probes.
13 p1620 A73-29254

The heat and mass transfer of a binary laminar boundary layer in the presence of simultaneous convection at a vertical permeable flat surface
13 p1708 A73-29350

Experimental investigation of the convection inversion process in the viscous sublayer of a turbulent boundary layer during blowing of carbon dioxide through a vertical porous heated surface under conditions of natural convection
13 p1708 A73-29407

Human thermoregulatory system examination under thermodynamic equilibrium based on conductive and convective metastable heat transfer from skin to environment
13 p1577 A73-29414

[ASME PAPER 73-AUT-J] Rough estimate of the heat transfer coefficient of a liquid in laminar and turbulent flow through plane ducts
14 p1744 A73-30012

Velocity profile determination in a turbulent boundary layer
14 p1746 A73-30795

Effectiveness of a gas screen in plasmatrons of axial configuration
15 p1917 A73-31191

Convective fluid motion and heat transfer in aircraft wing fuel tanks due to aerodynamic heating, comparing analytical with experimental results
15 p1957 A73-31643

Transient forced convection heat transfer from an isothermal flat plate.
15 p1957 A73-31664

Response-optimal heating of thin plates with constraints on the temperature stresses.
15 p1957 A73-31688

Experimental assembly for complex heat transfer studies
15 p1858 A73-31860

A procedure for simultaneous measurement of convective and radiant thermal fluxes in permeable walls
15 p1957 A73-31866

Heat transfer in the case of free convection of air between vertical surfaces
15 p1958 A73-31908

Natural convective heat transfer between vertical parallel plates - One plate with a uniform heat flux and the other thermally insulated.
15 p1958 A73-32057

Forced convective heat transfer of a gas with condensing vapor around a flat plate.

15 p1958 A73-32058

Effectiveness and heat transfer with full-coverage film cooling.

[ASME PAPER 73-GT-18] 16 p2086 A73-33495
The thermal regime and convective motions in the lower layers of the Venusian atmosphere

16 p2068 A73-33825

Thermal shielding by subliming volume reflectors in convective and intense radiative environments.

17 p2253 A73-34183

Experimental heat transfer investigations on modules mounting hybrid packages.

17 p2135 A73-34729

Russian book on radiative and complex heat transfer covering electromagnetic energy-matter interaction, modeling, convective and conductive transfer and thermodynamic equilibrium radiation

17 p2254 A73-34899

Effect of Reynolds number on nonstationary convective heat exchange in a tube with variable heat load.

17 p2255 A73-35191

Solid state convection role in moon from analysis of models with homogeneous initial distribution of radioactive heat sources

17 p2232 A73-35262

Book - Buoyancy effects in fluids.

17 p2155 A73-35336

Theoretical analysis of forced laminar convection heat transfer in the entrance region of an elliptic duct.

17 p2256 A73-35850

Convective heating in dust-laden hypersonic flows.

[AIAA PAPER 73-761] 18 p2371 A73-36376

Mass transfer effects on turbulent heating in the vicinity of slots.

18 p2371 A73-36381

[AIAA PAPER 73-766] Approximate solution of the problem of local heat transfer at a vertical plate under conditions of laminar mixed convection

18 p2371 A73-36649

Combined forced and free-convection over thin needles.

18 p2371 A73-36697

Some laboratory observations on convective plumes.

18 p2333 A73-36711

Fine scale structure and mixing within inversion capping convective boundary layer, proposing atmospheric model for sensible downward heat transfer

19 p2448 A73-38215

Heat transfer in an absorbing, emitting and scattering slug flow between parallel plates.

[ASME PAPER 73-HT-13] 20 p2625 A73-38568

Combined forced convection and radiation heat transfer in the thermal entrance region of a non-isothermal parallel plate channel - Optical thin gases.

[ASME PAPER 73-HT-14] 20 p2625 A73-38569

A tilted plate interferometer for heat transfer studies.

20 p2564 A73-38879

Bounding flow existence for turbulent convection in fluid and porous layers analysis between parallel plates based on calculus of variations in Banach spaces

20 p2626 A73-39012

Heat transfer through free convection of air between vertical plates, obtaining Nusselt and Grashof numbers, and temperature and pressure effects

20 p2628 A73-39407

Study of heat transfer in boundary layer taking into account the radiation at the surface.

20 p2507 A73-39420

Radiative and convective heat transfer in a magnetic field

20 p2628 A73-39608

Heat release by free convection from horizontal cylinders to CO₂ under near-critical conditions

20 p2628 A73-39613

Small surface plate calorimeter for convection and radiation heat transfer measurements from heated body in air

21 p2692 A73-39920

Asymmetric heat transfer in turbulent flow through a plane slot

21 p2790 A73-40398

Measuring the boundary layer temperature distributions using ablating specimens in an air plasma flow.

21 p2791 A73-41052

Unsteady convective heat transfer attending the cooling of gas in tubes.

21 p2791 A73-41053

Radiative-convective heat transfer in flows of hot air past a flat plate.

21 p2791 A73-41056

Convective heat transfer with allowance for three-dimensional heat sources in the fluid for turbulent flow in a plane slit

21 p2792 A73-41196

Steady-state heat transfer between fluids divided by a thin wall

21 p2792 A73-41224

On turbulent stress and the structure of young convective stars.

22 p2908 A73-42306

Effect of wall conduction on convective heat transfer with laminar boundary layer.

23 p3049 A73-43833

Forced convective heat transfer from isothermal sphere in steady incompressible flow at low Reynolds and various Prandtl numbers, obtaining mean Nusselt number

23 p3049 A73-43934

Jupiter radiative greenhouse model overestimation of lower cloud level temperature due to convective heat transport neglect, discussing rejection of water cumulus cloud possibility

24 p3129 A73-44439

Unsteady convective heat exchange for various hot-gas cooling laws in tubes

24 p3156 A73-45077

Determination of the temperature field in a perforated plate with convective heat transfer

24 p3157 A73-45171

CONVENTIONS

Satellite orbits allocation by international conventions to prevent interference with existing vehicles, noting international cooperation in communication frequencies allocation

04 p0524 A73-15157

CONVERGENCE

Equivalence theorems for nonlinear finite-difference methods.

01 p0069 A73-10074

An improved algorithm for the inversion of limb radiance measurements.

01 p0072 A73-10355

Mesh subdivision type influence on convergence properties of mixed triangular elements in plate bending analysis

01 p0115 A73-10745

Modified convergence criterion for boundary layers.

01 p0033 A73-10750

Accelerated convergence of sequences of quadrature approximations.

01 p0072 A73-11471

Functions of a generalized restricted variation and the convergence of their Fourier series and conjugate trigonometric series

02 p0188 A73-12551

The convergence of separation (Galerkin) formulations in the case of time-dependent equations

03 p0336 A73-13165

Convergence of consistently derived Timoshenko beam finite elements.

03 p0390 A73-13342

A modified conjugate gradient method for optimization problems.

04 p0471 A73-15216

On the prediction of the expansion coefficients in a variational calculation.

04 p0471 A73-15228

Relaxation algorithms for nonlinear system modal trajectory estimation by approximate step with lower triangular matrix inversions sequence, comparing convergence with Gauss-Newton method

04 p0472 A73-15265

Stability analysis of Riccati covariance equations of Kalman filter.

04 p0472 A73-15273

Comparison of the Powell 1, Powell 2, and Zangwill static optimization methods

06 p0670 A73-17859

Mean square error automatic equalizer for synchronous data transmission by gradient projection method for parameter optimization in discrete frequency domain, noting algorithm convergence

06 p0665 A73-18141

On weak convergence of empirical processes for random number of independent stochastic vectors.

06 p0718 A73-18502

On the convergence of random search algorithms in continuous time with applications to adaptive control.

06 p0671 A73-18623

On the convergence of the method of homogeneous linear approximations in problems of the theory of plasticity of inhomogeneous bodies.

07 p0906 A73-19022

An iterative procedure for the oscillatory laminar boundary layer.

07 p0809 A73-19035

Acceleration of the convergence in Nesbet's algorithm for eigenvalues and eigenvectors of large matrices.

07 p0844 A73-19271

Sundman power series convergence enhancement in three body problem by Poincare transformation

07 p0852 A73-20042

Some results of finite element applications in finite elasticity.

07 p0914 A73-20213

Convergence of difference methods for certain degenerating quasi-linear parabolic equations

09 p1111 A73-21919

Convergence of the solution for the far scattered field of a conducting cylinder of arbitrary cross-section.

09 p1050 A73-22397

Convergence to logarithmic distribution laws

09 p1112 A73-22884

Evaluation of the convergence rate in an integral limit theorem

09 p1112 A73-22885

Weak convergence of stepwise random processes

09 p1112 A73-22886

On the convergence of the finite element method for problems with singularity.

09 p1160 A73-22891

Rayleigh-Ritz solution of boundary value problem for plane compressible subsonic flow past aerofoil noting convergence

09 p1028 A73-22954

Numerical solution of Volterra integral equations.

09 p1113 A73-23020

Semivariational approximation for solution of parabolic differential equation with inhomogeneous mixed boundary conditions and abstract equation with operators, noting convergence and stability

09 p1113 A73-23025

Applications of the finite element method to the calculations of stress intensity factors.

09 p1162 A73-23185

Finite element analysis of curved structures, discussing shape functions generation method for convergence determination

09 p1165 A73-23439

Use of modal solutions in elastic wave propagation problems.

09 p1166 A73-23456

Contraction-mapping algorithm with guaranteed convergence.

10 p1242 A73-24034

On a method of adaptive control under conditions of great uncertainty.

10 p1199 A73-24036

Use of the least squares criterion in the finite element formulation.

10 p1243 A73-24295

Certain finitely converging algorithms for the solution of infinite systems of inequalities and their application in the theory of adaptive systems

10 p1192 A73-24486

Nonlinear dynamic feedback control system state variable observers reconstruction error convergence and digital simulation for performance

11 p1390 A73-25187

Maximum principle and uniform convergence for the finite element method.

11 p1390 A73-25435

Rayleigh quotient minimization and eigenvalue/eigenvector errors of mode convergence in dynamic structural analysis, using gradient algorithm and scaling transformation

11 p1438 A73-25497

[AIAA PAPER 73-361] Algorithm and convergence behavior of the local variation method for problems with partial derivatives

11 p1400 A73-26326

Accuracy and convergence of absolutely stable finite difference procedures for solution of multidimensional heat conductivity equation with discontinuous coefficients

11 p1452 A73-26327

Optimization problems with large parameters.

11 p1391 A73-26365

An iterative method for generalized nonlinear complementarity problems.

11 p1391 A73-26577

Superlinear convergent multistep procedure of the regula falsi and the Newton type

11 p1392 A73-26728

Rate of convergence of the distribution of the maximum of successive sums of independent random variables

12 p1516 A73-26958

A method for studying the completeness of systems of analytic functions

12 p1516 A73-26960

Quadratically convergent algorithms and one-dimensional search schemes.

12 p1517 A73-27118

Convergence of distributions of point complexes in Z/super m/ to Poisson processes

12 p1523 A73-27191

Multistep conjugate gradient search methods with memory, describing convergence of iterative procedure for functional minimization

12 p1485 A73-27617

Conditions for convergence of spectral decompositions corresponding to self-adjoint expansions of elliptic operators. IV - Negative-type theorems for arbitrary expansion of a general self-adjoint second-order elliptic operator

12 p1518 A73-27726

Application of Liapunov functions for studying the convergence of unconstrained minimization methods

13 p1657 A73-28018

Sound absorption in lined rectangular ducts with wall shear layers - Convergence of the numerical procedure to the analytical solution.

13 p1658 A73-28061

Shape function generation for high order conforming rectangular plate element in bending theory, noting rapid convergence of deflection and bending moments

13 p1691 A73-28087

The convergence theorems and their role in the theory of structures.

13 p1692 A73-28227

Effective use of the incremental stiffness matrices in nonlinear geometric analysis.

13 p1694 A73-28252

Rate of convergence of a class of methods of feasible directions.

13 p1649 A73-28609

A convergence theory for a class of nonlinear programming problems.

13 p1649 A73-28610

Stability of difference equations and convergence of iterative processes.

14 p1767 A73-29937

Numerical implementation of the Schwarz alternating procedure for elliptic partial differential equations.

14 p1768 A73-29938

Some efficient algorithms for solving systems of nonlinear equations.

14 p1768 A73-29939

Convergence of the net-point method for multidimensional quasi-linear heat-conduction problems

14 p1816 A73-30020

Some aspects of recent contributions to the mathematical theory of finite elements.

14 p1806 A73-30177

Stability and convergence of finite element methods for elastic structures vibration analysis, stressing application to mixed boundary value problems

14 p1807 A73-30185

Fourier decomposition for antenna near field reconstruction from far field pattern data, investigating numerical stability and convergence bounds

14 p1727 A73-30213

On numerical convergence of moment solutions of moderately thick wire antennas using sinusoidal basis functions.

14 p1734 A73-30216

Construction of a uniformly converging sequence of algebraic polynomials by the generalized method of least squares for a class of continuous functions

14 p1768 A73-30249

Convergence of a difference procedure for quasi-linear parabolic initial boundary-value problems in cylinder symmetry

14 p1769 A73-30422

Convergence of the arithmetic-geometric mean procedure for the complex variables and the calculation of the complete elliptic integrals with complex modulus.

14 p1769 A73-30423

Convergence of the Bubnov-Galerkin method for a type of nonlinear operator equation

15 p1898 A73-30966

Convergence of the upper relaxation method for solving variational-difference equations for elliptic equations in an arbitrary plane

15 p1898 A73-30967

Convergence, accuracy and stability of finite element approximations of a class of non-linear hyperbolic equations.

15 p1899 A73-32030

Book - Two-point boundary value problems: Shooting methods.

15 p1901 A73-32299

The Fredholm alternative in the case of linear approximation-regular operators

15 p1901 A73-32371

Rapidly convergent approximations to Dirichlet's problem for semilinear elliptic equations.

15 p1901 A73-32372

Small parameter series convergence evaluation in geometrically nonlinear problems by Cauchy majorants, applying to flat curvilinear beam deflection

16 p2074 A73-32689

Convergence of difference methods for second-order ordinary differential equations

16 p2031 A73-32821

Probability series weak uniform convergence based on Billingsley-Topsoe uniformity theorem, using Borel set theory for separable metric space

16 p2031 A73-33107

Numerical experience with algorithms for unconstrained minimization.

16 p2033 A73-33852

Nonlinear least squares calculations by Gauss-Newton and Levenberg, Marquardt and Morrison methods, discussing algorithm convergence rate and numerical computational scheme

16 p2033 A73-33854

Monotonically convergent approximate solutions for finite element eigenvalues in structural vibration and stability problems, assessing accuracies

16 p2083 A73-33949

Gradient methods with penalty functions for solution of optimal control with terminal constraints, noting convergence superiority of conjugate gradient algorithm

16 p2034 A73-33998

Nonlinear functional minimization under auxiliary constraints, discussing convergence conditions and iterative solution algorithm performance for least squares weighted sum problem

17 p2199 A73-34106

On the choice of relaxation parameters for nonlinear problems.

17 p2199 A73-34108

Variational principle with penalty for finite element solution of model Poisson equation with homogeneous Dirichlet boundary conditions, noting convergence

17 p2199 A73-34209

Iteration methods for finding all zeros of a polynomial simultaneously.

17 p2200 A73-34215

Remarks on the optimum rate of convergence of the on-line identification of non-stationary systems.

17 p2144 A73-34600

Kantorovich functional analysis algorithms providing rigorous theory for convergence of iterative methods to nonlinear functional equations on Banach spaces, emphasizing Newton method

17 p2163 A73-35268

Inconsistencies and S.O.R. convergence for the discrete Neumann problem.

17 p2202 A73-35519

Quasi-Newton methods for discretized non-linear boundary problems.

17 p2202 A73-35520

On the convergence of two-stage iterative processes for solving linear equations.

17 p2203 A73-35726

Convergence of matrix iterations subject to diagonal dominance.

17 p2203 A73-35727

Sensitivity of the numerical analysis of the three-fluid plasma mixed initial-boundary value problem.

18 p2338 A73-36160

Numerical solution of ordinary and retarded differential equations with discontinuous derivatives.

19 p2444 A73-37523

Acceleration of the convergence of functions related to the orientation of a Brownian particle in a laminar flow

19 p2419 A73-37536

Stability and convergence of streamline curvature flow analysis procedures.

19 p2421 A73-38190

Bounded spherical body wave diffraction field represented by diverging wave series expansion, examining Rayleigh hypothesis, Butrov algebraic solution and converging waves

19 p2406 A73-38339

A dual method for optimal control problems with initial and final boundary constraints.

19 p2446 A73-38376

Convergence of learning and adaptation algorithms

20 p2532 A73-38711

Convergence of Huber's method for heat conduction problems with change of phase.

20 p2626 A73-39100

Book - An analysis of the finite element method.

20 p2581 A73-39139

Computer-aided two-dimensional analysis of bipolar transistors.

20 p2536 A73-39410

Rate of convergence of the distribution of the maximum of successive sums of independent variously distributed random vectors toward the limiting law

20 p2583 A73-39476

Strong and weak convergence of the sequence of successive approximations for quasi-nonexpansive mappings.

21 p2724 A73-40297

The existence and convergence of subsequences of Pade approximants.

21 p2725 A73-40298

A finite algorithm for the minimum l-infinity solution to a system of consistent linear equations.

21 p2725 A73-40376

Nonlinear eigenvalue problem of square matrix of analytic functions of complex number lambda, comparing algorithms convergence by numerical tests

21 p2725 A73-40380

Free boundary problem involving elliptic differential equation, discussing iterative method instabilities inhibition of convergence

21 p2727 A73-40998

Pattern recognition learning machine design heuristics, discussing analysis, synthesis and convergence of algorithms

21 p2659 A73-41290

Convergence of perturbation-theory series in the problem of short-wave propagation through a randomly nonhomogeneous medium

21 p2657 A73-41514

Convergence of simplified hybrid displacement method for plate bending.

22 p2921 A73-42203

CONVERGENT-DIVERGENT NOZZLES

Accelerating the convergence of elastic-plastic stress analysis.

22 p2922 A73-42481

Convergence of the method of successive approximations in geometrically nonlinear problems

23 p2999 A73-44197

Topological modification and bounded length of decomposition series for convergence space

23 p3000 A73-44301

Convergence of the Bazley-Fox method in the problem of eigenvalues of a bilinear form relative to another bilinear form

24 p3109 A73-44649

Numerical analysis of pre- and post-critical response of elastic continua at finite strains.

24 p3150 A73-45227

Convergence of finite difference transient response computations for thin shells.

24 p3150 A73-45228

Skylab complex stiffened structure shell instability analysis by computer program, discussing convergence of finite difference formulation and eigenvalue calculation

24 p3144 A73-45234

Nonlinear difference schemes for linear partial differential equations.

24 p3106 A73-45332

Optimal convergence of iterative solution for system of linear equations with real roots based on matrix method

24 p3106 A73-45441

Convergence rate of two-real-parameter iterative solution of linear equations system based on matrix eigenvalues relationship

24 p3106 A73-45442

Strong plasma turbulence theory, discussing convergence of perturbation series formed with renormalized particle propagator

24 p3118 A73-45462

The exterior Neumann problem for the Helmholtz equation.

24 p3112 A73-45470

CONVERGENT NOZZLES

Development of flow in the entrance region of a converging channel.

07 p0810 A73-19103

The effect of nozzle inlet shape, lip thickness, and exit shape and size on subsonic jet noise.

[AIAA PAPER 73-187]

07 p0776 A73-20465

Effects of contraction geometry on non-isotropic free-stream turbulence.

08 p0955 A73-21438

Low velocity wind tunnel design with adjustable pressure gradient, determining contraction section wall contour to avoid boundary layer separation via velocity distribution improvement

11 p1347 A73-25714

CONVERGENT-DIVERGENT NOZZLES

Investigation of high-power quasi-steady arcs in strong axial gas flows

05 p0602 A73-16583

Theoretical study of a by-pass convergent-divergent nozzle

05 p0533 A73-17191

Transonic nozzle flow with a parabolic temperature distribution.

07 p0811 A73-19985

Relationship among various parameters used in ejector-nozzle performance estimates

07 p0776 A73-20097

Transonic nozzle flow with nonuniform gas properties.

08 p0925 A73-20719

Calculation of the relaxed one-dimensional flow of a gas in a convergent-divergent sonic nozzle

11 p1348 A73-25869

Study of disturbance reflection from the subsonic section of a Laval nozzle

11 p1411 A73-26437

Transonic similarity solution for aligned field MHD nozzle flow.

13 p1599 A73-28089

Two-dimensional calculation of revolution of the relaxed flow of a gas in a convergent-divergent sonic nozzle

13 p1563 A73-28563

Calculation of the flow of a two-phase mixture in a Laval nozzle with allowance for turbulent diffusion of particles

15 p1822 A73-31300

Characteristics of the heat exchange in the region of injection into a supersonic high-temperature flow

17 p2254 A73-34772

Approximate configuration factors for a gray nonisothermal gas-filled conical enclosure.

[AIAA PAPER 73-752]

18 p2370 A73-36368

Flow properties fluctuations in a convergent-divergent nozzle.

19 p2375 A73-37402

Thermodynamic expansion processes for argon plasma in a convergent-divergent nozzle.

22 p2894 A73-42632

The calculation of flow in nozzles using a time-marching technique based on the method of characteristics.

24 p3079 A73-44894

CONVERSION TABLES

Aircraft performance calculations in SI units, considering conversion factors for forces, pressures and specific fuel consumption

06 p0648 A73-18511

Metric technical, Imperial/British/ and SI dimensional systems, discussing conversion rules for mass, force, length, area, volume, density, moment of inertia and stress relationships

[SAWE PAPER 963]

19 p2499 A73-37881

CONVERTAPLANES

U V/STOL AIRCRAFT

CONVERTERS

Synthesis of active RC circuits by means of equivalent circuits of impedance converters

02 p0148 A73-11549

Analog simulation for transient and steady state performance of group-triggered cycloconverter supplying controlled slip induction motor, discussing commutation failures

03 p0253 A73-13932

Switching stepdown dc-to-dc converter with analog signal to discrete interval converter, hybrid micromodule and two-loop control subsystem, discussing circuitry and performance

03 p0283 A73-13935

Analysis and synthesis of automatic control systems with controlled converters.

10 p1198 A73-24019

Errors in the determination of random process characteristics with the aid of measuring converters with randomly varying parameters

11 p1341 A73-25024

Multi-Hundred Watt converter design considerations.

11 p1396 A73-26029

An optimal scheme for excitation of low-threshold magnetically modulated converters and analysis of their operation

13 p1591 A73-28855

Two terminal network immittance converters with feedback for passband and IC operational amplifier applications

23 p2959 A73-43515

Digital-computer aided analysis and synthesis of specialized functional diode converter circuits

23 p2959 A73-43579

CONVEXITY

Axiymmetric slow viscous flow past an arbitrary convex body of revolution.

02 p0153 A73-12040

Average monostatic scattering cross section for plane electromagnetic wave incident on ideally conducting convex body, considering wavelength relation to body dimensions

03 p0278 A73-14072

Method of branches and bounds as a regular method for the solution of irregular mathematical programming problems. I.

06 p0716 A73-17961

A nonlinear, nonconvex optimization problem

08 p0983 A73-20778

Uniform estimate of the residual term in the multidimensional limiting theorem for homogeneous Markov chains on the basis of a class of all measured convex sets. II

10 p1242 A73-23814

Best rational approximation and strict quasi-convexity.

13 p1649 A73-28602

Stress convexity domains for rigid perfectly plastic continuum, using directional derivative and distance function

14 p1811 A73-30483

Proof of B-completeness of locally convex spaces in series of quasi-reflective Banach spaces, generalizing Van Dulst theorem

15 p1900 A73-32205

Topology of tunneled locally convex spaces, considering Kelley theorem

15 p1900 A73-32206

Applications of a ray reflection model in the problem of highly rarefied gas flow past bodies.

17 p2094 A73-34549

A geometric solvability characteristic for some boundary value problems of linear elliptic-type equations and strongly elliptic second-order systems

20 p2583 A73-39498

Experiment on convex curvature effects in turbulent boundary layers.

21 p2676 A73-40245

On quasi-concave and strictly quasi-concave functions on a convex set relative to one of its nonvacant subsets

21 p2727 A73-41023

Convex approximation of the control process and a method for constructing generalized optimum regimes

21 p2727 A73-41064

The Minkowski problem generalized for ovals

23 p2999 A73-43613

The entropy rate admissibility criterion for solutions of hyperbolic conservation laws.

23 p3000 A73-44203

Geometrical properties of normed spaces, associated with the convexity and smoothness moduli of a unit sphere

24 p3106 A73-45353

CONVOLUTION INTEGRALS

Analysis of non-linear systems defined by their response to arbitrary disturbances.

01 p0028 A73-11456

A note on a general linear initial-boundary value problem.

06 p0716 A73-17980

Method of solving heat conduction problems with nonideal thermal contact

11 p1450 A73-25624

Digitally scanned spectral convolution by computerized filtering for noise spectra quality improvement with instrument signature removal

11 p1334 A73-26679

A numerical algorithm for identifying spread functions of shift-invariant imaging systems.

12 p1475 A73-27114

Extended Mellin transforms for boundary value problems, discussing inversion integral, operational properties convolution formulas, and application to circular sector steady state heat problem

13 p1648 A73-28422

Convolutional variational principles for stress distribution in anisotropic plates of linear viscoelastic material

16 p2077 A73-32981

Quantum signal superposition in radio communication, discussing Glauber convolution formula limitations and minimum three signal rule

20 p2529 A73-38924

Spectral theory and convolution systems of diagonal and nondiagonal discrete transformation filters on Abelian groups, comparing with computational simulations

23 p2957 A73-43311

CONVOLUTIONS [MATHEMATICS]

U CONVOLUTION INTEGRALS

CONVULSIONS

Influence of different motor regimes on the convulsive reactivity of the central nervous system.

05 p0542 A73-17178

Effect of stimulation of the mesencephalic reticular formation on the convulsive electrical activity of the brain

14 p1716 A73-30381

Effect of convulsions on certain aspects of the biosynthesis of proteins in the brain cortex

21 p2638 A73-40750

COOLANTS

NT ENGINE COOLANTS

COOLING

NT AIR COOLING

NT EVAPORATIVE COOLING

NT FILM COOLING

NT GAS COOLING

NT LIQUID COOLING

NT QUENCHING [COOLING]

NT RADIANT COOLING

NT REGENERATIVE COOLING

NT SODIUM COOLING

NT SUPERCOOLING

NT SURFACE COOLING

NT SWEAT COOLING

NT THERMOELECTRIC COOLING

Cooling modes effect on heat treated Ti-Nb alloys as function of Nb content, investigating alpha prime and double prime martensites

02 p0181 A73-12500

Charge carrier cooling in nonhomogeneous semiconductors by static electric field, plotting average electron temperature as function of current

04 p0484 A73-15569

Active control heat pipe performance for long life battery cooling.

[ASME PAPER 72-WA/HT-43] 04 p0518 A73-15813

The application of heat pipe techniques to electronic component cooling.

[ASME PAPER 72-WA/HT-42] 04 p0518 A73-15814

High temperature gas turbine engines rotor blades cooling, deriving generalized dimensionless relations for heat transfer data extension from static tests to operational conditions

05 p0607 A73-16797

Nonlinear aspects of cooling of a strongly anisotropic optical element of a laser.

06 p0702 A73-18579

Analysis of the thermal stress-strain state and cooling effectiveness of some turbine-blade designs

07 p0868 A73-20085

Carbon monoxide rotational transitions as dark cloud cooling mechanism during protostar formation

08 p1013 A73-21814

Cooling effects of CO IR opacity in stellar atmospheres of dwarfs and supergiants, considering application to sun and grain formation in cooler stars

09 p1142 A73-22031

The thermal future of the universe.

09 p1143 A73-22109

Thermal stresses in cooled gas turbine blade foils and roots with allowance for thermoelastic effects

09 p1136 A73-22568

Kinetics of transformation of carbon- and nitrogen-enriched austenite by carbonitriding in the gas phase

09 p1105 A73-23038

The cooling of a sunspot. I - A Carnot cycle and the hydromagnetic interactions. II - Convection zone models and the magnetic power supply.

10 p1279 A73-24137

High responsivity large surface liquid helium cooled IR bolometers based on carbon resistors and Ge and Si elements

11 p1368 A73-26510

A new type of helium-cooled bolometer.

11 p1368 A73-26511

Cooling systems for spaceborne infrared experiments.

11 p1453 A73-26515

Turbine blades cooling effectiveness for engines gas temperature energy gain compensation

12 p1532 A73-27090

Cooling of IC chips by heat conduction.

13 p1590 A73-28480

Carrier heating or cooling in semiconductor devices.

13 p1590 A73-28540

The heat loss of hot wires and heat films in steady flow

15 p1879 A73-32349

Experimental evaluation of the strength of elements of thin-walled pressure vessels during severe cooling

17 p2177 A73-34331

Cooling associated with minority carriers exclusion effect in semiconductors, discussing influence of electroconductivity and forbidden bandwidth

17 p2219 A73-35160

Electron cooling rates calculation based on measured impact cross sections of molecular oxygen for vibrational and low lying electronic excitation

24 p3086 A73-45123

COOLING FINS

Flow measurement on scale model of air cooling system for various blowing conditions and structure parameters, noting flow resistance of cooling fins

02 p0237 A73-11634

Study of the natural convection between two plane, vertical plates parallel and isothermal

02 p0238 A73-12795

Heat transfer characteristics of air conditioner finned tube heat exchanger surfaces from steady state heat balance, monitoring fluid temperature response at outlet

05 p0638 A73-16223

Vapor chamber fin radiator study for the potassium Rankine cycle.

11 p1451 A73-25991

COOLING SYSTEMS

Forced flow, single-phase helium cooling systems.

01 p0123 A73-11099

Thermal development of heat pipe cooled IC packages.

[ASME PAPER 72-WA/HT-44] 04 p0518 A73-15812

Survey of heat transfer techniques applied to electronic equipment.

[ASME PAPER 72-WA/HT-39] 04 p0518 A73-15816

Spaceborne IR systems cryogenic cooling, considering passive radiators and open or closed cycle cryogenic fluid systems

06 p0683 A73-18315

Aircraft and land vehicle electric generators and motors, noting semiconductor application and cooling systems

07 p0779 A73-20124

Russian book on space flight radiative heat transfer problems covering spacecraft thermal conditions, solar and planetary heat flux, radiant cooling and vacuum tests

09 p1166 A73-22348

Cryogenic cooling systems technology for spacecraft applications, comparing passive and phase-change coolers and closed cycle refrigerator for capacity and service life

10 p1285 A73-23790

Shock tubes with cryogenically cooled test section for experimental investigation of pressure and temperature pulse effects on cryogenic materials

10 p1203 A73-24267

Cryogenic applications for environment simulation.

11 p1344 A73-25580

Heat pipe cooling of electronic components for design requirements of high voltage insulation, small size, low temperature and protection from external heat sources

11 p1451 A73-25990

Heat pipe thermal control of spacecraft batteries.

11 p1309 A73-25992

Compact gas transpiration cooling system for thermal protection of hypersonic flight leading edges, discussing computer program

11 p1452 A73-26212

Influence of the turbine air cooling system on the characteristics of a turbojet engine during regulation of the latter

12 p1532 A73-27091

- Investigation of the throughput capacity of the longitudinal cooling ducts of gas turbine blades
12 p1532 A73-27093
- A cooled illuminator for studying ruby lasers
12 p1506 A73-27219
- Cryogenically cooled parametric amplifiers for 100 meter radio telescope low noise operation, describing system design and performance
12 p1481 A73-27780
- Miniature Stirling cycle refrigerators to cool IR detectors, discussing refrigerators with rhombic drive, thermal coupling to detector, triple expansion and Vuilleumier cycle
13 p1707 A73-29066
- Camera design with deep-cooled photographic emulsion for low intensity light photography, discussing gas filling and vacuum techniques for water condensation avoidance
14 p1753 A73-30275
- Thermosiphon evaporation-condensation-evaporation cycle cooling system operation and effectiveness in thermoelectric cooling and generator devices
14 p1713 A73-30950
- Simulation of a steady-state integrated human thermal system.
15 p1839 A73-32225
- AEGIS Demineralizer/Water Cooler - Design for availability.
16 p1989 A73-33608
- Thermosiphon technology advances covering open and closed single-phase natural convection and mixed convection systems, two phase systems and turbine blade cooling
17 p2254 A73-34352
- Four Space Shuttle wing leading edge concepts.
[AIAA PAPER 73-738] 18 p2359 A73-36355
- Baseplate heat pipe system for waste heat dispersion and temperature control of TWT microwaves amplifier in space shuttle communication equipment, discussing design and performance
[AIAA PAPER 73-755] 18 p2370 A73-36371
- Heat pipe and phase changing material /PCM/ sounding rocket experiment.
[AIAA PAPER 73-759] 18 p2371 A73-36374
- Heat transfer in rotating cylindrical enclosures with axial inflow and outflow of coolant.
19 p2504 A73-37877
- Development of a cryogenic heat pipe radiator for a detector cooling system.
[ASME PAPER 73-ENAS-47] 19 p2493 A73-37994
- Design and test of a self-controlled heat pipe radiator.
[ASME PAPER 73-ENAS-49] 19 p2435 A73-37996
- A cryogenic heat pipe for satellite sensor cooling.
[ASME PAPER 73-ENAS-50] 19 p2494 A73-37997
- High power transistor amplifier thermal design with heat sink convective and radiant cooling for low junction temperature and long service life
19 p2411 A73-38474
- Design modeling of external and internal cooling systems for bodies exposed to high temperature gas flow, discussing operation similarity conditions
20 p2628 A73-39419
- Investigation of different air-cooling methods for the first-stage disk of a two-stage gas turbine
21 p2754 A73-40397
- Dimensionless pressure method to account for air density variations in gas turbine cooling system design
21 p2677 A73-41051
- Construction techniques for an S-band high-power fluid-cooled TWT helix.
22 p2834 A73-42697
- Propagating thermal waves in force-cooled superconducting devices.
22 p2938 A73-42953
- Thermodynamics of an air-cooled gas-turbine stage
23 p3019 A73-43733
- The problem of extrapolating test data on the efficiency of turbine-blade cooling to actual conditions
23 p3020 A73-43741
- A physical-numerical model for the determination of the meteorological environmental effects produced by cooling towers
23 p3003 A73-43995
- Stability criteria for two phase transpiration, cooling system with equilibrium phase transition inside porous wall
24 p3156 A73-45079
- COORDINATE SYSTEMS**
U COORDINATES
COORDINATE TRANSFORMATIONS
Planar three body problem singularities due to binary collisions, regularizing equations of motion by Levi-Civita coordinate transformation
01 p0099 A73-10692
- Matrix transformations for spacecraft attitude determination.
02 p0228 A73-11905
- Coordinate transformation in arbitrarily dimensional spaces
04 p0443 A73-15509
- 'Barycentric' averaging of the hydro-dynamical equations with respect to coordinate systems with arbitrary vertical coordinate
04 p0473 A73-15697
- Harmonic frames of reference in Einstein's theory of gravitation.
05 p0598 A73-16791
- Planets geometric figure via visible site photography from spacecraft, noting coordinate transformation for conical projection surface
06 p0751 A73-18152
- Collinear theory of photogrammetry developed from projective equations in three dimensional space through singular transformation with 11 independent parameters
09 p1082 A73-22383
- Lunar surface reference points requirements for selenodetic coordinate system, analyzing coordinate transformations precision
10 p1277 A73-24087
- Computer realization of a method of scaling the gravity force
13 p1609 A73-29128
- Least squares method for geomagnetic potential transformation in spherical offset inclined dipole coordinates with Schmidt coefficients
14 p1749 A73-29982
- Minimum time response control problem of moving point in state space, determining piecewise-continuous vector function for optimal system transfer to coordinate reference point
15 p1931 A73-31231
- A solution operator for ordinary differential equations and its application in fluid dynamics
15 p1862 A73-31329
- Nomograms for determining horizontal coordinates of artificial earth satellites
16 p2063 A73-33662
- Matrix displacement solution to elastica problems of beams and frames.
16 p2082 A73-33906
- A new fundamental system of modified cylindrical functions for an annular region.
17 p2200 A73-34248
- Y-covariant formulation of the relativistic electrodynamics of material media
17 p2213 A73-35569
- Local Y-transformations in the electrodynamics of inhomogeneous accelerated media
17 p2213 A73-35570
- Transonic flow analysis using a streamline coordinate transformation procedure.
[AIAA PAPER 73-657] 18 p2261 A73-36211
- Plane coordinate transformations for area navigation based on existing VOR/DME network
18 p2336 A73-37043
- Transformation symmetry of x-space coordinates of geometric transors, tensors and M-objects with constant length dimensionality
20 p2594 A73-39729
- Transformation between orbital parameters in different coordinate systems of the general relativistic Schwarzschild problem.
22 p2886 A73-41967
- German monograph on display unit nonlinear interpolation approach based on higher order curve for reduced computer storage requirements covering Chebyshev approximation and coordinate transformations
22 p2830 A73-42738
- On the generalization of the Mangler transformation for axisymmetric boundary layers.
23 p2967 A73-43226
- COORDINATES**
NT ASTRONOMICAL COORDINATES
NT CARTESIAN COORDINATES
NT GEOCENTRIC COORDINATES
NT GEODETTIC COORDINATES
NT INERTIAL COORDINATES
NT LAGRANGE COORDINATES
NT POLAR COORDINATES
Algorithms for phase vector coordinates calculation of servomechanism, using measuring instrument data as starting information
01 p0028 A73-10676
- Curvilinear coordinates for deformation tensor and stress analysis of structures, using finite element method
02 p0231 A73-11812
- Center of mass coordinates of Baker-Nunn camera tracking stations from Geos 1 and Geos 2 optical flash data
04 p0437 A73-14785
- Thermal resistance /conductance shape factor/ prediction for thermal components, considering cylindrical and rotational coordinate systems
[AIAA PAPER 73-121] 05 p0640 A73-16877
- Coordinates correction for atmospheric refraction in aerial photography, noting effects of ground elevation, atmospheric pressure and temperature
08 p0969 A73-21709
- Kinematic problem of orientation in a rotating coordinate system
09 p1116 A73-22354
- Lunar surface reference points requirements for selenodetic coordinate system, analyzing coordinate transformations precision
10 p1277 A73-24087
- Coordinate systems standardization in stress analysis, considering vector orientation definitions
11 p1444 A73-26374
- Phase coordinates estimation optimization, deriving observable vector relations from sampling laws
12 p1524 A73-27417
- Problem of the legibility of records produced by strip chart recorders with curvilinear coordinate systems
14 p1754 A73-30875
- Astronautical coordinate systems definition and applications for flight mechanics problems involving earth curvature and motion effects
15 p1908 A73-32202
- View function in generalized curvilinear coordinates for specular reflection of radiation from a curved surface.
17 p2256 A73-35849
- Martian surface primary and secondary triangulation networks based on multiphotograph stereophotogrammetry and rectified photographs by Mariner 9, discussing control nets and points
19 p2479 A73-37227
- Mars physical ephemeris elements and aerographic coordinate system for Mariner 9 mapping
19 p2479 A73-37228
- The method of plane-axial vector coordinates in the determination of velocities in the general motion of a rigid solid
19 p2459 A73-37643
- Ellipsoidal coordinates - A natural coordinate system for calculations of laser irradiations of slabs.
20 p2572 A73-38972
- Proposal of a new criterion for evaluating the adequacy of models
21 p2669 A73-40499
- Relation between the fundamental solutions in cylindrical and spherical coordinates /with identical coordinate origins/ for certain equations of mathematical physics
21 p2753 A73-41025
- An iteration method of alternating directions for the Poisson difference equation in curvilinear orthogonal coordinates
24 p3105 A73-44650
- COPERNICUS SPACECRAFT**
U OAO 3
COPILOTS
U AIRCRAFT PILOTS
COPLANARITY
Two coplanar cracks in an infinitely long elastic strip bonded to semi-infinite elastic planes.
14 p1815 A73-30918
- COPOLYMERIZATION**
Stereo-enriched poly-alpha-amino acids - Synthesis under postulated prebiotic conditions.
06 p0661 A73-17940
- Study of the hardening and mechanical properties of polyester resins
18 p2327 A73-36468
- COPOLYMERS**
Low temperature dynamic mechanical properties of polyurethane-polyether block copolymers.
02 p0185 A73-12426
- Polyphosphazene fluoroelastomers preparation, properties and potential applications.
03 p0331 A73-13029
- Nylon copolymers dynamical mechanical properties temperature dependence, discussing alpha peak shifts, polyamides relaxation and ordered structure
13 p1646 A73-29526
- Fundamentals of fatigue and creep rupture of a thermoplastic.
17 p2197 A73-35345
- COPPER**
Structural changes in Kh18N9T steel during explosion welding
01 p0055 A73-10262
- Study of creep in copper and aluminum by the differential method of constant-rate temperature change
01 p0064 A73-10612
- Structured changes and phase transformations of welded joints of Ac alloy with Cu addition during welding thermal cycles
01 p0067 A73-11352
- Influence of the thickness of a copper coating on the critical current of a superconducting wire made from niobium-based alloys
01 p0089 A73-11435
- Determination of yield locus curves for copper and aluminum crystals with the aid of Knoop hardness measurements
02 p0181 A73-12364
- The influence of texture on the yield loci of copper and aluminum.
02 p0181 A73-12365
- Semihydrostatic hot extrusion for Ti plated Cu anode bar, noting metal bonding and current distribution
03 p0312 A73-13583
- Internal friction in polycrystalline copper foils after alpha-irradiation at 78 K
03 p0328 A73-14653
- Supersonic electrical-discharge copper vapor laser.
04 p0457 A73-14746

- Sliding friction welding of nonferrous Cu, wrought Al alloy and Ti, resting rubbing speed and axial pressure effects on equilibrium condition transition
08 p0973 A73-21238
- Investigation of the electrical explosion of conductors by holographic methods
10 p1248 A73-23507
- Amplitude-dependent anelasticity in aluminum and copper single crystals
10 p1231 A73-23693
- Diffraction study of fast electrons of the adsorption layer of oxygen on the surface of a film of epitaxial copper
10 p1259 A73-23767
- Cu annealability tests for assessing suitability for applications requiring low softening temperature, discussing recrystallization behavior and softness measures
11 p1379 A73-25130
- Optical resolution of DL-aspartic acid in the presence of optically active amino acid and copper /II/ ion.
11 p1324 A73-25146
- Effects of oxygen environment and surface diffused coatings on fatigue crack development in copper single crystals.
11 p1380 A73-25806
- Critical current value for a superconductor niobium-alloy wire as a function of its copper coating thickness.
11 p1409 A73-26062
- Low-energy positrons from metallic moderators in a back scattering mode.
11 p1402 A73-26544
- Amplitude-dependent anelasticity in aluminum and copper single crystals. II - Studies in amplitude range III during and after plastic deformation
11 p1385 A73-26567
- Absorption spectrum of Cu I in the vacuum ultraviolet.
12 p1526 A73-27122
- Copper deposition on ceramic plate, studying interdigital slow wave structure and thin film meander-line coupling impedance and dispersion characteristics
12 p1480 A73-27581
- The influence of the thermal properties of the heating-surface on the heat-transfer of bubble boiling
12 p1559 A73-27698
- Influence of deformation history on the yield locus and stress-strain behavior of aluminum and copper.
13 p1632 A73-28130
- Cu content comparison of Eaton meteorite to true extraterrestrial meteorites, determining dendritic structure and terrestrial origin from similarity to brass
13 p1684 A73-29179
- Holographic investigation of electrical explosions of conductors.
17 p2212 A73-35187
- Determination of ultramicro-impurities in CdS-type semiconductor materials - Determination of copper
17 p2220 A73-35558
- Emerging aerospace materials and fabrication techniques.
17 p2198 A73-35841
- The thermal and electrical conductivities of porous copper and stainless steel to elevated temperatures.
[ASME PAPER 73-HT-47]
20 p2575 A73-38572
- Emission spectra of ZnS-Cu single crystals
21 p2751 A73-40311
- Work hardening of copper, nickel, and alloy H31 by compression and explosion
21 p2707 A73-40705
- Some experiments on the influence of surface treatment on the Kapitza conductance between copper and He4 at temperatures from 1.2 to 2.0 K.
21 p2741 A73-41105
- Solubilization and accumulation of copper from elementary surfaces by Penicillium notatum.
21 p2648 A73-41217
- Quartz transformation to stishovite in shock loaded quartz-copper mixture, discussing relationship to short range order phase
22 p2848 A73-42497
- Technique for resistance brazing of thin copper conductors.
23 p2985 A73-43998
- COPPER ALLOYS**
NT BRASSES
NT BRONZES
NT MANGANIN [TRADEMARK]
Structure changes during ageing in aluminium 4 wt. % copper alloy studied by the channeling technique.
01 p0063 A73-10310
- Damping in copper-aluminum-nickel alloys and its causes
01 p0064 A73-10611
- Interaction of chromium carbide with copper-nickel melts
02 p0178 A73-11539
- Sn suppression of Al-Cu-Sn alloy aging at low temperatures, relating to Cu solubility decrease in alpha phase
02 p0179 A73-11599
- Advanced copper and copper alloy conducting wires with metallic coatings
03 p0312 A73-13582
- Cu and Cu-Sn base self lubricating composites, testing solid lubricants effects on friction coefficient, wear, electrical resistance, hardness, porosity and structure
04 p0454 A73-14996
- Solubility of zirconium and niobium in solid-state copper
04 p0464 A73-15495
- Mechanical properties and structure of certain internally oxidized copper alloys
04 p0464 A73-15500
- Vacancy trapping model inadequacy for aging retardation in Al-Cu-Cd alloys, noting Cd content and Cu solid solubility effects
05 p0587 A73-16576
- Investigation of precipitation morphology in Cu-Ti alloys
06 p0707 A73-18037
- Cu-Ni-Zu alloys high ambient temperature tensile and fatigue strengths due to recrystallization and precipitation produced fine grain microstructure, describing annealing and cold working process
06 p0711 A73-18751
- Dendritic solidification of Cu-Ni alloys. I - Initial growth of dendrite structure.
06 p0712 A73-18756
- Dendritic solidification of Cu-Ni alloys. II - The influence of initial dendrite growth temperature on microsegregation.
06 p0712 A73-18757
- Joining copper and copper alloys.
07 p0831 A73-20269
- Grain-boundary internal friction of copper-nickel alloys
09 p1099 A73-21965
- An electron microscopy study of precipitation in Cu-Ti sideband alloys.
10 p1234 A73-24434
- An investigation into the electron beam welding of five non-ferrous alloys.
11 p1372 A73-25125
- Constitution and phase relationships in copper-silver-aluminum ternary system.
11 p1385 A73-26566
- Russian papers on nonferrous metals and alloys metallurgy covering phase equilibria, strengthening, deformation and processing of Al, Mg, Cu and Ti alloys
12 p1510 A73-26902
- Stereometric microanalysis of conglomerate, colony and dispersed structures of binary eutectic Fe, Al, Cu and low melting alloys
13 p1631 A73-28109
- Unidirectional solidification formed interdendritic eutectic composition related to solidification variables, discussing Al-Cu and Al-Cu-Ni systems
13 p1632 A73-28131
- The Portevin-Le Chatelier effect in the case of alloys of copper with aluminum, gallium, germanium, arsenic, and indium
14 p1760 A73-30443
- Crystallostructural investigation of the eutectoid decomposition of copper-beryllium alloys - Ordering accompanied by formation of Cu2Be metastable solid solution
14 p1760 A73-30587
- Diffusion creep by dislocation climb in beryllium and Be-Cu single crystals.
14 p1761 A73-30633
- The wetting of carbon and carbides by copper alloys.
15 p1897 A73-31837
- Deformation and fracture behaviours of composites of copper and copper-chromium alloys reinforced with tungsten or molybdenum fibres.
16 p2025 A73-33022
- Thermodynamic analysis of the distribution of silver in the Cu-Cu2S system in the presence of Ni3S2 and FeS
17 p2188 A73-34556
- Limit of the two-phase region of Mo/Ni, Cu/ and Cu/Ni, Mo/ solid solutions in the Mo-Cu-Ni system
18 p2325 A73-36859
- Superplasticity and residual tensile properties of a microduplex copper-nickel-zinc alloy.
22 p2879 A73-42582
- Phase composition of Cu-Ni-O alloys with Ir additions, examining oxygen content influence on Ir distribution and solid solution formation
23 p2990 A73-43483
- Phase transformations in beta-Cu-Al during extremely rapid cooling from the melt
23 p2992 A73-43914
- Superconductivity of copper containing small amounts of niobium.
23 p3017 A73-44033
- The copper-boron eutectic - Unidirectionally solidified.
23 p2993 A73-44035
- The precipitation of titanium in copper and copper-nickel base alloys.
24 p3100 A73-45473
- COPPER CHLORIDES**
Effect of copper ions on the functional state of the neuromuscular apparatus
09 p1039 A73-22369
- Studies of a homogeneous copper catalyst for fuel cell air cathodes in acid media.
19 p2390 A73-38400
- COPPER COMPOUNDS**
NT COPPER CHLORIDES
NT COPPER SULFIDES
Optical resolution of aspartic acid by using copper complexes of optically active amino acids.
07 p0789 A73-20457
- Linear and nonlinear dielectric properties of tetrahedral structure crystals. III - Theory of dielectric properties of tetrahedral structure compounds
08 p0990 A73-20965
- Intergranular precipitation in the oriented bicrystals of aluminum-copper
09 p1105 A73-23039
- Coherent X ray emission from plasma generated by laser irradiation of copper sulfate doped thin gelatin layer
21 p2710 A73-40126
- COPPER SULFIDES**
High efficiency Cu2S-CdS-solar cells with improved thermal stability.
03 p0255 A73-14216
- Diffusion and conduction processes in CdS-Cu/x/S thin film photocells.
03 p0350 A73-14217
- Optical degradation and thermal restoration - New inputs to the mechanism of the photovoltaic effects in Cu2S-CdS heterojunctions.
03 p0350 A73-14218
- Cadmium sulfide/cuprous sulfide solar cell abrupt heterojunction band model description by two quasi-Fermi levels
03 p0350 A73-14219
- Investigations of the inhomogeneity of polycrystalline Cu/x/S-CdS solar cells.
03 p0255 A73-14222
- Thermodynamic analysis of the distribution of silver in the Cu-Cu2S system in the presence of Ni3S2 and FeS
17 p2188 A73-34556
- CORAL HEADS**
U CORAL REEFS
CORAL REEFS
Cenozoic coral and aragonitic fossil age determination by He, U, Th and Ru isotope retentivity consistency checks
13 p1609 A73-29178
- CORDAGE**
Large deformations of cord-reinforced multilayered axisymmetric shells.
20 p2621 A73-39542
- CORDITE**
U COLLOIDAL PROPELLANTS
U DOUBLE BASE PROPELLANTS
CORE FLOW
Natural convective heat transfer in cavities and horizontal circular tubes, considering boundary layer and core flow interaction effects
01 p0120 A73-10290
- Solar core stability via model including plain parallel stratified fluid layer with energy generation, noting age correlation with mixing phases during evolution
04 p0501 A73-15623
- Isentropic compressible flow equations for pressure and velocity distributions across vortex in axial core mass flow, noting atmospheric circulation and pressure effects
[AIAA PAPER 73-106]
05 p0529 A73-16866
- The effect of shear stress on the screw dislocation core structure in body-centred cubic lattices.
08 p0978 A73-21525
- Finite core model of self induced motions and stability of filament vortex rings in inviscid fluid under small sinusoidal perturbation
11 p1348 A73-26202
- Evolution of stars with suppressed core convection.
11 p1427 A73-26608
- Vortex core precession in water or air high swirl flows above critical Reynolds number
13 p1602 A73-29017
- Trailing vortex pair instability in inviscid incompressible fluid with rotating and nonrotating isolated and axial velocity jet core
18 p2300 A73-36628
- Mathematical approximation of turbulent cylindrical jets: Initial core - Velocity distribution
18 p2301 A73-36690
- Effect of combustion upon precessing vortex cores generated by swirl combustors.
22 p2934 A73-42781
- Nonlinear stability of cylindrical vortex enclosing a central jet of light or dense fluid.
24 p3080 A73-45452
- CORE SAMPLING**
The morphology, types and distribution of sizes of regolith particles in the Sea of Fertility.
02 p0214 A73-12241

Mossbauer spectroscopic analysis of Sea of Fertility regolith core samples, noting olivine content increase with depth
02 p0214 A73-12242

Trace elements profiles, notably Hg, from a preliminary study of the Apollo 15 deep-drill core.
02 p0220 A73-12477

Luna 20 and Apollo 16 core fines - Large-ion lithophile trace-element abundances.
05 p0546 A73-16828

Depth relationships for Apollo 14 and 15 core tubes and Apollo 15 drill core, noting sample recovery ratio
07 p0898 A73-19900

Depth variation of Apollo 15 deep drill fines trace elements from neutron activation analysis, noting KREEP abundance
10 p1278 A73-24113

Deep sea drilling core sample analysis methods and results relation to sediment age and fossil fauna and flora
11 p1325 A73-25462

Particle track densities in 100-200 micron crystalline grains from soil column returned from lunar highlands by Luna 20 and 16
12 p1541 A73-27487

Particle track record in Apollo 15 deep core from 54 to 80 cm depths.
13 p1686 A73-29566

Performance of a soil sample selection experiment on the surface of the moon by means of the automatic lunar station "Luna-20"
18 p2295 A73-36114

Paleomagnetic excursion recorded in latest Pleistocene deep-sea sediments, Gulf of Mexico.
18 p2313 A73-36513

Apollo 16 neutron stratigraphy.
18 p2354 A73-36514

CORE STORAGE

Ferrite core modular memory characteristics, considering bit capacity and printed circuit technology utilization
05 p0556 A73-16167

Address structure optimization and minimum access time and decoder terminals in nonvolatile core memory array design, noting binary notation for information storage
05 p0554 A73-16991

Design, manufacture and performance of Eole satellite computer core memory, noting circuit reliability and testing
07 p0796 A73-18959

Memory included linear stochastic system optimum control over finite time, using Liapunov-Krasovskii functionals
11 p1398 A73-25618

Computerized finite difference method with reduced core storage requirements for solving boundary value problem of forced random vibration of rotating beam
17 p2204 A73-35830

Electromagnetic core storage and switching elements design for Setun threshold ternary logic computer
19 p2408 A73-38562

Noise and stable operation conditions in associative memory devices
23 p2956 A73-43580

CORES

NT EARTH CORE
NT HONEYCOMB CORES
NT LUNAR CORE
NT MAGNETIC CORES
NT REACTOR CORES

Dielectric gradient waveguides inhomogeneous core layer, solving differential equation by perturbation method
09 p1065 A73-23113

CORIOLIS EFFECT

The effect of the Coriolis force on the stability of rotating magnetic stars.
01 p0103 A73-11034

Multicomponent plasmas with cations or anions in presence of Coriolis force, determining crossover frequencies for polarization reversal and mode coupling of waves
05 p0603 A73-16594

Vestibular reactions to Coriolis accelerations under hypoxia conditions
06 p0650 A73-17691

Theory of inertial atmospheric oscillations in low latitudes
06 p0691 A73-18729

Observations on perceived changes in aircraft attitude attending head movements made in a 2-g bank and turn.
07 p0785 A73-19485

Second kind conditional instability of resting atmosphere, noting Ekman boundary layer absence in rain area for given Coriolis parameter
08 p0985 A73-21379

On the demonstration and interpretation of the Coriolis effect.
09 p1120 A73-22475

Equivalence of the action of Coriolis accelerations to that of certain angular accelerations in their effects on the receptors of semicircular canals
12 p1463 A73-27718

The role of the Coriolis force on the stability of rotating magnetic stars and the origin of convective motions.
12 p1547 A73-27883

Prophylaxis and treatment of the motion sickness syndrome
13 p1580 A73-29410

Influence of stimulation of the vestibular analyzer under conditions of hypoxia on certain functions of the visual analyzer
15 p1835 A73-31516

Calculation of a Coriolis acceleration acting on semicircular canal receptors of man in rotating systems
15 p1835 A73-31518

Effectiveness of some hemodynamic indices in the detection of vestibulo-vegetative disorders under ordinary conditions and those of hypoxia
17 p2110 A73-34121

A numerical study in three space dimensions of Bénard convection in a rotating fluid.
17 p2151 A73-34855

Out-of-plane vibration and stability of curved tubes conveying fluid.
[ASME PAPER 72-WA/APM-36]
17 p2248 A73-35101

Visual-vestibular interaction and motion perception.
18 p2273 A73-36460

Allowance for the effects of the relief and of the Coriolis force in forecasting meteorological elements
22 p2883 A73-41954

An exact solution for the rotation of the atmosphere about the spheroidal earth.
22 p2848 A73-42541

CORK [MATERIALS]

Missile ablation shields erosion by high velocity dust, considering wind tunnel test data on phenolic cork for various dust materials, particle sizes and velocities
[AIAA PAPER 73-739]
11 p1388 A73-25509

CORN

Data handling and analysis for the 1971 corn blight watch experiment.
04 p0443 A73-15402

Effects of leaf age for four growth stages of cotton and corn plants on leaf reflectance, structure, thickness, water and chlorophyll concentrations and selection of wavelengths for crop discrimination.
05 p0571 A73-17128

Corn blight epiphytotic remote sensing, data acquisition and crop identification by photointerpretation and computer aided multispectral band scanner data analysis
20 p2556 A73-39836

CORNEA

Effect of steady magnetic fields up to 4,500 Oe on the mitotic activity of the corneal epithelium in mice
15 p1838 A73-31510

CORNERS

Measurements on separated supersonic boundary layer flows after an expansion corner.
01 p0003 A73-11135

Conical solutions for diffraction of plane pulse wave by three dimensional trihedron corner via boundary conditions reduction to eigenvalue problem, presenting sonic boom example
01 p0019 A73-11424

Determination of elastic stresses at notches and corners by integral equations.
02 p0234 A73-12075

Viscous compressible flow near right angle corner of two flat plates, presenting streamwise and secondary flow velocities and skin friction coefficient distribution
06 p0687 A73-18532

Corner pressures and fillet shock locations for symmetrical corners by an approximate method.
07 p0774 A73-19494

Existence of a corner-type steady flow for an ideal fluid with a free surface
13 p1605 A73-29554

The origin of secondary flow in turbulent flow along a corner.
14 p1744 A73-30164

Experimental investigation of the laminar flow along a straight 135-deg corner.
15 p1861 A73-31124

Supersonic and hypersonic two-dimensional laminar flow over a compression corner.
17 p2096 A73-35134

Numerical solution for the inviscid supersonic flow in the corner formed by two intersecting wedges.
[AIAA PAPER 73-675]
18 p2262 A73-36226

Flow of a mixture consisting of a fluid and gas bubbles past a corner
18 p2301 A73-37007

Numerical solution existence for three dimensional boundary layer equations governing corner flow in symmetry plane with critical pressure gradients
19 p2419 A73-37492

CORONA BOREALIS CONSTELLATION

Infrared measurements of R. Coronae Borealis through its 1972 March-June minimum.
05 p0627 A73-17391

CORONA DISCHARGES

U ELECTRIC CORONA CORONAGRAPHS

Polarization of the inner corona during the solar eclipse of March 7, 1970
01 p1002 A73-10939

Adaptation of the electronic camera to the coronagraph
02 p0170 A73-12544

Electron density distribution in a coronal condensation
07 p0902 A73-20321

Polarization of the inner corona at the total eclipse of March 7, 1970.
09 p1147 A73-22734

Electron-density distribution in a coronal condensation.
12 p1540 A73-27293

Results of observations of coronal condensation in photographic rays during the solar eclipse of Sept. 22, 1968
13 p1673 A73-28299

Space application of SEC vidicons - The OSO 7 coronagraph.
17 p2170 A73-35293

Solar eclipse of July 10, 1972 - Comparison of photographic-photometry and K-coronometer measurement data
20 p2611 A73-39589

Observational results on coronal condensation in photographic light during the September 22, 1968 solar eclipse.
21 p2779 A73-41543

CORONARY CIRCULATION

Left ventricular receptors activated by severe asphyxia and by coronary artery occlusion.
01 p0008 A73-10549

Non-invasive technique for diagnosing atrial septal defect and assessing shunt volume using directional Doppler ultrasound - Correlations with phasic flow velocity patterns of the shunt.
01 p0014 A73-11505

Nature of the conduction disturbance in selective coronary arteriography and left heart catheterization.
02 p0134 A73-12443

Maximal treadmill exercise electrocardiography - Correlations with coronary arteriography and cardiac hemodynamics.
02 p0136 A73-12821

Correlation of computer-quantitated treadmill exercise electrocardiogram with arteriographic location of coronary artery disease.
03 p0260 A73-13543

Radiotelemetry of direct bloodpressure measurements in aorta, pulmonary artery and heart.
03 p0271 A73-14291

Quantitative radionuclide angiocardiology for determination of chamber to chamber cardiac transit times.
04 p0409 A73-14767

Cardiocirculatory adaptation to chronic hypoxia. III - Comparative study of cardiac output, pulmonary and systemic circulation between sea level and high altitude residents.
04 p0410 A73-15523

Uses and limitations of stress testing in the evaluation of ischemic heart disease.
05 p0552 A73-17278

Correlation of electrocardiographic studies and arteriographic findings with angina pectoris.
05 p0546 A73-17279

Physiological tests for hypothalamus regions stimulation effects on coronary circulation, noting hypoxia and emotional stress effects
06 p0650 A73-17770

The reconstruction of three-dimensional objects from two orthogonal projections and its application to cardiac cineangiography.
06 p0657 A73-17801

Pattern of blood flow within the heart - A stable system.
08 p0930 A73-21214

Inability of the submaximal treadmill stress test to predict the location of coronary disease.
08 p0932 A73-21802

Distribution of systemic blood flow during cardiopulmonary bypass.
09 p1041 A73-22930

Left ventricular blood flow velocity in man studied with the Doppler ultrasonic flowmeter.
09 p1042 A73-23173

Coronary flow and left ventricular function during environmental stress.
09 p1047 A73-23380

Immediate hemodynamic effects of cardiac angiography in man.
10 p1179 A73-23841

Regional myocardial dynamics from single-plane coronary cineangiograms.
10 p1185 A73-24771

Unreliability of conventional electrocardiographic monitoring for arrhythmia detection in coronary care units.

12 p1465 A73-27891

Assessment of left heart function by noninvasive exercise test in normal subjects.

15 p1834 A73-31345

Nutritional circulation in the heart. IV - Effect of calcium chloride and potassium chloride on myocardial hemodynamics and clearance of rubidium-86.

16 p1973 A73-33990

Coronary atherosclerosis and ischemic myocardial damage.

18 p2275 A73-36538

Factors influencing coronary blood flow in the presence of coronary obstructive disease.

18 p2275 A73-36539

The prognosis of myocardial infarction.

18 p2276 A73-36549

Nonlinear analysis of aortic flow in living dogs.

21 p2638 A73-40640

The correlation of coronary angiography and the electrocardiographic response to maximal treadmill testing in 76 asymptomatic men.

22 p2806 A73-42342

The complications of coronary arteriography.

22 p2806 A73-42343

Early diagnosis of coronary heart disease; Proceedings of the Second Paavo Nurmi Symposium, Porvoo, Finland, September 9-11, 1971.

22 p2808 A73-42826

The early diagnosis of coronary heart disease - Critical review.

22 p2808 A73-42827

Preventive value of early diagnosis of coronary heart disease, noting importance of screening populations for genetic and environmental risk factors

22 p2808 A73-42828

Significance of arterial obstructive lesions in early diagnosis of coronary heart disease.

22 p2808 A73-42829

Indications and value of coronary arteriography.

22 p2808 A73-42830

The value of different angiographic procedures in coronary heart disease.

22 p2808 A73-42831

Emotionally induced increases in heart rate and plasma catecholamine and free fatty acids, noting relation to coronary heart disease

22 p2809 A73-42837

Measurement of coronary blood flow by radiocardiography - Study of 116 cases.

22 p2809 A73-42838

Coronary heart disease; Proceedings of the Second International Symposium, Frankfurt am Main, West Germany, June 1972.

22 p2809 A73-42856

Velocity distribution in aortic flow.

22 p2811 A73-43104

Measurement of left anterior descending coronary arterial blood flow - Technique, methods of blood flow analysis and correlation with angiography.

24 p3058 A73-44469

The presence in the heart of compounds which participate in the neurohumoral regulation of coronary circulation

24 p3059 A73-44769

Doppler echocardiography - The localization of cardiac murmurs.

24 p3064 A73-44947

Hemoglobin-oxygen equilibrium and coronary blood flow - An analog model.

24 p3064 A73-45060

Response of coronary blood flow to pH-induced changes in hemoglobin-O₂ affinity.

24 p3060 A73-45061

CORONAS

NT ELECTRIC CORONA

NT SOLAR CORONA

Search for coronal line emission from the Cygnus Loop.

05 p0626 A73-17380

Validity criteria for local thermodynamic equilibrium and coronal equilibrium.

08 p0992 A73-21007

X-ray and radio emission from stellar coronae.

16 p2052 A73-32827

High rotational velocity correlation with metal abundance interpreted by coronal mass loss rate in metal-poor stars

24 p3140 A73-45184

Single component wind model for stellar rotation dependent mass loss from hot corona with application to T Tauri star observations

24 p3140 A73-45186

CORPUSCULAR RADIATION

NT BETA PARTICLES

NT CYCLOTRON RADIATION

NT ELECTRON BEAMS

NT ELECTRON PRECIPITATION

NT ELECTRON RADIATION

NT ION CYCLOTRON RADIATION

NT PRIMARY COSMIC RAYS

NT RADIATION BELTS

NT SOLAR CORPUSCULAR RADIATION

NT SOLAR COSMIC RAYS

NT SOLAR ELECTRONS

NT SOLAR PROTONS

Distortion of particle trajectories by dynamic effects in the problem of two bodies with corpuscular emission

01 p0102 A73-10947

Corpuscular radiation as an upper atmospheric energy source.

02 p0205 A73-12289

Radial gradients and anisotropies due to galactic cosmic rays.

02 p0207 A73-12378

Muon densities in penetrating high energy particles, comparing with extensive air showers

02 p0210 A73-12683

Dynamical effects of the curvature of particle trajectories in the two-body problem with corpuscular radiation.

09 p1148 A73-22742

Useful penetration in an austenitic stainless steel, of electrons accelerated under a very high voltage /1500 to 2500 kV/

09 p1105 A73-23037

Interstellar and interplanetary dust grains orientation distribution function in anisotropic corpuscular or radiation fluxes

10 p1271 A73-23482

Investigation of geoeactive corpuscular particles and photoelectrons on board the Cosmos 261 satellite. V - Spectra of ionospheric photoelectrons and migration of the latter from the conjugate ionosphere

10 p1211 A73-23887

Radiation doses during a prolonged orbital space flight about the earth

14 p1721 A73-29867

Screen effect on the radiation heat transfer in an area of penetrating radiation

14 p1816 A73-30013

Search for sporadic radio emission from space at centimeter and decimeter wavelengths

14 p1798 A73-30261

Simultaneous measurements of ion concentration and corpuscular stream intensity at altitudes ranging from 10 to 79 km

18 p2345 A73-36121

Rocket investigation of the intensity and composition of the corpuscular radiation at altitudes 180 km up to the polar region.

18 p2345 A73-36137

Investigation of geoeactive corpuscles and photoelectrons with the Cosmos 261 satellite. V - Spectra of ionospheric photoelectrons and their transfer from the conjugate ionosphere.

20 p2550 A73-38906

A study of geoeactive corpuscles and photoelectrons on the Cosmos 261 satellite. VI - Epithelial electrons in the energy range from 30 to 150 eV in the region of the dayside and nightside polar cusps

21 p2686 A73-40909

Complex studies of corpuscular radiation in the upper atmosphere at midlatitudes during geomagnetic perturbations

21 p2760 A73-40918

High energy cosmic rays and elementary particles, discussing detection, sources, nature and properties

21 p2764 A73-41611

Measurement of the absolute vertical integral and differential cosmic-ray single-muon flux at 3.6 GeV and a measurement of the showerless penetrating particle-pair flux above 3.6 GeV.

22 p2903 A73-42440

Muon decay/transmission ratios at 60 and 850 mwe measured by scintillation counter

23 p3023 A73-43563

Spark calorimetry investigation of trident and extensive air showers muon component generated high energy penetrating particles at large zenith angles

23 p3024 A73-43565

CORRECTION

NT OPTICAL CORRECTION PROCEDURE

White noise signal correction for nonlinear nonstationary systems, using orthonormalized functionals

01 p0027 A73-10593

Rank-one and rank-two corrections to positive definite matrices expressed in product form.

09 p1113 A73-22956

Dynamical latitude correction requiring changes in ephemeris and time determination, discussing applicability to nutation of pole of earth figure

11 p1429 A73-26689

A generalization of the additive correction methods for the iterative solution of matrix equations.

17 p2203 A73-35729

Finite-boundary corrections to the coplanar waveguide analysis.

23 p2954 A73-44075

CORRELATION

NT ANGULAR CORRELATION

NT AUTOCORRELATION

NT CORRELATION COEFFICIENTS

NT CORRELATION DETECTION

NT CROSS CORRELATION

NT DATA CORRELATION

NT SIGNAL ANALYSIS

NT STATISTICAL CORRELATION

Full correlation ionospheric drift analysis for a general observing triangle.

01 p0036 A73-10330

Curves of spatial isocorrelations and space-time isocorrelations relative to longitudinal velocity fluctuations in a smooth circular duct

01 p0031 A73-10418

Correlation function for prediction of surface roughness induced supersonic boundary layer transition on blunt bodies, taking into account compressibility and centrifugal force effects

01 p0002 A73-10742

Analog computer regression line and correlation ratio determination for random stationary processes with time lag

01 p0028 A73-10928

Correlation theory for equations of motion of constant thickness shallow shell vibration under random loads

03 p0387 A73-13158

Correlation of noisy radiation reflected from a statistically uneven surface.

03 p0344 A73-14039

Fluctuations in the level and phase of a field in a waveguide with a random boundary

07 p0793 A73-19916

Some problems in methods for determining the parameters of scattering inhomogeneities

08 p0959 A73-21284

An investigation of the application of Taylor's hypothesis to atmospheric boundary layer turbulence.

09 p1114 A73-22331

Study of the time correlation of multifrequency-laser emission by the photon coincidence method

09 p1096 A73-22877

Analog computer regression line and correlation ratio determination for random stationary processes with time lag

10 p1201 A73-24188

Error analysis of correlation method for determining directional characteristics /angular power density/ of homogeneous random wave field

11 p1359 A73-25005

Determination of the statistical characteristics of signals parametrically affecting a dynamic plant

11 p1340 A73-25006

Estimate of the spectral density of a stationary random process by an indirect method

11 p1341 A73-25017

Comparative analysis of algorithms for measurement of correlation functions by the multiplication method /Review/

11 p1360 A73-25018

Shaping of the one-dimensional distribution and correlation function of a reference signal when checking statistical analyzers

11 p1360 A73-25022

Considerations concerning the solution of Chandrasekhar's system of equations in the case of MHD turbulence

11 p1404 A73-25700

Application of lasers, radioisotopes, and the correlation method for measuring flow velocity

12 p1495 A73-26847

Light scattering from independent particles - Non-gaussian correction to the clipped intensity correlation function.

13 p1658 A73-28208

Analysis of correlation functions of space-time wideband signals received by linear antennas.

13 p1591 A73-28657

Correlation and prediction of gaseous diffusion coefficients.

15 p1958 A73-31998

Correlation functions of the elastic field of quasi-isotropic composite materials under nonisotropic deformation

17 p2240 A73-34146

Analysis of the correlation properties of certain PSK signal systems

17 p2121 A73-34586

Transition probability approach to the theory of plasmas.

17 p2218 A73-35819

Ionospheric drift measurements. I - A new method for ionospheric drift measurements. II - The effect of random drift velocities upon the determination of ionospheric drift velocities.

18 p2304 A73-35989

Two-point correlation model and the redistribution of Reynolds stresses.

18 p2300 A73-36627

Some problems concerning the method of determining the parameters of scattering inhomogeneities.

19 p2424 A73-37913

Waveguide channel point source electric field level and phase derived by Rytov smooth perturbation technique, obtaining correlation functions, energy spectra and phase fluctuations

19 p2406 A73-38338

Image reconstruction from the modulus of the correlation function - A practical approach to the phase problem of coherence theory.

20 p2570 A73-38616

Correlation function of a laser beam near threshold.

20 p2571 A73-38631

- Correlative function formalism for neuron networks with limited communication channels and active-refractive-storing signal action 21 p2645 A73-41277
- A method of reducing the influence of interference on the operation of a correlation interferometer 21 p2667 A73-41511
- Correlometry of ergodic nonstationary random processes 24 p3074 A73-45095
- ### CORRELATION COEFFICIENTS
- Relationship between the various indices of geomagnetic activity and the interplanetary plasma parameters. 02 p0159 A73-12033
- Laser Doppler shift velocity correlation meter operation in turbulent flow analyzed by optical mixing theory 02 p0153 A73-12049
- Radioisotopic T-3 and T-4 thyroid function tests in the pig-tailed monkey /Macaca nemestrina/. 02 p0135 A73-12548
- The estimation of order and parameters in a process of stochastic differential equations with uncertain observations. 07 p0846 A73-20594
- Radiosonde soundings for typhoons and hurricanes isobaric surfaces heights, temperatures and humidities, calculating correlation coefficients between sea level pressure and other parameters 10 p1245 A73-23985
- Cross correlation coefficients for H, K and H beta lines of solar spectrum related to observed peculiarities from microphotometer intensity traces [AD-759889] 10 p1278 A73-24131
- Relationship of the sporadic Es layer parameters with the absorption of radio waves in the ionosphere 11 p1350 A73-25085
- Spatial correlation of the critical frequencies of the F2 layer on the basis of data from stationary mid-latitude stations 11 p1351 A73-25091
- Autocorrelation and cross correlation coefficients for maximum electron densities and total electron content in E and F regions and upper and lower ionosphere 11 p1351 A73-25093
- Pi 2 micropulsation period and frequency correlation coefficients for planetary magnetic activity Kp index and magnitude of accompanying auroral bay 11 p1357 A73-25930
- Correlation of the shift in the center of gravity of a focused light beam in a turbulent atmosphere 11 p1331 A73-26160
- Cometary brightness variations and conditions in interplanetary space. 14 p1789 A73-29779
- The estimation of extratropical cyclone parameters from satellite radiation measurements. 15 p1903 A73-31315
- The correlation between 10.7-cm /2800 MHz/ solar radio emission and chromospheric flares 15 p1926 A73-31646
- Experiments in objectivization of a forecasting method for lower cloud boundary altitudes 17 p2204 A73-34541
- Correlations among the parameters of the spherical model for eclipsing binaries. 17 p2236 A73-35778
- Serial correlation of physiological time series and its significance for a stress analysis 19 p2401 A73-38159
- Correlational relations between F2 critical frequency deviations and the solar activity cycle according to a number of high-latitude stations 20 p2555 A73-39176
- Correlation of random phases spaced over oscillation frequencies 20 p2531 A73-39457
- A meteorological and a geophysical example of the use of the scale autocorrelation coefficient to determine ratios of frequencies present in periodic phenomena. 22 p2883 A73-42542
- Statistical analysis for autocorrelation and cross correlation coefficients of mean annual total atmospheric ozone and relative sunspot number as solar activity indicator 23 p2976 A73-43883
- Space-time autocorrelation and cross correlation coefficients for transverse turbulent velocity fluctuations in pipe flow 24 p3080 A73-45451
- ### CORRELATION DETECTION
- Output signal-to-noise ratios in frequency measurement system using correlation detector. 01 p0018 A73-11183
- Incoherent optical correlation with a hologram - An example of identifying fingerprints 01 p0054 A73-11489
- Holographic correlation offers new possibilities for acoustical NDT. 04 p0446 A73-14675
- Performance of correlation receivers in the presence of impulse noise. 04 p0419 A73-15406
- The probability density function for the output of a cross-correlator with bandpass inputs. 06 p0665 A73-18139
- Sensor concept and algorithms for a completely strapdown autonomous navigation approach. 19 p2452 A73-38057
- UHF airborne antenna diversity combiner for signal reception using correlation technique for phase variation removal to improve SNR and gain 20 p2523 A73-38725
- Evaluation of the correctness of Gaussian approximation in noise immunity theory 23 p2954 A73-43519
- ### CORRELATION FUNCTIONS
- #### U CORRELATION
- #### CORRELATORS
- #### NT IMAGE CORRELATORS
- Variance estimate of random process second order moment by nonlinear correlator in presence of additive amplitude and phase modulated and normal noise processes 03 p0278 A73-14075
- Inertialess smoothing of multiplier signals in automatic control system under sinusoidal signal, noting analog simulation of inertialess synchronous detector for self adaptive control 09 p1069 A73-22654
- Photoresistor synchronous detector circuits with rectangular light pulse switching elements for capacitive and resistive loads 13 p1592 A73-28900
- Digital correlator-computer-pattern recognition system for VLF phenomena investigation, discussing electromagnetic waves structure and spectrum analysis 15 p1845 A73-32234
- Complementary MOS/silicon on sapphire LSI technology for high speed digital multiplier and correlator logical building blocks design, fabrication and subsystem array implementations 17 p2140 A73-35318
- Study of a correlator using two auxiliary noise sources 20 p2532 A73-39203
- Optimum processing for delay-vector estimation in passive signal arrays. 22 p2825 A73-42198
- ### CORROSION
- #### NT CAVITATION CORROSION
- #### NT ELECTROCHEMICAL CORROSION
- #### NT FRETTING CORROSION
- #### NT FUEL CORROSION
- #### NT INTERGRANULAR CORROSION
- #### NT RUSTING
- #### NT SCALE [CORROSION]
- #### NT STRESS CORROSION
- Ni-Cr-thoria alloy surface oxidation induced by sprayed coating of sodium sulfate for gas turbine blade hot corrosion investigation 04 p0468 A73-15316
- Book - Advances in corrosion science and technology. Volume 2. 06 p0704 A73-17506
- Microorganisms induced biological corrosion, considering oxidizing agents, inhibitors, protective coatings and cathodic protection 06 p0704 A73-17507
- Ellipsometric polarized light methods application to corrosion technology, discussing surface film optical properties and measurement techniques 06 p0704 A73-17508
- Nickel-base alloys hot corrosion mechanism due to sodium sulfate induced accelerated or catastrophic oxidation as result of protective oxide scale dissolution 06 p0712 A73-18763
- Calculation of the heat resistance of metals at variable temperatures 21 p2721 A73-41230
- Book - Advances in corrosion science and technology. Volume 3. 23 p2990 A73-43455
- Corrosion and deposition of steels and nickel-base alloys in liquid sodium. 23 p2990 A73-43456
- ### CORROSION PREVENTION
- Inhibition of stress corrosion cracking of AISI 4340 steel in 10% potassium nitrate solution at 100 C. 01 p0061 A73-10138
- Russian papers on metal corrosion and protection covering additives, annealing, polymer coatings, anodic polarization, electrodeposition, magnetic alloy coatings, etc 02 p0174 A73-12534
- Performance of an inhibitor-protector of steel against corrosion-fatigue failure at elevated temperatures and pressures. 02 p0182 A73-12700
- Corrosion fatigue of type 4140 high strength steel. 02 p0183 A73-12764
- Book - Corrosion and corrosion control: An introduction to corrosion science and engineering /2nd edition/. 03 p0321 A73-13125
- Practical protective atmospheres for molten magnesium. 03 p0323 A73-13267
- Microcorrosion studies with functional fluids. [ASLE PREPRINT 72LC-4C-1] 03 p0335 A73-14360
- Maraging steels galvanic corrosion reduction by two layer Fe-Cu protective coatings, presenting salt water stress corrosion/time-to-failure test results 06 p0705 A73-17799
- Evaluation of protective coatings for prevention of corrosion of high strength steels when subjected to extreme environments. 06 p0711 A73-18717
- Aircraft components solid film lubrication problems, discussing surface pretreatment, contamination susceptibility, corrosion prevention and aerosol applicability 07 p0842 A73-19554
- Protecting metals in corrosive high-temperature environments. 09 p1089 A73-23296
- Stress corrosion crack protection from coatings on high strength H-11 steel aerospace bolts. 10 p1232 A73-23874
- Corrosion fatigue considerations in engineering materials selection and design, discussing alleviation and control 11 p1442 A73-25802
- Chromium coated steels corrosion fatigue in normal conditions, aggressive media and high temperature environments 11 p1386 A73-26733
- Inert gas injection for W-Re thermocouple wire corrosion protection during temperature measurement in aggressive media 12 p1497 A73-27319
- Corrosion and corrosion prevention of light metal alloys. [NACE PAPER 114] 13 p1637 A73-29314
- Study of the structural and mechanical properties of polyvinyl-chloride pastes used as anticorrosion coatings 14 p1766 A73-30377
- Oxidizability of the IVT1 beta titanium alloy and its protection from gaseous corrosion 15 p1894 A73-32537
- Oxidizability of AN-type beta titanium alloys and their protection from gaseous corrosion 15 p1894 A73-32538
- Evaluation of additives for prevention of high temperature corrosion of superalloys in gas turbines. [ASME PAPER 73-GT-1] 16 p2047 A73-33479
- Filiform corrosion associated with commonly applied aircraft metal pretreatments and finishes. [SAE PAPER 730311] 17 p2717 A73-34671
- The relationship between relative oxide ion content of Na2SO4, the presence of liquid metal oxides and sulfidation attack. 20 p2575 A73-39022
- Carbon deposition and the role of reducing agents in hot-corrosion processes. 20 p2576 A73-39027
- ### CORROSION RESISTANCE
- #### NT OXIDATION RESISTANCE
- Corrosion behavior of sintered stainless steels. 01 p0065 A73-10815
- Demonstration of the inhibiting action of certain mineral iodides on the stress corrosion of type 18-10 low-carbon stainless steel 02 p0178 A73-11524
- Polyamide compounds stress corrosion properties and chemical resistance in different test fluids, discussing fluid effect on flaw development rate 02 p0184 A73-11583
- Investigation of the possibility for ultrasonic dispersion of certain corrosion inhibitors introduced in easily removable film coatings 02 p0184 A73-11643
- Effects of inhibitors PB-5 and of dialkyl-dimethyl ammonium chloride on the corrosion resistance and mechanical strength of structural materials during the cleaning of heat exchangers from scale by the hydrochloric acid method 02 p0174 A73-12537
- Influence of cerium and boron additions on the corrosion properties of Kh18N9TL steel 02 p0181 A73-12538
- Book - Corrosion and corrosion control: An introduction to corrosion science and engineering /2nd edition/. 03 p0321 A73-13125
- Ni-Mo-W alloys hardness rating and corrosion resistance to sulfuric and hydrochloric acids, discussing dispersion hardening, quenching and aging treatments 03 p0327 A73-14001
- Transitions in the friction coefficients, the wear rates, and the compositions of the wear debris produced in the unlubricated sliding of chromium steels. [ASLE PREPRINT 72LC-7B-2] 03 p0316 A73-14369
- Preparation and corrosion properties of a tantalum sputtered thick film. 04 p0456 A73-15759
- Glued metal joints polished samples interface corrosion under alternate immersions and withdrawals in baths of different compositions 04 p0468 A73-15991

Properties of a cobalt superalloy resistant to hot corrosion

05 p0588 A73-17247

Flat dendritic carbide effects on crack formation in Ti and Nb stabilized austenitic Cr-Ni corrosion resistant steels after heating to 1250 C

06 p0705 A73-17850

Resistance to hydroerosion of hard-faced maraging steels

06 p0706 A73-17881

Weldability, corrosion resistance and heat resistance increase in Nb alloyed steels, noting aging temperature effects and microstructure

06 p0706 A73-17886

Mechanical properties of heat and corrosion resistant nonmagnetic Ni-Cr-Nr spring alloys with W addition tested in aggressive and nitric acid base media

06 p0709 A73-18211

Effects of ash deposition on the fatigue strength of the working blade material in gas turbines

06 p0741 A73-18662

Investigation of the corrosion-erosion resistance of niobium alloys

06 p0711 A73-18668

Saturation of 1Kh18N9T steel with beryllium and corrosion resistance of the coating in a lithium melt

06 p0711 A73-18669

Development and properties of cobalt-base alloys with improved hot-corrosion resistance.

07 p0838 A73-19497

The effect of carbon on the hot corrosion of cobalt-base alloys.

07 p0838 A73-19498

The corrosion problem in aircraft structures.

07 p0840 A73-20452

On relationship between stress corrosion resistance and grain shape of extruded Al-Zn-Mg alloys with heavy section.

08 p0977 A73-21140

Potentiostatic study of iron meteorite corrosion.

09 p1139 A73-21857

Effect of addition of Bi on stress-corrosion cracking of Al-Mg alloy.

09 p1102 A73-22421

Stress corrosion cracking of commercial Al-Mg alloys and its prevention.

09 p1102 A73-22422

Titanium alloys corrosion resistance modification relative to nonoxidizing acid media by hydrogen reduction conditions or anodic dissociation curve alteration

09 p1104 A73-22965

The resistance of wrought high strength aluminum alloys to stress corrosion cracking.

10 p1232 A73-23872

Resistance of high strength structural steel to environmental stress corrosion cracking.

10 p1232 A73-23875

Investigation of the polar and protective properties of magnesium salts of organic acids

10 p1239 A73-24248

Si addition effect on Ni-Cr alloy calorized layer depth, microhardness, phase structure, chemical composition and scaling resistance

10 p1227 A73-24960

Composite material production by grinding Ni-Al-Ti alloy powder with other mixed powders, noting alloying elements effects on corrosion resistance and ductility

11 p1372 A73-25406

Production and properties of tungsten-wire reinforced NiCr 80 20

11 p1379 A73-25407

Hot gas environment fatigue analysis from corrosion viewpoint, considering gas-alloy reactions

11 p1383 A73-25833

Dynamic potential method of estimating the susceptibility of corrosion-resistant steels to intercrystalline corrosion

11 p1364 A73-26112

Recent developments in precipitation hardenable stainless steels.

13 p1637 A73-29271

Corrosion performance of new fastener coatings on operational military aircraft.

[NACE PAPER 115]

13 p1637 A73-29315

Compatible coatings for corrosion resistant aerospace fasteners.

[NACE PAPER 116]

13 p1638 A73-29316

Critical properties of exterior aircraft finish systems to protect fastener areas.

[NACE PAPER 117]

13 p1638 A73-29317

New inhibited elastomeric finish system designed by corrosion engineers to solve acute corrosion problems on military aircraft.

[NACE PAPER 118]

13 p1638 A73-29318

Corrosion properties and structural transformations of the N70M27 alloy containing vanadium and niobium

13 p1644 A73-29645

Mo and W alloying effects on low carbon chromium nickel steels intergranular corrosion resistance

13 p1644 A73-29648

Intergranular corrosion in iron and nickel base alloys.

15 p1888 A73-31739

Significance of intergranular corrosion in high-strength aluminum alloy products.

15 p1889 A73-31740

Ferritic martensitic stainless steels stress corrosion cracking, emphasizing heat treatment and environment conditions effects on corrosion resistance

15 p1891 A73-32170

High-temperature corrosion in gas turbines and steam boilers by fuel impurities. II - The sodium sulfate-magnesium sulfate-vanadium pentoxide system.

15 p1841 A73-32175

Investigation of the structure and corrosion behavior of alloys of the Ti-Ta-Cr system

15 p1895 A73-32542

Investigation of corrosion stability in alloys of the Ti-Ta-Nb system

15 p1895 A73-32543

International Congress on Metallic Corrosion, 5th, Tokyo, Japan, May 21-27, 1972, Proceedings.

15 p1895 A73-32564

Effect of chloride ions on the dissolution behavior of Fe-Ni alloys.

15 p1895 A73-32565

Study of multiple surface compound precipitation during passivation of D6AC-steel.

15 p1895 A73-32566

The passivation behaviour of the Ti-6Al-4V alloy.

15 p1895 A73-32567

Na2SO4-induced attack of Ni-20Cr-2TiO2.

15 p1896 A73-32575

Solid film lubricant corrosion study employing salt spray test with sulfur dioxide and synthetic sea water, examining molybdenum disulfide, antimony trioxide and graphite films

[ASLE PREPRINT 73AM-3C-4]

17 p2196 A73-34989

Synthesis of metal-ceramic and other heat-resistant coatings by the electrochemical method

18 p2319 A73-35890

Corrosion wear mechanism with emphasis on chemical and mechano-chemical reaction products formation and removal from friction surface /tribo-mechanical processes/

18 p2320 A73-36494

Titanium cathode blanks in electrolytic production of metals, noting titanium oxide nonstick properties, electron transmission and corrosion resistance

19 p2442 A73-37841

Mechanical and corrosion resistant properties of titanium castings.

19 p2442 A73-37947

Effects of small amounts of additional elements on directionality of stress corrosion resistance of the Al-Zn-Mg alloys.

19 p2442 A73-37948

The influence of heat treatment on the stress-corrosion susceptibility of a ternary Al-5.3 pct Zn-2.5 pct Mg alloy.

20 p2576 A73-39031

Corrosion characteristics and structural transformations in alloy N70M27 with vanadium and niobium.

21 p2720 A73-41038

Mo and W alloying effects on low carbon chromium nickel steels intergranular corrosion resistance

21 p2721 A73-41041

How composition affects properties of a ferritic stainless steel.

21 p2721 A73-41084

Mechanical properties of AFCT7 stainless steel bolts.

21 p2721 A73-41085

The fretting fatigue of titanium and some titanium alloys in a corrosive environment.

22 p2876 A73-42356

Exceptional hardness and corrosion resistance of Mo5Ru3 and W3Ru2 films.

22 p2866 A73-42581

International Metal Spraying Conference, 7th, London, England, September 10-14, 1973, Proceedings.

22 p2879 A73-42591

Mo content influence on heat resistant Ni base alloys corrosion and oxidation resistance and gamma-prime phase solution temperature and amount

23 p2989 A73-43435

Improvement of the corrosion-fatigue strength of aluminum alloys by exposure of the medium to a magnetic field

23 p2984 A73-43466

Aluminum brazed titanium honeycomb sandwich structure - A new system.

23 p2985 A73-44000

Development of corrosion resistant filler metals for brazing molybdenum.

23 p2986 A73-44004

Investigation of the possibility of obtaining an-desite-based alkali-resistant glass compositions for a continuous glass fiber

23 p2998 A73-44298

Research and development of aerospace adhesive bonded systems and concepts.

24 p3093 A73-44763

Selection of phosphate impregnants for graphite oxidation inhibition

24 p3104 A73-44954

CORROSION TESTS

NT SALT SPRAY TESTS

Influence of metallurgical factors on the corrosion cracking under tension of TA6V titanium alloy in an aqueous medium at ambient temperature

[ONERA, TP NO. 1100] 01 p0061 A73-10231

Stress corrosion cracking behavior of 18% Ni /300/ maraging steel.

01 p0066 A73-11295

Lifetime of Dural structural elements operating in aggressive media

02 p0180 A73-11794

Microstructure and microsegregation effects in the intergranular corrosion of austenitic stainless steel.

02 p0183 A73-12765

Evaluation of materials for underground exposure in extreme environments.

03 p0329 A73-13006

Corrosion tests for rocket propulsion system components materials for use with nitric acid-nitrogen tetroxide blend oxidizer

03 p0329 A73-13007

The influence of adhesive components on the corrosion of aluminum honeycomb.

03 p0321 A73-13038

Effects of hot-salt stress corrosion on titanium alloys.

03 p0323 A73-13268

Synergistic effects of anions in the corrosion of aluminum alloys.

03 p0325 A73-13729

Influence of microstructure on the corrosion behavior of Ti-2% Ni in hot acidic chloride solutions with particular reference to weld regions.

03 p0325 A73-13730

Maraging steels galvanic corrosion reduction by two layer Fe-Cu protective coatings, presenting salt water stress corrosion/time-to-failure test results

06 p0705 A73-17799

Fractographic aspects of the stress corrosion cracking of titanium in a methanol/HCl mixture.

06 p0705 A73-17800

High temperature behavior of superalloys exposed to sodium chloride. I - Mechanical properties. II - Corrosion.

06 p0713 A73-18766

Study of pitting corrosion and stress corrosion in stainless steels with the aid of alloys of very high purity

07 p0838 A73-19114

Scale effects on the fatigue and corrosion fatigue of steel

07 p0839 A73-19657

Crack corrosion of titanium in a solution of hot concentrated magnesium chloride

07 p0839 A73-20167

Inhibition of corrosion fatigue in 7075 aluminum alloys.

07 p0840 A73-20351

Temperature dependent pitting corrosion tests of Mo containing austenitic stainless steels

07 p0840 A73-20354

Ion gun sputter cleaning of thin film metal substrate for in situ corrosion studies by UHV transmission electron microscopy

08 p0990 A73-21616

Study of the formation process of corrosion cracks under tension in an aluminum alloy

[ONERA, TP NO. 1213] 09 p1098 A73-21925

Neutron radiography as a diagnostic tool in the study of corrosion in lithium-filled heat pipes.

09 p1079 A73-21991

Stress corrosion cracking characteristics and test data interpretation, considering pitting, brittle fracture, crack propagation, chemical environment and smooth and cracked specimens

10 p1232 A73-23868

Stress corrosion cracking behavior of nickel and nickel alloys.

10 p1232 A73-23870

Standardization, loading methods and environments for stress corrosion cracking tests, noting prevention of crevice, galvanic and hydrogen embrittlement effects

10 p1232 A73-23871

Overview of corrosion cracking of titanium alloys.

10 p1232 A73-23873

Hydrogen promoted corrosion of tungsten by oxygen in an electric field A field ion microscope study.

11 p1325 A73-25205

Determination of criteria for rain erosion testing of the standard arm radome.

11 p1335 A73-25298

The kinetic and dynamic aspects of corrosion fatigue in a gaseous hydrogen environment.

11 p1382 A73-25817

Aircraft structures aluminum alloys fatigue crack growth rate relationship to cracking mode, stress ratio, cyclic frequency and corrosive environment severity

11 p1382 A73-25826

Study on the superposition of intergranular corrosion and pitting corrosion by fatigue cracking of stainless steels.

11 p1383 A73-25831

- Use of soft X-ray spectroscopy to study corrosion and oxidation products on metals and alloys.
[NACE PAPER 124] 13 p1638 A73-29319
- Metallurgical and strength studies of heat resisting alloys for gas turbines after long term service.
13 p1625 A73-29519
- Al and Ti alloy corrosion and fretting fatigue in aqueous environment, noting protective oxide surface film effects
13 p1642 A73-29524
- Localized corrosion - Cause of metal failure; Proceedings of the Symposium, Atlantic City, N.J., June 27-July 2, 1971.
15 p1888 A73-31736
- Exfoliation corrosion of aluminum alloys.
15 p1888 A73-31737
- Simplified exfoliation testing of aluminum alloys.
15 p1888 A73-31738
- Significance of intergranular corrosion in high-strength aluminum alloy products.
15 p1889 A73-31740
- Pitting corrosion - A review of recent advances in testing methods and interpretation.
15 p1889 A73-31741
- Exfoliation corrosion testing of 7178 and 7075 aluminum alloys.
15 p1889 A73-31742
- International Congress on Metallic Corrosion, 5th, Tokyo, Japan, May 21-27, 1972, Proceedings.
15 p1895 A73-32564
- Notched austenitic stainless steel stress corrosion cracking tests in boiling magnesium chloride solutions, obtaining relationship between maximum stress and strain rate in graph
15 p1895 A73-32569
- Stress corrosion cracking of titanium alloys in hydrogen chloride.
15 p1896 A73-32573
- Effect of thermomechanical treatment on the stress corrosion cracking of metastable beta III titanium.
15 p1896 A73-32574
- Nickel-water heat pipes accelerated life testing, deriving corrosion model based on hydrogen evolution [AIAA PAPER 73-726] 18 p2369 A73-36343
- Estimation of corrosion damage levels in thin-walled structural elements by the punching method
18 p2320 A73-36825
- Effects of small amounts of additional elements on directionality of stress corrosion resistance of the Al-Zn-Mg alloys.
19 p2442 A73-37948
- Corrosiveness of naturally occurring sulfur compounds and organic peroxides in aviation turbine fuels toward Cu and Ag, detailing maximum tolerable ratios
20 p2600 A73-39637
- Application of the 'differential reflectometer' to materials research in corrosion, ordering and alloying.
21 p2719 A73-40897
- Pitting of titanium. I - Titanium-foil experiments. II - One-dimensional pit experiments.
23 p2991 A73-43521
- The stress corrosion of titanium materials - The present status of research
23 p2992 A73-43910
- CORRUGATED PLATES**
Investigation of the first forming phase of transverse corrugations
02 p0172 A73-11722
- Stretch formed corrugated Rene 41 panel development for space shuttle booster nose section hot area skin, discussing tooling and formation techniques [SAE PAPER 720873] 05 p0582 A73-16670
- Orthotropic panel flutter at arbitrary yaw angles - Experiment and correlation with theory.
[AIAA PAPER 73-192] 05 p0634 A73-16924
- Flange-to-web connection requirements on beams with corrugated webs.
10 p1223 A73-23632
- Scattering from a periodic corrugated surface - Semi-infinite alternately filled plates.
13 p1659 A73-28484
- Supersonic flow along a wavy wall in a channel
15 p1823 A73-31332
- CORRUGATED SHELLS**
Application of shell equations to an unsymmetrically loaded corrugated shell of revolution.
01 p0115 A73-10769
- Investigation of the elastoplastic characteristics of corrugated membranes under cyclic loading conditions
10 p1293 A73-24792
- CORRUGATING**
Surface wave characteristics of circular cylindrical corrugated and uniform dielectric rod excited in E sub 0-mode.
07 p0792 A73-19545
- Corrugated and uniform dielectric rod aerial excited in E sub 0-mode.
07 p0792 A73-19547
- Laser oscillation in leaky corrugated optical waveguides.
08 p0975 A73-21206
- General cavity analysis for corrugation in rectangular waveguide microwave filters, using admittance method with consideration for propagation modes
10 p1192 A73-23606
- Radiation characteristics of corrugated E-plane sectoral horns.
14 p1734 A73-30209
- Laser action from optically pumped epitaxial GaAs crystal waveguides with feedback provided by surface corrugation
21 p2713 A73-40455
- Diffraction grating model in terms of amplitude and phase modulation to explain angular spectrum of light reflection from corrugated surface for various incidence angles
21 p2740 A73-40790
- Tapered corrugated waveguide low-pass filters.
21 p2666 A73-41427
- Corrugated conical horn antenna feed design, discussing Newton-Raphson iterative solution and computer program for spherical hybrid mode eigenvalues
22 p2832 A73-42296
- CORSAIR AIRCRAFT**
U A-7 AIRCRAFT
CORTI ORGAN
Electron-microscopy investigation of Corti's organ after noise trauma
05 p0539 A73-16333
- Neuroanatomy of the auditory system.
14 p1715 A73-30280
- Corti organ lesion effects on signal perception in patients with noise induced hearing loss, correlating speech discrimination with age and sound level
19 p2396 A73-38182
- CORTICOSTEROIDS**
NT ALDOSTERONE
NT CORTISONE
NT HYDROXYCORTICOSTEROID
Corticosterone level and the binding capacity of blood plasma proteins under thermal effects
03 p0261 A73-13749
- Inhibition of the adrenocortical response to hypoxia by dexamethasone.
07 p0780 A73-19476
- Interrelations among the supranal glucocorticoid activity, the cardiovascular systems, and the electrolyte metabolism during prolonged work
11 p1317 A73-26085
- Diurnal rhythm of a corticosteroid reaction to ACTH and physical load
14 p1719 A73-30841
- Effect of prior adaptation to cold on the development of experimental hypertonia
21 p2636 A73-40209
- Activity of acid nucleases in eye tissues under the action of corticosteroid hormones
24 p3058 A73-44430
- CORTISONE**
Diurnal variations of plasma cortisol and glucose and of urinary excretion of free cortisol in man at rest
24 p3061 A73-45158
- CORUNDUM**
U ALUMINUM OXIDES
COSINE
U TRIGONOMETRIC FUNCTIONS
- COSMIC DUST**
NT INTERPLANETARY DUST
NT METEOROID DUST CLOUDS
NT ZODIACAL DUST
An upper limit on the OH abundance in the intercloud medium.
01 p0096 A73-10314
- Cool giant star-ejected high velocity dust grains interaction with interstellar clouds, discussing solid state defect accumulation, sputtering and grain and cloud heating
01 p0098 A73-10582
- A simple analytic approximation for dusty stromgren spheres.
01 p0104 A73-11047
- Cosmic black glassy spherules composition, mineralogy and physical properties compared to lunar fines, considering possible common origin
02 p0214 A73-12254
- Cosmic dust distribution measurement by satellites, relating accuracy to sensor calibration conditions and region characteristics
02 p0215 A73-12258
- Mesospheric cosmic dust concentration measurements from particle collection rocket flights, discussing interference from uplifted aerosols of terrestrial or cosmic origin
02 p0215 A73-12259
- Meteor shower and cosmic dust effects on twilight sky brightness from mountain top and balloon observations
02 p0215 A73-12261
- Extensive cosmic ray shower production by relativistic dust grain accelerated in interstellar space by galactic radiation pressure and subsequent magnetic processes
02 p0207 A73-12388
- Diffuse galactic FUV radiation and interstellar dust grains.
02 p0207 A73-12399
- Diffuse interstellar lines and bands interpreted as extinction structure due to impurities in cosmic dust grains, comparing theory with observation
02 p0225 A73-12807
- On the maximum value of the mass of a star.
04 p0500 A73-15525
- Interaction of stars with local dust formations.
04 p0503 A73-16008
- The infrared variability of a dust model for Seyfert galaxies.
05 p0624 A73-17311
- Rocket-borne instruments for cosmic dust particles detection in extraterrestrial space, noting collector foils and plates fabrication
06 p0748 A73-17768
- Radiation-driven efflux and circulation of dust in spiral galaxies.
07 p0875 A73-19345
- Spectrum of a dust-embedded Wolf-Rayet star in Cygnus OB2.
07 p0900 A73-20241
- Finson-Probstin model for dust comets applied to calibrated photographic plates of Comet Bennett, giving dust size distribution, emission rate and initial velocities
07 p0902 A73-20443
- Spiral arm structure as standing wave, of magnetically controlled star creation, considering various hydromagnetic models, dust and H I distributions
08 p1002 A73-20879
- Observations of circumstellar circular polarization in four more infrared stars.
08 p1013 A73-21813
- Galactic dust region molecular cloud effects on cloud chemical evolution, star and planetary formation and life development on planets
09 p1140 A73-21975
- The influence of dust upon the dynamics and thermal stability of planetary nebulae.
09 p1142 A73-22032
- Cosmic absorption of stellar light in the belt of a local system
09 p1148 A73-22861
- Carbon stars molecular band strength variations in two-micron spectral region due to thermal emission from circumstellar dust shell
09 p1149 A73-23129
- The interpretation of continuum and line absorption and radiation by circumstellar dust.
09 p1150 A73-23132
- IR galaxy model consisting of low energy cosmic or X rays at center of dust shell, discussing physical dimensions of radiating region
09 p1151 A73-23146
- The motion of dust and gas in the heads of comets with type II tails.
10 p1271 A73-23494
- Metallic dust particles in quasi circular solar orbit, discussing evolution, thermal evaporation, atomization and size
10 p1274 A73-23720
- Optical anomalies due to scattered disperse cosmic matter in upper atmosphere from Tungusk meteorite fall
10 p1213 A73-24681
- Production of metagalactic X-rays by relativistic dust grains.
10 p1270 A73-24907
- Critique of Anderson hypothesis of moon origin by condensation of material off median plane of initial solar nebula
11 p1428 A73-26664
- IR spectra of quasars and Seyfert galaxies interpreted as thermal radiation from dust envelopes around cores, considering graphite and silica dust particles
12 p1547 A73-27876
- Transition radiation production by relativistic electrons traversing cosmic grains as source of celestial X rays, discussing formation zone effect
14 p1787 A73-30730
- Production of astrophysical X-rays by transition radiation.
15 p1926 A73-31553
- Extinction and scattering by several types of silicate sphere of radius 0.05-1.0 micron, for the wavelength range 0.21-50 microns.
15 p1939 A73-32012
- Southern Milky Way early type star interstellar extinction curves, considering position with regard to galactic plane and local dust cloud conditions
15 p1939 A73-32046
- Moon surface physical properties from earth based observations and lunar soil samples, noting effects of cosmic dust and meteorite impacts
16 p2063 A73-33752
- Planetary cosmogony theory review emphasizing cold evolution through dust-gas protoplanetary cloud nucleosynthesis, discussing iron fractionation, organic compounds and planetary thermal history
16 p2066 A73-33793

Enhancement of upper atmospheric sodium from sporadic dust influxes.

16 p2010 A73-33917

Protoplanetary gas-dust cloud evolution and planetary formation, investigating earth initial state

17 p2227 A73-34408

Silicates and water identification in interstellar grains, considering possibility of iron and carbon components

17 p2227 A73-34410

Planetary accretion from grains in intersecting solar orbits, investigating velocity impact behavior of silicate particles

17 p2228 A73-34423

Stellar wind radiation damage in cosmic dust grains - Implications for the history of early accretion in the solar nebula.

17 p2228 A73-34424

Transition radiation from interstellar dust grains.

17 p2231 A73-34755

Metallic dust particles in quasi-circular solar orbit, discussing evolution, thermal evaporation, atomization and size

18 p2355 A73-36745

A survey of interstellar formaldehyde in dust clouds.

19 p2475 A73-37610

OH observations of sixteen interstellar dust clouds.

20 p2607 A73-39118

Helios probe design for solar wind acceleration mechanism, magnetic and electric fields, interplanetary dust and cosmic radiation

21 p2780 A73-40449

Interstellar extinction, relation to spatial dust distribution, light scattering by grains, diffuse absorption lines and polarization

21 p2772 A73-41247

Space research XIII: Proceedings of the Fifteenth Plenary Meeting, Madrid, Spain, May 10-24, 1972. Volumes I & 2.

21 p2687 A73-41325

Helicentric Pioneers 8 and 9 hyperbolic cosmic dust data suggesting cosmic dust origin of previously solar effect generated noise

21 p2775 A73-41410

Pioneers 8 and 9 cosmic dust data reliability, presenting sensor geometry, field of view, response function, instrument control and sensitivity

21 p2775 A73-41411

Near-earth micrometeorite flux measurement by rocket-borne acoustic detectors, noting consistency with previous observations

21 p2775 A73-41415

Solar atmosphere origin for submicrometer cosmic dust in ionosphere and noctilucent clouds, noting anomalously high atomic weight

21 p2775 A73-41416

Dust measurements in the upper atmosphere during and in the absence of noctilucent cloud display.

21 p2691 A73-41417

Mie scattering computation of cosmic dust flux in upper atmosphere from twilight luminance increase during meteor showers

21 p2775 A73-41418

Cometary atmospheric dust chemical composition and physical properties estimated from colorimetric, polarimetric and IR data, using models of optically thin polydisperse media

21 p2776 A73-41421

Comment on 'Anomalous hyperfine lines in formaldehyde in a dust cloud.'

22 p2904 A73-41755

On the infrared emission of H II regions due to dust.

22 p2908 A73-42314

Global coordinate systems for spherical collapsing and expanding Oppenheimer-Snyder dust cloud behavior after critical Schwarzschild radius attainment

22 p2908 A73-42438

Surface wind stress and threshold friction velocity required to raise dust on Mars, discussing mechanisms for production of strong winds in Ekman layer

22 p2912 A73-42981

Micrometeorite and cosmic dust studied for solar system and universe origin and evolution and for medium range weather forecasting, discussing cosmic matter infall to earth

22 p2913 A73-42988

Ion-grain collision cooling rate for hot gas above million K, discussing applications to supernova explosions, Seyfert nuclei and intergalactic matter within galactic clusters

22 p2916 A73-43121

Extinction and scattering cross sections of small planetesimal particles with iron cores and silicate mantles in circumstellar dust of young T Tauri stars

23 p3030 A73-43748

Accretion and electrostatic interaction of interstellar dust grains - Interstellar grit.

23 p3030 A73-43757

Normal galaxy central region dust content /mass/ estimates based on photoelectric measurements

23 p3035 A73-44235

Comet Bennett neutral sodium atom and dust particle distribution across head and tail measured by photometry of Na emission radial profile

24 p3133 A73-44560

Photometric study of a diffuse reinforcement observed in the zodiacal light at a distance of 100 solar radii from the sun

24 p3134 A73-44566

Scattered-light phenomena in interstellar space

24 p3137 A73-44824

Electron transitions in interstellar dust 4430 A line, indicating ferric oxide /alpha-hematite/ in type I supernovae

24 p3138 A73-44990

COSMIC GASES

NT INTERPLANETARY GAS

NT INTERSTELLAR GAS

Gas shell surrounding Galaxy with temperatures intermediate between corona and disk due to hot gas accretion from intergalactic space of Local Group

05 p0622 A73-17179

The motion of dust and gas in the heads of comets with type II tails.

10 p1271 A73-23494

Protoplanetary gas-dust cloud evolution and planetary formation, investigating earth initial state

17 p2227 A73-34408

Optical and radio observations of NGC 4258 anomalous arms indicating eruptive processes in galactic nucleus as possible source of spiral structure

20 p2605 A73-39057

Distribution of gases within Apollo 15 samples - Implications for the incorporation of gases within solid bodies of the solar system.

20 p2612 A73-39715

COSMIC NOISE

Photomultiplier operation pulse control in semiconductor circuit for background cosmic radiation noise error minimization in air shower station

02 p0171 A73-12688

A revised low-frequency cosmic noise spectrum.

04 p0500 A73-15516

Ionospheric propagation effects on riometer recorded cosmic radio emission spectra, noting temporal and frequency spectra dependence on ionospheric plasma turbulence scale

05 p0573 A73-16266

Characteristics of the VLF-noise spectrum during excitation of the earth-ionosphere resonator by cosmic sources.

10 p1188 A73-24222

Bremsstrahlung X-rays in the stratosphere and auroral activity on January 21 and February 3, 1969.

10 p1268 A73-24224

Structure of a noise-storm source according to observations of the eclipse of September 22, 1968 at the 1.37-m wavelength

16 p2057 A73-32704

Occurrence of IPDP events accompanied by cosmic noise absorption in the course of proton aurora substorms.

18 p2312 A73-36298

Particle precipitation in Brazilian geomagnetic anomaly during magnetic storms.

23 p2971 A73-43687

COSMIC PLASMA

Second-level population of a hydrogen atom in a plasma medium

01 p0085 A73-10950

Cygnus X-3 radio outburst as consequence of synchrotron radiation due to expanding relativistic plasma ejection, considering polarization, flux densities and spectral index

02 p0211 A73-11872

Hydrodynamic and kinetic instability and oscillations of plasma with non-Maxwellian particle velocity distribution, noting laboratory and cosmic plasmas

04 p0478 A73-15018

Frequency correlation measurement of pulsar spectral fine structure due to radio emission scattering by interstellar plasma

04 p0503 A73-16002

Turbulent plasma 'piles' in the nuclei of galaxies.

04 p0504 A73-16022

Effect of Thomson scattering on the emission spectrum of an optically semiopaque plasma.

04 p0493 A73-16024

Spectrum of small-scale inhomogeneities in the interplanetary plasma

06 p0747 A73-17529

Nonlinear mode-mode coupling of Alfvén waves in the interstellar medium.

06 p0730 A73-18465

Faraday rotation of polarized extragalactic radio sources interpretation as plasmas of mixed matter and antimatter

07 p0900 A73-20277

Heating of astrophysical plasma due to rotation.

08 p1007 A73-20957

Magnetic field in the plasmasphere of a compact star.

08 p1007 A73-21001

Ultrarelativistic cosmic plasma analysis of high density electron beams transport across strong magnetic fields with application to pulsar NP 0532 spectrum

08 p0999 A73-21334

Population of the second level of the hydrogen atom in a plasma medium.

09 p1130 A73-22744

Time dependent radio stars scintillation spectra with allowance for interplanetary plasma discontinuities velocity dispersion at small solar distances

10 p1274 A73-23716

Threshold energies of K-shell photoionization cross sections for various cosmic ionic species

10 p1251 A73-23756

Interplanetary plasma shock event of 8 March 1970 from Heos 1 data, noting magnetospheric compression and solar wind velocity at geosynchronous orbit

10 p1270 A73-24742

Cosmic dilute collisionless plasma physical properties, discussing plasma wave turbulence characteristics, particle acceleration, relativistic plasmas, synchrotron emission, pulsars and galactic nuclei

12 p1537 A73-26850

Anisotropic contact discontinuities at magnetospheric boundary and tail from MHD space plasma data analysis, suggesting sector boundary identification in interplanetary magnetic field

12 p1528 A73-27329

Existence of a new type of rotating equilibrium ellipsoids in the presence of a toroidal magnetic field

14 p1782 A73-30816

Russian book - Plasma astrophysics.

15 p1936 A73-31579

Spectrum of small-scale interplanetary plasma inhomogeneities.

16 p2058 A73-32753

Plasma near Venus - Comparison of results obtained with the aid of Venus 4 and Mariner 5

16 p2067 A73-33804

Waves in a plasma amid magnetic and gravitational fields

17 p2226 A73-34373

Experiment and observation of isotope and element separation in a plasma with cosmical applications.

17 p2216 A73-34420

On the role of plasma effects in the cosmic ray propagation and isotropization in the galaxy.

17 p2225 A73-35779

Observation and analysis of abrupt changes in the interplanetary plasma velocity and magnetic field.

18 p2351 A73-36265

Time dependent radio sources scintillation spectra with allowance for interplanetary plasma discontinuities velocity dispersion at small solar distances

18 p2355 A73-36741

High-frequency plasma turbulence in outer-space

19 p2481 A73-37341

Russian book on satellite measurement of magnetic fields and plasmas in interplanetary medium, magnetosphere, moon and Venus vicinity and geomagnetic field-solar wind interaction region

19 p2486 A73-37772

The propagation of an intense electromagnetic wave in a plasma.

19 p2469 A73-38087

Russian book - Stellar atmospheres and interplanetary plasma.

21 p2671 A73-40531

Quasar scintillations at an inhomogeneous interstellar plasma

21 p2767 A73-40535

Role of plasma effects in the propagation and isotropization of cosmic rays in the Galaxy

21 p2756 A73-40579

Annual review of astronomy and astrophysics. Volume 11.

21 p2771 A73-41234

Turbulence and scintillations in the interplanetary plasma.

21 p2748 A73-41235

Interaction of fast particles with waves in cosmic magnetoactive plasma.

21 p2748 A73-41248

Phase method of investigation of short time scale disturbances and motions in space plasma.

21 p2748 A73-41373

Effects of electrostatic instabilities on planetary and interstellar ions in the solar wind.

22 p2902 A73-41940

Hydromagnetic stability of a composite plasma in the presence of Hall currents.

22 p2894 A73-42439

Anisotropic contact discontinuities at magnetospheric boundary and tail from MHD space plasma data analysis, suggesting sector boundary identification in interplanetary magnetic field

23 p3008 A73-43227

COSMIC RADIATION

U COSMIC RAYS

COSMIC RADIO WAVES

U EXTRATERRESTRIAL RADIO WAVES

COSMIC RAY ALBEDO

Solar and geomagnetic modulation of low-energy secondary cosmic ray electrons.

12 p1533 A73-26977

Measurement of geomagnetic cutoff rigidities and particle fluxes below geomagnetic cutoff near Palestine, Texas.

Cosmic ray albedo neutron decay injection theory for proton belt, considering radial diffusion, atmospheric losses, geomagnetic models, atmospheric density, etc

Flux measurements of galactic cosmic-ray albedo neutrons by the Molnia 1 satellite in 1972

COSMIC RAY SHOWERS

Book - Cosmic rays: Selected readings in physics.

The possibility of a consistent explanation of various phenomena involving cosmic ray muons.

A search for the quark in extensive air showers, using a counter-controlled cloud chamber.

Extensive air showers on Jupiter, and its sporadic decimeter radio emission.

Data processing for radioastronomy and cosmic ray air shower arrays.

Extensive cosmic ray shower production by relativistic dust grain accelerated in interstellar space by galactic radiation pressure and subsequent magnetic processes

Nuclear-electron cascades longitudinal evolution calculation in ionization calorimeter for primary nucleons and pions, using Monte Carlo method

Ionization calorimeter study of cosmic ray hadrons inelastic collision cross sections and partial K-neutral pion inelasticity factor

Secondary cosmic ray shower charged particles angular distribution asymmetry in center-of-mass system and azimuthal plane related to single fireball formation

Energy spectrum, composition and anisotropy study of cosmic radiation from extensive air showers observation, using scintillation and Cerenkov detectors

Extensive air showers radio emission polarization, spatial distribution and electric field strength, noting geomagnetic mechanism effect

Electron and muon density fluctuations, trajectory distribution and azimuthal symmetry in cosmic ray air showers

Extensive air showers vertical distribution at aircraft heights, constructing integral spectrum based on particle number

Primary cosmic radiation energy spectrum approximation from air showers, high-energy hadrons and Proton 4 data

Cosmic radiation high energy hadron component relation to extensive electron-photon showers, comparing sampling events based on multicore structure and total energy

Extensive air shower spectra based on electron and muon number for given shower development mechanism and primary cosmic ray chemical composition

Extensive air shower characteristics and muon counts at different level observations relative to particle number and primary energy spectra

High energy cosmic ray interactions at one TeV, including X process, horizontal showers and muon poor showers

Energy spectrum of muon formed electromagnetic cascades in vertical cosmic radiation flux

Spectral calculations of electromagnetic and nuclear showers, studying cosmic ray muons interactions with matter

Muon densities in penetrating high energy particles, comparing with extensive air showers

Muon generated cascade showers in iron, using ionization calorimeter and hodoscope detectors

Photomultiplier operation pulse control in semiconductor circuit for background cosmic radiation noise error minimization in air shower station

Unorthodox ideas concerning the origin of cosmic radiation.

Cosmic-ray particle density

Nonconventional processes in anomalous cosmic-ray experiments.

Extensive air showers and Feynman scaling above 1000 GeV.

Cosmic ray electrons of E greater than 1 Gev - Some new measurements and interpretations.

Intensity and energy spectrum calculation of albedo electrons recorded in cosmic particle showers by gas discharge counters

Lateral distribution of u.h.f. radio emission associated with cosmic ray showers.

Cerenkov shower spectrometer with a conical radiator made of TF-5 glass

Secondary particles multiplicity law validity in cosmic ray showers highest energy interactions

Primaries of extensive air showers of cosmic radiation.

Cosmic ray bursts in 1970-1971 according to measurements in the stratosphere

Effect of rapidly rising proton-proton total cross sections on idealized extensive air showers.

Amplitude analysis of extensive air shower particle fluxes

Search for quarks using a flash-tube chamber.

Abundance and lateral distribution of muons in inclined showers.

Null correlation method for estimation of the primary energies of cosmic ray jets.

International Conference on Cosmic Rays, 12th, University of Tasmania, Hobart, Tasmania, Australia, August 16-25, 1971, Papers. Volume 7 & Invited and Rapporteur Papers.

Fast pulse VHF background noise measurements in site selection for radio detection of cosmic ray air showers

The lateral distribution of muons in near vertical EAS.

Calculations on the radio emission resulting from geomagnetic charge separation in an extensive air shower.

Electron calibration on a high-energy cosmic ray detector.

Large underground showers and multiple muons in association with E.A.S.

Photon lateral distribution sensitivity to longitudinal development of electron cascade via computer simulations of optical Cerenkov emission from cosmic ray showers

Muon production in large air showers, determining mean origin height via magnetic spectrography, distance from shower core, geomagnetic deflection and trajectory angles

Cosmic ray muon zenith angle distribution during horizontal air showers, discussing kaon and pion decay, spectrum characteristics, bremsstrahlung effects and flux upper limits

Electron calibration of a high-energy cosmic ray detector.

The multiplicity distribution of shower particles underground and the cosmic-ray primary spectrum.

Size spectra of extensive air showers and primary cosmic-ray spectrum.

Root-mean-square signal amplitude variation measurements of LF radio emission from extensive air showers by whip antenna

Comparison of calculated characteristics of extensive atmospheric showers with experimental results at various altitudes

A study of elementary acts of interaction between hadrons with energies of about 10 TeV

Preliminary results of the Pamir-20-71 experiment on interactions at energies of about 1000 TeV

High energy gamma quanta families and multiple generation processes in electron photon cascades detected by nuclear emulsion X ray chamber

Intercosmos 6 cosmic ray shower experiment using emulsion stack, spark chamber and scintillation counter to measure particle energy, angular distribution and production multiplicity

Intense air showers with an electron-photon core of complex structure

Certain problems in measuring Cerenkov light on the lakutsk extensive air shower device

The assembly edge effect and the spatial distribution of extensive air shower particles in an assembly with widely spaced detectors

Large transverse momenta and the structure of extensive air shower cores

An arrangement for studying horizontal air showers - Initial results

High energy gamma quanta families and multiple generation processes in electron photon cascades detected by nuclear emulsion X ray chamber

Intercosmos 6 cosmic ray shower experiment using emulsion stack, spark chamber and scintillation counter to measure particle energy, angular distribution and production multiplicity

Intense air showers with an electron-photon core of complex structure

Certain problems in measuring Cerenkov light on the lakutsk extensive air shower device

The assembly edge effect and the spatial distribution of extensive air shower particles in an assembly with widely spaced detectors

Large transverse momenta and the structure of extensive air shower cores

An arrangement for studying horizontal air showers - Initial results

Results of radio emission studies at frequencies of 32 and 58 MHz in extensive air showers on the assembly of Moscow State University

Extensive air showers and nuclear interaction characteristics at superhigh energies

Spatial electron distribution in extensive air showers at energies of one thousand to one billion TeV

Calculated characteristics of the electron and muon components of extensive air showers at the 690 g/sq cm level

Calculation of the fluctuations of the Cerenkov radiation of an electron-photon shower in the atmosphere

Fluctuations of the total path of charged particles in electron-photon showers caused by gamma-quanta with energies of 40, 60 and 200 m/c-squared/

The structure of the spatio-angular distribution function of electron-photon shower particles near the axis

Intensity variations of electron-photon shower particles in the atmosphere

Transition effects during the recording of the electron-photon component of extensive air showers

The energy spectrum of cosmic ray muons at sea level

Generation of high-energy muons in cosmic rays

Experimental characteristics of a muon stream with energies above 10 GeV, contained in an extensive air shower

Some characteristics of the muon component of extensive air showers at mountain level

Spark calorimetry investigation of trident and extensive air showers muon component generated high energy penetrating particles at large zenith angles

Identification of hadrons with 500 GeV energies in cosmic rays by using transitional emission

COSMIC RAYS

NT COSMIC RAY SHOWERS

NT PRIMARY COSMIC RAYS

NT SECONDARY COSMIC RAYS

NT SOLAR COSMIC RAYS

Book - Cosmic rays: Selected readings in physics.

Book - An introduction to the theory of plasma turbulence.

Thin polypropylene window proportional counters for the observation of cosmic soft X-rays.

Multiple scattering of cosmic ray muons in the range 10-70 GeV/c.

Properties of H I regions heated by X-rays and cosmic rays

Energy balance in the current sheath of a solar flare and the acceleration of cosmic rays by plasma waves

Galactic and extragalactic X and gamma ray sources identification from satellite, rocket and high altitude balloon observations, discussing radiation generation theories

Relativistic cosmic rays propagation, calculating abundances of Pt, Pb, actinides and superheavy groups as function of cosmic ray leakage time

01 p0092 A73-11027

High-energy cosmic gamma-ray observations from the OSO-3 satellite.

01 p0092 A73-11028

Observations of galactic cosmic-ray intensity at heliocentric radial distances of from 1.0 to 2.0 astronomical units.

01 p0093 A73-11044

International Conference on Cosmic Rays, 12th, University of Tasmania, Hobart, Tasmania, Australia, August 16-25, 1971, Papers. Volumes 1, 2, 3, 4, 5 & 6.

01 p0093 A73-11375

Observation of low-charge low-energy geomagnetically forbidden particles.

02 p0155 A73-11726

Cosmic ray muon component integral multiplicity calculations with allowance for angular distribution of secondary particles in elementary collision event on atmospheric boundary, using computer

02 p0205 A73-12172

Composition of relativistic cosmic rays near the earth and at the sources.

02 p0207 A73-12327

Radial gradients and anisotropies due to galactic cosmic rays.

02 p0207 A73-12378

Further evidence for a cosmic ray selection mechanism.

02 p0207 A73-12397

Cosmic diffuse soft X rays intensity distribution, taking interstellar absorption into account

02 p0207 A73-12402

Cosmic soft X rays observations by rocket-borne polypropylene window proportional counters, analyzing X ray sources spectra and intensity distributions

02 p0207 A73-12404

Cosmic-ray production of deuterium, He-3, lithium, beryllium, and boron in the galaxy.

02 p0208 A73-12412

Lunar rock C 14 production rate as function of depth, discussing solar and galactic cosmic radiation induced nuclear reactions

02 p0220 A73-12479

All-Union Conference on the Physics of Cosmic Rays, Moscow, USSR, October 26-November 2, 1970, Transactions.

02 p0208 A73-12651

High energy cosmic ray pions and nucleons interactions with atomic nuclei, using ionization calorimeter and spark chambers system

02 p0209 A73-12661

Cosmic ray particle high energy inelastic interactions, discussing pion and nucleon interaction angular and energy characteristics and muon production mechanism

02 p0209 A73-12664

Inelastic pionization cross section of cosmic ray hadrons with carbon nuclei at energies of 100 to 300 GeV

02 p0209 A73-12665

Meteorite apheia calculation from activity levels of accumulated cosmogenic radioisotope due to cosmic ray irradiation

02 p0221 A73-12690

Spectrum of the cosmic X- and gamma ray background in the energy range 1 keV-1 MeV.

02 p0210 A73-12730

The Os-Pt-Hg abundance peak in Ap stars and the problem of very heavy cosmic rays.

02 p0210 A73-12733

The spectrum of diffuse cosmic X-rays in the 20-125 keV range.

02 p0210 A73-12738

On the 4686-A He II line intensity in H II regions and the cosmic ray flux.

03 p0361 A73-13220

Near earth electron spectra applied to cosmic ray transport equation numerical solution extension to 1968-1970, providing models for modulation and gradients reproduction

03 p0361 A73-13362

The Fermi mechanism and the source spectrum of cosmic ray nuclei.

03 p0361 A73-13365

Cosmic ray produced neutron flux equilibrium for lunar surface compositions, calculating isotopic production rates as function of depth

03 p0364 A73-14105

Advances in solar and cosmic X-ray astronomy - A survey of experimental techniques and observational results.

03 p0364 A73-14167

On the altitude dependence of the atmospheric X-rays in the energy range 0.1-1 MeV.

03 p0365 A73-14441

The residual cosmic ray modulation at the 1954 solar minimum.

04 p0492 A73-14968

Cosmic-ray scintillations. I - Inside the magnetosphere.

04 p0492 A73-15526

Modulation of low-energy galactic cosmic rays over solar maximum /cycle 20/.

04 p0493 A73-15549

Disk-shaped diffusion model with inhomogeneous distribution of gas and heavy relativistic nuclei sources for galactic cosmic rays chemical composition

05 p0608 A73-16081

Russian book - Meteorological effects on cosmic rays.

05 p0608 A73-16125

Anomalous recurrent diurnal anisotropy in cosmic ray intensity with maximum along the garden hose direction.

05 p0608 A73-16142

Statistical multifactor analysis of the accuracy of continuously recorded cosmic-ray data

05 p0573 A73-16271

Variations of cosmic ray intensity in consequence of the corotation effect.

05 p0609 A73-16371

Galactic cosmic radiation He 3 and deuteron abundances interpretation from production cross sections and reaction kinematics

05 p0609 A73-16741

High energy /X ray, gamma ray and cosmic ray/ astronomy research impact on astrophysical and cosmological models

05 p0610 A73-16932

Cosmic ray number density modulation by off-ecliptic phenomena to explain interplanetary magnetic field measurements onboard Heos 1 and 2

05 p0611 A73-17186

Analysis of the isotopic composition of low-energy cosmic ray particles in plastic detectors, taking into account the elements boron, carbon, nitrogen, and oxygen

05 p0611 A73-17275

Pulsed galactic nuclei and the origin of cosmic rays.

05 p0611 A73-17308

Cosmic-ray evolution due to interactions with self-excited plasma waves.

05 p0612 A73-17385

Interplanetary cosmic ray low energy electron observation, explaining steep spectrum origin and time variations by model with spectral decomposition

05 p0612 A73-17386

Temporal and spatial changes in cosmic ray intensity increases preceding Forbush decreases

06 p0742 A73-17531

Barometric coefficients of the nucleon components of cosmic rays of various energies

06 p0742 A73-17550

A general study of the effect of collision parameters on the cosmic-ray fluxes in the atmosphere.

06 p0743 A73-17831

High energy astronomy research in space, discussing HEAO A and B, UV astronomy, X ray astronomy, gamma rays, cosmic rays, hot stars, stellar energy sources and elementary particles

06 p0743 A73-18016

Electromagnetic interactions of cosmic ray muons in iron. I - Search for a charge asymmetry.

06 p0743 A73-18386

Electromagnetic interactions of cosmic ray muons in iron. II - Momentum dependence of the interaction probabilities.

06 p0743 A73-18387

The stability of a self-gravitating, nonrotating gas layer with stellar, magnetic, and cosmic-ray components. II.

07 p0873 A73-19058

Cosmic radiation and research carried out on board the 001 prototype Concorde

07 p0784 A73-19211

Energy dependent time lag in the long-term modulation of cosmic rays.

07 p0869 A73-19252

The propagation of the energetic very heavy nuclei in the cosmic radiation.

07 p0870 A73-19340

Multiple production of hadrons at cosmic ray energies - Experimental results and theoretical concepts.

07 p0870 A73-19374

Harmonic analysis of solar wind geometry and geomagnetic activity levels during even and odd cycles based on cosmic ray intensity variations for 1900-1969 period

07 p0870 A73-19451

Similarity solution for equations of nonplanar relativistic flow from point energy source, applying to spherical shock propagation and cosmic ray generation

07 p0810 A73-19506

The heliocentric radial gradient in cosmic ray density and the 'Swinson' sidereal time variation.

07 p0870 A73-19671

Lunar rocks age determination by Ar isotopes technique, noting plagioclase gas retention and cosmic ray exposure characteristics

07 p0888 A73-19782

Lunar surface processes and cosmic ray characterization from Apollo 12-15 lunar sample analyses.

07 p0870 A73-19790

Cosmic-ray produced radioisotopes in Apollo 12 and Apollo 14 samples.

07 p0870 A73-19791

Study on the cosmic ray produced long-lived Mn-53 in Apollo 14 samples.

07 p0870 A73-19795

Cosmic ray exposure ages from Apollo 14 lunar rocks isotopic anomalies due to neutron capture effect in Gd, Br and Ba

07 p0871 A73-19803

Cosmic ray track densities of Apollo 14 breccias, igneous rock and soils from Fra Mauro, indicating surface residence times

07 p0871 A73-19871

Solar flare and galactic cosmic ray studies of Apollo 14 and 15 samples.

07 p0871 A73-19876

Charge assignment to cosmic ray heavy ion tracks in lunar pyroxenes.

07 p0872 A73-19877

Energy spectra of cosmic pions and nucleons at the top of the atmosphere.

07 p0872 A73-20015

Consequences of a universal cosmic-ray theory for gamma-ray astronomy.

07 p0872 A73-20154

Diffuse cosmic gamma rays - Present status of theory and observations.

07 p0872 A73-20186

The generation of the highest cosmic ray energies.

07 p0872 A73-20193

Charge dependence of the energy spectra of cosmic rays.

07 p0873 A73-20561

Evidence for differences in the energy spectra of cosmic ray nuclei.

07 p0873 A73-20562

Mean path length of high energy galactic cosmic rays in the galactic disk.

07 p0873 A73-20563

Clusters of galaxies and the cosmic light.

08 p1002 A73-20876

Cosmic-ray heating and molecular cooling of dense clouds.

08 p0997 A73-20899

Nonprimordial hypothesis for cosmic microwave background radiation generation by ordinary astronomical processes and subsequent thermalization by interaction with dust grains

08 p1008 A73-21152

Cosmic ray source composition calculated from diffusion-produced path length spreads

08 p0998 A73-21232

Galactic cosmic ray particle intensity decrease relationship to low energy proton flux increase based on interplanetary Zond 3 and Venera probes measurements

08 p0999 A73-21326

Ionization loss effects on cosmic ray lifetime in galactic interstellar medium, noting dependence on particle energy

08 p0999 A73-21335

Interstellar gas role in cosmic ray yearly variations determined from solar short wave radiation induced gas ionization

08 p0999 A73-21338

Solar modulation of cosmic ray intensity in stratosphere, examining relationship to sunspots group number and heliographic latitudes over 11 year period

08 p0999 A73-21339

Solar and magnetic fields characteristics relative to 11 year cosmic ray modulation in interplanetary space

08 p0999 A73-21340

Nonstationary and asymmetric cosmic ray modulation theory, discussing moving boundary problem and solar wind model with spherical singularity

08 p0999 A73-21341

Galactic cosmic ray modulation region evaluation from meteoroid orbit, velocity and radioactive dating data

08 p1000 A73-21342

Three dimensional cosmic ray anisotropy and density distribution at earth orbit and in interplanetary space with allowance for primary particle and nucleon energy spectrum

08 p1000 A73-21343

Solar active regions effects on galactic cosmic ray distribution and interplanetary magnetic field structure

08 p1000 A73-21344

Diurnal, sporadic and yearly variations in cosmic ray flux based on neutron component data, noting relation to solar activity cycles

08 p1000 A73-21345

Diffusion and stochastic variations of galactic cosmic rays in solar wind

08 p1000 A73-21346

Stratospheric cosmic ray short period variations at 30 km by spectral density method

08 p1000 A73-21351

Summary of daily observational results of solar phenomena, cosmic ray, geomagnetic variation, ionosphere, radio wave propagation and airtlow during October 1969 through December 1971.

08 p0961 A73-21393

Nuclear particle fluxes and radioactive isotopes production rate distribution from cosmic rays data along orbits, calculating iron meteorite dimensions prior to atmosphere entry

08 p1012 A73-21582

Solar neutrino flux prediction discrepancies with observation, considering cosmic ray background and flaws in calculation of capture rate

09 p1136 A73-21995

Statistical analysis of continuous neutron component intensity measurements in cosmic rays

09 p1137 A73-22020

Cosmic rays in a random magnetic field - Breakdown of the quasilinear derivation of the kinetic equation.

09 p1137 A73-22036

Forbush predecrease observation by superneutron monitors, interpreting cosmic ray depletion and rigidity dependence by model of interplanetary magnetic field propagating disturbance from sun

09 p1073 A73-22051

Cosmic gamma ray studies for metagalactic and remote galactic model construction as substitute for radio and X ray emission data

09 p1138 A73-22725

Properties of H I regions heated by X rays and cosmic rays.

09 p1147 A73-22730

Energy balance in the current sheet of a solar flare, and the acceleration of cosmic rays by plasma waves.

09 p1138 A73-22731

Cosmic gamma ray observations for choice between galactic and metagalactic models of cosmic ray origin, discussing proton nuclear component

09 p1138 A73-22952

IR galaxy model consisting of low energy cosmic or X rays at center of dust shell, discussing physical dimensions of radiating region

09 p1151 A73-23146

Isotopic and crystalline structure changes in lunar rock and meteorite constituents for cosmic ray nuclei intensity and energy spectrum

09 p1138 A73-23169

Chemical composition of the interstellar gas - X-ray determinations.

10 p1263 A73-23480

Some limits on cosmic-ray heating of H I clouds by magnetic stars.

10 p1263 A73-23487

Diffuse cosmic gamma rays observed at an equatorial balloon altitude.

10 p1263 A73-23491

Study of strong interactions between cosmic-ray hadrons and nuclei at 200 to 2000 GeV energies

10 p1264 A73-23816

All-Union Conference on the Physics of Cosmic Rays, Tiflis, Georgian SSR, October 18-21, 1971, Proceedings

10 p1265 A73-23901

Theory of cosmic ray transport with anisotropic particle scattering and convection

10 p1265 A73-23903

Investigation of cosmic-ray propagation in the interplanetary magnetic field on the basis of the kinetic equation

10 p1265 A73-23904

Solar wind effect on azimuthal and radial galactic cosmic ray currents, noting Forbush decreases relation to current structures

10 p1265 A73-23907

Particle motion diffusion model for cosmic ray propagation in Galaxy, investigating electron component energy spectra and background radio emission

10 p1265 A73-23908

Spatial variations of cosmic rays on the basis of data for the radioactivity of meteorites with known orbits

10 p1266 A73-23910

Cosmic ray, solar activity, supernova outbursts and geomagnetic field effects on atmospheric C-14 concentration

10 p1266 A73-23911

Problems of linear and nonlinear theory of cosmic ray modulation

10 p1266 A73-23913

A method for determining the polarization and energy spectrum of cosmic-ray gamma quanta

10 p1266 A73-23914

Relationship between the 27-day cosmic-ray variations and various solar-activity indices during the period from 1957 to 1970

10 p1266 A73-23918

Cosmic-ray anisotropy during the disturbed period from Oct. 25 to Nov. 10, 1968

10 p1267 A73-23919

Comparative characteristics of the soft component of solar and galactic cosmic rays on the basis of rocket and stratospheric measurements at Heis Island and Apatite Station

10 p1267 A73-23920

Frequency spectrum of cosmic ray intensity and solar activity variations

10 p1267 A73-23924

Energy spectrum of galactic cosmic rays beyond the region of modulation and the anisotropy of cosmic rays in the Galaxy

10 p1267 A73-23925

The Elbrus cosmic ray spectrograph

10 p1203 A73-23926

Polar coupling coefficients and generalization of the spectrographic method for studying cosmic-ray variations of magnetospheric and interplanetary origin

10 p1267 A73-23927

Analysis of the variations of cosmic rays of magnetospheric and interplanetary origins according to spectrographic data

10 p1267 A73-23928

Data processing technique and calculation procedure for cosmic rays hard particle and neutron components coupling coefficients

10 p1268 A73-23932

Altitude and latitude dependences of the partial coefficients and integral multiplicity of the cosmic-ray neutron component

10 p1268 A73-23933

Analysis of the quality of the cosmic ray data recorded by the neutron supermonitor at Krasnaia Pakhra

10 p1217 A73-23934

A mathematical model of the optimization of cosmic ray intensity observation data

10 p1268 A73-23935

North-south asymmetry in the increase of cosmic-ray intensity before magnetic storms.

10 p1268 A73-24212

Some aspects of measuring the differential cosmic-ray spectrum.

10 p1268 A73-24213

Tracks from extinct radioactivity, ancient cosmic rays, and calibration ions.

10 p1269 A73-24271

Solar quiet long-term modulation of cosmic ray intensity diurnal variation explained via interplanetary sector pattern changes

10 p1269 A73-24448

New data on the cosmic history of the Sikhote-Alin meteorite

10 p1281 A73-24462

Solar modulation of the galactic cosmic rays. III - Implications of the Compton-Getting coefficient.

10 p1269 A73-24726

Production of metagalactic X-rays by relativistic dust grains.

10 p1270 A73-24907

High energy astrophysics research at the Max-Planck-Institut.

11 p1411 A73-25139

A phenomenological study of cosmic ray propagation. I - The nuclei component.

11 p1412 A73-25263

Depth variation of cosmogenic noble gases in the approximately 120-kg Keyes chondrite.

11 p1418 A73-25587

Development of spark chambers for use in measurements of the charge spectrum of high energy cosmic rays.

11 p1363 A73-25961

High spatial resolution wire spark chamber system using electromagnetic delay line readout.

11 p1363 A73-25962

High spatial resolution MWPC systems using electromagnetic delay line readouts.

11 p1364 A73-25966

Geomagnetic latitude variation of cosmic radiation rates measured onboard Concorde SST prototypes, investigating solar flares

11 p1324 A73-26588

A measurement of cosmic-ray rigidity spectra above 5 GV/c of elements from hydrogen to iron.

11 p1414 A73-26612

Investigation of resonance integrals occurring in cosmic-ray diffusion theory.

11 p1414 A73-26615

Preliminary Pioneer-10 intensity gradients of galactic cosmic rays.

11 p1414 A73-26622

Sea level search for leptonic quarks in cosmic rays.

11 p1414 A73-26660

Cosmic ray electrons from 0.2 to 8 MeV - Pioneer 8 and 9 measurements of their spectrum, time variations, and interplanetary radial gradient.

12 p1533 A73-26976

Cosmic ray storm effect on midlatitude and polar neutron monitors, noting comparison with underground mu-meson telescopic observations at high rigidities

12 p1534 A73-27001

Metagalactic cosmic ray origin models and cosmic ray energy density around Galaxy, considering gamma ray flux, measurement from Magellanic Clouds

12 p1539 A73-27142

Criticism of Galactic cosmic ray production model with rotating magnetic white dwarfs, noting contrary evidence in magnetic field observations and decay theories

12 p1539 A73-27149

Means of measuring the linear polarization of cosmic gamma quanta by means of the Compton effect

12 p1496 A73-27204

Theory of cosmic ray transfer by anisotropically scattered particles

12 p1534 A73-27331

Modulation of galactic cosmic rays by a solar wind asymmetric with respect to the heliolatitude

12 p1534 A73-27332

Convection and diffusion transport equation of galactic cosmic ray electrons with energy loss and absorption allowance for supernova compressed halo models

12 p1535 A73-27635

Solar-terrestrial relations in the retrospective world interval from July 26 to August 14, 1972

12 p1535 A73-27766

Galactic and extragalactic radio emission and satellite observations of RF cosmic radiation and noise intensity

12 p1544 A73-27783

Path length distribution of cosmic rays from pulsar nebula complexes.

12 p1536 A73-27880

Radioactive spallation induced scintillator errors in satellite measurements of diffuse cosmic X ray spectrum, considering astrophysical implications

12 p1537 A73-27882

Statistical analysis of Forbush decreases and of cosmic-ray intensity increases preceding them.

13 p1670 A73-28701

East-west asymmetry of cosmic rays at sea level at geomagnetic latitudes from 50 N to 20 S.

13 p1670 A73-28702

Variation of the cosmic-ray gradient during the solar activity cycle.

13 p1670 A73-28721

Interplanetary radial gradients of galactic cosmic ray protons and helium nuclei - Pioneer 8 and 9 measurements from 0.75 to 1.10 AU.

14 p1786 A73-29951

Cosmic ray properties and origin, discussing pulsars and superstrong magnetic fields existence effects

14 p1787 A73-30233

Measurement of cosmic-ray muon charge ratio at sea level between energies of 10 and 1500 GeV.

14 p1787 A73-30455

Solar wind properties near and beyond Jupiter orbit, considering steady state wind extrapolation to large distances, cosmic ray modulation and interactions with planetary bodies

14 p1787 A73-30541

Low energy galactic cosmic ray exploration via space mission to Jupiter and Saturn, considering nuclear abundances and galactic evolution theories

14 p1787 A73-30542

Extragalactic X ray source data increase from Uhuru catalog publication, discussing relevance to X ray background

14 p1787 A73-30598

Outer solar system, including planetary atmospheres, natural satellites, solar wind, interstellar cosmic rays and spacecraft missions

14 p1800 A73-30616

The cosmic gamma-ray spectrum between 0.3 and 27 MeV measured on Apollo 15.

14 p1788 A73-30731

Interplanetary scintillations of cosmic rays.

14 p1788 A73-30752

Primordial cosmic ray abundance from rotating magnetic A stars with accelerating ionized interstellar gas particles

15 p1925 A73-31059

Gamma and cosmic ray astronomy review, covering balloon and rocket measurements, galactic and metagalactic source locations and radio source information

15 p1926 A73-31148

Composition of galactic cosmic rays with energy ranging between 10 and 30 MeV/nucleon.

15 p1926 A73-31355

Contribution of atmospheric multiple neutron production to the multiplicity distribution observed in cosmic ray neutron monitor.

15 p1926 A73-31385

The fluorine abundance in the galactic cosmic radiation.

15 p1926 A73-31552

Production of astrophysical X-rays by transition radiation.

15 p1926 A73-31553

Yearly and trimonthly variations in solar activity and cosmic-ray intensity

15 p1926 A73-31879

Large area focusing collector for the observation of cosmic X rays.

15 p1876 A73-31976

Ultrahigh energy photons, electrons, and neutrinos, the microwave background, and the universal cosmic-ray hypothesis.

15 p1927 A73-32004

On a possible mechanism responsible for the differential energy spectrum of relativistic electrons and non-linear low-frequency spectra of cosmic radio sources.

15 p1927 A73-32005

Energy losses of galactic cosmic rays in the interplanetary medium.

15 p1927 A73-32010

Cosmic abundance of boron.

15 p1942 A73-32648

Observations of cosmic X-ray sources by the MIT instrument on the OSO-7.

16 p2049 A73-32729

Time and space variations of cosmic-ray intensity increases prior to Forbush decreases.

16 p2052 A73-32755

Barometric coefficients of the nucleon component of cosmic rays of different energies.

16 p2052 A73-32774

Study on the charge and isotope composition of medium cosmic ray particles.

16 p2054 A73-33278

Charge and energy spectra of cosmic rays with Z equal to or greater than 30.

16 p2054 A73-33279

Study of high energy electrons at upper layers of atmosphere during magnetic perturbations.

16 p2054 A73-33282

Cosmic ray trapping region and characteristic exit time from Galaxy, discussing electronic component and chemical composition

16 p2054 A73-33286

The dynamical effects of cosmic rays in the Galaxy and the generation of the galactic magnetic field.

16 p2054 A73-33287

Gamma ray astronomical state-of-art, discussing cosmic gamma ray sources observation and diffuse radiation measurement

16 p2055 A73-33290

Muon observations, discussing high energy cosmic ray neutrino experiments and production via pion and kaon decay, neutrino interactions and nuclear collisions

16 p2055 A73-33291

Transient solar modulation of cosmic rays.

16 p2055 A73-33294

Galactic sources and the propagation of cosmic rays - A review of the light isotopes and the odd-Z elements.

16 p2055 A73-33295

Steady-state solar modulation of cosmic rays.

16 p2055 A73-33296

Geomagnetic effects on cosmic ray cut-off daily, seasonal and secular variations, considering north-south symmetry and magnetospheric models

16 p2055 A73-33297

Calculations of neutron flux spectra induced in the earth's atmosphere by galactic cosmic rays.

16 p2055 A73-33426

Time dependent worldwide distribution of atmospheric neutrons and of their products. I, II, III.

16 p2055 A73-33427

Calculated cosmic ray neutron monitor response to solar modulation of galactic cosmic rays.

16 p2056 A73-33444

Measurement of cosmic rays and searches for radiation belts near Venus

16 p2057 A73-33829

Interpretation of the charge ratio of cosmic ray muons.

17 p2223 A73-34242

Cosmic ray pulses conduction to interstellar gas by magnetic field, describing effects on sound vibration

17 p2223 A73-34369

Cosmic radiation intensity constancy from observations of cosmic ray induced transmutations in meteorites

17 p2223 A73-34419

Radial variation of magnetic fluctuations and the cosmic-ray diffusion tensor in the solar wind.

17 p2224 A73-34762

Search for small-scale anisotropy in the 2.7 K cosmic background radiation at a wavelength of 3.56 centimeters.

17 p2231 A73-34768

A new test for solar modulation theory - The 1972 May-July low-energy galactic cosmic-ray proton and helium spectra.

17 p2224 A73-34769

Observations of gamma-ray bursts of cosmic origin.

17 p2224 A73-34770

Cosmic ray bombardment of meteorites allowing solar system age estimation from spallation product concentration and subatomic particle track distribution

17 p2232 A73-34975

Radioactivities and He, Ne and Ar stable isotopes measured in meteorites for cosmic ray exposure ages

17 p2233 A73-35267

On the role of plasma effects in the cosmic ray propagation and isotropization in the galaxy.

17 p2225 A73-35779

Composition of low energy cosmic radiation from silicon to nickel.

17 p2225 A73-35787

Aluminum-26 in meteorites. VII - Ureilites, their unique radiation history.

17 p2237 A73-35803

Properties of cosmic X-ray sources.

18 p2343 A73-35924

Experimental methods of correlation between the trajectories of cosmic heavy ions and biological objects: Dosimetric results - Experiment Biostack on Apollo XVI and XVII.

18 p2270 A73-35946

The charge spectrum of heavy cosmic ray nuclei measured on board of Apollo 16/Biostack/ using plastic detectors.

18 p2344 A73-35987

Characteristics of the influence of the solar wind on cosmic-ray intensity during 1969

18 p2345 A73-36108

Simultaneous measurements of ion concentration and corpuscular stream intensity at altitudes ranging from 10 to 79 km

18 p2345 A73-36121

Preliminary results of the action of cosmic heavy ions on development of eggs of *Artemia salina*.

18 p2271 A73-36129

Periodic variations of the cosmic radiation. III - The 27-day variation.

18 p2345 A73-36180

Cosmic ray total ionization - 1970-1972.

18 p2347 A73-36293

Cosmic rays airborne dosimetry from Concorde aircraft, noting passenger and crew radiobiological hazards at supersonic flight altitudes

18 p2348 A73-36908

Evidence for the softening of the cosmic-ray electron spectrum at a few hundred GeV and the origin of the galactic-ridge X-radiation.

18 p2348 A73-37102

A search for laser-amplified cosmic ray tracks.

19 p2437 A73-37254

On the abundance of secondary nuclei in cosmic rays.

19 p2475 A73-37572

Interplanetary shock waves and cosmic rays.

19 p2476 A73-37759

Russian book on cosmogenic nuclear reactions in meteorites and asteroid and lunar surface layers covering vertical /depth/ distributions of isotopes and nuclear-active particles

19 p2486 A73-37775

Periodic analysis of arrival times in delayed cosmic-ray coincidences.

19 p2476 A73-38086

New data on the cosmic history of the Sikhote-Alin meteorite.

19 p2486 A73-38128

Kinetic equation for one particle cosmic ray distribution function in static random magnetic field on basis of diffusion theory

19 p2476 A73-38291

Search for magnetic monopoles in lunar material using an electromagnetic detector.

19 p2461 A73-38492

Cosmic sources of X rays and gamma rays

20 p2601 A73-39061

Nuclide production rates in stone meteorites and lunar samples by galactic cosmic radiation.

20 p2612 A73-39716

A survey on the recent measurements of the absolute vertical cosmic-ray muon flux at sea level.

20 p2603 A73-39825

Russian book - Certain problems concerning solar-terrestrial links and physics of the atmosphere.

21 p2730 A73-40102

The 27-day variations of the hard cosmic ray component and the atmospheric ozone X-layer according to IGY data

21 p2755 A73-40109

The relation between cosmic ray intensity variations and effects due to the electromagnetic complex

21 p2755 A73-40110

The question of the method of studying cosmic ray anisotropy

21 p2755 A73-40111

Frequency distribution of the parameters of the diurnal variation of the cosmic ray intensity

21 p2755 A73-40112

Investigation of solar activity and its association with cosmic ray variations

21 p2755 A73-40113

Seasonal variations of the barometric effect of the cosmic ray neutron component intensity

21 p2755 A73-40114

All-Union Conference on the Physics of Cosmic Rays, Apatity, USSR, December 12-15, 1972, Proceedings

21 p2755 A73-40576

Role of plasma effects in the propagation and isotropization of cosmic rays in the Galaxy

21 p2756 A73-40579

Nova and supernova stars as sources of relativistic particles

21 p2756 A73-40580

Effects of nuclear reactions with fast protons in a supernova shell and the origin of cosmic rays

21 p2756 A73-40581

Geomagnetic field, cosmic rays, and radiocarbon content in the earth's atmosphere

21 p2756 A73-40585

Cosmic ray intensity over the past 100,000 to 1,000,000 years and the Kr-81 isotope content in the atmosphere

21 p2756 A73-40586

Cosmic ray intensity variation observation during August 2-8, 1972, suggesting complex interactions

with interplanetary shock waves and magnetic field and magnetosphere

21 p2757 A73-40590

Ground level cosmic ray variations in August 1972, relating intensities and Forbush decreases with solar flares and shock wave parameters

21 p2757 A73-40591

A kinetic description of the interaction between cosmic rays and shock waves

21 p2758 A73-40596

The 11-year cycle of cosmic ray intensity in the stratosphere and its dependence on solar activity

21 p2758 A73-40597

Differences in the correlations of 27-day and 11-year cosmic ray variations with solar activity parameters

21 p2758 A73-40598

Investigation of isotropic and anisotropic effects of cosmic rays during October through November 1968

21 p2758 A73-40600

Diurnal, semidiurnal, and the eight-hour components of cosmic-ray anisotropy

21 p2758 A73-40601

Estimate of the spectrum of cosmic-ray variations in the high-energy range on the basis of subterranean observations

21 p2758 A73-40602

Analytical approach to the direct and inverse problems of cosmic ray action on the lower ionosphere

21 p2759 A73-40609

Research of short-period variations in cosmic rays at Moscow's latitude

21 p2759 A73-40610

A meson supertelescope using plastic scintillators and the coupling coefficients for it

21 p2701 A73-40611

Book on cosmic ray effective cut-off rigidities calculations in dipole and geomagnetic fields, using trajectory calculations of penumbra function

21 p2760 A73-40805

Al-26 and Na-22 measurements on Luna 16 samples by non-destructive gamma-gamma coincidence spectrometry.

21 p2774 A73-41405

Evidence for confinement of low-energy cosmic rays ahead of interplanetary shock waves.

21 p2763 A73-41504

Angular effects in the propagation of cosmic rays in the atmosphere.

21 p2764 A73-41629

Origin of cosmic rays, atomic nuclei, and pulsars in explosions of massive stars.

22 p2905 A73-41765

Low-energy cosmic ray protons from nuclear interactions of cosmic rays with the interstellar medium.

22 p2902 A73-41927

Frequency of heavy ions in space and their biologically important characteristics.

22 p2805 A73-42178

Solid state AgCl detectors for nuclear tracks with on- and off-response at choice - Applications to life sciences.

22 p2814 A73-42179

Measurements of absolute intensities of cosmic-ray muons in the vertical and greatly inclined directions at geomagnetic latitudes 16 N.

22 p2903 A73-42437

Measurement of the absolute vertical integral and differential cosmic-ray single-muon flux at 3.6 GeV and a measurement of the showerless penetrating particle-pair flux above 3.6 GeV.

22 p2903 A73-42440

The parallel diffusion of cosmic rays in a random magnetic field.

22 p2904 A73-43011

The abundances of galactic cosmic-ray carbon, nitrogen, and oxygen and their astrophysical implications.

22 p2914 A73-43012

On Kraichnan's direct interaction approximation applied to charged-particle transport in turbulent magnetic fields.

22 p2904 A73-43013

Contribution to the theory of cosmic-ray propagation with anisotropic particle scattering.

23 p3020 A73-43229

Modulation of galactic cosmic-rays by solar wind which is unsymmetric in solar latitude.

23 p3020 A73-43230

Study of low-energy heavy-nucleus track regression in plastic detectors /cellulose triacetate and polyethylene terephthalate/ and in low-sensitivity nuclear photoemulsion

23 p2981 A73-43567

Large wire spark chambers with an information output and storage system

23 p2982 A73-43570

Observation of cosmic-ray particles with Z greater than 35.

23 p3024 A73-43609

Galactic and extragalactic gamma ray bursts contribution to diffuse cosmic X ray flux, noting superposition of supernovae outbursts

23 p3025 A73-43957

Cosmic gamma ray studies for metagalactic and remote galactic model construction as substitute for radio and X ray emission data 23 p3025 A73-44325

A device for recording the energy spectrum and fluxes of electrons with energies greater than 100 MeV in cosmic rays 24 p3124 A73-44782

Scientific equipment for studying cosmic rays on Prognoz satellites. I 24 p3144 A73-44783

Physical characteristics of the set of scientific devices used to record the cosmic-ray ionizing component on 'Prognoz' satellites 24 p3089 A73-44784

Role of hydromagnetic waves in cosmic-ray confinement in the disk. I - Theory of behavior in general wave spectra. 24 p3124 A73-45040

Energy spectra of cosmic gamma-ray bursts. 24 p3125 A73-45053

Production of gamma radiation in dense interstellar clouds by cosmic-ray interactions. 24 p3125 A73-45054

Interstellar trace element ionization predictions by cosmic ray, X-ray and UV star models with hydrogen allowance, showing disagreement with satellite observation 24 p3125 A73-45056

Variations of three-dimensional anisotropy of cosmic rays during Forbush decreases. 24 p3125 A73-45102

Correlation length for interplanetary magnetic field fluctuations. 24 p3139 A73-45125

Absence of cosmic gamma-ray bursts in association with normal stellar flares. 24 p3127 A73-45492

COSMOGONY

U COSMOLOGY

COSMOLOGY

NT BIG BANG COSMOLOGY

NT HUBBLE DIAGRAM

Intergalactic matter existence experiments, discussing critical cosmological energy and matter density, neutral and ionized gas, clustering and hot media 01 p0094 A73-10060

Book - Cosmic rays: Selected readings in physics. 01 p0091 A73-10122

A non-uniform relativistic cosmological model. 01 p0098 A73-10581

The interaction of primordial gravitational waves with groups of galaxies. 01 p0098 A73-10585

Dynamics of gravitating systems against the neutrino background of the universe 01 p0100 A73-10712

Newtonian analysis of cosmological model for galactic accretion from small initial perturbation of central black hole 01 p0104 A73-11048

Hadron number density model to predict fossil quark abundance in big bang cosmology 01 p0104 A73-11098

Cosmological evolution from initial inhomogeneous and anisotropic universe to present structure, using general relativity for free gravitational field and waves 01 p0106 A73-11242

Pregalactic vortex motion decay calculation from kinetic equation of hot expanding universe model 01 p0106 A73-11307

The n-body problem with variable gravitational constant, and some dynamical consequences for large-scale cosmic systems. 01 p0107 A73-11327

Rotational perturbations in anisotropic cosmology. 01 p0107 A73-11328

Hydrodynamic motions and the vacuum stage in an anisotropic cosmological model 01 p0108 A73-11432

The evolution of galaxies - A heretical view. 02 p0211 A73-11592

Gravitational radiation effects on cosmological time scale and models from matter fractional conversion and mass loss rate profile analysis 02 p0205 A73-11873

Neutrino contribution to relativistic interacting matter-radiation cosmological models, presenting cosmological interpretation of quasars 02 p0218 A73-12410

Closed time as an explanation of the black body background radiation. 02 p0193 A73-12440

CP-noninvariance model of baryon asymmetry of universe, postulating kappa particle /neutral massive fermion/ 02 p0221 A73-12669

A galactic formation model based on post-big bang fragmentation. 02 p0224 A73-12740

Exact cosmological solutions in Brans and Dicke's scalar-tensor theory. II. 02 p0224 A73-12743

Condensation and protostar expansion hypotheses of stellar and galactic evolution in view of discoveries of quasars, central bodies and stellar associations 03 p0365 A73-12902

A finite expanding universe with matter injection. 03 p0342 A73-13291

Cosmological vacuum solutions in Brans and Dicke's scalar-tensor theory. 03 p0373 A73-13356

The redshifts of quasi-stellar objects and associated galaxies. 03 p0375 A73-13896

Hubble law correspondence in invariant mechanical theory of universe expansion to direct consequence of impulse conservation in inertially moving many body system 03 p0380 A73-14603

Radio source counts and redshifts in steady state cosmology. 04 p0497 A73-15048

Galaxy formation from amihilation-generated supersonic turbulence in the baryon-symmetric big-bang cosmology and the gamma-ray background spectrum. 04 p0499 A73-15353

Primordial turbulence and the formation of galaxies. 04 p0499 A73-15354

A hypothesis, unifying the structure and the entropy of the universe. 04 p0500 A73-15492

The universe as a black hole. 04 p0501 A73-15624

Orbital eccentricity of Mercury and the origin of the moon. 04 p0501 A73-15625

Gravitational origin of high energy interactions and general relativity equivalence principle for unitary symmetry, noting quantum geometrodynamics cosmological model 04 p0501 A73-15632

Cosmological deceleration parameter differences prediction from light evolution correction on diameter-red shift relation of cluster elliptical galaxies 04 p0502 A73-15689

Russian monograph on relativistic celestial mechanics covering celestial and solar system bodies motion, Riemann geometry, tensor analysis, N body problem and cosmology 04 p0502 A73-15969

X ray background radiation measurement in outer space for proof of Gamow hypothesis on universe chemical composition, indicating improved cosmological models 05 p0613 A73-16210

Book - The emerging universe: Essays on contemporary astronomy. 05 p0613 A73-16301

Planetary system formation likelihood disparaged, discussing planetary orbit stability, dark companions and life existence improbability 05 p0614 A73-16303

Cosmological models based on 18th and early 19th century physics for sky darkness resulting from universe expansion, speculating upon Olbers paradox resolution 05 p0614 A73-16308

Quantum cosmology for universe beginning and first microseconds, treating quantum gravitation, time and cycles, superspace and quantum foam 05 p0614 A73-16310

High energy /X ray, gamma ray and cosmic ray/ astronomy research impact on astrophysical and cosmological models [AIAA PAPER 73-197] 05 p0610 A73-16932

Expansion hypothesis and assumption of invisible intergalactic matter in galactic clusters stability theory, noting IR spectroscopy and radio observation 05 p0623 A73-17196

A comparative study of Brans-Dicke and general relativistic cosmologies in terms of observationally measurable quantities. 05 p0624 A73-17303

Nonzero radiation pressure inclusion into Einstein cosmological equations, discussing Friedmann models evolution from radiation state epoch to matter domination 05 p0624 A73-17304

The possibility that nongaseous hydrogen supplies the missing cosmological mass. 05 p0625 A73-17328

Cosmological aspects of order, relevance, and information theory. 06 p0749 A73-18002

Exploring the origin of the solar system by space missions to asteroids. 06 p0750 A73-18025

Influence of scalar and vector fields on the nature of a cosmological singularity 06 p0751 A73-18101

Book - The Titius-Bode Law of planetary distances: Its history and theory. 06 p0753 A73-18403

Organogenic elements in stars, interstellar matter, comets, meteorites and planets, discussing molecular

distribution and formation, prebiological chemical evolution, and terrestrial and extraterrestrial biology 06 p0754 A73-18430

High-frequency sound waves to eliminate a horizon in the mixmaster universe. 06 p0724 A73-18550

Space-time transformation for equation of relative motion of two bodies on gravitating matter background of Einstein-de Sitter universe 06 p0724 A73-18689

On the collisional absorption of radio waves in cosmology. 07 p0877 A73-19602

Origin of magnetic fields in the early universe. 07 p0877 A73-19607

Black hole creation via partial gravitational collapse of matter ejected by explosion within asymptotically Friedmannian space-time 07 p0900 A73-20182

Light elements D 2, He 3-4, Li 6-7, Be 9 and B 10-11 origin and history in universe, considering nucleosynthesis sites 08 p0997 A73-20885

A redshift magnitude relation for radiation universes. 08 p1007 A73-21002

Elemental synthesis during high temperature phase of expansion of big bang universes, obtaining universal baryon density relationship to primordial deuterium abundance 08 p1008 A73-21151

Nonprimordial hypothesis for cosmic microwave background radiation generation by ordinary astronomical processes and subsequent thermalization by interaction with dust grains 08 p1008 A73-21152

Papers on cosmology and nuclear fusion covering big bang and expanding universe models, conformal invariance, microwave astronomy, neutrino physics, gravitational constant, cosmic rays, etc 08 p1009 A73-21226

Gamow contributions to cosmology and primeval nucleosynthesis theories, discussing big bang model, residual cosmic black body radiation, stellar energy sources and cosmonumerology 08 p1009 A73-21227

Conformally invariant cosmological and physical models in terms of Einstein, Maxwell and Dirac equations 08 p1009 A73-21228

Microwave background radiation in terms of isotropy, universe mass density, sky brightness temperature spectra investigations and H distribution in intergalactic space 08 p1010 A73-21229

Friedman expanding universe model based on Gamow theory of weakly interacting black body radiation-filled space at 3 K temperature 08 p1010 A73-21230

Nucleocosmochronology and stellar nucleosynthesis models for Galaxy origin and solar system formation 08 p1010 A73-21231

Construction of the spinor field equations in cosmological space 08 p1010 A73-21271

Energy release mechanism during early universe expansion leading to distortion of relic black body spectrum, noting Comptonization effects 08 p1013 A73-21693

Monograph on Hamiltonian cosmology, considering cosmological models with Hamiltonian equations of motion, Bianchi universes, superspace concepts and quantum mechanical Hamiltonian construction 08 p0984 A73-21834

Neutrino hindrance of density irregularities growth in expanding radiation dominated cosmological model from numerical integration of perturbation equations 09 p1141 A73-22026

Nonzero neutrino rest mass to account for virial mass discrepancy in Coma cluster and missing cosmological mass needed to close universe 09 p1141 A73-22027

The thermal future of the universe. 09 p1143 A73-22109

Tidal, primordial turbulence and spinning core theories for galactic rotation origin, considering rotational waves, gravitational waves and wave excitations 09 p1143 A73-22123

Isotropic cosmological models of X ray background radiation, presenting observational constraints on source distribution and radiation mechanisms 09 p1138 A73-22869

Cosmic gamma ray observations for choice between galactic and metagalactic models of cosmic ray origin, discussing proton nuclear component 09 p1138 A73-22952

A new cosmological model - Formation of organic molecules, planets, and comets. 09 p1151 A73-23147

Universe isotropic state evolution from initial chaotic conditions, considering attractive and repulsive cosmological constants 10 p1271 A73-23526

New limit on small-scale irregularities of "blackbody" radiation.

10 p1272 A73-23543

Thermal instability caused primary interstellar dust cloud fragmentation and resulting star formation according to Peebles-Dicke hypothesis for cosmological origin of globular clusters

10 p1274 A73-23713

Multiple subuniverses concept for wide mean space density variations in closed universe, considering radio and optical observation possibility

10 p1275 A73-23822

Cosmological evolution from initial inhomogeneous and anisotropic universe to present structure, using general relativity for free gravitational field and waves

10 p1279 A73-24178

Reply to criticism of local fluctuation interpretation of radio source counts deviation from Euclidean distribution

10 p1280 A73-24273

Evolution of universe filled with cold baryons at cosmological singularity from Friedmann solution and equation of state for cold baryons

10 p1284 A73-24753

Friedmann expanding cosmological model with superimposed spherically symmetric inhomogeneity for gravitational lens and point light sources dispersion and motion effects on images

11 p1418 A73-25747

Critique of missing planet theory of asteroidal origin, considering mass required, Bode law and disruption forces

11 p1419 A73-25861

Hydrodynamic motions and the vacuum stage in an anisotropic cosmological model.

11 p1423 A73-26052

Gravitational instability of regular model-universes in a modified theory of general relativity.

11 p1423 A73-26106

The interaction of weak gravitational waves with a gas.

11 p1400 A73-26177

Construction of a general cosmological solution of the Einstein equation with a time singularity.

11 p1425 A73-26178

Observational constraints imposed by Brans-Dicke cosmologies.

11 p1426 A73-26413

Primordial random motions and angular momenta of galaxies and galaxy clusters.

11 p1427 A73-26601

Galaxies as local perturbations in homogeneous universe, considering galactic manufacture within Einstein theory context

12 p1539 A73-27141

Universe evolution explanation via interstellar deuterium investigation, discussing galactic gas chemical composition history

12 p1543 A73-27692

Dependence of the integrated background light on cosmology, galactic spectra, and galactic evolution.

13 p1671 A73-28035

Vortex motions of cosmic matter as cosmological evolution mechanism, considering galactic and solar system kinetics

13 p1681 A73-28780

Pb 205 as chronometer for s-process nucleosynthesis mechanism, discussing cosmochemistry implications and abundance at solidification

13 p1657 A73-28923

Universe rest energy density, isotropic background radiation energy and galactic kinetic energy

13 p1686 A73-29654

On the origin of comets and their importance for the cosmogony of the solar system.

14 p1794 A73-29836

Turbulence dissipation model for galactic origin, accounting for masses and angular momenta of large galaxies

14 p1796 A73-30002

Cosmological theories historical review, discussing observational background for big bang, steady state and astrophysical theories based on theoretical physics

14 p1797 A73-30059

Societa Astronomica Italiana, Meeting, 15th and Workshop on Rotation as a Phenomenon and Evolutionary Factor in the Universe, Università degli Studi, Bologna, Italy, October 8, 9, 1971, Proceedings

14 p1797 A73-30138

The sun rotation and the Brans-Dicke cosmology.

14 p1798 A73-30140

Einstein equations reduction to friction systems in homogeneous cosmological models, investigating Bianchi models solutions isotropization

14 p1798 A73-30327

The implications for geophysics of modern cosmologies in which G is variable.

14 p1799 A73-30525

Outer planet formation from gaseous solar nebula with absence of magnetic effects, discussing gravitational instabilities, gas capture onto planetary core and model construction

14 p1799 A73-30528

Elemental and isotopic abundances of the volatile elements in the outer planets.

14 p1799 A73-30529

Singularity and matter creation in cosmological models.

14 p1800 A73-30599

Cosmological arrow of time theory describing approach to equilibrium in closed systems, noting relation to cosmic expansion

15 p1933 A73-31310

Cosmological information from surveys of radio source spectra.

15 p1933 A73-31396

Russian book - Geochemistry and cosmochemistry of inert gas isotopes.

15 p1840 A73-31585

Solar system evolution and planets configuration regularity and geometrical shape considerations in terms of tidal dissipation, stray body collision and close approach

15 p1937 A73-31776

Bulk viscosity effects in imperfect fluid Friedmann cosmology, considering implications for singularity problem

15 p1939 A73-32011

Chemical fractionations in meteorites. VII - Cosmochemistry and cosmochemistry.

15 p1841 A73-32390

X ray background and emission mechanism nature, considering evolutionary effects and unresolved sources

16 p2051 A73-32747

A new theory of gravity.

16 p2036 A73-33123

Isotropic solution of Einstein gravitational equations for anisotropic homogeneous cosmological models with hydrodynamic energy-momentum tensor

16 p2071 A73-34051

Characteristics of the Bianchi-IX cosmological model from the viewpoint of the qualitative theory of differential equations

16 p2071 A73-34052

Trends in physics; General Conference, 2nd, Wiesbaden, West Germany, October 3-6, 1972, Lectures.

17 p2256 A73-34109

Spherically symmetric zero energy Einstein-de Sitter cosmological model validity for world geometry from observational data and invalidity of other models

17 p2225 A73-34110

Barnard star multiplanet system, discussing inclinations of planetary orbits and cosmogonic implications

17 p2229 A73-34430

Book - Meteorites and their origins.

17 p2229 A73-34470

Cosmic ray bombardment of meteorites allowing solar system age estimation from spallation product concentration and subatomic particle track distribution

17 p2232 A73-34975

The applications of relativistic kinetic theory to cosmological models - Some observational consequences.

17 p2234 A73-35616

On the origin of short-period comets.

17 p2234 A73-35620

Structure and evolutionary history of the solar system. III.

17 p2236 A73-35784

Book on large scale structure of space-time covering gravity roles, differential geometry, general relativity, gravitational collapse, black holes, spatially homogeneous cosmological models, etc

18 p2336 A73-35901

Thermal instability caused primary interstellar dust cloud fragmentation and resulting star formation according to Peebles-Dicke hypothesis for cosmological origin of globular clusters

18 p2355 A73-36738

Apollo program contributions to lunar cosmology and composition, discussing core-mantle structure, earth-moon gravitational system, mineral types and cosmological hypotheses

18 p2356 A73-37044

The luminosity function of quasars and its evolution - A comparison of optically selected quasars and quasars found in radio catalogs.

19 p2484 A73-37606

Observational nondifferentiability between expanding universe and static world models

19 p2484 A73-37607

A deduction of the inverse square law from Newtonian cosmology.

19 p2486 A73-38169

Absorber theory of radiation and the future of the universe.

19 p2460 A73-38172

The redshift-distance relation. V - Galaxy colors as functions of galactic latitude and redshift - Observed colors compared with predicted distributions for various world models.

19 p2487 A73-38504

Massive singlet f-meson gravitational field effects on gravitational collapse in universe model with ten to eightieth power aligned neutrons

20 p2605 A73-39016

Universe evolutionary model construction based on observations of high flux gravitational radiation generated within Milky Way Galaxy

20 p2609 A73-39434

The cosmological significance of molecular band strengths in the infrared spectra of elliptical galaxies.

20 p2609 A73-39447

On an eigenvalue problem in the kinematic approach to dynamo theories of cosmic magnetism.

20 p2609 A73-39571

On galaxy formation from primeval universal turbulence. II.

20 p2609 A73-39572

A Green Bank sky survey in search of radio sources at 1400 MHz. IV - Anisotropy and counts of radio sources.

20 p2610 A73-39574

Generation of magnetic fields in a matter-antimatter universe.

20 p2611 A73-39587

Scalar waves in the mixmaster universe. I - The Helmholtz equation in a fixed background.

21 p2766 A73-40317

A new estimate of the fluctuation of relic radiation in the universe

21 p2759 A73-40708

Cosmological singularity structures, taking into account initial singularity inevitability, uniform models, mixmaster model quantal limitations and physical processes

21 p2772 A73-41249

Model for galactic cluster formation after radiation decoupling from matter in Einstein-De Sitter universe, discussing turbulence in primeval cosmos

21 p2778 A73-41526

Gravitational radiation in the scalar-tensor gravitation theory.

22 p2885 A73-41718

Global coordinate systems for spherical collapsing and expanding Oppenheimer-Snyder dust cloud behavior after critical Schwarzschild radius attainment

22 p2908 A73-42438

On the problem of the initial state in the isotropic scalar-tensor cosmology of Brans-Dicke.

22 p2911 A73-42931

Cosmogonic prerequisites for the accumulation of volatile substances in the upper mantle of the earth

22 p2912 A73-42972

Micrometeorite and cosmic dust studied for solar system and universe origin and evolution and for medium range weather forecasting, discussing cosmic matter infall to earth

22 p2913 A73-42988

Cosmic deuterium abundance derived from measured HD/H2 ratio, noting derivation sensitivity to ionizing flux and to oxygen and carbon depletion

22 p2904 A73-43119

Primordial abundance values for heavy nuclei related to content of type 1 and 2 carbonaceous chondrites

23 p2950 A73-43752

Extrasolar planetary systems.

24 p3127 A73-44391

Effect of scalar and vector fields on the nature of the cosmological singularity.

24 p3132 A73-44493

Solar system cosmochemistry concerning element abundances, structure and composition of comets, planets, moon, exospheric dust and meteorites, protosolar magnetic field, nucleosynthesis and cosmic rays

24 p3134 A73-44569

COSMONAUTS

Peripheral blood composition changes in cosmonauts during 18- and 24-day space flights

12 p1463 A73-27710

Russian book - Optical phenomena in the atmosphere as observed from piloted spacecraft.

18 p2348 A73-35898

COSMOS SATELLITES

NT COSMOS 137 SATELLITE

NT COSMOS 381 SATELLITE

NT INTERCOSMOS SATELLITES

Ion concentration measurements in the earth's ionosphere at altitudes from 200 to 6000 km

02 p0164 A73-12462

Latitude-time variations of the total number of electrons and of its gradients in the ionosphere at high latitudes

02 p0164 A73-12474

Analysis of the orbit of Cosmos 316 /1969-108 A/.

02 p0225 A73-12824

Analysis of the orbit of Cosmos 268 rocket /1969-20B/.

04 p0496 A73-14964

Air density at heights near 200 km from the orbit of 1969-20B.

04 p0440 A73-14965

- Magnetic storm of March 8-10, 1970 from Cosmos-321 and ground observations. I - Morphology of the disturbance
08 p0959 A73-21290
- Space distribution of the intensity of excess radiation at low altitudes.
12 p1535 A73-27637
- Measurement of the ion density in the earth's ionosphere at altitudes from 200 to 6000 km.
15 p1874 A73-32612
- Latitudinal and time variations of total electron number and its gradients in the ionosphere at high latitudes.
15 p1874 A73-32625
- Extra-atmospheric observations of the luminosity of the sky from the Cosmos 51 and Cosmos 213 satellites. I - Method and calibration of the measurements
16 p2011 A73-32706
- Extra-atmospheric observations of the luminosity of the sky from the Cosmos 51 and Cosmos 213 satellites. II - Measurement data and their interpretation
16 p2001 A73-32707
- Spatial distribution of outgoing long wave radiation fluxes according to Cosmos-320 satellite data
20 p2555 A73-39188
- COSMOS 137 SATELLITE**
Formation and decay of a narrow band of energetic electrons in the earth's magnetosphere
08 p0998 A73-21305
- COSMOS 381 SATELLITE**
Cosmos 381 onboard ionospheric station signals received from magnetically conjugate region by ground wideband antennas
03 p0280 A73-14576
- COSPAR [COMMITTEE]**
U COMMITTEE ON SPACE RESEARCH
COSSERAT SURFACES
Certain generalizations of load-limit theorems for a Cosserat medium
01 p0114 A73-10573
- Shell and plate theory covering constitutive and equilibrium equations, Cosserat surfaces and uniqueness theorem
02 p0234 A73-1381
- A consistent approximation in the linear theory of elastic lattice-type shells.
03 p0393 A73-13780
- Axial shear vibrations of cylinders made of a micropolar elastic solid.
03 p0393 A73-13781
- The influence of the reference geometry on the response of elastic shells.
05 p0637 A73-17236
- Derivation of the linear shell theory from the theory of Cosserat medium.
06 p0763 A73-18454
- Homogeneous flat elastic plate theory in Cosserat surface context, considering application of general constitutive equations and extension to right circular cylindrical shells
07 p0908 A73-19085
- Crystal lattice dynamics, elasticity and piezoelectricity theories covering linear, Cosserat and strain gradient theories, acoustic and optical properties, etc
11 p1409 A73-26276
- Constraints theory for Cosserat surfaces with applications in thermomechanics and shell theory, investigating equilibrium laws transformation properties and constitutive equations restrictions
16 p2076 A73-32936
- The derivation of the mechanical balance equations of the Cosserat continuum on the basis of the energy equation and its behavior at the transition to rotating systems
16 p2080 A73-33240
- Molecular crystals with behavior predictable by discrete quasi-continuous Cosserat model based on system of oriented Newtonian particles with six degrees of freedom
21 p2739 A73-40573
- Equations of linear elastic theory of thin shells based on model of anisotropic Cosserat surface
24 p3147 A73-44744
- COST ANALYSIS**
Thin film and thick metal film technology comparison and production cost analysis, emphasizing thin film resistors application in hybrid circuits
01 p0026 A73-11399
- Superconducting magnet ac generators development, emphasizing conversion efficiency, manufacturing, relative costs, machine geometry and interwinding coupling factor effects
02 p0132 A73-11833
- Short haul twin jet passenger aircraft lak-40 for small airfields, noting flight characteristics and cost analysis
03 p0249 A73-13070
- Computerized operational simulation for space shuttle program in terms of flight units, launch rate, success probabilities and costs
03 p0381 A73-13298
- Satellite charges for a mixed pre-demand-assigned system.
03 p0276 A73-13901
- Private business aircraft economic aspects, discussing costs vs time savings and indirect advantages
03 p0401 A73-13997
- NASA space research costs balanced with scientific and technological achievements in relation to space law
04 p0524 A73-15156
- Cr heat vacuum decarburization equipment for stainless steel vacuum melting, noting cost analysis, vacuum pumping curve and desulfurization
04 p0455 A73-15745
- Book - The local service airline experiment.
05 p0534 A73-16360
- Technical and economical analysis of various QSTOL concepts
[DGLR PAPER 72-055]
06 p0647 A73-17675
- Management systems for quality cost accounting, time control and productivity analysis based on random time sampling technique
06 p0771 A73-17866
- Business aircraft operational costs, considering maintenance, repair and depreciation
06 p0771 A73-17998
- Electrical and isotope power from space for terrestrial use.
06 p0750 A73-18028
- A unified formulation of the theory of optimal plastic design with convex cost function.
06 p0763 A73-18343
- Some preliminary notions towards improved stochastic controller synthesis via transformed indices of performance.
06 p0681 A73-18817
- Management and cost of European-U.S. Aerosat program based on geostationary satellites for air/ground voice and data messages relay and aircraft position determination
07 p0905 A73-19174
- Benefit-cost analysis of delay reduction with STOL. [ASCE PREPRINT 1507]
08 p1025 A73-21000
- Development of maintenance policies in the operation of aircraft
10 p1174 A73-23655
- Fiber reinforced composite design and application within performance and cost parameters, considering composite structure cost reduction and functional redesign increase
10 p1238 A73-23968
- Aircraft and ground equipment damage during ground handling operations, discussing repair costs and out-of-service time
10 p1176 A73-24715
- Design of lowest-cost prestressed combined metallic systems
11 p1371 A73-25035
- Improvements in the use of FAA resources for system performance assurance.
12 p1561 A73-27364
- L-band satellite systems for mobile applications.
12 p1472 A73-27664
- Engineering economic considerations for a maritime-satellite service.
12 p1473 A73-27677
- Air transportation direct and indirect costs analysis, considering cruising speed, flight time, aircraft design and manufacture and fuel expenses
13 p1569 A73-28950
- A procedure for the minimization of the costs of a project in the case of a given project duration
15 p1959 A73-31224
- Land construction and cost studies for Chicago offshore airport site development in Lake Michigan using rock and sandfill dikes for protection against waves
15 p1857 A73-31536
- The utilization of solar energy to help meet our nation's energy needs.
15 p1832 A73-32193
- STOL short haul system development, discussing airport congestion, operational costs and environmental considerations
16 p1968 A73-33192
- Airborne photography with multispectral scanners for remote sensing of large area features, discussing cost and feasibility of computerized pattern recognition and automatic identification
16 p2015 A73-33361
- Computer program for Equipment Improvement Recommendation (EIR) evaluation relative to reliability, availability, inventory cost and total annual expenditure in Army engineering management decision making
16 p2089 A73-33653
- Equipment life cycle costs dependence on acquisition decision making, discussing stochastic computer simulation of failure times, repairs, inventory replacement and personnel availability
16 p2089 A73-33655
- Future technical developments and efficiency of helicopters and their derivatives
17 p2098 A73-34252
- VTOL jet transport aircraft commercial applications, describing lift engine system, hover flight control, engine failure problems and operating cost analysis
17 p2099 A73-34257
- How to be healthy, wealthy and wise through fastening analysis - The 'how to' of living with fasteners.
[SAE PAPER 730309]
17 p2177 A73-34669
- Economic and design advantages of aluminum precision forgings.
[SAE PAPER 730312]
17 p2177 A73-34672
- A reliability, cost and risk analysis of establishing and maintaining a space communications satellite network.
[ALAA PAPER 73-582]
18 p2288 A73-36074
- The impact of launch vehicle reliability on the financial risks associated with multiple payload space functions.
[ALAA PAPER 73-591]
18 p2358 A73-36079
- Requirements of an economic approach to maintenance.
18 p2373 A73-37142
- Impact of the space tug concept on space program economics.
19 p2490 A73-37192
- Air cushion landing system /ACLS/ design and drone flight tests for low cost unmanned military aircraft recovery, comparing with mid air retrieval system /MARS/
19 p2383 A73-37699
- Air freight handling equipment, techniques and costs in cargo terminals, including forklifts, pallets, containers, conveyor belts and warehouse configurations
19 p2418 A73-37821
- The weight/performance interface - An argument for weight control.
[SAWE PAPER 967]
19 p2385 A73-37884
- Electrolytic hydrogen fuel production with solid polymer electrolyte technology.
19 p2391 A73-38413
- Availability, maintenance and cost of communication satellite systems.
20 p2613 A73-38768
- Space shuttle program budget difficulties, discussing consequences of cost increase or program suspension
21 p2793 A73-40234
- Future technology and economy of jet-supported VTOL transport aircraft
21 p2793 A73-40448
- Lower bounds on the cost functional for systems governed by partial differential equations.
21 p2726 A73-40838
- Runway configuration improvement programming model.
[ASCE PREPRINT 2034]
22 p2839 A73-42864
- Hydrazine and methanol fuel cells comparison with hydrogen-air cells in terms of fuel costs and conversion efficiency, considering electric generators and automotive applications
24 p3057 A73-45025
- COST EFFECTIVENESS**
Optimization study of the satellite broadcasting system for television.
01 p0018 A73-11180
- Multisatellite systems for transoceanic aircraft communications and ATC, discussing day and night operations, cost-benefit optimization and adaptive techniques for capacity augmentation
01 p0018 A73-11201
- Low-cost fluid film bearings for gas turbine engines.
[SAE PAPER 720740]
02 p0174 A73-12006
- Reducing the cost of the R&D proposal process.
02 p0239 A73-12349
- Army studies cost effectiveness of communications satellites.
03 p0274 A73-13075
- Cost goals for silicon solar arrays for large scale terrestrial applications.
03 p0258 A73-14250
- Optical Characters Reading and facsimile terminals reduction of message preparation time for electrical transmission in Defense Communications System, considering cost effectiveness and maximum benefit
04 p0418 A73-15380
- Space shuttle cost effectiveness studies from viewpoint of combined civil and military payloads and simplified systems design
05 p0613 A73-16182
- Space shuttle missions and configurations, discussing payload, external tank, solid rocket engines, orbiter vehicle and alternate delivery system costs
05 p0627 A73-16183
- Jet engine condition monitoring without aids.
[SAE PAPER 720815]
05 p0606 A73-16640
- The cost-effectiveness of high altitude systems for regional resource assessment.
05 p0642 A73-17139
- Security system signal detector with time delay and prediction filters and optimal noise suppression, noting detection time dependence on cost effectiveness
06 p0679 A73-17806

Economic performance and cost problems in civil air transport maintenance and engineering quality control related to selling price trends

06 p0647 A73-17888

Space shuttle cost effectiveness from earth orbital mission analysis, discussing potential performance and shuttle derived high energy transportation system

06 p0756 A73-18017

Cost effectiveness and observation speed of small astronomical telescopes array with TV detection systems

06 p0693 A73-18240

Microwave small signal bipolar transistor evolution, design and applications, noting cost effectiveness and surface geometry control

09 p1064 A73-22499

Value engineering methodology for quality control and reliability, noting cost effectiveness

09 p1168 A73-22644

Large area wraparound contact silicon solar cell, application and development.

09 p1036 A73-22812

PCM and DPCM digital modulators design and performance comparison for sampling rate effects on quantizing noise, noting tradeoffs between cost and system efficiency

09 p1059 A73-23435

Cost effectiveness of planned aviation system improvements, considering ATC automation vs terminal aids, noise control, ground facilities, capacity and en-route situation

10 p1247 A73-24767

Noise abatement two-segment, precision and category I, II and III approaches considerations covering altimetry, cost and safety problems in ATC

10 p1247 A73-24768

Radio Technical Commission for Aeronautics, Annual Assembly Meeting, Washington, D.C., November 9, 10, 1972, Proceedings.

12 p1522 A73-27360

National aviation system improvement via cost effectiveness, considering FAA facilities and equipment program, ATC automation and terminal aids

12 p1522 A73-27365

Justification and calculation of the lifetimes and efficiency of new equipment

12 p1562 A73-27468

Calculation of single phase pressure drop in heat exchangers considering the change of fluid properties along the flow path.

12 p1559 A73-27694

Aircraft-airport system R and D program in terms of efficient planning, lighting and marking, geometric design, safety and pavements

13 p1598 A73-29103

Central regional airport planning, compatibility and construction/operational costs for freight/passenger transport service in response to future economic growth

13 p1598 A73-29109

Airport planning trends and engineering, discussing systems analysis, pavement design, modular terminal facilities, costs and economic efficiency

13 p1598 A73-29111

Cost effective land use mapping and resources inventory for Mississippi via high altitude color IR aerial photography and ERTS-1 multispectral imagery [AIAA PAPER 73-3]

13 p1610 A73-29300

General aviation aircraft technology developments based on military and transport aircraft design, considering cost, complexity and reliability

13 p1570 A73-29348

Space cost effectiveness through space shuttle orbiter programs based on payload recovery and reuse in routine round trip operations

14 p1803 A73-29941

Lower payload costs through refurbishment and module replacement.

14 p1803 A73-29944

Cost effective space shuttle solid rocket booster recovery parachute system planning, discussing model drop and structural load testings [AIAA PAPER 73-441]

15 p1825 A73-31427

Offshore airport planning, discussing selection economics from cost effective alternatives based on usage projection, community benefits and intrinsic and social costs

15 p1856 A73-31531

Netherlands international airport planning and site selection, discussing cost/benefit analysis experience from large coastal and offshore projects

15 p1959 A73-31535

Los Angeles offshore airport planning case study covering design, logistics problems and costs with allowance for airspace and environmental considerations peculiar to Southern California area

15 p1857 A73-31540

Offshore airport planning in Osaka-Bay, Japan - New Kansai International Airport.

15 p1857 A73-31542

San Diego offshore airport feasibility to meet future air traffic demands, evaluating sites for capacity, environmental impact, access and construction costs

15 p1857 A73-31543

ARINC-573 recording system - Application to maintenance

15 p1883 A73-32462

All-weather landing technology and economics, considering ground and airborne equipment and benefits and costs

15 p1859 A73-32553

Gimbaled electrostatic gyro inertial aircraft navigation system /GEANS/ designs balancing performance against cost of ownership

16 p2034 A73-33086

Air Force Increase Reliability of Operational Systems computer program and mathematical models for economic logistic resource allocations and cost effective system modification

16 p2088 A73-33627

Economic tradeoff study of design criteria cost effectiveness, applying to reusable nuclear shuttle /RNS/ engine concepts

16 p2035 A73-33650

Airborne air to air and air to ground fire control radar systems for all-weather fighter aircraft, emphasizing cost effectiveness through modularity and commonality

16 p1985 A73-34041

Hypersonic transports - Economics and environmental effects.

17 p2099 A73-34435

Cost/weight tradeoff ratios for fiber reinforced plastic aircraft structural components [SAE PAPER 730338]

17 p2257 A73-34689

STOL aircraft choice for air transportation in low passenger density areas, discussing market characteristics in U.S. and tradeoffs between airline operation and airfield costs

[SAE PAPER 730357]

17 p2209 A73-34705

Turbine powerplants for missiles - Cost improvement requirements.

[SAE PAPER 730364]

17 p2222 A73-34709

Helicopter design and production cost target and tradeoff considerations based on past programs, supplier quotations, government documents, estimating practices and functional requirements

[AHS PREPRINT 712]

17 p2257 A73-35058

Technological forecasting for microcomputer architecture and fabrication on LSI chip, considering cost effectiveness, pins number, packing density, power and speed factors

17 p2131 A73-35226

Custom LSI technology utilization in low volume avionic systems, discussing handcrafted chip design, full wafer, array logic and MOS cell approaches and costs

17 p2138 A73-35227

Thin configuration flat digital CRT display with electron beam control improvement for military avionics applications, discussing performance advantages and ownership cost

17 p2139 A73-35235

Computerized approach for aerospace electronic components standardization for procurement cost, logistics and warehousing problems reduction and reliability improvement

17 p2140 A73-35260

Monte Carlo simulation on CRT display for training and learning system reliability and early decision effects on life cycle cost effectiveness

17 p2140 A73-35261

Book - Zero-base budgeting: A practical management tool for evaluating expenses.

17 p2258 A73-35674

A concept for Space Shuttle payload ground operations.

[AIAA PAPER 73-615]

18 p2359 A73-36093

Offshore airport design, construction and operation on basis of cost/benefit considerations, emphasizing ATC problems generated by ILS localizer and glide path signal reflection

18 p2296 A73-36682

New constraints of military aviation

18 p2267 A73-36684

Variable pitch turboprop driven at constant speed through reduction gear to obtain cost-efficiency compromise for future STOL and business aircraft applications

18 p2343 A73-36998

Matrix formulation of reliability analysis and reliability-based design.

19 p2496 A73-37479

Financing the new generation of airports.

19 p2506 A73-37745

Strapped down inertial navigation systems.

19 p2452 A73-37876

Cost-effective radioisotope thermoelectric generator designs involving Cm-244 and Pu-238 heat sources.

19 p2455 A73-38389

The availability and cost of curium-244 from power reactor fuel reprocessing wastes.

19 p2457 A73-38430

Communication satellites future use in Europe, considering mission requirements, data transmission, specialized TV distribution, cost effectiveness and shuttle/tug launch system

[AAS PAPER 73-148]

20 p2521 A73-38596

Future communication satellite technology improvement, market expansion and cost effectiveness, considering foreign domestic, and international light-to-medium and high density systems

20 p2522 A73-38715

The effects of multipath on the design of ship board satellite communications antennas.

20 p2523 A73-38726

Optimization in the design of a 12 GHz low cost ground receiving system for broadcast satellites.

20 p2527 A73-38762

Strapdown inertial navigation with high speed digital computer, discussing attitude propagation algorithms and life cycle system cost advantages

21 p2734 A73-40036

Fog dispersal technique evaluation for cost effectiveness by statistical method, taking into account time dependent probability of natural visibility improvement

21 p2729 A73-40066

Design, performance, and cost considerations for solid-state arrays.

21 p2662 A73-40648

High resolution beam steering phased array radar antenna design by subarray techniques, using time delay circuit for cost effective driver control simplification

21 p2653 A73-40672

Experience with the NRC 10 ft. x 20 ft. V/STOL propulsion tunnel - Some practical aspects of V/STOL engine model testing.

21 p2672 A73-40855

Explosive and electrohydraulic forming techniques cost effectiveness in metal technology, considering welding methods and metal powder compaction

22 p2865 A73-41779

USA government and industry efforts on aircraft midair collision avoidance systems technology advancement, comparing cost effectiveness between airborne and ground based options

[ASME PAPER 73-1CT-49]

23 p3005 A73-43495

Maximum SNR performance calculation for heterodyne laser detection system with parameters optimization under assumed total cost

24 p3096 A73-44875

COST ESTIMATES

Secondary electron conduction /SEC/ vidicon television system for space astronomy, discussing data reduction requirements, costs and quasar spectrum observation

01 p0048 A73-10530

Aircraft industry design and development costs prediction, using Monte Carlo model to determine effect of poor estimates

02 p0238 A73-11860

Technological evolution of solar generators for terrestrial applications and sounding balloons, discussing environment caused problems and solutions, energy cost estimate and future prospects

03 p0258 A73-14253

Adaptive feedback control without complete plant identification, deriving vector cost function and algorithm for performance optimization

04 p0430 A73-15214

Two approaches to aircraft development - The USA and Europe.

13 p1568 A73-28177

Power plants, cost estimates, freighter missions, commercial feasibility and technology for nuclear air cushion vehicles

15 p1912 A73-32194

Cost estimating techniques for airframe weight-cost interface study for military aircraft design

[SAWE PAPER 969]

19 p2385 A73-37885

Curium 244 heat source design for multihundred watt radioisotope thermoelectric generator with Si-Ge thermocouples for energy conversion, noting low cost

19 p2457 A73-38429

Development costs for a nuclear electric propulsion stage.

19 p2458 A73-38434

Technological change measurement methodology for cost and production estimates with application to aircraft turbine engine development

23 p3020 A73-44219

COST REDUCTION

Theory and design of economical net solar flux radiometer adaptable to conventional short wave radiosonde system, discussing prototype instrument tests and modifications

01 p0045 A73-10386

Reducing the cost of the R&D proposal process.

02 p0239 A73-12349

Applying surface integrity principles in jet engine production.

03 p0312 A73-13272

Solar cell optical properties effects on electrical and thermal performance and cost savings in panel design optimization

03 p0255 A73-14226

Economic analysis of silicon solar cells production noting cost reduction from feasibility studies of edge defined film fed crystal growth in ribbon form

03 p0258 A73-14251

An assessment of some mixed-oxide systems as low-cost electrocatalysts for oxygen electrodes.

04 p0407 A73-15110

A compact low-cost electronic time division multiplexer.

04 p0417 A73-15295

Ferrous and nonferrous metal alloys melting and re-melting in plasma induction and beam furnaces, noting cost reduction and ingots homogeneity

04 p0455 A73-15748

Transport aircraft wheels and brakes operational cost minimization, discussing contributory roles of governmental regulations /FAA/, aircraft manufacturer, supplier and user

[SAE PAPER 720867]

05 p0534 A73-16650

Communication satellite application to shipping company operations for cost benefits and alleviation of distress alerting, search and rescue, and heavy weather damage problems

[AIAA PAPER 73-47]

06 p0755 A73-17625

Design of low-cost, refurbishable spacecraft for use with the Shuttle.

[AIAA PAPER 73-73]

06 p0756 A73-17638

Revolutionary implications of the space shuttle.

06 p0756 A73-18018

Continuous ultrasonic joining of thin plastic films

07 p0828 A73-18902

Energetically and financially economical hydrazine synthesis method based on ammonia oxidation by water solution of hydrogen peroxide

07 p0787 A73-19325

A description of two low cost turbo-compressors built for powered lift research.

07 p0867 A73-19942

Economical system design for remote data acquisition.

07 p0824 A73-19948

Structural fabrication of advanced metal-matrix composites.

[SME PAPER EM 72-108]

07 p0832 A73-20449

Distributed ATC with traffic information in cockpit, noting potential for cost and risk reduction and capacity increase based on system performance evaluation

07 p0850 A73-20600

Non-destructive testing in industry - Non-ferrous metals.

08 p0973 A73-21077

Computer systems configurations for design and engineering, considering graphic and conversational capability and cost and time reduction

09 p1168 A73-21949

Recoverable sounding rocket payload field refurbishment for data acquisition with time and monetary savings, noting micrometeorite collection experiments

[AIAA PAPER 73-301]

09 p1156 A73-23220

Hot die forging /gatorizing/ technique for Ti and heat resistant alloys jet engine parts, emphasizing material and cost savings

09 p1089 A73-23295

Logistics planning with cost reduction for NASA phased programs in conducting R and D and real time inventory control, discussing major activities and objectives

11 p1454 A73-25450

Automatic control system components optimization for minimal cost, demonstrating algorithm efficiency for servosystem

12 p1482 A73-26775

Counting operation based recursive digital filter hardware design in canonic and direct forms, emphasizing low cost, low speed and high flexibility

12 p1483 A73-27116

Precision low frequency adaptive MOSFET IC electronic oscillators with loose tolerance component timers for cost reduction

12 p1478 A73-27167

Shuttle payloads - Saving dollars by offsetting risks.

12 p1549 A73-27438

Three dimensional elastic stress analysis by finite element method within reasonable computer costs, noting problem simplification

13 p1693 A73-28240

Light-weight Al isogrid panel design with triangular reinforcement elements for aerospace structural applications, discussing load response characteristics, fabrication and cost reduction

13 p1624 A73-28906

Solar array cost reductions.

13 p1573 A73-29592

Arithmetic algorithms for error-coded operands.

15 p1899 A73-31349

Transage 129 Ti-Al-V-Sn-Zr alloy fabrication cost reduction through good cold formability and weldability with weight saving due to high strength and fatigue resistance

15 p1891 A73-32172

Light aircraft-borne low cost phased array X band radar and display design requirements for weather detection and ground mapping

15 p1909 A73-32451

French civil aviation inexpensive C band landing system with ILS angular coding and simplified on-board equipment for STOL and Alpine airports

15 p1910 A73-32467

Some aerodynamic problems applicable to the light aircraft

16 p1961 A73-32809

Avionics systems simplification for cost, weight and space reduction, considering ease of maintenance, failure points reduction and flight director/autopilot computers and couplers elimination

16 p1968 A73-33187

Aerodynamic study of a turbine designed for a small low-cost turbofan engine.

[ASME PAPER 73-GT-29]

16 p2048 A73-33500

Rigid lightweight honeycomb core radome development from materials and processes standpoint, discussing cost reduction and fabrication

[SAE PAPER 730310]

17 p2177 A73-34670

Development of a low-cost flight director system for general aviation.

[SAE PAPER 730331]

17 p2167 A73-34684

Navy development of low-cost supersonic turbojet engines.

[SAE PAPER 730362]

17 p2222 A73-34708

A simplified fuel control approach for low cost aircraft gas turbines.

17 p2222 A73-34725

C band low noise IC microwave amplifier for phased array module in multiple access communication links, discussing photofabrication for low cost batch processing

17 p2135 A73-34727

Unconventional digital avionics black box approach for cost reduction and reliability improvement in terms of packaging, component coding and hardware qualification programs multiplicity

17 p2137 A73-35205

Multifield multifrequency broadband constant index lens antenna with high power and variable polarization handling capabilities and low manufacturing cost advantage

17 p2137 A73-35206

LN-33 airborne inertial navigation system with low cost precision instruments and miniaturized digital computer, noting built-in calibration and test capability for minimizing maintenance

17 p2210 A73-35212

Low cost data processor and display for ICNI, DME/TACAN, LORAN or range/range difference radio navigation systems in aerospace applications

17 p2210 A73-35213

Avionics subsystems operational, functional and physical considerations, discussing cost, computer programming, common components, multiplexing and hardware design

17 p2139 A73-35249

Canadian domestic satellite system applications.

17 p2124 A73-35311

Thin film hybrid microwave integrated circuit.

17 p2141 A73-35323

Low cost beam current integrator for use with dc-accelerators in ion implantation experiments

17 p2175 A73-35759

A low-cost system for reproducing ERTS imagery.

18 p2315 A73-36018

Cost reductions in transportation to geosynchronous and lunar orbits by a swing station.

19 p2490 A73-37193

A digital simulation facility for air traffic control experimentation.

19 p2451 A73-37809

Structural composites on future fighter aircraft.

[AIAA PAPER 73-806]

19 p2388 A73-38371

Low cost modular power systems for multi mission earth observations.

19 p2494 A73-38435

Civil and military aircraft preventive maintenance, discussing on-condition and condition monitoring concepts for equipment reliability enhancement and cost reduction

20 p2544 A73-39275

Low cost airport surveillance and Localized Cable Radar with runway or taxiway vehicle guidance capability for ground traffic control, using solid state equipment

21 p2736 A73-40051

Planar phased array beam steering methods, emphasizing electronic driver and logic circuit sharing between phase shifters for cost reduction

21 p2652 A73-40666

Limited scan phased array antenna design, featuring electronic beam deflection from few beamwidths to twenty degrees with cost reduction

21 p2653 A73-40680

COSTS

NT AIRPLANE PRODUCTION COSTS

NT FREIGHT COSTS

COTTON

Effects of leaf age for four growth stages of cotton and corn plants on leaf reflectance, structure, thickness, water and chlorophyll concentrations and selection of wavelengths for crop discrimination.

05 p0571 A73-17128

COUETTE FLOW

Viscous steady Couette flow between two parallel flat walls with particle injection, obtaining velocity and temperature distribution

01 p0033 A73-10808

Sturm-Liouville solution of unsteady stratified two dimensional Couette flow equations of motion

03 p0292 A73-13304

Stability investigation in the case of an oscillating Couette flow. I Nonlinear theory. II - Linear theory [DFVLR-SONDDR-257]

05 p0563 A73-16098

Application of invariant imbedding techniques to flow instability problems.

[AD-756824]

05 p0591 A73-16608

Further results concerning the forces on a flat plate in a Couette flow.

08 p0926 A73-21402

A special form of Galerkin's method applied to heat transfer in plane Couette-Poiseuille flows.

[AD-757002]

08 p1023 A73-21412

Nonisothermal instability of flows of viscoelastic media

09 p1072 A73-22481

Electrically conducting unsteady viscoplastic plane channel Hartmann and Couette MHD flows in presence of uniform transverse magnetic field and time variable electric field

10 p1256 A73-24589

On the stability of plane Couette flow to infinitesimal disturbances.

11 p1346 A73-25158

Instability of density-stratified incompressible inviscid rotary Couette flow between corotating coaxial vertical cylinders due to gravitational effects

13 p1600 A73-28439

Test of statistical models for gases with and without internal energy states.

14 p1818 A73-30653

An upper bound on the stress in plane Couette flow. [ASME PAPER 73-FE-8]

17 p2152 A73-35007

Unsteady Couette flow in hydromagnetics.

17 p2154 A73-35121

An approximation for combined heat transfer in a radiatively absorbing and emitting gas.

18 p2370 A73-36366

Turbulent Couette flow statistical theory, applying stochastic analysis to Navier-Stokes equation

19 p2421 A73-37855

Non-steady, stratified Couette flow between concentric rotating spheres.

20 p2548 A73-39521

Experimental study of rotational MHD Couette flow in a coplanar field

21 p2747 A73-40886

Rarefied gas flows based on variational principle.

22 p2840 A73-41741

Heat transfer in plane Couette flow of rarefied gas between parallel plates, determining temperature jumps at plates from transfer equations

23 p3048 A73-43206

Prediction of stability of viscoelastic Couette flow based on network rupture hypothesis.

23 p2967 A73-43300

A variant of the Monte-Carlo method for solving the linear dynamics problems of a rarefied gas

24 p3076 A73-44660

On the instability of magnetohydrodynamic Couette flow via non-axisymmetric, oscillatory critical modes.

24 p3116 A73-45241

COULOMB COLLISIONS

Multiple scattering of cosmic ray muons in the range 10-70 GeV/c.

01 p0091 A73-10787

Secondary particles in pion-nucleon and coherent interactions, measuring momentum from multiple Coulomb scattering

02 p0209 A73-12666

Contribution of Coulomb collisions to plasma relaxation in the DECA mirror machine.

05 p0604 A73-17367

Coulomb collision induced mean-energy variations in homogeneous nonrelativistic plasma components, discussing two-component plasma and energy transfer rates

10 p1257 A73-24760

Spatially dependent electron relaxation near a thermionic emitting electrode.

14 p1713 A73-30473

Asymptotic form for the cross section for the Coulomb interacting rearrangement collisions.

14 p1777 A73-30551

Quantum correction to the electrical conductivity of a Coulomb plasma

14 p1781 A73-30584

Effect of collisions on the random electron density fluctuations in a plasma.

19 p2468 A73-37519

Electron-electron collisions and the electrical conductivity of metals at low temperatures

23 p3016 A73-44021

Computerized simulation of plasma particle collisions, using electric dipole expansion method for grid charge density and electrostatic force determination with Fourier transformation

24 p3116 A73-45027

COULOMB POTENTIAL

The anisotropic Kepler problem in two dimensions.

08 p0988 A73-21204

Calculation of the electron density in heterogeneous mixtures with allowance for the tunneling effect and for super-barrier reflection

Potential created by a test particle in one-, two- and three-dimensions in a flowing ion-electron plasma.

One-component two dimensional plasma, calculating equilibrium pair correlation function by Debye approximation for particle interaction via Coulomb potential

COULOMETRY

Determination of the value of blood oxygen capacity and of the oxyhemoglobin dissociation curves by polarographic coulombometry

COUNTDOWN

AEROS satellite launching from Western Test Range, describing time sequence of satellite and rocket countdowns and communication system activities coordinated by project management

COUNTERFLOW

Effect of counterflows of normal and superfluidic fluid on the second-sound velocity in helium II

On the deviation of the flame from the stagnation point in opposed-jet diffusion flames.

Penetration of retrorocket exhausts into subsonic counterflows.

Electromagnetic instability for plasma waves propagating perpendicular to uniform magnetic field in counterstreaming electron-ion plasmas based on linearized Vlasov-Maxwell equations

Magnetically induced collisionless coupling between counterstreaming laser-produced plasmas.

Study of a compact counterflow heat-exchanger with mercury at small Peclet numbers.

COUNTERMEASURES

NT CHAFF
NT ELECTRONIC COUNTERMEASURES
NT JAMMING

Laser guided weapon system optical countermeasures (OCM) vulnerability evaluation, discussing use of LED laser in computerized simulation at low cost

COUNTERS

NT CERENKOV COUNTERS
NT ELECTRON COUNTERS
NT GEIGER COUNTERS
NT NEUTRON COUNTERS
NT PARTICLE TELESCOPES
NT PROPORTIONAL COUNTERS
NT QUANTUM COUNTERS
NT RADIATION COUNTERS
NT SCINTILLATION COUNTERS
NT SPARK CHAMBERS

The analysis of particulate contaminants in hydraulic fluids.

Continuous flow condensation nucleus counter

Investigation of the scattered-light-flux magnitude dependence on the drop size in the aerosol photoelectric counter

Continuously recording cloud nuclei counter, describing diffusion chamber with separate functions of sample supersaturation and photoelectric droplets recording

Evaluation of the performance of a signal detection system by counting the overshoots of an internal threshold

Vertical plate steady flow thermal diffusion chamber for cloud condensation nucleus counter, featuring long available growth time for operation below 0.2 percent supersaturation

COUNTING CIRCUITS

A systematic approach to the problem of crossings by a random process.

Automatic pulse count recorder, discussing circuit, performance and applications to laboratory and clinic

Nonrecursive digital filter hardware design based on analysis of bit level counting operations in convolution, using fixed and floating point representations

Counting operation based recursive digital filter hardware design in canonic and direct forms, emphasizing low cost, low speed and high flexibility

Binary counters design based on TTL, DTL and ECL integrated circuits, giving circuit diagrams for 70 MHz 24 stage and 20 MHz dual 16 stage counters

Microwave tunnel diode ring counter with displaced nonlinear load line in multistage transistor driver and current switching configuration

A new technique for designing high-speed frequency counters.

Punched card controlled program units including readers, comparator circuits, pneumomechanical counters and fluidic feedback oscillators

COUPLED MODES

Random gust response statistics for coupled torsion-flapping rotor blade vibrations.

Sawtooth, solitary, and turbulent waves in a weakly ionized plasma.

Asymmetric eigenmodes in a simple model plasma-sphere.

Pulse propagation in a two-mode waveguide.

Higher-order scattering losses in dielectric waveguides.

Higher-order loss processes and the loss penalty of multimode operation.

Multicomponent plasmas with cations or anions in presence of Coriolis force, determining crossover frequencies for polarization reversal and mode coupling of waves

Nonlinear mode-mode coupling of Alfvén waves in the interstellar medium.

Mode-coupling and wave-particle interactions for unstable ion-acoustic waves.

Optical modulator based on coupled waveguides for integrated optical circuits, presenting design and dynamic characteristics

Study and development of a dye laser with coupled modes excited by a flash tube and emitting in the near infrared

An antiresonant ring interferometer for coupled laser cavities, laser output coupling, mode locking, and cavity dumping.

Ionogram traces production by mode coupling process in thin sporadic E layers, using calculated reflection and transmission coefficients for radio waves incidence

Mode coupling importance in midlatitude nonblanketing sporadic E layers from observations of ordinary and extraordinary blanketing frequencies

Influence of combinational coupling on the spectral and statistical properties of multimode fluctuations in a traveling-wave laser

Attitude stability of two elastically coupled spinning bodies.

Finite static deformations of elastic solids at constant temperature, discussing couples for different deformations

Coupled asymmetrical microstrip transmission lines odd and even mode wave impedances as functions of conductor strip width and spacing

Raman scattering from phonon bath using quantum mechanical model with random and stochastic Stokes and anti-Stokes coupled modes in light fields

Stability condition of an intense two-modes regime in a gas laser

Obliquely incident plane wave scattering from moving perfectly conducting cylinder, discussing mode coupling, Doppler shift and far field scattered power

Effects of attenuation on the stability characteristics in the case of combination resonances

Experimental evidence of a couple-stress effect.

Effect of torsion-flap-lag coupling on hingeless rotor stability.

[AHS PREPRINT 731] Propagation of VLF waves in the earth-ionosphere waveguide under nighttime ionospheres.

Direct nonlinear coupling of electromagnetic waves and electrostatic waves in a plasma - Experiment.

Interaction of parametrically coupled waves in nonequilibrium media /Survey/

Longitudinal-torsional vibrations of rotors

Perturbation analysis of holographic grating couplers in thin film waveguides, discussing coupling efficiency dependence on evanescent tail length, refractive index and gelatin film thickness

Coupled bending-twisting vibrations of a single boom flexible solar array and spacecraft.

Coupled mode analysis for solid travelling-wave amplifiers.

Noise in solid travelling-wave tubes using coupled-mode analysis.

Losses and impulse response of a parabolic index fiber with random bends.

TEM-TE coupled transmission line model for microstrip, calculating frequency-dependent wave dispersion curves for comparison with experiment

On coupled fields in stratified plasmas with tensor pressure perturbations.

On the observation of linear polarization of solar microwave bursts.

Energy conversion between longitudinal and transverse waves by mode-mode coupling in a relativistic plasma.

COUPLERS

NT ANTENNA COUPLERS
NT COUPLING CIRCUITS
NT DIPLEXERS

Perturbation theory for the surface-wave multistrip coupler.

French automatic beam coupler system for V/STOL and helicopter low speed and low altitude instrument approach

COUPLES

The effect of groupings of surface couples on flat plates

COUPLING

NT COUPLES
NT CROSS COUPLING
NT GYROSCOPIC COUPLING
NT MICROWAVE COUPLING
NT OPTICAL COUPLING
NT THERMODYNAMIC COUPLING

The theory of coupling of characteristic radio waves in the ionosphere.

Coupling function for the vertical muon telescope at 60-meters-water-equivalent depth.

Utilization of thermal phenomena in the construction of signal-energy converters for coupling automatic control devices belonging to different categories of the State Instrument System

Stability of coupled systems of nonlinear differential delayed-argument equations

A general theory of harmonic wave propagation in linear periodic systems with multiple coupling.

Mutual coupling in the signal-to-noise ratio optimization of antenna arrays.

Stellar explosive nucleosynthesis foundations in nuclear experiments and numerical schemes for solutions in limits of strong and weak coupling of abundances by nuclear reactions

On aeroacoustic coupling in free-stream turbulence manipulators.

COUPLING CIRCUITS

Nonlinear analysis of double feedback loop tracking system with coupling, obtaining steady state phase error probability density functions with application to satellite transponder

Time dependent and independent electric coupling between magnetosphere and ionosphere, discussing auroral arcs formation and magnetospheric plasma convection

Lambda/4 directional coupler in an inhomogeneous medium with deviations of even and odd mode parameters from the ideal value

A dc amplifier operating with a measuring bridge circuit

Mutual coupling, mainlobe reflected power and radiation patterns of periodic antenna arrays thinned by statistically selected element feeds

Panoramic measurement of the coupling impedance of delay systems by the heterodyne method

- Two coupled nonlinear oscillators driven by sinusoidal input, calculating fractional harmonic frequency pairs relationship to driving and resonance frequencies
13 p1659 A73-28487
- Analysis of commutator inverters with allowance for capacitive coupling to an ac amplifier
13 p1591 A73-28854
- Synthesis of a control coupling in a nonlinear servosystem
14 p1738 A73-30287
- Influence of tolerances on printed directional-coupler circuit parameters
15 p1850 A73-31498
- Russian book - Design and calculation of microwave stripline elements.
15 p1852 A73-32295
- Kirchhoff mode theory application to electrical network analysis with arbitrary branch couplings including ideal transformers and controlled sources
16 p1992 A73-32909
- Antenna coupling induced intersystem electromagnetic interference prediction, discussing tradeoffs between analysis level, input information, measurements, cost results and user requirements
22 p2822 A73-41795
- German monograph on microwave filters for communication channels separation at millimeter wavelengths covering coupling circuits design and resonant frequencies of coaxial resonator
22 p2827 A73-42701
- Extension of Kirchhoff's theory to coupled strip lines - Application to the calculation of band line couplers
24 p3068 A73-44975
- German book on HF technology, Volume 1, covering coupling filters, transmission lines, antennas, Lecher waves, waveguides, etc
24 p3073 A73-44999
- COUPLING COEFFICIENTS**
Experimental investigation of the coupling impedance in resonator chains with a positive mutual inductance coefficient
01 p0025 A73-10987
- Primary proton-air atom nuclei interaction study of negative and positive cosmic ray muon coupling coefficients with angular distribution allowance
02 p0205 A73-12173
- Study of bends in long distance waveguides - The case of metallic guides
04 p0427 A73-14900
- Polar coupling coefficients and generalization of the spectrographic method for studying cosmic-ray variations of magnetospheric and interplanetary origin
10 p1267 A73-23927
- Data processing technique and calculation procedure for cosmic rays hard particle and neutron components coupling coefficients
10 p1268 A73-23932
- Temperature dependence of the Na-23 quadrupole coupling constants in Rochelle salt.
11 p1409 A73-25875
- Coupling coefficients for resonant interaction between three waves with well-defined phases in cold magnetized plasma, applying to solar corona
11 p1405 A73-25917
- Mutual coupling effects in semi-infinite arrays.
14 p1734 A73-30202
- Effects of mirror reflectivity in a distributed-feedback laser.
16 p2024 A73-33081
- The theory of half-open ferrite microwave filters.
20 p2535 A73-38925
- A meson supertelescope using plastic scintillators and the coupling coefficients for it
21 p2701 A73-40611
- Numerical solution of edge effects of external coupling between elements in linear phased array of slots covered by dielectric slab, using scattering matrix
21 p2651 A73-40654
- Small arrays - Their analysis and their use for the design of array elements.
21 p2652 A73-40656
- Unsteady state coupled thermoelasticity problem solution based on reducing order of Laplace transform equation, using coupling coefficient as small parameter in series expansion
22 p2921 A73-42279
- Losses and impulse response of a parabolic index fiber with random bends.
23 p2987 A73-43989
- Optical directional coupler tolerance improvement by tapered propagation coefficients based on numerical model
23 p2955 A73-44113
- Coupling coefficient/frequency characteristics of rectangular dielectric waveguide channel dropping coupled line filter for millimeter wave
23 p2961 A73-44118
- COUPLINGS**
Technological and structural design ensuring optimum clearance and aerodynamic coupling of moving units /wing-aileron or aileron-trim tab/
02 p0129 A73-11648
- On the evaluation of tri-diagonal secular determinants.
02 p0188 A73-12606
- Influence of the nonlinear thermomechanical effect on the thermal stability of rubber-metallic couplings of vibration machines
04 p0509 A73-14981
- Control of the motion of a solid body with servo couplings
05 p0597 A73-16611
- Couplings effect on Liapunov stability estimation of higher order linear nonstationary systems, using aggregation method
05 p0599 A73-17084
- Isochromatic curves modeling for stress-strain state of doubly connected regions by optical polarization and photoelastic analysis, using isopach field method
05 p0578 A73-17092
- The influence of nonlinear couplings on the behaviour of the solution of the equations of motion of a mechanical system.
06 p0722 A73-17756
- Investigation of friction and wear mechanisms in a friction coupling with a small overlapping coefficient
15 p1882 A73-31599
- Qualitative analysis of the behavior of weakly coupled oscillators near the equilibrium position
19 p2458 A73-37191
- The load transfer problem in shafts coupled through a sleeve.
22 p2867 A73-42877
- COVALENT BONDS**
Covalent bond formation role in Ti strengthening by oxygen from evidence of alpha phase stabilization, ordered structures, abnormal resistivity and high activation energy
03 p0323 A73-13371
- Investigation of X-ray atomic scattering functions taking into consideration the tetrahedral covalent bonds in some semiconductors
06 p0736 A73-18217
- Static electric quadrupole interaction of Ta- and Hf-ions in barium and lead titanate.
07 p0862 A73-20018
- COVARIANCE**
Estimation of the statistical parameters of the Kalman-Bucy filter.
04 p0431 A73-15261
- A state covariance matrix computation algorithm for satellite orbit determination sequential filtering.
04 p0431 A73-15267
- Stability analysis of Riccati covariance equations of Kalman filter.
04 p0472 A73-15273
- Wiener and Kalman-Bucy filters design with error covariance bound for performance divergence prevention under stochastic processes with unknown signal and noise densities
07 p0806 A73-20603
- Covariance matrices and means of atmospheric Plank function profiles for application to temperature sounding from satellite measurements.
08 p0967 A73-21385
- Description of hydrodynamics in the theory of gravitation on the basis of covariant statistical equations
08 p0989 A73-21522
- Mean vector and covariance matrix estimation for training class sample statistics updating in pattern recognition, applying to crops or any category of objects
08 p0984 A73-21668
- Estimation of noise covariance matrices for a linear time-varying stochastic process.
10 p1201 A73-24053
- Kalman filtering of systems with parameter uncertainties - A survey.
13 p1597 A73-29569
- Mixed autoregressive moving average models parameters recursive joint identification and order determination extended for Kalman-Bucy filter transition and covariance parameters estimation
15 p1853 A73-31630
- An algebraic method for linear dynamical systems with stationary excitations.
16 p2076 A73-32919
- Explicit formulas for the representation of the Green's functions of covariant wave equations in the case of a weak gravitational field. I, II
16 p2038 A73-34021
- The transformational behaviour of perturbation theories.
18 p2352 A73-36421
- Kalman filter for rapid detection and adaptive estimation of state and covariance, deriving Bayes decision rule and algorithm for spacecraft tracking
19 p2410 A73-38030
- Suboptimal filter design for dynamic measurement systems, deriving bias and Kalman covariance formulae for error analysis and model sensitivity
19 p2410 A73-38031
- A conservative bound on the estimation error covariance matrix in the presence of correlated driving noise and correlated discrete measurement noise.
21 p2724 A73-40295
- Unsupervised learning of the Kalman filter.
21 p2664 A73-41109
- Standard sensitivity and covariance matrices for statistical estimation of overall performance.
23 p2962 A73-43279
- COVERINGS**
French D2A satellite construction, describing AG5 sheet covering and gold coating fabrication methods
07 p0829 A73-18912
- COWELL METHOD**
U NUMERICAL INTEGRATION
CRAB NEBULA
Nonlinear inverse compton radiation and the circular polarization of diffuse radiation from the crab nebula.
01 p0092 A73-11032
- Pulsar glitches and the metastability of the superfluid core.
02 p0211 A73-11895
- Energy distribution of relativistic electrons generated within radio sources with constant magnetic field and diffusion coefficient, discussing simplified model representation for Crab nebula
02 p0207 A73-12379
- Very long baseline interferometer observations of Taurus A and other sources at 121.6 MHz.
03 p0366 A73-12933
- Detection of 10-100 MeV gamma-rays from the Crab Nebula pulsar NP 0532.
03 p0362 A73-13847
- Sco X-1, Crab Nebula, extragalactic, thermal and diffuse background source X ray spectra
03 p0364 A73-13962
- A search for isolated radio pulses from the Crab Nebula at 151.5 MHz.
04 p0500 A73-15493
- The pulse shape of the Crab Nebula pulsar NP 0532 as a function of color.
04 p0501 A73-15685
- Crab Nebula evolution from 1054 supernova to neutron star and nebula expansion, discussing pulsar properties
05 p0614 A73-16304
- The excitation mechanism for the filaments in the Crab Nebula.
05 p0617 A73-16471
- A model of the Crab Nebula derived from dual-frequency radio measurements.
05 p0622 A73-17075
- Mechanisms of optical, X-ray and gamma-radiation from Crab pulsar.
05 p0611 A73-17314
- Observations of Taurus X-1 by the I-60 keV X-ray detector on the OSO-7.
07 p0868 A73-19064
- Recent supernova in NGC 5253 and the supernova rate.
07 p0900 A73-20238
- Radio brightness distribution in the Crab Nebula at the 3.55-cm and 1.28-cm wavelengths
07 p0901 A73-20309
- Very long baseline interferometry techniques for Crab Nebula pulsar observation at meter wavelengths
08 p1013 A73-21812
- The structure of the Crab Nebula. II - The spatial distribution of the relativistic electrons.
09 p1151 A73-23290
- The structure of the Crab Nebula. III - The radio filamentary radiation.
09 p1151 A73-23291
- Compton effect in charged particle under intense circularly polarized electromagnetic wave, noting application to Crab pulsar
10 p1271 A73-23485
- Pulsed gamma ray emission at 5-25 MeV from Crab Nebula pulsar, noting time-averaged energy flux with consideration for telescope efficiency
10 p1272 A73-23535
- Radio polarization and variability of pulsar NP 0532.
11 p1417 A73-25582
- The 1969 solar occultation of the Crab Nebula pulsar.
11 p1417 A73-25583
- Pulsar magnetospheres, braking index, polar caps, and period-pulse-width distribution.
11 p1428 A73-26618
- Radio-brightness distribution over the Crab Nebula at 3.55 and 1.28 cm.
12 p1539 A73-27281
- Supernova outbursts and the formation of relativistic objects. I
12 p1546 A73-27853
- Crab Nebula magnetic field origin and internal electron acceleration mechanism nature
13 p1673 A73-28225
- Observation of linear polarization of the Crab nebula during an occultation by the solar corona.
13 p1586 A73-29247
- Gamma-ray emission above 20 MeV from the Crab Nebula and NP 0532.
14 p1785 A73-29737
- Anticipated variability of Pulsar NP 0532 emission in the Crab nebula associated with angular velocity jumps
15 p1938 A73-31964

- Crab Nebula pulsar electromagnetic radiation emission model based on high energy electron circular motion around magnetic field lines
15 p1942 A73-32649
- Ionization and relative abundance of hydrogen and helium atoms in filaments of the Crab Nebula
16 p2057 A73-32712
- Supernovae remnant X radiation observations, discussing Crab Nebula, Cas A, SN 1572, Cygnus Loop, Vela X and Puppis A and possibilities from Uhuru catalog
16 p2050 A73-32735
- High energy gamma ray discrete source identification in Crab Nebula, pulsar NP 0532 and galactic regions from Apollo and TD-1 satellite measurements
16 p2051 A73-32750
- On the energy spectrum of relativistic electrons in the Crab Nebula.
19 p2475 A73-37619
- Faraday rotation patterns in Crab Nebula pulsar radio spectra for average signal and giant pulses, noting difference in linear polarization percentage
19 p2488 A73-38516
- The optical polarization of the Crab Nebula pulsar. I - A relativistic vector model.
19 p2488 A73-38517
- Optical polarization of the Crab Nebula pulsar. II - Observational results and fits by the relativistic vector model.
19 p2488 A73-38518
- Supernova outbursts and the formation of relativistic objects. I.
20 p2608 A73-39227
- Collisionless damping of hydromagnetic waves in relativistic plasma. I - Weak Landau damping - Heating of the Crab Nebula.
20 p2609 A73-39442
- Second-order plasma interaction in the Crab Nebula.
20 p2610 A73-39579
- X-ray studies of the Crab nebula occultations, 1974-75.
21 p2765 A73-40300
- Pulsed high-energy gamma rays from the Crab Nebula.
22 p2901 A73-41760
- Expected radiative variability of Crab-Nebula pulsar NP 0532, related to abrupt changes in angular velocity.
24 p3132 A73-44489
- CRABS**
- Light evoked changes in potential difference between inside and outside of cells in *Limulus* ommatidia, describing multistage model of generator potential
09 p1043 A73-23309
- Inhibitory interaction in the retina of *Limulus*.
09 p1043 A73-23311
- CRACK FORMATION**
- U CRACK INITIATION**
- CRACK INITIATION**
- Crack formation in orthogonally reinforced fiberglass plastics
01 p0067 A73-10482
- Crack initiation and propagation in glass fiber reinforced plastic materials, noting rod bending
02 p0231 A73-11810
- Impact fracture resistance of Cr-Mn-Si steel, investigating alloying effects on crack initiation and propagation
02 p0181 A73-12211
- Brittle crack initiation at the elastic-plastic interface.
02 p0182 A73-12752
- Cracking of Zircaloy as a result of unusual localized texturing.
02 p0183 A73-12756
- Stress history effect on incubation time for stress corrosion crack growth in AISI 4340 steel.
02 p0183 A73-12763
- Accommodation of the stress field at a grain boundary under heterogeneous shear by initiation of microcracks.
02 p0237 A73-12812
- Fatigue induced microstructural changes in metals and alloys, considering crystal lattice defects, crack formation and propagation, dislocations and strengthening effects
03 p0321 A73-13133
- Inhomogeneity of the structure and deformability of aluminum and aluminum-magnesium alloys
03 p0324 A73-13506
- Microstructural changes that drilling and reaming can cause in the bore holes in DTD 5014 /RR58 extrusions/.
03 p0325 A73-13573
- Crack initiation, acceleration, steady propagation and fatigue growth, considering Griffith criterion on fracture mechanics
04 p0507 A73-14705
- Techniques for smooth specimen simulation of the fatigue behavior of notched members.
04 p0453 A73-14862

- Fracture criteria in quasi-viscoelastic analysis of crack initiation and propagation in polymethyl methacrylate, noting thermal effects on stress intensity factor
04 p0512 A73-15237
- Formation of annular cracks in cylindrical samples intended for estimating resistance to crack propagation.
04 p0514 A73-15673
- Mathematical model for long term creep strength from creep tests, noting crack initiation and microstructural changes
04 p0517 A73-15952
- Fretting-fatigue mechanisms and the effect of direction of fretting motion on fatigue strength.
05 p0581 A73-16128
- Flat dendritic carbide effects on crack formation in Ti and Nb stabilized austenitic Cr-Ni corrosion resistant steels after heating to 1250 C
06 p0705 A73-17850
- Influence of local variations of yield strength on plastic zones at crack tips.
06 p0709 A73-18480
- Stress intensity factors and singularity power and strain energy release rate near localized cracks and inclusions in composite materials
06 p0764 A73-18489
- Effects of thermal treatment on the resistance of some steels to crack development and propagation
06 p0711 A73-18664
- Crack corrosion of titanium in a solution of hot concentrated magnesium chloride
07 p0839 A73-20167
- Acoustic emission weld monitoring of nuclear components.
07 p0832 A73-20274
- Mechanism by which hot cracks form during welding aluminum and its alloys.
08 p0977 A73-21236
- Study of the formation process of corrosion cracks under tension in an aluminum alloy [ONERA, TP NO. 1213]
09 p1098 A73-21925
- Transmission electron microscope study on initiation of fatigue crack in 18-8 austenitic steel.
09 p1104 A73-22523
- Apparatus for recording acoustic signals from cracks initiated in brittle materials.
09 p1086 A73-23165
- Mechanisms of stress corrosion cracking of titanium-aluminum alloys in methanol-HCl solutions.
09 p1106 A73-23166
- An electrochemical testing method for stress corrosion cracking by separating crack anode from cathode.
09 p1106 A73-23168
- Fatigue crack initiation and propagation in part through crack metal specimens under cyclic loading, discussing plasticity effects and surface wave interaction
09 p1163 A73-23253
- Surface crack slow growth onset investigation with near tip strain as ductile fracture criterion, measuring fracture strength
09 p1109 A73-23264
- Ductile fracture strain criteria from known stress-strain relationships, predicting microscopic crack and void nucleation strain
09 p1164 A73-23322
- Effect of mean stress on fatigue crack initiation and propagation /from different configurations of notch/.
09 p1164 A73-23323
- Metal fatigue crack nucleation behavior and dislocation microstructures, including slip band and extrusion-intrusion pairs
11 p1380 A73-25804
- Fatigue damage and dislocation structures in fcc metals surface layers, noting microcrack formation conditions
11 p1380 A73-25805
- Effects of oxygen environment and surface diffused coatings on fatigue crack development in copper single crystals.
11 p1380 A73-25806
- The effect of surface films on fatigue crack initiation.
11 p1381 A73-25810
- Oxygen and temperature effects on Ni base superalloys fatigue fracture, discussing trans- and intergranular crack propagation and initiation in single and polycrystals and surface coatings
11 p1382 A73-25818
- An ultrasonic device for the study of fatigue crack initiation in anodized aluminum alloys.
11 p1363 A73-25830
- The effect of fretting corrosion in fatigue crack initiation.
11 p1383 A73-25835
- Dissolution of Ti-6Al-4V at cathodic potentials in 5N HCl.
12 p1512 A73-27249
- Bending-produced cracks, stresses and fracture of rectangular cross section beam from brittle body homogeneous model
12 p1552 A73-27255

- A potential means of using acoustic emission for crack detection under cyclic-load conditions.
13 p1700 A73-29401
- Brittle fracture initiation characteristics of twin notches.
13 p1700 A73-29469
- Effects of specimen geometry and loading conditions on the crack tip plastic zone.
13 p1701 A73-29474
- Fatigue crack initiation and propagation in low stacking fault energy austenite steel related to plastic deformation induced gamma alpha transformation and martensite failure
13 p1640 A73-29481
- Crack initiation and propagation in notched plates subjected to cyclic inelastic strains.
13 p1701 A73-29489
- Correlation between notch sensitivity of a material and its non-propagating crack, under rotating bending stress.
13 p1641 A73-29493
- Some observations of crack initiation and propagation of notched specimens under creep conditions.
13 p1641 A73-29510
- An X-ray study of the stress corrosion of austenitic stainless steels.
13 p1625 A73-29521
- Stress gradient as one of the causes of the scale effect on the brittle fracture of materials.
13 p1703 A73-29614
- Experimental and theoretical investigation of the fracture of sheet materials in the presence of cracks.
13 p1703 A73-29625
- Finite element method investigation of branch and secondary crack formation and multiple fracture, solving sequences of boundary value problems and strain energy release rates
14 p1808 A73-30195
- Crack formation in orthogonally reinforced glass-fiber ware.
14 p1765 A73-30307
- Book - A course in continuum mechanics. Volume 4 - Elastic and plastic solids and the formation of cracks.
14 p1813 A73-30595
- Application of fiber optics to the observation of fatigue crack development
14 p1754 A73-30691
- High strength steel fracture characteristics in vacuum and gaseous medium, noting hydrogen adsorption effect on crack resistance
15 p1887 A73-31248
- A note on the use of a simple technique for failure prediction using resistance curves.
15 p1951 A73-31989
- German monograph on frictional fatigue failure covering microcrack initiation due to shear induced vibrational stresses
15 p1956 A73-32587
- Effect of additional alloying and heat treatment on the strength of steels
17 p2187 A73-34336
- Workhardening, slip band formation and crack initiation during fatigue of titanium.
17 p2190 A73-34882
- A microscopic study of crack initiation mechanisms in 7075 aluminum alloy sheets.
17 p2190 A73-34885
- Interdisciplinary communications problems of metal physicists, fracture mechanists, structural designers and reliability analysts for fatigue crack generation and growth
17 p2246 A73-34886
- Solid cadmium cracking of titanium alloys.
17 p2191 A73-35123
- A quantitative model of hydrogen induced grain boundary cracking.
17 p2191 A73-35124
- Fracture mechanics in materials selection and design.
18 p2363 A73-36483
- An automatic flash photomicrographic system for fatigue crack initiation studies.
18 p2316 A73-36588
- DC 10 airframe structure full scale fatigue tests for crack initiation and growth, residual strength and service life [AIAA PAPER 73-803]
19 p2379 A73-37463
- Metal fatigue studies of nucleation and crack propagation through plastic and elastic regimes
19 p2502 A73-38548
- Some specific features of crack initiation and development in heat-resistant alloys under various loading conditions
20 p2578 A73-39376
- Nature of the damage caused by laser radiation on the surfaces or in the bulk of transparent glasses.
20 p2573 A73-39687
- The interaction of creep and fatigue for a rotor steel /The William M. Murray Lecture, 1972/.
21 p2722 A73-41264
- Effect of a loading sequence on threshold stress intensity determination.
22 p2875 A73-42141

- Fatigue-crack initiation studied by electrical resistance measurements. 23 p2979 A73-43301
- Metal fatigue phases investigation including strain hardening under cyclic loads and microcrack nucleation due to dislocation formation under hydrostatic pressure 23 p2993 A73-43966
- Hydrogen-induced transformation and embrittlement in 18-8 stainless steel. 23 p2994 A73-44158
- Investigation of the initial stage of crack development during compression and tension of polymethylmethacrylate samples 23 p2998 A73-44278
- Determination of the magnitude and distribution of initial stresses in fiberglass-reinforced plastics. I 24 p3103 A73-44527
- 'Crack boundaries' in the case of unidirectional glass-fiber-reinforced plastic wound laminates under uniaxial and multiaxial stress 24 p3103 A73-44883
- The dynamic fracture toughness of carbon-carbon composites. 24 p3105 A73-45147
- Materials testing by sonic emission analysis /SEA/ 24 p3094 A73-45445
- CRACK PROPAGATION**
- Influence of the loading conditions on the propagation of fatigue cracks in D16T-alloy sheet samples 01 p0064 A73-10489
- The diffusion of point defects to a propagating crack tip. 01 p0116 A73-11000
- Statistical characteristics for duralumin sheets mechanical properties, fatigue life and crack growth 01 p0117 A73-11298
- Effect of various surface-active media on the changes taking place in the strength of U8 steel in the high-strength state. 01 p0066 A73-11337
- Fatigue crack propagation in stainless steel weldments at high temperature. 01 p0067 A73-11372
- Electron microanalysis of backfilled hot cracks in Inconel 600. 01 p0067 A73-11373
- Crack initiation and propagation in glass fiber reinforced plastic materials, noting rod bending 02 p0231 A73-11810
- Fracture resistance curve calculation from fracturing diagram, noting crack propagation in thin plate under tensile deformation 02 p0232 A73-11930
- On two coplanar cracks in an infinite transversely isotropic medium. 02 p0234 A73-12087
- The effects of frequency of loading and of nonreactive external media on growth of fatigue cracks. 02 p0235 A73-12132
- Engineering method of calculating the parameter of fracture toughness. 02 p0235 A73-12210
- Impact fracture resistance of Cr-Mn-Si steel, investigating alloying effects on crack initiation and propagation 02 p0181 A73-12211
- Growth of fatigue cracks in polycarbonate. 02 p0185 A73-12430
- Limiting crack propagation rates during a quasi-brittle failure 02 p0236 A73-12582
- Fracture mechanics equations for crack propagation braking by elliptic and circular holes at crack tip, noting stress concentration 02 p0237 A73-12586
- Stress history effect on incubation time for stress corrosion crack growth in AISI 4340 steel. 02 p0183 A73-12763
- Regression models for the effect of stress ratio on fatigue crack growth rate. 03 p0387 A73-13231
- On the probabilistic determination of scatter factors using Miner's rule in fatigue life studies. 03 p0388 A73-13237
- Stress redistribution model for anisotropic fiber reinforced laminates with internal cracks, assuming preferred directions to bonding planes and fiber orientation 03 p0334 A73-13333
- The fracture mechanics of slit-like cracks in anisotropic elastic media. 03 p0394 A73-13979
- The dynamic growth of a void in a plastic material and an application to fracture. 03 p0394 A73-13984
- Ni-Cr-Ti steel aircraft structural element fatigue life calculation based on failure mechanism involving crack propagation 03 p0394 A73-14011
- Hold-time effects on the elevated temperature fatigue-crack propagation of type 304 stainless steel. 03 p0328 A73-14448
- National Symposium on Fracture Mechanics, 5th, University of Illinois, Urbana, Ill., August 31-September 2, 1971, Proceedings. Part 1 - Stress analysis and growth of cracks. 04 p0505 A73-14676
- Stress intensity factor for an elliptical crack approaching the surface of a plate in bending. 04 p0505 A73-14677
- Fatigue crack growth data for various materials deduced from the fatigue lives of precracked plates. 04 p0506 A73-14684
- Fatigue threshold crack propagation in air and dry argon for a Ti6Al4V alloy. 04 p0459 A73-14685
- Extensive study of low fatigue crack growth rates in A533 and A508 steels. 04 p0459 A73-14686
- Fatigue crack propagation growth rates under a wide variation of Delta K for an ASTM A517 Grade F /T-1/ steel. 04 p0459 A73-14687
- Fatigue crack propagation of D6ac steel in air and distilled water. 04 p0459 A73-14688
- The effect of frequency upon the fatigue-crack growth of Type 304 stainless steel at 1000 F. 04 p0459 A73-14689
- Delay effects in fatigue crack propagation. 04 p0459 A73-14690
- Rayleigh waves for continuous monitoring of a propagating crack front. 04 p0452 A73-14691
- Rice energy line J integral fracture strength criterion applicability to crack tip elastoplastic testing for steel alloys 04 p0506 A73-14694
- Elastoplastic slip line analysis of specimen geometry effects on J fracture strength criterion for medium strength steel center cracked panel and bend bar 04 p0506 A73-14695
- Crack initiation, acceleration, steady propagation and fatigue growth, considering Griffith criterion on fracture mechanics 04 p0507 A73-14705
- Colloquium on Structural Reliability notes on 'Fatigue Lecture.' 04 p0507 A73-14706
- The design and development of fracture resistant structures. 04 p0507 A73-14712
- Applications of exoelectron emission to nondestructive evaluation of alloying, crack growth, fatigue, annealing, and grinding processes. 04 p0453 A73-14856
- The force on a crack deviating from its original plane. 04 p0509 A73-14950
- Acoustic emission source location using single and multiple transducer arrays. 04 p0448 A73-15121
- Frequency spectra of acoustic emissions generated by deforming metals and ceramics. 04 p0448 A73-15122
- Sonic degradation of thermally shocked ceramics. 04 p0448 A73-15124
- On the modified Westergaard equations for certain plane crack problems. 04 p0512 A73-15236
- Fracture criteria in quasi-viscoelastic analysis of crack initiation and propagation in polymethyl methacrylate, noting thermal effects on stress intensity factor 04 p0512 A73-15237
- Fourier transformations and Wiener-Hopf equations for stress intensity factor of crack propagation in linearly elastic homogeneous isotropic strip 04 p0512 A73-15238
- Plastic deformations and crack propagation in cylindrical and spherical shells under uniform pressure, calculating stress intensity factor 04 p0512 A73-15239
- Fatigue crack growth measurement on Al alloy wedge-opening-load specimens under constant amplitude sinusoidal loading, comparing data with existing crack propagation results 04 p0462 A73-15241
- Fractographic observations of fatigue crack tip behavior of age hardened Al-Zn-Mg-Cu alloy during static loading 04 p0462 A73-15242
- Fatigue crack propagation in terms of fracture mechanics concepts 04 p0462 A73-15298
- Accelerated method of estimating the growth rate of fatigue cracks. 04 p0514 A73-15671
- Method of repeatedly determining the fracture roughness with one specimen. 04 p0466 A73-15672
- Formation of annular cracks in cylindrical samples intended for estimating resistance to crack propagation. 04 p0514 A73-15673
- Stresses in laminated composites containing a broken layer. [ASME PAPER 72-WA/APM-14] 04 p0516 A73-15899
- Analysis of transverse cracks in an orthotropic strip with edge stiffeners. [ASME PAPER 72-WA/APM-4] 04 p0516 A73-15904
- The energy of crack propagation in carbon fibre-reinforced resin systems. 04 p0469 A73-15981
- A plastic-strip specimen for fatigue crack propagation studies in low yield strength alloys. 05 p0581 A73-16127
- Crack tip stress field variation via elastic pulses for crack path alteration and subsequent fracturing process termination, using photoelastic analysis 05 p0634 A73-16795
- Crack growth and failure of aluminum plate under in-plane shear. [ALAA PAPER 73-253] 05 p0635 A73-16975
- The probability of fracture as parameter of crack propagation under cyclic stress 05 p0635 A73-17065
- Torsional fatigue fixture for high temperature investigation of high strength steels crack growth rate in tensile mode 05 p0563 A73-17254
- Determination of constants in the equation for the fatigue-crack propagation rate with allowance for properties of the plastic zone 06 p0761 A73-17847
- Tensile tests and heat treatment for creep rupture and fracture strengths of heat resistant steel, noting crack initiation and propagation 06 p0706 A73-17884
- Crack problem of transversely isotropic strip. 06 p0762 A73-17986
- Influence of local variations of yield strength on plastic zones at crack tips. 06 p0709 A73-18480
- Growth of part-through thickness fatigue cracks in sheet polymethylmethacrylate. 06 p0714 A73-18481
- Method of analysis and prediction for variable amplitude fatigue crack growth. 06 p0709 A73-18482
- Subcritical crack growth of TRIP steels in air under static loads. 06 p0710 A73-18485
- Stress intensity factors and singularity power and strain energy release rate near localized cracks and inclusions in composite materials 06 p0764 A73-18489
- Materials cracking resistance characterization by fracture toughness determination as function of crack front speed 06 p0764 A73-18491
- Direct observation of tensile and fatigue cracks. 06 p0710 A73-18495
- Study of fatigue crack propagation by X-ray diffraction approach. 06 p0698 A73-18496
- The influence of stress intensity and microstructure on fatigue crack propagation in ferritic materials. 06 p0710 A73-18498
- Crack propagation measurements by surface gage of polymethyl methacrylate, epoxy resin and glass reinforced epoxy composites, conforming with Mott energy balance equation 06 p0714 A73-18499
- Effects of thermal treatment on the resistance of some steels to crack development and propagation 06 p0711 A73-18664
- Frequency dependent low cycle fatigue crack propagation. 06 p0713 A73-18767
- A note on the Cherepanov calculation of viscoelastic fracture. 07 p0908 A73-19090
- Nonlinear effect of initial stress on crack propagation between similar and dissimilar orthotropic media. 07 p0915 A73-20334
- Inhibition of corrosion fatigue in 7075 aluminum alloys. 07 p0840 A73-20351
- Crystal defect model of crack propagation in three dimensional solid, assuming nonlinear dependence of Young modulus on strain with term for time lag 08 p1017 A73-21025
- The fracture toughness and crack propagation properties of polyester resin casts and laminates. 08 p0983 A73-21595
- Study of the formation process of corrosion cracks under tension in an aluminum alloy [ONERA, TP NO. 1213] 09 p1098 A73-21925
- Mixed viscous-brittle fracture model of plastic crack distribution and propagation pattern in bcc polycrystal by electron raster microscope analysis 09 p1157 A73-21961
- On the influence of deformation rate on intergranular crack propagation in Type 304 stainless steel. 09 p1100 A73-22000
- Inhibition of a wedge-shaped crack by a plane buildup of edge dislocations 09 p1157 A73-22159

Influence of inclusion content on fatigue crack propagation in aluminum alloys. 09 p1101 A73-22409

Effect of thermomechanical processing on fatigue crack propagation. 09 p1102 A73-22415

Substructure formation around fatigue cracks and its role in the propagation of fatigue cracks in aluminum. 09 p1103 A73-22437

Acoustic emission for monitoring fatigue crack growth. 09 p1083 A73-22511

An electrochemical testing method for stress corrosion cracking by separating crack anode from cathode. 09 p1106 A73-23168

Book - Methods of analysis and solutions of crack problems: Recent developments in fracture mechanics; Theory and methods of solving crack problems. 09 p1161 A73-23176

A special theory of crack propagation. 09 p1161 A73-23177

Fracture mechanics of brittle matrix ductile fiber composites. 09 p1111 A73-23251

Fatigue crack growth under C.O.D. cycling. 09 p1163 A73-23252

Fatigue crack initiation and propagation in part through crack metal specimens under cyclic loading, discussing plasticity effects and surface wave interaction. 09 p1163 A73-23253

The role of fracture toughness in low-cycle fatigue crack propagation for high-strength alloys. 09 p1108 A73-23254

Artificial slow crack growth under constant stress - The R-curve concept in plane stress. 09 p1108 A73-23255

Plastic strain rates within discrete crack tip zones at running brittle cracks in mild steel plates, identifying twinning as main deformation mode. 09 p1163 A73-23258

Influence of material properties on dynamic fracture toughness of steels. 09 p1109 A73-23259

Tensile, fracture toughness and crack growth properties of a roll-extruded HP 9Ni-4Co-25C steel alloy. 09 p1109 A73-23260

Research and application problems in fracture of materials and structures in the United States Air Force. 09 p1163 A73-23261

Linear elastic and general yielding fracture mechanics compatibility, investigating crack opening displacement relationship to stress intensity factor. 09 p1109 A73-23263

Surface crack slow growth onset investigation with near tip strain as ductile fracture criterion, measuring fracture strength. 09 p1109 A73-23264

Effect of mean stress on fatigue crack initiation and propagation /from different configurations of notch/. 09 p1164 A73-23263

Thermal stresses in an elastic solid weakened by two coplanar circular cracks. 10 p1287 A73-23563

Stress corrosion cracking characteristics and test data interpretation, considering pitting, brittle fracture, crack propagation, chemical environment and smooth and cracked specimens. 10 p1232 A73-23868

Stress corrosion cracking of a high strength steel. 10 p1232 A73-23869

Moire fringe method for stationary and running cracks length and crack opening displacement measurements in composite materials. 10 p1240 A73-24287

Plastic strain as factor in crack propagation rate smoothing and branching rate reduction in elastic and elastoplastic materials. 10 p1291 A73-24362

Failure of high-strength welded structures with initial cracks. 10 p1225 A73-24368

Subcritical crack growth measurement during static loading of precracked Ti alloys in salt water, discussing arrested crack propagation at different stress intensities. 10 p1234 A73-24429

Al alloy stress intensity range estimation from surface fatigue striation incidence and modulus of elasticity, noting relationship to crack growth closure in fractography. 10 p1235 A73-24447

Investigation of stress state at fatigue crack tip by means of X-ray microbeam. 10 p1293 A73-24918

Electron fractography of fatigue failure and macrocrack propagation in dual phase Ti alloy during cyclic loading at minus 140 to plus 150 C. 10 p1236 A73-24931

Fatigue-crack growth in Type 304 stainless steel weldments at elevated temperatures. 11 p1379 A73-25131

Measurement of the critical crack displacement with the help of double-notched specimens. 11 p1434 A73-25325

Fatigue crack delay and arrest due to single peak tensile overloads. 11 p1441 A73-25555

[AIAA PAPER 73-325] The influence of environment and the surface layer on crack propagation and cyclic behavior. 11 p1380 A73-25807

Metal surfaces corrosion fatigue due to environmentally induced localized attack, discussing protective film growth, crack propagation hydrogen interaction and stresses. 11 p1381 A73-25811

Brittle cleavage crack propagation in crystals in terms of bonds acting between pairs of atoms, considering stress distribution around crack tip. 11 p1409 A73-25812

Stress and displacement fields around growing corrosion fatigue crack, discussing intensity factor, plastic zones, cyclic loading and fluid pressure effects. 11 p1381 A73-25813

Shear decohesion mechanism of fatigue crack propagation in ductile metals under cyclic loads, considering secondary microfracture and creep cavitation effects at elevated temperatures. 11 p1381 A73-25814

Corrosion fatigue and stress corrosion crack growth in high strength aluminum alloys, magnesium alloys, and titanium alloys exposed to aqueous solutions. 11 p1381 A73-25815

Gaseous environments compatibility with structural alloys under fatigue loading, presenting crack growth rate data. 11 p1381 A73-25816

The kinetic and dynamic aspects of corrosion fatigue in a gaseous hydrogen environment. 11 p1382 A73-25817

Environment enhanced corrosion fatigue crack growth and fracture mechanics, discussing inspection intervals to maintain structural integrity. 11 p1382 A73-25819

On the superposition model for environmentally-assisted fatigue crack propagation. 11 p1382 A73-25820

Corrosion fatigue crack propagation behavior in steels above/below stress intensity threshold within framework of linear elastic fracture mechanics. 11 p1382 A73-25821

Effect of cyclic stress form on corrosion fatigue crack propagation below K_{ISCC} in a high yield strength steel. 11 p1382 A73-25822

Aircraft structures aluminum alloys fatigue crack growth rate relationship to cracking mode, stress ratio, cyclic frequency and corrosive environment severity. 11 p1382 A73-25826

Corrosive aspects of the fatigue of rubber. 11 p1388 A73-25841

Crack growth rate due to steels and Ti and Ni alloys electrochemical dissolution, noting tensile stress intensity factor. 11 p1385 A73-26173

Energy flux into extending crack in elastic solid calculated in terms of stress intensity factor for plane and antiplane strain problems. 11 p1444 A73-26281

Crack propagation behavior in type 304 stainless steel weldments at elevated temperature. 11 p1375 A73-26357

Coarse grain Al alloys strength characteristics, crack resistance and specific energy of failure due to brittle fracture. 11 p1386 A73-26736

Crack propagation in some aluminum alloys with tensile stresses. 12 p1511 A73-26916

Stress-corrosion cracking of Ti-8Al-1Mo-1V in aqueous environments. I - The kinetics of subcritical crack propagation. II - Plastic zones, crack morphology, and fractography. 13 p1632 A73-28135

Elastic-plastic fracture by homogeneous microvoid coalescence tearing along alternating shear planes. 13 p1633 A73-28142

Body centered cubic lattice transition metals favored cleavage plane prediction for crack propagation. 13 p1635 A73-28261

Propagation of a brittle crack at constant and accelerating speeds. 13 p1635 A73-28755

Application of Papkovitch-Neuber potentials to a crack problem. 13 p1635 A73-28756

Crack propagation in an elastic solid subjected to general loading. III - Stress wave loading. 13 p1696 A73-28792

Symmetrical crack branching in polymethyl methacrylate plates, using method of caustics for stress intensity factor evaluation. 13 p1645 A73-28842

Elliptic notch interaction with nearby crack in elastic solid under longitudinal shear, obtaining stress intensity factor. 13 p1697 A73-28914

Application of fracture mechanics to the analysis of statically indeterminate structure. 13 p1700 A73-29466

Aluminum foils crack propagation observation with electron microscope during tensile tests, noting crystal dislocation role in ductile fracture process. 13 p1639 A73-29467

Brittle fracture strength and non-crack propagation. 13 p1639 A73-29470

Interaction of elasto-plastic cracks subjected to a uniform tensile stress in an infinite or a semi-infinite plate. 13 p1701 A73-29471

Parametric finite element stress analysis of multiple crack propagation in nonhomogeneous nonisotropic materials, using Griffith criterion. 13 p1701 A73-29472

The interaction of material and geometric aspects in the fracture of aluminum alloys. 13 p1640 A73-29475

Fracture toughness defined as work required for unit area crack extension, discussing toughness as function of material strength and strain characteristics. 13 p1640 A73-29478

Thin Al alloy sheet fracture toughness from crack growth resistance curves, discussing failure modes and critical stress intensities. 13 p1640 A73-29480

X-ray investigation of fatigue-crack growth - On critical strain for fracture at the crack tip. 13 p1625 A73-29482

Further consideration of crack propagation by oscillating crystal X-ray microbeam diffraction technique. 13 p1625 A73-29483

The effect of microstructure on fatigue crack propagation in Ti-6Al-6V-2Sn alloy. 13 p1640 A73-29484

A study of fatigue crack propagation in high strength aluminum alloys at high stresses. 13 p1640 A73-29488

Crack initiation and propagation in notched plates subjected to cyclic inelastic strains. 13 p1701 A73-29489

Fatigue crack propagation as successive stochastic processes and fatigue fracture toughness. 13 p1701 A73-29490

Random and program fatigue tests of Cr-Mo steel specimen with V-grooved notch. 13 p1641 A73-29494

Aspect of cumulative fatigue damage under multiaxial strain cycling. 13 p1701 A73-29497

Some observations of crack initiation and propagation of notched specimens under creep conditions. 13 p1641 A73-29510

The effect of elevated temperature upon the fatigue-crack propagation behavior of two austenitic stainless steels. 13 p1642 A73-29525

Experimental and theoretical investigation of the fracture of sheet materials in the presence of cracks. 13 p1703 A73-29625

Acoustic-emission detection techniques for high-cycle-fatigue testing. 14 p1751 A73-29772

Tape recorder instrumentation for structural dynamic load test data analysis, discussing cable crosstalk, lead length and electrical noise effects in crack propagation measurements. 14 p1751 A73-29775

Estimation of fatigue-crack propagation life in butt welds. 14 p1755 A73-30147

Fatigue crack propagation in butt welds containing joint penetration defects. 14 p1755 A73-30148

Effect of loading conditions on the propagation of fatigue cracks in sheet samples of D16T alloy. 14 p1759 A73-30314

Fatigue crack propagation in martensitic and austenitic steels. 14 p1761 A73-30632

Investigation of crack propagation in small samples under conditions of low-cyclic fatigue. 14 p1763 A73-30680

Effect of cooling /to -269 C/ on failure in K18N10T and K16N6 steels under impact bending. 14 p1763 A73-30692

Application of cylindrical specimens with a ring crack for determining the brittle strength in materials. 14 p1814 A73-30719

Dynamic singular boundary value problem of elastic body with propagating crack under concentrated force. 14 p1814 A73-30784

Fracture strength of fiber reinforced plastics, investigating crack propagation susceptibility, stress concentration and fracture mechanics. 14 p1767 A73-30821

Fracture mechanics approach to fatigue analysis in design. [ASME PAPER 73-DE-20] 14 p1763 A73-30823

Brittle fracture of a body with a crack under variable shear load

15 p1945 A73-31040

Semiinfinite and finite crack motion models comparison without loading restrictions, considering finite length dislocation pile up role and singular integral equation use

15 p1946 A73-31106

Brittle fracture and crack propagation prediction in unidirectionally fiber reinforced composites via Sc theory, comparing with stress intensity factor Kc concept

15 p1949 A73-31681

Fracture toughness evaluation by R-curve methods; Proceedings of the Symposium, Hawthorne, Calif., September 29-October 1, 1971.

15 p1950 A73-31982

Crack growth resistance curves /R-curves/ - Literature review.

15 p1950 A73-31983

R-curve determination using a crack-line-wedge-loaded /CLWL/ specimen.

15 p1950 A73-31984

Thin Al alloy sheet plane stress testing with zero K gradient specimen based on tapered double cantilever beam modification, considering fracture toughness and crack propagation

15 p1950 A73-31985

Fracture extension resistance /R-curve/ characteristics for three high-strength steels.

15 p1951 A73-31986

Plane stress fracture testing using center-cracked panels.

15 p1951 A73-31987

Comparison of R-curves determined from different specimen types.

15 p1951 A73-31988

A note on the use of a simple technique for failure prediction using resistance curves.

15 p1951 A73-31989

Effect of specimen thickness on the fracture surface energy of 100 axis tungsten single crystals.

15 p1891 A73-32022

Infinite elastically isotropic solid under external tensile stress, deriving condition for complete fracture from wedge crack

15 p1951 A73-32023

Self similar dynamic problems for elastic plane and half-plane with/without propagating crack, assuming application of instantaneous perturbation source or uniform stress field

15 p1952 A73-32078

Displacements and elastoplastic deformations at a crack edge under tension

15 p1954 A73-32105

Study on stress corrosion cracking of austenitic stainless steel under pulsating load.

15 p1895 A73-32570

Corrosion-fatigue crack growth in high-strength aluminum alloys with and without susceptibility to stress-corrosion cracking.

15 p1895 A73-32571

Stress corrosion cracking of titanium alloys in hydrogen chloride.

15 p1896 A73-32573

Two theoretical models of fatigue crack propagation.

16 p2079 A73-33200

The dynamic field of a growing plane elliptical shear crack.

16 p2082 A73-33907

Steady state diffraction of stress waves by semiinfinite running crack in elastic solid under dynamic loading, obtaining solution based on Wiener Hopf technique

16 p2082 A73-33910

System of arbitrarily oriented cracks in elastic bodies

17 p2240 A73-34144

A steadily moving longitudinal-shear crack with an infinitely narrow plastic zone

17 p2241 A73-34266

Elastic isotropic infinite body with interior tunneling crack under dynamic shear force perpendicular to crack propagation direction, obtaining solution via Mathieu functions

17 p2241 A73-34329

An experimental study of the heat generated in the plastic region of a running crack in different polymeric materials.

17 p2195 A73-34878

Effect of load sequences on crack propagation under random and program loading.

17 p2190 A73-34879

A numerical and experimental investigation of the use of J-integral.

17 p2246 A73-34880

Prior-to-failure extension of flaws under monotonic and pulsating loadings.

17 p2246 A73-34884

Interdisciplinary communications problems of metal physicists, fracture mechanists, structural designers and reliability analysts for fatigue crack generation and growth

17 p2246 A73-34886

Welded steel beam fatigue behavior evaluation via stable crack growth concepts, developing fracture mechanics model for cracks originating from pores

17 p2246 A73-34887

On the influence of single and multiple peak overloads on fatigue crack propagation in 7075-T6511 aluminum.

17 p2190 A73-34889

Role of stress in the stress corrosion cracking of a Mg-Al alloy.

17 p2191 A73-35100

On the opening of a finite crack normal to an interface.

17 p2250 A73-35122

Continuous monitoring of fatigue crack growth by acoustic emission techniques.

[TR-DE-73-2] 17 p2148 A73-35445

Viscoelastic fracture of solid propellant pressurization condition.

[SESA PAPER 2114A] 17 p2220 A73-35449

Acoustic emission instrumentation and application for plastic deformation, flaw detection monitoring of fatigue crack growth, stress corrosion and hydrogen embrittlement

17 p2175 A73-35670

Compliance measurement for determination of crack extension force, specimen dimensions and elastic constants in linear fracture mechanics, discussing instrumentation, precautions and data reduction

17 p2252 A73-35671

Fracture mechanics in materials selection and design.

18 p2363 A73-36483

The measurement and analysis of fatigue crack growth in cylindrical shapes.

18 p2363 A73-36486

On the physical justification of the term 'state of fatigue of materials under cyclic loading.'

18 p2364 A73-36592

Environment-assisted fracture in engineering alloys. I - Monotonic loading.

[ASME PAPER 73-MAT-R] 18 p2365 A73-36613

Fatigue and corrosion-fatigue crack propagation in intermediate-strength aluminum alloys.

[ASME PAPER 73-MAT-N] 18 p2323 A73-36615

Influence of the structural state of the surface layers on the resistance to crack propagation of steel products

18 p2366 A73-36819

A simple method for studying slow crack growth.

19 p2497 A73-37588

A path-independent integral for transient crack problems.

19 p2500 A73-38114

The motion of a brittle crack.

19 p2444 A73-38263

System for determining the critical range of stress-intensity factor necessary for fatigue-crack propagation.

19 p2501 A73-38297

Quantitative estimation of the fatigue crack propagation under varying load conditions.

19 p2501 A73-38346

Metal fatigue studies of nucleation and crack propagation through plastic and elastic regimes

19 p2502 A73-38548

Fracture toughness, ductility and cleavage mechanisms of crack extension in structural materials

19 p2502 A73-38550

A finite element approach to the critical cyclic stress required to propagate a crack.

20 p2615 A73-38639

Determination of the critical load for a compressed plate weakened by a circular hole and by cracks propagating toward the hole contour

20 p2617 A73-39263

Moisture effect on Ni steel fatigue crack propagation under low stresses

20 p2617 A73-39291

Designing equal-life minimum-weight truss structures

20 p2619 A73-39357

Brittleness of coated tungsten wire

20 p2577 A73-39361

Some specific features of crack initiation and development in heat-resistant alloys under various loading conditions

20 p2578 A73-39376

Stress singularities associated with a crack inclined to a bi-material interface.

20 p2620 A73-39531

Torsional and anti-plane strain delamination of an orthotropic layered composite.

20 p2622 A73-39549

Experimental error equation of stress intensity factor for fracture toughness and crack growth rate testing

21 p2785 A73-40635

Influence of preloading on the sustained load cracking behavior of maraging steels in hydrogen.

21 p2719 A73-40924

Effect of orthotropy on singular stresses produced near a crack tip by incident SH-waves.

21 p2786 A73-40933

Critical load analysis of strip /beam/ with arched crack under compressive stress and bending moments

21 p2786 A73-40985

A finite-element representation of stable crack-growth.

21 p2788 A73-41549

Fatigue behavior of stiffened flat panels

21 p2788 A73-41555

Heat resistant materials cracking and fracturing caused by ductility loss at high temperatures, discussing cavitation mechanisms, microcracks, creep tests and time dependence

21 p2722 A73-41576

Stopping of a wedge-shaped crack by a plane cluster of edge dislocations.

22 p2919 A73-42107

Progress in flaw growth and fracture toughness testing; Proceedings of the Sixth National Symposium on Fracture Mechanics, Philadelphia, Pa., August 28-30, 1972.

22 p2920 A73-42131

Application of strip model to crack tip resistance and crack closure phenomena.

22 p2875 A73-42132

Some observations on fracture under combined loading.

22 p2920 A73-42133

Interaction of cracks with rigid inclusions in longitudinal shear deformation. II - Further results.

22 p2920 A73-42134

Prior to failure extension of flaws in a rate sensitive Tresca solid.

22 p2880 A73-42136

Threshold for fatigue crack propagation and the effects of load ratio and frequency.

22 p2875 A73-42137

Overload effects on subcritical crack growth in austenitic manganese steel.

22 p2875 A73-42138

Effect of multiple overloads on fatigue crack propagation in 2024-T3 aluminum alloy.

22 p2875 A73-42139

Fatigue-crack growth under variable-amplitude loading in ASTM A514-B steel.

22 p2875 A73-42140

Fatigue and corrosion-fatigue crack growth of 4340 steel at various yield strengths.

22 p2875 A73-42142

Fatigue crack propagation and fracture toughness of 5Ni and 9Ni steels at cryogenic temperatures.

22 p2875 A73-42143

A method for measuring K sub Ic at very high strain rates.

22 p2866 A73-42148

Plane-stress fracture toughness and fatigue-crack propagation of aluminum alloy wide panels.

22 p2876 A73-42151

Structure of polymers and fatigue crack propagation.

22 p2880 A73-42152

The effect of plasticity and crack blunting on the stress distribution in orthotropic composite materials.

[ASME PAPER 73-APMW-2] 22 p2924 A73-42876

Fracture control - Past, present and future.

23 p3039 A73-43383

Titanium alloys mechanical, electrochemical and metallurgical parameters effects on stress corrosion cracking, discussing crack growth kinetics, failure features and component hazard minimization

23 p2990 A73-43457

Fracture mechanics and composite materials - A critical analysis.

23 p3040 A73-43628

Method for estimating fracture strength of specially orthotropic composite laminates.

23 p3040 A73-43630

Fracture behaviour of crystalline Al3Ni intermetallic fibres.

23 p2991 A73-43774

The stress pulses propagated as a result of the rapid growth of brittle fracture.

23 p3042 A73-43805

A review of fatigue crack growth in high strength aluminum alloys and the relevant metallurgical factors.

23 p2991 A73-43806

Fatigue crack growth retardation after single-cycle peak overload in Ti-6Al-4V titanium alloy.

23 p2992 A73-43809

Slow growth of cracks in a rate sensitive Tresca solid.

23 p2992 A73-43810

Fatigue crack growth detection by acoustic emission monitoring in correlation with stress intensity for high cycle fatigue Al alloy

23 p2992 A73-43814

Transmission of anti-plane shear waves past an interface crack in dissimilar media.

23 p3043 A73-43815

Acoustic emission from low-cycle high-stress-intensity fatigue.

23 p2992 A73-43816

Resistance to crack propagation in ceramics subjected to thermal shock.

23 p2997 A73-44031

On Papkovitch-Fadle solutions of crack problems relating to an elastic strip.

23 p3046 A73-44227

Fracture micromechanism characteristics and crack tip plastic zone formation effects on metal embrittlement, using elastoplasticity theory

23 p3047 A73-44277

Investigation of the initial stage of crack development during compression and tension of polymethylmethacrylate samples

23 p2998 A73-44278

Electronic logic device for crack arresting penthrate microcharge pulse initiation, including crack and stress wave propagation measurements

23 p3047 A73-44286

Free vibrational development of laser-induced cracks

24 p3095 A73-44510

Determination of lifetime characteristics from crack growth kinetics data

24 p3145 A73-44523

Shear crack stress intensity and displacement jump solution for half space under plane strain in form of singular integral equation

24 p3146 A73-44677

The dynamic fracture toughness of carbon-carbon composites.

24 p3105 A73-45147

A layered composite with a broken laminate.

24 p3151 A73-45301

Plastic relaxation of a shear crack near a planar interface.

24 p3152 A73-45403

CRACKING [FRACTURING]

NT STRESS CORROSION CRACKING

Inhibition of stress corrosion cracking of AISI 3430 steel in 10% potassium nitrate solution at 100 C.

01 p0061 A73-10138

Influence of metallurgical factors on the corrosion cracking under tension of TA6V titanium alloy in an aqueous medium at ambient temperature [ONERA, TP NO. 1100]

01 p0061 A73-10231

Stress corrosion cracking behavior of 18% Ni/300/maraging steel.

01 p0066 A73-11295

Effects of hot-salt stress corrosion on titanium alloys.

03 p0323 A73-13268

Cracking and corrosion of plastic materials under stress

03 p0334 A73-13592

A study of local stresses near surface flaws in bending fields.

04 p0505 A73-14678

Fatigue crack growth data for various materials deduced from the fatigue lives of precracked plates.

04 p0506 A73-14684

Fracture mechanics consideration of hydrogen sulfide cracking in high strength steels.

04 p0459 A73-14692

Rice path independent J integral fracture strength criterion estimation as function of crack size and elastoplastically adjusted load point displacement for Ni-Cr-Mo-V steel

04 p0506 A73-14696

Ductile fracture initiation, propagation, and arrest in cylindrical vessels.

04 p0506 A73-14697

Center cracked tension specimen geometry effects on plane stress fracture toughness of high strength Al, Ti and steel alloy sheets

04 p0460 A73-14699

Study by autoradiography at high resolution power of the role of hydrogen in the mechanism of cracking of TA6V titanium alloy in salt water

04 p0461 A73-15097

On the production of fatigue cracks for determining the work of rupture in bending tests.

04 p0450 A73-15670

Temperature distribution at a thermally insulated crack in a plate for various boundary conditions

05 p0640 A73-16774

Subsonic jet airframe fatigue cracking as function of load, geometry, material, joint performance and environment

05 p0636 A73-17200

Fractographic aspects of the stress corrosion cracking of titanium in a methanol/HCl mixture.

06 p0705 A73-17800

The linear thermoelastic problem of uniform heat flow disturbed by a two-dimensional crack in a strip.

06 p0762 A73-17985

The stress intensity factor of an edge crack in a finite elastic disc.

06 p0762 A73-17989

Edge crack in a strip of an elastic solid.

06 p0762 A73-17991

A comparison of hydrogen embrittlement and stress corrosion cracking in high-strength steels.

06 p0709 A73-18479

Probability of stress-corrosion fracture under random loading.

06 p0763 A73-18483

On the buckling of thin tensioned sheets with cracks and slots.

06 p0764 A73-18497

Stress intensity factors for nozzle corner cracks.

07 p0912 A73-19564

Surface fatigue crack morphology comparison to bulk crack developments, considering surface grains constraints by adjoining grains

09 p1103 A73-22441

Orthotropic material plane crack problem numerical solutions by polynomial approximation and modified mapping-collocation technique involving conformal mapping

09 p1161 A73-23178

Isotropic homogeneous elastic medium internal crack analysis based on Laurent series expansions of complex potentials consistent with displacements and stress-strain single valuedness

09 p1162 A73-23179

Asymptotic approximation to crack problems with emphasis on stress intensity factor, discussing interpolation procedure based on simplified problem form

09 p1162 A73-23180

Stress field singularities due to cracks in isotropic elastic bodies, assuming Hooke's law stress-strain relationship in integral equation representations

09 p1162 A73-23182

Mixed boundary value problems in solid contact and crack mechanics, discussing numerical solution of singular integral equations with simple and generalized Cauchy kernels

09 p1162 A73-23184

Applications of the finite element method to the calculations of stress intensity factors.

09 p1162 A73-23185

Finite element methods for elastic bodies containing cracks.

09 p1162 A73-23186

Study on the superposition of intergranular corrosion and pitting corrosion by fatigue cracking of stainless steels.

11 p1383 A73-25831

Crack toughness evaluation of hot pressed and forged beryllium.

11 p1384 A73-26169

A metallurgical approach to cracked solder joints.

11 p1375 A73-26355

Continuum mechanics analysis of local rupture and plastic strains near cracks and fractures, noting elastoplastic applications

12 p1551 A73-27251

Brittle failure of infinite plate with circular hole and radial cracks under two perpendicular uniformly distributed tensile loads

12 p1556 A73-27802

A hypothesis of non-propagating fatigue crack.

13 p1635 A73-28644

Plane strain elastic-plastic state and fracture in cracked blunt notched steel plates under tensile loads

13 p1701 A73-29477

Finite element method application to nonlinear, microscopic and ductile fracture mechanics covering crack tip singularity elastoplastic analysis and elastic constants of metal crystals

14 p1809 A73-30200

Two coplanar cracks in an infinitely long elastic strip bonded to semi-infinite elastic planes.

14 p1815 A73-30918

Critical stress intensity factors applied to glass reinforced polyester resin.

15 p1897 A73-31676

High strength Ti alloy cracking and brittle fracture prevention during aging by high heat rate treatment at 250-500 C

15 p1889 A73-31814

Lattice theory of fracture and crack creep.

15 p1890 A73-31927

Spherical debris - Its occurrence, formation and significance in rolling contact fatigue.

16 p2022 A73-34029

An overview of fatigue and fracture for design and certification of advanced high performance ships.

17 p2246 A73-34881

Tensile fracture of boron-epoxy composites with ordered filament packing geometry.

17 p2198 A73-35535

Two and three dimensional elasticity theory of linear fracture mechanics covering stress functions, finite element method and crack behavior in solids

17 p2252 A73-35669

Crack resistance tests of polymethyl methacrylate specimens under tensile stress

18 p2366 A73-36824

Influence of non-singular stress terms and specimen geometry on small-scale yielding at crack tips in elastic-plastic materials.

19 p2501 A73-38264

Plane crack problems for ideal fibre-reinforced materials.

21 p2787 A73-41014

Influence of stress intensity level during fatigue precracking on results of plane-strain fracture toughness tests.

22 p2876 A73-42149

Experimentally determined shape factors for deep part-through cracks in a thick-walled pressure vessel.

22 p2866 A73-42157

Stress-strain state of disk with internal rectilinear cracks under load, solving Fredholm equations

23 p3039 A73-43468

Fiber reinforced composite crack model performance prediction and tests, noting fiber volume fraction for maximum fracture toughness

23 p3040 A73-43629

Fracture analysis of surface- and through-cracked sheets and plates.

23 p3042 A73-43813

High strength Ti alloy cracking and brittle fracture prevention during aging by high heat rate treatment at 250-500 C

24 p3100 A73-45277

CRACKS

NT MICROCRACKS

NT SURFACE CRACKS

Axisymmetric thermoelasticity problem for an infinite body weakened by two parallel circular cracks

01 p0113 A73-10014

Two dimensional elasticity theory for radial crack effects on tensile stress concentration in circular elastic isotropic plate

01 p0117 A73-11092

Nonlinear stress properties in vicinity of crack tip, taking into account finite crack width effect by parabolic model

03 p0385 A73-13131

Stress intensity factors for internally pressurized thick-wall cylinders.

04 p0505 A73-14680

Crack shapes and stress intensity factors for edge-cracked specimens.

04 p0506 A73-14681

Elliptical, annular, through, part-through and irregularly shaped crack front curvature effect on stress intensity factor calibration

04 p0506 A73-14682

Some crack tip finite elements for plane elasticity.

04 p0506 A73-14683

Strength analyses for design with composite materials using metals technology.

04 p0507 A73-14713

The influence of anisotropy and crystalline slip on relaxation at a crack tip.

06 p0709 A73-18331

An assessment of factors influencing data obtained by the photoelastic stress freezing technique for stress fields near crack tips.

06 p0764 A73-18488

Dynamic stress intensity factor for an unbounded plate having collinear cracks.

[AD-758426] 06 p0764 A73-18492

The compressional modulus of a material permeated by a random distribution of circular cracks.

07 p0915 A73-20335

Distinguishing characteristics of pitting and crevice corrosion.

08 p0980 A73-21775

A cylindrical shell with an axial crack under skew-symmetric loading.

09 p1160 A73-22894

Some results of a study of the interaction between Rayleigh pulses and edge cracks

10 p1287 A73-23591

A mechanized eddy current scanning system for aircraft struts.

10 p1225 A73-24631

Elastic circular inclusion in an infinite plane containing two cracks.

13 p1696 A73-28749

Finite element method application to elastoplastic analysis of cracked metal plates, discussing plate thickness effects on plastic zone growth and stress distributions along crack tip

13 p1701 A73-29476

Stress distribution about defects such as rigid sharp-angled inclusions.

13 p1703 A73-29619

Effect on the stresses around a crack due to the presence of circular inclusion.

14 p1806 A73-30042

Influence on the stress-strain state of the way a concentrated force is applied to the tip of a crack in a plate

14 p1814 A73-30718

Influence of the diathermancy of an arc-shaped crack on the thermoelastic state of the area about the crack

14 p1814 A73-30720

Spatial problem of thermoelasticity of a body with an insulated external circular crack

14 p1814 A73-30725

Effect of a crack in an infinite plane containing a circular hole under uniform normal pressure.

15 p1947 A73-31333

Determination of stress intensity factors in cracked plates by the finite element method.

15 p1951 A73-32034

The stress field near a system of four symmetrically situated line cracks of equal length.

15 p1953 A73-32093

- Stresses in a symmetrically-laminar plate weakened by a central crack
17 p2240 A73-34145
- Limiting equilibrium of a plate weakened by two arbitrarily oriented cracks
19 p2494 A73-37186
- Application of dual integral equations to the problem of torsion of an elastic space, weakened by a conical crack of finite dimensions.
19 p2498 A73-37640
- Determination of the stress strain state of closed cylindrical shells and infinite plates with cracks
20 p2624 A73-39645
- Ellipsoidal crack and needle in an anisotropic elastic medium
21 p2783 A73-40187
- Stress distribution in thin circular plate with equiarmed cruciform crack, obtaining stress intensity factor and crack energy by numerical solution of Fredholm equation
21 p2785 A73-40932
- J-integral and equivalent energy method parameter relationship from elastic and inelastic stress concentration factors for notches and cracks
22 p2920 A73-42146
- Applications of the compliance concept in fracture mechanics.
22 p2920 A73-42154
- Determination of the limiting equilibrium of a brittle body weakened by a system of cracks whose form on a plane approaches a circular form
22 p2921 A73-42284
- Analysis of stress intensity factors for the tension of a centrally cracked strip with stiffened edges.
23 p2992 A73-43812
- CRANIUM**
NT INTRACRANIAL CAVITY
Orbit and superior orbital fissure acoustic window for cranium posterior structures imaging by echoencephalographic techniques
22 p2815 A73-42667
- CRASH INJURIES**
Helmets effectiveness evaluation from acceleration and impact tests, discussing test criteria and civilian and military standards
16 p1975 A73-33132
- Aircraft crash injury reduction through seat and restraint design, discussing dummy size considerations, seat belts, aircraft acceleration and injury types [SAE PAPER 730290]
17 p2114 A73-34655
- Aircraft evacuation and safety procedures during emergencies, discussing negative panic, flight crew training and impact injury minimization
18 p2268 A73-36849
- Severe intraabdominal injuries without abdominal protective rigidity after an air crash - Seat belt injury
20 p2517 A73-39209
- Design and analysis of an energy absorbing restraint system for light aircraft crash-impact.
[ASME PAPER 73-DET-111] 22 p2799 A73-42080
- CRASH LANDING**
NT DITCHING [LANDING]
Post-crash survival planning and procedures, discussing passenger instructions and control, crew training and rescue signalling devices
10 p1176 A73-24711
- Aircraft crash fire prevention and fighting in airports, discussing aircraft fuel system fail-safe design concepts and airport fire fighting equipment and procedures
15 p1859 A73-32366
- Airplane accident survival, discussing cabin safety, fire protection, crashworthiness, emergency evacuation and crash landing in water
17 p2097 A73-34079
- Development of airframe design technology for crashworthiness.
[SAE PAPER 730319] 17 p2101 A73-34677
- CRASHES**
NT CRASH LANDING
NT DITCHING [LANDING]
A consistent crashworthiness design approach for rotary-wing aircraft.
[AHS PREPRINT 781] 17 p2106 A73-35094
- CRATERING**
NT PROJECTILE CRATERING
Volatile-rich lunar soil - Evidence of possible cometary impact.
05 p0615 A73-16321
- Lunar micrometeoroid flux, calculating rocks survival time before impact damage and mass wasting rate by single particle abrasion
07 p0895 A73-19865
- Radar measurement of altitude profiles and reflected power for Martian topography and surface properties, noting heavy cratering
09 p1144 A73-22260
- Displaced mass, depth, diameter, and effects of oblique trajectories for impact craters formed in dense crystalline rocks.
10 p1276 A73-24077
- Moon - 'Ghost' craters formed during Mare filling.
17 p2236 A73-35746
- Lunar and terrestrial impact crater spherules.
17 p2236 A73-35749
- Martian cratering. IV - Mariner 9 initial analysis of cratering chronology.
19 p2477 A73-37207
- Ancient lunar mega-regolith and subsurface structure.
24 p3129 A73-44448
- CRATERS**
NT LUNAR CRATERS
NT METEORITE CRATERS
Interplanet variations in scale of crater morphology - Earth, Mars, Moon.
06 p0745 A73-17442
- Craters on photographs of the Mars surface taken by the Mariner 4 probe in 1965
16 p2069 A73-33835
- Comparison of Martian and lunar multiringed circular basins.
19 p2477 A73-37206
- CRAZING**
U SURFACE CRACKS
CREATINE
Importance of the Lohmann reaction in the response of the heart to anoxic aggression
02 p0133 A73-12152
- Serum creatine phosphokinase activity and urinary excretion of creatine and creatinine in man during acclimatization to high altitude and in high altitude natives.
11 p1315 A73-25333
- Study of nitrogen balance and creatine and creatinine excretion during recumbency and ambulation of five young adult human males.
18 p2278 A73-36786
- Influence of electric stimulation of the hypothalamus on catecholamine, phosphorated compound, and cholesterol levels
21 p2637 A73-40284
- CREATININE**
Serum creatine phosphokinase activity and urinary excretion of creatine and creatinine in man during acclimatization to high altitude and in high altitude natives.
11 p1315 A73-25333
- Study of nitrogen balance and creatine and creatinine excretion during recumbency and ambulation of five young adult human males.
18 p2278 A73-36786
- CREATION**
U CREATIVITY
CREATIVITY
Reflex act structural components interaction in terms of reflection, creativity and organism-environment relations, noting subjective and objective perception and attitude formation
04 p0410 A73-15798
- CREEP ANALYSIS**
Investigation of the interrelation between creep parameters in industrial aluminum during the first and second stages of creep
02 p0179 A73-11567
- Flat Ti alloy sheet creep under variable loads at 300-400 C comparing prediction with test data
03 p0328 A73-14016
- Stress analysis of thick walled hollow viscoelastic circular cylinder enclosed in elastic shell and subjected to nonlinear creep conditions, noting temperature effects
03 p0394 A73-14021
- Internal stress and dislocation structure of aluminum in high-temperature creep.
04 p0467 A73-15930
- High temperature steady state creep determination in Al by dip test technique interpreted in terms of slip and recovery activation energy due to effective and internal stress
04 p0467 A73-15933
- Deformation, displacement, and work bounds for structures in a state of creep and subject to variable loading.
[ASME PAPER 72-APM-U] 05 p0632 A73-16529
- A time hardening transient creep solution for steadily loaded uniaxial tension panels containing circular and elliptical holes under conditions of plane stress.
06 p0761 A73-17820
- A stochastic model of creep in the heat-resistant low-alloy CrMoV steel
06 p0705 A73-17846
- Creep of precipitation-hardened nickel-base alloy single crystals at high temperatures.
06 p0713 A73-18768
- A creep bending analysis of plates by the finite element method.
07 p0908 A73-19093
- The Castigliano variational equation in the theory of nonlinearly hereditary creep
07 p0912 A73-19322
- Theoretical and experimental prediction for pulsating creep failure.
07 p0917 A73-20489
- Multi-axial and reversing stress effects in dislocation creep - A mechanical equation of states.
08 p0980 A73-21781
- Correlation between pore formation at grain boundaries and internal friction during creep of nickel
09 p1099 A73-21970
- A strain criterion for failure of materials subjected to stress and temperature cycles
09 p1159 A73-22570
- Application of the extended Newton method to the creep analysis of shells of revolution.
11 p1432 A73-24998
- Nonlinear thermo-elastic-plastic and creep analysis by the finite element method.
[AIAA PAPER 73-358] 11 p1437 A73-25494
- Transient creep of shells of revolution.
11 p1444 A73-26336
- Cumulative creep formulas for construction steels at stepwise increasing temperatures
12 p1510 A73-26900
- Creep analysis of a thin-walled wing on the basis of the plate analogy
12 p1551 A73-27086
- Deformation of zero-moment shells subjected to internal pressure under creep conditions
12 p1551 A73-27179
- Nickel base alloys high temperature steady creep rate and stress relations
12 p1512 A73-27256
- Alloy creep due to temperature and tensile stress in absence of hardening
12 p1513 A73-27479
- Thermally activated low temperature creep of solids at constant load, considering creep curve stages and plastic deformation mechanism
13 p1635 A73-28263
- Creep analysis of transversely isotropic bodies subjected to time-dependent loading.
14 p1805 A73-29769
- Energy methods in plasticity theory extension to creep mechanics with respect to stress-strain rate tensors relationships
14 p1811 A73-30478
- Combined tension-torsion creep of polyethylene with abrupt changes of stress.
15 p1897 A73-31613
- Nonisothermal creep of chrome-nickel steel
15 p1890 A73-31830
- A high order finite element for completely incompressible creeping flow.
15 p1951 A73-32026
- Tensile creep in short fibre reinforced thermoplastics.
17 p2197 A73-35344
- Creep, self heating and failure of thermoplastics under pulsating tensile stress.
17 p2197 A73-35346
- A numerical method for creep deformation of solids.
18 p2365 A73-36612
- Finite element elastic-plastic-creep analysis of two-dimensional continuum with temperature dependent material properties.
19 p2496 A73-37483
- A model of strain hardening during high-temperature creep.
19 p2442 A73-38168
- Localized creep of a nonhomogeneous beam subjected to loads exceeding the true elastic limit
19 p2501 A73-38306
- Flow theoretical model for nonstationary creep in metals, using Galerkin method for approximate solution of boundary value problem
20 p2616 A73-39099
- Creep relaxation approximations and exact solutions, discussing rectangular beam pure bending, spherical shell internal pressure loading and thin circular tube bending
20 p2616 A73-39115
- Strain-hardening anisotropy and original anisotropy in creep
20 p2580 A73-39364
- Irishin linear theory for defect accumulation generalized for endurance limit of materials under noncyclic loads, examining time to failure under creep and relaxation conditions
20 p2624 A73-39644
- Cumulative creep formulas for construction steels at stepwise increasing temperatures
21 p2720 A73-41033
- The activation energy for creep of columbium /niobium/.
22 p2879 A73-42580
- Creep rate relationship in terms of stress and strain rate for anisotropic metal based on single crystal theory, applying to pressurized thin cylinder
23 p3045 A73-44167
- Dynamic strain ageing in creep of beta-NiAl.
24 p3100 A73-45331
- Constitutive equations, creep laws, stress functions, variational principles and differential operators in dynamic and static linear viscoelasticity theory
24 p3153 A73-45496
- CREEP BUCKLING**
The effect of variable temperature on creep collapse of a cylindrical shell under external pressure
07 p0913 A73-20070
- Pseudoelastic design method for bottle-crack stack instability performance prediction through failure by

- creep buckling, assessing effectiveness by comparison with measurements 12 p1514 A73-26876
- Non-linear creep buckling with random temperature variations. 23 p3045 A73-44166
- Creep buckling stability for deformable rod with initial deflection, determining perturbed and unperturbed motion of random and deterministic components 23 p3046 A73-44188
- Topography on satellite surfaces and the shape of asteroids. 24 p3129 A73-44446
- Optimum design of lattice structures in creep conditions with consideration of the Kempner-Hoff theory of buckling. 24 p3148 A73-45002

CREEP DIAGRAMS

- Surfaces of constant rate of energy dissipation and deformation velocity for arbitrary thin walled shell under steady creep with given strain hardening 02 p0233 A73-11937
- Frame photography for temporary creep in cylindrical Al alloy specimen necks under tensile loads, calculating creep diagrams 05 p0634 A73-16748
- Creep and creep-rupture-strength of titanium strengthened by molybdenum fibers 10 p1233 A73-24356
- Heat resistant nickel alloys creep rupture strength diagram, determining time to failure as function of loads 13 p1636 A73-29062
- Creep test diagrams plotted to estimate heat resistance for turbine blades design, predicting fatigue life with allowance for loading cycle form and duration 13 p1703 A73-29616
- Interpretation of tensile and compressive creep behaviour of two nickel alloys. 15 p1888 A73-31618
- Creep and recovery of polycarbonate. 17 p1294 A73-34525
- Heat resistant nickel alloys creep rupture strength diagram, determining time to failure as function of loads 18 p2325 A73-36894
- Discontinuous flow in steady-state creep of Al-Mg alloys at high temperatures. 23 p2995 A73-44162

CREEP PROPERTIES

- NT STEADY STATE CREEP**
- NT TENSILE CREEP**
- Processing conditions and sample dimensions and shapes effects on Ti alloy creep characteristics at room temperature 01 p0064 A73-10487
- Study of creep in copper and aluminum by the differential method of constant-rate temperature change 01 p0064 A73-10612
- Superplasticity in two phase compositions based on refractory compounds, noting creep rate dependence on concentration and electroconductivity 01 p0066 A73-11339
- Random stresses effect on dynamic creep properties of Ti alloy in high temperature air flow 02 p0180 A73-11625
- Possibility of using the method of time characteristics for solving applied problems concerning the bending of sandwich plates with allowance for creep of the materials 02 p0230 A73-11641
- Behavior of certain turbine-blade materials under asymmetric loading. 02 p0180 A73-12128
- Creep and durability of tungsten wire. 02 p0180 A73-12137
- The creep of materials being weakly strengthened in nonsteady temperature and force conditions. 02 p0180 A73-12138
- The relation between creep at room temperature and the characteristics of the stress-strain diagram in the case of metallic materials 02 p0181 A73-12366
- Calculation of the stress distribution in rotating disks in the case of unsteady creep with the aid of a digital computer 03 p0385 A73-13140
- Changes in the fine structure of heat-resistant nickel-chromium alloys during the creep process 03 p0324 A73-13505
- Stresses governing the high-temperature creep rate in single crystals with a bcc lattice 03 p0326 A73-13971
- Substructural changes during high-temperature creep deformation of aluminum single crystals 03 p0327 A73-13978
- Flat Ti alloy sheet creep under variable loads at 300-400 C comparing prediction with test data 03 p0328 A73-14016
- Zirconium carbide creep characteristics and limit at 2450-2810 K, examining test conditions effects on parameters 03 p0328 A73-14017

- Dimensionless results for plane stress creep behavior of thin disks with central rigid inserts under combined loading 03 p0396 A73-14644
- High temperature creep properties of recrystallized W-thoria alloy wires, noting dependence on temperature, grain structure and stress 04 p0463 A73-15306
- Nonlinear physical stress-strain relation for reticular polymers and fiberglass plastics under conditions of microcreep and elastic aftereffect 04 p0468 A73-15508
- Effect of accommodation coefficient on thermal creep flow of rarefied gas. 04 p0436 A73-15973
- Evaluation of multiaxial theories for room-temperature plasticity and elevated-temperature creep and relaxation of several metals. 06 p0759 A73-17599
- Creep characteristics and substructure disorientation in metals with an fcc lattice 06 p0706 A73-17904
- Creep in molybdenum single crystals at 0.57 of the melting temperature 06 p0708 A73-18047
- Quasi-static load acting on a rotating shaft in the presence of creep 07 p0830 A73-19309
- Low-frequency creep in CoNiFe films. 07 p0861 A73-19362
- [IEEE PAPER 7,1] The influence of scatter on some simple variable-stress creep predictions. 08 p1016 A73-20798
- A recovery creep model based on dislocation distributions. 08 p0980 A73-21777
- The effect of a dispersed phase on the creep properties of a Cr-Ni steel. 08 p0980 A73-21779
- A new explanation for the creep of domain boundaries with transverse constrictions 09 p1098 A73-21846
- High temperature creep in nickel and its alloys 09 p1108 A73-23229
- High temperature creep properties of PIOP polyimide - HMS graphite composites. 10 p1239 A73-23975
- Tensile creep modulus, creep lateral contraction ratio and torsional creep measurements on small non-rigid specimens. 10 p1218 A73-24120
- Discrete creep of AMg6 aluminum alloy subjected to repeated static loading 10 p1233 A73-24365
- Quantitative characterization of the substructure of AISI 316 stainless steel resulting from creep. 10 p1234 A73-24436
- Unsteady creep in a symmetrical cylindrical shell 10 p1293 A73-24793
- Udimet 700 creep behavior under cyclic tensile stresses at 925 C from hodograph of monotonic stress-strain relations, taking into account strain rate effects [AIAA PAPER 73-387] 11 p1439 A73-25516
- Shear decohesion mechanism of fatigue crack propagation in ductile metals under cyclic loads, considering secondary microfracture and creep cavitation effects at elevated temperatures 11 p1381 A73-25814
- Dislocation structure of subgrain boundaries in creep-deformed aluminium. 12 p1511 A73-27028
- Flattening and creep stability loss of nonlinear viscoelastic ring under external pressure 12 p1551 A73-27180
- Lunar rotation secular acceleration and tidal friction related to earth rotational velocity and creep properties 13 p1677 A73-28378
- Elastic and creep limits of heteroplastic micrograin metallic (duralumin/ materials in terms of stress-strain curve, sliding plane and stress hardening and relaxation 13 p1635 A73-28471
- Changes in the electrical resistance of heat-resistant EI 826 alloy in the presence of creep 13 p1636 A73-29065
- German monograph - Effect of creep strains at 700 C on the hardening characteristics of the steel X 8 Cr-NiMoNb 16 16 at room temperature. 13 p1637 A73-29281
- Nimonic and Mg alloys creep behavior interpretation by constitutive law, discussing recovery activation and strain hardening from microstructural behavior 13 p1642 A73-29515
- Low carbon steel S-N diagram for stresses ranging to fatigue limit, noting cyclic creep, macroplastic cyclic stress and fatigue failure 13 p1703 A73-29603
- High temperature tests of microalloying effect on creep and stress rupture characteristics of hot rolled and annealed Mo alloys 13 p1643 A73-29605

- Investigation of some principles in the processes of creep and fracture in heat-resistant materials. 13 p1643 A73-29626
- Processing conditions and sample dimensions and shapes effects on Ti alloy creep characteristics at room temperature 14 p1759 A73-30312
- Anomalous creep behavior of crystal bar alpha-Zr during dynamic strain aging at 723-823 K as function of temperature, stress and oxygen content 14 p1760 A73-30626
- Thoria particle dispersion TD-nickel creep and tensile deformation at elevated temperature dependence on grain size and L/D ratio 14 p1761 A73-30635
- German monograph - Effect of the transformation and heat treatment conditions on the mechanical properties and the creep characteristics of the alloy TiAl6V4. 14 p1762 A73-30668
- Grain-boundary sliding and recrystallization of Nimonic 108 during creep. 15 p1887 A73-31352
- A simple model of uniaxial creep recovery and stress relaxation based on residual-stress redistribution. 15 p1948 A73-31615
- Transition theory application to creep deformation, considering spherical shells 15 p1954 A73-32117
- Thermal creep of rarefied gas in a circular tube. 16 p2039 A73-33328
- Experimental investigation of the effect of vibrations on the creep of glassfiber-reinforced plastics in the presence of complex stress conditions 16 p2030 A73-33939
- Special features of high-temperature creep in metals with an fcc lattice 17 p2188 A73-34563
- On the stress analysis of creeping structures subject to variable loading. [ASME PAPER 72-APM-NNN] 17 p2250 A73-35115
- Fatigue and creep behavior of aluminum and titanium matrix composites. 17 p2193 A73-35543
- Cylindrical Poiseuille flow and thermal creep of a rarefied gas. 18 p2300 A73-36635
- Theory of hardening applicability to the description of deformation law singleness under various conditions of uniaxial tension 18 p2366 A73-36759
- The change in the electrical resistance of EI826 refractory alloy with creep. 18 p2325 A73-36897
- Short-term creep of OT4 alloy. 19 p2440 A73-37786
- Anisotropic nature of strain hardening during unsteady creep of alloy AK4-1 subject to combined tension and torsion 20 p2577 A73-39288
- Effect of porosity on creep in niobium carbide and other powder materials under uniaxial loads 20 p2578 A73-39381
- Effect of gas diffusion on creep behavior of polycarbonate. 20 p2580 A73-39403
- Effect of zirconium concentration on creep of niobium-zirconium alloys 20 p2579 A73-39739
- Changes in the disorientation of the substructure of a nickel-aluminum alloy under ultrasonic treatment and creep 20 p2579 A73-39748
- The influence of phase size on the creep of lamellar and particulate Al-CuAl2 eutectic composites. 21 p2719 A73-40896
- Designing a slender-wing-type cantilever plate under conditions of unsteady creep 23 p3042 A73-43728
- High temperature creep of lithium zinc silicate glass-ceramics. I - General behaviour and creep mechanisms. II - Compression creep and recovery. 23 p2997 A73-44030
- Steady-state creep characteristics of an Fe alloy containing 3.5 at.% Mo. 23 p2994 A73-44153
- Creep during the hot compression of titanium diboride powder 24 p3093 A73-44740
- Creep and aging characteristics of glass-fiber-reinforced plastics 24 p3104 A73-44885
- CREEP RESISTANCE**
- U CREEP STRENGTH**
- CREEP RUPTURE STRENGTH**
- Time characteristics of rupture and creep in metals during tension under hydrostatic pressure conditions 01 p0064 A73-10605
- Experimental estimation of the deformation criterion of long-term /creep/ strength. 02 p0180 A73-12130
- The influence of preliminary thermocycling on the high-temperature strength of austenitic steel. 02 p0180 A73-12139

Apparatus for investigations into long-term strength and creep of coated materials at temperatures above 1400 C in air.

02 p0150 A73-12219

The effect of small magnesium additions on microstructure and high-temperature properties of nickel-2 1/2 vol. % alumina.

03 p0326 A73-13966

Creep rupture under multi-axial states of stress.

03 p0327 A73-13981

Parametric-graphical method of cumulative creep damage evaluation for Cr-Mo-V steel in terms of postexposure rupture and hardness measurements

04 p0460 A73-14855

Characterization of age-hardenability and stress-rupture properties of some cobalt-base alloys.

04 p0465 A73-15579

The effect of alloying elements on creep rupture strength and microstructure of 12 percent chromium heat resisting steel.

04 p0465 A73-15581

High temperature strength and microstructure of nickel-base heat resisting No. 64BC alloy.

04 p0465 A73-15583

On the production of fatigue cracks for determining the work of rupture in bending tests.

04 p0450 A73-15670

Creep rupture testing of aluminum alloys to 100,000 hours.

05 p0581 A73-16133

Tensile tests and heat treatment for creep rupture and fracture strengths of heat resistant steel, noting crack initiation and propagation

06 p0706 A73-17884

Postirradiation mechanical properties of Types 304 and 304 + 0.15% titanium stainless steel.

06 p0710 A73-18545

Fracture in conditions of creep under complex loading

07 p0910 A73-19302

Theoretical and experimental prediction for pulsating creep failure.

07 p0917 A73-20489

Creep-rupture strength of OT4 alloy

07 p0840 A73-20511

Stress rupture behavior of a dispersion strengthened superalloy.

[ASME PAPER 72-MAT-G] 08 p0978 A73-21570

The influence of microstructure on creep properties of low alloy ferritic chromium-molybdenum-vanadium steel.

08 p0980 A73-21675

Some problems in the assessment of high temperature properties for engineering purposes.

08 p0981 A73-21782

Some empirical relationships between creep strain, stress, time and temperature in ICr-Mo-V rotor forgings.

08 p0981 A73-21783

The effect of niobium carbide on the creep rupture properties of austenitic stainless steels.

08 p0981 A73-21790

The influence of nickel content on the structure and high temperature properties of a 12% Cr Mo V Nb steel.

08 p0982 A73-21799

Certain regularities in the deformation and rupture of molybdenum-, niobium-, and tantalum-based high-melting-point alloys under programmed temperature changes

09 p1100 A73-22151

Deformation and rupture of molybdenum under conditions of creep

09 p1100 A73-22161

Ti based beta alloy strain hardening and failure characteristics, emphasizing initial deformation phase and microdefect onset and development

09 p1105 A73-23064

Heat resistant alloys stress-rupture strength tests for operating temperatures based on equivalent high temperatures damageability

09 p1106 A73-23156

Plane stress rupture criterion for age hardening materials during plastic deformation, calculating resistance to shear and torsion of solid and hollow round bars

09 p1106 A73-23157

Creep-rupture strength criterion in the case of interlayer shearing of oriented fiberglass plastics

10 p1240 A73-24355

Creep and creep-rupture-strength of titanium strengthened by molybdenum fibers

10 p1233 A73-24356

Stress redistribution and rupture due to creep in a uniformly stretched thin plate containing a circular hole.

[ASME PAPER 72-APM-KKK] 11 p1442 A73-25709

Deformation bounds for a creeping structure approaching rupture.

11 p1447 A73-26654

Loading time to failure and creep rupture strength from interatomic stochastic bond fracture

11 p1448 A73-26739

Transverse creep and stress-rupture of Borsic-aluminum composites and Borsic-aluminum composites containing stainless steel and titanium.

13 p1633 A73-28143

Heat resistant nickel alloys creep rupture strength diagram, determining time to failure as function of loads

13 p1636 A73-29062

Creep properties of low alloy steel in relation to microstructure.

13 p1641 A73-29509

Present situation of Japanese research on the long-time creep and creep rupture properties of steels.

13 p1642 A73-29513

Minimum creep lives of structural metallic materials at elevated temperatures.

13 p1701 A73-29514

Development of austenitic heat-resistant steel containing a high concentration of nitrogen.

13 p1642 A73-29516

Effects of small amounts of carbide-forming elements on the elevated temperature strength of austenitic stainless steel.

13 p1642 A73-29517

High temperature tests of microalloying effect on creep and stress rupture characteristics of hot rolled and annealed Mo alloys

13 p1643 A73-29605

Deformation criteria of failure under simple and composite stresses.

13 p1703 A73-29621

Al alloy rupturing analysis in complex stress state, noting sublimation and self diffusion values of activation energy in torsional to tensile state transition

13 p1643 A73-29624

Creep and fracture in OT-4 titanium alloy at temperatures from 400 to 550 C.

13 p1643 A73-29627

Effects of some carbide stabilizing elements on creep-rupture strength and microstructural changes of 18-10 austenitic steel.

14 p1761 A73-30627

Conditionally-instantaneous and long term strength of a longitudinally-transversely wound glass-fiber-reinforced plastic under biaxial compression

15 p1896 A73-30975

Testing machine to determine perforated plate biaxial tension creep rupture strength and fatigue life at high temperature

15 p1858 A73-31617

Diffusional creep and creep-degradation in dispersion-strengthened Ni-Cr base alloys.

16 p2025 A73-33111

A statistical method for evaluating structural reliability and minimum structural creep life at elevated temperature.

16 p2084 A73-33974

Short- and long-term strength characteristics of particulate-filled cast epoxy resin.

17 p2197 A73-35343

Fundamentals of fatigue and creep rupture of a thermoplastic.

17 p2197 A73-35345

High temperature tensile and stress rupture tests of tungsten /Nichrome laminar composites and tungsten alloy/ Inconel sheet and foil specimens

17 p2193 A73-35545

Heat resistant nickel alloys creep rupture strength diagram, determining time to failure as function of loads

18 p2325 A73-36894

Book - Elevated temperature properties as influenced by nitrogen additions to types 304 and 316 austenitic stainless steels.

18 p2325 A73-36971

Strain accumulation and rupture during creep under variable uniaxial tensile loading.

19 p2495 A73-37434

An arrangement for carrying out metal creep and stress-rupture strength tests under high vacuum conditions

20 p2545 A73-39384

The creep characteristics of the heat-resistant ferritic steels X 20 CrMoV 12 1 and X 18 CrMoNi V Nb 12 1 and their welded connections

22 p2872 A73-41780

Some patterns of deformation and failure of refractory alloys of molybdenum, niobium and tantalum during a programmed change of temperature.

22 p2874 A73-42101

The deformation and fracture of molybdenum under creep conditions.

22 p2874 A73-42109

Aluminum brazed titanium honeycomb sandwich structure - A new system.

23 p2985 A73-44000

Optimum design of lattice structures in creep conditions with consideration of the Kempner-Hoff theory of buckling.

24 p3148 A73-45002

CREEP STRENGTH

Mo addition effect on high temperature creep resistance and diffusion activation energy of Nb alloys tested in torsion and tension at 1100-1500 C in vacuum

03 p0328 A73-14018

Some factors affecting high-temperature strength of matrix in heat resisting alloys.

04 p0464 A73-15577

Mathematical model for long term creep strength from creep tests, noting crack initiation and microstructural changes

04 p0517 A73-15952

Effect of overheating on creep resistance in metastable alloys.

06 p0710 A73-18639

Temper embrittlement of pressure vessel steels.

07 p0839 A73-20271

The influence of prior fatigue deformation on creep behaviour.

08 p0979 A73-21672

Creep strength of low alloy ferritic steels at low strain rates as function of grain boundary structure and matrix deformation

08 p0979 A73-21673

Cr-Ni carbon steel testing for stress and temperature dependencies of secondary creep rate, noting grain boundary diffusion controlled mechanism

08 p0980 A73-21674

Creep strength in steel and high temperature alloys; Meeting, Sheffield, England, September 20-22, 1972, Preprints.

08 p0980 A73-21776

Mechanisms of transient and steady state creep in a gamma-prime hardened austenitic steel.

08 p0980 A73-21778

Steel and Ni-based alloys structural stability during long term high temperature creep, noting matrix structure dependence on initial dislocation and interparticle spacing

08 p0980 A73-21780

The effect of creep strain on stacking-fault precipitation in Nb-stabilized 20/25 austenitic stainless steels.

08 p0981 A73-21787

Stress varied creep of 20Cr-25Ni-Nb stabilised austenitic stainless steel.

08 p0981 A73-21788

The ageing and creep behaviour of a Cr-Ni-Mn austenitic steel.

08 p0981 A73-21791

The creep strength of 17 Cr-11 Ni-2.5 Mo austenitic steel stabilised by titanium.

08 p0982 A73-21792

The influence of some structural factors on the creep strength of wrought precipitation-hardened Ni-Cr alloys.

08 p0982 A73-21793

Irradiation creep in some austenitic stainless steels, nimonic PE16 alloy and nickel.

08 p0982 A73-21794

The influence of structure upon the notched creep strength of a nickel-base alloy.

08 p0982 A73-21795

Effects of composition and structure on the creep strength of molybdenum bearing ferritic steels.

08 p0982 A73-21796

Strengthening mechanisms in ferritic creep resistant steels.

08 p0982 A73-21797

Dispersion-strengthened ferritic alloys for high-temperature application.

08 p0982 A73-21798

High temperature creep resistance enhancement by stress relaxation or removal of unstable surface layers, increasing activation energy for different alloys

09 p1101 A73-22403

Consideration of creep probability in a low-alloyed heat-resistant CrMoV steel

11 p1384 A73-26111

Study of plasticity laws of polycrystalline metals at elevated temperatures - Specifically the influence of hydrostatic stress on creep.

13 p1641 A73-29506

A static-to-dynamic transition in creep of metallic materials under cyclic stress conditions as caused by an interaction of creep and creep recovery.

13 p1642 A73-29512

Investigation of the structure of turbine disc materials after use.

13 p1643 A73-29632

Time required for the destruction of a nonuniformly heated wall

15 p1953 A73-32098

Ten years' experience of UMCo-type alloys in a special steel foundry.

24 p3099 A73-45074

Influence of boron on the precipitation of carbides in Fe-Ni-Cr austenitic matrices

24 p3101 A73-45523

CREEP TESTS

Assembly for studying the characteristics of materials under cyclic loads at elevated temperatures

01 p0029 A73-10024

Deformation and failure of heat-resistant materials under conditions of thermal fatigue and creep as functions of the nature of the temperature change cycle and of the boundary conditions

01 p0063 A73-10478

Time characteristics of rupture and creep in metals during tension under hydrostatic pressure conditions
01 p0064 A73-10605

Investigation of creep in Kh18N10T steel at varying temperatures
01 p0066 A73-11094

Creep of wound orthotropic glass fiber reinforced plastic
03 p0335 A73-13745

Disordered precipitation effect on steady state creep rate of gamma prime Ni-Al-Ti single crystals
03 p0326 A73-13963

Creep life and strain estimation for Nimonic alloy by monitoring cavity density under optical microscope
03 p0326 A73-13965

Creep rupture under multi-axial states of stress.
03 p0327 A73-13981

Zirconium carbide creep characteristics and limit at 2450-2810 K, examining test conditions effects on parameters
03 p0328 A73-14017

Predictive testing in elevated temperature fatigue and creep - Status and problems.
04 p0453 A73-14853

Development and use of relaxation tests for study of the long-term creep of metals
[ONERA, TP NO. 1146]
04 p0511 A73-15095

Mathematical model for long term creep strength from creep tests, noting crack initiation and microstructural changes
04 p0517 A73-15952

Creep rupture testing of aluminum alloys to 100,000 hours.
05 p0581 A73-16133

Frame photography for temporary creep in cylindrical Al alloy specimen necks under tensile loads, calculating creep diagrams
05 p0634 A73-16748

Structural changes in molybdenum single crystals during high temperature creep
06 p0708 A73-18048

Creep tests and fracture mechanics for high temperature properties of steels and alloys under static load, noting discrepancies for brittle materials
07 p0840 A73-20510

The influence of scatter on some simple variable-stress creep predictions.
08 p1016 A73-20798

Low stress creep tests of niobium stabilized austenitic steels.
08 p0981 A73-21789

Four-section equipment for studying creep and long-term strength in deep cooling conditions.
09 p1086 A73-23067

Refractory materials cyclic elastoplastic tests under shear with holding creep, showing relationship between creep rate and recurrent static deformation
09 p1161 A73-23155

Influence of heat treatment on the high-temperature strength and creep of the NV10M5T3T niobium alloy
10 p1230 A73-23600

Fatigue and creep testing of unidirectional carbon fibre reinforced plastics.
10 p1238 A73-23965

Crippling allowables for elevated temperature and creep environments.
[AIAA PAPER 73-388]
11 p1439 A73-25517

Temperature dependence of the hardness and estimation of the creep of the Rh-18% Re alloy
12 p1509 A73-26899

Creep and long-term strength of molybdenum with a boron silicide coating in vacuum at temperatures from 1000 to 1400 C
12 p1512 A73-27257

Ti-Al-Sn alloy microstructure effects on low temperature creep, discussing creep stresses, activation energy and yield stress
13 p1632 A73-28127

Long term temperature control and calibration system for creep testing facility temperature drift monitoring and correction
13 p1597 A73-28841

Some observations of crack initiation and propagation of notched specimens under creep conditions.
13 p1641 A73-29510

Present situation of Japanese research on the long-time creep and creep rupture properties of steels.
13 p1642 A73-29513

Minimum creep lives of structural metallic materials at elevated temperatures.
13 p1701 A73-29514

Deformation and destruction of heat-resistant materials in conditions of thermal fatigue and creep as a function of the nature of the cyclic change in temperature and boundary conditions.
14 p1759 A73-30303

Diffusion creep by dislocation climb in beryllium and Be-Cu single crystals.
14 p1761 A73-30633

A high temperature vacuum assembly for precision creep tests
14 p1743 A73-30694

Diffusion-controlled processes in the homogeneity region of zirconium carbide
15 p1881 A73-31593

Testing machine to determine perforated plate biaxial tension creep rupture strength and fatigue life at high temperature
15 p1858 A73-31617

Nonlinear creep in glassfiber-reinforced plastics in the presence of some types of complex stress conditions
16 p2030 A73-33926

X-ray investigation of the fine crystalline structure of aluminum with creep
17 p2186 A73-34117

Durability of the Kh18N10T steel under the combined influence of creep and thermal cycling
17 p2187 A73-34335

The supporting effect of bending specimens under static load in the temperature range from 400 to 500 C
17 p2187 A73-34521

Room temperature creep of Borsic-aluminum composites.
17 p2189 A73-34644

The anisotropy of creep behaviour in oriented thermoplastics.
17 p2196 A73-35342

Creep in VT-14 titanium alloy under low-cycle load conditions
18 p2323 A73-36758

Creep tests and fracture mechanics for high temperature properties of steels and alloys under static load, noting discrepancies for brittle materials
19 p2440 A73-37785

Apparatus for creep and long-term strength testing of materials in aggressive media under irradiation
20 p2544 A73-39368

High temperature creep in magnesium strengthened by magnesia particles.
21 p2719 A73-40899

Temperature dependence of hardness and creep of alloy Rh 18Re.
21 p2720 A73-41032

The interaction of creep and fatigue for a rotor steel /The William M. Murray Lecture, 1972/.
21 p2722 A73-41264

Influence of initial transients on stress relaxation and creep measurements on visco-elastic materials.
22 p2868 A73-43172

The creep of sapphire filament with orientations close to the c-axis.
23 p2997 A73-44029

Additive distribution and formation of internal stress in fired magnesia.
23 p2998 A73-44133

Changes in surface structure during high-temperature creep flow.
23 p2994 A73-44159

Investigation of the softening processes in molybdenum and its alloys under conditions of creep
23 p2995 A73-44281

Influence of the type of loading on high-temperature creeping of zirconium carbide
23 p2998 A73-44287

A device for durability and creep testing of fiberglass-reinforced plastic pipes and shells in a complex stressed state
23 p2967 A73-44293

Fiberglass reinforced plastic laminate creep rate for ultrasonic vibrational and static tensile loads, showing nonlinear viscoelasticity and stress amplitude effects
24 p3102 A73-44504

CRESTATRONS

U TRAVELING WAVE TUBES

CRESTS

U WAVES

CREVASSES

NT GLACIERS

CREVICES

U CRACKS

CREWS

NT FLIGHT CREWS

Crew performance in extended operation under vibrational stress.
05 p0543 A73-16717

CRICKETS

NT TRIBOLIA

CRITERIA

NT STRUCTURAL DESIGN CRITERIA

CRITICAL EXPERIMENTS

Singular eigenfunction solution of the monoenergetic neutron transport equation for finite radially reflected critical cylinders.
24 p3109 A73-44700

CRITICAL FLICKER FUSION

Photopic luminous efficiency measured by critical flicker frequency method, noting dependence on intermittence frequency of light stimulus or overall radiance level
[AD-754344]
02 p0137 A73-12076

Effect of altitude acclimatization and simultaneous acclimatization to altitude and cold on critical flicker frequency at 11,000 ft. altitude in man.
02 p0135 A73-12562

Dynamic properties of vision. III - Twin flashes, single flashes and flickerfusion.
07 p0783 A73-20253

Cyclofusional stimulation effects on retinal image disparity in terms of central component and Panum fusional areas
07 p0783 A73-20265

Analysis of transient visual sensations above the flicker fusion frequency.
08 p0932 A73-21566

Binocular rivalry and binocular fusion of after-images.
11 p1318 A73-26200

Stabilized target visibility as a function of contrast and flicker frequency.
17 p2112 A73-34846

Visual field defects after missile injuries to the geniculate-striate pathway in man.
21 p2641 A73-41600

CRITICAL FLOW

Equations of motion for two dimensional steady conducting gas flow in transverse magnetic field, deriving flow equations for transcritical region via small perturbation theory
05 p0602 A73-16585

Critical flows in open vertical ducts filled with superfluid helium under pressure
05 p0599 A73-17230

Periodic semi-integral solutions of secondary unsteady convective flows in external force field for critical Rayleigh numbers by Liapunov-Schmidt method
10 p1204 A73-23584

Quasi-linear partial differential equations of nonlinear pulse shock wave propagation in two- and three-dimensional steady transonic gas flow near critical point
11 p1302 A73-25854

Application of the principle of corresponding states to two-phase choked flow.
11 p1349 A73-26744

Stability, solvability and adjoint conditions for time periodic perturbation solutions to subcritical bifurcating plane Poiseuille flow
15 p1863 A73-31340

Effect of intense injection on flow stability and turbulence development
15 p1864 A73-31857

Trapped wave vortex breakdown model for long weakly nonlinear wave propagation on critical flows in tubes of variable cross sections
16 p1998 A73-32796

On the existence of critical levels, with applications to hydromagnetic waves.
16 p2043 A73-33869

Critical flow speed divergence in aeroelastic systems stability loss, discussing statistical analysis using partial differential equation
17 p2250 A73-35119

High speed cinematographic study of mass flow rate of pressurized subcooled liquid nitrogen inward choked flow through radial gap at various stagnation pressures
21 p2740 A73-40634

Critical two phase He flow rates prediction based on homogeneous thermal equilibrium model, Henry-Fauske data and empirical correction factor curve
24 p3077 A73-44823

CRITICAL FREQUENCIES

The influence of chordal paths on signals propagating to the near antipode of an HF radio transmitter.
01 p0015 A73-10182

Ionospheric bottom side electron density profiles from measured monthly median values, using CCIR and ITS computer programs for critical frequencies
02 p0163 A73-12302

Problems in estimating the total electron content from Faraday rotation observations on geostationary satellites.
03 p0300 A73-13638

Electron concentration variation in E layer after sunrise, noting critical frequency deviations from Chapman law
05 p0568 A73-16216

Spatial variations in F2 layer critical frequencies
05 p0568 A73-16258

The theory of the reflection of low frequency radio waves in the ionosphere near critical coupling conditions.
05 p0551 A73-17052

Assessment of ISS topside sounder system by computer simulation.
05 p0579 A73-17168

Critical frequency gradients-geometric parameters equivalence coefficients for ionospheric layer with parabolic vertical ionization distribution for radio wave path determination
06 p0690 A73-17555

Fractional polarization constancy in pulsars to critical frequency with subsequent falloff
07 p0874 A73-19070

The computation of critical frequencies of waves of higher types in a hollow elliptical waveguide.
07 p0802 A73-20141

Analysis of dispersion equation of a two-layer elliptical waveguide in critical regime.
07 p0802 A73-20142

Estimating the accuracy of longitudinal interpolation of foF2 from shipboard observations
08 p0959 A73-21301

Nighttime electron density in the E region at auroral latitudes in sunspot maximum.
09 p1078 A73-22747

Equatorial anomaly in the F2 layer during local noon and the IGY and IQSY periods
11 p1350 A73-25089

Spatial correlation of the critical frequencies of the F2 layer on the basis of data from stationary mid-latitude stations
11 p1351 A73-25091

ISIS-1 satellite observations of the ionosphere at high southern latitudes.
11 p1353 A73-25753

A theoretical study of lunar variations in foF2 at low latitude.
11 p1354 A73-25764

F 2 layer characteristics forecasts by extrapolation of critical F 2 frequency data from Moscow, Sverdlovsk, Irkutsk, Alma-Ata and Salehard
12 p1490 A73-27338

Asymmetrical model for F 2 critical frequency variability analysis to determine dimensions and effective number of large scale ionospheric electron density inhomogeneities
13 p1608 A73-28707

Computerized simulation of Ionosphere Sounding Satellite topside sounder system techniques for observation of critical frequencies and apparent distance-frequency characteristic relation
13 p1586 A73-29248

Critical frequencies of electromagnetic wave propagation in H waveguides with a dielectric cross-piece
13 p1595 A73-29411

The relationship between the structure of the equatorial anomaly and the strength of the equatorial electrojet.
15 p1869 A73-31761

Critical frequency gradients-geometric parameters equivalence coefficients for ionospheric layer with parabolic vertical ionization distribution for radio wave path determination
16 p2002 A73-32779

F 2 critical frequency and maximum height at high southern latitudes explained via additional ionization provided by energetic particles
16 p2009 A73-33911

Enhancements of the electron concentration in the F2-layer at magnetic noon.
16 p2010 A73-33914

Ionospheric response to internal gravity waves observed at Delhi.
16 p2010 A73-33919

Evaluation of the accuracy of longitudinal interpolation of foF2 based on ship observations.
19 p2425 A73-37930

Mapping of foF2 by means of topside sounder satellites.
19 p2427 A73-38285

The determination of foF2 and hmF2 from satellite-borne probe data.
19 p2427 A73-38286

Reflection of powerful radio waves from the lower ionosphere
19 p2406 A73-38334

Application of mathematical methods for the description of the planetary distribution of ionosphere parameters
20 p2554 A73-39169

Correlational relations between F2 critical frequency deviations and the solar activity cycle according to a number of high-latitude stations
20 p2555 A73-39176

Functional relation between the F2-layer ionization state in daylight time and the zenith angle of the sun
20 p2555 A73-39178

Midlatitude F 2 layer critical frequency fluctuations as ionosphere disturbance criteria during magnetically quiet days
21 p2681 A73-40104

Measurement of attenuation of 9.303 MHz waves from ISIS-II through the ionosphere.
22 p2825 A73-42193

F 2 layer characteristics forecasts by extrapolation of critical F 2 frequency data from Moscow, Sverdlovsk, Irkutsk, Alma-Ata and Salehard
23 p2970 A73-43236

Appleton seasonal anomaly in E region maximum electron density investigated by critical frequency data statistical analysis, showing solar activity effects
23 p2979 A73-44006

F 2 region critical frequency variations during geomagnetic storms, noting correlation with main phase onset
24 p3082 A73-44728

Critical frequency evolution during F 2 region storms at middle and low latitudes, showing random global patterns and relation to neutral wind flow
24 p3087 A73-45205

CRITICAL LOADING

On the general solution of externally pressurized gas journal bearings.
[ASME PAPER 72-LUB-Q] 01 p0055 A73-10218

Load carrying capacity of ceramic spherical shells under external pressure
01 p0114 A73-10481

Temperature dependence of the critical shear stress in single crystals of Al-Mg alloys of various concentration at temperatures between 1.6 and 300 K
01 p0064 A73-10488

Certain generalizations of load-limit theorems for a Cosserat medium
01 p0114 A73-10573

Upper bounds to the load for the plane strain working of anisotropic metals.
01 p0057 A73-10696

Phase plane analysis of free vibration of rectangular plate loaded by in-plane compressive load, calculating critical load and amplitude in postbuckling region
01 p0115 A73-10770

Asymptotic method of determining critical buckling loads for strictly convex shallow shells of revolution
01 p0116 A73-10963

Approximate relationships between the behavior of plates under destabilizing and non-destabilizing loads.
01 p0117 A73-11120

Assessment of the stressed state of a material from the strain nomogram
02 p0229 A73-11618

Stress distribution in elastic shell of revolution under axisymmetrical loads, noting thickness distribution for uniform stress in critical edge loading zone
02 p0231 A73-11805

Study of the effect of small elastoplastic deformations on the load-bearing capacity of specimens with stress concentrators under repeated variable loading.
I. 02 p0235 A73-12202

Study of the effect of small elastoplastic deformations on the load-bearing capacity of specimens with stress concentrators under repeated variable loading.
II. 02 p0181 A73-12203

Elastic and plastic deformations of circular ring with initial machining produced stresses distributed across thickness, calculating critical load for static stability
02 p0236 A73-12581

Effect of transverse shear on limit load of cylindrical shells.
03 p0383 A73-12873

Evaluation of a two-pocket hydrostatic journal bearing suitable for use over a wide range of temperature.
03 p0311 A73-13204

Externally pressurized gas-lubricated journal bearings with herringbone grooves - Load capacity and stability analysis.
03 p0311 A73-13208

Stability of an idealized circular three-layer plate beyond the elastic limit
03 p0393 A73-13777

The gas liquid interface and the load capacity of helical grooved journal bearings.
03 p0314 A73-14334

Inelastic spherical shells elastic-plastic buckling, presenting numerical procedure for critical loads and stresses
04 p0508 A73-14942

Symmetrical bending for the general case of oscillating beams under transverse loads
04 p0511 A73-15174

Bifurcation of rings under concentrated centrally directed loads.
[ASME PAPER 72-WA/APM-37] 04 p0515 A73-15885

A technical note on the correspondence between Amontons' law and wear-scar data in a 4-ball machine.
05 p0581 A73-16108

The load carrying capacities of symmetrically loaded shallow shells.
05 p0631 A73-16120

Finite element limit analysis using linear programming.
05 p0631 A73-16124

Buckling of a long, axially compressed, thin cylindrical shell with random initial imperfections.
[ASME PAPER 72-APM-MMM] 05 p0632 A73-16532

Buckling of columns with variable moment of inertia.
05 p0633 A73-16538

Limit analysis of plates with piecewise linear yield surface.
06 p0758 A73-17398

Truncated conical shell buckling and stability beyond elastic limit, deriving lower critical loads by orthogonalization method
06 p0760 A73-17781

Coupled thermoelastic stability effect on critical thermal buckling of strip under compression in temperature field
06 p0765 A73-18686

A finite element, linear programming method for the limit analysis of thin plates.
07 p0906 A73-19026

CRITICAL LOADING

Decohesive load carrying capacity of elastoplastic bodies based on permissible discontinuities due to strain increase, relating to structural strength determination
07 p0908 A73-19082

Imperfection-sensitivity of a wide integrally stiffened panel under compression.
07 p0908 A73-19087

The critical rate of tensile stress application and its significance for characterizing the behavior of materials under impact loads
07 p0838 A73-19213

Extremal boundary value problems of plasticity theory
07 p0910 A73-19304

One dimensional elastoplastic system optimal design by stochastic programming, determining limiting stresses and random load distribution
07 p0914 A73-20151

Buckling load of shallow circular vaults, investigating boundary conditions, load intensity and interconnecting beam flexibility and spacing effects
07 p0916 A73-20434

Effect of major axis curvature on L-beam stability.
07 p0916 A73-20437

Structural service life from carrying capacity during rupturing stage, noting microstructural properties effect
07 p0917 A73-20504

Estimation of the fatigue characteristics of D16T and AVT1 aluminum alloys from the breaking stress
07 p0841 A73-20515

Use of chromoplastic models for the study of the behaviour of rectangular plates after buckling.
08 p1017 A73-20946

Artificial slow crack growth under constant stress - The R-curve concept in plane stress.
09 p1108 A73-23255

Cantilever cylindrical shells of rigid-plastic material, determining collapse loads under external pressure combined with end moment by numerical solution to limit analysis
[ASME PAPER 72-PVP-B] 09 p1164 A73-23271

Investigation of the load-carrying capacity of rotating disks by the method of optically sensitive coatings
10 p1291 A73-24364

A theory for the mechanical properties of metal-matrix composites at ultimate loading.
10 p1235 A73-24443

Probable collapse mechanisms in indefinite plates on an elastoplastic continuum.
11 p1434 A73-25217

Buckling analysis of elastically constrained conical shells under hydrostatic pressure by the collocation method.
[ATAA PAPER 73-364] 11 p1438 A73-25499

Buckling of partially debonded layered cylindrical shells.
[ATAA PAPER 73-366] 11 p1438 A73-25501

Spot welded stainless steel cylindrical shells post-critical loading behavior, analyzing equilibrium states dependence on axial loads and buckling forces
11 p1443 A73-26058

Stability of rectangular plates under mixed boundary conditions
12 p1552 A73-27372

Instability of asymmetric strongly convex thin shallow shells
12 p1553 A73-27414

Stability of cylindrical shells of variable thickness during torsion
12 p1553 A73-27462

Conditional margin of plastic strength for shaft-type elements subjected to torsion at low temperatures
12 p1554 A73-27478

Asymptotic method of determining the critical buckling loads of shallow strictly convex shells of revolution.
12 p1554 A73-27539

Postbuckling behavior of orthotropic skew plates.
13 p1697 A73-28813

Interfiber failure of unidirectional composite material.
13 p1702 A73-29538

Load-bearing capacity of ceramic spherical shells under external pressure.
14 p1810 A73-30306

Critical shear stress temperature dependence in Al-Mg single crystal alloys of various concentrations in the range 1.6-300 K.
14 p1759 A73-30313

Limit state solution to equilibrium equation of elliptical plate with Johansen yield condition under uniform load, using Abel differential equation
14 p1811 A73-30486

Limit equilibrium of thin-walled containers composed of joined conical sections
15 p1944 A73-30973

Critical load determination for nonsymmetrical stability losses of ring shaped plates clamped against bending
15 p1945 A73-31029

Integral equations for nondestructive determination of buckling loads for elastic plates and bars.
15 p1948 A73-31634

Critical stress intensity factors applied to glass reinforced polyester resin.

15 p1897 A73-31676

Technical studies and research on airport infrastructure

15 p1859 A73-32561

Influence of preliminary dynamic loading on the load-bearing capacity of cylindrical shells

16 p2075 A73-32693

Lateral instability of thin-walled beams - Considerations regarding methods of experimental investigation

16 p2081 A73-33372

The effect of transverse shear stresses on the yield surface for thin shells.

16 p2082 A73-33905

Inelastic buckling of eccentrically loaded columns.

17 p2240 A73-34180

Molybdenum bicrystals mechanical properties dependence on mismatch angle under bending with torsion and brittle cleavage under critical stresses

17 p2189 A73-34636

A note on bending-shear interaction in the limit analysis of cylindrical shells

17 p2243 A73-34650

Determination of the carrying capacity of axisymmetric shells under piecewise linear plasticity conditions

17 p2244 A73-34738

Buckling of rectangular plates with general variation in thickness.

[ASME PAPER 73-APM-10]

17 p2247 A73-35035

Determination of stiffness and critical loads of a circular plate from a simple bending test.

18 p2362 A73-36327

Limiting equilibrium of a circular plate with allowance for the shearing stress

18 p2363 A73-36405

Evaluation of the carrying capacity of reinforced plastics subjected to nonuniform heating

18 p2328 A73-36760

Nonlinear bending problem for a beam of variable rigidity

18 p2366 A73-36959

General methods of determining the limiting load in brute-force reliability tests

18 p2321 A73-37023

Limiting equilibrium of a plate weakened by two arbitrarily oriented cracks

19 p2494 A73-37186

Structural service life from carrying capacity during rupturing stage, noting microstructural properties effect

19 p2499 A73-37779

Evaluation of the fatigue properties of aluminum alloys D16T and AVT1 on the basis of limit stresses.

19 p2440 A73-37790

Effect of rivet spacing on crippling loads of joined aluminum angles.

19 p2499 A73-38009

System for determining the critical range of stress-intensity factor necessary for fatigue-crack propagation.

19 p2501 A73-38297

Localized creep of a nonhomogeneous beam subjected to loads exceeding the true elastic limit

19 p2501 A73-38306

A finite element approach to the critical cyclic stress required to propagate a crack.

20 p2615 A73-38639

Rigid-plastic collapse of compression-bent shallow shells.

20 p2616 A73-39114

Laterally restrained beam columns with uniform biaxial loading.

20 p2616 A73-39117

Determination of the critical load for a compressed plate weakened by a circular hole and by cracks propagating toward the hole contour

20 p2617 A73-39263

Elastoplastic strains and carrying capacity of shallow shells /Review/

21 p2786 A73-40976

Critical pressure and vibration frequencies of cylindrical shells with edges elastically reinforced in the axial direction

21 p2786 A73-40980

Influence of the geometrical configuration of a structure on its carrying capacity

21 p2786 A73-40982

Critical load analysis of strip /beam/ with arched crack under compressive stress and bending moments

21 p2786 A73-40985

Stability of a cylindrical shell of linearly variable thickness beyond the elastic limit

21 p2787 A73-41195

Nondestructive shell-stability estimation by a combined-loading technique.

21 p2708 A73-41266

Threshold for fatigue crack propagation and the effects of load ratio and frequency.

22 p2875 A73-42137

Overload effects on subcritical crack growth in austenitic manganese steel.

22 p2875 A73-42138

Effect of multiple overloads on fatigue crack propagation in 2024-T3 aluminum alloy.

22 p2875 A73-42139

Effect of a loading sequence on threshold stress intensity determination.

22 p2875 A73-42141

A method for measuring K sub Ic at very high strain rates.

22 p2866 A73-42148

An exact method for the study of the dynamic stability of supporting structures acted upon by periodic impulses.

22 p2927 A73-43031

Stability of nonlinearly elastic plates in the presence of random initial stresses

22 p2928 A73-43060

Dynamic stability of rotating disks loaded by a concentrated force

22 p2928 A73-43064

Fatigue crack growth retardation after single-cycle peak overload in Ti-6Al-4V titanium alloy.

23 p2992 A73-43809

Postcritical deformations in a multilayer plate under edge pressure

23 p3043 A73-43925

Experimental evaluation of the load capacity of smooth fiberglass-reinforced plastic shells under external hydrostatic pressure

23 p2998 A73-44191

Critical equilibrium of cylindrical shells made from an ideal rigid-plastic material with different yield points in tension and compression

23 p3047 A73-44280

Improved turbine blade attachment profiles with shoulder locks

23 p2986 A73-44291

Limit loads of circular plates under combined loading.

[ASME PAPER 73-APM-G]

23 p3047 A73-44379

Upper bounds to in-plane shear strength of unidirectional fiber-reinforced composites.

23 p3048 A73-44383

Lubricating properties of micropolar fluids in composite and step slider bearings, obtaining analytic expressions for load carrying capacity and skin friction

24 p3092 A73-44409

Surface buckling of a laminated medium

24 p3145 A73-44525

Load capacity of rings formed by winding of composites reinforced with high-modulus anisotropic fibers

24 p3093 A73-44528

Critical stresses of compressed cylindrical shells consisting of orthotropic layers with various orientations

24 p3145 A73-44529

Strip weakened by array of holes, investigating plastic zone initiation and propagation under uniaxial tension for load bearing capacity estimation

24 p3147 A73-44685

Generalized shear stress and shearing strain rate variables for thick circular plate, using von Mises yield criterion for limit load analysis

24 p3148 A73-44895

CRITICAL MACH NUMBER

U CRITICAL VELOCITY

U MACH NUMBER

CRITICAL MASS

Critical mass of cryogenic rocket propellants.

07 p0866 A73-20415

Magnetic stars formation from interstellar matter in presence of interstellar magnetic field, considering critical mass based on Chandrasekhar-Fermi virial theorem

14 p1799 A73-30426

Magnetic stars origin from gravitational collapse of ionized hydrogen clouds, discussing implications of interstellar magnetic fields and critical mass according to Chandrasekhar-Fermi virial theorem

20 p2605 A73-39058

CRITICAL PATH METHOD

Computer application for management of Skylab launch operations.

04 p0424 A73-14905

CRITICAL POINT

The effect of gravity on the thermal and caloric measurements for pure fluid substances at the critical point

03 p0400 A73-14634

Establishment of thermal equilibrium in a liquid near the critical point.

08 p1021 A73-20857

Prediction of height-velocity boundaries for rotorcraft by application of optimization techniques.

12 p1459 A73-27175

Possibility of gasdynamic effects at the critical point of the phase equilibrium

12 p1487 A73-27418

Experimental study of the heat transfer in the vicinity of the critical point during nonequilibrium physicochemical transformations and determination of the nitrogen recombination rate constant

18 p2287 A73-37013

Calibration of capsule platinum resistance thermometers at the triple point of water.

22 p2857 A73-42027

Critical slope of the vapor pressure curve of a pure substance.

22 p2932 A73-42506

Surface tension and interfacial density profile of fluids near the critical point.

24 p3110 A73-44986

CRITICAL PRESSURE

Temperature characteristics in the wall of an annular channel heated internally at supercritical pressures

01 p0123 A73-10861

Determination of the hydraulic resistance of throttles by short unsteady blowing

07 p0779 A73-20083

Inelastic buckling of shallow spherical shells under external pressure.

[ASME PAPER 72-PVP-6]

09 p1164 A73-23270

Numerical solution existence for three dimensional boundary layer equations governing corner flow in symmetry plane with critical pressure gradients

19 p2419 A73-37492

Critical pressure and vibration frequencies of cylindrical shells with edges elastically reinforced in the axial direction

21 p2786 A73-40980

Revision of high temperature and critical properties of cesium.

22 p2932 A73-42513

CRITICAL REYNOLDS NUMBER

U CRITICAL VELOCITY

U REYNOLDS NUMBER

CRITICAL SPEED

U CRITICAL VELOCITY

CRITICAL STRESS

U CRITICAL LOADING

CRITICAL TEMPERATURE

Unacclimatized male Caucasians lower critical temperature determination for subsequent investigation of ethnic variability in acute cold exposure responses

01 p0008 A73-10166

Predicting the critical boundary temperature of multidimensional explosives.

07 p0918 A73-19386

Influence of nickel on the superconductivity parameters of Nb3Al + Ni

09 p1098 A73-21845

Time delays and Q switching in homostucture and heterostructure injection lasers.

09 p1092 A73-22246

Critical transition temperatures and magnetic moment measurements of superconducting state of binary Be alloys

11 p1409 A73-25630

Investigation of a film boiling crisis in the presence of natural convection

11 p1451 A73-25734

Vanadium galliumide tape preparation and critical temperature and current as function of heat treatment temperature and applied magnetic field, considering pancake current capacity

13 p1669 A73-29069

Heat release by free convection from horizontal cylinders to CO2 under near-critical conditions

20 p2628 A73-39613

Magnetic properties of layered superconductors with a weak layer interaction

21 p2751 A73-40371

Revision of high temperature and critical properties of cesium.

22 p2932 A73-42513

Critical heat flux for two-phase flow of helium I.

24 p3155 A73-44822

CRITICAL VELOCITY

The applicability of Stokes expansions to reversed flow.

05 p0565 A73-16606

Negative Magnus forces in the critical Reynolds number regime.

05 p0533 A73-17212

Experimental investigation of flow stability during intense injection

06 p0643 A73-17462

Mathematical models for critical flow rates of annular two phase mixtures under various discharge conditions

06 p0688 A73-18563

Pressure distributions on circular cylinders at critical Reynolds numbers.

11 p1300 A73-25151

Gas jet flow at high subsonic velocities, determining stream function, contraction coefficient, convergence at critical velocity and pressure above obstacle

11 p1302 A73-26215

Critical rpm of a radial-flow turbine wheel of the closed type

14 p1814 A73-30685

Critical rpm of conical shells incorporated in turbine rotors

14 p1814 A73-30686

Gyroscopic moment effect on rotating shafts lowest critical velocity, plotting convergence characteristics

15 p1949 A73-31668

Elastic buckling instability of rotating rods and plates due to compressive stress under critical speed
15 p1955 A73-32161

Critical Reynolds number for nondelayed transition in environmental testing for internal and external fluid flows
16 p1999 A73-33146

Mathematical models for critical flow rates of annular two phase mixtures under various discharge conditions
16 p2000 A73-33588

Critical speeds for cantilever shafts.
18 p2320 A73-36700

Incompressible potential flow past sphere parallel to contact plane tangent as model to determine critical velocity for dissipation onset in superfluid liquid He II
19 p2421 A73-37853

Pressure distribution and boundary layer separation measurement on circular cylinder at critical subsonic velocities for various Reynolds and Mach numbers
21 p2632 A73-40476

Further experiments on balancing of a high-speed flexible rotor.
[ASME PAPER 73-DET-99] 22 p2865 A73-42077

Critical velocity for collapse of a shell of circular cross section without buckling.
[ASME PAPER 73-APM-W-31] 22 p2925 A73-42891

Critical velocities of the steady motion of a pliable thread in plane homogeneous flow
22 p2928 A73-43061

Increasing the critical rotational speed of the tail rotor drive shaft in SM-1 and SM-2 helicopters
24 p3057 A73-45195

Electromagnetic wave interaction with moving bounded plasmas.
24 p3069 A73-45409

CROCCO METHOD
Streamline curvature and velocity gradient behind curved shocks.
21 p2632 A73-40441

CROP GROWTH
Effects of leaf age for four growth stages of cotton and corn plants on leaf reflectance, structure, thickness, water and chlorophyll concentrations and selection of wavelengths for crop discrimination.
05 p0571 A73-17128

Solar activity effects on tree growth, farm crop yield, fish availability and human sickness trends, discussing indirect effects via meteorological factors
05 p0622 A73-17171

Russian book on mathematical models of biological systems covering biogeocenosis, optimal crop, chemostat cultivation, predator-victim society, trophic control, and life support systems
09 p1044 A73-22347

Multispectral reflectance scanning of crop image signatures during April-July growing season, examining time dependent image changes, discrimination tests and crop types
20 p2561 A73-39900

CROP IDENTIFICATION
Parametric and nonparametric classification techniques for pattern recognition in remote sensed data processing, noting crop identification
03 p0281 A73-14485

Supervised and unsupervised category identification and classification systems consistency with FRTS satellites high rate multispectral data requirements
05 p0572 A73-17142

Mean vector and covariance matrix estimation for training class sample statistics updating in pattern recognition, applying to crops or any category of objects
08 p0984 A73-21668

Natural resources research and development in Lesotho using FRTS imagery.
18 p2308 A73-36045

Corn blight epiphytotic remote sensing, data acquisition and crop identification by photointerpretation and computer aided multispectral band scanner data analysis
20 p2556 A73-39836

Adaptive multispectral scanner recognition via maximum likelihood classifier for agricultural crops, discussing error sources
20 p2559 A73-39877

Remotely sensed multispectral scanner data collection over agricultural area, discussing spatial resolution modification for crops and unresolved objects classification
20 p2559 A73-39882

Crop identification by microwave remote sensing obtained spectral response data from fields with corn, sorghum, soybeans and alfalfa
20 p2562 A73-39902

Photodensity and the impact of shifting agriculture on subtropical vegetation - A case study in the Bahamas.
20 p2562 A73-39905

Earth surveys by remote sensing in Israel.
21 p2685 A73-40816

Use of earth resources satellites for supranational inventories of forests and agricultural areas
23 p2972 A73-43779

CROP VIGOR

Remote sensing for healthier crops.
05 p0569 A73-16745

Reflectance and internal structure of leaves from several crops during a growing season.
11 p1352 A73-25566

Remote mapping of standing crop biomass for estimation of the productivity of the shortgrass prairie, Pawnee National Grasslands, Colorado.
20 p2562 A73-39907

Multi-stage acquisition of forest information from space and aircraft imagery and ground sampling.
21 p2687 A73-41334

CROPLANDS

U FARMLANDS

CROSS CORRELATION

Cross correlations between turbulent jet flow and noise from hot-film and acoustic signal measurement, using Proudman form of Lighthill integral
03 p0246 A73-13842

Two-channel direction finding with point source emission and spaced antennas reception, investigating cross correlation and background noise interference effects on accuracy
03 p0278 A73-14062

Auto and cross correlation functions of combined binary pseudorandom sequences in digital space communication systems
04 p0423 A73-15916

PM signal cross-correlated receiver output SNR in presence of random misalignments with respect to carrier frequency and signal arrival time
05 p0547 A73-16058

The probability density function for the output of a cross-correlator with bandpass inputs.
06 p0665 A73-18139

Auto- and cross-correlations of diffuse objects for coherent optical data processing, using single lensless Fresnel hologram
08 p0963 A73-21036

Spatial crosscorrelation in anisotropic sound fields.
08 p0987 A73-21125

Cross-correlation analysis of the AE index and the interplanetary magnetic field Bz component.
09 p1142 A73-22055

Cross correlation functions skewness of fading records, noting dispersion correlation with ionospheric irregularities horizontal drift
09 p1076 A73-22143

Cross correlation coefficients for H, K and H beta lines of solar spectrum related to observed peculiarities from microphotometer intensity traces
[AD-759889] 10 p1278 A73-24131

Dual magnetometer systems with cross correlation signal enhancement to overcome intrinsic sensor ambient noise and spacecraft magnetic field fluctuation effects on single detection performance
12 p1468 A73-27002

Monograph - Two causality correlation techniques applied to jet noise.
17 p2155 A73-35150

Huffman binary codes for pulse compression radar, evaluating ambiguity or cross correlation by computer program for replicas formation performance
17 p2131 A73-35221

Asymptotic behaviour of a scalar in an axisymmetric final period turbulent wake.
20 p2507 A73-39086

Experimental correlation techniques for the characterisation of vibration transmission paths.
20 p2617 A73-39267

A conservative bound on the estimation error covariance matrix in the presence of correlated driving noise and correlated discrete measurement noise.
21 p2724 A73-40295

A digital correlation spectrometer employing multiple-level quantization.
23 p2981 A73-43378

Modal analysis of turbulent correlations in compressible flow.
23 p2970 A73-44382

CROSS COUPLING
Effects of cross-coupling and of the edge effect on the characteristics of linear phased antenna arrays
02 p0146 A73-12021

Random antenna array design for narrow beam radiation and blind angle avoidance, determining mutual coupling effect on performance
04 p0416 A73-15059

Heuristic response strategies and operator performance errors as function of practice in cross coupled pursuit tracking control tasks
07 p0785 A73-19548

Periodic regime stability of two channel relay system as function of main channels identicalness and cross coupling symmetry, using Tsytkin method
09 p1063 A73-22340

Experimental investigations of coupling phenomena in a periodic linear antenna array
14 p1729 A73-30697

Roll coupling moment of deflected wing-body combination.
15 p1823 A73-31573

Cross coupling between effects of linear and angular acceleration on vestibular nystagmus.
18 p2272 A73-36441

Root trajectories method for stability analysis of two channel automatic control systems with antisymmetric and symmetric cross couplings
20 p2541 A73-38980

Analysis of the characteristics of radiating elements in antenna arrays on the basis of laws describing cross-coupling variations
21 p2661 A73-40195

Optimum cross-coupled tracker for pulse-Doppler radar.
21 p2649 A73-40328

Mutual coupling effects in circular arrays on cylindrical surfaces Aperture design implications and analysis.
21 p2653 A73-40674

Computer program for analysis of radiation pattern distortion and mutual coupling in antenna farms, allowing user specification by types or vertical cylindrical antenna dimensions
22 p2823 A73-41797

Interwire coupling noise and cable resonance equations for fast rise time signal switching at resonant frequencies
22 p2823 A73-41800

Multidimensional cross control stabilization of multiple link feedback control systems, applying 70 dc 70 ac power converter
22 p2836 A73-42603

Multicircuit structural analysis of linear multiple link control systems with dynamic interchannel cross couplings
22 p2836 A73-42608

Linearization technique for synthesis of nonlinear two dimensional automatic control systems with cross disturbances, imposing constraints on motion coordinate deviations
22 p2836 A73-42615

Use of cancellation techniques in the measurement of atmospheric crosspolarisation.
23 p2955 A73-44111

The effect of interaction of array elements with arbitrary amplitude distribution on the radiation pattern.
24 p3068 A73-44942

CROSS FAULTS

U GEOLOGICAL FAULTS

CROSS FLOW

Heat transfer and hydraulic resistance of single banks and systems of tubes in cross flow of gases and viscous liquids
01 p0120 A73-10289

Arc current, column electric field, mainstream velocity and applied transverse magnetic field relationships in magnetically balanced cross flow plasmas
01 p0084 A73-10738

Breakup and penetration of transverse liquid jets in supersonic air cross flow
[AIAA PAPER 72-1180] 03 p0293 A73-13475

Combustion mechanisms of fuel rich propellants in flow fields.
[AIAA PAPER 72-1145] 04 p0485 A73-14915

Determination of the turbulent exchange coefficients in the case of tube bundles in crossflow
11 p1448 A73-25109

Performance characteristics of a model VTOI. lift fan in crossflow.
11 p1301 A73-25782

Optical absorption cell with water vapor cross flow instrument designed for wall decontamination and open air meteorological simulation, examining thermodynamic parameters effects
11 p1367 A73-26318

Behavior of a weak turbulent jet in a cross flow
15 p1822 A73-31199

Spatially growing wave trails of an inviscid fluid discontinuity.
16 p2001 A73-33868

Turbulent jet deflection and impingement in confined cross flow occurring in gas turbine blade impingement cooling schemes
[ASME PAPER 73-FE-15] 17 p2152 A73-35012

Experiments on confined turbulent jets in cross flow.
[AIAA PAPER 73-647] 18 p2260 A73-36202

Cross flows in bounded three-dimensional turbulent boundary layers.
19 p2422 A73-38298

Freon-22 circular and flat jet propagation in air cross flow in wind tunnel, examining air-gas dynamic pressure ratio effects
21 p2676 A73-40405

An experimental investigation of a jet issuing from a wing in crossflow.
22 p2798 A73-43111

CROSS RELAXATION
Laser emission spectral theory, calculating cross relaxation in three and four level systems, monochromatic radiation effects on matter and laser action in inhomogeneous media
17 p2184 A73-34923

CROSS SECTIONS

Molecular beam study of the K+CH₃I reaction - Energy dependence of the detailed differential reactive cross section.

05 p0546 A73-16047

Effect of the cross sectional shape of specimens on their strength under transverse-bending impact loads

05 p0632 A73-16327

An aluminum waveguide of oval cross section, which can be wound on a drum, with favorable wave resistance transformations /ALFORM waveguide/

06 p0663 A73-17582

Non-linear bending of beams of variable cross-section.

08 p1016 A73-20831

Aerodynamic forces and moments estimation for slender bodies of circular and noncircular cross section without and with lifting surfaces at 0-90 degree angles of attack

09 p1030 A73-23468

Equivalence of geoelectric cross sections in the frequency probing method

14 p1750 A73-30835

Fluorescent cross sections and yields of CO₂/+ from threshold to 185 Å.

15 p1915 A73-31274

The optimization of the cross-sectional profile of rods and plates subjected to dynamic stress

16 p2080 A73-33241

High-transverse-momentum secondaries and rising total cross sections in cosmic-ray interactions.

19 p2476 A73-38292

CROSSED FIELD AMPLIFIERS

Theory of the signal suppression effect in an M-type TWT amplifier with preliminary modulation of the electron beam

01 p0025 A73-10983

Minimum noise coefficients of M-type microwave beam amplifiers with crossed fields taking into account distributed losses in slow wave structure

04 p0429 A73-15922

Platinotron crossed field microwave amplifier tube phase response characteristics, considering anode current fluctuations and statistical phase variations at constant operating conditions

06 p0674 A73-17823

The continuous-cathode /emitting-sole/ crossed-field amplifier.

11 p1339 A73-26694

Dual mode microwave tube parameters for ECM power amplifiers based on systems rationale analysis, considering TWT and injected-beam crossed field amplifier

14 p1736 A73-30621

Crossed field amplifier selection for application to pulsed radar transmitters, considering system operation effects, power supply regulation and droop limitation method

16 p1991 A73-33899

Mobile IC coherent radar with computerized display and calibration, incorporating cold cathode crossed field amplifier tube in transmitter amplifier stage

20 p2528 A73-38871

Reduction of noise in high-power crossed-field amplifiers.

21 p2665 A73-41114

Microwave cross field and traveling wave tube amplifier characteristics for ECM systems, discussing bandwidth, dual mode, modulation and size and weight tradeoffs

22 p2834 A73-42872

CROSSED FIELD GUNS

Investigation of the gun aspects of a rotating plasma source.

06 p0732 A73-18779

Calculation of the electron trajectories in helical beams produced by axisymmetric magnetron-type injection guns

23 p2961 A73-44346

CROSSED FIELDS

Measurement of the macroscopic velocity of the neutral component of weakly ionized gas in the crossed fields.

01 p0081 A73-10116

Working prototype image dissector photoelectron beam scanning by crossed electric and magnetic fields to measure beam density distribution in proton synchrotron

01 p0048 A73-10528

On the origin of small-scale type II irregularities in the equatorial electrojet.

02 p0157 A73-11760

Plasma inhomogeneity in crossed electromagnetic fields, comparing motion velocity to ion component transverse drift rate in polarized electric field

03 p0346 A73-13178

Equatorial electrojet currents effect on sporadic E layer near magnetic equator, noting cross field irregularities

07 p0819 A73-20066

Electron energy loss effect on cross-field electron streaming instability in low density high temperature plasmas, using high voltage theta pinch

07 p0859 A73-20192

On the steady flow of a non-equilibrium ionized gas around sharp corners in the presence of a crossed magnetic field.

08 p0992 A73-21009

Equatorial sporadic E and cross-field instability.

08 p0958 A73-21150

Low threshold unstable nonpotential oscillations of weakly ionized rotating plasma in crossed field centrifuge, noting MHD generator and ionospheric implications

09 p1124 A73-21891

Plasma diffusion across a magnetic field due to thermal vortices.

09 p1126 A73-22217

Study of antenna cross-polarization characteristics by using microwave holography

09 p1065 A73-23087

Analytical model of electron velocity, resonance and potential of plasma accelerated in crossed electric and magnetic fields

10 p1253 A73-23577

Periodic instability induced in semiconductor situated in crossed electric and magnetic fields via electron gas heating, deriving expressions for properties of steady nonlinear waves

10 p1261 A73-24764

Statistical velocity and temperature characteristics of turbulent electron beams in crossed HF electric and magnetic fields, comparing with Brillouin flow

10 p1258 A73-24880

Stability of a plasma rotating in crossed electric and magnetic fields

11 p1403 A73-25240

Long wavelength instability in a perpendicular shock.

11 p1406 A73-26557

Certain considerations concerning a magnetoplasma-dynamic flux in the one-dimensional hypothesis

12 p1527 A73-27061

Damping of a discharge in crossed fields - Application to the ionosphere in the auroral zone

13 p1611 A73-29562

Unified theory of type I and II irregularities in the equatorial electrojet.

14 p1748 A73-29973

Investigation of the radial structure of the oscillations of a plasma column situated in crossed fields in the presence of resonant cyclotron instability

14 p1781 A73-30579

Unified geometric and analytical treatment of magnetogasdynamical shocks. I - General solutions and theorems.

15 p1917 A73-31339

Motion of a sphere in a conducting fluid under the action of crossed electric and magnetic fields

15 p1917 A73-31405

Low threshold unstable nonpotential oscillations of weakly ionized rotating plasma in crossed field centrifuge, noting MHD generator and ionospheric implications

17 p2215 A73-34314

Cross-field instability as a mechanism for equatorial E region irregularities.

18 p2304 A73-35998

Ion cyclotron instability of a rotating plasma

18 p2340 A73-36671

Spread E occurrence relationship to blanketing frequency from cross field plasma instability mechanism

20 p2552 A73-38948

MPD annular duct flows in crossed external fields for arbitrary values of the Hall parameter

20 p2599 A73-39675

Statistical velocity and temperature characteristics of turbulent electron beams in crossed HF electric and magnetic fields, comparing with Brillouin flow

21 p2749 A73-41655

Self-sustaining Penning avalanche discharge in crossed electric and magnetic fields, discussing anode surface boundary effects and maximum discharge intensity conditions

23 p3015 A73-44345

Investigation of plasma acceleration in crossed electric and magnetic fields

24 p3115 A73-44751

Electron-molecule collision frequencies in a crossed electric and magnetic field.

24 p3118 A73-45476

CROSSLINKING

Finite deformation behavior of elastomers - Dependence of strain energy density on degree of crosslinking for SBR.

13 p1646 A73-29527

Synchronous communication satellite crosslink antenna design and tracking and acquisition procedures for Ka band frequencies, describing reflectors, paraboloids, and five horn feed system

16 p1977 A73-32721

Enhancement of polymer adhesion to metals by means of additives with crosslink systems

16 p2030 A73-33941

Studies on glass-reinforced epoxy resin using either Vulkadur A or a mixture of Vulkadur A and triethanolamine as crosslinking agent.

19 p2444 A73-38092

Cross-linking ambient curing mechanisms for air-drying oxidizable coatings, involving chemical film-forming reactions

20 p2580 A73-39636

On the dimensions of intramolecularly crosslinked polymer molecules. I - The synthesis and chemical characterization of intramolecularly crosslinked polystyrene molecules having a narrow distribution of molecular weight. II - The theoretical prediction of the dimensions in solution of intramolecularly crosslinked polystyrene molecules. III - The measurement of the dimensions of intramolecularly crosslinked polystyrene.

23 p3008 A73-43795

Molecular rupture mechanism, self reinforcement and failure modes of elastomeric materials dependence on strain, temperature, filler and crosslink density

23 p2997 A73-43808

CROSSOVERS

Crossover frequencies in multiconductor plasma.

16 p2041 A73-33333

A bilevel thin film hybrid circuit containing crossovers, resistors, capacitors, and integrated circuits.

21 p2669 A73-40773

CROSSTALK

Intelligible crosstalk and AM/PM transfer in commercial communications satellites. I

06 p0663 A73-17589

Intelligible crosstalk and AM/PM transfer in commercial communication satellites. II

08 p0937 A73-20773

HF CW ultrasonics, discussing elimination of electromagnetic leakage or crosstalk between transmitter and receiver by sampling technique

13 p1612 A73-28483

Combination and crosstalk distortions in microwave parametric systems.

13 p1583 A73-28665

Crosstalk compensation in optical beam transmission.

20 p2528 A73-38769

Use of magnetic materials for improvement of screening properties of different types of cables.

22 p2830 A73-41805

Crosstalk interference and regenerative amplifier noise effects on PCM signal transmission over twin- and four-conductor lines

23 p2954 A73-43784

CRUCIBLES

Nonstoichiometric yttria crucibles for cold wall Ti melting, noting single batches, cost reduction and alloy homogeneity

04 p0455 A73-15749

CRUDE OIL

The isolation of a series of acyclic isoprenoid alcohols from an ancient sediment - Approaches to a study of the diagenesis and maturation of pythol.

11 p1326 A73-25465

Proposed stratigraphic controls on the composition of crude oils reservoir in the Green River formation, Uinta Basin, Utah.

11 p1352 A73-25471

High-temperature corrosion in gas turbines and steam boilers by fuel impurities. II - The sodium sulfate-magnesium sulfate-vanadium pentoxide system.

15 p1841 A73-32175

Aircraft design for transporting arctic crude oil or liquid natural gas, examining air terminal requirements and handling specifications

21 p2634 A73-41172

CRUISING FLIGHT

Optimum position of the center of gravity of a passenger plane in cruising flight

02 p0129 A73-11649

Hypersonic flows in large-scale inlet models.

07 p0773 A73-19189

Icing conditions of modern transport aircraft according to cruise flight data

17 p2100 A73-34545

Air transportation economic efficiency as function of fuel consumption, cruising flight speed, altitude range and load factor /payload/

19 p2506 A73-38118

The evaluation of autonomous navigation systems for cruise vehicles.

20 p2587 A73-38811

[ALAA PAPER 73-874]

CRUSADER AIRCRAFT

U F-8 AIRCRAFT

CRUSTS

NT EARTH CRUST

NT LUNAR CRUST

Mars equatorial region crustal structure from Bouguer gravity anomalies computed by differencing free air gravity and topographically predicted gravity

20 p2612 A73-39710

CRYODEPOSITS

Spectral transmittance of cryodeposits on a transmitting substrate.

05 p0598 A73-16897

Optical effects of cryodeposits on low scatter mirrors.

18 p2336 A73-36349

[ALAA PAPER 73-732]

Liquid helium cryopump extension to gaseous hydrogen and helium pumping via adsorption on argon cryodeposit, obtaining gases partial pressures evolution

22 p2886 A73-41871

CRYOGENIC EQUIPMENT

Time dependence of carbon monoxide TEA laser emission at 77 K, presenting time resolved transitions spectral data

01 p0058 A73-10128

Cryoprobe with truncated circular cross sectioned Cu cone with copper slug heat sink for momentum flow rate measurement in hypersonic low density flow

01 p0003 A73-10755

Spaceborne IR systems cryogenic cooling, considering passive radiators and open or closed cycle cryogenic fluid systems

06 p0683 A73-18315

Cryogenic problems involved in the development of the structure of a hydrogen/oxygen rocket stage.

07 p0905 A73-18991

A cryogenic ultrahigh-vacuum pump with a small liquid-helium flow rate

07 p0830 A73-19288

Four-section equipment for studying creep and long-term strength in deep cooling conditions.

09 p1086 A73-23067

Cryogenic cooling systems technology for spacecraft applications, comparing passive and phase-change coolers and closed cycle refrigerator for capacity and service life

10 p1285 A73-23790

Shock tubes with cryogenically cooled test section for experimental investigation of pressure and temperature pulse effects on cryogenic materials

10 p1203 A73-24267

Cryogenic applications for environment simulation.

11 p1344 A73-25580

Principles of evacuated cryogenic insulations.

11 p1450 A73-25581

A compact demountable superleak-tight seal for low temperature experiments.

11 p1375 A73-26317

A cooled illuminator for studying ruby lasers

12 p1506 A73-27219

Cryogenically cooled parametric amplifiers for 100 meter radio telescope low noise operation, describing system design and performance

12 p1481 A73-27780

Cryogenic ultrahigh-vacuum pump with low liquid-helium consumption.

13 p1659 A73-28688

Aerospace cryogenic static seals.

13 p1624 A73-28800

Parameters and energy resolution of the KP303 field effect transistors at low temperatures

17 p2133 A73-34162

Cryogenic preamplifier with cooled GaAs junction FET in input stage, discussing application to sensor systems using high impedance cryogenically cooled optical detectors

17 p2137 A73-35219

Cryogenically cooled CO-He TEA laser.

19 p2437 A73-37253

Development of a cryogenic heat pipe radiator for a detector cooling system.

[ASME PAPER 73-ENAS-47]

19 p2493 A73-37994

A cryogenic heat pipe for satellite sensor cooling.

[ASME PAPER 73-ENAS-50]

19 p2494 A73-37997

50 kG gas cooled superconducting solenoid operated at 13 K.

21 p2702 A73-41103

Methods for cryogenic thermocouple thermometry.

22 p2857 A73-42029

Gold-iron alloys for low temperature thermocouples.

22 p2857 A73-42030

Reference data for thermocouple materials below the ice point.

22 p2857 A73-42031

Radio astronomical traveling wave maser with ruby or doped rutile single crystals, superconducting magnet, cryogenic equipment and low noise temperature

23 p2953 A73-43375

CRYOGENIC FLUID STORAGE

Thermal stresses in a spherical vessel filled with liquefied gas

07 p0917 A73-20507

High modulus filament wound vessels for cryogenic containers in spacecraft.

17 p2238 A73-34807

Thermal stresses in spherical reservoirs while filling with liquefied gas.

19 p2499 A73-37782

CRYOGENIC FLUIDS

NT FERMI LIQUIDS

NT FLOX

NT LIQUID HELIUM

NT LIQUID HELIUM 2

NT LIQUID HYDROGEN

NT LIQUID NITROGEN

NT LIQUID OXYGEN

NT SOLIDIFIED GASES

Supercavitating pumps for cryogenic liquids.

05 p0582 A73-17286

Atomization of cryogenic liquid droplets by shock waves

07 p0811 A73-19656

Investigation of a film boiling crisis in the presence of natural convection

11 p1451 A73-25734

Breakdown of a drop of cryogenic liquid by shock waves.

14 p1745 A73-30322

High speed cinematographic study of mass flow rate of pressurized subcooled liquid nitrogen inward choked flow through radial gap at various stagnation pressures

21 p2740 A73-40634

Complex flow in vapour columns over boiling cryogenic liquids.

21 p2740 A73-41102

Liquid-vapour equilibria research on systems of interest in cryogenics - A survey.

24 p3155 A73-44821

CRYOGENIC GYROSCOPES

Theory of cryogenic suspensions for navigational devices

20 p2566 A73-39353

Calculation of the force characteristics of the external spherical suspension of a cryogenic gyroscope

24 p3091 A73-50523

CRYOGENIC MAGNETS

Note on analysis of cryogenic suspensions for space vehicles.

12 p1524 A73-27633

CRYOGENIC ROCKET PROPELLANTS

Mono- and multipropellant, storable and cryogenic, liquid rocket propulsion engines developments including gas generators and engines

[AIAA PAPER 72-1104]

03 p0355 A73-13422

Cryogenic liquid O₂/H₂ reaction control systems for Space Shuttle

[AIAA PAPER 72-1155]

03 p0382 A73-13458

Cryogenic problems involved in the development of the structure of a hydrogen/oxygen rocket stage.

07 p0905 A73-18991

Critical mass of cryogenic rocket propellants.

07 p0866 A73-20415

Cryogenic propellants in rocket engines.

16 p2045 A73-33118

CRYOGENIC STORAGE

Thermal control and structures approach for fluorinated propulsion.

[AIAA PAPER 73-772]

18 p2360 A73-36386

CRYOGENICS

Facility for investigating low-cycle fatigue of alloys at cryogenic temperatures

01 p0029 A73-10491

Investigation of cryogenic stability and reliability of operation of Nb₃Sn coils in helium gas environment.

02 p0200 A73-11838

The influence of stress concentrators on the properties of steel in cryogenic technology.

02 p0181 A73-12213

Thermophysical properties of thermally insulating materials in the cryogenic temperature region.

04 p0520 A73-15938

Superconductivity theory and applications, considering cryogenic problems low-loss and magnetic properties and Josephson junction effect on low power technology

04 p0484 A73-15958

High performance cryogenic multilayer thermal insulation with plastic films coated by vapor deposited metal, discussing heat transfer mechanism for comparison with microsphere insulation

05 p0642 A73-17285

International Cryogenic Engineering Conference, 4th, Eindhoven, Netherlands, May 24-26, 1972, Proceedings.

07 p0922 A73-20401

The Solar Collector Thermal Power System - Its potential and development status.

09 p1035 A73-22792

Thermostable polymers for freezing and cryogenic temperatures, noting theory, methodology and preparation for science and industry

10 p1241 A73-24675

Vacuum technology at low temperatures; Proceedings of the Symposium, Denver, Colo., August 31, 1970.

11 p1398 A73-25578

Stud welding on 5083 aluminum and 9% Ni steel for cryogenic use.

11 p1375 A73-26352

Cooling systems for spaceborne infrared experiments.

11 p1453 A73-26515

Austenitic stainless steels at cryogenic temperatures. I - Structural stability and magnetic properties.

13 p1636 A73-29070

A unit for investigating the low-cycle fatigue of alloys at cryogenic temperatures.

14 p1743 A73-30316

Papers on heat transfer covering thermosiphon technology, flowing gas-solid mixtures, condensation, free convection, flow stability and cryogenic insulation

17 p2254 A73-34351

Cryogenic insulation heat transfer.

17 p2254 A73-34355

Development of a high capacity cryogenic heat pipe. [AIAA PAPER 73-729]

18 p2369 A73-36346

Absolute viscosity of air down to cryogenic temperatures and up to high pressures.

19 p2422 A73-38296

Some experiments on the influence of surface treatment on the Kapitza conductance between copper and He4 at temperatures from 1.2 to 2.0 K.

21 p2741 A73-41105

Investigation of nozzles with cryogenic suction of the boundary layer

21 p2678 A73-41221

Thermistors as cryogenic thermometers.

22 p2854 A73-41998

Germanium resistance thermometers for cryogenic temperature precision measurement, discussing design technology, resistance-temperature characteristics types, installation and measurement methods

22 p2854 A73-41999

Platinum resistance thermometry below 13.81 K.

22 p2854 A73-42002

A rhodium-iron resistance thermometer for use below 20 K.

22 p2855 A73-42004

Liquid helium temperature range thermometry using superconducting tunnel junction devices with temperature dependent I-V characteristics

22 p2856 A73-42018

A new type of charge trapping in MOS systems.

22 p2896 A73-42275

Josephson junction principles for superconducting metals at cryogenic temperatures, considering ultrasonic electronic measuring instruments and computer components

24 p3073 A73-45224

CRYOPUMPING

Test chamber for on board moving parts in ultrahigh vacuum.

01 p0030 A73-11148

Supercavitating pumps for cryogenic liquids.

05 p0582 A73-17286

Cryopumping use in clean ultrahigh vacuum technology, considering cold surface heat load, condensate layer growth rate and heat conductivity, cryosorption and cryotrapping

07 p0852 A73-20402

Adsorption characteristics of condensed Ar, C₂H₆, NH₃ and CO₂ layers with respect to cryopumping.

07 p0922 A73-20413

Cryopumping adsorption-desorption theory and cryosorption and condensation pumps, including bare surface, adsorbents and frozen deposit pumps

08 p0989 A73-21619

High and ultra-high vacuum by pumping with cryocooled surfaces.

11 p1398 A73-25579

Cryogenic applications for environment simulation.

11 p1344 A73-25580

Development of a vacuum chamber for ionospheric plasma simulation - Utilization of liquid helium cryopumping

22 p2838 A73-41869

Liquid helium cryopump extension to gaseous hydrogen and helium pumping via adsorption on argon cryodeposit, obtaining gases partial pressures evolution

22 p2886 A73-41871

CRYOSORPTION

U SORPTION

CRYOSTATS

A cryostat for measuring electrical values of semiconductor devices in the temperature range from 77 to 300 K

02 p0165 A73-11550

Experience in developing and using laboratory superconducting solenoids with fields up to 119 kOe

10 p1177 A73-23936

Cryostats with and without radiation passage through window into vacuum space in balloon-borne far IR instruments requiring cooling to liquid He temperature

11 p1453 A73-26516

The lattice heat conductivity of aluminum alloys during age-hardening.

13 p1636 A73-29068

Mariner Mars 1969 infrared spectrometer - Gas delivery system and Joule-Thomson cryostat.

21 p2702 A73-41101

Fiber glass reinforced plastics measurement for ratio of elastic modulus to mean thermal conduction for use in cryostat to resist large forces

21 p2723 A73-41106

Specifications of a cryostat for a vibrating sample magnetometer between 1.7 and 300 K

21 p2706 A73-41592

CRYSTAL DEFECTS

NT CRYSTAL DISLOCATIONS

NT EDGE DISLOCATIONS

NT FRENKEL DEFECTS

NT POINT DEFECTS

NT SCREW DISLOCATIONS

NT VACANCIES [CRYSTAL DEFECTS]

Effect of structural factors on the surface properties of single crystal silicon films

01 p0087 A73-10038

Nickel structure stabilization by multiply alternated thermocyclic treatment and isothermal annealing

01 p0062 A73-10253

Plastic strain anisotropy changes in single crystals of beryllium following programmed load application

01 p0064 A73-10610

Metallographic macro- and microstructural study of semiconductor compounds, discussing single crystal imperfections, polycrystals and semiconducting films

02 p0199 A73-11582

Fracture of nonlinear crystals (KDP and LiNbO₃) by radiation from a ruby laser.

02 p0176 A73-12112

Study of the composition of inclusions in synthetic diamond crystals by microanalysis.

02 p0185 A73-12691

Fatigue induced microstructural changes in metals and alloys, considering crystal lattice defects, crack formation and propagation, dislocations and strengthening effects

03 p0321 A73-13133

Liquation-induced microinhomogeneity of heat resistant submerged-arc-smelted steel 4Kh12N8G8MFB/EI4811

03 p0326 A73-13829

Stacking faults in alpha titanium alloys

03 p0327 A73-13977

Influence of lattice defects on EPR line-shapes in ruby.

06 p0734 A73-17794

Microwave method of investigating the quality of ruby boules.

06 p0734 A73-17813

Stacking faults effect on martensitic phase formation during steel hardening based on X ray diffraction analysis and Paterson theory

06 p0735 A73-18034

A note on fatigue crack starter defects produced by a pulsed laser.

06 p0710 A73-18500

Crystal defect model of crack propagation in three dimensional solid, assuming nonlinear dependence of Young modulus on strain with term for time lag

08 p0107 A73-21025

Investigations on 'doping stacking fault' pyramids.

08 p0995 A73-21479

Neutron bombardment radiative effects on thin metal plate stability, considering compressive force, lattice defects and critical flux relations

08 p1020 A73-21771

The effect of creep strain on stacking-fault precipitation in Nb-stabilized 20/25 austenitic stainless steels.

08 p0981 A73-21787

Inter crystalline molybdenum fracture

09 p1099 A73-21971

Annealing of discontinuities in deformed aluminum

09 p1100 A73-21973

Alloying elements effects on voids nucleation in irradiated Al alloys, tabulating defect concentration

09 p1101 A73-22175

High temperature mechanical properties measurements verifying metal polycrystal internal friction background origin in diffusion of vacancies formed under grain boundary loading

09 p1105 A73-23060

Ti based beta alloy strain hardening and failure characteristics, emphasizing initial deformation phase and microdefect onset and development

09 p1105 A73-23064

Electron microscopy study of Nb₃Sn strips

10 p1259 A73-23674

Energetic and structural models of microdefects in germanate glasses

10 p1240 A73-24465

Manifestation of the defect structure of cadmium telluride through high-temperature electrical conductivity

10 p1261 A73-24776

Effect of impurities and X-ray irradiation on the motion of pores in ionic crystals under the action of an external electric field

11 p1401 A73-25242

Brittle cleavage crack propagation in crystals in terms of bonds acting between pairs of atoms, considering stress distribution around crack tip

11 p1409 A73-25812

Investigation of radiation defects in silicon and germanium single crystals irradiated by 50-MeV electrons

11 p1410 A73-26449

Deformation and recrystallization of twin crystals in aluminum and magnesium alloys

12 p1510 A73-26913

High-cyclic fatigue curves for annealed metals from investigation of defect buildups, lattice distortions, microcrack nucleation and fatigue crack growth

12 p1552 A73-27253

Influence of plastic deformation on the electrical resistance of molybdenum single crystals

12 p1512 A73-27260

Metallic crystal growth and defects; All-Union Conference on Metallic Crystal Growth and Imperfections, 2nd, Kiev, Ukrainian SSR, June 15-18, 1970, Proceedings

13 p1631 A73-28101

Investigation of structure and imperfections in molybdenum single crystals grown by electron-beam zone refining techniques

13 p1631 A73-28106

Luminescence quenching and zero-phonon line broadening associated with defect interactions in diamond.

13 p1667 A73-28212

NiO-CoO solid solutions defect structure from high temperature measurements of integrated Bragg peak intensities

13 p1645 A73-28934

An X-ray study of hydrogen induced phenomena affecting mechanical behaviours of austenitic stainless steels.

13 p1625 A73-29522

Characteristics of the decomposition of an interstitial-impurities solid solution in molybdenum during recrystallization

14 p1760 A73-30589

Some problems in measuring the electrical properties of semiconductors

14 p1784 A73-30924

Concentration dependence of the degree of occupancy of a lattice element in cubic titanium oxycarbide

15 p1896 A73-31210

Investigation of defects in GaAs on the basis of the photoluminescence

15 p1923 A73-31717

An X-ray examination of deformation in beta Ti-V alloys.

17 p2189 A73-34642

Book - Advanced experimental techniques in the mechanics of materials.

17 p2176 A73-35834

High temperature investigations of the steady and nonequilibrium electrical conductivity of cadmium sulfide crystals

18 p2340 A73-36670

Influence of extended defects on the electron spectrum of semiconductors

19 p2470 A73-37952

Faulty structure in niobium single crystals deformed by rolling at 77 K

20 p2579 A73-39743

The influence of crystal defects in platinum on platinum resistance thermometry.

22 p2855 A73-42009

Influence of inhomogeneities in a nonlinear crystal on the conversion of an image by sum-frequency generation.

22 p2869 A73-42245

X-ray investigation of the mechanism of effects of alloying on defect formation in refractory metal alloys

22 p2877 A73-42454

Atomic diffusion mechanisms in multiphase and multicomponent alloys covering relaxation, crystal lattice atom exchange and motion along dislocation lines and to neighboring vacancies

23 p2989 A73-43439

Investigation of the substructure in molybdenum single crystals deformed by compression

23 p2991 A73-43712

Anisotropy of galvanomagnetic effects in laminarily inhomogeneous semiconductors

23 p3017 A73-44044

Defect structure introduced during operation of heterojunction GaAs lasers.

24 p3096 A73-44923

Dependence of electrical erosion on the interatomic bond strength in binary titanium alloys

24 p3101 A73-45514

CRYSTAL DISLOCATIONS

NT EDGE DISLOCATIONS

NT SCREW DISLOCATIONS

Dislocation damping in ultrasound-irradiated molybdenum single crystals

01 p0061 A73-10251

Dislocation density in Mo single crystals subject to uniaxial tensile stress or sphere-produced indentation, evaluating plastic strain level

01 p0063 A73-10484

Mosaic-angle and dislocation-density variations in polycrystalline aluminum alloys under tension

01 p0064 A73-10609

Cr, Ti, Ce, V and Nb carbide-forming additives effects on crystal dislocations growth and movement during strain hardening of Mn rich steel

01 p0066 A73-11345

Characteristics of the process of plastic deformation of bcc metals in the microyield zone

02 p0179 A73-11622

Statistical evaluation of strength of metals at brittle fracture.

02 p0235 A73-12133

The influence of oxygen concentration on the internal stress and dislocation arrangements in alpha titanium.

02 p0184 A73-12768

Effects of the state of the surface and of titanium films on the dislocation structure of surface layers in molybdenum single crystals

03 p0326 A73-13969

Dislocation dynamics in niobium-oxygen solid solutions.

04 p0462 A73-15303

Dislocation interstitial impurities interactions in high purity Mo, using dislocation damping techniques

04 p0462 A73-15304

The dependence of the lower yield strength in iron and steel on grain size and temperature.

04 p0463 A73-15308

Internal stress and dislocation structure of aluminum in high-temperature creep.

04 p0467 A73-15930

Stability of the dislocation structure in cold-deformed Kh18N12T and Kh16N9M2 steels during high-temperature aging

06 p0707 A73-17905

Cyclic endurance and alteration nature of the dislocation structure in nickel before and after programmed strengthening

06 p0707 A73-17906

Influence of annealing at near melting point temperatures on the substructure of aluminum single crystals

06 p0707 A73-18036

Mathematical models for yield point dependence on statistical arrangements of ordered precipitated phases, noting crystal dislocations interaction effect

06 p0735 A73-18044

Investigation of dislocation locking by interstitial impurities in bcc-lattice metals

06 p0708 A73-18055

The influence of anisotropy and crystalline slip on relaxation at a crack tip.

06 p0709 A73-18331

Dislocation structure of tungsten single crystals grown by electron-beam zone refining

07 p0841 A73-20523

The movement of Volterra disclinations and the associated mechanical forces.

08 p0995 A73-21627

Dislocation glide controlled by linear elastic obstacles - A thermodynamic analysis.

08 p1019 A73-21628

Observation of Bardeen-Herring sources in quenched magnesium

08 p0979 A73-21629

Electric resistance of hydraulically extruded and annealed beryllium

09 p1098 A73-21847

Thermal-activation parameters of plastic deformation in alpha-titanium single crystals

09 p1099 A73-21964

Certain two-dimensional problems with discontinuous displacements in the theory of elasticity and their application to problems of dislocation-surface propagation

09 p1158 A73-22358

Transmission electron microscope study on initiation of fatigue crack in 18-8 austenitic steel.

09 p1104 A73-22523

On the identification of the unknown functions in Drucker's work-hardening relation for plastic deformation of crystalline materials.

10 p1292 A73-24652

Additives alloying with cobalt, discussing allotropic transformation dependence, recrystallization, mobile dislocations, and iron deformation by twinning

11 p1408 A73-25322

Fatigue damage and dislocation structures in fcc metals surface layers, noting microcrack formation conditions

11 p1380 A73-25805

The influence of environment and the surface layer on crack propagation and cyclic behavior.

11 p1380 A73-25807

The effect of surface films on fatigue crack initiation.

11 p1381 A73-25810

Effect of high dislocation density on stress corrosion cracking and hydrogen embrittlement of type 304L stainless steel.

11 p1385 A73-26174

Change in the dislocation structure during fatigue of nickel prestrained by tension

11 p1386 A73-26732

Dislocation structure of subgrain boundaries in creep-deformed aluminum.

12 p1511 A73-27028

Austenitic steel dislocation density, X ray interference width and hardness changes due to intensified crystal fragmentation from biaxial elongation under tension

12 p1512 A73-27246

Sintering of refractory titanium carbide with varied bound nitrogen content, discussing crystal dislocation effects on initial stage compaction intensification in nonstoichiometric specimens

12 p1503 A73-27556

Dislocation structure and low-temperature plasticity of chromium alloys with rare earth metals

13 p1630 A73-28011

Effect of impurities on the substructure and dislocation formation in metal crystals grown from melts

13 p1631 A73-28103

Effect of the degree of purity on the dislocation structure of tungsten single crystals

13 p1631 A73-28104

Niobium mechanical twin formation and propagation, discussing continuous nucleation, matrix interface and dislocation core energies

13 p1632 A73-28132

Weak-beam high-resolution electron micrographs of plastic deformation-generated extended dislocations in Ge single crystals

13 p1668 A73-28222

Magnesium oxide crystal dislocation loop shrinkage rate measurement, suggesting oxygen ion diffusion as rate controlling process for dislocation climb

13 p1634 A73-28257

Crystallographic analysis of hexagonal vacancy type Al-Mg alloy cube plane dislocation loops produced by specimen deformation before quenching

13 p1634 A73-28260

Plastically deformed Fe-Si and Al alloys surface layer crystal dislocation density and plastic flow onset determination as function of depth

13 p1635 A73-28264

Temperature and rate dependence of the critical shearing stress in magnesium single crystals

13 p1636 A73-29056

The effect of neutron irradiation damage on the low temperature deformation characteristics of b.c.c. metals and their alloys.

13 p1638 A73-29454

Aluminum foils crack propagation observation with electron microscope during tensile tests, noting crystal dislocation role in ductile fracture process

13 p1639 A73-29467

Monotonic and cyclic prestrain influence on alpha-Ti fatigue life, suggesting twin/grain boundary dislocation interactions

13 p1640 A73-29486

An X-ray study of the stress corrosion of austenitic stainless steels.

13 p1625 A73-29521

Influence of alloying on the phase composition and properties of maraging stainless steels

13 p1644 A73-29647

Observation of dislocations and inclusions in neodymium-doped yttrium aluminium garnet by transmission electron microscopy.

14 p1782 A73-29744

Assessment of the degree of plastic deformation in a crater with ball imprint.

14 p1810 A73-30309

Dependence of the variation of the electronic dislocation drag force in a superconducting transition on the stress, temperature, and velocity.

14 p1783 A73-30341

Some basic solutions in strain gradient elasticity theory of an arbitrary order.

14 p1812 A73-30546

Dislocation structure of Ni₃Al intermetallic compound during various stages of deformation

14 p1760 A73-30591

Diffusion creep by dislocation climb in beryllium and Be-Cu single crystals.

14 p1761 A73-30633

Attenuation of an ultrasonic signal in aluminum deformed according to a harmonic law

14 p1764 A73-30857

Influence of ordering in a Ni₃Mn alloy on the magnitude of the critical shearing stresses

14 p1764 A73-30859

Enhanced strain aging of niobium by cyclic deformation.

15 p1890 A73-31990

Grain boundary dislocations in aluminum bicrystals after high-temperature deformation.

15 p1891 A73-32020

Dislocation-type mechanism of the influence of solid surface films on the deformation and fracture of metals

18 p2319 A73-35891

Certain law controlling the temperature dependence of the microdeformation of Fe-Cu-Ti, W, and W-Re bcc alloys

18 p2324 A73-36803

Some characteristics of the microplastic deformation of the surface layers of semiconductor crystals at temperatures below and above the thermal brittleness threshold

18 p2341 A73-36805

Influence of stresses on the nature of the distribution of dislocations in Kh18Ni9Ti steel at a temperature of 650 C

18 p2325 A73-36820

Critical shear stress temperature and rate dependence in magnesium single crystals.

18 p2325 A73-36888

Superconducting fluctuations in complexes of tetra-cyanoquinodimethane and structural imperfections.

19 p2482 A73-37387

Some details concerning plastic deformation mechanism of commercial titanium between -100 and 400 C

19 p2441 A73-37839

Study of the phenomenon of stress relaxation of flow in the case of titanium

19 p2442 A73-37840

Changes in the microhardness of lithium fluoride crystals subjected to cyclic elastic compression

19 p2470 A73-37954

A model of strain hardening during high-temperature creep.

19 p2442 A73-38168

Capillarity induced stresses effects on dislocations generation during early stage sintering, predicting plastic flow via modified Hirth method of surface nucleation

20 p2576 A73-39221

Vacancy precipitation in quenched and aged Zr-Al alloys and Zircaloy 2, obtaining evidence by transmission electron microscopy for detailed dislocation structure examination

20 p2578 A73-39488

Continuous decomposition of gamma solid solution in iron-nickel-titanium alloys

20 p2579 A73-39736

Dislocation structure of Ni₃Fe and Ni₃FeCr alloys in various stages of strain hardening

20 p2579 A73-39742

Effect of ultrasound on the dislocation structure and mechanical properties of molybdenum

20 p2579 A73-39745

Influence of electrically active impurities on the mobility of individual dislocations in germanium

21 p2751 A73-40370

Effect of alloying and phase composition on the properties of maraging stainless steels.

21 p2720 A73-41040

Field-ion-microscopic study of interstitial plasticity of tungsten microcrystals.

22 p2872 A73-41726

The nature of the high microhardness of surfaces strain-hardened by friction

23 p2984 A73-43467

Elementary mechanisms and physical models in plasticity and viscoplasticity

23 p3043 A73-43965

Metal fatigue phases investigation including strain hardening under cyclic loads and microcrack nucleation due to dislocation formation under hydrostatic pressure

23 p2993 A73-43966

Optical and polarization study of magnetization processes around individual dislocations in yttrium-iron garnet single crystals

23 p3017 A73-44024

The creep of sapphire filament with orientations close to the c-axis.

23 p2997 A73-44029

Mechanism of ordered dislocation structure formation in metals deformed under high hydrostatic pressure

23 p2993 A73-44043

Geometry, kinematics and dynamics of dislocations in non-linear continuum mechanics.

23 p3045 A73-44082

Dislocation plasticity theory for slip system in terms of constitutive equations for dislocation speeds and densities, extending to rigid viscoplastic body

23 p3046 A73-44226

Influence of dislocation density and aging on the yield point of Al-Cu-Mg-Mn alloys

23 p2995 A73-44285

Influence of ultrasonic vibrations on the mechanical properties and fine structure of aluminum and an aluminum-magnesium alloy

24 p3098 A73-44570

Dislocation locking by interstitial oxygen atoms and the temperature dependence of the yield point in niobium

24 p3099 A73-44574

Study of the deformation structure in alpha-SiC single crystals

24 p3099 A73-44741

CRYSTAL GROWTH

NT EPITAXY

NT HYDROTHERMAL CRYSTAL GROWTH
Doping additions dissociation effect on impurities distribution in grown semiconductor crystals of melts, calculating atomic and molecular concentration

02 p0201 A73-12356

Extended chain crystals of linear high polymers.

02 p0139 A73-12650

Terminal velocity equations for ice crystal growth forms and precipitation rates calculation in clouds, using drag coefficients, aspect ratios and densities

02 p0189 A73-12783

Economic analysis of silicon solar cells production noting cost reduction from feasibility studies of edge defined film fed crystal growth in ribbon form

03 p0258 A73-14251

The edge-defined, film-fed growth (EFG) of silicon single crystal ribbon for solar cell applications.

03 p0258 A73-14254

Growth of ternary composites from the melt. I, II.

04 p0463 A73-15310

Technology and properties of epitaxial GaAs layer grown from liquid phase, considering GaAs solubility in Ga

06 p0734 A73-17798

Titanium nitrides effect on austenite grains formation by high temperature fusion, considering electric arc and vacuum melting of structural steels

06 p0706 A73-17883

Influence of rare-earth metals on the grain growth process during recrystallization of heat-resistant steels

06 p0706 A73-17887

Dendritic solidification of Cu-Ni alloys. I - Initial growth of dendrite structure.

06 p0712 A73-18756

Determination of some kinetic recrystallization parameters of thin films by mathematical and graphical analysis of crystallite boundary shapes

07 p0861 A73-19329

Plagioclase and Ba-K phases from Apollo samples 12063 and 14310.

07 p0881 A73-19714

Crystallization behavior and glass formation of selected lunar compositions.

07 p0895 A73-19858

Dislocation structure of tungsten single crystals grown by electron-beam zone refining

07 p0841 A73-20523

Electrical conductivity of a directionally crystallized Al-Al₃Ni composition

09 p1099 A73-21972

Inhibition of a wedge-shaped crack by a plane buildup of edge dislocations

09 p1157 A73-22159

Effect of hafnium dioxide on grain growth and strength characteristics in niobium

09 p1108 A73-23233

Structure diagram, crystal growth, band structure, physical, optical and photoelectric properties of Al_{1/2}B_{1/2}V compounds, emphasizing CdSb-ZnSb solid solutions

10 p1258 A73-23566

Investigation of the growth surface of GaAs epitaxial films by chemical decoration and small-angle shadowing technique.

10 p1259 A73-23570

Grain growth inhibition by carbide additives in hard metal alloys of the ISO-K 10 type

10 p1231 A73-23688

Crystallography and morphology of as-grown and coarsened Al-Al₃Ni directionally solidified eutectic.

10 p1234 A73-24432

Investigation of the growth of the disperse structure of gold on a germanium surface

11 p1408 A73-25247

Pressure sensitization relation to electrical conductivity relaxation during isothermal isobaric annealing of CdTe crystals

12 p1531 A73-27196

Metallic crystal growth and defects; All-Union Conference on Metallic Crystal Growth and Imperfections, 2nd, Kiev, Ukrainian SSR, June 15-18, 1970, Proceedings

13 p1631 A73-28101

Effect of impurities on the substructure and dislocation formation in metal crystals grown from melts

13 p1631 A73-28103

Striated, cellular and dendritic substructure formation during growth of Fe-Ni alloy single crystals

13 p1631 A73-28107

Application of similarity criteria in calculations of a mobile magnetic field to be used for growth stimulation in single crystals of metals

13 p1667 A73-28108

Niobium mechanical twin formation and propagation, discussing continuous nucleation, matrix interface and dislocation core energies

13 p1632 A73-28132

Vapor-phase deposition of elementary boron at substrate temperatures in the range from 1100 to 1400 C

13 p1645 A73-28181

Grain growth of chemical vapour deposited tungsten-22 wt % rhenium alloy.

13 p1636 A73-28927

Some observations on grain boundary sliding in aluminum bicrystals deformed at elevated temperatures.

13 p1641 A73-29508

Ostwald ripening of transition-metal carbides in liquid nickel and cobalt

14 p1760 A73-30441

Strength and elastic characteristics of ammonium perchlorate whiskers grown with potassium permanganate additions, discussing crystal dislocations and physico-chemical properties

14 p1767 A73-30829

Experimental observations of dendritic duplex crystals grown in complex Ni base alloys.

15 p1890 A73-31841

Crystal growth by vapor transport of GeSe₂, GeSe₂, and GeTe and transport mechanism and morphology of GeTe.

15 p1842 A73-32652

Bubble domain memory materials production, processing and testing, discussing crystal growth, propagation margins, interaction effects and stroboscopic observations

16 p2044 A73-32864

Some properties of synthesized stephanite /Ag₂SbS₄/ specimens

17 p2219 A73-35551

Luminescence of CdS single crystals doped with various donors and acceptors

19 p2471 A73-37955

Book - Gallium arsenide microwave bulk and transit-time devices.

20 p2536 A73-39137

Growth mechanism of charged ice crystals in water vapor

21 p2742 A73-40123

Vapor-liquid-solid type growth in lunar glass covered breccia 15015, noting metallic iron stalks with bulbous tips of iron and sulfur mixture.

21 p2766 A73-40412

Stopping of a wedge-shaped crack by a plane cluster of edge dislocations.

22 p2919 A73-42107

Microdefects in dislocation-free silicon crystals.

22 p2896 A73-42276

Bcc and fcc metal crystal growth, determining thermodynamic and kinetic conditions, surface texture and favored crystal types

23 p2990 A73-43487

Special features of the structure and growth of pyrocarbon whiskers

23 p2996 A73-43624

Whisker junctions between growth structures on CdS layers.

23 p2997 A73-44027

The hardness of titanium-diboride single crystal grown from metal bath.

23 p2994 A73-44154

The effect of halide impurities on the mass production of metal whiskers by reduction.

24 p3098 A73-44401

CRYSTAL LATTICES

NT BODY CENTERED CUBIC LATTICES

NT CLOSE PACKED LATTICES

NT CUBIC LATTICES

NT FACE CENTERED CUBIC LATTICES

Low-temperature induced changes in the martensite crystalline structure of iron-aluminum-carbon alloys

01 p0064 A73-10607

Mosaic-angle and dislocation-density variations in polycrystalline aluminum alloys under tension

01 p0064 A73-10609

The thermally activated deformation of niobium-molybdenum and niobium-rhenium alloy single crystals.

02 p0179 A73-11574

Laser Raman spectrum of crystalline cyclopentened- $\text{sub } 0\text{'}$ and - $\text{sub } 10\text{'}$.

03 p0318 A73-13282

Neodymium energy level shifts in three oxygen-compensated sites of neodymium oxide-doped calcium fluoride crystals

03 p0349 A73-13288

Influence of electron concentration on the formation of phases with bcc, fcc, and hexagonal close packed lattices in certain transition-metal alloys

03 p0324 A73-13510

Investigation of hole scattering in surface inversion channels arising on a cleaved germanium surface

03 p0349 A73-13659

Constitutive analysis of elastic-plastic crystals at arbitrary strain.

03 p0394 A73-13983

X-ray spectral investigation of some vanadium compounds with a Cr_3Si structure

05 p0588 A73-17295

Effect of gamma irradiation on carbon redistribution processes in the martensite lattice

06 p0706 A73-17902

X ray K absorption spectra shifts/Begard additivity rule deviations/ in Fe-Cr, Fe-V, Fe-Ni and Fe-Co systems due to lattice characteristics and electron structure changes

06 p0707 A73-18039

Martensite transformation in an aged Fe-Ni-Ti alloy

06 p0708 A73-18052

Investigation of X-ray atomic scattering functions taking into consideration the tetrahedral covalent bonds in some semiconductors

06 p0736 A73-18217

Superlattice of voids in neutron-irradiated tungsten.

06 p0709 A73-18353

Electric properties of 5,12-6,11-tetraoxatetrasene crystals

07 p0862 A73-20007

Lattice dynamics, third-order elastic constants, and thermal expansion of titanium.

07 p0839 A73-20173

Nature of chemical bonds in metal-like compounds based on transition metals

07 p0841 A73-20519

New method of measuring rapidly varying pressures in the range below 500 atm

07 p0827 A73-20541

A new method of local X-ray structural analysis - The method of an X-ray beam converging in a solid angle

08 p0965 A73-21131

The investigation of the middle infrared absorption spectrum of DyVO_4 at low temperatures.

08 p0994 A73-21219

E resonance line broadening due to superhyperfine interactions in ruby, noting angular dependence of mosaic structure mechanism

09 p1132 A73-21954

Features of the structure and of plastic deformation in zirconium saturated with nitrogen and oxygen

09 p1099 A73-21967

Ni-Ti alloy aging effects on yield strength explained by internal strain due to lattice modulation and Ti rich region volume fraction

09 p1103 A73-22520

Crystallochemical analogy between europium, ytterbium, calcium, and barium in their alloys with manganese

09 p1135 A73-23235

Sheet, tecto-, ortho- and chain silicates crystal lattice breakdown under shock from ballistic range experiments, using Debye-Scherrer method for X ray diffraction studies

10 p1277 A73-24078

Fine structure of X-ray spectra of nickel and some of its alloys with a nickel arsenide lattice and lattices resembling it

10 p1259 A73-24152

Thermal oscillations of hexaboride atoms of some metals

10 p1261 A73-24777

Nb nitriding kinetics and external effects observations, noting nitrogen diffusion through crystal lattices

10 p1236 A73-24955

Mixed valencies and site occupancies of iron in silicate minerals from Moessbauer spectroscopy.

11 p1324 A73-25142

Preferred a axis orientation parallel to fiber axis in commercial carbon fibers due to lower surface energy of basal plane configuration

11 p1389 A73-25857

Lattice model calculation of elastic and thermodynamic properties at high pressure and temperature.

11 p1399 A73-25900

Determination of alpha plus gamma phase boundaries in Fe-Cr-Ni, Fe-Cr-Co, and Fe-Cr-Mn systems

11 p1384 A73-26108

Electrodynamics analysis of superconducting vortices interaction with cylindrical cavities /pinning/, calculating critical currents in type II superconductors in external magnetic field

11 p1409 A73-26191

Crystal lattice dynamics, elasticity and piezoelectricity theories covering linear, Cosserat and strain gradient theories, acoustic and optical properties, etc

11 p1409 A73-26276

Coherent production of electron-positron pairs and bremsstrahlung on a corundum crystal

11 p1410 A73-26447

Preparation and investigation of EuS thin films

11 p1410 A73-26672

Ion distribution in the crystal structure of complex spinel phases of the Mn-Fe-Ti-O system

11 p1386 A73-26674

Distribution coefficients and solubility curves of certain rare-earth elements in GaAs

12 p1531 A73-27194

Electron-diffraction study of amorphous condensates of barium titanate

12 p1531 A73-27198

Mechanical properties of strip molybdenum with a polygonized single-crystal structure

12 p1513 A73-27265

V and Cr thin film lattice parameter decrease with thinness, discussing vacuum effects and surface energies estimation

12 p1531 A73-27935

Anisotropy of gallium elasticity and thermal expansion

12 p1531 A73-27936

Some physical properties of stephanite in the phase transition region

13 p1667 A73-28002

Possibility of atom displacements in solids under the action of laser light pulses

13 p1626 A73-28003

Effect of impurities on the substructure and dislocation formation in metal crystals grown from melts

13 p1631 A73-28103

Effect of the degree of purity on the dislocation structure of tungsten single crystals

13 p1631 A73-28104

Study of the structure and properties of oriented tungsten single crystals

13 p1631 A73-28105

Investigation of structure and imperfections in molybdenum single crystals grown by electron-beam zone refining techniques

13 p1631 A73-28106

Striated, cellular and dendritic substructure formation during growth of Fe-Ni alloy single crystals

13 p1631 A73-28107

On the quadrupole interaction in the diamond structure.

13 p1667 A73-28213

A method for calculating the low temperature surface specific heat of a crystal lattice.

13 p1704 A73-28214

Dislocation structure in molybdenum single crystals after deformation at 293 and 400 deg K.

13 p1634 A73-28221

The effect of lattice disorder on the thermodynamic properties of the f.c. tetragonal beta-one NiZn alloys.

13 p1635 A73-28262

Determination of the boundaries of fluorite-type Y_2O_3 solid solutions in HfO_2

13 p1645 A73-28292

The lattice heat conductivity of aluminium alloys during age-hardening.

13 p1636 A73-29068

Theoretical interpretation of residual lattice strains induced in polycrystalline metals by plastic deformation.

13 p1639 A73-29460

Formation of oriented structures by action of a laser beam on metals.

14 p1760 A73-30325

Phenomenon of negative differential resistance in silicon carbide crystals

14 p1783 A73-30384

Some comments on the importance of third order contributions to the screening of the ionic potential and to the structural energy of metals.

14 p1783 A73-30432

Crystallostructural investigation of the eutectoid decomposition of copper-beryllium alloys - Ordering accompanied by formation of Cu_2Be metastable solid solution

14 p1760 A73-30587

Fatigue failure of a two-phase titanium alloy in vacuum

14 p1763 A73-30713

'Anomalous' alteration of the Moessbauer isomer shift of Te^{125} in defect diamond-like semiconductors

14 p1784 A73-30809

Influence of interstitial impurities on the formation of a cellular structure and on the properties of chromium

14 p1764 A73-30858

Influence of ordering in a NiMn alloy on the magnitude of the critical shearing stresses

14 p1764 A73-30859

Kinetics of changes in deformability of a heat-resistant nickel-base alloy

14 p1764 A73-30861

Empirical intermolecular potentials for N_2 and CO_2 from crystal data.

15 p1915 A73-31272

Transformations in crystalline boron during mechanical dispersion

15 p1897 A73-31600

Visible luminescence of Yb^{3+} and Er^{3+} during IR excitation

15 p1884 A73-31712

Effects of electron-phonon interaction in the luminescence spectra of transition and rare-earth impurities in crystals

15 p1885 A73-31715

Stimulation of nonradiating transitions during intense excitation by light

15 p1885 A73-31720

The Li donor, and binding of excitons at neutral donors and acceptors in crystals

15 p1924 A73-31722

Lattice theory of fracture and crack creep.

15 p1890 A73-31927

Perturbation solution for shock waves in a dissipative lattice.

15 p1913 A73-31937

Critical survey of studies of the equilibrium phase diagram of the Ti-W system

15 p1893 A73-32513

Structural transformations in two-phase titanium alloys

15 p1893 A73-32522

Phase and structural changes in titanium under impulsive loads

15 p1894 A73-32523

Influence of heating rate on the phase composition of the VT-3-I alloy

15 p1894 A73-32525

Neutron matter solidification in neutron star cores, discussing energy minimization through strongly interacting baryon system via arrangement into lattice structure

16 p2061 A73-33220

Niobium-gold alloys crystal structure, phase diagrams, peritectic crystallization and microhardness, noting intermetallics formation by solid state reactions

16 p2026 A73-33957

Oscillations of the magnetic susceptibility in n-type semiconductors with a chalcopyrite lattice

16 p2044 A73-34008

X-ray investigation of the fine crystalline structure of aluminum with creep

17 p2186 A73-34117

Ultrasound absorption coefficient measurement in semiconductor crystal lattices based on acoustoelectric effect

17 p2218 A73-34159

X ray data refinement on proteins, discussing backbone and side chain dihedral angles adjustment by least squares fitting to relieve atomic overlaps 17 p2112 A73-34893

The strength prediction problem of unidirectional fiberglass-reinforced plastics under transverse tension and shear 18 p2326 A73-36409

Low temperature tensile tests for strength and plasticity of pure bcc, hcp and fcc polycrystalline metals, indicating stacking fault energy role 18 p2324 A73-36804

X radiation arising during collisions between metal bodies 19 p2458 A73-37249

Structure and phase composition of welded joints of zirconium alloy with 2.5% Nb 19 p2439 A73-37266

Microstructural characteristics of the TA6V alloy as a function of thermomechanical treatments in alpha plus beta - Effects on the mechanical characteristics in tension 19 p2441 A73-37831

Nonlinear light scattering in crystals 19 p2462 A73-38539

Molecular crystals with behavior predictable by discrete quasi-continuous Cosserat model based on system of oriented Newtonian particles with six degrees of freedom 21 p2739 A73-40573

Binary and ternary Laves phases in systems composed of zirconium and transition metals of the V through VII groups of the periodic system 21 p2718 A73-40848

A study of the real structure of titanium mononitride in its homogeneity region 21 p2721 A73-41225

Russian book - The structure of zirconium alloys. 22 p2873 A73-41973

Drop forged Ti alpha-beta alloy textures after heat treatment, quenching, aging and surface machining 22 p2866 A73-42089

Microdefects in dislocation-free silicon crystals. 22 p2896 A73-42276

Structure of the phase diagrams of the ternary systems /Mo, W/ - /Ti, Zr, Hf, V, Nb, Ta/ - C 22 p2877 A73-42455

Atomic diffusion mechanisms in multiphase and multicomponent alloys covering relaxation, crystal lattice atom exchange and motion along dislocation lines and to neighboring vacancies 23 p2989 A73-43439

Microstructural characteristics of the plastic deformation and recrystallization of an aluminum alloy of various heterophase structure 23 p2991 A73-43489

Light absorption coefficient of disordered semiconductor with random field due to charged impurity centers in presence of constant external electric field 23 p3016 A73-43648

Postannealing isothermal decomposition products of Al-Mn alloys studied by transmission electron microscopy, revealing trigonal and hexagonal lattice diffraction patterns 23 p2993 A73-43916

EPR-line splitting in irradiated ruby containing impurities 23 p3017 A73-44039

Preparation of lanthanum sulfides using carbon disulfide as a sulfurizing agent and the change of these sulfides on heating in air. 23 p3018 A73-44130

Hydrogen-induced transformation and embrittlement in 18-8 stainless steel. 23 p2994 A73-44158

Diagram of continuous cooling transformation of a titanium alloy with 6 per cent Al, 6 per cent V, and 2 per cent Sn /TA 6-V 6-E 2/ homogenized in the beta /sub 0/ phase 23 p2995 A73-44177

Determination of the temperature fields of turbine disks and blades, using irradiated diamond indicators 23 p2987 A73-44294

Development and properties of CdP2S4 24 p3119 A73-44951

Chemical stability and features of the formation of complex nitrides of III-B subgroup elements /Al-B-N system/ 24 p3119 A73-44952

Certain properties of synthetic diamond crystals of various habits 24 p3104 A73-44970

Metal crystal lattice properties and chemical bond nature in terms of valence concept, analyzing p-electron cloud overlapping 24 p3119 A73-45178

Consideration of lattice translations in computer studies of grain-boundary coincidence. 24 p3120 A73-45405

Far-field analysis of nonlinear shock waves in a lattice. 24 p3112 A73-45412

Thermodynamics of white dwarf matter in crystalline phase. 24 p3143 A73-45435

CRYSTAL OPTICS

Synchronously pulsed high repetition rate IR up converter based on Nd-YAG pump laser and proustite nonlinear crystal, describing experimental arrangement and operation 01 p0044 A73-10133

Some optical properties of CaMoO4 single crystals 01 p0088 A73-10626

Spontaneous luminescence of ZnTe single crystals and mixed zinc cadmium telluride crystals at low temperatures, describing spectral lines 01 p0088 A73-10628

The laser's impact on crystal technology. 01 p0088 A73-11067

Accumulation of the light sum in alkali halide crystals under the action of laser emission 01 p0060 A73-11088

Liquid crystal optical and physical characteristics and applications to display design, emphasizing field effect and twisted nematic devices 02 p0201 A73-12083

Morphic effects. III - Effects of an external magnetic field on the long wavelength optical phonons. 02 p0201 A73-12638

Morphic effects. V - Time reversal symmetry and the mode properties of long wavelength optical phonons. 03 p0349 A73-12901

Linear and nonlinear optical properties of some ternary selenides. 03 p0350 A73-14458

Phononless lines shift and broadening during electron phonon interaction in lanthanum trifluoride-Nd crystal, obtaining temperature dependence of non-radiative transition probability 04 p0484 A73-15566

Light speed determination methods, considering He-Ne laser modulation at microwave frequency via intracavity electro-optic KDP crystal 05 p0575 A73-16341

Russian papers on phosphor crystal luminescence and nonlinear optics covering spectral line decomposition, GaAs laser and electromagnetic wave interaction 05 p0584 A73-16551

Phosphor crystals for electromagnetic emission recording based on optical and thermal effects on luminescent screens, considering optimal extinguishing and color alteration conditions 05 p0584 A73-16552

Extinction of photoluminescence by electron irradiation and energy transfer in molecular crystals 05 p0600 A73-16555

Electro-optical media for initial light radiation frequency shift maximum, analyzing circular light/modulating wave interactions 05 p0551 A73-16780

Light signal modulation by traveling wave in circular waveguide with coaxial KDP crystal 05 p0558 A73-16781

Cooperative luminescence in trivalent ytterbium and erbium ions in cadmium fluoride crystals 06 p0738 A73-18543

Second-harmonic conversion of laser radiation generated under free-oscillation conditions. 06 p0702 A73-18594

Maximum permissible pulse duration in second-harmonic generation in a KDP crystal. 06 p0703 A73-18595

High-power Y3Al5O12:Nd3+/ laser with an explosion-type lamp. 06 p0703 A73-18597

Quartz optical waveguide by ion implantation. 06 p0703 A73-18745

Discontinuities propagation in quasi-linear hyperbolic partial differential equation systems, noting MHD flow and crystal optics equations 07 p0850 A73-19016

Electrooptic liquid crystal devices - Principles and applications. 07 p0861 A73-19135

Numerical integration over Brillouin zone for solids spectral properties calculation, considering crystal optical spectra, phonon effects, IR absorption, electron emission and magnetic susceptibilities 07 p0861 A73-19266

Phase matching in second-harmonic generation using artificial periodic structures. 07 p0834 A73-19538

Crystal-field effects of iron and titanium in selected grains of Apollo 12, 14, and 15 rocks, glasses, and fine fractions. 07 p0881 A73-19710

Lunar plagioclase - A mineralogical study. 07 p0881 A73-19712

Twin laws, optic orientation, and composition of plagioclases from rocks 12051, 14053, and 14310. 07 p0881 A73-19713

Spectroscopy of optical centers of Nd3+/ in CaF2 and SrF2 crystals 07 p0836 A73-20203

Optical centers of Nd3+/ in calcium and strontium fluorophosphate crystals 07 p0836 A73-20204

Optical constants measurement for far IR materials of crystalline quartz, sapphire, Ge and Si at room temperature and 1.5 K 08 p0994 A73-21049

Laser optical double resonance and efficient infrared quantum counter upconversion in LaCB:Pr3+/ and LaF3:Pr3+/ 09 p1090 A73-21936

Production of a coherent submillimetric radiation by a heterodyne method 09 p1097 A73-23030

Color centers in gamma-irradiated ruby with vanadium additions 10 p1259 A73-24069

Two-photon excitation of luminescence in CaF2:Er3+/ crystals by a frequency-scanning laser employing organic dye solutions 10 p1227 A73-24075

Generation of the second harmonic of laser emission in organic crystals 10 p1228 A73-24583

Luminescence line width in ruby crystals of a laser resonator 12 p1505 A73-26892

Controllable liquid-crystal transparency for recording of holograms. 12 p1498 A73-27513

Reduction of the switching time of a liquid-crystal optical transparency. 12 p1498 A73-27514

Magneto-oscillatory absorption effect in SbI3 13 p1667 A73-28004

Specific characteristics of interband luminescence in crystals in the presence of intense laser radiation 13 p1628 A73-29049

Transient processes in second harmonic excitation by ultrashort laser light pulse train related to crystal length and phase matching 13 p1629 A73-29433

Thermal deformation of an injection laser crystal during the passage of pumping current pulses. 13 p1630 A73-29443

Detection of transient absorption in YAG laser crystals using combined laser. 14 p1756 A73-29930

Characteristics of the reflection spectra of CdS/x/Se/1-x/ mixed crystals in their exciton absorption region 14 p1783 A73-30578

Concentration dependence of the lasing parameters of a laser based on CaF2:Dy2+ crystals 15 p1884 A73-31221

Quantum theory of frequency conversion in nonlinear optics 15 p1886 A73-32330

Optical parametric oscillators. 16 p2023 A73-32857

Single crystals for optical applications - Problem of index homogeneity of double niobates Ba/x/Sr/1-x/Nb2O6 and Ba2NaNb5O15. 16 p2043 A73-32862

Coherent optical processing of linear phased array radar signals. 17 p2132 A73-35649

Use of a stable polarization modulator in a scanning spectrophotometer and ellipsometer. 17 p2175 A73-35751

Parameters of fast recombination centers in CdS single crystals and the effect of the parameters on photosensitivity 18 p2340 A73-36669

Investigation of 'external' self-focusing of ruby laser emission in CdS crystals 18 p2322 A73-36674

Effect of the surface condition on the reflection and luminescence spectra of CdS crystals 19 p2471 A73-37961

Amplitude stabilization of pulses from a Q-switched ruby laser by means of interaction with a non-linear medium. 20 p2570 A73-38614

Green function and Poynting vector calculation of solid angles of radiation outside and inside anisotropic crystal in laser light scattering experiments 20 p2591 A73-38617

Engineering design and optimization of the parameters of frequency doublers for the visible range. 20 p2573 A73-39685

Low pass wide and medium band far IR filter obtained by cooling crystalline material to liquid He or nitrogen temperatures, tabulating transmission characteristics 21 p2697 A73-40127

Angular dependence of optical scattering in mixed nematic-cholesteric liquid crystals. 21 p2751 A73-40453

Ruby coloring centers and orange coloration dependence in corundum crystals on additive Mg, Cr, V and Ti ions 21 p2752 A73-40560

Limitations for mode-locking enhancement of internal SHG in a laser. 21 p2714 A73-40759

- Light scattering from electrohydrodynamic turbulence in liquid crystals. 21 p2744 A73-41020
- Incident-light double-refracting interference microscope with variable wavefront shear. 21 p2703 A73-41134
- Crystal spectrometry of active regions on the sun. 21 p2706 A73-41602
- Approximate variational treatment of elastic scattering of electrons from semi-infinite lattices. 21 p2741 A73-41627
- Influence of inhomogeneities in a nonlinear crystal on the conversion of an image by sum-frequency generation. 22 p2869 A73-42245
- Phase fluctuations in a parametric light source operating inside a laser resonator. 22 p2869 A73-42246
- Some features of second-harmonic generation in a lithium metaniobate crystal. 22 p2896 A73-42247
- Generation of high-power light pulses at wavelengths 1.06 and 0.53 microns and their application in plasma heating. II - Neodymium-glass laser with a second-harmonic converter. 22 p2869 A73-42248
- Determination of valence electron plasma frequencies and optical permittivity in single crystals of trisulfide of antimony 22 p2897 A73-42648
- Noncollinear second harmonic generation in KDP. 22 p2871 A73-43078
- KRS5 - A new high-performance acousto-optical material 22 p2897 A73-43100
- Electrooptical modulator employing a barium titanate single crystal. I - Estimates of critical control voltages 23 p2987 A73-43571
- Distribution of hot phonons generated by laser radiation 23 p2988 A73-44020
- Optical orientation in a system of electrons and lattice nuclei within semiconductors - Experiment 23 p3016 A73-44022
- Optical orientation in a system of electrons and lattice nuclei within semiconductors - Theory 23 p3017 A73-44023
- Bulk and surface damage mechanisms of laser crystalline and nonlinear optical materials and thin films, noting plasma thresholds and surface polishing 23 p2989 A73-44210
- The behavior of nematic liquid crystals in the electric field 23 p3019 A73-44387
- ### CRYSTAL OSCILLATORS
- #### NT PIEZOELECTRIC CRYSTALS
- Quartz self-oscillator short term frequency instability lower limit estimation by calculating Q values and nonlinearity and resonator parameter fluctuation effects 03 p0284 A73-14064
- Short term instability of frequency standard using AFC of quartz crystal oscillator by phase locking to optically pumped Rb 87 vapor clock 05 p0583 A73-16071
- Crystal transverse modulators for laser Q-switching, discussing electro-optical properties of various materials 06 p0699 A73-17753
- High level quartz resonators and oscillators 07 p0798 A73-19177
- Certain features of the analysis of a crystal-controlled FM oscillator at high modulating voltage levels 12 p1477 A73-26872
- Selection of the parameters of a rectangular-pulse generator with quartz-crystal controlled frequency 12 p1481 A73-27587
- Generalized theory of nonlinear susceptibilities and linear electrooptic coefficients based on a three-dimensional anharmonic oscillator model. 14 p1756 A73-29926
- An optical parametric generator with a large length of nonlinear interaction and weak feedback 14 p1754 A73-30853
- Study of excitation conditions for a piezo-semiconductor oscillator by the electron modeling method 14 p1737 A73-30946
- Complementary MOS transistor inverter application to quartz oscillator in terms of frequency, temperature and supply voltage 23 p2960 A73-44112
- The frequency stability and noise of passive Rb standard. 23 p2965 A73-44137
- ### CRYSTAL STRUCTURE
- #### NT WIDMANSTATTEN STRUCTURE
- Nickel structure stabilization by multiply alternated thermocyclic treatment and isothermal annealing 01 p0062 A73-10253
- Role of the crystalline structure and orientation of single crystals in the formation of the external friction process 01 p0062 A73-10259
- On the ternary compound G in the Al-Mn-Cr system. 02 p0179 A73-11598
- The effect of crystallite size on the strength of carbon-graphite materials. 02 p0185 A73-12142
- Quadrilateral packet structure and lattice atom positions in single crystal ternary Re-Co-B alloy by X ray analysis 02 p0181 A73-12198
- The influence of texture on the yield loci of copper and aluminium. 02 p0181 A73-12365
- Thermal conductivity of polyethylene - The effects of crystal size, density and orientation on the thermal conductivity. 02 p0185 A73-12431
- Morphic effects. IV - Effects of an applied magnetic field on first-order photon-optical phonon interactions in non-magnetic crystals. 02 p0201 A73-12637
- Cracking of Zircaloy as a result of unusual localized texturing. 02 p0183 A73-12756
- Stress shock waves effect on polycrystalline metals grain structure, discussing strain rate critical value zones 03 p0386 A73-13147
- Inhomogeneity of the structure and deformability of aluminum and aluminum-magnesium alloys 03 p0324 A73-13506
- Effects of alloying on structural stability and cohesion between phases in oxide/metal composites. 03 p0326 A73-13964
- Grain boundary interface and crystal structure effect on elastic and plastic deformation and mechanical properties of metals at low and high temperatures 04 p0462 A73-15301
- Impurities and cooling rate effects on cast W structure during crystallization from optical metallography 04 p0466 A73-15668
- Metallographic orientation determinations on hexagonal polycrystals with the aid of the quantitative polarization equipment of the Neophot. 05 p0577 A73-16752
- Morphological, structural and electrical nonuniformities correlation in epitaxial GaAs films on planes, noting Miller indices effects on morphological and electrical properties 05 p0605 A73-17290
- Directional dependence of the thermal conductivity of crystal-oriented pyrolytic graphite at high temperatures. 06 p0713 A73-17405
- Creep characteristics and substructure disorientation in metals with an fcc lattice 06 p0706 A73-17904
- On supposedly five-co-ordinate titanium (IV) complexes - The crystal and molecular structure of C13Ti(CSH7O2). 06 p0661 A73-18266
- Diffusion in the titanium-aluminum system. I - Interdiffusion between solid Al and Ti or Ti-Al alloys. 06 p0709 A73-18332
- Anisotropy of piezoelectrical scattering in semiconductors with a wurtzite structure 06 p0738 A73-18648
- Grain size effects on iron substitutional alloys yield stress, investigating Hall-Petch relation 06 p0713 A73-18770
- Superrefractory Ni-based alloys mechanical properties enhancement through unidirectional solidification, considering grain boundary structure 07 p0838 A73-19116
- Experimental petrology and origin of Fra Mauro rocks and soil. 07 p0883 A73-19728
- Application of the fourth-order anharmonic theory to the prediction of equations of state at high compressions and temperatures. 07 p0851 A73-19925
- Linear and nonlinear dielectric properties of tetrahedral structure crystals. III - Theory of dielectric properties of tetrahedral structure compounds 08 p0990 A73-20965
- On the influence of grain size and vacancy annihilation on the Portevin-Le Chatelier-effect 08 p0977 A73-21021
- The effect of shear stress on the screw dislocation core structure in body-centred cubic lattices. 08 p0978 A73-21525
- Observations on the interaction of twins with grain boundaries in Mo-35 at.% Re alloy. 09 p1100 A73-21982
- Electron microscopic determination of orientation relationship and habit plane for Ti-Cu martensite. 09 p1101 A73-22406
- Ultrafine grained two-phase alloys fatigue properties as function of phase volume fractions and grain size, noting Coffin law type behavior from low cycle fatigue tests 09 p1102 A73-22411
- Fine grained ingot source Be ductility at 700 C as function of strain rate, noting superplastic behavior with grain boundary sliding at low strain rates 09 p1102 A73-22413
- The exciton energy spectrum in diamond and sphalerite type crystals 09 p1134 A73-22683
- Morphology and spontaneous crystallization conditions of silicides of the transition metals from solutions in metallic melts 09 p1104 A73-22976
- Useful penetration in an austenitic stainless steel, of electrons accelerated under a very high voltage /1500 to 2500 kV/ 09 p1105 A73-23037
- Intergranular precipitation in the oriented bicrystals of aluminum-copper 09 p1105 A73-23039
- Crystalline structure of the Cr3AlB4 compound 10 p1259 A73-24066
- Phase equilibria and crystal structure of intermediate phases in Er-Rh binary alloys 10 p1260 A73-24435
- Fabrication procedures, structure, and mechanical properties of BiTeI thin films 10 p1260 A73-24470
- Characteristics of the vibrational spectrum of laminar As2S3 semiconductors 11 p1408 A73-25244
- Influence of the intercrystalline structure on the diffusion of zinc in the symmetrical joints of bending of aluminum 11 p1379 A73-25324
- Earth mantle rutile-structure germanium dioxide elastic properties as function of pressure and temperature in single crystals 11 p1352 A73-25585
- Shock induced phase change in single crystal orthoclase at 115 kb, noting high pressure phase with hollandite-structure properties 11 p1352 A73-25586
- Rare earth-rhodium systems intermediate phase equilibria and crystal structures, using powder X ray diffraction technique 11 p1410 A73-26569
- Structure of beryllium boron hydrides BeBH5 and BeB2H8. 12 p1466 A73-27045
- X-ray structural investigations of Dy-Fe-Al system alloys in the region of 0 to 33 at. % dysprosium 12 p1512 A73-27243
- Crystalline structure of the TaCoB and NbCoB2 compounds 12 p1512 A73-27244
- Stereometric microanalysis of conglomerate, colony and dispersed structures of binary eutectic Fe, Al, Cu and low melting alloys 13 p1631 A73-28109
- Preparation of a rhombohedral boron carbide of the composition of B13C2 13 p1645 A73-28185
- A static-to-dynamic transition in creep of metallic materials under cyclic stress conditions as caused by an interaction of creep and creep recovery. 13 p1642 A73-29512
- Nickel niobide tested along crystal growth direction for twinning mode of intermetallic phase in tensile deformation, projecting crystallographic structure upon crystal plane 14 p1762 A73-30640
- German monograph - Elevation of the yield point and pronounced yield range of multicrystalline aluminum-magnesium alloys. 14 p1762 A73-30673
- Plastic crystals structural, thermodynamic and mechanical properties, noting high deformability due to molecular rotational freedom 15 p1923 A73-31415
- Mono- and polycrystalline barium titanate structural and physical properties, discussing thermally induced structural changes effects on polarization, permittivity and loss tangent 15 p1924 A73-31775
- Experimental observations of dendritic duplex crystals grown in complex Ni base alloys. 15 p1890 A73-31841
- Electrooptical-phase imaging device using nematic liquid crystals 16 p2013 A73-32881
- Phase equilibria in the metal-rich side of the Ta-N system. 16 p2025 A73-33110
- Phase constitution of the Ni-Cr-S alloy system between 600 and 850 C. 16 p2025 A73-33112
- The influence of prior thermal treatment of cast blocks on the coarse grain characteristics in extruded bars and profiles of alloys of the type AlCuSiMn 16 p2021 A73-33952
- Investigation of the effect of pressed-powder grain composition on the physico-mechanical properties of magnesia refractory materials 17 p2187 A73-34337

Use of cellulose crystallite structures with solid state strain gages for humidity and moisture measurement. 17 p2166 A73-34621

High temperature investigations of the steady and nonequilibrium electrical conductivity of cadmium sulfide crystals 18 p2340 A73-36670

A unified theory of thermoviscoplasticity of crystalline solids. 19 p2501 A73-38256

The preparation and anisotropic hardness of tantalum single crystals with principal orientations. 20 p2575 A73-38637

Structural changes during plastic deformation and annealing of tungsten single crystals 20 p2579 A73-39738

Russian book on radiation effects on ferroelectric crystals and ceramic materials covering changes in dielectric, piezoelectric and optical properties, structure and phase transitions 20 p2600 A73-39757

Photographic investigation of hailstone form, size and structure, determining layer growth from air bubble shape and spectrum 21 p2730 A73-40116

Instability of transverse electromagnetic waves in a drifting electron-hole plasma 21 p2751 A73-40368

Raman spectrum of PbZrO₃. 21 p2752 A73-40894

Structural transformations in molybdenum-carbon alloys during quenching and aging 22 p2874 A73-42091

Patterns of the structure of transition metal/interstitial element diagrams (Me - B, C, N, O, H) 22 p2877 A73-42452

Special features of the structure and growth of pyrocarbon whiskers 23 p2996 A73-43624

The stability of sapphire whiskers in nickel at elevated temperatures. I - General morphological and chemical stability. II - The kinetics of morphological changes over the temperature range 1100 to 1400 C. 23 p2986 A73-44032

Structural changes caused in glassy arsenic trisulfide and triselenide by penetrating radiation 23 p3017 A73-44042

Spatial orientation of phases in the Al-Al₃Ni eutectic system 24 p3099 A73-45169

CRYSTAL SURFACES

Effect of structural factors on the surface properties of single crystal silicon films 01 p0087 A73-10038

An 'ab initio' Gaussian orbital calculation of the /100/ surface of crystalline lithium hydride. 06 p0737 A73-18252

Laser-radiation-induced damage to the surface of lithium niobate and tantalate single crystals. 06 p0738 A73-18591

Surface photovoltage spectroscopy - A new approach to the study of high-gap semiconductor surfaces. 08 p0968 A73-21620

Work function measurements by the field emission retarding potential method. 09 p1133 A73-22196

Certain two-dimensional problems with discontinuous displacements in the theory of elasticity and their application to problems of dislocation-surface propagation 09 p1158 A73-22358

Work function of the principal faces of single crystals of rhenium solutions in molybdenum 10 p1231 A73-23818

Investigation of the growth of the disperse structure of gold on a germanium surface 11 p1408 A73-25247

Metal surfaces structure, chemical segregation, electronic properties, space charge and electrode behavior 11 p1381 A73-25809

Crystal surface topography investigation by scanning electron microscopy for dihedral angle measurements on thermally grooved grain boundaries 13 p1617 A73-28935

A study of the adsorption of oxygen on Ni(111) using Auger electron spectroscopy - Chemical shifts and valence spectra. 15 p1840 A73-31968

Axial alignment of basal planes in polyacrylonitrile base carbon fibers, increasing axial and radial microstructural textures via heat treatment temperature 17 p2198 A73-35837

Effect of atom self-diffusion on evaporation processes and porosity development in solid bodies during electron-beam treatment 18 p2320 A73-36900

Effect of the surface condition on the reflection and luminescence spectra of CdS crystals 19 p2471 A73-37961

Reflection of conductivity electrons from an atomically pure /110/ face of a tungsten crystal 21 p2751 A73-40367

Dynamic properties of surface layers in semiconductors 21 p2752 A73-40845

Combined LEED, Auger electron and flash desorption spectroscopy of metals on single crystal surfaces. 21 p2706 A73-41596

Excitation of surface molecular orbitals on the /100/ face of molybdenum 21 p2722 A73-41597

Influence of mechanical treatment of the resonator on the parameters of an electron-beam-pumped cadmium sulfide laser. 22 p2869 A73-42259

Some experiments to crystallize the metal thin films on quartz plates. 23 p3018 A73-44136

Oxygen-W/100/ surface interactions investigated simultaneously by secondary ion mass spectrometry (SIMS) and electron induced desorption (EID) 24 p3066 A73-45330

CRYSTALLINITY

The composition and crystalline structure of the minerals of regolith from the Sea of Fertility. 02 p0214 A73-12243

Impurity concentration relationship to electrons and holes density and potential fluctuations in completely compensated crystalline semiconductors with randomly distributed donors and acceptors 06 p0735 A73-17976

Fra Mauro crystalline rocks - Mineralogy, geochemistry and subsolidus reduction of the opaque minerals. 07 p0880 A73-19698

Crystalline structure of the Cr₃AlB₄ compound 10 p1259 A73-24066

Study of crystalline transformations at high temperature above 2000 K; International Colloquium, Odeillo, Pyrenees-Orientales, France, September 27-30, 1971, Proceedings 12 p1514 A73-27918

On a finite strain theory of elastic-inelastic materials. 13 p1692 A73-28167

CRYSTALLITES

Inter- and transcrystallite breakdown of steels and alloys under the action of various media /A review/ 01 p0062 A73-10258

The effect of crystallite size on the strength of carbon-graphite materials. 02 p0185 A73-12142

Determination of some kinetic recrystallization parameters of thin films by mathematical and graphical analysis of crystallite boundary shapes 07 p0861 A73-19329

CRYSTALLIZATION

NT RECRYSTALLIZATION

Nucleation during solidification and melting of metals and alloys 02 p0181 A73-12363

The solidification sequence in an 18-8 stainless steel, investigated by directional solidification. 02 p0184 A73-12769

Russian book on ultrasonic processing in metal crystallization covering design of vibrators and transducers and acoustic power measurement 02 p0175 A73-12800

The inhibition of the dendritic electrocrystallization of zinc from doped alkaline zincate solutions. 03 p0273 A73-13727

Purification, crystallization, and subunit structure of allosteric adenosine 5'-monophosphate nucleosidase. 03 p0273 A73-13807

Cummingtonite temperature dependent Mg and ferric ions order-disorder, estimating crystallization temperatures 03 p0375 A73-14104

Characteristics of the ingot crystallization process under conditions of melting in vacuum furnaces with a consumable electrode, and the stability of the cast structure in alloys of the Nb-Ti system 04 p0464 A73-15496

Phase equilibrium in the TeO₂-V₂O₅ system 05 p0589 A73-17173

Comparative study of the epitaxial growth in GaAs-I and GaP-I systems over a wide range of crystallization conditions 05 p0605 A73-17292

Stable or metastable phase crystallization rate of Cd-Sb liquid alloys as function of time, composition and temperature above liquidus line 05 p0605 A73-17294

Petrography and crystallization history of basalts 14310 and 14072. 07 p0879 A73-19685

Lunar rocks petrogenesis, determining liquidus and solidus temperatures and crystalline phases sequence in lunar samples and synthesized oxides and silicates 07 p0879 A73-19689

Experimental petrology and petrogenesis of Apollo 14 basalts. 07 p0880 A73-19690

Vapor phase crystallization in Apollo 14 breccia. 07 p0882 A73-19724

Crystallization behavior and glass formation of selected lunar compositions. 07 p0895 A73-19858

Electrical conductivity of a directionally crystallized Al-Al₃Ni composition 09 p1099 A73-21972

A new method for thermographic investigation of high-speed crystallization processes in high-melting-point metals 09 p1103 A73-22483

Morphology and spontaneous crystallization conditions of silicides of the transition metals from solutions in metallic melts 09 p1104 A73-22976

Thermophysical effects of solidification on dendritic structure and mechanical properties of cast stainless and low alloy carbon steels for different crystallization rates 09 p1107 A73-23198

Nonequilibrium crystallization of Al-Ru alloys 09 p1108 A73-23228

Effect of carbon on the fine structure of cast molybdenum 09 p1108 A73-23232

Investigation of the crystallization of metallic powders obtained by liquid-phase atomization 10 p1224 A73-24313

Property control in reinforced plastics through interface tailoring. 11 p1389 A73-26296

Phase structure and composition during the crystallization of eutectic-type alloys of the Ni-Cr system 12 p1509 A73-26897

Electrical conductivity of semiconductor glass crystals on an arsenic and lead selenide base 12 p1531 A73-27195

Influence of the physical properties of metal melts on the spheroidization of droplets in the process of their crystallization 12 p1503 A73-27551

Dendritic liquation of hypoeutectic binary, ternary and complex Fe- and Ni-base alloys dependence on phase diagram 13 p1631 A73-28102

Temperature conditions of aluminum alloy crystallization at cooling rates of 10,000 to 1,000,000 deg/sec 13 p1632 A73-28111

Crystallization of nickel-based alloys and indium-lithium system alloys at ultrahigh cooling rates 13 p1632 A73-28112

Dependence of the diffuse expansion characteristics of a crystallization zone on the vertical stability of the atmosphere 13 p1654 A73-28879

New method of thermographic investigation of rapid processes of crystallization of refractory metals. 15 p1891 A73-32070

Temperature dependent crystallization and density of Fe-Mn-C alloys with niobium at 1200-1500 C from gamma ray measurements 16 p2027 A73-34012

Cold rolling of polymers. III - Properties of rolled crystallized polycarbonates. 17 p2197 A73-35351

The gas carrier problem during the crystallization of metals from a gas phase 18 p2323 A73-35880

Experimental and theoretical investigation of the process of artificial crystallization and dissipation of supercooled clouds 18 p2332 A73-35919

Grain refinement in aluminium-zirconium and aluminium-titanium alloys by metastable phases. 19 p2440 A73-37444

Application of the method of straight lines to the solution of a modified Stefan problem 20 p2626 A73-39253

Investigation of the crystallization of polyethylene terephthalate 21 p2647 A73-40260

The possibility of crystallization of condensed combustion products in nozzles 21 p2753 A73-40697

Study of a chondrule extracted from Lot 118-111 of the lunar soil of Mare Fecunditatis 21 p2770 A73-41006

Structure and composition of phases during solidification of Ni-Cr alloys of the eutectic type. 21 p2720 A73-41030

Metastable phase diagrams of eutectic and peritectic alloys crystallization during rapid cooling from liquid state 22 p2877 A73-42458

Al-aluminum nickelide eutectic fiber composite impact strength dependence on crystallization rate, examining crack propagation rate relation to fiber spacing 23 p2996 A73-43437

Ni-based ternary alloy element segregation after addition of third element during crystallization, showing Si addition influence on segregation direction of Co, Cr and Mo 23 p2992 A73-43915

Quasi-steady Stefan problem solutions for nonlinear heat conduction in two phase /liquid-solid/ state crystallizer

24 p3158 A73-45501

CRYSTALLOGRAPHY

X-ray investigation of textures in thin films
01 p0050 A73-10800

Electron diffraction investigations of the short-range order in GaAs and GaP films
05 p0605 A73-17291

Crystallography and chemical trends of orthopyroxene-pigeonite from rock 14310 and coarse fine 12033.
07 p0881 A73-19703

Pyroxenes as recorders of lunar basalt petrogenesis - Chemical trends due to crystal-liquid interaction.
07 p0881 A73-19704

Crystallographic studies of lunar plagioclases from samples 14053, 14163, 14301, and 14310.
07 p0882 A73-19715

A new method of local X-ray structural analysis - The method of an X-ray beam converging in a solid angle
08 p0965 A73-21131

Crystallography and morphology of as-grown and coarsened Al-Al₃Ni directionally solidified eutectic.
10 p1234 A73-24432

Stony-iron meteorite shock histories, determining crystallographic character of kamacite in samples via back reflection X ray diffraction technique
11 p1419 A73-25780

Maximal finite groups of $n \times n$ integral matrices and complete groups of integral automorphisms of positive quadratic forms /Bravais types/
13 p1648 A73-28342

The relationship between thermal history, X-ray crystallographic structure and thermal properties of Pyco-bond rayon precursor carbon-carbon composites.
16 p2028 A73-33044

The relationship between thermal history, X-ray crystallographic structure and thermal properties of rayon precursor carbon-carbon composites A literature review.
16 p2028 A73-33045

The development and control of crystallographic texture in 3Al-2.5V titanium alloy tubing.
[SAE SP-378] 19 p2434 A73-37870

The effects of crystallographic texture on the mechanical and fracture properties of Ti-3Al-2.5V hydraulic tubing.
[SAE SP-378] 19 p2434 A73-37871

Fracture behaviour of crystalline Al₃Ni intermetallic fibres.
23 p2991 A73-43774

Some experiments to crystallize the metal thin films on quartz plates.
23 p3018 A73-44136

CRYSTALS

NT BICRYSTALS
NT BOULES
NT BRAVAIS CRYSTALS
NT CREATINE
NT CRYSTAL OSCILLATORS
NT CRYSTALLITES
NT DENDRITIC CRYSTALS
NT IONIC CRYSTALS
NT LIQUID CRYSTALS
NT METAL CRYSTALS
NT MIXED CRYSTALS
NT PIEZOELECTRIC CRYSTALS
NT POLYCRYSTALS
NT QUARTZ CRYSTALS
NT SINGLE CRYSTALS
NT WHISKERS [SINGLE CRYSTALS]

Geometric interpretation of conditions for resonant wave interactions valid under nondispersive conditions, noting relevance for acoustic waves in crystals and slowness vectors
11 p1400 A73-26278

Discrete /microscopic, atomic/, continuous /macroscopic, phenomenological/ and quasi-continuous models of elastic solids, exemplifying elastic crystals linear model
16 p2037 A73-33230

CSM

U COMMAND SERVICE MODULES

CUBIC LATTICES

NT BODY CENTERED CUBIC LATTICES
NT FACE CENTERED CUBIC LATTICES
Application of the fourth-order anharmonic theory to the prediction of equations of state at high compressions and temperatures.
07 p0851 A73-19925

Spectroscopy of optical centers of Nd³⁺ in CaF₂ and SrF₂ crystals
07 p0836 A73-20203

Study of the dynamic theory of BaTiO₃ in the cubic phase
07 p0864 A73-20612

Cast, annealed and hardened zirconium binary alloys cubic to hexagonal phase transitions from X ray and differential thermal analysis
10 p1233 A73-24318

Ferritic stainless steel transverse tension ridging mechanism in terms of CF and CC mixed texture bands, contradicting plastic buckling theory
13 p1633 A73-28147

Concentration dependence of the degree of occupancy of a lattice element in cubic titanium oxycarbide
15 p1896 A73-31210

Polarization plane rotation under magnetic field for IR waves in nonmagnetic semiconductors with cubic crystal lattices, explained by magneto-optical Faraday effect
17 p2219 A73-34342

Theory of the phase transition in group IV-VI compound semiconductors
21 p2751 A73-40369

CUES

A computer-generated display to isolate essential visual cues in landing.
05 p0595 A73-16704

Scalar perceptions with binocular cues of distance.
13 p1578 A73-28176

Scanning movements in space perception in terms of convergence role during cue conflict and cue isolation experiments
18 p2274 A73-36462

Effects of prestimulus cuing and target load variability on maintenance of response strategies in a visual search task.
19 p2402 A73-38378

Visual cues and six degree of freedom motion flight simulation for F-4 aircraft energy maneuvering performance, discussing pilot evaluations
[AIAA PAPER 73-934] 21 p2674 A73-40880

A comparison of the Ponzo illusion with a textural analogue.
21 p2639 A73-41180

CUESTAS

U RIDGES

CULTURE TECHNIQUES

Resistance of soil microorganisms to starvation.
02 p0136 A73-12627

Effect of cultural conditions on the fatty acid composition of *Thiobacillus novellus*.
03 p0261 A73-13599

The effect of temperature on the mitotic activity of human peripheral blood lymphocytes in a culture
07 p0781 A73-19649

Method for measuring the contractions of small hearts in organ culture.
08 p0933 A73-21218

Cinemicrographic study of the development of sub-surface colonies of *Staphylococcus aureus* in soft agar.
08 p0933 A73-21828

Russian book on mathematical models of biological systems covering biogeocenosis, optimal crop, chemostat cultivation, predator-victim society, trophic control, and life support systems
09 p1044 A73-22347

Automatic surface inoculation of agar trays.
09 p1045 A73-22550

Biochemical and morphological studies of lunar material effects on plant tissue culture cells, noting nonpathological increased cellular activity and chloroplast and cytoplasm changes
11 p1320 A73-26482

Response of tobacco tissue cultures growing in contact with lunar fines.
11 p1320 A73-26483

Fatty acids of *Pinus elliotii* tissues.
15 p1841 A73-32199

Survival of common bacteria in liquid culture under carbon dioxide at high temperatures.
15 p1837 A73-32650

Monitoring for microbial flora contamination on spacecraft surface, discussing cultural techniques and sampling methods for microorganisms detection and sterilization
16 p1976 A73-33698

Survival and mutability of *Chlorella* under various orientation in the earth's gravitational field.
18 p2270 A73-35997

Purification of *Synechococcus lvis* by equilibrium centrifugation and its synchronization by differential centrifugation.
18 p2274 A73-36503

Solubilization and accumulation of copper from elementary surfaces by *Penicillium notatum*.
21 p2648 A73-41217

On the multiplication of xerophilic micro-organisms under simulated Martian conditions.
22 p2803 A73-42165

CUMULATIVE DAMAGE

Optimal renewal algorithm for control plant with cumulative damage, using failure rate and renewal point spacing model
01 p0058 A73-11421

Comparison of scatter under program and random loading and influencing factors.
[DFVLR-SONDDR-259] 03 p0387 A73-13232

Random fatigue of 2024-T3 aluminum under two spectra with identical peak-probability density functions.
03 p0322 A73-13235

On the probabilistic determination of scatter factors using Miner's rule in fatigue life studies.
03 p0388 A73-13237

Cumulative fatigue damage tests of Al alloy, evaluating Miner cycle/stress ratio
03 p0325 A73-13571

The additivity of cumulative damage in the test or use environment.
04 p0507 A73-14716

Kinetic model considering cumulative fatigue damage interaction with chance overload on component or structure under probabilistic service load, discussing crack growth in composites
04 p0508 A73-14717

Visual display of fatigue damage by means of exoelectron emission.
04 p0446 A73-14748

Parametric-graphical method of cumulative creep damage evaluation for Cr-Mo-V steel in terms of postexposure rupture and hardness measurements
04 p0460 A73-14855

Structural reliability under cumulative fatigue damage and chance overload interaction, postulating kinetic fracture model based on probabilistic service load histories
04 p0512 A73-15243

Nondestructive screening and pulse damage mechanism for thermal second breakdown of semiconductor junction diodes
05 p0557 A73-16504

Early diagnosis of machine damage on the basis of the determination of rubbed-off materials in highly stressed lubricating oils - Employment of spectrographic methods for the analysis of the oil
05 p0582 A73-16998

Predicting failures with conducting-polymer fatigue-damage indicators.
06 p0759 A73-17598

Probability of stress-corrosion fracture under random loading.
06 p0763 A73-18483

Theoretical and experimental prediction for pulsating creep failure.
07 p0917 A73-20489

Book - Fundamentals of cyclic stress and strain.
08 p1020 A73-21836

High temperature fatigue sensor based on conductive composite device irreversible resistance increase resulting from cumulative strain damage
09 p1083 A73-22504

Plasticity and failure of heat-resistant materials at a low number of cycles of simultaneous fluctuations of temperature and load.
09 p1105 A73-23154

Cyclic stress, strain, and energy variations under cumulative damage tests in low-cycle fatigue.
11 p1379 A73-25132

Phenomenological approach to low-cycle fatigue fracture of a typical aircraft full scale component static test.
11 p1305 A73-25554

Cumulative damage theories for the prediction of life in the case of vibrational stresses. I - A critical overview
11 p1441 A73-25576

Damage accumulation hypotheses concerning lifetime prediction during vibrational loading. II - A critical review
11 p1384 A73-25849

Fatigue resistant design with fiber reinforced plastics /FRP/, discussing stress analysis, failure criteria, material anisotropy, multiaxial stress conditions and cumulative damage
12 p1515 A73-26880

Studies on fatigue damage caused by stresses below the endurance limit - The effect of program period and fatigue failure by stresses below the endurance limit.
13 p1692 A73-28197

Evaluation of torsional fatigue damage from changes in the fatigue properties and microhardness.
13 p1635 A73-28522

Choice of materials on the basis of random vibration and structural fatigue.
13 p1641 A73-29495

Machine parts fatigue life and linear cumulative damage at stresses below endurance limit, including plastic strain, microcracking and S-N curves
13 p1641 A73-29496

Aspect of cumulative fatigue damage under multiaxial strain cycling.
13 p1701 A73-29497

Fatigue damage by a stress below the endurance limit.
13 p1641 A73-29498

Cumulative damage and behavior of plastic strain in high and low cycle fatigue.
13 p1641 A73-29500

Evaluation of dissipation and damage in metals submitted to dynamic loading.
13 p1701 A73-29503

On fatigue damage and debonding of glass fiber reinforced plastics.
13 p1647 A73-29546

A mathematical model of damage accumulation in plastic isotropic materials. 14 p1810 A73-30301

Approximate determination of the reliability function of a digital computer 15 p1848 A73-31912

Environmental damage avoidance via climatic and mechanical factors simulation tests for vibration, humidity, temperature, sunlight, rain, salt spray, shock and altitude 16 p1997 A73-33377

Probabilistic fatigue design alternative to Miner's cumulative damage rule. 16 p2081 A73-33643

Lubricant testing as an aid to bearing damage analysis. [ASLE PREPRINT 73AM-3B-1] 17 p2178 A73-34983

Cumulative fatigue damage under complex strain histories. 18 p2364 A73-36593

The effect of stress amplitude below the fatigue limit on cumulative fatigue lives in perforated round specimens. 19 p2501 A73-38344

The impact resistance of glassfiber reinforced plastics under accumulation of fatigue damage. 20 p2580 A73-38645

Diagrams of cumulative damage during tension of polycrystalline metals 20 p2577 A73-39371

Il'ushin linear theory for defect accumulation generalized for endurance limit of materials under noncyclic loads, examining time to failure under creep and relaxation conditions 20 p2624 A73-39644

Prediction of failure processes in fiberglass-reinforced plastics by a seismoacoustic method. II - Features of damage buildup in woven fiberglass-reinforced plastics in uniaxial tension 24 p3102 A73-44507

CUMULONIMBUS CLOUDS

A note on the use of airborne 30-millimetre radar at long ranges. 04 p0423 A73-15699

Interpretation of numerical observations of meteorological satellites with infrared and monochromatic vision by means of high resolution satellites - The case of storm cloud systems 05 p0594 A73-17232

Time lapse stereo photogrammetry of ring vortex type circulation in cumulonimbus cloud tops of hail bearing storms 07 p0847 A73-19042

Turbulence energy spectra in thick convective cumulonimbus cloud zone, using aircraft measurements 08 p0984 A73-21186

Calculation of the growth and melting of ice particles and the radar signal reflection profiles in cumulonimbus clouds 13 p1653 A73-28878

Russian monograph on convective cumulus and cumulonimbus cloud physics covering atmospheric convection, meteorological field structure and dynamic-kinematic schemes 15 p1903 A73-31584

Influence of the vertical structure of the wind field on the development of cumulus and cumulonimbus clouds 18 p2332 A73-35920

Laboratory vortices in rotating, sheared flow. 19 p2420 A73-37664

Certain results of radar studies of the evolution of convective clouds 21 p2731 A73-40494

Penetration of thundercloud electric fields into the ionosphere and magnetosphere. I - Middle and subauroral latitudes. 24 p3085 A73-45118

CUMULUS CLOUDS

On a method of determining the interaction coefficient in convective clouds 01 p0074 A73-11273

Cloud characteristics in problems of radiation energetics in the earth's atmosphere. 02 p0159 A73-12146

Two dimensional deep convection primitive model of pressure perturbation in cumulus cloud with precipitation 02 p0189 A73-12781

Numerical simulation of precipitation development in supercooled cumuli. I, II. 05 p0594 A73-16572

Jet model of cloud convection - A numerical experiment 05 p0594 A73-17353

Vertical profiles of liquid water content and other cloud parameters for cumulus and cumulus cong clouds from aircraft measurements over Ukraine 08 p0985 A73-21454

An experimental investigation of the nature of changes in the intensity of precipitations from stratiform and cumuliform clouds 12 p1522 A73-27747

A three-dimensional model of cumulus cloud development. 14 p1771 A73-30764

A jet-stream model of cloud convection and a numerical experiment. 15 p1902 A73-31003

Russian monograph on convective cumulus and cumulonimbus cloud physics covering atmospheric convection, meteorological field structure and dynamic-kinematic schemes 15 p1903 A73-31584

Certain parameters of cumulus clouds as determined from sky photographs and from ground-based actinometric measurements 15 p1905 A73-31793

Solar radiation fluxes at the earth's surface in the presence of cumulus clouds 15 p1905 A73-31794

Spatial structure of the short-wave radiation field in stratocumulus and cumulus clouds 15 p1905 A73-31795

Cloud cover probability computation models, showing averaged values for direction of sighting and cumulus cloud cover estimations 15 p1905 A73-31797

Scheme for evaluating the influence of convective-cloud modifications aimed at controlling precipitations artificially, and the results of cumulus cloud structure investigations from aircraft 18 p2332 A73-35917

Influence of the vertical structure of the wind field on the development of cumulus and cumulonimbus clouds 18 p2332 A73-35920

Cumuli structure at various stages of development. 18 p2333 A73-36705

Numerical modeling of the dynamics and microphysics of warm cumulus convection. 19 p2447 A73-37658

A comparison between axisymmetric and slab-symmetric cumulus cloud models. 19 p2447 A73-37659

Structure of cumulus clouds during various development phases 20 p2583 A73-39186

Cumulus congestus cloud circulation velocity field measurement by balloon, comparing with radar, cameras, satellite and ground based observed meteorological model computations 21 p2728 A73-40060

Numerical one dimensional cumulus model of stratification and cloud depth-radius relations for convective layer prediction 21 p2729 A73-40068

Rate of growth of the upper boundary of cumulus clouds 21 p2730 A73-40117

Certain parameters of cellular convection according to observations by meteorological earth satellites and from a high mast 21 p2731 A73-40492

Numerical simulation of maritime warm cumulus by one dimensional cylindrical cloud model incorporating nucleation and raindrop breakup processes 22 p2883 A73-42546

Nonlinear theory of the formation and structure of the intertropical convergence zone. 23 p3001 A73-43586

Cumulus-scale vertical transport of mass, heat and momentum calculated from radar and rain gage precipitation measurement 23 p3002 A73-43596

Total ozone measurements in cloudy weather. 23 p2973 A73-43853

CURIE TEMPERATURE

Positive thermal coefficient of electrical resistance in BaTiO₃ single crystals near the Curie point 10 p1260 A73-24473

Investigation of phase transitions in BaTiO₃ 15 p1923 A73-31204

Quasistatic generation of harmonics in a ferroelectric crystal with a second order transition above the Curie point. 15 p1924 A73-32157

Highly permeable nickel-iron-molybdenum alloys containing 33 to 37% nickel 16 p2026 A73-33958

CURING

Characterization of an epoxy system for filament winding. 03 p0330 A73-13016

Computing pressure cure viscoelastic effects in solid propellants. 05 p0606 A73-17208

Syntactic foam from Pyrrone prepolymer and hollow carbon microsphere mixtures, discussing low curing shrinkage and high thermal stability 16 p2029 A73-33051

The effect of cure cycle on the mechanical properties of carbon-fibre/epoxide resin. 16 p2031 A73-33988

Cross-linking ambient curing mechanisms for air-drying oxidizable coatings, involving chemical film-forming reactions 20 p2580 A73-39636

CURIUM

NT CURIUM ISOTOPES

NT CURIUM 244

CURIUM ISOTOPES

NT CURIUM 244

Curium-248 in the early solar system. 24 p3143 A73-45348

CURIUM 244

Cost-effective radioisotope thermoelectric generator designs involving Cm-244 and Pu-238 heat sources. 19 p2455 A73-38389

Curium 244 heat source design for multithundred watt radioisotope thermoelectric generator with Si-Ge thermocouples for energy conversion, noting low cost 19 p2457 A73-38429

The availability and cost of curium-244 from power reactor fuel reprocessing wastes. 19 p2457 A73-38430

CURL (VECTORS)

NT VORTICITY

Vorticity equation advection, divergence and curl terms effects on vorticity changes over isobaric surfaces and on weather and cyclonic development in synoptic meteorology 13 p1653 A73-28745

CURRENT AMPLIFIERS

NT PHOTOMULTIPLIER TUBES

The use of operational amplifiers to generate precise current ratios for platinum resistance thermometry. 22 p2832 A73-42028

CURRENT DENSITY

Influence of the thickness of a copper coating on the critical current of a superconducting wire made from niobium-based alloys 01 p0089 A73-11435

Superconducting Mo-Re alloy thin film prepared by sputtering and deposition onto sapphire substrate, measuring transition temperature, critical current and magnetic field characteristics 02 p0200 A73-11841

Response of boron/epoxy composite materials to simulated lightning current. 03 p0331 A73-13025

The performance of recently developed high voltage high current power transistors. 03 p0283 A73-13944

Influence of the pinning forces for flux lines on the critical current density in magnetic fields of up to 10 Tesla in superconducting titanium-niobium alloys 03 p0328 A73-14654

Fuel cell air cathode for high current densities at low polarization and ambient temperature, noting performance improvement with pure oxygen supply 04 p0407 A73-15112

Radial anode current density distribution measurement in high current pulsed arcs in air on copper split anode, using Rogowski coils 06 p0723 A73-18357

Pressure, temperature, current density and potential difference fluctuations in subsonic flow of combustion products plasma, noting steadiness, ergodicity and distribution functions 06 p0732 A73-18616

Electromagnetic current and charge due to interaction between a gravitational and a free electromagnetic field. 06 p0732 A73-18715

Screw instability of a plasma with a distributed current 07 p0855 A73-19280

Effect of carrier multiplication in the collector junction of an alloyed transistor on the behavior of the transistor at high current densities 07 p0798 A73-19292

Design considerations for high-current-density superconducting saddle magnets for MHD. 07 p0852 A73-20405

Steady state hot toroidal Tokamaks plasma, calculating seed current density for bootstrap effect produced by neutral particle injection parameters control 08 p0991 A73-20814

Low-field tunnelling current in thin-oxide M.N.O.S. memory transistors. 08 p0946 A73-21115

Analysis of an inhomogeneous bulk 'S-shaped' negative differential conductivity element in a circuit containing reactive elements. 09 p1061 A73-21989

Calculation of the magnetic properties of a hydrogen molecule with the aid of the method of varying the vector potential and the method of varying the induced current 09 p1122 A73-22017

Gain-current relation for GaAs lasers with n-type and undoped active layers. 09 p1091 A73-22239

Transverse mode control in semiconductor lasers. 09 p1092 A73-22242

A limitation on repetition rate of pulsations of junction lasers due to the repetitively Q-switched mechanism. 09 p1093 A73-22253

Nonlinear properties of microwave avalanche diodes operated in IMPATT mode, discussing current density effect and power efficiency

09 p1063 A73-22489

Influence of the Hall effect on current structure in a plasma flow through a spatially periodic magnetic field

09 p1127 A73-22606

Comparison of the efficiency of photocells with stepwise and exponential distributions of the impurities in the doped layer

09 p1033 A73-22721

Current saturation and small-signal characteristics of GaAs field-effect transistors.

10 p1197 A73-24868

CdS-metal contact at higher current densities.

11 p1407 A73-24984

Photon rest mass limit determination from Galactic magnetic field measurements, utilizing maximum current density capability of plasmas

11 p1415 A73-25121

Measurement of point-discharge current density in the atmosphere.

11 p1354 A73-25767

Critical current value for a superconductor niobium-alloy wire as a function of its copper coating thickness.

11 p1409 A73-26062

Electromagnetic scattering by a transversely moving conducting cylinder of arbitrary cross section.

12 p1468 A73-27018

Electrohydrodynamic equation solutions for non-collinear current density and velocity vectors of unipolarly charged fluid flow in channel with wall-type electrodes

12 p1528 A73-27406

Highly disperse Fe powder electrodeposition on cathode, examining electrolyte concentration, acidity, current density and bath temperature effects on current efficiency for optimal deposition conditions

12 p1503 A73-27552

Screw instability in a plasma with a distributed current.

13 p1665 A73-28680

Vanadium galliumide tape preparation and critical temperature and current as function of heat treatment temperature and applied magnetic field, considering pancake current capacity

13 p1669 A73-29069

Properties and structure of Ti-Nb-base superconducting alloys

13 p1643 A73-29644

Split Langmuir probe measurements of current density and electric fields in an aurora.

14 p1748 A73-29970

Electron characteristics of sprayed vanadium-gallium alloys

15 p1922 A73-31178

Influence of heat treatment on the critical currents in binary alloys of niobium with zirconium and titanium

15 p1887 A73-31185

The passivation behaviour of the Ti-6Al-4V alloy.

15 p1895 A73-32567

High-frequency current states in small-size superconductors

16 p2044 A73-34066

Transistor design and thermal stability.

17 p2133 A73-34218

Temperature dependence of thermionic emission current density of Pt additive powdered zirconium carbide deposit on diode cathode working surface

17 p2109 A73-35171

Transient temperatures in a plate from a Gaussian distribution of normal heat flux and current flow with application to the free arc discharge.

17 p2255 A73-35843

Excitation of an open resonator by initial emission from a high current discharge

19 p2469 A73-37963

Computer-aided two-dimensional analysis of bipolar transistors.

20 p2536 A73-39410

Microarc current flow and potential drop through cold boundary layer near plasma electrodes in MHD generators

20 p2598 A73-39604

Numerical experiment in a study of the separation of a laminar boundary layer in an MHD channel

20 p2598 A73-39611

Linear theory of transverse-current instability in a plasma

21 p2746 A73-40521

Tungsten target surface contaminants produced fast ion current peak measured by ion collector in expanding laser produced plasma

21 p2716 A73-40972

Properties and structure of superconducting Ti-Nb alloys.

21 p2720 A73-41037

Correlation of ion and beam current densities in Kaufman thrusters.

22 p2900 A73-42636

Models of force-free magnetic fields in resistive media.

22 p2911 A73-42938

Bipolar transistor emitter efficiency calculation, considering heavy doping induced impurity profiles effects on current gain

23 p2958 A73-43451

Diffusionless theory of the current-voltage characteristics of a metal/monopolar semiconductor contact in the case of current limiting by an arbitrary space charge

23 p3015 A73-43621

Induced currents in a stationary plasma flow in an axially-symmetric magnetic field

23 p3010 A73-43663

Equilibrium configurations of electron beams in a plasma

23 p3014 A73-44338

Thermal and electrical properties of superconducting vanadium silicide tapes, plotting transition temperature vs heat treatment time and temperature and critical current vs current density

24 p3119 A73-44411

Investigation of plasma acceleration in crossed electric and magnetic fields

24 p3115 A73-44751

Influence of emitter current concentration effects on the temperature distribution in power transistors

24 p3072 A73-44930

CURRENT DISTRIBUTION

Multifrequency excitation of a wire antenna for an invariant radiation pattern.

01 p0023 A73-10190

Integral equations for current distribution and input impedances of curved thin symmetrical dipole antenna, noting Q factor of fourth wave antennas

01 p0017 A73-10216

Investigation of the structure of an electron beam formed by a high-perveance triode gun under controlled-current conditions

01 p0025 A73-10989

Semihydrostatic hot extrusion for Ti plated Cu anode bar, noting metal bonding and current distribution

03 p0312 A73-13583

Current distribution prediction in transient response of rotating disk electrode, noting mass transfer for cathodic reduction of ferricyanide

03 p0273 A73-13728

Antenna radiation pattern synthesis, discussing current phase and amplitude distribution determination by iterative and quadratures solutions respectively

03 p0284 A73-14059

Linear array antenna radiation pattern synthesis for minimum sidelobe level outside of given intervals, calculating current distribution

03 p0278 A73-14060

Calculation of the diffusion current of a finite-base semiconductor diode

03 p0284 A73-14322

Ion-current distributions around an electrically conductive body in ionized gas flow.

05 p0603 A73-17110

Ion density and current distribution measurements in hypersonic turbulent wakes behind sphere flown in ballistic range, using cylindrical electrostatic probes

06 p0645 A73-18135

Reflector antenna radiation pattern analysis by equivalent edge currents.

06 p0665 A73-18179

Thin walled open ended cylindrical antenna in cold magnetoplasma, calculating current distribution by approximations based on Wiener-Hopf procedure

06 p0729 A73-18193

Cross polarization definitions in terms of antenna pattern measurement coordinate system and source current distribution, considering relative merits

06 p0666 A73-18199

Analysis of antenna structures assembled from arbitrarily located straight wires.

06 p0668 A73-18441

Investigation of the influence of the emitter current on the collector junction capacitance of transistors

07 p0799 A73-19399

Numerical analysis of magnetohydrodynamic instabilities by the finite element method.

07 p0856 A73-19515

A possible mechanism for the change in the discharge current in CO₂ through the action of laser radiation.

07 p0836 A73-20137

Electrodynamic mathematical model for electroconductivity of nonuniform plasma with Hall effect, calculating current distribution from Riemann problem solution

08 p0992 A73-20863

Probability estimates of the accuracy of a solution to the problem of antenna synthesis in the case of an experimental determination of the direct operator of the problem

08 p0946 A73-21104

Convergence of the solution for the far scattered field of a conducting cylinder of arbitrary cross-section.

09 p1050 A73-22397

Measurement of the current distribution at the surface of a doublet immersed in an isotropic hot plasma

09 p1131 A73-23034

Solar wind effect on azimuthal and radial galactic cosmic ray currents, noting Forbush decreases relation to current structures

10 p1265 A73-23907

Imperfectly conducting circular loop antenna driving-point impedance derivation for uniform resistive loading, comparing differential and integral equation methods for current distribution calculation

10 p1191 A73-24899

Impedance comparisons for the asymmetrically driven thin cylindrical antenna.

11 p1329 A73-25663

Synthesis of a linear antenna in a class of piecewise-constant current-distribution functions

12 p1479 A73-27228

Aspects of the application of Rogovskii's coil to the measurement of steady currents in a plasma

12 p1528 A73-27306

Formation of current pulses in an inductive load by reactive two-terminal networks

12 p1481 A73-27586

A device for experiments on high-beta plasmas in a toroidal geometry

13 p1663 A73-28120

Screw instability in a plasma with a distributed current.

13 p1665 A73-28680

Analysis of primary currents in a three-phase/single-phase frequency converter with direct coupling and artificial commutation

13 p1592 A73-28940

Stability of a plasma cylinder containing axisymmetric opposite currents

13 p1666 A73-28952

Self consistent one dimensional plasma layer model with current layer at center described by Vlasov equation and nonexistent normal magnetic field component

14 p1796 A73-29870

Analytical solution to problems of eddy current distribution in a thin plate and a conducting spherical shell

14 p1774 A73-30029

Effect of linear load graduation in the end zones of an inductor on the longitudinal side effect in induction machines

15 p1832 A73-31410

Seasonal movement of the Sq current foci and related effects in the equatorial electrojet.

15 p1869 A73-31754

Solutions of boundary value problems of multilayer analogs of geoelectrics and hydrology.

15 p1872 A73-32040

Current distribution on an infinite tubular antenna immersed in a cold collisional magnetoplasma.

15 p1920 A73-32236

Dispersion equation for nonpotential oscillations and hydrodynamic instabilities in hot ion plasma with transverse current in magnetic field

15 p1920 A73-32304

Numerical computation of the current distribution and far-field-radiation pattern of the axial-mode helical aerial.

16 p1985 A73-34020

An integro-differential equation technique for the time-domain analysis of thin wire structures. I - The numerical method.

17 p2246 A73-34892

Use of the Singularity Expansion Method in electromagnetic transient scattering problems.

17 p2124 A73-35360

Current distribution of a dipole antenna of revolution in dissipative media.

17 p2141 A73-35366

General theoretical analysis of impedance loaded rectangular loop antennas.

17 p2141 A73-35368

Numerical computation of antenna patterns near a conducting elliptic cylinder.

17 p2126 A73-35608

General theoretical analysis of loop and folded dipole antennas.

17 p2142 A73-35646

Electric potential and current distribution in a rectangular sample of anisotropic material with application to the measurement of the principal resistivities by an extension of van der Pauw's method.

17 p2220 A73-35653

Measurement techniques for antennas in dissipative media.

17 p2143 A73-35685

Antenna radiation patterns from statistical phase synthesis of antenna arrays, estimating directivity loss for in- and out-of-phase initial current distribution

17 p2129 A73-35708

Investigation of the discharge structure in a rare gas alkali MHD generator plasma. II.

18 p2339 A73-36304

Current distribution at the zero line of the magnetic field and the turbulent resistance of a plasma

18 p2339 A73-36550

Injection and field processes in thin semiconductor films in the current jump region

18 p2341 A73-36723

Impedance and far field characteristics of a linear antenna near a conducting cylinder.

19 p2403 A73-37271

- Optimum windings for linear induction machines.
19 p2389 A73-38312
- Current and energy characteristics of an electron plasma in a magnetron diode
20 p2536 A73-39254
- Calculation of the current of a nonlinear element with inertia in the presence of a biharmonic input
20 p2537 A73-39454
- A numerical investigation of the current and density distributions for a non-equilibrium plasma in a segmented electrode duct.
21 p2748 A73-40926
- Perturbation of the magnetic configuration of a stellarator by a longitudinal current in the plasma.
21 p2750 A73-41678
- Insulated electrically thin dipole antenna with surrounding large wave number isotropic medium, discussing transmission line properties and current and charge distribution
22 p2829 A73-43183
- A theoretical and experimental study of the insulated loop antenna in a dissipative medium.
22 p2829 A73-43184
- Structure of currents in a stationary plasma jet in the presence of the Hall effect
23 p3010 A73-43664
- Stability of a plasma cylinder with counterstreaming axisymmetric currents.
23 p3013 A73-44304
- Dispersion equation for nonpotential oscillations and hydrodynamic instabilities in hot ion plasma with transverse current in magnetic field
24 p3114 A73-44612
- Oblique radiation of ultrasound by an electromagnetic-acoustical method.
24 p3109 A73-44697
- The effect of interaction of array elements with arbitrary amplitude distribution on the radiation pattern.
24 p3068 A73-44942
- Calculation of the nonstationary electric field, carrier concentration, and current distribution in semiconductor integrated circuits
24 p3119 A73-45177
- CURRENT REGULATORS**
Electron beam current fluctuation reduction by placing hot filament into Wheatstone bridge arm for temperature regulation in power supply for electron gun
17 p2176 A73-35776
- Dynamic properties of transistor current switches
22 p2833 A73-42369
- CURRENT SHEETS**
Energy balance in the current sheath of a solar flare and the acceleration of cosmic rays by plasma waves
01 p0092 A73-10936
- Particle motions in coronal streamers and type III radio bursts.
01 p0093 A73-11393
- Magnetic field strength change in equatorial plasmasphere, considering quiet ring current as equatorial sheet current extension of neutral sheet current in magnetospheric tail
02 p0155 A73-11732
- Consistency of fields and particle motion in the 'speiser' model of the current sheet.
02 p0157 A73-11901
- Time correlation between current sheet collapse in plasma focus and X ray production, investigating radiation intensity and distribution
02 p0197 A73-12061
- A phenomenological study of the steady-state current sheet speed in a magnetically driven shock tube.
03 p0288 A73-13809
- Current sheet model for sunspot structure, considering ohmic dissipation as decay mechanism
03 p0377 A73-14408
- Magnetic models of solar flares.
04 p0490 A73-14834
- Stability of a model current sheet with finite transverse field and finite flow velocity.
05 p0568 A73-16141
- Ion acceleration in the current sheath of a solar flare
07 p0872 A73-20320
- Parallel plate electromagnetic shock tube, investigating drive current, gas pressure and electrode material effects on electrode ablation and current sheet velocity
08 p0953 A73-21632
- Energy balance in the current sheet of a solar flare, and the acceleration of cosmic rays by plasma waves.
09 p1138 A73-22731
- Magnetotail model for magnetic field strength and particle drift in magnetic equatorial plane earth, using current sheet from satellite observations
11 p1357 A73-25929
- Ion acceleration in the current layer of a solar flare.
12 p1534 A73-27292
- The normal-tangential form of the equations for the electrodynamics of conducting media
12 p1525 A73-27806
- Instability of the current in the neutral sheet of the tail of the earth's magnetosphere.
13 p1608 A73-28715
- Field-aligned currents, plasma waves, and anomalous resistivity in the disturbed polar cusp.
14 p1747 A73-29964
- Instabilities in charge sheets and current sheets and their possible occurrence in the aurora.
15 p1873 A73-32235
- Structure of the current front and turbulent acceleration of ions in a pulsed plasma accelerator. I.
17 p2215 A73-34305
- Structure of current front and turbulent acceleration of ions in a plasma accelerator. II.
17 p2215 A73-34306
- Re-connection of magnetic lines of force - Evolution in incompressible MHD fluids.
18 p2338 A73-36181
- Self consistent geomagnetic tail current sheet model described by exact analytic solution of time independent Vlasov-Maxwell equations
18 p2351 A73-36274
- A mechanism for the growth phase of magnetospheric substorms.
21 p2682 A73-40157
- A magnetospheric field model incorporating the OGO 3 and 5 magnetic field observations.
23 p2972 A73-43693
- CURRENT STABILIZERS**
U CURRENT REGULATORS
CURRENTS (OCEANOGRAPHY)
U WATER CURRENTS
CURTISS-WRIGHT MILITARY AIRCRAFT
U MILITARY AIRCRAFT
CURVATURE
Effect of major axis curvature on I-beam stability.
07 p0916 A73-20437
- Effect of the curvature of a shallow spherical shell on its vibrations with losses
08 p1018 A73-21449
- Calculation of turbulent boundary layers and wall jets over curved surfaces.
11 p1348 A73-26383
- Influence of curvature on the vibrations of an oblate spherical shell with losses.
15 p1945 A73-31013
- Study in curvature of long distance wave guides - The case of helicoidal guides. I
15 p1842 A73-31360
- Two dimensional diffuser flow measurement and model calculation for curvature effects on wall pressure and boundary layer velocity distributions
17 p2152 A73-35002
- Curvature effects in extended stellar atmospheres - Pure absorption.
17 p2237 A73-35788
- Experiment on convex curvature effects in turbulent boundary layers.
21 p2676 A73-40245
- Colored aftereffects after prolonged inspection of convex lines of one color and concave lines of another color
21 p2640 A73-41303
- Curvature effects in extended stellar atmospheres - Absorption and scattering.
23 p3030 A73-43751
- Local form of the radiation condition - Application to curved dielectric structures.
24 p3069 A73-45257
- CURVE FITTING**
The functional form of rate curves for the high-temperature oxidation of dispersion-containing alloys forming Cr2O3 scales.
04 p0461 A73-14924
- Isochromatic curves modeling for stress-strain state of doubly connected regions by optical polarization and photoelastic analysis, using isopach field method
05 p0578 A73-17092
- Apollo 14 returned lunar rock fine thermal conductivity measurement as function of temperature under vacuum conditions, using least squares curve fitting method
07 p0895 A73-19856
- Shock and vibration disturbance identification based on structural system response, discussing linear programming, curve fitting, constraints, objective functions and applications
07 p0916 A73-20430
- Lamb dip measurements on low pressure CO laser vibrational-rotational lines, determining line widths, velocity-changing collision rate and saturation intensities with curve fitting
09 p1090 A73-22078
- Computerized normal loci plotting by orthogonal Chebyshev approximation, using minimum variance principle and Fisher test for regression curve selection
09 p1143 A73-22094
- Degrees of freedom elimination method shown equivalent to interpolation by splining by means of actual structure in curve connection for given points
09 p1166 A73-23465
- Subgrid resolution achievement by spline fitting during flow and force field sources conversion from Lagrangian distribution onto Eulerian grid and interpolation
10 p1248 A73-23603
- Book - Digital simulation of physical systems.
10 p1191 A73-23946
- Analytical fit of the transfer function of a logarithmic electrometer and correction for ambient temperature variations.
11 p1367 A73-26306
- Group data handling theorems on uniqueness of mathematical model for regression curve reconstruction in polynomial domain with small number of points
14 p1738 A73-30288
- Measurement of impedance transformation on practical dipoles.
17 p2128 A73-35690
- Aerodynamic coefficients determination for nonlinear equations of motion solution to fit experimental free flight data, obtaining starting solution by noniterative continuation method
18 p2263 A73-36307
- Oxygen and nitrogen thermodynamic state equation determination by least squares fitting to experimental PVT, isochoric heat capacity and saturation density data
21 p2740 A73-41104
- Curve fitting by application of splines under tension, discussing polynomial interpolation drawbacks and linear system solution for unknown second derivatives
24 p3070 A73-45090
- CURVED BEAMS**
Buckling of laterally loaded plates having initial curvature.
01 p0115 A73-10768
- Constant curvature beam finite elements for in-plane vibration.
05 p0637 A73-17371
- Comparison of the characteristic values and characteristic vibration forms of a circular ring beam, a circular ring disk, and a circular ring fiber. II
06 p0759 A73-17586
- Interaction curves for bending and axial forces of perfectly plastic curved I-beams.
06 p0762 A73-18339
- The use of straight beam finite elements for analysis of vibrations of curved beams.
07 p0909 A73-19100
- Finite element analysis of curved structures, discussing shape functions generation method for convergence determination
09 p1165 A73-23439
- Impact response of curved box beam-columns with large global and local deformations.
11 p1440 A73-25530
- Coupled twist-bending waves and natural frequencies of multispan curved beams.
14 p1815 A73-30914
- Russian book - Plane bending and tension of curvilinear thin-walled beams.
15 p1956 A73-32296
- Method for determining Young's dynamic modulus for curvilinear specimens
16 p2030 A73-33938
- Modes and frequencies of transversely isotropic slightly curved Timoshenko beams.
17 p2248 A73-35043
- On one-dimensional large-displacement finite-strain beam theory.
17 p2252 A73-35828
- On an anomaly of the theory of beams with directors
19 p2497 A73-37527
- Curved twisted space beam elements, expressing displacement function and inertia property by rotation and mass matrices
20 p2621 A73-39533
- In-plane vibration of continuous curved beams.
23 p3045 A73-44165
- Convergence of the method of successive approximations in geometrically nonlinear problems
23 p2999 A73-44197
- On the hybrid stress finite element model for incremental analysis of large deflection problems.
24 p3151 A73-45303
- CURVED PANELS**
Light weight beaded and tubular structural panels for heat shielded aerodynamic surfaces
11 p1438 A73-25504
- Theory of light deviation by sheets of circular cone geometry
11 p1397 A73-25565
- Graphite- and boron-epoxy composite curved panels, determining shear buckling stress and post-buckling strength by visual and photographic observations
13 p1699 A73-29308
- Cylindrically curved panels flutter characteristics in supersonic flow parallel to generators, investigating in-plane boundary conditions and panel geometry effects
15 p1949 A73-31652
- High frequency vibration of aircraft structures.
17 p2250 A73-35329
- Experimental investigation of the stability of oblique conical panels under the action of uniform external pressure
20 p2617 A73-39308
- Large deflections and stability of a long shallow orthotropic cylindrical panel under the action of a local load
20 p2618 A73-39312

- Investigation of the free vibrations of sectorial plates and conical panels by a theoretical-experimental method
20 p2618 A73-39314
- A natural frequency analogy between spherically curved panels and flat plates.
21 p2785 A73-40754
- CURVED SURFACES**
U CONTOURS
U SHAPES
U SURFACES
- CURVES [GEOMETRY]**
NT EPICYCLOIDS
Curved element for geometrical approximation of thin shell structures, deriving element stiffness equations in terms of nodal displacement degrees of freedom
03 p0389 A73-13325
- Interpolation theory over curved elements, with applications to finite element methods.
04 p0470 A73-15010
- The finite element method in domains with curved boundaries.
07 p0907 A73-19029
- Curved finite elements by the method of initial strains.
08 p1016 A73-20727
- Numerical evaluation of integrals around simple closed curves.
21 p2725 A73-40378
- CUSPS**
NT CUSPS [MATHEMATICS]
Dependence of the polar cusp on the north-south component of the interplanetary magnetic field.
18 p2351 A73-36273
- Seasonal and solar cycle dependence of the position of the cusp region of the magnetosphere.
20 p2555 A73-39828
- Thermal positive ions in the dayside polar cusp measured on the ISIS 1 satellite.
21 p2690 A73-41368
- Observations of electron fluxes and related variations of ionospheric plasma parameters in the south polar cusp.
21 p2690 A73-41369
- CUSPS [MATHEMATICS]**
NT DOUBLE CUSPS
Cusped wave fronts in anisotropic elastic plates.
07 p0907 A73-19079
- CUT-OFF**
Geomagnetic effects on cosmic ray cut-off daily, seasonal and secular variations, considering north-south symmetry and magnetospheric models
16 p2055 A73-33297
- Dielectric coaxial waveguide modal cut-off, dispersion and attenuation characteristics, discussing guide geometry and dielectric properties effects
24 p3069 A73-45407
- CUTANEOUS PERCEPTION**
U TOUCH
- CUTTERS**
NT DRILLS
- CUTTING**
NT METAL CUTTING
NT MILLING [MACHINING]
NT SPARK MACHINING
Optimal cutting conditions for working of reinforced plastic laminates, comparing with metals
18 p2319 A73-36471
- Laser cutting of aerospace materials.
[SME PAPER EM 73-214] 19 p2436 A73-38496
- CV-7 AIRCRAFT**
U DHC 5 AIRCRAFT
- CW RADAR**
U CONTINUOUS WAVE RADAR
- CYANAMIDES**
High strength properties and hardening of epoxy resin bonding materials using dicyaninediamides
10 p1239 A73-24094
- Microwave spectrum, structure, dipole moment and low frequency vibrations of dimethyl cyanamide.
24 p3066 A73-44771
- CYANATES**
The addition of tert-butyl hypochlorite to isocyanates.
13 p1580 A73-28022
- CYANIDES**
NT CYANOGEN
Intensity variation of CN bands with temperature in active nitrogen methylene chloride chemiluminescent reaction.
01 p0014 A73-10333
- Electric dipole moment of diatomic molecules by configuration interaction. V - Two states of $I_2(\Sigma_g^-)$ symmetry in CN.
04 p0477 A73-14816
- Radio telescope identification of interstellar isocyanic acid, methylacetylene and hydrogen isocyanide molecules from pure rotational transitions
06 p0751 A73-18229
- A shock tube determination of the CN ground state dissociation energy and the CN violet electronic transition moment.
08 p0989 A73-20789

- Asymmetric intensities of Zeeman components of electronic transitions of diatomic molecular spectra in sunspots, considering CN red lines
11 p1422 A73-25936
- Solar rotational and vibrational temperature based on turbulent velocity determined from CN molecular line profiles half widths
12 p1547 A73-27870
- Photo-induced isomerization of aryl isocyanides into cyanides.
13 p1580 A73-28200
- Laser induced fluorescence of CN radicals.
19 p2437 A73-37902
- CN red system line opacity codes for late star model atmosphere calculation
19 p2488 A73-38513
- Solar rotational and vibrational temperature based on turbulent velocity determined from CN molecular line profiles half widths
20 p2608 A73-39244
- CYANO COMPOUNDS**
NT CYANAMIDES
NT ISOCYANATES
Photoisomerization of 2-isocyno- and 2,x'-diisocyanobiphenyls in cyclohexane.
12 p1466 A73-27600
- Methylacetylene and isocyanic acid data from April 1972 and February 1973 observation of interstellar media in direction of Galactic center source Sgr B2
16 p2060 A73-33095
- One dimensional model of electron-phonon system exhibiting Peierls instability for tetrathiofulvalinium tetracyanoquinodimethane conductivity, considering high temperature superconductivity achievement via Peierls instability suppression
21 p2751 A73-40508
- CYANOGEN**
High temperature ionic and charged species reactions in hydrocarbon and cyanogen flames and additive combustion systems
22 p2819 A73-42770
- CYANOPHYTA**
U BLUE GREEN ALGAE
- CYBERNETICS**
Survival probability of a system with a Poisson flow of losses in life-sustaining elements
01 p0028 A73-11422
- Information processing in the visual system.
07 p0786 A73-20374
- Russian papers on cybernetic systems reliability and accuracy covering analog, hybrid and digital computers, electronic modeling, nonlinear control systems, computer and complex system design, etc
14 p1730 A73-30031
- Russian book - Applied mathematics and cybernetics.
20 p2541 A73-38977
- Application of cybernetic means and methods in studies of plasma physics and controlled thermonuclear synthesis
23 p3011 A73-43671
- Structural complexity and technical realization of formal neurons by means of magnetic current switches
24 p3063 A73-44901
- CYCLES**
NT ACTIVITY CYCLES [BIOLOGY]
NT BRAYTON CYCLE
NT CARNOT CYCLE
NT RANKINE CYCLE
NT SOLAR CYCLES
NT STIRLING CYCLE
NT STRESS CYCLES
NT SUNSPOT CYCLE
NT THERMODYNAMIC CYCLES
NT WORK-REST CYCLE
- CYCLIC ACCELERATORS**
NT BETATRONS
- CYCLIC HYDROCARBONS**
NT ANTHRACENE
Laser Raman spectrum of crystalline cyclopentane-d/sub 0/ and -d/sub 10/.
03 p0318 A73-13282
- Cool flame oxidation studies of acyclic and cyclic hydrocarbons.
05 p0606 A73-16691
- Projected states of open shell molecules - The pi-electron states of the cyclopentadienyl cation.
06 p0726 A73-18775
- Geochemical significance of perylene occurrence in marine sediments, discussing land organism biogenic pigment precursors and polycyclic aromatic hydrocarbon conversion
10 p1211 A73-24105
- C-13 nuclear magnetic resonance in organic geochemistry.
11 p1325 A73-25461
- A new approach to the isolation of milligram amounts of significant geochemical compounds.
11 p1325 A73-25463
- CYCLIC LOADS**
Assembly for studying the characteristics of materials under cyclic loads at elevated temperatures
01 p0029 A73-10024

- Influence of the loading conditions on the propagation of fatigue cracks in D16T-alloy sheet samples
01 p0064 A73-10489
- Unit for fatigue testing with a pulsating load at a specified force and deflection.
01 p0054 A73-11299
- Fatigue of duralumin under cyclic loads at ultrasonic frequencies
02 p0179 A73-11566
- Application of the theory of linear fracture mechanics to the assessment of turbine rotor strength
02 p0229 A73-11620
- Pulsating vertical load effect on friction force magnitude between two horizontal solid surfaces during initial phase of static to kinetic friction transition
02 p0172 A73-11797
- Structural and energetic analysis of fatigue failure in metals
02 p0232 A73-11929
- Behavior of certain turbine-blade materials under asymmetric loading.
02 p0180 A73-12128
- The effects of frequency of loading and of nonreactive external media on growth of fatigue cracks.
02 p0235 A73-12132
- Two coordinate oscillograph recording device with automatic reversing for stress-strain tests under static and cyclic loads
02 p0168 A73-12144
- Study of the effect of small elastoplastic deformations on the load-bearing capacity of specimens with stress concentrators under repeated variable loading. I.
02 p0235 A73-12202
- A method of estimating the probability of faults in material on cyclic loading.
02 p0236 A73-12221
- Growth of fatigue cracks in polycarbonate.
02 p0185 A73-12430
- Studies of fatigue in smooth AlCuMg specimens
03 p0321 A73-13134
- Thermomechanical dissipation analysis of thermoviscoelastic solids by finite elements.
03 p0389 A73-13326
- High frequency fatigue test assembly for glass fiber reinforced plastics specimens under symmetric tension-compression
03 p0288 A73-13747
- Low-cycle fatigue of titanium alloys.
03 p0327 A73-14007
- Large elasto-plastic deflection of a circular plate of mild steel under cyclic loading.
03 p0396 A73-14626
- The effect of frequency upon the fatigue-crack growth of Type 304 stainless steel at 1000 F.
04 p0459 A73-14689
- Colloquium on Structural Reliability notes on 'Fatigue Lecture.'
04 p0507 A73-14706
- An inelastic stress-strain law for elevated temperature and slowly time varying loads.
04 p0512 A73-15235
- Fatigue crack growth measurement on Al alloy wedge-opening-load specimens under constant amplitude sinusoidal loading, comparing data with existing crack propagation results
04 p0462 A73-15241
- Cyclic loads for decrease in relaxation softening of heat resistant Ni-Cr alloys, noting working temperature effects
06 p0706 A73-17885
- Cyclic endurance and alteration nature of the dislocation structure in nickel before and after programmed strengthening
06 p0707 A73-17906
- Growth of part-through thickness fatigue cracks in sheet polymethylmethacrylate.
06 p0714 A73-18481
- Method of analysis and prediction for variable amplitude fatigue crack growth.
06 p0709 A73-18482
- Dynamic stress intensity factor for an unbounded plate having collinear cracks.
[AD-758426] 06 p0764 A73-18492
- Borated steel fracture characteristics in the case of cyclic plane bending
06 p0711 A73-18663
- Method for increasing the fatigue strength of hardened steels
06 p0711 A73-18666
- Frequency dependent low cycle fatigue crack propagation.
06 p0713 A73-18767
- Behavior of austenitic stainless steels under continuous or repeated strain
07 p0838 A73-19115
- S-N fatigue curve analysis from ultimate tensile strength to cyclic elastic limit below fatigue limit, discussing load cycle zones and discontinuities
07 p0910 A73-19214
- The effect of grain size on the fatigue of an Al-Mg alloy.
07 p0839 A73-20114

A visco-plasto-elastic expression for stress-strain diagram of fiber reinforced plastics subjected to repeated low frequency loads.

07 p0915 A73-20329

Investigation of the low-cycle fatigue of light-alloy welds

07 p0833 A73-20506

Influence of low temperatures on the fatigue life of welds

07 p0833 A73-20508

Book - Fundamentals of cyclic stress and strain.

08 p1020 A73-21836

Effects of hold time on low-cycle fatigue behavior of AISI Type 304 stainless steel at 593 C.

09 p1102 A73-22417

Comparison of the fracture strength K_{IS} of aluminum (AK4-IT1, V95T1, and D16T) and titanium (VT8 and VT9) alloys under static and cyclic loads.

09 p1105 A73-23054

Consideration of the hysteresis behavior of a solid medium in a complex stress state under the conditions of simple cyclic loading.

09 p1161 A73-23059

Effect of loading frequency on fatigue strength of metals.

09 p1106 A73-23159

The effect of the structure of the titanium alloys VT3-1 and VT-18 on their fatigue resistance under asymmetrical cyclic loading.

09 p1106 A73-23164

Fatigue crack growth under C.O.D. cycling.

09 p1163 A73-23252

Fatigue crack initiation and propagation in part through crack metal specimens under cyclic loading, discussing plasticity effects and surface wave interaction

09 p1163 A73-23253

Discrete creep of AMg6 aluminum alloy subjected to repeated static loading

10 p1233 A73-24365

Investigation of the elastoplastic characteristics of corrugated membranes under cyclic loading conditions

10 p1293 A73-24792

Electron fractography of fatigue failure and macrocrack propagation in dual phase Ti alloy during cyclic loading at minus 140 to plus 150 C

10 p1236 A73-24931

Upper bounds to plastic strains in shake-down of structures subjected to cyclic loads.

11 p1434 A73-25216

Shear decohesion mechanism of fatigue crack propagation in ductile metals under cyclic loads, considering secondary microfracture and creep cavitation effects at elevated temperatures

11 p1381 A73-25814

Aircraft structures aluminum alloys fatigue crack growth rate relationship to cracking mode, stress ratio, cyclic frequency and corrosive environment severity

11 p1382 A73-25826

Service failures and fracture mechanisms under cyclic load at high temperature.

11 p1442 A73-25845

Corrosion fatigue due to static and cyclic stress, noting electrochemical adsorption theory

11 p1386 A73-26737

High frequency load tests for fatigue properties of glassand carbon fiber reinforced plastics and epoxy impregnated wood laminates

12 p1515 A73-26879

Kinetic strain criteria of cyclic failure at high temperatures

12 p1552 A73-27252

High-cyclic fatigue curves for annealed metals from investigation of defect buildups, lattice distortions, microcrack nucleation and fatigue crack growth

12 p1552 A73-27253

Procedure for studying fatigue failure features in metals under harmonic and complex loading at low temperatures

12 p1486 A73-27254

Damping properties of a composite material with monodirectional continual fibers

12 p1516 A73-27258

Thermal stresses arising in high-frequency fatigue tests

12 p1512 A73-27259

The changes in structural and mechanical properties of construction materials under loads

12 p1513 A73-27500

Studies on fatigue damage caused by stresses below the endurance limit - The effect of program period and fatigue failure by stresses below the endurance limit.

13 p1692 A73-28197

Method for the investigation of the fatigue strength of fiberglass produced by winding and loaded by inter-layer shear.

13 p1695 A73-28523

Relationship between the strain curves of a material subjected to static and to cyclic loads

13 p1698 A73-29055

Facility for conducting fatigue tests with sheet materials in cyclic tension

13 p1597 A73-29058

A potential means of using acoustic emission for crack detection under cyclic-load conditions.

13 p1700 A73-29401

The effect of plastic anisotropy in the low-cycle fatigue behavior of Zircaloy.

13 p1640 A73-29487

Cumulative damage and behavior of plastic strain in high and low cycle fatigue.

13 p1641 A73-29500

Life prediction of metals subjected to high temperature fatigue.

13 p1708 A73-29503

Evaluation of dissipation and damage in metals submitted to dynamic loading.

13 p1701 A73-29505

A static-to-dynamic transition in creep of metallic materials under cyclic stress conditions as caused by an interaction of creep and creep recovery.

13 p1642 A73-29512

Study on stress corrosion cracking of austenitic stainless steel under pulsating load.

13 p1642 A73-29523

Bonding characterization in reinforced composites.

13 p1702 A73-29536

Effect of loading frequency and directional anisotropy on the fatigue strength of grade AMg6BM aluminum alloy sheet.

13 p1643 A73-29606

Energy dissipation in metals in high-frequency fatigue tests. I.

13 p1643 A73-29630

Energy dissipation in metals in high-frequency fatigue tests. II.

13 p1643 A73-29631

Acoustic-emission detection techniques for high-cycle-fatigue testing.

14 p1751 A73-29772

Effect of loading conditions on the propagation of fatigue cracks in sheet samples of D16T alloy.

14 p1759 A73-30314

Optimisation theory of elastic-rigid bodies under repeated variable deformation.

14 p1812 A73-30495

Investigation of fatigue and brittle failure patterns in 15G2AFDps steel at low temperatures

14 p1762 A73-30678

Investigation of crack propagation in small samples under conditions of low-cyclic fatigue

14 p1763 A73-30680

Quantitative classification criterion for corrosion causes in metal under static and cyclic loads, examining failure mechanism

14 p1763 A73-30712

Fatigue failure of a two-phase titanium alloy in vacuum

14 p1763 A73-30713

Some plastic deformation laws for titanium under static and alternating loads

14 p1763 A73-30723

Influence of hydrogen on the failure of the VT3-1 titanium alloy in programmed cyclic loading

15 p1886 A73-31035

A test machine for fatigue under pulsed moving loads

15 p1855 A73-31144

Strains and stress-concentration factors in plates under out-of-phase biaxial cyclic loads.

15 p1948 A73-31614

Enhanced strain aging of niobium by cyclic deformation.

15 p1890 A73-31990

Study on stress corrosion cracking of austenitic stainless steel under pulsating load.

15 p1895 A73-32570

Nonlinear behavior of shells of revolution under cyclic loading.

16 p2075 A73-32791

Effect of load sequences on crack propagation under random and program loading.

17 p2190 A73-34879

On the stress analysis of creeping structures subject to variable loading.

[ASME PAPER 72-APM-NNN] 17 p2250 A73-35115
Cyclic stress-strain behavior - Analysis, experimentation, and failure prediction; Proceedings of the Symposium, Bal Harbour, Fla., December 7, 8, 1971.

18 p2364 A73-36584

Ni-Fe-Cr alloy and austenitic stainless steel cyclic stress-strain behavior at 70-1400 F

18 p2323 A73-36586

On the physical justification of the term 'state of fatigue of materials under cyclic loading.'

18 p2364 A73-36592

Engineering analysis of the inelastic stress response of a structural metal under variable cyclic strains.

18 p2364 A73-36594

Environment-assisted fracture in engineering alloys. II - Cyclic loading and future work.

[ASME PAPER 73-MAT-S] 18 p2365 A73-36614
The effect of hydrostatic pressure environment on the low cycle fatigue properties of a maraging steel.

[ASME PAPER 73-MAT-K] 18 p2323 A73-36616
The plastic bending of beams and their failure by low cycle fatigue.

18 p2365 A73-36617

Fatigue strength of materials under a two-frequency load /Review/

18 p2366 A73-36754

Creep in VT-14 titanium alloy under low-cycle load conditions

18 p2323 A73-36758

Relation of strain curves of material in static and cyclical loading.

18 p2366 A73-36887

Apparatus for fatigue tests on sheet materials subject to cyclical extension.

18 p2297 A73-36890

Fractography of stress corrosion in Ti-8Al tested in fatigue.

18 p2326 A73-36972

Strain accumulation and rupture during creep under variable uniaxial tensile loading.

19 p2495 A73-37434

Biaxial cyclic high-strain fatigue of aluminum alloy RR5K.

19 p2440 A73-37437

Fracture types in load-controlled low-cycle fatigue.

19 p2498 A73-37666

Investigation of low-cycle fatigue of welded joints in light alloys.

19 p2433 A73-37781

Effect of low temperature on the fatigue limit of welded joints.

19 p2433 A73-37783

Changes in the microhardness of lithium fluoride crystals subjected to cyclic elastic compression

19 p2470 A73-37954

Quantitative estimation of the fatigue crack propagation under varying load conditions.

19 p2501 A73-38346

A finite element approach to the critical cyclic stress required to propagate a crack.

20 p2615 A73-38639

Influence of cycle ratio on the elastic modulus of glassfiber reinforced plastics subjected to repeated tensile load.

20 p2580 A73-38644

Investigation of energy criteria for the failure by fatigue of some metals at low and high loading frequencies

20 p2577 A73-39354

Study of low-cycle fatigue of titanium-base alloys at a temperature of -196 C

20 p2577 A73-39375

Investigation of the transition zone structure in composite materials under cyclic loads

20 p2580 A73-39379

Yield criterion in plane stress state for description of second order effect relating to axial strain accumulation in cyclic torsion

20 p2624 A73-39568

A mixture theory of the response of a laminated plate to impulsive loads.

21 p2783 A73-40291

Flexibility matrix coefficients for disk loading under sinusoidal edge loading tabulation and derivation to accommodate boundary conditions

21 p2784 A73-40434

The response of viscoelastic materials to slow cyclic stresses.

21 p2789 A73-41689

The behavior of materials subjected to multiaxial cyclic stresses. I - Methods of calculation

22 p2917 A73-41781

Overload effects on subcritical crack growth in austenitic manganese steel.

22 p2875 A73-42138

Effect of multiple overloads on fatigue crack propagation in 2024-T3 aluminum alloy.

22 p2875 A73-42139

The cyclic elastoplastic torsion of the circular cylinder in the case of finite deformations

22 p2922 A73-42527

Testing set-up for cyclic torsion with tension on a small number of loading cycles.

22 p2861 A73-42530

German monograph on cyclic stress-strain curves and fracture strength of steels with various compositions covering plastic strain energy, S-N diagrams and test equipment

22 p2879 A73-42739

Thermal response of a viscoelastic rod under cyclic loading.

[ASME PAPER 73-APMW-39] 22 p2926 A73-42896

Parametric instability of clamped-clamped and clamped-simply supported columns under periodic axial load.

22 p2929 A73-43137

Fatigue failure analysis of low carbon steel endurance under cyclic loading with time dependent viscoelastic effects, using Hookes-Trouton laws

23 p3040 A73-43469

Fatigue crack growth retardation after single-cycle peak overload in Ti-6Al-4V titanium alloy.

23 p2992 A73-43809

Metal fatigue phases investigation including strain hardening under cyclic loads and microcrack nucleation due to dislocation formation under hydrostatic pressure

23 p2993 A73-43966

- Kinetics of the development of structural changes in iron in the presence of adsorption fatigue
23 p2995 A73-44224
- Nonlinear stress-strain hysteresis equation of cyclic straining for vibrating imperfectly elastic systems, using Masing principle
23 p3047 A73-44276
- Evaluation of the sensitivity of materials to stress concentrations in cyclic loading
23 p3047 A73-44279
- On the description of cyclic deformation processes using a more general elasto-plastic constitutive law.
24 p3147 A73-44683
- Behavior of materials under multiaxial vibrating loads. II - Experimental investigations
24 p3153 A73-45447
- CYCLOGENESIS**
Statistical analysis of satellite-observed trade wind cloud clusters in the western North Pacific.
23 p3003 A73-43980
- Cloud destabilization due to long wave radiative cooling resulting from IR radiative heat transfer in cloudy atmosphere, considering temperature inversion effects and cyclogenesis mechanism
24 p3108 A73-45016
- CYCLOHEXANE**
Mass spectrometry in structural and stereochemical problems. CCXVII - Electron impact promoted fragmentation of O-methyl oximes of some alpha, beta-unsaturated ketones and methyl substituted cyclohexanones.
10 p1186 A73-23550
- Photoisomerization of 2-isocyanato- and 2,x'-diisocyanobiphenyls in cyclohexane.
12 p1466 A73-27600
- CYCLONES**
NT CYCLOGENESIS
NT HURRICANES
NT TYPHOONS
Satellite pictures as aids for the determination of the structure of upper-level cyclones
05 p0593 A73-16347
- Blocking situations lasting less than five days over the Euro-Atlantic region in the 20-year period from 1951 through 1970
08 p0986 A73-21486
- Tropical cyclone track statistical forecasting comparing methods based on synoptic, empirical and combined data
10 p1245 A73-23984
- Rapid intensification and low-latitude weakening of tropical cyclones of the western North Pacific Ocean.
10 p1245 A73-23986
- Theory of cyclogenesis, taking into account condensation
13 p1653 A73-28744
- Some characteristics of stratiform St-Sc clouds in various synoptic situations
13 p1654 A73-28885
- The estimation of extratropical cyclone parameters from satellite radiation measurements.
15 p1903 A73-31315
- Some results of ozone observations by satellite on June 17 and 18, 1966
15 p1868 A73-31607
- Relation between the pressure at the center of a tropical cyclone and the dimension of its cloud system
15 p1904 A73-31610
- Relation between the average motion of cyclones and anticyclones and their shape.
15 p1906 A73-32255
- Some parameters of cyclonic cloud vortices.
18 p2333 A73-37053
- Meteorological satellite TV cloud cover photographs of cyclogenesis over Mediterranean Sea and cyclone arrival to European U.S.S.R. and Scandinavian Peninsula
18 p2334 A73-37074
- Comparison and synthesis of the characteristics of long- and short-duration blocking systems over the Euroatlantic region
19 p2447 A73-38124
- Numerical forecasting experiments based on the conservation of potential vorticity on isentropic surfaces.
21 p2728 A73-40053
- Wind speed variability /standard deviation difference/ over 16.25 km distance between observation sites compared to generalized models for varying conditions of cyclonic activity
23 p3004 A73-44267
- CYCLOTION FREQUENCY**
Influence of the degree of uniformity of the magnetic field on the emission of electron cyclotron frequency harmonics from a plasma
04 p0478 A73-15036
- Short-life mode of electrostatic electron cyclotron harmonic waves.
04 p0477 A73-15196
- Instability of a current-carrying plasma at cyclotron harmonics, and anomalous resistance
06 p0729 A73-18113
- Parametric action of high-power radiation on a plasma near the electron cyclotron frequencies
09 p1123 A73-21876

- Use of electron and proton beams for production of very low frequency and hydromagnetic emissions.
09 p1074 A73-22061
- Fast wave propagation and damping at the second harmonic of the ion cyclotron frequency.
09 p1128 A73-22631
- [TTU-SR-2]
Electron-cyclotron drift instability in high-beta plasmas, developing nonlinear theory based on wave kinetic equation for weak turbulence
10 p1255 A73-24263
- HF radio wave enhanced electron cyclotron frequency lines and ion plasma fluctuations due to artificial ionospheric excitation
12 p1490 A73-27008
- Microwave heating of electrons of a dense plasma column at frequencies higher than electron cyclotron frequency.
14 p1782 A73-30771
- Formation of fast electrons in a plasma under the influence of SHF power near harmonics of the electron cyclotron frequency
15 p1920 A73-32309
- Excitation of an electron semicyclotron wave and its harmonics during the interaction of high-current opposed electron beams
15 p1920 A73-32312
- Resonant absorption of an electromagnetic wave by an inhomogeneous magnetoactive plasma at electron cyclotron frequency harmonics
18 p2289 A73-36563
- Excitation of transverse extraordinary mode in an inhomogeneous magnetoplasma.
20 p2598 A73-39300
- Wave absorption by a plasma with a nonmonotonic longitudinal distribution of the concentration
21 p2746 A73-40524
- Interference structure of oscillating point charge near resonance cone in warm magnetized collisionless plasma, relating structure location to cyclotron frequency and plasma parameters
22 p2891 A73-42242
- Instability of a current-carrying plasma at cyclotron harmonics and the anomalous resistance.
24 p3114 A73-44502
- Production of fast plasma electrons by microwave power at harmonics of the electron cyclotron frequency.
24 p3114 A73-44617
- Excitation of electron-cyclotron waves by high-current counter-streaming electron beams.
24 p3115 A73-44620
- CYCLOTION RADIATION**
NT ION CYCLOTION RADIATION
Solar coronal plasma cyclotron radiation, taking into account temperature effects
01 p0096 A73-10309
- Quasi-linear interaction of whistler-mode waves and nonthermal electrons.
02 p0141 A73-12390
- Changes in the distribution function of magnetospheric particles associated with gyroresonant interactions.
03 p0303 A73-13882
- A target design for irradiation of NaI at high beam current.
07 p0853 A73-20469
- The effect of a metallic reflector upon cyclotron radiation.
08 p0990 A73-20813
- Use of electron and proton beams for production of very low frequency and hydromagnetic emissions.
09 p1074 A73-22061
- Coupled waves and particle scattering processes in ferromagnetic semiconductors and metals
09 p1133 A73-22677
- Normal Doppler shifted cyclotron radiation from a cold plasma.
18 p2338 A73-36189
- Jupiter satellite Io controlled decametric Alfvén wave emission pattern, considering relationship to coherent cyclotron radiation growth rate
21 p2764 A73-40168
- CYCLOTION RESONANCE**
Theory of electron cyclotron resonance heating. I - Short-time and adiabatic effects.
[AD-759528]
03 p0345 A73-14434
- Cyclotron resonance instability in a rotating plasma
04 p0479 A73-15042
- Experimental investigation of the kinetic instabilities in Gabor's alternative magnetron
04 p0481 A73-15610
- Microwave power absorption by a plasma outside the electron cyclotron resonance region.
06 p0733 A73-18795
- Electron cyclotron off-resonance heating rate in hot electron plasmas, comparing numerical calculation in terms of harmonic resonance with computerized simulation
07 p0856 A73-19519
- Intrinsic bandwidth of cyclotron resonance in the geomagnetic field.
07 p0792 A73-19532
- Transmission of electromagnetic waves through a conducting slab. IV - A simple multiple-reflection method.
07 p0852 A73-20172

- Absorption of electromagnetic waves by a magnetoactive plasma at parametric-resonance frequencies
09 p1124 A73-21889
- Cyclotron heating of plasmas with finite amplitude waves.
[TTU-SR-2]
09 p1128 A73-22630
- Influence of dispersion on the nonlinear evolution of quasi-monochromatic spiral waves in a magnetoactive plasma
09 p1130 A73-22708
- Frequency entrainment of a drift instability by nonlinear effects in a plasma.
10 p1253 A73-24114
- Experimental investigation of kinetic instabilities in the Gabor magnetron.
10 p1254 A73-24200
- Investigation of the radial structure of the oscillations of a plasma column situated in crossed fields in the presence of resonant cyclotron instability
14 p1781 A73-30579
- Quasi-classical calculation of the power output of a cyclotron resonance maser
14 p1758 A73-30944
- Saturation in cyclotron resonance heating of plasma.
16 p2042 A73-33339
- Absorption of electromagnetic waves at parametric resonances in a magnetoactive plasma.
17 p2215 A73-34312
- Simulation of gyroresonant electron-whistler interactions in the outer radiation belts.
18 p2347 A73-36296
- Cyclotron resonance in a weakly ionized hydrogen plasma with nitrogen, oxygen and air impurities
22 p2890 A73-41864
- The shape of the cyclotron absorption line in a weakly ionized plasma
23 p3011 A73-43794
- Cyclotron oscillations of a plasma in an inhomogeneous magnetic field
23 p3012 A73-44090
- Far IR grating spectrometer using InSb detector with narrow spectral band responsivity and tunability due to cyclotron resonance absorption in magnetic field
23 p2984 A73-44364
- Cyclotron resonance breakdown with submillimeter lasers.
24 p3095 A73-44586
- A new ion and electron detector for ion cyclotron resonance spectroscopy.
24 p3089 A73-44816
- CYGNUS CONSTELLATION**
Detection of a flux of gamma quanta in the direction of the Cygnus constellation
10 p1265 A73-23906
- Radial velocity measurements of the Cetus Arc nebula around Loop II.
19 p2483 A73-37571
- Variability of high-energy gamma-radiation sources
21 p2759 A73-40707
- CYLINDERS**
Comparative study of free jets and jets emitted in the wake of a cylinder with axis parallel to a hypersonic flow
01 p0002 A73-10417
- Effects of forced flow, noncondensables, and variable properties on film condensation of pure and binary vapors at the forward stagnation point of a horizontal cylinder.
01 p0122 A73-10806
- Determination of a time-dependent thermal stress on a finite cylinder
[DGLR PAPER 72-112]
02 p0230 A73-11671
- An investigation into the flow around a family of elliptically nosed cylinders at zero incidence at free-stream Mach numbers of 2.5 and 4.
02 p0129 A73-12507
- Stress intensity factors for internally pressurized thick-wall cylinders.
04 p0505 A73-14680
- Steady state aerodynamic characteristics of cylinders with spanwise protrusions, presenting wind tunnel drag and lift measurements in Reynolds number transition range
04 p0403 A73-14949
- Ionospheric plasma flow past a semi-infinite cylinder.
04 p0440 A73-14967
- Axial and transverse wave motions of inviscid perfect gas in isothermal solid-body rotation in cylinder
04 p0434 A73-15163
- Initial and boundary value problems for melting propagation from solid cylinder axis and sphere center, assuming pure conductive heat transfer
05 p0638 A73-16595
- Stabilization of flames formed behind cylinders wetted by liquid fuels in high velocity gas streams
[WSCIPAPER 72-38]
05 p0639 A73-16679
- Analysis and space-time reconstitution of the circumferential component of instantaneous velocity in immediate proximity to the wall of a cylinder
08 p0926 A73-21496

Electric and magnetic field shielding performance of nonmagnetic metallic cylinders, using Sommerfeld approximation

08 p0949 A73-21663

Approximate method for calculating heat transfer to yawed cylinders in laminar flow.

08 p1025 A73-21818

Elastoplastic deformation and stresses in clamped multilayer cylinders

10 p1287 A73-23593

Study of the fluctuations of wall pressures in transonic flow on a cone-cylinder group presenting a constriction

10 p1173 A73-24825

Frequencies and virtual masses of a liquid in a cavity formed by eccentric cylinders

11 p1347 A73-25391

One dimensional temperature equalization process in planar plate, infinitely long cylinder and sphere for range of Biot and Fourier numbers, estimating approximate solution error

11 p1452 A73-26372

Certain methods of numerical calculation in problems of microwave scattering from cylindrical obstacles

13 p1581 A73-28125

An integral equation approach to heat and mass transfer problem in an infinite cylinder.

13 p1705 A73-28431

Scattering by a gyrotropic cylinder coated with another gyrotropic layer.

13 p1586 A73-29232

Thermal stresses and couple-stresses in square cylinder with a circular hole.

14 p1815 A73-30919

Obliquely incident plane wave scattering from moving perfectly conducting cylinder, discussing mode coupling, Doppler shift and far field scattered power

15 p1845 A73-32238

Approximation nature and error magnitude in radial radiative heat flux within optically thin nongray isothermal gas cylinder

15 p1959 A73-32282

A method for calculating unsteady turbulent boundary layers in two- and three-dimensional flows.

17 p2154 A73-35135

The measurement and analysis of fatigue crack growth in cylindrical shapes.

18 p2363 A73-36486

The asymptotic analysis of canonical problems in high-frequency scattering theory. I - Stratified media above a plane boundary. II - The circular and parabolic cylinders.

22 p2886 A73-42347

CYLINDRICAL AFTERBODIES

U AFTERBODIES

U CYLINDRICAL BODIES

CYLINDRICAL ANTENNAS

Antenna synthesis via inverse electrodynamic problem solution for infinite impedance cylinder excited by traveling wave, noting directional antenna with rotating polarization

01 p0017 A73-10217

The integral equation and boundary conditions for a cylindrical antenna in a warm plasma.

04 p0429 A73-15482

Experimental investigations on the impedance behavior of a cylindrical antenna in a collisional magnetoplasma.

06 p0729 A73-18186

Dipole antenna coaxially mounted on a conducting cylinder.

06 p0666 A73-18189

Thin walled open ended cylindrical antenna in cold magnetoplasma, calculating current distribution by approximations based on Wiener-Hopf procedure

06 p0729 A73-18193

Corrugated and uniform dielectric rod aerial excited in E sub 0-mode.

07 p0792 A73-19547

Diffraction on an infinite grating made of cylindrical elements of random cross section

09 p1051 A73-22851

A local point method for problems of diffraction on an array

09 p1051 A73-22860

Measurement of the current distribution at the surface of a doublet immersed in an isotropic hot plasma

09 p1131 A73-23034

Resonances in circular arrays with dielectric sheet covers.

11 p1337 A73-25654

Impedance comparisons for the asymmetrically driven thin cylindrical antenna.

11 p1329 A73-25663

Tangential electric field near base driven cylindrical antenna surrounded by free space or by homogeneous isotropic dissipative medium from charge distribution measurement

11 p1329 A73-25665

Radiation properties of a composite-dielectric-rod aerial.

11 p1332 A73-26286

Dispersion characteristics of multiloop cylindrical spiral antennas with opposite winding

12 p1480 A73-27237

Radial mode analysis of electromagnetic wave propagation on slotted cylindrical structures.

14 p1727 A73-30208

Current distribution on an infinite tubular antenna immersed in a cold collisional magnetoplasma.

15 p1920 A73-32236

Impedance of a short cylindrical dipole antenna in a hot uniaxial plasma.

15 p1845 A73-32237

Oriental dependence of certain RF impedance probes in the ionosphere.

18 p2288 A73-36188

Synthesis of impedance-type cylindrical antenna arrays

21 p2661 A73-40197

Realized gain function for a cylindrical array of open-ended waveguides.

21 p2653 A73-40677

Integral equation analysis of cylindrical antennas having arbitrary surface impedance.

21 p2655 A73-41093

Gravitational radiation detection via computerized delay-dependent coincidence comparisons of squared time derivatives of output powers of Argonne and Maryland cylindrical antenna detectors

22 p2885 A73-41734

Computer program for analysis of radiation pattern distortion and mutual coupling in antenna farms, allowing user specification by types or vertical cylindrical antenna dimensions

22 p2823 A73-41797

Impedance and large signal excitation of satellite-borne antennas in the ionosphere.

22 p2831 A73-41835

Calculation of the early time radiated electric field from a linear antenna with a finite source gap.

22 p2832 A73-41856

Electromagnetic wave diffraction by a metallic cylinder surrounded by a plasma layer

22 p2892 A73-42336

CYLINDRICAL BODIES

NT ROTATING CYLINDERS

Linear MHD equations for inviscid medium under external forces, discussing magnetoacoustic wave generation by radially pulsating cylinder and sphere

02 p0196 A73-11605

Propagation of elastic waves in a cylindrical bar subject to a moving load on its lateral surface.

03 p0343 A73-13833

Jet-driven cylindrical cavity oscillators. [ASME PAPER 72-WA/FLCS-4]

04 p0409 A73-15862

Solution of the general heat-transfer problem for flow past cylindrical bodies by the Tolubinskii integral method.

06 p0766 A73-17407

Matched asymptotic expansions method application to slender cylindrical beams, calculating displacement far field by Navier-Stokes elasticity equation

07 p0913 A73-20075

Implosive and explosive welding of mono- and bimetallic duplex cylinders.

08 p0973 A73-21239

Cylinder surface roughness and transverse curvature effects on turbulent boundary layer in incompressible and compressible flows, deriving formula for skin friction coefficient

08 p0956 A73-21603

Cold collisionless plasma equations for electromagnetic waves absorption near lower hybrid resonance in inhomogeneous magnetized plasma contained in ideally conducting cylinder

09 p1125 A73-21906

An axisymmetrical nonstationary heat-conduction problem for a system of two cylinders contacting at the end faces

09 p1166 A73-22363

Convergence of the solution for the far scattered field of a conducting cylinder of arbitrary cross-section.

09 p1050 A73-22397

Experimental study of the heat transfer in the separation zones in front of cylindrical projections

10 p1294 A73-23587

Dissipation of mechanical energy in a deformable body during thermal diffusion processes

10 p1291 A73-24351

A direct method of interpreting gravity and magnetic anomalies - The case of a horizontal cylinder.

11 p1351 A73-25162

Torsional stress on micropolar prismatic nonsymmetrically elastic rotating cylindrical shaft with six degrees of freedom evaluated in terms of Saint Venant function

11 p1445 A73-26409

Investigation of the flutter of cylindrical panels in a supersonic gas flow

12 p1550 A73-26954

Electromagnetic scattering by a transversely moving conducting cylinder of arbitrary cross section.

12 p1468 A73-27018

Temperature field calculation for certain elements located in microwave channels

12 p1558 A73-27247

Stability of sheet metal drawn by a rigid stamp to cylindrical and conical shapes

12 p1503 A73-27476

Plane and cylindrical electromagnetic waves diffraction on infinitely long cylindrical bodies, calculating induced currents, diffraction patterns and near fields

13 p1582 A73-28654

Plane TE polarized electromagnetic wave diffraction on infinite conducting cylinder in nonhomogeneous medium, calculating far field diffraction patterns

13 p1582 A73-28656

Fracture strength of helically wound composite cylinders.

13 p1702 A73-29542

Mode factor and stress concentration parameter for sudden heating of solid cylinders and disks, noting thermal stability criterion with allowance for statistical strength

13 p1703 A73-29611

Elastoplastic torsion of a cylindrical bar of multiconnected section

14 p1805 A73-29762

Radiant heat transfer on circular-finned cylinders.

14 p1817 A73-30574

Failure under thermal loads of cylindrical bodies consisting of brittle materials

14 p1813 A73-30683

Application of cylindrical specimens with a ring crack for determining the brittle strength in materials

14 p1814 A73-30719

Vertical submersion of a floating cylindrical solid

15 p1861 A73-31283

Experimental investigation of the pressure distribution in constrained MHD flows past cylinders

15 p1917 A73-31401

The attenuation of ultrasonic waves in cylindrical work pieces with central bore-hole

15 p1882 A73-32053

Cold collisionless plasma equations for electromagnetic waves absorption near lower hybrid resonance in inhomogeneous magnetized plasma contained in ideally conducting cylinder

15 p1922 A73-32631

Planar free convection flow over horizontal cylinders with a small Grashof number under the influence of a planar wall

16 p2085 A73-33254

Similarity in the flow of a magnetized plasma around a plate and cylinder

17 p2215 A73-34260

Diffraction of a plane electromagnetic wave on arrays of periodically spaced cylinders

17 p2121 A73-34583

Torsion of a cylindrical shaft having an annular semicircular cutout

17 p2244 A73-34791

Torsional rigidities for bars under fully plastic torsion.

18 p2365 A73-36695

Turbulence measurements in interacting wakes.

18 p2301 A73-36698

Prediction of the lift and moment on a slender cylinder-segment wing-body combination.

19 p2377 A73-38007

Investigation of the flutter of cylindrical panels in a supersonic gas flow.

19 p2500 A73-38139

Solution of a nonlinear problem of heat conductivity concerning a multilayer cylindrical wall with a no-ideal thermal contact

20 p2627 A73-39257

A method of obtaining approximate solutions to unsteady-state heat conduction problems

20 p2627 A73-39258

Some three-dimensional boundary value problems for an elastic medium bounded by cylindrical surfaces

20 p2620 A73-39508

Radiative and convective heat transfer in a magnetic field

20 p2628 A73-39608

Van der Waals energy calculation from electromagnetic mode quantum energy in spheres and cylinders, considering finite boundary conditions, Green function techniques, and periodic lattices

20 p2538 A73-39706

Aerodynamic forces on a triangular cylinder.

21 p2782 A73-40003

Dynamics of cylindrical structures subjected to axial flow.

21 p2783 A73-40292

Nonsymmetric buckling of cylinders with axisymmetric thermal discontinuities.

21 p2784 A73-40425

Radiatively driven harmonic acoustic waves in vibrational equilibrium in closed cylindrical tube, deriving pressure response, radiative absorption coefficient and spectral detail

22 p2930 A73-42235

Experiments on radiatively driven harmonic acoustic waves in a confined gas.

22 p2930 A73-42236

Some investigation on base flow behind cylindrical bodies in incompressible flow.

22 p2797 A73-42997

Wave propagation and diffraction in bodies with noncircular cylindrical boundaries

23 p3045 A73-44181

Weak longitudinal waves in a nonlinear viscoelastic medium

23 p3045 A73-44182

Three dimensional elasticity solution for layer interaction and shear coupling and deflection effects of laminated anisotropic composite cylinders under bending

24 p3149 A73-45152

CYLINDRICAL CHAMBERS

A distribution of molecular flow in the interior of a cylindrical space-simulation chamber with spherical gas source

11 p1343 A73-25111

CYLINDRICAL SHELLS

Investigation of a deformation process in a heated elastoplastic cylindrical shell

01 p0112 A73-10006

Stress concentration at circular holes in a cylindrical shell of moderate thickness

01 p0114 A73-10480

Free vibration of prestressed cylindrical shells having arbitrary homogeneous boundary conditions.

01 p0114 A73-10730

Solution of stresses and strains for laminated monoclinic cylinders.

01 p0115 A73-10748

Aerodynamic generalized forces for supersonic shell flutter.

01 p0003 A73-10751

Optimal thickness of a cylindrical shell under external pressure

01 p0116 A73-10964

Dynamic stability of the state of moment stress in a cylindrical shell with allowance for inertia of the subcritical state

01 p0117 A73-11093

A semimomentless theory of asymmetrically structured cylindrical sandwich shells with a rigid compressible filler

01 p0118 A73-11406

Oscillations of nonshallow cylindrical shells loaded by distributed and concentrated masses

01 p0118 A73-11407

Stability of orthotropic circular cylindrical shells reinforced by annular ribs under external pressure

01 p0118 A73-11409

Temperature fields and stresses during local tempering of helical welds of a cylindrical shell

01 p0118 A73-11413

Spot welded stainless steel cylindrical strip shells supercritical behavior, analyzing equilibrium states dependence on axial loads and buckling forces

01 p0119 A73-11441

Experimental investigation of the behavior of cylindrical shells under dynamic loads

02 p0229 A73-11626

Helios solar probe structural adapter design for linking to booster rocket end stage, investigating orthotropic cylindrical shell carrying capacity [DGLR PAPER 72-101]

02 p0227 A73-11685

Designing of shells with a zero Gaussian curvature under an edge load applied to a portion of the shell contour

02 p0230 A73-11717

Stress analysis of cantilever thin walled cylindrical shell with concentrated force on free reinforcement ring, noting members rigidity relationship to internal stress concentration

02 p0230 A73-11718

Solution of axisymmetrical problems of the interaction between a cylindrical shell and an elastic filler by the finite difference method

02 p0231 A73-11806

Rigidly plastic cylindrical shell design for axial-load and lateral-pressure combinations with allowance for large deflections

02 p0231 A73-11808

Bulging of a circular cylindrical shell under axial compression

02 p0231 A73-11814

Stability of a cylindrical shell under the action of concentrated axial compression loads

02 p0231 A73-11815

Effect of the length on the stability of cylindrical shells compressed by longitudinal local forces

02 p0231 A73-11816

Circular cylindrical shell stability for thermal shock on end face, calculating critical thermal flux

02 p0232 A73-11818

Critical stress in an anisotropic cylindrical shell under nonuniform compression

02 p0233 A73-11938

Oscillations of open cylindrical shells of variable curvature

02 p0233 A73-11941

Discussion of the bending theory of cylindrical shells of orthogonally anisotropic structural material, by introducing the displacement function.

02 p0236 A73-12514

Elastoplastic stressed state of cylindrical shells weakened by a circular hole

02 p0237 A73-12590

Prediction of the response of a cylindrical shell to arbitrary or boundary-layer-induced random pressure fields.

02 p0237 A73-12601

Effect of transverse shear on limit load of cylindrical shells.

03 p0383 A73-12873

Vibrations of circular cylindrical shells subjected to nonuniform initial stress.

03 p0384 A73-12984

Parametric vibration of simply supported rectangular plate and cylindrical shell under random excitation, using Markov process theory and Fokker-Planck equation

03 p0388 A73-13318

On higher-order theory for thermoelastic analysis of heterogeneous orthotropic cylindrical shells.

03 p0389 A73-13327

Stability of fiberglass-reinforced cylindrical shell under the action of axial dynamic loads

03 p0392 A73-13746

Dynamic stability of a cylindrical shell in an acoustic medium.

03 p0393 A73-13834

Shear strains and elastic anisotropy of transversely isotropic cylindrical shell with circular hole under uniform internal pressure, using shallow shell equations

03 p0394 A73-14020

Vibrational frequency density analysis of thin spherical and cylindrical shells of revolution, using asymptotic integration method

03 p0394 A73-14051

Natural vibration frequency spectra of circular cylindrical and spherical shells of revolution, using Bessel function

03 p0395 A73-14052

Effect of a circular hole on the buckling of cylindrical shells loaded by axial compression.

03 p0395 A73-14181

Bending rigidity of an inflated circular cylindrical membrane of rubbery materials.

03 p0395 A73-14183

Transient interaction of a flexible ring-reinforced shell and a fluid medium.

03 p0395 A73-14197

Determination of critical stresses for elements of cylindrical shells in the plastic state

03 p0396 A73-14619

Ductile fracture initiation, propagation, and arrest in cylindrical vessels.

04 p0506 A73-14697

Determination of the natural oscillation frequencies of three-layer circular cylindrical shells by a numerical method

04 p0510 A73-15081

Application of the method of summary representations to problems of cylindrical shell oscillations

04 p0511 A73-15086

Analytical investigation of a cylindrical shell embedded in a soft medium.

04 p0511 A73-15172

Plastic deformations and crack propagation in cylindrical and spherical shells under uniform pressure, calculating stress intensity factor

04 p0512 A73-15239

Law governing the oscillations of a circular cylindrical shell of finite length containing a liquid with a variable level

04 p0434 A73-15505

Free vibration of cantilever circular cylindrical shells - A comparative study.

04 p0513 A73-15589

Russian book on orthotropic laminated cylindrical shells strength and optimal design covering glass ribbon reinforced zero moment shells and interlayer shear theory

04 p0514 A73-15702

Dynamic response of pressurized thin cylindrical shells subjected to torsional loads. [ASME PAPER 72-WA/PROD-6]

04 p0514 A73-15807

An approximate rigid-plastic analysis of shell intersections loaded dynamically. [ASME PAPER 72-WA/DE-1]

04 p0515 A73-15876

Singular solutions for shallow cylindrical shells. [ASME PAPER 72-WA/APM-27]

04 p0515 A73-15891

Propagation of harmonic waves in orthotropic circular cylindrical shells.

04 p0515 A73-15893

Dynamic response of a semi-infinite elastic cylinder containing an acoustic medium. [ASME PAPER 72-WA/APM-3]

04 p0516 A73-15905

Axial impact response of semiinfinite cylindrical membrane shell of helically oriented linearly elastic orthotropic fiber reinforced material, solving motion equations

05 p0631 A73-16112

Roots of the circular cylindrical shell characteristic equation.

05 p0632 A73-16499

Buckling of a long, axially compressed, thin cylindrical shell with random initial imperfections.

[ASME PAPER 72-APM-MMM] 05 p0632 A73-16532

On the determination of the centers of twist and of shear for cylindrical shell beams.

[ASME PAPER 72-APM-XX] 05 p0633 A73-16534

General instability of cylinders with inclined stiffeners under axial compression.

05 p0633 A73-16541

Two types of loss of stability and strength in cylindrical shells

05 p0634 A73-16747

Nonsteady heat conduction of multilayer cylindrical and conical shells in periodic radiation flux, calculating temperature distribution

05 p0640 A73-16798

Response of a cylindrical fiberglass-reinforced plastic shell to the action of an explosive load

05 p0635 A73-17079

A temperature extrapolation method for hollow cylinders.

05 p0641 A73-17119

Analysis of noncircular cylindrical shells.

06 p0758 A73-17446

Impact of a cylindrical shell against the surface of a compressible fluid

06 p0758 A73-17451

Dynamic behaviour of thin cylindrical shells subjected to high-speed travelling inner pressures.

06 p0758 A73-17518

Transversal vibrations of the thin shell of revolution produced by the thermal shock.

06 p0763 A73-18453

Nonlinear natural vibrations of rectangular plates and cylindrical panels.

06 p0765 A73-18640

Transient response of a plastically anisotropic cylinder in plane strain.

07 p0908 A73-19081

Homogeneous flat elastic plate theory in Cosserat surface context, considering application of general constitutive equations and extension to right circular cylindrical shells

07 p0908 A73-19085

Acoustic radiation from two concentric cylindrical shells.

07 p0851 A73-19958

Bending stress in an impulsively loaded cylindrical shell of exponentially varying thickness.

07 p0913 A73-19973

The effect of variable temperature on creep collapse of a cylindrical shell under external pressure

07 p0913 A73-20070

Steady-state heat conduction in slabs, cylindrical and spherical shells with non-uniform heat generation.

07 p0921 A73-20181

Effects of shearing force and rotary inertia to dynamical behaviours of thin cylindrical shells subjected to impulsive inner pressures.

07 p0915 A73-20286

Nonlinear multiple-scale solution of a cylindrical shell.

07 p0915 A73-20337

Plastic analysis of filled, reinforced, circular cylindrical shells.

08 p1015 A73-20672

On optimizing thermal stresses in cylindrical shells.

08 p1015 A73-20674

Solution of the asymmetric steady-state heat conduction problem for a two-layer hollow cylinder of finite length

08 p1021 A73-20995

Dispersion of axially symmetric waves in empty and fluid-filled cylindrical shells.

08 p0987 A73-21075

Axisymmetric deformation of a laminar, orthotropic, cylindrical shell

08 p1017 A73-21368

Viscoelastic strains in a thick-walled cylinder under the long-term effect of a gravitational load

08 p1017 A73-21371

Stability of the state of moment stress of a three-layer orthotropic cylindrical shell under uniform and nonuniform external pressure

08 p1018 A73-21374

Dynamic analysis of freely supported axisymmetric shells.

08 p1018 A73-21473

Dynamic behaviour of thin cylindrical shells collided with dampers.

08 p1019 A73-21527

Solution of the three-dimensional thermoelasticity problem for a long cylinder with mixed heating conditions

08 p1019 A73-21758

Elastic wave propagation in a cylindrical shell containing a filler

09 p1158 A73-22357

Characteristics of the motion of a system composed of a shell and fluid within the limits of hydraulic approximation

09 p1072 A73-22587

Determination of the optimal physical load in the local heating of a cylindrical shell

09 p1159 A73-22589

A cylindrical shell with an axial crack under skew-symmetric loading.

09 p1160 A73-22894

Calculation of the stress concentration produced by an internal pressure in the region where a cylindrical shell is connected to a branch pipe.

09 p1161 A73-23058

The effect of a transverse shear acting on the edge of a circular cutout in a simply supported circular cylindrical shell.

09 p1161 A73-23092

An evaluation of finite element methods for the computation of elastic stress intensity factors.

[ASME PAPER 72-PVP-19] 09 p1163 A73-23267

Cantilever cylindrical shells of rigid-plastic material, determining collapse loads under external pressure combined with end moment by numerical solution to limit analysis

[ASME PAPER 72-PVP-B] 09 p1164 A73-23271

An approximate rigid-plastic analysis of shell intersections loaded dynamically.

[ASME PAPER 72-WA/DE-1] 09 p1164 A73-23272

Effect of elastic displacements of a cylindrical shell on the vibrations of the free surface of a fluid

09 p1073 A73-23345

Vertical circular cylindrical shells buckling under axisymmetric compressive stress due to own structural weight, using Timoshenko elastic stability theory

09 p1166 A73-23459

Numerical solution of some boundary value problems for an isotropic cylindrical shell

10 p1288 A73-24060

Optimal conductive heating of hollow cylinder inner surface with temperature dependent thermal stress limits for internal/external surfaces

10 p1289 A73-24063

Stability analysis of axially compressed closed circular cylindrical shells with reinforcement rings

10 p1290 A73-24301

Stability of transversely isotropic cylindrical shells in nonuniform subcritical states

10 p1290 A73-24311

Method of variable directions for solving the equations of an isotropic cylindrical shell

10 p1292 A73-24501

Vibrations of segmented shells.

10 p1293 A73-24720

Unsteady creep in a symmetrical cylindrical shell

10 p1293 A73-24793

New arrangement for testing materials in the volume stressed state and at elevated temperatures /Exchange of experience/.

10 p1222 A73-24947

Nonlinear transient stress-waves in cylindrical and conical shells.

11 p1432 A73-24978

Thin walled elastoplastic cylindrical shells deformations investigation by elliptic quasi-linear equation systems

11 p1433 A73-25044

Experimental investigation of the stability of shells with holes

11 p1434 A73-25390

Stability of cylindrical shells with filler under axial compression and external pressure

11 p1435 A73-25396

Experimental investigation of oscillation damping in shells with holes

11 p1435 A73-25398

Nonlinear transient analysis of shells and solids of revolution by convected elements.

[AIAA PAPER 73-359] 11 p1437 A73-25495

Buckling of partially debonded layered cylindrical shells.

[AIAA PAPER 73-366] 11 p1438 A73-25501

A finite element method for nonaxisymmetric vibrations of pressurized shells of revolution partially filled with liquid.

[AIAA PAPER 73-399] 11 p1440 A73-25528

Vibration and flutter of cylindrical shells including the effects of stringer stiffening.

[AIAA PAPER 73-312] 11 p1441 A73-25543

Near field of scattering by a hollow semi-infinite cylinder and its application to sensor booms.

11 p1328 A73-25658

A method for obtaining stresses and displacements in thick cylindrical shells under arbitrary boundary conditions.

[ASME PAPER 72-APM-LLL] 11 p1442 A73-25708

Stress waves in finite longitudinally layered shells.

11 p1442 A73-25712

Spot welded stainless steel cylindrical shells post-critical loading behavior, analyzing equilibrium states dependence on axial loads and buckling forces

11 p1443 A73-26058

A corrected assessment of the cylindrical shell finite element of Bogner, Fox and Schmit when applied to arches.

11 p1443 A73-26090

Edge buckling of cylindrical shells with low in-plane shear moduli.

11 p1445 A73-26392

Effect on shell dynamics of a shell mass distributed within a shell surface area

11 p1446 A73-26461

On the buckling and postbuckling behavior of thin-walled circular cylinders.

[DFVLR-SONDDER-261] 12 p1550 A73-26843

Multilocal difference method for free vibration analysis of closed and open orthotropic noncircular cylindrical shells with supported curved edges

12 p1551 A73-27035

Stresses in bonded joints of circular cylindrical shells and panels

12 p1551 A73-27182

Determination of the stressed state of a circular cylindrical shell with stepwise variation in wall thickness along the generatrix under the action of a local load

12 p1552 A73-27261

Stability of a cylindrical anisotropic shell under the action of a ring load with allowance for subcritical deflection

12 p1553 A73-27373

Stability of cylindrical shells of variable thickness during torsion

12 p1553 A73-27462

Stability of a reinforced cylindrical shell during axial compression

12 p1553 A73-27463

Elastoplastic bending of a cylindrical shell according to the Prandtl-Reuss theory

12 p1554 A73-27472

On optimal thickness of a cylindrical shell loaded by external pressure.

12 p1554 A73-27540

A cylindrical shell model of the NASA-MPE barium ion cloud experiment.

12 p1492 A73-27607

Approximate dependences for the vibration frequencies of smooth cylindrical shells and for ones with concentrated inclusions

12 p1555 A73-27789

Influence of rotational inertia on the frequency spectrum of the natural vibrations of a cylindrical shell

12 p1556 A73-27801

Stressed state of multilayer spherical vessels, cylindrical tubes and circular disks consisting of a linear viscoelastic material

13 p1690 A73-27994

Criteria for finite element discretization of shells of revolution.

13 p1691 A73-28084

Vibration analysis of thick-walled hollow spheres and cylinders, determining periodic response and fundamental frequency as function of wave reflection number and dimensions

13 p1695 A73-28489

Calculation of the low natural frequencies of clamped cylindrical shells by asymptotic methods.

13 p1696 A73-28752

Buckling of unstiffened and ring stiffened cylindrical shells under axial compression.

13 p1696 A73-28758

Tensometric strain gage evaluation of stress analysis methods for hollow cylindrical shells under uniform internal pressure

13 p1698 A73-29057

Stresses in adhesive bonds of thin cylindrical shells

13 p1698 A73-29063

Nonlinear axisymmetric subcritical deformation effect on elastic stability of locally loaded thin circular cylindrical shells under free end compressive load

13 p1698 A73-29089

German monograph - A contribution to the stability calculation and the test of cylindrical shells of glass-fiber reinforced plastics under uniform external pressure.

13 p1646 A73-29280

Forced vibration solution and wind tunnel investigation of shallow cylindrical shells under moving pulsating pressure discontinuities, noting compression shock effects

13 p1703 A73-29602

Temperature fields in a hollow cylinder in presence of heat source under the boundary conditions of the second kind.

13 p1708 A73-29666

Finite difference solution for large deformations of cylindrical shells - A comparison with finite element solutions.

14 p1807 A73-30182

Stability criteria for rigid plastic cylindrical shells at yield point load as function of deformation rate and geometry changes

14 p1809 A73-30257

Minimum potential and complementary energy rate principle formulation for finite plastic deformation, applying to cylindrical shell under uniformly distributed internal load

14 p1809 A73-30258

Stress concentrations close to circular holes in a cylindrical shell of medium thickness.

14 p1810 A73-30305

Formulation of local stability problems of shells of revolution.

14 p1810 A73-30326

A comparison of theory and experiments on the dynamic plastic behavior of shells.

14 p1811 A73-30476

Buckling of viscoplastic cylindrical shells loaded by radial pressure impulse.

14 p1811 A73-30481

Buckling of circular cylindrical shells under compression. IV - Solutions based on the modified Flugge equations considering prebuckling edge rotations.

14 p1813 A73-30573

The contact problem of two coaxial cylindrical shells

14 p1813 A73-30663

On the weight minimization of supersonic, axisymmetric circular cylindrical shells of finite length.

14 p1814 A73-30709

Optimal conditions for residual stress reduction in a cylindrical shell by local annealing

14 p1814 A73-30721

Solution of the fundamental boundary value problems for a closed semiinfinite cylindrical shell

15 p1945 A73-31023

Hydraulic impact in a circular cylindrical shell

15 p1860 A73-31047

Hydrodynamics in weak gravitational fields - Small oscillations of an ideal liquid in a cylindrical vessel

15 p1861 A73-31280

On dynamic response of prestressed cylindrical shells - Green's tensor technique.

15 p1947 A73-31367

Stresses in a pressurized ribbed cylindrical shell with a reinforced hole.

15 p1948 A73-31621

Cylindrical panels buckling under nonuniform axial compression with various load distributions, basing analysis on Donnell equations and Galerkin method

15 p1948 A73-31635

Forced motion of cylindrical shells - A comparison of shell theory with elasticity theory.

15 p1949 A73-31651

Stability of a stochastically excited nonlinear cylindrical shell.

15 p1949 A73-31654

Stringer stiffened cylindrical shells stability characteristics under axial compression, using Donnell thin-shell and Vlasov thin-walled beam theories

15 p1949 A73-31656

Design of stiffened cylinders to resist axial compression.

15 p1950 A73-31921

Theory for cylindrical wavy shells via fiberglass-plastic models, noting application to wavy rod torsion problem

15 p1952 A73-32083

Influence of preliminary dynamic loading on the load-bearing capacity of cylindrical shells

16 p2075 A73-32693

Stress concentration near a cutout on the surface of an orthotropic cylindrical shell

16 p2075 A73-32694

The application of finite elements to the large deflection geometrically non-linear behaviour of cylindrical shells.

16 p2078 A73-32998

Curved rotational shell elements by the constraint method.

16 p2078 A73-33002

Torsional vibrations of shells of revolution of variable thickness.

16 p2081 A73-33682

Effect of transverse shear on the stability of an orthotropic cylindrical shell with an elastic filler under axial compression

16 p2082 A73-33931

Stability of composite-material cylindrical shells under unsteady heating and axial compression

16 p2083 A73-33934

Application of a technical theory to the calculation of three-layered vaulted shells with a continuous middle layer of polymer material

16 p2083 A73-33935

Dynamic stability of an orthotropic cylindrical shell allowing for transversal shear

16 p2083 A73-33937

Combined Rayleigh-Ritz and Lagrange multiplier technique for investigation of free vibrations of constrained cylindrical shell, considering axisymmetric mode

17 p2241 A73-34198

Book - Stresses in shells /2nd edition/.

17 p2242 A73-34469

A note on bending-shear interaction in the limit analysis of cylindrical shells

17 p2243 A73-34650

Wave propagation in uniform laminar cylindrical shells, discussing group and phase velocities on wave numbers in sandwich walls

17 p2243 A73-34734

Reaction of a cylindrical shell to periodic shock waves propagating in its interior

17 p2243 A73-34735

Stability of a cylindrical shell under dynamic axial load

17 p2244 A73-34739

Elastic semiinfinite cylindrical shell stress-strain state after axial impact against static rigid plane, obtaining solutions for small time values

17 p2244 A73-34740

Shell stability effects of holes from review of published studies, emphasizing cylindrical shells under uniformly distributed compression loads

17 p2244 A73-34789

Cylindrical shell postbuckling behavior under axial compression using multiple scale averaging technique, concluding predominance of diamond shaped postbuckling pattern

[ASME PAPER 73-APM-7] 17 p2247 A73-35032

Forced plane strain motion of cylindrical shells - A comparison of shell theory with elasticity theory.

[ASME PAPER 73-APM-9] 17 p2247 A73-35034

First-order frequency effects in supersonic panel flutter of finite cylindrical shells.

[ASME PAPER 73-APM-K] 17 p2249 A73-35106

Large amplitude forced vibrations of simply supported thin cylindrical shells.

[ASME PAPER 73-APM-Q] 17 p2249 A73-35107

On the buckling of cylinders in axial compression.

[ASME PAPER 72-APM-BBB] 17 p2250 A73-35113

On an accurate theory for circular cylindrical shells.

[ASME PAPER 73-APM-E] 17 p2250 A73-35114

Further experimental studies on buckling of integrally ring-stiffened cylindrical shells under axial compression.

17 p2250 A73-35441

Residual stresses and mechanical properties of circumferentially wrapped metal-metal composite cylinders fabricated from plasma sprayed Al reinforced with steel filaments

17 p2251 A73-35534

A new finite element method for analysing symmetrically loaded thin shells of revolution.

17 p2252 A73-35601

Probabilistic model for radiative transfer problems in cylindrical shell media with complete redistribution in frequency.

17 p2236 A73-35781

Inextensional approximations in cylindrical shells.

18 p2362 A73-36329

A contact problem for a transversely isotropic cylindrical shell of finite length

18 p2363 A73-36404

Limiting equilibrium of reinforced cylindrical shells

18 p2363 A73-36412

Stability of cylindrical shells during rapid loadings

18 p2365 A73-36599

Tensometric strain gage evaluation of stress analysis methods for hollow cylindrical shells under uniform internal pressure

18 p2366 A73-36889

Stresses in bonded joints of thin cylindrical shells.

18 p2366 A73-36895

Vibration of layered shells.

18 p2367 A73-37029

Straightforward design of a three-layer cylindrical shell

19 p2494 A73-37183

Influence of the structure of the material of a three-layered cylindrical shell on the natural frequencies

19 p2494 A73-37184

Nonlinear axisymmetric subcritical deformation effect on elastic stability of locally loaded thin circular cylindrical shells under free end compressive load

19 p2498 A73-37639

Nonlinear parametric vibrations of closed cylindrical shells

19 p2499 A73-37764

Application of the method of normal waves to the study of the oscillations of a cylindrical shell in contact with an elastic medium

20 p2615 A73-38984

Front-end collision of a partially liquid-filled cylindrical shell with a solid body

20 p2616 A73-39261

Inverse bending problems for two-layer orthotropic shallow shells

20 p2618 A73-39313

Numerical solution of problems of stability of three-layer cylindrical shells

20 p2620 A73-39503

Free vibration and buckling loads of anisotropic pressurized thin walled shells of revolution, considering cylinders, barrels and spherical sections

20 p2621 A73-39538

Buckling analysis of deformation and stress distribution in axially compressed longitudinally stiffened cylindrical shells, considering prebuckling deformation effects

20 p2621 A73-39539

Dynamic response of laminated composite circular cylindrical shells with freely supported or clamped edges.

20 p2621 A73-39543

Series analysis of cylindrical shells - New look at an old problem.

20 p2622 A73-39550

Determination of the stress strain state of closed cylindrical shells and infinite plates with cracks

20 p2624 A73-39645

Response of a cylindrical shell with filler to the action of a moving load

20 p2624 A73-39648

Optimum design of three-layer shells

20 p2625 A73-39655

Stability of the bending equilibrium of shells beyond the elastic limit

20 p2625 A73-39657

Effect of the yield point of the material on the stability of cylindrical shells under axial compression

20 p2625 A73-39658

The vibrations of non-circular cylindrical shells with initial stresses.

21 p2783 A73-40288

Frame of a cylindrical shell under the action of a concentrated radial force

21 p2783 A73-40388

Linearized characteristics method for supersonic flow past vibrating shells.

21 p2632 A73-40426

Stability of cylindrical shells beyond the elastic limit

21 p2786 A73-40979

Critical pressure and vibration frequencies of cylindrical shells with edges elastically reinforced in the axial direction

21 p2786 A73-40980

Elastoplastic stressed state of a long thick-walled cylinder subjected to the action of a magnetic field

21 p2786 A73-40981

Vibrations of a rotating solid body with a cavity partly filled with an arbitrary viscous fluid

21 p2677 A73-40988

Experimental investigation of a cylindrical shell loaded by a concentrated tangential force and a bending moment

21 p2787 A73-41193

Stability of a cylindrical shell of linearly variable thickness beyond the elastic limit

21 p2787 A73-41195

Temperature and stress fields in a cylindrical shell subjected to induction heat treatment

21 p2787 A73-41233

Nondestructive shell-stability estimation by a combined-loading technique.

21 p2708 A73-41266

Eigenmodes in vibrations of circular cylindrical shells with free boundaries, calculating frequencies from theory of inextensional vibrations

21 p2788 A73-41614

An approximation for the determination of the dynamic characteristics of long viscoelastic hollow cylinders

21 p2788 A73-41615

Free vibrations of fluid-conveying cylindrical shells. [ASME PAPER 73-DET-96]

22 p2919 A73-42075

Cylindrical circular shell vibrational frequencies, examining free surface or solid plane influence on shell natural vibrations in incompressible fluids

22 p2920 A73-42130

Local deformations arising in the contact between a cylindrical shell and a solid

22 p2921 A73-42281

The calculation of open circular cylindrical shells with the aid of partial discretization

22 p2922 A73-42528

Combined radial-axial large amplitude oscillations of hyperelastic cylindrical tubes.

22 p2923 A73-42637

The Morley-Koiter equations for thin-walled circular cylindrical shells. I - General solution for symmetrical shells of uniform thickness.

[ASME PAPER 73-APMW-22] 22 p2924 A73-42884

The Morley-Koiter equations for thin-walled circular cylindrical shells. II - Solution for a line loaded cylinder with close-spaced circumferential grooves.

[ASME PAPER 73-APMW-23] 22 p2925 A73-42885

Dynamic stability of transverse axisymmetric waves in circular/cylindrical shells.

[ASME PAPER 73-APMW-26] 22 p2925 A73-42887

Complex structural dynamic response reduction, discussing methods for mathematical models establishment and application to thin cylindrical shell

22 p2926 A73-42921

Computer analysis of clamped-clamped and clamped-supported cylindrical shells.

22 p2927 A73-42995

Contact pressure problem solution for circular cylindrical shell resting on circular Winklerian bases under external load in terms of Fourier expansion

22 p2928 A73-43053

Forced vibrations of a cylindrical shell in the presence of gas pressure fluctuations

22 p2928 A73-43057

Arbitrarily variable thickness cylindrical shell behavior under radial concentrated load calculated using Fourier series, differential equations and matrices

22 p2928 A73-43063

Limit pressures for cylindrical shells with two adjacent circular cut outs.

22 p2929 A73-43175

Evaluating the performance of shell-and-tube heat exchangers.

23 p3048 A73-43299

Cylindrical shell design with a frame-connected bottom and a system of concentrated forces applied to the bottom

23 p3042 A73-43726

Torsion of a cylindrical shell with a lateral surface containing an elastic circular inclusion

23 p3042 A73-43727

Stability under torsion of a moderately long cylindrical shell with different walls

23 p3042 A73-43738

Order of magnitude of the differences between theory and experiment in viscoplasticity under varying stress and temperature

23 p3044 A73-43971

Buckling of short viscoplastic cylindrical shells subjected to radial impulse.

23 p3045 A73-44080

Non-linear creep buckling with random temperature variations.

23 p3045 A73-44166

Numerical calculation of simply supported cylindrical shells of arbitrary cross section

23 p3046 A73-44192

Investigation of the stress-strain state at a strengthened hole in an orthotropic cylindrical shell

23 p3046 A73-44193

Critical equilibrium of cylindrical shells made from an ideal rigid-plastic material with different yield points in tension and compression

23 p3047 A73-44280

Dynamic buckling of an axially compressed cylindrical shell with discrete rings and stringers.

23 p3047 A73-44377

Nonlinear parametric vibrations of cylindrical shells prepared from composite materials

24 p3145 A73-44517

Power series solution to Volterra equations in nonlinear viscoelastic dynamic plate and shell theory with application to flexible cylindrical shell vibrations under periodic loads

24 p3145 A73-44518

Critical stresses of compressed cylindrical shells consisting of orthotropic layers with various orientations

24 p3145 A73-44529

Dynamic stability of a viscoelastic orthotropic cylindrical shell

24 p3146 A73-44532

Chebyshev solution to elliptical equilibrium equations of elastic reticular cylindrical and toroidal shells under distributed loads, applying to extensible fiber structures/tires/

24 p3146 A73-44652

On the problem of flexure of anisotropic cylindrical shells.

24 p3151 A73-45302

The problem of natural oscillations of a thin shell containing an elastoacoustic medium

24 p3152 A73-45359

CYLINDRICAL TANKS

Natural frequencies, forces and moments for liquid propellant sloshing in tilted cylindrical tank as function of tilt angle and liquid depth

03 p0293 A73-13314

Law governing the oscillations of a circular cylindrical shell of finite length containing a liquid with a variable level

04 p0434 A73-15505

Theoretical-experimental studies and research concerning the technical safety of the casing of a high-pressure cylindrical tank. I

04 p0454 A73-15657

Partial yielding of cylindrical pressure vessel with elastic modulus and yield function as arbitrary functions of radial coordinate, assuming elastoplastic strain hardening material

06 p0761 A73-17895

Transient Ekman and Stewartson layers in a rotating tank with a spinning cover.

10 p1210 A73-24840

Hydroelastic oscillations in a rigid circular cylinder in the presence of an elastic fluid surface covering

18 p2297 A73-36065

The use of glass-fiber-reinforced plastics for containers which are subjected to external pressure

24 p3147 A73-44881

CYLINDRICAL WAVES

Self focusing of two dimensional cylindrical waves propagating in inhomogeneous natural duct, noting tropospheric communications and ionospheric and sound propagation applications

02 p0142 A73-12527

Reflector antenna radiation pattern analysis by equivalent edge currents.

06 p0665 A73-18179

Self-similar cylindrical magnetogasdynamics and ionizing shock waves.

10 p1204 A73-23564

Time-dependent electromagnetic field scattering and diffraction by half plane during illumination by impulsive plane cylindrical or spherical wave

11 p1330 A73-25683

Scattering of a cylindrical wave in an elastic plate in the presence of an absolutely rigid cylindrical inclusion

12 p1551 A73-27240

Book - Mathematical problems in wave propagation theory.

12 p1524 A73-27625

- Plane and cylindrical electromagnetic waves diffraction on infinitely long cylindrical bodies, calculating induced currents, diffraction patterns and near fields
13 p1582 A73-28654
- Implicit predictor-corrector difference scheme for boundary value problem solution in propagation of spherical and cylindrical N waves /asymptotic pulse forms/
14 p1745 A73-30175
- Amplification of cylindrical electromagnetic waves reflected from a rotating body.
14 p1728 A73-30333
- Two dimensional wave problems in rotating elastic media.
19 p2460 A73-38183
- CYLINDROIDS**
U CYLINDRICAL BODIES
CYTOCHROMES
A salt-inhibited cytochrome c reductase obtained from the moderately halophilic bacterium, *Micrococcus halodenitrificans*.
03 p0261 A73-13598
- Informational biopolymer structure in early living forms.
06 p0652 A73-17946
- CYTOGENESIS**
Cytogenetic analysis of diploid and autotetraploid *Crepis capillaris* seeds following space travel on the 'Cosmos-368' artificial earth satellite
18 p2271 A73-36117
- Results of cytogenetic studies of seeds after their extended orbital flight aboard the Salyut orbital scientific station.
22 p2804 A73-42169
- Space flight factors effects on *Drosophila* development in terms of dominant, autosomal and sex-linked recessive lethals frequency, noting gametogenesis stage sensitivity
22 p2804 A73-42173
- CYTOLOGY**
Cytochemical-luminescence study of adrenal cortex proteins under the influence of ionizing radiation
02 p0134 A73-12354
- Biological, chemical and cytological methods of microorganism detection integrated into single instrument
03 p0272 A73-14320
- Results of electron microscopic studies in the rat brain under oxygen at high pressure.
11 p1314 A73-25330
- Mechanisms of secretion of neurohypophyseal hormones - Cellular and subcellular aspects
15 p1836 A73-32286
- CYTOPLASM**
Autoradiographic study of protein synthesis in perikaryons and of nitrogen migration into the axons of hypertrophic sympathetic neurons
13 p1574 A73-28296

D

D LINES

- On the minimum intensity of the Na D2-5890 A line in sunspot umbra /Research note/.
03 p0377 A73-14411
- Investigation of the chromosome in the D3 helium line at the eclipse of September 22, 1968.
04 p0503 A73-16014
- Interstellar molecular hydrogen cloud size and optical extinction by interstellar Na D and Ca lines, estimating molecular lifetime within dark cloud
06 p0752 A73-18230
- The damping of the NaD lines in the solar spectrum by atomic hydrogen.
06 p0753 A73-18239
- Increase of Na twilight emission after the earth's crossing of the orbital planes of Comets Halley and Encke.
07 p0899 A73-20063
- Isophotes comparison of quiescent and quasi-quietest solar prominences in D3 and H alpha lines, noting structural similarity from narrow band filter observation
12 p1545 A73-27836
- Rhodamine laser frequency locking using Faraday filter for tuning to sodium D lines
13 p1628 A73-29249
- The effect of comparison source reflectance on gas temperature measurement by Kuribaum's method and line reversal methods.
21 p2692 A73-39916
- The inversion of the mean and spatially resolved sodium D2 line profiles from the sun.
22 p2908 A73-42311

D REGION

- D-region parameters from the extraordinary component of partial reflections.
01 p0036 A73-10329
- Geomagnetic activity effects on D layer absorption from vertical soundings during solar flare induced sudden magnetic storms
01 p0039 A73-10415

- Symposium on D- and E-Region Ion Chemistry, University of Illinois, Urbana, Ill., July 6-8, 1971, Informal Record.
01 p0040 A73-10876
- D and E region aeronomy, discussing ionization sources, ion composition, water cluster ion formation and ratio of molecular oxygen and nitric oxide ions
01 p0040 A73-10877
- Ionization sources of the ionospheric D and E regions.
01 p0041 A73-10886
- Positive ion composition measurements in the D and E regions of the equatorial ionosphere.
01 p0041 A73-10889
- Positive ion composition measurements in disturbed D region, noting positive molecular oxygen ions as major source of water cluster ions
01 p0041 A73-10890
- Dependence of the D-region positive-ion composition on the atomic oxygen and atomic hydrogen concentrations.
01 p0041 A73-10891
- D-region negative-ion chemistry.
01 p0042 A73-10895
- Negative-ion composition measurements in the D and lower E regions.
01 p0042 A73-10896
- Equilibrium composite negative ion density profiles in nighttime D region from mass spectrometer measurements
01 p0042 A73-10897
- Ion composition dependent recombination coefficient loss rate changes in D region during solar flares, using electron density and X ray flux measurements
01 p0042 A73-10903
- Synoptic studies of D-region ionization changes and electron densities by the partial reflection differential absorption experiment.
01 p0042 A73-10904
- A comparison of two ground-based techniques for measuring D-region electron densities. I.
01 p0042 A73-10905
- A comparison of two ground-based techniques for measuring D-region electron densities. II.
01 p0042 A73-10906
- D and E ionospheric regions behavior, emphasizing water cluster ions formation, minor neutral constituents measurement and daytime ionization sources
01 p0043 A73-10912
- Observations of simultaneous auroral D and E layers with incoherent scatter radar.
01 p0043 A73-10998
- Rocket payload designs simulated by Monte Carlo method for aerodynamic properties during D region composition measurements
02 p0156 A73-11740
- Energetic metastable molecular oxygen as a source of ionization in the D region.
02 p0157 A73-11757
- Electron production rates and density profiles in D region during solar flares, presenting ionization vertical distribution model
02 p0206 A73-12304
- On D-region electron heating by a low-frequency terrestrial line current with ground return.
02 p0143 A73-12533
- Possibility of continuous monitoring of celestial X-ray sources through their ionization effects in the nocturnal D-region ionosphere.
03 p0361 A73-13361
- Bombardment of the polar-cap ionosphere by solar cosmic rays.
03 p0301 A73-13710
- D region HF radio wave noontime absorption correlation to winds and temperature in Northern Hemisphere during IQSY
03 p0304 A73-14593
- Absorption measurements at Calcutta compared with current D region models for atomic oxygen production and loss processes
03 p0305 A73-14594
- Nonsolar related D region semilunar variation effects on Omega navigation systems signal phase shift from harmonic analysis of VLF propagation data periodicities
04 p0416 A73-15062
- Chemical kinetics equations of lower ionosphere and D region particle interactions for aeronomic problems
05 p0569 A73-16396
- Contribution of hard solar X-ray radiation to D-region ionization.
05 p0611 A73-17172
- D region electron density profiles analytical determination from pulsed wave interaction measurements
07 p0791 A73-19242
- Lower ionosphere electron densities from rocket measurements employing LF radio propagation and DC probe techniques.
07 p0818 A73-19670
- Differential phase experiment on signal reflections from D region, noting systematic error in phase jitter calculation with pulse nonoverlap explanation
07 p0820 A73-20067

- Transition region response of the symmetric double probe and its application in the lower ionosphere.
09 p1080 A73-22101
- The influence of negative-ion changes in the D-region during sudden ionospheric disturbances.
09 p1075 A73-22126
- The negative-ion composition of the daytime D-region.
09 p1048 A73-22127
- Type variation of solar sudden field anomaly /SFA/ on 164 kHz as an indicator of seasonal structure changes in the D-region.
09 p1076 A73-22141
- Possibility of estimating the flux of energetic particles in the ionospheric D-region at sunrise and during the daytime.
10 p2122 A73-24219
- D-region recombination coefficients and the short wavelength X-ray flux during a solar flare.
11 p1356 A73-25914
- Energetic electron precipitation as a source of ionization in the night-time D-region over the mid-latitude rocket range, South Uist.
11 p1358 A73-26701
- The measurement of winds in the D-region of the ionosphere by the use of partially reflected radio waves.
11 p1358 A73-26707
- D layer electron density long term continuous monitoring, comparing FM-CW method application to partial reflection technique with conventional pulse method
12 p1474 A73-27765
- An analysis of seasonal changes in electron densities at middle latitudes in the lower D-region.
13 p1606 A73-28207
- Effective recombination coefficient in the ionospheric D-region.
13 p1608 A73-28711
- High power radio transmitter for structural investigation and electron concentration profiles of ionospheric D and E regions
13 p1583 A73-28725
- Ionospheric D region dissociation-recombination reaction constants derived from ion production rate data compiled during polar cap absorption
15 p1872 A73-31887
- Turbulent scattering phenomenological model for D region partial coherent reflection experiments with measurement noise, presenting amplitude and phase statistics
15 p1845 A73-32230
- Phase-difference distributions in a D-region partial-reflection experiment.
15 p1845 A73-32231
- D region partial reflection mechanism model based on multiple reflector concept, presenting electron density vertical distribution
15 p1845 A73-32233
- Experimental results of radio wave absorption measurements in Southwest Europe.
18 p2288 A73-35940
- The use of the LF A3 absorption measurements in studying the winter anomaly.
18 p2303 A73-35947
- The use of VLF propagation measurements for studies of magnetospheric and meteorological influences on the lower ionosphere.
18 p2303 A73-35953
- Some features of the equatorial D-region as revealed from the Langmuir probe experiments conducted at Thumba.
18 p2303 A73-35954
- D region electron density profiles from radio broadcast field strength measurements by rocket-borne passive RF spectrometers, using ray theory for wave propagation
18 p2303 A73-35956
- Ion and neutral composition measurements in the lower ionosphere.
18 p2303 A73-35960
- Evidence and characteristics of internal and planetary waves within the D-region plasma.
18 p2304 A73-35967
- Results of simultaneous in-situ-observations in Spain of electron concentration, neutral wind and air pressure in the D-region in different seasons and during an SID-event and their relevance to the winter-anomalous state of the atmosphere.
18 p2305 A73-36001
- Positive ion composition in the lower ionosphere during the Geminid meteorshower and the occurrence of a winter anomaly.
18 p2305 A73-36005
- Comparison of electron density profiles in the lower ionosphere at Equator and midlatitudes.
18 p2305 A73-36007
- Tromsø /Norway/ Auroral Observatory partial reflection experiment, considering data processing techniques, height resolution, phase detection, antenna arrays and D region drift measurements
18 p2315 A73-36009

Construction of D-region electron-density profiles by combined use of ground-based reflection and satellite-based transmission measurements.

18 p2306 A73-36016

D region electron and ion density profiles, recombination coefficient and electron detachment rate changes during solar eclipse

18 p2310 A73-36127

Meteorite ions in the D and E-regions.

18 p2310 A73-36132

Mean D-region electron density profiles derived by combination of rocket and radio wave propagation data.

21 p2686 A73-40831

D region electron density profiles at geomagnetic equator by rocket sounding, showing ionization production by Lyman alpha radiation and cosmic rays

21 p2690 A73-41361

Steady state coefficients in the D region during solar particle events.

21 p2760 A73-41372

On the detection of X-rays from celestial sources through their ionization of the terrestrial atmosphere.

21 p2762 A73-41394

Variations of the total amount of ozone and the behaviour of some ionospheric parameters in the winter time upper atmosphere.

23 p2976 A73-43885

DACRON [TRADEMARK]

Force-strain characteristics of dacron parachute suspension-line cord under dynamic loading conditions.

15 p1825 A73-31432

DAEMO [DATA ANALYSIS]

U DATA PROCESSING
U DATA REDUCTION
U DATA TRANSMISSION

DAMAGE

NT CUMULATIVE DAMAGE
NT EARTHQUAKE DAMAGE
NT FIRE DAMAGE
NT IMPACT DAMAGE
NT METEORITIC DAMAGE
NT PROTON DAMAGE
NT RADIATION DAMAGE
NT RAIN IMPACT DAMAGE

Aircraft and ground equipment damage during ground handling operations, discussing repair costs and out-of-service time

10 p1176 A73-24715

Survey of the civil responsibility for damages caused by aircraft noise in American and French law

19 p2506 A73-37998

DAMPING

NT ELASTIC DAMPING
NT LANDAU DAMPING
NT VIBRATION DAMPING
NT VISCOUS DAMPING

Review of nozzle damping in solid rocket instabilities.

[AIAA PAPER 72-1050] 03 p0353 A73-13381
Damping perturbation of high order nonlinear autonomous Liapunov system, reducing system equations integration to quadratures via transformation to lower order quasi-linear nonautonomous system

03 p0344 A73-14054

Plasma ion and electron modes nonlinear damping, presenting solution for Vlasov-Poisson system

04 p0480 A73-15195

Dislocation interstitial impurities interactions in high purity Mo, using dislocation damping techniques

04 p0462 A73-15304

On the damping of high-frequency motions in four-dimensional assimilation of meteorological data.

05 p0592 A73-16199

The damping of the NaD lines in the solar spectrum by atomic hydrogen.

06 p0753 A73-18239

Stability of incompletely damped mechanical systems

08 p1014 A73-20780

Treatment of dynamic snap-through problems by the direct Liapunov method

08 p1018 A73-21410

Three-dimensional theory of elastic stability in the presence of finite subcritical strains

10 p1290 A73-24302

Application of the complementary energy method to two non-conservative problems of elastic stability.

10 p1291 A73-24393

Cavity-backed panel resonance.

13 p1690 A73-28062

On some natures of the excitation and damping of the polar motion.

13 p1680 A73-28406

Ion-acoustic turbulence as MHD wave damping mechanism in weakly turbulent magnetosheath plasma at high and low frequencies

15 p1919 A73-31893

Damping of gravity stabilized satellite small rotary oscillations in circular orbit via stepwise change of moment of inertia

16 p2072 A73-33232

Altitude damping of space-stable inertial navigation systems.

16 p2034 A73-33403

Self excited whirl stability limits and frequencies of continuous rotors under gyroscopic, damping and hydrodynamic bearing film forces

16 p2022 A73-34035

Resonance damping of oscillations in a model of a spherical stellar cluster

17 p2226 A73-34367

High-frequency oscillation passage through a circuit with modulated damping

17 p2144 A73-34589

Reduction of helicopter control system loads with fixed system damping. [AHS PREPRINT 733]

17 p2105 A73-35069

Spinning HEOS-A2 satellite active deconing with pulse sequence from attitude reorientation system, discussing optimal control pulse number and timing

18 p2361 A73-36957

Material damping - An introductory review of mathematical models, measures and experimental techniques.

19 p2500 A73-38105

On the aerodynamic damping moment in pitch of a rigid helicopter rotor in hovering. I - Experimental phase.

19 p2387 A73-38281

Accurate approximate solutions to oscillatory problems with perturbing singular damping.

19 p2461 A73-38490

Column instability under nonconservative forces, with internal and external damping - Finite element using adjoint variational principles.

20 p2621 A73-39540

On the aerodynamic damping moment in pitch of a rigid helicopter rotor in hovering. II - Analytical phase.

21 p2631 A73-40087

Precession damping of solar probes by radiative forces.

21 p2737 A73-40767

The damping of electromagnetic waves in smooth, superconductive waveguides.

24 p3068 A73-44945

DAMPING FACTOR

U DAMPING

DAMPING IN PITCH

U DAMPING

U PITCH [INCLINATION]

DAMPING IN ROLL

U DAMPING

DAMPING IN YAW

U DAMPING

U YAW

DAMPING TESTS

Influence of temperature on the damping characteristics of heat resistant EP452 and EI696 steels in a uniform stress-strain state produced by tension and compression

10 p1233 A73-24358

Damping properties of soft viscoelastic materials for certain plane stress combinations

12 p1515 A73-27176

DAMPNESS

U MOISTURE CONTENT

DANGER

U HAZARDS

DARK ADAPTATION

Asymmetries related to cerebral dominance in returning the eyes to specified target positions in the dark.

03 p0261 A73-13760

Reduced illumination effects on visual acuity, color vision, dark adaptation, accommodation, visual fields and glare

05 p0540 A73-16480

Intrinsic light brightness and intensity estimation tests for foveal and peripheral retina under photopic and scotopic stimuli

07 p0783 A73-20257

Photochemical receptor mechanism of chromatic vision and scotopic contrast hue sensation due to cone and rod activity interaction

07 p0783 A73-20261

Duplex vision theory of photoreceptor/rods and cones/light and dark adaptation, discussing rhodopsin regeneration, bleaching and desensitization mechanisms

09 p1043 A73-23317

Frog retinal metabolism in photoreceptors during dark and light adaptation, using ERG, radiopneumetry, oxygen uptake polarography and pyridine spectrophotometric assay

09 p1044 A73-23319

Electroretinogram recovery cycle during light adaptation and after dark adaptation

10 p1181 A73-24518

Single unit and evoked potential responses in cat optic tract to paired light flashes.

11 p1317 A73-25647

Effects of prolonged dark adaptation on autokinetic movement.

11 p1324 A73-26322

Scotopic visibility curve in man obtained by the VER.

13 p1575 A73-28356

Scotopic electroretinography and visual evoked responses under adaptive illumination, comparing blind spot stray light with parafoveal stimulation

13 p1575 A73-28361

Accuracy of saccadic eye movements and maintenance of eccentric eye positions in the dark.

14 p1716 A73-30390

Eigenvectors of the sensitivity variations across the human central fovea.

22 p2810 A73-42957

Recovery of cone receptor activity in the frog's isolated retina.

22 p2810 A73-42962

Frog red rod dark adaptation from recorded receptor potentials of isolated retina, examining permanent sensitivity loss due to pigment bleaching

22 p2810 A73-42963

Eye function and the illumination of instrument dials in aircraft

22 p2817 A73-43133

DARKENING

NT LIMB DARKENING

DARKNESS

Involuntary eye movements in the presence and absence of points

18 p2276 A73-36568

DART TURBOPROP ENGINES

U TURBOPROP ENGINES

DATA ACQUISITION

Application of random time and frequency multiplexing to a data collection satellite.

01 p0018 A73-11182

Measuring equipment for multipoint data acquisition and recording, noting modular design of party-line system with programmed data processing

01 p0054 A73-11398

Preparation of information for programming machining operations during grinding of a blade profile by the continuous-shaping method

02 p0172 A73-11799

Lunar laser ranging system for experimental data acquisition, discussing preliminary design, SNR, photodetection method and data processing

02 p0141 A73-12245

Data acquisition, processing and retrieval in information system for product design and development, noting storage system for spring material data

03 p0400 A73-13238

Spacecraft techniques for lunar research.

04 p0448 A73-15182

The growing role of standards in the national and international coordination of space programs.

04 p0524 A73-15381

Acquisition time evaluation at different input SNR values for pseudonoise signal demodulation, noting common bandwidth detection system advantage

04 p0421 A73-15427

Moored radio telemetering buoy relay stations for North Pacific climatological data acquisition, noting optimum channel frequency for data transmission error rate reduction

04 p0421 A73-15429

Information management system breadboard data acquisition and control system.

04 p0425 A73-15461

Prototype data processing system design for automatic correlation of earth resources image data collected from remote sensors and gyrating vehicle platforms

04 p0426 A73-15776

Satellite-borne solid state multispectral image remote sensors with photodiode linear arrays for data acquisition, noting system performance and reliability advantages

04 p0451 A73-15781

French telemetry processing center, discussing data acquisition and reduction systems and application software

05 p0552 A73-17299

Space shuttle flight operations ground support systems for trajectory control and systems/mission management, discussing payloads data acquisition and transmission to user

06 p0755 A73-17620

Picture information acquisition, storage and transmission characteristics of film and vidicon systems for photographic reconnaissance of planets

06 p0750 A73-18010

Meteorological satellites data acquisition, storage, reproduction, recall, use and costs

06 p0664 A73-18023

Telemetry data acquisition, transmission lines and delayed time processings onboard spacecraft and at ground receiving stations and center, discussing multiplexing and computer control

07 p0795 A73-18953

European space operations control center subsystems for PCM telemetry data acquisition and processing

07 p0790 A73-18973

Acquisition and processing system of vibration measurements
07 p0807 A73-19001

National Congress on Reliability, Perros-Guirec, Cotes-du-Nord, France, September 20-22, 1972, Text of the Lectures
07 p0799 A73-19401

Acquisition and utilization of data of exploitation of equipment in the particular case of exposure to different environments
07 p0830 A73-19402

Economical system design for remote data acquisition.
07 p0824 A73-19948

Balloon-borne telescope-UV spectrometer for stellar spectrophotometric measurement with high spectral resolution, discussing system design and operation, image motion compensation and data acquisition
08 p0971 A73-21751

Airborne photogrammetric system with mapping and geodetic surveying data acquisition capability, discussing inertial navigation subsystem, terrain profile recorder and electronic distance measuring equipment
09 p1081 A73-22380

Automated vibration shaker calibration data acquisition and analysis system with minicomputer for working transfer standard voltage monitoring and acceleration level determination
09 p1070 A73-22508

Missile and spacecraft radio telemetry data acquisition site polarization diversity signal combiner transient response requirements, comparing bench test with flight test data
09 p1057 A73-23414

Predicting network for artificial satellite tracking data acquisition and preprocessing and orbit parameters computation
10 p1187 A73-23622

The Coude spectrum scanner at the Lowell Observatory.
11 p1360 A73-25069

Methodologies for the analysis of transport requirements with particular regard to the aeronautic case
12 p1561 A73-27070

Data aided phase locked loops for phase estimation improvement in coherent demodulator to obtain loop acquisition characteristics design flexibility
12 p1483 A73-27157

Data acquisition process to plan and engineer air traffic system, considering design aspects and piecemeal evolution
12 p1522 A73-27362

Radio astronomy telescope all sky survey procedure and data acquisition systems development for use with parametric amplifiers
12 p1544 A73-27781

Project VEMNO - North Sea-Baltic measuring network.
13 p1608 A73-28787

Real time microwave hologram data acquisition by double circular scanning of single sensor over recording aperture, presenting optical bench simulation
13 p1618 A73-29122

Four dimensional forecast assimilation of temperature data from Nimbus 4 SIRS radiance measurements, using two level model with geostrophic wind adjustment
15 p1902 A73-31314

Equatorial electrojet characteristics observation during 1967-1970 with POGO satellite-borne magnetometers, noting anomaly characterized by sharp negative V-signature in width and variable amplitude
15 p1870 A73-31768

Remote sensing in a circulatory survey of Boston Harbor.
16 p2003 A73-33356

A performance data acquisition and analysis system for turbine engine component testing.
17 p2146 A73-34610

The use of remote sensing for the detection of natural resources - Definition of the platforms, technical-organizational considerations
17 p2160 A73-34930

Earth resources monitoring from satellites, aircraft and ground stations for fast data acquisition and management
17 p2161 A73-34934

Participation of the Air Force Weather Service in the Fole experiment
17 p2206 A73-34940

Station Data Acquisition and Control System.
17 p2147 A73-35301

Remote control of planetary surface vehicles.
17 p2148 A73-35316

Data acquisition technique for Fabry-Perot spectroscopy, noting application to Brillouin spectra recording of solid Ne
17 p2171 A73-35403

Sabreliner Airborne Data Acquisition and Recording System /ADARS/ for communication with flight observers to evaluate research missions
17 p2174 A73-35582

Measurement of the radiation patterns of full-scale HF and VHF antennas.
17 p2128 A73-35689

The evolution of location and data collection systems in the United States.
[AIAA PAPER 73-584] 18 p2372 A73-36076

United States en route air traffic control systems.
19 p2451 A73-37810

A comparative evaluation of the application of several aircraft parameter identification methods to flight data - with emphasis on the development of rational evaluation criteria.
19 p2386 A73-38044

Data collection platforms, ground receiving and processing equipment for environmental study and management
[AAS PAPER 73-122] 20 p2520 A73-38583

GOES system data collection performance estimates.
20 p2525 A73-38743

Radiometric terrain mapping at 3 mm wavelength.
20 p2568 A73-39870

Remotely sensed multispectral scanner data collection over agricultural area, discussing spatial resolution modification for crops and unresolved objects classification
20 p2559 A73-39882

Multispectral scannery imagery in aerial photography of plant communities, discussing reflectance effects, digital processing, vegetation types, classification errors and spectrum analysis
20 p2561 A73-39901

Integration of remote sensing data into spatial information systems, discussing data specification, acquisition, storage, retrieval, processing, etc
21 p2658 A73-40820

Satellite techniques for automatic platforms location and data relay.
21 p2737 A73-41335

Pioneers 8 and 9 cosmic dust data reliability, presenting sensor geometry, field of view, response function, instrument control and sensitivity
21 p2775 A73-41411

ERTS-1 satellite-borne TV cameras and multispectral band scanners for remote sensing and data collection with applications in agriculture, forestry, and water resources survey
21 p2692 A73-41521

Simulator performance validation and improvement through recorded data.
[AIAA PAPER 73-938] 22 p2838 A73-41972

Mathematical model of spacecraft onboard digital guidance computer under data acquisition conditions, using imbedded Markov chains
23 p2955 A73-43261

National Center for Atmospheric Research collected synoptic meteorological data from earth surface, upper air and satellite observations for handling on computers
24 p3075 A73-45087

DATA ADAPTIVE EVALUATOR/MONITOR
U DATA PROCESSING
U DATA REDUCTION
U DATA TRANSMISSION

DATA ANALYSIS
U DATA PROCESSING
U DATA REDUCTION

DATA BASES
Image analysis techniques associated with automatic data base generation.
[AIAA PAPER 73-430] 12 p1499 A73-27823

VIEW - A distributed system for graphical analysis of large data bases.
[AIAA PAPER 73-431] 12 p1476 A73-27824

Computer data base use by industrial management for product design, development, manufacturing, testing and documentation coordination to achieve system communication and control improvement
17 p2257 A73-35215

Design concepts for an earth resources data management system.
[AAS PAPER 73-151] 20 p2521 A73-38597

DATA COLLECTION PLATFORMS
The evolution of location and data collection systems in the United States.
[AIAA PAPER 73-584] 18 p2372 A73-36076

DATA COMPRESSORS
U DATA REDUCTION
U DATA TRANSMISSION

DATA CONTROL SYSTEMS
U DATA SYSTEMS

DATA CONVERSION ROUTINES
NT SUBROUTINES

DATA CONVERTERS
NT ANALOG TO DIGITAL CONVERTERS
NT DIGITAL TO ANALOG CONVERTERS
A five-channel time-scale converter
09 p1064 A73-23007

Automatic measurement recorders with discrete output
13 p1617 A73-28858

A digital measurement converter of pulsed flows
13 p1591 A73-28872

Russian book on digital computer construction and operation covering data processing and conversion algorithms, memory, arithmetic and control devices, microprogramming, etc
13 p1588 A73-28948

Construction principles of a controlled universal functional converter for a hybrid computer
15 p1848 A73-31805

Akademiia Nauk SSSR, Astronomicheskii Sovet, Meeting of the Commission on Astronomical Instrument Engineering, Sverdlovsk, USSR, July 1-3, 1970, Proceedings
15 p1877 A73-32128

Angle to digital photoelectric converter for azimuthal telescope, discussing accuracy and temperature effects
15 p1877 A73-32132

A rotation angle-to-digital code photoelectric converter
15 p1877 A73-32133

A three-channel reversible data converter and its possible applications in astronomy
15 p1878 A73-32146

Design of a controlled general-purpose functional converter for a hybrid computer system.
24 p3071 A73-45349

DATA CORRELATION
NT SIGNAL ANALYSIS
Solar activity and the variations of the geomagnetic K sub p-index. I.
03 p0378 A73-14422

Accuracy of potential coefficients obtained from present and future gravity data.
04 p0438 A73-14796

Analytical correlation technique for air breathing and rocket engines combustor design and performance prediction based on hydrogen oxygen engines test data [AIAA PAPER 72-1074] 04 p0486 A73-14904

Prototype data processing system design for automatic correlation of earth resources image data collected from remote sensors and gyrating vehicle platforms
04 p0426 A73-15776

Turbulent space-time correlation measurements in a plane two-stream mixing layer at velocity ratio 0.3.
[AIAA PAPER 73-225] 05 p0566 A73-16951

Optimal correlation of sensor data with tracks in surveillance systems.
06 p0682 A73-18822

Search for 3C 191 ionization potential-red shift correlations to other quasar absorption lines
07 p0900 A73-20237

The challenge to unify treatment of high-temperature fatigue - A partisan proposal based on strainrange partitioning.
07 p0917 A73-20461

The estimation of order and parameters in a process of stochastic differential equations with uncertain observations.
07 p0846 A73-20594

Suggested interpretation of the correlations in intensity fluctuations in the lines Ca II H and K, magnesium b, and hydrogen H beta /Research note/
10 p1278 A73-24132

Flight test correlation technique for turbulent base heat transfer with low ablation.
11 p1453 A73-26671

Correlation of 'satellite estimates' of the equatorial electrojet intensity with ground observations at Addis Ababa.
15 p1870 A73-31771

An example of anticorrelation of auroral particles and electric fields.
18 p2312 A73-36297

Subsonic jet noise measurements on model jet rig in anechoic chamber, discussing correlation and prediction
19 p2473 A73-38106

Differences in the correlations of 27-day and 11-year cosmic ray variations with solar activity parameters
21 p2758 A73-40598

DATA HANDLING SYSTEMS
U DATA SYSTEMS

DATA LINKS
Two X-ray bursts /1 August 1967 and 30 January 1968/ and some associated VLF disturbances.
01 p0091 A73-10556

Experimental validation and design refinement program for air-ground-air data link based on automatic time division multiplex transmission of air traffic messages
02 p0190 A73-11852

Command and control for a missile air defense system. I - SAM-D communications.
04 p0417 A73-15377

TDM link with digitized voice channel and PCM telemetry sequence coding for error correction, comparing tested performance with prediction and computer simulation
04 p0419 A73-15401

Spin and three-axis stabilized geosynchronous tracking and data relay satellite system for telecommunication service to user spacecraft in low earth orbit
04 p0420 A73-15422

Digital link for bidirectional communication between manned spacecraft and ground terminal by synchronous communication relay satellite, noting coding parameters effects on error rate

04 p0421 A73-15426

Radio set design requirements for communication link between meteorological sensor platforms and spacecraft in Geostationary Operational Environmental Satellite System

04 p0421 A73-15432

Data link control procedures for error-free transmission channels, discussing serialization and synchronization techniques and reverse interrupt facilities in sequential machine model

05 p0551 A73-16802

Missile guidance and control systems optical linking, using fiber optics and light emitting diodes and photodetectors as optical/electrical transducers

06 p0757 A73-18324

French Guiana space center facilities for missile tracking, telemetry, data processing and transmission of command instructions, discussing PCM, PAM and PDM links equipment

07 p0807 A73-18942

Optical communications links with EDM digital data channels, examining signal optimal reception and noise stability

09 p1048 A73-22043

Decimicrometer band laser operated communication system to link earth observation satellites with geosynchronous satellites, discussing key technologies

09 p1055 A73-23393

A telecommunications link model for deep space - With applications to the HELIOS probe.

09 p1058 A73-23419

Error probability in an atmospheric twin-channel optical link.

10 p1190 A73-24628

Microelectronics developments and limitations, considering bipolar IC, metal-dielectric-semiconductor structures and optoelectronic communication links

12 p1480 A73-27267

ATC concepts and air/ground data link requirements for U.S. airspace structure in 1980s to support anticipated Los Angeles basin traffic densities in 1995

14 p1772 A73-29879

U.S. civil and military air-ground communications development history and expectations, considering information exchange, radar beacon transponders, digital communication and data links

14 p1725 A73-29880

The role of the airborne traffic situation display in future ATC systems.

14 p1773 A73-29897

Radio telemetry for strain measurements in turbines.

14 p1752 A73-30064

Payload/launcher radio compatibility, discussing RF link parameters choice, terminal devices quality and test schedule

14 p1742 A73-30113

Statistical computation of compatibility of tropospheric and satellite communication lines.

15 p1842 A73-30986

Spectral-energy dispersal in digital communication-satellite systems.

15 p1842 A73-31096

Output signal-to-noise ratio for a random-access repeater link with an ideal hard limiter.

15 p1844 A73-31733

Aircraft onboard data link and Aerosat equipment integration, considering antenna, duplexer, amplifier and receiver systems

15 p1846 A73-32428

Rain-attenuation measurements of millimetre waves over short paths.

15 p1848 A73-32647

Atmospheric refractivity effects on maximum antenna gain and correlation coefficient in design of microwave line of sight links for high reliability

16 p1981 A73-33704

The characteristics of millimeter wavelength satellite-to-ground space diversity links.

16 p1981 A73-33707

Automated discrete address radar beacon system and data link for ATC, describing simultaneous message decoding capacity, system specifications and implementation prognosis

17 p2208 A73-34612

Problems related to the operation of an air-ground data-link system

18 p2289 A73-36686

Recursive ideal observer detection of known M-ary signals in multiplicative and additive Gaussian noise.

19 p2407 A73-38385

Diversity combining of UHF signals under rapid fading conditions.

20 p2523 A73-38724

DCS - A global satellite environmental data collection system.

20 p2525 A73-38744

Airborne digital data link terminal for commercial airlines' use.

20 p2526 A73-38756

The universal data link system for air/ground communications.

20 p2526 A73-38757

The ARINC plan for implementing air/ground DATALINK.

20 p2527 A73-38758

ASTRO-DABS communication system with hybrid satellite and terrestrial discrete address beacon system for accurate aerial surveillance and navigation with reliable data link

20 p2527 A73-38759

The utility of data link to military aircraft communication - An operational view.

20 p2527 A73-38760

Variable data rate multimode quadriphase modem for PSK or QPSK operation in digital communication links, noting optimum overall system performance

20 p2527 A73-38764

Transmission strategy and optimal block size in high-speed data communication.

20 p2530 A73-39128

Binary error estimation in real time for channel quality monitoring, comparing upper and lower bounds with number of errors for bit sequence

21 p2656 A73-41170

Satellite techniques for automatic platforms location and data relay.

21 p2737 A73-41335

An evaluation of experimental errors in electromagnetic wave measurements aboard satellites.

22 p2844 A73-41911

Interconnecting computer network theory and system types, discussing data coordination and transformation, host computer links with system participants and network applications

23 p2957 A73-44389

DATA MANAGEMENT

Computer application for management of Skylab launch operations.

[AIAA PAPER 72-1083] 04 p0424 A73-14905

The Mariner Venus Mercury flight data subsystem.

04 p0425 A73-15423

Applications technology satellite data handling processing and interpretation for future earth survey, communications and meteorological satellite operational programs

08 p1014 A73-21593

Shuttle Orbiter fuel cell power system simulation, describing data management, programming and computational control

09 p1060 A73-22804

Management of a magnetic tape dubbing and evaluation station.

09 p1087 A73-23408

Principles of spacecraft telemetry data management.

11 p1333 A73-25351

Message organisation in the ground segment of an aeronautical satellite system.

12 p1472 A73-27668

Applications of vector and parallel computers to radar defense systems.

[AIAA PAPER 73-428] 12 p1476 A73-27822

A real-time simulator for image data systems.

17 p2147 A73-34903

Computer data base use by industrial management for product design, development, manufacturing, testing and documentation coordination to achieve system communication and control improvement

17 p2257 A73-35215

Station Data Acquisition and Control System.

17 p2147 A73-35301

Spacecraft systems design trade-offs for the Earth Resources Technology Satellite.

17 p2239 A73-35631

Environmental data - From sensors to users.

[AAS PAPER 73-138] 20 p2521 A73-38592

Design concepts for an earth resources data management system.

[AAS PAPER 73-151] 20 p2521 A73-38597

Remote sensing data management from a user's viewpoint.

[AAS PAPER 73-152] 20 p2521 A73-38598

Optimal utilization of redundant information in thermal radiation in thermophysical measurements.

[ECTP PAPER II-2] 22 p2931 A73-42408

National Center for Atmospheric Research collected synoptic meteorological data from earth surface, upper air and satellite observations for handling on computers

24 p3075 A73-45087

Research Aviation Facility collected aircraft data processing, merging and enhancement problems, software development and future resource requirements

24 p3070 A73-45088

DATA PROCESSING

NT BATCH PROCESSING

NT CENSORED DATA [MATHEMATICS]

NT CENTRAL ELECTRONIC MANAGEMENT

SYSTEM

NT DATA CORRELATION

NT DATA REDUCTION

NT DATA RETRIEVAL

NT DATA SMOOTHING

NT DATA STORAGE

NT KARHUNEN-LOEVE EXPANSION

NT MULTIPROCESSING [COMPUTERS]

NT OPTICAL DATA PROCESSING

NT PARALLEL PROCESSING [COMPUTERS]

NT SIGNAL ANALYSIS

NT SIGNAL PROCESSING

NT VOICE DATA PROCESSING

Multiband and multimultimultidigitized aerial photographs automatic processing by digital computer techniques and statistical pattern recognition algorithms

01 p0044 A73-10140

Automated system of storing and processing vector-cardiograms

01 p0012 A73-10660

Complex processing of discrete biological information

01 p0012 A73-10662

Application of the algorithm of a median for accuracy and reliability improvement in data processing

01 p0020 A73-10678

Measuring equipment for multipoint data acquisition and recording, noting modular design of party-line system with programmed data processing

01 p0054 A73-11398

Information processing 71; Proceedings of the Congress, Ljubljana, Yugoslavia, August 23-28, 1971. Volume 1 - Foundation and Systems. Volume 2 Applications.

01 p0020 A73-11451

Data processing for radioastronomy and cosmic ray air shower arrays.

01 p0020 A73-11455

Symbol ring as alphabetic element in information processing technique, defining address substitution operation

02 p0143 A73-11642

The onboard data processing system of the Helios probe

[DGLR PAPER 72-092] 02 p0228 A73-11700

Data acquisition, processing and retrieval in information system for product design and development, noting storage system for spring material data

03 p0400 A73-13238

Theoretical foundations of the development of a system of automated information processing for the problems of manufacturing-process design in the metalworking industry

03 p0400 A73-13240

Recording and data processing equipment proposed for scintillation measurements.

03 p0308 A73-13646

Decoding of thermoelement data for a flow with velocity, pressure, and temperature pulsations

03 p0308 A73-13667

Method for quantitative estimation of the functional state of the motor apparatus

03 p0268 A73-13822

Aircraft reference altitude computation from air data inputs, deriving algorithm for pressure gradient errors correction

03 p0308 A73-13915

Procedure for automatic statistical processing of experimental data in determining the rated current-voltage characteristic of TD-320 thyristors

03 p0285 A73-14325

Parametric and nonparametric classification techniques for pattern recognition in remote sensed data processing, noting crop identification

03 p0281 A73-14485

Automated procedures for mapping and display of digitized radar data.

03 p0281 A73-14522

Project Cloud Catcher weather radar data system revisions in radar set, echo pulse integrator, data logging and analysis and graphic displays

03 p0289 A73-14523

Data processing method for optimal prediction of spacecraft orbital elements, using dynamic and quadratic programming

03 p0379 A73-14555

Western Electronic Show and Convention, Los Angeles, Calif., September 19-22, 1972, Proceedings.

04 p0426 A73-14728

Problems of the synthesis of spacecraft onboard data computation units

05 p0553 A73-16417

Aircraft flight plan data processing in FORTRAN program to predict altitude and time conflicts, noting short CPU time

05 p0595 A73-16618

Computerized airlines reservations systems with real time conversational interactive characteristics, discussing initial design, simulation, measurement, stability, reliability and data processing techniques

05 p0551 A73-16806

Mathematical model for information search and retrieval under Poisson process requests, discussing data processing time minimization sorting algorithms

06 p0670 A73-17856

The use of model building in a production environment.

06 p0698 A73-18514

French Guiana space center facilities for missile tracking, telemetry, data processing and transmission

of command instructions, discussing PCM, PAM and PDM links equipment

07 p0807 A73-18942

Satellite data concentration, memorization, transmission and processing, discussing central computer control unit, ground stations peripheral links, magnetic tapes and system reliability

07 p0795 A73-18952

Telemetry data acquisition, transmission lines and delayed time processings onboard spacecraft and at ground receiving stations and center, discussing multiplexing and computer control

07 p0795 A73-18953

Third generation satellite PCM telemetry data processing with computer control for optimization and supervision, discussing system reliability, automatic control and diagnostic routine

07 p0795 A73-18954

Reliable, high performance magnetic tape recorder/reproducer for third generation telemetry data computer processing lines, noting human error possibility reduction

07 p0795 A73-18955

Computer for automatic equipment monitoring, operation control and breakdown diagnosis in telemetry data processing, discussing management routines and reliability

07 p0795 A73-18956

Circuit diagrams, electronic modules and design of PCM telemetry encoder for Eole satellite, noting data multiplexing and processing

07 p0789 A73-18957

European space operations control center subsystems for PCM telemetry data acquisition and processing

07 p0790 A73-18973

Prospero satellite orbital/operational performance and control, describing ground-satellite telemetry and data processing operations

07 p0905 A73-19142

Collection and processing of data for the establishment of route charges.

07 p0796 A73-19182

Applications technology satellite data handling processing and interpretation for future earth survey, communications and meteorological satellite operational programs

08 p1014 A73-21593

Simultaneous motor and verbal processing of visual information in a modified Stroop test.

09 p1044 A73-21896

Possibilities of optimal processing of capacitance fuel meter data

09 p1083 A73-22652

Eole project data processing organization and operations management, describing information acquisition and reduction

09 p1060 A73-23377

Contributions to the design of future on-board data processing systems for scientific space-craft experiments.

09 p1061 A73-23379

D-2A /Tournesol/ satellite data processing procedures for technological controls, operation in flight and scientific purposes

10 p1187 A73-23620

Predicting network for artificial satellite tracking data acquisition and preprocessing and orbit parameters computation

10 p1187 A73-23622

D-2A satellite experiments for sky mapping and radiation intensity measurement, discussing attitude correction processing

10 p1285 A73-23623

Data processing technique and calculation procedure for cosmic rays hard particle and neutron components coupling coefficients

10 p1268 A73-23932

Function generation technique based on variables stochastic representation and clocked random pulses in data processing operations, noting application to closed loop control systems

10 p1242 A73-24016

Fast and reliable automatic digital control components and transducers for data processing, display and storage, assessing technology development trends and preference over analog devices

10 p1199 A73-24028

Application of a digital computer in the processing and presentation of tensile test results.

10 p1192 A73-24569

Smithsonian Package for Algebraic and Symbolic Manipulation /SPASM/ computer program with generality and efficiency for Poisson series processing in celestial mechanics

10 p1283 A73-24667

Hybrid computer systems of high speed and accuracy

10 p1192 A73-24674

A BESM-3M computer program for processing photographic observations of extended objects

11 p1333 A73-25231

Personnel radiation protection technology and criteria review, discussing dosimeter specifications and automatic data processing

11 p1322 A73-25314

Principles of spacecraft telemetry data management.

11 p1333 A73-25351

Dynamics of changes in neuron activity regimes of the ascending auditory pathways

11 p1317 A73-26079

Forced guidance and distribution of practice in sequential information processing.

11 p1323 A73-26319

Optimum processor accuracy for radar altimetry for geodesy over sea, considering surface reflectivity, height variation additive noise and pointing errors

11 p1371 A73-26631

Pneumosomatic data transmission and processing based on pressurized gases and dynamic body interactions

12 p1460 A73-26771

Method of utilizing structural redundancy in a measuring system for processing experimental data with systematic errors

12 p1494 A73-26776

Devices for primary processing of information in controller machines, based on the principles of quantum magnetometry

12 p1495 A73-26778

Spatial-temporal analysis of asynchronous meteorological data

12 p1521 A73-27743

Redundant central processor system for fault tolerant real time operation in space applications, describing systems organization

[AIAA PAPER 73-424]

12 p1476 A73-27821

Side-looking pulse Doppler radar data presuming prior to correlation to obtain desired resolution performance with minimal digital storage

13 p1585 A73-29203

Book - Introduction to defense radar systems engineering.

13 p1587 A73-29677

The data processing architecture on the launch bases of the Directorate of Research and Test Methods

14 p1742 A73-30091

German ground operations network design, describing data system and flow with automatic handling of telemetry data, tracking data and operational information

14 p1727 A73-30098

Group data handling theorems on uniqueness of mathematical model for regression curve reconstruction in polynomial domain with small number of points

14 p1738 A73-30288

Experimental data processing system for EUROCONTROL scale model semiautomatic digital route control system for operational conditions simulation

15 p1907 A73-31132

A basis for four-dimensional /continuous/ processing of meteorological observation data, using a dynamic statistical approach

15 p1904 A73-31608

Decentralized coalition control in data processing systems

15 p1848 A73-31804

A punched tape recorder for observation data

15 p1878 A73-32142

Central digital measuring and data logging systems for electrical and nonelectrical analog signal conversion, display and recording

15 p1849 A73-32204

Bringing data processing to projects and tests of large antennas

15 p1846 A73-32430

Use of associative processors for radar data processing in air traffic control systems.

15 p1849 A73-32434

ATC radar information processing systems optimization, discussing hard- and software selection criteria

15 p1847 A73-32440

Functioning in multiprocessing of two 10020 computers at the Bretigny Eurocontrol Experimental Center

15 p1847 A73-32442

ATC system with radar data processing, discussing hardware and software organization, programmed logic integration possibilities and functional flexibility

15 p1909 A73-32445

MADAP - Implementation of a large size real time data processing system.

15 p1849 A73-32448

Real time information processing automated systems for ATC, considering reliability based on redundancy

15 p1910 A73-32483

Application of the visualization of radar information in television

15 p1911 A73-32484

The London Air Traffic Control Centre radar data processing system.

15 p1911 A73-32485

French monograph on numerical data processing organs for real time process control, describing modular computer design project

15 p1849 A73-32590

Iterative method for the statistical processing of measurements with incomplete information on the measurement error characteristics.

15 p1902 A73-32605

Book - Techniques involving extreme environment, nondestructive techniques, computer methods in metals research, and data analysis. Part 1.

16 p2017 A73-32696

Space missile test center development for checkout, launch and data processing for space boosters, intermediate and intercontinental range ballistic missiles and supersonic aircraft

16 p1993 A73-33087

Experimental educational noise surveys of rural, suburban, urban and industrial areas at various times of day, using computerized data processing

16 p2036 A73-33216

Quality assurance for the data processing industry.

16 p1985 A73-33614

Data processing for earth resources survey including data handling, preprocessing for instrument errors, decision making and data bank

17 p2161 A73-34941

Mathematical functional modular building block implementation in LSI microelectronics for signal and data processing, discussing primitive functions and 8-bit family design example

17 p2138 A73-35229

Spatial information coding in the human visual system - Psychophysical data.

17 p2116 A73-35240

Expanded built-in-test for advanced electrical systems for aircraft.

17 p2109 A73-35248

Evolution of the satellite telemetry data processing facility at the Goddard Space Flight Center.

17 p2123 A73-35300

Optical data storage and data processing, and holography in aerospace and electronic instrumentation.

17 p2131 A73-35382

Factors affecting processing mode in visual search.

17 p2117 A73-35493

Stationary target identification with radar beam for comet nucleus within coma, noting echo spatial extent and Doppler bandwidth effects on data processing

17 p2174 A73-35634

Digital data acquisition and processing from a remote magnetic observatory.

17 p2175 A73-35667

Measurement of the radiation patterns of full-scale HF and VHF antennas.

17 p2128 A73-35689

Book on experimental analysis covering measurement systems, engineering problems, data analysis, electro-optics and dimensional parameters

17 p2176 A73-35855

Hydrometeorological data processing and dissemination techniques and equipment, with emphasis on computerized regional centers and space-based systems

18 p2295 A73-35907

Problems associated with automation of the checking and processing of meteorological and climatological data

18 p2332 A73-35916

Tromsø /Norway/ Auroral Observatory partial reflection experiment, considering data processing techniques, height resolution, phase detection, antenna arrays and D region drift measurements

18 p2315 A73-36009

Computerized flight test data processing, emphasizing speed in turnaround and data analysis efficiency

18 p2266 A73-36070

Computerized processing system with real time control, data analysis and display capabilities for space shuttle checkout, servicing, launching and landing to reduce cost

[AIAA PAPER 73-601]

18 p2295 A73-36083

The value of data processing in the analysis of visual evoked potentials

18 p2279 A73-36911

Calculation of the plan for the transportation performance with the aid of electronic data processing

19 p2506 A73-38121

Digital filter tasks and applications, discussing recursive and transversal filters, waveforms, SNR, truncation errors and complex filtering

19 p2414 A73-38301

NAS enroute automated flight and radar data processing, describing communication facilities, computer complex, software, data entry, display function and ATC personnel interface

19 p2453 A73-38464

Optimal filtering and smoothing simulation results for CIRIS inertial and precision ranging data.

[AIAA PAPER 73-872]

20 p2587 A73-38809

A method of processing a priori information about a controlled plant with the aim of reducing the number of changing parameters of the dynamic characteristics

20 p2541 A73-38993

Optimal statistical solution methods in recognition, data processing, and control problems
20 p2532 A73-38997

Development of a program basis for statistical data processing on an analog-digital complex
20 p2532 A73-39392

Canadian remote sensing programs for ERTS data, describing receiving stations, data acquisition and processing facilities and techniques, digital system and aerial photography
20 p2545 A73-39913

Integration of remote sensing data into spatial information systems, discussing data specification, acquisition, storage, retrieval, processing, etc
21 p2658 A73-40820

Interpretation of hot-wire anemometer readings in a flow with velocity, pressure and temperature fluctuations.
21 p2705 A73-41317

Computer processing of RF neutral-hydrogen line observations carried out with a fixed antenna
21 p2659 A73-41468

A fixed point calibration procedure for precision platinum resistance thermometers.
22 p2857 A73-42026

Tape recording, off-line digitalization and time series analysis of dynamic field measurement analog data for computerized power spectral density calculation
22 p2859 A73-42197

The MINFAP system - First phase in the automation of the EUROCONTROL Maastricht Centre.
22 p2884 A73-42323

Theory and design of pipelined fast Fourier transform processors.
23 p2956 A73-43325

National Radio Astronomy Observatory interferometer system with rotating head video tape recording and computerized sampled data processing equipment for use with radio telescope
23 p2980 A73-43358

Large-scale systems and operations management decentralized conditional control in data processing systems.
23 p2956 A73-44333

Research Aviation Facility collected aircraft data processing, merging and enhancement problems, software development and future resource requirements
24 p3070 A73-45088

DATA PROCESSING EQUIPMENT
NT AIRBORNE/SPACEBORNE COMPUTERS
NT ANALOG COMPUTERS
NT COMPUTERS
NT DATA PROCESSING TERMINALS
NT DIGITAL COMPUTERS
NT HYBRID COMPUTERS
NT IBM 1130 COMPUTER
NT MINICOMPUTERS
NT PARALLEL COMPUTERS
NT SEQUENTIAL COMPUTERS

A brief summary of the meteorological research flight digital magnetic-tape data-recording and data-processing system.
04 p0450 A73-15700

French telemetry processing center, discussing data acquisition and reduction systems and application software
05 p0552 A73-17299

French computation center equipment for satellite orbit calculations and attitude corrections, describing links between teleprocessing and data transmission
05 p0555 A73-17300

Acquisition and processing system of vibration measurements
07 p0807 A73-19001

A five-channel time-scale converter
09 p1064 A73-23007

Microprogrammable processors applied to telemetry processing systems.
09 p1057 A73-23411

Eole experiment processing network for data pretreatment, system management aid and accuracy study and feasibility demonstration of fast response time operational system
10 p1187 A73-23619

Intercoms 2 satellite design, construction, on-board scientific instrumentation, ionospheric experiments and data processing equipment
10 p1217 A73-23886

An advanced computer communication network.
[AIAA PAPER 73-1414]
12 p1474 A73-27820

System of recording based on partial on-board processing
15 p1880 A73-32494

Development of a data-processing installation for the automatic quality control of spot-welding joints
16 p2019 A73-33222

Hybrid techniques for automatic imagery interpretation.
16 p2016 A73-33367

Processing of aircraft data.
17 p2132 A73-35583

Intercoms 2 satellite design, construction, on-board scientific instrumentation, ionospheric experiments and data processing equipment
20 p2565 A73-38905

DATA PROCESSING TERMINALS
Single channel per carrier FCM FDMA demand assignment satellite communications system /SPADE/ for INTELSTAT, discussing hardware and software introduction at first terminal
04 p0420 A73-15414

Data processing remote terminals for real time on-line computer communication systems, discussing design, characteristics and applications
05 p0551 A73-16801

Computer communication networks with programmable concentrators for combining multiple terminals, discussing structure, message handling and transmission, routing and reliability
05 p0551 A73-16805

Digital computer graphic data feeder with electric pulsed-voltage coordinate matrix and readout probe sensor for input data code coordinate selection
12 p1475 A73-26779

Terminal pointer hand controller and other recent teleoperator controller concepts - Technology summary and application to earth orbital missions.
19 p2397 A73-37326

ASCII code applications to alphanumeric display terminals.
21 p2655 A73-40835

Interconnecting computer network theory and system types, discussing data coordination and transformation, host computer links with system participants and network applications
23 p2957 A73-44389

DATA PROCESSORS
U DATA PROCESSING EQUIPMENT
DATA READOUT SYSTEMS
U DATA SYSTEMS
U DISPLAY DEVICES

DATA RECORDERS
High resolution image data sensors and recorders characteristics and performance limits, describing transmission system
04 p0449 A73-15385

A high-speed automatic strip-chart recorder
12 p1497 A73-27220

Automatic measurement recorders with discrete output
13 p1617 A73-28858

Thunderstorm activity determination on lightning discharge number recorders
14 p1754 A73-30792

Problem of the legibility of records produced by strip chart recorders with curvilinear coordinate systems
14 p1754 A73-30875

Conference on Video and Data Recording, University of Birmingham, Birmingham, England, July 10-12, 1973, Proceedings.
19 p2431 A73-38195

A new automatic ozone recorder for near-surface measurements working at 19 stations on a meridional chain between Norway and South Africa.
23 p2982 A73-43863

DATA RECORDING
Measuring equipment for multipoint data acquisition and recording, noting modular design of party-line system with programmed data processing
01 p0054 A73-11398

The data-handling problem with television recording of spectra.
02 p0170 A73-12340

Recording and data processing equipment proposed for scintillation measurements.
03 p0308 A73-13646

Standard format for reporting electron content data using magnetic tape.
03 p0308 A73-13655

Automatic digital image processing for remote sensing with ERTS, Skylab and NASA survey aircraft, considering image registration, projective transformation and ground truth information
03 p0309 A73-14487

A brief summary of the meteorological research flight digital magnetic-tape data-recording and data-processing system.
04 p0450 A73-15700

Large ruby laser radar for remote detection and recording of atmospheric scattering data, describing tracking mount, optics, electronic signal processing and display features
04 p0433 A73-15768

High data rate holographic recorder with six-channel acousto-optical modulator array as input composer and mode locked Ar laser as light source
06 p0694 A73-18311

The influence of recording speed on apexographic timing - A multi-observer study of precision and performance utilizing randomized tracings in multiple subjects.
07 p0785 A73-19932

Vibration test facilities and control techniques for application to industrial products, discussing shakers,

signal generation and amplification, and data recording and reduction
07 p0809 A73-20575

Some characteristics of the ionospheric irregularities over the magnetic equator derived from spaced fading records.
08 p0957 A73-20656

Technique for measuring time-base errors of magnetic instrumentation recorders/reproducers.
08 p0965 A73-21084

Solar cosmic ray flare recording in stratosphere in Murmansk and Antarctic regions during February-April 1969
08 p1000 A73-21347

Ionospheric electron density profile observation by partial reflection experiment, discussing radio signal amplitude and phase data recording sensitivity requirement
09 p1075 A73-22071

Effect of flutter on theoretical bit error rates for digital recording systems.
09 p1087 A73-23369

Magnetic tape recorder parameters effect on PCM telemetry bit error rate, discussing contribution factors and test methods
09 p1087 A73-23370

Management of a magnetic tape dubbing and evaluation station.
09 p1087 A73-23408

Analysis of the quality of the cosmic ray data recorded by the neutron supermonitor at Krasnaia Pakhra
10 p1217 A73-23934

High speed cinetheodolite for missile tracking incorporating LED /light emitting diode/ system for metric data recording
10 p1222 A73-24950

Photochromic glass as reversible optical recording storage medium, discussing image resolution, configuration improvements, merits and applications in holography, random access memory and displays
11 p1370 A73-26537

Method of studying the fatigue damage of metals with automatic data processing on a computer
13 p1597 A73-29053

Tape recorder instrumentation for structural dynamic load test data analysis, discussing cable crosstalk, lead length and electrical noise effects in crack propagation measurements
14 p1751 A73-29775

An integrated random access memory with full-current recording and readout
14 p1730 A73-30290

Equatorial scintillation variation with magnetic storm from ATS 3 VHF telemetry signal recordings, comparing with spread F observation
15 p1870 A73-31763

A portable millisecond-integration-time photoelectric photometer.
17 p2165 A73-34273

Method of recording the deformation diagram in thermal-fatigue tests.
17 p2165 A73-34278

Sabreliner Airborne Data Acquisition and Recording System /ADARS/ for communication with flight observers to evaluate research missions
17 p2174 A73-35582

Processing of aircraft data.
17 p2132 A73-35583

Antenna radiation pattern recording as functions of two simultaneous parameters, considering measurement time savings
17 p2129 A73-35699

Method of investigating fatigue damage of metals with automatic information processing by computer.
18 p2297 A73-36885

ICAO meeting reports on international aircraft accident investigation, onboard data recording, inquiry process and low-safety interface
19 p2506 A73-37738

The equipment for photoelectric photometry in the Graz observatory
20 p2565 A73-39068

Tape recording, off-line digitalization and time series analysis of dynamic field measurement analog data for computerized power spectral density calculation
22 p2859 A73-42197

Geophysical field cartographic isoline recording via least generalized course representation of observation points, discussing analytic functions and least squares method
22 p2850 A73-42734

Optimization of exposure time in linear hologram recording by pre-exposure or post-exposure.
22 p2862 A73-43090

Radio astronomical problems due to pulsar radiation dispersal by frequency dependent propagation velocity in interstellar medium, discussing signal reception and data recording techniques
23 p2953 A73-43368

Chromatic photosensitization of a variable-index material for the recording of high-efficiency phase holograms
24 p3091 A73-45011

DATA REDUCTION

NT DATA SMOOTHING

Tropical atmosphere radiative heating estimates for BOMEX /Barbados Oceanographic and Meteorological Experiment/ from direct radiation measurements, satellite images and surface and rawinsonde data

01 p0038 A73-10387

Secondary electron conduction /SEC/ vidicon television system for space astronomy, discussing data reduction requirements, costs and quasar spectrum observation

01 p0048 A73-10530

Filters for solar corona polarization observations, deriving equations for arbitrary settings to obtain data reduction with simplified polarization direction calculation

02 p0170 A73-12370

Dollen data reduction method for meridian-observed FK 4 star pairs right ascension and time determination, calculating instrument, personal and catalog errors

03 p0371 A73-13219

A program for plate reduction in the case of satellite observations with a satellite observation camera

03 p0274 A73-13254

Matrix method for direct reduction of astronomical X ray spectral data, taking into account detector resolution and fluorescent escape phenomena effects

03 p0361 A73-13366

A comparison of total electron content determined by the differential Doppler and the Faraday effects using radio signals from a geostationary satellite.

03 p0300 A73-13637

Data analysis criteria and instrumentation requirements for the transient measurement of mechanical impedance.

03 p0343 A73-13837

Analysis of some aspects of 25 chromospheric events. I - Reduction of the optical data. II - Discussion on the optical data.

03 p0364 A73-14414

Storm cell models from digital radar data.

03 p0338 A73-14510

Radar measurement of the atmospheric turbulence structure function.

03 p0279 A73-14537

Computerized weather radar data central processor design, implementation and programs for data reduction and calibration

03 p0281 A73-14548

Results concerning the movement of the instantaneous pole of rotation of the earth, using the data published by R. Vicente and S. Yumi

03 p0304 A73-14580

Status of data reduction and analysis methods for the worldwide geometric satellite triangulation program.

04 p0437 A73-14780

An empirically derived lunar gravity field.

04 p0498 A73-15184

Ways for increasing the efficiency of data transmission systems.

04 p0420 A73-15421

Real time programmable data compression system with minicomputers for operation between TV data acquisition ground stations and ATS satellites

04 p0425 A73-15442

A study of simple chromatogram - Compression algorithm efficiency.

04 p0449 A73-15445

Information-loss and risk-increase estimation during observational data reduction in successive estimation problems

05 p0589 A73-16299

A Green Bank sky survey in search of radio sources at 1400 MHz. III - Positions and flux densities of the GB radio sources.

05 p0622 A73-17070

The use of a simulator in a synthetic aperture radar data processing tradeoff study.

05 p0554 A73-17149

Transinformation and real time identification applied to the study of pilot workload

05 p0545 A73-17195

Analysing vibration and shock data. II - Processing and presentation of results.

05 p0637 A73-17234

Methods and techniques in spectral analysis of random-vibration data

05 p0637 A73-17271

French telemetry processing center, discussing data acquisition and reduction systems and application software

05 p0552 A73-17299

Apollo 17 spacecraft telemetered IR scanner remote sensing data, reduction, discussing use of interpolating and smoothing splines for restored image resolution improvement

06 p0696 A73-18807

Welded structural components fatigue behavior representation by characteristic curves derived from S-N diagrams, describing data reduction procedure

07 p0910 A73-19216

Identification of large structures using data from ambient and low level excitations.

07 p0916 A73-20431

Analysis procedure of gamma ray astronomy spark chamber data.

07 p0828 A73-20644

Testing of the Apollo 15 Metric Camera System.

08 p0968 A73-21703

Camera orientation with peripheral image coordinates of oblique circles.

08 p0968 A73-21704

Fine verticality readout accuracy test on film format of each photograph obtained by prime camera, describing aerial photogrammetric data reduction methods

08 p0969 A73-21708

Lateral distribution of u.h.f. radio emission associated with cosmic ray showers.

09 p1137 A73-22174

Recursive methods in on-line computer photogrammetric data reduction deriving algorithms for fixed and variable parameter numbers cases with matrix partitioning

09 p1059 A73-22381

Error analysis for the Mariner-6 and -7 occultation experiments.

09 p1146 A73-22428

On the use of running means in the power spectrum analysis of ionospheric data.

09 p1078 A73-22831

Redundant area encoding for relieving integration time requirement in airborne reconnaissance photograph transmission, discussing algorithms, display technique, data reduction and pictorial simulation

09 p1034 A73-23386

A mobile tone range/RDF system for telemetry tracking of sounding rockets.

09 p1057 A73-23412

On-board registration and redundancy reduction method for quasi-stationary Poisson processes.

09 p1058 A73-23420

The preprocessing of French laser observations from the ISAGEX program

10 p1187 A73-23621

Higher-order numerical differentiation of experimental information.

10 p1244 A73-24719

A description of the NAE T-33 turbulence research aircraft, instrumentation and data analysis.

11 p1306 A73-26269

Additional evidence for the existence of a very high energy solar particle component.

11 p1413 A73-26473

Asteroidal spectral reflectivity measurement with data reduction for various curve types, noting correlations with UVB color, orbital and physical property parameters and albedo

11 p1429 A73-26686

The use of sampling quantiles for the compression of telemetric transmission and the statistical handling of medical information.

12 p1465 A73-27646

Spatial-temporal analysis of asynchronous meteorological data

12 p1521 A73-27743

RAPID - A system for online radar data reduction and performance analysis.

12 p1476 A73-27825

Fraunhofer line data reduction and wavelengths identification in solar UV spectra recorded during flight of Skylark rocket SL 601

12 p1544 A73-27827

Electronic image enhancement in remote sensing by information content reduction before computer read-in, discussing electronic image transformations

12 p1501 A73-27961

Speech data rate reduction. I - Applicability of modern estimation theory. II - Applicability of sensitivity and error analysis.

13 p1585 A73-29201

Some aspects of nonorthogonal data analysis. I - Developing prediction equations.

13 p1650 A73-29298

Coronal densities and temperatures derived from monochromatic images in the red and green lines.

13 p1685 A73-29364

The problem of elaboration and classification of observational material for one-apparition comets.

14 p1790 A73-29793

Periodic comet Tempel-Tuttle orbital elements relation to Leonid meteor shower, using computer program for numerical integration

14 p1791 A73-29807

Period determination method for variable stars using interpolation in light curves, noting applicability to light curves with few branches

15 p1936 A73-31645

Artificial satellites photographic observations reduction by Turner and colineation methods, considering IBM 360 FORTRAN program application

15 p1843 A73-31648

Satellite rotation period determination from visual photometric observations reduction, noting solar and geomagnetic activity effects

15 p1843 A73-31649

Polarization observations of variable stars and extragalactic objects. I - Instruments and methods of ob-

servation and data processing. II - Polarization of the EV Lac flare

16 p2057 A73-32708

Waveform vector analysis of orthogonal electrocardiograms - Quantification and data reduction.

16 p1975 A73-33115

Microcomputer programs for data reduction and quality control chart work, using Olivetti P-101, HP 9100-B and Wang 700-A calculators

16 p1986 A73-33642

Compression of weather charts by the segmented Lynch-Davison code.

16 p1983 A73-33744

Evaluation of astrophysical hypotheses.

17 p2231 A73-34760

Empirical formula suitability for analysis of ionosonde data on blanketing sporadic E, noting time variation effects of limiting frequency and layer intensities

17 p2159 A73-34776

X ray data refinement on proteins, discussing backbone and side chain dihedral angles adjustment by least squares fitting to relieve atomic overlaps

17 p2112 A73-34893

Application of data compression techniques to spacecraft imaging systems.

17 p2122 A73-34910

Some results obtained in ESRO satellite data compression.

17 p2239 A73-34955

Signal conditioning, separation and parameter measurement in modular digital Elint analysis system for airborne, shipboard or ground based reconnaissance applications

17 p2137 A73-35207

Application of the SIT vidicon to astronomical measurements.

17 p2169 A73-35285

Development of data analysis in sound and vibration.

17 p2131 A73-35335

Modeling, instrumentation and data evaluation in clinical electroretinography, discussing Fourier analysis of sinusoidal light stimulation response in normal and abnormal humans

17 p2117 A73-35359

Experimental force data reduction equations solved by iterative method for multicomponent force transducers used in load tests, discussing wind tunnel balances

17 p2148 A73-35437

Airborne flight-test strain gage instrumentation from installation, calibration and data recording and reduction standpoint, discussing ground and airborne minicomputer use

17 p2148 A73-35442

Book on experimental analysis covering measurement systems, engineering problems, data analysis, electro-optics and dimensional parameters

17 p2176 A73-35855

Validation of digital radar landmass simulation utilizing terrain elevation data compression.

18 p2292 A73-36842

Quantitative study of an aerodynamic flow by holographic interferometry

18 p2317 A73-37082

Laboratory for the automatic treatment of analog signals

18 p2297 A73-37086

8-13-micron spectra of NGC 7027, BD +30.3639 deg, and NGC 6572.

18 p2357 A73-37104

Data compression techniques as a means of reducing the storage requirements for satellite data - A quantitative comparison.

19 p2405 A73-38196

Application of some data compression systems to ESRO satellite data.

20 p2524 A73-38735

Data compression in recursive estimation with applications to navigation systems.

[AIAA PAPER 73-901]

20 p2589 A73-38835

Thermal conductivity measurement for particulate materials in vacuum, comparing line and differential-line source methods in terms of test and data reduction times

20 p2565 A73-38882

Role of gas-surface interactions in the reduction of Ogo 6 neutral particle mass spectrometer data.

20 p2551 A73-38941

Minor planets and related objects. XII - Radar observations of 11685 Toro.

20 p2607 A73-39122

International Symposium on Remote Sensing of Environment, 8th, University of Michigan, Ann Arbor, Mich., October 2-6, 1972, Proceedings. Volumes 1 & 2.

20 p2556 A73-39829

An experimental model for the automated detection, measurement, and quality control of low-level cloud motion vectors from geosynchronous satellite data.

20 p2533 A73-39853

Performance evaluation of multispectral scanner classification methods.

20 p2559 A73-39876

Multispectral scanner data analysis by application of spectral radiance signature extension techniques based on preprocessing to reduce atmospheric and scanner look angle effects

20 p2559 A73-39880

Geomagnetic variation terms neglect in Chapman-Miller method, noting Bartels-Johnston method comparison and possible consequences for lunar tides

21 p2684 A73-40780

Post GARP Global Experiment programs, considering tropical vertical wind structure, satellite temperature measurement accuracy increase, data handling for real time and long term prediction

21 p2732 A73-40819

Diurnal density variations measured by the San Marco III satellite in equatorial orbit.

21 p2685 A73-40830

Interactive processing of map data produced by the Westerbork supersynthesis radio telescope.

21 p2778 A73-41534

Simulator performance validation and improvement through recorded data.

[AIAA PAPER 73-938]

22 p2838 A73-41972

Line intensities of CO₂ in the 2.0 micron region.

22 p2890 A73-42708

Recursive methods in photogrammetric data reduction.

22 p2862 A73-42825

Data reduction for annual, diurnal and satellite observation aberrations via rectangular coordinate method, discussing parallax, refraction, instrument eccentricity and computer applications

22 p2915 A73-43034

Automated data reduction of holographic interferometry translational measurement of diffusely reflecting rigid body by reconstructed virtual image processing on CDC 6600 computer

22 p2863 A73-43147

FORTH computer program for National Radio Astronomy Observatory telescope observed millimeter wave spectral line data reduction, summarizing language capabilities

23 p2956 A73-43380

Multidimensional scaling methods and data visualization /Review/

23 p2949 A73-43578

Anisotropic composite material swelling coefficients and elastic compliances data averaging and reduction, using tensor transformation and associated scalar invariants

23 p3041 A73-43636

Count of radio sources at a frequency of 86 MHz. I - Method of processing observations in the radio source survey by the East-West arm of the DKR-1000

23 p3035 A73-44230

Analysis of hurricane data using the variational optimization approach with a dynamic constraint.

23 p3004 A73-44258

Clusters of galaxies with a wide range of X-ray luminosities.

24 p3139 A73-45055

Vela 3 proton data analysis for compressions and rarefactions effects on solar wind density, temperature and velocity behavior

24 p3125 A73-45106

Smoothing and filtering of apparent surface distribution of galaxies.

24 p3143 A73-45363

DATA RETRIEVAL

Data acquisition, processing and retrieval in information system for product design and development, noting storage system for spring material data

03 p0400 A73-13238

Meteorological satellites data acquisition, storage, reproduction, recall, use and costs

06 p0664 A73-18023

A search for Encke's comet in ancient Chinese records - A progress report.

14 p1791 A73-29799

DATA SAMPLING

Mathematical model, digital filter design and phase error behavior derivation for higher order discrete phase locked loops

03 p0276 A73-13906

Absolute instability of nonlinear pulse-amplitude control systems - Frequency criteria.

04 p0430 A73-15204

Estimating the mean time until follow-up cutoff in a nonlinear sampled-data servosystem for irregular arrival of the signal.

04 p0430 A73-15205

Optimal equalization of discrete signals passed through a random channel.

04 p0420 A73-15418

Investigation of the dynamics of nonlinear sampled-data automatic control systems

05 p0560 A73-16296

Extremal control system efficiency enhancement by information storage, noting algorithms for sequential data storage

05 p0560 A73-16298

Estimation of the state vector of a plant by minimization of a distance in metric space when using discrete sampling

05 p0561 A73-17281

Digitalized or sampled data FM demodulator recursive algorithm synthesis and SNR performance comparison with optimum analog and conventional limiter discriminator demodulators

06 p0664 A73-17712

Iterative scheme for identifying linear systems from input/output samples or construction of rational z-transform approximations to sample data sequences

06 p0718 A73-18534

On the numerical reconstruction of images from a microwave hologram.

06 p0669 A73-18737

Compact digital coding of electrocardiographic data.

06 p0660 A73-18815

Adaptive trackers based on continuous learning theory.

06 p0682 A73-18821

Radio oscillators short term frequency instability, examining relations between time domain and frequency domain sample variance definitions

07 p0798 A73-19176

The estimation of order and parameters in a process of stochastic differential equations with uncertain observations.

07 p0846 A73-20594

Influence of coherence of sampling on the accuracy of linear statistical forecasting and on the optimal predictor dimension

08 p0985 A73-21452

Features of the application of the root-locus method to the study of sampled-data automatic systems on the basis of the w-transform

09 p1068 A73-22341

Linear decision rule for probabilistic signal estimation in image recognition problems with sampling

09 p1060 A73-22556

Equivalent number method of optimal interval selection for meteorological observations with independent statistical samplings

09 p1114 A73-22853

Wideband high-speed high-resolution analog to digital converters technology developments, discussing voltage addressable read-only memory concept and related data sampling

10 p1177 A73-23792

Book - Digital simulation of physical systems.

10 p1191 A73-23946

Analysis and synthesis of automatic control systems with controlled converters.

10 p1198 A73-24019

Study of recurrence relationships and their applications by the Laboratoire d'Automatique et de ses Applications Spatiales.

10 p1200 A73-24042

Optimal reconstruction of a stationary random process from discrete readings

10 p1202 A73-24611

Russian book on military application oriented automatic control systems design covering amplifiers, servo elements, stability, performance, optimization, and nonlinear and sampled data systems

10 p1203 A73-24972

Measurement of certain one-dimensional characteristics describing the evolution of the two-dimensional probability density of random processes when changing the interval between readings

11 p1340 A73-25004

Random analog signal quantization and reconstruction from discrete sample values by optimal filtration according to statistical criteria

11 p1341 A73-25013

Effect of time-quantization errors on the accuracy in periodogram analysis of random processes

11 p1360 A73-25015

Comparative analysis of algorithms for measurement of correlation functions by the multiplication method /Review/

11 p1360 A73-25018

The optimality of variable sampling schemes for a digital encoder.

11 p1327 A73-25194

Differential mode of operation for bucket-brigade circuits.

11 p1341 A73-25360

Single input n-th order linear constant discrete-time adaptive control systems, deriving phase canonical form sensitivity functions by z-transform

11 p1342 A73-26636

Asymmetric positively skewed distributions family for precipitation data analysis, using two-sample non-parametric test

12 p1520 A73-26804

Choice of the quantization step and sampling interval for analog measurement signals

12 p1482 A73-26848

Amplitude-modulated pulse code sequence demodulation using physically realizable linear filter for reconstruction of discrete sample message at optimum mean-square error level

12 p1467 A73-26943

An adaptive digital compensator for saturating control systems.

12 p1483 A73-27160

Phase coordinates estimation optimization, deriving observable vector relations from sampling laws

12 p1524 A73-27417

Analysis of the stochastic stability of pulsed control systems in the frequency domain

12 p1485 A73-27622

Verification of the 'potential' work capacity of dynamic systems by a frequency-time technique

12 p1485 A73-27946

Continuous analog signals optimal discretization involving selected quantization steps and sampling rates

13 p1595 A73-28017

Comparison of different methods of reconstitution of a signal furnished under a sampled form

13 p1582 A73-28475

Optimal data sampling in communication channels system, discussing algorithms for data transmission and control

13 p1587 A73-28870

Analysis of stability and periodic motions in nonlinear sampled-data systems by the root locus method.

15 p1854 A73-31690

Data sample analysis of anomalous in-flight behavior incidents for spacecraft reliability covering incident causes and occurrence time, effects on mission and corrective actions

16 p2073 A73-33625

Exhaust emissions analysis system for aircraft gas turbine engines.

17 p2146 A73-34615

Digital flight control systems data sampling rate selection effects on intersample ripple, spectral folding and distortion and system bandwidth

17 p2138 A73-35224

Magnitude error bounds for sampled-data frequency response obtained from the truncation of an infinite series.

17 p2145 A73-35640

Estimates of unknown parameter from quantized observations given as sequence of evenly distributed random values, noting optimal grouping equations for general distribution function

17 p2130 A73-35722

DONAR - A computer processing system to extend ultrasonic pulse-echo testing.

19 p2407 A73-37448

The fastest extremum search in sampled-data automatic control systems

20 p2539 A73-38695

An adaptive scheme for PCM transmission.

20 p2523 A73-38728

A general quadratic criterion for absolute stability of nonlinear automatic control systems and its application to sampled-data systems with pulse-width modulation

20 p2541 A73-38988

Statistically optimal sampled data terminal guidance algorithm for complex probabilistic multipurpose control system, using linearized equations

20 p2590 A73-39344

Calculation of processes taking place in digital automatic control systems with finite switch-closing times

20 p2543 A73-39477

The filtering of random sequences with gaps by optimal discrete filters with a constant memory volume

21 p2658 A73-40857

Speech scrambling by the matrixing of amplitude samples.

21 p2657 A73-41206

Synthesis of optimal sampled-data control systems in the presence of continuous disturbances.

23 p2965 A73-44332

DATA SMOOTHING

State augmentation procedure for fixed point smoothing algorithm derivation through known solutions of higher dimensional digital filtering problem

03 p0277 A73-13914

Power spectral density estimation by spline smoothing in the frequency domain.

04 p0471 A73-15254

Convergent iterative smoothing algorithm for aircraft stability parameter identification from measurement, using variational optimization procedure

09 p1067 A73-22233

A survey of data smoothing for linear and nonlinear dynamic systems.

10 p1243 A73-24546

Discrete-time fixed-lag smoothing algorithms.

10 p1243 A73-24547

Mean frequency response characteristics of graphical smoothing operator for latitude observations analysis

13 p1683 A73-29099

A computer program for plotting exponentially smoothed average control charts.

13 p1588 A73-29299

Automatic methods for smoothing and separation of characteristic points in an electrocardiographic signal

14 p1721 A73-30387

Program for triangular bending elements with derivative smoothing.

15 p1848 A73-32028

Optimal filtering and smoothing simulation results for CIRIS inertial and precision ranging data.

20 p2587 A73-38809

Suboptimal algorithms for nonlinear smoothing.

21 p2669 A73-40333

Application of precise heat-capacity data to the analysis of the temperature intervals of the International Practical Temperature Scale of 1968 in the region of 90 K. 22 p2852 A73-41977

Smoothing and filtering of apparent surface distribution of galaxies. 24 p3143 A73-45363

DATA STORAGE

Bell Laboratories laser optics development and technology applications, discussing CW lasers, light deflectors, holography, optical memories, pattern generator, remote blackboard and micrographics 01 p0060 A73-11213

Digital storage of graphs and curves and their representation on visual displays 01 p0021 A73-11484

Analysis of dynamic-excitation conditions for electroluminescent panels 03 p0282 A73-13658

High-data-rate, spacecraft tape recorders. 04 p0449 A73-15383

Extremal control system efficiency enhancement by information storage, noting algorithms for sequential data storage 05 p0560 A73-16298

Address structure optimization and minimum access time and decoder terminals in nonvolatile core memory array design, noting binary notation for information storage 05 p0554 A73-16991

Picture information acquisition, storage and transmission characteristics of film and vidicon systems for photographic reconnaissance of plants 06 p0750 A73-18010

Meteorological satellites data acquisition, storage, reproduction, recall, use and costs 06 p0664 A73-18023

Mechanical and electrical performance of satellite-borne magnetic tape recording system for computer data storage in radio telemetry 07 p0820 A73-18960

High resolution Mossbauer spectrometer design and applications, describing electromechanical Doppler shifter, control electronics and data storage 07 p0822 A73-19170

Storage and transmission of sequences of moving images 08 p0941 A73-21559

Amorphous semiconductors for switching, memory, and imaging applications. 09 p1132 A73-21984

Multicolor documentation type information holographic storage, recording, indexing, registration and reconstruction technology assessment and application, emphasizing displays and automatic test equipment systems 10 p1216 A73-23797

Computer executive system for design automation file network creation and monitoring to permit input/output operations, storage information updating and display [AIAA PAPER 73-355] 11 p1334 A73-25492

Digital computers with multistage storage in control systems, determining algorithms for data exchange between operative, superoperative and external memory devices 12 p1475 A73-26782

Effectiveness of analog storage in the detection of signals on a background of noise and strong random pulsed interference 12 p1467 A73-26942

An electrooptical method for storage of weak linear-FM signals 12 p1470 A73-27577

VIEW - A distributed system for graphical analysis of large data bases. 12 p1476 A73-27824

[AIAA PAPER 73-431] Method for synthesizing built-in control circuits of automatic systems with memory 12 p1476 A73-27899

Side-looking pulse Doppler radar data presuming prior to correlation to obtain desired resolution performance with minimal digital storage 13 p1585 A73-29203

Investigation of an analog memory for the computational-measurement complex of an electrodynamic model 13 p1588 A73-29420

Parachutes computer aided design and performance analysis system development and operation, presenting information storage and retrieval tasks mechanics [AIAA PAPER 73-484] 15 p1829 A73-31466

Limiting information capacity of a holographic system 15 p1879 A73-32317

Ultra high resolution electronic imaging and storage with the return beam vidicon. 17 p2136 A73-34904

Data processing for earth resources survey including data handling, preprocessing for instrument errors, decision making and data bank 17 p2161 A73-34941

Method of synthesizing built-in monitoring arrangements for automata with memory. 18 p2291 A73-36751

Large wire spark chambers with an information output and storage system 23 p2982 A73-43570

Maximum information capacity of a holograph system. 24 p3089 A73-44623

Angular selectivity of lithium niobate volume holograms. 24 p3092 A73-45424

DATA SYSTEMS

Considerations for an earth physics information-management service. 04 p0439 A73-14814

International legal problems concerning earth environmental survey system composed of ERT satellites, survey aircraft and ground data handling systems 04 p0521 A73-15129

Command and control for a missile air defense system. II - Implementation of system requirements. 04 p0418 A73-15378

Data handling and analysis for the 1971 corn blight watch experiment. 04 p0443 A73-15402

The Mariner Venus Mercury flight data subsystem. 04 p0425 A73-15423

Universal data system for image processing of earth resources observations, discussing input/output film, tape and multispectral data, interactive control and video color displays 05 p0555 A73-17155

Data collecting and sequencing equipment for Prospero satellite PCM telemetry system, describing encoders, programming unit and tape recorder for orbital data storage 09 p1051 A73-22918

Atmosphere Explorer for satellite observation of thermosphere, discussing design goals, spacecraft components and data system 13 p1687 A73-28627

Optimal data sampling in communication channels system, discussing algorithms for data transmission and control 13 p1587 A73-28870

German ground operations network design, describing data system and flow with automatic handling of telemetry data, tracking data and operational information 14 p1727 A73-30098

Aircraft integrated data systems (AIDS) utilization for airlines operational flight control and economic exploitation enhancement, discussing aircraft accident investigation, maintenance, navigability, etc 15 p1831 A73-32496

A review of some possible uses of remote sensing techniques in fishery research and commercial fisheries. 18 p2307 A73-36031

Environmental data - From sensors to users. [AAS PAPER 73-138] 20 p2521 A73-38592

Remote sensing data management from a user's viewpoint. [AAS PAPER 73-152] 20 p2521 A73-38598

DCS - A global satellite environmental data collection system. 20 p2525 A73-38744

Integration of remote sensing data into spatial information systems, discussing data specification, acquisition, storage, retrieval, processing, etc 21 p2658 A73-40820

DATA TRANSMISSION

NT AUTOMATIC PICTURE TRANSMISSION

Digital apparatus for telemetry of pressure 01 p0044 A73-10034

Application of random time and frequency multiplexing to a data collection satellite. 01 p0018 A73-11182

Optimal fixed message block size for computer communications. 01 p0019 A73-11454

The onboard data processing system of the Helios probe [DGLR PAPER 72-092] 02 p0228 A73-11700

Future NASA communication satellite technology applications in meeting national education, health care, culture and data transfer needs, considering ATS F and CTS spacecraft 02 p0143 A73-12846

Error probabilities estimates for digital communication systems using orthogonal multiposition signals in data transmission 03 p0278 A73-14029

A programmable four channel system for long-time radio telemetry of biomedical parameters. 03 p0270 A73-14280

Current and near future data transmission via satellites of the Intelsat network. 03 p0280 A73-14659

The use of tolerance detectors for data protection in the case of FM data transfer 04 p0415 A73-14773

The ERTS wideband image communication system. 04 p0418 A73-15382

High resolution image data sensors and recorders characteristics and performance limits, describing transmission system 04 p0449 A73-15385

Miniature biotelemetry giving 10 channels of wide-band biomedical data. 04 p0412 A73-15388

Low error rate transmission by iterative probabilistic threshold decoding, noting performance improvement over sequential and low density parity check code techniques from simulation 04 p0425 A73-15399

Performance of correlation receivers in the presence of impulse noise. 04 p0419 A73-15406

The transmission of low frequency medical data using delta modulation techniques. 04 p0412 A73-15408

Ways for increasing the efficiency of data transmission systems. 04 p0420 A73-15421

Data return maximization for unpredictable channel capacity, considering planetary entry probe to Venus or Jupiter with unknown atmospheric transmission characteristics 04 p0420 A73-15425

Message switching for multiplexing data of computer users with interactive access onto common facilities, evaluating traffic induced time delay performance 04 p0425 A73-15428

Geophysical data transmission from automatic stations in the antarctic via earth synchronous satellites. 04 p0421 A73-15430

Environmental data transmission from arctic data buoys via polar orbiting satellite. 04 p0421 A73-15431

Real time programmable data compression system with minicomputers for operation between TV data acquisition ground stations and ATS satellites 04 p0425 A73-15442

Communications technology satellite /CTS/ with transponder and TWT operating into steerable antenna, discussing experiments on TV broadcast, data transmission, FM and transportable terminals 04 p0422 A73-15446

Information management system breadboard data acquisition and control system. 04 p0425 A73-15461

Analysis of a dual mode digital synchronization system employing digital rate-locked loops. 05 p0549 A73-16369

Teleprocessing systems communication software functions and construction, considering network control, message preprocessing, queueing and error recovery in multiprogramming and multiprocessing environment 05 p0551 A73-16803

Datran TDM switching system with stored program controller and IC components providing reliability, flexibility and high channel capacity in data transmission 05 p0551 A73-16804

Computer communication networks with programmable concentrators for combining multiple terminals, discussing structure, message handling and transmission, routing and reliability 05 p0551 A73-16805

Mariner 9 Martian surface mapping, describing science instrumentation, orbit characteristics, mapping cycles sequence design and data telecommunications [AIAA PAPER 73-204] 05 p0630 A73-16938

French computation center equipment for satellite orbit calculations and attitude corrections, describing links between teleprocessing and data transmission 05 p0555 A73-17300

Transmission quality in noiseless multiple-access systems with feedback 06 p0679 A73-17855

Mean square error automatic equalizer for synchronous data transmission by gradient projection method for parameter optimization in discrete frequency domain, noting algorithm convergence 06 p0665 A73-18141

Atmospheric conditions effects on line-of-sight microwave PCM data transmission system performance, comparing predicted error probability vs predetection SNR with measurement 06 p0665 A73-18187

Applications for quantum amplifiers in simple digital optical communication systems. 06 p0668 A73-18404

Satellite data concentration, memorization, transmission and processing, discussing central computer control unit, ground stations peripheral links, magnetic tapes and system reliability 07 p0795 A73-18952

Telemetry data acquisition, transmission lines and delayed time processings onboard spacecraft and at ground receiving stations and center, discussing multiplexing and computer control 07 p0795 A73-18953

ERTS program, describing satellite design and imaging and data collection systems for real time or delayed taped transmission to ground stations

07 p0905 A73-19112

Common-bandwidth transmission of data signals and wide-band pseudonoise synchronization waveforms.

07 p0790 A73-19200

A study on accumulation of waveform distortions in PCM hybrid transmission.

07 p0791 A73-19369

The resistance of discrete phase modulation to random interference

07 p0793 A73-20023

Flawless operation probability for information transmission reliability of electronic logic circuits with binary data inputs

07 p0801 A73-20040

Increasing the traffic-capacity utilization factor of a telemetry channel

07 p0794 A73-20297

Storage and transmission of sequences of moving images

08 p0941 A73-21559

Holographic method of controlling the spatial-angular characteristics of laser emission

09 p1090 A73-21951

Synchronization theory for digital data transmission with random changes in channel characteristics

09 p1049 A73-22045

Cyclic binary coding and decoding circuits for high reliability data and command transmission, discussing analytical relations and design aspects

09 p1060 A73-22923

Radio telemetering trends in post-Apollo space programs, emphasizing service lifetimes and orbiting space station data bit generation rate

09 p1053 A73-23362

Hybrid coding/decoding scheme for deep space probes data transmission, estimating bit error probability for given SNR

09 p1054 A73-23376

Bandwidth as measure of dimensions added to signal space per unit time in digital transmission power spectral density computation, presenting comparison for telemetry signals

09 p1054 A73-23384

Amplitude-phase-keying with M-ary alphabets - A technique for bandwidth reduction.

09 p1054 A73-23385

Redundant area encoding for relieving integration time requirement in airborne reconnaissance photograph transmission, discussing algorithms, display technique, data reduction and pictorial simulation

09 p1054 A73-23386

Communication system for digital image processing services over Advanced Research Project Agency computer network, describing hardware facilities and software capacity

09 p1061 A73-23390

Multispectral imagery data compression for earth resources satellites, comparing performance of spectral-spatial-delta-interleave and Rice coding algorithms

09 p1055 A73-23391

Adaptive algorithm with error control for line by line encoder for image transmission, noting reconstructed image quality improvement

09 p1055 A73-23392

IR laser terrestrial communication system with 5 Mbit/sec digital data capacity, using intracavity optical frequency modulation or frequency shift keying modulation

09 p1055 A73-23394

Optical fiber waveguide operational principles, discussing information transfer rate capability, channel characteristics and input and output devices

09 p1055 A73-23396

High data rate hard decision digital IC sequential decoder for earth-orbiting satellite space missions, discussing computational efficiency of modified Fano algorithm

09 p1056 A73-23398

Digitally implemented clock acquisition loops for low SNR data signals.

09 p1056 A73-23405

Design philosophy and operation of hardware and data flow of TELFILE real time multiprogrammed telemetry system, discussing support of Minuteman III Weapons Systems

09 p1057 A73-23415

Comparing bandwidth requirements for digital baseband signals.

09 p1058 A73-23423

Intersymbol interference in binary communication systems with single-pole band-limiting filters.

10 p1186 A73-23498

The effect of carrier phase and timing on a single-sideband data signal.

10 p1187 A73-23500

Run length code for redundancy encoding of black-white facsimile picture data transmission to allow channel or storage capacity reduction and hardware simplification

10 p1188 A73-23741

High data rate YAG laser communication experimental systems with partial cavity dumping, orthogonal setup or harmonic mode locking, investigating internal modulation feasibility

11 p1378 A73-26246

Canadian telecommunications satellite system for TV, voice and analog or digital data transmission, describing space segment, satellite control and ground station network

11 p1431 A73-26259

A technique of modulating pulsed semiconductor lasers.

12 p1505 A73-27009

Ranging and data transmission using digital encoded FM-'chirp' surface acoustic wave filters.

12 p1470 A73-27571

Information transmission reliability enhancement via digital code group symbol transmission by wide-band linear FM radio signals

12 p1471 A73-27593

A modulator with inherent bandwidth limiting for use with a bi-phase PSK data transmission system.

12 p1472 A73-27663

The use of satellites for aircraft communications and air traffic control.

12 p1472 A73-27666

The operational requirements for a maritime satellite communication service.

12 p1473 A73-27676

Balloon-aircraft ranging, data, and voice experiment.

12 p1473 A73-27680

An advanced computer communication network. [AIAA PAPER 73-414]

12 p1474 A73-27820

Problems involving efficient transmission of informative parameters in the adaptive discretization of an analog signal

13 p1583 A73-28852

Evaluation of the noise immunity of pulsed systems for transmission of continuous messages with allowance for quantization and interpolation errors. I

13 p1584 A73-28891

Probability of error in selecting the information signal and the synchronization signal by frequency multiplication

13 p1584 A73-28892

Ranging and data transmission using digital encoded FM-'chirp' surface acoustic wave filters.

14 p1733 A73-29935

A simple error-protection approach in the case of a transmission of anisochronous data signals over time-division multiplex systems

14 p1726 A73-30071

Loss of information during central summation of local postsynaptic potentials

14 p1719 A73-30825

Reliability estimation technique for data transmission processes in remote control systems with redundancy, assuming Markovian randomness of signal input

15 p1854 A73-31806

Radar data digital relay from outlying stations to ATC centers for air traffic image integration, discussing computerized plotting and alphanumeric display techniques

15 p1847 A73-32435

German monograph on data transmission by laser covering analysis of electromagnetic wave diffraction by narrow slits via Mathieu function solution of boundary value problem

15 p1847 A73-32585

Small earth terminals for satellite communications.

16 p1979 A73-33084

Transmission of nerve pulses at the switching locations of the brain

16 p1973 A73-33424

Propagation studies and the development of terrestrial microwave radio relay systems above 10 GHz in the UK.

16 p1980 A73-33702

EHF radio wave limitations and potentialities for high speed data communications systems, considering applications in urban short range relays

16 p1981 A73-33705

Feasibility experiments for high capacity Hertzian cables to distribute and collect data within urban areas, using cylindrical mirrors

16 p1982 A73-33715

Compression of weather charts by the segmented Lynch-Davison code.

16 p1983 A73-33744

Comparing bandwidth requirements for binary baseband signals.

16 p1984 A73-33745

Phase modulated data transmission with partial pilot signals, interpolating reference demodulation signals at receiving end by maximum cross correlation

16 p1984 A73-33978

Quasi-optimal signal reception in asynchronous addressing communication systems with a time-frequency matrix

17 p2121 A73-34587

Encoding altimeter for coding, transmitting and displaying flight altitude information to air traffic controllers [SAE PAPER 730301]

17 p2167 A73-34663

Application of data compression techniques to spacecraft imaging systems.

17 p2122 A73-34910

Prototype TDMA system design for Intelsat 4 satellite, discussing separate synchronization and data bursts transmission feature for service quality and reliability improvement

17 p2122 A73-34967

Multiplex data bus techniques for digital avionics, discussing transmission media, modulation methods, remote control and reliability

17 p2138 A73-35231

TDM data bus and interface design for digital avionics system, considering standard remote terminal in terms of system parameters, operation and cost effectiveness

17 p2139 A73-35233

Application of multiplexing to the B-1 aircraft.

17 p2107 A73-35247

Station Data Acquisition and Control System.

17 p2147 A73-35301

The problem of applying information theory to efficient image transmission.

17 p2124 A73-35302

Wideband multidrop asynchronous TDM/FDM multichannel data distribution system for space station application, discussing analog and digital buses design

17 p2124 A73-35308

Canadian domestic satellite system applications.

17 p2124 A73-35311

Effect of bandlimiting on the noncoherent detection of Amplitude-Shift Keying /ASK/ signals.

17 p2125 A73-35377

The effects of cycle slips and phase jitter on the probability of bit error in suppressed carrier phase-shift keyed communications.

17 p2126 A73-35628

Maximum likelihood synchronizer for binary overlapping PCM/NRZ signals.

17 p2127 A73-35641

VM 256 - Experimental system of a 3-D radar installation

18 p2335 A73-37040

Increasing the utilization factor of the carrying capacity of a telemetry channel.

18 p2291 A73-37134

Data compression techniques as a means of reducing the storage requirements for satellite data - A quantitative comparison.

19 p2405 A73-38196

An error correction method for DPCM picture transmission

19 p2432 A73-38268

Probability of error in binary communication systems with causal band-limiting filters. I - Non-return-to-zero signal. II - Split-phase signal.

19 p2415 A73-38384

Canadian space programs in communications, navigation and atmospheric science, considering telephony, data transmission, TV broadcasting and remote sensing [AAS PAPER 73-118]

20 p2584 A73-38580

A proposed time division multiple access /TDMA/ satellite system for Anik I.

20 p2523 A73-38719

ML receiver for binary signals with intersymbol interference in Gaussian noise.

20 p2524 A73-38733

Application of some data compression systems to ESRO satellite data.

20 p2524 A73-38735

GOES system data collection performance estimates.

20 p2525 A73-38743

DCS - A global satellite environmental data collection system.

20 p2525 A73-38744

A digital communications system for manned spaceflight applications.

20 p2527 A73-38763

The effect of carrier recovery and bit timing errors in the coherent reception of 2 and 4 phase PSK signals.

20 p2527 A73-38766

Noise immunity of digital methods for the transmission of analog messages with an enhanced information content

20 p2531 A73-39463

New initiatives in engineering computer software sharing.

20 p2533 A73-39515

Maritime communications via satellites employing phased arrays.

21 p2649 A73-40330

Risk of estimation by data obtained via communication channel.

21 p2654 A73-40689

Data transmission system based on voice channels time division into blocks using cyclic code redundancy without appreciable loss in error correcting capability

21 p2655 A73-41044

A semiconductor-laser communication system using differential pulse position modulation.

21 p2656 A73-41094

- Symbol set for multiregenerated digital transmission featuring highly redundant timing for low frequency phase noise suppression
21 p2656 A73-41110
- Binary error estimation in real time for channel quality monitoring, comparing upper and lower bounds with number of errors for bit sequence
21 p2656 A73-41170
- Error detection and synchronization with pseudoternary codes for data transmission.
22 p2827 A73-42464
- Carrier-phase tracking-loop computer simulation and performance evaluation in high-speed SSB data transmission.
23 p2953 A73-43322
- Gilbert burst noise model for statistical analysis of nonindependent errors in digital data transmission systems, noting performance and utility in communication theory
23 p2954 A73-43986
- Visual and verbal coding in the interhemispheric transfer of information.
24 p3065 A73-45337
- Reliability estimation technique for data transmission processes in remote control systems with redundancy, assuming Markovian randomness of signal input
24 p3075 A73-45350
- DATING**
U CHRONOLOGY
U TIME MEASUREMENT
- DAWN CHORUS**
Preliminary findings of a petrel rocket experiment to investigate the VLF emission 'chorus' in the ionosphere.
02 p0141 A73-12319
- DAYGLOW**
Rocket measurements of low energy electrons and optical emissions in the dayglow and aurora.
01 p0036 A73-10346
- Rocket photometric observations of dayglow sky radiation in O green line, noting aerosol scattering coefficient and particle concentration
02 p0161 A73-12277
- Airglow height profiles of forbidden O I 6300 and 5577 A line emissions in morning ionosphere from rocket photometric measurement
04 p0444 A73-15542
- Dawn airglow far UV spectrum observed by scanning Ebert spectrophotometer aboard Aerobee rocket, obtaining altitude profiles at 100-244 km
07 p0814 A73-19247
- Fraunhofer line depth in daytime airglow
07 p0817 A73-19471
- Observations of the Helium II 304-A and Helium I 584-A atmospheric dayglow radiation.
10 p1213 A73-24735
- Ultra-violet argon dayglow lines in the atmosphere of Mercury.
11 p1421 A73-25916
- Second positive system of nitrogen bands in dayglow, according to Kosmos-224 data.
13 p1607 A73-28703
- Dayglow nitrogen ion 3914 A emission profiles for average solar activity at 110-240 km heights from Cosmos 224 observations
13 p1607 A73-28704
- Ionospheric nitrogen ion density from rocket-borne dayglow spectrometry, considering charge exchange with metastable oxygen ions and solar EUV photoionization as ionizing mechanisms
14 p1723 A73-29953
- UV dayglow in 750-1050 A region at 100-800 km observed with rocket-borne thin film filter photometer, solving radiative transfer problem for excitation process
15 p1867 A73-31077
- Depth of the Fraunhofer lines in the spectrum of the daytime sky.
15 p1873 A73-32061
- Photoelectron excitation of the Jupiter dayglow.
16 p2062 A73-33430
- Atomic collision processes applied to earth atmospheric physics and chemistry, Jovian ionospheric composition and terrestrial tropical UV dayglow
17 p2213 A73-34450
- Photometer for detection of sodium day airglow.
19 p2428 A73-37261
- TD 1 A astronomical satellite detection of UV dayglow emissions above F 2 peak in equatorial zone, considering Mg ions resonance scattering to account for emission features
20 p2551 A73-38940
- Enhancements of the photoelectron-excited dayglow during solar flares.
21 p2761 A73-41389
- Estimate of extreme ultraviolet dayglow of helium in the Martian atmosphere.
22 p2909 A73-42485
- DAYTIME**
Daytime laser radar measurements of the atmospheric sodium layer.
02 p0157 A73-11875
- Daytime sky brightness from atmospheric transmittance, noting single and multiple scattering calculations
11 p1352 A73-25603
- Correlation between the absolute brightness characteristic of day sky and the optical thickness of the atmosphere
11 p1353 A73-25605
- Optical characteristics of bright day sky in the visual region of the spectrum and the atmospheric aerosol
11 p1353 A73-25606
- Daytime cloudless sky glow, atmospheric transmittance, neutral polarization and aerosol optical characteristics in solar almucantar and vertical
11 p1353 A73-25608
- Polarization of the cloudless daytime sky in the 1.25- to 2.42-micron range
11 p1353 A73-25645
- Dayside polar aurorae during various substorm phases from IGY data, noting time of glow intensity maximum
12 p1490 A73-27343
- Preliminary results obtained with astrophotometer installed on Lunokhod II.
18 p2315 A73-35992
- Functional relation between the F2-layer ionization state in daylight time and the zenith angle of the sun
20 p2555 A73-39178
- Daytime applications of Raman technique of laser backscatter to measure atmospheric composition profiles
21 p2729 A73-40067
- Russian book - Scattered daytime sky light.
21 p2691 A73-41439
- Dayside polar aurorae during various substorm phases from IGY data, noting time of glow intensity maximum
23 p2970 A73-43240
- Vertical and latitudinal development of a seasonal anomaly in the daytime F2 region. I
24 p3083 A73-44791
- DC (CURRENT)**
U DIRECT CURRENT
DC 9 AIRCRAFT
DC9-30 refrigeration system diagnosis by computer.
16 p1969 A73-33654
- DC 10 AIRCRAFT**
Automated navigation system design for DC 10 long range version, emphasizing control display unit interface functions with pilot
05 p0594 A73-16050
- Flight simulator development in parallel with aircraft flight test A case study of the American Airlines DC-10 program.
05 p0562 A73-16664
- [SAE PAPER 720858]
DC-10 aircraft slide/raft system for emergency personnel evacuation, discussing certification test program for performance, reliability, seaworthiness and compliance with regulations
16 p1965 A73-32659
- Time compressed training program for DC-10 flight crews, emphasizing operational proficiency through specific behavioral objectives approach
16 p1966 A73-32663
- Integrated reliability and safety analysis of the DC-10 all-weather landing system.
16 p1969 A73-33641
- Certification program for the DC-10 slide/raft.
17 p2108 A73-35807
- DC 10 airframe structure full scale fatigue tests for crack initiation and growth, residual strength and service life
19 p2379 A73-37463
- [AIAA PAPER 73-803]
Guidance, control, and instrumentation progress on the McDonnell Douglas DC-10.
19 p2451 A73-37814
- The application of Armco 21-6-9 steel tubing to the DC-10 hydraulic system.
19 p2389 A73-37865
- DC-10 Twin design, discussing balance characteristics, loading limits and sample forms
19 p2386 A73-37891
- DE HAVILLAND AIRCRAFT**
NT DHC 5 AIRCRAFT
DHC-7 four engine turboprop transport aircraft, emphasizing quietness and STOL capability
18 p2266 A73-36067
- DE HAVILLAND DHC 5 AIRCRAFT**
U DHC 5 AIRCRAFT
DE LAVAL NOZZLES
U CONVERGENT-DIVERGENT NOZZLES
- DEACCLIMATIZATION**
U ACCLIMATIZATION
DEACTIVATION
Direct overtone excitation of hydrogen fluoride second vibrational level, measuring global deactivation rate by temperature tuned Nd-YAG laser excited fluorescence technique
06 p0703 A73-18750
- DEADWEIGHT**
U STATIC LOADS
DEAFNESS
U AUDITORY DEFECTS
DEBRIS
NT SPACE DEBRIS
- Transitions in the friction coefficients, the wear rates, and the compositions of the wear debris produced in the unlubricated sliding of chromium steels.
[ASLE PREPRINT 72LC-7B-2]
03 p0316 A73-14369
- Spherical debris - Its occurrence, formation and significance in rolling contact fatigue.
16 p2022 A73-34029
- Latitudinal distribution of a debris mantle on the Martian surface.
19 p2477 A73-37208
- DEBUGGING**
U CHECKOUT
DEBYE LENGTH
Instability of a weakly ionized plasma at wavelengths of the order of the Debye radius.
03 p0347 A73-14092
- Nonphysical noises and instabilities in plasma simulation due to a spatial grid.
07 p0854 A73-19267
- Expanded laser produced plasma Debye length from slab geometry, evaluating electron temperature for ion recombination rates
10 p1256 A73-24270
- Effect of Debye shielding on the ionization energy of air plasma components
13 p1667 A73-29164
- Screened potential Lorentz model for electrical conductivity of non-Debye plasma, investigating electron energy distribution function
17 p2214 A73-34127
- Weakly ionized continuum plasma turbulent shear flow and transport properties calculation, noting ratio of Debye shielding length to local integral scale
19 p2463 A73-37153
- Debye representation and multipole expansion of the quantized free electromagnetic field.
20 p2591 A73-38609
- One-component two dimensional plasma, calculating equilibrium pair correlation function by Debye approximation for particle interaction via Coulomb potential
23 p3013 A73-44172
- DEBYE TEMPERATURE**
U SPECIFIC HEAT
DEBYE-HUCKEL THEORY
Special features of Debye screening and the equation of state of a partially ionized plasma
06 p0730 A73-18551
- Debye screening and equation of state of a partially ionized plasma.
16 p2042 A73-33576
- DEBYE-SCHERER METHOD**
Sheet, tecto-, ortho- and chain silicates crystal lattice breakdown under shock from ballistic range experiments, using Debye-Scherer method for X ray diffraction studies
10 p1277 A73-24078
- DECAMETRIC WAVES**
Off-path transequatorial propagation in decametric waves. II - Application to the study by diffusion of ionospheric irregularities
01 p0017 A73-10334
- Type 3 bursts exciter duration and decay time constant from time profiles analysis in decimeter range, explaining coronal temperature
03 p0361 A73-13213
- Radio sources in decimeter wave range from astronomical model and radio observations, noting spectral characteristics dependence on electron energy spectra
04 p0496 A73-14824
- Decametre-wave radiation from Jupiter and solar activity.
04 p0491 A73-14956
- Jupiter southern equatorial band eruptive centers and decametric radio sources interrelationship, discussing reanimations responsible for Red Spot displacement sense
08 p1012 A73-21474
- Major planets nonthermal radio emission observations, noting powerful decametric sources related to Jupiter rotation and Io orbital motion
11 p1420 A73-25879
- Jupiter's decametric rotation period and the Source-A emission beam.
11 p1420 A73-25881
- Observations on the time and frequency structure of solar decameter radio bursts.
11 p1413 A73-25951
- Jovian decametric emission origin in cyclotron instability of weakly relativistic electrons trapped in magnetic field, considering group velocity in magnetospheric plasma
11 p1424 A73-26129
- Jupiter radiation reception at decametric wavelengths by Yagi antenna and radiometer, taking into account Io modulation effect
11 p1424 A73-26131
- Pulsar decametric radiation reception hindrance by SNR deterioration caused by bandwidth decrease and background radiation, discussing signal processing methods
11 p1426 A73-26474

- The geometry and dynamic spectra of Io-modulated Jovian decametric radio emissions. 12 p1540 A73-27327
- Fine structure of Jupiter's decametric source B. 19 p2482 A73-37389
- Jupiter satellite Io controlled decametric Alfvén wave emission pattern, considering relationship to coherent cyclotron radiation growth rate. 21 p2764 A73-40168

DECARBONATION

- Photo-decarbonylation of beta-styryl isocyanates. 12 p1466 A73-27225

DECARBOXYLATION

- Non-enzymic beta-decarboxylation of aspartic acid. 04 p0414 A73-16032
- Light enhanced decarboxylations by proteinoids. 06 p0661 A73-17941

DECARBURIZATION

- Cr heat vacuum decarburation equipment for stainless steel vacuum melting, noting cost analysis, vacuum pumping curve and desulfurization. 04 p0455 A73-15745

DECAY

- NT ALPHA DECAY
- NT BIOLUMINESCENCE
- NT CHEMILUMINESCENCE
- NT ELECTROLUMINESCENCE
- NT ELECTRON EMISSION
- NT FIELD EMISSION
- NT FLUORESCENCE
- NT HALF LIFE
- NT ION EMISSION
- NT LIGHT EMISSION
- NT LUMINESCENCE
- NT LUNAR LUMINESCENCE
- NT NEUTRON DECAY
- NT NEUTRON EMISSION
- NT NUCLEAR FISSION
- NT OPTICAL RESONANCE
- NT PARTICLE EMISSION
- NT PHOTOELECTRIC EFFECT
- NT PHOTOELECTRIC EMISSION
- NT PHOTOIONIZATION
- NT PHOTOLUMINESCENCE
- NT PHOTOPRODUCTION
- NT PLASMA DECAY
- NT RADIO EMISSION
- NT RADIOACTIVE DECAY
- NT SECONDARY EMISSION
- NT SELF SUSTAINED EMISSION
- NT SHOCK WAVE LUMINESCENCE
- NT SOLAR RADIO BURSTS
- NT SOLAR RADIO EMISSION
- NT SPECTRAL EMISSION
- NT STIMULATED EMISSION
- NT THERMAL EMISSION
- NT THERMIONIC EMISSION
- NT THERMOLUMINESCENCE
- NT TYPE 2 BURSTS
- NT TYPE 3 BURSTS
- NT TYPE 4 BURSTS
- NT TYPE 5 BURSTS
- NT X RAY FLUORESCENCE
- Mechanism of decay of ammonia in flame gases from an NH₃/O₂ flame. 16 p1976 A73-33345

DECAY RATES

- NT ELECTRON DECAY RATE
- Measurement of the local production of muons underground. 01 p0080 A73-11009
- Type 3 bursts exciter duration and decay time constant from time profiles analysis in decameter range, explaining coronal temperature. 03 p0361 A73-13213
- Bottleneck of 29/cm phonons in ruby. 04 p0484 A73-15471
- The swirling turbulent jet. 05 p0564 A73-16544
- [ASME PAPER 72-FF-18] Low speed wind tunnel test section anisotropic turbulence decay rates representation by power type laws, comparing with grid and nearly isotropic turbulence. 11 p1348 A73-26390
- Saint Venant principle investigation for plane problem of linear elastostatics for anisotropic media by energy method, calculating exponential stress decay constant lower bound. 15 p1946 A73-31102
- Swirl decay in circular pipe air flow in terms of angular and axial momenta, dimensionless parameter and velocity profiles. 16 p1999 A73-32825
- Decay of the kinetic energy of compressible micropolar fluids. 20 p2547 A73-39341
- Decay time of type III solar bursts observed at kilometric wavelengths. 21 p2762 A73-41497
- Time of flight spectral measurements of metastable lifetimes in molecular beams with different excited states. 24 p3089 A73-44814

DECCA NAVIGATION

- Comparison of medium-distance navigation systems. II 02 p0191 A73-12014

DECELERATION

- NT SPIN REDUCTION
- Meteor dust motion in the upper atmosphere and in the vicinity of the earth's orbit. 02 p0214 A73-12255
- Decelerator parachute systems for heavy loads recovery, discussing stress, stability and reliability assessment. 03 p0251 A73-14638
- [AIAA PAPER 72-798] Aerodynamic decelerator dynamics modeling for Viking lander parachute deployment, analyzing unfurling process with attention to longitudinal and rotational dynamics. 12 p1549 A73-27440
- Flow deceleration as mechanism of vortex ring formation, showing liquid mass variability and vortex clusters of spheroid and hemisphere shapes. 15 p1861 A73-31282
- Several computerized techniques to aid in the design and optimization of parachute deceleration and aerial-delivery systems. 15 p1829 A73-31470
- [AIAA PAPER 73-488] Test gas properties behind a decelerating shock wave in a shock tube. 16 p2000 A73-33319
- Analytical estimate of the effect of the motion of a small internal mass on the oscillation of a body decelerating in the atmosphere. 19 p2494 A73-38131

DECELERATORS

U BRAKES (FOR ARRESTING MOTION)

DECIMETER WAVES

- The role of energetic electrons in the correlation of meter and decimeter type III bursts with 4 keV X-ray emission. 01 p0093 A73-11391
- Properties of different groups of type IV solar radio bursts. 04 p0493 A73-16013
- Saturn 49.5 and 94.3 cm brightness temperature, considering magnetic field effects, synchrotron emission and atmosphere. 11 p1424 A73-26127
- Jupiter radio observations at 13 cm during 1969 and 1971 oppositions for circular polarization and flux density. 11 p1424 A73-26128
- A broadband antenna and multiplexer system in the decimeter-wave range for solar radio astronomy. 12 p1481 A73-27782
- Radar echo from a 'clear sky' in the decimeter radio wave range. 13 p1585 A73-29156
- Search for sporadic radio emission from space at centimeter and decimeter wavelengths. 14 p1798 A73-30261
- Development of moving type IV solar radio bursts and relation to expanding magnetic bottles from flare regions. 16 p2054 A73-33096
- Analysis of the Jovian electron radiation belts. II - Observations of the decimetric radiation. 19 p2475 A73-37622
- The brightness temperature of Venus and the absolute flux-density scale at 608 MHz. 19 p2489 A73-38527
- Pulsar searches at 408 MHz with Northern Cross radio telescope, comparing discovered objects with previously known pulsars. 21 p2778 A73-41532
- On the spectrum of the S- and B-components of solar radio emission at dm-wavelengths. 22 p2915 A73-43038
- Computer controlled steerable radio telescope construction and performance for decimeter and centimeter wavelength observations. 23 p2958 A73-43367
- Origination of Type-IV decimetric bursts in the solar corona. 23 p3036 A73-44248

DECISION ELEMENTS

U LOGICAL ELEMENTS

DECISION MAKING

- Flight personnel training meetings, covering decision making, cockpit personnel selection and instructor role analysis. 03 p0266 A73-13073
- Assessment and operational implications for ATC capital investment decision making by relative capacity estimating process using analytical models. 03 p0280 A73-13801
- Interactive aspects of man/learning system control teams. 05 p0543 A73-16708
- The prediction of team monitoring performance under conditions of varied team size and decision rules. 05 p0543 A73-16710
- A critique of remote sensing evaluation techniques. 05 p0571 A73-17129

Rapid processing of multispectral scanner data using linear techniques. 05 p0554 A73-17150

The use of model building in a production environment. 06 p0698 A73-18514

Fuzzy multi-stage decision-making, fuzzy state and terminal regulators and their relationship to non-fuzzy quadratic state and terminal regulators. 06 p0681 A73-18523

Outline of a new approach to the analysis of complex systems and decision processes. 06 p0671 A73-18622

Current status of models for the human operator as a controller and decision maker in manned aerospace systems. 07 p0787 A73-20587

R and D organizational resource allocation, discussing attributes of formal evaluation and selection model for management decision processes. 08 p1025 A73-20973

Electronic display devices for command, monitoring, surveillance, simulation and training in military applications, considering reliability, cost and performance specifications in procurement decision making. 08 p0965 A73-21245

State-of-art review in identification, state estimation and decision processes for time variant systems, discussing parametric, nonparametric, static and dynamic models. 10 p1197 A73-23635

A mathematical programming approach to identification and optimization of a class of unknown systems. 10 p1242 A73-23773

Regional airport systems study for San Francisco bay area, discussing commercial and general aviation future needs, environmental and economic aspects and alternative options. 11 p1454 A73-26125

Visual pattern matching - An investigation of some effects of decision task, auditory codability, and spatial correspondence. 13 p1579 A73-29123

Effect of mild acute hypoxia on a decision-making task. 14 p1717 A73-30514

Book - Interorganizational decision making. 15 p1960 A73-31577

Mathematical modeling technique for marketing reliability programs in terms of cost/performance assurance for use in management decision making. 16 p2089 A73-33638

Computer program for Equipment Improvement Recommendation (EIR) evaluation relative to reliability, availability, inventory cost and total annual expenditure in Army engineering management decision making. 16 p2089 A73-33653

Equipment life cycle costs dependence on acquisition decision making, discussing stochastic computer simulation of failure times, repairs, inventory replacement and personnel availability. 16 p2089 A73-33655

Multipurpose properties and conflict situations in automatic control systems. 16 p1992 A73-33666

Data processing for earth resources survey including data handling, preprocessing for instrument errors, decision making and data bank. 17 p2161 A73-34941

Aerospace industry project managers and support personnel authority perceptions based on assessment of situational factors surrounding decision making, tabulating empirical investigation statistics. 17 p2257 A73-35214

Book - Systems concepts: Lectures on contemporary approaches to systems. 17 p2258 A73-35572

A model of the human in a cognitive prediction task. 22 p2814 A73-42223

Information seeking with multiple sources of conflicting and unreliable information. 24 p3063 A73-44778

Representation of the computer-aided design process by a network of decision tables. 24 p3070 A73-45230

DECISION THEORY

NT STATISTICAL DECISION THEORY

Conjoint-measurement framework for the study of probabilistic information processing. 02 p0138 A73-12545

A very high speed hard decision sequential decoder. 04 p0424 A73-15398

Conference on Decision and Control and Symposium on Adaptive Processes, 11th, New Orleans, La., December 13-15, 1972, Proceedings. 07 p0805 A73-20576

Multiple input system with feedback loops and majority decision for performance optimization, discussing design principles and applications for structural synthesis and circuit design. 12 p1482 A73-26759

Truncated sequential life tests for a 3-way decision procedure.

15 p1883 A73-32260

A current turbine engine maintenance program and the experience and logic upon which it is based.

[ASME PAPER 73-GT-81] 16 p2049 A73-33526

Probabilistic analysis of sequential test plans.

16 p1986 A73-33636

Papers on optimal control and dynamic systems theory covering linear discrete systems observers, quasi-linearization, national economic policy, decision theory and closed loop formulation

17 p2143 A73-34360

Book - Zero-base budgeting: A practical management tool for evaluating expenses.

17 p2258 A73-35674

Synthesis problems of adaptive systems for processing information and accepting solutions

20 p2531 A73-38684

A criterion for a free choice of decisions involving continuous control systems

24 p3074 A73-45100

DECODERS

Minicomputer for real time sequential decoding of convolutional code transmission in space communication, discussing system design, performance and metric bias effect

01 p0020 A73-11185

Performance versus complexity of Viterbi and sequential decoding.

04 p0424 A73-15397

A very high speed hard decision sequential decoder.

04 p0424 A73-15398

Design, production, reliability analysis and testing of Eole satellite decoder for balloon sounding data, noting performance tests

07 p0790 A73-18966

High data rate hard decision digital IC sequential decoder for earth-orbiting satellite space missions, discussing computational efficiency of modified Fano algorithm

09 p1056 A73-23398

Binary cyclic code detection capability, polynomial description, coder-decoder circuits and error correction application

10 p1197 A73-23848

The application of integrated magnetic devices for circuit checking and error correcting.

10 p1198 A73-24021

Design principles for control systems of digital computers

14 p1730 A73-30035

Matrix, pyramid and rectangular decoder reliability and operational probability during short circuit/cut-off failures

14 p1736 A73-30566

DECODING

Error-erasure decoding of product codes.

01 p0020 A73-11296

Low error rate transmission by iterative probabilistic threshold decoding, noting performance improvement over sequential and low density parity check code techniques from simulation

04 p0425 A73-15399

Polynomial weights and code constructions.

06 p0671 A73-18143

Simulation of sequential decoding with phase-locked demodulation.

07 p0794 A73-20498

Random coding bound of information theory providing upper bound to decoding error probability for best code of given rate and block length

09 p1111 A73-22117

Hybrid coding/decoding scheme for deep space probes data transmission, estimating bit error probability for given SNR

09 p1054 A73-23376

A single channel command detector for deep space missions.

09 p1057 A73-23417

Cyclic binary codes circuit technology, discussing error types and decoding circuits for error detection and correction

11 p1332 A73-26254

The interpretation of signals from space.

11 p1428 A73-26661

Logic and computational complexity of decoders for BCH codes, discussing channel capacity, error correction and information theory

13 p1587 A73-29672

Algebraic decoding algorithms for block codes over q-ary input Q-ary output alphabet channel, presenting examples for Hamming, Lee or burst distance

14 p1730 A73-30501

Search properties of some sequential decoding algorithms.

22 p2829 A73-42706

DECOMPOSITION

NT GLYCOLYSIS

NT HYDROGENOLYSIS

NT PHOTODECOMPOSITION

NT PHOTODISSOCIATION

NT PHOTOLYSIS

NT PROPELLANT DECOMPOSITION

NT RADIOLYSIS

Shock layer measurements of decomposition reactions of water cluster ions.

01 p0014 A73-10900

On the decomposition of a dynamical system into non-interacting subsystems.

05 p0591 A73-16824

The adsorption and decomposition of CO on Pt(111).

08 p0937 A73-21617

Knudsen measurements of the decomposition and the heat of formation of manganese ditelluride.

09 p1048 A73-22442

Investigation of the morphology and decomposition kinetics of Co-Ni-Ti alloys

10 p1232 A73-24153

Electron absorption spectra of benzochromium-dicarbonyltriphenylphosphine and benzochromium-tricarbonyl and their application to studies of the decomposition kinetics of these compounds

10 p1186 A73-24457

Phenolic binder decomposition in silica-phenolic ablator, determining reaction mechanism from Arrhenius rate equations for various temperatures

11 p1452 A73-26376

Dissociation of semiconductor compounds under the action of a laser beam

11 p1378 A73-26675

Characteristics of martensite decomposition during the tempering of rhenium steels

12 p1509 A73-26894

Rate constants for the reactions of hydroxyl and hydroperoxyl radicals with ozone.

14 p1724 A73-30619

Influence of plastic deformation and of alloying with small additions of oxygen on the decomposition of the metastable beta phase in the TS6 alloy

15 p1894 A73-32526

Continuous decomposition of gamma solid solution in iron-nickel-titanium alloys

20 p2579 A73-39736

Decomposition of martensite during tempering of rhenium steels.

21 p2720 A73-41027

Topological modification and bounded length of decomposition series for convergence space

23 p3000 A73-44301

DECOMPRESSION

U PRESSURE REDUCTION

DECOMPRESSION SICKNESS

Effects of immersion with the head above water on tissue nitrogen elimination in man.

02 p0135 A73-12563

Gas phase separation following decompression in asymptomatic rats - Visual and ultrasound monitoring.

03 p0263 A73-14162

Pathogenesis of some respiration and circulation reactions to barometric pressure gradients

08 p0929 A73-20980

Analysis of some mechanisms of human stability to decompression of the lower portion of the body

08 p0930 A73-20987

Intravascular changes associated with hyperbaric decompression - Theoretical considerations using ultrasound.

09 p1045 A73-22534

EEG activity of rats compressed by inert gases to 700 feet and oxygen-helium to 4000 feet.

11 p1314 A73-25327

Incidence and severity of altitude decompression sickness in Navy hospital corpsmen.

13 p1576 A73-28511

Development of effective means for desaturation of the human organism as a prophylactic measure against altitude decompression disturbances

17 p2111 A73-34231

Effect of certain flight factors on crew efficiency

21 p2643 A73-40350

Absorption of gas bubbles in flowing blood.

22 p2806 A73-42414

DECONTAMINATION

NT SPACECRAFT STERILIZATION

Oxygen plasma for cleaning polymerized organic material contaminated oil-pumped channel electron multiplier arrays used as vacuum UV to visible radiation converters

01 p0054 A73-11237

Design principles for contamination abatement in scientific satellites.

02 p0136 A73-11991

The removal of impurities from hydrazine for control of contamination caused by rocket engine exhaust. [AIAA PAPER 72-1046]

03 p0351 A73-13379

Clean rooms and contamination-free zones in space technology

07 p0830 A73-19011

Removal of hydrocarbon contaminant film from spacecraft optical surfaces using a radiofrequency-excited oxygen plasma. [AIAA PAPER 72-263]

08 p0989 A73-21835

Alkali metal purification and handling for advanced space power systems.

11 p1310 A73-26004

Optical absorption cell with water vapor cross flow instrument designed for wall decontamination and

open air meteorological simulation, examining thermodynamic parameters effects

11 p1367 A73-26318

Spacecraft decontamination and sterilization by formaldehyde, beta-propiolactone, ethylene oxide, radiation and dry heat, noting effects on polymers

14 p1721 A73-30137

DECOUPLING

Non-interacting control of non-linear multivariable systems.

01 p0028 A73-11517

A decoupling supply network for small antenna arrays

02 p0145 A73-11825

Decoupling in a class of nonlinear systems by state variable feedback.

[ASME PAPER 72-AUT-V] 06 p0679 A73-17725

Scalar and block decoupling of time varying and invariant linear multivariable control systems, discussing sufficiency conditions, state estimation and order reduction possibility

08 p0950 A73-21089

Active RC filter synthesis with decoupling stage and third order element for minimizing impedance mismatching and overall capacitance

10 p1193 A73-23734

On the application of the method of decoupling of motions to the analysis and synthesis of nonlinear systems.

10 p1199 A73-24031

Decoupling longitudinal motions of an aircraft.

19 p2386 A73-38033

A sensitivity approach to the decoupling of linear systems with parameter disturbances.

19 p2412 A73-38034

DEEP DRAWING

Deep drawability of titanium sheets.

09 p1104 A73-22522

DEEP SCATTERING LAYERS

Meteorological structure of thin clear air scatter layers observed by ultra-high resolution radar.

03 p0338 A73-14529

DEEP SPACE

NT INTERPLANETARY SPACE

NT INTERSTELLAR SPACE

The zodiacal light as seen from the Pioneer F/G and Helios probes.

02 p0215 A73-12263

Simulation of rendezvous of a man in deep space.

03 p0288 A73-13569

Concatenated and hybrid coding system performance and implementation complexity for moderate speed deep space communication

09 p1056 A73-23401

DEEP SPACE NETWORK

Unified S-band ground system design and management for Apollo program, deep space and manned space flight network tracking and communications requirements

01 p0030 A73-11184

Australian east-west baseline interferometer observations at 2.3 GHz.

03 p0372 A73-13349

Improvements in deep-space tracking by use of third-order loops.

09 p1056 A73-23406

German command station for Helios solar probe, discussing antenna design, transmitter parameters, back-up operation and compatibility with deep space network

[DFVLR-SONDDR-263] 13 p1598 A73-29275

Low-noise microwave receiving systems in a worldwide network of large antennas.

23 p2958 A73-43376

DEFECTS

NT AUDITORY DEFECTS

NT CRYSTAL DEFECTS

NT CRYSTAL DISLOCATIONS

NT EDGE DISLOCATIONS

NT FRENKEL DEFECTS

NT INCLUSIONS

NT POINT DEFECTS

NT SCREW DISLOCATIONS

NT SURFACE DEFECTS

NT VACANCIES [CRYSTAL DEFECTS]

Determining the size of defects in standardizing sensitivity using a spherical reflector.

02 p0169 A73-12149

Gas path analysis applied to turbine engine condition monitoring.

[AIAA PAPER 72-1082] 03 p0354 A73-13405

Acoustic emission source location using single and multiple transducer arrays.

04 p0448 A73-15121

Simple test apparatus for a 100% defect-detection probability in ultrasonic surface scanning of plates and strips

09 p1070 A73-22219

Defect size determination by ultrasonic scanning with a relative threshold

09 p1088 A73-22220

Defect detection in solid materials with the aid of holographic vibration analysis

09 p1089 A73-23115

Comparative investigation of sensitivities of the xeroradiographic and the roentgenographic methods of flaw detection. 11 p1375 A73-26364

Fracture and flaws; Proceedings of the Thirteenth Annual Symposium, Albuquerque, N. Mex., March 1, 2, 1973. 18 p2363 A73-36482

Semiconductor failures due to oxide defects and diffusion faults, describing nematic liquid crystals application to pinholes detection in oxide layers 19 p2410 A73-38447

Progress in flaw growth and fracture toughness testing; Proceedings of the Sixth National Symposium on Fracture Mechanics, Philadelphia, Pa., August 28-30, 1972. 22 p2920 A73-42131

Failure stress levels of flaws in pressurized cylinders. 22 p2921 A73-42156

Ultrasonic determination of shape and size of hidden defects in solids. 23 p2984 A73-43298

DEFENSE COMMUNICATIONS SATELLITE SYSTEM

Army studies cost effectiveness of communications satellites. 03 p0274 A73-13075

Time Division Multiple Access for the defense satellite communications system. 17 p2124 A73-35307

DEFENSE COMMUNICATIONS SYSTEM (DCS)

Optical Characters Reading and facsimile terminals reduction of message preparation time for electrical transmission in Defense Communications System, considering cost effectiveness and maximum benefit 04 p0418 A73-15380

DEFENSE PROGRAM

Financial problems related to aircraft and ships development and production for Defense Department, stressing C-5A, Cheyenne helicopter and DD-963 class of automated destroyers 03 p0401 A73-13897

Electronic display devices for command, monitoring, surveillance, simulation and training in military applications, considering reliability, cost and performance specifications in procurement decision making 08 p0965 A73-21245

US Department of Defense aircraft system effectiveness tests survey questionnaire response data from component, subsystem and system suppliers 21 p2635 A73-41204

DEFLAGRATION

An experimental study of the low pressure limit for steady deflagration of ammonium perchlorate. 16 p2045 A73-33347

Deflagration in the combustion of hydrogen-fluorine mixtures. 16 p2045 A73-33349

Plane unsteady dispersion of gas behind deflagration wave moved by laser radiation with high flux density 20 p2573 A73-39281

Pressure waves generated by constant velocity deflagration flame in explosive hydrocarbon-air mixture for self-similar flow field 22 p2936 A73-42808

DEFLATING

U INFLATABLE STRUCTURES

U PRESSURE REDUCTION

DEFLECTION

Large deflection calculation of circular and annular strain hardenable rigid plastic plates under axisymmetric load, using Kirchhoff-Love hypothesis and Tresca flow condition 03 p0394 A73-14022

Electro-optical multiple transit laser beam deflection system using KDP crystals and quadrupole electrode arrangements 03 p0319 A73-14066

Short-term longitudinal dynamic stability of rods with allowance for clamping methods and for previous transverse deflection 05 p0632 A73-16329

Antenna beam focusing and deflection with the aid of a digital phase computer, in a radiation-fed electronically controlled antenna 06 p0673 A73-17580

Stress distribution on astronomical telescope mirror outer surface, calculating deflection and relief load 06 p0693 A73-18157

Computation of the deflections of straight beams with any variation of the moment of inertia by the method of the three unknowns. 10 p1287 A73-23617

Finite deflections of transversally-isotropic plates and shallow shells 15 p1953 A73-32089

Nonlinear behavior of shells of revolution under cyclic loading. 16 p2075 A73-32791

Application of the method of integrating matrices to the calculation of the natural vibrations of a propeller

blade with allowance for deflection in two planes and for torsion 21 p2783 A73-40389

Large deflection theory for viscoelastic anisotropic thin plates, deriving constitutive, plane stress, plate and nonlinear integrodifferential equations 22 p2923 A73-42638

Influence of initial deflections on the work of a rectangular plate subject to bending in its plane 24 p3150 A73-45244

On the hybrid stress finite element model for incremental analysis of large deflection problems. 24 p3151 A73-45303

DEFLECTORS

An analytical investigation of the impingement of jets on curved deflectors. 03 p0296 A73-14178

Programmable, digital, rapidly frequency-shift-keyed, high-frequency generators for driving acoustooptical light deflectors 05 p0586 A73-17239

Electro-optical laser beam deflector with lithium niobate for low resolution and high speed operation, discussing system design, construction and tests 06 p0700 A73-18296

Experimental results on the application of an x-y acousto-optic deflection system to wide band laser recorders. 06 p0701 A73-18312

Television rate laser raster scanner, discussing deflectors, beam-shaping and image-forming optics, electronic system and scanning beam frequency response 08 p0975 A73-21141

Television rate laser scanner with anisotropic Bragg device of paratellurite as acousto-optic horizontal deflector, noting operation efficiency and limiting resolution 08 p0975 A73-21142

Acoustooptical materials evaluation based on figures of merits and acoustic attenuation for laser beam deflection device design and fabrication 21 p2710 A73-40095

DEFOCUSING

Optical beam spread in a turbulent medium - Effect of the outer scale of turbulence. 07 p0851 A73-19274

Block defocused spherical Fabry-Perot interferometer. 08 p0964 A73-21038

Adiabatic following and the self-defocusing of light in rubidium vapor. 20 p2571 A73-38632

Experimental verification of the analysis of umbrella parabolic reflectors. 22 p2831 A73-41844

DEFORMATION

NT AXIAL STRAIN

NT ELASTIC BENDING

NT ELASTIC BUCKLING

NT ELASTIC DEFORMATION

NT PLASTIC DEFORMATION

NT STATIC DEFORMATION

NT TENSILE DEFORMATION

NT WAVE FRONT DEFORMATION

Investigation of the macroscopic rheonomic properties of a monodirectional fiberglass-reinforced plastic 01 p0067 A73-10002

Thermal diffusion theory for deformations of thin isotropic shells and plates subjected to nonuniform temperature and stress concentration fields 01 p0113 A73-10019

Renormalized Brueckner-Hartree-Fock theory generalization to calculate intrinsic states of many-body nuclear system with permanent deformation 01 p0079 A73-10243

Research performed on the thermomechanics of deformable solids at the Ukrainian Academy of Sciences 01 p0114 A73-10569

Deformation and stress analysis in continuum mechanics problems of solid bodies near singular points, noting applicability of linear theory of elasticity 01 p0118 A73-11404

The thermally activated deformation of niobium-molybdenum and niobium-rhenium alloy single crystals. 02 p0179 A73-11574

Curvilinear coordinates for deformation tensor and stress analysis of structures, using finite element method 02 p0231 A73-11812

Initially spherical water drops deformation under external flow for wide range of Weber and Bond numbers, investigating drag coefficient and Taylor instability 02 p0153 A73-12037

Yield and plastic flow theory for porous metal powder compacts and preforms, discussing stress-strain and deformation-densification relations 03 p0388 A73-13260

How deformation affects the mechanical properties of aluminum forgings. 03 p0322 A73-13266

Upper bound predictions of composite tensile strength as function of transitions from homogeneous to nonhomogeneous deformation [ASME PAPER 72-WA/PROD-8] 04 p0469 A73-15806

Affine and nonlinear transformations for aerial photography film deformation effects on photogrammetry accuracy 05 p0575 A73-16315

Introduction of two solving functions into the equations for nonshallow shells. 05 p0634 A73-16796

Deformation of silicates in some Fra Mauro breccias. 07 p0883 A73-19734

A contactless method of measuring the radial deformations of rotating shafts 07 p0827 A73-20533

On one-dimensional finite-strain beam theory - The plane problem. 08 p1018 A73-21405

Material resistance analogies, relating shear, force and strain factors for bar deformation in tension, compression, torsion and bending 09 p1157 A73-22162

Elastoplastic deformation and hardening function of perforated plates under in-plane tensile loads 09 p1164 A73-23346

Deformation of shells of revolution with attached rings under different local loads, deriving approximate expressions for stressed state 10 p1287 A73-23592

Fiber reinforced metal matrix composites mixing rule, determining tensile strength, deformation energy and flow curve 10 p1231 A73-23694

The effect of deformations in the measurement of the force and the couple of friction 11 p1374 A73-25871

Flexural/torsional deformations of material line in continuous body in terms of curvature and bending vectors, using Frenet-Serret equations 11 p1445 A73-26408

Field-ion microscopic study of the high-speed deformation of tungsten 12 p1509 A73-26838

The Castigliano variational equation and strain continuity relations for a thin shell 12 p1555 A73-27788

Examination of film deformation for aerial photography 12 p1500 A73-27960

Deformable solid as discretized body in classical continuum mechanics, deriving motion and constitutive equations 13 p1659 A73-28558

Effects of deformation on diffusion in iron-nickel and iron-chrome systems 14 p1760 A73-30379

Influence of heating on the intensity and energy of exoelectrons in deformed aluminum 14 p1765 A73-30889

Low temperature deformation of commercial Ti alloys. 16 p2024 A73-32848

A stress-strain relation for homogeneous and isotropic continua 16 p2035 A73-32934

Characteristic matrix method for automatic recognition and extraction of rigid body modes from inconsistent to natural force-deformation relationship of stress and strain elements 16 p2077 A73-32990

Non-linear problems of slender webs and of shallow shells. 16 p2078 A73-33006

Prediction of the deformation properties of polymer materials 17 p2194 A73-34268

Continuum mechanics - A brief review. 17 p2244 A73-34827

Dynamically-induced large deformations of multilayer, variable thickness shells. 18 p2362 A73-36317

Large deformations of cord-reinforced multilayered axisymmetric shells. 20 p2621 A73-39542

Deformation of shells with a circular axis and variable cross-section parameters 21 p2786 A73-40978

Material resistance analogies, relating shear, force and strain factors for bar deformation in tension, compression, torsion and bending 22 p2919 A73-42110

Transformation of a symmetric wave-type process of deformation into an asymmetric process in a plate during the development of a shock wave 22 p2927 A73-42930

Experimental investigation of the strength and deformability of vacuum-prepared fiberglass-reinforced plastic shells 22 p2881 A73-43062

Laws governing the behavior of the electrical resistance during process of inelastic-strain relaxation 23 p3040 A73-43574

- Cylindrical shell design with a frame-connected bottom and a system of concentrated forces applied to the bottom
23 p3042 A73-43726
- Deformation behaviour and deviation from the simple rule of mixture for the ultimate tensile strength in the cold rolled fibre-reinforced composites.
23 p2998 A73-44151
- Deformation history approach compared to internal variables introduced by solution of initial value problem for materials, obtaining constitutive equation
24 p3109 A73-44749
- Recrystallization and precipitation induced by high temperature deformation - Case of a weldable construction steel containing niobium
24 p3101 A73-45524
- DEGASSING**
- NT DEOXYGENATION**
- Moon flares due to lunar gas eruptions, investigating degassing in former geological epochs
02 p0212 A73-11950
- Restrictions on McElroy theory of Martian chaotic terrain production by permafrost withdrawal, calculating degassed water/carbon dioxide ratios in Mars and earth atmospheres
02 p0218 A73-12418
- Relationship between cavitation and decontamination during ultrasonic processing of aluminum and its magnesium alloys
04 p0454 A73-15663
- Electron beam float zone melting and vacuum degassing of niobium single crystals.
04 p0456 A73-15762
- Kinetics of the degassing of oxygen-containing niobium in flowing acetylene to form carbon monoxide
11 p1375 A73-26565
- Diffusion of hydrogen and deuterium in Ta, Nb, and V.
20 p2576 A73-39134
- The origin and evolution of the atmospheres of the terrestrial planets.
22 p2912 A73-42976
- DEGENERATION**
- Solvability of mixed boundary value problems for second-order parabolic equations with degeneration
08 p0983 A73-21126
- Structural characteristics of connections between medial efferent systems and spinal cord neurons
09 p1040 A73-22577
- Degeneracy phenomenon in minimax rational approximation behavior in neighborhood of approximating function pole
13 p1650 A73-29396
- Almost projective mapping of gravitational fields - Degenerate case
17 p2212 A73-35564
- A stable manifold theorem for degenerate fixed points with applications to celestial mechanics.
19 p2486 A73-37799
- Quasi-averages for Green functions construction in solving quantum statistical mechanics problems with degenerate equilibrium states
21 p2741 A73-41297
- DEGENERATIVE FEEDBACK**
- U NEGATIVE FEEDBACK**
- DEGRADATION**
- NT THERMAL DEGRADATION**
- Determination of degradation of nylon 66 using differential scanning calorimetry.
04 p0468 A73-14857
- Semiconductor device degradation by high amplitude current pulses.
05 p0557 A73-16505
- Degradation analysis of infrared and visible optoelectronics devices.
08 p0944 A73-20742
- QAO 2 satellite nickel-cadmium batteries with auxiliary electrodes for overcharge control, discussing operation and degradation mechanism
13 p1572 A73-29583
- Failure data evaluation, determining wear out, degradations, environments causing system failures, repairs, maintenance and sub par performers
16 p2021 A73-33649
- Intensity of mechanical influences and mechanical degradation of hard polymers
16 p2030 A73-33940
- Hydrolytic degradation of polymer electrical insulating materials in warm humid environments, noting relation to ester and ether linkage presence
17 p2197 A73-35349
- Bonding degradation in the tantalum nitride-chromium-gold metallization system.
19 p2435 A73-38440
- Group 3-5 compound light emitting diode degradation modes and mechanisms, discussing epoxy lenses, light transmission characteristics, time and temperature functions and surface passivation
19 p2439 A73-38457
- Biodegradation from evolution viewpoint as physiological function and fundamental cellular process regulating biological equilibrium, explained by intracellular digestion and phagocytic cells association
21 p2638 A73-41024
- DEGREES OF FREEDOM**
- Similar normal mode vibrations in certain conservative systems with two degrees-of-freedom.
02 p0193 A73-12515
- Convergence of consistently derived Timoshenko beam finite elements.
03 p0390 A73-13342
- Three-degree-of-freedom motions of a slender asymmetric cone in a hypersonic wind tunnel.
03 p0287 A73-13494
- Computerized multiple level substructuring analysis.
03 p0392 A73-13690
- N degrees of freedom system resonant vibration mode and frequencies determination from forced vibration of complementary body
04 p0509 A73-14979
- Structural comparison of articulated plane kinematic chains /PKC/ with the aid of graph theory
04 p0476 A73-15656
- Considerations concerning the orthogonality of the natural oscillation modes in elastic systems with many degrees of freedom
04 p0476 A73-15658
- Stability of a thin-wing model with one and two degrees of freedom
05 p0632 A73-16297
- Free vibrations in nonlinear systems with two degrees of freedom
05 p0599 A73-17087
- Discretized body defined as special system with finite degrees of freedom, describing mechanics in terms of constitutive and motion equations
06 p0723 A73-17894
- Calculus of variations for mathematical model of elastic shell with internal degrees of freedom, noting boundary and discontinuity conditions
06 p0766 A73-18877
- Free vibration of multi-degree-of-freedom nonlinear systems.
07 p0909 A73-19164
- Forced vibration of a class of non-linear two-degree-of-freedom oscillators.
07 p0851 A73-19165
- Monofrequent resonance oscillations with external excitation.
07 p0851 A73-19544
- Frequency response of a dynamic system with statistical damping.
08 p0950 A73-20715
- Construction of the frequency spectrum of a three-degree-of-freedom gyroscope with a flexible rotor shaft and elastic gimbal mountings
09 p1084 A73-22656
- Six degree of freedom guided sounding rocket flight simulations and trajectory program, discussing financial and technical feasibility
09 p1117 A73-23218
- Degrees of freedom elimination method shown equivalent to interpolation by splining by means of actual structure in curve connection for given points
09 p1166 A73-23465
- Signal flow graph methods for four and three degree of freedom linear conservative mechanical vibration systems solution, noting Chan-Mai method superiority
11 p1434 A73-25193
- Sensitivity of rotor blade vibration characteristics to torsional oscillations.
11 p1440 A73-25533
- Dynamical system of N degrees of freedom reduced to ideal resonance problem involving Hamiltonian function, presenting algorithm for calculating ignorable coordinates
11 p1423 A73-26071
- Elasticity theory of three dimensional system of particles in rectangular prismatic or tetrahedral net arrangement as topological model for finite element method
11 p1448 A73-26727
- Determination of the equilibrium positions of mechanisms with two degrees of freedom
12 p1524 A73-27465
- Kinetic phenomena in a Knudsen gas with rotational degrees of freedom
12 p1530 A73-27982
- Numerical study of the stochasticity of dynamical systems with more than two degrees of freedom.
13 p1648 A73-28425
- Normal coordinates in the analysis of the principal resonances of nonlinear vibrating systems with multiple degrees of freedom
13 p1695 A73-28557
- Influence of elastic deformations of the gimbal support on the motion of a three-degree-of-freedom astatic gyroscope
13 p1618 A73-29147
- Parametric vibrations of elastically connected two mass system with two degrees of freedom, considering dynamic response to excitation by external compression loads
13 p1700 A73-29391
- All order stability of Hamiltonian systems with two degrees of freedom.
14 p1773 A73-29756
- Viscosity coefficients and heat conductivity of dense gases with rotational degrees of freedom
15 p1915 A73-31022
- Gravitational stabilization of a two-body satellite.
15 p1943 A73-31916
- The geometrical stability of non-linear normal modes in two degree of freedom systems.
15 p1955 A73-32167
- Calculus of variations for mathematical model of elastic shell with internal degrees of freedom, noting boundary and discontinuity conditions
15 p1956 A73-32402
- Application of the finite element method to cases requiring the combination of elements possessing different numbers of degrees of freedom.
16 p2077 A73-32991
- Oscillations of a system with two degrees of freedom during resonance
17 p2213 A73-35591
- Book - Vibration of linear mechanical systems.
18 p2361 A73-35900
- Program of computation of spectral and modal matrices associated with a linear elastic system
18 p2364 A73-36493
- Calculation of hypersonic nonequilibrium nozzle flows with excited vibrational degrees of freedom
18 p2266 A73-37018
- Virtual motion principle implication for structural damping differential equations for cases of homogeneous, inhomogeneous and aerodynamic flutter for various degrees of freedom
20 p2616 A73-39098
- Quasi-dynamic system with eliminable generalized coordinates to define pseudo-degrees of freedom, identifying characteristics
20 p2594 A73-39537
- Configuration space and phase space of a system with an infinite number of degrees of freedom
20 p2594 A73-39640
- Excitation of parametric vibrations in stochastic systems with two degrees of freedom
20 p2594 A73-39641
- A streak technique for measuring the initial movement of a rocket with four unknown and two known degrees of motion.
21 p2696 A73-39986
- Washout circuit design for multi-degrees-of-freedom moving base simulators.
21 p2674 A73-40876
- SAFE - Six axis frequency evaluation of a motion simulator.
21 p2674 A73-40879
- Visual cues and six degree of freedom motion flight simulation for F-4 aircraft energy maneuvering performance, discussing pilot evaluations
21 p2674 A73-40880
- Reduction of the degrees of freedom in solving dynamic problems by the finite element method.
22 p2922 A73-42479
- Forced motion of lumped mass systems including the effect of axial force.
22 p2923 A73-42630
- Reduction of the sensitivity of optimal control systems by using two degrees of freedom.
23 p2962 A73-43285
- Vibrations of a three-degree-of-freedom gyroscope in transition through resonance
23 p2983 A73-44199
- On the stability limit of nonlinear resonances in multiple-degree-of-freedom vibrating systems.
24 p3146 A73-44681
- Ideal resonance problem for dynamic system of N degrees of freedom, obtaining global solution covering libration and circulation regimes under normality condition
24 p3141 A73-45287
- The evolution of periodic orbits close to homoclinic points.
24 p3142 A73-45296
- DEHYDRATED FOOD**
- Microbiological testing of Skylab foods.
12 p1464 A73-27075
- DEHYDRATION**
- Cardiovascular and temperature regulatory changes during progressive dehydration and euhydration.
01 p0008 A73-10165
- Optical and thermal properties of hydrated yttrium vanadates in aqueous solutions, showing decomposition during thermal dehydration
06 p0739 A73-18655
- Cardiovascular adjustments to progressive dehydration.
24 p3060 A73-45063
- DEICING**
- Installing the heater cable directly in the redesigned leading edge.
16 p1970 A73-32924
- DEIMOS**
- Mariner 9 television observations of Phobos and Deimos.
06 p0745 A73-17480
- Mariner 9 television observations of Phobos and Deimos. II.
19 p2479 A73-37222

DEKATRONS U COUNTERS DELAMINATING

On fracture toughness and its size dependence for steels showing thickness delamination.

06 p0709 A73-18476

Torsional and anti-plane strain delamination of an orthotropic layered composite.

20 p2622 A73-39549

DELAY

Measurement on a polarization interferometer of absolute and relative light wave delay in liquid dielectrics under the action of an electric field

07 p0823 A73-19332

Russian book on linear differential delay equations covering solvability theorems, solution properties, stable and unstable equations, first and second order equations, periodic equations, etc

18 p2329 A73-35897

DELAY CIRCUITS

Design and fabrication of helix-like strip meander line delay equalizer in printed circuit technology, noting group delay and insertion loss frequency responses

02 p0145 A73-11823

Selective amplifier with zero group delay in pass-band phase characteristics for sinusoidal frequency signal measurement

09 p1066 A73-23118

Parametric synchronization of self-oscillators with feedback delay and nonlinear circuit

11 p1337 A73-25429

Construction of verification tests for digital devices with delay elements

12 p1482 A73-26753

Panoramic measurement of the coupling impedance of delay systems by the heterodyne method

12 p1479 A73-27210

Frequency distortions of signals in frequency-modulated oscillators with a delayed feedback

17 p2130 A73-35714

Investigation of a stabilization system with a relay angular sensor

20 p2593 A73-39321

Tunnel diode different time constants two delay-line circuit, noting self oscillation range, constant pulse periods and hysteresis phenomenon elimination

21 p2660 A73-40099

DELAY LINES

NT ACOUSTIC DELAY LINES

NT DELAY LINES [COMPUTER STORAGE]

Automated system with CW signal and feedback to measure delay line group delay and transfer function frequency responses, detailing operation and errors

02 p0146 A73-11952

System design, breadboard construction and tests of slope reversal video processor based on tapped delay line estimation with timing discriminator

02 p0167 A73-11957

Channel equalization in presence of intersymbol interference, comparing sequential statistical, dynamic programming, delay line and minimum mean square error techniques

04 p0425 A73-15419

Use of a surface-acoustic-wave delay line to provide pseudocoherence in a clutter-reference pulse doppler radar.

08 p0939 A73-21113

Moving-target-indicator recursive radar filter using bucket-brigade circuits.

09 p1065 A73-23096

Group delay equalization in waveguide communications systems for signal regeneration with tapered meander transmission line

09 p1053 A73-23110

Differential mode of operation for bucket-brigade circuits.

11 p1341 A73-25360

High spatial resolution wire spark chamber system using electromagnetic delay line readout.

11 p1363 A73-25962

A multiwire proportional counter with integral readout delay line.

11 p1364 A73-25964

High spatial resolution MWPC systems using electromagnetic delay line readouts.

11 p1364 A73-25966

High-speed frequency count-down circuit using a tunnel diode and a delay line.

13 p1594 A73-29226

Calculation of dispersion in delay systems composed of resonator sequences with mixed excitation

14 p1733 A73-30028

Opto-acoustic signal processors extend radar and communication system capabilities.

14 p1729 A73-30675

Tapped delay line filter for optimal single pulse detection in band-limited PCM/NRZ system in presence of Gaussian noise

14 p1729 A73-30698

Single-loop delay line integrator SNR enhancement properties in additive zero mean correlated noise channels for finite signal observation times

16 p1979 A73-33406

Light pulse structure and bandwidth bounds in ruby laser with delay line inside variable effective length resonator

17 p2185 A73-35169

A study of the characteristics of surface charge transfer devices

20 p2534 A73-38854

Self and excited oscillations in a circuit composed of a non-linear element and a delay line.

24 p3075 A73-45487

DELAY LINES [COMPUTER STORAGE]

Analysis of the operation of devices for normalizing random signals

18 p2293 A73-36851

DELTA FUNCTION

Application of the Dirac delta function in the calculation of the bending of a rectangular beam with shear strain

03 p0384 A73-13130

An integral representation of the Dirac delta function for axisymmetric boundary value problems.

16 p2032 A73-33309

DELTA LAUNCH VEHICLE

The Delta launch vehicle for scientific and applications satellites.

01 p0111 A73-11159

Flight evaluation of a quartz-fiberfrax heat shield.

05 p0641 A73-17209

Digital control system development for the Delta launch vehicle.

20 p2613 A73-38786

DELTA MODULATION

A time-division multiplexed telemetry system using delta-modulation.

03 p0270 A73-14279

The transmission of low frequency medical data using delta modulation techniques.

04 p0412 A73-15408

Low cost electronic method of delaying speech signals based on adaptive delta modulators

05 p0552 A73-17375

Energy spectra of mixed discrete random processes in statistical multiplexing systems with pulse position, delta and pulse code modulation

06 p0668 A73-18390

Constant factor delta modulator with adaptive voltage feedback to error point in coder for SNR improvement and hunting characteristic removal

09 p1065 A73-23100

Delta modulation and differential PCM systems performance comparison at high sampling rates for color video signal coding

09 p1055 A73-23389

Application of some data compression systems to ESRO satellite data.

20 p2524 A73-38735

DELTA WINGS

Higher-order delta wings with flow separation at subsonic leading edges

02 p0127 A73-11581

Nonlinear characteristics of a slender triangular wing near an interface

02 p0127 A73-11630

The pressure on flat and anhedral delta wings with attached shock waves.

02 p0128 A73-12501

Application of an improved transpiration cooling concept to space shuttle type vehicles.

03 p0397 A73-13492

Lee-side vortices on delta wings at hypersonic speeds.

03 p0247 A73-14180

Rates of change of flutter Mach number and flutter frequency.

03 p0395 A73-14188

A new algorithm for three-dimensional method of characteristics.

03 p0337 A73-14201

The influence of a strake on the flow field of a delta wing/lamda 0.2/ at near-sonic velocities

03 p0248 A73-14385

Fighter aircraft maneuverability improvement at high subsonic speeds by slotted and unslotted leading- and trailing-edge flaps on delta wing

03 p0248 A73-14386

The aerodynamic characteristics of the thin delta wing fitted with a conical body in supersonic flow.

04 p0404 A73-15167

Study of a series of variable-geometry wings derived from delta wings of different aspect ratios. I - Aerodynamic characteristics of delta wings

04 p0404 A73-15651

Experimental determination of bound vortex lines and flow in the environment of the trailing edge of a slender delta wing

05 p0528 A73-16600

Similarity relationship for wing-like bodies at high Mach numbers.

05 p0532 A73-16937

Weight sensitivity of a space shuttle orbiter to thermal structural combined loads design criteria.

05 p0635 A73-16979

Convective heating on delta-wing Space-Shuttle boosters including interference effects.

05 p0533 A73-17202

Applications of shock expansion theory to the flow over non-conical delta wings.

06 p0645 A73-18512

Conically cambered triangular wings with reflex spanwise curvature.

08 p0925 A73-20938

Slender delta-wings for future subsonic passenger planes

09 p1027 A73-21992

Correlation of wing-body combination lift data.

09 p1028 A73-22435

Nonstationary flow downwash behind a delta wing during supersonic motion

11 p1299 A73-25046

Flutter of pairs of aerodynamically interfering delta wings.

11 p1301 A73-25545

[AIAA PAPER 73-314] Supersonic gas flow past the leeward side of a conical wing

11 p1304 A73-26439

Supersonic flow around a delta wing, taking into account flow separation at the leading edges

12 p1457 A73-27098

Separated flow past a slender delta wing at incidence.

15 p1821 A73-31121

Linear problem for delta and V-shaped wings

15 p1823 A73-31301

VTOL jet transport aircraft commercial applications, describing lift engine system, hover flight control, engine failure problems and operating cost analysis

17 p2099 A73-34257

Successive approximations for calculating supersonic flow past wings with subsonic leading edges

17 p2091 A73-34347

Investigation of the expansion side of a delta wing at supersonic speed.

18 p2263 A73-36312

Supersonic conical flow past delta and tapered structures, considering angle of attack, leading edges, flow separation, negative slope concept and pressure distribution

19 p2376 A73-37546

Effect of yaw on supersonic and hypersonic flow over delta wings.

19 p2377 A73-38008

Pressure fields over hypersonic wing-bodies at moderate incidence.

20 p2508 A73-39808

Sound propagation in rotating vortex flow downstream from delta wing in wind tunnel, discussing acoustic ray refraction by flow

22 p2839 A73-41715

Methods for calculating nonlinear flows with attached shock waves over conical wings.

22 p2796 A73-42562

DEMAGNETIZATION

The theoretical output of a ring core fluxgate sensor.

07 p0825 A73-20219

Plane film elements demagnetizing factor measurement from material-element hysteresis loop comparison

09 p1084 A73-22655

A determination of the intensity of the ancient lunar magnetic field.

12 p1542 A73-27494

Electron-beam welding of small components

12 p1504 A73-27989

DEMAND [ECONOMICS]

Methodologies for the analysis of transport requirements with particular regard to the aeronautic case

12 p1561 A73-27070

DEMINERALIZING

AEGIS Demineralizer/Water Cooler - Design for availability.

16 p1989 A73-33608

Low calcium diet produced chronic decalcification effect on osseous repair of experimentally induced cortical bone defect in chickens

18 p2270 A73-35981

DEMULATION

Complex detection - A waveform preserving technique for single-sideband demodulation.

04 p0415 A73-14989

Demodulation of pulse modulated signals using Kalman filtering techniques.

06 p0669 A73-18809

Digital phase locked loop for FM demodulation in real time, computing SNR for frequency offsets and sinusoidal modulation

09 p1054 A73-23373

Human visual evoked response signal decomposition by complex demodulation in terms of after-discharge time, envelope and frequency parameters

11 p1324 A73-26497

Amplitude-modulated pulse code sequence demodulation using physically realizable linear filter for reconstruction of discrete sample message at optimum mean-square error level

12 p1467 A73-26943

Experimental studies of a method of detecting microwave-modulated laser radiation in a photosensitive detector

13 p1628 A73-29415

- A nomographic comparison of coherent and non-coherent detection statistics. 16 p1980 A73-33415
- Phase modulated data transmission with partial pilot signals, interpolating reference demodulation signals at receiving end by maximum cross correlation 16 p1984 A73-33978
- DEMODULATORS**
- NT MODEMS
- NT PHASE DEMODULATORS
- NT PHASE LOCK DEMODULATORS
- FM threshold performance of the frequency demodulator with feedback. 03 p0276 A73-13903
- Digitalized or sampled data FM demodulator recursive algorithm synthesis and SNR performance comparison with optimum analog and conventional limiter discriminator demodulators 06 p0664 A73-17712
- A sampling FM wide-band demodulator useful for laser Doppler velocimeters. 06 p0673 A73-17786
- Direct frequency demodulation with CW Gunn and IMPATT oscillators. 07 p0795 A73-20554
- Kalman filtering theory application to optimal causal demodulator for pulse amplitude modulated signals in white Gaussian noise 09 p1067 A73-22116
- TDMA satellite telephonic communication network with preassigned channelled radio carrier, describing four phase demodulator and channel units regrouping 09 p1050 A73-22320
- Digital coherent demodulator techniques for moderate data rate PSK signal reception in real time, describing synchronous bandpass sampling receiver with IF signal A/D conversion 09 p1053 A73-23371
- Noise immunity evaluation for noncoherent demodulators or FSK and PSK signals in short wave channels, using minimum a priori information on additive noise properties 13 p1592 A73-28899
- Some investigations on frequency demodulating systems with fluidic jet deflection amplifiers. 13 p1572 A73-29046
- DENDRITIC CRYSTALS**
- The inhibition of the dendritic electrocrystallization of zinc from doped alkaline zincate solutions. 03 p0273 A73-13727
- Flat dendritic carbide effects on crack formation in Ti and Nb stabilized austenitic Cr-Ni corrosion resistant steels after heating to 1250 C 06 p0705 A73-17850
- Dendritic solidification of Cu-Ni alloys. I - Initial growth of dendrite structure. 06 p0712 A73-18756
- Dendritic solidification of Cu-Ni alloys. II - The influence of initial dendrite growth temperature on microsegregation. 06 p0712 A73-18757
- Thermophysical effects of solidification on dendritic structure and mechanical properties of cast stainless and low alloy carbon steels for different crystallization rates 09 p1107 A73-23198
- Investigation of the crystallization of metallic powders obtained by liquid-phase atomization 10 p1224 A73-24313
- Dendritic liquation of hypoeutectic binary, ternary and complex Fe- and Ni-base alloys dependence on phase diagram 13 p1631 A73-28102
- Striated, cellular and dendritic substructure formation during growth of Fe-Ni alloy single crystals 13 p1631 A73-28107
- Unidirectional solidification formed interdendritic eutectic composition related to solidification variables, discussing Al-Cu and Al-Cu-Ni systems 13 p1632 A73-28131
- Cu content comparison of Faton meteorite to true extraterrestrial meteorites, determining dendritic structure and terrestrial origin from similarity to brass 13 p1684 A73-29179
- Solidification structure and tensile properties of 2014 aluminum alloy welds. 14 p1755 A73-30149
- Experimental observations of dendritic duplex crystals grown in complex Ni base alloys. 15 p1890 A73-31841
- The influence of primary precipitates on the tensile strength of unidirectionally solidified /Fe, Cr/-Cr, Fe/7C3 in-situ grown composites containing 30 wt % Cr. 19 p2442 A73-38088
- Influence of magnesium on the structure of heat-resistant nickel-base alloys 21 p2718 A73-40485
- DENDRITIC DRAINAGE**
- U DRAINAGE PATTERNS
- DENTROGENATION**
- Development of effective means for desaturation of the human organism as a prophylactic measure against altitude decompression disturbances 17 p2111 A73-34231
- DENSE PLASMAS**
- Effect of electron-electron collisions on the thermal conductivity of a dense plasma. 11 p1402 A73-25120
- Quantum statistical mechanics of dense partially ionized hydrogen. 11 p1405 A73-25886
- Laser light pulse absorption in transient dense hot plasma generated around metallic anode tip by fast capacitive discharge in vacuum 13 p1664 A73-28460
- Role of stimulated Compton scattering in the interaction of laser radiation with a superdense plasma. 13 p1664 A73-28615
- Suppression of the flute instability of a dense plasma by a magnetic system of feedbacks in an open trap 13 p1666 A73-28953
- General radio-frequency properties of bounded plasma systems in connection with the production and heating of dense plasmas. 14 p1780 A73-30120
- Microwave heating of electrons of a dense plasma column at frequencies higher than electron cyclotron frequency. 14 p1782 A73-30771
- Longitudinal force exerted by circularly polarized high-powered laser radiation in a dense electron plasma. 15 p1917 A73-31091
- Heating of a high-density plasma with the aid of powerful electron beams 15 p1920 A73-32308
- The radiative properties of high density argon plasma in explosively driven shock waves. 16 p2040 A73-32907
- Electric properties of dense plasmas in high current pulsed discharge. 16 p2040 A73-32943
- Theory of light scattering from dense plasmas. 16 p2041 A73-33323
- Traveling regions of high solar wind density observed in early August 1972. 16 p2056 A73-33460
- Experimental observation of the high-density plasma-beam formation by continuous-flow Z-pinch. 17 p2217 A73-35523
- Anomalous heating of dense plasma by laser radiation. 17 p2218 A73-35823
- Measurement of electron-ion recombination rate of a dense high-temperature cesium plasma. 18 p2339 A73-36622
- Investigation of the performance of a coaxial accelerator in the production of a dense high-energy plasma 19 p2467 A73-37367
- High-speed interferometry of expanding and collapsing laser produced plasma. 21 p2744 A73-39964
- Stark broadening of high quantum number delta n = 1 transitions of carbon V and VI in a laser-produced plasma. 21 p2745 A73-40471
- Instability of an azimuthal ion beam in a dense plasma 21 p2746 A73-40522
- Electron concentrations calculated from the lower hybrid resonance noise band observed by Ogo 3. 22 p2901 A73-41912
- Dense argon plasma expansion into vacuum or low density partially ionized hydrogen plasma, examining momentum transfer, electron density and electric field effects 22 p2891 A73-42239
- The efficient inject of high microwave powers into the overdense magnetoactive plasma in the waveguide. 22 p2827 A73-42517
- Current-induced heating of a dense plasma during collective interactions in a high-current gas discharge 23 p3009 A73-43651
- Electrical conductivity of a plasma during collective interactions in a high-current gas discharge 23 p3009 A73-43652
- Some diagnostic methods for dense plasmas from high-pressure pulse discharges 23 p3011 A73-43667
- A magnetogasdynamic accelerometer for the simulation of micrometeoroids 23 p2966 A73-43781
- Suppression of the flute instability in a dense plasma in an open system by magnetic feedback. 23 p3013 A73-44305
- Volt-ampere characteristics of double electrical plasma probe measuring ionization level in low temperature dense plasma under interelectrode gap near-breakdown conditions 23 p2983 A73-44344
- Heating of a dense plasma by a powerful electron beam. 24 p3114 A73-44616
- Picosecond framing photography of a laser-produced plasma. 24 p3090 A73-44920
- Calculation of the Lyman-alpha asymmetry in a dense, partially-ionized hydrogen plasma. 24 p3116 A73-45323
- DENSIFICATION**
- The role of pore size in the ultimate densification achievable during P/M forging. 04 p0456 A73-15799
- Investigation in the sintering of Y2O3 powders in the temperature range 1000 to 1400 C. 04 p0457 A73-15987
- Development of a production technology for high-density metal-ceramic materials by the method of impregnating porous preforms with low-melting iron boride alloys 10 p1224 A73-24316
- DENSITOMETERS**
- NT MICRODENSITOMETERS
- Ejection time by ear densitogram and its derivative - Clinical and physiologic applications. 20 p2511 A73-38866
- DENSITY [MASS/VOLUME]**
- NT ATMOSPHERIC DENSITY
- NT GAS DENSITY
- NT SPACE DENSITY
- Intergalactic matter existence experiments, discussing critical cosmological energy and matter density, neutral and ionized gas, clustering and hot media 01 p0094 A73-10060
- Lunar interior density constraints from moon moment of inertia and mean density calculations and seismometer data on lunar crust mass and density 02 p0220 A73-12484
- New formulations of the corresponding states principle for the transport properties of pure dense fluids. 08 p1023 A73-21258
- Lunar soil density estimation from Lunar Orbiter photographic measurements of boulder tracks, determining friction angle 10 p1277 A73-24085
- Determination of the density of the surface covering of the moon from given surface temperatures during eclipse and lunar-night periods 16 p2063 A73-33754
- Internal structure and chemical composition of Mercury 16 p2066 A73-33796
- On the diurnal variations of total mass density, number density and temperature in the upper thermosphere. 21 p2682 A73-40170
- DENSITY [NUMBER/VOLUME]**
- NT ELECTRON DENSITY [CONCENTRATION]
- NT ELECTRON DENSITY PROFILES
- NT ELECTRON DISTRIBUTION
- NT ION DENSITY [CONCENTRATION]
- NT IONOSPHERIC ELECTRON DENSITY
- NT IONOSPHERIC ION DENSITY
- NT MAGNETOSPHERIC ELECTRON DENSITY
- NT MAGNETOSPHERIC ION DENSITY
- NT MAGNETOSPHERIC PROTON DENSITY
- NT METEOROID CONCENTRATION
- NT PACKING DENSITY
- NT PARTICLE DENSITY [CONCENTRATION]
- NT PLASMA DENSITY
- NT PROTON DENSITY [CONCENTRATION]
- NT SPACE DENSITY
- Number density estimation for neutral hydrogen hot component required for solar wind heating to satisfy observed proton temperature relationship to wind velocity 02 p0205 A73-11745
- The number-intensity distribution of X-ray sources observed by Uhuru. 14 p1788 A73-30733
- Interstellar matter observations, discussing densest stages spatial distribution near solar system and dense clouds 17 p2227 A73-34409
- On the diurnal variations of total mass density, number density and temperature in the upper thermosphere. 21 p2682 A73-40170
- DENSITY [RATE/AREA]**
- U FLUX DENSITY
- DENSITY DISTRIBUTION**
- A non-uniform relativistic cosmological model. 01 p0098 A73-10581
- Velocity, temperature and component concentration distributions in laminar boundary layer at blown surface for binary mixture flow 01 p0034 A73-10957
- Ionospheric bottom side electron density profiles from measured monthly median values, using CCIR and ITS computer programs for critical frequencies 02 p0163 A73-173202
- Sound propagation in a combustion can with axial temperature and density gradients. 02 p0238 A73-12608
- A search for density and pressure inversions in high-temperature, low-gravity model atmospheres. 03 p0366 A73-12935
- Square well fluid liquid-vapor interface density profiles from perturbation expansion in chemical

potential, comparing to BGYB and excess free energy minimization approaches

03 p0342 A73-13277

The relative merits of galactic density functions - An orbit computational viewpoint.

03 p0373 A73-13363

Computerized flying spot scanner/analyzer for automatic mensuration analysis of droplets, particles and cell preparations from 35 mm film density distributions

03 p0309 A73-14449

Nature of the density reversal beneath the lunar maria.

04 p0496 A73-14821

Resonance coupling of a transverse magnetic response to a transverse electric excitation by the axial density gradient of a bounded plasma.

05 p0601 A73-16364

Open spiral density wave propagation and distortion due to differential rotation in Lindblad resonance region

05 p0616 A73-16455

Closed form solutions for dust density and temperature distributions in shock layer of hypersonic wedge flow

05 p0533 A73-17115

Determination of the spatial distribution of a plasma with a microwave resonator.

06 p0727 A73-17423

Density-matrix method for a weakly ionized plasma.

06 p0730 A73-18373

Argon plasma density and energy distribution development during microwave radiation absorption at upper hybrid resonance

06 p0732 A73-18605

A new integral-variational method for calculation of relaxation regions behind shock and detonation waves.

07 p0809 A73-19050

Interpretation of Ogo 5 Lyman alpha measurements in the upper geocorona.

07 p0813 A73-19233

The luminosity function and density distribution of disk population stars.

07 p0876 A73-19358

Thermodynamic short range order models for dense substance equilibrium properties calculation, assuming molecular interaction independence and self similar radial function

07 p0851 A73-19397

Three-colour photometry in a field in the direction of the galactic anticentre near M 35.

08 p1005 A73-20923

Three dimensional cosmic ray anisotropy and density distribution at earth orbit and in interplanetary space with allowance for primary particle and nucleon energy spectrum

08 p1000 A73-21343

Measurement of spatial plasma-density distributions with the aid of an open barrel-shaped resonant cavity

09 p1124 A73-21879

Block diagram of transistorized phase instability meter for statistical analysis of one dimensional density distributions, noting two series connected identical delay lines

09 p1064 A73-23008

Density homogeneity in a laser cavity due to energy release.

09 p1098 A73-23450

Multiple subuniverses concept for wide mean space density variations in closed universe, considering radio and optical observation possibility

10 p1275 A73-23822

An exact solution for a collisionless flat galactic model.

10 p1275 A73-23826

Stress differences in the moon as an evidence for a cold moon.

10 p1277 A73-24084

Coronal polar plume observed electron density dependence on assumed density distribution normal to axis, analyzing errors in measurements

10 p1279 A73-24141

Ion-implanted bipolar transistor carrier concentration profiles.

10 p1194 A73-24155

On the relation between optical scale height and density scale height in a stellar atmosphere.

10 p1281 A73-24406

Solar Lyman alpha changes and related hydrogen density distribution at the earth's exobase (1969-1970).

10 p1269 A73-24736

The structure of the shock wave in the vicinity of the shock tube sidewall.

10 p1209 A73-24824

Shock wave determination of shear velocity at high pressures for understanding of planetary interior behavior with abrupt change in density from seismic interpretation

11 p1355 A73-25898

The solar wind and the temperature-density structure of the solar corona.

11 p1413 A73-25954

Density distribution of radiation from a source of limited size in a scattering medium.

11 p1400 A73-26193

Generalized van der Waals theories for surface tension and interfacial width.

11 p1400 A73-26214

Natural oscillations of density-stratified ideal incompressible liquid in rectangular vessel, solving oscillation equation for various density distributions

11 p1349 A73-26441

Emission from a point charge during motion along the plane boundary of a dielectric with periodically varying density

11 p1402 A73-26448

Feedback stabilization of a multimode two-stream instability.

11 p1406 A73-26556

Macroscopic equilibria of relativistic electron beams in plasmas.

11 p1407 A73-26561

The structure of the Eta Aquarid meteor stream.

11 p1426 A73-26573

Radar angels cross section statistical distribution model based on radar measurement and direct ornithological data on bird populations density

11 p1332 A73-26630

Inhomogeneous plasma density distribution relation to ambipolar diffusion and ionization balance processes of electron cooling, particle recombination and ground state, step wise and Penning ionization

12 p1527 A73-26932

Interplanetary scintillations observations from solar wind plasma density fluctuations power spectrum

12 p1533 A73-26980

An association of magnetospheric whistler dispersion characteristics with changes in local plasma density.

12 p1488 A73-26985

Electron-density distribution in a coronal condensation.

12 p1540 A73-27293

Possibility of gasdynamic effects at the critical point of the phase equilibrium

12 p1487 A73-27418

Explosion in detonating media with a variable initial density

12 p1487 A73-27419

Model for lateral variations of lunar density minimizing total shear strain energy of moon, noting gravitational potential equal to observed potential at surface

12 p1541 A73-27488

Explosion in a variable-density medium in the presence of variable counterpressure.

12 p1487 A73-27532

Velocity, temperature and component concentration distributions in laminar boundary layer at blown surface for binary mixture flow

12 p1487 A73-27533

Conditions for powder compaction over the deformation zone width during rolling

12 p1503 A73-27554

Improved three-dimensional mapping of the electron density distribution of the solar corona.

12 p1536 A73-27843

Dynamic figure of the moon and the density distribution in the lunar interior

12 p1546 A73-27866

Electric field interaction with polar molecules at varying density diffusing through solid body surface, deriving dispersion law for density and potential fluctuations

12 p1526 A73-27939

A probe system for spectrometric determination of temperature and concentration distributions in combustion gases.

13 p1612 A73-28432

A method for calculating the sedimentation characteristics of particles in linear dextrane-density gradients and its application to the separation of red blood cells according to the sedimentation rate

13 p1578 A73-28476

Instability of hydromagnetic perpendicular shocks in inhomogeneous fluids.

13 p1601 A73-28775

Entropy layer effects in constant pressure hypersonic boundary layers.

13 p1564 A73-28812

Water sources in lunar atmosphere, calculating minimum depth for existence from water density values

13 p1681 A73-28844

Shock wave large particle model of ion density discontinuity decay in nonisothermal plasma, assuming high electron temperature and Boltzmann distribution

13 p1667 A73-29171

Particle track record in Apollo 15 deep core from 54 to 80 cm depths.

13 p1686 A73-29566

Polar ionospheric electron density distribution near closed field line boundaries for ISIS 1 dayside passes, discussing geomagnetic storm effects

14 p1748 A73-29980

Shock wave propagation in atmospheres with spatially inhomogeneous density and temperature fields, using ideal polytropic gas model

14 p1750 A73-30654

Patterns of waves in galactic disks.

14 p1801 A73-30728

A microscopic theory of density fluctuations in partially ionized gases.

15 p1916 A73-31086

Clairaut equation solution for determination of equilibrium configuration of corotating masses, considering density distribution of fluid rotating planet

15 p1939 A73-32006

Density and temperature distributions in hypersonic sphere wakes.

15 p1824 A73-32150

Vacuum evaporation method for manufacturing neutral density filters with nonlinear density profiles.

15 p1914 A73-32380

Theory of light scattering from dense plasmas.

16 p2041 A73-33323

Axial distribution for a hot electron plasma.

16 p2041 A73-33325

Early-time model of laser plasma expansion.

16 p2042 A73-33340

A two-dimensional theoretical model for stratospheric ozone density distributions in the meridional plane. [AIAA PAPER 73-541]

16 p2008 A73-33571

Discreteness of the dimensions of lunar circular maria and thalassoids

16 p2065 A73-33788

An experiment in photographic eisdensitometry of the moon and planets

16 p2070 A73-33848

The lateral distribution of muons in near vertical EAS.

17 p2223 A73-34243

Measurement of plasma density distribution using an open barrel-shaped cavity.

17 p2215 A73-34303

A numerical study in three space dimensions of Bénard convection in a rotating fluid.

17 p2151 A73-34855

Classical fracture mechanics concepts, considering Griffith theory and modifications for ductile materials and strain energy density field

17 p2246 A73-34883

Vertical ozone profiles from observations of eclipsing satellites.

18 p2304 A73-35971

Atomic oxygen profiles determined by EUV absorption analysis.

18 p2308 A73-36049

Air density at heights near 200 km from the orbit of 1970-65D.

18 p2309 A73-36052

Density nonuniformities in a gas dynamic laser cavity.

18 p2321 A73-36174

Specie number density, pitot pressure, and flow visualization in the near field of two supersonic nozzle banks used for chemical laser systems.

18 p2322 A73-36200

Turbulence in stably stratified fluids - A review of laboratory experiments.

19 p2449 A73-38234

On steady wave profiles in solids.

19 p2461 A73-38262

Dynamical figure of the moon and the density distribution of the lunar interior.

20 p2608 A73-39240

Nonlinear model for plane unsteady flow resulting from collapse of homogeneous density region in heavy ideal density-stratified fluid

20 p2547 A73-39287

An approach to the determination of conditions impairing heat transfer under supercritical pressure

20 p2628 A73-39614

Study of turbulent wakes behind cones in hypersonic flight using Schlieren photograph correlation

21 p2696 A73-39983

Relativistic baryon effective masses and thresholds for strongly interacting superdense matter.

21 p2766 A73-40318

Numerical model for cold gaseous planets (Jupiter, Saturn, Uranus, Neptune) as remnants of star formation attempts, taking into account density fluctuations in collapse region

21 p2766 A73-40374

A numerical investigation of the current and density distributions for a non-equilibrium plasma in a segmented electrode duct.

21 p2748 A73-40926

Interaction of a shock wave with blunt bodies in supersonic flow

21 p2633 A73-41222

Inhomogeneous plasma density distribution relation to ambipolar diffusion and ionization balance processes of electron cooling, particle recombination and ground state, step wise and Penning ionization

22 p2891 A73-42266

An attempt to interpret the mean properties of the velocity field of young stars in terms of Lin's theory of spiral waves.

22 p2908 A73-42310

Rayleigh-Taylor problem of thermal instability of density-stratified layer of incompressible fluid heated

from above, considering oscillatory and nonoscillatory modes stability 23 p3048 A73-43346

Porous and dense layers in Nb-Ti-O system analyzed by X-ray spectroscopy, finding element content influence 23 p2990 A73-43481

Mean Reynolds stress tensor model for analytical prediction of turbulence structure of density-stratified atmospheric boundary layer 23 p3002 A73-43592

Ammonia density profiles and photochemical destruction above Jovian tropopause as function of eddy diffusion coefficient, considering background atmosphere scale height 23 p3028 A73-43601

The nighttime distribution of ozone in the low-latitude mesosphere. 23 p2975 A73-43881

On the theoretical model for vertical ozone density distributions in the mesosphere and upper stratosphere. 23 p2977 A73-43898

Density and velocity fluctuations in young nebulae of Orion type 23 p3035 A73-44232

Galactic protocluster radio emission detection, using adiabatic density perturbation theory of galactic evolution 23 p3037 A73-44256

Density variation and radiative exchange effects on convective instability of plane-parallel polytropic atmosphere heated from below with application to solar granulation 24 p3135 A73-44628

Similarity of flows arising during reflection of weak shock waves from a rigid wall and from a free surface 24 p3076 A73-44713

Surface tension and interfacial density profile of fluids near the critical point. 24 p3110 A73-44986

DENSITY MEASUREMENT

NT X RAY DENSITY MEASUREMENT

Density and temperature measurement in laminar boundary layer and free jet of hypersonic nozzles by electron beam probe. [ONERA, TP NO. 1131] 01 p0045 A73-10239

Plasma density measurement by a Langmuir probe in the presence of a magnetic field 01 p0082 A73-10428

Gas density measurements in a jet using Raman scattering. 01 p0050 A73-10763

Measurement of particle size, number density, and velocity using a laser interferometer. 01 p0053 A73-11226

Free jet expansion from concentric orifices into vacuum. 02 p0152 A73-11528

Turbulent gas mixing measurements using a laser schlieren technique. 03 p0296 A73-14202

The application of dual hologram interferometry to wind tunnel testing. [AIAA PAPER 73-210] 05 p0577 A73-16941

A neutral-potassium-beam measurement of plasma density. 05 p0604 A73-17364

Ion density and current distribution measurements in hypersonic turbulent wakes behind sphere flown in ballistic range, using cylindrical electrostatic probes 06 p0645 A73-18135

Atomic oxygen formation times obtained from measurements of electron density profiles behind shock waves in air. 07 p0853 A73-19510

Nitric oxide densities during sunrise derived from overhead emission measurement as function of altitude 09 p1074 A73-22065

The electron density experiment on-board the Ariel 4 satellite. 09 p1085 A73-22916

Use of lasers for local measurement of velocity components, species densities, and temperatures. 10 p1217 A73-23852

Level and density sensors using pneumatic repeaters 11 p1364 A73-26099

High temperature density measuring apparatus using the photon attenuation technique. 11 p1367 A73-26309

The open-source neutral-mass spectrometer on Atmosphere Explorer-C, -D, and -E. 13 p1616 A73-28628

Explorer satellite triaxial accelerometer system to determine neutral atmosphere density, monitoring orbit adjust propulsion thrust and measuring spacecraft roll, describing instrument calibration 13 p1688 A73-28631

Density measurements in high speed arc heated flows. 13 p1622 A73-29640

Millstone Hill Thomson scatter results for 1966 and 1967. 15 p1866 A73-31067

Test gas properties behind a decelerating shock wave in a shock tube. 16 p2000 A73-33319

Probe design for orbit-limited current collection. 16 p2041 A73-33320

Temperature dependent crystallization and density of Fe-Mn-C alloys with niobium at 1200-1500 C from gamma ray measurements 16 p2027 A73-34012

An evaluation of ionospheric probe performance. I - Evidence of contamination and clean-up of probe surfaces. II - The influence of vehicle wake effects on electron density and temperature measurements. 17 p2160 A73-34786

FM-CW method application to partial reflection measurements of ionospheric electron density to avoid man-made interference and interpretation difficulties from frequency spectrum broadening 18 p2305 A73-36008

Earth radiation pressure and the determination of density from atmospheric drag. 18 p2308 A73-36051

Drag density data from the Cannon Ball II and Muskel Ball satellites. 18 p2309 A73-36053

A comment on the measurement of atmospheric density by absorption of Lyman-alpha. 18 p2309 A73-36054

Interpretation of short period density changes shown by the drag of satellites. 18 p2310 A73-36133

Gas concentration measurement by coherent Raman antistokes scattering. [AIAA PAPER 73-702] 18 p2315 A73-36251

Density measurements in the equatorial atmosphere by means of the San Marco 3 satellite 19 p2426 A73-38151

Determination of local gas states from scattered laser light 19 p2438 A73-38270

Low value atmospheric density extremes evaluation covering ground elevations up to 15,000 feet for engine power calculation in aircraft design 21 p2729 A73-40063

On the possibility of measuring gas concentrations by stimulated anti-Stokes scattering. 21 p2699 A73-40458

Structure variations in the winter polar atmosphere. 21 p2685 A73-40827

Electron concentrations calculated from the lower hybrid resonance noise band observed by Ogo 3. 22 p2901 A73-41912

Changes in the distribution of density and radio scattering in the solar corona in 1971. 24 p3138 A73-45049

DEOXIDIZING

Kinetics of the degassing of oxygen-containing niobium in flowing acetylene to form carbon monoxide 11 p1375 A73-26565

Ni-base alloy powder metallurgy from production waste cuttings by oxidation and subsequent oxide reduction with hydrogen and calcium hydride 12 p1503 A73-27553

Phase equilibrium technique to measure oxygen solubility in liquid Co at 1510 to 1700 C, determining thermodynamic characteristics and deoxidation curves 23 p2990 A73-43482

DEOXYGENATION

Effect of antioxidants on the blood deoxygenation rate in animals exposed to altered atmospheres 12 p1465 A73-27702

DEOXYRIBONUCLEIC ACID

Russian book - Information macromolecules during radiation injury to cells. 04 p0410 A73-15707

DNA catabolism in rat tissues in response to transverse accelerations 06 p0650 A73-17679

Antiradial properties of DNA and of its denaturation products 06 p0656 A73-18875

Silk fibroin, collagen, glycoproteins, keratin and protamines formation in single evolutionary event by de novo synthesis of DNA 07 p0780 A73-19219

RNA and DNA of internal organs during a remote postreanimation period in animals with complete and incomplete functional recovery of the central nervous system 14 p1719 A73-30842

Protein and nucleic acid contents in animal tissues under hypokinesia 15 p1834 A73-31503

Effects of electromagnetic waves of the millimeter range on a cell and on some structural elements of a cell 23 p2949 A73-44095

Desoxyribonucleases in sweat gland secretion of 24 p3059 A73-44674

DEPENDENCE

NT SPATIAL DEPENDENCIES

NT TIME DEPENDENCE

DEPENDENT VARIABLES

Method of trigonometric sums in the metric theory of Diophantine approximations of dependent variables 13 p1648 A73-28343

Theory for errors, resolution, and separation of unknown variables in inverse problems, with application to the mantle and the crust in Southern Africa and Scandinavia. 13 p1607 A73-28621

Fractured solutions in the calculus of variations. 18 p2330 A73-36640

DEPLOYMENT

Analysis of deployment and inflation of large ribbon parachutes. [AIAA PAPER 73-451] 15 p1826 A73-31437

Development of a high-performance ringsail parachute cluster. [AIAA PAPER 73-468] 15 p1828 A73-31452

DEPOLARIZATION

Lunar maps from CW radar imagery by aperture synthesis method at long wavelengths, noting depolarized return from highland regions 04 p0417 A73-15178

Depolarization phase of the spatial velocity electrocardiogram in normal and ventricular overloading. 10 p1185 A73-24900

Cardiac action potential rising phase and generation mechanism, discussing pacemaker potential and slow depolarization initiating upstroke in spontaneously active cardiac cells 11 p1316 A73-25592

Phenomenological analysis of thermostimulated depolarization effects 13 p1668 A73-28463

Depolarisation with Cassegrainian and front-fed reflectors. 14 p1728 A73-30448

Catalytic effects in corrosion processes with hydrogen depolarization of multiphase magnesium alloys 14 p1764 A73-30827

Non-existence of linear polarization in type III solar bursts at 80 MHz. 16 p2053 A73-32962

Faraday depolarization of radio galaxies and quasars with simple spectra. 17 p2234 A73-35621

Measurements of F2, NO, and ONF Raman cross sections and depolarization ratios for diagnostics in chemical lasers. 18 p2322 A73-36978

Effect of the electrical stimulation of the sensorimotor cortex on the potentials of dorsal roots and on the depolarization of primary spinal afferents 22 p2807 A73-42652

DEPOLARIZERS

U DEPOLARIZATION

DEPOLYMERIZATION

Surface temperature measurement of regressing polymethyl methacrylate slabs burning in oxygen-nitrogen mixtures, discussing chemical mechanism for condensed phase depolymerization 13 p1707 A73-28994

DEPOSITION

NT ANODIZING

NT ELECTRODEPOSITION

NT ELECTROPLATING

NT VACUUM DEPOSITION

NT VAPOR DEPOSITION

Luminosity and frequency spectrum of radiation from spherically symmetric steady state accretion of interstellar gas onto nonrotating black hole at rest 10 p1272 A73-23534

Ionic machine tools for microelectronic manufacture, discussing ion jets properties, optics and construction and implantation, micromachining and deposition technologies 16 p1987 A73-33088

Physicochemistry of the deposition of gelatinous photographic emulsion layers on a substrate 21 p2647 A73-40268

DEPOSITS

Method for determining the thermal resistance of channel-wall deposits 08 p1022 A73-21198

Determination of the proneness of aviation oils to carbon deposition 19 p2472 A73-38491

Carbon deposition and the role of reducing agents in hot-corrosion processes. 20 p2576 A73-39027

DEPRECIATION

Business aircraft operational costs, considering maintenance, repair and depreciation 06 p0771 A73-17998

DEPRESSION

Alpha-delta sleep as replacement for delta sleep in various psychiatric patients with chronic fatigue and depression 09 p1045 A73-22694

Features of the evolution of depressions and their cloud systems over the Pacific Ocean. 18 p2334 A73-37061

DEPRESSIONS [TOPOGRAPHY]

U STRUCTURAL BASINS

DEPRESSURIZATION

U PRESSURE REDUCTION

DEPRIVATION

NT SENSORY DEPRIVATION

NT SLEEP DEPRIVATION

NT WATER DEPRIVATION

DEPTH

Tomosynthesis - A holographic method for variable depth display.

12 p1495 A73-26829

DEPTH MEASUREMENT

Magnetotelluric and geomagnetic depth sounding methods compared.

05 p0572 A73-17189

Depth sensing, camera and touch/force sensing systems for autonomous industrial robotics and planetary exploration

19 p2429 A73-37322

Application of a pulsed laser for measurements of bathymetry and algal fluorescence.

20 p2574 A73-39863

Analog scale model of radio interferometry depth sounding at centimeter wavelengths, examining glacier layer boundaries

24 p3082 A73-44750

DEPTH PERCEPTION

U SPACE PERCEPTION

DERIVATION CALCULUS

U DIFFERENTIAL CALCULUS

DERMATOLOGY

Soaps, detergents and surfactants dermatological hazards in personal hygiene use by spacecrews during long term space flight/Skylab/

[ASME PAPER 73-ENAS-26] 19 p2400 A73-37981

DESCENT

NT PARACHUTE DESCENT

DESCENT TRAJECTORIES

NT REENTRY TRAJECTORIES

Venus atmosphere wind velocity profiles from analysis of Venera 7 descent stage radial velocity measurements

05 p0612 A73-16086

Data on dynamics of the subcloud Venus atmosphere from Venera spaceprobe measurements

06 p0744 A73-17436

Some problems of optimal control of space-vehicle trajectories in the Martian atmosphere

10 p1247 A73-23878

Space shuttle ascent-flyback trajectory optimization with in-flight inequality constraints based on accelerated gradient parameters determination including attitude control angles

10 p1276 A73-24002

Guidance methods for heat-optimal three-dimensional descent paths of aerodynamic reentry bodies

11 p1430 A73-25350

Civil aircraft vertical plane navigation and guidance during climb and descent, discussing atmospheric, performance and passenger comfort constraints on flight path selection

13 p1656 A73-28075

Optimal descent maneuver with a limited-thrust engine for entry at a prescribed angle into the atmosphere of a planet

13 p1689 A73-29139

Optimization of descent maneuvers for a section of a satellite in a planetary orbit

15 p1931 A73-31227

Predicting descent rate for aircraft parachute flares.

[AIAA PAPER 73-482] 15 p1829 A73-31464

Longitudinal motion of a transport aircraft during steep landing approaches

17 p2100 A73-34482

Some problems in the optimal control of spacecraft trajectories in the Martian atmosphere.

20 p2589 A73-38897

DESERT ADAPTATION

Thermal factor and dehydration influences on protidic and lipidic catabolisms of young men with partial food deprivation in hot climate, discussing metabolic balances

08 p0934 A73-21248

On the mechanism of adaptation of micro-organisms to conditions of extreme low humidity.

22 p2803 A73-42164

On the multiplication of xerophilic micro-organisms under simulated Martian conditions.

22 p2803 A73-42165

DESERTS

Thermal structure of the sand desert from the data of IR aerophotography.

20 p2558 A73-39869

DESIGN

Book - Forging design handbook.

02 p0173 A73-11884

An algorithmically and physically oriented design approach. I - Problems analysis

09 p1087 A73-21900

DESIGN OF EXPERIMENTS

U EXPERIMENTAL DESIGN

DESORPTION

Book on surface ionization covering atomic and molecular ionization during thermal desorption from high melting point solid surfaces

03 p0345 A73-13996

High vacuum thermal desorption mass spectrometry for electron bombardment activated nitrogen desorption from W surface, discussing lambda state population

04 p0414 A73-14999

Mechanisms and kinetics of absorption and desorption reactions in systems of refractory metals with nitrogen, oxygen or carbon.

04 p0462 A73-15302

Investigation of gas sorption and desorption in polymer materials in the process of gaseous sterilization of such materials

06 p0656 A73-17681

Laser-induced fast thermal desorption from solid surfaces

06 p0699 A73-17914

Cryopumping adsorption-desorption theory and cryosorption and condensation pumps, including bare surface, adsorbents and frozen deposit pumps

08 p0989 A73-21619

Diffusion theory for adsorption and desorption of gas atoms at surfaces.

09 p1047 A73-22073

Coadsorption of oxygen and carbon monoxide on tungsten - Desorption spectra, electron stimulated desorption and field emission microscopy.

11 p1325 A73-25204

States of absorption, velocities of absorption, of desorption of oxygen on rhenium, and mechanisms of atomization and oxidation at high temperature and low pressure

13 p1580 A73-28451

Temperature dependence of the cross section of O⁺ ion desorption by electrons from an oxygen layer adsorbed on a tungsten surface

13 p1663 A73-28969

A new technique for Auger analysis of surface species subject to electron-induced desorption.

17 p2175 A73-35757

Molecular beam study of the desorption of cesium ions from tungsten crystals.

18 p2338 A73-36976

Chemisorption of CO on tungsten /100/- Combined flash desorption and electron stimulated desorption study. II.

18 p2287 A73-37033

Spatial distributions of H₂ desorbed from Fe, Pt, Cu, Nb, and stainless steel surfaces.

19 p2402 A73-37951

Combined Auger electron spectroscopy and electron impact desorption studies of silicon surfaces.

20 p2595 A73-39665

Spacecraft polyurethane foam jacket sterilization by gas method, discussing ethylene oxide and methyl bromide sorption and desorption

22 p2803 A73-42160

Temperature dependence of the cross section for electron-induced O⁺ desorption from tungsten.

23 p3008 A73-44321

DESPINNING

U SPIN REDUCTION

DESTABILIZATION

Destabilization of vapor film boiling around spheres.

08 p1024 A73-21641

Cloud destabilization due to long wave radiative cooling resulting from IR radiative heat transfer in cloudy atmosphere, considering temperature inversion effects and cyclogenesis mechanism

24 p3108 A73-45016

DESTRUCTIVE TESTS

Equations of the time-dependent strength of solid bodies

01 p0114 A73-10479

Lamellar tearing and the slice bend test.

07 p0832 A73-20275

Equations for the time-dependent strength of a solid.

14 p1810 A73-30304

Analysis of sudden death tests of bearing endurance.

[ASLE PREPRINT 73AM-3B-2]

17 p2179 A73-34984

DESYNCHRONIZED SLEEP

U RAPID EYE MOVEMENT STATE

DETECTION

NT AIRCRAFT DETECTION

NT CORRELATION DETECTION

NT FOREST FIRE DETECTION

NT HIGH ALTITUDE NUCLEAR DETECTION

NT RADAR DETECTION

NT SIGNAL DETECTION

NT TARGET RECOGNITION

DETECTORS

The use of electret films as time-of-arrival detectors for shock and detonation waves.

10 p1218 A73-24122

DETERGENTS

Studies of the electron transport chain of extremely halophilic bacteria. VIII - Respiration-dependent detergent dissolution of cell envelopes.

01 p0009 A73-10625

Influence of electron transport on the interaction between membrane lipids and Triton X-100 in Halobacterium cutirubrum.

15 p1841 A73-32024

Soaps, detergents and surfactants dermatological hazards in personal hygiene use by spacecrews during long term space flight/Skylab/

[ASME PAPER 73-ENAS-26] 19 p2400 A73-37981

Emission of aqueous solutions of rhodamine 6G with detergent additives in the presence of flash lamp excitation

21 p2711 A73-40305

DETERIORATION

Deterioration of impermeable alumina tubes in inert atmospheres at elevated temperatures.

12 p1515 A73-27032

DETERMINANTS

On the evaluation of tri-diagonal secular determinants.

02 p0188 A73-12606

Algorithms for finding the coefficients of polynomials of matrix determinants

13 p1587 A73-28864

General treatment of the evaluation of tri-diagonal secular determinants.

13 p1700 A73-29379

DETERMINATION

U MEASUREMENT

DETONABLE GAS MIXTURES

Explosion in detonating media with a variable initial density

12 p1487 A73-27419

Condition of the medium before the flame front during the initial phase of a combustion process

15 p1957 A73-31867

Permeable elastic piston models of shock wave formation before flame front during inflammable gas mixture combustion in channels

15 p1957 A73-31868

DETONATION

Detonation in a medium of variable density with allowance for variable back pressure

01 p0034 A73-10956

Prediction of the critical diameter of composite propellants.

[AIAA PAPER 72-1117] 03 p0351 A73-13432

Detonation propulsion system for missile/spacecraft maneuvering, determining performance characteristics by one dimensional computer calculations for various configurations

[AIAA PAPER 72-1161] 03 p0357 A73-13462

Detonation gun flame spray coatings, determining adhesive strength as function of coating thickness and process technological parameters

03 p0313 A73-14014

Investigation of the detonation characteristics of hexogen-filler systems

13 p1706 A73-28970

Detonation of explosives containing boron and its organic derivatives

13 p1669 A73-28971

Russian book - Transition of burning of compacted systems to detonation.

15 p1959 A73-32420

Explosive behavior of aluminized ammonium perchlorate.

16 p2045 A73-33346

Book - Gasdynamic theory of detonation.

17 p2253 A73-34297

Plastic bonded, thermally stable explosive for an Apollo experiment.

18 p2341 A73-36152

Annex 13, sabotage and malicious acts against aircraft - Practical problems.

19 p2506 A73-37740

Influence of nonexplosive liquids on the detonation rate of solid explosives

24 p3157 A73-45380

DETONATION WAVES

On self-similar blast waves headed by the Chapman-Jouguet detonation.

01 p0120 A73-10441

Blast wave theory extension to time variable energy input, considering application to laser induced blast waves

01 p0121 A73-10760

MHD detonation waves properties and propagation velocities within relativistic theory, discussing shock equations nontrivial solution existence and uniqueness

01 p0085 A73-11260

A new integral-variational method for calculation of relaxation regions behind shock and detonation waves.

07 p0809 A73-19050

Lateral expansion of a laser-supported detonation wave in a gas.

07 p0920 A73-19979

Investigation of the burnup process structure under spin conditions

07 p0923 A73-20424

- Difference schemes for two dimensional gas flows with detonation in frame of Lagrange variables, comparing point explosion with self similar solution
09 p1070 A73-21923
- Utilization of the detonation phenomenon for the deposition of coatings /Survey/
09 p1088 A73-22468
- Isolated reactive and nonreactive Mach stem structure in exothermic systems under conditions encountered behind detonation waves front
10 p1294 A73-23553
- Microwave reflection from detonation waves in equimolar C2H2-O2 at low pressures.
10 p1294 A73-23557
- Explosion gas dynamics experimental investigation, noting fast chemical reactions induced exothermic processes and detonation wave structure
10 p1295 A73-23853
- The use of electret films as time-of-arrival detectors for shock and detonation waves.
10 p1218 A73-24122
- Nearly spherical constant-power detonation waves as driven by focused radiation.
[AIAA PAPER 73-674] 18 p2322 A73-36225
- Detonation shock wave against metal surface with hemispherical notch, investigating expelled metal jet dimensions relation to notch radius and Reynolds number
19 p2433 A73-37515
- Chapman-Jouguet rule for real detonation waves
19 p2419 A73-37516
- Visualization of the shape and symmetry of detonation waves by a slit camera - Application to hollow charges
21 p2697 A73-39992
- Tungusk meteorite event with thermal radiation and severe blast wave attributed to black hole of substellar mass
22 p2909 A73-42488
- On detonation waves supported by diffusion flames.
22 p2936 A73-42810
- Time variation in the reaction-zone structure of two-phase spray detonations.
22 p2936 A73-42811
- Numerical study of the problem of explosion of a cylindrical charge of finite length
24 p3076 A73-44654
- Solid fuels combustion stability and shock wave induced detonations propagation stability in aerosols investigation based on one dimensional turbulence, using multistage mathematical models
24 p3157 A73-45383
- Laser supported gaseous detonation wave propagation above solid surface, calculating momentum transfer as functions of laser energy, pulse duration, and beam and target areas
24 p3097 A73-45455
- DETONATORS**
The utilization of detonating fuses on launchers.
07 p0865 A73-18996
- DEUTERIUM**
Thermal instability of nonuniform plasma in steady state D-T fusion reactor operated by charged particle heating with spatially uniform fuel injection
01 p0084 A73-10465
- Access to uncombined titanium through an inhibiting film in sublimation pumping of deuterium.
02 p0194 A73-12844
- Monte Carlo classical trajectory calculation of the rates of H and D-atom vibrational relaxation of HF and DF.
03 p0318 A73-13280
- Deuterium-hydrogen ratio in Jupiter.
05 p0623 A73-17182
- The abundance of CH3D and the D/H ratio in Jupiter.
07 p0874 A73-19066
- Exothermic deuterium-fluorine chain reaction pumping of high pressure pulsed carbon dioxide chemical transfer laser
07 p0835 A73-19631
- Deuterium content of lunar material.
07 p0887 A73-19774
- Elemental synthesis during high temperature phase of expansion of big bang universes, obtaining universal baryon density relationship to primordial deuterium abundance
08 p1008 A73-21151
- 327-MHz observations of the galactic center - Possible detection of a deuterium absorption line.
08 p1013 A73-21808
- Valence-bond study of the /H2, D2/ exchange reaction mechanism.
09 p1047 A73-22074
- Prohibited autodetachment in OD- formed by collisions of O- with D2.
09 p1048 A73-22075
- Universe evolution explanation via interstellar deuterium investigation, discussing galactic gas chemical composition history
12 p1543 A73-27692
- Access to uncombined titanium through an inhibiting film in sublimation pumping of deuterium.
13 p1581 A73-28929
- Deuterium in interstellar molecules.
14 p1802 A73-30749
- Pulsed laser irradiation effects on solid deuterium slab, deriving two-temperature electron-ion model
15 p1884 A73-31660
- Noble gas isotopes abundances for solar wind and outer convective zone of sun, emphasizing isotopic abundance of deuterium
17 p2228 A73-34416
- Diffusion of hydrogen and deuterium in Ta, Nb, and V.
20 p2576 A73-39134
- Chemisorption of H2 on W(211).
22 p2817 A73-42444
- Cosmic deuterium abundance derived from measured HD/H2 ratio, noting derivation sensitivity to ionizing flux and to oxygen and carbon depletion
22 p2904 A73-43119
- Jupiter HD absorption line measurement for model-independent number ratio D/H
22 p2916 A73-43125
- Early solar system deuterium abundance based on nebular chemical equilibrium, comparing with Jupiter atmosphere and meteorite data
24 p3131 A73-44468
- DEUTERIUM COMPOUNDS**
NT HEAVY WATER
Monte Carlo classical trajectory calculation of the rates of F-atom vibrational relaxation of HF and DF.
03 p0318 A73-13279
- Drift mobility of holes and electrons in perdeuterated anthracene single crystals.
12 p1531 A73-27688
- Monte Carlo calculations of reaction rates and energy distributions among reaction products. IV - F + HF/nu/ yields HF/nu-prime/ + F and F + DF/nu/ yields DF/nu-prime/ + F.
19 p2463 A73-37898
- HF and DF molecules vibrational relaxation investigation by recording IR radiation behind incident shock wave at 1500-5000 K
21 p2743 A73-40360
- Some reactions and hydroperoxyl and hydroxyl radicals at high temperatures.
22 p2898 A73-42754
- Catalytic efficiencies of atoms in the vibrational relaxation of HF and DF.
22 p2818 A73-42763
- DEUTERIUM OXIDES**
U HEAVY WATER
DEUTERIUM PLASMA
Cumulation-laser heating of two-temperature plasma, the recovered energy of nuclear fusion being taken into consideration.
04 p0480 A73-15596
- A neutral-potassium-beam measurement of plasma density.
05 p0604 A73-17364
- Thermal cumulation equations for concentric conductive laser heating of two temperature D-T plasma with nuclear fusion energy recovery
11 p1406 A73-26411
- Laser concentric conduction heating of two-temperature D-T plasma.
11 p1406 A73-26412
- Concentric laser cumulation of plasma with consideration of the heat of nuclear fusion.
13 p1667 A73-29393
- Electron-molecule collision ionization in hydrogen and deuterium.
14 p1776 A73-29700
- A high-temperature plasma state in a high-power microwave discharge
17 p2214 A73-34136
- Numerical analysis of the averaged equations of concentric laser cumulation of plasma with consideration of nuclear fusion energy.
17 p2216 A73-34323
- Simplified averaged equations of concentric laser compression of plasma.
24 p3117 A73-45427
- DEUTERON IRRADIATION**
Effect of irradiation on the absolute thermal emf of metals and alloys
06 p0706 A73-17901
- Intermediate energy nucleon-deuteron scattering theory.
14 p1776 A73-29766
- DEUTERONS**
Galactic cosmic radiation He 3 and deuterium abundances interpretation from production cross sections and reaction kinematics
05 p0609 A73-16741
- Backward elastic proton-deuteron differential cross sections at different energies, describing experimental setup
05 p0601 A73-17322
- DEVELOPERS (PHOTOGRAPHY)**
U PHOTOGRAPHIC DEVELOPERS
DEVITRIFICATION
U CRYSTALLIZATION
DEW
Numerical model for three dimensional air parcels trajectories computation from operational wind forecasts, deriving atmospheric moisture, dew and temperature distributions predictions
06 p0720 A73-18705
- DEWAR SYSTEMS**
U CRYOGENIC EQUIPMENT
DEWETTING
U DRYING
DEXTRANS
A method for calculating the sedimentation characteristics of particles in linear dextrane-density gradients and its application to the separation of red blood cells according to the sedimentation rate
13 p1578 A73-28476
- DHC 5 AIRCRAFT**
Buffalo aircraft fiberglass laminated polyester nose boom for mounting horizontal and vertical wind sensing probes, describing instruments and measurement procedures
17 p2174 A73-35576
- CC-115 /Buffalo/ aircraft air cushion landing system design, testing and implementation prognosis, discussing propeller design, power systems, wings and U.S.-Canadian project cooperation
19 p2381 A73-37687
- Buffalo aircraft modification for air cushion landing system, considering weight, performance, stability and control, configuration alternatives and ground maneuvering
19 p2382 A73-37688
- The aircraft modification phase of the joint U.S./Canadian ACLS program.
19 p2382 A73-37689
- Ground and flight testing of air cushion landing system /ACLS/ equipped CC-115 Buffalo aircraft for performance and stability/control characteristics
19 p2382 A73-37691
- DIABATIC PROCESSES**
U HEAT TRANSFER
DIABETES MELLITUS
Antidiabetic medications and aircrow
08 p0935 A73-21541
- Ribes Nigrum anthocyanosides in ophthalmology
18 p2280 A73-36935
- DIADEME SATELLITES**
Diademe satellite passive magnetic stabilization system, describing magnet and damper design
07 p0904 A73-18935
- DIAGNOSIS**
Certain aspects of the bionic analysis and control of dynamic systems
01 p0012 A73-10658
- Automated system of storing and processing vectorcardiograms
01 p0012 A73-10660
- Nonlinear method of analyzing electroencephalograms
01 p0012 A73-10661
- Non-invasive technique for diagnosing atrial septal defect and assessing shunt volume using directional Doppler ultrasound - Correlations with phasic flow velocity patterns of the shunt.
01 p0014 A73-11505
- Gas path analysis applied to turbine engine condition monitoring.
03 p0354 A73-13405
- [AIAA PAPER 72-1082] Diagnostic value of vectorcardiogram in strictly posterior infarction.
03 p0268 A73-13891
- Computerized ECG interpretation system for heart and circulatory disorder detection and diagnosis and health screening
03 p0272 A73-14660
- Clinical electrocardiographic and vectorcardiographic diagnosis of left posterior subdivision block, isolated or associated with RBBB.
04 p0409 A73-15200
- Numerical classification and coding of electrocardiograms.
04 p0412 A73-15647
- Clinical diagnosis of angina pectoris, implicating obstructive disease of coronary arteries and effects of paroxysmal events on heart rate and blood pressure
05 p0542 A73-17277
- Book - Peripheral vascular diseases: Diagnosis and management.
06 p0651 A73-17871
- Computer-controlled software diagnosis of an airborne computer.
08 p0940 A73-20677
- Fault isolation in complex systems via Bode diagram technique.
08 p0941 A73-20684
- Echocardiography status, potentialities and requirements in congenital heart disease diagnosis, considering feasibility in left ventricular performance evaluation
14 p1721 A73-30053
- Medical diagnosis of pilot performance disturbances from viewpoint of flight surgeon responsibilities
15 p1837 A73-31171
- A new method for diagnosing myocardial damage in patients with normal electrocardiograms and vector cardiograms.
16 p1973 A73-33375

- Digital computer diagnosis of cardiac arrhythmias in a singlelead electrocardiogram. 17 p2114 A73-34533
- Electrocardiographic diagnosis of sinus node rhythm variations and SA block. 18 p2274 A73-36520
- Intra-atrial and esophageal electrography in the diagnosis of complex arrhythmias. 18 p2274 A73-36525
- A diagnostic program - Problems of predicting myocardial infarction on a digital computer 20 p2516 A73-38998
- Automatic identification of cardiac rhythm and conductivity disturbances with the aid of digital computers 21 p2643 A73-40751
- Early diagnosis of coronary heart disease; Proceedings of the Second Paavo Nurmi Symposium, Porvoo, Finland, September 9-11, 1971. 22 p2808 A73-42826
- The early diagnosis of coronary heart disease - Critical review. 22 p2808 A73-42827
- Preventive value of early diagnosis of coronary heart disease, noting importance of screening populations for genetic and environmental risk factors 22 p2808 A73-42828
- The value of different angiographic procedures in coronary heart disease. 22 p2808 A73-42831
- Angina pectoris and ECG abnormalities in relation to prognosis of coronary heart disease in population studies in Finland. 22 p2809 A73-42836
- DIAGRAMS**
- NT BENDING DIAGRAMS
- NT BLOCK DIAGRAMS
- NT CIRCUIT DIAGRAMS
- NT CREEP DIAGRAMS
- NT FEYNMAN DIAGRAMS
- NT HERTZSPRUNG-RUSSELL DIAGRAM
- NT PHASE DIAGRAMS
- NT S-N DIAGRAMS
- NT STRESS-STRAIN DIAGRAMS
- DIALYSIS**
- Influence of nonideal flow conditions in haemodialysers on mass-transfer theories. 22 p2816 A73-42678
- DIAMAGNETISM**
- Magnetic susceptibility of amorphous semiconductors. 06 p0733 A73-17746
- High temperature-microwave spectrometer for Zeeman-effect measurements involving diamagnetic molecules 14 p1753 A73-30235
- Topology of induced lunar magnetic fields. 17 p2235 A73-35736
- Continuum theory of a slightly ionized plasma, diamagnetic effects. 19 p2468 A73-37522
- Diamagnetism of Penning discharge plasma as function of gas pressure, magnetic field strength and applied voltage, discussing plasma energetic lifetime and current characteristics 23 p3009 A73-43653
- DIAMANT LAUNCH VEHICLE**
- The liquefied ergol supply-trailers for DIAMANT B and EUROPA II launchers. 07 p0807 A73-18948
- Diamant launcher tilting system. 07 p0905 A73-18993
- Reinforced plastics role in construction and shielding of Diamant B satellite booster main components 07 p0905 A73-18995
- Satellite-equipment compartment separation system. 07 p0905 A73-18997
- Program objectives and propulsive, equipment case, attitude control, interstage, separation skirt and nose cone subassemblies of French Diamant B-P4 launch vehicle 10 p1285 A73-23654
- Manufacturing, integration and launching phases of Diamant B launcher inspection, discussing automatic control and testing bench structure and safety 14 p1742 A73-30104
- DIAMETERS**
- Influence of small local deviations in specimen diameter on conventional strain at maximum load in tensile test 11 p1380 A73-25448
- Considerations concerning the inadequacy of the classical concept of equivalent diameter in calculations of heat transfer in elliptical pipes 12 p1557 A73-26796
- Angular diameter calculation of Ellis atmospheric window via ionospheric wave ray tracing technique 15 p1844 A73-32048
- New determinations of the diameters of planets and satellites 16 p2066 A73-33792

- Geometric interpretation of the ratio of overall diameter to rim crest diameter for lunar and terrestrial craters. 22 p2909 A73-42498
- DIAMINES**
- Polyimidazopyrrolone model compounds. 15 p1840 A73-31572
- DIAMOND WINGS**
- U LOW ASPECT RATIO WINGS
- U SWEPT WINGS
- DIAMONDS**
- NT METEORITIC DIAMONDS
- Study of the composition of inclusions in synthetic diamond crystals by microanalysis. 02 p0185 A73-12691
- Shock wave generation for industrial applications in graphite to diamond conversion and incompatible materials bonding 07 p0850 A73-19048
- The use of a diamond heat sink for a high reliability IMPATT diode. 08 p0944 A73-20736
- The exciton energy spectrum in diamond and sphalerite type crystals 09 p1134 A73-22683
- Luminescence quenching and zero-phonon line broadening associated with defect interactions in diamond. 13 p1667 A73-28212
- On the quadrupole interaction in the diamond structure. 13 p1667 A73-28213
- Investigation of the turning process using diamond cutting tools on ML-5 magnesium alloy, with the application of mathematical methods in experiment planning 15 p1881 A73-31278
- Determination of the temperature fields of turbine disks and blades, using irradiated diamond indicators 23 p2987 A73-44294
- Effect of the characteristics of diamond grinding on the stressed state and strength of hard alloy VK6 24 p3094 A73-44968
- Ultrasonic treatment of nonmetallic materials with a diamond instrument 24 p3094 A73-44969
- Certain properties of synthetic diamond crystals of various habits 24 p3104 A73-44970
- Transient vibration processes during diamond grinding and their statistical evaluation 24 p3094 A73-44971
- DIAPHRAGM (ANATOMY)**
- Oxidation of amino acids by diaphragms from fed and fasted rats. 05 p0538 A73-16153
- 'Closing volumes' and decreased maximum flow at low lung volumes in young subjects. 09 p1041 A73-22929
- Volume-pressure characteristics of rib cage-diaphragm interaction in standing subjects during voluntary relaxation 20 p2518 A73-39778
- Force output of the diaphragm as a function of phrenic nerve firing rate and lung volume. 20 p2515 A73-39780
- Control of the duration of expiration. 21 p2642 A73-41635
- DIAPHRAGMS (MECHANICS)**
- Field distribution formulas for fast wave attenuation in thin walled tubular dielectric waveguide within external absorbing diaphragms 02 p0142 A73-12495
- Compressible boundary layer formation on shock tube walls after bursting of diaphragm separating gases at different pressures 03 p0293 A73-13527
- Piecewise linear approximation of thin walled rib and diaphragm reinforced conical beams under thermal field and axial loads, using limit stress-strain diagrams 07 p0913 A73-20096
- Image contrast in a microscope with synchronous scanning of the object by point or raster field diaphragms 13 p1616 A73-28771
- Field properties and losses in a three-mirror optical ring resonator with a Gaussian diaphragm 15 p1886 A73-32341
- Utilization of miniature diaphragm-leakport devices in fluidic applications. 20 p2511 A73-39752
- Diaphragm ejector pulse shortener for transforming periodic input signal into sharp pulses by adjusting vent areas of two fluid amplifiers 23 p2942 A73-43408
- The diaphragm-ejector proportional amplifier and its application to fluidic operational circuits. 23 p2943 A73-43409
- Small ejector system for fluidic subtracting network with diaphragm operated Schmitt trigger proportional amplifier and pneumatic signal generator, discussing construction and characteristics 23 p2943 A73-43410

- Opening time of brittle shock-tube diaphragms for dense fluids. 24 p3075 A73-44820
- DIASTOLE**
- Unusual diastolic heart beat in pericardial effusion. 03 p0259 A73-13059
- Structural conditions in the hypertrophied and failing heart. 22 p2807 A73-42685
- DIASTOLIC PRESSURE**
- Left ventricular end-diastolic pressures following selective coronary arteriography. 01 p0010 A73-11508
- Nature and significance of alterations in myocardial compliance. 22 p2808 A73-42689
- DIATOMIC GASES**
- Navier-Stokes approximation for gas dynamics equations of molecular oscillations in diatomic gas, noting relaxation pressure proportionality to energy density equilibrium deviation 02 p0152 A73-11602
- Measurements of temperatures of vibrationally excited N₂. 04 p0477 A73-14819
- Temperature dependence of diatomic gases thermal conductivity coefficient from shock tube tests, noting molecular gases above dissociation temperature 06 p0687 A73-18561
- Vibrational relaxation theory of diatomic and multiautomatic single component and gas mixture systems for molecular laser mechanisms, using oscillator simulation 09 p1097 A73-23331
- The Knudsen layer in a flow with two-temperature relaxation 10 p1250 A73-23580
- Classical dynamical investigations of reaction mechanism in three-body hydrogen-halogen systems. 13 p1581 A73-29427
- Test of statistical models for gases with and without internal energy states. 14 p1818 A73-30653
- Temperature dependence of diatomic gases thermal conductivity coefficient from shock tube tests, noting molecular gases above dissociation temperature 16 p2086 A73-33586
- Near continuum impact of an underexpanded jet plume on a wall. 17 p2096 A73-35137
- Collisional radiative processes and molecular lasers 23 p2988 A73-44013
- DIATOMIC MOLECULES**
- Calculations on energy transfer to a diatomic molecule in high-energy head-on collisions. 02 p0195 A73-12723
- Electric dipole moment of diatomic molecules by configuration interaction. V - Two states of $[2/\Sigma_{\text{g}}^{+}]$ / symmetry in CN. 04 p0477 A73-14816
- The formation of diatomic molecules in interstellar clouds. 05 p0625 A73-17333
- Diatomic molecule formation in interstellar medium via two body collision, calculating rate coefficients for radiative association 06 p0752 A73-18231
- Collision matrix elements near a pseudocrossing of potential energy curves. 06 p0726 A73-18249
- The charge transfer spectrum of $\text{Li}/\text{LiNa}^{+}$. 06 p0726 A73-18250
- Multiphoton excitations in vibrational-rotational states of diatomic molecules in an intense electromagnetic field. 08 p0990 A73-21003
- Diatomic molecules dissociation investigation from effective cross section measurement of slow atomic negative ions formation by molecules collisions with fast ions and atoms 08 p0990 A73-21694
- Double charge transfer spectroscopy of diatomic molecules. 09 p1122 A73-22118
- Asymmetric intensities of Zeeman components of electronic transitions of diatomic molecular spectra in sunspots, considering CN red lines 11 p1422 A73-25936
- Vibration-to-rotation and vibration-to-vibration energy transfer between diatomic molecules. 11 p1401 A73-25967
- Vibrational level populations in diatomic molecules during steady pumping 12 p1504 A73-26888
- Classical calculation of intensity distribution in the oscillatory-rotational spectra of diatomic molecules 15 p1916 A73-32338
- The variation of the electronic transition moment, Re, in the intensity theory of diatomic molecules. 15 p1916 A73-32392
- Dissociative recombination rate for CH positive ions in interstellar clouds 19 p2490 A73-38531

Computer checking of rotational line intensity factors for diatomic transitions. 21 p2744 A73-41212

Dissociation of diatomic molecules. I. 22 p2889 A73-42443

Electron scattering from diatomic molecules in the first Born approximation. 22 p2889 A73-42446

Precise measurements of diatomic dissociation rates in shock waves. 22 p2818 A73-42765

DICHROISM

A combined magnetic circular dichroism and electron paramagnetic resonance spectrometer. 02 p0167 A73-11951

Morphic effects. IV - Effects of an applied magnetic field on first-order photon-optical phonon interactions in non-magnetic crystals. 02 p0201 A73-12637

DICHROMATES

U CHROMATES

DICKE RADIOMETERS

Microwave noise measurement with Dicke type radiometers, discussing measurement error reduction 09 p1052 A73-23109

DICKE TYPE RADIOMETERS

U DICKE RADIOMETERS

DIELECTRIC CONSTANT

U PERMITTIVITY

DIELECTRIC MATERIALS

U DIELECTRICS

DIELECTRIC PERMEABILITY

Field distribution formulas for fast wave attenuation in thin walled tubular dielectric waveguide within external absorbing diaphragms 02 p0142 A73-12495

Electromagnetic wave diffraction by ideally conducting homogeneous bodies of revolution with arbitrary complex permittivity and permeability, using separation of variables method 05 p0547 A73-16054

DIELECTRIC POLARIZATION

Electrohydrodynamic heat pipe design based on electrode structure to orient and guide dielectric liquid phase flow, using polarization force in place of capillarity [ASME PAPER 72-WA/HT-35] 04 p0518 A73-15820

Some characteristics of isopotential curves of photoelectret state formation in compressed polycrystalline anthracene 05 p0605 A73-17176

Measurement on a polarization interferometer of absolute and relative light wave delay in liquid dielectrics under the action of an electric field 07 p0823 A73-19332

The elastic dielectric as oriented elastic continuum 13 p1658 A73-28163

Method of recording elastoplastic stress waves in solids with a dielectric sensor 13 p1618 A73-29059

A method of recording elastoplastic stress waves in solids by means of a dielectric pickup. 18 p2317 A73-36891

DIELECTRIC PROPERTIES

NT PERMITTIVITY

Unit for wideband measurements of dielectric parameters at millimeter wavelengths 01 p0050 A73-10794

Dielectric properties of cholesteric liquid crystals. 02 p0199 A73-11577

Thermal cycling and frequency tests for lunar soil dielectric constant, loss tangent and dc conductivity, noting moisture effects 02 p0220 A73-12481

Non polar thermosetting resins for high temperature electrical/electronic components. 03 p0332 A73-13035

The relationship between dielectric and mechanical properties of polymers. 03 p0332 A73-13036

Dispersion relations for electromagnetic radiation in random media. 05 p0597 A73-16494

Effects of ionizing radiation on dielectrically isolated junction field effect transistors. 05 p0558 A73-16524 [AD-757969]

Quantum theory of the dielectric constant of a magnetized plasma and astrophysical applications. I. 05 p0624 A73-17310

Book - Electronic properties of composite materials. 06 p0714 A73-17872

Emission of metals under the action of non-relativistic electrons 06 p0725 A73-18102

Excited molecules in a medium with a negative dielectric constant 06 p0725 A73-18105

Dielectric constant and molar polarizability of compressed gaseous and liquid fluorine. 06 p0661 A73-18124

Source excited dielectric wedge surface magnetic field local mode solution compared with plane wave method, noting inaccuracy near surface wave cutoff 06 p0666 A73-18197

Optical constitutive equation derivation for Tresca type plastic dielectrics, calculating birefringence and extinction angle in simple shear 06 p0723 A73-18458

Corrugated and uniform dielectric rod aerial excited in E sub 0-mode. 07 p0792 A73-19547

Dielectric properties of Apollo 14 lunar samples at microwave and millimeter wavelengths. 07 p0898 A73-19894

Dielectric properties of Apollo 14 lunar samples. 07 p0898 A73-19895

Measurement of the dielectric constant of polyvinyl chloride at very low frequencies, and influence of the superposition of a continuous voltage 08 p0942 A73-20648

Effect of dielectric loading on the radiation power of an axial slot antenna. 08 p0938 A73-20837

Book - Introduction to quantum electronics. 08 p0994 A73-20951

Linear and nonlinear dielectric properties of tetrahedral structure crystals. III - Theory of dielectric properties of tetrahedral structure compounds 08 p0990 A73-20965

The growth of dielectric aluminum and tantalum oxide layers 08 p0977 A73-21023

Influence of a constant electric field on the dielectric properties of polycrystalline BaTiO3 08 p0995 A73-21273

High resolution radar observation of Martian surface topography and scattering properties, noting dielectric constant and rms surface slope variations 09 p1144 A73-22261

Dielectric dispersion of irradiated BaTiO3 in the phase transition region 09 p1134 A73-22983

Electromagnetic wave propagation velocity modulation in dispersionless linear medium with dielectric constant variation in space and time, evaluating approximation with neglected multiple reflections 10 p1249 A73-24526

Lunar permafrost - Dielectric identification. 10 p1282 A73-24629

A quick accurate method to measure the dielectric constant of microwave integrated-circuit substrates. 10 p1197 A73-24866

Study of electromechanical coupling in a non-piezoelectric dielectric with a high dielectric constant 11 p1408 A73-25249

On nonlinear transformation and stabilization of beam-plasma instability. 11 p1404 A73-25274

Graphs for the design of laser mirrors at normal incidence. 13 p1627 A73-28598

On the propagation of electromagnetic waves through a time-varying dielectric layer. 14 p1726 A73-29932

Radiation patterns of dielectric loaded rectangular horns. 14 p1735 A73-30220

Multiplicity of dielectric local modes - Bound states of phonons with impurity centers 15 p1885 A73-31719

Investigation of the dielectric properties of terrestrial rocks at super-high frequencies for the purpose of improving accuracy for the composition of lunar material 16 p2064 A73-33771

Determination of the lunar albedo at the 6-m wavelength 16 p2064 A73-33772

Polyimide resin dielectric and mechanical properties, discussing syntactic foam composite with aluminum filler for radome construction 17 p2195 A73-34804

Dielectric properties of ferrites in the microwave band 17 p2141 A73-35548

Causes of changes in the properties of resite in aqueous and alkaline media 18 p2328 A73-36822

Dielectric anisotropy of new liquid-crystal mixtures and its effect on dynamic scattering. 21 p2665 A73-41115

A projection method in the problem of the excitation of a dielectric antenna 21 p2667 A73-41512

Illumination aftereffects due to semiconducting ferrite electron and ion motion, discussing dielectric properties and electron hole deficiencies 22 p2833 A73-42514

Measurements of the dielectric properties of seawater and NaCl solutions at 2.65 GHz. 22 p2849 A73-42549

A theoretical and experimental study of the insulated loop antenna in a dissipative medium. 22 p2829 A73-43184

Properties of laser mirrors at non-normal incidence. 22 p2872 A73-43186

High strength filaments for cables and lines, discussing bundle theory and comparing dielectric and tensile properties for glass, graphite and organic fibers 23 p2997 A73-43645

Electrical breakdown in interface zone between two dielectric insulators, studying premature breakdown dependence on dielectric constant, layer thickness and electric field conditions 23 p3006 A73-43673

Dielectric coaxial waveguide modal cut-off, dispersion and attenuation characteristics, discussing guide geometry and dielectric properties effects 24 p3069 A73-45407

DIELECTRICS

NT RADOME MATERIALS

Importance of Fresnel reflections in laser surface damage of transparent dielectrics. 01 p0076 A73-10131

Performance of a protruding-dielectric waveguide element in a phased array. 01 p0022 A73-10180

The destruction of reflecting dielectric coatings by laser radiation. 01 p0059 A73-10836

Role of absorbing inclusions in the fracture mechanism of transparent dielectrics by laser emission 01 p0026 A73-11291

Superconductor/exiton-dielectric phase transition in a semimetal 01 p0089 A73-11292

Large amplitude oscillations of a hollow spherical dielectric. 02 p0236 A73-12518

Hot-electron concept for Poole-Frenkel conduction in amorphous dielectric solids. 02 p0201 A73-12817

Influence of gamma irradiation on the surface properties of metal-dielectric-semiconductor structures 03 p0349 A73-13661

Natural frequencies of a rectangular waveguide filled with a piecewise-homogeneous dielectric 04 p0417 A73-15076

Metal-dielectric-semiconductor junction transistor HF response analysis by digital computer, deriving switching time as function of impurity concentration and electrode voltage 05 p0556 A73-16069

Higher-order scattering losses in dielectric waveguides. 05 p0549 A73-16366

Dielectric layers in the radiation field of microwave antennas 05 p0550 A73-16475

Radiation damage effects in microwave dielectric substrate materials. 05 p0557 A73-16507

Effect of boundary conditions on the radiative reflectance of dielectric coatings. 05 p0598 A73-16896 [AIAA PAPER 73-148]

The solution of Maxwell's equation for inhomogeneous dielectric slabs. 06 p0699 A73-17809

Radiation from an axial slot antenna coated with a homogeneous material. 06 p0665 A73-18138

Distortion of electromagnetic pulses undergoing total internal reflection from a moving dielectric half-space. 06 p0666 A73-18200

New interpretation of the equivalent circuit used in dielectric-degradation studies 07 p0796 A73-18893

Calculation of the asymptotic behaviour of the TDR step response related to the asymptotic behaviour of dielectrics in the frequency domain. 07 p0797 A73-19107

E-polarized plane wave diffraction by conducting wedge loaded with thin dielectric slab, obtaining Fresnel integral solution with application to cylindrical wave excitation 07 p0792 A73-19383

Surface wave characteristics of circular cylindrical corrugated and uniform dielectric rod excited in E sub 0-mode. 07 p0792 A73-19545

Radiation characteristics of waveguide-excited dielectric spheres with matched sphere-air boundary. 08 p0947 A73-21121

Quasi-static ion acoustic surface wave propagation along warm plasma layer-dielectric boundary 08 p0993 A73-21460

Dielectric breakdown of shock-loaded PZT 65/35. 09 p1132 A73-21927

Investigation of the dielectric waveguide modes in homostructure GaAs laser. 09 p1091 A73-22238

Internal equation numerical solution for excitation of multilayer arbitrary shape dielectric body of revolution, considering radome curvature effects on antenna radiation pattern 09 p1052 A73-23084

Dielectric gradient waveguides inhomogeneous core layer, solving differential equation by perturbation method 09 p1065 A73-23113

- Book - Optical waveguides. 09 p1066 A73-23274
- Procedure for recording stresses by dielectric sensors in the case of impulsive loads 10 p1219 A73-24367
- Tube waveguide for optical transmission. 10 p1196 A73-24624
- High temperature superconductivity in three dimensional systems of metals and nonmetals, discussing electron collectivization in metals, dielectrics, organic compounds, semiconductors and molecular crystals 10 p1261 A73-24692
- Loaded and artificial dielectric materials with variable permittivity for sandwich radomes, discussing weight saving, multiband coverage and cross polarization reduction 11 p1335 A73-25281
- Experimental study of electrical reflectors equipped with thin radomes 11 p1335 A73-25292
- Resonances in circular arrays with dielectric sheet covers. 11 p1337 A73-25654
- Reflection and transmission of radio waves at a dielectric slab with variable permittivity. 11 p1329 A73-25675
- Plane wave expansion approximation for wave field on dielectric wedge representing tapered antenna, considering lateral wave contribution 11 p1329 A73-25681
- Radiation properties of a composite-dielectric-rod aerial. 11 p1332 A73-26286
- Emission from a point charge during motion along the plane boundary of a dielectric with periodically varying density 11 p1402 A73-26448
- Intensity and displacement fields of microinhomogeneous medium with random permittivity tensor field described by step functions, using renormalization method 12 p1530 A73-26929
- Phenomenological analysis of thermostimulated depolarization effects 13 p1668 A73-28463
- Paraxial electromagnetic wave packets diffraction on thin conducting periodic structures and dielectric plate, noting packet width and phase front curvature changes 13 p1582 A73-28653
- Critical frequencies of electromagnetic wave propagation in H waveguides with a dielectric cross-piece 13 p1595 A73-29411
- Mechanism of damage of the surface of a transparent dielectric during illumination with short light pulses. 13 p1629 A73-29429
- Transient self focusing theory of high power laser pulse for homogeneous isotropic transparent solid dielectric with allowance for electrostriction and thermal effects 13 p1629 A73-29440
- High-resolution microwave holographic technique - Application to the imaging of objects obscured by dielectric media. 13 p1622 A73-29668
- IMEKO Symposium on Microwave Measurement, Budapest, Hungary, May 10-13, 1972, Proceedings. 14 p1733 A73-30054
- Radiation characteristics of a waveguide excited dielectric sphere backed by a metallic hemisphere. 14 p1728 A73-30225
- Modified radar cross section of a dielectric cylinder with conducting circumferential loop loading. 14 p1729 A73-30699
- Propagation constant and wave resistance in the case of coaxial and hollow conductors with lossy dielectric and magnetic materials 14 p1730 A73-30920
- Thin dielectric films as protective coatings for metallic mirrors and antireflective coatings for semiconductors and active laser materials 15 p1884 A73-31416
- Contribution to the theory of electron-beam stability in an inhomogeneous dielectric medium 15 p1920 A73-32302
- Scattering of electromagnetic waves by a disk positioned at the boundary between two media 15 p1846 A73-32318
- Theory of transient radiation in a waveguide with a piecewise-homogeneous dielectric filler 16 p1978 A73-32898
- Classical and natural conduction and deformation modes concepts for axisymmetric variational problems. 16 p2079 A73-33007
- Thermomechanical theory of ferromagnetic and dielectric materials magnetoelastic and electroelastic properties, using variational principles 16 p2037 A73-33228
- Transmission of isotropic light across a dielectric surface in two and three dimensions. 16 p2037 A73-33685
- Mechanism of failure in transparent organic-glass-type dielectrics under the action of laser radiation 16 p2030 A73-33927
- Current-voltage characteristic of a metal-dielectric contact with allowance for thermionic and field emission of electrons 16 p1972 A73-34010
- Interference patterns of a horizontal electric dipole over layered dielectric media. 17 p2123 A73-35270
- Local Y-transformations in the electrodynamics of inhomogeneous accelerated media 17 p2213 A73-35570
- Remote sensing of complex permittivity by multiple resonances in RCS. 17 p2128 A73-35692
- Capacitance of a field-effect MDS transistor gate 18 p2293 A73-36721
- Dielectric impulse pressure recorders consisting of organic glass, cellulose-ether film and muscovite mica, investigating shock wave profiles and electrode voltage amplitude 18 p2317 A73-36764
- Geometric deformation of spherical dielectric lens antennas 19 p2409 A73-37715
- An approximation method for calculating the attenuation characteristic of dielectric-lined circular waveguides. 19 p2404 A73-37723
- Cross focusing possibility between two coaxial laser beams in dielectrics with optical inhomogeneities and oscillatory waveguide characteristics, noting critical power role 20 p2572 A73-38848
- Carbon dioxide jet laser cutting technology and rate calculations for metals and dielectrics as function of laser power and material thermal properties 20 p2569 A73-39677
- Polarizability of interacting atoms - Relation to collision-induced light scattering and dielectric models. 21 p2742 A73-40211
- Reflection of a laser beam from an interface between isotropic dielectrics 21 p2714 A73-40569
- Numerical solution of edge effects of external coupling between elements in linear phased array of slots covered by dielectric slab, using scattering matrix 21 p2651 A73-40654
- Surface wave radiation pattern determination for solid state lasers, taking into account dielectric interface presence 21 p2716 A73-41113
- Extraction of Tscheysheff design data for the low-pass dielectric multilayer. 21 p2665 A73-41135
- Viscous dielectric materials for application in microwave microcircuits. 21 p2668 A73-41589
- Electrohydrodynamic Rayleigh-Taylor instabilities of a plane circular interface. 21 p2749 A73-41626
- Electromagnetic radiation excited by electric or magnetic line source near inhomogeneous dielectric layer, evaluating reflected and transmitted fields by saddle point technique 22 p2824 A73-41831
- Changes in the characteristics of giant laser radiation pulses and of luminous plasma during formation of damage regions on the surface or in the bulk of transparent dielectrics. 22 p2869 A73-42250
- Bounds on effective dielectric constant of inhomogeneous material. 22 p2896 A73-42263
- Interference filters for the VUV /1200-1900 Å/. 22 p2863 A73-43142
- Regularities in the behavior of semiconductors and dielectrics in connection with deviation from stoichiometry 23 p2959 A73-43479
- The role of absorbing impurities in laser-induced damage of transparent dielectrics. 23 p2959 A73-43512
- The superconductor-excitonic dielectric phase transition in a semimetal. 23 p3015 A73-43513
- Three layer semiconductor dielectric interface model of structural and electrical properties of silicon-silicon dioxide system involving amorphous regions 23 p3015 A73-43614
- Electromagnetic resonances and Q-factors of lossy dielectric spheres. 23 p2960 A73-44067
- Modified H guide for millimeter and submillimeter wavelengths. 23 p2960 A73-44072
- Stability of an electron beam in an inhomogeneous dielectric medium. 24 p3114 A73-44610
- Scattering of electromagnetic waves by a disk at the interface between two media. 24 p3067 A73-44624
- Local form of the radiation condition - Application to curved dielectric structures. 24 p3069 A73-45257
- ### DIENCEPHALON
- Brain stem reticular formation influence on lateral geniculate body neurons during eye movements, suggesting cortical oculomotor impulse influence mediation by perigeniculate nucleus 18 p2272 A73-36448
- Changes in respiration accompanying a diencephalic vegetative-vascular syndrome under the action of a hypoxic mixture 21 p2636 A73-40280
- ### DIES
- Consideration of a number of factors involved in determining the long-term strength of dies used for the extrusion of hollow sections of aluminum alloys 03 p0318 A73-14651
- ### DIESEL ENGINES
- Book - ASTM manual for rating motor, diesel, and aviation fuels. 06 p0740 A73-18402
- Book - Engine emissions: Pollutant formation and measurement. 19 p2474 A73-38321
- ### DIETS
- Diet, exercise, and glycogen changes in human muscle fibers. 01 p0007 A73-10160
- Arterial oxygen increase by high-carbohydrate diet at altitude. 01 p0007 A73-10164
- Hepatic lipogenesis in fasted, re-fed rats and mice - Response to dietary fats of differing fatty acid composition. 03 p0258 A73-13054
- Effect of high-fat diet on thermal acclimation with special reference to thyroid activity. 05 p0541 A73-16800
- Low calcium diet produced chronic decalcification effect on osseous repair of experimentally induced cortical bone defect in chickens 18 p2270 A73-35981
- Apollo diet evaluation - A comparison of biological and analytical methods including bioisolation of mice and gamma radiation of diet. 20 p2517 A73-39103
- ### DIFFERENCE EQUATIONS
- Difference procedures of monotonic type for nonlinear parabolic boundary value problems 01 p0069 A73-10072
- Iteration approach for elliptic /nonlinear/ difference operators in divergence form 01 p0069 A73-10075
- Numerical integration of a problem of a second-order equation with discontinuous coefficients 01 p0070 A73-10088
- Study of the oscillations of plates, shells and combined systems by the basis vector method with difference discretization 02 p0232 A73-11817
- Grid model to derive biharmonic difference operators with computer programming application, assessing errors in boundary conditions 02 p0236 A73-12512
- Difference approximations for boundary and eigenvalue problems for ordinary differential equations. 02 p0188 A73-12613
- Stability theory of difference approximations for mixed initial boundary value problems. II. 02 p0188 A73-12616
- Calculation of supercritical flow past airfoils by the Murman-Krupp difference method [DGLR PAPER 72-128] 03 p0248 A73-14387
- Two numerical methods for three-dimensional boundary layers. 04 p0433 A73-15003
- Variational-difference method for solving the third boundary value problem of an elliptic equation in a three-dimensional region with a smooth boundary 05 p0590 A73-16445
- A stability theory for perturbed difference equations. 05 p0590 A73-16491
- Application of the variational-difference method in solving the problems of torsion for rods of complex form 05 p0636 A73-17094
- Convergence of difference methods for certain degenerating quasi-linear parabolic equations 09 p1111 A73-21919
- Difference schemes for two dimensional gas flows with detonation in frame of Lagrange variables, comparing point explosion with self similar solution 09 p1070 A73-21923
- Recurrent orbit estimation biases by filtering, using method representing motion by finite difference equations 09 p1143 A73-22098
- A probabilistic approach to a differential-difference equation arising in analytic number theory. 10 p1241 A73-23643

Difference equations of elastic equilibrium for shells with variable characteristics in polar coordinates

11 p1433 A73-25027

Converse theorems for Liapunov stability and boundedness of nonlinear discrete-time systems described by difference equations

11 p1389 A73-25186

Admissible step sizes for Adams-Bashforth, Adams-Moulton, Nystrom and Milne-Simpson difference methods for initial value problems solution

11 p1392 A73-26729

Necessary and sufficient condition for stability of a class of difference-type boundary value problems

12 p1517 A73-26962

Necessary termination conditions for difference-differential rendezvous /pursuit with evasion/ game with functional goal set

12 p1524 A73-27401

Two-sided difference methods of solving linear boundary value problems for ordinary differential equations

13 p1647 A73-28341

The numerical treatment of natural eigenvalue problems of the 4th order according to the collocation method with a Lagrange polynomial approach

13 p1695 A73-28411

Numerical stability criteria for fourth order nonlinear difference equations, using discrete form of Liapunov direct method

13 p1649 A73-28699

Stability of difference equations and convergence of iterative processes.

14 p1767 A73-29937

Convergence of a difference procedure for quasi-linear parabolic initial boundary-value problems in cylinder symmetry

14 p1769 A73-30422

Fundamental solution to a single-parameter family of Laplace-parameter difference approximations on a plane

15 p1898 A73-30961

Convergence of the upper relaxation method for solving variational-difference equations for elliptic equations in an arbitrary plane

15 p1898 A73-30967

Synthesis of optimal discrete control systems with persisting perturbations

15 p1854 A73-31803

Corresponding function solutions of discrete mechanics problems based on difference polynomials, applying to Lagrange problem of string natural vibrations for distributed point masses

16 p2035 A73-32680

Estimates of the eigenvalues of a difference problem for a plate

16 p2074 A73-32690

Solutions of certain difference equations describing transformation of the temporal characteristics of radiation in a laser

16 p2024 A73-32891

A geometrical proof of the maximum principle for systems represented by difference-differential equations.

16 p2032 A73-33302

A difference method of solving boundary value problem for a parabolic-type quasi-linear integro-differential equation

16 p2034 A73-34070

Formulation of stable difference schemes for systems of initial-value partial differential equations.

17 p2200 A73-34284

The numerical derivation of a periodic solution of a second order differential difference equation.

17 p2203 A73-35728

Book - Analysis of discretization methods for ordinary differential equations.

18 p2329 A73-35904

On the Volterra series functional evaluation of the response of non-linear discrete-time systems.

22 p2837 A73-43069

Exponential stability theorems of multivalued difference equations for discrete dynamical systems

23 p3000 A73-44206

Synthesis of optimal sampled-data control systems in the presence of continuous disturbances.

23 p2965 A73-44332

Applicability of difference methods for solving Navier-Stokes equations at large Reynolds numbers

24 p3076 A73-44426

An iteration method of alternating directions for the Poisson difference equation in curvilinear orthogonal coordinates

24 p3105 A73-44650

A divergent difference scheme for calculation of steady supersonic flows with complex structures

24 p3053 A73-44651

Numerical study of the problem of explosion of a cylindrical charge of finite length

24 p3076 A73-44654

DIFFERENTIAL ALGEBRA

U DIFFERENTIAL CALCULUS
U MATRICES [MATHEMATICS]

DIFFERENTIAL AMPLIFIERS

Selective differential broadband precision amplifier for weak signals of galvanomagnetic sensor of magnetic induction indicator based on Hall effect

01 p0022 A73-10083

Overload tolerance formulas for differential voltage null measuring system with amplifier for trigger circuit drive

02 p0170 A73-12345

Design of active filter sections performing biquadratic transfer functions on the basis of a branched operational-amplifier configuration

07 p0796 A73-18895

A low-sensitivity third-order active filter constructed with DVCCS/DVCCS universal sources

07 p0796 A73-18897

A dc amplifier operating with a measuring bridge circuit

07 p0803 A73-20540

A charge amplifier for pressure measurements

07 p0827 A73-20543

Temperature measuring devices based on operational amplifier circuits, considering design and applications

09 p1085 A73-22924

An electrocardiograph amplifier which satisfies the stringent requirements of long-term monitoring of cardiac activity

10 p1184 A73-23849

Oscillatory operational amplifiers for control systems and computer technology

12 p1477 A73-26773

A low-velocity hot-wire anemometer.

12 p1496 A73-27055

Selectivity enhancement of certain low-sensitivity RC active networks.

14 p1738 A73-29711

Operational amplifier integrator for storage element in track-hold circuit, discussing drift rate reduction with large equal-value resistors from input terminal to ground

16 p1988 A73-33398

A pulse-width modulator operating on dc integral amplifiers

18 p2293 A73-36855

The equipment for photoelectric photometry in the Graz observatory

20 p2565 A73-39068

Possibilities of improving the characteristics of operational amplifiers by using thermostated input cascades

21 p2660 A73-40023

Noise characteristics in bipolar transistor differential amplifiers, discussing current sources, circuit configurations, feedback amplifiers and equivalent circuits

22 p2832 A73-41897

Two channel transistor amplifier design with negative capacitance correction for microelectrode applications

24 p3062 A73-44723

DIFFERENTIAL ANALYZERS

U ANALOG COMPUTERS

DIFFERENTIAL CALCULUS

Imbedding theorem for the spaces of functions whose mixed derivatives satisfy the multiple integral Hoelder condition

02 p0187 A73-12178

Trajectory deviation conditions in second order linear differential escape game

07 p0850 A73-19014

Necessary and sufficient conditions for differentiable nonscalar-valued functions to attain extrema.

10 p1243 A73-24537

Algorithm and convergence behavior of the local variation method for problems with partial derivatives

11 p1400 A73-26326

Differential coefficient computation for spacecraft orbital velocity component variations in case of universal elements utilization for orbit improvement problems

12 p1538 A73-26864

Matrix calculus operations and Taylor expansions.

14 p1769 A73-30410

Approximation of differentiable functions of numerous variables by Fourier sums in an L sub p metric

15 p1899 A73-31218

Derivatives of eigensolutions for a general matrix.

18 p2330 A73-36318

Construction of a transformation matrix and the differentiability of the formal solution of a system of partial differential equations

20 p2582 A73-39475

DIFFERENTIAL EQUATIONS

NT BIHARMONIC EQUATIONS

NT BLASIUS EQUATION

NT BURGER EQUATION

NT CAUCHY-RIEMANN EQUATIONS

NT CHANDRASEKHAR EQUATION

NT DUFFING DIFFERENTIAL EQUATION

NT ELLIPTIC DIFFERENTIAL EQUATIONS

NT FALKNER-SKAN EQUATION

NT FOKKER-PLANCK EQUATION

NT GAUSS EQUATION

NT HELMHOLTZ VORTICITY EQUATION

NT HYPERBOLIC DIFFERENTIAL EQUATIONS

NT LAME WAVE EQUATIONS

NT LIOUVILLE EQUATIONS

NT PARABOLIC DIFFERENTIAL EQUATIONS

NT PARTIAL DIFFERENTIAL EQUATIONS

NT POISSON EQUATION

NT VLASOV EQUATIONS

NT VORTICITY EQUATIONS

Conformal transformation of semiordered linear space via inclusion statement, considering second order differential operators

01 p0069 A73-10068

Equivalence theorems for nonlinear finite-difference methods.

01 p0069 A73-10074

Numerical integration of a problem of a second-order equation with discontinuous coefficients

01 p0070 A73-10088

Asymptotic properties of eigenvalues in the Sturm-Liouville problem of a class of equations with random coefficients

01 p0070 A73-10099

Construction of finite-difference schemes in engineering theory of elasticity on the basis integral representations of the resolvent functions

01 p0114 A73-10483

Rectangular plates with unidirectionally variable rigidity

01 p0114 A73-10572

On a new form for the differential equations of relative motion of the three-body problem.

01 p0099 A73-10690

Nonlinear axisymmetric flexural vibration equations of a cylindrically anisotropic circular plate.

01 p0115 A73-10756

Application of shell equations to an unsymmetrically loaded corrugated shell of revolution.

01 p0115 A73-10769

Asymptotic properties of solutions of certain linear systems of differential equations with random coefficients

01 p0070 A73-10913

Solutions and stability of a system of two first-order linear differential equations with variable coefficients

01 p0070 A73-10914

Study of a mixed problem for a third-order nonlinear differential equation with degeneration or singularity

01 p0070 A73-10920

Optimal control problems in differential games of pursuit and evasion involving deterministic, random and controlled motion

01 p0028 A73-11071

Finite difference solution to Vekua thin shell equations, using differential and equivalent energetic operators

01 p0116 A73-11076

Nonlinear differential equations with logarithmically small perturbations.

01 p0071 A73-11268

Boundary layer equation complete solution from first order differential equation graphic solution by Poincare method

01 p0034 A73-11360

Ordinary integrodifferential equations for dynamic and quasi-static problems of nonlinear viscoelasticity theory

01 p0119 A73-11431

Uniqueness of a solution to an inverse problem in the case of a second order equation with continuous boundary conditions: Regularized sums of a portion of eigenvalues - Factorization of the characteristic determinant

01 p0071 A73-11440

Second-order abstract and Schroedinger linear differential equations in Beurling spaces

02 p0186 A73-11570

Integration of a differential equation describing the bending of a physically nonlinear plate of variable thickness

02 p0231 A73-11811

Spectral analysis of integro-differential forms in spatial dynamic problems of the theory of elasticity

02 p0232 A73-11820

Conference on the Theory of Ordinary and Partial Differential Equations, Dundee, Scotland, March 28-31, 1972, Proceedings.

02 p0186 A73-11968

Singular elliptic perturbations of vanishing first-order differential operators.

02 p0186 A73-11970

The deficiency indices and spectrum associated with self-adjoint differential expressions having complex coefficients.

02 p0186 A73-11971

A Liapunov function for an autonomous second-order ordinary differential equation.

02 p0186 A73-11974

Construction of solutions and the application of the joining method to the solution of the Liapunov stability problem for a system of linear homogeneous differential equations with pi-periodic coefficients

02 p0193 A73-12189

Uniqueness and stability of positive periodic solutions of differential equations with a delayed argument
02 p0187 A73-12357

The effects of viscous friction on axial rotation of celestial bodies.
02 p0216 A73-12376

Difference approximations for boundary and eigenvalue problems for ordinary differential equations.
02 p0188 A73-12613

A note on modified optimal linear multistep methods.
02 p0188 A73-12614

Stability theory of difference approximations for mixed initial boundary value problems. II.
02 p0188 A73-12616

Asymptotic estimates for solutions of linear systems of ordinary differential equations having multiple characteristic roots.
02 p0188 A73-12625

A method for phenomenological analysis of ecological data.
02 p0188 A73-12629

Improved sixth-order Runge-Kutta formulas and approximate continuous solution of ordinary differential equations.
02 p0188 A73-12822

Variational aspects of oscillation phenomena for higher order differential equations.
[AD-758575] 02 p0188 A73-12823

Boundary value problems with a turning point.
03 p0336 A73-13066

Stress-strain diagrams for stability of structures under plastic bending, noting differential equations for rigidity characteristics
03 p0386 A73-13144

Tensor analysis for micropolar elastic body deformation and stresses, solving differential equations of thermoelasticity
03 p0386 A73-13153

Lyapunov functions for quadratic differential equations with applications to adaptive control.
03 p0336 A73-13520

On the almost-sure sample stability of systems with randomly time-varying delays.
03 p0285 A73-13898

Optimal control of observation processes, formulating solvability conditions in terms of ordinary differential equations
03 p0286 A73-14043

Liapunov function application to stability of unperturbed motion of system of differential equations with respect to part of variables
03 p0344 A73-14056

Oscillatory and asymptotic behavior of functional differential equations.
04 p0469 A73-14663

The behavior of a self-excited system acted upon by a sequence of random impulses.
04 p0469 A73-14664

A class of neutral functional differential equations.
04 p0469 A73-14666

Theorems on periodic noncritical approximate solutions of nonlinear oscillations differential equations
04 p0469 A73-14667

Stabilization of constraints and integrals of motion in dynamical systems.
04 p0470 A73-15002

The solution of linear, constant-coefficient, ordinary differential equations with APL.
04 p0470 A73-15008

Newtonian differential equations of Kepler motion, analyzing stability by numerical integration based on Floquet theorem and Runge-Kutta method
04 p0497 A73-15013

Extended validity of single segment stepwise integration schemes for solution of two-point boundary value problems.
04 p0510 A73-15015

Certain analytical solutions of the Cauchy problem for a disturbed loaded linear integrodifferential equation
04 p0470 A73-15080

Stability of the Bubnov-Galerkin method for unstable operator equations with variable coefficients
04 p0470 A73-15085

Algebraic and transfer-function criteria of fixed-time controllability of delay-differential systems.
04 p0430 A73-15212

Necessary and sufficient conditions of pointwise completeness of linear time-invariant delay-differential systems.
04 p0430 A73-15213

Hyperbolic equations and systems with multiple characteristics.
04 p0471 A73-15224

Governing equations for vibrating constrained-layer damping sandwich plates and beams.
[ASME PAPER 72-WA/APM-24] 04 p0515 A73-15892

On the stability of linear stochastic differential equations.
[ASME PAPER 72-WA/APM-16] 04 p0472 A73-15898

A multi-step method for the numerical integration of ordinary differential equations.
05 p0589 A73-16100

Existence theorem for integral manifolds of point mappings in resonant and nonresonant cases for differential equations systems with fast rotating phases
05 p0560 A73-16290

Phase space structure of neutral-type quasi-linear differential equations
05 p0589 A73-16294

Instability of the exponential discreteness characteristic of solutions to a system of differential equations, and the asymmetry of the near-reducibility ratio of a system of differential equations with an integral discreteness of solutions
05 p0590 A73-16335

Discrete Galerkin and related one-step methods for ordinary differential equations.
05 p0590 A73-16375

Control of functional differential equations of retarded and neutral type to target sets in function space.
[AD-758569] 05 p0561 A73-16486

Computer-aided solution of nonlinear differential equations in electrical engineering, using an extension of Wolinkin's procedure
06 p0669 A73-17595

The problem of the excitation of subharmonics and higher harmonics in circuits, determined by a nonlinear differential equation of second order
06 p0715 A73-17698

Construction of the equations of a programmed motion possessing extremal properties
06 p0722 A73-17715

Matrix transformation in hyperplanes method for successive solution of boundary value problems of multidimensional differential equations, using space-time functions
06 p0715 A73-17718

Applications of Jacobi polynomials to non-linear differential equation associated with generalized hypergeometric function.
06 p0716 A73-17791

Further exact and approximate considerations of the barrier problem.
06 p0716 A73-17981

Riemann-method solution of the Cauchy problem for a system of first-order equations with a degeneracy at the boundary
06 p0717 A73-18068

Representation of oscillations in piecewise-linear systems by the phase-shift-averaging method.
06 p0717 A73-18146

Comparing numerical methods for ordinary differential equations.
06 p0717 A73-18406

A simple interpolation algorithm for improvement of the numerical solution of a differential equation.
06 p0717 A73-18407

Multistep methods with variable matrix coefficients.
06 p0718 A73-18409

Kolmogorov's differential equations for non-stationary, countable state Markov processes with uniformly continuous transition probabilities.
06 p0718 A73-18501

Boundedness of infinitely extendable solutions to a system of two equations with quadratic right members, and the manifold of Liapunov's characteristic exponents of solutions to this system
06 p0718 A73-18679

Convergence of the small parameter method in deriving periodic solutions to ordinary neutral-type differential equations with small delay
06 p0718 A73-18680

Solution stability of autonomous differential equations with holomorphic members under perturbation by time dependent auxiliary functions
06 p0724 A73-18683

Multipoint boundary problem for differential equations with a deviating argument
06 p0718 A73-18685

Construction of a set of systems of second-order delayed-argument differential equations having a prescribed integral curve
06 p0718 A73-18687

Solution of a boundary problem for a second-order delayed-argument differential equation by the spline-function method
06 p0719 A73-18688

Boundary value problems for non-elliptic first-order systems of pseudo-differential operators.
06 p0719 A73-18699

Galerkin method for approximate solution of differential equation with boundary conditions, considering applicability to nonself-adjoint and nonlinear systems
06 p0765 A73-18725

Nonlinear time-varying control systems transformation, deriving conditions for existence of observable system representation and corresponding scalar differential equation
06 p0719 A73-18802

Identification of multivalued nonlinearities in a class of noisy time invariant dynamic systems.
06 p0681 A73-18811

Modeling of linear time-varying systems by linear time-invariant systems of lower order.
06 p0682 A73-18867

Estimate of the time of occurrence of discontinuities in the solution of a boundary value problem for a second order quasilinear hyperbolic system.
07 p0844 A73-19023

The determination of state-space representations for linear multivariable systems.
07 p0804 A73-19131

The finite element method with Lagrangian multipliers.
07 p0844 A73-19137

Methods of reducing continual nonlinear mechanics problems for deformable solids to discrete problems
07 p0910 A73-19303

A general scheme for solving ordinary differential equations under two-point boundary conditions.
07 p0845 A73-19546

An analytical method for certain weakly nonlinear periodic differential systems.
07 p0845 A73-20226

A proposal for the calculation of characteristic functions for certain differential and integral operators via initial-value methods.
07 p0845 A73-20490

Topologies for neutral functional differential equations.
07 p0845 A73-20493

Stability of difference approximations to differential equations.
07 p0845 A73-20494

Conditional stability and separation of solutions to differential equations.
07 p0845 A73-20496

An attainable sets approach to optimal control of functional differential equations with function space terminal conditions.
07 p0846 A73-20497

The estimation of order and parameters in a process of stochastic differential equations with uncertain observations.
07 p0846 A73-20594

Dual characterizations of optimal control systems governed by linear and nonlinear differential equations with dynamic constraints, using complementary variational principle in Hilbert space
07 p0846 A73-20598

Necessary condition for complete controllability with respect to arbitrary function for linear time-invariant differential equation system with time lag
08 p0950 A73-21092

Distributed parameter system a priori stochastic optimal control, deriving canonical differential equations from dynamic programming formulation for insight into feedback control problem
08 p0950 A73-21093

Book - Stochastic differential equations.
08 p0984 A73-21833

Nonoscillation of second-order, linear differential equations with retarded argument.
09 p1112 A73-22420

Second order differential equations with complex-valued coefficients.
09 p1112 A73-22425

Extremal targeting in a nonlinear rendezvous game
09 p1112 A73-22476

Optimal control system design with respect to vector quality criterion, noting linear system described by differential equations
09 p1068 A73-22560

Asymptotic behavior of the distribution of the solution of a stochastic differential equation with coefficients depending on the entire history of the process
09 p1112 A73-22844

Studies in the application of recurrence relations to special perturbation methods.
09 p1149 A73-22914

Periodic solution of a second-order non-linear differential equation.
09 p1113 A73-22985

Some oscillatory properties of solutions of fourth-order quasi-linear differential equations
09 p1113 A73-22986

Contribution to the numerical solution of differential equations by means of Runge-Kutta formulas with Newton-Cotes numbers weights
09 p1113 A73-22988

Optimal control problems in differential games of pursuit and evasion involving deterministic, random and controlled motion
09 p1113 A73-22996

The numerical solution of boundary value problems for second order functional differential equations by finite differences.
09 p1113 A73-23021

Matrix Riccati differential and quadratic algebraic equations in optimal control and filtering theory, discussing stabilizing solutions, asymptotic properties and computational techniques
09 p1069 A73-23102

Dielectric gradient waveguides inhomogeneous core layer, solving differential equation by perturbation method
09 p1065 A73-23113

Differential equations in terms of the osculatory elements of a solid for the motion of the solid about its center of mass

09 p1121 A73-23355

Combined-operations method for diffuse reflection by an isotropic, non-coherent scattering homogeneous sphere.

10 p1271 A73-23484

Nonstationary equations of the nonlinear theory of elasticity in Euler coordinates

10 p1287 A73-23590

Local extrapolation in the solution of ordinary differential equations.

10 p1241 A73-23641

A probabilistic approach to a differential-difference equation arising in analytic number theory.

10 p1241 A73-23643

Perturbed satellite motion differential equations, on basis of fixed center problem and perturbing forces with no force function

10 p1274 A73-23721

Boundary value problems for a nonlinear differential equation with a deviating argument of neutral type

10 p1241 A73-23742

Linear dependence of functions along the solutions of systems of differential equations and of a system with algebraic loci

10 p1241 A73-23743

Iterative optimum control function determination without directly solving the system dynamical equations.

10 p1242 A73-24033

Initial conditioned solutions of a second-order nonlinear conservative differential equation with a periodically varying coefficient.

10 p1244 A73-24706

Unsteady creep in a symmetrical cylindrical shell

10 p1293 A73-24793

Ambipolar drift, deformation, and diffusion of a plasma in a magnetic field.

11 p1402 A73-24989

A structural model of random processes and its invariant properties

11 p1340 A73-25007

Nonlinear delay-differential control systems described by periodic functional differential equations with small real parameter, investigating asymptotic stability in Liapunov sense

11 p1390 A73-25190

An approximate solution to a strongly non-linear, second-order, differential equation.

11 p1390 A73-25195

Analytical investigation of heat transfer in bodies with moving boundaries

11 p1450 A73-25622

Application of nonalgorithmic digital machines in modeling differential equations

11 p1334 A73-25633

Ordinary integrodifferential equations for dynamic and quasi-static problems of nonlinear viscoelasticity theory

11 p1443 A73-26066

Nonsingular differential equations derivation for parabolic, hyperbolic, elliptic and rectilinear orbit perturbations via simple osculating element coordinate transformations and Lagrange planetary equations

11 p1423 A73-26073

Calculation of functionals of the eigenfunctions in the boundary value problem of a system of linear ordinary differential equations

11 p1391 A73-26331

Differential equations for asymmetric bending of circular sandwich plates.

11 p1445 A73-26406

Stagnation conditions in systems with Coulomb friction

11 p1400 A73-26451

Application of the Chaplygin method to the solution of Volterra-type nonlinear integro-differential equations

11 p1391 A73-26521

Optimal inputs and sensitivities for parameter estimation.

11 p1391 A73-26579

Optimal control for functional differential systems through Krasovskii generalization for time delay systems and resulting Riccati equations numerical solution

11 p1392 A73-26581

Analytical properties of solutions to linear differential equations and systems

12 p1516 A73-26951

Method for successively increasing the step of numerical integration for systems of ordinary differential equations

12 p1516 A73-26952

Stability of the solutions of differential equations with a nonlinear potential operator in a Hilbert space

12 p1516 A73-26959

A boundary value problem for higher-order hyperbolic equations

12 p1516 A73-26961

On the formulation of the traction problem for the flow theory of plasticity.

12 p1551 A73-27046

Group properties and invariant solutions of the Bellman equation in the problem of optimal control synthesis for second-order systems

12 p1483 A73-27079

Stochastic equations of nonlinear filtering of random processes

12 p1518 A73-27222

Construction of asymptotic solutions to the Cauchy problem with an initial jump for nonlinear systems of integrodifferential equations containing a small parameter at the higher derivative

12 p1518 A73-27298

Solution of systems of nonlinear differential equations by the Newton-Raphson method

12 p1518 A73-27396

Necessary termination conditions for difference-differential rendezvous /pursuit with evasion/ game with functional goal set

12 p1524 A73-27401

Existence solution to linear differential rendezvous game of dynamic system with pursuit and evasion

12 p1524 A73-27402

Synthesis of an approximately optimal control for one class of controlled systems.

12 p1484 A73-27457

A uniqueness theorem for the solution of the inverse problem of spectral analysis in the case of a differential equation with periodic boundary conditions

12 p1518 A73-27727

Symposium on Ordinary Differential Equations, University of Minnesota, Minneapolis, Minn., May 29, 30, 1972, Proceedings.

12 p1519 A73-27919

Stability of coupled systems of nonlinear differential delayed-argument equations

12 p1525 A73-27947

Vibrations of a system with memory, non-linear elasticity, friction and relaxation.

13 p1690 A73-28055

Methods for the approximate computation of the periodic solutions of systems of nonlinear periodic differential equations

13 p1647 A73-28193

Two-sided difference methods of solving linear boundary value problems for ordinary differential equations

13 p1647 A73-28341

Nonoscillation and disconjugacy of systems of linear differential equations.

13 p1648 A73-28441

Characteristic initial value problem for class of differential equations, proving solution existence and uniqueness as generic properties

13 p1648 A73-28536

Singular perturbations for a nonlinear differential equation with a small parameter.

13 p1648 A73-28537

Estimating the eigenvalues of Sturm-Liouville problems by approximating the differential equation.

13 p1649 A73-28606

Differential equations for digital model of linear quadrupole, discussing digital simulation of analog radio equipment circuits

13 p1591 A73-28659

On an Euler-like method with exponential correction for initial-value problems.

13 p1650 A73-28799

Extremal controls in a nonlinear differential game

13 p1660 A73-29077

Conditions for evading a point in a second-order differential game

13 p1660 A73-29078

Differential game estimate of phase point pursuit of evading closed convex set for feedback control in irregular case

13 p1660 A73-29079

Classification theorem for analytical transformations of second order differential equations of motion at arbitrary resonance based on group theory

13 p1661 A73-29081

Periodic rectilinear solutions close to normal mode shapes of vibration of nonlinear conservative system described by differential equations generated by homogeneous potential systems

13 p1661 A73-29083

Arrangement of integral surfaces in weakly-nonlinear systems of differential equations

13 p1650 A73-29137

On the stability of numerical integration routines for ordinary differential equations.

13 p1650 A73-29397

Rayleigh-Ritz method for approximate solutions to nonlinear ordinary differential equations with nonlinear boundary conditions

13 p1650 A73-29399

Routh-Hurwitz method for optimal algebraic stability of ordinary differential equations of fourth order systems with linear control law

13 p1597 A73-29419

Book - Optimal control of differential and functional equations.

13 p1651 A73-29550

Zero sum differential game theory for two players, discussing strategies, stochastic versions and saddle value and points existence

13 p1651 A73-29650

Accuracy estimates for analog computer solutions to systems of ordinary linear equations and some algebraic equations

14 p1768 A73-30033

Method of reducing the order of a differential equation when studying transient processes in mechanical systems

14 p1774 A73-30286

Construction of finite difference diagrams of the engineering theory of elasticity, on the basis of integral representations of the resolvent functions.

14 p1810 A73-30308

Nonlinear vector matrix differential equations for automatic control systems dynamics, discussing stability, dissipativity and convergence

14 p1768 A73-30344

Some aspects of the asymptotic behavior of solutions of nonlinear differential equations with delayed argument

14 p1768 A73-30345

Boundary value problem of a system of ordinary differential equations with a complex parameter

14 p1768 A73-30346

Stress determination approximation in structural mechanics problems by linear first order differential equations reduction to linear algebraic equations

14 p1810 A73-30378

A survey of recent results in differential equations.

14 p1769 A73-30411

Numerical solutions by the continuation method.

14 p1769 A73-30454

An existence theorem for linear boundary value problems.

14 p1770 A73-30524

Application of the optimal linearization method to the heat transfer problem.

14 p1817 A73-30605

Delay and functional differential equations and their applications; Proceedings of the Conference, Park City, Utah, March 6-11, 1972.

14 p1770 A73-30753

Control of functional differential equations with function space boundary conditions.

14 p1770 A73-30754

Numerical methods for functional differential equations.

14 p1770 A73-30755

Oscillations of higher-order retarded differential equations generated by the retarded argument.

14 p1770 A73-30756

On asymptotic solutions of nonlinear differential equations with time lag.

14 p1770 A73-30759

Existence and uniqueness theorems for differential equations with deviating arguments of mixed type.

14 p1770 A73-30760

Oscillations of nonlinear functional differential equations generated by retarded actions.

14 p1770 A73-30761

Stability in the critical case of purely imaginary roots for neutral functional differential equations.

14 p1771 A73-30773

Fixed point theorems and dissipative processes.

14 p1771 A73-30774

Expansion of nonconjugate differential Dirac operators into a series of eigenvalues over the whole axis, and an analytical expression for a spectral matrix-function

14 p1771 A73-30787

Some questions of approximation in the variational difference method

14 p1771 A73-30830

Analysis of a system of differential equations with a small parameter at the higher derivatives

14 p1771 A73-30832

Extension of the Favard theory to the case of a system of linear differential equations with unbounded coefficients which are nearly periodic according to Levitan

14 p1771 A73-30837

Asymptotic solution of a system of linear differential equations with slowly varying coefficients in a complex domain

15 p1898 A73-31028

Asymptotic solution of a system of linear differential equations with slowly varying coefficients of the neutral type

15 p1898 A73-31036

Nonlinear differential equation solutions for prismatic body elastic equilibria in terms of deformation and stress tensor relations by small parameter method

15 p1945 A73-31042

Effects of motion of the equatorial plane on the orbital elements of an earth satellite.

15 p1930 A73-31112

Elimination of time and differential equation of trajectories in the problem of three restricted, circular, plane bodies

15 p1930 A73-31175

Boundary value problems for a first-order differential equation with operator coefficients and for the expansion of this equation in a series of its eigenvalues

15 p1899 A73-31216

Differential operators of constant force and a comparison of differential operators

15 p1899 A73-31217

Nonlocal continuance of solutions to vibration-stable differential equations

15 p1899 A73-31219

A solution operator for ordinary differential equations and its application in fluid dynamics

15 p1862 A73-31329

Uniqueness and existence estimates of third order differential equation solutions for nonlinear boundary value problem in fluid mechanics

15 p1863 A73-31363

Error investigations regarding the solution of the inhomogeneous natural boundary value problem by means of a Ritz approach with standardized coordinate functions

15 p1899 A73-31364

Book on perturbation methods for nonlinear differential equations covering canonical transformation theory, Hamiltonian and integrable systems, area preserve mapping and resonance problem

15 p1899 A73-31472

Differential and pseudodifferential operators with an infinite number of independent variables, and their applications

15 p1900 A73-32081

Multivariable linear passive systems

15 p1900 A73-32087

Lie group theory of differential equations in continuum mechanics, gas dynamics, heat conduction, biharmonic and second order quasi-linear equations

15 p1914 A73-32109

A periodic solution of a singular differential system with a retarded argument - Construction and approximate calculation

15 p1900 A73-32165

Book - Two-point boundary value problems: Shooting methods.

15 p1901 A73-32299

The method of penalty functions and necessary conditions of optimality for generalized solutions of the optimal control problem

15 p1901 A73-32367

A criterion for global existence in case of ordinary differential equations.

15 p1901 A73-32370

Spectral resolution of differential operators associated with symmetric hyperbolic systems.

15 p1901 A73-32373

Sturm comparison and separation theorems for linear, second order, self-adjoint, ordinary, differential equations and for first order systems.

15 p1902 A73-32377

Existence and uniqueness of solutions of boundary value problems for third order differential equations.

15 p1902 A73-32398

Convergence of difference methods for second-order ordinary differential equations

16 p2031 A73-32821

Differential equations with free boundaries in stochastic control problems

16 p2031 A73-32822

The iterative solution of two-point linear differential eigenvalue problems.

16 p2031 A73-32930

Extension of the Carathéodory theory to multivalued differential systems with nonlinear boundary conditions

16 p2031 A73-32932

Nonlinear shell theory, obtaining differential equilibrium equations and boundary conditions from three dimensional variational energy expression by kinematic hypothesis and Ritz method

16 p2078 A73-32996

New problems pertaining to nonlinear integro-differential equations with several independent variables. I - Search for solutions in the case of initial integral boundary conditions

16 p2032 A73-33172

Numerical integration errors due to differential equations instability for Kepler orbits, discussing error reduction procedure by substituting for time as independent variable

16 p2061 A73-33231

A geometrical proof of the maximum principle for systems represented by difference-differential equations.

16 p2032 A73-33302

Solutions of a class of random differential equations.

16 p2032 A73-33308

Periodic solutions of singularly perturbed equations arising from gyroscopic systems.

16 p2032 A73-33310

Regularity theorems for the solution of a second-order abstract linear differential equation

16 p2032 A73-33373

Characteristics of the Bianchi-IX cosmological model from the viewpoint of the qualitative theory of differential equations

16 p2071 A73-34052

A modified Butcher formula for integration of stiff systems of ordinary differential equations.

17 p2199 A73-34212

A new fundamental system of modified cylindrical functions for an annular region.

17 p2200 A73-34248

Book - Methods of nonlinear analysis. Volume 2.

17 p2200 A73-34453

Convergence of periodic solutions of differential equations for resonance circuits with nonlinear semiconductor capacitance

17 p2144 A73-34585

Multivalued solutions and the classification principle for nonlinear differential equations

17 p2200 A73-34628

On the distribution of the eigenvalues and the order of the eigenfunctions of a fourth-order singular boundary value problem.

17 p2201 A73-34823

Weighted residual processes in finite element with particular reference to some transient and coupled problems.

17 p2245 A73-34835

Russian book - Asymptotic and qualitative methods in the theory of nonlinear oscillations.

17 p2211 A73-34850

Prior-to-failure extension of flaws under monotonic and pulsating loadings.

17 p2246 A73-34884

A procedure for investigating the Liapunov stability of nonautonomous linear second-order systems.

[ASME PAPER 73-APM-31] 17 p2201 A73-35044

A perturbation method for obtaining approximate solutions of an equation with two small parameters

17 p2201 A73-35046

On an accurate theory for circular cylindrical shells.

[ASME PAPER 73-APM-E] 17 p2250 A73-35114

Numerical solution of the three-dimensional Navier-Stokes equations in integro-differential form - Flow about a finite body.

17 p2155 A73-35139

Boundary value problem of the E problem type for mixed equations of the second kind

17 p2203 A73-35588

Chemically reacting gas flow numerical calculations from stiff nonlinear ordinary differential equations solution in finite difference form

17 p2119 A73-35609

A computer program to find analytical solutions of second order linear differential equations.

17 p2132 A73-35611

The numerical derivation of a periodic solution of a second order differential difference equation.

17 p2203 A73-35728

Nonlinear boundary value problems and several Lyapunov functions.

17 p2203 A73-35730

A note on saddle point behavior for ordinary and functional differential equations.

17 p2204 A73-35733

Russian book on linear differential delay equations covering solvability theorems, solution properties, stable and unstable equations, first and second order equations, periodic equations, etc

18 p2329 A73-35897

Russian book - Linear differential equations with periodic coefficients and their applications.

18 p2329 A73-35903

Book - Analysis of discretization methods for ordinary differential equations.

18 p2329 A73-35904

Wazewski retract method application to boundary value problems for second order generalized differential equations, proving solutions existence

18 p2330 A73-36693

Oscillation theorems for a second order damped nonlinear differential equation.

18 p2330 A73-36694

Perturbed satellite motion differential equations derivation on basis of fixed center problem and perturbing forces with no force function, obtaining intermediate orbital elements

18 p2355 A73-36746

Differential games applied to some interception models

18 p2268 A73-37080

Numerical solution of ordinary and retarded differential equations with discontinuous derivatives.

19 p2444 A73-37523

Classification theorem for analytical transformations of second order differential equations of motion at arbitrary resonance based on group theory

19 p2445 A73-37632

Periodic solutions close to rectilinear normal mode shapes of vibration of nonlinear conservative system described by differential equations generated by homogeneous potential systems

19 p2459 A73-37634

Differential equations modelled on nonalgorithmic digital computers.

19 p2408 A73-38144

Nonlinear time-varying differential system stability and asymptotic stability study using equivalent inner product method, discussing global and regional stability

19 p2445 A73-38255

Accurate approximate solutions to oscillatory problems with perturbing singular damping.

19 p2461 A73-38490

Optimality and lower and upper bound conditions for multistep games with saddle point and minimax/maximin strategies, extending to differential games

20 p2539 A73-38678

Wave guide propagation of micropulsations out of the plane of the geomagnetic meridian.

20 p2529 A73-38937

An initial value method for the eigenvalue problem for systems of ordinary differential equations.

20 p2581 A73-38970

Lyapunov theory and perturbations of differential equations.

20 p2581 A73-38974

Some nonoscillation theorems for a second order nonlinear differential equation.

20 p2581 A73-38976

Bifurcations and certain qualitative characteristics of a phase-locked automatic frequency control system with a second-order filter

20 p2535 A73-38979

Investigation of the stability of solutions to a quasi-stationary system of linear differential equations with quasi-periodic coefficients

20 p2581 A73-38987

A study of systems with time-variable coefficients by the definite-integral method

20 p2542 A73-39037

Virtual motion principle implication for structural damping differential equations for cases of homogeneous, inhomogeneous and aerodynamic flutter for various degrees of freedom

20 p2616 A73-39098

Book on oscillation theory covering classical, abstract and complex theories, nonselfadjoint differential equations, hyperbolic and elliptic equations, Sturm-Picone theorem, etc

20 p2582 A73-39141

Solution of a multipoint problem about the eigenvalues and eigenfunctions of an ordinary linear differential operator using a decomposition technique

20 p2582 A73-39251

Application of the method of straight lines to the solution of a modified Stefan problem

20 p2626 A73-39253

Nonoscillation and oscillation of a linear differential equation of the n-th order

20 p2582 A73-39318

Normal third-order shapes of nonlinear oscillations

20 p2593 A73-39320

Differential equations for the vibrations of twisted rods with allowance for energy dissipation

20 p2619 A73-39372

Stochastic differential equation solutions for Markov processes with diffuse switching, including limit theorem on convergence

20 p2582 A73-39386

Boundary value problems for linear generalized differential equations and their adjoints.

20 p2582 A73-39402

Solution of a boundary-value problem for a second-order differential equation with a lagging argument by the method of spline functions - A scheme of increased accuracy

20 p2582 A73-39472

A numerical method in the analytic dynamics of gyrocompasses

20 p2566 A73-39499

Conditionally periodic oscillations in nonlinear systems

20 p2593 A73-39500

Differential equations of the asymmetrical mathematical theory of elasticity and their solution when Young's modulus varies according to an exponential law

20 p2620 A73-39505

Special periodic solutions and asymptotic properties of a class of quasi-linear differential equations with delayed argument

20 p2583 A73-39509

Mixed finite-difference scheme for a class of linear and nonlinear structural mechanics problems.

20 p2621 A73-39544

A singular boundary value problem for a system of ordinary differential equations

20 p2583 A73-39817

A practical means of calculating normal forms in problems involving nonlinear oscillations

21 p2738 A73-40178

Deviation of the solution of a quasi-linear wave equation from the solution of the linear equation in the region of continuous first derivatives

21 p2724 A73-40181

Dynamic programming method for constructing stable bridges based on mixed strategies in differential games of rendezvous-evasion

21 p2669 A73-40856

Compact integral varieties existence in certain meromorphic Pfaff differential equation systems

21 p2726 A73-40946

Integration of certain ordinary differential equations based on the approximation of continuous functions by linear functions

21 p2727 A73-41063

The solution and stability of a system of two first-order linear ordinary differential equations with variable coefficients

21 p2727 A73-41066

Necessary and sufficient conditions for solvability of certain boundary value problems for a second-order ordinary differential equation

21 p2727 A73-41272

On the evaluation of the principal value integral in the scattering problems.

21 p2728 A73-41475

Canonical differential equations from equilibrium and compatibility conditions for boundary loaded, shell of revolution, simplifying and transforming by canonical transformations

21 p2788 A73-41616

Wave amplitude calculation for propagation in inhomogeneous isotropic media by optical ray tracing consisting of integration of first and second order differential equations

22 p2885 A73-41817

Asymptotic properties of solutions to single-point and two-point problems with singular perturbations for systems of ordinary linear differential equations

22 p2882 A73-42473

A method for numerically solving second-order non-homogeneous linear differential equations with variable coefficients.

22 p2882 A73-42482

Solving linear boundary value problems by approximating the coefficients.

22 p2882 A73-42519

Numerical integration of shell equations using the field method.

[ASME PAPER 73-APMW-27] 22 p2925 A73-42888

Static and dynamic finite deformations of cables using rate equations.

23 p3042 A73-43804

Asymptotic mean value method for differential equations solution under given Lipschitz condition generalized via Liapunov procedure elimination

23 p2999 A73-44079

Unboundedness of solutions and comparison theorems for time-dependent quasilinear differential matrix inequalities.

23 p3000 A73-44202

Liapunov-like behavior and separation of solutions to nonlinear and linear differential equations

23 p3000 A73-44204

Representation of functions of Markov processes as solutions of stochastic equations.

23 p3000 A73-44207

Boundary value problem solutions uniqueness and existence for ordinary differential equations under Cauchy condition

23 p3000 A73-44209

On the Stepanov-almost periodic solution of an abstract differential equation.

24 p3105 A73-44420

Asymptotic solutions of second-order linear homogeneous differential equations in a Banach space in the case of a higher derivative having a small parameter

24 p3105 A73-44603

Application of stochastic differential equations in description of automatic control plants

24 p3074 A73-45098

Classical MHD differential equations solution for uniqueness and existence of shock wave structure based on thermodynamic potential concept

24 p3116 A73-45222

Differential and integral formulations of variational principles in mechanics, discussing Hoelder-Voss, d'Alembert-Lagrange, Gauss and Jourdain principles

24 p3110 A73-45246

Rectilinear trajectories of the three-body problem when the constant of line forces is zero

24 p3141 A73-45282

Numerical stabilization of all laws of conservation in the many body problem.

24 p3142 A73-45289

A Runge-Kutta Nystrom algorithm.

24 p3142 A73-45290

Numerical methods of boundary layer type for stiff systems of differential equations.

24 p3106 A73-45333

Multistep-multistage-multiderivative methods for ordinary differential equations.

24 p3106 A73-45334

Stability and small parameter perturbations of a critical neutral functional differential equation.

24 p3106 A73-45336

Solutions of boundary value problems with integral conditions for linear ordinary differential equations by the method of decomposition

24 p3106 A73-45351

Time-varying network analysis via matrix manipulation and Peano-Baker solution for second and higher order differential equations with periodic coefficients.

24 p3075 A73-45477

Reduction of systems of nonlinear differential equations to normal form

24 p3107 A73-45511

DIFFERENTIAL GEOMETRY
NT LIE GROUPS

NT RIEMANN MANIFOLD
NT SPINOR GROUPS
NT TENSOR ANALYSIS

Geometric programming with signomial transformation into equivalent posynomials minimized under inequality constraints and generalization by equilibrium solutions to reverse programs in larger class

11 p1391 A73-26576

Almost projective mapping of gravitational fields - Degenerate case

17 p2212 A73-35564

Bireductive spaces, Jordanian algebras, and spinor representations of non-Euclidean and quasi-non-Euclidean motions

17 p2212 A73-35566

Book on large scale structure of space-time covering gravity roles, differential geometry, general relativity, gravitational collapse, black holes, spatially homogeneous cosmological models, etc

18 p2336 A73-35901

DIFFERENTIAL INTERFEROMETRY

Differential interferometry for radio astronomy applications, discussing earth-based tracking of lunar rover relative to module, moon libration determination, Venus wind measurement, etc

02 p0218 A73-12416

The application of holography to sonic boom investigations.

11 p1371 A73-26633

Selenographic coordinates determination of ALSEP 12 and 14 telemetry transmitters via differential interferometric signal reception at two tracking stations, discussing instrument error reduction

20 p2603 A73-38894

Interferograms of high optical quality by double exposure.

21 p2695 A73-39963

DIFFERENTIAL OPERATORS

U DIFFERENTIAL EQUATIONS
U OPERATORS [MATHEMATICS]

DIFFERENTIAL THERMAL ANALYSIS

Study of creep in copper and aluminum by the differential method of constant-rate temperature change

01 p0064 A73-10612

Thermal analysis and its verification test of a small probe for space use.

01 p0052 A73-11147

North American Thermal Analysis Society, Annual Meeting, 3rd, Waco, Tex., February 7, 8, 1972, Proceedings.

01 p0015 A73-11446

High-temperature thermal analysis of high boron alloys using automatic optical pyrometry.

01 p0015 A73-11450

Book - Fundamentals of spacecraft thermal design.

02 p0237 A73-11885

The VDTA-3 apparatus for high-temperature differential thermal analysis

06 p0693 A73-18043

Thermal analysis-mass spectrometer computer system and its application to the evolved gas analysis of Green River shale and lunar soil samples.

08 p0936 A73-20824

Application of simultaneous DTA/TGA and DTA/MS analysis for predicting the flammability of composite textile fabrics and polymers.

09 p1110 A73-22515

Cast, annealed and hardened zirconium binary alloys cubic to hexagonal phase transitions from X ray and differential thermal analysis

10 p1233 A73-24318

Cast and annealed chromium-yttrium and chromium-lanthanum alloys peak solubility from metallographic, durometric and differential thermal analyses

12 p1512 A73-27245

An X-ray diffraction and DTA study of the ferroelectric transition in barium sodium niobate.

15 p1924 A73-31839

Aircraft engine fuel and oil differential temperature measurement via platinum probes, specifying sensor sensitivity, calibration, circuit operation and data reduction

17 p2165 A73-34607

Fast differential thermal analysis.

17 p2119 A73-34799

Differential calorimetry technique with heat link placement between samples for maintaining near equilibrium state to achieve accuracy in specific heat ratio measurement

17 p2175 A73-35753

Determination of the heat transfer coefficient for bodies of arbitrary shape at Re tending to 0

18 p2372 A73-37121

Ti rich corner of Ti-Al alloys phase diagrams investigated by differential thermal analysis and radiography for thermal resistance and intermetallic compounds existence

19 p2441 A73-37838

Differential method for determining specific heat

20 p2627 A73-39299

The nature of the interaction between scandium and aluminum in the aluminum-rich part of the Al-Sc system

21 p2718 A73-40486

DIFFERENTIATION [BIOLOGY]

Comparative physiological characteristics of functional relations among the hypothalamus and the olfactory and limbic systems of the brain

01 p0006 A73-10151

Differential housing /isolation vs aggregation/ as factor in postnatal development of mouse brain cell specificity and metabolism, noting relation to sleep behavior

03 p0264 A73-14259

Electrical operational and pneumatic /variometer/ differentiation recording of displaced volume derivative from pneumotachograph in spontaneous breathing

09 p1046 A73-22937

Free fall effects on differential growth and radiation sensitivity of higher plants in space flight and ground based clinostat experiments

22 p2804 A73-42172

DIFFERENTIATORS

Signal amplitude ratios measurement in automatic control applications by digital differential logometer, using time-pulse dividing circuits

01 p0022 A73-10082

Multichannel differential coincidence circuit in the nanosecond range

01 p0024 A73-10792

Differentiators and integrators with RC circuits for piezoelectric transducer signals, noting instrument errors and SNR

07 p0827 A73-20534

Electronic differentiator for aircraft flight data on-board calculation in performance gliding, discussing compensation method and vertical air velocity measuring instrument advantage

13 p1569 A73-28556

An improved method of triggering oscilloscopes for dynamic-strain measurements.

21 p2704 A73-41267

DIFFRACTION

NT ELECTRON DIFFRACTION
NT FRESNEL DIFFRACTION
NT PULSE DIFFRACTION
NT WAVE DIFFRACTION
NT X RAY DIFFRACTION

Stationary functionals for introducing eigenfunctions in diffraction theory of electrodynamic systems

03 p0337 A73-14080

Application of optical methods to the verification of microscopic data on polymer materials

04 p0468 A73-15693

Interference measurement techniques for small phase difference changes, noting diffraction and noise effects as limiting factors

10 p1222 A73-24945

Complex resonant frequencies calculation in external diffraction problems for arbitrary shaped bodies, noting Green function poles correspondence to eigenvalue zeros of integral equation

13 p1582 A73-28652

Effects of electron-microscope design features on the accuracy of the microprobe diffraction method

17 p2164 A73-34176

DIFFRACTION GRATINGS

U GRATINGS [SPECTRA]

DIFFRACTION LIMITED CAMERAS

Properties and fabrication of micro Fresnel zone plates.

17 p2173 A73-35434

DIFFRACTION PATHS

Bragg diffraction by standing ultrasonic waves with application to optical demultiplexing.

06 p0701 A73-18364

Bragg-diffraction imaging - A potential technique for medical diagnosis and material inspection.

13 p1614 A73-28582

DIFFRACTION PATTERNS

NT RAINBOWS

Off-axis polarization characteristics of Cassegrainian and front-fed paraboloidal antennas.

01 p0022 A73-10177

Incident plane wave fluctuations effect on diffraction pattern formed by scattering on reflecting sphere, calculating amplitude distribution in Fresnel and Fraunhofer regions

01 p0016 A73-10211

Full correlation ionospheric drift analysis for a general observing triangle.

01 p0036 A73-10330

Fresnel diffraction by a circular aperture illuminated with partially coherent light. I.

01 p0078 A73-11004

Holo-diagram coherent optics device for studying interference patterns of object near focal points representing illumination and/or observation points

01 p0053 A73-11220

Quantum mechanical interpretation for low intensity optical interference experiments with independent light sources and modulated light beams

01 p0078 A73-11250

Optical properties of the Apollo laser ranging retroreflector arrays.

02 p0141 A73-12250

Correlation analysis as applied to the observation of fluctuations of laser light diffracted on an ultrasonic wave in an inhomogeneous medium.

03 p0318 A73-12994

A dynamic holographic grating for a mode of operation with peaks

04 p0447 A73-14884

Special features of recording 'pure' phase /binary/ acoustic holograms

04 p0450 A73-15619

Bragg-diffraction imaging and its application for non destructive testing.

05 p0574 A73-16281

Edge diffraction cone detection by illuminating razor blade edge with laser beam, noting agreement with geometrical theory prediction

[AD-758568] 05 p0585 A73-16812

Wavelength dependence of moire patterns

05 p0577 A73-16822

Diffraction effects encountered in the measurement of bidirectional reflectance from square pyramids.

[AIAA PAPER 73-150] 05 p0598 A73-16898

Aperture fields and gain of open-ended parallel-plate waveguides.

06 p0676 A73-18178

Triangular obstacle caused microwave shadow zone diffraction pattern calculation by ray optics theory, comparing with scale model test results

06 p0666 A73-18201

Coherent intensity spatial filtering applied to inspection of photolithography masks for LSI.

06 p0694 A73-18288

An assessment of factors influencing data obtained by the photoelastic stress freezing technique for stress fields near crack tips.

06 p0764 A73-18488

Moire phenomena theory and applications extension by diffraction and Fourier optics

06 p0696 A73-18696

The formation and structure of precipitates in a dilute magnesium-neodymium alloy.

07 p0838 A73-19121

Holographic visualization of elastic waves

07 p0822 A73-19287

Diffractographic moire technique illustrated by determination of beam deflections.

08 p0106 A73-20797

Broadening of the measured frequency spectrum in a differential laser anemometer due to interference plane gradients.

08 p0967 A73-21596

The use of image quality criteria in designing a diffraction limited large space telescope.

08 p0969 A73-21730

Forms of carbon in the new Haverø urelite of Finland.

09 p1140 A73-21863

Characteristics of interference pattern formation during a self-reproduction process

09 p1096 A73-22858

Moire fringe method for stationary and running cracks length and crack opening displacement measurements in composite materials

10 p1240 A73-24287

A new interpretation of interferometric fringe patterns.

10 p1220 A73-24661

Geometrical diffraction theory for radiation pattern of extended vertical monopole antenna over infinitely conducting ground plane, noting back radiation level

11 p1329 A73-25662

Iron silicate disproportionation by ruby laser and static heating in resistance furnace, discussing X ray diffraction patterns

11 p1409 A73-25901

Gaussian light beam transmitted intensity derivation for thermal lensing in solids by vector Kirchhoff approach, obtaining time dependent shift in diffraction focus

11 p1377 A73-26228

Reflection plate interferometer with thin glass shearing plate replacing knife edge in Schlieren system, noting optimum operating range and fringe spacing

11 p1365 A73-26238

Improvement on moire technique for in-plane deformation measurements.

11 p1365 A73-26241

Image plane or optical system focal point location based on grain size variations from laser speckle patterns

11 p1378 A73-26245

Holographic nondestructive evaluation of interference fit fasteners.

11 p1366 A73-26247

Interference fringes and surface displacement interrelationship in holographic interferometry, discussing fringe localization, visibility and interpretation and postrecording techniques

11 p1369 A73-26530

Live fringes time averaging, fringe spoiling, stroboscopic and speckle pattern real time recording techniques in holographic interferometry for surface vibration modes analysis

11 p1369 A73-26531

Hologram interferometry and laser speckle methods - Further applications.

11 p1370 A73-26532

Fringe control in real time and double exposure holography for nondestructive testing of multilaminated and thin laminated structures and vibration analysis

11 p1370 A73-26541

Investigation of coherence with the aid of the diffraction shearing interferometer.

12 p1507 A73-27515

Moire techniques of incoherent and coherent light filtering, line multiplication and contrast amelioration in framework of physical optics and diffraction theory for stress analysis

13 p1612 A73-28470

Reference fringes in holographic interferometry.

13 p1616 A73-28599

Moire gauging by projected interference fringes.

13 p1616 A73-28600

Plane and cylindrical electromagnetic waves diffraction on infinitely long cylindrical bodies, calculating induced currents, diffraction patterns and near fields

13 p1582 A73-28654

Plane TE polarized electromagnetic wave diffraction on infinite conducting cylinder in nonhomogeneous medium, calculating far field diffraction patterns

13 p1582 A73-28656

Reference wave elimination in acoustic holographic experiments via boundary surface of medium having sound wave propagation used as hologram

13 p1616 A73-28687

Developments in the optical spatial filtering of superposed, crossed gratings.

13 p1620 A73-29302

IR seeing disks /blurred interference patterns of corrugated wave fronts/ speckles and intensity profiles from atmospheric turbulence models

15 p1929 A73-31061

Diffraction gratings manufacture by holographic recording of laser beam generated interference fringes on photosensitized surfaces, describing etching and metallization process

15 p1875 A73-31417

Thermal expansion coefficient measurement of diffusely reflecting samples by holographic interferometry.

15 p1877 A73-31980

Thermal expansion coefficient measurements of specularly reflecting samples.

15 p1877 A73-31981

Strain analysis of composites by moire methods.

15 p1956 A73-32269

Three-dimensional hologram recordings on photochrome glass with the application of an optical discoloration process. II

15 p1879 A73-32340

Speckle reference beam /by retro reflection/ holography for the real time visualisation of vibration patterns.

16 p2012 A73-32847

Experimental studies on the scattering pattern from a ruby laser rod.

16 p2023 A73-32875

Angle-of-arrival difference spectrum of a simple interferometer in turbulent air.

16 p2037 A73-33683

Josephson junction interference grating.

17 p2129 A73-34915

Interference patterns of a horizontal electric dipole over layered dielectric media.

17 p2123 A73-35270

Nondestructive optical contour mapping for non-contact testing of reflecting surface deformations from interference pattern due to monochromatic illumination of grating

17 p2172 A73-35419

Applications of the speckle pattern techniques to the visualization of modulation transfer functions and quantitative study of vibrations of mechanical structures.

17 p2173 A73-35433

Interferometric surface strain measurement with optical strain gage using laser-generated interference pattern with linear fringe motion-intensity relation [SESA PAPER 2158A]

17 p2173 A73-35453

Interference phenomena obtained by replacing the mirrors of a Michelson interferometer by Fabry-Perot couples

19 p2429 A73-37540

Analysis of a method for obtaining near-diffraction-limited information in the presence of atmospheric turbulence.

19 p2461 A73-38485

Application of method of fringe waves to problems of diffraction from bodies placed in a smoothly inhomogeneous medium.

20 p2529 A73-38919

Sampled aperture antenna array measurement of RF phase characteristics of diffraction pattern formed on ground by radio waves obliquely reflected from ionosphere

20 p2530 A73-39018

Angular distribution patterns of thick-film holograms.

20 p2567 A73-39701

Angular distribution patterns of thick-film holograms obtained by rigorous solution of the diffraction problem.

20 p2567 A73-39702

Measurement of change in a cross section and position of small particles by diffraction techniques.

21 p2695 A73-39959

Recording of diffraction patterns by X-ray pulses of materials subjected to a shock wave compression

21 p2695 A73-39967

Diffraction pattern scanning display technique using electron detector in microscope final image, discussing gold particle demonstration, lens configuration, illumination angle and sawtooth currents

21 p2700 A73-40466

Basic theoretical aspects of spherical phased arrays.

21 p2653 A73-40678

Incident-light double-refracting interference microscope with variable wavefront shear.

21 p2703 A73-41134

Interference patterns and operation of four unit interferometer consisting of beam splitter, mirrors and analyzer

21 p2704 A73-41261

Residual-stress measurement using surface displacements around an indentation.

21 p2704 A73-41265

Diffraction of a plane electromagnetic wave by a slit in a thick screen placed between two different media.

22 p2821 A73-41744

Fading characteristics and drift and anisotropy parameters of the ground diffraction pattern of the radio waves reflected from the equatorial ionosphere during spread F conditions.

22 p2825 A73-41929

German monograph on holographic interferometry for displacement and deformation determination of diffusely reflecting bodies covering wave front reconstruction methods and diffraction pattern characteristics

22 p2862 A73-42719

Investigation of the radiation properties of a laser without external feedback

22 p2871 A73-42971

Holographic thin-beam reconstruction technique for the study of 3-D refractive-index field.

22 p2862 A73-43087

Redundant speckle free hologram production without spurious background patterns, blocking intensity by cutting of lower order frequencies

22 p2862 A73-43089

Interference patterns from spatially separate holograms and holograms superimposed on same region of recording medium, comparing to double exposure holography performance

22 p2862 A73-43091

Fringe localization and visibility in hologram and classical broad source interferometry.

22 p2863 A73-43094

The effect of change of polarisation of the illuminating beam on the microstructure of speckles produced by a random diffuser.

22 p2871 A73-43095

Application of holographic subtraction to time-average hologram interferometry of vibrating objects.

22 p2863 A73-43141

Multiple-beam lateral-shear interferometer.

22 p2863 A73-43146

Three-dimensional diffraction calculations of laser resonator modes.

22 p2872 A73-43151

Study of laser radiation propagation and the diagnostics of a randomly inhomogeneous troposphere

23 p2954 A73-43572

Speckle effect use in laser photography for vibration and displacement measurement of mechanical systems, discussing diffraction patterns and measurement methods

23 p2982 A73-43675

Postannealing isothermal decomposition products of Al-Mn alloys studied by transmission electron microscopy, revealing trigonal and hexagonal lattice diffraction patterns

23 p2993 A73-43916

Electronic fringe-follower for interferometer.

23 p2983 A73-44086

Biaxial potassium niobate single crystal nonlinear optical coefficients determination by Marker fringe pattern method, using CW Nd doped yttrium-aluminum garnet laser

23 p3018 A73-44369

Measurement of optically induced refractive-index changes with sharp edged illumination pattern.

23 p2984 A73-44371

HF and molecular fluorine refractive indices in visible spectral region computed from interferometer fringe shift vs pressure measurements

24 p3113 A73-44983

Angular selectivity of lithium niobate volume holograms.

24 p3092 A73-45424

Investigation of the diffraction of strong shock waves on convex corners

24 p3081 A73-45536

DIFFRACTION PROPAGATION

Diffraction effects from cylindrical transducers in a piezo-electric medium of hexagonal symmetry /class C6v/6mm//.

07 p0822 A73-19108

Microwave transhorizon propagation in atmospheric evaporative duct layer by superdiffraction, using Monin-Obukhov similarity theory for computerized prediction

16 p1981 A73-33712

Derivation of diffraction coefficients for a thin wire of finite length.

23 p2955 A73-44106

DIFFRACTION TELESCOPES

U SPECTROSCOPIC TELESCOPES

DIFFRACTOMETERS

Determination of the instrumental profile of the DFS-13 diffraction spectrograph

11 p1363 A73-25615

Diffractionography versus holography - A stress analyst's comparison.

17 p2173 A73-35440

Diffractionographic techniques for vibration measurement.

[ASME PAPER 73-DET-116] 22 p2859 A73-42081

DIFFUSE RADIATION

A solution to the auxiliary equation of radiative transfer for a planetary atmosphere with molecular anisotropy.

01 p0097 A73-10352

Positive detection of an excess of low-energy diffuse X-rays at high galactic latitude.

[AD-760197] 01 p0092 A73-11029

Galactic-latitude dependence of low-energy diffuse X-rays.

[AD-760196] 01 p0092 A73-11030

Observations of soft X-rays - Two supernova remnants in the constellation Lupus and the diffuse background.

01 p0103 A73-11031

Nonlinear inverse Compton radiation and the circular polarization of diffuse radiation from the crab nebula.

01 p0092 A73-11032

Optical measurements of lunar albedo, angular illumination, diffuse and specular reflectance and scattering coefficients on Mare Foecunditatis regolith powder of various sizes

02 p0213 A73-12238

Relation of the diffuse reflectance remission function to the fundamental optical parameters.

02 p0193 A73-12350

On combined operations method for transfer problems in homogeneous, cylindrical media.

02 p0193 A73-12383

Invariant imbedding and Chandrasekhar's planetary problem of radiative transfer.

02 p0207 A73-12389

Diffuse galactic FUV radiation and interstellar dust grains.

02 p0207 A73-12399

Cosmic diffuse soft X rays intensity distribution, taking interstellar absorption into account

02 p0207 A73-12402

The spectrum of diffuse cosmic X-rays in the 20-125 keV range.

02 p0210 A73-12738

Granularity produced by a diffuser illuminated in partially coherent light

03 p0320 A73-14606

Diffuse radiation of a two-layer galaxy with carbon-silicate particles

05 p0617 A73-16460

Solution on a BESM-3M electronic computer of the equation for transfer of diffuse radiation in two-layer plane-parallel models of galaxies

05 p0617 A73-16461

Isotropic and incoherent light scattering by atomic slab, calculating Doppler effect induced diffuse radiation energy partial redistribution by Monte Carlo method

05 p0597 A73-16562

A study of the unidentified interstellar diffuse features.

05 p0626 A73-17379

Diffuse cosmic gamma rays - Present status of theory and observations.

07 p0872 A73-20186

Zonal and seasonal peculiarities in the influx of diffuse solar radiation

07 p0848 A73-20625

Radiation between finite surfaces with variable radiative characteristics.

08 p1021 A73-20794

Observations of spatial structure in the soft X-ray diffuse flux.

08 p0997 A73-20881

Auto- and cross-correlations of diffuse objects for coherent optical data processing, using single lensless Fresnel hologram

08 p0963 A73-21036

Holographic recording of focused images in multimode laser radiation

09 p1084 A73-22879

Optimum holographic recording of complex light fields generated by diffusive objects in presence of point sources, maximizing SNR or distortion-free diffraction level

09 p1084 A73-22880

Distribution of diffuse solar radiation over regions of the sky for various regions of the spectrum in the absence of cloudiness

09 p1138 A73-22994

Probabilistic model for the resolvent kernel in diffusion problems in spherical-shell media.

09 p1121 A73-23071

Equivalence relationships between diffuse radiation fields for finite slabs bounded by a perfect specular reflector and a perfect absorber.

09 p1121 A73-23072

Spectroscopy of tetrabenzoporphin molecules and possible astrophysical implications.

09 p1048 A73-23136

Combined-operations method for diffuse reflection by an isotropic, non-coherent scattering homogeneous sphere.

10 p1271 A73-23484

Diffuse cosmic gamma rays observed at an equatorial balloon altitude.

10 p1263 A73-23491

Millimeter wave imagery of complex three dimensional target by diffuse reflection with spatial filtering, discussing range, resolution and view field capabilities

10 p1188 A73-23798

Solar cosmic ray diffusion, convection, accumulation and acceleration as function of interplanetary medium perturbation and flare coordinates

10 p1266 A73-23909

Comment on: Holographic interferometry applied to measurements of small static displacements of diffusely reflecting surfaces.

11 p1360 A73-25064

Investigation of the diffuse glow of the clouds of dark absorbing matter in the region of the Aquila constellation

11 p1416 A73-25229

A phenomenological study of cosmic ray propagation. I - The nuclei component.

11 p1412 A73-25263

Collimator corrections to the measured diffuse X-ray background.

12 p1537 A73-27885

Parameter estimation for a specular-diffusion reflection model from the motion of "Proton" series satellites about their centers of mass

14 p1803 A73-29851

Diffuse background X ray origin theories with emphasis on soft flux in galactic plane and at poles

16 p2051 A73-32748

Extragalactic diffuse X ray background above 30 keV, discussing spectral breaks and bumps at various energies

16 p2051 A73-32749

Gamma ray astronomical state-of-art, discussing cosmic gamma ray sources observation and diffuse radiation measurement

16 p2055 A73-33290

Transmission of isotropic light across a dielectric surface in two and three dimensions.

16 p2037 A73-33685

Calculation of the diffuse reflection and transmission of light by a semiinfinite atmosphere

16 p2066 A73-33791

Description of small-scale fluctuations in the diffuse X-ray background.

17 p2224 A73-34753

Observations of soft X-rays - Upper limits on the flux from SN 1972E and measurements of the diffuse background in Centaurus.

17 p2224 A73-34754

Transition radiation from interstellar dust grains.

17 p2231 A73-34755

Numerical techniques in two- and three-dimensional radiation hydrodynamics.

17 p2255 A73-35596

Non-coherent scattering in transfer problems in spherical shell media. II - Frequency-dependent source function.

17 p2237 A73-35789

Apparent reflectance from a semi-infinite absorbing-scattering medium.

[AIAA PAPER 73-753] 18 p2337 A73-36369

Cosmic X-ray sources - A progress report.

19 p2474 A73-37149

Evidence for an interstellar or interplanetary source of diffuse He I 584 A radiation.

19 p2475 A73-37629

Diffuse parasitics gain thresholds of laser models for rectangular geometries, discussing radiation field and boundary conditions

21 p2710 A73-40145

Diffuse X and gamma radiation at 0.1-100 MeV, discussing nonthermal mechanisms, thermal emission from uniform intergalactic medium, isotropic background, galactic clusters, etc

21 p2760 A73-41246

Interstellar extinction, relation to spatial dust distribution, light scattering by grains, diffuse absorption lines and polarization

21 p2772 A73-41247

Light spectral width and constant frequency shift during spontaneous diffusion in ideal gas for fixed photon wave

22 p2885 A73-41721

Observations in linearly polarized light of the intensity of the diffuse 6180 A absorption band in 49 O, B, and A stars.

22 p2908 A73-42308

German monograph on holographic interferometry for displacement and deformation determination of diffusely reflecting bodies covering wave front reconstruction methods and diffraction pattern characteristics

22 p2862 A73-42719

The parallel diffusion of cosmic rays in a random magnetic field.

22 p2904 A73-43011

Automated data reduction of holographic interferometry translational measurement of diffusely reflecting rigid body by reconstructed virtual image processing on CDC 6600 computer

22 p2863 A73-43147

Matrix method evaluating an internal radiation field in a plane-parallel atmosphere.

23 p3030 A73-43754

Scattering and transmission functions of radiation by finite atmospheres with reflecting surfaces.

23 p3030 A73-43755

Galactic and extragalactic gamma ray bursts contribution to diffuse cosmic X ray flux, noting superposition of supernovae outbursts

23 p3025 A73-43957

Resonance scattering from interstellar and interplanetary helium.

24 p3140 A73-45188

DIFFUSERS

Subsonic centrifugal compressor efficient operating range extension by collector and diffuser blade cascades separation, presenting performance test results

02 p0204 A73-12792

Some effects of normal shock boundary layer interaction on the performance of straight walled conical diffusers.

[AIAA PAPER 72-1140] 03 p0243 A73-13446

Effects of transverse ribs on pressure recovery in two-dimensional subsonic diffusers.

[AIAA PAPER 72-1141] 03 p0243 A73-13447

Investigation of flow characteristics behind diffusers with large cone angles

03 p0245 A73-13671

Turbulent shear flow structure parameters in conical diffuser, investigating Reynolds number and turbulent kinetic energy effects

03 p0247 A73-14176

Performance of truncated conical diffusers with compressible flow.

03 p0249 A73-14641

Inverse problem approach to the design of short two-dimensional diffusers.

[ASME PAPER 72-WA/GT-6] 04 p0404 A73-15870

Application of external aerodynamic diffusion to reduce shrouded propeller noise.

05 p0528 A73-16623

Highly uniform inlet velocity profile influence on conical diffuser characteristics

07 p0774 A73-19615

Circular conical diffuser inlet velocity profile effect on efficiency, presenting experimental results for different cone angles and expansion ratios

07 p0774 A73-19616

A subsonic diffuser with moving walls for boundary-layer control.

08 p0953 A73-20723

A radial diffuser with a rotating boundary layer at the throat.

08 p0953 A73-20795

Turbulence in a conical diffuser with fully developed flow at entry.

11 p1345 A73-25057

Diffuser static pressure recovery coefficient for varying turbulence intensity at inlet, considering performance correlation with geometrical and/or velocity profile parameters

12 p1488 A73-27930

Flow analysis of three-dimensional diffuser for fluid amplifier.

13 p1603 A73-29033

Flow deflection characteristics of short pyramid wire gauze conical diffuser with high expansion ratio, showing satisfactory uniformity, pressure loss and flow steadiness

16 p2001 A73-34032

Two dimensional diffuser flow measurement and model calculation for curvature effects on wall pressure and boundary layer velocity distributions

[ASME PAPER 73-FE-2] 17 p2152 A73-35002

Further data on the pressure recovery performance of straight-channel, plane-divergence diffusers at high subsonic Mach numbers.

[ASME PAPER 73-FE-5] 17 p2152 A73-35005

Performance of low-aspect-ratio diffusers with fully developed turbulent inlet flows. I - Some experimental results.

[ASME PAPER 73-FE-12] 17 p2152 A73-35009

Performance of low-aspect-ratio diffusers with fully developed turbulent inlet flows. II - Development and application of a performance prediction method.

[ASME PAPER 73-FE-13] 17 p2152 A73-35010

Oscillatory flow phenomena in diffusers at low Reynolds numbers.

[ASME PAPER 73-FE-14] 17 p2152 A73-35011

Forces acting on conical diffusers and their relation to integral performance parameters.

[AIAA PAPER 73-686] 18 p2262 A73-36237

Relaxation of coherence requirements in holography.

21 p2695 A73-39961

Possibility of using an axial-flow impeller designed according to the law $\rho c_{sub} u/r = \text{const}$ as the primary pump

21 p2754 A73-40394

Some effects of pipe flow generated entry conditions on the performance of straight walled conical diffusers with high sub-sonic entry Mach number.

23 p2939 A73-43294

DIFFUSION

- NT AMBIPOLAR DIFFUSION
- NT ATMOSPHERIC DIFFUSION
- NT ELECTRON DIFFUSION
- NT GASEOUS DIFFUSION
- NT GASEOUS SELF-DIFFUSION
- NT IONIC DIFFUSION
- NT MAGNETIC DIFFUSION
- NT MOLECULAR DIFFUSION
- NT PARTICLE DIFFUSION
- NT PLASMA DIFFUSION
- NT SPECIES DIFFUSION
- NT SURFACE DIFFUSION
- NT THERMAL DIFFUSION
- NT TURBULENT DIFFUSION

DIFFUSION BONDING

U DIFFUSION WELDING

DIFFUSION COEFFICIENT

Activation energy volume relation to heat of fusion and lattice characteristics for vacancy diffusion along crystal grains in melting metals

01 p0087 A73-10256

High energy proton model for the inner radiation belt.

03 p0363 A73-13880

Propagation of solar cosmic rays in the solar wind.

04 p0491 A73-14837

Beta irradiation of silicon junction devices - Effects on diffusion length.

05 p0537 A73-16522

Study of the specific characteristics of the diffusion method for measuring turbulence characteristics under conditions of a free homogeneous jet

05 p0576 A73-16617

Diffusion coefficients and current velocities in coastal waters by remote sensing techniques.

05 p0572 A73-17141

Diffusion time of charged particles in a plasma with volume ionization.

06 p0726 A73-17417

Temperature and concentration effects on heterodiffusion coefficient of diffusion welded Mo-W alloy rods

06 p0707 A73-17907

Metal atom migration acceleration under radioactive radiation, showing diffusion coefficient dependence on free and coupling electron interactions

06 p0735 A73-18038

Heating of a plasma in stimulated scattering of laser radiation /Review/.

06 p0731 A73-18578

Diffusion on a particle in the shear flow of a viscous fluid - Approximation of the diffusion boundary layer.

07 p0809 A73-19021

Diffusion of hot electrons in n indium phosphide.

07 p0861 A73-19157

The diffusion coefficient during plastic deformation in AlMg5

08 p0977 A73-21019

Spun on arsenosilica films as sources for shallow arsenic diffusions with high surface concentration.

08 p0995 A73-21478

Plasma diffusion across a magnetic field due to thermal vortices.

09 p1126 A73-22217

Investigation of carbon- and manganese-diffusion processes in the metal-ceramic steel G13M

09 p1103 A73-22466

Study of the W-Ta-Re phase diagram by the diffusion layer method

09 p1108 A73-23236

Pulsed probe studies on the diffusion coefficient of an afterglow plasma across a magnetic field.

09 p1132 A73-23250

Determination of upper atmosphere parameters from measurements of the ambipolar diffusion coefficient by radar observations of meteor trails.

10 p1212 A73-24223

Multistage diffusion model of IC transistor electrical characteristics and impurity distributions as func-

tion of surface concentrations and junction depths during fabrication

10 p1196 A73-24606

Mathematical description by Gaussian error function for metals diffusive saturation and diffusion constants determination

10 p1236 A73-24952

A phenomenological study of cosmic ray propagation. I - The nuclei component.

11 p1412 A73-25263

Investigation of resonance integrals occurring in cosmic-ray diffusion theory.

11 p1414 A73-26615

Theory of cosmic ray transfer by anisotropically scattered particles

12 p1534 A73-27331

Modulation of galactic cosmic rays by a solar wind asymmetric with respect to the heliolatitude

12 p1534 A73-27332

Selection of a propagation model for computing the solar-proton injection spectrum

12 p1534 A73-27333

Titanium monoxide system cation self-diffusion coefficients, and quenched-in vacancy concentrations as function of stoichiometry, tabulating Arrhenius parameters

13 p1633 A73-28145

Magnesium oxide crystal dislocation loop shrinkage rate measurement, suggesting oxygen ion diffusion as rate controlling process for dislocation climb

13 p1634 A73-28257

A comparison of time-varying concentrations of air admixtures with those of the corresponding stationary cases

13 p1653 A73-28742

Determination of coefficients of vertical diffusion between 0 and 100 m with the help of radon and of ThB

13 p1655 A73-29342

Effects of deformation on diffusion in iron-nickel and iron-chrome systems

14 p1760 A73-30379

Determining unknown coefficients in a nonlinear heat conduction problem.

14 p1817 A73-30406

Determination of diffusion characteristics in the boundary and volume components of a diffusing hydrogen stream in a polycrystalline metal

14 p1763 A73-30716

Diffusion-controlled processes in the homogeneity region of zirconium carbide

15 p1881 A73-31593

Correlation and prediction of gaseous diffusion coefficients.

15 p1958 A73-31998

Gravity wave magnitudes and horizontal and vertical scales measured and applied to eddy diffusion coefficients in upper stratosphere

[AIAA PAPER 73-495] 16 p2005 A73-33538

Stratospheric mixing estimated from high altitude turbulence measurements.

[AIAA PAPER 73-497] 16 p2005 A73-33539

Monthly mean values of eddy diffusion coefficients in the lower stratosphere.

[AIAA PAPER 73-498] 16 p2005 A73-33540

A simple technique to estimate large-scale eddy coefficients in the stratosphere.

[AIAA PAPER 73-499] 16 p2005 A73-33541

On limits to Jupiter's magnetospheric diffusion rates.

17 p2224 A73-34511

Tracer diffusion of Ni-63 in Fe-17 wt pct Cr-12 wt pct Ni.

17 p2189 A73-34641

Radial variation of magnetic fluctuations and the cosmic-ray diffusion tensor in the solar wind.

17 p2224 A73-34762

Directional diffusion coefficients of solar protons inside and outside the bow shock.

17 p2224 A73-34781

Combined temperature, diffusion coefficient and density measurements of photoluminescent A10 releases.

18 p2303 A73-35949

Rocket sounding of upper atmosphere vertical wind profiles, shear, temperature distribution and diffusion coefficient for model atmosphere calculation

18 p2309 A73-36057

Coronal propagation of low-energy solar protons.

18 p2347 A73-36290

Kinetic equation for one particle cosmic ray distribution function in static random magnetic field on basis of diffusion theory

19 p2476 A73-38291

U.L.F geomagnetic power near $L = 4$. II - Temporal variation of the radial diffusion coefficient for relativistic electrons.

20 p2551 A73-38936

Diffusion of hydrogen and deuterium in Ta, Nb, and V.

20 p2576 A73-39134

Effect of gas diffusion on creep behavior of polycarbonate.

20 p2580 A73-39403

Influence of nonadiabatic effects during magnetic storms on the dynamics of proton belts

21 p2760 A73-40907

CAD for realization of an impurity distribution in a semiconductor.

21 p2753 A73-41095

The measurement of turbulent spectra and diffusion coefficients in the altitude region 95 to about 110 km.

21 p2688 A73-41341

Wave-induced eddy diffusion coefficients in the upper atmosphere of Mars.

22 p2906 A73-41903

Diffusion parameters of oxygen in alpha and beta titanium modifications

22 p2874 A73-42098

Interdiffusion in the titanium-zirconium system

22 p2874 A73-42099

Anomalous behaviour during interdiffusion in the system Nb-Mo.

22 p2876 A73-42340

State variables and transport coefficients of binary gaseous mixtures. III - The calculation of transport coefficients with the aid of consistent potential parameters

22 p2931 A73-42375

[DFVLR-SONDDR-280] Anomalous diffusion in a magnetized plasma.

22 p2894 A73-42483

German monograph - Doping profiles of boron-implanted silicon layers.

22 p2897 A73-42717

The parallel diffusion of cosmic rays in a random magnetic field.

22 p2904 A73-43011

Contribution to the theory of cosmic-ray propagation with anisotropic particle scattering.

23 p3020 A73-43229

Modulation of galactic cosmic-rays by solar wind which is unsymmetric in solar latitude.

23 p3020 A73-43230

Selection of a propagation model for calculating the injection spectrum of solar protons.

23 p3020 A73-43231

Estimate of the effect of photoionization and ion-molecule reactions on the diffusion coefficient in the ionosphere.

23 p2971 A73-43257

Impurity diffusion of iron in molybdenum.

23 p2994 A73-44157

Concentration contours in regions with both normal and enhanced diffusion coefficients.

24 p3120 A73-45404

DIFFUSION ELECTRODES

Concerning the stability of the triple-phase boundary in gas-diffusion electrodes of fuel cells.

21 p2636 A73-41320

DIFFUSION FLAMES

Multi-droplet combustion of liquid propellants.

01 p0089 A73-11114

Hydrocarbon fuels diffusion flame ignition characteristics in hypersonic ramjet engines, testing additives effect for thermal self-ignition improvement

03 p0398 A73-14132

On the deviation of the flame from the stagnation point in opposed-jet diffusion flames.

03 p0399 A73-14388

Soot particles oxidation by oxygen diffusion in laminar hydrocarbon flames, deriving kinetic expression from observed time dependent particle concentration variations

03 p0399 A73-14395

The stability of lifted turbulent diffusion and premixed flames.

[WSCI PAPER 72-39] 05 p0638 A73-16678

Radial concentration profiles of NO and combustion products formation in laminar diffusion flames, using vertical coaxial burner and quartz microprobe

06 p0740 A73-17730

A mathematical model of the opposed-jet diffusion flame - Effect of an electric field on concentration and temperature profiles.

07 p0918 A73-19388

IR absorption spectra of powdered graphite samples during treatment in laminar propane-butane diffusion flame zones

07 p0921 A73-19996

Streamline deflection by diffusion flame stabilized on Parker-Wolfhard burner, discussing flow visualization and Burke-Schumann flame sheet in Oseen flow

07 p0921 A73-20355

Some studies on opposed-jet diffusion flame considering general Lewis numbers.

07 p0921 A73-20357

A new criterion for the length of a gaseous turbulent diffusion flame.

11 p1449 A73-25372

Determination of the temperature of a methane-fluorine diffusion flame by means of the vibration-rotation spectrum of the HF molecule

11 p1453 A73-26586

Theoretical investigation on laminar boundary layer with combustion on a flat plate.

14 p1817 A73-30611

Combustion of droplets of liquid fuels - A review.

18 p2372 A73-37096

- Double-probe measurements of electron temperatures on low pressure diffusion flames - Criticism of the methods for determining the electron temperature from the double-probe current voltage characteristic. 18 p2317 A73-37097
- Formation of a nonstationary diffusive flame front during the ignition of a liquid fuel droplet. 19 p2471 A73-37507
- Aerodynamic and thermal structures of the laminar boundary layer over a flat plate with a diffusion flame. 22 p2933 A73-42774
- An analytical and experimental investigation of gravity effects upon laminar gas jet-diffusion flames. 22 p2933 A73-42775
- Refraction, convection, and diffusion flame effects in combustion-generated noise. 22 p2934 A73-42780
- Turbulent diffusion flame velocity, concentration, temperature and momentum flux measurements for hydrogen round jet in co-flowing air stream. 22 p2935 A73-42788
- Nitric oxide formation weightless in diffusion flame ethanol drop combustion as function of air temperature and diffusion and spray characteristics. 22 p2935 A73-42797
- Nitric oxide generation in turbulent diffusion flames, discussing limits for constant pressure turbulent reacting mixing zone between parallel flowing streams of fuel and oxidizer. 22 p2935 A73-42798
- Linear pyrolysis of various polymers under combustion conditions. 22 p2898 A73-42807
- On detonation waves supported by diffusion flames. 22 p2936 A73-42810
- Temperatures in low-pressure magnesium-vapor diffusion flames. 22 p2899 A73-42820
- DIFFUSION PUMPS**
- The performance characteristics of modern vacuum pumps. 21 p2707 A73-39915
- Photoluminescence and optical transmission of diffusion-pump oils. 21 p2698 A73-40139
- DIFFUSION THEORY**
- Comments on the conduction mechanism in Schottky diodes. 01 p0088 A73-10474
- Effects of transverse diffusion and transverse stored charge in alloy transistor base. 01 p0023 A73-10681
- Diffusion of radiation in a stellar shell expanding at a constant rate. 01 p0100 A73-10707
- Kinetics of the deactivation of the vibrations of highly excited oscillators in an inert gas medium with allowance for spontaneous emission. 02 p0194 A73-11607
- Theory of the electrodiffusion method for measuring the spectral characteristics of turbulent flows. 02 p0165 A73-11614
- On certain parabolic differential equations and an equivalent variational problem. 02 p0186 A73-11972
- Diffusion approximation for kinetic equation of repeatedly ionized plasma, calculating direct transitions between excited ion states. 03 p0344 A73-13180
- Vertical multijunction solar cells light generated current spectral response and I-V characteristics derivation from minority carrier diffusion equations. 03 p0254 A73-14208
- Critical analysis of Moushah-Susskind diffusion theory for magnetron diode electron transport, noting theoretical results discrepancy with experimental data. 05 p0556 A73-16064
- Disk-shaped diffusion model with inhomogeneous distribution of gas and heavy relativistic nuclei sources for galactic cosmic rays chemical composition. 05 p0608 A73-16081
- Diffusion in the titanium-aluminum system. I - Interdiffusion between solid Al and Ti or Ti-Al alloys. 06 p0709 A73-18332
- Diffusion in the titanium-aluminum system. II - Interdiffusion in the composition range between 25 and 100 at.% Ti. 06 p0709 A73-18333
- Diffusion equation for current carriers in solar cell with inhomogeneous internal electric field, determining photoelectric current in p-n junction. 07 p0778 A73-19299
- Turbulent jet diffusion and vortex models, noting velocity profile in mixing and turbulent boundary layers. 07 p0811 A73-19617
- A review of the diffusion path concept and its application to the high-temperature oxidation of binary alloys. 08 p0978 A73-21414
- Nonstationary radiation diffusion in a semiinfinite isotropically scattering medium. 08 p0985 A73-21453
- Book - Stochastic differential equations. 08 p0984 A73-21833
- On degenerate elliptic-parabolic operators of second order and their associated diffusions. 09 p1111 A73-21996
- Diffusion of charged particles in a random magnetic field. 09 p1137 A73-22035
- Diffusion theory for adsorption and desorption of gas atoms at surfaces. 09 p1047 A73-22073
- Unidirectional filament reinforced metal matrix composites compositional changes due to temperature induced interatomic diffusion, using diffusion equation finite difference solutions superposition technique. 09 p1101 A73-22404
- The structure of the Crab Nebula. II - The spatial distribution of the relativistic electrons. 09 p1151 A73-23290
- Particle motion diffusion model for cosmic ray propagation in Galaxy, investigating electron component energy spectra and background radio emission. 10 p1265 A73-23908
- A finite element method for non-self-adjoint problems. 10 p1243 A73-24292
- Boltzmann equation integral form derived tensorial formulation of monoenergetic neutron diffusion theory, evaluating components of diffusion coefficient tensor. 11 p1401 A73-25211
- A two-component model of the diurnal variations in the thermospheric composition. 11 p1354 A73-25758
- On optimal nonlinear estimation. I - Continuous observation. 12 p1517 A73-27147
- Determination of the diffusion length of excess carriers in semiconductors under a polyethylene film. 13 p1668 A73-28462
- Diffusion spreading of weak plasma inhomogeneities in the presence of two kinds of positive ions. 13 p1608 A73-28710
- Similarity theory of diffusion and the observed vertical spread in the diabatic surface layer. 13 p1655 A73-29339
- Diffusion of comets from parabolic into nearly parabolic orbits. 14 p1793 A73-29828
- New estimates of cometary disintegration times and the implications for diffusion theory. 14 p1794 A73-29829
- Dyadic formalism in two dimensional distributions in general relativity theory, discussing gravitational, diffusive, wave, Einstein and preservation equations. 14 p1776 A73-30942
- A priori estimates for solution operators of diffusion equations. 15 p1901 A73-32368
- Influence of diffusion on plasma parameters - A qualitative estimate and a physical interpretation. 16 p2040 A73-32941
- Time dependent diffusion equation for solar flare cosmic ray propagation through interplanetary space, specifying continuous emission curve shape and period. 16 p2053 A73-32966
- The numerical solution of quasilinear elliptic equations. 17 p2199 A73-34103
- Two dimensional half-jet mixing of dissociated air, investigating chemical rate and diffusion processes interaction effects on mixing layer thermodynamics. 17 p2156 A73-35503
- On the convective diffusion in tubes of circular section. 18 p2299 A73-36489
- Transport of charged particles in the earth's magnetosphere. 19 p2474 A73-37348
- Stability criteria for explicit finite difference solutions of the parabolic diffusion equation with nonlinear boundary conditions. 19 p2445 A73-38189
- Turbulent diffusion in Schwinger formulation of quantum field theory, deriving transition probabilities from Dyson and Saffman equations. 20 p2599 A73-39674
- Bilinear hydrodynamics and the Stokes-Einstein law. 21 p2676 A73-40218
- Contribution to the theory of wave propagation in a one-dimensional randomly inhomogeneous medium. 22 p2826 A73-42334
- Anisotropy of galvanomagnetic effects in laminarily inhomogeneous semiconductors. 23 p3017 A73-44044
- Random vibrations of elastic nonlinear nonautonomous systems with variable parameters. 24 p3112 A73-45502
- DIFFUSION WAVES**
- Quasi-linear theory of plasma waves resonant diffusion, proceeding from Vlasov equation to derive frequency, wavenumber and velocity by quantum methods. 01 p0086 A73-11492
- DIFFUSION WELDING**
- Diffusive thermal bonding of cermet elements on steel and iron substrates in vacuum. 02 p0172 A73-11537
- Diffusion welding of beryllium. I - Basic studies. 04 p0451 A73-14669
- Metal deformation processes, discussing hot working, fracture, hydrostatic extrusion, superplastic forming, diffusion bonding and powder fabrication. 04 p0452 A73-14742
- Diffusion welding of beryllium. II - The role of the microalloying elements. 06 p0704 A73-17597
- Temperature and concentration effects on heterodiffusion coefficient of diffusion welded Mo-W alloy rods. 06 p0707 A73-17907
- Surface preparation and heating and control processes in diffusion brazing and welding, illustrating with turboreactor construction. 06 p0698 A73-18695
- The yield point phenomenon in a Be-Al composite. 07 p0839 A73-20115
- Resistance diffusion bonding boron/aluminum composite to titanium. 19 p2435 A73-38004
- Aerospace applications of heat resistant alloy diffusion welding techniques, describing mechanical properties, metal bonding, surface cleaning, vacuum levels, temperature effects and microstructure. 20 p2569 A73-39246
- Anomalous behaviour during interdiffusion in the system Nb-Mo. 22 p2876 A73-42340
- Fabrication techniques for Ti alloys in aerospace applications, discussing hot forming, electron beam and diffusion welding under vacuum and stress relaxation annealing. 23 p2985 A73-43911
- DIFFUSIVITY**
- The diffusivity and solubility of oxygen in liquid tin and solid silver and the diffusivity of oxygen in solid nickel. 04 p0463 A73-15315
- Determination of the diffusivity-mobility ratio in highly degenerate semiconductors at low temperatures from linewidth measurements in junction lasers. 16 p1990 A73-33689
- Technique for measuring the diffusivity of hydrogen in titanium alloys. 22 p2878 A73-42505
- DIFLUORIDES**
- NT CALCIUM FLUORIDES**
- F-19 chemical shift tensor in group II difluorides. 05 p0546 A73-16046
- DIFLUORO COMPOUNDS**
- NT POLYTETRAFLUOROETHYLENE**
- Mass spectrometric studies of tetrafluorohydrate and the difluoroamino radical. 08 p0936 A73-21173
- Low frequency vibrations and molecular structure of /CH3/2NPF2. 11 p1326 A73-25567
- DIGESTING**
- An atomic absorption method for cation measurements in Kjeldahl digests of biological materials. 02 p0139 A73-12424
- Gamma time-dependency in Blaxter's compartmental model. 02 p0187 A73-12550
- DIGESTIVE SYSTEM**
- NT ESOPHAGUS**
- NT GASTROINTESTINAL SYSTEM**
- NT INTESTINES**
- NT PANCREAS**
- Digestive hemorrhages in aircrew - Individual and collective safety. 18 p2280 A73-36952
- Russian book - Mutual relationship of water and salt secretion functions in digestive and excretory organs under conditions of high temperature. 21 p2641 A73-41438
- DIGITAL COMMAND SYSTEMS**
- F-8 digital fly by wire control system development and flight testing, using Apollo lunar guidance computer and inertial measurement unit for angular rates and accelerations. 09 p1030 A73-22180
- Second order digital phase locked loop for Viking Orbiter 1975 command system, using filtered sequence of phase error polarity to correct system clocks. 09 p1053 A73-23372
- The multi-moded remote manipulator system. 19 p2416 A73-37314
- Redundant system design for advanced digital flight control. [AIAA PAPER 73-846] 20 p2585 A73-38785
- DIGITAL COMMUNICATION**
- U PULSE COMMUNICATION**
- DIGITAL COMPUTERS**
- NT IBM 1130 COMPUTER**
- NT MINICOMPUTERS**
- NT PARALLEL COMPUTERS**
- NT SEQUENTIAL COMPUTERS**

A comparison of analog and digital techniques for pattern recognition.

01 p0021 A73-11478

Airborne associative parallel array digital computer built with MOS LSI technology for size and weight reduction, discussing design and applications

04 p0424 A73-15065

Canadian E.R.T.S. data handling system.

04 p0424 A73-15384

Procedural formalization and methodology for automated problem solving in terms of digital program systems for algorithms generation, describing operational procedures

06 p0669 A73-17594

A cellular processor for task assignments in polymorphic, multiprocessor computers.

06 p0671 A73-18061

Control algorithm for digital computer operations organization in real time processing of variable priority assignment tasks, estimating memory storage requirements

07 p0796 A73-20049

Russian book - Dynamics of rocket control systems with onboard digital computers.

07 p0906 A73-20229

Construction of analytical formulas for functions of linear circuits by means of engineering-application digital computers

08 p0941 A73-21552

Topological design of thin-film resistors with the aid of a digital computer

09 p1066 A73-23119

The introduction of a digital computer on board ESRO scientific satellites.

09 p1061 A73-23378

Contributions to the design of future on-board data processing systems for scientific spacecraft experiments.

09 p1061 A73-23379

Communication system for digital image processing services over Advanced Research Project Agency computer network, describing hardware facilities and software capacity

09 p1061 A73-23390

Block coding for digital computer error detection and correction, considering applications for arithmetic operations, storage media and permanent hardware failure recognition

09 p1061 A73-23400

Fluidic setup corresponding to automatic control and digital computation circuits, discussing analog elements regulation and applications of logic subassemblies without moving parts

11 p1307 A73-25376

Nonalgorithmic design and coding system for digital mathematical machines for accuracy and speed compatible with digital and analog computer, respectively

11 p1334 A73-25626

Application of nonalgorithmic digital machines in modeling differential equations

11 p1334 A73-25633

Digital computer graphic data feeder with electric pulsed-voltage coordinate matrix and readout probe sensor for input data code coordinate selection

12 p1475 A73-26779

Digital computers with multistage storage in control systems, determining algorithms for data exchange between operative, superoperative and external memory devices

12 p1475 A73-26782

Traffic analysis by statistical tests for batch mode operated digital computer network design, considering user habits, and interarrival, waiting and partition times

12 p1475 A73-27159

The hyperelliptical and other new pseudo cylindrical equal area map projections.

13 p1608 A73-28845

Russian book on digital computer construction and operation covering data processing and conversion algorithms, memory, arithmetic and control devices, microprogramming, etc

13 p1588 A73-28948

Automation of plotting root-locus curves for automatic control systems

13 p1596 A73-29142

Application of analog and digital computers to fatigue testing.

13 p1622 A73-29547

Algorithms of formal selection for optimal control systems of digital computers

14 p1730 A73-30034

Design principles for control systems of digital computers

14 p1730 A73-30035

Algorithm for statistical error detection in digital control computers

14 p1730 A73-30038

Dynamic scheduling of large digital computer systems using adaptive control and clustering techniques.

14 p1730 A73-30039

Small digital computer program packet organization for central processor productivity and use coefficient

improvement, discussing graph-algorithm language for program splicing

15 p1848 A73-31694

Russian book - Problems in the synthesis of finite automata.

15 p1848 A73-31909

Approximate determination of the reliability function of a digital computer

15 p1848 A73-31912

Organization of checks of the central control unit in a digital process-control computer operating with fixed word length

16 p1986 A73-33665

Digital hardware and computer system for a digital image recorder.

17 p2131 A73-35280

Algorithm construction for the stabilization of a deformable spacecraft using an onboard digital computer

18 p2359 A73-36105

Differential equations modelled on nonalgorithmic digital computers.

19 p2408 A73-38144

A study of models of certain digital computer units with the aid of a digital computer

20 p2533 A73-39822

A computing digital phase meter

21 p2664 A73-41083

Russian book on accuracy of automatic systems using digital computers as control devices covering analysis and synthesis, stochastic inputs, system errors and operator methods

21 p2658 A73-41282

Certain problems in determining the capacity of digital computers

22 p2829 A73-41953

Error-correcting codes in computer arithmetic.

22 p2830 A73-42713

Mathematical model of spacecraft onboard digital guidance computer under data acquisition conditions, using imbedded Markov chains

23 p2955 A73-43261

DIGITAL DATA

Analysing vibration and shock data. II - Processing and presentation of results.

05 p0637 A73-17234

Technique for measuring time-base errors of magnetic instrumentation recorders/reproducers.

08 p0965 A73-21084

Internal additive noise generated by a random pulse process

08 p0939 A73-21395

Optical communications links with EDM digital data channels, examining signal optimal reception and noise stability

09 p1048 A73-22043

Digital FM signal receiver with postdetector integration, determining error probability as function of input SNR and noise stability

09 p1049 A73-22044

Synchronization theory for digital data transmission with random changes in channel characteristics

09 p1049 A73-22045

Effect of flutter on theoretical bit error rates for digital recording systems.

09 p1087 A73-23369

Comparing bandwidth requirements for digital baseband signals.

09 p1058 A73-23423

A new type of PSK anti-ambiguity system for satellite applications.

09 p1156 A73-23431

Hybrid computer systems of high speed and accuracy

10 p1192 A73-24674

Digital temperature-measuring device for medical applications

13 p1578 A73-28338

Automatic measurement recorders with discrete output

13 p1617 A73-28858

PCM mobile ground station design covering telemetry receivers, digital data magnetic recording and computer interface circuitry and software

14 p1742 A73-30112

Photoelectron statistics and calculation of the characteristics of optical communications lines

15 p1842 A73-31257

A fast access holographic memory.

16 p2012 A73-32868

Digitized weather radar data models of intense storm cells with 1-2 km resolution and 10 dBZ reflectivity

16 p1983 A73-33727

Multiplex data bus techniques for digital avionics, discussing transmission media, modulation methods, remote control and reliability

17 p2138 A73-35231

Digital data acquisition and processing from a remote magnetic observatory.

17 p2175 A73-35667

Probability of reception of discrete information with a specified reliability under conditions of random radio interference.

17 p2129 A73-35713

Recent developments in digital image processing at the Image Processing Laboratory of JPL.

19 p2429 A73-37324

Internal additive interference produced by a pulsed random process.

19 p2407 A73-38353

The filtering of random sequences with gaps by optimal discrete filters with a constant memory volume

21 p2658 A73-40857

Russian book on radio telemetry systems analysis and theory covering analog and digital data, signal processing, algebraic and trigonometric polynomials and discrete representations

22 p2824 A73-41879

Winds and wave motions 770-100 km/ as measured by a partial reflection radiowave system.

24 p3088 A73-45212

DIGITAL FILTERS

Digital filters applicable to electroencephalographic pattern recognition.

01 p0013 A73-11464

Mathematical model, digital filter design and phase error behavior derivation for higher order discrete phase locked loops

03 p0276 A73-13906

State augmentation procedure for fixed point smoothing algorithm derivation through known solutions of higher dimensional digital filtering problem

03 p0277 A73-13914

Pseudorandom noise for telemetry error rate measurement applications and limitations.

04 p0449 A73-15457

Application of a mathematical filter in the design of a spacecraft inertial stabilization system without a platform

05 p0630 A73-17005

An initialization technique for improved MTI performance in phased array radars.

06 p0664 A73-17790

Determination of the transfer function of a digital filter from the real part of the frequency response.

06 p0674 A73-17811

Improvement of frequency characteristics of digital filters.

08 p0945 A73-20801

Realization of two-dimensional state space digital filters.

09 p1068 A73-22398

Digital multiplicity filters analysis via Walsh functions, considering time discrete dyadic invariant systems

09 p1065 A73-23111

Digital phase locked loops with sequential loop filters - A case for coarse quantization.

09 p1054 A73-23374

The complex digital filter and its applications in digital signal processing.

09 p1058 A73-23425

Intersymbol interference in binary communication systems with single-pole band-limiting filters.

10 p1186 A73-23498

Weaver modulator with digital filter for single side-band transmission in radio communication and telemetry, discussing FORTRAN simulation for cost, computation time and accuracy

10 p1186 A73-23499

Best approximation in digital filtering

10 p1242 A73-23764

Synthesis of nonrecurrent digital filters utilizing the knowledge of the spectral characteristics of the input signal

10 p1195 A73-24421

Construction of discrete shaping filters for the digital simulation of linear Markov processes

11 p1340 A73-25011

Random analog signal quantization and reconstruction from discrete sample values by optimal filtration according to statistical criteria

11 p1341 A73-25013

Method of designing digital devices for bandpass filtration of signals

11 p1333 A73-25023

Iterative computer-aided design of optimum cascaded digital recursive filter, using unconstrained Fletcher-Powell algorithm for frequency domain synthesis

11 p1327 A73-25189

Digitally scanned spectral convolution by computerized filtering for noise spectra quality improvement with instrument signature removal

11 p1334 A73-26679

Nonrecursive digital filter hardware design based on analysis of bit level counting operations in convolution, using fixed and floating point representations

12 p1483 A73-27115

Counting operation based recursive digital filter hardware design in canonic and direct forms, emphasizing low cost, low speed and high flexibility

12 p1483 A73-27116

Range-gated moving target indicator with digital filters.

12 p1469 A73-27161

Microprogrammed digital filters for strapdown guidance application.

12 p1483 A73-27168

- A computer program for filter design having arbitrary magnitude specifications in the frequency domain. 13 p1587 A73-28085
- Quantization and roundoff errors in a digital MTI filter. 13 p1590 A73-28478
- Optimum mismatched filters for sidelobe suppression. 13 p1593 A73-29209
- A new concept for the realization of data models with integrated digital filters and modulators. 13 p1594 A73-29293
- Range and data transmission using digital encoded FM-'chirp' surface acoustic wave filters. 14 p1733 A73-29935
- German monograph - The design of digital filters with minimal storage word length for coefficients and state parameters. 14 p1737 A73-30667
- Tapped delay line filter for optimal single pulse detection in band-limited PCM/NRZ system in presence of Gaussian noise. 14 p1729 A73-30698
- Papers on digital signal processing covering digital filters, fast Fourier transform, finite word length effects, algorithms, and design and programming considerations. 15 p1855 A73-32425
- Bipolar LSI building blocks for digital filtering applications. 17 p2138 A73-35228
- Word length problems in the on-board computer implementation of digital flight control systems. 17 p2145 A73-35384
- Linear filtering of random signals according to the criterion of maximum signal-to-noise ratio. 17 p2145 A73-35719
- Digital filter tasks and applications, discussing recursive and transversal filters, waveforms, SNR, truncation errors and complex filtering. 19 p2414 A73-38301
- Probability of error in binary communication systems with causal band-limiting filters. I - Non-return-to-zero signal. II - Split-phase signal. 19 p2415 A73-38384
- Digital control of a pneumatic isolation system for inertial instrument testing. [AIAA PAPER 73-830] 20 p2543 A73-38775
- Design and analysis of a practical on-line filter to process gyrocompass data. [AIAA PAPER 73-841] 20 p2564 A73-38782
- The application of digital filters using observers to the design of an ICBM flight control system. [AIAA PAPER 73-845] 20 p2541 A73-38784
- Synthesis of digital filters for the control of short periodic angular oscillations of aerospace vehicles. 21 p2780 A73-40326
- An improved light gun tracking algorithm based on a recursive digital filter. 21 p2654 A73-40834
- Operation, design and applications of inductorless digital IC selective N-path filters. 21 p2664 A73-41099
- On the design of wave digital filters with low sensitivity properties. 22 p2835 A73-41950
- Signal processing; Specialists' Conference, Erlangen, West Germany, April 4-6, 1973, Reports. 23 p2952 A73-43308
- Spectral theory and convolution systems of diagonal and nondiagonal discrete transformation filters on Abelian groups, comparing with computational simulations. 23 p2957 A73-43311
- Applications of digital frequency warping to unequal bandwidth and Vernier spectrum analysis. 23 p2952 A73-43312
- Interpolation using finite duration impulse response digital filters. 23 p2952 A73-43313
- Digital LC branch filter transformation with direct element /adapter/ connections, considering gate number and passband attenuation distortion. 23 p2957 A73-43314
- Design and structure of a flexible recursive digital filter. 23 p2957 A73-43315
- Implementation problems of a multichannel digital filter in the case of beat frequencies in the MHz range. 23 p2957 A73-43316
- Digital filter bank with integrated FFT computer. 23 p2956 A73-43326
- Synthesis of a transverse digital filter defined in the complex plane. 24 p3072 A73-44973
- German book on digital systems for signal processing covering discrete linear systems characteristics and design, fast Fourier transformation, digital filters, multiplexing, etc. 24 p3074 A73-45000
- DIGITAL INTEGRATORS**
- Type and time of integration in precision digital video integrator for meteorological radar, describing equipment and operation [AD-751726] 03 p0281 A73-14521
- Project Cloud Catcher weather radar data system revisions in radar set, echo pulse integrator, data logging and analysis and graphic displays. 03 p0289 A73-14523
- Radio astronomy receiver with digital integrator for weak radio source detection, noting minimum detectable flux density. 05 p0552 A73-17166
- Operational algorithms for probabilistic digital integrators for Stieltjes integral and nonhypertranscendental functions. 09 p1060 A73-22555
- Realization of digital differential analyser on the basis of multifunction memory units. 10 p1198 A73-24018
- High-speed universal digital integrators with multistage increments as elements of automatic control systems. 12 p1475 A73-26781
- A portable millisecond-integration-time photoelectric photometer. 17 p2165 A73-34273
- DIGITAL NAVIGATION**
- VLF/Omega digital airborne area navigation system evaluation tests, discussing transmitting stations and system performance. 13 p1656 A73-28904
- Digital flight control systems data sampling rate selection effects on intersample ripple, spectral folding and distortion and system bandwidth. 17 p2138 A73-35224
- DIGITAL RADAR SYSTEMS**
- Storm cell models from digital radar data. 03 p0338 A73-14510
- Digitized radar experiments project for data acquisition and processing and weather forecasting techniques development, describing test bed configuration, equipment and operation. 03 p0288 A73-14515
- Application of pattern recognition techniques to digitized radar data. 03 p0279 A73-14517
- Radar sequential detector for digital processing of signal masked by noise, determining false alarm and detection probabilities and mean sampling time. 04 p0423 A73-15917
- Digital step transform for airborne radar linear FM signal pulse compression, reducing data memory requirements. 17 p2123 A73-35237
- Validation of digital radar landmass simulation utilizing terrain elevation data compression. 18 p2292 A73-36842
- Operational principles and testing of a digital radar target extractor. 19 p2404 A73-37584
- Secondary surveillance radar - Current usage and improvements. 19 p2451 A73-37808
- Airborne multimode radar digital data system using high transfer rate magnetic tape recording, discussing 8 track tape storage capacity, coding and logic circuits. 19 p2431 A73-38198
- A method of optimization of algorithms for secondary processing of radio signals. 21 p2656 A73-41129
- Russian book - Digital methods and systems in radar technology. 21 p2657 A73-41433
- DIGITAL SIMULATION**
- Transient variation of martian ground-atmosphere thermal boundary layer structure. 01 p0097 A73-10400
- Numerical simulations of the tropical air-sea planetary boundary layer. 01 p0073 A73-10496
- GREMEX - A management game for the new public administration. 01 p0124 A73-11007
- Three dimensional jet stream dynamics based on particle population evolution numerical simulation, interpreting solar system evolution. 02 p0218 A73-12415
- Digital simulation of random processes and its applications. 02 p0144 A73-12607
- Experimental verification of a digital computer simulation method for predicting gas turbine dynamic behaviour. 02 p0204 A73-12647
- Invariant poles feedback control of flexible highly variable spacecraft. 03 p0285 A73-13522
- Simulation of rendezvous of a man in deep space. 03 p0288 A73-13569
- Monte Carlo solution of structural dynamics. 03 p0391 A73-13681
- Cell averaging constant-false-alarm-rate radar receiver with noise estimated from logarithmic detector output, determining performance in Gaussian noise by Monte Carlo simulation. 03 p0277 A73-13910
- A digital simulation method for interconnected continuous systems. 03 p0281 A73-14479
- Impact loading on structures with random properties. 04 p0510 A73-15028
- Digital modeling of multipath induced monopulse angle tracking errors. 04 p0416 A73-15056
- Application of stochastic stability theory to model-reference systems. 04 p0430 A73-15215
- Digital simulation of imperfect second-order hybrid phase locked loop operating in RF interference background, determining phase error variance and probability density function. 04 p0422 A73-15438
- Numerical simulation of precipitation development in supercooled cumuli. I, II. 05 p0594 A73-16572
- Numerical simulation of high Mach number supercritical magnetosonic collisionless shock wave propagation perpendicular to magnetic field, considering cause of anomalous ion heating. 05 p0604 A73-17365
- An analysis of optimal control system algorithms. 06 p0670 A73-18059
- Fault insertion techniques and models for logic simulation. 06 p0671 A73-18062
- A simple method for precise attitude determination of a spinning spacecraft. 06 p0722 A73-18827
- Digital simulation of the Lunar Roving Vehicle navigation system. 06 p0722 A73-18828
- Variational algorithms for numerical simulation of collisionless plasma with point particles including electromagnetic interactions. 07 p0854 A73-19264
- Nonphysical noises and instabilities in plasma simulation due to a spatial grid. 07 p0854 A73-19267
- Equations of motion of the lunar roving vehicle. 07 p0808 A73-19490
- GARP Global Experiment design with satellite and balloon borne systems for meteorological observation and atmospheric research, discussing sounding data numerical simulation. 07 p0820 A73-20442
- Carre method for optimum overrelaxation factor determination in electron gun performance analysis by digital simulation, discussing choice of parameters for rapid iterative convergence. 08 p0990 A73-20836
- Numerical studies of two-dimensional vortex motion by a system of point vortices. 08 p0954 A73-21010
- Rossby wave barotropic instability effects on errors leading to large scale atmosphere predictability experiments by numerical simulation of two dimensional turbulence. 08 p0985 A73-21386
- Analog, digital and hybrid simulation of a planetary boundary layer meteorological forecast model. 09 p1114 A73-22333
- Digital simulation methodology for LSI computer design and technology assessment to assure competitive cost, schedule and implementation cycles in manufacturing. 10 p1191 A73-23793
- Book - Digital simulation of physical systems. 10 p1191 A73-23946
- Spinning Skylab space station dynamics, investigating motion stability from simplified models with flexible appendages by digital simulation. 10 p1286 A73-24003
- Spectral energy transfer models of turbulence decay compared with numerical simulation of three dimensional homogeneous isotropic turbulence, considering eddy viscosity and diffusion models. 10 p1246 A73-24252
- Numerical simulation of small amplitude whistler waves in thermal plasma, describing particle motion under self consistent and external magnet fields via Lorentz equation. 10 p1255 A73-24269
- Construction of discrete shaping filters for the digital simulation of linear Markov processes. 11 p1340 A73-25011
- Nonlinear dynamic feedback control system state variable observers reconstruction error convergence and digital simulation for performance. 11 p1390 A73-25187
- Simulation capability for dynamics of rotating counterweight space stations. [AIAA PAPER 73-320] 11 p1343 A73-25551
- Diagnostic simulation of a pneumatically controlled blowdown wind tunnel. 11 p1344 A73-26546
- Techniques for simulation of radar displays. 12 p1475 A73-27132
- A simulation model for a memory organization for a multiprocessor. 12 p1475 A73-27155

Differential equations for digital model of linear quadrupole, discussing digital simulation of analog radio equipment circuits

13 p1591 A73-28659

Design and simulation of an aircraft brake using a digital computer.

13 p1588 A73-29385

Generalized mathematical model for gas turbine dynamic behavior simulation based on one dimensional flow theory with functional integration for rotor speed time derivative

15 p1925 A73-31629

Digital simulation of physical systems using CSMP.

16 p1985 A73-33129

Charge transfer in overlapping gate charge-coupled devices.

16 p1988 A73-33396

Simulation of a multiple element test environment.

16 p1985 A73-33417

Simulated weather records experiment for polluted atmosphere effects on climatic change, using numerical circulation model

[AIAA PAPER 73-537]

16 p2007 A73-33568

Simulation of the compounder in a single base propellant (SBP) process.

17 p2220 A73-34819

Nonphysical self forces removal from electromagnetic plasma models by simulation algorithm, discussing optimization of particle orbit equations integration

17 p2216 A73-34895

Simulation results for a radar multipath angle error reduction method.

17 p2127 A73-35633

A simulation study for the design of an air terminal building.

17 p2149 A73-35826

Artificial earth satellite brightness attenuation and rotation periods from spectral analyses of photometric curves by mathematical simulation

18 p2315 A73-36142

Application of the Ornstein-Uhlenbeck stochastic process to the study of dynamic systems in an environment of stochastic disturbances.

18 p2330 A73-36829

Airport simulation program describing passenger flow and scheduling considerations, including automobile parking, baggage handling, rapid transit, arrival and departure peaks and passenger decisions

18 p2296 A73-36841

Computer models for air traffic control system simulation.

18 p2335 A73-36843

ACLS CC-115 model simulation, test analysis and correlation.

19 p2382 A73-37693

A digital simulation facility for air traffic control experimentation.

19 p2451 A73-37809

Application of digital computer APU modeling techniques to control system design.

19 p2392 A73-38416

Availability, maintenance and cost of communication satellite systems.

20 p2613 A73-38768

Study of control system effectiveness in alleviating vortex wake upsets.

[AIAA PAPER 73-833]

20 p2507 A73-38776

An attitude control system for earth observation spacecraft.

[AIAA PAPER 73-854]

20 p2585 A73-38792

System performance prediction by modeling test data in digital simulations.

[AIAA PAPER 73-880]

20 p2543 A73-38816

A diagnostic program - Problems of predicting myocardial infarction on a digital computer

20 p2516 A73-38998

Digital computer simulation program for North Atlantic hybrid navigation systems configurations, using covariance matrix error analysis for planned increase of commercial air traffic capacity

21 p2733 A73-40028

Nonlinear trajectory-following and control techniques in the terminal area using the Microwave Landing System Navigation Sensor.

21 p2734 A73-40038

Linear fire control predictor with non-Gaussian inputs, calculating on-target probability lower bounds for verification by digital simulation

21 p2649 A73-40332

The use of logic simulation in the design of a large computer system.

21 p2658 A73-41210

Computer simulation of complex electronic circuit equations derived from subcircuit equations combined with coupling equations, noting topological modification ease and run time savings

21 p2671 A73-41309

A model of diffusion in the respiratory unit.

21 p2645 A73-41638

Russian book on scale selection in modeling for analog and digital computers covering similarity theory, error formation, accuracy optimization, etc

22 p2829 A73-41883

Compartmental analysis of biological system with a digital computer.

22 p2829 A73-42228

Numerical simulation of maritime warm cumulus by one dimensional cylindrical cloud model incorporating nucleation and raindrop breakup processes

22 p2883 A73-42546

Certain algorithmic aspects of flight dynamics simulation on digital computers

23 p3038 A73-43262

An investigation of the numerical properties of the surface heat-balance equation.

23 p3004 A73-44265

Numerical simulation of three dimensional atmospheric turbulence with emphasis on kinetic energy transfer from large to small scales of motion with heat conversion

24 p3108 A73-45092

DIGITAL SPACECRAFT TELEVISION

Manned spacecraft digital TV system channel error correcting encoder and decoder performance test data including bit error rate versus SNR and decoding depth

04 p0419 A73-15400

Real time digital spacecraft TV with data compression/error correction test system, evaluating source encoding algorithm performance from processed picture quality

04 p0449 A73-15409

A DPCM codec using edge coding and line replacement.

04 p0422 A73-15443

DIGITAL SYSTEMS

NT DIGITAL NAVIGATION

NT DIGITAL RADAR SYSTEMS

Inherent limitations in digital incremental oscillator-analyser systems for mechanical vibration testing.

02 p0171 A73-12610

Extension of a portable tactical instrument approach and landing system.

03 p0340 A73-13574

Design of a digital adaptive control system for reentry vehicles.

03 p0286 A73-14482

A very accurate X-band rotary attenuator with an absolute digital angular measuring system.

03 p0310 A73-14498

A universal digital autopilot and integrated avionics system.

04 p0474 A73-14735

Spacecraft digital attitude control.

04 p0504 A73-14736

Spacecraft control hardware for use with digital processors.

04 p0424 A73-14737

Design of digital force function generator for aircraft tire load testing.

04 p0424 A73-15064

Digital phase locked loops for incoming signal phase tracking, predicting performance from nonlinear difference equation model for comparison with digital simulation

04 p0421 A73-15435

Digital vibration control systems for structural design dynamic testing and evaluation, discussing state of art and trends toward multichannel and multi-axis control

[SAE PAPER 720820]

05 p0553 A73-16628

A digital processing and analysis system for multispectral scanner and similar data.

05 p0554 A73-17147

Programmable, digital, rapidly frequency-shift-keyed, high-frequency generators for driving acoustooptical light deflectors

05 p0586 A73-17239

Programmable digital pulse generator for NMR applications based on master clock, several counters and inexpensive ICs

05 p0559 A73-17256

Digital Avionics Information System (DAIS)/development for military supersonic all-weather precision weapon delivery system, emphasizing modular design for different aircraft types

06 p0672 A73-17572

Applications for quantum amplifiers in simple digital optical communication systems.

06 p0668 A73-18404

Modeling and evaluating the performance of high data rate digital satellite communication systems with limiters.

06 p0669 A73-18830

German monograph - Synchronization of digital telephone networks by means of phase averaging with parameter transfer.

07 p0794 A73-20386

Dynamic response of digital-analog flow measurement system based on turbine driven pulse generator as sensor element

07 p0828 A73-20545

High efficiency microwave avalanche diode capability for digital applications, describing GHz rate 100 V pulse generator circuit

07 p0804 A73-20556

A modular approach to an automated digital test system.

08 p0940 A73-20678

Majority logic detection scheme of differentially phase-modulated waves.

08 p0937 A73-20802

Optimization of detection systems for quasi-classical optical signals

08 p0940 A73-21558

Interdigitated power junction transistor technology assessment for power gain, bandwidth and frequency performance, noting packaging effect and thin film module advantage

08 p0949 A73-21648

Time jitter in line regenerators with pattern dependent pulse waveforms.

09 p1062 A73-22301

A new analysis of the digital data transition tracking loop.

09 p1062 A73-22302

Digital quartz pressure transducer for FM signal output to interface with digital computer and telemetry, noting insensitivity to temperature and vibration interference effects

09 p1082 A73-22503

Calculation of the reliability of hierarchical systems with quorum redundancy

09 p1088 A73-22552

An approximate continuous representation of discrete control systems

09 p1068 A73-22564

Analysis of the mechanical and energetic characteristics in pulse-coded regulation of an asynchronous motor

09 p1037 A73-22939

640 Mbit/sec waveguide transmitter at 38 GHz.

09 p1065 A73-23095

Moving-target-indicator recursive radar filter using bucket-brigade circuits.

09 p1065 A73-23096

Digital phase locked loop for FM demodulation in real time, computing SNR for frequency offsets and sinusoidal modulation

09 p1054 A73-23373

Digital phase locked loops with sequential loop filters - A case for coarse quantization.

09 p1054 A73-23374

Subjective comparisons of analog and digital TV transmission system, considering spectral occupancy and picture quality

09 p1055 A73-23387

PCM and DPCM digital modulators design and performance comparison for sampling rate effects on quantizing noise, noting tradeoffs between cost and system efficiency

09 p1059 A73-23435

Digital microwave receiver with passive discriminator for precise and instantaneous pulsed RF signal frequency measurement

10 p1188 A73-24168

Statistical synthesis of digital parameter-measuring equipment and analysis of its efficiency

11 p1360 A73-25021

The optimality of variable sampling schemes for a digital encoder.

11 p1327 A73-25194

Digital electrode breakdown potential controller for spark source mass spectrometer automation, using radio frequency pulse amplitude sensing

11 p1367 A73-26315

Construction of verification tests for digital devices with delay elements

12 p1482 A73-26753

Digital measuring devices with a constant range of relative error variations

12 p1495 A73-26777

Unified approach to the performance analysis of linear modulation systems with coherent detection.

12 p1469 A73-27072

An adaptive digital compensator for saturating control systems.

12 p1483 A73-27160

A digital measurement converter of pulsed flows

13 p1591 A73-28872

Suppressing spurious signals in saturated switching systems.

13 p1595 A73-29394

Transient analysis of multiple-input integrated digital structures.

13 p1595 A73-29580

Digital circuits test equipment functional principles, considering time, instantaneous voltage and pulse height measurements

14 p1731 A73-29873

Approximate investigation of the dynamics of a digital phase-lock automatic frequency control system (DPAFC)

14 p1728 A73-30269

Probabilistic properties and spectral characteristics of the duobinary code in the baseband

14 p1729 A73-30897

Spectral-energy dispersal in digital communication-satellite systems.

15 p1842 A73-31096

Digital readout wind measurement and indicator system for data acquisition, processing and display in airports for aircraft wind information service
15 p1874 A73-31318

A high-accuracy digital star tracker for advanced planetary missions.
15 p1907 A73-31356

The influence of pulsed noise on the performance of incoherent digital communications systems
15 p1843 A73-31567

Digital correlator-computer-pattern recognition system for VLF phenomena investigation, discussing electromagnetic waves structure and spectrum analysis
15 p1845 A73-32234

Digital transmission techniques for ATC satellite system, considering technical and economic aspects of various coding systems
15 p1846 A73-32427

Radar data digital relay from outlying stations to ATC centers for air traffic image integration, discussing computerized plotting and alphanumeric display techniques
15 p1847 A73-32435

Single and dual path propagation at 18 GHz with application to the design of digital radio relay systems.
16 p1981 A73-33703

Methods for investigating the effects of multipath fading on 2-phase digital radio systems.
16 p1981 A73-33708

An approach to the analysis of performance of quasi-optimum digital phase-locked loops.
16 p1992 A73-33743

Solid state Digital Slip Sync Strobe/Camera Control System design for powered wind tunnel helicopter models testing
17 p2101 A73-34622

Real time digital videomagnetograph at the Aerospace San Fernando Solar Observatory.
17 p2168 A73-34909

Redundant system design and flight test evaluation for the TAGS digital control system.
17 p2131 A73-35062

Military aircraft onboard Digital Avionics Information System for computerized integration of navigation, guidance, weapon delivery, cockpit display, communication, flight control and energy management
17 p2136 A73-35202

Digital avionics systems software development trends, considering compatibility and cost problems in increased use of complex processing hardware, sensors and displays
17 p2137 A73-35203

Unconventional digital avionics black box approach for cost reduction and reliability improvement in terms of packaging, component coding and hardware qualification programs multiplicity
17 p2137 A73-35205

Signal conditioning, separation and parameter measurement in modular digital Elint analysis system for airborne, shipboard or ground based reconnaissance applications
17 p2137 A73-35207

Digital fly by wire flight control system with airborne digital processor for increased aircraft survivability, determining redundancy level to satisfy system performance
17 p2138 A73-35222

Flight test and demonstration of digital multiplexing in a fly-by-wire flight control system.
17 p2107 A73-35225

Information transfer system of digital avionics system, examining signal reduction by baseband time division multiplexing and video distribution systems
17 p2138 A73-35230

Liquid crystal approach to integrated programmable digital displays and aircraft control, considering flat panel digital-matrix display
17 p2139 A73-35234

Thin configuration flat digital CRT display with electron beam control improvement for military avionics applications, discussing performance advantages and ownership cost
17 p2139 A73-35235

Digitally integrated cockpit simulation facility for display systems and avionics to plan mission/human program and airborne equipment requirements
17 p2139 A73-35236

Preliminary progress with digital image-tubes at Cerro Tololo.
17 p2169 A73-35281

Techniques for digital-microwave hybrid real-time radar simulation.
17 p2131 A73-35303

Wideband multidrop asynchronous TDM/FDM multichannel data distribution system for space station application, discussing analog and digital buses design
17 p2124 A73-35308

B-1 aircraft electrical multiplex system.
17 p2110 A73-35309

Development of data analysis in sound and vibration.
17 p2131 A73-35335

A digital optimization device for directional charged particle measurements in space research.
19 p2428 A73-37148

A comparison of errors in linear digital models.
19 p2413 A73-38059

Recursive ideal observer detection of known M-ary signals in multiplicative and additive Gaussian noise.
19 p2407 A73-38385

Discrete address beacon system /DABS/ data links and digital communication between ground based ATC computer and aircraft for IFR-VFR conflict detection and safety separation
19 p2453 A73-38466

COS/MOS phase-locked-loop - A versatile building block for micro-power digital and analog applications.
20 p2534 A73-38657

Dynamics and stability of the algorithm of a digital adaptive system using a prediction technique
20 p2532 A73-38688

Airborne digital data link terminal for commercial airlines' use.
20 p2526 A73-38756

A digital communications system for manned spaceflight applications.
20 p2527 A73-38763

Variable data rate multimode quadriphase modem for PSK or QPSK operation in digital communication links, noting optimum overall system performance
20 p2527 A73-38764

Digital control system development for the Delta launch vehicle.
20 p2613 A73-38786

An organized approach to the digital autopilot design problem.
20 p2585 A73-38787

Design of a digital controller for spinning flexible spacecraft.
20 p2589 A73-38830

Digital information management system of navigation and flight data for post-1975 fighter aircraft.
20 p2589 A73-38832

Optimal detection of binary signals with an arbitrary distribution of state durations at the output of a binary symmetrical Markov channel
20 p2541 A73-38992

A method of analyzing transient processes in digital fluidic circuits
20 p2510 A73-39352

Calculation of processes taking place in digital automatic control systems with finite switch-closing times
20 p2543 A73-39477

Morphological indices of digital microelectronic structures
21 p2660 A73-40016

Fly-by-wire digital F-8C aircraft control system using Apollo guidance, navigation and control hardware, emphasizing interface design and fault detection
21 p2733 A73-40027

Thermally induced FM noise in Gunn oscillators and jitter in Gunn-effect digital devices.
21 p2660 A73-40096

Use of switching circuits as redundant multiplier elements in canonic digital networks.
21 p2658 A73-41209

Gunn effect digital functional device.
22 p2829 A73-42204

German monograph - Theoretical and experimental investigation of digital hydraulic positioning devices.
22 p2801 A73-42848

Use of a response surface to optimize digital telecommunication systems.
23 p2948 A73-43214

A digital system for receiving binary phase-coded signals
23 p2952 A73-43319

Digital fluidic systems application to binary signal transmission via system with fluid transmission lines and switching element-based transmitters and receivers
23 p2944 A73-43417

Compensation of an underdamped fluidic position control system by a digital pulse compensator.
23 p2944 A73-43420

The design of digital fluidic components and systems - A review.
23 p2945 A73-43433

Malfunction diagnostics in digital integrated-circuit devices
23 p2956 A73-43581

German book on digital systems for signal processing covering discrete linear systems characteristics and design, fast Fourier transformation, digital filters, multiplexing, etc
24 p3074 A73-45000

Digital communication system with known channel characteristics, discussing intersymbol interference dependence on signalling rate based on Nyquist criteria consideration
24 p3070 A73-45482

Attitude control for the Netherlands astronomical satellite /ANS/.
24 p3144 A73-45558

DIGITAL TECHNIQUES

Digital apparatus for telemetry of pressure
01 p0044 A73-10034

Self-compensating digital phase meter with discrete phase shifters
01 p0044 A73-10078

Design of digital phase meters with intermediate frequency converters
01 p0044 A73-10079

Signal amplitude ratios measurement in automatic control applications by digital differential logometer, using time-phase dividing circuits
01 p0022 A73-10082

Multiband and multiemulsion digitized aerial photographs automatic processing by digital computer techniques and statistical pattern recognition algorithms
01 p0044 A73-10140

On-line digital recording of stellar spectrum with photoelectron-counting spectrophotometer, noting discrimination against spurious signals from noise and pulse height distribution measurements
01 p0048 A73-10531

Photographic equipment for astronomical telescopes, considering mechanical devices for plate translation and rotation, guiding microscope and digitally controlled servomotors with incremental feedback
01 p0049 A73-10541

Prototype solid state radio sounder with digitization concept of multipulse integration for L.F. sounding of lower ionosphere, noting performance
01 p0043 A73-10909

Digital attitude sun sensor for ionosphere sounding satellite.
01 p0053 A73-11171

Digital image processing for the earth resources technology satellite data.
01 p0020 A73-11457

A discrete numerical approach to fluid dynamics.
01 p0071 A73-11461

A fast computational algorithm for optimum digital control systems.
01 p0021 A73-11463

Comparison of digital-signal multiplexing methods by means of sequencing
01 p0021 A73-11485

Device for measuring the instantaneous value of current and voltage in the operation of a pulsed plasma accelerator
02 p0196 A73-11792

Component errors of digital frequency meter with nonius estimation of measured quantity smaller digits
02 p0167 A73-11863

Automatic N/h, t/ profiles of the ionosphere with a digital ionosonde.
02 p0143 A73-12530

Multidimensional coding for telemetric transmission of work load factors in ergonomics research.
03 p0272 A73-14307

Automatic digital image processing for remote sensing with ERTS, Skylab and NASA survey aircraft, considering image registration, projective transformation and ground truth information
03 p0309 A73-14487

Automated procedures for mapping and display of digitized radar data.
03 p0281 A73-14522

Demonstration of digital three axis spacecraft control.
04 p0432 A73-14738

A digital echo suppressor for satellite circuits.
04 p0416 A73-14995

Digital image registration by correlation techniques.
04 p0449 A73-15413

Color image quantization error assessment from noninferior bit assignment determination for several coordinate systems by color shift comparison, using computer simulation
04 p0449 A73-15444

Numerical classification and coding of electrocardiograms.
04 p0412 A73-15647

Analysis of a dual mode digital synchronization system employing digital rate-locked loops.
05 p0549 A73-16369

A digitally controlled scanning device for a high resolution spectrograph.
05 p0576 A73-16439

Control of electro-hydraulic shaker by digital iteration techniques.
05 p0562 A73-16636

Two dimensional digital Fourier transform applications to picture processing, noting economy in computer storage
05 p0554 A73-17146

Noise magnitude calculation for intensity quantized hologram based on Laplace transform for nonlinear device analysis and Gaussian random process
05 p0579 A73-17220

He-Ne laser beam intrinsic third order intensity statistical correlation function measurement by digital technique for comparison with calculations
06 p0699 A73-17520

Digitalized or sampled data FM demodulator recursive algorithm synthesis and SNR performance comparison with optimum analog and conventional limiter discriminator demodulators
06 p0664 A73-17712

Digital and hybrid computational aspects of the discrete representation theorem of nonlinear estimation. 06 p0670 A73-17803

Compact digital coding of electrocardiographic data. 06 p0660 A73-18815

Reduced-order observers for linear discrete-time systems. 07 p0805 A73-20581

A digital instrument for measuring amplitude-time parameters of nanosecond-duration pulses 08 p0949 A73-21711

Digicon multichannel image tube photoelectron counter for astronomical spectroscopy, discussing design information density and accuracy, noise and quantum efficiency 08 p0971 A73-21747

State of the art in the techniques of digital phase modulation 09 p1050 A73-22317

High capacity digital concentrator of telephone circuits for a TDMA station /CELTIC/ 09 p1050 A73-22319

Digital pressure transducer based on vibrating cylinder frequency response to pressure changes, discussing operational principles and applications 09 p1082 A73-22502

Digital coherent demodulator techniques for moderate data rate PSK signal reception in real time, describing synchronous bandpass sampling receiver with IF signal A/D conversion 09 p1053 A73-23371

Discrete dynamic adaptive control algorithms for estimation of minimum loss function point trajectory characterizing system quality in nonstationary conditions 10 p1242 A73-24035

Application of a digital computer in the processing and presentation of tensile test results. 10 p1192 A73-24569

Higher-order numerical differentiation of experimental information. 10 p1244 A73-24719

Two dimensional signals Fourier transformations, discussing digital techniques application to linear and optical systems 11 p1397 A73-24993

Comparative analysis of algorithms for measurement of correlation functions by the multiplication method /Review/ 11 p1360 A73-25018

Design principles of digital devices for measuring time intervals /Survey/ 12 p1496 A73-27201

Satellite communication channels assignment to ships and aircraft, considering automated digital calling method for ship-to-shore communication 12 p1472 A73-27670

Digital computer aided control systems design, discussing components dynamic behavior mathematical modeling and control processes simulation 12 p1476 A73-27872

Quantizer functions and their use in the analyses of digital beamformer performance. 13 p1582 A73-28496

Digital single sideband mixing circuit for sum or difference frequency conversion in phase quadrature, using exclusive-or logic gates 13 p1593 A73-29117

Blocking oscillator multiple mode operation digital control by supply voltage regulation 13 p1593 A73-29119

Computer and digital techniques in ATC automation technology, considering functional organizations, terminal facilities and system capabilities to meet future needs 14 p1730 A73-29886

Multipath propagation in aircraft digital communication with ground terminal, modeling received signal for detection and estimation theories applications 14 p1726 A73-29902

NASTRAN digital computer program for static and dynamic structural analysis by finite element method, including nonlinear static and dynamic response 14 p1808 A73-30198

Control systems synthesis via digital computer techniques, describing numerical optimization procedure and analog simulation method 14 p1730 A73-30921

Noise rejection estimation for sinusoidal signal detectors which use information on zero-crossing moments 15 p1842 A73-31251

Digital image processing for information extraction. 15 p1875 A73-31800

Automatic measurement of intervals of shock wave transit across a base section 15 p1876 A73-31862

Central digital measuring and data logging systems for electrical and nonelectrical analog signal conversion, display and recording 15 p1849 A73-32204

Optimal digital modulation techniques for aeronautical communications via satellite, considering air navigational systems for transoceanic flight 15 p1847 A73-32480

Digital photoelectric tracking systems with accumulation of the mismatch signal 16 p1977 A73-32716

The application of digital techniques to a VOR signal generator. 16 p1979 A73-33405

Digital synchronization of synchronous collision prevention systems in aviation 17 p2207 A73-34480

Turbo and jet powered general aviation aircraft-borne weatherer memory radar system with digital processing technique to eliminate direct view storage tube [SAE PAPER 730316] 17 p2122 A73-34674

Digital attitude reference system for three-axis-stabilized earth oriented satellites, using gyrocompasses with solar and horizon sensors 17 p2209 A73-34875

Digital processing of Mariner 9 television data. 17 p2168 A73-34907

Two-way wideband microwave communication system oriented toward PCM-TDM digital technique for covering telephone, videophone and radio broadcasting services 17 p2123 A73-34968

Digital time division multiplexing for integrating avionics equipment, discussing electrical power control signal multiplexing 17 p2139 A73-35246

A technique for measuring small displacements in digital spectra. 17 p2170 A73-35297

TVAC - A television area correlator tracking system. 17 p2171 A73-35381

Limit cycles resulting from quantization in digital control systems. 17 p2145 A73-35642

Digital processing of stereoscopic image pairs. 19 p2432 A73-38534

Digital flight control design using implicit model following. [AIAA PAPER 73-844] 20 p2508 A73-38783

Signal filtering using hard-limited digital processing. II - Performance with a single target in a coloured-noise background. 20 p2530 A73-39126

Worldwide TV satellite systems, discussing transmission channels, power limitations, quality objectives, conversion and digital techniques 20 p2530 A73-39204

Vibration test techniques used to simulate transients and match shock spectra. 20 p2544 A73-39268

Spectra of signals with functional phase modulation in digital frequency synthesizers 20 p2537 A73-39461

Noise immunity of digital methods for the transmission of analog messages with an enhanced information content 20 p2531 A73-39463

Polarimetric mapping techniques using multichannel digital photometry via remote sensors, discussing terrain types, lunar topographic analysis and soil and vegetation mapping 20 p2568 A73-39860

Digitally switched phase shifter operating at metric wavelengths 21 p2662 A73-40544

Digital codings of multi-dimensional information sources and applications to image coding. 21 p2655 A73-41043

Tape recording, off-line digitalization and time series analysis of dynamic field measurement analog data for computerized power spectral density calculation 22 p2859 A73-42197

German monograph on display unit nonlinear interpolation approach based on higher order curve for reduced computer storage requirements covering Chebyshev approximation and coordinate transformations 22 p2830 A73-42738

Real-time identification using adaptive discrete model. 23 p2962 A73-43286

A digital correlation spectrometer employing multiple-level quantization. 23 p2981 A73-43378

Output pressure-displacement and flow pattern characteristics of digital limit Schrenk, wall attachment and nozzle receiver fluidic switches 23 p2945 A73-43426

An automated Dobson spectrophotometer. 23 p2982 A73-43855

Cascade n-phase transistorized stable multivibrator circuit design for digital and tool control clock applications 23 p2983 A73-44142

Digital microstress gauge for magneto-thermal gas transport studies. 24 p3089 A73-44815

DIGITAL TO ANALOG CONVERTERS

Automatic frequency control in the case of manually tuned oscillators 04 p0427 A73-14774

Viking lander vehicles ground reconstruction equipment for Martian surface digital magnetic tape video data conversion into high quality hard copy 06 p0683 A73-18321

Choice of the quantization step and sampling interval for analog measurement signals 12 p1482 A73-26848

Some problems associated with the construction of scanner employing a cathode-ray tube and programmed control 21 p2665 A73-41270

DIGITAL TRANSDUCERS

Linear response transistorized FM temperature measuring transducer with thermistor, noting low distortion and digital display convenience 01 p0044 A73-10032

Fast and reliable automatic digital control components and transducers for data processing, display and storage, assessing technology development trends and preference over analog devices 10 p1199 A73-24028

VHF and microwave surface acoustic wave band-pass filter design with impulse model for frequency response and interdigital transducer input admittance calculation 12 p1484 A73-27563

Ranging and data transmission using digital encoded FM-'chirp' surface acoustic wave filters. 12 p1470 A73-27571

DIGITIZERS

U ANALOG TO DIGITAL CONVERTERS

DIGITS

NT BINARY DIGITS

DIHEDRAL ANGLE

Pressure distribution and shock wave intensity variations in supersonic flow past two plane wings forming dihedral angle 03 p0245 A73-13623

Crystal surface topography investigation by scanning electron microscopy for dihedral angle measurements on thermally grooved grain boundaries 13 p1617 A73-28935

X ray data refinement on proteins, discussing backbone and side chain dihedral angles adjustment by least squares fitting to relieve atomic overlaps 17 p2112 A73-34893

DILATATION

U STRETCHING

DILATATIONAL WAVES

Elastic waves originating at the surface of a spherical opening in nonhomogeneous isotropic media. 01 p0116 A73-11065

Stability of waves and shock structure in generalised thermoelasticity at low temperatures. 20 p2624 A73-39564

DILUENTS

Measurement of the temperature dependence of the vibrational relaxation rate of HF and the effect of SF₆, N₂, and F₂ as diluents. 07 p0853 A73-19628

DIMENSIONAL ANALYSIS

Convection heat transfer in a contained fluid subjected to vibration. 03 p0398 A73-13547

Experimental investigations concerning pneumatic ejectors, with special reference to the effect of dimensional parameters on performance characteristics. 03 p0297 A73-14503

Television/computer dimensional analysis interface with special application to left ventricular cineangiograms. 06 p0657 A73-17860

Vector characteristics use in dimensional analysis, solving Huntley method inconsistencies 07 p0916 A73-20438

The dynamic response of a diaphragm-ejector amplifier. 08 p0929 A73-21830

Plasma production by laser, discussing basic equations, dimensional analysis, heating, focusing lens and targets 09 p1125 A73-22050

Book on experimental analysis covering measurement systems, engineering problems, data analysis, electro-optics and dimensional parameters 17 p2176 A73-35855

Metric technical, Imperial /British/ and SI dimensional systems, discussing conversion rules for mass, force, length, area, volume, density, moment of inertia and stress relationships [SAWE PAPER 963] 19 p2499 A73-37881

Solar mass, earth mass and kilogram re-examined for gravitational constants, discussing geocentric constant 20 p2613 A73-39750

Multidimensional scaling methods and data visualization /Review/ 23 p2949 A73-43578

DIMENSIONAL MEASUREMENT
Dimension-theory determination of the separation parameter for an incompressible magnetohydrodynamic boundary layer. 06 p0726 A73-17406
Displacement comparator based on laser interferometer with photoelectric counter for monitoring inside and outside dimensions of cylinder bores, shafts, spheres, etc 11 p1364 A73-26103
Saturn disk and ring dimensions, discussing photometric parameters, ice as ring constituent and ring models 11 p1425 A73-26139
Error in the interferometric measurement of length by the rotational movement of a mirror and multipass corner cube arrangement. 11 p1365 A73-26240
Application of an electronic image analyzer to dimensional measurements from neutron radiographs. 11 p1371 A73-26743
A kinematically designed mount for the precise location of specimens for holographic interferometry. 14 p1753 A73-30414
Some scale estimates of the three-dimensional structure of cloud fields from aircraft-based aerial photographs 24 p3107 A73-44962

DIMENSIONAL STABILITY
NT SHELL STABILITY
NT STRUCTURAL STABILITY
Construction materials selection for thermal dimensional stability in critically sensitive precision instruments and mechanical components, considering economic factors 01 p0066 A73-11293
Beryllium for nonstructural and structural applications in aerospace systems, considering high dimensional stability, mechanical and thermodynamic properties, and metal sintering techniques for production 07 p0828 A73-18904
Breakdown of the superheated Meissner state and spontaneous vortex nucleation in type II superconductors. 13 p1669 A73-29183

DIMENSIONLESS NUMBERS
NT FROUDE NUMBER
NT GRASHOF NUMBER
NT LEWIS NUMBERS
NT MACH NUMBER
NT NUSSELT NUMBER
NT PECLET NUMBER
NT PRANDTL NUMBER
NT RAYLEIGH NUMBER
NT REYNOLDS NUMBER
NT RICHARDSON NUMBER
NT SIMILARITY NUMBERS
NT STANTON NUMBER
NT STROUHAL NUMBER
Dimensionless results for plane stress creep behavior of thin disks with central rigid inserts under combined loading 03 p0396 A73-14644

DIMENSIONS
NT DEPTH
NT DIAMETERS
NT FILM THICKNESS
NT HEIGHT
NT LENGTH
NT SCALE HEIGHT
NT THICKNESS

DIMERS
Thermodynamic functions and molecular parameters of rhombic dimeric molecules of alkali metal halides 01 p0080 A73-10857
A shocktube study of the combustion of Sheldyne-H with additives. (WSCIPAPER 72-29) 05 p0639 A73-16686
Rotational spectral lines of water vapor dimers in the upper troposphere 13 p1609 A73-29152
Condensation in CO2 free jet expansions. I - Dimer formation. 21 p2743 A73-40937

DIMETHYLHYDRAZINES
Shock tube study of the effect of unsymmetric dimethyl hydrazine on the ignition characteristics of hydrogen-air mixtures. 18 p2372 A73-37098

DIODES
NT AVALANCHE DIODES
NT CESIUM DIODES
NT GERMANIUM DIODES
NT GUNN DIODES
NT JUNCTION DIODES
NT LIGHT EMITTING DIODES
NT PARAMETRIC DIODES
NT PHOTODIODES
NT PLASMA DIODES
NT SCHOTTKY DIODES
NT THERMIONIC DIODES
NT TUNNEL DIODES
NT VARACTOR DIODES

Diode behaviour in an electron-bombardment ion engine. 01 p0090 A73-10112
Negative resistance in metal-semiconductor-metal /MSM/ diodes. 01 p0023 A73-10579
Instability nature in Gunn diode type system with negative differential conductivity, presenting expressions for oscillation threshold and gain 01 p0088 A73-10629
Microwave-power attenuation in Gunn diodes 01 p0025 A73-10979
Series-connected operation of Gunn diodes in a coaxial resonator 01 p0025 A73-10980
Microwave amplifier design based on negative differential mobility in Gunn diodes 02 p0144 A73-11531
Microwave Gunn diode oscillators applications, noting use as Doppler radar and synchronized oscillators 02 p0144 A73-11532
Bidimensional and surface effects in a coplanar-contact Gunn diode 02 p0144 A73-11533
Light-emitting diode and liquid crystal applications to displays, discussing gas discharge plasma, electrophoretic, fluorescent and incandescent devices, electronic wristwatches and calculators 02 p0168 A73-12082
Coupling losses between cylindrical multimode fibers and laser diodes 04 p0458 A73-15321
Exact frequency dependent complex admittance of the MOS diode including surface states, Shockley-Read-Hall /SRH/ impurity effects, and low temperature dopant impurity response. 04 p0427 A73-15347
Wideband microwave device with diode and single component correction circuits Q factors measurement from frequency dependence of input traveling wave coefficients 04 p0429 A73-15927
Critical analysis of Moutaahan-Susskind diffusion theory for magnetron diode electron transport, noting theoretical results discrepancy with experimental data 05 p0556 A73-16064
Purity evaluation of n type GaAs LSA diodes from low-field temperature-dependent mobility. 05 p0556 A73-16435
Effect of ionizing radiation on Gunn diode amplifiers. 05 p0557 A73-16502
Transverse magnetic field effects on n-type GaAs Gunn diodes microwave power, coherence and dynamic I-V characteristics 05 p0558 A73-16784
GaAs Gunn diode LSA operation mode in multiloop circuit to extend high frequency limit 05 p0558 A73-16788
Investigation of surface states in the MOS system by gate controlled diode structure. 05 p0559 A73-17170
The current-voltage characteristics of boron implanted silicon diodes. 06 p0674 A73-17797
A diode model with a current-dependent series resistance 06 p0674 A73-17828
Investigation of regularities characterizing impact ionization within a high-field domain in Gunn diodes 06 p0675 A73-18076
Investigation of static and transient current-voltage characteristics of diodes made of nickel-modified silicon 06 p0676 A73-18248
Use of a semiconductor laser diode as a modulator of gas laser radiation. 06 p0702 A73-18592
Convolution and correlation by nonlinear interaction in a diode-coupled tapped delay line. 06 p0678 A73-18746
Light emitting diode pumped Nd-YAG laser analysis for pumping rate and output dependence on temperature, using circular and transverse intensity distribution 06 p0704 A73-18787
A diode-type shutter tube for ultrahigh-speed photography 06 p0679 A73-18854
Operation, fabrication and structural features of pulsed/CW microwave p-i-n diodes, presenting diode impedance and resistance as function of conduction current 07 p0797 A73-18898
Noise performance of gallium-arsenide and indium-phosphide injection-limited diodes. 07 p0798 A73-19158
Current spreading at contacts to planar Gunn devices. 07 p0799 A73-19343
A scanned light emitting diode display. 07 p0862 A73-19608

Gunn diode effect in n-type GaAs, discussing electron drift velocity relationship to electric field, I-V characteristics and fabrication 08 p0943 A73-20709
Gunn diode characteristics under large and small signal conditions, noting applications for FM oscillators and voltage tuned and magnetically tuned oscillators 08 p0943 A73-20711
The effects of device configuration in the degradation of GaP red light-emitting diodes. 08 p0944 A73-20743
GaAs Schottky-barrier diodes for ultrahigh-frequency communication systems. 08 p0945 A73-20808
Measurement of admittance of Gunn diodes in passive and active regions of bias voltage. 08 p0947 A73-21432
Equivalent circuit of unbent p-PbS point diodes 09 p1061 A73-22022
Doppler signal detection with negative-resistance diode oscillators. 09 p1062 A73-22321
Dynamic operating regime of multistage diode-capacitor storage networks 09 p1063 A73-22459
Thermal limitation for CW output power of a Gunn diode. 09 p1064 A73-23043
The effect of an interfacial layer on minority carrier injection in forward-biased silicon Schottky diodes. 09 p1135 A73-23044
Semiconductor electroluminescent diode displays. 10 p1218 A73-24118
Investigation of the synchronization of Gunn diode oscillators having a stripline resonance system. 12 p1480 A73-27448
Analog voltage squaring circuits with series-connected resistors shunted by semiconductor diodes or ladder network, discussing design, construction and operation principles 12 p1481 A73-27591
Analysis of the operation of a diode phase detector with allowance for the diode recovery time 13 p1591 A73-28866
Study of a read-only optical memory addressed by an array of electroluminescent diodes 14 p1755 A73-29726
Description of the measurement design and the measurement principle in the measurement of the chip impedance of coaxially mounted semiconductor diodes in the microwave range 14 p1733 A73-30058
Phenomenon of negative differential resistance in silicon carbide crystals 14 p1783 A73-30384
Theory of shot noise depression in a modified diode 14 p1597 A73-30943
An analog computer study of a thyristor inverter with opposite-parallel diodes under load switched-on between input throttles 15 p1851 A73-31697
Charge-storage diodes with an internal field in the base 15 p1851 A73-31774
Current-voltage characteristics of multispike diodes operating under conditions of explosive emission of electrons 15 p1852 A73-32315
Prolonged monitoring of experimental equipment with the aid of semiconductor emitters 17 p2133 A73-34152
Gallium phosphide with nitrogen doping from the gas phase 20 p2599 A73-38666
Current and energy characteristics of an electron plasma in a magnetron diode 20 p2536 A73-39254
Ultrahigh-speed unsaturated diode-transistor logic elements with a small logic differential 21 p2660 A73-40013
Analysis of limit cycles in a two-transistor saturable-core parallel inverter. 21 p2662 A73-40339
Threshold, spectral, and output power characteristics of GaAs/Ga_{1-x}Al_x/As single-heterostructure diode lasers. 21 p2713 A73-40462
Diode and ferrite phaser configurations for phased array antenna system, discussing digital and analog versions, driver requirements and design trends 21 p2663 A73-40665
Bias controlled step recovery diode as combined frequency multiplier and analog phase shifter for applications in microwave phased array antenna systems 21 p2663 A73-40668
The theory of the current-voltage characteristic of diodes fabricated out of compensated semiconductors 21 p2663 A73-40795
AM radio receiver diode resonance circuit design for large signal processing, considering FET pinch-off voltage effects and correct circuit parameter selection 21 p2664 A73-41089

- Accuracy of gallium arsenide diode thermometers in the range 4-300 K. 22 p2856 A73-42019
- Pulse burnout of microwave mixer diodes. 22 p2835 A73-42965
- The steady-state and transient performance of some large-scale vortex diodes. 23 p2942 A73-43407
- Digital-computer aided analysis and synthesis of specialized functional diode converter circuits. 23 p2959 A73-43579
- DIOPHANTINE EQUATION**
- Method of trigonometric sums in the metric theory of Diophantine approximations of dependent variables. 13 p1648 A73-28343
- DIOXIDES**
- NT CARBON DIOXIDE
- NT QUARTZ
- NT SILICON DIOXIDE
- DIPHOSPHATES**
- NT ADENOSINE DIPHOSPHATE [ADP]
- Studies on the metabolism of glucose-1,6-diphosphate in human erythrocytes. 21 p2639 A73-41139
- DIPLEXERS**
- Satellite S-band telemetry evanescent mode waveguide diplexer design with foreshortened bandpass filters to eliminate I junction and connecting flanges. 06 p0678 A73-18741
- DIPOLE ANTENNAS**
- The radiation efficiency of a dipole antenna located above an imperfectly conducting ground. 01 p0015 A73-10185
- The extended boundary condition solution of the dipole antenna of revolution. 01 p0016 A73-10186
- Multifrequency excitation of a wire antenna for an invariant radiation pattern. 01 p0023 A73-10190
- Radiation resistance of small electric and magnetic antennas in a cold uniaxial plasma. 01 p0081 A73-10194
- Integral equations for current distribution and input impedances of curved thin symmetrical dipole antenna, noting Q factor of fourth wave antennas. 01 p0017 A73-10216
- The EM field of a dipole transmitter in the two-layer medium air space-magnetoactive ionosphere. 01 p0035 A73-10299
- VLF-ELF radiation characteristics of a 90 degree-phased crossed-dipole array in a cold multicomponent magnetoplasma. 02 p0140 A73-11739
- Electromagnetic near field energy flow characteristics of dipole/monopole receiving rod antenna, investigating frequency dependence of antenna effective area shape. 02 p0145 A73-11824
- Tikhonov conditions of field excitation for dipole antenna radiation study in stratified gyrotropic medium. 02 p0147 A73-12470
- Theoretical analysis and experimental verification for multielement dipole antenna array of unequal parallel conductors, noting impedance characteristics desirable for broadband use. 02 p0148 A73-12853
- Analysis of an asymmetric dipole antenna with displaced feed points. 02 p0148 A73-12856
- Electromagnetic and electroacoustic mode radiation resistance of linear antennas in compressible electron plasma. 02 p0199 A73-12858
- The excitation of resonances by a dipole antenna inside a hollow cylindrical plasma. 03 p0346 A73-13695
- Book on electromagnetic field theory covering free space Maxwell equations, Lorentz force law, vector analysis, Laplace equation, lossless transmission lines and dipole antennas. 03 p0343 A73-13988
- Broad-band isotropic electromagnetic radiation monitor. 03 p0310 A73-14493
- Input resistance of a short dipole antenna in a warm uniaxial plasma. 04 p0429 A73-15480
- Radiation pattern of longitudinal magnetic dipole ideally conducting infinite circular cylinder parallel to infinite plane screen. 04 p0429 A73-15912
- Space wave field produced by a vertical electric dipole above a perfectly conducting sinusoidal ocean surface. 06 p0665 A73-18181
- Dipole antenna coaxially mounted on a conducting cylinder. 06 p0666 A73-18189
- Radiation patterns of linear equidistant fishbone-type dipole antenna array fed by long symmetrical transmission line. 06 p0677 A73-18392

- Calculated pattern of a vertical antenna with a finite radial-wire ground system. 07 p0792 A73-19384 [AD-756789]
- Waves in a hot uniaxial plasma excited by a current source. 07 p0860 A73-20477
- Scattering by perfectly conducting rotational bodies of arbitrary form excited by an obliquely incident plane wave or by a linear antenna. 09 p1052 A73-22959
- A new log-periodic structure with asymmetric dipole elements. 10 p1194 A73-24172
- Effect of edge reflections on the performance of antenna ground screens. 11 p1329 A73-25673
- Radiation properties of a composite-dielectric-rod aerial. 11 p1332 A73-26286
- Planar dipole antenna arrays directivity evaluation from spatial radiation density distribution, considering arbitrary aperture shape and amplitude loading. 12 p1469 A73-27040
- Electromagnetic fields due to dipole antennas over stratified anisotropic media. 12 p1523 A73-27146 [AD-756044]
- Synthesis of a linear antenna in a class of piecewise-constant current-distribution functions. 12 p1479 A73-27228
- A radiating element giving circularly polarized radiation over a large solid angle. 12 p1471 A73-27656
- Dipole antenna radiation in homogeneous plasma layer magnetized by normal uniform magnetic field, calculating radiation pattern. 13 p1583 A73-28661
- Receiving characteristics of antennas in an isotropic compressible plasma. 13 p1594 A73-29230
- Log periodic triangular dipole antenna design and electrical properties, noting improved frequency transition, gain and axial length reduction. 14 p1731 A73-29714
- On linear parasitic array of dipoles with reactive loading. 14 p1734 A73-30203
- Log periodic dipole antenna design procedure, discussing gain as function of transmission line characteristic impedance, half length/dipole radius ratio and geometric parameters. 14 p1734 A73-30206
- On numerical convergence of moment solutions of moderately thick wire antennas using sinusoidal basis functions. 14 p1734 A73-30216
- E-plane synthesis of dipole array antennas. 14 p1735 A73-30223
- Impedance of a short cylindrical dipole antenna in a hot uniaxial plasma. 15 p1845 A73-32237
- Tikhonov conditions of field excitation for dipole antenna radiation study in stratified gyrotropic medium. 15 p1847 A73-32621
- Shadow zone effect of electromagnetic wave propagation in stratified layer with vertical dipole source and square law dependent refractive index profile. 16 p1978 A73-32890
- Coaxial cable fed dipole antenna array for observation of coherent backscatter radar signal from ionospheric electron density irregularities in electrojet region. 16 p1987 A73-33117
- Size-reduced log-periodic dipole array antenna. 16 p1988 A73-33299
- Variation of the antenna radiation pattern during motion of the medium. 17 p2122 A73-34924
- Current distribution of a dipole antenna of revolution in dissipative media. 17 p2141 A73-35366
- Log-periodic dipole arrays - A numerical analysis. 17 p2141 A73-35367
- General theoretical analysis of loop and folded dipole antennas. 17 p2142 A73-35646
- Measurement techniques for antennas in dissipative media. 17 p2143 A73-35685
- Measurement of the radiation patterns of full-scale HF and VHF antennas. 17 p2128 A73-35689
- Measurement of impedance transformation on practical dipoles. 17 p2128 A73-35690
- On the relative response and absolute gain toward the zenith of HF field-expedient antennas - measured with an ionospheric sounder. 17 p2129 A73-35698
- Impedance and far field characteristics of a linear antenna near a conducting cylinder. 19 p2403 A73-37271
- Unidirectional small active antenna. 20 p2525 A73-38742

- Semiconducting ground influence on input impedance and radiation resistance of horizontal magnetic dipoles, covering short wave band for various antenna elevations and conductivity levels. 21 p2661 A73-40203
- Pulsar polarization measurements by multielement interferometer dipole antenna and DKR-1000 cross array radio telescope. 21 p2662 A73-40546
- Phased array element types comparison, discussing dipole and open-ended waveguide radiator designs with emphasis on driving point impedance accuracy and active element pattern. 21 p2663 A73-40649
- Wide-angle impedance matching of phased-array antennas - A survey of theory and practice. 21 p2652 A73-40659
- Straight wire monopole and dipole antenna near field coupling characteristics prediction, deriving mathematical model by method of moments for computerized analysis. 22 p2823 A73-41798
- Near fields of wire antennas by matrix methods. 22 p2830 A73-41827
- Analysis and design of circular antenna arrays by matrix methods. 22 p2830 A73-41828
- A cavity-backed dipole antenna with wide-bandwidth characteristics. 22 p2831 A73-41851
- Observation of extraordinary wave propagation near the lower hybrid resonance frequency. 22 p2895 A73-43023
- Insulated electrically thin dipole antenna with surrounding large wave number isotropic medium, discussing transmission line properties and current and charge distribution. 22 p2829 A73-43183
- Dipole antenna with variable capacitance diodes for wideband tuning, calculating and measuring input impedance frequency response. 23 p2960 A73-44110
- DIPOLE MOMENTS**
- NT ELECTRIC MOMENTS
- NT MAGNETIC MOMENTS
- Microinhomogeneous active medium effects on laser monopulse duration and energy, noting luminescence band random shift and directional diversity in dipole moments. 09 p1097 A73-23083
- On numerical convergence of moment solutions of moderately thick wire antennas using sinusoidal basis functions. 14 p1734 A73-30216
- Bose-Einstein condensation of dipole-active excitons and photons. 16 p2039 A73-34064
- Self consistent field calculations of CO positive ion dipole moment in ground state. 17 p2119 A73-35180
- Apollo 15 and 16 subsatellite magnetometer measurements of the lunar magnetic field. 18 p2349 A73-35944
- Nonradiative motion in a radiative gravitational field. 21 p2742 A73-41631
- Examination of a multiple dipole inverse cardiac generator, based on accurately determined model data. 22 p2813 A73-41961
- Microwave spectrum, structure, dipole moment and low frequency vibrations of dimethyl cyanamide. 24 p3066 A73-44771
- Dipole moment of water from Stark measurements of H₂O, HDO, and D₂O. 24 p3113 A73-44978
- DIPOLARS**
- An analysis of the acoustic power radiated by a point dipole source into a rectangular reverberation chamber. 02 p0194 A73-12603
- Sound directivity pattern radiated from small airfoils. 11 p1345 A73-24980
- Acoustic dipole source strength on flat plate and simple airfoil surfaces from local surface and far field acoustic pressure cross correlation. 11 p1345 A73-24982
- The photoionization cross section of magnesium near threshold. 14 p1776 A73-29699
- Dipole-quadrupole dispersion coefficient calculation for interactions of atomic pairs formed from hydrogen, alkali and rare gas atoms, using perturbation and variation methods. 23 p3007 A73-43522
- DIRAC EQUATION**
- Expansion of nonconjugate differential Dirac operators into a series of eigenvalues over the whole axis, and an analytical expression for a spectral matrix-function. 14 p1771 A73-30787
- Gravitational analogy of electromagnetic Aharonov-Bohm effect, considering massless Dirac equation for

weak gravitational fields arising from mass currents moving between particle beams

22 p2887 A73-42434

DIRECT CURRENT

High efficiency dc-to-dc converter with second non-saturable transformer for eliminating collector current spike to reduce electromagnetic interference and transistor damage

01 p0005 A73-10247

A new program for the dc one-dimensional analysis of semiconductor devices.

01 p0023 A73-10576

Time-averaged power stage models transient and frequency responses characterization and circuit component values derivation for switched dc-dc converters design

03 p0282 A73-13927

Magnetic pulse width modulator and power switch subsystem of switching-mode dc regulator, deriving describing function from transfer functions

03 p0282 A73-13928

Computer-aided design and graphics applied to the study of inductor-energy-storage dc-to-dc electronic power converters.

03 p0252 A73-13931

Switching stepdown dc-to-dc converter with analog signal to discrete interval converter, hybrid micromodule and two-loop control subsystem, discussing circuitry and performance

03 p0283 A73-13935

Reliable uninterrupted controlled transient voltage dc power supplies with active energy storage element, comparing three system configurations, design features and applications

03 p0253 A73-13946

Variation of dc domain threshold in a nematic liquid crystal under continual dynamic scattering.

06 p0739 A73-18794

A switching circuit for a low voltage, medium current dc power supply.

06 p0649 A73-18847

Analog-computer studies on microwave mixing in superconducting weak links.

07 p0863 A73-20103

A dc amplifier operating with a measuring bridge circuit

07 p0803 A73-20540

Direct current and voltage effects on plasma longitudinal oscillations, discussing frequency dependence and waves in semiconductors with ionic lattices

09 p1129 A73-22681

Semiconductor and semi-insulator resistivity measurements using a direct current four point probe apparatus with non-penetrating tips.

10 p1194 A73-24158

Analyses of techniques for measuring DC and AC electric fields in the magnetosphere.

11 p1352 A73-25316

The cause and effects of dc offset voltage in solid state ac power controllers.

17 p2109 A73-32525

Low cost beam current integrator for use with dc accelerators in ion implantation experiments

17 p2175 A73-35759

Electric power cell for producing direct/alternating current and shaft horsepower by direct electrochemical reaction of alkali metals with water

19 p2390 A73-38397

Electrical design requirements for electrolytic capacitors used in regulated low voltage DC power supplies.

21 p2663 A73-40772

Determination of work functions near melting points of refractory metals by using a direct-current arc.

21 p2722 A73-41563

The use of operational amplifiers to generate precise current ratios for platinum resistance thermometry.

22 p2832 A73-42028

DIRECT LIFT CONTROLS

Flight mechanics problems associated with landing approaches using direct lift control, as exemplified by the HFB 320 Hansa aircraft

17 p2100 A73-34496

Problems concerning the implementation of an integrated flight control system, giving particular attention to curved flight path profiles

17 p2208 A73-34498

DIRECT POWER GENERATORS

NT ALKALINE BATTERIES
NT FUEL CELLS
NT HYDROGEN OXYGEN FUEL CELLS
NT MAGNETOHYDRODYNAMIC GENERATORS

NT NICKEL ZINC BATTERIES
NT PHOTOELECTRIC GENERATORS
NT PRIMARY BATTERIES
NT RADIOISOTOPE BATTERIES
NT REGENERATIVE FUEL CELLS
NT SNAP 19
NT SNAP 27
NT SNAP 29
NT SOLAR CELLS
NT THERMIONIC CONVERTERS
NT THERMOELECTRIC GENERATORS

Direct nuclear-to-electric power conversion based on Sr 90 electron emission and collection system, noting spacecraft applications

09 p1119 A73-22828

Radioisotopic energy conversion by radiovoltaic effect, describing titanium-tritium sources and semiconductor converter

09 p1037 A73-23278

A model of a thermophotovoltaic radionuclide battery.

09 p1037 A73-23279

A hybrid motor - A high-speed and accuracy final actuator/automatic control element/.

10 p1177 A73-24025

DIRECTION FINDERS [RADIO]

U RADIO DIRECTION FINDERS

DIRECTIONAL ANTENNAS

NT DIPOLE ANTENNAS
NT HELICAL ANTENNAS
NT HORN ANTENNAS
NT LENS ANTENNAS
NT LOG PERIODIC ANTENNAS
NT LOOP ANTENNAS
NT PARABOLIC ANTENNAS
NT RADAR ANTENNAS
NT SLOT ANTENNAS
NT STEERABLE ANTENNAS
NT TWO REFLECTOR ANTENNAS
NT YAGI ANTENNAS

Antenna synthesis via inverse electrodynamic problem solution for infinite impedance cylinder excited by traveling wave, noting directional antenna with rotating polarization

01 p0017 A73-10217

Results of an experimental investigation of a two-mirror antenna with a modified counter reflector

02 p0146 A73-12019

Target angular characteristics of direction finding antenna in sidelobe region for wideband signals, using single coordinate measurement and amplitude scanning

02 p0146 A73-12023

Maximum likelihood estimate of carrier frequency and arrival direction of radio signals in background noise for large aperture antennas

03 p0278 A73-14081

Reciprocity theorem for antenna directivity pattern measurement of optical superheterodyne receiver for carbon dioxide laser radiation

03 p0284 A73-14084

Two channel multimode feed for circular horn tracking antenna applications, discussing channel patterns, coupling, isolation and frequency response

04 p0428 A73-15417

Annular energy vortex in the near field of a directional antenna

06 p0674 A73-17821

A relationship between the antenna synthesis for a given radiation pattern and the statistical synthesis of systems for spatial signal processing.

07 p0801 A73-20129

Application of equiangular conical antennas with thick leads

08 p0938 A73-20963

A new earth-station antenna for domestic satellite communications.

08 p0947 A73-21144

Some experimental results for a capacitively loaded V antenna.

08 p0939 A73-21431

The concentric double spherical reflector as an antenna for simple scanning over a limited angular range

10 p1187 A73-23739

Computer aided directivity measurements of large antennas in Fresnel zone

10 p1188 A73-24184

Thick walled multilayer wideband radomes for supporting high hydrostatic pressures and protecting weakly directional submarine antennas with circular polarization

11 p1336 A73-25305

Ring arrays as medium- and long-wave broadcast antennas

11 p1336 A73-25318

Mutual coupling, mainlobe reflected power and radiation patterns of periodic antenna arrays thinned by statistically selected element feeds

11 p1332 A73-26205

Zero-steering antenna system for receiving a signal close to the direction of strong interference.

11 p1332 A73-26284

Planar dipole antenna arrays directivity evaluation from spatial radiation density distribution, considering arbitrary aperture shape and amplitude loading

12 p1469 A73-27040

Algorithm for choosing the optimal disposition of radiating elements in a linear antenna array by the method of coordinate trials

12 p1479 A73-27232

Directional antenna formed by a system of two wires lying along the generatrices of a profiled impedance cylinder.

12 p1480 A73-27269

The disc antenna - A possible L-band aircraft antenna.

12 p1471 A73-27655

Satellite tracking interferometer systems with three steerable directional antennas mounted over azimuth mounts near Lichtenau /German Federal Republic/

14 p1742 A73-30100

Finding the approximate angular probability density function of wave arrival by using a directional antenna.

14 p1727 A73-30210

Mean value and variance of the directivity of randomly thinned array antennas

16 p1979 A73-33093

Effect of the amplitude-phase distribution of the field in the aperture of an antenna on its directional properties.

16 p1991 A73-33980

Antenna radiation patterns from statistical phase synthesis of antenna arrays, estimating directivity loss for in- and out-of-phase initial current distribution

17 p2129 A73-35708

Linear antenna directivity loss for fluctuating signal reception, noting effects of signal to noise ratio and antenna length

17 p2129 A73-35709

Contribution to the theory of synthesis of discrete antennas in the case of a uniform approach to a given radiation pattern.

17 p2130 A73-35717

Unidirectional small active antenna.

20 p2525 A73-38742

Lowering of average directive gain caused by cross-polarization radiation in an aperture antenna

20 p2537 A73-39456

Error signal of a scanning antenna with a sum-difference directional pattern

20 p2537 A73-39465

Directional properties of horn-parabolic antennas

21 p2661 A73-40193

Radiation patterns of directional end-on antennas, deriving formulas for side lobe levels and main lobe energy distribution

21 p2661 A73-40198

Beam steering system of the north-south array of the DKR-1000 FIAN radio telescope

21 p2662 A73-40542

Narrow-beam antennas using cylindrical columns of isotropic plasma.

21 p2665 A73-41124

Operation of a variable profile antenna with a plane periscopic reflector

21 p2666 A73-41444

Main-mirror aberrations in a variable-profile antenna and beam scanning by displacement of the primary radiating element

21 p2667 A73-41446

Calculation of the antenna noise temperature in the RATAN-600 radio telescope

21 p2667 A73-41448

Monitoring antenna parameters from radio-astronomical directions

21 p2667 A73-41459

DIRECTIONAL CONTROL

NT THRUST VECTOR CONTROL

Electro-optical multiple transit laser beam deflection system using KDP crystals and quadrupole electrode arrangements

03 p0319 A73-14066

Step input tracking experiment for testing human psychological refractory period, noting directional error correcting reaction time similarities with keyboard tasks

06 p0659 A73-18470

Algorithms for calculating Euler angles of moving objects

20 p2590 A73-39044

Reference indication and setting devices for circular mirror sections of the RATAN-600 radio telescope

21 p2675 A73-41452

Simultaneous statistical treatment of the readings of a directional gyroscope and a magnetic compass

24 p3089 A73-44547

DIRECTIONAL STABILITY

NT GYROSCOPIC STABILITY

Fine pointing performance characteristics of the Orbiting Astronomical Observatory [OAO-3].

20 p2587 A73-38807

Error analysis of a coupled inertial navigation system

22 p2884 A73-42358

DIRECTIVITY

Directivity and bandwidth of single-band and double-band Yagi arrays.

01 p0023 A73-10188

Piezoeactive material constants, vibration mode, radiation directivity and VHF and UHF operation of ultrasonic transducers

03 p0306 A73-12954

Phillips aerodynamic noise theory application to directional patterns of high speed hot jets, discussing convection laws and sound field-turbulence correspondence

06 p0684 A73-17654

The directivities and spectral contents of radiation of multidiode injection lasers.

09 p1097 A73-23049

A simulation of the directivity effect to be expected in hard X-ray flares. 10 p1268 A73-24143

Directivity of high-energy X-ray emission during flares. 10 p1270 A73-24774

Sound directivity pattern radiated from small airfoils. 11 p1345 A73-24980

Error analysis of correlation method for determining directional characteristics /angular power density/ of homogeneous random wave field 11 p1359 A73-25005

Antenna effective area lower limit based on photon limited localizability and Heisenberg uncertainty principle, deriving directivity dependence on area 11 p1338 A73-25672

Directivities of planar arrays with triangular arrangement of elements. 11 p1333 A73-26699

The significance of the elementary radiator directivity for the determination of the directive gain of linear arrays 12 p1468 A73-27039

Planar dipole antenna arrays directivity evaluation from spatial radiation density distribution, considering arbitrary aperture shape and amplitude loading 12 p1469 A73-27040

Series-fed antennas principal beam direction and grating lobes buildup as function of antenna and feed characteristics, considering frequency dependence 12 p1469 A73-27041

Horn-element antenna phase center position calculation for directivity characteristics by power series of radiation patterns 12 p1480 A73-27236

Evaluation of the directivity of gravitational wave radiators. 15 p1914 A73-31944

Mean value and variance of the directivity of randomly thinned array antennas 16 p1979 A73-33093

Radiating near-field power density and directivity reduction of tapered circular apertures. 22 p2829 A73-43181

DIRECTORIES

U INDEXES [DOCUMENTATION]

DIRICHLET PROBLEM

Finite element model for discontinuous potential flow field analysis leading to Dirichlet, Neumann and mixed boundary value problems solution 06 p0644 A73-17514

The finite element method in domains with curved boundaries. 07 p0907 A73-19029

The finite element method with Lagrangian multipliers. 07 p0844 A73-19137

Conducting medium flow in cylinder with nonconducting walls, solving nonlinear elliptic equation /Dirichlet problem/ by projective-iterative method 10 p1256 A73-24509

Equivalent formulations of quasilinear Dirichlet problem driven by positive sources, examining limiting and similarity singular solutions and uniqueness properties 10 p1250 A73-24785

Maximum principle and uniform convergence for the finite element method. 11 p1390 A73-25435

Lame problems in theory of elasticity, discussing reduction to Dirichlet sequence for Laplace equation 11 p1446 A73-26597

Solution in Dirichlet series to a system of linear partial differential equations 12 p1518 A73-27223

Point matching /collocation/ computation of transverse resonances by complex valued solutions of Helmholtz equation with Neumann or Dirichlet problems, applying to electromagnetic waveguides 13 p1581 A73-28076

Approximate solution of the Laplace and Poisson equations in weighted Hoelder spaces 13 p1647 A73-28340

Uniqueness theorems for the Dirichlet boundary value problem in the case of elliptic-parabolic differential equations and lower bounds for the smallest eigenvalue 14 p1767 A73-29765

The asymptotic behavior of the first real eigenvalue of a second order elliptic operator with a small parameter in the highest derivatives. 14 p1769 A73-30457

Single point solutions of Dirichlet boundary value problems by Monte Carlo and successive over-relaxation. 15 p1899 A73-32037

The Dirichlet boundary and initial value problem for hyperbolic differential equations 15 p1901 A73-32369

Rapidly convergent approximations to Dirichlet's problem for semilinear elliptic equations. 15 p1901 A73-32372

The numerical solution of quasilinear elliptic equations. 17 p2199 A73-34103

Variational principle with penalty for finite element solution of model Poisson equation with homogeneous Dirichlet boundary conditions, noting convergence 17 p2199 A73-34209

Simplified proof of error estimates for the least squares method for Dirichlet's problem. 17 p2199 A73-34210

On the iterative solution of Dirichlet problem for some mildly non-linear elliptic equations. 19 p2445 A73-38027

Finite difference approximation of the weak solution of a mildly nonlinear Dirichlet problem. 21 p2725 A73-40379

A priori L sub 2 error estimates for Galerkin approximations to parabolic partial differential equations. 21 p2725 A73-40383

Monograph - Singular perturbation problems for partial differential equations. 22 p2882 A73-42715

The axisymmetric Dirichlet problem of the static theory of elasticity in displacements for a region bounded by cylindrical and spherical surfaces 24 p3146 A73-44604

The Dirichlet and Neumann problems for parabolic equations with a Bessel operator in Dini spaces 24 p3106 A73-45510

DIRIGIBLES

U AIRSHIPS

DISASTERS

International law aspects of catastrophic disaster prohibition in terms of endangering earth environment /resources/ 04 p0522 A73-15137

DISCHARGE COEFFICIENT

Performance and noise generation studies of supersonic air ejectors. 03 p0290 A73-12972

Discharge coefficients for air outflow through a single orifice in the wall of a tube. 03 p0297 A73-14597

Mathematical models for critical flow rates of annular two phase mixtures under various discharge conditions 06 p0688 A73-18563

Long bore thick plate orifices performance in flow velocity measurement at low Reynolds numbers, calculating uncalibrated uncertainty in discharge coefficient 10 p1221 A73-24860

Mathematical models for critical flow rates of annular two phase mixtures under various discharge conditions 16 p2006 A73-33588

Herschel-type venturimeter discharge coefficients at low Reynolds number. 20 p2566 A73-39116

Incompressible flow planar-nozzle discharge coefficient computations for one dimensional inviscid flow, considering nozzle geometry, flow cross sections and turbulence 20 p2548 A73-39526

DISCHARGE TUBES

U GAS DISCHARGE TUBES

DISCOLORATION

Electrodeposited Au on TO-5 headers, discussing discoloration measurement and ultrasonic test for bondability from correlation between optical reflectivity and bond pull strength 19 p2435 A73-38441

DISCONNECT DEVICES

Sea survival after ejection and parachute descent, describing hand operated canopy connector release to free pilot from entanglement or dragging 16 p1974 A73-32665

Single point emergency equipment divestment system for instantaneous parachute harness, lap belt and leg restraint release, describing pyrotechnic actuation system 16 p1966 A73-32666

DISCONNECTORS

U DISCONNECT DEVICES

DISCONTINUITY

NT SHOCK DISCONTINUITY

One-dimensional electrohydrodynamic flows with a variable mobility coefficient - Evaporation and condensation discontinuities 01 p0077 A73-10954

Propagation of the discontinuities of the covariant derivative of the electromagnetic and of the curvature tensor in an electromagnetic and gravitational wave 01 p0079 A73-11261

Discontinuous variational problems in time optimal control of systems describable by ordinary differential equations, deriving Weierstrass optimality conditions 03 p0286 A73-14055

Electromagnetic scattering from a radially moving spherical discontinuity. 06 p0669 A73-18785

Discontinuities propagation in quasi-linear hyperbolic partial differential equation systems, noting MHD flow and crystal optics equations 07 p0850 A73-19016

Estimate of the time of occurrence of discontinuities in the solution of a boundary value problem for a second order quasilinear hyperbolic system. 07 p0844 A73-19023

Discontinuity conditions for two fluid model of liquid helium 2 from total energy and superfluid linear momentum balance and entropy production inequality postulations 07 p0850 A73-19106

Transmission zeros in microstrip discontinuities, considering structure effective width for TEM and higher modes 09 p1049 A73-22315

Operational methods for analysis of discontinuous systems with multiple lumped parameter attachments and concentrated forces, obtaining steady state closed form solutions 09 p1159 A73-22648

Application of the method of Bhatnagar-Gross-Krook-Morse to the Knudsen layer of a polyatomic gas which is solidified or in equilibrium - Expression of discontinuities of wall temperatures 09 p1072 A73-23033

Solvability of the mixed boundary value problem for higher-order parabolic quasi-linear equations with discontinuous and rapidly growing coefficients in the Orlich classes 11 p1392 A73-26599

One-dimensional electrohydrodynamic flows with variable mobility coefficient, evaporation and condensation jumps. 12 p1524 A73-27530

Atomic L2 and L3 vacancy states absolute width from photoelectron spectroscopy, investigating discontinuities, Auger intensity ratio and Coster-Kronig transition probability 13 p1662 A73-28189

Identification of interplanetary tangential and rotational discontinuities. 14 p1796 A73-29958

Interplanetary medium rotational discontinuities polarization, vorticity transport and angular momentum properties, implying solar wind velocity jump from magnetic field transverse perturbation 14 p1796 A73-29961

Stress hybrid model extension to stiffness matrix of element with discontinuous stress distribution, considering transverse shear strains in laminated plate layers 14 p1807 A73-30181

An invariant treatment of interfacial discontinuities in elastic composites. 15 p1954 A73-32121

Fractured solutions in the calculus of variations. 18 p2330 A73-36640

Equivalent filamentary current derivation for bi-static field diffracted by ring singularity based on geometrical theory 22 p2824 A73-41838

Two dimensional microstrip transmission line with step discontinuities, predicting microwave filtering behavior by broadband equivalent circuit for comparison with experiment 22 p2835 A73-42465

Lunar 25 km discontinuity seismically examined, discussing hypotheses with shock metamorphism lack and annealing of shock induced microcracks 24 p3131 A73-44470

Weak invariance conditions and synthesis algorithms for control systems with discontinuities on hypersurfaces in phase space 24 p3074 A73-44666

DISCRETE FUNCTIONS

A discrete numerical approach to fluid dynamics. 01 p0071 A73-11461

High-order necessary conditions of optimality for singular controls of discrete systems 06 p0679 A73-17717

Discrete maximum principle /local cross sections/ method applications to optimal control and mathematical programming 06 p0718 A73-18676

Minimum fuel control solution for linear discrete systems, discussing finite iterative algorithm based on dual problem of functional analysis 07 p0806 A73-20595

A discrete separation principle with a stochastic terminal constraint. 07 p0806 A73-20599

Fourier transformation of two-dimensional signals. I 09 p1119 A73-21899

Approximate solution of certain optimal-control and discrete-programming problems 09 p1068 A73-22561

Discrete Wiener-Hopf equations composed of the Fourier coefficients of piecewise Wiener functions 10 p1243 A73-24459

Maximum principle and uniform convergence for the finite element method. 11 p1390 A73-25435

An algorithmic procedure for determining discrete transfer matrices of controlled plants 12 p1485 A73-27624

- Correlation and indeterminate functions of signals with discrete frequency-time structure, noting linear frequency modulation of signal element
13 p1583 A73-28669
- Basic concepts of the mechanics of discretized bodies with an introduction to discrete element calculus.
14 p1775 A73-30548
- Continuously-discrete method for the construction of control devices
14 p1740 A73-30940
- Corresponding function solutions of discrete mechanics problems based on difference polynomials, applying to Lagrange problem of string natural vibrations for distributed point masses
16 p2035 A73-32680
- Limit cycles resulting from quantization in digital control systems.
17 p2145 A73-35642
- Optimal control of linear systems in the case of continuous and discrete controls
18 p2337 A73-36410
- A continuous-discrete method of design of control devices.
19 p2414 A73-38194
- Conditions of existence of steady representations for discrete linear systems given in terms of unsteady representations
21 p2669 A73-40497
- Russian book on mathematical theory of optimal control of discrete time systems covering multidimensional geometry, convex sets, Pontryagin maximum principle and dynamic programming
21 p2726 A73-40802
- Russian book on R-function method for solving boundary value problems of bending and vibration of thin plates with complex configurations
21 p2787 A73-41250
- Singular integral equations with a Carleman shift in the case of discrete coefficients and investigation of the Noetherian character of a class of linear operators with involution
24 p3105 A73-44425
- DISCRIMINATION**
NT BRIGHTNESS DISCRIMINATION
NT SENSORY DISCRIMINATION
NT TACTILE DISCRIMINATION
NT VISUAL DISCRIMINATION
- DISCRIMINATORS**
System design, breadboard construction and tests of slope reversal video processor based on tapped delay line estimation with timing discriminator
02 p0167 A73-11957
- Frequency discriminator use for range measurements with FM radar systems, deriving reflecting target distance relationship to output voltage
03 p0278 A73-14028
- Application of frequency discrimination technique to the analysis of electroencephalographic signals.
04 p0411 A73-15052
- Fast accurate phase lock loop with self calibrating frequency discriminator, showing dynamic response of frequency lock-up
06 p0675 A73-17843
- Delay-lock discriminator to measure spatial delay time of noiselike signal received by two spaced antennas
09 p1049 A73-22048
- Digital microwave receiver with passive discriminator for precise and instantaneous pulsed RF signal frequency measurement
10 p1188 A73-24168
- Amplitude discriminator with variable effective range design for use with/without digital computer in neuron pulsed activity analysis
10 p1184 A73-24516
- The BD-9 integral discriminator in the circuit of a scintillation-type fast neutron detector
12 p1497 A73-27207
- Characteristics of amplitude discriminators built with transistors operating in the avalanche mode
12 p1479 A73-27209
- Phase discriminator of a nonregulair signal.
12 p1480 A73-27270
- Transient processes in FM discriminators
20 p2537 A73-39458
- Uses of tunnel diodes for zero-transition discrimination in phasometric devices
23 p2959 A73-43477
- Zero-transition discrimination in phase-measuring devices with amplifier-limiters and tunnel diodes
23 p2959 A73-43478
- A phase discriminator with feedbacks
24 p3071 A73-44545
- Analysis of the detection characteristics of frequency discriminators with nonminimum-phase loops
24 p3071 A73-44597
- DISEASED VEGETATION**
U BLIGHT
- DISEASES**
NT AEROSINUSITIS
NT ARTERIOSCLEROSIS
NT ATAXIA
NT CANCER
NT CARBON MONOXIDE POISONING
- NT DIABETES MELLITUS
NT EDEMA
NT ENCEPHALITIS
NT EPILEPSY
NT HEART DISEASES
NT INFARCTION
NT INFECTIOUS DISEASES
NT KIDNEY DISEASES
NT LITHIASIS
NT PARALYSIS
NT PARKINSON DISEASE
NT PULMONARY LESIONS
NT RESPIRATORY DISEASES
NT SMALLPOX
NT TACHYCARDIA
NT THROMBOSIS
NT TOXIC DISEASES
NT TUBERCULOSIS
NT ULCERS
- DISHES**
U PARABOLIC REFLECTORS
- DISILICIDES**
Disilicides solubility in silver and tin melts, discussing ternary phase formation
02 p0181 A73-12367
- Mo disilicide-Ti disilicide system phase diagram based on metallographic, X ray structural and high temperature differential thermal analyses
05 p0587 A73-16846
- DISINFECTANTS**
U ANTISEPTICS
- DISINTEGRATION**
Investigation of the process of the explosive disintegration and simultaneous collision of n gravitating material points
05 p0619 A73-16844
- Explosive disintegration and simultaneous collision of n material gravitating points.
11 p1423 A73-26054
- DISKS**
Plane stress fields in isotropic disks due to singular and distributed loads, obtaining Fredholm integral equation solution via cubic spline function
16 p0209 A73-33238
- Experimental investigation of the development of a cavern in the case of unsteady gas-induced cavitation
22 p2841 A73-42128
- A note on the drag due to steady flow of a conducting fluid past a disk at high Hartmann number.
22 p2894 A73-42475
- DISKS (SHAPES)**
NT ACTUATOR DISKS
NT ROTATING DISKS
- Unsteady temperature and stress distribution in variable thickness disk under convective heat transfer with ambient medium, using approximation method
01 p0113 A73-10021
- Stress concentration in disk with radial slot and with outer boundary subject to arbitrary continuous load, using plane elasticity theory
01 p0117 A73-11095
- Displacement and stress determination in the case of the profile-planar viscoelastic disk
03 p0385 A73-13141
- Disks with inclined face, investigating effects of joint between hub and disk face on stress-strain state in elastic deformation range
03 p0394 A73-14012
- Dimensionless results for plane stress creep behavior of thin disks with central rigid inserts under combined loading
03 p0396 A73-14644
- Magnetohydrodynamic viscous flow induced by an oscillating disk.
06 p0728 A73-17792
- The stress intensity factor of an edge crack in a finite elastic disc.
06 p0762 A73-17989
- Impedance and radiation pattern of antennas above flat discs.
06 p0676 A73-18191
- The stress intensity factors of a radial crack in a point loaded disc.
07 p0918 A73-20567
- Anisotropic model of gravitational radiation enhancement from relativistic disk located in Galactic nucleus
09 p1149 A73-22946
- The disc antenna - A possible L-band aircraft antenna.
12 p1471 A73-27655
- Determining elasticity constants of disc-shaped specimens of material.
13 p1613 A73-28521
- Scattering of electromagnetic waves by a disk positioned at the boundary between two media
15 p1846 A73-32318
- Young elastic modulus determination in steel and alloy disks by contact method
17 p2177 A73-34338
- Disk formation by collapsing rotating gas cloud, considering free turbulence and intermittency effects on gravitational instability
17 p2227 A73-34413
- On the effects of uniform high suction on the rotationally symmetric flow of a conducting liquid near a stationary disc in the presence of a transverse magnetic field.
19 p2469 A73-38186
- Flexibility matrix coefficients for disk loading under sinusoidal edge loading tabulation and derivation to accommodate boundary conditions
21 p2784 A73-40434
- Solution of the mixed boundary value problem of plane elasticity theory with the aid of singular integral equations
21 p2785 A73-40931
- Stress-strain state of disk with internal rectilinear cracks under load, solving Fredholm equations
23 p3039 A73-43468
- Scattering of electromagnetic waves by a disk at the interface between two media.
24 p3067 A73-44624
- DISLOCATIONS [MATERIALS]**
NT CRYSTAL DISLOCATIONS
NT EDGE DISLOCATIONS
NT SCREW DISLOCATIONS
- Fatigue induced microstructural changes in metals and alloys, considering crystal lattice defects, crack formation and propagation, dislocations and strengthening effects
03 p0321 A73-13133
- Dynamic singularity in the continuum theory of dislocations
03 p0343 A73-13775
- The force on a crack deviating from its original plane.
04 p0509 A73-14950
- Dislocation-point defect interactions in fatigued pure aluminum
05 p0588 A73-17231
- A recovery creep model based on dislocation distributions.
08 p0980 A73-21777
- Steel and Ni-based alloys structural stability during long term high temperature creep, noting matrix structure dependence on initial dislocation and interparticle spacing
08 p0980 A73-21780
- Multi-axial and reversing stress effects in dislocation creep - A mechanical equation of states.
08 p0980 A73-21781
- Dislocation distributions during creep and recovery of a 20% Cr-35% Ni steel at 700 deg C.
08 p0981 A73-21784
- Void initiation and growth in Al alloys due to inclusions, presenting dislocation model for ductile fracture strength
09 p1109 A73-23256
- Semiinfinite and finite crack motion models comparison without loading restrictions, considering finite length dislocation pile up role and singular integral equation use
15 p1946 A73-31106
- Two theoretical models of fatigue crack propagation.
16 p2079 A73-33200
- Theory of disclinations. II - Continuous and discrete disclinations in anisotropic elasticity.
17 p2242 A73-34500
- Temperature dependent softening effect due to state transition and electronic drag coefficient for dislocations in pure two band superconductors
18 p2341 A73-36768
- Continuous distributions of dislocations in bonded half spaces.
21 p2742 A73-41666
- Micropolar elasticity solution for static plane boundary value problems in circular ring shaped region, considering Volterra dislocation example
21 p2789 A73-41670
- DISORDERS**
Eigenstate localization parameter calculation for wave functions in one dimensional disordered potential chain, considering extension to coupled oscillators and electromagnetic waves in stratified media
21 p2750 A73-40227
- DISORIENTATION**
Disorienting effects of aircraft catapult launchings.
07 p0785 A73-19480
- Study of Indian naval aircrew experiences and psychic factors in disorientation.
18 p2285 A73-36919
- Aircraft pilot spatial disorientation and illusory perceptual break-off sensations during flight associated with minor vestibular asymmetry
20 p2512 A73-39111
- Inverted posture illusion phenomenon in astronauts during weightless space flight, discussing vestibular organ function, acceleration effects and body gravitation sensing system
20 p2513 A73-39149
- DISPERSING**
A note on the angular dispersion of a fluid line element in isotropic turbulence.
01 p0032 A73-10443

Plane unsteady dispersion of gas behind deflagration wave moved by laser radiation with high flux density

20 p2573 A73-39281

Existence and uniqueness conditions for solid surface vaporization products dispersion into vacuum formulated for equations of motion of ideal gas under variable energy release

20 p2573 A73-39282

DISPERSION

Unsteady heat transfer in dispersion media at small values of time

08 p1021 A73-20994

An optimal algorithm for measuring the dispersion of a random process in the case of separate allowance for the influence of external and internal additive noise

09 p1051 A73-22462

Dispersion relation derivation and approximation applications for generalized optical potential use in analysis of energy dependence of empirical potential strength

14 p1774 A73-30237

Application of a holographic technique to the determination of the dispersity of a two-phase gas/liquid flow

18 p2318 A73-37122

Calculation of the radiative characteristics of polydisperse concentric spheres

20 p2531 A73-39728

DISPERSION PRECIPITATION HARDENING

U PRECIPITATION HARDENING

DISPERSIONS

NT AEROSOLS

NT COLLOIDAL PROPELLANTS

NT COLLOIDS

NT EMULSIONS

NT FOG

NT LIQUID-GAS MIXTURES

NT NUCLEAR EMULSIONS

NT PHOTOGRAPHIC EMULSIONS

NT SMOKE

Investigation of the possibility for ultrasonic dispersion of certain corrosion inhibitors introduced in easily removable film coatings

02 p0184 A73-11643

Obtaining of carbide and nitride dispersions in iron

13 p1633 A73-28182

Influence of oxidizer dispersity on the efficiency of combustion catalyzers

13 p1669 A73-28973

Light beam absorption correlation with axial dispersion of ink injected into turbulent water flow in pipe

17 p2156 A73-35509

Stepwise burning of non-volatile readily dispersible substances

19 p2503 A73-37502

Russian book on nonlinear waves in dispersive media covering unsteady waves, gravity waves in deep water, electromagnetic waves in nonlinear dielectric, etc

21 p2741 A73-41285

DISPLACEMENT

Determination of the strains and displacements for a rectangular shaped viscoelastic body

02 p0229 A73-11578

Structural design via finite element method, noting object discretization, displacement forms and nonlinear problems of deformable body mechanics

02 p0233 A73-11936

Transverse vibrations generated in a bracket bar by the reciprocating linear displacements of its seal which are damped in the course of time

02 p0235 A73-12127

Space-time finite element method for determining dynamic response of continuous media, using Hamilton principle for nodal displacements variations

03 p0389 A73-13320

Amplification of the displacement of Goos-Hanchen by interposition of thin films

03 p0320 A73-14605

Plane time-harmonic wave propagation through periodically arranged composite material, determining displacement mode shapes and dispersion relations by variational method [ASME PAPER 72-WA/APM-10]

04 p0516 A73-15902

Matched asymptotic expansions method application to slender cylindrical beams, calculating displacement far field by Navier-Stokes elasticity equation

07 p0913 A73-20075

Electrical measurement of mechanical forces and displacements, discussing transducers design and measurement standards and units

10 p1215 A73-23633

Shear stresses and displacements of each layer of elastic plate with multiple layers of varying rigidity resting on elastic Winklerian base

11 p1433 A73-25029

Solution of fundamental three-dimensional problems in the theory of elasticity for arbitrarily shaped bodies by way of a numerical realization of the method of integral equations

11 p1441 A73-25627

Russian book on linear truss systems potential strain energy and displacements covering matrix and graph-analytic methods, influence functions, simple and complex strains, etc

11 p1442 A73-25775

Variational principles application to finite element method in elastostatic and elastodynamic and elastodynamic small and finite displacement theories

14 p1806 A73-30178

Derivation of a normal displacement function for the triangular finite element of plates and shells

15 p1945 A73-31032

Determination of the displacement for a membrane stretched over a constant-curvature surface

16 p2076 A73-32935

On the stress analysis of creeping structures subject to variable loading. [ASME PAPER 72-APM-NNN]

17 p2250 A73-35115

On one-dimensional large-displacement finite-strain beam theory.

17 p2252 A73-35828

Thermal stresses in axially connected circular cylinders.

19 p2495 A73-37435

Numerical solutions of basic three-dimensional elasticity theory problems for bodies of arbitrary shape.

19 p2500 A73-38149

Deflection function for the asymmetrical bending of circular plates.

21 p2784 A73-40435

Telecontrol system for particle accelerator target displacement via micromotor electronic control with emphasis on adaptation to ultrahigh vacuum chamber simulating ionospheric plasma

22 p2838 A73-41868

Experimental verification of lower bound K sub Ic values utilizing the equivalent energy concept.

22 p2875 A73-42147

Computer analysis of clamped-clamped and clamped-supported cylindrical shells.

22 p2927 A73-42995

Multiphase incompressible half-space as simplified earth model for investigating surface displacements due to time- and depth-dependent heat sources

23 p2973 A73-43797

Displacements and rotations in micropolar elastic body with external loading and permanent distortions

24 p3149 A73-45004

DISPLACEMENT MEASUREMENT

A linear motion generator for physiological research.

01 p0011 A73-10173

Utilization of electro-optical methods in designing angular- and linear-displacement sensors

01 p0052 A73-11074

Fatigue strength of constructional materials and components of GTD-type compressors under conditions of fretting corrosion.

02 p0181 A73-12217

Displacement and stress determination in the case of the profile-planar viscoelastic disk

03 p0385 A73-13141

Some applications of interferometry in coherent light

05 p0586 A73-17321

Stress analysis of sharply notched plates and measurement of notch tip blunting.

06 p0764 A73-18487

Fast radial displacement of a toroidal plasma by a transverse magnetic field.

06 p0732 A73-18620

A modified sensor of linear accelerations, velocities, and displacements over a path of 0 to 1500 mm

07 p0826 A73-20527

Characteristics of the OT-series transformer-type transducers of linear displacements

07 p0779 A73-20528

Diffraction moire technique illustrated by determination of beam deflections.

08 p1016 A73-20797

Length measurement interferometry principles and limitations imposed by available coherent sources, discussing laser source techniques and fringe counting method

09 p1093 A73-22313

Some investigations on the methods of measuring 3-dimensional plastic deformations by laser.

09 p1086 A73-23321

Self-consistent and direct reading laser homodyne measurement technique.

11 p1360 A73-25063

Comment on: Holographic interferometry applied to measurements of small static displacements of diffusely reflecting surfaces.

11 p1360 A73-25064

Measurement of the critical crack displacement with the help of double-notched specimens

11 p1434 A73-25325

Stress and displacement fields around growing corrosion fatigue crack, discussing intensity factor, plastic zones, cyclic loading and fluid pressure effects

11 p1381 A73-25813

Improvement on moire technique for in-plane deformation measurements.

11 p1365 A73-26241

Interference fringes and surface displacement relationship in holographic interferometry, discussing fringe localization, visibility and interpretation and postrecording techniques

11 p1369 A73-26530

Application of double trigonometric series to the calculation of shell plates of variable thickness

11 p1446 A73-26600

Displacement and finite-strain fields in a sphere subjected to large deformations.

11 p1447 A73-26647

Myocardial contraction velocity and acceleration in man measured by ultrasound echocardiography differentiation.

12 p1461 A73-27026

Brittle fracture initiation characteristics of twin notches.

13 p1700 A73-29469

Measurement of gas quantities by liquid displacement.

14 p1723 A73-30048

Measuring accuracy of three-dimensional displacements in holographic interferometry.

14 p1752 A73-30154

Measurement of small movements and vibrations by laser photography.

16 p2013 A73-32879

Determination of displacements during compression of an oval seal ring

16 p2021 A73-33942

Measurement of the displacement of the electrical axis of an antenna with respect to its geometrical axis by using extraterrestrial radio emission sources

17 p2120 A73-34119

Distortionless recording in double-exposure holographic interferometry.

17 p2173 A73-35430

Diffraction versus holography - A stress analyst's comparison.

17 p2173 A73-35440

Interferometric surface strain measurement with optical strain gage using laser-generated interference pattern with linear fringe motion-intensity relation [SESA PAPER 2158A]

17 p2173 A73-35453

Determination of slope and strain contours by double-exposure shearing interferometry.

17 p2174 A73-35459

[SESA PAPER 2215A] Determination of stiffness and critical loads of a circular plate from a simple bending test.

18 p2362 A73-36327

Method of holography in nondestructive testing.

19 p2432 A73-38359

A system for continuous remote measurements and automatic recording of nonlinear displacements in testing structural materials in the field of reactor emission

20 p2566 A73-39369

Introduction of shear deformations into a thin plate displacement formulation.

22 p2923 A73-42559

Measuring characteristics of the displacement cardiograph.

22 p2815 A73-42676

German monograph on holographic interferometry for displacement and deformation determination of diffusely reflecting bodies covering wave front reconstruction methods and diffraction pattern characteristics

22 p2862 A73-42719

Ultrasonic transducer instrument with broad beam dispersal for blood vessel displacement recording in chronic animal experimentation

22 p2817 A73-43109

Application of holographic subtraction to time-average hologram interferometry of vibrating objects.

22 p2863 A73-43141

Automated data reduction of holographic interferometry translational measurement of diffusely reflecting rigid body by reconstructed virtual image processing on CDC 6600 computer

22 p2863 A73-43147

Speckle effect use in laser photography for vibration and displacement measurement of mechanical systems, discussing diffraction patterns and measurement methods

23 p2982 A73-43675

Elastomechanical model measurements conducted with the aid of holographic approaches in the case of a mirror cell

24 p3090 A73-44897

DISPLAY DEVICES

NT ANEMOMETERS

NT APPROACH INDICATORS

NT HEAD-UP DISPLAYS

NT HOT-FILM ANEMOMETERS

NT HOT-WIRE ANEMOMETERS

NT KINOFORM

NT PLAN POSITION INDICATORS

NT POSITION INDICATORS

NT RADARSCOPES

NT RADIO DIRECTION FINDERS

NT SONIC ANEMOMETERS

NT SPACECRAFT POSITION INDICATORS

NT SPEED INDICATORS

NT TACHOMETERS

Interactive pattern analysis and classification systems - A survey and commentary.

Digital storage of graphs and curves and their representation on visual displays

Computerized multichannel alphanumeric TV system for ATC operational information display, describing data acquisition, processor and software peripherals and video display subsystem

Electromechanical and electronic cockpit displays effectiveness in terms of aircraft control and psychological/physiological factors relating to pilot performance and workload

[DGLR PAPER 72-097]

Comparative simulator studies regarding a contact-analog channel display and conventional instrumentations

[DGLR PAPER 72-100]

Computer based data processing system with display for improving ultrasonic pulse echo NDT test equipment resolution and SNR

Light-emitting diode and liquid crystal applications to displays, discussing gas discharge plasma, electrophoretic, fluorescent and incandescent devices, electronic wristwatches and calculators

Liquid crystal optical and physical characteristics and applications to display design, emphasizing field effect and twisted nematic devices

Linear schlieren photography with concave mirror and variable ultrasonic source for high resolution display of acoustic free field pressure gradient on TV screen

FORTAN subroutine for X-Y plotting and display of two dimensional alphanumeric finite element mesh on line printer

Integrated engine diagnostics and displays for Navy aircraft of the 1980's.

[AIAA PAPER 72-1084]

Analysis of dynamic-excitation conditions for electro-optical-coupling switches in control circuits of electroluminescent panels

Book on passive IR sensing devices design and use in industrial and manufacturing problems solution covering detector types, display devices and reliability analysis

Automated procedures for mapping and display of digitized radar data.

Computer-mediated human communications in an air traffic control environment A preliminary design.

Visual display of fatigue damage by means of exoelectron emission.

An electronic multiband camera film viewer.

Automated navigation system design for DC 10 long range version, emphasizing control display unit interface functions with pilot

Improvements in solid state radiographic converter screens.

Application of graphic display to ultrasonic testing.

Ultrasonic isometric imaging.

Display of HF acoustic holograms utilizing liquid crystals.

A computer-generated display to isolate essential visual cues in landing.

Performance comparisons for joystick and track ball optimized control configurations operating in rate and position modes

Apparatus replicating and extending development work on real-time time-compressed radar observation processor and display system

High resolution radar target recognition, discussing effects of transfer curves of radar signal strength vs display luminance on operator performance

Universal data system for image processing of earth resources observations, discussing input/output film, tape and multispectral data, interactive control and video color displays

Recent advances in low light level field sequential color television.

Display of microwave pulse response via the real-time Fourier transform of the transfer function.

Radar engineering developments, discussing microwave and optical systems, plan position indicators, antennas, displays, receivers, transmitters, solid state IC devices and signal processing

Two-level computer system with main and display processors as scale working model for semiautomatic digital ATC en route control

Automated radar terminal systems [ARTS/.

A scanned light emitting diode display.

Moving radiography for photographic recording and display of transient or cyclic motion, emphasizing application to aircraft gas turbines under dynamic conditions

Test techniques for advanced avionics displays.

Holographic optical element for visual display applications.

Conference on Display Devices, New York, N.Y., October 11, 12, 1972, Conference Record.

Electronic display devices for command, monitoring, surveillance, simulation and training in military applications, considering reliability, cost and performance specifications in procurement decision making

Real time 3-D holographic display, discussing reusable thermoplastic photoconducting recording film and frequency compensation with short laser pulses and acousto-optic modulator

Nucleation film/electron beam recorder - Near-real-time display system.

Comparison of human operator critical tracking task performance with aural and visual displays.

Natural resources information system.

Fine vertically readout accuracy test on film format of each photograph obtained by prime camera, describing aerial photogrammetric data reduction methods

Amorphous semiconductors for switching, memory, and imaging applications.

PRADIS - An advanced programming system for 3-D-display.

Real time display, processing and image-data products production system for supporting Mariner 9 TV experiment, discussing computer algorithms

The image-readout system of the combination photographic and television scanners of the Mars-2 and Mars-3 automatic interplanetary space probes.

Redundant area encoding for relieving integration time requirement in airborne reconnaissance photograph transmission, discussing algorithms, display technique, data reduction and pictorial simulation

Visual display of the spatial distribution of colloidal particle beams.

Computerized interactive graphic display systems for three dimensional shape design

Semiconductor electroluminescent diode displays.

Design of control and display panels using computer algorithms.

Display system for monitoring automatically controlled STOL landing glide paths, discussing computer controlled simulation

Computer executive system for design automation file network creation and monitoring to permit input/output operations, storage information updating and display

Computer generated displays of structures in vibration.

Human factors aspects in aircraft electronic display systems, discussing cathode ray tubes (CRT) and light emitting diodes (LED) applications and characteristics

Real time quantitative display for visible and IR scanning radiometer in ITOS-D satellite-borne automatic picture transmission system with stations access to computers

Cockpit instrument display systems visibility and reliability requirements, discussing various illumination methods in terms of power consumption, cost and human factors engineering

European airbus A300B aircraft flight tests and on-board instrumentation in certification program, illustrating desk layout, control and display panels

Computer graphics applied to production structural analysis.

Digital temperature-measuring device for medical applications

Graphic display for ultrasonic nondestructive testing.

Curved landing approaches under visual and instrument flight conditions, investigating steep glide slope display configurations and flight control modes

Manual vs fully automatic landing concepts, discussing pilots abilities and limitations and primary requirements for displays

Automation of plotting root-locus curves for automatic control systems

Detection of informational constraints related to multi-variate visual displays.

Vertical aircraft flight control and navigation instrumentation avionics developments, emphasizing Inertial-lead Vertical Speed Indicator design and command and advisory information displays

Thick film multilayer IC for electro-optical applications, discussing package techniques, sealing materials, ultrathin printing cold cathode panel and liquid crystal displays

The role of the airborne traffic situation display in future ATC systems.

A data display device for switching and logic elements constructed from single-crystal ferromagnetic materials

A comparison of visual, auditory, and cutaneous tracking displays when divided attention is required to a cross-adaptive loading task.

Application of the visualization of radar information in television

The London Air Traffic Control Centre radar data processing system.

Graphical distribution in colors adapted to traffic control

Electronic integrated flight data displays for pilot workload reduction at takeoff, approach and landing, considering head-up and head-down and colored systems

Instrument-panel electronic display system

A light amplifier display device.

Monitor display to indicate aircraft position relation to desired flight profile during automatically controlled steep landing approaches with curved segments

Considerations concerning the design of an electronic landing display for STOL aircraft

Aircraft wake vortex avoidance system for safety management and capacity optimization in airport operations related to ATC, considering various sensors and display subsystem requirements

Application of advanced control system and display technology to general aviation.

Development of a low-cost flight director system for general aviation.

Visual scene simulation with computer generated images.

Scaled illustration of unit sphere geometry with navigation applications.

V/STOL aircraft pilot-in-loop flight control/display system to overcome pilot limitations with performance and decision making flexibility enhancement

The application of system analysis techniques for the solution of complex helicopter crew station design problems.

Integrated image and symbolic display hierarchy with increasing horizontal and vertical information content for superposition as helicopter aid in approach and precision hovering
[AHS PREPRINT 724] 17 p2168 A73-35065

Low cost data processor and display for ICNI, DME/TACAN, LORAN or range/range difference radio navigation systems in aerospace applications
17 p2210 A73-35213

Liquid crystal approach to integrated programmable digital displays and aircraft control, considering flat panel digital-matrix display
17 p2139 A73-35234

Thin configuration flat digital CRT display with electron beam control improvement for military avionics applications, discussing performance advantages and ownership cost
17 p2139 A73-35235

Digitally integrated cockpit simulation facility for display systems and avionics to plan mission/human program and airborne equipment requirements
17 p2139 A73-35236

Pattern recognition techniques suggested from psychological correlates of a model of the human visual system.
17 p2116 A73-35241

Monte Carlo simulation on CRT display for training and learning system reliability and early decision effects on life cycle cost effectiveness
17 p2140 A73-35261

The application of interactive graphics to the numerical methods used in structural analysis.
17 p2250 A73-35314

A low-cost system for reproducing ERTS imagery.
18 p2315 A73-36018

Pulsed-Doppler velocity isotach displays of storm winds in real time.
18 p2333 A73-36707

Real-time, three-dimensional, visual scene generation with computer generated images.
18 p2291 A73-36831

Optimal feedback control and Kalman filter design via an interactive computing and visual display system.
18 p2295 A73-36839

Validation of digital radar landmass simulation utilizing terrain elevation data compression.
18 p2292 A73-36842

Experimental evaluation of remote manipulator systems.
19 p2416 A73-37305

Sorcerer Apprentice head mounted display with wand for interaction with computer generated synthetic objects, describing creation of illusory three dimensional environment
19 p2397 A73-37323

Terminal pointer hand controller and other recent teleoperator controller concepts - Technology summary and application to earth orbital missions.
19 p2397 A73-37326

Two man crew cockpit design for commercial 737 jet transport aircraft, discussing pilot vision, control and display panels and avionics disposition
19 p2384 A73-37729

United States en route air traffic control systems.
19 p2451 A73-37810

The B.O.A.C. navigation procedures trainer.
19 p2418 A73-37874

ATC enroute automation program using radar tracking and computer readout system, describing terminal traffic control, wake vortices and aircraft spacing
19 p2453 A73-38439

Oakland airport oceanic ATC with input-output display device, describing minicomputer, CRT displays and data link system
19 p2454 A73-38471

Electroluminescent display device of integrated XY structure utilizing GaAlAs and GaAsP
20 p2536 A73-39202

Radiometric terrain mapping at 3 mm wavelength.
20 p2568 A73-39870

Rear projection holographic and interferometric viewing screens using deflected and scattered light, discussing microfilm reading applications, dichromated gelatin film and laser exposures
21 p2699 A73-40151

Diffraction pattern scanning display technique using electron detector in microscope final image, discussing gold particle demonstration, lens configuration, illumination angle and sawtooth currents
21 p2700 A73-40466

An improved light gun tracking algorithm based on a recursive digital filter.
21 p2654 A73-40834

ASCII code applications to alphanumeric display terminals.
21 p2655 A73-40835

A study of the statistical patterns of visual perception of a black and white raster image
21 p2644 A73-40861

The oculometer - A new approach to flight management research.
[AIAA PAPER 73-914] 21 p2702 A73-40862

Sensor data display simulator for airborne target acquisition with improved sensors, using TV scanning of film based imagery
[AIAA PAPER 73-921] 21 p2673 A73-40869

The Large Amplitude Multi-Mode Aerospace Research/LAMAR/Simulator.
[AIAA PAPER 73-922] 21 p2673 A73-40870

A visual display system approach for an advanced spaceflight simulator.
[AIAA PAPER 73-923] 21 p2673 A73-40871

A compound wide angle color visual display system and a high resolution, high sensitivity close circuit color television camera developed for wide angle color visual systems.
[AIAA PAPER 73-925] 21 p2702 A73-40872

Optical mosaics for large field visual simulation display systems.
[AIAA PAPER 73-926] 21 p2673 A73-40873

An approach to computer image generator for visual simulation.
[AIAA PAPER 73-928] 21 p2673 A73-40875

The possibility of using information theory in optics
21 p2740 A73-41100

Image tube systems for ground based and spaceborne astronomical observations, considering self scanning diode array, phosphor screen output devices, electronography, etc
21 p2703 A73-41239

Human recognition of dynamic pattern changes in numerical series displayed on spatiotemporal panels, discussing learning times and reactions to pattern disruptions
22 p2812 A73-41887

Effect of the information panel structure on operator activity
22 p2812 A73-41889

An engineering flight simulation visual display system.
[AIAA PAPER 73-924] 22 p2838 A73-41970

The MINFAP system - First phase in the automation of the EUROCONTROL Maastricht Centre.
22 p2884 A73-42323

Applications of liquid crystals to information display, fault detection, and medical thermography.
22 p2897 A73-42524

Performance and characteristics of smectic liquid crystal storage displays.
22 p2861 A73-42525

A multiplex cathode-ray-tube display with digital readout for a body plethysmograph.
22 p2815 A73-42666

German monograph on display unit nonlinear interpolation approach based on higher order curve for reduced computer storage requirements covering Chebyshev approximation and coordinate transformations
22 p2830 A73-42738

Kinoform production method combining pen-drum plotter with low pass spatial filter converting binary transmittance of precursory mask
22 p2862 A73-43088

Techniques for decreasing power and increasing legibility of electronic watches.
22 p2863 A73-43101

Eye function and the illumination of instrument dials in aircraft
22 p2817 A73-43133

Keeping track of sequential events - Implications for the design of displays.
23 p2948 A73-43215

Direct-display plasma density and temperature meter by the use of Langmuir probe.
23 p3015 A73-44367

National Center for Atmospheric Research utility plotting programs for computer graphics, two and three dimensional fields display and movie generation
24 p3070 A73-45089

DISPLAY SYSTEMS

U DISPLAY DEVICES

DISPOSAL

NT WASTE DISPOSAL

DISSIPATION

NT ENERGY DISSIPATION

NT OHMIC DISSIPATION

Experimental and theoretical investigation of the process of artificial crystallization and dissipation of supercooled clouds
18 p2332 A73-35919

DISSIPATORS

U DISSIPATION

DISSOCIATION

NT AUTOIONIZATION

NT GAS DISSOCIATION

NT PHOTODISSOCIATION

NT THERMAL DISSOCIATION

Doping additions dissociation effect on impurities distribution in grown semiconductor crystals of melts, calculating atomic and molecular concentration
02 p0201 A73-12356

Diatomic molecules dissociation investigation from effective cross section measurement of slow atomic negative ions formation by molecules collisions with fast ions and atoms
08 p0990 A73-21694

Mass spectrometric determination of the dissociation energies of AIC₂, AIZ₂, and AlAuC₂.
09 p1048 A73-23247

Dissociative recombination rate for CH positive ions in interstellar clouds
19 p2490 A73-38531

Dissociation of diatomic molecules. I.
22 p2889 A73-42443

DISSOLUTION

U DISSOLVING

DISSOLVING

A study of the extraction of oxygen from molybdenum by dissolving it in metallic carbon-containing melts in a vacuum
21 p2717 A73-40479

DISSYMMETRY

U ASYMMETRY

DISTANCE

NT DEBYE LENGTH

NT MISS DISTANCE

NT MISSILE RANGES

NT RADAR RANGE

NT RADIO RANGE

NT RANGE AND RANGE RATE TRACKING

NT REENTRY RANGE

Stellar distances, magnitude and mass measurements methods, noting distance to globular clusters and center of Galaxy
07 p0903 A73-20638

Galactic origin, distance and flux estimates of transient X ray sources, rejecting extragalactic and supernova event hypotheses
14 p1788 A73-30732

On the stability of the light-variations of RR Lyrae stars.
15 p1933 A73-31308

Distribution of satellite bodies according to their mean distances in the systems of the sun, Jupiter, Saturn and Uranus
17 p2231 A73-34598

DISTANCE MEASURING EQUIPMENT

NT ALTIMETERS

NT LASER RANGE FINDERS

NT OPTICAL RANGE FINDERS

NT RADIO ALTIMETERS

NT RANGE FINDERS

Rocket stages separation distance measurement by monitoring gamma ray flux variation, noting separation mechanisms and retromotor performances
01 p0052 A73-11166

Future of exclusive measurements of distances
02 p0190 A73-12012

Hyades stellar flux parallaxes for cosmic scale photometric distance determinations and calibration
03 p0372 A73-13248

Detection probability in the case of laser distance measurements involving moving targets
03 p0274 A73-13256

On automatic angle measurements and a proposition of their application into zenith distance measurements on the surface of the moon.
03 p0307 A73-13258

Extension of a portable tactical instrument approach and landing system.
03 p0340 A73-13574

The determination of distance, absorption, probable physical members and age for the open clusters Haffner 8, Haffner 6, Basel 11 and NGC 2374.
05 p0618 A73-16743

Cygnus X-3 radio source - Lower limit on size and upper limit on distance.
05 p0623 A73-17185

Minimum performance standards - Airborne distance measuring equipment (DME) operating within the radio-frequency range of 960-1215 megahertz.
07 p0849 A73-19575

Russian book on onboard distance measuring systems for flight vehicles covering design of cw and pulsed devices, modulators, error analysis, noise, logic elements, etc
07 p0825 A73-20378

Length measurement interferometry principles and limitations imposed by available coherent sources, discussing laser source techniques and fringe counting method
09 p1093 A73-22313

Prototype distance measuring instrument for modulated light beam transit time determination
11 p1367 A73-26308

The redshift-distance relation. IV - The composite nature of N galaxies, their Hubble diagram, and the validity of measured redshifts as distance indicators.
11 p1427 A73-26602

Microwave Landing System under U.S. national development plan for replacing ILS, discussing system requirements and design, precision DME and flare-out guidance
14 p1773 A73-29884

Exclusive distance measurements as substitute to combined distance difference and angular measurements in radio navigation, considering system accuracy and electromagnetic wave transmission
15 p1909 A73-32450

Frequency hopping principle for precision L band DME as complementary aid to microwave landing system

15 p1911 A73-32490

Remote measurement of the thickness, distance and velocity of objects by means of a piezoelectric laser beam deflector.

16 p2023 A73-32877

TACAN based SETAC and L band DME based DLS approach and landing systems for military aircraft, discussing time division multiplexing and antenna array

[DGLR PAPER 73-019] 17 p2208 A73-34493

Plane coordinate transformations for area navigation based on existing VOR/DME network

18 p2336 A73-37043

Doppler landing system based on standard DME for ILS replacement, describing development history and operational principles

19 p2450 A73-37385

Hybrid-inertial navigation with range updates in a relative grid.

[AIAA PAPER 73-873] 20 p2587 A73-38810

Fluidic vortex-type proximity sensor with analog to digital converter, optimizing output nozzle diameter and pressure by steepest ascent method

23 p2981 A73-43431

DISTANCE PERCEPTION U SPACE PERCEPTION DISTILLATION

Use of the fractional-distillation effect to increase the sensitivity of spectral analysis of metallic titanium

24 p3066 A73-45515

DISTORTION

NT FLOW DISTORTION
NT SIGNAL DISTORTION
NT SURFACE DISTORTION

Aerial photograph distortion due to sealed compartment temperature and pressure effects in terms of internal refraction

06 p0693 A73-18156

An analytic expression for the radial photogrammetric distortion of aerial photo cameras

10 p1219 A73-24479

Metric calibration of distortion in aerial mapping cameras, using laser, collimator and diffraction grating generated angularly accurate image points matrix

12 p1501 A73-27970

DISTRIBUTED AMPLIFIERS

A distributed amplifier using bipolar transistors in a common-base circuit

19 p2409 A73-37719

DISTRIBUTED PARAMETER SYSTEMS

Influence of tolerances on printed directional-coupler circuit parameters

15 p1850 A73-31498

A computational scheme used with the epsilon-technique in synthesizing optimal controls.

15 p1853 A73-31625

A distributed parameter model of the inertially loaded human spine.

18 p2281 A73-36429

Generalized Galerkin method for approximate solution of eigenvalue self-adjoint boundary value problems in stability analysis of mechanical distributed parameter systems

19 p2458 A73-37189

Certain methods of determining the dynamic characteristics of stochastic objects

20 p2540 A73-38710

Application of the averaging method to the study of oscillatory systems with distributed parameters and time lag

20 p2592 A73-38978

Series representation of the solution of nonlinear partial differential equations and its use in determining the dynamic characteristics of nonlinear plants with distributed parameters

20 p2581 A73-38986

Flow stabilization by methods of distributed automatic control

20 p2545 A73-39042

Suppression of free convection by a distributed automatic controller

20 p2626 A73-39043

Multiwave interactions in nonlinear distributed systems

20 p2593 A73-39511

The approximation problem in the synthesis of circuits with distributed RC parameters

21 p2670 A73-41128

Russian papers on vibration theory of lumped and distributed systems covering pendulums, virial theorem, electric filters, solids, Fourier series, degrees of freedom and sinusoidal waves

21 p2741 A73-41434

Bilateral estimates of the critical parameters of elastic systems experiencing flutter

22 p2921 A73-42280

Parametric amplification and generation of pulses in nonlinear distributed systems

22 p2826 A73-42333

French monograph - On the representation of linear dynamic systems with distributed parameters and its

application to the study of intrinsic properties of these systems.

22 p2837 A73-42746

Stability circle criteria extended to signal power gain mean-square criteria for nonlinear feedback distributed parameter system defined by transfer function

22 p2837 A73-43066

Optimal discrete-time feedback control of mixed distributed and lumped parameter systems.

22 p2837 A73-43072

Application of finite integral transformations to optimal control problems

23 p2963 A73-43576

L2-stability and L2-instability of linear time-invariant distributed feedback systems perturbed by a small delay in the loop.

23 p2964 A73-43822

Group properties and invariant solutions in the problem of the analytic design of controllers for a process with distributed parameters

24 p3074 A73-44661

Parameter evaluation method for lossy strip transmission lines, assuming microwave propagation in waveguide system with dielectric between two conducting plates

24 p3074 A73-45007

A method for qualitatively studying the oscillations and stability of systems with distributed parameters

24 p3111 A73-45354

DISTRIBUTION [PROPERTY]

NT ANGULAR DISTRIBUTION
NT ANTENNA RADIATION PATTERNS
NT BOLTZMANN DISTRIBUTION

NT CHARGE DISTRIBUTION
NT CURRENT DISTRIBUTION
NT DIFFRACTION PATTERNS

NT ELECTRON DENSITY PROFILES
NT ELECTRON DISTRIBUTION
NT ENERGY DISTRIBUTION

NT FLOW DISTRIBUTION
NT FORCE DISTRIBUTION
NT FREQUENCY DISTRIBUTION

NT HOLE DISTRIBUTION [ELECTRONICS]
NT HOLE DISTRIBUTION [MECHANICS]
NT INTERFERENCE LIFT

NT ION DISTRIBUTION
NT LOAD DISTRIBUTION [FORCES]
NT MASS DISTRIBUTION

NT MOMENT DISTRIBUTION
NT NEUTRON DISTRIBUTION
NT PRESSURE DISTRIBUTION

NT RADIAL DISTRIBUTION
NT RADIATION DISTRIBUTION
NT RAINBOWS

NT SIDELOBES
NT SPATIAL DISTRIBUTION
NT SPECTRAL ENERGY DISTRIBUTION

NT STAR DISTRIBUTION
NT STRESS CONCENTRATION
NT TEMPERATURE DISTRIBUTION

NT VELOCITY DISTRIBUTION
NT VERTICAL DISTRIBUTION

DISTRIBUTION FUNCTIONS

Radiation transfer within spectral line in symmetric isothermal medium, assuming spherical incoherent scattering characteristic and scattering angle-independent redistribution law

01 p0100 A73-10705

Distribution function of atomic level populations in a plasma

02 p0196 A73-11603

Determination of the molecular velocity distribution function in a molecular beam by the method of mechanical selection

02 p0194 A73-11606

Effects of the secular magnetic variation on the distribution function of inner-zone protons.

02 p0155 A73-11731

Free streaming electrons effect on spatial ballistic electron plasma wave echoes response, calculating echo electric fields and electron distribution function

02 p0197 A73-12065

Measurement of electron distribution function in a cesium plasma.

02 p0199 A73-12815

Changes in the distribution function of magnetospheric particles associated with gyroresonant interactions.

03 p0303 A73-13882

Solution of the Boltzmann equation for a fully ionized plasma in an oscillatory electric field and a steady magnetic field. VI - The first velocity moments of distribution function for a homogeneous plasma in a high-frequency electric field.

03 p0349 A73-14650

Distribution functions with fatigue analysis laws and safety predictions, noting life length and fleet assurance models

04 p0507 A73-14710

Statistical linearization of nonlinear single-mass mechanical system for given distribution function of random disturbances, noting amplitude frequency distribution

04 p0475 A73-14977

DISTRIBUTION FUNCTIONS

Partial differential equations with random coefficients and boundary conditions for stochastic processes in plasma, using parabolic equations for distribution function

04 p0479 A73-15037

H emission line shape of plasma radiation under anisotropic electric microfields, calculating field distribution function, dispersion and frequency

04 p0480 A73-15601

Measurement of the electron energy distribution function in a plasma with periodically varying parameters

04 p0481 A73-15615

Ion distribution function in plasma cylinder flow around thin plate in magnetic field under ionospheric conditions

04 p0481 A73-15617

Electron velocity distribution function in the ionosphere

05 p0568 A73-16252

Sphericity distribution function of galaxy-cluster members

05 p0617 A73-16459

Nonlinear damping of potential monochromatic waves in inhomogeneous plasma, obtaining resonance particle distribution function

06 p0728 A73-17967

Shot noise in diodes with a Schottky barrier in the case of a disturbed carrier distribution function

06 p0676 A73-18090

Pressure, temperature, current density and potential difference fluctuations in subsonic flow of combustion products plasma, noting steadiness, ergodicity and distribution functions

06 p0732 A73-18616

Energy distribution functions of kilovolt ions in a modified Penning discharge.

07 p0808 A73-20459

Probability estimates of the accuracy of a solution to the problem of antenna synthesis in the case of an experimental determination of the direct operator of the problem

08 p0946 A73-21104

Evaluation of the norm of the wave-impedance distribution function in the synthesis of an inhomogeneous line for wide-band matching

08 p0946 A73-21105

Iterative method for calculating hot carrier distributions in semiconductors.

08 p0994 A73-21221

Calculation of the moments of the electron spatial distribution function without allowance for ionization losses

08 p1000 A73-21514

Approximation of experimental rheological curves by distribution functions

08 p1019 A73-21592

Electron energy distribution function in CO laser discharge for elastic collisions, noting kinetic equation solution

09 p1089 A73-21914

Propagation of electronic longitudinal modes in a non-Maxwellian plasma.

09 p1126 A73-22278

Ultrarelativistic pulsar plasmas with one dimensional distribution functions in strong magnetic fields, considering dispersion ratios of plasma waves along magnetic lines

09 p1145 A73-22294

Convergence to logarithmic distribution laws

09 p1112 A73-22884

Evaluation of the convergence rate in an integral limit theorem

09 p1112 A73-22885

Weak convergence of stepwise random processes

09 p1112 A73-22886

Optimal self learning classification of point in set for image recognition systems, using proximity functions

09 p1060 A73-22944

The methods of time-variable systems analysis based on new trends in theory of these systems.

10 p1200 A73-24047

Boltzmann transport equation for plasma probe detector characteristics for Maxwellian and non-Maxwellian distribution functions of electrons in dc and ac electric fields

10 p1254 A73-24192

Measurement of electron energy distribution in a plasma with periodically varying parameters.

10 p1254 A73-24205

Ion distribution function in plasma cylinder flow around thin plate in magnetic field under ionospheric conditions

10 p1254 A73-24207

Electrostatic turbulence and ion thermalization in modified Penning discharge, investigating ion heating processes

10 p1251 A73-24259

Recent measurements of flow using nuclear magnetic resonance techniques.

10 p1185 A73-24855

Errors in the velocity-area method of measuring asymmetric flows in circular pipes.

10 p1221 A73-24861

Composite distribution function for absolute magnitudes of uniformly distributed galaxies

11 p1416 A73-25238

Approximation of empirical size distributions of cloud droplets and other aerosol particles

11 p1393 A73-25644

Analysis of the behavior of the electron velocity distribution function of beam interacting with a plasma

12 p1527 A73-26933

Book - Fourier analysis in probability theory.

12 p1517 A73-27051

Strengthening of Liapunov-type estimates / case where the distributions of members are close to the normal distribution/

12 p1517 A73-27190

Dynamics of strongly nonlinear beam-plasma interaction.

[IPPCZ-167]

12 p1529 A73-27434

Estimations for queuing and reliability theory

13 p1649 A73-28796

Derivation of a chain of equations for characteristic functions of a turbulent velocity field from the Hopf equation

14 p1744 A73-30021

A posteriori estimates of error distribution laws in the solution of linear algebraic equations by analog techniques

14 p1768 A73-30032

Electron energy distribution function in CO laser discharge for elastic collisions, noting kinetic equation solution

15 p1886 A73-32640

Book - Non-homogeneous boundary value problems and applications. Volume 3.

17 p2200 A73-34464

Electron energy distribution function validity for nonequilibrium plasma in presence of electric field verified for ionized cesium vapor positive column

17 p2216 A73-34551

On the identifiability of finite mixtures of Laguerre distributions.

18 p2330 A73-36984

Noise source distribution in subsonic jets.

19 p2472 A73-37290

Acceleration of the convergence of functions related to the orientation of a Brownian particle in a laminar flow

19 p2419 A73-37536

Integral transport equations for component distribution function of gas mixture with internal degrees of freedom and chemical reactions

19 p2463 A73-37847

The electron kinetics of a weakly ionized Lorentz plasma in arbitrarily oriented external electric and magnetic fields

20 p2596 A73-39192

Energy distribution functions of kilovolt ions in a modified Penning discharge.

20 p2597 A73-39197

Rate of convergence of the distribution of the maximum of successive sums of independent variously distributed random vectors toward the limiting law

20 p2583 A73-39476

Monte Carlo technique investigation of subclass number effects in nonoptimum parametric maximum likelihood classification procedure, defining distribution functions of representative subclasses

20 p2559 A73-39878

Green function hydrodynamic asymptotic behavior obtained via closed inhomogeneous linear equations, discussing distribution function kinetic equation, correlation function spectral distribution and adiabatic conditions

21 p2677 A73-40636

Asteroidal dust population model coinciding with spatial density demonstrating distribution below astrodynamical mass limit and larger time for distribution function extrapolation

21 p2776 A73-41422

Continuous distributions of dislocations in bonded half spaces.

21 p2742 A73-41666

Variation of electron velocity distribution function in the beam-plasma interaction.

22 p2891 A73-42267

Gaskinetic treatment of the Rayleigh problem in the case of moderately to greatly diluted gases

22 p2843 A73-42529

Concentration functions of finite-dimensional and infinite-dimensional random vectors

22 p2882 A73-42649

Frequency distribution functions of pulsars, supernovae and sunspot groups relationship to age and lifetime, considering stellar mass and initial luminosity

22 p2915 A73-43033

Higher order Compton-Getting anisotropies in particle population distribution function of low energy solar protons in interplanetary space

23 p3024 A73-43698

Gasdynamic equations for low temperature monatomic gas, showing Wigner distribution function independence of density gradient in agreement with nonequilibrium statistical thermodynamics concepts

23 p2939 A73-43704

Distribution function of relativistic electrons in a strong magnetic field.

23 p3011 A73-43753

Steady state exponential distribution function of outer radiation belt low energy protons in terms of adiabatic invariants

24 p3124 A73-44807

DISTRIBUTION MOMENTS

NT MEAN

NT STANDARD DEVIATION

NT VARIANCE (STATISTICS)

Calculation of the moments of the electron spatial distribution function without allowance for ionization losses

08 p1000 A73-21514

Choosing the optimal distribution of radar and optical observations of Venus

09 p1142 A73-22091

Liquid droplet and ice particle distribution in spatially homogeneous mixed clouds, solving kinetic coagulation equations via distribution function moments

21 p2730 A73-40119

DISTURBANCE THEORY

U PERTURBATION THEORY

DISTURBING FUNCTIONS

Circular orbit stability in restricted two body problem with secular variations, giving disturbing function secular terms to eighth order

02 p0222 A73-12710

A numerical investigation of secular terms of the planetary disturbing function.

03 p0372 A73-13351

Expansions of the derivatives of the disturbing function in planetary problems.

03 p0377 A73-14272

Solution of an inhomogeneous boundary value problem with continuous discrete parameters in the presence of discrete disturbances

04 p0470 A73-14934

Disturbing functions application to secular perturbation calculation for periodic comets with validity for any eccentricity and inclination

14 p1790 A73-29787

Basic theory for PROD, a program for computing the development of satellite orbits.

15 p1930 A73-31108

Synthesis of optimal discrete control systems with persisting perturbations

15 p1854 A73-31803

Determination of disturbances acting on a space vehicle from the liquid-disposal nozzle

21 p2781 A73-41199

Phase plane analysis of the commensurable restricted three-body problem.

22 p2912 A73-42942

Problem of synthesizing a control system in the case of a plant involving random jerky forces

23 p2963 A73-43577

Synthesis of optimal sampled-data control systems in the presence of continuous disturbances.

23 p2965 A73-44332

DISULFIDES

NT CARBON DISULFIDE

The additive action of some organic chlorides and sulfides in the four-ball lubricant test. [ASLE PREPRINT 72LC-3C-2]

03 p0316 A73-14357

Frictional behaviour of molybdenum disulfide in high vacuum.

04 p0454 A73-14997

A study on some metal-base self-lubricating composites containing tungsten disulfide. [ASLE PREPRINT 73AM-3C-1]

17 p2196 A73-34986

DITCHING (LANDING)

Multiple occupant flotation devices for commercial transport aircraft survivors sea ditching, discussing slide/raft design improvement for high density loading

16 p1974 A73-32658

Ventilated wet suit for naval aircrews protection against water exposure in aircraft accidents, describing neoprene foam and nylon liner construction with air ventilation

16 p1974 A73-32672

DITHERS

Frequency-agile coaxial magnetrons.

12 p1477 A73-26925

DIURESIS

The effect of prolonged immobilization on diuresis and water intake in rats.

01 p1320 A73-26489

Water and salt metabolism in hypokinesia-subjected animals

12 p1462 A73-27704

DIURNAL RHYTHMS

U CIRCADIAN RHYTHMS

DIURNAL VARIATIONS

6300 A night airglow emission over the magnetic equator.

01 p0036 A73-10344

Research of the emission at 5577 A in the period of 1958-1967 in Ashkhabad.

01 p0036 A73-10345

Natural variation of the radiation budget of the earth-atmosphere system as measured from satellites.

01 p0038 A73-10390

Nongray theory for temperature wave propagation without turbulent or convective motions, discussing diurnal waves simulation for planetary atmospheres

01 p0039 A73-10396

Transient variation of martian ground-atmosphere thermal boundary layer structure.

01 p0097 A73-10400

Ion composition and photochemistry of the E-region.

01 p0042 A73-10892

Comparative study of monthly and diurnal occurrences of whistlers and gyroelectric echoes in conjugate regions of Europe and South Africa

01 p0043 A73-11274

Studies of the lower ionosphere by means of VLF propagation over long distances

01 p0044 A73-11515

Diurnal latitudinal composition variations in light ion trough fromOGO mass spectrometric observations, noting magnetic storm effects

02 p0157 A73-11904

A sub-class of pi 1 micropulsations associated with the diurnal transit of the neutral sheet.

02 p0158 A73-11908

Diurnal effects in pc 1 hydromagnetic whistlers - An early afternoon source model.

02 p0158 A73-11909

The diurnal variations of hydrogen and oxygen constituents in the mesosphere and lower thermosphere.

02 p0158 A73-12026

Diurnal variation of the exospheric temperatures on Venus and Mars.

02 p0214 A73-12253

Turbopause effect on latitudinal diurnal variation of upper atmosphere neutral species, using turbulent diffusion coefficients and photochemical transport theory

02 p0161 A73-12278

Theoretical model of diurnal variations of the equatorial thermosphere at equinox.

02 p0162 A73-12290

Interaction between gravity waves and ionization in the ionospheric F region.

02 p0162 A73-12298

Characteristics of quiet as well as enhanced diurnal anisotropy of cosmic radiation.

03 p0360 A73-12876

The use of Faraday rotation measurements on geostationary satellites.

03 p0300 A73-13635

Diurnal and latitudinal variations and frequency dependence of scintillation due to ionospheric irregularities, using rms electron density fluctuation and transverse scale size model

03 p0275 A73-13643

A proposed ionospheric disturbance index.

03 p0300 A73-13651

Recent satellite measurements of the morphology and dynamics of the plasmasphere.

03 p0301 A73-13709

Inferring the interplanetary magnetic field by observing the polar geomagnetic field. [AD-755684]

03 p0373 A73-13712

Magnetospheric thermal plasma and hydrogen cation density profile characteristics in different local time regions explained by time-varying convection model

03 p0303 A73-13879

Local time variations of X ray substorm activity observed at auroral zone station, including atmospheric passage and energy spectrum measurements

03 p0363 A73-13889

Equatorial scintillation diurnal and seasonal variations and F region electron density irregularities, noting unusual post sunset behavior of Faraday rotation angle [AD-757291]

04 p0440 A73-14951

The residual cosmic ray modulation at the 1954 solar minimum.

04 p0492 A73-14968

VLF wave propagation properties in waveguide formed by ground and ionospheric shell, noting diurnal phase and amplitude anomalies due to ionospheric disturbances

04 p0416 A73-15060

Solar cycle control of the ionospheric E-region.

04 p0441 A73-15291

Two layer model for diurnal temperature variations analysis of radiative heat transfer between planetary lower atmosphere and underlying

04 p0473 A73-15574

Diurnal variation of the effective earth's radius factor /k/ over India and its influence on microwave propagation.

04 p0423 A73-15599

Diurnal variation of the effective earth's radius factor /k/ over India and its influence on microwave propagation.

04 p0423 A73-15928

Anomalous recurrent diurnal anisotropy in cosmic ray intensity with maximum along the garden hose direction. 05 p0608 A73-16142

Altitude variations of the sporadic E layer at geographical mid-latitudes 05 p0568 A73-16217

Diurnal and annual behavior of the radiation balance 05 p0609 A73-16218

Diurnal variability of temperature and of isobaric surface heights in the troposphere and lower stratosphere 05 p0593 A73-16241

Lunisolar tidal effects and motions in the F region 05 p0568 A73-16255

Temperature fluctuations in the ionospheric F region 05 p0568 A73-16256

Variations of cosmic ray intensity in consequence of the corotation effect. 05 p0609 A73-16371

VLF field diurnal variations and terminator crossing effect on signal path during transmission in earth-ionosphere waveguide 05 p0549 A73-16393

Rapid variations of Psi Per shell star H beta line, indicating shell and stellar atmosphere activity 05 p0617 A73-16466

Diurnal and seasonal variations in conditions for the occurrence of the F 1 layer over Middle Asia during the IQSY period 05 p0569 A73-16615

Theory of diurnal fluctuations of the earth's magnetic tail 05 p0620 A73-17011

Fluctuations of the ion concentration level in the terrestrial ionosphere at altitudes from 200 to 1300 km 05 p0570 A73-17012

E layer ionization diurnal exponent independence of seasons and station latitude ascertained by statistical tests 05 p0571 A73-17058

Analysis of the meteor wind data. 05 p0622 A73-17167

3C 120, BL Lacertae, and OJ 287 - Coordinated optical, infrared, and radio observations of intraday variability. 05 p0625 A73-17342

Diurnal amplitude variations of equatorial electrojet intensity as functions of solar activity, using 1958 South American observatory data 06 p0690 A73-17556

Seasonal variations in the solar and lunar daily geomagnetic variations. 07 p0813 A73-19024

Geomagnetic activity semiannual and diurnal variations due to interplanetary field southward component interaction with magnetosphere based on model ordered in solar equatorial coordinates 07 p0813 A73-19234

Thermosphere kinetic temperature diurnal variation from heat conduction equation periodic solution, determining heat sources from solar radiation atmospheric absorption 07 p0815 A73-19440

Solar proton flare prediction, examining diurnal rotation of axis connecting two stable spots and change in horizontal gradient of spots magnetic field 07 p0870 A73-19449

Lower ionospheric seasonal anomaly in electron density levels, noting diurnal and latitudinal characteristics at various heights 07 p0816 A73-19453

Auroral sporadic E layer diurnal distribution correlation to charged particle integral flux diurnal variations observed by satellite in winter, noting Kp index effect 07 p0816 A73-19455

Earth electrical conductivity radial distribution effect on solar quiet day geomagnetic field variations 07 p0816 A73-19466

Scattered twilight light variations at 5500 to 6600-A wavelengths according to spectral observations in 1962 through 1968 at Abastumani 07 p0817 A73-19587

Relationships between the equatorial electrojet and polar magnetic variations. 07 p0818 A73-19662

Geomagnetic variations with the period of a sidereal day. 07 p0818 A73-19672

Some characteristics of the ionospheric irregularities over the magnetic equator derived from spaced fading records. 08 p0957 A73-20656

Heating of the upper atmosphere during aurorae and auroral rays length. 08 p0957 A73-20663

Equivalent gravity wave mode approximation for main solar diurnal tide in rotating spherical dissipative atmosphere modeled by Newtonian cooling and Rayleigh friction 08 p0958 A73-20959

Equatorial sporadic E and cross-field instability. 08 p0958 A73-21150

Ion composition and photochemistry of the E region 08 p0958 A73-21282

Diurnal temperature variations in the thermosphere with solar activity 08 p0959 A73-21288

Magnetic storm of March 8-10, 1970 from Cosmos-321 and ground observations. I - Morphology of the disturbance 08 p0959 A73-21290

Diurnal, sporadic and yearly variations in cosmic ray flux based on neutron component data, noting relation to solar activity cycles 08 p1000 A73-21345

An analytical and numerical study of the Martian planetary boundary layer over slopes. 08 p1011 A73-21381

Summary of daily observational results of solar phenomena, cosmic ray, geomagnetic variation, ionosphere, radio wave propagation and airglow during October 1969 through December 1971. 08 p0961 A73-21393

Neutral thermosphere temperatures from density scale height measurements. 09 p1074 A73-22063

Phase and amplitude variations of 40-kHz radio waves propagating over a 7.1-Mm path. 09 p1049 A73-22134

A new look at the Martian 'violet haze' problem. II - 'Blue clearing' in 1969. 09 p1145 A73-22275

Effect of geomagnetic activity on occurrence of whistler atmospherics. 09 p1077 A73-22373

Drive and performance modification following multiple /light-light/ shifts in the photoperiod. 09 p1039 A73-22528

Catalog of geomagnetic activity indices for the years 1841-1864 and 1870 09 p1077 A73-22543

Ion composition in the E- and lower F-region above Kiruna during sunset and sunrise. 09 p1078 A73-22838

Cosmic-ray anisotropy during the disturbed period from Oct. 25 to Nov. 10, 1968 10 p1267 A73-23919

The diurnal wind variation in the lowest 1500 ft in central Oklahoma - June 1966-May 1967. 10 p1245 A73-23987

Solar cosmic ray anisotropy 27-day variations during IGY from global network stations neutron component data 10 p1268 A73-24237

Solar quiet long-term modulation of cosmic ray intensity diurnal variation explained via interplanetary sector pattern changes 10 p1269 A73-24448

Prenoon anomaly of ionization in the F region at the transition latitudes 11 p1350 A73-25090

Diurnal variations in electron density at heights of 160 to 200 km and electron temperature variations 11 p1351 A73-25095

The diurnal and semidiurnal barometric oscillations, global distribution and annual variation. 11 p1351 A73-25167

Measurement of the transparency of the atmospheric ground layer at different wavelengths 11 p1363 A73-25612

A two-component model of the diurnal variations in the thermospheric composition. 11 p1354 A73-25758

Anomalous diurnal changes of transequatorial VLF radio waves. 11 p1330 A73-25760

Measurement of point-discharge current density in the atmosphere. 11 p1354 A73-25767

Hourly and daily variations of H values for sunspot minimum, showing uncorrelated night time level departures and range implications for solar flares 11 p1355 A73-25772

A possible current system associated with the Sq variation. 11 p1356 A73-25910

A theoretical study of the ionospheric F region equatorial anomaly. I - Theory. II - Results in the American and Asian sectors. 11 p1356 A73-25919

Physical interpretation of the diurnal behavior of the TM and TE components of VLF fields in the far zone 11 p1331 A73-26152

Diurnal, seasonal and solar cycle changes in southern midlatitude ionosphere electron content from June 1965-August 1971 11 p1359 A73-26712

Results of ship-borne ionospheric absorption measurements on the North Atlantic during winter. 11 p1359 A73-26713

Seasonal and diurnal variations of forbidden oxygen and sodium lines emission, stressing nightglow zenith intensity fluctuations connection to F layer electric fields 12 p1489 A73-26992

Daily variation of geomagnetic field at the Indian stations under the electrojet during the period of the July 1966 proton flare. 12 p1534 A73-26998

Investigation of the phase variation of a NWC signal /22.3 kHz/ along a transequatorial path 12 p1469 A73-27339

Auroral atmosphere temperature variations relation to naturally auroral streamer length variations, assuming ionospheric current dissipation as heat source 12 p1491 A73-27344

Temperature variations in the upper atmosphere during a period of minimum solar activity from topside ionospheric sounding data 12 p1491 A73-27346

Day-to-day variability of the quiet-day solar-diurnal variations and the orientation of the interplanetary magnetic field 12 p1540 A73-27358

Diurnal thermospheric heat budget in terms of electron-ion recombination, photodissociation and neutral wind energy transfer and conductive and radiative cooling 12 p1492 A73-27604

Diurnal atomic hydrogen variation at exospheric temperatures as function of thermal ion and proton charge exchange with plasmasphere 12 p1492 A73-27612

Bactericidal activity of the integument of man at different times of the day 12 p1463 A73-27716

Daily altitude variations of medium frequency radio waves reflection in ionosphere over Tsamab, SW Africa, examining attenuation correlation with solar zenith angle 12 p1494 A73-27767

Diurnal tropopause maps divergence from average tropopause altitude profile, commenting on Eole experiment 13 p1605 A73-28073

On the comparison of diurnal nutation derived from separate series of latitude and time observations. 13 p1679 A73-28402

Diurnal variation of nightglow Na emission, noting linear intensity variation with time, oscillatory and anticovariation characteristics 13 p1610 A73-29337

Determination of coefficients of vertical diffusion between 0 and 100 m with the help of radon and of ThB 13 p1655 A73-29342

Daily variations of the characteristics of beating-type Pc3 /Bpc3/ pulsations. 13 p1611 A73-29661

Slow variations of pulsar intensities. 14 p1802 A73-30750

Anisotropy parameters of the ionospheric irregularities at Thumba during high solar activity period. 14 p1750 A73-30905

Diurnal variations of H-alpha nightglow emission intensity 15 p1867 A73-31261

Numerical study of the seasonal variations of the ionosphere. 15 p1867 A73-31381

Diurnal variations of the vertical component of the magnetic field in high latitude regions as a function of the east-west component of the interplanetary magnetic field 15 p1868 A73-31570

Equatorial Esq disappearance relationship to daily magnetic Sr variation inverted latitudinal profiles during magnetic quiet periods, considering counter electrojet current belt hypothesis 15 p1869 A73-31757

The field levels near midnight at low and equatorial geomagnetic stations. 15 p1869 A73-31758

The relationship between the structure of the equatorial anomaly and the strength of the equatorial electrojet. 15 p1869 A73-31761

POGO satellite observed electrojet signature data comparison with daily geomagnetic variation amplitude measurement at equatorial ground station in India 15 p1870 A73-31769

Earth deflections of vertical due to luni-solar gravitation changes determined by astronomical observation with Herstonmouex photographic zenith tube, noting semidiurnal tidal effects 15 p1937 A73-31779

Comparison of true and effective altitudes of the sporadic E layer 15 p1872 A73-31899

Study of traveling ionospheric perturbations 15 p1872 A73-31901

French monograph - Experimental study of conditions of resonance of tubes of forces of the terrestrial magnetic field. 15 p1874 A73-32594

Diurnal amplitude variations of equatorial electrojet intensity as functions of solar activity, using 1958 South American observatory data 16 p2002 A73-32780

Industrial work rhythm and between-day fluctuation studies 1920-1969, emphasizing industrial record and between-day fluctuations

16 p1975 A73-33160

Steady-state solar modulation of cosmic rays.

16 p2055 A73-33296

Geomagnetic effects on cosmic ray cut-off daily, seasonal and secular variations, considering north-south symmetry and magnetospheric models

16 p2055 A73-33297

Sky brightness observation of post-dusk effect in Spanish Sierra Nevada for relationship to predawn enhancement, noting insufficient evidence for quantitative analysis

16 p2008 A73-33880

Enhancements of the electron concentration in the F2-layer at magnetic noon.

16 p2010 A73-33914

Analysis of the parameters of solar-heat power sources with energy storage units

17 p2108 A73-34283

Diurnal, annual and solar cycle variations of hydroxyl and sodium nightglow intensities in the Europe-Africa sector.

17 p2160 A73-34785

A study of the time lag of the 27-day variation in the thermospheric density.

18 p2303 A73-35961

Latitudinal and temporal variability of temperature in the lower thermosphere.

18 p2304 A73-35991

Meteor radar study of tides in the 80 to 100 km altitude range.

18 p2305 A73-35999

The southern boundary region of the winter anomaly in ionospheric absorption in winter 1971/72 observed on board the cargo vessel 'Hanau' of Hapag-Lloyd moving between 10 deg and 55 deg N.

18 p2305 A73-36002

Some results obtained from the European Cooperation concerning studies of the winter anomaly in ionospheric absorption.

18 p2305 A73-36004

Electron-density profiles obtained from MF sounding at Tsunemb.

18 p2306 A73-36012

A study of the diurnal variation in the thermosphere as derived by satellite drag.

18 p2309 A73-36059

A model of formation of the mean diurnal state of the upper atmosphere and its diurnal variations.

18 p2311 A73-36147

Lunar tidal oscillations in the horizontal ionospheric drift at the Equator.

18 p2311 A73-36177

Diurnal and annual temperature variations in the 30-60 km region as indicated by statistical analysis of rocketsonde temperature data.

19 p2424 A73-37662

Ion composition and photochemistry of the E-region.

19 p2424 A73-37911

Variations in the temperature of the thermosphere in the course of the day and with solar activity.

19 p2424 A73-37917

Magnetic storm of March 8-10, 1970, according to ground-based and Kosmos-321 observations.

19 p2424 A73-37919

Photometric measurements of zenith night sky over Fritz Peak /CO/ for diurnal and seasonal variation of nightglow continuum

19 p2425 A73-38013

Ducted propagation of low-latitude whistlers deduced from simultaneous observations at multi-stations.

19 p2404 A73-38019

Density measurements in the equatorial atmosphere by means of the San Marco 3 satellite

19 p2426 A73-38151

Patterns of diurnal variation in the intraocular pressure of airline pilots.

20 p2512 A73-39107

Latitude distribution of the regularity in F2-region irregularities.

20 p2553 A73-39132

Statistical characteristics of the diurnal drift velocity variations in the F2 layer

20 p2554 A73-39160

Diurnal variations in the drift velocity and direction of the ionization inhomogeneities in the F layer

20 p2554 A73-39161

Effective altitudes of the F region in the IGY and IQSY periods

20 p2554 A73-39167

Latitudinal distribution change in the conditions for F1 layer occurrence from the solar-activity maximum to minimum

20 p2554 A73-39170

Midlatitude ionospheric disturbances

20 p2554 A73-39172

Stratifications in the F region of the ionosphere

20 p2554 A73-39174

Visual responsiveness repeat variability magnitude during prolonged sessions and time of day

20 p2513 A73-39479

Mesospheric ozone concentration night and day variations comparison, describing microwave radiometer and remote sensing and photochemical theories

20 p2557 A73-39857

Atomic oxygen and helium concentrations variation at 120 km in thermospheric composition models, discussing association with geomagnetic activity

21 p2679 A73-40074

Statistical analysis of daily, monthly, annual and seasonal activity of earth currents field, presenting tables of storms and disturbances

21 p2681 A73-40107

The nature of the polarization of geomagnetic micropulsations of Pi 2 type

21 p2681 A73-40108

The question of the method of studying cosmic ray anisotropy

21 p2755 A73-40111

Frequency distribution of the parameters of the diurnal variation of the cosmic ray intensity

21 p2755 A73-40112

Counter equatorial electrojet currents in the Indian zone.

21 p2682 A73-40162

On the diurnal variations of total mass density, number density and temperature in the upper thermosphere.

21 p2682 A73-40170

Topside ionospheric winter and summer diurnal electron density variations in Arctic regions as function of universal time, showing Ariel 3 measurements graphically

21 p2682 A73-40171

Criticism of Gribbin and Plagemann findings on universal time observations as evidence of day length and earth rotation rate changes due to 1972 solar storm

21 p2766 A73-40375

Diurnal, semidiurnal, and the eight-hour components of cosmic-ray anisotropy

21 p2758 A73-40601

Estimate of the spectrum of cosmic-ray variations in the high-energy range on the basis of subterranean observations

21 p2758 A73-40602

Axial symmetry of the magnetosphere and the noon recovery of polar cap absorption

21 p2759 A73-40608

Atmospheric structure and its variations in the region from 25 to 120 km.

21 p2683 A73-40628

Exospheric and thermospheric structure variations with solar activity, diurnal variation, geomagnetic activity, seasonal-latitudinal variations of He, H and density waves

21 p2683 A73-40630

Upper atmospheric models dealing with diurnal variation and latitudinal density dependence to derive time and space dependencies

21 p2683 A73-40631

Diurnal density variations measured by the San Marco III satellite in equatorial orbit.

21 p2685 A73-40830

Characteristic features of the solar diurnal variation according to data obtained by magnetic observatories in Kazakhstan

21 p2686 A73-40846

Equatorial thermospheric composition and its variations.

21 p2688 A73-41347

Thermospheric structural parameter diurnal variations from satellite orbit decay, rocket measurements of vertical temperature distribution and atmospheric component concentrations and incoherent scatter observations

21 p2688 A73-41348

Thermospheric density diurnal and seasonal variations from cosmos drag data, discussing amplitude, density distribution, coefficients of expansion, summer solstice spherical functions

21 p2689 A73-41351

Structure of the neutral atmosphere between 150 and 500 km.

21 p2689 A73-41352

Solar quiet dynamo region electric fields and currents diurnal and semidiurnal field components variations with latitude

21 p2689 A73-41357

Diurnal and seasonal variations of neutral winds and electric fields above 90 km in the vicinity of the auroral electrojet.

21 p2690 A73-41365

Geomagnetic disturbance diurnal variation /JDS/ component evolution and equatorial electrojet strength changes observation during magnetic storms by globally located stations at various latitudes

22 p2844 A73-41918

Diurnal and semidiurnal nitrogen density and temperature variations from thermosphere probe measurements.

22 p2845 A73-41926

A modified composite wave technique for OMEGA.

22 p2884 A73-42325

Diurnal cycles of the refractive index structure function coefficient.

22 p2849 A73-42545

Diurnal thermospheric and ionospheric variations from time dependent continuity equations for O⁺, H⁺, O₂⁺, and NO⁺ ions, motion and heat conduction equations

22 p2849 A73-42572

Absorption of vlf and elf waves in whistler mode - Sunrise and sunset effects.

22 p2849 A73-42622

Data reduction for annual, diurnal and satellite observation aberrations via rectangular coordinate method, discussing parallax, refraction, instrument eccentricity and computer applications

22 p2915 A73-43034

Study of phase changes of the NWC signal /22.3 kHz/ on a transequatorial path.

23 p2952 A73-43237

Auroral atmosphere temperature variations relation to nightly auroral streamer length variations, assuming ionospheric current dissipation as heat source

23 p2970 A73-43241

Temperature variations in the upper atmosphere during the solar activity minimum based on data of topside sounding of the ionosphere.

23 p2970 A73-43243

Day-to-day variability of quiet-day solar daily variations and the direction of the interplanetary magnetic field.

23 p3027 A73-43258

Diurnal harmonic oscillation instability of atmospheric boundary layer as mesoscale internal gravity waves generation mechanism in lower atmosphere, considering unsteady flow equations

23 p3001 A73-43589

The solar coronal green line as an index of cosmic ray modulation.

23 p3024 A73-43683

Ozone concentration studies and ozone flux measurements near the ground at Poona.

23 p2974 A73-43868

Martian W cloud diurnal brightening observation by Mariners 6 and 7 flyby missions, considering probable water ice formation

24 p3128 A73-44398

Mars seasonal effects from observations of contrast changes in blue light, discussing diurnal variations and UV contrast reversal

24 p3134 A73-44567

A numerical study of three-dimensional diurnal variations within the thermosphere.

24 p3082 A73-44731

Diurnal and semidiurnal variations in amplitude and phase of midlatitude ionosphere tidal motions, using sodium cloud drift rate

24 p3082 A73-44732

Diurnal ion composition variations in E region under quiet and perturbed solar conditions, using continuity equations for positive ions and electroneutrality equations

24 p3083 A73-44793

Short-time fluctuations of the VLF field along polar paths

24 p3067 A73-44809

The behaviour of the upper ionosphere over North America at sunset.

24 p3087 A73-45203

Thunderstorm excited cavity resonances between earth and ionosphere measured by solenoidal coil antenna, finding diurnal frequency variations related to solar and geomagnetic effects

24 p3088 A73-45211

DIVERGENCE

NT MAGNETIC CHARGE DENSITY

Cantilever beam dynamic stability under follower force, investigating divergence, flutter and autoparametric resonance relations

09 p1161 A73-23088

Vorticity equation advection, divergence and curl terms effects on vorticity changes over isobaric surfaces and on weather and cyclonic development in synoptic meteorology

13 p1653 A73-28745

DIVERGENT NOZZLES

German monograph on compressible turbulent boundary layer equations solution for heat transfer in divergent nozzle flow based on modified Patankar-Spalding difference method

13 p1605 A73-29276

DIVERTERS

Plasma confinement in a racetrack magnetic field with a diverter.

03 p0347 A73-14094

Investigation of the stability of plasma-jet motion in the magnetic field of a diverter

04 p0479 A73-15045

DIVIDING [MATHEMATICS]

Error maxima for division algorithm adaptiveness evaluation of damaged computer elements with corrective readjustments

19 p2408 A73-38563

DIVING [UNDERWATER]

Body thermotopography and some metabolic process characteristics in scuba divers under various underwater exposure conditions
05 p0545 A73-16734
Human respiration under increased pressures
12 p1461 A73-26924

DME-A SATELLITE

U EXPLORER 31 SATELLITE

DNA

U DEOXYRIBONUCLEIC ACID

DO-31 AIRCRAFT

The significance of the aerodynamic jet interference for the development and the testing of the V/STOL transport DO 31
[DGLR PAPER 72-106] 02 p0127 A73-11651

DOCKING

U SPACECRAFT DOCKING

DOCUMENT STORAGE

USAF WAVR file of epidemiologic data on medically waived flying personnel, describing computerized updating system
09 p1039 A73-22539

DOCUMENTATION

Effective development, documentation, and distribution of computer programs.
03 p0392 A73-13691

DOCUMENTS

NT BIBLIOGRAPHIES

NT HANDBOOKS

NT MANUALS

Holographic document data recording and storage for single- and multimaterial information processing system, emphasizing Fourier and carrier frequency photography techniques
16 p2013 A73-32873

DOGHOUSES

U PROTUBERANCES

DOMAIN WALL

Low-frequency creep in CoNiFe films.
[IEEE PAPER 7,1] 07 p0861 A73-19362
Wall contraction in Bloch wall films.
07 p0864 A73-20218

A new explanation for the creep of domain boundaries with transverse constrictions
09 p1098 A73-21846

Some principles of domain device designing for data processing and means of control.
10 p1198 A73-24022

DOMAINS

NT MAGNETIC DOMAINS

Infrared detection by reconfiguration of high field domains in CdS:Ag, Al.
06 p0733 A73-17500

Computer simulation model of field independent trapping effects on slow Gunn domains in gallium arsenide, noting double symmetry electron-ion density distributions
06 p0737 A73-18368

Elastic domain similar to half plane with perturbed boundaries, comparing small parameter method accuracy with exact solutions
11 p1446 A73-26467

A numerical conformal transformation method for harmonic mixed boundary value problems in polygonal domains.
24 p3107 A73-45544

DOMES [STRUCTURAL FORMS]

NT RADOMES

Geometric nonlinearity effects on rigid joint deformation of three dimensional skeletal structures, including roofing, cable and shallow dome systems
06 p0762 A73-18342

Axisymmetrical bending of circular plates and shallow spherical cupolas with allowance for physical and geometrical nonlinearities
20 p2618 A73-39310

DOMINANCE

NT EYE DOMINANCE

DONNELL EQUATIONS

Second order closed form asymptotic solution to Donnell type nonlinear equations of elastic homogeneous conical shells for displacement and stress resultants
11 p1447 A73-26650

Cylindrical panels buckling under nonuniform axial compression with various load distributions, basing analysis on Donnell equations and Galerkin method
15 p1948 A73-31635

DONOR MATERIALS

Investigation of the emission of donor-acceptor pairs and of their phonon echoes in CdS single crystals
01 p0088 A73-10634

Voltage and power relationships in lithium-containing solar cells.
03 p0257 A73-14241

Impurity concentration relationship to electrons and holes density and potential fluctuations in completely compensated crystalline semiconductors with randomly distributed donors and acceptors
06 p0735 A73-17976

Dependence of the current-voltage characteristic of a p-n-p drift triode on the donor concentration in the n-type base
06 p0675 A73-18081

Thermal free electron constant approximation in space charge current theory, considering I-V characteristics and ionized donor concentrations at injection levels
08 p0951 A73-21484

The Li donor, and binding of excitons at neutral donors and acceptors in crystals
15 p1924 A73-31722

Effect of donor density and temperature on the performance of stabilized transferred-electron devices.
17 p2134 A73-34220

Luminescence of CdS single crystals doped with various donors and acceptors
19 p2471 A73-37955

Relative performance of a variety of NF3/+/- hydrogen-donor transverse-discharge HF chemical-laser systems.
21 p2714 A73-40757

Observation of doping profiles in Gunn diodes with a scanning electron microscope using the beta-conductivity.
23 p2960 A73-43777

Theory of donor-acceptor radiative and Auger recombination in simple semiconductors.
23 p3016 A73-43796

DOORS

Graphite-epoxy composite door landing gear assembly for space shuttle orbiter, discussing design, analysis, fabrication and structural testing
16 p2029 A73-33058

HOPES

Summary of results of JPL lithium-doped solar cell development program.
03 p0257 A73-14240

DOPING [ADDITIVES]

U ADDITIVES

DOPPLER EFFECT

NT DOPPLER-FIZEAU EFFECT

Short period pulsating radio auroras properties, determining apparent Doppler characteristics of long period echo sequences
01 p0017 A73-10340

Some features of the Leiden radial velocity instrument.
01 p0047 A73-10516

Two-stream heterogeneous mixing measurements using laser Doppler velocimeter.
01 p0050 A73-10741

Orbit determination for the scientific satellite in Japan.
01 p0105 A73-11186

Remotely sensing strain-rate meter based on the Doppler shift of laser light.
02 p0168 A73-11961

Laser Doppler shift velocity correlation meter operation in turbulent flow analyzed by optical mixing theory
02 p0153 A73-12049

Turbulence measurements with a laser anemometer measuring individual realizations.
02 p0168 A73-12057

A modernized technique for ionospheric drifts with spectral analysis.
02 p0161 A73-12286

Laser Doppler anemometer theory and application to radial flow velocity measurement in oscillating boundary layer in front of blunt body
02 p0171 A73-12559

Surface gravities, Doppler broadening velocities, effective temperatures and metal abundances of K giants from narrow band photometry
03 p0371 A73-13224

On the apparent visual forms of relativistically moving objects.
03 p0343 A73-13294

Determination of solid-propellant transient regression rates using a microwave Doppler shift technique.
[AIAA PAPER 72-1118] 03 p0351 A73-13433

A comparison of total electron content determined by the differential Doppler and the Faraday effects using radio signals from a geostationary satellite.
03 p0300 A73-13637

A simple apparatus for signal reception of transit system satellites and principal results.
03 p0308 A73-13649

Atmospheric wind and temperature inhomogeneity induced sound wave refraction effects on acoustic sounder measurements, noting scattering volume displacement and Doppler shift
03 p0276 A73-13831

Atmospheric turbulence information in signal backscattered from pulsed radar, discussing Doppler power spectrum variance determination
03 p0279 A73-14528

High power radar for measurement of refractivity inhomogeneities in clear air turbulence from backscattered energy Doppler shift
03 p0338 A73-14530

Doppler turbulence spectrum and intensity measurement in stalactites region at base of cloud deck cooled by evaporation and destabilized by convection
03 p0339 A73-14539

The effects of a finite radar pulse volume on turbulence measurements.
03 p0279 A73-14540

DOPPLER EFFECT

Venera satellite parachute probe method for Doppler measurement of Venus atmosphere wind velocity and turbulence
03 p0379 A73-14566

Refinement of the gravity field by satellite-to-satellite Doppler tracking.
04 p0438 A73-14793

Gas velocity measurements within a compressor rotor passage using the laser Doppler velocimeter.
[ASME PAPER 72-WA/GT-2] 04 p0451 A73-15866

Doppler spectral width of radar signal reflected from sea surface as function of illuminated region dimensions, waviness scale and emission factors
04 p0423 A73-15913

Indeterminacy functions side maxima for phase manipulated signals with low sidelobe levels in autocorrelation functions, noting Doppler frequency shift effect
04 p0423 A73-15925

The Doppler frequency shift in ionospheric propagation of radio waves
05 p0548 A73-16260

Laser Doppler velocity measurements in a super-sonic flow without artificial seeding.
05 p0576 A73-16361

A signal simulator for testing laser-Doppler fluid-flow velocimeter systems.
05 p0562 A73-16442

Isotropic and incoherent light scattering by atomic slab, calculating Doppler effect induced diffuse radiation energy partial redistribution by Monte Carlo method
05 p0597 A73-16562

New laser technique for the identification of molecular transitions.
05 p0585 A73-16597

A study of vortex rings using a laser Doppler velocimeter.
[ALAA PAPER 73-105] 05 p0565 A73-16865

Measurements of turbulence-transport properties with a laser Doppler velocimeter.
[ALAA PAPER 73-169] 05 p0566 A73-16914

The ionospheric effects of geomagnetic sudden commencements as measured with an HF Doppler sounder at Hawaii.
05 p0571 A73-17062

Laser velocity meters - A comparative study.
05 p0580 A73-17265

Principles of synthetic-aperture radar
05 p0552 A73-17267

Ultrasonic Doppler locators for peripheral vessel blood circulation and myocardium and valvular motor activity measurements
06 p0656 A73-17682

A sampling FM wide-band demodulator useful for laser Doppler velocimeters.
06 p0673 A73-17786

Electromagnetic scattering from a radially moving spherical discontinuity.
06 p0669 A73-18785

Turbulent transport measurements with a laser Doppler velocimeter.
07 p0826 A73-20462

Doppler effect intermodulation distortion derivation by perturbation method for loudspeaker modeled with pulsating sphere, considering boundary condition and nonlinear effect in wave propagation
08 p0987 A73-21123

Effect of Doppler ambiguity on the measurement of turbulence spectra by laser Doppler velocimeter.
[AD-756047] 08 p0965 A73-21211

Broadening of the measured frequency spectrum in a differential laser anemometer due to interference plane gradients.
08 p0967 A73-21596

Flow velocity measurement method based on laser light frequency Doppler shift in scattering experiment on particle seeded liquid, presenting velocity profiles
09 p1094 A73-22314

Doppler signal detection with negative-resistance diode oscillators.
09 p1062 A73-22321

An optical Doppler meter of the velocity of a moving surface
09 p1096 A73-22970

Optically pumped gas laser steady state solution for population inversion, gain coefficient, radiative intensity and power output, noting Doppler broadening role
09 p1097 A73-23070

Doppler broadening of OI 1304 A multiplet in dissociative excitation of CO2 and O2.
10 p1251 A73-24243

Influence of the nonidentity of the antennas of a Doppler speed meter on the accuracy of its operation
10 p1195 A73-24386

Laser Doppler velocimeter configuration and operation, discussing applications and test results
10 p1229 A73-24856

Flow measurement in the presence of strong swirl using a laser Doppler anemometer.
10 p1221 A73-24857

Microwave Doppler flowmeter design and performance, discussing free flow monitoring of sand

from hopper and pneumatic conveying of alumina through steel pipe

10 p1221 A73-24859

Radiation source motion at supertuminal speed in vacuum, defining conditions for Vavilov-Cerenkov and Doppler effects

10 p1250 A73-24943

Remote measurement of wind speed by laser Doppler systems.

11 p1375 A73-25062

Line source functions with variable Doppler width and noncoherent scattering.

11 p1415 A73-25135

Image holography through convective fog.

11 p1361 A73-25365

A source of nonlinear distortions in acoustic emission

11 p1399 A73-26093

Laser dynamic theory with uniformly broadened and Doppler spectral lines based on nonlinear interactions between harmonic oscillations

12 p1506 A73-27139

Upper atmospheric temperatures from Doppler line widths. V - Auroral electron energy spectra and fluxes deduced from the 5577 and 6300 Å atomic oxygen emissions.

12 p1492 A73-27605

The vibrational frequency of Fe-57 atoms in Pt-Fe solid solution from measurements of the second-order Moessbauer Doppler shift.

13 p1634 A73-28258

Comparison of the coordinates of the pole as obtained by classical astrometry /IPMS, BIH/ and as obtained by Doppler measurements on artificial satellites /Dahlgren polar monitoring service/.

13 p1679 A73-28390

Measurement of Coanda flow in fluidic elements by a laser Doppler velocimeter method and a quantitative tracer method.

13 p1618 A73-29040

Problems of theory and practical application of Doppler-laser rate measuring devices in turbulent flow studies

13 p1628 A73-29169

A semicoherent detection and Doppler estimation statistic.

13 p1585 A73-29202

The comparison of a new constant temperature anemometer with several laser anemometer configurations.

13 p1620 A73-29268

Spectral analysis of the signal from the Laser Doppler Velocimeter - Turbulent flows.

14 p1752 A73-29919

Unified theory of type I and II irregularities in the equatorial electrojet.

14 p1748 A73-29973

Insensitivity of single particle time domain measurements to laser velocimeter 'Doppler ambiguity.'

15 p1875 A73-31671

Measurement using the Doppler effect of small velocities in flows occurring in the free convection of fluids.

15 p1864 A73-32069

The possibility of measuring gravitational redshift by means of earth satellites.

15 p1940 A73-32074

Obliquely incident plane wave scattering from moving perfectly conducting cylinder, discussing mode coupling, Doppler shift and far field scattered power

15 p1845 A73-32238

Geodetic control point accurate position determination by Navy navigation Doppler satellite observations with geociever and teletype tape

15 p1873 A73-32268

Two-component dual-scalar laser Doppler velocimeter with frequency burst signal readout.

15 p1880 A73-32383

Doppler VOR equipment, economics, blending function and antenna system, discussing ground measurement and monitoring, sideband generation and reference modulation

15 p1859 A73-32452

Doppler scanning landing guidance system based on linear array of equally spaced radiators with RF source commutation

15 p1912 A73-32502

Measurements of wind-induced Doppler shifts at 16 GHz over a long range bistatic scatter link.

16 p1983 A73-33726

Tunable-laser derivative spectroscopy on spectral lines with combined Doppler and collision broadening.

16 p2039 A73-33741

Comparison of determinations of the rotational velocity of Venus by radar, optical Doppler effect, and spot measurement methods

16 p2067 A73-33809

Normal Doppler shifted cyclotron radiation from a cold plasma.

18 p2338 A73-36189

The application of a scanning laser Doppler velocimeter to trailing vortex definition and alleviation.

[AIAA PAPER 73-680]

18 p2315 A73-36231

Measurements of aerosol size distributions with a laser Doppler velocimeter /LDV/.

[AIAA PAPER 73-705] 18 p2315 A73-36254

Pulsed-Doppler velocity isotach displays of storm winds in real time.

18 p2333 A73-36707

The remote sensing of wind velocity in the lower troposphere using an acoustic sounder.

19 p2427 A73-38208

Trans-horizon propagation techniques for examining disturbances in stratified tropospheric layers.

19 p2405 A73-38221

Measurements of artificial satellite signal Doppler spectrum.

19 p2407 A73-38351

VHF radar aurora echo Doppler spectral properties, discussing electron density irregularities, echo power spectra, drift velocity, two stream instability and convection hypothesis

20 p2553 A73-38962

Frequency-domain analysis of laser Doppler signals for estimation of turbulence parameters.

20 p2572 A73-39130

Demodulated Doppler signal analyzed for uniform steady flow, noting non-Gaussian phase fluctuations statistics

21 p2699 A73-40454

Geociever passive Doppler receiver precision capabilities and accuracy experience, noting portability, commercial availability, error sources enumerated and quantified

21 p2705 A73-41329

Studies of granular velocities. III - The influence of finite spectral and spatial resolution upon the measurement of granular Doppler shifts.

21 p2776 A73-41478

Sampling phase rotator for removal of Doppler shift in a lunar radar.

21 p2658 A73-41590

Angle and Doppler measurements of the quasi-coherent and incoherent components of microwave transhorizon signals.

22 p2824 A73-41859

Laser Doppler instrument for measurement of vibration of moving turbine blades.

22 p2869 A73-42297

Laser Doppler velocity measuring system parameters and SNR analysis, comparing photomultiplier, p-i-n and avalanche photodiode detectors for performance

22 p2825 A73-42298

Pulsed laser saturation spectroscopy - Observation of power broadening by optical nutations.

22 p2871 A73-43082

Confocal backscatter laser velocimeter with on-axis sensitivity.

22 p2864 A73-43162

The laser-Doppler velocimeter and its application to the measurement of turbulence.

23 p2982 A73-43937

Results of delay-time and Doppler-correction measurements obtained in radar observations of Venus during 1962, 1964, 1969, 1970, and 1972

23 p3037 A73-44252

A laser Doppler velocimeter for studying fast gas-dynamic flows

24 p3089 A73-44714

Laser Doppler interferometry for measuring small absorption coefficients.

24 p3090 A73-44924

Doppler echocardiography - The localization of cardiac murmurs.

24 p3064 A73-44947

Reducing the level of additive noise in the output signal of a laser velocimeter

24 p3096 A73-44958

DOPPLER NAVIGATION

Doppler TACAN navigation system for helicopters obtaining data through computer display method

10 p1247 A73-24475

Radome precision testing for fire control, missile aiming, Doppler navigation and bombing

11 p1335 A73-25277

A new approach to Doppler-inertial navigation /Doppler Beam Sampling/.

12 p1522 A73-27162

Doppler VOR area navigation operational principles, emphasizing bearing accuracy improvement compared to conventional VOR systems

15 p1909 A73-32456

Doppler landing system based on standard DME for ILS replacement, describing development history and operational principles

19 p2450 A73-37385

The evaluation of autonomous navigation systems for cruise vehicles.

[AIAA PAPER 73-874]

20 p2587 A73-38811

DOPPLER RADAR

Microwave Gunn diode oscillators applications, noting use as Doppler radar and synchronized oscillators

02 p0144 A73-11532

Acoustic-Doppler-radar scattering equation and general solution.

03 p0276 A73-13830

Doppler radar evidence of severe storm high-reflectivity cores acting as obstacles to airflow.

03 p0337 A73-14507

Measurement of wind gradients in convective storms by Doppler radar.

[AD-751716] 03 p0278 A73-14508

Uncertainties in coherent measurement of the mean frequency and variance of the Doppler spectrum from meteorological echoes.

03 p0279 A73-14525

Doppler radar measurements of the velocity field associated with a turbulent clear air layer.

03 p0338 A73-14532

Radar observations of intense undulance in an evaporating cloud layer.

03 p0339 A73-14541

Earth-moon mass ratio from Mariner 9 radio tracking data.

07 p0899 A73-20156

Doppler radar characteristics of precipitation at vertical incidence.

10 p1190 A73-24778

Utilization of the Doppler effect to measure the drift angle and the ground speed of an aircraft

11 p1305 A73-25797

FM laser noise effects on optical Doppler radar systems.

11 p1333 A73-26639

VHF Doppler spectra of radar echoes associated with a visual auroral form - Observations and implications.

12 p1468 A73-26996

Multiple target CW FM Doppler radar with solid state devices and CRT indicator, noting range resolution advantage over pulse radar

12 p1469 A73-27164

Quantization and roundoff errors in a digital MTI filter.

13 p1590 A73-28478

Detection of Doppler signals by a receiver which incorporates a counter of the number of excursions of additive noise.

13 p1583 A73-28728

Echo signal spectral compression in airborne FM Doppler radar measurement, allowing for flight trajectory and target surface characteristics

13 p1584 A73-28889

Amplitude modulation effects of the Doppler return at low altitudes.

13 p1586 A73-29223

Cloud research by radar, describing tracking, imaging and Doppler techniques

15 p1904 A73-31748

The Corail radar - Automatic equipment for runway surveillance

15 p1846 A73-32431

Radiogoniometric vectors superposition on ATC Doppler radar image, noting direction finding display availability and echoes identification

15 p1847 A73-32438

Computer analysis of reflected signals obtained during radar sounding of Venus

16 p2067 A73-33807

USAF Airborne Warning and Control System with overland download Doppler radar for low-fly aircraft detection in severe clutter environment, discussing design and performance

17 p2121 A73-34371

Doppler radar with polarization diversity.

17 p2122 A73-34862

Solid state null tracking Doppler radar ground velocity sensor for supersonic weapon delivery aircraft precision bombing, discussing design and test with computer simulation

17 p2137 A73-35209

Doppler radar measurements and observations of precipitation velocity fields.

17 p2125 A73-35361

Real-time estimates of mean velocity by averaging quantized phase displacements of Doppler radar echoes.

17 p2125 A73-35362

Stationary target identification with radar beam for comet nucleus within coma, noting echo spatial extent and Doppler bandwidth effects on data processing

17 p2174 A73-35634

Autocorrelation functions for meteorological scatterer velocity measurements in Doppler spectrum from linear, quadratic and logarithmic radar signal detectors

23 p2955 A73-44268

Meteorological Doppler radar for measurements of particle velocity and horizontal winds inside convective storms, discussing signal processing and multiple radar method

24 p3107 A73-44687

DOPPLER-FIZEAU EFFECT

Spiral structure and kinematics of the galaxy from a study of the H II regions - Fabry-Perot interference methods applied to ionized hydrogen.

01 p0096 A73-10297

DORMANT VEGETATION

U VEGETATION

DORNIER AIRCRAFT

NT DO-31 AIRCRAFT

DORNIER DO-31 AIRCRAFT
 U DO-31 AIRCRAFT
DOSAGE
 NT RADIATION DOSAGE
DOSIMETERS
 NT THRESHOLD DETECTORS [DOSIMETERS]
 New norms and standardization trends for dosimetry and protection against radiation
 11 p1322 A73-25311
 Solid state neutron radiation dosimeter for hands of medical and industrial personnel working with spontaneously fissionable fuels, describing Th foil detector and automatic spark counter
 11 p1361 A73-25312
 LiF albedo dosimeter for fast neutron and gamma irradiation measurement on personnel, using Cf-252 source for calibration
 11 p1361 A73-25313
 Personnel radiation protection technology and criteria review, discussing dosimeter specifications and automatic data processing
 11 p1322 A73-25314
 Papers on radiation dosimetric instruments and problems covering nuclear track recorders, ionization chambers, proportional counters, radiophotoluminescence, thermoluminescence, X rays, neutron equivalents, etc
 11 p1362 A73-25420
 Nuclear track etching in radiation and fast neutron dosimetry and health physics, discussing counter materials and fission and alpha particles and recoil nucleus recordings
 11 p1362 A73-25421
 Ionization vacuum chambers for radiation measurement, discussing secondary emission, Greening theory and dosimeters, electron beam monitors, pulse measurement, energy spectrometers and interface dosimetry applications
 11 p1362 A73-25422
 Delta ray particle track structure theory for radiation dosimetry and biological cell response to heavy ions, fast neutrons, stopped pions and mixed radiation fields
 11 p1323 A73-25423
 Dose equivalent determinations in neutron fields by means of moderator techniques
 11 p1362 A73-25424
 Radiophotoluminescence dosimetry for personnel monitoring, discussing thermoluminescence of phosphate and silver activated glasses, energy compensation filters and measurement techniques
 11 p1362 A73-25425
 Cosmic rays airborne dosimetry from Concorde aircraft, noting passenger and crew radiobiological hazards at supersonic flight altitudes
 18 p2348 A73-36908
 Apollo 14 and Apollo 16 heavy-particle dosimetry experiments
 19 p2396 A73-37150
 Proton dosimeter design for distributed body organs
 23 p2949 A73-43389
 A megaread plastic film dosimeter
 23 p2949 A73-44212
DOUBLE BASE PROPELLANTS
 NT DOUBLE BASE ROCKET PROPELLANTS
 The role of impurity particles in the combustion of double-base propellants
 01 p0089 A73-10639
 The service life of rocket motors filled with double base propellants
 [AIAA PAPER 72-1109] 03 p0351 A73-13424
 The thermal decomposition of nitroglycerin and its relation to the stability of CMDB propellants
 [WSCI PAPER 72-30] 05 p0605 A73-16685
 Measuring apparatus for residual effective stabilizer content in single and double base propellants by passing nitrogen dioxide through ground sample
 09 p1135 A73-22300
DOUBLE BASE ROCKET PROPELLANTS
 Considerations concerning the service life, handling and storage of double base solid propellant rocket motors
 [AIAA PAPER 72-1086] 03 p0351 A73-13408
 Aging mechanisms in composite-modified double-base propellants
 [AIAA PAPER 72-1089] 03 p0351 A73-13410
 U.S. double-base solid propellant tactical rockets of the 1940-1955 era
 [AIAA PAPER 73-274] 09 p1135 A73-23248
 The scope and methods of environmental testing of double-base propellant rocket motors - Choice of conditions and interpretation of results
 16 p2047 A73-33390
 Influence of acceleration on the combustion of solid propellants - Measurement and prediction of the effects
 16 p2045 A73-33391
DOUBLE CUSPS
 Gaussian variational equations for osculating elements of an arbitrary separable reference orbit
 15 p1930 A73-31113
DOUBLE PRECISION ARITHMETIC
 Roundoff and uncertain data error analysis, discussing hasty judgements, double precision, trajec-

tory problems, ill-posed problems, computer software and hardware flaws, etc
 01 p0021 A73-11460
DOUBLE SIDEBAND TRANSMISSION
 Required carrier-to-interference ratios for frequency sharing between frequency-modulation television signal and amplitude-modulation vestigial sideband television signal
 01 p0018 A73-11811
 Oscillator synchronization by FM signal for constant central frequency-sideband phase difference operation
 08 p0946 A73-21112
DOUGLAS AIRCRAFT
 NT A-4 AIRCRAFT
 NT DC 9 AIRCRAFT
 NT DC 10 AIRCRAFT
DOUGLAS DC-9 AIRCRAFT
 U DC 9 AIRCRAFT
DOUGLAS MILITARY AIRCRAFT
 U MILITARY AIRCRAFT
DOVAP
 U DOPPLER EFFECT
DOWN-CONVERTERS
 Comparison of an aluminum-coated phosphor layer and a Channeltron Electron Multiplier Array as extreme ultraviolet-to-visible image converters for use in space applications
 14 p1752 A73-30155
 Low-noise microwave down-converter with optimum matching at idle frequencies
 21 p2666 A73-41428
DOWNTIME
 Optimal time calculation for aging complex control system replacement with allowance for downtime losses
 05 p0554 A73-16989
 Aircraft and ground equipment damage during ground handling operations, discussing repair costs and out-of-service time
 10 p1176 A73-24715
DOWNWASH
 Induced drag of finite wing with antisymmetric incidence distribution due to rolling, deriving relations between wing lift distribution and induced downwash
 03 p0248 A73-14472
 Nonstationary flow downwash behind a delta wing during supersonic motion
 11 p1299 A73-25046
 Downwash-velocity potential method for oscillating surfaces
 13 p1564 A73-28803
 An improved nonlinear lifting-line theory
 13 p1564 A73-28817
DRACONID METEORIDS
 Investigation of the motion of periodic comet Giacobini-Zinner and the origin of the Draconid meteor showers of 1926, 1933 and 1946
 14 p1791 A73-29802
DRAFTING [DRAWING]
 Degrees of freedom elimination method shown equivalent to interpolation by splining by means of actual structure in curve connection for given points
 09 p1166 A73-23465
DRAG
 NT AERODYNAMIC DRAG
 NT FRICTION DRAG
 NT MINIMUM DRAG
 NT PRESSURE DRAG
 NT SATELLITE DRAG
 NT VISCOUS DRAG
 NT WAVE DRAG
 Drag coefficient for particles in rarefied, low Mach-number flows
 05 p0564 A73-16354
 Some evaluations of drag and bulk transfer coefficients over water bodies of different sizes
 06 p0720 A73-18328
 Experimental drag coefficients for evaporating and burning drops at elevated pressures
 13 p1707 A73-28998
 Impulsively started viscous flow past a finite flat plate with and without an applied magnetic field
 17 p2217 A73-35604
 Surface wind-geostrophic wind relationship at Salisbury Plain, England, deducing geostrophic drag coefficients for open sea
 21 p2732 A73-41571
 A note on the drag due to steady flow of a conducting fluid past a disk at high Hartmann number
 22 p2894 A73-42475
DRAG BALANCE
 U AERODYNAMIC BALANCE
 U LIFT DRAG RATIO
DRAG CHUTES
 Parawing-drag chute system operation on wind shear energy to maintain payload flight altitude
 11 p1305 A73-25787
DRAG COEFFICIENT
 U AERODYNAMIC COEFFICIENTS
 U AERODYNAMIC DRAG
DRAG DEVICES
 NT AERODYNAMIC BRAKES
 NT BALLUTES
 NT DRAG CHUTES

NT LEADING EDGE SLATS
 NT SPOILERS
 NT TRAILING-EDGE FLAPS
 NT WING FLAPS
 Decelerator sail erosion during interstellar vessel deceleration, using drag screens to improve vehicle mass ratio via propellant requirement reduction
 18 p2361 A73-37039
DRAG EFFECT
 U DRAG
DRAG MEASUREMENT
 Investigation of friction drag during gas flow in a tube with wall temperatures up to 2800 K
 06 p0686 A73-18126
 Experimental developments in V/STOL wind tunnel testing at the National Aeronautical Establishment
 18 p2265 A73-36774
 Jet engine exhaust plume effects on solid bodies, examining nozzle drag effects, nozzle geometry, plume entrainment and shape, wind tunnel tests and pressure effects
 20 p2626 A73-38651
 Tetrahedral Mylar plastic balloon drag coefficient measurement as function of Reynolds numbers from experimental free flight test data
 23 p3004 A73-44263
DRAG REDUCTION
 Drag reduction in non-Newtonian turbulent flow, considering viscosity change with strain in long-chain molecules/polymers/ fluid solutions
 01 p0034 A73-11134
 Aircraft aftbody/propulsion system integration for low drag
 [AIAA PAPER 72-1101] 03 p0243 A73-13420
 Flow visualization of the near-wall region in a drag-reducing channel flow
 06 p0685 A73-17709
 Monatomic gas flow around uniformly heated sphere for small Reynolds numbers, noting drag decrease due to thermal stresses
 06 p0646 A73-18884
 Hydrodynamic wind tunnel investigation of drag reduction and propulsion effect by flexible walls, observing boundary layer transition and turbulence
 09 p1071 A73-22207
 Turbulent friction drag of a dusty gas. I. Theoretical study
 09 p1072 A73-23325
 Base drag reduction on blunt based axisymmetric bodies by base burning, calculating inviscid flow field with heat addition around recirculating bubble
 11 p1449 A73-25347
 Monatomic gas flow around uniformly heated sphere for small Reynolds numbers, noting drag decrease due to thermal stresses
 15 p1824 A73-32409
 An investigation of the flow field and drag of helicopter fuselage configurations
 [AHS PREPRINT 700] 17 p2095 A73-35051
DRAGUERS
 U BRAKES [FOR ARRESTING MOTION]
 U DRAG DEVICES
DRAINAGE PATTERNS
 Statistical uniformity of hydrological data from series of river drainage pattern observations
 19 p2446 A73-38546
DRAWING
 Dependence of the deformability of the Kh17 high-chromium steel on texture
 03 p0326 A73-13827
 The tensile strength of pultruded carbon fibre/epoxy resin composite
 21 p2723 A73-40923
DRIFT
 Surface drift waves in a weakly ionized plasma
 03 p0347 A73-14090
 Utilization of the Doppler effect to measure the drift angle and the ground speed of an aircraft
 11 p1305 A73-25797
DRIFT [INSTRUMENTATION]
 Energy dissipation and drift angular velocity calculation for horizontal pendulum on vibrating base, using revised differential equation of motion
 01 p0079 A73-11417
 M.O.S.F.E.T. temperature-drift performance limitations
 04 p0427 A73-14983
 Systematic drift of a gyroscope with variable angular momentum in the gimbal suspension during vibrations of the frame
 09 p1084 A73-22657
 A condition for drift invariance with respect to acting accelerations in a two-degree-of-freedom gyroscope having arbitrary gas lubricated bearings on the main axis
 09 p1084 A73-22658
 Drift phenomena in shaken measurement systems prone to torsional vibrations. III
 09 p1086 A73-23116
 Strain gage measurement errors under long term installation conditions, considering drift, temperature and moisture effects, connection wires impedance and selector switch contact resistance
 10 p1219 A73-24568

Drift moments produced by rotor nonsphericity in a suspension system with an axially-symmetric field 11 p1367 A73-26453

Influence of clearances on the behavior of a gyroscope on a vibrating base 19 p2428 A73-37188

Long-term drift of some noble-and refractory-metal thermocouples at 1600 K in air, argon, and vacuum. 22 p2857 A73-42033

Measured drift of irradiated and unirradiated W3%Re/W25%Re thermocouples at a nominal 2000 K. 22 p2858 A73-42046

The travelling gradient approach to thermocouple research. 22 p2859 A73-42049

Comparison of temperature sensors for space instrumentation. 22 p2859 A73-42064

DRIFT RATE

Magnetic pumping of electrons in ohmic dissipation mechanism responsible for neoclassical plasma diffusion rate increase in banana regime 01 p0084 A73-10467

Hall mobility measurements on iron rich nickel ferrites from room temperature to 600 C. 02 p0199 A73-11725

Magnetospheric tail plasma sheet near earth structure explained via tangential magnetic field gradient drift velocity coupling to strong pitch-angle diffusion 02 p0157 A73-11898

E region electromagnetic east-west drift velocity measurement at magnetic equator by incoherent scatter radar 02 p0161 A73-12285

Thermal and near-thermal electron transport coefficients in O₂ determined with a time-of-flight swarm experiment using a drift-dwell-field technique. 03 p0344 A73-13276

Nonuniformities of the ion density at an altitude of 600 km in the ionosphere. 05 p0567 A73-16083

Anomaly configuration maps showing westward drift and positions of residual geomagnetic fields and eccentric dipoles during 1885-1965 period 06 p0689 A73-17544

Current induced drift rate of plasma electrons in electric and magnetic fields, noting electron velocities in turbulent heating of plasma 06 p0732 A73-18621

Study of the surface layer of drift currents in the laboratory 08 p0985 A73-21455

An indirect method for measuring equatorial electrojet currents and its relation to nonlinear saturation of type I instabilities. 09 p1075 A73-22070

Errors in measuring the angles of rotation of an object with a triaxial gyro-stabilized platform with allowance for its drift 09 p1115 A73-22343

Synchrotron emission, adiabatic invariant, and gradient drift of particles in a linearly inhomogeneous magnetic field 09 p1132 A73-23079

Precession motion stability and drift rates of gimbal gyroscope under angular and translational resonant base vibration 09 p1087 A73-23343

Direct measurements of plasma convection in the upper ionosphere 10 p1211 A73-23885

Multistatic incoherent scatter measurements of ionospheric drift velocity. 10 p1188 A73-24274

Drift mobilities of holes and electrons in naphthalene single crystals. 11 p1407 A73-24988

The causes of storm-time increases of the F-layer at mid-latitudes. 11 p1353 A73-25751

Ionosphere spatial resonance as result of internal gravity wave phase velocity equal to ionization irregularity drift rate 11 p1356 A73-25908

Correspondence of main trough ion temperatures with horizontal drift speed. 12 p1489 A73-27006

Effective 'radius of operation' of a system for measuring ionospheric drifts 12 p1490 A73-27341

Relationship between geomagnetic pulsations of diminishing period and the motion of plasma discontinuities in the magnetosphere 12 p1491 A73-27350

Equatorial ionospheric electron drift rate measurement over Thumba, deriving north-south component 13 p1609 A73-28921

Direct measurements of ion drift velocity in the upper ionosphere during a magnetic storm. I - Methodological aspects and some results of measurements in magnetically quiet periods. II - Results of measurements during the magnetic storm of November 3, 1967 14 p1746 A73-29863

Anomaly configuration maps showing westward drift and positions of residual geomagnetic fields and eccentric dipoles during 1885-1965 period 16 p2002 A73-32768

Solar wind density model from km-wave type III bursts. 16 p2053 A73-32965

Operational amplifier integrator for storage element in track-hold circuit, discussing drift rate reduction with large equal-value resistors from input terminal to ground 16 p1988 A73-33398

Strapdown electrostatic gyroscope spin axis precession drift rate calibration, using virtual work technique for modeling bearing torques on rotor 17 p2137 A73-35210

ESRO Geos geostationary satellite for measurement of magnetospheric plasma electric and magnetic fields and drift rate at various frequency regions via electron injection 17 p2176 A73-35816

Kinesonde studies of cesium ion clouds in the E-region. 18 p2304 A73-35988

Ionospheric drift measurements. I - A new method for ionospheric drift measurements. II - The effect of random drift velocities upon the determination of ionospheric drift velocities. 18 p2304 A73-35989

Lunar tidal oscillations in the horizontal ionospheric drift at the Equator. 18 p2311 A73-36177

Some problems concerning the method of determining the parameters of scattering inhomogeneities. 19 p2424 A73-37913

Velocity of weak inhomogeneities in the ionospheric plasma. 19 p2425 A73-37931

Direct measurements of plasma convection in the upper ionosphere. 20 p2550 A73-38904

On the validity of the gradual channel approximation for junction field effect transistors with drift velocity saturation. 20 p2535 A73-39006

Drift velocity measurements for small-scale inhomogeneities at various levels of the F2 layer 20 p2553 A73-39158

Investigation of the inhomogeneous structure of the ionosphere using observations of discrete cosmic radio emission sources and vertical soundings 20 p2553 A73-39159

Statistical characteristics of the diurnal drift velocity variations in the F2 layer 20 p2554 A73-39160

Diurnal variations in the drift velocity and direction of the ionization inhomogeneities in the F layer 20 p2554 A73-39161

Altitude distribution of the drift velocity and direction of ionosphere inhomogeneities over Ashkhabad in years of maximum and minimum solar activity 20 p2554 A73-39162

Investigation of the fine-structure inhomogeneities of the Es layer at oblique radio wave incidence 20 p2554 A73-39163

Interpretation of the results of drift measurements by the space diversity reception method 20 p2555 A73-39819

Drift tube and mass spectrometric measurement of molecular positive ion drift velocities in carbon dioxide 21 p2742 A73-40221

Fading characteristics and drift and anisotropy parameters of the ground diffraction pattern of the radio waves reflected from the equatorial ionosphere during spread F conditions. 22 p2825 A73-41929

Experimental investigation of current-driven ion wave turbulence in plasma. 22 p2890 A73-42224

Effective 'radius of action' of a device for measuring ionospheric drifts. 23 p2970 A73-43239

Relationship between geomagnetic PDP pulsations and the motion of plasma inhomogeneities in the magnetosphere. 23 p2970 A73-43247

Ionosphere dynamic process investigations, describing wind models, E region drift velocity curves and energy distribution chart 23 p2978 A73-43978

The drifts of a gyroscope mounted on the oscillating housing. 23 p2983 A73-44271

DRILLING

Machining precision in deep-hole boring by a feed-division technique 02 p0174 A73-12578

Microstructural changes that drilling and reaming can cause in the bore holes in DTD 5014 /RR58 extrusions/. 03 p0325 A73-13573

Design and characteristics of a single pass normal mode ruby oscillator-amplifier laser for hole drilling in metals. 06 p0700 A73-18277

Hole preparation in titanium and high strength steels. [SME PAPER IQ 72-208] 07 p0832 A73-20450

The drilling of a metal plate by a laser beam. [ASME PAPER 73-PROD-6] 16 p2019 A73-33535

Material processing with solid-state laser. [SME PAPER EM 73-213] 19 p2436 A73-38495

Kinetic effects in drilling with the CO₂ laser. 21 p2707 A73-40974

German monograph - Materials removal in the case of the drilling of holes with the aid of solid-state lasers. 22 p2866 A73-42699

DRILLS

Ultrasonic treatment of nonmetallic materials with a diamond instrument 24 p3094 A73-44969

DRINKING

The role of the amygdaloid nuclei in the regulation of water intake 21 p2636 A73-40278

DROGUE PARACHUTES

U DRAG CHUTES

DROGUES

U TOWED BODIES

DRONE AIRCRAFT

NT JINDIVIK TARGET AIRCRAFT

Intensive probing of clear air convective fields by radar and instrumented drone aircraft. 03 p0339 A73-14542

Aerial targets for weapon systems performance testing, discussing converted aircraft, pilotless drones and towed targets 09 p1168 A73-23120

Turana drone system design and development for Australian naval guns and guided weapons exercises, describing construction and operational details 09 p1032 A73-23122

Drone recovery surface impact and midair techniques involving parachutes and/or hot-air balloons, considering TALOS/Low Altitude Supersonic Target recovery capability [AIAA PAPER 73-465] 15 p1827 A73-31451

Development of an improved midair-retrieval parachute system for drone/RPV aircraft. [AIAA PAPER 73-469] 15 p1828 A73-31453

Drone launch and recovery reliability requirements for target, reconnaissance, air-to-air combat, high altitude endurance and defense suppression missions 19 p2381 A73-37681

DRONE HELICOPTERS

U DRONE AIRCRAFT

U HELICOPTERS

DRONE VEHICLES

NT DRONE AIRCRAFT

NT JINDIVIK TARGET AIRCRAFT

DROP SIZE

Pressure drop, gas content, liquid drop size and nozzle length effects on flow velocity and heat transfer in two phase nozzle flow 01 p0033 A73-10863

An electrostatic cloud droplet probe. 01 p0052 A73-11058

Meteorological parameters conducive to ice formation on aircraft, analyzing data statistics on atmospheric moisture content, temperature and drop size [DGLR PAPER 72-109] 02 p0130 A73-11660

A new Monte-Carlo simulation model for the temporal development of cloud droplet spectra. 02 p0144 A73-12782

Simultaneous quantitative measurements of rainfall rate and drop size distribution by X-band radar and drop distrometer /system Joss-Waldvogel/ at two rain gauge equipped places near to Bonn/West Germany. 03 p0338 A73-14520

Droplets size and velocity distribution in air-kerosene atomized spray flame as function of fuel-air ratio from double image high speed photographic measurements [ASME PAPER 72-WA/HT-25] 04 p0519 A73-15829

Fog droplet vaporization and fragmentation by a 10.6-micron laser pulse. [AD-758948] 06 p0698 A73-17494

Investigation of the scattered-light-flux magnitude dependence on the drop size in the aerosol photoelectric counter 06 p0691 A73-18734

Tests of coherence for the empirical laws of distribution of raindrops 08 p0938 A73-20966

Determination of criteria for rain erosion testing of the standard arm radome. 11 p1335 A73-25298

Approximation of empirical size distributions of cloud droplets and other aerosol particles 11 p1393 A73-25644

Precipitation drops initial growth and final size limits due to collision mechanism, investigating drop interactions by wind tunnel experiments 12 p1520 A73-26807

Diameter reduction rate and time dependence of corresponding temperature variation of liquid drop unsteady evaporation in rarefied ambient gas 12 p1558 A73-27392

Pressure drop, gas content, liquid drop size and nozzle length effects on flow velocity and heat transfer in two phase nozzle flow 12 p1560 A73-27912

Study of droplet size distribution in a two-phase stratiform cloud - A numerical experiment 13 p1653 A73-28877

Growth rate calculation for hygroscopic condensation nuclei in the presence and absence of a monolayer of a surface-active substance 13 p1654 A73-28880

The effect of the size distribution of the rain drops on the standard visibility 15 p1902 A73-31139

Drop size distribution resulting from liquid jet injection across a supersonic stream. 15 p1863 A73-31659

Study of the conditions defining the passivating action of surface-active substances on hygroscopic condensation nuclei 18 p2332 A73-35918

Light beam dispersal of fog with various drop sizes based on energy equation, considering cloud water content, cross wind effects and front velocity 18 p2337 A73-36561

A study of droplet spectra in fogs. 19 p2447 A73-37660

Condensation of drops in motion through a gravitation field 21 p2731 A73-40743

Determination of the size and the imaginary part of the refractive index of Al₂O₃ drops in a flame 22 p2932 A73-42724

Nitric oxide formation weightless in diffusion flame ethanol drop combustion as function of air temperature and diffusion and spray characteristics 22 p2935 A73-42797

Numerical solution of linearized kinetic equations for coagulation of cloud particles by the Monte-Carlo method 24 p3107 A73-44965

Clearing of a cloudy atmosphere containing water drops by intense monochromatic radiation 24 p3108 A73-45520

DROP TESTS

A comparison of neutral buoyancy and free fall for liquid propellant system zero-G simulations. [AIAA PAPER 72-1041] 03 p0287 A73-13376

Close range photogrammetry of objects moving at high speed. 09 p1081 A73-22377

Impact strength and fracture of carbon fiber composite beams. 10 p1238 A73-23972

Development of an improved midair-retrieval parachute system for drone/RPV aircraft. [AIAA PAPER 73-469] 15 p1828 A73-31453

Development and testing of ballute stabilizer/decelerators for aircraft delivery of a 500-lb munition. [AIAA PAPER 73-485] 15 p1829 A73-31467

An omnidirectional gliding ribbon parachute and control system. [AIAA PAPER 73-486] 15 p1829 A73-31468

DROP TRANSFER

Droplet transfer in two phase annular mist flow. II - Prediction of droplet transfer rate. 19 p2423 A73-38350

DROP WEIGHT TESTS

U DROP TESTS

DROPS (LIQUIDS)

NT RAINDROPS

Analysis of NO formation in single droplet combustion. 01 p0014 A73-10645

Multi-droplet combustion of liquid propellants. 01 p0089 A73-11114

Initially spherical water drops deformation under external flow for wide range of Weber and Bond numbers, investigating drag coefficient and Taylor instability 02 p0153 A73-12037

Ethanol condensation by homogeneous nucleation and growth of liquid droplets in steady state supersonic nozzle flow of ethanol-air and ethanol-nitrogen mixtures 02 p0153 A73-12051

Decomposition and hybrid combustion of hydrazine, MMH and UDMH as droplets in a combustion gas environment. 03 p0352 A73-14392

Experimental investigation of the evaporation rate of water droplets in atmospheres of air and carbon dioxide under conditions of a thermostatic droplet surface 04 p0517 A73-14881

Equilibrium shape and stability conditions of rotating inviscid liquid drop in electric field 04 p0476 A73-15165

Emitter efficiency increase in annular colloid microthrusters with single sharp tips for high specific charge of conducting liquid droplets under low potential 04 p0488 A73-15723

Hydrodynamic phenomena during high-speed collision between liquid droplet and rigid plane. [ASME PAPER 72-WA/FE-30] 04 p0435 A73-15850

Design and development of a high pressure facility for droplet combustion experiments. 05 p0562 A73-16440

Steady state spray combustion model, using Nukiyama-Ianassawa drop distribution function, Stokes drag and modified Priem-Heidmann or Spalding vaporization rate equations [WSCI PAPER 72-36] 05 p0639 A73-16680

Condensate droplets heat conductivity as function of drop geometry and vapor mass transport interaction with interior heat conduction, using finite difference method 06 p0768 A73-17920

Atomization of cryogenic liquid droplets by shock waves 07 p0811 A73-19656

Experimental study of water drop evaporation in a heated air flow 07 p0922 A73-20416

Evaporation rate and temperature of liquid drops calculated for low and high temperature aerosols 07 p0922 A73-20417

Phase transition effects at the collecting droplet surface on the capture coefficient magnitude 07 p0922 A73-20418

Quasi-stationary theory of hydrocarbon droplet ignition. I - Moment and limit of ignition 07 p0923 A73-20422

Brightness balancing spectrograph method for flame temperature measurement of liquid fuel drop 07 p0826 A73-20423

A method of calculating heat and mass transfer between liquid droplets and a gaseous phase in an acoustic wave field 08 p1022 A73-21196

Damage produced by high-speed liquid-drop impacts. 09 p1109 A73-21932

Assembly for measurement of free surface energy, contact angles, and melt densities by a lying drop technique 09 p1085 A73-23017

Continuously recording cloud nuclei counter, describing diffusion chamber with separate functions of sample supersaturation and photoelectric droplets recording 10 p1217 A73-23990

Influence of liquid circulation within a droplet on the vaporization rate and drag in a viscous flow 10 p1206 A73-24680

Investigation of metal droplet shaping during atomization 10 p1225 A73-24688

Features of the mechanism of vapor condensation from humid air in narrow channels and the hydrodynamics of two-phase flow during droplet condensation 11 p1451 A73-25735

Liquid droplet drag in vapor flow as function of drop vaporization rate, using Stokes formula 11 p1451 A73-25736

Dynamics and energetics of the explosive vaporization of fog droplets by a 10.6-micron laser pulse. 11 p1377 A73-26231

An approximate estimate of the reaction coefficient during the motion of a vaporizing droplet of fuel in a gas flow 12 p1532 A73-27088

Diameter reduction rate and time dependence of corresponding temperature variation of liquid drop unsteady evaporation in rarefied ambient gas 12 p1558 A73-27392

Differential difference equations for probability of water droplet electrization in weakly ionized medium during cloud and fog formation 13 p1654 A73-28883

Experimental drag coefficients for evaporating and burning drops at elevated pressures. 13 p1707 A73-28998

Temperature effects on liquid drop evaporation in an air flow 14 p1816 A73-30015

Breakdown of a drop of cryogenic liquid by shock waves. 14 p1745 A73-30322

Combustion of fuel vapor-drop-air systems. I - Open burner flames. II - Spherical flames in a vessel. 16 p2085 A73-33343

Combustion of droplets of liquid fuels - A review. 18 p2372 A73-37096

Ignition temperature of liquid fuel-fuel droplets 18 p2342 A73-37115

Quasi-stationary theory of hydrocarbon droplet ignition. II - Ignition limits of cold and hot droplets 18 p2372 A73-37117

Formation of a nonstationary diffusive flame front during the ignition of a liquid fuel droplet 19 p2471 A73-37507

Leidenfrost temperature - Its correlation for liquid metals, cryogenics, hydrocarbons, and water. [ASME PAPER 73-HT-F] 19 p2504 A73-37641

Droplet transfer in two phase annular mist flow. II - Prediction of droplet transfer rate. 19 p2423 A73-38350

Effects of thermal and mass diffusivities on the burning of fuel droplets. [AICHE PREPRINT 22] 20 p2626 A73-39249

Dynamic electron bunching theory applied to moving solid particles and liquid droplets, describing synchronization mechanism for mechanical particles in oscillating gas 20 p2598 A73-39494

Liquid droplet and ice particle distribution in spatially homogeneous mixed clouds, solving kinetic coagulation equations via distribution function moments 21 p2730 A73-40119

The possibility of crystallization of condensed combustion products in nozzles 21 p2753 A73-40697

Evaporation of a water drop 21 p2791 A73-40745

The slow unsteady settling of two fluid spheres along their line of centres. 22 p2840 A73-41742

The rapid cooling of a hot gas discharge by liquid sprays. 22 p2929 A73-41743

A note on residual drop and single drop formation. 22 p2840 A73-41748

Venus atmosphere water vapor phase transformation possibilities, discussing ice crystal and supercooled water drop formation 22 p2911 A73-42736

Experimental studies on the flame structure in the wake of a burning droplet. 22 p2937 A73-42816

High pressure burning rates of liquid alcohol and hydrocarbon fuels with droplet simulation by porous spheres, deriving surface temperature, pressure distribution and critical burning conditions 22 p2937 A73-42817

Liquid fuel spray burning characteristics in stabilizer disk wake of luminous hollow cone pressure jet flame, using spark photographic technique 22 p2937 A73-42819

Breakup of liquid drops due to convective flow in shocked sprays. 22 p2937 A73-42819

Charge transfer from a highly electrically stressed water surface during drop impact. 24 p3108 A73-45206

Analysis of the self-ignition of fuel droplets behind a reflected shock wave 24 p3121 A73-45390

DROPSONDES

Dropsonde for continuous temperature measurement during descent through lower atmospheric level, discussing receiving unit and data conversion unit 12 p1495 A73-26815

DROSOPHILA

Space flight factors effects on Drosophila development in terms of dominant, autosomal and sex-linked recessive lethals frequency, noting gametogenesis stage sensitivity 22 p2804 A73-42173

DROWSINESS

U SLEEP

DRUG THERAPY

U CHEMOTHERAPY

DRUGS

NT ACTINOMYCIN

NT ADRENERGICS

NT ANTIADRENERGICS

NT ANTIBIOTICS

NT ANTIIDIURETICS

NT ANTIINFECTIVES AND ANTIBACTERIALS

NT ANTIRADIATION DRUGS

NT CENTRAL NERVOUS SYSTEM STIMULANTS

NT CHOLINERGICS

NT CORTISONE

NT EPINEPHRINE

NT HEMOSTATICS

NT HISTAMINES

NT INSULIN

NT MOTION SICKNESS DRUGS

NT NARCOTICS

NT NOREPINEPHRINE

NT PENICILLIN

NT SEDATIVES

NT TRANQUILIZERS

Prediction of flight safety hazards from drug induced performance decrements with alcohol as reference substance. [DFVLR-SONDR-268] 03 p0269 A73-14158

Effect of hydrochlorothiazide on +Gz tolerance in normotensives. 03 p0269 A73-14159

DRUMLINS

U GLACIAL DRIFT
DRUMS (CONTAINERS)

Highly-stressed centrifuge and rotor drums made of reinforced plastics

01 p0056 A73-10308

DRY CELLS

NT NICKEL ZINC BATTERIES

DRY FRICTION

Control theory analysis of equilibrium state asymptotic stability of system with dry friction, applying to power driven gyrostabilizer

01 p0054 A73-11402

Effect of friction in suspension bearings on the motion of a gyroscope with a forced rotation of its base

01 p0054 A73-11415

Investigation of the friction and wear behavior of polytetrafluoro-ethylene composite materials as compared to synthetic carbon and sintered metal. I

06 p0714 A73-18449

Device for studying the effect of ultrasonic oscillations on contact interaction in high vacuum

07 p0822 A73-19295

Improvement of the friction and wear behavior of T-A6V alloy by a new anodic oxidation treatment

09 p1104 A73-22966

Stagnation conditions in systems with Coulomb friction

11 p1400 A73-26451

Dependence of the closeness of two contacting bodies on the load under a high contour-applied pressure with a plastic contact

15 p1880 A73-31143

DRY HEAT

Acclimatization to severe dry heat by brief exposures to humid heat.

03 p0267 A73-13700

Work-heat test comparisons of dry and wet heat and exercise programs for heat acclimatization

09 p1041 A73-22932

Spacecraft decontamination and sterilization by formaldehyde, beta-propiolactone, ethylene oxide, radiation and dry heat, noting effects on polymers

14 p1721 A73-30137

DRYING

NT DEHYDRATION

NT FREEZE DRYING

Survival of *Arthrobacter crystallopoietes* during prolonged periods of extreme desiccation.

07 p0782 A73-20026

Survival of soil bacteria during prolonged desiccation.

14 p1720 A73-30959

DTA [ANALYSIS]

U DIFFERENTIAL THERMAL ANALYSIS

DTMB-111 GROUND EFFECT MACHINE

U GROUND EFFECT MACHINES

DTMB-430 GROUND EFFECT MACHINE

U GROUND EFFECT MACHINES

DUAL SPIN SPACECRAFT

Attitude dynamics of a 'nearly-spherical' dual-spin satellite and orbital results for OSO-7.

02 p0227 A73-11600

Stability criteria for a free dual-spin satellite.

02 p0228 A73-12398

On the stability of dual-spin bodies with unbalancing mass.

03 p0381 A73-13364

Constant and variable amplitude limit cycles in dual-spin spacecraft.

03 p0382 A73-13493

The motion and stability of a dual-spin satellite during the momentum wheel spin-up maneuver.

[AIAA PAPER 73-142] 05 p0629 A73-16891

Maneuvering a tumbling dual-spin spacecraft - The recovery of OSO-7.

[AIAA PAPER 73-248] 05 p0630 A73-16971

Stable tumbling motions of a dual-spin satellite subject to gravitational torques.

17 p2237 A73-34177

Fuel-optimal angular momentum vector control for spinning and dual-spin spacecraft.

17 p2240 A73-35663

Dual and triple spin-stabilized deformable spacecraft attitude stability, comparing results based on Sturm theorem with Liapunov analysis

18 p2359 A73-36306

Dual spin spacecraft minimum energy and nutational dynamic trap states due to asymmetric or unbalanced rotors, analyzing single degree of freedom dynamic model

[AIAA PAPER 73-908] 20 p2614 A73-38842

Energy-sink analysis for asymmetric dual-spin spacecraft.

[AIAA PAPER 73-909] 20 p2614 A73-38843

On the use of a dual spin vehicle for scanning a celestial body.

[AIAA PAPER 73-910] 20 p2614 A73-38844

DUCTED FANS

Investigation of an axial-flow blower during variation of axial clearance and of blade mounting angles in the stator and rotor sections

02 p0131 A73-11791

Radiation properties of propeller and helicopter /free field/ rotors and fans and gas turbine compressors /ducted rotors/

02 p0131 A73-12611

Variable-pitch fans - Progress in Britain.

14 p1785 A73-29770

Variable-pitch fans - Hamilton Standard and the Q-fan.

14 p1785 A73-29771

Multibladed shrouded fan /Q-fan/ with rotary or piston engines as propulsion system for light/medium business aircraft, noting noise and drag reduction

14 p1785 A73-29996

Acoustic generation and propagation in annular ducts of axial flow fans, discussing techniques for in-duct fan noise modal distribution measurement

16 p1999 A73-32846

High bypass ratio quiet turbofan engine for STOL aircraft, emphasizing noise reducing design based on low-speed variable pitch fan concept

16 p2049 A73-34040

Aerodynamic design parameters effects on static performance of short ducted fans for helicopter tail rotor applications, comparing theoretical analysis and experimental results

[AHS PREPRINT 701] 17 p2104 A73-35052

Aircraft engine fan noise radiation from inlet and discharge ducts, describing wind tunnel tests and noise spectra at various blade tip speeds

19 p2472 A73-37288

Reduction of fan noise by annulus boundary layer removal.

22 p2795 A73-41713

DUCTED FLOW

NT KNUDSEN FLOW

Curves of spatial isocorrelations and space-time isocorrelations relative to longitudinal velocity fluctuations in a smooth circular duct

01 p0031 A73-10418

Pressure distributions in manifolds with return ducts.

01 p0032 A73-10699

Representation of a 1/N power law boundary layer in the sheared flow acoustic transmission problem.

01 p0033 A73-10783

The fourth annual Fairey lecture - The propagation of sound through moving fluids.

01 p0077 A73-10784

The optimisation of sound attenuation in lined ducts containing uniform, axial, subsonic, mean flow.

03 p0291 A73-12987

Sound propagation in sheared flow in a duct with transverse temperature gradients.

03 p0342 A73-12988

On the measurement of the local impedance of acoustical duct liners in the presence of grazing mean air flow.

03 p0342 A73-12989

Prediction of inlet duct overpressures resulting from engine surge.

[AIAA PAPER 72-1142] 03 p0243 A73-13448

Three-dimensional MHD duct flows with strong transverse magnetic fields. III - Variable-area rectangular ducts with insulating walls.

03 p0346 A73-13534

Monograph on hydrodynamics of nonisothermal laminar duct flows of real fluids with temperature dependent properties

03 p0295 A73-13998

Inverse Laval problem of three dimensional subsonic and supersonic flows in nozzles and ducts of variable cross section in terms of asymptotic series

03 p0246 A73-14046

Two numerical methods for three-dimensional boundary layers.

04 p0433 A73-15003

Numerical predictions of some three-dimensional boundary layers in ducts.

04 p0433 A73-15006

Calculation of interacting turbulent shear layers - Duct flow.

[ASME PAPER 72-WA/FE-25] 04 p0435 A73-15849

Secondary flow in the entrance region boundary layers of an expanding square duct.

[ASME PAPER 72-WA/FE-34] 04 p0404 A73-15851

The influence of combustor parameters on the combustion of particle-laden fuels in ducted flows.

[AIAA PAPER 73-177] 05 p0640 A73-16919

Effect of bulk-reacting liners on wave propagation in ducts.

[AIAA PAPER 73-227] 05 p0566 A73-16952

Critical flows in open vertical ducts filled with superfluid helium under pressure

05 p0599 A73-17230

Knudsen flow in a rectangular duct of finite length.

06 p0684 A73-17426

Three-dimensional MHD duct flows with strong transverse magnetic fields. IV - Fully insulated, variable-area rectangular ducts with small divergences.

06 p0728 A73-17704

Heat transfer in the thermal entrance region of rectangular channels with a circumference only partially heated

06 p0768 A73-17918

Temperature of a duct flow under conditions of unsteady-state heat transfer

06 p0769 A73-18131

Dynamics of axial heat transfer in turbulent duct flow

06 p0770 A73-18831

Mass transfer coefficient measurement in turbulent ducted flow, obtaining numerical solution to diffusion equation

06 p0770 A73-18835

Energy conserving finite difference approximation for solution of unaveraged Navier-Stokes equations of three dimensional incompressible turbulent flow in square duct

07 p0810 A73-19263

Heat transfer in two-dimensional turbulent confined flows.

07 p0920 A73-19570

Flow of a conductive fluid through a cylindrical duct with periodic deformations in the presence of an azimuthal magnetic field

07 p0858 A73-20073

A zero-streamwise-pressure-gradient, three-dimensional turbulent boundary layer in a 90 deg curved rectangular duct.

08 p0953 A73-20796

Experimental verification of the energy dissipation mechanism in acoustic dampers.

08 p1024 A73-21472

Flowfield calculations for some supersonic sections with ducted heat addition.

09 p1028 A73-23089

Unsteady MHD duct flow by the finite element method.

10 p1256 A73-24289

Acoustically induced vibrations of slender rods in a cylindrical duct with parallel flow.

11 p1432 A73-24983

Wall-less electromechanical flow structures developed similar to structures with fluid partially ducted at free sources by external forces

11 p1403 A73-25255

Asymptotic Nusselt numbers for dissipative non-Newtonian flow through ducts.

11 p1346 A73-25370

Investigation of the throughput capacity of the longitudinal cooling ducts of gas turbine blades

12 p1532 A73-27093

Effects of wall admittance changes on duct transmission and radiation of sound.

13 p1658 A73-28060

Heat transfer to laminar flow in vertical rounded corner square duct, noting wall shear stress parameter as laminarization criterion

13 p1704 A73-28428

Wing-fuselage junctions fairings compromise design, describing rotational eddies formation mechanism for unsteady ducted flow and wing root phenomena

13 p1564 A73-28836

Linear viscoelastic fluid parallel flow in straight duct of uniform cross section under axial pressure gradient

13 p1602 A73-28918

Free stream turbulence and transition in a circular duct.

13 p1602 A73-29014

Rough estimate of the heat transfer coefficient of a liquid in laminar and turbulent flow through plane ducts

14 p1744 A73-30012

Radiation from line vortex filaments exhausting from a two-dimensional semi-infinite duct.

14 p1744 A73-30168

Gas flow properties in curvilinear turbine ducts, considering pressure gradient, outer flow shear and Coriolis force on boundary layer

14 p1712 A73-30649

Velocity hodograph solvability and univalence problems in hydromechanics for profiles in duct, bounded flow and cascades

15 p1861 A73-31151

Influence of a longitudinal pressure gradient on turbulent diffusion in ducts

15 p1862 A73-31297

A simple estimate of the effect of ejector length on thrust augmentation.

15 p1824 A73-31745

The optimization of modal sound attenuation in ducts, in the absence of mean flow.

15 p1865 A73-32152

Longitudinal evolution of the velocity and pressure in a circular duct in pulsating flow

16 p1998 A73-32803

Identification and coding of fluid and electrical piping system functions.

[SAE AIR 1273] 16 p1970 A73-33019

Dynamic gas temperature measurements in a gas turbine transition duct exit.

[ASME PAPER 73-GT-7] 16 p2047 A73-33485

Approximation for thin boundary layers in the sheared flow duct transmission problem.

16 p2000 A73-33679

- The propagation and attenuation of sound in lined ducts containing uniform or 'plug' flow. 16 p1970 A73-33944
- Acoustic energy flow in lined ducts containing uniform or 'plug' flow. 16 p2038 A73-33945
- Some aspects of 'sound' attenuation in lined ducts containing inviscid mean flows with boundary layers. 16 p2049 A73-33946
- Study of gas-phase reactions in particle-laden, ducted flows. 17 p2150 A73-34194
- Pressure distributions in porous ducts of arbitrary cross section. [ASME PAPER 73-FE-9] 17 p2152 A73-35008
- Numerical solution procedure for calculating the unsteady, one-dimensional flow of compressible fluid /with allowance for the effects of heat transfer and friction/. [ASME PAPER 73-FE-30] 17 p2153 A73-35022
- Theoretical analysis of forced laminar convection heat transfer in the entrance region of an elliptic duct. 17 p2256 A73-35850
- Observation and calculation of a steady, laminar separated flow. 17 p2157 A73-35866
- Sound measurements within and in the radiated field of an annular duct with flow. 18 p2302 A73-37028
- On energy, group velocity and small damping of sound waves in ducts with shear flow. 18 p2302 A73-37031
- Noise of jets discharging from a duct containing bluff bodies. 19 p2472 A73-37291
- Incompressible potential flow past axisymmetric bodies in cylindrical pipes. 19 p2376 A73-37489
- Studies on the hydraulic loss in pipe bends - Results for 90-deg screw type elbows. 19 p2420 A73-37672
- On the stability of the conduction regime of natural convection in a vertical slot. 19 p2505 A73-38476
- Vibration of tubes containing flowing fluid. [MERL-TN-72-2] 20 p2616 A73-39147
- MPD annular duct flows in crossed external fields for arbitrary values of the Hall parameter. 20 p2599 A73-39675
- On the coexistence of laminar and turbulent flow in a narrow triangular duct. 20 p2549 A73-39813
- High-speed photographic observation of the propagation of a shockwave in a branched-tunnel system. 21 p2676 A73-39983
- Propagation of acoustic waves in a fluid flowing through a cylindrical duct. 21 p2677 A73-40944
- Attenuation of spiral modes in a circular and annular lined duct. 22 p2839 A73-41714
- The numerical prediction of streamer growth in MHD ducts. 22 p2894 A73-42558
- Unsteady aerodynamic loads on slender cones at free-stream Mach numbers from 0 to 22. [AIAA PAPER 73-998] 24 p3053 A73-44833
- A difference theory for noise propagation in an acoustically lined duct with mean flow. [AIAA PAPER 73-1007] 24 p3078 A73-44840
- Acoustic propagation in ducts with varying cross sections and sheared mean flow. [AIAA PAPER 73-1008] 24 p3078 A73-44841
- Sound interaction with a helical flow contained in an annular duct with radial gradients of flow, density and temperature. [AIAA PAPER 73-1010] 24 p3078 A73-44842
- Theoretical studies of sound emission from aircraft ducts. [AIAA PAPER 73-1012] 24 p3078 A73-44844
- Transmission and far field radiation of sound waves in and from lined ducts containing shear flow. [AIAA PAPER 73-1013] 24 p3078 A73-44845
- On aeroacoustic coupling in free-stream turbulence manipulators. [AIAA PAPER 73-1015] 24 p3054 A73-44847
- Laser Doppler velocimeter measurement of laminar velocity profiles for developing MHD flow in rectangular duct, noting inlet effects on flow development. 24 p3118 A73-45464
- Elevated temperature toughness and a dimensionless parameter involving the zero-ductility temperature. 04 p0459 A73-14670
- Ductile fracture initiation, propagation, and arrest in cylindrical vessels. 04 p0506 A73-14697
- Photographic and metallographic evidence of two stage ductile materials erosion mechanism under particle impact, describing impact velocity, particle size and angle effects. 07 p0839 A73-20225
- Lamellar tearing and the slice bend test. 07 p0832 A73-20275
- Effects of heat treatment on the properties of a molybdenum-carbon-nickel alloy and joints in it. 07 p0840 A73-20371
- Grain size effects on strength and ductility of two phase Ni-Cr and Ni-Mo alloys at high and low deformation temperatures. 09 p1101 A73-22164
- Fine grained ingot source Be ductility at 700 C as function of strain rate, noting superplastic behavior with grain boundary sliding at low strain rates. 09 p1102 A73-22413
- Effect of test temperature on energy of fracture of graphite. 09 p1110 A73-23062
- Effect of magnesium additions on the ductility of heat-resistant nickel alloys. 09 p1108 A73-23230
- Ductility of recrystallized molybdenum as a function of oxygen concentration and grain size. 09 p1108 A73-23231
- Fracture mechanics of brittle matrix ductile fiber composites. 09 p1111 A73-23251
- Void initiation and growth in Al alloys due to inclusions, presenting dislocation model for ductile fracture strength. 09 p1109 A73-23256
- Surface crack slow growth onset investigation with near tip strain as ductile fracture criterion, measuring fracture strength. 09 p1109 A73-23264
- Ductile fracture strain criteria from known stress-strain relationships, predicting microscopic crack and void nucleation strain. 09 p1164 A73-23322
- Composite material production by grinding Ni-Al-Ti alloy powder with other mixed powders, noting alloying elements effects on corrosion resistance and ductility. 11 p1372 A73-25406
- Mechanical properties of weld, base metal and coated columbium alloy Cb 752. 11 p1375 A73-26356
- Effect of prestraining on the brittleness of molybdenum. 12 p1511 A73-27058
- Solid fracture theories based on brittle region toughness parameter and absorbed specific fracture work factor above ductile-brittle transition respectively. 13 p1640 A73-29479
- Investigation of some principles in the processes of creep and fracture in heat-resistant materials. 13 p1643 A73-29626
- Strength and ductility of chromium-nickel-manganese steel as a function of carbon and nitrogen contents over the range 20-253 C. 14 p1759 A73-30315
- Enhanced ductility in metals /Superplasticity/. 17 p2240 A73-34113
- Relationship between K/Ic and plane-strain tensile ductility and microscopic mode of fracture. 17 p2190 A73-34876
- Fracture toughness, ductility and cleavage mechanisms of crack extension in structural materials. 19 p2502 A73-38550
- Heat resistant materials cracking and fracturing caused by ductility loss at high temperatures, discussing cavitation mechanisms, microcracks, creep tests and time dependence. 21 p2722 A73-41576
- Grain size effects on strength and ductility of two phase Ni-Cr and Ni-Mo alloys at high and low deformation temperatures. 22 p2875 A73-42112
- Unified plastic yield criterion for ductile solids. 22 p2923 A73-42555
- Influence of deformation on the strength and ductility of low-alloy chromium. 23 p2996 A73-44290
- Deformation characteristics and ductility of two-phase titanium alloys of laminated structure. 24 p3099 A73-44573
- DUCTS**
- NT ACOUSTIC DUCTS
- NT AIR DUCTS
- Magnetic duct field and induction distributions for liquid metal pump design, using Tozoni integral equations. 10 p1177 A73-23475
- The influence of the sea evaporation duct on the phase of the received field on a line-of-sight path. 16 p1981 A73-33713
- Russian book - Hydraulic ducts of control systems in aviation: The effects of external factors. Shop testing, and reliability. 19 p2389 A73-37766
- Electromagnetic scattering by discontinuities in weakly inhomogeneous parallel plane waveguides or ducts, noting edge diffraction singularities role from ray optical calculation. 20 p2528 A73-38847
- A numerical investigation of the current and density distributions for a non-equilibrium plasma in a segmented electrode duct. 21 p2748 A73-40926
- DUFFING DIFFERENTIAL EQUATION**
- Numerical computation of forced oscillations in coupled Duffing equations. 09 p1113 A73-23022
- Canonical perturbation theory solution for nonconservative dynamic systems equations of motion, considering Duffing and van der Pol equations. 10 p1283 A73-24665
- Quadratically coupled oscillators interaction at semiresonant frequencies, considering time dependent Duffing equation and frequency divider application. 13 p1661 A73-29375
- Stability of an almost periodic solution to a generalized Duffing equation. 20 p2593 A73-39493
- Comparison of the Kryloff-Bogoliuboff method and the refined elliptic function method. 22 p2882 A73-43071
- System stability analysis technique for nonlinear oscillation via Van der Pol and Duffing equations, noting ease of approximating higher harmonics. 23 p3007 A73-44085
- DUMMIES**
- Anthropometric dummy design improvements, detailing verisimilitude specifications for harness support in accident tests and design of chest, spine, shoulder and pelvic areas. 17 p2114 A73-34617
- Aircraft crash injury reduction through seat and restraint design, discussing dummy size considerations, seat belts, aircraft acceleration and injury types [SAE PAPER 730290] 17 p2114 A73-34655
- DUNES**
- Mars Hellespontus region identification from Mariner 9 photographs as wind produced dunes, considering albedo features. 19 p2477 A73-37210
- Reversing barchan dunes in lower Victoria Valley, Antarctica. 21 p2687 A73-41214
- DUNGEYS WIND SHEAR MECHANISM**
- U WIND SHEAR
- DUNITE**
- Lunar 'dunite', 'pyroxenite' and 'anorthosite.' 03 p0375 A73-14108
- DUOPLASMATRONS**
- A low-power MPD thruster of DuoPlasmatron type. 18 p2342 A73-36154
- DUPLEXERS**
- Override waveguide polarization duplexers based on metal grating or dielectric plate at Brewster angle, measuring performances in microwave circuit and with HCN IR laser. 23 p2960 A73-44071
- DUPPLICATING**
- U REPRODUCTION [COPYING]
- DURABILITY**
- Durability tests of a five-centimeter diameter ion thruster system. [AIAA PAPER 72-1151] 03 p0356 A73-13455
- Investigation of the durability of metals under conditions of transition from brittle to plastic failure. 10 p1235 A73-24456
- Durability of the Kh18N10Ti steel under the combined influence of creep and thermal cycling. 17 p2187 A73-34335
- Investigation of the durability of metals under conditions of a transition from brittle fracture to plastic flow. 19 p2442 A73-38138
- DUST**
- NT COSMIC DUST
- NT INTERPLANETARY DUST
- NT LUNAR DUST
- NT METEOROID DUST CLOUDS
- NT METEOROIDAL DUST BELT
- NT ZODIACAL DUST
- Return of normal stratospheric turbidity and a new short dust event during October 1971. 01 p0038 A73-10374
- Upper atmospheric dust concentrations in polar regions. 02 p0215 A73-12260
- Type II comet model for head and tail regions release of dust particles having wide size distribution. 04 p0494 A73-14759
- The use of a gas laser for sizing single particles of airborne dust. 05 p0584 A73-16444

- Martian dust storm from photometric observations on board the Automatic Interplanetary Station Mars 3
05 p0620 A73-17018
- Upper atmospheric dust particle temperature and related Na atom abundance seasonal variation based on energy budget and Na sublimation rate considerations
05 p0571 A73-17061
- Closed form solutions for dust density and temperature distributions in shock layer of hypersonic wedge flow
05 p0533 A73-17115
- Mariner 9 IR spectral features due to carbon dioxide, water vapor and silicate dust suspended in Mars atmosphere before/after planet-wide dust storm
06 p0746 A73-17482
- Mariner 9 S-band radio occultation measurements of Mars shape and atmospheric parameters, discussing global dust storm and equatorial surface pressure
06 p0746 A73-17487
- Atmospheric dust trace elements levels sampled in United Kingdom, considering natural origin
07 p0820 A73-20279
- A numerical model of thermal radiation in a dusty atmosphere.
08 p0960 A73-21383
- Ground based spectroscopic observation of carbon dioxide distribution on Mars surface, noting Tharsis region pressure anomaly, ridge slope and dust storm activity
09 p1144 A73-22262
- Mars dust storm observations at time of great oppositions, suggesting local time and space meteorological conditions and feedback processes favoring global dust spread
09 p1144 A73-22269
- Effect of the shape and orientation of atmospheric dust particles on the spectral position and form of the attenuation band
09 p1077 A73-22372
- Turbulent friction drag of a dusty gas. I - Theoretical study.
09 p1072 A73-23325
- Missile ablation shields erosion by high velocity dust, considering wind tunnel test data on phenolic cork for various dust materials, particle sizes and velocities
[AIAA PAPER 73-379] 11 p1388 A73-25509
- The radiation regime of the Martian surface and dusty atmosphere
11 p1418 A73-25628
- A model of a Martian Great dust storm.
11 p1418 A73-25715
- Mars photographic observations during opposition, analyzing polar caps, surface reliefs, dust storms and atmospheric optical thickness
12 p1542 A73-27498
- Test data obtained with an experimental gas turbine operated with kerosene combustion products artificially contaminated by dust
14 p1785 A73-30650
- Electrical breakdown caused by dust motion in low-pressure atmospheres - Considerations for Mars.
15 p1941 A73-32267
- Flow of a dust suspension over an ellipsoid of revolution.
17 p2091 A73-34348
- Convective heating in dust-laden hypersonic flows.
[AIAA PAPER 73-761] 18 p2371 A73-36376
- Mechanisms for Mars dust storms.
19 p2485 A73-37656
- Radiation regime of the surface and dust-filled atmosphere of Mars.
19 p2486 A73-38140
- Structure of dust storms from ITOS-I T.V. images obtained over Iraq and the Gulf of Persia.
20 p2584 A73-39854
- Portable respirable dust monitor for continuous concentration measurement by light scattering of gas laser cavity beam
21 p2708 A73-39923
- ### DUST COLLECTORS
- Rocket-borne instruments for cosmic dust particles detection in extraterrestrial space, noting collector foils and plates fabrication
06 p0748 A73-17768
- Noctilucent cloud sampling by a multi-experiment payload.
21 p2775 A73-41414
- Dust measurements in the upper atmosphere during and in the absence of noctilucent cloud display.
21 p2691 A73-41417
- ### DWARF STARS
- #### NT SUBDWARF STARS
- #### NT WHITE DWARF STARS
- Self-accretion of matter, red subluminoous stars and early evolution of low-mass stars.
02 p0225 A73-12808
- The luminosity function and density distribution of disk population stars.
07 p0876 A73-19358
- Dwarf binary component convective shell behavior under gravitational field periodic tidal action, noting conditions for thermal instability
08 p1012 A73-21548
- Cooling effects of CO IR opacity in stellar atmospheres of dwarfs and supergiants, considering application to sun and grain formation in cooler stars
09 p1142 A73-22031
- Elongated shells around novae and concentration near orbital planes resulting from perpetual matter losses, considering close dwarf binaries and recurrent novae
09 p1145 A73-22288
- The red dwarf stars of the UV Ceti-type in the neighbourhood of the sun.
15 p1935 A73-31480
- Shock waves in gas flows in close binary dwarf star systems
17 p2226 A73-34366
- ### DWELL
- Dwell times of thin exploding wires.
15 p1913 A73-31934
- ### DYADICS
- Event manifold curvature tensor as six dimensional bivector space via dyadic projections, applying to gravitational waves description
08 p0989 A73-21521
- Digital multiplicity filters analysis via Walsh functions, considering time discrete dyadic invariant systems
09 p1065 A73-23111
- Dyadic formalism in two dimensional distributions in general relativity theory, discussing gravitational, diffusive, wave, Einstein and preservation equations
14 p1776 A73-30942
- ### DYE LASERS
- Broadly tunable, narrow linewidth dye laser emission in the near infrared.
11 p1375 A73-25366
- Rhodamine laser frequency locking using Faraday filter for tuning to sodium D lines
13 p1628 A73-29249
- Observations of stimulated anti-Stokes radiation in barium vapour.
14 p1776 A73-29697
- Quenching of lasing and the short wave fluorescence in a 3,3 diethylthiatricarbocyanine dye laser
14 p1757 A73-30462
- Experimental studies of pulse lasers using organic-dye solutions covering the spectral range from 7,100 to 11,000 Å - Analysis of optimal generation conditions
17 p2184 A73-34918
- Investigation of the characteristics of organic compound lasers with dispersive resonators
17 p2184 A73-34920
- New algae mapping technique by the use of an airborne laser fluorosensor.
17 p2163 A73-35412
- Single mode operation of flashlamp pumped dye laser achieved after emission spectrum line narrowing by interference filter and successive quartz Fabry-Perot etalons
17 p2185 A73-35769
- Kinetics of bleaching in polymethine cyanine dyes.
17 p2186 A73-35793
- New improved laser dye for the blue-green spectral region.
17 p2186 A73-35800
- Difference frequency generation by optical mixing of two dye lasers in proustite.
19 p2438 A73-38165
- Tuning and bandwidth control of laser pumped continuous dye lasers for obtaining stable single axial mode operation
20 p2571 A73-38624
- Adiabatic following and the self-defocusing of light in rubidium vapor.
20 p2571 A73-38632
- Emission of aqueous solutions of rhodamine 6G with detergent additives in the presence of flash lamp excitation
21 p2711 A73-40305
- Dye laser operation at independently tunable wavelengths via utilization of holographic wavelength selectors in succession, discussing limitations on multiple frequency tuning range
21 p2713 A73-40460
- Excited state absorption spectroscopy of alkaline earths selectively pumped by tunable dye lasers. I - Barium arc spectra.
21 p2713 A73-40472
- Laser induced red-blue energy transfer upconversion in Pr(3+) doped lanthanum fluorides via excitation annihilation involving pairs of ions
21 p2715 A73-40934
- Study of excitation transfer in dye mixtures by measurements of gain spectra.
21 p2716 A73-40968
- Dye laser tuning with pellicles.
22 p2870 A73-42707
- Self diffraction of coherent wave radiation by absorption from excited levels of Nd laser light induced phase diffraction gratings in thin layer rhodamine
22 p2870 A73-42723
- Ultrashort pulses from mode-locked cw dye lasers.
22 p2871 A73-43079
- Quenching effects in flashlamp-excited polymethine dye lasers.
22 p2871 A73-43083
- Q switched Nd-YAG laser third harmonic for pumping dye laser, extending tunable output range to blue region
23 p2989 A73-44373
- Rapidly fading absorption induced in polymethine dyes by nanosecond pulses of ruby laser radiation
24 p3096 A73-44959
- Microwave optical double resonance spectra of CW dye laser pumped transitions in BaO
24 p3096 A73-44976
- Influence of photodecomposition on the emission of a lamp-pumped dye laser
24 p3098 A73-45518
- ### DYES
- Simultaneous two-wavelength selection in the N2 laser-pumped dye laser.
01 p0058 A73-10126
- Passive mode locking of the cw dye laser.
01 p0058 A73-10129
- An 11 megawatt 6.8 joule flashlamp pumped coaxial liquid dye laser.
02 p0175 A73-11956
- The generation of tunable near IR radiation using a nitrogen laser pumped dye laser.
03 p0318 A73-12869
- Combined nonlinear amplification and absorption role in ultrashort pulse generation of mode locked quasi-continuous dye laser in absence of short relaxation time
03 p0318 A73-12870
- Transient analysis of an electronically tunable dye laser. I - Simulation study.
03 p0320 A73-14457
- CW dye laser with dye solution pumped through simple nozzles to provide unconfined flowing thin streams with optical quality and long term stability
03 p0320 A73-14460
- The effect of pH on photobleaching of organic laser dyes.
03 p0320 A73-14462
- Organic dye lasers use as continuously tunable sources of coherent light, discussing molecular energy level systems and transitions
05 p0583 A73-16337
- Picosecond pulses from a passively mode-locked cw dye laser.
05 p0585 A73-17222
- Frequency shift in a mode-selected dye laser.
05 p0586 A73-17225
- Time dependence of the gain of an optically pumped solution of rhodamine 6G.
06 p0703 A73-18598
- The effect of an electric field on the active medium in a dye laser.
07 p0834 A73-19540
- Angular dispersion of an acoustooptic Bragg cell used in the wavelength tuning of an organic dye laser.
08 p0975 A73-21056
- Study and development of a dye laser with coupled modes excited by a flash tube and emitting in the near infrared
08 p0976 A73-21493
- A photochemical method of determining the optical pumping energy absorbed by rhodamine dyes under conditions corresponding to stimulated emission of radiation
09 p1095 A73-22668
- A tunable laser based on an organic dye solution and providing highly monochromatic, stable single-frequency emission
09 p1097 A73-23010
- Possibility of smoothly tuning the emission frequency of a mixed-dye laser
10 p1228 A73-24582
- Effect of concentration on laser threshold of organic dye laser.
10 p1229 A73-24695
- Direct measurement of the fluorescence energy yield of a rhodamine 6G solution with the aid of an Ar+ laser
11 p1377 A73-26146
- Superradiant waveguide dye laser pumped by flash lamps, noting power output and stable mode pattern insensitivity to disturbance and thermal effects
11 p1378 A73-26324
- Control of laser-pulse shape with the aid of an organic dye switch
18 p2322 A73-36558
- Advantages of using polymer bases as fixing agents in hydrotype printing
21 p2646 A73-40258
- Influence of certain wetting agents on the optical sensitization and retention of the photographic properties of a finished layer
21 p2647 A73-40271
- Compartmental analysis of biological system with a digital computer.
22 p2829 A73-42228
- The complications of coronary arteriography.
22 p2806 A73-42343
- ### DYNAMIC CHARACTERISTICS
- #### NT AERODYNAMIC DRAG

NT AERODYNAMIC STABILITY
NT AIRCRAFT STABILITY
NT ATTITUDE STABILITY
NT BOUNDARY LAYER STABILITY
NT COMBUSTION STABILITY
NT CONTROL STABILITY
NT DIRECTIONAL STABILITY
NT DRAG
NT DYNAMIC PRESSURE
NT DYNAMIC STABILITY
NT FLAME STABILITY
NT FLOW CHARACTERISTICS
NT FLOW DISTRIBUTION
NT FLOW STABILITY
NT FLOW VELOCITY
NT FREQUENCY STABILITY
NT FRICTION DRAG
NT GYROSCOPIC STABILITY
NT HOVERING STABILITY
NT INTERFERENCE LIFT
NT LIFT
NT LONGITUDINAL STABILITY
NT MAGNETOHYDRODYNAMIC STABILITY
NT MINIMUM DRAG
NT MOTION STABILITY
NT PRESSURE DRAG
NT ROTARY STABILITY
NT ROTOR LIFT
NT SATELLITE DRAG
NT SPACECRAFT STABILITY
NT TRANSIENT RESPONSE
NT VISCOUS DRAG
NT WAVE DRAG

Dynamic and thermodynamic effects addition to basic Boussinesq convection for convection in stars, discussing rotation, magnetic fields, radiative transfer and state equation 01 p0094 A73-10061

A study of the kinematic and dynamic characteristics in the wake behind a plate in an unbounded flow 01 p0032 A73-10620

Stress analysis and dynamic investigation of turbine blades from constrained torsion theory, calculating free torsional vibration frequencies 02 p0229 A73-11621

Application of electrical modeling in the analysis of the dynamic properties of temperature sensors 02 p0166 A73-11637

Dynamic characteristics of two bodies coupled by common axis, noting equations of motion of Lagrange gyroscopes system 02 p0192 A73-11766

Operators tolerated by the dynamics equations in the three-dimensional problem of elasticity theory 02 p0230 A73-11781

Spectral analysis of integro-differential forms in spatial dynamic problems of the theory of elasticity 02 p0232 A73-11820

Low temperature dynamic mechanical properties of polyurethane-polyether block copolymers. 02 p0185 A73-12426

Model studies of an electrohydraulic amplifier 03 p0258 A73-14617

Control of the motion of a solid body with servo couplings 05 p0597 A73-16611

On the decomposition of a dynamical system into non-interacting subsystems. 05 p0591 A73-16824

Three dimensional dynamic characteristics of solid particles suspended by polluted air flow in a turbine stage. [AIAA PAPER 73-140] 05 p0531 A73-16889

Influence of recombinations in the base contact and on the base surface upon static and dynamic characteristics of the p-n junction. 06 p0674 A73-17816

Nonlinear dynamic systems controllability theorem formulation and proof using matrix theory 06 p0716 A73-17853

Point plot recording instrument for instantaneous signal values measurement, discussing dynamic characteristics of constant plotting rate devices 06 p0693 A73-18168

A class of almost periodic motions in systems with impulses 06 p0724 A73-18681

Analytic construction of adaptive systems with stabilization of the dynamic characteristics. 07 p0805 A73-20039

Russian book - Dynamics of rocket control systems with onboard digital computers. 07 p0906 A73-20229

Dynamic analysis of tidal effects arising from hyperbolic close encounters of massive body past galaxy, calculating matter velocity field and galactic structure distortion 08 p1004 A73-20907

Reduction of phase non linearities in Traveling Wave Tubes (TWT). 09 p1062 A73-22305

Prediction models for surface and air transportation dynamic environments, considering broadband and

single frequency continuous and recurrent and intermittent discrete excitation modes 09 p1032 A73-22718

An 'orthogonalization' method for determining the dynamic characteristics of an elastic body from static vibration tests 09 p1161 A73-23090

The dynamic properties of unidirectional fibre reinforced composites in flexure and torsion. 10 p1240 A73-24279

Parachute opening dynamic analysis, taking into account risers, shrouds and canopy cloth elastic properties on opening history and loads 10 p1176 A73-24647

Unsteady aerodynamics of separating and reattaching flow on bodies of revolution. 10 p1173 A73-24816

Dynamic characteristics of space thin beams. 11 p1433 A73-25126

Multiple shaker resonance testing for structural dynamic characteristics, considering natural frequencies, mode shapes, damping and generalized masses [AIAA PAPER 73-402] 11 p1440 A73-25531

Terrain-vehicle dynamic interaction studies of a mobility concept /ELMS/ for planetary surface exploration. [AIAA PAPER 73-407] 11 p1343 A73-25536

Dynamic properties of graphite fiber honeycomb panels. [AIAA PAPER 73-326] 11 p1388 A73-25556

External static and dynamic characteristics of input-output sequences of logic elements 12 p1475 A73-26764

Principle of virtual work in the dynamics of systems having variable mass solids for constitutive elements 12 p1523 A73-27102

Laser dynamic theory with uniformly broadened and Doppler spectral lines based on nonlinear interactions between harmonic oscillations 12 p1506 A73-27139

Dynamic characteristics, stability and steady state accuracy for orbital gyroscope with digital control, noting bit density requirements of onboard computer 12 p1523 A73-27632

Application of Liapunov functions for studying the convergence of unconstrained minimization methods 13 p1657 A73-28018

Mass to wind and wind to mass adjustments in dynamic initialization for primitive equation model of atmospheric motion 13 p1652 A73-28270

Study of kinematic and dynamic characteristics in a wake behind a plate in an unbounded flow. 13 p1601 A73-28739

Nylon copolymers dynamical mechanical properties temperature dependence, discussing alpha peak shifts, polyamides relaxation and ordered structure 13 p1646 A73-29526

Dynamic properties of human and animal middle ear in terms of acoustic impedance, transfer function, impulse response, sound diffraction and reflex sensitivity 14 p1715 A73-30279

Time varying linear and constant bilinear dynamic systems state space structure, obtaining canonical decomposition by suitable choice of input/output interaction properties 14 p1739 A73-30778

A dynamic and aerodynamic analysis of an articulated autorotor decelerator system. [AIAA PAPER 73-463] 15 p1827 A73-31449

Simultaneous control of temperature and humidity in a confined space. I - Mathematical modeling of the dynamic behavior of temperature and humidity in a confined space. 15 p1959 A73-32597

Dynamic analysis procedure to locate vibration sources without simulated service tests, mapping structural surfaces at all frequencies via transfer function or mechanical impedance analysis 16 p2019 A73-33098

Study of the static and dynamic characteristics of a family of discrete pneumatic jet modules 16 p1971 A73-33670

Hydraulic jet amplifier design, considering selector static and dynamic characteristics, membrane attached plate, piston with feedback control and self oscillation elimination 16 p1971 A73-33672

Magnetohydrodynamics, hydrodynamics and dynamics of solar system model as contracting rotating cloud, discussing effects of turbulence 17 p2226 A73-34403

Dynamic behavior of satellites with large-area solar cell panels [DGLR PAPER 73-049] 17 p2239 A73-35485

Dynamic characteristics of a plasma diode under conditions of a low-voltage arc discharge. I - Theory of the dynamic characteristics 18 p2339 A73-36557

Application of the Ornstein-Uhlenbeck stochastic process to the study of dynamic systems in an environment of stochastic disturbances. 18 p2330 A73-36829

Probability method and algorithm for analyzing the dynamic precision of pulse generators 18 p2294 A73-37024

Analysis of some functional parameters of rotary hydrostatic engines under dynamic conditions by modeling on a computer 19 p2388 A73-37557

Application of the Gauss principle in the dynamics of systems having rigid solids of variable mass as constituent elements 19 p2459 A73-37652

Series representation of the solution of nonlinear partial differential equations and its use in determining the dynamic characteristics of nonlinear plants with distributed parameters 20 p2581 A73-38986

A method of processing a priori information about a controlled plant with the aim of reducing the number of changing parameters of the dynamic characteristics 20 p2541 A73-38993

The characteristics of hydraulic tensile-test machines of the pendulum type and their effect on the tensile test 20 p2545 A73-39629

Photoelastic investigation of dynamic stress conditions involving rapidly varying principal stress directions 21 p2695 A73-39965

Specific problems of the dynamics of composite systems 21 p2788 A73-41603

Dynamic behaviour of orthotropic plates using finite difference technique. 22 p2917 A73-41716

Dynamic operative image formation and function features during extrapolation tracking of visibly moving target, noting image reaction to operator performance 22 p2812 A73-41886

Human recognition of dynamic pattern changes in numerical series displayed on spatiotemporal panels, discussing learning times and reactions to pattern disruptions 22 p2812 A73-41887

Dynamic characteristics of a plasma diode with a low-voltage arc discharge. II - Experimental study of dynamic characteristics 22 p2833 A73-42386

Dynamics of quasigeostrophic flows and instability theory. 22 p2842 A73-42450

German monograph - Theoretical and experimental investigation of digital hydraulic positioning devices. 22 p2801 A73-42848

German monograph - Characteristics of motion of an elastically supported rotor with interior damping. 22 p2867 A73-42849

A model of the dynamic behavior of the coaxial-flow gaseous-core nuclear reactor. 23 p3005 A73-43387

Study of the parameters of three-dimensional holographic gratings in LiNbO3 crystals 23 p2987 A73-43717

Typical characteristics of dynamic systems nearly all of whose trajectories remain stable under steadily acting disturbances 24 p3109 A73-44424

Experimental study of the dynamic parameters of varactor diodes 24 p3072 A73-44929

DYNAMIC CONTROL

Certain aspects of the bionic analysis and control of dynamic systems 01 p0012 A73-10658

Programming and correcting control effects for prescribed interrelationship between variable states of dynamic control, noting system synthesis for programmed motion 01 p0027 A73-10667

Method of structural synthesis of multivariable systems for automatic control of plants with incomplete information 01 p0028 A73-10672

Liapunov vector functions in stability analysis of nonlinear dynamic distributed parameter, interconnected and multivariable systems 01 p0078 A73-11073

Effects of controller dynamics on the stability of a class of optimal control systems. 01 p0028 A73-11518

Variational method in the invariance problem for controlled systems. 02 p0149 A73-12117

Optimization of control and observation processes in dynamic systems under random perturbations. 02 p0149 A73-12118

Linear dynamic control system synthesis methods based on aggregation and suboptimal control by decomposition, minimizing quadratic performance criterion 02 p0149 A73-12124

Book on modal control theory and applications covering continuous and discrete time lumped param-

ter linear dynamic systems controllability and observability characteristics

03 p0285 A73-13989

Optimal control approximations for time delay systems.

03 p0286 A73-14195

Demonstration of digital three axis spacecraft control.

04 p0432 A73-14738

Optimal trajectory control system synthesis via Pontryagin maximum principle, taking into account system dynamics, control constraints and boundary conditions

04 p0429 A73-15201

On-line parameter estimation of nonlinear dynamic system with unknown impulsive inputs by Kalman filter with application to maneuvering spacecraft tracking

04 p0431 A73-15270

The mathematics of coordinated control of prosthetic arms and manipulators.

[ASME PAPER 72-WA/AUT-4] 04 p0414 A73-15884

Automatic control system synthesis for optimal correction, maximum accuracy and stability of linear unsteady final action systems under deterministic and random actions

05 p0561 A73-16420

On the dynamics of randomly excited nonlinear systems.

06 p0715 A73-17393

On an application of Lie group theory to the optimal control problem for linear dynamic systems with time-varying parameters.

06 p0679 A73-17954

Time-invariant single input/output controllable and observable tracking servosystem, discussing dynamic trajectory controller and cost functional selection for zero steady state error

06 p0680 A73-18516

Dynamic system optimal control problems with higher order state variable inequality constraints, obtaining solutions with boundary arcs and isolated points

06 p0680 A73-18519

Invariance conditions and controllability relation of linear and nonlinear dynamic systems, including composite systems and systems with deviating argument

06 p0724 A73-18678

Frequency domain synthesis algorithm for linear multivariable system via state variable feedback combined with input dynamics compensation, applying to decoupling and model matching

06 p0682 A73-18866

Evolution equations of motion for program manifold of continuous control system with given transient response

07 p0852 A73-20632

Algorithmic construction of optimal controllers on the basis of incomplete information about the state of the plant

09 p1068 A73-22562

Solution of the Fokker-Planck-Kolmogorov equation for a dynamic system with analytical characteristics

09 p1068 A73-22563

Optimal observation laws for certain controlled motions

09 p1069 A73-22565

Liapunov vector functions in stability analysis of nonlinear dynamic distributed parameter, interconnected and multivariable systems

09 p1121 A73-22998

Incomplete/complete feedback and off-on control moments for prescribed orientation of solid body in rotational motion

10 p1248 A73-23744

A first-approximation theory of discrete nonautonomous stabilization systems

10 p1248 A73-23745

Discrete dynamic adaptive control algorithms for estimation of minimum loss function point trajectory characterizing system quality in nonstationary conditions

10 p1242 A73-24035

Stabilization of linear dynamical systems with output feedback.

10 p1199 A73-24037

Existence solution to linear differential rendezvous game of dynamic system with pursuit and evasion

12 p1524 A73-27402

Optimization of the parameters of heterogeneous multipurpose controlled systems using standard elements.

12 p1484 A73-27456

Computerized adaptive flight control for helicopter dynamic systems based on identification and optimization methods

13 p1569 A73-28829

Application of the theory of Markov processes in state estimation of dynamic systems and in control of flight-vehicle oscillations

15 p1942 A73-31239

Construction of equations of motion for program manifold of continuous control system with given transient response

15 p1913 A73-31686

Contribution to the synthesis of optimum control of motion of a point mass in a spherical lamella of a central gravitational field with finite miss vectors noncollinear with respect to radius vector and velocity vector.

15 p1915 A73-32602

Papers on optimal control and dynamic systems theory covering linear discrete systems observers, quasi-linearization, national economic policy, decision theory and closed loop formulation

Application of the dynamic filtration method to spacecraft orientation control problems

18 p2359 A73-36104

An application of truncated power series controllers for optimization of dynamic systems.

19 p2413 A73-38040

Parallel algorithms for optimum nonlinear state estimation.

19 p2413 A73-38041

Controllability and stabilizability of decentralized dynamic systems.

19 p2413 A73-38045

A practical filter for noisy dynamic systems with unknown time-varying parameters.

19 p2410 A73-38047

Suboptimal design of a class of nonlinear controllers.

19 p2414 A73-38068

Application of digital computer APU modeling techniques to control system design.

19 p2392 A73-38416

Controllability and synthesis of optimal dynamic systems

20 p2591 A73-38672

Controllability conditions and optimization solution to finite control problem during prescribed time for lumped parameter system

20 p2591 A73-38673

Approximate synthesis theory in problems of optimization of automatic control systems

20 p2591 A73-38674

Optimal invariant solution for compensating circuit of nonlinear control system under disturbances, using unperturbed motion prediction

20 p2538 A73-38676

Construction of improving variations during the optimization of determinate and stochastic systems

20 p2539 A73-38677

Determination of an optimal dynamic system according to complex statistical criteria in the presence of constraints

20 p2539 A73-38680

Some problems in the analysis and synthesis of statistically optimal constrained control

20 p2539 A73-38681

Dynamics and stability of the algorithm of a digital adaptive system using a prediction technique

20 p2532 A73-38688

Synthesis of a class of optimal discrete systems for correcting the trajectories of dynamic systems

20 p2592 A73-38697

Correctness, regularization, and the maximum complexity principle in the statistical dynamics of automatic control systems

20 p2540 A73-38699

Determination of the structural features of nonlinear dynamic systems

20 p2540 A73-38709

Certain methods of determining the dynamic characteristics of stochastic objects

20 p2540 A73-38710

Choice of optimal parameters for flight-vehicle control systems in the presence of random disturbances

20 p2590 A73-38991

Some nonlinear problems in optimal control

20 p2541 A73-38995

A study of systems with time-variable coefficients by the definite-integral method

20 p2542 A73-39037

Optimal stabilization of moving control plants during multichannel measurement of their coordinates

20 p2542 A73-39039

Stability and dissipativity of control systems containing unsteady nonlinearities

20 p2542 A73-39041

On-off control of an unstable plant with time lag

20 p2542 A73-39345

Adaptive control of forced motions in discrete extremal systems with independent search

20 p2542 A73-39346

Optimal active damping of vibrations

20 p2594 A73-39638

Optimal motions of a spacecraft relative to its center of mass

21 p2781 A73-40903

Application of the method of slipping modulating functions for identification of plants with time lag

21 p2670 A73-40993

Analysis of the accuracy of a system for controlling vibration tests with sinusoidal excitation

21 p2674 A73-40996

Operator response to sinusoidally varying normal and emergency cycles in dynamic control task, testing anticipatory aversion response ability and error response

22 p2812 A73-41885

Drive logic computation for variable stability aircraft in-flight simulators with six independent controllers providing dynamic motion and ground, crosswind and special effects

[AIAA PAPER 73-933] 22 p2799 A73-41971

Liapunov vector functions for solving stability problems of complex multidimensional dynamic control systems with nonlinear interactions and delay

22 p2887 A73-42606

Optimal closed automatic control systems synthesis in terms of minimum integral square error of phase coordinates during transient response time

22 p2836 A73-42609

Structural sensitivity transfer matrix for dynamic multiple link control system response minimization with corrections within frequency range

22 p2836 A73-42613

Linearization technique for synthesis of nonlinear two dimensional automatic control systems with cross disturbances, imposing constraints on motion coordinate deviations

22 p2836 A73-42615

Quasi-autonomous dynamic control subsystem interrelation and location for nonlinear multiple link automatic control synthesis with iterative integration of motion equations

22 p2836 A73-42616

Optimal dynamic accuracy measurement complexing for combined data processing in multidimensional automatic control systems with various sensors

22 p2836 A73-42618

Synthesis of optimal discrete controls for a continuous plant over a fixed time interval

22 p2837 A73-42619

French monograph - On the representation of linear dynamic systems with distributed parameters and its application to the study of intrinsic properties of these systems.

22 p2837 A73-42746

Problem of synthesizing a control system in the case of a plant involving random jerky forces

23 p2963 A73-43577

Linear time variant multivariable decentralized system stabilization by feedback control laws with dynamic compensation

23 p2964 A73-43821

On the adaptive control of linear systems using the open-loop-feedback-optimal approach.

23 p2964 A73-43824

Discrete time composite system stability with nonperiodic sampling in terms of vector Liapunov functions and real symmetric matrix test

23 p2964 A73-43826

Exponential stability theorems of multivalued difference equations for discrete dynamical systems

23 p3000 A73-44206

Application of the sensitivity theory to an analysis of the high-frequency components of motion

24 p3074 A73-45096

Frequency methods for simulation, analysis and identification of multiply-connected dynamic systems with delay

24 p3074 A73-45097

DYNAMIC LOADS

NT AERODYNAMIC LOADS

NT BLAST LOADS

NT CYCLIC LOADS

NT GUST LOADS

NT IMPACT LOADS

NT LANDING LOADS

NT ROLLING CONTACT LOADS

NT SHOCK LOADS

NT THRUST LOADS

NT TRANSIENT LOADS

NT VIBRATORY LOADS

NT WING LOADING

Bending stresses propagating from the clamped support of an impulsively loaded beam.

01 p0115 A73-10753

Experimental investigation of the behavior of cylindrical shells under dynamic loads

02 p0229 A73-11626

Dynamic calculation of the stretching of a spring with allowance for redistribution of mass along its length

02 p0230 A73-11720

On approximate solutions for rigid-plastic structures subjected to dynamic loading.

02 p0236 A73-12520

Constitutive equation for shock waves under dynamic load in prismatic bar axially prestressed to plastic range

03 p0383 A73-12903

Dynamic loads intermittency effects on structural fatigue strength, discussing conditions for materials structural recovery during load pauses

03 p0385 A73-13137

Photoelastic methods of studying dynamic stress problems 03 p0306 A73-13163

Impulsive loading of liquid squeeze film plane circular bounding surfaces, showing fluid inertia effect on bonding strength and cavitation relationship to viscosity 03 p0292 A73-13305

Nonlinear responses for a circular plate subjected to a dynamic ring load. 03 p0388 A73-13319

Impulsive loading of rectangular plates with finite plastic deformations. 03 p0389 A73-13322

Stability of fiberglass-reinforced cylindrical shell under the action of axial dynamic loads 03 p0392 A73-13746

Propagation of elastic waves in a cylindrical bar subject to a moving load on its lateral surface. 03 p0343 A73-13833

Refractory alloys fatigue life up to 950 C under non-stationary loading, noting log-normal law distribution 03 p0327 A73-14010

Flat Ti alloy sheet creep under variable loads at 300-400 C comparing prediction with test data 03 p0328 A73-14016

Elastic force minimization during transient process in mechanical multimass system under time dependent external load 04 p0509 A73-14976

Minimum-weight plastic design of continuous beams subjected to one single moveable load. 04 p0510 A73-15030

Error effects in dynamic force measurements performed on materials testing pulsators 04 p0450 A73-15475

Transverse oscillations produced by dynamic loads in structural elements of parabolic arc shape 04 p0513 A73-15506

Transient axisymmetric response of a conical shell frustum. 04 p0513 A73-15585

An approximate rigid-plastic analysis of shell intersections loaded dynamically. [ASME PAPER 72-WA/DE-1] 04 p0515 A73-15876

Deformation, displacement, and work bounds for structures in a state of creep and subject to variable loading. [ASME PAPER 72-APM-U] 05 p0632 A73-16529

Influence of a moving load on the vibrational characteristics of plates 05 p0636 A73-17093

Minimum principles in the dynamics of isotropic rigid-plastic and rigid-viscoplastic continuous media. 06 p0757 A73-17396

Dynamic behaviour of thin cylindrical shells subjected to high-speed travelling inner pressures. 06 p0758 A73-17518

Linearized theory of dynamically loaded thin rigid viscoplastic rectangular plates transient response, investigating strain rate effect 06 p0760 A73-17760

A new approach to the mode approximation for impulsively loaded rigid-plastic structures. 06 p0760 A73-17764

Dynamic plastic deformation of rings under impulsive load. 06 p0761 A73-17817

Large deflexion elastic-plastic response of certain structures to impulsive load - Numerical solutions and experimental results. 06 p0761 A73-17818

Transient response of a plastically anisotropic cylinder in plane strain. 07 p0908 A73-19081

Stress wave propagation in a laminated plate under impulsive loads. 07 p0908 A73-19089

The effect of metal gripping during dynamic loading 08 p0973 A73-21132

Treatment of dynamic snap-through problems by the direct Liapunov method 08 p1018 A73-21410

Investigation of the deformation of a hollow sphere under an impulsive load on the basis of three-dimensional elasticity theory and shell theory 08 p1019 A73-21761

Book - Vibration of solids and structures under moving loads. 09 p1159 A73-22526

Lie operators admitted by Lamé equations in three dimensional dynamic elasticity theory for arbitrary particle velocity and displacement and linear stress-strain tensor relation 09 p1159 A73-22585

Influence of material properties on dynamic fracture toughness of steels. 09 p1109 A73-23259

An approximate rigid-plastic analysis of shell intersections loaded dynamically. [ASME PAPER 72-WA/DE-1] 09 p1164 A73-23272

Bonded joints under long-term dynamic load and their resistance to climatic effects 10 p1224 A73-24089

Determination of the initial stress-strain state of a shallow spherical shell under the action of a dynamic load 10 p1290 A73-24310

Machine for life testing materials under varying tension in working media with high temperatures and pressures. 10 p1204 A73-24946

Flow and velocity fields simulation by calculating dynamic loads in moving liquid from pressure distribution, viscosity and gravitational acceleration [AIAA PAPER 73-409] 11 p1441 A73-25537

An examination of dynamic fracture under biaxial-strain conditions. 12 p1550 A73-27022

Dynamic moire methods for the bending of plates. 12 p1550 A73-27023

Dynamic tensile deformation of viscoplastic filament without bending rigidity, displacement constraints and cross sectional area variations 12 p1552 A73-27300

Book - Introductory structural analysis with matrix methods. 12 p1554 A73-27548

Relative magnitudes of stresses caused by static and dynamic launch vehicle loads. 13 p1697 A73-28833

Lamb solution analog for dynamic problem of homogeneous isotropic elastic body with impulsive force applied to semi-infinite plane incision 13 p1698 A73-29088

A sandwich-transducer technique for measurement of internal dynamic stress. 14 p1751 A73-29773

A comparison of theory and experiments on the dynamic plastic behavior of shells. 14 p1811 A73-30476

Buckling of viscoplastic cylindrical shells loaded by radial pressure impulse. 14 p1811 A73-30481

Linearized constitutive equations for thin viscoplastic shell deflection under dynamic loads 14 p1811 A73-30488

Rate-type constitutive equations for plateau predictions in dynamic plasticity for stress, strain and particle velocity functions 14 p1812 A73-30492

Extremum principles in the dynamics of rigid-plastic bodies and mathematical programming. 14 p1813 A73-30547

Designs of statically undeterminable elastoplastic systems under complex loads 15 p1946 A73-31141

Force-strain characteristics of dacron parachute suspension-line cord under dynamic loading conditions. [AIAA PAPER 73-446] 15 p1825 A73-31432

Influence of preliminary dynamic loading on the load-bearing capacity of cylindrical shells 16 p2075 A73-32693

Dynamic analysis of viscoelastoplastic anisotropic shells. 16 p2075 A73-32787

Optimal design of layered structures under dynamic loading. 16 p2075 A73-32790

Forced extensional vibrations of isotropic elastic plates with time dependent body forces, surface tractions and nonhomogeneous boundary conditions, using Kane-Mindlin theory 16 p2076 A73-32920

Structural shock response spectrum analysis for maximum dynamic loads and damage potential determination 16 p2014 A73-33135

The optimization of the cross-sectional profile of rods and plates subjected to dynamic stress 16 p2080 A73-33241

Probabilistic fatigue design alternative to Miner's cumulative damage rule. 16 p2081 A73-33643

Steady state diffraction of stress waves by semi-infinite running crack in elastic solid under dynamic loading, obtaining solution based on Wiener Hopf technique 16 p2082 A73-33910

Stability of a cylindrical shell under dynamic axial load 17 p2244 A73-34739

Inertial motion of a plastic ring under the action of a pulsed load 17 p2244 A73-34797

Prior-to-failure extension of flaws under monotonic and pulsating loadings. 17 p2246 A73-34884

Static, dynamic and fatigue load influence on solid lubricant compact bearings. [ASLE PREPRINT 73AM-1A-1] 17 p2178 A73-34976

Reduction of helicopter control system loads with fixed system damping. [AHS PREPRINT 733] 17 p2105 A73-35069

An investigation of the vibratory and acoustic benefits obtainable by the elimination of the blade tip vortex. [AHS PREPRINT 735] 17 p2105 A73-35071

Dynamic mechanical loading of solid material resulting in stress levels with impulse process described by fluid flow equations with application to shock compression of mechanical mixtures 17 p2193 A73-35541

Skylab experience with Apollo docking/latching loads. [AIAA PAPER 73-613] 18 p2358 A73-36091

Stability of cylindrical shells during rapid loadings 18 p2365 A73-36599

Lamb solution analog for dynamic problem of homogeneous isotropic elastic body with impulsive force applied to semiinfinite plane incision 19 p2498 A73-37638

A path-independent integral for transient crack problems. 19 p2500 A73-38114

Dynamics of structural systems subjected to moving loads. II - Half-spaces, plates, and shells under the action of moving loads 20 p2617 A73-39304

The problem of wave propagation in physically nonlinear rods of finite length 20 p2618 A73-39315

Improved relations in the dynamics of moderately thick shells and plates under the action of massive moving loads 20 p2618 A73-39316

Successive approximation technique for dynamic-load problems of nonlinear viscoelastic systems 20 p2593 A73-39322

Response of a cylindrical shell with filler to the action of a moving load 20 p2624 A73-39648

Study of elastoplastic deformations in a two-layer shell under dynamic loads 20 p2625 A73-39653

Dynamic contact problem for the case of longitudinal shear strain 22 p2927 A73-43051

Procedure and device for the study of the behavior of metals subjected to dynamic torsional stresses 22 p2868 A73-43171

Dynamical bending resistance of circular piecewise nonhomogeneous rigid-plastic plates in terms of Tresca yield condition for pressure pulse loads 24 p3146 A73-44679

A lower bound theorem for dynamically loaded rigid-viscoplastic structures. 24 p3146 A73-44680

Elastic deformation of isotropic infinite plane with central circular inhomogeneity and elastokinetics of two bonded dissimilar half planes under uniformly moving body force 24 p3152 A73-45343

DYNAMIC MODELS

Book - Lectures in mathematical models of turbulence. 01 p0031 A73-10123

Isovolumic contraction dynamics in man according to two different muscle models. 01 p0007 A73-10158

A continuum analysis of a two-dimensional mechanical model of the lung parenchyma. 01 p0010 A73-10168

Reduced dimensionality for minimization of degrees of freedom of skeletal activity models for anthropomorphic locomotion system synthesis 01 p0013 A73-11052

Wave propagation in elastic laminates using a multi-continuum theory. 01 p0117 A73-11364

Simulation of unsteady gas exchange in internal combustion engines 02 p0202 A73-11632

Statistical mechanics of the Burgers model of turbulence. 02 p0153 A73-12039

Three dimensional jet stream dynamics based on particle population evolution numerical simulation, interpreting solar system evolution 02 p0218 A73-12415

Multiple production processes hydrodynamic-type models validated by high energy particle collision collective interactions 02 p0208 A73-12659

Dynamical model for evolution of melted spherical drop of homogeneous glassy material to explain observed glassy spherules in lunar dust 03 p0368 A73-13090

Application of the turbulent eddy diffusivity transport equation to the analysis of turbulent flow in the radial face seal. 03 p0293 A73-13315

Analysis of free turbulent mixing flows without a net momentum defect. 03 p0296 A73-14187

Dynamic modelling of the innovation cycle as applied to fluidics. 03 p0258 A73-14450

Test field model for nonstationary inhomogeneous turbulence with mean shearing velocity

04 p0434 A73-15164

Estimation of unmodeled forces on a low-thrust space vehicle.

04 p0504 A73-15272

Linear solar collector conversion efficiency over wide operating temperature range via model consisting of long pipe with energy injection at points along length

[ASME PAPER 72-WA/SOL-7] 04 p0408 A73-15802

A model for eddy conductivity and turbulent Prandtl number.

[ASME PAPER 72-WA/HT-13] 04 p0434 A73-15834

Nonlinear modeling and dynamic simulation of vehicle air cushion suspensions.

[ASME PAPER 72-WA/AUT-5] 04 p0406 A73-15883

A one-dimensional flow model for an air-augmented rocket.

05 p0607 A73-16848

Multivortex model for bodies of arbitrary cross-sectional shapes.

[AIAA PAPER 73-104] 05 p0529 A73-16864

Numerical analysis of eddy viscosity models in super-sonic turbulent boundary layers.

[AIAA PAPER 73-164] 05 p0566 A73-16910

Two dimensional jet stream dynamics from simulation particle population evolution in different collision models

05 p0623 A73-17301

An analytical fluid dynamic model of turbulent inlet flow.

[AIAA PAPER 73-138] 06 p0644 A73-17647

Fracture mechanism theories based on discrete and continuous models of solids, explaining Griffith brittle crack dynamics

06 p0760 A73-17776

Some averaged properties of wave solutions for a hypersonic thermal wave.

06 p0728 A73-17890

Discretized body defined as special system with finite degrees of freedom, describing mechanics in terms of constitutive and motion equations

06 p0723 A73-17894

Numerical prediction of the phenomenon of transition for a flow between two parallel planes

06 p0687 A73-18537

An adaptive bit synchronization algorithm under time-varying environment.

06 p0672 A73-18810

Identification of multivalued nonlinearities in a class of noisy time invariant dynamic systems.

06 p0681 A73-18811

An identification of time varying linear system without a priori information on variation of system parameters.

06 p0681 A73-18812

Pioneer Jupiter spacecraft magnetic field control with periodically updated magnetic model for tradeoffs in subsystem moments within allowed magnetic budget

[IEEE PAPER 41,4] 07 p0905 A73-19364

Radiation effects on state of gas behind strong shock wave, representing power density of non-relativistic fully ionized hydrogen plasma

07 p0920 A73-19508

Three dimensional models images information content increase in coherent light by interference shadow marking, noting automatic systems for distant objects recognition

07 p0824 A73-20140

Study on fracture mechanism for composite materials based on the concept of the change in Poisson's ratio.

07 p0915 A73-20328

Some studies on opposed-jet diffusion flame considering general Lewis numbers.

07 p0921 A73-20357

Dynamic system model identification computational considerations, discussing equation error methods based on regression analysis, maximum likelihood estimates and gradient dependent algorithms for optimization

07 p0845 A73-20428

An analytical method for the filtering error evaluation of sub-optimal filters in a noisy non-linear dynamic system.

08 p0950 A73-21091

Dynamic model of flow separation of plane fluid past body in channel with eddy wake formation

08 p0954 A73-21183

Pulsed magnetic system /terrella/ for model of earth radiation belts and geomagnetic field-solar wind interaction

08 p0960 A73-21309

Experiments on the seasonal variation of the general circulation in a statistical-dynamical model.

08 p0960 A73-21378

An algebraic algorithm for the design and analysis of linear dynamical systems.

08 p0984 A73-21468

Prediction models for surface and air transportation dynamic environments, considering broadband and

single frequency continuous and recurrent and intermittent discrete excitation modes

09 p1032 A73-22718

Nitric oxide formation and radical overshoot in premixed hydrogen flames.

10 p1294 A73-23558

Fiberglass reinforced plastics dynamic models, discussing stress-strain relationship, Poisson ratio and fatigue

10 p1288 A73-23962

Theoretical and practical aspects of an automatic hover control system for an unmanned tethered rotor-platform.

10 p1175 A73-24009

Stability theory of dynamic large scale system under structural perturbations based on comparison principle and vector Liapunov functions

10 p1248 A73-24039

Optimal filtering for systems described by linear partial differential equations.

10 p1200 A73-24050

Resonance phenomena associated with nonlinear vibrations of solid bodies

10 p1249 A73-24303

A four-level technique for estimation of tactical missile aerodynamic parameters.

10 p1172 A73-24538

A survey of data smoothing for linear and nonlinear dynamic systems.

10 p1243 A73-24546

Axisymmetric flow model of rotating inviscid incompressible fluid into point sink at low Rossby numbers, discussing selective withdrawal and blocking wave

11 p1345 A73-25053

Vertical distribution of viscosity and convection conditions in earth mantle, discussing shallow convection model and geophysical evidence for validity

11 p1356 A73-25906

Dynamic prediction model and optimal control of a commercial plant

12 p1561 A73-27081

Dynamic model of the interaction between the F region of the ionosphere and the plasmosphere

12 p1490 A73-27335

Aerodynamic decelerator dynamics modeling for Viking lander parachute deployment, analyzing unfurling process with attention to longitudinal and rotational dynamics

12 p1549 A73-27440

Solid body on elastic supports as model for helicopter stability and nonlinear oscillations analysis

12 p1459 A73-27791

Optimal estimation of the phase coordinates for a linear dynamic system

12 p1485 A73-27898

Verification of the 'potential' work capacity of dynamic systems by a frequency-time technique

12 p1485 A73-27946

Deformable body with reticular structure, studying microstructural transitions using physical model with isolated-valence bond coupling

13 p1690 A73-27992

Visual perception of motion in depth - Application of a vector model to three-dot motion patterns.

13 p1577 A73-28091

An explanation of the polar motion by a rigid core-mantle model.

13 p1679 A73-28398

Numerical study of the stochasticity of dynamical systems with more than two degrees of freedom.

13 p1648 A73-28425

A survey of the mean turbulent field closure models.

13 p1601 A73-28801

A forcing mechanism for spiral density waves in galaxies.

13 p1686 A73-29372

Ergatic modeling as dynamic goal-oriented physical process based on heuristic autonomous information-structured organization system with regulated model-human operator interaction

13 p1580 A73-29418

Investigation of an analog memory for the computational-measurement complex of an electrodynamic model

13 p1588 A73-29420

Mathematical models and identification of bilinear systems.

14 p1740 A73-30782

Generalisation and application of Rayleigh's theory of sound scattering

14 p1775 A73-30893

Dynamic structural model of transient processes of discrete jet element chain with duct joints

15 p1832 A73-31145

The period of nonlinear vibrations of autonomous dynamical systems of the order n

15 p1947 A73-31366

Dynamic parachute inflation model for dimensionless time and maximum force predictions at high altitudes

[AIAA PAPER 73-450] 15 p1826 A73-31436

Multi-parameter sensitivity analysis of linear dynamic systems through the second method of Liapunov.

15 p1854 A73-31632

Two component glass fiber reinforced plastic model describing stress-strain state via elastic properties analysis, internal energy production and Hooke's Law application

15 p1952 A73-32085

Film-cooling effectiveness in the near-slot region.

15 p1958 A73-32278

A theoretical analysis of the recovery factor for high-speed turbulent flow.

15 p1865 A73-32280

Memorization and model change, alpha-beta, adaptive model and Kalman type radar pursuit tracking techniques efficiency comparison

15 p1908 A73-32443

An algebraic method for linear dynamical systems with stationary excitations.

16 p2076 A73-32919

Early-time model of laser plasma expansion.

16 p2042 A73-33340

A wake and an eddy in a rotating, radial-flow passage. II - Flow model.

[ASME PAPER 73-GT-58] 16 p1964 A73-33513

Photochemical, radiative and dynamic modeling of the stratosphere.

[AIAA PAPER 73-527] 16 p2007 A73-33561

Applications of a ray reflection model in the problem of highly rarefied gas flow past bodies.

17 p2094 A73-34549

Finite element approximations in nonlinear thermoviscoelasticity.

17 p2245 A73-34829

A dynamic modeling method of unsteady flows in long fluid lines with turbulent bulk velocities.

[ASME PAPER 73-FE-18] 17 p2153 A73-35014

Polycarbonate as a model material for three-dimensional photoplasticity.

[ASME PAPER 73-APM-4] 17 p2247 A73-35029

A quantitative model of hydrogen induced grain boundary cracking.

17 p2191 A73-35124

IR laser induced change in atmospheric temperature as function of time, using kinetic model with input molecular energy transfer rates for thermal blooming

17 p2163 A73-35414

Russian book - Nonlinear oscillations and transient processes in machines.

18 p2319 A73-35895

A distributed parameter model of the inertially loaded human spine.

18 p2281 A73-36429

Optimal estimation of the phase coordinates of a linear dynamic system.

18 p2294 A73-36603

Use of continuous simulation models in application of remote sensing to hydrology.

18 p2292 A73-36840

The method of virtual powers in mechanics of continuous media. I - Theory of the second gradient

19 p2495 A73-37424

Stellar kinetic energy gain in spherical systems by transient external gravitational perturbations, computing dynamic models for compressive shocks

19 p2484 A73-37616

Preliminary results from dynamic model tests of an air cushion landing system.

19 p2382 A73-37694

Pulsed magnetic system /terrella/ as earth model with dipole magnetic field for laboratory simulation of geophysical phenomena

19 p2425 A73-37938

Discrete stochastic linear servomechanism with observation costs, deriving optimal control solution with extension to nonlinear systems suggested by dynamic population models

19 p2412 A73-38029

Some aspects of the inverted pendulum problem for modelling of locomotion systems.

19 p2460 A73-38035

Derivation of aggregation matrices for simplified models of linear dynamic systems and their applications for optimal control.

19 p2413 A73-38053

Precise attitude control of the Stanford relativity satellite.

19 p2494 A73-38080

A study on the dynamical behaviors of composite materials by dynamical model.

20 p2580 A73-38643

Quasi-dynamic system with eliminable generalized coordinates to define pseudo-degrees of freedom, identifying characteristics

20 p2594 A73-39537

Dynamical models of tailed radio sources in clusters of galaxies.

20 p2610 A73-39584

An experimental model for the automated detection, measurement, and quality control of low-level cloud motion vectors from geosynchronous satellite data.

20 p2533 A73-39853

Core coupling to mantle precession, discussing model with quantitative consideration of inertial and dissipative coupling torque superposition
21 p2764 A73-39929

Oscillating spherically symmetric charge-matter fluid for avoidance of singularities in gravitational collapse models
21 p2766 A73-40316

Dynamic model of economically efficient multipurpose plants
21 p2793 A73-40386

Vibration tests with rotors as a rotor identification problem
21 p2707 A73-40395

Comparison of the plane, cylindrical and spherical one-dimensional models of the free expansion of a collisionless plasma.
21 p2748 A73-40929

On the radiation from an aerodynamic acoustic dipole source
21 p2633 A73-40943

The partial molar thermodynamic magnitudes of oxygen and the nonstoichiometry of oxides - Model with interactions
21 p2791 A73-40950

Optical and mechanical models of interplanetary dust.
21 p2776 A73-41420

Elements of a model of oxygen interactions under low pressure with transition metals at high temperature
21 p2648 A73-41562

Rotation of the earth's magnetic field.
21 p2692 A73-41641

Dynamical evolution of an expanding gas cloud.
22 p2840 A73-41758

Gradient methods for extremum solutions of two-point boundary value problems of dynamics.
[ASME PAPER 73-DET-44] 22 p2916 A73-42069

An aeroelastic whirl phenomenon in turbomachinery rotors.
[ASME PAPER 73-DET-97] 22 p2900 A73-42076

The theory of elasticity of flexural-stiffness exhibiting, planar particle systems with a rectangular net
22 p2922 A73-42526

Experimental and theoretical studies of NO/x formation in a jet-stirred combustor.
22 p2820 A73-42793

Modeling methods for shock isolation systems for fragile equipment protection from HF effects generated by high loading rates and/or random multifrequency input displacement signatures
22 p2927 A73-42925

Flow patterns and velocity and shear stress distribution downstream of steady and pulsatile flow models for fluid dynamics of blood vessel branches
22 p2816 A73-43103

Dynamic model of interaction of the F-region of the ionosphere with the plasmasphere.
23 p2970 A73-43233

Elementary mechanisms and physical models in plasticity and viscoplasticity
23 p3043 A73-43965

A kinetic model of population inversion generation in a gas-discharge carbon monoxide laser
23 p2988 A73-44012

Critical two phase He flow rates prediction based on homogeneous thermal equilibrium model, Henry-Fauske data and empirical correction factor curve
24 p3077 A73-44823

Physical model selection for the balance preservation system in man
24 p3063 A73-44903

Dynamics of the balance preservation system of man
24 p3064 A73-44909

Damping of mechanical systems with the aid of viscoelastic liquids
24 p3109 A73-44915

Ideal resonance problem for dynamic system of N degrees of freedom, obtaining global solution covering libration and circulation regimes under normality condition
24 p3141 A73-45287

Vortex model for flames and free jets characteristic velocities based on three dimensional turbulent combustible flow
24 p3158 A73-45387

On the problem of nonlinear interactions in fluid dynamics.
24 p3080 A73-45449

DYNAMIC MODULUS OF ELASTICITY
Measurement of the flexural damping capacity and dynamic Young's modulus of metals and reinforced plastics.
08 p0967 A73-21594

Stress differentiation procedure for screen technique studies in dynamic photoelasticity, giving expressions for elastic modulus and Poisson ratio
13 p1703 A73-29613

Dynamic mechanical properties of graphite-epoxy and carbon-epoxy composites.
15 p1897 A73-31677

Investigation of the dynamic modulus of polymethyl methacrylate saturated by carbon dioxide
16 p2031 A73-33943

DYNAMIC PRESSURE
Possibility of obtaining mullite at high dynamic pressures
02 p0178 A73-11542

Deformations and stresses in a hollow sphere with spherical transversal isotropy under impulsive pressure.
07 p0913 A73-20116

Recovery of sounding rocket payloads by center-of-gravity position control.
[AIAA PAPER 73-294] 09 p1155 A73-23213

Dynamic viscous pressure interaction on a cone.
10 p1173 A73-24821

Study of the fluctuations of wall pressures in transonic flow on a cone-cylinder group presenting a constriction
10 p1173 A73-24825

Anomalous lower dynamic pressure in piezometer of pitot tube in liquid flow containing solid particles, using seeds in aqueous solution of calcium chloride
11 p1367 A73-26476

Stability of truncated conical shells under dynamic external pressure
18 p2363 A73-36413

Freon-22 circular and flat jet propagation in air cross flow in wind tunnel, examining air-gas dynamic pressure ratio effects
21 p2676 A73-40405

Transformation of meteorite material in experiments on explosively produced shock compression at pressures of 500 and 1000 kbar
24 p3137 A73-44710

DYNAMIC PROGRAMMING
Dynamic programming and a max-min problem in the theory of structures.
01 p0019 A73-10199

Optimal processes theory, discussing Pontryagin principle, special controls, dynamic programming, discrete systems, algorithms, identification and controllability
01 p0028 A73-11072

Trajectory optimization of pursuer vehicle for multitarget rendezvous, noting algorithm for dynamic programming
01 p0105 A73-11124

The optimum allocation of redundancy - An application of mathematical programming to system design.
01 p0071 A73-11199

Book on control engineering covering dynamic system state representation, finite and infinite dimensional optimization, dynamic programming, stochastic estimation, applications, etc
03 p0285 A73-13987

Data processing method for optimal prediction of spacecraft orbital elements, using dynamic and quadratic programming
03 p0379 A73-14555

Channel equalization in presence of intersymbol interference, comparing sequential statistical, dynamic programming, delay line and minimum mean square error techniques
04 p0425 A73-15419

The representation and matching of pictorial structures.
06 p0692 A73-17804

A partitioning algorithm with application in pattern classification and the optimization of decision trees.
06 p0670 A73-17805

Design of dynamic programming feedback controllers for multivariable time-invariant linear systems.
06 p0680 A73-18517

Optimal control of stochastic systems with continuous and discontinuous random disturbances, obtaining problem solution conditions for linear system via dynamic programming
07 p0805 A73-20038

An approximate method for the synthesis of optimal control of distributed systems.
07 p0806 A73-20596

An actively adaptive control for linear systems with random parameters via the dual control approach.
[AD-751587] 07 p0806 A73-20601

Investigation of the smoothness characteristics of the Bellman function on the basis of the equation of motion of the system in time-optimal problems. I. Linear case
07 p0806 A73-20633

The use of dynamic programming techniques for determining resource allocations among R/D projects - An example.
08 p1025 A73-20970

Distributed parameter system a priori stochastic optimal control, deriving canonical differential equations from dynamic programming formulation for insight into feedback control problem
08 p0950 A73-21093

Dynamic programming as applied to feature subset selection in a pattern recognition system.
08 p0941 A73-21666

Approximate solution of certain optimal-control and discrete-programming problems
09 p1068 A73-22561

Application of the principle of invariant imbedding in the solution of optimal control problems
09 p1069 A73-22722

Continuous analog of dynamic-programming allocation process
09 p1112 A73-22889

Optimal processes theory, discussing Pontryagin principle, special controls, dynamic programming, discrete systems, algorithms, identification and controllability
09 p1069 A73-22997

Optimization methods in control systems design, discussing nonlinear and linear programming, variational and maximum principles, dynamic programming and game and graph theories
10 p1242 A73-24032

An actively adaptive control for linear systems with random parameters via the dual control approach.
10 p1202 A73-24534

Sufficiently informative functions and the minimax feedback control of uncertain dynamic systems.
10 p1202 A73-24535

Solution of the stochastic control problem in unbounded domains.
10 p1203 A73-24705

Synthesis of broad-band arrays with arbitrary frequency-independent elements.
11 p1329 A73-25664

Temperature field in front of or behind gas turbine with additive white noise, deriving optimal filter for dynamic programming technique in random fields analysis
12 p1483 A73-27080

Use of the dynamic programming method for optimization of relay systems
13 p1596 A73-28853

An historical survey of computational methods in optimal control.
14 p1738 A73-30413

Use of the principle of invariant imbedding in solving an optimal control problem.
14 p1740 A73-30955

Study of the smoothness properties of the Bellman function in time-optimal problems, based on the equation of motion of the system. I - The linear case.
15 p1854 A73-31687

Optimal structural design of elastic rotating disks by dynamic programming
16 p2079 A73-33009

Book - Optimum structural design: Theory and applications.
17 p2242 A73-34350

Book - Methods of nonlinear analysis. Volume 2.
17 p2200 A73-34453

A constraining hyperplane technique for state variable constrained optimal control techniques.
19 p2413 A73-38036

Some numerical aspects of the solution of functional equations in dynamic programming
19 p2445 A73-38163

Prediction of the outcomes of myocardial infarction from formulas derived by the dynamic programming method
20 p2516 A73-39000

Dynamic programming method for constructing stable bridges based on mixed strategies in differential games of rendezvous-evasion
21 p2669 A73-40856

Convex approximation of the control process and a method for constructing generalized optimum regimes
21 p2727 A73-41064

Runway configuration improvement programming model.
[ASCE PREPRINT 2034] 22 p2839 A73-42864

Dynamic programming application to extremal fields topological singularity in optimal control theory for flight vehicle with state variables satisfying initial conditions and ordinary differential equations
22 p2917 A73-43030

Bellman dynamic programming principle for elastic-perfectly plastic beam structure design optimization with respect to cross-sections, span lengths and weight
24 p3148 A73-45003

DYNAMIC PROPERTIES
U DYNAMIC CHARACTERISTICS
DYNAMIC RESPONSE
Wave motion in an elastic solid due to a nonuniformly moving line load.
01 p0114 A73-10301

A simple Fourier analysis technique for measuring the dynamic response of manual control systems.
01 p0027 A73-10321

Study of the acoustic reflex in human beings. I - Dynamic characteristics.
01 p0013 A73-10828

Dynamic response of an on-off type secondary injection thrust vector control.
01 p0091 A73-11196

Analysis of non-linear systems defined by their response to arbitrary disturbances.
01 p0028 A73-11456

Dynamic study of a very-low-pressure sensor
02 p0165 A73-11591

Response of helicopter rotor blades to random loads near hover.

02 p0129 A73-12503

Response of a system of cascaded nonlinear springs

02 p0193 A73-12521

Dynamic errors in force measuring transducers, simulating unsteady processes by analog model with varying step function input signals

02 p0170 A73-12540

Nonlinear responses for a circular plate subjected to a dynamic ring load.

03 p0388 A73-13319

Space-time finite element method for determining dynamic response of continuous media, using Hamilton principle for nodal displacements variations

03 p0389 A73-13320

Finite element equations of motion of elastoplastic shell, applying theory to edge clamped circular plate dynamic response

03 p0389 A73-13321

Impulsive loading of rectangular plates with finite plastic deformations.

03 p0389 A73-13322

On the stability of steady-state response of certain nonlinear dynamic systems subjected to harmonic excitations.

03 p0393 A73-13792

Transient interaction of a flexible ring-reinforced shell and a fluid medium.

03 p0395 A73-14197

Static and dynamic behavior of spherical hydrostatic bearings - Theory and experiments.

[ASME PAPER 72-LUB-35] 03 p0315 A73-14344

Dynamic response of nonlinear media at large strains.

04 p0509 A73-14947

Mean field equations for dynamic response of homogeneous linearly elastic solids, obtaining formulation for ensemble averaged displacement and stress fields of composite

[ASME PAPER 72-WA/APM-28]

04 p0515 A73-15890

Dynamic response of a semi-infinite elastic cylinder containing an acoustic medium.

[ASME PAPER 72-WA/APM-3] 04 p0516 A73-15905

The dynamic properties of the acoustic middle ear reflex in nonanesthetized rabbits - Quantitative aspects of a polysynaptic reflex system.

05 p0539 A73-16249

Dynamic radiography - A new imaging technique using penetrating radiation.

05 p0573 A73-16278

Space-time dynamics of the impulse activity in human-brain neuron populations

05 p0540 A73-16692

Correction of the dynamic distortions of signals resulting from measurement information compression

05 p0577 A73-16986

Platinotron crossed field microwave amplifier tube phase response characteristics, considering anode current fluctuations and statistical phase variations at constant operating conditions

06 p0674 A73-17823

Fast accurate phase lock loop with self calibrating frequency discriminator, showing dynamic response of frequency lock-up

06 p0675 A73-17843

On forced vibrations in the linear theory of micropolar elasticity.

06 p0762 A73-17987

Power series method for accurate solution of eigenvalue problems and simultaneous equations representing static, dynamic and stability responses to structural design parameter changes

07 p0906 A73-19027

Calculation of the asymptotic behaviour of the TDR step response related to the asymptotic behaviour of dielectrics in the frequency domain.

07 p0797 A73-19107

Predictions of the dynamic response of the lung.

07 p0785 A73-19477

Dynamic response of a vertical cantilever structure in the natural wind.

07 p0823 A73-19565

Review of theories and experimental results pertaining to the dynamic behavior of porous bodies

07 p0912 A73-19905

Bending stress in an impulsively loaded cylindrical shell of exponentially varying thickness.

07 p0913 A73-19973

Forced motion of elastic cylindrical rods - A comparison of two theories.

07 p0915 A73-20284

Effects of shearing force and rotary inertia to dynamical behaviours of thin cylindrical shells subjected to impulsive inner pressures.

07 p0915 A73-20286

Response of nonlinear beam to random excitation.

07 p0916 A73-20436

Moving radiography for photographic recording and display of transient or cyclic motion, emphasizing application to aircraft gas turbines under dynamic conditions

07 p0832 A73-20451

Dynamic response of digital-analog flow measurement system based on turbine driven pulse generator as sensor element

07 p0828 A73-20545

Frequency response of a dynamic system with statistical damping.

08 p0950 A73-20715

Response time of metal-insulator-metal tunnel junctions.

08 p0945 A73-20844

On the mechanical response of a non-uniform piezoelectric transducer with elastic compliances having damping characteristics.

08 p0994 A73-20875

Impact-deflection by oblique fibers in sparsely reinforced composites.

08 p1018 A73-21408

Dynamic behaviour of thin cylindrical shells collided with dampers.

08 p1019 A73-21527

The dynamic response of a diaphragm-ejector amplifier.

08 p0929 A73-21830

Radar filter asymptotic efficiency analysis for pass-band and impulse response duration increase, considering realization of approximate Urkowitz filter with controlled memory

10 p1194 A73-23737

Applications of symbolic computing methods to the dynamic analysis of large systems.

10 p1192 A73-24029

Liapunov stability analysis and attitude response of a passively stabilized space system.

10 p1286 A73-24541

An optimal control problem for a class of distributed parameter systems.

10 p1202 A73-24549

On structure of the laminar boundary layer in the presence of a fluctuating free stream.

10 p1209 A73-24830

Linear or nonlinear dynamic systems response to arbitrary input functions, describing numerical computation method with provision for discontinuities

11 p1389 A73-25110

Sensitivity of rotor blade vibration characteristics to torsional oscillations.

[AIAA PAPER 73-404] 11 p1440 A73-25533

The spatial correlation method and a time-varying flexible structure.

[AIAA PAPER 73-406] 11 p1440 A73-25535

Aeroelastic dynamic response to shock induced flow separation, analyzing wing buffet components at high Mach number subsonic flow

[AIAA PAPER 73-308] 11 p1300 A73-25539

An exploratory investigation of the unsteady aerodynamic response of a two-dimensional airfoil at high reduced frequency.

[AIAA PAPER 73-309] 11 p1301 A73-25540

Vibrations of an Euler beam with a system of discrete masses, springs, and dashpots.

11 p1442 A73-25788

Experiments on the non-linear dynamic response of shells under blast waves.

11 p1446 A73-26492

The dependence of piezo-electric accelerometer response on method of attachments.

12 p1496 A73-26974

Response-optimum control of the angular and torsional oscillations of an elastic flying wing.

12 p1459 A73-27459

Differential equations of thermoelastic state for shells receiving a thermal shock at the surface

12 p1555 A73-27790

Flexural response of tapered beam on elastic-plastic foundation, solving in closed form to evaluate efficiency of numerical methods

12 p1557 A73-27932

Dynamically possible finite deformations of isotropic, incompressible, elastic-inelastic solids with temperature independent response.

13 p1695 A73-28416

The effect of strain rate and heat developed during deformation on the stress-strain curve of plastics.

[SESA PAPER 2088A] 13 p1646 A73-29303

Parametric vibrations of elastically connected two mass system with two degrees of freedom, considering dynamic response to excitation by external compression loads

13 p1700 A73-29391

Deformation mechanism and strength of metals under impulsive loading.

13 p1639 A73-29463

A variational method for micromechanics of composite materials.

13 p1702 A73-29534

Ionospheric model impulse response transfer functions phase and amplitude dependence on profile parameters and TE C, using ray tracing technique

14 p1728 A73-30231

Approximate investigation of the dynamics of a digital phase-lock automatic frequency control system /DPAFC/

14 p1728 A73-30269

On dynamic response of prestressed cylindrical shells - Green's tensor technique.

15 p1947 A73-31367

The dynamic plastic behavior of simply supported spherical shells.

15 p1948 A73-31369

Computerized six degree of freedom parachute deployment model for predicting entry vehicle-decelerator dynamic response to aerodynamic forces and physical property changes

[AIAA PAPER 73-460] 15 p1827 A73-31446

Generalized mathematical model for gas turbine dynamic behavior simulation based on one dimensional flow theory with functional integration for rotor speed time derivative

15 p1925 A73-31629

Asymmetric missile subharmonic response to nonlinear aerodynamic moments, considering spin and aerodynamic damping effects

15 p1943 A73-31667

Dynamic analysis of viscoelastoplastic anisotropic shells.

16 p2075 A73-32787

Critical study of the effects of gusts on an aircraft

16 p1961 A73-32808

Structural shock response spectrum analysis for maximum dynamic loads and damage potential determination

16 p2014 A73-33135

Satellite waves effects on dynamic behavior of resonant wave-triplet coupling from comparison with isolated triplet in explosive and decay instabilities

16 p2041 A73-33334

Behavior of a wing panel under transient conditions in a gas flow

17 p2091 A73-34139

Estimation of the response of a mechanical structure to arbitrary excitation

17 p2243 A73-34649

Dynamic behavior of light aircraft interaction with jet transport vortex on basis of accident records and computer simulation

[SAE PAPER 730296] 17 p2094 A73-34660

The dynamic behavior and compliance of a stream of cavitating bubbles.

[ASME PAPER 73-FE-34] 17 p2153 A73-35025

Nonstationary response of linear time-varying dynamical systems to random excitation.

[ASME PAPER 73-APM-6] 17 p2247 A73-35031

Forced plane strain motion of cylindrical shells - A comparison of shell theory with elasticity theory.

[ASME PAPER 73-APM-9] 17 p2247 A73-35034

The dynamic response of columns under short duration axial loads.

[ASME PAPER 73-APM-19] 17 p2248 A73-35040

The use and evaluation of shock spectra in the dynamic analysis of structures.

[ASME PAPER 73-APM-22] 17 p2248 A73-35041

Dynamic buckling of shallow spherical shells.

[ASME PAPER 73-APM-A] 17 p2249 A73-35104

Reflection characteristics of quasi-tapered anechoic chamber at VHF and EHF, evaluating broadband response, radar cross sections and field in quiet zone

17 p1219 A73-35701

Book - Dynamics and vibration of structures.

17 p2252 A73-35833

The dynamic-bias in radiation interrogation of two-phase flow.

17 p2256 A73-35846

Analytical investigation of compressibility and three-dimensionality on the unsteady response of an airfoil in a fluctuating flow field.

[AIAA PAPER 73-683] 18 p2262 A73-36234

The response of unsteady boundary-layer separation to impulsive changes of outer flow.

[AIAA PAPER 73-684] 18 p2298 A73-36235

Response of a rigid aircraft to nonstationary atmospheric turbulence.

18 p2267 A73-36305

Thin clamped hemispherical shell nonlinear dynamic response to suddenly applied pressure, deriving finite difference formulation of fourth order coupled nonlinear equations

18 p2362 A73-36310

Dynamically-induced large deformations of multilayer, variable thickness shells.

18 p2362 A73-36317

Engineering analysis of the inelastic stress response of a structural metal under variable cyclic strains.

18 p2364 A73-36594

Stationary high-current plasma accelerators

19 p2466 A73-37359

Nonlinear parametric vibrations of closed cylindrical shells

19 p2499 A73-37764

Determination of dynamic loads on elastic structures caused by external excitations

19 p2500 A73-38155

The selection of test frequencies for system fault diagnosis.

[AIAA PAPER 73-864] 20 p2586 A73-38802

Modal technique to obtain forced axisymmetric response of elastic spherical shells from free vibration

response relations, taking into account transverse shear and rotational inertia

20 p2621 A73-39541

Dynamic response of laminated composite circular cylindrical shells with freely supported or clamped edges.

20 p2621 A73-39543

Rotary inertia and energy dissipation effects on dynamic response of three layered symmetrical laminate beam with viscoelastic core vibrating in flexural mode, using variational calculus

20 p2623 A73-39555

Response of a cylindrical shell with filler to the action of a moving load

20 p2624 A73-39648

Prediction of the dynamic and quasi-static performance characteristics of flueric wall-attachment amplifiers.

20 p2511 A73-39756

Probabilistic and deterministic solutions of random vibration response problems.

21 p2783 A73-40294

Parametric study of multiple-layer damping treatments on beams.

21 p2785 A73-40752

Russian book - Introduction to the statistical dynamics of systems with possible disturbances.

21 p2669 A73-40775

Propagation of steady shock waves in non-linear thermoviscoelastic solids.

21 p2724 A73-41548

An approximation for the determination of the dynamic characteristics of long viscoelastic hollow cylinders

21 p2788 A73-41615

The response of viscoelastic materials to slow cyclic stresses.

21 p2789 A73-41689

Development of a thermistor type temperature probe for use at low absolute pressures.

22 p2856 A73-42016

A model to predict the mechanical impedance of the sitting primate during sinusoidal vibration.

[ASME PAPER 73-DET-78] 22 p2813 A73-42073

Dynamic properties of transistor current switches

22 p2833 A73-42369

Thermal response of a viscoelastic rod under cyclic loading.

[ASME PAPER 73-APMW-39] 22 p2926 A73-42896

Complex structural dynamic response reduction, discussing methods for mathematical models establishment and application to thin cylindrical shell

22 p2926 A73-42921

Certain algorithmic aspects of flight dynamics simulation on digital computers

23 p3038 A73-43262

Dynamic range and frequency response of the vortex rate sensor.

23 p2942 A73-43406

Periodic oscillations of a closed hydraulic throttle servomechanism with inertial and positional loads

23 p2945 A73-43739

Variational principles in dynamic thermoviscoelasticity.

24 p3151 A73-45306

Thin plate in two dimensional supersonic flow, deriving vibration amplitude response to shock pressure load by numerical analysis with Laplace transform

24 p3055 A73-45432

DYNAMIC STABILITY

NT AERODYNAMIC STABILITY

NT AIRCRAFT STABILITY

NT ATTITUDE STABILITY

NT BOUNDARY LAYER STABILITY

NT COMBUSTION STABILITY

NT CONTROL STABILITY

NT DIRECTIONAL STABILITY

NT FLAME STABILITY

NT FLOW STABILITY

NT FREQUENCY STABILITY

NT GYROSCOPIC STABILITY

NT HOVERING STABILITY

NT LONGITUDINAL STABILITY

NT MAGNETOHYDRODYNAMIC STABILITY

NT MOTION STABILITY

NT ROTARY STABILITY

NT SPACECRAFT STABILITY

Dynamic stability of the state of moment stress in a cylindrical shell with allowance for inertia of the subcritical state

01 p0117 A73-11093

Stability boundaries of solid rocket motors.

01 p0091 A73-11116

Development of dynamic modes of the loss of stability in elastic systems during intense loading over a finite interval of time

02 p0229 A73-11615

Externally pressurized gas-lubricated journal bearings with herringbone grooves - Load capacity and stability analysis.

03 p0311 A73-13208

Dynamic stability of a cylindrical shell in an acoustic medium.

03 p0393 A73-13834

Dynamic stability of gimbaled spiral-grooved thrust bearing.

[ASME PAPER 72-LUB-13] 03 p0313 A73-14329

A study of the stability of externally pressurized gas bearings with porous wall by Liapunov's direct method.

[ASME PAPER 72-LUB-18] 03 p0314 A73-14333

Experimental rotor unbalance response using hydrostatic gas lubrication.

[ASME PAPER 72-LUB-31] 03 p0315 A73-14341

Linear and nonlinear systems dynamic stability conditions for incomplete coefficients data, determining worst disturbance from Pontryagin principle

04 p0475 A73-14887

Stability of the solar system - Evidence from the asteroids.

04 p0497 A73-15179

Stability and uniqueness of initially straight elastic rods undergoing three dimensional deformations

04 p0514 A73-15682

Investigation of the dynamics of nonlinear sampled-data automatic control systems

05 p0560 A73-16296

Short-term longitudinal dynamic stability of rods with allowance for clamping methods and for previous transverse deflection

05 p0632 A73-16329

Study of the dynamics of the preliminary-damping system of a gravitationally stable satellite with allowance for constraints on its sensors and on the flexural vibrations of the stabilizer

05 p0628 A73-16406

Stability conditions for strongly flattened galaxy model with respect to axisymmetric disturbances of gaseous subsystem in finite isothermal layer

05 p0616 A73-16456

Dynamic stability of monosymmetrical thin-walled structures.

[ASME PAPER 72-APM-SS] 05 p0632 A73-16530

From theory to practical use of air cushions for transport of heavy loads in the factory

05 p0535 A73-16753

Three dimensional static and dynamic stability equations of viscoelastoplastic deformation under axial compression

05 p0635 A73-17078

Nonlinear stability analysis of nonhomogeneous self-gravitating unstable equilibrium stellar systems, using numerical techniques and water bag configurations

05 p0624 A73-17317

Rotating shafts dynamic stability, analyzing eigenvalue problem derived via energy equations based on virtual work principle

06 p0697 A73-17517

Transition effects on slender vehicle stability and trim characteristics.

[AIAA PAPER 73-126] 06 p0756 A73-17646

Reentry vehicle dynamic stability mechanism during boundary layer transition, using angle of attack divergence dependence on fluctuating pressure

[AIAA PAPER 73-180] 06 p0756 A73-17652

An iterative approach to nonlinear dynamic stability problems.

06 p0717 A73-18145

Equations of disturbed motion and equilibrium for solid body with incompressible fluid filled cavity, noting equilibrium position stability conditions

06 p0688 A73-18878

Stability of clusters of galaxies with mass loss to gravitational radiation.

07 p0873 A73-19053

The stability of a self-gravitating, nonrotating gas layer with stellar, magnetic, and cosmic-ray components. II.

07 p0873 A73-19058

Effects of collisions with neutrals on the dynamic stability of a finitely conducting hydromagnetic composite plasma in the presence of Hall currents.

07 p0858 A73-19600

Stability of clamped rectangular plates in uniform subsonic flow.

07 p0913 A73-19982

Analytic construction of adaptive systems with stabilization of the dynamic characteristics.

07 p0805 A73-20039

German monograph - The calculation of the stability limit of statically operating circular gas bearings, taking into account the effect of the supported mass.

07 p0832 A73-20390

Instability of shock waves in inhomogeneous gases.

07 p0812 A73-20445

RR Lyrae, W Virginis and RV Tauri population II variables, considering pulsation problem, instability mechanisms and He ionization

07 p0903 A73-20630

Some delinearization problems in the dynamics of complex vibrational systems

08 p0989 A73-21768

Cantilever beam dynamic stability under follower force, investigating divergence, flutter and autoparametric resonance relations

09 p1161 A73-23088

Free particle gravitating cylindrical model for gravitational kinetic instabilities, calculating natural

vibration spectrum and parameters for beam instability development

10 p1253 A73-23714

Stability of a gravitating fluid layer in the presence of a uniform magnetic field perpendicular to its boundary.

10 p1253 A73-23832

Experimental investigation of kinetic instabilities in the Gabor magnetron.

10 p1254 A73-24200

Influence of interaction on the stability and pulsations of rotating neutron stars

10 p1283 A73-24704

Stability predictions with the aid of energy expressions in the case of a turborotor with gyroscopic effects

11 p1432 A73-24999

Dynamic stability of cable in incompressible flow at angle of incidence, calculating characteristic lengths and vibration frequencies by singular perturbation theory

[AIAA PAPER 73-395] 11 p1440 A73-25524

Dynamic error of solid body-elastic rod pendulum system hinged on vibrating suspension point in terms of tensile rigidity finiteness

11 p1399 A73-26096

Stability of the regular precession of a symmetrical solid with an ellipsoidal cavity

11 p1401 A73-26469

Static and dynamic stability of simply supported imperfect beam resting on nonlinear elastic foundation under axial load

12 p1550 A73-27033

A new method for the study of the phenomenon of dynamic instability of thin-walled bars used in the construction of aeroplanes, ships and bridges.

12 p1551 A73-27063

Shallow spherical shell dynamic stability under axisymmetric loads, noting small HF vibrations effect on static stability

12 p1556 A73-27814

Stability of stochastic dynamical systems; Proceedings of the International Symposium, University of Warwick, Coventry, England, July 10-14, 1972.

12 p1519 A73-27920

Conditions for stability of incompressible elastic material obtained from small-amplitude plane sinusoidal waves superposed on finitely deformed state of material

13 p1696 A73-28753

Dependence of the diffuse expansion characteristics of a crystallization zone on the vertical stability of the atmosphere

13 p1654 A73-28879

Massive main sequence stars structure and evolution within core hydrogen burning models, giving mathematical relation and conditions for convective instability

13 p1682 A73-28979

Stellar evolution as succession of quasi-equilibrium states, investigating dynamic stability via hydrodynamic and state equations

13 p1682 A73-28980

Computer plotted dynamic stability and transient response of linear continuous systems described by high order differential equations of motion

13 p1661 A73-29144

Secular stability of an 8 solar mass star during central helium burning.

13 p1685 A73-29355

Numerical experiments on the stability of spherical stellar systems.

13 p1685 A73-29359

Pulsational instability of a star of 0.5 solar mass during core hydrogen burning.

13 p1685 A73-29362

Numerical integration of orbits for evolution of different configurations, discussing Titius-Bode law and stability limits of planetoid and hypothetical planet orbits

13 p1686 A73-29366

Cavity-like instability observed in quiescent prominence from H alpha slit-yaw pictures shown with Ca ion 8542 A spectra

13 p1670 A73-29371

All order stability of Hamiltonian systems with two degrees of freedom.

14 p1773 A73-29756

Influence of structural flexibility on the dynamic stability of rockets.

14 p1803 A73-30043

Relativistic stellar stability - An empirical approach.

14 p1801 A73-30740

Stability of elliptical cylinder consisting of perfect incompressible gravitating fluid subject to arbitrary perturbations

15 p1860 A73-31048

Upper and lower stability limits criterion for plane shock waves, based on Hugoniot curve positive slope

15 p1860 A73-31090

Russian book - Calculation and designing of gyroscopic stabilizers.

15 p1875 A73-31587

Stability analysis procedure for shock wave in steady compressible fluid flow, obtaining equations of motion

15 p1864 A73-32113

Equations of disturbed motion and equilibrium for solid body with incompressible fluid filled cavity, noting equilibrium position stability conditions

15 p1915 A73-32403

Complex roots onset in secular stellar spectrum extended to case with shell sources present, determining eigenvalues for different intensity and position parameters

16 p2058 A73-32830

Effects of attenuation on the stability characteristics in the case of combination resonances

16 p2080 A73-33260

Ranges of instability of the first and the second kind for vibrational systems with random parameter excitation

16 p2080 A73-33264

Newkirk effect - Thermally induced dynamic instability of high-speed rotors.

[ASME PAPER 73-GT-26] 16 p2047 A73-33499

Dynamic stability of an orthotropic cylindrical shell allowing for transversal shear

16 p2083 A73-33937

Effect of finite resistivity on the dynamic stability of a composite plasma.

17 p2214 A73-34074

Jupiter atmospheric circulation as manifestation of large scale convective instability generated by internal heat sources, considering Red Spot production

17 p2232 A73-34859

Helicopter turboshaft engine vibration reduction through engine-airframe interface compatibility design and torsional stability of drive trains with automatic fuel control

[AHS PREPRINT 774] 17 p2106 A73-35092

Free particle gravitating cylindrical model for gravitational kinetic instabilities, calculating natural vibration spectrum and parameters for beam instability development

18 p2340 A73-36739

Computation of the nonlinear dynamic stability functions of a reentry body in hypersonic flight

18 p2361 A73-37081

Qualitative analysis of the behavior of weakly coupled oscillators near the equilibrium position

19 p2458 A73-37191

Stability of nonlinear oscillations with unsteady impulsive excitation

19 p2459 A73-37650

Acoustic echo-sounding techniques and their application to gravity-wave, turbulence, and stability studies.

19 p2405 A73-38207

Forward scatter propagation measurements /trans-horizon and line-of-sight/ applied to specific forms of instabilities in layers.

19 p2406 A73-38247

Dual spin spacecraft minimum energy and nutational dynamic trap states due to asymmetric or unbalanced rotors, analyzing single degree of freedom dynamic model

[AIAA PAPER 73-908] 20 p2614 A73-38842

Instability of electromagnetic surface waves supported by a bounded plasma stream.

20 p2595 A73-38891

Stability of periodic oscillations of stars.

20 p2606 A73-39081

Integral parameters and pulsation frequencies for equilibrium configurations of rotating neutron stars, expanding energy characteristics into series of relativistic members

20 p2608 A73-39228

Equilibrium point asymptotic stability for nonlinear generalization of Onsager theory for entropy functions construction with applications to chemical reaction kinetics

20 p2627 A73-39338

Dynamic stability of a nonlinear beam subjected to both longitudinal and transverse excitation.

20 p2621 A73-39532

Stability of waves and shock structure in generalized thermoelasticity at low temperatures.

20 p2624 A73-39564

Excitation of parametric vibrations in stochastic systems with two degrees of freedom

20 p2594 A73-39641

Dynamic systems stability under influence of white noise-Gaussian random processes, discussing optical control, Markov processes, linear equations and vector fields

20 p2583 A73-39768

The photolytic stability of the Martian atmosphere.

21 p2764 A73-40159

Application of R-functions to a calculation of the dynamic stability of plates with a complex planform geometry

21 p2786 A73-40984

Tuned dampers for randomly excited dynamic systems.

[ASME PAPER 73-DET-70] 22 p2919 A73-42070

Spatial stability of incompressible two-dimensional Gaussian wake in steady viscous flow.

22 p2796 A73-42243

The stability of rotating supermassive stars.

22 p2907 A73-42304

Vibration and stability of nondivergent elastic systems.

22 p2922 A73-42551

Dynamic stability of transverse axisymmetric waves in circular/cylindrical shells.

[ASME PAPER 73-APMW-26] 22 p2925 A73-42887

The dynamic behavior of articulated pipes conveying fluid with periodic flow rate.

[ASME PAPER 73-APMW-32] 22 p2925 A73-42892

Stress amplification in a ring caused by dynamic instability.

[ASME PAPER 73-APMW-35] 22 p2925 A73-42893

An exact method for the study of the dynamic stability of supporting structures acted upon by periodic impulses.

22 p2927 A73-43031

Dynamic stability of rotating disks loaded by a concentrated force

22 p2928 A73-43064

Hydrodynamic equations for nonlinear stability of plasma ionization wave interactions in absence of magnetic field

23 p3012 A73-44040

A new method of analysing the stability of nonlinear dynamic systems.

23 p3006 A73-44084

Typical characteristics of dynamic systems nearly all of whose trajectories remain stable under steadily acting disturbances

24 p3109 A73-44424

Dynamic stability of a viscoelastic orthotropic cylindrical shell

24 p3146 A73-44532

Model for radiative dynamic instability of cloudy planetary atmosphere from coupling for case of radiative heating rate dependent cloud properties

24 p3132 A73-44534

Radiative instability model of cloud cover on equatorial beta plane to explain Jupiter bands zonal symmetry and meridional wavelength

24 p3132 A73-44535

On the stability limit of nonlinear resonances in multiple-degree-of-freedom vibrating systems.

24 p3146 A73-44681

Dynamics of the balance preservation system of man

24 p3064 A73-44909

Gaseous plasma thermal conductivity in dynamic equilibrium, relating particle binary correlation to shielding distance under temperature gradients

24 p3116 A73-45243

Book - Solid-state mechanics 3.

24 p3153 A73-45495

Ljapunov functions application to stability analysis of dynamic systems and elastic bodies, considering eigenfunction method, maximum principle and energy criterion

24 p3153 A73-45497

DYNAMIC STRUCTURAL ANALYSIS

Stress function for estimating mutual effects of strain and temperature fields in dynamic coupled thermoelasticity problem for thin circular plates

01 p0113 A73-10094

A linearized analysis for frictionally damped systems.

01 p0090 A73-10782

Dynamic edge effect in rods - Formulation of shortened problems

01 p0118 A73-11405

Experimental investigation of the behavior of cylindrical shells under dynamic loads

02 p0229 A73-11626

Determination of attenuation factors from experimental vibrograms of multifrequency attenuating oscillations

02 p0233 A73-11942

A numerical method considering the Bauschinger effect for large deflection analysis of elastic-plastic circular plates.

02 p0236 A73-12522

Free vibrations of elastic systems with discrete dynamic systems attached.

03 p0384 A73-12983

Flight-mechanical analysis of various flight states of conventional aircraft. VII - Mechanical principles: Rigid-body dynamics

03 p0250 A73-13074

Dynamic plastic tensile stress analysis based on equation of motion, kinematic equation and material law with conditions regarding disturbance propagation velocity

03 p0385 A73-13142

Rotatory inertia and hub radius effects on transverse vibrational characteristics of clamped Rayleigh beam, using Galerkin method

03 p0388 A73-13316

An approximate algorithm for the reanalysis of structures by the finite element method.

03 p0391 A73-13676

Monte Carlo solution of structural dynamics.

03 p0391 A73-13681

Perturbation and harmonic balance methods for nonlinear panel flutter.

03 p0395 A73-14182

Dynamic structural analysis large eigenvalue problems, presenting subspace iteration algorithm for arbitrary system size and bandwidth

04 p0509 A73-14944

Transient dynamic response of viscoelastic structures.

[SAE PAPER 720812] 05 p0634 A73-16649

Calculation of general surface-supporting structures with the aid of dynamic relaxation

06 p0758 A73-17516

Dynamic plastic deformation of rings under impulsive load.

06 p0761 A73-17817

Large deflexion elastic-plastic response of certain structures to impulsive load - Numerical solutions and experimental results.

06 p0761 A73-17818

Thermal stresses in an anisotropic plate with a circular hole.

07 p0914 A73-20199

Longitudinal vibration analysis of partially-filled ellipsoidal tanks.

07 p0914 A73-20215

Shock and vibration disturbance identification based on structural system response, discussing linear programming, curve fitting, constraints, objective functions and applications

07 p0916 A73-20430

Identification of large structures using data from ambient and low level excitations.

07 p0916 A73-20431

The state of the art of system identification of aerospace structures.

07 p0916 A73-20432

On the application of parameter identification to high-speed ground transportation systems.

07 p0808 A73-20433

Synthesis of two discrete vibratory systems using eigenvalue modification.

08 p1015 A73-20726

Derivatives of eigenvalues and eigenvectors in non-self-adjoint systems.

08 p0983 A73-20728

The method of internal force parameters in elastokinetics

08 p1016 A73-20782

Beams and membranes nonlinear vibrations via modified perturbation method based on Linstedt-Poincare technique

08 p1018 A73-21406

Improved finite elements for vibration analysis of tapered beams.

08 p1018 A73-21439

Dynamic analysis of freely supported axisymmetric shells.

08 p1018 A73-21473

Association Technique Maritime et Aeronautique, Session, 72nd, Ecole Nationale Supérieure de Techniques Avancées, Paris, France, May 15-19, 1972, Proceedings.

09 p1031 A73-22201

Dynamic analysis of helicopter structures

09 p1031 A73-22206

On the generalization of stress function procedure for dynamic analysis of plates.

09 p1158 A73-22395

Book - Vibration of solids and structures under moving loads.

09 p1159 A73-22526

Natural vibrations of laminated orthotropic spheres.

09 p1160 A73-22890

An approximate rigid-plastic analysis of shell intersections loaded dynamically.

[ASME PAPER 72-WA/DE-1] 09 p1164 A73-23272

Computation of the deflections of straight beams with any variation of the moment of inertia by the method of the three unknowns.

10 p1287 A73-23617

Vibration analysis of clamped, rectangular plates of generalized orthotropy.

10 p1291 A73-24387

Axisymmetric vibrations of circular plates with stepped thickness.

10 p1291 A73-24394

On the role of the adjoint problem in dissipative, nonconservative problems of elastic stability.

11 p1434 A73-25214

Probable collapse mechanisms in indefinite plates on an elastoplastic continuum.

11 p1434 A73-25217

Rayleigh quotient minimization and eigenvalue/eigenvector errors of mode convergence in dynamic structural analysis, using gradient algorithm and scaling transformation

[AIAA PAPER 73-361] 11 p1438 A73-25497

The state of the art in aeroelasticity of aerospace vehicles in Japan.

[AIAA PAPER 73-331] 11 p1305 A73-25560

Dynamic stiffness matrix method for determining natural frequencies of plane frame with axially loaded Timoshenko members of uniform mass distribution 11 p1446 A73-26494

Dual-beam polariscope and framing camera for dynamic photoelasticity. 12 p1496 A73-27025

Formulation of time variant stiffness matrices due to changing joint properties. 12 p1555 A73-27737

Mathematical observations in structural dynamics. 12 p1555 A73-27739

Free vibration of cantilever beam with/without tip mass and with nonlinear material properties, using perturbation and finite element techniques 12 p1556 A73-27928

First-excursion probability in non-stationary random vibration. 13 p1691 A73-28064

Natural frequencies of a beam considering support characteristics. 13 p1691 A73-28065

Dynamic structural response analysis with eigenvalue problem solution in terms of stiffness and mass matrices, discussing algorithm selection for efficient computation 13 p1691 A73-28081

The local solution approach in the finite element method. 13 p1692 A73-28232

The application of a curved, mixed-type shell element. 13 p1693 A73-28237

Geometrically nonlinear static and dynamic analysis of shells of revolution. 13 p1693 A73-28239

Computational efficiency of equilibrium models in eigenvalue analysis. 13 p1694 A73-28248

Complementary energy method in elastodynamics. 13 p1694 A73-28249

Line and rectangular plane finite element models for accurate and efficient dynamic vibration frequency analysis of frames and shear walls respectively 13 p1700 A73-29377

Behavior of random micro-structural systems. 13 p1701 A73-29530

Stress differentiation procedure for screen technique studies in dynamic photoelasticity, giving expressions for elastic modulus and Poisson ratio 13 p1703 A73-29613

Large amplitude vibrations of certain deformable bodies. II Plates and shells. 14 p1806 A73-30041

Matrix method analysis of stiffened plates free vibrations, deriving governing equation in stiffness matrix form by combining plane stress theory and lateral vibration equation 14 p1807 A73-30186

Frame structures dynamic analysis, comparing force method derived from stress and velocities variational principles with displacement method derived from Hamilton principle 14 p1807 A73-30188

Dynamic stress concentration at an elliptic hole due to plane SH-waves 15 p1947 A73-31331

Russian book - Strength of turbine wheels. 15 p1948 A73-31578

Computation of upper and lower bounds to the frequencies of elastic systems by the method of Lehmann and Maehly. 15 p1951 A73-32027

Free vibration of an inflated oblate spheroidal shell. 15 p1955 A73-32155

Application of stress functions to dynamic analysis of shallow shells. 16 p2077 A73-32987

Nonlinear dynamic problem concerning a cylinder with a slowly changing internal boundary 16 p2082 A73-33932

Method for determining Young's dynamic modulus for curvilinear specimens 16 p2030 A73-33938

Flexural wave mechanics - An analytical approach to the vibration of periodic structures forced by convected pressure fields. 16 p2083 A73-33947

Natural frequencies and normal modes of a four plate structure. 16 p2083 A73-33948

Influence of structural flexibility on attitude control of spacecraft 17 p2162 A73-34950

The use and evaluation of shock spectra in the dynamic analysis of structures. [ASME PAPER 73-APM-22] 17 p2248 A73-35041

On stability of large-scale systems under structural perturbations. 17 p2213 A73-35827

Book - Dynamics and vibration of structures. 17 p2252 A73-35833

Nonlinear transient responses of structures by the spatial finite-element method. 18 p2362 A73-36309

Dynamically-induced large deformations of multilayer, variable thickness shells. 18 p2362 A73-36317

Engineering analysis of the inelastic stress response of a structural metal under variable cyclic strains. 18 p2364 A73-36594

Aspects of the finite element method as applied to aero-space structures. [ISD-138] 18 p2365 A73-36725

Forecast of mode variation subsequent to structure modifications 18 p2367 A73-37083

Computer based analyses of the response of box type structures to random pressures. 19 p2497 A73-37485

Resonance methods for the dynamic study of deformable structures 19 p2497 A73-37556

Material damping - An introductory review of mathematical models, measures and experimental techniques. 19 p2500 A73-38105

Determination of dynamic loads on elastic structures caused by external excitations 19 p2500 A73-38155

Midwestern Mechanics Conference, 13th, University of Pittsburgh, Pittsburgh, Pa., August 13-15, 1973, Proceedings. 20 p2620 A73-39513

Free vibration of arches flexible in shear. 21 p2782 A73-40002

Dynamics of cylindrical structures subjected to axial flow. 21 p2783 A73-40292

Large amplitude flexural vibration of simply supported skew plates. 21 p2784 A73-40423

Russian book on elastic and thermoelastic waves in continuous deformable bodies covering steady and unsteady deformation dynamics, viscoelasticity and nonlinear elasticity using computer methods 21 p2785 A73-40800

Identification and simulation of antenna dynamics. 21 p2667 A73-41525

An approximation for the determination of the dynamic characteristics of long viscoelastic hollow cylinders 21 p2788 A73-41615

Finite element analysis of rotating shells. [ASME PAPER 73-DET-94] 22 p2919 A73-42074

Convergence of simplified hybrid displacement method for plate bending. 22 p2921 A73-42203

Book - Dynamics in engineering structures. 22 p2922 A73-42491

Vibration analysis of laminated plates and shells by a hybrid stress element. 22 p2923 A73-42566

Experimental determination of the transient uniaxial stress in a bar by dynamic photoplasticity. [ASME PAPER 73-APMW-37] 22 p2926 A73-42894

Complex structural dynamic response reduction, discussing methods for mathematical models establishment and application to thin cylindrical shell 22 p2926 A73-42921

Fuel tank wall response to hydraulic ram during the shock phase. 22 p2843 A73-43114

Book on engineering dynamics similarity and scaling methods covering blast waves and gas dynamics, transient loads, fluid-structure interaction, soil dynamics, thermal modeling, etc 23 p3039 A73-43460

Static and dynamic finite deformations of cables using rate equations. 23 p3042 A73-43804

Transmission of anti-plane shear waves past an interface crack in dissimilar media. 23 p3043 A73-43815

Dynamic buckling of an axially compressed cylindrical shell with discrete rings and stringers. 23 p3047 A73-44377

Large amplitude vibrations of elastically restrained rectangular plates. 23 p3048 A73-44380

Nonlinear transverse vibration analysis of a rectangular plate with lumped M-S-D systems. 23 p3048 A73-44384

Numerical approximation of quasi-static and dynamic problems in viscoelasticity by net-point and finite difference methods 24 p3144 A73-44505

Power series solution to Volterra equations in nonlinear viscoelastic dynamic plate and shell theory with application to flexible cylindrical shell vibrations under periodic loads 24 p3145 A73-44518

A minimum principle in dynamics of elastic-plastic continua at finite deformation. 24 p3146 A73-44678

Beck cantilever problem solution for quasi- and purely dynamic case by Euler or energy method under internal constraint 24 p3147 A73-44892

On response of initially stressed structures to random excitations. 24 p3150 A73-45229

DYNAMIC TESTS

Some experiments on dynamic and quasi-static forging of aluminum at elevated temperatures. [ASME PAPER 72-WA/MAT-1] 04 p0457 A73-15811

Digital vibration control systems for structural design dynamic testing and evaluation, discussing state of art and trends toward multichannel and multi-axis control [SAE PAPER 720820] 05 p0553 A73-16628

The determination of free-body responses of a structure from constrained test data. [AIAA PAPER 73-191] 05 p0635 A73-16928

Complete identification of some non-linear closed-loop systems. 06 p0681 A73-18525

Static and dynamic behavior of welded aluminum beams. 07 p0839 A73-20270

Measurement of the critical crack displacement with the help of double-notched specimens 11 p1434 A73-25325

Tape recorder instrumentation for structural dynamic load test data analysis, discussing cable crosstalk, lead length and electrical noise effects in crack propagation measurements 14 p1751 A73-29775

The use of elastic relaxation for testing aerospace equipment. 15 p1948 A73-31462

A dynamics approach to helicopter transmission noise reduction and improved reliability. [AHS PREPRINT 772] 17 p2106 A73-35090

An optimization technique utilizing the deflected gradient algorithm for dynamic testing of electromechanical equipment. 17 p2202 A73-35386

Two dimensional static, dynamic and three dimensional photoelasticity measurement techniques for stress intensity, factors determination in boundary value problems of fracture mechanics 17 p2252 A73-35673

Preliminary results from dynamic model tests of an air cushion landing system. 19 p2382 A73-37694

Design and testing of a 150 watt SNAP 19 high performance generator. [IECEC PAPER 739090] 19 p2458 A73-38437

Building a dynamic test complex near an inertial test facility and general test pad considerations. [AIAA PAPER 73-827] 20 p2543 A73-38772

An electromagnetic torsional vibrator. 20 p2544 A73-39271

Two wavelength variable sensitivity interferometry, extending static technique to real time dynamic testing 21 p2698 A73-40138

The influence of flaw density and flaw size distribution on the static and dynamic fatigue behaviour of graphite. 23 p2998 A73-44037

DYNAMO THEORY

On the dynamo action of the global convection in the solar convection zone. 05 p0627 A73-17387

Geomagnetic variations with the period of a sidereal day. 07 p0818 A73-19672

The possibility of disappearance of the earth's magnetic field during inversion 08 p0958 A73-21275

Turbulent dynamo theory based on functional analysis, noting equation with variational derivatives of characteristic functional 08 p0989 A73-21697

Response to critiques of paper on earth core paradox consisting of stratification inhibition on outer core fluid circulation needed for dynamo theory of geomagnetic field generation 09 p1077 A73-22193

Oscillation of the earth's inner core and its relation to the generation of geomagnetic field. 09 p1077 A73-22194

Star magnetic field origin in dynamo action associated with nuclear energy generation in stellar evolution, discussing effects on flares, chromosphere and coronal activities 10 p1271 A73-23489

Turbulent plasma dynamo mechanisms of magnetic field origin in astrophysics, noting Steenbeck and Parker theories 10 p1285 A73-24942

Geomagnetic field polarity reversal mechanism, interpreting frequency distribution by energy exchange between dynamo models and conversion between kinetic and magnetic energies 11 p1355 A73-25792

Nonlinear resistive boundary layer in rotating hydromagnetic flow related to earth dynamo theory, discussing steady solution uniqueness and numerical temporal stability 11 p1355 A73-25794



Ionospheric currents induced by solar wind interaction with planetary atmospheres.

11 p1412 A73-25921

Liquid core model with precessionally driven magnetoturbulence applied to moon, discussing tidal effects in outer solid and liquid shells.

12 p1541 A73-27489

Condensation of stars and magnetic field formation in protogalaxies

12 p1547 A73-27868

Alpha-omega dynamo problem of electrically conducting sphere magnetic field, obtaining eigenvalues from variational principle with free decay modes as trial functions

13 p1685 A73-29365

Lunar magnetic field model with primeval liquid shell dynamo driven by thermal convection or earth tidal motions

14 p1789 A73-29722

Outer solar system planetary and subplanetary objects magnetic field existence, discussing internal dynamo fields, externally driven dynamos and fossil fields

14 p1800 A73-30540

Numerical simulation of equatorial electric fields and magnetic variations based on global ionospheric dynamo and equatorial electrojet models

15 p1869 A73-31753

Three dimensional dynamo theory in the magnetosphere.

17 p2158 A73-34503

Dynamo theory of earth magnetic field generation, discussing earth core characteristics, electromagnetic induction processes and magnetic field energy sources

17 p2162 A73-35049

Numerical solutions of the kinematic dynamo problem.

19 p2460 A73-38102

Worldwide distribution of geomagnetic tides.

19 p2426 A73-38104

Star contraction and magnetic-field generation in protogalaxies.

20 p2608 A73-39242

On an eigenvalue problem in the kinematic approach to dynamo theories of cosmic magnetism.

20 p2609 A73-39571

Dynamo theory for geomagnetic field, emphasizing fluid flow symmetric and asymmetric velocity component relative magnitudes

21 p2679 A73-39930

Plasmaspheric quasistatic electric fields and plasma convection, discussing dynamic electric fields and magnetospheric field penetration to low latitudes

21 p2679 A73-40075

Solar quiet dynamo region electric fields and currents diurnal and semidiurnal field components variations with latitude

21 p2689 A73-41357

DYNAMOMETERS

Nonisothermal instability of flows of viscoelastic media

09 p1072 A73-22481

Fabrication of high precision strain gauge dynamometers and balances at the O.N.E.R.A. Modane Centre. [ONERA, TPNO. 1196]

22 p2839 A73-42217

DYNAMOS

U ROTATING GENERATORS

DYNODES

Cleaning and activation of beryllium-copper electron multiplier dynodes.

02 p0146 A73-11966

Multichannel secondary electron image intensifier design, using dynode and separate channel transmission

23 p2961 A73-44386

DYSON THEORY

Turbulent diffusion in Schwinger formulation of quantum field theory, deriving transition probabilities from Dyson and Saffman equations

20 p2599 A73-39674

DYSPROSIUM

Domain-wall related, natural, submillimeter-wave resonance in orthoferrites

06 p0736 A73-18114

Investigation of the lasing and luminescent properties of fluorite and strontium fluoride crystals containing bivalent dysprosium impurities

07 p0837 A73-20207

The investigation of the middle infrared absorption spectrum of DyVO₄ at low temperatures.

08 p0994 A73-21219

X-ray structural investigations of Dy-Fe-Al system alloys in the region of 0 to 33 at. % dysprosium

12 p1512 A73-27243

The magnetic characteristics of the alloys of palladium with gadolinium, dysprosium, and holmium

13 p1667 A73-28183

Investigation of the delay of stimulated emission from a CaF₂:Dy²⁺ laser relative to pumping pulses.

13 p1629 A73-29431

Concentration dependence of the lasing parameters of a laser based on CaF₂:Dy²⁺ crystals

15 p1884 A73-31221

E LAYERS

U E REGION

E REGION

NT SPORADIC E LAYER

Symposium on D- and E-Region Ion Chemistry, University of Illinois, Urbana, Ill., July 6-8, 1971, Informal Record.

01 p0040 A73-10876

D and E region aeronomy, discussing ionization sources, ion composition, water cluster ion formation and ratio of molecular oxygen and nitric oxide ions

01 p0040 A73-10877

Mass spectrometric measurements of minor constituents in the lower thermosphere.

01 p0041 A73-10880

Estimation of nitric oxide concentration in the lower E region from rocket and satellite measurements of electron densities and X-ray fluxes.

01 p0041 A73-10882

Ionization sources of the ionospheric D and E regions.

01 p0041 A73-10886

Positive ion composition measurements in the D and E regions of the equatorial ionosphere.

01 p0041 A73-10889

Ion composition and photochemistry of the E-region.

01 p0042 A73-10892

A nighttime ionospheric E-region model.

01 p0042 A73-10893

Negative-ion composition measurements in the D and lower E regions.

01 p0042 A73-10896

D and E ionospheric regions behavior, emphasizing water cluster ions formation, minor neutral constituents measurement and daytime ionization sources

01 p0043 A73-10912

Observations of simultaneous auroral D and E layers with incoherent scatter radar.

01 p0043 A73-10998

E region irregularities investigation via phase path measurements and radio wave ionospheric soundings, using model for undulatory variation of reflection height

02 p0158 A73-12028

Molecular nitrogen vibrational temperature in E and F regions, using positive ion data and model for ionic reaction rate and continuity equation numerical solution

02 p0161 A73-12279

Features of the ionospheric drift over the magnetic equator.

02 p0162 A73-12287

E region wind and density measurements by VHF radar and atmosphere temperature measurement by radio acoustic sounding technique, describing instrumentation and computerized data reduction

03 p0339 A73-14546

E region electron collision frequency vertical distribution from ground and rocket measurements of radio wave absorption and electron density respectively

03 p0304 A73-14562

Instabilities resulting from gravity wave perturbation of ionization via neutral-charged particle collisions in nighttime E region

03 p0305 A73-14595

Solar cycle control of the ionospheric E-region.

04 p0441 A73-15291

Geomagnetic storm effects in the nighttime E layer during increasing and maximal solar activities

05 p0568 A73-16215

Electron concentration variation in E layer after sunrise, noting critical frequency deviations from Chapman law

05 p0568 A73-16216

Planetary-scale fluctuations of pressure in the E-layer, f-min, and pressure in the stratosphere.

05 p0571 A73-17057

E layer ionization diurnal exponent independence of seasons and station latitude ascertained by statistical tests

05 p0571 A73-17058

Latitude, longitude and hemisphere effects on Appleton E layer seasonal anomaly from statistical analysis of critical frequency

05 p0571 A73-17059

Ionospheric electron density profiles model evaluation, considering E region height and thickness seasonal variation

05 p0571 A73-17063

Correlations between X-rays and UV ionizing radiation in the E region from data obtained during the solar eclipse of 25 February 1971

06 p0742 A73-17534

Vertical profiles of the effective collision number in the E and F regions of the ionosphere

06 p0689 A73-17552

Two-beam observations of ionospheric irregularity structure and velocity at Arecibo.

07 p0791 A73-19379

Lower ionosphere electron densities from rocket measurements employing LF radio propagation and DC probe techniques.

07 p0818 A73-19670

Ion composition and photochemistry of the E region

08 p0958 A73-21282

Study on the solar activity dependence of the E region peak electron density and some atmospheric parameters.

08 p0961 A73-21652

Metallic ion composition and electron density measurements in equatorial E region, considering three body reaction kinetics with dissociative ion-electron recombination

09 p1074 A73-22064

Nighttime electron density in the E region at auroral latitudes in sunspot maximum.

09 p1078 A73-22747

Ion composition in the E- and lower F-region above Kiruna during sunset and sunrise.

09 p1078 A73-22838

Field-aligned ionospheric E-region irregularities and sporadic E.

10 p1191 A73-24897

Statistical characteristics of E and F regions maximum electron density and ionization height, discussing electron content in vertical unit column in upper and lower ionosphere

11 p1351 A73-25092

Autocorrelation and cross correlation coefficients for maximum electron densities and total electron content in E and F regions and upper and lower ionosphere

11 p1351 A73-25093

Disturbances observation in E-F region and sporadic E layer by vertical ionospheric sounding during IQSY

11 p1351 A73-25098

Wide angle narrow band interference filter for detecting E region barium ion clouds against intense background

11 p1366 A73-26250

Total electron content measurements during visible auroras.

11 p1359 A73-26714

Polar cap E layer conductivity difference effects on ring currents associated with vertical current along lines of force at conjugate points

13 p1608 A73-28717

High power radio transmitter for structural investigation and electron concentration profiles of ionospheric D and E regions

13 p1583 A73-28725

Electric field and plasma density oscillations due to the high-frequency Hall current two-stream instability in the auroral E region.

14 p1748 A73-29971

Type I and II electron density irregularities due to two-stream and cross field instabilities in E region equatorial electrojet, considering wind shear role

15 p1869 A73-31755

Equatorial Esq disappearance relationship to daily magnetic Sr variation inverted latitudinal profiles during magnetic quiet periods, considering counter electrojet current belt hypothesis

15 p1869 A73-31757

Correlations between X-rays and ionizing ultraviolet radiation in the E-region, according to data from the solar eclipse of February 25, 1971.

16 p2052 A73-32758

Vertical profiles of the effective collision frequency in the E- and F-regions of the ionosphere.

16 p2002 A73-32776

Downward transport of nighttime Es layers into the lower E-region at Arecibo.

18 p2302 A73-35941

ALADDIN II ionospheric composition measurements, obtaining ion and neutral vertical density profiles and dynamic parameters for E region nighttime ion layering prediction model

18 p2303 A73-35958

Ion and neutral composition measurements in the lower ionosphere.

18 p2303 A73-35960

Kinesonde studies of cesium ion clouds in the E-region.

18 p2304 A73-35988

Cross-field instability as a mechanism for equatorial E region irregularities.

18 p2304 A73-35998

A rocket observation of the disturbed mid-latitude nighttime ionosphere.

18 p2308 A73-36048

Tentative E-region electron density profiles.

18 p2309 A73-36099

Joule heating effect due to currents in the equatorial electrojet as observed by rocket borne probes.

18 p2310 A73-36128

Simultaneous measurements of some ionospheric parameters at altitudes 100-170 km.

18 p2310 A73-36131

Meteoric ions in the D and E-regions.

18 p2310 A73-36132

- Ion composition and photochemistry of the E-region.**
19 p2424 A73-37911
- A phenomenological model of global ionospheric electron density in the E-, F1- and F2-regions.**
19 p2425 A73-38014
- Ionospheric inhomogeneity parameters and geoelectromagnetic field variations**
20 p2553 A73-39156
- Magnetic equatorial ionospheric characteristics, discussing E and F regions, diurnal drift variations, field strength, equatorial electrojet, spread F and sporadic E**
20 p2555 A73-39633
- Method of studying magnetic-ionospheric disturbances and solar flare effects on long-upset periods.**
20 p2555 A73-39767
- Temperature dependence for dissociative recombination of NO⁺ in E- and F-region models.**
21 p2684 A73-40787
- Radio frequency heating effects on electron density in the lower E region.**
22 p2845 A73-41930
- Characteristics of the redistribution of charged particles in the nighttime E region at mid-latitudes**
22 p2847 A73-42331
- E and F regions nitrogen vibration energy content by numerical integration of time dependent species continuity equation and species equation of motion**
22 p2848 A73-42537
- Appleton seasonal anomaly in E region maximum electron density investigated by critical frequency data statistical analysis, showing solar activity effects**
23 p2979 A73-44006
- Diurnal ion composition variations in E region under quiet and perturbed solar conditions, using continuity equations for positive ions and electroneutrality equations**
24 p3083 A73-44793
- E and F layers, discussing formation, collision processes and S and L geomagnetic variations**
24 p3087 A73-45204
- ISIS 2 scanning photometric analysis of E and F region airglow at O I 5577 Å, noting height difference of airglow components at midlatitudes and near equator**
24 p3088 A73-45214
- EAR**
NT COCHLEA
NT CORTI ORGAN
NT EARDRUMS
NT LABYRINTH
NT MIDDLE EAR
NT SEMICIRCULAR CANALS
NT VESTIBULES
A study of basilar membrane vibrations. I - Fuzziness-detection: A new method for the analysis of microvibrations with laser light.
01 p0013 A73-10973
- Some effects of cooling and heating areas of the head and neck on body temperature measurement at the ear.**
13 p1575 A73-28504
- Electrical activity of the external ear muscles in man /at rest and during identification of acoustic signals/**
14 p1719 A73-30843
- Ejection time by ear densitogram and its derivative - Clinical and physiologic applications.**
20 p2511 A73-38866
- EAR PRESSURE TEST**
Procedures for polarocochleography and for pressure measurement in the inner ear perilymph in acute experiments on animals
11 p1314 A73-25043
- EAR PROTECTORS**
A single number rating for effective noise reduction.
11 p1397 A73-25000
- Hearing conservation studies covering impulse noise produced threshold shift, damage risk criteria, ultrasound hazards and hearing protection**
17 p2117 A73-35326
- EARDRUMS**
Study of the acoustic reflex in human beings. I - Dynamic characteristics.
01 p0013 A73-10828
- EARLY STARS**
NT PROTOSTARS
NT T TAURI STARS
UV astronomy advances from rocket and satellite observations, discussing early stars, interstellar extinction and gas, galaxies and globular clusters
01 p0094 A73-10059
- Element abundances in O- and early B-stars.**
01 p0096 A73-10296
- LTE fine analysis of omicron-tw C Ma line profiles, showing chemical composition near Iota Her**
02 p0221 A73-12705
- Infrared excesses in early-type stars - Free-free emission.**
02 p0225 A73-12826
- Polarization of light by circumstellar material.**
02 p0226 A73-12828
- New ultraviolet line identifications for early-type stars.**
02 p0226 A73-12831
- A search for density and pressure inversions in high-temperature, low-gravity model atmospheres.**
03 p0366 A73-12935
- A search for He-weak stars in very young clusters.**
03 p0372 A73-13227
- A study of the unidentified interstellar diffuse features.**
05 p0626 A73-17379
- Optically thin stellar winds in early-type stars.**
07 p0873 A73-19061
- Luminosity classification of stars earlier than O9.**
07 p0875 A73-19120
- Stellar and interstellar K lines - Gamma Pegasi and Iota Herculis.**
08 p1003 A73-20882
- The interstellar reddening law in the ultraviolet deduced from filter photometry obtained by the OAO-2 satellite.**
09 p1141 A73-22029
- Infra-red observations of young stars. I - Stars in young clusters. II - T Tauri stars and the Orion population. III - Nebulous emission-line stars.**
09 p1143 A73-22112
- A non-LTE study of silicon line formation in early-type main-sequence atmospheres.**
10 p1272 A73-23532
- Near infra-red magnitudes of 248 early-type emission-line stars and related objects.**
11 p1415 A73-25172
- Electric conductivity in the atmosphere of early-type stars.**
11 p1427 A73-26575
- Dust emission nebulae around Orion O and B stars.**
11 p1427 A73-26606
- Massive X ray binaries consisting of early type star with neutron stars or black holes as companions**
12 p1535 A73-27597
- LTE and hydrogen and ionized He lines approximations for model atmosphere computations of hot early stars, discussing UV line blanketing**
13 p1686 A73-29367
- On the kinematics of a local component of the interstellar hydrogen gas possibly related to Gould's Belt.**
13 p1686 A73-29369
- RY Sct detection from search for binary systems with early type star and mass exchange for radio source candidacy**
14 p1789 A73-29736
- Stellar atmospheric conditions taking into account A5 and early stars, considering spectral characteristics, absorption spectra and spectrum prediction**
15 p1932 A73-31305
- Russian papers on young stellar complexes and astrolimate covering physical nature and activity of nonstationary stars, stellar evolution, T-associations and earth atmosphere optical instability**
15 p1934 A73-31418
- Relationship between T-associations and the interstellar medium in the northern region of the Monoceros complex**
15 p1934 A73-31421
- New directions and new frontiers in variable star research; Colloquium on Variable Stars, 5th, Bamberg, West Germany, August 31-September 3, 1971, Proceedings.**
15 p1934 A73-31476
- Southern Milky Way early type star interstellar extinction curves, considering position with regard to galactic plane and local dust cloud conditions**
15 p1939 A73-32046
- Early type stellar line spectra, discussing LTE, hydrogen and helium lines, stellar element abundance and O and B stars**
18 p2356 A73-36875
- The He I lambda 5876 line in O-star spectra.**
18 p2356 A73-36973
- IR astronomical objects, methods and instruments, discussing galactic and extragalactic sources, early and late stars, planetary nebulae, interstellar dust and hydrogen ion clouds**
20 p2605 A73-39060
- Observations of ultraviolet stellar spectra by the Utrecht Orbiting Stellar Spectrophotometer S59.**
21 p2769 A73-40811
- The near ultraviolet spectrum of early type stars obtained with S 59.**
21 p2769 A73-40825
- Detection of radio emission from V1016 Cygni.**
21 p2780 A73-41644
- Radio emission from HD167362 and VY2-2.**
21 p2780 A73-41645
- On turbulent stress and the structure of young convective stars.**
22 p2908 A73-42306
- An attempt to interpret the mean properties of the velocity field of young stars in terms of Lin's theory of spiral waves.**
22 p2908 A73-42310
- Extinction and scattering cross sections of small planetesimal particles with iron cores and silicate mantles in circumstellar dust of young T Tauri stars**
23 p3030 A73-43748
- Investigation of anomalously fast stars of early spectral class. III - Search for the He-3 isotope**
23 p3036 A73-44244
- Galactic structure in the direction of Cepheus**
24 p3140 A73-45191
- EARPHONES**
An earphone coupling system for acute physiological studies.
01 p0013 A73-10829
- EARTH (PLANET)**
Earth normal gravity field spherical harmonics in terms of Stokes constants from satellite orbit dynamics, comparing with Helmert system
03 p0305 A73-14613
- Book - Evolution of the protoplanetary cloud and formation of the earth and the planets.**
05 p0615 A73-16356
- Terrestrial thermal history from mathematical model of earth formation with low temperature dust and gas accumulation**
07 p0818 A73-19997
- Terrestrial gravitational models derived from satellite tracking and surface gravimetric data, comparing to 1969 Smithsonian Standard Earth II models**
21 p2773 A73-41326
- Extraterrestrial intelligent life existence possibility in terms of hypothesis involving earth as wilderness area or zoo with failure of interaction with other civilization**
24 p3058 A73-44554
- EARTH ALBEDO**
Polarization of near-infrared sunlight reflected by terrestrial clouds.
01 p0073 A73-10363
- The interaction between ground reflecting power and celestial brightness**
04 p0441 A73-15292
- Reflection and absorption of solar radiant energy by cloud layers.**
07 p0820 A73-20344
- Measurements of solar energy reflected by the earth and atmosphere from meteorological satellites.**
08 p0958 A73-21268
- On a possible relation between lunar transient phenomena and the earth-shine /Research note/.**
10 p1277 A73-24082
- On relationship between the earth-atmosphere system albedo and the earth's surface albedo.**
18 p2308 A73-36042
- Energy spectra and angular distribution measurement for 10-100 MeV earth albedo neutrons by balloon sounding at 116,000 ft**
21 p2761 A73-41380
- Measurements of the energy exchange between earth and space from satellites during the 1960's.**
22 p2851 A73-42858
- EARTH ATMOSPHERE**
NT D REGION
NT E REGION
NT EXOSPHERE
NT F REGION
NT F1 REGION
NT F2 REGION
NT FREE ATMOSPHERE
NT INNER RADIATION BELT
NT IONOSPHERE
NT LOWER ATMOSPHERE
NT LOWER IONOSPHERE
NT MAGNETOPAUSE
NT MAGNETOSPHERE
NT MESOPAUSE
NT MESOSPHERE
NT MIDLATITUDE ATMOSPHERE
NT OUTER RADIATION BELT
NT OZONOSPHERE
NT PROTON BELTS
NT RADIATION BELTS
NT SPORADIC E LAYER
NT STRATOPAUSE
NT THERMOSPHERE
NT TROPOPAUSE
NT TROPOSPHERE
NT UPPER IONOSPHERE
Analysis of a nonisothermal, spherical detector for monitoring the earth's radiative energy budget.
01 p0045 A73-10382
- Natural variation of the radiation budget of the earth-atmosphere system as measured from satellites.**
01 p0038 A73-10390
- Solar events and their effects on the earth surface in August, 1972**
01 p0097 A73-10469
- Russian book on physicochemical basis of space research covering near earth and interplanetary environmental factors and effects on spacecraft designs and materials**
02 p0211 A73-11886
- Composition of relativistic cosmic rays near the earth and at the sources.**
02 p0207 A73-12327
- Restrictions on McElroy theory of Martian chaotic terrain production by permafrost withdrawal, calculating degassed water/carbon dioxide ratios in Mars and earth atmospheres**
02 p0218 A73-12418
- Synthesis of a nonlinear control law for the motion of a space vehicle in the earth's atmosphere.**
05 p0627 A73-16077

Russian book - Meteorological effects on cosmic rays. 05 p0608 A73-16125

The field of a vertical electric dipole over a spherical earth having an atmosphere that is nonhomogeneous with height 05 p0549 A73-16390

Problems of realization of optimal trajectories for spacecraft entry into the dense layers of the earth's atmosphere 05 p0616 A73-16409

Some structure synthesis problems for systems controlling the three-dimensional motion of orbital-aircraft in the earth's atmosphere 05 p0594 A73-16418

The atmospheres of the earth and the terrestrial planets - Their origin and evolution. 06 p0749 A73-17868

Solar flare frequency and associated physical phenomena diversity, discussing earth atmosphere protective effects and impact on Concorde flights 07 p0784 A73-19210

Investigation of the time characteristics of the phase fluctuations of optical waves propagating through the earth atmosphere boundary layer 07 p0792 A73-19914

Effects of changes in the atmosphere on solar insolation. 08 p0958 A73-21269

Low latitude density variations in the earth's neutral atmosphere between 200 and 400 km, from August 1969 to May 1970. 09 p1079 A73-22840

Supersonic generation of atmospheric gravity waves, via atmospheric cooling by moon shadows during lunar eclipses, noting analogy to terminator action 10 p1211 A73-23825

Earth-atmosphere-ocean energy balance time dependent model equation, using Sellers radiation relationships and turbulent exchange coefficients for numerical solution 10 p1245 A73-23982

The radiation balance of the earth-atmosphere system - Recent results from satellite measurements 10 p1213 A73-24399

Lunar eclipses in astronomical history, discussing deviations from geometrical theory, earth atmospheric effects, photometric observations, lunar luminescence, etc 10 p1282 A73-24643

Optical anomalies due to scattered disperse cosmic matter in upper atmosphere from Tungusk meteorite fall 10 p1213 A73-24681

Book - Atmospheric optics. Volume 2. 13 p1680 A73-28513

Effect of instability of earth's atmosphere on results of solar granulation observations. 13 p1680 A73-28515

Terrestrial atmospheric general circulation theoretical and observational research, considering Reynolds or eddy stress distribution across horizontal and vertical surfaces 13 p1610 A73-29333

Acoustic-gravity modes and large-scale traveling ionospheric disturbances of a realistic, dissipative atmosphere. 14 p1748 A73-29977

Prebiological synthesis of organic compounds. 14 p1724 A73-30129

The annual radiation balance of the earth-atmosphere system during 1969-70 from Nimbus 3 measurements. 14 p1750 A73-30762

An analytic formula for heating due to ozone absorption. 14 p1750 A73-30767

Kinetic energy conversions by horizontal and vertical eddy processes from 5 years of hemispheric data. 15 p1873 A73-32253

Thermospheric wind effects on the distribution of helium and argon in the earth's upper atmosphere. 16 p2004 A73-33441

Mars blue haze, earth noctilucent clouds and Venus blue clouds, considering mechanism and condensate chemical composition for formation 16 p2069 A73-33833

The inertia tensor of the atmosphere, annual variations in its components, and variations in the earth's rotation 17 p2158 A73-34343

Atomic collision processes applied to earth atmospheric physics and chemistry, Jovian ionospheric composition and terrestrial tropical UV dayglow 17 p2213 A73-34450

On relationship between the earth-atmosphere system albedo and the earth's surface albedo. 18 p2308 A73-36042

Composition of the earth's atmosphere by shock-layer radiometry during the PAET entry probe experiment. 18 p2313 A73-36797

Nonequilibrium effects on shock-layer radiometry during earth entry. 18 p2338 A73-36798

Differential equations for ballistic motion of meteoric particles in earth atmosphere, noting orbit stability 19 p2480 A73-37237

Atmospheric sounding by satellite-borne remote sensors, discussing radiometric measurements of temperature, composition, and reflected and emitted radiation in visible, IR and microwave bands [AAS PAPER 73-125] 20 p2550 A73-38585

Numerical solution of hydrothermodynamics equations for atmospheric processes on a flat earth 20 p2584 A73-39471

The origin and evolution of the atmospheres of the terrestrial planets. 22 p2912 A73-42976

Russian book - Studies of the natural environment from manned orbital stations. 23 p2971 A73-43330

Visual observations of the earth and of the circumterrestrial space environment from manned orbital stations 23 p2971 A73-43331

Spectrophotometric investigations of the earth from manned orbital stations 23 p2979 A73-43333

EARTH AXIS

Polar motion from laser tracking of artificial satellites. 01 p0039 A73-10406

Astronomical determination of pole motions by procedures employed at international latitude stations 02 p0155 A73-11650

Results concerning the movement of the instantaneous pole of rotation of the earth, using the data published by R. Vicente and S. Yumi 03 p0304 A73-14580

Earth polar motion from revised station coordinates and data from additional Doppler satellite tracking stations 04 p0439 A73-14800

Tracking stations interdistances and solid-earth tidal perturbations determination by laser ranging to satellites 04 p0439 A73-14801

Theory of diurnal fluctuations of the earth's magnetic tail 05 p0620 A73-17011

On a relation between the variations of the rotational velocity of the earth and the anomalous behavior of the polar wobble around 1930. 07 p0877 A73-19603

Computerized precession and nutation matrix calculations of rectangular equatorial coordinates with longitude and inclination allowance for radar data processing 09 p1142 A73-22092

Spectrum of the earth's pole coordinates over the period from 1846 to 1971 10 p1274 A73-23723

A short periodic irregularity in earth's rotation and the motion of the earth's instantaneous pole 10 p1275 A73-23724

Relationship between the coefficients of spherical and ellipsoidal expansion of the gravity force in the case of the biaxial earth ellipsoid 11 p1352 A73-25431

Algorithm for locating a moving object 11 p1394 A73-26097

Dynamical latitude correction requiring changes in ephemeris and time determination, discussing applicability to nutation of pole of earth figure 11 p1429 A73-26689

Rotation of the earth; Proceedings of the Symposium, Morioka, Japan, May 9-15, 1971. 13 p1677 A73-28376

General considerations about the revision of all the calculations of the International Latitude Service. 13 p1678 A73-28379

Chandler polar motion due to elastic earth free nutation using models based on historical data 13 p1678 A73-28380

Power spectral analysis of Chandler wobble latitude variations over 70 year period, showing doubtfulness of two-peak resonance pattern in wobble 13 p1678 A73-28381

Earth axis 14 month variation with latitude/Eulerian nutation/as free vibration subject to damping, obtaining nonuniform drift rate from seven year interval observations 13 p1678 A73-28382

Analysis of the Chandler period of polar coordinates calculated by the Orlov method. 13 p1678 A73-28383

An interpretation of the ambiguity between annual terms obtained by time and latitude observations. 13 p1678 A73-28384

On the regularity of fluctuations in annual and secular polar motions. 13 p1678 A73-28385

Secular pole motion vs continental drift effects from geodetic, astronomical and time base observations 13 p1678 A73-28386

Non-periodic latitude variations and the secular motion of the earth's pole. 13 p1678 A73-28387

Washington observatory latitude variations observations compared with earth rotation pole secular variations from International Polar Motion Service data, suggesting seismic influences 13 p1678 A73-28388

Earth pole secular motion analyzed by latitude observations, suggesting northward drift of major continents 13 p1679 A73-28389

Comparison of the coordinates of the pole as obtained by classical astrometry/IPMS, BIH/ and as obtained by Doppler measurements on artificial satellites/Dahlgren polar monitoring service/. 13 p1679 A73-28390

Earth rotation axis motion determination through satellite tracking via laser range observation, estimating orbit computation error sources 13 p1656 A73-28392

Pole position studied with artificial earth satellites. 13 p1656 A73-28393

Earth polar motion and angular velocity sequential estimation in presence of unmodelled random accelerations, via Gauss-Markov process representation 13 p1679 A73-28397

An explanation of the polar motion by a rigid core-mantle model. 13 p1679 A73-28398

Earth axis displacement and continental drift related to lack of coincidence of core and mantle-crust centers of mass 13 p1679 A73-28399

Earth liquid core effect on axis annual nutation, deriving Z term for correction of International Latitude Service latitude variation data 13 p1606 A73-28400

On the comparison of diurnal nutation derived from separate series of latitude and time observations. 13 p1679 A73-28402

Polar wandering and the earth's dynamical evolution cycle. 13 p1679 A73-28403

Earth mantle convection theory, calculating polar secular wandering from inertia product change due to mass transfer 13 p1607 A73-28404

On the correlation between earthquake occurrence and disturbances in the path of the rotation pole. 13 p1607 A73-28405

On some natures of the excitation and damping of the polar motion. 13 p1680 A73-28406

Excitation of the Chandler wobble by large earthquakes. 13 p1607 A73-28407

On the relation between the rotation of the earth and solar activity. 13 p1680 A73-28408

Estimate of the influence of the seasonal redistribution of air masses on the motion of the earth's poles 15 p1939 A73-31967

Spectrum of the coordinates of the earth's pole during the period 1846-1971. 18 p2355 A73-36748

A short-period irregularity in the earth's rotation and the motion of the instantaneous pole. 18 p2355 A73-36749

Earth rotation measurements relative to reference frames and changes and mechanisms of axis orientation and spin rate 20 p2553 A73-39125

Motion of the inertia pole of the earth over a hundred years 23 p3037 A73-44255

Estimated seasonal redistribution of air masses affecting motion of earth's poles. 24 p3081 A73-44492

EARTH CORE

Analytical description of the geomagnetic field of past epochs and the determination of the magnetic-wave spectrum in the earth's core 08 p0959 A73-21297

Response to critiques of paper on earth core paradox consisting of stratification inhibition on outer core fluid circulation needed for dynamo theory of geomagnetic field generation 09 p1077 A73-22193

Oscillation of the earth's inner core and its relation to the generation of geomagnetic field. 09 p1077 A73-22194

High pressure physics and planetary interiors; Proceedings of the Conference, Houston, Tex., March 1-3, 1972. 11 p1419 A73-25876

The origin and chemical composition of the earth's core. 11 p1355 A73-25896

Bullen solid core model for earth and Venus vindicated by free earth oscillations records and detection of PKJKP seismic phase, discussing compressibility effects 11 p1421 A73-25897

Heat flow from earth core to mantle, discussing geomagnetic field generation by adiabatic MHD circu-

lation of outer core and core-mantle interfacial temperature gradients

12 p1492 A73-27482

Earth mantle-core mechanical and electromagnetic interactions influencing rotation rate random variations

13 p1679 A73-28396

An explanation of the polar motion by a rigid core-mantle model.

13 p1679 A73-28398

Earth axis displacement and continental drift related to lack of coincidence of core and mantle-crust centers of mass

13 p1679 A73-28399

Earth liquid core effect on axis annual nutation, deriving 2 term for correction of International Latitude Service latitude variation data

13 p1606 A73-28400

Terrestrial planetary core model concerning mantle-core iron oxide composition to avoid phase transition theory difficulties

15 p1867 A73-31100

Dynamo theory of earth magnetic field generation, discussing earth core characteristics, electromagnetic induction processes and magnetic field energy sources

17 p2162 A73-35049

Two layer cores in terrestrial planets with emphasis on Mars and Venus, discussing pressure at earth mantle-core boundary, equations of state and composition

17 p2235 A73-35743

Iron core age end in terrestrial planets via Ramsey phase change onset producing metallic state core with growth via radioactive heating

17 p2236 A73-35745

Satellite geodesy application to earth internal structure and gravity field relationship to geomagnetism, noting magnetic secular variation correspondence with large scale mass motion

18 p2302 A73-35932

Analytical description of the geomagnetic field of past epochs and determination of the spectrum of magnetic waves in the core of the earth.

19 p2425 A73-37926

Core coupling to mantle precession, discussing model with quantitative consideration of inertial and dissipative coupling torque superposition

21 p2764 A73-39929

Correction to calculation of temperature rise in connection with gravitational energy release accompanying rapid core formation from undifferentiated earth

22 p2848 A73-42499

EARTH CRUST

Earth crust materials high temperature lattice and radiative thermal conductivity from laser IR measurements, discussing single crystal and polycrystal forsterite-rich olivines and enstatite

05 p0569 A73-16378

A method for computing the gravitational attraction of three-dimensional bodies in a spherical or ellipsoidal earth.

05 p0569 A73-16379

A crustal-upper-mantle model for the Colorado plateau based on observations of crystalline rock fragments in the Moses Rock dike.

05 p0569 A73-16381

Earth crust inhomogeneities from high altitude aeromagnetic survey, noting informativeness loss increase with height

08 p0960 A73-21308

Crustal movements in tectonic areas.

11 p1352 A73-25564

Earth crustal conductivity structure from micropulsation activity cycle using magnetic variometer array

12 p1488 A73-26986

Theory for errors, resolution, and separation of unknown variables in inverse problems, with application to the mantle and the crust in Southern Africa and Scandinavia.

13 p1607 A73-28621

The effect of two periodic conductivity anomalies on geomagnetic micropulsation measurements.

13 p1607 A73-28622

Lower boundary of occurrence of magnetically active masses.

19 p2425 A73-37925

Earth crust inhomogeneities from high altitude aeromagnetic survey, noting information loss increase with height

19 p2425 A73-37937

EARTH CURRENTS

U TELLURIC CURRENTS

EARTH ENVIRONMENT

Space experience and ethics impact on world development, considering knowledge advancement, regional applications, economy stimulation, environment improvement and international cooperation

02 p0239 A73-11998

Legal problems for the protection of the earth's environment.

04 p0522 A73-15136

Earth environment pollution protection in space exploration, noting international law principles application

04 p0522 A73-15140

International law for earth environment protection against pollution by activities in outer space, noting International Court of Justice Advisory Opinion procedure

04 p0522 A73-15141

The control of the terrestrial environment from space: International collaboration, methods and technologies; International Conference on Space, 13th, Rome, Italy, March 22-24, 1973, Proceedings

17 p2160 A73-34926

Low altitude satellite networks for recording programmable earth atmosphere parameters related to terrestrial environment control

17 p2205 A73-34929

Skylark rocket measurement of earth atmosphere and ionosphere, examining payload capacity, camera image quality, cost, use of smaller rockets and practical applications

17 p2239 A73-34953

Remote sensing - The application of space technology to the survey of the earth and its environment.

19 p2423 A73-37497

Study of laser remote sensing techniques from space platforms.

[AAS PAPER 73-136]

20 p2521 A73-38591

EARTH FIGURE

U GEODESY

EARTH HYDROSPHERE

Earth-atmosphere-ocean energy balance time dependent model equation, using Sellers radiation relationships and turbulent exchange coefficients for numerical solution

10 p1245 A73-23982

On the torques due to tidal friction of the oceans and adjacent seas.

13 p1607 A73-28409

Passive microwave radiometry and its potential applications to earth resources surveys.

17 p2162 A73-34958

Prospects for physical oceanography from space.

18 p2306 A73-36024

EARTH LIMB

Atmospheric temperature profile determination by limb radiance inversion radiometer, discussing radiative transfer, instrument parameters and inversion process effects on retrievable information content

01 p0072 A73-10354

An improved algorithm for the inversion of limb radiance measurements.

01 p0072 A73-10355

Inference of stratospheric temperature structure from limb radiance profiles.

01 p0072 A73-10356

EARTH MANTLE

A crustal-upper-mantle model for the Colorado plateau based on observations of crystalline rock fragments in the Moses Rock dike.

05 p0569 A73-16381

Distribution of electrical conductivity in the earth's mantle from data on the secular variations of the geomagnetic field

08 p0959 A73-21295

Earth mantle rutile-structure germanium dioxide elastic properties as function of pressure and temperature in single crystals

11 p1352 A73-25585

Vertical distribution of viscosity and convection conditions in earth mantle, discussing shallow convection model and geophysical evidence for validity

11 p1356 A73-25906

Heat flow from earth core to mantle, discussing geomagnetic field generation by adiabatic MHD circulation of outer core and core-mantle interfacial temperature gradients

12 p1492 A73-27482

Earth mantle-core mechanical and electromagnetic interactions influencing rotation rate random variations

13 p1679 A73-28396

An explanation of the polar motion by a rigid core-mantle model.

13 p1679 A73-28398

Earth mantle convection theory, calculating polar secular wandering from inertia product change due to mass transfer

13 p1607 A73-28404

Theory for errors, resolution, and separation of unknown variables in inverse problems, with application to the mantle and the crust in Southern Africa and Scandinavia.

13 p1607 A73-28621

Terrestrial planetary core model concerning mantle-core iron oxide composition to avoid phase transition theory difficulties

15 p1867 A73-31100

POGO satellite observed electrojet current data comparison with ground measurement at Ibadan, discussing data ratios variation by upper earth mantle conductivity structure

15 p1870 A73-31772

Two layer cores in terrestrial planets with emphasis on Mars and Venus, discussing pressure at earth mantle-core boundary, equations of state and composition

17 p2235 A73-35743

Distribution of electric conductivity in the mantle of the earth, according to data on secular geomagnetic field variations.

19 p2425 A73-37924

Core coupling to mantle precession, discussing model with quantitative consideration of inertial and dissipative coupling torque superposition

21 p2764 A73-39929

The detection of 'intermediate' size magnetic anomalies in Cosmos 49 and OGO 2, 4, 6 data.

21 p2691 A73-41374

Cosmogonic prerequisites for the accumulation of volatile substances in the upper mantle of the earth

22 p2912 A73-42972

EARTH MOTION

A method of a determination of earth's motions around its mass center from simultaneous laser and photographic observations of artificial earth satellites made by two stations.

02 p0159 A73-12168

How to measure the earth's velocity with respect to absolute space.

05 p0615 A73-16363

Trigonometric series for earth rotation velocity around solar system center of mass

07 p0902 A73-20325

Trigonometric series for earth rotation velocity around solar system center of mass

12 p1540 A73-27297

Chandler polar motion due to elastic earth free nutation using models based on historical data

13 p1678 A73-28380

Secular pole motion vs continental drift effects from geodetic, astronomical and time base observations

13 p1678 A73-28386

EARTH MOVEMENTS

NT EARTHQUAKES

Some observations on the cenozoic volcano-tectonic evolution of the Great Basin, western United States.

05 p0570 A73-16841

Geopause satellite orbit, tracking, environment, gravity and station position properties and applications to earth and oceanographic dynamics studies

11 p1430 A73-25317

Crustal movements in tectonic areas.

11 p1352 A73-25564

The excess secular change in the obliquity of the ecliptic and its relation to the internal motion of the earth.

13 p1679 A73-28401

Worldwide sea level pulsations and interpellations relation to elevation and subsidence of oceanic ridge systems, discussing sea floor spreading hypotheses

17 p2164 A73-35858

Selected applications of a biaxial tiltmeter in the ground motion environment.

20 p2564 A73-38781

EARTH ORBITS

NT APOGEES

NT PERIGEEES

Earth satellites in resonance with the moon and the sun as objects of laser ranging - Analytical solution for their motion.

01 p0099 A73-10695

Chemical and nuclear space tugs in the earth orbital shuttle mission.

02 p0216 A73-12372

Resistojet and plasma propulsion system technology.

[AIAA PAPER 72-1124]

03 p0355 A73-13436

Solar electric propulsion for payloads earth orbit injection, discussing communication satellites and space shuttle/tug system applications

[AIAA PAPER 72-1126]

04 p0486 A73-14912

Earth orbital, lunar, and planetary missions of the space tug.

06 p0750 A73-18019

Linear perturbations of the coordinates of satellites in the normal gravitational field of the earth

09 p1143 A73-22099

Configuration control of dual satellite systems in earth orbit, obtaining equations of motion, deployment paths and force functions

10 p1276 A73-24008

Lunar orbit and mapping coordinates, discussing libration effects due to motion and surface features

13 p1681 A73-28947

Observations of the Saturn rings during the earth's passage through the ring plane in 1966

16 p02070 A73-33846

Differential equations for ballistic motion of meteoric particles in earth atmosphere, noting orbit stability

19 p2480 A73-37237

Earth-orbit mission considerations and Space Tug requirements.

19 p2490 A73-37302

Derivation of an approximate solution to the equation of geocentric motion of a space vehicle with a solar sail

19 p2492 A73-37849

Gravitational perturbations of equatorial orbits.

23 p3032 A73-43839

EARTH PLANETARY STRUCTURE

- On the possible differences in the bulk chemical composition of the earth and the moon forming in the circumterrestrial swarm. 03 p0370 A73-13110
- Magnetotelluric and geomagnetic depth sounding methods compared. 05 p0572 A73-17189
- The sources of phosphorus on the primitive earth - An inquiry. 06 p0651 A73-17933
- Range of earth structure nonuniqueness implied by body wave observations. 10 p1215 A73-24779
- The origin and chemical composition of the earth's core. 11 p1355 A73-25896
- Partitioning of potassium between silicates and sulphide melts - Experiments relevant to the earth's core. 11 p1355 A73-25902
- Magnetovariational frequency sounding of the earth, using the ratio of magnetic potentials. 12 p1491 A73-27352
- Russian book on inverse problems for hyperbolic differential equations covering functionals, uniqueness theorems, integral geometry and earth interior structure from seismological data. 15 p1899 A73-31581
- Papers on earth and planetary sciences, volume I covering earth planetary structure, red beds, planetary interiors, mineral deposits and order-disorder relationship in silicates. 17 p2158 A73-34356
- Protoplanetary gas-dust cloud evolution and planetary formation, investigating earth initial state. 17 p2227 A73-34408
- Book - Theory of the earth's gravity field. 17 p2162 A73-35148
- Frequency magnetovariational sounding of the earth, using the ratio of potentials. 23 p2970 A73-43249
- Multiphase incompressible half-space as simplified earth model for investigating surface displacements due to time- and depth-dependent heat sources. 23 p2973 A73-43797
- Physical relations of the asymmetric structure of the earth. 24 p3088 A73-45448
- EARTH RADIATION**
- U TERRESTRIAL RADIATION**
- EARTH RESOURCES**
- NT COAL
- NT CORN
- NT COTTON
- NT CRUDE OIL
- NT DESERTS
- NT FARM CROPS
- NT FORESTS
- NT GLACIERS
- NT GRANITE
- NT LAKES
- NT LAND ICE
- NT LAVA
- NT RIVERS
- NT ROCKS
- NT SANDS
- NT SANDSTONES
- NT SHALES
- NT VEGETATION
- NT WATER RESOURCES
- NT WETLANDS
- National reports on earth resources surveys at 1971 COSPAR meeting, including remote sensing techniques application in agriculture, forestry, geology and oceanography. 02 p0160 A73-12264
- International law aspects of catastrophic disaster prohibition in terms of endangering earth environment/resources. 04 p0522 A73-15137
- The evaluation, conservation, and international development of terrestrial resources from outer space. 04 p0523 A73-15143
- Information transfer satellite system (ITSS) design for earth resource and meteorological data collection and relay from remote sensing platforms. 04 p0419 A73-15404
- Remote sensing techniques in evaluating earth resources - A study of potential uses of remote sensing for Southeastern U.S. 05 p0642 A73-17131
- The cost-effectiveness of high altitude systems for regional resource assessment. 05 p0642 A73-17139
- In-depth exploration of the solar system and its utilization for the benefit of Earth. 06 p0751 A73-18029
- Natural resources information system. 08 p0961 A73-21707
- Skylab A solar and terrestrial observation and photography hardware, including solar observatory, microwave scanner, IR spectrometer and multispectral photographic facility. 13 p1612 A73-28276

- Cost effective land use mapping and resources inventory for Mississippi via high altitude color IR aerial photography and ERTS-1 multispectral imagery [AIAA PAPER 73-3]. 13 p1610 A73-29300
- Realism in environmental testing and control; Proceedings of the Nineteenth Annual Technical Meeting, Anaheim, Calif., April 2-5, 1973. 16 p1993 A73-33126
- The control of the terrestrial environment from space: International collaboration, methods and technologies; International Conference on Space, 13th, Rome, Italy, March 22-24, 1973, Proceedings. 17 p2160 A73-34926
- The use of remote sensing for the detection of natural resources - Definition of the platforms, technical-organizational considerations. 17 p2160 A73-34930
- Satellite remote monitoring of earth environment and natural resources by high resolution multispectral scanners for European requirements. 17 p2160 A73-34931
- Earth resources monitoring from satellites, aircraft and ground stations for fast data acquisition and management. 17 p2161 A73-34934
- Data processing for earth resources survey including data handling, preprocessing for instrument errors, decision making and data bank. 17 p2161 A73-34941
- Satellite imagery of land resources, discussing synoptic views, spatial dependence, closed loop information and sequential sampling. 17 p2161 A73-34945
- The preparatory phase of the German Earth Resources program. 18 p2372 A73-35934
- Remote sensing of ocean color as an index of biological and sedimentary activity. 18 p2307 A73-36030
- A review of some possible uses of remote sensing techniques in fishery research and commercial fisheries. 18 p2307 A73-36031
- Satellite imagery in national resource surveys and vegetation growth monitoring on mine dumps from ERTS-1 data. 18 p2311 A73-36151
- Optimum parameters of an infrared imaging system for aerial scanning of earth resources. 18 p2317 A73-36874
- Remote sensing of terrestrial resources. 19 p2426 A73-38176
- Equipment for checking of terrestrial resources. 19 p2431 A73-38177
- Computer processing of earth resources data from mono- and multispectral band scanners and IR photography. 19 p2431 A73-38178
- Photographic processing of aerial imagery for earth resources, discussing photographic developers, film and materials. 19 p2431 A73-38179
- The use of remote sensing in the USSR for the study of natural resources. 20 p2520 A73-38579
- [AAS PAPER 73-115]. 20 p2520 A73-38579
- Contributions of the EROS Program to the Department of the Interior's resources and management responsibilities. 20 p2550 A73-38588
- [AAS PAPER 73-130]. 20 p2550 A73-38588
- Design concepts for an earth resources data management system. 20 p2521 A73-38597
- [AAS PAPER 73-151]. 20 p2521 A73-38597
- EARTH RESOURCES OBSERVATION SATELLITES**
- U EROS (SATELLITES)**
- EARTH RESOURCES PROGRAM**
- Geology, hydrology, land use and transportation net of Dallas-Fort Worth area from Apollo 6 photographs, comparing with ground based data. 01 p0035 A73-10139
- The Earth Resources Program - International benefits from space. 01 p0043 A73-11107
- Digital image-processing activities in remote sensing for earth resources. 01 p0021 A73-11476
- Earth resources exploration with a sortie laboratory within the framework of the Post-Apollo Program /PAP/. 02 p0227 A73-11677
- [DGLR PAPER 72-080]. 02 p0227 A73-11677
- Earth resources remote survey methods capability assessment, considering radar and passive microwave imaging, IR and multispectral scanning and photographic and absorption spectrometric methods [DGLR PAPER 72-072]. 02 p0155 A73-11703
- Data handling and analysis for the 1971 corn blight watch experiment. 04 p0443 A73-15402
- Earth resources sensing technology - 24-channel multispectral sensor system development. 04 p0449 A73-15463
- Remote sensing of earth resources and the environment; Proceedings of the Seminar-in-Depth, Palo Alto, Calif., November 8, 9, 1971. 04 p0450 A73-15766

- Prototype data processing system design for automatic correlation of earth resources image data collected from remote sensors and gyrating vehicle platforms. 04 p0426 A73-15776
- Ocean color measurements utilizing a noon orbit for earth resources satellite applications. 04 p0445 A73-15778
- Optical design of an imaging spectral radiometer for earth resources applications. 04 p0451 A73-15780
- Remote sensing of earth resources; Proceedings of the Conference on Earth Resources Observation and Information Analysis Systems, Tullahoma, Tenn., March 13, 14, 1972. Volume 1. 05 p0571 A73-17126
- Earth resources remote sensors operation and potential, explaining atmospheric transmission and scattering and radiation polarization. 05 p0578 A73-17130
- Investigation of color detail, color analysis and false-color representation in satellite photographs. 05 p0578 A73-17136
- Social, economic and political factors associated with earth resources observation and information analyses. 05 p0642 A73-17137
- Automatic classification by sequential statistical variance and K-means clustering techniques for remote multispectral earth resource observation data. 05 p0555 A73-17154
- Universal data system for image processing of earth resources observations, discussing input/output film, tape and multispectral data, interactive control and video color displays. 05 p0555 A73-17155
- International space station program for global resources and ecological monitoring and management, reviewing US Skylab and Space Shuttle and USSR Soyuz projects. 06 p0757 A73-18026
- The earth resources experiment package on Skylab and proposed resource investigations. 09 p1082 A73-22389
- Skylab earth terrain camera for high resolution photography of areas covered by other Earth Resources Experiment Package sensors to aid in data interpretation. 12 p1500 A73-27958
- ERAF - Proposal for a European Earth Resources Aircraft. 13 p1569 A73-28786
- Apollo, Skylab and shuttle programs, discussing crews, tasks, national economic benefits and earth resources experiments effects. 15 p1941 A73-32544
- Organization, administration and technological aspects of ERTS system on international scale. 17 p2162 A73-34952
- Remote sensing technology - The 24-channel multispectral scanner. 17 p2171 A73-35365
- Need for and aspects of a cooperative European earth resources program. 18 p2372 A73-35933
- Teledetection of terrestrial resources by satellites. 18 p2373 A73-36390
- Remote sensing - The application of space technology to the survey of the earth and its environment. 19 p2423 A73-37497
- Water resources systems modelling today and its research opportunities. 19 p2426 A73-38074
- Earth studies from space and their legal problems. 19 p2506 A73-38267
- Sensor development - An overview of recent Canadian experience. 20 p2533 A73-38578
- [AAS PAPER 73-114]. 20 p2533 A73-38578
- Remote sensing data management from a user's viewpoint. 20 p2521 A73-38598
- [AAS PAPER 73-152]. 20 p2521 A73-38598
- An integrated resource survey using orbital imagery - An example from south-east Spain. 20 p2556 A73-39834
- Remote sensor role in international environmental management, considering monitoring of biosphere, atmosphere and oceans and UN action plan for natural resources. 20 p2629 A73-39837
- Test flight and configuration of Skylark based SL 1081 earth resources rocket prototype with two photographic cameras and earth albedo sensors. 20 p2615 A73-39874
- Earth surveys by remote sensing in Israel. 21 p2685 A73-40816
- Assessment of applications of space-borne remote sensing to hydrology and water resources - An overview. 21 p2686 A73-40832
- The use of Skylab and ERTS data in an integrated natural resources development programme. 23 p2973 A73-43785

EARTH RESOURCES SURVEY AIRCRAFT

International legal problems concerning earth environmental survey system composed of ERT satellites, survey aircraft and ground data handling systems
04 p0521 A73-15129
The utility of a low flying aircraft or helicopter when collecting ground data for regional resource surveys.
08 p0961 A73-21710
ERAP - Proposal for a European Earth Resources Aircraft.
13 p1569 A73-28786

EARTH RESOURCES SURVEY PROGRAM

Passive microwave radiometry and its potential applications to earth resources surveys.
17 p2162 A73-34958

EARTH RESOURCES TECHNOLOGY SATELLITE 1

Earth studies from space and their legal problems
19 p2506 A73-38267
Interdisciplinary research on the application of ERTS-1 data to the regional land use planning process.
20 p2563 A73-39910
ERTS-1 multispectral scanner analysis of Kansas reservoirs color and water content, discussing turbidity, gray coloration levels, water management possibilities and water sample data
20 p2563 A73-39912

An analysis of the earth's resources satellite /ERTS-1/ data.
22 p2850 A73-42732

Flight performance of the ERTS-1 spacecraft power system.
22 p2801 A73-42904

**EARTH RESOURCES TECHNOLOGY SATELLITES
NT EARTH RESOURCES TECHNOLOGY
SATELLITE 1**

The Earth Resources Program - International benefits from space.
01 p0043 A73-11107

Digital image processing for the earth resources technology satellite data.
01 p0020 A73-11457

The use of orbital photography for earth-resources satellite mission planning.
03 p0301 A73-13843

Automatic digital image processing for remote sensing with ERTS, Skylab and NASA survey aircraft, considering image registration, projective transformation and ground truth information
03 p0309 A73-14487

International legal problems concerning earth environmental survey system composed of ERT satellites, survey aircraft and ground data handling systems
04 p0521 A73-15129

Legal problems relating to the evaluation, conservation and development of earth resources by means of space objects.
04 p0523 A73-15144

Legal regulation of investigation of natural environment from outer space.
04 p0523 A73-15145

The ERTS wideband image communication system.
04 p0418 A73-15382

Canadian E.R.T.S. data handling system.
04 p0424 A73-15384

Supervised and unsupervised category identification and classification systems consistency with ERTS satellites high rate multispectral data requirements
05 p0572 A73-17142

ERTS two-inch RBV cameras performance characteristics.
05 p0579 A73-17144

Multispectral additive color viewer for ERTS satellite photography, discussing colorimetric measurement usefulness and photo processing and image density control effects on color characteristics
05 p0579 A73-17145

Remote sensing application to the fisheries environment.
06 p0690 A73-17606

[AIAA PAPER 73-12] ERTS program, describing satellite design and imaging and data collection systems for real time or delayed taped transmission to ground stations
07 p0905 A73-19112

ERTS return beam vidicon TV cameras and ground based electron beam recording system resolution and distortion characteristics from preflight and in-flight simulation and calibration studies
09 p1082 A73-22385

Multispectral imagery data compression for earth resources satellites, comparing performance of spectral-spatial-delta-interleave and Rice coding algorithms
09 p1055 A73-23391

Study of terrestrial resources by space objects and international law
11 p1454 A73-26295

The American space program for the future.
12 p1560 A73-27062

Remote sensing capability development program planning, discussing world participation in ERTS and alternatives
12 p1500 A73-27951

Photogrammetric solution for precision processing of E.R.T.S. images.
12 p1501 A73-27964

ERTS-1 satellite-borne high resolution multispectral radiometer scanner, discussing optical surface performance during exposure to direct and reflected sunlight
13 p1621 A73-29331

Book on earth satellites covering transmission technology, cost effectiveness and materials development for communication, meteorological, earth resources, navigational, research and military applications
15 p1944 A73-32292

Digital computer processing for automatic feature classification of ERTS-borne MSS and RBV imagery data, emphasizing interactive man-machine analysis for image enhancement
16 p1985 A73-33366

Monitoring earth's resources from space.
17 p2157 A73-34279

Simulated ERTS data for coastal management.
17 p2157 A73-34285

Key technological challenges of the Earth Resources Technology Satellite program.
17 p2161 A73-34943

ERTS-1 satellite-borne multispectral scanner photographic mapping of Israel vegetation, hydrology, geological structure, atmospheric phenomena and oceanography
17 p2162 A73-34947

Organization, administration and technological aspects of ERTS system on international scale
17 p2162 A73-34952

Spacecraft systems design trade-offs for the Earth Resources Technology Satellite.
17 p2239 A73-35631

Applications of ERTS data to oceanography and the marine environment.
18 p2302 A73-35935

A low-cost system for reproducing ERTS imagery.
18 p2315 A73-36018

The cartographic and scientific application of ERTS-1 imagery in polar regions.
18 p2306 A73-36019

Mapping of snow cover in the Swiss Alps from ERTS-1 imagery.
18 p2306 A73-36021

Applications of ERTS imagery to snow and glacier hydrology.
18 p2306 A73-36022

ERTS-1 MSS imagery - A tool for identifying soil associations.
18 p2306 A73-36023

New ways to monitor the mass and areal extent of snowcover.
18 p2307 A73-36025

Applications of the ERTS-1 satellite in remote sensing of water resource data in Canada.
18 p2307 A73-36026

EROS Program and ERTS-1 satellite applications to geophysical problems.
18 p2307 A73-36032

Natural resources research and development in Lesotho using ERTS imagery.
18 p2308 A73-36045

Satellite imagery in national resource surveys and vegetation growth monitoring on mine dumps from ERTS-1 data
18 p2311 A73-36151

The growth of remote sensing through the Nimbus and ERTS spacecraft.
19 p2430 A73-37712

The role of applications satellites in the management of the human environment.
19 p2424 A73-37713

Low cost modular power systems for multi mission earth observations.
19 p2494 A73-38435

Data collection platforms, ground receiving and processing equipment for environmental study and management
20 p2520 A73-38583

[AAS PAPER 73-122] Enhancement of Earth Resources Technology Satellite /ERTS/ and aircraft imagery using atmospheric corrections.
20 p2567 A73-39835

ERTS-1 satellite return beam vidicon and multispectral scanner comparative evaluation for image quality, considering response functions, resolution, measurability, detectability and image motion effects
20 p2563 A73-39909

The usefulness of ERTS-1 and supporting aircraft data for monitoring plant development in rangeland environments.
20 p2563 A73-39911

Canadian remote sensing programs for ERTS data, describing receiving stations, data acquisition and processing facilities and techniques, digital system and aerial photography
20 p2545 A73-39913

Expected results of hydrologic and geologic studies using ERTS imagery of the Atacama Desert, Altiplano, and Puna de Atacama, South America /Southwest Bolivia, Northwest Argentina, and Northern Chile/.
20 p2563 A73-39914

ERTS-1 satellite-borne multispectral scanner remote sensor for global pollution monitoring, geological and heat balance surveys, and storm and earthquake caused damage
21 p2692 A73-41520

ERTS-1 satellite-borne TV cameras and multispectral band scanners for remote sensing and data collection with applications in agriculture, forestry, and water resources survey
21 p2692 A73-41521

Suspended sediment observations from ERTS-1.
22 p2850 A73-42726

Use of earth resources satellites for supranational inventories of forests and agricultural areas
23 p2972 A73-43779

EARTH ROTATION

Astronomical evidence concerning non-gravitational forces in the earth-moon system.
02 p0217 A73-12385

Paleontological evidence on the earth's rotational history since early Precambrian.
02 p0217 A73-12387

On the initial distance of the moon forming in the circumterrestrial swarm.
03 p0369 A73-13108

The secular accelerations of the moon's orbital motion and the earth's rotation.
04 p0497 A73-15176

An effect of the solar wind on the earth's rotation
04 p0498 A73-15282

On a relation between the variations of the rotational velocity of the earth and the anomalous behavior of the polar wobble around 1930.
07 p0877 A73-19603

The heliocentric radial gradient in cosmic ray density and the 'Swinson' sidereal time variation.
07 p0870 A73-19671

The role of the satellite swarm in the origin of the earth's rotation.
08 p1012 A73-21579

Gravitational constant constancy from 1663-1972 earth rotation and 1943-1972 stellar occultations by moon, discussing various time scales used
09 p1079 A73-22948

Spectrum of the earth's pole coordinates over the period from 1846 to 1971
10 p1274 A73-23723

A short periodic irregularity in earth's rotation and the motion of the earth's instantaneous pole
10 p1275 A73-23724

The earth's rotation and atmospheric circulation. I - Seasonal variations.
13 p1606 A73-28282

Rotation of the earth; Proceedings of the Symposium, Morioka, Japan, May 9-15, 1971.
13 p1677 A73-28376

Past and future of research methods in problems of the earth's rotation.
13 p1677 A73-28377

Lunar rotation secular acceleration and tidal friction related to earth rotational velocity and creep properties
13 p1677 A73-28378

Non-periodic latitude variations and the secular motion of the earth's pole.
13 p1678 A73-28387

Washington observatory latitude variations observations compared with earth rotation pole secular variations from International Polar Motion Service data, suggesting seismic influences
13 p1678 A73-28388

Earth rotational accelerations magnitudes as obtained from astronomical observations, noting semimonthly lunar body tides effects
13 p1679 A73-28395

Earth mantle-core mechanical and electromagnetic interactions influencing rotation rate random variations
13 p1679 A73-28396

Earth polar motion and angular velocity sequential estimation in presence of unmodelled random accelerations, via Gauss-Markov process representation
13 p1679 A73-28397

An explanation of the polar motion by a rigid core-mantle model.
13 p1679 A73-28398

Earth liquid core effect on axis annual nutation, deriving Z term for correction of International Latitude Service latitude variation data
13 p1606 A73-28400

The excess secular change in the obliquity of the ecliptic and its relation to the internal motion of the earth.
13 p1679 A73-28401

On the comparison of diurnal nutation derived from separate series of latitude and time observations.
13 p1679 A73-28402

On the correlation between earthquake occurrence and disturbances in the path of the rotation pole.
13 p1607 A73-28405

On some natures of the excitation and damping of the polar motion.
13 p1680 A73-28406

On the relation between the rotation of the earth and solar activity. 13 p1680 A73-28408

On the torques due to tidal friction of the oceans and adjacent seas. 13 p1607 A73-28409

The implications for geophysics of modern cosmologies in which G is variable. 14 p1799 A73-30525

Discontinuous change in earth's spin rate following great solar storm of August 1972. 14 p1800 A73-30602

Earth deflections of vertical due to luni-solar gravitation changes determined by astronomical observation with Herstmonceux photographic zenith tube, noting semidiurnal tidal effects 15 p1937 A73-31779

Astronautical coordinate systems definition and applications for flight mechanics problems involving earth curvature and motion effects 15 p1908 A73-32202

The inertia tensor of the atmosphere, annual variations in its components, and variations in the earth's rotation 17 p2158 A73-34343

Speed variation in the earth's rotation and the baric field of the earth's Northern Hemisphere 17 p2159 A73-34637

Spectrum of the coordinates of the earth's pole during the period 1846-1971. 18 p2355 A73-36748

A short-period irregularity in the earth's rotation and the motion of the instantaneous pole. 18 p2355 A73-36749

Earth rotation measurements relative to reference frames and changes and mechanisms of axis orientation and spin rate 20 p2553 A73-39125

Core coupling to mantle precession, discussing model with quantitative consideration of inertial and dissipative coupling torque superposition 21 p2764 A73-39929

Criticism of Gribbin and Plagemann findings on universal time observations as evidence of day length and earth rotation rate changes due to 1972 solar storm 21 p2766 A73-40375

Simultaneous determination of pole coordinates and the nonuniformity of the earth's rotation 21 p2768 A73-40727

Errors on the dial of cosmic clocks 21 p2701 A73-40728

Rotation of the earth's magnetic field. 21 p2692 A73-41641

An exact solution for the rotation of the atmosphere about the spheroidal earth. 22 p2848 A73-42541

Linear array radio telescope for large aperture synthesis by using earth rotation to change relative orientation to radio source, discussing design and performance 23 p3028 A73-43352

Stanford radio telescope array with five paraboloid antennas for fast image forming interferometry, using earth rotation synthesis to produce sky continuous radiation brightness map 23 p2957 A73-43359

Southern Hemisphere earth rotational synthesis radio telescope array with paraboloids arranged as compound grating interferometer for astronomical radio sources mapping 23 p2958 A73-43361

An analytical expression for the secular variation of the geomagnetic field and a comparison of the activity of secular variations with some astronomical phenomena 23 p2973 A73-43793

Motion of the inertia pole of the earth over a hundred years 23 p3037 A73-44255

EARTH SATELLITES

NT AEROS SATELLITE
NT ALOUETTE 2 SATELLITE
NT APPLICATIONS TECHNOLOGY SATELLITES

NT ARIEL SATELLITES
NT ARIEL 4 SATELLITE
NT ASTRONOMICAL NETHERLANDS SATELLITE

NT ATS 1
NT ATS 3
NT ATS 5
NT ATS 6

NT BEACON SATELLITES
NT COMMUNICATION SATELLITES
NT COSMOS SATELLITES
NT COSMOS 137 SATELLITE

NT COSMOS 381 SATELLITE
NT DIADEME SATELLITES
NT EARTH RESOURCES TECHNOLOGY SATELLITE 1

NT EARTH RESOURCES TECHNOLOGY SATELLITES

NT ECHO 1 SATELLITE
NT ECHO 2 SATELLITE
NT ELEKTRON SATELLITES

NT ENVIRONMENTAL RESEARCH SATELLITES

NT EOLE SATELLITES
NT EROS [SATELLITES]
NT ESRO SATELLITES
NT ESRO 1 SATELLITE
NT ESRO 2 SATELLITE
NT ESRO 4 SATELLITE

NT EXPLORER SATELLITES
NT EXPLORER 31 SATELLITE
NT EXPLORER 35 SATELLITE
NT EXPLORER 43 SATELLITE

NT GEODETIC SATELLITES
NT GEOPHYSICAL SATELLITES
NT GEOS SATELLITES [ESRO]
NT GEOS 1 SATELLITE
NT GEOS 2 SATELLITE

NT GEOS-C SATELLITE
NT GOE SATELLITES
NT HELIOS SATELLITES
NT HEOS A SATELLITE

NT HEOS B SATELLITE
NT HEOS SATELLITES
NT INTEL SAT SATELLITES
NT INTERCOSMOS SATELLITES

NT ITOS 1
NT METEOROLOGICAL SATELLITES
NT METEOSAT SATELLITE
NT MOLNIYA SATELLITES
NT MOON

NT NAVIGATION SATELLITES
NT NIMBUS SATELLITES
NT NIMBUS 3 SATELLITE
NT NIMBUS 4 SATELLITE
NT NIMBUS 5 SATELLITE

NT OAO
NT OSO
NT OSO-7
NT PAGEOS SATELLITE

NT POGO
NT PROTON SATELLITES
NT PROTON 3 SATELLITE
NT PROTON 4 SATELLITE

NT RADIO ASTRONOMY EXPLORER SATELLITE
NT RELAY SATELLITES
NT SAN MARCO SATELLITE

NT SIRIO SATELLITE
NT SPUTNIK SATELLITES
NT SYMPHONIE SATELLITES
NT SYNCHRONOUS METEOROLOGICAL SATELLITE

NT SYNCOM SATELLITES
NT TELSTAR 1 SATELLITE
NT TIROS M
NT TIROS SATELLITES

NT TRANSIT SATELLITES
NT UHURU SATELLITE
NT VELA SATELLITES
NT VENERA SATELLITES

NT VENERA 4 SATELLITE
NT VENERA 6 SATELLITE
NT VENERA 7 SATELLITE

Subsatellite point coordinates calculation for artificial earth satellites with nearly circular orbits, noting ephemeris application 05 p0613 A73-16203

Equations of motion for precession theory of two rotor gyroscopes on earth satellites for orbit plane determination, noting noise spectrum transformation 05 p0628 A73-16407

An optimal orbit control system for a stationary artificial earth satellite 05 p0616 A73-16427

Application of Gauss' method to the determination of secular radiational perturbations of artificial earth satellites 09 p1143 A73-22100

Investigation of long-term periodic changes of the orbital elements of artificial earth satellites 10 p1283 A73-24699

Geopause satellite orbit, tracking, environment, gravity and station position properties and applications to earth and oceanographic dynamics studies 11 p1430 A73-25317

Precession, nutation and the choice of reference system for close earth satellite orbits. 11 p1423 A73-26067

Earth satellites and the gravitational potential. 12 p1539 A73-27148

Application of methods of mathematical statistics to study the motion of an artificial earth satellite about its center of mass 15 p1931 A73-31234

Intermediate orbit of an artificial earth satellite obtained by the averaging method - First order perturbations 15 p1936 A73-31644

Book on earth satellites covering transmission technology, cost effectiveness and materials development for communication, meteorological, earth resources, navigational, research and military applications 15 p1944 A73-32292

Nomograms for determining horizontal coordinates of artificial earth satellites 16 p2063 A73-33662

Night sky photographic evidence for natural retrograde earth satellites explanation for Vulcan type observations, considering group C orbit anomaly and terrestrial day length errors 16 p2071 A73-34000

The Space Shuttle and its utilization. 18 p2357 A73-35936

Artificial earth satellite brightness attenuation and rotation periods from spectral analyses of photometric curves by mathematical simulation 18 p2315 A73-36142

Study of cosmic rays by the Prognos satellites 21 p2756 A73-40577

Refutation of Bagby moonlet theory via analysis of supporting evidence 24 p3133 A73-44542

EARTH SHAPE

U GEODESY

EARTH SURFACE

Influence of haze layers upon remotely-sensed surface properties. 01 p0037 A73-10360

Calculation of the spectral, angular and altitudinal distributions of the thermal radiation field of the atmosphere and the earth's surface 01 p0040 A73-10871

The meteoroid influx and the maintenance of the solar system dust cloud. 03 p0365 A73-12889

Soyuz 9 spectrophotometry of earth surface features, comparing manned spacecraft-obtained and conventional spectrographs 03 p0304 A73-14564

Contribution to the problem of the geoelectric effects on lightning hazard 04 p0473 A73-15283

Topographic earth observations using radar techniques with a single flight. 04 p0419 A73-15403

Book - Calculation of wave propagation by nomograms - Frequencies above 30 MHz. 05 p0548 A73-16325

Orbital parameters optimization of circular orbit earth satellites network for continuous earth observation, using group theory 05 p0620 A73-17004

Isostasy and relief of the Earth, the Moon and Mars 07 p0878 A73-19661

Earth surface and background wind effects on mesoscale and large scale meteorological processes in free stably stratified atmosphere 07 p0848 A73-20343

Reflection from the earth's surface of shock waves generated by falling meteorites 08 p0958 A73-21065

Influence of atmospheric haze on the color of the underlying surface observed from a manned spacecraft 09 p1077 A73-24484

Sector structure of the interplanetary magnetic field, and magnetic disturbances in the circumpolar region 10 p1276 A73-23896

Earth surface magnetic field intensity variations in terms of magnetospheric resonator excitation, assuming three dimensional Alfvén waves 10 p1212 A73-24230

Photometric analysis of earth photographs from Zond space station, determining earth sidereal magnitude 10 p1281 A73-24477

One method of computing the meteorological variables for mesoscale processes. 11 p1394 A73-26192

Determination of the relative position of points on the earth surface with the aid of satellite observations 11 p1357 A73-26294

The occurrence of nitrate on the early earth and its role in the evolution of the prokaryotes. 11 p1320 A73-26490

Photographic experiments during a spacecraft flight lasting a number of days 13 p1611 A73-28008

Magnetic and gravitational potential anomalies due to uneven nonuniform material layers, using Fourier transforms 13 p1607 A73-28623

The spectral, angular, and altitudinal distributions of the earth and sky thermal radiation field. 13 p1607 A73-28695

Bibliography on the measurement of electrical parameters of layered lunar/earth surfaces. 13 p1619 A73-29221

Solar radiation fluxes at the earth's surface in the presence of cumulus clouds 15 p1905 A73-31794

Earth shape determination from ellipsoidal model, comparing with spherical functions 15 p1871 A73-31798

Wave polarizations of geomagnetic pulsations observed in high latitudes on the earth's surface. 16 p2003 A73-33440

- Aerological investigation of the volcanic beds of Kamchatka by polarizational and spectral methods
16 p1977 A73-33760
- Earth-flattening approximations in the theory of radio wave propagation near the surface of the earth.
16 p1984 A73-33916
- Scaled illustration of unit sphere geometry with navigation applications.
17 p2209 A73-34874
- Remote sensing with VHRR satellite imagery.
18 p2308 A73-36041
- On relationship between the earth-atmosphere system albedo and the earth's surface albedo.
18 p2308 A73-36042
- Reflection of meteorite generated shock waves from the earth's surface.
18 p2313 A73-36866
- Utilization of satellite radiation measurements in analyzing the temperature near the ground.
18 p2334 A73-37067
- Some characteristics of the surface scattering of the Sikhote-Alin meteorite shower
19 p2480 A73-37240
- Possible trend of the earth's evolution
19 p2481 A73-37242
- Russian book on electromagnetic wave propagation in ionosphere, covering atmospheric structure, electron concentration, waveguides and earth surface effects
19 p2424 A73-37773
- Determination of the shape of the earth's physical surface from the anomalies of the vertical gradient of gravitational acceleration
19 p2427 A73-38554
- Influence of the atmosphere on the gravity force and its potential at points on the earth's physical surface
19 p2428 A73-38555
- The radiation balance of the earth's surface and inclinations of isodioptric surfaces
19 p2428 A73-38556
- Airborne and spaceborne microwave imaging techniques for earth surface surveys, discussing resolution capabilities and applications for side-looking radar, microwave radiometers and scatterometers [AAS PAPER 73-111]
20 p2533 A73-38577
- Sector-patterned structure of interplanetary magnetic field and magnetic disturbances in the circumpolar region.
20 p2603 A73-38915
- Some results of spectrophotometric studies of natural formations from the manned spacecraft 'Soyuz-9'.
20 p2558 A73-39858
- Spacecraft television image comparison between earth and Mars surface features and geology, discussing mountain chains, deserts and tectonic mapping techniques
20 p2613 A73-39897
- Russian book - Chemistry of terrestrial and lunar basaltic rocks.
21 p2648 A73-41436
- Russian book - Studies of the natural environment from manned orbital stations.
23 p2971 A73-43330
- Visual observations of the earth and of the circumterrestrial space environment from manned orbital stations
23 p2971 A73-43331
- Satellite-borne photography of earth surface covering environment and flight dynamics effects, space photogrammetry principles, natural environment imagery interpretation and natural resource photography
23 p2971 A73-43332
- Spectrophotometric investigations of the earth from manned orbital stations
23 p2979 A73-43333
- Multiphase incompressible half-space as simplified earth model for investigating surface displacements due to time- and depth-dependent heat sources
23 p2973 A73-43797
- The precision of contour lines and contour intervals of large- and medium-scale maps.
23 p2979 A73-44123
- Meteoroids impact rate on lunar and earth surfaces for given geocentric and selenocentric velocity distributions, taking into account gravitational effects
24 p3131 A73-44461
- EARTH TIDES**
Lunar magnetic field model with primeval liquid shell dynamo driven by thermal convection or earth tidal motions
14 p1789 A73-29722
- EARTH-MARS TRAJECTORIES**
Objectives and first results of the Mars 2, Mars 3 and Mariner 9 planetary probes
01 p0103 A73-10996
- From earth to Mars orbit - Mariner 9 propulsion flight performance with analytical correlations.
[AIAA PAPER 72-1185]
03 p0382 A73-13478
- Mariner Mars 1971 orbiter spacecraft with sun-Canopus orientation as references, discussing mission objectives, trajectory characteristics, orbital operations, scientific instruments and system design
10 p1276 A73-24004
- Hohmann trajectories efficiency for interplanetary transfers of spacecraft between circular coplanar orbits, considering earth-Mars-earth flight and transition to parabolic trajectory
12 p1538 A73-27065
- Minimum time of Earth-to-Mars and Earth-to-Venus flights with an uncontrolled limited-power engine
14 p1795 A73-29856
- Viking type spacecraft rendezvous with the Martian moons.
19 p2482 A73-37401
- EARTH-MOON SYSTEM**
Lunar motion numerical analysis, discussing flaws due to inadequate solar system model and arithmetic-algebraic procedural deficiencies
01 p0099 A73-10694
- Earth satellites in resonance with the moon and the sun as objects of laser ranging - Analytical solution for their motion.
01 p0099 A73-10695
- A method of determining the center of mass of the moon from ground observations
01 p0100 A73-10840
- Structural and thermal design and fabrication of Lunokhod retro reflecting panel mounted on lunar surface for earth-moon distance determination by laser telemetry
02 p0176 A73-12251
- Astronomical evidence concerning non-gravitational forces in the earth-moon system.
02 p0217 A73-12385
- The origin of the moon - Theories involving joint formation with the earth.
02 p0217 A73-12386
- Paleontological evidence on the earth's rotational history since early Precambrian.
02 p0217 A73-12387
- Lunar surface cratering history from Apollo rock age data, implying earth-moon and solar system evolution mechanism
02 p0217 A73-12406
- On the initial distance of the moon forming in the circumterrestrial swarm.
03 p0369 A73-13108
- Geodesy information and accuracy obtainable by laser ranging from earth onto lunar retroreflector packages
04 p0495 A73-14810
- The secular accelerations of the moon's orbital motion and the earth's rotation.
04 p0497 A73-15176
- Four body problem reduction to three body problem via perturbation region, noting Moon-Earth-Sun system
05 p0623 A73-17198
- Earth-moon mass ratio from Mariner 9 radio tracking data.
07 p0899 A73-20156
- Effects of the sun and the moon on a near-equatorial synchronous satellite.
08 p1011 A73-21430
- Earth-moon system mass and angular momentum distribution anomaly, considering light gases association with Jupiter, Saturn, Uranus and Neptune satellites
11 p1419 A73-25793
- The implications for geophysics of modern cosmologies in which G is variable.
14 p1799 A73-30525
- Lunar origin dynamics, discussing earth-moon tidal evolution, capture probability, fragmentary collisions, precession and auxiliary models
14 p1800 A73-30550
- A method for determining the position of the moon's center of mass from earth-based observations.
15 p1927 A73-30976
- Forward precession motion of the moon caused by attraction to the earth and the sun
15 p1939 A73-31966
- Lunar evolution theory review covering separation from earth, capture by earth, formation by particle accumulation and core iron content approximation
16 p2065 A73-33781
- Photometric variability of counterglow radiance as evidence for dust cloud presence in earth-moon system region
18 p2351 A73-36183
- Earth-moon system angular momentum loss from paleontological data and earth rotational moment of inertia effect
18 p2354 A73-36509
- Inclination of the moon's orbit - The early history.
20 p2605 A73-39055
- On the theoretical possibility of the libration cloud.
22 p2911 A73-42936
- Translational-precessional motion of the moon in the gravitational field of the earth and sun.
24 p3132 A73-44491
- Periodic symmetric solution properties of restricted three body problem for case with lunar mass parameter tending to zero, discussing bifurcation orbit dynamics
24 p3141 A73-45286
- EARTH-MOON TRAJECTORIES**
Systematics of earth-to-moon trajectories. I
01 p0102 A73-10995
- Translunar flight plan of Luna 21 probe, describing Lunokhod structure and lunar descent procedure
08 p1007 A73-20974
- Selection of a trajectory for the return to earth from lunar orbit of an artificial satellite
18 p2351 A73-36106
- EARTH-VENUS TRAJECTORIES**
Minimum time of Earth-to-Mars and Earth-to-Venus flights with an uncontrolled limited-power engine
14 p1795 A73-29856
- EARTHQUAKE DAMAGE**
Engineering applications of geophysical phenomena covering earthquakes, volcanology, hydrology, glaciology and wind stress effects during severe storms
23 p2979 A73-44007
- EARTHQUAKES**
Use of associated matrices in deriving frequency equations for rods with variable rigidities and masses
05 p0636 A73-17082
- Application of the ambiguity function to seismic signatures.
06 p0690 A73-18009
- Nonstationary envelope process and first excursion probability.
06 p0762 A73-18341
- Seismicity as a guide to global tectonics and earthquake prediction.
11 p1352 A73-25563
- Crustal movements in tectonic areas.
11 p1352 A73-25564
- On the correlation between earthquake occurrence and disturbances in the path of the rotation pole.
13 p1607 A73-28405
- Excitation of the Chandler wobble by large earthquakes.
13 p1607 A73-28407
- Dispersed signal filtering and filtered signal duration relation to filter bandwidth and dispersiveness, isolating fundamental mode of Rayleigh waves from earthquake 650 km deep
21 p2648 A73-39931
- EEF**
U EXTERNALLY BLOWN FLAPS
EBULLITION
U BOILING
ECCENTRIC ORBITS
Stable longitudes for 12-hr eccentric orbit satellites.
01 p0095 A73-10104
- Eclipsing binary system orbital eccentricity deduction from observed epochs of light minima
02 p0223 A73-12734
- Interplanetary spacecraft transfer maneuver for hyperbolic trajectory change into eccentric orbit, using aerodynamic drag to obtain nearly circular orbit
03 p0379 A73-14571
- Calculus of variations for equations of relative motion of two satellites with unperturbed Kepler orbits of arbitrary eccentricity
05 p0620 A73-17006
- Photometric orbit and apsidal motion of DR Vulpeculae.
07 p0875 A73-19119
- Determination of the elements of an orbit from known values of the velocity vector at three different moments of time
08 p1012 A73-21550
- Mars polar regions layered deposits annual solar insolation variations due to eccentricity
13 p1687 A73-29674
- Systematic analysis of perturbations of orbits - The case of drag.
14 p1788 A73-29717
- Chebyshev polynomial series solution method for highly eccentric perturbed orbits of comets, using modified Hansen method of partial anomalies
14 p1790 A73-29783
- Investigation of the orbital stability of minor planets with cometary eccentricities.
14 p1794 A73-29839
- Evolution of the orbits of selected minor planets during an interval of 1000 years.
14 p1794 A73-29840
- A note on the relations between true and eccentric anomalies in the two-body problem.
15 p1930 A73-31116
- A study of commensurable motion in the asteroid belt.
20 p2606 A73-39075
- Apollo asteroid discovery, orbital peculiarities, future earth approaches, Apollo group ephemerides and distribution
21 p2765 A73-40299
- Determination of the orbital period of a satellite moving in the earth's gravitational field
23 p3027 A73-43268
- Fast computation of high eccentricity orbits by the stroboscopic method.
24 p3142 A73-45292

ECCENTRICITY

Orbital eccentricity of Mercury and the origin of the moon. 04 p0501 A73-15625

Effect of shroud eccentricity on suppression of flow induced vibrations. 13 p1690 A73-28059

Pallas evolution on basis of orbital eccentricity and inclination, discussing accumulation in asteroid belt in quiescent solar nebula, collisions and planetary gravitational encounters 17 p2229 A73-34428

The Taylor vortex regime in the flow between eccentric rotating cylinders. [ASME PAPER 73-LUBS-8] 17 p2181 A73-35391

Measurement of residual stresses in a cylinder. III - On the effect of eccentricity of holes bored out in Sachs method. 19 p2501 A73-38345

Finite journal bearings with stepwise discontinuity in hydrodynamic film shape, predicting optimal performance as function of step height, eccentricity and L/D ratios 23 p2984 A73-43293

ECCHELETTE GRATINGS

Echelle spectrographs design, applications and performance, discussing modified Czerny-Turner mounting and Schmidt camera arrangements 01 p0046 A73-10510

Prototype design of echelle grating spectrographs for Anglo-Australian 3.8 meter telescope Cassegrain focus, presenting main parameters 01 p0047 A73-10511

Spectroscopic telescope diffraction gratings, discussing fabrication methods and performance characteristics of echelle and Coude gratings 01 p0047 A73-10511

Blank pupil arrangement of coude spectrograph with echelle for 1.52 meter reflector, describing dispersions obtained, receivers used and electronic camera adaptation 01 p0048 A73-10523

The coude spectrograph and echelle scanner of the 2.7 m telescope at McDonald Observatory. 01 p0048 A73-10525

The data-handling problem with television recording of spectra. 02 p0170 A73-12340

A mechanically scanned interferometer-echelle spectrometer for the middle ultraviolet. 21 p2692 A73-39924

Hybrid numerical solution to electromagnetic wave scattering and diffraction with application to microstrip transmission lines, echelle gratings and dielectric step discontinuities in waveguides 22 p2828 A73-42844

ECCHELON FAULTS

U GEOLOGICAL FAULTS

ECHO SATELLITES

NT ECHO 1 SATELLITE

NT ECHO 2 SATELLITE

ECHO SUPPRESSORS

A digital echo suppressor for satellite circuits. 04 p0416 A73-14995

The staggering of pulse sequences in the case of a pulsed radar providing moving target indication 18 p2289 A73-36399

Telephone line echo reduction by adaptive filter compensation, using statistical speech-white noise relations 23 p2952 A73-43318

ECHO 1 SATELLITE

Measured physical and optical properties of the passive geodetic satellite /Pages/ and Echo 1. 04 p0446 A73-14809

ECHO 2 SATELLITE

Vertical ozone profiles from observations of eclipsing satellites. 18 p2304 A73-35971

ECHOCARDIOGRAPHY

Ultrasonic Doppler locators for peripheral vessel blood circulation and myocardium and valvular motor activity measurements 06 p0656 A73-17682

Estimation of left ventricular size by echocardiography. 09 p1046 A73-22999

Myocardial contraction velocity and acceleration in man measured by ultrasound echocardiography differentiation. 12 p1461 A73-27026

Multi-information recording and reproduction in the ultrasono-cardio-tomography. 13 p1579 A73-28581

Echocardiography status, potentialities and requirements in congenital heart disease diagnosis, considering feasibility in left ventricular performance evaluation 14 p1721 A73-30053

Book on echocardiography covering examination of mitral, aortic, tricuspid and pulmonary valves, ventricles, atrium, pericardial effusion, coronary artery disease and tumors 14 p1721 A73-30358

Echocardiographic detection of regional myocardial infarction - An experimental study. 15 p1839 A73-31997

Assessment of left ventricular dimensions and function by echocardiography. 16 p1973 A73-34038

A new technique for the study of left ventricular pressure-volume relations in man. 19 p2401 A73-38259

Echocardiographic evaluation of the hemodynamic effects of chronic aortic insufficiency with observations on left ventricular performance. 20 p2512 A73-38868

Detection of left ventricular asynergy by echocardiography. 20 p2512 A73-38869

Doppler echocardiography - The localization of cardiac murmurs. 24 p3064 A73-44947

Comparison of ultrasound and cineangiographic measurements of left ventricular performance in patients with and without wall motion abnormalities. 24 p3062 A73-45400

ECHOES

NT ANGELS

NT AURORAL ECHOES

NT CLUTTER

NT LUNAR ECHOES

NT LUNAR RADAR ECHOES

NT RADAR ECHOES

NT RADIO ECHOES

NT SIGNAL REFLECTION

NT VENUS RADAR ECHOES

Third order collisionless electron plasma echo signal wavelength and rise and fall rate about central position, comparing experiment with Vlasov equation theory 02 p0197 A73-12064

Free streaming electrons effect on spatial ballistic electron plasma wave echoes response, calculating echo electric fields and electron distribution function 02 p0197 A73-12065

Spatial plasma echoes of ion acoustic waves in low pressure He and Ne discharges in anode direction 03 p0348 A73-14622

Spatial echo and nonlinear interaction of waves in a plasma 04 p0478 A73-15035

Quasi-monochromatic radiation pulse reflection from rough surfaces, analyzing echoes statistical properties 09 p1120 A73-22575

Study of disturbance reflection from the subsonic section of a Laval nozzle 11 p1411 A73-26437

DONAR - A computer processing system to extend ultrasonic pulse-echo testing. 19 p2407 A73-37448

FM-CW ground and aircraft radar observations of clear air echo strata, examining turbulence levels, Richardson number, turbulent scattering, radar reflectance and power spectra 19 p2427 A73-38203

Acoustic echo-sounding techniques and their application to gravity-wave, turbulence, and stability studies. 19 p2405 A73-38207

Orbit and superior orbital fissure acoustic window for cranium posterior structures imaging by echoencephalographic techniques 22 p2815 A73-42667

ECLIPSES

NT LUNAR ECLIPSES

NT SOLAR ECLIPSES

Mutual phenomena of Jupiter's satellites in 1973-74. 07 p0875 A73-19260

The occultations and the mutual eclipses of the Galilean satellites of Jupiter 20 p2604 A73-39009

Mutual Jupiter satellite-satellite eclipses and occultation observations for improved ephemerides, albedo maps, radii and limb darkening estimation 24 p3130 A73-44454

The post-eclipse brightening of Io. 24 p3134 A73-44563

Posteclipse brightening of Io observed at 3500 and 4000 A suggested as transient partial covering of high-albedo material 24 p3134 A73-44564

ECLIPSING BINARY STARS

Mass-luminosity relation for eclipsing and visual binary stars, analyzing observational data by least squares method 02 p0218 A73-12409

Eclipsing binary system orbital eccentricity deduction from observed epochs of light minima 02 p0223 A73-12734

Polarimeter search for optical circular polarization in eclipsing binaries, magnetic Ap stars, planetary nebula, Hubble and Orion nebulae, M87 and Sirius 03 p0366 A73-12939

Narrow band and broadband light curves for Algol eclipsing binary from differential photometry, calculating reflection effect 03 p0366 A73-12940

MASS FLOW AND PERIOD CHANGES OF CONTACT BINARIES.

03 p0370 A73-13212

Orbital period variations of eclipsing binary TW Draconis caused by third body effect, apsidal motion and matter exchange 03 p0379 A73-14582

Determination of the coefficient of displacement of the line connecting the apsides in stellar models and comparison of it with observations 03 p0379 A73-14584

Secondary component minimum deepening in UV light curve of Beta Lyr eclipsing binary star, suggesting black hole model 04 p0501 A73-15637

The period and light curve of HZ Herculis. 04 p0501 A73-15683

Spectroscopic observations of HZ Herculis. 04 p0501 A73-15684

Stratification of the emission in the envelope of the eclipsing-binary Wolf-Rayet star V444 Cygni. 04 p0503 A73-16009

Solutions of the light curves of eclipsing binaries by the generalized method of least squares. 04 p0503 A73-16010

Gravity-darkening of the secondary component of RW monocerotus. 05 p0624 A73-17315

Spectroscopic observations of HZ Herculis and a model for Hercules X-1. 05 p0625 A73-17344

Observations of Vela XR-1 by the UCSD X-ray telescope on OSO-7. 05 p0627 A73-17390

Beta Persei decimetric-centimetric radio emission variations, relating observational data to continuous structural adjustment model based on starguakes hypothesis 05 p0627 A73-17392

Preliminary observations of variable polarization in epsilon Aurigae. 07 p0875 A73-19118

Photometric orbit and apsidal motion of DR Vulpeculae. 07 p0875 A73-19119

Least squares method for eclipsing binary stars minimum epoch, noting application to artificial and observed light curves 08 p1006 A73-20928

Spectral energy distribution, photometric gradients and Balmer discontinuities for eclipsing binary RZ Scutum from spectrograms with low dispersion in H-gamma line 10 p1273 A73-23707

Photometric and spectroscopic observations of eclipsing binary object BM Orionis interpreted in terms of thin disk model with collapsed star /black hole/ 11 p1415 A73-25072

Differential UBv photometry of beta Lyrac. III. 11 p1415 A73-25072

Two-color electrophotometry of RW in the Northern Crown 11 p1416 A73-25233

Photoelectric observations of the close binary system SZ Camelopardalis. 11 p1425 A73-26266

UBV photometry of 32 Cygni during the 1971 eclipse. 11 p1426 A73-26268

The spectrum and variability of Hercules X-1 observed by OSO-7. 11 p1428 A73-26626

Her X-1 optical counterpart observed for B magnitude, relating light curve scatter to 35-day cycle 11 p1428 A73-26627

Evidence for the binary nature of 2U 1700-37. 11 p1428 A73-26628

The light variation and orbital elements of VW Bootis. 11 p1429 A73-26680

The eclipsing binary system RU Ursae Minoris. 11 p1429 A73-26681

X ray sources in Centaurus X-3 and Hercules X-1 eclipsing binaries, determining upper and lower limits on physical parameters from assumption involving mass function 12 p1536 A73-27878

Nebular stage of Nova Delphini 1967. I 13 p1672 A73-28039

Photoelectric light curve of the Algol system TW Andromedae and the interpretation of its distortions by the effects of hot spots. 13 p1672 A73-28040

Close binaries structure and evolution, discussing model computations for H-R diagram and mass-luminosity relations 13 p1682 A73-28983

OA0-2 observations of HD 153919 = 2U 1700-37. 14 p1797 A73-30007

Variable star observations from outside the earth's atmosphere - Review and prospects. 15 p1935 A73-31488

OA0-2 observations of Beta Lyrac and a provisional interpretation. 15 p1935 A73-31489

X-ray pulse profile and celestial position of Hercules X51.
15 p1936 A73-31563

Quantitative analysis of the spectrum of beta Lyr. I-Variation of certain hydrogen and helium emission lines
16 p2057 A73-32710

Fundamental data for contact binaries - RZ Comae Berenices, RZ Tauri, and AW Ursae Majoris.
17 p2231 A73-34759

Correlations among the parameters of the spherical model for eclipsing binaries.
17 p2236 A73-35778

Spectral energy distribution, spectrophotometric gradients and Balmer discontinuities for eclipsing binary RZ Scuti from spectrograms with low dispersion in H gamma line
18 p2354 A73-36732

Measurement of the position and spectrum of Hercules X-1 from the OSO-7 satellite.
18 p2356 A73-36982

Hard X-ray spectrum of Hercules X-1.
19 p2475 A73-37388

Copernicus satellite observation of eclipsing binary Her X-1 to search for steady soft X ray flux strong enough to heat companion star
19 p2482 A73-37391

Evolutionary track calculation for 1.8 solar mass close binary systems, noting luminosity transfer to secondary from primary
19 p2483 A73-37569

Upper limits to the X-ray emission from Beta Persei during radio flares.
19 p2475 A73-37630

On the accretion model for X-ray double stars.
20 p2607 A73-39082

Mass-luminosity relations for unevolved stars in high mass eclipsing binaries and low mass visual binary systems for hydrogen and metal abundances of Population I stars
20 p2609 A73-39439

X ray source Hercules X-1 observation from Uhuru satellite, relating regular dips in intensity to orbital phase
20 p2602 A73-39440

The eclipsing contact binary VW Cephei.
20 p2610 A73-39577

Narrow-band photoelectric observations of the Wolf-Rayet type eclipsing binary star V444 Cyg in the continuum /4244 - 7512A/
21 p2768 A73-40717

Optical studies of Uhuru sources. VI - Photoelectric photometry of HD 153919 = 2U 1700-37.
22 p2905 A73-41766

The role of rotation in close binary systems of high mass.
22 p2909 A73-42584

Russian book on eclipsing binary stars covering limb darkening law, photometric eclipsing phases, computer applications and models
22 p2911 A73-42747

Light curve for eclipsing binary systems with an extensive atmosphere.
22 p2916 A73-43044

Cepheus X-4 X ray source observation by X ray telescope on OSO-7, confirming position by second telescope aboard
22 p2904 A73-43122

Sanduleak 160 variability confirmed, discussing double peaked optical variation, mass ratios and X ray eclipse
22 p2916 A73-43123

Photographic observations of the occultation of Beta Scorpii by Jupiter.
23 p3033 A73-43944

W-Ursa-Major stars
24 p3137 A73-44825

The unstable eclipsing giant system RZ Cancri.
24 p3143 A73-45438

The 35-day cycle of HZ Herculis.
24 p3143 A73-45491

ECLIPTIC

Gravitational constant anisotropy effects on planets with orbits close to ecliptic in solar system two body problem
01 p0099 A73-10689

The excess secular change in the obliquity of the ecliptic and its relation to the internal motion of the earth.
13 p1679 A73-28401

Imp-3 satellite measurement-based investigation of variability of interplanetary magnetic field component normal to plane of ecliptic during passage across sector field boundary
19 p2480 A73-37241

Enhanced scintillation sectors outside the plane of the ecliptic.
23 p3029 A73-43679

ECOLOGICAL SYSTEMS

U ECOLOGY

ECOLOGY

NT COASTAL ECOLOGY

A method for phenomenological analysis of ecological data.
02 p0188 A73-12629

Synchronous satellite ground track drift analysis for ecological survey application, discussing zonal, tesseral and sectorial harmonics and perturbation compensation
03 p0370 A73-13150

Social, economic and political factors associated with earth resources observation and information analyses.
05 p0642 A73-17137

International space station program for global resources and ecological monitoring and management, reviewing US Skylab and Space Shuttle and USSR Soyuz projects
06 p0757 A73-18026

Russian book on mathematical models of biological systems covering biogeocenosis, optimal crop, chemostat cultivation, predator-victim society, trophic control, and life support systems
09 p1044 A73-22347

Book - The economics of airborne emissions: The case for an air rights market.
12 p1561 A73-27399

Miami offshore airport project rejection reasons, citing commercial and marine ecological considerations
15 p1857 A73-31541

Rotary wing aircraft ecological advantages in logging, off shore oil exploration and short haul passenger transport for airport size reduction
16 p2088 A73-33185

Airborne remote sensing of Georgia tidal marshes.
16 p2003 A73-33359

A comprehensive remote sensing legend system for the ecological characterization and annotation of natural and altered landscapes.
20 p2557 A73-39851

RF fields as new ecological factor in environment pollution, considering radiation interaction with biological systems and increased use of electromagnetic spectrum
22 p2811 A73-41787

Solar activity cycles effects on physical and biological processes in helioterrestrial domain, discussing crops, tree growth, diseases and fishing
24 p3088 A73-45364

ECONOMIC ANALYSIS

Monopoly, concentration, and competition in the air transportation industry of the United States
01 p0124 A73-10568

Investigation of cryogenic stability and reliability of operation of Nb3Sn coils in helium gas environment.
02 p0200 A73-11838

Technical and economic analysis of nuclear power reactors application for international cargo ship and air transportation, noting feasibility study of airborne power plants
03 p0340 A73-13390

[AIAA PAPER 72-1061] Satellite charges for a mixed pre-demand-assigned system.
03 p0276 A73-13901

Economic analysis of silicon solar cells production noting cost reduction from feasibility studies of edge defined film fed crystal growth in ribbon form
03 p0258 A73-14251

Air traffic volume prediction by 1985, determining passenger growth factors for terminal pairs
07 p0923 A73-19348

Calculation and comparison of the economics of electrochemical fuel cells
11 p1410 A73-25346

Economic-mathematics approaches to prognostic air traffic computations
11 p1455 A73-26724

Aircraft integrated data systems /AIDS/ utilization for airlines operational flight control and economic exploitation enhancement, discussing aircraft accident investigation, maintenance, navigability, etc
15 p1831 A73-32496

Economic models for satellite system effectiveness.
16 p2073 A73-33618

Economic tradeoff study of design criteria cost effectiveness, applying to reusable nuclear shuttle /RNS/ engine concepts
16 p2035 A73-33650

Performance and economic advantages offered by a diffused semiconductor strain gage pressure transducer.
17 p2167 A73-34626

Requirements of an economic approach to maintenance.
18 p2373 A73-37142

New York offshore airport feasibility study.
19 p2418 A73-37750

Freighter airships economical and technological feasibility study, discussing performance requirements and design concepts
19 p2385 A73-37879

Resource exchange and allocation /a generalized thermodynamic approach/. II
20 p2629 A73-39351

Dynamic model of economically efficient multipurpose plants
21 p2793 A73-40386

Russian book - Economic efficiency and planning of air freight transportation.
21 p2793 A73-41294

Air carrier and general aviation airports system planning with emphasis on economic analysis of operation, ownership and finance
[ASME PAPER 73-ICT-33] 23 p2965 A73-43494

Optimal macroscopic control and resource exchange model for open market-like systems in economic and thermodynamic terms
24 p3154 A73-44665

ECONOMIC FACTORS

Construction materials selection for thermal dimensional stability in critically sensitive precision instruments and mechanical components, considering economic factors
01 p0066 A73-11293

STOL aircraft technology, operation and markets in view of future European air traffic development, discussing various lift devices, noise aspects and economic factors
[DGLR PAPER 72-054] 02 p0130 A73-11662

TV satellite system feasibility and design study for Germany, discussing technical and economic aspects
[DGLR PAPER 72-051] 02 p0140 A73-11664

Aircraft fault isolation based on pattern of cockpit indications - A human factors approach.
02 p0136 A73-11857

General optimization criteria with allowance for economic factors and their use in measurement technology
03 p0305 A73-12894

Airlines passenger transportation profitability, discussing relationships between service quality, load factor and operating costs
03 p0400 A73-13575

An acceptable exposure level for aircraft noise in residential communities.
03 p0250 A73-13838

Financial problems related to aircraft and ships development and production for Defense Department, stressing C-5A, Cheyenne helicopter and DD-963 class of automated destroyers
03 p0401 A73-13897

Private business aircraft economic aspects, discussing costs vs time savings and indirect advantages
03 p0401 A73-13997

Airlines responsibility and measures for aircraft noise abatement, considering economic and safety aspects
04 p0406 A73-14893

Composite materials technology for aircraft and spacecraft structures, discussing various fiber-matrix combinations mechanical properties and production volume/price relations
05 p0589 A73-16759

Social, economic and political factors associated with earth resources observation and information analyses.
05 p0642 A73-17137

Technology and operation of Olympus engine cycle on Concorde aircraft, discussing chemical and noise pollution and economic factors
05 p0536 A73-17190

Long range air transportation technical and economic future prospects, discussing passenger and cargo developments, noise reduction and SST technology
06 p0646 A73-17607

[AIAA PAPER 73-14] Economically viable and socially acceptable second-generation SST, discussing technological developments for range/payload, airport noise and sonic boom improvements
06 p0646 A73-17608

[AIAA PAPER 73-15] Book - Aviation law: Cases and materials.
06 p0771 A73-17870

Economic performance and cost problems in civil air transport maintenance and engineering quality control related to selling price trends
06 p0647 A73-17888

Energetically and financially economical hydrazine synthesis method based on ammonia oxidation by water solution of hydrogen peroxide
07 p0787 A73-19325

National Congress on Reliability, Perros-Guirec, Cotes-du-Nord, France, September 20-22, 1972, Text of the Lectures
07 p0799 A73-19401

Acquisition and utilization of data of exploitation of equipment in the particular case of exposure to different environments
07 p0830 A73-19402

Technology advancement effects on military and commercial transport aircraft development and production costs, considering airframes, engines and avionics
07 p0924 A73-20394

Mass air transportation development in Sweden, discussing flight scheduling, fare structure and quiet STOL aircraft introduction in 1980s
07 p0778 A73-20618

Technology and operation of Olympus engine cycle on Concorde aircraft, discussing chemical and noise pollution and economic factors
08 p0996 A73-21687

Six degree of freedom guided sounding rocket flight simulations and trajectory program, discussing financial and technical feasibility
[AIAA PAPER 73-299] 09 p1117 A73-23218

Charter air fleet maintenance economic management, discussing budget, manpower, time and materials control
09 p1168 A73-23243

U.S. industry R and D fund cutback caused problems survey by questionnaire, discussing problem minimization with consideration for economic market conditions
10 p1298 A73-24632

The satellite system as an integrated telecommunications switching center.
12 p1468 A73-27011

Cargo air transport means selection procedure, suggesting methods for economic evaluation of time savings
12 p1560 A73-27066

On-orbit checkout and repair as a factor in economical spacecraft design and operation.
12 p1549 A73-27439

Justification and calculation of the lifetimes and efficiency of new equipment
12 p1562 A73-27468

Unit batch size optimization in mass production, discussing labor efficiency, operational cycle length, unfinished volume and total cost
12 p1562 A73-27477

Multiple access system by time division with synchronization in the S2 TDMA satellite
13 p1584 A73-28908

Launching base creation process and economic factors, considering rocket firing safety, scientific requirements and financial investments criteria
14 p1741 A73-30080

Wind tunnel tests as part of rotary wing aircraft development, discussing technical and economic aspects
14 p1743 A73-30469

Helicopter use for urban transportation to meet economic growth needs and alleviate traffic congestion, considering IFR equipment and noise reduction
14 p1712 A73-30470

Design considerations for offshore airports.
15 p1856 A73-31527

Multi-purpose use potential of offshore airports.
15 p1856 A73-31528

Offshore airport planning, discussing selection economics from cost effective alternatives based on usage projection, community benefits and intrinsic and social costs
15 p1856 A73-31531

MGC 30 inertial navigation system for civil aviation, emphasizing economics and ease of maintenance
15 p1909 A73-32457

Canadian air transportation survey, outlining history of other modes, transportation investment trends, modal traffic distribution, STOL applications, airline social services and marketing
16 p2087 A73-33177

Large payload aircraft for Alaskan and Canadian gas-oil transportation, examining alternative pipeline economic factors and possible new North Canadian island fuel fields
16 p2088 A73-33183

Short haul V/STOL air transportation social and economic aspects in comparison with ground transportation modes, emphasizing convenience and frequency of service
16 p2088 A73-33193

Specific Behavior Objective approach to airline flight simulation, featuring duplicate training elimination and education time reduction
16 p1995 A73-33202

Avionics and human factors in flight simulator economics, interrelating aircraft design to simulation system
16 p1995 A73-33206

Utilization of realization to optimize the choices of reliability from the economic point of view
16 p2088 A73-33270

Selection of brazing solders according to technical requirements and economy
16 p2026 A73-33350

A current turbine engine maintenance program and the experience and logic upon which it is based.
[ASME PAPER 73-GT-81] 16 p2049 A73-33526

Some economic aspects of aviation safety.
16 p2089 A73-33648

Mechanical faster types, design considerations and economic factors, detailing nut and bolt joint assembly design, static and dynamic loads and production engineering
16 p2021 A73-33862

Design to detect and avoid failure - One airline's viewpoint.
17 p2097 A73-34081

Hypersonic transports - Economics and environmental effects.
17 p2099 A73-34435

Book - Satellite broadcasting.
17 p2121 A73-34473

Transport cargo aircraft design requirements and supporting ground system concepts in view of future market demands with emphasis on economic constraints
[SAE PAPER 730352] 17 p2102 A73-34700

Market economic environment change effects on air transport design and use, examining 747 operational requirements in terms of cargo load factor, passenger fares and labor costs
[SAE PAPER 730355] 17 p2103 A73-34703

New constraints of military aviation
18 p2267 A73-36684

Civil aviation environmental and economic aspects, discussing noise and air pollution, fuel consumption and airspace and ground space utilization
18 p2267 A73-36685

Aircraft noise in airport areas, discussing effects on environment and economics
18 p2373 A73-36949

Subsonic aircraft turbojet engines, discussing thermodynamic cycles, entry temperature increase, propulsion efficiency and economy improvements and ecological requirements
18 p2343 A73-36994

Impact of the space tug concept on space program economics.
19 p2490 A73-37192

On the cost benefits of air cushion landing gear to civil aviation.
19 p2381 A73-37685

'The hub of the wheel' - A project designer's view of weight.
[SAE PAPER 996] 19 p2386 A73-37895

Air transportation economic efficiency as function of fuel consumption, cruising flight speed, altitude range and load factor /payload/
19 p2506 A73-38118

Aircraft economics and its effect on propulsion system design.
[AIAA PAPER 73-808] 19 p2388 A73-38372

Small earth terminal applications for satellite communications.
[AAS PAPER 73-121] 20 p2543 A73-38582

World Bank support for airports.
22 p2938 A73-42317

ECONOMICS

NT DEMAND [ECONOMICS]

Apollo project management techniques transfer to socio-economic programs, discussing systems oriented approach to city planning, mass transportation, pollution control, public hygiene, etc
09 p1167 A73-21898

Book - The economics of airborne emissions: The case for an air rights market.
12 p1561 A73-27399

ECOSYSTEMS

The role of applications satellites in the management of the human environment.
19 p2424 A73-37713

EDDIES

U VORTICES

EDDINGTON APPROXIMATION

Time-dependent Yukawa-potentials of a class of weak gravitational fields.
02 p0193 A73-12182

The Eddington factor for radiative transfer in spherical geometry.
09 p1121 A73-23289

Note on the modified two-stream approximation of Sagan and Pollack.
24 p3123 A73-44438

EDDY CURRENTS

Ultrasonic sensing apparatus and eddy current method in NDT, noting radiography, sonics, penetrants and magnetic particles
01 p0057 A73-11001

Conductivity of 2024-T42 aluminum sheet solution heat treated at various temperatures.
02 p0168 A73-11986

Nondestructive eddy current tests of Al bronze alloy fillet size and flatwise distribution in Ti honeycomb sandwich panels
05 p0581 A73-16131

Influence of eddy currents on the rotation and orientation of an asymmetric artificial earth's satellite
08 p1014 A73-21547

Investigation of the sensitivity of a duct sensor to discontinuities in alternating fields of square-pulse or sinusoidal shape - Detectability of surface defects on nonmagnetic and ferromagnetic specimens. I
08 p0967 A73-21587

A mechanized eddy current scanning system for aircraft struts.
10 p1225 A73-24631

Eddy current testing - The present situation, results, new developments.
11 p1374 A73-26300

Analytical solution to problems of eddy current distribution in a thin plate and a conducting spherical shell
14 p1774 A73-30029

FFTF probe-type eddy-current flowmeter - Wet versus dry performance evaluation in sodium.
21 p2738 A73-40768

Oblique radiation of ultrasound by an electromagnetic-acoustical method.
24 p3109 A73-44697

EDDY DIFFUSION

U TURBULENT DIFFUSION

EDDY VISCOSITY

Analysis of free turbulent mixing flows without a net momentum defect.
03 p0296 A73-14187

A model for eddy conductivity and turbulent Prandtl number.
[ASME PAPER 72-WA/HT-13] 04 p0434 A73-15834

Eddy-viscosity distribution in thick axisymmetric turbulent boundary layers.
[ASME PAPER 72-WA/FE-18] 04 p0435 A73-15845

Free turbulent mixing in axial pressure gradients.
[ASME PAPER 72-WA/APM-31] 04 p0435 A73-15888

Numerical analysis of eddy viscosity models in supersonic turbulent boundary layers.
[AIAA PAPER 73-164] 05 p0566 A73-16910

Kinematic eddy viscosity at low Reynolds numbers.
05 p0567 A73-17111

Prandtl eddy viscosity model for incompressible coaxial jet far field velocity decay prediction with non-dimensional term inclusion
[AD-758488] 07 p0811 A73-19965

Repeated cascade structure and kinetic description for homogeneous turbulence spectrum, considering coupled hierarchies origin from transfer function and eddy viscosity development
07 p0812 A73-20472

Mixing length flow theory for turbulent boundary layer calculation, with allowance for mass transfer
08 p0953 A73-20721

Turbulent interface structure from eddy viscosity models, discussing equations of motion and Nee-Kovaszay and Prandtl models
10 p1205 A73-24253

Turbulent viscosity distribution in axisymmetric compressible wake and coaxial mixing flows via Navier-Stokes equations, taking into account pressure gradients
10 p1206 A73-24545

A model for investigating eddy viscosity effects on mesoscale cellular convection.
11 p1393 A73-25716

The wind profile very close to the ground.
14 p1772 A73-30904

A generalized theory for the turbulent mixing of axially symmetric compressible free jets.
17 p2156 A73-35505

An integral procedure for estimating boundary layer parameters and heat transfer in arbitrary pressure gradients.
[AIAA PAPER 73-700] 18 p2298 A73-36249

EDEMA

Effect of interstitial edema on distribution of ventilation and perfusion in isolated lung.
01 p0008 A73-10167

Age-related characteristics of pulmonary edema development during acute hypoxic hypoxia
10 p1180 A73-23939

Evaluation of positive end-expiratory pressure in hypoxic dogs.
20 p2515 A73-39781

Phase IV volume of the single-breath nitrogen washout curve on exposure to altitude.
20 p2518 A73-39783

EDGE DISLOCATIONS

Edge dislocation in an infinite anisotropic elastic medium under consideration of the core conditions.
03 p0392 A73-13774

High temperature tests for chemical vapor deposited W ring and tensile specimens mechanical properties, investigating slip traces and fracture surfaces
04 p0462 A73-15305

Anomalous slip in high-purity niobium single crystals deformed at 77 K in tension.
04 p0467 A73-15931

Creep in molybdenum single crystals at 0.57 of the melting temperature
06 p0708 A73-18047

Structural changes in molybdenum single crystals during high temperature creep
06 p0708 A73-18048

The behaviour of an edge dislocation in non-homogeneous anisotropic body with cracks.
07 p0915 A73-20285

Inhibition of a wedge-shaped crack by a plane buildup of edge dislocations
09 p1157 A73-22159

The analysis of dislocation systems by the finite element method.
10 p1290 A73-24298

Metal fatigue crack nucleation behavior and dislocation microstructures, including slip band and extrusion-intrusion pairs
11 p1380 A73-25804

Dislocation structure in molybdenum single crystals after deformation at 293 and 400 deg K.
13 p1634 A73-28221

A treatise on the stress-fields produced by moving dislocations Supplementary remarks and applications. 13 p1697 A73-28915

Workhardening, slip band formation and crack initiation during fatigue of titanium. 17 p2190 A73-34882

Edge dislocation in an anisotropic material with a surface layer. 20 p2593 A73-39342

A detailed investigation of slip line pattern and sub-surface dislocation structure of molybdenum single crystals. 21 p2722 A73-41566

Stopping of a wedge-shaped crack by a plane cluster of edge dislocations. 22 p2919 A73-42107

Plastic deformation and anisotropy of sapphire crystals via nonbasal plane slip under bending, obtaining stress-strain curves and flow stresses temperature dependence 23 p2997 A73-43772

Orientation dependent slip in polycrystalline titanium. 23 p2993 A73-44028

Influence of the offset on the experimental yield surfaces of metals - A theoretical evaluation. 24 p3147 A73-44747

EDGE LOADING

Rectangular plate stability under compression by uniformly distributed loads applied to two opposite simply supported edges with mixed boundary conditions at other edges 02 p0230 A73-11640

Designing of shells with a zero Gaussian curvature under an edge load applied to a portion of the shell contour 02 p0230 A73-11717

Stress distribution in elastic shell of revolution under axisymmetrical loads, noting thickness distribution for uniform stress in critical edge loading zone 02 p0231 A73-11805

Finite axisymmetric deformations of elastic membranes. 02 p0234 A73-12089

Effect of membrane forces on large deflection of simply supported rectangular plates. 03 p0389 A73-13323

Influence coefficients for end-loaded conical frustums. 07 p0913 A73-19983

Secondary terms of thin multilayer plate equations, involving edge and stress-strain state fluctuation effects on boundary condition formulation 08 p1019 A73-21766

The effect of a transverse shear acting on the edge of a circular cutout in a simply supported circular cylindrical shell. 09 p1161 A73-23092

Alternating method with combined analytical and numerical calculations for two dimensional edge and three dimensional surface crack problems 09 p1162 A73-23181

Book - Structural analysis of shells. 09 p1164 A73-23273

An elastic-plastic buckling solution using the incremental theory. 11 p1443 A73-26089

Edge buckling of cylindrical shells with low in-plane shear moduli. 11 p1445 A73-26392

Bending stresses and strains in anisotropic semi-infinite plates with arbitrary edge and surface loadings. 11 p1445 A73-26404

Torsion of an axisymmetrical anisotropic body with mixed boundary conditions on the edge surface 13 p1698 A73-29086

Unsymmetric wrinkling of circular plates. 14 p1812 A73-30522

Asymptotic solutions for shells with general boundary curves. 14 p1812 A73-30523

Nature of stresses in the internal vicinity of the edge of the joint surface in a compound body loaded under conditions of the plane problem of the theory of elasticity 15 p1950 A73-31827

Thin elastic orthotropic annular plate postbuckling behavior under planar edge compression loads, analyzing axisymmetric deformations via nondimensional equations and Keller-Reiss numerical method [ASME PAPER 73-APM-5] 17 p2247 A73-35030

Torsion of an axisymmetric anisotropic body with mixed boundary conditions on the side surface. 19 p2498 A73-37636

Two-dimensional problem in elasticity theory for a rectangle with mixed boundary conditions 19 p2499 A73-37761

Finite difference technique for elastic-plastic buckling of edge-loaded rectangular plates, finding bifurcation stresses via Hill and Prandtl-Reuss expressions 20 p2623 A73-39560

Flexibility matrix coefficients for disk loading under sinusoidal edge loading tabulation and derivation to accommodate boundary conditions 21 p2784 A73-40434

Mixed boundary value problem of thin isotropic plate under edge loading, examining bending moment applied to plate with intermittent edge clamping 22 p2928 A73-43065

Postcritical deformations in a multilayer plate under edge pressure 23 p3043 A73-43925

An examination of the edge effect in a cantilever beam. 24 p3152 A73-45371

EDGES

NT LEADING EDGES

NT SHARP LEADING EDGES

NT TRAILING EDGES

Dynamic edge effect in rods - Formulation of shortened problems 01 p0118 A73-11405

Edge diffraction cone detection by illuminating razor blade edge with laser beam, noting agreement with geometrical theory prediction [AD-758568] 05 p0585 A73-16812

A method for determining the stressed state of anisotropic plates with a nonsymmetrically reinforced edge 18 p2363 A73-36407

EDUCATION

NT ASTRONAUT TRAINING

NT FLIGHT TRAINING

NT PILOT TRAINING

NT SPACE FLIGHT TRAINING

Future NASA communication satellite technology applications in meeting national education, health care, culture and data transfer needs, considering ATS F and CTS spacecraft 02 p0143 A73-12846

Maintaining vitality and productivity in R & D - Steps to maintain high level staff performance. 10 p1298 A73-24633

Civil aviation medicine functional standardization and expansion, emphasizing preventive medicine, health education and operational safety 10 p1185 A73-24718

Engineering personnel, technical and flight instructors training for introduction to and effective utilization of new civil and military aircraft and weapon systems 13 p1624 A73-28789

Experimental educational noise surveys of rural, suburban, urban and industrial areas at various times of day, using computerized data processing 16 p2036 A73-33216

Design for teaching aerospace engineering at Texas A & M University. [AIAA PAPER 73-786] 19 p2505 A73-37456

A new approach to aircraft design education. [AIAA PAPER 73-787] 19 p2505 A73-37457

EDUCATIONAL TELEVISION

Satellite educational TV systems for underdeveloped countries, discussing installation problems, capital investments requirements and potential benefits 03 p0401 A73-14173

Educational radio and television satellite networks, considering computer networks, cable TV and NASA Applications Technology Satellites [ATS] utilization 09 p1056 A73-23397

Problems and possibilities related to transmissions by satellites covering large zones in Africa 11 p1454 A73-26274

Indian national educational communications program for information dissemination on health, family planning, hygiene and agriculture, discussing satellite TV development project [AAS PAPER 73-106] 20 p2629 A73-38576

Some developments in semi-direct broadcast satellites and community receiving systems. [AAS PAPER 73-155] 20 p2521 A73-38599

EKG [ELECTROENCEPHALOGRAMS]

U ELECTROENCEPHALOGRAPHY

EFFECTIVE PERCEIVED NOISE LEVELS

Osaka airport effective continuous perceived noise level measurements, area contour map and noise duration allowance vs aircraft distance diagram 03 p0249 A73-12977

A note on the quantity /effective/ perceived noisiness and units of perceived noise level. 04 p0406 A73-15587

Perceived level calculation methods for aircraft flyover noise scaling, rating jets, turboprops, piston aircraft and helicopters with frequency weighting functions, duration and tone corrections 10 p1175 A73-24391

Definitions and procedures for computing the effective perceived noise level for flyover aircraft noise. [SAE ARP 1071] 16 p1967 A73-33015

Noise certification of a transport airplane. 19 p2378 A73-37279

Perceived noise level ratings for helicopter noise, discussing blade slap, tail rotor whine, broadband noise and PNL rating shortcomings 22 p2798 A73-41708

EFFECTIVENESS

NT COST EFFECTIVENESS

NT SYSTEM EFFECTIVENESS

EFFECTORS

U CONTROL EQUIPMENT

EFFERENT NERVOUS SYSTEMS

Current views on the mechanism of the quantum-induced liberation of a mediator from the motor nerve endings of a skeletal muscle 01 p0009 A73-11023

Response of motoneurons of the spinal cord to gamma radiation - A cytochemical study. 03 p0262 A73-13808

Method for quantitative estimation of the functional state of the motor apparatus 03 p0268 A73-13822

Effect of hypercapnia on the electrical discharges of the bulbar respiratory neurons and motor neuron ganglia of respiratory muscles 05 p0541 A73-16735

Electrophysiological investigation of supraspinal motor control systems evolution through Cyclostoma-Primate series, noting preservation of reticulomotor neuron projection characteristics 07 p0781 A73-20001

Changes in hemodynamics and efferent sympathetic pulsation during pressor cardiovascular reflexes under conditions of acute hypoxic hypoxia 09 p1039 A73-22365

Structural characteristics of connections between medial efferent systems and spinal cord neurons 09 p1040 A73-22577

Cortico-pyramidal and cortico-extrapyramidal synaptic effects on lumbar motor neurons in monkeys 09 p1040 A73-22578

Investigation of evoked activity in the ventral horn of lumbar segments during the interaction of efferent extrapyramidal and cortical stimuli 09 p1040 A73-22579

Voluntary activation of individual motor units in man 10 p1181 A73-24519

Reflex excitability of spinal motor neurons in man under high atmospheric pressure 10 p1182 A73-24525

Organization of the activity of a group of motor neurons in man during voluntary contraction of a muscle 10 p1182 A73-24599

Functional and morphological structures of motor activity events, noting central integration ensemble of cerebrium transmitter sequences 11 p1314 A73-25200

Motor functions and control of sensorial messages of somatic origin 13 p1576 A73-29174

Intranuclear organization of the center median nucleus of the thalamus. 13 p1576 A73-29175

Anatomical and neurophysiological investigations of centrifugal control of retinal activity via efferent optic nerve fibers 14 p1714 A73-29875

Human average evoked potential distribution over scalp to associate cortical electrical activity with voluntary movement, reacting to EMG activity 14 p1714 A73-29990

Features of the influence of hypergravitation on the motor activity of the chicken embryo amnion developing under normal conditions and under conditions of constant rotation 14 p1715 A73-30022

Motor unit reactions of man to spinal and supraspinal inhibitory stimuli 19 p2395 A73-37943

Russian book - Electrical activity of the human brain in the process of motor action. 21 p2640 A73-41289

Spinal and spino-bulbo-spinal neuron mechanisms of somatic and visceromotor reflex transfer in the thoracic spinal cord 24 p3061 A73-45249

EFFICIENCY

NT COMBUSTION EFFICIENCY

NT COMPRESSOR EFFICIENCY

NT ENERGY CONVERSION EFFICIENCY

NT NOZZLE EFFICIENCY

NT POWER EFFICIENCY

NT PROPELLER EFFICIENCY

NT PROPULSION EFFICIENCY

NT THERMODYNAMIC EFFICIENCY

NT TRANSMISSION EFFICIENCY

Re-calculation of efficiency factors for radiation pressure. 02 p0225 A73-12804

Low energetic efficiency of semiconductor microwave scanning converters for radio images of fog obscured objects 05 p0556 A73-16072

A technique to retain the hologram reconstruction efficiency in elimination of the intense reference beam by the method of pre- or postexposure. 15 p1874 A73-31137

EFFUSIVES

NT LAVA

EGGS

Circaseptan /7-day/ oviposition rhythm and growth of Spring Tail, *Folsomia candida* /Collembola: Isotomidae/. 15 p1836 A73-32185

- AgCl detectors in the Biostack II experiment aboard Apollo 17. 18 p2314 A73-35986
- Preliminary results of the action of cosmic heavy ions on development of eggs of *Artemia salina*. 18 p2271 A73-36129
- EIGENFUNCTIONS**
U EIGENVECTORS
EIGENSTATES
U EIGENVECTORS
EIGENVALUES
- Asymptotic properties of eigenvalues in the Sturm-Liouville problem of a class of equations with random coefficients 01 p0070 A73-10099
- Taylor vortices nonoscillation theory for outward decrease of circulation square, investigating system eigenvalues [AD-754480] 01 p0033 A73-10779
- Dynamical edge effect in rods - Formulation of shortened problems 01 p0118 A73-11405
- Conical solutions for diffraction of plane pulse wave by three dimensional trihedron corner via boundary conditions reduction to eigenvalue problem, presenting sonic boom example 01 p0019 A73-11424
- Uniqueness of a solution to an inverse problem in the case of a second order equation with continuous boundary conditions: Regularized sums of a portion of eigenvalues - Factorization of the characteristic determinant 01 p0071 A73-11440
- A selfadjoint formulation of overdamped systems. 02 p0193 A73-12090
- Vibration of a square plate symmetrically supported at four points. 02 p0237 A73-12605
- Difference approximations for boundary and eigenvalue problems for ordinary differential equations. 02 p0188 A73-12613
- Asymptotic estimates for solutions of linear systems of ordinary differential equations having multiple characteristic roots. 02 p0188 A73-12625
- A variational principle for wave propagation in random media. 02 p0194 A73-12732
- The influence of axial load on eigenfrequencies of a vibrating lateral restraint cantilever. 03 p0384 A73-13115
- Hilbert space and calculus of variations for eigenvalue bounds of integral equations of elasticity and potential theories 03 p0387 A73-13162
- Bounds for eigenvalues in some vibration and stability problems. 03 p0390 A73-13341
- Eigenproblems condensation techniques consisting of combined finite element, Rayleigh-Ritz and power methods 03 p0337 A73-14190
- Dynamic structural analysis large eigenvalue problems, presenting subspace iteration algorithm for arbitrary system size and bandwidth 04 p0509 A73-14944
- Eigenvalues and eigenfunctions of electric and magnetic waves of shielded strip transmission line, calculating electromagnetic field in cylindrical waveguide 04 p0417 A73-15089
- Numerical determination of the sound field and the characteristic frequencies in a circular enclosure by the discretization method 04 p0476 A73-15375
- Proof of the eigenvalues 0 and -1 in the spectra of integral operators of two-dimensional elasticity theory 04 p0514 A73-15677
- Heat transfer in fully developed laminar flow between flat parallel boundary walls, deriving approximations to higher eigenvalues 05 p0563 A73-16101
- Eigenvalues of normal waves in a plane waveguide channel 05 p0549 A73-16385
- Roots of the circular cylindrical shell characteristic equation. 05 p0632 A73-16499
- Rotating shafts dynamic stability, analyzing eigenvalue problem derived via energy equations based on virtual work principle 06 p0697 A73-17517
- Comparison of eigenvalues and characteristic vibration modes of circular ring bars, circular ring disks, and circular ring fibers 06 p0758 A73-17584
- Comparison of the characteristic values and characteristic vibration forms of a circular ring beam, a circular ring disk, and a circular ring fiber. II 06 p0759 A73-17586
- Computational variants of the Lanczos method for the eigenproblem. 06 p0716 A73-17984
- Eigenvalues of a class of spherical wave functions. 06 p0665 A73-18177

- Power series method for accurate solution of eigenvalue problems and simultaneous equations representing static, dynamic and stability responses to structural design parameter changes 07 p0906 A73-19027
- Free vibration analysis of spinning structural systems. 07 p0907 A73-19032
- Kron algorithm for complex eigenvalue problems of damped vibrating mechanical systems, using Newton method 07 p0909 A73-19098
- Acceleration of the convergence in Nesbet's algorithm for eigenvalues and eigenvectors of large matrices. 07 p0844 A73-19271
- Stochastic linear system observer eigenvalue optimal placement with respect to quadratic error criterion for adaptation to digital computation and applicability to higher order system 07 p0849 A73-19966
- Thin elastic plate stability characteristic values control through elemental boundary forces variation, applying von Karman nonlinear differential equations system eigenvalue problem 07 p0915 A73-20289
- Stiffness matrix formulation and eigenvalue analysis for high order shallow shell finite element of rectangular plan 07 p0916 A73-20439
- A proposal for the calculation of characteristic functions for certain differential and integral operators via initial-value methods. 07 p0845 A73-20490
- Synthesis of two discrete vibratory systems using eigenvalue modification. 08 p1015 A73-20726
- Derivatives of eigenvalues and eigenvectors in non-self-adjoint systems. 08 p0983 A73-20728
- Use of matrix eigenvalues in the synthesis of symmetrical two terminal pair networks 08 p0947 A73-21397
- Simple iterative method for determining the eigenvalues of a Hermitian /real-symmetrical/ pair of matrices 09 p1111 A73-22107
- Characteristic indices of vanishing solutions to a gyro system with partial dissipation 09 p1081 A73-22352
- Matrix eigenvalue search algorithms of Rutishauser-Francis type, showing relationship to linear group decompositions 10 p1243 A73-24124
- Nonlinear singular multipoint boundary value problems. 10 p1243 A73-24161
- A finite element method for non-self-adjoint problems. 10 p1243 A73-24292
- Determination of eigenvalues in a class of waveguides of doubly connected cross section. 10 p1249 A73-24392
- Tube waveguide for optical transmission. 10 p1196 A73-24624
- Eigenvalue problem and stiffness optimization procedure for incremental flutter analysis, describing method use in computer graphics mode [AIAA PAPER 73-392] 11 p1439 A73-25521
- An automated procedure for computing flutter eigenvalues. [AIAA PAPER 73-393] 11 p1440 A73-25522
- Influence of a small bending stiffness on the lateral vibrations of a clamped rectangular membrane [DFVLR-SONDDR-226] 11 p1445 A73-26425
- Asymptotic behavior of the eigenvalues of self-conjugate expansions of the Schroedinger operator in a multidimensional bounded domain 11 p1391 A73-26463
- Calculation of eigenvalues and eigenvectors of normal matrix couples with the aid of Ritz iteration 11 p1392 A73-26726
- Book - Mathematical problems in wave propagation theory. 12 p1524 A73-27625
- A uniqueness theorem for the solution of the inverse problem of spectral analysis in the case of a differential equation with periodic boundary conditions 12 p1518 A73-27727
- Behavior of eigenfunctions and values in elliptical boundary value problems in a variable region 12 p1518 A73-27728
- Dynamic structural response analysis with eigenvalue problem solution in terms of stiffness and mass matrices, discussing algorithm selection for efficient computation 13 p1691 A73-28081
- A method for obtaining bounds on eigenvalues and eigenfunctions by solving non-homogeneous integral equations. 13 p1647 A73-28192
- Static force and displacement methods as eigenvalue problems. 13 p1694 A73-28246

- Computational efficiency of equilibrium models in eigenvalue analysis. 13 p1694 A73-28248
- On the eigenvalue problem for fluid sloshing in a half-space. 13 p1599 A73-28410
- The numerical treatment of natural eigenvalue problems of the 4th order according to the collocation method with a Lagrange polynomial approach 13 p1695 A73-28411
- The Rayleigh-Faber-Krahn theorem for the characteristic values associated with a class of nonlinear boundary value problems. 13 p1648 A73-28423
- Numerical study of the stochasticity of dynamical systems with more than two degrees of freedom. 13 p1648 A73-28425
- Estimating the eigenvalues of Sturm-Liouville problems by approximating the differential equation. 13 p1649 A73-28606
- Complex resonant frequencies calculation in external diffraction problems for arbitrary shaped bodies, noting Green function poles correspondence to eigenvalue zeros of integral equation 13 p1582 A73-28652
- Alpha-omega dynamo problem of electrically conducting sphere magnetic field, obtaining eigenvalues from variational principle with free decay modes as trial functions 13 p1685 A73-29365
- General treatment of the evaluation of tri-diagonal secular determinants. 13 p1700 A73-29379
- Kron's method - A consequence of the minimization of the primitive Lagrangian in the presence of displacement constraints. 13 p1700 A73-29381
- The employment of special methods of the matrix-eigenvalue theory in the calculation of the resistance to buckling according to Vianello 14 p1805 A73-29740
- Ritz method application to structural eigenvalue problems, considering plate buckling in box beams 14 p1805 A73-29741
- Uniqueness theorems for the Dirichlet boundary value problem in the case of elliptic-parabolic differential equations and lower bounds for the smallest eigenvalue 14 p1767 A73-29765
- Boundary value problem solutions for parallelogram and elliptical thin plates vibration frequencies and mode shapes based on eigenvalues domain dependence and parameter differentiation technique 14 p1810 A73-30408
- Standard algorithms application to modified matrix and least squares eigenvalues, determining quadratic forms and Gauss-Radau and Gauss-Lobatto quadrature rules coefficients 14 p1769 A73-30409
- Numerical solutions by the continuation method. 14 p1769 A73-30454
- The asymptotic behavior of the first real eigenvalue of a second order elliptic operator with a small parameter in the highest derivatives. 14 p1769 A73-30457
- Truncated general equations and a characteristic equation of a self-excited transistor oscillator 14 p1736 A73-30562
- Expansion of nonconjugate differential Dirac operators into a series of eigenvalues over the whole axis, and an analytical expression for a spectral matrix-function 14 p1771 A73-30787
- Eigenvalues asymptotic behavior in boundary value problems of infinitely expanding region of Euclidean space, applying results to continuous media stability investigation 15 p1860 A73-30964
- Boundary value problems for a first-order differential equation with operator coefficients and for the expansion of this equation in a series of its eigenvalues 15 p1899 A73-31216
- On the propagation of disturbances in a laminar boundary layer. I, II. 15 p1863 A73-31725
- Locally modified and unmodified structures eigenvalues and eigenvectors solutions, considering computational accuracy improvement and application to dynamic stiffness matrix equation 15 p1951 A73-32035
- Lower bounds to the frequencies of continuous elastic systems. 15 p1954 A73-32125
- Spectral resolution of differential operators associated with symmetric hyperbolic systems. 15 p1901 A73-32373
- Estimates of the eigenvalues of a difference problem for a plate 16 p2074 A73-32690
- The iterative solution of two-point linear differential eigenvalue problems. 16 p2031 A73-32930

Elastic viscously damped ten degree of freedom system with two torsion-elastically mutually pivotally joined rotors, determining eigenfrequencies by equations of motion numerical evaluation

16 p1968 A73-33235

Repetitively switched circuit analysis via matrix formalism and eigenvalue techniques with application to dc-dc converter

16 p1992 A73-33409

Monotonically convergent approximate solutions for finite element eigenvalues in structural vibration and stability problems, assessing accuracies

16 p2083 A73-33949

On the distribution of the eigenvalues and the order of the eigenfunctions of a fourth-order singular boundary value problem.

17 p2201 A73-34823

Instability analysis using the incremental stiffness matrices.

17 p2245 A73-34838

Unconditional stability in numerical time integration methods.

[ASME PAPER 73-APM-1]

17 p2201 A73-35027

Helicopter engineering applications of antiresonance theory, showing eigenvalue nature and matrix iteration determination of antiresonances [AHS PREPRINT 736]

17 p2105 A73-35072

Book - Variational analysis: Critical extremals and sursum extensions.

17 p2203 A73-35598

Mass condensation and simultaneous iteration for vibration problems.

17 p2252 A73-35605

Derivatives of eigensolutions for a general matrix.

18 p2330 A73-36318

Global stability and the restricted 3-body problem.

18 p2352 A73-36417

An iterative solution to the second order eigenvalue equation with periodic boundary conditions.

18 p2330 A73-36609

Variability of eigenvectors and eigenvalues of correlation matrices for vertical temperature profiles.

18 p2334 A73-37062

Generalized Galerkin method for approximate solution of eigenvalue self-adjoint boundary value problems in stability analysis of mechanical distributed parameter systems

19 p2458 A73-37189

A new approach to the 'inverse problem of optimal control theory' by use of a generalized performance index [GPI].

19 p2414 A73-38063

Eigenproblem solution by a combined Sturm sequence and inverse iteration technique.

19 p2408 A73-38188

Use of the eigenvalues of a matrix to synthesize symmetrical four-terminal networks.

19 p2415 A73-38355

Detuned single mode laser detailed balance and line width factor in threshold region expressed by Fokker-Planck equation and nonhermitian eigenvalue

20 p2571 A73-38622

An initial value method for the eigenvalue problem for systems of ordinary differential equations.

20 p2581 A73-38970

Book - An analysis of the finite element method.

20 p2581 A73-39139

Solution of a multipoint problem about the eigenvalues and eigenfunctions of an ordinary linear differential operator using a decomposition technique

20 p2582 A73-39251

Sylvester matrix equation analysis of rigidly connected beam gridworks with weak regularity and translational properties, considering iterative and eigenvalue-eigenvector solutions

20 p2621 A73-39534

On an eigenvalue problem in the kinematic approach to dynamo theories of cosmic magnetism.

20 p2609 A73-39571

Laser transient behavior analysis by quantum theory, obtaining density matrix equation solution in terms of exponentially decaying eigenmodes by truncation method

21 p2711 A73-40214

Nonlinear eigenvalue problem of square matrix of analytic functions of complex number lambda, comparing algorithms convergence by numerical tests

21 p2725 A73-40380

Branching solutions for superperson interacting boundary layers.

21 p2632 A73-40440

Pairs of positive solutions of nonlinear elliptic partial differential equations.

21 p2726 A73-40695

On the evaluation of the principal value integral in the scattering problems.

21 p2728 A73-41475

Transient heat conduction in laminated composites. [ASME PAPER 73-HT-R]

22 p2930 A73-42286

Corrugated conical horn antenna feed design, discussing Newton-Raphson iterative solution and computer program for spherical hybrid mode eigenvalues

22 p2832 A73-42296

Finite difference scheme for wave equation solution for wave propagation in layered composite materials, obtaining matrix eigenvalues with Floquet condition for various methods

[ASME PAPER 73-APMW-40]

22 p2926 A73-42897

Mathieu function eigenvalue computation based on Algol program, using Fourier series, Bessel functions, wave equations and elliptic domains

23 p2998 A73-43209

Numerical study of the unstable modes of a hyperbolic-tangent barotropic shear flow.

23 p3002 A73-43591

The eigenvalue solution of asymmetric-ridge waveguides using the mode-matching method.

23 p2955 A73-44146

Convergence of the Bazley-Fox method in the problem of eigenvalues of a bilinear form relative to another bilinear form

24 p3109 A73-44649

Stability of a potential vortex with a non-rotating and rigid-body rotating top-hat jet core.

24 p3055 A73-45309

Convergence rate of two-real-parameter iterative solution of linear equations system based on matrix eigenvalues relationship

24 p3106 A73-45442

EIGENVECTORS

Determination of the dynamic characteristics of a fluid in a moving vessel in the presence of a weak gravitational field by the eigenfunction expansion method

01 p0030 A73-10095

Dynamic edge effect in rods - Formulation of shortened problems

01 p0118 A73-11405

Stationary functionals for introducing eigenfunctions in diffraction theory of electrodynamic systems

03 p0337 A73-14080

Eigenvalues and eigenfunctions of electric and magnetic waves of shielded strip transmission line, calculating electromagnetic field in cylindrical waveguide

04 p0417 A73-15089

Eigenfunction expansions and scattering theory for perturbed elliptic partial differential equations.

06 p0719 A73-18698

On the relation between solar wind structure and solar wind rotational and tangential discontinuities.

07 p0869 A73-19231

Acceleration of the convergence in Nesbet's algorithm for eigenvalues and eigenvectors of large matrices.

07 p0844 A73-19271

A proposal for the calculation of characteristic functions for certain differential and integral operators via initial-value methods.

07 p0845 A73-20490

Derivatives of eigenvalues and eigenvectors in non-self-adjoint systems.

08 p0983 A73-20728

Optimized design - Characteristic vibration shapes and resonators.

08 p1017 A73-21191

Simple iterative method for determining the eigenvalues of a Hermitian /real-symmetrical/ pair of matrices

09 p1111 A73-22107

S matrix method featuring eigenenergy and eigenfunction trials number reduction for rapid numerical determination of bound states of partial-wave-projected Schroedinger equation

10 p1248 A73-23669

A case of application of the variational method in the theory of the eigenfunctions of nonlinear equations

11 p1391 A73-26076

Calculation of functionals of the eigenfunctions in the boundary value problem of a system of linear ordinary differential equations

11 p1391 A73-26331

Eigenfunction analysis for bending of clamped rectangular, orthotropic plates.

11 p1447 A73-26653

Calculation of eigenvalues and eigenvectors of normal matrix couples with the aid of Ritz iteration

11 p1392 A73-26726

Arched and spherical antenna arrays synthesis for given vectorial radiation patterns by numerical solution via algorithm using eigenfunctions

12 p1479 A73-27229

A uniqueness theorem for the solution of the inverse problem of spectral analysis in the case of a differential equation with periodic boundary conditions

12 p1518 A73-27727

Behavior of eigenfunctions and values in elliptical boundary value problems in a variable region

12 p1518 A73-27728

A method for obtaining bounds on eigenvalues and eigenfunctions by solving non-homogeneous integral equations.

13 p1647 A73-28192

Static force and displacement methods as eigenvalue problems.

13 p1694 A73-28246

Truncated general equations and a characteristic equation of a self-excited transistor oscillator

14 p1736 A73-30562

On the propagation of disturbances in a laminar boundary layer. I, II.

15 p1863 A73-31725

Locally modified and unmodified structures eigenvalues and eigenvectors solutions, considering computational accuracy improvement and application to dynamic stiffness matrix equation

15 p1951 A73-32035

Existence and uniqueness of positive eigenfunctions for a class of quasilinear elliptic boundary value problems of sublinear type.

15 p1900 A73-32181

On the distribution of the eigenvalues and the order of the eigenfunctions of a fourth-order singular boundary value problem.

17 p2201 A73-34823

An iterative solution to the second order eigenvalue equation with periodic boundary conditions.

18 p2330 A73-36609

Variability of eigenvectors and eigenvalues of correlation matrices for vertical temperature profiles.

18 p2334 A73-37062

Waveguide transitions especially for excitation of the H sub 11 mode in a circular waveguide

19 p2404 A73-37722

An initial value method for the eigenvalue problem for systems of ordinary differential equations.

20 p2581 A73-38970

Solution of a multipoint problem about the eigenvalues and eigenfunctions of an ordinary linear differential operator using a decomposition technique

20 p2582 A73-39251

Sylvester matrix equation analysis of rigidly connected beam gridworks with weak regularity and translational properties, considering iterative and eigenvalue-eigenvector solutions

20 p2621 A73-39534

Eigenstate localization parameter calculation for wave functions in one dimensional disordered potential chain, considering extension to coupled oscillators and electromagnetic waves in stratified media

21 p2750 A73-40227

Eigenvectors of the sensitivity variations across the human central fovea.

22 p2810 A73-42957

Eigenfunction calculation of injected carrier density in doped semiconductor filaments, relating negative eigenvalues to Suhl effect and lifetime dependence to bulk and surface recombination

23 p3016 A73-43674

Singular eigenfunction solution of the monoenergetic neutron transport equation for finite radially reflected critical cylinders.

24 p3109 A73-44700

Computational methods for studying acoustic propagation in nonuniform waveguides.

24 p3078 A73-44839

Eigenfunction expansions for randomly excited non-linear systems.

24 p3151 A73-45265

EIKONAL EQUATION

Conservation of quasiparticles in weakly turbulent plasmas.

06 p0076 A73-18273

Eikonal properties for real rays chromatic aberration formulas in terms of path length, image space and lens parameters

13 p1660 A73-28768

EINSTEIN EQUATIONS

On the integration of Einstein's equation for energy density inside a perfect fluid sphere.

01 p0076 A73-10250

A finite expanding universe with matter injection.

03 p0342 A73-13291

Design of a space probe for the experimental investigation of Einstein's theory of gravitation

03 p0381 A73-13296

Some consequences of the Mach-Einstein doctrine for celestial mechanics and geophysics

04 p0498 A73-15280

Nonzero radiation pressure inclusion into Einstein cosmological equations, discussing Friedmann models evolution from radiation state epoch to matter domination

05 p0624 A73-17304

Influence of scalar and vector fields on the nature of a cosmological singularity

06 p0751 A73-18101

Time /T-field/ solutions to Einstein equations of test particles and light rays in nonstatic spherically symmetric gravitational field

06 p0724 A73-18646

Time evolution of rotating incoherent matter with vanishing internal pressure by Einstein field equations

09 p1151 A73-23342

Gravitational waves - A progress report.

10 p1280 A73-24324

Model universe generalization to minisuperspace with Einstein equation solution and nondiagonal metric replacing wave equation, considering commutation relations for quantization in curved space

11 p1397 A73-25309

- Construction of a general cosmological solution of the Einstein equation with a time singularity.
11 p1425 A73-26178
- Observational constraints imposed by Brans-Dicke cosmologies.
11 p1426 A73-26413
- Stellar structure deviation from neutron star models, deriving equations for relativistic models with deviation from Einstein principle of equivalence
13 p1686 A73-29655
- Mach principle incorporation into general relativity, discussing application as selection rule in Einstein field equations solution and other gravitation theories
14 p1798 A73-30238
- Einstein equations reduction to friction systems in homogeneous cosmological models, investigating Bianchi models solutions isotropization
14 p1798 A73-30327
- First derivative discontinuities of space-time metric tensor in Einstein equations solution for nonisotropic and isotropic hypersurfaces, proving coordinate system existence for continuity
14 p1774 A73-30328
- Dyadic formalism in two dimensional distributions in general relativity theory, discussing gravitational, diffusive, wave, Einstein and preservation equations
14 p1776 A73-30942
- Kinematic invariants and their relation to chromometric invariants in Einstein's theory of gravitation
15 p1913 A73-31246
- Evaluation of the directivity of gravitational wave radiators.
15 p1914 A73-31944
- Electromagnetic emission in the general relativity theory. I
16 p1984 A73-34006
- Isotropic solution of Einstein gravitational equations for anisotropic homogeneous cosmological models with hydrodynamic energy-momentum tensor
16 p2071 A73-34051
- Characteristics of the Bianchi-IX cosmological model from the viewpoint of the qualitative theory of differential equations
16 p2071 A73-34052
- Einstein-Maxwell fields in conformal space, studying field equations, reducible electromagnetic field in space-time and constraints on metric tensor by Rainich conditions
17 p2212 A73-35560
- Superposition of Schwarzschild solutions and metric of a gravitational dipole
17 p2212 A73-35561
- Nonconformally plane relativistic recurrent-curvature spaces
17 p2212 A73-35567
- Book - Gravitational waves in Einstein's theory.
19 p2461 A73-38366
- The gravitational influence of a beam of light. I.
22 p2886 A73-42320
- Gravitational energy quantization model of noncharged particle based on proposed centrosymmetric metric with nonzero Einstein matter tensor and without Schwarzschild singularity
22 p2887 A73-42430
- Centrosymmetric metric generator of field models of particles, discussing Einstein tensor components representation
22 p2887 A73-42431
- Matter representation in general theory of relativity in terms of sourceless metric tensor and Einstein matter tensor, examining Mach principle status
22 p2887 A73-42435
- Effect of scalar and vector fields on the nature of the cosmological singularity.
24 p3132 A73-44493
- On a possible repulsive interaction in universal gravitation.
24 p3110 A73-45038
- ### EJECTION
- #### NT STELLAR MASS EJECTION
- Sea survival after ejection and parachute descent, describing hand operated canopy connector release to free pilot from entanglement or dragging
16 p1974 A73-32665
- ### EJECTION INJURIES
- Injuries induced by high speed ejection - An analysis of USAF noncombat operational experience.
16 p1966 A73-32664
- A method of determining spinal alignment and level of vertebral fracture during static evaluation of ejection seats.
16 p1967 A73-32676
- Surveillance of the vertebral column in pilots who have undergone an ejection
18 p2284 A73-36914
- ### EJECTION SEATS
- The 600 knot Yankee escape system.
05 p0534 A73-16200
- F/RP-101 ejection seat upgrade kit for performance improvement, discussing propulsion, trajectory control, snubber system and rapid recovery parachute opening
16 p1966 A73-32667
- UPSTARS - A single escape subsystem providing stabilization, retardation, and separation.
16 p1966 A73-32668
- ESCAPAC IE stabilized ejection seat for Navy S-3A and Air Force A-9A aircraft, describing propulsion, stabilization, separation and lateral divergence subsystems
16 p1966 A73-32669
- Stowable deployable autogyro aircrew vehicle escape rosette /SAVER/ conversion to flight vehicle for advanced escape rescue capability /AERCAB/ from hostile areas
16 p1966 A73-32674
- A method of determining spinal alignment and level of vertebral fracture during static evaluation of ejection seats.
16 p1967 A73-32676
- ### EJECTORS
- Performance and noise generation studies of supersonic air ejectors.
03 p0290 A73-12972
- Recent developments in large area ratio thrust augmentors.
03 p0357 A73-13470
- [AIAA PAPER 72-1174] Experimental investigations concerning pneumatic ejectors, with special reference to the effect of dimensional parameters on performance characteristics.
03 p0297 A73-14503
- Theoretical study of a by-pass convergent-divergent nozzle
05 p0533 A73-17191
- The prediction of the optimum performance of ejectors.
07 p0810 A73-19571
- Viking 75 Mars lander spacecraft mortar system design and environmental requirements, stressing manufacturing and qualification tests and parachute ejection
15 p1827 A73-31444
- [AIAA PAPER 73-458] Mortar design for parachute ejection and deployment into airstream to decelerate spacecraft and aircraft pilot escape modules, estimating hardware weight and reaction load
15 p1827 A73-31445
- [AIAA PAPER 73-459] A simple estimate of the effect of ejector length on thrust augmentation.
15 p1824 A73-31745
- Aerodynamic rig and wind tunnel developments of compound ejector thrust augmentor for V/STOL aircraft with combined Coanda and center injection flows
16 p2048 A73-33519
- [ASME PAPER 73-GT-67] Inlet state limitations and flow characteristics equations for supersonic ejector jet mixing duct
17 p2156 A73-35504
- An evaluation of hypermixing for VSTOL aircraft augmentors.
18 p2267 A73-36208
- [AIAA PAPER 73-654] Rumanian contributions regarding the application of the Coanda effect
19 p2387 A73-38303
- Diaphragm ejector pulse shortener for transforming periodic input signal into sharp pulses by adjusting vent areas of two fluid amplifiers
23 p2942 A73-43408
- The diaphragm-ejector proportional amplifier and its application to fluidic operational circuits.
23 p2943 A73-43409
- Small ejector system for fluidic subtracting network with diaphragm operated Schmitt trigger proportional amplifier and pneumatic signal generator, discussing construction and characteristics
23 p2943 A73-43410
- ### EKMAN LAYER
- #### U BOUNDARY LAYER TRANSITION
- ### ELASTIC ANISOTROPY
- Approximate method for solving boundary value problems in the mathematical theory of elasticity of an anisotropic medium
01 p0113 A73-10098
- Construction of a general solution for an elastic anisotropic shallow shell with arbitrary boundary conditions, and some of its applications
02 p0230 A73-11714
- Shear strains and elastic anisotropy of transversely isotropic cylindrical shell with circular hole under uniform internal pressure, using shallow shell equations
03 p0394 A73-14020
- Cusped wave fronts in anisotropic elastic plates.
07 p0907 A73-19079
- Nonuniformly heated anisotropic rods with variable elastic parameters
07 p0911 A73-19317
- Characteristics of elastic anisotropy and the textural development of sheet titanium
09 p1099 A73-21968
- Calculation of the elastic anisotropy of Ti-6Al-4V alloy sheet from pole figure data.
10 p1234 A73-24431
- Torsion of an axisymmetrical anisotropic body with mixed boundary conditions on the edge surface
13 p1698 A73-29086
- Saint Venant problem for a continuously inhomogeneous anisotropic beam
15 p1953 A73-32103
- The transverse vibration of spinning aeolotropic disk.
16 p2084 A73-34026
- Stress concentration on an ellipsoidal inhomogeneity in an anisotropic elastic medium
17 p2240 A73-34142
- Torsion of an axisymmetrical anisotropic body with mixed boundary conditions on the side surface.
19 p2498 A73-37636
- Ellipsoidal crack and needle in an anisotropic elastic medium
21 p2783 A73-40187
- Nonlinear stress-strain hysteresis equation of cyclic straining for vibrating imperfectly elastic systems, using Masing principle
23 p3047 A73-44276
- Numerical realization of a possible way of determining the tensor of elastic constants in an anisotropic body
24 p3144 A73-44506
- Process anisotropy of randomly reinforced fiberglass plastics
24 p3102 A73-44515
- Load capacity of rings formed by winding of composites reinforced with high-modulus anisotropic fibers
24 p3093 A73-44528
- Mixed boundary value problem solution for stress-strain state of anisotropic elastic cylinder and layer under joint torsion, using Fourier and Hankel transforms
24 p3146 A73-44676
- ### ELASTIC BARS
- The equivalence method and the finite-difference method in linear elasticity
03 p0383 A73-12909
- Determination of Young's modulus and of the Poisson coefficient by a method of resonant bars
04 p0462 A73-15247
- Stability and uniqueness of initially straight elastic rods undergoing three dimensional deformations
04 p0514 A73-15682
- Effect of external-load nonconservativeness on the stability of an idealized elastoplastic rod
05 p0635 A73-17076
- Experimental analysis of the low-temperature strength of notched bars
06 p0705 A73-17779
- Investigation of the stressed state of a rod with a cut under elastoplastic torsion
07 p0911 A73-19308
- Elastic wedge whose apex section is reinforced with a rod of variable cross section
07 p0911 A73-19313
- Nonuniformly heated anisotropic rods with variable elastic parameters
07 p0911 A73-19317
- Approximate solutions to some static and dynamic optimal structural design problems.
07 p0915 A73-20341
- Action of a concentrated force on an elastic ring pressed into a circular hole in an isotropic plate
09 p1165 A73-23357
- A numerical method for the analysis of longitudinal elastic-plastic stress wave propagation.
10 p1290 A73-24297
- Elastic impact against a beam with allowance for internal energy absorption
11 p1433 A73-25032
- Small parameter method, with the parameter proportional to the friction forces, in the case of forced vibrations of complex trusses
11 p1435 A73-25395
- Axially symmetric transient wave propagation in elastic rods with nonuniform section.
11 p1447 A73-26652
- A new method for the study of the phenomenon of dynamic instability of thin-walled bars used in the construction of aeroplanes, ships and bridges.
12 p1551 A73-27063
- Shock wave produced in a solid by means of supersonic thermal sources.
13 p1700 A73-29390
- Integral equations for nondestructive determination of buckling loads for elastic plates and bars.
15 p1948 A73-31634
- Antiplane elasticity boundary value problem solution for isotropic bars under tangential loads, considering twisting and bending
15 p1955 A73-32127
- Stability of a cylindrical shell under dynamic axial load
17 p2244 A73-34739
- Differential equations for the vibrations of twisted rods with allowance for energy dissipation
20 p2619 A73-39372
- Experimental study of the stressed state of an elastic beam undergoing transverse impact
20 p2620 A73-39385
- Problem of an elastic semiinfinite cover plate fastened to a linearly deformable base
20 p2624 A73-39646

- Vibrations of turbojet-engine components containing structural dampers of the type of sandwich rods
23 p3020 A73-43735
- Monofrequent oscillations in mechanical systems governed by second order hyperbolic differential equations with small non-linearities.
23 p3044 A73-44077
- The method of forces for thermoviscoelastic rod systems
24 p3148 A73-44918
- Shock wave propagation in colliding elastic bars under axial end-on impact, deriving closed form solution for curvilinear stress-strain characteristics
24 p3112 A73-45430
- Small transverse vibrations of a flexible rod under the action of a variable axial force
24 p3153 A73-45504

ELASTIC BENDING

- The analysis of nonlinear three dimensional frames.
03 p0391 A73-13684
- Three-dimensional finite-element analysis of laminated composites.
[AD-759453] 03 p0392 A73-13687
- Pure moment loading of axisymmetric finite element models.
09 p1158 A73-22391
- Stability of elastic bending and torsion of uniform cantilevered rotor blades in hover.
[AIAA PAPER 73-405] 11 p1440 A73-25534
- Transversely isotropic /anisotropic/ elastic beam bending and torsion, determining frequency dependent compliances by approximate analytic solution via variational method
11 p1447 A73-26655
- Multiphase composite material models for elastoplastic beam bending under loading and unloading, using stress-strain diagram in tension and compression
13 p1698 A73-29052
- Refined method of determining tangential stresses and testing the strength of cylinders subjected to transverse flexure.
13 p1703 A73-29635
- Oblique bending of a homogeneous orthotropic prismatic beam by a force couple in the quadratic theory of elasticity
14 p1815 A73-30785
- Deflection of a thin, nonlinearly heated, rectangular strip
15 p1946 A73-31142
- Russian book - Plane bending and tension of curvilinear thin-walled beams.
15 p1956 A73-32296
- Thermal stress in and bending of elastic rectangular plates from Kantorovich method combined with iterative techniques
16 p2077 A73-32993
- Multiphase composite material models for elastoplastic beam bending under loading and unloading, using stress-strain diagram in tension and compression
18 p2366 A73-36884
- Nonlinear bending of rectangular orthotropic plates.
19 p2500 A73-38116
- Effects of misalignment on the pre-macroyield region of the uniaxial stress-strain curve.
20 p2576 A73-39030
- Inverse bending problems for two-layer orthotropic shallow shells
20 p2618 A73-39313
- Convergence of simplified hybrid displacement method for plate bending.
22 p2921 A73-42203
- Helical wound composite cylindrical tube under pure bending, determining elastic response from boundary value problem solution
23 p3041 A73-43637
- Convergence of the method of successive approximations in geometrically nonlinear problems
23 p2999 A73-44197
- Three dimensional elasticity solution for layer interaction and shear coupling and deflection effects of laminated anisotropic composite cylinders under bending
24 p3149 A73-45152

ELASTIC BODIES

- Wave motion in an elastic solid due to a nonuniformly moving line load.
01 p0114 A73-10301
- Topologic group theory for stress analysis of non-linearly elastic body under complex load, representing loads set by Lie group
01 p0119 A73-11428
- Determination of the strains and displacements for a rectangular shaped viscoelastic body
02 p0229 A73-11578
- Dynamic calculation of the stretching of a spring with allowance for redistribution of mass along its length
02 p0230 A73-11720
- The equivalence method and the finite-difference method in linear elasticity
03 p0383 A73-12909

Tensor analysis for micropolar elastic body deformation and stresses, solving differential equations of thermoelasticity

- 03 p0386 A73-13153
- The stability theory of elastic bodies and the theory of thermal stresses of piecewise anisotropic bodies
03 p0386 A73-13156
- Singular solutions of the plane distortion problem of micropolar elasticity.
03 p0392 A73-13776
- Fourier transformations and Wiener-Hopf equations for stress intensity factor of crack propagation in linearly elastic homogeneous isotropic strip
04 p0512 A73-15238
- A closed-form solution of the propagation problem of an unloading shock wave in a bilinear elastic body.
04 p0513 A73-15595
- Mean field equations for dynamic response of homogeneous linearly elastic solids, obtaining formulation for ensemble averaged displacement and stress fields of composite
[ASME PAPER 72-WA/APM-28] 04 p0515 A73-15890
- Discretized elastic multipolar bodies equations of motion and conservation laws from variational formulation, considering virtual work, Betti principle and Somigliana formulæ
06 p0761 A73-17892
- On forced vibrations in the linear theory of micropolar elasticity.
06 p0762 A73-17987
- Extension of an interface flaw under the influence of transient waves.
07 p0908 A73-19080
- Methods of reducing continual nonlinear mechanics problems for deformable solids to discrete problems
07 p0910 A73-19303
- Extremal boundary value problems of plasticity theory
07 p0910 A73-19304
- Infinite triangular wedge, with a notch at its bisectrix, under the action of concentrated forces applied to the edges of the notch
07 p0911 A73-19312
- Bielayev's point in poroelastic bodies in contact.
08 p1016 A73-20829
- Longitudinal impact of a rigid body against a clamped rod
09 p1158 A73-22361
- Natural vibrations of laminated orthotropic spheres.
09 p1160 A73-22890
- Influence of Poisson's ratio on the condition of the finite element stiffness matrix.
09 p1160 A73-22892
- An 'orthogonalization' method for determining the dynamic characteristics of an elastic body from static vibration tests
09 p1161 A73-23090
- Stress field singularities due to cracks in isotropic elastic bodies, assuming Hookes law stress-strain relationship in integral equation representations
09 p1162 A73-23182
- Finite element methods for elastic bodies containing cracks.
09 p1162 A73-23186
- Thermoelastic boundary value problem for heat conduction in elastic bodies with linear and three dimensional inserts
10 p1290 A73-24305
- Elastic properties of materials strengthened by short unidirectional fibers
10 p1240 A73-24306
- Polymer chain model with internal rotations for elastic body stress-strain state, internal work, elastic energy and equations of motion
10 p1240 A73-24307
- Two dimensional statics for isotropic elastic body with inhomogeneous mechanical properties, discussing two-step solutions for differential equilibrium equation and boundary value problem
10 p1293 A73-24676
- Stress concentration in an anisotropic plate with an insert in pure bending
11 p1433 A73-25031
- On the role of the adjoint problem in dissipative, nonconservative problems of elastic stability.
11 p1434 A73-25214
- The elastic energy and character of quakes in solid stars and planets.
11 p1420 A73-25894
- Topologic group theory for stress analysis of non-linearly elastic body under complex load, representing loads set by Lie group
11 p1443 A73-26057
- Energy flux into extending crack in elastic solid calculated in terms of stress intensity factor for plane and antiplane strain problems
11 p1444 A73-26281
- Method of initial functions for the plane problem of a linearly orthotropic body in the theory of elasticity
11 p1445 A73-26457
- Variational aspect of the integration of partial differential equations for the oscillations of elastic bodies
12 p1517 A73-27097

Russian book - Design of structural elements with the use of electronic digital computers.

- 12 p1556 A73-27923
- Approximate method for solving dynamic problems in thermoviscoelasticity
13 p1690 A73-27993
- Dynamically possible finite deformations of isotropic, incompressible, elastic-inelastic solids with temperature independent response.
13 p1695 A73-28416
- Elastic unipolar discretized linear bodies, considering motion and constitutive equations, conservation laws, virtual work principle and uniqueness and reciprocity theorems
13 p1659 A73-28559
- A contribution to Hertz's theory of elastic impact.
13 p1696 A73-28748
- Application of Papkovitch-Neuber potentials to a crack problem.
13 p1635 A73-28756
- Crack propagation in an elastic solid subjected to general loading. III - Stress wave loading.
13 p1696 A73-28792
- Elliptic notch interaction with nearby crack in elastic solid under longitudinal shear, obtaining stress intensity factor
13 p1697 A73-28914
- Lamb solution analog for dynamic problem of homogeneous isotropic elastic body with impulsive force applied to semi-infinite plane incision
13 p1698 A73-29088
- Stability and convergence of finite element methods for elastic structures vibration analysis, stressing application to mixed boundary value problems
14 p1807 A73-30185
- Third basic boundary value problem of dynamics for a three-dimensional elastic body
14 p1810 A73-30383
- Optimisation theory of elastic-rigid bodies under repeated variable deformation.
14 p1812 A73-30495
- Book - A course in continuum mechanics. Volume 4 - Elastic and plastic solids and the formation of cracks.
14 p1813 A73-30595
- Dynamic singular boundary value problem of elastic body with propagating crack under concentrated force
14 p1814 A73-30784
- Bending of rectangular plates of variable thickness with edges reinforced by elastic ribs
14 p1815 A73-30796
- Numerical solution to the problem of elastic ring impact at a rigid obstacle
14 p1815 A73-30798
- Solution of three-dimensional contact problems in elasticity theory
14 p1775 A73-30831
- Static problem of elastic body with stresses at boundary, solving incompatible difference equations by explicit iteration methods
15 p1945 A73-31026
- Muskhelishvili elastodynamic theorem concerning natural stress-free state extension to three dimensional theory of inhomogeneous anisotropic elastic bodies
15 p1946 A73-31105
- The effect of couple-stresses on the stress concentration around an elliptic hole.
15 p1947 A73-31335
- Weak solutions existence and uniqueness for boundary value problem in linearized theory for mixtures of two isotropic incompressible elastic solids, obtaining differentiability conditions
15 p1947 A73-31336
- Computerized stress analysis of shock load induced circular elastic membrane interaction with fluid stream via method of characteristics related to aerodynamic decelerator design
[AIAA PAPER 73-443] 15 p1948 A73-31429
- Mass and stiffness matrices reduction in determining linearly elastic structure natural modes and frequencies with computational accuracy improvement
15 p1949 A73-31672
- Infinite elastically isotropic solid under external tensile stress, deriving condition for complete fracture from wedge crack
15 p1951 A73-32023
- Mathematical model of elastic flight body behavior in continuous medium based on combination solutions to aerodynamics, automatic control and elasticity theory problems
15 p1952 A73-32063
- Solution of certain classes of three-dimensional problems in elasticity theory with the aid of analytic functions
15 p1952 A73-32077
- Hadamard theorem on wave propagation existence in elastic body with infinitesimal stability condition proved by linear elliptical partial differential equations systems theory techniques
15 p1914 A73-32120
- Symmetric vector-type tensor functions of elastic bodies related to strain measure invariants, formulating limited hardness principle in terms of Poisson ratio
15 p1954 A73-32123

Application of extended variational principles to finite element analysis.

16 p2077 A73-32982

Ranges of instability of the first and the second kind for vibrational systems with random parameter excitation

16 p2080 A73-33264

Contraction of an elastic layer by girder slabs

17 p2240 A73-34148

A steadily moving longitudinal-shear crack with an infinitely narrow plastic zone

17 p2241 A73-34266

Elastic isotropic infinite body with interior tunneling crack under dynamic shear force perpendicular to crack propagation direction, obtaining solution via Mathieu functions

17 p2241 A73-34329

Elastic equilibrium of an ellipsoid under the action of concentrated loads

17 p2244 A73-34790

Approximate method based on the application of hydrodynamic analogy

17 p2244 A73-34794

A perturbation method for low-frequency fluid-structure interaction problems.

[ASME PAPER 72-APM-WWW] 17 p2248 A73-35102

Method of orthogonal projections for three-dimensional problems of elasticity theory

18 p2362 A73-36401

Lamb solution analog for dynamic problem of homogeneous isotropic elastic body with impulsive force applied to semiinfinite plane incision

19 p2498 A73-37638

Non-linear vibration of beams with time-dependent boundary conditions.

19 p2501 A73-38253

Calculation of bending vibrations in beams with the aid of a discrete model

20 p2615 A73-38982

Elastic bodies nonlinear thermomechanical stability under conditions of loaded equilibrium configuration, using Liapunov type energy-like functionals

20 p2615 A73-39010

Construction of a stress tensor according to Papkovitch-Filonenko-Borodich method

20 p2618 A73-39324

Thermoelasticity of coupled bodies in the case of stress-dependent heat transfer

20 p2618 A73-39327

Stability and postbuckling behavior of hyperelastic bodies at finite strain by the finite element method.

20 p2620 A73-39529

Two-dimensional contact problem for a prestressed elastic body

20 p2625 A73-39652

Mathematical modeling of spinning elastic bodies for modal analysis.

21 p2784 A73-40421

Proof for the existence of a solution to the fundamental quadrantal problem of dynamics for a three-dimensional elastic body, and approximate computation of the solution

22 p2918 A73-41951

The hydrodynamic analogy and its application to a two-dimensional problem in elasticity theory

22 p2921 A73-42282

Thermal stresses due to an internal source of heat in a solid elastic hemisphere with radiating curved surface and the plane base resting on a smooth rigid insulating plane surface.

22 p2932 A73-42469

The elliptical crack subjected to nonuniform shear loading.

[ASME PAPER 73-APMW-42] 22 p2926 A73-42898

Equilibrium of an elastic paraboloid of revolution under a concentrated load applied to its apex

22 p2927 A73-43052

Indentation of the semi-infinite elastic solid by a hot sphere.

22 p2929 A73-43174

Solution of spatial contact problems of the theory of elasticity.

23 p3040 A73-43585

Torsion of a cylindrical shell with a lateral surface containing an elastic circular inclusion

23 p3042 A73-43727

A new approach to optimal design of elastic structures.

23 p3042 A73-43798

A method for solving ill-posed integral equations of the first kind.

23 p2999 A73-43803

The stress pulses propagated as a result of the rapid growth of brittle fracture.

23 p3042 A73-43805

Constitutive equations of elastoplastic and elastoviscoplastic bodies based on thermodynamic state, considering deformation velocity and stress relaxation

23 p3043 A73-43967

Papkovitch-Neiber solution for stress-strain state of initially isotropic mixture of two elastic bodies

23 p3007 A73-44183

Some results of the application of the nondestructive ultrasonic method to the measurement of residual stresses

23 p2996 A73-44289

Numerical realization of a possible way of determining the tensor of elastic constants in an anisotropic body

24 p3144 A73-44506

Thermal stresses in rotationally symmetric semiinfinite elastic body with heat input along hole boundary and on plane bounding surface, reducing to solution of Fredholm equation

24 p3147 A73-44745

An elastoplastic strain-hardening material - Quasistatic evolution of the stress distribution

24 p3147 A73-44748

Displacements and rotations in micropolar elastic body with external loading and permanent distortions

24 p3149 A73-45004

Book - Solid-state mechanics 3.

24 p3153 A73-45495

Liapunov functions application to stability analysis of dynamic systems and elastic bodies, considering eigenfunction method, maximum principle and energy criterion

24 p3153 A73-45497

Longitudinal and transverse shock and acceleration waves propagation and decay in anisotropic and isotropic elastic bodies based on theory of singular surfaces

24 p3153 A73-45498

Solution of a mixed axisymmetric problem for an elastic ellipsoid of revolution by the method of p-analytic functions

24 p3153 A73-45509

ELASTIC BUCKLING

The application of Newton's method to the problem of elastic stability.

[ASME PAPER 72-APM-P] 05 p0632 A73-16531

Finite element analysis of the post-buckling behavior of structures.

[AIAA PAPER 73-255] 05 p0635 A73-16977

A finite element tensor approach to plate buckling and postbuckling.

07 p0907 A73-19028

Lateral vibration and stability relationship of elastically restrained circular plates.

07 p0913 A73-19967

Finite element analysis of buckling and post-buckling behaviors of arches with geometric imperfections.

07 p0914 A73-20211

Effect of major axis curvature on I-beam stability.

07 p0916 A73-20437

Application of the finite element method to the study of the elastic buckling of thin plates of any form

09 p1157 A73-22214

Application of general variational methods with discontinuous fields to bending, buckling, and vibration of beams.

11 p1435 A73-25436

Buckling analysis of elastically constrained conical shells under hydrostatic pressure by the collocation method.

[AIAA PAPER 73-364] 11 p1438 A73-25499

An elastic-plastic buckling solution using the incremental theory.

11 p1443 A73-26089

Advanced elastic postbuckling analysis by a perturbation procedure.

13 p1697 A73-28826

The employment of special methods of the matrix-eigenvalue theory in the calculation of the resistance to buckling according to Vianello

14 p1805 A73-29740

Integral equations for nondestructive determination of buckling loads for elastic plates and bars.

15 p1948 A73-31634

Elastic buckling instability of rotating rods and plates due to compressive stress under critical speed

15 p1955 A73-32161

Thin elastic orthotropic annular plate postbuckling behavior under planar edge compression loads, analyzing axisymmetric deformations via nondimensional equations and Keller-Reiss numerical method

[ASME PAPER 73-APM-5] 17 p2247 A73-35030

Laterally restrained beam columns with uniform biaxial loading.

20 p2616 A73-39117

Finite difference technique for elastic-plastic buckling of edge-loaded rectangular plates, finding bifurcation stresses via Hill and Prandtl-Reuss expressions

20 p2623 A73-39560

ELASTIC COLLISIONS

U ELASTIC SCATTERING

ELASTIC CONSTANTS

U ELASTIC PROPERTIES

ELASTIC CYLINDERS

Incompressible elastic circular cylinders quasi-equilibrated motions analysis, obtaining free and forced oscillations periods

02 p0191 A73-11573

Axial shear vibrations of cylinders made of a micropolar elastic solid.

03 p0393 A73-13781

Dynamic response of a semi-infinite elastic cylinder containing an acoustic medium.

[ASME PAPER 72-WA/APM-3] 04 p0516 A73-15905

Vibrations of circular cylinders of a perfectly conducting elastic material.

05 p0637 A73-17298

Solution of a contact problem for an infinite elastic cylinder with two contact areas by the method of triple integral equations

07 p0910 A73-19307

Forced motion of elastic cylindrical rods - A comparison of two theories.

07 p0915 A73-20284

Asymptotic approximation of an infinitely thin, elastic, nonlinear cylinder by a curvilinear medium

10 p1288 A73-23765

Potential energy method for boundary value problem of axisymmetric elastic contact of solid and hollow cylinders compressed by plane walls

10 p1289 A73-24064

Torsion of a circular-section bar weakened by two longitudinal circular-cylindrical cavities

10 p1293 A73-24702

Torsional stress on micropolar prismatic nonsymmetrically elastic rotating cylindrical shaft with six degrees of freedom evaluated in terms of Saint Venant function

11 p1445 A73-26409

Asymptotic pressure calculation of plane acoustic wave diffraction by infinitely long isotropic solid elastic circular cylinder in viscous liquid medium

13 p1583 A73-28863

Note on the application of the Tresca criterion to the problem of circular bending of an elastoplastic cylinder

14 p1811 A73-30485

Stress concentration determination near a small hole on a plate in three-dimensional representation

14 p1813 A73-30682

Stability of a cylindrical shell under dynamic axial load

17 p2244 A73-34739

Thermal stresses in axially connected circular cylinders.

19 p2495 A73-37435

Some new results for the vibrations of circular cylinders.

19 p2500 A73-38107

Measurement of residual stresses in a cylinder. III - On the effect of eccentricity of holes bored out in Sachs method.

19 p2501 A73-38345

Mixed boundary value problem solution for stress-strain state of anisotropic elastic cylinder and layer under joint torsion, using Fourier and Hankel transforms

24 p3146 A73-44676

ELASTIC DAMPING

Elastic damping properties of binary Mg and Al alloy systems with Cd, Mn, Ni, Si, Zr, Nd and Ca alloying

03 p0324 A73-13515

Acoustic model of HF damping and microstructure of dispersed aluminum oxide ceramics systems, using Hugoniot elastic limits for Young modulus and fracture determination

04 p0468 A73-15373

Effect of additive damping on transfer function characteristics of structures.

[SAE PAPER 720811] 05 p0634 A73-16641

Randomly separated ends scattering effect on linear and nonlinear coherent oscillations of elastic string by perturbation technique

06 p0723 A73-17900

Damping configurations that have a stabilizing influence on nonconservative systems.

07 p0908 A73-19088

Calculation of the deflections of fast-rotating rotors on elastic-damping supports with allowance for unilateral electromagnetic attraction forces

07 p0779 A73-20084

Damping properties of 1Kh13 and 2Kh13 high-chromium steels in a uniform stress-strain state in tension and compression at room and high temperatures

07 p0841 A73-20513

Dynamic behaviour of thin cylindrical shells collided with dampers.

08 p1019 A73-21527

Measurement of the flexural damping capacity and dynamic Young's modulus of metals and reinforced plastics.

08 p0967 A73-21594

A generalization of equations of the outline of a hysteresis loop for the case of an asymmetrical cycle.

09 p1161 A73-23152

Improving reliability and eliminating maintenance with elastomeric dampers for rotor systems.

10 p1175 A73-23950

Beam and plate flexural vibration damping by free or uncompressed rigid viscoelastic coatings applied on sides

10 p1293 A73-24794

Experimental investigation of hydrodynamic stability at rigid and elastic-damping surfaces

11 p1349 A73-26440

- Damping properties of soft viscoelastic materials for certain plane stress combinations 12 p1515 A73-27176
- Application of a variational method to dissipative, non-conservative problems of elastic stability. 13 p1700 A73-29376
- Dynamic mechanical properties of graphite-epoxy and carbon-epoxy composites. 15 p1897 A73-31677
- The damping properties of high-chrome steels 1Kh13 and 2Kh13 in a homogeneous stress state of tension-compression under the conditions of normal and elevated temperatures. 19 p2440 A73-37788
- Transverse oscillations of a beam lying on an elastic base under the action of a perturbation force which has several harmonics with frequencies close to the first natural frequency 20 p2620 A73-39512
- A numerical study of damping in viscoelastic sandwich beams. [ASME PAPER 73-DET-73] 22 p2919 A73-42071
- Improvement of damping capacity of structural members by introduced stress concentration. [ASME PAPER 73-DET-76] 22 p2919 A73-42072
- Damping of mechanical systems with the aid of viscoelastic liquids 24 p3109 A73-44915
- The motion of a body containing a liquid-filled cavity with elastic radial ribs and exhibiting perturbations relative to the longitudinal axis 24 p3112 A73-45513
- ELASTIC DEFORMATION**
- NT ELASTIC BENDING**
- NT ELASTIC BUCKLING**
- Combined heating and irradiation effects on body elastoplastic stress-strain state, deriving thermoradiative plasticity equations 01 p0112 A73-10004
- Shell designs by the theory of small elastoplastic deformations with allowance for the compressibility of material 01 p0112 A73-10005
- Investigation of a deformation process in a heated elastoplastic cylindrical shell 01 p0112 A73-10006
- Singular integral equations analysis of elasticity theory boundary value problem to determine axisymmetric thermoelastic stress-strain state of half space with cylindrical cavity 01 p0112 A73-10012
- Book - Deformations of fibre-reinforced materials. 01 p0113 A73-10148
- Elastic-plastic analysis on the structural elements with different values of stress concentration factor. 01 p0117 A73-11122
- Wave propagation in elastic laminates using a multi-continuum theory. 01 p0117 A73-11364
- The deformations and stresses in floating ice plates. 01 p0118 A73-11366
- Anisotropic beam elastic deformation under end loads, deriving coefficients for linear relation between cross sectional stresses and elastic deformation curvature 02 p0230 A73-11780
- Numerical solution to the problem of the elastoplastic stability of doubly connected plates with curvilinear boundaries 02 p0231 A73-11813
- Elastic deformation of a single-cavity hyperboloid of revolution under given forces at the boundary 02 p0233 A73-11939
- Small disturbance propagation in infinitely extended thermoelastic medium with initial finite homogeneous deformation, determining longitudinal and transverse wave propagation velocities 02 p0234 A73-12018
- Three-dimensional problem of the deformation instability of incompressible layered materials in the case of highly elastic strains 02 p0235 A73-12191
- Study of the effect of small elastoplastic deformations on the load-bearing capacity of specimens with stress concentrators under repeated variable loading. I. 02 p0235 A73-12202
- Study of the effect of small elastoplastic deformations on the load-bearing capacity of specimens with stress concentrators under repeated variable loading. II. 02 p0181 A73-12203
- Elastic deformation of lightweight mirrors. 02 p0236 A73-12375
- Elastic and plastic deformations of circular ring with initial machining produced stresses distributed across thickness, calculating critical load for static stability 02 p0236 A73-12581
- Stress concentration in a plane weakened by two different circular holes in the presence of small elastoplastic strains 02 p0237 A73-12585
- Elastoplastic stressed state of cylindrical shells weakened by a circular hole 02 p0237 A73-12590
- Mercury thermal stress and strain fields of elastic deformation from solar heating variations due to resonance rotation 02 p0223 A73-12721
- Elasto-plastic analysis of three-dimensional structures using the isoparametric element. 03 p0383 A73-12874
- The post-buckled behaviour of a thin-walled box beam in pure bending. 03 p0384 A73-13114
- The calculation of supporting planar-surface structures with the aid of the characteristic functions of correlated simplified basic problems 03 p0386 A73-13154
- Stress field and deformed shapes of liquid filled axisymmetric sessile neo-Hookean membrane during submergence to various depths 03 p0292 A73-13303
- A computational method for optimal structural design. I - Piecewise uniform structures. 03 p0390 A73-13337
- Lagrange equations of motion for ideal incompressible fluid flow under asymmetric deformation of expanding circular cylinders and spheres, calculating resistance forces 03 p0294 A73-13613
- A theoretical and numerical comparison of elastic nonlinear finite element methods. 03 p0392 A73-13689
- Disks with inclined face, investigating effects of joint between hub and disk face on stress-strain state in elastic deformation range 03 p0394 A73-14012
- Reversible instantaneous deformations and internal energy in viscoelastic incompressible fluids, using Oldroyd and De Witt hydrodynamic models 03 p0296 A73-14053
- Large elasto-plastic deflection of a circular plate of mild steel under cyclic loading. 03 p0396 A73-14626
- Calculus of variations for minimum energy method in elasticity theory of incompressible elastic body, calculating elastic deformations 04 p0509 A73-14980
- Theoretical formulation of finite-element methods in linear-elastic analysis of general shells. 04 p0510 A73-15026
- Stability of a transversely isotropic solid under large elastic deformation. 04 p0511 A73-15171
- Inflation-extension and eversion of a tube of incompressible isotropic elastic material. 04 p0512 A73-15234
- Grain boundary interface and crystal structure effect on elastic and plastic deformation and mechanical properties of metals at low and high temperatures 04 p0462 A73-15301
- Stability of thick circular plates subjected to compressive loads and finite strains 04 p0513 A73-15504
- Nonlinear physical stress-strain relation for reticular polymers and fiberglass plastics under conditions of microcreep and elastic aftereffect 04 p0468 A73-15508
- Elastic-plastic deformation in edge-notched tension specimens under plane stress conditions. [ASME PAPER 72-WA/MAT-3] 04 p0514 A73-15809
- An extension of the Grubin theory of elastohydrodynamic lubrication. 05 p0581 A73-16433
- Deformation, displacement, and work bounds for structures in a state of creep and subject to variable loading. [ASME PAPER 72-APM-U] 05 p0632 A73-16529
- A new algorithm for the computation of bending moments and deflections of straight beams. 05 p0637 A73-17325
- Calculation of general surface-supporting structures with the aid of dynamic relaxation 06 p0758 A73-17516
- Surface tractions, heat fluxes and body forces required for deformation of flat perforated thermoelastic circular plate into pierced spherical cap 06 p0759 A73-17757
- Book - On elastic stability under nonconservative loads. 06 p0762 A73-18275
- Extremum principles on time independent elastoplastic solids nonisothermal deformation properties based on yield function dependence on temperature 06 p0763 A73-18456
- Two dimensional indentation of elastic half space by rigid punch under slowly applied normal load for case with finite friction between surfaces 06 p0765 A73-18508
- Uniqueness of non-linear elastic equilibrium for prescribed boundary displacements and sufficiently small strains. 06 p0719 A73-18700
- Application of the finite element method to the solution of elastoplastic problems 06 p0766 A73-18726
- Approximate method of studying the symmetrical deformation of orthotropic bodies 07 p0911 A73-19311
- Deformations and stresses in a hollow sphere with spherical transversal isotropy under impulsive pressure. 07 p0913 A73-20116
- Some results of finite element applications in finite elasticity. 07 p0914 A73-20213
- Self-compensating strain measurement in rotating disks subjected to elastic and plastic deformation 07 p0826 A73-20516
- New method of measuring rapidly varying pressures in the range below 500 atm 07 p0827 A73-20541
- Curved finite elements by the method of initial strains. 08 p1016 A73-20727
- Non-linear bending of beams of variable cross-section. 08 p1016 A73-20831
- Viscoelastic strains in a thick-walled cylinder under the long-term effect of a gravitational load 08 p1017 A73-21371
- Load and support configurations associated with aspherical dioptr of revolution with variable thickness profile generating dioptrics deformed by elasticity 08 p0967 A73-21492
- Effects of thermal loading on foil and sheet composites with constituents of differing thermal expansivities. [ASME PAPER 72-MAT-E] 08 p0979 A73-21572
- Effects of thermal loading on fiber-reinforced composites with constituents of differing thermal expansivities. [ASME PAPER 72-MAT-F] 08 p0979 A73-21573
- Investigation of the deformation of a hollow sphere under an impulsive load on the basis of three-dimensional elasticity theory and shell theory 08 p1019 A73-21761
- Stress-strain state of a piecewise homogeneous plane with thin-walled elastic inclusions of finite length 08 p1019 A73-21765
- Elastic potentials application to second axisymmetric problem solution in micropolar elasticity, considering moments loaded seminifinite elastic body deformation and stress tensor components 09 p1157 A73-22170
- Certain two-dimensional problems with discontinuous displacements in the theory of elasticity and their application to problems of dislocation-surface propagation 09 p1158 A73-22358
- Axisymmetric deformation of an elastic layer containing coaxial circular slots 09 p1158 A73-22359
- Lie operators admitted by Lamé equations in three dimensional dynamic elasticity theory for arbitrary particle velocity and displacement and linear stress-strain tensor relation 09 p1159 A73-22585
- Strain boundary conditions and complex representations of joining conditions in the theory of shells with finite shear rigidity 09 p1159 A73-22588
- Stress distortion coefficient of uniaxial tension /compression/ of elastic isotropic medium with flattened ellipsoidal sensor from sensor stress recording 09 p1159 A73-22590
- Consideration of the hysteresis behavior of a solid medium in a complex stress state under the conditions of simple cyclic loading. 09 p1161 A73-23059
- An evaluation of finite element methods for the computation of elastic stress intensity factors. [ASME PAPER 72-PVP-19] 09 p1163 A73-23267
- Effect of elastic displacements of a cylindrical shell on the vibrations of the free surface of a fluid 09 p1073 A73-23345
- Small perturbation approximations of plane biaxial tensile deformation of semilinear elastic medium with cavity, using Piola-Kirchhoff stress functions 09 p1164 A73-23347
- Deformation of a spherical shell under the action of an unsteady spherical hydroacoustic wave 09 p1165 A73-23354
- Bifurcation of the equilibrium of a randomly inhomogeneous nonlinearly elastic plate 09 p1165 A73-23356
- Elastoplastic deformation and stresses in clamped multilayer cylinders 10 p1287 A73-23593
- Dependence of the coefficient of external friction on a normal load during elastic saturated contact 10 p1222 A73-23596
- Three-dimensional theory of elastic stability in the presence of finite subcritical strains 10 p1290 A73-24302
- Polymer chain model with internal rotations for elastic body stress-strain state, internal work, elastic energy and equations of motion 10 p1240 A73-24307

Stability of transversely isotropic cylindrical shells in nonuniform subcritical states

10 p1290 A73-24311

Circular cylindrical tube lap joints elastic strain relations based on plane contact problem reduction to Prandtl type equation in finite-span wing theory

10 p1225 A73-24363

Cylindrical metal projectile impact induced elastoplastic deformation, determining dynamic yield point by computer simulation of Taylor stress wave propagation model

10 p1292 A73-24529

Boundary conditions model calculations for thermoelastic deformations of continuum body with surface tractions on interface, discussing energy balance laws derivation for loading devices

10 p1292 A73-24659

Elastic deformation of an orthotropic semi-infinite plate with straight boundary asymmetric with respect to the elastic axes of the material under uniform partial loading.

10 p1293 A73-24922

Difference equations of elastic equilibrium for shells with variable characteristics in polar coordinates

11 p1433 A73-25027

Limiting deformability of lengthwise-crosswise wound fiberglass-reinforced plastics under conditionally instantaneous and prolonged biaxial compression

11 p1386 A73-25034

Thin walled elastoplastic cylindrical shells deformations investigation by elliptic quasi-linear equation systems

11 p1433 A73-25044

Experimental investigation of the stability of shells with holes

11 p1434 A73-25390

Experimental verification of the applicability of small elastoplastic deformation theory to the calculation of rotating disks

11 p1434 A73-25392

Linear elastic behavior of laminated plate with ribs reinforced by continuous unidirectional fibers under surface distributed loads orthogonal and parallel to plane

11 p1435 A73-25403

Incremental deformations in orthotropic laminated plates under initial stress.

[ASME PAPER 72-APM-VV] Influence of elastic deformations on the lasing-threshold characteristics of a ruby laser

11 p1376 A73-26141

Saint Venant principle for plane deformation of anisotropic elastic solid extended to analysis of fiber reinforced transversely isotropic composites

11 p1444 A73-26280

Displacement boundary value problem of linearized elastodynamics with superimposed small and large deformations in homogeneous anisotropic elastic solid, proving solution uniqueness theorem

11 p1444 A73-26282

Gradient decomposition and kinematic constitutive equations for elastoplastic material behavior under large strains

11 p1445 A73-26410

Method of initial functions for the plane problem of a linearly orthotropic body in the theory of elasticity

11 p1445 A73-26457

Antiplane deformation near a cut in a hardening elastoplastic material

11 p1445 A73-26458

Asymptotic analysis of the equations of oscillations and stability of bodies of revolution in the case of turning points

11 p1445 A73-26459

Hamilton variational principle for deriving equations of motion for small elastic displacements of thin circular rings, noting twist equation occurrence

11 p1446 A73-26493

Displacement and finite-strain fields in a sphere subjected to large deformations.

11 p1447 A73-26647

Shear stress and deformation inclusion in elastic plate bending finite element theory, discussing stiffness matrix improvement for thin shells

11 p1447 A73-26651

Axially symmetric transient wave propagation in elastic rods with nonuniform section.

11 p1447 A73-26652

Universal solutions for fiber-reinforced incompressible isotropic elastic materials.

11 p1447 A73-26656

Finite static deformations of elastic solids at constant temperature, discussing couples for different deformations

11 p1448 A73-26748

Pseudoelastic design method for bottle-crate stack instability performance prediction through failure by creep buckling, assessing effectiveness by comparison with measurements

12 p1514 A73-26876

Static and dynamic stability of simply supported imperfect beam resting on nonlinear elastic foundation under axial load

12 p1550 A73-27033

Deformation equations of a propeller blade and the orthogonality characteristics of its normal mode shapes of vibration

12 p1458 A73-27085

Investigation of the stress-strain state of spherical shells with an eccentric hole on the basis of the three-dimensional theory of elasticity by the finite element method

12 p1552 A73-27262

Large elastic flexural and elongation strains in a portion of tube prepared from a material with different resistance to tensile and compressive strains

12 p1552 A73-27369

Thin piezoelectric plate bending deformation and polarization theory in terms of piezoelectricity, electrostatics and elasticity equations for anisotropic body

12 p1552 A73-27371

Elastic and viscoelastic zero moment reinforced and weakened shells of composite materials, calculating deformation mode characteristics

12 p1553 A73-27375

Analysis of finite deformations of elastic solids by the finite element method.

13 p1692 A73-28229

Finite element theory of plates and shells including transverse shear strain effects.

13 p1693 A73-28235

On further application of the finite element method to three-dimensional elastic analysis.

13 p1693 A73-28241

Incremental solution of axisymmetric plate and shell finite deformation.

13 p1694 A73-28250

The splitting-up method and its application to elasticity problems.

13 p1694 A73-28254

Dynamically possible finite deformations of isotropic, incompressible, elastic-inelastic solids with temperature independent response.

13 p1695 A73-28416

Elastic and creep limits of heteroplastic micrograin metallic/duralumin materials in terms of stress-strain curve, sliding plane and stress hardening and relaxation

13 p1635 A73-28471

Finite deflection of a shallow spherical membrane.

13 p1697 A73-28815

Strain gage measurements of elastoplastic deformations under biaxial and triaxial stresses with application to cylindrical steel container

13 p1617 A73-28843

Method of recording elastoplastic stress waves in solids with a dielectric sensor

13 p1618 A73-29059

Investigation of the elastoplastic state of a spherical shell with a unreinforced circular hole

13 p1698 A73-29061

Nonlinear axisymmetric subcritical deformation effect on elastic stability of locally loaded thin circular cylindrical shells under free end compressive load

13 p1698 A73-29089

Application of paired integral equations to the problem of the torsion of an elastic space weakened by a conical slot of finite dimensions

13 p1698 A73-29090

Influence of elastic deformations of the gimbal support on the motion of a three-degree-of-freedom astatic gyroscope

13 p1618 A73-29147

Plane strain elastic-plastic state and fracture in cracked blunt notched steel plates under tensile loads

13 p1701 A73-29477

Finite deformation behavior of elastomers - Dependence of strain energy density on degree of crosslinking for SBR.

13 p1646 A73-29527

Stress-strain state of thin circular perforated Cu plate under uniform tensile load, showing applicability of small elastoplastic finite deformation theory

13 p1703 A73-29601

Hysteresis loop equation for calculation of elastoplastic deformations caused by forced vibrations, taking into account medium compressibility and inertial forces

13 p1703 A73-29609

Epoxy-thiocol binder viscoelastic deformation under short and long term loads, noting stress-strain linearity limit

13 p1647 A73-29610

Statistical displacement characteristics of random multiphase composite elastic structures in terms of stochastic Green functions and Neumann series

14 p1811 A73-30482

Some thermodynamic considerations of phenomenological theory of non-isothermal elastoplastic deformations.

14 p1811 A73-30490

Optimal shapes of simply supported vibrating elastic beams for maximum fundamental frequency under axial compressive load

14 p1812 A73-30494

Optimisation theory of elastic-rigid bodies under repeated variable deformation.

14 p1812 A73-30495

Nonlinear toroidal curved elastic sheet inflated by fluid at constant pressure, discussing existence, uniqueness and asymptotic behavior

14 p1812 A73-30520

Asymptotic solutions for shells with general boundary curves.

14 p1812 A73-30523

Initial plastic deformations due to surface defects, deriving corresponding elastic distortions and velocity fields of medium from equilibrium equations

14 p1812 A73-30544

Couple-stress effects near an interior hole of an infinite elastic plane subjected to a concentrated force.

14 p1813 A73-30593

Propagation of elastic Lamb waves in an initially stressed body

15 p1945 A73-31030

Nonlinear differential equation solutions for prismatic body elastic equilibria in terms of deformation and stress tensor relations by small parameter method

15 p1945 A73-31042

Thin flexible inextensible fiber reinforced compressible isotropic elastic materials under large elastic deformations, obtaining solutions to equilibrium and constitutive equations

15 p1946 A73-31101

Fredholm integral equation singularity method solution for calculating stresses and elastic displacements in bodies of revolution of arbitrary shape under torsional loads

15 p1947 A73-31327

Solution uniqueness for elasticity problem with modulus diversity based on deformation potential energy as convex function

15 p1950 A73-31826

Nature of stresses in the internal vicinity of the edge of the joint surface in a compound body loaded under conditions of the plane problem of the theory of elasticity

15 p1950 A73-31827

Elastic deformation of thin walled U-bars lateral stiffeners under torsion, eccentric tension and bending loads, determining vaulting stiffness by finite element method

15 p1950 A73-31906

Two component glass fiber reinforced plastic model describing stress-strain state via elastic properties analysis, internal energy production and Hookes Law application

15 p1952 A73-32085

Mixed boundary value problem solution for strip under elastic deformation due to external loads based on reduction to system of integrodifferential equations

15 p1952 A73-32088

Variational principles of three-dimensional linearized theory of elasticity problems with large initial deformations

15 p1953 A73-32091

Kinetic stress functions and the geometry of space in a deformed continuum

15 p1953 A73-32099

Displacements and elastoplastic deformations at a crack edge under tension

15 p1954 A73-32105

A variational principle for finite deformations of quasi-shallow shells.

15 p1955 A73-32162

Poisson's Ratio and the deflection of a viscoelastic plate.

15 p1956 A73-32342

Some considerations regarding the dynamics problem for an elastic space and the use of its solution

15 p1956 A73-32545

Deformation of a multilayer shell of revolution under nonisothermal loading

16 p2074 A73-32684

Aerodynamic and thermal problems related to wall deformations

16 p2076 A73-32801

On thermodynamics of deformations and variational methods in reversible thermoelasticity.

16 p2077 A73-32977

The analysis of three dimensional problems of elasticity by integral representation of displacement.

16 p2078 A73-33003

Classical and natural conduction and deformation modes concepts for axisymmetric variational problems.

16 p2079 A73-33007

Matrix theory algorithms for static stresses and elastic deformations in truss structures, deriving equilibrium equations in terms of forces, deformations and node displacements

16 p2080 A73-33258

Matrix displacement solution to elastica problems of beams and frames.

16 p2082 A73-33906

Thin shell elastoplastic deformation theory development for small strains, using Hooke's law to analyze hardening, stress and unloading

16 p2084 A73-34033

Shock wave structure in elastoplastic media

17 p2211 A73-34141

- Experimental evidence of a couple-stress effect.
17 p2241 A73-34200
- A unified approach to the solution of plane problems of magneto-elasticity with special reference to a hole in a thin infinite conducting plate.
17 p2211 A73-34346
- Stress analysis of composite materials with strong fibers in weak matrix, obtaining tensile stress boundary layer equations via elasticity theory and perturbation methods
[ASME PAPER 72-APM-TTT] 17 p2249 A73-35110
- On one-dimensional large-displacement finite-strain beam theory.
17 p2252 A73-35828
- On kinematics and statics of finite-strain force and moment stress elasticity.
17 p2252 A73-35829
- Dislocation-type mechanism of the influence of solid surface films on the deformation and fracture of metals
18 p2319 A73-35891
- Elastic-plastic expansion of 6061-T6 aluminum rings.
18 p2362 A73-36320
- Geometrically nonlinear axisymmetric deformation of toroidal shells
18 p2362 A73-36403
- Dirac's distribution in the study of statically indeterminate beams.
18 p2364 A73-36491
- A method of recording elastoplastic stress waves in solids by means of a dielectric pickup.
18 p2317 A73-36891
- Study of elastoplastic state of a spherical shell with round unsupported apertures.
18 p2366 A73-36893
- Axisymmetric deformation of soft spherical shells
18 p2367 A73-37139
- Elastic stresses in rotating orthotropic discs of variable thickness.
19 p2496 A73-37436
- On an anomaly of the theory of beams with directors
19 p2497 A73-37527
- Resonance methods for the dynamic study of deformable structures
19 p2497 A73-37556
- Nonlinear axisymmetric subcritical deformation effect on elastic stability of locally loaded thin circular cylindrical shells under free end compressive load
19 p2498 A73-37639
- Application of dual integral equations to the problem of torsion of an elastic space, weakened by a conical crack of finite dimensions.
19 p2498 A73-37640
- Non-singular control problems. II - Integral equation function-space method applied to the solution of optimization problems in the mechanics of deformable bodies.
19 p2498 A73-37649
- Autocompensatory strain measurement of rotating disks subjected to elastic and plastic deformation.
19 p2430 A73-37792
- Stress field in a sphere subjected to large deformations.
19 p2500 A73-38111
- Postbuckling behavior of circular rings with two or four concentrated loads.
19 p2501 A73-38251
- Constitutive equations for isotropic and anisotropic perfectly plastic materials derived from Clausius-Duhem inequality, considering thermal influences, plastic flow, entropy and elastic deformation
19 p2501 A73-38283
- Metal fatigue studies of nucleation and crack propagation through plastic and elastic regimes
19 p2502 A73-38548
- Group properties of the equations of strain theory of thermoplasticity
20 p2618 A73-39329
- Edge dislocation in an anisotropic material with a surface layer.
20 p2593 A73-39342
- Differential equations of the asymmetrical mathematical theory of elasticity and their solution when Young's modulus varies according to an exponential law
20 p2620 A73-39505
- Liquid jet development under gravity, discussing jet surface elastic film, axisymmetric membrane elastic deformations, liquid drop pressure variations and hydrostatic pressure
20 p2548 A73-39517
- Impact generated elastic strain low amplitude pulses propagating in filamentary composite rods, using Fourier transform technique and viscoelastic relation
20 p2623 A73-39557
- The elastic layer with a cylindrical hole subjected to a nonuniform axisymmetric radial displacement.
20 p2624 A73-39566
- Three-dimensional problem of the stability of fibers in a matrix in the presence of highly elastic strains
20 p2581 A73-39642
- Problem of an elastic semiinfinite cover plate fastened to a linearly deformable base
20 p2624 A73-39646
- Two-dimensional contact problem for a prestressed elastic body
20 p2625 A73-39652
- Study of elastoplastic deformations in a two-layer shell under dynamic loads
20 p2625 A73-39653
- Influence of a mixture of plasticizers, exhibiting a different mechanism of action, on the deformation of cellulose triacetate over a wide range of temperatures
21 p2647 A73-40264
- Nb electrical resistance change under elastic distortion due to lattice distortions and dimensional change
21 p2717 A73-40323
- Changes in the geometrical parameters of a radio-telescope parabolic mirror experiencing radially symmetric deformations
21 p2672 A73-40549
- Russian book on elastic and thermoelastic waves in continuous deformable bodies covering steady and unsteady deformation dynamics, viscoelasticity and nonlinear elasticity using computer methods
21 p2785 A73-40800
- Optimal design of linearly elastic vibrating structural members for minimized total mass and maximized fundamental frequency respectively, noting solution existence dependence on boundary conditions
21 p2785 A73-40840
- Finite plasticity theory in acoustic tensor calculation for elastic, viscoplastic and plastic wave propagation
21 p2740 A73-40947
- Plane strain and generalized plane stress problems for fibre-reinforced materials.
21 p2788 A73-41546
- Thermoelastic dilatational deformation in two perfectly bonded orthotropic half-planes, showing linear relations between elastic and homogeneous field
21 p2789 A73-41674
- Some further results of J-integral analysis and estimates.
22 p2920 A73-42144
- A comparison of the J-integral fracture criterion with the equivalent energy concept.
22 p2920 A73-42145
- J-integral and equivalent energy method parameter relationship from elastic and inelastic stress concentration factors for notches and cracks
22 p2920 A73-42146
- Local deformations arising in the contact between a cylindrical shell and a solid
22 p2921 A73-42281
- Effect of the elastic deformation of a gimbal suspension on the nutation oscillation frequency of a gyroscope
22 p2860 A73-42359
- Estimation of the effect of the internal properties of the material on the characteristics of string sensors
22 p2860 A73-42370
- A coupled thermo-elastic problem of a half-space under the action of a thermal shock on the bounding surface.
22 p2922 A73-42467
- Accelerating the convergence of elastic-plastic stress analysis.
22 p2922 A73-42481
- The cyclic elastoplastic torsion of the circular cylinder in the case of finite deformations
22 p2922 A73-42527
- Large deflection theory for viscoelastic anisotropic thin plates, deriving constitutive, plane stress, plate and nonlinear integrodifferential equations
22 p2923 A73-42638
- Generalized initial yield surfaces for unidirectional composites.
[ASME PAPER 73-APMW-24] 22 p2925 A73-42886
- Response function class for constitutive equations in nonlinear isothermal theory of elastic-plastic metals, discussing free energy and stress response as measure of deformation
[ASME PAPER 73-APMW-30] 22 p2925 A73-42890
- Second order cross stress study of elastic shear deformation, considering rotation invariant Cauchy tensor and Poynting effect
23 p3039 A73-43306
- Deformation and failure of boron-epoxy plate with circular hole.
23 p3040 A73-43631
- Calculation of the deformations of a propeller blade in flight
23 p3041 A73-43724
- Piecewise linear law of the relation between stresses and strains for large deformations
23 p3043 A73-43920
- Certain methods in the physically nonlinear theory of three-layer plates
23 p3043 A73-43921
- Constitutive equations of elastoplastic and elastoviscoplastic bodies based on thermodynamic state, considering deformation velocity and stress relaxation
23 p3043 A73-43967
- Classical viscoplasticity and Mandel plasticity theories comparison with emphasis on strain hardening, acceleration wave propagation and plastic and elastic deformations
23 p3043 A73-43968
- Thermodynamic treatment of plastic media with application to viscoplastic materials, elastoplastic deformation and entropy jump across weak shock waves
23 p3043 A73-43969
- Order of magnitude of the differences between theory and experiment in viscoplasticity under varying stress and temperature
23 p3044 A73-43971
- Plasticity theory algebraic structure with emphasis on plastic flow laws formulation by adjoint functions and elastoplastic media finite deformations
23 p3044 A73-43972
- Study of a dynamic problem in viscoelastoplasticity and ideal plasticity with conditions of friction at the boundary
23 p3044 A73-43973
- Mechanism of ordered dislocation structure formation in metals deformed under high hydrostatic pressure
23 p2993 A73-44043
- Geometry, kinematics and dynamics of dislocations in non-linear continuum mechanics.
23 p3045 A73-44082
- Complex elastoplastic torsion of cylindrical shafts
23 p3045 A73-44184
- Determination of the strained state of a thick elastoplastic plate with an elliptical hole
23 p3046 A73-44201
- The theory of distribution of elastic deformations in two-component composites
24 p3102 A73-44521
- The axisymmetric Dirichlet problem of the static theory of elasticity in displacements for a region bounded by cylindrical and spherical surfaces
24 p3146 A73-44604
- On the description of cyclic deformation processes using a more general elasto-plastic constitutive law.
24 p3147 A73-44683
- Static theory of plane micropolar strain for homogeneous orthotropic elastic solids, deriving existence and uniqueness theorems and reducing boundary value problems to Fredholm equations
24 p3147 A73-44684
- Numerical analysis of pre- and post-critical response of elastic continua at finite strains.
24 p3150 A73-45227
- Elastic deformation of isotropic infinite plane with central circular inhomogeneity and elastokinetics of two bonded dissimilar half planes under uniformly moving body force
24 p3152 A73-45343
- Application of the finite difference method to the elastic stability problem
24 p3152 A73-45357
- An examination of the edge effect in a cantilever beam.
24 p3152 A73-45371
- Reduced equilibrium equations solution for plane deformations of isotropic incompressible elastic media, using stress-strain relations
24 p3153 A73-45549
- Partial solutions of finite elasticity - Axially symmetric deformations.
24 p3154 A73-45550

ELASTIC MEDIA

- Singular integral equations analysis of elasticity theory boundary value problem to determine axisymmetric thermoelastic stress-strain state of half space with cylindrical cavity
01 p0112 A73-10012
- Utilization of polarized ultrasound in stress investigations
02 p0166 A73-11645
- Small disturbance propagation in infinitely extended thermoelastic medium with initial finite homogeneous deformation, determining longitudinal and transverse wave propagation velocities
02 p0234 A73-12018
- Edge dislocation in an infinite anisotropic elastic medium under consideration of the core conditions.
03 p0392 A73-13774
- The fracture mechanics of slit-like cracks in anisotropic elastic media.
03 p0394 A73-13979
- Finite element analysis of finite sized plates bonded to an elastic half space.
04 p0510 A73-15012
- Small vibrations of isotropic elastic medium under finite strain and with time proportional elongations in three mutually perpendicular directions
06 p0759 A73-17759
- The influence of viscosity on the stability of a relative motion of two media.
06 p0685 A73-17761
- The axisymmetric Boussinesq problem in the micropolar theory of elasticity.
06 p0760 A73-17763

Large amplitude waves in bounded media. I - Reflexion and transmission of large amplitude shockless pulses at an interface.

06 p0761 A73-17874

Wave propagation in a micro-isotropic, micro-elastic solid.

06 p0762 A73-17990

Propagation of one-dimensional, plane waves in a physically nonlinearly-elastic medium

06 p0765 A73-18691

Integrodifferential equation for three dimensional contact problem of elastic half space strengthened by elastic stringer, solving by Fourier series

06 p0766 A73-18876

Transient stresses induced by heating a plane boundary.

07 p0907 A73-19077

Integral representations for a nonhomogeneous region in couple stress theory of elasticity.

07 p0909 A73-19105

Two dynamic contact problems for a half-plane with elastic cover pieces

07 p0911 A73-19314

The compressional modulus of a material permeated by a random distribution of circular cracks.

07 p0915 A73-20335

The propagation and growth of acceleration waves in heat-conducting elastic materials.

07 p0917 A73-20441

Effect of diffusion on the growth and decay of acceleration waves in gases.

08 p0955 A73-21189

Steady temperature fields and stresses in a half-space heated by a linear inductive source

08 p1019 A73-21759

Axisymmetric deformation of an elastic layer containing coaxial circular slots

09 p1158 A73-22359

Nonisothermal instability of flows of viscoelastic media

09 p1072 A73-22481

Isotropic homogeneous elastic medium internal crack analysis based on Laurent series expansions of complex potentials consistent with displacements and stress-strain single valuedness

09 p1162 A73-23179

Small perturbation approximations of plane biaxial tensile deformation of semilinear elastic medium with cavity, using Piola-Kirchhoff stress functions

09 p1164 A73-23347

Thermal stresses in an elastic solid weakened by two coplanar circular cracks.

10 p1287 A73-23563

The propagation of waves from a cylindrical cavity.

10 p1289 A73-24282

The three-ring effect in flexible bunches of optical fibers

10 p1228 A73-24585

Stress distribution in a half-plane with a hole strengthened by an elastic insert

11 p1432 A73-25026

Small amplitude surface and plate waves propagation in incompressible biaxially stressed elastic media, obtaining dispersion equation for various phase velocities

11 p1434 A73-25166

Stress-strain state of a thermoelastic spheroidal insert in a thermal viscoelastic medium

11 p1434 A73-25388

Solution of fundamental three-dimensional problems in the theory of elasticity for arbitrarily shaped bodies by way of a numerical realization of the method of integral equations

11 p1441 A73-25627

A source of nonlinear distortions in acoustic emission

11 p1399 A73-26093

Amplification of a travelling wave in a non-homogeneous elastic medium.

11 p1400 A73-26407

Shock wave formation in an elastic half-space during one-dimensional nonlinear transient wave processes generated by a continuous force

11 p1445 A73-26456

Elastic domain similar to half plane with perturbed boundaries, comparing small parameter method accuracy with exact solutions

11 p1446 A73-26467

Universal solutions for fiber-reinforced incompressible isotropic elastic materials.

11 p1447 A73-26656

Two dimensional elasticity theory boundary value problem, for inhomogeneous laminar elastic medium, using Airy stress functions and power series expansion of inhomogeneity parameter

12 p1553 A73-27412

Ray method for solving dynamic problems in viscoelastoplastic media

12 p1553 A73-27415

Boundary value problem solution uniqueness in dynamic linear theory of hereditary-elastic rheologically composite media

12 p1555 A73-27793

Design of an infinite beam with an elastic base in a nonclassical formulation

12 p1555 A73-27796

The elastic dielectric as oriented elastic continuum

13 p1658 A73-28163

Chandler polar motion due to elastic earth free nutation using models based on historical data

13 p1678 A73-28380

Conditions for stability of incompressible elastic material obtained from small-amplitude plane sinusoidal waves superposed on finitely deformed state of material

13 p1696 A73-28753

Application of paired integral equations to the problem of the torsion of an elastic space weakened by a conical slot of finite dimensions

13 p1698 A73-29090

Mathematical theory of elasticity for stress concentration in homogeneous isotropic perfectly elastic composites with spherical inclusions, noting grain boundary stresses

13 p1702 A73-29535

On the concepts of viscous fluids, of elastic solids, and of heat conduction in relativity

13 p1661 A73-29555

Static electromagnetic field structure in elastic homogeneous medium for sources distributed by simple and double layers in terms of scalar and vector potentials

14 p1774 A73-30030

Spherical concentric shock wave excitation in elastic medium by hypersonic thermal wave in terms of displacements, particle velocity and stresses

14 p1817 A73-30252

Thermal stress in an anisotropic elastic half-space.

14 p1810 A73-30407

Stress distribution due to a Griffith crack at the interface of an elastic half plane and a rigid foundation.

14 p1815 A73-30917

Thin flexible inextensible fiber reinforced compressible isotropic elastic materials under large elastic deformations, obtaining solutions to equilibrium and constitutive equations

15 p1946 A73-31101

The ultrasonic pulse-echo technique as applied to adhesion testing.

15 p1882 A73-31673

Integrodifferential equation for three dimensional contact problem of elastic half space strengthened by elastic stringer, using Fourier series

15 p1956 A73-32401

Some considerations regarding the dynamics problem for an elastic space and the use of its solution

15 p1956 A73-32545

Vector field representation of curved elastic membranes oscillatory motions, particularizing equations of motion for small displacements from equilibrium configurations

16 p2076 A73-32937

Variational methods applied to nonconservative stability problems of elastic continua.

16 p2078 A73-32995

Relativistic elasticity theory for solids based on Cattaneo definitions for Riemann metric, considering hyper- and hypoelastic media

16 p2036 A73-33108

Discrete /microscopic, atomic/, continuous /macroscopic, phenomenological/ and quasi-continuous models of elastic solids, exemplifying elastic crystals linear model

16 p2037 A73-33230

Principle of virtual work and Piola theorem for motion and constitutive equations and boundary conditions of oriented elastic media, using point continuum mechanics assumptions

16 p2080 A73-33245

Circular elastic membrane stability against wrinkling under radial peripheral tension and transverse pressure loading, considering solutions via Foepl-Hencky theory

16 p2080 A73-33246

Propagation of thermoelastic waves in an undefined isotropic soil

16 p2081 A73-33369

Acceleration waves in simple elastic materials.

16 p2081 A73-33746

The mixed boundary value problem for the elastic half space.

16 p2081 A73-33901

The dynamic field of a growing plane elliptical shear crack.

16 p2082 A73-33907

Steady state diffraction of stress waves by semi-infinite running crack in elastic solid under dynamic loading, obtaining solution based on Wiener Hopf technique

16 p2082 A73-33910

Solution of the plane problem in elasticity theory for an incompressible material by the fractional step method

17 p2211 A73-34299

Solving some contact problems by electrical modeling

17 p2244 A73-34795

Propagation of stress gradient through an inclusion.

I. [ASME PAPER 73-APM-15] 17 p2247 A73-35038

Propagation of stress gradient through an inclusion.

II. [ASME PAPER 73-APM-16] 17 p2247 A73-35039

Stresses in an anisotropic half-space.

18 p2362 A73-36319

Application of dual integral equations to the problem of torsion of an elastic space, weakened by a conical crack of finite dimensions.

19 p2498 A73-37640

Numerical solutions of basic three-dimensional elasticity theory problems for bodies of arbitrary shape.

19 p2500 A73-38149

Linear dispersive shear waves in two-layer elastic medium.

19 p2461 A73-38185

Application of the method of normal waves to the study of the oscillations of a cylindrical shell in contact with an elastic medium

20 p2615 A73-38984

Symmetrical three-layer shells with a light-weight elastic filler

20 p2618 A73-39328

Some three-dimensional boundary value problems for an elastic medium bounded by cylindrical surfaces

20 p2620 A73-39508

Isotropic elastic material fracture and yield criteria in terms of frame-indifferent relation between stress and strain increments

20 p2623 A73-39563

Ellipsoidal crack and needle in an anisotropic elastic medium

21 p2783 A73-40187

Wave equation solutions for free plane standing wave fields formation in unbounded elastic media

21 p2740 A73-40794

Acceleration waves in ideal fluid mixtures with several temperatures.

22 p2929 A73-41772

Equations of an elastic medium with a large number of absolutely solid inclusions

22 p2921 A73-42278

Wave potentials for an elastic transversely isotropic medium

22 p2921 A73-42285

Effect of a Griffith crack on the distribution of stress in a semi-infinite two-dimensional medium.

22 p2922 A73-42470

Combined radial-axial large amplitude oscillations of hyperelastic cylindrical tubes.

22 p2923 A73-42637

An integral equation approach to the semi-infinite strip problem.

[ASME PAPER 73-APMW-5] 22 p2924 A73-42878

Elastic semispace motion under the action of a shock wave in a magnetic field

23 p3006 A73-43919

The problem of natural oscillations of a thin shell containing an elastoacoustic medium

24 p3152 A73-45359

ELASTIC MODULUS

U MODULUS OF ELASTICITY

ELASTIC PLATES

Stress concentration in disk with radial slot and with outer boundary subject to arbitrary continuous load, using plane elasticity theory

01 p0117 A73-11095

Long-wave approximation in problems of stability loss by impact

01 p0118 A73-11410

Sound generation at an elastic plate acting as an obstruction in a turbulent free jet

[DGLR PAPER 72-085] 02 p0152 A73-11667

Integration of a differential equation describing the bending of a physically nonlinear plate of variable thickness

02 p0231 A73-11811

Study of the oscillations of plates, shells and combined systems by the basis vector method with difference discretization

02 p0232 A73-11817

Generalized dynamic problem of thermoelasticity for an infinite plate with a circular hole

02 p0232 A73-11931

Stability characteristics of thin elastic plate with time varying temperature under transversal magnetic field, calculating buckling probability

02 p0234 A73-12016

Reduction of a three-dimensional quasi-static problem of thermoelasticity for plates to a two-dimensional problem by a symbolic method and by the method of passing to the limit

02 p0235 A73-12194

A numerical method considering the Bauschinger effect for large deflection analysis of elastic-plastic circular plates.

02 p0236 A73-12522

Stress concentration near a circular hole reinforced with a wide ring in the case of a nonlinear law of elasticity

02 p0236 A73-12584

Vibration of a square plate symmetrically supported at four points.

02 p0237 A73-12605

Interference grating production for viscoelasticity investigation by moire method, noting tensile tests of viscoelastic plates

03 p0306 A73-13159

Effect of membrane forces on large deflection of simply supported rectangular plates.

03 p0389 A73-13323

A method for including the effects of transverse shear and rotatory inertia on flexural motion of elastic plates.

04 p0510 A73-15074

Note on the thermal stresses in an elastic semi-circular disc due to an internal source of heat, the curved boundary being exposed to radiation while the straight insulated boundary is in contact with a smooth rigid surface.

04 p0511 A73-15173

Stability of thick circular plates subjected to compressive loads and finite strains

04 p0513 A73-15504

Velocity corrected theory of laminated plates applied to free plate strip vibrations.

04 p0513 A73-15588

Some finite element solutions for plate bending problems by simplified hybrid displacement method.

06 p0758 A73-17444

Stress analysis for homogeneous elastic disk under continuous and concentrated load distribution

06 p0760 A73-17783

The stress intensity factor of an edge crack in a finite elastic disc.

06 p0762 A73-17989

Edge crack in a strip of an elastic solid.

06 p0762 A73-17991

A couple-stresses elastic solution of an infinite tension plate bounded by an elliptical hole.

06 p0717 A73-18173

Tensor-linear approach to the stability problem of nonlinearly elastic isotropic plates

06 p0765 A73-18690

Cusped wave fronts in anisotropic elastic plates.

07 p0907 A73-19079

Homogeneous flat elastic plate theory in Cosserat surface context, considering application of general constitutive equations and extension to right circular cylindrical shells

07 p0908 A73-19085

Conservation of energy in random media, with application to the theory of sound absorption by an inhomogeneous flexible plate.

07 p0851 A73-19153

Notch induced stress concentrations at elastic rectangular core /inclusion/ in extended rectangular plate with rigidly supported edges, using finite element method

07 p0910 A73-19196

Some contact problems for an infinite plate strengthened by elastic cover pieces

07 p0910 A73-19305

Elastic wedge whose apex section is reinforced with a rod of variable cross section

07 p0911 A73-19313

Thermoelastic problem for plate with an elliptic insert in the case of nonideal thermal contact

07 p0911 A73-19316

Thin elastic plate stability characteristic values control through elemental boundary forces variation, applying von Karman nonlinear differential equations system eigenvalue problem

07 p0915 A73-20289

The stress intensity factor of an edge crack in a finite rotating elastic disc.

07 p0918 A73-20566

The stress intensity factors of a radial crack in a point loaded disc.

07 p0918 A73-20567

Postbuckling analysis of rectangular orthotropic plates.

08 p1015 A73-20673

Free vibrations of an infinite strip of variable thickness.

08 p1016 A73-20940

Lateral vibration and stability relationship of elastically restrained skew plates.

08 p1017 A73-20944

Vibration of four point-supported plates by a finite element method.

08 p1017 A73-20945

A problem for a half-plane with a finite vertical cut

08 p1019 A73-21722

On the generalization of stress function procedure for dynamic analysis of plates.

09 p1158 A73-22395

Difference iterative solution for two dimensional boundary value problem for rectangular elastic plate with rectangular cutout

09 p1159 A73-22584

Characteristics of the motion of a system composed of a shell and fluid within the limits of hydraulic approximation

09 p1072 A73-22587

A triangular plate bending element for contact problems.

09 p1160 A73-22899

Propagation of monochromatic waves in an initially stressed infinite micropolar elastic plate.

09 p1160 A73-23024

An elastic ribbon under the action of a nonuniform load

09 p1165 A73-23348

Bifurcation of the equilibrium of a randomly inhomogeneous nonlinearly elastic plate

09 p1165 A73-23356

A yield-surface corner lowers the buckling stress of an elastic-plastic plate under compression.

10 p1289 A73-24100

Allowance for diffraction occurring in the interaction between a weak shock wave and a plate

10 p1206 A73-24488

Shear stresses and displacements of each layer of elastic plate with multiple layers of varying rigidity resting on elastic Winklerian base

11 p1433 A73-25029

Shear stress and deformation inclusion in elastic plate bending finite element theory, discussing stiffness matrix improvement for thin shells

11 p1447 A73-26651

Influence of the shape of inclusions on the initial stage of failure of two-component composite materials

11 p1389 A73-26738

Scattering of a cylindrical wave in an elastic plate in the presence of an absolutely rigid cylindrical inclusion

12 p1551 A73-27240

Bending of a circular nonlinearly-elastic plate by a concentrated force

12 p1555 A73-27794

On moderately large deflection of multiply connected plates.

12 p1557 A73-27933

Vibration of simply supported-clamped skew plates at large amplitudes.

13 p1690 A73-28057

Triangular finite elements for plate bending with constant and linearly varying bending moments.

13 p1692 A73-28230

Finite element matrix formulation of post-buckling stability and imperfection sensitivity.

13 p1694 A73-28253

Postbuckling behavior of orthotropic skew plates.

13 p1697 A73-28813

Couple-stresses effects in vicinity of interface for infinite elastic plane with a rigid inclusion.

13 p1702 A73-29533

Large amplitude vibrations of certain deformable bodies. II Plates and shells.

14 p1806 A73-30041

Effect on the stresses around a crack due to the presence of circular inclusion.

14 p1806 A73-30042

A method of elastic-plastic analysis of largely deformed plate problems.

14 p1808 A73-30194

Stress concentration determination near a small hole on a plate in three-dimensional representation

14 p1813 A73-30682

Two coplanar cracks in an infinitely long elastic strip bonded to semi-infinite elastic planes.

14 p1815 A73-30918

Nonlinear vibrations of rectangular plates.

15 p1944 A73-31000

A new method for the Lebedev-Ufliand integral equation for contact problems of elasticity.

15 p1946 A73-31103

The large deflection and post-buckling behaviour of some laminated plates.

15 p1946 A73-31117

Integral equations for nondestructive determination of buckling loads for elastic plates and bars.

15 p1948 A73-31634

Accuracy of the finite element analysis for the elastic plate with a circular hole.

15 p1951 A73-32036

Self similar dynamic problems for elastic plane and half-plane with/without propagating crack, assuming application of instantaneous perturbation source or uniform stress field

15 p1952 A73-32078

The transition from thin plate to membrane in the case of a plate under uniform tension.

15 p1953 A73-32094

Stress distribution near holes

15 p1953 A73-32097

First fundamental problem of the theory of elasticity for a biplanar system of cuts

15 p1953 A73-32100

Poisson's Ratio and the deflection of a viscoelastic plate.

15 p1956 A73-32342

Forced extensional vibrations of isotropic elastic plates with time dependent body forces, surface tractions and nonhomogeneous boundary conditions, using Kane-Mindlin theory

16 p2076 A73-32920

Thermal stress in and bending of elastic rectangular plates from Kantorovich method combined with iterative techniques

16 p2077 A73-32993

Flexural vibrations of clamped orthotropic plates.

16 p2081 A73-33680

Equilibrium conditions for multilayer anisotropic viscoelastic plates in a complex stressed state

16 p2083 A73-33933

System of arbitrarily oriented cracks in elastic bodies

17 p2240 A73-34144

Stresses in a symmetrically-laminar plate weakened by a central crack

17 p2240 A73-34145

Free vibrations of multilayered composite plates.

17 p2241 A73-34192

Stress distribution near a circular hole on a plane consisting of a stochastically inhomogeneous material

17 p2244 A73-34798

Buckling of rectangular plates with general variation in thickness.

[ASME PAPER 73-APM-10] 17 p2247 A73-35035

Continuum theory for elastic laminates in terms of effective stiffness, deriving displacement and stress interface boundary conditions with illustrative wave propagation examples

[ASME PAPER 72-WA/APM-13] 17 p2249 A73-35112

A necessary condition for the nonoccurrence of von Mises yielding in impulsively loaded plates.

17 p2250 A73-35118

Stress concentration determination under biaxial tension in a plate weakened by a randomly-shaped hole

18 p2363 A73-36414

Contact problem for infinite elastic isotropic plate weakened by rectilinear cut with free, slipping and adhesive segments and uniformly distributed load at infinity

18 p2363 A73-36415

Limiting equilibrium of a plate weakened by two arbitrarily oriented cracks

19 p2494 A73-37186

Two-dimensional problem in elasticity theory for a rectangle with mixed boundary conditions

19 p2499 A73-37761

Contact problem of the elastic interaction between a plate and an elliptic insert

19 p2499 A73-37762

Boundary layer concept /attenuating stress-strain state with homogeneous boundary conditions/ incorporation into internal stress-strain state theory for orthotropic rectangular elastic plates

19 p2499 A73-37763

On a formulation of the bending of elastic plates.

19 p2500 A73-38112

Determination of kinetic stress functions in elastodynamic problems of plates

20 p2617 A73-39262

Certain approximations in the solution of shell and plate bending problems with allowance for physical and geometrical nonlinearity

20 p2618 A73-39311

Stress-concentration at a hole with periodic irregularities

20 p2619 A73-39334

Finite-element formulations for elastic plates by general variational statements with discontinuous fields.

20 p2623 A73-39558

Problem of an elastic semiinfinite cover plate fastened to a linearly deformable base

20 p2624 A73-39646

Buckling of continuous circular plates.

21 p2782 A73-40004

Flexural wave propagation in a thin plate with circular holes.

21 p2787 A73-41142

The stress field near a Griffith crack at the interface of two bonded dissimilar elastic half-planes.

21 p2789 A73-41672

Convergence of simplified hybrid displacement method for plate bending.

22 p2921 A73-42203

Large deflection theory for viscoelastic anisotropic thin plates, deriving constitutive, plane stress, plate and nonlinear integrodifferential equations

22 p2923 A73-42638

Stress distribution around an elliptic hole in an infinite micropolar elastic plate.

22 p2924 A73-42684

Asymptotic method for approximate elastodynamic plate theories derivation from elasticity equations with application to plate free extensional and forced flexural vibration frequency spectrum

[ASME PAPER 73-APMW-44] 22 p2926 A73-42900

Transformation of a symmetric wave-type process of deformation into an asymmetric process in a plate during the development of a shock wave

22 p2927 A73-42930

Stability of nonlinearly elastic plates in the presence of random initial stresses

22 p2928 A73-43060

Solution of plane problems of elasticity utilizing partitioning concepts.

[ASME PAPER 73-APM-C] 23 p3047 A73-44378
Large amplitude vibrations of elastically restrained rectangular plates.

23 p3048 A73-44380
Nonlinear transverse vibration analysis of a rectangular plate with lumped M-S-D systems.

23 p3048 A73-44384
Three-dimensional axisymmetric problem of a normal load concentrated on an elastic free-surface plate of constant thickness - Expression for the stresses in the vicinity of the load

24 p3149 A73-45218

ELASTIC PROPERTIES

NT AEROELASTICITY
NT AEROTHERMOELASTICITY
NT ANELASTICITY
NT DYNAMIC MODULUS OF ELASTICITY
NT ELASTOPLASTICITY
NT HYDROELASTICITY
NT HYPOELASTICITY
NT MAGNETOSTRICTION
NT MODULUS OF ELASTICITY
NT PHOTOELASTICITY
NT PHOTOVISCOELASTICITY
NT THERMOELASTICITY
NT THERMOVISCOELASTICITY
NT VISCOELASTICITY

Construction of finite-difference schemes in engineering theory of elasticity on the basis integral representations of the resolvent functions

01 p0114 A73-10483
Structural members optimal shaping in terms of stress concentration, analyzing plane elasticity boundary value problem

01 p0114 A73-10600
Shock waves existence and behavior in elastic non-conductors, investigating Hugoniot stress-strain curve properties

01 p0033 A73-10778
Approximate reduction of the equations of elasticity theory and electrodynamics for inhomogeneous media to Helmholtz equations

01 p0077 A73-10959
Reduction of integral equations in elasticity theory to infinite systems

01 p0116 A73-10960
Doubly-periodic problem in elasticity theory for an isotropic medium weakened by congruent groups of arbitrary holes

01 p0116 A73-10961
Effective solutions to the third and fourth boundary value problems of a sphere in the theory of elasticity

01 p0116 A73-11077
Elasticity theory contact problem for rectangle under compression loads, using Airy stress function for reduced linear algebraic equations system

01 p0117 A73-11090
Stress determination below thin elastic stiffeners partially braced to finite boundary of elastic half space

01 p0117 A73-11091
Two dimensional elasticity theory for radial crack effects on tensile stress concentration in circular elastic isotropic plate

01 p0117 A73-11092
Deformation and stress analysis in continuum mechanics problems of solid bodies near singular points, noting applicability of linear theory of elasticity

01 p0118 A73-11404
Asymptotic analysis of nonlinearly elastic and plastic thin rectilinear panels under combined bending and tensile stress

01 p0119 A73-11442
Operators tolerated by the dynamics equations in the three-dimensional problem of elasticity theory

02 p0230 A73-11781
Solution of axisymmetrical problems of the interaction between a cylindrical shell and an elastic filler by the finite difference method

02 p0231 A73-11806
Spectral analysis of integro-differential forms in spatial dynamic problems of the theory of elasticity

02 p0232 A73-11820
Elastic deformation of a single-cavity hyperboloid of revolution under given forces at the boundary

02 p0233 A73-11939
Linearly elastic materials theory covering kinematics, momentum balance, constitutive relation, boundary value problems and field equations

02 p0233 A73-11977
Existence theorems for boundary value problems of elasticity defined by unilateral constraints, developing abstract theory of functional inequalities

02 p0233 A73-11979
Boundary value problems of elasticity with unilateral constraints.

02 p0234 A73-11980
Impact and contact stress analysis in multilayer media.

02 p0234 A73-12072
Determination of elastic stresses at notches and corners by integral equations.

02 p0234 A73-12075

Finite axisymmetric deformations of elastic membranes.

02 p0234 A73-12089
Application of mathematical programming to the solution of extremal problems in two-dimensional elasticity theory

02 p0235 A73-12197
The effect of a preliminary plastic strain on the form of a mechanical hysteresis loop.

02 p0235 A73-12208
Stress concentration near a circular hole reinforced with a wide ring in the case of a nonlinear law of elasticity

02 p0236 A73-12584
Boundary value problem of Lamé equation in elasticity theory of two dimensional region with angular points, solving by Fredholm integral equation

02 p0237 A73-12591
Lunar librations results of Koziel reevaluated, noting elasticity effects and elastic strain perturbation on satellite

03 p0367 A73-13077
On optimal design of prestressed elastic structures.

03 p0384 A73-13119
Mathematical models for elastic solid bodies via similarity theory, noting rheoelectrical simulation for thermal stress analysis

03 p0386 A73-13146
The calculation of supporting planar-surface structures with the aid of the characteristic functions of correlated simplified basic problems

03 p0386 A73-13154
Mechanical properties and stress analysis of elastoplastic body, noting yield conditions and Bauschinger effect

03 p0386 A73-13155
The application of electrical analogy to the solution of problems of continuum mechanics

03 p0342 A73-13161
Hilbert space and calculus of variations for eigenvalue bounds of integral equations of elasticity and potential theories

03 p0387 A73-13162
Boundary-layer methods in microstructure theories of elasticity.

03 p0390 A73-13330
Elastic-plastic analysis of Saint-Venant torsion problem by a hybrid stress model.

03 p0390 A73-13338
An analysis of thermally-induced plane waves in elastic-plastic single crystals.

03 p0394 A73-13980
Constitutive analysis of elastic-plastic crystals at arbitrary strain.

03 p0394 A73-13983
Static boundary value problem of asymmetric elasticity for elastic isotropic media with small energy contribution to potential due to moment effects

03 p0394 A73-14050
Prediction tests for pulmonary elasticity model of expansion stresses in lung region restricted by obstructed airways

03 p0262 A73-14114
Some crack tip finite elements for plane elasticity.

04 p0506 A73-14683
Calculus of variations for minimum energy method in elasticity theory of incompressible elastic body, calculating elastic deformations

04 p0509 A73-14980
Electric and thermal conductivity, elastic properties, and resistance to bending of porous tungsten throughout the porosity range

04 p0464 A73-15371
Potential methods in the linear couple-stress theory of elasticity.

04 p0514 A73-15676
Proof of the eigenvalues 0 and -1 in the spectra of integral operators of two-dimensional elasticity theory

04 p0514 A73-15677
Buckling of continuously supported beams.

[ASME PAPER 72-WA/APM-34] 04 p0515 A73-15886
Thermodynamics and shocks in nonelastic mediums

04 p0520 A73-15994
Galerkin stress functions for non-local theories of elasticity.

05 p0631 A73-16123
Complex resilient-base structure designs incorporating the reaction to an external load

05 p0636 A73-17083
Studies in stress-relaxation and distensibility characteristics of small skin veins in vivo by a combined photoelectric-photographic and plethysmographic technique.

05 p0541 A73-17098
X-ray elastic constants of titanium and TiAl6V4

05 p0588 A73-17242
Calculation of X-ray elastic constants on the basis of single crystal coefficients of metals with a hexagonal structure

05 p0588 A73-17244
Numerical solution of elastoplastic problems by the method of local variations

06 p0760 A73-17777

The 'second' plane distortion problem of the theory of micropolar elasticity.

06 p0761 A73-17891
Contribution to the classical theory of solids with statistical structural characteristics

06 p0762 A73-17994
Collocated interfacial stress intensity factors for finite bi-material plates.

06 p0763 A73-18477
Variational methods in solid media linear theory of elasticity, discussing Rayleigh-Ritz method application to linear static, harmonic response and linearized stability problems

06 p0765 A73-18724
Possibility of using harmonic functions in the solution of problems in elasticity theory for inhomogeneous media

06 p0766 A73-18885
Laplace equation and elasticity theory problems solution via Fredholm integral equation, noting boundary value problems for discrete points of given curve

07 p0909 A73-19127
Elastic behavior of polymer-impregnated porous ceramics.

07 p0842 A73-19198
S-N fatigue curve analysis from ultimate tensile strength to cyclic elastic limit below fatigue limit, discussing load cycle zones and discontinuities

07 p0910 A73-19214
Extremal stresses in the first basic two-dimensional problem of elasticity theory for a half-plane

07 p0911 A73-19310
Microinhomogeneous plane with a circular hole in tension

07 p0911 A73-19320
Ultrasonic P and S waves velocity of Apollo 14 and 15 lunar igneous and breccia rocks for elastic properties determination, noting cracks distribution function

07 p0894 A73-19853
Lattice dynamics, third-order elastic constants, and thermal expansion of titanium.

07 p0839 A73-20173
Stress functions for the 'second' plane problem of micropolar elasticity.

07 p0914 A73-20198
Circular electric waveguide of minimum loss and elastic flexibility.

08 p0938 A73-20838
On the mechanical response of a non-uniform piezoelectric transducer with elastic compliances having damping characteristics.

08 p0994 A73-20875
Contact problem with one governing parameter in elasticity theory

08 p1017 A73-21099
Blood vessels simulation by muscle pump represented by elastically deformable pipe with valves, solving Navier-Stokes equation for viscous fluid flow

08 p0934 A73-21375
A model for the elastic properties of the lung and their effect on expiratory flow.

08 p0934 A73-21502
Dynamic yield, compressional, and elastic parameters for several lightweight intermetallic compounds.

09 p1099 A73-21926
Shock wave compression of iron-silicate garnet.

09 p1076 A73-22146
Elastic stiffness properties and structural designs of fiber composite materials, including laminate and plate problems

09 p1110 A73-22516
High modulus organic fiber/epoxide properties for reinforced composites, including strands, rings and filament wound vessels

09 p1110 A73-22518
On the convergence of the finite element method for problems with singularity.

09 p1160 A73-22891
Design of rotating discs of irregular outline.

09 p1161 A73-23051
Linear elastic and general yielding fracture mechanics compatibility, investigating crack opening displacement relationship to stress intensity factor

09 p1109 A73-23263
Hybrid stress finite element models for elastic continuum, discussing variational principle and macroscopic equilibrium

09 p1166 A73-23457
Buckling of a simply-supported beam between two unattached elastic foundations.

09 p1166 A73-23466
Nonstationary equations of the nonlinear theory of elasticity in Euler coordinates

10 p1287 A73-23590
Elastic circular ring stability under uniformly distributed equal radial concentrated forces

10 p1287 A73-23594
Contribution to the study of the elasticity of monocrystalline aluminum under very low stresses

10 p1231 A73-23771
On the elastic properties of fiber composite laminates with statistically dispersed fiber and ply orientations.

10 p1288 A73-23959

Nonlinear elastic behavior of unidirectional composite laminae.

10 p1289 A73-24283

Note on an approximate method for computing consistent conjugate stresses in elastic finite elements.

10 p1290 A73-24293

Elastic properties of materials strengthened by short unidirectional fibers

10 p1240 A73-24306

Temperature dependence of the adhesive strength and elasticity of some high-melting coatings

10 p1225 A73-24371

Parachute opening dynamic analysis, taking into account risers, shrouds and canopy cloth elastic properties on opening history and loads

10 p1176 A73-24647

Dynamic characteristics of space thin beams.

11 p1433 A73-25126

Polynomial solutions to the plane problem of electroelasticity theory

11 p1434 A73-25394

Optimum design of stressed skin structures using a sequence of linear programs method.

[AIAA PAPER 73-342]

11 p1436 A73-25481

Earth mantle rutile-structure germanium dioxide elastic properties as function of pressure and temperature in single crystals

11 p1352 A73-25585

Lattice model calculation of elastic and thermodynamic properties at high pressure and temperature.

11 p1399 A73-25900

The elastic constants of carbon-fibre composites.

11 p1389 A73-26045

Asymptotic analysis of nonlinearly elastic and plastic thin rectilinear panels under combined bending and tensile stress

11 p1443 A73-26060

Crystal lattice dynamics, elasticity and piezoelectricity theories covering linear, Cosserat and strain gradient theories, acoustic and optical properties, etc

11 p1409 A73-26276

Sommerfeld type radiation conditions for asymmetric theory of linear homogeneous and isotropic micropolar elasticity, applying to regular solution to infinite domain field equations

11 p1444 A73-26279

Lame problems in theory of elasticity, discussing reduction to Dirichlet sequence for Laplace equation

11 p1446 A73-26597

Elasticity theory of three dimensional system of particles in rectangular prismatic or tetrahedral net arrangement as topological model for finite element method

11 p1448 A73-26727

Fiber strength, fracture types and material elastic properties relationship to impact resistance in carbon fiber reinforced plastics

12 p1515 A73-26882

Approximate reduction of the equations of the theory of elasticity and electrodynamics for inhomogeneous media to the Helmholtz equations.

12 p1524 A73-27535

On the reduction of integral equations of the theory of elasticity to infinite systems.

12 p1554 A73-27536

Doubly-periodic problem of the theory of elasticity for an isotropic medium weakened by congruent groups of arbitrary holes.

12 p1554 A73-27537

Book - Mathematical problems in wave propagation theory.

12 p1524 A73-27625

Elastic-plastic fracture by homogeneous microvoid coalescence tearing along alternating shear planes.

13 p1633 A73-28142

On a finite strain theory of elastic-inelastic materials.

13 p1692 A73-28167

A theory of an elastic-plastic continuum with special emphasis to artificial graphite.

13 p1644 A73-28168

Variational treatment of the elastic constants of disordered materials.

13 p1692 A73-28169

High speed computing of elastic structures; Proceedings of the Symposium, Universite de Liege, Liege, Belgium, August 23-28, 1970. Volumes 1 & 2.

13 p1692 A73-28226

Analysis of stress intensity factor for surface-flawed tension plate.

13 p1692 A73-28231

Generalized Green function for infinite plate strip with free edges, noting application to elastic boundary value problems

13 p1695 A73-28560

Elastic circular inclusion in an infinite plane containing two cracks.

13 p1696 A73-28749

Elastic structures nonlinear free vibrations theory based on Hamilton principle and perturbation method, applying to beams and rectangular plates

13 p1696 A73-28751

A variant of the moment theory of elasticity for a one-dimensional continuous medium with a non-homogeneous periodic structure

13 p1698 A73-29085

Inelastic strain and hysteresis energy criteria for fatigue fracture of metals.

13 p1641 A73-29499

Mechanical strength of titanium alloys AT-2 and AT-3 and of their welded seams at extreme temperatures.

13 p1643 A73-29633

Fiberglass-reinforced plastics for glider laminate wing spars, describing elastic properties and strength characteristics

14 p1809 A73-30241

Stress formulation of the 'second' axially symmetric problem of micropolar theory of elasticity.

14 p1809 A73-30253

Construction of finite difference diagrams of the engineering theory of elasticity, on the basis of integral representations of the resolvent functions.

14 p1810 A73-30308

Solution of the first boundary value problem of statics in the moments theory of elasticity

14 p1810 A73-30382

Maxwell kinetic theory of gases with elasticity of shape /modulus of rigidity/ and obeying Hooke's law, deriving expressions for simple shear and relaxation time

14 p1745 A73-30477

Finite bending of incompressible hyperelastic plastic strip, analyzing stress and stored energy function

14 p1812 A73-30496

Some basic solutions in strain gradient elasticity theory of an arbitrary order.

14 p1812 A73-30546

Strength and elastic characteristics of ammonium perchlorate whiskers grown with potassium permanganate additions, discussing crystal dislocations and physico-chemical properties

14 p1767 A73-30829

Solution of three-dimensional contact problems in elasticity theory

14 p1775 A73-30831

Projection method in the shell theory and its realization on a computer

15 p1944 A73-30971

An iteration method of solving the three-dimensional problem for equations of the theory of elasticity in displacements

15 p1945 A73-31027

Note on volume integrals of the elastic field around an ellipsoidal inclusion.

15 p1946 A73-31104

Bulk elastic properties of excised lungs and the effect of a transpulmonary pressure gradient.

15 p1832 A73-31128

The use of elastic relaxation for testing aerospace equipment.

[AIAA PAPER 73-478]

15 p1948 A73-31462

Cast thermosetting epoxy resin linear elastic stress-strain characteristics under tension, compression, torsional and bending loads

15 p1897 A73-31619

Theoretical post-yielding behavior of composite laminates. I - Inelastic micromechanics.

15 p1897 A73-31678

Linear elastic fracture mechanics applicability to graphite-epoxy laminated fracture specimens configuration from fractographic studies

15 p1897 A73-31684

Finite element methods in continuum mechanics.

15 p1950 A73-31973

A numerical technique for determining the effect of singularities in finite difference solutions illustrated by application to plane elastic problems.

15 p1951 A73-32031

Book - Continuum mechanics and related problems of analysis.

15 p1952 A73-32076

Solution of certain classes of three-dimensional problems in elasticity theory with the aid of analytic functions

15 p1952 A73-32077

Variational principles of three-dimensional linearized theory of elasticity problems with large initial deformations

15 p1953 A73-32091

The stress field near a system of four symmetrically situated line cracks of equal length.

15 p1953 A73-32093

Solution to a three-dimensional mixed boundary value problem in the theory of elasticity

15 p1953 A73-32102

Hilbert space of states, considering variational principles, linear elasticity pointwise bounds for homogeneous/inhomogeneous problems and potential theory

15 p1954 A73-32112

Macroscopic elastic constant determination for randomly reinforced composite materials by equilibrium method

15 p1954 A73-32115

An invariant treatment of interfacial discontinuities in elastic composites.

15 p1954 A73-32121

An approach to the analysis of boundary value problems in the theory of functions and two-dimensional problems in the theory of elasticity

15 p1954 A73-32124

Russian book - Precision alloys with specific thermal-expansion and elastic properties

15 p1893 A73-32293

On the possibility of using harmonic functions for solving problems of the theory of elasticity of non-homogeneous media.

15 p1956 A73-32410

Nonlinear behavior of shells of revolution under cyclic loading.

16 p2075 A73-32791

Correlation functions of the elastic field of quasi-isotropic composite materials under nonisotropic deformation

17 p2240 A73-34146

Influence of the structure of a composite material on its elastic properties

17 p2194 A73-34269

Solution of the plane problem in elasticity theory for an incompressible material by the fractional step method

17 p2211 A73-34299

Application of the random walk method for solving problems in the theory of elasticity

17 p2241 A73-34332

Theory of disclinations. II - Continuous and discrete disclinations in anisotropic elasticity.

17 p2242 A73-34500

Effects of cold deformation and heat treatment on the elastic properties of niobium

17 p2188 A73-34562

Fracture toughness parameters and elastic-plastic analysis of non-moderate fracture conditions using finite element methods.

17 p2245 A73-34877

A nondestructive measurement of the elastic constants of unidirectional borsic fiber reinforced aluminum composites.

[SC-DC-72-1644]

17 p2182 A73-35439

On the fracture of high-strength metals in the stress fields of various stress-concentration factors.

[SESA PAPER 2163A]

17 p2191 A73-35454

Symmetric integral equations of the theory of elasticity

17 p2251 A73-35585

Use of Gq functions for the representation of solutions to equations of statics in the theory of elasticity

17 p2251 A73-35586

A class of particular solutions to three-dimensional equations of dynamics in the theory of elasticity

17 p2251 A73-35587

Two and three dimensional elasticity theory of linear fracture mechanics covering stress functions, finite element method and crack behavior in solids

17 p2252 A73-35669

Matrix method for the determination of the elastic and mechanical properties of reinforced plastics

18 p2327 A73-36475

Fracture mechanics in materials selection and design.

18 p2363 A73-36483

The median problem of the theory of elastic mobility with polar effects of spectral type.

18 p2364 A73-36492

The role of the elastic properties of brain and spine cavities in hyperemia compensation

18 p2276 A73-36572

The elastic properties of carbon fibres and their composites.

18 p2329 A73-37095

A version of the couple stress theory of elasticity for a one-dimensional continuous medium with inhomogeneous periodic structure.

19 p2498 A73-37635

A quantitative estimate of the effect of the parameters of oscillatory systems on the natural frequencies

19 p2498 A73-37653

Localized creep of a nonhomogeneous beam subjected to loads exceeding the true elastic limit

19 p2501 A73-38306

Book - Stress wave propagation in solids: An introduction.

19 p2502 A73-38363

Elastic properties of tantalum over the temperature range 4-300 K.

20 p2575 A73-38886

Unique relations between equilibrium and Galimov-Novozhilov stability equations of geometrically nonlinear elasticity theory based on Hooke's law

20 p2617 A73-39305

The symmetry method and its application to plane problems of elasticity theory

20 p2618 A73-39325

Some aspects of the approximation of functions of many variables, and effective direct methods for solving problems in elasticity theory

20 p2618 A73-39326

Study of the two-frequency natural oscillation regime of a circular membrane on a nonlinearly elastic base

20 p2593 A73-39501

Stability criteria for incompressible elastic isotropic materials subject to shearing displacement superimposed on homogeneous elastic deformation, discussing Cauchy stress and shear modulus

20 p2620 A73-39530

Stress singularities associated with a crack inclined to a bi-material interface.

20 p2620 A73-39531

Stability of the bending equilibrium of shells beyond the elastic limit

20 p2625 A73-39657

A photographic method for testing the impact strength of metals

21 p2696 A73-39991

Russian book on elasticity theory for multilayer media covering plate compression and bending under boundary contact conditions, Algol programming, tensile stress, functional equations, etc

21 p2782 A73-40175

Boundary residual methods limitation on elasticity problem solution accuracy, considering torsional stress analysis of square and hexagonal cylinders with circular hollow cores

21 p2784 A73-40431

Ceramic component strength degradation by projectile impacts in terms of momentum and elasticity relation

21 p2723 A73-40892

Solution of the mixed boundary value problem of plane elasticity theory with the aid of singular integral equations

21 p2785 A73-40931

Nonlinear elasticity of random inhomogeneous materials reinforced by grains or oriented fibers, using Kauderer stress relation

21 p2787 A73-40987

Polish book - Theory of coupled stresses.

21 p2787 A73-41219

Micropolar elasticity solution for static plane boundary value problems in circular ring shaped region, considering Volterra dislocation example

21 p2789 A73-41670

Elastic properties of alloys of the Ti-Al-Mo system as a function of the composition and heat treatment

22 p2874 A73-42095

Estimation of the effect of the internal properties of the material on the characteristics of string sensors

22 p2860 A73-42370

The theory of elasticity of flexural-stiffness exhibiting, planar particle systems with a rectangular net

22 p2922 A73-42526

On the integral equations of three-dimensional multiple inclusion problems.

22 p2924 A73-42682

German monograph - Characteristics of motion of an elastically supported rotor with interior damping.

22 p2867 A73-42849

Matrix methods application to stress in elastic structures, examining Mohr circles, design implications and orthogonality anisotropy

22 p2929 A73-43173

Statistical theory of solid heterogeneous materials, discussing constant elastic bounds, fiber reinforced cell model, thermal expansion and stress-strain relations

23 p3038 A73-43303

Book - Elasticity.

23 p3039 A73-43434

Solution of spatial contact problems of the theory of elasticity.

23 p3040 A73-43585

Anisotropic composite material swelling coefficients and elastic compliances data averaging and reduction, using tensor transformation and associated scalar invariants

23 p3041 A73-43636

High modulus carbon fiber reinforced epoxy composite elastic constant determination by ultrasonic wave propagation velocity measurement in immersion tank, discussing data error sources

23 p2985 A73-43642

Saint Venant continuity equation for identical formulation of Lamé equations and elasticity theory problem of stress-strain state in bodies of revolution

23 p3045 A73-44185

Perturbation method applications to elasticity theory three-dimensional problems, discussing differential operator construction via recursion relations

23 p3046 A73-44190

Turbine wheel strength, lifetime and safety margin calculations based on classical elasticity and plasticity theories

23 p3020 A73-44225

Influence of neutron bombardment on the mechanical properties of titanium and the magnitude of the programmed-hardening effect

23 p2995 A73-44284

Singular approximation in the calculation of the elastic properties of reinforced systems

24 p3145 A73-44514

Investigation of the elastic stiffness of niobium low-alloys subjected to small plastic strains

24 p3099 A73-44572

Elastomechanical model measurements conducted with the aid of holographic approaches in the case of a mirror cell

24 p3090 A73-44897

The static axisymmetric problem of the micropolar theory of elasticity and thermoelasticity

24 p3148 A73-44913

The governing equations and extremum principles of elasticity and plasticity generated from a single functional. I.

24 p3152 A73-45315

Structural analysis for idealized nonlinear material behavior.

24 p3152 A73-45316

ELASTIC SCATTERING

Use of the Glauber approximation in atomic collisions - A progress report.

02 p0195 A73-12649

Electron scattering by molecules with and without vibrational excitation. VI - Elastic scattering by CO at 6-80 eV.

03 p0344 A73-13284

Elastic scattering of negative pions from O-16 in the region of the $\pi/3, 3/\pi$ resonance.

04 p0477 A73-16037

Backward elastic proton-deuteron differential cross sections at different energies, describing experimental setup

05 p0601 A73-17322

Electron energy distribution function in CO laser discharge for elastic collisions, noting kinetic equation solution

09 p1089 A73-21914

On the analysis of glory scattering data for the extraction of information on the interatomic potential well.

09 p1122 A73-22072

Intermolecular potential energy curve crossing probabilities and associated phases determination for low energy elastic scattering cross section of He cations by Ne, noting rainbow effect

10 p1250 A73-23670

Influence of elastic collisions on the intensity of natural oscillations in a He-Ne laser

11 p1376 A73-25432

Low-temperature negative differential microwave conductivity in semiconductors following elastic scattering of electrons.

13 p1669 A73-28614

Application of the Poisson stochastic process for collision relaxation calculations in a nonequilibrium gas

15 p1915 A73-30968

Low-energy elastic differential scattering of He/ $++$ by He.

15 p1916 A73-32290

Electron energy distribution function in CO laser discharge for elastic collisions, noting kinetic equation solution

15 p1886 A73-32640

Elastic and inelastic scattering in orbital clustering.

18 p2357 A73-37109

Fredholm-uniformization computation of elastic scattering amplitudes in the presence of arbitrarily many open channels.

21 p2738 A73-40212

Approximate variational treatment of elastic scattering of electrons from semi-infinite lattices.

21 p2741 A73-41627

ELASTIC SHEETS

Temperature stresses in an elastic infinite strip due to sudden heating and heat transfer at the boundary of the strip

01 p0113 A73-10091

Nonlinear toroidal curved elastic sheet inflated by fluid at constant pressure, discussing existence, uniqueness and asymptotic behavior

14 p1812 A73-30520

Stresses in a fiber-reinforced elastic sheet containing a circular hole.

15 p1949 A73-31655

The non-linear theory of thin elastic sheets.

15 p1954 A73-32118

Effects of axisymmetric loads on inflated non-linear membranes.

23 p3045 A73-44081

On Papkovitch-Fadle solutions of crack problems relating to an elastic strip.

23 p3046 A73-44227

Partial solutions of finite elasticity - Axially symmetric deformations.

24 p3154 A73-45550

ELASTIC SHELLS

Basic behavioral characteristics of viscoelastic orthotropic shell prepared from a generalized thermohydrologically simple material

01 p0112 A73-10001

Bubnov-Galerkin method for natural vibration frequencies of thin elastic circular conical shell under thermal loading

01 p0113 A73-10015

Construction of a general solution for an elastic anisotropic shallow shell with arbitrary boundary conditions, and some of its applications

02 p0230 A73-11714

Stress distribution in elastic shell of revolution under axisymmetrical loads, noting thickness distribution for uniform stress in critical edge loading zone

02 p0231 A73-11805

Solution of axisymmetrical problems of the interaction between a cylindrical shell and an elastic filler by the finite difference method

02 p0231 A73-11806

Study of the oscillations of plates, shells and combined systems by the basis vector method with difference discretization

02 p0232 A73-11817

On bending and vibration of reinforced and bireinforced elastic and viscoelastic shells.

03 p0387 A73-13160

Computation and solution procedures for nonlinear analysis by combined finite element-finite difference methods.

03 p0391 A73-13685

Discretized body mechanics equilibrium, constitutive and motion equations application to elastic lattice type shell structures

03 p0393 A73-13779

A consistent approximation in the linear theory of elastic lattice-type shells.

03 p0393 A73-13780

Stress analysis of thick walled hollow viscoelastic circular cylinder enclosed in elastic shell and subjected to nonlinear creep conditions, noting temperature effects

03 p0394 A73-14021

Determination of the natural oscillation frequencies of three-layer circular cylindrical shells by a numerical method

04 p0510 A73-15081

Axial impact response of semiinfinite cylindrical membrane shell of helically oriented linearly elastic orthotropic fiber reinforced material, solving motion equations

05 p0631 A73-16112

Roots of the circular cylindrical shell characteristic equation.

05 p0632 A73-16499

The influence of the reference geometry on the response of elastic shells.

05 p0637 A73-17236

Calculation of general surface-supporting structures with the aid of dynamic relaxation

06 p0758 A73-17516

Derivation of the linear shell theory from the theory of Cosserat medium.

06 p0763 A73-18454

Calculus of variations for mathematical model of elastic shell with internal degrees of freedom, noting boundary and discontinuity conditions

06 p0766 A73-18877

A linear theory of thin elastic shells, based on conservation of a non-normal straight line.

07 p0908 A73-19091

Deformation of an elastic spherical shell with random initial imperfections

07 p0911 A73-19319

Stability of the axisymmetric form of motion of flexible shallow shells

09 p1164 A73-23344

Numerical solution of some boundary value problems for an isotropic cylindrical shell

10 p1288 A73-24060

Combined axial and torsional shear of a tube of incompressible isotropic elastic material.

10 p1291 A73-24336

Impact on a simple physical model of the head.

10 p1185 A73-24770

Nonlinear transient stress-waves in cylindrical and conical shells.

11 p1432 A73-24978

Asymptotic analysis of the equations of oscillations and stability of bodies of revolution in the case of turning points

11 p1445 A73-26459

Estimates for stress derivatives and error in interior equations for shells of variable thickness with applied forces.

11 p1446 A73-26548

Second order closed form asymptotic solution to Donnell type nonlinear equations of elastic homogeneous conical shells for displacement and stress resultants

11 p1447 A73-26650

Design of zero-moment axisymmetric tanks made of a reinforced hereditary-elastic material

12 p1551 A73-27181

Asymptotic distribution of the natural frequencies of elastic shells

12 p1524 A73-27452

Differential equations of thermoelastic state for shells receiving a thermal shock at the surface

12 p1555 A73-27790

One-dimensional zero-moment problem of a thin elastic shell of variable thickness

12 p1556 A73-27800

Geometrically nonlinear static and dynamic analysis of shells of revolution.

13 p1693 A73-28239

Perturbation techniques in the analysis of geometrically nonlinear shells.

13 p1694 A73-28251

Response functions for mathematical double membrane model of isotropic elastic shell in form of orientable two dimensional differentiable manifold

13 p1694 A73-28284

Free and forced vibration analysis of laminated ring structure with elastic inner, outer layers and core, obtaining natural frequency response by variational method

13 p1695 A73-28486

Calculation of the low natural frequencies of clamped cylindrical shells by asymptotic methods.

13 p1696 A73-28752

The static-geometric duality and a staggered mesh scheme in the numerical solution of some shell problems.

13 p1699 A73-29373

Apparent symmetry of certain thin elastic shells.

14 p1805 A73-29763

Large amplitude vibrations of certain deformable bodies. II Plates and shells.

14 p1806 A73-30041

Construction of refined applied theories for a truncated hollow cone of variable thickness

14 p1815 A73-30786

Traveling wave solutions of differential equations describing thin elastic shell oscillations due to point source

14 p1815 A73-30951

Solution of the fundamental boundary value problems for a closed semiinfinite cylindrical shell

15 p1945 A73-31023

Impact interaction between a soft shell and a hard obstacle

15 p1947 A73-31276

Analysis of the static deformations of flexible extensible gas-filled shells

15 p1947 A73-31279

Stability of a spherical shell containing an elastic filler

15 p1950 A73-31828

Calculus of variations for mathematical model of elastic shell with internal degrees of freedom, noting boundary and discontinuity conditions

15 p1956 A73-32402

Forced vibrations of elastic shells of revolution filled with liquid

16 p2074 A73-32687

Stress concentration near a cutout on the surface of an orthotropic cylindrical shell

16 p2075 A73-32694

Discrete approximations of elastic-plastic bodies by variational methods.

16 p2078 A73-32994

Curved rotational shell elements by the constraint method.

16 p2078 A73-33002

Nonlinear dynamic problem concerning a cylinder with a slowly changing internal boundary

16 p2082 A73-33932

Chernin type second order equation for complex stress function for elastic shells of revolution under lateral load and tilting moment

16 p2084 A73-34034

Asymptotic characteristics of the problem involving intrinsic asymmetrical vibrations of circular conical shells

17 p2241 A73-34267

Some properties of dynamic equation integrals from the theory of shells

17 p2244 A73-34736

Elastic semiinfinite cylindrical shell stress-strain state after axial impact against static rigid plane, obtaining solutions for small time values

17 p2244 A73-34740

Forced plane strain motion of cylindrical shells - A comparison of shell theory with elasticity theory.

[ASME PAPER 73-APM-9]

17 p2247 A73-35034

First-order frequency effects in supersonic panel flutter of finite cylindrical shells.

[ASME PAPER 73-APM-K]

17 p2249 A73-35106

A new finite element method for analysing symmetrically loaded thin shells of revolution.

17 p2252 A73-35601

Shells of revolution belonging to a spherical class subjected to local loads at the pole

18 p2362 A73-36402

Geometrically nonlinear axisymmetric deformation of toroidal shells

18 p2362 A73-36403

A contact problem for a transversely isotropic cylindrical shell of finite length

18 p2363 A73-36404

Book - Theory and design of shells on the basis of asymptotic analysis: A unifying approach to the variety of thick and thin elastic shell theories and problems.

18 p2367 A73-36967

Approximate method for solving a boundary value problem in the theory of zero-moment elastic spherical shells

18 p2367 A73-36988

Supercritical strains in nonlinear elastic shells

20 p2616 A73-39259

Certain approximations in the solution of shell and plate bending problems with allowance for physical and geometrical nonlinearity

20 p2618 A73-39311

Numerical solution of problems of stability of three-layer cylindrical shells

20 p2620 A73-39503

Modal technique to obtain forced axisymmetric response of elastic spherical shells from free vibration response relations, taking into account transverse shear and rotational inertia

20 p2621 A73-39541

Method for calculation of natural and induced oscillations in elastic shells of revolution which are filled with an ideal incompressible liquid

20 p2624 A73-39647

A note on the finite elastic inflation of a thin spherical shell.

21 p2789 A73-41688

Discretized solution of junction problems in shells.

22 p2917 A73-41740

Asymptotic distribution of the eigenfrequencies of elastic shells.

22 p2881 A73-41811

Determination of the stressed state near a curvilinear hole in a transversely isotropic spherical shell

23 p3043 A73-43924

Numerical calculation of simply supported cylindrical shells of arbitrary cross section

23 p3046 A73-44192

Traveling wave solutions of differential equations describing thin elastic shell oscillations due to point source

23 p3047 A73-44327

Nonlinear vibrations of viscoelastic cylinder with elastic shell under harmonic forces, showing steady state equilibrium stability conditions

24 p3145 A73-44530

Dynamic stability of a viscoelastic orthotropic cylindrical shell

24 p3146 A73-44532

Chebyshev solution to elliptical equilibrium equations of elastic reticular cylindrical and toroidal shells under distributed loads, applying to extensible fiber structures/tires/

24 p3146 A73-44652

Equations of linear elastic theory of thin shells based on model of anisotropic Cosserat surface

24 p3147 A73-44744

On the problem of flexure of anisotropic cylindrical shells.

24 p3151 A73-45302

Equilibrium of two elastic shallow shells of revolution which are connected by radial ribs

24 p3152 A73-45355

ELASTIC STABILITY

U DAMPING

ELASTIC SYSTEMS

A method of construction and the structure of asymptotic approximations of the solutions of nonlinear mixed boundary value problems in studies of multifrequency oscillation modes

01 p0076 A73-10097

Development of dynamic modes of the loss of stability in elastic systems during intense loading over a finite interval of time

02 p0229 A73-11615

Free vibrations of elastic systems with discrete dynamic systems attached.

03 p0384 A73-12983

Harmonic oscillations of elastic system with viscous damping, calculating maximum amplitude of third subharmonic

04 p0509 A73-19978

Considerations concerning the orthogonality of the natural oscillation modes in elastic systems with many degrees of freedom

04 p0476 A73-15658

The calculation of the natural vibration parameters of a damped system on the basis of the results of a vibration test in an exciter configuration

05 p0634 A73-16758

Group theory application to in-plane vibrations natural frequencies of nth order polygonal particle elastic system, obtaining analytical solution through eigenvalue problem simplification

05 p0599 A73-17373

Thin walled beam composed indeterminate elastic framed structures minimum weight design, obtaining solutions by nonlinear programming algorithm

07 p0912 A73-19951

Synthesis of two discrete vibratory systems using eigenvalue modification.

08 p1015 A73-20726

Satellites elastic structures equations of state for stability and attitude control systems analysis, deriving translational and rotational momentum equations for moving coordinate systems

08 p1014 A73-20779

Attitude stability of two elastically coupled spinning bodies.

10 p1286 A73-24543

Impact interaction of an absolutely hard body and an elastic two-mass system

11 p1400 A73-26455

Selection of optimal rigidities for elastic regions of a mechanical system with resonance oscillations

12 p1524 A73-27473

Solid body on elastic supports as model for helicopter stability and nonlinear oscillations analysis

12 p1459 A73-27791

Parametric vibrations of elastically connected two mass system with two degrees of freedom, considering dynamic response to excitation by external compression loads

13 p1700 A73-29391

Russian book on elastic structures vibration in aircraft covering integral equations for beams, damping principles and transcendental equations for flexural and torsional vibrations natural frequencies

14 p1810 A73-30354

Book - Optimal control theory for the damping of vibrations of simple elastic systems.

14 p1813 A73-30674

Spin stability of torque-free elastic dissipative systems with finite number of degrees of freedom, deriving Liapunov function via energy considerations

15 p1943 A73-31663

Computation of upper and lower bounds to the frequencies of elastic systems by the method of Lehmann and Maehly.

15 p1951 A73-32027

Lower bounds to the frequencies of continuous elastic systems.

15 p1954 A73-32125

Elastic viscously damped ten degree of freedom system with two torsion-elastically mutually pivotally joined rotors, determining eigenfrequencies by equations of motion numerical evaluation

16 p1968 A73-33235

Stability of motion in a controlled system consisting of two elastically butted bodies one of which has cavities partially filled with a liquid

17 p2243 A73-34733

Effect of a connecting plane link on the excitation and propagation of flexural oscillations in parallel plates

17 p2244 A73-34737

Program of computation of spectral and modal matrices associated with a linear elastic system

18 p2364 A73-36493

Calculation of a system of two infinite beams on an elastic base

19 p2495 A73-37190

Determination of dynamic loads on elastic structures caused by external excitations

19 p2500 A73-38155

A direct method of stability analysis for elastic circulatory systems.

20 p2621 A73-39535

Optimal active damping of vibrations

20 p2594 A73-39638

Bilateral estimates of the critical parameters of elastic systems experiencing flutter

22 p2921 A73-42280

Vibration and stability of nondivergent elastic systems.

22 p2922 A73-42551

Normal modes of elastically connected circular plates.

22 p2929 A73-43140

A method for qualitatively studying the oscillations and stability of systems with distributed parameters

24 p3111 A73-45354

Equilibrium of two elastic shallow shells of revolution which are connected by radial ribs

24 p3152 A73-45355

Random vibrations of elastic nonlinear nonautonomous systems with variable parameters

24 p3112 A73-45502

ELASTIC WAVES

NT AERODYNAMIC NOISE

NT AIRCRAFT NOISE

NT BAROCLINIC WAVES

NT CAPILLARY WAVES

NT COHERENT ACOUSTIC RADIATION

NT COMPRESSION WAVES

NT DETONATION WAVES

NT DILATATIONAL WAVES

NT ELECTROSTATIC WAVES

NT ENGINE NOISE

NT GRAVITY WAVES

NT IONIC WAVES

NT JET AIRCRAFT NOISE

NT LAMB WAVES

NT LOVE WAVES

NT MACH CONES

NT MAGNETOACOUSTIC WAVES

NT MAGNETOELASTIC WAVES

NT MAGNETOHYDRODYNAMIC STABILITY

NT MAGNETOHYDRODYNAMIC WAVES

NT MICROSEISMS

NT NOISE [SOUND]

NT NORMAL SHOCK WAVES

NT OBLIQUE SHOCK WAVES

NT P WAVES
 NT PHONON BEAMS
 NT PHONONS
 NT PLASMA WAVES
 NT POLARIZED ELASTIC WAVES
 NT RAYLEIGH WAVES
 NT RIEMANN WAVES
 NT ROCKET ENGINE NOISE
 NT S WAVES
 NT SEISMIC WAVES
 NT SHOCK WAVES
 NT SONIC BOOMS
 NT SOUND WAVES
 NT STRESS WAVES
 NT THERMAL NOISE
 NT TOLLMEIN-SCHLICHTING WAVES
 NT ULTRASONIC RADIATION
 NT UNLOADING WAVES
 Some numerical experiments with Dafermos's method for nonlinear hyperbolic equations.
 01 p0069 A73-10071
 Elastic waves originating at the surface of a spherical opening in nonhomogeneous isotropic media.
 01 p0116 A73-11065
 Scheme for calculating the process of elastic wave propagation in a composite beam
 02 p0233 A73-11943
 Diffraction of elastic waves by two coplanar and parallel rigid strips.
 02 p0234 A73-12088
 Elastic surface waves - Many new applications.
 02 p0193 A73-12598
 Two-dimensional unsteady flow by hydraulic analogy.
 03 p0295 A73-13769
 Propagation of elastic waves in a cylindrical bar subject to a moving load on its lateral surface.
 03 p0343 A73-13833
 The effect of polarity on the diffraction of plane elastic waves by a cylindrical cavity.
 03 p0396 A73-14627
 Thermoelastic wave propagation in a transversally isotropic circular cylinder
 04 p0512 A73-15501
 Elastic waves in an infinite cylinder with micropolar structure
 04 p0513 A73-15502
 Elastic wave propagation in a circular cylinder subjected to finite deformation Compressible material
 04 p0513 A73-15503
 Elastic wave propagation in filamentary composite materials.
 05 p0631 A73-16122
 Crack tip stress field variation via elastic pulses for crack path alteration and subsequent fracturing process termination, using photoelastic analysis
 05 p0634 A73-16795
 Boundary value problems of elastic wave diffraction by spherical cavities, using vector equation of motion solutions
 05 p0636 A73-17091
 Large amplitude waves in bounded media. I - Reflexion and transmission of large amplitude shockless pulses at an interface.
 06 p0761 A73-17874
 Note on the wave propagation problems in isotropic discretized bodies.
 06 p0723 A73-17893
 Scattering of a transverse elastic wave by an elastic sphere in a solid medium.
 06 p0737 A73-18351
 Stress-induced rotation of polarization directions of elastic waves in slightly anisotropic materials.
 07 p0908 A73-19083
 On the reflection of harmonic waves in fiber-reinforced materials.
 07 p0909 A73-19096
 Elastic waves induced fluctuating stresses in turbulent parallel mean flow, deriving hyperbolic relations consistent with Taylor frozen field hypothesis
 07 p0810 A73-19109
 Holographic visualization of elastic waves
 07 p0822 A73-19287
 MHD shock wave decay in oblique magnetic field, considering shock and rarefaction waves interaction
 07 p0858 A73-20071
 Theory of excitation of microwave elastic waves by multilayer transducers /considering the effect of metallic and insulator layers/.
 07 p0801 A73-20139
 Dispersion of axially symmetric waves in empty and fluid-filled cylindrical shells.
 08 p0987 A73-21075
 Propagation of a transverse harmonic wave in a plate with a statistically rough circular hole
 08 p1020 A73-21770
 Elastic wave propagation in a cylindrical shell containing a filler
 09 p1158 A73-22357
 One-dimensional finite amplitude wave propagation in a compressible elastic half-space.
 09 p1160 A73-22895
 A continuum mixture theory of wave propagation in laminated and fiber reinforced composites.
 09 p1160 A73-22897

Apparatus for recording acoustic signals from cracks initiated in brittle materials.
 09 p1086 A73-23165
 Use of modal solutions in elastic wave propagation problems.
 09 p1166 A73-23456
 Continuum theory of wave propagation in laminated composites.
 10 p1287 A73-23565
 Elastic wave analysis in nondestructive testing.
 10 p1292 A73-24630
 Rigorous analogies between elastic and electromagnetic systems.
 10 p1250 A73-24873
 Geometrical theory for flexure waves in shells.
 11 p1432 A73-24977
 Sommerfeld type radiation conditions for asymmetric theory of linear homogeneous and isotropic micropolar elasticity, applying to regular solution to infinite domain field equations
 11 p1444 A73-26279
 Amplification of a travelling wave in a non-homogeneous elastic medium.
 11 p1400 A73-26407
 Shock attenuation in a shock tube due to boundary layer.
 12 p1486 A73-27174
 The use of surface-elastic-wave reflection gratings in large time-bandwidth pulse-compression filters.
 12 p1480 A73-27566
 Surface elastic wave microwave bandpass filter for miniaturized frequency synthesizer in satellite communications systems, noting insertion loss and sidelobe reduction
 12 p1484 A73-27573
 Nonlinear wave propagation processes in elastic tubes
 13 p1692 A73-28165
 Concentric, uniform elastic spherical wave excited by thermal explosion of the envelope.
 14 p1816 A73-30251
 Quasi-monochromatic viscoelastic waves energy velocity equivalence to phase velocity for medium represented by standard linear solid or Maxwell model
 15 p1955 A73-32176
 Planar pressure waves propagation across wall with elastically supported and damped edges, considering induced gas flow characteristics behind wall
 16 p2000 A73-33257
 Propagation of thermoelastic waves in an undefined isotropic soil
 16 p2081 A73-33369
 Book on wave propagation in continuous media covering Hamilton principle, energy theorems, elastic waves, electromagnetic and hydromagnetic waves, Green function and nonlinear effects
 17 p2211 A73-34280
 Book - Diffraction of elastic waves and dynamic stress concentrations.
 17 p2242 A73-34468
 Acceleration wave propagation in a nonlinear viscoelastic solid.
 [ASME PAPER 73-APM-2]
 17 p2247 A73-35028
 Phase velocity dispersion for transverse normal elastic wave propagation through sandwiched CdS and molten quartz or germanium layers
 18 p2340 A73-36672
 Diffraction of waves at finite bodies of revolution
 19 p2458 A73-37182
 Visualization of surface elastic waves on structural materials.
 19 p2432 A73-37449
 Analysis of pressure waves as a mean of diagnosing vascular obstructions.
 19 p2398 A73-37524
 Two dimensional wave problems in rotating elastic media.
 19 p2460 A73-38183
 Application of the method of normal waves to the study of the oscillations of a cylindrical shell in contact with an elastic medium
 20 p2615 A73-38984
 An integral-equation approach to dispersion relations for guided elastic surface waves.
 20 p2592 A73-39048
 Dispersion curve computation for elastic acoustic waves propagation in /001/-cut cubic free anisotropic plate, noting relationship with slowness curves for bulk waves
 20 p2616 A73-39050
 Propagation of mechanical waves in the solar atmosphere
 20 p2606 A73-39078
 Thermodynamic formation of negative /rarefaction/ shock waves in single-phase viscous fluids by approximate continuum model
 21 p2790 A73-40251
 Russian book on elastic and thermoelastic waves in continuous deformable bodies covering steady and unsteady deformation dynamics, viscoelasticity and nonlinear elasticity using computer methods
 21 p2785 A73-40800
 Russian book on wave propagation in stratified media covering elastic and electromagnetic fields,

waveguides, whispering galleries, diffraction rays, caustic surfaces, etc
 21 p2741 A73-41279
 Thermoelastic wave propagation in a random medium and some related problems.
 21 p2789 A73-41667
 Vibrational relaxation of oxygen in an unsteady expansion wave.
 22 p2889 A73-42441
 Book - Ultrasonic investigation of mechanical properties.
 22 p2861 A73-42575
 Pressure waves generated by constant velocity deflagration flame in explosive hydrocarbon-air mixture for self-similar flow field
 22 p2936 A73-42808
 High frequency vibrations and waves in laminated orthotropic plates.
 22 p2928 A73-43135
 Transverse elastic wave propagation in CdS crystal wafer coated on both sides with AgBr, titanium oxide, Si or polystyrene
 23 p3017 A73-44038

ELASTICITY

U ELASTIC PROPERTIES

ELASTICIZERS

U PLASTICIZERS

ELASTODYNAMICS

NT ELASTIC DAMPING

NT ELASTOHYDRODYNAMICS

Linearization method for analytic solution of oscillatory motion differential equations of elastic nonlinear system, studying combinations of free and forced vibrations
 01 p0075 A73-10093
 Uniqueness and continuous dependence for the equations of elastodynamics without strain energy function.
 01 p0115 A73-10777
 Generalized dynamic problem of thermoelasticity for an infinite plate with a circular hole
 02 p0232 A73-11931
 Linearly elastic materials theory covering kinematics, momentum balance, constitutive relation, boundary value problems and field equations
 02 p0233 A73-11977
 On the semi-discrete Galerkin method for hyperbolic problems and its application to problems in elastodynamics.
 04 p0471 A73-15222
 On the uniqueness of singular solutions to boundary-initial value problems in linear elastodynamics.
 04 p0512 A73-15226
 Three dimensional analysis in series form for statics and dynamics of simply supported rectangular plates of micropolar elastic material, obtaining free vibration frequencies
 07 p0917 A73-20565
 The method of internal force parameters in elastokinetics
 08 p1016 A73-20782
 One-dimensional finite amplitude wave propagation in a compressible elastic half-space.
 09 p1160 A73-22895
 A continuum mixture theory of wave propagation in laminated and fiber reinforced composites.
 09 p1160 A73-22897
 Rigorous analogies between elastic and electromagnetic systems.
 10 p1250 A73-24873
 Thermoelastic response of a cylinder in the generalised dynamical theory of thermoelasticity.
 11 p1433 A73-25161
 Direct time numerical integration of spatially discretized linear elastodynamics integral equations, comparing one-step algorithms for stability and accuracy in terms of frequency spectrum
 11 p1435 A73-25439
 Crystal lattice dynamics, elasticity and piezoelectricity theories covering linear, Cosserat and strain gradient theories, acoustic and optical properties, etc
 11 p1409 A73-26276
 Displacement boundary value problem of linearized elastodynamics with superimposed small and large deformations in homogeneous anisotropic elastic solid, proving solution uniqueness theorem
 11 p1444 A73-26282
 Solution of the dynamic problem of thermoelasticity for a circular plate with allowance for the finite velocity of heat propagation
 12 p1552 A73-27263
 Differential equations of thermoelastic state for shells receiving a thermal shock at the surface
 12 p1555 A73-27790
 Boundary value problem solution uniqueness in dynamic linear theory of hereditary-elastic rheologically composite media
 12 p1555 A73-27793
 Approximate method for solving dynamic problems in thermoviscoelasticity
 13 p1690 A73-27993
 Complementary energy method in elastodynamics.
 13 p1694 A73-28249

German book - Elastostatics and elastokinetics in matrix notation: The procedure of transmission matrices.

13 p1695 A73-28300

Lamb solution analog for dynamic problem of homogeneous isotropic elastic body with impulsive force applied to semi-infinite plane incision

13 p1698 A73-29088

Variational principles application to finite element method in elastostatic and elastodynamic and elastodynamic small and finite displacement theories

14 p1806 A73-30178

On the uniqueness of solutions of stress equations of motion of the Beltrami-Michell type.

14 p1809 A73-30254

A uniqueness theorem for a system of stress equations of motion in linear elasticity.

14 p1809 A73-30255

Existence of generalized tensorial fields in linear asymmetric elastodynamics.

14 p1809 A73-30256

Third basic boundary value problem of dynamics for a three-dimensional elastic body

14 p1810 A73-30383

Dynamic singular boundary value problem of elastic body with propagating crack under concentrated force

14 p1814 A73-30784

Muskhelishvili elastodynamic theorem concerning natural stress-free state extension to three dimensional theory of inhomogeneous anisotropic elastic bodies

15 p1946 A73-31105

Forced motion of cylindrical shells - A comparison of shell theory with elasticity theory.

15 p1949 A73-31651

Book - Continuum mechanics and related problems of analysis.

15 p1952 A73-32076

Self similar dynamic problems for elastic plane and half-plane with/without propagating crack, assuming application of instantaneous perturbation source or uniform stress field

15 p1952 A73-32078

Variational principles of three-dimensional linearized theory of elasticity problems with large initial deformations

15 p1953 A73-32091

Kinetic stress functions and the geometry of space in a deformed continuum

15 p1953 A73-32099

Some considerations regarding the dynamics problem for an elastic space and the use of its solution

15 p1956 A73-32545

Half plane stress boundary value problems in elastodynamics, obtaining similarity solutions in terms of analytic functions via integral transforms

16 p2082 A73-33903

An assumed stress hybrid finite element model for linear elastodynamic analysis.

17 p2241 A73-34189

Stability of motion in a controlled system consisting of two elastically butted bodies one of which has cavities partially filled with a liquid

17 p2243 A73-34733

Dual principles of elastodynamics finite element applications.

17 p2245 A73-34833

Symmetric integral equations of the theory of elasticity

17 p2251 A73-35585

A class of particular solutions to three-dimensional equations of dynamics in the theory of elasticity

17 p2251 A73-35587

On kinematics and statics of finite-strain force and moment stress elasticity.

17 p2252 A73-35829

Lamb solution analog for dynamic problem of homogeneous isotropic elastic body with impulsive force applied to semiinfinite plane incision

19 p2498 A73-37638

Determination of dynamic loads on elastic structures caused by external excitations

19 p2500 A73-38155

A study on the dynamical behaviors of composite materials by dynamical model.

20 p2580 A73-38643

Automatic control theory and systems representation in framework of unilateral mechanics, using canonical elastodynamic and elastostatic equations

20 p2540 A73-38703

Determination of kinetic stress functions in elastodynamic problems of plates

20 p2617 A73-39262

Improved relations in the dynamics of moderately thick shells and plates under the action of massive moving loads

20 p2618 A73-39316

Proof for the existence of a solution to the fundamental quadrantal problem of dynamics for a three-dimensional elastic body, and approximate computation of the solution

22 p2918 A73-41951

Asymptotic method for approximate elastodynamic plate theories derivation from elasticity equations with

application to plate free extensional and forced flexural vibration frequency spectrum

[ASME PAPER 73-APMW-44] 22 p2926 A73-42900

Dynamic contact problem for the case of longitudinal shear strain

22 p2927 A73-43051

Synthesis of optimal control of the longitudinal motion of an elastic tank containing liquid

22 p2843 A73-43059

Numerical approximation of quasi-static and dynamic problems in viscoelasticity by net-point and finite difference methods

24 p3144 A73-44505

Elastic deformation of isotropic infinite plane with central circular inhomogeneity and elastokinetics of two bonded dissimilar half planes under uniformly moving body force

24 p3152 A73-45343

Liapunov functions application to stability analysis of dynamic systems and elastic bodies, considering eigenfunction method, maximum principle and energy criterion

24 p3153 A73-45497

ELASTOHYDRODYNAMICS

Elastohydrodynamic lubrication in rolling and sliding contacts.

[ASME PAPER 72-LUB-K] 01 p0055 A73-10222

An elastohydrodynamic analysis of the sleeve type high pressure seal.

[ASME PAPER 72-LUB-M] 01 p0055 A73-10224

Inlet shear heating in elastohydrodynamic lubrication.

[ASME PAPER 72-LUB-21] 03 p0314 A73-14336

Elastohydrodynamic traction characteristics of 5P4E polyphenyl ether.

[ASME PAPER 72-LUB-40] 03 p0335 A73-14347

Elastohydrodynamic lubrication in rolling and sliding contacts.

[ASME PAPER 72-LUB-K] 03 p0315 A73-14351

The application of elastohydrodynamic lubrication in gear tooth contacts.

03 p0317 A73-14375

Feasibility study of a slanted 'O-ring' as a high pressure rotary seal.

[ASME PAPER 72-WA/DE-14] 04 p0457 A73-15873

An extension of the Grubin theory of elastohydrodynamic lubrication.

05 p0581 A73-16433

A review of thermoelastohydrodynamic lubrication in rolling and sliding contacts.

07 p0831 A73-20223

Nonlinear wave propagation processes in elastic tubes

13 p1692 A73-28165

Frictional traction in elastohydrodynamic lubrication.

13 p1623 A73-28198

German monograph - Investigations regarding the elastohydrodynamic lubricant film thickness in the case of elliptical Hertzian contact surfaces.

13 p1625 A73-29287

Elastohydrodynamic principles applied to the design of helicopter components.

[AHS PREPRINT 770] 17 p2248 A73-35088

Some observations of the relationship between film thickness and load in high Hertz pressure sliding elastohydrodynamic contacts.

[ASME PAPER 73-LUB-D] 19 p2433 A73-37450

Contribution to the theory of high-frequency pulsations caused by instability of the combustion process in a solid-propellant rocket engine

21 p2753 A73-40391

Stability of a flow bounded by elastic walls

24 p3079 A73-44898

ELASTOMERS

NT CHLOROPRENE RESINS

NT THIOPLASTICS

NT VITON RUBBER [TRADEMARK]

NT VULCANIZED ELASTOMERS

On some relation between the mechanical properties and the bond strength of elastomer to solid inclusion in solid propellant.

01 p0090 A73-11117

The fracture energy and some mechanical properties of a polyurethane elastomer.

02 p0185 A73-12641

Age control evaluation of Buna N elastomers by ANA Bulletin 438, using shelf aging and crashed aircraft case studies

03 p0331 A73-13026

Thermally conducting alumina and boron nitride filled silicone and polysulfide elastomer sheet materials for electrical insulation and heat sink applications

03 p0331 A73-13028

Polyphosphazene fluoroelastomers preparation, properties and potential applications.

03 p0331 A73-13029

Thermal conductance of gasket materials for spacecraft joints.

[AIAA PAPER 73-119] 05 p0640 A73-16875

Elastomer compatibility considerations relative to O-ring and sealant selection.

[SAE AIR 786 A] 08 p0982 A73-20691

Improving reliability and eliminating maintenance with elastomeric dampers for rotor systems.

10 p1175 A73-23950

Hydrolytic reversion of elastomeric potting compounds.

13 p1646 A73-29274

New inhibited elastomeric finish system designed by corrosion engineers to solve acute corrosion problems on military aircraft.

[NACE PAPER 118] 13 p1638 A73-29318

Finite deformation behavior of elastomers - Dependence of strain energy density on degree of crosslinking for SBR.

13 p1646 A73-29527

A molecular theory of elastomer deformation and rupture.

13 p1646 A73-29528

Elastomeric and ceramic coatings for aircraft and missile radomes protection in subsonic and supersonic rain erosion environments

16 p2027 A73-33031

Low-cost fabrication and installation of ablative heat shields for the space shuttle orbiter.

16 p2072 A73-33060

Pressure vessels filament winding with inflatable mandrel in reinforced elastomer, discussing use of balloon as liner

16 p2018 A73-33068

How to select shaft seal materials.

[ASLE PREPRINT 73AM-6E-2] 17 p2196 A73-34990

The effects of environment on performance of fluoroelastomers in seal applications.

[ASLE PREPRINT 73AM-8B-2] 17 p2179 A73-34994

Sikorsky CH-53D helicopter main rotor head design, considering spherical elastomeric bearing, microstructural analysis, flight and ground fatigue tests and forging techniques

[AHS PREPRINT 713] 17 p2104 A73-35059

Modulus reinforcement in elastomer composites. I - Inorganic fillers.

18 p2328 A73-36980

Modulus reinforcement in elastomer composites. II - Polymeric fillers.

18 p2328 A73-36981

Feasibility study of skirt configurations and materials for an ACLS aircraft.

19 p2443 A73-37696

Mechanical properties of polymeric solids.

19 p2444 A73-38549

Molecular rupture mechanism, self reinforcement and failure modes of elastomeric materials dependence on strain, temperature, filler and crosslink density

23 p2997 A73-43808

ELASTOPLASTICITY

Combined heating and irradiation effects on body elastoplastic stress-strain state, deriving thermoradiative plasticity equations

01 p0112 A73-10004

Shell designs by the theory of small elastoplastic deformations with allowance for the compressibility of material

01 p0112 A73-10005

Investigation of a deformation process in a heated elastoplastic cylindrical shell

01 p0112 A73-10006

Reflection of plane stress waves in an elastoplastic medium with a variable yield limit

01 p0114 A73-10570

Elastic-plastic analysis on the structural elements with different values of stress concentration factor.

01 p0117 A73-11122

Stability of orthotropic circular cylindrical shells reinforced by annular ribs under external pressure

01 p0118 A73-11409

Numerical solution to the problem of the elastoplastic stability of doubly connected plates with curvilinear boundaries

02 p0231 A73-11813

Study of the effect of small elastoplastic deformations on the load-bearing capacity of specimens with stress concentrators under repeated variable loading. I.

02 p0235 A73-12202

Elastoplastic stressed state of cylindrical shells weakened by a circular hole

02 p0237 A73-12590

Brittle crack initiation at the elastic-plastic interface.

02 p0182 A73-12752

Elasto-plastic analysis of three-dimensional structures using the isoparametric element.

03 p0383 A73-12874

Effect of residual or characteristic stresses on the deformation of plates

03 p0385 A73-13143

Finite element equations of motion of elastoplastic shell, applying theory to edge clamped circular plate dynamic response

03 p0389 A73-13321

A simple finite element model for elastic-plastic plate bending.

03 p0391 A73-13680

Computation and solution procedures for nonlinear analysis by combined finite element-finite difference methods.

03 p0391 A73-13685

Rice energy line J integral fracture strength criterion applicability to crack tip elastoplastic testing for steel alloys

04 p0506 A73-14694

Elastoplastic slip line analysis of specimen geometry effects on J fracture strength criterion for medium strength steel center cracked panel and bend bar

04 p0506 A73-14695

Rice path independent J integral fracture strength criterion estimation as function of crack size and elastoplastically adjusted load point displacement for Ni-Cr-Mo-V steel

04 p0506 A73-14696

Inelastic spherical shells elastic-plastic buckling, presenting numerical procedure for critical loads and stresses

04 p0508 A73-14942

Minimum potential principles application to elastoplastic analysis of nonhardening materials, using quadratic programming

04 p0509 A73-14948

Elastic-plastic analysis of stresses near fastener holes.

[AIAA PAPER 73-252] 05 p0635 A73-16974

A numerical solution of an elastoplastic thick-walled tube subjected to thermal loading.

[AIAA PAPER 73-256] 05 p0635 A73-16978

Effect of external-load nonconservativeness on the stability of an idealized elastoplastic rod

05 p0635 A73-17076

Time variable stress-strain state of viscoelastoplastic hollow sphere under internal pressure, using piecewise linear differential law

05 p0635 A73-17080

Numerical solution of elastoplastic problems by the method of local variations

06 p0760 A73-17777

Large deflexion elastic-plastic response of certain structures to impulsive load - Numerical solutions and experimental results.

06 p0761 A73-17818

Partial yielding of cylindrical pressure vessel with elastic modulus and yield function as arbitrary functions of radial coordinate, assuming elastoplastic strain hardening material

06 p0761 A73-17895

Application of the finite element method to the solution of elastoplastic problems

06 p0766 A73-18726

On the convergence of the method of homogeneous linear approximations in problems of the theory of plasticity of inhomogeneous bodies.

07 p0906 A73-19022

Transient response of a plastically anisotropic cylinder in plane strain.

07 p0908 A73-19081

Decohesive load carrying capacity of elastoplastic bodies based on permissible discontinuities due to strain increase, relating to structural strength determination

07 p0908 A73-19082

Extremal boundary value problems of plasticity theory

07 p0910 A73-19304

Investigation of the stressed state of a rod with a cut under elastoplastic torsion

07 p0911 A73-19308

Axisymmetric buckling of uniformly loaded spherical caps undergoing plastic deformation.

07 p0913 A73-19971

Analysis of the elastoplastic bending of profiles whose cross sections are asymmetric with respect to the bending plane

07 p0913 A73-20090

One dimensional elastoplastic system optimal design by stochastic programming, determining limiting stresses and random load distribution

07 p0914 A73-20151

Elastoplastic analysis by matrix displacement or finite element method, presenting various direct and iterative solution techniques

08 p1016 A73-20776

Determination of stresses during pure elastoplastic bending and torsion

09 p1157 A73-22163

Longitudinal impact of a rigid body against a clamped rod

09 p1158 A73-22361

Fatigue life prediction and design optimization for solar cell interconnectors based on elastoplastic material stress distribution calculation by finite element methods

09 p1036 A73-22809

Refractory materials cyclic elastoplastic tests under shear with holding creep, showing relationship between creep rate and recurrent static deformation

09 p1161 A73-23155

Applications of the finite element method to the calculations of stress intensity factors.

09 p1162 A73-23185

Conical shell inversion - An approximate energy analysis.

[ASME PAPER 72-PVP-4] 09 p1163 A73-23266

On the elastoplastic problem of cantilever subject to combined bending and twisting.

09 p1164 A73-23320

Elastoplastic deformation and hardening function of perforated plates under in-plane tensile loads

09 p1164 A73-23346

Biharmonic coupling solutions of Saint Venant equation for elastoplastic plane under unequal loads, using Kolosov-Muskhelishvili functions and conformal mapping

09 p1165 A73-23350

Nonstationary equations of the nonlinear theory of elasticity in Euler coordinates

10 p1287 A73-23590

A yield-surface corner lowers the buckling stress of an elastic-plastic plate under compression.

10 p1289 A73-24100

Elasto-plastic stress analysis of prismatic bar under combined bending and torsion.

10 p1289 A73-24160

Stresses in a partly yielded notched bar - An assessment of three alternative programs.

10 p1290 A73-24294

A numerical method for the analysis of longitudinal elastic-plastic stress wave propagation.

10 p1290 A73-24297

The analysis of dislocation systems by the finite element method.

10 p1290 A73-24298

Plastic strain as factor in crack propagation rate smoothing and branching rate reduction in elastic and elastoplastic materials

10 p1291 A73-24362

Investigation of the elastoplastic characteristics of corrugated membranes under cyclic loading conditions

10 p1293 A73-24792

Some finite extremum principles in piecewise linear elasto-plasticity.

11 p1434 A73-25215

Probable collapse mechanisms in indefinite plates on an elastoplastic continuum.

11 p1434 A73-25217

Nonlinear transient analysis of shells and solids of revolution by convected elements.

[AIAA PAPER 73-359] 11 p1437 A73-25495

Gradient decomposition and kinematic constitutive equations for elastoplastic material behavior under large strains

11 p1445 A73-26410

Antiplane deformation near a cut in a hardening elastoplastic material

11 p1445 A73-26458

Biharmonic solutions of problems for elastoplastic bodies in the presence of nonuniformity of the stress field

11 p1446 A73-26598

Elastic and elastoviscoplastic unloading waves propagation in semiinfinite bar under axial impact stress, considering bilinear stress-strain curve

11 p1447 A73-26646

Continuum mechanics analysis of local rupture and plastic strains near cracks and fractures, noting elastoplastic applications

12 p1551 A73-27251

Boundary value problems in elastoplastic plate theory, obtaining solution through reduction to operator equations

12 p1552 A73-27370

Ray method for solving dynamic problems in viscoelastoplastic media

12 p1553 A73-27415

Elastoplastic bending of a cylindrical shell according to the Prandtl-Reuss theory

12 p1554 A73-27472

Flexural response of tapered beam on elastic-plastic foundation, solving in closed form to evaluate efficiency of numerical methods

12 p1557 A73-27932

Extension of the hodograph method for the one-dimensional elastic-plastic wave propagation.

13 p1696 A73-28646

Multiphase composite material models for elastoplastic beam bending under loading and unloading, using stress-strain diagram in tension and compression

13 p1698 A73-29052

Investigation of the elastoplastic state of a spherical shell with a unreinforced circular hole

13 p1698 A73-29061

Interaction of elasto-plastic cracks subjected to a uniform tensile stress in an infinite or a semi-infinite plate.

13 p1701 A73-29471

Finite element method application to elastoplastic analysis of cracked metal plates, discussing plate thickness effects on plastic zone growth and stress distributions along crack tip

13 p1701 A73-29476

Extension of Mandel inequalities to plastic acceleration wave velocities in a finitely deformed medium

13 p1703 A73-29553

Stress-strain state of thin circular perforated Cu plate under uniform tensile load, showing applicability of small elastoplastic finite deformation theory

13 p1703 A73-29601

Elastoplastic torsion of a cylindrical bar of multiconnected section

14 p1805 A73-29762

Finite difference solution for large deformations of cylindrical shells - A comparison with finite element solutions.

14 p1807 A73-30182

Finite element static structural analysis for small elastoplastic strains and geometric nonlinearities, considering total Lagrangian and incremental moving coordinate formulations

14 p1807 A73-30189

Nonlinear thermal elastoplastic structural analysis, using principle of virtual work in finite element method

14 p1808 A73-30192

A method of elastic-plastic analysis of largely deformed plate problems.

14 p1808 A73-30194

Finite element method application to nonlinear, microscopic and ductile fracture mechanics covering crack tip singularity elastoplastic analysis and elastic constants of metal crystals

14 p1809 A73-30200

Note on the application of the Tresca criterion to the problem of circular bending of an elastoplastic cylinder

14 p1811 A73-30485

Normal impact of a cone against an elastoplastic membrane

14 p1815 A73-30789

Study of the elastoplastic stressed state and plastic zones of a plate with a circular hole under tension

14 p1815 A73-30794

Designs of statically undeterminable elastoplastic systems under complex loads

15 p1946 A73-31141

Rectangular cross section isotropic elastoplastic material behavior under combined compressive and bending stresses with allowance for work hardening

16 p2076 A73-32931

Discrete approximations of elastic-plastic bodies by variational methods.

16 p2078 A73-32994

Thin shell elastoplastic deformation theory development for small strains, using Hooke's law to analyze hardening, stress and unloading

16 p2084 A73-34033

Shock wave structure in elastoplastic media

17 p2211 A73-34141

Book - Computer methods in structural analysis.

17 p2251 A73-35473

Multiphase composite material models for elastoplastic beam bending under loading and unloading, using stress-strain diagram in tension and compression

18 p2366 A73-36884

Study of elastoplastic state of a spherical shell with round unsupported apertures.

18 p2366 A73-36893

Finite element elastic-plastic-creep analysis of two-dimensional continuum with temperature dependent material properties.

19 p2496 A73-37483

A procedure for solving problems of elasto-plastic flow.

19 p2496 A73-37484

Inhomogeneous yield limit effect on elastic-plastic boundary of circular cylinder in torsion, considering radial and angular dependencies

19 p2498 A73-37651

Minimum principles and some theorems on the elastoplastic equilibrium of bodies subjected to nonstationary physical and thermal effects

19 p2499 A73-37765

Influence of non-singular stress terms and specimen geometry on small-scale yielding at crack tips in elastic-plastic materials.

19 p2501 A73-38264

A study on the dynamical behaviors of composite materials by dynamical model.

20 p2580 A73-38643

Stress-concentration at a hole with periodic irregularities

20 p2619 A73-39334

The incremental theory of three dimensional transient thermoelastoplasticity - Formulation and solution.

20 p2622 A73-39552

Elastoplastic strains and carrying capacity of shallow shells /Review/

21 p2786 A73-40976

Stability of cylindrical shells beyond the elastic limit

21 p2786 A73-40979

Elastoplastic stressed state of a long thick-walled cylinder subjected to the action of a magnetic field

21 p2786 A73-40981

Stability of a cylindrical shell of linearly variable thickness beyond the elastic limit

21 p2787 A73-41195

Determination of the stresses for pure elastic-plastic flexure and torsion. 22 p2919 A73-42111

Elastic-plastic wave reflection and refraction obtained by method of singular surfaces, discussing interface and plastic deformation effects [ASME PAPER 73-APMW-38] 22 p2926 A73-42895

Slow growth of cracks in a rate sensitive Tresca solid. 23 p2992 A73-43810

Potential theory-based relationships between plastic deformation and strain hardening properties of elastoviscoplastic and elastoplastic media, considering specific entropy and free energy contributions 23 p3045 A73-44099

Complex elastoplastic torsion of cylindrical shafts 23 p3045 A73-44184

Determination of the strained state of a thick elastoplastic plate with an elliptical hole 23 p3046 A73-44201

A minimum principle in dynamics of elastic-plastic continua at finite deformation. 24 p3146 A73-44678

An elastic-plastic analysis of a bar under repeated axial loading. 24 p3151 A73-45307

Plasticity theory development taking into account thermodynamics of elastoplastic materials, considering existence theorems for plastic flow and variational principle for equilibrium problems solution 24 p3153 A73-45500

ELASTOSTATICS

Solution of the thermoelasticity problem for half-spaces with boundary conditions divided by circular lines 01 p0113 A73-10013

Large amplitude oscillations of a hollow spherical dielectric. 02 p0236 A73-12518

Static analysis of beams with random material or environmental characteristics, deriving probability functions for beam descriptors 04 p0509 A73-14945

Contribution to the classical theory of solids with statistical structural characteristics 06 p0762 A73-17994

Three dimensional analysis in series form for statics and dynamics of simply supported rectangular plates of micropolar elastic material, obtaining free vibration frequencies 07 p0917 A73-20565

A comparison of first and second order axially symmetric finite elements. 09 p1158 A73-22399

Two dimensional statics for isotropic elastic body with inhomogeneous mechanical properties, discussing two-step solutions for differential equilibrium equation and boundary value problem 10 p1293 A73-24676

Finite static deformations of elastic solids at constant temperature, discussing couples for different deformations 11 p1448 A73-26748

Static force and displacement methods as eigenvalue problems. 13 p1694 A73-28246

German book - Elastostatics and elastokinetics in matrix notation: The procedure of transmission matrices. 13 p1695 A73-28300

Elastostatic invariance in the composite plane. 13 p1696 A73-28747

Variational principles application to finite element method in elastostatic and elastodynamic and elastodynamic small and finite displacement theories 14 p1806 A73-30178

Solution of the first boundary value problem of statics in the moments theory of elasticity 14 p1810 A73-30382

Static problem of elastic body with stresses at boundary, solving incompatible difference equations by explicit iteration methods 15 p1945 A73-31026

Saint Venant principle investigation for plane problem of linear elastostatics for anisotropic media by energy method, calculating exponential stress decay constant lower bound 15 p1946 A73-31102

Variational principles of three-dimensional linearized theory of elasticity problems with large initial deformations 15 p1953 A73-32091

Solution to a three-dimensional mixed boundary value problem in the theory of elasticity 15 p1953 A73-32102

Symmetric integral equations of the theory of elasticity 17 p2251 A73-35585

Use of Gq functions for the representation of solutions to equations of statics in the theory of elasticity 17 p2251 A73-35586

On kinematics and statics of finite-strain force and moment stress elasticity. 17 p2252 A73-35829

Automatic control theory and systems representation in framework of unilateral mechanics, using canonical elastodynamic and elastostatic equations 20 p2540 A73-38703

Relation between the fundamental solutions in cylindrical and spherical coordinates /with identical coordinate origins/ for certain equations of mathematical physics 21 p2753 A73-41025

The plane elastostatic solution for a symmetrically loaded crack in a strip composite. 21 p2789 A73-41669

Numerical approximation of quasi-static and dynamic problems in viscoelasticity by net-point and finite difference methods 24 p3144 A73-44505

The axisymmetric Dirichlet problem of the static theory of elasticity in displacements for a region bounded by cylindrical and spherical surfaces 24 p3146 A73-44604

The static axisymmetric problem of the micropolar theory of elasticity and thermoelasticity 24 p3148 A73-44913

Application of the finite difference method to the elastic stability problem 24 p3152 A73-45357

ELBOW [ANATOMY]

EMG measurement on male adults for muscular relaxation reaction time interval from light stimulus onset to elbow flexor response 03 p0267 A73-13699

ELDO LAUNCH VEHICLE

ELDO equatorial launching base for Europa 2 vehicle, discussing launch site and telemetry facilities and logistics management/organizational aspects 14 p1741 A73-30077

ELECTRETS

Some characteristics of isopotential curves of photoelectret state formation in compressed polycrystalline anthracene 05 p0605 A73-17176

The use of electret films as time-of-arrival detectors for shock and detonation waves. 10 p1218 A73-24122

Carnauba wax electrets manufactured under the simultaneous action of magnetic and electric fields 12 p1523 A73-27103

Foil-electret transducer arrays for real-time acoustical holography. 13 p1614 A73-28583

ELECTRIC ANALOGIES

U ANALOGIES

ELECTRIC APPLIANCES

U ELECTRIC EQUIPMENT

ELECTRIC ARCS

NT MERCURY ARCS

Electrical conductivity and total radiant power of air plasma. 01 p0081 A73-10121

Ar and Kr continuous wave ion lasers with electric arc discharge, noting quartz, graphite and beryllium oxide gas discharge tubes 01 p0059 A73-10714

Arc current, column electric field, mainstream velocity and applied transverse magnetic field relationships in magnetically balanced cross flow plasmas 01 p0084 A73-10738

The measurement of plasma transport properties in a free-burning electric arc. 05 p0603 A73-16763

Heat removal in a sectioned channel of an electric-arc plasmatron 06 p0731 A73-18572

Numerical calculations for the turbulent arc constrictor. 07 p0858 A73-19960

Influence of the thermal effect of the gas on the motion of an electric arc in a transverse magnetic field 07 p0858 A73-20081

Ar plasma diagnostics from stabilized arc emission spectra, noting thermodynamic equilibrium in central zone of arc channel 08 p0992 A73-20855

Electric arc motion during initiation by plasma injection between static electrodes in dc circuit, applying to pulsed arc commutator design 09 p1131 A73-22938

Low temperature plasma electric arc discharge generators, noting electrode interaction, energy losses and high enthalpy efficiencies 10 p1253 A73-23516

Biased wall heat transfer in electric arc chamber, noting I-V characteristics and electron current saturation in superimposed axial flow 12 p1560 A73-27700

Computer simulation of arc heaters for production of flow with high enthalpy. 13 p1707 A73-29023

Research on ignition and combustion in oxygen systems. 13 p1708 A73-29402

Effectiveness of a gas screen in plasmatrions of axial configuration 15 p1917 A73-31191

Heat removal in the sectionized channel of an electrode-type plasmatron. 16 p2042 A73-33597

Heat conductivity measurements for a hydrogen plasma in a stabilized electric arc 17 p2214 A73-34129

Low temperature plasma electric arc discharge generators, noting electrode interaction, energy losses and high enthalpy efficiencies 17 p2217 A73-35196

Microarc current flow and potential drop through cold boundary layer near plasma electrodes in MHD generators 20 p2598 A73-39604

Determination of work functions near melting points of refractory metals by using a direct-current arc. 21 p2722 A73-41563

Turbulence generation by supersonic nozzle gas flow interaction with plasmas, discussing high current electric arc in axis 22 p2895 A73-43166

ELECTRIC BATTERIES

NT ALKALINE BATTERIES

NT NICKEL CADMIUM BATTERIES

NT NICKEL ZINC BATTERIES

NT PRIMARY BATTERIES

NT SILVER ZINC BATTERIES

NT STORAGE BATTERIES

Circuitry for battery cell control and protection from overcharge and over-discharge for long service life operation 03 p0253 A73-13937

Electronically conducting oxides as cathodes or interconnection materials in high-temperature fuel cell batteries. 04 p0407 A73-15111

Carbon-PTFE fuel cell electrode for hydrogen-KOH-air batteries for operation over long time periods, discussing rolling technique and industrialization possibilities 04 p0407 A73-15114

Active control heat pipe performance for long life battery cooling. [ASME PAPER 72-WA/HT-43] 04 p0518 A73-15813

Battery charge regulator for Eole meteorological balloons power supply, describing printed circuit design and construction 07 p0778 A73-18970

Physical and thermal constraints on batteries of electrochemical power supply systems onboard satellites, sounding and booster rockets and balloons 07 p0778 A73-18977

An approach to performance assessment and management of a large solar array/battery power system. 09 p1035 A73-22775

A solar array and battery electrical power subsystem for the shuttle-launched modular space station. 09 p1153 A73-22783

Computer simulation concept for a large solar array/battery power system. 09 p1060 A73-22803

A power and load priority control concept as applied to a Brayton cycle turbo-electric generator. 11 p1309 A73-25984

Solar cell battery operational performance test equipment and computerized simulation programs for post-1975 satellite and space station systems integration and design 11 p1309 A73-25986

Solar/battery space station power plants combined with nuclear configurations, discussing rectified alternator current, direct energy transfer, and high voltage dc sources 11 p1311 A73-26008

A 25 kW solar array/battery design for an earth-orbiting space station. 11 p1311 A73-26010

Space shuttle orbiter power system requirements and design tradeoffs, comparing fuel cells, solar array/battery and radioisotope Brayton cycle and cryogenic fueled turboalternators 11 p1312 A73-26017

Power system for a 4.1 kilowatt synchronous satellite. 11 p1312 A73-26023

Battery-powered electric propulsion for north-south stationkeeping. 17 p2222 A73-34872

High-temperature batteries. 17 p2110 A73-35594

Stable high energy nonaqueous lithium-organic electrolyte batteries, discussing discharge rates, temperature effects, energy density and voltage regulation 19 p2390 A73-38396

Electric power cell for producing direct/alternating current and shaft horsepower by direct electrochemical reaction of alkali metals with water 19 p2390 A73-38397

Theory and performance of a tritium battery for the microwatt range. 21 p2737 A73-39922

Silver powder anode, perylene-iodide cathode and ionically conductive solid cyanide-iodide electrolyte battery construction and performance tests [ECS PAPER 12] 21 p2635 A73-40841

ELECTRIC BRIDGES

NT WHEATSTONE BRIDGES

NT WIRE BRIDGE CIRCUITS

Investigation of residual resistance in semiconductor switches used to commutate the measuring circuits of alternating-current bridge networks

01 p0022 A73-10080

An accurate bridge method for impedance measurements of impatt diodes.

03 p0281 A73-13175

High power inverter with commutator of single LC network and steering SCR capable of multiple high voltage dc bridge operation

03 p0253 A73-13936

Inductance and magnetic reversal losses in pulse operated communication, describing bridge circuit for comparing test sample current with capacitor voltage/time characteristics

05 p0559 A73-17241

A modified sensor of linear accelerations, velocities, and displacements over a path of 0 to 1500 mm

07 p0826 A73-20527

Prefabricated strain gage bridge instrumentation for flight testing under time and environment installation restrictions, including tail vibration, wing load and tail boom tests

09 p1083 A73-22506

Automatic measurement recorders with discrete output

13 p1617 A73-28858

Constant current and temperature hot-wire anemometer systems evaluation via ratio of changes in bridge balance to heat transfer changes between sensor and environment

13 p1620 A73-29257

Reflectometric bridge in Q band /8 mm/ - Power detected in an unbalanced bridge

19 p2403 A73-37532

Summation of the output power from two Gunn diodes

21 p2659 A73-40008

Equivalent circuits for differential bridge quartz filter inductance evaluation in mass production

24 p3071 A73-44600

ELECTRIC CHARGE

NT ELECTRIC DIPOLES

NT ELECTROSTATIC CHARGE

NT ION CHARGE

NT SPACE CHARGE

NT TRAVELING CHARGE

The effect of the surface electric charge on the gain of a solid-state traveling-wave amplifier

01 p0023 A73-10429

Radiation-driven efflux and circulation of dust in spiral galaxies.

07 p0875 A73-19345

A charge amplifier for pressure measurements

07 p0827 A73-20543

Electrometric amplifiers for inductive measurement of charges

08 p0949 A73-21713

Electric charges on stainless steel surfaces - The effects of hydrogen, charged particles, illumination, and electric fields on the work function.

09 p1133 A73-22195

Electromagnetic field of rotating charged oblate ellipsoid of revolution with infinite conductivity and vacuum or infinite magnetic susceptibility

10 p1252 A73-24344

Transient processes in an inductive energy storage element for a plasma injector

12 p1460 A73-26931

Carnauba wax electrets manufactured under the simultaneous action of magnetic and electric fields

12 p1523 A73-27103

Growth mechanism of charged ice crystals in water vapor

21 p2742 A73-40123

Oscillating spherically symmetric charge-matter fluid for avoidance of singularities in gravitational collapse models

21 p2766 A73-40316

Transients in inductive energy-storage devices for plasma injectors.

22 p2891 A73-42265

Charged black hole collisions as gravitational radiation sources in terms of conservation of mass and surface area

22 p2908 A73-42428

ELECTRIC CHOPPERS

Optimum operation conditions of thyatron generator circuit in electroacoustic system for excitation of quartz piezoelectric vibrators in ultrasonic NDT

02 p0168 A73-12147

Analysis of commutator inverters with allowance for capacitive coupling to an ac amplifier

13 p1591 A73-28854

ELECTRIC CIRCUITS

U CIRCUITS

ELECTRIC COILS

NT MAGNETIC COILS

Electric coil systems for magnetic field simulation, discussing field size and characteristics and coil configurations

16 p1997 A73-33383

ELECTRIC CONDUCTORS

Geometrical theory to approximate HF electromagnetic wave diffraction from moving conducting strip under incident field

01 p0016 A73-10192

HF microwave scattering by perfectly conducting four-sided involuted pyramid, deriving principally polarized radar cross section at small aspect angles [AD-753370]

01 p0016 A73-10193

Differing roles of electron scattering processes in the thermodynamics of metals in the normal and superconducting states

01 p0088 A73-10613

Superconducting magnetic systems reliability engineering and design, noting combined conductors for uncontrolled transition prevention in normal state under subcritical currents

01 p0005 A73-10616

Radially conducting cone wave spectrum calculation for noncophasal excitation, noting circularly polarized TEM and elliptically polarized TM wave amplitudes

03 p0278 A73-14058

Multilayer thin film microcircuit and printed circuit conductors partial capacitance and potential coefficients, using matrix method for approximate calculation

03 p0284 A73-14070

Diffraction of a two-dimensional electromagnetic field by an ideally conducting plane with a boundless rectilinear slit

04 p0423 A73-15608

Electromagnetic wave diffraction by ideally conducting homogeneous bodies of revolution with arbitrary complex permittivity and permeability, using separation of variables method

05 p0547 A73-16054

Ion-current distributions around an electrically conductive body in ionized gas flow.

05 p0603 A73-17110

On a set of continuous wave electromagnetic inverse scattering boundary conditions.

06 p0664 A73-18136

Averaged boundary conditions for a grid consisting of nonparallel and nonrectilinear conductors placed on a nonplane surface.

07 p0801 A73-20127

Transmission of electromagnetic waves through a conducting slab. IV - A simple multiple-reflection method.

07 p0852 A73-20172

Scattering by perfectly conducting rotational bodies of arbitrary form excited by an obliquely incident plane wave or by a linear antenna.

09 p1052 A73-22959

Investigation of the electrical explosion of conductors by holographic methods

10 p1248 A73-23507

Diffraction of a two-dimensional electromagnetic field on an ideally conducting plane with an infinite straight slit.

10 p1188 A73-24198

Edge condition of a perfectly conducting wedge with its exterior region divided by a resistive sheet.

11 p1329 A73-25676

Correction to 'The echo area of a perfectly conducting prolate spheroid.'

11 p1330 A73-25684

Electromagnetic scattering by a transversely moving conducting cylinder of arbitrary cross section.

12 p1468 A73-27018

Magnetoelastic vibration of electrically conducting thin shells and plates in steady magnetic field from asymptotic integration of electrodynamics equations

12 p1553 A73-27413

Coupled asymmetrical microstrip transmission lines odd and even mode wave impedances as functions of conductor strip width and spacing

12 p1481 A73-27582

Determination of the time interval for orientation of conducting nonmagnetic oblong bodies by a homogeneous alternating magnetic field

13 p1571 A73-28467

Alpha-omega dynamo problem of electrically conducting sphere magnetic field, obtaining eigenvalues from variational principle with free decay modes as trial functions

13 p1685 A73-29365

Analytical solution to problems of eddy current distribution in a thin plate and a conducting spherical shell

14 p1774 A73-30029

Integral equation formulation for electromagnetic scattering by conducting cylinders, investigating coupling between complementary boundary value problem and nonuniqueness consequences on numerical resolution

14 p1727 A73-30215

Holographic investigation of electrical explosions of conductors.

17 p2212 A73-35187

Numerical computation of antenna patterns near a conducting elliptic cylinder.

17 p2126 A73-35608

A reliable Teflon cell with many electrical leads for pressures up to 40 kilobars.

17 p2175 A73-35761

A high-speed /subsecond/ system for accurate thermophysical measurements at high temperatures. [AIAA PAPER 73-743]

18 p2316 A73-36359

Application of the four-probe method to the determination of the resistance of thin films deposited on various substrates

19 p2470 A73-37953

System for measuring the thermal diffusivity of electrically conducting materials at high temperatures

19 p2432 A73-38543

Reflection and transmission of plane waves at a boundary between two conducting media.

21 p2655 A73-41047

Diffraction of a plane electromagnetic wave by a perfectly conducting elliptic cylinder.

22 p2822 A73-41749

Electromagnetic inverse boundary conditions determination of profile and material surface characteristics of conducting circular cylindrical shape scatterer

22 p2824 A73-41834

Plane transient electromagnetic wave propagation in a generalized conducting medium.

22 p2886 A73-41965

Electromagnetic field equations in operator form for anisotropic conducting media

22 p2886 A73-42212

ELECTRIC CONNECTORS

Metal stripline connector technology to fabricate flexible silicon solar cell arrays, noting cost reduction

03 p0256 A73-14232

One-dimensional periodic superconducting weak-link systems.

04 p0484 A73-16040

Thermodynamic optimization of current leads into low temperature regions.

13 p1707 A73-29067

Field penetration through a flush mounted coaxial aperture - Variational calculation.

17 p2127 A73-35630

The lightning arrestor-connector concept - Description and data.

19 p2408 A73-37270

Electric connector reliability assessment model based on operating conditions and failure modes analysis without using MTBF

21 p2665 A73-41208

ELECTRIC CONTACTS

A reliable all-silver front contact for silicon solar cells.

03 p0256 A73-14230

Solar cells and generator technology for the Helios sun probe.

03 p0256 A73-14235

Metallic contact resistance and friction behavior under microdisplacement for lead/gold surfaces with lubricant or oxide film, noting consistency with Greenwood theory [ASLE PREPRINT 72LC-6B-1]

03 p0316 A73-14364

Analysis of the resistance of reed contacts to shock and vibration impacts

05 p0559 A73-17237

Influence of recombinations in the base contact and on the base surface upon static and dynamic characteristics of the p-n junction.

06 p0674 A73-17816

Electrical contacts to ion cleaned n-type gallium arsenide.

07 p0797 A73-19136

Characteristics of a gallium-arsenide travelling-wave amplifier with Schottky-barrier contacts.

08 p0946 A73-21118

Large area wraparound contact silicon solar cell, application and development.

09 p1036 A73-22812

Development and investigation of fine-grain metal ceramic contacts of silver/graphite and silver/nickel/graphite composition for low-voltage device applications

10 p1225 A73-24320

CdS-metal contact at higher current densities.

11 p1407 A73-24984

Ag- or Cu-based fiber reinforced composite materials for springs in electrical contact devices, investigating mechanical strength and contact and wear resistances

11 p1387 A73-25410

Friction, wear, and noise of slip ring and brush contacts for synchronous satellite use.

11 p1374 A73-26211

Implication of contact thermalization effect in two-valley semiconductors for the high frequency device performance.

14 p1783 A73-29929

Electrolytically deposited noble-metal layers in the electronic industry

16 p1987 A73-32945

- Electric contact materials technology, discussing intermetallics, ordered alloys, metal matrix composites and silver, gold and platinum based dispersion hardened alloys manufacture and properties
16 p2027 A73-32946
- A user-oriented guide to the design and application of solid state relays.
17 p2132 A73-34089
- Properties of a superconducting point contact connected to a resonator.
17 p2220 A73-35725
- Series resistance of rectangular and cylindrical semiconductor photocells with linear and circular contacts and thin base, noting dependence on contact strip width
24 p3058 A73-45251
- ELECTRIC CONTROL**
- An advanced concept in electrical power distribution control and management.
03 p0253 A73-13945
- Electric power processing, distribution and control for advanced aerospace vehicles.
03 p0253 A73-13947
- Model studies of an electrohydraulic amplifier
03 p0258 A73-14617
- Advanced aerospace power distribution and control techniques.
04 p0408 A73-15389
- Control of electro-hydraulic shaker by digital iteration techniques.
05 p0562 A73-16636
- [SAE PAPER 720823]
Possibility of affecting the coagulation of droplets in warm clouds and fog by electrical methods
06 p0719 A73-17840
- A low-sensitivity third-order active filter constructed with DVCCS/DVCCS universal sources
07 p0796 A73-18897
- Electrically controlled microwave polarization transformer
09 p1064 A73-22675
- Micromovement servocontrollers in closed loop system, using piezoelectric device, ceramic element actuators and rotary switch derived logic control signal
10 p1199 A73-24027
- Design and performance of electrically regulated phase shifter comprising rectangular waveguide section containing two ferrite resonators magnetized at ferromagnetic-resonance frequency
12 p1477 A73-26945
- System of electric control of surveillance of the control surfaces of the Concorde
15 p1830 A73-32475
- Load transfer between AC sources within relay ratings through circuit design.
17 p2133 A73-34094
- Application of distributed p-n and p-i-n structures in the development of integrated circuits for electrically controlled SHF devices
20 p2535 A73-38856
- Beam steering system of the north-south array of the DKR-1000 FIAN radio telescope
21 p2662 A73-40542
- Use of two-stage condenser braking of the single-motor drive for the mirror sections of the RATAN-600 radio telescope
21 p2675 A73-41450
- Indicator and setting devices for circular-mirror sections of the RATAN-600 radio telescope
21 p2675 A73-41451
- Electrical control of particulate pollutants from flames.
22 p2935 A73-42799
- Charged particle track detector design with electric field control of nuclear photoemulsion sensitivity, discussing microcrystals, trajectory recording and proton irradiation
23 p2982 A73-43569
- Electrooptical modulator employing a barium titanate single crystal. I - Estimates of critical control voltages
23 p2987 A73-43571
- ELECTRIC CORONA**
- Electric corona assessment of Skylab spacecraft high voltage electrical/electronic equipment and instruments, considering operating temperature and environment contaminants effects
17 p2109 A73-35256
- Tuned loop antenna for radio observation of electrostatic spark and corona discharges generated during oil tanker cleaning operations
23 p2945 A73-43960
- ELECTRIC CURRENT**
- NT ALTERNATING CURRENT
NT ARC DISCHARGES
NT AURORAL ELECTROJETS
NT BEAM CURRENTS
NT DIRECT CURRENT
NT EDDY CURRENTS
NT ELECTRIC ARCS
NT ELECTRIC CORONA
NT ELECTRIC DISCHARGES
NT ELECTRIC SPARKS
NT ELECTRODELESS DISCHARGES
NT ELECTROJETS
- NT EQUATORIAL ELECTROJET
NT GAS DISCHARGES
NT GLOW DISCHARGES
NT HIGH CURRENT
NT IONOSPHERIC CURRENTS
NT LIGHTNING
NT MERCURY ARCS
NT PENNING DISCHARGE
NT RADIO FREQUENCY DISCHARGE
NT RING CURRENTS
NT TELLURIC CURRENTS
NT THRESHOLD CURRENTS
NT TOROIDAL DISCHARGE
NT TOWNSEND DISCHARGE
- Theoretical and experimental study of the H.F. current associated with a plasma wave.
01 p0081 A73-10118
- Effect of heterogeneity and Hall current on the MHD power generator.
01 p0005 A73-10434
- Superconducting magnetic systems reliability engineering and design, noting combined conductors for uncontrolled transition prevention in normal state under subcritical currents
01 p0005 A73-10616
- Nonthermal X-radiation and electric currents in solar flares
01 p0092 A73-10937
- Device for measuring the instantaneous value of current and voltage in the operation of a pulsed plasma accelerator
02 p0196 A73-11792
- Double discharge TEA carbon dioxide laser trigger circuit, using plastic materials with selected dielectric constant and resistivity for trigger current increase
02 p0175 A73-11958
- Effects of Hall currents and collisions with neutrals on the dynamic stability of a composite hydromagnetic plasma.
03 p0346 A73-13292
- The diffusion-driven current in a toroidal resistive plasma.
03 p0348 A73-14433
- Current trapping in toroidal high current discharges.
03 p0348 A73-14435
- Current near the insulator wall in plasma accelerators.
03 p0348 A73-14437
- Estimates of dense plasma heating by stable intense electron beams.
03 p0348 A73-14438
- Passage of electric current through an illuminated semiconductor under conditions where the anisotropy parameters, the electrical conductivity, and the relaxation time are nonuniform. I
04 p0484 A73-15641
- Mathematical model for electric current in granulated media, establishing temperature dependence of tunneling conductivity for tunnel junction with metallic inclusions in oxide layer
06 p0736 A73-18117
- Forward biased P-N junction photoelectric current shown resulting from photovoltaic, photoresistive and electric injection currents superposition
06 p0738 A73-18544
- Preswitching and postswitching phenomena in amorphous semiconducting films.
06 p0739 A73-18800
- Hall current effects on waves in an electrically conducting rotating fluid.
07 p0854 A73-19104
- Polarization dependence of a photoelectric current during the modulated illumination of a system composed of an electrolyte, a porous pigment film, and a metal
07 p0851 A73-19473
- Steady nonlinear Ekman-Hartmann boundary layer on flat surface, evaluating pumping and electric current as functions of Rossby number and magnetic interaction parameter
07 p0856 A73-19512
- Effects of collisions with neutrals on the dynamic stability of a finitely conducting hydromagnetic composite plasma in the presence of Hall currents.
07 p0858 A73-19600
- Geomagnetic variations with the period of a sidereal day.
07 p0818 A73-19672
- Photocurrent pulse shape in thin organic semiconductor films
07 p0862 A73-20008
- Fine structure in the optical-absorption edge of silicon.
07 p0863 A73-20175
- Dependence of He-Ne laser output power on discharge current, gas pressure and tube radius.
08 p0976 A73-21462
- Discharge current dependence of saturation parameter of a He-Ne gas laser.
08 p0976 A73-21463
- Transient photocurrent pulse shapes and transit times in insulators with uniform and exponential trapped space charge in excitation layer or insulator surface
09 p1119 A73-21945
- Nonthermal X rays and electric currents in solar flares.
09 p1138 A73-22732
- Hall current effects in the Lewis magnetohydrodynamic generator.
09 p1130 A73-22823
- Quantum mechanical formalism for unitary transformations of wave functions, gauge transformations and current conservation, discussing use of gauge invariant atomic orbitals
10 p1251 A73-24245
- Carbon dioxide laser active medium excitation by ionizing radiation from external source during electric current passage, discussing gain dependence on pressure and mixture
10 p1229 A73-24756
- Alternating spectral oscillations of nonequilibrium photoelectron current in p-InSb in the presence of a quantizing magnetic field
10 p1261 A73-24763
- Electric current in pressurized N₂, CO₂, and their mixtures under conditions of strong ionization by an electron beam
10 p1230 A73-24883
- CdS-metal contact at higher current densities.
11 p1407 A73-24984
- Determination of attachment center parameters in semiconductors from the temperature dependence of the photocurrent
11 p1408 A73-25248
- Electrodynamics analysis of superconducting vortices interaction with cylindrical cavities /pinning/, calculating critical currents in type II superconductors in external magnetic field
11 p1409 A73-26191
- Parametron circuit current fluctuations analysis via successive approximation solution of nonlinear differential equation, investigating operational mode stability
11 p1400 A73-26452
- Comparison of methods of photomultiplier photocurrent recording in measurements of weak luminous fluxes
12 p1495 A73-26866
- The kinetic reflection coefficient in a formula for the current at a plasma/semiconductor interface in the case of an inelastic mechanism of electron energy relaxation
12 p1527 A73-26928
- Thermal noise calculation of single-carrier space-charge-limited current in a non-insulating solid.
12 p1530 A73-27029
- Aspects of the application of Rogowski's coil to the measurement of steady currents in plasma
12 p1528 A73-27306
- Diffraction of electromagnetic waves on reflectors with parameters that vary periodically in time
12 p1470 A73-27583
- Threshold of appearance of anomalous resistance for field-aligned currents in the magnetosphere.
13 p1608 A73-28726
- An empirical function between the resistance and the temperature of a carbon thermometer for 0.3 to 4.2 K.
13 p1618 A73-29071
- Electrical model for calculation of resistance strain gage errors due to grid-grid and grid-body shunt currents
13 p1622 A73-29617
- Influence of the difference in effective masses on the efficiency of heterojunction solar cells.
14 p1713 A73-30000
- NMR measurements of the speed of vortices in flux flow in a type II superconductor.
14 p1783 A73-30433
- Earth magnetosphere ion acoustic turbulence generation by longitudinal currents and electric fields, relating turbulence induced current dissipation to plasma heating
15 p1872 A73-31894
- Potential distribution in a two-gas thermionic converter at current saturation.
15 p1832 A73-32638
- Selection, application, and inspection of electric overcurrent protective devices.
16 p1987 A73-33016
- [SAE ARP 1199]
Josephson junction interference grating.
17 p2219 A73-34915
- Precise and rapid measurements of small currents from high impedance sources.
17 p2143 A73-35775
- Injection currents in semiconductors with deep polarizable impurity centers
18 p2341 A73-37046
- Load currents in missile circuits excited by a plane polarized field.
19 p2409 A73-37272
- Medium-velocity and electric-current concepts in restricted relativity
19 p2459 A73-37535
- Current carriers and electron impurity centers in ferrimagnetic semiconductors - The case of weak interaction
19 p2471 A73-37959

Horizontal electric fields and currents caused by depths-to-surface oceanic water exchange in geomagnetic field, discussing electric field distribution and magnetic field distortion

19 p2426 A73-38175

A study of the effect of the emitter current on the barrier capacitance of a transistor collector junction.

II

20 p2536 A73-39395

Electrical current in electron-beam ionized N₂ and CO₂.

21 p2749 A73-41658

Kinetic reflection coefficient at a plasma-semiconductor boundary for inelastic electron energy relaxation.

22 p2891 A73-42262

German monograph - Investigation of time-variable currents in Al-Al₂O₃-Al thin-film structures.

22 p2897 A73-42855

Models of force-free magnetic fields in resistive media.

22 p2911 A73-42938

Generation of electrical current by impact in metallic and semiconductor bodies

23 p3015 A73-43476

Experimental investigation of a 'poloidal' current in a plasma flow in an inhomogeneous axially-symmetric magnetic field

23 p3010 A73-43657

Induced currents in a stationary plasma flow in an axially-symmetric magnetic field

23 p3010 A73-43663

Fall-off of base component of I/T at low currents in a bipolar transistor.

23 p2961 A73-44148

Electric field observations by incoherent scatter radar in the auroral zone.

24 p3085 A73-45117

ELECTRIC DIPOLES

The relation between momentum transfer and capture and total scattering cross sections for ion-dipole collisions.

02 p0195 A73-12842

Vertical electric dipole excited electromagnetic fields in triple layer medium with plane boundaries, noting waveguide thickness effect on electromagnetic wave propagation

05 p0549 A73-16386

Propagation of radio waves in a triple-layer medium with spheroidal boundary surfaces

05 p0549 A73-16388

Vertical electric dipole excited electromagnetic field in earth-ionosphere waveguide, using Galerkin method for VLF electromagnetic wave propagation equation

05 p0549 A73-16389

The field of a vertical electric dipole over a spherical earth having an atmosphere that is nonhomogeneous with height

05 p0549 A73-16390

Space wave field produced by a vertical electric dipole above a perfectly conducting sinusoidal ocean surface.

06 p0665 A73-18181

Stability criteria for dipole domains in Gunn diodes

10 p1193 A73-23726

Nonstationary emission from dipole sources in a plasma with a diagonal permittivity tensor

14 p1780 A73-30263

Scattering of electromagnetic waves by a disk positioned at the boundary between two media

15 p1846 A73-32318

Electric dipole motion in Einstein unitary field with electrostatic potential as function of polar coordinates, deriving law of motion from Clausen integral formula

16 p2037 A73-33371

Interference patterns of a horizontal electric dipole over layered dielectric media.

17 p2123 A73-35270

Limitations of the dipole concept in electrocardiographic interpretation.

18 p2281 A73-36517

Nonlinear radiation reaction field effects on operator self-field and oscillating dipole, taking into account one-atom spontaneous emission and superradiance theories

20 p2590 A73-38607

Excitation of the earth-ionosphere waveguide by point dipoles at satellite heights.

20 p2528 A73-38846

Scattering of electromagnetic waves by a disk at the interface between two media.

24 p3067 A73-44624

Computerized simulation of plasma particle collisions, using electric dipole expansion method for grid charge density and electrostatic force determination with Fourier transformation

24 p3116 A73-45027

ELECTRIC DISCHARGES

NT ARC DISCHARGES

NT ELECTRIC ARCS

NT ELECTRIC CORONA

NT ELECTRIC SPARKS

NT ELECTRODELESS DISCHARGES

NT GAS DISCHARGES

NT GLOW DISCHARGES

NT LIGHTNING

NT MERCURY ARCS

NT PENNING DISCHARGE

NT RADIO FREQUENCY DISCHARGE

NT TOROIDAL DISCHARGE

NT TOWNSEND DISCHARGE

Fluctuation characteristics of dense plasmas from high-current discharges produced by electric explosion of metallic wires in vacuum

01 p0086 A73-11283

Q-switching of a CO₂ laser with the aid of an active gas cell

02 p0175 A73-11617

Electric discharge CO mixing gas dynamic laser, noting nitrogen molecules vibrational excitation and mixing with cold CO in supersonic expansion with population inversion

02 p0175 A73-12050

High power carbon dioxide electric discharge convection laser operation in closed cycle mode with combined dc and RF excitation and aerodynamic stabilization techniques

02 p0178 A73-12749

Oscillation modes and cathode potential drop in plasma generated by continuous electric discharge at low pressure between anode and cold cathode

03 p0346 A73-13603

Investigation of fluctuation and wave phenomena in argon low-current low-pressure discharges, taking place under the influence of a 'brief' axial magnetic field

03 p0348 A73-14623

Low current mercury vapor discharge positive column plasma continuous radiation measurements as function of pressure, current density and temperature at 2300-14,000 Å

03 p0348 A73-14624

High current low voltage magnetically confined hollow cathode discharge for vacuum evaporation and ionization, noting vacuum deposition of quartz and copper

04 p0455 A73-15755

Characteristics of a vacuum discharge triggered by an electron beam.

06 p0722 A73-17424

Effects of contaminants in CO₂ lasers.

[AIAA PAPER 73-52]

06 p0699 A73-17628

The development of magnetohydrodynamic flow due to the passage of an electric current past a sphere immersed in a fluid.

06 p0728 A73-17705

The emission spectrum of the silent electric discharge in ammonia and hydrazine vapor

06 p0723 A73-17916

Experimental study of argon ion laser discharge at high current.

[AD-754727]

06 p0701 A73-18361

Unstable resonators for CO₂ electric-discharge convection lasers.

06 p0703 A73-18747

Stability of an electrical discharge surrounded by a free vortex.

07 p0848 A73-19514

Comparison of theory and experiment for a transversely excited high-pressure CO₂ laser.

[AD-756053]

07 p0835 A73-19637

Parametric studies of pulsed HF lasers using transverse excitation.

[AD-760268]

07 p0835 A73-19641

Investigation of the structure of a high-current discharge in a lithium plasma.

08 p0992 A73-20853

Influence of an external electric field on the initial phase of the explosion of wires in a vacuum

09 p1119 A73-21883

High energy and power carbon dioxide laser with nitrogen and He mixtures, transverse electric discharge excitation and modular construction, noting efficiency and gain

09 p1090 A73-22081

A simple device for measuring the characteristics of double Langmuir probes in a periodic pulse discharge

10 p1257 A73-24691

Measurement of point-discharge current density in the atmosphere.

11 p1354 A73-25767

Steady conditions of a radiating self-constricted high-current discharge in a plasma

11 p1406 A73-26333

Nitrogen laser with a transverse discharge

12 p1506 A73-27215

Gasdynamic laser with a high water vapor content.

12 p1507 A73-27510

Semiconductor lasers pumped by pulsed electric discharge in vacuum.

13 p1626 A73-28545

Maximum loads on pulse-discharge light sources producing short flashes.

13 p1629 A73-29437

Performance comparison of pulsed discharge and E-beam controlled CO₂ lasers.

14 p1756 A73-29918

High frequency discharges sustained either on a cavity resonance or on a plasma resonance

14 p1779 A73-29923

High-pressure CO₂-N₂ laser excited by electric discharge controlled by means of electron beam.

14 p1757 A73-30260

Ionization instability in CO₂ laser discharges.

15 p1885 A73-32258

Electric properties of dense plasmas in high current pulsed discharge.

16 p2040 A73-32943

Effect of an external electric field on exploding wires in vacuum.

17 p2211 A73-34307

Pressure dependency of the NF₃-H₂ transverse-discharge pulse-initiated HF chemical laser.

17 p1886 A73-35790

Theoretical investigation of the CO supersonic electric discharge laser.

[AIAA PAPER 73-623]

18 p2321 A73-36171

Study of a linear noncylindrical discharge by holographic interferometry

20 p2597 A73-39198

Plasma stability of electric discharges in molecular gases.

21 p2744 A73-40220

Spectral discharge plasma emission analysis with controlled electrical synchronization of laser vaporized microsamples of steel and wolframite

21 p2711 A73-40302

Point discharge current measurements in trees and metal points during storms, discussing implications for structure of electrified clouds

21 p2684 A73-40779

Fluctuation characteristics of a dense plasma of high current discharges produced by electric explosion of metallic wires.

23 p3009 A73-43504

ELECTRIC ENERGY STORAGE

Computer-aided design and graphics applied to the study of inductor-energy-storage dc-to-dc electronic power converters.

03 p0252 A73-13931

Dynamic operating regime of multistage diode-capacitor storage networks

09 p1063 A73-22459

A nickel-hydrogen secondary cell for synchronous orbit application.

09 p1033 A73-22753

Space station solar array-energy storage-power control and distribution system based on regenerative fuel cell integrated with life support system

09 p1153 A73-22784

A regenerative fuel cell system for modular space station integrated electrical power.

19 p2390 A73-38402

ELECTRIC EQUIPMENT

Allowance for the correlation of factors in the method of priorities for electrical system optimization

05 p0560 A73-16272

Total irradiance calibrations using electrically calibrated radiometer, discussing lamp detector alignment procedures

11 p1366 A73-26252

Hydrolytic reversion of elastomeric potting compounds.

13 p1646 A73-29274

Performance measurements of aircraft electrical systems having highly distorted voltage and current waveforms.

17 p2135 A73-34604

Expanded built-in-test for advanced electrical systems for aircraft.

17 p2109 A73-35248

Electric corona assessment of Skylab spacecraft high voltage electrical/electronic equipment and instruments, considering operating temperature and environment contaminants effects

17 p2109 A73-35256

ELECTRIC EQUIPMENT TESTS

Evaluation of Intelstat IV nickel-cadmium cells.

13 p1572 A73-29582

Nickel-cadmium cells for low earth orbit applications.

13 p1572 A73-29584

Long-life, high energy Ni-Cd aerospace cells.

13 p1572 A73-29585

Sealed silver oxide zinc cells for orbiting and planetary missions.

13 p1572 A73-29586

Electric trim systems - Design and certification considerations under FAR 23.677/CAM 3.337-2.

[SAE PAPER 730299]

17 p2101 A73-34662

ELECTRIC FIELD STRENGTH

Some peculiarities of the development of the magnetic storm on March, 5-10, 1970.

01 p0036 A73-10342

Simultaneous upper atmospheric measurements of electric field at points differing in altitude by balloon-borne instruments

02 p0156 A73-11736

Free streaming electrons effect on spatial ballistic electron plasma wave echoes response, calculating echo electric fields and electron distribution function

02 p0197 A73-12065

On D-region electron heating by a low-frequency terrestrial line current with ground return.

02 p0143 A73-12533

Extensive air showers radio emission polarization, spatial distribution and electric field strength, noting geomagnetic mechanism effect

02 p0209 A73-12672

Injun 5 observations of magnetospheric electric fields and plasma convection.

03 p0303 A73-13875

Rocket sounding for space charge distribution and electric field strength in stratosphere and mesosphere, noting vertical distribution of atmospheric conductivity

05 p0570 A73-17013

Ion-acoustic oscillations effect on turbulent plasma electric conductivity within weak external electric field

06 p0729 A73-17973

Recent studies of magnetospheric electric field emissions above the electron gyrofrequency.

07 p0815 A73-19254

Electron-beam excitation of finite-sized plasma near the lower-hybrid frequency.

[TTU-SR-2]

09 p1129 A73-22638

A method for studying the action of high-intensity electric fields on microorganisms

10 p1184 A73-24419

Breakdown criteria for streamer formation, electrostatic field analysis and laboratory high voltage experiments on aircraft initiation of lightning strikes

10 p1175 A73-24558

Collective interactions and electrical conductivity of plasma in strong electric fields.

11 p1406 A73-26554

Result of medium- and long-wave observations at distances of about 7500 km

12 p1474 A73-27768

The normal-tangential form of the equations for the electrodynamics of conducting media

12 p1525 A73-27806

Electron temperature in a weakly ionized plasma during a nonlinear skin effect

12 p1530 A73-27979

Nonlinear theory of parametric wave instability in a plasma

12 p1530 A73-27981

Nonequilibrium ionization in magnetohydrodynamic conversion generators

13 p1571 A73-28071

A mode theory of radio wave propagation in an inhomogeneous atmosphere with jointed-segment N-profile.

13 p1586 A73-29227

Approximate near field parameters computation from Kirchhoff boundary values of antenna aperture field intensity

14 p1733 A73-30072

Energy partitioning of gaseous ions in an electric field.

14 p1776 A73-30246

The turbulent heating of ions and related efficiencies in a current carrying plasma.

15 p1916 A73-31081

Longitudinal force exerted by circularly polarized high-powered laser radiation in a dense electron plasma.

15 p1917 A73-31091

Field-dependent carrier transport in non-crystalline semiconductors.

15 p1924 A73-32021

The Pioneer 9 electric field experiment. III - Radial gradients and storm observations.

17 p2230 A73-34513

Electric field intensity of the lightning return stroke.

17 p2163 A73-35464

Electron emission of InSe crystals in strong electric fields

17 p2219 A73-35555

D region electron density profiles from radio broadcast field strength measurements by rocket-borne passive RF spectrometers, using ray theory for wave propagation

18 p2303 A73-35956

An example of anticorrelation of auroral particles and electric fields.

18 p2312 A73-36297

Analysis of methods for measuring electric field intensities in the magnetosphere

19 p2481 A73-37340

Propagation curves of an ionospheric wave at night for the broadcasting range.

19 p2404 A73-37915

Emission of longitudinal waves from a charge in an external high-frequency electric field in a magnetoelectric plasma

19 p2470 A73-38331

Waveguide channel point source electric field level and phase derived by Rytov smooth perturbation technique, obtaining correlation functions, energy spectra and phase fluctuations

19 p2406 A73-38338

Influence of electric field strength on effective carrier mobility in polycrystalline CdSe thin films

20 p2536 A73-39200

Influence of electrically active impurities on the mobility of individual dislocations in germanium

21 p2751 A73-40370

Simple expressions for the electric and magnetic field strengths between the elements of an infinite array.

22 p2831 A73-41849

Electromagnetic field equations in operator form for anisotropic conducting media

22 p2886 A73-42212

Book - Avalanche-diode microwave oscillators.

22 p2833 A73-42490

Radiating near-field power density and directivity reduction of tapered circular apertures.

22 p2829 A73-43181

Electrical conductivity of a plasma during collective interactions in a high-current gas discharge

23 p3009 A73-43652

Electrical breakdown in interface zone between two dielectric insulators, studying premature breakdown dependence on dielectric constant, layer thickness and electric field conditions

23 p3006 A73-43673

Non-linear propagation of VLF waves in a magnetoplasma including the effect of ions.

23 p3012 A73-44143

Electrical field distribution in the human body.

23 p2950 A73-44216

Ionospheric electric field measurements with a spin stabilized detector.

24 p3090 A73-44818

ELECTRIC FIELDS

Glow discharge electron guns for welding.

01 p0055 A73-10113

Computed secondary-electron and electric field distributions in an electron-beam-controlled gas-discharge laser.

01 p0058 A73-10130

Multiquantum ionization of a molecule represented by a nonorthogonal wave function system

01 p0080 A73-10622

Arc current, column electric field, mainstream velocity and applied transverse magnetic field relationships in magnetically balanced cross flow plasmas

01 p0084 A73-10738

Periodic structure of the electric field in a stratified plasma with tensor conductivity

01 p0085 A73-10955

Experimental study of the inverse Faraday effect in plasmas

02 p0196 A73-11587

Ionizing potential wave analysis for gas breakdown, noting photoionization role in avalanche propagation and velocity, electron densities and temperature as function of electric field

02 p0197 A73-12063

Observation and interpretation of ionization drift measurements in the F region at St-Santin-Nancay.

02 p0161 A73-12284

Horizontal and vertical drift motions in F 2 region caused by electrostatic and geomagnetic fields

02 p0162 A73-12294

Determination of the ionospheric density and temperature using a double probe electric field detector.

02 p0164 A73-12310

Electric fields and conductivities derived from wake measurements on a rocket.

02 p0164 A73-12311

Space discharge instability in carbon dioxide laser pumping by ionization source and electric field for time difference in heat removal and gas heating

02 p0177 A73-12553

Electrostatic autopilot using atmosphere electric field lines for stabilization and guidance, applying to remotely piloted vehicles

02 p0191 A73-12595

Magnetic horizontal component variations on quiet days, suggesting effect of electric field reversal at equatorial electrojet ionospheric region

03 p0299 A73-12949

Electric field in a segmented MHD generator for a finite conductivity of the walls at the channel inlet

03 p0346 A73-13621

Noise measurement in p-n junction surface of Si semiconductor wafer under transverse electric field, noting reverse current contribution

03 p0350 A73-13665

Effect of illumination on the form of current-voltage characteristics of SbSI in the paraelectric region

03 p0350 A73-13756

Magnetospheric structure studies during 1969-1971, discussing bow shock magnetosheath, magnetopause, polar cusps, electric fields and trapped particle composition

03 p0302 A73-13852

Electromagnetic wave observation in interplanetary medium and in magnetosphere, emphasizing magnetic and electric field measurements

03 p0374 A73-13855

Dc electric field measurement with rocket-borne double probes and by satellite and balloon observation, noting ionospheric fields, magnetospheric plasma and auroras

03 p0302 A73-13874

Acceleration of auroral particles by electric double layers.

03 p0303 A73-13877

Plasma convection in the vicinity of the geosynchronous orbit.

03 p0303 A73-13878

Parametric instability of a spatially modulated plasma.

03 p0347 A73-14089

Solution of the Boltzmann equation for a fully ionized plasma in an oscillatory electric field and a steady magnetic field. VI - The first velocity moments of distribution function for a homogeneous plasma in a high-frequency electric field.

03 p0349 A73-14650

Laser beam self focusing possibility in GaAs, considering nonlinearity mechanism of intervalley carrier transfer due to applied dc field

04 p0458 A73-14874

The effect of an electric field induced by a time-dependent ring current on the particle drift motion.

04 p0440 A73-14954

Kinetic and dispersion equations for collisionless plasma interaction with HF magnetic and electric fields, noting conical, drift and cyclotron instabilities prevention

04 p0478 A73-15019

Interaction of an intense electron beam with a homogeneous and a nonhomogeneous plasma

04 p0478 A73-15031

Parametric electron-beam instability in a spatially periodic electric field

04 p0479 A73-15043

A numerical computer method for computing the electrostatic field and electron paths of focusing optoelectronic systems

04 p0448 A73-15078

Equilibrium shape and stability conditions of rotating inviscid liquid drop in electric field

04 p0476 A73-15165

Magnetospheric electric fields convective motions measurement by Ba ion cloud tracking and symmetric double probe floating potential technique

04 p0442 A73-15333

Electric field and plasma observations in the magnetosphere.

04 p0442 A73-15334

Time dependent and independent electric coupling between magnetosphere and ionosphere, discussing auroral arcs formation and magnetospheric plasma convection

04 p0442 A73-15335

Two substorm studies of relations between westward electric fields in the outer plasmasphere, auroral activity, and geomagnetic perturbations.

04 p0444 A73-15545

Charge carrier cooling in nonhomogeneous semiconductors by static electric field, plotting average electron temperature as function of current

04 p0484 A73-15569

H emission line shape of plasma radiation under anisotropic electric microfields, calculating field distribution function, dispersion and frequency

04 p0480 A73-15601

Boltzmann transport equation for plasma probe detector characteristics for Maxwellian and non-Maxwellian distribution functions of electrons in dc and ac electric fields

04 p0480 A73-15602

Excitation of electromagnetic waves in a plasma with the aid of longitudinal electric fields

04 p0481 A73-15606

Application of the Stark effect to the determination of the fields in the region of microwave/plasma interaction

04 p0423 A73-15611

Numerical integration of equations of Ba cloud motion in ionosphere with end shorting, noting critical electric field for motion stability

04 p0445 A73-15649

MIS and Schottky barrier microstrip devices consisting of microstrip transmission line fabricated on semiconductor substrate, causing capacitance dependence on electric field

05 p0559 A73-16818

Study of VLF and ELF noises observed by Alouette 2.

05 p0552 A73-17163

Instrument suspended from tethered balloon for oceanic measurement of average lower atmosphere vertical electric field profile

05 p0579 A73-17251

Quantum electrodynamical models of coherent plasma electron-positron pair production and pulsed radiation in electric field, relating to pulsars

05 p0626 A73-17383

On the transport properties of charged particles in one dimension in random electric fields.

05 p0612 A73-17384

Motion of plasmoids in a toroidal magnetic multipole.

06 p0727 A73-17421

Numerical simulation of a plasma. I - General description of the model

06 p0727 A73-17574

Density and electric field oscillations of plasma in stellarator, considering magnetic field strength effect,

stabilization by ionic collisions and energy pumping mechanism

06 p0728 A73-17968

Investigation of regularities characterizing impact ionization within a high-field domain in Gunn diodes

06 p0675 A73-18076

Plasma instability in terms of electron oscillations due to parametric interaction with UHF electric field, noting inverse Cerenkov effect for electrons

06 p0729 A73-18111

Electric vector peak and rms magnitude determination for near field polarization ellipse, relating to radiation hazard criteria

06 p0667 A73-18202

Low-resistance CdTe films exhibiting a constant emf under the action of an ac field

06 p0737 A73-18222

Conversion of trapped charged particles into untrapped particles in a high-frequency electric field.

06 p0732 A73-18608

Electrostatic field effects on the fatigue of steel in

06 p0711 A73-18661

Monte Carlo simulation for electron diffusion in Cd Te, noting effects of applied electric field near threshold value for negative differential mobility

06 p0739 A73-18799

Observed relationships between electric fields and auroral particle precipitation.

07 p0814 A73-19237

A semiempirical model of large-scale magnetospheric electric fields.

07 p0814 A73-19238

Moment equations of temperature and high latitude spread F instability in presence of north-south electric field, relating to maximum Pedersen current and barium cloud deformation

07 p0814 A73-19243

Diffusion equation for current carriers in solar cell with inhomogeneous internal electric field, determining photoelectric current in p-n junction

07 p0778 A73-19299

Measurement on a polarization interferometer of absolute and relative light wave delay in liquid dielectrics under the action of an electric field

07 p0823 A73-19332

On the form and stability of electric-field profiles within a negative differential mobility semiconductor.

07 p0799 A73-19344

A mathematical model of the opposed-jet diffusion flame - Effect of an electric field on concentration and temperature profiles.

07 p0918 A73-19388

Changes in the durability and lifetime of polymer films under simultaneous exposures to an electric field and mechanical loading

07 p0842 A73-19394

Influence of an electric field on the laser-induced impurity photoconductivity of gallium selenide

07 p0861 A73-19398

Ionosphere heating effects produced by transverse electric field, discussing strong nighttime source

07 p0815 A73-19431

Magnetospheric and ionospheric potential electric fields, using variational process based on transverse/longitudinal conductivity ratios in plasma

07 p0815 A73-19433

Magnetospheric electric fields estimation from electron fluxes intensity on early daylight side

07 p0816 A73-19460

The effect of an electric field on the active medium in a dye laser.

07 p0834 A73-19540

Static electric quadrupole interaction of Ta- and Hf-ions in barium and lead titanate.

07 p0862 A73-20018

Transmission of electromagnetic waves through a conducting slab. IV - A simple multiple-reflection method.

07 p0852 A73-20172

Variation of atmospheric electric field during aurorae.

07 p0820 A73-20216

The a.c. losses of non-ideal type II superconductors under parallel configurations of electric currents and magnetic fields.

07 p0864 A73-20403

Anomalous plasma ion heating by parametric excitation of lower hybrid instabilities, using long wavelength oscillating electric field

[AD-759477] 07 p0860 A73-20482

Auroral particle influx behavior and electric field aligned electron precipitation observation by Ba release and electrostatic probe in rocket and satellite experiments

08 p0957 A73-20662

On near-field distributions along the leaky coaxial cable.

08 p0937 A73-20804

Experimental study of influence of an electric field on a laminar flame.

08 p1021 A73-20864

Influence of a constant electric field on the dielectric properties of polycrystalline BaTiO₃

08 p0995 A73-21273

Calculation of the field amplitude and phase velocity of low-frequency waves in the earth's spherical waveguide

08 p0939 A73-21285

Concentrations of carriers and electric field along an insulating or semiconducting sample: Developments of steady solutions up to the second order Case of weak potentials

08 p0995 A73-21443

Observation of beam-plasma interaction in a toroidal plasma in a large electric field.

08 p0993 A73-21631

Electric and magnetic field shielding performance of nonmagnetic metallic cylinders, using Sommerfeld approximation

08 p0949 A73-21663

Particle and energy fluxes across magnetic field in axisymmetric toroidal magnetic traps and plasmas with weak collisions, calculating radial electric field

08 p0993 A73-21695

Parametric instability of an electron beam modulated by an external electrostatic field

09 p1123 A73-21878

Influence of an external electric field on the initial phase of the explosion of wires in a vacuum

09 p1119 A73-21883

Dwell times of exploding tungsten wires in air.

09 p1119 A73-21929

Relations between ionospheric electric fields and energetic trapped and precipitating electrons.

09 p1073 A73-22056

Charge separation induced vertical electric field calculated for wind motion periodic with height, latitude and longitude at magnetic equator, noting relationship to electrojet

09 p1074 A73-22067

Characteristics of the electric field far from and close to a radiating antenna around the lower hybrid resonance in the ionospheric plasma.

09 p1049 A73-22277

Analytical and computer simulation of two ion species RF heated magnetoplasmas response to driving electric fields near lower hybrid frequency, observing parametric instabilities

[TTU-SR-2] 09 p1129 A73-22640

Study of antenna cross-polarization characteristics by using microwave holography

09 p1065 A73-23087

Zero-mass scalar and electrostatic fields with the central symmetry in the general relativity.

09 p1121 A73-23148

Stability criteria for dipole domains in Gunn diodes

10 p1193 A73-23726

Origin of the external electric field detected near animals and men

10 p1184 A73-23942

Variational determination of electric field induced by charge separation in near wake of negatively charged body moving at mesothermal speeds in collisionless plasma

10 p1254 A73-24116

Space discharge instability in carbon dioxide laser pumping by ionization source and electric field for time difference in heat removal and gas heating

10 p1228 A73-24182

Boltzmann transport equation for plasma probe detector characteristics for Maxwellian and non-Maxwellian distribution functions of electrons in dc and ac electric fields

10 p1254 A73-24192

Excitation of electromagnetic waves in a plasma by longitudinal electric fields.

10 p1254 A73-24196

Determination of field strength in a microwave-plasma interaction by means of the Stark effect.

10 p1254 A73-24201

Electromagnetic wave reflection at interface between anisotropic Vlasov plasma and vacuum with external magnetic field, deriving electric and magnetic field characteristics

10 p1255 A73-24260

Low-frequency parametric instabilities of magnetized plasmas with two ion species.

10 p1255 A73-24261

Measurement of the horizontal component of the electrostatic field intensity in the lower atmosphere

10 p1219 A73-24400

Experimental observation of Wannier levels in semi-insulating gallium arsenide.

10 p1260 A73-24638

Relationship of southward-drifting auroral arcs to the magnetospheric electric field and substorm activity.

10 p1213 A73-24734

Magnetospheric substorms correlation with interplanetary magnetic field, discussing balloon and satellite electric field measurements

10 p1215 A73-24784

Electric field in the plasma sheath at the electrodes and the Bohm condition

10 p1258 A73-24879

Strict calculation of static fields in devices for periodic electrostatic focusing /PEF/ of electron beams

10 p1197 A73-24882

On the origin of the electric field of polarization in a gravitational plasma.

11 p1350 A73-24990

Hydrogen promoted corrosion of tungsten by oxygen in an electric field A field ion microscope study.

11 p1325 A73-25205

Effect of impurities and X-ray irradiation on the motion of pores in ionic crystals under the action of an external electric field

11 p1401 A73-25242

Vacuum state of a relativistic system interacting with an external field

11 p1397 A73-25245

Electrostatic turbulence parametric excitation by electric field with frequency near plasma frequency, accounting for saturation electric field in anomalous plasma heating via electron trapping theory

11 p1403 A73-25256

Analyses of techniques for measuring DC and AC electric fields in the magnetosphere.

11 p1352 A73-25316

Polynomial solutions to the plane problem of electroelasticity theory

11 p1434 A73-25394

Light absorption coefficient of disordered semiconductor within external dc field, discussing electron states near band boundaries

11 p1408 A73-25427

Tangential electric field near base driven cylindrical antenna surrounded by free space or by homogeneous isotropic dissipative medium from charge distribution measurement

11 p1329 A73-25665

Investigation of heat transfer in a rarefied molecular gas with the aid of the Senfleben effect

11 p1453 A73-26445

Current and fields reduced in plasmas by relativistic electron beams with arbitrary radial and axial density profiles.

11 p1407 A73-26560

Carnauba wax electrets manufactured under the simultaneous action of magnetic and electric fields

12 p1523 A73-27103

The periodic structure of an electric field in stratified plasma with tensor conductivity.

12 p1529 A73-27531

Longitudinal magnetospheric currents contribution to auroral electrojet from satellite observation data, noting magnetosphere electric field excitation of meridional Pedersen and Hall currents

12 p1493 A73-27650

Determination of the effect of electric fields on the ionosphere, based on the behavior of the F₂-layer above geomagnetically conjugate points

12 p1493 A73-27760

Perpendicular and parallel electric fields in the ionosphere during a magnetospheric substorm

12 p1494 A73-27776

Electric field interaction with polar molecules at varying density diffusing through solid body surface, deriving dispersion law for density and potential fluctuations

12 p1526 A73-27939

The channel flow of an electrically conducting Prandtl-Eyring fluid in a magnetic and an electric field

13 p1663 A73-28161

The elastic dielectric as oriented elastic continuum

13 p1658 A73-28163

Improved uniform-field electrode profiles for TEA laser and high-voltage applications.

13 p1626 A73-28366

Method of experimental study of fields in electromagnetic resonators - Application to helicoidal resonators

13 p1589 A73-28472

Aerosol particle downward motion in vertical electric field, discussing stability of major axis orientation of ellipsoid of revolution

13 p1654 A73-28881

The orientations of ice crystal models during a fall in an electric field

13 p1654 A73-28882

Particle diffusion rate due to poloidal magnetic field component in low beta symmetric toroidal plasma, discussing losses induced by electrostatic field fluctuations

14 p1778 A73-29693

Electrostatic and magnetic fields methods comparison for small angle scanning of electron beam, considering particle trajectories, field energy and circuit electrical parameters

14 p1732 A73-29913

Split Langmuir probe measurements of current density and electric fields in an aurora.

14 p1748 A73-29970

Electric field and plasma density oscillations due to the high-frequency Hall current two-stream instability in the auroral E region.

14 p1748 A73-29971

Equatorial spread F formation convective electric fields generation by neutral winds and conductivity caused by metallic ion concentrations

14 p1749 A73-29988

Secondary source method solutions for media interface integral equations of electrostatic fields in piecewise homogeneous anisotropic media
14 p1774 A73-30027

Detection of a feedback in a plasma-electron beam system
14 p1781 A73-30585

Effect of induced axial electric field on a relativistic electron beam pulse propagating through a plasma.
14 p1777 A73-30661

Structured discharges in high frequency plasmas.
14 p1782 A73-30770

Equivalence of geoelectric cross sections in the frequency probing method
14 p1750 A73-30835

Electron current estimation along auroral zone-plasma neutral sheet field line from steady state one dimensional model
15 p1866 A73-31065

Motion of a sphere in a conducting fluid under the action of crossed electric and magnetic fields
15 p1917 A73-31405

Electrical conductivity and total emission coefficient of air plasma.
15 p1918 A73-31657

Magnetic dip equator region ionospheric drifts and electric fields measurements and experimental techniques
15 p1868 A73-31752

Numerical simulation of equatorial electric fields and magnetic variations based on global ionospheric dynamo and equatorial electrojet models
15 p1869 A73-31753

Flame propagation in a transverse electric field
15 p1957 A73-31869

Plasma and fields in the vicinity of a rapidly moving body in the presence of an external magnetic field
15 p1919 A73-31880

Magnetospheric electric field under quiet conditions on the basis of ground-based observations of whistlers
15 p1872 A73-31903

The electric field and structure of a weakly ionized plasma in the vicinity of a small charged body
15 p1921 A73-32322

Kinetic instability of a plasma located in an SHF field
15 p1921 A73-32332

The effect of polar magnetic sub-storms on the equatorial sporadic E.
15 p1874 A73-32596

Continuum analysis of the photoionization chamber in the transition from low to high rates of ionization.
16 p2015 A73-33321

Effect of a sheath on the fields of a probe in a hot magnetized plasma.
16 p2041 A73-33330

Ion-ion instability induced by ac electric fields.
16 p2042 A73-33336

Additional results from an Ogo 6 experiment concerning ionospheric electric and electromagnetic fields in the range 20 Hz to 540 kHz.
16 p2003 A73-33438

Theory of the oscillations and stability of a semiconductor plasma with a small number of carriers in a strong electric field
16 p2042 A73-33734

Sudden disappearance of Es-q and the reversal of the equatorial electric fields.
16 p2008 A73-33879

Characteristics change of Gunn diodes with uniaxial stress and temperature.
16 p1991 A73-33996

Fluctuation theory of the two-dimensional mixed state of superconductors of the first kind
16 p2044 A73-34068

Parametric instability of an electron beam modulated by an external electrostatic field.
17 p2215 A73-34302

Operational aspects of coaxial plasma accelerator with gas preionization by induction electric field introduced into interelectrode gap via longitudinal slits in external electrode
17 p2215 A73-34304

Effect of an external electric field on exploding wires in vacuum.
17 p2211 A73-34307

The ionospheric electric field during substorms - An interpretation based on non-uniform reconnection in the geomagnetic tail.
17 p2159 A73-34512

Electron energy distribution function validity for nonequilibrium plasma in presence of electric field verified for ionized cesium vapor positive column
17 p2216 A73-34551

Diffusive motion of initially ellipsoidal plasma irregularities or ion clouds in upper atmosphere, considering space charge electric field effects
17 p2160 A73-34787

Solving some contact problems by electrical modeling
17 p2244 A73-34795

Generation-recombination noise and the microwave emission from InSb.
17 p2219 A73-34912

Currents in Florida lightning return strokes.
17 p2163 A73-35465

Effect of an electric field on the negative photoconductivity of high-resistance ZnTe-CdTe crystals
17 p2219 A73-35552

Field penetration through a flush mounted coaxial aperture - Variational calculation.
17 p2127 A73-35630

A method for solving the problem of irradiation in anisotropic plasma.
17 p2217 A73-35724

ESRO Geos geostationary satellite for measurement of magnetospheric plasma electric and magnetic fields and drift rate at various frequency regions via electron injection
17 p2176 A73-35816

Cross-field instability as a mechanism for equatorial E region irregularities.
18 p2304 A73-35998

Generalized representation of electric fields in interaction gaps of klystrons and traveling-wave tubes.
18 p2292 A73-36595

Injection and field processes in thin semiconductor films in the current jump region
18 p2341 A73-36723

Probe measurement of the electrostatic field in the ionosphere and magnetosphere
18 p2314 A73-37026

Ruby laser light spark ion-electron currents in gap between copper plates under electric field
18 p2322 A73-37047

Study of plasma systems with a closed electron drift and a distributed electric field
19 p2466 A73-37357

Traveling longitudinal electrostatic waves excitation in warm nonuniform plasma by external HF electric fields, using kinetic theory
19 p2468 A73-37857

Computations of the field amplitude and phase velocity of low-frequency waves in a spherical surface waveguide.
19 p2404 A73-37914

Horizontal electric fields and currents caused by depths-to-surface oceanic water exchange in geomagnetic field, discussing electric field distribution and magnetic field distortion
19 p2426 A73-38175

Low-frequency flute instabilities of a bounded plasma column.
20 p2595 A73-38889

Lunar thermal ionosphere acceleration and detection within lunar electric field for electric potential of moon in solar wind or magnetosheath
20 p2604 A73-38933

Explorer 45 /S3-A/ symmetrical floating probes for plasmopause dc electric fields, discussing plasma sheaths, noise storms, whistlers, electric field strength and orbit configuration
20 p2552 A73-38954

Plasma wave observations near the plasmopause with the S3-A satellite.
20 p2552 A73-38956

Structural determination of electric field conditions in ionizing shock waves.
20 p2596 A73-38964

Structural determination of electric field conditions in ionizing shock waves.
20 p2596 A73-38965

Non-turbulent electric fields in soliton and shock-like structures in magnetized plasmas.
20 p2596 A73-38967

The electron kinetics of a weakly ionized Lorentz plasma in arbitrarily oriented external electric and magnetic fields
20 p2596 A73-39192

Plasmaspheric quasistatic electric fields and plasma convection, discussing dynamic electric fields and magnetospheric field penetration to low latitudes
21 p2679 A73-40075

Statistical analysis of daily, monthly, annual and seasonal activity of earth currents field, presenting tables of storms and disturbances
21 p2681 A73-40107

Electric field in an MHD channel of rectangular cross section in the presence of the Hall effect
21 p2744 A73-40183

Probability distribution of electric fields in thermal and nonthermal plasmas.
21 p2744 A73-40216

Contribution to the theory of electromagnetic fluctuations of a plasma situated in a weak SHF electric field
21 p2746 A73-40517

Parametric excitation of oscillations in an electron plasma
21 p2746 A73-40518

Parametric excitation of ion-acoustic oscillations in a plasma situated in an alternating electric field and a constant magnetic field
21 p2746 A73-40519

Electron-acoustic and ion-cyclotron parametric instabilities of a plasma in an alternating electric field. I, II
21 p2746 A73-40520

Rocket measurements of electric field and optical aurora during weak PCA event, noting rocket passage through discrete auroral forms
21 p2684 A73-40781

Solar quiet dynamo region electric fields and currents diurnal and semidiurnal field components variations with latitude
21 p2689 A73-41357

Diurnal and seasonal variations of neutral winds and electric fields above 90 km in the vicinity of the auroral electrojet.
21 p2690 A73-41365

Electrohydrodynamic Rayleigh-Taylor instabilities of a plane circular interface.
21 p2749 A73-41626

Electric field in an electrode sheath and the Bohm criterion.
21 p2749 A73-41654

Static fields for periodic electrostatic focusing of electron beams.
21 p2668 A73-41657

Calculation of the early time radiated electric field from a linear antenna with a finite source gap.
22 p2832 A73-41856

Barium cloud release near equatorial plane for investigating interaction with ambient medium and electric and magnetic field properties in outer radiation belt
22 p2852 A73-41932

Balloon and VLF whistler measurements of electric fields, equatorial electron density, and precipitating particles during a barium cloud release in the magnetosphere.
22 p2845 A73-41934

Preliminary analysis of NASA optical data obtained in barium ion cloud experiment of September 21, 1971.
22 p2846 A73-41937

Nature of the anomaly of the electrical conductivity of a magnetized plasma
22 p2892 A73-42381

Ambipolar diffusion generator based on self generated electric fields in premixed ionized methane flame, comparing with opposite caloelectric effects
22 p2895 A73-42773

Observation of extraordinary wave propagation near the lower hybrid resonance frequency.
22 p2895 A73-43023

Effect of an electric field on the ignition of a reacting binary gas mixture
23 p3009 A73-43441

Charged particle track detector design with electric field control of nuclear photoemulsion sensitivity, discussing microcrystals, trajectory recording and proton irradiation
23 p2982 A73-43569

Investigation of the influence of a nonuniform high-frequency electric field on the parameters of a helium-neon laser
23 p2987 A73-43575

Light absorption coefficient of disordered semiconductor with random field due to charged impurity centers in presence of constant external electric field
23 p3016 A73-43648

Electric polarization of a plasma beam in an axially symmetrical magnetic field
23 p3009 A73-43655

A computational study of the diffusion of meteor trains using a self-consistent model for the space-charge electric field.
23 p3029 A73-43684

Quantum transport theory of high-field conduction in semiconductors.
23 p3016 A73-43775

Linear external electric field approximation for intervalley scattering effects on nondegenerate semiconductor surface electroconductivity
23 p3017 A73-44045

Theory of parametric resonance in a spatially modulated plasma
23 p3013 A73-44334

The behavior of nematic liquid crystals in the electric field
23 p3019 A73-44387

The possibility of field emission from metal surface with a Q-switched laser pulse.
24 p3095 A73-44404

Plasma instability in terms of electron oscillations due to parametric interaction with UHF electric field, noting inverse Cerenkov effect for electrons
24 p3114 A73-44500

Computation of plane-meridional fields of non-homogeneous coaxial cables
24 p3067 A73-44598

Electric field observations by incoherent scatter radar in the auroral zone.
24 p3085 A73-45117

Penetration of thundercloud electric fields into the ionosphere and magnetosphere. I - Middle and subauroral latitudes.
24 p3085 A73-45118

Probe electric field measurements near a midlatitude ionospheric barium release.
24 p3085 A73-45119

Polar cap electric field measurements by balloons indicating ionospheric convection control by interplanetary magnetic field

24 p3086 A73-45135

Calculation of the nonstationary electric field, carrier concentration, and current distribution in semiconductor integrated circuits

24 p3119 A73-45177

Charge transfer from a highly electrically stressed water surface during drop impact.

24 p3108 A73-45206

The determination of whistler nose-frequency and minimum group delay and its implication for the measurement of the east-west electric field and tube content in the magnetosphere.

24 p3087 A73-45210

Transient ion neutralization by electrons.

24 p3111 A73-45411

A new electric field effect in silicon solar cells.

24 p3058 A73-45426

Electron-molecule collision frequencies in a crossed electric and magnetic field.

24 p3118 A73-45476

ELECTRIC FILTERS

NT BANDPASS FILTERS

NT DIGITAL FILTERS

NT INFRARED FILTERS

NT LINEAR FILTERS

NT LOW PASS FILTERS

NT MICROWAVE FILTERS

NT OPTICAL FILTERS

NT RADAR FILTERS

NT RADIO FILTERS

NT TRACKING FILTERS

NT ULTRAVIOLET FILTERS

NT WAVEGUIDE FILTERS

Loss compensation in the case of filters with additional resistors

03 p0284 A73-14124

Security system signal detector with time delay and prediction filters and optimal noise suppression, noting detection time dependence on cost effectiveness

06 p0679 A73-17806

Design of active filter sections performing biquadratic transfer functions on the basis of a branched operational-amplifier configuration

07 p0796 A73-18895

Design of selective third-order active RC filters exhibiting high Q values at low Q sensitivities

07 p0796 A73-18896

A low-sensitivity third-order active filter constructed with DVCCS/DVCCS universal sources

07 p0796 A73-18897

Requirements specification for ac and dc current carrying filter networks for electromagnetic interference reduction, noting RLC circuits

08 p0942 A73-20697

Use of matrix eigenvalues in the synthesis of symmetrical two terminal pair networks

08 p0947 A73-21397

Theoretical fundamentals of constructing parametric filters equivalent to linear filters

09 p1063 A73-22451

Amplitude predistortion and deemphasis filters, measuring channel noise immunity enhancement by mean square deviation

10 p1195 A73-24379

Active RC filter circuit design based on Pukhov generalized two subcircuit model, determining complex transfer function

10 p1195 A73-24511

Differential mode of operation for bucket-brigade circuits.

11 p1341 A73-25360

Discrete wideband FM signals optimal filter synthesis by coupling two nonlinear servosystems

12 p1467 A73-26869

Use of the eigenvalues of a matrix to synthesize symmetrical four-terminal networks.

19 p2415 A73-38355

Equivalent circuits for differential bridge quartz filter inductance evaluation in mass production

24 p3071 A73-44600

ELECTRIC FUSES

Self healing fuse for fast acting current overload protection of electric circuits, discussing design and performance

03 p0283 A73-13942

Selection, application, and inspection of electric overcurrent protective devices.

16 p1987 A73-33016

ELECTRIC GENERATORS

NT AC GENERATORS

NT ALKALINE BATTERIES

NT DIRECT POWER GENERATORS

NT DYNAMOMETERS

NT FUEL CELLS

NT HYDROGEN OXYGEN FUEL CELLS

NT MAGNETOHYDRODYNAMIC GENERATORS

NT NICKEL ZINC BATTERIES

NT PHOTOELECTRIC GENERATORS

NT PRIMARY BATTERIES

NT RADIOISOTOPE BATTERIES

NT REGENERATIVE FUEL CELLS

NT ROTATING GENERATORS

NT SNAP 19

NT SNAP 27

NT SNAP 29

NT SOLAR AUXILIARY POWER UNITS

NT SOLAR CELLS

NT SOLAR GENERATORS

NT THERMIONIC CONVERTERS

NT THERMOELECTRIC GENERATORS

NT TURBOGENERATORS

High efficiency dc-to-dc converter with second non-saturable transformer for eliminating collector current spike to reduce electromagnetic interference and transistor damage

01 p0005 A73-10247

Electrical power source for spacecraft reentry trajectory control system, thermal protection and radio communication based on reentry vehicle external surfaces utilization as generator electrodes

01 p0111 A73-11174

Solar cell generator design for Helios solar probe, considering thermal stresses at sun proximity and sufficient power generating capacity at orbital apogee [DGLR PAPER 72-091]

02 p0131 A73-11663

Synchronous electric generators with superconducting field windings, discussing fundamental characteristics, operating modes, refrigeration and cryogenic equipment and applications

02 p0132 A73-11834

Electric generator inside turbojet or turbofan aircraft engine to reduce need for external gearbox, simplifying nacelle assembly and increasing aircraft design flexibility

[AIAA PAPER 72-1056]

03 p0252 A73-13387

Design point characteristics of a 500 - 2500 watt isotope-Brayton power system.

[AIAA PAPER 72-1059]

03 p0252 A73-13388

Nuclear rocket engine reactor utilization as energy center for propulsion, attitude control, refrigeration and scientific experiments, emphasizing dual mode electrical power generation

[AIAA PAPER 72-1091]

03 p0340 A73-13412

Dual mode applications of nuclear rocket engine for spacecraft propulsion and electrical power generation, considering payloads and missions competitiveness with nondual system

[AIAA PAPER 72-1092]

03 p0341 A73-13413

Reliable uninterrupted controlled transient voltage dc power supplies with active energy storage element, comparing three system configurations, design features and applications

03 p0253 A73-13946

Electric power processing, distribution and control for advanced aerospace vehicles.

03 p0253 A73-13947

Technology assessment of superconductivity application to windings of electric machinery

07 p0863 A73-20108

Aircraft and land vehicle electric generators and motors, noting semiconductor application and cooling systems

07 p0779 A73-20124

Narrow band and broad band step-recovery diode frequency multipliers for microwave power generation.

08 p0947 A73-21138

Investigation of the output characteristic and errors of a reversible, contactless, dc tachometric generator designed on the basis of a synchronous machine

09 p1033 A73-22342

Spacecraft dynamic solar electric power/thermal control system with cold liquid flow and regenerator cooling for energy conversion efficiency and weight characteristics improvements

09 p1153 A73-22785

Concepts for application of 500- to 2500-W Brayton power systems for shuttle-launched missions.

09 p1154 A73-22794

Slip parameter for electrodynamic generators with unsteady flow.

09 p1037 A73-22825

Recent technology advances in the NASA-Lewis Research Center Brayton program.

09 p1037 A73-23249

The Gicodyne 400 power generator using a radioisotopic source with thermodynamic conversion

09 p1038 A73-23283

Theoretical possibility of converting the kinetic energy of an ionized gas flow into electricity

10 p1177 A73-23473

Autonomous composite power system with electrochemical generator, ion exchange membrane and storage battery

11 p1308 A73-25625

Evaluation testing of a closed Brayton-cycle electrical-power-conversion system.

11 p1309 A73-25983

A 6 kWe organic Rankine power conversion system for space applications.

11 p1310 A73-26006

Solar array concept for a portable retractable oriented power system.

11 p1310 A73-26007

An integrated system for space station power, life support, and propulsion.

11 p1311 A73-26009

A modular Space Station/Base electrical power system - Requirements and design study.

11 p1311 A73-26015

Design criteria and candidate electrical power systems for a reusable Space Shuttle booster.

11 p1311 A73-26016

Computerized design of electromagnetic systems in electric power conversion and electromechanical devices, noting mathematical models for electromagnetic field calculations

11 p1313 A73-26114

Observation of Raman scattering by SO₂ in a generating plant stack plume.

13 p1607 A73-28547

Large area silicon solar array development.

13 p1573 A73-29593

150 KVA integrated drive generator for aircraft electrical systems.

17 p2109 A73-35253

Power-generation potential of various IMPATT structures from a scaling approximation.

21 p2668 A73-41591

ELECTRIC IGNITION

Electroexplosive device pin-pin firing frequency mathematical modeling and prediction based on RF impedance data obtained nondestructively by automatic network analyzer

22 p2822 A73-41793

Effect of an electric field on the ignition of a reacting binary gas mixture

23 p3009 A73-43441

ELECTRIC IMPULSES

U ELECTRIC PULSES

ELECTRIC LEADS

U ELECTRIC WIRE

ELECTRIC MOMENTS

Electric dipole moment of diatomic molecules by configuration interaction. V - Two states of $|2/\Sigma_{\text{g}}^{\pm}|$ symmetry in CN.

04 p0477 A73-14816

ELECTRIC MOTORS

NT MICROMOTORS

NT SYNCHRONOUS MOTORS

NT TORQUE MOTORS

Flooded rotor, direct current acyclic motor, with superconducting field winding.

02 p0132 A73-11829

Analogue simulation for transient and steady state performance of group-triggered cycloconverter supplying controlled slip induction motor, discussing commutation failures

03 p0253 A73-13932

Speed-torque characteristics of a solar cell motor.

04 p0406 A73-15068

Computer control algorithms for transient response optimization in on/off motor control system synthesis

06 p0741 A73-17963

Technology assessment of superconductivity application to windings of electric machinery

07 p0863 A73-20108

Aircraft and land vehicle electric generators and motors, noting semiconductor application and cooling systems

07 p0779 A73-20124

Correlation analysis of the accuracy of the machining of micromachine components

09 p1088 A73-22660

Analysis of the mechanical and energetic characteristics in pulse-coded regulation of an asynchronous motor

09 p1037 A73-22939

Start/stop motor incremental motion system design for optimal control with minimized energy dissipation and operating temperature under inertial and constant torque load

10 p1198 A73-24023

Variable-reluctance stepping motor performance capabilities for point-to-point positional control.

10 p1199 A73-24024

A hybrid motor - A high-speed and accuracy final actuator/automatic control element/

10 p1177 A73-24025

Automation of thermal design calculations for electrical machines

11 p1313 A73-26115

Investigation of new elements and equipment configurations in stable-frequency, alternating-current, electrical power supply systems employing primary power plants consisting of engines with varying rotational speed

12 p1460 A73-26785

System for automatic regulation of the constant-absolute-slip mode of an asynchronous electrical actuating element with frequency-modulation control by a thyristor converter

12 p1460 A73-26786

A positional, asynchronous, thyristor-based, electrical servo actuating element with directional shaping of the phase trajectories

12 p1460 A73-26787

Hot environment lubrication failures of sleeve bearing diester lubricant system in small electric motors, using reliability-temperature accelerated tests

[ASME PAPER 73-DE-13]

14 p1767 A73-30819

Effect of linear load gradation in the end zones of an inductor on the longitudinal side effect in induction machines

15 p1832 A73-31410

Electromagnetic inductive microsystems with synchronization. I Determination of the characteristic functional magnitudes. II - Determination of the magnetic field in a region with linear and nonlinear media

16 p1992 A73-33664

Variable speed single- and multi-quadrant drives using thyristor electronic regulating unit with static converter motor and frequency changers

16 p1971 A73-33961

Use of two-stage condenser braking of the single-motor drive for the mirror sections of the RATAN-600 radio telescope

21 p2675 A73-41450

ELECTRIC NETWORKS

New transistor squaring stage with a 'smooth' parabolic characteristic for realizing a simple high-precision parabolic multiplier

01 p0024 A73-10924

Parameter selection scheme for unit measuring frequency deviation as function of voltage, resistance and circuit sensitivity

02 p0149 A73-11864

Mathematical model selection rules for stability studies of linear mechanical or passive electrical network systems with arbitrary degrees of freedom

08 p0987 A73-20787

Feedback loop and forward path electronic circuits, discussing two port network representation

10 p1201 A73-24384

Application of the invariant of a homographic transformation to measure the series resistance of semiconductor elements

11 p1336 A73-25319

Application of similarity theory to the calculation of certain characteristics of an electrical explosion of wires

12 p1523 A73-26937

Formation of current pulses in an inductive load by reactive two-terminal networks

12 p1481 A73-27586

Stationary multiport networks frequency response and representation by equivalent circuits

13 p1589 A73-28122

Automatic measurement of the Q factor of stationary bipolar networks and multiports

13 p1589 A73-28123

Nonlinear distortions of series-connected two-port networks

15 p1850 A73-31253

Electrical network analysis and synthesis problems concerning sensitivity characteristics relationship to circuit parameters and structure determination to satisfy behavioral requirements respectively

21 p2670 A73-41074

Application of similitude theory to exploding wire experiments.

22 p2886 A73-42271

ELECTRIC POTENTIAL

NT BIOELECTRIC POTENTIAL

NT CONTACT POTENTIALS

NT COULOMB POTENTIAL

NT LOW VOLTAGE

NT PHOTOVOLTAGES

NT SPIKE POTENTIALS

Electric potential and particle concentration of a plasma in the proximity of a projectile moving rapidly toward the plasma

01 p0086 A73-11289

Device for measuring the instantaneous value of current and voltage in the operation of a pulsed plasma accelerator

02 p0196 A73-11792

Multilayer thin film microcircuit and printed circuit conductors partial capacitance and potential coefficients, using matrix method for approximate calculation

03 p0284 A73-14070

Ionospheric plasma flow past a semi-infinite cylinder.

04 p0440 A73-14967

Magnetospheric electric fields convective motions measurement by Ba ion cloud tracking and symmetric double probe floating potential technique

04 p0442 A73-15333

Emitter efficiency increase in annular colloid microthrusters with single sharp tips for high specific charge of conducting liquid droplets under low potential

04 p0488 A73-15723

Bubbles and operating voltage effects in electrochemical machining of tungsten carbide and discharge machining of glass

[ASME PAPER 72-WA/PROD-21]

04 p0456 A73-15804

Determination of the optimal structure of a unit measuring the effective value of a nonsinusoidal periodic voltage

05 p0560 A73-16330

Nonlinear analysis for local microwave oscillator voltage waveform across nonlinear junction of Schott-

ky barrier mixer diode, comparing results with analog simulation

06 p0677 A73-18740

Influence of repeated voltage applications on the reliability of a system

07 p0800 A73-19417

Characteristic functions of potential distribution on sphere with longitude dependent conductivity for application to ionosphere electrodynamics

07 p0816 A73-19444

The theoretical output of a ring core fluxgate sensor.

07 p0825 A73-20219

Investigation of the operation of a polarographic sensor under the action of surge-type polarizing voltage, using an electric analog

08 p0965 A73-21107

Potentiostatic study of iron meteorite corrosion.

09 p1139 A73-21857

Direct current and voltage effects on plasma longitudinal oscillations, discussing frequency dependence and waves in semiconductors with ionic lattices

09 p1129 A73-22681

Threshold voltage of nonuniformly doped MOS structures.

09 p1064 A73-23046

Induction flowmeter theory in a T-tube of circular section.

10 p1220 A73-24619

Strict calculation of static fields in devices for periodic electrostatic focusing /PEF/ of electron beams

10 p1197 A73-24882

Electron-neutral particle collisions effect on potential of test charge moving at velocity lower than plasma electrons, using BGK model and Lorentz collision operator

11 p1404 A73-25260

Calculation of the rotor potential of an electrostatic gyroscope

11 p1364 A73-26098

Dissolution of Ti-6Al-4V at cathodic potentials in 5N HCl.

12 p1512 A73-27249

Applied electrical potential effect on heat transfer to tube immersed in highly ionized flow of atmospheric pressure Ar plasma

12 p1529 A73-27696

Simplified Hartree-Fock approximation for complex atom opacity efficient calculation based on homogeneous one-electron orbital equation solution with effective potential optimization

13 p1662 A73-28455

Voltage-locked diode oscillators. II - The effect of harmonics on the locking range.

14 p1734 A73-30074

Asymptotic behavior of a kinetic model of the solar wind

14 p1787 A73-30424

Behavior of the electrode potential of a metal under conditions of fretting corrosion

14 p1763 A73-30711

Ionization oscillations in a plasma in the presence of negative ions

15 p1920 A73-32319

Exo-electron emission during heterogeneous catalysis /the effect of external electric potentials/.

15 p1842 A73-32599

Use of emissive probes in plasma density measurements.

16 p2011 A73-32725

Electric dipole motion in Einstein unitary field with electrostatic potential as function of polar coordinates, deriving law of motion from Clausen integral formula

16 p2037 A73-33371

The field-effect transistor as a resistance varying linearly in time

17 p2141 A73-35547

An accurate method for determining electron beam welding voltages.

19 p2435 A73-38001

Effect of secondary emission of the potential of a metallic body in the electron radiation belts of the earth.

20 p2601 A73-38875

Lunar thermal ionosphere acceleration and detection within lunar electric field for electric potential of moon in solar wind or magnetosheath

20 p2604 A73-38933

Signal to noise ratios of inertial detector of mixture of stationary, normal, random and harmonic voltages, varying RC circuit time constants

20 p2537 A73-39459

Effective interchange effects between the ions in metals

21 p2721 A73-41141

Static fields for periodic electrostatic focusing of electron beams.

21 p2668 A73-41657

Electric potential and particle concentration of a plasma in the vicinity of a rapidly moving charge.

23 p3009 A73-43510

Electrooptical modulator employing a barium titanate single crystal. I - Estimates of critical control voltages

23 p2987 A73-43571

Atmospheric oscillations. V - The propagator matrix and the transmission of an electrostatic potential along the geomagnetic field lines.

23 p2971 A73-43686

Uniaxial pressure effects on diode structures volt-ampere characteristics, examining potential barrier height and photo emf changes

23 p2960 A73-43787

Some experiments on a voltage-induced optical waveguide in LiNbO3.

23 p3019 A73-44374

An analytical solution of the problem of a frequency tripler employing a varactor diode with an arbitrary voltage-charge characteristic

24 p3072 A73-44927

Silicon Zener diodes used as temperature sensors

24 p3090 A73-44937

Determination of the voltage distribution in the interelectrode space of a grid probe immersed in a Maxwellian plasma

24 p3116 A73-45328

ELECTRIC POWER

Effect of heterogeneity and Hall current on the MHD power generator.

01 p0005 A73-10434

Rotating electrical machine superconducting field winding design requirements in terms of size, magnetic energy storage, power level, rotation speed and pole number

02 p0132 A73-11828

TWT power gain, efficiency and output variations compensation methods during electron beam switching between pulsed and CW modes

02 p0148 A73-12570

Power Processing and Electronics Specialists Conference, Atlantic City, N.J., May 22, 23, 1972, Record.

03 p0252 A73-13926

Voltage and power relationships in lithium-containing solar cells.

03 p0257 A73-14241

Practical and precise means of microwave power meter calibration transfer.

03 p0310 A73-14499

Newly developed bolometer mounts for the short millimeter wave region.

03 p0310 A73-14500

Advanced aerospace power distribution and control techniques.

04 p0408 A73-15389

Solar cells with Si Schottky function diode, discussing fabrication and barrier metal and thickness effects on output power and energy conversion efficiency

05 p0538 A73-16816

Effect of dielectric loading on the radiation power of an axial slot antenna.

08 p0938 A73-20837

Electrical Power Subsystem definition for shuttle launched modular space station.

09 p1153 A73-22781

The phosphoric acid fuel cell, a long life power source for the low to medium wattage range.

09 p1037 A73-22821

Laser energy transfer - An analytic survey of high power applications.

09 p1096 A73-22822

High power microwave tubes design trends, considering output capacity and quality, bandwidth, gain, linearity, low noise and intermodulation performance factors

11 p1339 A73-26691

Book - Microwave power measurement.

12 p1480 A73-27425

The Canadian/U.S. High-Power Communications Technology Satellite.

12 p1472 A73-27669

Microwave transmitter tubes for surface-based and airborne radar applications, considering ATC, output power, stability, spectrum, size, weight, reliability, maintainability and cost requirements

13 p1590 A73-28532

ECM systems with TWT dual moding to provide distinct CW and pulsed microwave power levels, evaluating performance beyond octave in bandwidth

16 p1990 A73-33849

Digital time division multiplexing for integrating avionics equipment, discussing electrical power control signal multiplexing

17 p2139 A73-35246

The cause and effects of dc offset voltage in solid state ac power controllers.

17 p2109 A73-35255

Josephson junction mixing of monochromatic sources at two microwave frequencies, noting output power dependence on dc bias

18 p2340 A73-36624

Measurement technique for large-signal admittance of IMPATT diodes.

19 p2409 A73-37427

- On the design of wave digital filters with low sensitivity properties. 22 p2835 A73-41950
- ELECTRIC POWER CONVERSION**
- U ELECTRIC GENERATORS**
- ELECTRIC POWER PLANTS**
- NT NUCLEAR POWER PLANTS**
- The role of solar cell technology in the satellite solar power station. 03 p0258 A73-14252
- Electrical and isotope power from space for terrestrial use. 06 p0750 A73-18028
- Thermionic fuel elements for in-core reactor power plant space applications, summarizing operating and environmental requirements and technology development. 09 p1036 A73-22819
- Exploratory investigation of an electric power plant utilizing a gaseous core reactor with MHD conversion. 09 p1119 A73-22829
- Near-equatorial synchronous orbit Satellite Solar Power Station system with photovoltaic cell arrays energy conversion into microwave power for transmission to earth. 10 p1285 A73-23601
- Satellite electric power station for conversion of solar energy to microwaves beamed to earth, discussing structural design, flight control, transportation and technology assessment. 10 p1178 A73-24554
- Solar/battery space station power plants combined with nuclear configurations, discussing rectified alternator current, direct energy transfer, and high voltage dc sources. 11 p1311 A73-26008
- Nuclear thermionic power plants in the 50-300 kW range. 11 p1396 A73-26027
- Thermal mapping at electrical power generating sites for outfall from fossil or nuclear fuel plants, considering airborne application. 16 p2015 A73-33360
- Some major terrestrial applications of solar energy. 17 p2110 A73-35312
- Multispectral survey of power plant thermal effluents in Lake Michigan. 20 p2558 A73-39862
- ELECTRIC POWER SUPPLIES**
- NT SPACECRAFT POWER SUPPLIES**
- Russian book on electrical power supply devices for radio systems covering design of rectifiers, transformers, current limiters, voltage regulators, filters, converters and inverters. 02 p0133 A73-12863
- United States SST electrical power system evaluation. [AIAA PAPER 72-1055] 03 p0252 A73-13386
- Pulse width amplitude converter design and performance for ion engine high voltage power supply, noting oscillator, modulator and circuit protection. 04 p0489 A73-15733
- Fuel cells for improved electrical power supply. [AIAA PAPER 73-82] 06 p0649 A73-17641
- Electrical power subsystem for the Synchronous Meteorological Satellite (SMS). 09 p1154 A73-22789
- Spacecraft nuclear power source optimization, considering radioisotope and reactor heat sources, cryogenic cooler cycle types and spacecraft design. 09 p1118 A73-22799
- Computer simulation concept for a large solar array/battery power system. 09 p1060 A73-22803
- Improvement of the static and dynamic accuracy of a dual-loop control system for an electric actuating element with a proportional velocity controller. 09 p1037 A73-22940
- Investigation of new elements and equipment configurations in stable-frequency, alternating-current, electrical power supply systems employing primary power plants consisting of engines with varying rotational speed. 12 p1460 A73-26785
- Primary cells hybridization with sealed nickel cadmium batteries for power supply operation over wide temperature ranges and discharge rates. 13 p1573 A73-29588
- Russian book on civil aviation aircraft and helicopter equipment covering navigation, automatic control, electrical and oxygen systems and aircraft instruments. 15 p1829 A73-31548
- Strain gage circuit with exponential pulsed power supply for data recovery in presence of high amplitude electrical noise. 17 p2167 A73-34625
- The role of the auxiliary power unit in future airplane secondary power systems. [SAE PAPER 730381] 17 p2108 A73-34720
- Computer analysis of the influence of solid state distribution on aircraft power generation. 17 p2109 A73-35250

Flight-critical fail-operative and endurance tests for SST electrical power system. 17 p2109 A73-35252

Runway lighting emergency power supplies for low visibility, comparing single supply backed by automatic generator with separate cable and duplicate supplies. 22 p2839 A73-42318

Fixed installation ground electrical power supply system for aircraft service, discussing motor-alternators, plant control cubicles, selector and busbar switchboxes and fault protection devices. 24 p3075 A73-45156

ELECTRIC POWER TRANSMISSION

An advanced concept in electrical power distribution control and management. 03 p0253 A73-13945

Electric power processing, distribution and control for advanced aerospace vehicles. 03 p0253 A73-13947

Advanced flight control systems - Power-by-wire and fly-by-wire. 11 p1306 A73-26272

Lossless electric energy transmission via superconductivity above 20 K, noting intense magnetic field generation. 12 p1531 A73-27689

Thunderstorm activity determination on lightning discharge number recorders. 14 p1754 A73-30792

Identification and coding of fluid and electrical piping system functions. [SAE AIR 1273] 16 p1970 A73-33019

Superconducting Josephson junction power flow relations dependence on harmonically or subharmonically phase locked autonomous frequency. 20 p2536 A73-39411

Theory of power rectification and harmonic generation processes at super-high frequencies. 22 p2800 A73-42213

ELECTRIC PROPULSION

NT ELECTROMAGNETIC PROPULSION

NT ELECTROSTATIC PROPULSION

NT ION PROPULSION

NT PLASMA PROPULSION

NT SOLAR ELECTRIC PROPULSION

Investigation of the fitness for space travel of the electric propulsion plant ESKA 18. [DGLR PAPER 72-087] 02 p0131 A73-11694

NASA technology program for auxiliary and primary electric propulsion systems, noting flight tests and solar arrays. [AIAA PAPER 72-1127] 03 p0355 A73-13437

Electric propulsion and its space applications; Workshop, 2nd, Toulouse, France, June 21-23, 1972, Proceedings. 04 p0487 A73-15712

Development of electrical propulsion in the Federal Republic of Germany. 04 p0487 A73-15713

ESRO electric propulsion research program, discussing colloid and field emission thruster concepts for different exhaust velocity ranges. 04 p0487 A73-15714

Cs ion bombardment and contact ionization engines in French space program for communication and geostationary satellites electric propulsion. 04 p0488 A73-15715

Colloid thruster propellants selection for semiconductor liquids with suitable electrochemical properties via cyclic voltametry. 04 p0485 A73-15724

Quasi-steady MPD thruster research at Rome University. 04 p0489 A73-15730

Transfer from a standby to a stationary orbit using electric propulsion. 04 p0505 A73-15740

Hydrogen resistojets for primary propulsion of communications satellites. 04 p0489 A73-15741

German book - Flight propulsion systems: Principles, systematics, and technology of aeronautical and astronautical propulsion systems. 05 p0606 A73-16355

Principle of operations and characteristics of electric propulsion devices - Application to satellite stabilization. I. 05 p0608 A73-17193

Optimization of multiple target electric propulsion trajectories. [AIAA PAPER 73-205] 06 p0748 A73-17658

Electric propulsion systems for satellite station-keeping, discussing developments in colloid thrusters and diagnostic equipment for performance measurement. 07 p0867 A73-19222

Operational principle and characteristics of electric propulsion systems. II - Application to satellite stabilization. 07 p0906 A73-20247

Thermionic reactor power systems design for spacecraft auxiliary power supply and electrical

propulsion, discussing performance and design guidelines for various applications. 09 p1118 A73-22798

Space propulsion future assessment, discussing space shuttle and tug, NERVA project and electric and photon propulsion. 10 p1262 A73-23611

Thermionic reactor systems for electric propulsion. 11 p1395 A73-26025

Battery-powered electric propulsion for north-south station-keeping. 17 p2222 A73-34872

Utilization of electric propulsion systems in communications satellites. [DGLR PAPER 73-048] 17 p2126 A73-35484

Trajectory of a solar-electric propelled vehicle passing through the shadow cone of a celestial body. 21 p2779 A73-41556

ELECTRIC PULSES

Automatic pulse count recorder, discussing circuit, performance and applications to laboratory and clinic. 01 p0012 A73-10663

Processing power for a low voltage source-pulse load system. 03 p0253 A73-13939

Holograms of spark discharges produced by nanosecond electrical pulses. 03 p0309 A73-14100

Semiconductor device degradation by high amplitude current pulses. 05 p0557 A73-16505

Separate generation of odd and even harmonics of a fundamental frequency, with the aid of pulse circuits. 06 p0663 A73-17576

Radial anode current density distribution measurement in high current pulsed arcs in air on copper split anode, using Rogowski coils. 06 p0723 A73-18357

Analysis of voltage steps with a time resolution of 12 picoseconds. 08 p0962 A73-20833

A simple device for measuring the characteristics of double Langmuir probes in a periodic pulse discharge. 10 p1257 A73-24691

Electrical explosion of wires at high energy input rates. 12 p1523 A73-26936

Investigation of a pulsed laser utilizing an exploding-film Q switch. 12 p1507 A73-27504

Pulse rebalance gyro electronic system with hybrid microcircuitry for digitizing sensor inputs to computer. 13 p1589 A73-28047

Semiconductor lasers pumped by pulsed electric discharge in vacuum. 13 p1626 A73-28545

Microwave pulse excited argon ion laser. 14 p1758 A73-30472

Some operational aspects of an inductively loaded transistorized pulse amplifier at short time intervals. 15 p1851 A73-31831

Electric properties of dense plasmas in high current pulsed discharge. 16 p2040 A73-32943

Strain gage circuit with exponential pulsed power supply for data recovery in presence of high amplitude electrical noise. 17 p2167 A73-34625

Transient temperature response of semiconductor devices under pulsed power operation. 17 p2135 A73-34728

Self calibrating automatic equipment for pulsed and CW RF testing of phase, amplitude and frequency characteristics of pulsed electronic devices. 20 p2535 A73-38870

Effect of ionizing radiation on second breakdown. 20 p2599 A73-39007

An investigation of pulsed GTA welding variables. 21 p2708 A73-41254

Exploding wires with high energy input. 22 p2886 A73-42270

Pulse burnout of microwave mixer diodes. 22 p2835 A73-42965

ELECTRIC RELAYS

Analysis of a defect of electromagnetic relays used in an electronic assembly. 07 p0799 A73-19406

Periodic regime stability of two channel relay system as function of main channels identicalness and cross coupling symmetry, using Tsypkin method. 09 p1063 A73-22340

An electronic relay constructed according to the principle of amplifiers with a controlled amplitude characteristic. 12 p1477 A73-26791

Use of the dynamic programming method for optimization of relay systems. 13 p1596 A73-28853

Annual National Relay Conference, 21st, Oklahoma State University, Stillwater, Okla., May 1, 2, 1973, Proceedings. 17 p2132 A73-34088

A user-oriented guide to the design and application of solid state relays. 17 p2132 A73-34089

- Electric relay contacts physical characteristics and state changes during dry circuit, low level, intermediate and power switchings 17 p2132 A73-34090
- Electric relay operating envelope definition and test plan for contact contamination and deterioration and resistance determination through controlled environmental changes 17 p2132 A73-34091
- The hazards of transferring loads between phases, sources and ground. 17 p2133 A73-34092
- Military specifications provisions regarding load transfer. 17 p2133 A73-34093
- Load transfer between AC sources within relay ratings through circuit design. 17 p2133 A73-34094
- Investigation of a stabilization system with a relay angular sensor 20 p2593 A73-39321
- The accuracy and operational stability of a transistorized time-delay relay with an RC network 21 p2668 A73-41640
- Four terminal, optically isolated, zero crossing arc relay. 22 p2834 A73-42913
- Development of a hybrid microelectronics solid state relay for 2500 volts isolation and -120 C to 80 C thermal cycling range. 22 p2835 A73-42914
- ELECTRIC ROCKET ENGINES**
- NT CESIUM ENGINES
- NT ELECTROSTATIC ENGINES
- NT ELECTROTHERMAL ENGINES
- NT ION ENGINES
- NT PLASMA ENGINES
- NT RESISTOJET ENGINES
- Pulsed electric thrusters theoretical and experimental radiation intensities and spectra, estimating interference with onboard satellite communication systems [AIAA PAPER 73-263] 05 p0608 A73-16984
- Estimation and correction of electric thruster misalignment effects on a geostationary satellite. 17 p2238 A73-34866
- ELECTRIC SPARKS**
- Zener diodes for overvoltage spark protection circuits in automatic control and measuring equipment operating in explosive environment 02 p0147 A73-12175
- Holograms of spark discharges produced by nanosecond electrical pulses. 03 p0309 A73-14100
- Wear resistant coatings deposition by spark discharge alloying of machine part surfaces, examining surface hardening process and assessing state of art 08 p0946 A73-21083
- Wear-resistant surfaces through electrical spark hardening 11 p1371 A73-24992
- Commutation of spark gaps with the aid of a pulsed gas laser emitting in the ultraviolet range 12 p1506 A73-27211
- Temporal characteristics of spark gaps with discharge initiation by a laser flare 12 p1506 A73-27212
- Strength characteristics of layers obtained by spark-alloying steels with high-melting metals 12 p1512 A73-27264
- The ignition of solid materials in oxygen by electrical sparks. 19 p2504 A73-38275
- A multichannel-discharge of high light intensity and short duration 21 p2695 A73-39971
- Time constants of spark discharges initiated by a gas-laser beam of 0.3371 micron wavelength. 22 p2869 A73-42257
- Tuned loop antenna for radio observation of electrostatic spark and corona discharges generated during oil tanker cleaning operations 23 p2945 A73-43960
- ELECTRIC STIMULI**
- Investigation of the recovery dynamics of the mimic muscle function and choice of an optimal bioelectric stimulation program with the aid of an electronic digital computer 01 p0012 A73-10656
- Structural change in the paradoxical phase of sleep due to the stimulation of the reticular formation and hypothalamus on a background of deep slow sleep 01 p0009 A73-11081
- Changes of the free radical concentration in the cerebral cortex depending on the functional state of the cerebrum 01 p0009 A73-11082
- The role of extrinsic vagal innervation in the motility of the smooth-muscle portion of the esophagus - Electromyographic study in the cat and the baboon 03 p0262 A73-13785
- Correlation between the voltage-time curves of H- and M-responses of a human muscle during various functional states of the spinal center 03 p0262 A73-13819
- The effect of time of electrical stimulation of the carotid sinus on the amount of reduction in arterial pressure. 03 p0265 A73-14648
- Characteristic of collicular responses to stimulation of various sections of the visual afferent pathway in cats 05 p0539 A73-16332
- Intercortical functional connections in lower monkeys, Macacus rhesus, exhibited by evoked responses 05 p0540 A73-16693
- Utilization extent of the muscle apparatus capabilities during maximum voluntary force exertion 05 p0541 A73-16696
- Three channel transistorized pulse generator for electric stimuli used in electrophysiological studies 05 p0543 A73-16739
- Influence of different motor regimes on the convulsive reactivity of the central nervous system. 05 p0542 A73-17178
- Functional organization of the mechanisms of presynaptic inhibition evoked by stimulation of cutaneous afferents 07 p0781 A73-20003
- Electrical stimulation effects of human eye on photic threshold for square wave vision as function of wavelength, orientation and spatial frequency 07 p0783 A73-20260
- Investigation of evoked activity in the ventral horn of lumbar segments during the interaction of efferent extrapyramidal and cortical stimuli 09 p1040 A73-22579
- Examination of responses evoked in the sensory cortex by thalamic stimulation. 10 p1178 A73-23772
- Neuron analyzer technique for poststimulus histogram plotting of neuron excitation as function of stimulus onset time 10 p1183 A73-23811
- Effect of electrostimulation on hemodynamic shifts during prolonged hypokinesia 10 p1180 A73-23940
- Functional state of the cerebral cortex and of the mesencephalic reticular formation during prolonged action of impulsive and stable noise 10 p1181 A73-24334
- Short-term latent reactions of the lateral geniculate body neurons in the rat to electrical stimulation of the optical tract 10 p1182 A73-24595
- Posture responses of upper limb muscles during electric stimulation of the vestibular apparatus 11 p1317 A73-26087
- Late visual cortical region reactions during the convergence of light stimulation and electrocutaneous stimulation 13 p1576 A73-29073
- Effect of stimulation of the mesencephalic reticular formation on the convulsive electrical activity of the brain 14 p1716 A73-30381
- Neurophysiological characteristics of isolated structures of the cerebral cortex 14 p1718 A73-30570
- Space flight exercise regimen proposals, exploring moving picture/electric muscle stimuli program as earth gravity simulator in weightlessness 15 p1838 A73-31515
- Acquisition of signal concepts under conditions of aversion activation. I - Theoretical part and form interpretation test 16 p1972 A73-33091
- Role of specific and nonspecific thalamic nuclei in the genesis of certain slow rhythms on the human electrocorticogram 19 p2395 A73-37939
- Evoked potentials in the hypothalamus in response to stimulation of the vagus and sciatic nerves 19 p2395 A73-37941
- Motor unit reactions of man to spinal and supraspinal inhibitory stimuli 19 p2395 A73-37943
- Effect of stimulation of the hypothalamus on the pH of arterial and venous blood 21 p2637 A73-40281
- Effect of stimulation of certain hypothalamic structures on systemic and pulmonary circulation 21 p2637 A73-40282
- Influence of electric stimulation of the hypothalamus on catecholamine, phosphorylated compound, and cholesterol levels 21 p2637 A73-40284
- Evoked potentials in the hypothalamus and mesencephalic reticular formation upon stimulation of the vagus nerve 21 p2640 A73-41263
- Loudness changes resulting from an electrically induced middle-ear reflex. 22 p2811 A73-41815
- Effect of the electrical stimulation of the sensorimotor cortex on the potentials of dorsal roots and on the depolarization of primary spinal afferents 22 p2807 A73-42652
- Neuronal activity of the sensorimotor and visual cortex in rabbits during development of a summation focus in the reticular formation 24 p3058 A73-44550
- The energetic metabolism and some reactions of the cardiovascular system during multichannel electrical stimulation and voluntary stressing of muscles 24 p3059 A73-44670
- ELECTRIC STRAIN GAGES**
- U STRAIN GAGES**
- ELECTRIC SWITCHES**
- NT THERMOSTATS**
- Magnetic energy storage and transfer from coil into resistive load with superconducting switch, discussing voltage and circuit conditions for full normalization 02 p0200 A73-11830
- Superconducting magnet for a Ku-band maser. 02 p0200 A73-11835
- Magnetic pulse width modulator and power switch subsystem of switching-mode dc regulator, deriving describing function from transfer functions 03 p0282 A73-13928
- The IHTS - A new building block for power conditioners. 03 p0282 A73-13934
- Subnanosecond pulse-front shaping with the aid of switches based on chalcogenide glass 10 p1196 A73-24614
- Inexpensive fast solid state current drive circuit for injection lasers, using parallel conventional transistor switches operated at avalanche breakdown for pulse generation 16 p2024 A73-33400
- Electric relay contacts physical characteristics and state changes during dry circuit, low level, intermediate and power switchings 17 p2132 A73-34090
- The hazards of transferring loads between phases, sources and ground. 17 p2133 A73-34092
- Load transfer between AC sources within relay ratings through circuit design. 17 p2133 A73-34094
- Calculation of processes taking place in digital automatic control systems with finite switch-closing times 20 p2543 A73-39477
- Fixed installation ground electrical power supply system for aircraft service, discussing motor-alternators, plant control cubicles, selector and busbar switchboxes and fault protection devices 24 p3075 A73-45156
- ELECTRIC TERMINALS**
- Nonleaking battery terminals design for polyphenylene oxide plastic cased Ag-Zn battery for synchronous satellite applications, describing life tests under thermal and electrical cycling 09 p1034 A73-22757
- TDM data bus and interface design for digital avionics system, considering standard remote terminal in terms of system parameters, operation and cost effectiveness 17 p2139 A73-35233
- Two-terminal current-fed negative admittance incorporating field effect transistors. 23 p2961 A73-44145
- ELECTRIC WELDING**
- NT ARC WELDING
- NT ELECTRON BEAM WELDING
- NT ELECTROSLAG WELDING
- NT GAS TUNGSTEN ARC WELDING
- NT PLASMA ARC WELDING
- Bibliography on Resistance Welding, 1950-1971. 01 p0058 A73-11374
- Adaptation of resistance welding techniques to hot staking. 07 p0831 A73-20268
- Joining copper and copper alloys. 07 p0831 A73-20269
- ELECTRIC WIRE**
- NT EXPLODING WIRES**
- Advanced copper and copper alloy conducting wires with metallic coatings 03 p0312 A73-13582
- Analysis of wire antennas in the presence of a conducting half-space. II - The horizontal antenna in free space. 03 p0276 A73-13694
- Analysis of antenna structures assembled from arbitrarily located straight wires. 06 p0668 A73-18441
- Electrical explosion of tungsten wires in a vacuum. 06 p0724 A73-18782
- Influence of wave currents on the windings of electrical equipment during short circuiting 09 p1037 A73-22942
- Junction discontinuities in wire antennas and scatterers, obtaining constraint on junction currents via equivalent charge distribution representation 11 p1329 A73-25666
- Investigation with an electron microscope of the structure of wires prepared from the 60T superconducting alloy 12 p1509 A73-26841

- An integro-differential equation technique for the time-domain analysis of thin wire structures. I - The numerical method. 17 p2246 A73-34892
- Studies of the renewal of stress relaxation on a high-grade steel wire subjected to stress corrosion after being treated for total elimination of relaxation 19 p2497 A73-37553
- Failure analysis of wire bonds. 19 p2436 A73-38446
- Investigation of temperature pulsations accompanying the heating of a laminar sample by alternating and pulsating currents 23 p3048 A73-43446
- ELECTRIC WIRING**
U ELECTRIC WIRE
U WIRING
- ELECTRICAL BREAKDOWN**
U ELECTRICAL FAULTS
U ELECTRICAL CONDUCTIVITY
U ELECTRICAL RESISTIVITY
U ELECTRICAL ENERGY
U ELECTRIC POWER
- ELECTRICAL ENGINEERING**
Computer-aided solution of nonlinear differential equations in electrical engineering, using an extension of Wolinkin's procedure 06 p0669 A73-17595
- Electrical engineering - Service to mankind; Proceedings of the Southeast Region 3 Conference, Louisville, Ky., April 30-May 2, 1973. 17 p2142 A73-35626
- ELECTRICAL FAULTS**
NT SHORT CIRCUITS
- Analytical method for diagnostic and checkout testing of logic element faults in complex combinational circuits 01 p0026 A73-10035
- The degradation of MOS transistors resulting from junction avalanche breakdown. 01 p0023 A73-10648
- Reducing the smoke hazard in small transformer failures. 03 p0252 A73-13572
- Breakdown phenomena in reverse biased silicon solar cells. 03 p0256 A73-14234
- Nondestructive screening and pulse damage mechanism for thermal second breakdown of semiconductor junction diodes 05 p0557 A73-16504
- Semiconductor device degradation by high amplitude current pulses. 05 p0557 A73-16505
- Adaptation of the P-N junction burnout model to circuit analysis codes. 05 p0557 A73-16506
- New interpretation of the equivalent circuit used in dielectric-degradation studies 07 p0796 A73-18893
- Fault isolation in complex systems via Bode diagram technique. 08 p0941 A73-20684
- The breakdown mechanism and methods for measuring breakdown voltages in insulated-gate MOS field-effect transistors 08 p0946 A73-21081
- Dielectric breakdown of shock-loaded PZT 65/35. 09 p1132 A73-21927
- Reversible thermal breakdown as a switching mechanism in chalcogenide glasses. 09 p1133 A73-21986
- Drift of the breakdown voltage in highly doped planar junctions. 09 p1064 A73-23047
- Role of static electricity in the incidents recorded during the F11 firing [ONERA, TP NO. 1214] 10 p1285 A73-23750
- Sequential systems fault detection methods based on topological description and Boolean analysis of internal variables, obtaining fanout free equivalent network by tree expansion 10 p1201 A73-24055
- Breakdown criteria for streamer formation, electrostatic field analysis and laboratory high voltage experiments on aircraft initiation of lightning strikes 10 p1175 A73-24558
- Methods of constructing control and diagnosis tests for homogeneous microelectronic circuits 12 p1476 A73-26757
- Multiple-fault detection in large logical networks. 13 p1588 A73-29296
- Laser-induced shock effects in Plexiglas and 6061-T6 aluminum. 15 p1956 A73-32259
- Electrical breakdown caused by dust motion in low-pressure atmospheres - Considerations for Mars. 15 p1941 A73-32267
- Fault ambiguity repair optimization (FARO) computer program for electronic circuit card group replacement strategy, using FORTRAN IV for SPEC-TRA 70/55 batch processing 16 p1990 A73-33626

- Device for nondestructive measurement of secondary-breakdown parameters in transistors 17 p2133 A73-34161
- Semiconductor failures due to oxide defects and diffusion faults, describing nematic liquid crystals application to pinholes detection in oxide layers 19 p2410 A73-38447
- Effect of ionizing radiation on second breakdown. 20 p2599 A73-39007
- Properties of a light-modified-breakdown detector in GaAs. 22 p2864 A73-43164
- Electrical breakdown in interface zone between two dielectric insulators, studying premature breakdown dependence on dielectric constant, layer thickness and electric field conditions 23 p3006 A73-43673
- Possible causes of failures in pulse-switched thyristors 24 p3072 A73-44933
- Parameters of low-power transistors in the avalanche mode of operation 24 p3072 A73-44934
- ELECTRICAL IMPEDANCE**
NT CONTACT RESISTANCE
NT ELECTRICAL RESISTANCE
NT REACTANCE
NT SKIN RESISTANCE
- Radiation resistance of small electric and magnetic antennas in a cold uniaxial plasma. 01 p0081 A73-10194
- Integral equations for current distribution and input impedances of curved thin symmetrical dipole antenna, noting Q factor of fourth wave antennas 01 p0017 A73-10216
- Operating characteristics of cylindrical thin film weak link circuits used as the sensing element in ultra-sensitive magnetometer systems. 02 p0200 A73-11845
- Resonances of an antenna associated with the excitation of ion Bernstein modes. 02 p0198 A73-12071
- X band microstripline slot antenna measurement for input impedance and radiation pattern dependence on slot-to-reflector spacing, applying to array design 02 p0141 A73-12100
- Theoretical analysis and experimental verification for multielement dipole antenna array of unequal parallel conductors, noting impedance characteristics desirable for broadband use 02 p0148 A73-12853
- Analysis of an asymmetric dipole antenna with displaced feed points. 02 p0148 A73-12856
- Electromagnetic and electroacoustic mode radiation resistance of linear antennas in compressible electron plasma. 02 p0199 A73-12858
- Nodal admittance matrix method for first and second derivative network sensitivity, noting applicability to network analysis at discrete frequencies 03 p0286 A73-14000
- Schwartz method application to stripline fields and impedance calculations for different cross sections and internal conductor dimensions 03 p0278 A73-14078
- CW microwave oscillations of reach-through p-n-p barrier injection transit time /BARITT/ diodes, calculating small signal impedance and noise measure for comparison with experiment 04 p0427 A73-15347
- Exact frequency dependent complex admittance of the MOS diode including surface states, Shockley-Read-Hall /SRH/ impurity effects, and low temperature dopant impurity response. 04 p0427 A73-15347
- Input resistance of a short dipole antenna in a warm uniaxial plasma. 04 p0429 A73-15480
- Input impedance of a thin biconical antenna vertically buried near the air-ground interface. 05 p0548 A73-16162
- Method of calculating high-frequency parameters of m.o.s. transistors in the nonpinchoff region 05 p0556 A73-16163
- Threshold value of the input impedance of a propagating-wave fed, long radiator series 05 p0559 A73-17240
- Gain correlation with sidelight and plasma impedance properties of a CO₂ laser discharge. 06 p0700 A73-18137
- Low-frequency loop antenna arrays - Ground reaction and mutual interaction. 06 p0665 A73-18176
- Experimental investigations on the impedance behavior of a cylindrical antenna in a collisional magnetoplasma. 06 p0729 A73-18186
- Impedance and radiation pattern of antennas above flat discs. 06 p0676 A73-18191
- High-frequency physical equivalent circuit of junction transistors in common collector configuration. 06 p0682 A73-18843

- Calculated pattern of a vertical antenna with a finite radial-wire ground system. 07 p0792 A73-19384 [AD-756789]
- Inverse problem of diffraction for a reactance plane 07 p0793 A73-19919
- Application of impedance treatment to diffraction problems for rectangular waveguide. 07 p0802 A73-20143
- Determination of the influence of the earth on the active component of the input impedance of loop antennas 08 p0947 A73-21400
- Some experimental results for a capacitively loaded V antenna. 08 p0939 A73-21431
- Equivalent circuit of unbent p-PbS point diodes 09 p1061 A73-22022
- Impedance of an ion-sheathed spherical probe in a warm, isotropic plasma. 09 p1127 A73-22431
- General cavity analysis for corrugation in rectangular waveguide microwave filters, using admittance method with consideration for propagation modes 10 p1192 A73-23606
- Equivalent circuits of diodes in millimeter and sub-millimeter wave frequencies. 10 p1193 A73-23667
- Feedback in amplifier circuits synthesis and analysis, discussing energy transfer, source impedance and terminals 10 p1201 A73-24383
- Immittance functions realizability by passive normal bipoles based on poles and zeros dislocations 10 p1202 A73-24415
- Dispersion equation and spectrum conversions for slow wave excitation and propagation in plane waveguide with homogeneous isotropic impedance 10 p1190 A73-24601
- Imperfectly conducting circular loop antenna driving-point impedance derivation for uniform resistive loading, comparing differential and integral equation methods for current distribution calculation 10 p1191 A73-24899
- Radome insertion phase delay errors due to element impedance, frequency uncertainty, power instability and heat effects 11 p1327 A73-25278
- Computerized large signal model of IMPATT diode, calculating output power and admittance as function of frequency and amplitude 11 p1336 A73-25320
- Efficiency transition point for inductively loaded monopole. 11 p1337 A73-25364
- Impedance comparisons for the asymmetrically driven thin cylindrical antenna. 11 p1329 A73-25663
- Effect of edge reflections on the performance of antenna ground screens. 11 p1329 A73-25673
- Calculation of the y-parameters of an integrated-circuit amplifier by reducing the matrix of an n-terminal network to the matrix of a two terminal pair network 11 p1338 A73-26102
- A current-excited large-signal analysis of IMPATT devices and its circuit implications. 12 p1478 A73-27112
- Copper deposition on ceramic plate, studying interdigital slow wave structure and thin film meander-line coupling impedance and dispersion characteristics 12 p1480 A73-27581
- Coupled asymmetrical microstrip transmission lines odd and even mode wave impedances as functions of conductor strip width and spacing 12 p1481 A73-27582
- Diffraction of electromagnetic waves on reflectors with parameters that vary periodically in time 12 p1470 A73-27583
- Wave resistance determination in synthesis of oscillatory circuits with homogeneous line segments for given resonant frequencies spectrum 13 p1591 A73-28660
- Description of the measurement design and the measurement principle in the measurement of the chip impedance of coaxially mounted semiconductor diodes in the microwave range 14 p1733 A73-30058
- On numerical convergence of moment solutions of moderately thick wire antennas using sinusoidal basis functions. 14 p1734 A73-30216
- Computer evaluation of large low-frequency antennas. 14 p1735 A73-30227
- Radiating slot antenna immittance reactive term due to energy storage in feeding waveguide, discussing resonance characteristics 15 p1849 A73-31097
- Wideband negative resistance by synthesizing parallel tank converter circuit, discussing input and load admittance 15 p1853 A73-31258
- Influence of the substrate on the transfer admittance of a saturated MOS transistor 15 p1850 A73-31495

Performance and possibilities of application of an electromagnetic comparator 15 p1883 A73-32056

Impedance of a short cylindrical dipole antenna in a hot uniaxial plasma. 15 p1845 A73-32237

Size-reduced log-periodic dipole array antenna. 16 p1988 A73-33299

Antenna admittance determination of electron density. 17 p2121 A73-34187

Effect of upper sideband impedance on a lower sideband up-converter. 17 p2123 A73-34971

General theoretical analysis of impedance loaded rectangular loop antennas. 17 p2141 A73-35368

General theoretical analysis of loop and folded dipole antennas. 17 p2142 A73-35646

Gunn diode parameters from a small signal analysis. 17 p2142 A73-35651

Measurement of impedance transformation on practical dipoles. 17 p2128 A73-35690

Antenna impedance measurement with Weissfloch transformer between terminals and point in input transmission line for achieving high precision. 17 p2129 A73-35704

Oriental dependence of certain RF impedance probes in the ionosphere. 18 p2288 A73-36188

Impedance and far field characteristics of a linear antenna near a conducting cylinder. 19 p2403 A73-37271

Measurement technique for large-signal admittance of IMPATT diodes. 19 p2409 A73-37427

Enhancement of the sensitivity of microwave admittance measurements through the use of 'matching' two-ports 19 p2409 A73-37717

Synthesis of impedance-type cylindrical antenna arrays 21 p2661 A73-40197

Semiconducting ground influence on input impedance and radiation resistance of horizontal magnetic dipoles, covering short wave band for various antenna elevations and conductivity levels 21 p2661 A73-40203

Phased array element types comparison, discussing dipole and open-ended waveguide radiator designs with emphasis on driving point impedance accuracy and active element pattern 21 p2663 A73-40649

The design of a wide band wide scan-angle waveguide radiating element. 21 p2652 A73-40660

Multimode phased array element for wide scan angle impedance matching. 21 p2652 A73-40661

Integral equation analysis of cylindrical antennas having arbitrary surface impedance. 21 p2655 A73-41093

Elaborated attenuation computation for elliptic waveguide with corrected expressions for axial and transverse surface impedances and TE and TM modes 21 p2656 A73-41112

Electromagnetic interference in military transport aircraft, discussing RF terminal voltage and current, radiated field, fuselage attenuation and power supply impedance measurements 22 p2821 A73-41693

Electroexplosive device pin-pin firing frequency mathematical modeling and prediction based on RF impedance data obtained nondestructively by automatic network analyzer 22 p2822 A73-41793

Impedance and large signal excitation of satellite-borne antennas in the ionosphere. 22 p2831 A73-41835

Impedance properties of a longitudinal slot antenna in the broad face of a rectangular waveguide. 22 p2831 A73-41845

Input admittance or impedance and effective height measurement for small metal antennas of prolate and oblate spheroidal and spherical shape, noting transient response 22 p2829 A73-43180

Two terminal network immittance converters with feedback for passband and IC operational amplifier applications 23 p2959 A73-43515

VLF input impedance of a loop antenna embedded in the magnetosphere. 23 p2954 A73-43700

Finite-boundary corrections to the coplanar waveguide analysis. 23 p2954 A73-44075

Dipole antenna with variable capacitance diodes for wideband tuning, calculating and measuring input impedance frequency response 23 p2960 A73-44110

Investigation of the input impedance of an emitter-input transistor amplifier at near-cutoff frequencies 24 p3072 A73-44935

Utilization of the impedance variation of the plasma of a CO₂ laser for frequency stabilization on the 'Lamb dip' 24 p3096 A73-45223

ELECTRICAL INSULATION

Electrohydrodynamic stability of insulating fluids subjected to a unipolar injection 01 p0086 A73-11361

Thermally conducting alumina and boron nitride filled silicone and polysulfide elastomer sheet materials for electrical insulation and heat sink applications 03 p0331 A73-13028

An advanced printed circuit board system having outstanding resistance to humid environments. 03 p0281 A73-13047

Thermophysical and electrical properties of powdered boron carbonitride as high temperature insulating and refractory material at 1800-2020°C 10 p1241 A73-24687

Foamed Al production from Al powder mixture with aluminum hydroxide and orthophosphoric acid, discussing mechanical, thermal conductivity and electrical insulating properties 10 p1236 A73-24919

Heat pipe cooling of electronic components for design requirements of high voltage insulation, small size, low temperature and protection from external heat sources 11 p1451 A73-25990

Thermophysical properties of high temperature electrical insulating materials on the basis of non-metallic compounds with high melting point [ECTP PAPER D2-3] 14 p1766 A73-30436

Hydrolytic stability of electrical insulation materials. 17 p2197 A73-35348

Hydrolytic degradation of polymer electrical insulating materials in warm humid environments, noting relation to ester and ether linkage presence 17 p2197 A73-35349

Insulated electrically thin dipole antenna with surrounding large wave number isotropic medium, discussing transmission line properties and current and charge distribution 22 p2829 A73-43183

A theoretical and experimental study of the insulated loop antenna in a dissipative medium. 22 p2829 A73-43184

Electrical breakdown in interface zone between two dielectric insulators, studying premature breakdown dependence on dielectric constant, layer thickness and electric field conditions 23 p3006 A73-43673

ELECTRICAL LEADS

U ELECTRIC CONDUCTORS

ELECTRICAL MEASUREMENT

NT COULOMETRY

NT POLAROGRAPHY

Self-compensating digital phase meter with discrete phase shifters 01 p0044 A73-10078

Design of digital phase meters with intermediate frequency converters 01 p0044 A73-10079

Quadrature phase splitter with indications of the quadrature and equality of output voltage amplitudes 01 p0022 A73-10081

Problem of using the magnetoresistance effect to measure transferred SHF power 01 p0023 A73-10215

Unit for wideband measurements of dielectric parameters at millimeter wavelengths 01 p0050 A73-10794

Alloying profile measurer for epitaxial films 01 p0050 A73-10799

Thermophysical properties of arc-cast tungsten using the TPRC multi-property apparatus (direct heating method). 01 p0067 A73-11483

A cryostat for measuring electrical values of semiconductor devices in the temperature range from 77 to 300 K 02 p0165 A73-11550

Device for measuring the instantaneous value of current and voltage in the operation of a pulsed plasma accelerator 02 p0196 A73-11792

Ti-Al-V alloys as differential measurement method for metallurgical processing and microstructure effects on superconducting critical temperature and magnetic permeability/susceptibility 02 p0200 A73-11843

AC studies of a superconducting Nb-52 at. % Ti alloy. 02 p0200 A73-11844

Measuring hybrid parameters of composite transistors. 02 p0148 A73-12855

Relaxation of excess populations in the lower laser level CO₂/100/. 03 p0318 A73-13278

Measurement of the dc plasma electric resistivity perpendicular to the magnetic surface. 04 p0482 A73-15959

ELECTRICAL MEASUREMENT

Determination of the optimal structure of a unit measuring the effective value of a nonsinusoidal periodic voltage 05 p0560 A73-16330

Magnetotelluric and geomagnetic depth sounding methods compared. 05 p0572 A73-17189

Instrument circuitry, calibration and errors in p-n junction capacitance measurement 06 p0691 A73-17399

Measurement of dielectric constant of nonmagnetic materials in a waveguide system with an unknown movable reflecting load. 06 p0696 A73-18618

Electrical measurements, metallographic microscopy and chemical analysis for failure analysis 07 p0800 A73-19409

Transistor tester circuit design with mutually independent collector-emitter voltage, collector current, generator and load resistance adjustment for arbitrary operating point selection 07 p0803 A73-20303

The breakdown mechanism and methods for measuring breakdown voltages in insulated-gate MOS field-effect transistors 08 p0946 A73-21081

The bus-probe and multiprobe methods of measuring Hall mobility in semiconductor layers of nonuniform depth 08 p0995 A73-21272

Measurement of amplifier noise. 08 p0949 A73-21623

Electrometric amplifiers for inductive measurement of charges 08 p0949 A73-21713

A system for the evaluation of solar cell samples. 09 p1033 A73-22438

Measurement of the current distribution at the surface of a doublet immersed in an isotropic hot plasma 09 p1131 A73-23034

An apparatus for measuring and recording the electrical resistance of metal specimens during mechanical testing. 09 p1070 A73-23066

Electrical measurement of mechanical forces and displacements, discussing transducers design and measurement standards and units 10 p1215 A73-23633

Semiconductor and semi-insulator resistivity measurements using a direct current four point probe apparatus with non-penetrating tips. 10 p1194 A73-24158

Measurement of the horizontal component of the electrostatic field intensity in the lower atmosphere 10 p1219 A73-24400

High voltage phase meter with electrostatic logometer for loss angle measurements in capacitors and power cables during operation 12 p1495 A73-26790

Book - Microwave power measurement. 12 p1480 A73-27425

Result of medium- and long-wave observations at distances of about 7500 km 12 p1474 A73-27768

Employment of mode theory and ray theory for the interpretation of very-long-wave measurements at medium distances 12 p1474 A73-27769

GEOS geostationary satellite experiments for dc magnetic fields, dc/ac electric fields and plasma resonances, thermal plasma, electrons and protons 12 p1499 A73-27775

Magnetic coil type electrical measurement indicating instruments accuracy dependence on manufacturing tolerances, discussing error reducing design methods 12 p1499 A73-27873

Stochastic-ergodic electronic U-functionmeter for signal electrical characteristics measurement, discussing design, operational features and applications 12 p1499 A73-27874

Automatic measurement of the Q factor of stationary bipolar networks and multiports 13 p1589 A73-28123

VLF atmospheric measurement and geophysical analysis, discussing meteorological, geoelectric and propagation aspects 13 p1582 A73-28151

Digital circuits test equipment functional principles, considering time, instantaneous voltage and pulse height measurements 14 p1731 A73-29873

Some problems in measuring the electrical properties of semiconductors 14 p1784 A73-30924

Central digital measuring and data logging systems for electrical and non-electrical analog signal conversion, display and recording 15 p1849 A73-32204

Passive alpha structure Ti base alloys with Al, Mn, Sn, Nb, Cr or Mo, investigating dissolution characteristics by chronoamperometric measurement using sulfuric acid 15 p1895 A73-32568

Measurement of external Q factor of microwave oscillators using frequency pulling or frequency locking.

15 p1852 A73-32646

Absolute calibration of antennas at extremely low frequencies.

17 p2128 A73-35686

Precise and rapid measurements of small currents from high impedance sources.

17 p2143 A73-35775

Semiconductor carrier mobility measurements with Hall generator, calculating sample geometry and finite dimension electrical contact effects on error

19 p2430 A73-37718

Rocket measurements of electric field and optical aurora during weak PCA event, noting rocket passage through discrete auroral forms

21 p2684 A73-40781

Diffusion profile measurements in the base of a microwave transistor.

21 p2668 A73-41560

Electromagnetic interference and compatibility control in aircraft communication, discussing RF current, voltage, impedance and SNR measurement techniques

22 p2821 A73-41692

Fatigue-crack initiation studied by electrical resistance measurements.

23 p2979 A73-43301

ELECTRICAL PROPERTIES

NT ANTIFERROELECTRICITY
NT CAPACITANCE
NT CARRIER MOBILITY
NT CHARGE DISTRIBUTION
NT CONTACT RESISTANCE
NT DIELECTRIC PROPERTIES
NT ELECTRIC MOMENTS
NT ELECTRICAL IMPEDANCE
NT ELECTRICAL RESISTANCE
NT ELECTRICAL RESISTIVITY
NT ELECTRON MOBILITY
NT ELECTRORECTION
NT FERROELECTRICITY
NT HOLE MOBILITY
NT INDUCTANCE
NT IONOSPHERIC CONDUCTIVITY
NT MAGNETORESISTIVITY
NT PERMITTIVITY
NT PHOTOCONDUCTIVITY
NT PHOTOVOLTAIC EFFECT
NT PIEZOELECTRICITY
NT PLASMA CONDUCTIVITY
NT POLARIZATION CHARACTERISTICS
NT PYROELECTRICITY
NT REACTANCE
NT SKIN RESISTANCE
NT SUPERCONDUCTIVITY

Influence of gamma-radiation on the electrical properties of a real germanium surface

01 p0087 A73-10039

Determination of the complete set of physical parameters of Schottky-barrier diodes

01 p0022 A73-10041

Diode behaviour in an electron-bombardment ion engine.

01 p0090 A73-10112

A new program for the dc one-dimensional analysis of semiconductor devices.

01 p0023 A73-10576

The growth and electrical characteristics of epitaxial layers of zinc sulphide and of zinc selenide on p-type gallium phosphide.

01 p0088 A73-10683

Electrical evaluation of doped and undoped cobalt chromite as the interconnection material for high-temperature, zirconia-electrolyte, fuel-cell batteries.

[ECS PAPER 16] 01 p0006 A73-10724

St. of the ac small-signal dynamic characteristic of p-n silicon diodes

01 p0024 A73-10921

Structure and electrical characteristics of epitaxial palladium silicide contacts on single crystal silicon and diffused P-N diodes.

02 p0147 A73-12045

Investigation of the electrical parameters and meteorological elements of the atmosphere close to the ground during thunderstorm and thunderstorm-free periods

02 p0189 A73-12589

Polyimide 2080 molded composites mechanical, thermal and electrical properties, discussing processing techniques

03 p0329 A73-13005

Engineering support activities for the Apollo 17 Surface Electrical Properties Experiment.

04 p0428 A73-15390

Aging effects on electrical and radiation characteristics of discrete semiconductors.

05 p0557 A73-16510

Electrical properties of electron-irradiated GaAs.

05 p0604 A73-16516

Morphological, structural and electrical nonuniformities correlation in epitaxial GaAs films on planes, noting Miller indices effects on morphological and electrical properties

05 p0605 A73-17290

Book - Electronic properties of composite materials.

06 p0714 A73-17872

Aircraft radome design mechanical, electrical and aerodynamic requirements, taking into account lightning hazards, electrostatic surface charges and plastic components deformations

06 p0648 A73-17997

Certain electrophysical properties of zinc oxide base semiconductor ceramics with admixtures of transition-metal oxides

06 p0735 A73-18079

Control of the electrical properties of a surface with the aid of adsorption of molecules/Stability of surface parameters and slow relaxation/

06 p0735 A73-18083

Influence of low-temperature heat treatment on the electrical and recombination properties of silicon-silicon dioxide systems

06 p0736 A73-18085

Electrical characteristics of the plasma in a CO laser.

06 p0703 A73-18614

Grain size analysis, optical reflectivity measurements, and determination of high-frequency electrical properties for Apollo 14 lunar samples.

07 p0898 A73-19897

Electric properties of 5,12-6,11-tetraoxatetrasene crystals

07 p0862 A73-20007

Microstrip transmission line microwave IC, discussing electrical characteristics, dielectric and conductor materials, photo-etching processes, connection fabrication and circuit encapsulation

08 p0942 A73-20702

Fabrication, electrical properties and reliability of thin film capacitors, noting surface irregularity and impurity effects on reliability

08 p0946 A73-21082

Characterization of p-n junctions under the influence of a time varying mechanical strain.

08 p0951 A73-21481

Electrical properties of InAs to very high pressures.

08 p0995 A73-21535

Application circuits for amorphous semiconductor switching devices with thin film active components, discussing electrical characteristics

09 p1061 A73-21990

Electrical properties of MOS capacitors with oxide grown in the presence of HCl.

09 p1062 A73-22308

Circuit diagram and electrical characteristics of semiconductor memory cell consisting of thyristor and n-p-n transistors, noting parameters stability

09 p1063 A73-22460

Room temperature electrical properties and dopant precipitation for SiGe thermoelectric alloys.

09 p1134 A73-22758

Properties of silicon implanted with boron ions through thermal silicon dioxide.

09 p1064 A73-23040

The electrical properties of anodically grown silicon dioxide films.

09 p1064 A73-23042

Multistage diffusion model of IC transistor electrical characteristics and impurity distributions as function of surface concentrations and junction depths during fabrication

10 p1196 A73-24606

Electrically stabilized alumina as ceramic material for radome applications, tabulating dielectric, thermal and mechanical properties and firing conditions

11 p1408 A73-25287

Fabrication and physical, mechanical and electrical properties of inorganic composite material for aircraft radomes

11 p1387 A73-25288

Experimental study of electrical reflectors equipped with thin radomes

11 p1335 A73-25292

Mechanical, thermal and electrical properties of machinable glass ceramics, discussing application as electromagnet window materials

11 p1387 A73-25293

Electrical characteristics of hardenable metallic lens or radome with near unity refractive index at out-of-band frequencies

11 p1338 A73-25670

Output power saturation with a discharge current in powerful continuous argon lasers.

11 p1377 A73-26179

On the electrical properties of nonstoichiometric oxides alpha-Nb2O5, MnO, and CoO at high temperature

13 p1634 A73-28202

Stratiform cloud electrical characteristic changes under solid carbon dioxide seeding in aircraft experiments

13 p1654 A73-28884

Bibliography on the measurement of electrical parameters of layered lunar/earth surfaces.

13 p1619 A73-29221

Log periodic triangular dipole antenna design and electrical properties, noting improved frequency transition, gain and axial length reduction

14 p1731 A73-29714

Russian book on aeronautical electric and electronic materials covering physicochemical properties of magnetic, dielectric, conductor, semiconductor, polymer, ferritic, thin film and composite materials

14 p1766 A73-30357

Influence of heating to high temperatures in vacuum on the electrophysical properties of niobium single crystals

14 p1763 A73-30722

Some problems in measuring the electrical properties of semiconductors

14 p1784 A73-30924

Effect of oxygen on the structure and properties of Bi2Te3-based alloys

15 p1923 A73-31209

Enhancement of the electrical strength of deposited aluminum oxide coatings by electrophoretically filling the pores

15 p1881 A73-31212

Russian book - Physics of carbographite materials.

15 p1897 A73-31583

Single crystal mechanical and electrophysical properties in refractory compounds, including temperature effects, microhardness, resistivity, heat transfer, deformation and Hall effect

15 p1898 A73-32241

Electrical properties of semiconductors with non-spherical radiation damage regions.

16 p2044 A73-33198

Heat conductivity and electrical properties of vanadium-alloyed titanium at 100 to 350 K

17 p2188 A73-34554

Moldability, storage stability and thermal, mechanical and electrical properties of epoxy molding compounds for electronic devices

17 p2196 A73-35340

The Apollo 17 Surface Electrical Properties Experiment antenna performance.

17 p2171 A73-35370

Some properties of synthesized stephanite /Ag5SbS4/ specimens

17 p2219 A73-35551

Electrical properties of single-crystal films of p-type PbTe

17 p2219 A73-35556

The electrical properties of phosphorus doped silicon layers obtained by ion implantation through a passivating oxide.

17 p2220 A73-35654

Mechanical, thermal and electrical properties of polymers as functions of temperature, radiation and frequency for cryogenic environment material and design selection

19 p2443 A73-37525

Transit satellite-borne radioisotope thermoelectric generators launch aboard Scout missile into circular polar orbit, obtaining electrical and thermal data

19 p2494 A73-38394

Unidirectional small active antenna.

20 p2525 A73-38742

High-molecular compounds and recording of information on thermoplastic films

21 p2646 A73-40253

Certain properties of semiconductor glasses from the Ge-As-Se-Te system

21 p2752 A73-40749

High temperature platinum resistance thermometry.

22 p2855 A73-42005

Heterojunction injection lasers [Review/.

22 p2869 A73-42244

Approximate nonlinear theory of orotron as SHF hybrid-type monotron oscillator, calculating output power and efficiency as function of tube electrical parameters and geometry

22 p2826 A73-42338

Some electric and spectroscopic properties of the radiofrequency plasma in a steady magnetic field.

23 p3012 A73-43831

Fluctuation characteristics of the electric component of the troposphere.

24 p3084 A73-44940

ELECTRICAL RESISTANCE

NT CONTACT RESISTANCE

NT SKIN RESISTANCE

Investigation of residual resistance in semiconductor switches used to commutate the measuring circuits of alternating-current bridge networks

01 p0022 A73-10080

Controlled low-resistance shunt method for determining the volt-ampere characteristics of composite superconductors

01 p0088 A73-10617

Automatic two-coordinate compensator for resistance-measurement studies of steels and special alloys

02 p0167 A73-11867

The thermal and electrical conductivities of tantalum at high temperatures.

03 p0322 A73-13182

Impurities effect on platinum resistance thermometers temperature reading accuracy, presenting empirical formula for approximate error estimate as function of operational conditions

03 p0307 A73-13193

Pre-threshold conductance and polarization effects in amorphous semiconductor switches.

04 p0427 A73-15343

Nonlinear harmonic analysis of reflex klystrons with high electron conductance, using average method in second approximation

05 p0556 A73-16065

Low temperature tests for magnetic field and temperature effects on differential resistance of lead alloy superconductors, calculating viscous friction coefficient

06 p0736 A73-18116

Distributed base resistance effect on stripline geometry transistor input characteristic, using equivalent circuit with pseudo-junction having high saturation current

06 p0677 A73-18396

Plasma sheath capacitance and resistance in double inverse pinch device from I-V measurements with Langmuir probe, noting relationship to plasma temperature and density

06 p0696 A73-18784

Si varactor diode series resistance resonance measurements in UHF band, noting approximate invariance with frequency

06 p0678 A73-18842

Cubic /four-index/ theory of thermal noises in nonlinear resistances

07 p0792 A73-19910

The low temperature strain sensitivity of MOS transistors.

08 p0948 A73-21476

Resistive MOS-gated diode light sensor.

08 p0948 A73-21477

Electric resistance of hydraulically extruded and annealed beryllium

09 p1098 A73-21847

Matthiessen's rule and the electric resistance of solid solutions of silicon in iron at high temperatures

09 p1104 A73-22602

Calculation of series and shunt resistances on the basis of the current-voltage characteristics of a solar cell

09 p1033 A73-22720

An apparatus for measuring and recording the electrical resistance of metal specimens during mechanical testing.

09 p1070 A73-23066

Electrical resistance and emissivity of certain transition metals and alloys in the high-temperature range

10 p1230 A73-23520

Positive thermal coefficient of electrical resistance in BaTiO₃ single crystals near the Curie point

10 p1260 A73-24473

Synthesis of RC gyrator circuits with a constant characteristic resistance

10 p1196 A73-24608

Application of the invariant of a homographic transformation to measure the series resistance of semiconductor elements

11 p1336 A73-25319

Solar cell dark I-V characteristics and their applications.

11 p1310 A73-26003

Rhenium solubility determination for deformed and annealed Re-Al alloy at 500 and 600 C by microstructural analysis and hardness and electrical resistance measurements

12 p1510 A73-26907

Influence of plastic deformation on the electrical resistance of molybdenum single crystals

12 p1512 A73-27260

A simple method for obtaining a constant input resistance in broadband amplifiers

13 p1590 A73-28572

Threshold of appearance of anomalous resistance for field-aligned currents in the magnetosphere.

13 p1608 A73-28726

Changes in the electrical resistance of heat-resistant EI 826 alloy in the presence of creep

13 p1636 A73-29065

Electrical model for calculation of resistance strain gage errors due to grid-grid and grid-body shunt currents

13 p1622 A73-29617

Resistance of superconductors near the critical field Hc2

14 p1784 A73-30813

Temperature dependence of the electrical resistance of superconducting Ti-Nb and Ti-Nb-Zr alloys subjected to working by hydrostatic pressure

15 p1887 A73-31186

Electrical resistance of tungsten-rhenium cermet alloys

15 p1892 A73-32243

German monograph - The spontaneous anisotropy of the resistance in nickel - Measurements involving single crystals of nickel and diluted nickel alloys between 4.2 and 358 K.

15 p1896 A73-32582

A contribution to the proof of the formula for resistance noise

16 p1978 A73-32910

Experimental studies and applications of vanadium oxides.

16 p2044 A73-33471

Hall effect and electrical resistance in Ni, Co and Ni-Co alloys

16 p2027 A73-34009

Electrical resistivity and emissivity of some transition metals and alloys in the high-temperature range.

17 p2191 A73-35200

Design of nonlinear resistive networks with prescribed input-output behavior.

17 p2145 A73-35378

The field-effect transistor as a resistance varying linearly in time

17 p2141 A73-35547

Resistance anomaly in semiconductor barium and strontium niobates

17 p2219 A73-35554

New methods for studying gas solid reaction kinetics using automated resistance monitoring.

17 p2175 A73-35756

Factors affecting the results of strain gauge measurements performed by electrical resistance strain gauges

18 p2316 A73-36473

Method for plotting frequency cutoff measurements for GaAs varactor diodes.

18 p2292 A73-36596

Some electron structure characteristics of W-Re solid solutions

18 p2325 A73-36809

The change in the electrical resistance of EI826 refractory alloy with creep.

18 p2325 A73-36897

Ion implanted megohm silicon monolithic IC resistors with buried n-guard layer protection against slice-to-slice variations of fixed surface charge

20 p2537 A73-39416

Variation of the electrical resistance of ordered Ni₃Mn alloy during irradiation by fission fragments

20 p2600 A73-39733

Electrical resistance variation kinetics in deformed beryllium after annealing

20 p2579 A73-39746

Influence of hydrogen, alcohols, and moisture on the ultimate strength and electrical resistance of tungsten and steel wire samples

21 p2721 A73-41227

A survey of thermometric characteristics of recently produced Allen-Bradley/Ohmite resistors.

22 p2854 A73-41996

Germanium resistance thermometers - Resistance vs. temperature and thermal time constant characteristics.

22 p2854 A73-42000

Representation of the temperature-resistance characteristic of germanium thermometers below 30 K.

22 p2854 A73-42001

The specific resistance of blood at body temperature.

22 p2807 A73-42670

Fatigue-crack initiation studied by electrical resistance measurements.

23 p2979 A73-43301

Local resistance variations caused by membrane potential shifts in the interior of the horizontal retina cell

24 p3061 A73-45250

Series resistance of rectangular and cylindrical semiconductor photocells with linear and circular contacts and thin base, noting dependence on contact strip width

24 p3058 A73-45251

Influence of heat treatment on the posistor effect of semiconductive BaTiO₃-ceramic.

24 p3120 A73-45367

ELECTRICAL RESISTIVITY

NT IONOSPHERIC CONDUCTIVITY

NT MAGNETORESISTIVITY

NT PHOTOCONDUCTIVITY

NT PLASMA CONDUCTIVITY

NT SUPERCONDUCTIVITY

Difference of thermal properties between threshold type and memory type chalcogenide glass semiconductors.

01 p0087 A73-10432

Microstructure, hardness, electrical resistivity and thermal properties of Ni alloys with Al and Ta, noting composition of heat resistant alloys

01 p0067 A73-11436

Conductivity of 2024-T42 aluminum sheet solution heat treated at various temperatures.

02 p0168 A73-11986

Lunar magnetic field measurements, electrical conductivity calculations and thermal profile inferences.

03 p0369 A73-13103

Third harmonic generation in Ge induced by conduction nonlinearity during bulk heating of charge carriers by microwave fields

03 p0350 A73-14077

The mechanism of stage III recovery of electron irradiated molybdenum.

04 p0461 A73-14870

Temperature dependence of impurity resistivity in dilute Al-based Ti, V, Fe, Cu, Zn alloys between 78 and 930 K.

04 p0461 A73-14875

Experimental study of millimeter-wave characteristics of hot electrons in n-type GaAs by electrodeless method.

05 p0558 A73-16525

Macroscopic inhomogeneities in amorphous semiconductors - Contactless conductivity.

05 p0605 A73-16570

De Gaston decharger with ionizing radiation for temporary jet fuel conductivity increase and charge density reduction, discussing theory, design and tests [SAE PAPER 720864]

05 p0537 A73-16673

Material variability as measured by low temperature electrical resistivity.

05 p0588 A73-17287

Surrounding wall electrical resistivity effects on plasma pinch stabilized by outer region force-free current flow, deriving instability growth rate

05 p0604 A73-17363

Resistivity of doped polycrystalline silicon films.

06 p0733 A73-17745

On the origin of strongly conducting states in thin insulator films.

06 p0734 A73-17812

Electrical properties of evaporated mercury telluride films.

06 p0734 A73-17815

Determination of the specific surface resistance of thin metallic layers in the microwave range, based on transmission coefficient measurements

06 p0737 A73-18221

Investigation of the electrical resistivity of zirconium and hafnium nitrides

06 p0714 A73-18559

Conduction electrons collective wave properties in metals, discussing energy structure, ground state, Fermi surface and quasi-particle concept for crystal conductivity

06 p0739 A73-18674

Optical and electrical properties of proton-bombarded p-type GaAs.

06 p0739 A73-18786

Body centered cubic transition metal stage 3 electrical resistivity recovery mechanism from experiment on recrystallized and stress-relieved plastically deformed Nb wire

07 p0839 A73-20112

Low-frequency current oscillations in high-resistivity, Au-doped silicon junctions with two Schottky contacts.

07 p0864 A73-20190

Magnetic field dependence of the surface resistance of pure and impure superconducting aluminum at photon energies near the energy gap.

07 p0864 A73-20573

Shock deformation of K-state in Ni-Cr alloys.

08 p0979 A73-21626

Electronic conduction and switching in chalcogenide glasses.

09 p1133 A73-21985

High temperature fatigue sensor based on conductive composite device irreversible resistance increase resulting from cumulative strain damage

09 p1083 A73-22504

Electrical and structural properties of low-temperature bismuth films

09 p1133 A73-22603

Certain physical properties of Nd-Sb system alloys and their correlation with the phase diagram

09 p1134 A73-22679

Concentrational dependence of resistivity in solid disordered binary alloys of nontransition metals

09 p1104 A73-22687

Light-induced potential and resistance changes in vertebrate photoreceptors.

09 p1043 A73-23313

Temperature dependent heat conductivity, Lorentz number and electrical resistivity of high melting Ti, Zr, Nb, Cr, Mo and W carbides and borides at 300-1200 K

10 p1230 A73-23519

Semiconductor and semi-insulator resistivity measurements using a direct current four point probe apparatus with non-penetrating tips.

10 p1194 A73-24158

Interpretation of quench-sensitivity in Al-Zn-Mg-Cu alloys.

10 p1235 A73-24442

Imperfectly conducting circular loop antenna driving-point impedance derivation for uniform resistive loading, comparing differential and integral equation methods for current distribution calculation

10 p1191 A73-24899

Pressure shocks in thermally and electrically conducting viscous gas, discussing growth equation and radiation effects

11 p1403 A73-25164

Edge condition of a perfectly conducting wedge with its exterior region divided by a resistive sheet.

11 p1329 A73-25676

Determination of the resistivity of nickel and of some of its alloys as a function of pressure up to 60 kbar

11 p1384 A73-25873

Calculations of electrical transport properties of liquid metals at high pressures.

11 p1399 A73-25899

Microstructure, hardness, electrical resistivity and thermal properties of Ni alloys with Al and Ta, noting composition of heat resistant alloys

11 p1384 A73-26063

Temperature and concentration dependence of the electrical resistivity of solid alloys in the magnesium-cadmium system

11 p1386 A73-26570

Effect of neutron irradiation on the structure and properties of zirconium carbide

12 p1512 A73-27200

Integral emittance of silicon alloyed with iron, cobalt, and nickel in the temperature range from 900 to 1750 C

12 p1513 A73-27309

Magnetovariational frequency sounding of the earth, using the ratio of magnetic potentials

12 p1491 A73-27352

Transonic similarity solution for aligned field MHD nozzle flow.

13 p1599 A73-28089

Investigation at the Moscow University of the thermal characteristics of material

13 p1704 A73-28426

Atmospheric moisture effects on hematitic sandstone, pyrite and galena electrical resistivity, noting comparison with semiconductors and insulators

13 p1609 A73-28847

The electrical resistivity of transition metals at high temperatures.

14 p1759 A73-29746

Field-aligned currents, plasma waves, and anomalous resistivity in the disturbed polar cusp.

14 p1747 A73-29964

The thermal conductivity of a number of alloys at elevated temperatures.

[ECTP PAPER B1-4]

14 p1760 A73-30435

High-speed /subsecond/ simultaneous measurement of specific heat, electrical resistivity, and hemispherical total emittance of Ta-10/wt.%W alloy in the range 1500 to 3200 K.

[ECTP PAPER D2-4]

14 p1760 A73-30437

The perturbation of alternating geomagnetic fields by discontinuities with high conductivity contrasts.

15 p1871 A73-31780

Electrophysical properties of TiC-Nb, TiC-Ta, TiC-Mo, and TiC-W cermets

15 p1892 A73-32242

Heat treatment effects upon the properties of PAN base carbon fibers.

16 p2028 A73-33040

Thermal properties of rhenium single crystals at high temperatures.

16 p2026 A73-33581

Effect of finite resistivity on the dynamic stability of a composite plasma.

17 p2214 A73-34074

Certain thermophysical properties of isotropic pyrolytic graphite

17 p2253 A73-34132

Certain physical properties of a new alloy of the nickel-rhenium-molybdenum system

17 p2186 A73-34137

Electrical properties and photoconductivity of CdS thin films obtained in a hydrogen atmosphere

17 p2219 A73-34281

Simultaneous measurement of specific heat, electrical resistivity, and hemispherical total emittance of niobium-1 /wt. %/ zirconium alloy in the range 1500 to 2700 K by a transient /subsecond/ technique.

17 p2187 A73-34499

Temperature dependent heat conductivity, Lorentz number and electrical resistivity of high melting Ti, Zr, Nb, Cr, Mo and W carbides and borides at 300-1200 K

17 p2191 A73-35199

Electric potential and current distribution in a rectangular sample of anisotropic material with application to the measurement of the principal resistivities by an extension of van der Pauw's method.

17 p2220 A73-35653

Electrical conductivity, internal temperatures and thermal evolution of the moon.

17 p2235 A73-35741

Calculation of components, electrical conductivity, and total radiative source strength of nitrogen plasma in local thermodynamic equilibrium.

[AIAA PAPER 73-744]

18 p2339 A73-36360

High temperature investigations of the steady and nonequilibrium electrical conductivity of cadmium sulfide crystals

18 p2340 A73-36670

A study of electrical conductivity inhomogeneities in CdS single crystals

18 p2341 A73-36963

Application of the four-probe method to the determination of the resistance of thin films deposited on various substrates

19 p2470 A73-37953

Influence of intervalley scattering on the size effect in the electrical conductivity of semiconductors

19 p2471 A73-37956

Calculation of the base layer conductivity of a transistor structure

20 p2535 A73-38859

The effect of vanadium, niobium, and tantalum on the electrical resistance of nickel

20 p2578 A73-39396

Detuning of Wheatstone-bridge circuit during the measurement with wire strain gages - Influence and elimination of undesired effects on detuning

20 p2566 A73-39630

NiO and CoO single crystal thermal conductivities, reporting specific heat and electrical resistivity near magnetic transition

20 p2600 A73-39826

Nb electrical resistance change under elastic distortion due to lattice distortions and dimensional change

21 p2717 A73-40323

Texture and anisotropy of the properties of titanium sheet

21 p2719 A73-40852

AC conductivities of amorphous Ge-As-Te and Ge-As-Se systems.

21 p2753 A73-41119

The influence of crystal defects in platinum on platinum resistance thermometry.

22 p2855 A73-42009

Electrical resistivity and thermal conductivity of alloys of the tungsten-molybdenum system.

[ECTP PAPER B1-6]

22 p2876 A73-42402

Frequency magnetovariational sounding of the earth, using the ratio of potentials.

23 p2970 A73-43249

Generation of electrical current by impact in metallic and semiconductor bodies

23 p3015 A73-43476

Laws governing the behavior of the electrical resistance during process of inelastic-strain relaxation

23 p3040 A73-43574

Superconductivity of copper containing small amounts of niobium.

23 p3017 A73-44033

Effects of additions of Al and Ti on electrical resistivities of oxide films of Fe-18 Cr sealing alloy.

23 p2986 A73-44152

On the process of precipitation in Mg-Ce alloy.

23 p2994 A73-44155

Analyses of some potential problems in cylindrical coordinates in connection with four-point probe technique.

23 p3018 A73-44368

ELECTRICALLY SUSPENDED GYROSCOPES

U ELECTROSTATIC GYROSCOPES

ELECTRICITY

NT ALTERNATING CURRENT

NT ATMOSPHERIC ELECTRICITY

NT AURORAL ELECTROJETS

NT ELECTROJETS

NT EQUATORIAL ELECTROJET

NT GEOELECTRICITY

NT IONOSPHERIC CURRENTS

NT STATIC ELECTRICITY

NT TELLURIC CURRENTS

ELECTRIFICATION

Thunderstorm electrification by the inductive charging mechanism. I - Particle charges and electric fields.

II - Possible effects of updraft on the charge separation process.

23 p3002 A73-43599

ELECTRO-OPTICAL EFFECT

High-repetition-rate optical pulse generator using a Fabry-Perot electro-optic modulator.

01 p0058 A73-10127

Electro-optical multiple transit laser beam deflection system using KDP crystals and quadrupole electrode arrangements

03 p0319 A73-14066

Nonlinear interaction between circular coherent light and modulating electromagnetic waves in presence of quadratic electrooptical effect, noting frequency shift

04 p0459 A73-15921

Electrooptic liquid crystal devices - Principles and applications.

07 p0861 A73-19135

Quasi-stationary emission from ruby and neodymium-glass lasers

08 p0976 A73-21718

Optical damage and internal fields in pyroelectrics.

10 p1260 A73-24531

Twisted nematic liquid-crystal electro-optic devices with areas of reverse twist.

11 p1337 A73-25357

Superposition method for potential distribution in plane tetrode field with unipotential and bipotential grids, noting electro-optical effect in cylindrical lenses

13 p1591 A73-28667

Investigation of some electrooptical properties of liquid crystals

14 p1784 A73-30854

Ultrafast spark gaps for electro-optical device control, discussing trigger system design and performance

06 p0693 A73-18276

in terms of delay, jitter and internal voltage time response

16 p2013 A73-32874

Stimulated entropy /temperature/ scattering and its effect on stimulated Mandel'shtam-Brillouin scattering.

22 p2868 A73-41720

Electrooptical modulator employing a barium titanate single crystal. I - Estimates of critical control voltages

23 p2987 A73-43571

Some experiments on a voltage-induced optical waveguide in LiNbO3.

23 p3019 A73-44374

ELECTRO-OPTICAL PHOTOGRAPHY

Electro-optical multiband cameras for spaceborne remote sensing, discussing optical multiplexing, return beam vidicon, intensifier vidicon storage tube, image spectrophotometer and dissector

04 p0450 A73-15770

Carrier-frequency photography - Principle and application of lattice-coded image tracing

06 p0692 A73-17574

Ultrahigh-speed electronic camera - CELER 2-500

06 p0696 A73-18856

Contribution of 1- and 5-nsec frame-type motion-picture photography to the study of dense plasmas

06 p0696 A73-18857

Implementation of the 1975 Mars Viking Lander camera.

08 p0970 A73-21741

Utilization for high speed cinematography of phased-locked CW lasers

21 p2709 A73-39954

ELECTRO-OPTICS

Propagation of submillimeter-band electromagnetic waves in the drifting plasma of a solid

01 p0017 A73-10976

The laser's impact on crystal technology.

01 p0088 A73-11067

Utilization of electro-optical methods in designing angular- and linear-displacement sensors

01 p0052 A73-11074

Light-emitting diode and liquid crystal applications to displays, discussing gas discharge plasma, electrophoretic, fluorescent and incandescent devices, electronic wristwatches and calculators

02 p0168 A73-12082

Microelectronic metal-dielectric-semiconductor devices for physical properties of multilayer multiphase systems, noting field effect transistors, integrated circuits and electro-optical elements

03 p0349 A73-13656

Electrooptical model of the first retina layers of a visual analyzer

03 p0267 A73-13657

Analysis of dynamic-excitation conditions for electrooptical-coupling switches in control circuits of electroluminescent panels

03 p0282 A73-13658

A numerical computer method for computing the electrostatic field and electron paths of focusing optoelectronic systems

04 p0448 A73-15078

Electro-optical, magneto-optical, absorptional and acousto-optical light modulation, noting Kerr effect, Faraday rotation and light absorption

04 p0458 A73-15348

Muller matrix derivation for microwave light modulation studies in quasi-homogeneous magneto-optical and electrooptical media, taking into account finite light speed

04 p0459 A73-15923

A graph-analytical method for precalculation of the moments of solar transition through the field of view of electrooptical systems

05 p0575 A73-16313

Electro-optical and acousto-optical methods of laser beam modulation and deflection with emphasis on various modulator and deflector types

05 p0583 A73-16340

Electro-optical media for initial light radiation frequency shift maximum, analyzing circular light/modulating wave interactions

05 p0551 A73-16780

Electro-optical fiducial system for shock wave interferometry relating impact time to free surface motion

05 p0580 A73-17261

Crystal transverse modulators for laser Q-switching, discussing electro-optical properties of various materials

06 p0699 A73-17753

A model of image-shape analysis based on fiber-optics elements and on the principle of photoelectric conversion

06 p0671 A73-18084

Annual Electro-Optical Systems Design Conference, 4th, New York, N.Y., September 12-14, 1972, Proceedings of the Technical Program.

06 p0693 A73-18276

Real time coherent electro-optic two dimensional on-line spatial light modulator role in optical data processing system

06 p0693 A73-18286

Electro-optical laser beam deflector with lithium niobate for low resolution and high speed operation, discussing system design, construction and tests
06 p0700 A73-18296

Electro-optical multiplexers and demultiplexers for time-multiplexed PCM laser communication systems.
06 p0700 A73-18297

The selection and design of electro-optical instruments for outer planet exploration.
06 p0695 A73-18320

High-frequency electro-optic prism deflector with application to optical demultiplexing and multiplexing.
06 p0701 A73-18363

Bismuth germanate and silicate single crystals refractive index and electro-optic coefficient measurement
06 p0737 A73-18367

Electro-optic contrast observations in single-domain epitaxial films of bismuth titanate.
06 p0739 A73-18748

Service life estimation of electro-optic devices and degradation kinetics, noting reliability of light transmitters and receivers
07 p0800 A73-19407

Russian book - Optoelectronic devices in spacecraft.
07 p0825 A73-20379

Degradation analysis of infrared and visible optoelectronics devices.
08 p0944 A73-20742

Television raster laser raster scanner, discussing deflectors, beam-shaping and image-forming optics, electronic system and scanning beam frequency response
08 p0975 A73-21141

A study of optical image sensors for the large space telescope.
08 p0971 A73-21742

Pulse amplitude modulation of a CO₂ laser in an electro-optic thin-film waveguide.
09 p1098 A73-23337

Electro-optical transient sampling analyzer with neon laser and hydrogen thyratron pulse generator and minimum optical and electrical jitter
11 p1377 A73-26244

Stabilized two-pulse operation of the phase-modulated, frequency-doubled laser.
12 p1504 A73-26831

Single-frequency ruby laser with electrooptical Q switching and smooth frequency tuning
12 p1504 A73-26886

An optimal electrooptical method of signal processing in coherent pulse reception
12 p1468 A73-26947

Optoelectronic step-up voltage transformer with optical coupling electrical isolation, using light emitting diode and semiconductor film with high photovoltage levels
12 p1496 A73-26964

Microelectronics developments and limitations, considering bipolar IC, metal-dielectric-semiconductor structures and optoelectronic communication links
12 p1480 A73-27267

An electrooptical method for storage of weak linear-FM signals
12 p1470 A73-27577

Electrooptical and piezoelectric alignment of a composite resonator in a semiconductor laser
13 p1627 A73-28764

The illumination distribution in the image plane from the radiation of a plane-parallel plate with the actual ray paths taken into consideration.
13 p1621 A73-29325

Thick film multilayer IC for electro-optical applications, discussing package techniques, sealing materials, ultrathick printing cold cathode panel and liquid crystal displays
13 p1669 A73-29395

Some limiting parameters of an optoelectronic device for determining the orientation of a spacecraft with respect to the sun
14 p1803 A73-29872

Generalized theory of nonlinear susceptibilities and linear electrooptic coefficients based on a three-dimensional anharmonic oscillator model.
14 p1756 A73-29926

Utilization of optical-frequency carriers for low- and moderate-bandwidth channels.
14 p1728 A73-30418

A tunnel diode trigger with an optical output
14 p1737 A73-30797

The effect of unmodulated sunlight on the integral voltage sensitivity of some radiation detectors.
14 p1754 A73-30954

Russian book - Radiation receivers of automatic electron optics devices.
15 p1875 A73-31588

A rotation angle-to-digital code photoelectric converter
15 p1877 A73-32133

European Electro-Optics Markets and Technology Conference, 1st, Geneva, Switzerland, September 13-15, 1972, Proceedings.
16 p2022 A73-32851

Electrooptical-phase imaging device using nematic liquid crystals
16 p2013 A73-32881

Hybrid optoelectronics - High frequency modulation and detection of light by semiconductor sources and sensors.
16 p1978 A73-32886

Electrooptical Q-switching /EQQS/ in solid-state laser resonators
17 p2184 A73-34917

Book on experimental analysis covering measurement systems, engineering problems, data analysis, electro-optics and dimensional parameters
17 p2176 A73-35855

An electrooptical modulator based on a coaxial shaped resonator
18 p2322 A73-36856

The scope for electron-optical devices for the optimal processing of composite signals in communications systems.
18 p2290 A73-37127

Application of a Thomson mass spectrograph with an electron-optical recorder to the investigation of the mechanism of plasmoid acceleration
19 p2467 A73-37370

The sensitivity of optoelectronic scanning systems with out-of-phase connection of the radiation detector elements.
20 p2564 A73-38850

The equipment for photoelectric photometry in the Graz observatory
20 p2565 A73-39068

Electroluminescent display device of integrated XY structure utilizing GaAlAs and GaAsP
20 p2536 A73-39202

Metal-insulator-semiconductor-insulator-metal information storage system with optical write and read operations.
20 p2533 A73-39683

Flashlamp pumped CW mode-locked dye laser picosecond light pulse duration measurement by electro-optical streak camera
21 p2694 A73-39946

Spatial resolution of an incoherent-to-coherent converter using bismuth germanium oxide.
22 p2863 A73-43098

Electrooptical radio spectrograph design for high resolution in time and frequency based on photographic film recording density and coherent optical processing data rate
23 p2980 A73-43374

Small signal duality theory of linear optoelectronic circuits with optical coupling for equivalent circuit computerized design and analysis
23 p2963 A73-43615

Theory for the steady-state operation of a thin-film regenerative optron
23 p2959 A73-43617

ELECTROACOUSTIC TRANSDUCERS

NT LOUDSPEAKERS

NT MICROPHONES

An earphone coupling system for acute physiological studies.
01 p0013 A73-10829

Acoustic field of an infinite annular cylindrical transducer partially coated with an acoustically soft material
01 p0077 A73-10927

Generation and detection of helical surface waves at cylindrical bodies by means of contactless electrodynamic transducers
01 p0051 A73-10974

Optimum operation conditions of thyatron generator circuit in electroacoustic system for excitation of quartz piezoelectric vibrators in ultrasonic NDT
02 p0168 A73-12147

Conversion of electromagnetic into acoustic energy via indium films.
06 p0734 A73-17834

Theory of excitation of microwave elastic waves by multilayer transducers /considering the effect of metallic and insulator layers/.
07 p0801 A73-20139

Microsonics /acoustic surface waves/ technology developments covering materials, heteroepitaxial systems, propagation, electron phonon interaction, acoustic amplifiers and waveguides, electromechanical transducers and signal processing
10 p1223 A73-23782

Sound field of an infinite circular cylindrical transducer partially coated with an acoustically compliant layer.
10 p1249 A73-24187

Surface acoustic wave multistrip components and their applications.
12 p1484 A73-27567

Application of acoustic surface-wave technology to spread spectrum communications.
12 p1470 A73-27570

Ranging and data transmission using digital encoded FM-'chirp' surface acoustic wave filters.
12 p1470 A73-27571

Potential applications of acoustic matched filters to air-traffic control systems.
12 p1522 A73-27572

Foil-electret transducer arrays for real-time acoustical holography.
13 p1614 A73-28583

Acoustical hologram recording by electrostatic transducers using rigid backplate electrode insulated with thin dielectric film transparent to ultrasonic radiation
13 p1614 A73-28584

Russian book on electroacoustic and electromechanical devices for sound recording and measurement covering human auditory system, microphones, loudspeakers, hydrophones, geophones, etc
22 p2832 A73-41882

Ultrasonic pulse techniques based on acoustic velocity for inert gas thermometry, discussing electroacoustic transducer response time, temperature sensitivity and momentary contact coupling technique
22 p2854 A73-41994

Microwave acoustic surface wave devices design tradeoffs, considering propagation losses, air loading, beam steering and diffraction, and transducer effects in curves and data
22 p2833 A73-42399

ELECTROACOUSTIC WAVES

Electromagnetic and electroacoustic mode radiation resistance of linear antennas in compressible electron plasma.
02 p0199 A73-12858

Coupled wave equations for propagation in generally inhomogeneous compressible magnetoplasma.
03 p0345 A73-13069

Influence of nonlinear polarization on the ultrasonic gain factor in piezosemiconductors
05 p0605 A73-16821

Saturation and acoustoelectric oscillations of a photocurrent in CdS and CdSe
06 p0737 A73-18218

Structure of the current front of an electron-acoustic wave in a plasma
15 p1920 A73-32301

Nonlinear ion-acoustic and electron-acoustic waves of a plasma in a magnetic field
15 p1921 A73-32324

Ultrasound absorption coefficient measurement in semiconductor crystal lattices based on acoustoelectric effect
17 p2218 A73-34159

Structure of the current front of an electron-acoustic wave in a plasma.
24 p3114 A73-44609

ELECTROCARDIOGRAMS

U ELECTROCARDIOGRAPHY

ELECTROCARDIOGRAPHY

Computation of solutions to the inverse problem of electrocardiography.
01 p0013 A73-11465

Atrioventricular block response to exercise and intraventricular conduction at rest.
01 p0010 A73-11506

Q waves and coronary arteriography in cardiomyopathy.
01 p0010 A73-11507

Nature of the conduction disturbance in selective coronary arteriography and left heart catheterization.
02 p0134 A73-12443

Maximal treadmill exercise electrocardiography - Correlations with coronary arteriography and cardiac hemodynamics.
02 p0136 A73-12821

Practical exercise test for physical fitness and cardiac performance.
03 p0259 A73-13540

Exercise electrocardiography and vasoregulatory abnormalities.
03 p0260 A73-13541

Correlation of computer-quantitated treadmill exercise electrocardiogram with arteriographic location of coronary artery disease.
03 p0260 A73-13543

Diagnostic value of vectorcardiogram in strictly posterior infarction.
03 p0268 A73-13891

P wave of electrocardiogram in early ischaemic heart disease.
03 p0268 A73-13892

Multichannel PDM-FM biomedical radio telemetry system for ECG, respiratory rate and oxygen consumption during exercise, considering transmitter and receiver design
03 p0269 A73-14278

Blood flow and pressure and ECG data acquisition and transmission via radio telemetry system with electromagnetic flowmeter
03 p0270 A73-14283

Electro-rheocardiotelemetric device for complex monitoring of the dynamics and efficiency of cardiac contraction.
03 p0271 A73-14292

Voltage controlled subcarrier oscillator design and performance for FM/FM multiplex telemetry system for ECG recording during exercise
03 p0271 A73-14293

Telemetrical measurements during sport performance on sportsmen with cardiac arrhythmias.

03 p0271 A73-14294

A remotely operated ECG telemeter for chronic implantation in rats.

03 p0272 A73-14303

Multichannel telemetry of physiological parameters/body temperature, ECG, EEG/ in the rat. I - Design and methods.

03 p0272 A73-14305

Multichannel telemetry of physiological parameters/body temperature, ECG, EEG/ in the rat. II - Applications in neuropharmacology.

03 p0272 A73-14306

Telemetry of cardiovascular parameters on fighter aircraft flying pilots.

03 p0272 A73-14309

Computerized ECG interpretation system for heart and circulatory disorder detection and diagnosis and health screening

03 p0272 A73-14660

Clinical electrocardiographic and vectorcardiographic diagnosis of left posterior subdivision block, isolated or associated with RBBB.

04 p0409 A73-15200

Elevated ST segments with exercise in ventricular aneurysm.

04 p0410 A73-15643

Use of an on-line computer in a study of cardiac arrhythmia.

04 p0412 A73-15644

Numerical classification and coding of electrocardiograms.

04 p0412 A73-15647

Computer-aided ECG analysis and research in a clinical setting.

04 p0412 A73-15648

Book - Understanding electrocardiography: Physiological and interpretive concepts.

05 p0542 A73-16359

Study of intraventricular conduction times in patients with left bundle-branch block and left axis deviation and in patients with left bundle-branch block and normal QRS axis using His bundle electrograms.

05 p0540 A73-16582

Uses and limitations of stress testing in the evaluation of ischemic heart disease.

05 p0552 A73-17278

Correlation of electrocardiographic studies and arteriographic findings with angina pectoris.

05 p0546 A73-17279

Prolonged control of cardiac bioelectrical activity in man in ground experiments and during spaceflight

06 p0657 A73-17694

Compact digital coding of electrocardiographic data.

06 p0660 A73-18815

Intermittent trifascicular block - Different mechanisms of conduction disturbances in the bundle branches.

07 p0780 A73-19152

Orthogonal versus planar vector-electrocardiography.

07 p0785 A73-19930

A method for electrocardiogram recording in Rhesus monkeys

08 p0934 A73-21324

Electromagnetic 60 Hz interference in ECG recordings, discussing sources, identifying tests, elimination and ECG amplifier design

10 p1183 A73-23648

Heart activity characteristics in a human operator during a control process

10 p1183 A73-23806

An electrocardiograph amplifier which satisfies the stringent requirements of long-term monitoring of cardiac activity

10 p1184 A73-23849

Cardiac potential measuring and recording instrument with 240 probes, presenting circuit and block diagrams

10 p1184 A73-24422

Depolarization phase of the spatial velocity electrocardiogram in normal and ventricular overload.

10 p1185 A73-24900

Portable electro-phonocardiograph using magnetic tape recorder equipped with patient's voice print.

11 p1323 A73-25475

Cardiac activity potentials, P-R interval and impulse propagation across atrioventricular node, ventricular conduction and Purkinje fiber-muscle junctions

11 p1316 A73-25598

Familial syndrome of midsystolic click and late systolic murmur.

11 p1317 A73-25697

Temporal sequence of right and left atrial contractions during spontaneous sinus rhythm and paced left atrial rhythm.

11 p1317 A73-25699

Electrocardiographic evidence of left atrial hypertension in acute myocardial infarction.

11 p1319 A73-26287

Angina pectoris in men - Prognostic significance of selected medical factors.

11 p1319 A73-26288

Computer analysis of the orthogonal electrocardiogram and vectorcardiogram in 939 cases with hypertensive cardiovascular disease.

11 p1324 A73-26361

Unreliability of conventional electrocardiographic monitoring for arrhythmia detection in coronary care units.

12 p1465 A73-27891

Relationship between ventricular premature contractions on routine electrocardiography and subsequent sudden death from coronary heart disease.

14 p1715 A73-30051

Immediate and remote prognostic significance of fascicular block during acute myocardial infarction.

14 p1715 A73-30052

A rapid method for frontal plane axis determination in scalar electrocardiograms.

14 p1721 A73-30063

Automatic methods for smoothing and separation of characteristic points in an electrocardiographic signal

14 p1721 A73-30387

The information content of successive RR-interval times in the ECG - Preliminary results using factor analysis and frequency analysis.

14 p1722 A73-30883

Plasma electrolytes, pH, and ECG during and after exhaustive exercise.

15 p1834 A73-31347

Polarcardiographic responses to maximal exercise and to changes in posture in healthy middle-aged men.

16 p1972 A73-33114

Waveform vector analysis of orthogonal electrocardiograms - Quantification and data reduction.

16 p1975 A73-33115

Phase progression of the QRS complexes in electrocardiograms versus the inscribing directions of the QRS loops in vectorcardiograms.

16 p1975 A73-33116

A new method for diagnosing myocardial damage in patients with normal electrocardiograms and vector cardiograms.

16 p1973 A73-33375

Digital computer diagnosis of cardiac arrhythmias in a single-lead electrocardiogram.

17 p2114 A73-34533

Automatic recognition of electrocardiographic patterns

17 p2116 A73-34964

Automatic cataloging of electrocardiographic patterns

17 p2116 A73-34965

Cardiovascular responses to sudden strenuous exercise - Heart rate, blood pressure, and ECG.

17 p2112 A73-35461

Advances in electrocardiography; Proceedings of the Symposium, Emory University, Atlanta, Ga., May 10-13, 1971.

18 p2274 A73-36516

Limitations of the dipole concept in electrocardiographic interpretation.

18 p2281 A73-36517

Intracellular-extracellular action potentials - Considerations for the formation of wavefronts and their detection on the body surface.

18 p2282 A73-36518

Physiologic correlates and clinical comparisons of isopotential surface maps with other electrocardiographic methods.

18 p2282 A73-36519

Electrocardiographic diagnosis of sinus node rhythm variations and SA block.

18 p2274 A73-36520

QRS abnormalities in AV block - Variations and their significance.

18 p2274 A73-36521

Identification of the sites of atrioventricular conduction defects by means of His bundle electrography and atrial pacing.

18 p2282 A73-36522

The differential electrocardiographic manifestations of hemiblocks, bilateral bundle branch block, and trifascicular blocks.

18 p2274 A73-36523

The clinical causes and mechanisms of intraventricular conduction disturbances.

18 p2274 A73-36524

Intra-atrial and esophageal electrography in the diagnosis of complex arrhythmias.

18 p2274 A73-36525

Current status of correlations between vectorcardiogram and hemodynamic data.

18 p2274 A73-36526

Diagnostic power of the Q wave - Critical assay of its significance in both detection and localization of myocardial deficit.

18 p2274 A73-36527

Mid- and late changes in the QRS complex.

18 p2274 A73-36528

The pathogenesis and clinical significance of primary T-wave abnormalities.

18 p2274 A73-36529

Central nervous system influence upon electrocardiographic waveforms.

18 p2275 A73-36530

Electrocardiographic alterations in the presence of angina pectoris.

18 p2282 A73-36542

Electrocardiographic diagnosis of myocardial infarction - Pitfalls of a graphic technique.

18 p2282 A73-36544

Comparative value of both hypoxic and positive pressure breathing tests for detection of premature beats.

18 p2280 A73-36944

Detection of left ventricular asynergy by echocardiography.

20 p2512 A73-38869

Variations of heart rate during sleep as a function of the sleep cycle.

20 p2514 A73-39762

Automatic identification of cardiac rhythm and conductivity disturbances with the aid of digital computers

21 p2643 A73-40751

Examination of a multiple dipole inverse cardiac generator, based on accurately determined model data.

22 p2813 A73-41961

P wave analysis in 2464 orthogonal electrocardiograms from normal subjects and patients with atrial overload.

22 p2806 A73-42341

The correlation of coronary angiography and the electrocardiographic response to maximal treadmill testing in 76 asymptomatic men.

22 p2806 A73-42342

Russian book - Integral topograms of heart potentials.

22 p2807 A73-42489

Polyparametric information of the electrocardiogram in injured tissue.

22 p2809 A73-42834

Ischemic heart disease prediction via exercise ECG tests, discussing work load standardization

22 p2809 A73-42835

Angina pectoris and ECG abnormalities in relation to prognosis of coronary heart disease in population studies in Finland.

22 p2809 A73-42836

Signal processing in medical technology

23 p2948 A73-43317

Transient S-T elevation detected by 24-hour ECG monitoring during normal daily activity.

23 p2946 A73-43492

Ischemic polarcardiographic changes induced by exercise - A new criterion.

24 p3060 A73-44946

ELECTROCATALYSTS

Nitrogen-containing active carbon as the cathode catalyst in acid fuel cells.

04 p0407 A73-15107

Cobalt phosphide CoP₃ as a catalyst for electrochemical H₂ oxidation in acid fuel cells.

04 p0407 A73-15108

Organic compounds catalytic activity comparison for use in fuel cell, noting superiority of dihydrodibenzo-tetraazaannulene cobalt complex

04 p0407 A73-15109

An assessment of some mixed-oxide systems as low-cost electrocatalysts for oxygen electrodes.

04 p0407 A73-15110

Bipolar noble-metal free electrodes for fuel cells with acid electrolytes.

04 p0407 A73-15113

Raney-Ni catalysts preparation for carbon-PTFE fuel cell electrodes from Ni-Al alloy, discussing rolling technique suitability and electrode characteristics

04 p0407 A73-15115

Transition metals nitrides, carbides and silicides applications as electrocatalysts in fuel cells for economic operation, considering hydrogen, formaldehyde and formic acid oxidation

04 p0414 A73-16038

ELECTROCHEMICAL CELLS

NT ALKALINE BATTERIES

NT ELECTRIC BATTERIES

NT FUEL CELLS

NT HYDROGEN OXYGEN FUEL CELLS

NT NICKEL CADMIUM BATTERIES

NT NICKEL ZINC BATTERIES

NT PRIMARY BATTERIES

NT REGENERATIVE FUEL CELLS

NT SILVER ZINC BATTERIES

NT STORAGE BATTERIES

Circuitry for battery cell control and protection from overcharge and over-discharge for long service life operation

03 p0253 A73-13937

The diffusivity and solubility of oxygen in liquid tin and solid silver and the diffusivity of oxygen in solid nickel.

04 p0463 A73-15315

Russian book - Power systems of spacecraft.

04 p0408 A73-15704

Kinetics of the formation of passivating nickel hydroxide layers on nickel carbonyl

07 p0788 A73-20397

- A nickel-hydrogen secondary cell for synchronous orbit application. 09 p1033 A73-22753
- Calculation and comparison of the economics of electrochemical fuel cells 11 p1410 A73-25346
- An electrochemical cell equivalent circuit for storage battery/power system calculations by digital computer. 11 p1309 A73-25985
- Intersociety Energy Conversion Engineering Conference, 8th, University of Pennsylvania, Philadelphia, Pa., August 13-16, 1973, Proceedings and Addendum. 19 p2390 A73-38386
- ELECTROCHEMICAL CORROSION**
- Synergistic effects of anions in the corrosion of aluminum alloys. 03 p0325 A73-13729
- Microcorrosion studies with functional fluids. [ASLE PREPRINT 72LC-4C-1] 03 p0335 A73-14360
- The role of electrochemical processes in the fretting corrosion of metals 06 p0710 A73-18660
- Composition of anolyte within pit anode of austenitic stainless steels in chloride solution. 07 p0840 A73-20352
- Distinguishing characteristics of pitting and crevice corrosion. 08 p0980 A73-21775
- Potentiostatic study of iron meteorite corrosion. 09 p1139 A73-21857
- Third elements effect on electrical erosion of steels noting influence of atmospheric composition 09 p1104 A73-22967
- Galvanic interaction between active and passive titanium. 09 p1106 A73-23167
- Stress corrosion cracking of a high strength steel. 10 p1232 A73-23869
- Standardization, loading methods and environments for stress corrosion cracking tests, noting prevention of crevice, galvanic and hydrogen embrittlement effects 10 p1232 A73-23871
- Overview of corrosion cracking of titanium alloys. 10 p1232 A73-23873
- Corrosion and electrochemical characteristics of oxidized steels Kh15N5D2T and Kh15N4AM3. 10 p1236 A73-24926
- On the nature of films over corrosion pits in stainless steel. 11 p1378 A73-24975
- Crack growth rate due to steels and Ti and Ni alloys electrochemical dissolution, noting tensile stress intensity factor 11 p1385 A73-26173
- Corrosion fatigue due to static and cyclic stress, noting electrochemical adsorption theory 11 p1386 A73-26737
- Factors controlling the corrosion behavior of titanium and titanium-nickel alloys in saline solutions. [NACE PAPER 64] 13 p1637 A73-29311
- Corrosion and corrosion prevention of light metal alloys. [NACE PAPER 114] 13 p1637 A73-29314
- Book on fretting corrosion covering contacting surface theory, damage characteristics, wear variables effect, fatigue, adhesion and electrochemical properties, etc 13 p1643 A73-29575
- Catalytic effects in corrosion processes with hydrogen depolarization of multiphase magnesium alloys 14 p1764 A73-30827
- Effect of chloride ions on the dissolution behavior of Fe-Ni alloys. 15 p1895 A73-32565
- An electrochemical model for hot-salt stress-corrosion of titanium alloys. 17 p2189 A73-34643
- A test procedure to evaluate the relative susceptibility of materials to stress corrosion cracking. 17 p2191 A73-35125
- The hydrogen evolution reaction on Ti-6Al-4V in acidic solutions of NaCl-HCl. 19 p2402 A73-37585
- Temperature-humidity acceleration of metal-electrolysis failure in semiconductor devices. 19 p2411 A73-38450
- Pitting of titanium. I - Titanium-foil experiments. II - One-dimensional pit experiments. 23 p2991 A73-43521
- The stress corrosion of titanium materials - The present status of research 23 p2992 A73-43910
- ELECTROCHEMICAL MACHINING**
- Analysis of electrolytes for electrochemical polishing of steel with cationite application 02 p0174 A73-12536
- Bubbles and operating voltage effects in electrochemical machining of tungsten carbide and discharge machining of glass [ASME PAPER 72-WA/PROD-21] 04 p0456 A73-15804
- Maximum metal removal rate in ECM. [SME PAPER MR 72-537] 06 p0697 A73-18092
- Electrochemical machining application to aircraft gas turbine engine components manufacture, discussing removal rate, accuracy and surface finish capability [SME PAPER MR 72-536] 06 p0697 A73-18093
- Application of inverse boundary value problems in the theory of dimensional electrochemical working 15 p1881 A73-31153
- Sodium chloride electrolyte data at high temperatures and pressures. [ASME PAPER 73-PROD-1] 16 p1971 A73-33532
- High feed rate electrochemical machining Fe in aqueous NaCl, using high supply voltage, electrolyte pressures and flow velocities [ASME PAPER 73-PROD-3] 16 p1971 A73-33533
- Electrochemical thinning of a metal disk rotating on a floating self-moulded cathode. 17 p2182 A73-35766
- ELECTROCHEMICAL OXIDATION**
- Electrode kinetic studies on the anodic oxidation of methanol. 04 p0406 A73-15102
- Studies of the anodic oxidation of hydrazine in an alkali electrolyte and of the side reaction of ammonia formation during the decomposition of hydrazine 04 p0407 A73-15103
- Cobalt phosphide CoP3 as a catalyst for electrochemical H2 oxidation in acid fuel cells. 04 p0407 A73-15108
- Transition metals nitrides, carbides and silicides applications as electrocatalysts in fuel cells for economic operation, considering hydrogen, formaldehyde and formic acid oxidation 04 p0414 A73-16038
- Chemical and electrolytic coatings for satellite surface thermal control, discussing surface anodic oxidation treatment of adhesive Au platings on Al alloys 07 p0829 A73-18910
- Directly excited subsonically flowing CW gas laser with carbon monoxide and dioxide generation as reaction products formed by organic molecule electrochemical oxidation 09 p1091 A73-22084
- The electrical properties of anodically grown silicon dioxide films. 09 p1064 A73-23042
- Anodic oxidation and stress corrosion cracking /SCC/ of titanium alloys. I - Factors affecting SCC and their influence on the anodic behavior of alloy Ti-6Al-6V-2.5Sn. 17 p2187 A73-34524
- Molybdenum-oxygen-sulfur fuel cell anode catalysts capable of oxidizing low cost fuels in acid electrolytes 19 p2390 A73-38401
- Theory of successive electron transfer steps in cyclic voltammetry Application to oxygen pseudocapacitance on platinum. 21 p2636 A73-40843
- Properties of anodic oxide films formed in the anodization of silicon nitride. [ECS PAPER 81] 21 p2702 A73-40844
- ELECTROCHEMISTRY**
- NT COULOMETRY
- NT ELECTROLYSIS
- Effect of temperature and polarization rate on the electrochemical behavior of titanium alloys in a sulfuric medium 02 p0178 A73-11523
- The inhibition of the dendritic electrocrystallization of zinc from doped alkaline zincate solutions. 03 p0273 A73-13727
- Metallurgical, chemical and electrochemical production and refining of refractory metals, including titanium, fluorotitanates and artificial rutile 04 p0465 A73-15660
- Colloid thruster propellants selection for semiconductor liquids with suitable electrochemical properties via cyclic voltametry 04 p0485 A73-15724
- Physical and thermal constraints on batteries of electrochemical power supply systems onboard satellites, sounding and booster rockets and balloons 07 p0778 A73-18977
- Some problems in the theory of an electrochemical velocity sensor for current-conducting fluids 08 p0965 A73-21106
- Autonomous composite power system with electrochemical generator, ion exchange membrane and storage battery 11 p1308 A73-25625
- Comparative properties, main characteristics, and areas of application of electrochemical transducers 12 p1459 A73-26767
- Chemotronic /electrochemical/ transducers of nonelectrical quantities in automatic control 12 p1459 A73-26768
- Pitting corrosion - A review of recent advances in testing methods and interpretation. 15 p1889 A73-31741
- Investigations of the electrochemical processes in titanium alloys as applied to stress-corrosion crack tip state in sea water. 15 p1896 A73-32572
- High-temperature batteries. 17 p2110 A73-35594
- Electric power cell for producing direct/alternating current and shaft horsepower by direct electrochemical reaction of alkali metals with water 19 p2390 A73-38397
- Silver powder anode, perylene-iodide cathode and ionically conductive solid cyanide-iodide electrolyte battery construction and performance tests [ECS PAPER 12] 21 p2635 A73-40841
- Problems experienced in continuous recording of surface ozone by the electrochemical method at Poona. 23 p2982 A73-43864
- ELECTROCONDUCTIVITY**
- Radiation and conductivity of a high current constricted discharge plasma. 01 p0081 A73-10119
- Electrical conductivity and total radiant power of air plasma. 01 p0081 A73-10121
- Superplasticity in two phase compositions based on refractory compounds, noting creep rate dependence on concentration and electroconductivity 01 p0066 A73-11339
- Collisionless plasma flow over a conducting sphere. 02 p0158 A73-11919
- Thermal cycling and frequency tests for lunar soil dielectric constant, loss tangent and dc conductivity, noting moisture effects 02 p0220 A73-12481
- Lunar magnetic field measurements, electrical conductivity calculations and thermal profile inferences. 03 p0369 A73-13103
- Electron-ion collision frequency and electrical conductivity of non-Debye plasma formed in high pressure discharge from Ar, Kr and Xe tubes 03 p0345 A73-13176
- Kinetic theory for calculation of low temperature homogeneous plasma electric conductivity in magnetic field, noting monotonic decrease 03 p0346 A73-13177
- The thermal and electrical conductivities of tantalum at high temperatures. 03 p0322 A73-13182
- Calculation of the complex conductivity of a monopolar semiconductor with a finite-injection contact 03 p0349 A73-13662
- Thermal conductivity and hot magnetic poles of pulsars. 03 p0374 A73-13796
- Electronically conducting oxides as cathodes or interconnection materials in high-temperature fuel cell batteries. 04 p0407 A73-15111
- Electric and thermal conductivity, elastic properties, and resistance to bending of porous tungsten throughout the porosity range 04 p0464 A73-15371
- Passage of electric current through an illuminated semiconductor under conditions where the anisotropy parameters, the electrical conductivity, and the relaxation time are nonuniform. I 04 p0484 A73-15641
- Electrical conductivity of very thin gold films. 04 p0484 A73-15948
- Magnetotelluric and geomagnetic depth sounding methods compared. 05 p0572 A73-17189
- Millimeter-wave investigation of electronic conduction in semiconducting III-V compounds. 06 p0737 A73-18366
- Si and silicon carbide effects on silicided graphite thermal and electrical conductivities 06 p0714 A73-18558
- Earth electrical conductivity radial distribution effect on solar quiet day geomagnetic field variations 07 p0816 A73-19466
- The induced magnetic field of the moon - Conductivity profiles and inferred temperature. 07 p0892 A73-19835
- Electrical conductivity and Moessbauer study of Apollo lunar samples. 07 p0898 A73-19896
- Experimental investigation of the electrical conductivity of a coaxial high-temperature jet with dispersed particles of Ti 07 p0858 A73-20010
- Residual conductivity in unannealed amorphous germanium. 07 p0864 A73-20455
- Single-phonon contribution to the hopping conductivity of amorphous solids. 08 p0994 A73-20955
- Electrical and thermal conductivities of a relativistic degenerate plasma. 08 p0992 A73-21161

Distribution of electrical conductivity in the earth's mantle from data on the secular variations of the geomagnetic field

08 p0959 A73-21295

Electrical conductivity of a directionally crystallized Al-Al3Ni composition

09 p1099 A73-21972

Lunar interior temperature profiles from olivine and pyroxene electrical conductivity data, indicating high temperature accretion from hydrogen depleted material

09 p1148 A73-22874

Electronic configuration and electrical conductivity in ceramics.

09 p1135 A73-23000

Direct measurements of the electrical conductivity and relaxation time of ionized air in the stratosphere and mesosphere

10 p1211 A73-23890

Conduction mechanisms in resistive films deposited by the silk-screen process

10 p1259 A73-24412

Manifestation of the defect structure of cadmium telluride through high-temperature electrical conductivity

10 p1261 A73-24776

Electrical conductivity of condensed molecular hydrogen in the giant planets.

11 p1420 A73-25885

Influence of a powerful electromagnetic wave on the electrical conductivity of a semiconductor

11 p1409 A73-26165

Collective interactions and electrical conductivity of plasma in strong electric fields.

11 p1406 A73-26554

Electric conductivity in the atmosphere of early-type stars.

11 p1427 A73-26575

Optimal electrical conductivity and mechanical properties of Cu-Mg-Fe-Si-Zr and Be-B containing heat resistant Al alloys, comparing to Cu at room and elevated temperatures

12 p1511 A73-26918

Earth crustal conductivity structure from micropulsation activity cycle using magnetic variometer array

12 p1488 A73-26986

Electrical conductivity of semiconductor glass crystals on an arsenic and lead selenide base

12 p1531 A73-27195

Pressure sensitization relation to electrical conductivity relaxation during isothermal isobaric annealing of CdTe crystals

12 p1531 A73-27196

Astronomical, geochemical and geophysical data and constraints for lunar evolution, considering remanent magnetization, electrical conductivity and early evolution model

12 p1541 A73-27491

Nonlinear integral equations for the electrodynamics of conducting media

12 p1525 A73-27805

The normal-tangential form of the equations for the electrodynamics of conducting media

12 p1525 A73-27806

Some physical properties of stephanite in the phase transition region

13 p1667 A73-28002

The effect of two periodic conductivity anomalies on geomagnetic micropulsation measurements.

13 p1607 A73-28622

Ground-wave perturbation over a transition zone between two different sections.

13 p1583 A73-28798

Plane electromagnetic wave diffraction by ideally conducting circular cylinder in far and bright spot zones, using Green theorem for field calculation

13 p1583 A73-28851

CW NMR millidegree thermometer using oscillator to detect resonance, noting Curie law, magnetogyric ratio, spin-lattice relaxation time and low electrical conductivity

13 p1618 A73-29072

High-temperature electrical conductivity relaxations induced in CdTe crystals by variations in cadmium vapor pressure

15 p1923 A73-31201

Engineering technique for secondary-medium parameter calculation in the substitution circuits of flat, linear induction MHD machines with side busbars

15 p1832 A73-31411

Electrical conductivity and total emission coefficient of air plasma.

15 p1918 A73-31657

Plane boundary layer equations of asymmetric MHD incompressible fluid motion for case of high and low electroconductivity

15 p1919 A73-31829

Field-dependent carrier transport in non-crystalline semiconductors.

15 p1924 A73-32021

Transport coefficients of ionized argon.

16 p2039 A73-33318

Sodium chloride electrolyte data at high temperatures and pressures.

[ASME PAPER 73-PROD-1] 16 p1971 A73-33532

Si and silicon carbide effects on silicided graphite thermal and electrical conductivities

16 p2030 A73-33584

Electrical conductivity variations in organic semiconductors in the melting temperature region

16 p2044 A73-34005

Screened potential Lorentz model for electrical conductivity of non-Debye plasma, investigating electron energy distribution function

17 p2214 A73-34127

Cooling associated with minority carriers exclusion effect in semiconductors, discussing influence of electroconductivity and forbidden bandwidth

17 p2219 A73-35160

Effect of adsorption on the electrical conductivity of thin vanadium films

17 p2220 A73-35557

Mesospheric positive ion observation via measurement of polar electrical conductivities by subsonic parachute-borne blunt probe system launched on meteorological rockets

18 p2305 A73-36006

Analysis of thick rectangular waveguide windows with finite conductivity.

18 p2292 A73-36605

Distribution of electric conductivity in the mantle of the earth, according to data on secular geomagnetic field variations.

19 p2425 A73-37924

Influence of intervalley scattering on the size effect in the electrical conductivity of semiconductors

19 p2471 A73-37956

Distribution of a monochromatic electromagnetic field and of temperature in a plane conductor with temperature dependent conductivity

19 p2471 A73-38340

The thermal and electrical conductivities of porous copper and stainless steel at elevated temperatures.

[ASME PAPER 73-HT-47] 20 p2575 A73-38572

Direct measurements of the electrical conductivity and relaxation time of ionized air in the stratosphere and mesosphere.

20 p2551 A73-38909

Ionic dissociation energy in polymeric electrical conductivity behavior, taking into account conductivity, viscosity, dissociation energy, dielectric constant, gas constant and absolute temperature

20 p2581 A73-39667

Semiconducting ground influence on input impedance and radiation resistance of horizontal magnetic dipoles, covering short wave band for various antenna elevations and conductivity levels

21 p2661 A73-40203

Amorphous material conduction, discussing glass transparency relation to electronic properties, semiconducting glasses and switching behavior

21 p2723 A73-40272

One dimensional model of electron-phonon system exhibiting Peierls instability for tetrathiofulvalinium tetracyanoquinodimethane conductivity, considering high temperature superconductivity achievement via Peierls instability suppression

21 p2751 A73-40508

Rotation of an electrically conducting fluid with a free surface in a rotating field

21 p2747 A73-40885

Thermal contraction of a system of glassfibre and epoxy resin between 300 and 77 K.

21 p2724 A73-41107

Electrical conductivity and superconductivity of vanadium, niobium, and chromium solid solutions

22 p2873 A73-41963

Optical and electrical properties of doped semiconductors in a strong electromagnetic field.

22 p2896 A73-42252

Nature of the anomaly of the electrical conductivity of a magnetized plasma

22 p2892 A73-42381

Investigation of the electron concentration behind strong shock waves

22 p2893 A73-42385

Theoretical studies and experimental verifications of thermal and electrical conductivity, molecular diffusivity and viscosity of a partially ionized suspension in an electric field.

22 p2894 A73-42512

Electrical conductivity of a plasma during collective interactions in a high-current gas discharge

23 p3009 A73-43652

Observation of doping profiles in Gunn diodes with a scanning electron microscope using the beta-conductivity.

23 p2960 A73-43777

Conductivity of Type II superconductors near the transition temperature

23 p3016 A73-44019

Electron-electron collisions and the electrical conductivity of metals at low temperatures

23 p3016 A73-44021

Linear external electric field approximation for intervalley scattering effects on nondegenerate semiconductor surface electroconductivity

23 p3017 A73-44045

Temperature dependence of dc electroconductivity of CdSe single crystals and compressed micron parti-

cle size powders, noting pressure and annealing effects on powder conductivity

23 p3018 A73-44372

Experimental study of shocked-plasma flows with a double search-coil conductivity probe.

24 p3113 A73-44402

Ac electroconductivity of polycrystalline Co-Fe ferrite as function of temperature, composition and frequency at 1 kHz-200 MHz

24 p3119 A73-44403

ELECTRODELESS DISCHARGES

Electromagnetic fields in electrodeless discharges of arbitrary length.

[TTU-SR-2] 09 p1128 A73-22635

Plasma excitation by HF field in carbon dioxide-argon flow under low pressure, noting disappearance of striations

10 p1253 A73-24072

Influence of the magnetic field on electrodeless-discharge plasmas

23 p3009 A73-43654

ELECTRODEPOSITION

NT ELECTROPLATING

Russian papers on metal corrosion and protection covering additives, annealing, polymer coatings, anodic polarization, electrodeposition, magnetic alloy coatings, etc

02 p0174 A73-12534

Metallographic investigation of electrodeposited iron-nickel-chromium alloys

02 p0174 A73-12535

Study of polarization during electrodeposition of tungsten simultaneously with nickel

02 p0174 A73-12539

Preparation and high-temperature properties of carbon fiber-Ni composites.

03 p0321 A73-12919

Influence of gas carburizing on the structure and properties of electrolytically deposited chromium

11 p1375 A73-26734

Highly disperse Fe powder electrodeposition on cathode, examining electrolyte concentration, acidity, current density and bath temperature effects on current efficiency for optimal deposition conditions

12 p1503 A73-27552

Corrosion performance of new fastener coatings on operational military aircraft.

13 p1637 A73-29315

Techniques for fabrication of composite materials.

16 p2017 A73-32699

Electrolytically deposited noble-metal layers in the electronic industry

16 p1987 A73-32945

Structure, strength, and fracture of electrodeposited nickel and Ni-Co alloys.

16 p2025 A73-33113

Comparative evaluation of the wear resistance of electrolytic and plasma chromium coatings

18 p2318 A73-35883

Synthesis of metal-ceramic and other heat-resistant coatings by the electrochemical method

18 p2319 A73-35890

Electrodeposited Au on TO-5 headers, discussing discoloration measurement and ultrasonic test for bondability from correlation between optical reflectivity and bond pull strength

19 p2435 A73-38441

The mechanism of electrical erosion in composite materials during electric arc alloying

24 p3093 A73-44743

Wear resistant abrasive and dry lubricant cobalt-chromium carbide composite material coatings obtained by electrolytic codeposition

24 p3094 A73-45073

ELECTRODERMAL RESPONSE

U GALVANIC SKIN RESPONSE

ELECTRODES

NT ANODES

NT CATHODES

NT CELL ANODES

NT CELL CATHODES

NT COLD CATHODES

NT DIFFUSION ELECTRODES

NT DYNODES

NT HOLLOW CATHODES

NT HOT CATHODES

NT PHOTOCATHODES

NT PHOTOMULTIPLIER TUBES

NT PLASMA ELECTRODES

NT THERMIONIC CATHODES

NT TUBE CATHODES

NT TUBE GRIDS

Current distribution prediction in transient response of rotating disk electrode, noting mass transfer for cathodic reduction of ferricyanide

03 p0273 A73-13728

Influence of structural perturbations applied to platinum and gold on kinetic processes at the electrode.

04 p0407 A73-15105

An assessment of some mixed-oxide systems as low-cost electrocatalysts for oxygen electrodes.

04 p0407 A73-15110

Bipolar noble-metal free electrodes for fuel cells with acid electrolytes. 04 p0407 A73-15113

Carbon-PTFE fuel cell electrode for hydrogen-KOH-air batteries for operation over long time periods, discussing rolling technique and industrialization possibilities 04 p0407 A73-15114

Raney-Ni catalysts preparation for carbon-PTFE fuel cell electrodes from Ni-Al alloy, discussing rolling technique suitability and electrode characteristics 04 p0407 A73-15115

Reliability of electromyographic measurements by means of surface electrodes 04 p0412 A73-15520

Electric forces in electrostatic gyroscope for rotor gravity center displacement, taking into account mutual effects of electrode pairs 05 p0577 A73-16994

Motion of a magnetized conducting liquid between two plane electrodes in a transverse magnetic field 06 p0727 A73-17472

Morphology and capacity of a cadmium electrode - Studies on a simulated pore. [ECS PAPER 68] 06 p0649 A73-17744

Kinetics of the formation of passivating nickel hydroxide layers on nickel carbonyl 07 p0788 A73-20397

Some problems in the theory of an electrochemical velocity sensor for current-conducting fluids 08 p0965 A73-21106

A method for electrocardiogram recording in Rhesus monkeys 08 p0934 A73-21324

An implantable glass electrode used for pH measurement in working skeletal muscle. 08 p0935 A73-21510

Performances of the better metallic electrodes in cesium thermionic converters. 09 p1036 A73-22817

Technique for the implantation of long-term diagnostic electrodes in the amygdaloid complex of the human brain 09 p1046 A73-22857

Electric arc motion during initiation by plasma injection between static electrodes in dc circuit, applying to pulsed arc commutator design 09 p1131 A73-22938

Calculation of the rotor potential of an electrostatic gyroscope 11 p1364 A73-26098

Digital electrode breakdown potential controller for spark source mass spectrometer automation, using radio frequency pulse amplitude sensing 11 p1367 A73-26315

Inductive flow meter sensor design for optimal electrode diameter to ensure signal quality and impedance matching, proposing circuit diagram 13 p1611 A73-28019

Improved uniform-field electrode profiles for TEA laser and high-voltage applications. 13 p1626 A73-28366

Effects of target-electrode polarity and of the position of the focal plane of the lens on the characteristics of a discharger with laser ignition 13 p1627 A73-28964

QAO 2 satellite nickel-cadmium batteries with auxiliary electrodes for overcharge control, discussing operation and degradation mechanism 13 p1572 A73-29583

Sealed nickel zinc cells with nonsintered and supplementary oxygen recombination electrodes and layer structure inorganic separators 13 p1572 A73-29587

Behavior of the electrode potential of a metal under conditions of fretting corrosion 14 p1763 A73-30711

Errors due to electrode-instrument wear during the electric-erosion treatment of cavities 15 p1881 A73-31146

Preparation of porous electrodes from titanium nitrides 15 p1881 A73-31592

Electrode reactions of aromatic amines in solvents containing fused AlCl3. 15 p1841 A73-32224

Technique for extemporaneously obtaining an electroencephalogram 18 p2286 A73-36937

Parametric measurements on a CO2 TEA laser with electrodes which have a Rogowsky profile 19 p2438 A73-37999

A numerical investigation of the current and density distributions for a non-equilibrium plasma in a segmented electrode duct. 21 p2748 A73-40926

Effects of target-electrode polarity and focal-plane position on a laser-triggered gap. 23 p2989 A73-44316

ELECTRODYNAMICS
NT ELECTROHYDRODYNAMICS
NT ELECTROMECHANICS
NT QUANTUM ELECTRODYNAMICS

Antenna synthesis via inverse electrodynamic problem solution for infinite impedance cylinder excited by traveling wave, noting directional antenna with rotating polarization 01 p0017 A73-10217

Equations for matrix elements in Euclidean quantum electrodynamics 01 p0076 A73-10621

Approximate reduction of the equations of elasticity theory and electrodynamics for inhomogeneous media to Helmholtz equations 01 p0077 A73-10959

International system of units applicability to constitutive equations of four dimensional relativistic electrodynamics 03 p0341 A73-12896

Scattering of a light pulse by a spherical particle 03 p0343 A73-13752

Complex transmission coefficient of waveguide with two arbitrarily spaced infinitely thin plane parallel inhomogeneities, using Galerkin method for single-parameter approximation of electrodynamic problem 03 p0278 A73-14057

Stationary functionals for introducing eigenfunctions in diffraction theory of electrodynamic systems. 03 p0337 A73-14080

Electrodynamic models for radio attenuation in ice by electromagnetic absorption and reflection from ice sheet interfaces, noting radar sounding 04 p0445 A73-15572

Electrodynamics of anisotropic media with space and time dispersion. 06 p0723 A73-17787

Electromagnetic wave reflection by two level medium analog of moving molecular beam, considering fields penetration and surface impedance effects 06 p0668 A73-18647

Characteristic functions of potential distribution on sphere with longitude dependent conductivity for application to ionosphere electrodynamics 07 p0816 A73-19444

Electromagnetic wave propagation in a circular waveguide with spirally conducting inserts 07 p0793 A73-19920

Dynamics of the current sheath in a pulsed electrodynamic plasma accelerator 09 p1125 A73-21910

Certain properties of an electron plasma in a strong electromagnetic field 09 p1130 A73-22704

Plane strain dynamics on magneto-thermoviscoelastic materials, noting conductivity, heat sources, potential and rotation 11 p1433 A73-25163

Electrodynamic analysis of superconducting vortices interaction with cylindrical cavities /pinning/, calculating critical currents in type II superconductors in external magnetic field 11 p1409 A73-26191

Ladderton oscillator /klystron/ cavity dispersion characteristics via electrodynamic analysis of dispersion equation for surface wave operation and coupled modes 12 p1477 A73-26948

Approximate reduction of the equations of the theory of elasticity and electrodynamics for inhomogeneous media to the Helmholtz equations. 12 p1524 A73-27535

Russian papers on mathematical physics boundary value problems covering electrodynamics, electromagnetic fields in conducting channels and ferromagnetic cylinders, heat transfer, shell theory, etc 12 p1525 A73-27803

Nonlinear integral equations for the electrodynamics of conducting media 12 p1525 A73-27805

The normal-tangential form of the equations for the electrodynamics of conducting media 12 p1525 A73-27806

Electron kinetics and stationary emission from semiconductor lasers 12 p1508 A73-27983

Investigation of an analog memory for the computational-measurement complex of an electrodynamic model 13 p1588 A73-29420

Integral equations for piecewise-homogeneous media in the solution of boundary value problems of electrodynamics 15 p1913 A73-31693

Current-shell dynamics in a pulsed electrodynamic plasma accelerator. 15 p1922 A73-32635

Dolapchiev-Mangeron-Tsenov analytical mechanics equations extension to potential force systems, applying to electric charge motion in electromagnetic field 16 p2035 A73-32681

Thermomechanical theory of ferromagnetic and dielectric materials magnetoelastic and electroelastic properties, using variational principles 16 p2037 A73-33228

The relation of tests with electrodynamic vibrators to the Woehler testing technique 16 p2037 A73-33379

Nonlinear theory of wave interaction in a plasma 16 p2042 A73-33735

Variation of the antenna radiation pattern during motion of the medium 17 p2122 A73-34924

Y-covariant formulation of the relativistic electrodynamics of material media 17 p2213 A73-35569

Local Y-transformations in the electrodynamics of inhomogeneous accelerated media 17 p2213 A73-35570

Estimate of error in the solution of interior problems of microwave electrodynamics. 17 p2143 A73-35706

Fluctuations in plasma and nonlinear susceptibilities. 17 p2217 A73-35817

Dynamics of the emission of semiconductor lasers whose refractive index depends on the emission intensity 18 p2322 A73-36560

Effect of near-electrode processes on plasma behavior in electrodynamic accelerators 19 p2467 A73-37365

Rectangular waveguide loaded by a semiinfinite chain of ferrite spheres 19 p2406 A73-38341

Application of method of fringe waves to problems of diffraction from bodies placed in a smoothly inhomogeneous medium. 20 p2529 A73-38919

The laws of conservation of energy and momentum during emission of electromagnetic waves /photons/ in a medium and the energy-momentum tensor in macroscopic electrodynamics 21 p2739 A73-40447

Some integral characteristics of an MHD channel at finite magnetic Reynolds numbers 21 p2747 A73-40889

Maxwell integral equations in problems of wave scattering by moving media 22 p2826 A73-42376

Electromagnetic theory of Fresnel holograms in the first perturbation theory approximation 22 p2862 A73-42927

ELECTRODYNAMOMETERS
U DYNAMOMETERS
ELECTROENCEPHALOGRAM
U ELECTROENCEPHALOGRAPHY
ELECTROENCEPHALOGRAPHY

Stability criteria in manifestations of the activity of the central nervous system in humans 01 p0006 A73-10152

Nonlinear method of analyzing electroencephalograms 01 p0012 A73-10661

Digital filters applicable to electroencephalographic pattern recognition. 01 p0013 A73-11464

Variations of evoked potentials during various mental stress situations 03 p0268 A73-13825

Development of wakefulness-sleep cycles and associated EEG patterns in mammals. 03 p0264 A73-14263

Three channel FM telemetry system for long term EEG monitoring, discussing routine clinical operation results 03 p0271 A73-14298

Telemetered EEG and neuronal spike activity in olfactory bulb and amygdala in free moving rabbits. 03 p0271 A73-14299

Multichannel telemetry of physiological parameters /body temperature ecg, eeg/ in the rat. I - Design and methods. 03 p0272 A73-14305

Multichannel telemetry of physiological parameters /body temperature, EKG, EEG/ in the rat. II - Applications in neuropharmacology. 03 p0272 A73-14306

EEG alterations by short time stress due to delayed speech feedback during reading, noting alpha and beta wave changes 03 p0265 A73-14473

A hybrid broad-band EEG frequency analyzer for use in long-term experiments. 04 p0411 A73-14847

Source locations of pattern-specific components of human visual evoked potentials. I - Component of striate cortical origin. II - Component of extrastriate cortical origin. 04 p0409 A73-15024

Application of frequency discrimination technique to the analysis of electroencephalographic signals. 04 p0411 A73-15052

Status and prospects of EEG spectral analysis. 04 p0411 A73-15278

New developments in EEG signal processing. 04 p0411 A73-15279

Application of multichannel rheography to physiological studies on a centrifuge 06 p0657 A73-17693

Statistical correlation between human mental activity and EEG beta rhythm wave energy and frequency characteristics

06 p0653 A73-18159

Visual evoked responses elicited by rapid stimulation.

06 p0654 A73-18350

Rabbit hippocampal neuron activity relation to theta-wave phases from cell potential and extracellular recording analyses

07 p0782 A73-20005

German monograph - Vigilance prognosis with the aid of a computer analysis of the spontaneous electroencephalogram.

07 p0786 A73-20391

Relation between the frequency-amplitude characteristics of cerebral electrical activity and gonadotropin hormone excretion levels at various stages of ontogenesis

08 p0930 A73-21319

The effects of Dalmane /flurazepam hydrochloride/ on human EEG characteristics.

08 p0931 A73-21464

Non-Gaussian properties of the EEG during sleep.

08 p0931 A73-21465

Application of the numerical study of random time series to the analysis of the electroencephalogram of the normal infant

08 p0935 A73-21540

Influence of a low-intensity ultrahigh-frequency electromagnetic field on the bioelectrical activity of the brain in rabbits

09 p1044 A73-22367

Modification of the electroencephalograph EEG-1 for polygraphy

09 p1044 A73-22370

Alpha-delta sleep as replacement for delta sleep in various psychiatric patients with chronic fatigue and depression

09 p1045 A73-22694

Reaction time method using EEG monitored paroxysm controlled auditory stimuli for responsiveness/consciousness/evaluation of spike wave burst onset during epileptic seizures

09 p1040 A73-22695

Technique for the implantation of long-term diagnostic electrodes in the amygdaloid complex of the human brain

09 p1046 A73-22857

Biopotential alpha and theta rhythms of neocortex and hippocampus of milk drinking cats after food and water deprivation

09 p1040 A73-22862

Correlation analysis of the bioelectrical activity of the brain during mental work

10 p1178 A73-23678

Hippocampus contribution to conditioned reflexes, memory, voluntary motions, orientation and emotional reactions, noting theta rhythm in stimuli response

10 p1180 A73-24326

Functional state of the cerebral cortex and of the mesencephalic reticular formation during prolonged action of impulsive and stable noise

10 p1181 A73-24334

Features of the spontaneous and evoked neuronal activity of deep brain structures in man during voluntary movements

10 p1181 A73-24517

Brain tissue functional organization based on models for cell pseudorandom behavior, information processing, learning and memory, considering spontaneous wave and unit firing

11 p1314 A73-25143

EEG activity of rats compressed by inert gases to 700 feet and oxygen-helium to 4000 feet.

11 p1314 A73-25327

Nature and significance of periodic electrical activity variations in the neocortex and the hippocampus during the paradoxical phase of sleep

11 p1317 A73-26083

Influence of synchronized sleep upon spontaneous and induced discharges of single units in visual system.

11 p1319 A73-26223

The operational control of the alpha component in the electroencephalogram by means of auditory feedback

11 p1324 A73-26549

Comparative analysis of the electrical activity of the cortex and of cerebral subcortical formations in the process of the alteration of conditioned reactions

12 p1461 A73-27104

Emotional stimulation traces in the spectra of EEG and cutaneous-galvanic reaction of man under normal conditions and in the case of memory impairment

12 p1461 A73-27106

Physiological nature of the electroencephalographic and vegetative components of human conditioned reactions

12 p1462 A73-27107

Photostimulation significance in electroencephalographic examinations of pilots and aviation school applicants

12 p1465 A73-27717

Theoretical models of the generation of steady-state evoked potentials, their relation to neuroanatomy and their relevance to certain clinical problems.

13 p1574 A73-28354

Behavioral and electrophysiological correlates during flash-frequency discrimination learning in monkeys.

14 p1714 A73-29989

Human average evoked potential distribution over scalp to associate cortical electrical activity with voluntary movement, reacting to EMG activity

14 p1714 A73-29990

Effect of stimulus uncertainty on the pupillary dilation response and the vertex evoked potential.

14 p1714 A73-29991

Alpha wave peak amplitude dependence on blocking pattern after stimulation during habituation-pseudoconditioning, conditioning and extinction

14 p1714 A73-29992

Simultaneous recording of acceleration and brain waves.

14 p1721 A73-29995

Effect of stimulation of the mesencephalic reticular formation on the convulsive electrical activity of the brain

14 p1716 A73-30381

Sleep behaviour as a biorhythm.

16 p1972 A73-33158

Automatic analysis and classification of electroencephalograms

17 p2116 A73-34966

Changes in the electrical activity of the brain and in some thermoregulation indices of nonanesthetized male cats during cooling

18 p2276 A73-36569

On correlation between the changes in cerebellar bioelectric activity and the adaptive reactions under the effect of accelerations.

18 p2279 A73-36915

Technique for extemporaneously obtaining an electroencephalogram

18 p2286 A73-36937

Role of specific and nonspecific thalamic nuclei in the genesis of certain slow rhythms on the human electrocorticogram

19 p2395 A73-37939

A study of evoked slow activities in man which follow a voluntary movement and articulated speech

20 p2514 A73-39759

Visually evoked cortical potentials to patterned stimuli in monkey and man.

20 p2514 A73-39760

Variations of heart rate during sleep as a function of the sleep cycle.

20 p2514 A73-39762

Similarities and differences concerning the sleep of two baboons, Papio hamadryas and Papio papio

20 p2514 A73-39764

Contingent negative variation expectancy waveform relation to human psychic state in response to visual and imperative acoustic stimuli

20 p2516 A73-39804

High-frequency synchronized activity of the amygdaloid complex as an EEG indicator of certain psychophysiological states

21 p2636 A73-40277

Clinical applications of spectral analysis and extraction of features from electroencephalograms with slow waves in adult patients.

21 p2638 A73-41011

Symmetry of the visual evoked potential in normal subjects.

21 p2638 A73-41012

Variations in the motor potential with force exerted during voluntary arm movements in man.

21 p2638 A73-41013

Russian book - Electrical activity of the human brain in the process of motor action.

21 p2640 A73-41289

Effect of the stimulation of nonspecific thalamic nuclei on spontaneous and evoked spindles in the auditory cortex

22 p2802 A73-41958

Influence of small electromagnetic-field fluctuations on the bioelectric activity of the human brain

22 p2813 A73-41964

Estimate of integrative cerebral activity using an orientation response example

22 p2807 A73-42651

Statistical treatment of evoked cerebral potentials during experiments on a Dnepri-1 computer

22 p2814 A73-42657

Signal processing in medical technology

23 p2948 A73-43317

Some physiological mechanisms of alpha-rhythm frequency fluctuations in man under conditions of relative rest

24 p3059 A73-44717

Application of factor analysis to the encephalographic characterization of sleep

24 p3062 A73-44722

Cortical and intracortical study of the frontal visual evoked potential in photosensitive Papio papio

24 p3061 A73-45159

Comparison of visual evoked potentials to stationary and to moving patterns.

24 p3061 A73-45168

ELECTROEROSION

U SPARK MACHINING

ELECTROEXPLOSIVE DEVICES

U INITIATORS [EXPLOSIVES]

ELECTROFORMING

Thin Ni shell electroforming for applications in structural tests, discussing plating bath composition, Al and wax mandrels preparation

22 p2867 A73-42999

ELECTROGENERATORS

U ELECTRIC GENERATORS

ELECTROHYDRAULIC CONTROL

U ELECTRIC CONTROL

U HYDRAULIC CONTROL

ELECTROHYDRAULIC FORMING

Explosive and electrohydraulic forming techniques cost effectiveness in metal technology, considering welding methods and metal powder compaction

22 p2865 A73-41779

ELECTROHYDRODYNAMICS

One-dimensional electrohydrodynamic flows with a variable mobility coefficient - Evaporation and condensation discontinuities

01 p0077 A73-10954

Electrohydrodynamic stability of insulating fluids subjected to a unipolar injection

01 p0086 A73-13611

Wave motion of low-tension interfaces with electrical double layers.

02 p0196 A73-12038

Equations of motion in electrohydrodynamics of multiphase one dimensional flow, noting shock wave propagation and attenuation

03 p0346 A73-13611

Polar ionospheric ion escape /polar wind/ hydrodynamic model equations, discussing singularities and critical points in terms of reduced Mach number

04 p0444 A73-15546

Electrohydrodynamic heat pipe design based on electrode structure to orient and guide dielectric liquid phase flow, using polarization force in place of capillarity

[ASME PAPER 72-WA/HT-35] 04 p0518 A73-15820

Electrohydrodynamic shock wave evolution in steady gas flow with positive space charge in electric field

06 p0733 A73-18881

One dimensional steady electrohydrodynamic duct flow with shock waves for continuous and discontinuous electric fields

06 p0733 A73-18882

One-dimensional electrogasdynamic flow with shock waves in the case of a small parameter of the electrohydraulic interaction

06 p0733 A73-18883

Stability of an electrical discharge surrounded by a free vortex.

07 p0848 A73-19514

Slip parameter for electrogasdynamic generators with unsteady flow.

09 p1037 A73-22825

Electrohydrodynamic equation solutions for non-collinear current density and velocity vectors of unipolarly charged fluid flow in channel with wall-type electrodes

12 p1528 A73-27406

Propagation of unipolarly charged jets in hydrodynamic flows

12 p1528 A73-27407

One-dimensional electrohydrodynamic flows with variable mobility coefficient, evaporation and condensation jumps.

12 p1524 A73-27530

Propagation of electrohydrodynamic surface waves in a conducting fluid.

13 p1663 A73-28160

Heat pipe substituting polarization electrohydrodynamic force effects for capillarity to collect, guide and pump working fluid condensate liquid phases

13 p1705 A73-28434

Two dimensional incompressible steady potential electrohydrodynamic flows past flat dielectric plate, using quasi one dimensional and boundary layer approximation

13 p1664 A73-28442

Electrohydrodynamic shock wave evolution in steady gas flow with positive space charge in electric field

15 p1921 A73-32406

One dimensional steady electrohydrodynamic duct flow with shock waves for continuous and discontinuous electric fields

15 p1921 A73-32407

One-dimensional electro-gasdynamic flow with shock waves and a small electrohydraulic interaction parameter.

15 p1921 A73-32408

Light scattering from electrohydrodynamic turbulence in liquid crystals.

21 p2744 A73-41020

Electrohydrodynamic Rayleigh-Taylor instabilities of a plane circular interface. 21 p2749 A73-41626

ELECTROJETS
NT AURORAL ELECTROJETS
NT EQUATORIAL ELECTROJET
Distance to the subsolar point of the magnetosphere boundary for various magnetic activity indices 15 p1932 A73-31266
Simultaneous growth of high-latitude positive bay and DR-field in the course of proton aurora substorm. 24 p3127 A73-45215

ELECTROKINETICS
Kinetics of impact-radiation ionization and recombination. 22 p2892 A73-42344

ELECTROLUMINESCENCE
Hologram reconstruction by incoherent light. II - Experimental results. 01 p0045 A73-10431
Two component magnetic pulsed modulator for electroluminescent and laser diodes, using ac source with nonresonance input capacitance charge 01 p0059 A73-10793
Analysis of dynamic-excitation conditions for electro-optical-coupling switches in control circuits of electroluminescent panels 03 p0282 A73-13658
Degradation analysis of infrared and visible optoelectronics devices. 08 p0944 A73-20742
Semiconductor electroluminescent diode displays. 10 p1218 A73-24118
Theory of spontaneous and stimulated electroluminescence of ZnS-Mn layers 10 p1261 A73-24766
Human factors aspects in aircraft electronic display systems, discussing cathode ray tubes (CRT) and light emitting diodes (LED) applications and characteristics 11 p1324 A73-26500
A new zero-beat indicator and its use in frequency measurements 13 p1617 A73-28859
Study of a read-only optical memory addressed by an array of electroluminescent diodes 14 p1755 A73-29726
Optoelectronic semiconductor components under the influence of ionizing radiation 14 p1733 A73-30070
A tunnel diode trigger with an optical output 14 p1737 A73-30797
A light amplifier display device. 16 p2013 A73-32882
Group 3-5 compound light emitting diode degradation modes and mechanisms, discussing epoxy lenses, light transmission characteristics, time and temperature functions and surface passivation 19 p2439 A73-38457
Degradation studies of diffused GaAs electroluminescent diodes subjected to mechanical stress. 19 p2439 A73-38458
Gallium phosphide with nitrogen doping from the gas phase 20 p2599 A73-38666
Electroluminescent display device of integrated XY structure utilizing GaAlAs and GaAsP 20 p2536 A73-39202
A technique for the investigation of deep-level states in diffused p-n junction devices - Application to GaAs electroluminescent diodes. 20 p2536 A73-39412
Emission spectra of ZnS.Cu single crystals 21 p2751 A73-40311
Theory for the steady-state operation of a thin-film regenerative optron 23 p2959 A73-43617

ELECTROLUMINESCENT LAMPS
U ELECTROLUMINESCENCE

ELECTROLYSIS
NT COULOMETRY
Oxygen from electrolyzed lunar rocks - A discussion of the energetics. 03 p0253 A73-14169
Titanium cathode blanks in electrolytic production of metals, noting titanium oxide nonstick properties, electron transmission and corrosion resistance 19 p2442 A73-37841
Electrolytic hydrogen fuel production with solid polymer electrolyte technology. 19 p2391 A73-38413

ELECTROLYTE METABOLISM
Renal vascular response to saline infusion from radioactive Xe washout and sodium excretion concentration data 01 p0008 A73-10170
Cation exchange binding of rubidium and cesium by rat liver cell microsomes. 02 p0135 A73-12549
Cardiovascular reflexes evoked by potassium ion stimulation of the heart under conditions of spinal deafferentation and intact innervation 03 p0262 A73-13820
Effects of an hyperoxic hypobaric environment on renin-aldosterone in normal man. 08 p0934 A73-21503

Changes in total plasma content of electrolytes and proteins with maximal exercise. 08 p0934 A73-21507

Relation of electrolyte disturbances to cardiac arrhythmias. 08 p0933 A73-21807

Energy requirements of ouabain-sensitive Na-K positive ion membrane pump during norepinephrine induced thermogenesis of brown adipose tissue in cold-exposed hamsters 09 p1040 A73-22649

Effect of actinomycin D on aldosterone-mediated changes in electrolyte excretion. 09 p1040 A73-22650

Electrogenic potassium inward transport involvement in mechanism of enhanced repolarization, correlating cardiac excitation with Na, K and Ca ions transfer and active ion transport 11 p1316 A73-25594

Sinoatrial node pacemaker cell functions, discussing ionic and metabolic principles, electrical activity, membranar effects of neurohormonal control factors and cardioactive drug effects 11 p1316 A73-25595

Interrelations among the suprarenal gluco-corticoid activity, the cardiovascular systems, and the electrolyte metabolism during prolonged work 11 p1317 A73-26085

Water and salt metabolism in hypokinesia-subjected animals 12 p1462 A73-27704

Changes caused by illumination in the Na+, K+ adenosine-triphosphatase and n-nitrophenyl-phosphatase activities of the external segments of the retina 13 p1574 A73-28294

Plasma electrolytes, pH, and ECG during and after exhaustive exercise. 15 p1834 A73-31347

Transudual fluxes of Na, K, and water in the human eccrine sweat gland. 15 p1836 A73-31923

Blood electrolytes and exercise in relation to temperature regulation in man. 18 p2280 A73-36983

Sodium Na-24 and potassium K-42 availability for sweat production after intravenous injection and their handling by sweat glands. 19 p2395 A73-37757

Effect of hypothermia on renal sodium reabsorption. 21 p2641 A73-41623

Effect of altitude on renin-aldosterone system and metabolism of water and electrolytes. 22 p2806 A73-42420

Oxygen affinity and electrolyte distribution of human blood - Changes induced by propranolol. 24 p3062 A73-44689

ELECTROLYTES
NT ANOLYTES
NT ION EXCHANGE MEMBRANE ELECTROLYTES
NT MOLTEN SALT ELECTROLYTES
Electrical evaluation of doped and undoped cobalt chromite as the interconnection material for high-temperature, zirconia-electrolyte, fuel-cell batteries. [ECS PAPER 16] 01 p0006 A73-10724
Calcium stabilized zirconia electrolyte with appreciable oxygen ionic diffusivity used as permeation membrane for oxygen leak source 02 p0167 A73-11955
Analysis of electrolytes for electrochemical polishing of steel with cationite application 02 p0174 A73-12536
Studies of the anodic oxidation of hydrazine in an alkali electrolyte and of the side reaction of ammonia formation during the decomposition of hydrazine 04 p0407 A73-15103
Bipolar noble-metal free electrodes for fuel cells with acid electrolytes. 04 p0407 A73-15113
Thermodynamic properties of gases dissolved in electrolyte solutions. 07 p0789 A73-20642
Solid polymer electrolyte fuel cell technology application to space shuttle orbiter requirements, noting 2000 hours maintenance free life and thermal stability 09 p1035 A73-22786
Study of the wear resistance of nitrated electrolytic chromium coatings on certain alloy steels 10 p1223 A73-24065
Investigation of the growth of the disperse structure of gold on a germanium surface 11 p1408 A73-25247
Sodium chloride electrolyte data at high temperatures and pressures. [ASME PAPER 73-PROD-1] 16 p1971 A73-33532
Silver powder anode, perylene-iodide cathode and ionically conductive solid cyanide-iodide electrolyte battery construction and performance tests [ECS PAPER 12] 21 p2635 A73-40841

ELECTROLYTIC CELLS
Hydrogen-air electrolytic fuel cell stack and auxilliary systems for use with methanol feedstock hydrogen generator 04 p0408 A73-15117
High temperature zirconium dioxide electrolyte fuel cell systems design and operation with methane or gasoline as fuel, evaluating performance characteristics 04 p0408 A73-15118
Transition metals nitrides, carbides and silicides applications as electrocatalysts in fuel cells for economic operation, considering hydrogen, formaldehyde and formic acid oxidation 04 p0414 A73-16038
Balloon-borne phosphoric anhydride electrolytic gage measurement of water vapor mixing ratio to 35 km, noting decrease to minimum near tropopause 16 p2008 A73-33884
Stable high energy nonaqueous lithium-organic electrolyte batteries, discussing discharge rates, temperature effects, energy density and voltage regulation 19 p2390 A73-38396
Thermoelectric effects and power calculation of solid electrolyte silver-silver iodide-silver thermocell as function of impurity ion concentration and temperature 21 p2636 A73-40842

ELECTROLYTIC GRINDING
U ELECTROCHEMICAL MACHINING

ELECTROLYTIC POLARIZATION
Galvanic interaction between active and passive titanium. 09 p1106 A73-23167
Ionic current mechanisms for cardiac muscle repolarization time course of Purkinje fibers and other heart cells, relating charge transfer data to earlier studies 11 p1316 A73-25593

ELECTROLYTIC POLISHING
U ELECTROPOLISHING

ELECTROMAGNETIC ABSORPTION
NT AURORAL ABSORPTION
NT PHOTOABSORPTION
NT POLAR CAP ABSORPTION
NT ULTRAVIOLET ABSORPTION
NT X RAY ABSORPTION
Geomagnetic activity effects on D layer absorption from vertical soundings during solar flare induced sudden magnetic storms 01 p0039 A73-10415
Anomalous absorption of electromagnetic radiation at double the plasma frequency. 01 p0082 A73-10425
Neoclassical theory of Landau damping and ion and electron transit-time magnetic pumping (TTMP) in toroidal geometry. 01 p0083 A73-10459
Winter anomaly in ionospheric absorption of radio waves on 1.725 MHz during sunspot minimum. 01 p0043 A73-10910
A simple analytic approximation for dusty stromgren spheres. 01 p0104 A73-11047
Low-sidelobe paraboloidal antenna with microwave absorber. 01 p0018 A73-11054
The velocity of a wave packet in an anisotropic absorbing medium. 01 p0079 A73-11494
Auroral X-ray and conjugate ionospheric absorption observations of an electron precipitation event accompanying a sudden impulse in the geomagnetic field. 02 p0157 A73-11759
Measurements of energetic particle fluxes during a slowly varying absorption event by two co-ordinated rocket flights. 02 p0206 A73-12314
Investigation of the radio wave absorption spectrum of atmospheric water vapor in the 1.15 to 1.5-mm range 02 p0142 A73-12487
The effects of ions of VLF and ELF propagation in an abnormally ionized atmosphere. 02 p0143 A73-12851
Combined nonlinear amplification and absorption role in ultrashort pulse generation of mode locked quasi-continuous dye laser in absence of short relaxation time 03 p0318 A73-12870
Morphic effects. V - Time reversal symmetry and the mode properties of long wavelength optical phonons. 03 p0349 A73-12901
Parametric instability and anomalous heating due to electromagnetic waves in plasma. 03 p0345 A73-13060
The absorption by the interstellar medium of 80 MHz radio emission from galactic supernova remnants. 03 p0372 A73-13346
D region HF radio wave noontime absorption correlation to winds and temperature in Northern Hemisphere during IQSY 03 p0304 A73-14593

Absorption measurements at Calcutta compared with current D region models for atomic oxygen production and loss processes

03 p0305 A73-14594

Spectral line shape for interband light absorption with excitons formation in incompletely ordered semiconductor, taking into account interaction with random electrostatic field

04 p0483 A73-14879

Electro-optical, magneto-optical, absorptional and acousto-optical light modulation, noting Kerr effect, Faraday rotation and light absorption

04 p0458 A73-15348

Electrodynamical models for radio attenuation in ice by electromagnetic absorption and reflection from ice sheet interfaces, noting radar sounding

04 p0445 A73-15572

Application of the Stark effect to the determination of the fields in the region of microwave/plasma interaction

04 p0423 A73-15611

Radio-wave absorption in the lower ionosphere and stratospheric effects

05 p0569 A73-16265

Error analysis of Wentzel-Kramers-Brillouin approximation for electromagnetic wave reflection from nonuniform absorbing half space

05 p0549 A73-16392

Emission risetime fluctuations in a gas laser with nonlinear resonant absorption

06 p0700 A73-18104

Domain-wall related, natural, submillimeter-wave resonance in orthoferrites

06 p0736 A73-18114

Surface absorption coefficient of electromagnetic wave incident on plasma boundary, considering particle specular reflection and density-frequency relation

06 p0732 A73-18642

Optical and electrical properties of proton-bombarded p-type GaAs.

06 p0739 A73-18786

Microwave power absorption by a plasma outside the electron cyclotron resonance region.

06 p0733 A73-18795

Absorption of light at oblique incidence on a plasma layer.

07 p0854 A73-19262

Ionospheric anomalies in the night mesosphere after geomagnetic storms.

07 p0817 A73-19543

Far infrared properties of lunar rock.

07 p0897 A73-19886

Problem of the influence of absorption on the amplitude fluctuations of submillimeter radio waves in the atmosphere

07 p0793 A73-19922

Mid-latitude winter anomalies in radio absorption and stratospheric temperature distribution - Observations concerning the influence of auroral and magnetic activity.

07 p0819 A73-20058

Reflection and absorption of solar radiant energy by cloud layers.

07 p0820 A73-20344

Dependence of characteristics of a gas laser on the parameters of an intracavity absorber.

08 p0974 A73-20953

Absorption measurements of carbon monoxide laser radiation by water vapor.

08 p0974 A73-21033

Absorption of electromagnetic waves by a magnetoactive plasma at parametric-resonance frequencies

09 p1124 A73-21889

Cold collisionless plasma equations for electromagnetic waves absorption near lower hybrid resonance in inhomogeneous magnetized plasma contained in ideally conducting cylinder

09 p1125 A73-21906

Effect of the shape and orientation of atmospheric dust particles on the spectral position and form of the attenuation band

09 p1077 A73-22372

Solution of equations for one-dimensional propagation of a monochromatic light pulse in absorbing media

09 p1095 A73-22623

Measurement of effective collision frequency in RF heating through parametric instabilities.

[TTU-SR-2] 09 p1128 A73-22634

Cosmic absorption of stellar light in the belt of a local system

09 p1148 A73-22861

The structure and reactions of visual pigments.

09 p1042 A73-23306

Absorption of laser emission by He-CO₂ mixtures, CO₂ and NH₃ gases, and water vapors

10 p1227 A73-24074

Determination of field strength in a microwave-plasma interaction by means of the Stark effect.

10 p1254 A73-24201

Signal reflection height seasonal variations effect on radio waves absorption estimation from vertical ionospheric sounding

10 p1188 A73-24242

Experimental observation of Wannier levels in semi-insulating gallium arsenide.

10 p1260 A73-24638

Ionospheric radio wave absorption coefficient correlation with solar activity Wolf number in IGY, IGC and IQSY

11 p1327 A73-25083

Vertical distribution of absorption of cosmic radio emission and radio waves in ionosphere and lower ionosphere based on electron density profiles

11 p1327 A73-25084

Relationship of the sporadic Es layer parameters with the absorption of radio waves in the ionosphere

11 p1350 A73-25085

Light absorption coefficient of disordered semiconductor within external dc field, discussing electron states near band boundaries

11 p1408 A73-25427

Russian book - Scattering and absorption of light in the atmosphere.

11 p1392 A73-25602

On the solar Lyman alpha control of the ionospheric absorption at 2775 kHz.

11 p1412 A73-25770

Enhanced laser-light absorption by optical resonance in inhomogeneous plasma.

11 p1405 A73-25970

Absorption and amplification of electromagnetic waves in a nonstationary magnetoactive plasma with allowance for spatial dispersion

11 p1405 A73-26151

Indirect transitions in thin quantized semiconductor films

11 p1410 A73-26450

Results of ship-borne ionospheric absorption measurements on the North Atlantic during winter.

11 p1359 A73-26713

Interstellar light absorption and distribution of stars about the star cluster NGC 6834

12 p1537 A73-26854

Interstellar light absorption and distribution of stars about the star cluster NGC 7654

12 p1537 A73-26855

Interstellar light absorption in the Orion constellation area

12 p1537 A73-26856

Absorption of microwaves by a plasma in a magnetic field in the presence of a large effect due to longitudinal inhomogeneity

12 p1467 A73-26934

A study of ionospheric absorption in conjugate regions produced by storm sudden commencements and sudden impulses in the geomagnetic field.

12 p1489 A73-26994

Application of the collisionless absorption of an extraordinary wave to the determination of plasma electron temperatures

12 p1528 A73-27302

Absorption of the microwave energy in a magnetoactive plasma.

12 p1529 A73-27433

Method of calculating the temperature dependence of the integral intensity of light absorption by local vibrations in crystals

12 p1525 A73-27937

Laser light pulse absorption in transient dense hot plasma generated around metallic anode tip by fast capacitive discharge in vacuum

13 p1664 A73-28460

Absorption of He-Ne laser radiation by an iodine molecule beam

13 p1627 A73-28773

Investigation of the absorption and emission of electron-beam-induced waves in an inhomogeneous magnetoactive plasma

13 p1666 A73-28958

Absorption of waves by a two-dimensionally inhomogeneous plasma in the vicinity of singularity points

13 p1666 A73-28960

Specific characteristics of interband luminescence in crystals in the presence of intense laser radiation

13 p1628 A73-29049

Reflection and transmission of a narrow beam of light in a thick turbid medium layer with isotropic scattering and absorption

13 p1609 A73-29158

Frequency fluctuations in a gas laser with nonlinear absorption.

13 p1629 A73-29430

Optical absorption spectrum of excited Cr³⁺/ions in yttrium aluminum garnet.

13 p1629 A73-29432

Detection of transient absorption in YAG laser crystals using combined laser.

14 p1756 A73-29930

Gas absorption lines detection based on multiple light passage through absorbing medium during generation process, noting radiation spectra of neodymium glass laser

14 p1757 A73-30331

Determination of the main details of the band structure of semiconductors from edge absorption data

14 p1783 A73-30366

The values of ionospheric absorption of VLF electromagnetic waves in middle geomagnetic latitudes.

15 p1868 A73-31523

Calculation of ionospheric N₂/ profiles with the use of radio-wave absorption data

15 p1871 A73-31883

Frequency dependence of radio-wave absorption in a reflecting layer

15 p1844 A73-31884

Electron concentrations increase observed at 60-90 km altitudes during anomalous winter radio wave absorption, noting association with upward aerosol transport decrease

15 p1844 A73-31889

Anomalous winter time absorption of radio waves in the middle latitude ionosphere

15 p1844 A73-31900

Investigation of the absorption of laser radiation in a laser spark in air

15 p1885 A73-32313

Anomalous absorption of superhigh-frequency waves in a plasma at frequencies close to the upper hybrid frequency

15 p1846 A73-32323

Cold collisionless plasma equations for electromagnetic waves absorption near lower hybrid resonance in inhomogeneous magnetized plasma contained in ideally conducting cylinder

15 p1922 A73-32631

Rain-attenuation measurements of millimeter waves over short paths.

15 p1848 A73-32647

Determination of changes in the reflection coefficient of absorbing coatings in the millimeter wavelength band

17 p2120 A73-34156

Absorption of electromagnetic waves at parametric resonances in a magnetoactive plasma.

17 p2215 A73-34312

Light beam absorption correlation with axial dispersion of ink injected into turbulent water flow in pipe

17 p2156 A73-35509

Electromagnetic wave absorbers and anechoic chambers through the years.

17 p2128 A73-35683

Observations of the entry of solar protons into the magnetosphere by use of riometers.

18 p2344 A73-35930

The use of the LF A3 absorption measurements in studying the winter anomaly.

18 p2303 A73-35947

Solar Lyman alpha control of the A3 ionospheric absorption on 2775 kHz.

18 p2288 A73-35948

The southern boundary region of the winter anomaly in ionospheric absorption in winter 1971/72 observed on board the cargo vessel 'Hanau' of Hapag-Lloyd moving between 10 deg and 55 deg N.

18 p2305 A73-36002

Spatial extent of the winter anomaly in absorption.

18 p2305 A73-36003

Some results obtained from the European Cooperation concerning studies of the winter anomaly in ionospheric absorption.

18 p2305 A73-36004

Unusual LF radio absorption events during a major meteor shower.

18 p2289 A73-36302

Resonant absorption of an electromagnetic wave by an inhomogeneous magnetoactive plasma at electron cyclotron frequency harmonics

18 p2289 A73-36563

Hot-electron production and anomalous microwave absorption near the plasma frequency.

19 p2469 A73-38289

Relationship between anomalous radio absorption and the solar zenith angle during periods of sudden ionospheric disturbances

19 p2406 A73-38327

Refractive index of n-type gallium arsenide.

20 p2599 A73-38892

B-2 installation for radio wave absorption measurements in the ionosphere at two frequencies simultaneously by the A/I pulse method

20 p2566 A73-39165

Estimation of the absorptive capacity of atmospheric haze from the brightness of clouds

20 p2583 A73-39183

Two-photon absorption in cadmium sulfide selenide single crystals employing pulsed ruby laser, discussing optical pumping, absorption anisotropy, ray refraction and luminous intensity

20 p2573 A73-39682

Carrier-frequency distance dependence of a pulse propagating in a two-level system.

21 p2649 A73-40224

Stimulated emission in multiple-photon-pumped xenon and argon excimers.

21 p2713 A73-40456

GaAs two-photon absorption coefficient obtained from transmission measurements with Q switched Nd-YAG laser, noting thermal self focusing

21 p2713 A73-40459

Wave absorption by a plasma with a nonmonotonic longitudinal distribution of the concentration
21 p2746 A73-40524

Electromagnetic absorption in magnetized cold plasma, discussing definition and use of velocity-dependent collision frequencies with Legendre polynomials as weighting functions
21 p2654 A73-40818

Chromium-ytterbium energy transfer in silicate glass.
21 p2752 A73-40963

Energy of an equilibrium fluctuating electromagnetic field in matter
21 p2741 A73-41515

The frequency stabilization of gas lasers.
22 p2868 A73-41698

Stimulated entropy /temperature/ scattering and its effect on stimulated Mandel'shtam-Brillouin scattering.
22 p2868 A73-41720

Sonic wave excitation by optical radiation, considering electrostriction effect and radiation absorption with subsequent intensity inhomogeneity-caused pressure gradients
22 p2868 A73-41898

Sudden commencement and sudden impulse absorption events at high latitudes.
22 p2845 A73-41928

Midday recovery of HF absorption during PCA events relationship to satellite observation of solar proton latitudinal variations
22 p2846 A73-41943

Observations of the ionospheric absorption at oblique incidence during the IASY.
22 p2847 A73-42195

Optical and electrical properties of doped semiconductors in a strong electromagnetic field.
22 p2896 A73-42252

Microwave absorption by a magnetoplasma with a strong longitudinal inhomogeneity.
22 p2891 A73-42268

Effect of the absorbers upon the thermal structure of a LTE atmosphere, hydrogen and helium.
22 p2908 A73-42309

The production of plasma by lasers on targets in the gaseous state
22 p2892 A73-42350

Contribution to the theory of parametric instability of a bounded homogeneous plasma
22 p2892 A73-42380

Absorption of vlf and elf waves in whistler mode - Sunrise and sunset effects.
22 p2849 A73-42622

Absorption of whistler waves during night.
22 p2850 A73-42623

Self diffraction of coherent wave radiation by absorption from excited levels of Nd laser light induced phase diffraction gratings in thin layer rhodamine
22 p2870 A73-42723

Bee image detection by ommatidium based on physical model using electromagnetic analysis of light absorption in photoreceptor
23 p2946 A73-43344

Light absorption coefficient of disordered semiconductor with random field due to charged impurity centers in presence of constant external electric field
23 p3016 A73-43648

Particle precipitation in Brazilian geomagnetic anomaly during magnetic storms.
23 p2971 A73-43687

Nonlinear dissipation of electromagnetic waves in a plasma
23 p3012 A73-44017

Absorption and emission of waves generated by an electron beam in an inhomogeneous magnetoplasma.
23 p3013 A73-44310

Wave absorption near singular points in a two-dimensional inhomogeneous plasma.
23 p3013 A73-44312

Plasma-electromagnetic wave interactions in toroidal discharge chamber, noting possibility of collisionless wave absorption due to conversion to longitudinal plasma waves at hybrid resonance
23 p3014 A73-44340

Fluctuations of the radiation rise time in a gas laser with nonlinear resonant absorption.
24 p3095 A73-44494

Absorption of laser radiation in a laser spark in air.
24 p3095 A73-44621

Radiant-conductive heat transfer in a plane layer of an absorbing and scattering medium
24 p3155 A73-44754

Determination of the transmittance of an optically not dense plasma by an intracavity method
24 p3115 A73-44762

Laser Doppler interferometry for measuring small absorption coefficients.
24 p3090 A73-44924

Rapidly fading absorption induced in polymethine dyes by nanosecond pulses of ruby laser radiation
24 p3096 A73-44959

Interior radiances in optically deep absorbing media. II - Rayleigh scattering.
24 p3111 A73-45319

Dielectric coaxial waveguide modal cut-off, dispersion and attenuation characteristics, discussing guide geometry and dielectric properties effects
24 p3069 A73-45407

ELECTROMAGNETIC COMPATIBILITY
Book - Topics in intersystem electromagnetic compatibility.
14 p1729 A73-30596

Statistical computation of compatibility of tropospheric and satellite communication lines.
15 p1842 A73-30986

Signal bandwidth consideration for electromagnetic compatibility specifications, comparing broad and narrow band measurements performance by computerized simulation
16 p1979 A73-33169

Book - A handbook series on electromagnetic interference and compatibility.
17 p2121 A73-34462

Intrasystem electromagnetic compatibility analysis program.
17 p2131 A73-35251

A rational basis for determining the EMC capability of a system.
20 p2528 A73-38770

Intrasystem electromagnetic compatibility analysis program.
20 p2528 A73-38771

Symposium on Electromagnetic Interference in Aircraft, London, England, February 15, 1973, Proceedings.
22 p2821 A73-41691

Electromagnetic interference and compatibility control in aircraft communication, discussing RF current, voltage, impedance and SNR measurement techniques
22 p2821 A73-41692

Aircraft communication and electronic equipment design for interference control to meet electromagnetic compatibility specification requirements
22 p2821 A73-41695

Electromagnetic compatibility specifications for aircraft communication and electronic equipment, discussing control and test plans, test facilities, cost effectiveness and British standard
22 p2821 A73-41696

Electromagnetic compatibility program for modern aircraft communication and electronic equipment design, discussing control plan, interference specification, cable separation and final testing
22 p2821 A73-41697

International Electromagnetic Compatibility Symposium, New York, N.Y., June 20-22, 1973, Record.
22 p2822 A73-41785

Overview of Department of Defense Electromagnetic Radiation Hazards Standardization Program.
22 p2822 A73-41790

A rational basis for determining the EMC capability of a system.
22 p2823 A73-41802

Electromagnetic shielding techniques and testing for environment and instrument protection from radio emission and noise
22 p2823 A73-41804

A quantitative estimate of the electromagnetic compatibility of high-frequency leads in electronic equipment
24 p3071 A73-44596

ELECTROMAGNETIC CONTROL
U ELECTROMAGNETS
U REMOTE CONTROL
ELECTROMAGNETIC DEDUCTION
U MAGNETIC INDUCTION
ELECTROMAGNETIC FIELDS
NT FAR FIELDS
Kinetic theory of electromagnetic fluctuations in an anisotropic plasma half-space
01 p0082 A73-10210

Relative equilibrium of a mass of charged particles /electrons/ subject to its own gravitation and uniformly rotating about an axis
01 p0082 A73-10267

The EM field of a dipole transmitter in the two-layer medium air space-magnetoactive ionosphere
01 p0035 A73-10299

Saturn rings formation explanation by electromagnetic effects, presenting mathematical model
01 p0097 A73-10551

Propagation of the discontinuities of the covariant derivative of the electromagnetic and of the curvature tensor in an electromagnetic and gravitational wave
01 p0079 A73-11261

Electromagnetic near field energy flow characteristics of dipole/monopole receiving rod antenna, investigating frequency dependence of antenna effective area shape
02 p0145 A73-11824

Tikhonov conditions of field excitation for dipole antenna radiation study in stratified gyrotropic medium
02 p0147 A73-12470

Electromagnetic field, polarization and population inversion equations for spiked emission operation analysis in single mode laser
02 p0177 A73-12694

Plasma inhomogeneity in crossed electromagnetic fields, comparing motion velocity to ion component transverse drift rate in polarized electric field
03 p0346 A73-13178

Relative importance of forces of interaction which create, between the grains of a very thin metallic film, the radiation of thermodynamic equilibrium on the one hand, and zero oscillations of the field on the other hand
03 p0349 A73-13605

Analysis of wire antennas in the presence of a conducting half-space. II - The horizontal antenna in free space.
03 p0276 A73-13694

Scattering of a light pulse by a spherical particle
03 p0343 A73-13752

Book on electromagnetic field theory covering free space Maxwell equations, Lorentz force law, vector analysis, Laplace equation, lossless transmission lines and dipole antennas
03 p0343 A73-13988

Schwartz method application to stripline fields and impedance calculations for different cross sections and internal conductor dimensions
03 p0278 A73-14078

Evaluation and reduction on the electromagnetic fields associated with a solar array.
03 p0256 A73-14233

Electrodynamic sailing - Beating into the solar wind.
04 p0487 A73-15073

Diffraction of a two-dimensional electromagnetic field by an ideally conducting plane with a boundless rectilinear slit
04 p0423 A73-15608

Parametric excitation of high-frequency potential oscillations in a cold magnetoactive plasma by the field of an electromagnetic wave
04 p0481 A73-15612

Shadowgraph photography for electromagnetic excitation of shock waves in normal pressure gas, noting plasma and shock compressed regions in shock tube
04 p0434 A73-15618

Invariant criterion generalization for pure gravitational waves in tetrad formulation of general relativity theory, noting electromagnetic field energy tensor
04 p0476 A73-15638

Vertical electric dipole excited electromagnetic fields in triple layer medium with plane boundaries, noting waveguide thickness effect on electromagnetic wave propagation
05 p0549 A73-16386

Propagation of radio waves in a triple-layer medium with spheroidal boundary surfaces
05 p0549 A73-16388

Vertical electric dipole excited electromagnetic field in earth-ionosphere waveguide, using Galerkin method for VLF electromagnetic wave propagation equation
05 p0549 A73-16389

The field of a vertical electric dipole over a spherical earth having an atmosphere that is nonhomogeneous with height
05 p0549 A73-16390

VLF field diurnal variations and terminator crossing effect on signal path during transmission in earth-ionosphere waveguide
05 p0549 A73-16393

Diffraction of waves generated by a magnetic-dipole current system on a variable-radius sphere
05 p0550 A73-16397

MHD-rotation of a conducting fluid in a rotationally symmetric electromagnetic field
05 p0603 A73-16590

Structure of the pulsations of the earth's electromagnetic field as a random function of time
06 p0689 A73-17541

Book - Microwave transmission.
06 p0663 A73-17670

Diffraction of the emission field of a horizontal dipole on a circular hole in a plane screen in the presence of a circular disk coaxial with the hole
06 p0664 A73-17716

The solution of Maxwell's equation for inhomogeneous dielectric slabs.
06 p0699 A73-17809

Annular energy vortex in the near field of a directional antenna
06 p0674 A73-17821

The electromagnetic perturbation fields of conductivity anomalies within the earth.
06 p0690 A73-17925

The red-shifts and the patterns of electromagnetic waves in quasistellar objects.
06 p0750 A73-18015

Excited molecules in a medium with a negative dielectric constant
06 p0725 A73-18105

Aperture fields and gain of open-ended parallel-plate waveguides.
06 p0676 A73-18178

Space wave field produced by a vertical electric dipole above a perfectly conducting sinusoidal ocean surface.
06 p0665 A73-18181

Magnetic current annular ring near field, noting application to coaxially driven parallel monopole arrays analysis

06 p0666 A73-18198

Physiological effects of microwave electromagnetic fields on human and animal organisms, considering etiology, diagnostics and prophylaxis

06 p0659 A73-18256

Density-matrix method for a weakly ionized plasma.

06 p0730 A73-18373

Electromagnetic current and charge due to interaction between a gravitational and a free electromagnetic field.

06 p0732 A73-18715

Radio wave propagation in stratified media with nonuniform boundaries and varying electromagnetic parameters - Full wave analysis.

07 p0791 A73-19261

Three layer atmospheric model for neutral gas motion-produced ionosphere and magnetosphere currents, electromagnetic field and charged particle concentration perturbations

07 p0815 A73-19432

Single point thunderstorm ranging method based on two radio frequencies field intensity spectral components ratio

07 p0847 A73-19439

Surface wave characteristics of circular cylindrical corrugated and uniform dielectric rod excited in E sub 0-mode.

07 p0792 A73-19545

Fluctuations in the level and phase of a field in a waveguide with a random boundary

07 p0793 A73-19916

A semiconductor in a microwave electromagnetic field and in a steady magnetic field

07 p0862 A73-20012

Calculation of the deflections of fast-rotating rotors on elastic-damping supports with allowance for unilateral electromagnetic attraction forces

07 p0779 A73-20084

Averaged boundary conditions for a grid consisting of nonparallel and nonrectilinear conductors placed on a nonplane surface.

07 p0801 A73-20127

Multiphoton excitations in vibrational-rotational states of diatomic molecules in an intense electromagnetic field.

08 p0990 A73-21003

Radiation fields in the Schwarzschild background.

08 p0988 A73-21202

A series expansion of a magnetic vector-potential calculated for a ring with a current

08 p0959 A73-21298

Electromagnetic pulse penetration through small apertures.

08 p0940 A73-21664

Electromagnetic field configuration about aligned rotating magnetic star from relativistic model of rotating magnetosphere

09 p1142 A73-22034

Influence of a low-intensity ultrahigh-frequency electromagnetic field on the bioelectrical activity of the brain in rabbits

09 p1044 A73-22367

Influence of ultrasound and of a superhigh-frequency electromagnetic field in the three-centimeter band on the oxidative phosphorylation of liver and kidney mitochondria

09 p1044 A73-22368

Electromagnetic fields in electrodeless discharges of arbitrary length.

09 p1128 A73-22635

Certain properties of an electron plasma in a strong electromagnetic field

09 p1130 A73-22704

Study of the influence of weak electromagnetic field gradients on man

09 p1046 A73-22850

Nonlinear theory of a relativistic monotron

09 p1065 A73-23086

Unified transducers of quantitative and geometrical parameters of different media based on the use of integral properties of electromagnetic fields.

10 p1217 A73-24014

Diffraction of a two-dimensional electromagnetic field on an ideally conducting plane with an infinite straight slit.

10 p1188 A73-24198

Parametric excitation of high-frequency electrostatic oscillations in a cold magnetoactive plasma by an electromagnetic wave.

10 p1254 A73-24202

Shadowgraph photography for electromagnetic excitation of shock waves in normal pressure gas, noting plasma and shock compressed regions in shock tube

10 p1205 A73-24208

Electromagnetic field of rotating charged oblate ellipsoid of revolution with infinite conductivity and vacuum or infinite magnetic susceptibility

10 p1252 A73-24344

Radiative losses in a magnetostatic and intense electromagnetic field.

10 p1270 A73-24908

Generalized electromagnetic torque on a vacuum pulsar model.

10 p1284 A73-24914

Error analysis of correlation method for determining directional characteristics /angular power density/ of homogeneous random wave field

11 p1359 A73-25005

Study of the Rayleigh zone of circular radiating apertures

11 p1328 A73-25283

Edge condition of a perfectly conducting wedge with its exterior region divided by a resistive sheet.

11 p1329 A73-25676

Physical interpretation of the diurnal behavior of the TM and TE components of VLF fields in the far zone.

11 p1331 A73-26152

Influence of field inhomogeneity on the intrinsic spectral linewidth of a laser

11 p1332 A73-26166

Problem of the reflection of pulse signals from a moving mirror

11 p1332 A73-26167

Integral equation for electromagnetic field in diffuse boundary plasma, noting anomalous skin effect

11 p1405 A73-26184

Combined electromagnetic and gravitational field equations derivation with explicit interaction term and tensors for curved space-times unrestrained in Einstein-Maxwell equations framework

11 p1401 A73-26658

Electromagnetic fields due to dipole antennas over stratified anisotropic media.

[AD-756044]

12 p1523 A73-27146

Propagation of low-frequency electromagnetic waves in the spherical waveguide formed by the earth and the ionosphere

12 p1469 A73-27340

Russian papers on mathematical physics boundary value problems covering electrodynamics, electromagnetic fields in conducting channels and ferromagnetic cylinders, heat transfer, shell theory, etc

12 p1525 A73-27803

Russian book on quantum radio physics, Volume 1 covering photons and nonlinear media, matter-radiation interaction, electromagnetic fields, relaxation, emission, solid state physics, etc

12 p1508 A73-27924

Nonlinear propagation of electromagnetic waves in a weakly ionized plasma.

13 p1665 A73-28677

Effect of radial profile of a charged particle pulse on the electromagnetic wake in a plasma.

14 p1779 A73-29710

Russian book - Methods for calculating electromagnetic fields by electronic digital computers.

14 p1774 A73-30026

Static electromagnetic field structure in elastic homogeneous medium for sources distributed by simple and double layers in terms of scalar and vector potentials

14 p1774 A73-30030

Approximate near field parameters computation from Kirchhoff boundary values of antenna aperture field intensity

14 p1733 A73-30072

Analysis of EH inhomogeneities and singular H inhomogeneities in a rectangular-section waveguide

14 p1729 A73-30560

Physical and psychological effects of electromagnetic fields on human and animal central nervous system

14 p1718 A73-30571

Determination of electromagnetic field correlators for a contained plasma

15 p1916 A73-31037

Field properties and losses in a three-mirror optical ring resonator with a Gaussian diaphragm

15 p1886 A73-32341

Tikhonov conditions of field excitation for dipole antenna radiation study in stratified gyrotropic medium

15 p1847 A73-32621

Dolapchiev-Mangeron-Tsenov analytical mechanics equations extension to potential force systems, applying to electric charge motion in electromagnetic field

16 p2035 A73-32681

Structure of pulsations of the electromagnetic field of the earth as a random function of time.

16 p2001 A73-32765

Additional results from an Ogo 6 experiment concerning ionospheric electric and electromagnetic fields in the range 20 Hz to 540 kHz.

16 p2003 A73-33438

Application of the momentum translation method to multiphoton ionization of hydrogen by intense electromagnetic fields.

16 p2039 A73-33864

Effect of the amplitude-phase distribution of the field in the aperture of an antenna on its directional properties.

16 p1991 A73-33980

Theory of electromagnetic field scattering in gases

16 p1984 A73-34007

Visualization of the amplitude-phase structure of electromagnetic fields in the millimeter and submillimeter ranges

17 p2121 A73-34158

Plasma hydrodynamics in high frequency electromagnetic field, discussing hydrodynamic equations, small perturbations, plasma equilibrium and movement in field

17 p2216 A73-34341

Interference patterns of a horizontal electric dipole over layered dielectric media.

17 p2123 A73-35270

Einstein-Maxwell fields in conformal space, studying field equations, reducible electromagnetic field in space-time and constraints on metric tensor by Rainich conditions

17 p2212 A73-35560

Numerical computation of antenna patterns near a conducting elliptic cylinder.

17 p2126 A73-35608

Poincare sphere representation of partially polarized electromagnetic field, calculating power reception by antenna for field intensity measurement

17 p2128 A73-35681

Spectral characteristics of the scatter field from a rotating impedance cylinder in uniform motion.

17 p2129 A73-35707

Book - Electromagnetic wave propagation.

17 p2130 A73-35857

Interaction of a strong shock wave with electromagnetic field.

19 p2464 A73-37157

Series expansion of the magnetic vector-potential computed for a current carrying ring.

19 p2425 A73-37927

Distribution of a monochromatic electromagnetic field and of temperature in a plane conductor with temperature dependent conductivity

19 p2471 A73-38340

Rectangular waveguide loaded by a semiinfinite chain of ferrite spheres

19 p2406 A73-38341

Electromagnetic wave propagation in inhomogeneous multilayered structures of arbitrarily varying thickness - Generalized field transforms.

19 p2461 A73-38379

Electromagnetic wave propagation in inhomogeneous multilayered structures of arbitrary thickness - Full wave solutions.

19 p2461 A73-38380

Debye representation and multipole expansion of the quantized free electromagnetic field.

20 p2591 A73-38609

Orthogonal operators and phase space distributions in quantum optics.

20 p2591 A73-38629

Explorer 45 mission objectives discussing magnetospheric ring current, magnetic storm detection, particle energy and interactions, electric and magnetic fields measurements, etc

20 p2614 A73-38949

Boundaries effect on dispersion interaction between molecules in bounded region, applying method to two oscillators between conducting plates

20 p2538 A73-39705

The relation between cosmic ray intensity variations and effects due to the electromagnetic complex

21 p2755 A73-40110

The momentum-energy tensor of an electromagnetic field

21 p2739 A73-40446

Rotation of a cylinder in a conducting fluid in an axial magnetic field

21 p2747 A73-40883

Directional plasma transport equations derived from Boltzmann equation by averaging of velocity space subset, applying to plasma confinement by external time dependent electromagnetic fields

21 p2748 A73-41127

Energy of an equilibrium fluctuating electromagnetic field in matter

21 p2741 A73-41515

Electromagnetic radiation excited by electric or magnetic line source near inhomogeneous dielectric layer, evaluating reflected and transmitted fields by saddle point technique

22 p2824 A73-41831

Equivalent filamentary current derivation for bi-static field diffracted by ring singularity based on geometrical theory

22 p2824 A73-41838

Electromagnetic field equations in operator form for anisotropic conducting media

22 p2886 A73-42212

Results of the application of the physical modeling method to a study of the tangential component of the magnetic field of a linear inductor on the surface of a massive ferromagnetic body

22 p2800 A73-42214

Electromagnetic flowmeters with point electrodes and finite length insulating liners, discussing performance numerical analysis accuracy by comparison with exact analytic solutions

22 p2860 A73-42300

Gravitational analogy of electromagnetic Aharonov-Bohm effect, considering massless Dirac equation for weak gravitational fields arising from mass currents moving between particle beams 22 p2887 A73-42434

Polarizable particle entrainment in electromagnetic field consisting of wave packets propagating in opposite directions 22 p2889 A73-43099

Propagation of low-frequency electromagnetic waves in a spherical earth-ionosphere waveguide. 23 p2952 A73-42328

Wave propagation through a highly restrained solid-state plasma. 23 p3012 A73-44141

Coherence of an electromagnetic field propagating in a weakly guiding fiber. 24 p3097 A73-45416

ELECTROMAGNETIC INTERACTIONS

NT PLASMA-ELECTROMAGNETIC INTERACTION

Interaction of opposed beams of electromagnetic waves in a transparent nonlinear medium 01 p0016 A73-10208

Effect of a neutrino-photon interaction on the solar-neutrino flux. 02 p0205 A73-12165

Nonlinear interaction between a spontaneous radiation field and the active media of high-gain gas laser amplifiers 02 p0177 A73-12489

Relative importance of forces of interaction which create, between the grains of a very thin metallic film, the radiation of thermodynamic equilibrium on the one hand, and zero oscillations of the field on the other hand 03 p0349 A73-13605

German monograph on parametric amplification in inverted material covering nonlinear interaction between electromagnetic field and paramagnetic material, dielectric resonator and pumping field strength 03 p0282 A73-13816

Magnetic semiconductor materials compositions and magnetoelectric characteristics, discussing magnetic-electric interactions, fabrication techniques and applications for magnetically controllable diodes, temperature sensors, etc 04 p0483 A73-15323

Nonlinear interaction between circular coherent light and modulating electromagnetic waves in presence of quadratic electrooptical effect, noting frequency shift 04 p0459 A73-15921

Electromagnetic interactions of cosmic ray muons in iron. I - Search for a charge asymmetry. 06 p0743 A73-18386

Electromagnetic interactions of cosmic ray muons in iron. II - Momentum dependence of the interaction probabilities. 06 p0743 A73-18387

On the detection of gravitational radiation by its interaction with electromagnetic fields. 07 p0852 A73-20227

On the definitions of parameters in ferrite-electromagnetic wave interactions. 09 p1062 A73-22323

On the interaction of the electromagnetic field with electron beams in resistive wall waveguides 09 p1062 A73-22324

Nonlinear theory of Ubitron microwave oscillator device using fast electromagnetic wave-fast electron beam interaction in spatially periodic magnetostatic field 11 p1332 A73-26164

Earth mantle-core mechanical and electromagnetic interactions influencing rotation rate random variations 13 p1679 A73-28396

Russian book on radiative and complex heat transfer covering electromagnetic energy-matter interaction, modeling, convective and conductive transfer and thermodynamic equilibrium radiation 17 p2254 A73-34899

Time domain current interaction coefficients for sheet antenna structures. 17 p2142 A73-35647

Generalized representation of electric fields in interaction gaps of klystrons and traveling-wave tubes. 18 p2292 A73-36595

Optical pulses interaction with two level atom spins, determining sub-cooperation limit in resonant absorbers 20 p2591 A73-38625

Network analysis of infinite regular antenna arrays, discussing unified approach based on electromagnetic interaction among subarrays as distinguished from boundary value problem solution 21 p2651 A73-40651

Metal oxide absorption coefficients for use in intense laser interaction with solids. 21 p2715 A73-40961

Interaction of fast particles with waves in cosmic magnetoactive plasma. 21 p2748 A73-41248

Mathematics of interaction between blood and electromagnetic fields. 22 p2802 A73-41788

Antenna coupling induced intersystem electromagnetic interference prediction, discussing tradeoffs between analysis level, input information, measurements, cost results and user requirements 22 p2822 A73-41795

Straight wire monopole and dipole antenna near field coupling characteristics prediction, deriving mathematical model by method of moments for computerized analysis 22 p2823 A73-41798

ELECTROMAGNETIC INTERFERENCE

NT ATMOSPHERICS

NT BLACKOUT (PROPAGATION)

NT COSMIC NOISE

NT CROSSTALK

NT DAWN CHORUS

NT ELECTROMAGNETIC NOISE

NT HISS

NT IONOSPHERIC NOISE

NT IONOSPHERICS

NT JAMMING

NT RADIO FREQUENCY INTERFERENCE

NT SHOT NOISE

NT SUDDEN ENHANCEMENT OF ATMOSPHERICS

NT THERMAL NOISE

NT WHISTLERS

NT WHITE NOISE

Double-reverse-scatter interference in optical fiber communication systems. 01 p0018 A73-11217

Quantum mechanical interpretation for low intensity optical interference experiments with independent light sources and modulated light beams 01 p0078 A73-11250

Two-channel direction finding with point source emission and spaced antennas reception, investigating cross correlation and background noise interference effects on accuracy 03 p0278 A73-14062

Hazard and interference avoidance in implant telemetry, discussing leakage currents, muscle interference, magnetic influence, high frequency noise, electrode and respiratory artifacts, etc 03 p0271 A73-14295

Channel equalization in presence of intersymbol interference, comparing sequential statistical, dynamic programming, delay line and minimum mean square error techniques 04 p0425 A73-15419

Pulsed electric thrusters theoretical and experimental radiation intensities and spectra, estimating interference with onboard satellite communication systems [AIAA PAPER 73-263] 05 p0608 A73-16984

The resistance of discrete phase modulation to random interference 07 p0793 A73-20023

Requirements specification for ac and dc current carrying filter networks for electromagnetic interference reduction, noting RLC circuits [SAE ARP 1172] 08 p0942 A73-20697

Measuring the off-duty factor of chaotic pulsed interference on a Gaussian noise background 09 p1050 A73-22338

Possibility of holographic observation of the interference of independent weakly degenerate fields 09 p1084 A73-22670

Electromagnetic 60 Hz interference in ECG recordings, discussing sources, identifying tests, elimination and ECG amplifier design 10 p1183 A73-23648

Combinational noise and interference effects during frequency conversion, noting mathematical methods 10 p1189 A73-24376

Linear codes and transverse equalization for limiting the effects of intersymbolic interference in the transmission of digital signals 10 p1189 A73-24416

Method of increasing the noise immunity of optical communications lines 10 p1190 A73-24615

Influence of laser field polarization on nonlinear interference effects. 11 p1377 A73-26180

Wide angle narrow band interference filter for detecting E region barium ion clouds against intense background 11 p1366 A73-26250

Multipaths by diffusion on the ground and application to the transmission of digital messages affected by jumps of the carrier frequency 14 p1725 A73-29732

Effect of multipath on ranging error for an airplane-satellite link. 14 p1725 A73-29892

Application of acoustic surface-wave technology to spread spectrum communications. 14 p1733 A73-29934

Book - A handbook series on electromagnetic interference and compatibility. 17 p2121 A73-34462

Domestic communication satellite systems with microwave transmission links and coast-to-coast earth stations and receivers, detailing design and interference problems 18 p2289 A73-36776

Electromagnetic interference caused by a solar array. 18 p2269 A73-36958

Interference phenomena obtained by replacing the mirrors of a Michelson interferometer by Fabry-Perot couples 19 p2429 A73-37540

ML receiver for binary signals with intersymbol interference in Gaussian noise. 20 p2524 A73-38733

The domain analysis of intersymbol interference effects on phase shift keyed (PSK) and quadrature phase shift keyed (QPSK) communication systems. 20 p2524 A73-38734

High-bit-rate transmissions through a channelized repeater. 20 p2526 A73-38753

Performance estimate for coherent QPSK with random intersymbol interference due to time-varying scatter. 20 p2527 A73-38765

Probability of error in a bandlimited quadriphase communication system. 21 p2649 A73-40334

Performance degradation plots for comparison of signal fading and intersymbol interference effects in two-component specular multipath digital microwave communication channel 21 p2649 A73-40336

The estimate feedback equalizer - A suboptimum nonlinear receiver. 21 p2656 A73-41165

Combined effects of intersymbol, interchannel, and co-channel interferences in M-ary CPSPK systems. 21 p2656 A73-41167

Symposium on Electromagnetic Interference in Aircraft, London, England, February 15, 1973, Proceedings. 22 p2821 A73-41691

Electromagnetic interference in military transport aircraft, discussing RF terminal voltage and current, radiated field, fuselage attenuation and power supply impedance measurements 22 p2821 A73-41693

Aircraft communication and electronic equipment design for interference control to meet electromagnetic compatibility specification requirements 22 p2821 A73-41695

Electromagnetic compatibility program for modern aircraft communication and electronic equipment design, discussing control plan, interference specification, cable separation and final testing 22 p2821 A73-41697

The coupling of high frequency electromagnetic energy into large systems. 22 p2822 A73-41792

Microelectronic circuitry for monitoring stray electromagnetic energy coupled into electroexplosive device, using fiber optic transmission with photovoltaic energy conversion to eliminate wiring caused interference 22 p2822 A73-41794

Antenna coupling induced intersystem electromagnetic interference prediction, discussing tradeoffs between analysis level, input information, measurements, cost results and user requirements 22 p2822 A73-41795

Prediction methods for the susceptibility of solid state devices to interference and degradation from microwave energy. 22 p2823 A73-41796

Computer program for analysis of radiation pattern distortion and mutual coupling in antenna farms, allowing user specification by types or vertical cylindrical antenna dimensions 22 p2823 A73-41797

Radio receiver intermodulation characteristics description by generic model, discussing frequency/distance separation criteria to avoid interference, signal measurement procedure and application to equipment standards 22 p2823 A73-41801

Cepstrum signal processing with complex algorithm involving Fourier transforms and logarithm for multipath interference distortion reduction in single sideband or multiplexed transmission channels 23 p2953 A73-43321

Digital communication system with known channel characteristics, discussing intersymbol interference dependence on signalling rate based on Nyquist criteria consideration 24 p3070 A73-45482

ELECTROMAGNETIC MEASUREMENT

NT ELECTROMAGNETIC NOISE MEASUREMENT

An electromagnetic comparator system with improved possibilities in regard of sorting and recording of absolute test parameters 01 p0056 A73-10588

Antennas for measurement of microwave electromagnetic field by a light-modulated scattering technique.

01 p0025 A73-11055

Conference on Precision Electromagnetic Measurements, 13th, Boulder, Colo., June 26-29, 1972, Proceedings.

03 p0309 A73-14490

Accuracy limitation in measurements of HF field intensities for protection against radiation hazards.

03 p0310 A73-14491

Broad-band isotropic electromagnetic radiation monitor.

03 p0310 A73-14493

Electromagnetic measurement at submillimeter wavelengths for solids and liquids absorption and refraction and atmospheric gases and plasmas emission based on Fourier transform spectrometry

03 p0310 A73-14496

A technique for making dispersion relation measurements of electrostatic waves.

04 p0450 A73-15554

Optimal distribution of resources in automatic detector-meters determining number of random concentrated radio noises in assigned frequency range

04 p0423 A73-15926

External field electromagnetic measurement of blood flow - An alternative approach to the solution of the baseline problem.

04 p0414 A73-15992

Study of VLF and ELF noises observed by Alouette 2.

05 p0552 A73-17163

Cross polarization definitions in terms of antenna pattern measurement coordinate system and source current distribution, considering relative merits

06 p0666 A73-18199

Antenna-aperture distributions from holographic type of radiation-pattern measurement.

06 p0668 A73-18443

Measurement of the attenuation of an electromagnetic wave in a bounded hot electron plasma.

07 p0860 A73-20478

Electromagnetic measurement of frequency and amplitude of mechanical vibration, based on echo signal phase modulation, explaining heterodyne detection system

07 p0827 A73-20532

Open resonator operating at 337-micron wavelength.

09 p1097 A73-23094

Lunar permafrost - Dielectric identification.

10 p1282 A73-24629

Comparison of methods of photomultiplier photocurrent recording in measurements of weak luminous fluxes

12 p1495 A73-26866

Bibliography on the measurement of electrical parameters of layered lunar/earth surfaces.

13 p1619 A73-29221

Support scattering effects on low-gain satellite antenna pattern measurements.

14 p1735 A73-30218

Laboratory measurements of electromagnetic properties of atmospheric gases at millimeter wavelengths.

16 p1983 A73-33731

Poincare sphere representation of partially polarized electromagnetic field, calculating power reception by antenna for field intensity measurement

17 p2128 A73-35681

Radio anechoic chamber reflectivity level evaluation, comparing antenna pattern method and free space voltage standing wave ratio technique

17 p2128 A73-35684

Antenna gain calibration on a ground reflection range.

17 p2128 A73-35688

Measurement of the radiation patterns of full-scale HF and VHF antennas.

17 p2128 A73-35689

Linear phased array antenna focused in Fresnel region, noting radiation pattern indoor measurement simplicity advantage over far field observation in performance monitoring

17 p2128 A73-35694

Effect of scattering on radiometer measurements of attenuation in rain.

19 p2403 A73-37426

Search for magnetic monopoles in lunar material using an electromagnetic detector.

19 p2461 A73-38492

Electromagnetic interference in military transport aircraft, discussing RF terminal voltage and current, radiated field, fuselage attenuation and power supply impedance measurements

22 p2821 A73-41693

Antenna radiation-pattern measurement using model aircraft.

22 p2831 A73-41841

Experimental determination of the field parameters in a sectorial horn aperture with the aid of a passive probe

22 p2826 A73-42337

Comparison of plethysmographic and electromagnetic flow measurements.

23 p2950 A73-44215

Phase-sensitive method of electromagnetic flaw detection.

24 p3093 A73-44696

ELECTROMAGNETIC NOISE

NT ATMOSPHERIC

NT COSMIC NOISE

NT DAWN CHORUS

NT HISS

NT IONOSPHERIC NOISE

NT IONOSPHERICS

NT SHOT NOISE

NT SUDDEN ENHANCEMENT OF ATMOSPHERICS

NT THERMAL NOISE

NT WHISTLERS

NT WHITE NOISE

Poisson model of atmospheric noise from lightning discharges as function of thunderstorm distribution and propagation conditions, calculating statistics for narrow band receiver

02 p0142 A73-12528

Correlation of noisy radiation reflected from a statistically uneven surface.

03 p0344 A73-14039

Noise characteristics, channel capacities, power requirements and transmission efficiencies of various semiconductor transmitter designs for FM directional radio systems

03 p0284 A73-14125

Optimal distribution of resources in automatic detector-meters determining number of random concentrated radio noises in assigned frequency range

04 p0423 A73-15926

Operating modes of a phase-loop AFC system with a low control circuit time lag under the action of additive harmonic noise

05 p0560 A73-16292

Optimal currents, voltages and frequencies for noise measurement in HF transistors for reliability prediction and failure analysis, noting diffusion alloyed and planar transistors

06 p0675 A73-18078

Noise of local oscillators of high capacity radio links

07 p0798 A73-19179

Noise immunity of autocorrelated reception of singly phase-shift-keyed signals

07 p0794 A73-20298

The effect of impulsive noise on FSK digital communication.

08 p0938 A73-20834

Possible explanation for nonthermal radio noise from binary stars.

08 p1003 A73-20883

Microwave noise measurement with Dicke type radiometers, discussing measurement error reduction

09 p1052 A73-23109

Amplitude predistortion and deemphasis filters, measuring channel noise immunity enhancement by mean square deviation

10 p1195 A73-24379

Interference measurement techniques for small phase difference changes, noting diffraction and noise effects as limiting factors

10 p1222 A73-24945

Radio Astronomy Explorer /RAE/. I - Observations of terrestrial radio noise.

11 p1356 A73-25920

Friction, wear, and noise of slip ring and brush contacts for synchronous satellite use.

11 p1374 A73-26211

FM laser noise effects on optical Doppler radar systems.

11 p1333 A73-26639

Evaluation of the efficiency of the polarization selection method in suppressing fluctuating polarization noise

12 p1468 A73-26946

Radio noise contaminated area avoidance by vehicles dependent on navigation or communication radio receivers, giving equations and curves for navigational problem

12 p1523 A73-27887

The first two receivers for the radio astronomy programme on the 100 meter radiotelescope - An assessment of performance.

13 p1581 A73-28000

Direct-reading measurement of receiver-noise parameters.

13 p1590 A73-28531

Noise at large RF amplitudes in IMPATT oscillators.

14 p1731 A73-29713

The influence of pulsed noise on the performance of incoherent digital communications systems

15 p1843 A73-31567

Atmospheric refractivity fluctuation caused transit time variation effects on propagation noise and frequency stability in microwave radio link signal reception at 36 GHz

16 p1982 A73-33714

Strain gage circuit with exponential pulsed power supply for data recovery in presence of high amplitude electrical noise

17 p2167 A73-34625

French book - Theory of communication: Signals, noises, and modulations.

17 p2123 A73-35149

Quadratic antenna systems and noise excited antennas.

17 p2128 A73-35682

Effectiveness of certain easily realizable rank algorithms for detections of signals against a background of noise.

17 p2130 A73-35720

Book - Low-noise electronic design.

17 p2143 A73-35825

Noise processes in a homing radar seeker.

18 p2290 A73-37088

Noise immunity of autocorrelation reception of single PSK signals.

18 p2291 A73-37135

Plasma wave observations near the plasmopause with the S3-A satellite.

20 p2552 A73-38956

Noise characteristics in bipolar transistor differential amplifiers, discussing current sources, circuit configurations, feedback amplifiers and equivalent circuits

22 p2832 A73-41897

Noise factor of a multiple-circuit input device

23 p2953 A73-43518

Noise immunity of quasi-optimal noncoherent reception during resynchronization with respect to time and frequency

24 p3067 A73-44590

ELECTROMAGNETIC NOISE MEASUREMENT

Noise measurement in p-n junction surface of Si semiconductor wafer under transverse electric field, noting reverse current contribution

03 p0350 A73-13665

Evaluation of the noise and dynamic range of transistorized selective RC amplifiers with controlled tuning

13 p1591 A73-28868

Experimental measurement of ambiguity noise in a laser anemometer.

13 p1622 A73-29641

Fast pulse VHF background noise measurements in site selection for radio detection of cosmic ray air showers

16 p1984 A73-33924

Book - A handbook series on electromagnetic interference and compatibility.

17 p2121 A73-34462

Radio noise from towns - Measured from an airplane.

19 p2404 A73-37675

Low noise Si multijunction IMPATT diode measurements for large signal FM X band oscillator performance

21 p2668 A73-41588

Interwire coupling noise and cable resonance equations for fast rise time signal switching at resonant frequencies

22 p2823 A73-41800

Electromagnetic shielding techniques and testing for environment and instrument protection from radio emission and noise

22 p2823 A73-41804

A square-law voltmeter based on elements with a thermal coupling

24 p3071 A73-44544

Investigation of low-frequency noise in MOS transistors

24 p3071 A73-44593

ELECTROMAGNETIC PROPAGATION U ELECTROMAGNETIC WAVE TRANSMISSION

ELECTROMAGNETIC PROPERTIES

NT ABSORPTIVITY

NT BIREFRINGENCE

NT BRIGHTNESS

NT COLOR

NT DICHROISM

NT ELECTRICAL PROPERTIES

NT ELECTROMAGNETIC ABSORPTION

NT FARADAY EFFECT

NT LUMINOSITY

NT OPACITY

NT OPTICAL PROPERTIES

NT OPTICAL REFLECTION

NT PHOTOCONDUCTIVITY

NT PHOTOELASTICITY

NT PHOTOELECTRIC EFFECT

NT PHOTOELECTRIC EMISSION

NT PHOTOIONIZATION

NT PHOTOVISCOELASTICITY

NT PHOTOVOLTAIC EFFECT

NT RADIANCE

NT REFLECTANCE

NT REFRACTIVITY

NT SKY BRIGHTNESS

NT STELLAR LUMINOSITY

NT TRANSMISSIVITY

NT TRANSMITTANCE

NT TRANSPARENCY
NT TURBIDITY

Influence of fluctuations on the electromagnetic properties of the Josephson tunnel junction.

06 p0733 A73-17425

High spatial resolution wire spark chamber system using electromagnetic delay line readout.

11 p1363 A73-25962

High spatial resolution MWPC systems using electromagnetic delay line readouts.

11 p1364 A73-25966

The general form of constitutive equations in relativistic physics.

13 p1658 A73-28374

The consideration of environmental effects in the development of environment-resistant systems

16 p2019 A73-33385

Explorer 35 lunar studies, discussing orbit characteristics, circumlunar magnetic field, surface electromagnetic properties and solar wind model

16 p2065 A73-33782

Fluctuations in plasma and nonlinear susceptibilities.

17 p2217 A73-35817

An electromagnetic torsional vibrator.

20 p2544 A73-39271

Pure two band superconductor theory, discussing thermodynamic and electromagnetic properties, London group, mixed state, critical field and weak field penetration

21 p2753 A73-41299

ELECTROMAGNETIC PROPULSION

Realization of a geostationary orbit by means of an electromagnetic propulsion system /quasi-steady MPD/

17 p2239 A73-34954

ELECTROMAGNETIC PULSES

Distortion of electromagnetic pulses undergoing total internal reflection from a moving dielectric half-space.

06 p0666 A73-18200

External self focusing of converging short duration pulsed light beams, analyzing resultant focal points trebling, nonlinear focus motion and intensity distribution

06 p0702 A73-18590

Pulsed magnetic system /terrella/ for model of earth radiation belts and geomagnetic field-solar wind interaction

08 p0960 A73-21309

Investigation of the sensitivity of a duct sensor to discontinuities in alternating fields of square-pulse or sinusoidal shape - Detectability of surface defects on nonmagnetic and ferromagnetic specimens. I

08 p0967 A73-21587

Parallel plate electromagnetic shock tube, investigating drive current, gas pressure and electrode material effects on electrode ablation and current sheet velocity

08 p0953 A73-21632

Electromagnetic pulse penetration through small apertures.

08 p0940 A73-21664

Problem of the reflection of pulse signals from a moving mirror

11 p1332 A73-26167

Ionospheric and pulse compression induced distortions in chirped Gaussian electromagnetic pulses

14 p1728 A73-30232

Modeling of pulsed propagation problems of radio waves excited by an infinite electric current filament in homogeneous dispersing media

15 p1853 A73-31496

An investigation of the reflection of electromagnetic pulses from moving plasmas.

16 p2041 A73-33199

Pulsed magnetic system /terrella/ as earth model with dipole magnetic field for laboratory simulation of geophysical phenomena

19 p2425 A73-37938

Observation of zero-degree pulse propagation in a resonant medium.

20 p2570 A73-38602

Higher conservation laws and coherent pulse propagation.

20 p2570 A73-38603

Coupled superradiance master equations - Application to fluctuations in coherent pulse propagation in resonant media.

20 p2571 A73-38627

Influence of vibrational, rotational, and reorientational relaxation on pulse amplification in molecular amplifiers.

21 p2742 A73-40217

Carrier-frequency distance dependence of a pulse propagating in a two-level system.

21 p2649 A73-40224

Protection of radiometers from pulse interference

21 p2705 A73-41463

Circumvention design of active circuitry and passive shielding for electromagnetic pulse environment with application to Minuteman ICBM system

22 p2822 A73-41786

Pulse scattering from a sphere coated with an inhomogeneous sheath.

22 p2824 A73-41852

ELECTROMAGNETIC RADIATION

NT AIRGLOW

NT BLACK BODY RADIATION

NT BREMSSTRAHLUNG

NT CERENKOV RADIATION

NT COHERENT ELECTROMAGNETIC RADIATION

NT COHERENT LIGHT

NT COMET TAILS

NT CYCLOTRON RADIATION

NT DAYGLOW

NT DECA-METRIC WAVES

NT DECIMETER WAVES

NT ELECTROMAGNETIC PULSES

NT ELECTROMAGNETIC SURFACE WAVES

NT EXTRATERRESTRIAL RADIO WAVES

NT FAR INFRARED RADIATION

NT FAR ULTRAVIOLET RADIATION

NT GALACTIC RADIO WAVES

NT GAMMA RAYS

NT GEIGESCHNEIN

NT GEOCORONAL EMISSIONS

NT H WAVES

NT INFRARED RADIATION

NT LIGHT [VISIBLE RADIATION]

NT LIGHT BEAMS

NT LONG WAVE RADIATION

NT LYMAN ALPHA RADIATION

NT MICROWAVE EMISSION

NT MICROWAVES

NT MILLIMETER WAVES

NT MODULATED CONTINUOUS RADIATION

NT MONOCHROMATIC RADIATION

NT NEAR INFRARED RADIATION

NT NEAR ULTRAVIOLET RADIATION

NT NIGHTGLOW

NT NONEQUILIBRIUM RADIATION

NT PHONON BEAMS

NT PHOTON BEAMS

NT PLANETARY RADIATION

NT POLARIZED ELECTROMAGNETIC RADIATION

NT POLARIZED LIGHT

NT RADIO BURSTS

NT RADIO EMISSION

NT RADIO WAVES

NT SHORT WAVE RADIATION

NT SKY RADIATION

NT SKY WAVES

NT SOLAR RADIO BURSTS

NT SOLAR RADIO EMISSION

NT SOLAR X-RAYS

NT SUBMILLIMETER WAVES

NT SUNLIGHT

NT SYNCHROTRON RADIATION

NT TERRESTRIAL RADIATION

NT THERMAL RADIATION

NT TROPOSPHERIC RADIATION

NT TWILIGHT GLOW

NT TYPE 2 BURSTS

NT TYPE 3 BURSTS

NT TYPE 4 BURSTS

NT TYPE 5 BURSTS

NT ULTRAVIOLET RADIATION

NT X RAYS

NT ZODIACAL LIGHT

Incidence of a plane electromagnetic wave on a moving shock wave in an ionized gas

01 p0016 A73-10205

Light waves interaction in nonlinear medium, noting operational principles and optical properties of parametric optical generators with semiconductors

01 p0059 A73-10717

Transition radiation from a plasma boundary.

01 p0085 A73-11063

Collision between an electromagnetic wave and a gravitational wave packet

01 p0019 A73-11280

Book - Radiation and scattering of waves.

02 p0192 A73-11882

Electromagnetic self induced vibrations in homogeneous unbounded electron beam moving with time dependent velocity, noting longitudinal and transverse wave generation

02 p0198 A73-12102

Energy spectrum of muon formed electromagnetic cascades in vertical cosmic radiation flux

02 p0209 A73-12681

Electromagnetic and electroacoustic mode radiation resistance of linear antennas in compressible electron-plasma.

02 p0199 A73-12858

Radiation from a magnetic line source in a compressible and anisotropic plasma half-space.

03 p0345 A73-12996

Electromagnetic wave observation in interplanetary medium and in magnetosphere, emphasizing magnetic and electric field measurements

03 p0374 A73-13855

Eigenvalues and eigenfunctions of electric and magnetic waves of shielded strip transmission line, calculating electromagnetic field in cylindrical waveguide

04 p0417 A73-15089

Excitation of electromagnetic waves in a plasma with the aid of longitudinal electric fields

04 p0481 A73-15606

ELECTROMAGNETIC RADIATION

Electromagnetic-emission energy flux during the development of beam instability in a magnetically confined plasma

04 p0481 A73-15607

Thermally induced stress waves in an elastic layer. [ASME PAPER 72-WA/APM-22]

04 p0516 A73-15894

Study of the dispersion curve of polarizations excited by Raman diffusion in the presence of damping

04 p0476 A73-15997

Maxwell equations in a spherically symmetric black-hole background and radiation by a radially moving charge.

05 p0597 A73-16470

Dispersion relations for electromagnetic radiation in random media.

05 p0597 A73-16494

Phosphor crystals for electromagnetic emission recording based on optical and thermal effects on luminescent screens, considering optimal extinguishing and color alteration conditions

05 p0584 A73-16552

Incoherent radiation from relativistic electrons with power energetic spectrum.

05 p0611 A73-17313

Electromagnetic radiation caused by the two-stream instability in a bounded plasma.

06 p0726 A73-17416

Resonance and propagation theory for all electromagnetic wave types in plasmas of ionosphere and interplanetary space, discussing stability and oscillations

06 p0689 A73-17505

Drift instabilities in nonuniform streaming plasmas.

07 p0855 A73-19337

Diffraction of a plane electromagnetic wave at an array of circular cylinders with a spiral slot

07 p0793 A73-19917

Diffraction of plane electromagnetic wave at anisotropic halfspace in free space and in planar waveguide.

07 p0793 A73-20126

Electromagnetic radiation from charges in weak gravitational fields.

07 p0852 A73-20179

Focusing of EM waves in plasmas by inhomogeneous magnetic fields.

08 p0993 A73-21205

Influence of radiation damping on the motion of a charge in a uniform magnetic field and in the field of a plane electromagnetic wave

08 p0989 A73-21516

Mathematical model for nonlinear interactions between HF waves and LF acoustic waves applied to electromagnetic wave stability in plasmas and dielectrics

09 p1128 A73-22614

Excitation of electromagnetic waves in a plasma by longitudinal electric fields.

10 p1254 A73-24196

Electromagnetic energy in the two-stream instability in a magnetized plasma.

10 p1254 A73-24197

Electromagnetic wave instability characteristics during propagation oblique to electron stream in cold electron-ion plasma

10 p1255 A73-24268

Vector and tensor radiation from Schwarzschild relativistic circular geodesics.

10 p1249 A73-24346

Wave amplification during the reflection from a rotating 'black hole'

10 p1283 A73-24752

Relativistic particle beam stability and electromagnetic oscillations in plasma rectangular waveguide under longitudinal magnetic field

10 p1258 A73-24887

EM induction in a semi-infinite solid, impulsively moving in a uniform magnetic field.

11 p1397 A73-25371

Influence of a powerful electromagnetic wave on the electrical conductivity of a semiconductor

11 p1409 A73-26165

A numerical method for solving the stationary diffraction problem of electromagnetic waves on bodies of revolution

11 p1332 A73-26332

Emission from a point charge during motion along the plane boundary of a dielectric with periodically varying density

11 p1402 A73-26448

Changes in the mean energy of an electron in the field of a plane wave with allowance for radiation damping

12 p1526 A73-26969

Emission of 'soft' photons in the field of a strong electromagnetic wave

12 p1468 A73-26972

Diffraction of electromagnetic waves on reflectors with parameters that vary periodically in time

12 p1470 A73-27583

Short time constant limits of pulse duration on electromagnetic energy emission as function of frequency, applying to extragalactic radio astronomy observations

12 p1547 A73-27884

Spontaneous-emission feedback in a three-level quantum system - A case of conflict between semiclassical and quantum theories of radiation.

13 p1659 A73-28375

HF CW ultrasonics, discussing elimination of electromagnetic leakage or crosstalk between transmitter and receiver by sampling technique

13 p1612 A73-28483

Plane electromagnetic wave diffraction by ideally conducting circular cylinder in far and bright spot zones, using Green theorem for field calculation

13 p1583 A73-28851

Overview of the biological effects of electromagnetic radiation.

13 p1580 A73-29211

Radiation from travelling wave circular loop antenna in compressible electron plasma.

14 p1731 A73-29709

Study of two types of turnstile aerial immersed in a warm plasma.

14 p1731 A73-29712

Book - Statistical mechanics, kinetic theory, and stochastic processes.

14 p1774 A73-29947

Direct nonlinear coupling of electromagnetic waves and electrostatic waves in a plasma - Theory.

14 p1781 A73-30656

Russian book - Asymptotic theory of diffraction of electromagnetic waves by finite structures.

15 p1845 A73-32294

Reflection of electromagnetic waves from a moving plasma

15 p1846 A73-32303

Electromagnetic emission during surface wave excitation by a relativistic electron beam in a plasma

15 p1921 A73-32321

Crab Nebula pulsar electromagnetic radiation emission model based on high energy electron circular motion around magnetic field lines

15 p1942 A73-32649

Diffraction of an electromagnetic wave on a plane hologram

16 p2011 A73-32823

The problem of interaction between a relativistic electron beam and plasma in a waveguide

16 p2040 A73-32899

Electromagnetic emission in the general relativity theory. I

16 p1984 A73-34006

The Compton effect in a medium near a Cerenkov cone

17 p2120 A73-34115

Book on wave propagation in continuous media covering Hamilton principle, energy theorems, elastic waves, electromagnetic and hydromagnetic waves, Green function and nonlinear effects

17 p2211 A73-34280

Diffraction of a plane electromagnetic wave on arrays of periodically spaced cylinders

17 p2121 A73-34583

Nonphysical self forces removal from electromagnetic plasma models by simulation algorithm, discussing optimization of particle orbit equations integration

17 p2216 A73-34895

Gravitational and electromagnetic shock waves

17 p2212 A73-35048

Excitation of electromagnetic waves in a plasma with a relativistic electron beam.

17 p2216 A73-35159

Y-covariant formulation of the relativistic electrodynamics of material media

17 p2213 A73-35569

Five wave interaction - A possibility for enhancement of optical or microwave radiation by nonlinear coupling to explosively unstable plasma waves.

17 p2218 A73-35821

Diffraction of waves at finite bodies of revolution

19 p2458 A73-37182

Nonsinusoidal EM waves - State of development

19 p2403 A73-37432

Statistical acceleration of ultrarelativistic electrons by random electromagnetic waves.

19 p2462 A73-37558

Russian book on electromagnetic wave propagation in ionosphere, covering atmospheric structure, electron concentration, waveguides and earth surface effects

19 p2424 A73-37773

Direct nonlinear coupling of electromagnetic waves and electrostatic waves in a plasma - Experiment.

19 p2469 A73-37860

Survey of the present status of neoclassical radiation theory.

20 p2590 A73-38604

Charged particle acceleration in strong dipole fields.

20 p2595 A73-39077

Calculation of the radiative characteristics of polydisperse concentric spheres

20 p2531 A73-39728

Instability of transverse electromagnetic waves in a drifting electron-hole plasma

21 p2751 A73-40368

The laws of conservation of energy and momentum during emission of electromagnetic waves/photons in

a medium and the energy-momentum tensor in macroscopic electrodynamics

21 p2739 A73-40447

Nonthermal electromagnetic and thermal X ray sources of accelerated electrons during solar flares

21 p2761 A73-41384

Relativistic particle beam stability and electromagnetic oscillations in plasma rectangular waveguide under longitudinal magnetic field

21 p2749 A73-41662

Electromagnetic radiation hazard test facility, instrumentation, and weapon system susceptibility evaluation for providing environment protection and military standards

22 p2822 A73-41791

An evaluation of experimental errors in electromagnetic wave measurements aboard satellites.

22 p2844 A73-41911

Influence of small electromagnetic-field fluctuations on the bioelectric activity of the human brain

22 p2813 A73-41964

Incident electromagnetic wave reflection in inhomogeneous plasma with local nonlinearity, discussing reflection point shift and dielectric permittivity effect

22 p2892 A73-42328

Parametric amplification and generation of pulses in nonlinear distributed systems

22 p2826 A73-42333

Computer simulation of the acceleration of charged particles captured by plane electromagnetic waves

22 p2826 A73-42378

Electromagnetic theory of Fresnel holograms in the first perturbation theory approximation

22 p2862 A73-42927

Collision between an electromagnetic wave and a gravitational wave packet.

23 p3006 A73-43501

Amplification of electromagnetic and gravitational waves during scattering on a rotating black hole

23 p3034 A73-44008

Reflection of electromagnetic waves from a moving plasma.

24 p3067 A73-44611

ELECTROMAGNETIC SCATTERING

NT HALOS

NT IONOSPHERIC F-SCATTER PROPAGATION

NT LIGHT SCATTERING

NT MICROWAVE SCATTERING

NT MIE SCATTERING

NT RAMAN SPECTRA

NT RAYLEIGH SCATTERING

NT THOMSON SCATTERING

NT X RAY SCATTERING

Kinetic theory of scattering by a plasma cylinder.

01 p0081 A73-10136

Discussion of radiative-transfer methods applied to electromagnetic reflection from turbulent plasma.

01 p0081 A73-10196

Nonlinear interaction of two monochromatic Langmuir waves

01 p0016 A73-10209

P, T invariance of electromagnetic interaction and the circular polarization of planetary emission

01 p0092 A73-10940

Average monostatic scattering cross section for plane electromagnetic wave incident on ideally conducting convex body, considering wavelength relation to body dimensions

03 p0278 A73-14072

Modeling of the radar scattering characteristics of aircraft.

04 p0416 A73-15057

Geometrical optics calculation of radar cross sections.

04 p0416 A73-15058

A system-synthesis approach to the inverse problem of scattering by smooth, convex-shaped scatterers for the high-frequency case.

04 p0423 A73-15484

Higher-order scattering losses in dielectric waveguides.

05 p0549 A73-16366

Scattering of electromagnetic waves from a turbulent plasma slab.

06 p0729 A73-18120

On a set of continuous wave electromagnetic inverse scattering boundary conditions.

06 p0664 A73-18136

On the analysis of scattering and antenna problems using the singularity expansion technique.

06 p0665 A73-18184

Monte Carlo computer technique for one-dimensional random media.

06 p0665 A73-18188

Scattering by nonconcentric circular plasma cylinders with axial magnetic fields.

06 p0729 A73-18204

Electromagnetic scattering from a radially moving spherical discontinuity.

06 p0669 A73-18785

Arbitrary source emitted electromagnetic radiation in anisotropic stratified media, evaluating transverse and scattered fields and plane wave response

07 p0791 A73-19382

Application of the Lorentz lemma to the calculation of diffraction mode excitation coefficients

07 p0793 A73-19918

Inverse problem of diffraction for a reactance plane

07 p0793 A73-19919

Nonstationary radiation diffusion in a semiinfinite isotropically scattering medium

08 p0985 A73-21453

Hemispherical reflectivity and transmissivity of an absorbing, isotropically scattering slab with a reflecting boundary.

08 p1025 A73-21643

Convergence of the solution for the far scattered field of a conducting cylinder of arbitrary cross-section.

09 p1050 A73-22397

P, T invariance of electromagnetic interaction, and circular polarization of planetary radiation.

09 p1138 A73-22735

A local point method for problems of diffraction on an array

09 p1051 A73-22860

Scattering by perfectly conducting rotational bodies of arbitrary form excited by an obliquely incident plane wave or by a linear antenna.

09 p1052 A73-22959

Spectra of short-term fluctuations of line-of-sight signals - Electromagnetic and acoustic.

10 p1190 A73-24893

Field scattered by rough surface generated by stationary random process, constructing two dimensional density from given marginals and correlation coefficient

11 p1328 A73-25656

Near field of scattering by a hollow semi-infinite cylinder and its application to sensor booms.

11 p1328 A73-25658

Loaded multiport electromagnetic scatterer modal analysis, presenting current resonating procedure

11 p1328 A73-25659

Junction discontinuities in wire antennas and scatterers, obtaining constraint on junction currents via equivalent charge distribution representation

11 p1329 A73-25666

Kirchhoff and small perturbation methods identity in composite model calculation for rough surface electromagnetic scattering of circularly polarized wave by perfectly conducting body

11 p1329 A73-25678

Time-dependent electromagnetic field scattering and diffraction by half plane during illumination by impulsive plane cylindrical or spherical wave

11 p1330 A73-25683

Linear polarization and spectrum of PSR0833-45 and the effects of scattering.

11 p1419 A73-25748

Electromagnetic wave scattering by an inhomogeneous magnetoplasma column moving in the axial direction.

11 p1407 A73-26700

Electromagnetic scattering by a transversely moving conducting cylinder of arbitrary cross section.

12 p1468 A73-27018

The influence of the scattering by plasma oscillation on the spectrum of emission from semi-opaque plasma

12 p1529 A73-27869

Scattering by a gyrotropic cylinder coated with another gyrotropic layer.

13 p1586 A73-29232

The scattering matrix of a double truncated corner in a waveguide

14 p1726 A73-30073

Integral equation formulation for electromagnetic scattering by conducting cylinders, investigating coupling between complementary boundary value problem and nonuniqueness consequences on numerical resolution

14 p1727 A73-30215

Support scattering effects on low-gain satellite antenna pattern measurements.

14 p1735 A73-30218

On the scattering cross section of passive linear arrays.

14 p1735 A73-30229

Rayleigh-fast Fourier transformation techniques for electromagnetic scattering over rough sinusoidal surface, comparing numerical validity with perturbation, physical optics and integral equation methods

14 p1728 A73-30230

Modified radar cross section of a dielectric cylinder with conducting circumferential loop loading.

14 p1729 A73-30699

Resonant scattering from inhomogeneous nonspherical targets.

14 p1775 A73-30906

A microscopic theory of density fluctuations in partially ionized gases.

15 p1916 A73-31086

Phenomena of scattering of electromagnetic and gravitational wave packets in the gravitational field of a black hole

15 p1932 A73-31245

Dispersion of electromagnetic waves on a weak isolated inhomogeneity.

15 p1843 A73-31522

Russian book - Scattering and attenuation of electromagnetic radiation by atmospheric particles.

15 p1843 A73-31586

Kinetics of stimulated scattering of Langmuir waves by plasma ions

15 p1919 A73-31708

General properties of electromagnetic scattering by inhomogeneous anisotropic composite obstacles of arbitrary shape.

15 p1844 A73-31930

Scattering of electromagnetic waves by a disk positioned at the boundary between two media

15 p1846 A73-32318

Scattering of electromagnetic radiation from a black hole.

16 p2060 A73-33120

Asymptotic development method for the determination of the field reflected by a random surface

16 p1984 A73-33966

Theory of electromagnetic field scattering in gases

16 p1984 A73-34007

An integro-differential equation technique for the time-domain analysis of thin wire structures. I - The numerical method.

17 p2246 A73-34892

Use of the Singularity Expansion Method in electromagnetic transient scattering problems.

17 p2124 A73-35360

Spectral characteristics of the scatter field from a rotating impedance cylinder in uniform motion.

17 p2129 A73-35707

Emission of an isothermal, isotropically scattering medium.

18 p2336 A73-36324

The interaction between atmospheric microstructure and acoustic and electromagnetic waves.

19 p2406 A73-38242

On the noniterative solution of integral equations for scattering of electromagnetic waves.

19 p2407 A73-38381

A generalized extinction theorem and its role in scattering theory.

20 p2591 A73-38613

General remarks concerning theories dealing with scattering and diffraction in random media.

20 p2528 A73-38845

Electromagnetic scattering by discontinuities in weakly inhomogeneous parallel plane waveguides or ducts, noting edge diffraction singularities role from ray optical calculation

20 p2528 A73-38847

Application of method of fringe waves to problems of diffraction from bodies placed in a smoothly inhomogeneous medium.

20 p2529 A73-38919

Influence of scattering by plasma oscillations on the spectrum of a semitransparent plasma.

20 p2597 A73-39243

Rotational line structure in three-photon scattering by symmetric top molecules.

20 p2574 A73-39723

Contribution to the theory of electromagnetic fluctuations of a plasma situated in a weak SHF electric field

21 p2746 A73-40517

Diffraction of a plane electromagnetic wave by a perfectly conducting elliptic cylinder.

22 p2822 A73-41749

Iterative and matrix inversion techniques for antenna electromagnetic radiation and scattering prediction compared for computer storage and execution time

22 p2823 A73-41799

Improved point-matching method with application to scattering from a periodic surface.

22 p2824 A73-41833

Electromagnetic inverse boundary conditions determination of profile and material surface characteristics of conducting circular cylindrical shape scatterer

22 p2824 A73-41834

Scattering of electromagnetic waves from rough oscillating surfaces using spectral Fourier method.

22 p2824 A73-41855

Unsteady, combined radiation and conduction in an absorbing, scattering, and emitting medium.

[ASME PAPER 73-HT-J]

22 p2930 A73-42288

Electromagnetic wave diffraction by a metallic cylinder surrounded by a plasma layer

22 p2892 A73-42336

The asymptotic analysis of canonical problems in high-frequency scattering theory. I - Stratified media above a plane boundary. II - The circular and parabolic cylinders.

22 p2886 A73-42347

Maxwell integral equations in problems of wave scattering by moving media

22 p2826 A73-42376

E-polarized electromagnetic scattering by conducting circular cylinder coated with plasma sheath during spacecraft reentry flight under plane wave incidence

22 p2827 A73-42466

The efficient inject of high microwave powers into the overdense magnetoactive plasma in the waveguide.

22 p2827 A73-42517

Reflection function for an isotropically scattering finite medium.

22 p2887 A73-42565

An exact solution on the propagation of small disturbances in a radiating grey gas with isotropic scattering.

22 p2932 A73-42570

Papers on computer techniques for electromagnetic radiation and scattering problems via integral equation formulation covering iterative and variational methods and antenna patterns

22 p2827 A73-42839

Numerical solution of electromagnetic scattering problems.

22 p2827 A73-42841

Integral equation solutions of three-dimensional scattering problems.

22 p2827 A73-42842

Variational and iterative methods for waveguides and arrays.

22 p2834 A73-42843

Hybrid numerical solution to electromagnetic wave scattering and diffraction with application to microstrip transmission lines, echelle gratings and dielectric step discontinuities in waveguides

22 p2828 A73-42844

On an integral equation governing the reflection of electromagnetic waves by a random surface

22 p2888 A73-42948

Derivation of diffraction coefficients for a thin wire of finite length.

23 p2955 A73-44106

Scattering of electromagnetic waves by a disk at the interface between two media.

24 p3067 A73-44624

Lunar electromagnetic scattering. I - Propagation parallel to the diamagnetic cavity axis.

24 p3139 A73-45109

Enhanced scattering and decay of electromagnetic waves in the ionosphere.

24 p3086 A73-45130

Lagrangian analysis of multiple scatter in acoustic and electromagnetic reflexion.

24 p3111 A73-45394

ELECTROMAGNETIC SHIELDING

NT RADIO FREQUENCY SHIELDING

Electromagnetic systems of noise-immunized nuclear-precession sensors

06 p0692 A73-17562

Electric and magnetic field shielding performance of nonmagnetic metallic cylinders, using Sommerfeld approximation

08 p0949 A73-21663

Fundamental and parasitic modes of a shielded microstrip transmission line

09 p1052 A73-23085

Electromagnetic systems of noiseproof nuclear precession sensors.

16 p2011 A73-32786

Environmental effects on EMI gaskets.

16 p1987 A73-33153

Book - A handbook series on electromagnetic interference and compatibility.

17 p2121 A73-34462

Circumvention design of active circuitry and passive shielding for electromagnetic pulse environment with application to Minuteman ICBM system

22 p2822 A73-41786

Prediction of RS01 design requirements for MIL-STD-461A.

22 p2823 A73-41803

Use of magnetic materials for improvement of screening properties of different types of cables.

22 p2830 A73-41805

ELECTROMAGNETIC SHOCK TUBES

U SHOCK TUBES

ELECTROMAGNETIC SPECTRA

NT BALMER SERIES

NT D LINES

NT ELECTRONIC SPECTRA

NT FRAUNHOFER LINES

NT H ALPHA LINE

NT H BETA LINE

NT H GAMMA LINE

NT H LINES

NT INFRARED SPECTRA

NT K LINES

NT LINE SPECTRA

NT LYMAN SPECTRA

NT MICROWAVE SPECTRA

NT PASCHEN SERIES

NT RADIO SPECTRA

NT RAMAN SPECTRA

NT RYDBERG SERIES

NT SOLAR SPECTRA

NT STELLAR SPECTRA

NT TELLURIC LINES

NT UVB SPECTRA

NT ULTRAVIOLET SPECTRA

NT VIBRATIONAL SPECTRA

NT X RAY SPECTRA

Some new techniques for processing remotely obtained images by self-generated spectral masks.

01 p0078 A73-11219

Russian book on spectral composition-dependent photoconductivity in Hg doped amorphous Se films covering effect of quasi-macroscopic centers in semiconductors

02 p0201 A73-12864

Study of bends in long distance waveguides - The case of metallic guides

04 p0427 A73-14900

Optical fibre guide measurements with short coherent light pulses.

14 p1756 A73-30056

Laser spectrometer for combination scattering, recording polarized spectra with thermoelectrically cooled photomultiplier by photon count

17 p2164 A73-34164

RF fields as new ecological factor in environment pollution, considering radiation interaction with biological systems and increased use of electromagnetic spectrum

22 p2811 A73-41787

ELECTROMAGNETIC SURFACE WAVES

Electromagnetic wave radiation and reflection at guiding structure discontinuity, calculating TE mode surface wave by boundary perturbation technique

14 p1727 A73-30214

Surface wave radiation pattern determination for solid state lasers, taking into account dielectric interface presence

21 p2716 A73-41113

ELECTROMAGNETIC WAVE FILTERS

NT ELECTRIC FILTERS

NT INFRARED FILTERS

NT MICROWAVE FILTERS

NT OPTICAL FILTERS

NT RADAR FILTERS

NT ULTRAVIOLET FILTERS

NT WAVEGUIDE FILTERS

Reconstruction of analog signals and choice of sampling rates in telemetry.

09 p1058 A73-23421

Design procedures for matched and broadbanding filters for scanning tests.

11 p1341 A73-25074

Wide angle narrow band interference filter for detecting E region barium ion clouds against intense background

11 p1366 A73-26250

Acoustic matched filters applications for multisubscriber band spread communication in ATC systems

14 p1733 A73-29936

Study of a narrow-band interference filter at various angles of incidence

16 p2012 A73-32844

Interference filters for the VUV (1200-1900 A).

22 p2863 A73-43142

Certain problems of frequency settling in ideal filters

23 p2959 A73-43514

German book on HF technology, Volume 1, covering coupling filters, transmission lines, antennas, Lecher waves, waveguides, etc

24 p3073 A73-44999

ELECTROMAGNETIC WAVE TRANSMISSION

NT DOUBLE SIDEBAND TRANSMISSION

NT HALOS

NT IONOSPHERIC F-SCATTER PROPAGATION

NT IONOSPHERIC PROPAGATION

NT LIGHT SCATTERING

NT LIGHT TRANSMISSION

NT MANDELSTAM REPRESENTATION

NT MICROWAVE ATTENUATION

NT MICROWAVE TRANSMISSION

NT MULTIPATH TRANSMISSION

NT RADAR TRANSMISSION

NT RADIO ATTENUATION

NT RADIO TRANSMISSION

NT SCATTER PROPAGATION

NT SHORT WAVE RADIO TRANSMISSION

NT SINGLE SIDEBAND TRANSMISSION

NT TELEVISION TRANSMISSION

NT TRANSEQUATORIAL PROPAGATION

Transport phenomena in turbulent plasma with electromagnetic waves.

01 p0081 A73-10117

Geometrical theory to approximate HF electromagnetic wave diffraction from moving conducting strip under incident field

01 p0016 A73-10192

Propagation of electromagnetic waves in a plasma with a sheared magnetic field

01 p0081 A73-10206

Electromagnetic wave transmission through 8-12 micron atmospheric window, investigating particulate matter effects on radiation energy extinction

01 p0037 A73-10372

Amplitude modulation of electromagnetic waves by acoustic waves in a dispersive plasma - Modified theory.

01 p0083 A73-10455

Propagation of submillimeter-band electromagnetic waves in the drifting plasma of a solid

01 p0017 A73-10976

Experimental investigation of millimeter-band electromagnetic wave propagation in a waveguide filled with n-type InSb under a magnetic field

01 p0017 A73-10977

Energy transfer between interacting electromagnetic waves propagating in half space media, applying to acoustic surface wave excitation by electromagnetic converter

02 p0140 A73-11568

Plane electromagnetic wave diffraction by periodic grid of dielectric cylindrical filaments, determining reflection and transmission coefficients of radome composite materials

02 p0141 A73-12024

Dual integral equations and diffraction of electromagnetic waves by a thin conducting strip.

02 p0141 A73-12101

The influence of atmospheric layer structure on space - Earth links.

03 p0275 A73-13653

Study of bends in long distance waveguides - The case of metallic guides

04 p0427 A73-14900

Influence of carrier drift on the propagation of electromagnetic wave in a solid-state plasma.

04 p0480 A73-15473

Propagation of electromagnetic waves in media which vary slowly with position and time.

[AD-753304] 04 p0423 A73-15483

Strong electromagnetic waves in semiconductors under conditions of inelastic scattering of current carriers by optical phonons.

04 p0484 A73-15568

Electromagnetic wave diffraction by ideally conducting homogeneous bodies of revolution with arbitrary complex permittivity and permeability, using separation of variables method

05 p0547 A73-16054

Distance measurement by means of modulated light.

05 p0575 A73-16342

Eigenvalues of normal waves in a plane waveguide channel

05 p0549 A73-16385

Vertical electric dipole excited electromagnetic fields in triple layer medium with plane boundaries, noting waveguide thickness effect on electromagnetic wave propagation

05 p0549 A73-16386

Propagation of electromagnetic waves in a rarefied plasma which has been placed in an alternating magnetic field.

06 p0726 A73-17402

Electrodynamics of anisotropic media with space and time dispersion.

06 p0723 A73-17787

Wave normal and ray propagation in lossless positive bianisotropic media.

06 p0723 A73-17875

Applications of conformal mappings to the diffraction of electromagnetic waves by a grating.

06 p0665 A73-18182

A new approach to the problem of wave fluctuations in localized smoothly varying turbulence.

06 p0665 A73-18183

Reflection and transmission of electromagnetic waves obliquely incident on a relativistically moving uniaxial plasma slab.

06 p0665 A73-18185

Diffraction of an arbitrary plane electromagnetic wave by a half-plane.

06 p0667 A73-18203

Diffraction of electromagnetic plane wave by an infinite slit embedded in an anisotropic plasma.

06 p0668 A73-18356

Electromagnetic wave reflection by two level medium analog of moving molecular beam, considering fields penetration and surface impedance effects

06 p0668 A73-18647

Nonlinear propagation theory for electromagnetic waves in a weakly ionized plasma

07 p0854 A73-19277

Dispersion equations for E and H waves in multilayer plasma, defining amplitudes correlation for incident, transmitted and reflected waves

07 p0855 A73-19278

Noncoherent reflection of electromagnetic waves from a plasma layer

07 p0855 A73-19281

Collision effects on electromagnetic wave propagation in a plasma generated by a moving ionization source

07 p0858 A73-19906

Electromagnetic wave propagation in a circular waveguide with spirally conducting inserts

07 p0793 A73-19920

Complex wave existence in some two-layer isotropic structures

07 p0793 A73-19921

Wave attenuation in superconducting elliptical waveguides

07 p0793 A73-19924

Transmission of electromagnetic waves through a conducting slab. IV - A simple multiple-reflection method.

07 p0852 A73-20172

Oblique electromagnetic wave propagation with respect to double stream in plasma, calculating unstable wave oscillation frequency and growth rate dependence on stream direction

08 p0993 A73-21633

Book - Theory of ionospheric waves.

08 p0962 A73-21838

Electromagnetic propagation in bianisotropic stratified media, obtaining Maxwell and constitutive equations in operator form

09 p0149 A73-22312

Algorithm for numerical calculation of transmitted and reflected electromagnetic waves, noting multiple reflections for inertial inhomogeneities

09 p0163 A73-22458

Propagation through a slab of irregularities in a magneto-ionic medium.

09 p0151 A73-22647

Diffraction on an infinite grating made of cylindrical elements of random cross section

09 p0151 A73-22851

Influence of absorption on the optical properties of solids - Propagation of uniform, plane, heterogeneous electromagnetic waves in isotropic and homogeneous mediums

09 p1121 A73-22963

Obliquely incident electromagnetic wave propagation through plane-stratified weakly ionized plasma with electron density inhomogeneity scale length comparable with mean free path

09 p1052 A73-23077

Conversion of the wave spectrum in a medium with smooth spatial-temporal fluctuations

09 p1052 A73-23082

Electromagnetic wave propagation velocity modulation in dispersionless linear medium with dielectric constant variation in space and time, evaluating approximation with neglected multiple reflections

10 p1249 A73-24526

Dispersion equation of parametric longitudinal LF instability of electromagnetic wave propagation in bunched electron beam in metallic waveguide

10 p1257 A73-24876

International Conference on Electromagnetic Windows, 2nd, Ecole Nationale Supérieure de Techniques Avancées, Paris, France, September 8-10, 1971, Proceedings. Volume 1, 2 & 3

11 p1334 A73-25276

Electromagnetic window for a trajectory radar

11 p1327 A73-25280

Integral equation numerical solution by minimum mean-squared estimator for atmospheric electromagnetic refractivity profile from satellite radar tracking data, noting iterative procedure convergence

11 p1330 A73-25686

Excitation and damping-mechanism of waves and resonances in bounded magnetoactive media. [IPPCZ-167]

12 p1528 A73-27431

Application of series to an investigation of a plane electromagnetic wave in a ferromagnetic half-space

12 p1474 A73-27804

Electron temperature in a weakly ionized plasma during a nonlinear skin effect

12 p1530 A73-27979

Reflection of plane heterogeneous and uniform electromagnetic waves and the reflected wave displacement

13 p1658 A73-28072

Finite element method for solution of Laplace or wave equation in cylindrical coordinates through base matrices, applying to electromagnetic wave propagation in waveguides

13 p1581 A73-28077

Paraxial electromagnetic wave packets diffraction on thin conducting periodic structures and dielectric plate, noting packet width and phase front curvature changes

13 p1582 A73-28653

Plane and cylindrical electromagnetic waves diffraction on infinitely long cylindrical bodies, calculating induced currents, diffraction patterns and near fields

13 p1582 A73-28654

Plane TE polarized electromagnetic wave diffraction on infinite conducting cylinder in nonhomogeneous medium, calculating far field diffraction patterns

13 p1582 A73-28656

Nonlinear propagation of electromagnetic waves in a weakly ionized plasma.

13 p1665 A73-28677

Dispersion equations for E and H waves in multilayer plasma, defining amplitudes correlation for incident, transmitted and reflected waves

13 p1665 A73-28678

Incoherent reflection of electromagnetic waves from a plasma layer.

13 p1665 A73-28681

Critical frequencies of electromagnetic wave propagation in H waveguides with a dielectric cross-piece

13 p1595 A73-29411

Electromagnetic wave reflection and transmission by slant air/dielectric interface in rectangular waveguide investigated by Green function technique

14 p1724 A73-29706

On the propagation of electromagnetic waves through a time-varying dielectric layer.

14 p1726 A73-29932

Radial mode analysis of electromagnetic wave propagation on slotted cylindrical structures.

14 p1727 A73-30208

The Stiles-Crawford effect - Explanation and consequences.

14 p1717 A73-30396

On the effect of electron-neutral particle collisions upon the refraction of high-frequency radio waves by the lower atmosphere and ionosphere of Mars.

15 p1929 A73-31078

Concept of phase centre of an array applied to elevation-angle measurements.

15 p1842 A73-31098

Electromagnetic wave propagation through a gas lens.

15 p1913 A73-31136

Electromagnetic instability in a counterstreaming plasma.

15 p1919 A73-31928

Reflection and transmission of electromagnetic waves obliquely incident on a relativistically moving isotropic plasma slab.

15 p1919 A73-31947

Electromagnetic wave propagation in p-type Ge and Si semiconductor plasmas, studying dispersion, cyclotron resonance, and kinetic equations

15 p1925 A73-32214

Exclusive distance measurements as substitute to combined distance difference and angular measurements in radio navigation, considering system accuracy and electromagnetic wave transmission

15 p1909 A73-32450

Book - Applications of the electromagnetic reciprocity principle.

15 p1915 A73-32577

Shadow zone effect of electromagnetic wave propagation in stratified layer with vertical dipole source and square law dependent refractive index profile

16 p1978 A73-32890

Average intensity of the normal wave during super-refraction

16 p1978 A73-32897

Eddy power flow of electromagnetic waves.

16 p1980 A73-33690

Nonlinear radial electron beam focusing in plasma under beam-plasma instability, showing irreversibility conditions dependence on electromagnetic wave propagation mode

16 p2043 A73-34056

Annual Southwestern Conference and Exhibition, 25th, Houston, Tex., April 4-6, 1973, Record.

17 p2124 A73-35357

Plane monochromatic electromagnetic waves in general relativity theory

17 p2212 A73-35562

A method for solving the problem of irradiation in anisotropic plasma.

17 p2217 A73-35724

Book - Electromagnetic wave propagation.

17 p2130 A73-35857

Transformation, transmission, and reflection of plasma waves in the presence of a tangential velocity discontinuity

18 p2339 A73-36551

Nonlinear expansion of arbitrarily polarized electromagnetic waves in gyrotropic media

18 p2340 A73-36961

Note regarding the propagation of electromagnetic fields through slots in cylinders.

19 p2403 A73-37273

Electromagnetic load propagation for an oblique incidence in a nonhomogeneous magnetized plasma

19 p2468 A73-37447

Calculation of reflection and transmission coefficients for a class of one-dimensional wave propagation problems in inhomogeneous media.

19 p2459 A73-37587

The propagation of an intense electromagnetic wave in a plasma.

19 p2469 A73-38087

Waves and turbulence in stable layers and their effects on EM propagation; Proceedings of the Third Symposium, La Jolla, Calif., June 5-15, 1972. Parts 1 & 2.

19 p2447 A73-38202

Theory of electromagnetic wave in a nonuniformly moving magnetoactive plasma

19 p2406 A73-38328

Excitation of electromagnetic waves propagating along a magnetic field in a cold plasma by a beam of phased oscillators

19 p2406 A73-38330

Phase characteristics of a rectangular waveguide with symmetrically arranged, transversely magnetized ferrite layers

19 p2407 A73-38342

Electromagnetic wave propagation in inhomogeneous multilayered structures of arbitrarily varying thickness - Generalized field transforms.

19 p2461 A73-38379

Electromagnetic wave propagation in inhomogeneous multilayered structures of arbitrary thickness - Full wave solutions.

19 p2461 A73-38380

On the noniterative solution of integral equations for scattering of electromagnetic waves.

19 p2407 A73-38381

Effects of dispersion on steady state electromagnetic shock profiles.

20 p2595 A73-38864

Instability of electromagnetic surface waves supported by a bounded plasma stream.

20 p2595 A73-38891

Reflection and transmission of plane waves at a boundary between two conducting media.

21 p2655 A73-41047

Russian book on wave propagation in stratified media covering elastic and electromagnetic fields, waveguides, whispering galleries, diffraction rays, caustic surfaces, etc

21 p2741 A73-41279

Dispersion equation of parametric longitudinal LF instability of electromagnetic wave propagation in bounded electron beam in metallic waveguide

21 p2744 A73-41651

Diffraction of a plane electromagnetic wave by a slit in a thick screen placed between two different media.

22 p2821 A73-41744

Diffraction of a plane electromagnetic wave by a perfectly conducting elliptic cylinder.

22 p2822 A73-41749

Dispersion relations for parallel-plane waveguide containing transversely magnetized uniaxial and warm plasma in relative motion.

22 p2824 A73-41857

Propagation of electromagnetic waves through turbulent plasma using transport theory.

22 p2824 A73-41860

Plane transient electromagnetic wave propagation in a generalized conducting medium.

22 p2886 A73-41965

Steady-state solutions for relativistically strong electromagnetic waves in plasmas.

22 p2891 A73-42238

Kinetic theory of electromagnetic waves in an electron plasma characterized by slowly changing parameters

22 p2892 A73-42327

Energy propagation lines in the diffraction of a plane electromagnetic wave by a slot in a conductive plane

22 p2826 A73-42353

Containment stability of charged particles captured by a plane electromagnetic wave propagating at a slowly varying velocity

22 p2826 A73-42377

Possible emission of transverse electromagnetic waves in an isotropic plasma

22 p2893 A73-42390

Nonlinear propagation of electromagnetic waves in a plasma containing random irregularities.

22 p2894 A73-42398

Diurnal cycles of the refractive index structure function coefficient.

22 p2849 A73-42545

Reflection and transmission of electromagnetic waves at a moving magnetoplasma half-space.

22 p2896 A73-43179

Wave propagation through a highly restrained solid-state plasma.

23 p3012 A73-44141

Guided propagation of very low frequency electromagnetic waves in irregularities of electronic density in the vicinity of the constant velocity mode

24 p3067 A73-44726

Coherence of an electromagnetic field propagating in a weakly guiding fiber.

24 p3097 A73-45416

ELECTROMAGNETIC WAVES

U ELECTROMAGNETIC RADIATION

ELECTROMAGNETICS

U ELECTROMAGNETISM

ELECTROMAGNETISM

NT MAGNETOSTATICS

Rigorous analogies between elastic and electromagnetic systems.

10 p1250 A73-24873

Computerized design of electromagnetic systems in electric power conversion and electromechanical devices, noting mathematical models for electromagnetic field calculations

11 p1313 A73-26114

A simplified method for the in vitro calibration of electromagnetic flowmeters.

12 p1464 A73-27027

Electromagnetic inductive microsystems with synchronization. I Determination of the characteristic functional magnitudes. II - Determination of the magnetic field in a region with linear and nonlinear media

16 p1992 A73-33664

Analysis of force interaction in magnetoelectric torque sensors

22 p2860 A73-42364

ELECTROMAGNETS

NT SUPERCONDUCTING MAGNETS

On the phenomenon of parametric resonance of a nonlinear vibrator under the action of electromagnetic force.

04 p0429 A73-15598

Electromagnetic systems of noise-immunized nuclear-precession sensors

06 p0692 A73-17562

Pulsed magnetic system /terrella/ for model of earth radiation belts and geomagnetic field-solar wind interaction

08 p0960 A73-21309

Electromagnetic systems of noiseproof nuclear precession sensors.

16 p2011 A73-32786

Pulsed magnetic system /terrella/ as earth model with dipole magnetic field for laboratory simulation of geophysical phenomena

19 p2425 A73-37938

ELECTROMECHANICAL DEVICES

Application of the VEDS-200A electrodynamic vibrator to fatigue tests in symmetric tension and compression

01 p0029 A73-10492

Special features of the calculation of electromechanical instrument servosystems with velocity feedbacks

02 p0148 A73-11861

On the phenomenon of parametric resonance of a nonlinear vibrator under the action of electromagnetic force.

04 p0429 A73-15598

Electromechanical techniques for rapid frequency tuning of lasers.

05 p0584 A73-16443

Time optimal control for vibrationless starting of electromechanical devices with moving parts, noting linear magnetic circuit

06 p0649 A73-18383

High resolution Mossbauer spectrometer design and applications, describing electromechanical Doppler shifter, control electronics and data storage

07 p0822 A73-19170

Failure analysis and reliability estimation methodology for electromechanical mosaic printer

07 p0800 A73-19419

Electronic six-channel phase shifter

08 p0950 A73-21715

Computerized design of electromagnetic systems in electric power conversion and electromechanical devices, noting mathematical models for electromagnetic field calculations

11 p1313 A73-26114

Opticomechanical system of an automatic stellar electrophotometer

12 p1495 A73-26865

The use of a type VEDS-200A vibrostand for fatigue tests under conditions of symmetrical tension-compression.

14 p1743 A73-30317

Continuously-discrete method for the construction of control devices

14 p1740 A73-30940

Organization of a reliability study on an electromechanical product

16 p1970 A73-33271

An optimization technique utilizing the deflected gradient algorithm for dynamic testing of electromechanical equipment.

17 p2202 A73-35386

Electro-mechano-hydraulic servovalve system, calculating dynamic frequency response in vibrating accelerated field under external disturbance

19 p2388 A73-37670

A continuous-discrete method of design of control devices.

19 p2414 A73-38194

Russian book on electroacoustic and electromechanical devices for sound recording and measurement covering human auditory system, microphones, loudspeakers, hydrophones, geophones, etc

22 p2832 A73-41882

Some general observations on the tuning characteristics of 'electromechanically' tuned Gunn oscillators.

23 p2960 A73-44070

ELECTROMECHANICS

Study of electromechanical coupling in a non-piezoelectric dielectric with a high dielectric constant

11 p1408 A73-25249

Wall-less electromechanical flow structures developed similar to structures with fluid partially ducted at free sources by external forces

11 p1403 A73-25255

ELECTROMETERS

Electrometric amplifiers for inductive measurement of charges

08 p0949 A73-21713

Modification and updating of the bioelectric DS2C amplifier for a FET input.

09 p1046 A73-22936

Analytical fit of the transfer function of a logarithmic electrometer and correction for ambient temperature variations.

11 p1367 A73-26306

ELECTROMIGRATION

A statistical model for electromigration induced failure in thin film conductors.

08 p0944 A73-20745

ELECTROMOTIVE FORCES

On the potential difference between two immiscible media.

04 p0483 A73-15106

Resultant value of the inertial emf during thermal convection in a rotating plasma

04 p0481 A73-15604

Low-resistance CdTe films exhibiting a constant emf under the action of an ac field

06 p0737 A73-18222

Thermal emf of indium antimonide of a p- and-n type of conductivity at room temperature

06 p0738 A73-18652

Determination of the frequency and amplitude of an external force that induces resonance in a linear system with variable parameters

07 p0792 A73-19908

A contactless method of measuring the radial deformations of rotating shafts

07 p0827 A73-20533

Texture and anisotropy of the thermal emf of sheet titanium

09 p1099 A73-21969

Inertial emf due to thermal convection in a rotating plasma.

10 p1254 A73-24194

Quasi-periodic oscillations in a nonautonomous oscillator

14 p1728 A73-30268

Titanium carbide nitride and zirconium niobium carbide solid solutions electromotive forces, examining temperature-concentration dependencies, carbide and carbonitride conductivity mechanisms, resistivity and Hall effect

18 p2325 A73-36964

Turbulent mean emf in presence of nonvanishing mean conducting fluid flow, modifying Green tensor of induction equation for constant strain rate velocity fields

23 p2969 A73-44050

Linear system resonance effects in single loop controlled frequency tank circuit with variable capacitor under variable or constant emf

24 p3074 A73-44591

ELECTROMYOGRAMS

U ELECTROMYOGRAPHY

ELECTROMYOGRAPHS

U ELECTROMYOGRAPHY

ELECTROMYOGRAPHY

Peripheral electromyography spike and ventral root unit discharge intervals during tonic vibration reflex of cat soleus motoneuron

01 p0008 A73-10410

Electromyographic study on human standing posture in experimental hypogravic state.

01 p0013 A73-11211

Muscular activity control mechanism interactions in vertical posture maintenance from stabilogram, mechanogram and electromyogram data

02 p0137 A73-12119

EMG measurement on male adults for muscular relaxation reaction time interval from light stimulus onset to elbow flexor response

03 p0267 A73-13699

Variability of normal glabellar and supraorbital reflexes in man

03 p0261 A73-13748

The role of extrinsic vagal innervation in the motility of the smooth-muscle portion of the esophagus - Electromyographic study in the cat and the baboon

03 p0262 A73-13785

Method for quantitative estimation of the functional state of the motor apparatus

03 p0268 A73-13822

EMG from smooth musculature /uterus, ureter, gut/ in unrestrained animals monitored by telemetry.

03 p0271 A73-14297

Reliability of electromyographic measurements by means of surface electrodes

04 p0412 A73-15520

Contributions of quick and slow muscle fibers to changes in the electrical activity of skeletal muscles in rats under acute and chronic effects of cold

08 p0931 A73-21323

Possibility of modeling the relationship between the intracellular potential of individual muscle fibers and the overall electromyogram for tonic muscles

10 p1179 A73-23810

- Electromyographic alterations in articular muscles during emotional shifts
10 p1180 A73-24328
- Posture responses of upper limb muscles during electric stimulation of the vestibular apparatus
11 p1317 A73-26087
- Human average evoked potential distribution over scalp to associate cortical electrical activity with voluntary movement, reacting to EMG activity
14 p1714 A73-29990
- Technique for recording muscle biopotentials by means of implanted electrodes
15 p1839 A73-31799
- Electromyographic study of repetitive fasciculation potentials in triceps and adductor pollicis in normal subjects and patients with motor neuron diseases, noting postcontraction pause
20 p2514 A73-39761
- Variations in the motor potential with force exerted during voluntary arm movements in man.
21 p2638 A73-41013
- Conditional computer analysis of the onset-to-onset duration of spikes from the electromyographic interference pattern of extraocular muscles.
22 p2802 A73-41731
- Signal/noise ratio in the recording of human nerve-action potentials.
22 p2814 A73-42372
- Reflex arch lability in rabbits at synchronous maximum frequency of electromyographic and muscle stretching vibration measurement
22 p2807 A73-42659
- Action of stable and pulsed noise on the processes of skeletal muscle excitation
22 p2815 A73-42662
- ELECTRON ACCELERATORS**
- NT BETATRONS**
- Interaction of an intense electron beam with a homogeneous and a nonhomogeneous plasma
04 p0478 A73-15031
- Crab Nebula magnetic field origin and internal electron acceleration mechanism nature
13 p1673 A73-28225
- Particle acceleration by a moving laser focus, focusing front or ultrashort laser pulse front.
14 p1757 A73-30338
- Pair production near energy threshold by electron oscillation and acceleration to relativistic velocities at laser beam focus with plasma wave excitation
23 p2989 A73-44121
- ELECTRON ATTACHMENT**
- Negative oxygen molecular ion formation in low energy electron collision and attachment obtaining capture cross section and resonance width
14 p1777 A73-30775
- ELECTRON AVALANCHE**
- The degradation of MOS transistors resulting from junction avalanche breakdown.
01 p0023 A73-10648
- Ionizing potential wave analysis for gas breakdown, noting photoionization role in avalanche propagation and velocity, electron densities and temperature as function of electric field
02 p0197 A73-12063
- Drift of the breakdown voltage in highly doped planar junctions.
09 p1064 A73-23047
- Study of the behavior of a monostable transistor circuit in the avalanche mode
10 p1195 A73-24413
- Avalanche mode I-V characteristics of diffused and alloyed junction transistors at large collector currents
10 p1196 A73-24609
- Confirmation of an electron avalanche causing laser-induced bulk damage at 1.06 micron.
11 p1377 A73-26227
- Characteristics of amplitude discriminators built with transistors operating in the avalanche mode
12 p1479 A73-27209
- Avalanche transistor circuit with controlled S shaped I-V characteristics, discussing equivalent circuits and operating points stability
13 p1591 A73-28731
- A simple theory of breakdown for nonlignit gases in fields of any frequencies ranging from low to optical
13 p1663 A73-29165
- Inexpensive fast solid state current drive circuit for injection lasers, using parallel conventional transistor switches operated at avalanche breakdown for pulse generation
16 p2024 A73-33400
- Continuous uniform excitation of medium-pressure CO₂ laser plasmas by means of controlled avalanche ionization.
17 p2183 A73-34207
- Avalanche properties of low-power epitaxially-planar transistors
18 p2293 A73-36719
- Silicon-on-sapphire thin film junction diodes, investigating second breakdown onset delay time and minimum energy dependence on high resistivity side heating
20 p2536 A73-39415

- Surface and bulk laser-damage statistics and the identification of intrinsic breakdown processes.
21 p2714 A73-40758
- Optimum design of electron beam-semiconductor linear low-pass amplifiers. II - Output capabilities.
23 p2958 A73-43454
- Self-sustaining Penning avalanche discharge in crossed electric and magnetic fields, discussing anode surface boundary effects and maximum discharge intensity conditions
23 p3015 A73-44345
- Switching transients in conducting channel-broadened p-n-p-n structure thyristors, predicting voltage change during current growth avalanche phase and settling at saturation point
24 p3072 A73-44932
- Parameters of low-power transistors in the avalanche mode of operation
24 p3072 A73-44934

ELECTRON BEAM WELDING

- Glow discharge electron guns for welding.
01 p0055 A73-10113
- Vibrational and energy spectra of welding electron beam interacting with beam produced plasma, noting interaction length effect on instability
04 p0454 A73-15609
- Some fatigue properties of welded high temperature alloys.
08 p0978 A73-21241
- Problems in electron-beam welding of non-ferrous metals.
08 p0973 A73-21243
- Effect of process variables on partial penetration electron beam welding.
10 p1223 A73-23629
- Vibrational and energy spectra of welding electron beam interacting with beam produced plasma, noting interaction length effect on instability
10 p1224 A73-24199
- An investigation into the electron beam welding of five non-ferrous alloys.
11 p1372 A73-25125
- Localized hydrogen in titanium welds.
11 p1375 A73-26358
- Electron-beam welding of small components
12 p1504 A73-27989
- Precipitation in EB welded beryllium ingot sheet.
14 p1759 A73-30146
- Book - Welding and welding technology.
17 p2177 A73-34454
- An accurate method for determining electron beam welding voltages.
19 p2435 A73-38001
- Scribe line technique detects incomplete fusion in EB welds.
21 p2708 A73-41251
- Application of electron beam welding to aircraft turbine engine parts.
22 p2866 A73-42196
- Fabrication techniques for Ti alloys in aerospace applications, discussing hot forming, electron beam and diffusion welding under vacuum and stress relaxation annealing
23 p2985 A73-43911

ELECTRON BEAMS

- Computed secondary-electron and electric field distributions in an electron-beam-controlled gas-discharge laser.
01 p0058 A73-10130
- Electron beam pumped super radiant light source.
01 p0058 A73-10311
- Working prototype image dissector photoelectron beam scanning by crossed electric and magnetic fields to measure beam density distribution in proton synchrotron
01 p0048 A73-10528
- Flying-spot scanned or computer controlled electron beam fabrication system for generating high packing density pattern of LSI microelectronic circuit components
01 p0023 A73-10548
- Capture of plasma electrons by the field of a wave that is excited by an ion beam
01 p0084 A73-10632
- Relativistic dispersion equation for a circular waveguide with a rotating tubular electron beam, allowing for the effect of the space charge
01 p0017 A73-10982
- Theory of the signal suppression effect in an M-type TWT amplifier with preliminary modulation of the electron beam
01 p0025 A73-10983
- Two-beam TWT /electron-wave TWT/ under large input-signal conditions - Effects of parameters
01 p0025 A73-10985
- Experimental investigation of a test-model two-beam TWT /electron-wave TWT/
01 p0025 A73-10986
- Analysis of a dual-signal balanced TWT amplifier
01 p0025 A73-10988
- Investigation of the structure of an electron beam formed by a high-perveance triode gun under controlled-current conditions
01 p0025 A73-10989

- Energy spectra of modulated relativistic electron beam as function of plasma density at beam-plasma interaction region boundary
01 p0086 A73-11284

- Transfer equations for high-energy electrons and photons in magnetic fields.
01 p0080 A73-11309
- Heating of plasma by high-energy electrons, and nonthermal X-ray emission in solar flares.
01 p0093 A73-11313
- Equilibrium model for force-free relativistic electron beam, obtaining solution with maximum beam radius and maximum axial current
02 p0198 A73-12070
- Electromagnetic self induced vibrations in homogeneous unbounded electron beam moving with time dependent velocity, noting longitudinal and transverse wave generation
02 p0198 A73-12102
- Electron beam heating test arrangement for high temperature testing of refractory materials in vacuum, describing temperature control systems
02 p0150 A73-12220
- Injection of an electron beam into a plasma confined by a conducting shell.
03 p0347 A73-14093
- Incoherent excitation of plasma oscillations by an almost-monoenergetic relativistic beam.
03 p0347 A73-14102
- Electron beam technique for evaporating titanium and silicon oxides antireflection coatings on solar cells, noting humidity and thermal resistances and UV radiation darkening
03 p0256 A73-14228
- Estimates of dense plasma heating by stable intense electron beams.
03 p0348 A73-14438
- Amplification of signal by Cerenkov resonance interaction.
04 p0415 A73-14958
- Quasi-linear equations for uniform plasma instabilities connected with potential oscillations, noting non-relativistic electron beam relaxation and abnormal plasma resistance
04 p0477 A73-15017
- Interaction of an intense electron beam with a homogeneous and a nonhomogeneous plasma
04 p0478 A73-15031
- Influence of external high-frequency modulation of the electron beam on ion heating during beam-plasma interaction
04 p0478 A73-15032
- Investigation of a dense plasma produced by an electron beam in a magnetic mirror
04 p0479 A73-15040
- Parametric electron-beam instability in a spatially periodic electric field
04 p0479 A73-15043
- Multifrequency modulation of electron beam for instability oscillations control and energy transfer to plasma particles
04 p0479 A73-15044
- Physical phenomena of controlled experiments in earth magnetosphere using test particles, radio emission and electron and ion beams
04 p0443 A73-15342
- Use of an electron beam for low-temperature plasma measurement in the magnetosphere and interplanetary space.
04 p0450 A73-15553
- Electromagnetic-emission energy flux during the development of beam instability in a magnetically confined plasma
04 p0481 A73-15607
- The deposition of multicomponent phases by ion plating.
04 p0456 A73-15758
- Preparation of alloy deposits by continuous electron beam evaporation from a single rod-fed source.
04 p0456 A73-15761
- Electron beam float zone melting and vacuum degassing of niobium single crystals.
04 p0456 A73-15762
- Minimum noise coefficients of M-type microwave beam amplifiers with crossed fields taking into account distributed losses in slow wave structure
04 p0429 A73-15922
- O-type synchronous electron beam waves interaction with electrostatically structured traveling wave, noting linear gain dependence on beam current and magnetic field
05 p0556 A73-16066
- Landau attenuation in a plasma excited by a monochromatic electron beam
05 p0601 A73-16394
- Investigation of a gallium arsenide laser pumped by an electron beam
05 p0584 A73-16553
- Electron beam fabrication of submillimeter diameter mixer diodes for millimeter and submillimeter wavelengths.
05 p0559 A73-16811
- Experimental observation of heating of a hydrogen plasma by a relativistic electron beam.
05 p0603 A73-17161

- Electromagnetic radiation caused by the two-stream instability in a bounded plasma. 06 p0726 A73-17416
- Characteristics of a vacuum discharge triggered by an electron beam. 06 p0722 A73-17424
- Combined plasma heating by an electron beam and an intense ion-cyclotron wave 06 p0729 A73-18106
- Waveguide resonator structure of an electron-beam-pumped semiconductor laser. 06 p0702 A73-18584
- Collective processes in the passage of high-current relativistic beams through a gas and a plasma. 06 p0732 A73-18714
- Difference frequency generation using non-linear interaction between a modulated electron beam and a collisionless plasma. 06 p0733 A73-18839
- Alternating current instability produced by the two-stream instability. 07 p0857 A73-19528
- Electron-beam-controlled CO₂ laser amplifiers. 07 p0835 A73-19639
- Dislocation structure of tungsten single crystals grown by electron-beam zone refining 07 p0841 A73-20523
- Rotational temperature measurements in nitrogen at hypersonic flow using an electron beam technique [ONERA, TP NO. 1206] 07 p0853 A73-20605
- High-energy electron-beam deposition onto a hot graphite surface. 08 p0990 A73-21210
- Ultrarelativistic cosmic plasma analysis of high-density electron beams transport across strong magnetic fields with application to pulsar NP 0532 spectrum 08 p0999 A73-21334
- Electron admittance and efficiency of the output cavity of a klystron 08 p0948 A73-21557
- Accelerated generation of deflecting voltages by the functional beam-control method 08 p0967 A73-21589
- Observation of beam-plasma interaction in a toroidal plasma in a large electric field. 08 p0993 A73-21631
- Ultrarelativistic electrons beam steady injection into plasma filled half space, using weak turbulence theory for assumed beam excited oscillations interaction 08 p0994 A73-21698
- An X-ray tube emitting soft and hard radiation with controlled focusing 08 p0969 A73-21721
- Parametric instability of an electron beam modulated by an external electrostatic field 09 p1123 A73-21878
- Quasi-linear relaxation of a monoenergetic relativistic electron beam in an external magnetic field 09 p1124 A73-21903
- Excitation of low-frequency oscillations by an electron beam in a hot plasma confined in a magnetic mirror 09 p1125 A73-21907
- Acceleration of ions during the formation of an electron beam from a stationary vacuum-arc plasma 09 p1125 A73-21909
- Experimental investigation of the excitation functions of thallium atoms 09 p1121 A73-21952
- Use of electron and proton beams for production of very low frequency and hydromagnetic emissions. 09 p1074 A73-22061
- The calibration of electrostatic analyzers and channel electron multipliers using laboratory simulated omnidirectional electron beams. 09 p1080 A73-22104
- Time behavior of the internal Q switching in GaAs lasers under electron-beam excitation. 09 p1092 A73-22245
- Semiconductor electron-beam-pumped lasers of the radiating mirror type. 09 p1092 A73-22248
- On the interaction of the electromagnetic field with electron beams in resistive wall waveguides 09 p1062 A73-22324
- Starting conditions for backward-wave tubes with preliminary modulation of the electron beam 09 p1063 A73-22453
- Experimental investigation of the excitation of Ar II and Kr II during electron-ion collisions 09 p1122 A73-22593
- Electron-beam excitation of finite-sized plasma near the lower-hybrid frequency. [TTU-SR-2] 09 p1129 A73-22638
- Kinetic theory of the spatial instability of a radially bounded plasma-electron beam system with a given radially nonhomogeneous plasma configuration 09 p1129 A73-22688
- Investigation of the heating mechanism for the electron component of a plasma under beam-instability conditions in a mirror confinement system 09 p1130 A73-22703
- Nonlinear theory of the interaction of a monoenergetic beam with a dense plasma 09 p1130 A73-22706
- Nonlinear theory of a relativistic monotron 09 p1065 A73-23086
- Recrystallization of electron-beam-melted tungsten with tantalum and zirconium carbide additions 09 p1106 A73-23189
- Structure and properties of electron-beam-melted 1Kh12N3M3B steel 09 p1107 A73-23194
- Nanosecond pulse amplification in electron-beam-pumped CO₂ amplifiers. 09 p1097 A73-23336
- Spontaneous Cerenkov emission of longitudinal waves produced by single particle and cylindrical electron beam moving inside magnetosphere along magnetic field 10 p1269 A73-24722
- Dispersion equation of parametric longitudinal LF instability of electromagnetic wave propagation in bounded electron beam in metallic waveguide 10 p1257 A73-24876
- Experimental investigation oscillations in a synthesized plasma jet 10 p1257 A73-24877
- Statistical velocity and temperature characteristics of turbulent electron beams in crossed HF electric and magnetic fields, comparing with Brillouin flow 10 p1258 A73-24880
- Strict calculation of static fields in devices for periodic electrostatic focusing /PEF/ of electron beams 10 p1197 A73-24882
- Electric current in pressurized N₂, CO₂, and their mixtures under conditions of strong ionization by an electron beam 10 p1230 A73-24883
- Observation of stationary acceleration of ions to energies of 2 to 20 keV in a nonisothermal plasma 10 p1258 A73-24888
- Measurement of the potential distribution in the vicinity of an electron beam with the aid of a thermal probe 10 p1258 A73-24889
- Stimulated emission due to the interaction between a relativistic high-current beam and a plasma 11 p1403 A73-25241
- Quasi-optical diffraction-type radiation generator 11 p1331 A73-26159
- Nonlinear theory of Ubitron microwave oscillator device using fast electromagnetic wave-fast electron beam interaction in spatially periodic magnetostatic field 11 p1332 A73-26164
- A plasma-beam discharge laser. 11 p1377 A73-26181
- Contribution to the nonlinear theory of kinetic instability of an electron beam in plasma. 11 p1405 A73-26183
- Current and fields reduced in plasmas by relativistic electron beams with arbitrary radial and axial density profiles. 11 p1407 A73-26560
- Macroscopic equilibria of relativistic electron beams in plasmas. 11 p1407 A73-26561
- The possibility of microfission explosions by laser or relativistic electron-beam high-density compression. 11 p1378 A73-26657
- Stability of a magneto-active plasma with a relativistic electron beam, situated in a high-frequency electric field 12 p1527 A73-26927
- Analysis of the behavior of the electron velocity distribution function of beam interacting with a plasma 12 p1527 A73-26933
- Study of the effect of a plasma on the microwave radiation of a helical beam in a waveguide 12 p1527 A73-26935
- Braking of electron beams in a plasma with a high level of Langmuir turbulence 12 p1527 A73-26956
- Electron-beam ionized pulsed CO₂ laser 12 p1506 A73-27216
- Dynamics of strongly nonlinear beam-plasma interaction. [IPPCZ-167] 12 p1529 A73-27434
- Possible utilization of a vapor, formed by the action of a high-power electron beam on a target, as an active medium for stimulated emission of light. 12 p1507 A73-27517
- KGP-2 - An electron-beam pumped cadmium sulfide laser. 12 p1507 A73-27520
- Electron-beam tube with a semiconductor target - A n-electron-beam-pumped scanning laser. 12 p1508 A73-27526
- Investigation of the heating of electrons of a dense beam-plasma discharge in strong magnetic fields 12 p1529 A73-27942
- Two-stream instability heating of plasmas by relativistic electron beams. 13 p1663 A73-28186
- Contribution to the theory of the natural vibration spectra of a nonequilibrium resonant cavity 13 p1589 A73-28290
- Apparatus and techniques for electron beam fluorescence probe measurements. 13 p1612 A73-28365
- The possibility of storing laser radiation scattered by an electron beam. 13 p1627 A73-28662
- Intermittent generation of microwave oscillations through a plasma-beam interaction. 13 p1583 A73-28664
- Interaction between a monoenergetic nonrelativistic electron beam and the surface potential oscillations of a plasma 13 p1666 A73-28955
- Investigation of the feasibility of the injection of electrons into heliotron-type closed magnetic mirror configurations 13 p1666 A73-28957
- Investigation of the absorption and emission of electron-beam-induced waves in an inhomogeneous magnetoactive plasma 13 p1666 A73-28958
- Translational temperature and atomic velocity distribution functions in rarefied binary gas jets by electron beam excited Doppler line measurement 13 p1618 A73-29163
- Measurement of rarefied gas flow rates from the drift of an ion mark produced by an electron beam 13 p1619 A73-29167
- Electrostatic and magnetic fields methods comparison for small angle scanning of electron beam, considering particle trajectories, field energy and circuit electrical parameters 14 p1732 A73-29913
- Performance comparison of pulsed discharge and E-beam controlled CO₂ lasers. 14 p1756 A73-29918
- Ionospheric plasma waves instabilities induced by energetic electron beam fired perpendicular to magnetic field 14 p1747 A73-29967
- Instabilities in a system of a plasma and an intense relativistic electron beam. 14 p1780 A73-30122
- Interaction between a plasma and an electron beam modulated by low-frequency oscillations. 14 p1780 A73-30335
- Plasma heating by an intense electron beam. 14 p1781 A73-30553
- Detection of a feedback in a plasma-electron beam system 14 p1781 A73-30585
- Relativistic electron beam focusing by neutral gas filled conical guide tube, comparing efficiency, fluence gain, energy loss and pressure variation predictions with experiments 14 p1777 A73-30658
- Effect of induced axial electric field on a relativistic electron beam pulse propagating through a plasma. 14 p1777 A73-30661
- Investigation of low-frequency instabilities in a linear plasma betatron 14 p1782 A73-30805
- Magnetic neutralization and discharge neutralization of an electron beam injected into a magnetoactive plasma 14 p1782 A73-30807
- Theory of shot noise depression in a modified diode 14 p1737 A73-30943
- Quasi-classical calculation of the power output of a cyclotron resonance maser 14 p1758 A73-30944
- Investigation of the structure of electron bands in In_{1-x}/Ga_x/As_{1-y}/P_y on the basis of luminescence 15 p1923 A73-31716
- Third-order treatment of combined effects of space charge and external fields on cylindrical ion and electron beams. 15 p1915 A73-31933
- Contribution to the theory of electron-beam stability in an inhomogeneous dielectric medium 15 p1920 A73-32302
- Heating of a high-density plasma with the aid of powerful electron beams 15 p1920 A73-32308
- Excitation of an electron semicyclotron wave and its harmonics during the interaction of high-current opposed electron beams 15 p1920 A73-32312
- Limitation of beam instability as a result of the capture of plasma electrons by the wave 15 p1920 A73-32320
- Electromagnetic emission during surface wave excitation by a relativistic electron beam in a plasma 15 p1921 A73-32321
- Quasilinear relaxation of a monoenergetic relativistic electron beam in an external magnetic field. 15 p1922 A73-32628
- Electron-beam excitation of low-frequency waves in a hot plasma confined in a mirror machine. 15 p1922 A73-32632
- Ion acceleration in the formation of an electron beam in a vacuum arc. 15 p1922 A73-32634

Secondary electrons and energy per ion-pair in a thermal gas for electron, proton and X-ray ionization. 16 p2052 A73-32826

The problem of interaction between a relativistic electron beam and plasma in a waveguide. 16 p2040 A73-32899

Dynamic stabilization of plasmas by means of a high-frequency-modulated electron beam. 16 p2041 A73-33326

Nonlinear radial electron beam focusing in plasma under beam-plasma instability, showing irreversibility conditions dependence on electromagnetic wave propagation mode. 16 p2043 A73-34056

Nonlinear frequency shift and damping stabilization mechanisms of unstable plasma waves in hot beam-cold plasma system. 16 p2043 A73-34058

Effects of electron-microscope design features on the accuracy of the microprobe diffraction method. 17 p2164 A73-34176

Generation of intense infrared radiation from an electron beam propagating through a rippled magnetic field. 17 p2214 A73-34204

Parametric instability of an electron beam modulated by an external electrostatic field. 17 p2215 A73-34302

Excitation of electromagnetic waves in a plasma with a relativistic electron beam. 17 p2216 A73-35159

A three-dimensional picture of the development of instability during the interaction of a modulated electron beam with a plasma. 17 p2216 A73-35170

Electron-beam irradiated discharges for initiating high-pressure pulsed chemical lasers. [AIAA PAPER 73-645] 18 p2322 A73-36259

Entry of a high-frequency longitudinal field into a nonequilibrium plasma. 18 p2339 A73-36554

Interaction between a tubular electron beam and a plasma. 18 p2339 A73-36555

Effect of atom self-diffusion on evaporation processes and porosity development in solid bodies during electron-beam treatment. 18 p2320 A73-36900

Deceleration of electron beams in a plasma with a high level of Langmuir turbulence. 19 p2469 A73-38133

Electron beams as carriers of optical coherence. 20 p2570 A73-38621

Ionization of a neutral medium by an electron beam. 20 p2597 A73-39279

Free atom and molecule energy levels studied by electron scattering spectroscopy, discussing energy losses, monochromated electron beams, particle resonance and electric fields. 20 p2520 A73-39635

On the diffraction of dense electron beams in quantum mechanics. 20 p2595 A73-39766

An accelerated electron beam position and shape meter. 21 p2699 A73-40172

Variable pulse-length electron beam CO₂ laser. 21 p2716 A73-40973

Coupled mode analysis for solid travelling-wave amplifiers. 21 p2665 A73-41121

Dispersion equation of parametric longitudinal LF instability of electromagnetic wave propagation in bounded electron beam in metallic waveguide. 21 p2744 A73-41651

Oscillations in a synthesized plasma jet. 21 p2749 A73-41652

Statistical velocity and temperature characteristics of turbulent electron beams in crossed HF electric and magnetic fields, comparing with Brillouin flow. 21 p2749 A73-41655

Static fields for periodic electrostatic focusing of electron beams. 21 p2668 A73-41657

Electrical current in electron-beam ionized N₂ and CO₂. 21 p2749 A73-41658

Steady-state acceleration of ions to 2-20 keV in a nonisothermal plasma. 21 p2749 A73-41663

Measurement of the potential distribution near an electron beam using a thermionic probe. 21 p2749 A73-41664

Theory of eigenmode spectra of a nonequilibrium resonator. 22 p2830 A73-41814

Wave spectrum analysis of electron beam-plasma longitudinal electrostatic fluctuations, finding triplet wave line shape and intensity and dispersion relations. 22 p2891 A73-42240

Divergence of the output radiation of electron-beam-pumped 'radiating mirror' lasers. 22 p2869 A73-42258

Stability of a magnetoactive plasma with a relativistic electron beam in an RF electric field. 22 p2891 A73-42261

Variation of electron velocity distribution function in the beam-plasma interaction. 22 p2891 A73-42267

Effect of a plasma on the microwave radiation from a helical beam in a waveguide. 22 p2892 A73-42269

Optimum design of electron beam-semiconductor linear low-pass amplifiers. II - Output capabilities. 23 p2958 A73-43454

Energy spectra of modulated relativistic electron beam as function of plasma density at beam-plasma interaction region boundary. 23 p3009 A73-43505

Observation of doping profiles in Gunn diodes with a scanning electron microscope using the beta-conductivity. 23 p2960 A73-43777

Interaction of a monoenergetic nonrelativistic electron beam with electrostatic surface oscillations in a plasma. 23 p3013 A73-44307

Electron injection through the diverter in a heliotron. 23 p3013 A73-44309

Absorption and emission of waves generated by an electron beam in an inhomogeneous magnetoplasma. 23 p3013 A73-44310

Equilibrium configurations of electron beams in a plasma. 23 p3014 A73-44338

Ion acceleration by relativistic electron beam extracted from discharge plasma, discussing proton acceleration and beam composition and energy distribution. 23 p3014 A73-44339

Calculation of the electron trajectories in helical beams produced by axisymmetric magnetron-type injection guns. 23 p2961 A73-44346

Combined heating of a plasma by an electron beam and an intense ion-cyclotron wave. 24 p3114 A73-44495

Stability of an electron beam in an inhomogeneous dielectric medium. 24 p3114 A73-44610

Heating of a dense plasma by a powerful electron beam. 24 p3114 A73-44616

Excitation of electron-cyclotron waves by high-current counter-streaming electron beams. 24 p3115 A73-44620

Electron beam concentration enhanced by a laser-produced plasma. 24 p3115 A73-44921

Experimental determination of the nonlinear interaction in a one dimensional beam-plasma system. 24 p3117 A73-45458

Nonlinear saturation of the relativistic beam-plasma instability in the presence of ion density fluctuations. 24 p3118 A73-45465

ELECTRON BOMBARDMENT

Diode behaviour in an electron-bombardment ion engine. 01 p0090 A73-10112

Control of electron bombardment ion engine for stationary satellite. 01 p0090 A73-11110

Comparison of data on irradiation of germanium by 1- and 28-MeV electrons. 02 p0201 A73-12592

High and low thrust systems for primary and auxiliary spacecraft propulsion, noting electron bombardment electrostatic thruster for north-south station-keeping. 03 p0355 A73-13435

Total electron backscatter and backemission yields from metals bombarded at several angles by 0.4 to 1.4 MeV electrons. 05 p0604 A73-16514

Magnetophotocconductivity of semi-insulating GaAs and its behavior upon electron bombardment. 06 p0738 A73-18369

Some characteristics of a miniature pulsed laser with electron excitation. 07 p0836 A73-20136

Electron bombardment ion rocket engine with large diameter and divergent magnetic field for efficiency improvement, considering application as source in plasma wind tunnel. 07 p0868 A73-20486

Evidence of fireball phenomena in hollow cathode of electron bombardment ion thrusters. 09 p1136 A73-23462

Volatilization studies on a terrestrial basalt and their applicability to volatilization from the lunar surface. 10 p1275 A73-23738

Design and performance of deflected-beam electron-bombarded semiconductor amplifiers. 12 p1478 A73-27113

Nickel single crystal target ionization by high-voltage electron beam bombardment, using time of flight mass spectroscopic analysis. 13 p1663 A73-28666

Optical study of charge exchange collisions between He⁺ and CO₂. 16 p2039 A73-33675

A new technique for Auger analysis of surface species subject to electron-induced desorption. 17 p2175 A73-35757

Cathodoluminescence of ruby 0.05 wt % at high temperatures. 21 p2752 A73-40797

Influence of mechanical treatment of the resonator on the parameters of an electron-beam-pumped cadmium sulfide laser. 22 p2869 A73-42259

Oxygen-W/100/ surface interactions investigated simultaneously by secondary ion mass spectrometry (SIMS) and electron induced desorption (EID). 24 p3066 A73-45330

ELECTRON BUNCHING

Hypotheses for excess background radiation at 200-500 km, suggesting single high energy electrons or electron clusters. 08 p0999 A73-21336

Electron admittance and efficiency of the output cavity of a klystron. 08 p0948 A73-21557

Emission from a bunch of charged particles in multiple transit through a cylindrical resonant cavity. 09 p1061 A73-21885

Optimal electron grouping arrangements in multi-resonator klystrons. 14 p1736 A73-30565

Allowance for the influence of the space charge in the kinematic theory of microwave devices. 15 p1850 A73-31491

Dynamic electron bunching theory applied to moving solid particles and liquid droplets, describing synchronization mechanism for mechanical particles in oscillating gas. 20 p2598 A73-39494

Monoenergetic particle beam bunching instabilities in homogeneous plasma due to secondary emission wave interactions. 22 p2890 A73-41813

ELECTRON CAPTURE

Capture of plasma electrons by the field of a wave that is excited by an ion beam. 01 p0084 A73-10632

Some parameters affecting the poleward boundary of trapped electrons. 03 p0363 A73-13869

Direct nuclear-to-electric power conversion based on Sr 90 electron emission and collection system, noting spacecraft applications. 09 p1119 A73-22828

Use of translational energy measurements in the evaluation of the energetics for dissociative attachment processes. 10 p1251 A73-24244

Limitation of beam instability as a result of the capture of plasma electrons by the wave. 15 p1920 A73-32320

On electron trapping in ion sound waves in turbulent plasma. 16 p2040 A73-32800

Determination of hole and electron traps from capacitance measurements. 24 p3119 A73-44405

ELECTRON COLLISIONS

U ELECTRON SCATTERING

ELECTRON COUNTERS

On-line digital recording of stellar spectrum with photoelectron-counting spectrophotometer, noting discrimination against spurious signals from noise and pulse height distribution measurements. 01 p0048 A73-10531

High voltage square pulse oscillator and recording circuit for negative and positive autoelectron emission properties. 01 p0024 A73-10795

Channel electron multiplier prepared from shaped glass tubing with inner conductive coating, discussing electron and photon detection characteristics. 02 p0146 A73-11954

Cleaning and activation of beryllium-copper electron multiplier dynodes. 02 p0146 A73-11966

Intensity and energy spectrum calculation of albedo electrons recorded in cosmic particle showers by gas discharge counters. 07 p0823 A73-19429

Digicon multichannel image tube photoelectron counter for astronomical spectroscopy, discussing design information density and accuracy, noise and quantum efficiency. 08 p0971 A73-21747

Diffraction pattern scanning display technique using electron detector in microscope final image, discussing gold particle demonstration, lens configuration, illumination angle and sawtooth currents. 21 p2700 A73-40466

A new ion and electron detector for ion cyclotron resonance spectroscopy. 24 p3089 A73-44816

ELECTRON DECAY RATE
Trapped electrons decay to ground state via nonthermal process in lunar samples during thermoluminescence emission at lunar day temperatures, proposing quantitative model 03 p0369 A73-13101

Influence of atom-atom collisions on electron density decay in laser-produced helium plasmas. 16 p2041 A73-32944

ELECTRON DENSITY [CONCENTRATION]
NT **ELECTRON DENSITY PROFILES**
NT **IONOSPHERIC ELECTRON DENSITY**
NT **MAGNETOSPHERIC ELECTRON DENSITY**
Electron density measurements in time varying plasmas with a microwave reflectometer system. 01 p0044 A73-10120

Three-dimensional effects on electron density in a blunt body laminar boundary layer. 01 p0002 A73-10731

Electron density measurement in a pulsed ablation accelerator plasma. 02 p0198 A73-12110

Collisional-radiative coefficients and population coefficients of hydrogen plasma. 02 p0198 A73-12347

Electron and muon density fluctuations, trajectory distribution and azimuthal symmetry in cosmic ray air showers 02 p0209 A73-12673

Alloy hardening and softening in binary molybdenum alloys as related to electron concentration. 03 p0323 A73-13300

Influence of electron concentration on the formation of phases with bcc, fcc, and hexagonal close packed lattices in certain transition-metal alloys 03 p0324 A73-13510

Determination of exospheric electron content from group delay and Faraday rotation observations of geostationary satellite signals. 03 p0300 A73-13636

Application of electron content observations in navigational ranging. 03 p0275 A73-13654

Investigation of electronic and gasdynamic parameters of hypersonic wakes behind models moving in argon. 03 p0296 A73-14099

Electron-ion density fluctuations in turbulent highly ionized Ar plasma, comparing experimental results with theory based on quasi-static formulation of Boltzmann equation 04 p0479 A73-15192

Interstellar magnesium abundances and electron density in the direction of Orion and Cassiopeia. 04 p0502 A73-15976

Recombination radio lines in H I regions. 04 p0504 A73-16026

Laser plasma generation with high electron densities by photoionization from flashlamp or coherent UV source from harmonic generation or gas lasers 05 p0601 A73-16362

Electron density reduction in high temperature air via boron powder aerosol, presenting shock tube data for temperature range 2800-4200 K and pressure range 1-2 atm [AIAA PAPER 73-261] 05 p0603 A73-16982

Impurity concentration relationship to electrons and holes density and potential fluctuations in completely compensated crystalline semiconductors with randomly distributed donors and acceptors 06 p0735 A73-17976

Computer simulation model of field independent trapping effects on slow Gunn domains in gallium arsenide, noting double symmetry electron-ion density distributions 06 p0737 A73-18368

Electrical characteristics of the plasma in a CO laser. 06 p0703 A73-18614

Concentration dependence of the hardness of nonstoichiometric group IV and V transition metal carbides 06 p0710 A73-18658

Electron density distribution in a coronal condensation 07 p0902 A73-20321

Threadlike solar coronal streamer observation at 20 July 1963 eclipse, noting electron density from photometric analysis 08 p1002 A73-20763

Solar plasma electron density and temperature measurement by Mars 2 and Mars 3 orbiter-borne retarding potential analyzers, considering solar wind shock front interaction role 09 p1126 A73-22263

Determination of the electron concentration in the boundary layer of air mixed with ablation products of an asbestos plastic 09 p1128 A73-22622

Nonequilibrium transport process calculation by theoretical microscopic model for interaction between

ionized gas and solid particles in suspension, noting free electron concentration change 09 p1130 A73-22826

Electron intensities over auroral arcs from rocket flight, noting electron phase-space density increase with northward progress 09 p1078 A73-22833

Obliquely incident electromagnetic wave propagation through plane-stratified weakly ionized plasma with electron density inhomogeneity scale length comparable with mean free path 09 p1052 A73-23077

Flux magnitude and single transition probabilities as function of electron density and temperature in relaxation model ionization and recombination channels 10 p1253 A73-23503

Investigation of the electrical explosion of conductors by holographic methods 10 p1248 A73-23507

Microwave reflection from detonation waves in equimolar C2H2-O2 at low pressures. 10 p1294 A73-23557

Development and properties of the halo in pinch plasmas 10 p1253 A73-23673

Coronal polar plume observed electron density dependence on assumed density distribution normal to axis, analyzing errors in measurements 10 p1279 A73-24141

Simultaneous determination of the electron temperature and density in the chromospheric-coronal transition region of the sun. 10 p1281 A73-24409

Kinetic equations for time behavior of electron concentration and proton, electron and H I atom temperatures in ionized hydrogen medium 10 p1282 A73-24492

Microwave cavity measurements of electron densities in a shock tube. 10 p1220 A73-24620

Optical orientation of metastable He-3 atoms and its influence on the electron density and on the emission of helium atoms in a plasma 10 p1257 A73-24755

Formula approximating Fermi-Dirac integrals for electron gas density, pressure and internal energy, discussing pressure ionization effect on equation of state in stellar interiors 11 p1417 A73-25261

Spectroscopic measurement method for the electron temperature and density of a focusing discharge of the 'plasma focusing' type 11 p1404 A73-25270

Electronic charge densities in semiconductors. 11 p1408 A73-25374

On the stability of finite difference schemes in transient semiconductor problems. 11 p1408 A73-25438

The 1969 solar occultation of the Crab Nebula pulsar. 11 p1417 A73-25583

Solar corona electron densities and temperatures as function of distance from solar center during 22 September 1968 eclipse 12 p1538 A73-26860

Solar corona streamers polarization, intensity and electron density and temperature during 22 September 1968 total eclipse 12 p1533 A73-26861

Absorption of microwaves by a plasma in a magnetic field in the presence of a large effect due to longitudinal inhomogeneity 12 p1467 A73-26934

Study on ionizing shock waves in argon. III - Thermodynamic properties of the plasma. 12 p1527 A73-27173

Electron-density distribution in a coronal condensation. 12 p1540 A73-27293

Improved three-dimensional mapping of the electron density distribution of the solar corona. 12 p1536 A73-27843

Flare-produced coronal MHD-fast-mode wavefronts and Moreton's wave phenomenon. 12 p1536 A73-27848

Search for quarks using a flash-tube chamber. 13 p1670 A73-28210

Determination of the parameters of a fluctuating plasma from the modulation of microwave signals 13 p1666 A73-28961

Observation of linear polarization of the Crab nebula during an occultation by the solar corona. 13 p1586 A73-29247

Coronal densities and temperatures derived from monochromatic images in the red and green lines. 13 p1685 A73-29364

Time behavior of hydrogen discharge in ST-Tokamak based on measured radial electron temperature and density profiles and ohmic-heating current and voltage 14 p1778 A73-29691

Electrostatic waves in warm random plasmas. 14 p1779 A73-29708

Electron density phase velocity, drift rate and ion temperatures from radar echoes power spectrum near equatorial electrojet 14 p1748 A73-29972

Possibility of electron concentration determination in a plasma with the aid of a gas laser with a nonlinearly rotating absorption cell 14 p1781 A73-30465

The determination of plasma electron density from refraction measurements. 15 p1916 A73-31085

Zone of Poynting vector rotation toward the direction of an applied magnetic field for a wave incident on an inhomogeneous plasma 15 p1919 A73-31707

Effect of H2O, SF6 and CCl3F additions on the electron concentration in highly heated air 15 p1840 A73-31852

Calculation of the electron density in heterogeneous mixtures with allowance for the tunneling effect and for super-barrier reflection 15 p1915 A73-31854

The possible nature of the fine structure of sporadic radio emission from the sun and other cosmic sources having a high density of electromagnetic radiation 15 p1926 A73-31876

High-resolution survey of thermal sources of radio emission at the 8.2-mm wavelength 15 p1938 A73-31952

Pulsar radio emission limiting polarization resulting from passage through magnetoactive plasma, discussing electron density effects 15 p1844 A73-32003

Measurement of density and temperature of a hydrogen plasma using an argon laser. 15 p1920 A73-32257

Ionization oscillations in a plasma in the presence of negative ions 15 p1920 A73-32319

The electric field and structure of a weakly ionized plasma in the vicinity of a small charged body 15 p1921 A73-32322

Model of the chromosphere and the transition layer between the chromosphere and solar corona 16 p2057 A73-32703

The prevalence of second harmonic radiation in type III bursts observed at kilometric wavelengths. 16 p2053 A73-32964

Solar wind density model from km-wave type III bursts. 16 p2053 A73-32965

Test gas properties behind a decelerating shock wave in a shock tube. 16 p2000 A73-33319

Probe design for orbit-limited current collection. 16 p2041 A73-33320

Effect of a sheath on the fields of a probe in a hot magnetized plasma. 16 p2041 A73-33330

Traveling regions of high solar wind density observed in early August 1972. 16 p2056 A73-33460

Recombination rate measurements in nitrogen. 16 p2039 A73-33673

Reflection coefficient of an electromagnetic wave by a plasma column of variable electron density in a waveguide. 16 p1984 A73-33994

Theory of the anomalous skin effect in a plasma with a diffuse boundary 16 p2043 A73-34060

Antenna admittance determination of electron density. 17 p2121 A73-34187

Flux magnitude and single transition probabilities as function of electron density and temperature in relaxation model ionization and recombination channels 17 p2217 A73-35183

Holographic investigation of electrical explosions of conductors. 17 p2212 A73-35187

Late B6 stars line spectra, atmospheric electron density, microturbulence velocity, excitation temperature, flux envelopes and energy distributions 17 p2233 A73-35612

A discussion of the distribution of interstellar matter close to the sun. 17 p2234 A73-35619

Electron temperature and density in the He-Cd12 positive column used for an I+/laser. 17 p2186 A73-35798

A density scale for the interplanetary medium from observations of a type II solar radio burst out to 1 astronomical unit. 18 p2348 A73-37113

Laminar boundary layers in low pressure argon plasma. 19 p2464 A73-37163

Electromagnetic interactions with turbulent plasmas. 19 p2465 A73-37167

Corner expansion flow of ionized argon, calculating electron density, plasma density and recombination rate constant for comparison with measurements 19 p2465 A73-37177

- Effect of collisions on the random electron density fluctuations in a plasma. 19 p2468 A73-37519
- The electron energy and number densities of the Jovian radiation belt. I. 19 p2475 A73-37621
- Protonospheric columnar electron content determination. I - Analysis. 19 p2426 A73-38017
- Gas discharge plasma diagnostics based on polarization frequency of a submillimeter laser radiation 20 p2598 A73-39622
- Local thermodynamic equilibrium validity limits in short spaced cesium plasmas, discussing electron density and temperature, Maxwell and Boltzmann distributions and total pressure 20 p2599 A73-39673
- Studies of collisional preionization in large pinch vessels. 21 p2748 A73-40927
- Determination of electron density and electron collision frequency in a plasma by an RF nonimmersive probe. 21 p2748 A73-40953
- Electron concentrations calculated from the lower hybrid resonance noise band observed by Ogo 3. 22 p2901 A73-41912
- Chromospheric hydrogen and helium spectral lines investigation in solar flares determining plasma and ionization temperatures, energy spectra and electron density 22 p2903 A73-42066
- Dense argon plasma expansion into vacuum or low density partially ionized hydrogen plasma, examining momentum transfer, electron density and electric field effects 22 p2891 A73-42239
- Microwave absorption by a magnetoplasma with a strong longitudinal inhomogeneity. 22 p2891 A73-42268
- Investigation of the electron concentration behind strong shock waves 22 p2893 A73-42385
- Langmuir probe signal analysis of root-mean-square electron density fluctuations in turbulent Ar plasma jet 22 p2893 A73-42394
- Interferometric measurement of thermodynamic variables of rare gas plasmas produced by shock waves 22 p2896 A73-43168
- Pulsars radio observations of magnetic field, electron density and neutral hydrogen atoms in interstellar space 23 p3028 A73-43369
- Concentration effect in semiconductors with bipolar conductivity in an alternating external magnetic field 23 p3017 A73-44046
- Determination of the parameters of a fluctuating plasma from modulation of a microwave signal. 23 p3013 A73-44313
- High-resolution survey of thermal radio sources at 8.2 mm. 24 p3131 A73-44477
- Solar Fe 13 coronal lines relative intensity calculation as function of electron density from cross sections for collisional excitation by protons 24 p3136 A73-44635
- A theory of the origin of the split pair burst emission from the solar corona. 24 p3123 A73-44646
- Changes in the distribution of density and radio scattering in the solar corona in 1971. 24 p3138 A73-45049
- A 337-micron HCN laser interferometer for plasma diagnostics. 24 p3097 A73-45410
- ELECTRON DENSITY PROFILES**
- Computed secondary-electron and electric field distributions in an electron-beam-controlled gas-discharge laser. 01 p0058 A73-10130
- D-region parameters from the extraordinary component of partial reflections. 01 p0036 A73-10329
- Electron temperature measurement in collisional plasma with double probe, noting electron and ion density distribution near isolated electrode under floating potential 01 p0085 A73-10866
- A comparison of two ground-based techniques for measuring D-region electron densities. I. 01 p0042 A73-10905
- A comparison of two ground-based techniques for measuring D-region electron densities. II. 01 p0042 A73-10906
- Changes of electron density with zenith angle, with the sunspot cycle, and during eclipses. 01 p0043 A73-10907
- Electron density profiles in the equatorial lower ionosphere at Thumba. 01 p0043 A73-10908
- Changes of lower ionosphere electron concentrations with solar activity. 02 p0159 A73-12029
- Radioastronomical measurements of ionospheric electron content. 02 p0159 A73-12031
- Ionospheric electron density profiles calculation from ionograms via nomograph relating gradients of possible and actual height in given frequency interval of integration 02 p0159 A73-12184
- The standard profile of the mid-latitude F region of the ionosphere as deduced from bottomside and top-side ionograms. 02 p0163 A73-12301
- Electron production rates and density profiles in D region during solar flares, presenting ionization vertical distribution model 02 p0206 A73-12304
- Preliminary findings of a petrel rocket experiment to investigate the VLF emission 'chorus' in the ionosphere. 02 p0141 A73-12319
- Latitude-time variations of the total number of electrons and of its gradients in the ionosphere at high latitudes 02 p0164 A73-12474
- Automatic N/h, t/ profiles of the ionosphere with a digital ionosonde. 02 p0143 A73-12530
- Minimized calculation errors in phase ionosonde true height reduction technique for electron density profile, noting lowest observable radio frequency 02 p0143 A73-12531
- Study on ionizing shock waves in argon. I - Precursor phenomena. 04 p0436 A73-15974
- Study on ionizing shock waves in argon. II - Ionization relaxation. 04 p0436 A73-15975
- Characteristics of interplanetary electron irregularities according to observations in 1967-1969. 04 p0503 A73-16015
- Temporal variations of the recombination coefficient and electron density profile in the lower ionosphere 05 p0568 A73-16261
- Atmospheric diffusion, radio meteor trail radius and electron density distribution effects on radar echoes time position, noting recorder resolution increase 05 p0617 A73-16613
- Ionospheric electron density profiles model evaluation, considering E region height and thickness seasonal variation 05 p0571 A73-17063
- Vertical distribution of electron concentration in the Northern Hemisphere at the geomagnetic pole /from top-side and ground-based ionospheric sounding data/ 06 p0689 A73-17554
- Scattering of microwaves by a stratified overdense plasma at high collision frequencies. 06 p0732 A73-18780
- D region electron density profiles analytical determination from pulsed wave interaction measurements 07 p0791 A73-19242
- Atomic oxygen formation times obtained from measurements of electron density profiles behind shock waves in air. 07 p0853 A73-19510
- Lower ionosphere electron densities from rocket measurements employing LF radio propagation and DC probe techniques. 07 p0818 A73-19670
- Global electron density distributions from the Ariel 3 satellite at mid-latitudes during quiet magnetic periods. 07 p0819 A73-20054
- Study on the electron density profile in the F1 region. 08 p0961 A73-21653
- Propagation of backward surface wave along an annular plasma guide with azimuthal electron density variation. 09 p1125 A73-21930
- Aurora and the poleward edge of the main ionospheric trough. 09 p1073 A73-22058
- Ionospheric electron density profile observation by partial reflection experiment, discussing radio signal amplitude and phase data recording sensitivity requirement 09 p1075 A73-22071
- Electromagnetic fields in electrodeless discharges of arbitrary length. 09 p1128 A73-22635
- [TTU-SR-2] The standard electron density profile of the F2-layer at noon. 09 p1078 A73-22746
- Possibility of estimating the flux of energetic particles in the ionospheric D-region at sunrise and during the daytime. 10 p1212 A73-24219
- Ionization front propagation velocity as function of microwave power density, showing dependence on precursor electron density profiles 10 p1251 A73-24257
- Some results of ionospheric measurements based on observations of geophysical rocket signals from spaced points and observations of signals reflected by space objects 11 p1350 A73-25077
- Ionospheric vertical electron density profiles from geophysical rocket-borne microwave dispersing interferometer 11 p1350 A73-25079
- Diurnal variations in electron density at heights of 160 to 200 km and electron temperature variations 11 p1351 A73-25095
- Calculation of the N/h' profiles in the ionosphere from two magnetotonic components 11 p1351 A73-25096
- The topside ionosphere at mid-latitudes during local sunrise. 11 p1353 A73-25757
- Three-dimensional analytical model of the electron density distribution in a quiet ionosphere 12 p1490 A73-27334
- Time dependent studies of the aurora. I - Ion density and composition. 12 p1492 A73-27601
- An inversion method for the determination of the electron density profile of the ionosphere on the basis of satellite tracking data 12 p1494 A73-27772
- Electron temperature measurement in recombination collisional plasma with double probe, noting electron and ion density distribution near isolated electrode under floating potential 12 p1499 A73-27916
- Group delay times of magnetoionic components for horizontal electron density profiles in magnetic meridian plane, noting comparison with ionospheric sounding data 13 p1608 A73-28708
- High power radio transmitter for structural investigation and electron concentration profiles of ionospheric D and E regions 13 p1583 A73-28725
- Ionospheric model impulse response transfer functions phase and amplitude dependence on profile parameters and TE C, using ray tracing technique 14 p1728 A73-30231
- Electron density characteristics in magnetized hydrogen arcs in the case of a deviation of the ion temperature from the electron temperature 14 p1780 A73-30419
- Diffraction spectra and electron density distributions of interatomic graphitizing carbon molecule bonds as polymer combinations, using diffractometer and scintillation counter recording 14 p1767 A73-30839
- Ionospheric electron density profiles calculation method based on oblique backscatter ionograms, presenting virtual height vs frequency 15 p1873 A73-32229
- Latitudinal and time variations of total electron number and its gradients in the ionosphere at high latitudes. 15 p1874 A73-32625
- Vertical electron density distribution at the geomagnetic pole in the Northern Hemisphere /from data of topside and ground-based soundings of the ionosphere/. 16 p2002 A73-32778
- D region electron density profiles from radio broadcast field strength measurements by rocket-borne passive RF spectrometers, using ray theory for wave propagation 18 p2303 A73-35956
- Estimation of H/+ / fluxes at the polar regions. 18 p2304 A73-35969
- Comparison of electron density profiles in the lower ionosphere at Equator and midlatitudes. 18 p2305 A73-36007
- Electron-density profiles obtained from MF sounding at Tsunbe. 18 p2306 A73-36012
- Construction of D-region electron-density profiles by combined use of ground-based reflection and satellite-based transmission measurements. 18 p2306 A73-36016
- Electron density profiles from ionograms - Comparisons with rocket profiles. 18 p2306 A73-36017
- Tentative E-region electron density profiles. 18 p2309 A73-36099
- Latitude distribution of the regularity in F2-region irregularities. 20 p2553 A73-39132
- Study of a linear noncylindrical discharge by holographic interferometry 20 p2597 A73-39198
- Ground based and rocket techniques for vertical ionospheric electron density distribution measurement, considering incoherent scatter, partial reflection, wave interaction, and Faraday rotation 21 p2685 A73-40809
- The total electron content of the ionosphere and its horizontal gradients, measured on the basis of recordings of satellite signals at scattered points 21 p2686 A73-40910

Electron density in a locally ionized plasma afterglow.

21 p2748 A73-40970

D region electron density profiles at geomagnetic equator by rocket sounding, showing ionization production by Lyman alpha radiation and cosmic rays

21 p2690 A73-41361

Rocket measurements of electron concentration and electron temperature in the polar ionosphere.

21 p2690 A73-41367

Ionospheric slab thickness relationship to electron density profile shape, plasma and neutral constituents scale heights and electron to ion temperature ratio

22 p2846 A73-41947

Ionospheric electron density profiles and contour plots above F layer maximum from vertical sounding and Faraday rotation techniques

22 p2851 A73-42984

An iterative mathematical technique for deriving electron-density profiles from multifrequency riometer data.

22 p2828 A73-43177

Three-dimensional analytical model of electron density distribution of the quiet ionosphere.

23 p2970 A73-43232

Effect of modified thermal conductivity on the temperature distribution in the protonosphere.

24 p3082 A73-44727

Calculation of a model of the neutral atmosphere of Mars above 140 km from ionospheric data

24 p3137 A73-44785

Formation of the sporadic E layer and the nighttime E region of the ionosphere at midlatitudes

24 p3083 A73-44794

Comparative analysis of rocket measurements of n sub e /h/ and of ground-based vertical sounding data

24 p3083 A73-44795

ELECTRON DETECTORS

U ELECTRON COUNTERS

ELECTRON DIFFRACTION

Use of LEED, Auger emission spectroscopy and field ion microscopy in microstructural studies.

02 p0171 A73-12843

The growth process of oxide layers during the initial oxidation of a 80Ni-20Cr alloy.

03 p0321 A73-12917

Electron diffraction investigations of the short-range order in GaAs and GaP films

05 p0605 A73-17291

Investigations on 'doping stacking fault' pyramids.

08 p0995 A73-21479

Diffraction study of fast electrons of the adsorption layer of oxygen on the surface of a film of epitaxial copper

10 p1259 A73-23767

Quasi-optical diffraction-type radiation generator

11 p1331 A73-26159

Electron-diffraction study of amorphous condensates of barium titanate

12 p1531 A73-27198

Determination of the temperature dependence of the Debye-Waller factor for thin gold films by electron diffraction observations

12 p1532 A73-27944

Electron diffraction study of a noncrystalline Zr-Ni phase.

20 p2575 A73-39021

On the diffraction of dense electron beams in quantum mechanics.

20 p2595 A73-39766

Diffraction pattern scanning display technique using electron detector in microscope final image, discussing gold particle demonstration, lens configuration, illumination angle and sawtooth currents

21 p2700 A73-40466

ELECTRON DIFFUSION

Magnetic pumping of electrons in ohmic dissipation mechanism responsible for neoclassical plasma diffusion rate increase in banana regime

01 p0084 A73-10467

The electron diffusion scattering cross section of cesium atoms

01 p0080 A73-10852

Calculation of the diffusion current of a finite-base semiconductor diode

03 p0284 A73-14322

Critical analysis of Mouthaan-Susskind diffusion theory for magnetron diode electron transport, noting theoretical results discrepancy with experimental data

05 p0556 A73-16064

Heating of a plasma in stimulated scattering of laser radiation /Review/.

06 p0731 A73-18578

Monte Carlo simulation for electron diffusion in Cd Te, noting effects of applied electric field near threshold value for negative differential mobility

06 p0739 A73-18799

Diffusion of hot electrons in n indium phosphide.

07 p0861 A73-19157

Diffusion effects in the double injection negative-resistance problem.

08 p0948 A73-21483

Diffusion processes electron mechanism in metal-metal and metal-nonmetal systems, using configurational model for valence electrons localization

10 p1236 A73-24951

Brownian motion of electrons in time-dependent magnetic fields.

11 p1403 A73-25124

Energetic electron production and loss model for Jupiter radiation belt, considering drive mechanisms for electron diffusion from solar wind

11 p1424 A73-26130

Low energy auroral electron pitch angle diffusion in postbreakup aurora due to injected particle loss in closed magnetic field lines

12 p1488 A73-26987

The diffusion cross section for scattering of electrons by cesium atoms.

12 p1526 A73-27902

Experimental study of the diffusion of electrons of conduction by superficial defects of thin gold films

13 p1668 A73-28453

Ion and electron diffusion in nonisothermal ionospheric F layer, analyzing ionization balance equations

15 p1871 A73-31882

Coulomb drift of electrons from a mirror confinement system in the case of a positive plasma potential

15 p1920 A73-32306

Splitting of an ionospheric layer by ambipolar diffusion.

18 p2313 A73-36388

Ionospheric sounding by ATS-3 emitted signal polarization measurement during partial solar eclipse of 10 July 1972, noting electron content decrease and diffusion rate

23 p2972 A73-43697

Low-pressure gas breakdown with CO2 laser radiation.

24 p3095 A73-44589

Coulomb loss of electrons from a mirror device with a positive plasma potential.

24 p3114 A73-44614

The relation between the diffusivity-mobility ratio and the linewidth of spontaneous emission in degenerate semiconductors at relatively high temperatures.

24 p3120 A73-45488

ELECTRON DISTRIBUTION

NT ELECTRON DENSITY PROFILES

Free streaming electrons effect on spatial ballistic electron plasma wave echoes response, calculating echo electric fields and electron distribution function

02 p0197 A73-12065

Ionospheric bottom side electron density profiles from measured monthly median values, using CCIR and ITS computer programs for critical frequencies

02 p0163 A73-12302

Thermal and near-thermal electron transport coefficients in O2 determined with a time-of-flight swarm experiment using a drift-dwell-drift technique.

03 p0344 A73-13276

Electron excitation and auroral emission parameters.

04 p0440 A73-14959

Boltzmann transport equation for plasma probe detector characteristics for Maxwellian and non-Maxwellian distribution functions of electrons in dc and ac electric fields

04 p0480 A73-15602

Space-time distribution of excess carriers and their space charge in doped semiconductors.

06 p0734 A73-17814

Two dimensional simulation of nonlinear ion-sound instability in current carrying collisionless plasma due to modification of electron distribution function

06 p0730 A73-18464

Global electron concentration disturbances in low and middle latitude F2 during magnetic storm

07 p0815 A73-19435

Magnetospheric quasi-stationary pinch effect and filamentary structure due to electron streams parallel to geomagnetic field lines

07 p0816 A73-19464

Computerized simulation for nonlinear evolution of whistler instabilities in anisotropic collisionless plasmas with various Maxwellian electron distributions

07 p0857 A73-19523

Intracavity breakdown in CO and CO2 lasers.

07 p0835 A73-19638

Electron-hole processes in CaF2 crystals doped with rare-earth ions

07 p0837 A73-20208

Iterative method for calculating hot carrier distributions in semiconductors.

08 p0994 A73-21221

Calculation of the moments of the electron spatial distribution function without allowance for ionization losses

08 p1000 A73-21514

Computer simulation of semiconductor devices.

08 p0948 A73-21534

Storms and the seasonal anomaly in the topside ionosphere.

09 p1075 A73-22132

Computer simulation of ion heating by pulsed microwaves.

09 p1129 A73-22642

Boltzmann transport equation for plasma probe detector characteristics for Maxwellian and non-Maxwellian distribution functions of electrons in dc and ac electric fields

10 p1254 A73-24192

The circular polarization of sources of synchrotron radiation.

10 p1270 A73-24901

Ion and electron distributions in the boundary layer of hypersonic vehicles.

11 p1404 A73-25290

Numerical analysis of the properties of an avalanche diode in the avalanche multiplication range

11 p1337 A73-25321

Dynamics of strongly nonlinear beam-plasma interaction.

[IPPCZ-167] 12 p1529 A73-27434

Negative horizontal gradients of the integral electron content of the ionosphere - A comparison of satellite and ionosonde data

12 p1494 A73-27774

Abundance and lateral distribution of muons in inclined showers.

13 p1670 A73-28371

Low-energy electron experiment for Atmosphere Explorer-C and -D.

13 p1689 A73-28642

Effect of plasma inhomogeneity on the relaxation of the electron distribution function in the electrode area of a low voltage arc

13 p1667 A73-28963

Consideration on the 'equilibrium' electrons distribution function for a homogeneous, high-frequency, fully ionized plasma.

14 p1779 A73-29998

Anisotropy and energy spectra of newly-generated photoelectrons

15 p1867 A73-31265

Axial distribution for a hot electron plasma.

16 p2041 A73-33325

Satellite studies of magnetospheric substorms on August 15, 1968. VI - Ogo 5 energetic electron observations - Pitch angle distributions in the nighttime magnetosphere.

16 p2056 A73-33454

Unpaired electrons and charge carriers in oxide semiconductor glasses based on the oxides of titanium, vanadium, and phosphorus

20 p2599 A73-39394

A two-dimensional numerical analysis of a silicon n-p-n transistor.

20 p2536 A73-39413

Field aligned electron anisotropies observed by the ESRO 1 A/Aurorae/ satellite.

21 p2691 A73-41370

Intense air showers with an electron-photon core of complex structure

23 p3022 A73-43545

Distribution function of relativistic electrons in a strong magnetic field.

23 p3011 A73-43753

Effect of plasma inhomogeneity on the relaxation of the electron distribution near the electrodes in a low-voltage arc.

23 p3013 A73-44315

Calculation of the nonstationary electric field, carrier concentration, and current distribution in semiconductor integrated circuits

24 p3119 A73-45177

Redistribution of charged particles and self-distribution of high-amplitude electromagnetic waves in a plasma.

24 p3117 A73-45413

Experimental determination of the nonlinear interaction in a one dimensional beam-plasma system.

24 p3117 A73-45458

ELECTRON EMISSION

NT FIELD EMISSION

NT PHOTOELECTRIC EMISSION

NT SECONDARY EMISSION

Effect of visible light on exoelectron emission

01 p0045 A73-10264

High voltage square pulse oscillator and recording circuit for negative and positive autoelectron emission properties

01 p0024 A73-10795

Polarization of relativistic-electron emission in the case of Compton scattering at turbulent plasma oscillations

01 p0085 A73-10949

Production of different non-thermal electron groups in small solar flares.

03 p0364 A73-13959

Visual display of fatigue damage by means of exoelectron emission.

04 p0446 A73-14748

Applications of exoelectron emission to nondestructive evaluation of alloying, crack growth, fatigue, annealing, and grinding processes.

04 p0453 A73-14856

The early detection of fatigue damage by exoelectron emission and acoustic emission.

04 p0453 A73-14858

- Theory of dynamic charge current and capacitance characteristics in MIS systems containing distributed surface traps. 04 p0427 A73-15345
- Type 3 radio bursts correlation with solar flares and electron events from OGO 5, IMP 5 and Explorer 35 observations 05 p0610 A73-17047
- Emission of metals under the action of non-relativistic electrons 06 p0725 A73-18102
- Miniaturized second generation night vision image intensifier system operation and performance based on secondary photoelectron emission 06 p0694 A73-18300
- Parametric radiation of relativistic electron bundles in a waveguide with a stratified dielectric filling. 07 p0802 A73-20145
- Polarized radiation of relativistic electrons scattered by plasma turbulence. 09 p1130 A73-22743
- Direct nuclear-to-electric power conversion based on Sr 90 electron emission and collection system, noting spacecraft applications 09 p1119 A73-22828
- Thermionic constants and electron reflection for Ta/100 by the Shelton retarding field method. 10 p1259 A73-23695
- Sources of spurious background in the Spectracon. 14 p1732 A73-29907
- Natural exoelectron emission from anorthositic rocks supplied by the Luna-20 automatic interplanetary station 14 p1802 A73-30833
- Influence of heating on the intensity and energy of exoelectrons in deformed aluminum 14 p1765 A73-30889
- Current-voltage characteristics of multispike diodes operating under conditions of explosive emission of electrons 15 p1852 A73-32315
- Exo-electron emission during heterogeneous catalysis (the effect of external electric potentials). 15 p1842 A73-32599
- Use of emissive probes in plasma density measurements. 16 p2011 A73-32725
- Temperature dependence of thermionic emission current density of Pt additive powdered zirconium carbide deposit on diode cathode working surface 17 p2109 A73-35171
- Electron emission of In2Se crystals in strong electric fields 17 p2219 A73-35555
- Extraction of electrons from a plasma in the presence of a gas in the high-voltage gap 20 p2598 A73-39606
- Exploding wires as a source of flash X-rays. 21 p2738 A73-39975
- Pulsed Langmuir probe measurements of hollow cathode plasma discharge electron emission in terms of secondary, thermionic and field components 21 p2747 A73-40793
- Natural exoelectron emission of anorthositic rocks returned by the automatic interplanetary station Luna-20. 23 p3028 A73-43583
- The possibility of field emission from metal surface with a Q-switched laser pulse. 24 p3095 A73-44404
- ### ELECTRON ENERGY
- #### NT ELECTRON STATES
- Variations of the auroral electron energy spectra during substorms. 01 p0036 A73-10339
- Rocket measurements of low energy electrons and optical emissions in the dayglow and aurora. 01 p0036 A73-10346
- Electron temperature measurement in collisional plasma with double probe, noting electron and ion density distribution near isolated electrode under floating potential 01 p0085 A73-10866
- The role of energetic electrons in the correlation of meter and decimeter type III bursts with 4 keV X-ray emission. 01 p0093 A73-11391
- Revised calculations of F region ambient electron heating by photoelectrons. 02 p0157 A73-11751
- The application of Langmuir probes to the measurement of very low electron temperatures. 02 p0158 A73-11912
- Rocket-borne instrumentation to measure ionospheric electron temperature with good spatial resolution. 02 p0167 A73-11953
- The global morphology of electron temperature in the topside ionosphere, as measured by an a.c. Langmuir probe. 02 p0158 A73-12027
- Probe measurements of positive ions and electron temperatures in high latitude rocket flights. 02 p0159 A73-12032
- Ionospheric electron and ion temperature profile measurements with satellite- and rocket-borne probes, comparing merits and discrepancies 02 p0163 A73-12303
- Determination of the ionospheric density and temperature using a double probe electric field detector. 02 p0164 A73-12310
- Measurements of energetic particle fluxes during a slowly varying absorption event by two co-ordinated rocket flights. 02 p0206 A73-12314
- Relativistic electron radio emission models, calculating magnetic bremsstrahlung spectra from galactic electron space-energy distributions 02 p0208 A73-12459
- On D-region electron heating by a low-frequency terrestrial line current with ground return. 02 p0143 A73-12533
- Measurement of electron distribution function in a cesium plasma. 02 p0199 A73-12815
- Ion density and electron temperature calculations for metallic plasma population inversion possibility by near resonant charge exchange with inert gas ions 02 p0194 A73-12847
- Near earth electron spectra applied to cosmic ray transport equation numerical solution extension to 1968-1970, providing models for modulation and gradients reproduction 03 p0361 A73-13362
- The pre-midnight asymmetry in the 40 keV electron flux profiles and its relation to magnetospheric substorms. 03 p0363 A73-13866
- Production of different non-thermal electron groups in small solar flares. 03 p0364 A73-13959
- Pulse discharge plasma in Ar with gas ionization level near unity, noting plasma cylinder parameters, electron temperature and I-V characteristics 03 p0347 A73-14091
- Molecular gas presence effect on electron energy balance in atomic gases, noting inelastic collisions loss factor in heated Ar plasma containing nitrogen molecules 03 p0347 A73-14098
- Electron temperature elevation compared to gas temperature in hydrocarbon flames, discussing energy exchange mechanism 03 p0352 A73-14394
- Solar corona X-ray emission from O VII and Ne IX ions by rocket-borne Bragg spectrometers observations, determining electron temperature from resonance lines intensity 03 p0364 A73-14418
- Theory of electron cyclotron resonance heating. I - Short time and adiabatic effects. 03 p0345 A73-14434
- Trapped and precipitated electron energy spectra in relativistic electron precipitation events (REP), discussing bremsstrahlung measurements deductions 03 p0304 A73-14591
- Study of electronic spectroscopy at low energy on graphite [ONERA, TP NO. 1181] 03 p0336 A73-14607
- Radio sources in decimeter wave range from astronomical model and radio observations, noting spectral characteristics dependence on electron energy spectra 04 p0496 A73-14824
- Velocity distribution of plasma electrons in the negative H2- and He-glow with superimposed longitudinal magnetic field. 04 p0477 A73-14897
- Electron density and temperature measurements in the lower ionosphere as deduced from the warm plasma theory of the H.F. quadrupole probe. 04 p0480 A73-15199
- Charge carrier cooling in nonhomogeneous semiconductors by static electric field, plotting average electron temperature as function of current 04 p0484 A73-15569
- Measurement of the electron energy distribution function in a plasma with periodically varying parameters 04 p0481 A73-15615
- Determination of plasma electron temperature from the reversal of radial ambipolar electric field in a longitudinal magnetic field. 05 p0602 A73-16584
- ESRO 1A satellite-borne Langmuir probe measurement for anisotropy in ionospheric thermal electron temperature relative to geomagnetic field 05 p0571 A73-17053
- Interplanetary cosmic ray low energy electron observation, explaining steep spectrum origin and time variations by model with spectral decomposition 05 p0612 A73-17386
- Electron energy distribution in a low-temperature plasma. 06 p0727 A73-17419
- Electron acceleration in the outer radiation belt 06 p0742 A73-17527
- Effects of non-Maxwellian electron energy distributions on the orbital limited current-voltage characteristics of cylindrical and spherical Langmuir probes under collisionless conditions. 06 p0730 A73-18463
- Experiments of magnetohydrodynamic conversion with ionization out of equilibrium 06 p0730 A73-18541
- Temperature dependence of the ion recombination coefficient in a hydrocarbon flame plasma 06 p0731 A73-18553
- Current induced drift rate of plasma electrons in electric and magnetic fields, noting electron velocities in turbulent heating of plasma 06 p0732 A73-18621
- Melchey thermodynamica hypotheses based on average electron energy for examination of equilibrium and steady state conditions in semiconductor p-n junctions 06 p0770 A73-18840
- Propagation anisotropies of solar flare protons and electrons at low energies in interplanetary space. 07 p0869 A73-19227
- Comparison of Te and Ti from Ogo 6 and from various incoherent scatter radars. 07 p0790 A73-19241
- Intensity and energy spectrum calculation of albedo electrons recorded in cosmic particle showers by gas discharge counters 07 p0823 A73-19429
- Ionospheric electrons and neutral particles temperature and concentration profiles explanation by electron gas cooling due to atomic oxygen excitation, calculating heat flow 07 p0815 A73-19441
- Solar energetic particles and wide-band continuum storms from metric to hectometric frequencies. 07 p0870 A73-19663
- Photoelectron layer detection above sunlit lunar surface with ion-electron spectrometer in Apollo 14 charged particle lunar environment experiment, noting energy spectra 07 p0895 A73-19859
- Secondary electron emission characteristics of lunar surface films. 07 p0871 A73-19861
- Energy loss measurements with 60 keV electrons in the case of amorphous and polycrystalline selenium and tellurium and the determination of optical constants 07 p0862 A73-20017
- Electron energy loss effect on cross-field electron streaming instability in low density high temperature plasmas, using high voltage theta pinch 07 p0859 A73-20192
- Measurements of the structure of an ionizing shock wave in a hydrogen-helium mixture. 07 p0813 A73-20475
- Collision cross sections for electrons with atmospheric species. 08 p0957 A73-20659
- On the radio optical depth of the layer where the temperature equals the brightness temperature. 08 p1002 A73-20761
- Solar soft X-ray bursts data recorded by satellite telemetry, considering production by thermal plasma and nonrelativistic electrons with power law energy distribution 08 p0996 A73-20765
- The effect of a metallic reflector upon cyclotron radiation. 08 p0990 A73-20813
- Influence of inelastic energy losses by electrons on the development of ionization instability in a plasma. 08 p0992 A73-20852
- Measurements of the electron temperatures in M42 from the profiles of H-alpha, forbidden N II, H-beta, and forbidden O III. 08 p1004 A73-20906
- The heating of the solar corona. I - Observation of ion energies in the transition zone. 08 p1005 A73-20919
- Heating of charged particles by electric waves. 08 p0993 A73-21233
- Rapid injection of energetic particles into the gap between the inner and outer radiation belts 08 p0998 A73-21300
- Formation and decay of a narrow band of energetic electrons in the earth's magnetosphere 08 p0998 A73-21305
- X-ray emission of coronal condensations during the eclipse on 20 May 1966 and its connection with optical and radio observations. 08 p0998 A73-21310
- Waves in magnetoactive plasma in the presence of a distinct transverse ion velocity 09 p1125 A73-21904
- Electron energy distribution function in CO laser discharge for elastic collisions, noting kinetic equation solution 09 p1089 A73-21914
- Wave functions and energies of the autoionization states of the cesium atom 09 p1122 A73-21976

- X-ray temperature measurements of laser produced plasmas in large radiation fields. 09 p1125 A73-22024
- Ogo 6 measurements of supercooled plasma in the equatorial exosphere. 09 p1074 A73-22066
- Modulation Langmuir probe and incoherent scatter radar measurements of ionospheric electron temperature. 09 p1075 A73-22128
- Solar plasma electron density and temperature measurement by Mars 2 and Mars 3 orbiter-borne retarding potential analyzers, considering solar wind shock front interaction role 09 p1126 A73-22263
- Energy absorption in cold inhomogeneous plasmas - The Herlofson paradox. 09 p1126 A73-22276
- Ion cyclotron instability in current-carrying plasmas with anisotropic temperatures. 09 p1127 A73-22284
- Nonlinear theory of plasma heating by parametric instabilities. 09 p1128 A73-22633
- [TTU-SR-2] Measurement of the electron temperature of a quasi-stationary pulsed glow-discharge plasma in highly overcharged gaps 09 p1129 A73-22663
- Enhanced energetic electron intensities at 100 km altitude and a whistler propagating through the plasmasphere. 09 p1079 A73-22839
- Flux magnitude and single transition probabilities as function of electron density and temperature in relaxation model ionization and recombination channels 10 p1253 A73-23503
- Determination of the electron temperature of a plasma by sounding with an extraordinary wave along a magnetic field 10 p1253 A73-23504
- Analytical model of electron velocity, resonance and potential of plasma accelerated in crossed electric and magnetic fields 10 p1253 A73-23577
- Investigation of geosynchronous corpuscular particles and photoelectrons on board the Cosmos 261 satellite. V - Spectra of ionospheric photoelectrons and migration of the latter from the conjugate ionosphere 10 p1211 A73-23887
- The asymptotic behavior of the supersonic solutions of the two-fluid solar wind equations. 10 p1268 A73-24147
- Measurement of electron energy distribution in a plasma with periodically varying parameters. 10 p1254 A73-24205
- Electron and proton acceleration in the outer regions of the magnetosphere during polar substorms. 10 p1268 A73-24227
- Electron temperature profile in stagnation region flow of blunt bodies with consideration of ionization recombination in shock layer 10 p1296 A73-24256
- Electron-cyclotron drift instability in high-beta plasmas, developing nonlinear theory based on wave kinetic equation for weak turbulence 10 p1255 A73-24263
- Expanded laser produced plasma Debye length from slab geometry, evaluating electron temperature for ion recombination rates 10 p1256 A73-24270
- Simultaneous determination of the electron temperature and density in the chromospheric-coronal transition region of the sun. 10 p1281 A73-24409
- Statistical velocity and temperature characteristics of turbulent electron beams in crossed HF electric and magnetic fields, comparing with Brillouin flow 10 p1258 A73-24880
- Thermal conductivity of the plasma electron component across the magnetic field 10 p1258 A73-24890
- Vertical electron density and temperature data from geophysical rocket borne Langmuir probes and electrode traps 11 p1350 A73-25078
- Recombination coefficient, heat flux, ionization balance and photoelectron kinetic energy from ionospheric electron temperature and density profiles and solar UV absorption data 11 p1350 A73-25081
- Calculation of electron energy flux distributions in noble gases. 11 p1401 A73-25144
- Electron-neutral particle collisions effect on potential of test charge moving at velocity lower than plasma electrons, using BGK model and Lorentz collision operator 11 p1404 A73-25260
- Spectroscopic measurement method for the electron temperature and density of a focusing discharge of the 'plasma focusing' type 11 p1404 A73-25270
- The transport coefficients and material functions of a plasma with different electron and gas temperatures 11 p1404 A73-25343
- Energetic electron production and loss model for Jupiter radiation belt, considering drive mechanisms for electron diffusion from solar wind 11 p1424 A73-26130
- Retarding field electron spectrometer for low kinetic energy electron analysis, discussing design, construction and performance in terms of resolution, sensitivity, luminosity and SNR 11 p1366 A73-26301
- Temperature-waves in connection with drift type instabilities in a Q-plasma. 11 p1406 A73-26558
- A note on the heating of magnetoplasma by magnetic perturbations. 11 p1407 A73-26659
- Solar corona electron densities and temperatures as function of distance from solar center during 22 September 1968 eclipse 12 p1538 A73-26860
- The kinetic reflection coefficient in a formula for the current at a plasma/semiconductor interface in the case of an inelastic mechanism of electron energy relaxation 12 p1527 A73-26928
- Changes in the mean energy of an electron in the field of a plane wave with allowance for radiation damping 12 p1526 A73-26969
- Cosmic ray electrons from 0.2 to 8 MeV - Pioneer 8 and 9 measurements of their spectrum, time variations, and interplanetary radial gradient. 12 p1533 A73-26976
- Heos 2 magnetometer observations of magnetosheath high and low energy electron flux during magnetopause boundary crossings in polar regions 12 p1489 A73-27004
- Gunn microwave oscillators electron temperature dependent noise in absence of 1/f type, considering thermal or Johnson noise augmented by carriers hopping 12 p1478 A73-27111
- Dependence of the light yield of a plastic scintillator on the energy of protons and electrons 12 p1496 A73-27206
- Application of the collisionless absorption of an extraordinary wave to the determination of plasma electron temperatures 12 p1528 A73-27302
- Influence of a transverse electron-temperature gradient on the plasma flow in an axisymmetric magnetic field 12 p1528 A73-27305
- Upper atmospheric temperatures from Doppler line widths. V - Auroral electron energy spectra and fluxes deduced from the 5577 and 6300 A atomic oxygen emissions. 12 p1492 A73-27605
- Probe device for measuring local parameters of ionized gas flow. 12 p1499 A73-27915
- Electron temperature measurement in recombination collisional plasma with double probe, noting electron and ion density distribution near isolated electrode under floating potential 12 p1499 A73-27916
- Two-flow instability of interpenetrating ion beams propagating in the same direction along an external magnetic field 12 p1529 A73-27941
- Effect of a magnetic field on the soft X-ray radiation of a laser plasma 12 p1530 A73-27977
- Electron temperature in a weakly ionized plasma during a nonlinear skin effect 12 p1530 A73-27979
- Low-energy electron experiment for Atmosphere Explorer-C and -D. 13 p1689 A73-28642
- Relaxation to Maxwellian distribution of electrons near low voltage Cs arc plasma discharge cathode 13 p1666 A73-28962
- Time behavior of hydrogen discharge in ST-Tokamak based on measured radial electron temperature and density profiles and ohmic-heating current and voltage 14 p1778 A73-29691
- Measurement of electron temperature in the ionosphere by the high-frequency probe method 14 p1746 A73-29861
- Ionospheric electron density and temperature measurement by cylindrical Langmuir probes onboard Interkosmos 2 satellite 14 p1746 A73-29862
- Band structure, electron energy distribution and emission efficiency of negative electron affinity secondary emitters and cold cathodes 14 p1732 A73-29912
- Earth radiation belts energetic electrons quiet equilibrium structure based on balance between pitch angle scattering loss and inward radial diffusion 14 p1786 A73-29965
- Auroral electrons of energy less than 1 keV observed at rocket altitudes. 14 p1748 A73-29969
- Existence of geomagnetically trapped electrons at altitudes below the inner radiation belt. 14 p1749 A73-29985
- Seasonal and sunspot cycle variations of F region electron temperatures and protonospheric heat fluxes. 14 p1749 A73-29986
- A nonlinear theory for the parametric instability with comparable electron and ion temperatures. 14 p1779 A73-30119
- Electron density characteristics in magnetized hydrogen arcs in the case of a deviation of the ion temperature from the electron temperature 14 p1780 A73-30419
- Spatially dependent electron relaxation near a thermionic emitting electrode. 14 p1713 A73-30473
- French monograph - Analysis of the functioning of the differential probe for measurement of electronic temperature in the ionosphere. 14 p1753 A73-30672
- Universality of the power spectra of relativistic electrons generated in a turbulent plasma 14 p1782 A73-30808
- Influence of heating on the intensity and energy of exoelectrons in deformed aluminum 14 p1765 A73-30889
- A critical study on the reliability of electron temperature measurements with a Langmuir probe. 15 p1871 A73-31835
- Ionization instability in CO2 laser discharges. 15 p1885 A73-32258
- Hydrodynamic theory of high-amplitude ionization waves 15 p1921 A73-32326
- Relativistic electron radio emission models, calculating magnetic bremsstrahlung spectra from galactic electron space-energy distributions 15 p1927 A73-32609
- Waves in a magnetoplasma with an isolated transverse ion velocity component. 15 p1922 A73-32629
- Electron energy distribution function in CO laser discharge for elastic collisions, noting kinetic equation solution 15 p1886 A73-32640
- Electron acceleration in the outer radiation belt. 16 p2051 A73-32752
- Secondary electrons and energy per ion-pair in a thermal gas for electron, proton and X-ray ionization. 16 p2052 A73-32826
- Probe design for orbit-limited current collection. 16 p2041 A73-33320
- Nonlinear evolution of the decay instability in a plasma with comparable electron and ion temperatures. 16 p2041 A73-33324
- Errors in ion and electron temperature measurements due to grid plane potential nonuniformities in retarding potential analyzers. 16 p2016 A73-33436
- Temperature dependence of the ion recombination coefficient for a hydrocarbon flame. 16 p2042 A73-33578
- Recombination rate measurements in nitrogen. 16 p2039 A73-33673
- Screened potential Lorentz model for electrical conductivity of non-Debye plasma, investigating electron energy distribution function 17 p2214 A73-34127
- Book - Low energy electron collisions in gases: Swarm and plasma methods applied to their study. 17 p2213 A73-34461
- Electron energy distribution function validity for nonequilibrium plasma in presence of electric field verified for ionized cesium vapor positive column 17 p2216 A73-34551
- Flux magnitude and single transition probabilities as function of electron density and temperature in relaxation model ionization and recombination channels 17 p2217 A73-35183
- Determination of electron temperature of a plasma by probing the extraordinary wave along a magnetic field. 17 p2217 A73-35184
- Electron gun with concentric hemispherical anode and space charge limited thermionic emitter for potential field simulation, measuring electron energy distribution for comparison with calculation 17 p2143 A73-35764
- High resolution nondispersive electron energy analyzer for electron spectroscopy for chemical analysis, using spherical mirror and grid retarding potential field as filters 17 p2176 A73-35770
- Electron temperature and density in the He-CD12 positive column used for an I/+ laser. 17 p2186 A73-35798
- Low energy electron fluxes and spectra correlation with auroral forms from weather satellite electrostatic measurements 18 p2304 A73-35964
- Electron temperature profile and its solar activity dependence in the middle latitude region. 18 p2308 A73-36047

Electron temperature and emission measure variations in the solar corona.

18 p2350 A73-36062

Simultaneous measurements of some ionospheric parameters at altitudes 100-170 km.

18 p2310 A73-36131

Rocket measurements of electron density and electron temperature at sunset.

18 p2311 A73-36148

Solar wind heat transport in the vicinity of the earth's bow shock.

18 p2346 A73-36269

Splitting of an ionospheric layer by ambipolar diffusion.

18 p2313 A73-36388

Procedure for measuring plasma electron energies from the bremsstrahlung with the aid of Cerenkov detectors

18 p2339 A73-36566

Energy transport by photoelectrons in the early morning ionosphere.

18 p2348 A73-37027

Double-probe measurements of electron temperatures on low pressure diffusion flames - Criticism of the methods for determining the electron temperature from the double-probe current voltage characteristic.

18 p2317 A73-37097

Evidence for the softening of the cosmic-ray electron spectrum at a few hundred GeV and the origin of the galactic-ridge X-radiation.

18 p2348 A73-37102

Laminar boundary layers in low pressure argon plasma.

19 p2464 A73-37163

Measurement of nonisotropic electron velocity distributions by laser scattering.

19 p2465 A73-37166

Satellite retarding potential trap contamination relationship to electron and ion temperatures evaluation, discussing Langmuir probes, sweep frequency and plasma density

19 p2429 A73-37373

Rocket measurement of photoelectrons in the ionosphere by K-9 M-40.

19 p2474 A73-37379

Model experiment on solar flares and the neutral sheet. III.

19 p2475 A73-37383

Comparison of electron and electronic temperatures in recombining nozzle flow of ionized nitrogen-hydrogen mixture. I, II.

19 p2462 A73-37441

The electron energy and number densities of the Jovian radiation belt. I.

19 p2475 A73-37621

Cooling and heating of electrons during the decay and development of a cesium discharge plasma

19 p2469 A73-37962

Investigation of geoeactive corpuscles and photoelectrons with the Cosmos 261 satellite. V - Spectra of ionospheric photoelectrons and their transfer from the conjugate ionosphere.

20 p2550 A73-38906

Effect of an isotropic nonequilibrium plasma on electron temperature measurements.

20 p2552 A73-38947

The electron kinetics of a weakly ionized Lorentz plasma in arbitrarily oriented external electric and magnetic fields

20 p2596 A73-39192

Ionization of a neutral medium by an electron beam

20 p2597 A73-39279

A semiempirical description of the structure of metals

20 p2577 A73-39295

Photoelectron energy spectra for atomic and molecular binding energies, examining spectrum signatures, angular distribution, autoionization, rare gases, carbon monoxide and cyanocobalamin

20 p2520 A73-39634

Free atom and molecule energy levels studied by electron scattering spectroscopy, discussing energy losses, monochromated electron beams, particle resonance and electric fields

20 p2520 A73-39635

Combined Auger electron spectroscopy and electron impact desorption studies of silicon surfaces.

20 p2595 A73-39665

Local thermodynamic equilibrium validity limits in short spaced cesium plasmas, discussing electron density and temperature, Maxwell and Boltzmann distributions and total pressure

20 p2599 A73-39673

New tubes and techniques for flash X-ray diffraction and high contrast radiography.

21 p2696 A73-39974

Thermal electron energy distribution measurements in the ionosphere.

21 p2681 A73-40156

Asymptotic electron terms of colliding identical heavy nuclei

21 p2742 A73-40353

Electron temperature and ionization state in laser produced plasmas.

21 p2745 A73-40470

Temperature gradient in gaseous nebulae

21 p2768 A73-40716

Theory of a steady-state nonisothermal positive column in a magnetic field.

21 p2748 A73-40954

The determination of ionospheric charged particle temperatures from in situ measurements

21 p2690 A73-41362

Rocket measurements of electron concentration and electron temperature in the polar ionosphere.

21 p2690 A73-41367

Nonthermal electromagnetic and thermal X ray sources of accelerated electrons during solar flares

21 p2761 A73-41384

Study of surface by spectrometry of slow electrons

21 p2706 A73-41598

Statistical velocity and temperature characteristics of turbulent electron beams in crossed HF electric and magnetic fields, comparing with Brillouin flow

21 p2749 A73-41655

Transverse electron thermal conductivity for a plasma in a magnetic field.

21 p2749 A73-41665

Effects of interhemisphere transport on plasma temperatures at low latitudes.

22 p2844 A73-41919

Ionospheric slab thickness relationship to electron density profile shape, plasma and neutral constituents scale heights and electron to ion temperature ratio

22 p2846 A73-41947

Apparatus and methods for the precise determination of Boltzmann temperature.

22 p2856 A73-42021

Temperature measurements in the thermosphere and ionosphere.

22 p2847 A73-42063

Theoretical and experimental investigations of the electron temperature in laser-produced plasmas.

22 p2891 A73-42249

Kinetic reflection coefficient at a plasma-semiconductor boundary for inelastic electron energy relaxation.

22 p2891 A73-42262

On the determination of electron temperature in diffusion-dominated non-L.T.E. plasmas.

22 p2896 A73-43167

Electron temperature of regions of the formation of recombinational continua on the sun - Temperature of the carbon emission regions

23 p3036 A73-44246

Relaxation to Maxwellian distribution of electrons near low voltage Cs arc plasma discharge cathode

23 p3013 A73-44314

Relaxation of longitudinal and transverse temperatures in a plasma with directional motion of electrons

23 p3014 A73-44336

Solar wind and magnetosheath electron temperature measurements by triaxial electron analyzer onboard Ogo-5, presenting data for bow shock

24 p3125 A73-45112

Simultaneous in situ electron temperature comparison of Alouette 2 probe and plasma resonance data.

24 p3086 A73-45129

Pulsed argon laser discharge oscillographic electron temperature and time variations measurement, obtaining short and long pulse regime emission characteristics

24 p3097 A73-45516

Spectrometer design with particle preacceleration for measuring energy spectra of secondary electrons and photoelectrons with high resolution

24 p3092 A73-45553

ELECTRON FLUX

U ELECTRONS

U FLUX (RATE)

ELECTRON FLUX DENSITY

Electron-density and energetic-electron measurements of the midlatitude lower ionosphere during winter.

01 p0041 A73-10888

Angular distributions of auroral electrons in the energy range 0.8 to 16 keV.

02 p0155 A73-11734

Measurements of energetic particle fluxes during a slowly varying absorption event by two co-ordinated rocket flights.

02 p0206 A73-12314

Extensive air shower spectra based on electron and muon number for given shower development mechanism and primary cosmic ray chemical composition

02 p0209 A73-12677

The pre-midnight asymmetry in the 40 keV electron flux profiles and its relation to magnetospheric substorms.

03 p0363 A73-13866

Pitch angles and spectra of particles in the outer zone near noon.

[AD-758531]

03 p0363 A73-13867

Auroral precipitating electron angular distributions from polar orbiting satellite OVI-18 measurements, indicating pitch-angle diffusion due to particle-wave interactions

03 p0363 A73-13868

Fokker-Planck equation for solar atmosphere modulation of galactic proton and electron flux at earth, including convection, diffusion and adiabatic deceleration effects

07 p0870 A73-19576

Evidence for a common origin of the electrons responsible for the impulsive X-ray and type III radio bursts.

08 p0996 A73-20766

Modulation of auroral electron fluxes and the geomagnetic pulsations during the storm of March 8, 1970

08 p0959 A73-21291

Measurement of auroral Birkeland currents and energetic particle fluxes.

09 p1073 A73-22057

Simultaneous observations of low energy electron fluxes and the polar red emission at 6300 A.

09 p1075 A73-22137

Fluxes of electrons with energies above 80 MeV at the equator on the basis of measurements by the Cosmos 490 satellite

10 p1265 A73-23897

Contribution of pion production by primary cosmic-ray nucleons to the interstellar electron-positron flux.

10 p1269 A73-24348

Twilight airglow. I - Photoelectrons and forbidden O I 5577-angstrom radiation.

10 p1214 A73-24737

On the secondary production of galactic cosmic ray electrons.

10 p1270 A73-24910

Calculation of electron energy flux distributions in noble gases.

11 p1401 A73-25144

Solar and geomagnetic modulation of low-energy secondary cosmic ray electrons.

12 p1533 A73-26977

The results of measurements of the intensity of cosmic rays by the automatic station 'Venera-7'.

12 p1535 A73-27638

Characteristics of electron and high-energy proton flares.

12 p1536 A73-27849

Study of the directional distribution of energetic electrons and protons in the morning sector of the auroral zone during enhanced particle flux

13 p1606 A73-28153

The photoelectron-spectrometer experiment on Atmosphere Explorer.

13 p1689 A73-28641

Energy spectra and pitch angle distributions of precipitating incident and backscattered electron fluxes in auroral arcs

14 p1747 A73-29968

Low energy electron fluxes and spectra correlation with auroral forms from weather satellite electrostatic measurements

18 p2304 A73-35964

Intensity variations of low-energy protons and electrons in the outer magnetosphere at the sudden onset of a magnetic storm

18 p2309 A73-36109

Modulation of auroral electron fluxes and geomagnetic pulsations during the storm of March 8, 1970.

19 p2424 A73-37920

Electron fluxes with energies greater than 80 MeV at the equator based on measurement data from the Cosmos-490 satellite.

20 p2601 A73-38916

Dynamic variations in intensity and energy spectra of electrons in the inner radiation belt.

20 p2601 A73-38934

Electron flux variation measurements in the upper atmosphere at altitudes of 200 to 500 km

20 p2554 A73-39168

Influence of a sudden compression of the magnetosphere on outer zone electron fluxes measured at arbitrary pitch-angle.

21 p2682 A73-40161

Fluxes of electrons with energies greater than 10 MeV at heights from 200 to 500 km

21 p2758 A73-40603

Satellite counting of excess radiation measured as ionospheric electron and proton intensity dependent on geomagnetic activity, discussing proton energy spectra and electron albedo

21 p2758 A73-40604

A study of geoeactive corpuscles and photoelectrons on the Cosmos 261 satellite. VI - Epithelial electrons in the energy range from 30 to 150 eV in the region of the dayside and nightside polar cusps

21 p2686 A73-40909

Dependence of high-energy electron fluxes at an altitude of 200 to 300 km on threshold rigidity

21 p2686 A73-40917

The aurora oval in the region of influx of electrons into the earth's atmosphere

21 p2686 A73-40919

Observations of electron fluxes and related variations of ionospheric plasma parameters in the south polar cusp.

21 p2690 A73-41369

- Results of solar plasma electron observations on Mars-2 and Mars-3 spacecraft. 22 p2906 A73-41941
- Large transverse momenta and the structure of extensive air shower cores 23 p3022 A73-43548
- Spatial electron distribution in extensive air showers at energies of one thousand to one billion TeV 23 p3022 A73-43552
- Calculated characteristics of the electron and muon components of extensive air showers at the 690 g/sq cm level 23 p3022 A73-43553
- A device for recording the energy spectrum and fluxes of electrons with energies greater than 100 MeV in cosmic rays 24 p3124 A73-44782
- Relativistic electron belt formation mechanism hypothesis based on Cosmos 137 data on electron intensity near geomagnetic shell L equal to 2.8 24 p3124 A73-44808
- ELECTRON GAS**
- Cold matter consisting of atomic nuclei submerged in electron-neutron gas, relating subnuclear density relation to existence and binding energy of neutron-rich nuclei 01 p0081 A73-11310
- Description of classical homogeneous systems in terms of dressed particles. II - Application to the Debye plasma 02 p0199 A73-12722
- Electron impulse interactions of heat in semiconductors 04 p0483 A73-15470
- Microwave heating of a plasma and longitudinal electronic thermal conductivity in a magnetic field. 06 p0732 A73-18606
- Ionospheric electrons and neutral particles temperature and concentration profiles explanation by electron gas cooling due to atomic oxygen excitation, calculating heat flow 07 p0815 A73-19441
- Effects of Compton scattering in a moving gas 07 p0853 A73-20308
- Electron heat conductivity along a magnetic field in a decaying plasma 09 p1124 A73-21887
- Nonstationary distribution of the electron-ion gas in the ionosphere. 10 p1212 A73-24239
- Periodic instability induced in semiconductor situated in crossed electric and magnetic fields via electron gas heating, deriving expressions for properties of steady nonlinear waves 10 p1261 A73-24764
- Formula approximating Fermi-Dirac integrals for electron gas density, pressure and internal energy, discussing pressure ionization effect on equation of state in stellar interiors 11 p1417 A73-25261
- Description of the photoelectron interaction with ambient electrons in the ionosphere. 11 p1357 A73-25927
- Ionospheric electron-ion gas distribution, allowing for diffusion, recombination and vertical drift 11 p1357 A73-26081
- Compton-scattering effects in a moving gas. 12 p1526 A73-27280
- Neutron stars physical model, deriving mass-density-energy relationships for degenerate electron gas 13 p1682 A73-28985
- Quantization effects in semiconductor inversion and accumulation layers. 13 p1669 A73-29291
- Ion Mach number of ion shock embedded in collisional shock wave propagating in electron proton gas plasma 14 p1777 A73-30660
- Electron thermal conductivity along the magnetic field in an afterglow. 17 p2215 A73-34310
- Polarization operator of a superconducting electron gas - The Kohn anomalies and charge screening in superconductors 18 p2337 A73-36666
- Kinetic theory of a collision-dominated plasma. 21 p2749 A73-41618
- Magnetic susceptibility of a degenerate electron gas - Interaction of nuclear magnetic moments in normal metals and superconductors 23 p3016 A73-43709
- ELECTRON GUNS**
- Glow discharge electron guns for welding. 01 p0055 A73-10113
- Design and modeling of periodic magnetic systems for SHF devices. I, II 01 p0025 A73-10981
- Investigation of the structure of an electron beam formed by a high-perveance triode gun under controlled-current conditions 01 p0025 A73-10989
- Traveling wave tube for satellite applications. 03 p0281 A73-13174
- Parametric electron-beam instability in a spatially periodic electric field 04 p0479 A73-15043
- Carre method for optimum overrelaxation factor determination in electron gun performance analysis by digital simulation, discussing choice of parameters for rapid iterative convergence 08 p0990 A73-20836
- High power linear beam microwave klystrons, coupled cavity TWTs and hybrid tubes design and operation, considering electron gun and focusing system 11 p1339 A73-26693
- Reliability testing of high-perveance three-electrode guns 15 p1851 A73-32215
- Ultra high resolution electronic imaging and storage with the return beam vidicon. 17 p2136 A73-34904
- Electron gun with concentric hemispherical anode and space charge limited thermionic emitter for potential field stimulation, measuring electron energy distribution for comparison with calculation 17 p2143 A73-35764
- Electron beam current fluctuation reduction by placing hot filament into Wheatstone bridge arm for temperature regulation in power supply for electron gun 17 p2176 A73-35776
- Reduction of noise in high-power crossed-field amplifiers. 21 p2665 A73-41114
- ELECTRON IMPACT**
- Oxygen emission volume rate in auroras due to direct electron impact excitation, obtaining integral cross sections and quenching rates 01 p0036 A73-10336
- Ionization cross sections for H₂, N₂, and CO₂ clusters by electron impact. 01 p0080 A73-10563
- A possible method for estimating any indirect process in the production of the O⁺/IS⁺ atoms in aurora. 02 p0157 A73-11902
- Vibrational excitation in CO by electron impact in the energy range 10-90 eV. 04 p0477 A73-14770
- Dissociative excitation of molecular hydrogen by electron impact. 05 p0600 A73-16596
- Impact and bremsstrahlung photoionization due to precipitating electrons in the lower ionosphere. 08 p0957 A73-20657
- Ionization of 6s- and 5p-electrons of the cesium atom by electron impact 09 p1122 A73-21977
- Excitation of autoionization states of the cesium atom by electron impact 09 p1122 A73-21978
- Mass spectrometry in structural and stereochemical problems. CCXVII - Electron impact promoted fragmentation of O-methyl oximes of some alpha, beta-unsaturated ketones and methyl substituted cyclohexanones. 10 p1186 A73-23550
- Electron impact excitation rates calculation for He I and II transitions, comparing measured, theoretical and semiempirical impact cross sections 10 p1251 A73-24133
- Electron impact ionization, three body recombination and thermal energy balance effects on gas discharge positive column between plane parallel walls 10 p1255 A73-24265
- Energy and angular correlations of the scattered and ejected electrons in the electron-impact ionization of argon. 10 p1252 A73-24340
- Electron impact excitation of H₂. 12 p1526 A73-27687
- Temporal development of longitudinal plasma current radial profile, obtaining effective collision frequency estimation for electron heating, hot plasma production conditions and stability restoration force 14 p1777 A73-29685
- Autoionizing transitions in N₂ and H₂ produced by electron impact. 14 p1776 A73-29695
- Electron-molecule collision ionization in hydrogen and deuterium. 14 p1776 A73-29700
- Excitation of atomic nitrogen by electron impact. 16 p2038 A73-33099
- Photoelectron excitation of the Jupiter dayglow. 16 p2062 A73-33430
- Electron impact excitation of N₂. I, II. 16 p2039 A73-33866
- Chemisorption of CO on tungsten /100/- Combined flash desorption and electron stimulated desorption study. II. 18 p2287 A73-37033
- Combined Auger electron spectroscopy and electron impact desorption studies of silicon surfaces. 20 p2595 A73-39665
- Atmospheric CO production from electron impact on carbon dioxide, considering lightning, radioactivity, discharges, photoelectrons, auroral particles, cosmic rays and solar wind 21 p2680 A73-40079
- Fluorescence efficiencies of electrons in second positive bands of N₂ and first negative bands of N₂⁺. 21 p2682 A73-40164
- Kinetics of impact-radiation ionization and recombination. 22 p2892 A73-42344
- Electron cooling rates calculation based on measured impact cross sections of molecular oxygen for vibrational and low lying electronic excitation 24 p3086 A73-45123
- ELECTRON INTENSITY**
- U ELECTRON FLUX DENSITY**
- ELECTRON INTERACTIONS**
- U ELECTRON SCATTERING**
- ELECTRON IONIZATION**
- U IONIZATION**
- ELECTRON IRRADIATION**
- Comparison of data on irradiation of germanium by 1- and 28-MeV electrons 02 p0201 A73-12592
- Luminescence excitation by protons and electrons, applied to Apollo lunar samples. 03 p0369 A73-13098
- Irradiation of solar cell candidates for the ATS-F solar cell flight experiment. 03 p0257 A73-14245
- Electron irradiated float-zone Si solar cell I-V performance degradation due to photon irradiation, noting base region minority carrier lifetime role 03 p0257 A73-14246
- The effect of boron concentration on radiation damage in silicon solar cells. 03 p0258 A73-14249
- The mechanism of stage III recovery of electron irradiated molybdenum. 04 p0461 A73-14870
- Electrical properties of electron-irradiated GaAs. 05 p0604 A73-16516
- Beta irradiation of silicon junction devices - Effects on diffusion length. 05 p0537 A73-16522
- Extinction of photoluminescence by electron irradiation and energy transfer in molecular crystals 05 p0600 A73-16555
- On the point defect production in electron-irradiated molybdenum. 06 p0705 A73-17832
- Luminescence of lunar material excited by electrons. 07 p0897 A73-19881
- Characteristics of infrared photodetectors produced by radiation doping. 09 p1079 A73-21934
- Silicon solar cells radiation damage from orbital flight and electron and proton irradiation laboratory test data, discussing radiation hardening by Li doping 09 p1036 A73-22811
- Useful penetration in an austenitic stainless steel, of electrons accelerated under a very high voltage /1500 to 2500 kV/ 09 p1105 A73-23037
- Investigation of radiation defects in silicon and germanium single crystals irradiated by 50-MeV electrons 11 p1410 A73-26449
- Electrical properties of semiconductors with non-spherical radiation damage regions. 16 p2044 A73-33198
- Kinetics of recovery of luminescence properties of gallium arsenide single crystals irradiated with high-energy electrons. 20 p2574 A73-39697
- Effective recombination levels in N- and P-type silicon irradiated by 4.5 MeV electrons. 21 p2753 A73-41558
- Fading of thermoluminescence induced in lunar fines. 22 p2915 A73-43027
- EPR-line splitting in irradiated ruby containing impurities 23 p3017 A73-44039
- Influence of radiation on the current-voltage characteristic of tunnel diodes /Survey/ 24 p3072 A73-44926
- ELECTRON MICROSCOPES**
- Electron-microscopic investigations of metal oxide powders 02 p0178 A73-11543
- Scanning electron microscope investigation of interaction between pyrolytic carbon fibers and oxidizer, noting periodic variations of carbon chemical activity in radial direction 02 p0185 A73-12556
- Limiting resolution of reconstructed image of focused hologram in electron microscopes as function of aberration and spatial coherence 03 p0309 A73-14088
- Holography without fringes in the electron microscope. 04 p0447 A73-15049

Scanning and transmission type electron microscopes, discussing operating principles, image quality, resolution and applications
05 p0575 A73-16311

Electron-microscopy investigation of Corti's organ after noise trauma
05 p0539 A73-16333

Quartz light pipe for scanning electron microscope, noting photomultiplier voltage reduction and indefinite service life
05 p0580 A73-17259

Scanning electron microscope operation and application to technology research and electronic components and circuits failure and reliability analysis
07 p0797 A73-18922

Defects analysis and the possibilities brought by the scanning electron microscope
07 p0823 A73-19408

Ion gun sputter cleaning of thin film metal substrate for in situ corrosion studies by UHV transmission electron microscopy
08 p0990 A73-21616

Scanning electron microscope for heat transfer surfaces characterization, noting Inconel surface roughness change in convective heat transfer experiment
08 p1025 A73-21642

A new explanation for the creep of domain boundaries with transverse constrictions
09 p1098 A73-21846

An electron microscopy study of precipitation in Cu-Ti sideband alloys.
10 p1234 A73-24434

Interpretation of quench-sensitivity in Al-Zn-Mg-Cu alloys.
10 p1235 A73-24442

Metallic and nonmetallic surface investigation by scanning electron microscopy, discussing operational features and applications to wear, fracture and corrosion studies
11 p1361 A73-25107

Crystal surface topography investigation by scanning electron microscopy for dihedral angle measurements on thermally grooved grain boundaries
13 p1617 A73-28935

Responses of indigenous microorganisms to soil incubation as viewed by transmission electron microscopy of cell thin sections.
14 p1714 A73-29724

Observation of dislocations and inclusions in neodymium-doped yttrium aluminium garnet by transmission electron microscopy.
14 p1782 A73-29744

Electron-microscopic investigation of the spatial distribution parameters of second-phase precipitation in aging nickel-base alloys
14 p1764 A73-30862

Twin-jet thinning techniques for transmission electron microscopy observation of tantalum and niobium.
15 p1891 A73-31995

Scanning electron microscope analysis of Ti-Al-V specimens under simultaneous fatigue and fretting loads
15 p1883 A73-32148

Application of a scanning electron microscope in powder investigations
15 p1892 A73-32239

The analysis of defects and the possibilities brought by the scanning electron microscope
16 p2019 A73-33272

Effects of electron-microscope design features on the accuracy of the microprobe diffraction method
17 p2164 A73-34176

A microscopic study of crack initiation mechanisms in 7075 aluminum alloy sheets.
17 p2190 A73-34885

Study of fretting wear in titanium, Monel-400, and cobalt-25 percent molybdenum using scanning electron microscopy.
[ASLE PREPRINT 73AM-8A-3]
17 p2190 A73-34993

Some details concerning plastic deformation mechanism of commercial titanium between -100 and 400 C
19 p2441 A73-37839

Screening of metallization step coverage on integrated circuits.
19 p2411 A73-38456

Chromatic aberration effects on inelastic image resolution for high voltage electron microscopes
21 p2702 A73-40789

Phase contrast transfer damping functions for various beam apertures in high resolution electron microscopy
21 p2702 A73-40949

A non-contacting length comparator with 10 nanometer precision.
21 p2704 A73-41257

Field electron emission microscopic study of titanium
24 p3098 A73-44474

ELECTRON MOBILITY

Studies of the electron transport chain of extremely halophilic bacteria. VIII - Respiration-dependent detergent dissolution of cell envelopes.
01 p0009 A73-10625

Thermal and near-thermal electron transport coefficients in O₂ determined with a time-of-flight swarm experiment using a drift-dwell-drift technique.
03 p0344 A73-13276

The equation of state of a dense metal vapor plasma and electron mobility
06 p0730 A73-18552

Concentration and mobility of electrons in indium-doped zinc oxide crystals
07 p0862 A73-20016

Photosensitized inhibitor formation in isolated, aging chloroplasts.
07 p0784 A73-20453

Gunn diode effect in n-type GaAs, discussing electron drift velocity relationship to electric field, I-V characteristics and fabrication
08 p0943 A73-20709

Finite difference calculation for Gunn effect mathematical model, noting negative slope in electron drift velocity versus electric field characteristics for microwave oscillation
08 p0943 A73-20710

Relaxation in a two-temperature plasma with directed motion of electrons
09 p1127 A73-22601

Effect of shielding on charge carrier mobility in compensated materials
09 p1133 A73-22674

Drift mobilities of holes and electrons in naphthalene single crystals.
11 p1407 A73-24988

Drift mobility of holes and electrons in perdeuterated anthracene single crystals.
12 p1531 A73-27688

Boltzmann transport equation solution for electron mobility in ellipsoidal valleys of n-type GaAs and GaP, taking into account arbitrary magnetic fields and scattering mechanisms
13 p1668 A73-28217

Unified theory of type I and II irregularities in the equatorial electrojet.
14 p1748 A73-29973

Russian book - Electrons and holes in semiconductors: Energy spectrum and dynamics.
15 p1852 A73-32298

Equation of state of a plasma of a dense metal vapor and the electron mobility.
16 p2042 A73-33577

Determination of the diffusivity-mobility ratio in highly degenerate semiconductors at low temperatures from linewidth measurements in junction lasers.
16 p1990 A73-33689

Experimental investigation of current-driven ion wave turbulence in plasma.
22 p2890 A73-42224

Illumination aftereffects due to semiconducting ferrite electron and ion motion, discussing dielectric properties and electron hole deficiencies
22 p2833 A73-42514

ELECTRON MULTIPLIERS
U PHOTOMULTIPLIER TUBES
ELECTRON OPTICS

Two-beam TWT /electron-wave TWT/ under large input-signal conditions - Effects of parameters
01 p0025 A73-10985

Experimental investigation of a test-model two-beam TWT /electron-wave TWT/
01 p0025 A73-10986

Nucleation film/electron beam recorder - Near-real-time display system.
08 p0965 A73-21247

Electron-optical investigations of discharge in air and carbon dioxide in the nanosecond range
10 p1219 A73-24469

Strict calculation of static fields in devices for periodic electrostatic focusing /PEF/ of electron beams
10 p1197 A73-24882

Quasi-optical diffraction-type radiation generator
11 p1331 A73-26159

Book on semiconductor opto-electronics covering solids optical constants, classical and quantum mechanical dispersion theory, absorption processes, magneto-optical and photo-electrical effects, etc
12 p1531 A73-27449

Application of the regularization method to the solution of the inverse problem in potential theory for electron-optical systems
13 p1662 A73-29681

Some aspects of the design and performance of a small high-contrast channel image intensifier.
14 p1751 A73-29909

Pick-up storage tube having an electronic shutter, automatic exposure control, wobbling correction, and slow scanning.
14 p1751 A73-29911

Optoelectronic semiconductor components under the influence of ionizing radiation
14 p1733 A73-30070

German book on physical foundations of electronics covering charged particle motions in electric and magnetic fields, relativistic effects, electron and ion optics, etc
14 p1736 A73-30597

Telescope equipment for future astronomical observatory, favoring array of computerized electronic imaging small telescopes vs single large reflector
14 p1754 A73-30916

Russian book - Radiation receivers of automatic electron optics devices.
15 p1875 A73-31588

Electron-optical image transfer using opaque photocathodes with electromagnetic lens in image tubes
17 p2136 A73-34905

Storage tube with silicon target captures very fast transients.
21 p2661 A73-40228

Static fields for periodic electrostatic focusing of electron beams.
21 p2668 A73-41657

Improvement of the electron optics of X-ray image-intensifiers.
23 p2982 A73-43678

ELECTRON ORBITALS

Projectile structure effects on neon K X-ray production by fast, highly ionized argon beams.
04 p0476 A73-14769

Ionization of 6s- and 5p-electrons of the cesium atom by electron impact
09 p1122 A73-21977

Quantum mechanical formalism for unitary transformations of wave functions, gauge transformations and current conservation, discussing use of gauge invariant atomic orbitals
10 p1251 A73-24245

Structure of beryllium boron hydrides BeBH₅ and BeB₂H₈.
12 p1466 A73-27045

Simplified Hartree-Fock approximation for complex atom opacity efficient calculation based on homogeneous one-electron orbital equation solution with effective potential optimization
13 p1662 A73-28455

ESCA study of fractional monolayer quantities of chemisorbed gases on tungsten.
14 p1724 A73-30421

Thermophysical properties of high temperature electrical insulating materials on the basis of non-metallic compounds with high melting point [ECTP PAPER D2-3]
14 p1766 A73-30436

Application of an extended method of calculation to rare-earth atoms and ions in the 4fN configuration
14 p1784 A73-30852

Electronic structure of ferric iron octahedrally coordinated to oxygen.
18 p2341 A73-37049

Temperature aspects of Landau orbital ferromagnetism in white dwarfs and neutron stars.
20 p2610 A73-39573

Ti-V alloys elastic modulus and paramagnetic susceptibility, considering composition vs property curve salient point indications of changes in interatomic bonding energy and electron structure
21 p2718 A73-40487

Energy level transitions in Ca XVII and Ti XIX UV spectra, basing identifications on extrapolation method
22 p2914 A73-43016

Nonlinear saturation of the gradient drift instability in the equatorial electrojet.
24 p3087 A73-45141

Metal crystal lattice properties and chemical bond nature in terms of valence concept, analyzing p-electron cloud overlapping
24 p3119 A73-45178

ELECTRON OSCILLATIONS

Oscillator strengths and ground-state photoionization cross-sections for Mg+ and Ca+.
01 p0104 A73-11043

Short-life mode of electrostatic electron cyclotron harmonic waves.
04 p0477 A73-15196

Vibrational and energy spectra of welding electron beam interacting with beam produced plasma, noting interaction length effect on instability
04 p0454 A73-15609

Plasma instability in terms of electron oscillations due to parametric interaction with UHF electric field, noting inverse Cerenkov effect for electrons
06 p0729 A73-18111

Solid material ion source discharge chamber with cathode sputtering-introduced metal vapor, based on conventional ion source with electrons oscillating in magnetic field
08 p0993 A73-21515

Parametric action of high-power radiation on a plasma near the electron cyclotron frequencies
09 p1123 A73-21876

'Flux quantization' type of oscillation effects in a normal metal
09 p1130 A73-22709

ELECTRON MICROSCOPY
U ELECTRON MICROSCOPES

Vibrational and energy spectra of welding electron beam interacting with beam produced plasma, noting interaction length effect on instability

10 p1224 A73-24199

Parametric instability in a plasma placed in non-homogeneous magnetic field.

11 p1407 A73-26563

A note on the heating of magnetoplasma by magnetic perturbations.

11 p1407 A73-26659

Quasi-linear theory of a parametrically unstable magnetoactive plasma

14 p1782 A73-30806

Contribution to the theory of electron-beam stability in an inhomogeneous dielectric medium

15 p1920 A73-32302

Parametric excitation of ion-acoustic oscillations in a plasma situated in an alternating electric field and a constant magnetic field

21 p2746 A73-40519

Nonlinear interacting longitudinal and transverse electron oscillations due to plasma density inhomogeneity in HF hybrid resonance region

21 p2750 A73-41683

Determination of valence electron plasma frequencies and optical permittivity in single crystals of trisulfide of antimony

22 p2897 A73-42648

Pair production near energy threshold by electron oscillation and acceleration to relativistic velocities at laser beam focus with plasma wave excitation

23 p2989 A73-44121

Influence of Langmuir electron oscillations on the degree of neutralization of an ion beam

23 p3014 A73-44342

Plasma instability in terms of electron oscillations due to parametric interaction with UHF electric field, noting inverse Cerenkov effect for electrons

24 p3114 A73-44500

Stability of an electron beam in an inhomogeneous dielectric medium.

24 p3114 A73-44610

ELECTRON PARAMAGNETIC RESONANCE

Electron spin resonance of ultraviolet radiation induced defects in ZnO thermal control coating pigment.

01 p0088 A73-11276

A combined magnetic circular dichroism and electron paramagnetic resonance spectrometer.

02 p0167 A73-11951

EPR in alpha-particle bombarded silicon single crystals

02 p0201 A73-12171

Electron spin resonance of manganous ions in frozen methanol solution.

04 p0414 A73-15025

F-19 chemical shift tensor in group II difluorides.

05 p0546 A73-16046

Effect of alkali-earth oxides on the optical and EPR spectra of irradiated alkali silicate glass

05 p0589 A73-17296

Influence of lattice defects on EPR line-shapes in ruby.

06 p0734 A73-17794

Microwave method of investigating the quality of ruby boules.

06 p0734 A73-17813

Evidence of lunar surface oxidation processes - Electron spin resonance spectra of lunar materials and simulated lunar materials.

07 p0893 A73-19840

Magnetic phases in lunar material and their electron magnetic resonance spectra - Apollo 14.

07 p0894 A73-19847

Confirmation of electronic paramagnetic resonance of the existence of an ordered phase in the zirconium-calcium system

09 p1135 A73-23031

Study by electronic paramagnetic resonance of the molecular dissociation in an oxygen plasma

13 p1664 A73-28566

Some aspects of the exchange-interaction and dipole-dipole broadening of the individual hyperfine components of the EPR spectrum

14 p1775 A73-30580

Electron paramagnetic resonance of Fe³⁺/ in forsterite/Mg₂SiO₄.

15 p1923 A73-31273

Unpaired electrons and charge carriers in oxide semiconductor glasses based on the oxides of titanium, vanadium, and phosphorus

20 p2599 A73-39394

Electron paramagnetic resonance studies of a viscous nematic liquid crystal. II - Evidence counter to a second-order phase change.

22 p2897 A73-42711

EPR-line splitting in irradiated ruby containing impurities

23 p3017 A73-44039

ELECTRON PATHS

U ELECTRON TRAJECTORIES

ELECTRON PHONON INTERACTIONS

Investigation of the phonon drag effect in n-GaAs.

04 p0482 A73-14866

The influence of the electron-phonon scattering on the total energy distribution of field emitted electrons from tungsten.

04 p0477 A73-15000

Radiation of phonons by metallic films.

04 p0483 A73-15465

Observation of Kohn-type anomalies in the electron-phonon interaction on the Fermi surface of degenerate semiconductors.

04 p0483 A73-15469

Electron impulse interactions of heat in semiconductors

04 p0483 A73-15470

Phononless lines shift and broadening during electron phonon interaction in lanthanum trifluoride-Nd crystal, obtaining temperature dependence of non-radiative transition probability

04 p0484 A73-15566

Non-ohmic transport and phonon amplification in polar semiconductors.

04 p0484 A73-16035

Single-phonon contribution to the hopping conductivity of amorphous solids.

08 p0994 A73-20955

Temperature dependent thermal conductivity coefficient and electron and phonon components for group IV-VI transition metal diborides at 2300 K, using Wiedemann-Frantz law

10 p1236 A73-23518

Microsonics /acoustic surface waves/ technology developments covering materials, heteroepitaxial systems, propagation, electron phonon interaction, acoustic amplifiers and waveguides, electromechanical transducers and signal processing

10 p1223 A73-23782

Influence of a powerful electromagnetic wave on the electrical conductivity of a semiconductor

11 p1409 A73-26165

On the quadrupole interaction in the diamond structure.

13 p1667 A73-28213

French monograph on metal-semiconductor junction electron tunneling effect covering phonon interaction mechanisms, control and characterization problems

13 p1669 A73-29290

Model of degenerate semiconductor transition to superconducting state in terms of electron interactions with phonons of low-lying spectral branch

14 p1783 A73-30343

Effects of electron-phonon interaction in the luminescence spectra of transition and rare-earth impurity ions in crystals

15 p1885 A73-31715

Interaction of nearly monochromatic LA phonons with excitons in CdS crystals

15 p1924 A73-31718

Multiplicity of dielectric local modes - Bound states of phonons with impurity centers

15 p1885 A73-31719

Temperature dependent thermal conductivity coefficient and electron and phonon components for group IV-VI transition metal diborides at 2300 K, using Wiedemann-Frantz law

17 p2196 A73-35198

Theory of quantum oscillations of the Nernst-Ettingshausen thermomagnetic coefficient in semiconductors

20 p2599 A73-39397

One dimensional model of electron-phonon system exhibiting Peierls instability for tetrathiofulvalinium tetracyanoquinodimethane conductivity, considering high temperature superconductivity achievement via Peierls instability suppression

21 p2751 A73-40508

Effect of high pressure on the superconducting transition temperature of Pd-H.

21 p2753 A73-41126

Quantum transport theory of high-field conduction in semiconductors.

23 p3016 A73-43775

Electron-electron collisions and the electrical conductivity of metals at low temperatures

23 p3016 A73-44021

ELECTRON PHOTOGRAPHY

Electroradiography technique involving photoproduction of free electrons via Townsend avalanche amplification in diode /triode/ gap, noting increased quantum efficiency

23 p2950 A73-44214

ELECTRON PHOTON CASCADES

Multilayer X ray film chamber for gamma quanta energy spectrum determination by primary photon impact and absorber calorimetric methods

02 p0208 A73-12660

Ionization calorimeter measurement of energy transfer to electron photon cascade secondary particles during hadron interaction with lead nuclei

02 p0209 A73-12662

Cosmic radiation high energy hadron component relation to extensive electron-photon showers, comparing sampling events based on multicore structure and total energy

02 p0209 A73-12676

High energy muon energy and angular distributions from electron-photon cascades, using emulsion chamber with X ray films

02 p0209 A73-12680

Spectral calculations of electromagnetic and nuclear showers, studying cosmic ray muons interactions with matter

02 p0210 A73-12682

Muon generated cascade showers in iron, using ionization calorimeter and hodoscope detectors

02 p0210 A73-12684

Electron photon shower particle flux transition effect on ionization chamber and scintillation counter readings

02 p0210 A73-12685

K-neutral pion energy fractions and inelasticity coefficients at primary energies of 100-1500 GeV during cosmic ray hadron-target interaction

02 p0210 A73-12689

Calculation of the moments of the electron spatial distribution function without allowance for ionization losses

08 p1000 A73-21514

Electron calibration of a high-energy cosmic ray detector.

21 p2703 A73-41150

Particle number fluctuations and transient effects in electron-photon showers in lead at energies above 20 GeV

23 p3021 A73-43531

Preliminary results of the Pamir-20-71 experiment on interactions at energies of about 1000 Tev

23 p3021 A73-43534

High energy gamma quanta families and multiple generation processes in electron photon cascades detected by nuclear emulsion X ray chamber

23 p3021 A73-43536

Intense air showers with an electron-photon core of complex structure

23 p3022 A73-43545

Calculation of the fluctuations of the Cerenkov radiation of an electron-photon shower in the atmosphere

23 p3022 A73-43554

Fluctuations of the total path of charged particles in electron-photon showers caused by gamma-quanta with energies of 40, 60 and 200 m/c-squared/

23 p3023 A73-43555

The structure of the spatio-angular distribution function of electron-photon shower particles near the axis

23 p3023 A73-43556

Intensity variations of electron-photon shower particles in the atmosphere

23 p3023 A73-43557

Transition effects during the recording of the electron-photon component of extensive air showers

23 p3023 A73-43558

The energy spectrum of cosmic ray muons at sea level

23 p3023 A73-43559

Generation of high-energy muons in cosmic rays

23 p3023 A73-43560

Semiautomatic recorder for photometry of black spots produced by electron-photon cascades on RT-6 type X-ray films

23 p2982 A73-43568

ELECTRON PLASMA

Third order collisionless electron plasma echo signal wavelength and rise and fall rate about central position, comparing experiment with Vlasov equation theory

02 p0197 A73-12064

Free streaming electrons effect on spatial ballistic electron plasma wave echoes response, calculating echo electric fields and electron distribution function

02 p0197 A73-12065

The integral equation and boundary conditions for a cylindrical antenna in a warm plasma.

[AD-760102] 04 p0429 A73-15482

Stable electron density fluctuations in a plasma in the presence of a high-frequency electric field.

04 p0444 A73-15539

Quantum theory of the dielectric constant of a magnetized plasma and astrophysical applications. I.

05 p0624 A73-17310

Stochastic kinetic theory of strong wave-plasma interaction. I - Kinetic equations.

05 p0603 A73-17323

Stimulated Compton scattering of laser radiation by electron plasma, determining electrons diffusion coefficient and velocity distribution function

06 p0700 A73-17970

Kadomtsev-Nedospasov helical instability during a strong pinch effect in an electron-hole plasma

06 p0729 A73-18119

Electron cyclotron off-resonance heating rate in hot electron plasmas, comparing numerical calculation in terms of harmonic resonance with computerized simulation

07 p0856 A73-19519

Measurement of the attenuation of an electromagnetic wave in a bounded hot electron plasma.

07 p0860 A73-20478

Electron plasma oscillation due to beam plasma interaction with standing wave formation between electrodes, observing temporal growth rate during beam modulation removal

08 p0992 A73-21005

Simultaneous suppression of an electron plasma wave and an ion acoustic wave by beam modulation.

08 p0992 A73-21006

Electrical and thermal conductivities of a relativistic degenerate plasma.

08 p0992 A73-21161

Nonlinear frequency correction to plasma instability at half harmonics of electron gyrofrequency as observed byOGO 5 near geomagnetic equator outside plasmopause

09 p1075 A73-22069

Microwave heating and resonant diffusion of electron plasmas, considering relativistic theory and Fokker-Planck equation

[TTU-SR-2] 09 p1129 A73-22641

Certain properties of an electron plasma in a strong electromagnetic field

09 p1130 A73-22704

Expanded laser produced plasma Debye length from slab geometry, evaluating electron temperature for ion recombination rates

10 p1256 A73-24270

Internal instabilities derived for electron plasma with electrons rotating about axis of symmetry parallel to confining external magnetic field

10 p1256 A73-24449

Satellite-borne electrostatic wave topside ionosphere sounder for electron plasma resonance measurement, discussing data spectra preservation, frequency synthesizer and gain-change mechanism features

11 p1339 A73-26629

Stability of a magneto-active plasma with a relativistic electron beam, situated in a high-frequency electric field

12 p1527 A73-26927

Parametric instabilities and harmonic generation in Tonks-Dattner resonances in inhomogeneous bounded electron plasma layer

13 p1665 A73-28791

Receiving characteristics of antennas in an isotropic compressible plasma.

13 p1594 A73-29230

Radiation from travelling wave circular loop antenna in compressible electron plasma.

14 p1731 A73-29709

Parametric instabilities and anomalous absorption and heating of plasmas.

14 p1779 A73-30118

Comparison of the hot-electron plasmas produced using two different plasma sources in a magnetic mirror compression experiment.

14 p1781 A73-30657

Microwave heating of electrons of a dense plasma column at frequencies higher than electron cyclotron frequency.

14 p1782 A73-30771

Longitudinal force exerted by circularly polarized high-powered laser radiation in a dense electron plasma.

15 p1917 A73-31091

Axial distribution for a hot electron plasma.

16 p2041 A73-33325

Edge instability of transverse electromagnetic waves in a weakly ionized plasma

17 p2214 A73-34249

Instability of plasma waves with nonlinear Landau effect.

17 p2215 A73-34296

Electrostatic waves with frequencies above the gyrofrequency in a plasma with a loss-cone.

17 p2218 A73-35831

Simulation of gyroresonant electron-whistler interactions in the outer radiation belts.

18 p2347 A73-36296

Parametric decay of obliquely incident electromagnetic waves into ion acoustic and electron plasma waves in vicinity of resonance

20 p2595 A73-38874

Current and energy characteristics of an electron plasma in a magnetron diode

20 p2536 A73-39254

Electron plasma wave shocks in a collisionless plasma.

20 p2598 A73-39301

Modification of weak turbulence theory due to perturbed orbit effects. II - Nonlinear Landau damping of electron plasma waves.

20 p2598 A73-39302

Parametric excitation of oscillations in an electron plasma

21 p2746 A73-40518

Nonlinear parametric electron plasma instability due to cyclotron harmonic Bernstein wave interaction in strong electric field

21 p2747 A73-40791

Rocket experiments on nonlinear wave-wave interaction in the ionospheric plasma.

21 p2685 A73-40823

New dispersion relation for a strongly magnetized degenerate electron plasma with anisotropic pressure.

22 p2890 A73-42237

Electron wave excitation and propagation in low density large volume plasmas near electron Langmuir frequency

22 p2891 A73-42241

Stability of a magnetoactive plasma with a relativistic electron beam in an RF electric field.

22 p2891 A73-42261

Kinetic theory of electromagnetic waves in an electron plasma characterized by slowly changing parameters

22 p2892 A73-42327

Nonlinear development and Fourier analysis of the whistler mode instability.

22 p2893 A73-42391

Shielding of moving test particles in warm, isotropic plasma.

22 p2893 A73-42392

The influence of electron plasma formation on superbroadening in light filaments.

22 p2871 A73-43077

Theory of parametric resonance in a spatially modulated plasma

23 p3013 A73-44334

Kadomtsev-Nedospasov helical instability in a strong pinch effect in an electron-hole plasma.

24 p3114 A73-44503

ELECTRON PRECIPITATION

Precipitation patterns in the Arctic ionosphere determined from airborne observations.

01 p0036 A73-10341

Multidiscipline study of perturbations observed on March 8, 1970 in the midnight sector

01 p0036 A73-10343

Rocket measurements of electron fluxes in the upper atmosphere at midlatitudes.

01 p0041 A73-10887

Auroral X-ray and conjugate ionospheric absorption observations of an electron precipitation event accompanying a sudden impulse in the geomagnetic field.

02 p0157 A73-11759

Auroral particle precipitation patterns from satellite observations, discussing electron and proton penetration from magnetosheath plasma and magnetotail

02 p0163 A73-12308

High-latitude precipitation of low-energy particles as observed by ESRO I A.

02 p0206 A73-12312

Precipitation of auroral and ring current particles by artificial plasma injection.

03 p0301 A73-13711

Low energy auroral electron and proton precipitation patterns from polar orbiting ESRO 1A satellite, noting discontinuities, flux distribution valleys, latitudinal crossover and Kp dependence

03 p0362 A73-13864

Pitch angles and spectra of particles in the outer zone near noon.

[AD-758531] 03 p0363 A73-13867

Auroral precipitating electron angular distributions from polar orbiting satellite OV1-18 measurements, indicating pitch-angle diffusion due to particle-wave interactions

03 p0363 A73-13868

Airborne photometric measurements of auroral emissions, indicating soft zone and superimposed energetic electron precipitation

03 p0363 A73-13870

A theory on the latitude and local time distribution of precipitating electrons during a sudden commencement.

03 p0304 A73-13885

Trapped and precipitated electron energy spectra in relativistic electron precipitation events /REP/, discussing bremsstrahlung measurements deductions

03 p0304 A73-14591

Auroral-zone X-ray measurements at Kiruna in 1970.

04 p0492 A73-15100

Precipitation of low-energy electrons at high latitudes - Effects of interplanetary magnetic field and dipole tilt angle.

04 p0493 A73-15531

Observed relationships between electric fields and auroral particle precipitation.

07 p0814 A73-19237

Photoelectron precipitation induced dissociation of atmospheric nitrogen molecules during moderate solar activity

07 p0816 A73-19459

Impact and bremsstrahlung photoionization due to precipitating electrons in the lower ionosphere.

08 p0957 A73-20657

Auroral particle influx behavior and electric field aligned electron precipitation observation by Ba release and electrostatic probe in rocket and satellite experiments

08 p0957 A73-20662

Relations between ionospheric electric fields and energetic trapped and precipitating electrons.

09 p1073 A73-22056

Measurement of auroral Birkeland currents and energetic particle fluxes.

09 p1073 A73-22057

Balloon observations of auroral-zone X-rays in conjugate regions.

09 p1137 A73-22135

Simultaneous observations of low energy electron fluxes and the polar red emission at 6300 A.

09 p1075 A73-22137

Results of volley flights of radio probes on the Kolak peninsula during periods of magnetic disturbances in March and April 1971

10 p1267 A73-23929

Auroral arcs oval configuration by all-sky photography from Arctica 2, considering difference in dayside and nightside halves from electron precipitation observations

10 p1214 A73-24745

On the morphology of auroral-zone X-ray events. II - Events during the early morning hours.

11 p1354 A73-25762

On the morphology of auroral-zone X-ray events. III - Large-scale observations in the midnight-to-morning sector.

11 p1354 A73-25763

Energetic electron precipitation as a source of ionization in the night-time D-region over the mid-latitude rocket range, South Uist.

11 p1358 A73-26701

Total electron content measurements during visible auroras.

11 p1359 A73-26714

Midlatitude bremsstrahlung X rays, VLF propagation disturbances and electron precipitation during magnetospheric substorm

12 p1468 A73-26983

Low energy auroral electron pitch angle diffusion in postbreakup aurora due to injected particle loss in closed magnetic field lines

12 p1488 A73-26987

Distributions and characteristics of high-latitude field-aligned electron precipitation.

12 p1534 A73-26988

On the longitudinal extension of electron precipitation during magnetospheric substorms.

13 p1606 A73-28152

Energy spectra and pitch angle distributions of precipitating incident and backscattered electron fluxes in auroral arcs

14 p1747 A73-29968

Auroral electrons of energy less than 1 keV observed at rocket altitudes.

14 p1748 A73-29969

Electron precipitation patterns and substorm morphology.

16 p2056 A73-33434

Red auroras in the morning sector.

16 p2004 A73-33446

Convection dominated electrons in auroral zone, discussing plasma sheet as magnetospheric electron source, convection electron spatial distribution and convection-precipitation coupling

17 p2223 A73-34358

Observation of quasitrapped and precipitating electrons at midlatitude.

18 p2344 A73-35927

An investigation on the spatial distribution of the quasi-trapped energetic electrons observed on board the satellite 'Shinsei.'

18 p2344 A73-35929

Large-scale auroral-zone electron precipitation event, briefly interrupted during a negative magnetic impulse.

18 p2344 A73-35951

Time dependent studies of the aurora. II - Spectroscopic morphology.

18 p2311 A73-36185

An example of anticorrelation of auroral particles and electric fields.

18 p2312 A73-36297

Satellite and ground-based observations during the onset phase of the 2 November 1969 PCA event.

19 p2426 A73-38016

Whistler-mode hiss at low and medium frequencies in the dayside-cusp ionosphere.

20 p2529 A73-38935

Auroral arc mechanism of solar wind intrusion and electron and proton energization and precipitation in magnetosphere from Isis photometric and spectrometric observations

20 p2553 A73-39124

A comparison of the latitudinal variation of auroral absorption at different longitudes.

21 p2684 A73-40785

Latitude and local time dependence of precipitated low-energy electrons at high latitudes.

22 p2901 A73-41914

Rocket observations of electron precipitation in a westward-traveling surge.

22 p2902 A73-41915

Balloon and VLF whistler measurements of electric fields, equatorial electron density, and precipitating particles during a barium cloud release in the magnetosphere.

22 p2845 A73-41934

Azimuthal drift and precipitation of electrons into the South Atlantic geomagnetic anomaly during an SC magnetic storm. 22 p2846 A73-41946

Auroral electron and proton flux density, energy spectra, acceleration and precipitation mechanisms and turbulent diffusion from rocket and satellite measurements 22 p2850 A73-42748

Electron precipitation caused auroral zone bremsstrahlung X rays classification with respect to magnetic storm phases 22 p2851 A73-42750

Particle precipitation in Brazilian geomagnetic anomaly during magnetic storms. 23 p2971 A73-43687

Critique of Lukina theory of number of auroral arc orientations related to characteristic precipitation zones 24 p3084 A73-44799

Simultaneous observations of auroras from the South Pole Station and of precipitating electrons by Isis I. 24 p3126 A73-45115

ELECTRON PRESSURE
On coupled fields in stratified plasmas with tensor pressure perturbations. 24 p3115 A73-44625

ELECTRON PROBES
Petrochemistry and chemical features of lunar glassy spherules. 03 p0273 A73-13089

Characterization of boron carbide with an electronic microprobe 13 p1645 A73-28346

Apparatus and techniques for electron beam fluorescence probe measurements. 13 p1612 A73-28365

Study of surface by spectrometry of slow electrons 21 p2706 A73-41598

The detectability limits of thin coatings measured with the electron microprobe. 23 p2985 A73-43917

ELECTRON RADIATION
NT BETA PARTICLES
NT ELECTRON BEAMS
The transient highly excited solar flare plasma. 03 p0364 A73-13960

Solar electrons and alpha particles during polar-cap absorption events. 04 p0493 A73-15558

Solar corona properties and nuclear reactions in flares from August 1972 OSO 7 observation, noting hard X ray bursts from electron streams 04 p0502 A73-15971

Auroral electron spectrum space-time dynamics during magnetospheric substorms, using X ray bremsstrahlung balloon data 07 p0815 A73-19437

Relativistic electron bremsstrahlung suppression in isotropic plasma, noting analogy to synchrotron radiation 10 p1252 A73-23476

Direct observations of low-energy solar electrons associated with a Type III solar radio burst. 10 p1268 A73-24145

Electron pitch angle distributions throughout the magnetosphere as observed on Ogo 5. 10 p1213 A73-24732

Cosmic ray trapping region and characteristic exit time from Galaxy, discussing electronic component and chemical composition 16 p2054 A73-33286

Solar electrons, Galactic electron radiation modulation and spectrum of high energy cosmic ray electrons 16 p2055 A73-33293

ELECTRON RECOMBINATION
NT RADIATIVE RECOMBINATION
Instabilities and small-signal response of double injection structures with deep traps. 02 p0146 A73-12042

The effect of surface recombination velocity on the performance of vertical multi-junction solar cell. 03 p0255 A73-14214

Influence of recombinations in the base contact and on the base surface upon static and dynamic characteristics of the p-n junction. 06 p0674 A73-17816

Disturbed ionospheric electron and ion kinetics, detailing dissociative recombination as regulating process for temporal evolution 07 p0816 A73-19454

The continuity and Poisson's equations for semiconductors with many coexisting kinds of multiple energy-level defects. 09 p1133 A73-22306

Flux magnitude and single transition probabilities as function of electron density and temperature in relaxation model ionization and recombination channels 10 p1253 A73-23503

Radiative and dielectronic recombination coefficients for complex ions. 16 p2038 A73-32842

Non-thermal ionization and recombination processes during solar flares. 16 p2052 A73-32958

Generation-recombination noise and the microwave emission from InSb. 17 p2219 A73-34912

Flux magnitude and single transition probabilities as function of electron density and temperature in relaxation model ionization and recombination channels 17 p2217 A73-35183

Voltage-to-frequency converters with an avalanche-recombination discharge diode 22 p2832 A73-42357

ELECTRON RING ACCELERATORS
U STORAGE RINGS [PARTICLE ACCELERATORS]
ELECTRON SCATTERING
Many-body effects at metal-semiconductor junctions. I - Surface plasmons and the electron-electron screened interaction. 01 p0087 A73-10147

Differing roles of electron scattering processes in the thermodynamics of metals in the normal and superconducting states 01 p0088 A73-10613

The electron diffusion scattering cross section of cesium atoms 01 p0080 A73-10852

Nonthermal X-radiation and electric currents in solar flares 01 p0092 A73-10937

Use of the Glauber approximation in atomic collisions - A progress report. 02 p0195 A73-12649

Electron-ion collision frequency and electrical conductivity of non-Debye plasma formed in high pressure discharge from Ar, Kr and Xe tubes 03 p0345 A73-13176

One-electron model for charge exchange in ion-atom collisions. 03 p0344 A73-13283

Electron scattering by molecules with and without vibrational excitation. VI - Elastic scattering by CO at 6-80 eV. 03 p0344 A73-13284

E region electron collision frequency vertical distribution from ground and rocket measurements of radio wave absorption and electron density respectively 03 p0304 A73-14562

Close coupled calculations of electron-hydrogen atom scattering using a noniterative integral equation technique. 04 p0477 A73-14818

Electron scattering effect on spectral line profiles from characteristic electron density estimates for astronomical objects with rapid radial matter outflow, using Monte Carlo method 04 p0499 A73-15362

Theory of scattering of electrons in a non-degenerate-semiconductor-surface inversion layer by surface-oxide charges. 06 p0733 A73-17747

Metal atom migration acceleration under radioactive radiation, showing diffusion coefficient dependence on free and coupling electron interactions 06 p0735 A73-18038

Instability of a current-carrying plasma at cyclotron harmonics, and anomalous resistance 06 p0729 A73-18113

Density-matrix method for a weakly ionized plasma. 06 p0730 A73-18373

Investigation of the temperature dependence of the anisotropy parameter K in n-Si and n-Ge by using magneto-plasma waves 07 p0861 A73-19327

Possibilities of using a quadrupole probe in the 0 to 1000-Hz range to measure the collision frequencies of charged particles in the ionosphere 08 p0957 A73-20654

Collision cross sections for electrons with atmospheric species. 08 p0957 A73-20659

Experimental investigation of the excitation of Ar II and Kr II during electron-ion collisions 09 p1122 A73-22593

Matthiessen's rule and the electric resistance of solid solutions of silicon in iron at high temperatures 09 p1104 A73-22602

Coupled waves and particle scattering processes in ferromagnetic semiconductors and metals 09 p1133 A73-22677

Theory of fluctuations and particle scattering in ferromagnetic semiconductors and metals 09 p1134 A73-22678

Nonthermal X rays and electric currents in solar flares. 09 p1138 A73-22732

Partially ionized nonideal plasma model electron-ion interactions, equilibrium, equations of state and thermodynamic quantities 10 p1252 A73-23501

Energy and angular correlations of the scattered and ejected electrons in the electron-impact ionization of argon. 10 p1252 A73-24340

The thermal radiation spectra of supermassive stars and X-ray sources. 10 p1270 A73-24902

Effect of electron-electron collisions on the thermal conductivity of a dense plasma. 11 p1402 A73-25120

Vacuum state of a relativistic system interacting with an external field 11 p1397 A73-25245

Electron-neutral particle collisions effect on potential of test charge moving at velocity lower than plasma electrons, using BGK model and Lorentz collision operator 11 p1404 A73-25260

Description of the photoelectron interaction with ambient electrons in the ionosphere. 11 p1357 A73-25927

Analysis of the static modes of a magnetron with allowance for electron-velocity scatter 11 p1332 A73-26163

Metal-poor stars. IV - The evolution of red giants. 12 p1540 A73-27328

Solar corona anomalous polarization degree and E vector vibration direction, interpreting discrepancy from Thomson scattering prediction by scattered electron velocity effects 12 p1545 A73-27845

The diffusion cross section for scattering of electrons by cesium atoms. 12 p1526 A73-27902

Electron kinetics and stationary emission from semiconductor lasers 12 p1508 A73-27983

Carrier heating or cooling in semiconductor devices. 13 p1590 A73-28540

Low-temperature negative differential microwave conductivity in semiconductors following elastic scattering of electrons. 13 p1669 A73-28614

Observation of the effects of rotational transitions in the resonant scattering of electrons from N₂. 14 p1776 A73-29696

Spatially dependent electron relaxation near a thermionic emitting electrode. 14 p1713 A73-30473

Asymptotic form for the cross section for the Coulomb interacting rearrangement collisions. 14 p1777 A73-30551

Negative oxygen molecular ion formation in low energy electron collision and attachment obtaining capture cross section and resonance width 14 p1777 A73-30775

On the absorption of microwave through laboratory plasma. 14 p1782 A73-30800

On the effect of electron-neutral particle collisions upon the refraction of high-frequency radio waves by the lower atmosphere and ionosphere of Mars. 15 p1929 A73-31078

Studies of galvanomagnetic and thermomagnetic phenomena in selenium and tellurium doped InSb. 15 p1924 A73-32159

Ionospheric electron thermal conductivity obtained for power law dependence of electron-neutral collision frequency dependence on velocity 16 p2010 A73-33923

The kinetic characteristics of the electrons of the anisothermal homogeneous steady neon plasma in the ionization level range from 10 to the minus 9th power to 0.01 16 p2043 A73-34022

Book - Low energy electron collisions in gases: Swarm and plasma methods applied to their study. 17 p2213 A73-34461

Partially ionized nonideal plasma model electron-ion interactions, equilibrium equations of state and thermodynamic quantities 17 p2216 A73-35181

D region electron and ion density profiles, recombination coefficient and electron detachment rate changes during solar eclipse 18 p2310 A73-36127

Temperature dependent softening effect due to state transition and electronic drag coefficient for dislocations in pure two band superconductors 18 p2341 A73-36768

Influence of intervalley scattering on the size effect in the electrical conductivity of semiconductors 19 p2471 A73-37956

A tensor surface harmonic expansion of the collision integral for a weakly ionized plasma. I 20 p2596 A73-39193

Free atom and molecule energy levels studied by electron scattering spectroscopy, discussing energy losses, monochromated electron beams, particle resonance and electric fields 20 p2520 A73-39635

Slow electron scattering near focused beam of Q-switched ruby laser, investigating scattering probability dependence on electron impact parameter 21 p2712 A73-40354

Approximate variational treatment of elastic scattering of electrons from semi-infinite lattices. 21 p2741 A73-41627

Electron scattering from diatomic molecules in the first Born approximation. 22 p2889 A73-42446

- Singlet s-wave electron-hydrogen scatter below first excitation threshold, computing phase shift in Feshbach operator and static exchange approximation
22 p2890 A73-43127
- Electron-electron collisions and the electrical conductivity of metals at low temperatures
23 p3016 A73-44021
- Linear external electric field approximation for intervalley scattering effects on nondegenerate semiconductor surface electroconductivity
23 p3017 A73-44045
- Instability of a current-carrying plasma at cyclotron harmonics and the anomalous resistance.
24 p3114 A73-44502
- Electron cooling rates calculation based on measured impact cross sections of molecular oxygen for vibrational and low lying electronic excitation
24 p3086 A73-45123
- ELECTRON SPIN**
- Relative equilibrium of a mass of charged particles /electrons/ subject to its own gravitation and uniformly rotating about an axis
01 p0082 A73-10267
- Spin saturation and pump depletion in continuous spin-flip Raman oscillation.
03 p0319 A73-14452
- Projected states of open shell molecules - The pi-electron states of the cyclopentadienyl cation.
06 p0726 A73-18775
- Internal instabilities derived for electron plasma with electrons rotating about axis of symmetry parallel to confining external magnetic field
10 p1256 A73-24449
- Influence of magnetic spin resonance in optically transparent magnetic materials on the nature of laser radiation
16 p2024 A73-34001
- Laser-pumped tunable spin-flip InSb Raman lasers in terms of low field operation, linewidth measurement technique, power output and applications
20 p2571 A73-38623
- Spin contamination in unrestricted Hartree-Fock calculations.
22 p2889 A73-42442
- Optical orientation in a system of electrons and lattice nuclei within semiconductors - Experiment
23 p3016 A73-44022
- Optical orientation in a system of electrons and lattice nuclei within semiconductors - Theory
23 p3017 A73-44023
- ELECTRON SPIN RESONANCE**
- U ELECTRON PARAMAGNETIC RESONANCE**
- ELECTRON STATES**
- Arrhenius rate law for thermally activated processes, deriving master equation based on rates of transition between quantum states
03 p0397 A73-13289
- Indirect interaction of nuclear spins through valence band electrons in semiconductors
03 p0350 A73-13754
- Electric dipole moment of diatomic molecules by configuration interaction. V - Two states of $^2\Sigma/\Sigma_{g/u}$ symmetry in CN.
04 p0477 A73-14816
- Gold high temperature thermoelectric properties from electron model based on scattering resulting from d band-Fermi level relative position changes
04 p0463 A73-15313
- Shot noise in a Schottky barrier diode in the presence of surface electronic states at the contact
06 p0675 A73-18077
- Projected states of open shell molecules - The pi-electron states of the cyclopentadienyl cation.
06 p0726 A73-18775
- Oxygen anions excited electronic states, analyzing energy curves and wave functions via configuration-interaction results obtained by multiconfiguration self consistent field techniques
07 p0853 A73-19333
- Nature of chemical bonds in metal-like compounds based on transition metals
07 p0841 A73-20519
- Multiphoton excitations in vibrational-rotational states of diatomic molecules in an intense electromagnetic field.
08 p0990 A73-21003
- Wave functions and energies of the autoionization states of the cesium atom
09 p1122 A73-21976
- Excitation of autoionization states of the cesium atom by electron impact
09 p1122 A73-21978
- Experimental study of the relaxation of excited states in a decaying alkaline plasma
10 p1256 A73-24576
- Auroral He precipitation flux and charge state measurements for auroral ions source location by comparison with ionospheric and solar wind ion abundances
10 p1215 A73-24783
- Light absorption coefficient of disordered semiconductor within external dc field, discussing electron states near band boundaries
11 p1408 A73-25427

- The role of surface states in the formation of a Schottky barrier at a metal/gallium arsenide contact
18 p2341 A73-36717
- Theoretical assignments of the low-lying electronic states of carbon dioxide.
19 p2462 A73-37583
- Low energy gamma ray spectrum following muon capture by oxygen 16 leading to bound states of nitrogen 16
21 p2743 A73-40475
- Influence of the surface level on the differential slope of the semilogarithmic current-voltage characteristic of Schottky diodes
23 p2960 A73-43620
- Allowance for electron degeneration in a pseudopotential model of a nonideal plasma
24 p3115 A73-44759

ELECTRON SWEEPING**U SWEEP FREQUENCY****ELECTRON TELESCOPES****U PARTICLE TELESCOPES****ELECTRON TEMPERATURE****U ELECTRON ENERGY****ELECTRON TRAJECTORIES**

Shadowing of electron azimuthal-drift motions near the noon magnetopause.
02 p0164 A73-12442

A numerical computer method for computing the electrostatic field and electron paths of focusing optoelectronic systems
04 p0448 A73-15078

Thermal conductivity of superconducting layer in intermediate state with Andreev electron excitation trajectories in magnetic field, using Green function and impurity distribution technique
22 p2896 A73-41728

Calculation of the electron trajectories in helical beams produced by axisymmetric magnetron-type injection guns
23 p2961 A73-44346

Thermalization and transport of photoelectrons - A comparison of theoretical approaches.
24 p3086 A73-45124

ELECTRON TRANSFER

Transfer equations for high-energy electrons and photons in magnetic fields.
01 p0080 A73-11309

Gunn diodes - Physical principles and simulation calculations
02 p0144 A73-11529

Indium phosphide as a new material for microwave /transferred electron effect/ oscillators.
02 p0199 A73-11536

Material concerns, fabrication procedure, cooling techniques, performance and stability characteristics of transferred electron microwave amplifiers and oscillators
03 p0282 A73-13893

Phase diagrams and properties of binary alloys of refractory metals, taking into account the electronic structure of the atoms of the components
03 p0328 A73-14652

Design and performance of transferred electron amplifiers using distributed equalizer networks.
07 p0803 A73-20553

On the theory of tunnelling in electron and proton transfer reactions.
09 p1133 A73-22199

Design criteria for high gain, wide band, microwave amplifiers.
09 p1062 A73-22304

Computer simulations of the large signal characteristics of supercritical GaAs transferred electron amplifiers.
09 p1063 A73-22492

Book - Transferred electron devices.
09 p1066 A73-23299

J-band transferred-electron oscillators.
10 p1196 A73-24863

Overlength modes of transferred-electron oscillators.
11 p1337 A73-25359

Convection and diffusion transport equation of galactic cosmic ray electrons with energy loss and absorption allowance for supernova compressed halo models
12 p1535 A73-27635

Implication of contact thermalization effect in two-valley semiconductors for the high frequency device performance.
14 p1783 A73-29929

Electron current estimation along auroral zone-plasma neutral sheet field line from steady state one dimensional model
15 p1866 A73-31065

Influence of electron transport on the interaction between membrane lipids and Triton X-100 in Halobacterium cutirubrum.
15 p1841 A73-32024

French monograph - Contribution to the study of background noise in Gunn effect diodes.
15 p1852 A73-32589

Microwave capabilities of transferred-electron devices.
16 p1986 A73-32720

Effect of donor density and temperature on the performance of stabilized transferred-electron devices.
17 p2134 A73-34220

Quenched-domain mode oscillation in waveguide circuits.
17 p2136 A73-34969

Titanium cathode blanks in electrolytic production of metals, noting titanium oxide nonstick properties, electron transmission and corrosion resistance
19 p2442 A73-37841

Theory of successive electron transfer steps in cyclic voltammetry Application to oxygen pseudocapacitance on platinum.
21 p2636 A73-40843

Theoretical study of primary photosynthesis processes in higher plants and algae
23 p2946 A73-43707

High temperature electron transfer and Bi and Sb ion valency pair predictions in ordered perovskite-type oxides, using lattice constants
23 p3017 A73-44129

Predicted electron transport coefficients and operating characteristics of CO₂-N₂-He laser mixtures.
24 p3097 A73-45420

ELECTRON TRANSITIONS

Multiquantum ionization of a molecule represented by a nonorthogonal wave function system
01 p0080 A73-10622

Multiphonon transition theory for electron transitions probability between conduction and forbidden bands, noting semiconductor surface states with long relaxation time
01 p0089 A73-11438

Infrared excesses in early-type stars - Free-free emission.
02 p0225 A73-12826

The valence states of 3d - Transition elements in Apollo 11 and 12 rocks.
03 p0369 A73-13097

Diffusion approximation for kinetic equation of repeatedly ionized plasma, calculating direct transitions between excited ion states
03 p0344 A73-13180

Arrhenius rate law for thermally activated processes, deriving master equation based on rates of transition between quantum states
03 p0397 A73-13289

He odd parity states computed via Hylleraas trial wave function with nonlinear parameters, considering mass-polarization correction and electron transitions
05 p0600 A73-16599

Direct measurement of the lifetimes and predissociation probabilities for rotational levels of the OH and OD A-2Sigma⁺ states.
05 p0601 A73-17341

Stimulated collisions in collision processes with transitions between atomic levels and free and bound states, noting population density stabilization
06 p0725 A73-17910

Studies of the potential-curve-crossing problem. II - General theory and a model for close crossings.
06 p0726 A73-18263

CW operation in some CO lines below 5.0 microns.
06 p0704 A73-18892

Gain measurements on CO P-branch transitions in a C₂H₂-O₂ flame.
07 p0788 A73-19634

Electron and X ray transitions between conduction band and bound level and between two bound levels in transition metals, investigating edge singularity and spectrum shape
07 p0864 A73-20614

A shock tube determination of the CN ground state dissociation energy and the CN violet electronic transition moment.
08 p0989 A73-20789

Carbon monoxide rotational transitions as dark cloud cooling mechanism during protostar formation
08 p1013 A73-21814

Molecular model with two interacting terms for time evolution of nonradiative transitions, obtaining expression for energy level populations
09 p1123 A73-22876

Electron impact excitation rates calculation for He I and II transitions, comparing measured, theoretical and semiempirical impact cross sections
10 p1251 A73-24133

A plasma laser operating on molecular electronic transitions
10 p1228 A73-24454

CsI optical and photoemission spectra computed from first order allowed transitions between Bloch-wave states, using energy band data
11 p1407 A73-24987

Asymmetric intensities of Zeeman components of electronic transitions of diatomic molecular spectra in sunspots, considering CN red lines
11 p1422 A73-25936

Indirect transitions in thin quantized semiconductor films
11 p1410 A73-26450

Changes in the mean energy of an electron in the field of a plane wave with allowance for radiation damping
12 p1526 A73-26969

Emission of 'soft' photons in the field of a strong electromagnetic wave 12 p1468 A73-26972

Ar laser output characteristics variation due to mutual influence of 4880 and 5145 Å transitions, solving ion density formation rate equations 13 p1628 A73-29184

Autoionizing transitions in N₂ and H₂ produced by electron impact. 14 p1776 A73-29695

Observation of the effects of rotational transitions in the resonant scattering of electrons from N₂. 14 p1776 A73-29696

Observations of stimulated anti-Stokes radiation in barium vapour. 14 p1776 A73-29697

Determination of the main details of the band structure of semiconductors from edge absorption data 14 p1783 A73-30366

Ionization transitions from the 8/2P_{1/2} level of a cesium atom in a low-temperature plasma 14 p1781 A73-30460

Stark broadening of high-principal-quantum-number n-alpha lines of hydrogen. 14 p1777 A73-30552

Observations of formamide at 6 cm in Sagittarius B2. 15 p1933 A73-31377

Detection of interstellar thioformaldehyde. 15 p1933 A73-31378

Stimulation of nonradiating transitions during intense excitation by light 15 p1885 A73-31720

Quantum losses during excitation of ruby luminescence 15 p1924 A73-31721

The variation of the electronic transition moment, Re, in the intensity theory of diatomic molecules. 15 p1916 A73-32392

Theory of the threshold of an injection laser operating at the experimental band tails 17 p2184 A73-34922

Vacuum UV radiation of electron beam excited high pressure Xe laser, measuring optical gain due to diatomic state-repulsive ground state transitions 17 p2186 A73-35794

Electron transitions of molecules in a plasma laser. 19 p2438 A73-38135

Oscillator strength calculations for vibrational transitions of X-A electronic system of interstellar CH positive ion, noting agreement with astrophysical observations of line spectra 19 p2488 A73-38512

Fredholm-uniformization computation of elastic scattering amplitudes in the presence of arbitrarily many open channels. 21 p2738 A73-40212

Computer checking of rotational line intensity factors for diatomic transitions. 21 p2744 A73-41212

Longitudinal alignment of working levels in a helium-neon laser 22 p2870 A73-42412

Quantum-beat g-value measurements on transitions from levels of aligned fast ions. 22 p2890 A73-42974

Energy level transitions in Ca XVII and Ti XIX UV spectra, basing identifications on extrapolation method 22 p2914 A73-43016

High order nonlinear effects in a gas laser - Saturation anomaly observable on a J equals 1 - J equals 2 transition 22 p2871 A73-43084

Theory of donor-acceptor radiative and Auger recombination in simple semiconductors. 23 p3016 A73-43796

Two level atomic inelastic transitions in plasma with damping for static, Weisskopf, adiabatic, exponential and Purcell/Born particle regions 23 p3008 A73-44014

Theoretical possibilities for the creation of a gamma laser /gazer/ using nuclear transitions 23 p2988 A73-44092

Hartree-Fock model for metal to insulator transition in vanadium oxide based on electronic band structure at zero and finite temperatures 23 p2961 A73-44163

Neutral Fe line profiles for low-lying transitions measured from solar disk center to limb by double pass spectrometer, considering limb darkening effect 24 p3135 A73-44626

Proton collisional excitation in the ground configuration of Fe⁺12. 24 p3123 A73-44634

Rotational line overlap in CO₂ laser transitions. 24 p3096 A73-44872

Dipole moment of water from Stark measurements of H₂O, HDO, and D₂O. 24 p3113 A73-44978

Electron transitions in interstellar dust 4430 Å line, indicating ferric oxide /alpha-hematite/ in type I supernovae 24 p3138 A73-44990

ELECTRON TUBES

NT CAMERA TUBES

NT CATHODE RAY TUBES

NT CELESCOPES

NT HELITRONS

NT IMAGE DISSECTOR TUBES

NT IMAGE ORTHICONS

NT KLYSTRONS

NT MAGNETRONS

NT MICROWAVE OSCILLATORS

NT MICROWAVE TUBES

NT PICTURE TUBES

NT PLANOTRONS

NT RETURN BEAM VIDICONS

NT THERMIONIC DIODES

NT THYRATRONS

NT TRAVELING WAVE TUBES

NT VACUUM TUBE OSCILLATORS

NT VIDICONS

Long life 100 W triode for ATC and telemetry transponders. 09 p1066 A73-23427

ELECTRON TUNNELING

Investigation of the tunnel characteristics of deposited superconducting Nb₃Sn films 01 p0089 A73-11290

The superconductor maser - A calculation of the gain from the two-level model and the BCS theory, and some new experimental results. 02 p0175 A73-11848

Superconducting tunnel junctions as phonon sources and detectors. 04 p0428 A73-15466

Experimental results on absolute phonon detection sensitivity of superconducting tunnelling junctions. 04 p0483 A73-15467

Book - Superconductive tunnelling and applications. 05 p0556 A73-16357

Josephson tunneling devices - A new technology with potential for high-performance computers. 06 p0735 A73-18066

Mathematical model for electric current in granulated media, establishing temperature dependence of tunneling conductivity for tunnel junction with metallic inclusions in oxide layer 06 p0736 A73-18117

Tunneling observation of bound states in a normal metal-superconductor sandwich. 07 p0862 A73-19606

Electron tunnelling into amorphous germanium and silicon. 07 p0864 A73-20454

Response time of metal-insulator-metal tunnel junctions. 08 p0945 A73-20844

Low-field tunnelling current in thin-oxide M.N.O.S. memory transistors. 08 p0946 A73-21115

Study of the geometrical resonances of superconducting tunnel junctions. 08 p0994 A73-21207

Dynamic behavior of Josephson tunnel junctions in the subnanosecond range. 09 p1132 A73-21941

On the theory of tunnelling in electron and proton transfer reactions. 09 p1133 A73-22199

A search for stimulated emission of radiation from superconducting tunnel junctions. 09 p1135 A73-23341

Photoconductor-metal contact at higher densities. 11 p1407 A73-24985

Tunneling transmission through the equatorial lower ionosphere of ELF and VLF electromagnetic waves. 11 p1358 A73-26702

A transport equation treatment of tunnelling in semiconductors. 13 p1668 A73-28218

French monograph on metal-semiconductor junction electron tunneling effect covering phonon interaction mechanisms, control and characterization problems 13 p1669 A73-29290

Calculation of the electron density in heterogeneous mixtures with allowance for the tunneling effect and for super-barrier reflection 15 p1915 A73-31854

Theory for the inelastic tunneling effect in normal metals 16 p2027 A73-34063

The problem of electron-pair tunneling in a sound field in superconductors 16 p2045 A73-34069

Determination of the dispersion relation in tunnel structures - Influence of the barrier shape and validity of the WK B approximation. 17 p2220 A73-35655

Detection of optical and infrared radiation with dc-biased electron-tunneling metal-barrier-metal diodes. 17 p2143 A73-35792

Influence of the reflection forces and the tunnel effect on the current-voltage characteristic of a metal-semiconductor contact with a Schottky barrier 18 p2340 A73-36668

ELECTRON-ION RECOMBINATION

Current-voltage characteristic of a real diode with a Schottky barrier, allowing for tunneling through the spatial charge region 18 p2293 A73-36718

Superconductor-semiconductor Schottky barrier diode video detector with proper doping and electron tunneling to obtain high degree nonlinearity in I-V characteristics 21 p2662 A73-40463

Liquid helium temperature range thermometry using superconducting tunnel junction devices with temperature dependent I-V characteristics 22 p2856 A73-42018

Investigation of tunnel characteristics of sputtered superconducting Nb₃Sn films. 23 p3015 A73-43511

Shot noise of a real Schottky-barrier diode during tunneling through the space charge region 23 p2960 A73-43619

Influence of the image force and tunnel effect on shot noise in diodes with a Schottky barrier 23 p2960 A73-43715

Evolution of the shape of the current-voltage characteristics of n-p-n and p-n-p three-layer degenerate semiconductor structures 24 p3119 A73-44607

ELECTRON-ION RECOMBINATION

NT RADIATIVE RECOMBINATION

Electron-ion recombination in cryogenic helium plasmas. 01 p0084 A73-10565

Recombination of electrons with positive ions of the H₃O⁺ /H₂O/n series. 01 p0014 A73-10901

Electron velocity distribution function in the ionosphere 05 p0568 A73-16252

Temperature dependence of the ion recombination coefficient in a hydrocarbon flame plasma 06 p0731 A73-18553

Dissociative recombination at elevated temperatures. IV - N₂⁺ /+/- dominated afterglows. 07 p0853 A73-19149

Characteristics of ionization-recombination processes in a plasma discharge diode 09 p1124 A73-21884

Resonant enhancement of photoexcited nitrogen trap n-type GaAs laser electron-hole recombination probability by crystal composition variation and gamma conduction band degeneration 09 p1093 A73-22255

Characteristics of the diffuse /tenous/ interstellar medium determined from radio recombination lines. 09 p1150 A73-23137

Electron temperature profile in stagnation region flow of blunt bodies with consideration of ionization recombination in shock layer 10 p1296 A73-24256

Expanded laser produced plasma Debye length from slab geometry, evaluating electron temperature for ion recombination rates 10 p1256 A73-24270

Ionospheric electron-ion gas distribution, allowing for diffusion, recombination and vertical drift 11 p1357 A73-26081

Diurnal thermospheric heat budget in terms of electron-ion recombination, photodissociation and neutral wind energy transfer and conductive and radiative cooling 12 p1492 A73-27604

Temperature dependence of the cross section of O⁺ ion desorption by electrons from an oxygen layer adsorbed on a tungsten surface 13 p1663 A73-28969

Influence of atom-atom collisions on electron density decay in laser-produced helium plasmas. 16 p2041 A73-32944

Temperature dependence of the ion recombination coefficient for a hydrocarbon flame. 16 p2042 A73-33578

Laboratory methods for study of aeronomical reactions of excited ions. 16 p2009 A73-33894

Approximation to the collisional-radiative recombination coefficient in a partially ionized gas. 17 p2213 A73-34197

Ionization and recombination in a plasma diode. 17 p2215 A73-34308

Measurement of electron-ion recombination rate of a dense high-temperature cesium plasma. 18 p2339 A73-36622

Corner expansion flow of ionized argon, calculating electron density, plasma density and recombination rate constant for comparison with measurements 19 p2465 A73-37177

Recombination and negative ion role in high-frequency gas discharges 21 p2743 A73-40366

Measurements of recombination of electrons with HCO⁺ ions. 23 p3007 A73-43530

Role of electron processes in the vaporization mechanism and in the formation of binary semiconductor alloy compositions with ion bonds 23 p3016 A73-43711

Temperature dependence of the cross section for electron-induced O⁺ desorption from tungsten.

23 p3008 A73-44321

Intensity of charged particle recombination on the surface of certain borides of high-melting-point metals in a weakly ionized hydrogen plasma

24 p3098 A73-44418

Transient ion neutralization by electrons.

24 p3111 A73-45411

ELECTRONIC AMPLIFIERS

U AMPLIFIERS

ELECTRONIC CONTROL

A linear motion generator for physiological research.

01 p0011 A73-10173

Electronic programming timer with crystal oscillator, IC counters and memory core matrix for event sequence radio control during spacecraft or rocket launchings

01 p0020 A73-11167

Flight test of narrow band television system.

01 p0052 A73-11169

Photomultiplier operation pulse control in semiconductor circuit for background cosmic radiation noise error minimization in air shower station

02 p0171 A73-12688

Trends in helicopter guidance and control systems with bad weather capability.

03 p0340 A73-13921

Transient analysis of an electronically tunable dye laser. I - Simulation study.

03 p0320 A73-14457

Digital control mounts on jet engine.

05 p0608 A73-17249

Antenna beam focusing and deflection with the aid of a digital phase computer, in a radiation-fed electronically controlled antenna

06 p0673 A73-17580

Microwelding equipment with automatic wire breaking and ball melting blocks and electronically controlled wire feeding, noting heating plate with thyristor temperature control

06 p0683 A73-18433

Electronically controlled phased arrays for radar tracking systems, considering military, earth resources and planetary topography applications

06 p0677 A73-18447

French satellites attitude stabilization and control systems, describing electronic sensor and servocontrol circuitry

07 p0904 A73-18967

Optimal planning of technological systems maintenance according to a reliability criterion

07 p0830 A73-19126

High resolution Mossbauer spectrometer design and applications, describing electromechanical Doppler shifter, control electronics and data storage

07 p0822 A73-19170

Electronic six-channel phase shifter

08 p0950 A73-21715

Sensitivity of variable-amplifier circuits to variation of the controlled parameters

09 p1069 A73-22651

Radio-guidance algorithms applied to the control of spacecrafts descending in the earth's atmosphere

10 p1247 A73-23880

Conditions for termination of tracking in electronic servo systems

10 p1202 A73-24610

Design and performance of the TACSAT power subsystem.

11 p1312 A73-26020

A positional, asynchronous, thyristor-based, electrical servo actuating element with directional shaping of the phase trajectories

12 p1460 A73-26787

An electronic relay constructed according to the principle of amplifiers with a controlled amplitude characteristic

12 p1477 A73-26791

Iris photometer electronic control system, presenting NGC 1778 cluster stars photoelectric UVB magnitudes

12 p1498 A73-27723

Mean risk determination in radio-electronic device control

14 p1735 A73-30291

Electronic control units, discussing automanual transfer, integral desaturation, proportional and compensatory action, position regulation with incorporated memory and computer applications

14 p1737 A73-30923

Variable speed single- and multi-quadrant drives using thyristor electronic regulating unit with static converter motor and frequency changers

16 p1971 A73-33961

An electronically tuned Gunn oscillator circuit.

17 p2134 A73-34222

Automatic electronic feedback control systems for active wing/external store flutter suppression

17 p2107 A73-35244

Demand-assignment multiple-access control techniques.

17 p2144 A73-35304

Electronically-regulated power supplies for microwave backward-wave oscillators.

17 p2142 A73-35643

Algorithms for radio guidance with application to control of landing of spacecraft in the earth's atmosphere.

20 p2590 A73-38899

Analysis of the control circuit of a seeing measurement device

20 p2565 A73-39069

Slit electronic camera with scanned memory used in high speed cineradiography

21 p2694 A73-39942

Optical diffraction grating design and production, discussing application of interferometry and electronics to ruling engine control

21 p2698 A73-40136

Time scanned array radar with time delay or phase gradient for electronic beam steering control by signal

21 p2652 A73-40669

Limited scan phased array antenna design, featuring electronic beam deflection from few beamwidths to twenty degrees with cost reduction

21 p2653 A73-40680

A single-plane electronically scanned antenna for airborne radar applications.

21 p2653 A73-40684

Physical design considerations for airborne electronic-scanning antennas.

21 p2654 A73-40685

Analysis of the accuracy of a system for controlling vibration tests with sinusoidal excitation

21 p2674 A73-40996

Adjustment of a variable-profile antenna

21 p2675 A73-41456

An electronically synchronized drum-type film camera

21 p2706 A73-41580

Dynamic behaviour and z-transform stability analysis of dc/dc regulators with a non linear P.W.M. control loop.

22 p2837 A73-42912

Four terminal, optically isolated, zero crossing ac relay.

22 p2834 A73-42913

Logic-controlled solid-state switchgear for 270 volt dc.

22 p2802 A73-42915

Bilateral power conditioner with common filters and transistor control circuits for battery charge and discharge functions onboard near earth orbit spacecraft

22 p2802 A73-42916

The application of standardized control and interface circuits to three dc to dc power converters.

22 p2802 A73-42918

Spectrophotometer design for total ozone measurement for Dobson instrument replacement, describing spectrograph, reads, electronic control, photon counter, readout system and accuracy

23 p2982 A73-43852

Electronic logic device for crack arresting penthrile microcharge pulse initiation, including crack and stress wave propagation measurements

23 p3047 A73-44286

Electronically tunable microwave bandpass filters

24 p3071 A73-44606

Voltage controlled attenuator circuit for acoustic signal duration and repetition control in hearing examinations

24 p3064 A73-44910

ELECTRONIC COUNTERMEASURES

NT CHAFF

Linear rapid frequency settling time solid state voltage controlled oscillators /VCO/ for electronic countermeasure and B-scan tracking radar applications

01 p0024 A73-10723

Comparing ECM antennas - Horns vs spirals.

02 p0147 A73-12568

Designing limiter/detectors for ECM receivers.

02 p0143 A73-12569

Phase and amplitude balance - Key to image rejection mixers.

02 p0148 A73-12571

Electronic warfare tactics against remotely piloted unmanned aircraft used for reconnaissance or weapons delivery, considering onboard countermeasures

04 p0418 A73-15379

Varactor or YIG tuned Gunn effect microwave oscillators for ECM applications, noting low noise octave tuning and high sweep rates

06 p0675 A73-17842

Frequency response of helix and coupled cavity traveling wave tubes and amplifiers power output, discussing electronic countermeasures and space communications

11 p1339 A73-26692

Dual mode microwave tube parameters for ECM power amplifiers based on systems rationale analysis, considering TWT and injected-beam crossed field amplifier

14 p1736 A73-30621

Simulation of a multiple element test environment.

16 p1985 A73-33417

Experimental autostabilized tethered rotor platform for reconnaissance, communications and ECM, discussing control system effectiveness from flight test results

16 p1969 A73-33736

ECM systems with TWT dual moding to provide distinct CW and pulsed microwave power levels, evaluating performance beyond octave in bandwidth

16 p1990 A73-33849

Optimal Markov sequence signal detection in correlated FM random electronic countermeasure background noise

20 p2529 A73-38929

Microwave cross field and traveling wave tube amplifier characteristics for ECM systems, discussing bandwidth, dual mode, modulation and size and weight tradeoffs

22 p2834 A73-42872

Octave-bandwidth, acoustic M/W frequency-memory loop.

22 p2834 A73-42873

Remotely piloted vehicle /RPV/ for reconnaissance, electronic warfare systems, target acquisition, weapon delivery, air-air combat and different combinations

24 p3057 A73-45399

ELECTRONIC EQUIPMENT

NT AVALANCHE DIODES

NT ELECTRONIC FILTERS

NT ELECTRONIC MODULES

NT ELECTRONIC PACKAGING

NT ELECTRONIC RECORDING SYSTEMS

NT ELECTRONIC TRANSDUCERS

NT FIELD EFFECT TRANSISTORS

NT GALLIUM ARSENIDE LASERS

NT GERMANIUM DIODES

NT JUNCTION DIODES

NT JUNCTION TRANSISTORS

NT METAL OXIDE SEMICONDUCTORS

NT MICROMODULES

NT MINIATURE ELECTRONIC EQUIPMENT

NT MIS [SEMICONDUCTORS]

NT NEURISTORS

NT PARAMETRIC DIODES

NT PHOTODIODES

NT PHOTOTRANSISTORS

NT PHOTOVOLTAIC CELLS

NT RUBY LASERS

NT SEMICONDUCTOR DEVICES

NT SEMICONDUCTOR LASERS

NT SILICON TRANSISTORS

NT SOLID STATE DEVICES

NT SOLID STATE LASERS

NT SPACECRAFT ELECTRONIC EQUIPMENT

NT THERMISTORS

NT THERYSTORS

NT TRANSISTOR AMPLIFIERS

NT TRANSISTORS

NT VARACTOR DIODES

NT VARISTORS

Blank pupil arrangement of coude spectrograph with echelette for 1.52 meter reflector, describing dispersions obtained, receivers used and electronic camera adaptation

01 p0048 A73-10523

The development of a device for measuring fuel consumption

02 p0165 A73-11521

The system approach to the design of engineering systems from the standpoint of reliability and efficiency

02 p0145 A73-11547

Adaptation of the electronic camera to the coronagraph

02 p0170 A73-12544

Russian book on electrical power supply devices for radio systems covering design of rectifiers, transformers, current limiters, voltage regulators, filters, converters and inverters

02 p0133 A73-12863

Non polar thermosetting resins for high temperature electrical/electronic components.

03 p0332 A73-13035

Time-averaged power stage models transient and frequency responses characterization and circuit component values derivation for switched dc-dc converters design

03 p0282 A73-13927

Computer-aided design and graphics applied to the study of inductor-energy-storage dc-to-dc electronic power converters.

03 p0252 A73-13931

Book - Fundamentals of nuclear hardening of electronic equipment.

03 p0283 A73-13990

The application of heat pipe techniques to electronic component cooling.

[ASME PAPER 72-WA/HT-42] 04 p0518 A73-15814

Survey of heat transfer techniques applied to electronic equipment.

[ASME PAPER 72-WA/HT-39] 04 p0518 A73-15816

Thermal stability improvement of variable inductance electronic circuits for analog magnitudes conversion to frequencies, noting instrument errors compensation

05 p0577 A73-16987

Low cost electronic method of delaying speech signals based on adaptive delta modulators
03 p0552 A73-17375

Electronic creation of still and animated complex images, discussing techniques for supplying computer with object description
06 p0669 A73-17474

The design of electronic equipment for biotelemetry using microcircuit techniques.
06 p0673 A73-17674

Electronics associated with ultrahigh-speed photographic equipment
06 p0679 A73-18855

Ultrahigh-speed electronic camera - CELER 2-500
06 p0696 A73-18856

Digital-computer analysis of linear electronic circuits by the method of structural numbers
07 p0804 A73-18894

Scanning electron microscope operation and application to technology research and electronic components and circuits failure and reliability analysis
07 p0797 A73-18922

Satellite-borne vidicon camera and associated control and telemetry electronics for imagery and dimensional parameters of sparks generated by gamma radiation
07 p0822 A73-18987

Some effects of temperature on material properties and device reliability.
07 p0797 A73-19134

Analysis of a defect of electromagnetic relays used in an electronic assembly
07 p0799 A73-19406

Application of the analysis of correspondences to the study of the reliability of electronic components
07 p0800 A73-19412

Influence of repeated voltage applications on the reliability of a system
07 p0800 A73-19417

Stress and strength theory application to mechanical failure of electronic equipment, showing Weibull law use in reliability analysis
07 p0800 A73-19420

Heat exchanger for dissipating heat due to energy losses in enclosed dust-proof electronic equipment
07 p0921 A73-20125

IR radiometers for free jets sound emission mechanism probing, describing optical and electronic equipment
07 p0825 A73-20164

[ONERA, TP NO. 1212]

A method for evaluating the circuit reliability of electronic equipment
07 p0802 A73-20299

Characteristics of beam- and membrane-type strain-gauge sensors of linear acceleration
07 p0826 A73-20529

Metallization failures caused by organic adhesives used in hybrid microelectronic devices.
08 p0944 A73-20747

Electrical components heat dissipation via thermal radiation, determining nonlinear temperature dependence from Stefan-Boltzmann law
08 p1020 A73-20775

Electronic equipment burn-in for repairable equipment.
08 p0945 A73-20949

Electronic display devices for command, monitoring, surveillance, simulation and training in military applications, considering reliability, cost and performance specifications in procurement decision making
08 p0965 A73-21245

Electronic system reliability improvement by partitioning into functional parallel redundant blocks
10 p1193 A73-23651

Electronic equipment thermal management for energy dissipation rejection, summarizing heat pipe, phase-change heat transfer and high pressure gas convection techniques
10 p1295 A73-23789

Book - Heat transfer in microelectronic equipment: A practical guide.
10 p1194 A73-23900

Electronic systems for time constant and altitude error compensation of rate of climb indicator used in high performance glider flight
10 p1222 A73-24916

Heat pipe cooling of electronic components for design requirements of high voltage insulation, small size, low temperature and protection from external heat sources
11 p1451 A73-25990

Equivalent continuous sound level determination from instantaneous sonic intensity measurement during representative time period, describing electron measuring device and circuitry
11 p1367 A73-26416

Electronic equipment computerized radiation hardness assurance program for retaliatory or deterrent missile system, discussing supplier data monitoring, verification test and radiation shield assurance
11 p1342 A73-26637

Design principles of digital devices for measuring time intervals /Survey/
12 p1496 A73-27201

Stochastic-ergodic electronic U-functionmeter for signal electrical characteristics measurement, discussing design, operational features and applications
12 p1499 A73-27874

Pulse rebalance gyro electronic system with hybrid microcircuitry for digitizing sensor inputs to computer
13 p1589 A73-28047

Automatic electronic pendulum astrolabe featuring altitude and azimuth tracking mechanisms, azimuth setter and 180 degree turning mechanism
13 p1612 A73-28394

Prediction of optimal maintenance for devices
13 p1625 A73-29136

Development of a new kind of Lallemand camera.
14 p1751 A73-29905

Russian book on aeronautical electric and electronic materials covering physicochemical properties of magnetic, dielectric, conductor, semiconductor, polymer, ferritic, thin film and composite materials
14 p1766 A73-30357

Application of human engineering principles and techniques in the design of electronic production equipment.
14 p1722 A73-30497

Electronic systems as piloting aids in Concorde SST, discussing flight controls, trim computer, autostabilizer, autopilot and automatic engine control
15 p1830 A73-32474

Technologies applicable to the development of an onboard L-band transmitter
15 p1852 A73-32481

Limitations in the use of all-electric systems for vital application in civil aircraft.
15 p1852 A73-32492

Electronic integrated flight data displays for pilot workload reduction at takeoff, approach and landing, considering head-up and head-down and colored systems
15 p1831 A73-32506

NEREM 72; Northeast Electronics Research and Engineering Meeting, Boston, Mass., October 30-November 3, 1972, Record. Part 1 - Technical Papers.
16 p1986 A73-32717

Comparative testing and evaluation of conformal coating materials and processes.
16 p2018 A73-33062

Design and service environment standardization /Military electronic equipment/.
16 p2087 A73-33143

Repairable electronic system random failure and repair time related to simulator time available for operation, analyzing MTBF and repair rates
16 p1996 A73-33207

Considerations concerning the design of an electronic landing display for STOL aircraft
17 p2146 A73-34478

Second generation supersonic transport, discussing fuel costs, changing markets, travel patterns, electronic displays and sound suppressor development [SAE PAPER 730349]
17 p2102 A73-34697

Moldability, storage stability and thermal, mechanical and electrical properties of epoxy molding compounds for electronic devices
17 p2196 A73-35340

Book - Low-noise electronic design.
17 p2143 A73-35825

Some considerations for Space Tug launch site support operations.
18 p2360 A73-36502

[AIAA PAPER 73-620]

Method of estimating the circuit reliability of electronic devices.
18 p2294 A73-37136

Conference on Electron Device Techniques, New York, N.Y., May 1, 2, 1973, Record.
22 p2833 A73-42691

Radio telescope array of interferometers formed by fixed and movable antennas operating on rotational aperture synthesis for radiation observation, emphasizing electronic system stability
23 p2957 A73-43360

Josephson junction principles for superconducting metals at cryogenic temperatures, considering ultrasensitive electronic measuring instruments and computer components
24 p3073 A73-45224

ELECTRONIC EQUIPMENT TESTS

Analytical method for diagnostic and checkout testing of logic element faults in complex combinational circuits
01 p0026 A73-10035

Mathematical formulation for classification, realization and evaluation of electronic components and systems reliability tests
01 p0023 A73-10647

Reliability-performance comparisons between tube and transistor power modules for ground-based and airborne radar applications
01 p0024 A73-10718

Discrete systems for automatic control of electronic equipment under conditions of its manufacture
02 p0146 A73-11865

Microelectronic technologies for SAM-D system, discussing thick film hybrid circuits and microstrip applications
02 p0148 A73-12594

ELECTRONIC EQUIPMENT TESTS

Printed circuit and electronic component solderability tests subsequent to adverse environment exposure, comparing electroplated materials with pressure leveled solder and Cu and Be coatings
03 p0333 A73-13046

Reducing the smoke hazard in small transformer failures.
03 p0252 A73-13572

Thermal design and tests of transcendent solid state power thyristor, rectifier and transistor devices, using heat pipe-silicon wafer construction
03 p0283 A73-13940

Attempt at estimating the parameters of soldering processes
04 p0454 A73-15349

Analytical techniques for the determination of equipment probability of survival to radiation stress.
05 p0596 A73-16509

Enhancing testability of large-scale integrated circuits via test points and additional logic.
06 p0674 A73-17802

Transistor tester circuit design with mutually independent collector-emitter voltage, collector current, generator and load resistance adjustment for arbitrary operating point selection
07 p0803 A73-20303

Test programs design for versatile avionics shop test system /VAST/, discussing compiler problems alleviation by on-station program patching capability
08 p0962 A73-20688

A procedure for the evaluation and failure analysis of M.O.S. memory circuits using the scanning electron microscope in potential contrast mode.
08 p0943 A73-20730

Possibilities of determining the testverse bias current and voltage in semiconductor devices by a nondestructive method
09 p1061 A73-21979

LSI computer design and fabrication for Space Ultrareliable Modular Computer Demonstration Vehicle, discussing assembly, physical and electrical characteristics and electronic testing procedures
10 p1191 A73-23794

Construction of verification tests for digital devices with delay elements
12 p1482 A73-26753

Checkout and failure diagnostics of an incompletely homogeneous two-dimensional structure
12 p1482 A73-26754

Diagnostic tests and failure checkout for interconnected combinational micrologic circuit components in manufacturing process, tabulating individual failure functions
12 p1474 A73-26755

Diagnosis of switching devices in the case where faults are represented by tests of individual elements
12 p1476 A73-26756

Methods of constructing control and diagnosis tests for homogeneous microelectronic circuits
12 p1476 A73-26757

Automatic checkout and monitoring in the AN TPQ-27 radar system.
13 p1585 A73-29210

Measurement equipment for the PCM transmission system KPK 30/32
14 p1736 A73-30373

Construction of a diagnostic sequence of tests of a combination automaton
15 p1848 A73-31913

Reliability testing functions for memory elements
15 p1848 A73-31914

Doppler scanning landing guidance system based on linear array of equally spaced radiators with RF source commutation
15 p1912 A73-32502

The role of temperature in the environmental acceptance testing of electronic equipment.
16 p1989 A73-33606

Computerized analysis of reliability or failure rate function data from electronic component and equipment operation and testing, using hazard plotting technique
16 p1989 A73-33613

Testing of spacecraft in long-term storage.
16 p2073 A73-33615

Tactical weapon system final test for random failures, discussing electronic component defects effects and semiconductor device screening for system reliability improvement
16 p1990 A73-33624

Concept and system of the versatile avionic shop test /VAST/ system.
16 p1986 A73-33634

Prolonged monitoring of experimental equipment with the aid of semiconductor emitters
17 p2133 A73-34152

Device for nondestructive measurement of secondary-breakdown parameters in transistors
17 p2133 A73-34161

Book - Compatibility and testing of electronic components.
17 p2134 A73-34573

Computerized automatic microwave testing with pulse measurements of phase and power from Reliable

- Advanced Solid State Radar phased array modules, discussing system design
17 p2135 A73-34724
- Experimental heat transfer investigations on modules mounting hybrid packages.
17 p2135 A73-34729
- Electric corona assessment of Skylab spacecraft high voltage electrical/electronic equipment and instruments, considering operating temperature and environment contaminants effects
17 p2109 A73-35256
- Operational principles and testing of a digital radar target extractor
19 p2404 A73-37584
- Process control stress test of MOS IC circuit susceptibility to charge spreading with channel formation
19 p2436 A73-38452
- Concepts of high-capacity communications satellites.
20 p2613 A73-38714
- Recent test results - A strapdown IMU utilizing hydrodynamic spin bearing rate sensors and pulse rebalance loops.
20 p2564 A73-38833 [AIAA PAPER 73-898]
- Self calibrating automatic equipment for pulsed and CW RF testing of phase, amplitude and frequency characteristics of pulsed electronic devices
20 p2535 A73-38870
- IR test data evaluation for printed circuits using computer techniques, discussing testing time reduction and efficiency optimization, programming language and error analysis
20 p2567 A73-39769
- Equipment for measuring cross-modulation distortions in high-frequency power transistors
21 p2660 A73-40014
- A method of locating defective elements in large phased arrays.
21 p2653 A73-40682
- Electromagnetic compatibility specifications for aircraft communication and electronic equipment, discussing control and test plans, test facilities, cost effectiveness and British standard
22 p2821 A73-41696
- Electromagnetic compatibility program for modern aircraft communication and electronic equipment design, discussing control plan, interference specification, cable separation and final testing
22 p2821 A73-41697
- Helix support, focusing, fabrication and performance tests of miniature traveling wave tubes (TWT), using rare earth-cobalt (RAECO) magnets
22 p2834 A73-42696
- Malfunction diagnostics in digital integrated-circuit devices
23 p2956 A73-43581
- Parameters of low-power transistors in the avalanche mode of operation
24 p3072 A73-44934
- ELECTRONIC FILTERS**
Multiple overlapping signal decomposition in noisy environment by inverse filtering, considering tradeoff between resolution and output SNR, and optimum pulse duration
03 p0277 A73-13908
- Equivalent, filter realization and threshold CNR determination for optimum design of extended range phase locked loop
04 p0421 A73-15436
- Operating modes of a phase-loop AFC system with a low control circuit time lag under the action of additive harmonic noise
05 p0560 A73-16292
- Low-pass filters and their realization by means of active circuits with operational amplifiers
06 p0673 A73-17723
- Nonlinear filter with a Pi-shaped amplitude-frequency characteristic
08 p0946 A73-21110
- Synthesis of functions for polynomial linear-phase amplifiers with feedback
08 p0947 A73-21396
- Matched filters for extracting synchronization in signaling, nonreturn-to-zero and split phase PCM systems, using finite-time-duration trigonometric pulse synthesis
09 p1056 A73-23402
- Synthesis of gyrator RC filters from the cascaded model
10 p1193 A73-23729
- Active RC filter synthesis with decoupling stage and third order element for minimizing impedance mismatching and overall capacitance
10 p1193 A73-23734
- A computer program for filter design having arbitrary magnitude specifications in the frequency domain.
13 p1587 A73-28085
- Active analog bandpass RC and LC filters design calculation by wave parameters
13 p1592 A73-28875
- Selectivity enhancement of certain low-sensitivity RC active networks.
14 p1738 A73-29711
- Active LC, RC and C/gyrator/ filters design, operation, tolerance, cost and noise characteristics
14 p1736 A73-30375
- Application of the describing-function approach to radio engineering problems. II
15 p1853 A73-31254
- Synthesis of the functions of polynomial linear-phase feedback amplifiers.
19 p2410 A73-38354
- Electronic integrated HF selective gyrator for TV IF filter development
21 p2661 A73-40230
- Degradation of probability of error due to IF filtering.
21 p2649 A73-40335
- Synthesis of reactive ladder filters with uniform losses, discussing iterative solution for nonlinear equations and low, high and band pass filters loss compensation
21 p2662 A73-40498
- Polynomial approximations of the characteristics of low-sensitivity filters
21 p2666 A73-41315
- Bilateral power conditioner with common filters and transistor control circuits for battery charge and discharge functions onboard near earth orbit spacecraft
22 p2802 A73-42916
- The effect of amplifier gain-bandwidth product on the performance of active filters.
24 p3073 A73-45393
- ELECTRONIC LEVELS**
U ELECTRON ENERGY
U ENERGY LEVELS
ELECTRONIC MODULES
NT MICROMODULES
Minicomputer based CAMAC modular system for astronomical telescope instrumentation, discussing hardware and software interfaces, squad scaler, photoelectric photometer, Michelson interferometer and multichannel spectrometers
01 p0019 A73-10547
- Reliability-performance comparisons between tube and transistor power modules for ground-based and airborne radar applications
01 p0024 A73-10718
- The IHTS - A new building block for power conditioners.
03 p0282 A73-13934
- Ferrite core modular memory characteristics, considering bit capacity and printed circuit technology utilization
05 p0556 A73-16167
- A cellular processor for task assignments in polymorphic, multiprocessor computers.
06 p0671 A73-18061
- Design of a fault-tolerant, modular computer with dynamic redundancy.
06 p0671 A73-18064
- Circuit diagrams, electronic modules and design of PCM telemetry encoder for Eole satellite, noting data multiplexing and processing
07 p0789 A73-18957
- A wide-band low-shape-factor amplifier module using an acoustic surface-wave bandpass filter.
07 p0804 A73-20557
- A modular approach to an automated digital test system.
08 p0940 A73-20678
- CAMAC - A proposed standard for astronomical instrumentation.
08 p0972 A73-21755
- High energy and power carbon dioxide laser with nitrogen and He mixtures, transverse electric discharge excitation and modular construction, noting efficiency and gain
09 p1090 A73-22081
- Solar cell generator technology development based on German AEROS satellite project and work on roll-up structure discussing module concepts and test results
09 p1033 A73-22439
- Cutpoint cellular switching array synthesis by combined cascade simplification rule, noting algorithm efficiency increase
09 p1065 A73-23101
- LSI computer design and fabrication for Space Ultrareliable Modular Computer Demonstration Vehicle, discussing assembly, physical and electrical characteristics and electronic testing procedures
10 p1191 A73-23794
- Complementary MOS LSI microprogrammed digital computer design, for Space Ultrareliable Modular Computer Demonstration Vehicle, discussing instruction operation codes, I/O peripherals and software support
10 p1191 A73-23795
- Standard flexible LSI logic cell arrays with uniform interconnections as fourth generation computer components, discussing microprograms and algorithms for arithmetic operations
10 p1198 A73-24017
- Fault-tolerance in the modular spacecraft computer.
12 p1475 A73-27130
- A simulation model for a memory organization for a multiprocessor.
12 p1475 A73-27155
- French monograph on numerical data processing organs for real time process control, describing modular computer design project
15 p1849 A73-32590
- An integrated, modular approach to automatic testing and data monitoring.
16 p1986 A73-33632
- Electronic Components Conference, 23rd, Washington, D.C., May 14-16, 1973, Proceedings.
17 p2135 A73-34726
- Experimental heat transfer investigations on modules mounting hybrid packages.
17 p2135 A73-34729
- Aircraft onboard computerized avionics and electrical systems architecture for information flow and control with maximum efficiency, flexibility, modularity and minimum maintenance
17 p2137 A73-35204
- Signal conditioning, separation and parameter measurement in modular digital EMI analysis system for airborne, shipboard or ground based reconnaissance applications
17 p2137 A73-35207
- Custom LSI technology utilization in low volume avionics systems, discussing handcrafted chip design, full wafer, array logic and MOS cell approaches and costs
17 p2138 A73-35227
- Mathematical functional modular building block implementation in LSI microelectronics for signal and data processing, discussing primitive functions and 8-bit family design example
17 p2138 A73-35229
- Optimal modular redundancy over a set of configurations for attaining specified system availability and reliability requirements.
17 p2139 A73-35257
- A method of computer design of microelectronic equipment
20 p2534 A73-38952
- ELECTRONIC PACKAGING**
Calculation of the temperature field of the heated zone of a complex shape consisting of a chassis with parts mounted on it.
06 p0766 A73-17412
- IC reliability enhancement by molded dual in-line packaging (DIP) technique, considering mold shrinkage effects on failure rates during temperature cycling tests
08 p0944 A73-20737
- IC plastic package performance prediction, discussing procedure to estimate degradation rate due to moisture effects
08 p0944 A73-20738
- Reliability aspects of plastic encapsulated integrated circuits.
08 p0944 A73-20739
- Forced air cooling of dual-in-line packages.
10 p1193 A73-23607
- Microwave electronic packaging with integrated multifunction assemblies, considering stripline choice for transmission line
11 p1338 A73-26113
- Thermal/electrical design of spaceborne microelectronic components.
13 p1588 A73-28046
- Thick film multilayer IC for electro-optical applications, discussing package techniques, sealing materials, ultrathick printing cold cathode panel and liquid crystal displays
13 p1669 A73-29395
- Microwave power transistors - The present and the future.
15 p1852 A73-32275
- Electrolytically deposited noble-metal layers in the electronic industry
16 p1987 A73-32945
- Epoxy adhesive materials evaluation for microelectronic assemblies of hermetically sealed hybrid circuits with semiconductor chips and thin film substrates
16 p1989 A73-33468
- Mechanical design of microwave integrated circuit enclosures.
16 p1989 A73-33469
- Fault ambiguity repair optimization (FARO) computer program for electronic circuit card group replacement strategy, using FORTRAN IV for SPEC-TRA 70/55 batch processing
16 p1990 A73-33626
- Microwave-package measurements at the Q band.
16 p1991 A73-34019
- Unconventional digital avionics black box approach for cost reduction and reliability improvement in terms of packaging, component coding and hardware qualification programs multiplicity
17 p2137 A73-35205
- Optimum thermal design of electronic packages cooled by free air convection.
17 p2141 A73-35387

- Torque and thermal cycling as methods of testing reliability of reflow-soldered chip-to-substrate joints.
19 p2436 A73-38445
- Long term life tests for thermal shock cycles effects on plastic encapsulated semiconductor device reliability, presenting salt atmosphere testing data for silicone package
19 p2471 A73-38454
- High-reliability plastic package for integrated circuits.
19 p2411 A73-38455
- Some considerations on solder flow-up into plated-through holes.
23 p2986 A73-44002
- ELECTRONIC PHOTOGRAPHY**
U ELECTRO-OPTICAL PHOTOGRAPHY
ELECTRONIC RECORDING SYSTEMS
Colour separation and electronic analysis of Gemini V and Apollo spacecraft photography.
01 p0045 A73-10275
- Automatic technique for extending magnetograms and for determining variometer sensitivity
05 p0573 A73-16267
- Developments in the electronic imaging techniques; Proceedings of the Seminar-in-Depth, San Mateo, Calif., October 16, 17, 1972.
17 p2167 A73-34901
- ELECTRONIC SIGNAL MEASUREMENT**
U SIGNAL MEASUREMENT
ELECTRONIC SPECTRA
Study of electronic spectroscopy at low energy on graphite
[ONERA, TP NO. 1181]
03 p0336 A73-14607
- Electronic spectra of pyroxenes and interpretation of telescopic spectral reflectivity curves of the moon.
07 p0897 A73-19885
- Electron-spectroscopic investigations of two modifications of the alloy steel Kh18N10T
09 p1104 A73-22690
- Processing the spectra of semiconductor detectors in a semiautomatic system containing data storage elements and a computer
09 p1085 A73-23005
- Electron absorption spectra of benzochromium-dicarbonyltriphenylphosphine and benzochromium-tricarbonyl and their application to studies of the decomposition kinetics of these compounds
10 p1186 A73-24457
- Temperature-induced changes of the electron-vibration spectrum of $\text{LaAlO}_3\text{-Cr}^{3+}$ crystals
10 p1260 A73-24578
- An evaluation of molecular constants and transition probabilities for the NH free radical.
11 p1402 A73-26582
- Anisotropy and energy spectra of newly-generated photoelectrons
15 p1867 A73-31265
- Effects of electron-phonon interaction in the luminescence spectra of transition and rare-earth impurity ions in crystals
15 p1885 A73-31715
- Multiplicity of dielectric local modes - Bound states of phonons with impurity centers
15 p1885 A73-31719
- Low energy electron fluxes and spectra correlation with auroral forms from weather satellite electrostatic measurements
18 p2304 A73-35964
- Influence of extended defects on the electron spectrum of semiconductors
19 p2470 A73-37952
- Charge transport bands in the electronic spectra of Fe/III/ complexes with certain oxygen-containing ligands
21 p2751 A73-40310
- An X-ray spectral study of the electronic structure of nonstoichiometric titanium carbide
21 p2721 A73-41226
- ELECTRONIC STRUCTURE**
U ATOMIC STRUCTURE
ELECTRONIC SWITCHES
U SWITCHING CIRCUITS
ELECTRONIC TRANSDUCERS
Linear response transistorized FM temperature measuring transducer with thermistor, noting low distortion and digital display convenience
01 p0044 A73-10032
- Stable optico-mechanical Q-factor modulator for a laser resonator
01 p0059 A73-10797
- A modified sensor of linear accelerations, velocities, and displacements over a path of 0 to 1500 mm
07 p0826 A73-20527
- Properties of electrocapillary transducers and possibilities of their application in vibration measurements
07 p0826 A73-20530
- Unified transducers of quantitative and geometrical parameters of different media based on the use of integral properties of electromagnetic fields.
10 p1217 A73-24014
- Comparative properties, main characteristics, and areas of application of electrochemical transducers
12 p1459 A73-26767
- Chemotronic /electrochemical/ transducers of nonelectrical quantities in automatic control
12 p1459 A73-26768
- Dynamic katathermometer for measuring the cooling effect of an ambient medium
15 p1838 A73-31512
- An integrated-circuit solar aspect sensor for spacecraft use.
16 p2013 A73-32884
- Optimization and data analysis of the Frascati gravitational-wave detector.
20 p2565 A73-39013
- ELECTRONICS**
Power Processing and Electronics Specialists Conference, Atlantic City, N.J., May 22, 23, 1972, Record.
03 p0252 A73-13926
- Western Electronic Show and Convention, Los Angeles, Calif., September 19-22, 1972, Proceedings.
04 p0426 A73-14728
- National Electronics Conference, 28th, Chicago, Ill., October 9-11, 1972, Proceedings. Volume 27.
04 p0416 A73-15051
- German book on physical foundations of electronics covering charged particle motions in electric and magnetic fields, relativistic effects, electron and ion optics, etc
14 p1736 A73-30597
- Electronics in the automation of services; International Congress on Electronics, 20th, Rome, Italy, March 28-31, 1973, Proceedings
17 p2122 A73-34960
- NAECON 73; Proceedings of the National Aerospace Electronics Conference, Dayton, Ohio, May 14-16, 1973.
17 p2136 A73-35201
- Electrical engineering - Service to mankind; Proceedings of the Southeast Region 3 Conference, Louisville, Ky., April 30-May 2, 1973.
17 p2142 A73-35626
- ELECTRONOGRAPHY**
Electronography application to telescope and auxiliary instrumentation designs for astronomical photometry, considering spectracon and suitable image tubes
01 p0049 A73-10537
- Electronographic photometry of very weak stars of extragalactic origin with shift towards red, discussing accuracy limitation causes
01 p0049 A73-10538
- Electronographic image tubes for stellar field photometry.
01 p0049 A73-10539
- Electronographic image receptor advantages in spectrography, noting linearity, efficiency and detection threshold and receiver noise absence
01 p0049 A73-10540
- Ruby laser radiation removal of glowing spot from Kron electronograph image tube
05 p0580 A73-17260
- Image intensifier systems and their applications to astronomy.
08 p0971 A73-21743
- Magnetically focused electronographic cameras for far UV imagery and spectrography in astronomical and optical geophysical observations from sounding rockets and space vehicles
08 p0971 A73-21744
- Photo-electronic image devices; Proceedings of the Fifth Symposium, Imperial College of Science and Technology, London, England, September 13-17, 1971.
14 p1751 A73-29903
- Electronographic image tube development at the Royal Greenwich Observatory.
14 p1732 A73-29908
- The oblique electron lens.
18 p2316 A73-36597
- Electronographic observations of the forbidden O II ratio in the core of the Orion Nebula.
24 p3140 A73-45183
- ELECTRONS**
NT CONDUCTION ELECTRONS
NT FREE ELECTRONS
NT HIGH ENERGY ELECTRONS
NT HOT ELECTRONS
NT PHOTOELECTRONS
NT PI-ELECTRONS
NT POLARONS
NT SOLAR ELECTRONS
L-beta /2/ and K-alpha X ray spectra of niobium and carbon in NbC compound, assuming collectivized valence electrons
02 p0180 A73-12174
- Analysis of the Jovian electron radiation belts. II - Observations of the decimetric radiation.
19 p2475 A73-37622
- ELECTROPHORESIS**
On the electrophoretic behavior of thermal polymers of amino acids.
06 p0661 A73-17939
- The effect of iontophoretically applied acetylcholine upon the cat's retinal ganglion cells.
14 p1715 A73-30061
- Enhancement of the electrical strength of deposited aluminum oxide coatings by electrophoretically filling the pores
15 p1881 A73-31212
- Influence of the magnetic field on electrodeless-discharge plasmas
23 p3009 A73-43654
- ELECTROPHOTOMETERS**
Photoelectric determination of radial velocities.
01 p0047 A73-10517
- Minicomputer based CAMAC modular system for astronomical telescope instrumentation, discussing hardware and software interfaces, squad scaler, photoelectric photometer, Michelson interferometer and multichannel spectrometers
01 p0019 A73-10547
- Photometric investigations of magnetic stars.
08 p1006 A73-20925
- Photoelectric observation of variable star V725 Sagittarii for significant magnitude and period changes since 1935
09 p1146 A73-22449
- Spectroelectrophotometer for atmospheric optical measurements in the near infrared region of the spectrum
11 p1362 A73-25610
- Photoelectric observations of the close binary system SZ Camelopardalis.
11 p1425 A73-26266
- Opticomechanical system of an automatic stellar electrophotometer
12 p1495 A73-26865
- The automatic telescope AZT-11
15 p1877 A73-32130
- Electrophotometer control system for the AZT-24 telescope
15 p1877 A73-32131
- Automatic stellar electrophotometer with photon counting
15 p1878 A73-32136
- High speed photoelectric photometer for night sky scanning
15 p1878 A73-32137
- Extra-atmospheric observations of the luminosity of the sky from the Cosmos 51 and Cosmos 213 satellites. I - Method and calibration of the measurements
16 p2001 A73-32706
- Extra-atmospheric observations of the luminosity of the sky from the Cosmos 51 and Cosmos 213 satellites. II - Measurement data and their interpretation
16 p2001 A73-32707
- A high-resolution photoelectric spectrophotometer at the coude focus of a 2.6-m telescope
16 p2011 A73-32714
- Optimum astronomical photoelectric photometry - Terrestrial operations in the UV-IR band up to 1 micron wavelength.
16 p2011 A73-32829
- Electrophotometric equipment in the Stara Zagora Observatory
16 p2016 A73-33663
- A portable millisecond-integration-time photoelectric photometer.
17 p2165 A73-34273
- The signal-to-noise ratio of a photodetector with a virtual cathode.
17 p2168 A73-35172
- ISIS-II scanning auroral photometer.
19 p2428 A73-37256
- ISIS-2 red line photometer for global distribution mapping of atomic oxygen 6300 A emission in airglow and auroras, discussing atomic excitation processes in upper atmosphere
19 p2428 A73-37257
- Photometer for detection of sodium day airglow.
19 p2428 A73-37261
- Application of a photoelectric area scanner to various astronomical problems
19 p2430 A73-37605
- CIE interlaboratory comparison of measurements of photocell spectral sensitivity.
21 p2698 A73-40141
- Optimum detection of an optical image on a photoelectric surface.
21 p2650 A73-40338
- Extra-atmospheric photoelectric study of the brightness of the earth's atmosphere
21 p2686 A73-40912
- ELECTROPHOTOMETRY**
Linear photoelectric scanning techniques for achieving high resolution, comparing with two dimensional scanning at telescope or of electronographic images
02 p0169 A73-12332
- Photoelectric measurement of twilight sky brightness distribution for separation of primary brightness component, noting possibility of secondary component due to dust
07 p0818 A73-19593
- Galactic structure at high galactic latitudes.
08 p1011 A73-21365
- Two-color electrophotometry of RW in the Northern Crown
11 p1416 A73-25233

- Photometric characteristics of the star AC Hercules
12 p1537 A73-26851
- Two-color electrophotometric observations of the BD Dra variable
12 p1537 A73-26852
- Photometry and some characteristics of spiral Seyfert galaxies beyond the nucleus boundary
15 p1938 A73-31951
- Application of the SIT vidicon to astronomical measurements.
17 p2169 A73-35285
- The effect of toroidal magnets on the sensitivity of photomultipliers.
21 p2699 A73-40410
- Narrow-band photoelectric observations of the Wolf-Rayet type eclipsing binary star V444 Cyg in the continuum /4244 - 7512A/
21 p2768 A73-40717
- The absorption cross sections of N₂, O₂, CO, NO, CO₂, N₂O, CH₄, C₂H₄, C₂H₆, and C₄H₁₀ from 180 to 700 Å.
22 p2890 A73-42992
- Normal galaxy central region dust content /mass/ estimates based on photoelectric measurements
23 p3035 A73-44235
- Photometry and some features of Seyfert spiral galaxies beyond the nuclear region.
24 p3131 A73-44476
- Photoelectric and visual observation of the total eclipse of the moon of August 6, 1971.
24 p3134 A73-44568
- ELECTROPHYSICS**
NT ELECTRO-OPTICS
- Influence of vacuum conditions in fabrication on the structure and electrophysical properties of epitaxial silicon films on sapphire
06 p0736 A73-18089
- Electrophysical properties of BiTeI thin films
10 p1259 A73-24154
- ELECTROPHYSIOLOGY**
An earphone coupling system for acute physiological studies.
01 p0013 A73-10829
- Structural organization and electrophysiological properties of the intercentral functional systems of the hypothalamic region of the brain
01 p0009 A73-11024
- Cat optic tract and geniculate unit responses corresponding to human visual masking effects.
02 p0134 A73-12161
- A new method to measure non-uniformity in the intact heart.
04 p0412 A73-15645
- Mathematical analysis of body surface potentials.
04 p0412 A73-15646
- Derivation of a function of nerve-fiber distribution according to fiber diameters on the basis of electrophysiological measurements
04 p0413 A73-15787
- Genesis mechanism of slow cortical after-discharges during brain injury by radiation
05 p0539 A73-16331
- Book - Understanding electrocardiography: Physiological and interpretive concepts.
05 p0542 A73-16359
- Electroretinography /ERG/, electro-oculography /EOG/, visual evoked response /VER/ and electric evoked response /EER/ procedures for electrophysiological investigation of visual system
05 p0542 A73-16484
- Study of intraventricular conduction times in patients with left bundle-branch block and left axis deviation and in patients with left bundle-branch block and normal QRS axis using His bundle electrograms.
05 p0540 A73-16582
- Three channel transistorized pulse generator for electric stimuli used in electrophysiological studies
05 p0545 A73-16739
- Electrographic data pertinent to exposures in a pressure chamber to moderate hypoxia levels
06 p0657 A73-17684
- Intermittent trifascicular block - Different mechanisms of conduction disturbances in the bundle branches.
07 p0780 A73-19152
- Modulated light transmission for electrical isolation in a multichannel physiological monitoring system.
07 p0785 A73-19482
- Evoked potential correlates of expected stimulus intensity.
08 p0930 A73-21225
- Effect of heparin on blood platelet aggregation and thrombosis under the action of direct electric current
08 p0931 A73-21321
- Relation of electrolyte disturbances to cardiac arrhythmias.
08 p0933 A73-21807
- Electrophysiological investigation of noise rejection in an auditory system receiving sound from a localized source
09 p1040 A73-22580
- Polysensory responses and sensory interaction in pulvinar and related postero-lateral thalamic nuclei in cat.
09 p1040 A73-22696
- Rapid eye movement analyzer.
09 p1045 A73-22697
- Caloric vestibular stimulation via UHF-microwave irradiation.
10 p1178 A73-23650
- Alternative mechanisms of apparent supernormal atrioventricular conduction.
10 p1184 A73-23843
- Sinusoidal stimuli induced electrical activity of hippocampus in waking rhesus monkeys and baboons
10 p1180 A73-24330
- Electrophysiological study of the topographic organization of Deiters' lateral vestibular nucleus
10 p1181 A73-24515
- Papers on cardiac electrophysiology covering heart cells, membrane mechanism, molecular structure, excitation-contraction coupling, muscular ion transport, synaptic and atrioventricular transmissions, healing, etc
11 p1315 A73-25588
- Single unit and evoked potential responses in cat optic tract to paired light flashes.
11 p1317 A73-25647
- Human visual evoked response signal decomposition by complex demodulation in terms of after-discharge time, envelope and frequency parameters
11 p1324 A73-26497
- A comparison of electrophysiological and psychophysical temporal modulation transfer functions of human vision.
13 p1575 A73-28360
- Intranuclear organization of the center median nucleus of the thalamus.
13 p1576 A73-29175
- Processing of auditory information by medial superior-olivary neurons.
14 p1715 A73-30281
- Retinal receptive fields - Correlations between psychophysics and electrophysiology.
14 p1717 A73-30397
- Sensory versus perceptual isolation - A comparison of their electrophysiological effects.
14 p1722 A73-30517
- German monograph - Comparative investigations regarding the phenomenon of force potentiation in the case of the heart muscle of cold-blooded and warm-blooded animals.
14 p1719 A73-30669
- Electrophysiological evidence that abnormal early visual experience can modify the human brain.
15 p1838 A73-31371
- Memory fixation during sleep, discussing EEG, EOG, EMG and ECG recordings for differences between light and paradoxal sleep
15 p1835 A73-31749
- Mechanisms of secretion of neurohypophyseal hormones - Cellular and subcellular aspects
15 p1836 A73-32286
- Russian book - Methods of studying eye movements.
15 p1840 A73-32417
- Physiologic correlates and clinical comparisons of isopotential surface maps with other electrocardiographic methods.
18 p2282 A73-36519
- Investigation of the distribution of synaptic inputs on an analog model of the motoneurons
19 p2399 A73-37942
- Probabilistic statistical methods for analysis of impulse flows in nerves
20 p2516 A73-39002
- A universal preamplifier for bioelectric signals
21 p2643 A73-40345
- An assembly for electrophysiological and thermometric studies
22 p2815 A73-42663
- Shaping device for frequency analysis of electrical processes in peripheral neural stems and ganglia
22 p2815 A73-42664
- Relation between vibratory sensibility and electric signal of living body.
22 p2816 A73-42680
- Investigation of complex and hypercomplex receptive fields of visual cortex of the cat as spatial frequency filters.
22 p2810 A73-42958
- Rectifier-like color dependent phase shifts in electrophysiological responses to different colored stimuli at evoked potential and single neuron levels
22 p2810 A73-42961
- Structurally functional properties of the dendrites of central neurons
23 p2947 A73-43926
- Electrical field distribution in the human body.
23 p2950 A73-44216
- Anatomic and functional organization of the ventral anterior and reticular nuclei of the thalamus
24 p3059 A73-44675
- Electronic simulation and analog computer studies of the influence of temperature on the process of nerve impulse shaping
24 p3062 A73-44725
- Intracellular measurements in a closed hyperbaric chamber.
24 p3065 A73-45072
- ELECTROPLATING**
Effect of the quality of electrolytic chromium plating on the endurance of steel
02 p0173 A73-11926
- Printed circuit and electronic component solderability tests subsequent to adverse environment exposure, comparing electroplated materials with pressure leveled solder and Cu and Be coatings
03 p0333 A73-13046
- Electro-gilding of coverings and light alloy component parts for satellites D2 and EOLE.
07 p0829 A73-18911
- Theory and performance of plated thermocouples.
22 p2859 A73-42051
- ELECTROPLETHYSMOGRAPHY**
Stroke volume measurement from an integral rheogram of human body
24 p3062 A73-44719
- ELECTROPOLISHING**
Analysis of electrolytes for electrochemical polishing of steel with cationite application
02 p0174 A73-12536
- Surface preparation and pit propagation in stainless steels.
03 p0325 A73-13726
- Effects of electropolishing on the tunneling current in aluminum-aluminum-oxide-aluminum diodes.
06 p0678 A73-18744
- Influence of electrolytic polishing on the stress-concentration sensitivity of some alloys in fatigue
23 p2995 A73-44283
- ELECTROREFINING**
Electron beam refined niobium melting temperature determination from black body brightness change
10 p1230 A73-23508
- Molybdenum metal by the aluminothermic reduction of calcium molybdate.
10 p1234 A73-24430
- Electron beam refined niobium melting temperature determination from black body brightness change
17 p2191 A73-35188
- ELECTRORETINOGRAPHY**
ERG late photoreceptor potential components time course in macaque monkey cones and rods, noting pure cone foveal response
03 p0261 A73-13761
- Electroretinography /ERG/, electro-oculography /EOG/, visual evoked response /VER/ and electric evoked response /EER/ procedures for electrophysiological investigation of visual system
05 p0542 A73-16484
- Linearity of the horizontal component of the electro-oculogram.
07 p0784 A73-19125
- Light-induced potential and resistance changes in vertebrate photoreceptors.
09 p1043 A73-23313
- Retinal S-potential receptive field relationship to light energy and wavelength, considering cone and rod potentials, ganglion cells and vision
09 p1043 A73-23314
- The electroretinogram, as analyzed by microelectrode studies.
09 p1047 A73-23318
- Frog retinal metabolism in photoreceptors during dark and light adaptation, using ERG, radiospirometry, oxygen uptake polarography and pyridine spectrophotometric assay
09 p1044 A73-23319
- Electroretinogram recovery cycle during light adaptation and after dark adaptation
10 p1181 A73-24518
- Electrical and metabolic manifestations of receptor and higher-order neuron activity in vertebrate retina.
13 p1574 A73-28353
- Cone spectral sensitivity studied with an ERG method.
13 p1575 A73-28358
- A comparison of electrophysiological and psychophysical temporal modulation transfer functions of human vision.
13 p1575 A73-28360
- Scotopic electroretinography and visual evoked responses under adaptive illumination, comparing blind spot stray light with parafoveal stimulation
13 p1575 A73-28361
- New method of stimulation for the study of photoreceptors.
13 p1578 A73-28362
- Stimulus luminance-duration relationship of adapting light effect in human electroretinography, referring to Bunsen-Roscoe and Bloch constant law
13 p1575 A73-28363
- The macular and paramacular local electroretinograms of the human retina and their clinical application.
13 p1575 A73-28364
- Oscillatory waves in intraretinally recorded electroretinograms in primates, considering electrode depth, stimulus duration and intensity and background illumination, anesthesia and tetrodotoxin effects
14 p1717 A73-30393
- Localized electroretinography capable of maintaining constant light scattering with small angular dimensions

- sions by employing Ulbricht principle of uniformly illuminated sphere 17 p2116 A73-34963
- Modeling, instrumentation and data evaluation in clinical electroretinography, discussing Fourier analysis of sinusoidal light stimulation response in normal and abnormal humans 17 p2117 A73-35359
- Local resistance variations caused by membrane potential shifts in the interior of the horizontal retina cell 24 p3061 A73-45250
- ELECTROSEISMIC EFFECT**
U ELECTRIC CURRENT
U SEISMIC WAVES
ELECTROSLAG REFINING
The reactions of titanium and silicon with Al₂O₃-CaO-CaF₂ slags in the ESR process. 04 p0455 A73-15744
- The feasibility of producing superalloy electrosag remelted hollows. 04 p0455 A73-15744
- Microstructural features of Cr12NiWMoVTi /S760/ steel after electrosag remelting 24 p3100 A73-45170
- ELECTROSLAG WELDING**
Metallographic investigation and notch, tensile and hardness tests for electrosag welding of austenitic stainless steels 07 p0831 A73-19949
- Book - Welding and welding technology. 17 p2177 A73-34454
- Structure and phase composition of a maraging-steel weld 21 p2718 A73-40737
- Influence of a magnetic field on the weld-seam structure during electrosag welding of titanium alloys 21 p2707 A73-40891
- Effect of technological and metallurgical treatment on the properties of electrosag-welded joints in heat resistant steels 22 p2865 A73-41778
- ELECTROSTATIC CHARGE**
Electrostatic autopilot using atmosphere electric field lines for stabilization and guidance, applying to remotely piloted vehicles 02 p0191 A73-12595
- The electrostatic charging tendencies of jet fuel filtration equipment. [SAE PAPER 720866] 05 p0582 A73-16672
- De Gaston decharger with ionizing radiation for temporary jet fuel conductivity increase and charge density reduction, discussing theory, design and tests. [SAE PAPER 720864] 05 p0537 A73-16673
- Kinetics of electrostatic image formation during exposure of electrophotographic layers 07 p0823 A73-19331
- Electrostatic charge induction on aircraft due to charged atmosphere and friction effects, noting lightning protection, fuel container shielding and charge removal methods 11 p1307 A73-26722
- Electrostatic charging of the lunar surface and possible consequences. 16 p2062 A73-33463
- Potential created by a test particle in one-, two- and three-dimensions in a flowing ion-electron plasma. 20 p2596 A73-38969
- An analytical solution of the problem of a frequency tripler employing a varactor diode with an arbitrary voltage-charge characteristic 24 p3072 A73-44927
- ELECTROSTATIC ENGINES**
Electrostatic ion thrusters of the DFVLR Braunschweig for primary propulsion. 04 p0488 A73-15717
- Linear slit colloid electrostatic thruster development and testing, discussing emitter geometry, gap design, exhaust velocity, operating voltage and power efficiency relationships 04 p0488 A73-15725
- Planetary exploration with electrically propelled vehicles. 06 p0750 A73-18021
- ELECTROSTATIC EROSION**
U SPARK MACHINING
ELECTROSTATIC FIELDS
U ELECTRIC FIELDS
ELECTROSTATIC GYROSCOPES
Electric forces in electrostatic gyroscope for rotor gravity center displacement, taking into account mutual effects of electrode pairs 05 p0577 A73-16994
- Calculation of the rotor potential of an electrostatic gyroscope 11 p1364 A73-26098
- Influence of the orthogonal axes of the suspension of an electrostatic gyroscope at zero rotor potential 13 p1618 A73-29148
- Gimbaled electrostatic gyro inertial aircraft navigation system /GEANS/ designs balancing performance against cost of ownership 16 p2034 A73-33086
- Strapdown electrostatic gyroscope spin axis precession drift rate calibration, using virtual work technique for modeling bearing torques on rotor 17 p2137 A73-35210
- The position of the axis of rotation of a free gyroscope ball rotor 18 p2317 A73-36852
- The effect of the rotor pattern on the accuracy of the photoelectric angle-measuring system of a gimbaless electrostatic gyroscope. 18 p2317 A73-36873
- Low cost strapdown inertial navigator with miniature electrostatically suspended gyros, discussing system performance goal in terms of position, velocity and attitude errors 21 p2734 A73-40037
- ELECTROSTATIC PLASMA**
U PLASMAS (PHYSICS)
ELECTROSTATIC PROBES
Plasma density measurement by a Langmuir probe in the presence of a magnetic field 01 p0082 A73-10428
- An electrostatic cloud droplet probe. 01 p0052 A73-11058
- The application of Langmuir probes to the measurement of very low electron temperatures. 02 p0158 A73-11912
- Rocket-borne instrumentation to measure ionospheric electron temperature with good spatial resolution. 02 p0167 A73-11953
- The global morphology of electron temperature in the topside ionosphere, as measured by an a.c. Langmuir probe. 02 p0158 A73-12027
- Spherical probe measurements of dense weakly ionized plasma parameters, noting ionization, recombination and secondary surface effects on probe characteristics 02 p0198 A73-12109
- Transverse ion temperature measurements in plasma stream wind tunnel simulating ionospheric conditions, using cylindrical Langmuir probe and collimator-collection device [ONERA, TP NO. 1180] 02 p0151 A73-12813
- Measurement of electron distribution function in a cesium plasma. 02 p0199 A73-12815
- Boundary-value problem for a Langmuir probe in a dense plasma. 06 p0727 A73-17420
- Ion density and current distribution measurements in hypersonic turbulent wakes behind sphere flown in ballistic range, using cylindrical electrostatic probes 06 p0645 A73-18135
- Effects of non-Maxwellian electron energy distributions on the orbital limited current-voltage characteristics of cylindrical and spherical Langmuir probes under collisionless conditions. 06 p0730 A73-18463
- Plasma sheath capacitance and resistance in double inverse pinch device from I-V measurements with Langmuir probe, noting relationship to plasma temperature and density [AD-760249] 06 p0696 A73-18784
- Experimental and numerical studies of flush electrostatic probes in hypersonic ionized flows. II - Theory. 07 p0858 A73-19961
- Continuum electrostatic probe theory with magnetic field. 07 p0860 A73-20476
- Characteristics of a spherical electrostatic probe in a weakly ionized plasma. 08 p0993 A73-21390
- Ion saturation currents to planar Langmuir probes in a collision-dominated flowing plasma. 08 p0993 A73-21597
- A comparative experimental study of electron and positive-ion current collection by a cylindrical Langmuir probe under orbital-limited conditions. 08 p0967 A73-21598
- Transition region response of the symmetric double probe and its application in the lower ionosphere. 09 p1080 A73-22101
- The calibration of electrostatic analyzers and channel electron multipliers using laboratory simulated omnidirectional electron beams. 09 p1080 A73-22104
- Modulation Langmuir probe and incoherent scatter radar measurements of ionospheric electron temperature. 09 p1075 A73-22128
- Pulsed probe studies on the diffusion coefficient of an afterglow plasma across a magnetic field. 09 p1132 A73-23250
- Measurement of the horizontal component of the electrostatic field intensity in the lower atmosphere 10 p1219 A73-24400
- Electrostatic probe theories and measurements in flame plasmas. 10 p1220 A73-24621
- A simple device for measuring the characteristics of double Langmuir probes in a periodic pulse discharge 10 p1257 A73-24691
- Vertical electron density and temperature data from geophysical rocket borne Langmuir probes and electrode traps 11 p1350 A73-25078
- Electrostatic toroidal analyzer for studying charged particle fluxes in outer space 12 p1496 A73-27203
- Probe device for measuring local parameters of ionized gas flow. 12 p1499 A73-27915
- Cylindrical electrostatic probes onboard Explorer C, D and E, presenting I-V characteristics of collector 13 p1688 A73-28636
- Ionospheric electron density and temperature measurement by cylindrical Langmuir probes onboard Interkosmos 2 satellite 14 p1746 A73-29862
- Split Langmuir probe measurements of current density and electric fields in an aurora. 14 p1748 A73-29970
- French monograph - Analysis of the functioning of the differential probe for measurement of electronic temperature in the ionosphere. 14 p1753 A73-30672
- Ion current at the forward stagnation region of an electrically conducting body. 15 p1918 A73-31669
- A critical study on the reliability of electron temperature measurements with a Langmuir probe. 15 p1871 A73-31835
- Probe design for orbit-limited current collection. 16 p2041 A73-33320
- Transient current overshoot to electrostatic probes in continuum, slightly ionized plasmas. 16 p2041 A73-33331
- Multiring probe in a flowing ionospheric plasma. 17 p2214 A73-34199
- Cylindrical probe in a glowing-discharge nitrogen plasma at medium pressures 17 p2215 A73-34261
- Electron depletion in the wake of ionospheric spacecraft - A comparison between results from Langmuir probes and antennas. 17 p2159 A73-34783
- Some features of the equatorial D-region as revealed from the Langmuir probe experiments conducted at Thumba. 18 p2303 A73-35954
- Inflight electrostatic probe measurements of the effect of chemical injection on the properties of the re-entry flow field. 18 p2338 A73-36243
- Probe measurement of the electrostatic field in the ionosphere and magnetosphere 18 p2314 A73-37026
- Continuum thick sheath probe studies in hypersonic ionized boundary layers. 19 p2375 A73-37164
- A review of electrostatic probe response in a flowing, low density plasma. 19 p2465 A73-37165
- Application of cylindrical Langmuir probes to streaming plasma diagnostics. 19 p2469 A73-37862
- Comparison of Langmuir double probe and laser scattering measurements of plasma parameters. 20 p2595 A73-38880
- Explorer 45 /S3-A/ symmetrical floating probes for plasma dc electric fields, discussing plasma sheaths, noise storms, whistlers, electric field strength and orbit configuration 20 p2552 A73-38954
- Pulsed Langmuir probe measurements of hollow cathode plasma discharge electron emission in terms of secondary, thermionic and field components 21 p2747 A73-40793
- The determination of ionospheric charged particle temperatures from in situ measurements. 21 p2690 A73-41362
- Direct-display plasma density and temperature meter by the use of Langmuir probe. 23 p3015 A73-44367
- Ionospheric electric field measurements with a spin stabilized detector. 24 p3090 A73-44818
- The inadequate reference electrode, a widespread source of error in plasma probe measurements. 24 p3115 A73-44873
- Simultaneous in situ electron temperature comparison of Alouette 2 probe and plasma resonance data. 24 p3086 A73-45129
- Experimental investigation of the low-frequency capacitive response of a plasma sheath. 24 p3117 A73-45408
- ELECTROSTATIC PROPULSION**
NT ION PROPULSION
High and low thrust systems for primary and auxiliary spacecraft propulsion, noting electron bombardment electrostatic thruster for north-south station-keeping [AIAA PAPER 72-1123] 03 p0355 A73-13435
- Correlation of ion and beam current densities in Kaufman thrusters. 22 p2900 A73-42636

ELECTROSTATIC SHIELDING

Electrostatic charge induction on aircraft due to charged atmosphere and friction effects, noting lightning protection, fuel container shielding and charge removal methods

11 p1307 A73-26722

ELECTROSTATIC WAVES

Two-dimensional investigation of absolute instabilities in mirror plasmas.

01 p0083 A73-10458

Role of trapped particles in plasma waves and instabilities.

02 p0197 A73-12967

Magnetospheric observations in OGO-5 plasma wave experiment, emphasizing electrostatic wave particles interaction with plasma

03 p0303 A73-13883

LF spectrum of plasma oscillations from amplitude modulation of plasma SHF radiation, noting Langmuir and magnetoacoustic waves interaction

04 p0478 A73-15034

Short-life mode of electrostatic electron cyclotron harmonic waves.

04 p0477 A73-15196

A technique for making dispersion relation measurements of electrostatic waves.

04 p0450 A73-15554

Electrostatic ion cyclotron waves in an anisotropic plasma.

05 p0611 A73-17305

A specific feature of surface waves at the boundary of inhomogeneous plasma.

06 p0730 A73-18466

The sideband instability of electrostatic waves in an inhomogeneous medium.

07 p0858 A73-19667

Parametric excitation of circularly polarized and Langmuir waves in a magnetized plasma.

07 p0859 A73-20197

Large-amplitude stabilization of the drift instability.

07 p0860 A73-20481

Non-local asymptotic treatment of the stability of an inhomogeneous confined plasma.

08 p0991 A73-20819

Electrostatic turbulence at colliding plasma streams as the source of ion heating in the solar wind.

08 p0997 A73-20886

Heating of charged particles by electric waves.

08 p0993 A73-21233

Effect of the plasma inhomogeneity on the nonlinear damping of monochromatic waves.

09 p1126 A73-22281

Nonlinear interactions between Langmuir waves in a weakly inhomogeneous plasma

10 p1253 A73-23576

Half-harmonic modes for different frequency ranges and wave vectors from infinite homogeneous plasma model for high frequency electrostatic wave propagation in magnetosphere

10 p1213 A73-24733

Turbulent loss mechanism of ring current protons in plasmopause vicinity via electrostatic drift cyclotron loss cone waves

10 p1270 A73-24743

Electrostatic turbulence parametric excitation by electric field with frequency near plasma frequency, accounting for saturation electric field in anomalous plasma heating via electron trapping theory

11 p1403 A73-25256

Unstable Langmuir or ion acoustic wave saturation in collisionless plasma due to electron trapping, estimating amplitude via adiabatic and sudden approximation

11 p1404 A73-25258

The ion cyclotron drift loss-cone instability with a coexisting cold plasma.

11 p1404 A73-25271

A photon rest mass and the propagation of longitudinal electric waves in interstellar and intergalactic space.

11 p1417 A73-25562

Refraction by the electromagnetic pump of parametrically generated electrostatic waves.

11 p1405 A73-25973

Parametric excitation of Langmuir oscillations in the ionosphere in a field of powerful radio waves

11 p1331 A73-26153

Plasma low density regions caused by Langmuir turbulence, discussing energy dissipation of long wave oscillations and wave collapse

11 p1406 A73-26185

Long wavelength instability in a perpendicular shock.

11 p1406 A73-26557

Satellite-borne electrostatic wave topside ionosphere sounder for electron plasma resonance measurement, discussing data spectra preservation, frequency synthesizer and gain-change mechanism features

11 p1339 A73-26629

Electrostatic waves in warm random plasmas.

14 p1779 A73-29708

Field-aligned currents, plasma waves, and anomalous resistivity in the disturbed polar cusp.

14 p1747 A73-29964

Direct nonlinear coupling of electromagnetic waves and electrostatic waves in a plasma - Theory.

14 p1781 A73-30656

Excitation of an electron semicyclotron wave and its harmonics during the interaction of high-current opposed electron beams

15 p1920 A73-32312

Lineshape of stable electrostatic fluctuations in a beam plasma system.

16 p2042 A73-33338

Instability of plasma waves with nonlinear Landau effect.

17 p2215 A73-34296

Electrostatic waves with frequencies above the gyrofrequency in a plasma with a loss-cone.

17 p2218 A73-35831

Absorption and transformation of electrostatic surface waves in the transition layer of a magneto-active plasma.

19 p2467 A73-37438

Wavenumber space analysis of oscillations in weakly non-uniform magnetoplasmas.

19 p2468 A73-37442

Traveling longitudinal electrostatic waves excitation in warm nonuniform plasma by external HF electric fields, using kinetic theory

19 p2468 A73-37857

Low-frequency flute instabilities of a hollow cathode arc discharge - Theory and experiment.

19 p2468 A73-37858

Direct nonlinear coupling of electromagnetic waves and electrostatic waves in a plasma - Experiment.

19 p2469 A73-37860

The theory of parametric excitation of electrostatic surface waves in a plasma layer

20 p2597 A73-39194

Nonlinear theory of a quasi-monochromatic electrostatic wave packet in an inhomogeneous plasma

21 p2745 A73-40363

Trapped-particle scattering by electrostatic turbulence in toroidal plasmas.

21 p2749 A73-41675

Effects of electrostatic instabilities on planetary and interstellar ions in the solar wind.

22 p2902 A73-41940

Wave spectrum analysis of electron beam-plasma longitudinal electrostatic fluctuations, finding triplet wave line shape and intensity and dispersion relations

22 p2891 A73-42240

Electrostatic waves with frequencies exceeding the gyrofrequency in the magnetosphere.

22 p2851 A73-42933

Propagation mode with fine structure interpreted as quasi-cylindrical electrostatic wave interference with cold plasma field from potential measurements near point source antenna

22 p2895 A73-43021

Anisotropic turbulent distributions for waves with a nondecay-type dispersion law

23 p3012 A73-44018

Langmuir wave attenuation in collisionless plasma of variable density due to field generated by resonant particle currents moving toward lower density region

23 p3015 A73-44349

Excitation of electron-cyclotron waves by high-current counter-streaming electron beams.

24 p3115 A73-44620

Diffusion of ring current particles by low-frequency long-wavelength electrostatic oscillations.

24 p3126 A73-45128

Enhanced scattering and decay of electromagnetic waves in the ionosphere.

24 p3086 A73-45130

Neutron emission from laser produced plasmas and collisionless electrostatic shock waves.

24 p3116 A73-45242

Wave-wave contribution to the high-frequency resistivity of nonequilibrium plasma.

24 p3117 A73-45457

ELECTROSTATICS

Large amplitude oscillations of a hollow spherical dielectric.

02 p0236 A73-12518

A numerical computer method for computing the electrostatic field and electron paths of focusing optoelectronic systems

04 p0448 A73-15078

Application of linear feedback control theory techniques to continuum dominated by electrostatic and gravitational fields.

06 p0680 A73-18004

Electrostatic getter-ion pump performance.

08 p0989 A73-21618

Strict calculation of static fields in devices for periodic electrostatic focusing /PEF/ of electron beams

10 p1197 A73-24882

Explanation of the accident to the Europa II F 11 launcher by phenomena of electrostatic origin

11 p1431 A73-25749

Thin piezoelectric plate bending deformation and polarization theory in terms of piezoelectricity, electrostatics and elasticity equations for anisotropic body

12 p1552 A73-27371

The geometrical factor of large aperture hemispherical electrostatic analyzers.

20 p2564 A73-38877

Static fields for periodic electrostatic focusing of electron beams.

21 p2668 A73-41657

An electrostatic suspension method for determining photoionization energies of solids.

23 p3015 A73-43447

Accretion and electrostatic interaction of interstellar dust grains - Interstellar grit.

23 p3030 A73-43757

Electrostatic Hellmann-Feynman theorem applied to long-range interatomic forces - The hydrogen molecule.

24 p3113 A73-44981

ELECTROSTRICTION

Measurement on a polarization interferometer of absolute and relative light wave delay in liquid dielectrics under the action of an electric field

07 p0823 A73-19332

Damage produced by laser radiation in optical materials. II

22 p2868 A73-41824

Sonic wave excitation by optical radiation, considering electrostriction effect and radiation absorption with subsequent intensity inhomogeneity-caused pressure gradients

22 p2868 A73-41898

ELECTROTHERMAL ENGINES

NT PLASMA ENGINES

NT RESISTOJET ENGINES

Electrothermal hydrazine thruster analyses and performance evaluation.

04 p0486 A73-14917

Book on aerospace propulsion covering nozzle, combustors and diffusers flow, space power generation, electrothermal engines, chemical rockets and central force fields

14 p1785 A73-30361

ELEKTRON SATELLITES

Electron acceleration in the outer radiation belt

06 p0742 A73-17527

Earth outer radiation belt and unstable radiation zone dynamics during IQSY magnetically quiet and disturbed period based on Elektron-series satellite data

12 p1535 A73-27636

Electron acceleration in the outer radiation belt.

16 p2051 A73-32752

ELEMENT ABUNDANCE

U ABUNDANCE

ELEMENTARY EXCITATIONS

NT EXCITONS

NT MAGNONS

NT PHONON BEAMS

NT PHONONS

NT PLASMONS

NT POLARONS

ELEMENTARY PARTICLE INTERACTIONS

NT ELECTRON CAPTURE

NT NUCLEAR CAPTURE

NT NUCLEON-NUCLEON INTERACTIONS
CP-noninvariance model of baryon asymmetry of universe, postulating kappa particle /neutral massive fermion/

02 p0221 A73-12669

Interaction lengths of energetic pions and protons in iron.

08 p0990 A73-21523

Study of strong interactions between cosmic-ray hadrons and nuclei at 200 to 2000 GeV energies

10 p1264 A73-23816

A low-background counter telescope for recording alpha particles in μ , alpha/-reactions

21 p2699 A73-40173

Reactions of pseudoscalar meson production by neutrinos on nucleons near the threshold in the range of high transferred impulses

23 p3008 A73-43544

ELEMENTARY PARTICLES

NT ALPHA PARTICLES

NT ANTINEUTRINOS

NT ANTIPARTICLES

NT ANTIPROTONS

NT BARYONS

NT BETA PARTICLES

NT CONDUCTION ELECTRONS

NT DEUTERONS

NT ELECTRONS

NT FAST NEUTRONS

NT FERMIONS

NT FREE ELECTRONS

NT GRAVITONS

NT HADRONS

NT HIGH ENERGY ELECTRONS

NT HOT ELECTRONS

NT LEPTONS

NT LIGHT BEAMS

NT MESONS

NT NEUTRINOS

NT NEUTRON BEAMS

NT NEUTRONS

NT NUCLEONS

NT PHOTOELECTRONS

NT PHOTONS
NT PI-ELECTRONS
NT PIONS
NT POLARONS
NT POSITRONS
NT PROTONS
NT QUARKS
NT RECOIL PROTONS
NT SOLAR ELECTRONS
NT SOLAR PROTONS
NT THERMAL NEUTRONS

Construction of the spinor field equations in cosmological space

08 p1010 A73-21271

Russian book on elementary particle counters covering gas discharge /Geiger-Muller/, scintillation, Cerenkov and semiconductor counters and matter-radiation interactions

15 p1880 A73-32418

High energy cosmic rays and elementary particles, discussing detection, sources, nature and properties

21 p2764 A73-41611

ELEVATION

Preliminary results of the determination of altitudes on Mars from CO₂ 2-micron wavelength bands aboard the Mars 3 interplanetary automatic station

13 p1673 A73-28288

Low value atmospheric density extremes evaluation covering ground elevations up to 15,000 feet for engine power calculation in aircraft design

21 p2729 A73-40063

Semiconducting ground influence on input impedance and radiation resistance of horizontal magnetic dipoles, covering short wave band for various antenna elevations and conductivity levels

21 p2661 A73-40203

Preliminary results of Martian altitude determinations with CO₂ bands /2 micron wavelength/ from the automatic interplanetary space station Mars 3.

22 p2905 A73-41807

ELEVATION ANGLE

Fraunhofer zone distribution functions for azimuth and elevation angles of radio waves reflected from inhomogeneous ionospheric scattering layer

03 p0278 A73-14071

Brightness and polarization of the sky in the solar almucantar in the near infrared region of the spectrum

11 p1353 A73-25604

Selection of stars for observations from the lunar surface by the method of equal altitudes

15 p1938 A73-31963

Experimental verification of the possibility of beam scanning in a variable profile antenna by radial displacement of the primary radiating element

21 p2667 A73-41469

Selection of stars for observation from the lunar surface by the method of equal altitudes.

24 p3132 A73-44488

ELEVONS

Epoxy adhesive bonding of Concorde light alloy sandwich structure elevons, discussing surface treatment, polymerization and ultrasonic testing

13 p1623 A73-28468

Elevon ribs and spars made of flat Rene 41 caps based on hot structure concept for thermal environment

16 p2072 A73-33061

ELLIPSOIDS

Three linear invariant relations in the problem of motion of a heavy solid body with a liquid filler

02 p0153 A73-11773

Ellipsoidlike deformations of tubelike balloons - Asymptotic solution with boundary layer. [ASME PAPER 72-WA/APM-29]

04 p0515 A73-15889

Stress concentration in rotating orthotropic elliptic disks solution via Chen-Hsu modification of stress function for bounded plates

08 p1017 A73-20943

Stability of the libration points of a triaxial ellipsoid under constantly acting disturbances in the first approximation

09 p1143 A73-22093

Relationship between the coefficients of spherical and ellipsoidal expansion of the gravity force in the case of the biaxial earth ellipsoid

11 p1352 A73-25431

A direct integral equation method for the potential flow about arbitrary bodies.

13 p1563 A73-28083

Aerosol particle downward motion in vertical electric field, discussing stability of major axis orientation of ellipsoid of revolution

13 p1654 A73-28881

Existence of a new type of rotating equilibrium ellipsoids in the presence of a toroidal magnetic field

14 p1782 A73-30816

Note on volume integrals of the elastic field around an ellipsoidal inclusion.

15 p1946 A73-31104

Potential flow induced aerodynamic forces and moments on triaxial ellipsoids, using Lagally theorem based on source, sink and doublet distribution imaging method

15 p1823 A73-31641

Stress concentration on an ellipsoidal inhomogeneity in an anisotropic elastic medium

17 p2240 A73-34142

Elastic equilibrium of an ellipsoid under the action of concentrated loads

17 p2244 A73-34790

Similarity parameters and approximate relations for the axisymmetric supersonic flow past an ellipsoid

18 p2266 A73-37019

Ellipsoidal coordinates - A natural coordinate system for calculations of laser irradiations of slabs.

20 p2572 A73-38972

Ellipsoidal crack and needle in an anisotropic elastic medium

21 p2783 A73-40187

Forced convection of a fluid inside an ellipsoidal cavity

21 p2791 A73-40740

About the stability of the libration points of a rotating triaxial ellipsoid in a degenerate case.

23 p3032 A73-43838

Solution of a mixed axisymmetric problem for an elastic ellipsoid of revolution by the method of p-analytic functions

24 p3153 A73-45509

ELLIPSOMETERS

Ellipsometric polarized light methods application to corrosion technology, discussing surface film optical properties and measurement techniques

06 p0704 A73-17508

Use of a stable polarization modulator in a scanning spectrophotometer and ellipsometer.

17 p2175 A73-35751

ELLIPTIC DIFFERENTIAL EQUATIONS

Existence of solutions of certain nonlinear elliptic boundary-value problems

01 p0069 A73-10067

Iteration approach for elliptic /nonlinear/ difference operators in divergence form

01 p0069 A73-10075

Explicit alternating-direction methods of solving the boundary value problem for a fourth-order self-conjugate elliptical differential equation with variable coefficients

01 p0070 A73-10915

Singular elliptic perturbations of vanishing first-order differential operators.

02 p0186 A73-11970

Elliptic partial differential equations may be related by a change of independent variables.

02 p0186 A73-11975

The representation of functions determined by a class of hypoelliptic operators

02 p0187 A73-12180

Integral bounds of generalized derivative solutions of second-order equations of elliptic type in the L_p metric and certain related embedding theorems

02 p0187 A73-12181

The method of variable directions for solving a boundary-value problem for a self-conjugate elliptic fourth-order differential equation with variable coefficients

02 p0187 A73-12190

Analog-analytic construction of supercritical flows past profiles [DGLR PAPER 72-129]

03 p0248 A73-14384

Integral representation of positive solutions of linear elliptic and parabolic differential equations with constant coefficients

04 p0470 A73-14898

Variational-difference method for solving the third boundary value problem of an elliptic equation in a three-dimensional region with a smooth boundary

05 p0590 A73-16445

Necessary conditions for optimal controls of elliptic or parabolic problems.

05 p0590 A73-16487

Comparison and maximum theorems for systems of quasilinear elliptic differential equations.

06 p0717 A73-18171

Eigenfunction expansions and scattering theory for perturbed elliptic partial differential equations.

06 p0719 A73-18698

Pointwise bounds for smooth film profiles Reynolds equation solution based on elliptic equations maximum principle, considering journal bearings

07 p0845 A73-20484

On degenerate elliptic-parabolic operators of second order and their associated diffusions.

09 p1111 A73-21996

A numerical method for the solution of an elliptic fourth-order differential equation with variable coefficients

10 p1243 A73-24059

Solution of the stochastic control problem in unbounded domains.

10 p1203 A73-24705

Conditions for convergence of spectral decompositions corresponding to self-adjoint expansions of elliptic operators. IV - Negative-type theorems for arbitrary expansion of a general self-adjoint second-order elliptic operator

12 p1518 A73-27726

Integral estimates of the derivatives of solutions of elliptic homogeneous linear equations of arbitrary order with variable coefficients in the metric L_p, p ranging between 1 and infinity, and some of their applications

12 p1519 A73-27819

Improperly posed initial value problems for self-adjoint hyperbolic and elliptic equations.

13 p1648 A73-28424

Automation of a solution to the general boundary value problem of a plane self-conjugate elliptic equation

13 p1650 A73-29129

Uniqueness theorems for the Dirichlet boundary value problem in the case of elliptic-parabolic differential equations and lower bounds for the smallest eigenvalue

14 p1767 A73-29765

Numerical implementation of the Schwarz alternating procedure for elliptic partial differential equations.

14 p1768 A73-29938

The asymptotic behavior of the first real eigenvalue of a second order elliptic operator with a small parameter in the highest derivatives.

14 p1769 A73-30457

On the connection between the elliptic equations of the Navier-Stokes type and the theory of harmonic functionals.

14 p1769 A73-30521

Convergence of the upper relaxation method for solving variational-difference equations for elliptic equations in an arbitrary plane

15 p1898 A73-30967

Poisson formula analogs for a class of higher-order elliptic-type differential equations with a singular line in the case of a half-space

15 p1898 A73-31020

Existence and uniqueness of positive eigenfunctions for a class of quasilinear elliptic boundary value problems of sublinear type.

15 p1900 A73-32181

Rapidly convergent approximations to Dirichlet's problem for semilinear elliptic equations.

15 p1901 A73-32372

Singularities of solutions to linear, second order, analytic elliptic equations in two independent variables. II - The piecewise regular boundary.

15 p1901 A73-32374

The numerical solution of quasilinear elliptic equations.

17 p2199 A73-34103

Book - Non-homogeneous boundary value problems and applications. Volume 3.

17 p2200 A73-34464

Russian book - Linear and nonlinear boundary value problems.

17 p2201 A73-34640

Finite element formulation of nonlinear boundary-value problems.

17 p2201 A73-34831

Hopscotch method for one-space dimensional bending beam elliptic differential equation solution, noting mesh ratio stability range

17 p2251 A73-35518

Boundary value problems with a normal derivative for a mixed-type equation with discontinuous coefficients

17 p2203 A73-35584

A generalization of the additive correction methods for the iterative solution of matrix equations.

17 p2203 A73-35729

Theorems concerning isomorphisms for elliptic boundary value problems with nonnormal boundary conditions

18 p2329 A73-36164

On the iterative solution of Dirichlet problem for some mildly non-linear elliptic equations.

19 p2445 A73-38027

Improvable estimates in some non-well-posed problems for a system of elliptic equations.

20 p2581 A73-38975

Book on oscillation theory covering classical, abstract and complex theories, nonselfadjoint differential equations, hyperbolic and elliptic equations, Sturm-Picone theorem, etc

20 p2582 A73-39141

Asymptotic representation of the fundamental solution of an elliptic equation with a small parameter in the presence of a higher derivative

20 p2582 A73-39474

A geometric solvability characteristic for some boundary value problems of linear elliptic-type equations and strongly elliptic second-order systems

20 p2583 A73-39498

Gevrey hypoelliptic differential operators for subelliptic boundary value problems, considering relationship to size of derivative fractional loss in subelliptic estimate

20 p2583 A73-39626

Pairs of positive solutions of nonlinear elliptic partial differential equations.

21 p2726 A73-40695

- Free boundary problem involving elliptic differential equation, discussing iterative method instabilities inhibition of convergence
21 p2727 A73-40998
- The method of the false transient for the solution of coupled elliptic equations.
21 p2727 A73-41473
- The integrals of the system of Navier-Stokes equations for axisymmetric motion of an incompressible fluid
22 p2841 A73-42123
- Monograph - Singular perturbation problems for partial differential equations.
22 p2882 A73-42715
- The Minkowski problem generalized for ovals
23 p2999 A73-43613
- Boundary value problems for elliptic equations in domains with an unlimited boundary
23 p2999 A73-43622
- Differential operator hypoellipticity, taking into account necessary and sufficient conditions for existence based on Ehrenpreis-Palamodov theorem
23 p3000 A73-44205
- A maximum principle and gradient bounds for linear elliptic equations.
24 p3105 A73-44421
- Chebyshev solution to elliptic equilibrium equations of elastic reticular cylindrical and toroidal shells under distributed loads, applying to extensible fiber structures /tires/
24 p3146 A73-44652
- Efficient subroutines for the solution of general elliptic and parabolic partial differential equations.
24 p3106 A73-45093
- The Cauchy problem and a general representation of solutions to an elliptic-type fourth-order equation with analytic coefficients
24 p3106 A73-45508
- ELLIPTIC FUNCTIONS**
A maximum principle for nondiagonal quasi-linear elliptic systems
01 p0071 A73-11267
- Ultraelliptic integrals degeneration to elliptic integrals in Goriachev-Chaplygin equation of rotating body, noting asymptotic approach to limiting motion
02 p0191 A73-11761
- The representation of functions determined by a class of hypoelliptic operators
02 p0187 A73-12180
- A method of solution of Vlasov's equation - Application to a nonlinear overall theory of the galactic rotation and of the galactic spiral structure
03 p0380 A73-14608
- Satellite motion in the equatorial plane of an oblate primary body and apsidal line shift evaluation.
04 p0498 A73-15296
- Jacobi-Hamilton equation of motion of mass point, using elliptic functions for harmonic potential
05 p0597 A73-16467
- Fractional exponents of an elliptic operator and parabolic differential equations in spaces of Hölder-continuous functions
08 p0983 A73-21250
- An approximate solution to a strongly non-linear, second-order, differential equation.
11 p1390 A73-25195
- Out-of-plane motion about libration points - Non-linearity and eccentricity effects.
11 p1423 A73-26069
- Direct numerical solution of three-dimensional equations containing elliptic operators.
13 p1647 A73-28080
- Some aspects of recent contributions to the mathematical theory of finite elements.
14 p1806 A73-30177
- Convergence of the arithmetic-geometric mean procedure for the complex variables and the calculation of the complete elliptic integrals with complex modulus.
14 p1769 A73-30423
- Approximate solutions and applications of hodograph equations in elliptic diabolic flow.
14 p1745 A73-30428
- Hyperbolic equation initial-boundary problem in finite cylinder solved via elliptic boundary problem with parameter
14 p1770 A73-30545
- Comparison of the Kryloff-Bogoliuboff method and the refined elliptic function method.
22 p2882 A73-43071
- ELLIPTIC INTEGRALS**
U ELLIPTIC FUNCTIONS
ELLIPTIC CYLINDERS
The parameters of an infinite homogeneous elliptical cylinder determined from its gravity effects.
03 p0380 A73-14612
- A system-synthesis approach to the inverse problem of scattering by smooth, convex-shaped scatterers for the high-frequency case.
04 p0423 A73-15484
- Cut-off frequency calculation for TE and TM modes in doubly ridged circular and elliptical microwave waveguides, using Mathieu function and eigenfunctions
06 p0669 A73-18736

- The computation of critical frequencies of waves of higher types in a hollow elliptical waveguide.
07 p0802 A73-20141
- Analysis of dispersion equation of a two-layer elliptical waveguide in critical regime.
07 p0802 A73-20142
- Stability of elliptical cylinder consisting of perfect incompressible gravitating fluid subject to arbitrary perturbations
15 p1860 A73-31048
- Numerical computation of antenna patterns near a conducting elliptic cylinder.
17 p2126 A73-35608
- Diffraction of a plane electromagnetic wave by a perfectly conducting elliptic cylinder.
22 p2822 A73-41749
- ELLIPTICAL GALAXIES**
A survey of elliptical galaxies at 6 cm.
13 p1685 A73-29361
- The cosmological significance of molecular band strengths in the infrared spectra of elliptical galaxies.
20 p2609 A73-39447
- ELLIPTICAL ORBITS**
NT APHELIONS
NT APOGEES
NT INTERPLANETARY TRANSFER ORBITS
NT PERIGEEES
NT PERIHELIONS
NT TRANSFER ORBITS
- Effects of gravity-gradient torque on the rotational motion of a triaxial satellite in a precessing elliptic orbit.
01 p0099 A73-10685
- Elliptical orbits of mass point under Newtonian gravitational forces of two fixed centers with different mass in Cartesian coordinates as function of time
02 p0211 A73-11776
- Analytical expressions for postmaneuver velocity and transfer impulse optimizing elliptic-to-hyperbolic orbital transfer
02 p0219 A73-12453
- Nearly-optimal single impulsive transfers between coplanar elliptical satellite orbits with identical pericenter altitude
03 p0372 A73-13299
- Complex variable analysis for exact solution to Kepler equation for elliptical and hyperbolic orbits based on canonical solutions to Riemann problem
03 p0376 A73-14269
- The transition from elliptic to hyperbolic orbits in the two-body problem by slow loss of mass.
03 p0377 A73-14273
- Optimum elliptic orbit characteristics of planetary artificial satellite based on earth-planet-earth flight
03 p0379 A73-14572
- Molnaya 1 satellite slow neutron monitor with photomultiplier scanned scintillator, noting limiting effect of geomagnetic perturbations
07 p0823 A73-19428
- Linear perturbations of the coordinates of satellites in the normal gravitational field of the earth
09 p1143 A73-22099
- Stability of planar oscillations of a satellite in an elliptic orbit.
10 p1287 A73-24663
- Periodic solutions of the third sort for restricted problem of three bodies and their stability.
11 p1423 A73-26068
- Nonsingular differential equations derivation for parabolic, hyperbolic, elliptic and rectilinear orbit perturbations via simple osculating element coordinate transformations and Lagrange planetary equations
11 p1423 A73-26073
- Hohmann trajectories efficiency for interplanetary transfers of spacecraft between circular coplanar orbits, considering earth-Mars-earth flight and transition to parabolic trajectory
12 p1538 A73-27065
- The effect of the ellipticity of Jupiter's orbit on the capture of comets to short-period orbits.
14 p1794 A73-29831
- Nonlinear two-dimensional oscillations of a satellite in an elliptic orbit
14 p1803 A73-29854
- Optimal control synthesis in the observation problem. I, II
14 p1802 A73-30788
- Optimal transfer between weakly elliptic orbits with a supplementary accuracy requirement and with allowance for nonsphericity
15 p1931 A73-31229
- Optimal transfer between coplanar elliptic orbits with the aid of tangential impulses applied at the apsidal points
15 p1931 A73-31232
- Analytical expressions for postmaneuver velocity and transfer impulse optimizing elliptic-to-hyperbolic orbital transfer
15 p1941 A73-32603
- Elliptical orbit of two coupled material points in Newtonian central gravitation field, discussing flexible weightless filament coupling, equations of motion and sinusoidal oscillations
20 p2608 A73-39319

- Evolution of a 'class two' family of periodic orbits in the general planar problem of three bodies.
23 p3031 A73-43835
- The stability of gravitating systems with a quadratic potential. II - The stability of models of spherically symmetric and axisymmetric clusters with elliptic orbits of particles
23 p3035 A73-44236
- Influence of nongravitational effects on the evolution of dust particles moving along elliptic orbits around the sun
23 p3036 A73-44251
- Parameter distribution of small periodic librations about the equilateral points of the elliptic restricted problem.
24 p3141 A73-45283
- Elliptic restricted three body problem equations derived from linear variational equations with periodic coefficients describing motion near libration centers
24 p3141 A73-45284
- Isosceles case of rectilinear restricted three body problem with two equal mass primaries in rectilinear ellipses, deriving escape and collision conditions
24 p3141 A73-45285
- Stability of Lagrange solutions to the three-dimensional elliptic problem of three bodies
24 p3111 A73-45299
- ELLIPTICAL POLARIZATION**
Electric vector peak and rms magnitude determination for near field polarization ellipse, relating to radiation hazard criteria
06 p0667 A73-18202
- Restoring the orthogonality of two polarizations in radio communication systems. II.
10 p1190 A73-24623
- Flush mountable elliptically polarized low silhouette blade antenna for aircraft, describing polarization and radiation characteristics
12 p1478 A73-27043
- Daily variations of the characteristics of beating-type Pc3/Bpc3/ pulsations.
13 p1611 A73-29661
- Polarization cascade matrix describing arbitrary elliptically polarized microwave transmission through inclined grating of parallel wires
13 p1587 A73-29669
- Polarization characteristics of phased arrays of elliptically polarized elementary radiators
21 p2664 A73-41082
- ELLIPTICITY**
Spherical analysis of the geomagnetic field during the epoch of 1965 from ground data up to $n = 23$. I
06 p0689 A73-17545
- Stressed state of an isotropic elliptical plate weakened by elliptical holes
08 p1020 A73-21767
- Spherical analysis of the geomagnetic field of the 1965 epoch to $n = 23$ from ground-based data. I.
16 p2002 A73-32769
- ELONGATION**
An analysis of the breaking elongation in high velocity impact of the power law hardening materials.
01 p0117 A73-11123
- EMBOLISMS**
NT AEROEMBOLISM
The complications of coronary arteriography.
22 p2806 A73-42343
- EMBRITTEMENT**
Temper embrittlement response and toughness of a rare earth treated Ni-Cr-Mo steel.
02 p0183 A73-12762
- High strength alloys hydrogen embrittlement mechanisms and effects and preventive measures, considering steel decarburization, stress corrosion cracking, hydride sheath formation and failure modes
03 p0328 A73-14425
- Embrittlement of N18K8M3TiU maraging steel after prolonged cooling from high temperatures
06 p0706 A73-17882
- A comparison of hydrogen embrittlement and stress corrosion cracking in high-strength steels.
06 p0709 A73-18479
- Ferritic chromium steels embrittlement under high temperature aging, using hardness measurements, impact tests and electron metallography
06 p0712 A73-18762
- Environmental hydrogen embrittlement of an alpha-beta titanium alloy - Effect of hydrogen pressure.
06 p0713 A73-18769
- Temper embrittlement of pressure vessel steels.
07 p0839 A73-20271
- Lattice dilatation and hydrogen embrittlement cracking.
07 p0840 A73-20353
- High strength TRIP /transformation induced plasticity/ steels hydrogen embrittlement susceptibility under cathodic charging, gaseous hydrogen environment and loading conditions
09 p1102 A73-22410
- Loading mode effects on high strength steel hydrogen embrittlement, considering stress tensor invariants and interstitial diffusion relationships
09 p1102 A73-22414
- Causes of embrittlement in the 11Kh18M steel
09 p1107 A73-23195

Effects of composition on embrittlement of austenitic stainless steels.

10 p1230 A73-23628

Effect of high dislocation density on stress corrosion cracking and hydrogen embrittlement of type 304L stainless steel.

11 p1385 A73-26174

Embrittlement of 2-14Cr-1Mo steel weld metal by postweld heat treatment.

11 p1375 A73-26354

Radiation-induced strengthening and embrittlement in aluminum.

14 p1761 A73-30628

Oxygen in titanium alloyed with aluminum and zirconium

15 p1889 A73-31812

Cleavage fracture in alpha phase Ti, considering embrittling species effects on electronic band structure

20 p2578 A73-39490

Temperature dependent chemisorption effects on hydrogen embrittlement of steel, showing strength-ductility correlation

22 p2874 A73-42106

The influence of testing temperature and thermal history on the intergranular embrittlement and penetration of aluminum by liquid gallium.

23 p2993 A73-44026

Fracture micromechanism characteristics and crack tip plastic zone formation effects on metal embrittlement, using elastoplasticity theory

23 p3047 A73-44277

Oxygen in alloys of titanium with aluminum and zirconium.

24 p3100 A73-45275

EMBRYOLOGY

Embryonic chick heart cell age dependent electrophysiological studies, discussing structure, metabolism, ATPase activity, membrane potential and cell interactions

11 p1315 A73-25589

Histological studies on the vestibular organ of frog embryos and larvae after the influence of simulated weightlessness.

18 p2270 A73-35979

EMBRYOS

Features of the influence of hypergravitation on the motor activity of the chicken embryo amnion developing under normal conditions and under conditions of constant rotation

14 p1715 A73-30022

EMERGENCIES

Physically or mentally disabled passengers handling on scheduled, charter and group flights, discussing rules for attendants, seating and emergency procedures

10 p1176 A73-24709

Pilot incapacitation as cause for aircraft operational risks, discussing flight crews education for emergency situations handling

10 p1185 A73-24717

Aircraft evacuation and safety procedures during emergencies, discussing negative panic, flight crew training and impact injury minimization

18 p2268 A73-36849

Flight deck management and pilot operation priorities in high pressure and emergency situations, using integrated aircraft-environment mental model

19 p2384 A73-37731

EMERGENCY LIFE SUSTAINING SYSTEMS

Development of neurosurgical instrumentation and procedures for emergency use in null and low-gravity environments - A speculative approach.

11 p1323 A73-25342

Influence of the packing and of certain conditions of usage on the medications in portable emergency medicine stores

12 p1465 A73-27720

Single point emergency equipment divestment system for instantaneous parachute harness, lap belt and leg restraint release, describing pyrotechnic actuation system

16 p1966 A73-32666

Behavioral stress response RE - Passenger briefings and emergency warning systems on commercial airlines.

18 p2285 A73-36922

EMISSION

NT BIOLUMINESCENCE
NT CHEMILUMINESCENCE
NT ELECTROLUMINESCENCE
NT ELECTRON EMISSION
NT FIELD EMISSION
NT FLUORESCENCE
NT HYDROXYL EMISSION
NT ION EMISSION
NT LIGHT EMISSION
NT LUMINESCENCE
NT LUNAR LUMINESCENCE
NT MICROWAVE EMISSION
NT NEUTRON EMISSION
NT OPTICAL RESONANCE
NT PARTICLE EMISSION
NT PHOTOELECTRIC EFFECT
NT PHOTOELECTRIC EMISSION
NT PHOTOIONIZATION
NT PHOTOLUMINESCENCE

NT RADIO BURSTS

NT RADIO EMISSION

NT SECONDARY EMISSION
NT SELF SUSTAINED EMISSION
NT SHOCK WAVE LUMINESCENCE
NT SOLAR RADIO BURSTS
NT SOLAR RADIO EMISSION
NT SPECTRAL EMISSION
NT SPONTANEOUS EMISSION
NT STIMULATED EMISSION
NT THERMAL EMISSION
NT THERMIONIC EMISSION
NT THERMOLUMINESCENCE
NT TYPE 3 BURSTS
NT TYPE 3 BURSTS
NT TYPE 4 BURSTS
NT TYPE 5 BURSTS
NT X RAY FLUORESCENCE

EMISSION SPECTRA

Time dependence of carbon monoxide TEA laser emission at 77 K, presenting time resolved transitions spectral data

01 p0058 A73-10128

Preliminary report on the infrared spectrum of Nova Serpentis 1970.

01 p0095 A73-10269

The IR emission spectrum of N2 excited under auroral conditions.

01 p0036 A73-10337

Investigation of the emission of donor-acceptor pairs and of their phonon echoes in CdS single crystals

01 p0085 A73-10634

Nature of the emission of UV Ceti-type stars

01 p0100 A73-10708

Global nitric oxide and gamma emission measurements with Ebert-Fastie scanning spectrometer on-board polar orbiting OGO 4 satellite

01 p0040 A73-10878

A vertical profile of OH in the mesosphere.

01 p0041 A73-10883

The consequences of grains in the atmospheres of late-type stars. I - Intrinsic polarization, infrared excesses, and emission lines.

01 p0103 A73-11035

Michelson interferometer on Mariner 9 space probe for thermal emission spectrum measurement, discussing spectral resolution, external vibration problem and instrument performance

01 p0054 A73-11228

Possibility of O III 304-A emissions in the extreme ultraviolet airglow.

02 p0157 A73-11755

Atomic oxygen concentration from the forbidden OI 5577 A line emission at the auroral zone latitude.

02 p0158 A73-11916

Experimental study of the luminous front produced by a coaxial plasma accelerator.

02 p0197 A73-12060

The infrared reflection, emission and absorption spectra of regolith from the Sea of Fertility and its scattering coefficient.

02 p0213 A73-12237

Extensive air showers vertical distribution at aircraft heights, constructing integral spectrum based on particle number

02 p0209 A73-12674

Spectrum of stimulated radiation in a flat-mirror resonator.

02 p0177 A73-12695

Variation of emission-line strengths across M31.

03 p0366 A73-12928

Luminescence excitation by protons and electrons, applied to Apollo lunar samples.

03 p0369 A73-13098

Photometric search for H alpha optical emission in Sco X-1 nebulosity region for linking companion radio sources to X ray source

03 p0373 A73-13374

Electron excitation and auroral emission parameters.

04 p0440 A73-14959

Correcting the OH contribution in emission line measurements in the night airglow filter photometry.

04 p0440 A73-14969

H I clouds with spin temperatures less than 25 K. II - Physical properties of two neutral hydrogen clouds.

04 p0500 A73-15517

H emission line shape of plasma radiation under anisotropic electric microfields, calculating field distribution function, dispersion and frequency

04 p0480 A73-15601

Spectroscopic observations of HZ Herculis.

04 p0501 A73-15684

Astrophysical CO isotopic constituents from H II regions line emissions, determining relative abundances

04 p0502 A73-15688

Observations of maser radio sources with an angular resolution of 0.0002 sec.

04 p0503 A73-16001

Stratification of the emission in the envelope of the eclipsing-binary Wolf-Rayet star V444 Cygni.

04 p0503 A73-16009

Effect of Thomson scattering on the emission spectrum of an optically semiopaque plasma.

04 p0493 A73-16024

Possibility of emission-line polarization in diffuse nebulae with a C + E spectrum

05 p0617 A73-16462

Investigation of a gallium arsenide laser pumped by an electron beam

05 p0584 A73-16553

An estimate of radiative emission from an isothermal xenon plasma at temperatures up to 50,000 K.

05 p0602 A73-16561

O stars line spectra from high dispersion photographic spectrograms at 3059-6683 A, tabulating absorption and emission lines identifications, equivalent widths and profiles

05 p0618 A73-16742

Vertical distribution of minor atmospheric constituents as derived from air-borne measurements of atmospheric emission and absorption infrared spectra. [AIAA PAPER 73-103]

05 p0570 A73-16863

The distribution of redshifts of quasi-stellar objects and related emission-line objects.

05 p0626 A73-17376

Search for coronal line emission from the Cygnus Loop.

05 p0626 A73-17380

The emission spectrum of the silent electric discharge in ammonia and hydrazine vapor

06 p0723 A73-17916

Plasma heating, emission spectrum distortion and light pressure effects under stimulated Compton scattering, noting upper bound of cosmic maser brightness temperature

06 p0729 A73-18110

Emission spectrum of a polyhedral-resonator laser pumped by long pulses.

06 p0702 A73-18380

Midinfrared emission spectra of Apollo 14 and 15 soils and remote compositional mapping of the moon.

07 p0897 A73-19888

Solar two-component atmospheric model for prediction of Ca II emission arches in spectrogram of strong lines near limb from kinetic equilibrium calculation

08 p1001 A73-20753

Ar plasma diagnostics from stabilized arc emission spectra, noting thermodynamic equilibrium in central zone of arc channel

08 p0992 A73-20855

Spectroscopic observations of the Cygnus X-1 optical candidate.

08 p1003 A73-20895

Study of the galactic structure from observations of interstellar calcium. I - Analysis of radial velocities

08 p1004 A73-20909

Aperture synthesis study of neutral hydrogen in the galaxies NGC 6946 and IC 342.

08 p1005 A73-20914

Spatial spectroscopic diagnostic of planetary nebulae. III - Numerical investigation of local absolute monochromatic energies and local absolute energies in spherically symmetric models.

08 p1010 A73-21313

Bennett comet head spectrophotometry over 352-612 millimicrons, identifying CN, CH, C2 and Na emission features

08 p1010 A73-21315

On the source of the 3840 A persistent emission by meteors.

08 p1010 A73-21318

High resolution spectra of the stratosphere between 30 and 200/cm.

08 p0961 A73-21533

Problem of the selective mechanism for the excitation of the C III 5696-A line in the spectra of certain stars. I

08 p1012 A73-21549

Energy release mechanism during early universe expansion leading to distortion of relic black body spectrum, noting Comptonization effects

08 p1013 A73-21693

The transfer of radiation from a flame to its fuel.

08 p1025 A73-21822

A discussion of the new variations observed in the nucleus of the Seyfert galaxy NGC 3516.

09 p1140 A73-22004

Broad-band laser emission from optically pumped PbS/1-x/Se/x.

[AD-759091]

09 p1092 A73-22249

PbTe-SaTe stripe junction diode lasers, discussing fabrication, electrical properties, and mode characteristics from emission spectra, polarization, mirror illumination and far field pattern measurements

[AD-759093]

09 p1092 A73-22250

Mesa-structure-geometry double-heterostructure injection lasers.

09 p1093 A73-22251

Emission spectrum of a source moving along a stable circular orbit near a rotating 'black hole'

09 p1145 A73-22295

An effective cross section method of accounting for the selectivity of emission and absorption in a hot gas

09 p1123 A73-22613

Spectral properties of laser crystal materials, noting deactivation energy storage in nonuniformly widened luminescence band

09 p1095 A73-22671

A relationship between photoemission-determined valence band gaps in semiconductors and insulators and ionicity parameters.

09 p1134 A73-22903

Measurements of some hydrogen-oxygen-nitrogen compounds in the stratosphere from Concorde 002.

09 p1079 A73-22947

Influence of thermo-optical distortions on the emission spectrum of a rhodamine 6G laser with incoherent pumping

09 p1096 A73-22972

ScO X-1 hard X rays and optical emission time variations from simultaneous observations, using balloon-borne counter telescopes

10 p1263 A73-23493

Determination of emission spectra of the sky in the infrared between 45 and 500 micrometer using an interferometer aboard an airplane

10 p1210 A73-23749

Interpretation of K X-ray emission spectra and chemical bonding in oxides of Mg, Al and Si using quantitative molecular orbital theory.

10 p1211 A73-24107

H emission line shape of plasma radiation under anisotropic electric microfields, calculating field distribution function, dispersion and frequency

10 p1254 A73-24191

Quasar characteristics, considering emission or absorption lines, red shift, optical intensity variation, unipolar generator representation and relativistic particle production

10 p1280 A73-24322

CsI thin film photoemission spectra resolution maximization, rejecting localized ionic state transitions model

11 p1407 A73-24986

CsI optical and photoemission spectra computed from first order allowed transitions between Bloch-wave states, using energy band data

11 p1407 A73-24987

Investigation of the relationship between 'edge' and exciton emission in CdS single crystals

11 p1408 A73-25246

Solar disk emission lines in Ca II H and K line wings from high resolution spectral observations

11 p1422 A73-25934

Simplified photoionization analysis of quasar emission spectra.

11 p1427 A73-26616

Averaged nighttime altitude profile of atmospheric emission at 6300 A

12 p1491 A73-27345

Emission core widths of K Ca II line in umbra and penumbra of sunspots near solar disk center, noting relationship to stellar luminosity

12 p1545 A73-27835

The influence of the scattering by plasma oscillation on the spectrum of emission from semi-opaque plasma

12 p1529 A73-27869

Emission field structure during transverse mode synchronization in a laser

13 p1626 A73-28005

The position of the emission lines of some lasers in the absorption spectrum of the earth's atmosphere.

13 p1626 A73-28174

Second positive system of nitrogen bands in daylight, according to Kosmos-224 data.

13 p1607 A73-28703

Dayglow nitrogen ion 3914 A emission profiles for average solar activity at 110-240 km heights from Cosmos 224 observations

13 p1607 A73-28704

German monograph - Determination of the OH-concentration distribution in a axisymmetric methane/oxygen flame.

13 p1708 A73-29279

Diurnal variation of nightglow Na emission, noting linear intensity variation with time, oscillatory and anticovariation characteristics

13 p1610 A73-29337

Spectral width of stationary emission from a laser with a spectrally inhomogeneous solid active element

14 p1757 A73-30266

Spatial distribution of H alpha emission in the earth's upper atmosphere, the variations of the emission during a solar cycle, and the dependence of the emission on geomagnetic perturbations

15 p1867 A73-31262

Predawn enhancement of 6300 A forbidden OI nightglow emission from observations at Abastumani

15 p1867 A73-31263

Investigation of the hydrogen in the upper atmosphere and geocorona from observations of the H-alpha emission line in the nightglow spectrum /Survey/

15 p1867 A73-31267

Spectral investigations of UV Ceti-type flare stars and search for new variables of this type carried out at Crimea.

15 p1934 A73-31479

Spectra of solar flares from 8.5 A to 16 A.

16 p2053 A73-32960

Spectral characteristics of quasar OQ172 with large red shift, considering absorption and emission spectra and Lyman alpha radiation

16 p2070 A73-33925

Single mode operation of flashlamp pumped dye laser achieved after emission spectrum line narrowing by interference filter and successive quartz Fabry-Perot etalons

17 p2185 A73-35769

Electron temperature and emission measure variations in the solar corona.

18 p2350 A73-36062

Time dependent studies of the aurora. II - Spectroscopic morphology.

18 p2311 A73-36185

Profiles of emission lines in Be stars. II - Interpretation of the long-period V/R variation.

19 p2484 A73-37615

Hydroxyl emission band high resolution spectra in airglow, examining doublet state ratio and rotational temperatures, vibration-rotation levels, temperature sensitivity and Boltzmann equilibrium

20 p2551 A73-38946

Relation between coronal 5303-A intensity, recurrent geomagnetic storms, and solar sector structure.

20 p2553 A73-38960

Line widths of CaII K2 and H-alpha and the chromospheres of late stars

20 p2606 A73-39073

Experimental results concerning the time decay of the line emission in luminescent plasmas of medium-pressure inert-gas discharges

20 p2596 A73-39191

Influence of scattering by plasma oscillations on the spectrum of a semitransparent plasma.

20 p2597 A73-39243

Comet 1969 g emission spectrum observation with 200-inch telescope, obtaining isotope ratio C-12/C-13

20 p2609 A73-39432

Emission of infrared molecular hydrogen lines from a cooled-gas laser.

20 p2574 A73-39694

Ruby laser with a wide emission spectrum.

20 p2574 A73-39696

Emission spectrum of a Q-switched ruby laser and its dependence on the density of the bleachable filter

21 p2711 A73-40304

Emission of aqueous solutions of rhodamine 6G with detergent additives in the presence of flash lamp excitation

21 p2711 A73-40305

Emission spectra of ZnS:Cu single crystals

21 p2751 A73-40311

Chromium-ytterbium energy transfer in silicate glass.

21 p2752 A73-40963

Cw degradation at 300 K of GaAs double-heterostructure junction lasers. I - Emission spectra. II - Electronic gain.

21 p2715 A73-40964

Evidence of features in atmospheric spectra at around 8 per cm of probable solar origin.

21 p2687 A73-41079

An X-ray spectral study of the electronic structure of nonstoichiometric titanium carbide

21 p2721 A73-41226

Kinetics of the generation spectrum of a photodissociation iodine laser.

22 p2868 A73-41722

Comment on 'Anomalous hyperfine lines in formaldehyde in a dust cloud.'

22 p2904 A73-41755

Excitation of the CO fourth positive system by the dissociative recombination of CO₂⁺ ions.

22 p2843 A73-41904

Short duration temperature measurements by infrared emission-absorption.

22 p2853 A73-41990

Temperature measurement, monitoring, and control on a Michelson interferometer for ambient-temperature emission spectroscopy.

22 p2856 A73-42025

Radiation field frequency dependent source function for two level atom, noting different stimulated emission and absorption line profiles

22 p2907 A73-42205

Measurement of the atmospheric brightness temperature at submillimeter wavelengths

22 p2847 A73-42330

Expected gamma ray emission spectra from the lunar surface as a function of chemical composition.

22 p2903 A73-42494

Measurements of hydrogen-helium radiation at shock-layer temperatures appropriate for Jupiter entry.

22 p2938 A73-42993

The temperature and ammonia profiles in the Jovian atmosphere from inversion of the Jovian emission spectrum.

22 p2915 A73-43017

Line identification and profiles in emission spectra of Wolf-Rayet stars from microphotometer tracings at high dispersion, noting effects of companion stars

23 p3026 A73-43196

O, Of, Oe and Wolf-Rayet star comparison in terms of emission and absorption line spectra, noting relationship to evolutionary status on H-R diagram

23 p3026 A73-43197

Planetary nebulae nuclei emission line spectral features similarity to spectra of Population I Wolf-Rayet and O-type stars

23 p3026 A73-43199

Wolf-Rayet stars continuous and line spectral features interpretation by model involving wide emission lines due to Doppler effect in rapidly expanding envelope

23 p3026 A73-43201

Average nighttime vertical profile of the 6300 A atmospheric emission.

23 p2970 A73-43242

High angular resolution very long baseline interferometry for emission spectra and angular size determination and structure mapping of galactic and extragalactic radio sources

23 p2980 A73-43355

On the emission coefficient of uranium plasmas.

23 p3005 A73-43388

Electron temperature of regions of the formation of recombinational continua on the sun - Temperature of the carbon emission regions

23 p3036 A73-44246

Optical characteristics of phononless lines

24 p3109 A73-44427

Plasma heating, emission spectrum distortion and light pressure effects under stimulated Compton scattering, noting upper bound of cosmic maser brightness temperature

24 p3114 A73-44499

Comet Bennett neutral sodium atom and dust particle distribution across head and tail measured by photometry of Na emission radial profile

24 p3133 A73-44560

Solar coronal Fe XIII 10747 A emission line resonance polarization observations during 12 November 1966 eclipse, discussing magnetic field effects

24 p3135 A73-44633

Spatial relationship between 5303-A and H alpha components of a loop prominence system.

24 p3123 A73-44640

Chemiluminescence spectra from cool and blue flames - Electronically excited formaldehyde.

24 p3066 A73-45163

EMISSIONITY

Computed total radiation properties of compressed oxygen between 100 and 1000 K.

01 p0122 A73-10809

CO2 plasma emissivity at temperatures from 7000 to 9000 K in the spectral range of 2100 to 10,000 A

01 p0085 A73-10854

Radiation heat transfer in isothermal adjoin plate system with directionally emitting and nondiffuse reflecting surfaces, considering surface roughness effects

01 p0123 A73-11140

Luminous flames thermal radiation total emissivity analysis, considering water vapor, carbon dioxide and soot particles overlapping spectral bands [WSCI PAPER 72-41]

05 p0638 A73-16677

Laboratory determinations of water surface emissivity.

06 p0691 A73-18713

Combustion molecular gases radiative heat transfer, emissivity and absorptivity calculation, presenting high speed computer routine

06 p0770 A73-18832

White and black paints for satellite thermal control coatings, discussing space environment radiation effects on emissivity and solar absorptance

07 p0841 A73-18909

Measurements of the emissivity of materials fabricated by powder- and plasma-metallurgy techniques

09 p1103 A73-22472

On the detection of H2 from interstellar clouds in the wavelength range 4.4 to 28.2 microns.

09 p1148 A73-22870

The emissivity of a system consisting of a semitransparent isothermal coating and a flat opaque substrate

10 p1294 A73-23514

Electrical resistance and emissivity of certain transition metals and alloys in the high-temperature range

10 p1230 A73-23520

The radiative capacity of a CO2 plasma at temperatures 7000-9000 K in the spectral interval 2100-10,000 A.

12 p1529 A73-27904

Thermal properties of rhodium single crystals at high temperatures.

16 p2026 A73-33581

Certain thermophysical properties of isotropic pyrolytic graphite

17 p2253 A73-34132

Radiating power of a system consisting of a semitransparent isothermal coating and a flat non-transparent substrate.

17 p2212 A73-35194

Electrical resistivity and emissivity of some transition metals and alloys in the high-temperature range.

17 p2191 A73-35200

- Experimental investigation of the integral hemispherical emissivity of refractory metals and alloys.
20 p2593 A73-39426
- Surface microwave emissivities dependence on humidity, vegetable cover and surface structure, considering water influence on sand emissivity
20 p2556 A73-39839
- Utilization of thermal infra-red ground measurements for determination of adequate surveying periods in remote sensing.
20 p2558 A73-39868
- The emittance of blackbody cavities.
22 p2930 A73-41981
- The emissivities of liquid metals at their fusion temperatures.
22 p2930 A73-41983
- Combined lidar and radiometric measurements of cirrus clouds for IR emissivity, optical thickness and albedo
23 p3003 A73-43600
- Spectral emissivity of skin and pericardium.
23 p2950 A73-44213
- EMISSOGRAPHS**
U ACTINOMETERS
U RECORDING INSTRUMENTS
- EMITTANCE**
Influence of refractive index on emittance from semi-infinite absorbing scattering media.
[AIAA PAPER 73-147] 05 p0598 A73-16895
- High-speed /subsecond/ simultaneous measurement of specific heat, electrical resistivity, and hemispherical total emittance of Ta-10/wt.%W alloy in the range 1500 to 3200 K.
[ECTP PAPER D2-4] 14 p1760 A73-30437
- Simultaneous measurement of specific heat, electrical resistivity, and hemispherical total emittance of niobium-1 /wt. %/ zirconium alloy in the range 1500 to 2700 K by a transient /subsecond/ technique.
17 p2187 A73-34499
- Emittance of an isothermal, isotropically scattering medium.
18 p2336 A73-36324
- Theory and measurement of emittance properties for radiation thermometry applications.
22 p2886 A73-41982
- High temperature thermophysical properties of tungsten.
[ECTP PAPER D1-5] 22 p2876 A73-42405
- Emittance measurement of Surveyor 3 spacecraft aluminum support tubing returned from moon by Apollo 12, noting lunar environment effects from control sample data
24 p3139 A73-45110
- EMITTERS**
NT THERMIONIC CATHODES
NT THERMIONIC EMITTERS
- Emitter efficiency increase in annular cold microthrusters with single sharp tips for high specific charge of conducting liquid droplets under low potential
04 p0488 A73-15723
- Ion engines with ion emission from liquid metal drops under electric field, noting emitter I-V characteristics and engine design
04 p0488 A73-15726
- A study of the effect of the emitter current on the barrier capacitance of a transistor collector junction.
II 20 p2536 A73-39395
- Bipolar transistor emitter efficiency calculation, considering heavy doping induced impurity profiles effects on current gain
23 p2958 A73-43451
- EMOTIONAL FACTORS**
Psychological and physiological components of biorhythm cycles governing periodic variations in physical, emotional and intellectual performance
05 p0544 A73-16720
- Physiological tests for hypothalamus regions stimulation effects on coronary circulation, noting hypoxia and emotional stress effects
06 p0650 A73-17770
- Emotional stresses during a space flight
07 p0785 A73-19297
- Electromyographic alterations in articular muscles during emotional shifts
10 p1180 A73-24328
- Experimental study of emotional stress in operators
II p1321 A73-25038
- Utilization of human voice for estimation of man's emotional stress and state of attention.
II p1322 A73-25329
- Psychopharmacology in treating psychiatric diseases, negative emotions, and nerve stimulation, discussing tranquilizers synthesis and effects
12 p1465 A73-27497
- Changes in blood-flow distribution during acute emotional stress in dogs.
13 p1576 A73-28533
- Emotional overstress effects on the indices of the blood coagulation system in monkeys
14 p1719 A73-30846
- A device for the continuous measurement of subjective changes
16 p1975 A73-33090
- The mechanisms of the occurrence of emotional stress in man.
18 p2279 A73-36920
- The effect of social-emotional environmental stress on the functional state of the neocortical structures of rhesus monkeys
19 p2394 A73-37755
- Bioelectric and vegetative components of conditioned reflexes of 'negative-emotional type'
20 p2515 A73-39797
- Experimental analysis of conditions for onset of emotional stress
20 p2516 A73-39800
- Effect of a subjective ambiguity estimate concerning the duration of work on activity regulation
22 p2812 A73-41892
- Emotionally induced increases in heart rate and plasma catecholamine and free fatty acids, noting relation to coronary heart disease
22 p2809 A73-42837
- The effect of anxiety control on the level of information processing
23 p2946 A73-43848
- EMOTIONS**
Hippocampus contribution to conditioned reflexes, memory, voluntary motions, orientation and emotional reactions, noting theta rhythm in stimuli response
10 p1180 A73-24326
- Participation of cholinergic mechanisms in negative human emotions
20 p2515 A73-39799
- Sentography - Dynamic forms of communication of emotion and qualities.
23 p2949 A73-44180
- EMPLOYEE RELATIONS**
Comparison of the job attitudes of personnel in three air traffic control specialties.
20 p2517 A73-39108
- EMULSIONS**
NT NUCLEAR EMULSIONS
NT PHOTOGRAPHIC EMULSIONS
- Emulsion and suspension effective viscosity dependence on dispersed phase volume concentration and particle interactions in two phase flows
13 p1580 A73-28465
- ENAMELS**
Surface properties improvement of Al products by metal coatings, noting corrosion prevention, anodic coatings, enameling and brazing
03 p0312 A73-13580
- Porcelain enamels for heat resistant alloys low temperature fatigue strength and high temperature vibration damping increase
[SAE PAPER 720809] 05 p0633 A73-16629
- Damping of glass-like materials at high temperatures.
20 p2580 A73-39272
- ENCAPSULATING**
Causes of defects arising in semiconductor devices encapsulated with plastic
04 p0427 A73-15350
- Reliability tests on miniature ceramic capacitors encapsulated by epoxy-novolac block polymer compounds
06 p0677 A73-18398
- Reliability aspects of plastic encapsulated integrated circuits.
08 p0944 A73-20739
- Superalloys oxidation behavior under long term exposure to high temperatures for suitability as Co-60 heat sources encapsulation materials
08 p0978 A73-21415
- A bonding-wire failure mode in plastic encapsulated integrated circuits.
19 p2410 A73-38442
- High-reliability plastic package for integrated circuits.
19 p2411 A73-38455
- Large-signal lumped modelling and characterization of an IMPATT diode.
24 p3073 A73-45478
- ENCEPHALITIS**
Remote sensing application to habitat of mosquito vectors of disease, considering St. Louis and Venezuelan encephalitis strains and human filariasis
20 p2520 A73-39866
- ENCKE METHOD**
Studies in the application of recurrence relations to special perturbation methods. II - Comparison of the Encke and Cowell methods of integration in the restricted three-body problem.
10 p1283 A73-24668
- Encke comet icy nucleus core-mantle evolutionary model, investigating mantle sublimation, fading and capture time approximation for nongravitational forces effect in terms of mass output
14 p1793 A73-29822
- ENCLOSURE**
Mechanical design of microwave integrated circuit enclosures.
16 p1989 A73-33469
- ENCLOSURES**
Approximate configuration factors for a gray nonisothermal gas-filled conical enclosure.
[AIAA PAPER 73-752] 18 p2370 A73-36368
- Noise reduction by enclosures to block airborne and structure-borne acoustic paths, developing models for insertion loss in different frequency ranges
22 p2888 A73-42924
- ENCODERS**
U CODERS
ENCODING
U CODING
ENCOUNTERS
Approximate method to determine collision probabilities, hyperbolas, and direct and retrograde ellipses during single close encounters in three body planetary problem
01 p0099 A73-10693
- END MORAINES**
U GLACIAL DRIFT
- ENDFIRE ARRAYS**
NT YAGI ANTENNAS
- ENDOCRINE GLANDS**
NT ADRENAL GLAND
NT GONADS
NT PANCREAS
NT PINEAL GLAND
NT PITUITARY GLAND
NT THYROID GLAND
- ENDOCRINE SECRETIONS**
NT ALDOSTERONE
NT HORMONES
NT HYDROXYCORTICOSTEROID
NT INSULIN
NT PITUITARY HORMONES
NT THYROXINE
- Multiple hormonal responses to graded exercise in relation to physical training.
03 p0263 A73-14116
- Human endocrine-metabolic responses to graded oxygen pressures.
07 p0785 A73-19479
- Binding of Melatonin to human and rat plasma proteins.
10 p1182 A73-24657
- Physiological time zone entrainment and stressor effects during prolonged C-141 transmeridian flights, using endocrine-metabolic indices in urine specimens
13 p1574 A73-28283
- Mechanisms of secretion of neurohypophyseal hormones - Cellular and subcellular aspects
15 p1836 A73-32286
- Endocrine studies during a 14-day continuous exposure to 5.2% O₂ in N₂ at pressure equivalent to 100 FSW /4 ata/.
18 p2279 A73-36795
- Physiologic cost of prolonged double-crew flights in C-5 aircraft.
21 p2644 A73-41152
- ENDOCRINE SYSTEMS**
Hypothalamo-adenohypophysis-adrenal neurosecretory system under hyperthermia
14 p1719 A73-30847
- Correlational inter-relationships between the neuroendocrinal system and the genotype in the formation of protective reactions of the organism
15 p1835 A73-31875
- ENDOGENOUS CONDITIONS**
U PHYSIOLOGY
- ENDOLYMPH**
Endolymph fluid mechanics in semicircular canals approximated by rigid torus filled with incompressible Newtonian fluid
18 p2281 A73-36430
- ENDOTHELIUM**
Mathematical model of collateral blood vessels caliber changes due to hydrodynamic drag /shear stress/ effects on vascular endothelium
22 p2817 A73-43105
- ENDOTOXINS**
Effects of endotoxin on monoamine metabolism in the rat.
01 p0009 A73-11100
- ENDURANCE**
The long term performance characteristics of a SNAP-19 generator operating under vacuum conditions.
11 p1396 A73-26038
- Optimal duration of endurance performance on the cycle ergometer in relation to maximal oxygen intake.
15 p1836 A73-32397
- ENERGY ABSORPTION**
NT AURORAL ABSORPTION
NT ELECTROMAGNETIC ABSORPTION
NT MOLECULAR ABSORPTION
NT NEUTRON THERMALIZATION
NT PHOTOABSORPTION
NT POLAR CAP ABSORPTION
NT SELF ABSORPTION
NT THERMAL ABSORPTION
NT THERMALIZATION [ENERGY ABSORPTION]
NT ULTRAVIOLET ABSORPTION
NT X RAY ABSORPTION
- Gamma ray dose and energy absorption buildup factors approximation based on geometrical progression formula as function of source energy and medium atomic number
06 p0704 A73-17445

- Energy absorption inelastic surface mechanisms effect on I-V characteristics profile for bounded semiconductor with negative differential conductivity 06 p0735 A73-17974
- Energy absorption in cold inhomogeneous plasmas - The Herlofson paradox. 09 p1126 A73-22276
- A photochemical method of determining the optical pumping energy absorbed by rhodamine dyes under conditions corresponding to stimulated emission of radiation 09 p1095 A73-22668
- Efficiency of the microwave energy absorption in a plasma at high magnetic fields. 10 p1257 A73-24627
- Absorption of the microwave energy in a magnetoactive plasma. [IPPCZ-167] 12 p1529 A73-27433
- Solid fracture theories based on brittle region toughness parameter and absorbed specific fracture work factor above ductile-brittle transition respectively 13 p1640 A73-29479
- Comprehensive theory of r.f. energy absorption by a hot ion-electron plasma cylinder excited by an arbitrary electromagnetic field. 15 p1916 A73-31080
- Absorption of hydromagnetic waves in the plasma layer of the magnetospheric tail 15 p1872 A73-31902
- Parachute webbing designs for opening shock energy absorption and force limitation, discussing drop tower and ballistic piston test results for various designs 16 p2018 A73-33066
- Nickel-titanium memory material stress measurement methods, energy absorption capacity and cyclic response, discussing nickel foil surface temperature sensing devices 17 p2166 A73-34616
- Laser energy absorption by plasma for controlled thermonuclear fusion, comparing uses of electrically pumped gas, chemical and solid state lasers 17 p2185 A73-35379
- Comparison of optimized active and passive vibration absorbers. 19 p2435 A73-38084
- Fracture toughness and absorbed energy measurements in impact tests on brittle materials. 19 p2500 A73-38094
- Observation of zero-degree pulse propagation in a resonant medium. 20 p2570 A73-38602
- Off-resonance microwave-created plasmas. 20 p2597 A73-39196
- Quiet-time solar neutron flux upper limit from OGO-6 neutron detector, evaluating solar cosmic ray acceleration, nuclear reaction and energy region 21 p2763 A73-41498
- Parametric instabilities of weakly turbulent plasma, determining collision frequencies characterizing high frequency electric field energy absorption 21 p2750 A73-41681
- Design and analysis of an energy absorbing restraint system for light aircraft crash-impact. [ASME PAPER 73-DET-111] 22 p2799 A73-42080
- ### ENERGY ABSORPTION FILMS
- Polarization dependence of a photoelectric current during the modulated illumination of a system composed of an electrolyte, a porous pigment film, and a metal 07 p0851 A73-19473
- Heating of a substance by short laser pulses 10 p1230 A73-24885
- Piezoelectric sound pressure sensor for damping measurement of structural element coatings under intense acoustic loads 13 p1618 A73-29060
- Piezoelectric sound pressure sensor for damping measurement of structural element coatings under intense acoustic loads 18 p2317 A73-36892
- Theory of successive electron transfer steps in cyclic voltammetry Application to oxygen pseudocapacitance on platinum. 21 p2636 A73-40843
- Heating with short laser pulses. 21 p2717 A73-41660
- ### ENERGY BANDS
- #### NT CONDUCTION BANDS
- #### NT FORBIDDEN BANDS
- Theory of dynamic charge and capacitance characteristics in MIS systems containing discrete surface traps. 04 p0427 A73-15344
- Theory of dynamic charge current and capacitance characteristics in MIS systems containing distributed surface traps. 04 p0427 A73-15345
- Nonequilibrium plasma wave scattering cross section dependence on energy bands shape and field orientation in semiconductors 06 p0735 A73-17975
- The plane-wave method in the study of helium atoms physisorbed on graphite 07 p0843 A73-20000
- Formation and decay of a narrow band of energetic electrons in the earth's magnetosphere 08 p0998 A73-21305
- CsI optical and photoemission spectra computed from first order allowed transitions between Bloch-wave states, using energy band data 11 p1407 A73-24987
- Electronic charge densities in semiconductors. 11 p1408 A73-25374
- Pressure effects on contact potential in diode p-n junction, discussing potential barrier height variation, minority carrier concentration changes and relative position of energy bands 11 p1338 A73-26520
- Investigation of the structure of electron bands in In_{1-x}Ga_xAs_{1-y}P_y on the basis of luminescence 15 p1923 A73-31716
- Thermal conductivity and temperature dependence of energy gaps in niobium samples containing large amounts of impurity atoms 16 p2027 A73-34061
- Formulation of the basic approximations of the field theory of static current-voltage characteristics of quasi-monopolar semiconductors 18 p2341 A73-36724
- A technique for the investigation of deep-level states in diffused p-n junction devices - Application to GaAs electroluminescent diodes. 20 p2536 A73-39412
- Pure two band superconductor theory, discussing thermodynamic and electromagnetic properties, London group, mixed state, critical field and weak field penetration 21 p2753 A73-41299
- ### ENERGY BUDGETS
- #### NT ATMOSPHERIC HEAT BUDGET
- Analysis of a nonisothermal, spherical detector for monitoring the earth's radiative energy budget. 01 p0045 A73-10382
- Natural variation of the radiation budget of the earth-atmosphere system as measured from satellites. 01 p0038 A73-10390
- Numerical simulations of the tropical air-sea planetary boundary layer. 01 p0073 A73-10496
- Power control unit for the scientific satellite. 01 p0111 A73-11165
- Self-similar flows with increasing energy. II - Isothermal flow. 02 p0238 A73-12091
- The radiation budget of the earth-atmosphere system as measured from the Nimbus 3 satellite /1969-1970/. 02 p0160 A73-12266
- Global distributions of thermal energy content and losses in thermosphere, discussing energy sources, continuity equations and transport mechanisms for heat balance 02 p0162 A73-12288
- Oscillations of spacecraft with on-off attitude control under constant perturbation moment, calculating energy expenditures for desired orientation maintenance 03 p0383 A73-14559
- Relativistic equations of balance in continuum mechanics. 04 p0476 A73-15223
- Energy balance, motion and constitutive equations of polar fluids, considering entropy inequality, viscosity and dissipation rate 04 p0434 A73-15679
- Motion, constitutive and energy balance equations for materials with microstructure, considering elastic bodies 04 p0514 A73-15680
- Certain problems and results of theoretical and experimental research on the energetics of general atmospheric circulation 05 p0593 A73-16237
- Aircraft performance augmentation by energy management instruments or systems, considering energy/rate meter and algorithm for real time onboard flight path optimization [AIAA PAPER 73-228] 05 p0536 A73-16953
- Long-range energy-state maneuvers for minimum time to specified terminal conditions. [AIAA PAPER 73-229] 05 p0536 A73-16954
- Energy management in aerial combat weapon systems maneuvering and delivery tactics, computing optimal feedback control laws for supersonic aircraft minimum time turning trajectories [AIAA PAPER 73-231] 05 p0536 A73-16956
- Radiation balance mapping with multispectral scanner data. 05 p0572 A73-17158
- Fusion plasma confined by nonpenetrating uniform magnetic field, calculating temperature and density effects on energy balance instabilities from particle conservation equations 05 p0604 A73-17366
- New interpretation of the equivalent circuit used in dielectric-degradation studies 07 p0796 A73-18893
- Glider soaring flight energy budget analysis, discussing rate of climb indicator error compensation 08 p0968 A73-21656
- Energy dissipation sources during reinforced plastic fracture, investigating fiber debonding energetics, toughness and crack propagation resistance 10 p1238 A73-23971
- Earth-atmosphere-ocean energy balance time dependent model equation, using Sellers radiation relationships and turbulent exchange coefficients for numerical solution 10 p1245 A73-23982
- Energy balance in the chromosphere-corona transition region. 10 p1279 A73-24138
- The radiation balance of the earth-atmosphere system - Recent results from satellite measurements 10 p1213 A73-24399
- Reaction equilibrium and energy balance in thermonuclear fusion propulsion for interstellar space flight, discussing nuclear fuel and ion temperature effects 10 p1262 A73-24544
- Boundary conditions model calculations for thermoelastic deformations of continuum body with surface tractions on interface, discussing energy balance laws derivation for loading devices 10 p1292 A73-24659
- Unsteady uniform-length turbulent flow of incompressible fluid in circular pipe studied via Reynolds and turbulence energy balance equations 10 p1210 A73-24851
- An observational study of the vertical profile of the high frequency fluctuations of the wind in the atmospheric boundary layer. 11 p1393 A73-25691
- Effect of polymer additions on some energy balance components in a turbulent flow 11 p1349 A73-26433
- Energy relations for turbulent flow in rough pipes. 13 p1604 A73-29265
- Earth radiation belts energetic electrons quiet equilibrium structure based on balance between pitch angle scattering loss and inward radial diffusion 14 p1786 A73-29965
- A simple integration method for the momentum and energy theorem of boundary layer theory 14 p1745 A73-30300
- Energy balance during moderate exercise at altitude. 15 p1833 A73-31343
- Instrumental theory in absolute radiometry 15 p1875 A73-31500
- Energy and momentum theorems in magnetospheric processes. 15 p1871 A73-31846
- Kinetic energy conversions by horizontal and vertical eddy processes from 5 years of hemispheric data. 15 p1873 A73-32253
- Considerations concerning the quasi-geostrophic model equations for an energetically open system 15 p1907 A73-32360
- The derivation of the mechanical balance equations of the Cosserat continuum on the basis of the energy equation and its behavior at the transition to rotating systems 16 p2080 A73-33240
- Book on energy equations for small and large scale atmospheric motion covering laminar and turbulent flow and space-time scales for atmospheric energy balance 17 p2158 A73-34463
- The atmospheric aerosol and its significance for the energy budget of the atmosphere 17 p2159 A73-34749
- On the temperature of the Jovian thermosphere. 17 p2232 A73-34860
- Numerical study on the effects controlling the low-level jet. 18 p2335 A73-37100
- Multispectral remote sensing of elements of water and radiation balances. 20 p2558 A73-39864
- ### ENERGY CONVERSION
- #### NT SATELLITE SOLAR ENERGY CONVERSION
- Approximate conditions to account for spring mass redistribution with kinetic energy conversion into strain energy over small critical time interval 02 p0230 A73-11795
- Time-averaged power stage models transient and frequency responses characterization and circuit component values derivation for switched dc-dc converters design 03 p0282 A73-13927
- Analysis of limit cycles in a two-transistor saturable-core parallel inverter. 03 p0252 A73-13929
- Computer-aided design and graphics applied to the study of inductor-energy-storage dc-to-dc electronic power converters. 03 p0252 A73-13931

Switching stepdown dc-to-dc converter with analog signal to discrete interval converter, hybrid micromodule and two-loop control subsystem, discussing circuitry and performance

03 p0283 A73-13935

Electric power processing, distribution and control for advanced aerospace vehicles.

03 p0253 A73-13947

Laser energy conversion into electrical energy with photovoltaic cells, noting Si and GaAs cells power efficiencies improvement compared to operation in sunlight

03 p0254 A73-14210

Energy conversion in the atmospheric boundary layer

04 p0441 A73-15286

Synchronous satellite solar power station for solar energy conversion to microwaves for transmission to earth discussing technical, economic and social aspects

[ASME PAPER 72-WA/SOL-6] 04 p0408 A73-15801

Analysis of optimal conditions for energy conversion in an MHD-generator channel

05 p0602 A73-16586

German book - New energy systems for space flight.

06 p0741 A73-17668

Satellite solar power station for solar energy conversion and transmission to earth via microwave beam, discussing technology status and weight and cost projections

06 p0750 A73-18027

Electrical and isotope power from space for terrestrial use.

06 p0750 A73-18028

Experiments of magnetohydrodynamic conversion with ionization out of equilibrium

06 p0730 A73-18541

Random forcing effects on numerical weather predictability, assessing atmospheric variables computational space truncation impact

06 p0720 A73-18701

Irreversible thermodynamics and losses in energy conversion, discussing N-port storage representation, flux rate, power flow and electro-caloric and state space relations

07 p0779 A73-20396

Intersociety Energy Conversion Engineering Conference, 7th, San Diego, Calif., September 25-29, 1972, Proceedings.

09 p1033 A73-22751

Satellite solar power station for solar energy conversion into electricity and transmission to ground receiving stations via microwave beams

09 p1035 A73-22791

The Solar Collector Thermal Power System - Its potential and development status.

09 p1035 A73-22792

Satellite solar power station systems engineering study, examining basic concept technical and economic feasibility

09 p1154 A73-22814

Slip parameter for electrogasdynamic generators with unsteady flow.

09 p1037 A73-22825

Direct nuclear-to-electric power conversion based on Sr 90 electron emission and collection system, noting spacecraft applications

09 p1119 A73-22828

Exploratory investigation of an electric power plant utilizing a gaseous core reactor with MHD conversion.

09 p1119 A73-22829

Radioisotopic energy conversion by radiovoltaic effect, describing titanium-tritium sources and semiconductor converter

09 p1037 A73-23278

The Gicodyne 400 power generator using a radioisotopic source with thermodynamic conversion

09 p1038 A73-23283

Near-equatorial synchronous orbit Satellite Solar Power Station system with photovoltaic cell arrays energy conversion into microwave power for transmission to earth

10 p1285 A73-23601

Vibrationally-excited nitrogen in the upper atmosphere.

10 p1212 A73-24226

Satellite electric power station for conversion of solar energy to microwaves beamed to earth, discussing structural design, flight control, transportation and technology assessment

10 p1178 A73-24554

Parawing-drag chute system operation on wind shear energy to maintain payload flight altitude

11 p1305 A73-25787

Energy 70; Proceedings of the Fifth Intersociety Energy Conversion Engineering Conference, Las Vegas, Nev., September 21-25, 1970. Volumes 1 & 2.

11 p1308 A73-25976

Utilization of thermal phenomena in the construction of signal-energy converters for coupling automatic control devices belonging to different categories of the State Instrument System

12 p1459 A73-26765

Certain considerations concerning a magnetoplasma dynamic flux in the one-dimensional hypothesis

12 p1527 A73-27061

Principles of photovoltaic solar energy conversion.

13 p1573 A73-29591

Studies on barotropic and baroclinic energy conversions in wave number regime.

14 p1772 A73-30901

The feasibility of a satellite solar power station.

16 p1970 A73-32718

Intersociety Energy Conversion Engineering Conference, 8th, University of Pennsylvania, Philadelphia, Pa., August 13-16, 1973, Proceedings and Addendum.

19 p2390 A73-38386

A solar engine using the thermal expansion of metals.

19 p2392 A73-38473

Some photoelectrical characteristics of photoelectric converters with a p-i-n structure

20 p2510 A73-39448

Russian book - Physical bases of thermionic energy conversion.

22 p2890 A73-41876

Theory of power rectification and harmonic generation processes at super-high frequencies

22 p2800 A73-42213

Finite element analysis on L-L type vibration energy concentrator/divider considering its design.

23 p2961 A73-44138

Numerical simulation of three dimensional atmospheric turbulence with emphasis on kinetic energy transfer from large to small scales of motion with heat conversion

24 p3108 A73-45092

Energy conversion between longitudinal and transverse waves by mode-mode coupling in a relativistic plasma.

24 p3116 A73-45240

ENERGY CONVERSION EFFICIENCY

Plasma jet acceleration by plasma injectors with capacitive and inductive energy storage for instantaneous breaking of charging circuit, noting energy conversion efficiency

02 p0196 A73-11712

Superconducting magnet ac generators development, emphasizing conversion efficiency, manufacturing, relative costs, machine geometry and interwinding coupling factor effects

02 p0132 A73-11833

The pressure-jet helicopter propulsion system.

02 p0130 A73-11858

Secondary ionisation and its possible bearing on the performance of a solar cell.

02 p0132 A73-12048

Design and practical aspects of maximum efficiency silicon solar cells for satellite applications.

03 p0254 A73-14205

An experimental investigation into the feasibility of higher efficiency silicon solar cells.

03 p0254 A73-14206

Silicon violet solar cell energy conversion efficiency improvement through extended spectral response and increased fill factor

03 p0254 A73-14212

High efficiency Cu₂S-CdS-solar cells with improved thermal stability.

03 p0255 A73-14216

Investigations of the inhomogeneity of polycrystalline Cu_x/S-CdS solar cells.

03 p0255 A73-14222

Submicrosecond pulses from a hydrogen-fluorine laser with high energy density and quantum efficiency.

03 p0320 A73-14454

The effect of pH on photobleaching of organic laser dyes.

03 p0320 A73-14462

H₂/O₂-fuel cells supplied with a H₂/N₂-mixture and air.

04 p0408 A73-15116

Linear solar collector conversion efficiency over wide operating temperature range via model consisting of long pipe with energy injection at points along length

[ASME PAPER 72-WA/SOL-7] 04 p0408 A73-15802

Solar cells with Si Schottky function diode, discussing fabrication and barrier metal and thickness effects on output power and energy conversion efficiency

05 p0538 A73-16816

Fuel cells for improved electrical power supply.

[AIAA PAPER 73-82] 06 p0649 A73-17641

Conversion of electromagnetic into acoustic energy via indium films.

06 p0734 A73-17834

Second-harmonic conversion of laser radiation generated under free-oscillation conditions.

06 p0702 A73-18594

An efficient electrical CO₂ laser using preionization by ultraviolet radiation.

06 p0704 A73-18797

Doping dependence of photon yield as a function of excitation energy in optically-excited n-type GaAs at 300 K.

06 p0704 A73-18844

Fast solid state IR detection photodiodes design, properties and utilization, investigating high speed response conditions and quantum efficiency

06 p0678 A73-18853

Cylindrical laser resonators with partial radial radiation and strong axial energy focusing, relating low-loss cavity modes to Gaussian beam modes

07 p0833 A73-19273

A reliable high efficiency atmospheric pressure CO₂ laser.

07 p0836 A73-20194

HF chemical lasers kinetics, radiative interactions and gas dynamics, deriving closed form solutions for excited states populations

08 p0976 A73-21671

High energy and power carbon dioxide laser with nitrogen and He mixtures, transverse electric discharge excitation and modular construction, noting efficiency and gain

09 p1090 A73-22081

A system for the evaluation of solar cell samples.

09 p1033 A73-22438

Development and application of a 0.14 gm piezoelectric accelerometer.

09 p1083 A73-22507

Wave transformation in warm magnetoplasma slab with parabolic density profile and two lower hybrid layers, discussing long wavelength energy tunneling and conversion efficiency

09 p1129 A73-22637

Comparison of the efficiency of photocells with stepwise and exponential distributions of the impurities in the doped layer

09 p1033 A73-22721

Hydrogen-oxygen fuel cell as reliable electric power supply for space shuttle mission requirements, assessing technological developments

09 p1035 A73-22777

Spacecraft dynamic solar electric power/thermal control system with cold liquid flow and regenerator cooling for energy conversion efficiency and weight characteristics improvements

09 p1153 A73-22785

Laser energy transfer - An analytic survey of high power applications.

09 p1096 A73-22822

A model of a thermophotovoltaic radionuclide battery.

09 p1037 A73-23279

Radiophotovoltaic devices power and energy conversion efficiency limits, investigating phosphors deterioration and nuclide layer optimal thickness

09 p1037 A73-23280

Development of thermionic radioisotope batteries.

09 p1038 A73-23281

Testing of the improved SNAP 19-primary power for advanced space missions.

09 p1038 A73-23285

Theoretical possibility of converting the kinetic energy of an ionized gas flow into electricity

10 p1177 A73-23473

Efficiency of the microwave energy absorption in a plasma at high magnetic fields.

10 p1257 A73-24627

Thermodynamic cycle processes in liquid propellant rocket engines, taking into account combustion products chemical dissociation, wall and nozzle heat losses, friction effects, etc

10 p1263 A73-24700

Review of liquid-metal magnetohydrodynamic spacecraft energy conversion cycles.

11 p1308 A73-25977

Evaluation testing of a closed Brayton-cycle electrical-power-conversion system.

11 p1309 A73-25983

Concept for a high voltage solar array with integral power conditioning.

11 p1310 A73-26001

66 kWe ZrH reactor-organic Rankine power systems for large manned orbiting space systems.

11 p1311 A73-26014

Status of silicon germanium air-vac converter development.

11 p1312 A73-26032

Performance of the thermoelectric converter for the zirconium hydride reactor thermoelectric space power supply.

11 p1396 A73-26036

Computerized design of electromagnetic systems in electric power conversion and electromechanical devices, noting mathematical models for electromagnetic field calculations

11 p1313 A73-26114

Hydrogen fluoride chemical laser with high voltage pulse initiation in simple transverse discharge geometry, measuring maximum energy output and corresponding efficiency

11 p1378 A73-26323

Influence of the spectral characteristics of liquid filters on the thermal regime and efficiency of a neodymium-glass laser

12 p1505 A73-26891

Qualitative analysis of MHD energy conversion efficiency

12 p1460 A73-27321

Efficiencies of Schottky-barrier GaAs and both complementary structures of Si IMPATT diodes.

13 p1595 A73-27579

Historical development of solar cells.

13 p1573 A73-29590

Solar array cost reductions. 13 p1573 A73-29592

Research plans for solar power in space. 13 p1573 A73-29594

Solar energy conversion development relative to Department of Defense space power requirements. 13 p1573 A73-29595

Performance comparison of pulsed discharge and E-beam controlled CO₂ lasers. 14 p1756 A73-29918

High-power high-efficiency operation of Read-type IMPATT-diode oscillators. 14 p1736 A73-30447

CdTe thin film fabrication by direct synthesis of vacuum evaporated Cd and Te, noting solar cell efficiency increase after storage in room temperature excicator 14 p1713 A73-30475

Optical parametric oscillators. 16 p2023 A73-32857

Design considerations of high-efficiency GaAs IMPATT diodes. 17 p2134 A73-34219

Two terminal large signal circular coupled wideband TRAPATT diode microwave amplifiers, noting negative resistance characteristics and dc-to-rf conversion efficiency 17 p2140 A73-35321

Solar energy conversion into thermal, chemical or electric energy, discussing high efficiency collector design with thin film for absorber and glass envelope improvement [AIAA PAPER 73-710] 18 p2269 A73-36331

A computer study of the design and operating performance of a photovoltaic cell for thermophotovoltaic energy conversion applications. 19 p2391 A73-38405

An analysis of linear focused collectors for solar power. 19 p2391 A73-38409

Exploratory study of several advanced nuclear-MHD power plant systems. 19 p2455 A73-38411

Isotope organic Rankine cycle electric power systems for the 150 to 1500 watj range. 19 p2456 A73-38414

Multihundred watt radioisotope thermoelectric generator design for on-pad and orbital conditions, discussing configurations, Pu-238 heat source and operating characteristics 19 p2456 A73-38419

Multihundred watt power supply with Si-Ge thermoelectric couples for Pu-238 source heat energy conversion into electric power, discussing computer model for performance projection 19 p2456 A73-38422

Multilayer foil insulated Si-Ge thermoelectric converters with multihundred watt power capacity, presenting thermal performance stability under vacuum operating conditions 19 p2392 A73-38423

Design of a nuclear isotope heat source assembly for a spaceborne mini-Brayton power module. 19 p2457 A73-38431

Engineering design and optimization of the parameters of frequency doublers for the visible range. 20 p2573 A73-39685

High power carbon dioxide-nitrogen gasdynamic laser vibration kinetics model, suggesting closed cycle photon generator engine for energy conversion to work 21 p2710 A73-40094

Fluorescence efficiencies of electrons in second positive bands of N₂ and first negative bands of N₂⁺. 21 p2682 A73-40164

High quantum efficiency IR up-conversion into visible photons through three wave interactions in nonlinear medium, using laser pump light feedback technique 21 p2699 A73-40464

Rotation of a cylinder in a conducting fluid in an axial magnetic field 21 p2747 A73-40883

Direct conversion of thermonuclear plasma energy by high magnetic compression and expansion. 21 p2750 A73-41676

The problem of extrapolating test data on the efficiency of turbine-blade cooling to actual conditions 23 p3020 A73-43741

Quantum yield of metastable oxygen atoms and molecules via ozone photolysis by UV absorption, noting uncertainties in secondary reaction kinetics 23 p2951 A73-43899

Complete photon conversion in backward-traveling-wave parametric amplification and oscillation. 23 p2955 A73-44108

Electroradiography technique involving photoproduction of free electrons via Townsend avalanche amplification in diode /triode/ gap, noting increased quantum efficiency 23 p2950 A73-44214

Hydrazine and methanol fuel cells comparison with hydrogen-air cells in terms of fuel costs and conver-

sion efficiency, considering electric generators and automotive applications 24 p3057 A73-45025

Theoretical study of a photodissociation model in polyatomic molecules 24 p3113 A73-45326

Pulsed high output double discharge TEA carbon dioxide laser with multiple electrodes and gas preionization in cavity, noting energy conversion efficiency 24 p3098 A73-45551

ENERGY CONVERTERS

U DIRECT POWER GENERATORS

ENERGY DENSITY

U FLUX DENSITY

ENERGY DISSIPATION

Application of the averaging method to the problem of plane wave propagation in a dissipative heat conducting medium 01 p0075 A73-10086

Dynamics of angular motions of a solid body carrying a rotating rotor, with allowance for energy dissipation 01 p0075 A73-10087

Electromagnetic wave transmission through 8-12 micron atmospheric window, investigating particulate matter effects on radiation energy extinction 01 p0037 A73-10372

The magnitude and character of the radiation induced vertical circulation of the troposphere. 01 p0039 A73-10394

The effect of radiative and viscous dissipation of the propagation of forced planetary waves in the vicinity of critical levels. 01 p0039 A73-10395

A linear harmonic analysis of atmospheric motion with radiative dissipation. 01 p0039 A73-10399

Estimation of the global circulation characteristics of planetary atmospheres with various hypotheses concerning the nature of dissipation 01 p0040 A73-10868

Measurements of microturbulent pulsations of the wind velocity derivative in the ground layer of the atmosphere 01 p0074 A73-10870

Internal friction and heat release in engineering and tool steels in the presence of intense ultrasonic oscillations 01 p0065 A73-10926

Stabilization of the relative equilibrium and steady motion of a mechanical system by partial dissipation forces 01 p0077 A73-10953

Energy dissipation and drift angular velocity calculation for horizontal pendulum on vibrating base, using revised differential equation of motion 01 p0079 A73-11417

Integrated subnanosecond circuits with low power dissipation and few components 01 p0021 A73-11487

Turbulent non-Newtonian liquid power dissipation steadiness during motion as function of viscous forces balanced variation 02 p0152 A73-11571

Model coil test results for a pulsed superconducting magnet energy storage system. 02 p0132 A73-11831

Energy balance and field equations of dissipative atmosphere oscillations for zonal semidiurnal Pedersen region, using K-Hermiticity 02 p0158 A73-11907

Surfaces of constant rate of energy dissipation and deformation velocity for arbitrary thin walled shell under steady creep with given strain hardening 02 p0233 A73-11937

Nonlinear waves in a multicomponent plasma with weak dissipation. 02 p0198 A73-12103

Transverse vibrations generated in a bracket bar by the reciprocating linear displacements of its seal which are damped in the course of time. 02 p0235 A73-12127

The effect of a preliminary plastic strain on the form of a mechanical hysteresis loop. 02 p0235 A73-12208

A method of estimating the probability of faults in material on cyclic loading. 02 p0236 A73-12221

Alfven waves nonlinear damping mechanism due to magnetosonic wave dissipation, presenting nonlinear coupling rates 02 p0217 A73-12401

Algorithms for spacecraft trajectory optimization programs for orbit perturbations caused by random measurement errors and minimum mathematical expectancy of energy dissipation 02 p0220 A73-12468

Limiting crack propagation rates during a quasi-brittle failure 02 p0236 A73-12582

The fracture energy and some mechanical properties of a polyurethane elastomer. 02 p0185 A73-12641

A procedure for the determination of hysteresis losses at a point of a body in the case of variable stresses 03 p0306 A73-13149

Thermomechanical dissipation analysis of thermoviscoelastic solids by finite elements. 03 p0389 A73-13326

On a heat transfer problem in the laminar flow in a tube 03 p0398 A73-13772

Molecular gas presence effect on electron energy balance in atomic gases, noting inelastic collisions loss factor in heated Ar plasma containing nitrogen molecules 03 p0347 A73-14098

High pressure stage efficiency of the turbines of modern turbojets 03 p0359 A73-14137

On similarity solution of an unsteady laminar boundary layer along a flat plate. 03 p0297 A73-14314

Wear and energy dissipation of contacts vibrated at high frequencies, analyzing mechanism of fretting wear [ASME PAPER 72-LUB-20] 03 p0314 A73-14335

Study of electronic spectroscopy at low energy on graphite [ONERA, TP NO. 1181] 03 p0336 A73-14607

Compressible flow characteristic generalizations, considering flow with/without heat transfer and losses in terms of empirical loss coefficient or heat transfer coefficient [ASME PAPER 72-WA/PWR-1] 04 p0434 A73-15803

Thermodynamic determination of power loss in hydraulic components. [ASME PAPER 72-WA/FE-22] 04 p0435 A73-15848

The energy of crack propagation in carbon fibre-reinforced resin systems. 04 p0469 A73-15981

The significance of impact data for brittle non-metallic materials. 04 p0469 A73-15985

Boron fiber-aluminum alloy matrix composite structure Charpy impact energy absorbing capacity explained via energy dissipation of matrix by plastic deformation 05 p0588 A73-16111

Progressive waves analysis, considering nonlinear convective, dissipative and dispersive effects 05 p0528 A73-16756

Coupled thermoelasticity with a finite heat propagation rate 05 p0634 A73-16770

Evidence for the existence of adiabatic energy loss in interplanetary space from observations of the decay of the February 25-March 2, 1969 series of solar cosmic ray events. 05 p0611 A73-17048

Influence of ionization losses on the conditions of cosmic ray generation on the sun 06 p0742 A73-17530

The influence of viscosity on the stability of a relative motion of two media. 06 p0685 A73-17761

Gravitational contraction and energy dissipation and compensation in stellar nuclear reactions, noting He thermonuclear reactions and nucleosynthesis 06 p0751 A73-18158

Accelerated life tests of microelectronic components by operational power dissipation, noting efficiency and profitability 07 p0799 A73-19404

Flow velocity fluctuation intensity relationship to turbulent energy dissipation based on Kolmogoroff similarity hypothesis 07 p0811 A73-19624

Cubic /four-index/ theory of thermal noises in nonlinear resistances 07 p0792 A73-19910

Energy loss measurements with 60 keV electrons in the case of amorphous and polycrystalline selenium and tellurium and the determination of optical constants 07 p0862 A73-20017

Superconductors HF properties and losses measurement and separation techniques, discussing applications to filters, oscillators, mixers, transmission lines and radiation detection 07 p0863 A73-20106

Heat exchanger for dissipating heat due to energy losses in enclosed dust-proof electronic equipment 07 p0921 A73-20125

Electron energy loss effect on cross-field electron streaming instability in low density high temperature plasmas, using high voltage theta pinch 07 p0859 A73-20192

Electromagnetic loss-cone instability of a plasma. 07 p0859 A73-20196

Evolution of scattered star clusters due to dissipation 07 p0901 A73-20316

German monograph on collective dissipation processes in collisionless shock waves in high ion temperature plasma, using laser beam scattering technique 07 p0837 A73-20387

- Power frequency losses in superconductors.
07 p0864 A73-20404
- Neutrino energy loss in neutron star matter.
07 p0902 A73-20444
- Calculation of the natural and forced vibrations of circular plates with allowance for energy dissipation in the material
07 p0917 A73-20501
- Heating of the upper atmosphere during aurorae and auroral rays length.
08 p0957 A73-20663
- Electrical components heat dissipation via thermal radiation, determining nonlinear temperature dependence from Stefan-Boltzmann law
08 p1020 A73-20775
- Energy loss of charged particles in Maxwellian plasmas.
08 p0992 A73-20823
- Influence of inelastic energy losses by electrons on the development of ionization instability in a plasma.
08 p0992 A73-20852
- Equivalent gravity wave mode approximation for main solar diurnal tide in rotating spherical dissipative atmosphere modeled by Newtonian cooling and Rayleigh friction
08 p0958 A73-20959
- Mass variation laws in light of Tsolkovski hypothesis, considering particle separation rates and thermal energy losses for actual jet engines
08 p1014 A73-21182
- Atmospheric gamma ray spectra from balloon spectrometer scintillator measured energy loss spectra
08 p0998 A73-21280
- Ionization loss effects on cosmic ray lifetime in galactic interstellar medium, noting dependence on particle energy
08 p0999 A73-21335
- Frequency dependence of losses by radio-wave scattering at turbulent discontinuities in the troposphere
08 p0939 A73-21398
- Experimental verification of the energy dissipation mechanism in acoustic dampers.
08 p1024 A73-21472
- Energy release mechanism during early universe expansion leading to distortion of relic black body spectrum, noting Comptonization effects
08 p1013 A73-21693
- Plasma-ion beam nonlinear interaction for beam velocity exceeding electrons thermal velocity, noting plasma heating and beam energy dissipation
08 p0994 A73-21696
- Satellite-caused energy dissipation via tides in spinning planet leading to orbital decay induced destruction or escape or to stable synchronism
09 p1142 A73-22041
- Loss analysis and design improvement for a continuous dye laser.
09 p1090 A73-22080
- Monte Carlo simulation of a model ionosphere. II - Energy flow and energy dissipation.
09 p1075 A73-22129
- Ultrarelativistic plasma momentum loss perpendicular to pulsar magnetic field, considering synchrotron compression of electrons leading to emission mechanisms
09 p1144 A73-22172
- Supernova explosions in close binary systems
09 p1145 A73-22289
- On the interaction of the electromagnetic field with electron beams in resistive wall waveguides
09 p1062 A73-22324
- Characteristic indices of vanishing solutions to a gyro system with partial dissipation
09 p1081 A73-22352
- Lower-hybrid-resonance heating of a plasma in a parallel-plate waveguide.
09 p1129 A73-22639
- The influence of substrate properties on microwave losses in thin films of semiconductors.
09 p1064 A73-23041
- Thermal limitation for CW output power of a Gunn diode.
09 p1064 A73-23043
- Effect of test temperature on energy of fracture of graphite.
09 p1110 A73-23062
- Conical shell inversion - An approximate energy analysis.
09 p1163 A73-23266
- [ASME PAPER 72-PVP-4] The influence of diameter on the burning velocity of strands of solid propellant.
10 p1261 A73-23560
- Semiconductor diode mixer for millimeter-wave frequencies.
10 p1193 A73-23665
- Energy dissipation sources during reinforced plastic fracture, investigating fiber debonding energetics, toughness and crack propagation resistance
10 p1238 A73-23971
- Start/stop motor incremental motion system design for optimal control with minimized energy dissipation and operating temperature under inertial and constant torque load
10 p1198 A73-24023
- Lifetime of solar flare particles in coronal storage regions.
10 p1268 A73-24144
- Dissipation of mechanical energy in a deformable body during thermal diffusion processes
10 p1291 A73-24351
- Time decay of weak shock waves in shock tubes based on energy rate of change balance with energy dissipation at walls and at shock front
10 p1206 A73-24389
- Spectroscopic study of the vibrational-energy dissipation of the I2 molecule excited by a He-Ne laser
10 p1228 A73-24577
- Turbulent loss mechanism of ring current protons in plasmopause vicinity via electrostatic drift cyclotron loss cone waves
10 p1270 A73-24743
- Auroral oval spectral features as basis for particle precipitation and energy deposition determination
10 p1215 A73-24782
- Radiative losses in a magnetostatic and intense electromagnetic field.
10 p1270 A73-24908
- Elastic impact against a beam with allowance for internal energy absorption
11 p1433 A73-25032
- Radome material technology in UK, summarizing permittivity, loss tangent, internal phase difference, attenuation, aberration, cross polarization and pattern distortion measurements and environmental tests
11 p1336 A73-25308
- Edge condition of a perfectly conducting wedge with its exterior region divided by a resistive sheet.
11 p1329 A73-25676
- An observational study of the vertical profile of the high frequency fluctuations of the wind in the atmospheric boundary layer.
11 p1393 A73-25691
- Heating effects due to radiative energy loss from acoustic waves in solar atmosphere, estimating temperature difference between radiative equilibrium and empirical model
11 p1421 A73-25931
- Energetic solar particles and their relation to optical flares.
11 p1413 A73-25952
- Plasma low density regions caused by Langmuir turbulence, discussing energy dissipation of long wave oscillations and wave collapse
11 p1406 A73-26185
- Photoneutrino energy losses in strong magnetic fields.
11 p1402 A73-26415
- Nutation dampers vs precession dampers for asymmetric spinning spacecraft.
11 p1432 A73-26670
- Damping properties of a composite material with monodirectional continual fibers
12 p1516 A73-27258
- Evolution of open star clusters through dissipation.
12 p1539 A73-27288
- On the stabilization of relative equilibrium and steady-state motion of a mechanical system by partial dissipation forces.
12 p1524 A73-27529
- Analysis of the energy losses during dynamic hot pressing of reinforced metals
12 p1503 A73-27557
- Convection and diffusion transport equation of galactic cosmic ray electrons with energy loss and absorption allowance for supernova compressed halo models
12 p1535 A73-27635
- Nonadiabatic condition effects on ultrarelativistic electron energy losses in geomagnetic trap in remote magnetosphere regions
12 p1535 A73-27649
- Electron impact excitation of H2O.
12 p1526 A73-27687
- Design of temperature-controlled substrates for hybrid microcircuits.
13 p1588 A73-28044
- Effect of adaptation to cold on the energy characteristics of muscular activity
13 p1574 A73-28295
- Estimates of global circulation characteristics of planetary atmospheres.
13 p1607 A73-28692
- Measurements of turbulent microfluctuations of the wind-velocity derivative in the surface layer.
13 p1653 A73-28694
- Dynamic losses in a transistorized switch operating on an active-capacitance load
13 p1593 A73-28944
- Turbulent flow energy transfer paths and irreversible dissipation as internal thermal energy analyzed by Reynolds convention for turbulent velocity
13 p1605 A73-29267
- Application of a variational method to dissipative, non-conservative problems of elastic stability.
13 p1700 A73-29376
- Evaluation of dissipation and damage in metals submitted to dynamic loading.
13 p1701 A73-29505
- Bonding characterization in reinforced composites.
13 p1702 A73-29536
- Resonant frequency, fatigue and energy dissipation relations for endurance limit determination in Al alloy specimens under vibrational loads
13 p1643 A73-29618
- Energy dissipation in metals in high-frequency fatigue tests. I.
13 p1643 A73-29630
- Energy dissipation in metals in high-frequency fatigue tests. II.
13 p1643 A73-29631
- Irreversible thermodynamics with internal inertia - Principle of stationary total dissipation.
14 p1817 A73-30484
- Fixed point theorems and dissipative processes.
14 p1771 A73-30774
- Magnetic field induced energy dissipation in conducting fluid isotropic turbulent flow velocity pulsations, noting Joule dissipation effect on damping
15 p1917 A73-31403
- Proportional counter energy deposition spectral quality prediction from experimental data, using folding procedure to produce composite energy absorption distributions for biological materials
15 p1839 A73-31549
- Spin stability of torque-free elastic dissipative systems with finite number of degrees of freedom, deriving Liapunov function via energy considerations
15 p1943 A73-31663
- Biological order, structure and instabilities in terms of irreversible thermodynamic processes, entropy, dissipative structures, randomness, abiogenesis, hierarchic organization, chemical reactions and molecular biology
15 p1835 A73-31824
- Amplified laser absorption - Detection of nitric oxide.
15 p1885 A73-31844
- Earth magnetosphere ion acoustic turbulence generation by longitudinal currents and electric fields, relating turbulence induced current dissipation to plasma heating
15 p1872 A73-31894
- Perturbation solution for shock waves in a dissipative lattice.
15 p1913 A73-31937
- Evolution of satellite resonances by tidal dissipation.
15 p1938 A73-31950
- Energy losses of galactic cosmic rays in the interplanetary medium.
15 p1927 A73-32010
- A theoretical analysis of the recovery factor for high-speed turbulent flow.
15 p1865 A73-32280
- Algorithms for spacecraft trajectory optimization programs for orbit perturbations caused by random measurement errors and minimum mathematical expectancy of energy dissipation
15 p1942 A73-32618
- Effect of ionization losses on cosmic-ray generation conditions on the sun.
16 p2052 A73-32754
- Book - Gasdynamic theory of detonation.
17 p2253 A73-34297
- Theoretical and experimental work on losses in 2-D turbine cascades with supersonic outlet flow.
17 p2092 A73-34377
- General solution to the subsonic through-flow problem in a turbomachine including losses.
17 p2092 A73-34385
- Decay of the magnetic storm ring current by the charge-exchange mechanism.
17 p2159 A73-34782
- Current distribution of a dipole antenna of revolution in dissipative media.
17 p2141 A73-35366
- Dielectric properties of ferrites in the microwave band
17 p2141 A73-35548
- On the explosive instabilities of waves in plasmas with special regard to dissipation and phase effects.
17 p2218 A73-35820
- Effect of temperature on true energy dissipation in heat resistant E1893 nickel alloy
18 p2324 A73-36766
- Solar wind-geomagnetic field interaction simulation by plasma flow and magnetic dipole, proving collisionless dissipation presence
19 p2481 A73-37339
- Calculation of forced and free oscillations of round plates taking into account the dissipation of energy in the material.
19 p2499 A73-37776
- Atmospheric gamma ray spectra from balloon spectrometer scintillator measured energy loss spectra
19 p2476 A73-37909
- Some properties of horizontally homogeneous, statistically steady turbulence in a stratified fluid.
19 p2449 A73-38236
- Frequency dependence of the loss when radio waves are scattered by turbulent inhomogeneities in the troposphere.
19 p2407 A73-38356

Energy-sink analysis for asymmetric dual-spin spacecraft.

[AIAA PAPER 73-909] 20 p2614 A73-38843

Existence and uniqueness conditions for solid surface vaporization products dispersion into vacuum formulated for equations of motion of ideal gas under variable energy release

20 p2573 A73-39282

Investigation of energy criteria for the failure by fatigue of some metals at low and high loading frequencies

20 p2577 A73-39354

Differential equations for the vibrations of twisted rods with allowance for energy dissipation

20 p2619 A73-39372

Rotary inertia and energy dissipation effects on dynamic response of three layered symmetrical laminate beam with viscoelastic core vibrating in flexural mode, using variational calculus

20 p2623 A73-39555

Free atom and molecule energy levels studied by electron scattering spectroscopy, discussing energy losses, monochromated electron beams, particle resonance and electric fields

20 p2520 A73-39635

A mechanism for the growth phase of magneto-spheric substorms.

21 p2582 A73-40157

Relationship between the hydraulic losses of a centrifugal wheel and the energy imparted by the wheel to the fluid by circulation in the relative motion

21 p2676 A73-40407

Hole-type confocal active optical cavity resonator loss distribution, discussing Fresnel zone oscillation type intensity within resonator and diffraction at cavity

21 p2714 A73-40559

Sealed-off waveguide carbon dioxide laser, investigating gas mixture and pressure effects on power gain and output and optical properties effects on losses

21 p2715 A73-40763

Energy losses of solar cosmic rays in interplanetary space.

21 p2763 A73-41503

Structure of ionizing shock waves with radiative energy loss.

22 p2841 A73-42200

Correction to calculation of temperature rise in connection with gravitational energy release accompanying rapid core formation from undifferentiated earth

22 p2848 A73-42499

Book - Ultrasonic investigation of mechanical properties.

22 p2861 A73-42575

German monograph - Model of a parallel shock wave with turbulent dissipation in a hot plasma.

22 p2895 A73-42718

Requirements of switching devices in dc-to-dc converters.

22 p2801 A73-42908

Multiperipherism and Landau hydrodynamic models of multiple particle collision processes with inhomogeneous and homogeneous energy liberation spaces

23 p3008 A73-43543

Computerized simulation of isotropic three dimensional turbulence velocity field growth and energy decay based on Navier-Stokes equation numerical integration

23 p3001 A73-43588

Radiation production and energy deposition by ring current protons precipitated into the mid-latitude upper atmosphere.

23 p3024 A73-43685

Vibrations of turbojet-engine components containing structural dampers of the type of sandwich rods

23 p3020 A73-43735

The effect of dissipation on the vertical propagation of planetary waves in the vicinity of critical levels.

23 p3032 A73-43906

Mixed finite element models for nonlinear thermomechanical responses of continuous dissipative media based on Oden variational principle and theory of thermoplastically simple materials

23 p3044 A73-44049

Electromagnetic resonances and Q-factors of lossy dielectric spheres.

23 p2960 A73-44067

Why Syrovatskii's mechanism of dynamic dissipation of magnetic fields does not work.

24 p3136 A73-44642

Gravitational radiation emission by star tidally deformed by black hole, computing energy loss rate

24 p3138 A73-45037

Energy balance and change in body weight and body water in man during a 2-day cold exposure.

24 p3060 A73-45059

Thermalization and transport of photoelectrons - A comparison of theoretical approaches.

24 p3086 A73-45124

On the problem of nonlinear interactions in fluid dynamics.

24 p3080 A73-45449

On the integration of Einstein's equation for energy density inside a perfect fluid sphere.

01 p0076 A73-10250

Troposphere turbulence kinetic energy dependence on height and scales of motions, presenting vertical energy profiles

01 p0074 A73-10869

Energy balance in the current sheath of a solar flare and the acceleration of cosmic rays by plasma waves

01 p0092 A73-10936

Computation of the sound energy radiated from turbulent flows

[DGLR PAPER 72-074] 02 p0153 A73-11699

Some exact statistics of two-dimensional viscous flow with random forcing.

02 p0153 A73-12041

Midlatitude excess radiation energy density relation to primary cosmic ray background from spectrum measurement data

02 p0208 A73-12460

Cosmic radiation high energy hadron component relation to extensive electron-photon showers, comparing sampling events based on multicore structure and total energy

02 p0209 A73-12676

High energy muon energy and angular distributions from electron-photon cascades, using emulsion chamber with X ray films

02 p0209 A73-12680

Measurement of electron distribution function in a cesium plasma.

02 p0199 A73-12815

A relation between the energy distribution of the main flow and the corresponding fluctuating quantities in boundary layers

03 p0292 A73-13171

Energy flux intensity in IR bands of selectively radiating molecular gas nonisothermal layer from radiative transfer equation and mathematical model

03 p0396 A73-13183

Effect of reagent vibrational excitation on reaction rate and product energy distribution in $F + HCl$ yields $HF + Cl$.

03 p0273 A73-13290

Energy distribution among reaction products. VII - $H + F_2$.

04 p0414 A73-14820

The influence of the electron-phonon scattering on the total energy distribution of field emitted electrons from tungsten.

04 p0477 A73-15000

Radiation energy distribution in laser pulse heating of moving plasma without reflection, noting thermal wave propagation

04 p0481 A73-15605

Measurement of the electron energy distribution function in a plasma with periodically varying parameters

04 p0481 A73-15615

Image quality and energy distribution for mirror cone and toroidal annular mirror optical coordinators in wide angle measuring instruments

05 p0575 A73-16318

Surveillance radar cosecant reflectors electromagnetic energy emission distribution, discussing design and directional characteristics

05 p0550 A73-16474

Electron energy distribution in a low-temperature plasma.

06 p0727 A73-17419

Annular energy vortex in the near field of a directional antenna

06 p0674 A73-17821

Noise figures, detection probabilities and scintillation energy distributions in second generation image intensifier tubes

06 p0676 A73-18299

Argon plasma density and energy distribution development during microwave radiation absorption at upper hybrid resonance

06 p0732 A73-18605

Chemical laser studies of vibrational energy distributions - The equal-gain and zero-gain temperature techniques.

07 p0834 A73-19629

Secondary electron emission characteristics of lunar surface films.

07 p0871 A73-19861

Energy distribution functions of kiloelectron ions in a modified Penning discharge.

07 p0808 A73-20459

Solar soft X-ray bursts data recorded by satellite telemetry, considering production by thermal plasma and nonrelativistic electrons with power law energy distribution

08 p0996 A73-20765

Effects of changes in the atmosphere on solar insolation.

08 p0958 A73-21269

Application of the numerical study of random time series to the analysis of the electroencephalogram of the normal infant

08 p0935 A73-21540

Particle and energy fluxes across magnetic field in axisymmetric toroidal magnetic traps and plasmas with weak collisions, calculating radial electric field

08 p0993 A73-21695

Electron energy distribution function in CO laser discharge for elastic collisions, noting kinetic equation solution

09 p1089 A73-21914

Symmetry properties of energy zones in rhombohedral-system crystals

09 p1134 A73-22682

Energy balance in the current sheet of a solar flare, and the acceleration of cosmic rays by plasma waves.

09 p1138 A73-22731

Assembly for measurement of free surface energy, contact angles, and melt densities by a lying drop technique

09 p1085 A73-23017

A unified approach to the theory of double injection in solids with traps uniformly and non-uniformly distributed in the energy band gap.

09 p1135 A73-23045

Radiation energy distribution in laser pulse heating of moving plasma without reflection, noting thermal wave propagation

10 p1254 A73-24195

Measurement of electron energy distribution in a plasma with periodically varying parameters.

10 p1254 A73-24205

Electrostatic turbulence and ion thermalization in modified Penning discharge, investigating ion heating processes

10 p1251 A73-24259

Coulomb collision induced mean-energy variations in homogeneous nonrelativistic plasma components, discussing two-component plasma and energy transfer rates

10 p1257 A73-24760

Measurement of the ion energy distribution resulting from the turbulent heating of a plasma.

11 p1404 A73-25269

Influence of vertical wind shear on the development of convective cloudiness

11 p1393 A73-25640

On the product rotational state distribution in exoergic atom-diatom molecule reactions.

11 p1402 A73-25968

The continuous-cathode /emitting-sole/ crossed-field amplifier.

11 p1339 A73-26694

Stability of sheet metal drawn by a rigid stamp to cylindrical and conical shapes

12 p1503 A73-27476

Observation and first evaluation of geomagnetic pulsations near the polar aurora zone in connection with the occurrence of si's and ssc's

12 p1494 A73-27778

Solar radio burst of 7 August 1972, discussing peak flux density, magnetic field intensity, energy distribution and polarization degree

12 p1536 A73-27850

Troposphere turbulence kinetic energy dependence on height and scales of motions, presenting vertical energy profiles

13 p1653 A73-28693

A survey of the mean turbulent field closure models.

13 p1601 A73-28801

Universe rest energy density, isotropic background radiation energy and galactic kinetic energy

13 p1686 A73-29654

Band structure, electron energy distribution and emission efficiency of negative electron affinity secondary emitters and cold cathodes

14 p1732 A73-29912

Energy partitioning of gaseous ions in an electric field.

14 p1776 A73-30246

Evolution of the CO vibrational energy distribution in a transverse flow laser.

15 p1864 A73-31313

Uses of the equation of pulsation energy balance in the theory of MHD flows in channels and tubes

15 p1917 A73-31404

Midlatitude excess radiation energy density relation to primary cosmic ray background from spectrum measurement data

15 p1927 A73-32610

Electron energy distribution function in CO laser discharge for elastic collisions, noting kinetic equation solution

15 p1886 A73-32640

Acoustic energy flow in lined ducts containing uniform or 'plug' flow.

16 p2038 A73-33945

Electron energy distribution function validity for nonequilibrium plasma in presence of electric field verified for ionized cesium vapor positive column

17 p2216 A73-34551

Satellite monitoring of climate parameters, discussing energy transfer in atmosphere, energy distribution, radiation balance, climatic models

17 p2205 A73-34928

Cryptosteady flow energy separation mechanisms, considering bearing friction and rotor torque effects and rotor nozzle proportion equations [ASME PAPER 73-FE-24] 17 p2153 A73-35019
Electron gun with concentric hemispherical anode and space charge limited thermionic emitter for potential field simulation, measuring electron energy distribution for comparison with calculation 17 p2143 A73-35764

Energy characteristics of a coaxial plasma source 19 p2467 A73-37363

Monte Carlo calculations of reaction rates and energy distributions among reaction products. IV - F + HF/nu/ yields HF/nu-prime/ + F and F + DF/nu/ yields DF/nu-prime/ + F. 19 p2463 A73-37898

Hot-electron production and anomalous microwave absorption near the plasma frequency. 19 p2469 A73-38289

The balance of turbulence energy and its components in incompressible turbulent boundary layers 20 p2546 A73-39096

Homogeneous anisotropic to isotropic turbulence convergence based on shear flow component measurements of turbulence energy distribution in axisymmetric flow 20 p2546 A73-39097

Energy distribution functions of kilovolt ions in a modified Penning discharge. 20 p2597 A73-39197

Ionization of a neutral medium by an electron beam 20 p2597 A73-39279

Radiation patterns of directional end-on antennas, deriving formulas for side lobe levels and main lobe energy distribution 21 p2661 A73-40198

Energy of an equilibrium fluctuating electromagnetic field in matter 21 p2741 A73-41515

The Marsta micro-meteorological field project - Profile measurement system and some preliminary data. 21 p2732 A73-41567

An operational approach to the energy of gravitational waves. 22 p2888 A73-42929

Pion-nucleon interaction structure based on negative pion beam data from Serpukhov accelerator, showing secondary particle energy distribution asymmetry 23 p3021 A73-43537

Ionosphere dynamic process investigations, describing wind models, E region drift velocity curves and energy distribution chart 23 p2978 A73-43978

ENERGY EXCHANGE

U ENERGY TRANSFER

ENERGY LEVELS

NT ATOMIC ENERGY LEVELS

NT ELECTRON STATES

NT GROUND STATE

NT INTERMOLECULAR FORCES

NT MOLECULAR ENERGY LEVELS

Two stage analytical model for mechanism of heavy nuclei acceleration in solar flares, considering ion Fermi acceleration to higher energies 03 p0362 A73-13720

Analysis of some aspects of 25 chromospheric events. I - Reduction of the optical data. II - Discussion on the optical data. 03 p0364 A73-14414

Electrical properties of electron-irradiated GaAs. 05 p0604 A73-16516

A search for the solar Sr-87 content and the solar Rb/Sr ratio. 05 p0620 A73-17027

Charge carriers concentration growth and decay for semiconductor model with independent capture centers, determining capture level activation energy 07 p0861 A73-19328

Calorimetric measurements of laser energy and power. 08 p0963 A73-20872

Ionization energy of adhesion levels and heat-generation centers in the microplasma volume in germanium p-n junctions 08 p0995 A73-21274

The continuity and Poisson's equations for semiconductors with many coexisting kinds of multiple energy-level defects. 09 p1133 A73-22306

Probability model of mode interactions, radiation density and output gain of gas laser channels with common lower energy level in active medium 10 p1227 A73-24071

Energetic and structural models of microdefects in germanate glasses 10 p1240 A73-24465

Determination of the basic characteristics of an impurity level by Hall effect measurements 13 p1668 A73-28461

Relaxation rates of lower laser levels in CO₂. 13 p1626 A73-28544

Theory for the susceptibility of quantum systems with degenerate levels 13 p1659 A73-28759

Classical mechanics-quantum mechanics relations and analogies, considering symmetry groups, Casimir invariants, energy levels and quantization 14 p1774 A73-30239

Multiplicity of dielectric local modes - Bound states of phonons with impurity centers 15 p1885 A73-31719

A study of the adsorption of oxygen on Ni(111)/using Auger electron spectroscopy - Chemical shifts and valence spectra. 15 p1840 A73-31968

Dual spin spacecraft minimum energy and nutational dynamic trap states due to asymmetric or unbalanced rotors, analyzing single degree of freedom dynamic model [AIAA PAPER 73-908] 20 p2614 A73-38842

Current and energy characteristics of an electron plasma in a magnetron diode 20 p2536 A73-39254

Carrier-frequency distance dependence of a pulse propagating in a two-level system. 21 p2649 A73-40224

Probability balance equations for energy level population analysis of ultrashort pulse solid state laser generation and amplification 21 p2712 A73-40309

Asymptotic electron terms of colliding identical heavy nuclei 21 p2742 A73-40353

Longitudinal alignment of working levels in a helium-neon laser 22 p2870 A73-42412

Level populations in plasmas - RF discharges and sonic channel. 22 p2895 A73-42994

Si and Ge doping characteristics and energy levels in vapor phase epitaxially grown GaAs from sample photoluminescence spectra 23 p3018 A73-44370

Determination of hole and electron traps from capacitance measurements. 24 p3119 A73-44405

ENERGY LOSSES

U ENERGY DISSIPATION

ENERGY METHODS

NT BERNSTEIN ENERGY PRINCIPLE

NT STRAIN ENERGY METHODS

Validity of averaging methods for certain systems with periodic solutions. 01 p0070 A73-10273

The effect of the Coriolis force on the stability of rotating magnetic stars. 01 p0103 A73-11034

Structural and energetic analysis of fatigue failure in metals 02 p0232 A73-11929

Saturn ring dynamics via numerical simulations of jet streams, discussing non-Maxwellian velocity distribution and energy consumption decrease with thickness 03 p0373 A73-13355

Gravitational equations derivation identical to electromagnetic Maxwell equations, noting nonviolation of energy conservation 03 p0373 A73-13358

Static boundary value problem of asymmetric elasticity for elastic isotropic media with small energy contribution to potential due to moment effects 03 p0394 A73-14050

Calculus of variations for minimum energy method in elasticity theory of incompressible elastic body, calculating elastic deformations 04 p0509 A73-14980

Method of determining the energy of fracture of aluminum alloys during impact-bend tests with sharp notches. 04 p0466 A73-15675

Rotating shafts dynamic stability, analyzing eigenvalue problem derived via energy equations based on virtual work principle 06 p0697 A73-15717

Determination of properties of cold stars in general relativity by a variational method. 07 p0874 A73-19065

Some diagnostic applications of wind speed and component spectra for mesoscale through synoptic scale frequencies. 09 p1114 A73-22336

Finite element methods for elastic bodies containing cracks. 09 p1162 A73-23186

An exact solution for a collisionless flat galactic model. 10 p1275 A73-23826

Application of the complementary energy method to two non-conservative problems of elastic stability. 10 p1291 A73-24393

Energy method for unsteady flow stability analysis, exemplifying by oscillatory Stokes layer and impulsively heated fluid layer 10 p1208 A73-24806

Stability predictions with the aid of energy expressions in the case of a turborotor with gyroscopic effects 11 p1432 A73-24999

Comparison and oscillation theory for Lienard's equation with positive damping. 11 p1391 A73-26367

Deformation bounds for a creeping structure approaching rupture. 11 p1447 A73-26654

Integral parameters and pulsation frequencies for equilibrium configurations of rotating neutron stars, expanding energy characteristics into series of relativistic members 12 p1546 A73-27854

Complementary energy method in elastodynamics. 13 p1694 A73-28249

Influence of niobium on the magnetic properties of high-titanium Al-Ni-Co alloys - Second communication. 13 p1637 A73-29244

Energy variational principle formulation for stability determination of scalar-pressure toroidal plasma, writing potential energy as one dimensional integral 14 p1778 A73-39689

Homogeneous and composite solid propellants, discussing rocket motor performance, energetics, smokeless exhaust, energy-weight relations and cost 14 p1784 A73-30135

Dispersion relation derivation and approximation applications for generalized optical potential use in analysis of energy dependence of empirical potential strength 14 p1774 A73-30237

Minimum-energy terminal state control of first order linear hyperbolic systems in one spatial variable using the method of characteristics. 14 p1769 A73-30453

Energy methods in plasticity theory extension to creep mechanics with respect to stress-strain rate tensors relationships 14 p1811 A73-30478

An iteration method of solving the three-dimensional problem for equations of the theory of elasticity in displacements 15 p1945 A73-31027

Saint Venant principle investigation for plane problem of linear elastostatics for anisotropic media by energy method, calculating exponential stress decay constant lower bound 15 p1946 A73-31102

Stability analysis of shell-like structures by complementary energy. 16 p2078 A73-33000

Single-fluid model of the distant solar wind. 16 p2056 A73-33459

Numerical analysis of the averaged equations of concentric laser cumulation of plasma with consideration of nuclear fusion energy. 17 p2216 A73-34323

Dual principles of elastodynamics finite element applications. 17 p2245 A73-34833

Inextensional approximations in cylindrical shells. 18 p2362 A73-36329

Elastic bodies nonlinear thermomechanical stability under conditions of loaded equilibrium configuration, using Liapunov type energy-like functionals 20 p2615 A73-39010

Acoustical radiation reaction by conservation of energy and Dirac prescription methods and derivation of acoustic index of refraction for system of soft spheres 20 p2592 A73-39049

Integral parameters and pulsation frequencies for equilibrium configurations of rotating neutron stars, expanding energy characteristics into series of relativistic members 20 p2608 A73-39228

A difference-energy method of studying the stability of rectangular plates in shear 20 p2617 A73-39306

Determination of the resistance of VT-14 alloy to brittle fracture 21 p2722 A73-41232

The behavior of materials subjected to multiaxial cyclic stresses. I - Methods of calculation 22 p2917 A73-41781

Determination of the deflections and stresses in a small-aspect-ratio wing by the displacement method 23 p3041 A73-43723

Inertia effects in MHD lubricated hydrostatic thrust bearing under axial magnetic field investigated by energy integral method, obtaining flow velocity and load carrying capacity 24 p3092 A73-44410

A lower bound theorem for dynamically loaded rigid-viscoplastic structures. 24 p3146 A73-44680

Beck cantilever problem solution for quasi- and purely dynamic case by Euler or energy method under internal constraint 24 p3147 A73-44892

The evolution of periodic orbits close to homoclinic points.

24 p3142 A73-45296

ENERGY REQUIREMENTS

Heating and cooling mechanisms, ionization processes, time-dependent models and energy requirements of interstellar H I regions

01 p0091 A73-10064

Oxygen from electrolyzed lunar rocks - A discussion of the energetics.

03 p0253 A73-14169

Space shuttle orbiter applications to manned high energy missions from low earth orbit, considering refueling requirements, aerobraking and overall mission capability

[AIAA PAPER 73-206]

05 p0630 A73-16939

Threshold pump energy value of liquid lasers in quasi-steady-state operation

06 p0699 A73-17915

Surface topography of the inner planets as related to planetary origins.

06 p0749 A73-18005

Energy requirements of ouabain-sensitive Na-K positive ion membrane pump during norepinephrine induced thermogenesis of brown adipose tissue in cold-exposed hamsters

09 p1040 A73-22649

Temperature, testing rate and substrate choice effects on characteristic energy required to produce separation and failure of adhesively bonded pieces

11 p1443 A73-26203

The utilization of solar energy to help meet our nation's energy needs.

15 p1832 A73-32193

Forming energy in rigid-plastic materials unsteady molding processes, obtaining nonlinear equations solution by iterative procedure

16 p2037 A73-33237

Characteristics of thin-film metal arrays for laser-beam information storage.

22 p2869 A73-42254

ENERGY SOURCES

Thermal convection in a horizontal fluid layer with uniform volumetric energy sources.

01 p0120 A73-10442

Homogeneous gas sphere model light scattering for different energy source distributions in planetary and stellar atmospheres

01 p0100 A73-10704

Nuclear energy sources in superdense celestial bodies.

01 p0106 A73-11311

Corpuscular radiation as an upper atmospheric energy source.

02 p0205 A73-12289

Nuclear rocket engine reactor utilization as energy center for propulsion, attitude control, refrigeration and scientific experiments, emphasizing dual mode electrical power generation

[AIAA PAPER 72-1091]

03 p0340 A73-13412

Processing power for a low voltage source-pulse load system.

03 p0253 A73-13939

Cost goals for silicon solar arrays for large scale terrestrial applications.

03 p0258 A73-14250

Electrodynamic sailing - Beating into the solar wind.

04 p0487 A73-15073

Geothermal energy extraction from hot rocks via deep dry wells by pressurized water circulation, solving numerically fluid flow, heat transport and rock fracture equations

05 p0569 A73-16382

German book - New energy systems for space flight.

06 p0741 A73-17668

Gravitational energy conversion into rotational energy in contraction process for pulsars, quasars and galactic radio emission energy sources

07 p0898 A73-19934

Stellar formation and cloud collision energy dissipations as energy sources for self gravitating shock waves maintenance in Galactic spiral theory

09 p1141 A73-22008

Thermoelectric radioisotope generators and nuclear thermoelectronic reactors, noting anaerobic self contained reliable operation and suitability for underwater energy sources

09 p1032 A73-22203

The phosphoric acid fuel cell, a long life power source for the low to medium wattage range.

09 p1037 A73-22821

An integrated radiation physics computer code system.

11 p1334 A73-25997

Solar array concept for a portable retractable oriented power system.

11 p1310 A73-26007

Design criteria and candidate electrical power systems for a reusable Space Shuttle booster.

11 p1311 A73-26016

EUV and radio observation of energy flux from corona into chromosphere, considering coronal holes as source of high energy streams of solar wind

12 p1545 A73-27839

Some major terrestrial applications of solar energy.

17 p2110 A73-35312

Energy supply in acute cold-exposed dogs.

18 p2278 A73-36655

Synthesis of the optimal characteristics of the engines of multiengine systems

19 p2388 A73-37187

Quasar and galactic nuclei energy source models, considering supermassive rotating magnetoplasma body, black hole and compact star cluster with flares and collisions

20 p2609 A73-39570

Non-thermal solar wind heating by supra-thermal ions.

21 p2763 A73-41499

Configurations of hot white dwarfs with nuclear energy sources

23 p3025 A73-44360

Ergosphere concept extended to classical mechanics from relativistic black hole mechanics

24 p3142 A73-45341

ENERGY SPECTRA

NT ELECTRONIC SPECTRA

NT NEUTRON SPECTRA

Variations of the auroral electron energy spectra during substorms.

01 p0036 A73-10339

The possibility of a consistent explanation of various phenomena involving cosmic ray muons.

01 p0092 A73-10789

Rocket measurements of electron fluxes in the upper atmosphere at midlatitudes.

01 p0041 A73-10887

High-energy cosmic gamma-ray observations from the OSO-3 satellite.

01 p0092 A73-11028

Positive detection of an excess of low-energy diffuse X-rays at high galactic latitude.

[AD-760197]

01 p0092 A73-11029

Galactic-latitude dependence of low-energy diffuse X-rays.

[AD-760196]

01 p0092 A73-11030

Energy spectra of modulated relativistic electron beam as function of plasma density at beam-plasma interaction region boundary

01 p0086 A73-11284

Absorbing boundary propagation model for solar cosmic rays energy spectrum kink time behavior, using Gleeson-Ng theory

[AD-756355]

02 p0205 A73-11753

Proton energy spectra from recent rocket measurements in the night and morning time auroral zone.

02 p0206 A73-12315

Flux and energy spectra of solar protons observed aboard the ESRO 2 satellite in 1968-1969.

02 p0206 A73-12316

Radiation belt low energy protons intensity and spectrum variations during geomagnetic storms from Molniya 1 satellite measurements, interpreting results in terms of electric field effects

02 p0206 A73-12318

Study of energy spectra of primary cosmic rays at very high energies on the proton series of satellites.

02 p0207 A73-12328

Particle multiplicity and momentum spectra for high energy inelastic nuclear interactions in Wilson chamber with polyethylene target

02 p0208 A73-12655

Inelasticity factor dependence on particle energy spectra to explain nucleon flux calculations and Proton satellite data, considering scattering cross sections

02 p0208 A73-12658

Multilayer X ray film chamber for gamma quanta energy spectrum determination by primary photon impact and absorber calorimetric methods

02 p0208 A73-12660

Secondary particles in pion-nucleon and coherent interactions, measuring momentum from multiple Coulomb scattering

02 p0209 A73-12666

Energy spectrum, composition and anisotropy study of cosmic radiation from extensive air showers observation, using scintillation and Cerenkov detectors

02 p0209 A73-12671

Primary cosmic radiation energy spectrum approximation from air showers, high-energy hadrons and Proton 4 data

02 p0209 A73-12675

Extensive air shower spectra based on electron and muon number for given shower development mechanism and primary cosmic ray chemical composition

02 p0209 A73-12677

Extensive air shower characteristics and muon counts at different level observations relative to particle number and primary energy spectra

02 p0209 A73-12678

Energy spectrum of muon formed electromagnetic cascades in vertical cosmic radiation flux

02 p0209 A73-12681

Uniformly rotating stars with hydrogen- and metallic-line blanketed model atmospheres.

02 p0222 A73-12712

Spectrum of the cosmic X- and gamma ray background in the energy range 1 keV-1 MeV.

02 p0210 A73-12730

Studies of the chemical composition of cosmic rays with Z = 3-30 at high and low energies.

02 p0210 A73-12737

The spectrum of diffuse cosmic X-rays in the 20-125 keV range.

02 p0210 A73-12738

Cross spectral analysis for auroral pulsations coherency in spatially separated patches, noting TV image recording of frequency and energy spectra

03 p0298 A73-12879

Near earth electron spectra applied to cosmic ray transport equation numerical solution extension to 1968-1970, providing models for modulation and gradients reproduction

03 p0361 A73-13362

The Fermi mechanism and the source spectrum of cosmic ray nuclei.

03 p0361 A73-13365

Existence in the laminar boundary layer of a natural instability not predicted by theory and connected to a wall deformation

03 p0294 A73-13576

Field dynamics equilibrium equation for particle rotational motion in gravitational field of central body, noting energy spectra of stationary orbits

03 p0374 A73-13751

Pitch angles and spectra of particles in the outer zone near noon.

[AD-758531]

03 p0363 A73-13867

Local time variations of X ray substorm activity observed at auroral zone station, including atmospheric passage and energy spectrum measurements

03 p0363 A73-13889

Quasi-stable energy spectrum of isotropic turbulence.

03 p0297 A73-14444

Trapped and precipitated electron energy spectra in relativistic electron precipitation events [REP], discussing bremsstrahlung measurements deductions

03 p0304 A73-14591

Radio sources in decimeter wave range from astronomical model and radio observations, noting spectral characteristics dependence on electron energy spectra

04 p0496 A73-14824

Vibrational and energy spectra of welding electron beam interacting with beam produced plasma, noting interaction length effect on instability

04 p0454 A73-15609

Derivation of a function of nerve-fiber distribution according to fiber diameters on the basis of electrophysiological measurements

04 p0413 A73-15787

Steady axisymmetric ring current models computed with energy density distribution parameters variations for effects on magnetic field and particle belt parameters

05 p0609 A73-16144

High energy primary cosmic ray particles total energy and mass spectra measurement

05 p0609 A73-16370

Enrichment of heavy nuclei in the 17 April 1972 solar flare.

05 p0609 A73-16571

Incoherent radiation from relativistic electrons with power energetic spectrum.

05 p0611 A73-17313

Small Magellanic Cloud X-1 X ray source binary nature, occultation, energy spectrum and intensity from Uhuru satellite observation

05 p0626 A73-17345

Frequency spectra of the inner and outer structures of wind waves at different stages of wave development

05 p0594 A73-17359

Interplanetary cosmic ray low energy electron observation, explaining steep spectrum origin and time variations by model with spectral decomposition

05 p0612 A73-17386

Dependence of the length of polar rays on the auroral activity level

06 p0690 A73-17558

Directional measurements of the solar wind by the ESRO HEOS 1 probe, S 58-73

06 p0749 A73-17863

Energy spectra of mixed discrete random processes in statistical multiplexing systems with pulse position, delta and pulse code modulation

06 p0668 A73-18390

Effects of non-Maxwellian electron energy distributions on the orbital limited current-voltage characteristics of cylindrical and spherical Langmuir probes under collisionless conditions.

06 p0730 A73-18463

Energy spectra of Cs+ ions scattered from the surface of a tungsten single crystal.

06 p0726 A73-18615

Long-term variations of total and polarized fluxes, absolute energy distribution, and line strength of BL Lacertae and four quasi-stellar sources.

07 p0873 A73-19051

Observations of Taurus X-1 by the 1-60 keV X-ray detector on the OSO-7.

07 p0868 A73-19064

Cosmic ray electrons of E greater than 1 GeV - Some new measurements and interpretations.

07 p0869 A73-19226

Intensity and energy spectrum calculation of albedo electrons recorded in cosmic particle showers by gas discharge counters

07 p0823 A73-19429

Turbulent energy variations in unsteadily moving flow with structural shift, emphasizing formation of vortices with various inertia scales

07 p0811 A73-19620

Photoelectron layer detection above sunlit lunar surface with ion-electron spectrometer in Apollo 14 charged particle lunar environment experiment, noting energy spectra

07 p0895 A73-19859

Photoemission from lunar surface fines and the lunar photoelectron sheath.

07 p0895 A73-19860

Energy spectra of cosmic pions and nucleons at the top of the atmosphere.

07 p0872 A73-20015

Quasi two dimensional turbulence model of energy spectra and potential enstrophy transfer in synoptic large scale quasi-horizontal atmospheric motions

07 p0820 A73-20342

Charge dependence of the energy spectra of cosmic rays.

07 p0873 A73-20561

Evidence for differences in the energy spectra of cosmic ray nuclei.

07 p0873 A73-20562

Energy dependence of primary cosmic ray nuclei abundance ratios.

07 p0873 A73-20564

Electron and X ray transitions between conduction band and bound level and between two bound levels in transition metals, investigating edge singularity and spectrum shape

07 p0864 A73-20614

The energy spectrum of small-scale solar magnetic fields.

08 p1003 A73-20888

Turbulence energy spectra in thick convective cumulonimbus cloud zone, using aircraft measurements.

08 p0984 A73-21186

Atmospheric gamma ray spectra from balloon spectrometer scintillator measured energy loss spectra

08 p0998 A73-21280

Primary cosmic rays energy spectrum at 100-1000 TeV from Proton 4 satellite data

08 p0999 A73-21329

Primary cosmic ray particles disappearance and proton spectrum slope rise in 1 TeV energy region from Proton satellites data

08 p0999 A73-21330

Primary cosmic rays alpha particles and protons energy spectra similarity and intensity difference at .05 to 1.6 TeV, using Proton satellites data

08 p0999 A73-21331

Three dimensional cosmic ray anisotropy and density distribution at earth orbit and in interplanetary space with allowance for primary particle and nucleon energy spectrum

08 p1000 A73-21343

Solar neutrino problem - No low energy He-3 + He-3 resonance.

08 p1000 A73-21530

Linear FM pulses in chirp radar transmitter, calculating and plotting bounds on amplitude, energy and power spectra for electromagnetic compatibility analysis

08 p0949 A73-21665

A possible cosmic ray primary particle energy spectrum above 10 TeV and its astrophysical implications.

08 p1000 A73-21824

Double charge transfer spectroscopy of diatomic molecules.

09 p1122 A73-22118

The exciton energy spectrum in diamond and sphalerite type crystals

09 p1134 A73-22683

Isotopic and crystalline structure changes in lunar rock and meteorite constituents for cosmic ray nuclei intensity and energy spectrum

09 p1138 A73-23169

An estimate of the energy spectrum of gamma rays from the central region of the Galaxy and some implications.

10 p1263 A73-23486

Energy spectrum and time variations of hard X-rays from Cyg X-1.

10 p1263 A73-23488

Observation of structure in the X-ray spectrum of Puppi A.

10 p1264 A73-23548

A method for determining the polarization and energy spectrum of cosmic-ray gamma quanta

10 p1266 A73-23914

Solar proton energy spectra recorded in stratosphere during two solar cycles, approximating generation spectra by power law

10 p1266 A73-23917

Energy spectrum of galactic cosmic rays beyond the region of modulation and the anisotropy of cosmic rays in the Galaxy

10 p1267 A73-23925

Vibrational and energy spectra of welding electron beam interacting with beam produced plasma, noting interaction length effect on instability

10 p1224 A73-24199

Some aspects of measuring the differential cosmic-ray spectrum.

10 p1268 A73-24213

Latitudinal energy distribution of geomagnetic disturbances.

10 p1212 A73-24229

Energy and angular correlations of the scattered and ejected electrons in the electron-impact ionization of argon.

10 p1252 A73-24340

High energy astrophysics research at the Max-Planck-Institut.

11 p1411 A73-25139

Calculation of electron energy flux distributions in noble gases.

11 p1401 A73-25144

On the morphology of auroral-zone X-ray events. II - Events during the early morning hours.

11 p1334 A73-25762

Retarding field electron spectrometer for low kinetic energy electron analysis, discussing design, construction and performance in terms of resolution, sensitivity, luminosity and SNR

11 p1366 A73-26301

Primordial random motions and angular momenta of galaxies and galaxy clusters.

11 p1427 A73-26601

X ray source identified with galaxy NGC 5128 located at center of radio source Cen A, noting 3.4 keV low energy cutoff in X ray spectrum

11 p1427 A73-26603

Hydrogen and helium isotopes differential energy spectra during solar flare particle acceleration related to nuclear interaction processes

11 p1414 A73-26610

A measurement of cosmic-ray rigidity spectra above 5 GV/c of elements from hydrogen to iron.

11 p1414 A73-26612

Evidence for the binary nature of 2U 1700-37.

11 p1428 A73-26628

Cosmic ray electrons from 0.2 to 8 MeV - Pioneer 8 and 9 measurements of their spectrum, time variations, and interplanetary radial gradient.

12 p1533 A73-26976

The first results of balloon measurements during the solar proton events in the period from August 2 to August 10, 1972

12 p1535 A73-27777

Low momentum integral muon spectrum at sea level near the geomagnetic equator.

13 p1670 A73-28211

Specific characteristics of interband luminescence in crystals in the presence of intense laser radiation

13 p1628 A73-29049

Charged stopping pions from nuclear-electromagnetic cascades in rock, calculating number and energy spectra by Monte Carlo method

13 p1671 A73-29667

Energy spectra and pitch angle distributions of precipitating incident and backscattered electron fluxes in auroral arcs

14 p1747 A73-29968

Iron energy spectra due to acceleration at neutron star surface vs primary cosmic rays

14 p1787 A73-30618

On the atmospheric kinetic energy spectrum and its estimation at some selected stations.

14 p1750 A73-30763

Universality of the power spectra of relativistic electrons generated in a turbulent plasma

14 p1782 A73-30808

Influence of heating on the intensity and energy of exoelectrons in deformed aluminum

14 p1765 A73-30889

Mars 3 solar wind probe of upper Mars atmosphere, showing plasma interaction with ionosphere measured by energy spectra

15 p1930 A73-31150

Anisotropy and energy spectra of newly-generated photoelectrons

15 p1867 A73-31265

On a possible mechanism responsible for the differential energy spectrum of relativistic electrons and non-linear low-frequency spectra of cosmic radio sources.

15 p1927 A73-32005

Null correlation method for estimation of the primary energies of cosmic ray jets.

15 p1927 A73-32149

Russian book - Electrons and holes in semiconductors: Energy spectrum and dynamics.

15 p1852 A73-32298

Dependence of the length of auroral rays on auroral activity level.

16 p2002 A73-32782

Charge and energy spectra of cosmic rays with Z equal to or greater than 30.

16 p2054 A73-33279

Solar proton, helium, and medium nuclei /Z from 6 to 9/ observed from the IMP-VI satellite.

16 p2054 A73-33280

Charge and energy spectra of particles with E from 0.2 to 30 MeV/nuc in the January 25, 1971 solar flare.

16 p2054 A73-33281

Calculations of neutron flux spectra induced in the earth's atmosphere by galactic cosmic rays.

16 p2055 A73-33426

Investigation of the lunar surface by the method of the scattering of radio waves emitted by lunar satellites

16 p2064 A73-33773

A new test for solar modulation theory - The 1972 May-July low-energy galactic cosmic-ray proton and helium spectra.

17 p2224 A73-34769

The effects of the observational system and the method of interpolation on the computation of spectra.

17 p2201 A73-34852

High resolution nondispersive electron energy analyzer for electron spectroscopy for chemical analysis, using spherical mirror and grid retarding potential field as filters

17 p2176 A73-35770

Medium-range forecasting of large-scale atmospheric circulation components on the basis of a nonlinear spectral model

18 p2331 A73-35910

Differential energy spectrum of low-energy protons in the inner regions of the radiation belt

18 p2345 A73-36110

Sounding balloon nuclear emulsion chamber recording of energy spectra and angular distribution of incoming and outgoing proton fluxes in atmosphere

18 p2310 A73-36124

Upper atmospheric turbulence kinetic energy spectrum from radio meteor trails observations, noting relationship to structure function for isotropic turbulence

18 p2312 A73-36288

Simple universal equilibrium spectrum.

18 p2300 A73-36634

Evidence for the softening of the cosmic-ray electron spectrum at a few hundred GeV and the origin of the galactic-ridge X-radiation.

18 p2348 A73-37102

Energetic neutrons leaking from the top of the atmosphere.

19 p2474 A73-37299

Rocket measurement of photoelectrons in the ionosphere by K-9 M-40.

19 p2474 A73-37379

On the energy spectrum of relativistic electrons in the Crab Nebula.

19 p2475 A73-37619

Multipoint distribution calculation of the isotropic turbulent energy spectrum.

19 p2421 A73-37854

Atmospheric gamma ray spectra from balloon spectrometer scintillator measured energy loss spectra

19 p2476 A73-37909

Turbulence spectra, length scales and structure parameters in the stable surface layer.

19 p2448 A73-38216

Turbulence spectra at scales smaller than 1 meter.

19 p2449 A73-38241

Waveguide channel point source electric field level and phase derived by Rytov smooth perturbation technique, obtaining correlation functions, energy spectra and phase fluctuations

19 p2406 A73-38338

Dynamic variations in intensity and energy spectra of electrons in the inner radiation belt.

20 p2601 A73-38934

Ring current particle distributions during the magnetic storms of December 16-18, 1971.

20 p2552 A73-38952

Energy spectra and pitch angle distributions of storm-time and substorm injected protons.

20 p2552 A73-38953

Proton flux density and differential energy spectra recorded by solid state proton detectors and three-axis fluxgate magnetometer aboard Explorer 45 at plasmopause

20 p2552 A73-38955

Energy spectra of velocity pulsations in a turbulent boundary layer on a permeable plate

20 p2547 A73-39286

Photoelectron energy spectra for atomic and molecular binding energies, examining spectrum signatures, angular distribution, autoionization, rare gases, carbon monoxide and cyanocobalamin

20 p2520 A73-39634

Free atom and molecule energy levels studied by electron scattering spectroscopy, discussing energy losses, monochromated electron beams, particle resonance and electric fields

20 p2520 A73-39635

Energy spectrum of transition metals in the superconducting state 20 p2600 A73-39727

New tubes and techniques for flash X-ray diffraction and high contrast radiography. 21 p2696 A73-39974

Differential energy spectra of low-energy/less than 8.5 MeV per nucleon/ heavy cosmic rays during solar quiet times. 21 p2755 A73-40509

Determination and interpretation of solar proton spectra at the earth and in the source 21 p2756 A73-40584

Complete hydrogen and helium particle spectra from 30- to 60-MeV proton bombardment of nuclei with $A = 12$ to 209 and comparison with the intranuclear cascade model. 21 p2744 A73-41019

Energy spectra and angular distribution measurement for 10-100 MeV earth albedo neutrons by balloon sounding at 116,000 ft 21 p2761 A73-41380

Lunar orbital gamma ray measurements from Apollo 15 and Apollo 16. 21 p2762 A73-41397

Angular effects in the propagation of cosmic rays in the atmosphere. 21 p2764 A73-41629

Inertial range differences between Kolmogoroff energy spectrum formula for turbulence and modified Navier-Stokes equation, considering mu value deductibility 22 p2840 A73-41733

Prediction and measurement of the proportionality constant in statistical energy analysis of structures. 22 p2918 A73-41821

Chromospheric hydrogen and helium spectral lines investigation in solar flares determining plasma and ionization temperatures, energy spectra and electron density 22 p2903 A73-42066

Frequency of heavy ions in space and their biologically important characteristics. 22 p2805 A73-42178

Size spectra of extensive air showers and primary cosmic-ray spectrum. 22 p2903 A73-42427

Comparison of calculated characteristics of extensive atmospheric showers with experimental results at various altitudes 22 p2903 A73-42733

Auroral electron and proton flux density, energy spectra, acceleration and precipitation mechanisms and turbulent diffusion from rocket and satellite measurements 22 p2850 A73-42748

The abundances of galactic cosmic-ray carbon, nitrogen, and oxygen and their astrophysical implications. 22 p2914 A73-43012

Calorimeter for picosecond laser pulses. 22 p2872 A73-43153

Energy spectra of modulated relativistic electron beam as function of plasma density at beam-plasma interaction region boundary 23 p3009 A73-43505

The energy spectrum of cosmic ray muons at sea level 23 p3023 A73-43559

Energy spectrum and angular distribution of outer space muons and the processes of their production in the 1 TeV energy range 23 p3024 A73-43564

Energy spectra of localized elementary excitations for dilute solutions of He 3 atoms in superfluid He 4 using Feynman type wave function, considering Raman scattering 23 p3007 A73-44173

A device for recording the energy spectrum and fluxes of electrons with energies greater than 100 MeV in cosmic rays 24 p3124 A73-44782

Energy spectra of cosmic gamma-ray bursts. 24 p3125 A73-45053

Spectrometer design with particle preacceleration for measuring energy spectra of secondary electrons and photoelectrons with high resolution 24 p3092 A73-45553

ENERGY STORAGE

NT ELECTRIC ENERGY STORAGE

Influence of the parameters of the accelerating circuit of an injector with inductive energy storage on the process of plasma-cluster acceleration 02 p0196 A73-11633

Plasma jet acceleration by plasma injectors with capacitive and inductive energy storage for instantaneous breaking of charging circuit, noting energy conversion efficiency 02 p0196 A73-11712

Magnetic energy storage and transfer from coil into resistive load with superconducting switch, discussing voltage and circuit conditions for full normalization 02 p0200 A73-11830

Model coil test results for a pulsed superconducting magnet energy storage system. 02 p0132 A73-11831

Reliable uninterrupted controlled transient voltage dc power supplies with active energy storage element, comparing three system configurations, design features and applications 03 p0253 A73-13946

High strength straight filament superflywheel configurations with improved energy storage capability for vehicle, tool and power supply applications 04 p0475 A73-14744

Large-scale applications of superconducting coils. 07 p0863 A73-20107

Irreversible thermodynamics and losses in energy conversion, discussing N-port storage representation, flux rate, power flow and electro-caloric and state space relations 07 p0779 A73-20396

Spectral properties of laser crystal materials, noting deactivation energy storage in nonuniformly widened luminescence band 09 p1095 A73-22671

Laminated composites displacement equations of motion, obtaining stored kinetic and strain energy and free harmonic waves dispersion normal and along layers 09 p1161 A73-23117

Mechanical energy storage by flywheel with magnetic fluid hermetic seal and bearing, using anisotropic and whisker materials 11 p1399 A73-25979

A power and load priority control concept as applied to a Brayton cycle turbo-electric generator. 11 p1309 A73-25984

Transient processes in an inductive energy storage element for a plasma injector 12 p1460 A73-26931

The possibility of storing laser radiation scattered by an electron beam. 13 p1627 A73-28662

Radiating slot antenna immittance reactive term due to energy storage in feeding waveguide, discussing resonance characteristics 15 p1849 A73-31097

Charge-storage diodes with an internal field in the base 15 p1851 A73-31774

Analysis of the parameters of solar-heat power sources with energy storage units 17 p2108 A73-34283

Chemical laser and molecular amplifiers characteristics covering population inversion and vibrational energy generation, storage, distribution and transfer 18 p2321 A73-35902

Computer-aided design and graphics applied to the study of inductor-energy-storage dc-to-dc electronic power converters. 21 p2635 A73-40340

Transients in inductive energy-storage devices for plasma injectors. 22 p2891 A73-42265

ENERGY STORAGE DEVICES

U ENERGY STORAGE

ENERGY TRANSFER

Hemispheric synoptic analysis of upper stratospheric warming for energy transformations in troposphere and lower and middle stratosphere 01 p0072 A73-10141

IR radiative energy transfer in gases, applying spectroscopic band absorption information 01 p0120 A73-10291

Blast wave theory extension to time variable energy input, considering application to laser induced blast waves 01 p0121 A73-10760

Energy transfer between impurity molecules in the presence of relaxation 01 p0080 A73-11243

Energy transfer between interacting electromagnetic waves propagating in half space media, applying to acoustic surface wave excitation by electromagnetic converter 02 p0140 A73-11568

On the plasma sheet contribution to the force balance requirements in the geomagnetic tail. 02 p0156 A73-11746

Electromagnetic near field energy flow characteristics of dipole/monopole receiving rod antenna, investigating frequency dependence of antenna effective area shape 02 p0145 A73-11824

Magnetic energy storage and transfer from coil into resistive load with superconducting switch, discussing voltage and circuit conditions for full normalization 02 p0200 A73-11830

Steady state conditions for maximal and minimal energy transfer between any load form and any system displacement shape, examining coincidence and resonance 02 p0194 A73-12604

Ionization calorimeter measurement of energy transfer to electron photon cascade secondary particles during hadron interaction with lead nuclei 02 p0209 A73-12662

K-neutral pion inelasticity factor measurement for nucleon interactions in carbon corresponding to primary neutron energy transferred to pions 02 p0209 A73-12663

Calculations on energy transfer to a diatomic molecule in high-energy head-on collisions. 02 p0195 A73-12723

Numerical model of energy transfer in carbon monoxide-nitrogen laser, considering electron-molecule excitation and vibration-vibration exchange 02 p0178 A73-12816

Enhanced N2 vibrational temperatures in the thermosphere. 03 p0298 A73-12881

Alfven wave induced bulk velocity amplitudes in lower solar atmosphere, discussing relationship between energy flux, bulk velocity, wavelengths and scale height 03 p0360 A73-12944

A problem of coupling between the vibration of a thin plate and an acoustic field in a fluid 03 p0383 A73-12982

Plane Poiseuille flow with small amplitude modulated pressure gradient, noting disturbance shear wave and stability from energy transfer calculation 03 p0293 A73-13530

Averaged equations of cumulative-laser heating of plasma in Z-pinch with consideration of the recovery of the energy of nuclear fusion. 03 p0347 A73-13782

Averaged equations of cumulative-laser heating of two-temperature plasma in Z-pinch taking into account the nuclear fusion energy. 03 p0347 A73-13783

Astronomical applications of general relativity, considering energy and matter outbursts, black holes and Kerr and Schwarzschild metrics 03 p0374 A73-13895

Electron temperature elevation compared to gas temperature in hydrocarbon flames, discussing energy exchange mechanism 03 p0352 A73-14394

Shock-tube study of vibrational energy transfers in the CO2-N2 and the CO2-CO systems. 03 p0345 A73-14442

Multifrequency modulation of electron beam for instability oscillations control and energy transfer to plasma particles 04 p0479 A73-15044

Mass transport and energy of impulse compression wave traces in atmosphere due to radiation, inner friction, gravity and rotation effects 04 p0440 A73-15285

One dimensional analysis of saturation spectral lines for energy transfer in plasma waves interaction, noting Landau damping effect on parametric instability 04 p0482 A73-15650

Extinction of photoluminescence by electron irradiation and energy transfer in molecular crystals 05 p0600 A73-16555

Boundary layer characteristics with radiant energy transfer under adverse pressure gradient. 05 p0530 A73-16874

[AIAA PAPER 73-117] Heat pipe operation in a gravity field with liquid pool pumping. 05 p0640 A73-16876

[AIAA PAPER 73-120] Rotating black holes - Locally nonrotating frames, energy extraction, and scalar synchrotron radiation. 05 p0625 A73-17331

Confined plasma diffusion due to growing or nonlinearly saturated LF ion waves causing energy transfer from electrons to ions in slabs 05 p0604 A73-17368

Biophysical properties of vibration energy transfer to human body structure, noting harmful effects dependence on frequency range 06 p0657 A73-17748

Thermal conductivity and resonant multipole interactions. 06 p0725 A73-18121

Optimum R.F.-power transport in Nd-limited gallium-arsenide travelling-wave amplifiers. 07 p0798 A73-19159

Laser-excited vibrational energy transfer studies of HF, CO, and NO. 07 p0834 A73-19627

CW and pulsed deuterium fluoride-carbon dioxide transfer chemical laser with molecular vibrational energy transfer for population inversion to obtain high power output 07 p0834 A73-19630

A kinetic model and computer simulation for a pulsed DF-CO2 chemical transfer laser. 07 p0835 A73-19632

On the transmission of the energy in an incompressible magnetohydrodynamic wave into a conducting solid. 07 p0858 A73-20029

Transfer of Yb3+/ excitation energy to TR3+/ in CaF2 and BaF2 crystals 07 p0837 A73-20206

Calculation of probabilities of energy transfer - Application to the vibrational relaxation of the C5 radical in the presence of argon 07 p0854 A73-20608

Flares, magnetic configurations, and magnetic energy release. 08 p0996 A73-20764

The macroscopic high-frequency quantum generator and detector of the gravitational radiation. 08 p0987 A73-21017

Energy transport over turbulence spectrum of free atmosphere, using aircraft experiments 08 p0984 A73-21187

Heating of laser-induced plasmas in helium. 09 p1125 A73-21998

Monte Carlo simulation of a model ionosphere. II - Energy flow and energy dissipation. 09 p1075 A73-21229

Kinetics of the excitation of molecular vibrations by infrared laser radiation 09 p1094 A73-22597

Relaxation in a two-temperature plasma with directed motion of electrons 09 p1127 A73-22601

Enhanced energy transfer to a cylindrical plasma by an Alfvén wave. 09 p1128 A73-22629

Laser energy transfer - An analytic survey of high power applications. 09 p1096 A73-22822

Viscous energy transfer from elliptical orifice originated laminar three dimensional jet, using boundary layer assumptions in jet mixing region 09 p1072 A73-22827

Images and sound rays in the numerical calculation of echograms 09 p1121 A73-23104

Recent experimental and theoretical investigations of infrared and microwave molecular spectra of astronomical interest /Introductory report/. 09 p1123 A73-23127

Density homogeneity in a laser cavity due to energy release. 09 p1098 A73-23450

Isothermal wall conical cavity radiant energy streaming, determining annular baffle effects by Monte Carlo method 10 p1295 A73-23835

Energy transfer between impurity molecules during relaxation. 10 p1251 A73-24180

Spectral energy transfer models of turbulence decay compared with numerical simulation of three dimensional homogeneous isotropic turbulence, considering eddy viscosity and diffusion models 10 p1246 A73-24252

Extraction of energy and charge from a black hole. 10 p1280 A73-24342

Feedback in amplifier circuits synthesis and analysis, discussing energy transfer, source impedance and terminals 10 p1201 A73-24383

Coulomb collision induced mean-energy variations in homogeneous nonrelativistic plasma components, discussing two-component plasma and energy transfer rates 10 p1257 A73-24760

Negative energy mode loss to positive energy mode in positive-negative energy wave interactions within magnetized plasma, considering ion acoustic waves 11 p1402 A73-25123

Radiative slip between two adjacent absorbing-emitting gases and its application to air pollution. 11 p1353 A73-25722

Geomagnetic field polarity reversal mechanism, interpreting frequency distribution by energy exchange between dynamo models and conversion between kinetic and magnetic energies 11 p1355 A73-25792

Vibration-to-rotation and vibration-to-vibration energy transfer between diatomic molecules. 11 p1401 A73-25967

Energy flux into extending crack in elastic solid calculated in terms of stress intensity factor for plane and antiplane strain problems 11 p1444 A73-26281

Implicit difference method of temperature determination in problems of radiative gasdynamics 11 p1348 A73-26329

Thermodynamic methods applied to self gravitating n-body systems for different boundary conditions, considering energy transfer 11 p1427 A73-26604

Vibrational level populations in diatomic molecules during steady pumping 12 p1504 A73-26888

EUV and radio observation of energy flux from corona into chromosphere, considering coronal holes as source of high energy streams of solar wind 12 p1545 A73-27839

Short time constant limits of pulse duration on electromagnetic energy emission as function of frequency, applying to extragalactic radio astronomy observations 12 p1547 A73-27884

Energy transfer from a pulsed thermal source to He II below 0.3 K. 13 p1658 A73-28191

Pulsation energy calculations in axisymmetric turbulent jet flows of incompressible fluids with a zero excess impulse 13 p1600 A73-28448

Radiative transport in stars, considering radiation field, transfer equation and radiative heat equation 13 p1683 A73-28988

Optimization of energy transfer in cascaded fluid jet deflection amplifiers. 13 p1571 A73-29045

New estimate of annual poleward energy transport by Northern Hemisphere oceans. 13 p1610 A73-29225

Energy and diffusive mass transport relation to thermospheric circulation, composition, temperature and mass density from three dimensional two constituent magnetic storm model 14 p1748 A73-29975

Calculation of radiant energy transfer by the Galerkin method 15 p1956 A73-30963

The excitation of atomic oxygen to the 0/1 S/ level by energy transfer from N₂/A 3 Sigma u+/- molecules in aurora. 15 p1866 A73-31075

Histochemical investigation of some energy metabolism characteristics in a rat heart after acute fatigue 15 p1834 A73-31393

Effect of prolonged hypokinesia on certain energy transfer characteristics in skeletal muscles and some internal organs 15 p1834 A73-31505

Interacting continuum theory concerning steady shock wave in composite materials, discussing energy interaction terms error correction effects on Hugoniot relations 15 p1949 A73-31685

Superexchange potential and kinetic energy theory in molecular orbital and configurational interaction approximation for three center four electron model of ferrimagnetic materials 15 p1924 A73-32156

Quasi-monochromatic viscoelastic waves energy velocity equivalence to phase velocity for medium represented by standard linear solid or Maxwell model 15 p1955 A73-32176

Eddy power flow of electromagnetic waves. 16 p1980 A73-33690

Two fluid models for solar wind heating under boundary conditions, considering enhanced energy transfer between electrons and protons in kinetic theory calculations 17 p2224 A73-34515

Effect of a connecting plane link on the excitation and propagation of flexural oscillations in parallel plates 17 p2244 A73-34737

Russian book on radiative and complex heat transfer covering electromagnetic energy-matter interaction, modeling, convective and conductive transfer and thermodynamic equilibrium radiation 17 p2254 A73-34899

Satellite monitoring of climate parameters, discussing energy transfer in atmosphere, energy distribution, radiation balance, climatic models 17 p2205 A73-34928

Vibrational relaxation in the HF-HCl, HF-HBr, HF-HI, and HF-DF systems. 17 p2119 A73-35176

Laser power and vibrational energy transfer in CO₂ lasers. 17 p2185 A73-35177

IR laser induced change in atmospheric temperature as function of time, using kinetic model with input molecular energy transfer rates for thermal blooming 17 p2163 A73-35414

Kinetic energy transfer during multiple jet mixing from primary jet array to secondary stream for various velocity ratios 17 p2156 A73-35511

Planetary atmospheric entry vehicles shock layer energy transport with nongray radiation, using optical thick-thin approximation for radiative transfer in temperature distribution calculation 18 p2369 A73-36334

[AIAA PAPER 73-715] The correlation between the kinematic structure of the flow and the energy transfer in the rotors of fluid flow machines 18 p2299 A73-36487

Effect of aerosols on the transfer of solar energy through realistic model atmospheres. I - Non-absorbing aerosols. 18 p2333 A73-36704

Energy transport by photoelectrons in the early morning ionosphere. 18 p2348 A73-37027

On energy, group velocity and small damping of sound waves in ducts with shear flow. 18 p2302 A73-37031

Thermal instabilities and energy relations in convective shells of slowly rotating stars 19 p2481 A73-37346

Decay of the kinetic energy of compressible micropolar fluids. 20 p2547 A73-39341

Atmospheric gravity waves and the energy of the jet stream. 21 p2729 A73-40091

Relationship between the hydraulic losses of a centrifugal wheel and the energy imparted by the wheel to the fluid by circulation in the relative motion 21 p2676 A73-40407

The momentum-energy tensor of an electromagnetic field 21 p2739 A73-40446

Laser induced red-blue energy transfer upconversion in Pr³⁺/doped lanthanum fluorides via excitation annihilation involving pairs of ions 21 p2715 A73-40934

Chromium-rare-earth energy transfer in YAlO₃. 21 p2752 A73-40957

Chromium-ytterbium energy transfer in silicate glass. 21 p2752 A73-40963

Effect of training with eccentric muscle contractions on skeletal muscle metabolites. 21 p2641 A73-41523

Linear convective modes and the energy transport in stellar convection zones. 22 p2905 A73-41761

Acoustic turbulence generation of shock waves in compressed gas or plasma excited by random potential forces based on energy transfer along spectrum 22 p2840 A73-41809

Energy propagation lines in the diffraction of a plane electromagnetic wave by a slot in a conductive plane 22 p2826 A73-42353

Measurements of the energy exchange between earth and space from satellites during the 1960's. 22 p2851 A73-42858

Stress amplification in a ring caused by dynamic instability. [ASME PAPER 73-APMW-35] 22 p2925 A73-42893

Influence of fiber property variation on composite failure mechanisms. 23 p2996 A73-43643

Single particle approximation analysis of particle velocity changes influence on plasma motion across nonhomogeneous magnetic field, examining energy exchange between particles 23 p3010 A73-43662

Transition of a low-pressure plasma into a highly ionized state 23 p3013 A73-44335

Relaxation of longitudinal and transverse temperatures in a plasma with directional motion of electrons 23 p3014 A73-44336

Radial and vertical force balance in primitive solar nebula, describing techniques for gravitational potential and gas opacity computation for energy transport 23 p3127 A73-44392

Tropospheric vertical energy transfer due to terrestrial and atmospheric water vapor and carbon dioxide radiation calculated for vertical atmospheric temperature and composition distributions 24 p3082 A73-44736

Northern summer tropical upper tropospheric large scale flow dynamics, energy exchange diagram and limited area numerical weather prediction problems 24 p3108 A73-45094

Energy deposition of protons in molecular nitrogen and applications to proton auroral phenomena. 24 p3126 A73-45116

Electron cooling rates calculation based on measured impact cross sections of molecular oxygen for vibrational and low lying electronic excitation 24 p3086 A73-45123

A numerical, thermo-mechanical model for the welding and subsequent loading of a fabricated structure. 24 p3150 A73-45231

Transfer of energy to light ions from the ion-acoustic-wave instability developed in a heavy-ion plasma. 24 p3117 A73-45406

Excitation mechanisms in He-Cd and He-Zn ion lasers. 24 p3097 A73-45418

ENGINE ANALYZERS

Portable self contained computerized in-aircraft engine analyzer with cassette tape resident program control and digital display and punched card indicators [AIAA PAPER 72-1080] 03 p0307 A73-13403

ENGINE CONTROL

NT ROCKET ENGINE CONTROL

NT TURBOJET ENGINE CONTROL

Control of electron bombardment ion engine for stationary satellite. 01 p0090 A73-11110

Digital control mounts on jet engine. 05 p0608 A73-17249

Minicomputer application to in-flight control of A300-B airbus engines, describing computational procedure for low pressure compressor stage RPM limit /N 1 limit/ 15 p1831 A73-32477

The use of a hybrid computer in the optimization of gas turbine control parameters. [ASME PAPER 73-GT-13] 16 p2047 A73-33491

Control of turbofan lift engines for VTOL aircraft. [ASME PAPER 73-GT-20] 16 p2047 A73-33496

- Potential payoffs of variable geometry engines in fighter aircraft. 17 p2099 A73-34436
- Integrated Propulsion Control System program. [SAE PAPER 730359] 17 p2222 A73-34707
- T700 fuel and control system - A modern system today for tomorrow's helicopters. [AHS PREPRINT 771] 17 p2109 A73-35089
- Turbine engine control system design based on linearized and nonlinear mathematical models accounting for thermodynamic performance. 18 p2343 A73-36995
- Application of digital computer APU modeling techniques to control system design. 19 p2392 A73-38416
- Optical diffraction grating design and production, discussing application of interferometry and electronics to ruling engine control. 21 p2698 A73-40136
- Airframe/propulsion system interactions - An important factor in supersonic aircraft flight control. [AIAA PAPER 73-831] 21 p2634 A73-40501
- The vapour core pump vortex inlet valve. 23 p2941 A73-43393
- ### ENGINE COOLANTS
- Additives for heat transfer reduction in the propellant combinations N2O4-MMH and N2O4-A-50. [AIAA PAPER 72-1132] 03 p0352 A73-13439
- Experiments on a shrouded, parallel disk system with rotation and coolant throughflow. [AD-759594] 08 p1023 A73-21256
- Air/water mist spray coolant for high gas temperature and pressure environment at gas turbine inlet. 17 p2221 A73-34388
- Heat transfer in rotating cylindrical enclosures with axial inflow and outflow of coolant. 19 p2504 A73-37877
- ### ENGINE DESIGN
- #### NT ROCKET ENGINE DESIGN
- Pegasus vectored thrust turbofan engine for Harrier class VISTOL aircraft, describing design and operational details. 01 p0090 A73-10200
- Synerjet composite rocket-air breathing propulsion system for reusable spacecraft mission profile optimization, discussing multimode operation and performance capabilities. 01 p0112 A73-11300
- A rapid matching procedure for twin-spool turbobfans. 02 p0202 A73-11593
- Development of pulsed hydrogen/oxygen attitude-control engines. [DGLR PAPER 72-077] 02 p0202 A73-11689
- Design study for long-lived compact 750 kW industrial gas turbine, discussing optimal aerodynamic proportioning and size determination. [ONERA, TP NO. 1174] 02 p0204 A73-12791
- Computer programs for air cooled gas turbine engine design and performance prediction, noting aerodynamic effect of turbine coolant. 02 p0129 A73-12848
- Possibilities of rationalizing the design of flow-through turbomachine components. 03 p0353 A73-13239
- Electric generator inside turbojet or turbofan aircraft engine to reduce need for external gearbox, simplifying nacelle assembly and increasing aircraft design flexibility. [AIAA PAPER 72-1056] 03 p0252 A73-13387
- Engine technology for large subsonic nuclear powered aircraft. [AIAA PAPER 72-1062] 03 p0353 A73-13391
- One-millipound colloid thruster system development. [AIAA PAPER 72-1153] 03 p0356 A73-13456
- Recent developments in large area ratio thrust augmentors. [AIAA PAPER 72-1174] 03 p0357 A73-13470
- Integrated engine-airframe design with fuselage boundary layer ingestion for subsonic-transonic cruise, discussing STOL thrust control via variable pitch fan for landing. 03 p0251 A73-14128
- Development of the Olympus turbojet to meet supersonic civil transport requirements. 03 p0359 A73-14131
- Stoichiometric gas turbines - Development problems. 03 p0359 A73-14146
- Aircraft engine development in terms of money, manpower, facilities and knowledge, discussing project organization and scheduling. 03 p0251 A73-14469
- Engine concepts for space applications. 03 p0360 A73-14475
- Russian book - VTOL aircraft power plants. 04 p0487 A73-15706
- Russian book on aerodynamic design of axial flow turbomachine blades covering direct and inverse problems for axisymmetric flow in axial turbomachines. 04 p0404 A73-15709
- Conformal mapping for Cs ion engine beam optical system with laminar flux, calculating design parameters for current limitation by Cs flow. 04 p0488 A73-15722
- Ion engines with ion emission from liquid metal drops under electric field, noting emitter I-V characteristics and engine design. 04 p0488 A73-15726
- Thermodynamic considerations for the design of a sonic-boom reducing powerplant. [ASME PAPER 72-WA/AERO-3] 04 p0404 A73-15907
- Army 1500 shp advanced technology engine development program, discussing in components design and fabrication, air leakage losses, environmental testing and maintainability oriented design. [SAE PAPER 720828] 05 p0606 A73-16627
- Airbreathing engines for Space Shuttle. [SAE PAPER 720805] 05 p0607 A73-16647
- The evolution and development status of the ALF 502 turbofan engine. [SAE PAPER 720840] 05 p0607 A73-16654
- TF34 and F101 turbofan engines for Navy S-3A ASW aircraft and USAF B-1 strategic bomber, respectively, discussing design features, manufacturing techniques and testing procedures. [SAE PAPER 720841] 05 p0607 A73-16655
- F100/F401 augmented turbofan engines - High thrust-to-weight propulsion systems. [SAE PAPER 720842] 05 p0607 A73-16657
- A testing procedure for flame arrestors for marine spark ignition engines. [WSCI PAPER 72-34] 05 p0563 A73-16681
- Development trends in design methods for aircraft engine compressors. II - Centrifugal-flow compressors. 06 p0741 A73-17996
- Lubricants thermophysical properties effects on gas turbine engine design, considering thermal stability, vapor pressure, autoignition, load capacity and bearing life. 07 p0843 A73-19563
- Development trends in aircraft-engine compressor design methods. III. 07 p0867 A73-19605
- A description of two low cost turbo-compressors built for powered lift research. 07 p0867 A73-19942
- TF-34 turbofan engines for S-3A and AX aircraft respectively, discussing technological development, and components and characteristic features. 07 p0868 A73-20350
- Space shuttle air breathing gas turbine engine design, modification, weight and test requirements associated with launch, space residence and reentry. 07 p0906 A73-20463
- Designing turbomachine blades for forced vibrations under various excitation conditions. 07 p0917 A73-20503
- Influence of a change in the throughput of the power turbine on the parameters of a dual-shaft gas turbine engine. 10 p1262 A73-23599
- Combustor design effect on jet aircraft engine exhaust pollutants reduction during hydrocarbon fuel burning. 10 p1263 A73-24556
- Performance of an auxiliary power unit on anhydrous hydrazine. 11 p1308 A73-25980
- A reappraisal of design methods for inward flow radial gas turbines. 11 p1411 A73-26370
- Analysis of the operational parameters of a bypass turbojet. 12 p1532 A73-27069
- A modern mechanical laboratory for the support of aircraft engine design. 12 p1486 A73-27385
- Concorde Olympus 593 axial flow turbojet engine design, detailing variable geometry intake and exhaust nozzles, noise abatement, combustion chamber, gearing and fuel system. 13 p1669 A73-28156
- Design and evaluation of combustors for reducing aircraft engine pollution. 13 p1670 A73-28932
- Protective coating systems for Navy aircraft turbine engines. [NACE PAPER 113] 13 p1637 A73-29313
- GT-D-350 gas turbine engine for Soviet Mi-2 twin engine helicopter, describing compressor, combustion chamber, turbine, reduction gear, exhaust, starting, lubrication, deicing and fuel systems. 14 p1785 A73-30450
- Russian book - Pioneers rocket engineering: Selected works /1929-1945/. 15 p1943 A73-31576
- Inlet duct sonic fatigue induced by the multiple pure tones of a high bypass ratio turbofan. 16 p2046 A73-33141
- Aircraft produced environmental noise and air pollution, discussing related aircraft power plant technology evolution. 16 p2047 A73-33191
- Low emissions combustion for the regenerative gas turbine. I - Theoretical and design considerations. [ASME PAPER 73-GT-11] 16 p2086 A73-33489
- Aerodynamic study of a turbine designed for a small low-cost turbofan engine. [ASME PAPER 73-GT-29] 16 p2048 A73-33500
- High bypass ratio quiet turbofan engine for STOL aircraft, emphasizing noise reducing design based on low-speed variable pitch fan concept. 16 p2049 A73-34040
- Experiments on the design of a small axial turbine. 17 p2092 A73-34379
- Effect of 'bulk' heat transfers in aircraft gas turbines on compressor surge margins. 17 p2221 A73-34382
- Potential payoffs of variable geometry engines in fighter aircraft. 17 p2099 A73-34436
- Market trends and technical progress in small gas turbine engines for general aviation and executive aircraft and helicopters. 17 p2256 A73-34447
- 'Quiet' aspects of the Pratt & Whitney Aircraft JT15D turbofan. [SAE PAPER 730289] 17 p2101 A73-34654
- Engine cycle considerations for future transport aircraft. [SAE PAPER 730345] 17 p2222 A73-34693
- Noise reduction modifications in JT3D and JT8D gas turbine engine by single stage fan replacements. [SAE PAPER 730346] 17 p2222 A73-34694
- Profitable transport engines for the environment of the eighties. [SAE PAPER 730347] 17 p2257 A73-34695
- Civil STOL aircraft engine thrust reverser and fast selection control system designs for high performance, low specific weight and acoustic compatibility requirements. [SAE PAPER 730358] 17 p2222 A73-34706
- Navy development of low-cost supersonic turbojet engines. [SAE PAPER 730362] 17 p2222 A73-34708
- Turbine powerplants for missiles - Cost improvement requirements. [SAE PAPER 730364] 17 p2222 A73-34709
- Review of engine maintenance concepts applied to wide body jets. [SAE PAPER 730375] 17 p2178 A73-34714
- Status of current development activity related to STOL propulsion noise reduction. [SAE PAPER 730377] 17 p2222 A73-34716
- Design studies of low-noise propulsive-lift airplanes. [SAE PAPER 730378] 17 p2103 A73-34717
- Realization of a geostationary orbit by means of an electromagnetic propulsion system /quasi-steady MPD/. 17 p2239 A73-34954
- Application of compressibility correction to calculation of flow in inlets. 18 p2265 A73-36395
- Subsonic aircraft turbojet engines, discussing thermodynamic cycles, entry temperature increase, propulsion efficiency and economy improvements and ecological requirements. 18 p2343 A73-36994
- Turbine engine control system design based on linearized and nonlinear mathematical models accounting for thermodynamic performance. 18 p2343 A73-36995
- Variable pitch turbofan driven at constant speed through reduction gear to obtain cost-efficiency compromise for future STOL and business aircraft applications. 18 p2343 A73-36998
- Aircraft installation requirements and considerations for variable pitch fan engines. [AIAA PAPER 73-807] 19 p2379 A73-37465
- Space shuttle liquid propellant reusable rocket engine design, discussing regenerative cooling, fuel pump, oxidizer turbopumps and electronic control systems. 19 p2492 A73-37597
- Calculating the fundamental oscillations in turboengine blades with different types of excitation. 19 p2499 A73-37778
- Turbofan suction noise level measurements, discussing octave noise analysis, angular velocity distributions, discharge coefficient, takeoff and landing operations. 19 p2473 A73-37816
- Book - Engine emissions: Pollutant formation and measurement. 19 p2474 A73-38321
- Aircraft economics and its effect on propulsion system design. [AIAA PAPER 73-808] 19 p2388 A73-38372
- A solar engine using the thermal expansion of metals. 19 p2392 A73-38473
- Optimum propulsion system design for advanced technology commercial transport, emphasizing low noise and emission, performance, reliability, maintainability and economics. [AIAA PAPER 72-760] 20 p2600 A73-38648

- RB-211 turbofan engine development, in-service problems and modifications for performance improvement 20 p2600 A73-39660
- High power carbon dioxide-nitrogen gasdynamic laser vibration kinetics model, suggesting closed cycle photon generator engine for energy conversion to work 21 p2710 A73-40094
- Small-scale suppressor of the aerodynamic noise of a subsonic gas jet 21 p2754 A73-40404
- A method of complex design of the meridional form of the air flow path of a multistage axial-flow compressor 21 p2633 A73-40477
- Dimensionless pressure method to account for air density variations in gas turbine cooling system design 21 p2677 A73-41051
- Experimental investigation of a gas-augmented water-jet engine model 22 p2841 A73-42126
- Acoustic investigation of the engine-over-the-wing concept using a D-shaped nozzle. [AIAA PAPER 73-1030] 24 p3122 A73-44860
- Aircraft gas turbine engines with single crystal blades to avoid conventional casting grain boundary weakness and premature damage 24 p3094 A73-45155
- ENGINE FAILURE**
- A method of early failure detection for gas turbines. 05 p0581 A73-16186
- Investigation of iron content of lubricating oil using a ferrograph and an emission spectrometer. 10 p1218 A73-24165
- Prediction of height-velocity boundaries for rotorcraft by application of optimization techniques. 12 p1459 A73-27175
- Fluidic control modules with temperature sensor and thrust reverser pneumatic actuator for aerospace system applications, investigating reliability test data. 16 p1971 A73-33477
- Macrofractographic studies of fatigue fractures in aircraft engine elements 21 p2754 A73-41593
- Principal failures of turbines during turbine engine operation 24 p3122 A73-45196
- ENGINE INLETS**
- Contribution to the problem of suction of foreign bodies into engine intakes [DGLR PAPER 72-107] 02 p0202 A73-11687
- Method for increasing wind tunnel Mach number for large-scale inlet testing. 03 p0287 A73-13416
- A method of testing full-scale inlet/engine systems at high angles of attack and yaw at transonic velocities. [AIAA PAPER 72-1097] 03 p0287 A73-13417
- Aircraft engine inlets total pressure fluctuations and distortion factors, presenting extreme-value statistical method for maximum distortion level probability estimate [AIAA PAPER 72-1100] 03 p0354 A73-13419
- Inlet produced flow distortion effect on compressor stability and engine stall, presenting unified theoretical analysis technique for compatible inlet/engine design [AIAA PAPER 72-1115] 03 p0355 A73-13430
- Boundary layer bleed system design for supersonic inlets, discussing bleed hole geometry effects on boundary layer velocity profile and inlet efficiency [AIAA PAPER 72-1138] 03 p0243 A73-13445
- Prediction of inlet duct overpressures resulting from engine surge. [AIAA PAPER 72-1142] 03 p0243 A73-13448
- Development of aft inlets for a ramjet powered missile. 03 p0246 A73-14133
- Inlet-combustor interface problems in scramjet engines. 03 p0360 A73-14153
- A procedure for estimating maximum time-variant distortion levels with limited instrumentation. [AIAA PAPER 72-1099] 04 p0432 A73-14908
- Results of an experimental program for the development of sonic inlets for turbofan engines. [AIAA PAPER 73-222] 06 p0645 A73-17664
- Ceramics replacement for Ni-Cr superalloys to improve automotive gas turbine performance by increasing inlet temperature, considering material selection 15 p1897 A73-31250
- Inlet duct sonic fatigue induced by the multiple pure tones of a high bypass ratio turbofan. 16 p2046 A73-33141
- Pressure measurements for establishing inlet/engine compatibility. 17 p2221 A73-34609
- Noise reducing choked /sonic/ inlet design for V/STOL jet aircraft, discussing aerodynamic theoretical and experimental studies 19 p2375 A73-37295
- Evaluation of F-15 inlet dynamic distortion. [AIAA PAPER 73-784] 19 p2379 A73-37454
- F-12 series aircraft propulsion system performance and development. [AIAA PAPER 73-821] 19 p2380 A73-37473
- Inlet geometry and axial Mach number effects on fan noise propagation. [AIAA PAPER 73-1022] 24 p3122 A73-44854
- ENGINE MONITORING INSTRUMENTS**
- The development of a device for measuring fuel consumption 02 p0165 A73-11521
- Integrated engine diagnostics and displays for Navy aircraft of the 1980's. [AIAA PAPER 72-1084] 03 p0354 A73-13406
- A method of early failure detection for gas turbines. 05 p0581 A73-16186
- Jet engine condition monitoring without aids. [SAE PAPER 720815] 05 p0606 A73-16640
- Book - Aircraft Instruments: Principles and applications. 06 p0693 A73-18075
- Condition monitoring - A new technology for aircraft engine maintenance 12 p1486 A73-27389
- Concorde engine monitoring instrumentation, discussing start cycle, temperature sensors and indicators and nozzle position indicators 14 p1754 A73-30931
- Jet engine malfunction diagnosis - The sensing problem, candidate solutions and experimental results. 17 p2222 A73-35243
- Some designs using sheathed thermocouple wire for jet engine applications. 22 p2858 A73-42042
- Trends of design in gas turbine temperature sensing equipment. 22 p2858 A73-42043
- Utilization of semiartificial thermocouples in gas-turbine engine tests 23 p2982 A73-43743
- ENGINE NOISE**
- NT ROCKET ENGINE NOISE**
- NASA Quiet Engine Program review and test results, discussing noise reduction technology application to transport aircraft 02 p0204 A73-12845
- An experimental study on noise reduction of axial flow fans. 03 p0241 A73-12961
- Subsonic aircraft noise - A solution by the wider application of today's new engines. 03 p0249 A73-13062
- Jet noise suppression for commercial CTOL, STOL and SST aircraft, discussing various devices effectiveness 03 p0251 A73-14130
- Noise sources analysis for high and low bypass ratio turbofan engines, considering jet, compressor, fan and turbine sound generation mechanisms 03 p0359 A73-14138
- The aeroplane as a threat to the environment. 03 p0251 A73-14468
- Engine noise reduction by fan blade tip speed reduction and high lift coefficient operation, presenting full scale test results 06 p0740 A73-17571
- Current Pratt & Whitney engine noise reduction programs. [AIAA PAPER 73-8] 06 p0740 A73-17603
- Ducts, nacelles, power source components and cabin noise sources identified for aircraft noise control research, considering prerequisites for quiet operations [SAE AIR 1079] 08 p0928 A73-20698
- Aircraft turboengine noise, discussing noise level/power output relations 10 p1262 A73-23861
- Jet aircraft engine noise reduction. 10 p1263 A73-24555
- A single number rating for effective noise reduction. 11 p1397 A73-25000
- Recent advances in aircraft noise reduction. 13 p1570 A73-29104
- Reduction of aircraft noise during stationary runs 13 p1570 A73-29651
- Concorde engine noise reduction at takeoff, initial climb and landing, discussing noise sources research and exhaust system nozzle modifications 14 p1785 A73-30930
- Aircraft engine noise reduction state of art, discussing FAA requirements, Concorde, DC-9 and Bertin Aladin II aircraft 16 p1967 A73-32970
- Standard indoor method of collection and presentation of the bare turboshaft engine noise data for use in helicopter installations. [SAE ARP 1279] 16 p2046 A73-33020
- Technology developments effect on jet aircraft design, discussing flight controls, engine noise suppression, supercritical aerodynamics and composite structures 16 p1968 A73-33188
- High, bypass fan engines for quiet propulsion and optimal aircraft performance in military and commercial applications 16 p2046 A73-33190
- Ground and air transportation noise propagation and effects, including aircraft engines, airfoils, sonic booms, auto traffic, railroads, subways, seismic noise and vibration 17 p2100 A73-34460
- Progress in the development of optimally quiet turboprop engines and installations. [SAE PAPER 730287] 17 p2221 A73-34652
- New low-pressure-ratio fans for quiet business aircraft propulsion. [SAE PAPER 730288] 17 p2221 A73-34653
- 'Quiet' aspects of the Pratt & Whitney Aircraft JT15D turbofan. [SAE PAPER 730289] 17 p2101 A73-34654
- Shrouded Q-FAN propulsor for light aircraft, discussing propulsion system performance, weight, noise and cost trends [SAE PAPER 730323] 17 p2221 A73-34680
- A dynamics approach to helicopter transmission noise reduction and improved reliability. [AHS PREPRINT 772] 17 p2106 A73-35090
- Jet aircraft noise research, emphasizing pure jet mixing noise, shock wave associated noise, and tail-pipe noise produced in engine or nozzle exit plane 17 p2096 A73-35332
- Jet engine noise reduction technology and design, discussing sonic pressure probes, high bypass turbofan engines, noise source fluctuations and far field measurements 19 p2472 A73-37287
- Aircraft engine fan noise radiation from inlet and discharge ducts, describing wind tunnel tests and noise spectra at various blade tip speeds 19 p2472 A73-37288
- Recent studies of fan noise generation and reduction. 19 p2473 A73-37293
- Combustion noise prediction techniques for small gas turbine engines. 19 p2473 A73-37296
- Noise from turbomachinery. [AIAA PAPER 73-815] 19 p2473 A73-37469
- Optimum propulsion system design for advanced technology commercial transport, emphasizing low noise and emission, performance, reliability, maintainability and economics [AIAA PAPER 72-760] 20 p2600 A73-38648
- Rolls-Royce RB-211 jet engine noise reduction program, considering fan, compressor, turbine and tail-pipe noise and acoustic linings and powerplant configurations 22 p2900 A73-41717
- Conventional and high frequency hearing of naval aircrewmembers as a function of noise exposure. 23 p2949 A73-43500
- Swirling flow effect on jet noise suppression based on acoustic field and engine thrust measurements with and without stationary swirl vanes in exhaust nozzle [AIAA PAPER 73-1003] 24 p3077 A73-44836
- Noise generation by turbulent combustion, discussing sound power, spectral content, enclosure effect, and importance in turbopropulsion system core engine noise [AIAA PAPER 73-1023] 24 p3155 A73-44855
- Turbofan engine core noise prediction and measurement, considering sources from flow passage obstructions, combustion chamber and turbine noise due to interaction with upstream turbulence [AIAA PAPER 73-1026] 24 p3122 A73-44857
- Low frequency noise generation within aircraft gas turbine engine core portion, discussing sources prediction, model and full scale engine tests, and future technology [AIAA PAPER 73-1027] 24 p3122 A73-44858
- Aircraft noise reduction alternatives for operational aircraft, noting noise generation upstream of final nozzle, reengining, refanning and suppressor techniques 24 p3123 A73-45374
- ENGINE PARTS**
- Automated test stands for full scale aircraft structure and engine parts fatigue tests, noting equipment for programmed static and dynamic loading 02 p0166 A73-11629
- Low-cost fluid film bearings for gas turbine engines. [SAE PAPER 720740] 02 p0174 A73-12006
- Applying surface integrity principles in jet engine production. 03 p0312 A73-13272
- Hydrogen oxygen propulsion component design and hot firing tests for space shuttle auxiliary systems and upper stage applications [AIAA PAPER 72-1156] 04 p0486 A73-14918
- Improved M50 aircraft bearing steel through advanced vacuum melting processes. 04 p0455 A73-15746
- Electrochemical machining application to aircraft gas turbine engine components manufacture, discussing removal rate, accuracy and surface finish capability [SME PAPER MR 72-536] 06 p0697 A73-18093
- Solid propellant rocket engines - Design and development of components in refractory and stratified materials. 07 p0867 A73-18992

- TF-34 turbofan engines for S-3A and AX aircraft respectively, discussing technological development, and components and characteristic features
07 p0868 A73-20350
- Probability theory for vibrational strength of turbomachine parts, calculating statistical maximum stress for given stress distribution conditions
07 p0917 A73-20502
- Hot die forging/gatorizing/ technique for Ti and heat resistant alloys jet engine parts, emphasizing material and cost savings
09 p1089 A73-23293
- Superalloys processing technology for aircraft gas turbine applications, discussing developments in eutectics and powder metallurgy for increased operating temperatures
13 p1636 A73-28931
- Improved corrosion protection for solid rocket propulsion systems.
13 p1645 A73-29273
- GTD-350 gas turbine engine for Soviet Mi-2 twin engine helicopter, describing compressor, combustion chamber, turbine, reduction gear, exhaust, starting, lubrication, deicing and fuel systems
14 p1785 A73-30450
- German monograph on bypass turbojet propulsion systems with jet mixing covering engine parts, thrust characteristics and fuel consumption
14 p1785 A73-30671
- Balancing equipment for jet engine components, compressors, and turbine - Rotating type for measuring unbalance in one or more than one transverse planes.
[SAE ARP 587A] 16 p1993 A73-33013
- Remanufacture of jet engine compressor components.
[ASME PAPER 73-GT-43] 16 p2048 A73-33504
- Silicon nitride materials for gas turbine components.
[ASME PAPER 73-GT-47] 16 p2048 A73-33508
- Hot isostatic pressing of titanium alloys for turbine engine components.
[ASME PAPER 73-GT-63] 16 p2019 A73-33516
- A performance data acquisition and analysis system for turbine engine component testing.
17 p2146 A73-34610
- Probability theory for vibrational strength of turbomachine parts, calculating statistical maximum stress for given stress distribution conditions
19 p2499 A73-37777
- Macrofractographic studies of fatigue fractures in aircraft engine elements
21 p2754 A73-41593
- Application of electron beam welding to aircraft turbine engine parts.
22 p2866 A73-42196
- ### ENGINE STARTERS
- Use of cycloconverters and variable speed alternators as engine starters.
01 p0006 A73-11511
- AC starter generator featuring variable-to-constant frequency conversion by cycloconverters as switching device for use with aircraft engines
24 p3057 A73-45154
- ### ENGINE TESTING LABORATORIES
- Russian book on jet engine testing covering tests in research and development, design, production and maintenance, test laboratories and stands and automation
04 p0487 A73-15708
- ### ENGINE TESTS
- NT COLD FLOW TESTS
- NT PREFIRED TESTS
- NT SPACE ELECTRIC ROCKET TESTS
- NT STATIC FIRING
- Investigation of the influence of technological factors on the endurance of gas-turbine engine rotor blades
01 p0114 A73-10477
- The construction of an operational model of the high-frequency ionic propulsion system RIT 10 M
[DGLR PAPER 72-088] 02 p0202 A73-11672
- Development of pulsed hydrogen/oxygen attitude-control engines
[DGLR PAPER 72-077] 02 p0202 A73-11689
- Investigation of the fitness for space travel of the electric propulsion plant ESKA 18
[DGLR PAPER 72-087] 02 p0131 A73-11694
- Gas turbine engine hot part equivalent accelerated tests duration determination by analytical method based on Larson-Miller parametric description of long term strength
02 p0236 A73-12216
- Experimental verification of a digital computer simulation method for predicting gas turbine dynamic behaviour.
02 p0204 A73-12647
- Survey of ONERA and SNPE work on combustion instability in solid propellant rockets.
[AIAA PAPER 72-1052] 03 p0353 A73-13383
- An altitude test facility for large turbofan engines.
[AIAA PAPER 72-1069] 03 p0287 A73-13396
- Propellants selection to provide an air simulant for hot gas testing or ramjets.
[AIAA PAPER 72-1070] 03 p0351 A73-13397
- Diagnostic instrumentation on J-85 engines for gas path and vibration analysis, noting flight test program and installation of remote pressure transducers and signal conditioners
[AIAA PAPER 72-1081] 03 p0308 A73-13404
- Integrated engine diagnostics and displays for Navy aircraft of the 1980's.
[AIAA PAPER 72-1084] 03 p0354 A73-13406
- Method for increasing wind tunnel Mach number for large-scale inlet testing.
[AIAA PAPER 72-1096] 03 p0287 A73-13416
- A method of testing full-scale inlet/engine systems at high angles of attack and yaw at transonic velocities.
[AIAA PAPER 72-1097] 03 p0287 A73-13417
- The Viking Orbiter 1975 beryllium INTERGEN rocket engine assembly.
[AIAA PAPER 72-1131] 03 p0382 A73-13438
- A description of the design, testing and application of the 'Waxwing' apogee boost motor for the 'Black Arrow' satellite launcher, with particular reference to development problems.
[AIAA PAPER 72-1134] 03 p0355 A73-13441
- Durability tests of a five-centimeter diameter ion thruster system.
[AIAA PAPER 72-1151] 03 p0356 A73-13455
- TF-30-P1 engine mixed flow augmentor test for combustion instability under operation with abnormal fuel zone combination, comparing with predicted pressure oscillations from model
[AIAA PAPER 72-1206] 03 p0358 A73-13489
- An automated jet-engine-blade inspection system.
03 p0312 A73-13524
- Development of the Olympus turbojet to meet supersonic civil transport requirements.
03 p0359 A73-14131
- The S4-Modane hypersonic wind-tunnel - Its use for air breathing engine tests
[ONERA, TP NO. 1103] 03 p0288 A73-14140
- Estimation of engine emissions at altitude through ground testing.
04 p0485 A73-14892
- Instrumentation and measurement for determination of emissions from jet engines in altitude test cells.
[AIAA PAPER 72-1068] 04 p0432 A73-14902
- Electrothermal hydrazine thruster analyses and performance evaluation.
[AIAA PAPER 72-1152] 04 p0486 A73-14917
- Gas turbine engine swirl-can combustor pollution tests of nitrogen oxides, unburned hydrocarbons and carbon monoxide levels for elevated temperature performance
[AIAA PAPER 72-1201] 04 p0485 A73-14921
- Linear slit collod electrostatic thruster development and testing, discussing emitter geometry, gap design, exhaust velocity, operating voltage and power efficiency relationships
04 p0488 A73-15725
- Airbreathing engines for Space Shuttle.
[SAE PAPER 720805] 05 p0607 A73-16647
- TF34 and F101 turbofan engines for Navy S-3A ASW aircraft and USAF B-1 strategic bomber, respectively, discussing design features, manufacturing techniques and testing procedures
[SAE PAPER 720841] 05 p0607 A73-16655
- Space shuttle bipropellant reaction control system /RCS/ engine design, characteristics and tests, emphasizing reusability and minimum servicing
[SAE PAPER 720839] 05 p0607 A73-16668
- Operation modes simulation of single stage gas turbine at subcritical and supercritical gas flow, noting scale model tests
05 p0532 A73-17024
- Rapid continuous evaluation of thruster performance dependence on system parameters using thrust balance for measurement, noting suitability for electric microthruster characterization
05 p0579 A73-17253
- Engine noise reduction by fan blade tip speed reduction and high lift coefficient operation, presenting full scale test results
06 p0740 A73-17571
- Afterburning turbojet engine exhaust emission products measurement under simulated flight conditions, determining Mach number and altitude effects on pollutants formation
[AIAA PAPER 73-98] 06 p0740 A73-17643
- L 17 satellite booster development from Emerald stage, discussing gas generator, Valois thruster engine and assembly tests, combustion instability and launching results
07 p0905 A73-18990
- Sound pressure level spectra measurements for four- and three-engine jet transport during concrete and grassy surface runup and flyover
[SAE AIR 1216] 08 p0927 A73-20693
- Astrobee F sounding rocket system design and development, describing advanced propulsion technology test program and results
[AIAA PAPER 73-300] 09 p1156 A73-23219
- Thermodynamic performance analysis of gas turbine power plants with intercooler. II - Performance of intercooling-regeneration-reheat type and precise calculation method.
11 p1411 A73-26343
- An-2R aircraft conversion to flying test bed for feasibility studies of jet engine use in agricultural aircraft, describing structural design modifications
12 p1458 A73-26823
- Study of the effect of technical factors on the fatigue limit of the working blades of gas turbine motors.
14 p1810 A73-33032
- Balancing equipment for jet engine components, compressors, and turbine - Rotating type for measuring unbalance in one or more than one transverse planes.
[SAE ARP 587A] 16 p1993 A73-33013
- The scope and methods of environmental testing of double-base propellant rocket motors - Choice of conditions and interpretation of results.
16 p2047 A73-33390
- Low emissions combustion for the regenerative gas turbine. II - Experimental techniques, results, and assessment.
[ASME PAPER 73-GT-12] 16 p2086 A73-33490
- Flight testing of the JT15D in the CF-100.
18 p2268 A73-36775
- Trimming and checking aircraft gas-turbine engines with the aid of the ratio of total pressure behind the turbine to total pressure in front of the compressor
21 p2754 A73-40403
- Experimental investigation of a gas-liquid thruster model with a ballasting-reinforced thrust
22 p2841 A73-42127
- Utilization of semiautomatic thermocouples in gas-turbine engine tests
23 p2982 A73-43743
- Low frequency noise generation within aircraft gas turbine engine core portion, discussing sources prediction, model and full scale engine tests, and future technology
[AIAA PAPER 73-1027] 24 p3122 A73-44858
- ### ENGINEERING
- Book - Statistical design and analysis of engineering experiments.
17 p2200 A73-34456
- Book on experimental analysis covering measurement systems, engineering problems, data analysis, electro-optics and dimensional parameters
17 p2176 A73-35855
- Engineering applications of geophysical phenomena covering earthquakes, volcanology, hydrology, glaciology and wind stress effects during severe storms
23 p2979 A73-44007
- ### ENGINEERING DEVELOPMENT
- ### U PRODUCT DEVELOPMENT
- ### ENGINEERING MANAGEMENT
- Book - Management of engineering design.
05 p0642 A73-16351
- Performance control in government R&D projects - The measurable effects of performing required management and engineering techniques.
08 p1025 A73-20971
- Engineering management for the Dallas/Fort Worth Airport.
13 p1708 A73-29110
- Resources management logistics support of research and development laboratories.
13 p1709 A73-29574
- Computer program for Equipment Improvement Recommendation /EIR/ evaluation relative to reliability, availability, inventory cost and total annual expenditure in Army engineering management decision making
16 p2089 A73-33653
- NAECON 73; Proceedings of the National Aerospace Electronics Conference, Dayton, Ohio, May 14-16, 1973.
17 p2136 A73-35201
- A survey of behavioral science contributions to laboratory management.
17 p2257 A73-35216
- Management approach to integration of B-1 avionics, discussing engineering problems, flight tests, electronic equipment and interface requirements
17 p2137 A73-35218
- Management and control of flight test programs of the Western Region FAA.
23 p3050 A73-44053
- Management of Air Force test and evaluation activities.
23 p3050 A73-44055
- The role of a military flight test engineer in test management.
23 p3051 A73-44062
- ### ENGINES
- NT AIR BREATHING ENGINES
- NT BOOSTER ROCKET ENGINES
- NT BRISTOL-SIDDELEY BS 53 ENGINE
- NT BRISTOL-SIDDELEY VIPER ENGINE
- NT CESIUM ENGINES
- NT DIESEL ENGINES
- NT ELECTRIC ROCKET ENGINES
- NT ELECTROSTATIC ENGINES
- NT ELECTROTHERMAL ENGINES
- NT GAS TURBINE ENGINES
- NT HELICOPTER ENGINES
- NT HYBRID PROPELLANT ROCKET ENGINES

NT HYDRAZINE ENGINES
 NT HYDROGEN OXYGEN ENGINES
 NT INTERNAL COMBUSTION ENGINES
 NT ION ENGINES
 NT J-33 ENGINE
 NT J-85 ENGINE
 NT JET ENGINES
 NT LIQUID PROPELLANT ROCKET ENGINES
 NT LITHERGOL ROCKET ENGINES
 NT MICROROCKET ENGINES
 NT NUCLEAR ENGINE FOR ROCKET VEHICLES
 NT NUCLEAR LIGHTBULB ENGINES
 NT NUCLEAR ROCKET ENGINES
 NT PISTON ENGINES
 NT PLASMA ENGINES
 NT PULSED JET ENGINES
 NT PULSEJET ENGINES
 NT RAMJET ENGINES
 NT RESTARTABLE ROCKET ENGINES
 NT RETROCKET ENGINES
 NT REUSABLE ROCKET ENGINES
 NT ROCKET ENGINES
 NT SOLID PROPELLANT ROCKET ENGINES
 NT SUPERSONIC COMBUSTION RAMJET ENGINES
 NT TF-30 ENGINE
 NT TF-34 ENGINE
 NT TURBINE ENGINES
 NT TURBOFAN ENGINES
 NT TURBOJET ENGINES
 NT TURBOPROP ENGINES
 NT TURBOROCKET ENGINES
 NT UPPER STAGE ROCKET ENGINES
 NT VERNIER ENGINES
 NT WANKEL ENGINES
ENGLISH CHANNEL

Effects of local conductivity anomalies on the magnetic fields of micropulsations. I - Electromagnetic induction in the English Channel. II - Effect of subterranean conductivity anomalies.
 19 p2425 A73-38012

ENLARGING
 U EXPANSION
ENSKOG-CHAPMAN THEORY
 U CHAPMAN-ENSKOG THEORY
ENSTATITE

Earth crust materials high temperature lattice and radiative thermal conductivity from laser IR measurements, discussing single crystal and polycrystal fosterite-rich olivines and enstatite
 05 p0569 A73-16378

Electron microscopy of some experimentally shocked counterparts of lunar minerals.
 07 p0885 A73-19750

Evidence for solar flare rare gases in the Khor Temiki aubritic.
 21 p2764 A73-40231

ENTHALPY
 Solid-solid phase transitions determined by differential scanning calorimetry.
 01 p0014 A73-11062

Enthalpy driving forces for gas cooling data correlation in convective heat transfer in reacting turbulent boundary layers with mass injection
 [ASME PAPER 72-WA/HT-31] 04 p0519 A73-15824

Enthalpy and heat capacity of boron carbide in the temperature range 273-2600 K.
 06 p0714 A73-17415

Numerical analysis of far turbulent wakes in ideal gas, determining hydrodynamic field moments, turbulence levels and mean square enthalpy fluctuations
 06 p0643 A73-17454

Enthalpy and heat capacity of graphite in the temperature interval between 273 and 3650 K.
 06 p0714 A73-18557

Enthalpy and specific heat of the orthophosphates of lanthanum, neodymium, and yttrium at high temperatures
 06 p0738 A73-18654

Enthalpy and specific heat of tantalum carbide in the range 273-3600 K.
 08 p0977 A73-20865

Mass spectrometric determination of the dissociation energies of AlC₂, Al₂C₂, and AlAuC₂.
 09 p1048 A73-23247

Temperature dependence of the activity and solubility of carbon in pure nickel
 11 p1384 A73-26110

Enthalpy restoration coefficient in a three-dimensional laminar boundary layer
 11 p1303 A73-26434

Investigation of the enthalpy and heat capacity of niobium carbide based materials at high temperatures
 12 p1513 A73-27310

Experimental investigation of the enthalpy of titanium oxides at temperatures ranging from 500 to 2000 K
 12 p1513 A73-27325

Computer simulation of arc heaters for production of flow with high enthalpy.
 13 p1707 A73-29023

Variation with temperature of free enthalpy of formation of certain carbides
 15 p1898 A73-32644

Enthalpy and specific heat of graphite in the temperature range 273-3650 K.
 16 p2030 A73-33583

Dynamics of step heat waves in gases and plasmas.
 20 p2592 A73-38863

Friction, heat transfer and material removal in a turbulent boundary layer of a compressible high-enthalpy gas under conditions of marked nonisothermicity, injection and negative pressure gradient.
 20 p2628 A73-39422

Some thermophysical properties of titanium in the neighborhood of the melting point.
 22 p2878 A73-42508

ENTIRE FUNCTIONS

A method for studying the completeness of systems of analytic functions
 12 p1516 A73-26960

Improvement to Klineberg's method for the calculation of viscous-inviscid interactions in supersonic flow.
 21 p2632 A73-40429

ENTRAINMENT

Polarizable particle entrainment in electromagnetic field consisting of wave packets propagating in opposite directions
 22 p2889 A73-43099

ENTRENCHED STREAMS

U STREAMS

ENTROPY

Computerized correlation analysis of single and multiple neuron pulse activity, considering temporal, sequential and entropy characteristics
 01 p0012 A73-10653

Solid-solid phase transitions determined by differential scanning calorimetry.
 01 p0014 A73-11062

Liapunov function relation to entropy production in irreversible processes, noting thermodynamic constraints on kinetic equation functions
 02 p0191 A73-11613

Collisionless plasma compression shock waves thermodynamics, noting entropy variations along shock adiabat under plasma heating in magnetic field
 02 p0198 A73-12552

The influence of planetary vorticity gradient and vertical entropy gradient on the stability of an atmospheric shear layer.
 04 p0441 A73-15288

A hypothesis, unifying the structure and the entropy of the universe.
 04 p0500 A73-15492

Relativistic thermodynamics of simple heat conducting fluids.
 05 p0641 A73-17235

The local form of the entropy inequality in neoclassical thermodynamics.
 06 p0768 A73-17897

Thermodynamics of self assembly - An empirical example relating entropy and evolution.
 06 p0651 A73-17932

Band position predictions in schlieren visualization of hypersonic entropy wake behind blunt bodies, assuming bow shock geometry
 07 p0775 A73-19970

Thermodynamic probability and statistical interpretations of entropy, with particular attention to information theory, negentropy and Boltzmann-Gibbs theory
 08 p1022 A73-21234

Perturbation method for linearizing equations of supersonic flow over conical bodies, obtaining potential velocity and entropy solutions
 10 p1171 A73-23615

Collisionless plasma compression shock waves thermodynamics, noting entropy variations along shock adiabat under plasma heating in magnetic field
 10 p1254 A73-24179

Numerical computation for entropy layer on blunt nosed cone in terms of shock layer fraction for given free stream and Mach number
 11 p1299 A73-25113

Critique of theory on monotonic entropy of black hole as linear function of area, considering gravitational energy and compression to singularity
 11 p1418 A73-25650

Entropy minimum principle applied to boundary value problem of non-linear heat conduction.
 11 p1452 A73-26342

Taking into account heat-transfer irreversibility in calculating the total change in entropy of individual substances
 12 p1557 A73-26939

Asymmetric mechanics of turbulent flows - Energy and entropy
 12 p1487 A73-27411

The vibrational frequency of Fe-57 atoms in Pt-Fe solid solution from measurements of the second-order Moessbauer Doppler shift.
 13 p1634 A73-28258

Entropy supply for classical and relativistic heat conducting fluids, assuming linearity for momentum and energy supplies
 13 p1704 A73-28286

Entropy layer effects in constant pressure hypersonic boundary layers.
 13 p1564 A73-28812

Maximum information compression and minimum entropy of random process, using Karhunen-Loeve basis
 13 p1596 A73-28869

Second law of thermodynamics revision to include only spontaneous processes made to yield work, discussing heat flow, solutes diffusion and Gibbs free energy
 14 p1816 A73-29735

Contact binary star evolution, discussing adiabatic convection zone entropy, mass flow and relative frequency
 15 p1928 A73-31054

Local potential variational method for analytic approximation of stagnation in plane flow, discussing generalized entropy method for accuracy improvement
 15 p1957 A73-31665

Biological order, structure and instabilities in terms of irreversible thermodynamic processes, entropy, dissipative structures, randomness, abiogenesis, hierarchic organization, chemical reactions and molecular biology
 15 p1835 A73-31824

The principle of minimum entropy applied to boundary value problem of non-linear heat conduction.
 16 p2084 A73-32984

Remarks on the optimum rate of convergence of the on-line identification of non-stationary systems.
 17 p2144 A73-34600

Discontinuity of the vortex on a shock in thermodynamic variables
 17 p2154 A73-35047

Equivalency and macrophysical validity of Thomson and Clausius theorems for second law of thermodynamics, considering Caratheodory theorem relative to entropy and temperature properties
 19 p2504 A73-37654

Information processes in control systems, discussing stability, state reproduction, invariance, entropy balance and statistical physics analogies
 20 p2539 A73-38698

Equilibrium point asymptotic stability for nonlinear generalization of Onsager theory for entropy functions construction with applications to chemical reaction kinetics
 20 p2627 A73-39338

Stimulated entropy /temperature/ scattering and its effect on stimulated Mandel'shtam-Brillouin scattering.
 22 p2868 A73-41720

Irreversible heat transfer in the total entropy change for a pure substance.
 22 p2930 A73-42273

Critical slope of the vapor pressure curve of a pure substance.
 22 p2932 A73-42506

Thermodynamic treatment of plastic media with application to viscoplastic materials, elastoplastic deformation and entropy jump across weak shock waves
 23 p3043 A73-43969

The entropy rate admissibility criterion for solutions of hyperbolic conservation laws.
 23 p3000 A73-44203

MHD partial differential equations solution via hyperbolic system indicating shock wave structure existence satisfying Rankine-Hugoniot relation and entropy condition
 24 p3116 A73-45221

ENVIRONMENT EFFECTS

Developments in space medicine.
 06 p0649 A73-17569

Psychological and psychophysiological factors of human performance in manned space missions, considering environmental effects of space flight and man-machine system
 06 p0650 A73-17775

Carbon dioxide concentration, pH and nutrient concentration effects on blue-green algae relative abundance to green algae in lakes
 06 p0655 A73-18577

An adaptive bit synchronization algorithm under time-varying environment.
 06 p0672 A73-18810

Space deployed expandable structures, discussing vehicular and environmental constraint effects on design, large structure requirements, and applications
 07 p0828 A73-18905

Friction in ultrahigh vacuum, discussing test program definition and testing machine design taking into account space environment effects
 07 p0829 A73-18907

Some effects of temperature on material properties and device reliability.
 07 p0797 A73-19134

Mountain inhabitants physiological characteristics due to altitude effects, investigating human tolerance and adaptation to ambient environment
 07 p0784 A73-19212

IC plastic package performance prediction, discussing procedure to estimate degradation rate due to moisture effects
 08 p0944 A73-20738

Determination of the influence of the earth on the active component of the input impedance of loop antennas

08 p0947 A73-21400

Russian book on aircraft natural-climatic environmental factors covering geographic region adverse effects on design, performance and maintenance

09 p1031 A73-22349

Investigation of certain indices of higher nervous activity in man during prolonged stay in a water environment

09 p1039 A73-22364

Influence of environment on the appearance of fatigue striations in various alloys

09 p1104 A73-22716

High altitude chamber effect on thyroid stimulating hormone and thyroxine concentrations, noting shift from extra to intravascular

09 p1041 A73-22926

Predicting heart rate response to work, environment, and clothing.

09 p1046 A73-22931

Coronary flow and left ventricular function during environmental stress.

09 p1047 A73-23380

Bonded joints under long-term dynamic load and their resistance to climatic effects

10 p1224 A73-24089

Atmospheric corrosion fatigue tests for environmental conditions and superimposed stress wave effects on Cr-Mo steel fatigue life under rotating bending

10 p1235 A73-24917

Aviation medicine assessment of environment effects on pilot responsiveness, task performance and flight safety predictability, considering temperature, oxygen, gravity, acceleration, pressure and stress effects

11 p1321 A73-25039

Implications of psychoanalytic factors for Air Force operations.

11 p1323 A73-25340

Pneumatic sensors without contact

11 p1308 A73-25381

Complex mixture analysis - Geochemical and environmental applications of a compound classifier based on computer analysis of low resolution mass spectra.

11 p1326 A73-25464

Gravitational effects on biological systems in terms of animal body size, age, sex and posture as factors affecting acceleration tolerance

11 p1315 A73-25573

The influence of environment and the surface layer on crack propagation and cyclic behavior.

11 p1380 A73-25807

Metal surfaces corrosion fatigue due to environmentally induced localized attack, discussing protective film growth, crack propagation hydrogen interaction and stresses

11 p1381 A73-25811

Gaseous environments compatibility with structural alloys under fatigue loading, presenting crack growth rate data

11 p1381 A73-25816

The kinetic and dynamic aspects of corrosion fatigue in a gaseous hydrogen environment.

11 p1382 A73-25817

Oxygen and temperature effects on Ni base superalloys fatigue fracture, discussing trans- and intergranular crack propagation and initiation in single and polycrystals and surface coatings

11 p1382 A73-25818

Environment enhanced corrosion fatigue crack growth and fracture mechanics, discussing inspection intervals to maintain structural integrity

11 p1382 A73-25819

On the superposition model for environmentally-assisted fatigue crack propagation.

11 p1382 A73-25820

Frequency and environmental interactions in the fatigue of aluminum alloys.

11 p1382 A73-25824

The effect of environmental relative humidity upon the ultrasonic fatigue endurance of an age hardening aluminum alloy.

11 p1382 A73-25825

Hot gas environment fatigue analysis from corrosion viewpoint, considering gas-alloy reactions

11 p1383 A73-25833

Analytical model for radioisotope thermoelectric generator performance prediction in air and vacuum, taking into account modified heat transfer rates

11 p1312 A73-26031

Results and prospects of microbiological studies in outer space.

11 p1320 A73-26487

Construction of fuel and oil quantity sensors for high-performance aircraft.

13 p1619 A73-29204

Effect of microstructure and environment on stress corrosion of 7075 aluminum alloy. [NASA PAPER 97]

13 p1637 A73-29312

Al and Ti alloy corrosion and fretting fatigue in aqueous environment, noting protective oxide surface film effects

13 p1642 A73-29524

The evolution of lignin - Experiments and observations.

13 p1577 A73-29649

Terrestrial and extraterrestrial stable organic molecules.

14 p1724 A73-30131

High temperature solid lubricants lubricating and environmental stability characteristics, discussing ball and journal bearings wear test results [ASME PAPER 73-DE-9]

14 p1767 A73-30818

Viking aerodynamic decelerator for Mars lander mission in 1976, discussing mortared disk-gap-band parachute, qualification flight tests and atmospheric environment effects

[AIAA PAPER 73-442]

15 p1825 A73-31428

London third airport planning, discussing site selection, large scale urbanization, land use and reclamation, operational aspects and environmental factors

15 p1857 A73-31539

Los Angeles offshore airport planning case study covering design, logistics problems and costs with allowance for airspace and environmental considerations peculiar to Southern California area

15 p1857 A73-31540

Ferritic martensitic stainless steels stress corrosion cracking, emphasizing heat treatment and environmental conditions effects on corrosion resistance

15 p1891 A73-32170

Book - Aircraft noise: Should the Noise and Number Index be revised.

15 p1830 A73-32414

Book - Aircraft noise: Selection of runway sites for Maplin Airport.

15 p1839 A73-32415

Histochemical correlates of changes in the primate brain associated with varying environmental light conditions.

15 p1837 A73-32600

Book - Techniques involving extreme environment, nondestructive techniques, computer methods in metals research, and data analysis. Part I.

16 p2017 A73-32696

Comparative testing and evaluation of conformal coating materials and processes.

16 p2018 A73-33062

A standard psychophysiological preparation for the study of environmental stress.

16 p1975 A73-33130

Measured thermal response to the MJL-STD 210B cold atmosphere.

16 p2034 A73-33140

Design and service environment standardization /Military electronic equipment/.

16 p2087 A73-33143

Environmental effects on EMI gaskets.

16 p1987 A73-33153

Concorde aircraft design, testing and projected environmental impact, discussing flight tests, sonic booms, atmospheric pollution, ATC problems and fueling

16 p1968 A73-33182

Rotary wing aircraft ecological advantages in logging, off shore oil exploration and short haul passenger transport for airport size reduction

16 p2088 A73-33185

Aircraft produced environmental noise and air pollution, discussing related aircraft power plant technology evolution

16 p2047 A73-33191

STOL short haul system development, discussing airport congestion, operational costs and environmental considerations

16 p1968 A73-33192

Environmental damage avoidance via climatic and mechanical factors simulation tests for vibration, humidity, temperature, sunlight, rain, salt spray, shock and altitude

16 p1997 A73-33377

The consideration of environmental effects in the development of environment-resistant systems

16 p2019 A73-33385

The simulation of environmental effects in military technology

16 p1997 A73-33386

Vibration and shock stresses in the case of ballistic rockets. II - Measurement, evaluation, simulation

16 p2072 A73-33388

Automatic detection radar with false alarm rate regulation capability in log-normal and Weibull clutter under severe environments

16 p1980 A73-33412

Failure data evaluation, determining wear out, degradations, environments causing system failures, repairs, maintenance and sub par performers

16 p2021 A73-33649

The effects of adverse environmental conditions on the resin-glass interface of epoxy composites.

16 p2031 A73-33989

An initial estimate of aircraft emissions in the stratosphere in 1990. [AIAA PAPER 73-508]

16 p2011 A73-34046

Electric relay operating envelope definition and test plan for contact contamination and deterioration and resistance determination through controlled environmental changes

17 p2132 A73-34091

Anodic oxidation and stress corrosion cracking /SCC/ of titanium alloys. I - Factors affecting SCC and their influence on the anodic behavior of alloy Ti-6Al-6V-2Sn.

17 p2187 A73-34524

Filiform corrosion associated with commonly applied aircraft metal pretreatments and finishes. [SAE PAPER 730311]

17 p2177 A73-34671

Rain erosion of reinforced plastics for aerospace applications in terms of drop size, impact angle and velocity effects and protective coatings

17 p2195 A73-34806

The potential application of carbon fibres to spacecraft.

17 p2238 A73-34811

Space radiation environment effects on Intelat 4 design, emphasizing trapped electrons and protons influences on solar cell shielding requirements

17 p2108 A73-34864

The effects of environment on performance of fluoroclastomers in seal applications. [ASLE PREPRINT 73AM-8B-2]

17 p2179 A73-34994

Hydrolytic degradation of polymer electrical insulating materials in warm humid environments, noting relation to ester and ether linkage presence

17 p2197 A73-35349

On relationship between the earth-atmosphere system albedo and the earth's surface albedo.

18 p2308 A73-36042

Laser measurement of high-altitude aircraft emissions.

[AIAA PAPER 73-704]

18 p2315 A73-36253

Optical stability of coatings exposed to four years space environment on OSO-III.

[AIAA PAPER 73-734]

18 p2336 A73-36351

Environment-assisted fracture in engineering alloys. I - Monotonic loading.

[ASME PAPER 73-MAT-R]

18 p2365 A73-36613

Environment-assisted fracture in engineering alloys. II - Cyclic loading and future work.

[ASME PAPER 73-MAT-S]

18 p2365 A73-36614

Civil aviation environmental and economic aspects, discussing noise and air pollution, fuel consumption and airspace and ground space utilization

18 p2267 A73-36685

Microwave equipment reliability design for aerospace environment applications, considering vibration, shock, humidity and temperature effects and frequency stability

18 p2293 A73-36778

Aircraft noise in airport areas, discussing effects on environment and economics

18 p2373 A73-36949

Developments in Canada related to remotely manned systems.

19 p2416 A73-37317

Consequences of aircraft noise reduction alternatives on communities around airports. [AIAA PAPER 73-818]

19 p2380 A73-37471

Internal operational environment effects on pilot errors in commercial aircraft flights in terms of man machine interface and flight deck design

19 p2384 A73-37728

Environmental considerations for offshore airports.

19 p2417 A73-37742

New York offshore airport feasibility study. [FAA-RD-73-45]

19 p2418 A73-37750

Environment effects on tape recorder design for in-flight data collection in military aircraft

19 p2431 A73-38197

Mechanism of hydrocarbon formation in combustion processes.

19 p2402 A73-38322

Multihundred watt radioisotope thermoelectric generator heat source materials compatibility with the thermochemical environment, considering maximum operational and reentry temperatures

19 p2457 A73-38427

Moisture effect on Ni steel fatigue crack propagation under low stresses

20 p2617 A73-39291

Geophysical effects of Concorde sonic boom.

20 p2509 A73-39624

ILS capability improvements on localizer and glide-slope antenna arrays and monitors, considering effects of reflecting objects on or near aerodrome and terrain

21 p2736 A73-40049

Interaction between radiation effects, gravity and other environmental factors in Tribolium confusum.

21 p2643 A73-40808

Water damage in polyester/glass laminates. II - Microscopic evidence.

21 p2723 A73-40921

Influence of hydrogen, alcohols, and moisture on the ultimate strength and electrical resistance of tungsten and steel wire samples

21 p2721 A73-41227

Skylab 1 medical experiments concerning astronaut physiological responses and work capability as affected by exposure to space flight environment
21 p2778 A73-41519

The coupling of high frequency electromagnetic energy into large systems.
22 p2822 A73-41792

A new conceptual model for components in measurement/control systems - Practical application to thermocouples.
22 p2859 A73-42050

The effect of variable environment temperature on heat transfer in extended surfaces.
23 p3048 A73-43296

Fluidic logic circuits applications under adverse environmental conditions, considering sequential control devices and rocket engine roll axis numerical control
23 p2941 A73-43394

Environmental effects on fracture resistant and biaxial fatigue design of aircraft structures.
23 p3042 A73-43811

Evaluating structural adhesives under sustained load in a hostile environment.
24 p3093 A73-44767

Emitance measurement of Surveyor 3 spacecraft aluminum support tubing returned from moon by Apollo 12, noting lunar environment effects from control sample data
24 p3139 A73-45110

ENVIRONMENT MANAGEMENT
The role of applications satellites in the management of the human environment.
19 p2424 A73-37713

Data collection platforms, ground receiving and processing equipment for environmental study and management
[AAS PAPER 73-122] 20 p2520 A73-38583

Contributions of the EROS Program to the Department of the Interior's resources and management responsibilities.
[AAS PAPER 73-130] 20 p2550 A73-38588

Environmental data - From sensors to users.
[AAS PAPER 73-138] 20 p2521 A73-38592

Remote sensor role in international environmental management, considering monitoring of biosphere, atmosphere and oceans and UN action plan for natural resources
20 p2629 A73-39837

ENVIRONMENT MODELS
Prediction models for surface and air transportation dynamic environments, considering broadband and single frequency continuous and recurrent and intermittent discrete excitation modes
09 p1032 A73-22718

Environment models and algorithm for obtaining statistically optimal proportions estimates for category mixtures in multispectral sensor data processing
20 p2559 A73-39883

ENVIRONMENT POLLUTION
NT AIR POLLUTION
NT WATER POLLUTION
The aeroplane as a threat to the environment.
03 p0251 A73-14468

International Conference on Transportation and the Environment, Washington, D.C., May 31-June 2, 1972, Proceedings. Part 1.
04 p0405 A73-14889

Space law provisions concerning terrestrial and celestial bodies environmental contamination, advocating establishment of international code of conduct and control authority
04 p0522 A73-15138

Space and terrestrial pollution definitions, discussing control and preventive measures by national and international public and private organizations
04 p0522 A73-15139

German book - Deutsche Gesellschaft fur Luft- und Raumfahrt, 1971 Yearbook.
05 p0528 A73-16755

The measurement of environmental pollution with the aid of aircraft and satellites
[DFVLR-SONDDR-247] 05 p0570 A73-16767

Hazardous gas detection system for analysis of gases escaping during cryogenic loading in Apollo-Saturn launch tests, discussing utilization for environment pollution detection
05 p0578 A73-17135

Realism in environmental testing and control; Proceedings of the Nineteenth Annual Technical Meeting, Anaheim, Calif., April 2-5, 1973.
16 p1993 A73-33126

Hypersonic transports - Economics and environmental effects.
17 p2099 A73-34435

Oil spread over Arctic ice, considering spread rate and oil slick size attainment for pollution potential during spills on tundra or pack ice
[AIAA PAPER 73-701] 18 p2312 A73-36250

Contributions of the DFVLR to environmental research and environment protection. II - Noise control, water environment protection, nature and landscape, environmental protection techniques
19 p2506 A73-38266

Energy supply and its effect on aircraft of the future. II - Liquid-hydrogen-fueled aircraft: Prospects and design issues.
[AIAA PAPER 73-809] 19 p2388 A73-38373

RF fields as new ecological factor in environment pollution, considering radiation interaction with biological systems and increased use of electromagnetic spectrum
22 p2811 A73-41787

Vacuum effects on materials and environment contamination - Screening method and results obtained at CNES
22 p2880 A73-41873

A physical-numerical model for the determination of the meteorological environmental effects produced by cooling towers
23 p3003 A73-43995

ENVIRONMENT PROTECTION
Climatic impact assessment for high-flying aircraft fleets.
04 p0436 A73-14672

Legal problems for the protection of the earth's environment.
04 p0522 A73-15136

International law aspects of catastrophic disaster prohibition in terms of endangering earth environment /resources/
04 p0522 A73-15137

Space law provisions concerning terrestrial and celestial bodies environmental contamination, advocating establishment of international code of conduct and control authority
04 p0522 A73-15138

Space and terrestrial pollution definitions, discussing control and preventive measures by national and international public and private organizations
04 p0522 A73-15139

Earth environment pollution protection in space exploration, noting international law principles application
04 p0522 A73-15140

International law for earth environment protection against pollution by activities in outer space, noting International Court of Justice Advisory Opinion procedure
04 p0522 A73-15141

Earth environment damage potential of space program side effects, discussing environmental protection from international responsibility viewpoint
04 p0522 A73-15142

Assessment of emission control technology for turbine-engine aircraft.
[ASME PAPER 72-WA/GT-8] 04 p0490 A73-15872

Legal aspects of water pollution detection through remote sensing.
05 p0642 A73-17138

Protective coating systems for Navy aircraft turbine engines.
[NACE PAPER 113] 13 p1637 A73-29313

Honolulu International Airport reef runway.
15 p1857 A73-31538

Lightning protection for boron and graphite fibers in epoxy resins for aircraft composite structures
16 p1967 A73-33032

Lightning protection for boron and graphite reinforced plastic composite aircraft structures, discussing zonal design concept and channel intermittent contact with protrusions on surface
16 p1968 A73-33034

F-14 aircraft boron-epoxy and graphite-epoxy composite structure production protection against degradation by lightning discharges, discussing design, processing and tests
16 p2028 A73-33035

Factors affecting the survivability of stressed bonds in adverse environments.
16 p2017 A73-33055

Inverse condemnation of airspace, discussing real property concept relation to aircraft noise, pollution and environment protection
16 p2087 A73-33103

Lightning simulation testing in aerospace.
16 p1994 A73-33145

The consideration of environmental effects in the development of environment-resistant systems
16 p2019 A73-33385

Reduction of nitrogen oxide emissions from a gas turbine by fuel modifications.
16 p2045 A73-33483

[ASME PAPER 73-GT-5] 16 p2045 A73-33483

Contributions of the DFVLR to environmental research and environment protection. II - Noise control, water environment protection, nature and landscape, environmental protection techniques
19 p2506 A73-38266

Aircraft noise consideration for environmental compatibility, airport development, short haul and supersonic air transport and legislation and regulation problems
19 p2387 A73-38368

[AIAA PAPER 73-795] 19 p2387 A73-38368

Circumvention design of active circuitry and passive shielding for electromagnetic pulse environment with application to Minuteman ICBM system
22 p2822 A73-41786

Electromagnetic radiation hazard test facility, instrumentation, and weapon system susceptibility evaluation for providing environment protection and military standards
22 p2822 A73-41791

Electromagnetic shielding techniques and testing for environment and instrument protection from radio emission and noise
22 p2823 A73-41804

Optical radar measurements of meteorological parameters and air pollution related to environment protection, using Raman effect and resonance and Mie scattering
24 p3096 A73-44896

ENVIRONMENT SIMULATION
NT ACOUSTIC SIMULATION
NT ALTITUDE SIMULATION
NT SPACE ENVIRONMENT SIMULATION
NT THERMAL SIMULATION
NT WEIGHTLESSNESS SIMULATION
Image transformation in visual condition simulators of aircraft training equipment
01 p0029 A73-10666

Powered model wind tunnel investigation to determine performance trends with nacelle location.
[AIAA PAPER 72-1114] 03 p0243 A73-13429

Lumped parameter network modeling for spacecraft surface thermal environment analysis, discussing computer program and application to Skylab ATM
07 p0919 A73-19496

Flow and velocity fields simulation by calculating dynamic loads in moving liquid from pressure distribution, viscosity and gravitational acceleration
[AIAA PAPER 73-409] 11 p1441 A73-25537

Microwave radiometric observations of simulated sea surface conditions.
11 p1355 A73-25774

Optical absorption cell with water vapor cross flow instrument designed for wall decontamination and open air meteorological simulation, examining thermodynamic parameters effects
11 p1367 A73-26318

Electric discharge and microbiological experiments in simulated Jovian atmosphere for investigation of Jupiter life prospects
11 p1319 A73-26478

Stable-member mounted instrument environment simulation model development.
11 p1395 A73-26638

Laboratory modeling of 'vaporization-condensation and spilling' type processes taking place on the lunar surface
13 p1672 A73-28118

Lunar soil models for equipment environmental testing, using vibrationally compacted volcanic granular materials
13 p1606 A73-28119

Laboratory simulation of development of super-booms by atmospheric turbulence.
13 p1568 A73-28495

A rapidly convergent procedure for computing large-scale condensation in a dynamical weather model.
13 p1655 A73-29338

Icy cometary nuclei laboratory simulation by sublimation of dust particle containing ice and frozen electrolyte mixtures in high vacuum at low temperature
14 p1793 A73-29823

Influence of transient conditions on the overall service life of turbine blades
14 p1785 A73-30676

Realism in environmental testing and control; Proceedings of the Nineteenth Annual Technical Meeting, Anaheim, Calif., April 2-5, 1973.
16 p1993 A73-33126

Lightning simulation testing in aerospace.
16 p1994 A73-33145

The simulation of the atmospheric surface layer with volumetric flow control.
16 p1994 A73-33152

Problems and methods of simulating the environment; Annual Meeting, Karlsruhe, West Germany, September 27-29, 1972, Reports
16 p1997 A73-33376

Environmental damage avoidance via climatic and mechanical factors simulation tests for vibration, humidity, temperature, sunlight, rain, salt spray, shock and altitude
16 p1997 A73-33377

Climate simulation via environmental test chambers examining mechanical, thermal and pressure effects to determine functional component suitability
16 p1997 A73-33382

Vibration and shock stresses in the case of ballistic rockets. II - Measurement, evaluation, simulation
16 p2072 A73-33388

The scope and methods of environmental testing of double-base propellant rocket motors - Choice of conditions and interpretation of results.
16 p2047 A73-33390

Simulation of a multiple element test environment.
16 p1985 A73-33417

Probabilistic Monte Carlo computerized simulation of surface to air missile systems reaction time from

aircraft attack in non-jamming environment and over flat terrain

16 p1985 A73-3418

Simulated ERTS data for coastal management.

17 p2157 A73-34285

Thermal synthesis of amino acids from a simulated primitive atmosphere.

17 p2117 A73-34572

Simulation of airport traffic flows with interactive graphics.

17 p2147 A73-34821

Measurement techniques for antennas in dissipative media.

17 p2143 A73-35685

Hyperballistics range erosion tests, describing dust, rain and ice simulation, dust and water fixed grid screens and shadowgraph and laser photography [AIAA PAPER 73-765]

18 p2295 A73-36380

High current lightning simulation testing of composite materials.

18 p2296 A73-36713

Summer Computer Simulation Conference, Montreal, Canada, July 17-19, 1973, Proceedings. Volumes 1 & 2.

18 p2291 A73-36826

Application of the Ornstein-Uhlenbeck stochastic process to the study of dynamic systems in an environment of stochastic disturbances.

18 p2330 A73-36829

Real-time, three-dimensional, visual scene generation with computer generated images.

18 p2291 A73-36831

Computation of launch vehicle system requirements using hybrid computer.

18 p2360 A73-36838

Use of continuous simulation models in application of remote sensing to hydrology.

18 p2292 A73-36840

A survey of the simulator technique for designing a radiating element in a phased-array antenna.

21 p2652 A73-40657

Telecontrol system for particle accelerator target displacement via micromotor electronic control with emphasis on adaptation to ultrahigh vacuum chamber simulating ionospheric plasma

22 p2838 A73-41868

Development of a vacuum chamber for ionospheric plasma simulation - Utilization of liquid helium cryopumping

22 p2838 A73-41869

Soil microbiological tests to evaluate Antarctica as Mars environment model for quarantine standards

21 p2803 A73-42162

On the multiplication of xerophilic micro-organisms under simulated Martian conditions.

22 p2803 A73-42165

A magnetogasdynamic accelerometer for the simulation of micrometeoroids

23 p2966 A73-43781

ENVIRONMENTAL SIMULATORS

NT LUNAR GRAVITY SIMULATOR

NT SOLAR SIMULATORS

NT SPACE SIMULATORS

Airlines flight safety management, discussing visual systems simulator /VSS/ for Tristar systems environmental and cycling endurance ground tests

10 p1176 A73-24710

The simulation of environmental effects in military technology

16 p1997 A73-33386

GDC/EOSS - Real-time visual and motion simulators for evaluation of fire control and electro-optical guidance systems.

21 p2673 A73-40867

An approach to computer image generator for visual simulation.

21 p2673 A73-40875

ENVIRONMENTAL CHAMBERS

U TEST CHAMBERS

ENVIRONMENTAL CONTROL

Book - Corrosion and corrosion control: An introduction to corrosion science and engineering /2nd edition/.

03 p0321 A73-13125

The Ranque-Hilsch vortex tube and its application to spacecraft environmental control systems.

03 p0287 A73-13313

Handbook on mechanical face seals covering applications, operational capabilities, design, environmental control, handling, installation, malfunctions, auxiliary equipment, optical flats, etc

03 p0313 A73-13995

Clean rooms and contamination-free zones in space technology

07 p0830 A73-19011

Airport noise control and minimization for community and airline industry interests by technology application and legal-political approaches

11 p1455 A73-26350

Electric relay operating envelope definition and test plan for contact contamination and deterioration and resistance determination through controlled environmental changes

17 p2132 A73-34091

Advanced aircraft power systems utilizing coupled APU/ECS.

[SAE PAPER 730380]

17 p2108 A73-34719

The control of the terrestrial environment from space: International collaboration, methods and technologies; International Conference on Space, 13th, Rome, Italy, March 22-24, 1973, Proceedings

17 p2160 A73-34926

Low altitude satellite networks for recording programmable earth atmosphere parameters related to terrestrial environment control

17 p2205 A73-34929

The use of remote sensing for the detection of natural resources - Definition of the platforms, technical-organizational considerations

17 p2160 A73-34930

Description of the docking module ECS for the Apollo-Soyuz Test Project.

[ASME PAPER 73-ENAS-21]

19 p2493 A73-37977

Reverse osmosis for recovering and recycling water in Space Station Prototype Environmental Thermal Control/Life Support System Integrated Water and Waste Management

[ASME PAPER 73-ENAS-22]

19 p2400 A73-37978

Space Shuttle Orbiter Environmental Control and Life Support System for atmosphere revitalization, crew life support, thermal conditioning and airlock support

[ASME PAPER 73-ENAS-23]

19 p2400 A73-37979

Apollo Lunar Module environmental control system - Mission performance and experience.

[ASME PAPER 73-ENAS-28]

19 p2400 A73-37983

Apollo command and service module environmental control system - Mission performance and experience.

[ASME PAPER 73-ENAS-29]

19 p2493 A73-37984

Gas management system for control, bleeding, evacuating and radiological and pressure monitoring of He atmosphere in multihundred watt heat source

19 p2457 A73-38428

A numerical analysis of some practical aspects of airborne urea seeding for warm fog dispersal at airports.

21 p2728 A73-40056

A gas density control system for X-ray proportional counters in space.

22 p2851 A73-41699

Spectrum control procedures for the National Radio Astronomy Observatory.

23 p2953 A73-43381

Use of earth resources satellites for supranational inventories of forests and agricultural areas

23 p2972 A73-43779

ENVIRONMENTAL ENGINEERING

German monograph - Investigations concerning perception levels and transferred vibrational forces in the case of a vertical action of periodic vibrational mixtures on man.

03 p0268 A73-13818

Technology for man 72; Proceedings of the Sixteenth Annual Meeting, Los Angeles, Calif., October 17-19, 1972.

05 p0542 A73-16701

Acquisition and utilization of data of exploitation of equipment in the particular case of exposure to different environments

07 p0830 A73-19402

Heavy marine structure engineering in offshore airport planning, discussing construction types and conditions, environmental factors, materials, methods and equipment

15 p1856 A73-31533

Canadian government planning for second land based or offshore jet airport in Toronto area, considering environmental and community factors

15 p1858 A73-31545

Realism in environmental design criteria - MIL-STD-210B.

16 p2034 A73-33139

Need for and aspects of a cooperative European earth resources program.

18 p2372 A73-35933

Vibrations in environmental engineering; Proceedings of the Symposium, Imperial College of Science and Technology, London, England, July 4, 5, 1973.

20 p2544 A73-39265

ENVIRONMENTAL LABORATORIES

A three-dimensional model of cumulus cloud development.

14 p1771 A73-30764

NAFEC test facilities.

23 p2966 A73-44063

ENVIRONMENTAL QUALITY

NT WATER QUALITY

ENVIRONMENTAL RESEARCH SATELLITES

Satellite remote monitoring of earth environment and natural resources by high resolution multispectral scanners for European requirements

17 p2160 A73-34931

NOAA environmental satellites with IR remote sensors for detection of upwelling off Mexican Pacific Coast and cold water eddies in Sargasso Sea

20 p2560 A73-39890

ENVIRONMENTAL SURVEYS

International legal problems concerning earth environmental survey system composed of ERT satellites, survey aircraft and ground data handling systems

04 p0521 A73-15129

Environmental data transmission from arctic data buoys via polar orbiting satellite.

04 p0421 A73-15431

Improved Tiros Operational Satellite and future near-polar orbiting environmental system, discussing scanning radiometer and vidicon and automatic picture transmission camera remote sensors

16 p2015 A73-33352

Thermal mapping at electrical power generating sites for outfall from fossil or nuclear fuel plants, considering airborne application

16 p2015 A73-33360

Remote sensing using microwave radiometry.

17 p2174 A73-35639

Applications of ERTS data to oceanography and the marine environment.

18 p2302 A73-35935

Remote sensing - The application of space technology to the survey of the earth and its environment.

19 p2423 A73-37497

Data collection platforms, ground receiving and processing equipment for environmental study and management

[AAS PAPER 73-122]

20 p2520 A73-38583

DCS - A global satellite environmental data collection system.

20 p2525 A73-38744

Development of a practical remote sensing water quality monitoring system.

20 p2567 A73-39830

Regional land inventory systems development in the Houston area.

20 p2629 A73-39832

Remote sensing applications in the Metropolitan Washington Council of Governments.

20 p2556 A73-39833

An integrated resource survey using orbital imagery - An example from south-east Spain.

20 p2556 A73-39834

NASA environmental applications demonstrations in southeastern United States.

20 p2557 A73-39848

A comprehensive remote sensing legend system for the ecological characterization and annotation of natural and altered landscapes.

20 p2557 A73-39851

Thermal activity of the Usón Caldera based on infrared and photographic aerial survey.

20 p2561 A73-39895

Monitoring levels of existing environmental impact utilizing remote sensing techniques.

20 p2562 A73-39908

Anthropogenic CO sources and urban concentrations, considering meteorological factors, nonanthropogenic sources, temporal variations and background levels in remote areas

21 p2729 A73-40080

Earth surveys by remote sensing in Israel.

21 p2685 A73-40816

Remote measurement of salinity in an estuarine environment.

22 p2850 A73-42730

Book - The surveillance science: Remote sensing of the environment.

23 p2971 A73-43605

ENVIRONMENTAL TEMPERATURE

U AMBIENT TEMPERATURE

ENVIRONMENTAL TESTS

NT CORROSION TESTS

NT HIGH TEMPERATURE TESTS

NT LOW TEMPERATURE TESTS

NT SALT SPRAY TESTS

NT UNDERWATER TESTS

Space simulation chamber tests of thermal louver model for spacecraft temperature control

01 p0110 A73-11150

Non-metallic materials selection, processing and environmental behavior; Proceedings of the Fourth National Technical Conference and Exhibition, Palo Alto, Calif., October 17-19, 1972.

03 p0328 A73-13001

Evaluation of materials for underground exposure in extreme environments.

03 p0329 A73-13006

The effect of environmental factors on seal performance of VITON E-60C fluoroelastomer.

03 p0331 A73-13027

A study of environmental degradation of adhesive bonded titanium structures in Army helicopters.

03 p0332 A73-13039

Printed circuit and electronic component solderability tests subsequent to adverse environment exposure, comparing electroplated materials with pressure leveled solder and Cu and Be coatings

03 p0333 A73-13046

An advanced printed circuit board system having outstanding resistance to humid environments.

03 p0281 A73-13047

Propulsion unit, components, environmental tests and development problems of Swedish air to ground missile rocket engine operating on liquid propellants [AIAA PAPER 72-1102] 03 p0355 A73-13421

Material evaluation under direct rocket exhaust impingement. [AIAA PAPER 72-1167] 03 p0287 A73-13465

Development and application of magnetic bearings. 03 p0313 A73-13924

Heat flow meter and calorimeter measurements of heat transfer between human body and environment under various climatic conditions for temperature regulation studies 03 p0268 A73-14123

Solar array and supporting technologies development, discussing manufacturing, handling, design qualification tests in space environment and comparison between fold-up and roll-up types 03 p0257 A73-14237

Further observed degradation on the LES-6 synchronous solar cell experiment. 03 p0258 A73-14247

Fatigue crack propagation of D6ac steel in air and distilled water. 04 p0459 A73-14688

Apollo program predictive testing for man machine and environmental capabilities in terms of engineering, qualification, manufacturing, maintenance and training aspects 04 p0453 A73-14863

Computer-controlled environmental test systems - Criteria for selection, installation, and maintenance. [SAE PAPER 720819] 05 p0562 A73-16638

Thermal conductivity measurements of porous materials in several gaseous environments at subatmospheric pressures. [AIAA PAPER 73-95] 05 p0640 A73-16858

Evaluation of protective coatings for prevention of corrosion of high strength steels when subjected to extreme environments. 06 p0711 A73-18717

Vibration, radiation and thermal vacuum test procedures and facilities for evaluating spacecraft reliability during launching and in space environment 07 p0807 A73-18999

Features of the influence of the ambient medium on the friction of plastics against metal during intermittent travel 09 p1089 A73-22855

Thermal conductivity of mixed-composition plasma-sprayed coatings. 09 p1111 A73-23464

Radome material technology in UK, summarizing permittivity, loss tangent, internal phase difference, attenuation, aberration, cross polarization and pattern distortion measurements and environmental tests 11 p1336 A73-25308

Environmental stress cracking of epoxy adhesives. 11 p1388 A73-25840

Life processes in ammonia - Anomalous germination behavior of onion seed in ammonia and amines. 11 p1321 A73-26491

Corrosion and corrosion prevention of light metal alloys. [NACE PAPER 114] 13 p1637 A73-29314

Test assembly for structural component members under different climatic conditions 14 p1743 A73-30689

Viking 75 Mars lander spacecraft mortar system design and environmental requirements, stressing manufacturing and qualification tests and parachute ejection [AIAA PAPER 73-458] 15 p1827 A73-31444

Phenomena associated with bench and thermal-vacuum testing of superconductors - Heat pipes. 16 p2084 A73-33131

MIL-STD-810 uniform test methods for determining military equipment environmental resistance, discussing inadequacies, misapplications and planned revision for improvement 16 p2087 A73-33144

Lightning simulation testing in aerospace. 16 p1994 A73-33145

Critical Reynolds number for nondelayed transition in environmental testing for internal and external fluid flows 16 p1999 A73-33146

A closed-loop automatic control system for high-intensity acoustic test systems. 16 p1994 A73-33147

The significance of the climate factor air velocity in environmental simulation 16 p1997 A73-33381

Missile and explosive environmental tests for mechanical properties, outlining test facilities, climatological effects, salt spray, vibration, shock, dropping, vacuum effects and crack propagation 16 p1997 A73-33387

The scope and methods of environmental testing of double-base propellant rocket motors - Choice of conditions and interpretation of results. 16 p2047 A73-33390

Aeros satellite simulated environmental testing for thermal behavior under space vacuum, temperature

and solar radiation conditions, comparing results with mathematical model calculations 16 p1997 A73-33392

Satellite systems space environmental simulation tests, discussing thermal models design, temperature field and error calculations by computerized data processing 16 p1998 A73-33393

The role of temperature in the environmental acceptance testing of electronic equipment. 16 p1989 A73-33606

Accelerated testing of air-to-air guided missiles. 16 p2073 A73-33612

Hydrolytic stability of electrical insulation materials. 17 p2197 A73-35348

High current lightning simulation testing of composite materials. 18 p2296 A73-36713

SkyLab medical experiments altitude test crew observations. [ASME PAPER 73-ENAS-30] 19 p2400 A73-37985

SkyLab Medical Experiments Altitude Test /SMEAT/ facility design and operation. [ASME PAPER 73-ENAS-44] 19 p2401 A73-37991

Test stand for the propulsion systems of the 'Symphonie' communications satellite in vacuum 19 p2419 A73-38271

Multihundred watt radioisotope thermoelectric generator full scale thermal performance, vibration, shock, acoustic, acceleration and magnetic field tests 19 p2456 A73-38421

Multilayer foil insulated Si-Ge thermopile design for multihundred watt radioisotope thermoelectric generator to withstand launch environments, evaluating performance under shock and vibration loads 19 p2392 A73-38424

Pulmonary function in man after short-term exposure to ozone. 21 p2642 A73-40001

Technical progress on new vibration and acoustic tests for proposed MIL-STD-810C, 'environmental test methods.' 21 p2674 A73-41200

US Department of Defense aircraft system effectiveness tests survey questionnaire response data from component, subsystem and system suppliers 21 p2635 A73-41204

Commercial aircraft system effectiveness survey questionnaire response data concerning various tests in manufacturing and operational environments 21 p2635 A73-41205

ENVIRONMENTS

NT AEROSPACE ENVIRONMENTS

NT CHROMOSPHERE

NT DEEP SPACE

NT EARTH ENVIRONMENT

NT EXTRATERRESTRIAL ENVIRONMENTS

NT HIGH ALTITUDE ENVIRONMENTS

NT HIGH GRAVITY ENVIRONMENTS

NT HIGH TEMPERATURE ENVIRONMENTS

NT INNER RADIATION BELT

NT INTERPLANETARY SPACE

NT INTERSTELLAR SPACE

NT IONOSPHERE

NT JUPITER ATMOSPHERE

NT LOW TEMPERATURE ENVIRONMENTS

NT LOWER IONOSPHERE

NT LUNAR ATMOSPHERES

NT LUNAR ENVIRONMENT

NT MAGNETOPAUSE

NT MAGNETOSPHERE

NT MARINE ENVIRONMENTS

NT MARS ATMOSPHERE

NT MARS ENVIRONMENT

NT MESOPAUSE

NT MESOSPHERE

NT MIDLATITUDE ATMOSPHERE

NT PLANETARY ATMOSPHERES

NT PLANETARY ENVIRONMENTS

NT ROTATING ENVIRONMENTS

NT SOLAR ATMOSPHERE

NT SPACECRAFT ENVIRONMENTS

NT STELLAR ATMOSPHERES

NT THERMAL ENVIRONMENTS

ENZYME ACTIVITY

Effects of exercise on activity of heart and muscle mitochondria. 01 p0006 A73-10135

Hydroxyindole-O-methyl transferases in rat pineal, retina and Harderian gland. 02 p0136 A73-12644

Properties of phosphoribulokinase from *Thiobacillus neapolitanus*. 03 p0261 A73-13597

A salt-inhibited cytochrome c reductase obtained from the moderately halophilic bacterium, *Micrococcus halodentificans*. 03 p0261 A73-13598

Purification, crystallization, and subunit structure of allosteric adenosine 5'-monophosphate nucleosidase. 03 p0273 A73-13807

Evolution of ribonuclease in relation to polypeptide folding mechanisms. 04 p0409 A73-15047

Myosin ATPase and fiber composition from trained and untrained rat skeletal muscle. 05 p0538 A73-16155

Effects of physical training on cardiac actomyosin adenosine triphosphatase activity. 05 p0539 A73-16157

Functional dependence of the ciliary epithelium ATPase activity and intracellular pressure on the autonomic nervous system. 05 p0539 A73-16248

Mechanisms of certain functional shifts during change in the blood of the content level of external pancreatic-gland secretion components 05 p0541 A73-16700

Action of Freon-114B2 on the activity of lactate-dehydrogenase iso-enzymes 06 p0650 A73-17696

Light enhanced decarboxylations by proteinoids. 06 p0661 A73-17941

A mechanism for polypeptide synthesis on a protein template. 06 p0652 A73-17943

Myeloperoxidase, the peroxidase of a primitive cell - Its reaction with Fe and H2O2. 06 p0652 A73-17944

Trypsinogen activation peptides - An example of molecular epigenesis. 06 p0652 A73-17947

Solvent effects on enzymes - Implications for extraterrestrial life. 06 p0652 A73-17948

Transglucosidase activity of heart-muscle per-glucosylase 08 p0930 A73-21136

Action of a serum protein on muscular contraction. 08 p0930 A73-21200

Morphometric and histochemical investigation on human right atrial and mitral papillary muscle. 08 p0930 A73-21215

Effects of an hyperoxic hypobaric environment on renin-aldosterone in normal man. 08 p0934 A73-21503

Effect of training on enzyme activity and fiber composition of human skeletal muscle. 08 p0935 A73-21508

Effects of experimental conditions on parameter estimated when using the Hill model 09 p1044 A73-21872

Acetylcholinesterase activity of hypothalamic and cortical structures under pharmacological effects 10 p1182 A73-24597

Serum creatine phosphokinase activity and urinary excretion of creatine and creatinine in man during acclimatization to high altitude and in high altitude natives. 11 p1315 A73-25333

Apparent paradoxical patterns of anaerobic glycolysis and hexokinase activity in the red blood cells of acutely bled rats, with evidence that the responses were in part hormone-dependent. 11 p1315 A73-25568

Changes caused by illumination in the Na⁺, K⁺ adenosine-triphosphatase and n-nitrophenylphosphatase activities of the external segments of the retina 13 p1574 A73-28294

Ape peculiarities of whole-blood transketolase activity in healthy persons 15 p1833 A73-31164

Fibrinolytic activity of urine in healthy persons 15 p1833 A73-31165

Influence of ribonuclease on changes in the membrane potential of muscle fibers evoked by stimulation of the sympathetic nerve 15 p1833 A73-31166

Influence of electron transport on the interaction between membrane lipids and Triton X-100 in *Halobacterium cutirubrum*. 15 p1841 A73-32024

Histochemical correlates of changes in the primate brain associated with varying environmental light conditions. 15 p1837 A73-32600

Activity variations of some renal enzymes during stepwise increased hypoxia 18 p2277 A73-36582

Glycolytic intermediates and adenosine phosphates in rat liver at high altitude /3,800 m/. 20 p2514 A73-39602

Starch hydrolysis in man - An intraluminal process not requiring membrane digestion. 20 p2519 A73-39789

Relationship between cyclic AMP, phosphodiesterase activity, calcium and contraction in intestinal smooth muscle. 21 p2638 A73-41130

Studies on the metabolism of glucose-1,6-diphosphate in human erythrocytes. 21 p2639 A73-41139

Effect of hind-limb immobilization on contractile and histochemical properties of skeletal muscle. 21 p2642 A73-41624

- Ribonucleic acid /RNA/ polymerase and adenyl cyclase in cardiac hypertrophy and cardiomyopathy.
22 p2808 A73-42687
- Influence of histotoxic hypoxia on the activity of lactic dehydrogenase isoenzymes in neurons and neuroglia of various sections of the central nervous system
24 p3058 A73-44429
- Activity of acid nucleases in eye tissues under the action of corticosteroidal hormones
24 p3058 A73-44430
- Desoxyribonucleases in sweat gland secretion of man
24 p3059 A73-44674
- Lactate origins and renewal in blood plasma, considering metabolism, enzymatic resynthesis and final excretion in urine
24 p3061 A73-45157

ENZYMES

- NT HEXOKINASE
NT NUCLEASE
NT OXIDASE
NT TRYPSIN
Quaternary structure /subunit composition/ of human ceruloplasmin
11 p1316 A73-25638

EOLE SATELLITES

- Electro-gilding of coverings and light alloy component parts for satellites D2 and EOLE.
07 p0829 A73-18911
- Eole satellite gravity gradient stabilized pointing control system, discussing implementation by eddy current, inertia and magnetic hysteresis devices
07 p0904 A73-18936
- The balloon launch stations of the EOLE program.
07 p0807 A73-18951
- Circuit diagrams, electronic modules and design of PCM telemetry encoder for Eole satellite, noting data multiplexing and processing
07 p0789 A73-18957
- Design, manufacture and performance of Eole satellite computer core memory, noting circuit reliability and testing
07 p0796 A73-18959
- Design and performance of VHF telemetry transmitter and remote controlled radio receiver for Eole satellite, noting production technology and block diagram
07 p0790 A73-18961
- Design and performance of UHF transmitter and receiver system for two way links between Eole satellite and constant ceiling balloons
07 p0790 A73-18962
- Antenna design for Eole satellite radio communications with balloons, noting wave polarization and sea reflection effects
07 p0797 A73-18963
- Design, production, reliability analysis and testing of Eole satellite decoder for balloon sounding data, noting performance tests
07 p0790 A73-18966
- Eole meteorological balloon scientific instruments, describing pressure sensor and electronic circuit design for signal transmission via satellite
07 p0821 A73-18969
- Eole project data processing organization and operations management, describing information acquisition and reduction
09 p1060 A73-23377
- Eole experiment processing network for data pretreatment, system management aid and accuracy study and feasibility demonstration of fast response time operational system
10 p1187 A73-23619
- Eole meteorological balloon sounding experiment in Southern Hemisphere, discussing mean circulation, eddy diffusion and data collection and satellite tracking system
15 p1904 A73-31723
- Participation of the Air Force Weather Service in the Eole experiment
17 p2206 A73-34940
- EOLE balloon clusters horizontal trajectories as indicators of southern hemisphere atmospheric circulation, estimating rms divergence as function of scale
19 p2424 A73-37661
- EOSINOPHILS
Physiological shifts in the human organism under increased neuropsychic stresses
19 p2393 A73-37392
- EPHEMERIDES
NT PLANET EPHEMERIDES
A semiautomatic tracking device for satellites
02 p0190 A73-12013
- Improved orbit and ephemeris of the periodic Comet Reinmuth 1 for its apparition in 1972-73.
03 p0370 A73-13197
- Utilization of computers in practical astronomy
03 p0372 A73-13243
- Earth polar motion from revised station coordinates and data from additional Doppler satellite tracking stations
04 p0439 A73-14800

- Subsatellite point coordinates calculation for artificial earth satellites with nearly circular orbits, noting ephemeris application
05 p0613 A73-16203
- Definitive orbit of the comet 1937 V Finsler.
08 p0102 A73-21580
- Influence of ephemerides errors on various determinations using laser lunar ranging
11 p1417 A73-25266
- The geometry and dynamic spectra of Io-modulated Jovian decametric radio emissions.
12 p1540 A73-27327
- Observations of comets at the Crimean Astrophysical Observatory.
14 p1789 A73-29780
- Comet orbit and ephemeris calculations with reference to position and magnitude to facilitate reobservation with long focus telescopes
14 p1789 A73-29782
- Selection of stars for observations from the lunar surface by the method of equal altitudes
15 p1938 A73-31963
- The application of the method of equal heights to the determination of astronomical azimuth
19 p2490 A73-38557
- Study of the redshift structure of the Coma cluster.
20 p2610 A73-39580
- Selection of stars for observation from the lunar surface by the method of equal altitudes.
24 p3132 A73-44488

EPHEMERIS TIME

- Eclipse calculations of lunar features.
01 p0095 A73-10294
- Determination of lunar orbital elements by the method of equal altitudes.
03 p0372 A73-13247
- Mars shape determination from radio occultation measurements by Mariner 9 probe of signal extinction time and spacecraft ephemeris
06 p0747 A73-17488
- Dynamical latitude correction requiring changes in ephemeris and time determination, discussing applicability to nutation of pole of earth figure
11 p1429 A73-26689

EPICYCLOIDS

- Epicyclic motion of stars at different regions of the galaxy.
03 p0379 A73-14586
- Stress-singularities due to uniformly distributed loads along straight boundaries.
13 p1696 A73-28757

EPIDEMIOLOGY

- An epidemiological survey of risk factors for ischemic heart disease in 42,804 men. I - Serum cholesterol value.
04 p0409 A73-15521
- USAF WAVR file of epidemiologic data on medically waived flying personnel, describing computerized updating system
09 p1039 A73-22539
- Risk factors for developing myocardial infarction and other diseases - The 'Men born in 1913' study.
14 p1716 A73-30352
- Prevention of the atherosclerotic diseases - Opportunities for military medicine.
14 p1718 A73-30518
- Air-transport, a main cause of smallpox epidemics today.
18 p2283 A73-36791

EPIDERMIS

- Time-temperature safety thresholds for human epidermal injury related to materials thermal properties
05 p0637 A73-16138
- Mitotic activity in dorsal epidermis of Rana pipiens.
07 p0784 A73-20456

EPILEPSY

- Changes of the free radical concentration in the cerebral cortex depending on the functional state of the cerebrum
01 p0009 A73-11082
- Reaction time method using EEG monitored paroxysm controlled auditory stimuli for responsiveness /consciousness/ evaluation of spike wave burst onset during epileptic seizures
09 p1040 A73-22695
- Effect of stimulation of the mesencephalic reticular formation on the convulsive electrical activity of the brain
14 p1716 A73-30381

EPINEPHRINE

- NT NOREPINEPHRINE
CNS epinephrine tone, a possible etiology for the threshold in susceptibility to oxygen toxicity seizures.
03 p0263 A73-14156
- Role of adrenalin and alpha-receptor deactivation in reactions of hemopoietic organs to stress
07 p0781 A73-19644

EPITAXY

- The growth and electrical characteristics of epitaxial layers of zinc sulphide and of zinc selenide on p-type gallium phosphide.
01 p0088 A73-10683
- Alloying profile measurer for epitaxial films
01 p0050 A73-10799

- Bidimensional and surface effects in a coplanar-contact Gunn diode
02 p0144 A73-11533

- Determination of the dopant concentration profile in epitaxial GaAs by the method of the differential capacitance of a Schottky diode
02 p0145 A73-11548

- Structure and electrical characteristics of epitaxial palladium silicide contacts on single crystal silicon and diffused P-N diodes.
02 p0147 A73-12045

- Experimental approaches to well controlled studies of thin-film nucleation and growth.
02 p0201 A73-12633

- Metal-semiconductor system phase diagram for temperature dependence of substrate surface epitaxial film thickness during single crystal growth, determining equilibrium saturation time
04 p0483 A73-14880

- Morphological, structural and electrical nonuniformities correlation in epitaxial GaAs films on planes, noting Miller indices effects on morphological and electrical properties
05 p0605 A73-17290

- Comparative study of the epitaxial growth in GaAs-I and GaP-I systems over a wide range of crystallization conditions
05 p0605 A73-17292

- Technology and properties of epitaxial GaAs layer grown from liquid phase, considering GaAs solubility in Ga
06 p0734 A73-17798

- Influence of vacuum conditions in fabrication on the structure and electrophysical properties of epitaxial silicon films on sapphire
06 p0736 A73-18089

- Solid-phase epitaxial growth of Si mesas from Al metallization.
06 p0738 A73-18650

- Electro-optic contrast observations in single-domain epitaxial films of bismuth titanate.
06 p0739 A73-18748

- Low-temperature epitaxy of Ge films by sputter deposition.
06 p0739 A73-18777

- Criteria for evaluating semiconductor materials in epiplanar technology applications
08 p0994 A73-21079

- Structure, composition and photoelectrical properties of cadmium sulfide and selenide epitaxial films subjected to heat treatment
14 p1784 A73-30856

- Ge-doped p-type epitaxial GaAs for microwave device application.
15 p1923 A73-31399

- Avalanche properties of low-power epitaxially-planar transistors
18 p2293 A73-36719

- Double heterostructure lasers for optical communications systems
20 p2572 A73-38664

- Laser action from optically pumped epitaxial GaAs crystal waveguides with feedback provided by surface corrugation
21 p2713 A73-40455

- Optical waveguides in GaAs-AlGaAs epitaxial layers.
21 p2752 A73-40969

- High power GaAs double-drift IMPATT devices.
22 p2834 A73-42693

- A new vapor growth method for GaP using a single flat temperature zone.
24 p3119 A73-44412

- Measurement of the p-n junction depth in photocells with epitaxial layers
24 p3058 A73-45254

EPITHELIUM

- Functional dependence of the ciliary epithelium AT-Pase activity and intraocular pressure on the autonomic nervous system.
05 p0539 A73-16248

- Modified rhodopsin in the pigment epithelium.
07 p0783 A73-20263

- Effect of steady magnetic fields up to 4,500 Oe on the mitotic activity of the corneal epithelium in mice
15 p1838 A73-31510

EPNL

- U EFFECTIVE PERCEIVED NOISE LEVELS

EPOCHS

- U TIME MEASUREMENT

EPOXIDES

- U EPOXY COMPOUNDS

EPOXY COMPOUNDS

- NT ETHYLENE OXIDE

- NT HYOSCINE

- High modulus organic fiber/epoxide properties for reinforced composites, including strands, rings and filament wound vessels
09 p1110 A73-22518

- Graphite- and boron-epoxy composite curved panels, determining shear buckling stress and post-buckling strength by visual and photographic observations [SESA PAPER 2030A]
13 p1699 A73-29308

EPOXY RESINS

Investigation of the rheological properties of a model material based on the 'Epidian 2' epoxy resin
01 p0068 A73-10571

Carbon fibre adhesion to organic matrices.
[ONERA, TP NO. 1173] 01 p0068 A73-11499

Glass reinforced epoxy structure for a lightweight superconducting dipole magnet.
02 p0232 A73-11836

Randomly oriented glass fibre reinforced epoxy composites tensile strength properties as function of fibre volume fraction
02 p0185 A73-12427

Glass bead reinforced epoxy and polyester resins mechanical properties as function of volume fraction and interfacial bond strength, discussing beads chemical surface treatment effects
02 p0185 A73-12428

Moisture effects on the high-temperature strength of fibre-reinforced resin composites.
03 p0328 A73-13002

Characterization of an epoxy system for filament winding.
03 p0330 A73-13016

Fiber strength of S-glass/epoxy composites under biaxial loading.
03 p0330 A73-13017

Design, development, fabrication and qualification load testing of high modulus graphite-epoxy reflector support truss for ATS F and G
03 p0330 A73-13021

Graphite-epoxy composite missile adapter design, fabrication, tooling, bonded assembly and costs, comparing with boron-aluminum material
03 p0331 A73-13022

Graphite-epoxy composite properties, fabrication and tests for light weight low distortion spacecraft antenna reflector applications
03 p0331 A73-13023

Filament wound boron/epoxy rocket motor chamber fabrication and hydroproof, burst and firing tests, including failure and deformation evaluation
03 p0331 A73-13024

Response of boron/epoxy composite materials to simulated lightning current.
03 p0331 A73-13025

Effects of process and test variables on the properties of carbon-fibre/epoxide-resin composites.
03 p0335 A73-13800

The energy of crack propagation in carbon fibre-reinforced resin systems.
04 p0469 A73-15981

Tensile properties of PRD-49 fiber in epoxy matrix.
05 p0588 A73-16118

Effect of specimen geometry on fatigue strength of boron and glass epoxy composites.
05 p0588 A73-16139

Crack propagation measurements by surface gage of polymethyl methacrylate, epoxy resin and glass reinforced epoxy composites, conforming with Mott energy balance equation
06 p0714 A73-18499

Properties of pultruded composites containing high modulus graphite fibers.
06 p0715 A73-18719

The Kaiser effect in stress wave emission testing of carbon fibre composites.
07 p0843 A73-20185

Hybrid composite of carbon and glass fiber reinforced epoxy resin, testing mechanical properties and optimal fibrous modulus ratios and volume fraction
07 p0844 A73-20327

Epoxy resins thermal mechanical properties, considering difference between toughness and flexibility in terms of temperature and loading rate insensitivities
10 p1237 A73-23952

Filament-wound vessel from an organic fiber-epoxy system.
10 p1237 A73-23958

Feasibility evaluation of graphite/epoxy composite materials to helicopter transmission housing.
10 p1238 A73-23969

Bearing materials from graphite fiber composites.
10 p1238 A73-23974

High modulus graphite fiber-epoxy composite shear strength and structural observation by X ray and electron diffraction and surface dark field electron microscopy
10 p1239 A73-23977

High strength properties and hardening of epoxy resin bonding materials using dicyaninediamides
10 p1239 A73-24094

Effects of shear damage on the torsional behaviour of carbon fibre reinforced plastics.
10 p1240 A73-24280

The effect of specimen and testing variables on the fracture of some fibre reinforced epoxy resins.
10 p1240 A73-24281

Development of loaded resin one-piece radomes
11 p1387 A73-25294

Effects of prestressing boron/epoxy prepreg on composite strength properties.
[AIAA PAPER 73-382] 11 p1388 A73-25512

Environmental stress cracking of epoxy adhesives.
11 p1388 A73-25840

The impact toughness of discontinuous boron-reinforced epoxy composites.
11 p1389 A73-26046

A compact demountable superleak-light seal for low temperature experiments.
11 p1375 A73-26317

Carbon fiber reinforced epoxy resins mechanical properties, correlating test parameters with observed failure mechanism
12 p1515 A73-26878

The effect of fibre-matrix interface strength on the impact and fracture properties of carbon-fibre-reinforced epoxy resin composites.
12 p1515 A73-26922

High strength glass fibre-resin composites.
13 p1645 A73-28498

Limit of linear viscoelastic behavior - An energy criterion.
13 p1700 A73-29465

Epoxy-thiocol binder viscoelastic deformation under short and long term loads, noting stress-strain linearity limit
13 p1647 A73-29610

Bakelite lacquer and epoxy and phenol-formaldehyde solidified resin binders strength at high temperatures
14 p1766 A73-30687

Cast thermosetting epoxy resin linear elastic stress-strain characteristics under tension, compression, torsional and bending loads
15 p1897 A73-31619

Dynamic mechanical properties of graphite-epoxy and carbon-epoxy composites.
15 p1897 A73-31677

Tensile and compressive strength trend prediction for anisotropic boron-epoxy composites from off axis tests
15 p1897 A73-31682

Linear elastic fracture mechanics applicability to graphite-epoxy laminated fracture specimens configuration from fractographic studies
15 p1897 A73-31684

Orthotropic characteristics of glass-fibre-epoxy laminates under plane stress.
15 p1897 A73-31698

Lightning protection for boron and graphite fibers in epoxy resins for aircraft composite structures
16 p1967 A73-33032

F-14 aircraft boron-epoxy and graphite-epoxy composite structure production protection against degradation by lightning discharges, discussing design, processing and tests
16 p2028 A73-33035

Epoxy resin adhesive for metal-to-metal and honeycomb sandwich bonding, featuring high flow during cure for high structural strength
16 p2029 A73-33054

Graphite-epoxy composite door landing gear assembly for space shuttle orbiter, discussing design, analysis, fabrication and structural testing
16 p2029 A73-33058

Investigation of mounting discrete chip components for hybrid microelectronic applications.
16 p1989 A73-33467

Epoxy adhesive materials evaluation for microelectronic assemblies of hermetically sealed hybrid circuits with semiconductor chips and thin film substrates
16 p1989 A73-33468

The effect of cure cycle on the mechanical properties of carbon-fibre/epoxide resin.
16 p2031 A73-33988

The effects of adverse environmental conditions on the resin-glass interface of epoxy composites.
16 p2031 A73-33989

Investigation of the bond strength between layers of textile materials
17 p2194 A73-34333

The processability of unidirectional prepreps in aerospace applications.
17 p2195 A73-34808

Moldability, storage stability and thermal, mechanical and electrical properties of epoxy molding compounds for electronic devices
17 p2196 A73-35340

An improved epoxy resin formulation for multi-layer circuit boards.
17 p2196 A73-35341

Short- and long-term strength characteristics of particulate-filled cast epoxy resin.
17 p2197 A73-35343

Chemo-rheology of two high temperature epoxy resins.
17 p2197 A73-35347

Micromechanic stresses in photoelastic composite coupons.
[SESA PAPER 2175A] 17 p2251 A73-35456

Carbon, boron and glass fiber-epoxy resin composites fracture processes, predicting fracture strength of aligned fibrous composites via linear elastic fracture mechanics concepts
17 p2198 A73-35530

Tensile fracture of boron-epoxy composites with ordered filament packing geometry.
17 p2198 A73-35535

Fiber orientation effects on fatigue failure of aligned short fiber composite materials.
17 p2198 A73-35546

Graphite fiber optimization and evaluation efforts for utilization as fiber-epoxy composites reinforcement in tensile-critical applications
17 p2198 A73-35838

Development and problems of testing prepreps for the purposes of the Czechoslovakian aircraft industry
18 p2327 A73-36469

The elastic properties of carbon fibres and their composites.
18 p2329 A73-37095

Boron epoxy, polyimide and aluminum composite materials for cost effective high performance aircraft and turbine engine structures, assessing development and application status
19 p2443 A73-37892

Studies on glass-reinforced epoxy resin using either Vulkadur A or a mixture of Vulkadur A and triethanolamine as crosslinking agent.
19 p2444 A73-38092

Group 3-5 compound light emitting diode degradation modes and mechanisms, discussing epoxy lenses, light transmission characteristics, time and temperature functions and surface passivation
19 p2439 A73-38457

Temperature dependence of adhesive fracture of epoxy resin.
20 p2580 A73-38642

The tensile strength of pultruded carbon fibre/epoxy resin composite.
21 p2723 A73-40923

Thermal contraction of a system of glassfibre and epoxy resin between 300 and 77 K.
21 p2724 A73-41107

Response of glass-fiber-reinforced epoxy specimens to high rates of tensile loading.
23 p2996 A73-43385

Deformation and failure of boron-epoxy plate with circular hole.
23 p3040 A73-43631

Some important aspects in testing high-modulus fiber composite tubes in axial tension.
23 p2996 A73-43639

Influence of fiber property variation on composite failure mechanisms.
23 p2996 A73-43643

Improved mechanical properties of composites reinforced with neutron-irradiated carbon fibers.
24 p3104 A73-45143

Theoretical post-yielding behavior of composite laminates. II - Inelastic macromechanics.
24 p3104 A73-45145

Acoustic emission produced during burst tests of filament-wound bottles.
24 p3094 A73-45146

Vibration characteristics of aluminum plates reinforced with boron-epoxy composite material.
24 p3149 A73-45148

EQUATIONS OF MOTION

NT EULER EQUATIONS OF MOTION
NT HELMHOLTZ VORTICITY EQUATION
NT HYDRODYNAMIC EQUATIONS
NT KINEMATIC EQUATIONS
NT KINETIC EQUATIONS
NT NAVIER-STOKES EQUATION
NT REYNOLDS EQUATION

Dynamics of angular motions of a solid body carrying a rotating rotor, with allowance for energy dissipation
01 p0075 A73-10087

Equations of motion integral properties-based construction of Liapunov functions used to derive sufficient conditions for perturbed nonlinear system solution stability
01 p0075 A73-10090

Linearization method for analytic solution of oscillatory motion differential equations of elastic nonlinear system, studying combinations of free and forced vibrations
01 p0075 A73-10093

A universal three-angle basis for rotational kinematic analysis, simulation and control.
01 p0109 A73-10108

Low order models representing realizations of turbulence.
01 p0032 A73-10450

The equations of motion of gyroscopes in general relativity
01 p0098 A73-10559

On a new form for the differential equations of relative motion of the three-body problem.
01 p0099 A73-10690

Planar three body problem singularities due to binary collisions, regularizing equations of motion by Levi-Civita coordinate transformation
01 p0099 A73-10692

Investigation of conditions corresponding to the existence of an energy integral in the generalized n-body problem with variable masses
01 p0077 A73-10918

A solution to the problem of the third integral of motion. I.
01 p0106 A73-11318

Determination of gimbal errors in an astatic gyroscope with allowance for drift

01 p0054 A73-11416

Multiple correction procedure for motion control ensuring arrival at final state without complete initial state information

01 p0079 A73-11419

The relation between three-dimensional and two-dimensional problems in the mechanics of continuous media

01 p0119 A73-11430

Equations of motion for nonuniformly heated gas past hot bodies, noting gas heating between two parallel flat surfaces with different temperatures

02 p0152 A73-11612

Calculation of the energy and force process parameters in magnetic-pulse forming of complex shaped elements

02 p0172 A73-11646

Ultraelliptic integrals degeneration to elliptic integrals in Goriachev-Chaplygin equation of rotating body, noting asymptotic approach to limiting motion

02 p0191 A73-11761

Investigation of a moving angular-velocity hodograph in the symmetrical solution to the problem of the motion of a body having a fixed point

02 p0191 A73-11762

Time dependence of the basic variables in the symmetric solution to the problem of the motion of a body having a fixed point

02 p0191 A73-11763

Equations of motion for Kovalevskaya gyroscope uniform rotation about axes differing from inertia ellipsoid principal axes, noting sufficient stability conditions

02 p0167 A73-11765

Dynamic characteristics of two bodies coupled by common axis, noting equations of motion of Lagrange gyroscopes system

02 p0192 A73-11766

Equations of motion of composite space pendulum formed by gyroscopes with Cardan suspension, noting equations integrability

02 p0192 A73-11767

Newtonian force field effect on gyroscope motion for coordinate axes coincident with inertia tensor axes, solving equations of motion by energy integral

02 p0192 A73-11769

New solutions of the problem of the motion of a gyroscope in a central Newtonian force field

02 p0192 A73-11770

Regular gyrostator precession in a central Newtonian field of forces

02 p0192 A73-11771

Three linear invariant relations in the problem of motion of a heavy solid body with a liquid filler

02 p0153 A73-11773

Precession equations of a triaxial power-driven gyrostabilizer

02 p0167 A73-11775

Equations of motion of solid body about fixed point with nonholonomic constraint, noting potential forces field effect

02 p0193 A73-12195

Algorithms for equations of oscillatory motion about moving center, noting disturbing force effect on vibrational frequency

02 p0193 A73-12196

The effects of viscous friction on axial rotation of celestial bodies.

02 p0216 A73-12376

Response of a system of cascaded nonlinear springs

02 p0193 A73-12521

MHD equations for velocity distribution of magnetic field motion in conducting fluid, noting evolution equations of geomagnetic field

02 p0164 A73-12555

On the evaluation of tri-diagonal secular determinants.

02 p0188 A73-12606

Equations of motion for steady state spherically symmetric flow of polytropic gases into or out of neutron stars, black holes or Schwarzschild singularities

02 p0223 A73-12729

Flight-mechanical analysis of various flight states of conventional aircraft. VII - Mechanical principles: Rigid-body dynamics

03 p0250 A73-13074

Correlation theory for equations of motion of constant thickness shallow shell vibration under random loads

03 p0387 A73-13158

Boundary value problem for flow equation of multiphase viscous fluid with given velocity distribution, noting equations of motion for incompressible micropolar fluid flow

03 p0291 A73-13164

Finite element equations of motion of elastoplastic shell, applying theory to edge clamped circular plate dynamic response

03 p0389 A73-13321

On the stability of dual-spin bodies with unbalancing mass.

03 p0381 A73-13364

Constant and variable amplitude limit cycles in dual-spin spacecraft.

03 p0382 A73-13493

Equations of motion in electrohydrodynamics of multiphase one dimensional flow, noting shock wave propagation and attenuation

03 p0346 A73-13611

Long wave disturbance propagation analysis via equations of motion from mathematical model of liquid-gas mixture, determining velocity, pressure and density perturbation propagation

03 p0294 A73-13612

Lagrange equations of motion for ideal incompressible fluid flow under asymmetric deformation of expanding circular cylinders and spheres, calculating resistance forces

03 p0294 A73-13613

Equations of motion for flexible cables.

03 p0343 A73-13706

Air-space analogies - The velocity limits in aeronautics and astronautics

03 p0374 A73-13765

Discretized body mechanics equilibrium, constitutive and motion equations application to elastic lattice type shell structures

03 p0393 A73-13779

Liapunov function application to stability of unperturbed motion of system of differential equations with respect to part of variables

03 p0344 A73-14056

Equilibrium motions of rigid spinning satellite in circular orbit around central body subject to gravitational torque

03 p0376 A73-14268

On the stability of triangular points of equilibrium in the restricted elliptic problem

03 p0376 A73-14270

Error sources in numerical integration of spacecraft equations of motion in solar and planetary gravitational fields, suggesting methods for improving accuracy

03 p0379 A73-14553

Existence theorem for nonlinear oscillatory equations of motion transformation into normal form, noting quasi-periodic functions with arbitrary frequencies

04 p0475 A73-14888

Stability of the motion of a nonautonomous gyrostator

04 p0475 A73-14932

Stabilization of constraints and integrals of motion in dynamical systems.

04 p0470 A73-15002

Newtonian differential equations of Kepler motion, analyzing stability by numerical integration based on Floquet theorem and Runge-Kutta method

04 p0497 A73-15013

Satellite motion in the equatorial plane of an oblate primary body and apsidal line shift evaluation.

04 p0498 A73-15296

Numerical integration of equations of Ba cloud motion in ionosphere with end shorting, noting critical electric field for motion stability

04 p0445 A73-15649

Equations of motion for mathematical models of turbine rotors with elastic shaft in unsteady operation, calculating resonant angular velocity

04 p0514 A73-15654

Energy balance, motion and constitutive equations of polar fluids, considering entropy inequality, viscosity and dissipation rate

04 p0434 A73-15679

Motion, constitutive and energy balance equations for materials with microstructure, considering elastic bodies

04 p0514 A73-15680

Theoretical low-speed particles collision with symmetrical and cambered aerofoils.

[ASME PAPER 72-WA/FE-35] 04 p0404 A73-15852

Equations of motion for precession theory of two rotor gyroscopes on earth satellites for orbit plane determination, noting noise spectrum transformation

05 p0628 A73-16407

Numerical integration of rotating body dynamic and kinematic equations, noting orthogonalization, normalization and error minimization methods

05 p0595 A73-16423

Jacobi-Hamilton equation of motion of mass point, using elliptic functions for harmonic potential

05 p0597 A73-16467

Control of the motion of a solid body with servo couplings

05 p0597 A73-16611

Equations for the compass motion of a triaxial gyrostabilizer in gyrocompass operation

05 p0577 A73-16993

Accelerated numerical integration of the equations of motion of celestial mechanics

05 p0619 A73-17002

Calculus of variations for equations of relative motion of two satellites with unperturbed Kepler orbits of arbitrary eccentricity

05 p0620 A73-17006

Construction of the equations of a programmed motion possessing extremal properties

06 p0722 A73-17115

The properties of a solution of the equations of motion of a mechanical system subject to irregular /singular/ perturbations.

06 p0722 A73-17155

The influence of nonlinear couplings on the behaviour of the solution of the equations of motion of a mechanical system.

06 p0722 A73-17156

Discretized elastic multipolar bodies equations of motion and conservation laws from variational formulation, considering virtual work, Betti principle and Somigliana formulae

06 p0761 A73-17892

Note on the wave propagation problems in isotropic discretized bodies.

06 p0723 A73-17893

Discretized body defined as special system with finite degrees of freedom, describing mechanics in terms of constitutive and motion equations

06 p0723 A73-17894

Solution of the low-altitude satellite equations.

06 p0757 A73-18072

A class of almost periodic motions in systems with impulses

06 p0724 A73-18681

Space-time transformation for equation of relative motion of two bodies on gravitating matter background of Einstein-de Sitter universe

06 p0724 A73-18689

Equations of disturbed motion and equilibrium for solid body with incompressible fluid filled cavity, noting equilibrium position stability conditions

06 p0688 A73-18878

Relations between the first integrals of a non-holonomic mechanical system and of the corresponding system freed of constraints.

07 p0850 A73-19013

Evaluation of gravity anomalies directly from satellite observations.

07 p0813 A73-19025

Equations of motion for mechanical system with imposed servo couplings, discussing Gauss variational principle applicability for system analysis

07 p0851 A73-19128

Necessary condition of optimality for some problems of optimal control theory

07 p0844 A73-19296

Resonances and certain cases of integrability of the motion of a heavy solid about a fixed point

07 p0851 A73-19469

Equations of motion of the lunar roving vehicle.

07 p0808 A73-19490

Monofrequent resonance oscillations with external excitation.

07 p0851 A73-19544

Flight vehicle equations of motion with variable information, noting flight control algorithm for random variable with given probability

07 p0849 A73-20077

The generation of the highest cosmic ray energies.

07 p0872 A73-20193

An exact helical wave solution to the equations of magnetohydrodynamics.

07 p0859 A73-20233

Evolution equations of motion for program manifold of continuous control system with given transient response

07 p0852 A73-20632

Investigation of the smoothness characteristics of the Bellman function on the basis of the equation of motion of the system in time-optimal problems. I Linear case

07 p0806 A73-20633

On the third integral of motion in stellar dynamics. I. On the analytical study of Saturn's satellites, Enceladus-Dione

08 p1002 A73-20849

Equation of motion and bubble size distribution function for nucleate boiling, noting balance equation for two phase fluid

08 p1022 A73-21096

Rocket rectilinear motion, comparing Meshcherskii and Gantmacher-Levin equations in light of contact interaction hypothesis

08 p1014 A73-21181

Integration of the equations of meteorology. III - Integration in time

08 p0986 A73-21485

Electron admittance and efficiency of the output cavity of a klystron

08 p0948 A73-21557

Monograph on Hamiltonian cosmology, considering cosmological models with Hamiltonian equations of motion, Bianchi universes, superspace concepts and quantum mechanical Hamiltonian construction

08 p0984 A73-21834

Investigation of the motion of the medium near the point of contact of shock waves in linear and nonlinear formulations

09 p1070 A73-21921

Literary theory of the motion of a satellite in the tesseral-harmonic field of the earth's gravitational potential at small eccentricities

09 p1143 A73-22097

- Equations of motion of ideally conducting medium in MHD approximation, solving under constant magnetic field and magnetic-hydrodynamic pressure equilibrium 09 p1126 A73-22280
- The motion of a dynamically unbalanced gyroscopic linear-acceleration integrator 09 p1081 A73-22344
- On the demonstration and interpretation of the Coriolis effect. 09 p1120 A73-22475
- Asymptotic scheme for a class of partial differential equations 09 p1112 A73-22477
- Equation of motion derived for laser resonator with frequency dispersion effect on emission kinetics and spectral features, analyzing unsteady /transient/ processes 09 p1094 A73-22596
- Investigation of the motion of a body of variable mass within a multibody gravitational field with the aid of a regularizing variable 09 p1121 A73-22852
- Laminated composites displacement equations of motion, obtaining stored kinetic and strain energy and free harmonic waves dispersion normal and along layers 09 p1161 A73-23117
- Conformal invariance of the equations of motion in curved spaces. 10 p1241 A73-23637
- Perturbed satellite motion differential equations, on basis of fixed center problem and perturbing forces with no force function 10 p1274 A73-23721
- Motion equation solutions for three flattened spheroids with coincident equatorial symmetry planes in Lagrange form by Duboshin transforms 10 p1274 A73-23722
- On the application of the method of decoupling of motions to the analysis and synthesis of nonlinear systems. 10 p1199 A73-24031
- Turbulent interface structure from eddy viscosity models, discussing equations of motion and Nee-Kovaszny and Prandtl models 10 p1205 A73-24253
- Coherent state systems for groups of motions of Hermitian bounded homogeneous regions in terms of Bergman kernels 10 p1249 A73-24463
- Calculation of higher-order perturbations in the motion of celestial bodies 10 p1282 A73-24482
- Canonical perturbation theory solution for nonconservative dynamic systems equations of motion, considering Duffing and van der Pol equations 10 p1283 A73-24665
- Radiative losses in a magnetostatic and intense electromagnetic field. 10 p1270 A73-24908
- Explicit and implicit difference schemes for solving complex equations of motion, deriving approximation stability conditions 11 p1397 A73-25033
- Vertical two axis gyroscopically stabilized equations of motion analysis by averaging method 11 p1360 A73-25048
- Russian book on rockets as control plants covering dynamics equations of motion for different configurations, linearization and matrix description of rockets 11 p1429 A73-25175
- Reduction of a gyrostabilizer problem to that of a rigid body. [ASME PAPER 72-APM-QQ] 11 p1398 A73-25704
- Relationship of spatial and planar problems in the mechanics of continuous media. 11 p1443 A73-26059
- Hamilton variational principle for deriving equations of motion for small elastic displacements of thin circular rings, noting twist equation occurrence 11 p1446 A73-26493
- Stable-member mounted instrument environment simulation model development. 11 p1395 A73-26638
- Flight-mechanics analysis of various flight conditions of conventional aircraft. VII - Mechanical foundations: Dynamic equations of motion of the translational motion of a rigid body 11 p1307 A73-26725
- Resonant oscillations of conservative system with nonlinear component, obtaining differential equations of motion solution 11 p1448 A73-26731
- Satellite ascent transfer trajectories equations of motion numerical integration, replacing time parameter by regularizing independent variable for gravitational singularity elimination [DFVLR-SONDDR-283] 12 p1537 A73-26822
- Differential equations of motion for analog model of M-type TWT performance, proposing block diagram for electron phase and trajectory and field distribution calculations 12 p1478 A73-26950
- Asymmetric mechanics of turbulent flows - Energy and entropy 12 p1487 A73-27411
- Control system equations of motion construction based on program manifold, determining multidimensional piecewise continuous controller vectors under assigned inequalities 12 p1484 A73-27455
- Differential equations of thermoelastic state for shells receiving a thermal shock at the surface 12 p1555 A73-27790
- A method of studying oscillatory systems subject to the action of external periodic forces in the nonresonant case 12 p1525 A73-27812
- Normal coordinates in the analysis of the principal resonances of nonlinear vibrating systems with multiple degrees of freedom 12 p1695 A73-28557
- Deformable solid as discretized body in classical continuum mechanics, deriving motion and constitutive equations 12 p1659 A73-28558
- Elastic unipolar discretized linear bodies, considering motion and constitutive equations, conservation laws, virtual work principle and uniqueness and reciprocity theorems 12 p1659 A73-28559
- Clamped orthotropic triangular plates free nonlinear vibrations, solving equations of motion in first order approximation by von Karman plate theory 12 p1697 A73-28808
- The use of averaged flow equations of motion in turbomachinery aerodynamics. 12 p1603 A73-29047
- Stabilization of steady motions of mechanical systems with respect to some of the variables 12 p1660 A73-29076
- Classification theorem for analytical transformations of second order differential equations of motion at arbitrary resonance based on group theory 12 p1661 A73-29081
- Small perturbation evolutionary motion equations for forced vibrations of quasi-linear two frequency autonomous systems at resonance 12 p1661 A73-29082
- Computer plotted dynamic stability and transient response of linear continuous systems described by high order differential equations of motion 12 p1661 A73-29144
- A method of integrating the equations of motion in special coordinates and the elimination of a discontinuity in the theory of the motion of periodic comet Wolf. 12 p1790 A73-29790
- Nongravitational effects on comets - The current status. 12 p1791 A73-29797
- Nongravitational forces and periodic comet Giacobini-Zinner. 12 p1791 A73-29803
- On the uniqueness of solutions of stress equations of motion of the Beltrami-Michell type. 12 p1809 A73-30254
- A uniqueness theorem for a system of stress equations of motion in linear elasticity. 12 p1809 A73-30255
- Existence of generalized tensorial fields in linear asymmetric elastodynamics. 12 p1809 A73-30256
- Zero tangential acceleration points on bodies moving in three dimensional Euclidean space, considering helical-spherical and rotating-spherical motion 12 p1775 A73-30707
- Elimination of time and differential equation of trajectories in the problem of three restricted, circular, plane bodies 12 p1930 A73-31175
- Slow motions of bodies in gas mixtures 12 p1861 A73-31198
- Minimum time response control problem of moving point in state space, determining piecewise-continuous vector function for optimal system transfer to coordinate reference point 12 p1931 A73-31231
- On the establishment and solution of equations of motion of an electrically conducting fluid set in motion by the slow and uniform rotation of walls of a ring-shaped receiver, in the presence of an axial magnetic field, in the case where the mean value of the intensity of the currents induced in a straight section takes a nonzero value 12 p1918 A73-31569
- Intermediate orbit of an artificial earth satellite obtained by the averaging method - First order perturbations 12 p1936 A73-31644
- Construction of equations of motion for program manifold of continuous control system with given transient response 12 p1913 A73-31686
- Study of the smoothness properties of the Bellman function in time-optimal problems, based on the equation of motion of the system. I - The linear case. 12 p1854 A73-31687
- Normal mode solution to the equations of motion of a flexible airplane. 15 p1950 A73-31747
- Resonances and some cases of integrability of the motion of a heavy rigid body about a fixed point. 15 p1914 A73-32068
- Stability analysis procedure for shock wave in steady compressible fluid flow, obtaining equations of motion 15 p1864 A73-32113
- The non-linear theory of thin elastic sheets. 15 p1954 A73-32118
- Equations of disturbed motion and equilibrium for solid body with incompressible fluid filled cavity, noting equilibrium position stability conditions 15 p1915 A73-32403
- Vector field representation of curved elastic membranes oscillatory motions, particularizing equations of motion for small displacements from equilibrium configurations 16 p2076 A73-32937
- Elastic viscously damped ten degree of freedom system with two torsion-elastically mutually pivotally joined rotors, determining eigenfrequencies by equations of motion numerical evaluation 16 p1968 A73-33235
- Principle of virtual work and Piola theorem for motion and constitutive equations and boundary conditions of oriented elastic media, using point continuum mechanics assumptions 16 p2080 A73-33245
- Electric dipole motion in Einstein unitary field with electrostatic potential as function of polar coordinates, deriving law of motion from Clausen integral formula 16 p2037 A73-33371
- Equations of motion for systems with nonlinear, second-order, nonholonomic connections 17 p2211 A73-34147
- Book - Lectures on fluid mechanics. 17 p2150 A73-34457
- Book on energy equations for small and large scale atmospheric motion covering laminar and turbulent flow and space-time scales for atmospheric energy balance 17 p2158 A73-34463
- Some properties of dynamic equation integrals from the theory of shells 17 p2244 A73-34736
- Finite element method application to solution of structural dynamics problems, considering equations of motion and vibration mode shapes 17 p2245 A73-34836
- Influence of structural flexibility on attitude control of spacecraft 17 p2162 A73-34950
- Optimal pursuit-evasive conflicts with guidance systems containing time delays. 17 p2145 A73-35380
- Dynamic behavior of satellites with large-area solar cell panels [DGLR PAPER 73-049] 17 p2239 A73-35485
- Book - Vibration of linear mechanical systems. 18 p2361 A73-35900
- Aerodynamic coefficients determination for nonlinear equations of motion solution to fit experimental free flight data, obtaining starting solution by noniterative continuation method 18 p2263 A73-36307
- Perturbed satellite motion differential equations derivation on basis of fixed center problem and perturbing forces with no force function, obtaining intermediate orbital elements 18 p2355 A73-36746
- Motion equation solutions for three flattened spheroids with coincident equatorial symmetry planes in Lagrange form by Duboshin transforms 18 p2355 A73-36747
- Forces acting on a small body in an arbitrary incompressible fluid flow and equations of motion of a two-phase medium 18 p2302 A73-37008
- Vibration of layered shells. 18 p2367 A73-37029
- Differential equations for ballistic motion of meteoric particles in earth atmosphere, noting orbit stability 19 p2480 A73-37237
- Diffusion of a vertical jet into a fluid medium of arbitrary density 19 p2420 A73-37547
- On stabilization of steady-state motions of mechanical systems with respect to a part of the variables. 19 p2459 A73-37631
- Classification theorem for analytical transformations of second order differential equations of motion at arbitrary resonance based on group theory 19 p2445 A73-37632
- Small perturbation evolutionary motion equations for forced vibrations of quasi-linear two frequency autonomous systems at resonance 19 p2445 A73-37633
- Third integral of motion and the velocity field for a quasi-Newtonian potential. I 19 p2486 A73-37848

Derivation of an approximate solution to the equation of geocentric motion of a space vehicle with a solar sail

19 p2492 A73-37849

Ion trajectories in plasma focusing devices based on numerical integration of three dimensional equations of motion

19 p2468 A73-37856

Flight-mechanics analysis of various flight conditions of conventional aircraft. VIII/1 - Mechanical foundations: Kinematic equations of motion of a rigid body

19 p2387 A73-38123

Optimal stabilization of moving control plants during multichannel measurement of their coordinates

20 p2542 A73-39039

Virtual motion principle implication for structural damping differential equations for cases of homogeneous, inhomogeneous and aerodynamic flutter for various degrees of freedom

20 p2616 A73-39098

Existence and uniqueness conditions for solid surface vaporization products dispersion into vacuum formulated for equations of motion of ideal gas under variable energy release

20 p2573 A73-39282

Elliptical orbit of two coupled material points in Newtonian central gravitation field, discussing flexible weightless filament coupling, equations of motion and sinusoidal oscillations

20 p2608 A73-39319

Equations of motion for ideal isotropic viscoplastic medium in axisymmetric space, determining conditions for flow core existence

20 p2619 A73-39336

Motion of a rigid-plastic beam in a resistant medium under the action of a local load

20 p2620 A73-39470

Investigation of the motion of a gyroscopic pendulum on a randomly vibrating base

20 p2566 A73-39504

Motion of a solid body having a cavity completely filled with two immiscible liquids

20 p2547 A73-39507

Equations of perturbed motion of a body with a liquid-containing cavity when the normal to the free liquid surface deviates sizably from the axis of the cavity

20 p2547 A73-39510

Deviation of the solution of a quasi-linear wave equation from the solution of the linear equation in the region of continuous first derivatives

21 p2724 A73-40181

Small oscillations of a heavy solid body about a stationary point and certain cases of the existence of 'linear integrals'

21 p2738 A73-40188

Statistical dynamics formulation of motion equations for particle system in gravitational interaction with neither gas law nor hydromagnetic effects, applying to solar system evolution

21 p2766 A73-40313

Self-similar solutions of the plasma equations

21 p2747 A73-40553

The effect of magnetic mass on Alfvén waves.

21 p2701 A73-40624

Computerized simultaneous numerical integration of motion equations for solar system, star cluster and galaxies, considering radar observations of moon, Mercury, Venus, Mars and Icarus

21 p2772 A73-41241

Approximate estimation of the possibility of using the viscoelasticity hypothesis for the formulation of an equation of motion for a liquid with polymer additions

22 p2841 A73-42122

Wave potentials for an elastic transversely isotropic medium

22 p2921 A73-42285

Properties of galactic orbits and motion integrals of high-velocity stars. II - Periodic and nonperiodic orbits in the 2nd Schmidt potential

22 p2907 A73-42303

Effect of the elastic deformation of a gimbal suspension on the nutation oscillation frequency of a gyroscope

22 p2860 A73-42359

German book on rocket propulsion theory covering orbital mechanics, equations of motion, performance parameters and nuclear, electric and chemical propulsion types

22 p2909 A73-42493

Forced motion of lumped mass systems including the effect of axial force.

22 p2923 A73-42630

German monograph - A contribution to the investigation of the stability of pipelines with flowing liquids according to the method of finite elements.

22 p2924 A73-42737

German monograph - Characteristics of motion of an elastically supported rotor with interior damping.

22 p2867 A73-42849

German monograph - The computation of periodic motions of multipath nonlinear systems.

22 p2888 A73-42854

Prediction of satellite motion by a combined method of recurrent relations

23 p3027 A73-43267

A note on relative motion in the general three-body problem.

23 p3031 A73-43834

Evolution of a 'class two' family of periodic orbits in the general planar problem of three bodies.

23 p3031 A73-43835

The global solution of the problem of the critical inclination.

23 p3031 A73-43836

Sandwich shells nonlinear theory with stress-strain relations in tensor notation, using Hamilton principle for equations of motion and boundary conditions

23 p3044 A73-44078

Stability of a biaxial gyroframe on a vibrating base in resonance conditions

23 p3007 A73-44186

Analysis of the perturbed motion of a solid with cavities partially filled with liquid

23 p2969 A73-44198

Motion of a solid with a nonholonomic constraint at a fixed point

23 p3007 A73-44200

Velocity field determination in meridional plane of potential field using third isolating integral of motion

23 p3035 A73-44238

Rectilinear trajectories of the three-body problem when the constant of line forces is zero

24 p3141 A73-45282

Numerical stabilization of all laws of conservation in the many body problem.

24 p3142 A73-45289

The restricted problem of three bodies with rigid dumb-bell satellite.

24 p3142 A73-45300

A simple theory of the anomalous Hall effect in semiconductors.

24 p3120 A73-45329

Continuity equation and equations of motion for ideal plastic body based on von Mises yield condition, considering stress discontinuity and boundary value problems

24 p3153 A73-45499

EQUATIONS OF STATE

NT HUGONIOT EQUATION OF STATE

Equations of state and dissociation equilibrium for CsCl plasma, noting thermodynamic model for phase transitions of liquid metal into nonideal ion plasma

01 p0084 A73-10851

Relation of the equation of state of compressed gases with the optical complex and the specific refraction - Virial coefficients of carbon dioxide

01 p0080 A73-10856

A standard format for mathematical models of fluid power systems.

02 p0132 A73-12001

Densities of compressed liquid methane, and the equation of state.

02 p0238 A73-12630

The state of ionization in nova shells.

02 p0222 A73-12706

Relativistic spheres of hadron gas with zero baryon number constructed from Hagedorn hadronic equation of state, considering sphere stability properties

03 p0370 A73-13211

A fourth-order nonlinear equation of state - Application to the determination of the elastic moduli of single-crystal and polycrystalline solids

03 p0350 A73-14601

State and integral equations formulations for signal design problem of channels with known time dispersion and additive white Gaussian noise

04 p0419 A73-15405

Subnuclear density state equation for minimum mass and binding energy of neutron star converting into white dwarf

04 p0502 A73-15978

Existence theorems for multidimensional control systems with lower-dimensional controls.

05 p0561 A73-16489

Introduction of two solving functions into the equations for nonshallow shells.

05 p0634 A73-16796

Use of approximations of thermodynamic functions in gasdynamics calculations

06 p0644 A73-17470

Special features of Debye screening and the equation of state of a partially ionized plasma

06 p0730 A73-18551

The equation of state of a dense metal vapor plasma and electron mobility

06 p0730 A73-18552

Statistical mechanics and virial functions for equation of state of dense gas with spherical nonpolar molecules, calculating compressibility factor for methane and Ar

06 p0726 A73-18555

Radiation effects on state of gas behind strong shock wave, representing power density of non-relativistic fully ionized hydrogen plasma

07 p0920 A73-19508

Application of the fourth-order anharmonic theory to the prediction of equations of state at high compressions and temperatures.

07 p0851 A73-19925

Satellites elastic structures equations of state for stability and attitude control systems analysis, deriving translational and rotational momentum equations for moving coordinate systems

08 p1014 A73-20779

Equation of state of a mixture of nonideal, chemically reacting gases.

08 p0936 A73-20856

New formulations of the corresponding states principle for the transport properties of pure dense fluids.

08 p1023 A73-21258

Constitutive equation for electronic circuits without topologically dependent variables, noting numerical analysis of equations of state for nonlinear circuits

08 p0951 A73-21551

Multi-axial and reversing stress effects in dislocation creep - A mechanical equation of states.

08 p0980 A73-21781

Initial circuit equation transformation into equation of variable states, noting linear and nonlinear circuits in static and dynamic regimes

09 p1068 A73-22452

Partially ionized nonideal plasma model electron-ion interactions, equilibrium, equations of state and thermodynamic quantities

10 p1252 A73-23501

Orthogonal polynomials for computerized construction of equations of state for substances under thermodynamic restrictions

10 p1293 A73-23505

S matrix method featuring eigenergy and eigenfunction trials number reduction for rapid numerical determination of bound states of partial-wave-projected Schroedinger equation

10 p1248 A73-23669

Gravitational collapse with a physical singularity on an isotropic hypersurface

10 p1283 A73-24751

Evolution of universe filled with cold baryons at cosmological singularity from Friedmann solution and equation of state for cold baryons

10 p1284 A73-24753

Formula approximating Fermi-Dirac integrals for electron gas density, pressure and internal energy, discussing pressure ionization effect on equation of state in stellar interiors

11 p1417 A73-25261

Isentropic compression of fused quartz and liquid hydrogen to several Mbar.

11 p1398 A73-25884

Quantum statistical mechanics of dense partially ionized hydrogen.

11 p1405 A73-25886

Equation of state and phase diagram of dense hydrogen.

11 p1399 A73-25890

Ground state energy of solid molecular hydrogen at high pressure.

11 p1401 A73-25891

On identifying transfer functions and state equations for linear systems.

11 p1342 A73-26641

Application of the principle of corresponding states to two-phase choked flow.

11 p1349 A73-26744

Formation and solution of the equations of state of electronic circuits

12 p1485 A73-27623

Equations of planet figures solved for third order accuracy, covering flattening, density distribution, Jupiter and Saturn models and gravitational moments corrections for radii

12 p1546 A73-27860

Equations of state and dissociation equilibrium for CsCe plasma, noting thermodynamic model for phase transitions of liquid metal into nonideal ion plasma

12 p1529 A73-27901

Connection between the equation of state of compressed gases with an optical complex and the specific refraction - The virial coefficients of carbon dioxide.

12 p1526 A73-27906

An equation for thermal expansion coefficient at high pressures.

13 p1673 A73-28206

Kinetic equations for the Green functions describing equilibrium states of a gas.

13 p1662 A73-28551

Stellar evolution as succession of quasi-equilibrium states, investigating dynamic stability via hydrodynamic and state equations

13 p1682 A73-28980

Neutron stars physical model, deriving mass-density-energy relationships for degenerate electron gas

13 p1682 A73-28985

Equation of state of matter at supernuclear densities deduced from particle interactions nature and effective baryon mass spectrum

14 p1777 A73-30739

Differentially rotating neutron star models calculation for given state equation, examining mass increase

relationship to rotational rigidity relaxation via Ostriker-Tassoul instability criterion

15 p1929 A73-31093

Active networks state equations with singular A matrix, considering algebraic method of reduction to equivalent set of equations with nonsingular A matrix

16 p1992 A73-32912

Optimal curved pursuit trajectories of point mass in three dimensional space, establishing search technique via Pontryagin principle calculations and equations of state

16 p2061 A73-33269

The magnetohydrodynamic stability of white dwarfs and neutron stars.

16 p2062 A73-33573

Debye screening and equation of state of a partially ionized plasma.

16 p2042 A73-33576

Equation of state of a plasma of a dense metal vapor and the electron mobility.

16 p2042 A73-33577

Statistical mechanics and virial functions for equation of state of dense gas with spherical nonpolar molecules, calculating compressibility factor for methane and Ar

16 p2039 A73-33580

Partially ionized nonideal plasma model electron-ion interactions, equilibrium equations of state and thermodynamic quantities

17 p2216 A73-35181

Orthogonal polynomials for computerized construction of equations of state for substances under thermodynamic restrictions

17 p2255 A73-35185

Two layer cores in terrestrial planets with emphasis on Mars and Venus, discussing pressure at earth mantle-core boundary, equations of state and composition

17 p2235 A73-35743

Validity of CGL equations in solar wind problems.

18 p2347 A73-36291

Neighboring extremals for optimal control problems.

18 p2294 A73-36308

Jupiter and Saturn interior structure models based on state equations and transport properties of hydrogen and helium at high pressures and temperatures

18 p2354 A73-36644

New vapour pressure measurements for argon and nitrogen and a new method for establishing rational vapour pressure equations.

19 p2461 A73-38200

Equations of planet figures solved for third order accuracy, covering flattening, density distribution, Jupiter and Saturn models and gravitational moments corrections for radii

20 p2608 A73-39234

Russian papers on thermophysical properties, similarity method application to thermodynamics, gaseous and liquid equations of state covering metal structures, specific heat measurement, etc

20 p2627 A73-39292

Smoothed distribution function of equilibrium states and probability of particle occurrence in thermodynamic systems, using Liouville equation

20 p2627 A73-39294

Thermodynamic properties of air and thermal equation of state as function of pressure and temperature from piezometer measurement

20 p2627 A73-39298

Oxygen and nitrogen thermodynamic state equation determination by least squares fitting to experimental PVT, isochoric heat capacity and saturation density data

21 p2740 A73-41104

State-change equations relating generalized load increment to response of constraint connected bars, deriving compatibility and equilibrium equations and matrix coefficients

21 p2788 A73-41604

Ehrenfest equations for thermostatic equilibrium in classical body second order phase changes using caloric equations of state, relating specific heat discontinuities and equilibrium manifold

22 p2885 A73-41737

A new determination of the second virial coefficient of carbon dioxide at temperatures between 0 and 150 C, and an evaluation of its reliability.

22 p2932 A73-42507

Stress relaxation and mechanical equation of state in austenitic stainless steels.

22 p2878 A73-42578

Real gas turbocompressor calculations based on equations of state for fundamental thermodynamic processes in ideal gas

22 p2797 A73-42645

Least squares methods for thermal equations of state parameters of substances and solutions, taking into account phase equilibrium lines

24 p3155 A73-44753

Allowance for electron degeneration in a pseudopotential model of a nonideal plasma

24 p3115 A73-44759

Line of symmetry for the classical equation of state.

24 p3110 A73-44987

EQUATORIAL ELECTROJET

On the origin of small-scale type II irregularities in the equatorial electrojet.

02 p0157 A73-11760

Features of the ionospheric drift over the magnetic equator.

02 p0162 A73-12287

Magnetic horizontal component variations on quiet days, suggesting effect of electric field reversal at equatorial electrojet ionospheric region

03 p0299 A73-12949

Equatorial region radio wave enhanced absorption by resonant coupling to electrojet irregularities and damped upper hybrid modes

04 p0423 A73-15548

Diurnal amplitude variations of equatorial electrojet intensity as functions of solar activity, using 1958 South American observatory data

06 p0690 A73-17556

Electron drift instabilities in turbulent equatorial electrojet from radar echo observations at 50 MHz

07 p0814 A73-19244

Generation of small-scale irregularities in the equatorial electrojet.

07 p0814 A73-19245

Relationships between the equatorial electrojet and polar magnetic variations.

07 p0818 A73-19662

Equatorial electrojet currents effect on sporadic E layer near magnetic equator, noting cross field irregularities

07 p0819 A73-20066

Equatorial sporadic E and cross-field instability.

08 p0958 A73-21150

Charge separation induced vertical electric field calculated for wind motion periodic with height, latitude and longitude at magnetic equator, noting relationship to electrojet

09 p1074 A73-22067

An indirect method for measuring equatorial electrojet currents and its relation to nonlinear saturation of type I instabilities.

09 p1075 A73-22070

Low latitude equatorial electrojet analysis based on three dimensional electric field equation for ionosphere and magnetosphere

10 p1211 A73-24215

Daily variation of geomagnetic field at the Indian stations under the electrojet during the period of the July 1966 proton flare.

12 p1534 A73-26998

Equatorial electrojet, according to Kosmos-321 measurements.

13 p1670 A73-28716

Electron density phase velocity, drift rate and ion temperatures from radar echoes power spectrum near equatorial electrojet

14 p1748 A73-29972

Unified theory of type I and II irregularities in the equatorial electrojet.

14 p1748 A73-29973

Numerical simulation of equatorial electric fields and magnetic variations based on global ionospheric dynamo and equatorial electrojet models

15 p1869 A73-31753

Seasonal movement of the Sq current foci and related effects in the equatorial electrojet.

15 p1869 A73-31754

Type I and II electron density irregularities due to two-stream and cross field instabilities in E region equatorial electrojet, considering wind shear role

15 p1869 A73-31755

Equatorial electrojet. I - Development of a model including winds and instabilities. II - Use of the model to study the equatorial ionosphere.

15 p1904 A73-31756

Study of ULF geomagnetic variations in connection with the equatorial electrojet /the Chad-Central African Republic magnetic project/

15 p1869 A73-31760

The relationship between the structure of the equatorial anomaly and the strength of the equatorial electrojet.

15 p1869 A73-31761

Equatorial electrojet characteristics observation during 1967-1970 with POGO satellite-borne magnetometers, noting anomaly characterized by sharp negative V-signature in width and variable amplitude

15 p1870 A73-31768

POGO satellite observed electrojet signature data comparison with daily geomagnetic variation amplitude measurement at equatorial ground station in India

15 p1870 A73-31769

The electrojet field from satellite and surface observations in the Indian equatorial region.

15 p1870 A73-31770

Correlation of 'satellite estimates' of the equatorial electrojet intensity with ground observations at Addis Ababa.

15 p1870 A73-31771

POGO satellite observed electrojet current data comparison with ground measurement at Ibadan, discussing data ratios variation by upper earth mantle conductivity structure

15 p1870 A73-31772

POGO satellite observation of electrojet profiles compared with H variation around measurements, interpreting data by classical band current model

15 p1871 A73-31773

The effect of polar magnetic sub-storms on the equatorial sporadic E.

15 p1874 A73-32596

Diurnal amplitude variations of equatorial electrojet intensity as functions of solar activity, using 1958 South American observatory data

16 p2002 A73-32780

Cross-field instability as a mechanism for equatorial E region irregularities.

18 p2304 A73-35998

Joule heating effect due to currents in the equatorial electrojet as observed by rocket borne probes.

18 p2310 A73-36128

Lunar tidal oscillations in the horizontal ionospheric drift at the Equator.

18 p2311 A73-36177

Semi-annual modulation of earth's magnetic field in the equatorial electrojet region.

18 p2311 A73-36187

Convective amplification of type I irregularities in the equatorial electrojet.

20 p2551 A73-38938

Magnetic equatorial ionospheric characteristics, discussing E and F regions, diurnal drift variations, field strength, equatorial electrojet, spread F and sporadic E

20 p2555 A73-39633

Effects of propagation parallel to the magnetic field on the Type I electrojet irregularity instability.

21 p2682 A73-40160

Counter equatorial electrojet currents in the Indian zone.

21 p2682 A73-40162

Geomagnetic disturbance diurnal variation /DS/ component evolution and equatorial electrojet strength changes observation during magnetic storms by globally located stations at various latitudes

22 p2844 A73-41918

Sunspot cycle effects on solar and lunar tide-produced diurnal and seasonal variations in equatorial electrojet

24 p3124 A73-44730

Nonlinear saturation of the gradient drift instability in the equatorial electrojet.

24 p3087 A73-45141

EQUATORIAL ORBITS

NT STATIONARY ORBITS

Beyond the horizon ionospheric propagation experiment from an equatorial orbiting satellite to a middle latitude station.

03 p0274 A73-12892

Satellite motion in the equatorial plane of an oblate primary body and apsidal line shift evaluation.

04 p0498 A73-15296

Satellite motion near the equatorial plane of a slowly rotating planet

05 p0617 A73-16468

Small oscillations of gravity gradient satellite in circular near-equatorial orbit, discussing operational efficiency of magnetic damping systems

12 p1549 A73-27648

Motion of a satellite in the equatorial plane of a spheroid.

15 p1929 A73-31107

Optimal orbital transfer in the equatorial plane of an axisymmetric planet with a supplementary accuracy requirement

15 p1931 A73-31228

Diurnal density variations measured by the San Marco III satellite in equatorial orbit.

21 p2685 A73-40830

Some useful results on initial node locations for near-equatorial circular satellite orbits.

23 p3031 A73-43837

Gravitational perturbations of equatorial orbits.

23 p3032 A73-43839

EQUATORS

NT MAGNETIC EQUATOR

UHF airborne measurement of equatorial ionospheric scintillation fading.

03 p0275 A73-13647

Secor equatorial network evaluation of satellite geodesy program, discussing range data and geocentric coordinate computation and adjustments

04 p0437 A73-14782

On the effect of the vertical drift in the equatorial F region.

04 p0443 A73-15476

Characteristics of spectra of pi2-type geomagnetic pulsations along the meridional profile

06 p0689 A73-17543

On the variance spectra and spatial coherences of equatorial winds.

07 p0846 A73-19038

Theoretical vertical profiles of minor ions at the Equator.

07 p0819 A73-20053

Properties of geomagnetic PI2 pulsation spectra along a meridional profile.

16 p2001 A73-32767

- Analysis of VHF/UHF frequency dependence, space, and polarization properties of ionospheric scintillation in the equatorial region. 20 p2525 A73-38741
- A possible connection between variation in the rotational period of Jupiter's central zone and variation in its equatorial diameter. 21 p2779 A73-41545
- ### EQUILIBRIUM
- The equivalence method and the finite-difference method in linear elasticity 03 p0383 A73-12909
- Auditory rail task for acoustic stimuli effects on human equilibrium under axisymmetric intermittent tone exposure, discussing acoustic energy effect on vestibular receptors 03 p0260 A73-13551
- On the evolution toward equilibrium in the kinetic theory of gases 05 p0599 A73-17229
- Equilibrium attitude transitions of a three-rotor gyrost in a circular orbit. 11 p1431 A73-26379
- Determination of the equilibrium positions of mechanisms with two degrees of freedom 12 p1524 A73-27465
- Principle of virtual work and Piola theorem for motion and constitutive equations and boundary conditions of oriented elastic media, using point continuum mechanics assumptions 16 p2080 A73-33245
- Numerical methods for solving some problems of the theory of plasma equilibrium in toroidal configurations. 21 p2750 A73-41680
- ### EQUILIBRIUM DIAGRAMS
- #### U PHASE DIAGRAMS
- ### EQUILIBRIUM EQUATIONS
- Relative equilibrium of a mass of charged particles /electrons/ subject to its own gravitation and uniformly rotating about an axis 01 p0082 A73-10267
- Time evolution and functional form of magneto-static equilibria in axisymmetry. 01 p0082 A73-10452
- Local hydromagnetic toroidal equilibria without symmetry. 01 p0083 A73-10457
- One-fluid MHD model for beta and flow effects on stationary axisymmetric self consistent toroidal equilibria, using Bennett relation 01 p0083 A73-10460
- Existence of solutions in nonlinear shallow shell theory 01 p0116 A73-10962
- Axisymmetric problem of the equilibrium of a cylindrical film under hydrostatic pressure 01 p0035 A73-11412
- Equilibrium equations in theory of anisotropic shells and plates with arbitrary boundary conditions under external loads, noting thin walled reinforced shells 02 p0231 A73-11807
- Equilibrium equations for rotating conical shells under centrifugal forces and compression loads, calculating revolutions number and stability limits 02 p0232 A73-11819
- Calculus of variations and finite difference method for equilibrium equations in axisymmetric plastic shell design 02 p0232 A73-11821
- Shell and plate theory covering constitutive and equilibrium equations, Cosserat surfaces and uniqueness theorem 02 p0234 A73-11981
- Rods theory covering constitutive equations, boundary value problems, variational formulation of equilibrium problems and uniqueness theorems 02 p0234 A73-11982
- The influence of axial load on eigenfrequencies of a vibrating lateral restraint cantilever. 03 p0384 A73-13115
- Resonant frequencies of free vibrating plate via finite difference method, noting difference equations for plate equilibrium 03 p0391 A73-13345
- Field dynamics equilibrium equation for particle rotational motion in gravitational field of central body, noting energy spectra of stationary orbits 03 p0374 A73-13751
- Discretized body mechanics equilibrium, constitutive and motion equations application to elastic lattice type shell structures 03 p0393 A73-13779
- Equilibrium equation for weightless flexible two dimensional sail in inviscid supersonic airstream, noting centred isentropic compression 03 p0246 A73-13789
- Stability of a transversely isotropic solid under large elastic deformation. 04 p0511 A73-15171
- Relativistic equations of balance in continuum mechanics. 04 p0476 A73-15223

- Uniqueness of non-linear elastic equilibrium for prescribed boundary displacements and sufficiently small strains. 06 p0719 A73-18700
- Melehy thermodynamics hypotheses based on average electron energy for examination of equilibrium and steady state conditions in semiconductor p-n junctions 06 p0770 A73-18840
- Equations of disturbed motion and equilibrium for solid body with incompressible fluid filled cavity, noting equilibrium position stability conditions 06 p0688 A73-18878
- On the convergence of the method of homogeneous linear approximations in problems of the theory of plasticity of inhomogeneous bodies. 07 p0906 A73-19022
- Deformation of an elastic spherical shell with random initial imperfections 07 p0911 A73-19319
- Thermodynamic short range order models for dense substance equilibrium properties calculation, assuming molecular interaction independence and self similar radial function 07 p0851 A73-19397
- Some results of finite element applications in finite elasticity. 07 p0914 A73-20213
- Privileged equilibria of a collisionless homogeneous or inhomogeneous plasma. 07 p0860 A73-20480
- Equilibrium method for stress concentration around hole in plate under tension, comparing with Kolosov-Muskhelishvili potential method 08 p1015 A73-20699
- On one-dimensional finite-strain beam theory - The plane problem. 08 p1018 A73-21405
- Intermittence effects in the equilibrium range of developing wind waves 08 p0986 A73-21458
- Tokamak axisymmetric toroidal plasma filament equilibrium in conducting circular and elliptic cylinder for pressure and current distributions, using numerical MHD equation integration 09 p1123 A73-21877
- Bifurcation of the equilibrium of a randomly inhomogeneous nonlinearly elastic plate 09 p1165 A73-23356
- A finite element method for non-self-adjoint problems. 10 p1243 A73-24292
- Nonlinear problem for a plane continuous medium in Euler coordinates 10 p1292 A73-24489
- Reaction equilibrium and energy balance in thermonuclear fusion propulsion for interstellar space flight, discussing nuclear fuel and ion temperature effects 10 p1262 A73-24544
- Uniform variable transverse magnetic field effects on convective instability of plane electrically conducting layer, reducing perturbed equilibrium equations to linear ordinary differential equations 10 p1256 A73-24593
- Two dimensional statics for isotropic elastic body with inhomogeneous mechanical properties, discussing two-step solutions for differential equilibrium equation and boundary value problem 10 p1293 A73-24676
- Difference equations of elastic equilibrium for shells with variable characteristics in polar coordinates 11 p1433 A73-25027
- The effect of deformations in the measurement of the force and the couple of friction 11 p1374 A73-25871
- Equilibrium stability of liquid filled body with closed internal cavity partially filled with ideal homogeneous incompressible fluid under gravitation 11 p1401 A73-26470
- Principle of virtual work in the dynamics of systems having variable mass solids for constitutive elements 12 p1523 A73-27102
- On the existence of solutions of the nonlinear theory of shallow shells. 12 p1554 A73-27538
- Polydynamic equilibrium equation for steady particle motion along stationary orbits in central body attraction field, comparing with Schroedinger wave equation 13 p1657 A73-28001
- On further application of the finite element method to three-dimensional elastic analysis. 13 p1693 A73-28241
- Static force and displacement methods as eigenvalue problems. 13 p1694 A73-28246
- Computational efficiency of equilibrium models in eigenvalue analysis. 13 p1694 A73-28248
- Perturbation techniques in the analysis of geometrically nonlinear shells. 13 p1694 A73-28251

- Some remarks on the thermal equilibrium equation of hot-wire probes. 13 p1613 A73-28528
- Integral relations for an equilibrium toroidal plasma filament with a noncircular cross section 13 p1665 A73-28951
- Instability of equilibrium figures consisting of several isolated components rotating jointly 13 p1684 A73-29141
- Consideration on the 'equilibrium' electrons distribution function for a homogeneous, high-frequency, fully ionized plasma. 14 p1779 A73-29998
- Incremental formulation for problems with geometric and material nonlinearities. 14 p1808 A73-30190
- Perturbation method in the analysis of geometrically nonlinear and stability problems. 14 p1808 A73-30196
- Equilibrium equations for vortex lines with allowance for interaction with boundary of ideal superconductor, calculating extremum values of magnetic field 14 p1774 A73-30342
- Finite element analysis with improved accuracy for rectangular plate bending element. 14 p1810 A73-30456
- Limit state solution to equilibrium equation of elliptical plate with Johansen yield condition under uniform load, using Abel differential equation 14 p1811 A73-30486
- Equilibrium equations for static computations of symmetrical plates with large number of rods, point supports or holes 14 p1815 A73-30814
- Existence of a new type of rotating equilibrium ellipsoids in the presence of a toroidal magnetic field 14 p1782 A73-30816
- General solution of an equation system on plate equilibrium 15 p1945 A73-31033
- Clairaut equation solution for determination of equilibrium configuration of corotating masses, considering density distribution of fluid rotating planet 15 p1939 A73-32006
- The stress field near a system of four symmetrically situated line cracks of equal length. 15 p1953 A73-32093
- Maximum equilibrium pressure of a plasma in a three-dimensional system with helical geometry 15 p1920 A73-32305
- Equations of disturbed motion and equilibrium for solid body with incompressible fluid filled cavity, noting equilibrium position stability conditions 15 p1915 A73-32403
- Three-dimensional turbulent boundary layer - Calculations and experiments 16 p1961 A73-32806
- Constraints theory for Cosserat surfaces with applications in thermomechanics and shell theory, investigating equilibrium laws transformation properties and constitutive equations restrictions 16 p2076 A73-32936
- Nonlinear shell theory, obtaining differential equilibrium equations and boundary conditions from three dimensional variational energy expression by kinematic hypothesis and Ritz method 16 p2078 A73-32996
- Matrix theory algorithms for static stresses and elastic deformations in truss structures, deriving equilibrium equations in terms of forces, deformations and node displacements 16 p2080 A73-33258
- Tokamak axisymmetric toroidal plasma filament equilibrium in conducting circular and elliptic cylinder for pressure and current distributions, using numerical MHD equation integration 17 p2215 A73-34301
- Mendional geometries for orthotropic shells with bending suppressed for different loading conditions, deriving shell configurations for combined loading via equilibrium equations 17 p2243 A73-34530
- On kinematics and statics of finite-strain force and moment stress elasticity. 17 p2252 A73-35829
- Method of orthogonal projections for three-dimensional problems of elasticity theory 18 p2362 A73-36401
- Limiting equilibrium of a circular plate with allowance for the shearing stress 18 p2363 A73-36405
- A relaxation method for solving nonlinear stress equilibrium problems. 18 p2365 A73-36611
- Numerical study on the effects controlling the low-level jet. 18 p2335 A73-37100
- Limiting equilibrium of a plate weakened by two arbitrarily oriented cracks 19 p2494 A73-37186
- Thermal stresses in axially connected circular cylinders. 19 p2495 A73-37435

Non-singular control problems. II - Integral equation functionspace method applied to the solution of optimization problems in the mechanics of deformable bodies. 19 p2498 A73-37649

Minimum principles and some theorems on the elastoplastic equilibrium of bodies subjected to nonstationary physical and thermal effects 19 p2499 A73-37765

Smoothed distribution function of equilibrium states and probability of particle occurrence in thermodynamic systems, using Liouville equation 20 p2627 A73-39294

Unique relations between equilibrium and Galimov-Novozhilov stability equations of geometrically nonlinear elasticity theory based on Hooke's law 20 p2617 A73-39305

Moderate-thickness plate equilibrium equations and boundary value problems, discussing successive approximation method, static bending and potential energy 20 p2618 A73-39317

Resource exchange and allocation /a generalized thermodynamic approach/. I 20 p2629 A73-39349

Resource exchange and allocation /a generalized thermodynamic approach/. II 20 p2629 A73-39351

The stability of steady motions of systems with quasi-cyclic coordinates and the stability of mechanical equilibrium under the action of a magnetic field 21 p2738 A73-40177

Algorithm for deriving the equilibrium equations of an electric circuit on the basis of logic rules 21 p2670 A73-41307

Ehrenfest equations for thermostatic equilibrium in classical body second order phase changes using caloric equations of state, relating specific heat discontinuities and equilibrium manifold 22 p2885 A73-41737

In-plane free vibrations of tapered oval rings, determining normal modes and resonant frequencies from differential force and moment equilibrium equations 22 p2918 A73-41818

Equations of an elastic medium with a large number of absolutely solid inclusions 22 p2921 A73-42278

The Morley-Koiter equations for thin-walled circular cylindrical shells. II - Solution for a line loaded cylinder with close-spaced circumferential grooves. [ASME PAPER 73-APMW-23] 22 p2925 A73-42885

Convergence of the method of successive approximations in geometrically nonlinear problems 23 p2999 A73-44197

Equilibrium of a toroidal plasma with noncircular cross section. 23 p3013 A73-44303

Equilibrium configurations of electron beams in a plasma 23 p3014 A73-44338

Maximum equilibrium pressure of a plasma in a spatial system with helical symmetry. 24 p3114 A73-44613

Allowance for electron degeneration in a pseudopotential model of a nonideal plasma 24 p3115 A73-44759

On response of initially stressed structures to random excitations. 24 p3150 A73-45229

Reduced equilibrium equations solution for plane deformations of isotropic incompressible elastic media, using stress-strain relations 24 p3153 A73-45549

Partial solutions of finite elasticity - Axiially symmetric deformations. 24 p3154 A73-45550

EQUILIBRIUM FLOW

NT FROZEN EQUILIBRIUM FLOW

Aerodynamics of blunt bodies in hypersonic stream at the angle of attack. 01 p0003 A73-11133

Temperature and heat flux distributions in incompressible turbulent equilibrium boundary layers. 04 p0520 A73-15942

Plane equilibrium turbulent boundary layer with longitudinal pressure gradient 07 p0811 A73-19619

Nonstationary wave propagation in equilibrium liquid-vapor flow, noting pressure jumps due to expansion 10 p1204 A73-23513

Equilibrium three-dimensional turbulent boundary layer on the end wall of a curved channel. 13 p1602 A73-29015

Calculation of the basic characteristics of turbulent flows in a state of structural equilibrium 13 p1604 A73-29168

Nonstationary wave propagation in equilibrium liquid-vapor flow, noting pressure jumps due to expansion 17 p2155 A73-35193

Simple universal equilibrium spectrum. 18 p2300 A73-36634

Some characteristics of two-phase nozzle flows 18 p2265 A73-37005

Non-reacting and equilibrium chemically reacting turbulent boundary-layer flows. 19 p2421 A73-38187

Velocity wave interaction and helical turbulence equilibrium spectra for two dimensional and three dimensional flow with quadratic energy and enstrophy states 20 p2549 A73-39812

EQUILIBRIUM METHODS

Constant curvature beam finite elements for in-plane vibration. 05 p0637 A73-17371

Principle of virtual work and equations of shells 14 p1805 A73-29761

Nonlinear bending problem for a beam of variable rigidity 18 p2366 A73-36959

Elastic bodies nonlinear thermomechanical stability under conditions of loaded equilibrium configuration, using Liapunov type energy-like functionals 20 p2615 A73-39010

EQUINOXES

Theoretical model of diurnal variations of the equatorial thermosphere at equinox. 02 p0162 A73-12290

F region neutral wind profiles and electron densities measured at midlatitude station during equinox months for medium sunspot year 16 p2009 A73-33888

EQUIPMENT

Equipment life cycle costs dependence on acquisition decision making, discussing stochastic computer simulation of failure times, repairs, inventory replacement and personnel availability 16 p2089 A73-33655

EQUIPMENT SPECIFICATIONS

Circuit parameters and performance of monolithic IC operational amplifiers, noting data sheets with voltage and temperature ranges and frequency response characteristics 06 p0672 A73-17450

IR tracking system for automatic target acquisition, discussing analyzer operation principles, closed loop characteristics, spectral field and equipment specifications 07 p0789 A73-18945

Solar, stellar and IR sensors, discussing structural, optical and electronic design features, operational requirements and performance specifications 07 p0821 A73-18984

Basic specification research for the main instruments of light aircraft 07 p0825 A73-20248

Crew station lighting - Commercial aircraft. [SAE ARP 1161] 08 p0925 A73-20692

General requirements for aerospace powered mobile ground support equipment. [SAE ARP 1247] 08 p0952 A73-20694

Fluidics test methods and instrumentation. [SAE ARP 1254] 08 p0928 A73-20695

VHF preamplifier with FET for resolving crosstalk and overload problems comparing designed and observed specifications 09 p1066 A73-23429

Aircraft maintenance for safety and reliability, considering design requirements, human errors, fault diagnosis, redundancy, failure mode analysis, service data statistics and equipment specifications 10 p1174 A73-23759

Personnel radiation protection technology and criteria review, discussing dosimeter specifications and automatic data processing 11 p1322 A73-25314

IR thermographic scanners and viewers operational principles, equipment performance specifications and thermal radiation distribution 13 p1611 A73-28020

Realism in environmental design criteria - MIL-STD-210B. 16 p2034 A73-33139

Design and service environment standardization /Military electronic equipment/. 16 p2087 A73-33143

Specifying maintainability-demonstration-test parameters. 16 p2020 A73-33635

Nuclear hardness assurance and radiation specifications for overall system assurance, listing electronic component failure modes 16 p2035 A73-33651

Military specifications provisions regarding load transfer. 17 p2133 A73-34093

How to be healthy, wealthy and wise through fastening analysis - The 'how to' of living with fasteners. [SAE PAPER 730309] 17 p2177 A73-34669

Aerosat program for civil aviation needs established by Seventh Air Navigation Conference of ICAO, discussing airborne equipments specification development [AAS PAPER 73-120] 20 p2520 A73-38581

Indoor azimuth reference systems specifications, characteristics and results, discussing optical win-

dows, theodolites, reflectors, bulk monument structure measurements and rocket applications [AIAA PAPER 73-842] 21 p2671 A73-40505

Specifications of a cryostat for a vibrating sample magnetometer between 1.7 and 300 K 21 p2706 A73-41592

Aircraft communication and electronic equipment design for interference control to meet electromagnetic compatibility specification requirements 22 p2821 A73-41695

Electromagnetic compatibility specifications for aircraft communication and electronic equipment, discussing control and test plans, test facilities, cost effectiveness and British standard 22 p2821 A73-41696

Prediction of RS01 design requirements for MIL-STD-461A. 22 p2823 A73-41803

EQUIPOTENTIALS

Graphoanalytic method of calculating plane potential flows 09 p1029 A73-23106

Gaussian curvature of smoothed equipotential surfaces from satellite orbit dynamics. 13 p1611 A73-29659

Electric potential and current distribution in a rectangular sample of anisotropic material with application to the measurement of the principal resistivities by an extension of van der Pauw's method. 17 p2220 A73-35653

Damping in a strip waveguide with a central conductor composed of two equipotential strips 23 p2959 A73-43517

EQUIVALENCE

Equivalence theorems for nonlinear finite-difference methods. 01 p0069 A73-10074

Equivalence rule and transonic flows involving lift. [AIAA PAPER 73-88] 06 p0644 A73-17642

Two quadratic cost functionals equivalence conditions derivation in terms of system parameters and weighting matrices for optimal control law generation 11 p1341 A73-25196

An equivalence theorem on best approximation of continuous functions by algebraic polynomials. 15 p1902 A73-32376

EQUIVALENT CIRCUITS

Operating characteristics of cylindrical thin film weak link circuits used as the sensing element in ultra-sensitive magnetometer systems. 02 p0200 A73-11845

Large-signal behaviour of R.F. power transistors. I - Analysis of the equivalent circuit. 05 p0559 A73-17125

Equivalent circuits for microwave frequency converter design, noting small and large signal operation and power efficiency of variable capacity diode circuit 06 p0673 A73-17578

Book - Transistor circuit design. 06 p0673 A73-17672

A diode model with a current-dependent series resistance 06 p0674 A73-17828

Quasi-linear equivalent circuit for harmonic LC oscillator design with FET transistor, using effective transconductance method 06 p0675 A73-17829

Circuit model for characterizing the nearly linear behavior of avalanche diodes in amplifier circuits. [AD-757849] 06 p0677 A73-18738

High-frequency physical equivalent circuit of junction transistors in common collector configuration. 06 p0682 A73-18843

New interpretation of the equivalent circuit used in dielectric-degradation studies 07 p0796 A73-18893

IMPATT diode microwave oscillator performance analysis for I-V characteristics, output power, efficiency and starting current from equivalent circuit 08 p0943 A73-20707

IMPATT diode anomalous microwave oscillation mode performance analysis, calculating I-V variation, power and efficiency from equivalent circuit 08 p0943 A73-20708

Nonlinear filter with a Pi-shaped amplitude-frequency characteristic 08 p0946 A73-21110

Equivalent circuit of unbent p-PbS point diodes 09 p1061 A73-22022

Equivalent circuits of diodes in millimeter and sub-millimeter wave frequencies. 10 p1193 A73-23667

Active RC filter circuit design based on Pukhov generalized two subcircuit model, determining complex transfer function 10 p1195 A73-24511

J-band transferred-electron oscillators. 10 p1196 A73-24863

Equivalent circuit analysis of noise in bulk semiconductor devices. 10 p1197 A73-24869

An electrochemical cell equivalent circuit for storage battery/power system calculations by digital computer. 11 p1309 A73-25985

- Automation of thermal design calculations for electrical machines 11 p1313 A73-26115
- Resonant bipolar linear networks representation by matched equivalent circuits 13 p1589 A73-28121
- Stationary multiport networks frequency response and representation by equivalent circuits 13 p1589 A73-28122
- A bipolar transistor model for high frequencies 13 p1589 A73-28124
- Spectral analysis of a physical system which can be represented by a stationary linear active electronic network 13 p1589 A73-28474
- Avalanche transistor circuit with controlled S shaped I-V characteristics, discussing equivalent circuits and operating points stability 13 p1591 A73-28731
- Modulation functions and transmission coefficients for static frequency converter representation in form of equivalent multipole networks for reactive loads 13 p1592 A73-28939
- Measurement of semiconductor junction parameters using lock-in amplifiers. 13 p1595 A73-29578
- The features of disk shape piezoelectric ceramic transducer equivalent circuit. 14 p1754 A73-30892
- Equivalent circuit HF model of MOS transistor active region based on transient response equation, voltage and structural parameters 15 p1850 A73-31492
- Influence of the substrate on the transfer admittance of a saturated MOS transistor 15 p1850 A73-31495
- Bucket-brigade shift-register operation-exact correlation between experimental data and a computer model. 16 p1988 A73-33397
- Small-signal modelling and characterization of microwave transistors. 16 p1990 A73-33687
- Microwave-package measurements at the Q band. 16 p1991 A73-34019
- Book - Design of modern transistor circuits. 17 p2134 A73-34458
- Solving some contact problems by electrical modeling 17 p2244 A73-34795
- State-space analysis of a magnetically tuned IMPATT oscillator lumped model. 17 p2136 A73-34973
- The effects of the microwave structure parameters on the behavior of X-band Gunn oscillator. 17 p2142 A73-35650
- Negative resistance oscillators, predicting fundamental, harmonic and subharmonic locking characteristics by nonlinear models and equivalent circuit. 19 p2410 A73-38307
- Equivalent circuit and transfer function of the multimode glass fiber with random mode conversions. 20 p2521 A73-38658
- Bipolar transistor base region noise current correlation with effective voltage, proposing equivalent circuit 20 p2538 A73-39597
- Analysis of limit cycles in a two-transistor saturable-core parallel inverter. 21 p2662 A73-40339
- Electronic circuit optimization via Powell iterative method, describing search techniques, matrix methods and transistor hybrid equivalent circuit application 21 p2671 A73-41313
- High loop gain operational amplifiers voltage changes as slewing rates using nonlinear circuit model, discussing equivalent circuits, frequency characteristics and bandwidth 22 p2832 A73-41896
- Noise characteristics in bipolar transistor differential amplifiers, discussing current sources, circuit configurations, feedback amplifiers and equivalent circuits 22 p2832 A73-41897
- Equivalent circuit modeling of insulator shunting errors in high temperature sheathed thermocouples. 22 p2858 A73-42045
- Two dimensional microstrip transmission line with step discontinuities, predicting microwave filtering behavior by broadband equivalent circuit for comparison with experiment 22 p2835 A73-42465
- Linearized stability analysis and design of a flyback dc-dc boost regulator. 22 p2801 A73-42910
- Junction or Schottky gate type FET power gain and high frequency limitations from y parameters calculation, using analog RC transmission line as equivalent network 23 p2963 A73-43452
- Small signal duality theory of linear optoelectronic circuits with optical coupling for equivalent circuit computerized design and analysis 23 p2963 A73-43615
- TEM-TE coupled transmission line model for microstrip, calculating frequency-dependent wave dispersion curves for comparison with experiment 23 p2964 A73-44073
- IMPATT diode frequency-independent small-signal equivalent circuit incorporated with negative resistance element and white noise source for terminal behavior prediction 23 p2964 A73-44074
- A quantitative estimate of the electromagnetic compatibility of high-frequency leads in electronic equipment 24 p3071 A73-44596
- Equivalent circuits for differential bridge quartz filter inductance evaluation in mass production 24 p3071 A73-44600
- Efficient numerical solution of the transmission-line equivalent-circuit model of a semiconductor. 24 p3119 A73-45261
- Large-signal lumped modelling and characterization of an IMPATT diode. 24 p3073 A73-45478
- Parametric oscillations in an oscillating circuit utilizing negative resistance. 24 p3075 A73-45479
- Tunnel diode equivalent circuit analysis based on empirical expressions for composite T-V characteristics, predicting series resistance effect on switching time 24 p3073 A73-45485
- ERBIUM**
- Cooperative luminescence in trivalent ytterbium and erbium ions in cadmium fluoride crystals 06 p0738 A73-18543
- ERBIUM ALLOYS**
- Phase equilibria and crystal structure of intermediate phases in Er-Rh binary alloys 10 p1260 A73-24435
- ERGODIC PROCESS**
- Steady ergodic Markovian random function construction 01 p0071 A73-11271
- Ergodic behaviour of nonlinear hydromagnetic waves in a cold collisionless plasma. 01 p0087 A73-11496
- Power spectral density estimation by spline smoothing in the frequency domain. 04 p0471 A73-15254
- Ergodicity criteria of homogeneous Markov chains in a special phase space. I, II 07 p0844 A73-19326
- Measurement of certain one-dimensional characteristics describing the evolution of the two-dimensional probability density of random processes when changing the interval between readings 11 p1340 A73-25004
- Certain aspects of the asymptotic behavior of generalized random systems with complete connections 15 p1901 A73-32208
- Statistical analysis of two dimensional turbulence, noting probability characteristics ergodicity with respect to class of two dimensional characteristic functions with converging mean squares 23 p2968 A73-43475
- Automorphism groups of W algebras operating in Hilbert space with application to noncommutative dynamic systems analysis and ergodic theory 23 p2999 A73-44102
- Signal analysis using stochastic-ergodic principles, discussing PCM correlation procedures, analog-digital signal conversion and measurement methods 23 p2983 A73-44149
- Correlogram of ergodic nonstationary random processes 24 p3074 A73-45095
- ERGONOMICS**
- Muscle, skin and esophageal temperature measurement during transient and steady state phases of negative work exercise on bicycle ergometer 03 p0262 A73-14112
- Telemetry and ergometry associated to the measure of oxygen consumption during sports events. 03 p0270 A73-14285
- Laddermill and ergometry - A comparative summary. 11 p1322 A73-25183
- ERGONOMICS**
- U HUMAN FACTORS ENGINEERING**
- EROS [SATELLITES]**
- EROS Program and ERTS-1 satellite applications to geophysical problems. 18 p2307 A73-36032
- EROSION**
- NT WATER EROSION**
- NT WIND EROSION**
- Erosion, transportation and the nature of the maria. 03 p0368 A73-13083
- Verification of a comprehensive thrust chamber compatibility model for liquid rocket engines. [ALAA PAPER 72-1078] 03 p0354 A73-13401
- Erosive burning rate perturbation in colloidal propellant slab combustor channel as function of lateral velocity gradient and chamber pressure [ALAA PAPER 72-1108] 03 p0351 A73-13423
- Hydrodynamic phenomena during high-speed collision between liquid droplet and rigid plane. [ASME PAPER 72-WA/FE-30] 04 p0435 A73-15850
- Theoretical low-speed particles collision with symmetrical and cambered aerofoils. [ASME PAPER 72-WA/FE-35] 04 p0404 A73-15852
- Investigation of the corrosion-erosion resistance of niobium alloys 06 p0711 A73-18668
- Simulated microscale erosion on the lunar surface by hypervelocity impact, solar wind sputtering, and thermal cycling. 07 p0896 A73-19867
- Photographic and metallographic evidence of two stage ductile materials erosion mechanism under particle impact, describing impact velocity, particle size and angle effects 07 p0839 A73-20225
- Possibility of improving the erosive activity of a cavitation bubble by the combined effect of continuous and pulsed sound 08 p0955 A73-21448
- Damage produced by high-speed liquid-drop impacts. 09 p1109 A73-21932
- Third elements effect on electrical erosion of steels noting influence of atmospheric composition 09 p1104 A73-22967
- Cavitation erosion in geometrically similar nozzles with lead and plastic liners, presenting expressions for erosion rates dependence on scale 10 p1206 A73-24669
- Determination of criteria for rain erosion testing of the standard arm radome. 11 p1335 A73-25298
- Missile ablation shields erosion by high velocity dust, considering wind tunnel test data on phenolic cork for various dust materials, particle sizes and velocities [ALAA PAPER 73-379] 11 p1388 A73-25509
- Investigation of a low-pressure arc erosion plasma 14 p1781 A73-30459
- Possibility of enhancing the erosive activity of a cavitation void under the simultaneous action of continuous and pulsed sound. 15 p1860 A73-31012
- Errors due to electrode-instrument wear during the electric-erosion treatment of cavities 15 p1881 A73-31146
- Sand erosion tests and protective coatings for aircraft jet and turbojet engines and helicopter compressor airfoils 16 p2046 A73-33029
- A survey and comparison of methods for predicting the profile loss of turbine blades. 17 p2093 A73-34391
- Wind tunnel and flight tests for Saturn S-2 stage polyurethane spray foam insulation erosion under aerodynamic heating, shear stress and static pressure [ALAA PAPER 73-740] 18 p2326 A73-36357
- Hyperballistics range erosion tests, describing dust, rain and ice simulation, dust and water fixed grid screens and shadowgraph and laser photography [ALAA PAPER 73-765] 18 p2295 A73-36380
- Decelerator sail erosion during interstellar vessel deceleration, using drag screens to improve vehicle mass ratio via propellant requirement reduction 18 p2361 A73-37039
- Latitudinal distribution of a debris mantle on the Martian surface. 19 p2477 A73-37208
- Mariner 9 evidence for wind erosion in the equatorial and mid-latitude regions of Mars. 19 p2477 A73-37209
- Martian sandstorms and wind erosion, discussing theoretical calculation methods and wind tunnel experiments 19 p2478 A73-37211
- Wind erosion in the Martian polar regions. 19 p2478 A73-37214
- Some results in the erosion of prestressed materials due to water-jet impact. 19 p2443 A73-38299
- The mechanism of electrical erosion in composite materials during electric arc alloying 24 p3093 A73-44743
- Mechanism of erosive burning of solid rocket propellants. 24 p3121 A73-45385
- ERROR ANALYSIS**
- Signal interpolation errors in adaptive-discretization systems 01 p0015 A73-10029
- Effect of inhomogeneity of normal specimens on measurement error estimation in devices with an incompletely closed magnetic system 01 p0044 A73-10085
- Inexpensive solar radiation measuring instruments comparison to standard solarimeter for mean and weekly errors 01 p0044 A73-10146
- Influence of additive and multiplicative noise on the accuracy in measuring the angular position of a source of radiation by systems with pulse-width modulation 01 p0017 A73-10212

Reynolds equation time dependent numerical integration errors due to phase shifts, indicating correction by extrapolated Crank-Nicolson scheme [ASME PAPER 72-LUB-L] 01 p0055 A73-10223

Atmospheric temperature profile determination by limb radiance inversion radiometer, discussing radiative transfer, instrument parameters and inversion process effects on retrievable information content 01 p0072 A73-10354

The effects of aerosols on the outgoing terrestrial radiation. 01 p0072 A73-10357

Extraterrestrial solar flux attenuation and photodissociation cross sections effects on errors in photochemical kinetic model calculations 01 p0014 A73-10369

Atmospheric ozone distribution from remote sensing with spaceborne IR interferometer spectrometer, estimating error due to cloud cover 01 p0038 A73-10384

Electronographic photometry of very weak stars of extragalactic origin with shift towards red, discussing accuracy limitation causes 01 p0049 A73-10538

The accuracy of measurements of star transits 01 p0098 A73-10553

Accuracy of the determination of the spectral density of a vibrational process with the aid of a spectrum analyzer 01 p0077 A73-10677

Application of the algorithm of a median for accuracy and reliability improvement in data processing 01 p0020 A73-10678

A comparison of two ground-based techniques for measuring D-region electron densities. I. 01 p0042 A73-10905

Approximate relationships between the behavior of plates under destabilizing and non-destabilizing loads. 01 p0117 A73-11120

Comparison of Kalman filter and stepwise methods for real time orbit determination. 01 p0105 A73-11187

Certain problems of dynamics and accuracy of gyroscopes in gimballs. 01 p0053 A73-11197

Verification of an approximation method for calculating multiple scattering of sky radiation. 01 p0074 A73-11236

Mean error probability during diversity reception at extremal group frequencies under random noise conditions 01 p0019 A73-11262

Roundoff and uncertain data error analysis, discussing hasty judgements, double precision, trajectory problems, ill-posed problems, computer software and hardware flaws, etc 01 p0021 A73-11460

Artificial viscosity truncation error analysis for finite difference analogs of linear advection equations 01 p0035 A73-11466

Thermocouple circuits for measurement of unsteady temperatures in gases by the two-thermoreceiver method and an analysis of thermocouple circuit errors 02 p0166 A73-11710

Mathematical model and error equations of inertial navigation system with two leveled accelerometers, comparing with three component and pendulum gyroscopic systems 02 p0190 A73-11778

Intermediate resistance standards for low resistivity resistance thermometer calibration, discussing accuracy requirements and error analysis 02 p0167 A73-11866

Position locus by measurement of the ascension speed of a real or fictitious star 02 p0190 A73-12011

Evaluation of the coefficients of the effect of errors in the original information and in the model of optimization results. 02 p0149 A73-12122

Russian book - Study of the theory of differentiable functions of many variables and its applications. IV. 02 p0187 A73-12176

Weighted estimates of the error in the grid method of solving the Laplace and Poisson equations 02 p0187 A73-12177

Inaccuracy sources in winds calculation from thermospheric models, considering neutral air motions due to global pressure variations 02 p0189 A73-12293

Tropospheric and ionospheric refraction errors in satellite tracking over the Indian sub-continent. 02 p0141 A73-12299

Estimation of gravity field harmonics in the presence of spin-axis direction error using radio tracking data. 02 p0164 A73-12373

Iteration method for statistical treatment of measurements when information on measurement error characteristics is incomplete 02 p0219 A73-12455

Multipole sine-cosine azimuth patterns for wide aperture Adcock direction finders, determining spacing and reradiation errors and array pickup factor 02 p0142 A73-12529

Minimized calculation errors in phase ionosonde true height reduction technique for electron density profile, noting lowest observable radio frequency 02 p0143 A73-12531

Total-pressure averaging in pulsating flows. 02 p0171 A73-12618

Upper bounds for long range numerical weather forecasts errors due to inadequate knowledge of frictional constants, heating and initial conditions 02 p0189 A73-12777

Dollen data reduction method for meridian-observed FK 4 star pairs right ascension and time determination, calculating instrument, personal and catalog errors 03 p0371 A73-13219

Radio aurora aspect sensitivity from radar VHF measurement error analysis 03 p0300 A73-13692

Binary noncoherent FSK communication under influence of bandpass Gaussian noise and linear FM jamming waveform, deriving error probability 03 p0276 A73-13905

Real time linear and nonlinear motion desmearing of imagery telemetered from airborne platform, discussing inverse filter error analysis and analog simulation 03 p0276 A73-13907

Effects of a finite-width decision threshold on binary CPSK and FSK communication systems. 03 p0277 A73-13911

Error probabilities estimates for digital communication systems using orthogonal multiposition signals in data transmission 03 p0278 A73-14029

A brief comparison of the accuracy of time-dependent integration schemes for the Reynolds equation. [ASME PAPER 72-LUB-L] 03 p0297 A73-14352

Accuracy limitation in measurements of HF field intensities for protection against radiation hazards. 03 p0310 A73-14491

Radar measurement errors due to rain attenuation compensation and improper system calibration, discussing error reduction procedures 03 p0279 A73-14518

A modified coefficient for the weather radar equation. 03 p0279 A73-14526

Error sources in numerical integration of spacecraft equations of motion in solar and planetary gravitational fields, suggesting methods for improving accuracy 03 p0379 A73-14553

Statistical data processing method for accuracy evaluation of satellite orbit parameters obtained from onboard measurements of two stars angular positions 03 p0379 A73-14554

Structural reliability definition and determination in terms of survival probability concept, discussing analytical errors effect on design and applications to aerospace vehicles 04 p0508 A73-14724

Propagation of errors in orbits computed from density layer models. 04 p0438 A73-14790

Geopotential coefficient error model using Geos 2 tracking data and SAO 1969 standard earth 04 p0439 A73-14797

Satellite borne Ku-band pulsed radar altimeter for altitude measurement above ocean surface, evaluating random and bias errors due to instrument, propagation and geometry 04 p0446 A73-14805

Optimum detection and signal design for channels with non-but near-Gaussian additive noise. 04 p0415 A73-14988

The performance of a noncoherent FSK receiver preceded by a bandpass limiter. 04 p0416 A73-14992

A second-order accurate difference method for systems of hyperbolic partial differential equations. 04 p0470 A73-15007

Note on symmetric decomposition of some special symmetric matrices. 04 p0470 A73-15014

Digital modeling of multipath induced monopulse angle tracking errors. 04 p0416 A73-15056

Certain algorithms and error assessments for the approximate analytical solution of boundary value problems 04 p0470 A73-15090

An adaptive Kalman filter using decomposition of the innovations sequence. 04 p0431 A73-15258

Estimation of the statistical parameters of the Kalman-Bucy filter. 04 p0431 A73-15261

An error sensitivity analysis for nonlinear second order filters. 04 p0431 A73-15269

An autonomous navigation technology system. 04 p0474 A73-15274

Application of adaptive tuning of filters to exoatmospheric target tracking. 04 p0498 A73-15275

Optimal processing of the backscatter signal in determining the structure of atmospheric inhomogeneities. 04 p0417 A73-15325

Low error rate transmission by iterative probabilistic threshold decoding, noting performance improvement over sequential and low density parity check code techniques from simulation 04 p0425 A73-15399

Manned spacecraft digital TV system channel error correcting encoder and decoder performance test data including bit error rate versus SNR and decoding depth 04 p0419 A73-15400

Performance of correlation receivers in the presence of impulse noise. 04 p0419 A73-15406

Comparison of coherent and noncoherent detection of phase continuous binary FM signals. 04 p0420 A73-15410

Digital link for bidirectional communication between manned spacecraft and ground terminal by synchronous communication relay satellite, noting coding parameters effects on error rate 04 p0421 A73-15426

Color image quantization error assessment from noninferior bit assignment determination for several coordinate systems by color shift comparison, using computer simulation 04 p0449 A73-15444

Pseudorandom noise for telemetry error rate measurement applications and limitations. 04 p0449 A73-15457

Error effects in dynamic force measurements performed on materials testing pulsators 04 p0450 A73-15475

Analysis of the accuracy of a determination of the reciprocal azimuths of a geodesic line 04 p0443 A73-15510

Determination of the mean square errors of functions of variables in uniquely determinate geodetic constructions 04 p0443 A73-15511

Error minimization methods for Planck law remote measurements of single and two color temperature, considering multiple wavelengths 04 p0445 A73-15773

Error analysis of ionospheric parameter measurement by satellite transmitted or reflected multiple frequency pulsed radiation signal, using perturbation method 05 p0547 A73-16051

A multi-step method for the numerical integration of ordinary differential equations. 05 p0589 A73-16100

Finite element model use for deducing errors magnitude in stress-strain properties obtained from laboratory compression test results 05 p0631 A73-16175

Statistical multifactor analysis of the accuracy of continuously recorded cosmic-ray data 05 p0573 A73-16271

Analysis of the effect of errors in determining the orbit parameters of a satellite on the accuracy of prediction of its motion 05 p0614 A73-16312

Almost-coherent detection of phase-shift-keyed signals using an injection-locked oscillator. 05 p0549 A73-16368

Discrete Galerkin and related one-step methods for ordinary differential equations. 05 p0590 A73-16375

Error analysis of Wentzel-Kramers-Brillouin approximation for electromagnetic wave reflection from nonuniform absorbing half space 05 p0549 A73-16392

On the probability of error and the expected Bhattacharyya distance in multiclass pattern recognition. 05 p0554 A73-16814

Numerical calculation of cumulative probability from the moment-generating function. 05 p0591 A73-16815

The attitude measuring system of the AEROS satellite. 05 p0629 A73-16849

Thermal conductivity measurements of porous materials in several gaseous environments at subatmospheric pressures. [AIAA PAPER 73-95] 05 p0640 A73-16858

Analytical approach to orbit determination in the presence of model errors. [AIAA PAPER 73-170] 05 p0619 A73-16915

The determination of free-body responses of a structure from constrained test data. [AIAA PAPER 73-191] 05 p0635 A73-16928

Lateral velocity measurement error analysis in inertial guidance system, noting automatic compensation of mass imbalance effects 05 p0596 A73-16992

A Green Bank sky survey in search of radio sources at 1400 MHz. III - Positions and flux densities of the GB radio sources. 05 p0622 A73-17070

Convergence and error estimation of Svirskii approximation method for determining circular plate deflections 05 p0635 A73-17081

Rapid processing of multispectral scanner data using linear techniques. 05 p0554 A73-17150

Order c-square bulk stress derivation for force-free spherical particles suspension in Newtonian ambient fluid with uniform viscosity, noting error bounds 06 p0722 A73-17701

Digital transmission performance on fading dispersive diversity channels. 06 p0664 A73-17711

Optimal sampling and quantization rates for analog signal by mean-square-error estimates and information content quantitative measure, describing probabilistic properties estimation 06 p0664 A73-17854

Error incidence probability for system control reliability determination, assuming error function as Markov process 06 p0680 A73-17956

Accuracy of the moon potential computation based on integral formulae 06 p0751 A73-18151

Central projection parameter determination of photographed objects 06 p0693 A73-18153

Errors in the predicted gain of pyramidal horns. 06 p0676 A73-18180

Ancillary information effects on photointerpretation performance under four imagery system operation modes, noting identification accuracy independence on information variables 06 p0658 A73-18245

Relationship between conventional-control-theory figures of merit and quadratic performance index in optimal control theory for a single-input/single-output system. 06 p0680 A73-18445

Use of numerical guidance at the National Weather Service's National Meteorological Center. 06 p0720 A73-18703

Heuristic response strategies and operator performance errors as function of practice in cross coupled pursuit tracking control tasks 07 p0785 A73-19548

Differential phase experiment on signal reflections from D region, noting systematic error in phase jitter calculation with pulse nonoverlap explanation 07 p0820 A73-20067

Computerized static and dynamic structural analysis, discussing modeling, programs, input preparation, solution algorithms, numerical errors, output interpretation and applications 07 p0914 A73-20209

An analytical method for certain weakly nonlinear periodic differential systems. 07 p0845 A73-20226

Vector characteristics use in dimensional analysis, solving Huntley method inconsistencies 07 p0916 A73-20438

Connecting measured objects with sensors measuring the parameters of vibrational motion 07 p0826 A73-20531

Wiener and Kalman-Bucy filters design with error covariance bound for performance divergence prevention under stochastic processes with unknown signal and noise densities 07 p0806 A73-20603

Majority logic detection scheme of differentially phase-modulated waves. 08 p0937 A73-20802

An analytical method for the filtering error evaluation of sub-optimal filters in a noisy non-linear dynamic system. 08 p0950 A73-21091

Second-order corrections for ionospheric radio-wave propagation 08 p0939 A73-21287

Rossby wave barotropic instability effects on errors leading to large scale atmosphere predictability experiments by numerical simulation of two dimensional turbulence 08 p0985 A73-21386

Measurement of amplifier noise. 08 p0949 A73-21623

Jupiter astrolabe observations analysis, investigating corrections for defective illumination, instrumental comparisons and systematic errors 09 p1140 A73-22002

Digital FM signal receiver with postdetector integration, determining error probability as function of input SNR and noise stability 09 p1049 A73-22044

Recurrent orbit estimation biases by filtering, using method representing motion by finite difference equations 09 p1143 A73-22098

Random coding bound of information theory providing upper bound to decoding error probability for best code of given rate and block length 09 p1111 A73-22117

Investigation of the output characteristic and errors of a reversible, contactless, dc tachometric generator designed on the basis of a synchronous machine 09 p1033 A73-22342

Error analysis for the Mariner-6 and -7 occultation experiments. 09 p1146 A73-22428

Stress miscalculation due to resistance strain gage errors, deriving expressions for stress-strain error relationships 09 p1083 A73-22505

Error analysis of approximate formula for transform of rarefied gas particle reflection from homogeneous anisotropic random surface 09 p1123 A73-22615

Possibilities of optimal processing of capacitance fuel meter data 09 p1083 A73-22652

A quality criterion test for tubes intended for measurement of acoustic absorption and impedance coefficients 09 p1121 A73-23105

Drift phenomena in shaken measurement systems prone to torsional vibrations. III 09 p1086 A73-23116

Low level wind measurement error as it affects sounding rocket dispersion. [ALAA PAPER 73-296] 09 p1116 A73-23215

Effect of flutter on theoretical bit error rates for digital recording systems. 09 p1087 A73-23369

Magnetic tape recorder parameters effect on PCM telemetry bit error rate, discussing contribution factors and test methods 09 p1087 A73-23370

Hybrid coding/decoding scheme for deep space probes data transmission, estimating bit error probability for given SNR 09 p1054 A73-23376

L orthogonal signaling scheme transmission bandwidth tradeoff with error probability performance of associated receiver used for data detection 09 p1054 A73-23383

Range instrumentation system timing error sources classification and uncertainty reduction for comparison of telemetry inertial guidance data with radar and optical data 09 p1057 A73-23413

Intersymbol interference in binary communication systems with single-pole band-limiting filters. 09 p1186 A73-23498

Accuracy studies of the numerical method of characteristics for axisymmetric, steady supersonic flows. 09 p1171 A73-23602

Microwave system with direct, AM, FM and pulse propagation techniques for swept-frequency group delay measurement, discussing error sources and various distortions 09 p1193 A73-23610

Local extrapolation in the solution of ordinary differential equations. 09 p1241 A73-23641

Spline approximation to the solution of the Volterra integral equation of the second kind. 09 p1241 A73-23642

Magnetic field intensity and invariant shell parameters computer programs, assessing error in expansion coefficients 09 p1276 A73-23888

Alternative algorithmic scheme for spherical harmonics series summation, noting high speed and precision loss at high resolution in comparison with conventional methods 09 p1246 A73-23993

Retroflecting satellite with laser range finder for Martian roving vehicle navigation, discussing error analysis and minimization by measurement geometry choice through nonlinear programming 09 p1247 A73-24005

A comparison of the effectiveness of some adaptive optimal filtering techniques applied to the gyrocompassing problem. 09 p1201 A73-24052

Calibration of a hot-wire anemometer for velocity perturbation measurement. 09 p1218 A73-24121

Coronal polar plume observed electron density dependence on assumed density distribution normal to axis, analyzing errors in measurements 09 p1279 A73-24141

Instrumental polarization concerning magnetographic measurements. 09 p1218 A73-24148

Problems of accuracy in the representation of values by stochastic sequences 09 p1202 A73-24418

Spacecraft transmitted TV picture geometrical distortion in terms of root-mean-square errors, considering applications to ESSA-7, Surveyor-7 and Mariner 4 data samples 09 p1219 A73-24485

Optimal reconstruction of a stationary random process from discrete readings 09 p1202 A73-24611

Error probability in an atmospheric twin-channel optical link. 09 p1190 A73-24628

Studies in the application of recurrence relations to special perturbation methods. II - Comparison of the Encke and Cowell methods of integration in the restricted three-body problem. 09 p1283 A73-24668

Errors in the velocity-area method of measuring asymmetric flows in circular pipes. 09 p1221 A73-24861

An analytical expression for the limits of error in the measurement of reflection-coefficient phase. 09 p1190 A73-24867

Further studies of backscattering from a finite cone. 09 p1191 A73-24898

Error analysis of correlation method for determining directional characteristics /angular power density/ of homogeneous random wave field 09 p1359 A73-25005

Problem of forming classes of input processes in the study of errors in devices for statistical measurements 09 p1359 A73-25014

Effect of time-quantization errors on the accuracy in periodogram analysis of random processes 09 p1360 A73-25015

Effect of measuring-device error on the accuracy of the determination of the mathematical expectation and dispersion of a stationary random process 09 p1360 A73-25016

Errors in the determination of random process characteristics with the aid of measuring converters with randomly varying parameters 09 p1341 A73-25024

Nonlinear dynamic feedback control system state variable observers reconstruction error convergence and digital simulation for performance 09 p1390 A73-25187

Photometric error of the NA-MK-25 camera field 09 p1361 A73-25250

Influence of ephemerides errors on various determinations using laser lunar ranging 09 p1417 A73-25266

Influence of fabrication inaccuracies on the axis deviation of an airborne radome 09 p1328 A73-25295

Direct time numerical integration of spatially discretized linear elastodynamics integral equations, comparing one-step algorithms for stability and accuracy in terms of frequency spectrum 09 p1435 A73-25439

Rayleigh quotient minimization and eigenvalue/eigenvector errors of mode convergence in dynamic structural analysis, using gradient algorithm and scaling transformation 09 p1438 A73-25497

Analytical and Monte Carlo analysis of rms beam pointing errors of planar phased arrays with isotropic elements 09 p1328 A73-25660

Correction to 'The echo area of a perfectly conducting prolate spheroid.' 09 p1330 A73-25684

On the origin of oscillations appearing in shock profiles calculated by difference methods 09 p1390 A73-25868

Dynamic error of solid body-elastic rod pendulum system hinged on vibrating suspension point in terms of tensile rigidity finiteness 09 p1399 A73-26096

Error analysis of a generator with a uniform probability distribution of instantaneous values 09 p1331 A73-26100

Active cavity radiometer as pyroheliometer for accurate radiation scale definition, determining measurement uncertainty through error analysis on quasi-equilibrium of power balance 09 p1365 A73-26236

Calibrations of the airglow photometers and spectrometers. 09 p1365 A73-26237

Automatic sensor with parabola null test and ray intercept error measurement for optical system wave front error determination, noting interferometric sensitivity 09 p1365 A73-26242

Thermoanemometer errors in turbulent wind velocity pulsations measurement 09 p1367 A73-26436

Errors associated with Rodrigues-Hamilton parameters /vector space basis quaternions/ calculation by numerical integration of kinematic equations of moving body orientation 09 p1400 A73-26454

Linear system modeling via optimal finite dimensional approximation based on Sard generalized spline, giving error bounds 09 p1391 A73-26580

Optimum processor accuracy for radar altimetry for geodesy over sea, considering surface reflectivity, height variation additive noise and pointing errors
11 p1371 A73-26631

LORAN range difference location system, deriving exact straight line of position on plane or spherical surface with computer-generated error maps
11 p1333 A73-26642

Method of utilizing structural redundancy in a measuring system for processing experimental data with systematic errors
12 p1494 A73-26776

Inertial air navigation system error minimization, using discrete-sampled position fixing and star sighting data in computerized calculations
12 p1522 A73-26821

Error curve in radiometric beta backscatter measurement of coatings thickness via digital computation
12 p1495 A73-26846

Beta estimation accuracy for reentry vehicles using a priori target information with 6-component state vectors to reduce computation time
12 p1548 A73-27131

Chetaev concept for experiments with small measurement errors and mathematical model instability and lability properties, applying to biological existence struggle and spacecraft reentry
12 p1524 A73-27405

An analysis of the effectiveness of ways of increasing the accuracy of a treatment
12 p1503 A73-27467

Book - Numerical methods for unconstrained optimization.
12 p1518 A73-27549

Errors of the formal theory of amplifiers with a feedback
12 p1481 A73-27594

Solvability of the boundary value problem in the theory of shallow shells of revolution and estimation of errors in the approximate solution
12 p1556 A73-27813

Some error estimates for approximate solutions of nonlinear integral Hammerstein-type equations
12 p1519 A73-27818

Solar microwave emission height determination from latitude shift, noting precision comparable with observation based on rate of motion in longitude
12 p1536 A73-27842

Gaussian quadrature formula derivation by integration of linear interpolation operator replacing Hermitian polynomial with vanishing derivative for error minimization
13 p1647 A73-28194

Dual analysis principle application to accuracy verification of finite element solutions of problems in continuum mechanics
13 p1693 A73-28233

Bounds upon the growth rate of errors in quasi-nondivergent prediction models.
13 p1652 A73-28271

General considerations about the revision of all the calculations of the International Latitude Service.
13 p1678 A73-28379

An interpretation of the ambiguity between annual terms obtained by time and latitude observations.
13 p1678 A73-28384

Earth rotation axis motion determination through satellite tracking via laser range observation, estimating orbit computation error sources
13 p1656 A73-28392

Light scattering by atmospheric aerosols.
13 p1653 A73-28517

A study of systematic errors in measurements with the constant-temperature anemometer in high-turbulence flows with and without hot-wire signal linearization.
13 p1613 A73-28529

Quadrature errors upper bound estimates for Gauss-Legendre, Newton-Cotes and Gauss-Laguerre formulas
13 p1649 A73-28603

Estimating the eigenvalues of Sturm-Liouville problems by approximating the differential equation.
13 p1649 A73-28606

The Ritz-Galerkin procedure for nonlinear control problems.
13 p1649 A73-28607

Theory for errors, resolution, and separation of unknown variables in inverse problems, with application to the mantle and the crust in Southern Africa and Scandinavia.
13 p1607 A73-28621

Error estimates for turbulent flow characteristics by visualization and solid particle photography
13 p1601 A73-28738

On an Euler-like method with exponential correction for initial-value problems.
13 p1650 A73-28799

Evaluation of the noise immunity of pulsed systems for transmission of continuous messages with allowance for quantization and interpolation errors. I
13 p1584 A73-28891

Probability of error in selecting the information signal and the synchronization signal by frequency multiplication
13 p1584 A73-28892

Speech data rate reduction. I - Applicability of modern estimation theory. II - Applicability of sensitivity and error analysis.
13 p1585 A73-29201

Computer program analysis of errors in mutual orientation elements on aerial photographs with different lengthwise overlaps, discussing error minimization
13 p1621 A73-29324

Simulated flight tests of a digitally autopiloted STOL-craft on a curved approach with scanning microwave guidance.
[ASME PAPER 73-AUT-L] 13 p1657 A73-29413

Exponential bounds for error and equivocation based on Markov chain observations.
13 p1651 A73-29600

Errors of the gravitational stabilization system of a satellite with gyrodamping
14 p1803 A73-29869

Effect of multipath on ranging error for an airplane-satellite link.
14 p1725 A73-29892

Thermal diffusivity measuring technique for hazardous materials.
14 p1752 A73-29914

Accuracy estimates for analog computer solutions to systems of ordinary linear equations and some algebraic equations
14 p1768 A73-30033

Algorithm for statistical error detection in digital control computers
14 p1730 A73-30038

A priori evaluation of the position finding system of the Guiana Space Center /CSG/ by the application of Kalman's algorithm
14 p1727 A73-30092

Methods of evaluation of tracking procedures used at the French Guiana Space Center
14 p1727 A73-30093

Measuring accuracy of three-dimensional displacements in holographic interferometry.
14 p1752 A73-30154

Some aspects of recent contributions to the mathematical theory of finite elements.
14 p1806 A73-30177

Quadrature errors effect on finite element method solutions accuracy, considering stiffness matrix numerical stability
14 p1806 A73-30179

Finite element method round-off errors relation to fundamental equations conditioning, considering round-off errors effect on precision of method of substructures
14 p1806 A73-30180

Numerical methods for functional differential equations.
14 p1770 A73-30755

Errors due to electrode-instrument wear during the electric-erosion treatment of cavities
15 p1881 A73-31146

A simulative study of correlated error propagation in various finite-precision arithmetics.
15 p1899 A73-31350

Error investigations regarding the solution of the inhomogeneous natural boundary value problem by means of a Ritz approach with standardized coordinate functions
15 p1899 A73-31364

Accurate flux densities at 8.87 GHz of 195 radio sources.
15 p1933 A73-31379

Instrumental theory in absolute radiometry
15 p1875 A73-31500

The influence of pulsed noise on the performance of incoherent digital communications systems
15 p1843 A73-31567

Russian book - Calculation and designing of gyroscopic stabilizers.
15 p1875 A73-31587

Optimal and linear sub-optimal control of second-order saturating control systems.
15 p1853 A73-31626

Interacting continuum theory concerning steady shock wave in composite materials, discussing energy interaction terms error correction effects on Hugoniot relations
15 p1949 A73-31685

Tilt-table alignment for inertial-platform maintenance without a surveyed site.
15 p1858 A73-31728

Maximum likelihood M-ary detection theory application to incoherent optical system model based on photodetectors governed by Laguerre counting statistics, deriving error probability
15 p1875 A73-31734

Convergence criteria for reverse error coefficient expansion under transient conditions for tracking servo system with open loop transfer function
15 p1854 A73-31735

Estimation of errors arising in calculations of the fluxes and influxes of thermal radiation due to errors in the initial meteorological parameters
15 p1905 A73-31786

Approximate determination of the reliability function of a digital computer
15 p1848 A73-31912

Software design and implementation for real time power spectral analysis on IBM-1130 8K-core computer, discussing coherence and cross spectra estimation and arithmetic errors
15 p1848 A73-32032

Locally modified and unmodified structures eigenvalues and eigenvectors solutions, considering computational accuracy improvement and application to dynamic stiffness matrix equation
15 p1951 A73-32035

Potentialities of lunar laser ranging for measuring tectonic motions.
15 p1873 A73-32201

Approximation nature and error magnitude in radial radiative heat flux within optically thin nongray isothermal gas cylinder
15 p1959 A73-32282

French monograph - Study and preparation of algorithms of coordination in the structures of hierarchized control systems.
15 p1855 A73-32592

Iterative method for the statistical processing of measurements with incomplete information on the measurement error characteristics.
15 p1902 A73-32605

Galerkin variational method combination with least squares error distribution technique for application in plate and shell theory
16 p2077 A73-32992

Modified finite difference procedures for structural mechanics, discussing interior and boundary discretization errors and accuracy improvement
16 p2079 A73-33012

The analytical aspects of the reduction of boundary errors in the case of numerical weather predictions
16 p2034 A73-33074

Quality assurance for the data processing industry.
16 p1985 A73-33614

System effectiveness and the one error per man per day expectation.
16 p2020 A73-33647

Synthesis of a universal cell with increased reliability for the realization of an iterative automatic system
16 p1986 A73-33667

Optimal receiver design for discrete information in the presence of non-Gaussian noise
16 p1990 A73-33669

An approach to the analysis of performance of quasi-optimum digital phase-locked loops.
16 p1992 A73-33743

Monotonically convergent approximate solutions for finite element eigenvalues in structural vibration and stability problems, assessing accuracies
16 p2083 A73-33949

Error probability of binary optical communications in turbulent atmosphere - Experimental results.
16 p1984 A73-33995

Safety in operation and human error.
17 p2097 A73-34077

Information systems enabling pilots to report incidents involving safety, including human fallibility and system errors in construction, operation and regulation
17 p2256 A73-34087

Comparison of the solutions obtained by Tikhonov's and Sparrow's methods for the inverse unsteady-heat-conductivity problem
17 p2253 A73-34134

Simplified proof of error estimates for the least squares method for Dirichlet's problem.
17 p2199 A73-34210

On the numerical computation of parabolic problems for preceding times.
17 p2199 A73-34211

Note on error bounds for numerical integration.
17 p2200 A73-34214

An error analysis of a method for solving matrix equations.
17 p2200 A73-34216

Systematic elevation errors in maps of the lunar edge zone
17 p2230 A73-34594

Deformation of a selenodetic reference system due to errors in lunar rotation constants
17 p2230 A73-34595

The effect of forecast error accumulation on four-dimensional data assimilation.
17 p2205 A73-34853

The human side of quality assurance /as viewed from helicopter manufacturing experiences/.
[AHS PREPRINT 751] 17 p2180 A73-35079

Flux-corrected transport - A minimum-error finite-difference technique designed for vector solution of fluid equations.
17 p2202 A73-35145

Some aspects of numerical integration.
17 p2202 A73-35372

Rapid estimation and detection of impulse inputs under continuity constraints for space vehicles.

17 p2144 A73-35375

Effect of bandlimiting on the noncoherent detection of Amplitude-Shift Keying /ASK/ signals.

17 p2125 A73-35377

Improvement of absolute accuracy for a multiple bounce reflectometer through a detailed effort to reduce systematic errors.

17 p2172 A73-35420

Searching for many targets - An analysis of speed and accuracy.

17 p2118 A73-35498

Testing and calibration of aircraft sensors and systems.

17 p2174 A73-35580

Spline interpolation techniques for approximation of boundary value problem solutions, relating approximation error norm to interpolation error norm from variational formulation

17 p2203 A73-35607

Simulation results for a radar multipath angle error reduction method.

17 p2127 A73-35633

Shop level maintenance of inertial platforms without a surveyed site.

17 p2148 A73-35644

Accurate measurement of antenna gain and polarization at reduced distances by an extrapolation technique.

17 p2127 A73-35676

Spatial statistics of instrument-limited angular measurement errors in phased array radars.

17 p2128 A73-35687

The generalized multiprobe reflectometer and its application to automated transmission line measurements.

17 p2143 A73-35691

Antenna impedance measurement with Weissfloch transformer between terminals and point in input transmission line for achieving high precision

17 p2129 A73-35704

Estimate of error in the solution of interior problems of microwave electrodynamics.

17 p2143 A73-35706

Medium-range forecasting of large-scale atmospheric circulation components on the basis of a nonlinear spectral model

18 p2331 A73-35910

Comparison of three techniques for solving the radiative transport equation.

[ALAA PAPER 73-751] 18 p2337 A73-36367

Computer models for air traffic control system simulation.

18 p2335 A73-36843

Statistical models for rounding-off error studies in linear algebraic problems

18 p2292 A73-37144

Whole aircraft and component design optimization, discussing criteria, constraints and performance prediction accuracy during feasibility analysis and project design

19 p2378 A73-37410

Numerical solution of ordinary and retarded differential equations with discontinuous derivatives.

19 p2444 A73-37523

Computer program for aircraft navigation error synthesis with evaluation of component error distribution on traffic control system effectiveness to provide cost effective guidance

19 p2452 A73-37875

Second-order corrections for radio-wave propagation through the ionosphere.

19 p2404 A73-37916

Suboptimal filter design for dynamic measurement systems, deriving bias and Kalman covariance formulae for error analysis and model sensitivity

19 p2410 A73-38031

System error analysis and algorithms for a strap-down navigation system.

19 p2452 A73-38058

A comparison of errors in linear digital models.

19 p2413 A73-38059

Intermittency of the small-scale structure of atmospheric turbulence. II.

19 p2448 A73-38213

Sampling, quantization and channel errors in differential pulse code modulation systems, discussing SNR, quantizer levels, standard PCM systems, reconstruction filters and bit errors

19 p2407 A73-38383

Probability of error in binary communication systems with causal band-limiting filters. I - Non-return-to-zero signal. II - Split-phase signal.

19 p2415 A73-38384

Ground based aircraft collision avoidance systems, discussing three dimensional tracking, aircraft velocity vector determination, radar systems and tracking errors

19 p2454 A73-38470

Precise positions of radio sources. IV - Improved solutions and error analysis for 59 sources.

19 p2488 A73-38510

Correctness of the solution of signal filtration and reconstruction problems by an analog computer

20 p2522 A73-38702

Error rate of a 4-phase coherent PSK satellite channel with non-Gaussian interference.

20 p2523 A73-38721

Information content subsetting of highly correlated error sources.

[ALAA PAPER 73-867] 20 p2586 A73-38805

An analysis of recent advances in autonomous navigation for near earth applications.

[ALAA PAPER 73-875] 20 p2587 A73-38812

Assessment of fine stabilization problems for the LST.

[ALAA PAPER 73-881] 20 p2587 A73-38817

Magnetic field intensity and invariant shell parameters computer programs, assessing errors in expansion coefficients

20 p2603 A73-38907

Equations for the instrumental errors of a type of inertial navigation system

20 p2590 A73-39045

Transformation of random signals by circuits containing a majoritarian element

20 p2542 A73-39046

Convergence of Huber's method for heat conduction problems with change of phase.

20 p2626 A73-39100

Respiratory nitrogen elimination - A potential source of error in closed-circuit spirometry.

20 p2512 A73-39113

Evaluation of the noise immunity of pulse systems for continuous message transmission allowing for quantization and interpolation errors. II

20 p2531 A73-39462

Digital computer simulation program for North Atlantic hybrid navigation systems configurations, using covariance matrix error analysis for planned increase of commercial air traffic capacity

21 p2733 A73-40028

Horizontal aircraft maneuver strategy for maximum miss distance and minimum course deviation, examining filtering techniques, collision avoidance system and signal error analysis

21 p2734 A73-40032

Navy Transit Navigation System precision improvements for stationary and nonstationary users, considering uncertainties due to satellite position and instrumentation errors and user motion

21 p2734 A73-40039

Redundant independent guidance, navigation and control system application to space shuttle, estimating channel output divergence due to sensor bias and scale factor errors

21 p2735 A73-40043

CIE interlaboratory comparison of measurements of photocell spectral sensitivity.

21 p2698 A73-40141

A conservative bound on the estimation error covariance matrix in the presence of correlated driving noise and correlated discrete measurement noise.

21 p2724 A73-40295

Pulse-position modulation based on energy detection.

21 p2649 A73-40329

Probability of error in a bandlimited quadrature communication system.

21 p2649 A73-40334

Degradation of probability of error due to IF filtering.

21 p2649 A73-40335

A priori L sub 2 error estimates for Galerkin approximations to parabolic partial differential equations.

21 p2725 A73-40383

Evaluation of various analytical models for buckling and vibration of stiffened shells.

21 p2784 A73-40424

Boundary residual methods limitation on elasticity problem solution accuracy, considering torsional stress analysis of square and hexagonal cylinders with circular hollow cores

21 p2784 A73-40431

Experimental error equation of stress intensity factor for fracture toughness and crack growth rate testing

21 p2785 A73-40635

On the effects of eliminating the passive elements from a thinned array.

21 p2652 A73-40655

Risk of estimation by data obtained via communication channel.

21 p2654 A73-40689

Errors on the dial of cosmic clocks

21 p2701 A73-40728

The quantity of initial-parameter information contained in trajectory measurements

21 p2726 A73-40916

Combined effects of intersymbol, interchannel, and co-channel interferences in M-ary CPSS systems.

21 p2656 A73-41167

Binary error estimation in real time for channel quality monitoring, comparing upper and lower bounds with number of errors for bit sequence

21 p2656 A73-41170

Optical communication system performance with tracking error induced signal fading.

21 p2657 A73-41171

Use of switching circuits as redundant multiplier elements in canonic digital networks.

21 p2658 A73-41209

Russian book on accuracy of automatic systems using digital computers as control devices covering analysis and synthesis, stochastic inputs, system errors and operator methods

21 p2658 A73-41282

Measurement accuracy achievable in photographic isochromatic pictures

21 p2706 A73-41605

Russian book on scale selection in modeling for analog and digital computers covering similarity theory, error formation, accuracy optimization, etc

22 p2829 A73-41883

An evaluation of experimental errors in electromagnetic wave measurements aboard satellites.

22 p2844 A73-41911

Effect of radiometric errors on accuracy of temperature-profile measurement by the spectral-scanning method.

22 p2853 A73-41988

Representation of the temperature-resistance characteristic of germanium thermometers below 30 K.

22 p2854 A73-42001

Instrumentation errors in nuclear resonance thermometry.

22 p2856 A73-42023

Error accumulation in thermocouple thermometry.

22 p2859 A73-42052

A few error detection codes for decision feedback system and error characteristics of channels.

22 p2835 A73-42192

On an asymptotic property of the least-mean-square-error design criterion in pattern recognition.

22 p2835 A73-42274

Electromagnetic flowmeters with point electrodes and finite length insulating liners, discussing performance numerical analysis accuracy by comparison with exact analytic solutions

22 p2860 A73-42300

Error analysis of a coupled inertial navigation system

22 p2884 A73-42358

A new determination of the second virial coefficient of carbon dioxide at temperatures between 0 and 150 C, and an evaluation of its reliability.

22 p2932 A73-42507

Determination of nongravitational forces in the motion of comets. I - Analysis of observation errors

22 p2910 A73-42643

Doublet ratio method for abundance determination application to interstellar multiple clouds, considering column density error due to velocity distribution simplification

22 p2910 A73-42703

Evaluation of error bounds in an optimization problem using the finite-element method.

[ASME PAPER 73-APMW-15] 22 p2924 A73-42882

Numerical method for computer generated kinoform image reconstruction error minimization, comparing with random phase method

22 p2863 A73-43148

Increase of error in range correction with elapsed time, evaluated by ray tracing through radiosonde-generated atmospheric models.

22 p2828 A73-43176

An optimality condition for assessing systematic errors

23 p2999 A73-43264

Evaluation of the accuracy of predicting the motion parameters of low-orbit artificial earth satellites

23 p3027 A73-43266

Suppression of equichannel interference in the case of binary phase shift keying employing a limiter

23 p2953 A73-43324

Resolution of point sources of light as analyzed by quantum detection theory.

23 p2987 A73-43523

Gilbert burst noise model for statistical analysis of nonindependent errors in digital data transmission systems, noting performance and utility in communication theory

23 p2954 A73-43986

Optimum mean-square decision feedback equalization.

23 p2964 A73-43988

Numerical stability of various summation schemes in a floating-type R subset

23 p2999 A73-44098

The precision of contour lines and contour intervals of large- and medium-scale maps.

23 p2979 A73-44123

Results of delay-time and Doppler-correction measurements obtained in radar observations of Venus during 1962, 1964, 1969, 1970, and 1972

23 p3037 A73-44252

Climatic means finite time average estimation standard error calculation by stochastic model with application to long range forecasting

23 p3004 A73-44264

Aerodynamic effects due to configuration of X-wire anemometers.
[ASME PAPER 73-APM-P] 23 p2984 A73-44375

Automatic integration algorithm for computer calculation of definite integral within specified tolerance, discussing computation failures and algorithm reliability
23 p2957 A73-44390

Refutation of Bagby moonlet theory via analysis of supporting evidence
24 p3133 A73-44542

A method for accurately compensating for the effects of the error beam of the NRAO 300-ft radio telescope at 21-cm wavelength.
24 p3067 A73-44581

The inadequate reference electrode, a widespread source of error in plasma probe measurements.
24 p3115 A73-44873

Determination of performance precision and informativeness of electronic models of the sensory system of man
24 p3064 A73-44911

Numerical convective schemes based on accurate computation of space derivatives.
24 p3105 A73-45026

Computerized structural analysis by finite element method, discussing round-off and truncation errors with emphasis on inherited error effects minimization
24 p3150 A73-45233

Extremum principles and error bound for a non-linear boundary value problem in the theory of laminar boundary layers.
24 p3080 A73-45340

Computational assessment of the numerical influence of the cutting step size and evaluation equation on the precision of experimental and analytical residual-stress determinations
24 p3153 A73-45446

ERROR CORRECTING DEVICES

Schmidt and Maksutov spectrographic cameras, discussing correcting devices for mirror aberrations
01 p0047 A73-10512

Theory of multistep coding and its application to multiphase-modulation communication systems.
01 p0018 A73-11053

Minicomputer for real time sequential decoding of convolutional code transmission in space communication, discussing system design, performance and metric bias effect
01 p0020 A73-11185

Error-erasure decoding of product codes.
01 p0020 A73-11296

Aircraft reference altitude computation from air data inputs, deriving algorithm for pressure gradient errors correction
03 p0308 A73-13915

Estimation of unmodeled forces on a low-thrust space vehicle.
04 p0504 A73-15272

A very high speed hard decision sequential decoder.
04 p0424 A73-15398

Manned spacecraft digital TV system channel error correcting encoder and decoder performance test data including bit error rate versus SNR and decoding depth
04 p0419 A73-15400

Real time digital spacecraft TV with data compression/error correction test system, evaluating source encoding algorithm performance from processed picture quality
04 p0449 A73-15409

Source encoding with fixed ward length and synchronous bit rate.
04 p0425 A73-15420

An amplitude-steered, electronically despun antenna for the synchronous meteorological satellite.
04 p0428 A73-15453

Data link control procedures for error-free transmission channels, discussing serialization and synchronization techniques and reverse interrupt facilities in sequential machine model
05 p0551 A73-16802

Periodic attitude control of a slowly spinning spacecraft.
[AIAA PAPER 73-246] 05 p0596 A73-16970

Nonlinear conversion of a measured value aimed at reducing the influence of dependent errors
05 p0577 A73-16985

Correction of the dynamic distortions of signals resulting from measurement information compression
05 p0577 A73-16986

Code correcting nonsymmetrical bursts of errors during data exchange between computers.
06 p0670 A73-17962

Pretransmission normalization procedure to suppress transmission error accumulation in receivers of differential PCM systems
09 p1055 A73-23388

Block coding for digital computer error detection and correction, considering applications for arithmetic operations, storage media and permanent hardware failure recognition
09 p1061 A73-23400

Optimum strategy for the correction of orbit-injection errors of arbitrary orientation.
09 p1151 A73-23451

A combined coding and modulation approach for communication over dispersive channels.
10 p1186 A73-23496

Range-azimuth-coupling aberrations in pulse-scanned imaging systems.
10 p1188 A73-23833

Airborne atmospheric temperature measurements correction for sensor response lag, deriving numerical scheme based on sensing systems wind tunnel calibration
10 p1217 A73-23991

The application of integrated magnetic devices for circuit checking and error correcting
10 p1198 A73-24021

Modeling of a bubble-memory organization with self-checking translators to achieve high reliability.
10 p1192 A73-24872

The dual-aperture counterwound log-spiral antenna direction-finder system.
11 p1338 A73-25669

Reduction of ILS errors caused by building reflections.
11 p1330 A73-25784

Cyclic binary codes circuit technology, discussing error types and decoding circuits for error detection and correction
11 p1332 A73-26254

Adaptive control for correction of flexible linear array phase error with resistance strain gages and ferrite phase shifter, noting radiation pattern performance
11 p1332 A73-26283

Holographic approach to real time correction of optical instruments images, discussing restoration by spatial frequency filtering
11 p1370 A73-26535

Dynamic AGC correction for angle signal variations in monopulse radar receivers with reference signal, analyzing signal statistics
12 p1469 A73-27163

Magnetic coil type electrical measurement indicating instruments accuracy dependence on manufacturing tolerances, discussing error reducing design methods
12 p1499 A73-27873

Solid ultrasonic cylindrical lens design for off-axis aberration minimization for focusing properties improvement, using method analogous to chromatic aberration correction in optics
13 p1612 A73-28491

Flat circular acoustic transducer for pressure spectrum analysis, deriving flow noise response correction factor in terms of polynomial coefficients and frequency-dependent constants
13 p1613 A73-28492

Long term temperature control and calibration system for creep testing facility temperature drift monitoring and correction
13 p1597 A73-28841

Atmospheric effects on ocean surface temperature sensing from the NOAA satellite scanning radiometer.
13 p1610 A73-29195

Algorithms of formal selection for optimal control systems of digital computers
14 p1730 A73-30034

A simple error-protection approach in the case of a transmission of anisochronous data signals over time-division multiplex systems
14 p1726 A73-30071

Algebraic decoding algorithms for block codes over q-ary input Q-ary output alphabet channel, presenting examples for Hamming, Lee or burst distance
14 p1730 A73-30501

Linear transformations of variable in system of normal equation in differential correction processes, reducing process to algorithm
15 p1930 A73-31115

Surveillance and correction of gas analysis devices and the analysis evaluation with the aid of a process computer
16 p2014 A73-33223

Numerical integration errors due to differential equations instability for Kepler orbits, discussing error reduction procedure by substituting for time as independent variable
16 p2061 A73-33231

Estimation and correction of electric thruster misalignment effects on a geostationary satellite.
17 p2238 A73-34866

TVAC - A television area correlator tracking system.
17 p2171 A73-35381

Corrections for response errors in a three-component propeller anemometer.
18 p2316 A73-36710

Design principles for phase-measuring attachments with automatic error corrections
18 p2294 A73-36999

An error correction method for DPCM picture transmission
19 p2432 A73-38268

Error maxima for division algorithm adaptiveness evaluation of damaged computer elements with corrective readjustments
19 p2408 A73-38563

Applications of error-correcting codes to TDMA satellite communications.
20 p2526 A73-38751

Design and analysis of a practical on-line filter to process gyrocompass data.
[AIAA PAPER 73-841] 20 p2564 A73-38782

Competitive evaluation of failure detection algorithms for strapdown redundant inertial instruments.
[AIAA PAPER 73-853] 20 p2585 A73-38791

Evaluation of burst error correcting codes using a simple partitioned Markov chain model.
21 p2656 A73-41168

Error-correcting codes in computer arithmetic.
22 p2830 A73-42713

ERROR DETECTION CODES

Theory of multistep coding and its application to multiphase-modulation communication systems.
01 p0018 A73-11053

Minicomputer for real time sequential decoding of convolutional code transmission in space communication, discussing system design, performance and metric bias effect
01 p0020 A73-11185

Error-erasure decoding of product codes.
01 p0020 A73-11296

Design of communication systems using short-constraint-length convolutional codes.
04 p0419 A73-15396

Performance versus complexity of Viterbi and sequential decoding.
04 p0424 A73-15397

TDM link with digitized voice channel and PCM telemetry sequence coding for error correction, comparing tested performance with prediction and computer simulation
04 p0419 A73-15401

Source encoding with fixed ward length and synchronous bit rate.
04 p0425 A73-15420

Modular arithmetic weight and cyclic shifting.
05 p0554 A73-17100

Code correcting nonsymmetrical bursts of errors during data exchange between computers.
06 p0670 A73-17962

Convolutional coding for multiple-access satellite communication.
09 p1056 A73-23399

Block coding for digital computer error detection and correction, considering applications for arithmetic operations, storage media and permanent hardware failure recognition
09 p1061 A73-23400

Concatenated coding for deep space interplanetary communication with low data rate and SNR, comparing performance of three binary codes
09 p1058 A73-23424

A combined coding and modulation approach for communication over dispersive channels.
10 p1186 A73-23496

Run length code for redundancy encoding of black-white facsimile picture data transmission to allow channel or storage capacity reduction and hardware simplification
10 p1188 A73-23741

Binary cyclic code detection capability, polynomial description, coder-decoder circuits and error correction application
10 p1197 A73-23848

Cyclic binary codes circuit technology, discussing error types and decoding circuits for error detection and correction
11 p1332 A73-26254

Sphere packings constructed from BCH and Justesen codes.
13 p1584 A73-28919

Algebraic decoding algorithms for block codes over q-ary input Q-ary output alphabet channel, presenting examples for Hamming, Lee or burst distance
14 p1730 A73-30501

Arithmetic algorithms for error-coded operands.
15 p1899 A73-31349

Organization of checks of the central control unit in a digital process-control computer operating with fixed word length
16 p1986 A73-33665

Signal set design for bandwidth constrained multiple phase amplitude shift keyed (MPASK) communication system, considering minimum error probability for given energy/noise ratio
20 p2522 A73-38717

Applications of error-correcting codes to TDMA satellite communications.
20 p2526 A73-38751

Ships inertial navigation system automated degradation detection and isolation, specifying decision error probabilities as function of degradation magnitude and observation time
[AIAA PAPER 73-849] 20 p2585 A73-38788

Transmission strategy and optimal block size in high-speed data communication.
20 p2530 A73-39128

Digital codings of multi-dimensional information sources and applications to image coding.
21 p2655 A73-41043

- Data transmission system based on voice channels time division into blocks using cyclic code redundancy without appreciable loss in error correcting capability 21 p2655 A73-41044
- Evaluation of burst error correcting codes using a simple partitioned Markov chain model. 21 p2656 A73-41168
- A few error detection codes for decision feedback system and error characteristics of channels. 22 p2835 A73-42192
- Error detection and synchronization with pseudoternary codes for data transmission. 22 p2827 A73-42464
- Error-correcting codes in computer arithmetic. 22 p2830 A73-42713

ERROR FUNCTIONS

- Mathematical description by Gaussian error function for metals diffusive saturation and diffusion constants determination 10 p1236 A73-24952
- Error curve in radiometric beta backscatter measurement of coatings thickness via digital computation 12 p1495 A73-26846
- A posteriori estimates of error distribution laws in the solution of linear algebraic equations by analog techniques 14 p1768 A73-30032

ERROR SIGNALS

- A simple Fourier analysis technique for measuring the dynamic response of manual control systems. 01 p0027 A73-10321
- Synthesis of a system with a Pi-shaped amplitude-frequency characteristic and a 'zero' equivalent phase-frequency characteristic 07 p0794 A73-20293
- The effect of impulsive noise on FSK digital communication. 08 p0938 A73-20834
- Block quantizers for encoding pictures at low bit rates, noting maximum nonstationary error signal incurred at block edges 10 p1186 A73-23497
- Constant-Q pulsed feedback electronics for strapped-down gyro systems. 11 p1342 A73-26635
- Unified approach to the performance analysis of linear modulation systems with coherent detection. 12 p1469 A73-27072
- A simple error-protection approach in the case of a transmission of anisochronous data signals over time-division multiplex systems 14 p1726 A73-30071
- Multi balance measurement of flow systems. 16 p2016 A73-33656
- Synthesis of a system of pi-shaped amplitude-frequency and 'zero' equivalent phase-frequency characteristics. 18 p2291 A73-37130
- Sampling, quantization and channel errors in differential pulse code modulation systems, discussing SNR, quantizer levels, standard PCM systems, reconstruction filters and bit errors 19 p2407 A73-38383
- Influence of low-frequency periodic interference on the operation of a complex system with variable structure 20 p2539 A73-38694
- Large scale telescope pointing stability augmentation system, using control moment gyro gimbal servo error signal to command momentum augmentation system [AIAA PAPER 73-868] 20 p2587 A73-38806
- Problems in the theory and practice of the self-tuning of compensating signals in complex control systems 20 p2541 A73-38994
- Error signal of a scanning antenna with a sum-difference directional pattern 20 p2537 A73-39465
- Time domain analysis of human operator manual control function for second order oscillatory divergent system with error signals for compensatory tracking 21 p2634 A73-40090

ERRORS

- NT INSTRUMENT ERRORS
- NT PHASE ERROR
- NT PILOT ERROR
- NT POSITION ERRORS
- NT RANDOM ERRORS
- NT RANGE ERRORS
- NT ROOT-MEAN-SQUARE ERRORS
- NT TRUNCATION ERRORS
- NT VELOCITY ERRORS

ERTS

- U EARTH RESOURCES TECHNOLOGY SATELLITES

ERTS-A

- U EARTH RESOURCES TECHNOLOGY SATELLITE I

ERYTHROCYTES

- NT RETICULOCYTES
- Biochemical processes during the maturation of erythrocytes - Further results with regard to the action site of the respiratory inhibitor F from reticulocytes in the respiratory chain 02 p0134 A73-12510

- A criterion for oxygen supply optimality in tissues and the capillary circulation rate 03 p0268 A73-13821
- Differentiations and maturations in red and white blood cells construction in red bone marrow, noting hematopoietic system formation from single source cell 06 p0649 A73-17473
- Red cell flexibility and pressure-flow relations in isolated lungs. 09 p1041 A73-22927
- Apparent paradoxical patterns of anaerobic glycolysis and hexokinase activity in the red blood cells of acutely bled rats, with evidence that the responses were in part hormone-dependent. 11 p1315 A73-25568
- A method for calculating the sedimentation characteristics of particles in linear dextrane-density gradients and its application to the separation of red blood cells according to the sedimentation rate 13 p1578 A73-28476
- Investigation of some blood characteristics in albino rats subjected to 60-day hypokinesia 15 p1834 A73-31502
- Responses to graded hypoxia at high and low 2,3-diphosphoglycerate concentrations. 17 p2112 A73-35460
- Red cell volume with changes in plasma osmolality during maximal exercise. 18 p2277 A73-36654
- Erythropoietin production in dogs exposed to high altitude and carbon monoxide. 20 p2513 A73-39599
- Studies on the metabolism of glucose-1,6-diphosphate in human erythrocytes. 21 p2639 A73-41139
- Hemoglobin molecule oxygenation mechanism in various animals, discussing erythrocytes as hemoglobin carriers, ecological factors and physicochemical conditions 23 p2947 A73-43929
- Oxygen affinity and electrolyte distribution of human blood - Changes induced by propranolol. 24 p3062 A73-44689
- Determination of the size distribution function of erythrocytes by the spectral transparency method 24 p3065 A73-45521
- Erythrocyte volume in acidified venous blood from exercising limbs. 24 p3062 A73-45557

ESAKI DIODES

U TUNNEL DIODES

ESCAPE

- Three body problem of stellar system subjected to isoenergetic variations, evaluating escape and ejection parameters 08 p1005 A73-20920
- The escape of H2 from Titan. 17 p2232 A73-34861
- Three body problem triple close approaches within escape mechanism, discussing method to control numerical integrations accuracy 24 p3141 A73-45281
- Isosceles case of rectilinear restricted three body problem with two equal mass primaries in rectilinear ellipses, deriving escape and collision conditions 24 p3141 A73-45285

ESCAPE CAPSULES

- Unmanned rendezvous applications for space rescue. 01 p0105 A73-11156
- B-1 bomber crew integrated escape module for safe recovery throughout aircraft operational envelope, discussing capsule configuration and flight tests [AIAA PAPER 73-440] 15 p1825 A73-31426
- Mortar design for parachute ejection and deployment into airstream to decelerate spacecraft and aircraft pilot escape modules, estimating hardware weight and reaction load [AIAA PAPER 73-459] 15 p1827 A73-31445
- Development of a high-performance ringsail parachute cluster. [AIAA PAPER 73-468] 15 p1828 A73-31452
- Experimental investigation and correlation of the ground impact acceleration characteristics of a full scale capsule and a 1/4 scale model aircraft emergency crew escape capsule system. [AIAA PAPER 73-480] 15 p1829 A73-31463

ESCAPE ROCKETS

- The 600 knot Yankee escape system. 05 p0534 A73-16200

ESCAPE SYSTEMS

- Unmanned rendezvous applications for space rescue. 01 p0105 A73-11156
- The 600 knot Yankee escape system. 05 p0534 A73-16200
- Concorde emergency power supply, oxygen and escape systems design and operational features 14 p1713 A73-30929
- A 14.2-ft-Do variable-porosity conical ribbon chute for supersonic application. [AIAA PAPER 73-472] 15 p1828 A73-31456
- Relative merit of the disc-gap-band parachute applied to individual aircrew member escape. [AIAA PAPER 73-483] 15 p1829 A73-31465

- Survival and Flight Equipment Association, Annual Symposium, 10th, Phoenix, Ariz., October 2-5, 1972, Proceedings. 16 p1965 A73-32653

- UPSTARS - A single escape subsystem providing stabilization, retardation, and separation. 16 p1966 A73-32668

- Stowable deployable autogyro aircrew vehicle escape rotoseat (SAVER) conversion to flight vehicle for advanced escape rescue capability /AERCAB/ from hostile areas 16 p1966 A73-32674

- Certification program for the DC-10 slide/raft. 17 p2108 A73-35807

ESCAPE VELOCITY

- Sighting methods during flights from the moon to the earth 18 p2351 A73-36107
- Derivation of an approximate solution to the equation of geocentric motion of a space vehicle with a solar sail 19 p2492 A73-37849
- Oscillatory motion existence in expanding n-body gravitational systems with distance bound and particle escape 23 p3034 A73-44208

ESG [GYROSCOPES]

U ELECTROSTATIC GYROSCOPES

ESKERS

U GLACIAL DRIFT

ESOPHAGUS

- The role of extrinsic vagal innervation in the motility of the smooth-muscle portion of the esophagus - Electromyographic study in the cat and the baboon 03 p0262 A73-13785
- Intra-atrial and esophageal electrography in the diagnosis of complex arrhythmias. 18 p2274 A73-36525

ESRO SATELLITES

- NT ESRO 1 SATELLITE
- NT ESRO 2 SATELLITE
- NT ESRO 2 SATELLITE
- NT GEOS SATELLITES [ESRO]
- NT HEOS A SATELLITE
- NT HEOS B SATELLITE
- NT HEOS SATELLITES
- ESRO I/A/B observations at high latitudes of trapped and precipitating protons with energies above 100 keV. 03 p0362 A73-13863
- Electron-proton spectrometer for the GEOS satellite. 06 p0692 A73-17826
- Stellar UV observations with spectrophotometer onboard ESRO TD-1A satellite in retrograde near polar orbit 07 p0875 A73-19259
- Preliminary results of a spectrophotometric survey of the sky in the ultraviolet with the aid of the TD-1 A satellite 08 p0967 A73-21499
- Modularised power conditioning units for high power satellite applications. 09 p1035 A73-22806
- The introduction of a digital computer on board ESRO scientific satellites. 09 p1061 A73-23378
- ESRO Aerosat L-band communication techniques experiments with stratospheric balloon-borne transponders relaying ground station signals to aircraft flying over sea 12 p1498 A73-27672
- Some results obtained in ESRO satellite data compression. 17 p2239 A73-34955
- Application of some data compression systems to ESRO satellite data. 20 p2524 A73-38735
- Stratospheric temperature measuring instrument development for Tiros N satellites and ESRO geostationary meteorological satellite development for cloud photography 23 p3004 A73-44103
- ESRO 1 SATELLITE
- A satellite-borne positive ion mass spectrometer. 14 p1753 A73-30415
- ESRO I /Aurorae/ satellite observations of aurora, magnetosphere-ionosphere interaction at high latitudes and auroral particle flux density 24 p3087 A73-45207
- ESRO 2 SATELLITE
- Monograph - Satellite-borne instrument for the measurement of soft solar X-rays. 01 p0045 A73-10150
- ESRO 4 SATELLITE
- A short description of the ESRO-IV satellite. 03 p0381 A73-13274
- Esro 4 performance of abandoned TD-2 experiments for particle measurements over polar regions, describing satellite construction, thermal control, power supply, attitude control and measurement 10 p1285 A73-23748
- The role of the Project Manager in the management of satellite projects. 11 p1454 A73-26262

ESTERS

NT CELLULOSE NITRATE
NT GLUTAMATES
NT ISOCYANATES
NT LACTATES
NT NITROGLYCERIN
NT POLYCARBONATES
NT POLYESTERS
NT POLYETHYLENE TEREPHTHALATE
NT STEARATES
NT URETHANES

Investigation of anti wear additives under various loads and at different sliding speeds.
[ASLE PREPRINT 72LC-3C-4]

Hydrolysis of a disiloxane/ester fluid in a simulated hydraulic system at 275 F.
[ASLE PREPRINT 72LC-6C-1]

Nonhydrocarbon liquid lubricants based on phosphate and neopentyl esters, perfluoroalkyl and polyphenyl ethers, silicone and perfluorotriazines, discussing performance testing techniques

Perchlorate degradation of ethyl oleate in solid propellants.

Amine phosphates as antiwear additives in neopentyl polyol esters.
[ASLE PREPRINT 73AM-9A-1]

Investigation of the photosensitivity of polyvinylcinnamate

Investigation of the spectral properties of sensitized polyvinylcinnamate

Investigation of the antistatic properties of lacquer coatings based on quaternary polyvinylpyridine salts

ESTIMATES

NT COST ESTIMATES

Weighted estimates of the error in the grid method of solving the Laplace and Poisson equations

Integral bounds of generalized derivative solutions of second-order equations of elliptic type in the L_p metric and certain related embedding theorems

Problems of accuracy in the representation of values by stochastic sequences

Features of the engineering theory for combined estimates of automatic control system reliability and lifetime

Several estimates in the theory of stochastic integals

Asymptotic behavior of some statistical estimates. II - Limit theorems for a-posteriori density and Bayesian estimates

Strengthening of Liapunov-type estimates /case where the distributions of members are close to the normal distribution/

Quadrature errors upper bound estimates for Gauss-Legendre, Newton-Cotes and Gauss-Laguerre formulas

A priori estimates for solution operators of diffusion equations.

Estimates of unknown parameter from quantized observations given as sequence of evenly distributed random values, noting optimal grouping equations for general distribution function

ESTIMATING

NT ORBITAL POSITION ESTIMATION

Assessment and operational implications for ATC capital investment decision making by relative capacity estimating process using analytical models

Mathematical algorithm using invariant imbedding method for accurate range and range rate estimates in terms of pulse Doppler radar ambiguity resolution

Pulse pair estimation of Doppler spectrum parameters.

Symposium on Nonlinear Estimation Theory and its Applications, 3rd, San Diego, Calif., September 11-13, 1972, Proceedings.

Air Force weapon system procurement needs, considering industry technological capabilities, nonlinear estimation in cruise navigation and nonlinear systems design, test and implementation

An application of Bayes-law estimation to nonlinear phase demodulation.

Power spectral density estimation by spline smoothing in the frequency domain.

Computerized parameter estimation by jump detection scheme for nonlinear atmosphere density and temperature profile tracking

Evaluation of the performance of a variance estimation algorithm using order statistics.

Estimation of the statistical parameters of the Kalman-Bucy filter.

A higher measurement space filter for passive tracking.

Relaxation algorithms for nonlinear system modal trajectory estimation by approximate step with lower triangular matrix inversions sequence, comparing convergence with Gauss-Newton method

Information-loss and risk-increase estimation during observational data reduction in successive estimation problems

State estimation of nonlinear system by applying stochastic approximation method.

Reduced-order observers for linear discrete-time systems.

The estimation of order and parameters in a process of stochastic differential equations with uncertain observations.

Scalar and block decoupling of time varying and invariant linear multivariable control systems, discussing sufficiency conditions, state estimation and order reduction possibility

Estimation theory and system state and parameter identification, developing algorithms for optimum linear sequential and nonlinear filters

Optimal inputs and sensitivities for parameter estimation.

Viterbi algorithm for recursive optimal estimation of state sequence of discrete time finite state Markov process observed in memoryless noise

Beta estimation accuracy for reentry vehicles using a priori target information with 6-component state vectors to reduce computation time

On optimal nonlinear estimation. I - Continuous observation.

Empirical estimation of the service life of injection lasers from short-term tests.

Optimal estimation of the phase coordinates for a linear dynamic system

A minimax filter for systems with large plant uncertainties using measurements corrupted by colored noise.

Cone-bounded nonlinearities and mean-square bounds - Estimation upper bound.

An adaptive estimation algorithm for time-varying bit synchronizers.

A scheme for estimating aircraft velocity directly from airborne range measurements.

Optimal estimation of the phase coordinates of a linear dynamic system.

A conservative bound on the estimation error covariance matrix in the presence of correlated driving noise and correlated discrete measurement noise.

Radar altimeter signal propagation delay estimation, calculating and plotting noise fluctuation characteristics as function of aircraft ground speed, altitude and other parameters

ESTIMATORS

Satellite attitude control estimators and observers, discussing applications to reaction wheel, spinning attitude and drag-free satellite translation control systems

Best linear unbiased estimator of the parameter of the Rayleigh distribution. I - Small sample theory for censored order statistics.

Trajectory optimization for the nonlinear combined estimation and control problem.

A consistent shape parameter estimator for the Weibull distribution.

Polynomial estimators for systems with polynomial nonlinearities.

High-altitude photographs of the Oregon coast.

Wetlands mapping in New Jersey.

Remote measurement of salinity in an estuarine environment.

Remote sensing of estuarine circulation dynamics.

ETCHING

Thin film CdS solar cell stability improvement by etching, noting cuprous sulfide oxidation effects on degradation from short term tests at high temperature

Microstrip transmission line microwave IC, discussing electrical characteristics, dielectric and conductor materials, photo-etching processes, connection fabrication and circuit encapsulation

Miniature pressure transducers with a silicon diaphragm.

Nuclear track etching in radiation and fast neutron dosimetry and health physics, discussing counter materials and fission and alpha particles and recoil nucleus recordings

Use of Sirtl etch for silicon-slice evaluation.

Competitive oxidation and pyrolysis of ethane in the presence of low concentrations of oxygen

Reactions of O(1D) with methane and ethane.

ETHERS

NT POLYPHENYL ETHER

A review of the perfluoroalkyl ether class of greases.

Nonhydrocarbon liquid lubricants based on phosphate and neopentyl esters, perfluoroalkyl and polyphenyl ethers, silicone and perfluorotriazines, discussing performance testing techniques

Ethanol condensation by homogeneous nucleation and growth of liquid droplets in steady state supersonic nozzle flow of ethanol-air and ethanol-nitrogen mixtures

Effects of ethyl alcohol on pilot performance.

Effects of a synchronizer phase-shift on circadian rhythms in response of mice to ethanol or ouabain.

Nitric oxide formation weightless in diffusion flame ethanol drop combustion as function of air temperature and diffusion and spray characteristics

Investigation of the possibility of using acetylated oxethylcellulose as a film forming substance for a moving-picture film base

Inhibition of the first limit of the hydrogen-oxygen reaction by ethyl bromide.

Combustion of stabilized ethylene within a supersonic flow by a Mach configuration

The gas-phase reaction of perchloric acid with ethylene.

Reaction H + C2H4 - Investigation into the effects of pressure, stoichiometry, and the nature of the third body species.

Chemisorption of H2 on W(211).

Spacecraft decontamination and sterilization by formaldehyde, beta-propiolactone, ethylene oxide, radiation and dry heat, noting effects on polymers

Incidence and severity of altitude decompression sickness in Navy hospital corpsmen.

U THERMOELECTRIC COOLING

EUCLIDEAN GEOMETRY

NT ANALYTIC GEOMETRY

NT ANGLES [GEOMETRY]

NT BRAGG ANGLE

NT CARTESIAN COORDINATES

NT CHORDS [GEOMETRY]

NT CIRCLES [GEOMETRY]

NT EPICYCLOIDS

NT HEXAGONS

NT OBLATE SPHEROIDS

NT PARABOLAS
NT PARALLELEPIPEDS
NT POINTS [MATHEMATICS]
NT POLYGONS
NT POLYHEDRONS
NT PROJECTIVE GEOMETRY
NT PROLATE SPHEROIDS
NT PYRAMIDS
NT QUADRANTS
NT RHOMBOHEDRONS
NT SPHEROIDS
NT TETRAHEDRONS
NT TORUSES
NT TRIANGLES

Hubble law from constant light velocity in Euclidean space, noting red shift equation and Einstein gravitational shift

03 p0379 A73-14577

Existence and conical intersection theorems for extremum conditions of Euclidean space subset function, noting discrete objects optimality conditions

05 p0589 A73-16334

Sphere packings constructed from BCH and Justesen codes.

13 p1584 A73-28919

Zero tangential acceleration points on bodies moving in three dimensional Euclidean space, considering helical-spherical and rotating-spherical motion

14 p1775 A73-30707

Schwarzschild solution indeterminacy as indicator of physical singularity analogous to intrinsically singular vertex of cone in Euclidean space

21 p2741 A73-41630

EUCLIDEAN SPACE

U EUCLIDEAN GEOMETRY

EULER BUCKLING

Beck cantilever problem solution for quasi- and purely dynamic case by Euler or energy method under internal constraint

24 p3147 A73-44892

EULER EQUATIONS OF MOTION

A note on the flow regimes in the unsteady, rectilinear flow of a perfect gas.

01 p0034 A73-11005

Selection of the measurement frequency in the determination of satellite orientation

05 p0630 A73-17007

High subsonic flow past airfoils at 2 deg angle of attack, describing relaxation method for hyperbolic Euler equations conversion to parabolic form

06 p0645 A73-17738

Differential equations in terms of the osculatory elements of a solid for the motion of the solid about its center of mass

09 p1121 A73-23355

Periodic small parameter solutions of rotary gyroscope motions about axis of ellipsoid of inertia, using Euler-Poisson equations

10 p1220 A73-24678

Impact interaction between a soft shell and a hard obstacle

15 p1947 A73-31276

Implicit finite difference scheme for Eulerian fluid dynamics of time dependent one dimensional polytropic gas flow, noting numerical stability

17 p2151 A73-34894

Bilinear hydrodynamics and the Stokes-Einstein law.

21 p2676 A73-40218

EULER-LAGRANGE EQUATION

Dynamic programming and a max-min problem in the theory of structures.

01 p0019 A73-10199

An action principle in general relativistic magnetohydrodynamics.

01 p0079 A73-11258

Energy dissipation and drift angular velocity calculation for horizontal pendulum on vibrating base, using revised differential equation of motion

01 p0079 A73-11417

Lagrange equations of motion for ideal incompressible fluid flow under asymmetric deformation of expanding circular cylinders and spheres, calculating resistance forces

03 p0294 A73-13613

Lagrange description of equations for finite deflections of incompressible plastic shells, classifying stress-strain relations

06 p0760 A73-17778

The variational derivative of degenerate Lagrange densities.

06 p0718 A73-18504

Powered-flight trajectory optimization for an inertial-guidance ballistic vehicle.

08 p1011 A73-21427

Subgrid resolution achievement by spline fitting during flow and force field sources conversion from Lagrangian distribution onto Eulerian grid and interpolation

10 p1248 A73-23603

Motion equation solutions for three flattened spheroids with coincident equatorial symmetry planes in Lagrange form by Duboshin transforms

10 p1274 A73-23722

Gaussian variational equations for osculating elements of an arbitrary separable reference orbit.

15 p1930 A73-31113

Motion equation solutions for three flattened spheroids with coincident equatorial symmetry planes in Lagrange form by Duboshin transforms

18 p2355 A73-36747

On the modal equations of large amplitude flexural vibration of beams, plates, rings and shells.

19 p2501 A73-38254

The Lagrange function for a gas bubble in an inhomogeneous flow

21 p2676 A73-40206

Integrals for optimal flight over a spherical earth.

22 p2884 A73-42561

EUROPA

Ten-micron eclipse observations of Io, Europa, and Ganymede.

11 p1424 A73-26133

Jupiter satellite Europa polar cap from photoelectric observation of occultations by satellite Io

21 p2687 A73-41077

EUROPA LAUNCH VEHICLES

NT EUROPA 2 LAUNCH VEHICLE

NT EUROPA 3 LAUNCH VEHICLE

Explanation of the accident to the Europa II F 11 launcher by phenomena of electrostatic origin

11 p1431 A73-25749

Space-flight qualification of solid-propellant units in the example of the cold-gas generator for the booster rocket Europa I/II

16 p2047 A73-33394

Strap-down inertial guidance systems study.

18 p2335 A73-36955

EUROPA 2 LAUNCH VEHICLE

Effect of the guidance reserve of the Europa II third stage on the consumption of propellants for stationing

04 p0504 A73-15294

The liquefied ergol supply-trailers for DIAMANT B and EUROPA II launchers.

07 p0807 A73-18948

Operational set up of Europa II launch vehicle control units.

07 p0808 A73-19005

Role of static electricity in the incidents recorded during the F11 firing [ONERA, TP NO. 1214]

10 p1285 A73-23750

ELDO equatorial launching base for Europa 2 vehicle, discussing launch site and telemetry facilities and logistics management/organizational aspects

14 p1741 A73-30077

Europa 2 Inertial Guidance System technology assessment covering design features, sensor, computer and interface units, first launch failure causes and need for improvements

24 p3108 A73-44694

EUROPA 3 LAUNCH VEHICLE

Considerations on transfer into geostationary orbit using ion propulsion - Application to the Europa III booster

04 p0505 A73-15742

Italian contributions to present aerospace activities; Conference, 2nd, Turin, Italy, June 9, 10, 1972, Proceedings

12 p1548 A73-27376

EUROPA III - Description of the work performed during the preparatory phase and characteristics of the booster

12 p1548 A73-27377

Europa 3 booster heat shields configuration selection factors and design, considering mechanical and electrical interfaces with vehicle equipment

12 p1548 A73-27378

The influence of the concept of a launcher on the layout of a launch base, and on the organization of test flights and operational launches

14 p1804 A73-30103

Utilization of PCM telemetry for the control of the Europa III launcher

14 p1804 A73-30111

Europa III heat shields - Aerothermodynamic analysis and design.

18 p2361 A73-36954

EUROPE

Secular variation of the stratospheric ozone layer over middle Europe during the solar cycles from 1951 to 1972.

04 p0445 A73-15635

Satellite remote monitoring of earth environment and natural resources by high resolution multispectral scanners for European requirements

17 p2160 A73-34931

Need for and aspects of a cooperative European earth resources program.

18 p2372 A73-35933

Statistical characteristics of the temperature field near the ground for Europe.

18 p2334 A73-37070

EUROPEAN AIRBUS

The technical evolution of air transport in the seventies - European contribution to this evolution

02 p0238 A73-11702

Russian book on passenger aircraft and air transport design covering technical and economic efficiency,

airbus concept, weight and size problems and aft-mounted engine design

07 p0777 A73-20377

Optimization and design of the rear fuselage of the A 300 B aircraft structure.

10 p1288 A73-23799

European airbus A300B aircraft flight tests and on-board instrumentation in certification program, illustrating desk layout, control and display panels

13 p1568 A73-28159

A-300 B airbus active and passive operational monitoring systems, considering visual and aural routine functional indicators, emergency warning devices and flight data recorders

15 p1830 A73-32458

The safety, the reliability, and redundancy in the automatic flight control system of the A300-B Airbus

15 p1830 A73-32459

ARINC-573 recording system - Application to maintenance

15 p1883 A73-32462

Minicomputer application to in-flight control of A300-B airbus engines, describing computational procedure for low pressure compressor stage RPM limit/N 1 limit/

15 p1831 A73-32477

EUROPEAN SPACE PROGRAMS

Scientific mission and German and U.S. plans/design for Helios cooperative solar probe, stressing advanced technology requirements

01 p0110 A73-11103

Physical contents and financial underpinning of future French and European space research programs, noting meteorology, satellite communication and R and D planning

01 p0125 A73-11254

Experience obtained so far in connection with the German scientific spacecraft program

02 p0227 A73-11654

Weather satellite Meteosat operational features and objectives, describing instrumentation, communication, data acquisition and processing facilities

02 p0227 A73-11695

Heos 2 satellite instrumentation and space exploration objectives, considering earth and interplanetary magnetic fields, electron and proton energies, solar radiation and wind, cosmic dust and micrometeoroids

02 p0228 A73-11949

The Meteosat system - Europe space contribution to global atmosphere observation.

03 p0381 A73-13275

Polish space research and prospects, discussing Intercosmos and Intersputnik participation and studies in space physics, communications, meteorology, geodesy, biology, radiology and medicine

04 p0521 A73-15021

Juridical problems connected with European network of telecommunication satellites, discussing satellite direct transmission

04 p0497 A73-15146

CERS/ESRO role, nonmember states participation and experimental systems in European telecommunication satellites program

04 p0523 A73-15147

European space conference, discussing space program priorities relative to applications or research satellites, communication satellites, launch vehicles and facilities and participation in post-Apollo program

04 p0523 A73-15151

ESRO electric propulsion research program, discussing colloid and field emission thruster concepts for different exhaust velocity ranges

04 p0487 A73-15714

High performance three axis attitude control system of TD1/A European scientific satellite, describing control circuits, logic, ancillaries and packaging procedure

07 p0904 A73-18968

European space operations control center subsystems for PCM telemetry data acquisition and processing

07 p0790 A73-18973

German scientific research satellite Aeros, discussing program planning and management, mission analysis, attitude control, power supplies, test methods, yo-yo despin and ground operations systems

08 p0154 A73-21658

The Federal Republic's AEROS Satellite Programme.

08 p1026 A73-21659

ELDO and ESRO space research activities review, stressing increased European cooperation, negotiations with U.S. and project budgeting vs national priorities

11 p1455 A73-26420

Italian contributions to present aerospace activities; Conference, 2nd, Turin, Italy, June 9, 10, 1972, Proceedings

12 p1548 A73-27376

EUROPA III - Description of the work performed during the preparatory phase and characteristics of the booster

12 p1548 A73-27377

Europa 3 booster heat shields configuration selection factors and design, considering mechanical and electrical interfaces with vehicle equipment
12 p1548 A73-27378

Meteosat geosynchronous satellite for European meteorological space program, discussing picture taking, data broadcasting and rebroadcasting, central control station and peripheral terminals
12 p1549 A73-27380

Sortie module/pallet scientific European space program based on system performing orbital zero-g or earth/celestial bodies observation platforms functions
12 p1549 A73-27381

European space tug conception evolution, discussing docking system
12 p1549 A73-27382

Meteosat - Project of a European geostationary meteorological satellite - Status: 9/15/1972
13 p1689 A73-28743

ERAF - Proposal for a European Earth Resources Aircraft
13 p1569 A73-28786

Space shuttle missions relationship to post-Apollo, European and joint European-U.S. space exploration programs
13 p1690 A73-29387

European telephony traffic and Eurovision TV program exchanges via three-axis stabilized communications satellite with fold out solar panel arrays
14 p1724 A73-29715

German ground operations network design, describing data system and flow with automatic handling of telemetry data, tracking data and operational information
14 p1727 A73-30098

The German Central-Ground-Station concept motivation and its multipurpose and automation aspects
14 p1742 A73-30099

Satellite payloads preparation and launching methods in European space programs, evaluating firing range apparatus and firing range/satellite interfaces
14 p1804 A73-30106

Theoretical and practical design aspects on spacecraft propellant and pressurant loading systems
14 p1742 A73-30107

European geostationary communication satellite system for telephone and TV transmission, discussing stabilization, command and power subsystems, modulation methods, power budgets, satellite configurations, etc
14 p1728 A73-30431

UN accomplishments in space law, discussing ERSO and ELDO application satellites and international agreements
14 p1819 A73-30898

European telecommunication satellite program implementation and preoperational phase regulation, stressing international constraints
14 p1819 A73-30900

The German aeronomy satellite Aeros
15 p1943 A73-32178

Italian SIRIO satellite cross polarization signal measurements aided by ground station antenna system using narrow bandwidth
16 p1983 A73-33725

The orbital test satellite for the European Communication Satellites Programme - Performance and growth capability.
[DGLR PAPER 73-044]
17 p2126 A73-35481

Communications system of the Symphonie satellite and special transmission parameters
[DGLR PAPER 73-056]
17 p2126 A73-35489

Transponder for European communications satellite systems/ECS and OTS program/
[DGLR PAPER 73-057]
17 p2126 A73-35490

The preparatory phase of the German Earth Resources program.
18 p2372 A73-35934

Communication satellites future use in Europe, considering mission requirements, data transmission, specialized TV distribution, cost effectiveness and shuttle/tug launch system
[AAS PAPER 73-148]
20 p2521 A73-38596

Design of the 14/11 GHz repeater for the European Orbital Test Satellite.
20 p2525 A73-38745

The Netherlands astronomical satellite/ANSI.
22 p2917 A73-42291

EUROPEAN SPACE RESEARCH ORGANIZATION
SAT
NT ERSO 1 SATELLITE
NT ERSO 2 SATELLITE
EUROPEUM
NT EUROPIUM ISOTOPES
Crystallochemical analogy between europium, yttrium, calcium, and barium in their alloys with manganese
09 p1135 A73-23235

Europium anomaly in plagioclase feldspar - Experimental results and semiquantitative model.
16 p1976 A73-32902

EUROPIUM COMPOUNDS

Optimum thickness for thermomagnetic laser writing on Fe doped EuO films on quartz substrate
06 p0702 A73-18372

Preparation and investigation of EuS thin films
11 p1410 A73-26672

EUROPIUM ISOTOPES
High resolution spectroscopic analysis for photospheric Eu II lines with spectrum synthesis techniques, determining solar isotopic composition and abundance
10 p1278 A73-24129

EUTECTIC ALLOYS
Refinement of primary silicon crystals in a hypereutectic Al-20% Si alloy by sulphur addition.
02 p0179 A73-11597

Growth of ternary composites from the melt. I, II.
04 p0463 A73-15310

Microstructure alignment in Ni-In system eutectic alloys due to directional solidification
04 p0463 A73-15312

Directionally solidified NiAl-Cr and NiAl-Mo eutectic composites microstructural stability as function of time and temperature
06 p0711 A73-18753

Morphological factors influencing the initial stages of coarsening in the Al-Al3Ni eutectic composite.
06 p0712 A73-18761

Electrical conductivity of a directionally crystallized Al-Al3Ni composition
09 p1099 A73-21972

Determination of the composition of Ni-NiMo eutectic by the zone recrystallization method
09 p1108 A73-23239

Crystallography and morphology of as-grown and coarsened Al-Al3Ni directionally solidified eutectic.
10 p1234 A73-24432

Heat resistant and refractory materials contact eutectic melting for surface coating production
10 p1227 A73-24967

Composite materials; Meeting, 2nd, Konstanz, West Germany, March 15, 16, 1972, Technical Reports
11 p1372 A73-25401

Directionally solidified eutectic high temperature alloys.
11 p1379 A73-25404

Mechanical properties at high temperature of Ni-based unidirectionally solidified eutectic: Ni-Ni3Ta.
11 p1379 A73-25405

Bivariant eutectic alloys located on liquidus surface within Ni-Nb-Cr-Al quaternary, permitting production of aligned delta Ni-Nb lamellae within nichrome matrix containing Ni-Al fcc precipitate
12 p1509 A73-26845

Phase structure and composition during the crystallization of eutectic-type alloys of the Ni-Cr system
12 p1509 A73-26897

Investigation of the sintering of binary alloys with limited solubility in the solid state. I - Concentration dependence of shrinkage during sintering of two-component systems with a eutectic type of phase diagram
12 p1503 A73-27558

Stereometric microanalysis of conglomerate, colony and dispersed structures of binary eutectic Fe, Al, Cu and low melting alloys
13 p1631 A73-28109

Unidirectional solidification formed interdendritic eutectic composition related to solidification variables, discussing Al-Cu and Al-Cu-Ni systems
13 p1632 A73-28131

Ti-Pd phase diagram eutectoid region configuration determination through alloy thin foil arc melting preparation and microstructure examination by electron microscopy
13 p1633 A73-28146

Directionally solidified eutectic alloy composites for high temperature turbine blade and vane applications, considering morphology, crystallography and thermal stability properties
13 p1635 A73-28778

Superalloys processing technology for aircraft gas turbine applications, discussing developments in eutectics and powder metallurgy for increased operating temperatures
13 p1636 A73-28931

Precipitation and dispersion hardened alloys, fiber reinforced metal matrix composites, carbon-carbon composites, and dispersed system, eutectics application in aerospace industry
14 p1759 A73-30067

Eutectic superalloys strengthened by aligned delta, Ni3Cb lamellae, gamma-prime, Ni3Al precipitates and reduced interlamellar spacing.
16 p2026 A73-33425

Direct observation of the failure of a fibre reinforced composite.
17 p2192 A73-35529

Observations on the directional solidification of cobalt-base alloys strengthened by carbide fibres.
19 p2443 A73-38249

Structures and properties of cobalt base-TaC eutectic alloys.
20 p2575 A73-39020

Partitioning of stress between fiber and matrix during tensile deformation of the Al-Al3Ni eutectic composite.
20 p2576 A73-39024

Carbide reinforcement in two directionally solidified alloyed nickel eutectic alloys.
20 p2576 A73-39028

The influence of phase size on the creep of lamellar and particulate Al-CuAl2 eutectic composites.
21 p2719 A73-40896

Structure and composition of phases during solidification of Ni-Cr alloys of the eutectic type.
21 p2720 A73-41030

Experimental aspects of the mechanical behavior of fiber composites produced by oriented solidification [ONERA, TP NO. 1205]
22 p2876 A73-42215

Metastable phase diagrams of eutectic and peritectic alloys crystallization during rapid cooling from liquid state
22 p2877 A73-42458

Phase diagrams of ruthenium and rhodium systems with carbon
22 p2878 A73-42461

Metastable phases produced by laser melt quenching.
22 p2878 A73-42576

The relation between the internal thermal resistance of transistors and the method of alloying.
23 p2960 A73-43677

The copper-boron eutectic - Unidirectionally solidified.
23 p2993 A73-44035

Influence of small beryllium, titanium, and zirconium additions on the structure and properties of Al9 alloy
24 p3098 A73-44571

Spatial orientation of phases in the Al-Al3Ni eutectic system
24 p3099 A73-45169

EUTECTIC DIAGRAMS
U PHASE DIAGRAMS
EUTECTICS
NT EUTECTIC ALLOYS
Evaluation of materials for sliding at 600F-1800F in air.
[ASLE PREPRINT 72LC-7C-2]
03 p0317 A73-14371

Mechanical behaviour of unidirectionally solidified composites.
[ONERA, TP NO. 1147]
08 p0983 A73-21676

Thermal stability of the microstructure in the eutectic composition Al-Al3Ni
09 p1099 A73-21966

Crystallostructural investigation of the eutectoid decomposition of copper-beryllium alloys - Ordering accompanied by formation of Cu2Be metastable solid solution
14 p1760 A73-30587

Morphology of the structure and the microhardness of Al/Ni, Cu, Be, Fe, Co eutectic compositions
14 p1760 A73-30588

Hot-pressed eutectics of oxides and metal fibers.
21 p2723 A73-40895

EUTROPHICATION
Eutrophication assessment using remote sensing techniques.
20 p2558 A73-39861

EVACUATING [TRANSPORTATION]
DC-10 aircraft slide/raft system for emergency personnel evacuation, discussing certification test program for performance, reliability, seaworthiness and compliance with regulations
16 p1965 A73-32659

Airplane accident survival, discussing cabin safety, fire protection, crashworthiness, emergency evacuation and crash landing in water
17 p2097 A73-34079

Certification program for the DC-10 slide/raft.
17 p2108 A73-35807

Aircraft evacuation and safety procedures during emergencies, discussing negative panic, flight crew training and impact injury minimization
18 p2268 A73-36849

International Congress of Aeronautical and Space Medicine, 20th, Nice, France, September 18-21, 1972, Reports
18 p2284 A73-36901

EVACUATING [VACUUM]
The evacuating and outgassing of a vacuum UV spectrophotometer for rockets
10 p1220 A73-24683

EVANESCENCE
Evanescent fields produced by totally reflected beams.
22 p2824 A73-41853

EVAPORATION
NT PROPELLANT EVAPORATION
NT TRANSPIRATION
One-dimensional electrohydrodynamic flows with a variable mobility coefficient - Evaporation and condensation discontinuities
01 p0077 A73-10954

A new experimental method for the investigation of fuel spray evaporation.
[AIAA PAPER 72-1148]
03 p0356 A73-13453

The evaporation of various lubricant fluids in vacuum.
[ASLE PREPRINT 72LC-6C-2]

Investigation of high-temperature evaporation of heat-resistant ceramic coatings on metals

Laser beam evaporation of dense substances, examining luminous flux densities with gasdynamic equations

Heat and mass transfer during the evaporation of liquids from capillary porous bodies situated in a hot air flow

One-dimensional electrohydrodynamic flows with variable mobility coefficient, evaporation and condensation jumps.

The determination of the evaporation from a class-A pan by means of empirical evaporation formulas

Experimental drag coefficients for evaporating and burning drops at elevated pressures.

Temperature effects on liquid drop evaporation in an air flow

The influence of the sea evaporation duct on the phase of the received field on a line-of-sight path.

Evaporation of metallic targets caused by intense optical radiation.

Analysis of the heat transfer associated with the evaporation of a fluid film on a rotating disk

Evaporation of metallic targets caused by intense optical radiation.

EVAPORATION RATE

Forced convection droplet evaporation with finite vaporization kinetics and liquid heat transfer.

Ultrahigh vacuum quartz spring microbalance for determination of evaporation rate and vapor pressure.

Experimental investigation of the evaporation rate of water droplets in atmospheres of air and carbon dioxide under conditions of a thermostatic droplet surface

High current low voltage magnetically confined hollow cathode discharge for vacuum evaporation and ionization, noting vacuum deposition of quartz and copper

The effect of substrate temperature on the structure of titanium carbide deposited by activated reactive evaporation.

The deposition of multicomponent phases by ion plating.

Preparation of alloy deposits by continuous electron beam evaporation from a single rod-fed source.

Suppression of evaporation of hydrocarbon liquids and fuels by aqueous films.

Upper atmospheric dust particle temperature and related Na atom abundance seasonal variation based on energy budget and Na sublimation rate considerations

Experimental study of water drop evaporation in a heated air flow

Evaporation rate and temperature of liquid drops calculated for low and high temperature aerosols

Phase transition effects at the collecting droplet surface on the capture coefficient magnitude

Diameter reduction rate and time dependence of corresponding temperature variation of liquid drop unsteady evaporation in rarefied ambient gas

Comet nuclei gas liberation, perihelion mass loss and photometric property dependence on water ice evaporation rate and nongravitational effects

Molybdenum evaporation rates in oxygen, air, and water vapor at high temperatures and low pressures

Evaporation rate and vapor pressure of selected polymeric lubricating oils.

A general expression for the rate of evaporation of a layer of liquid on a solid body.

Evaporation of a water drop

Preparation of liquid fuels by evaporation from a hot wall

Evaporative cooling

NT FILM COOLING

NT SWEAT COOLING

Doppler turbulence spectrum and intensity measurement in stalactites region at base of cloud deck cooled by evaporation and destabilized by convection

A study of mist cooling /1st Report - Investigation of mist cooling/.

Physical conditions of heat transfer and design of heat pipes for the evaporation mode of operation at moderate temperatures

EVASIVE ACTIONS

Optimal control problems in differential games of pursuit and evasion involving deterministic, random and controlled motion

Pursuit-evasion reconnaissance game with evader reconnoitering target from close distance with guaranteed safe escape from pursuer

Pursuit/evasion game problem with two pursuers to one evader, discussing coalition tactic based on open loop and closed loop conjugate points difference

Trajectory deviation conditions in second order linear differential escape game

Approach and evasion games in conflict controlled system with nonlinear control, deriving necessary condition for winning

Optimal control problems in differential games of pursuit and evasion involving deterministic, random and controlled motion

Necessary termination conditions for difference-differential rendezvous /pursuit with evasion/ game with functional goal set

Existence solution to linear differential rendezvous game of dynamic system with pursuit and evasion

Conditions for evading a point in a second-order differential game

Differential game estimate of phase point pursuit of evading closed convex set for feedback control in irregular case

Optimal evasive tactics against a proportional navigation missile with time delay.

Optimal pursuit-evasive conflicts with guidance systems containing time delays.

Dynamic programming method for constructing stable bridges based on mixed strategies in differential games of rendezvous-evasion

Eviction

U LUNAR ORBITS

U ORBIT PERTURBATION

U SOLAR GRAVITATION

EVENING

Magnetic storm inflation analysis from Explorer 45 and ground observation data, noting proton penetration into magnetosphere evening quadrant

Events

NT CONSECUTIVE EVENTS

EVOLUTION (DEVELOPMENT)

NT ABIOTIC GENESIS

NT BIOLOGICAL EVOLUTION

NT GALACTIC EVOLUTION

NT LUNAR EVOLUTION

NT PLANETARY EVOLUTION

NT STELLAR EVOLUTION

Sleep and the maturing nervous system; Proceedings of the Symposium on the Maturation of Brain Mechanisms Related to Sleep Behavior, Boiling Springs, Pa., June 21-24, 1970.

Morphological, physiological and pharmacological investigations of rat cerebellar cortex synaptic structure and function maturation and neurotransmitter receptivity development

Maturing neuronal subsystems - The dendrites of spinal motoneurons.

Differential housing /isolation vs aggregation/ as factor in postnatal development of mouse brain cell specificity and metabolism, noting relation to sleep behavior

Developmental changes in neurochemistry during the maturation of sleep behavior.

Development of wakefulness-sleep cycles and associated EEG patterns in mammals.

Wakefulness and sleep states in developing organism, discussing REM sleep deprivation effects on

behavior, brain excitability, pharmacology and biochemistry

Evolution of ribonuclease in relation to polypeptide folding mechanisms.

An evolutionary thermal model for the Cynus Loop.

A hypothesis, unifying the structure and the entropy of the universe.

Universe evolution model, considering quasar number density, radio source counts and big-bang cosmologies

Cardiac output and oxygen transport in early ontogenesis

Atomic, molecular, cellular, genetic, multicellular, neural, mental, social and suprasocial levels of evolution, discussing systems constituents, interactions and selective focus

Organic compounds in the Murchison meteorite.

Cosmochemical evolution of large organic molecules - Illustrative laboratory simulations for porphyrins.

The equilibrium, stability and evolution of a rotating magnetized gaseous disk.

Experimental models of communication at the molecular and microsystemic levels.

On the evolution of turbulent magnetic fields in a collision dominated plasma.

Numerical experiments by Monte Carlo method to examine comet orbits evolution within solar system, noting Trojan, horseshoe and Jupiter-Saturn midrange orbits

The luminosity function of quasars and its evolution - A comparison of optically selected quasars and quasars found in radio catalogs.

The asteroid belt and its evolution.

Evolution (liberation)

NT GAS EVOLUTION

EXACTNESS

U PRECISION

EXAMINATION

NT EYE EXAMINATIONS

EXCAVATION

NT TUNNELING [EXCAVATION]

EXCHANGING

NT CHARGE EXCHANGE

NT GAS EXCHANGE

NT ION EXCHANGING

NT RESONANCE CHARGE EXCHANGE

NT SPIN EXCHANGE

EXCITATION

NT ACOUSTIC EXCITATION

NT ATOMIC EXCITATIONS

NT HARMONIC EXCITATION

NT MOLECULAR EXCITATION

NT SELF EXCITATION

NT WAVE EXCITATION

Effect of excited states of atomic oxygen ions on the reaction rates and thermal balance in the F-region.

On the regularity of fluctuations in annual and secular polar motions.

Ranges of instability of the first and the second kind for vibrational systems with random parameter excitation

Continuous uniform excitation of medium-pressure CO₂ laser plasmas by means of controlled avalanche ionization.

Excited states

U EXCITATION

EXCITONS

Superconductor/exiton-dielectric phase transition in a semimetal

Condensation of excitons in momentum space under the influence of optical pumping.

Spectral line shape for interband light absorption with excitons formation in incompletely ordered semiconductor, taking into account interaction with random electrostatic field

Exciton-phonon interaction in recrystallized CdTe layers

The exciton energy spectrum in diamond and sphalerite type crystals

Giant polaritons and selfinduced transparency of Frenkel-excitons. 10 p1249 A73-24694

Investigation of the relationship between 'edge' and exciton emission in CdS single crystals 11 p1408 A73-25246

Exciton absorption band splitting in the PbI₂ spectrum 12 p1532 A73-27945

International Conference on the Physics of Semiconductors, 11th, Warsaw, Poland, July 25-29, 1972, Proceedings. Volumes 1 & 2. 14 p1783 A73-30572

Characteristics of the reflection spectra of CdS/xSe/1-x/ mixed crystals in their exciton absorption region 15 p1885 A73-31714

Quantum oscillators employing the luminescence of self-localized excitons in condensed inert gases 15 p1924 A73-31718

Interaction of nearly monochromatic LA phonons with excitons in CdS crystals 16 p2039 A73-34064

Bose-Einstein condensation of dipole-active excitons and photons 17 p2218 A73-34118

Scattering of a nonlocalized exciton on phonons in thin quantized semiconductor films 23 p3015 A73-43513

The superconductor-excitonic dielectric phase transition in a semimetal. 20 p1267 A73-27934

EXCRETION

Renal vascular response to saline infusion from radioactive Xe washout and sodium excretion concentration data 01 p0008 A73-10170

Serum creatine phosphokinase activity and urinary excretion of creatine and creatinine in man during acclimatization to high altitude and in high altitude natives. 01 p0121 A73-10644

Circadian rhythm of urinary calcium excretion during immobilization. 03 p0382 A73-13467

Study of nitrogen balance and creatine and creatinine excretion during recumbency and ambulation of five young adult human males. 03 p0358 A73-13487

Russian book - Mutual relationship of water and salt secretion functions in digestive and excretory organs under conditions of high temperature. 03 p0308 A73-13568

Lactate origins and renewal in blood plasma, considering metabolism, enzymatic resynthesis and final excretion in urine 04 p0436 A73-14672

EXECUTIVE AIRCRAFT

U GENERAL AVIATION AIRCRAFT 04 p0405 A73-14890

U PASSENGER AIRCRAFT 04 p0432 A73-14891

EXERCISE (PHYSIOLOGY)

Comparative evaluation of the general and specific efficiencies of athletes under normal barometric pressure and in the process of training and acclimatization under highland conditions of Pamir 04 p0485 A73-14892

Muscle, skin and esophageal temperature measurement during transient and steady state phases of negative work exercise on bicycle ergometer 04 p0490 A73-15868

Pulse duration-frequency modulation multichannel biotelemetry system for physiological parameter assessment during exercise, noting circuit diagrams of radio transmitter and receiver 05 p0608 A73-16859

Telemetry and ergometry associated to the measure of oxygen consumption during sports events. 05 p0578 A73-17135

Telemetry of venous blood pressure at rest and at muscle activity during running. 06 p0767 A73-17655

Postural effects on respiration, pulmonary ventilation, oxygen uptake and inhalation and exhalation volumes during asana /yoga gymnastics/ exercises executed by athletes 06 p0645 A73-17657

Aerobic capacity of relatively sedentary males. 07 p0812 A73-20338

Effect of exercise on the response time in an identification problem 07 p0868 A73-20359

EXERTION

U PHYSICAL WORK 07 p0921 A73-20361

EXHAUST DIFFUSERS

Basic flow characteristics of a linear aerospike nozzle segment. 09 p1136 A73-22216

Joint operation of the last gas-turbine stage and a diagonal diffuser 10 p1263 A73-24556

Investigation of two-dimensional cavity diffusers. 11 p1411 A73-26423

EXHAUST FLOW SIMULATION

NT ATMOSPHERIC ENTRY SIMULATION 11 p1411 A73-26424

NT FLIGHT SIMULATION 11 p1411 A73-26424

Rocket exhaust plume ground test facilities and scaling for in-flight conditions simulation and separation in supersonic flow 04 p0414 A73-14903

Gas turbine combustion rig simulation of pollutant carbon and nitrogen oxide emissions as function of air-fuel mixing, metallic additions and chamber design 06 p0767 A73-17732

Wind tunnel simulation of jet exhaust in low speed testing of Franco-German Alpha-Jet trainer and fire support aircraft 16 p1993 A73-32802

Aircraft turbine engine exhaust emissions under simulated high altitude, supersonic free-stream flight conditions. 17 p2223 A73-35625

EXHAUST GASES

Nongray atmospheric model to assess radiative effects of water vapor and carbon dioxide layer injected into lower stratosphere by SST and HST exhaust gases 01 p0038 A73-10388

Manganese additive effects on emissions from a model gas turbine combustor. 01 p0121 A73-10644

Titan III convective base heating from solid rocket motor exhaust plumes. 03 p0382 A73-13467

Gas turbine engine exhaust emissions measurement data scatter, investigating temperature and humidity effects and emission variations in tailpipe plane 03 p0358 A73-13487

Laser measurement of turbulence in exhaust jets. 03 p0308 A73-13568

Climatic impact assessment for high-flying aircraft fleets. 04 p0436 A73-14672

The impact of aircraft emissions upon air quality. 04 p0405 A73-14890

Monitoring and modeling of airport air pollution. 04 p0432 A73-14891

Estimation of engine emissions at altitude through ground testing. 04 p0485 A73-14892

Aircraft turbine engine emissions and the possibilities for control. 04 p0490 A73-15868

Assessment of emission control technology for turbine-engine aircraft. 04 p0490 A73-15872

Turbojet exhaust reactions in stratospheric flight. 05 p0608 A73-16859

Atmospheric dispersion of aircraft exhaust. 05 p0570 A73-16860

Hazardous gas detection system for analysis of gases escaping during cryogenic loading in Apollo-Saturn launch tests, discussing utilization for environment pollution detection 05 p0578 A73-17135

Afterburning turbojet engine exhaust emission products measurement under simulated flight conditions, determining Mach number and altitude effects on pollutants formation 06 p0740 A73-17643

Noise characteristics of combustion augmented high speed jets. 06 p0767 A73-17655

A study of the rarefaction of the interaction between an exhaust plume and a hypersonic external flow. 06 p0645 A73-17657

Emissions from continuous combustion systems; Proceedings of the Fifteenth Symposium, Warren, Mich., September 27, 28, 1971. 06 p0767 A73-17726

Effects of fuel injection method on gas turbine combustor emissions. 06 p0768 A73-17735

Effect of operating variables on pollutant emissions from aircraft turbine engine combustors. 06 p0768 A73-17736

Control and reduction of aircraft turbine engine exhaust emissions. 06 p0768 A73-17737

Refraction of acoustic duct waveguide modes by exhaust jets. 07 p0812 A73-20338

Emissions from and within an Allison J-33 combustor. 07 p0868 A73-20359

Exhaust emission reduction through two-stage combustion. 07 p0921 A73-20361

Aviation and atmospheric pollution - The real dimension of the problem and its solutions 09 p1136 A73-22216

Combustor design effect on jet aircraft engine exhaust pollutants reduction during hydrocarbon fuel burning 10 p1263 A73-24556

Emissions from and within an Allison J-33 combustor. II - The effect of inlet air temperature. 11 p1411 A73-26423

Effects of prevaporized fuel on exhaust emissions of an experimental gas turbine combustor. 11 p1411 A73-26424

Gas turbine engine exhaust pollutants consisting of unburned hydrocarbons, nitric oxide, carbon dioxide, nitrogen dioxide and carbon monoxide 12 p1467 A73-27934

Design and evaluation of combustors for reducing aircraft engine pollution. 13 p1670 A73-28932

Exhaust cloud rise and growth for Apollo Saturn engines. 15 p1906 A73-31920

Low emissions combustion for the regenerative gas turbine. I - Theoretical and design considerations. 16 p2086 A73-33489

Low emissions combustion for the regenerative gas turbine. II - Experimental techniques, results, and assessment. 16 p2086 A73-33490

Concentration of OH and NO in YJ93-GE-3 engine exhausts measured in situ by narrow-line UV absorption. 16 p2045 A73-33546

Aircraft exhaust plume dispersion and flight corridor concentration profiles in stratosphere as function of flight frequency and scale dependent diffusion 16 p2046 A73-33565

Experimental study of the condensed phase in the combustion products of metallized solid propellants 16 p2086 A73-33965

An initial estimate of aircraft emissions in the stratosphere in 1990. 16 p2011 A73-34046

The geometry and physical properties of exhaust clouds generated during the static firing of large rocket engines. 17 p2253 A73-34349

Parameters controlling nitric oxide emissions from gas turbine combustors. 17 p2221 A73-34474

Exhaust emissions analysis system for aircraft gas turbine engines. 17 p2146 A73-34615

Nitric oxide emissions from tube combustor burning premixed gaseous propane-air mixture, considering inlet conditions for equivalence ratios 17 p2222 A73-35468

Parametric test results of a swirl-can combustor. 17 p2222 A73-35471

Laser measurement of high-altitude aircraft emissions. 18 p2315 A73-36253

Nitrogen oxide turbojet emissions minimization with hydrogen compared to kerosene /JP/ fuels due to flammability limits, burning velocity and introduction in combustor as gas 19 p2473 A73-37498

Book - Engine emissions: Pollutant formation and measurement. 19 p2474 A73-38321

Mechanism of hydrocarbon formation in combustion processes. 19 p2402 A73-38322

Jet engine exhaust plume effects on solid bodies, examining nozzle drag effects, nozzle geometry, plume entrainment and shape, wind tunnel tests and pressure effects 20 p2626 A73-38651

Small-scale suppressor of the aerodynamic noise of a subsonic gas jet 21 p2754 A73-40404

The effects of catalysis in measuring the temperature of incompletely-burned gases with noble-metal thermocouples. 22 p2857 A73-42035

Emissions from and within an Allison J-33 combustor. II - The effect of inlet air temperature. 23 p3019 A73-43327

EXHAUST JETS

U EXHAUST GASES

EXHAUST NOZZLES

NT CONVERGENT-DIVERGENT NOZZLES

NT PLUG NOZZLES

NT SPIKE NOZZLES

NT TURBINE EXHAUST NOZZLES

Criteria concerning the adaptation of the rear components of a propulsion system to the subsonic and transonic altitude flight 02 p0128 A73-11690

Thrust nozzle optimization including boundary-layer effects. 02 p0129 A73-12508

Implementing the design of airplane engine exhaust systems. 03 p0355 A73-13427

Directional devices for noise reduction of high speed jets 03 p0359 A73-14142

Flyover and static tests to investigate external flow effect on jet noise for nonsuppressor and suppressor exhaust nozzles. 05 p0531 A73-16927

Relationship among various parameters used in ejector-nozzle performance estimates 07 p0776 A73-20097

Performance of jet V/STOL tactical aircraft nozzles. 16 p1969 A73-33523

- Velocity decay and acoustic characteristics of various nozzle geometries with forward velocity.
[AIAA PAPER 73-629] 18 p2263 A73-36256
- Vortex sheet model of directional acoustic wave radiation near nozzle exit from supersonic helium jet shear layer instability
21 p2677 A73-40617
- Determination of disturbances acting on a space vehicle from the liquid-disposal nozzle
21 p2781 A73-41199
- Experimental study on optimization parameters of a supersonic jet ejector thrust augmentor.
22 p2798 A73-43113
- The effects of the exit velocity profile on the flow of a circular jet exhausting normal to the free stream.
23 p2969 A73-44125

EXHAUST SYSTEMS

- Theoretical studies of sound emission from aircraft ducts.
[AIAA PAPER 73-1012] 24 p3078 A73-44844

EXHAUST VELOCITY

- Linear slit colloid electrostatic thruster development and testing, discussing emitter geometry, gap design, exhaust velocity, operating voltage and power efficiency relationships
04 p0488 A73-15725
- Space charge neutralized Hall ion microthrusters, discussing ion exhaust velocity, thrust and efficiency relationships
04 p0489 A73-15729
- Liquid propellant rockets, discussing effective exhaust velocity, nozzle expansion, chamber pressure effects on equilibrium performance and kinetic recombinations
14 p1784 A73-30136
- Coaxial Ar plasma accelerator for spacecraft propulsion, discussing quasi-steady state I-V characteristics and exhaust velocity
19 p2466 A73-37180
- Combustion noise prediction techniques for small gas turbine engines.
19 p2473 A73-37296
- The effects of the exit velocity profile on the flow of a circular jet exhausting normal to the free stream.
23 p2969 A73-44125

EXHAUSTION

- Histochemical investigation of some energy metabolism characteristics in a rat heart after acute fatigue
15 p1834 A73-31393

EXISTENCE THEOREMS

- Existence of solutions of certain nonlinear elliptic boundary-value problems
01 p0069 A73-10067
- Existence and stability of the secondary periodic solution figuring in Navier-Stokes type evolution problems
[ONERA, TP NO. 1172] 01 p0033 A73-10780
- Existence theorem for nonlinear parabolic equations of evolution in real Banach space
01 p0071 A73-11270
- Second-order abstract and Schroedinger linear differential equations in Beurling spaces
02 p0186 A73-11570
- Existence conditions of precessional motions of gyroscope with fixed point, assuming constant time function and unit vector coincident with gravity force direction
02 p0192 A73-11772
- Existence theorems for boundary value problems of elasticity defined by unilateral constraints, developing abstract theory of functional inequalities
02 p0233 A73-11979
- Existence and uniqueness of heat equation two phase free boundary problem classical solutions
03 p0336 A73-12922
- Existence theorems for Navier-Stokes equations periodic solution bifurcation in convection between two horizontal plates at different time periodical temperature
[ONERA, TP NO. 1179] 03 p0343 A73-13602
- Stress equations solutions existence near Mikowski solution for asymptotic behavior, demonstrating flat space-time stability
[AD-756017] 03 p0344 A73-14604
- A class of neutral functional differential equations.
04 p0469 A73-14666
- Existence theorem for nonlinear oscillatory equations of motion transformation into normal form, noting quasi-periodic functions with arbitrary frequencies
04 p0475 A73-14888
- Note on symmetric decomposition of some special symmetric matrices.
04 p0470 A73-15014
- Necessary and sufficient conditions of pointwise completeness of linear time-invariant delay-differential systems.
04 p0430 A73-15213
- Hyperbolic equations and systems with multiple characteristics.
04 p0471 A73-15224
- Functional analysis approach of the partial differential equation arising from non-linear filtering theory.
04 p0472 A73-15263

- Existence theorem for integral manifolds of point mappings in resonant and nonresonant cases for differential equations systems with fast rotating phases
05 p0560 A73-16290
- Existence and conical intersection theorems for extremum conditions of Euclidean space subset function, noting discrete objects optimality conditions
05 p0589 A73-16334
- Control of functional differential equations of retarded and neutral type to target sets in function space.
[AD-758569] 05 p0561 A73-16486
- Existence theorems for multidimensional control systems with lower-dimensional controls.
05 p0561 A73-16489
- Existence of analytic solutions of partial differential equations with constant coefficients in an arbitrary number of variables
05 p0591 A73-17246
- Boundary value problem for subsonic gas flow, proving existence theorem for gas dynamics problem solution
06 p0645 A73-18069
- Nonlinear time-varying control systems transformation, deriving conditions for existence of observable system representation and corresponding scalar differential equation
06 p0719 A73-18802
- The existence and the numerical evaluation of generalized solutions of semilinear initial value problems
07 p0845 A73-20288
- Feedback law choice for autonomy properties of controlled object, noting existence and uniqueness theorems
08 p0951 A73-21127
- The use of operators with degenerated kernel for nonlinear system investigation.
10 p1242 A73-24043
- Unsteady discrete linear systems semisteady realizations existence conditions and matrices elements determination methods
10 p1202 A73-24414
- Algorithm for solution of inverse Stefan problem for flow characteristics determination, stating necessary and sufficient conditions for solution existence and uniqueness
11 p1452 A73-26328
- An existence proof for permanent capillary gravity waves with general vortex distributions
11 p1349 A73-26747
- Existence and stability of the solution of the Volterra nonlinear integral equation
12 p1517 A73-27101
- Minimum fuel problem link to Kalman controllability theorem, deriving solution based on state transition and controllability matrices
12 p1517 A73-27152
- On the existence of solutions of the nonlinear theory of shallow shells.
12 p1554 A73-27538
- Global solutions to a class of nonlinear hyperbolic systems of equations.
13 p1647 A73-28024
- Characteristic initial value problem for class of differential equations, proving solution existence and uniqueness as generic properties
13 p1648 A73-28536
- Generalized smoothing spline functions for operators.
13 p1649 A73-28604
- Book - Optimal control of differential and functional equations.
13 p1651 A73-29550
- Some aspects of the asymptotic behavior of solutions of nonlinear differential equations with delayed argument
14 p1768 A73-30345
- Stability considerations for a Volterra integral equation with discontinuous nonlinearity.
14 p1769 A73-30403
- An existence theorem for linear boundary value problems.
14 p1770 A73-30524
- Oscillations of higher-order retarded differential equations generated by the retarded argument.
14 p1770 A73-30756
- The infinite time quadratic cost problem for certain classes of infinite dimensional control systems.
14 p1770 A73-30758
- Existence and uniqueness theorems for differential equations with deviating arguments of mixed type.
14 p1770 A73-30760
- Center of forces existence and related configurations for given law of force, rejecting Wintner conjecture
15 p1913 A73-31109
- Weak solutions existence and uniqueness for boundary value problem in linearized theory for mixtures of two isotropic incompressible elastic solids, obtaining differentiability conditions
15 p1947 A73-31336
- Uniqueness and existence estimates of third order differential equation solutions for nonlinear boundary value problem in fluid mechanics
15 p1863 A73-31363

- Feedback law choice for autonomy properties of controlled object, noting existence and uniqueness theorems
15 p1855 A73-32062
- Hadamard theorem on wave propagation existence in elastic body with infinitesimal stability condition proved by linear elliptical partial differential equations systems theory techniques
15 p1914 A73-32120
- Existence and uniqueness of positive eigenfunctions for a class of quasilinear elliptic boundary value problems of sublinear type.
15 p1900 A73-32181
- A criterion for global existence in case of ordinary differential equations.
15 p1901 A73-32370
- Liapunov functions and boundedness and global existence of solutions.
15 p1901 A73-32375
- Existence and uniqueness of solutions of boundary value problems for third order differential equations.
15 p1902 A73-32398
- New problems pertaining to nonlinear integro-differential equations with several independent variables. I - Search for solutions in the case of initial integral boundary conditions
16 p2032 A73-33172
- Optimal control solution existence for relaxed linear systems with strictly convex Hamiltonian
16 p1992 A73-33303
- Periodic solutions of singularly perturbed equations arising from gyroscopic systems.
16 p2032 A73-33310
- Regularity theorems for the solution of a second-order abstract linear differential equation
16 p2032 A73-33373
- Simplified proof of error estimates for the least squares method for Dirichlet's problem.
17 p2199 A73-34210
- Overall existence of a solution of the Cauchy problem for the system of equations with Liouville-Newton partial derivatives
17 p2201 A73-35045
- Computation of the exponential of a matrix. I - Theoretical considerations.
17 p2203 A73-35521
- The numerical derivation of a periodic solution of a second order differential difference equation.
17 p2203 A73-35728
- On the existence of an optimal solution of the epsilon variational problem.
18 p2330 A73-36641
- Wazewski retract method application to boundary value problems for second order generalized differential equations, proving solutions existence
18 p2330 A73-36693
- Oscillation theorems for a second order damped nonlinear differential equation.
18 p2330 A73-36694
- Numerical solution existence for three dimensional boundary layer equations governing corner flow in symmetry plane with critical pressure gradients
19 p2419 A73-37492
- An optimal feedback control law for regulator problems with linear state inequality constraints.
19 p2413 A73-38060
- Oscillations in nonlinear feedback systems.
19 p2414 A73-38069
- Some nonoscillation theorems for a second order nonlinear differential equation.
20 p2581 A73-38976
- Complementary variational principle existence condition and duality in linear and quadratic programming in Hilbert space setting, considering relationship to Kuhn-Tucker saddle point theory
21 p2724 A73-40296
- The existence and convergence of subsequences of Pade approximants.
21 p2725 A73-40298
- Pairs of positive solutions of nonlinear elliptic partial differential equations.
21 p2726 A73-40695
- Optimal design of linearly elastic vibrating structural members for minimized total mass and maximized fundamental frequency respectively, noting solution existence dependence on boundary conditions
21 p2785 A73-40840
- Compact integral varieties existence in certain meromorphic Pfaff differential equation systems
21 p2726 A73-40946
- Necessary and sufficient conditions for solvability of certain boundary value problems for a second-order ordinary differential equation
21 p2727 A73-41272
- The existence of a minimal surface with a free boundary of a given length
22 p2885 A73-41774
- Proof for the existence of a solution to the fundamental quadrantal problem of dynamics for a three-dimensional elastic body, and approximate computation of the solution
22 p2918 A73-41951

Local and global theorems of existence and uniqueness for solutions to nonlinear singular integral equations on a denumerable set of contours
22 p2882 A73-42472

Optimal feedback control solution existence and uniqueness conditions for asymptotic stability, discussing relationships with Pontryagin equations and linear regulator problem with quadratic cost functionals
22 p2837 A73-43070

Classical mechanics Noether theorem and variational calculus for optimal control, noting Pontryagin maximum principle equations first integral solution existence condition
22 p2837 A73-43073

Quasi-periodic solutions existence, uniqueness and asymptotic behavior to quasi-linear parabolic equations, demonstrating vanishing conditions at boundary
23 p3049 A73-43611

The Minkowski problem generalized for ovoidals
23 p2999 A73-43613

An existence and uniqueness theorem for the solution of a stochastic integrodifferential equation
23 p2999 A73-44101

Differential operator hypoellipticity, taking into account necessary and sufficient conditions for existence based on Ehrenpreis-Palamodov theorem
23 p3000 A73-44205

Boundary value problem solutions uniqueness and existence for ordinary differential equations under Cauchy condition
23 p3000 A73-44209

Static theory of plane micropolar strain for homogeneous orthotropic elastic solids, deriving existence and uniqueness theorems and reducing boundary value problems to Fredholm equations
24 p3147 A73-44684

Classical MHD differential equations solution for uniqueness and existence of shock wave structure based on thermodynamic potential concept
24 p3116 A73-45222

On global existence and uniqueness theorems for gravitational systems.
24 p3141 A73-45280

On the existence, uniqueness, and stability of solutions of a new boundary layer problem concerning certain nonlinear integral-differential polyvibratory systems. I
24 p3106 A73-45395

Plasticity theory development taking into account thermodynamics of elastoplastic materials, considering existence theorems for plastic flow and variational principle for equilibrium problems solution
24 p3153 A73-45500

EXITS [DOORS]
U DOORS

EXO BIOLOGY
Viking Mars program for surface mapping and exploration, atmospheric composition investigation and life evidence search, discussing orbiter and lander phases
01 p0105 A73-11155

Book - Theory and experiment in exobiology. Volume 2.
03 p0265 A73-14315

Protobiological developments in terms of extraterrestrial life search and roles of nitriles and urea in prebiological chemical evolution
03 p0265 A73-14319

Biological, chemical and cytological methods of microorganism detection integrated into single instrument
03 p0272 A73-14320

Quarantine necessity, protocol and effectiveness for Mars samples, emphasizing risks of foreign replicating agent introduction to earth biosphere
03 p0272 A73-14321

Developments in space medicine.
06 p0649 A73-17569

Space exploration and the origin of life.
06 p0651 A73-17930

Organic compounds in the Murchison meteorite.
06 p0752 A73-18234

Solar system other planets suitability for terrestrial organisms, noting life forms possible existence on Venus, Mars and Jupiter
06 p0654 A73-18349

The organic analysis and carbon chemistry of lunar samples: Their significance for exobiology; Proceedings of the Conference, University of Maryland, College Park, Md., October 26-28, 1971.
06 p0753 A73-18410

Indigenous lunar organic compound search, considering prebiological chemistry and composition possibility in deeper region under surface
06 p0655 A73-18428

Organogenic elements in stars, interstellar matter, comets, meteorites and planets, discussing molecular distribution and formation, prebiological chemical evolution, and terrestrial and extraterrestrial biology
06 p0754 A73-18430

Survival of micro-organisms on the moon.
07 p0780 A73-19111

Electric discharge and microbiological experiments in simulated Jovian atmosphere for investigation of Jupiter life prospects
11 p1319 A73-26478

Results and prospects of microbiological studies in outer space.
11 p1320 A73-26487

Estimating the number of terrestrial organisms on the moon.
11 p1320 A73-26488

International literature survey of microbiological space research for 1930-1970, discussing high altitude balloon, rocket and satellite experiments, weightlessness effects, mutagenesis, etc
15 p1838 A73-31501

Russian papers on populated cosmos covering space exploration impact on human civilization, extraterrestrial life, space medicine and biology, solar system, space law, etc
19 p2393 A73-37398

Space-related research in mycology concurrent with the first decade of manned space exploration.
20 p2513 A73-39478

Life origin hypothesis based on interstellar molecular concentration in gas clouds, examining radical types and molecular Doppler spectra
21 p2638 A73-41080

Life sciences and space research XI; Proceedings of the Fifteenth Plenary Meeting, Madrid, Spain, May 10-24, 1972.
22 p2803 A73-42158

Developments in the analysis of planetary quarantine requirements.
22 p2803 A73-42159

Organic geochemical analysis of lunar samples with emphasis on detecting biologically significant organogenic elements, projecting techniques to Mars soil analysis
22 p2803 A73-42163

EXOSKELETONS
A technique for extracting Radiolaria from radiolarian cherts.
11 p1324 A73-25141

Amino acid composition significance in sedimentary fossil skeletal protein calcification, discussing diagenetic temperature effects
11 p1326 A73-25470

Upper Cretaceous Spumellariina from the Great Valley Sequence, California coast ranges.
13 p1605 A73-28023

EXOSPHERE
Diurnal variation of the exospheric temperatures on Venus and Mars.
02 p0214 A73-12253

Drag derived density analysis for geomagnetic disturbances effect in thermosphere, noting atmospheric reaction time delay and exospheric temperature increment per unit Kp
02 p0161 A73-12280

Transmission and reflection of magnetospheric whistlers in the ionosphere and lower exosphere at high latitudes.
03 p0298 A73-12884

Determination of exospheric electron content from group delay and Faraday rotation observations of geostationary satellite signals.
03 p0300 A73-13636

Pitch angles and spectra of particles in the outer zone near noon.
03 p0363 A73-13867

[AD-758531] The effect of photoelectrons on kinetic polar wind models.
05 p0572 A73-17159

Ogo 6 measurements of supercooled plasma in the equatorial exosphere.
09 p1074 A73-22066

Ionospheric and plasma sheet particle densities, fluxes and bulk velocities along auroral magnetic field line for collisionless ion-exosphere model
09 p1079 A73-22842

Dispersion of the direction of the angular momentum vector of sounding rocket payloads due to atmosphere exit and certain vehicle activities.
09 p1116 A73-23212

[AIAA PAPER 73-293] On empirical models of the upper atmosphere in the polar regions.
11 p1356 A73-25915

Diurnal atomic hydrogen variation at exospheric temperatures as function of thermal ion and proton charge exchange with plasmasphere
12 p1492 A73-27612

Neutral hydrogen distribution in the upper atmosphere of the earth
14 p1747 A73-29871

Atmospheric models for 110-2000 km region, considering composition, temperature profiles, thermosphere and exosphere variations, density and boundary condition computation, etc
21 p2683 A73-40629

Exospheric and thermospheric structure variations with solar activity, diurnal variation, geomagnetic activity, seasonal-latitudinal variations of He, H and density waves
21 p2683 A73-40630

Energetic dissociative recombination oxygen atom production and exospheric redistribution for high/low solar conditions in terms of ballistic trajectories and neutral density models
24 p3086 A73-45131

EXOTHERMIC REACTIONS
Study of exothermic processes in shock ignited gases by the use of laser shear interferometry.
05 p0640 A73-16920

Application of the method of matched asymptotic expansions to calculate the steady-state thermal propagation of an exothermic reaction front in a condensed medium
09 p1167 A73-22616

Isolated reactive and nonreactive Mach stem structure in exothermic systems under conditions encountered behind detonation waves front
10 p1294 A73-23553

Transverse discharge pulsed CO₂ chemical transfer laser.
10 p1227 A73-23840

Explosion gas dynamics experimental investigation, noting fast chemical reactions induced exothermic processes and detonation wave structure
10 p1295 A73-23853

Asymptotic analysis of the steady propagation of a successive two-stage exothermal reaction front in a condensed medium
13 p1707 A73-29166

Free convection and thermal explosion in reactive systems.
17 p2255 A73-35662

Graphite oxidation at low temperature in subsonic air.
18 p2326 A73-36352

[AIAA PAPER 73-735] Nonequilibrium velocity distributions and reaction rates in fast highly exothermic reactions.
19 p2402 A73-37897

Investigations into the mechanism of exothermically reacting nickel-aluminum spraying materials.
22 p2879 A73-42595

EXPANDABLE STRUCTURES
NT BALLOONS
NT BALLUTES
NT BEACON SATELLITES
NT HIGH ALTITUDE BALLOONS
NT INFLATABLE STRUCTURES
NT METEOROLOGICAL BALLOONS
NT SKYHOOK BALLOONS
NT TETHERED BALLOONS

Space deployed expandable structures, discussing vehicular and environmental constraint effects on design, large structure requirements, and applications
07 p0828 A73-18905

EXPANSION
NT GAS EXPANSION
NT KARHUNEN-LOEVE EXPANSION
NT PRANDTL-MEYER EXPANSION
NT THERMAL EXPANSION

Expansion hypothesis and assumption of invisible intergalactic matter in galactic clusters stability theory, noting IR spectroscopy and radio observation
05 p0623 A73-17196

Global coordinate systems for spherical collapsing and expanding Oppenheimer-Snyder dust cloud behavior after critical Schwarzschild radius attainment
22 p2908 A73-42438

EXPANSION WAVES
U ELASTIC WAVES

EXPECTANCY HYPOTHESIS
Algorithms for spacecraft trajectory optimization programs for orbit perturbations caused by random measurement errors and minimum mathematical expectancy of energy dissipation
02 p0220 A73-12468

Taking into account correlation when forecasting the parameters of failure-free operation of radio equipment.
15 p1849 A73-30994

Algorithms for spacecraft trajectory optimization programs for orbit perturbations caused by random measurement errors and minimum mathematical expectancy of energy dissipation
15 p1942 A73-32618

The asymptotic dispersion characteristics of the best unbiased linear estimate obtained by the uniform division of the observation interval for the unknown mathematical expectation of a stationary random process
18 p2329 A73-36162

EXPECTATION
Statistical expectation application to risk density functions and fee/incentive-element relationships for contract incentive structuring, considering C-5A procurement
08 p1025 A73-20958

EXPERIMENTAL DESIGN
NT FACTORIAL DESIGN

System design, hardware and software of RF interference measurement experiment regarding microwave frequency optimal sharing between ATS-F satellite and terrestrial relay telecommunication
04 p0422 A73-15460

- Book - Sequential analysis and optimal design.
05 p0590 A73-16352
- Macroscopic systems response to gravitational radiation for detector design and calibration, noting accessibility to people unfamiliar with general relativity
06 p0724 A73-18549
- Search of optimal biological conservation conditions for a heart, using methods of mathematical experiment planning
07 p0781 A73-19648
- GARP Global Experiment design with satellite and balloon borne systems for meteorological observation and atmospheric research, discussing sounding data numerical simulation
07 p0820 A73-20442
- Proposed new test for aptitude screening of air traffic controller applicants.
09 p1045 A73-22535
- Effect of process variables on partial penetration electron beam welding.
10 p1223 A73-23629
- Productivity estimates of the strategic airlift system by the use of simulation.
10 p1297 A73-23774
- Chetaev concept for experiments with small measurement errors and mathematical model instability and lability properties, applying to biological existence struggle and spacecraft reentry
12 p1524 A73-27405
- Temporal and spatial features in detecting one- and two-dimensional constraints in complementary visual displays.
13 p1578 A73-28095
- Skylab experiments through airlock studying earth atmosphere, particles, background sky light, solar spectra, nebulae, stars and galaxies
13 p1617 A73-28945
- Investigation of the turning process using diamond cutting tools on ML-5 magnesium alloy, with the application of mathematical methods in experiment planning
15 p1881 A73-31278
- Book - Statistical design and analysis of engineering experiments.
17 p2200 A73-34456
- The superiority of the pair-comparisons method for scaling visual illusions.
17 p2118 A73-35497
- Book on experimental analysis covering measurement systems, engineering problems, data analysis, electro-optics and dimensional parameters
17 p2176 A73-35855
- Coaxial hydrogen and erosion pulsed plasma accelerators in vacuum, discussing experiment design, discharge characteristics and practical applications
19 p2466 A73-37361
- Analysis of methods for selecting significant attributes in the classification of patterns
20 p2532 A73-38999
- Experimental design to produce visible-reflective IR ratio image from ERTS data for geological mapping of iron compounds
20 p2561 A73-39899
- Visually perceived motion in depth resulting from proximal changes. I, II.
21 p2640 A73-41186
- Application of cybernetic means and methods in studies of plasma physics and controlled thermonuclear synthesis
23 p3011 A73-43671
- Response surface /descriptive function/ methodology design for human performance research, discussing central composite design, observations at experimental points and orthogonal blocking
24 p3062 A73-44773
- Response surface methodology analysis of training transfer in pursuit rotor tracking task, relating three independent variables through multiple-regression prediction equations
24 p3063 A73-44774
- EXPIRATION**
Bronchial tree model simulation of pressure-flow-volume relationships during expiration, using gas physics and lung physiology and anatomy data
01 p0011 A73-10169
- Evaluation of positive end-expiratory pressure in hypoxemic dogs.
20 p2515 A73-39781
- Control of the duration of expiration.
21 p2642 A73-41635
- EXPIRED AIR**
Effects of immersion with the head above water on tissue nitrogen elimination in man.
02 p0135 A73-12563
- A model for the elastic properties of the lung and their effect on expiratory flow.
08 p0934 A73-21502
- 'Closing volumes' and decreased maximum flow at low lung volumes in young subjects.
09 p1041 A73-22929
- Carbon monoxide content in the exhaled air and carboxyhemoglobin in the blood of subjects equipped with an isolating protective garment
12 p1463 A73-27712

- Validation of open-circuit method for the determination of oxygen consumption.
17 p2117 A73-35462
- Temperature of exhaled air of healthy subjects
18 p2277 A73-36583
- Steady-state equality of respiratory gaseous N2 in resting man.
18 p2278 A73-36660
- Phase IV volume of the single-breath nitrogen washout curve on exposure to altitude.
20 p2518 A73-39783
- Anaerobic threshold and respiratory gas exchange during exercise.
20 p2519 A73-39785
- A system for automatic end-tidal gas sampling at rest and during exercise.
20 p2519 A73-39794
- Peak expiratory flow rate and rate of change of pleural pressure.
21 p2642 A73-41636
- Influence of expiratory flow limitation on the pattern of lung emptying in normal man.
22 p2807 A73-42422
- A rapid method for determining the CO2 transport characteristics in man by using a capnograph and a multichannel respirator
22 p2815 A73-42665
- Differences between inspired and expired minute volumes of nitrogen in man.
24 p3060 A73-45069
- EXPLODING CONDUCTOR CIRCUITS**
U CIRCUITS
U EXPLODING WIRES
EXPLODING CONDUCTORS
U EXPLODING WIRES
EXPLODING WIRES
Fluctuation characteristics of dense plasmas from high-current discharges produced by electric explosion of metallic wires in vacuum
01 p0086 A73-11283
- The formation of primary gas discharge zones in electrical wire explosions
06 p0723 A73-17911
- Electrical explosion of tungsten wires in a vacuum.
06 p0724 A73-18782
- Influence of an external electric field on the initial phase of the explosion of wires in a vacuum
09 p1119 A73-21883
- Dwell times of exploding tungsten wires in air.
09 p1119 A73-21929
- Investigation of the electrical explosion of conductors by holographic methods
10 p1248 A73-23507
- Electrical explosion of wires at high energy input rates
12 p1523 A73-26936
- Application of similarity theory to the calculation of certain characteristics of an electrical explosion of wires
12 p1523 A73-26937
- Dwell times of thin exploding wires.
15 p1913 A73-31934
- Effect of an external electric field on exploding wires in vacuum.
17 p2211 A73-34307
- Holographic investigation of electrical explosions of conductors.
17 p2212 A73-35187
- Exploding wires as a source of flash X-rays.
21 p2738 A73-39975
- Kerr-cell studies of exploding wires in vacuum.
21 p2738 A73-39996
- Near-infrared radiation intensity from restrikes of exploding wires.
21 p2740 A73-40955
- Exploding wires with high energy input.
22 p2886 A73-42270
- Application of similitude theory to exploding wire experiments.
22 p2886 A73-42271
- Fluctuation characteristics of a dense plasma of high current discharges produced by electric explosion of metallic wires.
23 p3009 A73-43504
- EXPLORATION**
NT LUNAR EXPLORATION
NT MINERAL EXPLORATION
NT OIL EXPLORATION
NT SPACE EXPLORATION
EXPLORER SATELLITES
NT EXPLORER 31 SATELLITE
NT EXPLORER 35 SATELLITE
NT EXPLORER 43 SATELLITE
NT RADIO ASTRONOMY EXPLORER SATELLITE
Atmosphere Explorer mission of lower thermosphere and ionosphere physics investigation, discussing orbit selection
13 p1687 A73-28626
- Atmosphere Explorer for satellite observation of thermosphere, discussing design goals, spacecraft components and data system
13 p1687 A73-28627
- The open-source neutral-mass spectrometer on Atmosphere Explorer-C, -D, and -E.
13 p1616 A73-28628

- A neutral-atmosphere composition experiment for the Atmosphere Explorer-C, -D, and -E.
13 p1687 A73-28629
- Explorer satellite triaxial accelerometer system to determine neutral atmosphere density, monitoring orbit adjust propulsion thrust and measuring spacecraft roll, describing instrument calibration
13 p1688 A73-28631
- Atmosphere Explorer pressure measurements - Ion gauge and capacitance manometer.
13 p1688 A73-28632
- The magnetic ion-mass spectrometer on Atmosphere Explorer.
13 p1688 A73-28633
- Bennett ion-mass spectrometer onboard Explorer C and E, describing operation, data outputs, calibration and data interpretation techniques
13 p1688 A73-28634
- Planar retarding potential analyzer onboard Explorer satellite for ion temperature and ion/electron concentration investigation
13 p1688 A73-28635
- Cylindrical electrostatic probes onboard Explorer C, D and E, presenting I-V characteristics of collector.
13 p1688 A73-28636
- EUV spectrophotometer onboard Atmosphere Explorer satellites, discussing design, aeronomical mission objectives, constraints and economic factors
13 p1688 A73-28637
- An extreme UV photometer for solar observations from Atmosphere Explorer.
13 p1688 A73-28638
- Conventional filter photometer onboard Explorer satellite for 3000-7500 Å airglow and auroral thermospheric emission features monitoring
13 p1688 A73-28639
- Atmosphere Explorer satellite-borne two channel fixed grating Ebert spectrometer for measurement of airglow at 2150 Å, yielding altitude profiles of nitric oxide density
13 p1689 A73-28640
- The photoelectron-spectrometer experiment on Atmosphere Explorer.
13 p1689 A73-28641
- Low-energy electron experiment for Atmosphere Explorer-C and -D.
13 p1689 A73-28642
- Three axis fluxgate magnetometer/analog to digital converter system onboard Explorer D and E for measuring magnetic fields in auroral zone and equatorial electrojet
13 p1689 A73-28643
- Explorer 45 mission objectives discussing magnetospheric ring current, magnetic storm detection, particle energy and interactions, electric and magnetic fields measurements, etc
20 p2614 A73-38949
- Explorer 45 /S3-A/ symmetrical floating probes for plasmopause dc electric fields, discussing plasma sheaths, noise storms, whistlers, electric field strength and orbit configuration
20 p2552 A73-38954
- EXPLORER 31 SATELLITE**
Ion angular distribution around Explorer 31, discussing observed ion flux relation to ionospheric parameters derived from ambient ion and electron measurements
09 p1075 A73-22136
- EXPLORER 35 SATELLITE**
Explorer 35 lunar studies, discussing orbit characteristics, circumlunar magnetic field, surface electromagnetic properties and solar wind model
16 p2065 A73-33782
- EXPLORER 43 SATELLITE**
Observations of noise bands associated with the upper hybrid resonance by the Imp 6 radio astronomy experiment.
12 p1468 A73-26995
- EXPLOSIONS**
NT AERIAL EXPLOSIONS
NT CHEMICAL EXPLOSIONS
NT GAS EXPLOSIONS
NT NUCLEAR EXPLOSIONS
NT THERMONUCLEAR EXPLOSIONS
Zener diodes for overvoltage spark protection circuits in automatic control and measuring equipment operating in explosive environment
02 p0147 A73-12175
- Black hole creation via partial gravitational collapse of matter ejected by explosion within asymptotically Friedmannian space-time
07 p0900 A73-20182
- Explosion gas dynamics experimental investigation, noting fast chemical reactions induced exothermic processes and detonation wave structure
10 p1295 A73-23853
- Concentric, uniform elastic spherical wave excited by thermal explosion of the envelope.
14 p1816 A73-30251
- Critical behaviour in chemically reacting systems. I - Difficulties with the Semenov theory. II - An exactly soluble model.
16 p1976 A73-33342
- Free convection and thermal explosion in reactive systems.
17 p2255 A73-35662

On the stabilization of explosive instabilities by non-linear frequency shifts. 17 p2218 A73-35822

Photographic laboratory studies of explosions. 21 p2706 A73-41553

Numerical study of the problem of explosion of a cylindrical charge of finite length 24 p3076 A73-44654

EXPLOSIVE DEVICES

NT DETONATORS

NT INITIATORS [EXPLOSIVES]

NT SHAPED CHARGES

The possibility of microfission explosions by laser or relativistic electron-beam high-density compression. 11 p1378 A73-26657

Investigation of a pulsed laser utilizing an exploding-film Q switch. 12 p1507 A73-27504

Pyrotechnic explosive power devices and systems for aerospace applications. 16 p2045 A73-33106

Calibration of Sandia Laboratories' 19-foot diameter explosively driven blast simulator. 16 p1994 A73-33136

Gas dynamic models of high speed explosive impacts of solid bodies, discussing metal cavity lining, buckling and hypersonic jet phenomena 19 p2433 A73-37514

Annex 13, sabotage and malicious acts against aircraft - Practical problems. 19 p2506 A73-37740

Electroexplosive device pin-pin firing frequency mathematical modeling and prediction based on RF impedance data obtained nondestructively by automatic network analyzer 22 p2822 A73-41793

Microelectronic circuitry for monitoring stray electromagnetic energy coupled into electroexplosive device, using fiber optic transmission with photovoltaic energy conversion to eliminate wiring caused interference 22 p2822 A73-41794

EXPLOSIVE FORMING

Mechanical properties of base and coating metals for explosive plating, noting heat treatment for strain hardening prevention 03 p0312 A73-13584

Dynamic response of nonlinear media at large strains. 04 p0509 A73-14947

Explosive forming for axisymmetric dished shells without clamped blank around edge, discussing design parameters, formability limits and optimization techniques [SME PAPER MF 72-237] 06 p0698 A73-18095

A comparison of the effects of explosive forming and static deformation on the mechanical properties of pressure vessel steels. 10 p1225 A73-24426

Explosive shock hardening effects on roller steel fatigue strength, surface hardness and wear resistance 14 p1755 A73-30318

Working of titanium by high energy due to detonation of an explosive charge 19 p2433 A73-37836

Explosive metal forming, considering energy cost, operational speed, achievable tolerances in symmetrical or nonsymmetrical shapes, production quantities and lead time for die preparation 20 p2569 A73-39405

Fine structure of an explosion-hardened chromium-nickel-manganese austenitic steel 21 p2718 A73-40484

Work hardening of copper, nickel, and alloy H31 by compression and explosion 21 p2707 A73-40705

Explosive and electrohydraulic forming techniques cost effectiveness in metal technology, considering welding methods and metal powder compaction 22 p2865 A73-41779

Compacting of metallic powders by plane high-explosive charges. I 24 p3092 A73-44414

EXPLOSIVE GASES

U FLAMMABLE GASES

EXPLOSIVE WELDING

Structural changes in Kh18N9T steel during explosion welding 01 p0055 A73-10262

Russian book on physics of explosive hardening and welding covering high velocity inelastic collisions, shock wave generation, strengthening mechanisms of metals, etc 02 p0173 A73-11892

A new uncomplicated method for the simultaneous determination of various parameters in explosive welding 06 p0698 A73-18446

Weld quality of explosive welded industrial metals, noting role of thermal processes and materials thermophysical properties 07 p0831 A73-19995

Implosive and explosive welding of mono- and bimetallic duplex cylinders. 08 p0973 A73-21239

Small-scale explosion seam welding. 10 p1223 A73-23626

Fiber reinforced metal production by explosive welding, discussing fiber winding upon metal foils 11 p1372 A73-25353

An ultrasonic technique for the inspection of magnetic and explosive welds, using a facsimile recording system. 12 p1502 A73-27037

Production of a niobium-stainless steel bimetal by explosion welding 14 p1755 A73-30386

Explosive and electrohydraulic forming techniques cost effectiveness in metal technology, considering welding methods and metal powder compaction 22 p2865 A73-41779

The effect of cold and hot rolling on the microstructure and fracture characteristics of titanium-to-steel explosion welds. 23 p2985 A73-43912

EXPLOSIVES

NT CELLULOSE NITRATE

NT TRINITROTOLUENE

The determination of moisture in propellant charge powders and solid propellants 02 p0202 A73-11565

Detonation propulsion system for missile/spacecraft maneuvering, determining performance characteristics by one dimensional computer calculations for various configurations [AIAA PAPER 72-1161] 03 p0357 A73-13462

Predicting the critical boundary temperature of multidimensional explosives. 07 p0918 A73-19386

Explosive systems with reactant fuel consumption, deriving asymptotic stability, with application to self heating chemical reaction via Liapunov functions 07 p0919 A73-19393

Convective combustion of porous explosives 07 p0920 A73-19990

Detonation of explosives containing boron and its organic derivatives 13 p1669 A73-28971

Ballistite burning rate in sonic gas flow in supersonic conical nozzles as function of flow velocity and combustion chamber pressure 13 p1706 A73-28972

Regularities in the burning of condensed systems within a field of mass forces at moderate pressures 13 p1706 A73-28975

Thermal diffusivity measuring technique for hazardous materials. 14 p1752 A73-29914

Russian book - Transition of burning of compacted systems to detonation. 15 p1959 A73-32420

Missile and explosive environmental tests for mechanical properties, outlining test facilities, climatological effects, salt spray, vibration, shock, dropping, vacuum effects and crack propagation 16 p1997 A73-33387

Plastic bonded, thermally stable explosive for an Apollo experiment. 18 p2341 A73-36152

Method of observing processes in the interior of explosives 21 p2695 A73-39966

Influence of nonexplosive liquids on the detonation rate of solid explosives 24 p3157 A73-45380

EXPONENTIAL FUNCTIONS

NT LOGARITHMS

Almost sure exponential bounds for stochastic operator systems, with applications to randomly sampled control. 01 p0027 A73-10426

The solution of linear, constant-coefficient, ordinary differential equations with APL. 04 p0470 A73-15008

Matrix exponential series approach to distributed parameter systems. 06 p0719 A73-18803

Methods of quadratic Liapunov vector-function construction for linear systems 12 p1525 A73-27895

On an Euler-like method with exponential correction for initial-value problems. 13 p1650 A73-28799

Uniqueness of Chebyshev approximation representation by ratios of exponential functions with restricted number of zeros 13 p1651 A73-29400

Computation of the exponential of a matrix. I - Theoretical considerations. 17 p2203 A73-35521

Methods of constructing quadratic Liapunov vector functions for linear systems. 18 p2330 A73-36600

Differential equations of the asymmetrical mathematical theory of elasticity and their solution when Young's modulus varies according to an exponential law 20 p2620 A73-39505

Study of a method of exponential control of a spacecraft rendezvous 21 p2781 A73-40905

EXPORTS

U INTERNATIONAL TRADE

EXPOSURE

Theoretical and experimental automatic exposure control study. 04 p0451 A73-15775

A triple-exposure technique to reduce recording time in stroboscopic holographic interferometry. 05 p0576 A73-16557

Criterion for the choice of exposure time in atmospheric turbulence investigation with an optical wave. 06 p0691 A73-17497

Aerial camera automatic exposure control design and operation, discussing maxima-minima metering and average brightness measurement techniques 12 p1501 A73-27965

A direct approach to reduce recording time in stroboscopic holographic interferometry. 19 p2429 A73-37541

Optimization of exposure time in linear hologram recording by pre-exposure or post-exposure. 22 p2862 A73-43090

EXPRESSIONS [MATHEMATICS]

U FORMULAS [MATHEMATICS]

EXTARS

Binary stars as X-ray sources. 01 p0102 A73-10969

Possibility of continuous monitoring of celestial X-ray sources through their ionization effects in the nocturnal D-region ionosphere. 03 p0361 A73-13361

Photometric search for H alpha optical emission in Sco X-1 nebulosity region for linking companion radio sources to X ray source 03 p0373 A73-13374

Sco X-1, Crab Nebula, extragalactic, thermal and diffuse background source X ray spectra 03 p0364 A73-13962

On the circular polarization of Sco X-1 and the adjacent sky. 04 p0501 A73-15634

The period and light curve of HZ Herculis. 04 p0501 A73-15683

Scorpius X-1 representation via old-nova model consisting of standing shock and X ray source formed by mass accretion at white dwarf surface 07 p0874 A73-19063

Particle injection in the Cygnus X-3 radio outburst. 11 p1419 A73-25859

The spectrum and variability of Hercules X-1 observed by OSO-7. 11 p1428 A73-26626

Her X-1 optical counterpart observed for B magnitude, relating light curve scatter to 35-day cycle 11 p1428 A73-26627

Massive X ray binaries consisting of early type star with neutron stars or black holes as companions 12 p1535 A73-27597

OAO-2 observations of HD 153919 = 2U 1700-37. 14 p1797 A73-30007

High-speed UVB photometry of Scorpius X-1 flares. 14 p1801 A73-30646

Variable X ray sources Cyg X-1, Cen X-3 and Sco X-1 behavioral analysis from Uhuru satellite data, considering pulsating white dwarf model for Cen X-3 15 p1935 A73-31483

Uhuru observed galactic X ray sources, discussing whole-galaxy X ray emission, Sco X-1 type binary sources and emissions in GX263+2 and Small Magellanic Cloud 16 p2049 A73-32728

Sco X-1 noncorrelation of radio with optical or X ray intensities, noting paucity of simultaneous observations of other X ray sources 16 p2050 A73-32732

Sco X 1, Cygnus and galactic center X ray sources radio observations, discussing identification, properties and variabilities 16 p2050 A73-32733

Compact X ray source models from statistical analysis of Uhuru catalog sources with respect to luminosities, lifetimes and stellar populations 16 p2050 A73-32737

HZ Hercules periodically pulsating variable extar in binary system detected by Uhuru satellite, detailing X ray emission, rotation pattern and mass exchange mechanism 16 p2059 A73-32948

The beaming of radiation from an accreting magnetic neutron star and the X-ray pulsars. 17 p2225 A73-35618

Balloon observations of Sco X-1 in the energy interval 17-106 keV. 17 p2225 A73-35783

Measurement of the position and spectrum of Hercules X-1 from the OSO-7 satellite. 18 p2356 A73-36982

Cosmic X-ray sources - A progress report. 19 p2474 A73-37149

Hard X-ray spectrum of Hercules X-1. 19 p2475 A73-37388

Copernicus satellite observation of eclipsing binary Her X-1 to search for steady soft X ray flux strong enough to heat companion star

19 p2482 A73-37391

Zeeman effect in the X-ray star candidates HD 77581 and theta super 2 Orionis.

19 p2482 A73-37399

Bragg spectroscopy of Scorpius X-1 in search of the Fe XXV emission lines.

19 p2485 A73-37627

On the accretion model for X-ray double stars.

20 p2607 A73-39082

Solar radio frequency radiation characteristics, considering flare stars, pulsars, X ray sources, Antares types, novae, red supergiants and stars with gas and dust envelopes

20 p2613 A73-39749

Optical studies of Uhuru sources. VI - Photoelectric photometry of HD 153919 = 2U 1700-37.

22 p2905 A73-41766

Observations of the highly variable X-ray source GX 339-4.

22 p2905 A73-41767

Sanduleak 160 variability confirmed, discussing double peaked optical variation, mass ratios and X ray eclipse

22 p2916 A73-43123

Long-term X-ray observations of Scorpius X-1 by OSO-III.

24 p3138 A73-45045

Infrared and X-ray variability of Cyg X-3.

24 p3143 A73-45347

The 35-day cycle of HZ Herculis.

24 p3143 A73-45491

EXTERNAL STORES

Active flutter control - An adaptable application to wing/store flutter.

[AIAA PAPER 73-194] 05 p0531 A73-16930

Calculation of forces on stores in the vicinity of aircraft.

09 p1028 A73-22433

Automatic electronic feedback control systems for active wing/external store flutter suppression

17 p2107 A73-35244

Space shuttle external tank, discussing Orbiter engine, propellant conditioning, solid rocket boosters structural support, environment effects and safe disposals

19 p2492 A73-37598

Aircraft-store separation design for angular momentum increase of external weapon with internally mounted spinning flywheel

20 p2508 A73-38652

EXTERNALLY BLOWN FLAPS

V/STOL hydraulic controls including internal and external blown jet flap and augmentor wing, describing integrated flight control actuator packages and aircraft configuration

17 p2108 A73-35851

Mechanisms of externally blown flap noise.

[AIAA PAPER 73-1029] 24 p3056 A73-44859

EXTINCTION

NT INTERSTELLAR EXTINCTION

Electromagnetic wave transmission through 8-12 micron atmospheric window, investigating particulate matter effects on radiation energy extinction

01 p0037 A73-10372

Extinction of photoluminescence by electron irradiation and energy transfer in molecular crystals

05 p0600 A73-16555

IR and thermal extinction spectra of luminescence and photoconductivity of zinc cadmium sulfide solid solution films doped with Cu and Cl

06 p0738 A73-18643

The interpretation of continuum and line absorption and radiation by circumstellar dust.

09 p1150 A73-23132

A generalized extinction theorem and its role in scattering theory.

20 p2591 A73-38613

Dynamic effects on ignitability limits of solid propellants subjected to radiative heating.

22 p2899 A73-42813

Extinction coefficient / point source light loss due to atmospheric scattering/ significance in reduction of night airglow data

24 p3082 A73-44734

EXTINGUISHERS

U FIRE EXTINGUISHERS

EXTINGUISHING

Depressurization extinguishment of composite solid propellants - Influence of composition and catalysts.

[AIAA PAPER 72-1136] 03 p0352 A73-13443

Extinguishment of composite propellants at low pressures.

[AIAA PAPER 73-175] 05 p0640 A73-16918

Mathematical model for extinguishing gunpowder combustion via pressure variations, assuming gunpowder surface dependence on combustion rates

09 p1167 A73-22617

Flame quenching, extinction, propagation, convection and ignition limits in premixed gas mixtures

13 p1707 A73-29003

EXTRACTION

NT SOLVENT EXTRACTION

A technique for extracting Radiolaria from radiolarian cherts.

11 p1324 A73-25141

EXTRAGALACTIC LIGHT

U EXTRATERRESTRIAL RADIATION

U LIGHT [VISIBLE RADIATION]

EXTRAGALACTIC MEDIA

U INTERGALACTIC MEDIA

EXTRAGALACTIC RADIO SOURCES

NT RADIO GALAXIES

Radio interferometry observation of extragalactic radio sources for geodetic survey of baseline between antenna sites in Massachusetts and West Virginia

01 p0039 A73-10405

Observation of compact objects of cosmic radio emission with maximum angular resolution at the 3.55-cm wavelength

01 p0092 A73-10931

A preferred orientation of extragalactic double radio sources.

02 p0217 A73-12405

Radio source counts and redshifts in steady state cosmology.

04 p0497 A73-15048

Observations of extragalactic variable sources at 2.8 and 4.5 cm wavelength.

04 p0500 A73-15515

Observations of the radio source PKS0123-01 at 5000, 408, and 80 MHz.

06 p0754 A73-18627

Positions and some identifications for 111 sources of about 1 flux unit at 408 MHz.

06 p0754 A73-18628

The radio continuum of the Large Magellanic Cloud. III - The sources at 11 cm wavelength.

06 p0754 A73-18631

The radio continuum of the Large Magellanic Cloud. IV - Spectra of sources.

06 p0754 A73-18632

Evidence for ejection of radio sources from supernova remnants.

07 p0873 A73-19056

7.8-GHz flux density measurements of variable radio sources.

07 p0876 A73-19355

Faraday rotation of polarized extragalactic radio sources interpretation as plasmas of mixed matter and antimatter

07 p0900 A73-20277

Results of radio source observations at short millimeter wavelengths

07 p0901 A73-20310

Intensity variations in a complete sample of radio sources at 2,300 MHz.

07 p0902 A73-20558

H flux density observations for 21 cm absorption spectrum in front of Cyg X-3

07 p0902 A73-20560

Virgo A nucleus compact radio source observation from February 1971 to August 1972, noting absence of intensity or size variations

08 p1004 A73-20898

Multifrequency polarization observations of eight extragalactic sources.

08 p1008 A73-21156

Observations of compact radio-emitting objects at 3.55 cm with maximum angular resolution.

09 p1147 A73-22726

The Parkes 2700 MHz survey. IV - Catalogue for the south polar cap zone, declinations -75 deg to -90 deg.

10 p1275 A73-23751

Observations of radio sources at short millimeter wavelengths.

12 p1539 A73-27282

31.4-GHz flux density measurements of variable radio sources.

12 p1540 A73-27426

Galactic and extragalactic radio emission and satellite observations of RF cosmic radiation and noise intensity

12 p1544 A73-27783

Short time constant limits of pulse duration on electromagnetic energy emission as function of frequency, applying to extragalactic radio astronomy observations

12 p1547 A73-27884

Cosmological information from surveys of radio source spectra.

15 p1933 A73-31396

Galactic and extragalactic X ray observations at 20-500 keV, considering supernova remnants, Sco-1 and Cyg 1 type sources, M31, Magellanic Clouds and Crab Nebula

16 p2049 A73-32731

Uhuru extragalactic X ray observations including normal galaxies, quasars, giant radio galaxies, Seyferts and galactic clusters

16 p2050 A73-32741

The properties of extragalactic X-ray sources from visible light observations.

16 p2050 A73-32742

Extragalactic X ray source physical properties, discussing thermal bremsstrahlung X ray generation by synchrotron mechanism or by Compton scattering

16 p2051 A73-32743

Extragalactic X-ray sources and their contribution to the diffuse background /Invited paper/.

16 p2051 A73-32744

Soft X ray background observations at 0.1-10 keV, considering interstellar absorption effects, galactic radiation and extragalactic components

16 p2051 A73-32745

Variable radio emission from the extragalactic supernova 1970g in M101.

16 p2060 A73-33094

Extragalactic radio phenomena.

16 p2054 A73-33288

The velocity of separation of the components of extragalactic radio sources.

16 p2062 A73-33572

Absorption of ultrahigh energy photons in the universe

17 p2223 A73-34368

Extragalactic radio sources modeled as bubbles of relativistic plasma rising through hot gas, producing galactic clusters X ray emission

18 p2353 A73-36508

Synchrotron model limitations for optical pulsars and compact extragalactic objects, considering NP 0532, PKS 2134+004, OQ 208 and NGC 10608

19 p2485 A73-37618

Extragalactic radio sources identification with galaxies and quasars by high sensitivity and resolution astronomical telescopes, obtaining angular structure maps and radio spectra

23 p3028 A73-43347

Very-long-baseline interferometry techniques applied to problems of geodesy, geophysics, planetary science, astronomy, and general relativity.

23 p2980 A73-43354

High angular resolution very long baseline interferometry for emission spectra and angular size determination and structure mapping of galactic and extragalactic radio sources

23 p2980 A73-43355

Radio spectra and mapping of extragalactic radio sources including radio galaxies and quasars with high angular resolution, noting energy sources and red shift

23 p3029 A73-43625

Galactic protocluster radio emission detection, using adiabatic density perturbation theory of galactic evolution

23 p3037 A73-44256

An all-sky catalogue of strong radio sources at 408 MHz.

24 p3144 A73-45560

EXTRAPOLATION

Accelerated convergence of sequences of quadrature approximations.

01 p0072 A73-11471

Generalized and modified parametric methods for extrapolating results of long term high temperature strength tests for service life determination

02 p0181 A73-12205

Wind tunnel experimental verification of flight vehicles aerodynamic characteristics during preliminary design stage, discussing correction procedures for model data extrapolation to full scale parameters [SAE PAPER 720861]

05 p0528 A73-16665

Solar cell fatigue life prediction by statistical analysis and extrapolation for determining failure probability curve as function of stress and time

09 p1036 A73-22808

Local extrapolation in the solution of ordinary differential equations.

10 p1241 A73-23641

An operational upper air analysis using the variational method.

10 p1244 A73-23645

Validity of zeta Oph cloud carbon isotope abundance extrapolation to dense dusty regions of Galactic center and Orion Nebula

10 p1275 A73-23824

Accurate measurement of antenna gain and polarization at reduced distances by an extrapolation technique.

17 p2127 A73-35676

Multidimensional linear extrapolation in problems of optimal design and control

20 p2539 A73-38687

Dynamic operative image formation and function features during extrapolation tracking of visibly moving target, noting image reaction to operator performance

22 p2812 A73-41886

EXTRASENSORY PERCEPTION

Clairvoyant perception of target material in three states of consciousness.

03 p0260 A73-13555

EXTRASOLAR PLANETS

Protoplanet cloud model for cosmic OH and water masers in H II regions to account for anomalous hydrogen deficiency, discussing pumping mechanisms and chemical composition

04 p0497 A73-14974

Planetary system formation likelihood disparaged, discussing planetary orbit stability, dark companions and life existence improbability

05 p0614 A73-16303

Extrasolar life in light of stars, planets, and living systems nuclear, gravitational, electromagnetic and weak interactions 05 p0539 A73-16306

Barnard star multiplanet system, discussing inclinations of planetary orbits and cosmogonic implications 17 p2229 A73-34430

Lifes possible origin on earth from extraterrestrial organisms, discussing galactic intelligent life and intelligent signals from extrasolar planets 21 p2639 A73-41175

Extrasolar planetary systems. 24 p3127 A73-44391

Barnard star proper motion and planetary system orbital analysis, indicating massive planet companions in inclined orbits 24 p3133 A73-44556

EXTRATERRESTRIAL ENVIRONMENTS

NT CHROMOSPHERE

NT DEEP SPACE

NT INTERPLANETARY SPACE

NT INTERSTELLAR SPACE

NT JUPITER ATMOSPHERE

NT LUNAR ATMOSPHERES

NT LUNAR ENVIRONMENT

NT MARS ATMOSPHERE

NT MARS ENVIRONMENT

NT PLANETARY ATMOSPHERES

NT PLANETARY ENVIRONMENTS

NT SOLAR ATMOSPHERE

NT STELLAR ATMOSPHERES

Rocket-borne instruments for cosmic dust particles detection in extraterrestrial space, noting collector foils and plates fabrication 06 p0748 A73-17768

EXTRATERRESTRIAL LIFE

Interstellar flight and intelligence in the Universe. 03 p0370 A73-13198

Book - Theory and experiment in exobiology. Volume 2. 03 p0265 A73-14315

Protobiochemical developments in terms of extraterrestrial life search and roles of nitriles and urea in prebiological chemical evolution 03 p0265 A73-14319

Biological, chemical and cytological methods of microorganism detection integrated into single instrument 03 p0272 A73-14320

Quarantine necessity, protocol and effectiveness for Mars samples, emphasizing risks of foreign replicating agent introduction to earth biosphere 03 p0272 A73-14321

Planetary system formation likelihood disparaged, discussing planetary orbit stability, dark companions and life existence improbability 05 p0614 A73-16303

Extrasolar life in light of stars, planets, and living systems nuclear, gravitational, electromagnetic and weak interactions 05 p0539 A73-16306

Space exploration and the origin of life. 06 p0651 A73-17930

Solvent effects on enzymes - Implications for extraterrestrial life. 06 p0652 A73-17948

Solar system other planets suitability for terrestrial organisms, noting life forms possible existence on Venus, Mars and Jupiter 06 p0654 A73-18349

Search for biogenic structures and viable organisms in lunar samples - A review. 06 p0654 A73-18416

Survival of micro-organisms on the moon. 07 p0780 A73-19111

Optimal search strategy to investigate probability of habitable systems with civilization transmitting detectable signals 08 p1013 A73-21645

Historical treatment and inconclusiveness of evidence of extraterrestrial life traces and organic matter in carbonaceous and other meteorites 09 p1146 A73-22545

Electric discharge and microbiological experiments in simulated Jovian atmosphere for investigation of Jupiter life prospects 11 p1319 A73-26478

Chemical volatilization as a technique for the detection of extraterrestrial biopolymers and possible metabolic products. 11 p1319 A73-26479

The interpretation of signals from space. 11 p1428 A73-26661

Liquid ammonia life existence in universe, considering halogen and silicon life chemistry 11 p1326 A73-26662

Extraterrestrial messenger probe recognition from inhabited planet via message involving home constellation binary coded signals 14 p1796 A73-29946

Chemical evolution before life from carbonaceous meteorites composition, noting porphyrins, optically active substances and isoprenoid hydrocarbons 14 p1715 A73-30130

Extraterrestrial life existence evidence, discussing biochemical properties, evolution and mental and moral characteristics of extraterrestrial life 17 p2113 A73-35657

Extraterrestrial life detection from imaging observations on lunar samples and meteorites, discussing application to Mars surface 17 p2113 A73-35804

Russian papers on populated cosmos covering space exploration impact on human civilization, extraterrestrial life, space medicine and biology, solar system, space law, etc 19 p2393 A73-37398

Space-related research in mycology concurrent with the first decade of manned space exploration. 20 p2513 A73-39478

Viking Mars 1975 soft landing and search for extraterrestrial life, considering lander transmission of atmospheric and surface data 21 p2766 A73-40414

Amino acids in the Murchison meteorite. 21 p2771 A73-41010

Life origin hypothesis based on interstellar molecular concentration in gas clouds, examining radical types and molecular Doppler spectra 21 p2638 A73-41080

Lifes possible origin on earth from extraterrestrial organisms, discussing galactic intelligent life and intelligent signals from extrasolar planets 21 p2639 A73-41175

Directed Panspermia theory of terrestrial bioevolution, suggesting microorganism transmission to earth by intelligent technologically advanced civilization via spacecraft 24 p3058 A73-44553

Extraterrestrial intelligent life existence possibility in terms of hypothesis involving earth as wilderness area or zoo with failure of interaction with other civilization 24 p3058 A73-44554

Communication possibilities between earth and technologically advanced galactic civilizations, discussing radio astronomy requirements, technology differences and communication distance estimates 24 p3133 A73-44555

Project Cyclops investigation of extraterrestrial civilization signal detection, discussing microwave apparatus, frequency bands, antenna arrays and research implementation proposals 24 p3134 A73-44561

EXTRATERRESTRIAL MATTER

NT COSMIC GASES

NT COSMIC PLASMA

NT INTERPLANETARY GAS

NT INTERSTELLAR GAS

A device for working with extraterrestrial material in an inert-gas medium 02 p0151 A73-12465

An ultrahigh-vacuum arrangement for studying extraterrestrial material 02 p0151 A73-12466

Solar wind, meteoritic, and cometary carbon sources for moon, discussing lunar atmospheric steady state carbon component sustained by meteoritic and cometary carbon vaporization 06 p0754 A73-18427

Organogenic elements in stars, interstellar matter, comets, meteorites and planets, discussing molecular distribution and formation, prebiological chemical evolution, and terrestrial and extraterrestrial biology 06 p0754 A73-18430

Terrestrial and extraterrestrial stable organic molecules. 14 p1724 A73-30131

An apparatus for work with extraterrestrial water in an inert gas atmosphere. 15 p1859 A73-32615

Ultrahigh-vacuum apparatus for studying extraterrestrial material. 15 p1859 A73-32616

Preliminary measurements of spherules of the Pontina Plain and of micrometeorites of Apollo 12 and related impact studies. 21 p2775 A73-41412

Ablation debris and primary micrometeoroids in the stratosphere. 21 p2775 A73-41419

EXTRATERRESTRIAL RADIATION

NT EXTRATERRESTRIAL RADIO WAVES

NT GALACTIC RADIATION

NT GALACTIC RADIO WAVES

NT GEGENSCHIEIN

NT INTERSTELLAR RADIATION

NT LUNAR RADIATION

NT PLANETARY RADIATION

NT PRIMARY COSMIC RAYS

NT RADIO BURSTS

NT SOLAR CORPUSCULAR RADIATION

NT SOLAR COSMIC RAYS

NT SOLAR ELECTRONS

NT SOLAR PROTONS

NT SOLAR RADIATION

NT SOLAR RADIO BURSTS

NT SOLAR RADIO EMISSION

NT SOLAR WIND

NT SOLAR X-RAYS

NT STELLAR RADIATION

NT STELLAR WINDS

NT SUNLIGHT

NT TYPE 2 BURSTS

NT TYPE 3 BURSTS

NT TYPE 4 BURSTS

NT TYPE 5 BURSTS

NT ZODIACAL LIGHT

Search for gravitational radiation of extraterrestrial origin. 01 p0097 A73-10424

Astronomical telescope research programs, emphasizing spectrographic instrumentation to detect and record extragalactic light sources spectra 01 p0046 A73-10502

New interpretations of extraterrestrial Lyman-alpha observations. 02 p0206 A73-12323

Annual Conference on Nuclear and Space Radiation Effects, 9th, University of Washington, Seattle, Wash., July 24-27, 1972, Proceedings. 05 p0557 A73-16501

The radiation environments of outer-planet missions. 05 p0617 A73-16511

Electrostatic toroidal analyzer for studying charged particle fluxes in outer space 12 p1496 A73-27203

Extraterrestrial ultraviolet radiation and the parameter of the HI medium near the sun 20 p2601 A73-39074

EXTRATERRESTRIAL RADIO WAVES

NT GALACTIC RADIO WAVES

NT RADIO BURSTS

NT SOLAR RADIO BURSTS

NT SOLAR RADIO EMISSION

NT TYPE 2 BURSTS

NT TYPE 3 BURSTS

NT TYPE 4 BURSTS

NT TYPE 5 BURSTS

Observation of compact objects of cosmic radio emission with maximum angular resolution at the 3.55-cm wavelength 01 p0092 A73-10931

Cosmic radio wave anomalous absorption height dependence on zenith distance in midlatitude ionosphere during solar flare emission from polarization study 03 p0365 A73-14561

Intensity variations in a complete sample of radio sources at 2,300 MHz. 07 p0902 A73-20558

Observations of compact radio-emitting objects at 3.55 cm with maximum angular resolution. 09 p1147 A73-22726

Vertical distribution of absorption of cosmic radio emission and radio waves in ionosphere and lower ionosphere based on electron density profiles 11 p1327 A73-25084

Anomalous absorption of cosmic radio emission in the auroral zone during the IQSY 11 p1411 A73-25087

Search for sporadic radio emission from space at centimeter and decimeter wavelengths 14 p1798 A73-30261

Measurement of the displacement of the electrical axis of an antenna with respect to its geometrical axis by using extraterrestrial radio emission sources 17 p2120 A73-34119

EXTRATERRESTRIAL RESOURCES

Extraterrestrial propellant resupply for advanced manned missions. 02 p0221 A73-12599

Space exploration and celestial bodies natural resources exploitation legislation proposals evaluation 04 p0523 A73-15152

UN space treaty proposals relating to moon and other celestial bodies natural resources utilization 04 p0524 A73-15158

In-depth exploration of the solar system and its utilization for the benefit of Earth. 06 p0751 A73-18029

EXTRATERRESTRIAL ROVING VEHICLES

U ROVING VEHICLES

EXTRAVEHICULAR ACTIVITY

Apollo 14 mission, discussing extravehicular activities time and payload increase via enlarged propellant tanks 03 p0368 A73-13085

Dynamics of an astronaut's movement on a tether towards a spacecraft and a spacecraft control concept based on the variable-structure systems theory 05 p0628 A73-16411

An experimental investigation of attitude control systems for astronaut maneuvering units. [AIAA PAPER 73-250] 05 p0563 A73-16973

Mercury, Gemini and Apollo space suits, discussing glove development, boot design, portable life support equipment and extravehicular mobility 16 p1976 A73-34025

Analysis of the extravehicular activity of an astronaut 18 p2281 A73-36116

Some psychological and engineering aspects of the extravehicular activity of astronauts. 22 p2814 A73-42167

EXTREMA

U RANGE [EXTREMES]

EXTREMELY HIGH FREQUENCIES

Absorption in the 220 GHz atmospheric window.

04 p0418 A73-15394

Synchronous communication satellite crosslink antenna design and tracking and acquisition procedures for Ka band frequencies, describing reflectors, paraboloids, and five horn feed system

16 p1977 A73-32721

EHF radio wave limitations and potentialities for high speed data communications systems, considering applications in urban short range relays

16 p1981 A73-33705

EXTREMELY LOW FREQUENCIES

ELF signal generation by solar protons observed via tape recording of north-south horizontal geomagnetic field variations in 3-75 Hz resonance range

05 p0571 A73-17064

Characteristics of the VLF-noise spectrum during excitation of the earth-ionosphere resonator by cosmic sources.

10 p1188 A73-24222

OGO 5 observation of ULF geomagnetic fluctuation at polar cusp boundaries in terms of ionospheric drift wave and Kelvin-Helmholtz instabilities

10 p1214 A73-24744

Effects of stress wave form and cycle frequency on low cycle corrosion fatigue.

11 p1382 A73-25823

Steady ELF plasmaspheric hiss, studying whistler mode turbulence, band limitation, power spectra and peak intensities

12 p1488 A73-26984

Explorer 45 search coil magnetometer detection of ELF signals during magnetic storms, noting signal variation with storm phases and satellite magnetospheric position

20 p2552 A73-38957

EXTREMELY LOW RADIO FREQUENCIES

Influence of an important region of the ionospheric layer on ELF propagation characteristics

01 p0016 A73-10203

Equipment for determining the amplitude-frequency characteristics of nonlinear elements in the range of low and extra-low frequencies

01 p0023 A73-10679

Tunneling transmission through the equatorial lower ionosphere of ELF and VLF electromagnetic waves.

11 p1358 A73-26702

Numerical solution of the problem of transmission of ELF waves through the lower ionosphere.

13 p1582 A73-28651

Absolute calibration of antennas at extremely low frequencies.

17 p2128 A73-35686

EXTREMUM VALUES

NT LIMITS [MATHEMATICS]

NT MAXIMA

An extremum principle for three-dimensional compressible inviscid flows.

01 p0031 A73-10427

Application of mathematical programming to the solution of extremal problems in two-dimensional elasticity theory

02 p0235 A73-12197

Algorithm for automatic optimal control of radio telescope parabolic antenna with extremal characteristic in radiation pattern, noting quasi-steady and steady operation

02 p0147 A73-12497

Worst inputs and a bound on the highest peak statistics of a class of non-linear systems.

02 p0188 A73-12602

Aircraft engine inlets total pressure fluctuations and distortion factors, presenting extreme-value statistical method for maximum distortion level probability estimate

03 p0354 A73-13419

Multichannel communication system in adaptive system with automatic channel selection based on random parameter extremum criterion for maximum usage time of extremal channel

03 p0278 A73-14063

Extremum value methods for design, production, testing and maintenance of components and system with low failure probability

04 p0507 A73-14709

Calculus of variations for functional conditional extremum, determining minimum drag shape for body of revolution in hypersonic flow

04 p0403 A73-14886

A new method of obtaining Q solutions to extremal problems in certain special classes of analytic functions associated with functions whose real part is positive in a circle

04 p0470 A73-15083

On the maximum value of the mass of a star.

04 p0500 A73-15525

Existence and conical intersection theorems for extremum conditions of Euclidean space subset function, noting discrete objects optimality conditions

05 p0589 A73-16334

Asymmetric principal stress bounds in terms of symmetric part of tensor, considering existence conditions and maximum shear and normal stresses

[ASME PAPER 72-APM-QQ] 05 p0633 A73-16535
Absolute minima determination for homogeneous polynomial real valued goal function under equality constraints, solving nonlinear programming problem by penalty function method

06 p0716 A73-17851

Method of branches and bounds as a regular method for the solution of irregular mathematical programming problems. I.

06 p0716 A73-17961

Extremum principles on time independent elastoplastic solids nonisothermal deformation properties based on yield function dependence on temperature

06 p0763 A73-18456

Pointwise bounds for smooth film profiles Reynolds equation solution based on elliptic equations maximum principle, considering journal bearings

07 p0845 A73-20484

Some extremum principles for pipe flow in magnetohydrodynamics.

08 p0993 A73-21403

Extremum criteria for Gato differentiable mappings in hypercomplex domains derived for nonlinear Chebyshev problems, extending results to partially ordered sets of operators

09 p1112 A73-22581

Sturm-Liouville problem monotone proper function zeros lower and upper bounds evaluation using Barta inequality and Schwartz iteration

09 p1113 A73-23026

Scalar sequence spaces theory extension to vectorial sequence spaces based on bounded ensemble concept

10 p1241 A73-23763

Necessary and sufficient conditions for differentiable nonscalar-valued functions to attain extrema.

10 p1243 A73-24537

An upper bound solution for rectangular plate in plane stress compression.

10 p1292 A73-24640

A priori bounds for some bifurcation problems in fluid dynamics.

10 p1207 A73-24786

Porous layer strongly nonlinear heat transfer curve bounds numerical computation by variational method, using boundary layer analysis

11 p1448 A73-25055

Some finite extremum principles in piecewise linear elastoplasticity.

11 p1434 A73-25215

Upper bounds to plastic strains in shake-down of structures subjected to cyclic loads.

11 p1434 A73-25216

Variational method for a generalized class of functionals and its application to aeromechanics problems

11 p1304 A73-26438

Bounds on mean excitation energies-Lamb shift, stopping power, straggling, and grazing collision of high-energy charged particle.

12 p1526 A73-27128

Variational treatment of the elastic constants of disordered materials.

13 p1692 A73-28169

A method for obtaining bounds on eigenvalues and eigenfunctions by solving non-homogeneous integral equations.

13 p1647 A73-28192

Quadrature errors upper bound estimates for Gauss-Legendre, Newton-Cotes and Gauss-Laguerre formulas

13 p1649 A73-28603

Book - Variational analysis: Critical extremals and turman extensions.

17 p2203 A73-35598

Neighboring extremals for optimal control problems.

18 p2294 A73-36308

The fastest extremum search in sampled-data automatic control systems

20 p2539 A73-38695

Low value atmospheric density extremes evaluation covering ground elevations up to 15,000 feet for engine power calculation in aircraft design

21 p2729 A73-40063

Lower bounds on the cost functional for systems governed by partial differential equations.

21 p2726 A73-40838

Gradient methods for extremum solutions of two-point boundary value problems of dynamics.

[ASME PAPER 73-DET-44] 22 p2916 A73-42069

Complementary variational principles and error bounds for biharmonic boundary value problems.

22 p2921 A73-42433

Dynamic programming application to extremal fields topological singularity in optimal control theory for flight vehicle with state variables satisfying initial conditions and ordinary differential equations

22 p2917 A73-43030

Level transgressions and extremal values of continuous stochastic signals

23 p2952 A73-43310

Performance criteria selection for complex system parameter optimization based on minimum deviation from extremal values

23 p2963 A73-43737

The governing equations and extremum principles of elasticity and plasticity generated from a single functional. I.

24 p3152 A73-45315

Extremum principles and error bound for a nonlinear boundary value problem in the theory of laminar boundary layers.

24 p3080 A73-45340

EXTRUDING

Hot extrusion and filled billet techniques to process superalloy powder metallurgy products into complex shapes, bars or wire

01 p0056 A73-10284

Hot extrusion and properties of rods from sintered molybdenum and tungsten blanks.

01 p0065 A73-10817

Means of improving the quality of heat-resistant metals and their alloys

03 p0324 A73-13504

Semihydrostatic hot extrusion for Ti plated Cu anode bar, noting metal bonding and current distribution

03 p0312 A73-13583

Consideration of a number of factors involved in determining the long-term strength of dies used for the extrusion of hollow sections of aluminum alloys

03 p0318 A73-14651

Effect of hydrostatic extrusion on the composition and properties of Nb3Sn compounds.

06 p0736 A73-18213

The influence of a thoria dispersion on preferred orientation in nickel alloys.

08 p0977 A73-21012

Linearized hydrodynamic instability initiation in polymer melts extrusion, examining Weissenberg number role in melt fracture onset

10 p1241 A73-24655

Unconventional processes for faster extrusion of aluminum hard alloys

16 p2021 A73-33951

The influence of prior thermal treatment of cast blocks on the coarse grain characteristics in extruded bars and profiles of alloys of the type AlCuSiMn

16 p2021 A73-33952

Stepped aluminum extrusions - Designing for business aircraft.

[SAE PAPER 730308] 17 p2177 A73-34668

Production of extruded tube hollows for titanium 3Al-2.5V hydraulic tubing.

[SAE SP-378] 19 p2434 A73-37869

Application of the hydrostatic extrusion process toward production of 3Al-2.5V titanium alloy hydraulic tubing.

[SAE SP-378] 19 p2434 A73-37873

The fabrication of fiber-reinforced composites with the aid of high-speed extrusion presses

19 p2435 A73-38272

Aluminum and aluminum alloys extrusion processes, discussing form shape, weldability, hardening and metal transformations

21 p2707 A73-41067

EYE [ANATOMY]

NT CORNEA

NT FOVEA

NT NYSTAGMUS

NT OCULOMOTOR NERVES

NT PUPILS

NT RETINA

Functional dependence of the ciliary epithelium ATPase activity and intraocular pressure on the autonomic nervous system.

05 p0539 A73-16248

Electrical stimulation effects of human eye on photic threshold for square wave vision as function of wavelength, orientation and spatial frequency

07 p0783 A73-20260

Meridional amblyopia - Evidence for modification of the human visual system by early visual experience.

08 p0931 A73-21562

Book - Physiology of photoreceptor organs.

09 p1042 A73-23301

The structural organization of the compound eye in insects.

09 p1042 A73-23302

Vertebrate photoreceptor cell /rods and cones/ development and structure, discussing light pathway, ciliary connective and microtubules, outer and inner segments, etc.

09 p1042 A73-23303

The morphological organization of the vertebrate retina.

09 p1042 A73-23304

Light evoked changes in potential difference between inside and outside of cells in Limulus ommatidia, describing multistage model of generator potential

09 p1043 A73-23310

Dioptric apparatus of arthropod compound eyes, describing optical characteristics of apposition eye

09 p1043 A73-23310

Inhibitory interaction in the retina of Limulus.

09 p1043 A73-23311

- Optical properties of vertebrate eyes.
09 p1043 A73-23312
Investigation of the exchange between the blood and the intraocular fluid with the aid of radioactive phosphorus
10 p1185 A73-24520
Two visual systems in the frog.
21 p2640 A73-41302
Activity of acid nucleases in eye tissues under the action of corticosteroidal hormones
24 p3058 A73-44430
- EYE DISEASES**
NT ASTIGMATISM
NT CATARACTS
NT GLAUCOMA
Idiopathic central serous retinopathy /cho-
roidopathy/ in flying personnel.
[AD-754147]
03 p0269 A73-14164
Congenital and acquired color vision defects,
discussing color blindness incidence, defect nomen-
clature and eye tests
05 p0540 A73-16482
Laser speckle for determining ametropia and ac-
commodation response of the eye.
11 p1377 A73-26232
Binocular color resolution capability of the eyes as a
function of the characteristics of vision during
anisometropia
15 p1832 A73-30999
Vein wall changes as the main cause of acute
disturbance of blood circulation in the Vena centralis
retinae system
15 p1833 A73-31173
Frontal eye-field lesions in monkeys.
18 p2272 A73-36446
The significance of retinal pathology in ageing air-
crew.
18 p2285 A73-36925
Possibilities of barotherapy in ophthalmology
21 p2637 A73-40349
Ocular antigens. IV - A comparative study of the lo-
calisation of immunogenic determinants of ocular
structural glycoproteins in connective tissues of vari-
ous organs.
22 p2802 A73-41729
Fluorescent angiographic technique for fundus oculi
23 p2946 A73-43788
- EYE DOMINANCE**
Asymmetries related to cerebral dominance in
returning the eyes to specified target positions in the
dark.
03 p0261 A73-13760
Eye dominance measurement relationship to image
sharpness or visual acuity from binocular and
monocular tests, obtaining dominance normal distribu-
tion
09 p1039 A73-21893
Monocular contribution to binocular vision in nor-
mals and amblyopes.
13 p1575 A73-28359
Amplitude of visual suppression during the control
of binocular rivalry.
17 p2117 A73-35491
Frequency analysis of spatio-temporal visually
evoked cortical potentials during binocular rivalry.
17 p2118 A73-35645
Asymmetry in perception - Attention versus other
determinants.
24 p3065 A73-45338
- EYE EXAMINATIONS**
Ocular tonus measurements for glaucoma detection
in flying personnel, discussing subsequent test
procedures in case of abnormal findings
02 p0134 A73-12158
Visual function as sum of visual acuity and visual
field, considering role of resolution and detection
tasks in retinal function examinations
05 p0539 A73-16478
Congenital and acquired color vision defects,
discussing color blindness incidence, defect nomen-
clature and eye tests
05 p0540 A73-16482
Monocular and binocular clues interaction in depth
perception and spatial orientation, discussing stereop-
sis testing
05 p0542 A73-16483
Electroretinography /ERG/, electro-oculography
/EOG/, visual evoked response /VER/ and electric
evoked response /EER/ procedures for elec-
trophysiological investigation of visual system
05 p0542 A73-16484
Dichromatic convergence points obtained by sub-
tractive colour matching.
19 p2398 A73-37420
Visual field defects after missile injuries to the
geniculo-striate pathway in man.
21 p2641 A73-41600
- EYE MOVEMENTS**
NT NYSTAGMUS
Extraretinal feedback and visual localization.
01 p0008 A73-10437
Influence of observing strategies and stimulus varia-
bles on watchkeeping performances.
01 p0012 A73-10771
- A combined photoelectric method for detecting eye
movements.
02 p0137 A73-12079
Variability of normal glabellar and supraorbital
reflexes in man
03 p0261 A73-13748
Asymmetries related to cerebral dominance in
returning the eyes to specified target positions in the
dark.
03 p0261 A73-13760
Visual receptive fields sensitive to absolute and
relative motion during tracking.
04 p0409 A73-15072
Mislocation of visual stimuli during voluntary sac-
cades.
05 p0541 A73-17174
A new illusion - The underestimation of distance
during pursuit eye movements.
06 p0656 A73-17575
The superior colliculus of the brain.
06 p0654 A73-18347
Mechanical modeling of eye muscle dynamics.
06 p0660 A73-18816
Linearity of the horizontal component of the elec-
tro-oculogram.
07 p0784 A73-19125
Two dimensional eye movement recording using a
photo-electric matrix method.
07 p0786 A73-20259
Saccadic suppression for structured background as
function of visual image pattern and threshold detec-
tion elevation in central nervous system
07 p0783 A73-20267
Central nervous system stresses effects estimation,
discussing ocular positioning movements functional
significance and psychological processes
08 p0935 A73-21542
The nature of the optimum muscular performance
achieved in the execution of fast eye rotations.
10 p1185 A73-24772
Adjustment of saccade characteristics during head
movements.
11 p1319 A73-26222
After-effects of movement contingent on direction
of gaze.
11 p1324 A73-26721
Implications of measurement of eye fixations for a
psychophysics of form perception.
13 p1577 A73-28092
Apparent motion of stimuli presented stroboscopically
during pursuit movement of the eye.
13 p1577 A73-28093
Monocular fixation tests and prediction model for
time course of aftereffect of eye turn on autokinetic il-
lusion direction
13 p1578 A73-28098
Scalar perceptions with binocular cues of distance.
13 p1578 A73-28176
New method of stimulation for the study of pho-
toreceptors.
13 p1578 A73-28362
Eye movements during visual search and memory
search.
13 p1579 A73-29125
Saccadic eye movement control system, investigat-
ing response characteristics to variously timed pulse
stimuli
14 p1716 A73-30389
Accuracy of saccadic eye movements and main-
tenance of eccentric eye positions in the dark.
14 p1716 A73-30390
Accommodation of the eye during sleep and
anesthesia.
14 p1716 A73-30391
Voluntary small saccadic eye movements in
presence of stationary visible target, considering
scanning function of fixation saccades
14 p1717 A73-30394
Normal fixation of eccentric targets.
15 p1837 A73-31018
Asymmetry of otolith responses in fish
15 p1834 A73-31507
Russian book - Methods of studying eye move-
ments.
15 p1840 A73-32417
Residual visual function after brain wounds involv-
ing the central visual pathways in man.
16 p1975 A73-33218
Temporal factors of movements in visual af-
tereffects
17 p2115 A73-34843
Movement perception during voluntary saccadic
eye movements.
17 p2112 A73-34845
Stabilized target visibility as a function of contrast
and flicker frequency.
17 p2112 A73-34846
The effect of colour on time delays in the human
oculomotor system.
17 p2112 A73-34847
Influence of stimulus symmetry on visual scanning
patterns.
17 p2118 A73-35494
- Cerebral control of eye movements and motion per-
ception; Proceedings of the Symposium, Freiburg im
Breisgau, West Germany, July 20-22, 1971.
18 p2271 A73-36432
The behavior of eye movement motoneurons in the
alert monkey.
18 p2271 A73-36433
Unit activity in the brainstem related to eye move-
ment - Possible inputs to the motor nuclei.
18 p2271 A73-36434
Supranuclear connections to oculomotor nuclei in
terms of stimulus relation to eye movements
18 p2271 A73-36435
Pontine reticular formation as origin of neural
mechanism generating saccades and nystagmus quick
phases in horizontal plane, investigating effects of
various brain lesions
18 p2271 A73-36436
Vestibular and cerebellar control of oculomotor
functions.
18 p2271 A73-36438
Cholinergic activation of vestibular neurones lead-
ing to rapid eye movements in the mesencephalic cat.
18 p2272 A73-36439
Vestibular and spinal control of eye movements.
18 p2272 A73-36440
Some functional characteristics of the superior col-
liculus of the Rhesus monkey.
18 p2272 A73-36442
Optomotor integration in the colliculus superior of
the cat.
18 p2272 A73-36443
The role of the superior colliculus in visually-
evoked eye movements.
18 p2272 A73-36445
Frontal eye-field lesions in monkeys.
18 p2272 A73-36446
Cerebellar ablations and spontaneous eye move-
ments in monkey.
18 p2272 A73-36447
Brain stem reticular formation influence on lateral
geniculate body neurons during eye movements, sug-
gesting cortical oculomotor impulse influence media-
tion by perigeniculate nucleus
18 p2272 A73-36448
Saccade correlated events in the lateral geniculate
body.
18 p2272 A73-36449
Neurophysiological correlates of eye movements in
the visual cortex.
18 p2272 A73-36450
Supranuclear structures regulating binocular eye
and head movements.
18 p2272 A73-36451
Central programming and peripheral feedback dur-
ing eye-head coordination in monkeys.
18 p2273 A73-36452
The control of eye movements in the saccadic
system.
18 p2273 A73-36453
Rabbit optokinetic reactions and retinal direction-
selective cells /A preliminary model/.
18 p2273 A73-36455
Investigations of the eye tracking system through
stabilized retinal images.
18 p2273 A73-36456
Eye movements necessary for continuous percep-
tion during stabilization of retinal images.
18 p2273 A73-36461
Scanning movements in space perception in terms
of convergence role during cue conflict and cue isola-
tion experiments
18 p2274 A73-36462
Visual perception of direction and voluntary sac-
cadic eye movements.
18 p2274 A73-36463
Involuntary eye movements in the presence and
absence of points
18 p2276 A73-36568
Gaze-positioning eye movement perturbations dur-
ing somnolence states
18 p2280 A73-36950
The interaction between horizontal and vertical eye-
rotations in tracking tasks.
19 p2394 A73-37417
Cockpit layout effects on pilot and flight crew ac-
tivities, using in-flight observation, photography and
pilot eye movement evaluation
19 p2384 A73-37733
Human miniature eye movement relationship to
visibility and saccades position-correcting reflex func-
tion and suppression
21 p2637 A73-40411
The oculometer - A new approach to flight manage-
ment research.
[AIAA PAPER 73-914]
21 p2702 A73-40862
Effect of eye movements on backward masking and
perceived location.
21 p2639 A73-41184
Visual search, complex backgrounds, mental coun-
ters, and eye movements.
21 p2639 A73-41185

Individual and simultaneous tracking of a step input by the horizontal saccadic eye movement and manual control systems.

22 p2811 A73-41735

Visual perception of relative object dimension during monocular and binocular rod equalization experiment in various visual field restriction conditions, recording eye movements and focusing characteristics

22 p2812 A73-41890

Recognition of component differences in two-dimensional oculomotor tracking tasks.

22 p2810 A73-42959

Signal and noise in the human oculomotor system.

22 p2810 A73-42964

Eye movements of trained inspectors recorded during visual inspection of colored slides of IC chips, determining performance with emphasis on speed

23 p2947 A73-43212

Visual evoked potentials to changes in the motion of a patterned field.

24 p3061 A73-45167

EYE PROTECTION

Retinal damage thresholds for multiple pulse lasers. [AD-758530]

11 p1315 A73-25341

Retinal damage from repeated subthreshold exposures using a ruby laser photocoagulator.

13 p1576 A73-28508

Analysis of multiwavelength observations of optical scintillation.

17 p2212 A73-35418

Laser hazards and safety performance standards, discussing ocular and skin damage and exposure limits and operational regulation

20 p2517 A73-39205

EYEPIECES

A proposed standard mechanical interface for Cassegrain acquisition-guider heads.

01 p0029 A73-10546

F

F CENTERS

U COLOR CENTERS

F DISPLAYS

U F REGION

F LAYER

U F REGION

F REGION

NT F1 REGION

NT F2 REGION

Off-path transequatorial propagation in decametric waves. II - Application to the study by diffusion of ionospheric irregularities

01 p0017 A73-10334

Infrasound in the ionosphere generated by severe thunderstorms.

01 p0040 A73-10826

Ionic reaction mechanism for F region nitrogen vibrational temperature, using positive ion composition

01 p0042 A73-10894

Processes leading to 6300 Å radiation during determinations of O(1D) quenching by nitrogen and oxygen molecules in F region, using model of neutral atmosphere composition

[AD-754996]

02 p0156 A73-11742

Revised calculations of F region ambient electron heating by photoelectrons.

02 p0157 A73-11751

Molecular nitrogen vibrational temperature in E and F regions, using positive ion data and model for ionic reaction rate and continuity equation numerical solution

02 p0161 A73-12279

Incoherent scatter observations of meridional winds in the 150-225 km region.

02 p0161 A73-12283

Observation and interpretation of ionization drift measurements in the F region at St-Santin-Nancay.

02 p0161 A73-12284

E region electromagnetic east-west drift velocity measurement at magnetic equator by incoherent scatter radar

02 p0161 A73-12285

Features of the ionospheric drift over the magnetic equator.

02 p0162 A73-12287

Effects of vertical mass motions on the composition structure in the thermosphere.

02 p0162 A73-12291

Statistical properties of traveling ionospheric disturbances in F region from phase height and angle of arrival data

02 p0162 A73-12296

Interaction between gravity waves and ionization in the ionospheric F region.

02 p0162 A73-12298

The standard profile of the mid-latitude F region of the ionosphere as deduced from bottomside and topside ionograms.

02 p0163 A73-12301

Rocket sounding of ionospheric electron density and temperature profiles during moderate auroral event, noting field-aligned motion of irregularities in F region

02 p0163 A73-12309

Electron density fluctuations during periods of scattered reflections at the ionospheric F-region maximum ionization level

02 p0164 A73-12359

Wavelike structure of magnetic field-aligned irregularities detected by phase interferometry.

03 p0300 A73-13696

On the effect of the vertical drift in the equatorial F region.

04 p0443 A73-15476

Equatorward shift of the polar F layer irregularity zone as a function of the Kp index.

04 p0445 A73-15557

Unisolar tidal effects and motions in the F region

05 p0568 A73-16255

Temperature fluctuations in the ionospheric F region

05 p0568 A73-16256

Electron density increase in the F region after proton bursts

05 p0609 A73-16257

Lower F region ionospheric wave dispersion observation for horizontal phase and group velocities relationship to period, considering interpretation by internal gravity wave hypothesis

05 p0552 A73-17056

Vertical profiles of the effective collision number in the E and F regions of the ionosphere

06 p0689 A73-17552

Vertical distribution of electron concentration in the Northern Hemisphere at the geomagnetic pole /from top-side and ground-based ionospheric sounding data/

06 p0689 A73-17554

Two-beam observations of ionospheric irregularity structure and velocity at Arecibo.

07 p0791 A73-19379

Global electron concentration disturbances in low and middle latitude F2 during magnetic storm

07 p0815 A73-19435

Dipolar coordinate system for geomagnetic field dipole approximation in studies of diffusion and heat conduction in F region and outer ionosphere

07 p0816 A73-19452

Coupling between the F-region and protonosphere - Numerical solution of the time-dependent equations.

07 p0818 A73-19665

Ionospheric winds in the F-region and their effects on the limiting periods of gravity waves.

07 p0818 A73-19673

Theoretical vertical profiles of minor ions at the Equator.

07 p0819 A73-20053

Ogo 6 measurements of supercooled plasma in the equatorial exosphere.

09 p1074 A73-22066

Experimental observations of the amplitudes of Es and F-region reflections and their comparison with the thin-layer model for Es.

09 p1076 A73-22138

Some effects of the equatorial ionosphere on terrestrial HF radiocommunication.

09 p1051 A73-22500

Effect of excited states of atomic oxygen ions on the reaction rates and thermal balance in the F-region.

09 p1078 A73-22832

Ion composition in the E- and lower F-region above Kiruna during sunset and sunrise.

09 p1078 A73-22838

Multistatic incoherent scatter measurements of ionospheric drift velocity.

10 p1188 A73-24274

Ogo 6 retarding potential analyzer observation of vertical and longitudinal gradients in ion concentrations below F region peak near magnetic equator

10 p1214 A73-24738

Empirical model for F layer electron density irregularities responsible for VHF/UHF amplitude scintillation, considering geomagnetic latitude, local time, season and sunspot effects

10 p1190 A73-24895

Prenoon anomaly of ionization in the F region at the transition latitudes

11 p1350 A73-25090

Statistical characteristics of E and F regions maximum electron density and ionization height, discussing electron content in vertical unit column in upper and lower ionosphere

11 p1351 A73-25092

Autocorrelation and cross correlation coefficients for maximum electron densities and total electron content in E and F regions and upper and lower ionosphere

11 p1351 A73-25093

Results of an investigation of the ionospheric effect of a sudden commencement of a magnetic storm

11 p1351 A73-25097

Disturbances observation in E-F region and sporadic E layer by vertical ionospheric sounding during IQSY

11 p1351 A73-25098

Aeros meteorological research satellite for F region aeronomic parameters and solar UV radiation measurements, discussing performance since launch

11 p1430 A73-25442

The causes of storm-time increases of the F-layer at mid-latitudes.

11 p1353 A73-25751

Structure at the poleward edge of a mid-latitude F-region trough.

11 p1353 A73-25756

Small scale loop structuring of F region ionogram traces due to HF ray propagation through irregularities

11 p1354 A73-25766

A diffusion model for the electron density distribution along the earth's magnetic field in an F-region plasma cloud.

11 p1354 A73-25768

The day-sector polar F-layer during a magnetospheric substorm.

11 p1356 A73-25918

Physics and chemistry of upper atmospheres.

11 p1425 A73-26209

The nature of seasonal changes in the effects of magnetic storms on mid-latitude F-layer electron concentration.

11 p1358 A73-26708

Magnetic control of near equatorial neutral thermosphere, calculating F region ionization anomaly and molecular nitrogen and atomic oxygen density latitudinal variations

12 p1489 A73-26997

Correspondence of main trough ion temperatures with horizontal drift speed.

12 p1489 A73-27006

Dynamic model of the interaction between the F region of the ionosphere and the plasmosphere

12 p1490 A73-27335

Influence of a variable ionospheric-protonospheric plasma flow on the nighttime F region of the ionosphere

12 p1490 A73-27336

Midlatitudinal standard ionospheric profile to construct F-region noon electron density profiles and thermal response to solar activity changes

12 p1493 A73-27761

Studies of the equatorial anomaly in the F region and outer ionosphere with the aid of spherical ion traps

14 p1746 A73-29860

Seasonal and sunspot cycle variations of F region electron temperatures and protonospheric heat fluxes.

14 p1749 A73-29986

Millstone Hill Thomson scatter results for 1966 and 1967.

15 p1866 A73-31067

Equatorial spread-F irregularities observed at Nairobi and on the transequatorial path Lindau-Tsumeb.

15 p1870 A73-31765

Signal fading and topside electron density profile observation over VHF transequatorial path between Europe and Southern Africa, noting great circle F transmission role

15 p1844 A73-31766

Ion and electron diffusion in nonisothermal ionospheric F layer, analyzing ionization balance equations

15 p1871 A73-31882

Vertical profiles of the effective collision frequency in the E- and F-regions of the ionosphere.

16 p2002 A73-32776

Vertical electron density distribution at the geomagnetic pole in the Northern Hemisphere /from data of topside and ground-based soundings of the ionosphere/.

16 p2002 A73-32778

F region neutral wind profiles and electron densities measured at midlatitude station during equinox months for medium sunspot year

16 p2009 A73-33888

Atomic nitrogen ion density measurements for loss rate coefficient of N+ reaction with oxygen at 150-220 km

16 p2009 A73-33892

Proton whistlers in the ionospheric F-region over the South American equatorial area.

18 p2304 A73-35970

Neutral winds in the F-region obtained from new models of density and temperature.

18 p2309 A73-36056

Thermospheric observations combining chemical seeding and ground-based techniques. II - Ionospheric drifts and the Sq current system.

18 p2311 A73-36186

Distortions of the nightside ionosphere during magnetospheric substorms.

18 p2312 A73-36279

F-layer and 6300-Å measurements in the day sector of the auroral oval.

18 p2312 A73-36281

Arbitrary propagation of HM waves along the F region.

18 p2312 A73-36285

Energy transport by photoelectrons in the early morning ionosphere.

18 p2348 A73-37027

A phenomenological model of global ionospheric electron density in the E-, F1- and F2-regions. 19 p2425 A73-38014

Vertical sounding investigation of ionospheric ionization inhomogeneity sizes, orientation, elongation degree and drift rate, determining F region electron density fluctuations 20 p2553 A73-39155

Diurnal variations in the drift velocity and direction of the ionization inhomogeneities in the F layer 20 p2554 A73-39161

Effective altitudes of the F region in the IGY and IQSY periods 20 p2554 A73-39167

Gravity waves in the F region of the ionosphere 20 p2554 A73-39173

Stratifications in the F region of the ionosphere 20 p2554 A73-39174

Magnetic equatorial ionospheric characteristics, discussing E and F regions, diurnal drift variations, field strength, equatorial electrojet, spread F and sporadic E 20 p2555 A73-39633

Method of studying magnetic-ionospheric disturbances and solar flare effects on long-upset periods. 20 p2555 A73-39767

Interpretation of the results of drift measurements by the space diversity reception method 20 p2555 A73-39819

Midlatitude F 2 layer critical frequency fluctuations as ionosphere disturbance criteria during magnetically quiet days 21 p2681 A73-40104

Measurement of the dispersion of waves in the ionosphere. 21 p2682 A73-40232

Maintenance of the F-region at night - Incoherent scatter measurements at a mid-latitude station. 21 p2683 A73-40776

Midlatitude spread F relationship to F region trough formation, considering multiple reflections emanating from steep ionization contours 21 p2684 A73-40784

Temperature dependence for dissociative recombination of NO+/- in E- and F-region models. 21 p2684 A73-40787

Dependence of high-energy electron fluxes at an altitude of 200 to 300 km on threshold rigidity 21 p2686 A73-40917

Ionospheric research by rocket, satellite and ground based methods, discussing ion and neutral chemistry, stratospheric-ionospheric coupling, ionospheric thermal structure, etc 21 p2689 A73-41358

Seasonal variation of atmospheric composition in the F region as a function of solar activity. 21 p2690 A73-41360

F region disturbances in wake of burnt-out Black Brant rocket body, discussing electron depletion from ground based Digisonde 21 p2690 A73-41363

A current mechanism for the formation of inhomogeneities resulting in the ionospheric spread F region at high latitudes 21 p2692 A73-41508

The combined use of satellite differential Doppler and ground-based measurements for ionospheric studies. 22 p2843 A73-41837

Periodically structured Pc 1 micropulsations during the recovery phase of intense magnetic storms. 22 p2844 A73-41913

Radio source signal scintillation correlation with high power HF transmitter caused F region electron density fluctuations 22 p2825 A73-41920

A nonstationary model of charged-particle diffusion in a gravitational field 22 p2902 A73-41955

E and F regions nitrogen vibration energy content by numerical integration of time dependent species continuity equation and species equation of motion 22 p2848 A73-42537

Ionospheric electron density profiles and contour plots above F layer maximum from vertical sounding and Faraday rotation techniques 22 p2851 A73-42984

Dynamic model of interaction of the F-region of the ionosphere with the plasmasphere. 23 p2970 A73-43233

Effect of changing ionospheric-protonospheric plasma flow on the nighttime F-region of the ionosphere. 23 p2970 A73-43234

On the large scale vertical movements of the F-layer and its effects on the total electron content over low latitude during the magnetic storm of 25 May 1967. 23 p2972 A73-43699

Effect of neutral winds on ionospheric F-region at a pair of conjugate stations in low latitude. 24 p3082 A73-44729

The behaviour of the upper ionosphere over North America at sunset. 24 p3087 A73-45203

E and F layers, discussing formation, collision processes and S and L geomagnetic variations 24 p3087 A73-45204

Nighttime meridional neutral winds near 350 km at low to mid-latitudes. 24 p3087 A73-45209

ISIS 2 scanning photometric analysis of E and F region airglow at O I 5577 A, noting height difference of airglow components at midlatitudes and near equator 24 p3088 A73-45214

F 1 REGION

Diurnal and seasonal variations in conditions for the occurrence of the F 1 layer over Middle Asia during the IQSY period 05 p0569 A73-16615

Estimation of the seasonal variation of the gas composition of the atmosphere at the height of the F1 layer from data on the developmental conditions of the layer 08 p0958 A73-21281

Study on the electron density profile in the F1 region. 08 p0961 A73-21653

Ambipolar diffusion in the F1-region of the ionosphere. 11 p1357 A73-25928

Estimation of the seasonal variation of the gas composition of the height of the F1-layer from data on the conditions of its development. 19 p2424 A73-37910

Latitudinal distribution change in the conditions for F1 layer occurrence from the solar-activity maximum to minimum 20 p2554 A73-39170

F 2 REGION

Geomagnetic control over evolution of F2-layer at sunrise. 02 p0159 A73-12183

Horizontal and vertical drift motions in F 2 region caused by electrostatic and geomagnetic fields 02 p0162 A73-12294

Spatial variations in F2 layer critical frequencies 05 p0568 A73-16258

Role of the sporadic E layer in short radio wave propagation at frequencies exceeding the maximum usable frequencies of the F2 layer 05 p0548 A73-16264

Estimating the accuracy of longitudinal interpolation of foF2 from shipboard observations 08 p0959 A73-21301

The standard electron density profile of the F2-layer at noon. 09 p1078 A73-22746

Equatorial anomaly in the F2 layer during local noon and the IGY and IQSY periods 11 p1350 A73-25089

Spatial correlation of the critical frequencies of the F2 layer on the basis of data from stationary mid-latitude stations 11 p1351 A73-25091

Forecast maps for seasonal variations in the geometrical parameters of the F2 layer 11 p1351 A73-25094

ISIS-1 satellite observations of the ionosphere at high southern latitudes. 11 p1353 A73-25753

A theoretical study of lunar variations in foF2 at low latitude. 11 p1354 A73-25764

A theoretical study of the ionospheric F region equatorial anomaly. I - Theory. II - Results in the American and Asian sectors. 11 p1356 A73-25919

Analytical model of the unsteady nighttime F2 region of the ionosphere at mid-latitudes. 12 p1490 A73-27337

F 2 layer characteristics forecasts by extrapolation of critical F 2 frequency data from Moscow, Sverdlovsk, Irkutsk, Alma-Ata and Salekhard 12 p1490 A73-27338

Determination of the effect of electric fields on the ionosphere, based on the behavior of the F2-layer above geomagnetically conjugate points 12 p1493 A73-27760

Shimazaki formula corrected for F 2 layer altitude estimation for 2-30 MHz field intensity and transmission losses calculations 12 p1493 A73-27762

Asymmetrical model for F 2 critical frequency variability analysis to determine dimensions and effective number of large scale ionospheric electron density inhomogeneities 13 p1608 A73-28707

Variations of the global values of F2-layer thickness and the parameters of the neutral atmosphere. 13 p1608 A73-28722

Numerical study of the seasonal variations of the ionosphere. 15 p1867 A73-31381

The relationship between the structure of the equatorial anomaly and the strength of the equatorial electrojet. 15 p1869 A73-31761

Semi-annual variation in the true height of the F2-peak in low latitudes /at Puerto Rico/. 15 p1869 A73-31762

The low-latitude and equatorial outer ionosphere during the magnetic storm of January 2-4, 1964 15 p1871 A73-31881

F 2 critical frequency and maximum height at high southern latitudes explained via additional ionization provided by energetic particles 16 p2009 A73-33911

The behaviour of the topside ionosphere during magnetically disturbed conditions. 16 p2010 A73-33912

Enhancements of the electron concentration in the F2-layer at magnetic noon. 16 p2010 A73-33914

Atmospheric composition changes and the F2-layer seasonal anomaly. 16 p2010 A73-33915

Ionospheric response to internal gravity waves observed at Delhi. 16 p2010 A73-33919

Neutral wind velocities calculated from temperature measurements during a magnetic storm and the observed ionospheric effects. 18 p2311 A73-36150

Evaluation of the accuracy of longitudinal interpolation of foF2 based on ship observations. 19 p2425 A73-37930

Mapping of foF2 by means of topside sounder satellites. 19 p2427 A73-38285

The determination of foF2 and hmF2 from satellite-borne probe data. 19 p2427 A73-38286

Height distribution of O+ and H+ ions in the ionosphere F2 region. I 19 p2427 A73-38333

TD 1 A astronomical satellite detection of UV dayglow emissions above F 2 peak in equatorial zone, considering Mg ions resonance scattering to account for emission features 20 p2551 A73-38940

Latitude distribution of the regularity in F2-region irregularities. 20 p2553 A73-39132

Correlation of variations in the horizontal component of the geomagnetic field with drift in the ionosphere 20 p2553 A73-39154

Drift velocity measurements for small-scale inhomogeneities at various levels of the F2 layer 20 p2553 A73-39158

Statistical characteristics of the diurnal drift velocity variations in the F2 layer 20 p2554 A73-39160

Altitude distribution of the drift velocity and direction of ionosphere inhomogeneities over Ashkhabad in years of maximum and minimum solar activity 20 p2554 A73-39162

Application of mathematical methods for the description of the planetary distribution of ionosphere parameters 20 p2554 A73-39169

Midlatitude ionospheric disturbances 20 p2554 A73-39172

Correlational relations between F2 critical frequency deviations and the solar activity cycle according to a number of high-latitude stations 20 p2555 A73-39176

Altitude dependence of F 2 layer electron density annual anomaly, discussing summer-winter density discrepancies and noontime critical frequencies 20 p2555 A73-39177

Functional relation between the F2-layer ionization state in daylight time and the zenith angle of the sun 20 p2555 A73-39178

Variations in the M/3000/F2 coefficient as a function of the solar energy entering the earth's atmosphere 20 p2555 A73-39179

Neutral air wind influences deduced from solar cycle changes in the F2 region equatorial anomaly. 21 p2679 A73-39932

Location in magnetic latitude and local time of the tropical ultraviolet bands seen from Apollo 16. 21 p2684 A73-40788

Analytical model of the nocturnal nonstationary F2-region of the ionosphere at middle latitudes. 23 p2970 A73-43235

F 2 layer characteristics forecasts by extrapolation of critical F 2 frequency data from Moscow, Sverdlovsk, Irkutsk, Alma-Ata and Salekhard 23 p2970 A73-43236

F 2 region critical frequency variations during geomagnetic storms, noting correlation with main phase onset 24 p3082 A73-44728

Vertical and latitudinal development of a seasonal anomaly in the daytime F2 region. I 24 p3083 A73-44791

Relationship of the sporadic F2 layer with certain features of the ionosphere and magnetosphere at subauroral latitudes 24 p3083 A73-44792

- Critical frequency evolution during F 2 region storms at middle and low latitudes, showing random global patterns and relation to neutral wind flow
24 p3087 A73-45205
- F-80 AIRCRAFT**
U T-33 AIRCRAFT
- F-4 AIRCRAFT**
Critical skills and procedures isolation within replacement air group/RAG/ training for F-4 pilot performance prediction
05 p0544 A73-16723
Identifying pilot error potential in the F-4 aircraft.
05 p0545 A73-16731
Toward the development of a criterion for fleet effectiveness in the F-4 fighter community.
13 p1579 A73-28512
Visual cues and six degree of freedom motion flight simulation for F-4 aircraft energy maneuvering performance, discussing pilot evaluations
[AIAA PAPER 73-934] 21 p2674 A73-40880
- F-8 AIRCRAFT**
F-8 digital fly by wire control system development and flight testing, using Apollo lunar guidance computer and inertial measurement unit for angular rates and accelerations
09 p1030 A73-22180
Surface effect take-off and landing system for high performance aircraft.
19 p2382 A73-37695
Fly-by-wire digital F-8C aircraft control system using Apollo guidance, navigation and control hardware, emphasizing interface design and fault detection
21 p2733 A73-40027
- F-110 AIRCRAFT**
U F-4 AIRCRAFT
- F-14 AIRCRAFT**
F-14 aircraft boron-epoxy and graphite-epoxy composite structure production protection against degradation by lightning discharges, discussing design, processing and tests
16 p2028 A73-33035
F-14 replacement for Phantom aircraft for escort missions, fleet defence, interdiction and close support, discussing airborne refuelling capability and composite materials applications
24 p3056 A73-44695
- F-15 AIRCRAFT**
C-5 program developments and alterations in terms of defense requirements and cost problems, discussing objectives and management policies in F-15 and B-1 projects
01 p0124 A73-11069
F-15 air superiority fighter aircraft flight testing, describing air inlet, flight control, landing gear, flaps, speed brake and cockpit layout
09 p1030 A73-22178
F-15 fighter aircraft development, discussing design and functional features of power plant, flight control system, landing gear, flaps, speed brakes and cockpit
09 p1031 A73-22198
Pressure measurements for establishing inlet/engine compatibility.
17 p2221 A73-34609
Evaluation of F-15 inlet dynamic distortion.
[AIAA PAPER 73-784] 19 p2379 A73-37454
- F-111 AIRCRAFT**
Concept and conduct of proof test of F-111 production aircraft.
03 p0317 A73-14467
- FAB [PROGRAMMING LANGUAGE]**
U FORTRAN
- FABRICATION**
NT SPACE MANUFACTURING
Fabrication of porous tungsten foils for contact ionization of cesium
[ONERA, TP NO. 1113] 01 p0055 A73-10234
Twisted, multifilament Nb₃Sn superconductive ribbon.
01 p0087 A73-10245
Flying-spot scanned or computer controlled electron beam fabrication system for generating high packing density pattern of LSI microelectronic circuit components
01 p0023 A73-10548
Spiral wrap - A technique for fabricating thick-wall carbon composites.
01 p0057 A73-11294
Josephson tunnel junction fabrication technology evaluation in terms of electrode materials, native oxide and artificial barriers, noting factors affecting stability and I-V characteristics
02 p0200 A73-11846
Uniform junction microwave transistor fabrication by automatically controlled diffusion technique, using low temperature phosphosilicate glass films on silicon wafers
02 p0147 A73-12164
Rocket nozzles fabrication technology, discussing construction materials and manufacturing processes
[AIAA PAPER 72-1191] 03 p0358 A73-13481
Preparations and properties of boron and silicon carbide filaments
03 p0334 A73-13588

- Operation, fabrication, characterization, I-V performance and application of transient voltage suppressor using metal oxide varistor
03 p0283 A73-13941
Tables summarizing Si solar cell fabrication parameters, complex design evolution and performance achievement
03 p0254 A73-14204
Heat resistant Ni and Cr alloys powder metallurgy, discussing inert and solute gas atomization, rotating electrode and gatorizing processes for powder fabrication
04 p0461 A73-15023
Raney-Ni catalysts preparation for carbon-PTFE fuel cell electrodes from Ni-Al alloy, discussing rolling technique suitability and electrode characteristics
04 p0407 A73-15115
Synthesis and fabrication of high purity hafnium nitride and hafnium carbide.
04 p0455 A73-15752
Electron beam fabrication of submicrometer diameter mixer diodes for millimeter and submillimeter wavelengths.
05 p0559 A73-16811
Industrial manufacturing of stratospheric balloons.
07 p0829 A73-18998
Semiconductor radiation detectors fabrication methods, discussing p-n junctions diffusion and ion implantation techniques and surface barrier, dE/dx, chessboard and rod type counters
07 p0822 A73-19172
Structural fabrication of advanced metal-matrix composites.
[SME PAPER EM 72-108] 07 p0832 A73-20449
Microstrip transmission line microwave IC, discussing electrical characteristics, dielectric and conductor materials, photo-etching processes, connection fabrication and circuit encapsulation
08 p0942 A73-20702
IC reliability enhancement by molded dual in-line packaging (DIP) technique, considering mold shrinkage effects on failure rates during temperature cycling tests
08 p0944 A73-20737
Welding and fabrication of non-ferrous metals; Proceedings of the International Conference, Eastbourne, Sussex, England, May 2, 3, 1972, Volume 1.
08 p0973 A73-21235
Mechanical behaviour of unidirectionally solidified composites.
[ONERA, TP NO. 1147] 08 p0983 A73-21676
Aircraft structural components in-house or subcontracted fabrication, discussing technical performance, economic and manpower aspects
10 p1297 A73-23521
Microwave characteristics of ion-implanted bipolar transistors.
10 p1194 A73-24156
Steel wire, boron or carbon filament reinforced Al alloys shaped parts fabrication, discussing sintering, pressure impregnation and filament winding processes
11 p1373 A73-25415
Light-weight Al isogrid panel design with triangular reinforcement elements for aerospace structural applications, discussing load response characteristics, fabrication and cost reduction
13 p1624 A73-28906
Heterojunction laser diode fabrication procedures operation and details, considering peak power levels, wavelengths and operating temperatures for CW and pulsed operations
14 p1736 A73-30575
Transage 129 Ti-Al-V-Sn-Zr alloy fabrication cost reduction through good cold formability and weldability with weight saving due to high strength and fatigue resistance
15 p1891 A73-32172
Book - MOS integrated circuits: Theory, fabrication, design and systems applications of MOS LSI.
15 p1852 A73-32579
Utilization of realization to optimize the choices of reliability from the economic point of view
16 p2088 A73-33270
Braided honeycomb structure design, fabrication and aerospace applications covering brazing methods, filler metal selection, nondestructive testing, sandwich designs, aircraft and spacecraft structures, etc
17 p2177 A73-34100
Rigid lightweight honeycomb core radome development from materials and processes standpoint, discussing cost reduction and fabrication
[SAE PAPER 730310] 17 p2177 A73-34670
C band low noise IC microwave amplifier for phased array module in multiple access communication links, discussing photofabrication for low cost batch processing
17 p2135 A73-34727
Physical and chemical analysis of germanium tunnel diodes.
17 p2219 A73-34865
Low loss light guiding polymer thin film with continuously adjustable refractivity, discussing fabrication and refractivity and scattering loss measurements
17 p2172 A73-35423

- Preparation and RF properties of MIS mesa varactors.
19 p2409 A73-37720
Book - RCA COS/MOS technology.
20 p2533 A73-38653
Fundamentals of COS/MOS integrated circuits.
20 p2534 A73-38655
Injection-modulation devices as elements of integrated circuits
20 p2534 A73-38855
Selection of conditions for the fabrication of planar n-p-n silicon transistors with the application of the ion-beam alloying method
20 p2535 A73-38858
Fabrication methods for beryllium spacecraft components.
20 p2615 A73-39775
Morphological indices of digital microelectronic structures
21 p2660 A73-40016
A bilevel thin film hybrid circuit containing cross-overs, resistors, capacitors, and integrated circuits.
21 p2669 A73-40773
Material preparation and fabrication techniques for the production of high reliability thermocouple devices.
22 p2858 A73-42040
High temperature core thermocouple development for the Nuclear Rocket Engine Program (Rover).
22 p2885 A73-42047
The design, fabrication, and evaluation of a silicon junction field-effect photodetector.
23 p2981 A73-43453
V groove MOS transistor fabrication by preferential silicon etching and masking process with noncritical alignment tolerances
23 p2960 A73-44115
Diffusion treatment of CdS and ZnO crystals and their applications in microwave acoustics.
24 p3120 A73-45433
- FABRICS**
NT DACRON [TRADEMARK]
NT FELTS
NT GAUZE
NT PARACHUTE FABRICS
Attempts at using fiberglass cloth as skin for aircraft
02 p0185 A73-12450
Advances in glass fiber fabrics for plastic reinforcement.
03 p0330 A73-13014
Influence of aging on the mechanical properties of polyester glass-resin laminated fabrics
03 p0334 A73-13591
Thermal analysis of combustion of fabric in oxygen-enriched atmospheres.
[ASME PAPER 72-WA/HT-22] 04 p0519 A73-15832
Fire retardance of mixtures of inert gases and oxygen.
09 p1045 A73-22532
Asbestos-textolite coating required thickness calculation with allowance for aerodynamic heating, discussing softening mechanisms
09 p1110 A73-23057
Recent developments in commercial fire resistant fibrous materials.
11 p1389 A73-26419
Relationship between structure and strength for CVD carbon infiltrated substrates. III - Fabric lay-up substrates.
13 p1645 A73-29272
Bending vibration test of glass-textolites, noting temperature effect on vibration damping properties
13 p1647 A73-29607
Effect of lasting high temperatures on the mechanical properties and microstructure of bonded glass mat with an aluminophosphate binder
15 p1896 A73-31213
High strength fiber woven cloth materials for inflatable structure, discussing characteristics assembly methods and tests
[AIAA PAPER 73-448] 15 p1826 A73-31434
Bioassay method for thermal protective clothing fabrics evaluation, measuring skin damage with various fabric combinations under exposure to calibrated flame source
16 p1974 A73-32671
High modulus graphite fabrics production processes for applications in composite aerospace materials reinforcement, discussing winding, creeling, sizing, drawing, reeling and weaving
17 p2182 A73-35840
Feasibility study of skirt configurations and materials for an ACLS aircraft.
19 p2443 A73-37696
- FABRY-PEROT INTERFEROMETERS**
High-repetition-rate optical pulse generator using a Fabry-Perot electro-optic modulator.
01 p0058 A73-10127
High resolution apparatus at the focus of large telescopes
01 p0049 A73-10532
Improved mount and alignment procedures for a rapid-scan Fabry-Perot interferometer.
06 p0691 A73-17498

Experimental verification and assessment of an infra-red radiation modulator based on a Fabry-Perot etalon. 07 p0825 A73-20373

Block defocused spherical Fabry-Perot interferometer. 08 p0964 A73-21038

The use of solid etalon devices as narrow band interference filters. 08 p0970 A73-21736

A tunable laser based on an organic dye solution and providing highly monochromatic, stable single-frequency emission 09 p1097 A73-23010

Interferometric investigations of the A21 nebula (YM29, Medusa) 10 p1273 A73-23704

Fabry-Perot interferometer with etalon for studying gas movements and planetary nebulae in Large Magellanic Cloud by spectral analysis from pressure scanning 11 p1361 A73-25176

Use of the Fabry-Perot etalon to study absorption spectra of the atmosphere 11 p1363 A73-25613

Lowest-order mode selection in a laser interferometer. 12 p1504 A73-26842

Interferometry of the Medusa nebula A21 /YM 29/. 18 p2354 A73-36729

Interference phenomena obtained by replacing the mirrors of a Michelson interferometer by Fabry-Perot couples 19 p2429 A73-37540

A mechanically scanned interferometer-echelle spectrometer for the middle ultraviolet. 21 p2692 A73-39924

Submillimeter wave spectroscopy with a vacuum Fabry-Perot interferometer 22 p2852 A73-41782

Interference filters for the VUV /1200-1900 A/. 22 p2863 A73-43142

Fabry-Perot etalon with evaporated Schott glass as a spacer-layer. 22 p2863 A73-43143

FABRY-PEROT LASERS
U LASERS

FABRY-PEROT SPECTROMETERS
Long slit spectrographs /Focal reducers - Fabry-Perot spectrographs - Array spectrographs/ 01 p0049 A73-10535

Nebular Fabry-Perot, Pepsios, and Sisam monochromators. 08 p0964 A73-21039

A Fabry-Perot acoustic surface vibration detector-application to acoustic holography. 13 p1622 A73-29422

Data acquisition technique for Fabry-Perot spectroscopy, noting application to Brillouin spectra recording of solid Ne 17 p2171 A73-35403

FACE [ANATOMY]
NT NOSE [ANATOMY]

FACE CENTERED CUBIC LATTICES
Use of a plastic deformation design model of polycrystalline material in the analysis of loading surface transformation 01 p0112 A73-10008

Amorphous magnetism in F.C.C. Vicalloy II. 01 p0087 A73-10242

Activity of carbon and solubility of carbides in the fcc Fe-Mo-C, Fe-Cr-C, and Fe-V-C alloys. 02 p0183 A73-12755

Pseudo-subgrain-boundaries in stainless steel. 04 p0461 A73-14872

Creep characteristics and substructure disorientation in metals with an fcc lattice 06 p0706 A73-17904

Thermodynamic stability of ordered phase atomic structure state for antiphase domain formation, noting superstructures in face centered and body centered cubic solutions 06 p0736 A73-18118

The dependence of the notch sensitivity of Waspaloy at 1000-1400 deg F on the gamma prime phase. 08 p0979 A73-21571

[ASME PAPER 72-MAT-J] Mechanisms of transient and steady state creep in a gamma-prime hardened austenitic steel. 08 p0980 A73-21778

Metal fcc polycrystals macroscopic plasticity theory based on discrete aggregate model, predicting stress-strain curves for partial load cycles 09 p1160 A73-22896

Fine precipitate within coarse gamma-prime particles in cast Ni-base superalloy during elevated temperature exposure 10 p1235 A73-24446

Fatigue damage and dislocation structures in fcc metals surface layers, noting microcrack formation conditions 11 p1380 A73-25805

Bivariant eutectic alloys located on liquidus surface within Ni-Nb-Cr-Al quaternary, permitting production

of aligned delta Ni-Nb lamellae within nichrome matrix containing Ni-Al fcc precipitate 12 p1509 A73-26845

Solubility of vanadium and tungsten in alpha and gamma phases in the Fe-V and Fe-W binary systems 12 p1513 A73-27683

Electron-microscopic investigation of the spatial distribution parameters of second-phase precipitation in aging nickel-base alloys 14 p1764 A73-30862

Kinetics of gamma-prime phase precipitation in steel N3672lu2 15 p1887 A73-31322

Temperature dependence of the single-crystal elastic constants of Co-rich Co-Fe alloys. 15 p1890 A73-31926

Eutectic superalloys strengthened by aligned delta, Ni3Cb lamellae, gamma-prime, Ni3Al precipitates and reduced interlamellar spacing. 16 p2026 A73-33425

Special features of high-temperature creep in metals with an fcc lattice 17 p2188 A73-34563

Study of the behavior of metallic single crystals - Application to the tension of the fcc single crystal 19 p2495 A73-37425

The effect of molybdenum on gamma prime coarsening and on elevated-temperature hardness in some experimental nickel-base superalloys. 20 p2576 A73-39029

Stabilized gamma phase U-Nb-Zr alloy observation by electron microscopy, noting displacement reaction role in transition phase formation 20 p2578 A73-39489

Continuous decomposition of gamma solid solution in iron-nickel-titanium alloys 20 p2579 A73-39736

Study of the mechanism of plastic deformation of aging nickel-aluminum alloys with a large volume fraction of gamma prime phase 20 p2579 A73-39740

Calculation of the physicochemical constants of metals associated with the strength of interatomic bonds 22 p2874 A73-42097

Mo content influence on heat resistant Ni base alloys corrosion and oxidation resistance and gamma-prime phase solution temperature and amount 23 p2989 A73-43435

Bcc and fcc metal crystal growth, determining thermodynamic and kinetic conditions, surface texture and favored crystal types 23 p2990 A73-43487

Stability of the gamma-prime Co3Ti compound in simple and complex cobalt alloys. 24 p3099 A73-45075

FACSIMILE COMMUNICATION
NT AUTOMATIC PICTURE TRANSMISSION
Optical Characters Reading and facsimile terminals reduction of message preparation time for electrical transmission in Defense Communications System, considering cost effectiveness and maximum benefit 04 p0418 A73-15380

A method for reproducing pictures transmitted by meteorological satellites. 04 p0449 A73-15452

Run length code for redundancy encoding of black-white facsimile picture data transmission to allow channel or storage capacity reduction and hardware simplification 10 p1188 A73-23741

The facsimile camera - Its potential as a planetary lander imaging system. 12 p1495 A73-26875

Investigation of a planar analyzing system employing laser illumination for facsimile transmitters 13 p1627 A73-28857

Communications and position fixing experiments using the ATS satellites. 21 p2733 A73-40024

FACSIMILE TRANSMISSION
U FACSIMILE COMMUNICATION

FACTOR ANALYSIS
On evaluation of aircraft noise around air-bases by factor analysis. 03 p0249 A73-12957

Allowance for the correlation of factors in the method of priorities for electrical system optimization 05 p0560 A73-16272

Application of the analysis of correspondences to the study of the reliability of electronic components 07 p0800 A73-19412

An innovation index based on factor analysis. 08 p1026 A73-21700

The information content of successive RR-interval times in the ECG - Preliminary results using factor analysis and frequency analysis. 14 p1722 A73-30883

Book - Statistical design and analysis of engineering experiments. 17 p2200 A73-34456

Application of factor analysis to the encephalographic characterization of sleep 24 p3062 A73-44722

FACTORIAL DESIGN
Productivity estimates of the strategic airlift system by the use of simulation. 10 p1297 A73-23774

Response surface /descriptive function/ methodology design for human performance research, discussing central composite design, observations at experimental points and orthogonal blocking 24 p3062 A73-44773

Response surface methodology analysis of training transfer in pursuit rotor tracking task, relating three independent variables through multiple-regression prediction equations 24 p3063 A73-44774

Performance prediction in a single-operator simulated surveillance system. 24 p3063 A73-44775

Prediction equation validity for response surface methodology analysis of surveillance tracking by human operators, comparing variance and regression procedures 24 p3063 A73-44776

FACTORIES
U INDUSTRIAL PLANTS

FACULAE
Physical properties of solar chromospheric plages. I - Line profiles of the CaII H, K, and infrared triplet lines. 01 p0108 A73-11385

Trapped gravity waves velocity oscillations in solar plages under magnetic field, comparing with Bilderberg continuum atmosphere 01 p0108 A73-11386

Behavior of carbon monoxide in the upper photosphere. 04 p0504 A73-16027

Flares, magnetic configurations, and magnetic energy release. 08 p0996 A73-20764

On the annual variation of solar faculae. 16 p2053 A73-33073

Photospheric faculae and the solar oblateness - A reply to 'Faculae and the solar oblateness' by R. H. Dicke. 19 p2488 A73-38520

Determination of the temperature behavior in a photospheric facula through the solution of an integral equation by the gradient-random search method 21 p2759 A73-40721

FADING
NT SELECTIVE FADING
NT SIGNAL FADING

FAHRENHEIT TEMPERATURE SCALE
U TEMPERATURE SCALES

FAIL-SAFE SYSTEMS
Stochastic behaviour of a complex system with standby redundancy. 01 p0023 A73-10649

United States SST electrical power system evaluation. [AIAA PAPER 72-1055] 03 p0252 A73-13386

Self healing fuse for fast acting current overload protection of electric circuits, discussing design and performance 03 p0283 A73-13942

Reliability of systems with shifting redundancy in servicing a random demand flow 05 p0560 A73-16274

Automation of reliability evaluation procedures through CARE - The computer-aided reliability estimation program. 06 p0670 A73-18058

Design of a fault-tolerant, modular computer with dynamic redundancy. 06 p0671 A73-18064

Fail-safe aircraft composite structures, achieving crack arrestment by integral buffer strips in primary load carrying laminates 06 p0764 A73-18494

A general model for the study of fault tolerance and diagnosis. 06 p0672 A73-18808

Modulated light transmission for electrical isolation in a multichannel physiological monitoring system. 07 p0785 A73-19482

Autonomous power subsystem design for an Outer Planet Spacecraft. 09 p1154 A73-22805

Artificial slow crack growth under constant stress - The R-curve concept in plane stress. 09 p1108 A73-23255

Ram air turbines for aircraft emergency power supply, discussing design, performance and control 10 p1177 A73-23525

Figure of merit for fault-tolerant space computers. 10 p1192 A73-24870

The concept of coverage and its effect on the reliability model of a repairable system. 10 p1226 A73-24871

Fault-tolerance in the modular spacecraft computer. 12 p1475 A73-27130

Redundant central processor system for fault tolerant real time operation in space applications, describing systems organization [AIAA PAPER 73-424] 12 p1476 A73-27821

- Concorde emergency power supply, oxygen and escape systems design and operational features
14 p1713 A73-30929
- A unified method for analyzing mission reliability for fault tolerant computer systems.
15 p1901 A73-32261
- An ILS sensor for fail operative autoland systems - The Bendix RIA-32A.
15 p1880 A73-32461
- Independent Landing Monitor for economic Category 3 operation with fail-operational autoland, fog dissipation or fail-passive autoland plus visibility augmentation
15 p1911 A73-32499
- Quad redundant fly by wire servocontrol system design and tests in F-8C high speed jet aircraft, using fail/safe hydraulic actuators
16 p1970 A73-33080
- Heavy lift helicopter rotor blade design including airfoils, fiberglass skin, titanium spar, fail-safety and aerodynamic and structural features
[AHS PREPRINT 710] 17 p2104 A73-35056
- Heavy lift helicopter rotor hub design and fatigue test technology, using fail-safe criteria, finite element analysis and fracture mechanics
[AHS PREPRINT 784] 17 p2180 A73-35097
- Flight-critical fail-operative and endurance tests for SST electrical power system
17 p2109 A73-35252
- The lightning arrestor-connector concept - Description and data.
19 p2408 A73-37270
- Redundant system design for advanced digital flight control.
[AIAA PAPER 73-846] 20 p2585 A73-38785
- Computerized synthesis of optimal fault-diagnosable logical circuits capable of detecting and repairing faulty modules for circuit reliability and availability improvements
21 p2669 A73-40687
- A failure tolerant power subsystem for outer planet spacecraft.
22 p2801 A73-42902
- The robustness of reliability predictions for series systems of identical components.
22 p2867 A73-42967
- Reliability of some redundant systems with repair.
22 p2867 A73-42968
- Equivalence of redundant systems with respect to time to failure.
22 p2867 A73-42970
- Ram air turbine with hydraulic pitch change servo regulated speed as emergency power source for aircraft control in event of main engine failure
24 p3058 A73-45475
- FAILURE**
NT ENGINE FAILURE
NT FAILURE ANALYSIS
NT STRUCTURAL FAILURE
NT SYSTEM FAILURES
- FAILURE ANALYSIS**
Thermal cycle influence in heat resistant materials plastic strain and time to failure for different stress and temperature conditions
01 p0112 A73-10009
- Analytical method for diagnostic and checkout testing of logic element faults in complex combinational circuits
01 p0026 A73-10035
- Deformation and failure of heat-resistant materials under conditions of thermal fatigue and creep as functions of the nature of the temperature change cycle and of the boundary conditions
01 p0063 A73-10478
- Statistical method of determining the load or stress distribution from the failure characteristics of mechanical systems
01 p0118 A73-11370
- Optimal renewal algorithm for control plant with cumulative damage, using failure rate and renewal point spacing model
01 p0058 A73-11421
- Reliability and failure sequence characteristics of automatic system, using input rarefaction of Markov renewal process
01 p0058 A73-11423
- Influence of high-temperature annealing on the rupture characteristics of zirconium carbide
02 p0178 A73-11541
- The generalized gamma distribution and the power distribution as element lifetime distributions
02 p0145 A73-11584
- Generalized gamma distribution with a negative shape parameter as a model of the lifetime distribution of electrical elements with a single-maximum failure rate
02 p0145 A73-11585
- Aircraft fault isolation based on pattern of cockpit indications - A human factors approach.
02 p0136 A73-11857
- Glass laminates and high strength oriented fiberglass reinforced plastics failure mechanism in tension and bending, noting equalizing effect through proper cohesion characteristics between layers
02 p0185 A73-12134
- Engineering method of calculating the parameter of fracture toughness.
02 p0235 A73-12210
- A versatile silver oxide-zinc battery for synchronous orbit and planetary missions.
02 p0133 A73-12622
- Application of the Monte Carlo technique to fatigue-failure analysis under random loading.
03 p0388 A73-13236
- Analyzing failures of metal components.
03 p0323 A73-13270
- Solid propellant rocket service life prediction based on propellant grain structural failure analysis, discussing surveillance program rationale for various conditions
[AIAA PAPER 72-1085] 03 p0354 A73-13407
- Failure criterion for a propellant of a spherical solid rocket motor.
[AIAA PAPER 72-1088] 03 p0351 A73-13409
- Failure phenomena relationship to kinetic equation for defect buildup from brittle fracture analysis of composite glass fiber reinforced plastic in uniaxial eccentric tension
03 p0394 A73-14008
- Ni-Cr-Ti steel aircraft structural element fatigue life calculation based on failure mechanism involving crack propagation
03 p0394 A73-14011
- Aircraft gas turbine mainshaft ball bearings fatigue life estimation via failure distribution
[ASME PAPER 72-LUB-10] 03 p0313 A73-14328
- Fatigue scoring - A new form of lubricant failure.
[ASLE PREPRINT 72LC-3B-1] 03 p0316 A73-14356
- Failure probability distribution models for reliability analysis, considering selection criteria based on application
04 p0507 A73-14708
- Weibull flaw distribution models for fracture strength and failure analysis of brittle materials and fiber reinforced composites
04 p0468 A73-14726
- Discussion of the Colloquium on Structural Reliability.
04 p0468 A73-14727
- Failure detection in solid propellants.
[AIAA PAPER 72-1087] 04 p0485 A73-14906
- Prediction of failure for a multiple load-path system under random loading.
04 p0510 A73-15075
- Probability model and causal approach to failure mechanisms and reliability of control system elements applied to IC
04 p0424 A73-15208
- Failure diagnostics in mathematical simulators of automatic control systems.
04 p0430 A73-15209
- Monograph on structural element and structures reliability covering structural design, failure analysis and reinforced element collapse under moment and force loads
04 p0472 A73-15694
- A finite element based procedure for simulating the transient response and failure of a two-dimensional continuum with nonlinear material characteristics.
[ASME PAPER 72-WA/DE-4] 04 p0515 A73-15875
- Investigations into film failure /transition point/ of lubricated concentrated contacts.
05 p0580 A73-16103
- A technical note on the correspondence between Amontons' law and wear-scar data in a 4-ball machine.
05 p0581 A73-16108
- Critical failure conditions in thin film lubrication - Preliminary results.
05 p0581 A73-16109
- Optimal experimental measurements of anisotropic failure tensors.
05 p0631 A73-16113
- Analytical techniques for the determination of equipment probability of survival to radiation stress.
05 p0596 A73-16509
- Extending the life and recycle capability of earth storable propellant systems.
[SAE PAPER 720837] 05 p0629 A73-16631
- Crack growth and failure of aluminum plate under in-plane shear.
[AIAA PAPER 73-253] 05 p0635 A73-16975
- Predicting failures with conducting-polymer fatigue-damage indicators.
06 p0759 A73-17598
- Enhancing testability of large-scale integrated circuits via test points and additional logic.
06 p0674 A73-17802
- Fault insertion techniques and models for digital logic simulation.
06 p0671 A73-18062
- Optimal currents, voltages and frequencies for noise measurement in HF transistors for reliability prediction and failure analysis, noting diffusion alloyed and planar transistors
06 p0675 A73-18078
- Nonstationary envelope process and first excursion probability.
06 p0762 A73-18341
- A general model for the study of fault tolerance and diagnosis.
06 p0672 A73-18808
- Scanning electron microscope operation and application to technology research and electronic components and circuits failure and reliability analysis
07 p0797 A73-18922
- Failure causes probability and accelerated life test conditions for ceramic capacitors, noting product selection by modified quality control procedures
07 p0799 A73-19405
- Analysis of a defect of electromagnetic relays used in an electronic assembly
07 p0799 A73-19406
- Defects analysis and the possibilities brought by the scanning electron microscope
07 p0823 A73-19408
- Electrical measurements, metallographic microscopy and chemical analysis for failure analysis
07 p0800 A73-19409
- Help derivable from failure analyses for the definition of a reliability evaluation model applicable to large-scale integrated circuits
07 p0800 A73-19411
- Mathematical models for failure rates of electronic components, considering tantalum condensers, Zener diodes and n-p-n Si transistors
07 p0830 A73-19413
- Estimation of reliability in storage - Optimal test procedure
07 p0830 A73-19415
- Failure analysis and reliability estimation methodology for electromechanical mosaic printer
07 p0800 A73-19419
- Stress and strength theory application to mechanical failure of electronic equipment, showing Weibull law use in reliability analysis
07 p0800 A73-19420
- Reliability of thin nickel-chromium resistance layers deposited by sublimation under vacuum on a glass substrate
07 p0862 A73-19424
- Metal surface active properties effects on fracture characteristics and deformation and failure conditions
07 p0912 A73-19472
- Metal tongues in trailing edge of surface pits near fracture path end in rolling contact fatigue of failed ball bearings
07 p0831 A73-20158
- Fault isolation in complex systems via Bode diagram technique.
08 p0941 A73-20684
- A procedure for the evaluation and failure analysis of M.O.S. memory circuits using the scanning electron microscope in potential contrast mode.
08 p0943 A73-20730
- Operational amplifier microcircuits intermittent failure due to input offset voltage drift, describing testing and analysis methods
08 p0944 A73-20740
- Degradation of MNOS memory transistor characteristics and failure mechanism model.
08 p0944 A73-20741
- A statistical model for electromigration induced failure in thin film conductors.
08 p0944 A73-20745
- Thin film nickel-chromium resistor failures in integrated circuits.
08 p0944 A73-20746
- Bayesian MFR life test sampling plans.
08 p0973 A73-20950
- The use of macroscopic failure diagrams to determine the quality of materials.
08 p0977 A73-21148
- Experimental investigation of the failure mechanism of fiber-reinforced composites subjected to uniaxial tension.
09 p1156 A73-21874
- Investigation of the failure characteristics of electrically heated samples of heat-resistant steels and alloys in a high-pressure oxidizing flow
09 p1069 A73-21980
- The average duration of the failed state in the interval between adjacent tests of a periodically verified standby radio system with z-multiple redundancy
09 p1051 A73-22464
- A strain criterion for failure of materials subjected to stress and temperature cycles
09 p1159 A73-22570
- Solar cell fatigue life prediction by statistical analysis and extrapolation for determining failure probability curve as function of stress and time
09 p1036 A73-22808
- An investigation into the relationships of fatigue fracture and inelastic deformation of metals in torsion.
09 p1161 A73-23052
- Aircraft maintenance for safety and reliability, considering design requirements, human errors, fault diagnosis, redundancy, failure mode analysis, service data statistics and equipment specifications
10 p1174 A73-23759
- Filament-wound vessel from an organic fiber-epoxy system.
10 p1237 A73-23958

Failure of high-strength welded structures with initial cracks 10 p1225 A73-24368

Failure analysis and heat resistance optimization factors of reinforced metal sheet under thermal cycling 10 p1233 A73-24369

Comparative analysis of optimal failure search procedures, considering criteria, failure extent, initial data, reliability and compatibility 10 p1226 A73-24696

Electron fractography of fatigue failure and macrocrack propagation in dual phase Ti alloy during cyclic loading at minus 140 to plus 150 C 10 p1236 A73-24931

Probable collapse mechanisms in indefinite plates on an elastoplastic continuum. 11 p1434 A73-25217

An experiment to correlate the thermal stress failure level to modulus of rupture in ceramic materials. 11 p1387 A73-25304

A statistical theory for failure of brittle materials under combined stresses. 11 p1439 A73-25511

Damage accumulation hypotheses concerning lifetime prediction during vibrational loading. II - A critical review 11 p1384 A73-25849

A metallurgical approach to cracked solder joints. 11 p1375 A73-26355

Book - Engineering means in automatic control. 12 p1481 A73-26751

Questionnaire approach for technical diagnostics problem formulation covering hardware failure analysis coding, combinational switching device synthesis and optimal program construction 12 p1482 A73-26752

Construction of verification tests for digital devices with delay elements 12 p1482 A73-26753

Checkup and failure diagnostics of an incompletely homogeneous two-dimensional structure 12 p1482 A73-26754

Diagnostic tests and failure checkout for interconnected combinational micrologic circuit components in manufacturing process, tabulating individual failure functions 12 p1474 A73-26755

Diagnosis of switching devices in the case where faults are represented by tests of individual elements. 12 p1476 A73-26756

Methods of constructing control and diagnosis tests for homogeneous microelectronic circuits 12 p1476 A73-26757

Glass fiber reinforced polyester laminates mechanical properties evaluation for structural design, considering failure criteria in terms of fiber debonding and resin and gel coat cracking 12 p1515 A73-26877

Fatigue resistant design with fiber reinforced plastics /FRP/, discussing stress analysis, failure criteria, material anisotropy, multiaxial stress conditions and cumulative damage 12 p1515 A73-26880

Kinetic strain criteria of cyclic failure at high temperatures 12 p1552 A73-27252

Procedure for studying fatigue failure features in metals under harmonic and complex loading at low temperatures 12 p1486 A73-27254

Book - Reliability concepts in engineering manufacture. 12 p1502 A73-27398

Statistical distribution of the failure of injection lasers. 12 p1508 A73-27524

Output radiation influence on catastrophic and slow degradation process in heterojunction injection lasers, noting service life dependence on current density 12 p1508 A73-27525

Book - Linear methods for unconstrained optimization. 12 p1518 A73-27549

Brittle failure of infinite plate with circular hole and radial cracks under two perpendicular uniformly distributed tensile loads 12 p1556 A73-27802

Strain hardening and instability in biaxially stretched sheets. 13 p1623 A73-28139

Minimax failure detection and identification in redundant gyro and accelerometer systems. 13 p1616 A73-28832

Analytical elasticity methods for airfield pavement structural stress-strain, failure and reliability performance evaluation 13 p1598 A73-29106

Brittle fracture strength and non-crack propagation. 13 p1639 A73-29470

Interfiber failure of unidirectional composite material. 13 p1702 A73-29538

A reliability analysis of fatigue limits based on large sample quantal response data. 13 p1702 A73-29548

Deformation and destruction of heat-resistant materials in conditions of thermal fatigue and creep as a function of the nature of the cyclic change in temperature and boundary conditions. 14 p1759 A73-30303

Some characteristics of the failure by fatigue of mild steel in vacuum 14 p1763 A73-30681

Application of fiber optics to the observation of fatigue crack development 14 p1754 A73-30691

Prediction of failures and efficiency characteristics of a system 14 p1740 A73-30799

Hot environment lubrication failures of sleeve bearing diester lubricant system in small electric motors, using reliability-temperature accelerated tests [ASME PAPER 73-DE-13] 14 p1767 A73-30819

Reliability analysis of time to failure distribution of redundant system with failing elements number as periodic function of time 15 p1880 A73-30998

Influence of hydrogen on the failure of the VT-1 titanium alloy in programmed cyclic loading 15 p1886 A73-31035

A note on the use of a simple technique for failure prediction using resistance curves. 15 p1951 A73-31989

Failure criterion for metallic materials in the case of multiaxial vibrational stress 15 p1952 A73-32045

Evaluation of composite failures through fracture signal analysis. 15 p1879 A73-32250

Truncated sequential life tests for a 3-way decision procedure. 15 p1883 A73-32260

Expected value and variance of failure time in redundant systems. 15 p1901 A73-32264

Failure retardation mechanism in plastic titanium alloys 15 p1894 A73-32529

German monograph on frictional fatigue failure covering microcrack initiation due to shear induced vibrational stresses 15 p1956 A73-32587

Protective helmets performance evaluation for design optimization, considering failure analysis from aircraft accident reports 16 p1973 A73-32655

Phenomena associated with bench and thermal-vacuum testing of super conductors - Heat pipes. 16 p2084 A73-33131

Analyses of flight model spacecraft performance during thermal-vacuum tests. 16 p2072 A73-33149

Repairable electronic system random failure and repair time related to simulator time available for operation, analyzing MTBF and repair rates 16 p1996 A73-33207

The analysis of defects and the possibilities brought by the scanning electron microscope 16 p2019 A73-33272

Investigation of mounting discrete chip components for hybrid microelectronic applications. 16 p1989 A73-33467

Computerized analysis of reliability or failure rate function data from electronic component and equipment operation and testing, using hazard plotting technique 16 p1989 A73-33613

Time dependent stress-strength models for non-electrical and electrical systems. I. 16 p2020 A73-33621

Analysis of early failures in unequal size samples. 16 p2020 A73-33622

Tactical weapon system final test for random failures, discussing electronic component defects effects and semiconductor device screening for system reliability improvement 16 p1990 A73-33624

Censored sample size selection for life tests. [AD-758315] 16 p2033 A73-33630

Operational readiness and maintenance testing of the B-1 strategic bomber. 16 p1969 A73-33631

Computerized total On-Line Testing System with diagnostic error visibility and preventive and corrective maintenance functions in multiprogramming mode, discussing design features 16 p1986 A73-33633

Concept and system of the versatile avionics shop test/VAST/ system. 16 p1986 A73-33634

A designer's approach to the fatigue failure mechanism. 16 p2081 A73-33644

Failure data evaluation, determining wear out, degradations, environments causing system failures, repairs, maintenance and sub par performers 16 p2021 A73-33649

Mechanism of failure in transparent organic-glass-type dielectrics under the action of laser radiation 16 p2030 A73-33927

Forecasting failures with acoustic emission. 16 p2022 A73-33992

Inter crystalline failure in recrystallized low-alloyed molybdenum alloys 17 p2189 A73-34577

Some physicochemical characteristics of failure in tempered high strength steels 17 p2189 A73-34580

New relationships between stress testing, failure and reliability. 17 p2178 A73-34730

Failure analysis used to vindicate JANITX components. 17 p2135 A73-34731

Detection of random chip defects in monolithic microcircuits. 17 p2135 A73-34732

Lubricant testing as an aid to bearing damage analysis. [ASLE PREPRINT 73AM-3B-1] 17 p2178 A73-34983

A test procedure to evaluate the relative susceptibility of materials to stress corrosion cracking. 17 p2191 A73-35125

CPU design for command and control system with programmable read-only control memory, discussing self microdiagnostics for control store error detection 17 p2144 A73-35258

Tension-tension low cycle fatigue failure mechanism in uniaxially and biaxially reinforced boron fiber-aluminum alloy composites, considering matrix plasticity role 17 p2193 A73-35544

The plastic bending of beams and their failure by low cycle fatigue. 18 p2365 A73-36617

Yielding and failure of metals in a complex state of stress 18 p2366 A73-36756

Failure analysis of wire bonds. 19 p2436 A73-38446

Semiconductor failures due to oxide defects and diffusion faults, describing nematic liquid crystals application to pinholes detection in oxide layers 19 p2410 A73-38447

Metal oxide semiconductor/large scale integration circuit failure analysis and diagnosis, discussing short circuits, cholesteric liquid crystal coloring and aluminum anodization 19 p2411 A73-38448

Analysis of integrated circuit failure modes and failure mechanisms derived from high temperature operating life tests. 19 p2411 A73-38449

Failure detection and isolation methods for redundant gimbal inertial measurement units. [AIAA PAPER 73-851] 20 p2585 A73-38790

Competitive evaluation of failure detection algorithms for strapdown redundant inertial instruments. 20 p2585 A73-38791

The selection of test frequencies for system fault diagnosis. [AIAA PAPER 73-864] 20 p2586 A73-38802

Il'ushin linear theory for defect accumulation generalized for endurance limit of materials under noncyclic loads, examining time to failure under creep and relaxation conditions 20 p2624 A73-39644

High-speed photographic study of failure processes in composite materials. 21 p2723 A73-39988

A method of locating defective elements in large phased arrays. 21 p2653 A73-40682

Computerized synthesis of optimal fault-diagnosable logical circuits capable of detecting and repairing faulty modules for circuit reliability and availability improvements 21 p2669 A73-40687

Risk analysis and reliability based design for probabilistic approach implementation for safety and performance of structures and structural components 21 p2788 A73-41650

Failure detection and isolation techniques for gimbal and strapdown inertial systems examining redundant system reliability relationship to MTBF [AIAA PAPER 73-852] 22 p2884 A73-41969

Failure stress levels of flaws in pressurized cylinders. 22 p2921 A73-42156

Assuring reliability program effectiveness. 22 p2938 A73-42199

High power airborne radar CW tube-transmitter interface failures due to design, maintenance, handling and environment effects 22 p2834 A73-42875

Failure diagnosis using quadratic programming. 22 p2867 A73-42966

The robustness of reliability predictions for series systems of identical components. 22 p2867 A73-42967

Fatigue failure analysis of low carbon steel endurance under cyclic loading with time dependent viscoelastic effects, using Hooke's-Trouton laws
23 p3040 A73-43469

Fatigue failure predictions for plates with holes and edge notches.
23 p3047 A73-44350

Prediction of failure processes in fiberglass-reinforced plastics by a seismocoustic method. II - Features of damage buildup in woven fiberglass-reinforced plastics in uniaxial tension
24 p3102 A73-44507

Europa 2 Inertial Guidance System technology assessment covering design features, sensor, computer and interface units, first launch failure causes and need for improvements
24 p3108 A73-44694

Possible causes of failures in pulse-switched thyristors
24 p3072 A73-44933

Reliability estimation for repairable and nonrepairable flight vehicles, considering nomographs for failure rate and probability of defined requirements satisfaction
24 p3057 A73-45197

FAILURE MODES

Characteristics of the fatigue curve of plastics.
02 p0185 A73-12699

Failure mechanisms in transversely loaded boron-aluminum.
02 p0184 A73-12861

Response of boron/epoxy composite materials to simulated lightning current.
03 p0331 A73-13025

Observations of failure modes in carbon composite materials.
03 p0332 A73-13042

Analyzing failures of metal components.
03 p0323 A73-13270

The effects of matrix and interface modification on local fractures of carbon fibers in epoxy.
03 p0335 A73-13982

High strength alloys hydrogen embrittlement mechanisms and effects and preventive measures, considering steel decarburization, stress corrosion cracking, hydride sheath formation and failure modes
03 p0328 A73-14425

Relationships between failure modes and fatigue scatter.
04 p0460 A73-14721

Stresses in laminated composites containing a broken layer.
[ASME PAPER 72-WA/APM-14]
04 p0516 A73-15899

Thermal collapse theory of hydrodynamic oil lubrication films failure for slider bearing, noting frictional forces role
05 p0580 A73-16105

Failure modes of hybrid microcircuits in thick films.
07 p0800 A73-19410

Reliability aspects of plastic encapsulated integrated circuits.
08 p0944 A73-20739

Failure analysis of semiconductor device bonds under on-off operation, noting fatigue testing machine for accelerated life tests
08 p0972 A73-20744

Ti based beta alloy strain hardening and failure characteristics, emphasizing initial deformation phase and microdefect onset and development
09 p1105 A73-23064

Plastic strain rates within discrete crack tip zones at running brittle cracks in mild steel plates, identifying twinning as main deformation mode
09 p1163 A73-23258

Carbon-carbon composites and bulk graphite fracture toughness and failure modes determination from single-edge-notched specimen responses under three-point bending
10 p1239 A73-24276

Effects of beryllium additions on the microstructure and the type of failure in Al-Mg alloys
10 p1233 A73-24423

Modeling of a bubble-memory organization with self-checking translators to achieve high reliability.
10 p1192 A73-24872

Carbon fiber reinforced epoxy resins mechanical properties, correlating test parameters with observed failure mechanism
12 p1515 A73-26878

Maximum loads on pulse-discharge light sources producing short flashes.
13 p1629 A73-29437

A theoretical study of fracture and yield conditions derived from hypo-elasticity.
13 p1639 A73-29464

Thin Al alloy sheet fracture toughness from crack growth resistance curves, discussing failure modes and critical stress intensities
13 p1640 A73-29480

Low carbon steel S-N diagram for stresses ranging to fatigue limit, noting cyclic creep, macroplastic cyclic stress and fatigue failure
13 p1703 A73-29603

The effects of out-of-phase biaxial-strain cycling on low-cycle fatigue.
14 p1806 A73-29774

Mechanism of breakdown in the interface region of glass reinforced polyester by artificial weathering.
15 p1898 A73-31838

Fatigue behaviour of ribbon-reinforced composites.
15 p1898 A73-31840

Characteristics of failure in alpha-titanium alloys at high temperatures
15 p1894 A73-32536

Factors affecting the survivability of stressed bonds in adverse environments.
16 p2017 A73-33055

Hydrofluidic component and system reliability.
16 p1971 A73-33478

Aircraft design for operational safety, discussing risk elimination, failure modes, maintenance analysis and fault diagnosis
17 p2098 A73-34083

Fatigue and fracture of advanced composite materials.
[SAE PAPER 730337]
17 p2194 A73-34688

Relationship between K_{Ic} and plane-strain tensile ductility and microscopic mode of fracture.
17 p2190 A73-34876

Prior-to-failure extension of flaws under monotonic and pulsating loadings.
17 p2246 A73-34884

Failure modes and accelerated life test methods for despun antenna bearings.
[ASLE PREPRINT 73AM-1A-4]
17 p2178 A73-34979

Broadband TWT microwave amplifier failure modes in airborne systems related to physical mechanism, fabrication processes and field operator handling
17 p2140 A73-35259

Creep, self heating and failure of thermoplastics under pulsating tensile stress.
17 p2197 A73-35346

Failure modes in composites; Proceedings of the Symposium, Boston, Mass., May 8-11, 1972.
17 p2191 A73-35526

Failure mode multiplicity in Al-stainless steel and Al-W metal matrix composites under various loading conditions
17 p2191 A73-35527

Direct observation of the failure of a fibre reinforced composite.
17 p2192 A73-35529

Brass matrix composites tensile strain characteristics and fracture mode dependence on fiber volume fraction and properties
17 p2192 A73-35531

Borsic/Ti-Al-W composite properties, fracture modes and fabrication, discussing tensile strength and temperature dependence of longitudinal strength
17 p2192 A73-35532

Failure mechanisms in impact loaded carbon and glass fiber reinforced plastics, discussing specimen geometry, notch presence, fiber type, fiber orientation and hybridization effects
17 p2198 A73-35538

Fiber orientation effects on fatigue failure of aligned short fiber composite materials.
17 p2198 A73-35546

Polymers fatigue life under cyclic deformation, discussing stress-strain and failure behavior as function of reversed stress cycle frequency
18 p2328 A73-36587

Matrix formulation of reliability analysis and reliability-based design.
19 p2496 A73-37479

Reliability physics 1973; Proceedings of the Eleventh Annual Symposium, Las Vegas, Nev., April 3-5, 1973.
19 p2410 A73-38438

A bonding-wire failure mode in plastic encapsulated integrated circuits.
19 p2410 A73-38442

Solid tantalum capacitor failure modes, discussing slug impurities, dielectric imperfections, short circuits, scintillation shorts, anodizing, soldering, screening methods and cost reduction
19 p2410 A73-38443

An elusive open-circuit failure mode in thin-film chip resistors.
19 p2410 A73-38444

Analysis of integrated circuit failure modes and failure mechanisms derived from high temperature operating life tests.
19 p2411 A73-38449

Temperature-humidity acceleration of metal-electrolysis failure in semiconductor devices.
19 p2411 A73-38450

Improve reliability of electron devices through optimized coverage of surface topography.
19 p2411 A73-38453

Screening of metallization step coverage on integrated circuits.
19 p2411 A73-38456

Pulsed RF life of an L-band power transistor.
19 p2411 A73-38460

High reliability manufacturing technology for COS/MOS IC devices, discussing failure mechanisms and MIL-STD-883 and MIL-M-38510 tests for quality control
20 p2534 A73-38656

Electric connector reliability assessment model based on operating conditions and failure modes analysis without using MTBF
21 p2665 A73-41208

Prediction methods for the susceptibility of solid state devices to interference and degradation from microwave energy.
22 p2823 A73-41796

Properties of a light-modified-breakdown detector in GaAs.
22 p2864 A73-43164

Response of glass-fiber-reinforced epoxy specimens to high rates of tensile loading.
23 p2996 A73-43385

Titanium alloys mechanical, electrochemical and metallurgical parameters effects on stress corrosion cracking, discussing crack growth kinetics, failure features and component hazard minimization
23 p2990 A73-43457

Compressive strength and failure modes of unidirectional composites.
23 p3041 A73-43634

Some important aspects in testing high-modulus fiber composite tubes in axial tension.
23 p2996 A73-43639

Influence of fiber property variation on composite failure mechanisms.
23 p2996 A73-43643

Molecular rupture mechanism, self reinforcement and failure modes of elastomeric materials dependence on strain, temperature, filler and crosslink density
23 p2997 A73-43808

Principal failures of turbines during turbine engine operation
24 p3122 A73-45196

FAIRCHILD MILITARY AIRCRAFT U MILITARY AIRCRAFT FAIRINGS

Wing-fuselage junctions fairings compromise design, describing rotational eddies formation mechanism for unsteady ducted flow and wing root phenomena
[ONERA, TP NO. 1217]
13 p1564 A73-28836

FALKNER-SKAN EQUATION

On some solutions of the Falkner-Skan equation.
02 p0154 A73-12797

On the uniqueness of solutions of the Falkner-Skan equation.
02 p0154 A73-12798

Reverse flow solutions of the Falkner-Skan equation for a lambda greater than one.
02 p0154 A73-12799

Nonsimilar flows between the solution branches of the Falkner-Skan equation.
05 p0567 A73-17116

Bifurcated small parameter perturbation solutions in boundary layer theory, applying to Falkner-Skan equation and instability in stratified shear flow
16 p2001 A73-33871

FALLOUT

Possible correlation between the concentration and density of alpha-radioactive fallouts and types of meteorological processes
09 p1115 A73-22995

Diffusion and fallout of pollutants emitted by aircraft engines.
19 p2474 A73-38323

FALLOW FIELDS

U FARMLANDS

FANLIFT DEVICES

U LIFT FANS

FANS

An experimental study on noise reduction of axial flow fans.
03 p0241 A73-12961

Compressor or fan location at intake or outflow side of compressible flow plant, considering power and size requirements with and without heat exchange
14 p1711 A73-30297

Fan acoustic measurements by hot-wire anemometers in anechoic chamber, discussing turbulent flow characteristics, noise spectra, wire velocity spectra and blade tip shape
19 p2472 A73-37289

FAR FIELDS

Incident plane wave fluctuations effect on diffraction pattern formed by scattering on reflecting sphere, calculating amplitude distribution in Fresnel and Fraunhofer regions
01 p0016 A73-10211

Optical modeling of antenna radiation patterns by radio holograms of aperture fields
02 p0146 A73-12020

Optical properties of the Apollo laser ranging retroreflector arrays.
02 p0141 A73-12250

Fiber-dispersion measurements with a mode-locked krypton laser.
02 p0177 A73-12574

Far field steady inviscid flow behavior of hyper-sonic blunt axisymmetric slender body, obtaining unsteady two dimensional solution with cylindrical symmetry 03 p0242 A73-13310

Far-field simulation of circular antenna arrays on the analog/hybrid computer 03 p0277 A73-13985

Fraunhofer zone distribution functions for azimuth and elevation angles of radio waves reflected from inhomogeneous ionospheric scattering layer 03 p0278 A73-14071

An experimental study of unstable confocal CO2 resonators. 03 p0320 A73-14456

Granularity produced by a diffuser illuminated in partially coherent light 03 p0320 A73-14606

Receiving characteristics of antennas in the case of coherent and incoherent radiation 04 p0427 A73-14775

Diffraction of a two-dimensional electromagnetic field by an ideally conducting plane with a boundless rectilinear slit 04 p0423 A73-15608

Special features of recording 'pure' phase /binary/ acoustic holograms 04 p0450 A73-15619

Far field solution for stress wave attenuation and dispersion in composite materials, noting pulse shape 05 p0633 A73-16340

Transformation of the hypersonic compressible Navier-Stokes equations. 05 p0567 A73-17120

Errors in the predicted gain of pyramidal horns. 06 p0676 A73-18180

Theory of double parasitic loop counterpoise antenna radiation patterns. 06 p0666 A73-18190

Acoustic results obtained with upper-surface-blowing lift-augmentation systems. 07 p0776 A73-20458

The effect of nozzle inlet shape, lip thickness, and exit shape and size on subsonic jet noise. [AIAA PAPER 73-187] 07 p0776 A73-20465

Waves in a hot uniaxial plasma excited by a current source. 07 p0860 A73-20477

Power reduction and fluctuations caused by narrow laser beam motion in the far field. 08 p0975 A73-21059

On the near- and far-field radiation patterns generated by the non-linear interaction of two separate and non-planar monochromatic sources. 08 p0988 A73-21469

Laser beam steering in confocal unstable resonators, interpreting mirror misalignment effects as far field dependence on magnification and Fresnel number from mode solution 09 p1090 A73-22076

Convergence of the solution for the far scattered field of a conducting cylinder of arbitrary cross-section. 09 p1050 A73-22397

Diffraction on an infinite grating made of cylindrical elements of random cross section 09 p1051 A73-22851

Near-field technique for inferring aperture antenna radiation patterns. 09 p1052 A73-22960

Performance of an unstable repetitive pulsed CO2 laser oscillator. 09 p1098 A73-23338

'Farfield' behavior of solutions to partial differential equations asymptotic expansions and maximal rates of decay along a ray. 10 p1241 A73-23700

Diffraction of a two-dimensional electromagnetic field on an ideally conducting plane with an infinite straight slit. 10 p1188 A73-24198

Optimization of the loop-coupled log-periodic antenna. 11 p1337 A73-25652

Field pattern of two identical nonstaggered parallel circular loop antennas. 11 p1337 A73-25667

Reconstruction of an antenna radiation pattern from field values available within a limited sector of angles in the Fresnel region 12 p1479 A73-27227

Circular aperture antenna with quadratic phase distortions, deriving near and far field patterns in terms of linear combinations of Bessel and Lommel functions 12 p1479 A73-27233

Phase and amplitude only scanned acoustical holograms, noting Fraunhofer diffraction region reconstructed images 13 p1615 A73-28592

Plane TE polarized electromagnetic wave diffraction on infinite conducting cylinder in nonhomogeneous medium, calculating far field diffraction patterns 13 p1582 A73-28656

Plane electromagnetic wave diffraction by ideally conducting circular cylinder in far and bright spot zones, using Green theorem for field calculation 13 p1583 A73-28851

Waveguide laser mode patterns in the near and far field. 14 p1756 A73-30157

Radiation characteristics of corrugated E-plane sectoral horns. 14 p1734 A73-30209

Fourier decomposition for antenna near field reconstruction from far field pattern data, investigating numerical stability and convergence bounds 14 p1727 A73-30213

The use of the terms nearfield and farfield in ultrasonic non-destructive testing 15 p1882 A73-32052

Obliquely incident plane wave scattering from moving perfectly conducting cylinder, discussing mode coupling, Doppler shift and far field scattered power 15 p1845 A73-32238

Spectral moving frame representation of jet noise by far field acoustic pressure autocorrelation and density function 16 p2000 A73-33681

Numerical computation of the current distribution and far-field-radiation pattern of the axial-mode helical aerial. 16 p1985 A73-34020

Probe compensated near-field measurements on a cylinder. 17 p2127 A73-35678

Impedance and far field characteristics of a linear antenna near a conducting cylinder. 19 p2403 A73-37271

The ultimate noise barrier - Far field radiated aerodynamic noise. 19 p2375 A73-37278

A quantum treatment of spontaneous emission without photons. 20 p2594 A73-38611

Shielding of a moving test charge in a turbulent plasma. 20 p2599 A73-39722

On the effects of eliminating the passive elements from a thinned array. 21 p2652 A73-40655

Pattern measurements of phased-arrayed antennas by focusing into the near zone. 21 p2653 A73-40681

Narrow beam phased array of identical isotropic elements, estimating far field beam width with consideration for element position error effects 22 p2831 A73-41839

Computer techniques for scatterer shape from far field data/inverse scattering/ via remote sensing, with application to antenna radiation pattern synthesis and holography 22 p2828 A73-42845

Measurements of the distribution of sound source intensities in turbulent jets. [AIAA PAPER 73-989] 24 p3053 A73-44826

Transmission and far field radiation of sound waves in and from lined ducts containing shear flow. [AIAA PAPER 73-1013] 24 p3078 A73-44845

Far field effects of weak spatially periodic inhomogeneities. [AIAA PAPER 73-1036] 24 p3109 A73-44864

Far-field analysis of nonlinear shock waves in a lattice. 24 p3112 A73-45412

Theory of a corner-driven loop antenna immersed in a warm plasma. 24 p3070 A73-45486

FAR INFRARED RADIATION

French monograph - Contribution to the experimental study of the integrated intensity of the translational absorption bands induced in pressurized rare-gas mixtures. 01 p0080 A73-10601

A simple analytic approximation for dusty stromgren spheres. 01 p0104 A73-11047

Far IR brightness temperature, opacity and emissivity of Jupiter, Venus, Mars and Saturn 05 p0626 A73-17348

Far IR molecular lasers evaluation, discussing excitation, line assignment, relaxation, frequency measurement and development predictions 07 p0835 A73-19636

Far infrared properties of lunar rock. 07 p0897 A73-19886

Far infrared and Raman spectroscopic investigations of lunar materials from Apollo 11, 12, 14, and 15. 07 p0897 A73-19889

Balloon measurements of the far-infrared background radiation. [AD-757848] 07 p0825 A73-20177

Night sky background radiation measurement by far IR radiometer carried on rocket launched from Hawaii 07 p0825 A73-20187

Optical constants measurement for far IR materials of crystalline quartz, sapphire, Ge and Si at room temperature and 1.5 K [AD-760151] 08 p0994 A73-21049

FAR ULTRAVIOLET RADIATION

Evidence for polarised radiation from the sun in the far infrared. 08 p1000 A73-21419

RCW 117 and DR 15 observed in the far infrared. 08 p1012 A73-21531

Excitation mechanism of the far-infrared sulfur dioxide molecular laser. [AD-760378] 09 p1090 A73-21938

Balloon observations of galactic and extragalactic objects at 100 microns. 09 p1150 A73-23134

Galactic nuclei and QSO far IR radiation luminosity explanation by nonthermal maser emission due to gas molecules in dense clouds 09 p1150 A73-23145

Far IR mapping of lunar surface during 19 December 1964 eclipse, discussing thermal contours and Apollo observed regions 10 p1282 A73-24644

Low frequency vibrations and molecular structure of /CH3/2NPF2. 11 p1326 A73-25567

Balloon-borne Newtonian telescope with parabolic pyrex primary mirror for far IR observation of celestial sources 11 p1368 A73-26504

A new type of helium-cooled bolometer. 11 p1368 A73-26511

Problems and design of black-body references. 11 p1401 A73-26514

Far infrared broad band interferometry. 11 p1369 A73-26518

Further measurements of the submillimeter background at balloon altitude. 13 p1606 A73-28188

On the observability of far infrared line emission originating from the interstellar medium. 13 p1686 A73-29368

Jupiter He abundance determination methods, considering mean density, spectral line broadening and stellar occultations with emphasis on far IR emission 14 p1799 A73-30533

Thermal imaging through hazes and fogs in the middle and far infrared windows - Some experimental results. 16 p2016 A73-33997

Far-infrared observations of galactic nuclei. 17 p2232 A73-34771

Bandpass filter with cooled InSb detector for measurement of far IR radiation and temperature-vs-wavelength characteristics of Hg arc lamp 17 p2176 A73-35774

Ground based photometry of planets, stars and galactic nebulae at 34 microns 19 p2489 A73-38529

Remote sensing of stratospheric gases using submillimetre radiation. 20 p2557 A73-39856

Low pass wide and medium band far IR filter obtained by cooling crystalline material to liquid He or nitrogen temperatures, tabulating transmission characteristics 21 p2697 A73-40127

Carbon dioxide laser pumped dielectric and metallic far IR waveguide, discussing size, mirror coupling and gas medium 21 p2713 A73-40461

Materials suitable for making far infrared high-pass transmission filters. 21 p2701 A73-40692

H II region OH maser source pumping by far IR radiation-induced population inversions between Lambda doublet levels 21 p2759 A73-40712

Far IR laser lines measurements in carbon dioxide laser pumped ethylene glycol, dimethyl ether, formic acid, and monomethyl amine, using grating spectrometer and Golay-cell detector 21 p2715 A73-40765

Observations of far infrared atmospheric windows at 44/cm and 50/cm from Pikes Peak. 21 p2780 A73-41647

Submillimeter wave spectroscopy with a vacuum Fabry-Perot interferometer 22 p2852 A73-41782

Far IR grating spectrometer using InSb detector with narrow spectral band responsivity and tunability due to cyclotron resonance absorption in magnetic field 23 p2984 A73-44364

FAR ULTRAVIOLET RADIATION

NT LYMAN ALPHA RADIATION

Optical, far UV and radio spectra observations and results for solar spicules, considering morphology, spectroscopic properties and dynamic models 01 p0094 A73-10055

Solar active regions analysis on far UV spectroheliograms obtained by OSO 4 satellite, investigating transition zone structure 01 p0098 A73-10560

Possibility of O III 304-A emissions in the extreme ultraviolet airglow. 02 p0157 A73-11755

Annual and sub-annual effects of EUV heating. I - Harmonic analysis. II Comparison with density variations.

02 p0158 A73-11914

Diffuse galactic FUV radiation and interstellar dust grains.

02 p0207 A73-12399

Apollo 16 ultraviolet astronomy observations.

02 p0220 A73-12475

EUV emitting plasma structure of solar quiet and active atmospheres, noting extreme departures from LTE

03 p0363 A73-13952

Solar rotation as measured in EUV chromospheric and coronal lines.

[AD-759854]

03 p0377 A73-14403

Side-viewing detector for a vacuum ultraviolet reflectometer.

03 p0309 A73-14430

Extreme ultraviolet observations of solar flares.

04 p0490 A73-14831

The spectra of highly ionized aluminum /Al VI-X/ in the extreme-ultraviolet and soft X-ray regions.

04 p0492 A73-15369

Molecular branching-ratio method for intensity calibration of optical systems in the vacuum ultraviolet.

05 p0597 A73-16495

The mechanism of vacuum ultraviolet emission from the Lewis-Rayleigh nitrogen afterglow.

05 p0600 A73-16560

Solar flares EUV observations by OSO 5 three band grating spectrophotometer, discussing flare intensity time dependence with superimposed impulsive bursts

05 p0610 A73-17044

Extreme-ultraviolet emission from solar prominences.

05 p0612 A73-17337

Analysis of the extreme-ultraviolet quiet solar spectrum.

05 p0625 A73-17338

Observations of the He II 304-A radiation in the night sky.

07 p0869 A73-19232

Global mean thermosphere temperature profiles as function of solar EUV flux, considering neutral gas heating and ionospheric electron temperature

07 p0869 A73-19246

Dawn airglow far UV spectrum observed by scanning Ebert spectrophotometer aboard Aerobee rocket, obtaining altitude profiles at 100-244 km

07 p0814 A73-19247

Use of MgF₂ and LiF photocathodes in the extreme ultraviolet.

08 p0964 A73-21048

Ultraviolet photometry from the Orbiting Astronomical Observatory. VII alpha squared Canum Venaticorum.

08 p1008 A73-21158

Magnetically focused electronographic cameras for far UV imagery and spectrography in astronomical and optical geophysical observations from sounding rockets and space vehicles

08 p0971 A73-21744

Aberrations, astigmatism and coma control for far UV stellar spectrograph design by grating shape and ruling space modification

08 p0972 A73-21752

The extreme-ultraviolet spectrum of Fe XV in a solar flare.

09 p1137 A73-22039

The problem of laser sources of radiation in the far-ultraviolet and X-ray regions of the spectrum

09 p1094 A73-22600

Solar rotation as determined from OSO-4 EUV spectroheliograms.

10 p1278 A73-24127

Observations of the Helium II 304-A and Helium I 584-A atmospheric dayglow radiation.

10 p1213 A73-24735

Broad band solar EUV absorption in the earth's upper atmosphere.

10 p1214 A73-24747

High resolution rocket EUV solar spectrograph.

11 p1360 A73-25059

Solar activity variation of XUV emission segregation into quiet sun and active region components via correlations of sunspots with observed fluxes and intensities

11 p1415 A73-25173

Extreme ultraviolet line intensities from the sun.

11 p1425 A73-26201

Utilization of vacuum ultraviolet radiation for measurement of humidity pulsations

12 p1521 A73-26966

Photoabsorption cross sections of H₂, D₂, N₂, O₂, Ar, Kr, and Xe at the 584-A line of neutral helium.

12 p1465 A73-26989

Absorption spectrum of Cu I in the vacuum ultraviolet.

12 p1526 A73-27122

Optical space astronomy and goals of the large space telescope.

12 p1497 A73-27436

Far UV scanning spectrometer aboard Apollo 17 CSM to measure lunar atmospheric composition, observing spectral albedo, LEM atmosphere, and galactic and solar system atmospheres

12 p1497 A73-27485

EUV spectrophotometer onboard Atmosphere Explorer satellites, discussing design, aeronautical mission objectives, constraints and economic factors

13 p1688 A73-28637

An extreme UV photometer for solar observations from Atmosphere Explorer.

13 p1688 A73-28638

Reflectance and optical constants of evaporated osmium in the vacuum ultraviolet from 300 to 2000 Å.

13 p1660 A73-28936

An analysis of the solar extreme-ultraviolet spectrum between 50 and 300 Å.

14 p1801 A73-30742

UV dayglow in 750-1050 Å region at 100-800 km observed with rocket-borne thin film filter photometer, solving radiative transfer problem for excitation process

15 p1867 A73-31077

Far ultraviolet reflectivity of lunar dust samples - Apollo 11, 12, and 14.

15 p1932 A73-31270

The extreme-ultraviolet spectrum of a solar active region.

15 p1936 A73-31560

Spectrophotometric results from the Copernicus satellite. VI - Extinction by grains at wavelengths between 1200 and 1000 Å.

15 p1936 A73-31561

Quantum oscillators employing the luminescence of self-localized excitons in condensed inert gases

15 p1885 A73-31714

Study of the influence of various parameters on the method used for determining the attenuation lengths through photoelectric yield measurements in the far ultraviolet

15 p1878 A73-32211

Arc plasmas as radiation standards in the vacuum ultraviolet.

16 p2036 A73-32942

Observations of the inner F and K coronas below 2220-Å wavelength.

16 p2060 A73-32954

The extreme ultraviolet emissions of solar flares - A comparison between OSO-6 spectroheliograph observations and SFDs.

16 p2053 A73-32959

Space observations of the variability of solar irradiance in the near and far ultraviolet.

16 p2062 A73-33428

Ultraviolet proximity focused converters for use in a satellite SEC-TV system.

17 p2170 A73-35296

VUV radiometry with hydrogen arcs. I - Principle of the method and comparisons with blackbody calibrations from 1650 Å to 3600 Å.

17 p2212 A73-35425

Vacuum UV radiation of electron beam excited high pressure Xe laser, measuring optical gain due to diatomic state-repulsive ground state transitions

17 p2186 A73-35794

Atomic oxygen profiles determined by EUV absorption analysis.

18 p2308 A73-36049

Fluorescence excitation and photoelectron spectra of CO₂ induced by vacuum ultraviolet radiation between 185 and 716 angstroms.

18 p2346 A73-36266

The Harvard experiment on OSO-6 - Instrumentation, calibration, operation, and description of observations.

18 p2357 A73-37108

Observation of the absolute intensity and the centre-to-limb variations of the sun in the vacuum ultraviolet region.

19 p2482 A73-37376

The absorption spectrum of Rb I between 350 and 810 Å.

19 p2462 A73-37623

The effect of solar activity on temperatures in the equatorial mesosphere.

19 p2426 A73-38015

A comparison of the efficiency and focused stray light characteristics of a conventionally ruled- and a holographically produced-concave diffraction grating in the vacuum ultraviolet.

19 p2431 A73-38164

NBS radiometric calibration services extended to far UV spectrum with dc high power hydrogen wall stabilized arc as primary standard of spectral radiance

21 p2703 A73-41256

Neutral composition and its variations in the lower thermosphere.

21 p2688 A73-41349

Solar corona observations in white light by OSO 7 and in XUV by Naval Research Laboratory, discussing contributions from other observatories and satellites

21 p2773 A73-41383

Further observations of the structure of the chromosphere-corona transition region from limb and disk intensities.

21 p2779 A73-41537

The far-ultraviolet spectrum of Jupiter.

22 p2905 A73-41769

Incompatibility of solar EUV fluxes and incoherent scatter measurements at Arecibo.

22 p2902 A73-41923

Estimate of extreme ultraviolet dayglow of helium in the Martian atmosphere.

22 p2909 A73-42485

French monograph - Preliminary photometric study in the far ultraviolet of the zodiacal and galactic emission.

22 p2910 A73-42716

Interference filters for the VUV /1200-1900 Å/.

22 p2863 A73-43142

Apollo 16 far-ultraviolet camera/spectrograph - Instrument and operations.

22 p2864 A73-43165

Vacuum-UV radiation of laser-produced plasmas.

23 p3008 A73-43340

Looking at the solar system in the far-ultraviolet.

23 p3034 A73-44220

FARADAY EFFECT

Experimental study of the inverse Faraday effect in plasmas

02 p0196 A73-11587

Morphic effects. III - Effects of an external magnetic field on the long wavelength optical phonons.

02 p0201 A73-12638

Traveling ionospheric disturbance analysis based on quasi-periodic perturbations in satellite transmitted VHF signal Faraday rotation, obtaining wave-like variations in electron content

03 p0300 A73-13634

The use of Faraday rotation measurements on geostationary satellites.

03 p0300 A73-13635

Determination of exospheric electron content from group delay and Faraday rotation observations of geostationary satellite signals.

03 p0300 A73-13636

A comparison of total electron content determined by the differential Doppler and the Faraday effects using radio signals from a geostationary satellite.

03 p0300 A73-13637

Problems in estimating the total electron content from Faraday rotation observations on geostationary satellites.

03 p0300 A73-13638

A receiver design for the ATS-F radio beacon experiment.

03 p0275 A73-13640

Computed effects of the ionosphere/protonosphere distribution on VHF signals from ATS-F/G.

03 p0275 A73-13641

Characteristics of large scale ionospheric irregularities.

03 p0300 A73-13652

Electro-optical, magneto-optical, absorptional and acousto-optical light modulation, noting Kerr effect, Faraday rotation and light absorption

04 p0458 A73-15348

Faraday effect in n-GaAs in the intermediate doping region

07 p0862 A73-20009

Faraday rotation of polarized extragalactic radio sources interpretation as plasmas of mixed matter and antimatter

07 p0900 A73-20277

On the procedures of measuring microwave Faraday rotation in semiconductors.

08 p0994 A73-21016

Multifrequency polarization observations of eight extragalactic sources.

08 p1008 A73-21156

Faraday pulsations and circular polarization of optical radiation from cosmic sources in terms of angle between interstellar dust orientation vector and galactic plane

10 p1273 A73-23709

Quantum theory of line formation in a magnetic field.

10 p1249 A73-24134

Electron content measurements - A method for resolving the n-pi ambiguity.

10 p1214 A73-24746

Possibilities and some results of studying the ionosphere by the method of 'incoherent' scattering of radio waves

11 p1350 A73-25088

Total electron content measurements during visible auroras.

11 p1359 A73-26714

Consideration of the different wave paths of the ordinary and extraordinary component in the calculation of electron density and collision frequency with the aid of the Faraday experiment

12 p1494 A73-27773

Faraday effect of incoherently scattered radar signals.

13 p1583 A73-28712

Rhodamine laser frequency locking using Faraday filter for tuning to sodium D lines 13 p1628 A73-29249

Total electron content of the equatorial ionosphere. 15 p1865 A73-31063

Magneto-optic investigation of MnBi films. 15 p1924 A73-31943

Non-existence of linear polarization in type III solar bursts at 80 MHz. 16 p2053 A73-32962

Faraday rotation based total ionospheric electron content information for correction of near real time satellite position determination errors, using spherically stratified ionospheric model 16 p2035 A73-33414

Helical antenna for satellite transmission. 16 p1980 A73-33686

Polarization plane rotation under magnetic field for IR waves in nonmagnetic semiconductors with cubic crystal lattices, explained by magneto-optical Faraday effect 17 p2219 A73-34342

Periodic Faraday bias and lock-in phenomena in a laser gyro. 17 p2172 A73-35413

Faraday depolarization of radio galaxies and quasars with simple spectra. 17 p2234 A73-35621

Faraday pulsations and circular polarization of optical radiation from cosmic sources in terms of angle between interstellar dust orientation vector and galactic plane 18 p2354 A73-36734

Protonospheric columnar electron content determination. I - Analysis. 19 p2426 A73-38017

Faraday rotation patterns in Crab Nebula pulsar radio spectra for average signal and giant pulses, noting difference in linear polarization percentage 19 p2488 A73-38516

Polarization characteristics of a regenerative laser with a Faraday cell and a partial polarizer 22 p2870 A73-42721

Ionospheric electron density profiles and contour plots above F layer maximum from vertical sounding and Faraday rotation techniques 22 p2851 A73-42984

The slab thickness of the mid-latitude ionosphere. 23 p2972 A73-43694

On the observation of linear polarization of solar microwave bursts. 24 p3136 A73-44644

Periodic variations in geostationary satellite polarisation observations. 24 p3082 A73-44735

FARADAY ROTATION

U FARADAY EFFECT

FARM CROPS

NT CORN

NT COTTON

The use of stress situations in vegetation for detecting ground conditions on aerial photographs. 03 p0301 A73-13844

FARMLANDS

Data handling and analysis for the 1971 corn blight watch experiment. 04 p0443 A73-15402

FAST FOURIER TRANSFORMATIONS

Signal processing; Specialists' Conference, Erlangen, West Germany, April 4-6, 1973, Reports 23 p2952 A73-43308

Theory and design of pipelined fast Fourier transform processors. 23 p2956 A73-43325

Digital filter bank with integrated FFT computer 23 p2956 A73-43326

German book on digital systems for signal processing covering discrete linear systems characteristics and design, fast Fourier transformation, digital filters, multiplexing, etc 24 p3074 A73-45000

Stress wave calculations in composite plates using the fast Fourier transform. 24 p3150 A73-45232

FAST NEUTRONS

Power frequency losses in superconductors. 07 p0864 A73-20404

LiF albedo dosimeter for fast neutron and gamma irradiation measurement on personnel, using Cf-252 source for calibration 11 p1361 A73-25313

Delta ray particle track structure theory for radiation dosimetry and biological cell response to heavy ions, fast neutrons, stopped pions and mixed radiation fields 11 p1323 A73-25423

An integrated radiation physics computer code system. 11 p1334 A73-25997

The BD-9 integral discriminator in the circuit of a scintillation-type fast neutron detector 12 p1497 A73-27207

Time dependent worldwide distribution of atmospheric neutrons and of their products. I, II, III. 16 p2055 A73-33427

A low-background counter telescope for recording alpha particles in n, α -reactions 21 p2699 A73-40173

FAST NUCLEAR REACTORS

NT FAST TEST REACTORS

FAST TEST REACTORS

Real-time X-ray inspection system for fast flux test facility fuel. 23 p2966 A73-44169

FASTENERS

NT BOLTS

NT LOCKS [FASTENERS]

Elastic-plastic analysis of stresses near fastener holes. 05 p0635 A73-16974

[AIAA PAPER 73-252] Criteria for self loosening of fasteners under vibration. II. 08 p0972 A73-20948

Criteria for self loosening of fasteners under vibration. III. 10 p1222 A73-23524

A synthesis procedure for mechanically fastened joints in advanced composite materials. 11 p1437 A73-25486

[AIAA PAPER 73-348] Holographic nondestructive evaluation of interference fit fasteners. 11 p1366 A73-26247

Corrosion performance of new fastener coatings on operational military aircraft. 11 p1637 A73-29315

[NACE PAPER 115] Compatible coatings for corrosion resistant aerospace fasteners. 13 p1638 A73-29316

[NACE PAPER 116] Critical properties of exterior aircraft finish systems to protect fastener areas. 13 p1638 A73-29317

[NACE PAPER 117] Mechanical faster types, design considerations and economic factors, detailing nut and bolt joint assembly design, static and dynamic loads and production engineering 16 p2021 A73-33862

How to be healthy, wealthy and wise through fastening analysis - The 'how to' of living with fasteners. 17 p2177 A73-34669

[SAE PAPER 730309]

FATIGUE [BIOLOGY]

NT FLIGHT FATIGUE

NT MUSCULAR FATIGUE

Airline flight and ground personnel fatigue and orthostatic hypotension syndrome manifested by variations in retinal arterial pressure and brain circulation 02 p0134 A73-12156

Energy balance and lactic acid production in the exercising rabbit. 05 p0538 A73-16156

Visual work duration and intensity effects on optic papillae expansions and shape alterations, noting differences between trained and untrained subjects 05 p0540 A73-16694

Alpha-delta sleep as replacement for delta sleep in various psychiatric patients with chronic fatigue and depression 09 p1045 A73-22694

Fatigue levels of cerebral hemispheres in response to visual task and test stimuli, noting left hander reduced performance capacity 09 p1040 A73-22925

Ergonomic endurance limits, physiological strains and fatigue assessment in video coding information task performance as function of work shift time length 11 p1323 A73-25649

German monograph - Investigation concerning a consideration of the human circadian rhythm by means of a variable working time. 13 p1580 A73-29283

Gaze-positioning eye movement perturbations during somnolence states 18 p2280 A73-36950

Amplitude variations of acoustically evoked potentials as a function of signal information and fatigue due to stress 19 p2396 A73-38161

FATIGUE [MATERIALS]

NT BENDING FATIGUE

NT METAL FATIGUE

NT THERMAL FATIGUE

Estimating the median fatigue limit for very small up-and-down quantal response tests and for S-N data with runouts. 03 p0387 A73-13230

Regression models for the effect of stress ratio on fatigue crack growth rate. 03 p0387 A73-13231

Structural reliability under cumulative fatigue damage and chance overload interaction, postulating kinetic fracture model based on probabilistic service load histories 04 p0512 A73-15243

The probability of fracture as parameter of crack propagation under cyclic stress 05 p0635 A73-17065

Subsonic jet airframe fatigue cracking as function of load, geometry, material, joint performance and environment 05 p0636 A73-17200

Growth of part-through thickness fatigue cracks in sheet polymethylmethacrylate. 06 p0714 A73-18481

High temperature fatigue sensor based on conductive composite device irreversible resistance increase resulting from cumulative strain damage 09 p1083 A73-22504

Corrosion fatigue: Chemistry, mechanics and microstructure; Proceedings of the International Conference, University of Connecticut, Storrs, Conn., June 14-18, 1971. 11 p1380 A73-25801

Corrosion fatigue considerations in engineering materials selection and design, discussing alleviation and control 11 p1442 A73-25802

Stress and displacement fields around growing corrosion fatigue crack, discussing intensity factor, plastic zones, cyclic loading and fluid pressure effects 11 p1381 A73-25813

The effect of fretting corrosion in fatigue crack initiation. 11 p1383 A73-25835

Surface damage under fretting fatigue as function of applied normal load and clamping pressure 11 p1383 A73-25836

Corrosive aspects of the fatigue of rubber. 11 p1388 A73-25841

Application of some aspects of low-cycle fatigue research in structural design. 11 p1443 A73-25846

Fatigue resistant design with fiber reinforced plastics (FRP), discussing stress analysis, failure criteria, material anisotropy, multiaxial stress conditions and cumulative damage 12 p1515 A73-26880

Book on fretting corrosion covering contacting surface theory, damage characteristics, wear variables effect, fatigue, adhesion and electrochemical properties, etc 13 p1643 A73-29575

Composite material design criteria, discussing fatigue, stress concentration, safety factors, scaling effects and load characteristics 16 p1967 A73-33028

Two theoretical models of fatigue crack propagation. 16 p2079 A73-33200

Spherical debris - Its occurrence, formation and significance in rolling contact fatigue. 16 p2022 A73-34029

An overview of fatigue and fracture for design and certification of advanced high performance ships. 17 p2246 A73-34881

Interdisciplinary communications problems of metal physicists, fracture mechanists, structural designers and reliability analysts for fatigue crack generation and growth 17 p2246 A73-34886

Creep, self heating and failure of thermoplastics under pulsating tensile stress. 17 p2197 A73-35346

Cyclic stress-strain behavior - Analysis, experimentation, and failure prediction; Proceedings of the Symposium, Bal Harbour, Fla., December 7, 8, 1971. 18 p2364 A73-36584

Japan Congress on Materials Research, 16th, Osaka, Japan, August 1972, Proceedings. 20 p2575 A73-38636

The impact resistance of glassfiber reinforced plastics under accumulation of fatigue damage. 20 p2580 A73-38645

FATIGUE DIAGRAMS

U S-N DIAGRAMS

FATIGUE LIFE

Investigation of the influence of technological factors on the endurance of gas-turbine engine rotor blades 01 p0114 A73-10477

Physical fatigue limit of hardened steels 01 p0063 A73-10485

Explosive shock hardening effects on roller steel fatigue strength, surface hardness and wear resistance 01 p0056 A73-10493

Statistical characteristics for duralumin sheets mechanical properties, fatigue life and crack growth 01 p0117 A73-11298

Effect of the quality of electrolytic chromium plating on the endurance of steel 02 p0173 A73-11926

Structural and energetic analysis of fatigue failure in metals 02 p0232 A73-11929

Hybrid fluid film and rolling element bearings for long fatigue life and gas bearings for high temperature operation in gas turbine applications [SAE PAPER 720739] 02 p0173 A73-12005

Experimental estimation of the deformation criterion of long-term/creep/strength. 02 p0180 A73-12130

Effect of diamond smoothing on the surface finish and fatigue strength of E1961 steel. 02 p0174 A73-12141

The influence of test temperature on the fatigue strength of Zhs6K alloy. 02 p0181 A73-12204

Fatigue strength of constructional materials and components of GTD-type compressors under conditions of fretting corrosion.

02 p0181 A73-12217

A temperature-programmed apparatus for fatigue testing metals.

02 p0150 A73-12218

A method of estimating the probability of faults in material on cyclic loading.

02 p0236 A73-12221

Characteristics of the fatigue curve of plastics.

02 p0185 A73-12699

Changes in microhardness as a basis of service life estimates for smooth AlCuMg specimens

03 p0321 A73-13135

Effect of a single plastic deformation on the fatigue behavior of metals

03 p0322 A73-13136

Dynamic loads intermittency effects on structural fatigue strength, discussing conditions for materials structural recovery during load pauses

03 p0385 A73-13137

Comparison of scatter under program and random loading and influencing factors.

[DFVLR-SONDDR-259] 03 p0387 A73-13232

Investigation of fatigue life and residual strength of wing panel for reliability purposes.

03 p0387 A73-13233

Application of the Monte Carlo technique to fatigue-failure analysis under random loading.

03 p0388 A73-13236

On the probabilistic determination of scatter factors using Miner's rule in fatigue life studies.

03 p0388 A73-13237

Recording of metal hardening during fatigue testing at elevated temperatures.

03 p0307 A73-13287

Low-cycle fatigue of titanium alloys.

03 p0327 A73-14007

Refractory alloys fatigue life up to 950 C under non-stationary loading, noting log-normal law distribution

03 p0327 A73-14010

Ni-Cr-Ti steel aircraft structural element fatigue life calculation based on failure mechanism involving crack propagation

03 p0394 A73-14011

Aircraft gas turbine mainshaft ball bearings fatigue life estimation via failure distribution

[ASME PAPER 72-LUB-10] 03 p0313 A73-14328

Analysis of an arched outer-race ball bearing considering centrifugal forces.

[ASME PAPER 72-LUB-28] 03 p0314 A73-14339

A new criterion for predicting rolling-element fatigue lives of through-hardened steels.

[ASME PAPER 72-LUB-32] 03 p0328 A73-14342

Optimal speed sharing characteristics of a series-hybrid bearing.

[ASME PAPER 72-LUB-39] 03 p0315 A73-14346

Fatigue crack growth data for various materials deduced from the fatigue lives of precracked plates.

04 p0506 A73-14684

Distribution functions with fatigue analysis laws and safety predictions, noting life length and fleet assurance models

04 p0507 A73-14710

Evaluation of a reliability analysis method for fatigue life of aircraft structures.

04 p0452 A73-14715

Kinetic model considering cumulative fatigue damage interaction with chance overload on component or structure under probabilistic service load, discussing crack growth in composites

04 p0508 A73-14717

Statistical stress concentration effects in composites.

04 p0468 A73-14718

Relationships between failure modes and fatigue scatter.

04 p0460 A73-14721

An investigation of fatigue life performance in lap-type solder joints.

04 p0452 A73-14852

Local stress-strain response of notched members to predict fatigue life of stress relieved and as-received weldments with internal cavities

04 p0453 A73-14864

Surface effects during fretting fatigue of Ti-6Al-4V.

04 p0461 A73-14998

Fretting-fatigue mechanisms and the effect of direction of fretting motion on fatigue strength.

05 p0581 A73-16128

Effect of specimen geometry on fatigue strength of boron and glass epoxy composites.

05 p0588 A73-16139

Porcelain enamels for heat resistant alloys low temperature fatigue strength and high temperature vibration damping increase

[SAE PAPER 720809] 05 p0633 A73-16629

Tensile and compressive prestressing effects on notched steel cantilever beam specimens low cycle fatigue life

06 p0764 A73-18490

Method for increasing the fatigue strength of hardened steels

06 p0711 A73-18666

Cu-Ni-Zu alloys high ambient temperature tensile and fatigue strengths due to recrystallization and precipitation produced fine grain microstructure, describing annealing and cold working process

06 p0711 A73-18751

Frequency dependent low cycle fatigue crack propagation.

06 p0713 A73-18767

The influence of fretting and geometric stress concentrations on the fatigue strength of clamped joints.

07 p0912 A73-19572

The effect of grain size on the fatigue of an Al-Mg alloy.

07 p0839 A73-20114

Fatigue life of aircraft structures

07 p0914 A73-20246

Hole preparation in titanium and high strength steels.

[SME PAPER IQ 72-208] 07 p0832 A73-20450

Influence of low temperatures on the fatigue life of welds

07 p0833 A73-20508

Durability of foil-type tensometric sensors under varying load conditions

07 p0827 A73-20536

Low cycle torsion fatigue, determining empirical relationship between strain amplitude and fatigue life

08 p0977 A73-21020

Evaluating the variation in fatigue properties of aluminum alloys due to variable loads by using secondary fatigue curves.

08 p0977 A73-21147

Book - Fundamentals of cyclic stress and strain.

08 p1020 A73-21836

Influence of the frequency of the tension-compression cycle on the fatigue life of D16T alloy

09 p1100 A73-22153

Solar cell fatigue life prediction by statistical analysis and extrapolation for determining failure probability curve as function of stress and time

09 p1036 A73-22808

Fatigue life prediction and design optimization for solar cell interconnectors based on elastoplastic material stress distribution calculation by finite element methods

09 p1036 A73-22809

An investigation into the relationships of fatigue fracture and inelastic deformation of metals in torsion.

09 p1161 A73-23052

Bonded joints under long-term dynamic load and their resistance to climatic effects

10 p1224 A73-24089

Fatigue properties of sandwich material with a honeycomb filler

10 p1289 A73-24097

Influence of notch and thread rolling on the fatigue strength of samples prepared from VT3-1 and VT16 alloys

10 p1233 A73-24370

Increasing the fatigue strength of metals by optimizing the thermal regime during strain hardening

10 p1226 A73-24799

Atmospheric corrosion fatigue tests for environmental conditions and superimposed stress wave effects on Cr-Mo steel fatigue life under rotating bending

10 p1235 A73-24917

Machine for life testing materials under varying tension in working media with high temperatures and pressures.

10 p1204 A73-24946

Carbon and stainless steels chemical composition effects on diffusion layer structure and fatigue strength after diffusive boring

10 p1236 A73-24954

Effect of heat treatment on the fatigue properties of unwoven fiberglass-reinforced plastics

11 p1386 A73-25047

Cumulative damage theories for the prediction of life in the case of vibrational stresses. I - A critical overview

11 p1441 A73-25576

Effects of stress wave form and cycle frequency on low cycle corrosion fatigue.

11 p1382 A73-25823

An ultrasonic device for the study of fatigue crack initiation in anodized aluminum alloys.

[AD-760070] 11 p1363 A73-25830

Neutron irradiation effects on room and high temperature fatigue behavior of stainless steel, noting fatigue life enhancement at low temperature and strains

11 p1383 A73-25832

Fretting fatigue in titanium helicopter components.

11 p1383 A73-25837

Ti alloy coating and surface treatment to prolong fatigue life by eliminating fretting damage, discussing design parameters selection, screening and strength tests and performance evaluation

11 p1383 A73-25838

Damage accumulation hypotheses concerning lifetime prediction during vibrational loading. II - A critical review

11 p1384 A73-25849

Certain fatigue phenomena in aeronautical structures with stiffened shells

12 p1553 A73-27394

Cast microstructure and fatigue behavior of a high strength aluminum alloy /KO-1/.

13 p1633 A73-28137

Studies on fatigue damage caused by stresses below the endurance limit - The effect of program period and fatigue failure by stresses below the endurance limit.

13 p1692 A73-28197

Method for the investigation of the fatigue strength of fiberglass produced by winding and loaded by inter-layer shear.

13 p1695 A73-28523

Rotating bending fatigue tests on Al coated steels, investigating electroplating, hot dip and spraying production methods effects on fatigue strength

13 p1635 A73-28645

Effect of tensile prestrain on fatigue strength of aluminum alloy in high cycle fatigue.

[ASME PAPER 72-MAT-N] 13 p1636 A73-29199

Residual surface stress changes dependence on fatigue life and steel specimen size during rotating bending fatigue tests from X ray diffraction study

13 p1625 A73-29485

Monotonic and cyclic prestrain influence on alpha-Ti fatigue life, suggesting twin/grain boundary dislocation interactions

13 p1640 A73-29486

Fatigue crack propagation as successive stochastic processes and fatigue fracture toughness.

13 p1701 A73-29490

The effect of wave form and cyclic frequency on the fatigue life of aluminium alloys.

13 p1640 A73-29491

Choice of materials on the basis of random vibration and structural fatigue.

13 p1641 A73-29495

Machine parts fatigue life and linear cumulative damage at stresses below endurance limit, including plastic strain, microcracking and S-N curves

13 p1641 A73-29496

A method for the calculation of the fatigue life of unnotched and notched specimens loaded with alternating stresses.

13 p1641 A73-29501

Life prediction of metals subjected to high temperature fatigue.

13 p1708 A73-29503

A reliability analysis of fatigue limits based on large sample quantal response data.

13 p1702 A73-29548

Effect of loading frequency and directional anisotropy on the fatigue strength of grade AMg6BM aluminum alloy sheet.

13 p1643 A73-29606

Creep test diagrams plotted to estimate heat resistance for turbine blades design, predicting fatigue life with allowance for loading cycle form and duration

13 p1703 A73-29616

Resonant frequency, fatigue and energy dissipation relations for endurance limit determination in Al alloy specimens under vibrational loads

13 p1643 A73-29618

Study of the effect of technical factors on the fatigue limit of the working blades of gas turbine motors.

14 p1810 A73-30302

Physical fatigue limit of hardened steels.

14 p1759 A73-30310

Explosive shock hardening effects on roller steel fatigue strength, surface hardness and wear resistance

14 p1755 A73-30318

Scale effect in fatigue and in corrosion fatigue of steel.

14 p1760 A73-30324

Some characteristics of the failure by fatigue of mild steel in vacuum

14 p1763 A73-30681

Testing machine to determine perforated plate biaxial tension creep rupture strength and fatigue life at high temperature

15 p1858 A73-31617

Exfoliation corrosion of aluminum alloys.

15 p1888 A73-31737

Determination of fatigue strength of welded joints with artificial flaws by radiographic examination

15 p1882 A73-32051

Properties of HSLA steels, with and without molybdenum.

15 p1891 A73-32169

German monograph on frictional fatigue failure covering microcrack initiation due to shear induced vibrational stresses

15 p1956 A73-32587

A statistical analysis of product reliability due to random vibration.

16 p2020 A73-33637

Probabilistic fatigue design alternative to Miner's cumulative damage rule.

16 p2081 A73-33643

A designer's approach to the fatigue failure mechanism.

16 p2081 A73-33644

Hot fatigue strength during fluctuating axial tension of PER 7 and IN 100 superalloys 16 p2026 A73-33971

Fatigue life of structural components under random loading 17 p2242 A73-34520

Fatigue and fracture of advanced composite materials. [SAE PAPER 730337] 17 p2194 A73-34688

Prior-to-failure extension of flaws under monotonic and pulsating loadings. 17 p2246 A73-34884

On the influence of single and multiple peak overloads on fatigue crack propagation in 7075-T6511 aluminum. 17 p2190 A73-34889

Analysis of sudden death tests of bearing endurance. [ASLE PREPRINT 73AM-3B-2] 17 p2179 A73-34984

Recognition and control of abusive machining effects on helicopter components. [AHS PREPRINT 750] 17 p2180 A73-35078

Performance, structural reliability and fatigue life of glass fiber-epoxy twin beam helicopter rotor blades [AHS PREPRINT 782] 17 p2106 A73-35095

Fiber orientation effects on fatigue failure of aligned short fiber composite materials. 17 p2198 A73-35546

Polymers fatigue life under cyclic deformation, discussing stress-strain and failure behavior as function of reversed stress cycle frequency 18 p2328 A73-36587

Applications of finite element stress analysis and stress-strain properties in determining notch fatigue specimen deformation and life. 18 p2364 A73-36591

Cumulative fatigue damage under complex strain histories. 18 p2364 A73-36593

Fatigue strength of materials under a two-frequency load /Review/ 18 p2366 A73-36754

High strength steel strain hardening residual stresses, discussing rolling treatment, complex strengthening, fatigue strength, asymmetric stress cycles and torsional stress 18 p2323 A73-36762

Fatigue of fibre-reinforced plastics - A review. 18 p2329 A73-37094

Effect of low temperature on the fatigue limit of welded joints. 19 p2433 A73-37783

Statistical characteristics of the fatigue strength of heat-resistant 1Kh18N9T steel under steady and programmed loading conditions at high temperatures 20 p2577 A73-39355

Designing equal-life minimum-weight truss structures 20 p2619 A73-39357

Influence of thermal cutting and its quality on the fatigue strength of steel. 21 p2722 A73-41253

The behavior of materials subjected to multiaxial cyclic stresses. I - Methods of calculation 22 p2917 A73-41781

Criteria relating to the fatigue life of steels subjected to alternating loads under conditions of uniaxial and biaxial static strain. 22 p2874 A73-42102

Effect of the frequency of cyclic tension-compression on the fatigue limit of alloy D16T. 22 p2874 A73-42103

German monograph - Lifetime detection in the case of acoustically loaded structures on the basis of the appropriate form of vibration. 22 p2924 A73-42741

Influence of structural changes arising during the hardening process on element lifetime 23 p2984 A73-43438

Improvement of the corrosion-fatigue strength of aluminum alloys by exposure of the medium to a magnetic field 23 p2984 A73-43466

Fracture mechanics and composite materials - A critical analysis. 23 p3040 A73-43628

The influence of flaw density and flaw size distribution on the static and dynamic fatigue behaviour of graphite. 23 p2998 A73-44037

Influence of heat treatment and surface quality on the endurance of E1961 steel 23 p2995 A73-44288

Fatigue failure predictions for plates with holes and edge notches. 23 p3047 A73-44350

The effect of the intermediate principal stress on triaxial fatigue of 7075-T6 aluminum alloy. 23 p3047 A73-44351

Static and fatigue strength of the KhN40MDTlu /EP 543/ alloy after various hardening treatments 24 p3098 A73-44475

Correlation between the static and fatigue strength of reinforced plastics 24 p3102 A73-44509

Acoustic fatigue resistance of aircraft structures at elevated temperatures. [AIAA PAPER 73-994] 24 p3056 A73-44829

Toward reliable composites - An examination of design methodology. 24 p3094 A73-45144

Behavior of materials under multiaxial vibrating loads. II - Experimental investigations 24 p3153 A73-45447

FATIGUE TESTING MACHINES

Facility for investigating low-cycle fatigue of alloys at cryogenic temperatures 01 p0029 A73-10491

High frequency fatigue test assembly for glass fiber reinforced plastics specimens under symmetric tension-compression 03 p0288 A73-13747

Error effects in dynamic force measurements performed on materials testing pulsators 04 p0450 A73-15475

Torsional fatigue fixture for high temperature investigation of high strength steels crack growth rate in tensile mode 05 p0563 A73-17254

High frequency equipment for studying fatigue in sheet materials in conditions of plane stress and elevated temperatures. 08 p0952 A73-21149

Device for investigating the mechanical characteristics of materials in a complex stressed state 09 p1070 A73-22167

Four-section equipment for studying creep and long-term strength in deep cooling conditions. 09 p1086 A73-23067

Machine for life testing materials under varying tension in working media with high temperatures and pressures. 10 p1204 A73-24946

A new fretting fatigue testing machine. 11 p1544 A73-25839

A servo-controlled axial fatigue machine with strain rate feedback for testing polymers and composites. 11 p1544 A73-26311

Testing machine for thermal fatigue with variable constraint ratio. 13 p1611 A73-28195

Method of studying the fatigue damage of metals with automatic data processing on a computer 13 p1597 A73-29053

Facility for conducting fatigue tests with sheet materials in cyclic tension 13 p1597 A73-29058

Application of analog and digital computers to fatigue testing. 13 p1622 A73-29547

Machine for investigating the fatigue and inelasticity of metals with programmed load changes both at room and at elevated temperatures. 13 p1599 A73-29636

A unit for investigating the low-cycle fatigue of alloys at cryogenic temperatures. 14 p1743 A73-30316

A test machine for fatigue under pulsed moving loads 15 p1855 A73-31144

Testing assembly for sheet metals and welded joints under static and low-cycle biaxial tension under low temperature conditions 15 p1855 A73-31147

An inexpensive, full-scale aircraft fatigue test system. [SAE PAPER 730341] 17 p2102 A73-34692

A study of thermal ratcheting using closed-loop, servo-controlled test machines. 18 p2296 A73-36585

Method of investigating fatigue damage of metals with automatic information processing by computer. 18 p2297 A73-36885

Apparatus for fatigue tests on sheet materials subject to cyclical extension. 18 p2297 A73-36890

A device for the investigation of the mechanical characteristics of materials under a complex stress system. 22 p2838 A73-42115

Fatigue test apparatus for metals at ultrasonic frequencies consisting of transducers, strain amplitude monitor, cooling circuit and static stress mechanism, discussing S-N response 22 p2867 A73-43169

Method of determining the susceptibility of metals to brittle fracture under shock loads 23 p2965 A73-43470

FATIGUE TESTS

Test results of fatigue at elevated temperatures on aeronautical materials. [ONERA, TP NO. 1098] 01 p0061 A73-10229

Influence of the loading conditions on the propagation of fatigue cracks in D16T-alloy sheet samples 01 p0064 A73-10489

Application of the VEDS-200A electrodynamic vibrator to fatigue tests in symmetric tension and compression 01 p0029 A73-10492

Unit for fatigue testing with a pulsating load at a specified force and deflection. 01 p0054 A73-11299

Fatigue crack propagation in stainless steel weldments at high temperature. 01 p0067 A73-11372

Fatigue of duralumin under cyclic loads at ultrasonic frequencies 02 p0179 A73-11566

Fatigue strength and stress-rupture strength of KhN77TiUR and KhN70VMTlu steels with a protective coating 02 p0180 A73-11628

Automated test stands for full scale aircraft structure and engine parts fatigue tests, noting equipment for programmed static and dynamic loading 02 p0166 A73-11629

Lifetime of Dural structural elements operating in aggressive media 02 p0180 A73-11794

Simultaneous manifestation of temper brittleness and hydrogen embrittlement during low-cycle fatigue of high-strength structural steel 02 p0180 A73-11927

Behavior of certain turbine-blade materials under asymmetric loading. 02 p0180 A73-12128

Experimental investigation of stresses in plates acted on by acoustic loads. 02 p0235 A73-12135

The influence of preliminary thermocycling on the high-temperature strength of austenitic steel. 02 p0180 A73-12139

A temperature-programmed apparatus for fatigue testing metals. 02 p0150 A73-12218

Growth of fatigue cracks in polycarbonate. 02 p0185 A73-12430

Performance of an inhibitor-protector of steel against corrosion-fatigue failure at elevated temperatures and pressures. 02 p0182 A73-12700

Corrosion fatigue of type 4140 high strength steel. 02 p0183 A73-12764

Machine components dimensioning and testing for fatigue strength, presenting methods for service life determination 03 p0385 A73-13132

Studies of fatigue in smooth AlCuMg specimens 03 p0321 A73-13134

Probabilistic aspects of fatigue; Proceedings of the Symposium, Atlantic City, N.J., June 27-July 2, 1971. 03 p0387 A73-13228

New method for the statistical evaluation of constant stress amplitude fatigue-test results. 03 p0387 A73-13229

Random fatigue of 2024-T3 aluminum under two spectra with identical peak-probability density functions. 03 p0322 A73-13235

Recording of metal hardening during fatigue testing at elevated temperatures. 03 p0307 A73-13287

Cumulative fatigue damage tests of Al alloy, evaluating Miner cycle/stress ratio 03 p0325 A73-13571

Microstructural changes that drilling and reaming can cause in the bore holes in DTD 5014 /RR58 extrusions/. 03 p0325 A73-13573

Resonance type facility using dynamic hysteresis loop method to test metal fatigue and anelasticity in torsion at room and high temperatures 03 p0288 A73-14025

Fatigue scoring - A new form of lubricant failure. [ASLE PREPRINT 72LC-3B-1] 03 p0316 A73-14356

Size effect in fatigue testing of metals explained, considering implications for bending, torsion and axial loading 03 p0396 A73-14646

Fatigue threshold crack propagation in air and dry argon for a Ti6Al-4V alloy. 04 p0459 A73-14685

Extensive study of low fatigue crack growth rates in A533 and A508 steels. 04 p0459 A73-14686

Fatigue crack propagation of D6ac steel in air and distilled water. 04 p0459 A73-14688

Delay effects in fatigue crack propagation. 04 p0459 A73-14690

Rayleigh waves for continuous monitoring of a propagating crack front. 04 p0452 A73-14691

The relationship between design allowances and load induced micromechanical damage in composite materials. 04 p0508 A73-14719

Visual display of fatigue damage by means of exoelectron emission. 04 p0446 A73-14748

Predictive testing in elevated temperature fatigue and creep - Status and problems. 04 p0453 A73-14853

Applications of exoelectron emission to nondestructive evaluation of alloying, crack growth, fatigue, annealing, and grinding processes. 04 p0453 A73-14856

The early detection of fatigue damage by exoelectron emission and acoustic emission. 04 p0453 A73-14858

Verification of structural integrity of pressure vessels by acoustic emission and periodic proof testing. 04 p0453 A73-14859

Techniques for smooth specimen simulation of the fatigue behavior of notched members. 04 p0453 A73-14862

Airframe structural testing and safety design for military aircraft, discussing static, dynamic and fatigue tests and environmental effects. 04 p0454 A73-14865

Fatigue crack growth measurement on Al alloy wedge-opening-load specimens under constant amplitude sinusoidal loading, comparing data with existing crack propagation results. 04 p0462 A73-15241

Fractographic observations of fatigue crack tip behavior of age hardened Al-Zn-Mg-Cu alloy during static loading. 04 p0462 A73-15242

Critical thickness effect of fatigue notched specimens on stress intensity factor and fracture toughness behavior of Ti-Al-V alloys. 04 p0462 A73-15244

Low-cycle fatigue behavior of quenched and tempered UNI 38NiCrMo4 steel. 04 p0462 A73-15300

Investigation of the effect of vacuum environment on the fatigue and fracture behavior of 7075-T6. 04 p0466 A73-15764

A plastic-strip specimen for fatigue crack propagation studies in low yield strength alloys. 05 p0581 A73-16127

Low cycle fatigue tests of medium strength Al alloys, showing agreement with Manson-Halford fatigue life-strain relation. 05 p0586 A73-16135

Predicting failures with conducting-polymer fatigue-damage indicators. 06 p0759 A73-17598

Determination of constants in the equation for the fatigue-crack propagation rate with allowance for properties of the plastic zone. 06 p0761 A73-17847

Cyclic endurance and alteration nature of the dislocation structure in nickel before and after programmed strengthening. 06 p0707 A73-17906

Thermal fatigue resistance of borided alloy KhN70VMYuT. 06 p0709 A73-18215

Fatigue and fracture basic research at the Langley Research Center. 06 p0764 A73-18486

Direct observation of tensile and fatigue cracks. 06 p0710 A73-18495

A note on fatigue crack starter defects produced by a pulsed laser. 06 p0710 A73-18500

Electrostatic field effects on the fatigue of steel in vacuum. 06 p0711 A73-18661

Effects of ash deposition on the fatigue strength of the working blade material in gas turbines. 06 p0741 A73-18662

S-N fatigue curve analysis from ultimate tensile strength to cyclic elastic limit below fatigue limit, discussing load cycle zones and discontinuities. 07 p0910 A73-19214

Welded structural components fatigue behavior representation by characteristic curves derived from S-N diagrams, describing data reduction procedure. 07 p0910 A73-19216

Effects of surface roughness and form factor on rolling contact fatigue. 07 p0831 A73-20119

Metal tongues in trailing edge of surface pits near fracture path end in rolling contact fatigue of failed ball bearings. 07 p0831 A73-20158

Inhibition of corrosion fatigue in 7075 aluminum alloys. 07 p0840 A73-20351

A new method of measurement to determine the stress-strain relation in a bending fatigue specimen. 07 p0917 A73-20488

Investigation of the low-cycle fatigue of light-alloy welds. 07 p0833 A73-20506

Estimation of the fatigue characteristics of D16T and AVT1 aluminum alloys from the breaking stress. 07 p0841 A73-20515

Low cycle torsion fatigue, determining empirical relationship between strain amplitude and fatigue life. 08 p0977 A73-21020

Some fatigue properties of welded high temperature alloys. 08 p0978 A73-21241

Variable-load endurance criteria for steels under conditions of uniaxial and biaxial static tension. 09 p1100 A73-22152

Device for endurance testing of materials at low temperatures. 09 p1070 A73-22168

Influence of inclusion content on fatigue crack propagation in aluminum alloys. 09 p1101 A73-22409

Ultrafine grained two-phase alloys fatigue properties as function of phase volume fractions and grain size, noting Coffin law type behavior from low cycle fatigue tests. 09 p1102 A73-22411

Effects of hold time on low-cycle fatigue behavior of AISI Type 304 stainless steel at 593 C. 09 p1102 A73-22417

Substructure formation around fatigue cracks and its role in the propagation of fatigue cracks in aluminum. 09 p1103 A73-22437

Surface fatigue crack morphology comparison to bulk crack developments, considering surface grains constraints by adjoining grains. 09 p1103 A73-22441

Acoustic emission for monitoring fatigue crack growth. 09 p1083 A73-22511

Transmission electron microscope study on initiation of fatigue crack in 18-8 austenitic steel. 09 p1104 A73-22523

Influence of environment on the appearance of fatigue striations in various alloys. 09 p1104 A73-22716

An apparatus for measuring and recording the electrical resistance of metal specimens during mechanical testing. 09 p1070 A73-23066

Heat resistant alloys stress-rupture strength tests for operating temperatures based on equivalent high temperatures damageability. 09 p1106 A73-23156

Effect of loading frequency on fatigue strength of metals. 09 p1106 A73-23159

The effect of the structure of the titanium alloys VT3-1 and VT-18 on their fatigue resistance under asymmetrical cyclic loading. 09 p1106 A73-23164

Fatigue and creep testing of unidirectional carbon fibre reinforced plastics. 10 p1238 A73-23965

Character and magnitude determination of residual stresses in surface layers of rolling bodies. 10 p1289 A73-24068

Difference of the plastic deformation of the surface and internal layers of polycrystalline iron under fatigue loading. 10 p1233 A73-24183

Investigation of stress state at fatigue crack tip by means of X-ray microbeam. 10 p1293 A73-24918

Electron fractography of fatigue failure and macrocrack propagation in dual phase Ti alloy during cyclic loading at minus 140 to plus 150 C. 10 p1236 A73-24931

Varying-temperature test installation for the interior design of the Concorde. 11 p1342 A73-25103

Welded joints fatigue properties, considering porosity, nonmetallic occlusions and cracks effects. 11 p1372 A73-25105

Fatigue-crack growth in Type 304 stainless steel weldments at elevated temperatures. 11 p1379 A73-25131

Cyclic stress, strain, and energy variations under cumulative damage tests in low-cycle fatigue. 11 p1379 A73-25132

Low temperature vacuum fatigue testing facility for materials testing under space environment conditions. 11 p1343 A73-25445

Phenomenological approach to low-cycle fatigue fracture of a typical aircraft full scale component static test. 11 p1305 A73-25554

[ALAA PAPER 73-324] Frequency and environmental interactions in the fatigue of aluminum alloys. 11 p1382 A73-25824

Effect of water vapor on fatigue behavior of an aluminum-boron composite. 11 p1383 A73-25828

The effect of vacuum on the high temperature, low cycle fatigue behavior of structural metals. 11 p1383 A73-25834

Damage accumulation hypotheses concerning lifetime prediction during vibrational loading. II - A critical review. 11 p1384 A73-25849

Structural failures in light weight solar cell arrays under thermal cycling. 11 p1310 A73-25999

Fretting fatigue strength of several materials combinations. 11 p1385 A73-26335

High frequency load tests for fatigue properties of glassand carbon fiber reinforced plastics and epoxy impregnated wood laminates. 12 p1515 A73-26879

Fatigue and impact tests on composite propeller blades made of glass- and carbon fiber reinforced plastics, noting comparison with measured vibratory strains. 12 p1458 A73-26881

Thermal stresses arising in high-frequency fatigue tests. 12 p1512 A73-27259

Stability of a multivariable discrete system for controlling a fatigue testing process with random loading. 12 p1557 A73-27949

Studies on fatigue damage caused by stresses below the endurance limit - The effect of program period and fatigue failure by stresses below the endurance limit. 13 p1692 A73-28197

Evaluation of torsional fatigue damage from changes in the fatigue properties and microhardness. 13 p1635 A73-28522

A hypothesis of non-propagating fatigue crack. 13 p1635 A73-28644

Method of studying the fatigue damage of metals with automatic data processing on a computer. 13 p1597 A73-29053

Relationship between the strain curves of a material subjected to static and to cyclic loads. 13 p1698 A73-29055

A potential means of using acoustic emission for crack detection under cyclic-load conditions. 13 p1700 A73-29401

X-ray investigation of fatigue-crack growth - On critical strain for fracture at the crack tip. 13 p1625 A73-29482

Further consideration of crack propagation by oscillating crystal X-ray microbeam diffraction technique. 13 p1625 A73-29483

The effect of plastic anisotropy in the low-cycle fatigue behavior of Zircaloy. 13 p1640 A73-29487

Statistical definition of fatigue behavior of strength of low alloy steels. 13 p1641 A73-29492

Correlation between notch sensitivity of a material and its non-propagating crack, under rotating bending stress. 13 p1641 A73-29493

Random and program fatigue tests of Cr-Mo steel specimens with V-grooved notch. 13 p1641 A73-29494

Aspect of cumulative fatigue damage under multiaxial strain cycling. 13 p1701 A73-29497

Fatigue damage by a stress below the endurance limit. 13 p1641 A73-29498

Cumulative damage and behavior of plastic strain in high and low cycle fatigue. 13 p1641 A73-29500

Fatigue analysis considering rotating principal stress axes for aluminum alloy 2024-T351. 13 p1641 A73-29502

Effect of temperature and strain rate on the high temperature, low cycle fatigue behaviour of a 17Cr-10Ni-2Mo stainless steel. 13 p1708 A73-29504

The effect of elevated temperature upon the fatigue-crack propagation behavior of two austenitic stainless steels. 13 p1642 A73-29525

On fatigue damage and debonding of glass fiber reinforced plastics. 13 p1647 A73-29546

Energy dissipation in metals in high-frequency fatigue tests. I. 13 p1643 A73-29630

Energy dissipation in metals in high-frequency fatigue tests. II. 13 p1643 A73-29631

High frequency model U-20P fatigue testing unit with program control of the specimen vibration amplitude. 13 p1599 A73-29637

Acoustic-emission detection techniques for high-cycle-fatigue testing. 14 p1751 A73-29772

The effects of out-of-phase biaxial-strain cycling on low-cycle fatigue. 14 p1806 A73-29774

Effect of loading conditions on the propagation of fatigue cracks in sheet samples of D16T alloy. 14 p1759 A73-30314

The use of a type VEDS-200A vibrostand for fatigue tests under conditions of symmetrical tension-compression. 14 p1743 A73-30317

- Fatigue behaviour of ribbon-reinforced composites.
15 p1898 A73-31840
- Scanning electron microscope analysis of Ti-Al-V specimens under simultaneous fatigue and fretting loads
15 p1883 A73-32148
- Wing spar static and fatigue tests and S-N curve for lifetime measurement of root sections of small trainer and passenger aircraft
15 p1955 A73-32190
- Some findings from a preliminary fatigue experiment with model light-alloy specimens
15 p1955 A73-32191
- A method of programmed fatigue tests with short-time overloads.
17 p2165 A73-34277
- Method of recording the deformation diagram in thermal-fatigue tests.
17 p2165 A73-34278
- Heat treated polyacrylonitrile filament produced carbon fiber strengthened after fatigue testing, noting maximum strengthening effect after 1000 load cycles
17 p2194 A73-34635
- Workhardening, slip band formation and crack initiation during fatigue of titanium.
17 p2190 A73-34882
- Static, dynamic and fatigue load influence on solid lubricant compact bearings.
[ASLE PREPRINT 73AM-1A-1]
- Heavy lift helicopter rotor hub design and fatigue test technology, using fail-safe criteria, finite element analysis and fracture mechanics
[AHS PREPRINT 784]
- Fundamentals of fatigue and creep rupture of a thermoplastic.
17 p2197 A73-35345
- Tension-tension low cycle fatigue failure mechanism in uniaxially and biaxially reinforced boron fiber-aluminum alloy composites, considering matrix plasticity role
17 p2193 A73-35544
- An automatic flash photomicrographic system for fatigue crack initiation studies.
18 p2316 A73-36588
- The effect of load interaction and sequence on the fatigue behavior of notched coupons.
18 p2364 A73-36589
- Cyclic inelastic deformation and the fatigue notch factor.
18 p2364 A73-36590
- On the physical justification of the term 'state of fatigue of materials under cyclic loading.'
18 p2364 A73-36592
- The plastic bending of beams and their failure by low cycle fatigue.
18 p2365 A73-36617
- Method of investigating fatigue damage of metals with automatic information processing by computer.
18 p2297 A73-36885
- Relation of strain curves of material in static and cyclical loading.
18 p2366 A73-36887
- Fractography of stress corrosion in Ti-8Al tested in fatigue.
18 p2326 A73-36972
- Biaxial cyclic high-strain fatigue of aluminum alloy RR58.
19 p2440 A73-37437
- DC 10 airframe structure full scale fatigue tests for crack initiation and growth, residual strength and service life
[AIAA PAPER 73-803]
- Weldbonding/rivetbonding - Application testing of thin gauge aircraft components.
[AIAA PAPER 73-805]
- Fracture types in load-controlled low-cycle fatigue.
19 p2498 A73-37666
- Investigation of low-cycle fatigue of welded joints in light alloys.
19 p2433 A73-37781
- Evaluation of the fatigue properties of aluminum alloys D16T and AVTI on the basis of limit stresses.
19 p2440 A73-37790
- Investigation of fatigue strength of DIT alloy with due regard to dispersion of results.
19 p2440 A73-37791
- System for determining the critical range of stress-intensity factor necessary for fatigue-crack propagation.
19 p2501 A73-38297
- The effect of stress amplitude below the fatigue limit on cumulative fatigue lives in perforated round specimens.
19 p2501 A73-38344
- Quantitative estimation of the fatigue crack propagation under varying load conditions.
19 p2501 A73-38346
- Metal fatigue studies of nucleation and crack propagation through plastic and elastic regimes
19 p2502 A73-38548
- Influence of cycle ratio on the elastic modulus of glassfiber reinforced plastics subjected to repeated tensile load.
20 p2580 A73-38644
- A fatigue test program for the wing of the Jantar SZD-37 sailplane
20 p2509 A73-39245
- Investigation of energy criteria for the failure by fatigue of some metals at low and high loading frequencies
20 p2577 A73-39354
- Experimental investigation of changes in the fracture toughness of aluminum alloys
20 p2577 A73-39359
- High-frequency fatigue tests at low temperatures
20 p2619 A73-39363
- Study of low-cycle fatigue of titanium-base alloys at a temperature of -196 C
20 p2577 A73-39375
- Fatigue life under random loading with varying mean stress and rms value.
20 p2622 A73-39553
- Experimental error equation of stress intensity factor for fracture toughness and crack growth rate testing
21 p2785 A73-40635
- The interaction of creep and fatigue for a rotor steel /The William M. Murray Lecture, 1972/.
21 p2722 A73-41264
- Fatigue behavior of stiffened flat panels
21 p2788 A73-41555
- A unit for fatigue testing of materials at low temperatures.
22 p2838 A73-42116
- Effect of multiple overloads on fatigue crack propagation in 2024-T3 aluminum alloy.
22 p2875 A73-42139
- Fatigue-crack growth under variable-amplitude loading in ASTM A514-B steel.
22 p2875 A73-42140
- Fatigue crack propagation and fracture toughness of 5Ni and 9Ni steels at cryogenic temperatures.
22 p2875 A73-42143
- Structure of polymers and fatigue crack propagation.
22 p2880 A73-42152
- Monograph - Fatigue and stochastic loadings.
22 p2923 A73-42673
- Fatigue-crack initiation studied by electrical resistance measurements.
23 p2979 A73-43301
- Fatigue failure analysis of low carbon steel endurance under cyclic loading with time dependent viscoelastic effects, using Hooke's-Trouton laws
23 p3040 A73-43469
- Characterization of composites for the purpose of reliability evaluation.
23 p3040 A73-43627
- A review of fatigue crack growth in high strength aluminum alloys and the relevant metallurgical factors.
23 p2991 A73-43806
- Fatigue crack growth retardation after single-cycle peak overload in Ti-6Al-4V titanium alloy.
23 p2992 A73-43809
- Environmental effects on fracture resistant and biaxial fatigue design of aircraft structures.
23 p3042 A73-43811
- Fatigue crack growth detection by acoustic emission monitoring in correlation with stress intensity for high cycle fatigue Al alloy
23 p2992 A73-43814
- Acoustic emission from low-cycle high-stress-intensity fatigue.
23 p2992 A73-43816
- FATS
NT CHOLINE
FATTY ACIDS
NT OLEIC ACID
Hepatic lipogenesis in fasted, re-fed rats and mice - Response to dietary fats of differing fatty acid composition.
03 p0258 A73-13054
- Effect of cultural conditions on the fatty acid composition of *Thiobacillus novellus*.
03 p0261 A73-13599
- Effect of hypoxia on free fatty acid metabolism during exercise.
05 p0540 A73-16609
- Spin-labeling studies on the membrane of a facultative thermophilic bacillus.
07 p0782 A73-20027
- Effect of low temperature on metabolism of rat liver slices and epididymal fat pads.
07 p0782 A73-20170
- Serum tryptophan level after carbohydrate ingestion - Selective decline in non-albumin-bound tryptophan coincident with reduction in serum free fatty acids.
12 p1464 A73-27975
- Exogenous free fatty acid effects on hypoxic myocardial function in isolated isometric rat papillary muscles
13 p1577 A73-29572
- Fatty acids of *Pinus elliottii* tissues.
15 p1841 A73-32199
- Reactions of singlet oxygen with pine pollen.
19 p2402 A73-38295
- FFA metabolism in thyroidectomized and normal dogs during rest and acute cold exposure.
20 p2515 A73-39787
- Serum tryptophan level after carbohydrate ingestion - Selective decline in non-albumin-bound tryptophan coincident with reduction in serum free fatty acids.
21 p2640 A73-41218
- Emotionally induced increases in heart rate and plasma catecholamine and free fatty acids, noting relation to coronary heart disease
22 p2809 A73-42837
- FAULT MECHANICS
U FRACTURE MECHANICS
FBFM [MODULATION]
U FEEDBACK FREQUENCY MODULATION
FCC LATTICES
U FACE CENTERED CUBIC LATTICES
FEASIBILITY ANALYSIS
Feasibility study for direct TV transmission and reception via satellite, discussing technical and economic aspects
[DGLR PAPER 72-050]
- Feasibility analysis of MIS sandwich structure for pulsed laser based on calculation for field distribution and TE and TM modes in optical cavity
09 p1093 A73-22254
- Management aspects of the development of the Ariel 4 satellite.
09 p1168 A73-22915
- Low altitude orbit feasibility study of integrated SNAP 29/Agenda satellite configuration, comparing with solar cell power system
11 p1396 A73-26040
- High data rate YAG laser communication experimental systems with partial cavity dumping, orthogonal setup or harmonic mode locking, investigating internal modulation feasibility
11 p1378 A73-26246
- Design considerations for offshore airports.
15 p1856 A73-31527
- San Diego offshore airport feasibility to meet future air traffic demands, evaluating sites for capacity, environmental impact, access and construction costs
15 p1857 A73-31543
- Reduction of nitrogen oxide emissions from a gas turbine by fuel modifications.
16 p2045 A73-33483
- Feasibility experiments for high capacity Hertzian cables to distribute and collect data within urban areas, using cylindrical mirrors
16 p1982 A73-33715
- Exploratory development of composite missile fuselages.
17 p2181 A73-35354
- Easing international language difficulties via an accommodating software design.
18 p2288 A73-36092
- Whole aircraft and component design optimization, discussing criteria, constraints and performance prediction accuracy during feasibility analysis and project design
19 p2378 A73-37410
- Structural optimization by methods of feasible directions.
19 p2496 A73-37478
- Analysis of pressure waves as a mean of diagnosing vascular obstructions.
19 p2398 A73-37524
- An offshore airport in Sydney region - Review of a 1972 feasibility study.
19 p2418 A73-37744
- Freighter airships economical and technological feasibility study, discussing performance requirements and design concepts
[SAWE PAPER 951]
- Feasibility analysis of satellite solar/thermal power generation and transmission to earth, describing Brayton cycle heat engine for initial energy conversion
19 p2391 A73-38404
- Feasibility of satellite solar power station technology concepts, discussing cost analysis, energy conversion efficiency, weight, space environment and microwave transmission
20 p2510 A73-39247
- Application of silicon photoelectric converters in solar orientation sensors
20 p2510 A73-39449
- FEDERAL BUDGETS
Airport and Airway Development Act trust fund surplus, discussing expenditure policy determination and incentive plan provisions to expedite improvements
12 p1561 A73-27367
- Space shuttle program budget difficulties, discussing consequences of cost increase or program suspension
21 p2793 A73-40234
- FEDERAL REPUBLIC OF GERMANY
U GERMANY
FEED SYSTEMS
Selection of a surface tension propellant management system for the Viking 75 Orbiter.
[AIAA PAPER 72-1042]
- Contamination damage avoidance concepts for propulsion feed system components.
07 p0868 A73-20470
- Cryogenic propellants in rocket engines.
16 p2045 A73-33118

FEEDBACK

- NT NEGATIVE FEEDBACK
- NT NONLINEAR FEEDBACK
- NT POSITIVE FEEDBACK
- NT SENSORY FEEDBACK

Changes in ventilatory patterns after ablation of various respiratory feedback mechanisms.

01 p0007 A73-10162

Acoustic feedback phenomena in the case of a subsonic and supersonic free jet which impinges on an obstacle

[DGLR PAPER 72-084]

02 p0127 A73-11683

Parasitic oscillations in external excitation oscillators due to internal feedback in transistor, investigating frequency dependence of stability coefficient in common emitter stage

03 p0284 A73-14032

Parametric synchronization of self-oscillators with feedback delay and nonlinear circuit

11 p1337 A73-25429

Spontaneous-emission feedback in a three-level quantum system - A case of conflict between semiclassical and quantum theories of radiation.

13 p1659 A73-28375

Detection of a feedback in a plasma-electron beam system

14 p1781 A73-30585

Hodograph construction by root trajectory method to provide maximum information on linear feedback systems dynamics

14 p1740 A73-30945

Interaction of self-excited vibrations in mechanical vibrational systems

19 p2494 A73-37181

FEEDBACK AMPLIFIERS

Low noise regenerative amplifier with direct coupling to load, noting optimal use at moderately high frequencies

03 p0284 A73-14033

Selectivity evaluation for reflection and transmission regenerative amplifiers of complex design

03 p0284 A73-14034

Low-pass filters and their realization by means of active circuits with operational amplifiers

06 p0673 A73-17723

Synthesis of functions for polynomial linear-phase amplifiers with feedback

08 p0947 A73-21396

Feedback in amplifier circuits synthesis and analysis, discussing energy transfer, source impedance and terminals

10 p1201 A73-24383

A low-velocity hot-wire anemometer.

12 p1496 A73-27055

Design of sinusoidal and pulsed signal amplification stages with emitter high-frequency compensation.

12 p1480 A73-27273

Errors of the formal theory of amplifiers with a feedback

12 p1481 A73-27594

SNR improvement by negative feedback and deterioration by positive feedback in amplifiers, discussing input circuit thermal noise

13 p1591 A73-28735

Evaluation of the noise and dynamic range of transistorized selective RC amplifiers with controlled tuning

13 p1591 A73-28868

Reduction of nonlinear distortions in a two-port network exhibiting a small nonlinearity

13 p1592 A73-28894

Synthesis of regenerative amplifiers with isothermal approximation of the amplitude-frequency characteristics

13 p1592 A73-28896

Optimal feedback characteristics of transistor amplifiers

14 p1736 A73-30372

Self-stabilizing power amplifiers with combination-type negative feedback

14 p1736 A73-30564

Instability of feedback systems containing several time-varying nonlinear amplifiers.

19 p2414 A73-38078

Synthesis of the functions of polynomial linear-phase feedback amplifiers.

19 p2410 A73-38354

Parallel resonator with a resistance and a frequency dependent negative resistance realized with a single operational amplifier.

19 p2411 A73-38356

Analysis of a resonant amplifier with stagger-tuned circuits at the input and output

20 p2538 A73-39466

Determination of optimal regimes of a common-emitter transistor cascade which ensure minimal distortions

21 p2659 A73-40012

Noise characteristics in bipolar transistor differential amplifiers, discussing current sources, circuit configurations, feedback amplifiers and equivalent circuits

22 p2832 A73-41897

Two terminal network immittance converters with feedback for passband and IC operational amplifier applications

23 p2959 A73-43515

Crosstalk interference and regenerative amplifier noise effects on PCM signal transmission over twin- and four-conductor lines

23 p2954 A73-43784

Aspects of field-effect transistor applications in amplifier stages with feedback

24 p3072 A73-44936

FEEDBACK CIRCUITS

Resonant feedback loops and impedance matching network analysis of pulsed and CW transistor microwave power oscillators

01 p0024 A73-10722

FM threshold performance of the frequency demodulator with feedback.

03 p0276 A73-13903

FM noise spectrum measurement in feedback harmonic oscillators with crystal or transmission cavity resonators as discriminator for frequency stability

05 p0556 A73-16164

Linear time-invariant feedback systems with multiple inputs and outputs, deriving necessary and sufficient conditions for stable closed loop impulse response

05 p0561 A73-16493

Feedback networks for RC oscillators with maximum frequency stability

06 p0673 A73-17581

Transmission quality in noiseless multiple-access systems with feedback

06 p0679 A73-17855

Analysis of parametron oscillation characteristics based on the collector-junction capacitance of the transistor.

10 p1193 A73-23666

Feedback loop and forward path electronic circuits, discussing two port network representation

10 p1201 A73-24384

Effect of nonlinearity in the feedback loop of a recirculation comb filter.

10 p1203 A73-24935

Constant-Q pulsed feedback electronics for strapped-down gyro systems.

11 p1342 A73-26635

Frequency characteristics of directional loop-type bandpass filters

12 p1477 A73-26870

SNR improvement by negative feedback and deterioration by positive feedback in amplifiers, discussing input circuit thermal noise

13 p1591 A73-28735

Charge transfer semiconductor devices operational principles and possible structures with two or three phases, discussing efficiency, regeneration circuitry and noise and dissipation problems

14 p1731 A73-29727

Phase effect in RC transistor oscillator with single transistor or tube as amplifying element, determining vibration frequency, reverse communication amplification and frequency dependence

14 p1737 A73-30793

Operational modes of the feedback circuit of an asynchronous logical network

14 p1731 A73-30939

Effect of nonlinearity in a coherent pulse integrator on signal-to-noise gain.

15 p1842 A73-30988

Nonlinear distortions of series-connected two-port networks

15 p1850 A73-31253

HYPHA analog-to-digital converters with phase-locked loops.

16 p1991 A73-32719

Dynamic analyses of hybrid bio/mechanical networks with feedback characterization.

16 p1975 A73-33161

Book - Solid state electronic circuits: For engineering technology.

18 p2292 A73-35899

Modes of operation of the feedback loop in an asynchronous logical network.

19 p2414 A73-38193

Feedback in microminiaturized transistor amplifiers

21 p2659 A73-40010

Graphical analysis of traveling-wave-tube oscillator with external feedback loop.

21 p2663 A73-41046

The estimate feedback equalizer - A suboptimum nonlinear receiver.

21 p2656 A73-41165

Voltage-to-frequency converters with an avalanche-recombination discharge diode

22 p2832 A73-42357

A phase discriminator with feedbacks

24 p3071 A73-44545

FEEDBACK CONTROL

NT CASCADE CONTROL

A simple Fourier analysis technique for measuring the dynamic response of manual control systems.

01 p0027 A73-10321

Almost sure exponential bounds for stochastic operator systems, with applications to randomly sampled control.

01 p0027 A73-10426

Photographic equipment for astronomical telescopes, considering mechanical devices for plate translation and rotation, guiding microscope and digitally controlled servomotors with incremental feedback

01 p0049 A73-10541

Investigation of a class of nonsearching extremal-control systems with pulse frequency modulation

01 p0027 A73-10594

Synthesis of a magnetoelastic control medium for stabilization of hydrodynamic flows

01 p0084 A73-10669

Experimental satellite for attitude control. I - System design.

01 p0111 A73-11188

Analysis of an altitude control system of a low flying vehicle.

01 p0075 A73-11195

Non-interacting control of non-linear multivariable systems.

01 p0028 A73-11517

Effects of controller dynamics on the stability of a class of optimal control systems.

01 p0028 A73-11518

Special features of the calculation of electromechanical instrument servosystems with velocity feedbacks

02 p0148 A73-11861

Automated system with CW signal and feedback to measure delay line group delay and transfer function frequency responses, detailing operation and errors

02 p0146 A73-11952

Construction of Lyapunov functions for nonstationary systems containing memoryless nonlinearities.

02 p0193 A73-12123

A new circle criterion for the stability of nonlinear control system.

02 p0149 A73-12346

A graphical test for checking the stability of a linear time-invariant feedback system.

03 p0285 A73-13519

Invariant poles feedback control of flexible highly variable spacecraft.

03 p0285 A73-13522

German monograph - Application of estimation procedures for the characteristic parameters of controlled systems on the basis of measurements on the closed control loop.

03 p0285 A73-13811

Mathematical model, digital filter design and phase error behavior derivation for higher order discrete phase locked loops

03 p0276 A73-13906

Switching stepdown dc-to-dc converter with analog signal to discrete interval converter, hybrid micromodule and two-loop control subsystem, discussing circuitry and performance

03 p0283 A73-13935

Book on linear optimal control theory covering systems analysis, state reconstruction, stochastic nature and feedback control

03 p0286 A73-13992

Dynamic modelling of the innovation cycle as applied to fluidics.

03 p0258 A73-14450

Analog signal to discrete time interval converter /ASD/TIC/ feedback control for high performance aerospace power supply conditioning

[AIAA PAPER 72-1057]

04 p0486 A73-14901

Nonlinear analysis of double feedback loop tracking system with coupling, obtaining steady state phase error probability density functions with application to satellite transponder

04 p0429 A73-14994

Adaptive feedback control without complete plant identification, deriving vector cost function and algorithm for performance optimization

04 p0430 A73-15214

The nonlinear analysis and design constraints of a multi-filter phase-lock loop.

04 p0421 A73-15434

Digital phase locked loops for incoming signal phase tracking, predicting performance from nonlinear difference equation model for comparison with digital simulation

04 p0421 A73-15435

Equivalent, filter realization and threshold CNR determination for optimum design of extended range phase locked loop

04 p0421 A73-15436

Fredholm operator theory application to linear feedback system input-output stability in terms of origin encirclement counting in complex plane

05 p0561 A73-16488

Need for within-trial feedback as a function of task similarity in adaptive training of manual control.

05 p0543 A73-16709

Application of the control configured vehicle concept to a Space Shuttle configuration.

[AIAA PAPER 73-158]

05 p0629 A73-16905

Optimal flight control system design for aircraft with large flight envelopes, using optimal control theory with limited measurement feedback [AIAA PAPER 73-159] 05 p0535 A73-16906

Active flutter control - An adaptable application to wing/store flutter. [AIAA PAPER 73-194] 05 p0531 A73-16930

Energy management in aerial combat weapon systems maneuvering and delivery tactics, computing optimal feedback control laws for supersonic aircraft minimum time turning trajectories [AIAA PAPER 73-231] 05 p0536 A73-16956

Soft constraint trajectory optimization formulation as real time optimal feedback guidance method for multiborn orbital maneuvers [AIAA PAPER 73-249] 05 p0596 A73-16972

Combinational servosystem with a self-adjusting loop 05 p0561 A73-17250

Continuous measurement of internal friction and modulus with a regenerative feedback loop and composite oscillator. 05 p0559 A73-17255

Suboptimal feedback control of linear gyroscopic systems. 06 p0679 A73-17568

Decoupling in a class of nonlinear systems by state variable feedback. [ASME PAPER 72-AUT-V] 06 p0679 A73-17725

The method of Lyapunov functions in control problems for distributed-parameter systems /A survey/. 06 p0723 A73-17953

Application of linear feedback control theory techniques to continuum dominated by electrostatic and gravitational fields. 06 p0680 A73-18004

A new method of calculating controller constants according to an optimal modulus criterion 06 p0680 A73-18169

Switching time dependence on input signal amplitude in self adaptive servosystem with open and closed control loops 06 p0680 A73-18382

Describing functions, circle criteria and multiple-loop feedback systems. 06 p0680 A73-18444

Design of dynamic programming feedback controllers for multivariable time-invariant linear systems. 06 p0680 A73-18517

Periodic oscillations in feedback systems with combined pulse modulation. 06 p0680 A73-18518

Complete identification of some non-linear closed-loop systems. 06 p0681 A73-18525

Rayleigh scattering influence on stimulated Raman effect, determining occurrence conditions for absolute instability due to feedback 06 p0702 A73-18593

Application of pole-placement theory to helicopter stabilization systems. 06 p0682 A73-18819

Absolute stability of nonlinear systems with a constraint on the derivative - Some extensions. 06 p0682 A73-18820

Properties of linear time-invariant multivariable systems subject to arbitrary output and state feedback. 06 p0682 A73-18865

Frequency domain synthesis algorithm for linear multivariable system via state variable feedback combined with input dynamics compensation, applying to decoupling and model matching 06 p0682 A73-18866

An algorithm for the assignment of closed-loop poles using output feedback in large linear multivariable systems. 06 p0672 A73-18869

IR tracking system for automatic target acquisition, discussing analyzer operation principles, closed loop characteristics, spectral field and equipment specifications 07 p0789 A73-18945

Type L linear multivariable systems with state integral feedback control, deriving optimal conditions for zero steady state error compensatory tracking by frequency domain techniques 07 p0805 A73-19133

A stabilized mode-locked Nd:YAlG laser using electronic feedback. 07 p0834 A73-19537

Experimental determination of the structure of plants with recycling 07 p0805 A73-20045

Absolute stability of nonlinear control systems with nonstationary nonlinearities and tachometric feedback 07 p0805 A73-20046

A computerized flutter solution procedure. 07 p0914 A73-20214

Feedback control of ionization instability in MHD generators. 07 p0779 A73-20395

State of the art and survey of learning control applications. 07 p0806 A73-20590

Feedback regulators for jump parameter systems with state and control dependent transition rates. 07 p0806 A73-20597

On the adaptive control of linear systems using the open-loop-feedback-optimal approach. 07 p0806 A73-20602

Synthesis of nonsearching self-adjusting systems by the root-locus method. II 07 p0807 A73-20637

Distributed parameter system a priori stochastic optimal control, deriving canonical differential equations from dynamic programming formulation for insight into feedback control problem 08 p0950 A73-21093

Feedback law choice for autonomy properties of controlled object, noting existence and uniqueness theorems 08 p0951 A73-21127

Film boiling heat transfer feedback control, comparing experimental process dynamics with analytical transfer function 08 p1024 A73-21526

On the control of linear systems using two level periodic output feedback. 09 p1067 A73-22231

Application of four methods for approximating optimal feedback gains. 09 p1067 A73-22234

Feedback control theory as general network analysis tool based on circuit decomposition 09 p1067 A73-22303

Equivalence of systems that follow a stochastic principle of computation 09 p1059 A73-22554

Optimal control problems under conditions of a priori indeterminateness 09 p1069 A73-22566

Mathematical model of equilibrium and steady state stability of pulse frequency modulation feedback systems of second kind with time delay filters 09 p1069 A73-22723

Improvement of the static and dynamic accuracy of a dual-loop control system for an electric actuating element with a proportional velocity controller 09 p1037 A73-22940

Constant factor delta modulator with adaptive voltage feedback to error point in coder for SNR improvement and hunting characteristic removal 09 p1065 A73-23100

First order phase locked loop statistical transient behavior in presence of noise from differential equation numerical solution, noting correlation with computer simulation 09 p1056 A73-23404

Digitally implemented clock acquisition loops for low SNR data signals. 09 p1056 A73-23405

Incomplete/complete feedback and off-on control moments for prescribed orientation of solid body in rotational motion 10 p1248 A73-23744

Vehicle coordinate-parametric control problems and some solution methods. 10 p1198 A73-24007

All-weather aircraft landing automation, discussing efficient optimal feedback control law selection based on trajectory termination or terminal control requirements 10 p1247 A73-24010

Function generation technique based on variables stochastic representation and clocked random pulses in data processing operations, noting application to closed loop control systems 10 p1242 A73-24016

Pneumatic controller with two cascade amplification stages and mechanical solid state gain adjustment variable feedback system 10 p1177 A73-24020

Micromovement servocontrollers in closed loop system, using piezoelectric device, ceramic element actuators and rotary switch derived logic control signal 10 p1199 A73-24027

The design of optimally parameter insensitive control systems. 10 p1199 A73-24030

Stabilization of linear dynamical systems with output feedback. 10 p1199 A73-24037

An adaptive convex feedback method for linear control systems with quadratic performance index. 10 p1199 A73-24038

New criteria for bounded-input-bounded-output and asymptotic stability of nonlinear systems. 10 p1199 A73-24041

Trajectory optimization for the nonlinear combined estimation and control problem. 10 p1200 A73-24044

Model reduction of multivariable control systems by means of matrix continued fractions. 10 p1200 A73-24046

Feedback control system transfer function matrix synthesis, determining design specifications for required compensation filters from compatibility conditions 10 p1200 A73-24049

Determination of changes in the properties and recognition of random processes with a complicated structure. 10 p1201 A73-24057

Linear multivariable control systems - A survey. 10 p1201 A73-24058

An actively adaptive control for linear systems with random parameters via the dual control approach. 10 p1202 A73-24534

Sufficiently informative functions and the minimax feedback control of uncertain dynamic systems. 10 p1202 A73-24535

A four-level technique for estimation of tactical missile aerodynamic parameters. 10 p1172 A73-24538

Nonlinear dynamic feedback control system state variable observers reconstruction error convergence and digital simulation for performance 11 p1390 A73-25187

Advanced flight control systems - Power-by-wire and fly-by-wire. 11 p1306 A73-26272

A servo-controlled axial fatigue machine with strain rate feedback for testing polymers and composites. 11 p1344 A73-26311

Instrument providing dc voltage corresponding to amplitude of uniform pulse train, using differential comparator as sensing element and closed loop control scheme 11 p1313 A73-26316

Feedback stabilization of a multimode two-stream instability. 11 p1406 A73-26556

Multiple input system with feedback loops and majority decision for performance optimization, discussing design principles and applications for structural synthesis and circuit design 12 p1482 A73-26759

Oscillatory operational amplifiers for control systems and computer technology 12 p1477 A73-26773

Rational methods for controlling multistable elements on the basis of an analysis of the preferential domains of steady states 12 p1482 A73-26774

Evaluation of glide paths for landing a VTOL airplane using linear regulator theory. 12 p1458 A73-27154

Data aided phase locked loops for phase estimation improvement in coherent demodulator to obtain loop acquisition characteristics design flexibility 12 p1483 A73-27157

An adaptive digital compensator for saturating control systems. 12 p1483 A73-27160

Practical quadratic optimal control for systems with large parameter variations. 12 p1483 A73-27166

Some features of the application of controlled-gain transistors. 12 p1480 A73-27271

Correlation analysis of systems with stochastic inertial elements. 12 p1484 A73-27458

Synthesis of searchless self-adjusting systems based on the root locus method. I. 12 p1484 A73-27460

Analysis of the distortions of an FM signal in a servo loop with external control 12 p1470 A73-27576

Verification of the 'potential' work capacity of dynamic systems by a frequency-time technique 12 p1485 A73-27946

Frequency method of synthesis for an active dynamic vibration damper 12 p1525 A73-27948

Linear systems with aftereffects of delayed feedback described by differential equations, obtaining optimal control solution in terms of parameters and boundary value problem 12 p1486 A73-27950

Suppression of the flute instability of a dense plasma by a magnetic system of feedbacks in an open trap 13 p1666 A73-28953

Differential game estimate of phase point pursuit of evading closed convex set for feedback control in irregular case 13 p1660 A73-29079

High gain hydromechanical servomechanism with multispring, mass damping and feedback control, deriving transfer function response, with application to aircraft control surface actuator design 13 p1596 A73-29150

Linear and nonlinear first order closed loop tracking radar systems, predicting noise performance by Gaussian signal amplitude fluctuation modeling 13 p1585 A73-29206

The sensitivity of nominally time-optimal control systems to parameter variation. 13 p1597 A73-29567

A first-harmonic method for nonlinear distributed-parameter systems subjected to deterministic or stochastic loads 14 p1738 A73-29707

Synthesis of a control coupling in a nonlinear servosystem 14 p1738 A73-30287

Stability considerations for a Volterra integral equation with discontinuous nonlinearity. 14 p1769 A73-30403

A criterion for the bounded-input, bounded-output stability of time-varying nonlinear systems. 14 p1738 A73-30404

Inverse problem of linear optimal control. 14 p1738 A73-30451

Nonlinear feedback systems and weakly stationary stochastic processes. 14 p1739 A73-30503

Suboptimal terminal feedback control of nonstationary, nonlinear systems. 14 p1739 A73-30507

Necessary and sufficient conditions for stability for n -input, n -output convolution feedback systems with a finite number of unstable poles. 14 p1739 A73-30509

An upper bound for the singular parameter in a stable, singularly perturbed system. 14 p1770 A73-30592

Near optimal control laws and controller realization for multilevel feedback and time optimal control design and simulation 14 p1739 A73-30780

Optimal control synthesis in the observation problem. I, II 14 p1802 A73-30788

Regulators providing control system autonomy 14 p1740 A73-30938

Mathematical model of equilibrium and steady state stability of pulse frequency modulation feedback systems of second kind with time delay filters 14 p1740 A73-30956

Automatic control of positive feedback depth and its application for stabilization of high Q -factor circuit characteristics 15 p1853 A73-31494

Integral action in the optimal control of linear systems with some inaccessible state variables. 15 p1854 A73-31631

Synthesis of searchless selfadjusting systems on the basis of the root-locus method. II. 15 p1854 A73-31691

Aided tracking as applied to high accuracy pointing systems. 15 p1854 A73-31726

Convergence criteria for reverse error coefficient expansion under transient conditions for tracking servo system with open loop transfer function 15 p1854 A73-31735

A method of assigning noise-resistant analog-to-digital converters 15 p1848 A73-31915

Feedback law choice for autonomy properties of controlled object, noting existence and uniqueness theorems 15 p1855 A73-32062

Intensity of thermal fluctuations of plasma flute instabilities in open confinement systems in the presence of a feedback system 15 p1920 A73-32307

The influence of a feedback system on the plasma flux in a closed-drift accelerator /CDA/ 15 p1920 A73-32311

Pilot-electronics-control surfaces as feedback loop for aircraft flight control, discussing instruments, pilot training and aircraft flying qualities 15 p1830 A73-32472

Simultaneous control of temperature and humidity in a confined space. III Feedback control synthesis via optimal control theory. 15 p1855 A73-32549

Book - Principles of biological regulation: An introduction to feedback systems. 15 p1840 A73-32576

Simultaneous control of temperature and humidity in a confined space. II - Feedback control synthesis via classical control theory. 15 p1855 A73-32598

Effects of mirror reflectivity in a distributed-feedback laser. 16 p2024 A73-33081

A closed-loop automatic control system for high-intensity acoustic test systems. 16 p1994 A73-33147

Remote feedback stabilization of ion acoustic type instability in plasma with LF density modulation, noting Van der Pol approach agreement and crossed field diffusion decrease 16 p2041 A73-33327

Single-loop delay line integrator SNR enhancement properties in additive zero mean correlated noise channels for finite signal observation times 16 p1979 A73-33406

Gated phase locked loop tracking device for maximum likelihood estimation of pulsed sinusoid imbedded in noise, predicting phase noise performance 16 p1980 A73-33408

Control of turbofan lift engines for VTOL aircraft. [ASME PAPER 73-GT-20] 16 p2047 A73-33496

Hydraulic jet amplifier design, considering selector static and dynamic characteristics, membrane attached plate, piston with feedback control and self oscillation elimination 16 p1971 A73-33672

Determining the stability of nonlinear systems. 16 p2033 A73-33699

An approach to the analysis of performance of quasi-optimum digital phase-locked loops. 16 p1992 A73-33743

Papers on optimal control and dynamic systems theory covering linear discrete systems observers, quasi-linearization, national economic policy, decision theory and closed loop formulation 17 p2143 A73-34360

Closed loop formulations of optimal control problems for minimum sensitivity. 17 p2144 A73-34363

Automated terminal area ATC operations under FAA ten year plan, investigating analytical model of pilot-aircraft control loop decision making by computer program 17 p2206 A73-34437

Problems concerning the implementation of an integrated flight control system, giving particular attention to curved flight path profiles [DGLR PAPER 73-030] 17 p2208 A73-34498

Separate surfaces for automatic flight controls. [SAE PAPER 730304] 17 p2101 A73-34665

State space attitude control synthesis for a satellite with flexible appendages. 17 p2239 A73-34951

V/STOL aircraft pilot-in-loop flight control/display system to overcome pilot limitations with performance and decision making flexibility enhancement [AHS PREPRINT 722] 17 p2105 A73-35063

Automatic electronic feedback control systems for active wing/external store flutter suppression 17 p2107 A73-35244

Feedback control configured vehicles ride control system design for B-52 aircraft load alleviation and mode stabilization during flight through atmospheric turbulence 17 p2107 A73-35245

Book - Introduction to servomechanism system design. 17 p2110 A73-35275

Limit cycle stability determination for nonlinear system with single loop feedback, using describing function method and z transform 17 p2202 A73-35517

Simulation results for a radar multipath angle error reduction method. 17 p2127 A73-35633

Fracture mechanics testing systems, discussing closed loop assembly, programming, readout and fail-safe units and fully automated computer-controlled technique 17 p2175 A73-35672

Neighboring extremals for optimal control problems. 18 p2294 A73-36308

Construction and testing of a gas-loaded, passive-control, variable-conductance heat pipe. [AIAA PAPER 73-727] 18 p2369 A73-36344

Thermal control flight experiment onboard ATS-F to evaluate feedback controlled variable conductance heat pipe performance in space environment [AIAA PAPER 73-757] 18 p2370 A73-36372

Central programming and peripheral feedback during eye-head coordination in monkeys. 18 p2273 A73-36452

A study of thermal ratcheting using closed-loop, servo-controlled test machines. 18 p2296 A73-36585

A closed-loop automatic control system for high-intensity acoustic test systems. 18 p2296 A73-36712

Optimal feedback control and Kalman filter design via an interactive computing and visual display system. 18 p2295 A73-36839

Technological survey of machine intelligence for real time autonomous manipulation with computer recognition sensory feedback and programmed task control to eliminate human operator 19 p2417 A73-37330

Design of decoupled multivariable control systems. 19 p2412 A73-38032

Decoupling longitudinal motions of an aircraft. 19 p2386 A73-38033

A comparative study of two basic approaches to extremum control. 19 p2413 A73-38037

On the use of singular perturbation methods in the solution of variational problems. 19 p2386 A73-38038

An application of truncated power series controllers for optimization of dynamic systems. 19 p2413 A73-38040

Controllability and stabilizability of decentralized dynamic systems. 19 p2413 A73-38045

Stabilization of multivariable systems with constant-gain output feedback. 19 p2413 A73-38046

Feedback controller design for multivariable systems by linear programming. 19 p2454 A73-38052

A hybrid fluidic directional gyro. 19 p2430 A73-38055

An optimal feedback control law for regulator problems with linear state inequality constraints. 19 p2413 A73-38060

Output feedback for linear multivariable systems with parameter uncertainty. 19 p2413 A73-38061

A computational algorithm for design of regulators for linear jump parameter systems. 19 p2408 A73-38066

Oscillations in nonlinear feedback systems. 19 p2414 A73-38069

On the stabilization of aided track pointing systems. 19 p2404 A73-38070

A study of a feedback fluidic jet oscillator. I, II. 19 p2389 A73-38077

Regulators guaranteeing the autonomy of a controlled system. 19 p2414 A73-38192

COS/MOS phase-locked-loop - A versatile building block for micro-power digital and analog applications. 20 p2534 A73-38657

Results and problems of a theory of final-position control systems with a nonstationary singular feedback 20 p2540 A73-38707

An approach to the synthesis of separate surface automatic flight control systems. [AIAA PAPER 73-834] 20 p2508 A73-38777

Digital flight control design using implicit model following. [AIAA PAPER 73-844] 20 p2508 A73-38783

The application of digital filters using observers to the design of an ICBM flight control system. [AIAA PAPER 73-845] 20 p2541 A73-38784

A 'type one' servo explicit model following adaptive scheme. [AIAA PAPER 73-862] 20 p2586 A73-38800

Optimal stabilization of moving control plants during multichannel measurement of their coordinates 20 p2542 A73-39039

Amplitude stability and distortion in thermistor-controlled oscillators. 20 p2535 A73-39131

Investigation of a stabilization system with a relay angular sensor 20 p2593 A73-39321

Reproduction of a useful signal by linear feedback systems 20 p2543 A73-39506

The effect of valve area gain on the performance of the hydraulic servomechanism. 20 p2511 A73-39755

Space shuttle ascent guidance, using quadratic performance index and reference trajectory kinematics to obtain optimal time-varying feedback control gain 21 p2735 A73-40044

Passive stochastic feedback stability. I - A general theory. II - Applications. 21 p2669 A73-40450

Generation of microsecond pulses with controllable pulse width in a ruby laser 21 p2713 A73-40527

Phase-locked loop operation in the presence of impulsive and Gaussian noise. 21 p2656 A73-41166

Impulse analysis of subharmonic oscillations in control systems with thyristor convertors. 22 p2835 A73-42299

Multidimensional cross control stabilization of multiple link feedback control systems, applying 70 dc 70 ac power converter 22 p2836 A73-42603

Multicircuit structural analysis of linear multiple link control systems with dynamic interchannel cross couplings 22 p2836 A73-42608

Optimal closed automatic control systems synthesis in terms of minimum integral square error of phase coordinates during transient response time 22 p2836 A73-42609

Problems of the theory of multidimensional combined systems with a common output 22 p2836 A73-42611

Structural sensitivity transfer matrix for dynamic multiple link control system response minimization with corrections within frequency range 22 p2836 A73-42613

Linearization technique for synthesis of nonlinear two dimensional automatic control systems with cross disturbances, imposing constraints on motion coordinate deviations 22 p2836 A73-42615

Quasi-autonomous dynamic control subsystem interrelation and location for nonlinear multiple link au-

Automatic control synthesis with iterative integration of motion equations

22 p2836 A73-42616

Optimal dynamic accuracy measurement complexing for combined data processing in multidimensional automatic control systems with various sensors

22 p2836 A73-42618

Analysis of transient oscillations in nonlinear control systems.

22 p2837 A73-43019

Optimal feedback control solution existence and uniqueness conditions for asymptotic stability, discussing relationships with Pontryagin equations and linear regulator problem with quadratic cost functionals

22 p2837 A73-43070

Optimal discrete-time feedback control of mixed distributed and lumped parameter systems.

22 p2837 A73-43072

Development of pilot-in-the-loop analysis. [AIAA PAPER 72-898]

22 p2817 A73-43110

Increase of closed-loop nominal trajectory likelihood in uncertain systems.

23 p2962 A73-43280

Synthesis of feedback systems with large plant ignorance for prescribed time domain tolerances.

23 p2962 A73-43282

Synthesis of parameter and state insensitive feedback systems with constraints based on piecewise constant linear control laws.

23 p2962 A73-43288

Real-time identification using adaptive discrete model.

23 p2962 A73-43286

Design of discrete model reference adaptive systems using the positivity concept.

23 p2962 A73-43287

Design of multivariable adaptive model following control systems.

23 p2962 A73-43288

Adaptive equalization with recursive noncanonical scanning filters

23 p2953 A73-43323

A study of a fluidic open loop damping flight stability augmentation system.

23 p2941 A73-43396

Servomechanism design techniques and applications - Aerospace problems.

23 p2945 A73-43450

Periodic oscillations of a closed hydraulic throttle servomechanism with inertial and positional loads

23 p2945 A73-43739

Nonlinear regulator theory and an inverse optimal control problem.

23 p2963 A73-43820

Linear time variant multivariable decentralized system stabilization by feedback control laws with dynamic compensation

23 p2964 A73-43821

L2-stability and L2-instability of linear time-invariant distributed feedback systems perturbed by a small delay in the loop.

23 p2964 A73-43822

On the adaptive control of linear systems using the open-loop-feedback-optimal approach.

23 p2964 A73-43824

Optimum mean-square decision feedback equalization.

23 p2964 A73-43988

Suppression of the flute instability in a dense plasma in an open system by magnetic feedback.

23 p3013 A73-44305

Closed loop linear control system synthesis possibility under condition of incomplete information on state vector with application to aircraft longitudinal motion

23 p2965 A73-44329

Synthesis of cascaded multiple-loop feedback systems with large plant parameter ignorance.

24 p3073 A73-44584

Discrete time invariant bilinear systems analysis for controllability, using decomposition by multiplicative feedback and linear compensation loops

24 p3073 A73-44585

Thermal flute perturbations in an open plasma device with feedback.

24 p3114 A73-44615

Effect of a feedback system on the plasma flux in an accelerator with closed electron drift.

24 p3115 A73-44619

Stabilization of unstable plants through automatic search

24 p3074 A73-44662

Adaptive array based on feedback concept for interference rejection, discussing processing of modulated signal with CW reference system

24 p3067 A73-44737

Nonminimum-phase difficulties in multivariable-control-system design.

24 p3074 A73-45258

Effect of unity-rank feedback on the transfer-function matrix of a multivariable system.

24 p3075 A73-45263

Compensation method for non-linear systems having jump and hysteresis properties.

24 p3075 A73-45555

FEEDBACK FREQUENCY MODULATION

Frequency distortions of signals in frequency-modulated oscillators with a delayed feedback.

17 p2130 A73-35714

Application of the method of equivalent nonlinear systems to noise rejection analysis in FM tracking receivers

20 p2537 A73-39451

FEEDFORWARD CONTROL

Cascade phase-lock loops for the generation of harmonic and subharmonic components.

04 p0421 A73-15433

Frequency domain synthesis algorithm for linear multivariable system via state variable feedback combined with input dynamics compensation, applying to decoupling and model matching

06 p0682 A73-18866

Model reduction of multivariable control systems by means of matrix continued fractions.

10 p1200 A73-24046

Synthesis of two-level controller for a class of linear plants in an unknown environment.

23 p2963 A73-43289

State-space matrix rank test in locating zeros of linear multivariable systems, noting application to feedforward regulators

23 p2964 A73-43828

FEEDING [SUPPLYING]

Microwelding equipment with automatic wire breaking and ball melting blocks and electronically controlled wire feeding, noting heating plate with thyristor temperature control

06 p0683 A73-18433

High feed rate electrochemical machining Fe in aqueous NaCl, using high supply voltage, electrolyte pressures and flow velocities [ASME PAPER 73-PROD-3]

16 p1971 A73-33533

FEEDING DEVICES

U ANTENNA FEEDS

FEEL

U SENSORY FEEDBACK

FELDSPARS

Trace-element variation of individual plagioclase and hornblende phenocrysts.

04 p0414 A73-14986

Mineralogical evidence for subsolidus vapor-phase transport of alkalis in lunar basalts.

07 p0880 A73-19693

Lunar plagioclase and pyroxene observation for lamella thicknesses by X ray diffraction, noting twinning, exsolution and crystal disorder effects

07 p0788 A73-19711

Lunar plagioclase - A mineralogical study.

07 p0881 A73-19712

Twin laws, optic orientation, and composition of plagioclases from rocks 12051, 14053, and 14310.

07 p0881 A73-19713

Plagioclase and Ba-K phases from Apollo samples 12063 and 14310.

07 p0881 A73-19714

Crystallographic studies of lunar plagioclases from samples 14053, 14163, 14301, and 14310.

07 p0882 A73-19715

On the amount of ferric iron in plagioclases from lunar igneous rocks.

07 p0882 A73-19716

Interlaboratory comparison for solar flare track density data on feldspars in individual sections of lunar rock 14310, noting depth dependence and irradiation history

07 p0896 A73-19878

Luminescence of lunar material excited by electrons.

07 p0897 A73-19881

Petrography, mineralogy and composition of plagioclase and pyroxenes of Washougal howardite by density and refraction measurements

09 p1139 A73-21853

Shock induced phase change in single crystal orthoclase at 115 kb, noting high pressure phase with hollandite-structure properties

11 p1352 A73-25586

Optical and chemical analysis of iron in Luna 20 plagioclase.

13 p1674 A73-28305

Fossil track and thermoluminescence studies of Luna 20 material.

13 p1675 A73-28312

Inert gases in a terra sample - Measurements in six grain-size fractions and two single particles from Luna 20.

13 p1675 A73-28318

Compositional and X-ray data for Luna 20 feldspar.

13 p1677 A73-28334

Europium anomaly in plagioclase feldspar - Experimental results and semiquantitative model.

16 p1976 A73-32902

Liquid anorthite viscosity and thermal expansion at 1450-1620 C and 820-950 C, noting agreement with Bottinga-Weill model predictions

20 p2555 A73-39718

Study by the method of nuclear tracking of the soil of Mare Fecunditatis /Luna 16/

21 p2770 A73-41002

Study of a chondrule extracted from Lot 118-111 of the lunar soil of Mare Fecunditatis

21 p2770 A73-41006

FELSITE

U IGNEOUS ROCKS

FELTS

The development and properties of a polyacrylonitrile /PAN/ fiber based carbon felt

16 p2028 A73-33041

FENCES [BARRIERS]

Use of surface fences to measure wall shear stress in three-dimensional boundary layers.

15 p1874 A73-31118

FERMI LIQUIDS

White dwarfs model based on zero temperature Fermi gas theory, determining mass-radius relation and limit mass

13 p1682 A73-28982

FERMI STATISTICS

U QUANTUM STATISTICS

FERMI SURFACES

The mechanism of the metallic adhesion bond.

01 p0087 A73-10473

Cadmium sulfide/cuprous sulfide solar cell abrupt heterojunction band model description by two quasi-Fermi levels

03 p0350 A73-14219

Observation of Kohn-type anomalies in the electron-phonon interaction on the Fermi surface of degenerate semiconductors.

04 p0483 A73-15469

Absorption coefficient due to band-band optical transitions in heavily doped semiconductor, obtaining electron and hole quasi-Fermi levels

06 p0738 A73-18586

Conduction electrons collective wave properties in metals, discussing energy structure, ground state, Fermi surface and quasi-particle concept for crystal conductivity

06 p0739 A73-18674

The anisotropy of carrier lifetime in graphite.

08 p0982 A73-21220

URCA process and the evolution of carbon stellar core.

13 p1673 A73-28173

Energy spectrum of transition metals in the superconducting state

20 p2600 A73-39727

FERMI-DIRAC STATISTICS

U QUANTUM STATISTICS

FERMIONS

NT ANTINEUTRINOS

NT BARYONS

NT FAST NEUTRONS

NT LEPTONS

NT NEUTRONS

NT PROTONS

NT RECOIL PROTONS

NT SOLAR PROTONS

NT THERMAL NEUTRONS

CP-noninvariance model of baryon asymmetry of universe, postulating kappa particle /neutral massive fermion/

02 p0221 A73-12669

Fermions spin polarization reversal for HF high intensity gravitational waves generation and detection, suggesting superconducting metals for waves receiver

04 p0476 A73-15633

FERRIC IONS

Fe ions optical transition lines in solar flares soft X ray spectra, noting continuum emission near 8A

03 p0367 A73-12945

Cummingtonite temperature dependent Mg and ferric ions order-disorder, estimating crystallization temperatures

03 p0375 A73-14104

Myceloperoxidase, the peroxidase of a primitive cell - Its reaction with Fe and H2O2.

06 p0652 A73-17944

On the amount of ferric iron in plagioclases from lunar igneous rocks.

07 p0882 A73-19716

Mixed valencies and site occupancies of iron in silicate minerals from Moessbauer spectroscopy.

11 p1324 A73-25142

Conditions of Cr IX and Fe XI luminescence in the corona

13 p1683 A73-29094

Electron paramagnetic resonance of Fe3+/ in forsterite /Mg2SiO4/.

15 p1923 A73-31273

Electronic structure of ferric iron octahedrally coordinated to oxygen.

18 p2341 A73-37049

Bragg spectroscopy of Scorpius X-1 in search of the Fe XXV emission lines.

19 p2485 A73-37627

FERRIMAGNETIC MATERIALS

Microwave integrated circuits on a ferrite substrate.

08 p0942 A73-20704

Microwave filters with single crystal YIG sample as ferrimagnetic resonators, determining magnetic field and temperature effects on resonator cut-off frequency 08 p0942 A73-20705

High power latching ferrite phase shifters for AEGIS. 13 p1591 A73-28620

Superexchange potential and kinetic energy theory in molecular orbital and configurational interaction approximation for three center four electron model of ferrimagnetic materials 15 p1924 A73-32156

Current carriers and electron impurity centers in ferrimagnetic semiconductors - The case of weak interaction 19 p2471 A73-37959

FERRIMAGNETISM

Optical and polarization study of magnetization processes around individual dislocations in yttrium-iron garnet single crystals 23 p3017 A73-44024

FERRITES

Recent advances in diode and ferrite phaser technology for phased-array radars. II. 01 p0024 A73-10720

Hall mobility measurements on iron rich nickel ferrites from room temperature to 600 C. 02 p0199 A73-11725

Ferrite core modular memory characteristics, considering bit capacity and printed circuit technology utilization 05 p0556 A73-16167

Domain-wall related, natural, submillimeter-wave resonance in orthoferrites 06 p0736 A73-18114

The distribution of chromium between ferrite and austenite and the thermodynamics of the alpha/gamma equilibrium in the Fe-Cr and Fe-Mn systems. 06 p0712 A73-18759

Calibration procedure for instruments to measure the delta ferrite content of austenitic stainless steel weld metal. 07 p0832 A73-20272

Microwave integrated circuits on a ferrite substrate. 08 p0942 A73-20704

Certain resonance properties of nickel-cadmium ferrites 08 p0995 A73-21513

Modulation type microwave receiver with selective filter and ferrite resonator in waveguide coupling 08 p0949 A73-21561

The effect of a dispersed phase on the creep properties of a Cr-Ni steel. 08 p0980 A73-21779

On the definitions of parameters in ferrite-electromagnetic wave interactions. 09 p1062 A73-22323

Magnetic permeability dependence on temperature and composition of hexaferrites with various Sc ion contents 09 p1134 A73-22982

Megabit capacity ferrite core memories for scientific satellites, using three dimensional organization with pulse program adapted for buffer application 09 p1087 A73-23426

Features of the domain structure of cobalt-doped lithium ferrite when changing the direction of easy magnetization 10 p1260 A73-24508

Paramagnetic resonance line broadening in ferrite garnets with small additions of rare-earth elements 10 p1261 A73-24703

Design and performance of electrically regulated phase shifter comprising rectangular waveguide section containing two ferrite resonators magnetized at ferromagnetic-resonance frequency 12 p1477 A73-26945

Phase transformations in the bismuth ferrites BiFeO₃ and Bi₂FeO₉ 12 p1531 A73-27199

Al, Sr or Co effects on kinetics of grain boundary ferrite allotriomorph formation relative to iron alloys, noting displacement of TTT curve 13 p1632 A73-28129

Delta ferrite and martensite formation in stainless steels. 14 p1759 A73-30145

Activation energy measurement for static strain aging rate controlling process in ferritic chromium steel 14 p1762 A73-30642

Utilization of hydrostatic compression at high pressures as a means of improving the properties of acoustic nickel ferrite 14 p1765 A73-30890

Ferrite component for waveguide commutator used as microwave switching element and modulator, noting application in navigation instruments and avionics. 15 p1849 A73-30995

Mossbauer and X-ray spectral studies of a nickel-cobalt ferrite subjected to thermomagnetic treatment 15 p1886 A73-31034

High pressure-sintering preparation of barium ferrites, discussing temperature and compression effects on density and magnetic properties 16 p2044 A73-32947

Dielectric properties of ferrites in the microwave band 17 p2141 A73-35548

Magnetodynamic and magnetostatic surface waves in a ferrite layered structure 19 p2470 A73-37724

Ferrite thick film deposition by arc plasma spraying, discussing apparatus, process and film properties after annealing 19 p2435 A73-38096

Rectangular waveguide loaded by a semiinfinite chain of ferrite spheres 19 p2406 A73-38341

Phase characteristics of a rectangular waveguide with symmetrically arranged, transversely magnetized ferrite layers 19 p2407 A73-38342

Experimental characteristics of certain types of semi-open, multi-circuit microwave ferrite filters. 20 p2535 A73-38920

The theory of half-open ferrite microwave filters. 20 p2535 A73-38925

Microstrip junction circulators with fixed ferrite disks, achieving broadband impedance matching between center conductor and transmission line by transformer on alumina substrate 20 p2538 A73-39668

Diode and ferrite phaser configurations for phased array antenna system, discussing digital and analog versions, driver requirements and design trends 21 p2663 A73-40665

Thermometric applications of ferrite permeability dependence on temperature, describing thermometer for magnetically levitated substrate 21 p2702 A73-41108

A method for thermal stabilization of the parameters of devices with ferrite cores 22 p2833 A73-42371

Illumination aftereffects due to semiconducting ferrite electron and ion motion, discussing dielectric properties and electron hole deficiencies 22 p2833 A73-42514

Influence of ion ordering on the induced anisotropy in Li-Fe ferrites 23 p3018 A73-44175

Ac electroconductivity of polycrystalline Co-Fe ferrite as function of temperature, composition and frequency at 1 kHz-200 MHz 24 p3119 A73-44403

FERRITIC STAINLESS STEELS

Delta-ferrite alteration in steel 1Kh16N4B during homogenization 03 p0326 A73-13828

Ferritic chromium steels embrittlement under high temperature aging, using hardness measurements, impact tests and electron metallography 06 p0712 A73-18762

The influence of scatter on some simple variable-stress creep predictions. 08 p1016 A73-20798

Creep strength of low alloy ferritic steels at low strain rates as function of grain boundary structure and matrix deformation 08 p0979 A73-21673

The influence of microstructure on creep properties of low alloy ferritic chromium-molybdenum-vanadium steel. 08 p0980 A73-21675

Effects of composition and structure on the creep strength of molybdenum bearing ferritic steels. 08 p0982 A73-21796

Strengthening mechanisms in ferritic creep resistant steels. 08 p0982 A73-21797

Dispersion-strengthened ferritic alloys for high-temperature application. 08 p0982 A73-21798

Structural evolution of an austenitic-ferritic stainless steel by keeping it between 600 and 1150 C 12 p1514 A73-27986

Ferritic stainless steel transverse tension ridging mechanism in terms of CF and CC mixed texture bands, contradicting plastic buckling theory 13 p1633 A73-28147

Pitting corrosion - A review of recent advances in testing methods and interpretation. 15 p1889 A73-31741

Ferritic martensitic stainless steels stress corrosion cracking, emphasizing heat treatment and environmental conditions effects on corrosion resistance 15 p1891 A73-32170

The creep characteristics of the heat-resistant ferritic steels X 20 CrMoV 12 1 and X 18 CrMoNi V Nb 12 1 and their welded connections 22 p2872 A73-41780

Gas metal arc welding of 9% Ni steel using ferritic filler metal. 22 p2866 A73-42226

Intergranular corrosion of iron-nickel-chromium alloys. 23 p2990 A73-43458

FERROELECTRICITY

Phenomenological theory of antiferroelectricity and ferroelectricity applied to NaNbO₃ and the system KNbO₃-NaNbO₃. 06 p0737 A73-18354

Contribution to the theory of the resonant thermal self-stabilization in ferroelectric vibrational systems 08 p0948 A73-21519

Dielectric breakdown of shock-loaded PZT 65/35. 09 p1132 A73-21927

Optical damage and internal fields in pyroelectrics. 10 p1260 A73-24531

Investigation of phase transitions in BaTiO₃ 15 p1923 A73-31204

An X-ray diffraction and DTA study of the ferroelectric transition in barium sodium niobate. 15 p1924 A73-31839

Quasistatic generation of harmonics in a ferroelectric crystal with a second order transition above the Curie point. 15 p1924 A73-32157

High speed serial multiplexed holographic recording for large capacity random access memories, using piezoelectric deflector and ferroelectric ceramic array modulators 16 p2013 A73-32872

Attempt at an interpretation of thermal reversals in the spontaneous polarization of ferroelectric microdomains 19 p2470 A73-37537

Papers on adaptive electronic devices, circuits and systems covering logic nets, solid state and ferroelectric devices and memory devices and artificial intelligence 20 p2535 A73-39135

Russian book on radiation effects on ferroelectric crystals and ceramic materials covering changes in dielectric, piezoelectric and optical properties, structure and phase transitions 20 p2600 A73-39757

Spectral determination of rare-earth components in Seignette-ceramic and piezoceramic materials 21 p2752 A73-40555

FERROMAGNETIC FILMS

Some principles of domain device designing for data processing and means of control. 10 p1198 A73-24022

Motion of a magnetizable fluid in the lubrication film of a cylindrical bearing 10 p1225 A73-24586

Wave devices built with ferromagnetic and electrically conducting film strips 12 p1460 A73-26772

Magneto-optic investigation of MnBi films. 15 p1924 A73-31943

FERROMAGNETIC MATERIALS

NT FERROMAGNETIC FILMS

NT MAGNETITE

NT PERMALLOYS [TRADEMARK]

Automatic two-coordinate compensator for resistance-measurement studies of steels and special alloys 02 p0167 A73-11867

Influence of the magnetic field on the heat transfer of a ferromagnetic viscoplastic fluid 03 p0347 A73-14323

Leakage field methods of defect detection. 04 p0447 A73-14929

Vanadium isotopic composition and the concentrations of it and ferromagnesian elements in lunar material. 07 p0889 A73-19797

Stability of a ferromagnetic plate within a gas flow in the presence of a magnetic field 08 p0989 A73-21723

Coupled waves and particle scattering processes in ferromagnetic semiconductors and metals 09 p1133 A73-22677

Theory of fluctuations and particle scattering in ferromagnetic semiconductors and metals 09 p1134 A73-22678

Spin relaxation times in ferromagnetic materials with magnetic anisotropy, discussing temperature effects and energy considerations 09 p1134 A73-22686

Investigation of the conversion characteristic of a ferromagnetic rod probe subjected to the simultaneous influence of longitudinal and transverse magnetic fields 13 p1617 A73-28867

Application of the superregeneration principle to a ferromagnetic amplifier 13 p1592 A73-28910

A data display device for switching and logic elements constructed from single-crystal ferromagnetic materials 14 p1731 A73-30941

Thermomechanical theory of ferromagnetic and dielectric materials magnetoelastic and electroelastic properties, using variational principles 16 p2037 A73-33228

The effect of vanadium, niobium, and tantalum on the electrical resistance of nickel 20 p2578 A73-39396

Results of the application of the physical modeling method to a study of the tangential component of the magnetic field of a linear inductor on the surface of a massive ferromagnetic body
22 p2800 A73-42214

FERROMAGNETIC RESONANCE
Control of the frequency of Gunn-effect oscillators by a magnetic field
01 p0024 A73-10978
Analog computer study of the effect of initial conditions on the excitation and sustaining of lower harmonic oscillations in a single-phase electroferromagnetic oscillatory circuit
02 p0147 A73-12352
Certain resonance properties of nickel-cadmium ferrites
08 p0995 A73-21513
Design and performance of electrically regulated phase shifter comprising rectangular waveguide section containing two ferrite resonators magnetized at ferromagnetic-resonance frequency
12 p1477 A73-26945
Use of an yttrium-iron garnet sphere as the tuning element in Gunn oscillators
12 p1481 A73-2592
Apollo lunar fines ferromagnetic resonance spectral line shape anomaly and anisotropy energy attributed to Fe particles with body centered cubic structure
13 p1684 A73-29177
Analysis of processes occurring during no-load operation of a ferroresonant voltage regulator with an improved shape of the output voltage curve
24 p3057 A73-44608

FERROMAGNETISM
Temperature-dependent hyperfine interactions in Fe2B.
06 p0734 A73-17833
Electromagnetic interactions of cosmic ray muons in iron. II - Momentum dependence of the interaction probabilities.
06 p0743 A73-18387
Magnetic phases in lunar material and their electron magnetic resonance spectra - Apollo 14.
07 p0894 A73-19847
Characteristics of the OT-series transformer-type transducers of linear displacements
07 p0779 A73-20528
Application of series to an investigation of a plane electromagnetic wave in a ferromagnetic half-space
12 p1474 A73-27804
An optimal scheme for excitation of low-threshold magnetically modulated converters and analysis of their operation
13 p1591 A73-28855
Laser threshold behavior analogy with thermodynamic ferromagnetic order-disorder phase transition, using self consistent field theory
20 p2571 A73-38628
Temperature aspects of Landau orbital ferromagnetism in white dwarfs and neutron stars.
20 p2610 A73-39573
Effect of small perturbations on the behavior of thermodynamic variables near the point of a phase transition of the second kind
21 p2790 A73-40445
Magnetic investigations of lunar soil delivered by A15 Luna 16.
21 p2773 A73-41399
Nuclear magnetic resonance thermometry.
22 p2856 A73-42022
Experimental study of the adiabatic invariant of self-oscillating processes
23 p3006 A73-43850

FERROUS METALS
Ferrous and nonferrous metal alloys melting and remelting in plasma induction and beam furnaces, noting cost reduction and ingots homogeneity
04 p0455 A73-15748
Investigation of the detectability of defects in the ultrasonic testing of joints obtained by friction welding.
09 p1088 A73-22299
Interaction of interstitial impurities with iron-subgroup metals in as-cast molybdenum-based dilute solid solutions
22 p2873 A73-42090

FERRY SPACECRAFT
Evolution of the Space Shuttle. I.
16 p2074 A73-34024

FET (TRANSISTORS)
U FIELD EFFECT TRANSISTORS

FETUSES
Cardiac output and oxygen transport in early ontogenesis
05 p0541 A73-16738

FEYNMAN DIAGRAMS
Extensive air showers and Feynman scaling above 1000 GeV.
06 p0743 A73-18325

FFT
U FAST FOURIER TRANSFORMATIONS

FIBER OPTICS
Future optical communication systems problems, potentialities and development prospects, considering bandwidth, laser modulation, directionality, fiber

transmission, reception, detection, power and efficiency
01 p0018 A73-11066
Measurement of the angular distribution of light scattered from a glass fiber optical waveguide.
01 p0078 A73-11215
Optical power handling capacity of low loss optical fibers as determined by stimulated Raman and Brillouin scattering.
01 p0078 A73-11216
Double-reverse-scatter interference in optical fiber communication systems.
01 p0018 A73-11217
Optical communication systems with glass fiber waveguide, using semiconductor lasers and photodiodes as transmitters and receivers respectively
01 p0019 A73-11486
Book - Light transmission optics.
02 p0192 A73-11881
Fiber-dispersion measurements using a mode-locked krypton laser.
02 p0177 A73-12574
Pyrometer for measurement of surface temperature distribution on a rotating turbine blade.
02 p0171 A73-12617
Coupling losses between cylindrical multimode fibers and laser diodes
04 p0458 A73-15321
A model of image-shape analysis based on fiber-optics elements and on the principle of photoelectric conversion
06 p0671 A73-18084
Missile guidance and control systems optical linking, using fiber optics and light emitting diodes and photodetectors as optical/electrical transducers
06 p0757 A73-18324
Pulse broadening in multimode fibres excited by GaAs lasers.
07 p0833 A73-19155
Wave propagation along radially inhomogeneous glass fibres.
08 p0937 A73-20832
Photomultiplier pairs arrays operation as solar magnetograph detector using fiber optics, comparing to photographic methods
08 p0970 A73-21737
Optical fiber waveguide operational principles, discussing information transfer rate capability, channel characteristics and input and output devices
09 p1055 A73-23396
Analysis of electromagnetic-wave modes in lens-like media.
10 p1248 A73-23834
Optical fiber element image microcontrast dependence on fiber lightguide output and light-tight shell illuminance difference
10 p1228 A73-24584
The three-ring effect in flexible bunches of optical fibers
10 p1228 A73-24585
Tube waveguide for optical transmission.
10 p1196 A73-24624
Low loss fiber optics communication technology with almost infinite bandwidth potential, discussing transmission lines, light sources, detectors, integrated circuits, systems and applications
11 p1399 A73-26118
Glass fiber optical waveguides for laser communications.
11 p1376 A73-26119
Optical fiber breaking stress distributions obtained by a cantilever method.
11 p1344 A73-26312
Glass fiber for optical communication with existing light source and detector devices, assessing materials and fabrication technology for capacity, attenuation and environmental requirements
13 p1585 A73-29114
Optical fibre guide measurements with short coherent light pulses.
14 p1756 A73-30056
Utilization of optical-frequency carriers for low- and moderate-bandwidth channels.
14 p1728 A73-30418
Samarium oxide neodymium oxide activated glass fiber output power under lasing conditions
14 p1766 A73-30468
Application of fiber optics to the observation of fatigue crack development
14 p1754 A73-30691
Monomode optical fiber waveguide propagation attenuation due to random curvature, analyzing radiation losses for clad cores with uniform and gradient refractive index profiles
14 p1729 A73-30695
Code division multiplexing system for multiple signal binary transmission in branched glass fiber optical communication network
14 p1729 A73-30696
Recent progress in fibres for optical communications.
16 p2023 A73-32863

Fiber laser amplifier properties and light dispersion due to fiber structure and materials in optical communication
16 p2024 A73-32883
Multichannel quick-response photoelectric micropycrometer
17 p2164 A73-34173
A new lidar for meteorological application.
18 p2333 A73-36708
Equivalent circuit and transfer function of the multimode glass fiber with random mode conversions.
20 p2521 A73-38658
Multimode glass fiber as transmission medium for digital signals.
20 p2521 A73-38659
Glass fiber transmission characteristics as optical waveguides for communication systems, considering transit time and attenuation
20 p2522 A73-38660
Using the new fundamental system of modified cylindrical functions for designing optical core fiber waveguides with cladding of finite thickness.
20 p2522 A73-38661
Detachable liquid filled capillary waveguide connector for glass fiber multimode optical transmission lines, discussing propagation efficiency as function of dimensional tolerances
20 p2522 A73-38662
Determining the absorption coefficients of low-loss bulk glass materials.
20 p2563 A73-38663
Use of laser amplifiers in a glass-fiber communications system.
20 p2522 A73-38667
A pulse-regenerating optical transmission line.
20 p2522 A73-38668
Microelectronic circuitry for monitoring stray electromagnetic energy coupled into electroexplosive device, using fiber optic transmission with photovoltaic energy conversion to eliminate wiring caused interference
22 p2822 A73-41794
Propagation of optical pulses through clad fiber - Modified theory.
22 p2828 A73-43163
Losses and impulse response of a parabolic index fiber with random bends.
23 p2987 A73-43989
Leaky rays cause failure of geometric optics on optical fibres.
23 p2955 A73-44105
Glass and plastic optical fiber properties, performance, limitations and applications
23 p3007 A73-44211

FIBER ORIENTATION
Impact-deflection by oblique fibers in sparsely reinforced composites.
08 p1018 A73-21408
Interfiber failure of unidirectional composite material.
13 p1702 A73-29538
Theory and experiments of compressive strength of unidirectionally fiber-reinforced composite materials.
13 p1702 A73-29539
Conditions for rational arrangement of reinforcing fibres in materials and structures.
13 p1702 A73-29540
Steel reinforcement fiber arrangement and volume content influence on aluminum composites strength and fatigue resistance at room and elevated temperatures
14 p1766 A73-30710
Brittle fracture and crack propagation prediction in unidirectionally fiber reinforced composites via Sc theory, comparing with stress intensity factor Kc concept
15 p1949 A73-31681
Orthotropic characteristics of glass-fibre-epoxy laminates under plane stress.
15 p1897 A73-31698
On the transverse strength of fiber-reinforced materials.
[ASME PAPER 72-APM-EEE] 17 p2249 A73-35111
Tensile creep in short fibre reinforced thermoplastics.
17 p2197 A73-35344
Alleviation of stress concentration with analogue reinforcement.
[SESA PAPER 2102] 17 p2250 A73-35446
Filament orientation effect on Al and Ti matrix composite tensile properties, using boron, boric and silicon carbide fibers
17 p2192 A73-35533
Tensile fracture of boron-epoxy composites with ordered filament packing geometry.
17 p2198 A73-35535
Fiber orientation effects on fatigue failure of aligned short fiber composite materials.
17 p2198 A73-35546
The strength prediction problem of unidirectional fiberglass-reinforced plastics under transverse tension and shear
18 p2326 A73-36409

- An improved method of production for high strength fibre-reinforced thermoplastics.
18 p2329 A73-37092
- Studies on the impact resistance of composite plates.
18 p2367 A73-37093
- Fibrous composite materials orthogonal shear properties related to laminate construction, discussing shear load tests, fiber orientation, boron, graphite, aluminum and titanium properties [SAWE PAPER 993]
19 p2443 A73-37893
- Plastic deformation anisotropy and work-hardening of composite materials.
19 p2444 A73-38261
- Carbide reinforcement in two directionally solidified alloyed nickel eutectic alloys.
20 p2576 A73-39028
- Anisotropy of the mechanical properties of aluminum hardened by a stainless steel grid.
20 p2578 A73-39382
- Interaction of cracks with rigid inclusions in longitudinal shear deformation. II - Further results.
22 p2920 A73-42134
- Study of the existence of compact laminar for certain complex analytical laminated structures.
23 p2999 A73-44097
- The strength of unidirectionally reinforced plastics subjected to tension at an angle to the direction of reinforcement
24 p3102 A73-44511
- Process anisotropy of randomly reinforced fiberglass plastics
24 p3102 A73-44515
- Mechanical properties of unidirectionally reinforced polyester and epoxy resin laminates under combined stresses perpendicular or parallel to glass fiber direction
24 p3104 A73-44886
- Whiskers as reinforcing component of composite materials, process-technical alignment methods
24 p3104 A73-44888
- FIBER STRENGTH**
- Investigation of structural changes during the heat treatment of carbonized fibers with the aid of a scanning electron microscope
01 p0068 A73-11246
- The fracture energy of carbon-fibre reinforced glass.
01 p0068 A73-11500
- Creep and durability of tungsten wire.
02 p0180 A73-12137
- Tensile, compressive and shear strength and absolute modulus of PRD fibers from reinforced plastic honeycomb and filament wound strand tests
03 p0330 A73-13015
- Fiber strength of S-glass/epoxy composites under biaxial loading.
03 p0330 A73-13017
- Fracture toughness of duplex structures. I - Tough fibers in a brittle matrix.
04 p0460 A73-14700
- High strength straight filament superflywheel configurations with improved energy storage capability for vehicle, tool and power supply applications
04 p0475 A73-14744
- Tensile properties of PRD-49 fiber in epoxy matrix.
05 p0588 A73-16118
- High strength and low density graphite fiber yarn for reinforcement in structural composite components on heavily loaded flight vehicles
06 p0715 A73-18716
- Variational bounds of unidirectional fiber-reinforced composites.
09 p1157 A73-21931
- Elastic stiffness properties and structural designs of fiber composite materials, including laminate and plate problems
09 p1110 A73-22516
- High modulus organic fiber/epoxide properties for reinforced composites, including strands, rings and filament wound vessels
09 p1110 A73-22518
- High modulus organic fibre composites in aircraft applications.
09 p1110 A73-22519
- High modulus graphite fiber-epoxy composite shear strength and structural observation by X ray and electron diffraction and surface dark field electron microscopy
10 p1239 A73-23977
- Reinforcement of magnesium with boron and tantalum filaments.
10 p1234 A73-24437
- Effects of prestressing boron/epoxy prepreg on composite strength properties.
11 p1388 A73-25512
- Stability of micromorphology of carbon fibres and their interstitial compounds.
11 p1389 A73-25858
- Optical fiber breaking stress distributions obtained by a cantilever method.
11 p1344 A73-26312

- Fiber strength, fracture types and material elastic properties relationship to impact resistance in carbon fiber reinforced plastics
12 p1515 A73-26882
- High strength glass fibre-resin composites.
13 p1645 A73-28498
- Method for the investigation of the fatigue strength of fiberglass produced by winding and loaded by inter-layer shear.
13 p1695 A73-28523
- High strength fiber woven cloth materials for inflatable structure, discussing characteristics assembly methods and tests [AIAA PAPER 73-448]
15 p1826 A73-31434
- Stability of metal-based composite materials
15 p1888 A73-31596
- The development and properties of a polyacrylonitrile (PAN)/ fiber based carbon felt
16 p2028 A73-33041
- High modulus graphite fiber preparation from polyacrylonitrile yarn, discussing graphitization, properties and stabilization oxidation treatment
16 p2028 A73-33042
- Heat treated polyacrylonitrile filament produced carbon fiber strengthened after fatigue testing, noting maximum strengthening effect after 1000 load cycles
17 p2194 A73-34635
- High strength organic fiber PRD-49 reinforced plastics compared to materials reinforced with glass, graphite and boron, discussing weight required to achieve Al faced sandwich performance
17 p2194 A73-34802
- Noncumulative fracture mode of unidirectional boron filament-aluminum matrix composite under axial tension, measuring critical filament stress
17 p2193 A73-35542
- Determination of rated strength characteristics of fiberglass in zones of stress concentration.
18 p2328 A73-36883
- Fracture mechanics of carbon fibers at high temperatures due to fine structure, discussing effects of ribbon unbending during extension
19 p2444 A73-38089
- The effect of elevated temperatures on the mechanical properties of B-Al composites.
19 p2442 A73-38095
- Strength of fibrous composite materials.
19 p2502 A73-38551
- Partitioning of stress between fiber and matrix during tensile deformation of the Al-Al3Ni eutectic composite.
20 p2576 A73-39024
- Properties of boron fibers and of boron-aluminum composites in uniaxial compression
20 p2580 A73-39358
- Three-dimensional problem of the stability of fibers in a matrix in the presence of highly elastic strains
20 p2581 A73-39642
- Hot-pressed eutectics of oxides and metal fibers.
21 p2723 A73-40895
- High-temperature internal friction in boron fibers
22 p2880 A73-41957
- Analysis of the test methods for high modulus fibers and composites; Proceedings of the Symposium, San Antonio, Tex., April 12, 13, 1972.
23 p2996 A73-43626
- Upper bounds to in-plane shear strength of unidirectional fiber-reinforced composites.
23 p3048 A73-44383
- Mechanical properties of boron fibers
24 p3102 A73-44524
- Whiskers as reinforcing component of composite materials, process-technical alignment methods
24 p3104 A73-44888
- Improved mechanical properties of composites reinforced with neutron-irradiated carbon fibers.
24 p3104 A73-45143

FIBERGLASS

U GLASS FIBERS

FIBERS

- NT CARBON FIBERS
- NT DACRON [TRADEMARK]
- NT GLASS FIBERS
- NT METAL FIBERS
- NT NYLON [TRADEMARK]
- NT RAYON
- NT REINFORCING FIBERS
- Properties and fabrication of cermet fibers from refractory compounds and of porous materials based on these fibers
02 p0178 A73-11538
- Recent developments in commercial fire resistant fibrous materials.
11 p1389 A73-26419
- Low-temperature internal friction in boron fibers
14 p1766 A73-30380
- Flame resistant and nonflammable textile fibers.
17 p2198 A73-35839
- Fibrous composite materials orthogonal shear properties related to laminate construction, discussing shear load tests, fiber orientation, boron, graphite, aluminum and titanium properties [SAWE PAPER 993]
19 p2443 A73-37893

Local form of the radiation condition - Application to curved dielectric structures.
24 p3069 A73-45257

FIBRIN

- Fibrinolytic activity of urine in healthy persons
15 p1833 A73-31165

FIBRINOGEN

- Emotional overstress effects on the indices of the blood coagulation system in monkeys
14 p1719 A73-30846

FIBROBLASTS

NT COLLAGENS

FIBROUS MATERIALS

U FIBERS

FIDUCIARIES

- Electro-optical fiducial system for shock wave interferometry relating impact time to free surface motion
05 p0580 A73-17261

FIELD COILS

- Feasibility model of airborne ac synchronous generator with rotating superconducting field winding, comparing predicted performance, size and weight with conventional technology
02 p0131 A73-11827

- Rotating electrical machine superconducting field winding design requirements in terms of size, magnetic energy storage, power level, rotation speed and pole number
02 p0132 A73-11828

- Flooded rotor, direct current acyclic motor, with superconducting field winding.
02 p0132 A73-11829

- Three-phase-synchronous alternator with a superconducting field winding.
02 p0132 A73-11832

- Synchronous electric generators with superconducting field windings, discussing fundamental characteristics, operating modes, refrigeration and cryogenic equipment and applications
02 p0132 A73-11834

- A 12-coil superconducting 'bumpy torus' magnet facility for plasma research.
02 p0150 A73-11839

- Aircraft power supply alternators with superconductive field windings, calculating specific weights and performance characteristics
07 p0779 A73-20408

FIELD EFFECT TRANSISTORS

- A two-dimensional analysis of gallium arsenide junction field effect transistors with long and short channels.
02 p0147 A73-12047

X-band GaAs FET.

- Microelectronic metal-dielectric-semiconductor devices for physical properties of multilayer multiphase systems, noting field effect transistors, integrated circuits and electro-optical elements
03 p0281 A73-13173

- Analysis of a Schmitt trigger employing a field transistor at the input
03 p0284 A73-14324

- Arsenic emitter silicon bipolar transistor and gallium arsenide FET transistor devices for low noise microwave amplification to 10 GHz
04 p0426 A73-14731

- M.O.S.F.E.T. temperature-drift performance limitations.
04 p0427 A73-14983

- Effects of ionizing radiation on dielectrically isolated junction field effect transistors.
[AD-757969]
05 p0558 A73-16524

- Book - Advances in electronics and electron physics. Volume 31.
05 p0558 A73-16601

- Current saturation mechanisms in junction field-effect transistors.
05 p0558 A73-16605

- Simple mathematical model of shift of threshold voltage induced in an m.o.s. transistor by testing at elevated temperatures.
05 p0560 A73-17324

- Book - Transistor circuit design.
06 p0673 A73-17672

- Quasi-linear equivalent circuit for harmonic LC oscillator design with FET transistor, using effective transconductance method
06 p0675 A73-17829

- MOS field effect components integration on Si operation, performance and application to logic circuits
07 p0797 A73-18916

- A two-dimensional numerical FET model for dc, ac, and large-signal analysis.
07 p0799 A73-19342

- Reliability design of type 2N 3966 field effect elements
07 p0801 A73-19421

- Matching of capacitive sensors to low-noise amplifiers based on field effect transistors
07 p0802 A73-20296

- X- and Ku-band amplifiers with GaAs Schottky-barriers field-effect transistors.
07 p0803 A73-20555

The breakdown mechanism and methods for measuring breakdown voltages in insulated-gate MOS field-effect transistors

Low-field tunnelling current in thin-oxide M.N.O.S. memory transistors.

Design a 4 to 8 GHz FET amplifier with a 7 dB NF.
Modification and updating of the bioelectric DS2C amplifier for a FET input.

Amplitude selector for linear transistorized devices
A linear voltage-tunable distributed null device.

VHF preamplifier with FET for resolving crosstalk and overload problems comparing designed and observed specifications

MOSFET devices with trapezoidal gates - I-V characteristics and magnetic sensitivity.

Current saturation and small-signal characteristics of GaAs field-effect transistors.

Self excited LC and RC oscillator networks based on FETs, discussing frequency tuning and FM methods

Steady state mathematical theory for the insulated gate field effect transistor.

A nanovolt-level MOSFET reversing switch for low temperature applications.

Book - Introduction to semiconductor devices: Diodes, bipolar transistors, JFETs, IGFETs, SCRs and integrated circuits.

Precision low frequency adaptive MOSFET IC electronic oscillators with loose tolerance component timers for cost reduction

A two-dimensional mathematical model of the insulated-gate field-effect transistor.

Influence of the parasitic capacitance of a field effect transistor and of the input capacitance of the amplifier on the null shift of a modulator

Null level of a field-effect-transistor modulator of small constant-voltage signals

The extension of self-registered gate and doped-oxide diffusion technology to the fabrication of complementary MOS transistors.

Analog transducers based on monocrystalline silicon semiconductor piezoresistivity properties, describing various piezo-FET circuits

The insulated-gate field-effect transistor - A bipolar transistor in disguise.

Book - The physics and circuit properties of transistors.

Avalanche injection effects in MIS structures and realization of n-channel enhancement type MOS FETs.

Thermal noise behavior of a FET as a function of the doping profile of the gate-channel junction

Bucket-brigade shift-register operation-exact correlation between experimental data and a computer model.

Parameters and energy resolution of the KP303 field effect transistors at low temperatures

The KP303 field transistor in a soft gamma radiation spectrometer

Book - Design of modern transistor circuits.

Experimental gain and noise parameters of microwave GaAs FET's in the L and S bands.

Cryogenic preamplifier with cooled GaAs junction FET in input stage, discussing application to sensor systems using high impedance cryogenically cooled optical detectors

Performance and advantages of FET's as microwave solid state amplifiers.

The field-effect transistor as a resistance varying linearly in time

Book - Solid state electronic circuits: For engineering technology.

Charge carrier mobility distribution along the channel of an MDS field transistor

Capacitance of a field-effect MDS transistor gate

Matching of capacitive pickups to low-noise junction-gate field-effect transistor amplifiers.

Electrical properties and simplified theory of a particular junction field-effect transistor operating with a forward gate-source bias.

FET for AM large signal processing and regulation without distortion in resonant circuits, discussing characteristics and harmonic analysis

Low-frequency 1/f noise in MOSFET's.

Threshold voltage stability improvement of p- and n-channel SNOS FET by annealing silicon nitride in oxygen or steam prior to gate deposition

Book - RCA COS/MOS technology.

Fundamentals of COS/MOS integrated circuits.

Design and application of low noise GaAs FET amplifiers.

Injection-modulation devices as elements of integrated circuits

On the validity of the gradual channel approximation for junction field effect transistors with drift velocity saturation.

Present state and future prospects of the design of large-scale integrated circuits using MIS transistors

Acoustic surface wave energy detection via combination of MOSFET array and ZnO overlay piezoelectric transducer, deriving signal processing technique

AM radio receiver diode resonance circuit design for large signal processing, considering FET pinch-off voltage effects and correct circuit parameter selection

CODYMOS frequency dividers achieve low power consumption and high frequency.

Junction or Schottky gate type FET power gain and high frequency limitations from y parameters calculation, using analog RC transmission line as equivalent network

The design, fabrication, and evaluation of a silicon junction field-effect photodetector.

Complementary MOS transistor inverter application to quartz oscillator in terms of frequency, temperature and supply voltage

V groove MOS transistor fabrication by preferential silicon etching and masking process with noncritical alignment tolerances

Two-terminal current-fed negative admittance incorporating field effect transistors.

Investigation of low-frequency noise in MOS transistors

Aspects of field-effect transistor applications in amplifier stages with feedback

FIELD EMISSION

The influence of the electron-phonon scattering on the total energy distribution of field emitted electrons from tungsten.

The effect of stress on metal semiconductor junctions.

Work function measurements by the field emission retarding potential method.

Current-voltage characteristic of a metal-dielectric contact with allowance for thermionic and field emission of electrons

Evanescent fields produced by totally reflected beams.

The possibility of field emission from metal surface with a Q-switched laser pulse.

Field electron emission microscopic study of titanium

FIELD INTENSITY METERS

Injun 5 observations of magnetospheric electric fields and plasma convection.

FIELD IONIZATION SOURCES

U BRUSHES

FIELD MODE THEORY

Coupled mode analysis for solid travelling-wave amplifiers.

Corrugated conical horn antenna feed design, discussing Newton-Raphson iterative solution and computer program for spherical hybrid mode eigenvalues

FIELD STRENGTH

NT ELECTRIC FIELD STRENGTH

NT MAGNETIC FLUX

Accuracy limitation in measurements of HF field intensities for protection against radiation hazards.

Single point thunderstorm ranging method based on two radio frequencies field intensity spectral components ratio

Ionospheric electron density changes caused by strong radio waves induced plasma heating

Short period geomagnetic pulsations with gradual amplitude increase and abatement, noting latitudinal variation

Low-field tunnelling current in thin-oxide M.N.O.S. memory transistors.

A special purpose computer for the study of fading signals.

Determination of field strength in a microwave-plasma interaction by means of the Stark effect.

Propagating radio wave field strength from double knife edge diffraction signals

A method for smoothing level fluctuations caused by echoes in the case of FM directional radio links

Intensity and displacement fields of microinhomogeneous medium with random permittivity tensor field described by step functions, using renormalization method

Shimazaki formula corrected for F 2 layer altitude estimation for 2-30 MHz field intensity and transmission losses calculations

Method of experimental study of fields in electromagnetic resonators - Application to helical resonators

Average intensity of the normal wave during superrefraction

Dependence of laser-induced breakdown field strength on pulse duration.

On the detection of X-rays from celestial sources through their ionization of the terrestrial atmosphere.

Bounds on effective dielectric constant of inhomogeneous material.

Field THEORY [ALGEBRA]

NT QUADRATIC EQUATIONS

Absolute continuity of estimates corresponding to uniform Gaussian fields

Extendibility over the entire plane and the functional equation of a scalar product of Hecke L-series of two quadratic fields

Field THEORY [PHYSICS]

Classical mechanics and field theory derivation based on material points motion in space, discussing space-time metric, electromagnetic and gravitational fields and quantum mechanics

Turbulent wake flow behind two dimensional flat plate trailing edge investigated by Nee-Kovaszny turbulent shear flow differential field theory

Spinorial solution associated to a radially symmetric radiation field in general relativity.

Book - Radiation and scattering of waves.

Consistency of fields and particle motion in the 'speiser' model of the current sheet.

A finite expanding universe with matter injection.

Mean field equations for dynamic response of homogeneous linearly elastic solids, obtaining formulation for ensemble averaged displacement and stress fields of composite

[ASME PAPER 72-WA/APM-28]

A force field theory. I - Laminar flow instability.

Influence of scalar and vector fields on the nature of a cosmological singularity

06 p0751 A73-18101

Electromagnetic current and charge due to interaction between a gravitational and a free electromagnetic field.

06 p0732 A73-18715

Distortion corrections in geophysically traced gravitational, magnetic and geoelectric field maps, discussing automation

07 p0816 A73-19442

German monograph on logarithmic spiral antennas radiation field theory, extending boundary value solution for cylindrical linear antenna to curved structure by segmentwise linearization

07 p0801 A73-19577

Radiation fields in the Schwarzschild background.

08 p0988 A73-21202

Backscattering of a scalar wave field by an ideally reflecting object situated near the caustic surface

09 p1052 A73-23081

Zero-mass scalar and electrostatic fields with the central symmetry in the general relativity.

09 p1121 A73-23148

Subgrid resolution achievement by spline fitting during flow and force field sources conversion from Lagrangian distribution onto Eulerian grid and interpolation

10 p1248 A73-23603

Field of attraction of a singularity of a nonlinear recurrence of the second order - Method of determination of the boundary

11 p1389 A73-25137

Method of calculation of radioelectric performances of airborne radomes

11 p1327 A73-25282

Plane wave expansion approximation for wave field on dielectric wedge representing tapered antenna, considering lateral wave contribution

11 p1329 A73-25681

Combined electromagnetic and gravitational field equations derivation with explicit interaction term and tensors for curved space-times unrestrained in Einstein-Maxwell equations framework

11 p1401 A73-26658

Certain quantum-gravitational effects in central classical fields

12 p1538 A73-26970

Emission of 'soft' photons in the field of a strong electromagnetic wave

12 p1468 A73-26972

On Maxwell-type equations in the theory of inertial-gravitational field.

13 p1657 A73-28025

Mach principle incorporation into general relativity, discussing application as selection rule in Einstein field equations solution and other gravitation theories

14 p1798 A73-30238

A note on the use of the finite difference method for predicting steady state sound fields.

16 p2036 A73-33217

Electric dipole motion in Einstein unitary field with electrostatic potential as function of polar coordinates, deriving law of motion from Clausen integral formula

16 p2037 A73-33371

Theory of electromagnetic field scattering in gases

16 p1984 A73-34007

A generalization of the equations governing the evolution of a particle distribution in a random force field.

17 p2213 A73-34449

Existence of thermodynamic limits in some models of quantum field theory

17 p2254 A73-34633

Nonphysical self forces removal from electromagnetic plasma models by simulation algorithm, discussing optimization of particle orbit equations integration

17 p2216 A73-34895

Perturbation theory for field moments in an inhomogeneous medium.

17 p2123 A73-35151

Einstein-Maxwell fields in conformal space, studying field equations, reducible electromagnetic field in space-time and constraints on metric tensor by Rainich conditions

17 p2212 A73-35560

Formulation of the basic approximations of the field theory of static current-voltage characteristics of quasi-monopolar semiconductors

18 p2341 A73-36724

Kinematic theory of magnetic field reconnection rate for analysis of turbulent flows in solar photosphere, flare phenomena and galaxy

19 p2467 A73-37439

Survey of the present status of neoclassical radiation theory.

20 p2590 A73-38604

Nonlinear radiation reaction field effects on operator self-field and oscillating dipole, taking into account one-atom spontaneous emission and superadiance theories

20 p2590 A73-38607

Finite-element formulations for elastic plates by general variational statements with discontinuous fields.

20 p2623 A73-39558

Generation of magnetic fields in a matter-antimatter universe.

20 p2611 A73-39587

Nonrelativistic effects in phenomenology of gravitation, describing gravitational field as curvature-tensor field within equivalence principle limits

21 p2766 A73-40352

The momentum-energy tensor of an electromagnetic field

21 p2739 A73-40446

Phased array analysis by circuit and field theory approaches, discussing boundary value problems formulation and solutions for systems with current carrying and aperture elements

21 p2651 A73-40650

A two-dimensional field induced by travelling sources.

21 p2740 A73-41016

Russian book - Statistical physics and quantum field theory.

21 p2741 A73-41296

Pure two band superconductor theory, discussing thermodynamic and electromagnetic properties, London group, mixed state, critical field and weak field penetration

21 p2753 A73-41299

Representation method for force free magnetic field class, including current free fields and applications to solar fields

21 p2779 A73-41536

Nonradiative motion in a radiative gravitational field.

21 p2742 A73-41631

Centrosymmetric metric generator of field models of particles, discussing Einstein tensor components representation

22 p2887 A73-42431

Nonsingular unified field model for charged particle described by interrelation of gravitational mass, global energy and effective charge, considering comparison with Reissner metric

22 p2887 A73-42432

A new method of analysing the stability of nonlinear dynamic systems.

23 p3006 A73-44084

Effect of scalar and vector fields on the nature of the cosmological singularity.

24 p3132 A73-44493

Tidal generation of magnetic fields in binary celestial systems, calculating growth times

24 p3134 A73-44578

A new electric field effect in silicon solar cells.

24 p3058 A73-45426

FIGHTER AIRCRAFT

NT F-4 AIRCRAFT

NT F-8 AIRCRAFT

NT F-14 AIRCRAFT

NT F-15 AIRCRAFT

NT F-111 AIRCRAFT

NT HARRIER AIRCRAFT

NT JAGUAR AIRCRAFT

Aft-end design criteria and performance prediction methods applicable to air superiority fighters having twin buried engines and dual nozzles.

[AIAA PAPER 72-1111] 03 p0250 A73-13426

Optimum design for air superiority fighter, noting conventional, delta and coupled canard wing configurations and SAAB Viggen aircraft

03 p0250 A73-13922

Fighter aircraft maneuverability improvement at high subsonic speeds by slotted and unslotted leading- and trailing-edge flaps on delta wing

[DGLR PAPER 72-126] 03 p0248 A73-14386

Control configured vehicle /CCV/ concept application to fighter aircraft design for combat maneuver capabilities and versatility enhancement, using fly by wire technology

[SAE PAPER 720854] 05 p0535 A73-16662

Control configured vehicle /CCV/ technology application for fighter aircraft combat control versatility enhancement, presenting F-4 analytical, simulation and wind tunnel test performance results

[AIAA PAPER 73-160] 05 p0535 A73-16907

Decomposition strategies for one on one aerial dog-fight game models with reinforcement learning

[AIAA PAPER 73-233] 05 p0536 A73-16958

Volvo RM8 turbofan engine for Viggen fighter and ground attack aircraft, emphasizing low fuel consumption for long range cruise and high thrust/weight ratio

05 p0608 A73-17099

Nonlinear programming in design of control systems with specified handling qualities.

07 p0777 A73-20588

USAF experience in lightweight fighter aircraft acquisition as illustration of requests for industrial proposals simplification and source selection process streamlining

09 p1168 A73-21947

Fighter aircraft survivable flight control system design and flight test philosophy, present status and

trends, considering fly-by-wire and power-by-wire systems

09 p1030 A73-22177

Air battle fighter aircraft design, discussing required performance characteristics in terms of lethality, maneuverability, range, visibility, handling qualities, sortie rate, reparability and fire control

09 p1031 A73-22197

Preliminary design of aircraft structures to meet structural integrity requirements.

[AIAA PAPER 73-374] 11 p1439 A73-25506

Experimental tests on scale models of conical variable geometry propulsion nozzle with short petals for fighter aircraft, discussing aerodynamic and thrust coefficients

12 p1533 A73-27388

SOKO Galeb 3 cantilever low wing trainer-fighter monoplane with Bristol-Siddeley Viper 20 turbojet engine, describing flight control, loading gear, fuel system and avionics

14 p1712 A73-30240

Conceptual study of high performance V/STOL fighters.

[ASME PAPER 73-GT-66] 16 p1969 A73-33518

Lift engine bleed flow management for a V/STOL fighter reaction control system.

[ASME PAPER 73-GT-70] 16 p2048 A73-33521

Performance of jet V/STOL tactical aircraft nozzles.

[ASME PAPER 73-GT-77] 16 p1969 A73-33523

Potential payoffs of variable geometry engines in fighter aircraft.

17 p2099 A73-34436

YF-12 aircraft flight loads measurement program with strain gage bridges in fuselage, fuel tanks, control surfaces and left wing

17 p2107 A73-35444

New constraints of military aviation

18 p2267 A73-36684

A parameter optimisation technique applied to the design of flight control systems.

19 p2378 A73-37409

Compatibility of maneuver load control and relaxed static stability.

[AIAA PAPER 73-791] 19 p2379 A73-37458

The F-12 series aircraft aerodynamic and thermodynamic design in retrospect.

[AIAA PAPER 73-820] 19 p2380 A73-37472

F-12 series aircraft propulsion system performance and development.

[AIAA PAPER 73-821] 19 p2380 A73-37473

Flight testing the F-12 series aircraft.

[AIAA PAPER 73-823] 19 p2380 A73-37475

VFW-FOKKER VAK-191B VTOL fighter aircraft structural and aerodynamic design, describing airframe construction, power plant arrangement, flight controls, hydraulic and electrical systems

19 p2387 A73-38167

Computerized optimization of interrelated airframe/engine design parameters against variable criteria to satisfy performance constraints in air superiority fighter design

[AIAA PAPER 73-800] 19 p2388 A73-38370

Structural composites on future fighter aircraft.

[AIAA PAPER 73-806] 19 p2388 A73-38371

Digital information management system of navigational and flight data for post-1975 fighter aircraft.

[AIAA PAPER 73-897] 20 p2589 A73-38832

Cobra P-530 air superiority fighter adaption to ground attack for international requirements for multipurpose aircraft, discussing avionics for multimission version

21 p2634 A73-40301

FIGURE OF MERIT

Features selection by heuristic method with figure of merit in pattern recognition

01 p0021 A73-14488

Relationship between conventional-control-theory figures of merit and quadratic performance index in optimal control theory for a single-input/single-output system.

06 p0680 A73-18445

Pressure-induced optical distortion in laser windows.

09 p1090 A73-21937

Ordinal relationships between measures of the 'accuracy' and 'value' of probability forecasts - Preliminary results.

10 p1244 A73-23646

Figure of merit for fault-tolerant space computers.

10 p1192 A73-24870

Injection frequency locking of the avalanche transit-time oscillator.

13 p1594 A73-29292

Heat pipe operation and characteristics, considering working fluid properties, choice and figure of merit

16 p2086 A73-34043

Acoustooptic materials evaluation based on figures of merits and acoustic attenuation for laser beam deflection device design and fabrication

21 p2710 A73-40095

Comparison of temperature sensors for space instrumentation.

22 p2859 A73-42064

FILAMENT WINDING

- Characterization of an epoxy system for filament winding. 03 p0330 A73-13016
- Acoustic emission during burst tests of filament wound composite pressure bottles as function of pressure, microscopic damage and winding parameters 03 p0331 A73-13031
- Effect of heat treatment on filament wound carbon composites. 03 p0332 A73-13043
- Tensile properties of PRD-49 fiber in epoxy matrix. 05 p0588 A73-16118
- Relationship between structure and strength for CVD carbon infiltrated substrates. II - Three dimensional woven, tufted and needled substrates. 06 p0715 A73-18718
- Material design concepts for filament-wound, graphite-graphite heatshields Further analysis. 08 p1020 A73-21819
- Filament-wound vessel from an organic fiber-epoxy system. 10 p1237 A73-23958
- Fiber reinforced metal production by explosive welding, discussing fiber winding upon metal foils 11 p1372 A73-25353
- Determination of the mechanical characteristics of fiberglass-strengthened plastics in the winding state 13 p1644 A73-27998
- Method for the investigation of the fatigue strength of fiberglass produced by winding and loaded by inter-layer shear. 13 p1695 A73-28523
- Fracture strength of helically wound composite cylinders. 13 p1702 A73-29542
- Two dimensional analysis of yielding to fracture process in angle-ply filament wound laminates under biaxial tension and compression 13 p1702 A73-29543
- Pressure vessels filament winding with inflatable mandrel in reinforced elastomer, discussing use of balloon as liner 16 p2018 A73-33068
- Development of advanced composite rocket motor chambers using boron and graphite fibers. 17 p2194 A73-34803
- High modulus filament wound vessels for cryogenic containers in spacecraft. 17 p2238 A73-34807
- Edgewise tape wound reinforced plastic ablative components for rocket motors to provide balance between optimum char strength, heat flow and insulation characteristics 17 p2195 A73-34809
- High strength continuous filament wound carbon fiber reinforced plastic performance evaluation for use in light weight rocket motors 17 p2195 A73-34810
- Rational winding of vessels with nonlinear winding programs 18 p2319 A73-36470
- Prediction and control of macroscopic fabrication stresses in hoop wound, fiberglass rings. 23 p3041 A73-43638
- Experimental investigations regarding optimally designed three-layer wound glass fiber/plastic tubes under internal pressure 24 p3147 A73-44882
- 'Crack boundaries' in the case of unidirectional glass-fiber-reinforced plastic wound laminates under uniaxial and biaxial stress 24 p3103 A73-44883
- Acoustic emission produced during burst tests of filament-wound bottles. 24 p3094 A73-45146

FILAMENT WOUND CONSTRUCTION

U FILAMENT WINDING

FILAMENTS

- Solar active region growth in terms of magnetic flux emergence in shape of new arch filament system 03 p0367 A73-12946
- Tidal generation of narrow intergalactic filaments from computer simulations, discussing alternative models 03 p0372 A73-13353
- The magnetic structure of arch filament systems. 03 p0378 A73-14415
- One-dimensional periodic superconducting weak-link systems. 04 p0484 A73-16040
- The excitation mechanism for the filaments in the Crab Nebula. 05 p0617 A73-16471
- Cellular or filamentary structure of galactic magnetic fields, noting correlations between rotations of radio sources and angular separation 08 p1002 A73-20880
- Thermal characteristics of constantan, Ni-Cr-Fe, Ni-Mo, Ce-Al-Fe and Ni-Cr alloy filaments for high temperature strain gages 11 p1362 A73-25456

- Laser beam transformation into light filament in inhomogeneous weakly absorbing media from Gaussian beam propagation analysis 14 p1758 A73-30466

FILLERS

- Solution of axisymmetrical problems of the interaction between a cylindrical shell and an elastic filler by the finite difference method 02 p0231 A73-11806
- Factors affecting coefficient of friction and wear of friction materials for brakes, discussing fillers use as reinforcements and friction modifiers 05 p0580 A73-16106
- Static-geometric analogy and complex transformation in the theory of three-layer shells with a light-weight filler 07 p0912 A73-19470
- Mineral filler reinforcement value in polyolefins, stressing composite properties at high temperatures 10 p1237 A73-23963
- Preparation and performance characteristics of flammable and inflammable polyimide foams as sandwich fillers 10 p1239 A73-24098
- Stress-strain state in the filler of a three-layer strip under local loading 10 p1291 A73-24354
- Investigation of the detonation characteristics of hexogen-filler systems 13 p1706 A73-28970
- Static-geometric analogy and complex transformation in the theory of three-layered shells with light fillers. 15 p1952 A73-32072
- The role of a porous filler structure in strengthening polymers 16 p2030 A73-33929
- Investigation of the thermophysical and antifriction characteristics of polyethylene composites. III - The effect of fillers on the heat conductivity of polyethylene 16 p2030 A73-33930
- Effect of transverse shear on the stability of an orthotropic cylindrical shell with an elastic filler under axial compression 16 p2082 A73-33931
- Modulus reinforcement in elastomer composites. I - Inorganic fillers. 18 p2328 A73-36980
- Modulus reinforcement in elastomer composites. II - Polymeric fillers. 18 p2328 A73-36981
- Symmetrical three-layer shells with a light-weight elastic filler 20 p2618 A73-39328
- Investigation of the dross molding process for titanium carbide 23 p2991 A73-43490
- Development of corrosion resistant filler metals for brazing molybdenum. 23 p2986 A73-44004
- The relationship of certain mechanical and thermophysical properties of polymer composites with the reduced filler concentration 24 p3102 A73-44512

FILLETS

- Corner pressures and fillet shock locations for symmetrical corners by an approximate method. 07 p0774 A73-19494

FILLING

- Filling tests in single and double arm plenum configuration models used in gasdynamic laser systems, noting wave controlled unsteady flow processes 09 p1030 A73-23447

FILM BOILING

- Analytical study of the sensitivity of a sensor for studying pulsations of the heat-transfer coefficient in a boiling high-temperature layer 01 p0051 A73-10864
- Oscillation effects upon film boiling from a sphere. 03 p0398 A73-13548
- Stagnation-point free-convection film boiling on a hemisphere. 05 p0638 A73-16353
- Laminar film boiling on inclined isothermal flat plates. 05 p0641 A73-17107
- The study of disperse regimes with film boiling of liquid nitrogen in tubes. 07 p0922 A73-20409
- The study of film boiling crises and transient boiling of cryogenic liquids. 07 p0922 A73-20410
- Film boiling heat transfer feedback control, comparing experimental process dynamics with analytical transfer function 08 p1024 A73-21526
- Destabilization of vapor film boiling around spheres. 08 p1024 A73-21641
- Investigation of a film boiling crisis in the presence of natural convection 11 p1451 A73-25734

- Heat transfer during helium boiling in narrow channels of different orientations 13 p1661 A73-29405

- Flow film boiling heat transfer correlations - Parametric study with data comparisons. [ASME PAPER 73-HT-50] 20 p2626 A73-38574

FILM CONDENSATION

- Effects of forced flow, noncondensables, and variable properties on film condensation of pure and binary vapors at the forward stagnation point of a horizontal cylinder. 01 p0122 A73-10806
- The effect of noncondensable gas on laminar film condensation of liquid metals. [ASME PAPER 72-WA/HT-9] 04 p0520 A73-15836
- Features of the mechanism of vapor condensation from humid air in narrow channels and the hydrodynamics of two-phase flow during droplet condensation 11 p1451 A73-25735
- Electron-diffraction study of amorphous condensates of barium titanate 12 p1531 A73-27198
- Condensation of cesium from an incident shock wave in cesium vapors 12 p1528 A73-27323
- Linear stability theory applied to stability characteristics of laminar condensate film flow along inclined wall, noting critical Reynolds number for disturbance amplification 12 p1559 A73-27697
- Laminar film condensation on the inside of slender, rotating truncated cones. 15 p1958 A73-32279

FILM COOLING

- Scaling of performance and thermal environment in fuel-vortex cooled rocket engines. [AIAA PAPER 72-1075] 03 p0354 A73-13399
- Heat transfer to film-cooled combustion chamber liners. [ASME PAPER 72-WA/HT-32] 04 p0518 A73-15823
- A proposed method for calculating film-cooled wall temperatures in gas turbine combustion chambers. [ASME PAPER 72-WA/HT-24] 04 p0519 A73-15830
- Liquid film cooling on hypersonic slender bodies. 10 p1172 A73-24540
- Air injection from wall slot into turbulent boundary layer of high temperature gas channel flow, calculating film cooling effectiveness in flat plate 13 p1706 A73-28675
- Film-cooling effectiveness in the near-slot region. 15 p1958 A73-32278
- Effectiveness and heat transfer with full-coverage film cooling. [ASME PAPER 73-GT-18] 16 p2086 A73-33495
- Effect of adverse pressure gradient on film cooling effectiveness. [AIAA PAPER 73-697] 18 p2368 A73-36246
- Investigation of multiple slot film cooling to a blunt nose cone. [AIAA PAPER 73-698] 18 p2368 A73-36247
- Film effectiveness and heat transfer coefficient downstream of a metered injection slot. [ASME PAPER 73-HT-31] 20 p2625 A73-38570
- The turbulent boundary layer with stepwise varying boundary conditions at a permeable surface. 20 p2628 A73-39423
- Effectiveness of film cooling of an adiabatic wall downstream of the perforated section. 20 p2628 A73-39424
- Gas turbine nozzle guide vane trailing edge protection by air films cooling, measuring gas temperatures with chromel-alumel thermocouples 20 p2600 A73-39425
- Effectiveness of film cooling in a curvilinear channel formed by guide vanes 23 p3048 A73-43442

FILM THICKNESS

- The effect of oxide thickness on the hot salt stress corrosion susceptibility of Ti-6Al-4V. 01 p0061 A73-10137
- Elastohydrodynamic lubrication in rolling and sliding contacts. [ASME PAPER 72-LUB-K] 01 p0055 A73-10222
- Influence of the thickness of a copper coating on the critical current of a superconducting wire made from niobium-based alloys 01 p0089 A73-11435
- Inlet shear heating in elastohydrodynamic lubrication. [ASME PAPER 72-LUB-21] 03 p0314 A73-14336
- Elastohydrodynamic lubrication in rolling and sliding contacts. [ASME PAPER 72-LUB-K] 03 p0315 A73-14351
- Metal-semiconductor system phase diagram for temperature dependence of substrate surface epitaxial film thickness during single crystal growth, determining equilibrium saturation time 04 p0483 A73-14880
- An extension of the Grubin theory of elastohydrodynamic lubrication. 05 p0581 A73-16433
- Electrical properties of evaporated mercury telluride films. 06 p0734 A73-17815

- Optimum thickness for thermomagnetic laser writing on Fe doped EuO films on quartz substrate
06 p0702 A73-18372
- Effects of electropolishing on the tunneling current in aluminum-aluminum-oxide-aluminum diodes
06 p0678 A73-18744
- Aircraft components solid film lubrication problems, discussing surface pretreatment, contamination susceptibility, corrosion prevention and aerosol applicability
07 p0842 A73-19554
- An X-ray monitor for measurement of a titanium tritide target thickness.
07 p0809 A73-20466
- Surface oxide transistor with MIS and base contacts, investigating I-V characteristics as function of oxide thickness and contact separation distance
08 p0948 A73-21480
- Asbestos-textolite coating required thickness calculation with allowance for aerodynamic heating, discussing softening mechanisms
09 p1110 A73-23057
- Thickness dependence of effective coupling factors of ZnO thin-film surface-wave transducers.
09 p1086 A73-23097
- Frequency and environmental interactions in the fatigue of aluminum alloys.
11 p1382 A73-25824
- Critical current value for a superconductor niobium-alloy wire as a function of its copper coating thickness.
11 p1409 A73-26062
- Error curve in radiometric beta backscatter measurement of coatings thickness via digital computation
12 p1495 A73-26846
- Reversible recording of holograms on chalcogenide glass films
12 p1495 A73-26940
- German monograph - Investigations regarding the elastohydrodynamic lubricant film thickness in the case of elliptical Hertzian contact surfaces.
13 p1625 A73-29287
- Use of interferential filters for optical control during deposition of reflecting coatings
17 p2183 A73-34171
- An analysis and prediction of lubricant film starvation in rolling contact systems.
[ASLE PREPRINT 73AM-3B-4]
- 17 p2179 A73-34985
- Self-acting and hydrodynamic shaft seals.
17 p2179 A73-34999
- Experimental study on the interference of inertia and friction forces in turbulent lubrication.
[ASME PAPER 73-LUBS-12]
- 17 p2181 A73-35393
- A reflectance analog computer for the determination of thin film optical properties.
17 p2132 A73-35773
- Oil spills - Measurements of their distributions and volumes by multifrequency microwave radiometry.
17 p2164 A73-35806
- Some observations of the relationship between film thickness and load in high Hertz pressure sliding elastohydrodynamic contacts.
[ASME PAPER 73-LUB-D]
- 19 p2433 A73-37450
- Investigation of the hypervelocity impact on thin plastics and metal foils
21 p2696 A73-39990
- The steady-state thickness of a liquid water film on the surface of halitones of various shapes
21 p2730 A73-40118
- Titanium oxide film dissolution indication by tempering colors and weld tensile strength dependence on film thickness and temperature
21 p2717 A73-40480
- Optimal thick layer nitriding of Ti alloys, discussing boundary conditions, film, hydrogen effect and mechanical properties
21 p2707 A73-40739
- Properties of anodic oxide films formed in the anodization of silicon nitride.
[ECS PAPER 81]
- 21 p2702 A73-40844
- Comparison of experimental microlayer thickness results.
21 p2793 A73-41690
- The imaging properties and aberrations of thick transmission holograms.
22 p2864 A73-43185
- The detectability limits of thin coatings measured with the electron microprobe.
23 p2985 A73-43917
- Thickness of liquid film on a rotating disk.
23 p2969 A73-44128
- Measurement of the p-n junction depth in photocells with epitaxial layers
24 p3058 A73-45254
- The flow of a viscous liquid down a variable incline.
24 p3080 A73-45368
- FILMS**
- Metallic contact resistance and friction behavior under microdisplacement for lead/gold surfaces with lubricant or oxide film, noting consistency with Greenwood theory
[ASLE PREPRINT 72LC-6B-1]
- 03 p0316 A73-14364
- Review of recent advances in bonded solid film lubrication at high temperatures.
07 p0842 A73-19552
- Characterization of passivation films formed at the surface of stainless steels in magnesium chloride solutions
08 p0976 A73-20650
- FILTRING**
- U FILTRATION**
- FILTERS**
- Canonical expansions of random processes, discussing discrete and continuous set transformations for spectral representation and shaping filters in time domain
01 p0068 A73-10027
- An algebraic algorithm for the design and analysis of linear dynamical systems.
08 p0984 A73-21468
- Dispersed signal filtering and filtered signal duration relation to filter bandwidth and dispersiveness, isolating fundamental mode of Rayleigh waves from earthquake 650 km deep
21 p2648 A73-39931
- FILTRATION**
- NT SPATIAL FILTERING**
- Hyperfiltration technique applied to wash water reclamation at elevated temperatures.
19 p2400 A73-37982
- [ASME PAPER 73-ENAS-27]
- Experimental investigation of the filtration characteristics of porous materials used in boundary-layer control systems
22 p2841 A73-42119
- Ultrafiltration by a compacted clay membrane. I - Oxygen and hydrogen isotopic fractionation. II - Sodium ion exclusion at various ionic strengths.
23 p2973 A73-43845
- FIN STABILIZERS**
- U FINIS**
- U STABILIZERS (FLUID DYNAMICS)**
- FINANCIAL MANAGEMENT**
- Physical contents and financial underpinning of future French and European space research programs, noting meteorology, satellite communication and R and D planning
01 p0125 A73-11254
- Financial problems related to aircraft and ships development and production for Defense Department, stressing C-5A, Cheyenne helicopter and DD-963 class of automated destroyers
03 p0401 A73-13897
- Satellite charges for a mixed pre-demand-assigned system.
03 p0276 A73-13901
- Financing of route installations and services to aircraft in flight, suggesting international rules for rental collection
06 p0771 A73-17862
- Collection and processing of data for the establishment of route charges.
07 p0796 A73-19182
- ELDO and ESRO space research activities review, stressing increased European cooperation, negotiations with U.S. and project budgeting vs national priorities
11 p1455 A73-26420
- Status of funded improvements to the National Aviation System and planned improvements not yet funded.
12 p1561 A73-27363
- An appraisal of the funding provisions of the Airport and Airways Development Act of 1970 to implement system improvements.
12 p1561 A73-27366
- Launching base creation process and economic factors, considering rocket firing safety, scientific requirements and financial investments criteria
14 p1741 A73-30080
- The financing of essential communication, navigation and terminal aids.
17 p2257 A73-34535
- Book - Zero-base budgeting: A practical management tool for evaluating expenses.
17 p2258 A73-35674
- Financing the new generation of airports.
19 p2506 A73-37745
- Air carrier and general aviation airports system planning with emphasis on economic analysis of operation, ownership and finance
[ASME PAPER 73-ICT-33]
- 23 p2965 A73-43494
- FINE STRUCTURE**
- X-ray fine structure of dense plasma in a co-axial accelerator.
01 p0086 A73-11493
- Preliminary results of the third flight of the Soviet stratospheric solar observatory.
02 p0216 A73-12335
- LTE fine analysis of omicron-tv C Ma line profiles, showing chemical composition near iota Her
02 p0221 A73-12705
- Magnetograph instrumentation and measurements, presenting solar magnetic field fine structure observations
04 p0496 A73-14829
- Atmospheric transmittance calculation from 0.76-micron oxygen band fine structure parameters
04 p0473 A73-15571
- Frequency correlation measurement of pulsar spectral fine structure due to radio emission scattering by interstellar plasma
04 p0503 A73-16002
- Sunspot fine structure from photographs taken on U.S.S.R. Stratospheric Solar Station, noting high Rayleigh resolution of small elements
05 p0621 A73-17031
- Solution of the transfer equation for interlocked multiplets by probabilistic method.
05 p0599 A73-17320
- Experiment on the geometry of the fine-structure regions in fully turbulent fluid.
06 p0684 A73-17703
- Selective reabsorption leading to multiple oscillations in the 8446-A atomic-oxygen laser.
07 p0834 A73-19335
- Interactions among multiple lines in the 8446-A atomic-oxygen laser.
07 p0834 A73-19336
- Petrology and chemistry of some Apollo 14 lunar samples.
07 p0882 A73-19721
- Fine structure in the optical-absorption edge of silicon.
07 p0863 A73-20175
- Fine structure of the temperature stratification in the troposphere and stratosphere.
07 p0848 A73-20348
- Fine structures of mutually normalized rare-earth patterns of chondrites.
07 p0789 A73-20620
- On the size of the structure elements in the solar chromosphere.
08 p1001 A73-20754
- Solar cosmic rays propagation between shock front and solar flare hot plasma, examining fine structure from Explorer 34 and Venera 6 data
08 p0999 A73-21328
- Fine structure of the Jupiter radio bursts.
08 p1013 A73-21646
- Fine structure of Pc 1 pulsations. I - Experimental evidence.
09 p1074 A73-22068
- Effect of carbon on the fine structure of cast molybdenum
09 p1108 A73-23232
- On the small-scale structure of solar magnetic fields.
10 p1279 A73-24135
- Fine structure of X-ray spectra of nickel and some of its alloys with a nickel arsenide lattice and lattices resembling it
10 p1259 A73-24152
- Studies of the atmospheric fine structure with the aid of microwave propagation experiments
10 p1213 A73-24682
- Morphological and experimental excitation models of cardiac muscle ultrastructure, transmission activity and intercellular contact relationships
11 p1315 A73-25590
- Solar Fraunhofer spectral lines having simple Zeeman triplet splitting with large Lande g-factors tabulated, noting missing lines in identification
11 p1421 A73-25932
- Observations on the time and frequency structure of solar decimeter radio bursts.
11 p1413 A73-25951
- Spectral investigation of the chromosphere. II.
12 p1544 A73-27829
- Fine bright umbral spot structures from photographic line spectra observation of sunspot, noting magnetic field strength, outflow velocity and photospheric temperature
12 p1545 A73-27834
- The relation between tensile bond strength and crystalline properties of the adhesive on the steel-nylon 12-steel system.
13 p1642 A73-29531
- Pulsar positions, polarization characteristics, intensity and fine structure, considering models explaining rotating neutron stars, galactic magnetic fields and electron densities and temperature
14 p1800 A73-30549
- The possible nature of the fine structure of sporadic radio emission from the sun and other cosmic sources having a high density of electromagnetic radiation
15 p1926 A73-31876
- Plasma fine velocity structure and dynamics from diffraction pattern of interplanetary radio sources scintillation
15 p1919 A73-31959
- Test for detection of fine structure of the solar wind velocity.
15 p1927 A73-32015
- Theory of satellite structures on spectral-line profiles.
15 p1915 A73-32289
- Microwave-propagation studies regarding the isotropy characteristics of the turbulent fine structure of the refractive index in the troposphere
15 p1874 A73-32361
- A test for revealing the fine-scale velocity structure of the solar wind
16 p2059 A73-32888

- Morphological and kinematic study of the fine structures of a sunspot**
16 p2052 A73-32956
- Fine structure in the sunspot spectrum - 2 to 70 years.**
17 p2230 A73-34514
- Structural formations in the interplanetary medium**
19 p2481 A73-37342
- Fine structure of Jupiter's decametric source B.**
19 p2482 A73-37389
- Fracture mechanics of carbon fibers at high temperatures due to fine structure, discussing effects of ribbon unbending during extension**
19 p2444 A73-38089
- Turbulence spectra at scales smaller than 1 meter.**
19 p2449 A73-38241
- H alpha line contrast profiles evaluation from solar chromosphere supergranulation observations, obtaining chromospheric fine structure characteristics**
20 p2606 A73-39072
- Investigation of the fine-structure inhomogeneities of the Es layer at oblique radio wave incidence**
20 p2554 A73-39163
- Rotational line structure in three-photon scattering by symmetric top molecules.**
20 p2574 A73-39723
- Rocket measurements of electric field and optical aurora during weak PCA event, noting rocket passage through discrete auroral forms**
21 p2684 A73-40781
- Observation of 9.0-micron line emission from Ar III in NGC 7027 and NGC 6572.**
22 p2910 A73-42704
- Quantum-beat g-value measurements on transitions from levels of aligned fast ions.**
22 p2890 A73-42974
- Propagation mode with fine structure interpreted as quasi-cylindrical electrostatic wave interference with cold plasma field from potential measurements near point source antenna**
22 p2895 A73-43021
- CW single mode He-Ne laser intensity fine structure fluctuations correlation measurement near threshold by digital correlator, obtaining higher order relaxation rates**
22 p2871 A73-43085
- Plasma fine velocity structure and dynamics from diffraction pattern of interplanetary radio sources scintillation**
24 p3132 A73-44484

FINES

- Luna 16 powdery regolith specimens magnetic properties, giving specific susceptibility, remanent magnetization and structure related recession**
02 p0213 A73-12236
- Cosmic black glassy spherules composition, mineralogy and physical properties compared to lunar fines, considering possible common origin**
02 p0214 A73-12254
- Petrochemistry and chemical features of lunar glassy spherules.**
03 p0273 A73-13089
- Interferometric studies on Apollo 11 and Apollo 12 lunar glass objects.**
03 p0369 A73-13096
- Luna 20 and Apollo 16 core fines - Large-ion lithophile trace-element abundances.**
05 p0546 A73-16828
- Lunar fines thermal diffusivity measurement, calculating lunar surface temperature distribution [AIAA PAPER 73-40]**
06 p0767 A73-17622
- An evaluation of pyrolytic techniques with regard to the Apollo 11, 12 and 14 lunar samples analyses.**
06 p0753 A73-18411
- Low molecular weight compounds of organogenic elements on Apollo 11 and 12 fines and breccias obtained by vacuum pyrolysis, acid hydrolysis and crushing**
06 p0654 A73-18418
- Apollo 11, 12 and 14 surface fines analysis by fluorescent technique for porphyrins content**
06 p0753 A73-18419
- Amino acid search in lunar fines, considering terrestrial source contamination, bound and free amino acids, processing and analysis contamination**
06 p0754 A73-18422
- Apollo 14 fines examination for indigenous amino acids or amino acid convertible materials, optimizing gas-liquid chromatographic systems for separation and flame ionization**
06 p0662 A73-18423
- Pyrolysis system with high sensitivity medium-resolution mass spectroscopy to quantify ions pyrolyzed in lunar fines, confirming presence of indigenous lower hydrocarbons**
06 p0662 A73-18431
- Reflection spectra of lunar dust grains with amorphous coatings.**
07 p0876 A73-19583
- Crystallography and chemical trends of orthopyroxene-pigeonite from rock 14310 and coarse fine 12033.**
07 p0881 A73-19703
- Crystallographic studies of lunar plagioclases from samples 14053, 14163, 14301, and 14310.**
07 p0882 A73-19715

- Chondrules in Apollo 14 samples and size analyses of Apollo 14 and 15 fines.**
07 p0882 A73-19720
- Mineralogy and origin of Fra Mauro fines and breccias.**
07 p0883 A73-19726
- Mineralogy, petrology, and chemical composition of lunar samples 15085, 15256, 15271, 15471, 15475, 15476, 15535, 15555, and 15556.**
07 p0883 A73-19727
- Apollo 14 glasses of impact origin and their parent rock types.**
07 p0883 A73-19735
- Chromatographic and mineralogical study of Apollo 14 fines.**
07 p0884 A73-19743
- Study of excess Fe metal in the lunar fines by magnetic separation, Moessbauer spectroscopy, and microscopic examination.**
07 p0788 A73-19745
- Major, minor, and trace element data for some Apollo 11, 12, 14, and 15 samples.**
07 p0886 A73-19759
- Rare earths and other trace elements in Apollo 14 samples.**
07 p0886 A73-19760
- Precise determination of rare-earth elements in the Apollo 14 and 15 samples.**
07 p0886 A73-19762
- Deuterium content of lunar material.**
07 p0887 A73-19774
- Sulphur concentrations and isotope ratios in lunar samples.**
07 p0887 A73-19775
- K-Ar dating of lunar fines - Apollo 12, Apollo 14, and Luna 16.**
07 p0888 A73-19781
- Trapped solar wind noble gases in Apollo 12 lunar fines 12001 and Apollo 11 breccia 10046.**
07 p0871 A73-19800
- Inert gases from Apollo 12, 14, and 15 fines.**
07 p0889 A73-19801
- A comparison of noble gases released from lunar fines (no. 15601.64) with noble gases in meteorites and in the earth.**
07 p0889 A73-19806
- Noble gases concentration profiles in lunar fines and minerals, investigating thermal release patterns**
07 p0889 A73-19807
- Atmospheric Ar-40 in lunar fines.**
07 p0890 A73-19808
- Survey of lunar carbon compounds. II - The carbon chemistry of Apollo 11, 12, 14, and 15 samples.**
07 p0890 A73-19818
- Amino acid precursors in lunar fines from Apollo 14 and earlier missions.**
07 p0891 A73-19820
- Amino acid analyses of Apollo 14 samples.**
07 p0891 A73-19821
- Spectrofluorometric search for porphyrins in Apollo 14 surface fines.**
07 p0891 A73-19823
- Some surface characteristics and gas interactions of Apollo 14 fines and rock fragments.**
07 p0891 A73-19831
- Remanent magnetization of Apollo 14 rocks and fines, discussing iron contribution and early internal magnetic field**
07 p0892 A73-19837
- Apollo 14 and 15 igneous rock, fines and breccia intrinsic and structure-sensitive magnetic parameters**
07 p0893 A73-19842
- Temperature-dependent magnetic properties of individual glass spherules, Apollo 11, 12, and 14 lunar samples.**
07 p0893 A73-19844
- Apollo 14 samples with Fe-bearing minerals examined by Mossbauer spectroscopy, noting parallelism with Apollo 11 and 12 samples**
07 p0893 A73-19845
- Nuclear magnetic resonance properties of lunar samples.**
07 p0893 A73-19846
- Apollo 14 returned lunar rock fine thermal conductivity measurement as function of temperature under vacuum conditions, using least squares curve fitting method**
07 p0895 A73-19856
- Photoemission from lunar surface fines and the lunar photoelectron sheath.**
07 p0895 A73-19860
- Secondary electron emission characteristics of lunar surface fines.**
07 p0871 A73-19861
- Radiation effects in soils from five lunar missions.**
07 p0896 A73-19875
- Thermoluminescence of individual grains and bulk samples of lunar fines.**
07 p0897 A73-19883
- Spectral emission of natural and artificially induced thermoluminescence in Apollo 14 lunar sample 14163.147.**
07 p0897 A73-19884
- Far infrared properties of lunar rock.**
07 p0897 A73-19886

- Quantitative size and shape analyses of Apollo 14 and 15 fines by computer evaluation of scanning electron microscope images**
07 p0898 A73-19898
- Mechanical properties of lunar soil - Density, porosity, cohesion, and angle of internal friction.**
07 p0898 A73-19902
- On-surface and laboratory size measurements of fine lunar particles.**
07 p0900 A73-20184
- Distribution of methane and carbide in Apollo 11 fines.**
07 p0900 A73-20188
- Apollo 14 lunar fines thermal radiation properties as function of bulk density, illumination angle and wavelength, calculating solar albedo and total emittance**
10 p1277 A73-24080
- Depth variation of Apollo 15 deep drill fines trace elements from neutron activation analysis, noting KREEP abundance**
10 p1278 A73-24113
- Apollo 12 fines vacuum thermal conductivity as function of temperature for different densities, comparing to terrestrial basalt under vacuum and pressure**
11 p1425 A73-26137
- Green spherules from Apollo 15 - Inferences about their origin from inert gas measurements.**
12 p1541 A73-27490
- Oxide minerals in lithic fragments from Luna 20 fines.**
13 p1674 A73-28306
- Inert gases in a terra sample - Measurements in six grain-size fractions and two single particles from Lunar 20.**
13 p1675 A73-28318
- Oxygen and bulk element abundances in Luna 20 fines from instrumental neutron activation analysis, noting comparison with Apollo lunar soil samples**
13 p1676 A73-28320
- Siderophile and volatile elements in Luna 20 fine soil and breccia samples from radiochemical neutron activation analysis, noting comparing with Apollo 16 results**
13 p1676 A73-28325
- Comparison of the magnetic properties of glass from Luna 20 with similar properties of glass from the Apollo missions.**
13 p1677 A73-28332
- Apollo lunar fines ferromagnetic resonance spectral line shape anomaly and anisotropy energy attributed to Fe particles with body centered cubic structure**
13 p1684 A73-29177
- Far ultraviolet reflectivity of lunar dust samples - Apollo 11, 12, and 14.**
15 p1932 A73-31270
- Trapped solar wind noble gases and exposure age of Luna 16 lunar fines.**
21 p2770 A73-41001
- O-18/O-16 ratios in Luna 16 fines.**
21 p2770 A73-41003
- Helium, neon and argon in Level C of Luna 16 fines.**
21 p2770 A73-41004
- Formation of lunar carbide from lunar iron silicates.**
21 p2780 A73-41643
- Fading of thermoluminescence induced in lunar fines.**
22 p2915 A73-43027

**FINGER LAKES
U LAKES
FINERS**

- Fingerprint patterns incidence relation in congenital vitium cordis patients, using Henry dactyloscopic classification**
01 p0009 A73-11800
- A device for the continuous measurement of subjective changes**
16 p1975 A73-33090
- Effect of skin wetting on finger cooling and freezing.**
20 p2518 A73-39779

**FINISHES
NT ENAMELS
NT LACQUERS**

- Aircraft surface primers and finishes composition, pretreatment and application, discussing epoxy, acrylic and polyurethane primers mechanical and chemical properties**
10 p1237 A73-23522
- Critical properties of exterior aircraft finish systems to protect fastener areas.**
13 p1638 A73-29317
- New inhibited elastomeric finish system designed by corrosion engineers to solve acute corrosion problems on military aircraft.**
13 p1638 A73-29318
- FINITE DIFFERENCE THEORY**
Equivalence theorems for nonlinear finite-difference methods.
01 p0069 A73-10074
- A general circulation model of the atmosphere suitable for long period integrations.**
01 p0072 A73-10143

Construction of finite-difference schemes in engineering theory of elasticity on the basis integral representations of the resolvent functions

01 p0114 A73-10483

Finite difference solution to Vekua thin shell equations, using differential and equivalent energetic operators

01 p0116 A73-11076

Artificial viscosity truncation error analysis for finite difference analogs of linear advection equations

01 p0035 A73-11466

Finite difference method for boundary layer flow, noting truncation errors due to nonuniform grid

01 p0035 A73-11468

An explicit difference method for steady supersonic flow [DGLR PAPER 72-066]

02 p0127 A73-11670

Finite difference method for transverse elliptical cross section effect of spiral shell on stress concentration

02 p0231 A73-11802

Solution of axisymmetrical problems of the interaction between a cylindrical shell and an elastic filler by the finite difference method

02 p0231 A73-11806

Calculus of variations and finite difference method for equilibrium equations in axisymmetric plastic shell design

02 p0232 A73-11821

Vibration of a square plate symmetrically supported at four points.

02 p0237 A73-12605

The equivalence method and the finite-difference method in linear elasticity

03 p0383 A73-12909

Calculation of the stress distribution in rotating disks in the case of unsteady creep with the aid of a digital computer

03 p0385 A73-13140

Application of a pseudo-viscous method to the calculation of the steady supersonic flow past a waisted body.

03 p0242 A73-13335

Resonant frequencies of free vibrating plate via finite difference method, noting difference equations for plate equilibrium

03 p0391 A73-13345

A discussion of the Marsh matrix technique applied to fluid flow problems.

03 p0244 A73-13563

Determination of the flow past a cylinder and a sphere in the presence of an incident shock wave

03 p0294 A73-13615

Computation and solution procedures for nonlinear analysis by combined finite element-finite difference methods.

03 p0391 A73-13685

Transient response of inelastic shells of revolution.

03 p0392 A73-13686

Finite difference theory for bending stress concentration in shells of revolution, noting constitutive equation for thermal stress analysis

03 p0393 A73-13793

Two numerical methods for three-dimensional boundary layers.

04 p0433 A73-15003

A second-order accurate difference method for systems of hyperbolic partial differential equations.

04 p0470 A73-15007

Calculation methods of three-dimensional boundary layers with and without rotation of the walls. [ONERA, TP NO. 1135]

04 p0403 A73-15093

Finite difference technique for numerical calculation of two dimensional stratified incompressible fluid flows

04 p0433 A73-15162

Stability of Richtmyer type difference schemes in any finite number of space variables and their comparison with multistep Strang schemes.

04 p0471 A73-15233

Practical techniques for estimating the accuracy of finite-difference solutions to parabolic equations. [ASME PAPER 72-WA/APM-12]

04 p0472 A73-15900

Evaluation of numerical viscosity effects in transonic flow calculations. [AIAA PAPER 73-131]

05 p0530 A73-16884

A method for solving moving boundary problems in heat flow using cubic splines or polynomials.

06 p0768 A73-17979

Convergent finite difference schemes for nonlinear parabolic equations.

06 p0717 A73-18405

The treatment of natural boundary conditions in the finite element and finite difference methods.

07 p0907 A73-19033

Energy conserving finite difference approximation for solution of unaveraged Navier-Stokes equations of three dimensional incompressible turbulent flow in square duct

07 p0810 A73-19263

A computational method for low Mach number unsteady compressible free convective flows.

07 p0918 A73-19268

Automatic optimization of Symbolic Algol programs. I - General principles.

07 p0796 A73-19269

A two-dimensional numerical FET model for dc, ac, and large-signal analysis.

07 p0799 A73-19342

A direct method for solving Poisson's equation.

07 p0845 A73-19574

Numerical method of transient heat conduction with temperature dependent thermal properties.

07 p0921 A73-20118

Longitudinal vibration analysis of partially-filled ellipsoidal tanks.

07 p0914 A73-20215

Stability of difference approximations to differential equations.

07 p0845 A73-20494

Finite difference calculation for Gunn effect mathematical model, noting negative slope in electron drift velocity versus electric field characteristics for microwave oscillation

08 p0943 A73-20710

Convergence of difference methods for certain degenerating quasi-linear parabolic equations

09 p1111 A73-21919

Finite difference programs with grid self adjustment for steady or unsteady problems with arbitrary boundaries and without coordinate hierarchy, noting computer time saving

09 p1071 A73-22400

Stability of certain finite-difference schemes for solving heat conduction equations with a nonself-conjugate elliptic operator

09 p1167 A73-22582

Thin panels stresses diffusion analysis, comparing Bleich, variational, Conway finite difference and finite element methods

09 p1159 A73-22717

Certain properties of functions with a non-zero difference quotient

09 p1112 A73-22887

The numerical solution of boundary value problems for second order functional differential equations by finite differences.

09 p1113 A73-23021

A note on the stability of an iterative finite-difference method for hyperbolic systems.

10 p1241 A73-23639

Numerical study of the flow of a viscous incompressible fluid around a circular cylinder

10 p1171 A73-23766

Application of a variational difference method to the calculation of forced vibrations of shells of revolution

10 p1292 A73-24487

Application of the extended Newton method to the creep analysis of shells of revolution.

11 p1432 A73-24998

Explicit and implicit difference schemes for solving complex equations of motion, deriving approximation stability conditions

11 p1397 A73-25033

An evaluation of cell type finite difference methods for solving viscous flow problems.

[AD-757443]

11 p1345 A73-25112

Viscous flow over a cone at moderate incidence. I - Hypersonic tip region.

11 p1300 A73-25114

On the stability of finite difference schemes in transient semiconductor problems.

11 p1408 A73-25438

Steady state mathematical theory for the insulated gate field effect transistor.

11 p1338 A73-25789

On the origin of oscillations appearing in shock profiles calculated by difference methods

11 p1390 A73-25868

An elastic-plastic buckling solution using the incremental theory.

11 p1443 A73-26089

Accuracy and convergence of absolutely stable finite difference procedures for solution of multidimensional heat conductivity equation with discontinuous coefficients

11 p1452 A73-26327

Implicit difference method of temperature determination in problems of radiative gasdynamics

11 p1348 A73-26329

Admissible step sizes for Adams-Bashforth, Adams-Moulton, Nystrom and Milne-Simpson difference methods for initial value problems solution

11 p1392 A73-26729

Comparison of grids and difference approximations for numerical weather prediction over a sphere.

12 p1519 A73-26803

Multilocal difference method for free vibration analysis of closed and open orthotropic noncircular cylindrical shells with supported curved edges

12 p1551 A73-27035

Sound absorption in lined rectangular ducts with wall shear layers - Convergence of the numerical procedure to the analytical solution.

13 p1658 A73-28061

Direct numerical solution of three-dimensional equations containing elliptic operators.

13 p1647 A73-28080

Transient cooling of a solid cylinder by combined convection and radiation at its surface.

13 p1704 A73-28086

Computer programs for analysis of shells of revolution based on numerical integration and finite difference procedures

13 p1693 A73-28236

Incremental solution of axisymmetric plate and shell finite deformation.

13 p1694 A73-28250

The mechanical interpretation of high accuracy multi-point difference methods for plates and shells.

13 p1694 A73-28255

An evaluation of finite difference and finite element techniques for analysis of general shells.

13 p1694 A73-28256

Approximate solution of the Laplace and Poisson equations in weighted Hoelder spaces

13 p1647 A73-28340

Two-sided difference methods of solving linear boundary value problems for ordinary differential equations

13 p1647 A73-28341

A two-dimensional mathematical model of the insulated-gate field-effect transistor.

13 p1590 A73-28543

A numerical method for highly accelerated laminar boundary-layer flows.

13 p1600 A73-28608

The static-geometric duality and a staggered mesh scheme in the numerical solution of some shell problems.

13 p1699 A73-29373

Book - Computer fluid dynamics: Recent advances.

14 p1744 A73-29743

Convergence of the net-point method for multidimensional quasi-linear heat-conduction problems

14 p1816 A73-30020

Implicit predictor-corrector difference scheme for boundary value problem solution in propagation of spherical and cylindrical N waves /asymptotic pulse forms/

14 p1745 A73-30175

Finite difference solution for large deformations of cylindrical shells - A comparison with finite element solutions.

14 p1807 A73-30182

Incremental formulation for problems with geometric and material nonlinearities.

14 p1808 A73-30190

Incremental solution procedures for finite element nonlinear structural analysis, considering combined material and geometric nonlinearities

14 p1808 A73-30193

Construction of finite difference diagrams of the engineering theory of elasticity, on the basis of integral representations of the resolvent functions.

14 p1810 A73-30308

Convergence of a difference procedure for quasi-linear parabolic initial boundary-value problems in cylinder symmetry

14 p1769 A73-30422

Some questions of approximation in the variational difference method

14 p1771 A73-30830

Numerical solution of the viscous flow in the entrance region of parallel plates.

14 p1746 A73-30907

The conservative method of flows and the calculation of a viscous heat conducting gas flow past a body of finite size

15 p1821 A73-30962

A numerical technique for determining the effect of singularities in finite difference solutions illustrated by application to plane elastic problems.

15 p1951 A73-32031

A consistent finite-difference model for the two-dimensional continuum.

15 p1954 A73-32122

Stability and oscillation characteristics of finite-element, finite-difference, and weighted-residuals methods for transient two-dimensional heat conduction in solids.

[ASME PAPER 73-HT-E]

15 p1958 A73-32277

Book - Two-point boundary value problems: Shooting methods.

15 p1901 A73-32299

Convergence of difference methods for second-order ordinary differential equations

16 p2031 A73-32821

Application of an irregular mesh finite difference approximation to the plate buckling problem.

16 p2079 A73-33008

Modified finite difference procedures for structural mechanics, discussing interior and boundary discretization errors and accuracy improvement

16 p2079 A73-33012

A note on the use of the finite difference method for predicting steady state sound fields.

16 p2036 A73-33217

The use of a finite difference technique to predict cascade, stator, and rotor deviation angles and optimum angles of attack. 16 p1963 A73-33488
 Numerical representation of inlet and exit boundary conditions in transient cascade flow. 16 p2048 A73-33511
 Finite-difference approximations of the Navier-Stokes equations applied to a geophysical flow. I. II - Three-dimensional approximations on a region homeomorphic to a plane region. III - Three-dimensional approximations over the totality of a spherical region represented by means of a regular polyhedron. 16 p2009 A73-33886
 The numerical solution of quasilinear elliptic equations. 17 p2199 A73-34103
 Some computational techniques for the nonlinear least squares problem. 17 p2199 A73-34105
 On the numerical computation of parabolic problems for preceding times. 17 p2199 A73-34211
 Solution of the plane problem in elasticity theory for an incompressible material by the fractional step method. 17 p2211 A73-34299
 Implicit finite difference scheme for Eulerian fluid dynamics of time dependent one dimensional polytropic gas flow, noting numerical stability. 17 p2151 A73-34894
 A finite difference solution of the two and three-dimensional incompressible turbulent boundary layer equations. 17 p2153 A73-35016
 An assessment of three-dimensional turbulent boundary layer prediction methods. 17 p2153 A73-35020
 Numerical solution procedure for calculating the unsteady, one-dimensional flow of compressible fluid /with allowance for the effects of heat transfer and friction/. 17 p2153 A73-35022
 Uniqueness requirements for calculated jump conditions across embedded shock waves based on relaxation methods, comparing to time dependent finite difference calculation. 17 p2154 A73-35130
 Viscous flow over spinning cones at angle of attack. 17 p2096 A73-35132
 Finite difference solution of Prandtl boundary layer equations for steady incompressible laminar and turbulent boundary layer flows. 17 p2154 A73-35136
 Alternating direction implicit finite difference computational method for solving two dimensional Navier-Stokes equations for high and low speed flows. 17 p2202 A73-35140
 Linearized implicit schemes for the computation of viscous incompressible flow - with applications. 17 p2155 A73-35141
 A new shock capturing numerical method with applications to some simple supersonic flow fields. 17 p2096 A73-35144
 Flux-corrected transport - A minimum-error finite-difference technique designed for vector solution of fluid equations. 17 p2202 A73-35145
 Inconsistencies and S.O.R. convergence for the discrete Neumann problem. 17 p2202 A73-35519
 Numerical studies of viscous, incompressible flow through an orifice for arbitrary Reynolds number. 17 p2157 A73-35602
 Chemically reacting gas flow numerical calculations from stiff nonlinear ordinary differential equations solution in finite difference form. 17 p2119 A73-35609
 A generalization of the additive correction methods for the iterative solution of matrix equations. 17 p2203 A73-35729
 Computerized finite difference method with reduced core storage requirements for solving boundary value problem of forced random vibration of rotating beam. 17 p2204 A73-35830
 Book - Analysis of discretization methods for ordinary differential equations. 18 p2329 A73-35904
 Finite-difference solution of the incompressible three-dimensional boundary layer equations for a blunt body. 18 p2259 A73-36156
 On the solution of the unsteady Navier-Stokes equations including multicomponent finite rate chemistry. 18 p2259 A73-36157
 Computation of three dimensional flows about aircraft configurations. 18 p2259 A73-36158
 Sensitivity of the numerical analysis of the three-fluid plasma mixed initial-boundary value problem. 18 p2338 A73-36160
 Finite difference theory predictions for turbulent boundary layer swirling flames, discussing flow simulation, turbulence models and flame size, shape and stability characteristics. 18 p2367 A73-36206
 Numerical solution for the inviscid supersonic flow in the corner formed by two intersecting wedges. 18 p2262 A73-36226
 On viscous and wind tunnel wall effects in transonic flows over airfoils. 18 p2263 A73-36261
 Thin clamped hemispherical shell nonlinear dynamic response to suddenly applied pressure, deriving finite difference formulation of fourth order coupled nonlinear equations. 18 p2362 A73-36310
 A serial CSDT predictor-corrector technique for the hybrid computer solution of partial differential equations. 18 p2291 A73-36425
 Solution by characteristics at fixed time interval of the equations of one dimensional unsteady flow. 18 p2300 A73-36608
 A relaxation method for solving nonlinear stress equilibrium problems. 18 p2365 A73-36611
 A numerical method for creep deformation of solids. 18 p2365 A73-36612
 Finite element and finite difference energy techniques for the numerical solution of partial differential equations. 18 p2330 A73-36827
 Approximate method for solving a boundary value problem in the theory of zero-moment elastic spherical shells. 18 p2367 A73-36988
 Thermal models of inhomogeneously accreted meteorite parent bodies. 18 p2356 A73-37048
 Thermal stresses in axially connected circular cylinders. 19 p2495 A73-37435
 Stability criteria for explicit finite difference solutions of the parabolic diffusion equation with nonlinear boundary conditions. 19 p2445 A73-38189
 Stability and convergence of streamline curvature flow analysis procedures. 19 p2421 A73-38190
 Practical calculations of transitional boundary layers. 19 p2423 A73-38479
 Numerical study of viscous flow in a cavity. 20 p2545 A73-38971
 Viscous flow over a cone at moderate incidence. II - Supersonic boundary layer. 20 p2507 A73-39093
 A difference-energy method of studying the stability of rectangular plates in shear. 20 p2617 A73-39306
 Numerical solution of quasi-static problems in viscoelasticity theory. 20 p2619 A73-39332
 Numerical solution of hydrothermodynamics equations for atmospheric processes on a flat earth. 20 p2584 A73-39471
 Mixed finite-difference scheme for a class of linear and nonlinear structural mechanics problems. 20 p2621 A73-39544
 An approximate solution for bending of anisotropic laminated plates. 20 p2623 A73-39554
 Finite difference technique for elastic-plastic buckling of edge-loaded rectangular plates, finding bifurcation stresses via Hill and Prandtl-Reuss expressions. 20 p2623 A73-39560
 Finite difference approximation of the weak solution of a mildly nonlinear Dirichlet problem. 21 p2725 A73-40379
 Heat pipe theory and design, discussing typical operating conditions and heat transfer capacity from flow equations solution by finite difference method. 21 p2792 A73-41059
 Application of a general finite-difference method to boundary layer flows. 21 p2678 A73-41686
 Dynamic behaviour of orthotropic plates using finite difference technique. 22 p2917 A73-41716
 Calculation of the two-dimensional turbulent wake behind a thin obstacle. 22 p2796 A73-42222
 The use of singularity programming in finite-difference and finite-element computations of temperature. 22 p2930 A73-42287
 Higher order accuracy finite difference algorithms for quasi-linear, conservation law hyperbolic systems. 22 p2882 A73-42518
 Stability of the De Vogelaere method for timewise numerical integration. 22 p2882 A73-42557
 Finite difference and truncation method comparison for supersonic conical flow equations solution, obtaining flow field and shock wave shape. 22 p2796 A73-42574

Finite difference scheme for wave equation solution for wave propagation in layered composite materials, obtaining matrix eigenvalues with Floquet condition for various methods. 22 p2926 A73-42897
 Convergent stable three-time level implicit numerical model for phase change problems, evaluating temperature dependent coefficients of parabolic equations at intermediate level. 22 p2937 A73-42951
 On the construction of accurate difference schemes for hyperbolic partial differential equations. 23 p3000 A73-43208
 Free point method finite difference solution for two dimensional nonstationary hydrodynamic problem of continuous media, demonstrating feasibility by plasma pinch effect calculation. 23 p2968 A73-43799
 Static and dynamic finite deformations of cables using rate equations. 23 p3042 A73-43804
 Zonally symmetric global general circulation models with and without the hydrologic cycle. 23 p2978 A73-43981
 Numerical approximation of quasi-static and dynamic problems in viscoelasticity by net-point and finite difference methods. 24 p3144 A73-44505
 A divergent difference scheme for calculation of steady supersonic flows with complex structures. 24 p3053 A73-44651
 Investigation of some theoretical point-explosion problems by the difference method. 24 p3076 A73-44656
 A difference theory for noise propagation in an acoustically lined duct with mean flow. 24 p3078 A73-44840
 Design criteria for finite-difference models for eddy diffusion with winds that guarantee stability, mass conservation, and nonnegative masses. 24 p3085 A73-45018
 Numerical convective schemes based on accurate computation of space derivatives. 24 p3105 A73-45026
 Numerical solution of a nonlinear inverse heat-conduction problem. 24 p3156 A73-45084
 Efficient subroutines for the solution of general elliptic and parabolic partial differential equations. 24 p3106 A73-45093
 On the choice of second-order difference schemes furnishing shock profiles without oscillation. 24 p3110 A73-45217
 Mixed finite-difference scheme for analysis of simply supported thick plates. 24 p3150 A73-45226
 Convergence of finite difference transient response computations for thin shells. 24 p3150 A73-45228
 Skylab complex stiffened structure shell instability analysis by computer program, discussing convergence of finite difference formulation and eigenvalue calculation. 24 p3144 A73-45234
 Nonlinear difference schemes for linear partial differential equations. 24 p3106 A73-45332
 Application of the finite difference method to the elastic stability problem. 24 p3152 A73-45357
FINITE ELEMENT METHOD
 Application of finite element methods to lubrication - An engineering approach. 01 p0055 A73-10221
 [ASME PAPER 72-LUB-N] Mesh subdivision type influence on convergence properties of mixed triangular elements in plate bending analysis. 01 p0115 A73-10745
 On a semi-variational method for parabolic equations. I. 02 p0186 A73-11589
 Some problems in the substantiation and application of discrete large-element design schemes for complex zero-moment shells. 02 p0230 A73-11716
 Curvilinear coordinates for deformation tensor and stress analysis of structures, using finite element method. 02 p0231 A73-11812
 Structural design via finite element method, noting object discretization, displacement forms and nonlinear problems of deformable body mechanics. 02 p0233 A73-11936
 Elastic deformation of lightweight mirrors. 02 p0236 A73-12375
 Axial compression buckling of single metal fiber embedded in plastic matrix, using photoelastic stress analysis and finite element method. 02 p0236 A73-12432
 Finite element technique application for determining velocity field of three dimensional fluid continuum and pressure distribution of lubrication film described by Reynolds equation. 03 p0289 A73-12872

Elasto-plastic analysis of three-dimensional structures using the isoparametric element.

03 p0383 A73-12874

Space-time finite element method for determining dynamic response of continuous media, using Hamilton principle for nodal displacements variations

03 p0389 A73-13320

Finite element equations of motion of elastoplastic shell, applying theory to edge clamped circular plate dynamic response

03 p0389 A73-13321

Curved element for geometrical approximation of thin shell structures, deriving element stiffness equations in terms of nodal displacement degrees of freedom

03 p0389 A73-13325

Thermomechanical dissipation analysis of thermoviscoelastic solids by finite elements.

03 p0389 A73-13326

A finite element analogue of the modified Rayleigh-Ritz method for vibration problems.

03 p0390 A73-13336

Elastic-plastic analysis of Saint-Venant torsion problem by a hybrid stress model.

03 p0390 A73-13338

Bounds for eigenvalues in some vibration and stability problems.

03 p0390 A73-13341

Convergence of consistently derived Timoshenko beam finite elements.

03 p0390 A73-13342

Finite element analysis of thick, thin and sandwich plates, considering quadrilateral elements with allowance for transverse shear effect

03 p0390 A73-13344

An approximate algorithm for the reanalysis of structures by the finite element method.

03 p0391 A73-13676

A finite element analysis of an axisymmetrically loaded orthotropic shell of revolution.

03 p0391 A73-13677

A simple finite element model for elastic-plastic plate bending.

03 p0391 A73-13680

On the conforming cubic triangular element for plate bending.

03 p0391 A73-13682

Computation and solution procedures for nonlinear analysis by combined finite element-finite difference methods.

03 p0391 A73-13685

Three-dimensional finite-element analysis of laminated composites.

[AD-759453]

03 p0392 A73-13687

A theoretical and numerical comparison of elastic nonlinear finite element methods.

03 p0392 A73-13689

A strain energy basis for studies of element stiffness matrices.

03 p0395 A73-14184

Eigenproblems condensation techniques consisting of combined finite element, Rayleigh-Ritz and power methods

03 p0337 A73-14190

Finite elements for axisymmetric solids under arbitrary loadings with nodes on origin.

03 p0395 A73-14192

Application of finite-element methods to lubrication - An engineering approach.

[ASME PAPER 72-LUB-N]

03 p0315 A73-14353

Flexibility matrix derived and applied to finite element production for thin walled open tubes under torsion, taking into account warping constraints

03 p0395 A73-14470

Analysis of the forced vibrations of composite linear systems by the stiff finite elements method

03 p0396 A73-14600

Finite element method for calculating temperature distributions in complex structures, taking into account heat transfer by radiation, conduction and convection

03 p0400 A73-14632

Finite element displacement analysis of a lung.

03 p0273 A73-14661

Some crack tip finite elements for plane elasticity.

04 p0506 A73-14683

Plate bending analysis using 12 degrees of freedom isoparametric and assumed-stress hybrid plate element theory

04 p0508 A73-14943

Dynamic response of nonlinear media at large strains.

04 p0509 A73-14947

Hypermatrix solution of large sets of symmetric positive-definite linear equations.

04 p0470 A73-15009

Interpolation theory over curved elements, with applications to finite element methods.

04 p0470 A73-15010

Finite element analysis of finite sized plates bonded to an elastic half space.

04 p0510 A73-15012

Note on symmetric decomposition of some special symmetric matrices.

04 p0470 A73-15014

Theoretical formulation of finite-element methods in linear-elastic analysis of general shells.

04 p0510 A73-15026

Impact loading on structures with random properties.

04 p0510 A73-15028

A finite element based procedure for simulating the transient response and failure of a two-dimensional continuum with nonlinear material characteristics.

[ASME PAPER 72-WA/DE-4]

04 p0515 A73-15875

Finite element limit analysis using linear programming.

05 p0631 A73-16124

Insulating materials fireproofing effectiveness prediction by finite element method for combined time dependent convective-radiative boundary conditions

05 p0637 A73-16132

Finite element model use for deducing errors magnitude in stress-strain properties obtained from laboratory compression test results

05 p0631 A73-16175

Variational principle application to oneself adjoint lifting surface integral equation from finite element viewpoint, considering two dimensional flat plate

[AIAA PAPER 73-87]

05 p0529 A73-16852

Finite element analysis of unsteady incompressible flow around an oscillating obstacle of arbitrary shape.

[AIAA PAPER 73-91]

05 p0529 A73-16855

Elastic-plastic analysis of stresses near fastener holes.

[AIAA PAPER 73-252]

05 p0635 A73-16974

Finite element analysis of the post-buckling behavior of structures.

[AIAA PAPER 73-255]

05 p0635 A73-16977

Finite element analysis of nonlinear vibration of beam columns.

05 p0636 A73-17118

Leading-edge force features of the aerodynamic finite element method.

05 p0533 A73-17213

Constant curvature beam finite elements for in-plane vibration.

05 p0637 A73-17371

Some finite element solutions for plate bending problems by simplified hybrid displacement method.

06 p0758 A73-17444

Indirect structural analysis by finite element method.

06 p0758 A73-17447

Finite element model for discontinuous potential flow field analysis leading to Dirichlet, Neumann and mixed boundary value problems solution

06 p0644 A73-17514

Limit design in the absence of a given layout - A finite element, zero-one programming approach.

06 p0762 A73-18340

Application of the finite element method to the solution of elastoplastic problems

06 p0766 A73-18726

A finite element, linear programming method for the limit analysis of thin plates.

07 p0906 A73-19026

A finite element tensor approach to plate buckling and postbuckling.

07 p0907 A73-19028

The finite element method in domains with curved boundaries.

07 p0907 A73-19029

The quadratic programming approach to the finite element method.

07 p0907 A73-19030

Free vibration analysis of spinning structural systems.

07 p0907 A73-19032

The treatment of natural boundary conditions in the finite element and finite difference methods.

07 p0907 A73-19033

A creep bending analysis of plates by the finite element method.

07 p0908 A73-19093

The use of straight beam finite elements for analysis of vibrations of curved beams.

07 p0909 A73-19100

The finite element method with Lagrangian multipliers.

07 p0844 A73-19137

Automated generation and condensation of large mass- and rigidity-matrices

07 p0909 A73-19175

Comparative considerations concerning parametric stress concentration studies involving finite elements and complex stress functions

07 p0910 A73-19208

Methods of reducing continual nonlinear mechanics problems for deformable solids to discrete problems

07 p0910 A73-19303

Finite-element analysis of shells of revolution by two doubly curved quadrilateral elements.

07 p0912 A73-19368

Numerical solution of the Navier-Stokes equations by the finite element method.

07 p0810 A73-19501

Numerical analysis of magnetohydrodynamic instabilities by the finite element method.

07 p0856 A73-19515

Analysis of flow of viscous fluids by the finite-element method.

07 p0811 A73-19953

Finite element analysis of buckling and post-buckling behaviors of arches with geometric imperfections.

07 p0914 A73-20211

Finite element displacement method for large amplitude free flexural vibrations of beams and plates.

07 p0914 A73-20212

Some results of finite element applications in finite elasticity.

07 p0914 A73-20213

Stiffness matrix formulation and eigenvalue analysis for high order shallow shell finite element of rectangular plan

07 p0916 A73-20439

Large deflection, geometrically non-linear finite element analysis of circular arches.

08 p1015 A73-20670

Curved finite elements by the method of initial strains.

08 p1016 A73-20727

Elastoplastic analysis by matrix displacement or finite element method, presenting various direct and iterative solution techniques

08 p1016 A73-20776

Vibration of four point-supported plates by a finite element method.

08 p1017 A73-20945

Improved finite elements for vibration analysis of tapered beams.

08 p1018 A73-21439

Calculation of the stability of rectangular plates in an air flow by the finite-element method

08 p1018 A73-21512

Application of the finite element method to the study of the elastic buckling of thin plates of any form

09 p1157 A73-22214

Finite element stress field solution of the problem of Saint Venant torsion.

09 p1158 A73-22390

Pure moment loading of axisymmetric finite element models.

09 p1158 A73-22391

Axisymmetric triangular finite elements for the scalar Helmholtz equation.

09 p1120 A73-22392

On the generalization of stress function procedure for dynamic analysis of plates.

09 p1158 A73-22395

Large deflection analysis of plates and shallow shells using the finite element method.

09 p1158 A73-22396

A comparison of first and second order axially symmetric finite elements.

09 p1158 A73-22399

Stacked membrane elements for plate and shell analysis, noting spurious shear components suppression

09 p1159 A73-22401

Thin panels stresses diffusion analysis, comparing Bleich, variational, Conway finite difference and finite element methods

09 p1159 A73-22717

On the convergence of the finite element method for problems with singularity.

09 p1160 A73-22891

Influence of Poisson's ratio on the condition of the finite element stiffness matrix.

09 p1160 A73-22892

A deficiency in current finite elements for thin shell applications.

09 p1160 A73-22893

Optimal beam frequencies by the finite element displacement method.

09 p1160 A73-22898

A triangular plate bending element for contact problems.

09 p1160 A73-22899

Finite element method for solution of two dimensional flow equations with applications to passive advection and nonlinear gravity wave problems, noting computing time

09 p1113 A73-22955

Book - Methods of analysis and solutions of crack problems: Recent developments in fracture mechanics; Theory and methods of solving crack problems.

09 p1161 A73-23176

Applications of the finite element method to the calculations of stress intensity factors.

09 p1162 A73-23185

Finite element methods for elastic bodies containing cracks.

09 p1162 A73-23186

An evaluation of finite element methods for the computation of elastic stress intensity factors.

[ASME PAPER 72-PVP-19]

09 p1163 A73-23267

Optimization of finite element grids based on minimum potential energy.

[ASME PAPER 72-PVP-3]

09 p1163 A73-23268

Finite element analysis of curved structures, discussing shape functions generation method for convergence determination

09 p1165 A73-23439

Explicit addition of rigid-body motions in curved finite elements. 09 p1165 A73-23441

Stress-strain relations for materials with different tension, compression yield strengths. 09 p1166 A73-23452

Hybrid stress finite element models for elastic continuum, discussing variational principle and macroscopic equilibrium 09 p1166 A73-23457

Temperature dependent combined hardening theory within plasticity formulations for finite element analysis of aerospace vehicle engines under plastic strain and cyclic fatigue 09 p1166 A73-23463

Application of the finite element method to the study of the stability of plane structures 10 p1287 A73-23618

A finite element collocation method for quasilinear parabolic equations. 10 p1241 A73-23638

Finite-element method applied to heat conduction in solids with nonlinear boundary conditions. 10 p1295 A73-23778

Unsteady MHD duct flow by the finite element method. 10 p1256 A73-24289

Bending and vibration of multilayer sandwich beams and plates. 10 p1289 A73-24290

A finite element method for block adjustment problems of photogrammetry. 10 p1218 A73-24291

A finite element method for non-self-adjoint problems. 10 p1243 A73-24292

Note on an approximate method for computing consistent conjugate stresses in elastic finite elements. 10 p1290 A73-24293

Stresses in a partly yielded notched bar - An assessment of three alternative programs. 10 p1290 A73-24294

Use of the least squares criterion in the finite element formulation. 10 p1243 A73-24295

Finite element solution algorithm for viscous incompressible fluid dynamics. 10 p1243 A73-24296

The analysis of dislocation systems by the finite element method. 10 p1290 A73-24298

A photoelastic and finite-element investigation of a nonsymmetrical plug-hatch configuration. 10 p1293 A73-24721

A numerical solution of the Navier-Stokes equations using the finite element technique. 11 p1345 A73-25116

Maximum principle and uniform convergence for the finite element method. 11 p1390 A73-25435

Application of general variational methods with discontinuous fields to bending, buckling, and vibration of beams. 11 p1435 A73-25436

Finite element method for structural analysis, discussing theory for isoparametric stress quadrilateral plate bending elements with curved boundaries 11 p1435 A73-25437

Structure statistical identification method based on experimental measurements of natural frequencies and mode shapes to modify finite element model structural parameters [AIAA PAPER 73-339] 11 p1436 A73-25479

Optimum design of stressed skin structures using a sequence of linear programs method. [AIAA PAPER 73-342] 11 p1436 A73-25481

Linear programming and gradient search algorithms for minimum weight design of finite element structures, applying to bar truss problems [AIAA PAPER 73-343] 11 p1436 A73-25482

Interdisciplinary computer analyses of three-dimensional solids defined by polyhedral surfaces. [AIAA PAPER 73-354] 11 p1437 A73-25491

Nonlinear thermo-elastic-plastic and creep analysis by the finite element method. [AIAA PAPER 73-358] 11 p1437 A73-25494

Nonlinear transient analysis of shells and solids of revolution by convected elements. [AIAA PAPER 73-359] 11 p1437 A73-25495

Computer generated displays of structures in vibration. [AIAA PAPER 73-362] 11 p1334 A73-25498

Linear elastic finite element stress analysis of lap and tapered adhesive joint bonding of composite to metal substrate [AIAA PAPER 73-371] 11 p1438 A73-25505

Aeroelastic structural weight optimization under strength and flutter constraints, using finite element and displacement methods to describe equations of motion in matrix form [AIAA PAPER 73-389] 11 p1439 A73-25518

A finite element method for nonaxisymmetric vibrations of pressurized shells of revolution partially filled with liquid. [AIAA PAPER 73-399] 11 p1440 A73-25528

A corrected assessment of the cylindrical shell finite element of Bogner, Fox and Schmit when applied to arches. 11 p1443 A73-26090

Galerkin finite element method for vibration problems. 11 p1445 A73-26389

Shear stress and deformation inclusion in elastic plate bending finite element theory, discussing stiffness matrix improvement for thin shells 11 p1447 A73-26651

Elasticity theory of three dimensional system of particles in rectangular prismatical or tetrahedral net arrangement as topological model for finite element method 11 p1448 A73-26727

Contribution to the theory of the finite element method applied to the overall stress analysis of a fuselage 12 p1551 A73-27084

Investigation of the stress-strain state of spherical shells with an eccentric hole on the basis of the three-dimensional theory of elasticity by the finite element method 12 p1552 A73-27262

Application of the finite-element method to the study of heat problems 12 p1558 A73-27397

Study of the rigidity of rectangular plates during bending by the finite-element method 12 p1553 A73-27461

Optimum design of composite shells subject to natural frequency constraints. 12 p1554 A73-27734

Static, vibration and buckling analysis of axisymmetric circular plates using finite elements. 12 p1555 A73-27738

The mathematical foundations of the finite element method with applications to partial differential equations; Proceedings of the Symposium, University of Maryland, Baltimore, Md., June 26-30, 1972. 12 p1519 A73-27921

Discrete flexural analyses of rectangular plates of abruptly varying stiffnesses. 12 p1556 A73-27926

Finite element method for solution of Laplace or wave equation in cylindrical coordinates through base matrices, applying to electromagnetic wave propagation in waveguides 13 p1581 A73-28077

Finite element method applied to analysis of flow over a spillway crest. 13 p1563 A73-28078

On the unity of the constant strain/constant moment finite element methods. 13 p1691 A73-28079

Criteria for finite element discretization of shells of revolution. 13 p1691 A73-28084

Shape function generation for high order conforming rectangular plate element in bending theory, noting rapid convergence of deflection and bending moments 13 p1691 A73-28087

The convergence theorems and their role in the theory of structures. 13 p1692 A73-28227

Finite element incremental solutions for geometrically nonlinear problems based on second variations of variational functionals, discussing numerical integration and variational principles 13 p1692 A73-28228

Analysis of finite deformations of elastic solids by the finite element method. 13 p1692 A73-28229

Triangular finite elements for plate bending with constant and linearly varying bending moments. 13 p1692 A73-28230

The local solution approach in the finite element method. 13 p1692 A73-28232

Dual analysis principle application to accuracy verification of finite element solutions of problems in continuum mechanics 13 p1693 A73-28233

Finite element method analysis of thin shells, discussing reference surface geometry and membrane and bending theory 13 p1693 A73-28234

Finite element theory of plates and shells including transverse shear strain effects. 13 p1693 A73-28235

The application of a curved, mixed-type shell element. 13 p1693 A73-28237

Triangular elements descriptive of sandwich panels for finite element analysis of symmetric panels, comparing numerical solutions to experimental data and analytical results 13 p1693 A73-28238

Three dimensional elastic stress analysis by finite element method within reasonable computer costs, noting problem simplification 13 p1693 A73-28240

On further application of the finite element method to three-dimensional elastic analysis. 13 p1693 A73-28241

Automatic mesh generation in two and three dimensional inter-connected domains. 13 p1693 A73-28242

Automatic system for kinematic analysis (ASKA) / computer programs for structural finite element solution, discussing design concepts, element types, user interface and computation time 13 p1693 A73-28243

Static force and displacement methods as eigenvalue problems. 13 p1694 A73-28246

Computational efficiency of equilibrium models in eigenvalue analysis. 13 p1694 A73-28248

Complementary energy method in elastodynamics. 13 p1694 A73-28249

Perturbation techniques in the analysis of geometrically nonlinear shells. 13 p1694 A73-28251

Finite element matrix formulation of post-buckling stability and imperfection sensitivity. 13 p1694 A73-28253

The splitting-up method and its application to elasticity problems. 13 p1694 A73-28254

An evaluation of finite difference and finite element techniques for analysis of general shells. 13 p1694 A73-28256

Effect of out-of-planeness of membrane quadrilateral finite elements. 13 p1697 A73-28818

Computer aided design with finite element method for two and three dimensional curved line and surface approximation and representation on interactive graphic console 13 p1587 A73-28850

Line and rectangular plane finite element models for accurate and efficient dynamic vibration frequency analysis of frames and shear walls respectively 13 p1700 A73-29377

A finite element study of the vibration of trapezoidal plates. 13 p1700 A73-29378

Parametric finite element stress analysis of multiple crack propagation in nonhomogeneous nonisotropic materials, using Griffith criterion 13 p1701 A73-29472

Finite element method application to elastoplastic analysis of cracked metal plates, discussing plate thickness effects on plastic zone growth and stress distributions along crack tip 13 p1701 A73-29476

An algorithm for numerical integration in triangular domains. 14 p1806 A73-30047

Some aspects of recent contributions to the mathematical theory of finite elements. 14 p1806 A73-30177

Variational principles application to finite element method in elastostatic and elastodynamic and elastodynamic small and finite displacement theories 14 p1806 A73-30178

Quadrature errors effect on finite element method solutions accuracy, considering stiffness matrix numerical stability 14 p1806 A73-30179

Finite element method round-off errors relation to fundamental equations conditioning, considering round-off errors effect on precision of method of substructures 14 p1806 A73-30180

Stress hybrid model extension to stiffness matrix of element with discontinuous stress distribution, considering transverse shear strains in laminated plate layers 14 p1807 A73-30181

Finite element models for continuum structural analysis, considering variational principles, element base functions and general purpose computer program 14 p1807 A73-30183

Equivalent finite element model derivation from plate bending triangular element, assumed stress hybrid method and elements with polynomial deflection function 14 p1807 A73-30184

Stability and convergence of finite element methods for elastic structures vibration analysis, stressing application to mixed boundary value problems 14 p1807 A73-30185

Numerical time integration methods in shell transient response finite element analysis, considering conditionally stable explicit and unconditionally or conditionally stable implicit schemes 14 p1807 A73-30187

Finite element static structural analysis for small elastoplastic strains and geometric nonlinearities, considering total Lagrangian and incremental moving coordinate formulations 14 p1807 A73-30189

Progress in nonlinear finite element analysis using asymptotic solution techniques. 14 p1808 A73-30191

Nonlinear thermal elastoplastic structural analysis, using principle of virtual work in finite element method

14 p1808 A73-30192

Incremental solution procedures for finite element nonlinear structural analysis, considering combined material and geometric nonlinearities

14 p1808 A73-30193

Finite element method investigation of branch and secondary crack formation and multiple fracture, solving sequences of boundary value problems and strain energy release rates

14 p1808 A73-30195

Finite element analysis programs for general applications, considering state of art

14 p1808 A73-30197

NASTRAN digital computer program for static and dynamic structural analysis by finite element method, including nonlinear static and dynamic response

14 p1808 A73-30198

Finite element method application to nonlinear, microscopic and ductile fracture mechanics covering crack tip singularity elastoplastic analysis and elastic constants of metal crystals

14 p1809 A73-30200

Finite element analysis of sweptback wing structures based on beam theory, presenting low aspect ratio models

14 p1809 A73-30201

Finite element analysis with improved accuracy for rectangular plate bending element

14 p1810 A73-30456

Basic concepts of the mechanics of discretized bodies with an introduction to discrete element calculus

14 p1775 A73-30548

The transient response of non-uniform, non-homogeneous beams

14 p1813 A73-30664

Derivation of a normal displacement function for the triangular finite element of plates and shells

15 p1945 A73-31032

Impact interaction between a soft shell and a hard obstacle

15 p1947 A73-31276

Effect of openings on stresses in rigid pavements

15 p1856 A73-31387

Book - Advances in applied mechanics. Volume 12.

15 p1950 A73-31972

Finite element methods in continuum mechanics

15 p1950 A73-31973

A high order finite element for completely incompressible creeping flow

15 p1951 A73-32026

Program for triangular bending elements with derivative smoothing

15 p1848 A73-32028

Convergence, accuracy and stability of finite element approximations of a class of non-linear hyperbolic equations

15 p1899 A73-32030

Discrete element development for anisotropic plates via bicubic Hermite interpolation functions, considering patch generation from boundary geometry data

15 p1951 A73-32033

Determination of stress intensity factors in cracked plates by the finite element method

15 p1951 A73-32034

Accuracy of the finite element analysis for the elastic plate with a circular hole

15 p1951 A73-32036

Bonded structural connections analysis by finite element method, presenting stress distribution in adhesive

15 p1952 A73-32038

Stability and oscillation characteristics of finite element, finite-difference, and weighted-residuals methods for transient two-dimensional heat conduction in solids

[ASME PAPER 73-HT-E]

15 p1958 A73-32277

Dynamic analysis of viscoelastoplastic anisotropic shells

16 p2075 A73-32787

The finite element method in shell stability analysis

16 p2075 A73-32789

Blocking procedure for large scale structural analysis in conjunction with plane truss using stiffness matrix method, considering computer subroutines in finite element method

16 p1985 A73-32793

The behaviour with diminishing curvature of strain-based arch finite elements

16 p2076 A73-32921

Variational principles in nonlinear continuum mechanics

16 p2036 A73-32979

Application of extended variational principles to finite element analysis

16 p2077 A73-32982

Finite element methods by variational principles with relaxed continuity requirement

16 p2031 A73-32985

Mixed variational principles based on stationary potential energy concept applied to finite element method in thin shell theory

16 p2077 A73-32986

Application of stress functions to dynamic analysis of shallow shells

16 p2077 A73-32987

A survey of finite element methods in continuum mechanics

16 p2036 A73-32988

Ring finite elements for axisymmetric and non axisymmetric thin shell analysis

16 p2077 A73-32989

Application of the finite element method to cases requiring the combination of elements possessing different numbers of degrees of freedom

16 p2077 A73-32991

Discrete approximations of elastic-plastic bodies by variational methods

16 p2078 A73-32994

Thin plates and shells post-buckling behavior analysis by discrete element method, noting computer program capabilities

16 p2078 A73-32997

The application of finite elements to the large deflection geometrically non-linear behaviour of cylindrical shells

16 p2078 A73-32998

Incremental variational method for the large displacement analysis of shells with geometric imperfections

16 p2078 A73-32999

Curved rotational shell elements by the constraint method

16 p2078 A73-33002

The analysis of three dimensional problems of elasticity by integral representation of displacement

16 p2078 A73-33003

Finite element analysis of coupled vibration of tapered twisted blades

16 p2078 A73-33005

A variational approach to grid optimization in the finite element method

16 p2079 A73-33010

Viscoelastic body stress-strain state under quasi-static loads, obtaining boundary value problem solution via finite element method

16 p2080 A73-33244

Stress calculation for plates and beams via finite element method, improving accuracy by smoothing stress and strain distributions at element boundaries

16 p2080 A73-33262

Iterative finite element method for minimum weight structural design with respect to buckling constraints applied to beam and orthogonal frame design

16 p2082 A73-33908

Optimum finite element idealization characterization based on displacement formulation, system potential energy true minimum, stiffness matrix gradients and geometry considerations

16 p2082 A73-33909

Monotonically convergent approximate solutions for finite element eigenvalues in structural vibration and stability problems, assessing accuracies

16 p2083 A73-33949

Matrix analysis of multilayered and sandwich shells by the finite element method

16 p2083 A73-33968

An assumed stress hybrid finite element model for linear elastodynamic analysis

17 p2241 A73-34189

Variational principle with penalty for finite element solution of model Poisson equation with homogeneous Dirichlet boundary conditions, noting convergence

17 p2199 A73-34209

Finite element analysis of inflatable shells

17 p2242 A73-34528

Strongly curved finite element for shell analysis

17 p2242 A73-34529

A comparison of structural test results with predictions of finite element analysis

[SAE PAPER 730340]

17 p2102 A73-34691

Study of a stationary flow of rigidly plastic material by the numerical finite element method

17 p2244 A73-34796

Finite element methods in continuum mechanics; Advanced Study Institute, Lisbon, Portugal, September 7-17, 1971, Lectures

17 p2244 A73-34826

Theory of conjugate projections in finite element analysis

17 p2201 A73-34828

Finite element approximations in nonlinear thermoviscoelasticity

17 p2245 A73-34829

The finite element method in fluid mechanics

17 p2151 A73-34830

Finite element formulation of nonlinear boundary-value problems

17 p2201 A73-34831

Dual principles of elastodynamics finite element applications

17 p2245 A73-34833

Isoparametric element forms in finite element analysis

17 p2245 A73-34834

Weighted residual processes in finite element with particular reference to some transient and coupled problems

17 p2245 A73-34835

Finite element method application to solution of structural dynamics problems, considering equations of motion and vibration mode shapes

17 p2245 A73-34836

Vibration analysis of finite element systems

17 p2245 A73-34837

Fracture toughness parameters and elastic-plastic analysis of non-moderate fracture conditions using finite element methods

17 p2245 A73-34877

A numerical and experimental investigation of the use of J-integral

17 p2246 A73-34880

Unconditional stability in numerical time integration methods

[ASME PAPER 73-APM-1]

17 p2201 A73-35027

The integration of NASTRAN into helicopter airframe design/analysis

[AHS PREPRINT 780]

17 p2106 A73-35093

Computational considerations in application of the finite element method for analysis of unsteady flow around airfoils

17 p2096 A73-35138

The application of interactive graphics to the numerical methods used in structural analysis

17 p2250 A73-35314

A new finite element method for analysing symmetrically loaded thin shells of revolution

17 p2252 A73-35601

Stiffness matrix displacement analysis via curved elements for plane stress and thin plate bending problems

17 p2252 A73-35606

Two and three dimensional elasticity theory of linear fracture mechanics covering stress functions, finite element method and crack behavior in solids

17 p2252 A73-35669

A jet-wing lifting-surface theory using elementary vortex distributions

[AIAA PAPER 73-652]

18 p2260 A73-36207

Nonlinear transient responses of structures by the spatial finite-element method

18 p2362 A73-36309

A finite-element method for calculating aerodynamic coefficients of a subsonic airplane

18 p2265 A73-36394

Applications of finite element stress analysis and stress-strain properties in determining notch fatigue specimen deformation and life

18 p2364 A73-36591

Aspects of the finite element method as applied to aero-space structures

[ISD-138]

18 p2365 A73-36725

Finite element and finite difference energy techniques for the numerical solution of partial differential equations

18 p2330 A73-36827

Calculation of the natural frequencies and the principal modes of helicopter blades

18 p2367 A73-37090

Finite element elastic-plastic-creep analysis of two-dimensional continuum with temperature dependent material properties

19 p2496 A73-37483

Calculation of the eigenfrequencies for a shaft/bearing system with the aid of transfer matrices

19 p2433 A73-37548

Bounds on the spectral and maximum norms of the finite element stiffness, flexibility and mass matrices

19 p2500 A73-38110

A computational technique for the efficient handling of large matrices

19 p2445 A73-38191

General theory of constrained continuous media and plastic materials, deriving Huber-Mises yield condition by finite element method

19 p2501 A73-38304

A finite element approach to the critical cyclic stress required to propagate a crack

20 p2615 A73-38639

Book - An analysis of the finite element method

20 p2581 A73-39139

A method of obtaining approximate solutions to unsteady-state heat conduction problems

20 p2627 A73-39258

Analysis of rarefied gas flow through an arbitrary cross section by the finite element method

20 p2549 A73-39528

Stability and postbuckling behavior of hyperelastic bodies at finite strain by the finite element method

20 p2620 A73-39529

Dynamic stability of a nonlinear beam subjected to both longitudinal and transverse excitation

20 p2621 A73-39532

Column instability under nonconservative forces, with internal and external damping - Finite element using adjoint variational principles

20 p2621 A73-39540

In-plane and lateral displacements triangular elements represented by cubic and quintic polynomials for folded plate structural analysis

20 p2622 A73-39545

The incremental theory of three dimensional transient thermoplasticity - Formulation and solution

20 p2622 A73-39552

Finite-element formulations for elastic plates by general variational statements with discontinuous fields.

20 p2623 A73-39558

Square plate symmetrically supported at four diagonal points, evaluating fundamental vibration frequency with accuracy by finite element method

21 p2783 A73-40293

Some results of fuselage calculations on a digital computer by the finite-element method

21 p2783 A73-40387

A finite-element representation of stable crack-growth.

21 p2788 A73-41549

Hybrid finite methods for linear and nonlinear unsteady heat conduction problems

21 p2793 A73-41617

Finite element program for flight structure analysis.

22 p2917 A73-41739

Discretized solution of junction problems in shells.

22 p2917 A73-41740

Finite element analysis of rotating shells.

[ASME PAPER 73-DET-94]

22 p2919 A73-42074

Convergence of simplified hybrid displacement method for plate bending.

22 p2921 A73-42203

The use of singularity programming in finite-difference and finite-element computations of temperature.

[ASME PAPER 73-HT-K]

22 p2930 A73-42287

Reduction of the degrees of freedom in solving dynamic problems by the finite element method.

22 p2922 A73-42479

Accelerating the convergence of elastic-plastic stress analysis.

22 p2922 A73-42481

Book - The finite element method: Fundamentals and applications.

22 p2882 A73-42492

The theory of elasticity of flexural-stiffness exhibiting, planar particle systems with a rectangular net

22 p2922 A73-42526

Buckling of segments of toroidal shells.

22 p2923 A73-42553

Introduction of shear deformations into a thin plate displacement formulation.

22 p2923 A73-42559

Vibration of beams with overhangs.

22 p2923 A73-42563

German monograph - A contribution to the investigation of the stability of pipelines with flowing liquids according to the method of finite elements.

22 p2924 A73-42737

Stirring factors in combustion chambers - A finite-element model of mixing along an 'information flow path.'

22 p2934 A73-42784

Evaluation of error bounds in an optimization problem using the finite-element method.

[ASME PAPER 73-APMW-15]

22 p2924 A73-42882

Book - Elasticity.

23 p3039 A73-43434

Mixed finite element models for nonlinear thermomechanical responses of continuous dissipative media based on Oden variational principle and theory of thermoplastically simple materials

23 p3044 A73-44049

Finite element analysis on L-L type vibration energy concentrator/divider considering its design.

23 p2961 A73-44138

Numerical calculation of simply supported cylindrical shells of arbitrary cross section

23 p3046 A73-44192

Theoretical studies of sound emission from aircraft ducts.

[AIAA PAPER 73-1012]

24 p3078 A73-44844

Fundamentals of the theory of plastic flow in discretized bodies

24 p3110 A73-44917

Theoretical post-yielding behavior of composite laminates. II - Inelastic macromechanics.

24 p3104 A73-45145

Numerical analysis of pre- and post-critical response of elastic continua at finite strains.

24 p3150 A73-45227

On response of initially stressed structures to random excitations.

24 p3150 A73-45229

A numerical, thermo-mechanical model for the welding and subsequent loading of a fabricated structure.

24 p3150 A73-45231

Computerized structural analysis by finite element method, discussing round-off and truncation errors with emphasis on inherited error effects minimization

24 p3150 A73-45233

Free vibration of square plates under different boundary conditions, determining opening geometry effects on fundamental frequencies by grid framework model with finite difference operators

24 p3151 A73-45266

Vibration of rectangular plates with mixed boundary conditions.

24 p3151 A73-45268

On the hybrid stress finite element model for incremental analysis of large deflection problems.

24 p3151 A73-45303

Optimization of fiber reinforced composite structures.

24 p3151 A73-45304

FINITE-STATE MACHINES

U TURING MACHINES

FINNED BODIES

Dual frequency antenna design using hollow fin as TE mode waveguide with sidewall radiating elements, calculating attenuation for comparison with experiment

01 p0023 A73-10189

Reentry vehicle finned roll rate control - Aerodynamic and flight dynamic analysis.

[AIAA PAPER 73-183]

05 p0531 A73-16923

A study of fin-induced laminar interactions on sharp and spherically blunted cones.

[AIAA PAPER 73-235]

05 p0532 A73-16960

Fish like slender body propulsion and flow theory, discussing fin surface-body thickness interaction, vortex sheets, trailing edges and lifting force

11 p1301 A73-25852

Infinitesimal deflections of finned surfaces of revolution fixed along the edge with respect to points in space

12 p1552 A73-27299

Radiant heat transfer on circular-finned cylinders.

14 p1817 A73-30574

A Riemann-Hilbert problem for a heat conduction in a finned surface.

23 p3049 A73-44051

FINS

NT COOLING FINS

Shock impingement caused by boundary layer separation ahead of blunt fins.

[AIAA PAPER 73-236]

05 p0532 A73-16961

Two-dimensional temperature fields in straight rectangular fins

06 p0768 A73-17921

Laminar flow heat transfer from wedge-shaped bodies with limited heat conductivity.

08 p1023 A73-21257

Experimental investigation of the Magnus effect at a finned body of revolution of large aspect ratio at a Mach number of 4

08 p0927 A73-21604

Computerized method for designing plate type sounding rocket fins.

[AIAA PAPER 73-285]

09 p1155 A73-23205

Turbulent heat transfer to a fin leading edge - Flight test results.

11 p1303 A73-26405

A new conception of modeling the process of heat transfer on a surface with artificial roughnesses and microfins

12 p1557 A73-26798

The effect of variable environment temperature on heat transfer in extended surfaces.

23 p3048 A73-43296

FIRE CONTROL

Reliability tests on fire control airborne radars prototypes, measuring MTBF

07 p0800 A73-19416

Radome precision testing for fire control, missile aiming, Doppler navigation and bombing

11 p1335 A73-25277

Airborne air to air and air to ground fire control radar systems for all-weather fighter aircraft, emphasizing cost effectiveness through modularity and commonality

16 p1985 A73-34041

Linear fire control predictor with non-Gaussian inputs, calculating on-target probability lower bounds for verification by digital simulation

21 p2649 A73-40332

GDC/EOSS - Real-time visual and motion simulators for evaluation of fire control and electro-optical guidance systems.

[AIAA PAPER 73-919]

21 p2673 A73-40867

Optimal SAM defense system - An application of optimal control concept to operations research.

23 p2964 A73-43823

FIRE CONTROL CIRCUITS

TWT for air-to-air missile fire control radar transmitter application, considering high average power, RF gain and PPM focusing requirements

14 p1737 A73-30624

Modeling the human in a time-varying anti-aircraft tracking loop.

19 p2401 A73-38071

FIRE DAMAGE

Fire retardance of mixtures of inert gases and oxygen.

09 p1045 A73-22532

FIRE EXTINGUISHERS

Fire suppression for shipboard machinery spaces - Extinguishing and inerting with Halon 1301.

[WSCI PAPER 72-33]

05 p0639 A73-16682

Full-scale fire tests on a simulated aircraft carrier flight deck.

[WSCI PAPER 72-31]

05 p0639 A73-16684

A study of Halon 1301 /CBrF3/ toxicity under simulated flight conditions.

09 p1045 A73-22537

German book - Fire protection technology in aviation. Volume 1 - Foundations of aviation and fire-protection technology.

17 p2098 A73-34124

A study of Halon 1301 /CBrF3/ toxicity under simulated flight conditions.

18 p2285 A73-36930

FIRE FIGHTING

Fire suppression for shipboard machinery spaces - Extinguishing and inerting with Halon 1301.

[WSCI PAPER 72-33]

05 p0639 A73-16682

Full-scale fire tests on a simulated aircraft carrier flight deck.

[WSCI PAPER 72-31]

05 p0639 A73-16684

Characterization and suppression of aircraft and fuel fires.

[WSCI PAPER 72-26]

05 p0639 A73-16688

Some results of studies of the boundary atmospheric layer and AN-2 aircraft flight conditions in a forest fire area

13 p1655 A73-29192

Aircraft crash fire prevention and fighting in airports, discussing aircraft fuel system fail-safe design concepts and airport fire fighting equipment and procedures

15 p1859 A73-32366

Space technology utilization for firefighters breathing equipment development, discussing design and field testing program

[ASME PAPER 73-ENAS-24]

19 p2400 A73-37980

All-wheel drive fire fighting equipment evolution under impact of wide bodied aircraft introduction

20 p2545 A73-39661

FIRE PREVENTION

An intumescent coating for improved fuel fire protection of heat sensitive articles.

02 p0185 A73-12642

A testing procedure for flame arrestors for marine spark ignition engines.

[WSCI PAPER 72-34]

05 p0563 A73-16681

Laser system for fire detection based on heat induced air refractive index changes and smoke induced light transmission loss, using photocell detectors

06 p0699 A73-17751

Habitable atmospheres which do not support combustion.

10 p1183 A73-23562

Flame suppression technique using halogen compounds with hydrogen and carbon, considering bromotrifluoromethane application in propane spray cloud seeding

12 p1521 A73-26818

Airborne fire protection equipment.

13 p1568 A73-28171

Aircraft crash fire prevention and fighting in airports, discussing aircraft fuel system fail-safe design concepts and airport fire fighting equipment and procedures

15 p1859 A73-32366

Airplane accident survival, discussing cabin safety, fire protection, crashworthiness, emergency evacuation and crash landing in water

17 p2097 A73-34079

German book - Fire protection technology in aviation. Volume 1 - Foundations of aviation and fire-protection technology.

17 p2098 A73-34124

Russian book - safety measures in aviation industry.

18 p2281 A73-35869

Investigation of flame expansion inhibition in air-dispersed systems

19 p2503 A73-37506

Fire protection and insurance in airport hangars, discussing governmental safety codes, fire prevention systems, aircraft vs building values and legislative proposals

20 p2544 A73-39214

Fire hazard reduction in corporate aircraft oxygen system, covering hoses, regulators, manifolds, cylinders, leakage, combustion conditions and servicing procedures

20 p2518 A73-39215

FIREBALLS

Multiple meson production in 250 GeV nucleon-nucleon collisions in LiH targets, noting 40 per cent formation of heavy meson cluster fireballs

02 p0208 A73-12653

Cometary structure from ground based observations of meteor showers, noting fireball characteristics difference

04 p0495 A73-14763

Evidence of fireball phenomena in hollow cathode of electron bombardment ion thrusters.

09 p1136 A73-23462

Cooling of the heated region formed during breakdown of air by laser radiation

17 p2183 A73-34262

Fireball spectral data reduction for self absorption, Fe abundance, excitation temperatures, relaxation time and optical thickness effects

22 p2915 A73-43043

- Events in a photoemulsion indicating the formation of superheavy fireballs 23 p3021 A73-43535
- FIREPROOFING**
 Insulating materials fireproofing effectiveness prediction by finite element method for combined time dependent convective-radiative boundary conditions 05 p0637 A73-16132
 Recent developments in commercial fire resistant fibrous materials. 11 p1389 A73-26419
 New fire resistant polymers - Poly(phosphazenes). 17 p2197 A73-35356
 Book - Flame retardancy of polymeric materials. Volume 1. 18 p2287 A73-37123
 Inorganic flame retardants, considering antimony, phosphorus, boron, aluminum, nitrogen, iron and sulfur compounds 18 p2287 A73-37124
 Inorganic flame retardants and their mode of action. 18 p2288 A73-37125
 Fire retardation of polyvinyl chloride and related polymers. 18 p2329 A73-37126
- FIRES**
 NT FOREST FIRES
- FIREWORKS**
 U PYROTECHNICS
- FIRING (IGNITING)**
 NT ROCKET FIRING
 NT STATIC FIRING
 NT TEST FIRING
 Hypergol rocket engines restart difficulties investigation via cold flow and hot firing tests, simulating worst case environmental conditions [AIAA PAPER 72-1160] 03 p0357 A73-13461
- FISH**
 U FISHES
- FISHES**
 Solar activity effects on tree growth, farm crop yield, fish availability and human sickness trends, discussing indirect effects via meteorological factors 05 p0622 A73-17171
 Remote sensing application to the fisheries environment. [AIAA PAPER 73-12] 06 p0690 A73-17606
 A review of some possible uses of remote sensing techniques in fishery research and commercial fisheries. 18 p2307 A73-36031
- FISHTAILING**
 U YAW
- FISSILE MATERIALS**
 U FISSIONABLE MATERIALS
- FISSION PRODUCTS**
 Post impact behavior of mobile reactor core containment systems. 07 p0850 A73-20468
 Variation of the electrical resistance of ordered Ni3Mn alloy during irradiation by fission fragments 20 p2600 A73-39733
 Nuclear meteorology as branch of atmospheric physics, examining natural and artificial fission products, nuclear explosion effects, atmospheric purification and radioactive tracers for meteorological process investigation 21 p2730 A73-40115
- FISSIONABLE MATERIALS**
 Solid state neutron radiation dosimeter for hands of medical and industrial personnel working with spontaneously fissionable fuels, describing Th foil detector and automatic spark counter 11 p1361 A73-25312
 A photoneutron antimony-124-beryllium system for fissile materials assay. 21 p2738 A73-40769
- FITNESS**
 NT FLIGHT FITNESS
 NT PHYSICAL FITNESS
- FITTING**
 Classification of fitting operations in airframe assembly 02 p0172 A73-11647
- FITZGERALD-LORENTZ CONTRACTION**
 U LORENTZ CONTRACTION
- FIXED POINT ARITHMETIC**
 Nonrecursive digital filter hardware design based on analysis of bit level counting operations in convolution, using fixed and floating point representations 12 p1483 A73-27115
- FIXED POINTS (MATHEMATICS)**
 State augmentation procedure for fixed point smoothing algorithm derivation through known solutions of higher dimensional digital filtering problem 03 p0277 A73-13914
 Nonlinear algorithms for the local solution of an equation with a fixed point in a product of Banach spaces 08 p0984 A73-21489
 The stationary-phase method for a double integral with an arbitrarily located stationary point 09 p1048 A73-21918
 Fixed point theorems and dissipative processes. 14 p1771 A73-30774

- A stable manifold theorem for degenerate fixed points with applications to celestial mechanics. 19 p2486 A73-37799
 The variable metric algorithm for non-definite quadratic functions. 21 p2727 A73-40999
 A fixed point calibration procedure for precision platinum resistance thermometers. 22 p2857 A73-42026
- FIXED WINGS**
 Pressure distribution and shock wave intensity variations in supersonic flow past two plane wings forming dihedral angle 03 p0245 A73-13623
 Rotary and fixed wing aircraft growth factors from implicit differentiation of gross weight relative to fixed weight [SAWE PAPER 952] 19 p2385 A73-37880
- FIXED-WING AIRCRAFT**
 U AIRCRAFT CONFIGURATIONS
 U FIXED WINGS
- FLAME CALORIMETERS**
 The spectral comparison method for temperature measurement in two-phase flames. 22 p2853 A73-41987
- FLAME FRONTS**
 U FLAME PROPAGATION
- FLAME HOLDERS**
 Some peculiarities of flames stabilized in pulsating streams. 10 p1294 A73-23551
- FLAME INTERACTION**
 U CHEMICAL REACTIONS
 U FLAME PROPAGATION
- FLAME IONIZATION**
 Ultrasonic waves generation by plasma of activated flame, presenting sound pressure and light emission graphs 01 p0086 A73-11272
 Temperature dependence of the ion recombination coefficient in a hydrocarbon flame plasma 06 p0731 A73-18553
 Experimental study of influence of an electric field on a laminar flame. 08 p1021 A73-20864
 Electrostatic probe theories and measurements in flame plasmas. 10 p1220 A73-24621
 KCl ionization and diffusion in premixed flames with uniform temperature and composition, studying gas velocity and photometry 13 p1707 A73-28995
 Temperature dependence of the ion recombination coefficient for a hydrocarbon flame. 16 p2042 A73-33578
 Instrumentation and techniques for measuring emissions. 19 p2432 A73-38324
 High temperature ionic and charged species reactions in hydrocarbon and cyanogen flames and additive combustion systems 22 p2819 A73-42770
 Ambipolar diffusion generator based on self generated electric fields in premixed ionized methane-air flame, comparing with opposite caloelectric effects 22 p2895 A73-42773
 Carbon particles size distribution and charged fraction in acetylene-oxygen flame using molecular beam system and electron microscopy, noting particle interaction formation mechanism 22 p2936 A73-42801
 Kinetics of formation of chloride ions in atmospheric pressure flames by way of the reversible reaction $\text{HCl} + \text{e}^- / \text{yields} \text{H} + \text{Cl}^-$. 24 p3085 A73-44991
- FLAME PROBES**
 Spectrum sensitive high amplification solar blind UV sensor for flame surveillance in jet engine environments at 1000 F, using miniature Geiger-Mueller tube 22 p2861 A73-42694
 A comparison of the sensitivity of atomic-fluorescent and atomic-absorption flame photometry 22 p2862 A73-42720
 Determination of the size and the imaginary part of the refractive index of Al_2O_3 drops in a flame 22 p2932 A73-42724
 Determination of dissociation energies for some alkaline earth /hydro-/ oxides in CO/N_2 flames. 24 p3156 A73-44985
- FLAME PROPAGATION**
 On self-similar blast waves headed by the Chapman-Jouguet detonation. 01 p0120 A73-10441
 Turbulent flame velocities in premixed sprays. I - Experimental study. 01 p0121 A73-10635
 Turbulent flame velocities in premixed sprays. II - Theoretical analysis. 01 p0121 A73-10636
 A critical discussion of theories of flame spread across solid and liquid fuels. 01 p0121 A73-10643

- Analysis of NO formation in single droplet combustion. 01 p0014 A73-10645
- Analysis of the problem of the thermal propagation of a flame by the method of joining asymptotic expansions 01 p0123 A73-10958
 Normal flame velocity in aerodisperse systems 01 p0123 A73-11245
 Application of basic research to the study of combustion in turbine combustion chambers [DGLR PAPER 72-058] 02 p0237 A73-11693
 Asymptotic analysis of premixed burning with large activation energy. 03 p0397 A73-13531
 On the deviation of the flame from the stagnation point in opposed-jet diffusion flames. 03 p0399 A73-14388
 Amplification of turbulence level by a flame and turbulent flame velocity. 03 p0399 A73-14391
 Flame propagation in premixed propane /air or propane/ oxygen vortex rings, describing normal and schlieren photographic techniques 03 p0399 A73-14399
 Unflanged electrode spark ignition tests for minimum energy to trigger gas mixtures explosion, using spark energy relation for outward propagating quasi-spherical flame 03 p0399 A73-14400
 Transport phenomena of reactive fluid flow in heterogeneous combustion processes. [ASME PAPER 72-WA/HT-30] 04 p0519 A73-15825
 Combustion chamber temperature profiles analytical derivation from simultaneous radiative and turbulent diffusion heat transfer of turbulent flame front [ASME PAPER 72-WA/HT-27] 04 p0519 A73-15827
 The influence of atmospheric oxygen on velocity of flame spread along a solid. [ASME PAPER 72-WA/HT-23] 04 p0519 A73-15831
 Smoke and fire propagation in compartment spaces. [WSCI PAPER 72-32] 05 p0639 A73-16683
 Theory of steady-state burning of porous propellants by means of a gas-penetrative mechanism. [AIAA PAPER 73-221] 06 p0767 A73-17663
 Gain measurements on CO P-branch transitions in a $\text{C}_2\text{H}_2\text{-O}_2$ flame. 07 p0788 A73-19634
 The transfer of radiation from a flame to its fuel. 08 p1025 A73-21822
 Application of the method of matched asymptotic expansions to calculate the steady-state thermal propagation of an exothermic reaction front in a condensed medium 09 p1167 A73-22616
 One dimensional model for spark ignition Wankel engine combustion, presenting unsteady turbulent flame propagation equations 09 p1136 A73-22824
 Computation of time-dependent laminar flame structure. 10 p1294 A73-23552
 Determination of burning velocity by double ignition in a closed vessel. 10 p1294 A73-23559
 Two zone model of multizone condensed system combustion, showing front velocity dependence on leading heat zone and dispersion depth 10 p1294 A73-23589
 Normal flame velocity in aerosol systems. 10 p1295 A73-24185
 A new criterion for the length of a gaseous turbulent diffusion flame. 11 p1449 A73-25372
 New phenomena during the burning of condensed systems 12 p1559 A73-27454
 Analysis of the problem of thermal flame propagation by the method of matched asymptotic expansions. 12 p1559 A73-27534
 Representative shear wave passage through plane flame front, determining wave refraction and modification, flame generated turbulence and noise and perturbation of front 13 p1707 A73-28993
 Laminar flame propagation in hydrogen, oxygen, nitrogen mixtures. 13 p1707 A73-29001
 Flame quenching, extinction, propagation, convection and ignition limits in premixed gas mixtures 13 p1707 A73-29003
 Asymptotic analysis of the steady propagation of a successive two-stage exothermal reaction front in a condensed medium 13 p1707 A73-29166
 Homogeneous turbulent forward and inverted flame front structure during hydrocarbon combustion, investigating gas flow velocity distribution, activation energy levels and burning zone boundaries 14 p1818 A73-30871
 Condition of the medium before the flame front during the initial phase of a combustion process 15 p1957 A73-31867

- Permeable elastic piston models of shock wave formation before flame front during inflammable gas mixture combustion in channels 15 p1957 A73-31868
- Flame propagation in a transverse electric field 15 p1957 A73-31869
- Condition for flameout from a burning droplet 18 p2372 A73-37116
- Investigation of flame expansion inhibition in air-dispersed systems 19 p2503 A73-37506
- Formation of a nonstationary diffusive flame front during the ignition of a liquid fuel droplet 19 p2471 A73-37507
- Chapman-Jouguet rule for real detonation waves 19 p2419 A73-37516
- Determination of a combustion wave in a conical supersonic flow 19 p2503 A73-37551
- A study on opposing jets in air stream and their flame. I - A structure of two dimensional opposing jets in the state without flames. 19 p2377 A73-37945
- Oxygen index flammability test relationship to flame spread model for polystyrene film burning rate as function of gas velocity and film thickness 19 p2504 A73-38274
- Plane unsteady dispersion of gas behind deflagration wave moved by laser radiation with high flux density 20 p2573 A73-39281
- Argon laser application in a study of velocity in flames 20 p2573 A73-39620
- Quasi-steady gas-phase flame theory in unsteady burning of a homogeneous solid propellant. 21 p2790 A73-40430
- Burning gunpowder interaction with an acoustic field in the presence of balanced chemical reactions behind the flame 21 p2791 A73-40699
- An analytical and experimental investigation of gravity effects upon laminar gas jet-diffusion flames. 22 p2933 A73-42775
- Centrifugal force effects on flame spread and extinction limits of fuel-air mixture combustion with laminar, turbulent and buoyant bubble transport 22 p2933 A73-42776
- Inhibition of the first limit of the hydrogen-oxygen reaction by ethyl bromide. 22 p2898 A73-42777
- Reaction of H atoms with CH₂Cl₂ - Application to the inhibition of flames. 22 p2819 A73-42779
- Pressure waves generated by constant velocity deflagration flame in explosive hydrocarbon-air mixture for self-similar flow field 22 p2936 A73-42808
- Ignition and flame spreading over a solid fuel - Non-similar theory for a hot oxidizing boundary layer. 22 p2936 A73-42809
- Experimental studies on the flame structure in the wake of a burning droplet. 22 p2937 A73-42816
- Effect of pressure on the flame propagation velocity in a turbulent flow 23 p3019 A73-43730
- Deviations from the Le Chatelier principle for flame propagation limits 24 p3155 A73-44716
- The theory of free ambient fires - The convectively mixed combustion of fuel reservoirs. 24 p3156 A73-45161
- Vortex model for flames and free jets characteristic velocities based on three dimensional turbulent combustible flow 24 p3158 A73-45387
- FLAME QUENCHING**
- U EXTINGUISHING
- U QUENCHING [COOLING]
- FLAME SPRAYING**
- Detonation gun flame spray coatings, determining adhesive strength as function of coating thickness and process technological parameters 03 p0313 A73-14014
- Alloy or metal coated composite powder thermal spraying applications, discussing bonding properties, wear resistance, low friction applications and abrasability 22 p2866 A73-42593
- FLAME STABILITY**
- The stability of lifted turbulent diffusion and premixed flames. [WSCI PAPER 72-39] 05 p0638 A73-16678
- Stabilization of flames formed behind cylinders wetted by liquid fuels in high velocity gas streams [WSCI PAPER 72-38] 05 p0639 A73-16679
- Extension of combustion in the supersonic flow downstream of a pilot flame stabilized with the help of a Mach configuration 06 p0769 A73-18539
- Streamline deflection by diffusion flame stabilized on Parker-Wolfhard burner, discussing flow visualization and Burke-Schumann flame sheet in Oseen flow 07 p0921 A73-20355
- Some peculiarities of flames stabilized in pulsating streams. 10 p1294 A73-23551
- Instability of free shear layers adjacent to a vibrating flame surface. 10 p1296 A73-24804
- Aerodynamic characteristics of torus shaped cascades involved in flame stabilization process of reheat devices for jet engines 11 p1453 A73-26595
- Finite difference theory predictions for turbulent boundary layer swirling flames, discussing flow simulation, turbulence models and flame size, shape and stability characteristics [AIAA PAPER 73-651] 18 p2367 A73-36206
- Experimental investigation of premixed swirling jet flames - Combustion characteristics. 19 p2504 A73-37946
- Effects of thermal and mass diffusivities on the burning of fuel droplets. [AICHE PREPRINT 22] 20 p2626 A73-39249
- Combustion in high speed swirling flow in gas turbine combustion chamber, discussing flame stability, pressure measurements and chamber configuration 22 p2935 A73-42790
- Liquid fuel spray burning characteristics in stabilizer disk wake of luminous hollow cone pressure jet flame, using spark photographic technique 22 p2937 A73-42818
- Combustion noise radiation by open turbulent flames. [AIAA PAPER 73-1025] 24 p3156 A73-44856
- Propane-air flame stabilization via combustion product recirculation due to transverse gas jet injection, increasing fuel-air ratio 24 p3123 A73-45379
- Gaseous fuel combustion in water flow by introducing fuel-oxygen mixture in stagnation region behind body for flame stabilization 24 p3158 A73-45386
- Investigation of the mechanism of reverse jet flame stabilization for a heterogeneous mixture. 24 p3158 A73-45388
- FLAME TEMPERATURE**
- Convective heat transfer coefficients at stagnation point of blunt body immersed in flames of fuel gases combustion with pure oxygen 01 p0122 A73-10807
- The investigation of the effect of acoustic oscillations on the combustion process of gaseous fuel 03 p0396 A73-12955
- Electron temperature elevation compared to gas temperature in hydrocarbon flames, discussing energy exchange mechanism 03 p0352 A73-14394
- Fuel-rich and stoichiometric carbon monoxide-nitrous oxide premixed laminar flames with varying water contents, determining flame temperature by line reversal method 03 p0399 A73-14396
- Multistage ignition behind second and third cool flames of hydrocarbon combustion, presenting graphs of propane mixtures ignition limits 03 p0400 A73-14401
- The influence of fuel preparation and operating conditions on flame radiation in a gas turbine combustor. [ASME PAPER 72-WA/HT-26] 04 p0519 A73-15828
- Cool flame oxidation studies of acyclic and cyclic hydrocarbons. 05 p0606 A73-16691
- Ignition analysis of adiabatic, homogeneous systems including reactant consumption. [AIAA PAPER 73-215] 05 p0640 A73-16945
- The cool-flame oxidation of n-heptane. I - The kinetic features of the reaction. 07 p0918 A73-19385
- A mathematical model of the opposed-jet diffusion flame - Effect of an electric field on concentration and temperature profiles. 07 p0918 A73-19388
- Brightness balancing spectrograph method for flame temperature measurement of liquid fuel drop 07 p0826 A73-20423
- A mass spectrometric investigation of reactions involving tungsten and molybdenum with potassium-seeded H₂/O₂ flames. 10 p1186 A73-23554
- A mass spectrometric investigation of reactions involving vanadium and chromium with potassium-seeded H₂/O₂ flames. 10 p1186 A73-23555
- Determination of the temperature of a methane-fluorine diffusion flame by means of the vibration-rotation spectrum of the HF molecule 11 p1453 A73-26586
- A system for instantaneous measurement of flame temperature 12 p1557 A73-27071
- Modeling the ignition and cool-flame limits of acetaldehyde oxidation. 13 p1581 A73-28999
- German monograph - Determination of the OH-concentration distribution in a axisymmetric methane/oxygen flame. 13 p1708 A73-29279
- The combustion of the n-pentenes in the cool flame region. 16 p2085 A73-33341
- Experimental measurement of heat transfer to a cylinder immersed in a large aviation-fuel fire. [ASME PAPER 73-HT-2] 20 p2625 A73-38565
- The spectral comparison method for temperature measurement in two-phase flames. 22 p2853 A73-41987
- Turbulent diffusion flame velocity, concentration, temperature and momentum flux measurements for hydrogen round jet in co-flowing air stream 22 p2935 A73-42788
- Laminar combustion of polymethylmethacrylate in O₂/N₂ mixtures. 22 p2898 A73-42805
- Temperatures in low-pressure magnesium-vapor diffusion flames. 22 p2899 A73-42820
- Development of a mathematical model for vortex configuration in jets and flames. 24 p3157 A73-45376
- Study of the spatial development of oxidation and combustion reactions by means of image photoelectric receivers, and of a thermometric method 24 p3091 A73-45398
- FLAMEOUT**
- Combustion mechanisms of fuel rich propellants in flow fields. [AIAA PAPER 72-1145] 04 p0485 A73-14915
- Condition for flameout from a burning droplet 18 p2372 A73-37116
- FLAMES**
- NT DIFFUSION FLAMES
- NT PREMIXED FLAMES
- Design of an extremely sensitive flame-photometer for analyses in the picogram range using a lock-in amplifier 01 p0051 A73-10925
- Line and continuous excitation sources for measuring wavelength dependence, angular distribution and polarization of scattered light intensity in turbulent and laminar flames 03 p0396 A73-12925
- The oscillations of supersonic gas flows 03 p0289 A73-12953
- German monograph - Axisymmetric free jets and free-jet flames and a numerical procedure for calculating them. 03 p0398 A73-13810
- Luminous flames thermal radiation total emissivity analysis, considering water vapor, carbon dioxide and soot particles overlapping spectral bands [WSCI PAPER 72-41] 05 p0638 A73-16677
- Stroboscopic investigation of the effect of standing acoustic waves on turbulent flames 07 p0920 A73-19992
- Absorption spectrum analysis of free Cu, Ca, Na, Zn, Ni and Cr atom concentration in acetylene air flame zones 14 p1817 A73-30458
- Combustion of fuel vapor-drop-air systems. I - Open burner flames. II - Spherical flames in a vessel. 16 p2085 A73-33343
- Spectroscopic investigations of the combustion zone of flame jets of compacted systems 19 p2402 A73-37508
- Recirculation and mixing characteristics prediction for enclosed turbulent jet flames in flow regions, using similarity parameters 22 p2934 A73-42782
- Two modes of interaction of NaOH and SO₂ in gases from fuel-lean H₂-air flames. 22 p2820 A73-42802
- Burner dimension and flame size effects on relative contributions of luminous soot and nonluminous molecular band radiations from combustion fires 23 p3048 A73-43329
- Chemiluminescence spectra from cool and blue flames - Electronically excited formaldehyde. 24 p3066 A73-45163
- FLAMMABILITY**
- Analysis of the problem of the thermal propagation of a flame by the method of joining asymptotic expansions 01 p0123 A73-10958
- Analysis of volatile combustion products and a study of their toxicological effects. 02 p0138 A73-12429
- Flammability comparisons of glass-reinforced unsaturated polyester moldings in various laboratory-scale tests. 08 p0983 A73-21820
- Application of simultaneous DTA/TGA and DTA/MS analysis for predicting the flammability of composite textile fabrics and polymers. 09 p1110 A73-22515
- Recent developments in commercial fire resistant fibrous materials. 11 p1389 A73-26419
- Evaluation of the smoke and flammability characteristics of polymer systems. 12 p1515 A73-27143

- Analysis of the problem of thermal flame propagation by the method of matched asymptotic expansions. 12 p1559 A73-27534
- Flame resistant and nonflammable textile fibers. 17 p2198 A73-35839
- Self extinguishing properties of polyester-glass laminates with reduced flammability due to polyvinyl chloride and antimony trioxide additives. 18 p2327 A73-36478
- Book - Flame retardancy of polymeric materials. Volume 1. 18 p2287 A73-37123
- Inorganic flame retardants, considering antimony, phosphorus, boron, aluminum, nitrogen, iron and sulfur compounds. 18 p2287 A73-37124
- Inorganic flame retardants and their mode of action. 18 p2288 A73-37125
- Fire retardation of polyvinyl chloride and related polymers. 18 p2329 A73-37126
- Oxygen index flammability test relationship to flame spread model for polystyrene film burning rate as function of gas velocity and film thickness. 19 p2504 A73-38274

FLAMMABLE GASES

- Flammable fuel-air mixture ignition by transient turbulent hot inert gas jet, calculating minimum required jet size. 03 p0399 A73-14390
- A new criterion for the length of a gaseous turbulent diffusion flame. 11 p1449 A73-25372
- Spectroscopic studies of low-pressure hydrogen-fluorine flames. 22 p2898 A73-42760

FLANGES

- Flange-to-web connection requirements on beams with corrugated webs. 10 p1223 A73-23632
- High vacuum coaxial and coaxial push-pull rotary motion feedthroughs with continuous well shielded low noise cable mounted on vacuum flange. 11 p1344 A73-26314

FLAP CONTROL

- U AIRCRAFT CONTROL
U FLAPS [CONTROL SURFACES]

FLAPPING

- Random gust response statistics for coupled torsion-flapping rotor blade vibrations. 01 p0004 A73-10046
- Model tests on unsteady rotor wake effects. 07 p0773 A73-19191
- Plane subsonic jet free boundaries flapping measurements from oppositely placed hot-wire probes. 11 p1346 A73-25251

FLAPS [CONTROL SURFACES]

- NT JET FLAPS
NT LEADING EDGE SLATS
NT TRAILING-EDGE FLAPS
NT WING FLAPS
- Hydraulic system on de Havilland Twin Otter STOL aircraft for flaps, wheel brakes and nose wheel steering, noting power supply mounting. 03 p0252 A73-13350
- Flap noise measurements for STOL configurations using external upper surface blowing. [AIAA PAPER 72-1203] 04 p0487 A73-14922
- Conformal mapping for potential flow about airfoils with attached flap. 07 p0773 A73-19192
- Symmetrical airfoils optimized for small flap deflection. 10 p1174 A73-24915
- A study of stall-induced flap-lag instability of hingeless rotors. [AHS PREPRINT 730] 17 p2095 A73-35066
- Analysis of the aerodynamic characteristics of devices for increasing wing lift. III - Influence of ground proximity on the aerodynamic characteristics of the flaps. 18 p2266 A73-37022
- An aerodynamic entry control technique utilizing the yaw flap concept. [AIAA PAPER 73-888] 20 p2588 A73-38824

FLARES

- UV Cet-type variable star quiet state and flare spectra, discussing flare mechanism relation to magnetic effects and star evolutionary position. 01 p0102 A73-10970
- X ray intensity observations of Cygnus X-3 by Uhuru satellite before/during September 1972 radio flare. 02 p0210 A73-11554
- Moon flares due to lunar gas eruptions, investigating degassing in former geological epochs. 02 p0212 A73-11950
- Importance of high time resolution in flare star observations. 03 p0373 A73-13373
- Activity in flare stars of the solar neighborhood. 08 p1013 A73-21773

- White dwarf flares UVB energy spectra, assuming mechanism of nonthermal bremsstrahlung due to fast electrons. 09 p1146 A73-22296
- High-speed UVB photometry of Scorpius X-1 flares. 14 p1801 A73-30646
- Predicting descent rate for aircraft parachute flares. [AIAA PAPER 73-482] 15 p1829 A73-31464
- Evidence of active and ancient volcanism on Mars - A review. 17 p2233 A73-35482

FLASH

- Visible light flash emission due to strong shock wave of laser spark, investigating strong external magnetic field effect and time variation of luminous intensity. 06 p0700 A73-17966
- Dynamic properties of vision. III - Twin flashes, single flashes and flickerfusion. 07 p0783 A73-20253
- Observations and theoretical reconstruction of the green flash. 11 p1351 A73-25168
- On the generation of umbral flashes and running penumbral waves. 24 p3136 A73-44638

FLASH BLINDNESS

- Flashblindness recovery following exposure to constant energy adaptive flashes. 13 p1579 A73-28505

FLASH LAMPS

- An 11 megawatt 6.8 joule flashlamp pumped coaxial liquid dye laser. 02 p0175 A73-11956
- Laser plasma generation with high electron densities by photoionization from flashlamp or coherent UV source from harmonic generation or gas lasers. 05 p0601 A73-16362
- A tunable flashlamp-pumped dye ring laser of extremely narrow bandwidth. 09 p0191 A73-22083
- Maximum loads on pulse-discharge light sources producing short flashes. 13 p1629 A73-29437
- Airport lighting systems as visual landing aids, discussing runway disposition, brightness levels, beam orientation, visibility factors and flashing lights. 16 p1993 A73-32974
- Radiation pulse development time instability in electro-optically Q switched lasers due to flash lamp output fluctuations. 22 p2870 A73-42722
- Quenching effects in flashlamp-excited polymethine dye lasers. 22 p2871 A73-43083

FLASH POINT

- Hydrolysis of a disiloxane/ester fluid in a simulated hydraulic system at 275 F. [ASLE PREPRINT 72LC-6C-1] 03 p0335 A73-14365

FLASH TUBES

U FLASH LAMPS

FLASH WELDING

- Bibliography on Resistance Welding, 1950-1971. 01 p0058 A73-13734

FLAT PLATES

- Unsteady viscous flow due to the impulsive motion of a flat plate, with special reference to the initial period. 01 p0031 A73-10422
- Hydrodynamic stability of boundary layers with surface suction. 01 p0033 A73-10749
- Flow and heat transfer on a flat plate normal to a two-dimensional laminar jet issuing from a nozzle of finite height. 01 p0033 A73-10804
- Turbulent wake flow behind two dimensional flat plate trailing edge investigated by Nee-Kovaszny turbulent shear flow differential field theory. 01 p0004 A73-11137
- Perturbed bifurcation and buckling of circular plates. 02 p0186 A73-11973
- Study of the natural convection between two plane, vertical plates parallel and isothermal. 02 p0238 A73-12795
- The boundary layer of particulate gas flow. 03 p0289 A73-12914
- A numerical analysis for chemical non-equilibrium boundary layer of dissociated gases over a flat plate with arbitrary catalyticity. 03 p0291 A73-13068
- Free stream turbulence effect on flat plate boundary layer turbulent behavior, considering Reynolds stress dependence on turbulence intensity. 03 p0292 A73-13170
- Similarity solution of boundary layer flow due to uniform streaming past infinite flat plate with uniform suction at plate surface. 03 p0292 A73-13306
- Matrix analysis of local instability in plates, stiffened panels and columns. 03 p0390 A73-13339

- Numerical solution for a flat plate experiencing a ground effect. 03 p0245 A73-13721

- Flutter of flat rectangular sandwich type panels in a supersonic, coplanar gas flow, with arbitrary direction. 03 p0392 A73-13768

- Flow conditions at inlet and exit of a flat plate cascade at supersonic velocities. 03 p0246 A73-14139

- On similarity solution of an unsteady laminar boundary layer along a flat plate. 03 p0297 A73-14314

- Inertia and energy effects in the developing gas film between two parallel flat plates. [ASME PAPER 72-LUB-33] 03 p0297 A73-14343

- On the weight optimization problem for supersonic rectangular flat panels with specified flutter speed. 04 p0511 A73-15170

- Flow induced vibration of cantilever mounted flat plates in an enclosed passage. An experimental investigation. 04 p0513 A73-15590

- Hypersonic rarefied flow past an insulated flat plate with suction/injection. 04 p0520 A73-15939

- Application of Olfe's modified differential approximation to the radiation-layer problem on a flat plate. [DFVLR-SONDDR-254] 04 p0520 A73-15946

- Hydromagnetic stability of a laminary boundary layer in a flow past a planar plate. 05 p0601 A73-16096

- Variational principle application to nonself adjoint lifting surface integral equation from finite element viewpoint, considering two dimensional flat plate. [AIAA PAPER 73-87] 05 p0529 A73-16852

- Numerical computation of the hypersonic rarefied flow near the sharp leading edge of a flat plate. [AIAA PAPER 73-200] 05 p0531 A73-16934

- Initial conditions for the hypersonic shock/boundary layer interaction problem. [AIAA PAPER 73-201] 05 p0532 A73-16935

- Shockwave-boundary layer interference heating analysis. [AIAA PAPER 73-237] 05 p0532 A73-16962

- Experimental results on the intermittent properties of the boundary layer pressure field during transition. [AIAA PAPER 73-243] 05 p0566 A73-16967

- Laminar film boiling on inclined isothermal flat plates. 05 p0641 A73-17107

- Ion-current distributions around an electrically conductive body in ionized gas flow. 05 p0603 A73-17110

- Supersonic boundary layer on a permeable surface. 05 p0534 A73-17268

- Numerical solution to kinetic equations of rarefied supersonic steady gas flow normal to plate by method of characteristics. 06 p0643 A73-17461

- Measurements of base pressure upon a plate and a wedge in the 2.8 to 6.8 Mach number range [DFVLR-SONDDR-256] 06 p0645 A73-17740

- Impedance and radiation pattern of antennas above flat discs. 06 p0676 A73-18191

- Solutions of thermal boundary layer equations when temperature gradient at the moving flat plate in parabolic flow is prescribed. 06 p0769 A73-18251

- Thermal boundary layer thickness for laminar forced convection to flat plates with uniform heating and uniform wall temperature. 06 p0769 A73-18260

- Viscous compressible flow near right angle corner of two flat plates, presenting streamwise and secondary flow velocities and skin friction coefficient distribution. 06 p0687 A73-18532

- Transmission of microwave through perforated flat plates of finite thickness. 06 p0669 A73-18735

- An extension of the modified Oseen solution for laminar viscous flow past a semi-infinite flat plate. 06 p0688 A73-18849

- Initial postbuckling behavior of optimally designed columns and plates. 07 p0908 A73-19084

- Homogeneous flat elastic plate theory in Cosserat surface context, considering application of general constitutive equations and extension to right circular cylindrical shells. 07 p0908 A73-19085

- The influence of the accommodation coefficients on the flow variables in the viscous interaction region of a hypersonic slip-flow boundary layer. [DFVLR-SONDDR-267] 07 p0773 A73-19206

- Characteristics of the unsteady shock-induced laminar boundary layer on a flat plate. 07 p0810 A73-19505

- Stationary vortices behind a flat plate normal to the freestream in incompressible flow. 07 p0775 A73-19974

- Unsteady motion of a viscous electrically conducting fluid around a flat plate in the case of orthogonal fields 07 p0858 A73-19999
- On the theory of optimal, constant thickness fibre-reinforced plates. II. 08 p1016 A73-20830
- Skin friction and heat flux in the impingement region of a low speed air jet upon a normal flat plate. 08 p0925 A73-20941
- Free molecular flow past a flat plate in the presence of a nontrivial gas-surface interaction. 08 p0926 A73-21401
- Further results concerning the forces on a flat plate in a Couette flow. 08 p0926 A73-21402
- Linearized solutions to supersonic laminar boundary layer structure near flat plate with slot injection, using triple deck separation theory 08 p0956 A73-21524
- Heat transfer through the unsteady laminar boundary layer on a semi-infinite flat plate. I - Theoretical considerations. II - Experimental results from an oscillating plate. 08 p1024 A73-21635
- Parabolic flow over a flat plate with wave disturbance in the main stream. 09 p1071 A73-21950
- Approximate calculation of a thermal boundary layer at a flat plate with allowance for a magnetic field 09 p1167 A73-22859
- Determination of tensile stresses in wide flat samples 09 p1165 A73-23359
- Temperature recovery coefficients during turbulent flow of liquid in a circular pipe 10 p1204 A73-23509
- Effect of jet turbulence on the flow in a wall boundary layer 10 p1205 A73-23586
- An experimental study of combined forced- and free-convective heat transfer from flat plates to air at low Reynolds numbers. 10 p1295 A73-23777
- Free convection from a semi-infinite flat plate inclined at a small angle to the horizontal. 10 p1296 A73-24339
- Evaluation of the characteristics of the boundary layer in transitional flow on a flat plate 10 p1296 A73-24497
- Flow near an accelerated plate in the presence of a magnetic field. 10 p1206 A73-24528
- Some heat transfer measurements in compressible turbulent boundary layers. 10 p1296 A73-24648
- An extended boundary-layer analysis of the impulsive motion of a flat plate in a viscous fluid. 10 p1208 A73-24809
- Transient viscous laminar incompressible flow pattern after sudden vanishing of semiinfinite flat plate based on two dimensional unsteady boundary layer equations with boundary conditions 10 p1208 A73-24811
- Incompressible boundary layer flow over semi-infinite plate with impulsive heat transfer, obtaining numerical solution for time dependent boundary layer growth 10 p1296 A73-24812
- Unsteady boundary layer and wake near the trailing edge of a flat plate. 10 p1173 A73-24826
- Unsteady boundary layer over a flat plate started from rest. 10 p1209 A73-24829
- Unsteady turbulent boundary layer flow past infinite flat plates with free stream acceleration or deceleration, computing characteristics by finite difference method 10 p1209 A73-24834
- Visualization experiments on unsteady viscous flows around cylinders and plates. 10 p1174 A73-24836
- Acoustic dipole source strength on flat plate and simple airfoil surfaces from local surface and far field acoustic pressure cross correlation 11 p1345 A73-24982
- Unsteady boundary layer flow of homogeneous viscous fluid in nonrotating environment or bounded by oscillating flat plates, determining velocity field by exact solutions 11 p1346 A73-25165
- Transpiration and natural convection - The vertical-flat-plate problem. 11 p1449 A73-25219
- Noise reduction for subsonic fluid flow over flat plate via interposition of secondary fluid layer at trailing edge 11 p1300 A73-25386
- Parametric excitation of Tollmein-Schlichting waves in a boundary layer 11 p1347 A73-25430
- The stability of simply supported rectangular surfaces in uniform subsonic flow. [ASME PAPER 72-APM-ZZ] 11 p1441 A73-25702
- Perturbation solutions to laminar boundary layer flow over flat plate with small hump downstream of leading edge, using Blasius equation 11 p1302 A73-25855
- Laminar free convection flow of an electrically conducting fluid from an inclined isothermal plate. 11 p1452 A73-26369
- One dimensional temperature equalization process in planar plate, infinitely long cylinder and sphere for range of Biot and Fourier numbers, estimating approximate solution error 11 p1452 A73-26372
- Initial conditions for the hypersonic-shock/boundary-layer interaction problem. 11 p1303 A73-26384
- Hydrogen ignition in flat rotating disk phase of stellar formation, determining central conditions from total mass and adiabatic constant 12 p1542 A73-27575
- Compressive buckling analysis and design of stiffened flat plates with multilayered composite reinforcement. 12 p1554 A73-27736
- Analysis of stress intensity factor for surface-flawed tension plate. 13 p1692 A73-28231
- Natural vibrations of thin, prismatic flat-walled structures. 13 p1694 A73-28247
- Incremental solution of axisymmetric plate and shell finite deformation. 13 p1694 A73-28250
- A note on the effect of Hall currents on hydromagnetic flow near an accelerated plate. 13 p1664 A73-28617
- Air injection from wall slot into turbulent boundary layer of high temperature gas channel flow, calculating film cooling effectiveness in flat plate 13 p1706 A73-28675
- Effects of free stream velocity profile on turbulent boundary layer, with some reference to the effects of free stream turbulence. 13 p1602 A73-29013
- Equilibrium three-dimensional turbulent boundary layer on the end wall of a curved channel. 13 p1602 A73-29015
- Wall effects on the motion of a two-dimensional jet switching between two parallel flat plates. 13 p1571 A73-29043
- Structure of the wall zone of a longitudinal disperse flow over a plane plate 14 p1711 A73-30014
- Plate-injection into a separated supersonic boundary layer. 14 p1711 A73-30172
- Theoretical investigation on laminar boundary layer with combustion on a flat plate. 14 p1817 A73-30611
- The effect of groupings of surface couples on flat plates 14 p1814 A73-30703
- Velocity profile determination in a turbulent boundary layer 14 p1746 A73-30795
- Solution of the plane problem of rarefied-gas aerodynamics on the basis of the Boltzmann kinetic equation 15 p1822 A73-31244
- Strains and stress-concentration factors in plates under out-of-phase biaxial cyclic loads. 15 p1948 A73-31614
- Transient forced convection heat transfer from an isothermal flat plate. 15 p1957 A73-31664
- Experimental investigation of longitudinal flow over a flat plate during strong blowing of a foreign gas under isothermal conditions 15 p1957 A73-31856
- Investigation of boundary layer flow on a flat porous plate with a regulated pressure gradient in the outer flow 15 p1864 A73-31873
- Forced convective heat transfer of a gas with condensing vapor around a flat plate. 15 p1958 A73-32058
- Leading edge effects on displacement thickness and skin friction variations of unsteady boundary layer on flat plate under impulsive motion in viscous fluid 16 p1962 A73-32927
- The numerical integration of the Navier-Stokes equations for the two-dimensional incompressible flow along a planar plate 16 p2000 A73-33261
- On the solution of magnetohydrodynamic elastico-viscous flow past a plane porous plate. 16 p2042 A73-33370
- Some effects of variable surface temperature on heat transfer to a partially porous flat plate. [ASME PAPER 73-GT-4] 16 p2086 A73-33482
- Continuum gas plasma boundary layer flow over flat plate, obtaining ion sheath characteristics and downstream solutions by asymptotic and characteristics methods 17 p2149 A73-34186
- Experimental study of turbulent boundary layer along a flat plate with linear increase of roughness height. 17 p2151 A73-34537
- Variational methods for vibratory bending equations of asymmetrical sandwich plates with mode families in terms of displacement ratios, taking into account inertia effects 17 p2243 A73-34548
- Impulsively started viscous flow past a finite flat plate with and without an applied magnetic field. 17 p2217 A73-35604
- Slightly ionized low density hypersonic flow about a sharp plate and its diagnostics. [AIAA PAPER 73-690] 18 p2262 A73-36241
- Velocity distribution in hypersonic helium flow near the leading edge of a flat plate. [AIAA PAPER 73-691] 18 p2262 A73-36242
- Reynolds number effects on the shock wave - Turbulent boundary layer interaction at transonic speeds. [AIAA PAPER 73-661] 18 p2298 A73-36262
- Thermal modeling of a plate with coupled heat transfer modes. [AIAA PAPER 73-748] 18 p2370 A73-36364
- Approximate solution of the problem of local heat transfer at a vertical plate under conditions of laminar mixed convection 18 p2371 A73-36649
- Magnetohydrodynamical steady aligned flow past an oblique flat plate at a high Reynolds number. 18 p2300 A73-36664
- The singularity at boundary layer separation due to mass injection. 18 p2301 A73-36696
- Calculation of turbulent boundary layers over flat plates with different phenomenological theories of turbulence and variable turbulent Prandtl number. 18 p2301 A73-36699
- Laminar boundary layers along an infinite flat plate with oblique suction. 19 p2420 A73-37646
- A variational principle for the laminar boundary layer theory. 19 p2421 A73-38026
- On Blasius's equation governing flow in the boundary layer on a flat plate. 19 p2421 A73-38101
- A tilted plate interferometer for heat transfer studies. 20 p2564 A73-38879
- Steady separated flow over finite flat plate in linearly decelerated free stream, using numerical solution of two dimensional Navier-Stokes equation 20 p2546 A73-39089
- Stability of a compressible boundary layer with regard to a localized disturbance 20 p2547 A73-39285
- Strouhal number and flat plate oscillation in an air stream. 21 p2782 A73-40125
- A natural frequency analogy between spherically curved panels and flat plates. 21 p2785 A73-40754
- Radiative-convective heat transfer in flows of hot air past a flat plate. 21 p2791 A73-41056
- Hot-wire investigation of the steady laminar wake behind a thin flat plate placed perpendicularly to a uniform flow. 21 p2703 A73-41118
- Fatigue behavior of stiffened flat panels 21 p2788 A73-41555
- Application of a general finite-difference method to boundary layer flows. 21 p2678 A73-41686
- On unsteady flow of an elastico-viscous fluid past an infinite plate with variable suction. 22 p2840 A73-41747
- Gaskinetic treatment of the Rayleigh problem in the case of moderately to greatly diluted gases 22 p2843 A73-42529
- Aerodynamic and thermal structures of the laminar boundary layer over a flat plate with a diffusion flame. 22 p2933 A73-42774
- A general conclusion regarding the large amplitude flexural vibration of beams and plates. 23 p3039 A73-43305
- Nonstationary mass transfer during the longitudinal flow of a nonlinearly viscous fluid past a flat plate and the forward stagnation point 23 p2967 A73-43440
- Thermal response of an unsteady laminar boundary layer on a flat plate due to step changes in wall temperature and in wall heat flux. 23 p3049 A73-43802
- Heat transfer rate and flow field and pressure distribution behind flat plate backward facing step in hypersonic flow 23 p3049 A73-43832
- Effect of wall conduction on convective heat transfer with laminar boundary layer. 23 p3049 A73-43833
- Heat transfer from a hypersonic turbulent boundary layer on a flat plate. 23 p3049 A73-43933

Boundary layer on flat plate in shear flow, calculating induced pressure gradients near leading edge and far downstream 24 p3080 A73-45369

Compressible laminar boundary layer differential equations solution for incident viscous gas flow on flat plate at high flow velocity 24 p3080 A73-45471

FLAT SURFACES

Equations of motion for nonuniformly heated gas past hot bodies, noting gas heating between two parallel flat surfaces with different temperatures 02 p0152 A73-11612

Investigation of a laminar boundary layer on a continuously moving smooth surface with allowance for heat transfer 02 p0153 A73-11786

Russian book - Study of the theory of differentiable functions of many variables and its applications. IV. 02 p0187 A73-12176

Partial optical coherence theory based Greenspan modification for calculation of sound power radiation from statistically vibrating flat surfaces 03 p0384 A73-12991

Wind tunnel study of flow structure and turbulent wakes on base surfaces of sharp or blunt edged flat bodies at various Mach and Reynolds numbers 06 p0643 A73-17456

Steady nonlinear Ekman-Hartmann boundary layer on flat surface, evaluating pumping and electric current as functions of Rossby number and magnetic interaction parameter 07 p0856 A73-19512

Large particle method for calculation of transonic supercritical vortex flow fields around flat and axisymmetric bodies 11 p1302 A73-26330

Simplification of one-dimensional heat-conduction problems in the case of impulsive radiative heating of flat bodies 12 p1558 A73-27317

Geometrical characteristics of flat-faced bodies of revolution. 22 p2842 A73-42425

Oblique radiation of ultrasound by an electromagnetic-acoustical method. 24 p3109 A73-44697

FLATTENING

Planetary masses, dynamic flattening and orbital elements determination by perturbation analysis for disturbed planet, space probe and satellite 11 p1420 A73-25882

FLAW DETECTION

U NONDESTRUCTIVE TESTS

FLEET BALLISTIC MISSILES

NT POSEIDON MISSILES

FLEXIBILITY

The flexible solar array - A spacecraft electrical power source technology option. 09 p1154 A73-22790

Epoxy resins thermal mechanical properties, considering difference between toughness and flexibility in terms of temperature and loading rate insensitivities 10 p1237 A73-23952

Influence of the flexibility of the walls on the oscillations of the liquid masses of storage tanks 12 p1487 A73-27395

Effects of flexibility on a momentum-stabilised communication-satellite attitude control system. 15 p1942 A73-31099

Bounds on the spectral and maximum norms of the finite element stiffness, flexibility and mass matrices. 19 p2500 A73-38110

Flexibility matrix coefficients for disk loading under sinusoidal edge loading tabulation and derivation to accommodate boundary conditions 21 p2784 A73-40434

Effect of support flexibility on the fundamental frequency of vibrating beams. 22 p2918 A73-41966

FLEXIBLE BODIES

Dynamics of flexible satellites with active attitude control. 02 p0228 A73-11994

Flexible satellite with three axisymmetrical bodies spinning at different rates about common axis of symmetry, deriving stability conditions based on Sturm theorem 02 p0228 A73-11997

Flexible rotor balancing of a high-speed gas turbine engine. [SAE PAPER 720741] 02 p0203 A73-12007

Equations of motion for flexible cables. 03 p0343 A73-13706

Flexible circular solar array for power to weight ratio increase at satellite outer surface, noting central supported structure superiority 03 p0257 A73-14239

About the motion of a heavy flexible string attached to the satellite in the central field of attraction. 03 p0376 A73-14267

Rotating flexible shaft stability criterion development by perturbation method, considering internal and external friction and rotor inertia loading moments effects 11 p1444 A73-26368

Liapunov stability analysis of spinning flexible spacecraft. 11 p1431 A73-26378

Influence of structural flexibility on the dynamic stability of rockets. 14 p1803 A73-30043

Torsion of a reversible flexible wire shaft 15 p1946 A73-31140

Normal mode solution to the equations of motion of a flexible airplane. 15 p1950 A73-31747

Procedure for the simulation of sonic fields, particularly for fatigue tests 16 p1997 A73-33384

State space attitude control synthesis for a satellite with flexible appendages. 17 p2239 A73-34951

Attitude control of a large flexible spacecraft using three-axis mass expulsion control. [AIAA PAPER 73-893] 20 p2588 A73-38829

Design of a digital controller for spinning flexible spacecraft. [AIAA PAPER 73-894] 20 p2589 A73-38830

Mathematical modeling of spinning elastic bodies for modal analysis. 21 p2784 A73-40421

Coupled bending-twisting vibrations of a single boom flexible solar array and spacecraft. 21 p2781 A73-40619

Further experiments on balancing of a high-speed flexible rotor. [ASME PAPER 73-DET-99] 22 p2865 A73-42077

Some results of experimental investigations of turbulent flow in flexible tubes 22 p2841 A73-42120

A new approach to gust alleviation of a flexible aircraft using an open loop device [ONERA, TP NO. 1236] 22 p2799 A73-42219

FLEXIBLE WINGS

NT PARAWINGS
Analysis of flight vehicle response to nonstationary atmospheric turbulence including wing bending flexibility. 05 p0535 A73-16921

The spatial correlation method and a time-varying flexible structure. 11 p1440 A73-25535

Rogallo variable geometry flexible cambered wing structure and aerodynamic performance for low speed agricultural flight applications 13 p1568 A73-28027

Improved aircraft capability through variable camber. 19 p2378 A73-37275

Influence of wing flexibility on sailplane loading by individual gusts 21 p2635 A73-41577

FLEXING

Bending and flexing of the Apollo 15 mass spectrometer boom. 05 p0636 A73-17210

The dynamic properties of unidirectional fibre reinforced composites in flexure and torsion. 10 p1240 A73-24279

Flexural/torsional deformations of material line in continuous body in terms of curvature and bending vectors, using Frenet-Serret equations 11 p1445 A73-26408

Discrete flexural analyses of rectangular plates of abruptly varying stiffnesses. 12 p1556 A73-27926

Flexural response of tapered beam on elastic-plastic foundation, solving in closed form to evaluate efficiency of numerical methods 12 p1557 A73-27932

Borsic-aluminum composites fracture and flexural behavior from Charpy impact and slow bend tests 17 p2192 A73-35537

On the flexural vibration frequencies of statically loaded beams. 18 p2367 A73-37091

On the modal equations of large amplitude flexural vibration of beams, plates, rings and shells. 19 p2501 A73-38254

Large amplitude flexural vibration of simply supported skew plates. 21 p2784 A73-40423

FLEXORS

EMG measurement on male adults for muscular relaxation reaction time interval from light stimulus onset to elbow flexor response 03 p0267 A73-13699

FLEXOWRITERS [TRADEMARK]

U AUTOMATIC TYPEWRITERS

FLICKER

Mathematical description of some visual inertia effects 04 p0413 A73-15786

Tilt discrimination and motion aftereffect independence of flicker rate of stroboscopically illuminated contours visual stimuli 06 p0660 A73-18624

FLICKER FLICKER FREQUENCY

U CRITICAL FLICKER FUSION

FLIGHT ALTITUDE

Analysis of an altitude control system of a low flying vehicle. 01 p0075 A73-11195

Aircraft reference altitude computation from air data inputs, deriving algorithm for pressure gradient errors correction 03 p0308 A73-13915

Aircraft flight plan data processing in FORTRAN program to predict altitude and time conflicts, noting short CPU time 05 p0595 A73-16618

IR radiation source shape and size effects on aerial IR surveys at various flight altitudes, noting spectral composition change with height 05 p0578 A73-17140

Upper atmosphere thermodynamic and circulation characteristics for high altitude aircraft flights, including geomagnetic disturbance factors 07 p0847 A73-19298

Parawing-drag chute system operation on wind shear energy to maintain payload flight altitude 11 p1305 A73-25787

Analytical estimates of the accuracy of spacecraft autonomous navigation based on measurements of flight altitude and zenith-distance inertial-space reference point. 12 p1523 A73-27647

M-15 agricultural turbojet aircraft design for slow low level flight, tabulating dimensions, weights and performance data 13 p1568 A73-28026

Pilot operation practices for helicopter noise level reduction, with emphasis on flight altitude increase and routing over noise insensitive areas 17 p2099 A73-34442

Icing conditions of modern transport aircraft according to cruise flight data 17 p2100 A73-34545

Encoding altimeter for coding, transmitting and displaying flight altitude information to air traffic controllers [SAE PAPER 730301] 17 p2167 A73-34663

Laser measurement of high-altitude aircraft emissions. [AIAA PAPER 73-704] 18 p2315 A73-36253

Cosmic rays airborne dosimetry from Concorde aircraft, noting passenger and crew radiobiological hazards at supersonic flight altitudes 18 p2348 A73-36908

Air transportation economic efficiency as function of fuel consumption, cruising flight speed, altitude range and load factor/payload/ 19 p2506 A73-38118

FLIGHT CHARACTERISTICS

Short haul twin jet passenger aircraft Iak-40 for small airfields, noting flight characteristics and cost analysis 03 p0249 A73-13070

Long-duration flight performance of medium large unpressurized stratospheric balloons. 04 p0406 A73-15099

Flight evaluation of a quartz-fiberfrax heat shield. 05 p0641 A73-17209

Recent advances and applications in the prediction of pilot acceptance of aircraft flying qualities. 07 p0777 A73-20586

Test pilots role in aircraft flying qualities evaluation, discussing spin and longitudinal stability testing 09 p1031 A73-22181

Flight research to develop airworthiness standards for civil aircraft. 09 p1031 A73-22184

Air battle fighter aircraft design, discussing required performance characteristics in terms of lethality, maneuverability, range, visibility, handling qualities, sortie rate, reparability and fire control 09 p1031 A73-22197

Study of the influence of asymmetries on the flight behaviour of a sounding rocket. [AIAA PAPER 73-283] 09 p1155 A73-23203

Aerodyne flight vehicle testing for hover flight characteristics during remote control by radio with pilot commands, noting reliability and attitude control 13 p1569 A73-28785

Aerodyne unmanned wingless reconnaissance aircraft, covering hovering capacity, internal flow duct for conventional flight, flight test results and stability characteristics 17 p2098 A73-34255

Russian book - Aerodynamics and flight dynamics of turbojet aircraft / 2nd revised and enlarged ed./ 17 p2104 A73-34900

A frequency response approach to flying qualities criteria and flight control system design. [AHS PREPRINT 740] 17 p2105 A73-35073

The C-401, a STOL transport for many applications 17 p2107 A73-35666

Teledetection experiments using balloons 17 p2176 A73-35815

Pulsejet engines operational characteristics compared to turbojet engines, noting flight speed limit due to interaction between unsteady gas flow and combustion process 18 p2342 A73-36063

- Space shuttle orbiter and subsystem design, discussing crew cabin, payload accommodations, flight characteristics and aerothermodynamics [AIAA PAPER 73-604] 18 p2358 A73-36085
- An in-flight investigation of the influence of flying qualities on precision weapons delivery. [AIAA PAPER 73-783] 19 p2378 A73-37453
- NAS enroute automated flight and radar data processing, describing communication facilities, computer complex, software, data entry, display function and ATC personnel interface 19 p2453 A73-38464
- Effects of certain flight parameters and of certain structural parameters on helicopter main-rotor blade flutter 21 p2635 A73-41581
- Program plan to develop airworthiness standards for STOL aircraft. 24 p3056 A73-44994
- FLIGHT CLOTHING**
- Laundrying in space - A summary of recent developments. [ASME PAPER 73-ENAS-43] 19 p2401 A73-37990
- FLIGHT CONDITIONS**
- Meteorological effects on SST operations during various flight phases, considering ATC and communications aspects 01 p0074 A73-10348
- Functional state alteration of the visual analyzer in pilots 06 p0659 A73-18257
- Nonlinear programing in design of control systems with specified handling qualities. 07 p0777 A73-20588
- Statistical turbulence model of meteorological and topographical aircraft flight conditions for low altitude critical air turbulence /LO-LOCAT/ environment 13 p1569 A73-28831
- Some results of studies of the boundary atmospheric layer and AN-2 aircraft flight conditions in a forest fire area 13 p1655 A73-29192
- PB-75 flight guidance system for subsonic commercial transport aircraft operation under Category IIIA conditions, describing cruise and ILS operation 15 p1911 A73-32500
- Relation between turbulence in a clear sky and the evolution of the baric field 17 p2204 A73-34543
- Some characteristics of pilot's performance under complicated flight conditions. 18 p2285 A73-36921
- Transport aircraft external operational environment factors, discussing navigation, ATC, airspace, flight and pilot workload conditions 19 p2450 A73-37727
- Flight-mechanics analysis of various flight conditions of conventional aircraft. VIII/1 - Mechanical foundations: Kinematic equations of motion of a rigid body 19 p2387 A73-38123
- FLIGHT CONTROL**
- NT AUTOMATIC FLIGHT CONTROL
- NT AUTOMATIC LANDING CONTROL
- NT FLY BY WIRE CONTROL
- NT POINTING CONTROL SYSTEMS
- NT THRUST VECTOR CONTROL
- A complex approach to flight vehicle control system designs 01 p0074 A73-10673
- Reentry trajectory optimization at superorbital velocities by aerodynamic lift control, using Pontryagin maximum principle 01 p0105 A73-11127
- Ground control facilities and organization of Helios space probe mission and flight operations system based on U.S.-German cooperation 03 p0381 A73-13297
- Trends in helicopter guidance and control systems with bad weather capability. 03 p0340 A73-13921
- Fiberglass reinforced composite material application to light weight ballistic damage tolerant military helicopter flight control components previously vulnerable to small arms fire 04 p0452 A73-14722
- Hydraulic and flight control system for Space Shuttle Orbiter. [SAE PAPER 720838] 05 p0537 A73-16630
- Optimal flight control system design for aircraft with large flight envelopes, using optimal control theory with limited measurement feedback [AIAA PAPER 73-159] 05 p0535 A73-16906
- A statistical analysis of pilot control during a simulation of STOL landing approaches. [AIAA PAPER 73-182] 05 p0536 A73-16922
- Flight control techniques for advanced commercial transports. [AIAA PAPER 73-30] 06 p0647 A73-17618
- Optimal 3-dimensional minimum time turns for an aircraft. 06 p0648 A73-18377
- Airships design, constructional and operational characteristics, discussing aerodynamics, flight control, performance and trim 06 p0648 A73-18510
- Flight vehicle equations of motion with variable information, noting flight control algorithm for random variable with given probability 07 p0849 A73-20077
- A flight control system for STOL aircraft. 07 p0777 A73-20171
- F-15 air superiority fighter aircraft flight testing, describing air inlet, flight control, landing gear, flaps, speed brake and cockpit layout 09 p1030 A73-22178
- F-15 fighter aircraft development, discussing design and functional features of power plant, flight control system, landing gear, flaps, speed brakes and cockpit 09 p1031 A73-22198
- Comparison of conventional flight control systems with a modern integrated flight control system 10 p1175 A73-23762
- Ballistic-tolerant helicopter flight control components from plastic composite materials. 10 p1237 A73-23964
- International Federation of Automatic Control, World Congress, 5th, Paris, France, June 12-17, 1972, Proceedings. Part 2 - Transportation, aeronautics and space, ship automation, and control components. Part 3 - Ecology and systems engineering; Large scale, sensitivity, optimization and adaptation theory. Part 4 - Education, feedback, regulators, linear and nonlinear systems; Identification, differential games, discrete and stochastic systems. 10 p1198 A73-24001
- Dynamics of variable sweep wing aircraft in the course of changing geometry. 10 p1175 A73-24012
- Parallel-redundant flight control systems, discussing sensor bias and combined control computer input effects on controllability and steady state modal response 11 p1342 A73-25783
- Hydraulic powered integrated actuator package /IAP/ for V/STOL aircraft flight control, noting advantages in system weight, mechanical complexity and power loss reduction 11 p1313 A73-26271
- Advanced flight control systems - Power-by-wire and fly-by-wire. 11 p1306 A73-26272
- Stability of symmetric flight vehicles in oblique flow 12 p1548 A73-27076
- Controlling the angular motions of a flight vehicle with the aid of flywheels 12 p1522 A73-27083
- Practical quadratic optimal control for systems with large parameter variations. 12 p1483 A73-27166
- Analytical design of manual control systems for flight bodies 12 p1549 A73-27896
- Electronic differentiator for aircraft flight data on-board calculation in performance gliding, discussing compensation method and vertical air velocity measuring instrument advantage 13 p1569 A73-28556
- Computerized adaptive flight control for helicopter dynamic systems based on identification and optimization methods 13 p1569 A73-28829
- Curved landing approaches under visual and instrument flight conditions, investigating steep glide slope display configurations and flight control modes 13 p1569 A73-28901
- Modelling and identification theory - A flight control application. 14 p1739 A73-30777
- Pilot-electronics-control surfaces as feedback loop for aircraft flight control, discussing instruments, pilot training and aircraft flying qualities 15 p1830 A73-32472
- Commercial aircraft flight control instrumentation for safe and efficient flight path management, emphasizing aircrew work load relief under stressful air traffic conditions 15 p1830 A73-32473
- Aircraft integrated data systems /AIDS/ utilization for airlines operational flight control and economic exploitation enhancement, discussing aircraft accident investigation, maintenance, navigability, etc 15 p1831 A73-32496
- Head-up displays for flight control information on velocity vector, angle of attack, glide path slope and ground reference data, considering VFR and IFR conditions 15 p1831 A73-32507
- Aircraft flight control head-up display system design, equipment installation particulars, performance tests and merits evaluation 15 p1831 A73-32508
- Technology developments effect on jet aircraft design, discussing flight controls, engine noise suppression, supercritical aerodynamics and composite structures 16 p1968 A73-33188
- Book - Flight dynamics of rigid and elastic airplanes. Parts 1 & 2. 17 p2099 A73-34451
- Flight control problems during STOL landing approaches, considering navigation aids, pilot work load and flight safety 17 p2207 A73-34483
- Terminal and flight control navigation guidance systems for restricted and short takeoff and landing aircraft air traffic and approach techniques [RAE-TM-AVIONICS-135/BLEU/] 17 p2100 A73-34490
- Flight-path control device for generating curvilinear flight path profiles using microwave landing systems [DGLR PAPER 73-016] 17 p2208 A73-34492
- Problems concerning the implementation of an integrated flight control system, giving particular attention to curved flight path profiles [DGLR PAPER 73-030] 17 p2208 A73-34498
- High reliability solid state force sensors for flight control systems. 17 p2165 A73-34603
- Development of a low-cost flight director system for general aviation. [SAE PAPER 730331] 17 p2167 A73-34684
- V/STOL aircraft pilot-in-loop flight control/display system to overcome pilot limitations with performance and decision making flexibility enhancement [AHS PREPRINT 722] 17 p2105 A73-35063
- Low cost manufacturing methods for highly reliable ballistic-tolerant composite helicopter flight control components. [AHS PREPRINT 754] 17 p2180 A73-35082
- Aerospace multiprocessor for A-7D aircraft digital fly by wire flight control, discussing design requirements, software development and reliability 17 p2107 A73-35223
- Digital flight control systems data sampling rate selection effects on intersample ripple, spectral folding and distortion and system bandwidth 17 p2138 A73-35224
- Station Data Acquisition and Control System. 17 p2147 A73-35301
- Analytical design of aircraft manual control systems. 18 p2267 A73-36601
- A parameter optimisation technique applied to the design of flight control systems. 19 p2378 A73-37409
- Compatibility of maneuver load control and relaxed static stability. [AIAA PAPER 73-791] 19 p2379 A73-37458
- Flight deck management and pilot operation priorities in high pressure and emergency situations, using integrated aircraft-environment mental model 19 p2384 A73-37731
- Simplification of navigation and flight control systems without compromising integrity. 19 p2452 A73-37826
- On the use of singular perturbation methods in the solution of variational problems. 19 p2386 A73-38038
- Modern control techniques applied to energy conservation flight control systems. 19 p2392 A73-38415
- Digital flight control design using implicit model following. [AIAA PAPER 73-844] 20 p2508 A73-38783
- The application of digital filters using observers to the design of an ICBM flight control system. [AIAA PAPER 73-845] 20 p2541 A73-38784
- Redundant system design for advanced digital flight control. [AIAA PAPER 73-846] 20 p2585 A73-38785
- Digital control system development for the Delta launch vehicle. [AIAA PAPER 73-847] 20 p2613 A73-38786
- 'Bank-to-turn steering' for highly maneuverable missiles. [AIAA PAPER 73-860] 20 p2586 A73-38798
- A practical load relief control system designed with modern control techniques. [AIAA PAPER 73-863] 20 p2508 A73-38801
- STOL passenger aircraft ride smoothing control system based on vertical and lateral acceleration limits for design flight condition of 7 fps rms gust velocity [AIAA PAPER 73-885] 20 p2509 A73-38821
- An aerodynamic entry control technique utilizing the yaw flap concept. [AIAA PAPER 73-888] 20 p2588 A73-38824
- Choice of optimal parameters for flight-vehicle control systems in the presence of random disturbances. 20 p2590 A73-38991
- Integrated hydraulic flight control actuator packages replacing mechanical linkages for aerodynamic surface control during V/STOL operation 20 p2510 A73-39015
- A Lie algebra of visual piloting 20 p2590 A73-39038
- Airframe/propulsion system interactions - An important factor in supersonic aircraft flight control. [AIAA PAPER 73-831] 21 p2634 A73-40501
- Flight simulation requirement in artificial stabilizer design for VTOL aircraft flight control system, noting agreement with flight tests 22 p2838 A73-41751

A study of a fluidic open loop damping flight stability augmentation system.

23 p2941 A73-43396

On problems of flight over an extended angle-of-attack range.

24 p3056 A73-44692

FLIGHT CREWS

Fatigue in flight personnel during long flights

02 p0137 A73-12153

Psychological and medical viewpoint for hijacker handling, discussing air crew training program [AD-757130]

02 p0138 A73-12564

Radiation problems of supersonic flight - The operators' viewpoint.

05 p0542 A73-16624

Renal lithiasis among civil operating aircrew

08 p0931 A73-21536

Renal lithiasis among military operating aircrew

08 p0931 A73-21537

Proteinuria and civil aviation aircrew

08 p0931 A73-21538

Proteinuria and military aircrew

08 p0931 A73-21539

Civil aircraft commander and crew duties and rights in air piracy cases, discussing international agreements and national legal provisions

10 p1297 A73-23683

Pilot incapacitation as cause for aircraft operational risks, discussing flight crews education for emergency situations handling

10 p1185 A73-24717

Neurological fatigue-indices of flight crews of long-range and military transport aviation

11 p1321 A73-25040

Incidence and severity of altitude decompression sickness in Navy hospital corpsmen.

13 p1576 A73-28511

Relative merit of the disc-gap-band parachute applied to individual aircrew member escape. [AIAA PAPER 73-483]

15 p1829 A73-31465

A comparison and analysis of head sizes of Navy aircrew to the standard anthropometric data.

16 p1974 A73-32656

U-2 and SR-71 aircrews physiological training for high altitude and supersonic flight hazards, discussing pressure suits, ejection seats, parachutes and survival and life support equipment

16 p1974 A73-32657

Time compressed training program for DC-10 flight crews, emphasizing operational proficiency through specific behavioral objectives approach

16 p1966 A73-32663

Ventilated wet suit for naval aircrews protection against water exposure in aircraft accidents, describing neoprene foam and nylon liner construction with air ventilation

16 p1974 A73-32672

Informative parameters of the psychophysiological state of flight personnel when working with indicators

17 p2114 A73-34237

Physical energy expenditure in long-haul cabin crew.

18 p2283 A73-36793

The significance of retinal pathology in ageing aircrew.

18 p2285 A73-36925

Current aspects of the cochlear function in members of flight crews

18 p2286 A73-36940

Digestive hemorrhages in aircrew - Individual and collective safety

18 p2280 A73-36952

Psychophysiological characteristic of the activity of military-transport-aviation flight crews during low-altitude flights

19 p2397 A73-37196

Sleep loss in air cabin crew.

20 p2517 A73-39109

Crew discipline factors in aircraft accident statistics, linking pilot-related accidents to crew carelessness, flight regulation infractions and unfamiliarity with flight conditions

20 p2509 A73-39216

Airline flight crew management and coordination procedures, outlining self-discipline philosophies and criteria, flight training and simulation, and performance records

20 p2509 A73-39217

Physiologic cost of prolonged double-crew flights in C-5 aircraft.

21 p2644 A73-41152

Developments as regards maximum visual acuity with age among cockpit crew members.

21 p2645 A73-41164

Conventional and high frequency hearing of naval aircrewmembers as a function of noise exposure.

23 p2949 A73-43500

FLIGHT FATIGUE

Fatigue in flight personnel during long flights

02 p0137 A73-12153

Neurological fatigue-indices of flight crews of long-range and military transport aviation

11 p1321 A73-25040

The effects of fatigue on health and flight safety.

17 p2113 A73-34080

Lone woman pilot sleep patterns and sleep disruptions on global flight across time zones

17 p2115 A73-34745

FLIGHT FITNESS

Carpenter reconstructive valvuloplasty technique of mitral valve insertion from viewpoint of pilots return to flying duties

02 p0138 A73-12157

Renal lithiasis among military operating aircrew

08 p0931 A73-21537

Proteinuria and military aircrew

08 p0931 A73-21539

Antidiabetic medications and aircrew

08 p0935 A73-21541

USAF WAVR file of epidemiologic data on medically waived flying personnel, describing computerized updating system

09 p1039 A73-22539

The role of vestibulometry in medical evaluation of flight personnel

10 p1183 A73-23821

Photostimulation significance in electroencephalographic examinations of pilots and aviation school applicants

12 p1465 A73-27717

Naval aviator training program dropouts identification in terms of physiological, safety, security, social, self-esteem and self-actualization needs

14 p1722 A73-30513

Detection of atherosclerosis in examinations of flight personnel

18 p2284 A73-36913

Surveillance of the vertebral column in pilots who have undergone an ejection

18 p2284 A73-36914

Clinical psychology diagnostic methods in military aviation medicine, considering neurotic symptoms and psychosomatic disorders in flight fitness examinations

22 p2817 A73-43129

Evaluation of the physical conditions of individual airmen

23 p2949 A73-43790

FLIGHT HAZARDS

Liability under international law for damages caused by space objects

01 p0124 A73-10567

Prediction of flight safety hazards from drug induced performance decrements with alcohol as reference substance.

03 p0269 A73-14158

Grand Tour missions to the outer solar system with Saturn /Intermediate 20/.

06 p0750 A73-18024

The aircraft wake turbulence problem.

06 p0648 A73-18149

Contribution to the protection of flight vehicles against lightning effects

06 p0648 A73-18436

U-2 and SR-71 aircrews physiological training for high altitude and supersonic flight hazards, discussing pressure suits, ejection seats, parachutes and survival and life support equipment

16 p1974 A73-32657

Safety and survival in manned space laboratory, discussing experimental and environment hazard elimination

16 p2071 A73-32673

Lightning protection for aircraft canopy, discussing simulation tests, safety margins, side puncture, corona streamer and pilot physiological reactions

16 p1968 A73-33036

Ocular hazard from viewing the sun unprotected and through various windows and filters.

21 p2698 A73-40143

Estimation of the biological danger of the very high energy component of space radiation.

22 p2805 A73-42180

FLIGHT INSTRUMENTS

NT APPROACH INDICATORS

NT ATTITUDE INDICATORS

NT AUTOMATIC PILOTS

NT FLIGHT TEST INSTRUMENTS

NT HORIZON SCANNERS

NT RADIO ALTIMETERS

Book - Aircraft Instruments: Principles and applications.

06 p0693 A73-18075

Basic specification research for the main instruments of light aircraft

07 p0825 A73-20248

Electronic integrated flight data displays for pilot workload reduction at takeoff, approach and landing, considering head-up and head-down and colored systems

15 p1831 A73-32506

Sabreliner Airborne Data Acquisition and Recording System (ADARS) for communication with flight observers to evaluate research missions

17 p2174 A73-35582

Internal operational environment effects on pilot errors in commercial aircraft flights in terms of man machine interface and flight deck design

19 p2384 A73-37728

FLIGHT LOAD RECORDERS

YF-12 aircraft flight loads measurement program with strain gage bridges in fuselage, fuel tanks, control surfaces and left wing

17 p2107 A73-35444

FLIGHT MECHANICS

Flight-mechanical analysis of various flight states of conventional aircraft. VII - Mechanical principles: Rigid-body dynamics

03 p0250 A73-13074

Russian book on celestial and space flight mechanics covering trajectory and orbit evolution problems, resonance effects, relative motion dynamics and mathematical treatment

09 p1146 A73-22350

Exact analytical solutions for orbits of bodies with atmospheric drag.

09 p1152 A73-23454

Remarks on the ISO international standards relating to 'Terms and Symbols for Flight Dynamics'

10 p1174 A73-23657

Flight-mechanics analysis of various flight conditions of conventional aircraft. VII - Mechanical foundations: Dynamic equations of motion of the translational motion of a rigid body

11 p1307 A73-26725

Astronautical coordinate systems definition and applications for flight mechanics problems involving earth curvature and motion effects

15 p1908 A73-32202

Book - Flight dynamics of rigid and elastic airplanes. Parts 1 & 2.

17 p2099 A73-34451

Flight mechanics problems associated with landing approaches using direct lift control, as exemplified by the HFB 320 Hansa aircraft

[DGLR PAPER 73-024]

17 p2100 A73-34496

Analysis of the use of an auxiliary wing on a helicopter

18 p2268 A73-37021

Flight-mechanics analysis of various flight conditions of conventional aircraft. VIII/1 - Mechanical foundations: Kinematic equations of motion of a rigid body

19 p2387 A73-38123

Dynamic programming application to extremal fields topological singularity in optimal control theory for flight vehicle with state variables satisfying initial conditions and ordinary differential equations

22 p2917 A73-43030

Russian book - Studies of spacecraft flight dynamics.

23 p3027 A73-43260

Certain algorithmic aspects of flight dynamics simulation on digital computers

23 p3038 A73-43262

FLIGHT OPTIMIZATION

Flight vehicle /FV/ control optimization taking into account control-function and phase-coordinate constraints

05 p0594 A73-16415

Optimal 3-dimensional minimum time turns for an aircraft.

06 p0648 A73-18377

Russian book - Mechanics of optimal spatial motion of flight vehicles in the atmosphere.

07 p0777 A73-20380

Space shuttle ascent-flyback trajectory optimization with in-flight inequality constraints based on accelerated gradient parameters determination including attitude control angles

10 p1276 A73-24002

Airport computerized departure control for check-in, load control, cargo and catering operations, discussing load optimization and passenger acceptance control /LOPAC/ system

11 p1343 A73-25210

Accelerating search-variable metric algorithm combination for space shuttle atmospheric flight optimization, comparing with cubic fit-golden section method

13 p1650 A73-28825

The sensitivity of optimal flight paths to variations in aircraft and atmospheric parameters.

19 p2386 A73-38051

Horizontal aircraft maneuver strategy for maximum miss distance and minimum course deviation, examining filtering techniques, collision avoidance system and signal error analysis

21 p2734 A73-40032

A new approach to gust alleviation of a flexible aircraft using an open loop device [ONERA, TP NO. 1236]

22 p2799 A73-42219

Integrals for optimal flight over a spherical earth.

22 p2884 A73-42561

Optimal landing flare control of aircrafts with sensitivity consideration.

23 p2940 A73-43284

FLIGHT PATHS

NT GLIDE PATHS

Sonic boom avoidance by flight path maneuvers, investigating shock front development in curved flight

02 p0130 A73-11856

Wind shear near the ground and aircraft operations.

03 p0337 A73-13702

- Application of the graphic flight path design program /FPDP/ for fast interactive trajectory design. [AIAA PAPER 73-113] 05 p0619 A73-16871
- Aircraft performance augmentation by energy management instruments or systems, considering energy/rate meter and algorithm for real time onboard flight path optimization [AIAA PAPER 73-228] 05 p0536 A73-16953
- Long-range energy-state maneuvers for minimum time to specified terminal conditions. [AIAA PAPER 73-229] 05 p0536 A73-16954
- Flight-path characteristics for few re-entry trajectories. 05 p0623 A73-17297
- Optimum flight paths of rocket powered vehicles for general thrust law. 06 p0756 A73-17742
- Dispersion of the direction of the angular momentum vector of sounding rocket payloads due to atmosphere exit and certain vehicle activities. [AIAA PAPER 73-293] 09 p1116 A73-23212
- Maximum range flight path during climb with specified fuel supply and variable lift coefficient, solving differential equations system by conjugate gradient procedure 10 p1175 A73-24542
- An optimal control approach to terminal area air traffic control. 11 p1394 A73-25786
- Determination of the turn start point coordinates for modern commercial aircraft 11 p1307 A73-26723
- Suprememory gradient-restoration algorithm in flight-path optimization problems 12 p1548 A73-27082
- Civil aircraft vertical plane navigation and guidance during climb and descent, discussing atmospheric, performance and passenger comfort constraints on flight path selection 13 p1656 A73-28075
- Pilot operation practices for helicopter noise level reduction, with emphasis on flight altitude increase and routing over noise insensitive areas 17 p2099 A73-34442
- Helicopter operations in London area, describing controlled airspace, helicopter routes and heliport approach and takeoff procedures 17 p2206 A73-34446
- Monitor display to indicate aircraft position relation to desired flight profile during automatically controlled steep landing approaches with curved segments 17 p2207 A73-34477
- Flight-path control device for generating curvilinear flight path profiles using microwave landing systems [DGLR PAPER 73-016] 17 p2208 A73-34492
- Problems concerning the implementation of an integrated flight control system, giving particular attention to curved flight path profiles [DGLR PAPER 73-030] 17 p2208 A73-34498
- The permissible scale of spatial averaging of geopotential values in the stratosphere where the impact of wind on the flight of a supersonic aircraft is taken into account 17 p2100 A73-34546
- Concorde aircraft introduction into airline network, discussing time gain over various routes, operating costs, passenger service, departure and arrival problems, maintenance, etc [SAE PAPER 73051] 17 p2102 A73-34699
- Accurate aircraft trajectory predictions applied to future en-route air traffic control. 18 p2335 A73-37041
- On the generation of accurate trajectory predictions for air traffic control purposes. 18 p2336 A73-37042
- The sensitivity of optimal flight paths to variations in aircraft and atmospheric parameters. 19 p2386 A73-38051
- Time, space, and energy management in the airways traffic control medium. 22 p2884 A73-42324
- ### FLIGHT PERFORMANCE
- #### U FLIGHT CHARACTERISTICS
- #### FLIGHT PLANS
- Collection and processing of data for the establishment of route charges. 07 p0796 A73-19182
- Air traffic control by programmed navigation. 07 p0849 A73-19349
- Flight planning and navigation for thermal-IR surveys. 07 p0849 A73-20019
- Translunar flight plan of Luna 21 probe, describing Lunokhod structure and lunar descent procedure 08 p1007 A73-20974
- Aircraft operations computerized simulation for commercial flight schedules evaluation and optimization, describing operational modeling and programming 10 p1203 A73-23685
- Automation of the print-out of strips of flight plans for air traffic control 15 p1847 A73-32441
- Air traffic control, discussing man machine systems, multipath with ILS, target indicator radars and flight progress strip preparation 17 p2206 A73-34086
- #### FLIGHT RECORDERS
- System for in-flight recording of the rotational speed of the turbine of a jet engine 07 p0828 A73-20546
- Pilot error evaluation in aircraft accidents, discussing human failure factors and flight and cockpit voice recorder evidence 17 p2115 A73-34748
- Engraved foil, photographic and EM flight recorders in aircraft accident investigations, discussing readout, processing and analysis 18 p2317 A73-36848
- #### FLIGHT RULES
- ##### NT INSTRUMENT FLIGHT RULES
- ##### NT VISUAL FLIGHT RULES
- Effects of noise curfew on airline operations. [AIAA PAPER 73-798] 19 p2379 A73-37461
- #### FLIGHT SAFETY
- Russian book on Il-18 aircraft practical aerodynamics covering aerodynamic characteristics, performance, controllability, stability and flight safety 04 p0406 A73-15968
- The role of the test pilot in evaluating auto landing systems. II. 09 p1115 A73-22183
- Human threats to air safety; Proceedings of the Twenty-fifth Annual International Air Safety Seminar, Washington, D.C., October 16-18, 1972. 10 p1176 A73-24707
- Airlines flight safety management, discussing visual systems simulator /VSS/ for Tristar systems environmental and cycling endurance ground tests 10 p1176 A73-24710
- Airfield requirements for flight safety enhancement, considering approach and takeoff path obstructions, runway conditioning, glide slope information and radio aids 10 p1203 A73-24713
- Aviation medicine assessment of environment effects on pilot responsiveness, task performance and flight safety predictability, considering temperature, oxygen, gravity, acceleration, pressure and stress effects 11 p1321 A73-25039
- A flight control simulator - A computer system for the training of flight control personnel 13 p1598 A73-29100
- External tracking, telemetry and concepts of free flight time, of safety corridor and of destruction time limit for ballistic missile flight tests safety 14 p1804 A73-30095
- Definition, philosophy, and development of safety interventions in flight at the Guiana Space Center 14 p1804 A73-30096
- The safety, the reliability, and redundancy in the automatic flight control system of the A300-B Airbus 15 p1830 A73-32459
- Commercial aircraft flight control instrumentation for safe and efficient flight path management, emphasizing aircrew work load relief under stressful air traffic conditions 15 p1830 A73-32473
- Study of the integrity of an equipment - Application to radio altimeters for category III landing 15 p1880 A73-32493
- Analysis of the reliability of airborne material in an airline company - Objectives and methods 15 p1831 A73-32495
- Meteorological satellites in the service of aeronautics 15 p1907 A73-32562
- Safety and survival in manned space laboratory, discussing experimental and environment hazard elimination 16 p2071 A73-32673
- Air piracy suppression measures adopted 23 September 1971 at Montreal international convention, discussing prevention and punishment provisions 16 p2087 A73-32972
- Data sample analysis of anomalous in-flight behavior incidents for spacecraft reliability covering incident causes and occurrence time, effects on mission and corrective actions 16 p2073 A73-33625
- Safety management of air to surface nuclear short range attack missile /SRAM/ at fabrication, testing and operation levels 16 p2073 A73-33640
- Outlook on safety; Proceedings of the Thirtieth Annual Technical Symposium, London, England, November 14-16, 1972. 17 p2097 A73-34076
- Man machine systems for flight safety, studying accidents, human factors in system design and implementation of personnel 17 p2113 A73-34078
- The effects of fatigue on health and flight safety. 17 p2113 A73-34080
- Aircraft performance relationship to safety margins improvement, discussing accelerate stop, approach control, airworthiness, landing and coordination 17 p2097 A73-34082
- Aircraft design for operational safety, discussing risk elimination, failure modes, maintenance analysis and fault diagnosis 17 p2098 A73-34083
- Low level wind shear and clear air turbulence effects on flight safety and aircraft accidents 17 p2098 A73-34084
- Safety in the accident prone flight phases of take-off, approach and landing. 17 p2098 A73-34085
- Information systems enabling pilots to report incidents involving safety, including human fallibility and system errors in construction, operation and regulation 17 p2256 A73-34087
- Flight control problems during STOL landing approaches, considering navigation aids, pilot work load and flight safety 17 p2207 A73-34483
- General aviation pilot operational profile study, discussing implications for airman certification standards, flight safety regulations and aircraft design [SAE PAPER 730334] 17 p2115 A73-34687
- Hypoglycemia in airline pilots. 18 p2278 A73-36790
- Behavioral stress response RE - Passenger briefings and emergency warning systems on commercial airlines. 18 p2285 A73-36922
- Sudden incapacitation in flight - 1 Jan. 1966-30 Nov. 1971. 20 p2512 A73-39112
- Safe flying, skilled personnel and aircraft maintenance assurance via safety equipment, initial and recurrent training, protective clothing and shelter from inclement weather, maintenance scheduling, etc 20 p2518 A73-39212
- Runway condition effects on landing safety, discussing surface friction, approach control, skidding, directional control, water and ice conditions, tires and brakes 20 p2509 A73-39220
- Eye function and the illumination of instrument dials in aircraft 22 p2817 A73-43133
- Aviation law development regarding ATC influence on legal liability for aircraft accidents, analyzing controller error influence on liability determination 24 p3159 A73-45444
- #### FLIGHT SIMULATION
- Comparative simulator studies regarding a contact-analog channel display and conventional instrumentations [DGLR PAPER 72-100] 02 p0150 A73-11680
- An altitude test facility for large turbofan engines. [AIAA PAPER 72-1069] 03 p0287 A73-13396
- Variable stability simulation techniques for non-linear rate-dependent systems. 03 p0285 A73-13521
- Interactive real time simulation for scheduling and monitoring of STOL aircraft in the terminal area. [AIAA PAPER 73-163] 05 p0535 A73-16909
- A statistical analysis of pilot control during a simulation of STOL landing approaches. [AIAA PAPER 73-182] 05 p0536 A73-16922
- Six degree of freedom guided sounding rocket flight simulations and trajectory program, discussing financial and technical feasibility [AIAA PAPER 73-299] 09 p1117 A73-23218
- Evaluation of Intelsat IV nickel-cadmium cells. 13 p1572 A73-29582
- Thrust measurement bench for afterbody and hot and cold jet nozzle simulated tests in Sigma 4 wind tunnel 16 p1993 A73-32820
- Flight Simulation Symposium, 2nd, London, England, May 16, 17, 1973, Proceedings. 16 p1995 A73-33201
- Specific Behavior Objective approach to airline flight simulation, featuring duplicate training elimination and education time reduction 16 p1995 A73-33202
- Airline flight simulation program, examining visual system capacity for replacement of in-flight training with pilot learning transfer estimation and simulation effectiveness appraisal 16 p1995 A73-33204
- Flight simulation visual image innovations, including closed circuit television, motion pictures and computer generated imagery with wide angle presentation and day/night realizations 16 p1995 A73-33205
- VTOL and STOL projects flight simulation trials for autostabilization, head-up displays and flight controls effectiveness in handling qualities improvement and pilot workload reduction 16 p1996 A73-33209
- Digital V/STOL flight simulation test procedures for aircraft navigation, guidance and control, detailing dis-

- play device panels, flight path simulation and software configuration 17 p2210 A73-35853
- Initial development of an ablative leading edge for the Space Shuttle orbiter. [AIAA PAPER 73-739] 18 p2369 A73-36356
- Summer Computer Simulation Conference, Montreal, Canada, July 17-19, 1973, Proceedings. Volumes 1 & 2. 18 p2291 A73-36826
- Skylab Mission Simulator Facility software, describing electric power systems, solar measurements, display panels, earth resource sensors and spacecraft environmental control 18 p2296 A73-36832
- A study of Halon 1301 /CBrF₃/ toxicity under simulated flight conditions. 18 p2285 A73-36930
- Simulation concepts for a full-sized Shuttle manipulator system. 19 p2416 A73-37310
- A digital computer flight simulation of an ACLS vehicle. 19 p2383 A73-37705
- Fixed base simulation of variable stability T-33 handling qualities, considering pilot performance in pitch tracking during atmospheric turbulence 19 p2386 A73-38072
- Physiological cost in 36- and 48-hour simulated flights. 20 p2512 A73-39101
- An aerodynamic test facility with free molecular flow and high stagnation temperature 20 p2545 A73-39615
- The oculometer - A new approach to flight management research. [AIAA PAPER 73-914] 21 p2702 A73-40862
- The Large Amplitude Multi-Mode Aerospace Research /LAMAR/ Simulator. [AIAA PAPER 73-922] 21 p2673 A73-40870
- A visual display system approach for an advanced spaceflight simulator. [AIAA PAPER 73-923] 21 p2673 A73-40871
- Optical mosaics for large field visual simulation display systems. [AIAA PAPER 73-926] 21 p2673 A73-40873
- Visual cues and six degree of freedom motion flight simulation for F-4 aircraft engine maneuvering performance, discussing pilot evaluations [AIAA PAPER 73-934] 21 p2674 A73-40880
- Flight simulation requirement in artificial stabilizer design for VTOL aircraft flight control system, noting agreement with flight tests 22 p2838 A73-41751
- An engineering flight simulation visual display system. [AIAA PAPER 73-924] 22 p2838 A73-41970
- Certain algorithmic aspects of flight dynamics simulation on digital computers 23 p3038 A73-43262
- FLIGHT SIMULATORS**
- NT COCKPIT SIMULATORS**
- Image transformation in visual condition simulators of aircraft training equipment 01 p0029 A73-10666
- Flight simulator development in parallel with aircraft flight test A case study of the American Airlines DC-10 program. [SAE PAPER 720858] 05 p0562 A73-16664
- A proposed design for the construction of a VTOL simulator 08 p0952 A73-21249
- Experimental approach for utilization of cathode ray tube piloting instruments 15 p1831 A73-32509
- Airline flight simulator programs for aircraft type conversion training, outlining flight instructor training, certification and instructional aids 16 p1995 A73-33203
- Avionics and human factors in flight simulator economics, interrelating aircraft design to simulation system 16 p1995 A73-33206
- Repairable electronic system random failure and repair time related to simulator time available for operation, analyzing MTBF and repair rates 16 p1996 A73-33207
- The simulator industry and its contribution to military training requirements. 16 p1996 A73-33208
- A flight research program to define VTOL visual simulator requirements. 16 p1996 A73-33210
- Royal Aircraft Establishment Aerodynamics Flight Division flight simulators for V/STOL and helicopters, emphasizing handling, aircraft mathematical models and cockpit simulation 16 p1996 A73-33211
- BOAC computer aided flight simulators, detailing simulator systems history, Boeing 747 training adaptation, and simulation types 16 p1996 A73-33212
- Flight simulator evaluation of control moment usage and requirements for V/STOL aircraft. [AHS PREPRINT 743] 17 p2147 A73-35076

- Experimental developments in V/STOL wind tunnel testing at the National Aeronautical Establishment. 18 p2265 A73-36774
- Computerized design for moving-base three man aircraft flight simulator servocontrol, considering disturbance torques, damping ratios, natural frequencies, load acceleration and smoothness 18 p2296 A73-36833
- Aircraft flight simulator with coordinated adaptive filter derived from continuous steepest descent method 18 p2295 A73-36836
- Ambient temperature rise effects on pilot performance in a flight simulator 18 p2287 A73-36948
- Cockpit mock-ups and simulator design for pilot workload assessment for Concorde program and V/STOL research 19 p2384 A73-37735
- Corporate aircraft design and operational problems, including supercritical wing and wasp-waist body design, airport private/airline interfaces, noise criteria, flight simulation and ATC 20 p2509 A73-39218
- A short description of the NAE airborne simulator feel system. 21 p2672 A73-40854
- A compound wide angle color visual display system and a high resolution, high sensitivity close circuit color television camera developed for wide angle color visual systems. [AIAA PAPER 73-925] 21 p2702 A73-40872
- An approach to computer image generator for visual simulation. [AIAA PAPER 73-928] 21 p2673 A73-40875
- Washout circuit design for multi-degrees-of-freedom moving base simulators. [AIAA PAPER 73-929] 21 p2674 A73-40876
- Motion cue method featuring coordinated adaptive washout circuitry in flight simulator using nonlinear filter, discussing heave, yaw and six degrees of freedom application [AIAA PAPER 73-930] 21 p2674 A73-40877
- Human motion perception in motion drive logic design for flight simulation discussing feedback control, angular velocity and degrees of freedom [AIAA PAPER 73-931] 21 p2674 A73-40878
- SAFE - Six axis frequency evaluation of a motion simulator. [AIAA PAPER 73-932] 21 p2674 A73-40879
- Drive logic computation for variable stability aircraft in-flight simulators with six independent controllers providing dynamic motion and ground, crosswind and special effects [AIAA PAPER 73-933] 22 p2799 A73-41971
- Simulator performance validation and improvement through recorded data. [AIAA PAPER 73-938] 22 p2838 A73-41972
- Program plan to develop airworthiness standards for STOL aircraft. 24 p3056 A73-44994
- Total In-Flight Simulator for X-22A aircraft based on variable stability-and-control system concept for reliability design 24 p3057 A73-45153
- FLIGHT STABILITY TESTS**
- Helicopter automatic flight control system design, testing and development, noting stability and control augmentation and attitude retention units 13 p1656 A73-28903
- Separate surfaces for automatic flight controls. [SAE PAPER 730304] 17 p2101 A73-34665
- FLIGHT STRESS**
- Effect of hydrochlorothiazide on +Gz tolerance in normotensives. 03 p0269 A73-14159
- Aviation medicine assessment of environment effects on pilot responsiveness, task performance and flight safety predictability, considering temperature, oxygen, gravity, acceleration, pressure and stress effects 11 p1321 A73-25039
- Further sleep problems in airline pilots on world-wide schedules. 18 p2283 A73-36792
- Physiologic cost of prolonged double-crew flights in C-5 aircraft. 21 p2644 A73-41152
- FLIGHT STRESS [BIOLOGY]**
- NT SPACE FLIGHT STRESS**
- Favorable effect of flight on pilots exhibiting degenerative arteriopathy of the lower limbs 02 p0137 A73-12151
- Fatigue in flight personnel during long flights 02 p0137 A73-12153
- Aerodynamic pumping-caused spinal fractures in two pilots during high speed flight 02 p0137 A73-12154
- Reactions of the cardiovascular system of pilots with atherosclerosis symptoms under professional activity conditions 06 p0657 A73-17689
- The biodynamic aspects of low altitude, high speed flight. 06 p0659 A73-18471

- Russian book - Tissue, oxygen in the presence of extremal flight factors. 07 p0780 A73-19425
- Physiological time zone entrainment and stressor effects during prolonged C-141 transmeridian flights, using endocrine-metabolic indices in urine specimens. 13 p1574 A73-28283
- Effects of flying and of time changes on menstrual cycle length and on performance in airline stewardesses. 13 p1576 A73-28509
- Towards an objective assessment of cockpit workload. I - Physiological variables during different flight phases. 14 p1718 A73-30515
- Commercial aircraft flight control instrumentation for safe and efficient flight path management, emphasizing aircrew work load relief under stressful air traffic conditions 15 p1830 A73-32473
- Military aircraft pilot in-flight consciousness loss etiologies, discussing rapid decompression, hypoxia, dysbarism, seizure, improper maneuver, vasovagal syncope, acceleration sensitivity, etc 17 p2115 A73-34747
- The role of the sympathetic section of the vegetative nervous system in the training of the organism for the influence of statokinetic irritants. 18 p2279 A73-36903
- Study of Indian naval aircrew experiences and psychic factors in disorientation. 18 p2285 A73-36919
- Psychophysiological characteristic of the activity of military-transport-aviation flight crews during low-altitude flights 19 p2397 A73-37196
- Pulmonary volume, respiration rate and alveolar air carbon dioxide content measurements in pilots during flight, noting hyperventilation occurrence 19 p2392 A73-37197
- Pilot workload immediate, duty day and long term period evaluation from heart rate, subjective, psychological, biochemical stress and sleep pattern measurements 19 p2398 A73-37734
- Physiological cost in 36- and 48-hour simulated flights. 20 p2512 A73-39101
- Studies of pilot performance. III - Validation of objective performance measures for rotary-wing aircraft. 21 p2644 A73-41154
- Stress and strain in student helicopter pilots. 21 p2644 A73-41155
- Individual personality variability difficulties in measurement of human psychophysiological reactions to flight stress, emphasizing psychological interview and evaluation methods 22 p2817 A73-43130
- FLIGHT SURGEONS**
- Medical diagnosis of pilot performance disturbances from viewpoint of flight surgeon responsibilities 15 p1837 A73-31171
- FLIGHT TEST INSTRUMENTS**
- Prefabricated strain gage bridge instrumentation for flight testing under time and environment installation restrictions, including tail vibration, wing load and tail boom tests 09 p1083 A73-22506
- Airborne flight-test strain gage instrumentation from installation, calibration and data recording and reduction standpoint, discussing ground and airborne minicomputer use 17 p2148 A73-35442
- FLIGHT TEST VEHICLES**
- A flight research program to define VTOL visual simulator requirements. 16 p1996 A73-33210
- FLIGHT TESTS**
- NT FLIGHT STABILITY TESTS**
- A French collision-avoidance system of time-frequency type - Critical analysis of test results [ONERA, TP NO. 1086] 01 p0074 A73-10227
- Flight test of narrow band television system. 01 p0052 A73-11169
- Reinforced all-plastic quadrant molded missile airframes design, fabrication and flight testing 03 p0333 A73-13052
- Diagnostic instrumentation on J-85 engines for gas path and vibration analysis, noting flight test program and installation of remote pressure transducers and signal conditioners [AIAA PAPER 72-1081] 03 p0308 A73-13404
- NASA technology program for auxiliary and primary electric propulsion systems, noting flight tests and solar arrays [AIAA PAPER 72-1127] 03 p0355 A73-13437
- Remote CAT detection by IR scanning of atmospheric temperature profiles, discussing flight tests design and results 04 p0450 A73-15767
- Flight and wind tunnel investigation of the effects of Reynolds number on installed boattail drag at subsonic speeds. [AIAA PAPER 73-139] 05 p0530 A73-16888

Functional state alteration of the visual analyser in pilots 06 p0659 A73-18257

Effect of low heat-shield ablation rates on flight test turbulent base pressure. 07 p0920 A73-19975

Russian book - Methods and equipment for in-flight aircraft strength tests. 07 p0777 A73-20376

1972 report to the aerospace profession; Proceedings of the Sixteenth Symposium, Beverly Hills, Calif., September 28-30, 1972. 09 p1030 A73-22176

F-15 air superiority fighter aircraft flight testing, describing air inlet, flight control, landing gear, flaps, speed brake and cockpit layout 09 p1030 A73-22178

F-8 digital fly by wire control system development and flight testing, using Apollo lunar guidance computer and inertial measurement unit for angular rates and accelerations 09 p1030 A73-22180

Test pilots role in aircraft flying qualities evaluation, discussing spin and longitudinal stability testing 09 p1031 A73-22181

The role of the test pilot in evaluating auto landing systems. I. 09 p1115 A73-22182

The role of the test pilot in evaluating auto landing systems. II. 09 p1115 A73-22183

Flight research to develop airworthiness standards for civil aircraft. 09 p1031 A73-22184

Arava STOL turboprop passenger aircraft flutter flight test program, describing measurement instrumentation and data recording system 09 p1031 A73-22185

Generator of rectilinear vibrations for the study of structures at low frequency [ONERA, TP NO. 1185] 09 p1084 A73-22713

A rocket system for hypersonic, high Reynolds number aerothermodynamic research. [AIAA PAPER 73-304] 09 p1156 A73-23223

Missile and spacecraft radio telemetry data acquisition site polarization diversity signal combiner transient response requirements, comparing bench test with flight test data 09 p1057 A73-23414

Certain results of flight tests of a model ion thruster employing contact ionization of cesium on tungsten 10 p1262 A73-23892

A method of measuring the thrust, the polar, and the performance of an aircraft on the basis of flight tests 10 p1175 A73-24494

The SNAP-19 radioisotopic thermoelectric generator experiment - Flight performance on the Nimbus III observatory. 11 p1396 A73-26037

Turbulent heat transfer to a fin leading edge - Flight test results. 11 p1303 A73-26405

Flight test correlation technique for turbulent base heat transfer with low ablation. 11 p1453 A73-26671

European airbus A300B aircraft flight tests and on-board instrumentation in certification program, illustrating desk layout, control and display panels 13 p1568 A73-28159

Coaxial anode for background suppression in X-ray proportional counters. 13 p1612 A73-28367

Aerodyne flight vehicle testing for hover flight characteristics during remote control by radio with pilot commands, noting reliability and attitude control 13 p1569 A73-28785

Flight tests of approach path angles and airspeed effects on landing of spoiler equipped light aircraft 13 p1569 A73-28830

Simulated flight tests of a digitally autopiloted STOL-craft on a curved approach with scanning microwave guidance. [ASME PAPER 73-AUT-L] 13 p1657 A73-29413

Sealed aircraft battery with integral power conditioner. 13 p1573 A73-29589

External tracking, telemetry and concepts of free flight time, of safety corridor and of destruction time limit for ballistic missile flight tests safety 14 p1804 A73-30095

B-1 bomber crew integrated escape module for safe recovery throughout aircraft operational envelope, discussing capsule configuration and flight tests [AIAA PAPER 73-440] 15 p1825 A73-31426

Viking aerodynamic decelerator for Mars lander mission in 1976, discussing mortared disk-gap-band parachute, qualification flight tests and atmospheric environment effects 15 p1825 A73-31428

Low altitude flight test phase of Viking decelerator system development, considering low density environment loading condition simulation method [AIAA PAPER 73-455] 15 p1826 A73-31441

Viking 75 Mars lander parachute high altitude qualification flight tests for camera, telemetry and radar performance, using ground based computer-radar monitoring system 15 p1826 A73-31442

Viking 75 lander deceleration system qualification flight tests at expected Mars conditions, discussing design requirements and full scale vehicle simulation in earth atmosphere [AIAA PAPER 73-457] 15 p1827 A73-31443

Development of a high-performance ringsail parachute cluster. [AIAA PAPER 73-468] 15 p1828 A73-31452

Development of an improved midair-retrieval parachute system for drone/RPV aircraft. [AIAA PAPER 73-469] 15 p1828 A73-31453

Random/turbulent/excitation of flutter in wind tunnel dynamic models and flight test aircraft, comparing prediction and damping measurement results [ONERA, TP NO. 1234] 15 p1830 A73-31638

The MADGE system - Operational results and stretch potential. 15 p1912 A73-32505

Experimental approach for utilization of cathode ray tube piloting instruments 15 p1831 A73-32509

Space missile test center development for checkout, launch and data processing for space boosters, intermediate and intercontinental range ballistic missiles and supersonic aircraft 16 p1993 A73-33087

Concorde aircraft design, testing and projected environmental impact, discussing flight tests, sonic booms, atmospheric pollution, ATC problems and fueling 16 p1968 A73-33182

Aerodyne unmanned wingless reconnaissance aircraft, covering hovering capacity, internal flow duct for conventional flight, flight test results and stability characteristics 17 p2098 A73-34255

Flight test studies of the formation and dissipation of trailing vortices. [SAE PAPER 730295] 17 p2094 A73-34659

Electric trim systems - Design and certification considerations under FAR 23.677 /CAM 3.337-2/. [SAE PAPER 730299] 17 p2101 A73-34662

Redundant system design and flight test evaluation for the TAGS digital control system. [AHS PREPRINT 721] 17 p2131 A73-35062

Management approach to integration of B-1 avionics, discussing engineering problems, flight tests, electronic equipment and interface requirements 17 p2137 A73-35218

Flight test and demonstration of digital multiplexing in a fly-by-wire flight control system. 17 p2107 A73-35225

Ground and flight test results for standard VOR and double parasitic loop counterpoise antennas. 17 p2129 A73-35700

Computerized flight test data processing, emphasizing speed in turnaround and data analysis efficiency 18 p2266 A73-36070

Thermal control flight experiment onboard ATS-F to evaluate feedback controlled variable conductance heat pipe performance in space environment [AIAA PAPER 73-757] 18 p2370 A73-36372

Orbiting Astronomical Observatory heat pipe flight performance data. 18 p2370 A73-36373

Flight testing of the JT15D in the CF-100. 18 p2268 A73-36775

B-52 control configured vehicles ride control analysis and flight test. [AIAA PAPER 73-782] 19 p2378 A73-37452

An in-flight investigation of the influence of flying qualities on precision weapons delivery. [AIAA PAPER 73-783] 19 p2378 A73-37453

Development of an Air Cushion Landing System. [AIAA PAPER 73-812] 19 p2379 A73-37468

Flight testing the F-12 series aircraft. [AIAA PAPER 73-823] 19 p2380 A73-37475

Space shuttle program, discussing master planning schedule, vehicle design, payloads and initial flight tests 19 p2491 A73-37592

Space Shuttle development, qualification, acceptance and horizontal/vertical flight tests for Orbiter, solid rocket motor and drop tank element subsystems 19 p2492 A73-37602

Ground and flight testing of air cushion landing system /ACLS/ equipped CC-115 Buffalo aircraft for performance and stability/control characteristics 19 p2382 A73-37691

LA-4 aircraft air cushion landing system ACLS development tests covering static and mobile ground tests, flight tests and performance from and to various surfaces 19 p2382 A73-37692

A comparative evaluation of the application of several aircraft parameter identification methods to flight data - with emphasis on the development of rational evaluation criteria. 19 p2386 A73-38044

Simulated flight tests of a digitally autopiloted STOL-craft on a curved approach with scanning microwave guidance. 19 p2386 A73-38049

Some results of flight tests of an ion-engine model using surface ionization of cesium on tungsten. 20 p2600 A73-38911

Navy Transit navigation satellite system, discussing flight test for feasibility of military application to YP-3C Antisubmarine Warfare Weapons System aircraft 21 p2735 A73-40040

Sonic bang investigations associated with the Concorde's test flying. 21 p2635 A73-41174

VAK 191B. 22 p2798 A73-41752

Flight tests of load factors for multicornered-equipped gliders of various designs during pullout and looping maneuvers 22 p2799 A73-41866

Society of Flight Test Engineers, National Symposium, 3rd, Arlington, Tex., September 11-14, 1972, Proceedings. 23 p3050 A73-44052

Management and control of flight test programs of the Western Region FAA. 23 p3050 A73-44053

Management and control of flight test programs at U.S. Army Aviation Systems Command. 23 p3050 A73-44054

Management and control of flight test programs of the Naval Air Systems Command. 23 p3050 A73-44056

Management and control of commercial flight test programs. 23 p3050 A73-44057

Management and control of military and commercial flight test programs at Bell Helicopter Company. 23 p3050 A73-44058

Management and control of military flight test programs at McDonnell Douglas St. Louis, Missouri. 23 p3050 A73-44059

Flight test programs management and control, considering weapon systems performance tests relative to contractual requirements, personnel allocation and supporting facilities 23 p3051 A73-44060

Air Force Prototype Program management. 23 p3051 A73-44061

The role of a military flight test engineer in test management. 23 p3051 A73-44062

The capabilities of army test facilities. 23 p2966 A73-44064

Naval test and evaluation capabilities for aircraft, emphasizing organizational relationships 23 p3051 A73-44066

Tetrahedral Mylar plastic balloon drag coefficient measurement as function of Reynolds numbers from experimental free flight test data 23 p3004 A73-44263

Comparison of aircraft noise measured in flight test and in the NASA Ames 40-by 80-foot wind tunnel. [AIAA PAPER 73-1047] 24 p3056 A73-44871

FLIGHT TIME

Aircraft flight plan data processing in FORTRAN program to predict altitude and time conflicts, noting short CPU time 05 p0595 A73-16618

Optimal 3-dimensional minimum time turns for an aircraft. 06 p0648 A73-18377

Physical energy expenditure in long-haul cabin crew. 18 p2283 A73-36793

FLIGHT TRAINING

NT SPACE FLIGHT TRAINING

Image transformation in visual condition simulators of aircraft training equipment 01 p0029 A73-10666

Flight personnel training meetings, covering decision making, cockpit personnel selection and instructor role analysis 03 p0266 A73-13073

Performance measurement system for combat crew flight training in complex aircraft weapon systems, identifying training research goals 05 p0544 A73-16726

The isolation of critical elements within selected maneuvers during primary flight training. 05 p0544 A73-16727

U-2 and SR-71 aircrews physiological training for high altitude and supersonic flight hazards, discussing pressure suits, ejection seats, parachutes and survival and life support equipment 16 p1974 A73-32657

Time compressed training program for DC-10 flight crews, emphasizing operational proficiency through specific behavioral objectives approach 16 p1966 A73-32663

FAA General Aviation Crashworthiness Program. [SAE PAPER 730293] 17 p2257 A73-34657

Aircraft evacuation and safety procedures during emergencies, discussing negative panic, flight crew training and impact injury minimization 18 p2268 A73-36849

- Objectives of training in relation to accident prevention. 18 p2284 A73-36850
- Design and application of a part-task trainer to teach formation flying in USAF Undergraduate Pilot Training. [AIAA PAPER 73-935] 21 p2674 A73-40881
- Stress and strain in student helicopter pilots. 21 p2644 A73-41155

FLIGHT VEHICLES

- A complex approach to flight vehicle control system designs 01 p0074 A73-10673
- Analysis of the longitudinal perturbed motion of a ground-effect flight vehicle 02 p0128 A73-11785
- Terrestrial prototype of a lunar hopping transporter. [ASME PAPER 72-WA/AUT-7] 04 p0433 A73-15882
- Flight vehicle /FV/ control optimization taking into account control-function and phase-coordinate constraints 05 p0594 A73-16415
- Wind tunnel experimental verification of flight vehicles aerodynamic characteristics during preliminary design stage, discussing correction procedures for model data extrapolation to full scale parameters [SAE PAPER 720861] 05 p0528 A73-16665
- Analysis of flight vehicle response to nonstationary atmospheric turbulence including wing bending flexibility. [AIAA PAPER 73-181] 05 p0535 A73-16921
- Stochastically optimal terminal control system synthesis for loss function dependence on finite phase coordinates of dynamic system, considering soft landing of flight vehicle 07 p0805 A73-20037
- Flight vehicle equations of motion with variable information, noting flight control algorithm for random variable with given probability 07 p0849 A73-20077
- Accelerations of points on a flight vehicle during short-period motion 07 p0777 A73-20095
- Stability of symmetric flight vehicles in oblique flow 12 p1548 A73-27076
- Aerodyne flight vehicle testing for hover flight characteristics during remote control by radio with pilot commands, noting reliability and attitude control 13 p1569 A73-28785
- Detection of flight vehicle transition from base measurements. 13 p1706 A73-28834
- Stowable deployable autogyro aircraft escape rotoescape /SAVER/ conversion to flight vehicle for advanced escape rescue capability /AERCAB/ from hostile areas 16 p1966 A73-32674
- Time and fuel consumption optimal nutation damping and attitude-angular velocity control of spin-stabilized flight vehicles 16 p2072 A73-33234
- Flight vehicle extensive attitude control theory, deriving kinematic relations for optimal control moment selection to ensure required rotation 21 p2780 A73-40385
- Reliability estimation for repairable and nonrepairable flight vehicles, considering nomographs for failure rate and probability of defined requirements satisfaction 24 p3057 A73-45197
- FLIP-FLOPS**
- Jet interaction in a simplified model of a bistable fluid amplifier. [ASME PAPER 72-WA/FLCS-6] 04 p0409 A73-15863
- An experimental study of flow fields in bistable fluid amplifiers. [ASME PAPER 72-WA/FLCS-9] 04 p0409 A73-15864
- Miniaturized unistable and bistable fluidic switching elements performance characteristics, considering vibration, velocity, pressure and laminar/turbulent flow effects on switching time and stability 13 p1571 A73-28482
- Reduction of power requirements in dynamic elements based on bipolar transistor 21 p2660 A73-40022
- Application of fluidic shift-register modules for sequential control of pneumatic sequential circuits. 23 p2943 A73-43412
- FLOATING**
- Vertical submersion of a floating cylindrical solid 15 p1861 A73-31283
- FLOATING POINT ARITHMETIC**
- Nonrecursive digital filter hardware design based on analysis of bit level counting operations in convolution, using fixed and floating point representations 12 p1483 A73-27115
- A simulative study of correlated error propagation in various finite-precision arithmetics. 15 p1899 A73-31350
- FLOATS**
- Multiple occupant flotation devices for commercial transport aircraft survivors sea ditching, discussing slide/raft design improvement for high density loading 16 p1974 A73-32658
- Large floating ocean platforms for US Navy bases, discussing concrete construction techniques and costs for different configurations 19 p2418 A73-37749
- FLOCCULATING**
- Protoplanet formation models with floccule accumulation, discussing momentum considerations and supersonically turbulent collapsing gas cloud 05 p0625 A73-17318
- FLOOD PLAINS**
- The use of near-infrared photography in the analysis of surface morphology of an Argentine alluvial floodplain. 22 p2850 A73-42728
- FLOQUET THEOREM**
- Newtonian differential equations of Kepler motion, analyzing stability by numerical integration based on Floquet theorem and Runge-Kutta method 04 p0497 A73-15013
- Propagation in periodically loaded waveguides with higher symmetries. 09 p1063 A73-22490
- Newton method relationship to Floquet theory for nonlinear vibration problems, considering Van der Pol equation periodic solutions for breathing and bending modes [ASME PAPER 73-APMW-20] 22 p2924 A73-42883
- Finite difference scheme for wave equation solution for wave propagation in layered composite materials, obtaining matrix eigenvalues with Floquet condition for various methods [ASME PAPER 73-APMW-40] 22 p2926 A73-42897
- FLORA**
- U PLANTS [BOTANY]**
- FLOTATION SYSTEMS**
- U FLOATS**
- FLOW CHARACTERISTICS**
- NT BOUNDARY LAYER STABILITY
- NT FLAME STABILITY
- NT FLOW DISTRIBUTION
- NT FLOW STABILITY
- NT FLOW VELOCITY
- NT MAGNETOHYDRODYNAMIC STABILITY
- Unsteady viscous flow due to the impulsive motion of a flat plate, with special reference to the initial period. 01 p0031 A73-10422
- Simulation of the flow past turbomachine blades in the study of plane-cascade vibrations 01 p0029 A73-10494
- A note on the flow regimes in the unsteady, rectilinear flow of a perfect gas. 01 p0034 A73-11005
- Integral method of calculating a semibounded laminar jet 02 p0153 A73-11784
- Self-similar flows with increasing energy. II - Isothermal flow. 02 p0238 A73-12091
- Incompressible flow characteristics and temperature transverse behavior in completely turbulent wall boundary layer 03 p0292 A73-13172
- Hypersonic turbulent boundary layer flow parameters and heat transfer during blowing of coolant air and He through slot 03 p0242 A73-13186
- Far field steady inviscid flow behavior of hypersonic blunt axisymmetric slender body, obtaining unsteady two dimensional solution with cylindrical symmetry 03 p0242 A73-13310
- Base resistance of axisymmetric bodies with a variable angle of attack - Analysis and interpretation of the physical phenomenon 03 p0242 A73-13375
- Axisymmetric gas-particle flows maximum thrust nozzle design, investigating particle size, nozzle geometry and heat transfer coefficient effects [AIAA PAPER 72-1189] 03 p0357 A73-13479
- Observations on the macroscopic structure of a near turbulent wake with a Mach number M sub infinity equal 2.3 [ONERA, TP NO. 1176] 03 p0244 A73-13577
- Supersonic nozzle design for prescribed flight trajectory and variable gas flow parameters, solving variational problem of optimal contour for given Mach number 03 p0244 A73-13616
- Pressure distribution and shock wave intensity variations in supersonic flow past two plane wings forming dihedral angle 03 p0245 A73-13623
- Flow parameter iterative formulas for laminar incompressible viscous fluid flow between two parallel disks rotating at same angular velocity 03 p0295 A73-13625
- Investigation of flow characteristics behind diffusers with large cone angles 03 p0245 A73-13671
- Acoustic and shock waves interaction in axisymmetric gas flow through variable section channel, calculating flow characteristics variations via isentropic theory of steady flow 03 p0295 A73-13673
- Theoretical analysis of the flow through a particular wall-attachment fluidic component. 03 p0295 A73-13767
- Flow conditions at inlet and exit of a flat plate cascade at supersonic velocities. 03 p0246 A73-14139
- Survey of some current aerodynamic problems pertaining to supersonic air intakes [ONERA, TP NO. 1102] 03 p0247 A73-14150
- Compressible flow characteristic generalizations, considering flow with/without heat transfer and losses in terms of empirical loss coefficient or heat transfer coefficient [ASME PAPER 72-WA/PWR-1] 04 p0434 A73-15803
- Basic flow characteristics of a linear aerospike nozzle segment. [ASME PAPER 72-WA/AERO-2] 04 p0405 A73-15908
- Experiments on flow about a yawed circular cylinder. [ASME PAPER 72-FE-2] 05 p0527 A73-16546
- Experimental results on the intermittent properties of the boundary layer pressure field during transition. [AIAA PAPER 73-243] 05 p0566 A73-16967
- Theoretical study of a by-pass convergent-divergent nozzle 05 p0533 A73-17191
- Mach numbers up to 30 obtained in a continuous operating wind tunnel 05 p0533 A73-17194
- Solid particle transport effect on structure and axial speed characteristics of two phase submerged turbulent jet 06 p0684 A73-17455
- Wind tunnel study of flow structure and turbulent wakes on base surfaces of sharp or blunt edged flat bodies at various Mach and Reynolds numbers 06 p0643 A73-17456
- Turbulent flow characteristics of an impinging jet. 07 p0810 A73-19569
- Flow characteristics in air injection through porous surface of blunt bodies, noting blowing parameter effect on boundary layer flow 07 p0774 A73-19622
- Sharply defined upper limit existence for lunar ash flow with heat transfer, presenting altitude dependence of pressure, gas density, temperature and velocity distributions 07 p0895 A73-19864
- Parameter calculations for a supersonic axisymmetric flow near its expansion center 07 p0775 A73-20093
- Numerical solutions to flow and heat transfer characteristics of free convection micropolar flow with Newtonian solvent substructure 08 p1023 A73-21260
- Computer calculation of the characteristics of multistage gas turbines 09 p1136 A73-22567
- Flow characteristics of spherically capped gas bubbles buoyancy induced motion in liquids, discussing Reynolds and Froude number effects 10 p1205 A73-23854
- Optimum operational flow characteristics derivation for control valves based on frequency distribution of relative pressure drop occurring in practical applications 10 p1223 A73-24015
- Flow stress dependence on grain size in microstrain region of Ni strip machined to produce different grain sizes 10 p1235 A73-24444
- Some characteristics of the flow downstream of a blunt trailing edge in the presence of a neighbouring wall. 10 p1173 A73-24818
- Unsteady turbulent boundary layer flow past infinite flat plates with free stream acceleration or deceleration, computing characteristics by finite difference method 10 p1209 A73-24834
- Joint operation of the last gas-turbine stage and a diagonal diffuser 11 p1299 A73-25050
- Natural convection in a sloping porous layer. 11 p1449 A73-25220
- Spectra of turbulent pulsations in velocity, temperature, and their correlations for air flow in a circular pipe 11 p1301 A73-25744
- Algorithm for solution of inverse Stefan problem for flow characteristics determination, stating necessary and sufficient conditions for solution existence and uniqueness 11 p1452 A73-26328
- Theory on blades of axial, mixed, and radial turbomachines by inverse method. 11 p1303 A73-26340
- Approximate calculation of flow parameters during interaction of supersonic jets 11 p1304 A73-26443
- Thermodynamic theory of heat conducting fluids with constitutive quantities dependence on rate of density, gradient, velocity and temperature 11 p1453 A73-26746

Influence of the shape of a body on the characteristics of a self-similar axisymmetric wake
12 p1457 A73-26953

Flow at the trailing edges of a blade cascade at variable M and Re numbers
12 p1457 A73-27096

Application of certain generalized data from wind-tunnel tests with plane subsonic compressor cascades to the calculation of the characteristic flow regimes in supersonic cascades
12 p1458 A73-27480

Approximate method for solving a boundary value problem describing gas flow during strong blowing
12 p1458 A73-27811

Fuel-air turbulent mixing process in double concentric jet type burner, measuring average velocity, pressure distribution, turbulence intensity and shear stress
13 p1601 A73-28648

Error estimates for turbulent flow characteristics by visualization and solid particle photography
13 p1601 A73-28738

Effect of solidity on rocket pump inducer performance.
13 p1624 A73-29011

Flow analysis of three-dimensional diffuser for fluid amplifier.
13 p1603 A73-29033

Flow visualization of two and three dimensional wall jets on circular cylinder, observing flow characteristics sensitivity to curved boundary
13 p1603 A73-29038

Turbulent jet noise generation theory relationship between flow and acoustic characteristics, obtaining intensity expression with velocity space-time derivatives for moving and stationary coordinates
13 p1603 A73-29138

Calculation of the basic characteristics of turbulent flows in a state of structural equilibrium
13 p1604 A73-29168

Features of flow-parameter measurement by a cylindrical probe in the vaneless diffuser of a small centrifugal compressor
13 p1568 A73-29552

Providing a model of flow round a turbine blade when investigating the vibration of flat blading.
14 p1743 A73-30319

Theoretical investigation on laminar boundary layer with combustion on a flat plate.
14 p1817 A73-30611

Heat transfer to a cylindrical laminar liquid jet ejecting into a gas.
14 p1817 A73-30612

Gas flow properties in curvilinear turbine ducts, considering pressure gradient, outer flow shear and Coriolis force on boundary layer
14 p1712 A73-30649

Determination of the shape of a plane supersonic nozzle
15 p1822 A73-31196

Wake flow model of Viking 75 entry vehicle for different angles of attack at free stream Mach numbers 0.2-3.95
15 p1823 A73-31459

[AIAA PAPER 73-475]

Bow shock waves and flow field preceding pointed slender bodies subject to supersonic flow, analyzing wave distance from body and frozen flow characteristics
16 p1962 A73-33249

Planar pressure waves propagation across wall with elastically supported and damped edges, considering induced gas flow characteristics behind wall
16 p2000 A73-33257

Flow deflection characteristics of short pyramid wire gauze conical diffuser with high expansion ratio, showing satisfactory uniformity, pressure loss and flow steadiness
16 p2001 A73-34032

VTOL and helicopter design considerations, including nonsymmetrical rotor flow characteristics, rotor types, airspeed capacities, compound helicopters, tilt wing and tilt rotor aircraft
17 p2099 A73-34259

Mixing and structural characteristics of turbulent pulsating jets based on hot-wire anemometer velocity measurement data
17 p2157 A73-35513

Chemically reacting gas flow numerical calculations from stiff nonlinear ordinary differential equations solution in finite difference form
17 p2119 A73-35609

Finite difference theory predictions for turbulent boundary layer swirling flames, discussing flow simulation, turbulence models and flame size, shape and stability characteristics
18 p2367 A73-36206

[AIAA PAPER 73-651]

Investigation of two-dimensional cavity diffusers.
18 p2262 A73-36236

[AIAA PAPER 73-685]

Investigation of laminar flow in a porous pipe with variable wall suction.
18 p2299 A73-36342

[AIAA PAPER 73-725]

Solution by characteristics at fixed time interval of the equations of one dimensional unsteady flow.
18 p2300 A73-36608

Reentry vehicle ablating control surface gap and slot regions flow characteristics prediction based on quasi-

one-dimensional compressible flow finite difference solution
18 p2265 A73-36663

[AIAA PAPER 73-742]

Magnetohydrodynamical steady aligned flow past an oblique flat plate at a high Reynolds number.
18 p2300 A73-36664

Flow properties fluctuations in a convergent-divergent nozzle.
19 p2375 A73-37402

A study of a feedback fluidic jet oscillator. I, II.
19 p2389 A73-38077

Influences of the shape of a body on the characteristics of a self-similar axisymmetric wake.
19 p2377 A73-38129

Turbulent flow development characteristics in channel inlets.
19 p2421 A73-38184

Thin steady two dimensional potential flow with free and/or rigid boundaries in presence of gravity, determining outer and inner expansions characteristics
20 p2546 A73-39085

Prediction of the dynamic and quasi-static performance characteristics of fluoric wall-attachment amplifiers.
20 p2511 A73-39756

Russian book on turbomachinery using compressible and incompressible working fluids covering gas and fluid flow equations, energy losses in axial and radial flow stages, etc
21 p2633 A73-40807

Some integral characteristics of an MHD channel at finite magnetic Reynolds numbers
21 p2747 A73-40889

Simulation of the flow past a high-altitude ion-concentration sensor
21 p2633 A73-41223

Study of flow around an airfoil with a spoiler at Mach numbers ranging from 0.5 to 2.3
21 p2634 A73-41584

Creeping flow of Newtonian fluids in curved rectangular channels.
22 p2840 A73-41745

Experimental investigation of hydrodynamic stability for flows past simple membrane surfaces
22 p2840 A73-42117

Experimental investigation of the development of a cavern in the case of unsteady gas-induced cavitation
22 p2841 A73-42128

Flow of a viscous gas at a slot with strong suction
22 p2796 A73-42283

Reattachment of a separated boundary layer to a convex surface.
22 p2843 A73-42554

Recirculation and mixing characteristics prediction for enclosed turbulent jet flames in flow regions, using similarity parameters
22 p2934 A73-42782

Statistical analysis of two dimensional turbulence, noting probability characteristics ergodicity with respect to class of two dimensional characteristic functions with converging mean squares
23 p2968 A73-43475

Classification of methods for solving the direct problem of axisymmetric flow calculation in turboengines
23 p3020 A73-43736

Total shock-tube working time in the investigation of the discharge through holes in the end face
24 p3076 A73-44755

Transonic equation for flow in apertures between compressor and turbine blades, examining gas dynamic and geometric parameter influence on near-sonic flow
24 p3054 A73-45024

A biparametric method for laminar boundary layer calculations
24 p3079 A73-45173

FLOW CHARTS

Prediction of failure for a multiple load-path system under random loading.
04 p0510 A73-15075

FLOW COEFFICIENTS

NT DISCHARGE COEFFICIENT

One-dimensional electrohydrodynamic flows with a variable mobility coefficient - Evaporation and condensation discontinuities
01 p0077 A73-10954

Flow parameters and cylinder elongation effects on turbulent boundary layer characteristics for compressible fluid flow, calculating velocity distribution
08 p0956 A73-21602

One-dimensional electrohydrodynamic flows with variable mobility coefficient, evaporation and condensation jumps.
12 p1524 A73-27530

Rotating stall in an isolated rotor row and a single-stage compressor.
17 p2093 A73-34386

FLOW DEFLECTION

Calculation of the flow of a viscous compressible fluid past a parabolic obstacle
01 p0002 A73-10238

[ONERA, TP NO. 1129]

Axisymmetric slow viscous flow past an arbitrary convex body of revolution.
02 p0153 A73-12040

Boundary layer growth of a micropolar fluid.
02 p0154 A73-12093

Similarity solution of boundary layer flow due to uniform streaming past infinite flat plate with uniform suction at plate surface
03 p0292 A73-13306

An analytical investigation of the impingement of jets on curved deflectors.
03 p0296 A73-14178

Streamline deflection by diffusion flame stabilized on Parker-Wolfhard burner, discussing flow visualization and Burke-Schumann flame sheet in Oseen flow
07 p0921 A73-20355

Simulation of velocity profiles by shaped gauze screens.
08 p0953 A73-20717

On the shearing flow of a fluid, heavy or not, with constant vortex, around a thin profile placed under a free line, in linear theory
08 p0926 A73-21490

Numerical study of the flow of a viscous incompressible fluid around a circular cylinder
10 p1171 A73-23766

The force acting from the direction of a flow of liquid on a thin curved body of circular cross section
11 p1348 A73-26427

Supersonic gas flow past the leeward side of a conical wing
11 p1304 A73-26439

Convective heat transfer in the region of interaction between a supersonic overexpanded jet and an oblique obstacle
12 p1458 A73-27324

Flows with wakes about a zero-incidence symmetric profile
13 p1599 A73-28069

Two dimensional incompressible steady potential electrohydrodynamic flows past flat dielectric plate, using quasi one dimensional and boundary layer approximation
13 p1664 A73-28442

Perforated water tunnel to decrease wall effect on deflected cavitation flow, studying suction coefficient, pressure losses and blowing parameters
13 p1597 A73-28450

The input characteristic due to the interaction of jets of beam-deflection amplifier.
13 p1571 A73-29037

Investigation of high-temperature gas flow around axisymmetric bodies in the presence of several discontinuity surfaces
13 p1708 A73-29404

The nature of viscous flow around the forward stagnation point in the presence of strong injection of a gas through the surface of a slender pointed body
15 p1821 A73-31043

Reynolds stresses in plane-parallel flows disturbed by Tollmein-Schlichting waves
15 p1861 A73-31193

Longitudinal rarefied diatomic and monatomic gas flows past elongated plates
15 p1822 A73-31293

Boundary layer separation in a steady plane-parallel incompressible fluid flow
15 p1864 A73-32110

Qualitative study of flow deviation by a wall cavity
16 p1962 A73-32811

Criteria regarding the predetermination of the laminar-turbulent boundary layer transition in the case of flows about body contours
16 p1965 A73-33750

Flow deflection characteristics of short pyramid wire gauze conical diffuser with high expansion ratio, showing satisfactory uniformity, pressure loss and flow steadiness
16 p2001 A73-34032

Turbulent jet deflection and impingement in confined cross flow occurring in gas turbine blade impingement cooling schemes
17 p2152 A73-35012

[ASME PAPER 73-FE-15]

Generalized expressions for secondary vorticity using intrinsic co-ordinates.
18 p2299 A73-36506

Steady-state solutions to the problem of viscous incompressible fluid flow past a body
19 p2419 A73-37244

On a stagnation condition for combining or branching inviscid flows.
20 p2546 A73-39091

Influence of suction on the supercavitation flow behind a body in a porous tube
22 p2841 A73-42125

Investigations on fluidic jet deflection amplifiers in dc- and ac networks.
23 p2942 A73-43400

Fluidic jet deflection anemometer design and tests of directional wind velocity measurement in rain/sand environments
23 p2981 A73-43429

FLOW DISTORTION

Aircraft engine inlets total pressure fluctuations and distortion factors, presenting extreme-value statistical method for maximum distortion level probability estimate
03 p0354 A73-13419

[AIAA PAPER 72-1100]

Inlet produced flow distortion effect on compressor stability and engine stall, presenting unified theoretical analysis technique for compatible inlet/engine design [AIAA PAPER 72-1115] 03 p0355 A73-13430

Inlet flow distortion induced axial flow compressor stall, converting stagnation pressure and temperature maps into vorticity maps via Crocco theorem [AIAA PAPER 72-1116] 03 p0243 A73-13431

A procedure for estimating maximum time-variant distortion levels with limited instrumentation. [AIAA PAPER 72-1099] 04 p0432 A73-14908

Three-dimensional MHD duct flows with strong transverse magnetic fields. IV - Fully insulated, variable-area rectangular ducts with small divergences. 06 p0728 A73-17704

Inlet air flow distortion in high hub/tip ratio mixed flow turbomachines, using modified actuator disc theory 08 p0925 A73-20784

An experimental investigation of three-dimensionality of wall jet flows. 08 p0956 A73-21831

Parabolic flow over a flat plate with wave disturbance in the main stream. 09 p1071 A73-21950

Performance characteristics of a model VTOL lift fan in crossflow. 11 p1301 A73-25782

Nonlinear development of disturbances in a plane-parallel Poiseuille flow 15 p1861 A73-31285

Upstream attenuation and quasi-steady rotor lift fluctuations in asymmetric flows in axial compressors. [ASME PAPER 73-GT-30] 16 p2048 A73-33501

Support wire disturbances in near viscous wakes of slender supersonic bodies. 18 p2295 A73-36155

Evaluation of F-15 inlet dynamic distortion. [AIAA PAPER 73-784] 19 p2379 A73-37454

FLOW DISTRIBUTION

Low Reynolds number flow past a transverse cylinder at Mach two. 01 p0003 A73-10758

The fourth annual Fairley lecture - The propagation of sound through moving fluids. 01 p0077 A73-10784

Numerical calculation of supersonic opposing jet directed upstream against supersonic main stream by the use of time-dependent finite-difference method. 01 p0003 A73-11130

An empirical flowfield analysis technique for preliminary evaluation of inlet systems operating in a vehicle generated flowfield. 01 p0003 A73-11132

On the multi-parameter characteristic perturbation method - Application to nonlinear supersonic nonequilibrium flow over a wedge. 01 p0004 A73-11425

Numerical method for describing turbulent, compressible, subsonic separated jet flows. 01 p0035 A73-11467

Numerical calculations of the flow field of low Reynolds number viscous flow with or without real-gas-effects in slender-channel-nozzles. [DGLR PAPER 72-110] 02 p0152 A73-11674

Ideal dissociating/nondissociating gas reentry flow fields hydrodynamic stability for various free stream and disturbance conditions 03 p0242 A73-13312

Application of a pseudo-viscous method to the calculation of the steady supersonic flow past a waisted body. 03 p0242 A73-13335

Supersonic mixing and combustion of confined coaxial hydrogen-air streams. [AIAA PAPER 72-1178] 03 p0397 A73-13473

Three dimensional flow pattern from two dimensional supersonic inviscid gas flows around wedged body 03 p0245 A73-13675

The influence of a strake on the flow field of a delta wing /lambda 0.2/ at near-sonic velocities [DGLR PAPER 72-125] 03 p0248 A73-14385

Convective transport terms effect on laminar flow-field of Newtonian fluid between rotating cylinders, using adapted finite difference solution technique 03 p0298 A73-14643

An experimental study of flow fields in bistable fluid amplifiers. [ASME PAPER 72-WA/FLCS-9] 04 p0409 A73-15864

Planar jet vortex growth control by excitation through transverse periodic disturbances, studying jet flow field by visualization via hydrogen bubble technique [ASME PAPER 72-WA/APM-21] 04 p0435 A73-15895

Pollutant formation in reacting turbulent jet flow field with recirculation, presenting methane-air system pointwise properties determination by numerical analysis [WSCI PAPER 72-21] 05 p0638 A73-16676

Finite element analysis of unsteady incompressible flow around an oscillating obstacle of arbitrary shape. [AIAA PAPER 73-91] 05 p0529 A73-16855

Annular truncated plug nozzle flowfield and base pressure characteristics. [AIAA PAPER 73-137] 05 p0530 A73-16887

Numerical solution of viscous reacting blunt body flows of a multicomponent mixture. [AIAA PAPER 73-202] 05 p0532 A73-16936

Gudunov-method computation of the flow field associated with a sonic-boom focus. [AIAA PAPER 73-240] 05 p0536 A73-16965

Finite element model for discontinuous potential flow field analysis leading to Dirichlet, Neumann and mixed boundary value problems solution 06 p0644 A73-17514

Experiment on the geometry of the fine-structure regions in fully turbulent fluid. 06 p0684 A73-17703

High Reynolds number steady separated flow past a wedge of negative angle. 06 p0685 A73-17710

Calculation of the mean parameters of an inhomogeneous flow by the method of sections 06 p0645 A73-17720

Pressure surfaces and flow lines geometry of three dimensional parallel steady flow, noting geodesics formation on surfaces of constant pressure 06 p0686 A73-18174

Radiating-conducting thick-transparent normal shock solution. 07 p0919 A73-19507

Turbulent mixing at homogeneous wakes boundary, using heat conduction equivalence 07 p0810 A73-19610

Detachment of the outer shock from underexpanded rocket plumes. 07 p0920 A73-19977

Transonic nozzle flow with nonuniform gas properties. 08 p0925 A73-20719

Generalization of J. K. Lunde's method for determining the flow around models in a rectangular-section test tank 08 p0955 A73-21195

Further results concerning the forces on a flat plate in a Couette flow. 08 p0926 A73-21402

Some remarks on the behaviour of surface source distributions near the edge of a body. 08 p0926 A73-21437

Calculation of forces on stores in the vicinity of aircraft. 09 p1028 A73-22433

Flowfield calculations for some supersonic sections with ducted heat addition. 09 p1028 A73-23089

Contributions to the kinematics of type I tails of comets. 10 p1271 A73-23477

Experimental investigation of turbulent flow structure in a circular pipe with delivery through a porous wall 10 p1204 A73-23512

Subgrid resolution achievement by spline fitting during flow and force field sources conversion from Lagrangian distribution onto Eulerian grid and interpolation 10 p1248 A73-23603

Transient viscous laminar incompressible flow pattern after sudden vanishing of seminfinit flat plate based on two dimensional unsteady boundary layer equations with boundary conditions 10 p1208 A73-24811

Transient Ekman and Stewartson layers in a rotating tank with a spinning cover. 10 p1210 A73-24840

Hydrodynamic visualization technique application to unsteady flow patterns around models and analysis of boundary layers, separation and wakes 10 p1174 A73-24842

Nonstationary flow downwash behind a delta wing during supersonic motion 11 p1299 A73-25046

A distribution of molecular flow in the interior of a cylindrical space-simulation chamber with spherical gas source 11 p1343 A73-25111

Transpiration and natural convection - The vertical-flat-plate problem. 11 p1449 A73-25219

Viscous incompressible Jeffery-Hamel fluid flow in divergent channel, discussing secondary supercritical flow, winding and vortex formation 11 p1346 A73-25223

Flow and velocity fields simulation by calculating dynamic loads in moving liquid from pressure distribution, viscosity and gravitational acceleration [AIAA PAPER 73-409] 11 p1441 A73-25537

Large particle method for calculation of transonic supercritical vortex flow fields around flat and axisymmetric bodies 11 p1302 A73-26330

Study of flow around a rotating circular cylinder. 11 p1302 A73-26337

Nonvortical axisymmetric flow of inviscid ideal incompressible fluid from partial differential equations solution 12 p1486 A73-27242

Mechanisms influencing the distribution of precipitation within baroclinic disturbances. 13 p1652 A73-28266

The wave patterns produced by a moving body in a compressible, density-stratified fluid. 13 p1606 A73-28273

Conjugating a Chaplygin operator with a differential operator in gasdynamics 13 p1563 A73-28443

Using a single hot-wire probe in three-dimensional turbulent flow fields. 13 p1600 A73-28526

Structure of the wall zone of a longitudinal dispersive flow over a plane plate 14 p1711 A73-30014

Nonlinear effects in steady supersonic dissipative gasdynamics. II - Three-dimensional axisymmetric flow. 14 p1711 A73-30167

The theory of fluctuating flow fields near walls. 14 p1746 A73-30704

The conservative method of flows and the calculation of a viscous heat conducting gas flow past a body of finite size 15 p1821 A73-30962

Probability distribution of the concentration and intermittency in turbulent jets 15 p1862 A73-31286

Flows past thin blunt bodies with shock layer separation 15 p1822 A73-31291

Calculation of the resultant moment of the hydrodynamic forces on jet profiles 15 p1824 A73-32000

Solutions of boundary value problems of multilayer-analogs of geoelectrics and hydrology. 15 p1872 A73-32040

Solution of the direct problem on mixed subsonic and supersonic flow of a gas in a nozzle of finite length. 15 p1824 A73-32067

Power law recompression of fully developed centered gas expansion, obtaining flow distribution via closed form integral solution based on similarity theory 16 p2000 A73-33317

On the unsteady supersonic cascade with a subsonic leading edge - An exact first order theory. [ASME PAPER 73-GT-15] 16 p1963 A73-33492

Interface effects between a moving supersonic blade cascade and a downstream diffuser cascade. [ASME PAPER 73-GT-23] 16 p1964 A73-33497

Calculation of flows past wings without thickness in the presence of developing vortex sheets 16 p1965 A73-33963

Similarity in the flow of a magnetized plasma around a plate and cylinder 17 p2215 A73-34260

Applications of a ray reflection model in the problem of highly rarefied gas flow past bodies. 17 p2094 A73-34549

Three-dimensional flow field in rocket pump inducers. I - Measured flow field inside the rotating blade passage and at the exit. [ASME PAPER 73-FE-33] 17 p2095 A73-35024

An investigation of the flow field and drag of helicopter fuselage configurations. [AHS PREPRINT 700] 17 p2095 A73-35051

A note on compressible flow through a vortex swirl cup. 17 p2154 A73-35120

Near continuum impact of an underexpanded jet plume on a wall. 17 p2096 A73-35137

Boundary condition calculation procedures for inviscid supersonic flow fields. 17 p2155 A73-35143

A new shock capturing numerical method with applications to some simple supersonic flow fields. 17 p2096 A73-35144

Experimental investigation of turbulent flow structure in a circular tube with expansion through a porous wall. 17 p2155 A73-35192

Computation of three dimensional flows about aircraft configurations. 18 p2259 A73-36158

Three-dimensional compressible boundary layer flow over a yawed cone. [AIAA PAPER 73-634] 18 p2260 A73-36193

Turbulent flow fields with two dynamically significant scales. [AIAA PAPER 73-646] 18 p2297 A73-36201

Flow field measurements in an asymmetric axial corner at $M = 12.5$. [AIAA PAPER 73-676] 18 p2297 A73-36227

Inflight electrostatic probe measurements of the effect of chemical injection on the properties of the reentry flow field. [AIAA PAPER 73-692] 18 p2338 A73-36243

Engineering analysis of hypersonic lifting body windward surface inviscid and viscous flow fields at high angles of incidence. [AIAA PAPER 73-637] 18 p2263 A73-36257

Investigation of the expansion side of a delta wing at supersonic speed. 18 p2263 A73-36312

Viscous effects in massively-ablating planetary entry body flow fields. 18 p2264 A73-36335 [ALAA PAPER 73-716]

Investigation of laminar flow in a porous pipe with variable wall suction. 18 p2299 A73-36342 [ALAA PAPER 73-725]

Monatomic and diatomic gas supersonic flow field calculation for sharp leading edge by BGK and ordinate models 18 p2265 A73-36631

Magnetohydrodynamical steady aligned flow past an oblique flat plate at a high Reynolds number. 18 p2300 A73-36664

Gas expelled from a strongly underexpanded nozzle upstream into a hypersonic flow 18 p2265 A73-37010

A modulation technique for measuring small disturbances in the upstream flow field of a sharp leading edge in a rarefied hypersonic flow. 19 p2377 A73-37714

Equations of motion for ideal isotropic viscoplastic medium in axisymmetric space, determining conditions for flow core existence 20 p2619 A73-39336

Self-similar flows behind shock waves in a gravitational field 21 p2676 A73-40190

Structure of the base flow in a four-nozzle cluster rocket engine 21 p2754 A73-40392

Supersonic gas flow pattern at blunt body of revolution with attached shock wave 21 p2632 A73-40400

Boundary-layer plasma of a re-entry vehicle - A comparison of prediction models and flight measurements. 21 p2632 A73-40420

Gaskinetic treatment of the Rayleigh problem in the case of moderately to greatly diluted gases 22 p2843 A73-42529

Finite difference and truncation method comparison for supersonic conical flow equations solution, obtaining flow field and shock wave shape 22 p2796 A73-42574

Influence of nonideal flow conditions in haemodialysis on mass-transfer theories. 22 p2816 A73-42678

Analytical modeling of a spherical combustor including recirculation. 22 p2934 A73-42783

Flow patterns and velocity and shear stress distribution downstream of steady and pulsatile flow models for fluid dynamics of blood vessel branches 22 p2816 A73-43103

Helium bubble survey of an opening parachute flowfield. 22 p2798 A73-43112

Output pressure-displacement and flow pattern characteristics of digital limit Schrenk, wall attachment and nozzle receiver fluidic switches 23 p2945 A73-43426

Thickness of liquid film on a rotating disk. 23 p2969 A73-44128

Similarity of flows arising during reflection of weak shock waves from a rigid wall and from a free surface. 24 p3076 A73-44713

Acoustic wave propagation in axisymmetric swirling subsonic jet flow, obtaining directivity patterns for spinning and nonspinning modes from wave equation numerical integration 24 p3077 A73-44837 [ALAA PAPER 73-1004]

Flow field over pointed wedges in isoenergetic flow of thermally and calorically perfect gases with nonuniform incident supersonic flow, noting attached shock formation 24 p3056 A73-45547

FLOW EQUATIONS

NT HELMHOLTZ VORTICITY EQUATION
NT VON KARMAN EQUATION
NT VORTICITY EQUATIONS
Modified convergence criterion for boundary layers.

Characteristics of the quiet solar wind beyond the earth's orbit. 01 p0033 A73-10750

Relativistic gas dynamics problems reduction to equivalent Newtonian flow via transformation of governing equations 01 p0034 A73-11138

A solution of the three-dimensional unsteady compressible boundary layer equations. 01 p0004 A73-11356

Exact vorticity solutions of the incompressible Navier-Stokes equations. 01 p0034 A73-11358

Boundary layer equation complete solution from first order differential equation graphic solution by Poincare method 01 p0034 A73-11360

A boundary value problem for a system of temperature boundary layer equations 01 p0123 A73-11433

German book on plasma physics covering MHD equations for incompressible and compressible flow, shock waves, electrical and thermal conductivity, viscosity, flow stability, turbulence, etc 02 p0196 A73-11894

Wing-tip vortex breakdown and dissipation, deriving closed form transcendental solutions for viscous core flow quasi-cylindrical momentum integral equations 02 p0128 A73-12036

Wave motion of low-tension interfaces with electrical double layers. 02 p0196 A73-12038

Reverse flow solutions of the Falkner-Skan equation for a lambda greater than one. 02 p0154 A73-12799

Boundary value problem for flow equation of multiphase viscous fluid with given velocity distribution, noting equations of motion for incompressible micropolar fluid flow 03 p0291 A73-13164

Micropolar model of blood steady flow through rigid circular tubes, presenting equations solutions and velocity profiles 03 p0266 A73-13302

Sturm-Liouville solution of unsteady stratified two dimensional Couette flow equations of motion 03 p0292 A73-13304

A discussion of the Marsh matrix technique applied to fluid flow problems. 03 p0244 A73-13563

Steady transverse plane magnetogasdynamics flows. 03 p0346 A73-13693

Closed form linearized solutions of plane laminar jets boundary layer equations based on Legendre functions 03 p0297 A73-14628

Energy balance, motion and constitutive equations of polar fluids, considering entropy inequality, viscosity and dissipation rate 04 p0434 A73-15679

Navier-Stokes equation solutions for steady laminar viscous flow of incompressible fluid with mixed no-slip and no-shear conditions 05 p0563 A73-16097

Equations of motion for two dimensional steady conducting gas flow in transverse magnetic field, deriving flow equations for transcritical region via small perturbation theory 05 p0602 A73-16585

Isentropic compressible flow equations for pressure and velocity distributions across vortex in axial core mass flow, noting atmospheric circulation and pressure effects 05 p0529 A73-16866 [ALAA PAPER 73-106]

Flow of a gas in a flat channel at a diminishing flow rate 05 p0533 A73-17090

Flow equations of a multiphase mixture with one coherent liquid or gaseous phase. 06 p0685 A73-17758

Solutions of thermal boundary layer equations when temperature gradient at the moving flat plate in parabolic flow is prescribed. 06 p0769 A73-18251

On generalized hydrodynamic equations used in heat transfer theory. 06 p0688 A73-18834

Electrohydrodynamic shock wave evolution in steady gas flow with positive space charge in electric field 06 p0733 A73-18881

Similarity solution for equations of nonplanar relativistic flow from point energy source, applying to spherical shock propagation and cosmic ray generation 07 p0810 A73-19506

Flow equation for axisymmetric compressible fluid flow in conical turbine stage, calculating radial distribution of flow velocity 07 p0868 A73-20088

Method of approximate calculation of the laminar boundary layer outside of vibrational equilibrium 08 p1023 A73-21259

Calculation of the transonic flow around an airfoil, taking account of the exact law of compressibility 09 p1027 A73-22210

Finite element method for solution of two dimensional flow equations with applications to passive advection and nonlinear gravity wave problems, noting computing time 09 p1113 A73-22955

Perturbation method for linearizing equations of supersonic flow over conical bodies, obtaining potential velocity and entropy solutions 10 p1171 A73-23615

Unsteady MHD duct flow by the finite element method. 10 p1256 A73-24289

Tensorial expansions for the plastic flow of partially compressible media. 10 p1290 A73-24325

Weakly rarefied gas flow described by simplified Barnett equations, analyzing boundary layer structure 10 p1172 A73-24491

Transonic gas flow in rotating turbomachine cascade channels, reducing flow equations to second order differential equation 10 p1172 A73-24507

Turbulent Hartmann flow based on differential equations for steady isothermic turbulent motion of incompressible electrically conducting fluid in magnetic field 10 p1256 A73-24591

Similarity solutions of unsteady, compressible plane and axisymmetric laminar boundary layer equations. 10 p1208 A73-24807

Turbulent wake development in oscillating flow, deriving flow equations for sinusoidally time dependent orifice flow 10 p1208 A73-24814

Universal equations of the three-dimensional laminar boundary layer in the unsteady state and their treatment 10 p1209 A73-24820

Equations for nonlinear Benard convection with rotation for fluid layer, investigating asymptotic solution for two dimensional cells at large Rayleigh and Taylor numbers 11 p1448 A73-25052

Fluid turbulence equations for large molecular drift velocity gradients in rarefied gas, near surface and stellar system motions, using Predvoditelev hydrodynamic equations 11 p1347 A73-25733

Boundary-value problem for a system of equations with a temperature boundary layer. 11 p1452 A73-26055

Equations for finitely-dimensional probability distributions of pulsating variables in a turbulent flow 13 p1599 A73-28287

The use of averaged flow equations of motion in turbomachinery aerodynamics. 13 p1603 A73-29047

Optimization of turbulence models by means of a logical search algorithm. 14 p1744 A73-29931

Derivation of a chain of equations for characteristic functions of a turbulent velocity field from the Hopf equation 14 p1744 A73-30021

Book - Computational fluid dynamics. 14 p1745 A73-30359

Approximate solutions and applications of hodograph equations in elliptic diabolic flow. 14 p1745 A73-30428

Chandrasekhar equations for axisymmetric MHD flows generalized for steady and unsteady flows 14 p1781 A73-30701

Momentum and moment of momentum differential equations of turbulent flow, reviewing and extending Mattioli theory to three dimensional flow 15 p1865 A73-32119

Electrohydrodynamic shock wave evolution in steady gas flow with positive space charge in electric field 15 p1921 A73-32406

Hagen-Poiseuille flow stability with superimposed rigid rotation, deriving perturbed differential flow equations from Navier-Stokes and continuity equations 16 p1999 A73-33253

Book - Physical fluid dynamics. 17 p2151 A73-34472

A dynamic modeling method of unsteady flows in long fluid lines with turbulent bulk velocities. [ASME PAPER 73-FE-18] 17 p2153 A73-35014

Inlet state limitations and flow characteristics equations for supersonic ejector jet mixing duct 17 p2156 A73-35504

The effect of nonlinear transformations on the computation of weak solutions. 18 p2330 A73-36610

Some transient MHD-flows with finite magnetic Reynolds numbers. 19 p2470 A73-38319

Linearized models of two dimensional steady air flow around mountain obstacle for constant temperature gradients and invariant velocity 21 p2731 A73-40741

Equations for the finite-dimensional probability distributions of pulsating variables in a turbulent flow. 22 p2840 A73-41810

Approximate estimation of the possibility of using the viscoelasticity hypothesis for the formulation of an equation of motion for a liquid with polymer additions 22 p2841 A73-42122

Finite difference and truncation method comparison for supersonic conical flow equations solution, obtaining flow field and shock wave shape 22 p2796 A73-42574

A divergent difference scheme for calculation of steady supersonic flows with complex structures 24 p3053 A73-44651

Transonic equation for flow in apertures between compressor and turbine blades, examining gas dynam-

ic and geometric parameter influence on near-sonic flow

24 p3054 A73-45024

A method of calculating a chemically nonequilibrium flow of gas in a heated tube under conditions close to the equilibrium or frozen state

24 p3081 A73-45527

Moment equation solutions for plane nonisothermal Poiseuille gas flow slip rate and temperature and pressure gradients in terms of molecular models

24 p3081 A73-45541

FLOW FIELDS

U FLOW DISTRIBUTION

FLOW GEOMETRY

Some characteristics of the passage of a circular nonuniformity zone through the working wheel grid of an axial-flow compressor

02 p0203 A73-11709

Experiment on the geometry of the fine-structure regions in fully turbulent fluid.

06 p0684 A73-17703

Turbulent boundary layer separation in supersonic air flow around flat rectangular plate, calculating flow geometry and pressure distribution

07 p0775 A73-20082

Determination of the shape of jets flowing off the walls of an asymmetrically positioned bucket

07 p0776 A73-20098

A reappraisal of design methods for inward flow radial gas turbines.

11 p1411 A73-26370

Spiral flows with multiple circulation in channels of simple shape

15 p1861 A73-31284

Stationary isothermal gas flow subject to self gravitation, finding subsonic regime oscillatory solutions for plane parallel, spherical and rotational symmetric cases

16 p2058 A73-32832

Free surface shape of MHD flow due to constant mass source expansion into uniform magnetic field as function of time

16 p2041 A73-33329

Prediction of flow outlet angle in blade rows with conical stream surfaces.

[ASME PAPER 73-GT-32]

16 p2048 A73-33502

Geometry of relaxing gas flows.

18 p2299 A73-36330

Boundary-layer separation at a free streamline. III - Axisymmetric flow and the flow downstream of separation.

20 p2549 A73-39806

Experiment on convex curvature effects in turbulent boundary layers.

21 p2676 A73-40245

Analysis of gas flow in multinozzle jets

21 p2631 A73-40393

FLOW MEASUREMENT

Cryoprobe with truncated circular cross sectioned Cu cone with copper slug heat sink for momentum flow rate measurement in hypersonic low density flow

01 p0003 A73-10755

Flow measurement on scale model of air cooling system for various blowing conditions and structure parameters, noting flow resistance of cooling fins

02 p0237 A73-11634

Some characteristics of the passage of a circular nonuniformity zone through the working wheel grid of an axial-flow compressor

02 p0203 A73-11709

Quasi-steady heat transfer equation for frequency response of wedge shaped hot film sensors for flow temperature, velocity and turbulence measurement

02 p0166 A73-11711

Thermoanemometer with automatically stabilized temperature of its sensitive element and output signal linearization

02 p0170 A73-12344

Rotor unsteady wakes three dimensional flow analysis by wave front averaging technique, using constant temperature hot-wire anemometer

02 p0129 A73-12504

Laser Doppler anemometer theory and application to radial flow velocity measurement in oscillating boundary layer in front of blunt body

02 p0171 A73-12559

The statistical evaluation of the measurement of viscosity of a non-Newtonian liquid.

03 p0306 A73-12899

Hot-wire anemometers calibration characteristics for steady channel turbulent air flow measurement, noting linearization error analysis

03 p0306 A73-13166

Conditionally sampled measurements near the outer edge of a turbulent boundary layer.

03 p0293 A73-13526

Turbulent shear flow structure parameters in conical diffuser, investigating Reynolds number and turbulent kinetic energy effects

03 p0247 A73-14176

Turbulent properties of a compressible boundary layer.

03 p0296 A73-14177

Telemetric measurement of local blood flow by heat conduction probes.

03 p0270 A73-14282

Respiratory air flow telemetry during exercise, discussing flowmeter working conditions and equipment testing

03 p0270 A73-14286

Radio telemetric measurements of oxygen consumption during exercise via respiratory air flow and oxygen partial pressure monitors, considering water vapor and temperature

03 p0270 A73-14288

The measurement of a pulsating air flow using a sharp-edged orifice meter.

[ASME PAPER 72-WA/FE-36]

04 p0451 A73-15853

An experimental study of flow fields in bistable fluid amplifiers.

[ASME PAPER 72-WA/FLCS-9]

04 p0409 A73-15864

External field electromagnetic measurement of blood flow - An alternative approach to the solution of the baseline problem.

04 p0414 A73-15992

Finite fringe holographic interferometry applied to a right circular cone at angle of attack.

[ASME PAPER 72-APM-PP]

05 p0527 A73-16528

Study of the specific characteristics of the diffusion method for measuring turbulence characteristics under conditions of a free homogeneous jet

05 p0576 A73-16617

A method for measuring the sublayer velocity profile of a liquid with polymer additive.

[AIAA PAPER 73-39]

06 p0692 A73-17621

Measurements in a transitional/turbulent Mach 10 boundary layer at high-Reynolds numbers.

[AIAA PAPER 73-165]

06 p0645 A73-17649

Dynamic response of digital-analog flow measurement system based on turbine driven pulse generator as sensor element

07 p0828 A73-20545

Experimental investigation of two-dimensional, supersonic flow impingement on a normal surface.

08 p0925 A73-20720

A zero-streamwise-pressure-gradient, three-dimensional turbulent boundary layer in a 90 deg curved rectangular duct.

08 p0953 A73-20796

A new probe for measurement of velocity and flow direction in separated flows.

08 p0963 A73-20871

Devices for dynamic recording of volumetric blood flow rates lower than 1 ml per minute

08 p0934 A73-21325

Experimental method for analyzing the unsteady flow in a transonic aircraft compressor

09 p1028 A73-22715

Development of a procedure for measuring the degree of turbulence at the axis of a free two-phase jet by a thermal-diffusion method

09 p1167 A73-22847

Optimal measurement location for integrating pipe flowmeters, exemplifying by linearly integrating ultrasonic flowmeter

09 p1086 A73-23114

Solar wind flow vector from detection of unshocked wind by plasma detector aboard ATS-5 during 8 March 1970 geomagnetic storm

10 p1270 A73-24741

Spatial amplitude distribution of vibrating ribbon two dimensional wake mean, periodic and random velocity components measured in uniform flow by hot-wire anemometry

10 p1173 A73-24828

Modern developments in flow measurement; Proceedings of the International Conference, Harwell, Berks., England, September 21-23, 1971.

10 p1220 A73-24852

Variable area, positive displacement, turbine type, electromagnetic and pressure difference flowmeters, noting reliability, repeatability and accuracy

10 p1221 A73-24853

State of art of water flow measurement by weirs and flumes in artificial channels

10 p1221 A73-24854

Recent measurements of flow using nuclear magnetic resonance techniques.

10 p1185 A73-24855

Flow measurement in the presence of strong swirl using a laser Doppler anemometer.

10 p1221 A73-24857

An evaluation of optical anemometers for volumetric flow measurement of liquids and gases.

10 p1221 A73-24858

Long bore thick plate orifices performance in flow velocity measurement at low Reynolds numbers, calculating uncalibrated uncertainty in discharge coefficient

10 p1221 A73-24860

Errors in the velocity-area method of measuring asymmetric flows in circular pipes.

10 p1221 A73-24861

The response of a hot-wire anemometer in flows of gas mixtures.

10 p1222 A73-24971

Conditional sampling and other measurements in a plane turbulent wake.

11 p1299 A73-25056

Problems in constructing aerodynamically active elements - Converters of input and output signals in automatic control systems

12 p1459 A73-26769

Calculation of the moisture content correction in measuring the quantity of gas flowing through an orifice

12 p1498 A73-27595

Dynamic measurement of the basic quantities of fluidics

12 p1461 A73-27596

Experimental studies on high speed performance of two-dimensional turbine cascades.

13 p1566 A73-29019

Measurement of Coanda flow in fluidic elements by a laser Doppler velocimeter method and a quantitative tracer method.

13 p1618 A73-29040

Turbulent interface detector using a multiple array of single hot wires.

13 p1619 A73-29252

The unpolarized electrode in a pulsating Poiseuille pipe flow.

13 p1620 A73-29258

The application of photon correlation spectroscopy to the measurement of turbulent flows.

13 p1622 A73-29421

Features of flow-parameter measurement by a cylindrical probe in the vaneless diffuser of a small centrifugal compressor

13 p1568 A73-29552

Three dimensional turbulent boundary layers prediction methods and flow measurements, considering swept and slender wings

14 p1744 A73-30173

Behavior of a weak turbulent jet in a cross flow

15 p1822 A73-31199

Turbulent source flow between parallel stationary and co-rotating disks.

15 p1862 A73-31337

Insensitivity of single particle time domain measurements to laser velocimeter 'Doppler ambiguity.'

15 p1875 A73-31671

Experimental investigation of a turbulent boundary layer on a porous plate with intense injection

15 p1824 A73-31858

Interaction between an ionized metal vapor flow and a body at Mach numbers equal to or larger than unity

15 p1919 A73-31863

Two-component dual-scatter laser Doppler velocimeter with frequency burst signal readout.

15 p1880 A73-32383

Multi balance measurement of flow systems.

16 p2016 A73-33656

Theory of mass flow measurement - Its advantages and instrumentation related to same.

17 p2166 A73-34619

Mixing and structural characteristics of turbulent pulsating jets based on hot-wire anemometer velocity measurement data

17 p2157 A73-35513

Three-dimensional hypersonic transitional/turbulent mean flow profiles.

18 p2260 A73-36194

Flow field measurements in an asymmetric axial corner at M = 12.5.

18 p2297 A73-36227

Turbulent correlation measurements in a two-stream mixing layer.

18 p2298 A73-36311

Mass flux measurements and correlations in the back flow region of a nozzle plume.

18 p2342 A73-36348

Techniques for studying the aerodynamic characteristics of the bronchial tree of man

18 p2282 A73-36576

Quantitative study of an aerodynamic flow by holographic interferometry

18 p2317 A73-37082

Application of a holographic technique to the determination of the dispersivity of a two-phase gas/liquid flow

18 p2318 A73-37122

Measurements of internal waves and turbulence in two-dimensional stratified shear flows.

19 p2422 A73-38238

Flow measurements over compression corner in supersonic separated laminar boundary layers with hot-wire probes

21 p2631 A73-40247

The vorticity equation as an angular momentum equation.

22 p2842 A73-42349

Measurement of coronary blood flow by radiocardiography - Study of 116 cases.

22 p2809 A73-42838

Use of a fluidic distributor for the calibration of unsteady flow probes.

23 p2945 A73-43430

Equipment for measuring local plasma flow parameters by a thermoanemometer probe 24 p3089 A73-44761

Comparison of results obtained with various sensors used to measure fluctuating quantities in jets. [AIAA PAPER 73-1043] 24 p3079 A73-44867

Introduction of the viscous force sensing fluctuating probe technique, with measurement in the mixing zone of a circular jet. [AIAA PAPER 73-1044] 24 p3090 A73-44868

Measurement of turbulence transport properties in a supersonic boundary-layer flow using laser velocimeter and hot-wire anemometer techniques. [AIAA PAPER 73-1045] 24 p3090 A73-44869

Measurements of the structure of the Reynolds stress in a turbulent boundary layer. 24 p3079 A73-45310

FLOW PATTERNS

U FLOW DISTRIBUTION

FLOW RATE

U FLOW VELOCITY

FLOW REGULATORS

NT FUEL FLOW REGULATORS

Rectangular channel mixed boundary layer flow patterns dependence on inlet edge configurations, channel geometry and hydrodynamic flow core parameters 13 p1601 A73-28737

FLOW RESISTANCE

NT AERODYNAMIC DRAG

NT FRICTION DRAG

NT VISCOUS DRAG

Heat transfer and hydraulic resistance of single banks and systems of tubes in cross flow of gases and viscous liquids 01 p0120 A73-10289

Flow and heat transfer on a flat plate normal to a two-dimensional laminar jet issuing from a nozzle of finite height. 01 p0033 A73-10804

Flow measurement on scale model of air cooling system for various blowing conditions and structure parameters, noting flow resistance of cooling fins 02 p0237 A73-11634

Lagrange equations of motion for ideal incompressible fluid flow under asymmetric deformation of expanding circular cylinders and spheres, calculating resistance forces 03 p0294 A73-13613

Empirical formulae for the universal functions M sub m/μ and N/μ in the resistance law for a barotropic and diabatic planetary boundary layer. 04 p0473 A73-15696

Optimization of drag minimums including effects of flow separation. [ASME PAPER 72-WA/AERO-1] 04 p0405 A73-15909

Weak normal shock wave interactions with materials, investigating incident pressure ratio, thickness, perforation diameter, close area and flow resistance effects on acoustic reflectance [AIAA PAPER 73-244] 05 p0598 A73-16968

Monatomic gas flow around uniformly heated sphere for small Reynolds numbers, noting drag decrease due to thermal stresses 06 p0646 A73-18884

Velocity and resistance profiles for unsteady turbulent flow in rough pressure channels, using Prandtl hypothesis 07 p0811 A73-19614

Determination of the hydraulic resistance of throttles by short unsteady blowing 07 p0779 A73-20083

Simulation of velocity profiles by shaped gauze screens. 08 p0953 A73-20717

Heat transfer, adiabatic enthalpy /temperature/ of the wall, and hydrodynamic resistance associated with the turbulent and laminar flow of a compressible fluid in a circular tube. 08 p0954 A73-20858

Theoretical study of a flow-resistance gas heater. 08 p1023 A73-21436

Variational formalism of a quasi-linear compressible fluid flow with heat exchange. 13 p1602 A73-29022

Experimental investigation of the velocity structure and of hydraulic resistances in unsteady forced turbulent flows 15 p1862 A73-31287

Monatomic gas flow around uniformly heated sphere for small Reynolds numbers, noting drag decrease due to thermal stresses 15 p1824 A73-32409

Fluidic strain gages based on detection of flow resistance or pressure drop changes due to elongation, comparing various type gage factors 20 p2564 A73-38873

Friction, heat transfer and material removal in a turbulent boundary layer of a compressible high-enthalpy gas under conditions of marked nonisothermicity, injection and negative pressure gradient. 20 p2628 A73-39422

Laminar steady state flow resistor design featuring temperature independence achieved with flattened core capillary tube 20 p2511 A73-39754

Mathematical model of collateral blood vessels caliber changes due to hydrodynamic drag /shear stress/ effects on vascular endothelium 22 p2817 A73-43105

The steady-state and transient performance of some large-scale vortex diodes. 23 p2942 A73-43407

Fluid pad resistor for linear laminar flow resistance between parallel plates with emphasis on fluidic circuits application 23 p2945 A73-43425

FLOW SEPARATION

U BOUNDARY LAYER SEPARATION

U SEPARATED FLOW

FLOW STABILITY

NT BOUNDARY LAYER STABILITY

NT FLAME STABILITY

NT MAGNETOHYDRODYNAMIC STABILITY

Unstable operation and rotating stall in axial flow compressors. [ONERA, TP NO. 1090] 01 p0001 A73-10228

Rigid and free boundaries effects on radiative heat transfer stabilization of fluid layer against Benard thermal convection 01 p0120 A73-10397

Thermal convection in a horizontal fluid layer with uniform volumetric energy sources. 01 p0120 A73-10442

Nonlinear waves on interface of two incompressible inviscid fluids of different densities and arbitrary surface tension analyzed by multiple scales method 01 p0032 A73-10445

Synthesis of a magnetoelastic control medium for stabilization of hydrodynamic flows 01 p0084 A73-10669

Stability of rotating stratified flow produced by tangential injection of high pressure gas into closed cylindrical vessel filled with gas of different density 01 p0033 A73-10752

Stability criteria for unsteady motion of incompressible Cosserat fluid in arbitrary time dependent domain, using Liapunov function 01 p0033 A73-10776

Vibrational instability of plane-parallel convective motion in a vertical duct 01 p0034 A73-10966

Electrohydrodynamic stability of insulating fluids subjected to a unipolar injection 01 p0086 A73-11361

Stability of a nonstationary circular jet of ideal incompressible fluid 02 p0152 A73-11609

Nonlinear baroclinic instability of a continuous zonal flow of viscous fluid. 02 p0153 A73-12035

Flow stability of ideal compressible and incompressible fluids, solving Navier-Stokes equation for rotating liquid with free boundary in gravitational field 02 p0154 A73-12692

Experimental investigation of the pressure and velocity fluctuations in a sound-affected free jet 03 p0290 A73-12965

The stability of oscillatory Stokes layers. 03 p0291 A73-13065

Nonclassical flow theory for continuum mechanics with asymmetrical stress concentration, noting rheological problems in laminar high polymers flow, hydrodynamic instability and turbulent flow 03 p0291 A73-13152

Incompressible fluid turbulent boundary layer flow stability, considering effect of high polymer additives 03 p0291 A73-13168

Ideal dissociating/nondissociating gas reentry flow fields hydrodynamic stability for various free stream and disturbance conditions 03 p0242 A73-13312

A feasibility study for definition of inlet flow quality and development criteria. [AIAA PAPER 72-1098] 03 p0243 A73-13418

Inlet produced flow distortion effect on compressor stability and engine stall, presenting unified theoretical analysis technique for compatible inlet/engine design [AIAA PAPER 72-1115] 03 p0355 A73-13430

Plane Poiseuille flow with small amplitude modulated pressure gradient, noting disturbance shear wave and stability from energy transfer calculation 03 p0293 A73-13530

Boundary conditions for temperature perturbations in stability problems of compressible gas flows 03 p0245 A73-13672

Three dimensional ideal incompressible fluid flows under small velocity perturbation, using Euler equations linearized with respect to steady flow 03 p0296 A73-14048

Nonlinear instability of two dimensional unbounded incompressible viscous fluid flows under periodic small perturbation 03 p0296 A73-14049

Optimal stabilization conditions of turboreactor combustor initial recirculation zone determined by hydraulic analogy technique, describing vorticity generation and mass flow rates [ONERA, TP NO. 1105] 03 p0359 A73-14126

Study of the waves configuration in an axial-flow supersonic compressor [ONERA, TP NO. 1104] 03 p0246 A73-14135

Extension of the Miles-Howard theorem to the circular flows of a compressible fluid. 03 p0297 A73-14443

Stability of nonrotationally symmetric disturbances for inviscid flow between rotating cylinders in the presence of an axial magnetic field. 04 p0433 A73-14899

A procedure for estimating maximum time-variant distortion levels with limited instrumentation. [AIAA PAPER 72-1099] 04 p0432 A73-14908

Helmholtz-Rayleigh instability of nondivergent horizontal flows in a barotropic atmosphere 04 p0441 A73-15287

The influence of planetary vorticity gradient and vertical entropy gradient on the stability of an atmospheric shear layer. 04 p0441 A73-15288

Stability investigation in the case of an oscillating Couette flow. I Nonlinear theory. II - Linear theory [DFVLR-SONDDR-257] 05 p0563 A73-16098

Particular variation of the velocity of the driver gas in a shock tube with electromagnetic blowing with two gases 05 p0601 A73-16429

Application of invariant imbedding techniques to flow instability problems. [AD-756824] 05 p0591 A73-16608

Aircraft wake dissipation by sinusoidal instability and vortex breakdown. [AIAA PAPER 73-107] 05 p0529 A73-16867

A force field theory. I - Laminar flow instability. 05 p0567 A73-17103

Hartmann flow stability of conducting incompressible viscous fluid between parallel plates at arbitrary Reynolds numbers under transverse magnetic field 06 p0727 A73-17453

Experimental investigation of flow stability during intense injection 06 p0643 A73-17462

Instability of a two-layer geostrophic flow with an antisymmetric velocity profile in the upper layer 06 p0691 A73-18728

Investigation of auto-oscillations of a continuous medium, occurring at loss of stability of a stationary mode. 07 p0809 A73-19018

Time-periodic solution of the system of boundary layer equations. 07 p0809 A73-19019

Spatial stability of stagnation water boundary layer with heat transfer. 07 p0919 A73-19503

Nonlinear thermal convection in electrically conducting Boussinesq fluid subject to temperature gradient and magnetic field, calculating flow stability limit by energy method 07 p0920 A73-19513

Steady almost parallel flows linear stability, using multiple scales method for perturbation waves analysis [ONERA, TP NO. 1235] 07 p0811 A73-20072

Planetary boundary layer flow of a stable atmosphere over the globe. 08 p0960 A73-21380

On the simplest example of the barotropic instability of Rossby wave motion. 08 p0985 A73-21388

Prediction of aeroelastic instabilities in turbines 09 p1135 A73-22204

Experimental study of the laminar-turbulent transition on a concave wall in a parallel flow 09 p1071 A73-22450

Nonisothermal instability of flows of viscoelastic media 09 p1072 A73-22481

Instability, transition, and turbulence in buoyancy-induced flows. 10 p1205 A73-23859

Linearized hydrodynamic instability initiation in polymer melts extrusion, examining Weissenberg number role in melt fracture onset 10 p1241 A73-24655

Recent research on unsteady boundary layers; Symposium, Universite du Quebec, Quebec, Canada, May 24-28, 1971, Proceedings. Volumes 1 & 2 10 p1207 A73-24801

Instability of free shear layers adjacent to a vibrating flame surface. 10 p1296 A73-24804

Energy method for unsteady flow stability analysis, exemplifying by oscillatory Stokes layer and impulsively heated fluid layer 10 p1208 A73-24806

Transient flows, effects of unsteady surface conditions on stability, and flow separation in buoyancy induced flows. 10 p1208 A73-24817

Hydrodynamic theory of heat transfer between a stabilized gas suspension flow and channel walls.

10 p1297 A73-24968

A note on the structure of thermal convection in a slightly slanted slot.

10 p1297 A73-24969

On Howard's technique for perturbing neutral solutions of the Taylor-Goldstein equation.

11 p1345 A73-25157

On the stability of plane Couette flow to infinitesimal disturbances.

11 p1346 A73-25158

Finite core model of self induced motions and stability of filament vortex rings in inviscid fluid under small sinusoidal perturbation

11 p1348 A73-26202

Hydrodynamic stability of density-stratified spiral flows.

11 p1348 A73-26388

Oscillations arising when parallel flows of a viscous liquid lose stability relative to periodic long-wave disturbances

11 p1349 A73-26430

Nonlinear behavior of capillary liquid jets ejected from nonsymmetric nozzles, showing effect on flow stability

11 p1349 A73-26432

Feedback stabilization of a multimode two-stream instability.

11 p1406 A73-26556

On oscillatory instability of plane-parallel convective motion in a vertical channel.

12 p1559 A73-27542

Linear stability theory applied to stability characteristics of laminar condensate film flow along inclined wall, noting critical Reynolds number for disturbance amplification

12 p1559 A73-27697

Two-flow instability of interpenetrating ion beams propagating in the same direction along an external magnetic field

12 p1529 A73-27941

The stability of Poiseuille flow - An analysis of two- and three-dimensional disturbances.

13 p1600 A73-28418

Instability of density-stratified incompressible inviscid rotary Couette flow between corotating coaxial vertical cylinders due to gravitational effects

13 p1600 A73-28439

Two dimensional opposing incompressible viscous fluid jets impingement, investigating stagnation surface stability characteristics

13 p1603 A73-29036

Stability of a two-layer fluid model to non-geostrophic disturbances.

13 p1610 A73-29334

Linear stability to axisymmetric perturbations of compressible nondissipative swirling flow, noting Richardson number role

13 p1605 A73-29374

The stability of a thermally radiating stratified shear layer.

14 p1816 A73-30169

Asymptotic solution of initial value problem for weakly nonlinear wave system including dispersive and diffusive effects related to plane Poiseuille flow instability

14 p1744 A73-30171

On the stability of natural convection boundary layer flow over horizontal and slightly inclined surfaces.

14 p1817 A73-30608

Investigation of the stability of a hollow vortex bounded by a rigid wall

15 p1861 A73-31156

Reynolds stresses in plane-parallel flows disturbed by Tollmein-Schlichting waves

15 p1861 A73-31193

Modification of Sygne's criterion for stratified shear flow for spatially growing disturbances.

15 p1862 A73-31334

Determination, by a wall probe, of the changing regime of the flow between two off-center cylinders with very close radii

15 p1863 A73-31568

Effect of intense injection on flow stability and turbulence development

15 p1864 A73-31857

Hagen-Poiseuille flow stability with superimposed rigid rotation, deriving perturbed differential flow equations from Navier-Stokes and continuity equations

16 p1999 A73-33253

Stability of a viscous fluid between rotating cylinders with axial flow and pressure gradient round the cylinders.

16 p2000 A73-33312

Bifurcated small parameter perturbation solutions in boundary layer theory, applying to Falkner-Skan equation and instability in stratified shear flow

16 p2001 A73-33871

Nonlinear algebraic equations in continuum mechanics.

17 p2199 A73-34102

Papers on heat transfer covering thermosiphon technology, flowing gas-solid mixtures, condensation, free convection, flow stability and cryogenic insulation

17 p2254 A73-34351

Natural convection flow equations and stability of laminar and transition flows, external and free boundary flows and boundary layer regimes

17 p2254 A73-34354

Book - Physical fluid dynamics.

17 p2151 A73-34472

The instability due to acoustic radiation striking a vortex sheet on a supersonic stream.

17 p2151 A73-34824

Harmonic and impulsive acoustic source-produced sound propagation across vortex sheet separating two subsonic fluids, investigating instability waves

17 p2151 A73-34825

Foppl vortices stability for two dimensional inviscid irrotational steady flow past circular cylinder

17 p2154 A73-35117

Development and effects of super-critical Taylor-vortex flow in a lightly-loaded journal bearing. [ASME PAPER 73-LUBS-4]

17 p2181 A73-35390

The role of jet stability in edgetone generation. [AIAA PAPER 73-628]

18 p2263 A73-36255

Trailing vortex pair instability in inviscid incompressible fluid with rotating and nonrotating isolated and axial velocity jet core

18 p2300 A73-36628

Velocity profiles in steady and unsteady rotating flows for a finite cylindrical geometry. II.

18 p2300 A73-36629

Concentrated vortex nonlinear oscillations, discussing vortex ring and helical vortex filament stability, mode shape and frequency changes and standing and traveling wave solutions

18 p2301 A73-37004

Generation of time-periodic secondary convective flows

18 p2301 A73-37006

Stability of stratified shear flows.

19 p2421 A73-38226

Linear viscous stability theory for stably stratified shear flow - A review.

19 p2421 A73-38227

Observed generation of an atmospheric gravity wave by shear instability in the mean flow of the planetary boundary layer.

19 p2448 A73-38229

Instabilities in buoyancy-driven boundary-layer flows in a stably stratified medium.

19 p2422 A73-38231

Laboratory observations of shear-layer instability in a stratified fluid.

19 p2422 A73-38232

Numerical investigation of internal waves in jet streams including nonlinear effects.

19 p2449 A73-38233

Hydrodynamics of stratified fluids - The applicability of linear theory.

19 p2422 A73-38243

On the stability of the conduction regime of natural convection in a vertical slot.

19 p2505 A73-38476

Flow stabilization by methods of distributed automatic control

20 p2545 A73-39042

Non-parallel flow corrections for the stability of shear flows.

20 p2546 A73-39092

Study of the stability of a perturbed conducting gas flow in a magnetic field at arbitrary Reynolds magnetic numbers

20 p2597 A73-39276

Taylor vortex occurrences between rotating eccentric cylinders

20 p2547 A73-39284

Stability of parallel flow of a dusty gas in an annulus.

20 p2548 A73-39523

Stationary water flow stability through 90-deg bend with rectangular cross section, noting preserved laminar structure of flow along convex wall

20 p2549 A73-39565

Overheat instability in a flow of electrically conducting incompressible medium under conditions of an internal boundary value problem

20 p2598 A73-39605

Wave dispersion equation for large eccentric elliptic jet stability calculations for noise suppression, using approximate Mathieu functions

20 p2549 A73-39807

Two types of instability of steady convective motion caused by internal heat sources

21 p2789 A73-40192

Global stability of time-dependent flows - Impulsively heated or cooled fluid layers.

21 p2790 A73-40249

Russian book - Convective stability of an incompressible fluid.

21 p2790 A73-40417

The dynamic stability of a pipe conveying a pulsatile flow.

21 p2678 A73-41671

Experimental investigation of hydrodynamic stability for flows past simple membrane surfaces

22 p2840 A73-42117

On the stability of a class of plasma flows with helical flow and field lines.

22 p2892 A73-42351

Dynamics of quasigeostrophic flows and instability theory.

22 p2842 A73-42450

Prediction of stability of viscoelastic Couette flow based on network rupture hypothesis.

23 p2967 A73-43300

Capillary breakup length and stability of Newtonian and viscoelastic cylindrical liquid jets in terms of dimensionless viscosity and relaxation time

23 p2967 A73-43307

Large amplitude baroclinic waves generation via instabilities of two layer fluid in rapidly rotating cylinder compared with mathematical model based on quasigeostrophic equations

23 p3001 A73-43590

Numerical study of the unstable modes of a hyperbolic-tangent barotropic shear flow.

23 p3002 A73-43591

Stability of a flow bounded by elastic walls

24 p3079 A73-44898

Spatial and temporal stability of laminar axisymmetric jet and wake shear layers in viscous and inviscid flow

24 p3079 A73-45308

Stability of a potential vortex with a non-rotating and rigid-body rotating top-hat jet core.

24 p3055 A73-45309

Nonlinear stability of cylindrical vortex enclosing a central jet of light or dense fluid.

24 p3080 A73-45452

FLOW THEORY

NT MIXING LENGTH FLOW THEORY

Method of calculating vortex-free flow around hydrodynamic cascades composed of arbitrary profiles

02 p0128 A73-11788

Conference on Mechanics, Berlin, East Germany, October 13-15, 1971, Reports

03 p0386 A73-13151

Nonclassical flow theory for continuum mechanics with asymmetrical stress concentration, noting rheological problems in laminar high polymers flow, hydrodynamic instability and turbulent flow

03 p0291 A73-13152

A feasibility study for definition of inlet flow quality and development criteria.

[AIAA PAPER 72-1098]

03 p0243 A73-13418

Practical application of boundary layer theory to flow and heat transfer problems in turbomachines.

03 p0398 A73-14145

A theoretical analysis of non-isentropic flow of a compressible, viscous gas in narrow passages.

[ASLE PREPRINT 72LC-3A-1]

03 p0297 A73-14355

Transonic profile theory - Critical comparison of various procedures

03 p0247 A73-14377

Theoretical investigation of transition phenomena in the boundary layer on an infinite swept wing

[DGLR PAPER 72-124]

03 p0248 A73-14379

Statistical transfer theory in non-homogeneous turbulence.

04 p0520 A73-15937

Sinusoidal thermal wave propagation in horizontal fluid layer with small Prandtl number, deriving induced mean flow from nonlinear equation solution by perturbation approach

05 p0591 A73-16188

Unsteady compressible potential flow around lifting bodies - General theory.

[AIAA PAPER 73-196]

05 p0531 A73-16931

Nonsimilar flows between the solution branches of the Falkner-Skan equation.

05 p0567 A73-17116

On unsteady forced flow against a rotating disk.

06 p0643 A73-17394

Upwelling of a stratified fluid in a rotating annulus - Steady state. I - Linear theory.

06 p0684 A73-17702

Applications of shock expansion theory to the flow over non-conical delta wings.

06 p0645 A73-18512

Analysis of internally generated sound in continuous materials. III - The momentum potential field description of fluctuating fluid motion as a basis for a unified theory of internally generated sound.

07 p0909 A73-19097

A correction to 'lifting-line theory as a singular perturbation problem.'

07 p0775 A73-19964

Asymptotic theory of the Boltzmann equation at large Knudsen number.

07 p0853 A73-20473

Inlet air flow distortion in high hub/tip ratio mixed flow turbomachines, using modified actuator disc theory

08 p0925 A73-20784

Special relativity theory for steady irrotational ideal gas flow, noting subsonic, supersonic and transonic flow calculations based on small perturbation theory 08 p0926 A73-21128

Boundary layer theory approximation for hydrodynamic parameters of unsteady laminar boundary layer on body moving in incompressible fluid 08 p0956 A73-21546

Steady nonviscous nonheat-conducting plane flow of compressible fluid, calculating entropy, speed and pressure under assumption of variable pressure along streamlines 09 p1071 A73-22419

Transonic airfoils - Recent developments in theory, experiment, and design. 10 p1171 A73-23856

Three dimensional boundary layer theory, applying Navier-Stokes equations to Newtonian fluids continuous flow over solid bodies or through finite ducts 10 p1171 A73-23863

Prandtl's boundary-layer theory from the viewpoint of a mathematician. 10 p1172 A73-23866

Wall-less electromechanical flow structures developed similar to structures with fluid partially ducted at free sources by external forces 11 p1403 A73-25255

Fish like slender body propulsion and flow theory, discussing fin surface-body thickness interaction, vortex sheets, trailing edges and lifting force 11 p1301 A73-25852

A linearized potential flow theory for airfoils with spoilers. 11 p1301 A73-25853

On the formulation of the traction problem for the flow theory of plasticity. 12 p1551 A73-27046

Asymmetric mechanics of turbulent flows - Energy and entropy 12 p1487 A73-27411

Finite element method applied to analysis of flow over a spillway crest. 13 p1563 A73-28078

Steady universal motions of a Navier-Stokes fluid - The case when the velocity magnitude is constant on a Lamb surface. 13 p1599 A73-28285

A Hamiltonian theory for weakly interacting vortices. 13 p1609 A73-28917

Two dimensional flow of viscous incompressible fluid, discussing formulation in analytic functions with applications to flows past elliptic cylinder and flat plates 13 p1603 A73-29048

Rotating flow evolution in long circular tubes, deriving mathematical formulation for laminar and turbulent flow 14 p1745 A73-30296

Two dimensional incompressible turbulent boundary layer flow theory, considering Bradshaw turbulence field and Felsch integral methods 14 p1745 A73-30298

Application of the energy equation for turbulence in the theory of jet flows 15 p1862 A73-31288

Linearized theory of finite conductivity steady ideal MGD flow past thin wedge in aligned magnetic field, using Fourier integral transform 15 p1917 A73-31338

German book - Theoretical gasdynamics. Volume I - Theory of the flows of compressible media. 15 p1863 A73-31474

Special relativity theory for steady irrotational ideal gas flow, noting subsonic, supersonic and transonic flow calculations based on small perturbation theory 15 p1864 A73-32060

Trapped wave vortex breakdown model for long weakly nonlinear wave propagation on critical flows in tubes of variable cross sections 16 p1998 A73-32796

Stratified Taylor column model for topography effect on slow rotating baroclinic flow, considering Jupiter Red Spot and oceanic observations 16 p1998 A73-32797

Numerical solution for the flow of a fluid in a heated closed cavity. 16 p2084 A73-32929

Laminar-turbulent transition in incompressible boundary layer flow from stability theoretical viewpoint, considering pressure gradient, free stream turbulence and wall roughness effects 16 p1999 A73-33229

Subsonic compressible airfoil cascade flow calculations by series, iterative, matrix and streamline curvature methods, discussing transonic and supersonic cases [ASME PAPER 73-GT-9] 16 p1963 A73-33487

The computation and utilization of Busemann's analysis of potential flow in an impeller. [ASME PAPER 73-GT-45] 16 p1964 A73-33506

Analyticity of the plane steady state solutions of the Navier-Stokes equation. 17 p2150 A73-34324

Book - Lectures on fluid mechanics. 17 p2150 A73-34457

Book - Foundations of fluid flow theory. 17 p2151 A73-34466

Calculation of the flow on a cone at high angle of attack. [AIAA PAPER 73-636] 18 p2260 A73-36195

On the higher approximations of the supersonic projectile theory. [AIAA PAPER 73-669] 18 p2262 A73-36220

A kernel function method for computing steady and oscillatory supersonic aerodynamics with interference. [AIAA PAPER 73-670] 18 p2262 A73-36221

Linear theory for chemically reacting flows. [AIAA PAPER 73-688] 18 p2298 A73-36239

Statistical theory of weakly interacting perturbations and low amplitude turbulence in fluids, considering diffusion, dispersive and acoustic wave characteristics and plasma instabilities 18 p2299 A73-36504

Generalized expressions for secondary vorticity using intrinsic co-ordinates. 18 p2299 A73-36506

Newtonian method of relativistic gas dynamics for steady gas, shock wave, nozzle, Prandtl-Meyer flow and photon gas applications 18 p2300 A73-36632

Recent progress in boundary layer research. [AIAA PAPER 73-780] 19 p2419 A73-37451

Three dimensional boundary layer flow with streamwise vorticity decay, deriving solutions as expansions in terms of eigenfunctions 19 p2420 A73-37851

Turbulent Couette flow statistical theory, applying stochastic analysis to Navier-Stokes equation 19 p2421 A73-37855

Stability of stratified shear flows. 19 p2421 A73-38226

Hydrodynamics of stratified fluids - The applicability of linear theory. 19 p2422 A73-38243

Bounding flow existence for turbulent convection in fluid and porous layers analysis between parallel plates based on calculus of variations in Banach spaces 20 p2626 A73-39012

Nonlinear streaming effects associated with viscous incompressible fluid near oscillating cylinder, considering theory based on outer-inner expansion technique with Stokes drift correction 20 p2546 A73-39088

On a stagnation condition for combining or branching inviscid flows. 20 p2546 A73-39091

Flow theoretical model for nonstationary creep in metals, using Galerkin method for approximate solution of boundary value problem 20 p2616 A73-39099

Decay of the kinetic energy of compressible micropolar fluids. 20 p2547 A73-39341

Two dimensional flow theory of Weis-Fogh lift generation in inviscid motions of insect wings involving viscous effects 21 p2631 A73-40244

Closed-form lift and moment for Osborne's unsteady thin-airfoil theory. 21 p2632 A73-40442

Rarefied gas flows based on variational principle. 22 p2840 A73-41741

Asymptotic unsteady three dimensional flow analysis in axial turbine cascade theory, assuming infinite blade number and unity pitch/chord ratio [ONERA, TP NO. 1249] 22 p2796 A73-42220

Monograph - Quasi homogeneous approximations for the calculation of wings with curved subsonic leading edges flying at supersonic speeds. 22 p2797 A73-42675

Navier-Stokes equation formulation in parabolic coordinates for flow in trailing vortex, obtaining asymptotic expansions for stream function and angular momentum 23 p2939 A73-43205

Poiseuille flow at arbitrary Knudsen numbers and tangential momentum accommodation 24 p3079 A73-45313

Linearized theory of two and three dimensional incompressible viscous flows based on locally unstable velocity profiles related to boundary layer instability mechanism 24 p3081 A73-45546

FLOW VELOCITY

NT SOLAR WIND VELOCITY

An experimental study of the dynamic lift on a cylinder subjected to a high Reynolds number flow perpendicular to its axis. [ONERA, TP NO. 1073] 01 p0001 A73-10226

Arc current, column electric field, mainstream velocity and applied transverse magnetic field relationships in magnetically balanced cross flow plasmas 01 p0084 A73-10738

Exact vorticity solutions of the incompressible Navier-Stokes equations. 01 p0034 A73-11358

Confined laminar jet mixing in a circular channel with arbitrary entrance velocity distribution. [AD-758578] 01 p0034 A73-11363

Number density estimation for neutral hydrogen hot component required for solar wind heating to satisfy observed proton temperature relationship to wind velocity 02 p0205 A73-11745

Flow rate sensor selectivity and additivity transformation functions for two component gas-liquid flowmeter with constrictive device 02 p0167 A73-11868

Integral transformations and conformal mapping for velocity distribution of steady two dimensional potential flow along given profile curve 03 p0241 A73-12904

Measurements of pressure and velocity fluctuations in turbulent pipe flow 03 p0290 A73-12963

Experimental investigation of the pressure and velocity fluctuations in a sound-affected free jet 03 p0290 A73-12965

Boundary value problem for flow equation of multiphase viscous fluid with given velocity distribution, noting equations of motion for incompressible micropolar fluid flow 03 p0291 A73-13164

Micropolar model of blood steady flow through rigid circular tubes, presenting equations solutions and velocity profiles 03 p0266 A73-13302

Conditionally sampled measurements near the outer edge of a turbulent boundary layer. 03 p0293 A73-13526

Existence in the laminar boundary layer of a natural instability not predicted by theory and connected to a wall deformation 03 p0294 A73-13576

Decoding of thermoanemometer data for a flow with velocity, pressure, and temperature pulsations 03 p0308 A73-13667

Turbulent flow velocity pulsations damping in wind tunnel chamber by wire grids, calculating grid turbulence effect 03 p0245 A73-13670

Boltzmann equation model approach for prediction of velocity profiles and gas flow rates through trapezoidal microgaps [ASME PAPER 72-LUB-15] 03 p0297 A73-14331

Observation and spectral analysis of instantaneous signals of velocity fluctuation in the laminar boundary layer 03 p0297 A73-14602

The starting transient of solid-propellant rocket motors with high internal gas velocities. [AIAA PAPER 72-1119] 04 p0486 A73-14909

Ionospheric plasma flow past a semi-infinite cylinder. 04 p0440 A73-14967

Numerical predictions of some three-dimensional boundary layers in ducts. 04 p0433 A73-15006

Calculation of interacting turbulent shear layers - Duct flow. [ASME PAPER 72-WA/FE-25] 04 p0435 A73-15849

Influences of free stream turbulence on mean velocities of turbulent boundary layer without pressure gradient. 04 p0435 A73-15972

Effect of accommodation coefficient on thermal creep flow of rarefied gas. 04 p0436 A73-15973

Rotating paraboloid of revolution in viscous conducting fluid, calculating flow velocity and magnetic field from MHD equations 05 p0601 A73-16172

Numerical solution of laminar jet mixing with and without free stream. 05 p0564 A73-16174

Particular variation of the velocity of the driver gas in a shock tube with electromagnetic blowing with two gases 05 p0601 A73-16429

The swirling turbulent jet. [ASME PAPER 72-FE-18] 05 p0564 A73-16544

Mathematical prediction for pressure distribution over arbitrary thin airfoil in inviscid potential and real fluid flows, determining velocity increment at leading edge 05 p0527 A73-16593

A study of vortex rings using a laser Doppler velocimeter. [AIAA PAPER 73-105] 05 p0565 A73-16865

Turbulent space-time correlation measurements in a plane two-stream mixing layer at velocity ratio 0.3. [AIAA PAPER 73-225] 05 p0566 A73-16951

Kinematic eddy viscosity at low Reynolds numbers. 05 p0567 A73-17111

Diffusion coefficients and current velocities in coastal waters by remote sensing techniques. 05 p0572 A73-17141

Application of constant temperature anemometry in measurement of intra-arterial blood flow velocity. 05 p0545 A73-17274

Hot wire measurement of velocity gradients in a fluid flow. 06 p0692 A73-17626
 [AIAA PAPER 73-50] Airfoil profile determination in inverse hydromechanics problem for given flow velocity distribution, discussing univalent solvability conditions 06 p0686 A73-18067
 Eddy cavitation flow past a wedge 06 p0686 A73-18071
 Viscous compressible flow near right angle corner of two flat plates, presenting streamwise and secondary flow velocities and skin friction coefficient distribution 06 p0687 A73-18532
 Mathematical models for critical flow rates of annular two phase mixtures under various discharge conditions 06 p0688 A73-18563
 On generalized hydrodynamic equations used in heat transfer theory. 06 p0688 A73-18834
 Velocity distribution of quasi-steady and steady flow of ideal incompressible fluids with congruent streamlines, investigating conditions for vortex and irrotational flow 07 p0809 A73-19017
 Two-dimensional turbulent jets at a porous wall. 07 p0811 A73-19613
 Highly uniform inlet velocity profile influence on conical diffuser characteristics 07 p0774 A73-19615
 Flow velocity fluctuation intensity relationship to turbulent energy dissipation based on Kolmogoroff similarity hypothesis 07 p0811 A73-19624
 Second derivatives of the flutter velocity and the optimization of aircraft structures. 07 p0912 A73-19952
 Prandtl eddy viscosity model for incompressible coaxial jet far field velocity decay prediction with non-dimensional term inclusion 07 p0811 A73-19965
 Flow of an ideal incompressible ponderable fluid around a thin profile placed under a free line. I, II 07 p0811 A73-19998
 Flow equation for axisymmetric compressible fluid flow in conical turbine stage, calculating radial distribution of flow velocity 07 p0868 A73-20088
 Possible construction of semiempirical turbulent flow theories 07 p0812 A73-20092
 Spiral flows in finite rotating annular tubes. 07 p0812 A73-20435
 Strain-gauge sensor of flow velocity and fluid discharge 07 p0828 A73-20544
 Unsteady laminar flow in a pipe with arbitrarily changing flow rate. 08 p0954 A73-20867
 Impurity transport in a cylinder in the case of a time-dependent flow rate and gas exchange with the wall 08 p1022 A73-20998
 Velocity distribution of the turbulent motion of a fluid between two plane-parallel walls 08 p0954 A73-21175
 Effect of Doppler ambiguity on the measurement of turbulence spectra by laser Doppler velocimeter. [AD-756047] 08 p0965 A73-21211
 Analysis and space-time reconstruction of the circumferential component of instantaneous velocity in immediate proximity to the wall of a cylinder 08 p0926 A73-21496
 Swirl injector driven air flow in cylindrical tube, measuring flow velocity and turbulent stress tensor components 08 p0956 A73-21601
 Flow parameters and cylinder elongation effects on turbulent boundary layer characteristics for compressible fluid flow, calculating velocity distribution 08 p0956 A73-21602
 Central shock position in supersonic jet impinging on wall, noting flow velocity dependence on pressure 08 p0927 A73-21605
 Discrete vortex scheme of a wing of finite span 08 p0927 A73-21611
 Multiphase flow past thin symmetrical airfoil, applying three velocity model with incident two phase and reflected particle flow components 09 p1027 A73-21993
 Temperature distribution in gas flow about a linear source of heat variable periodically in function of time. 09 p1166 A73-22169
 Flow velocity measurement method based on laser light frequency Doppler shift in scattering experiment on particle seeded liquid, presenting velocity profiles 09 p1094 A73-22314
 Graphoanalytic method of calculating plane potential flows 09 p1029 A73-23106
 Left ventricular blood flow velocity in man studied with the Doppler ultrasonic flowmeter. 09 p1042 A73-23173

Boundary layer efficiency as working fluid in ram-jets for high aircraft speeds, obtaining external efficiency as function of boundary layer parameters and flow rate 09 p1073 A73-23360
 Perturbation method for linearizing equations of supersonic flow over conical bodies, obtaining potential velocity and entropy solutions 10 p1171 A73-23615
 Hot-wire anemometer probe operation in constant current in continuous high-temperature hypersonic turbulent boundary layer, computing velocity and temperature fluctuations 10 p1205 A73-24254
 Breakup length maximum and decrease achievement in laminar viscous jet with velocity increase, discussing effects of ambient gas 10 p1206 A73-24255
 The initial flow past an impulsively started circular cylinder. 10 p1172 A73-24338
 On the response of laminar boundary layers to periodic changes in free-stream speed. 10 p1207 A73-24803
 Incompressible turbulent axisymmetrical impulsive air injection at moderate pressure into stagnant surroundings, measuring flow velocity distribution 10 p1210 A73-24849
 Diffusion aluminizing of Ni and Ni-base alloys by gas circulation method, investigating gas flow velocity effect relationship to specimen weight gain 10 p1226 A73-24957
 Considerations concerning the solution of Chandrasekhar's system of equations in the case of MHD turbulence 11 p1404 A73-25700
 On the turbulent thermal diffusion parallel to a plane wall for y/δ equals 2 to 300 11 p1451 A73-25870
 The force acting from the direction of a flow of liquid on a thin curved body of circular cross section 11 p1348 A73-26427
 Oscillations arising when parallel flows of a viscous liquid lose stability relative to periodic long-wave disturbances 11 p1349 A73-26430
 NASA use of liquid and gaseous oxygen under extreme pressure, temperature and flow rate conditions, discussing safety requirements in terms of structural and chemical compatibility 11 p1410 A73-26525
 Application of lasers, radioisotopes, and the correlation method for measuring flow velocity 12 p1495 A73-26847
 A low-velocity hot-wire anemometer. 12 p1496 A73-27055
 The limits and the nature of the onset of influence of thermogravitational forces on turbulent flow and heat transfer in vertical tubes 12 p1487 A73-27313
 Electrohydrodynamic equation solutions for non-collinear current density and velocity vectors of unipolarly charged fluid flow in channel with wall-type electrodes 12 p1528 A73-27406
 Dynamic measurement of the basic quantities of fluids 12 p1461 A73-27596
 A direct integral equation method for the potential flow about arbitrary bodies. 13 p1563 A73-28083
 Steady universal motions of a Navier-Stokes fluid - The case when the velocity magnitude is constant on a Lamb surface. 13 p1599 A73-28285
 Rain fall deceleration effect on flow velocity of infinitely deep water mass, solving Navier-Stokes equations via Laplace transforms 13 p1600 A73-28419
 Using a single hot-wire probe in three-dimensional turbulent flow fields. 13 p1600 A73-28526
 The influence of acoustic disturbances on the mechanics in shear layer behind a circular cylinder in air flow. 13 p1563 A73-28530
 Flow of viscous fluid at small Reynolds numbers past a porous body. 13 p1601 A73-28625
 Approximate shock-free transonic solution for a symmetric profile at zero incidence. 13 p1564 A73-28823
 Effects of free stream velocity profile on turbulent boundary layer, with some reference to the effects of free stream turbulence. 13 p1602 A73-29013
 The thick turbulent boundary layers on rotating cylinders in axial flow. 13 p1602 A73-29016
 The input characteristic due to the interaction of jets of beam-deflection amplifier. 13 p1571 A73-29037
 Measurement of rarefied gas flow rates from the drift of an ion mark produced by an electron beam 13 p1619 A73-29167

Problems of theory and practical application of Doppler-laser rate measuring devices in turbulent flow studies 13 p1628 A73-29169
 Turbulence measurements with the split-film anemometer probe. 13 p1619 A73-29253
 Hot-wire anemometric velocity measurements in nonisothermal turbulent flows, compensating for local temperature effects on downstream wire 13 p1620 A73-29255
 Interpretation of hot-film anemometer response in a non-isothermal field. 13 p1620 A73-29256
 The unpolarized electrode in a pulsating Poiseuille pipe flow. 13 p1620 A73-29258
 An attempt to characterize the 'turbulence burst phenomena' using digital time series analysis. 13 p1604 A73-29260
 Free parallel shear flow approximation by velocity discontinuity involving Kelvin-Helmholtz waves longer than shear layer thickness 13 p1605 A73-29448
 Density measurements in high speed arc heated flows. 13 p1622 A73-29640
 Measurement of gas quantities by liquid displacement. 14 p1723 A73-30048
 Two-dimensional bubbles in slow viscous flows. II. 14 p1744 A73-30170
 An accurate method for solving some theoretical problems of spatial supersonic gas flows 14 p1712 A73-30826
 Transport effects in a turbulent flowing plasma - The moment relations. 15 p1916 A73-31082
 Velocity hodograph solvability and univalence problems in hydromechanics for profiles in duct, bounded flow and cascades 15 p1861 A73-31151
 Flow deceleration as mechanism of vortex ring formation, showing liquid mass variability and vortex clusters of spheroid and hemisphere shapes 15 p1861 A73-31282
 Velocity structure of a flow in a magnetic field periodically varying along the flow 15 p1918 A73-31413
 An approximate method for the calculation of the velocities induced by a wing oscillating in subsonic flow 15 p1824 A73-31905
 Plasma fine velocity structure and dynamics from diffraction pattern of interplanetary radio sources scintillation 15 p1919 A73-31959
 Measurement using the Doppler effect of small velocities in flows occurring in the free convection of fluids. 15 p1864 A73-32069
 The heat loss of hot wires and heat films in steady flow 15 p1879 A73-32349
 Longitudinal evolution of the velocity and pressure in a circular duct in pulsating flow 16 p1998 A73-32805
 Galactic neutral hydrogen observations along loop III, noting loop effects on gas velocity distribution 16 p2058 A73-32835
 Stability of a viscous fluid between rotating cylinders with axial flow and pressure gradient round the cylinders. 16 p2000 A73-33312
 Poiseuille flow and thermal creep of a rarefied gas between parallel plates. 16 p2085 A73-33315
 The significance of the climate factor air velocity in environmental simulation 16 p1997 A73-33381
 On the unsteady supersonic cascade with a subsonic leading edge - An exact first order theory. II. [ASME PAPER 73-GT-16] 16 p1964 A73-33493
 Mathematical models for critical flow rates of annular two phase mixtures under various discharge conditions 16 p2000 A73-33588
 Computerized stream-curvature method for calculation velocity distribution and stream surface twist effects for three dimensional flow through gas turbine blade passage 17 p2092 A73-34378
 Effect of axial velocity variation on deviation for compressor cascades. 17 p2092 A73-34383
 Flight test studies of the formation and dissipation of trailing vortices. [SAE PAPER 730295] 17 p2094 A73-34659
 Laser anemometer for the measurement of air flow velocities 17 p2167 A73-34775
 A dynamic modeling method of unsteady flows in long fluid lines with turbulent bulk velocities. [ASME PAPER 73-FE-18] 17 p2153 A73-35014

An assessment of three-dimensional turbulent boundary layer prediction methods. [ASME PAPER 73-FE-25] 17 p2153 A73-35020

Out-of-plane vibration and stability of curved tubes conveying fluid. [ASME PAPER 72-WA/APM-36] 17 p2248 A73-35101

Critical flow speed divergence in aeroelastic systems stability loss, discussing statistical analysis using partial differential equation 17 p2250 A73-35119

Alternating direction implicit finite difference computational method for solving two dimensional Navier-Stokes equations for high and low speed flows 17 p2202 A73-35140

Turbulent flow research, discussing time domain analysis of velocity, displacement and pressure, potential flow models of vortices, and shear flow turbulence 17 p2155 A73-35330

Kinetic energy transfer during multiple jet mixing from primary jet array to secondary stream for various velocity ratios 17 p2156 A73-35511

Time evolution of pulsating air jets from schlieren photography and velocity measurements, using motor driven piston 17 p2157 A73-35514

Turbulent mixing of cylindrical jet with parallel stream in terms of mixing length concepts and velocity profiles 17 p2157 A73-35515

Velocity distribution in hypersonic helium flow near the leading edge of a flat plate. [AIAA PAPER 73-691] 18 p2262 A73-36242

Turbulence measurements in interacting wakes. 18 p2301 A73-36698

Certain vortical flows with variable vorticity past a circular cylinder 18 p2302 A73-37009

Experimental investigation of the velocities in the turbulent wake behind bodies of revolution 18 p2266 A73-37017

Parametric analysis of turbulent wall jets. 19 p2376 A73-37491

The velocity profile in the wall region of a turbulent boundary layer 19 p2420 A73-37554

Studies on the hydraulic loss in pipe bends - Results for 90-deg screw type elbows. 19 p2420 A73-37672

Velocity distributions of rough wall turbulent boundary layers without pressure gradient. 19 p2422 A73-38284

Cross flows in bounded three-dimensional turbulent boundary layers. 19 p2422 A73-38298

Potential created by a test particle in one-, two- and three-dimensions in a flowing ion-electron plasma. 20 p2596 A73-38969

Asymptotic behaviour of a scalar in an axisymmetric final period turbulent wake. 20 p2507 A73-39086

Flow through non-uniform gauze screens. 20 p2508 A73-39811

Dynamo theory for geomagnetic field, emphasizing fluid flow symmetric and asymmetric velocity component relative magnitudes 21 p2679 A73-39930

Respirator cartridge filter efficiency under cyclic and steady-flow conditions. 21 p2643 A73-40408

Formation of a plasma focus in erosion-type plasma accelerators. I 21 p2746 A73-40525

Experimental study of conductivity, velocity, and temperature distributions in a submerged jet of low-temperature plasma 21 p2747 A73-40575

Contribution to the study of the development of a jet issuing from a nozzle of small elongation and confined between two lateral walls 21 p2677 A73-40620

Problems of the aerodynamics of satellites with uniaxial orientation 21 p2781 A73-40902

On the radiation from an aerodynamic acoustic dipole source 21 p2633 A73-40943

Turbulent incompressible plane wall jet flow in still air, examining maximum velocity, total thickness and inner length scale with parametric analysis 21 p2678 A73-41191

Interpretation of hot-wire anemometer readings in a flow with velocity, pressure and temperature fluctuations. 21 p2705 A73-41317

Turbulent flow velocity pulsations damping in wind tunnel chamber by wire grids, calculating grid turbulence effect 21 p2633 A73-41319

Noise from an isolated rotor due to inflow turbulence. 22 p2795 A73-41711

A note on residual drop and single drop formation. 22 p2840 A73-41748

Experimental investigations of the effects of polymer additions on the kinematic characteristics of a plane turbulent flow in a tube with variable wall roughness 22 p2841 A73-42121

Calculation of the maximum attainable efficiency of a moving compressor blade cascade 22 p2797 A73-42646

The dynamic behavior of articulated pipes conveying fluid with periodic flow rate. [ASME PAPER 73-APMW-32] 22 p2925 A73-42892

Experimental investigation of turbulent flow characteristics in a rotating channel 23 p2968 A73-43443

Experimental investigation of a turbulent boundary layer on a triangular plate with a wedge 23 p2939 A73-43473

Precise method for solving certain problems of the theory of three-dimensional supersonic gas flows. 23 p2939 A73-43582

The effects of the exit velocity profile on the flow of a circular jet exhausting normal to the free stream. 23 p2969 A73-44125

Interaction between flows with different velocities in the solar wind 24 p3124 A73-44780

Critical two phase He flow rates prediction based on homogeneous thermal equilibrium model, Henry-Fauske data and empirical correction factor curve 24 p3077 A73-44823

Hypersonic flow velocity measurements using laser velocimeter. [AIAA PAPER 73-1046] 24 p3090 A73-44870

Study of the steady flow of an incompressible viscous fluid around a cylinder in rotation 24 p3079 A73-45219

Influence of velocity pulsations on the range of stable combustion of homogeneous mixtures 24 p3157 A73-45382

Compressible laminar boundary layer differential equations solution for incident viscous gas flow on flat plate at high flow velocity 24 p3080 A73-45471

FLOW VISUALIZATION

NT NUMERICAL FLOW VISUALIZATION

Free jet expansion from concentric orifices into vacuum. 02 p0152 A73-11528

Application of the moire effect for studying flows of a continuous medium 02 p0230 A73-11721

A new dimension in front-light laser photography. 03 p0309 A73-14199

Flame propagation in premixed propane /air or propane/ oxygen vortex rings, describing normal and schlieren photographic techniques 03 p0399 A73-14399

Visualization study of flow in axial flow inducer. [ASME PAPER 72-FE-33] 05 p0565 A73-16547

Flow visualization of the near-wall region in a drag-reducing channel flow. 06 p0685 A73-17709

Thermal tagging for laminar and turbulent liquid flow shadowgraph visualization by ND glass laser beam 06 p0696 A73-18573

The use of aerosols for the visualization of flow phenomena. 06 p0683 A73-18837

Visualization of boundary layer flow patterns around protuberances using an optical-surface indicator technique. 07 p0808 A73-19530

Band position predictions in schlieren visualization of hypersonic entropy wake behind blunt bodies, assuming bow shock geometry 07 p0775 A73-19970

Streamline deflection by diffusion flame stabilized on Parker-Wolfhard burner, discussing flow visualization and Burke-Schumann flame sheet in Oseen flow 07 p0921 A73-20355

Visualization of thermal fields in saturated porous media by the Christiansen effect. 08 p0963 A73-21030

Pattern of blood flow within the heart - A stable system. 08 p0930 A73-21214

Experiments on a shrouded, parallel disk system with rotation and coolant throughflow. [AD-759594] 08 p1023 A73-21256

Species separation in swirling expansion jet of gases mixture. 08 p0956 A73-21774

Dense air plasma compression and heating by TNT explosive charge, noting shock tube flow patterns 10 p1203 A73-23515

Book - Annual review of fluid mechanics. Volume 5. 10 p1205 A73-23851

Liquid and gas flow visualization methods, discussing water tests and hydraulic analogies [ONERA, TP NO. 1222] 10 p1172 A73-23864

Visualization experiments on unsteady viscous flows around cylinders and plates. 10 p1174 A73-24836

Hydrodynamic visualization technique application to unsteady flow patterns around models and analysis of boundary layers, separation and wakes 10 p1174 A73-24842

An investigation of unsteady aerodynamics on an oscillating airfoil. [AIAA PAPER 73-318] 11 p1301 A73-25549

Flow visualization of two and three dimensional wall jets on circular cylinder, observing flow characteristics sensitivity to curved boundary 13 p1603 A73-29038

Study of the effects of geometrical parameters on the characteristics of air jet flow by some optical methods. 13 p1618 A73-29039

Visualization of unsteady flow over oscillating airfoils. 13 p1620 A73-29270

Book - Illustrated experiments in fluid mechanics - The NCFMF book of film notes. 14 p1743 A73-29725

HF laser flow visualization with an infrared television system. 15 p1874 A73-31357

Parachute gore shape and flow visualization during transient and steady-state conditions. 15 p1828 A73-31458

Photographic studies of the transition between continuum and free molecular flow. 15 p1864 A73-31935

Investigation of a gas flow on an aeroballistic track by holographic methods 15 p1879 A73-32328

Qualitative study of flow deviation by a wall cavity 16 p1962 A73-32811

Thermal tagging for laminar and turbulent liquid flow shadowgraph visualization by Nd glass laser beam 16 p2016 A73-33598

Development of a turbulent mixing region in a liquid 17 p2150 A73-34265

Book - Flow visualization: Optical methods of analyzing fluid flows. 17 p2165 A73-34459

Flight test studies of the formation and dissipation of trailing vortices. [SAE PAPER 730295] 17 p2094 A73-34659

Application of the hydrogen-bubble technique for velocity measurements in thin liquid films. [ASME PAPER 73-APM-8] 17 p2153 A73-35033

A detailed experimental analysis of dynamic stall on an unsteady two-dimensional airfoil. [AHS PREPRINT 702] 17 p2095 A73-35053

Dense air plasma compression and heating by TNT explosive charge, noting shock tube flow patterns 17 p2147 A73-35195

Specie number density, pitot pressure, and flow visualization in the near field of two supersonic nozzle banks used for chemical laser systems. [AIAA PAPER 73-642] 18 p2322 A73-36200

Supersonic, turbulent boundary layer separation measurements at Reynolds number of 10,000,000 to 100,000,000. [AIAA PAPER 73-665] 18 p2261 A73-36216

Investigation of two-dimensional cavity diffusers. [AIAA PAPER 73-685] 18 p2262 A73-36236

Experimental investigation of the velocities in the turbulent wake behind bodies of revolution 18 p2266 A73-37017

Quantitative study of an aerodynamic flow by holographic interferometry 18 p2317 A73-37082

Smoke visualization of three-dimensional flow patterns in a nominally two-dimensional wake. 19 p2375 A73-37423

High-speed photography of laser-induced cavities in liquids 21 p2709 A73-39968

Visualization of gas flows by means of high-speed holography 21 p2696 A73-39978

Aeroballistic gas flow investigation using holographic device to schlieren systems. 21 p2696 A73-39981

Holographic interferometry applied to aerodynamics. 21 p2696 A73-39984

Study of turbulent wakes behind cones in hypersonic flight using Schlieren photograph correlation 21 p2696 A73-39985

High speed cinematographic study of mass flow rate of pressurized subcooled liquid nitrogen inward choked flow through radial gap at various stagnation pressures 21 p2740 A73-40634

Complex flow in vapour columns over boiling cryogenic liquids. 21 p2740 A73-41102

French monograph - Contribution to the experimental study of a boundary layer trap in a supersonic air inlet. 22 p2797 A73-42740

- Helium bubble survey of an opening parachute field. 22 p2798 A73-43112
- Axial vortex and Coanda vortex flow controllers. 23 p2941 A73-43392
- Investigation of the flow pattern in the wall region of a turbulent boundary layer during injection with a positive pressure gradient 24 p3079 A73-45080

FLOWMETERS

NT HOT-WIRE FLOWMETERS
NT RHEOMETERS

Non-invasive technique for diagnosing atrial septal defect and assessing shunt volume using directional Doppler ultrasound - Correlations with phasic flow velocity patterns of the shunt.

Flow rate sensor selectivity and additivity transformation functions for two component gas-liquid flowmeter with constrictive device 01 p0014 A73-11505

Blood flow and pressure and ECG data acquisition and transmission via radio telemetry system with electromagnetic flowmeter 02 p0167 A73-11868

The measurement of a pulsating air flow using a sharp-edged orifice meter. [ASME PAPER 72-WA/FE-36] 04 p0451 A73-15853

A signal simulator for testing laser-Doppler flow-velocity systems. 05 p0562 A73-16442

A new probe for measurement of velocity and flow direction in separated flows. 08 p0963 A73-20871

Optimal measurement location for integrating pipe flowmeters, exemplifying by linearly integrating ultrasonic flowmeter 09 p1086 A73-23114

Left ventricular blood flow velocity in man studied with the Doppler ultrasonic flowmeter. 09 p1042 A73-23173

Induction flowmeter theory in a T-tube of circular section. 10 p1220 A73-24619

Modern developments in flow measurement; Proceedings of the International Conference, Harwell, Berks., England, September 21-23, 1971. 10 p1220 A73-24852

Variable area, positive displacement, turbine type, electromagnetic and pressure difference flowmeters, noting reliability, repeatability and accuracy 10 p1221 A73-24853

Laser Doppler velocimeter configuration and operation, discussing applications and test results 10 p1229 A73-24856

Microwave Doppler flowmeter design and performance, discussing free flow monitoring of sand from hopper and pneumatic conveying of alumina through steel pipe 10 p1221 A73-24859

State of art of flowmetering, discussing acceptability factors, weirs, laser Doppler velocity method, ultrasonic type, pressure difference technique and turbine and electromagnetic devices 10 p1221 A73-24862

A simplified method for the in vitro calibration of electromagnetic flowmeters. 12 p1464 A73-27027

Inductive flow meter sensor design for optimal electrode diameter to ensure signal quality and impedance matching, proposing circuit diagram 13 p1611 A73-28019

Theory of mass flow measurement - Its advantages and instrumentation related to same. 17 p2166 A73-34619

A flowmeter to measure cloud liquid content. 17 p2174 A73-35578

The application of a scanning laser Doppler velocimeter to trailing vortex definition and alleviation. [AIAA PAPER 73-680] 18 p2315 A73-36231

FFTF probe-type eddy-current flowmeter - Wet versus dry performance evaluation in sodium. 21 p2738 A73-40768

Electromagnetic flowmeters with point electrodes and finite length insulating liners, discussing performance numerical analysis accuracy by comparison with exact analytic solutions 22 p2860 A73-42300

Comparison of plethysmographic and electromagnetic flow measurements. 23 p2950 A73-44215

FLOX

Investigations in connection with the preliminary development of a FLOX-polyethylene hybrid propulsion system [DGLR PAPER 72-086] 02 p0202 A73-11676

Thermal control and structures approach for fluorinated propulsion. [AIAA PAPER 73-772] 18 p2360 A73-36386

FLUCTUATION THEORY

Periodically correlated random processes to model additive and multiplicative rhythmic phenomena, discussing structural properties and theorems 01 p0075 A73-10028

Statistical theory of light propagation in a turbulent medium /Survey/ 02 p0141 A73-12485

Power reduction and fluctuations caused by narrow laser beam motion in the far field. 08 p0975 A73-21059

Fluctuation theory for isothermal and nonisothermal semibounded plasma, obtaining correlation functions, dispersion laws and damping coefficients 09 p1129 A73-22689

Application of the fluctuation model of superplasticity to calculate the surface tension of metals during phase transformations 10 p1235 A73-24455

Influence of elastic collisions on the intensity of natural oscillations in a He-Ne laser 11 p1376 A73-25432

Focused laser irradiance fluctuations in a turbulent medium. 11 p1376 A73-25874

Fluctuation theory of the two-dimensional mixed state of superconductors of the first kind 16 p2044 A73-34068

Fluctuations in plasma and nonlinear susceptibilities. 17 p2217 A73-35817

Nonlinear wave interaction and fluctuations in plasma. 17 p2217 A73-35818

Transition probability approach to the theory of plasmas. 17 p2218 A73-35819

Fluctuation model of superplasticity and surface tension of a metal at a phase transition. 19 p2442 A73-38137

Frequency spectra of strong fluctuations of laser radiation in a turbulent atmosphere 19 p2406 A73-38337

Polarization of signals which are reflected from a group of independently fluctuating targets. 20 p2529 A73-38927

Influence of a random transport-velocity component on the space-time correlations of signal fluctuations 23 p2954 A73-43647

FLUERIC

An analytical and empirical basis for the design of turbulence amplifiers. I - Analysis and experimental confirmation. [ASME PAPER 72-WA/FLCS-1] 04 p0408 A73-15859

An analytical model for the response of fluoric wall attachment amplifiers. 16 p1970 A73-33474

Effect of contamination on fluoric system reliability. 16 p1971 A73-33476

Single axis analog fluoric accelerometer using mercury as solid proof mass, describing differential gas pressure outputs, porous cylindrical configuration and hydrostatic pressure gradients 19 p2389 A73-38076

Prediction of the dynamic and quasi-static performance characteristics of fluoric wall-attachment amplifiers. 20 p2511 A73-39756

A hot gas actuator for missile control. 23 p2942 A73-43398

FLUID AMPLIFICATION

U FLUID AMPLIFIERS

FLUID AMPLIFIERS

NT JET AMPLIFIERS

Theoretical analysis of the flow through a particular wall-attachment fluidic component. 03 p0295 A73-13767

Model studies of an electrohydraulic amplifier 03 p0258 A73-14617

An analytical and empirical basis for the design of turbulence amplifiers. II - Empirical relationships and design procedure. [ASME PAPER 72-WA/FLCS-2] 04 p0408 A73-15860

Jet interaction in a simplified model of a bistable fluid amplifier. [ASME PAPER 72-WA/FLCS-6] 04 p0409 A73-15863

An experimental study of flow fields in bistable fluid amplifiers. [ASME PAPER 72-WA/FLCS-9] 04 p0409 A73-15864

Work carried out by Societe Bertin under contract to CNES in the field of fluidic control 07 p0904 A73-18938

The dynamic response of a diaphragm-ejector amplifier. 08 p0929 A73-21830

Pneumatic controller with two cascade amplification stages and mechanical solid state gain adjustment variable feedback system 10 p1177 A73-24020

Flow analysis of three-dimensional diffuser for fluid amplifier. 13 p1603 A73-29033

A study of frequency selection and jumping peculiar to some fluidic oscillations. 13 p1603 A73-29034

Response of a jet to a pressure gradient and its relation to edgetones. 13 p1603 A73-29035

The input characteristic due to the interaction of jets of beam-deflection amplifier. 13 p1571 A73-29037

A study of switching process and design parameters of supersonic fluidic amplifiers. 13 p1571 A73-29042

Optimization of energy transfer in cascaded fluid jet deflection amplifiers. 13 p1571 A73-29045

Some investigations on frequency demodulating systems with fluidic jet deflection amplifiers. 13 p1572 A73-29046

The effectiveness of flow control devices and circuits. 16 p1970 A73-33473

An analytical model for the response of fluoric wall attachment amplifiers. 16 p1970 A73-33474

A model for the prediction of the time delay characteristics of turbulence amplifiers. 19 p2389 A73-38075

Prediction of the dynamic and quasi-static performance characteristics of fluoric wall-attachment amplifiers. 20 p2511 A73-39756

Axial vortex and Coanda vortex flow controllers. 23 p2941 A73-43392

Pneumatic fluidic operational amplifier application to proportional position servomechanism with hydraulic actuator for high force output, considering working fluid and Reynolds number effects 23 p2941 A73-43397

Turbulence amplifier with transition process control for multi-input fluid logic OR device operation at very low pressures and flow rates 23 p2942 A73-43399

An experimental investigation of the induced turbulence in laminar channel flow due to a transverse ion current and its applications to fluidic turbulence amplifiers. 23 p2942 A73-43402

Oil hydraulic fluidic amplifier mathematical model and computerized design for power consumption optimization at high pressures, testing performance dependence on viscosity 23 p2942 A73-43405

Diaphragm ejector pulse shortener for transforming periodic input signal into sharp pulses by adjusting vent areas of two fluid amplifiers 23 p2942 A73-43408

The diaphragm-ejector proportional amplifier and its application to fluidic operational circuits. 23 p2943 A73-43409

Small ejector system for fluidic subtracting network with diaphragm operated Schmitt trigger proportional amplifier and pneumatic signal generator, discussing construction and characteristics 23 p2943 A73-43410

Fluidic logic circuit universal block with turbulence amplifiers for control of servomechanisms, comparing with use of conventional fluid logical elements 23 p2943 A73-43414

Signal transmission in analog fluidic systems mainly with respect to noise influence. 23 p2944 A73-43421

Of fluid mechanics and fluidics and of analysis and physical insight. 23 p2945 A73-43432

FLUID BOUNDARIES

NT GAS-SOLID INTERFACES

NT JET BOUNDARIES

NT LIQUID-LIQUID INTERFACES

NT LIQUID-SOLID INTERFACES

NT LIQUID-VAPOR INTERFACES

Thermal convection in a horizontal fluid layer with uniform volumetric energy sources. 01 p0120 A73-10442

Nonlinear waves on interface of two incompressible inviscid fluids of different densities and arbitrary surface tension analyzed by multiple scales method 01 p0032 A73-10445

Wave coupling at a collisionless plasma discontinuity. 02 p0198 A73-12408

Determination of the statistical characteristics of temperature fluctuation in pool boiling. 08 p1022 A73-21252

Calculation of one-dimensional hydrodynamic in Eulerian coordinates 09 p1070 A73-21922

Two approximate methods for describing the steady motions of an incompressible viscous fluid with a free boundary 09 p1072 A73-22619

Effect of elastic displacements of a cylindrical shell on the vibrations of the free surface of a fluid 09 p1073 A73-23345

Parallel magnetic field effect upon plane interface stability between two conducting viscous fluids in uniform relative motion, obtaining neutral shear flow stability curves
11 p1402 A73-25054

Steady doubly periodic convection regimes in horizontal fluid layer heated at lower surface, considering branching from state of rest
12 p1559 A73-27420

Classical solutions to the second boundary value problem for the unsteady free convection equations
12 p1559 A73-27421

Kerr metric properties and astrophysical implications, presenting perfect fluid boundaries family in weak field approximation and photon orbits behavior in equatorial plane
14 p1798 A73-30143

Artificial viscosity related to shocks for studying anomalous wall heating and solution behavior at interface by substituting Rankine-Hugoniot equation
14 p1775 A73-30908

Investigation of the stability of a hollow vortex bounded by a rigid wall
15 p1861 A73-31156

Development of convection in horizontal layers of a non-Newtonian fluid
16 p2084 A73-32679

Two dimensional wedge flow singularities for free and fixed boundaries at flow separation points, applying to water entry problem
16 p1999 A73-32928

Numerical solution for the flow of a fluid in a heated closed cavity.
16 p2084 A73-32929

On the Oseen limiting movements around a rectilinear profile placed under a free line
19 p2459 A73-37526

Suppression of free convection by a distributed automatic controller
20 p2626 A73-39043

Global stability of time-dependent flows - Impulsively heated or cooled fluid layers.
21 p2790 A73-40249

FLUID DYNAMICS

NT AERODYNAMICS

NT AEROTHERMODYNAMICS

NT ELASTOHYDRODYNAMICS

NT ELECTROHYDRODYNAMICS

NT GAS DYNAMICS

NT HYDRODYNAMICS

NT MAGNETOHYDRODYNAMICS

NT RAREFIED GAS DYNAMICS

NT ROTOR AERODYNAMICS

Determination of the dynamic characteristics of a fluid in a moving vessel in the presence of a weak gravitational field by the eigenfunction expansion method
01 p0030 A73-10095

Linear solutions for heat propagation in relativistic fluid dynamics
01 p0076 A73-10266

Stability criteria for unsteady motion of incompressible Cosserat fluid in arbitrary time dependent domain, using Liapunov function
01 p0033 A73-10776

A discrete numerical approach to fluid dynamics.
01 p0071 A73-11461

Wave front propagation velocity definition valid for classical and relativistic fluid dynamics
02 p0152 A73-11572

Convection heat transfer in a contained fluid subjected to vibration.
03 p0398 A73-13547

A discussion of the Marsh matrix technique applied to fluid flow problems.
03 p0244 A73-13563

An analytical fluid dynamic model of turbulent inlet flow.
06 p0644 A73-17647

[AIAA PAPER 73-138] French monograph - Determination and utilization of the laws of viscoelastic fluid behavior.
06 p0686 A73-18098

Boundary value problems of viscous fluid dynamic system generated by Navier-Stokes equations, using Hopf theory
06 p0724 A73-18634

Establishment of thermal equilibrium in a liquid near the critical point.
08 p1021 A73-20857

Investigation of the motion of the medium near the point of contact of shock waves in linear and nonlinear formulations
09 p1070 A73-21921

Fluid dynamical method for computing spherical star cluster evolution based on Fourier transformation of Liouville-Boltzmann equation
10 p1273 A73-23612

Finite element solution algorithm for viscous incompressible fluid dynamics.
10 p1243 A73-24296

A priori bounds for some bifurcation problems in fluid dynamics.
10 p1207 A73-24786

The motion of a viscous, stratified fluid subjected to forced oscillations.
10 p1210 A73-24844

The dynamical effect of inertial waves on the gyroscopic motion of a body containing several eccentrically located liquid-filled cylinders.
11 p1346 A73-25224

Fluid turbulence equations for large molecular drift velocity gradients in rarefied gas, near surface and stellar system motions, using Predvoditelev hydrodynamic equations
11 p1347 A73-25733

Natural oscillations of density-stratified ideal incompressible liquid in rectangular vessel, solving oscillation equation for various density distributions
11 p1349 A73-26441

A new conception of modeling the process of heat transfer on a surface with artificial roughnesses and microfins
12 p1557 A73-26798

Piezoelectric gages for fluid dynamic multicomponent force measurements, discussing quartz transducers, measurement accuracy and capability for rapidly fluctuating forces measurement
12 p1499 A73-27871

High Reynolds number fluid dynamics and heat and mass transfer in real concentrated particulate two-phase systems.
13 p1704 A73-28427

Viscous fluid sloshing in rectangular vessel, studying forced oscillations, ejected flow and frequency equation based on Navier-Stokes equations and boundary conditions
13 p1600 A73-28444

Two dimensional flow of viscous incompressible fluid, discussing formulation in analytic functions with applications to flows past elliptic cylinder and flat plates
13 p1603 A73-29048

Turbulent shear research, considering nondimensional data correlation, governing equations solution for parameters, statistical and experimental methods for structure determination
13 p1604 A73-29259

Book - Computer fluid dynamics: Recent advances.
14 p1744 A73-29743

Book - Computational fluid dynamics.
14 p1745 A73-30359

A solution operator for ordinary differential equations and its application in fluid dynamics
15 p1862 A73-31329

German book - Similarity laws and model rules of aerodynamics.
15 p1863 A73-31475

Book - Foundations of fluid flow theory.
17 p2151 A73-34466

Book - Physical fluid dynamics.
17 p2151 A73-34472

Computational Fluid Dynamics Conference, Palm Springs, Calif., July 19, 20, 1973, Proceedings.
17 p2095 A73-35126

Viscous fluid dynamic problem solution method implementation in Eulerian code AZTEC within continuum mechanics-kinetic theory union, preserving conservation properties throughout time integration
17 p2155 A73-35142

Russian book - Fundamentals of the dynamics and heat and mass transfer of fluids under conditions of weightlessness.
18 p2297 A73-35868

Turbulent flow fields with two dynamically significant scales.
18 p2297 A73-36201

[AIAA PAPER 73-646] The correlation between the kinematic structure of the flow and the energy transfer in the rotors of fluid flow machines
18 p2299 A73-36487

Diffusion of a vertical jet into a fluid medium of arbitrary density
19 p2420 A73-37547

Compressible fluid dynamic theory, using stress tensors to derive constitutive equations for plane homogeneous and shear flows
19 p2420 A73-37644

Multipoint distribution calculation of the isotropic turbulent energy spectrum.
19 p2421 A73-37854

Oscillating spherically symmetric charge-matter fluid for avoidance of singularities in gravitational collapse models
21 p2766 A73-40316

Motion of a two-component stratified gas-liquid flow in a horizontal pipe
21 p2677 A73-40989

Book on engineering dynamics similarity and scaling methods covering blast waves and gas dynamics, transient loads, fluid-structure interaction, soil dynamics, thermal modeling, etc
23 p3039 A73-43460

FLUID FILMS

Pressure distribution vs porosity and load variation with permeability for squeeze fluid films in porous metal journal bearings
[ASME PAPER 72-LUB-P] 01 p0055 A73-10219

Analysis of face deformation effects on gas film seal performance.
01 p0055 A73-10246

Hybrid fluid film and rolling element bearings for long fatigue life and gas bearings for high temperature operation in gas turbine applications
[SAE PAPER 720739] 02 p0173 A73-12005

Low-cost fluid film bearings for gas turbine engines.
[SAE PAPER 720740] 02 p0174 A73-12006

Finite element technique application for determining velocity field of three dimensional fluid continuum and pressure distribution of lubrication film described by Reynolds equation
03 p0289 A73-12872

Computer-aided design of externally pressurized bearings.
03 p0311 A73-13202

The performance of a four-pocket conical hydrostatic bearing.
03 p0311 A73-13206

Impulsive loading of liquid squeeze film plane circular bounding surfaces, showing fluid inertia effect on bonding strength and cavitation relationship to viscosity
03 p0292 A73-13305

Spiral groove thrust bearing with load carrying lubricating oil film between stationary and rotating surfaces, discussing design, manufacturing and applications
03 p0313 A73-13925

Basic relationships in turbulent lubrication and their extension to include thermal effects.
[ASME PAPER 72-LUB-16] 03 p0314 A73-14332

The gas liquid interface and the load capacity of helical grooved journal bearings.
[ASME PAPER 72-LUB-19] 03 p0314 A73-14334

Thermohydrodynamic phenomena in fluid film lubrication.
[ASME PAPER 72-LUB-25] 03 p0314 A73-14338

Inertia and energy effects in the developing gas film between two parallel flat plates.
[ASME PAPER 72-LUB-33] 03 p0297 A73-14343

Optimal speed sharing characteristics of a series-hybrid bearing.
[ASME PAPER 72-LUB-39] 03 p0315 A73-14346

A hero-jet driven porous spherical hydrostatic gas bearing gyro.
[ASME PAPER 72-LUB-41] 03 p0315 A73-14348

Experiments on the stability of various water-lubricated fixed geometry hydrodynamic journal bearings at zero load.
[ASME PAPER 72-LUB-46] 03 p0315 A73-14350

The role of compressional viscoelasticity in the lubrication of rolling contacts.
[ASME PAPER 72-LUB-O] 03 p0315 A73-14354

On the influence of the contact pattern on the sealing capacity and the power loss of hydrodynamic lip seals.
[ASLE PREPRINT 72LC-7A-1] 03 p0316 A73-14367

The application of elastohydrodynamic lubrication in gear tooth contacts.
03 p0317 A73-14375

Russian book - Heat transfer in liquid films.
04 p0517 A73-15710

Investigations into film failure /transition point/ of lubricated concentrated contacts.
05 p0580 A73-16103

Thermal collapse theory of hydrodynamic oil lubrication films failure for slider bearing, noting frictional forces role
05 p0580 A73-16105

Suppression of evaporation of hydrocarbon liquids and fuels by aqueous films.
[WSCI PAPER 72-27] 05 p0639 A73-16687

Cylindrical pores in viscous incompressible liquid film, considering existence duration and pore wall motion under surface tension forces
07 p0923 A73-20420

Analysis of the shrouded Rayleigh step pad for an incompressible fluid film with the centrifugal inertia effect included.
09 p1089 A73-23103

Fluid film lubrication fluid mechanical theory, considering non-Newtonian fluids, turbulence, inertia and elastohydrodynamic effects in various bearing types
10 p1223 A73-23858

Unbalance vibration of a rotor-bearing system supported by floating-ring journal bearings.
13 p1623 A73-28647

Nonlinear stability of a liquid film adjacent to a supersonic stream.
14 p1711 A73-30166

Self excited whirl stability limits and frequencies of continuous rotors under gyroscopic, damping and hydrodynamic bearing film forces
16 p2022 A73-34035

An analysis and prediction of lubricant film starvation in rolling contact systems.
[ASLE PREPRINT 73AM-3B-4] 17 p2179 A73-34985

Self-acting and hydrodynamic shaft seals.
17 p2179 A73-34999

Analytical study of pressure balancing in gas film seals. 17 p2180 A73-35000

Application of the hydrogen-bubble technique for velocity measurements in thin liquid films. [ASME PAPER 73-APM-8] 17 p2153 A73-35033

An analytical and experimental investigation of turbulent flow in bearing films including convective fluid inertia forces. [ASME PAPER 73-LUBS-1] 17 p2181 A73-35388

On the possibilities of improving the accuracy of the evaluation of inertia forces in laminar and turbulent films. [ASME PAPER 73-LUBS-3] 17 p2181 A73-35389

Turbulent lubrication theory - Application to design. [ASME PAPER 73-LUBS-10] 17 p2181 A73-35392

Application of energy model of turbulence to calculation of lubricant flows. [ASME PAPER 73-LUBS-18] 17 p2181 A73-35397

Calculation of pressure, shear, and flow in lubricating films for high speed bearings. [ASME PAPER 73-LUBS-21] 17 p2182 A73-35399

Heat transfer in the case of turbulent and laminar trickle films 19 p2505 A73-38477

A general expression for the rate of evaporation of a layer of liquid on a solid body. 19 p2505 A73-38483

Unified thermodynamics of dissipative structures and coherence in nonlinear optics. 20 p2571 A73-38633

Liquid jet development under gravity, discussing jet surface elastic film, axisymmetric membrane elastic deformations, liquid drop pressure variations and hydrostatic pressure 20 p2548 A73-39517

The steady-state thickness of a liquid water film on the surface of hailstones of various shapes 21 p2730 A73-40118

Comparison of experimental microlayer thickness results. 21 p2793 A73-41690

Finite journal bearings with stepwise discontinuity in hydrodynamic film shape, predicting optimal performance as function of step height, eccentricity and L/D ratios 23 p2984 A73-43293

Rayleigh-Taylor problem of thermal instability of density-stratified layer of incompressible fluid heated from above, considering oscillatory and nonoscillatory modes stability 23 p3048 A73-43346

Thickness of liquid film on a rotating disk. 23 p2969 A73-44128

Analysis of the heat transfer associated with the evaporation of a fluid film on a rotating disk 24 p3156 A73-45078

The flow of a viscous liquid down a variable incline. 24 p3080 A73-45368

Preparation of liquid fuels by evaporation from a hot wall 24 p3158 A73-45389

FLUID FILTERS

The electrostatic charging tendencies of jet fuel filtration equipment. [SAE PAPER 720866] 05 p0582 A73-16672

Relative efficiencies of filters and impactors for collecting stratospheric particulate matter. 17 p2167 A73-34863

FLUID FLOW

NT ADIABATIC FLOW
NT AIR CURRENTS
NT AIR FLOW
NT AIR JETS
NT ANNULAR FLOW
NT AXIAL FLOW
NT AXISYMMETRIC FLOW
NT BAROTROPIC FLOW
NT BASE FLOW
NT BELTRAMI FLOW
NT BLASIUS FLOW
NT BLOOD FLOW
NT BOUNDARY LAYER FLOW
NT BOUNDARY LAYER SEPARATION
NT CAPILLARY FLOW
NT CASCADE FLOW
NT CAVITATION FLOW
NT CHANNEL FLOW
NT COAXIAL FLOW
NT COMBUSTIBLE FLOW
NT COMPRESSIBLE FLOW
NT CONICAL FLOW
NT CONTINUUM FLOW
NT CONVECTIVE FLOW
NT CORE FLOW
NT COUETTE FLOW
NT COUNTERFLOW
NT CRITICAL FLOW
NT CROSS FLOW
NT DUCTED FLOW
NT EQUILIBRIUM FLOW
NT FREE FLOW
NT FREE MOLECULAR FLOW
NT FROZEN EQUILIBRIUM FLOW
NT FUEL FLOW

NT GAS FLOW
NT HARTMANN FLOW
NT HELICAL FLOW
NT HYPERSONIC FLOW
NT HYPERVELOCITY FLOW
NT INCOMPRESSIBLE FLOW
NT INLET FLOW
NT INVISCID FLOW
NT ISOTHERMAL FLOW
NT JET FLOW
NT JET MIXING FLOW
NT JET STREAMS [METEOROLOGY]
NT KNUDSEN FLOW
NT LAMINAR FLOW
NT LIQUID FLOW
NT MAGNETOHYDRODYNAMIC FLOW
NT MASS FLOW
NT MERIDIONAL FLOW
NT MOLECULAR FLOW
NT MULTIPHASE FLOW
NT NONEQUILIBRIUM FLOW
NT NONNEWTONIAN FLOW
NT NONUNIFORM FLOW
NT NOZZLE FLOW
NT ONE DIMENSIONAL FLOW
NT ORIFICE FLOW
NT OSCILLATING FLOW
NT PARALLEL FLOW
NT PERIPHERAL JET FLOW
NT PIPE FLOW
NT PLASTIC FLOW
NT POTENTIAL FLOW
NT PROPELLANT TRANSFER
NT RADIAL FLOW
NT REATTACHED FLOW
NT RECIRCULATIVE FLUID FLOW
NT REVERSED FLOW
NT SECONDARY FLOW
NT SEPARATED FLOW
NT SHEAR FLOW
NT SINGLE-PHASE FLOW
NT SLIP FLOW
NT SMALL PERTURBATION FLOW
NT SOLIDS FLOW
NT STAGNATION FLOW
NT STEADY FLOW
NT STEAM FLOW
NT STOKES FLOW
NT STRATIFIED FLOW
NT SUBCRITICAL FLOW
NT SUBSONIC FLOW
NT SUPERCAVITATING FLOW
NT SUPERCRITICAL FLOW
NT SUPERSONIC FLOW
NT SUPERSONIC JET FLOW
NT THREE DIMENSIONAL FLOW
NT TRANSITION FLOW
NT TRANSONIC FLOW
NT TRESKA FLOW
NT TURBULENT FLOW
NT TWO DIMENSIONAL FLOW
NT TWO PHASE FLOW
NT UNIFORM FLOW
NT UNSTEADY FLOW
NT VERTICAL AIR CURRENTS
NT VISCOUS FLOW
NT WALL FLOW
NT WATER FLOW
NT WEDGE FLOW

Infinite Prandtl number fluids with constraint characterized by Taylor number heated from below, choosing boundary conditions for laminar convection 03 p0293 A73-13329

Sinusoidal thermal wave propagation in horizontal fluid layer with small Prandtl number, deriving induced mean flow from nonlinear equation solution by perturbation approach 05 p0591 A73-16188

Solution of the general heat-transfer problem for flow past cylindrical bodies by the Tolubinskii integral method. 06 p0766 A73-17407

Hot wire measurement of velocity gradients in a fluid flow. [AIAA PAPER 73-50] 06 p0692 A73-17626

Optimal stabilization of the Rayleigh-Taylor instability in the multiarm fluid pendulum. 09 p1119 A73-21942

Noise reduction for subsonic fluid flow over flat plate via interposition of secondary fluid layer at trailing edge 11 p1300 A73-25386

Calculation of single phase pressure drop in heat exchangers considering the change of fluid properties along the flow path. 12 p1559 A73-27694

Boundary layer separation in a steady plane-parallel incompressible fluid flow 15 p1864 A73-32110

The effectiveness of flow control devices and circuits. 16 p1970 A73-33473

Conference on Heat and Fluid Flow in Steam and Gas Turbine Plant, University of Warwick, Coventry, England, April 3-5, 1973, Proceedings. 17 p2092 A73-34376

Book - Flow visualization: Optical methods of analyzing fluid flows. 17 p2165 A73-34459

Application of the generalized Galerkin method to the computation of fluid flows. 17 p2154 A73-35133

Dynamic mechanical loading of solid material resulting in stress levels with impulse process described by fluid flow equations with application to shock compression of mechanical mixtures 17 p2193 A73-35541

The effect of nonlinear transformations on the computation of weak solutions. 18 p2330 A73-36610

Flow of a mixture consisting of a fluid and gas bubbles past a corner 18 p2301 A73-37007

Horizontal electric fields and currents caused by depths-to-surface oceanic water exchange in geomagnetic field, discussing electric field distribution and magnetic field distortion 19 p2426 A73-38175

Vortex interaction with plane in viscous fluid, discussing free parameter related to insufficient boundary conditions for solving Navier-Stokes equations 20 p2547 A73-39289

Dynamo theory for geomagnetic field, emphasizing fluid flow symmetric and asymmetric velocity component relative magnitudes 21 p2679 A73-39930

Free vibrations of fluid-conveying cylindrical shells. [ASME PAPER 73-DET-96] 22 p2919 A73-42075

FLUID INJECTION

NT GAS INJECTION
NT LIQUID INJECTION
NT WATER INJECTION

An experimental investigation of the downstream effects of upstream boundary-layer injection. 01 p0002 A73-10732

Stability boundaries of solid rocket motors. 01 p0091 A73-11116

Hypersonic rarefied flow past an insulated flat plate with suction/injection. 04 p0520 A73-15939

Linearized solutions to supersonic laminar boundary layer structure near flat plate with slot injection, using triple deck separation theory 08 p0956 A73-21524

Electric arc motion during initiation by plasma injection between static electrodes in dc circuit, applying to pulsed arc commutator design 09 p1131 A73-22938

Plate-injection into a separated supersonic boundary layer. 14 p1711 A73-30172

Magnetohydrodynamic boundary layer control with suction or injection. 15 p1864 A73-31931

Effectiveness and heat transfer with full-coverage film cooling. [ASME PAPER 73-GT-18] 16 p2086 A73-33495

Numerical stability of boundary layers with massive blowing. 18 p2298 A73-36321

The singularity at boundary layer separation due to mass injection. 18 p2301 A73-36696

Increasing the transport capacity in a viscous fluid flow by the injection method 19 p2420 A73-37552

Film effectiveness and heat transfer coefficient downstream of a metered injection slot. [ASME PAPER 73-HT-31] 20 p2625 A73-38570

Hot-wire anemometer investigation of turbulent boundary layers at a permeable plate with injection. 21 p2678 A73-41055

An experimental study of strong injection at axisymmetrical bodies of revolution. 21 p2633 A73-41057

Heat transfer from an enclosed rotating disk with uniform suction and injection. 22 p2938 A73-42998

FLUID JET AMPLIFIERS

U FLUID AMPLIFIERS

U JET AMPLIFIERS

FLUID JETS

NT AIR JETS
NT FREE JETS
NT GAS JETS
NT HYDRAULIC JETS
NT VAPOR JETS

Performance of liquid jet pumps at elevated temperatures. 03 p0317 A73-14502

Jet deviation fluidic analog amplifiers, noting industrial application to pressure, flow rate and dimensional measurements 11 p1308 A73-25379

Nonlinear behavior of capillary liquid jets ejected from nonsymmetric nozzles, showing effect on flow stability 11 p1349 A73-26432

Parameter calculation for laminar incompressible fluid jet expanding in gradient slipstream along moving surface, determining velocity distribution in jet axis 13 p1601 A73-28736

Dynamic structural model of transient processes of discrete jet element chain with duct joints
15 p1832 A73-31145

A study of a feedback fluidic jet oscillator. I, II.
19 p2389 A73-38077

Cavitation and boiling bubble growth, collapse and damage effects, discussing liquid jet formation temperature effects, glycerol, ethanol and water solutions and bubble geometry
20 p2548 A73-39516

Liquid jet development under gravity, discussing jet surface elastic film, axisymmetric membrane elastic deformations, liquid drop pressure variations and hydrostatic pressure
20 p2548 A73-39517

The initial development of a submerged laminar round jet.
20 p2550 A73-39815

Conducting fluid jets in a transverse magnetic field
21 p2747 A73-40888

Capillary breakup length and stability of Newtonian and viscoelastic cylindrical liquid jets in terms of dimensionless viscosity and relaxation time
23 p2967 A73-43307

A hot gas actuator for missile control.
23 p2942 A73-43398

Investigations on fluidic jet deflection amplifiers in dc- and ac networks.
23 p2942 A73-43400

Fluidic jet deflection anemometer design and tests of directional wind velocity measurement in rain/sand environments
23 p2981 A73-43429

FLUID LOGIC
Systematic method of designing fluidic-pneumatic control circuits.
02 p0133 A73-12646

Fluidic system design based on miniaturized modular high power fluidic logic elements, discussing applications in production process control
10 p1177 A73-23761

Fluidic setup corresponding to automatic control and digital computation circuits, discussing analog elements regulation and applications of logic subassemblies without moving parts
11 p1307 A73-25376

Book on fluid power control covering servovalve orifices discharge characteristics, flow forces, hydraulic and pneumatic servomechanisms, fluid logic and sequential circuits
11 p1313 A73-26258

Miniaturized unistable and bistable fluidic switching elements performance characteristics, considering vibration, velocity, pressure and laminar/turbulent flow effects on switching time and stability
13 p1571 A73-28482

Fluidic programmer for nuclear engine application.
19 p2454 A73-38054

A model for the prediction of the time delay characteristics of turbulence amplifiers.
19 p2389 A73-38075

Turbulence amplifier with transition process control for multi-input fluid logic OR device operation at very low pressures and flow rates
23 p2942 A73-43399

Hybrid fluid logic systems for integrated circuits using static and dynamic logical elements, considering fluidic circuits design with redundancy
23 p2943 A73-43411

Systems engineering approach to pneumatic hybrid automatic/manual control system with fluid logical elements and reduced air consumption
23 p2943 A73-43413

Some practical methods for development of modular fluidic devices.
23 p2943 A73-43415

FLUID MECHANICS
NT AERODYNAMICS
NT AEROTHERMODYNAMICS
NT ELASTOHYDRODYNAMICS
NT ELECTROHYDRODYNAMICS
NT FLUID DYNAMICS
NT GAS DYNAMICS
NT HYDRODYNAMICS
NT HYDROMECHANICS
NT HYDROSTATICS
NT MAGNETOHYDRODYNAMICS
NT MAGNETOHYDROSTATICS
NT PNEUMATICS
NT RAREFIED GAS DYNAMICS
NT ROTOR AERODYNAMICS

Boundary value problems with variable boundaries for a special differential equation
03 p0337 A73-14630

Energy balance, motion and constitutive equations of polar fluids, considering entropy inequality, viscosity and dissipation rate
04 p0434 A73-15679

Association Technique Maritime et Aeronautique, Session, 72nd, Ecole Nationale Supérieure de Techniques Avancées, Paris, France, May 15-19, 1972, Proceedings.
09 p1031 A73-22201

Kinetic equation derived for collective linear fluid oscillations development, applying to longitudinal and transverse wave propagation in fluids
09 p1072 A73-22574

Method of integral equations in the statistical theory of fluids
09 p1121 A73-22724

Book - Annual review of fluid mechanics. Volume 5.
10 p1205 A73-23851

Fluid film lubrication fluid mechanical theory, considering non-Newtonian fluids, turbulence, inertia and elastohydrodynamic effects in various bearing types
10 p1223 A73-23858

Parametric instabilities and harmonic generation in Tonks-Dattner resonances in inhomogeneous bounded electron plasma layer
13 p1665 A73-28791

Book - Illustrated experiments in fluid mechanics - The NCFMF book of film notes.
14 p1743 A73-29725

Some computation-steeple in fluid mechanics.
14 p1745 A73-30412

Uniqueness and existence estimates of third order differential equation solutions for nonlinear boundary value problem in fluid mechanics
15 p1863 A73-31363

A criterion for global existence in case of ordinary differential equations.
15 p1901 A73-32370

Heat transfer to flowing gas-solid mixtures.
17 p2254 A73-34353

Book - Lectures on fluid mechanics.
17 p2150 A73-34457

The finite element method in fluid mechanics.
17 p2151 A73-34830

An approximate method for the solution of a class nonlinear equations in fluid mechanics and magnetohydrodynamics.
17 p2216 A73-35018

[ASME PAPER 73-FE-22] Fluid mechanics of mixing; Proceedings of the Joint Meeting, Georgia Institute of Technology, Atlanta, Ga., June 20-22, 1973.
17 p2156 A73-35501

Endolymph fluid mechanics in semicircular canals approximated by rigid torus filled with incompressible Newtonian fluid
18 p2281 A73-36430

Book - Hydraulic systems and maintenance.
20 p2510 A73-39142

Statistical continuum mechanics and constitutive theories governing microfluid behavior, noting relations with aid of tables
20 p2547 A73-39343

Midwestern Mechanics Conference, 13th, University of Pittsburgh, Pittsburgh, Pa., August 13-15, 1973, Proceedings.
20 p2620 A73-39513

Green function hydrodynamic asymptotic behavior obtained via closed inhomogeneous linear equations, discussing distribution function kinetic equation, correlation function spectral distribution and adiabatic conditions
21 p2677 A73-40636

Of fluid mechanics and fluidics and of analysis and physical insight.
23 p2945 A73-43432

Method of integral equations in statistical theory of liquids.
23 p3007 A73-44324

FLUID POWER
A standard format for mathematical models of fluid power systems.
02 p0132 A73-12001

A fundamental method for evaluating the contaminant tolerance of fluid power control valves.
02 p0132 A73-12003

Book on fluid power control covering servovalve orifices discharge characteristics, flow forces, hydraulic and pneumatic servomechanisms, fluid logic and sequential circuits
11 p1313 A73-26258

Oil hydraulic button vortex valve optimization experiment for power consumption reduction, noting Reynolds number effects on turn down and pressure ratios
23 p2942 A73-43404

Oil hydraulic fluidic amplifier mathematical model and computerized design for power consumption optimization at high pressures, testing performance dependence on viscosity
23 p2942 A73-43405

FLUID ROTOR GYROSCOPES
Russian book on hydrodynamic gyroscope theory and design covering casing angular velocity, cavity fluid motion, induction removal, noise levels and threshold sensitivity
04 p0450 A73-15705

One degree of freedom fluid suspension gyros, direct drive gimbal motors and microelectronic control assemblies review, noting miniature inertial platforms availability
07 p0820 A73-18941

A hybrid fluidic directional gyro.
19 p2430 A73-38055

FLUID SWITCHING ELEMENTS

Contactless switch for three stage gas flow using symmetric jet booster based on Coanda effect
09 p1037 A73-22848

Fluidic system design based on miniaturized modular high power fluidic logic elements, discussing applications in production process control
10 p1177 A73-23761

Miniaturized unistable and bistable fluidic switching elements performance characteristics, considering vibration, velocity, pressure and laminar/turbulent flow effects on switching time and stability
13 p1571 A73-28482

The switching of wall-reattachment fluidic devices.
13 p1571 A73-29041

A study of switching process and design parameters of supersonic fluidic amplifiers.
13 p1571 A73-29042

Wall effects on the motion of a two-dimensional jet switching between two parallel flat plates.
13 p1571 A73-29043

Accuracy of switching pressure of fluidic OR-NOR device.
13 p1571 A73-29044

The effectiveness of flow control devices and circuits.
16 p1970 A73-33473

An analytical model for the response of fluidic wall attachment amplifiers.
16 p1970 A73-33474

Fluidic component performance and circuit reliability.
16 p1971 A73-33475

Effect of contamination on fluidic system reliability.
16 p1971 A73-33476

Fluidic programmer for nuclear engine application.
19 p2454 A73-38054

A model for the prediction of the time delay characteristics of turbulence amplifiers.
19 p2389 A73-38075

A study of a feedback fluidic jet oscillator. I, II.
19 p2389 A73-38077

A method of analyzing transient processes in digital fluidic circuits
20 p2510 A73-39352

Prediction of the dynamic and quasi-static performance characteristics of fluidic wall-attachment amplifiers.
20 p2511 A73-39756

The initial development of a submerged laminar round jet.
20 p2550 A73-39815

A periodicity phenomenon occurring instantly when a standing ultrasonic wave is switched off
21 p2738 A73-39982

Turbulence amplifier with transition process control for multi-input fluid logic OR device operation at very low pressures and flow rates
23 p2942 A73-43399

Digital fluidic systems application to binary signal transmission via system with fluid transmission lines and switching element-based transmitters and receivers
23 p2944 A73-43417

Output pressure-displacement and flow pattern characteristics of digital limit Schrenk, wall attachment and nozzle receiver fluidic switches
23 p2945 A73-43426

Use of a fluidic distributor for the calibration of unsteady flow probes.
23 p2945 A73-43430

FLUID TRANSMISSION LINES
New arrangement for testing materials in the volume stressed state and at elevated temperatures /Exchange of experience/.
10 p1222 A73-24947

A dynamic modeling method of unsteady flows in long fluid lines with turbulent bulk velocities.
17 p2153 A73-35014

[ASME PAPER 73-FE-18] A simple yet theoretically based time domain model for fluid transmission line systems.
17 p2153 A73-35021

[ASME PAPER 73-FE-27] Digital fluidic systems application to binary signal transmission via system with fluid transmission lines and switching element-based transmitters and receivers
23 p2944 A73-43417

Theoretical and experimental investigation of fluidic signal and noise filters with application to DC and AC fluidic systems.
23 p2944 A73-43418

The design of digital fluidic components and systems - A review.
23 p2945 A73-43433

FLUID TRANSPARATION
U TRANSPARATION
FLUIDIC CIRCUITS
NT FLIP-FLOPS

Some incompressible jet flow and reattachment effects in fluidic control elements.
06 p0687 A73-18513

Fluidic circuits fabrication and design technology for rocket guidance and attitude control
07 p0778 A73-18939

- Fluidic setup corresponding to automatic control and digital computation circuits, discussing analog elements regulation and applications of logic subassemblies without moving parts
11 p1307 A73-25376
- Jet deviation fluidic analog amplifiers, noting industrial application to pressure, flow rate and dimensional measurements
11 p1308 A73-25379
- The effectiveness of flow control devices and circuits.
16 p1970 A73-33473
- Fluidic component performance and circuit reliability.
16 p1971 A73-33475
- Effect of contamination on fluieric system reliability.
16 p1971 A73-33476
- Fluidic control modules with temperature sensor and thrust reverser pneumatic actuator for aerospace system applications, investigating reliability test data
16 p1971 A73-33477
- Hydrofluidic component and system reliability.
16 p1971 A73-33478
- Fluidic programmer for nuclear engine application.
19 p2454 A73-38054
- A method of analyzing transient processes in digital fluidic circuits
20 p2510 A73-39352
- Utilization of miniature diaphragm-leakport devices in fluidic applications.
20 p2511 A73-39752
- Cranfield Fluidics Conference, 5th, University of Uppsala, Uppsala, Sweden, June 13-16, 1972, Proceedings. Volumes 1 & 2.
23 p2941 A73-43390
- Use of fluidics in explosive component fabrication.
23 p2941 A73-43391
- Fluidic logic circuits applications under adverse environmental conditions, considering sequential control devices and rocket engine roll axis numerical control
23 p2941 A73-43394
- Fluidic bolometer type sensor for reaction wheel control to maintain spacecraft and rocket vehicle attitude relative to sun, discussing design, simulation and tests
23 p3038 A73-43395
- A study of a fluidic open loop damping flight stability augmentation system.
23 p2941 A73-43396
- The steady-state and transient performance of some large-scale vortex diodes.
23 p2942 A73-43407
- The diaphragm-ejector proportional amplifier and its application to fluidic operational circuits.
23 p2943 A73-43409
- Small ejector system for fluidic subtracting network with diaphragm operated Schmitt trigger proportional amplifier and pneumatic signal generator, discussing construction and characteristics
23 p2943 A73-43410
- Hybrid fluid logic systems for integrated circuits using static and dynamic logical elements, considering fluidic circuits design with redundancy
23 p2943 A73-43411
- Application of fluidic shift-register modules for sequential control of pneumatic sequential circuits.
23 p2943 A73-43412
- Fluidic logic circuit universal block with turbulence amplifiers for control of servomechanisms, comparing with use of conventional fluid logical elements
23 p2943 A73-43414
- Some practical methods for development of modular fluidic devices.
23 p2943 A73-43415
- Theoretical and experimental investigation of fluidic signal and noise filters with application to DC and AC fluidic systems.
23 p2944 A73-43418
- Fluidic circuits application to stochastic computer with analog to digital converter and logic gates for arithmetic operations
23 p2944 A73-43419
- A flexible automatic typewriting system using three tape readers.
23 p2944 A73-43422
- Fluid pad resistor for linear laminar flow resistance between parallel plates with emphasis on fluidic circuits application
23 p2945 A73-43425
- Fluidic linear nozzle-flapper valve accelerometer for ship motion sensing, describing circuit configuration and performance tests
23 p2981 A73-43428
- The design of digital fluidic components and systems - A review.
23 p2945 A73-43433

FLUIDICS

NT FLUERICs

- Fluidic ignition system with two-component aerodynamic resonance heating /pneumatic match/ and hand pump for solid propellant sounding rocket engine
[AIAA PAPER 72-1197] 03 p0252 A73-13486

Dynamic modelling of the innovation cycle as applied to fluidics.

- 03 p0258 A73-14450
- Acoustic properties of fluid mixtures for ultrasonic delay lines, noting temperature and composition effects on water-glycol mixture parameters
03 p0280 A73-14620
- Fluidic system for precision positioning of cylindrical machine parts and length and angle measurements, using nozzle jet impingement system for pressure symmetry sensing
05 p0538 A73-17248
- A fluidic transducer of rotor-shaft torque
06 p0692 A73-17836
- Fluidics test methods and instrumentation.
[SAE ARP 1254] 08 p0928 A73-20695
- Fluidic sensing of rotational speed using spur gears.
08 p0928 A73-21829
- Some limitations on the use of fluidic pulse width and pulse position modulation for phase measurement.
08 p0929 A73-21832
- Fluidics terminology and vocabulary development and practical use, describing control functions and symbols
11 p1307 A73-25378
- Pneumatic and fluidic automatic controls, investigating peripheral elements and systems feed
11 p1308 A73-25380
- Problems in constructing aerodynamically active elements - Converters of input and output signals in automatic control systems
12 p1459 A73-26769
- Pneumosomatic data transmission and processing based on pressurized gases and dynamic body interactions
12 p1460 A73-26771
- Dynamic measurement of the basic quantities of fluidics
12 p1461 A73-27596
- Fluid machinery and fluidics; Proceedings of the Second International Symposium, Tokyo, Japan, September 4-9, 1972. Volumes 1 & 2 - Fluid machinery. Volume 3 - Fluidics. Volume 4 - General lectures, discussions, events.
13 p1602 A73-29004
- Measurement of Coanda flow in fluidic elements by a laser Doppler velocimeter method and a quantitative tracer method.
13 p1618 A73-29040
- Some investigations on frequency demodulating systems with fluidic jet deflection amplifiers.
13 p1572 A73-29046
- Speed control for an air motor using fluidic techniques.
[ASME PAPER 73-DE-35] 14 p1713 A73-30824
- Use of fluidic and pneumatic elements to determine the composition of a gas mixture
16 p1970 A73-33025
- A study of a feedback fluidic jet oscillator. I, II.
19 p2389 A73-38077
- Fluidic strain gages based on detection of flow resistance or pressure drop changes due to elongation, comparing various type gage factors
20 p2564 A73-38873
- Long range fluidic acoustic sensors cross air currents and temperature gradient effects on operational characteristics and resolution, and prototype design for industrial applications
20 p2511 A73-39753
- Russian book - Aerohydrodynamic methods for measuring input parameters of automatic systems: Fluidic measuring elements.
21 p2704 A73-41288
- Cranfield Fluidics Conference, 5th, University of Uppsala, Uppsala, Sweden, June 13-16, 1972, Proceedings. Volumes 1 & 2.
23 p2941 A73-43390
- Pneumatic fluidic operational amplifier application to proportional position servocontrol with hydraulic actuator for high force output, considering working fluid and Reynolds number effects
23 p2941 A73-43397
- Compensation of an underdamped fluidic position control system by a digital pulse compensator.
23 p2944 A73-43420
- Punched card controlled program units including readers, comparator circuits, pneumomechanical counters and fluidic feedback oscillators
23 p2944 A73-43424
- Optimal parameters on fluidic noncontact sensors for drives of exact positioning.
23 p2945 A73-43427
- Fluidic vortex-type proximity sensor with analog to digital converter, optimizing output nozzle diameter and pressure by steepest ascent method
23 p2981 A73-43431
- Of fluid mechanics and fluidics and of analysis and physical insight.
23 p2945 A73-43432

FLUIDIZED BED PROCESSORS

- Carbon and pyrolytic graphite isothermal chemical vapor deposited (CVD) composite coated and free standing products fluid bed manufacturing and applications
03 p0333 A73-13053

Compound heat exchange between a high temperature gas-fluidized bed and a solid surface.

08 p1022 A73-21251

FLUIDS

- Light scattering from an inhomogeneous fluid.
01 p0077 A73-10971
- The specific isochoric heat capacity of pure fluids on the dew curve and the boiling curve
03 p0400 A73-14633

FLUORESCENCE

- NT X RAY FLUORESCENCE
- Polychromatic X-ray diffraction - A rapid and versatile technique for the study of solids under high pressure and high temperature.
01 p0054 A73-11482
- Cross sections for the production of excited products in the photoionization of N₂, O₂, CO, and N₂O by 58.4-nm radiation.
02 p0157 A73-11752
- Dynamics of the CO₂ atmospheric pressure laser with transverse pulse excitation.
02 p0177 A73-12435
- Laser induced infrared fluorescence - Thermal heating, mass diffusion, and collisional relaxation in SF₆.
03 p0318 A73-13281
- Q switched ruby laser emission absorption by diatomic Rb vapor, noting molecular fluorescence intensity changes
04 p0458 A73-15560
- Spectrophotofluorometers for returned lunar samples and geological materials organic analyses, discussing optical component performance and calibration to avoid instrumental artifacts effect on spectra
06 p0662 A73-18415
- Apollo 11, 12 and 14 surface fines analysis by fluorescent technique for porphyrins content
06 p0753 A73-18419
- Cooperative luminescence in trivalent ytterbium and erbium ions in cadmium fluoride crystals
06 p0738 A73-18543
- Direct overtone excitation of hydrogen fluoride second vibrational level, measuring global deactivation rate by temperature tuned Nd-YAG laser excited fluorescence technique
06 p0703 A73-18750
- Saturation resonances by magnetic mode crossing in optical pumping with a multimode gas laser.
07 p0837 A73-20606
- Application of the method of polarization ultraviolet fluorescence microscopy to study giant muscle fibers Balanus rostratus Hock
08 p0930 A73-21135
- Prolonged luminescence of complex molecules in the gas phase
09 p1123 A73-23334
- Laser application for remote analysis of gaseous air pollutants emission based on Raman scattering, resonance fluorescence or absorption measurements
11 p1375 A73-25399
- Influence of excitation power on the energetic characteristics of phthalimide solutions
11 p1376 A73-26143
- Direct measurement of the fluorescence energy yield of a rhodamine 6G solution with the aid of an Ar+ laser
11 p1377 A73-26146
- Apparatus and techniques for electron beam fluorescence probe measurements.
13 p1612 A73-28365
- Quenching of lasing and the short wave fluorescence in a 3,3 diethylthiatricarbocyanine dye laser
14 p1757 A73-30462
- Fluorescent cross sections and yields of CO₂+/+ from threshold to 185 Å.
15 p1915 A73-31274
- Upper level populations in optically excited cesium vapor
15 p1914 A73-32337
- Spectroscopic laser methods of automatic gas analysis based on Raman backscattering, resonance fluorescence or absorption measurements for atmospheric pollutant and exhaust gas detection
16 p2023 A73-32876
- Effect of nitrite and nitrate on chlorophyll fluorescence in green algae.
16 p1973 A73-33226
- Recent measurements of stratospheric reactions by flash photolysis resonance fluorescence.
[AIAA PAPER 73-502] 16 p2005 A73-33543
- Vibrational relaxation in the HF-HCl, HF-HBr, HF-HI, and HF-DF systems.
17 p2119 A73-35176
- New algae mapping technique by the use of an airborne laser fluorosensor.
17 p2163 A73-35412
- Kinetics of bleaching in polymethine cyanine dyes.
17 p2186 A73-35793
- Fluorescence excitation and photoelectron spectra of CO₂ induced by vacuum ultraviolet radiation between 185 and 716 angstroms.
18 p2346 A73-36266
- Laser induced fluorescence of CN radicals.
19 p2437 A73-37902

A test of Jaynes' neoclassical theory - Incoherent resonance fluorescence from a coherently excited state. 20 p2570 A73-38605

Application of a pulsed laser for measurements of bathymetry and algal fluorescence. 20 p2574 A73-39863

Flash photography using laser excited fluorescent tracers. 21 p2709 A73-39969

Real time nitrogen dioxide and nitric oxide pollution measurement by molecular fluorescence induced by argon laser beam 21 p2671 A73-40135

Fluorescence efficiencies of electrons in second positive bands of N2 and first negative bands of N2+/. 21 p2682 A73-40164

Stimulated emission in multiple-photon-pumped xenon and argon excimers. 21 p2713 A73-40456

Satellite ultraviolet measurements of nitric oxide fluorescence with a diffusive transport model. 22 p2845 A73-41925

A comparison of the sensitivity of atomic-fluorescent and atomic-absorption flame photometry. 22 p2862 A73-42720

High order nonlinear effects in a gas laser - Saturation anomaly observable on a J equals 1 - J equals 2 transition 22 p2871 A73-43084

Theoretical study of a photodissociation model in polyatomic molecules 24 p3113 A73-45326

FLUORESCENT EMISSION
U FLUORESCENCE
FLUORIDES
NT BARIUM FLUORIDES
NT BORON FLUORIDES
NT CADMIUM FLUORIDES
NT CALCIUM FLUORIDES
NT CHLORINE FLUORIDES
NT DIFLUORIDES
NT HYDROFLUORIC ACID
NT LANTHANUM FLUORIDES
NT LITHIUM FLUORIDES
NT MAGNESIUM FLUORIDES
NT NITROGEN FLUORIDES
NT STRONTIUM FLUORIDES
NT SULFUR FLUORIDES
Lubricating characteristics of polyimide bonded graphite fluoride and polyimide thin films. 03 p0317 A73-14372

Optical properties of Nd3+/- in lanthanum oxyfluoride single crystals 07 p0837 A73-20205

Absorption of CO2 laser radiation by carbonyl fluoride. 21 p2715 A73-40958

FLUORINE
Molecular fluorine concentration and pressure change monitor based on UV absorption spectrum during chemical reactants mixing, noting measurement accuracy 02 p0168 A73-11967

Monte Carlo classical trajectory calculation of the rates of F-atom vibrational relaxation of HF and DF. 03 p0318 A73-13279

Effect of reagent vibrational excitation on reaction rate and product energy distribution in F + HCl yields HF + Cl. 03 p0273 A73-13290

Submicrosecond pulses from a hydrogen-fluorine laser with high energy density and quantum efficiency. 03 p0320 A73-14454

Dielectric constant and molar polarizability of compressed gaseous and liquid fluorine. 06 p0661 A73-18124

Exothermic deuterium-fluorine chain reaction pumping of high pressure pulsed carbon dioxide chemical transfer laser 07 p0835 A73-19631

Development of special graphites for lithium hydride/fluorine rocket engines 09 p1110 A73-23019

Pulsed laser utilizing a fluorine and hydrogen mixture. 13 p1629 A73-29434

The fluorine abundance in the galactic cosmic radiation. 15 p1926 A73-31552

Fluorine in lunar samples - Implications concerning lunar fluorapatite. 15 p1941 A73-32388

Deflagration in the combustion of hydrogen-fluorine mixtures. 16 p2045 A73-33349

Experimental studies of chemically reactive F + H2/ flow in supersonic free jet mixing layers. 18 p2321 A73-36198

[AIAA PAPER 73-640]

Branched-chain mechanism of propane-oxygen-fluorine explosions. 22 p2819 A73-42778

HF and molecular fluorine refractive indices in visible spectral region computed from interferometer fringe shift vs pressure measurements 24 p3113 A73-44983

FLUORINE COMPOUNDS
NT BARIUM FLUORIDES
NT BORON FLUORIDES
NT CADMIUM FLUORIDES
NT CALCIUM FLUORIDES
NT CARBON TETRAFLUORIDE
NT CHLORINE FLUORIDES
NT DIFLUORIDES
NT DIFLUORO COMPOUNDS
NT FLUORIDES
NT FLUORINE ORGANIC COMPOUNDS
NT FLUORITE
NT FLUORO COMPOUNDS
NT FLUOROCARBONS
NT FLUOROHYDROCARBONS
NT HYDROFLUORIC ACID
NT LANTHANUM FLUORIDES
NT LITHIUM FLUORIDES
NT MAGNESIUM FLUORIDES
NT NITROGEN FLUORIDES
NT POLYTETRAFLUOROETHYLENE
NT STRONTIUM FLUORIDES
NT SULFUR FLUORIDES
NT TETRAFLUOROETHYLENE
Optical centers of Nd3+/- in calcium and strontium fluorophosphate crystals 07 p0836 A73-20204

Chromatographic separation of niobium from titanium, tungsten, molybdenum, and vanadium on the fluoroform of the AV-16 anion exchanger 20 p2520 A73-39820

Spectroscopic studies of low-pressure hydrogen-fluorine flames. 22 p2898 A73-42760

FLUORINE ORGANIC COMPOUNDS
NT CARBON TETRAFLUORIDE
NT FLUOROCARBONS
NT FLUOROHYDROCARBONS
Polyphosphazene fluoroclastomers preparation, properties and potential applications. 03 p0331 A73-13029

Vibrational spectra and structure of tetrakis(trifluoromethyl)hydrazine in the crystalline and fluid states. 04 p0414 A73-16036

Gas-liquid chromatography of trifluoroacetyl derivatives of cyclitols. 11 p1325 A73-25150

Flame suppression technique using halogen compounds with hydrogen and carbon, considering bromotrifluoromethane application in propane spray cloud seeding 12 p1521 A73-26818

FLUORINE-LIQUID OXYGEN
U FLOX
FLUORITE
Investigation of the lasing and luminescent properties of fluorite and strontium fluoride crystals containing bivalent dysprosium impurities 07 p0837 A73-20207

Determination of the boundaries of fluorite-type Y2O3 solid solutions in HfO2 13 p1645 A73-28292

Stimulation of nonradiating transitions during intense excitation by light 15 p1885 A73-31720

FLUORO COMPOUNDS
NT CARBON TETRAFLUORIDE
NT DIFLUORO COMPOUNDS
NT FLUORINE ORGANIC COMPOUNDS
NT FLUOROCARBONS
NT FLUOROHYDROCARBONS
NT POLYTETRAFLUOROETHYLENE
A review of the perfluoroalkyl ether class of greases. 07 p0843 A73-19558

Nonhydrocarbon liquid lubricants based on phosphate and neopentyl esters, perfluoroalkyl and polyphenyl ethers, silicone and perfluorotriazines, discussing performance testing techniques 07 p0843 A73-19559

Vibrational spectrum of bis(trifluoromethyl) trioxide. 15 p1841 A73-32221

The effects of environment on performance of fluoroclastomers in seal applications. [ASLE PREPRINT 73AM-8B-2] 17 p2179 A73-34994

FLUOROCARBONS
Effect of H2O, SF6 and CCl3F additions on the electron concentration in highly heated air 15 p1840 A73-31852

Polytetrafluoroethylene and fluorinated ethylene-propylene grease lubricants. [ASLE PREPRINT 73AM-1A-2] 17 p2195 A73-34977

FLUOROHYDROCARBONS
NT CARBON TETRAFLUORIDE
A study of Halon 1301 / CBrF3 toxicity under simulated flight conditions. 09 p1045 A73-22537

FLUTTER ANALYSIS
High-temperature low pressure hose assembly, convoluted-, tetrafluoroethylene-, for aerospace. [SAE ARP 1227] 16 p1970 A73-33017

FLUOROSCOPY
Spectrofluorometric search for porphyrins in Apollo 14 surface fines. 07 p0891 A73-19823

Electrofluoroplanigraphy for human body layer single-plane sections synchronization, using X ray tomography and TV imaging followed by roentgenogram electronic summation 21 p2645 A73-41216

FLUTTER
NT PANEL FLUTTER
NT SUBSONIC FLUTTER
NT SUPERSONIC FLUTTER
NT TRANSONIC FLUTTER
Effects of tape flutter on notch noise loading test performance of predetection recording of a frequency modulated carrier. 09 p1087 A73-23367

Effect of flutter on theoretical bit error rates for digital recording systems. 09 p1087 A73-23369

Strouhal number and flat plate oscillation in an air stream. 21 p2782 A73-40125

FLUTTER ANALYSIS
Flutter analysis method for unsteady aerodynamic forces on wings and rotating blades under harmonic vibrations and uniform flow [ONERA, TP NO. 1099] 01 p0001 A73-10230

Aerodynamic generalized forces for supersonic shell flutter. 01 p0003 A73-10751

Selective reinforcement of wing structure for flutter prevention. 03 p0392 A73-13705

Rates of change of flutter Mach number and flutter frequency. 03 p0395 A73-14188

Beams subjected to follower force within the span. 04 p0508 A73-14938

Stability of a thin-wing model with one and two degrees of freedom 05 p0632 A73-16297

Orthotropic panel flutter at arbitrary yaw angles - Experiment and correlation with theory. [AIAA PAPER 73-192] 05 p0634 A73-16924

Aeroelastic instabilities of hingeless helicopter blades. 05 p0536 A73-16929

Active flutter control - An adaptable application to wing/store flutter. [AIAA PAPER 73-194] 05 p0531 A73-16930

The effects of various parameters on an aeroelastic optimization problem. 06 p0758 A73-17565

An automated method for determining the flutter velocity and the matched point. [AIAA PAPER 73-195] 06 p0645 A73-17656

Approximative calculation of flutter regions for collision body systems in phase space, noting fluttering duration as function of post-impact velocity recovery factor 06 p0725 A73-18880

Damping configurations that have a stabilizing influence on nonconservative systems. 07 p0908 A73-19088

Second derivatives of the flutter velocity and the optimization of aircraft structures. 07 p0912 A73-19952

A computerized flutter solution procedure. 07 p0914 A73-20214

Stability of a ferromagnetic plate within a gas flow in the presence of a magnetic field. 08 p0989 A73-21723

Arava STOL turboprop passenger aircraft flutter flight test program, describing measurement instrumentation and data recording system 09 p1031 A73-22185

Cantilever beam dynamic stability under follower force, investigating divergence, flutter and autparametric resonance relations 09 p1161 A73-23088

Helicopter main-rotor blade flutter in steady inclined flight 10 p1174 A73-23662

The effect of servomechanical control and stability systems on the flutter behavior of aircraft [DFVLR-SONDDR-272] 11 p1304 A73-25349

Gradient optimization of structural weight for specified flutter speed. 11 p1439 A73-25519

Numerical procedure for determining optimal member sizes of aircraft structural components with weight minimization and flutter speed lower bound [AIAA PAPER 73-391] 11 p1439 A73-25520

Eigenvalue problem and stiffness optimization procedure for incremental flutter analysis, describing method use in computer graphics mode. [AIAA PAPER 73-392] 11 p1439 A73-25521

An automated procedure for computing flutter eigenvalues. [AIAA PAPER 73-393] 11 p1440 A73-25522

Parametric studies of the wing flutter behavior of a STOL transport. 11 p1304 A73-25523
[AIAA PAPER 73-394]
Analysis of stall flutter of a helicopter rotor blade. 11 p1305 A73-25532
[AIAA PAPER 73-403]
Vibration and flutter of cylindrical shells including the effects of stringer stiffening. 11 p1441 A73-25543
[AIAA PAPER 73-312]
Flutter of pairs of aerodynamically interfering delta wings. 11 p1301 A73-25545
[AIAA PAPER 73-314]
Active flutter suppression - B-52 controls configured vehicle. 11 p1305 A73-25552
[AIAA PAPER 73-322]
The theoretical and experimental methods used in France for flutter prediction. 11 p1305 A73-25558
[AIAA PAPER 73-329]
Flutter technology in the United Kingdom - A survey. 11 p1441 A73-25559
[AIAA PAPER 73-330]
The state of the art in aeroelasticity of aerospace vehicles in Japan. 11 p1305 A73-25560
[AIAA PAPER 73-331]
In-flight flutter testing methods for determining aircraft structure natural frequencies and vibration damping ratios with air flow 11 p1306 A73-26593
[ONERA, TP NO. 1224]
Investigation of the flutter of cylindrical panels in a supersonic gas flow 12 p1550 A73-26954
Linear aerodynamic model incorporating torsional oscillations about two dimensional airfoil midchord for stall flutter description 13 p1697 A73-28814
Theoretical investigation on stall flutter of an airfoil [the case of trailing edge stall]. 13 p1566 A73-29027
Semiempirical method for flutter prediction of unsteady lift and aerodynamic forces acting on oscillating airfoil in stall regime, using separation function 13 p1566 A73-29029
Random /turbulent/ excitation of flutter in wind tunnel dynamic models and flight test aircraft, comparing prediction and damping measurement results 15 p1830 A73-31638
[ONERA, TP NO. 1234]
Cylindrically curved panels flutter characteristics in supersonic flow parallel to generators, investigating in-plane boundary conditions and panel geometry effects 15 p1949 A73-31652
A numerical integration method for the determination of flutter speeds. 15 p1955 A73-32163
Approximate calculation of flutter regions for collision body systems in phase space, noting fluttering duration as function of post-impact velocity recovery factor 15 p1915 A73-32405
Rayleigh-Ritz coefficient application in variational principle calculations of instability and flutter load of nonconservative systems 16 p2031 A73-32980
Out-of-plane vibration and stability of curved tubes conveying fluid. 17 p2248 A73-35101
[ASME PAPER 72-WA/APM-36]
Automatic electronic feedback control systems for active wing/external store flutter suppression 17 p2107 A73-35244
Alteration of a static vibration result by rigidizing some degrees of freedom 18 p2361 A73-36066
Investigation of the flutter of cylindrical panels in a supersonic gas flow. 19 p2500 A73-38139
A direct method of stability analysis for elastic circularity systems. 20 p2621 A73-39535
Flutter-divergence transition criteria in certain viscoelastic polygenic systems. 20 p2623 A73-39556
Effects of certain flight parameters and of certain structural parameters on helicopter main-rotor blade flutter 21 p2635 A73-41581
Bilateral estimates of the critical parameters of elastic systems experiencing flutter 22 p2921 A73-42280
The dynamic behavior of articulated pipes conveying fluid with periodic flow rate. 22 p2925 A73-42892
[ASME PAPER 73-APMW-32]
FLUX [RATE PER UNIT AREA]
U FLUX DENSITY
FLUX [RATE]
NT HEAT FLUX
NT MAGNETIC FLUX
NT SOLAR FLUX
Interplanetary dust particle flux curves, number densities and size distributions from zodiacal light investigations 02 p0215 A73-12262
Irreversible thermodynamics and losses in energy conversion, discussing N-port storage representation,

flux rate, power flow and electro-caloric and state space relations 07 p0779 A73-20396

Theorems on symmetries and flux conservation in radiative transfer using the matrix operator theory. 08 p1020 A73-20791

The entropy rate admissibility criterion for solutions of hyperbolic conservation laws. 23 p3000 A73-44203

FLUX DENSITY

NT CURRENT DENSITY
NT ELECTRON FLUX DENSITY
NT ILLUMINANCE
NT IRRADIANCE
NT LUMINANCE
NT LUMINOUS INTENSITY
NT NEUTRON FLUX DENSITY
NT PARTICLE FLUX DENSITY
NT PHOTON DENSITY
NT PROTON FLUX DENSITY
NT RADIANCE
NT RADIANT FLUX DENSITY
NT SOLAR CONSTANT
NT SOLAR FLUX DENSITY
NT SOUND INTENSITY

Intergalactic matter existence experiments, discussing critical cosmological energy and matter density, neutral and ionized gas, clustering and hot media 01 p0094 A73-10060

Navier-Stokes approximation for gas dynamics equations of molecular oscillations in diatomic gas, noting relaxation pressure proportionality to energy density equilibrium deviation 02 p0152 A73-11602

Midlatitude excess radiation energy density relation to primary cosmic ray background from spectrum measurement data 02 p0208 A73-12460

Sealed cylindrical high energy density Ni-Cd batteries, discussing electrode design and performance characteristics 09 p1034 A73-22754

High energy density long life Ni-Cd battery systems for synchronous satellites, discussing radiation protection, charge and discharge control electronics and temperature control 09 p1034 A73-22756

Radio-echo measurements of the flux of the Quadrantid, Perseid and Geminid meteor streams. 11 p1415 A73-25169

Modification of the two-flow approximation in radiant-transfer calculations 11 p1450 A73-25623

Direct measurement of the fluorescence energy yield of a rhodamine 6G solution with the aid of an Ar+ laser 11 p1377 A73-26146

Absorption and amplification of electromagnetic waves in a nonstationary magnetoactive plasma with allowance for spatial dispersion 11 p1405 A73-26151

The turbulent heating of ions and related efficiencies in a current carrying plasma. 15 p1916 A73-31081

Midlatitude excess radiation energy density relation to primary cosmic ray background from spectrum measurement data 15 p1927 A73-32610

High energy density silver-hydrogen cells for space and terrestrial applications. 19 p2391 A73-38403

Optical waveguide refractive index control process for glass film during deposition by sputtering power density variance 21 p2665 A73-41116

Radiating near-field power density and directivity reduction of tapered circular apertures. 22 p2829 A73-43181

FLUX MAPPING

U FLUX DENSITY
U MAPPING

FLUX QUANTIZATION

Low-frequency applications of superconducting quantum interference devices. 07 p0863 A73-20101

'Flux quantization' type of oscillation effects in a normal metal 09 p1130 A73-22709

Alternating spectral oscillations of nonequilibrium photoelectron current in p-InSb in the presence of a quantizing magnetic field 10 p1261 A73-24763

Gravitational energy quantization model of noncharged particle based on proposed centrosymmetric metric with nonzero Einstein matter tensor and without Schwarzschild singularity 22 p2887 A73-42430

FLUXES

Fluxless brazing of aluminum using protective gas. 23 p2985 A73-43997

FLUXMETERS

U MAGNETIC MEASUREMENT
U MEASURING INSTRUMENTS

FLY BY WIRE CONTROL

Control configured vehicle /CCV/ concept application to fighter aircraft design for combat maneuver capabilities and versatility enhancement, using fly by wire technology 05 p0535 A73-16662
[SAE PAPER 720854]

Fighter aircraft survivable flight control system design and flight test philosophy, present status and trends, considering fly-by-wire and power-by-wire systems 09 p1030 A73-22177

F-8 digital fly by wire control system development and flight testing, using Apollo lunar guidance computer and inertial measurement unit for angular rates and accelerations 15 p1830 A73-32475

Advanced flight control systems - Power-by-wire and fly-by-wire. 11 p1306 A73-26272

System of electric control of surveillance of the control surfaces of the Concorde 15 p1830 A73-32475

Quad redundant fly by wire servocontrol system design and tests in F-8C high speed jet aircraft, using fail/safe hydraulic actuators 16 p1970 A73-33080

Redundant system design and flight test evaluation for the TAGS digital control system. 17 p2131 A73-35062
[AHS PREPRINT 721]

Tactical aircraft guidance system for CH-47B helicopter utilizing fly by wire control system, describing design, display devices, flight instruments, computer configuration and crew duties 17 p2210 A73-35084
[AHS PREPRINT 761]

Digital fly by wire flight control system with airborne digital processor for increased aircraft survivability, determining redundancy level to satisfy system performance 17 p2138 A73-35222

Aerospace multiprocessor for A-7D aircraft digital fly by wire flight control, discussing design requirements, software development and reliability 17 p2107 A73-35223

Flight test and demonstration of digital multiplexing in a fly-by-wire flight control system. 17 p2107 A73-35225

Redundant system design for advanced digital flight control. 20 p2585 A73-38785
[AIAA PAPER 73-846]

Fly-by-wire digital F-8C aircraft control system using Apollo guidance, navigation and control hardware, emphasizing interface design and fault detection 21 p2733 A73-40027

FLYBY MISSIONS

NT GRAND TOURS

NT MARINER VENUS-MERCURY 1973

Trajectory analysis for swingby technique using Jovian gravitational field for leaving plane of ecliptic along heliocentric orbit and for solar flyby at specified distance 03 p0378 A73-14552

Estimating trajectory correction requirements for multiple outer planet missions. 05 p0623 A73-17205

Major planets gravitational fields models from flyby spacecraft measurements, discussing Red Spot and Jupiter effect on Galilean satellites 14 p1799 A73-30531

Imaging as primary exploration tool for outer planets and satellites, considering flyby and orbital imaging for planetary atmospheres 14 p1800 A73-30536

Cometary Science Working Group, Meeting, Williams Bay, Wis., June 9-11, 1971, Proceedings. 15 p1941 A73-32413

Planetary flybys resulting in heliocentric orbits normal to the ecliptic with fixed perihelia. 22 p2909 A73-42628

Martian W cloud diurnal brightening observation by Mariners 6 and 7 flyby missions, considering probable water ice formation 24 p3128 A73-44398

FLYING BEDSTEAD AIRCRAFT

U FLYING PLATFORMS

FLYING PERSONNEL

NT AIRCRAFT PILOTS

NT COSMONAUTS

NT FLIGHT CREWS

NT TEST PILOTS

Thoracic X ray photography technique for tubercular lesion detection in flight personnel, comparing to standard radiography and radiocopy 02 p0137 A73-12155

Ocular tonus measurements for glaucoma detection in flying personnel, discussing subsequent test procedures in case of abnormal findings 02 p0134 A73-12158

Flight personnel training meetings, covering decision making, cockpit personnel selection and instructor role analysis 03 p0266 A73-13073

Idiopathic central serous retinopathy /cho-roidopathy/ in flying personnel. 03 p0269 A73-14164
[AD-754147]

Performance measurement system for combat crew flight training in complex aircraft weapon systems, identifying training research goals

05 p0544 A73-16726

Human factor role in flying personnel errors, noting man machine system performance and medical service engagement

06 p0659 A73-18258

USAF WAVR file of epidemiologic data on medically waived flying personnel, describing computerized updating system

09 p1039 A73-22539

The role of vestibulometry in medical evaluation of flight personnel

10 p1183 A73-23821

Effects of flying and of time changes on menstrual cycle length and on performance in airline stewardesses.

13 p1576 A73-28509

Aircraft cabin altitude hypoxia effects on mother, embryo and fetus during first trimester of pregnancy in air hostesses and women passengers

14 p1718 A73-30519

Responsibility for ischemic cardiopathies in civil aviation flight personnel

18 p2284 A73-36902

Detection of atherosclerosis in examinations of flight personnel

18 p2284 A73-36913

Psychotechnical selection of flight crews in South Vietnam

18 p2284 A73-36918

Visual problems among senior flight personnel.

18 p2285 A73-36924

Glaucoma development in aging flight personnel.

18 p2285 A73-36926

Binocular vision variation with age in flight crews

18 p2285 A73-36928

Information yield of the Annual Medical Examination for Flying.

20 p2517 A73-39110

Evaluation of the physical conditions of individual airmen

23 p2949 A73-43790

FLYING PLATFORM STABILITY

U AERODYNAMIC STABILITY

U FLYING PLATFORMS

FLYING PLATFORMS

An-2R aircraft conversion to flying test bed for feasibility studies of jet engine use in agricultural aircraft, describing structural design modifications

12 p1458 A73-26823

Experimental autostabilized tethered rotor platform for reconnaissance, communications and ECM, discussing control system effectiveness from flight test results

16 p1969 A73-33736

Large space vehicles - Platforms for second generation in-situ wake observations.

21 p2781 A73-40901

FLYING QUALITIES

U FLIGHT CHARACTERISTICS

FLYING SPOT SCANNERS

Computerized flying spot scanner/analyzer for automatic mensuration analysis of droplets, particles and cell preparations from 35 mm film density distributions

03 p0309 A73-14449

Computer aided recognition of objects shapes on aerial photographs, discussing image derivatives and histograms use and flying spot scanner principle

07 p0825 A73-20165

Electron-beam tube with a semiconductor target - An electron-beam-pumped scanning laser.

12 p1508 A73-27526

FLYING WING AIRCRAFT

U TAILLESS AIRCRAFT

FLYWHEELS

High strength straight filament superflywheel configurations with improved energy storage capability for vehicle, tool and power supply applications

04 p0475 A73-14744

Mechanical energy storage by flywheel with magnetic fluid hermetic seal and bearing, using anisotropic and whisker materials

11 p1399 A73-25979

Controlling the angular motions of a flight vehicle with the aid of flywheels

12 p1522 A73-27083

Aircraft-store separation design for angular momentum increase of external weapon with internally mounted spinning flywheel

20 p2508 A73-38652

FOAMS

Analysis of volatile combustion products and a study of their toxicological effects.

02 p0138 A73-12429

Preparation and performance characteristics of flammable and inflammable polyimide foams as sandwich fillers

10 p1239 A73-24098

Foamed Al production from Al powder mixture with aluminum hydroxide and orthophosphoric acid,

discussing mechanical, thermal conductivity and electrical insulating properties

10 p1236 A73-24919

Syntactic foam from Pyrrone prepolymer and hollow carbon microsphere mixtures, discussing low curing shrinkage and high thermal stability

16 p2029 A73-33051

Polyimide resin dielectric and mechanical properties, discussing syntactic foam composite with aluminum filler for radome construction

17 p2195 A73-34804

FOCI

Multiple mirror telescope consisting of six Cassegrainian telescopes combined for common focal surface, noting light gathering power equivalent to 180 inch standard telescope

08 p0970 A73-21738

FOCUSING

NT DEFOCUSING

NT SELF FOCUSING

Auxiliary instruments for 4-m reflectors related to astronomical telescope focal positions, discussing correlators, cameras, sensitometers, film, rotator-adaptor, guider, echelle spectrograph and photometers

01 p0046 A73-10504

Basic instrumentation components for prime, Cassegrain and coude focal positions of Anglo-Australian telescope, discussing acquisition and guiding, photography, photometry and spectrography

01 p0046 A73-10506

Intermediate dispersion spectrograph instrument design for Cassegrain focus of Anglo-Australian telescope, discussing optical and mechanical layouts and remote control

01 p0046 A73-10509

Prototype design of echelle grating spectrographs for Anglo-Australian 3.8 meter telescope Cassegrain focus, presenting main parameters

01 p0047 A73-10511

Converging lens effect of air jet for upstream moving waves, describing experimental procedure

03 p0290 A73-12968

Sporadic E cloud focusing of radio waves as interpretation of observed short duration bursts accompanied by rapid phase variation

03 p0280 A73-14592

Charged particle beams focusing in combined dual spiral system with uniform magnetic field along axis, applying to imaging of flat object

05 p0556 A73-16067

Gudunov-method computation of the flow field associated with a sonic-boom focus.

05 p0536 A73-16965

Distortion of near-sonic shocks by layers with weak thermal fluctuations.

05 p0537 A73-17374

Antenna beam focusing and deflection with the aid of a digital phase computer, in a radiation-fed electronically controlled antenna

06 p0673 A73-17580

Cylindrical laser resonators with partial radial radiation and strong axial energy focusing, relating low-loss cavity modes to Gaussian beam modes

07 p0833 A73-19273

Focusing of EM waves in plasmas by inhomogeneous magnetic fields.

08 p0993 A73-21205

An X-ray tube emitting soft and hard radiation with controlled focusing

08 p0969 A73-21721

Properties of magnetic focusing systems for picture tubes

10 p1194 A73-23850

Strict calculation of static fields in devices for periodic electrostatic focusing /PEF/ of electron beams

10 p1197 A73-24882

Correlation of the shift in the center of gravity of a focused light beam in a turbulent atmosphere

11 p1331 A73-26160

Solid ultrasonic cylindrical lens design for off-axis aberration minimization for focusing properties improvement, using method analogous to chromatic aberration correction in optics

13 p1612 A73-28491

Sensitivity and resolution in holographic interferometry of focused images

13 p1616 A73-28766

Effects of target-electrode polarity and of the position of the focal plane of the lens on the characteristics of a discharger with laser ignition

13 p1627 A73-28964

A Lallemand electronic camera focused by a superconducting magnetic coil.

14 p1751 A73-29904

Particle acceleration by a moving laser focus, focusing front or ultrashort laser pulse front.

14 p1757 A73-30338

Relativistic electron beam focusing by neutral gas filled conical guide tube, comparing efficiency, fluence gain, energy loss and pressure variation predictions with experiments

14 p1777 A73-30658

Experimental investigation of the plasma focus in erosion-source plasma accelerators. I

15 p1921 A73-32325

Mapping with coherent-radiation focused synthetic-aperture side-looking radar.

16 p2015 A73-33357

Linear phased array antenna focused in Fresnel region, noting radiation pattern indoor measurement simplicity advantage over far field observation in performance monitoring

17 p2128 A73-35694

Large parabolic reflector microwave antenna astigmatism effects on radiation pattern, discussing focusing procedure for phase error reduction

17 p2143 A73-35695

A comparison of the efficiency and focused stray light characteristics of a conventionally ruled- and a holographically produced-concave diffraction grating in the vacuum ultraviolet.

19 p2431 A73-38164

Optimal pumping focusing in parametric single-resonator lasers

19 p2439 A73-38336

Cross focusing possibility between two coaxial laser beams in dielectrics with optical inhomogeneities and oscillatory waveguide characteristics, noting critical power role

20 p2572 A73-38848

Technical and experimental investigations of a plasma focus neutron source

21 p2744 A73-39976

Czerny-Turner monochromator design using small spherical mirror off-axis angles to eliminate multiply dispersed light, discussing mirror types and focal length

21 p2697 A73-40129

Changes in the geometrical parameters of a radio-telescope parabolic mirror experiencing radially symmetric deformations

21 p2672 A73-40549

Pattern measurements of phased-arrayed antennas by focusing into the near zone.

21 p2653 A73-40681

Phase errors at the aperture of a curvilinear antenna during displacement of the primary radiating element from the focal point

21 p2667 A73-41447

Static fields for periodic electrostatic focusing of electron beams.

21 p2668 A73-41657

Effects of target-electrode polarity and focal-plane position on a laser-triggered gap.

23 p2989 A73-44316

Comparative focusing properties of spherical and plane microwave zone plate antennas.

24 p3069 A73-45480

FOETUSES

U FETUSES

FOG

Fog droplet vaporization and fragmentation by a 10.6-micron laser pulse.

06 p0698 A73-17494

[AD-758948] Possibility of affecting the coagulation of droplets in warm clouds and fog by electrical methods

06 p0719 A73-17840

A radiative-conductive model for the prediction of radiation fog.

06 p0720 A73-18327

Image holography through convective fog.

11 p1361 A73-25365

Dynamics and energetics of the explosive vaporization of fog droplets by a 10.6-micron laser pulse.

11 p1377 A73-26231

Differential difference equations for probability of water droplet electrization in weakly ionized medium during cloud and fog formation

13 p1654 A73-28883

Atmospheric air characteristics classification as haze, foggy haze, fog and drizzle from light scattering matrix on basis of aerosol condensation

13 p1654 A73-29159

Fog frequency and characteristics at the site of the proposed New York offshore airport, as compared with those at J. F. Kennedy International Airport - A preliminary report.

15 p1903 A73-31546

Thermal imaging through hazes and fogs in the middle and far infrared windows - Some experimental results.

16 p2016 A73-33997

Analysis of visibility conditions during aircraft landing in radiation fog

17 p2204 A73-34540

Light beam dispersal of fog with various drop sizes based on energy equation, considering cloud water content, cross wind effects and front velocity

18 p2337 A73-36561

A study of droplet spectra in fogs.

19 p2447 A73-37660

Operative visibility limits over the airports of Milan Linate and Malpensa in the 1960-1969 decade

19 p2447 A73-38125

A numerical analysis of some practical aspects of airborne urea seeding for warm fog dispersal at airports.

21 p2728 A73-40056

Fog dispersal technique evaluation for cost effectiveness by statistical method, taking into account time dependent probability of natural visibility improvement

21 p2729 A73-40066

FOILS [MATERIALS] NT METAL FOILS

FOKKER AIRCRAFT

VFW-FOKKER VAK-191B VTOL fighter aircraft structural and aerodynamic design, describing airframe construction, power plant arrangement, flight controls, hydraulic and electrical systems

19 p2387 A73-38167

VAK 191B.

22 p2798 A73-41752

FOKKER BOND TESTERS

U ADHESION TESTS

FOKKER-PLANCK EQUATION

Parametric vibration of simply supported rectangular plate and cylindrical shell under random excitation, using Markov process theory and Fokker-Planck equation

03 p0388 A73-13318

Application of stochastic stability theory to model-reference systems.

04 p0430 A73-15215

Transient phenomena in a phase-locked loop with a noisy reference.

04 p0421 A73-15437

Emission risetime fluctuations in a gas laser with nonlinear resonant absorption

06 p0700 A73-18104

Fokker-Planck equation for solar atmosphere modulation of galactic proton and electron flux at earth, including convection, diffusion and adiabatic deceleration effects

07 p0870 A73-19576

Numerical studies of the transport of solar protons in interplanetary space.

07 p0870 A73-19664

Trapped electrons instability in Tokamak configuration, calculating plasma wave propagation modes via Fokker-Planck equation

08 p0991 A73-20815

Transient analysis of phase-locked tracking systems in the presence of noise.

09 p1066 A73-22113

Nonlinear system analysis based on Fokker-Planck equation, simplifying solution sequence for steady state or variance of states combination

09 p1111 A73-22114

Kinetic theory of a two-dimensional magnetized plasma. II - Balescu-Lenard limit.

09 p1126 A73-22282

Solution of the Fokker-Planck-Kolmogorov equation for a dynamic system with analytical characteristics

09 p1068 A73-22563

Solar flare particle propagation - Comparison of a new analytic solution with spacecraft measurements.

10 p1269 A73-24727

Theory of cosmic ray transfer by anisotropically scattered particles

12 p1534 A73-27331

On the transport of charged particles in turbulent fields - Comparison of an exact solution with the quasilinear approximation.

15 p1916 A73-31083

Intermittency in fully developed turbulence as a consequence of the Navier-Stokes equations.

15 p1860 A73-31092

A generalization of the equations governing the evolution of a particle distribution in a random force field.

17 p2213 A73-34449

Elastic and inelastic scattering in orbital clustering.

18 p2357 A73-37109

Detuned single mode laser detailed balance and line width factor in threshold region expressed by Fokker-Planck equation and nonhermitian eigenvalue

20 p2571 A73-38622

Quantum mechanics /semiclassical/ theory investigation of shot and thermal noise effects on laser behavior, deriving Fokker-Planck equations for field probability distribution

21 p2711 A73-40215

Asymptotic forms of solutions to nonrelativistic Compton Fokker-Planck equation for bremsstrahlung X ray spectra changes due to Compton scattering in emitting gas

22 p2904 A73-43018

Small angle multiple backscattering from randomly spaced cylindrical plasma cloud striations, obtaining ray density via Fokker-Planck transport equation

22 p2896 A73-43182

Contribution to the theory of cosmic-ray propagation with anisotropic particle scattering.

23 p3020 A73-43229

Fluctuations of the radiation rise time in a gas laser with nonlinear resonant absorption.

24 p3095 A73-44494

Eigenfunction expansions for randomly excited non-linear systems.

24 p3151 A73-45265

FOLDING STRUCTURES

Development of a deployable and selfrigidizing solar cell array for the multikilowatt range.

11 p1310 A73-26002

In-plane and lateral displacements triangular elements represented by cubic and quintic polynomials for folded plate structural analysis

20 p2622 A73-39545

FOLIAGE

Theoretical and experimental investigations of the coefficients of reflection from plant foliages at small slip angles

22 p2847 A73-42332

FOOD INTAKE

Hypothalamic norepinephrine - Circadian rhythms and the control of feeding behavior.

02 p0134 A73-12417

Resistance of soil microorganisms to starvation.

02 p0136 A73-12627

U.S. manned space flight food system development experience assessment, covering Mercury, Gemini, Apollo and manned orbiting laboratory programs

03 p0269 A73-14168

Organ and body mass changes in restrained and fasted domestic fowl.

04 p0409 A73-14975

Effect of hypergravity on the circadian rhythms of white rats.

[ASME PAPER 72-WA/BHF-14]

04 p0410 A73-15877

Hypobaric hypoxia - Within-subject transition effects in albino rats.

06 p0649 A73-17525

Gas-chromatography investigation of volatile metabolites in man on reduced food rations and during starvation

06 p0657 A73-17690

Thermal factor and dehydration influences on protidic and lipidic catabolisms of young men with partial food deprivation in hot climate, discussing metabolic balances

08 p0934 A73-21248

Drive and performance modification following multiple light-light/ shifts in the photoperiod.

09 p1039 A73-22528

Biopotential alpha and theta rhythms of neocortex and hippocampus of milk drinking cats after food and water deprivation

09 p1040 A73-22862

Nutrition systems for pressure suits.

20 p2517 A73-39105

FORBIDDEN BANDS

Multiphonon transition theory for electron transitions probability between conduction and forbidden bands, noting semiconductor surface states with long relaxation time

01 p0089 A73-11438

Planetary nebulae NGC 7635, 7008, 1514, 650-1, 7139, 3587, 6781 and 6543 monochromatic images, centering filters on H alpha, N II and O III forbidden lines

02 p0221 A73-12703

Quasi-discrete acceptor states in zero forbidden gap n-type semiconductors, showing noncompensation at low temperatures

04 p0484 A73-15567

Some optical properties of solid solutions in the 2GaAs-ZnSiAs2 section

05 p0605 A73-16612

Twilight airglow. I - Photoelectrons and forbidden O I 5577-angstrom radiation.

10 p1214 A73-24737

Kinematics of the Huyghenian region of the Orion Nebula.

11 p1427 A73-26605

Seasonal and diurnal variations of forbidden oxygen and sodium lines emission, stressing nightglow zenith intensity fluctuations connection to F layer electric fields

12 p1489 A73-26992

Twilight enhancement of forbidden-OI 6300 A airglow.

15 p1868 A73-31382

Cooling associated with minority carriers exclusion effect in semiconductors, discussing influence of electroconductivity and forbidden bandwidth

17 p2219 A73-35160

Determination of the dispersion relation in tunnel structures - Influence of the barrier shape and validity of the WKB approximation.

17 p2220 A73-35655

An atlas of low-latitude 6300-A forbidden O I night airglow from Ogo 4 observations.

22 p2845 A73-41924

Variations in the distribution and physical properties of Perseid meteors.

22 p2914 A73-43015

Electronographic observations of the forbidden O II ratio in the core of the Orion Nebula.

24 p3140 A73-45183

FORBIDDEN TRANSITIONS

Airglow height profiles of forbidden O I 6300 and 5577 A line emissions in morning ionosphere from rocket photometric measurement

04 p0444 A73-15542

Measurements of the electron temperatures in M42 from the profiles of H-alpha, forbidden N II, H-beta, and forbidden O III.

08 p1004 A73-20906

A proposed correction to the solar abundances of carbon and oxygen utilizing new and accurate theoretical forbidden transition probabilities.

16 p2060 A73-32952

Measurement of turbulent HF fields in a high-current rectilinear gas discharge from the intensity of forbidden HeI lines

23 p3011 A73-43669

FORBUSH DECREASES

Prediction of proton flares and Forbush effects.

04 p0491 A73-14843

Anomalous recurrent diurnal anisotropy in cosmic ray intensity with maximum along the garden hose direction.

05 p0608 A73-16142

Temporal and spatial changes in cosmic ray intensity increases preceding Forbush decreases

06 p0742 A73-17531

Speed of propagation of shock waves responsible for geomagnetic storms and Forbush decreases

06 p0689 A73-17548

Record-breaking cosmic ray storm stemming from solar activity in August 1972.

08 p0996 A73-20664

Characteristics of cosmic ray variations near the solar equator plane

08 p0998 A73-21299

Forbush prederecrease observation by superneutron monitors, interpreting cosmic ray depletion and rigidity dependence by model of interplanetary magnetic field propagating disturbance from sun

09 p1073 A73-22051

Solar wind effect on azimuthal and radial galactic cosmic ray currents, noting Forbush decreases relation to current structures

10 p1265 A73-23907

Problems of linear and nonlinear theory of cosmic ray modulation

10 p1266 A73-23913

Forbush decreases and their relation to solar activity and the parameters of the interplanetary medium

10 p1267 A73-23921

Analysis of the variations of cosmic rays of magnetospheric and interplanetary origins according to spectrographic data

10 p1267 A73-23928

The first results of balloon measurements during the solar proton events in the period from August 2 to August 10, 1972

12 p1535 A73-27777

Statistical analysis of Forbush decreases and of cosmic-ray intensity increases preceding them.

13 p1670 A73-28701

Time and space variations of cosmic-ray intensity increases prior to Forbush decreases.

16 p2052 A73-32755

Propagation velocity of shock waves causing geomagnetic storms and Forbush decreases.

16 p2002 A73-32772

Transient solar modulation of cosmic rays.

16 p2055 A73-33294

Interplanetary shock waves and cosmic rays.

19 p2476 A73-37759

Characteristics of cosmic-ray variations near the solar equatorial plane.

19 p2476 A73-37928

The Forbush effect in the nuclear component of primary cosmic rays in August 1972

21 p2757 A73-40588

Ground level cosmic ray variations in August 1972, relating intensities and Forbush decreases with solar flares and shock wave parameters

21 p2757 A73-40591

Investigation of shock waves responsible for Forbush decreases

21 p2757 A73-40595

Variations of three-dimensional anisotropy of cosmic rays during Forbush decreases.

24 p3125 A73-45102

FORBUSH EFFECT

U FORBUSH DECREASES

FORCE DISTRIBUTION

Fourier transformation for stress analysis of anisotropic shells under concentrated forces, solving shallow shell equations via MacDonald functions

01 p0118 A73-11408

Buoyancy distribution of slender axisymmetric bodies of higher order in the case of compressible subsonic flow

02 p0127 A73-11681

Effect of the length on the stability of cylindrical shells compressed by longitudinal local forces

02 p0231 A73-11816

Elastic deformation of a single-cavity hyperboloid of revolution under given forces at the boundary

02 p0233 A73-11939

Equations of motion of solid body about fixed point with nonholonomic constraint, noting potential forces field effect

02 p0193 A73-12195

Oscillatory point force generated motion in inviscid incompressible rotating stratified fluid, obtaining closed form solutions via Fourier transforms

03 p0296 A73-14313

Design of digital force function generator for aircraft tire load testing.

04 p0424 A73-15064

Expansion of the force function of two homogeneous spheroids with noncoincident symmetry planes.

04 p0503 A73-16021

Multivortex model for bodies of arbitrary cross-sectional shapes.

[AIAA PAPER 73-104]

05 p0529 A73-16864

Leading-edge force features of the aerodynamic finite element method.

05 p0533 A73-17213

A new measurement device for measuring harmonic forces

06 p0695 A73-18434

Infinite triangular wedge, with a notch at its bisectrix, under the action of concentrated forces applied to the edges of the notch

07 p0911 A73-19312

Numerical experiments on probability distribution of random force in stellar gravitational systems, noting agreement with Chandrasekhar and von Neumann theory

08 p1003 A73-20884

The movement of Volterra disclinations and the associated mechanical forces.

08 p0995 A73-21627

Operational methods for analysis of discontinuous systems with multiple lumped parameter attachments and concentrated forces, obtaining steady state closed form solutions

09 p1159 A73-22648

Elastic circular ring stability under uniformly distributed equal radial concentrated forces

10 p1287 A73-23594

Acoustic streaming and forces generated on circular cylinder in radially oscillatory incompressible fluid, considering steady and unsteady flow

10 p1174 A73-24847

The effect of deformations in the measurement of the force and the couple of friction

11 p1374 A73-25871

Composite solid with two contacting or bonded half planes of different elastic moduli, considering interplane force transmission from stress distribution calculation

11 p1443 A73-26277

Estimates for stress derivatives and error in interior equations for shells of variable thickness with applied forces.

11 p1446 A73-26548

Singular nonaxisymmetric shallow shell equation solutions for concentrated normal and tangential forces and bending and twisting moments

12 p1550 A73-27034

Nongravitational force variation with heliocentric distances computed for long and short period comets, deriving force law from water snow vaporization rate

12 p1540 A73-27428

Bending of a circular nonlinearly-elastic plate by a concentrated force

12 p1555 A73-27794

Influence on the stress-strain state of the way a concentrated force is applied to the tip of a crack in a plate

14 p1814 A73-30718

Dynamic singular boundary value problem of elastic body with propagating crack under concentrated force

14 p1814 A73-30784

A parachute snatch force theory incorporating line disengagement impulses.

[AIAA PAPER 73-464]

15 p1827 A73-31450

A technique for the calculation of the opening-shock forces for several types of solid cloth parachutes.

[AIAA PAPER 73-477]

15 p1829 A73-31461

On kinematics and statics of finite-strain force and moment stress elasticity.

17 p2252 A73-35829

Shock wave generation by moving distributed non-diffusive force, solving initial value problem for single fluid model to obtain supersonic force field velocity

18 p2299 A73-36323

Equivalence rule and transonic flow theory involving lift.

18 p2264 A73-36328

Forces acting on a small body in an arbitrary incompressible fluid flow and equations of motion of a two-phase medium

18 p2302 A73-37008

Changes in whole body force transmission of dogs exposed repeatedly to vibration.

20 p2512 A73-39106

The symmetry method and its application to plane problems of elasticity theory

20 p2618 A73-39325

Method of studying thermal fatigue from the parameters of the hysteresis loop in temperature-force coordinates

20 p2619 A73-39362

Thermoelastic dilatational deformation in two perfectly bonded orthotropic half-planes, showing linear relations between elastic and homogeneous field

21 p2789 A73-41674

The effects of speed and radial flow on the axial force on an enclosed rotating disc.

21 p2754 A73-41685

An exact method for the study of the dynamic stability of supporting structures acted upon by periodic impulses.

22 p2927 A73-43031

Dynamic stability of rotating disks loaded by a concentrated force

22 p2928 A73-43064

Investigation on the optimum tightening force of bolted joint in torque control method.

23 p2986 A73-44140

Solution of boundary value problems in thermoviscoelasticity with allowance for mass forces exhibiting a potential

23 p3046 A73-44196

Radial and vertical force balance in primitive solar nebula, describing techniques for gravitational potential and gas opacity computation for energy transport

24 p3127 A73-44392

Formation of a pseudoliquidified layer during combustion of condensed systems with solid nonagglomerating additives in a field of mass forces

24 p3121 A73-44705

Calculation of the force characteristics of the external spherical suspension of a cryogenic gyroscope

24 p3091 A73-45023

Structural analysis for idealized nonlinear material behavior.

24 p3152 A73-45316

Optimal force transmission by flexure-clamped boundaries.

24 p3152 A73-45317

FORCE FIELDS

U FIELD THEORY [PHYSICS]

FORCE-FREE MAGNETIC FIELDS

Equilibrium model for force-free relativistic electron beam, obtaining solution with maximum beam radius and maximum axial current

02 p0198 A73-12070

Resistive diffusion of force-free magnetic fields in a passive medium.

11 p1428 A73-26620

Representation method for force free magnetic field class, including current free fields and applications to solar fields

21 p2779 A73-41536

Models of force-free magnetic fields in resistive media.

22 p2911 A73-42938

Resistive diffusion of force-free magnetic fields in a passive medium. II - A nonlinear analysis of the one-dimensional case.

22 p2914 A73-43009

The topological association of H alpha structures and magnetic fields.

24 p3136 A73-44639

FORCED CONVECTION

Forced convection droplet evaporation with finite vaporization kinetics and liquid heat transfer.

01 p0122 A73-10803

Forced flow, single-phase helium cooling systems.

01 p0123 A73-11099

Combined forced and free-convection heat transfer from vertical thin needles in a uniform stream.

02 p0238 A73-12052

Carbon dioxide turbulent flow heat transfer in single phase near-critical region under forced and free convection

03 p0396 A73-13185

Unsteady laminar natural and forced convection at transparent medium boundary layer radiating surface, noting turbulence effects on heat exchange

03 p0397 A73-13187

Forced convective heat transfer to supercritical water flowing in tubes.

04 p0520 A73-15945

Combined free and forced laminar convection in inclined tubes.

05 p0564 A73-16173

Thermal boundary layer thickness for laminar forced convection to flat plates with uniform heating and uniform wall temperature.

06 p0769 A73-18260

Thermo-acoustic oscillations in forced convection heat transfer to supercritical pressure water.

08 p1022 A73-21253

Analysis and space-time reconstitution of the circumferential component of instantaneous velocity in immediate proximity to the wall of a cylinder

08 p0926 A73-21496

Destabilization of vapor film boiling around spheres.

08 p1024 A73-21641

Mode of thickening of a low morning convective layer in clear sky

09 p1115 A73-23036

Periodic semi-integral solutions of secondary unsteady convective flows in external force field for

critical Rayleigh numbers by Liapunov-Schmidt method

10 p1204 A73-23584

Forced air cooling of dual-in-line packages.

10 p1193 A73-23607

An experimental study of combined forced- and free-convective heat transfer from flat plates to air at low Reynolds numbers.

10 p1295 A73-23777

Electronic equipment thermal management for energy dissipation rejection, summarizing heat pipe, phase-change heat transfer and high pressure gas convection techniques

10 p1295 A73-23789

Unsteady three dimensional laminar incompressible boundary layer with free and forced convection, determining flow and temperature fields adjacent to heated body

10 p1208 A73-24810

Interaction of free and forced convection in horizontal tubes in the transition regime.

11 p1448 A73-25153

Forced convection heat transfer in laminar boundary layer at low Prandtl numbers.

11 p1452 A73-26123

One method of computing the meteorological variables for mesoscale processes.

11 p1394 A73-26192

Solutions of some Fredholm integral equations using fractional integration, with an application to a forced convection problem.

13 p1704 A73-28413

Experiments in magneto-fluid-mechanic natural and forced heat transfer from horizontal hot-film probes.

13 p1620 A73-29254

Effects of buoyancy and of acceleration owing to thermal expansion on forced turbulent convection in vertical circular tubes - Criteria of the effects, velocity and temperature profiles, and reverse transition from turbulent to laminar flow.

14 p1818 A73-30614

Transient forced convection heat transfer from an isothermal flat plate.

15 p1957 A73-31664

Forced convective heat transfer of a gas with condensing vapor around a flat plate.

15 p1958 A73-32058

Theoretical analysis of forced laminar convection heat transfer in the entrance region of an elliptic duct.

17 p2256 A73-33580

Combined forced and free-convection over thin needles.

18 p2371 A73-36697

Combined forced convection and radiation heat transfer in the thermal entrance region of a non-isothermal parallel plate channel - Optical thin gases. [ASME PAPER 73-HT-14]

20 p2625 A73-38569

Forced convection of a fluid inside an ellipsoidal cavity

21 p2791 A73-40740

Forced convective heat transfer from isothermal sphere in steady incompressible flow at low Reynolds and various Prandtl numbers, obtaining mean Nusselt number

23 p3049 A73-43934

FORCED OSCILLATION

U FORCED VIBRATION

FORCED VIBRATION

Heating of a viscoelastic beam subjected to transverse vibrations

01 p0112 A73-10003

Linearization method for analytic solution of oscillatory motion differential equations of elastic nonlinear system, studying combinations of free and forced vibrations

01 p0075 A73-10093

Incompressible elastic circular cylinders quasi-equilibrated motions analysis, obtaining free and forced oscillations periods

02 p0191 A73-11573

Non-linear vibration of rotating cantilever blades treated by the Ritz averaging process.

02 p0232 A73-11859

Dynamics of flexible satellites with active attitude control.

02 p0228 A73-11994

Large amplitude oscillations of a hollow spherical dielectric.

02 p0236 A73-12518

Nonlinear responses for a circular plate subjected to a dynamic ring load.

03 p0388 A73-13319

Analysis of the forced vibrations of composite linear systems by the stiff finite elements method

03 p0396 A73-14600

N degrees of freedom system resonant vibration mode and frequencies determination from forced vibration of complementary body

04 p0509 A73-14979

Self-excited and forced vibrations of an aeroelastic system subject to a follower force.

04 p0513 A73-15597

Spectral analysis of the vibrations of mechanical systems with continuous mass which have a finite number of attached concentrated masses

04 p0476 A73-15659

On the forced vibration of a rectangular plate. [ASME PAPER 72-WA/DE-20]

04 p0514 A73-15838

The calculation of the natural vibration parameters of a damped system on the basis of the results of a vibration test in an exciter configuration

05 p0634 A73-16758

On forced vibrations in the linear theory of micropolar elasticity.

06 p0762 A73-17987

Forced vibration of a class of non-linear two-degree-of-freedom oscillators.

07 p0851 A73-19165

German monograph - Harmonically excited forced oscillations of a spring/mass system with controlled Coulomb damping.

07 p0851 A73-19581

Nonlinear longitudinal oscillations of relativistic plasma.

07 p0859 A73-20217

Forced motion of elastic cylindrical rods - A comparison of two theories.

07 p0915 A73-20284

Identification of large structures using data from ambient and low level excitations.

07 p0916 A73-20431

On the application of parameter identification to high-speed ground transportation systems.

07 p0808 A73-20433

Calculation of the natural and forced vibrations of circular plates with allowance for energy dissipation in the material

07 p0917 A73-20501

Designing turbomachine blades for forced vibrations under various excitation conditions

07 p0917 A73-20503

Velocity ratio in the analysis of linear dynamical systems.

08 p0988 A73-21467

Prediction of aeroelastic instabilities in turbines

09 p1135 A73-22204

Recursive solution for steady forced vibration modes of tenses string under concentrated harmonic forces

09 p1120 A73-22583

Numerical computation of forced oscillations in coupled Duffing equations.

09 p1113 A73-23022

Application of a variational difference method to the calculation of forced vibrations of shells of revolution

10 p1292 A73-24487

Calculation of forced vibrations in damped centrifugal pumps with a given level of rotor imbalance

10 p1263 A73-24673

The motion of a viscous, stratified fluid subjected to forced oscillations.

10 p1210 A73-24844

Small parameter method, with the parameter proportional to the friction forces, in the case of forced vibrations of complex trusses

11 p1435 A73-25395

Application of the harmonic balance method for studying oscillations of nonlinear systems with distributed parameters

11 p1400 A73-26464

On combined frequency oscillations of the forced Van der Pol oscillator.

11 p1339 A73-26696

A method of studying oscillatory systems subject to the action of external periodic forces in the nonresonant case

12 p1525 A73-27812

Frequency method of synthesis for an active dynamic vibration damper

12 p1525 A73-27948

Effect of shroud eccentricity on suppression of flow induced vibrations.

13 p1690 A73-28059

Methods for the approximate computation of the periodic solutions of systems of nonlinear periodic differential equations

13 p1647 A73-28193

The Rayleigh-Faber-Krahn theorem for the characteristic values associated with a class of nonlinear boundary value problems.

13 p1648 A73-28423

Analytical approximation of high order Galerkin solutions to ordinary differential equations describing forced oscillations of systems with polynomial nonlinearities, considering first-order harmonic effects

13 p1648 A73-28440

Viscous fluid sloshing in rectangular vessel, studying forced oscillations, ejected flow and frequency equation based on Navier-Stokes equations and boundary conditions

13 p1600 A73-28444

Free and forced vibration analysis of laminated ring structure with elastic inner, outer layers and core, obtaining natural frequency response by variational method

13 p1695 A73-28486

Small perturbation evolutionary motion equations for forced vibrations of quasi-linear two frequency autonomous systems at resonance

13 p1661 A73-29082

Analysis of self-excited and forced vibrations of a rectangular plate on many supports in supersonic flow.

13 p1700 A73-29392

Forced vibration solution and wind tunnel investigation of shallow cylindrical shells under moving pulsating pressure discontinuities, noting compression shock effects

13 p1703 A73-29602

Hysteresis loop equation for calculation of elastoplastic deformations caused by forced vibrations, taking into account medium compressibility and inertial forces

13 p1703 A73-29609

Note on forced vibration of a non-homogeneous cone with spherical caps.

14 p1814 A73-30708

On the vibrations of a rotor with rotating inequality and with variable rotating speed.

15 p1883 A73-32216

Investigation of forced oscillations of the plasma potential in a closed electron-drift accelerator (CDA)

15 p1920 A73-32310

Forced vibrations of elastic shells of revolution filled with liquid

16 p2074 A73-32687

Forced extensional vibrations of isotropic elastic plates with time dependent body forces, surface tractions and nonhomogeneous boundary conditions, using Kane-Mindlin theory

16 p2076 A73-32920

Flexural wave mechanics - An analytical approach to the vibration of periodic structures forced by convected pressure fields.

16 p2083 A73-33947

Reaction of a cylindrical shell to periodic shock waves propagating in its interior

17 p2243 A73-34735

Large amplitude forced vibrations of simply supported thin cylindrical shells.

[ASME PAPER 73-APM-Q]

17 p2249 A73-35107

Computerized finite difference method with reduced core storage requirements for solving boundary value problem of forced random vibration of rotating beam

17 p2204 A73-35830

Small perturbation evolutionary motion equations for forced vibrations of quasi-linear two frequency autonomous systems at resonance

19 p2445 A73-37633

Stability of nonlinear oscillations with unsteady impulsive excitation

19 p2459 A73-37650

Calculation of forced and free oscillations of round plates taking into account the dissipation of energy in the material.

19 p2499 A73-37776

Calculating the fundamental oscillations in turboengine blades with different types of excitation.

19 p2499 A73-37778

Two-frequency unsteady forced oscillations of a beam

20 p2593 A73-39502

Transverse oscillations of a beam lying on an elastic base under the action of a perturbation force which has several harmonics with frequencies close to the first natural frequency

20 p2620 A73-39512

Modal technique to obtain forced axisymmetric response of elastic spherical shells from free vibration response relations, taking into account transverse shear and rotational inertia

20 p2621 A73-39541

Free and forced nonlinear oscillations of anisotropic orthotropic annular plate with free inner boundary and fixed immovable outer boundary

20 p2623 A73-39561

Method for calculation of natural and induced oscillations in elastic shells of revolution which are filled with an ideal incompressible liquid

20 p2624 A73-39647

A method for selecting a nonlinear clutch in a system undergoing vibration forced by polyharmonic excitation

21 p2708 A73-41583

Sinusoidal response of composite-material plates with material damping.

[ASME PAPER 73-DET-120]

22 p2919 A73-42082

Resonant oscillations of intermediate frequency in a stratified atmosphere.

22 p2848 A73-42539

Forced motion of lumped mass systems including the effect of axial force.

22 p2923 A73-42630

Forced vibrations of a cylindrical shell in the presence of gas pressure fluctuations

22 p2928 A73-43057

Study and calculation of the vibrations of a rotating rotor with allowance for clearances in the bearings

23 p3041 A73-43725

Vibrations of a three-degree-of-freedom gyroscope in transition through resonance

23 p2983 A73-44199

The drifts of a gyroscope mounted on the oscillating housing.

23 p2983 A73-44271

Nonlinear vibrations of viscoelastic cylinder with elastic shell under harmonic forces, showing steady state equilibrium stability conditions

24 p3145 A73-44530

Driven electrostatic plasma oscillations in a closed electron drift accelerator.

24 p3114 A73-44618

Thin plate in two dimensional supersonic flow, deriving vibration amplitude response to shock pressure load by numerical analysis with Laplace transform

24 p3055 A73-45432

Small transverse vibrations of a flexible rod under the action of a variable axial force

24 p3153 A73-45504

FORCED VIBRATORY MOTION EQUATIONS

U FORCED VIBRATION

FOREARM

Human forearm-muscle blood supply regimes after 'static' exercise with increasing stress

10 p1181 A73-24522

Mechanism of working hyperemia condition alteration in the forearm muscles of man under increased loads

18 p2276 A73-36570

Control of forearm skin blood flow during periods of steadily increasing skin temperature.

18 p2278 A73-36657

FOREBODIES

NT NOSE CONES

NT NOSES [FOREBODIES]

NT ROCKET NOSE CONES

High Reynolds number experimental data for forebody axial force.

09 p1030 A73-23453

FORECASTING

NT LONG RANGE WEATHER FORECASTING

NT NUMERICAL WEATHER FORECASTING

NT PERFORMANCE PREDICTION

NT PREDICTION ANALYSIS TECHNIQUES

NT STATISTICAL WEATHER FORECASTING

NT TECHNOLOGICAL FORECASTING

NT WEATHER FORECASTING

Computerized short- and long term ionospheric propagation forecasting for HF communications, frequency scheduling and broadcasting circuits

09 p1048 A73-21983

Determination of the information-forecasting indices of biometeorological phenomena

13 p1579 A73-28861

Solar flare forecasting method developed and applied at Crimean observatory, using magnetic instability model for active regions

21 p2762 A73-41391

FORECASTS

U FORECASTING

FOREIGN BODIES

Contribution to the problem of suction of foreign bodies into engine intakes

02 p0202 A73-11687

FOREIGN POLICY

NT INTERNATIONAL COOPERATION

NT INTERNATIONAL RELATIONS

FORENSIC SCIENCES

U LAW [JURISPRUDENCE]

FOREST FIRE DAMAGE

U FIRE DAMAGE

FOREST FIRE DETECTION

Detection of small fires and mapping of large forest fires by infrared imagery.

20 p2562 A73-39904

FOREST FIRES

Some results of studies of the boundary atmospheric layer and AN-2 aircraft flight conditions in a forest fire area

13 p1655 A73-29192

FORESTS

Airborne remote sensing for forestry and agricultural land imagery and water pollution detection, discussing use of color films and picture processing

17 p2161 A73-34933

Remote sensing applications in agriculture and forestry including land inventories, soil classification and water resources detection

17 p2162 A73-34948

Land use classification in the southeastern forest region by multispectral scanning and computerized mapping.

20 p2557 A73-39849

Automatic terrain mapping by texture recognition.

20 p2568 A73-39873

FORGING

Fundamental principles of powder preform forging.

01 p0056 A73-10278

Processing and properties of powder forgings.

01 p0056 A73-10279

Potential titanium airframe applications.

01 p0063 A73-10285

Book - Forging design handbook.

02 p0173 A73-11884

Minimum deformation forging of prealloyed steel powder for weapon components, discussing mechanical properties, processing and cost analysis
03 p0322 A73-13265

How deformation affects the mechanical properties of aluminum forgings.
03 p0322 A73-13266

Warm forging of steels for increased precision and mechanical properties.
03 p0323 A73-13269

The role of pore size in the ultimate densification achievable during P/M forging.
04 p0456 A73-15799

Compression tests for plastic deformation and fracturing of Al alloy powder at hot working temperatures, noting limiting deformations in forging
[ASME PAPER 72-WA/MAT-5] 04 p0456 A73-15808

Some experiments on dynamic and quasi-static forging of aluminum at elevated temperatures.
[ASME PAPER 72-WA/MAT-1] 04 p0457 A73-15811

Some empirical relationships between creep strain, stress, time and temperature in 1Cr-Mo-V rotor forgings.
08 p0981 A73-21783

Microstructural control of Ti-6Al-4V forgings.
09 p1085 A73-22495

Hot die forging /gatorizing/ technique for Ti and heat resistant alloys jet engine parts, emphasizing material and cost savings
09 p1089 A73-23295

Crack toughness evaluation of hot pressed and forged beryllium.
11 p1384 A73-26169

The role of micropores in the fracture of forged sintered steel.
13 p1639 A73-29468

Book - Forging of powder metallurgy preforms.
15 p1891 A73-32195

Economic and design advantages of aluminum precision forgings.
17 p2177 A73-34672

[SAE PAPER 730312] Mechanical and corrosion resistant properties of titanium castings.
19 p2442 A73-37947

Incremental forging of parts with cross-ribs.
[SME PAPER MF 73-164] 19 p2437 A73-38503

Drop forged Ti alpha-beta alloy textures after heat treatment, quenching, aging and surface machining
22 p2866 A73-42089

Hot closed-die forging of powder titanium
24 p3093 A73-44739

FORM FACTORS
Effects of surface roughness and form factor on rolling contact fatigue.
07 p0831 A73-20119

A microscopic theory of density fluctuations in partially ionized gases.
15 p1916 A73-31086

Determination of heat flow shape factors for hollow, regular polygonal prisms.
23 p3049 A73-44164

FORM PERCEPTION
U SPACE PERCEPTION

FORMALDEHYDE
Physical conditions in interstellar hydroxyl and formaldehyde clouds.
01 p0100 A73-10790

Radiant flux densities of Cygnus X-3, observing OH and formaldehyde absorption
02 p0210 A73-11560

4830 MHz observations of the formaldehyde molecule in the direction of discrete radio sources.
03 p0371 A73-13214

Radio spectroscopy superiority for interstellar cloud chemical composition studies, detecting formaldehyde, X-ogen, HNC and other exotic molecular species
05 p0546 A73-16305

The kinematical distribution of dark clouds surveyed in the 4830 MHz H2CO line.
08 p1004 A73-20904

H I absorption in the galactic center region and between galactic longitudes 350 deg and 359 deg.
09 p1141 A73-22009

Interferometric observations of formaldehyde absorption in front of strong galactic sources.
09 p1150 A73-23139

On the kinematics of a local component of the interstellar hydrogen gas possibly related to Gould's Belt.
13 p1686 A73-29369

Spacecraft decontamination and sterilization by formaldehyde, beta-propiolactone, ethylene oxide, radiation and dry heat, noting effects on polymers
14 p1721 A73-30137

Investigation of a low-pressure arc erosion plasma
14 p1781 A73-30459

Interferometric observations of formaldehyde absorption in front of strong galactic sources.
14 p1801 A73-30735

Detection of interstellar thioformaldehyde.
15 p1933 A73-31378

The absence of formaldehyde radiation toward cold regions of the galactic plane - Further investigation.
15 p1936 A73-31554

Homogeneously catalyzed formaldehyde condensation to carbohydrates. II - Instabilities and Cannizzaro effects.
15 p1841 A73-32200

Branched-chain carbohydrate structures resulting from formaldehyde condensation.
15 p1842 A73-32550

Formaldehyde gas as a sterilant.
16 p1976 A73-33694

A survey of interstellar formaldehyde in dust clouds.
19 p2475 A73-37610

Comment on 'Anomalous hyperfine lines in formaldehyde in a dust cloud.'
22 p2904 A73-41755

New formaldehyde base disinfectants.
23 p2948 A73-43276

Chemiluminescence spectra from cool and blue flames - Electronically excited formaldehyde.
24 p3066 A73-45163

FORMAT
A standard format for mathematical models of fluid power systems.
02 p0132 A73-12001

Standard format for reporting electron content data using magnetic tape.
03 p0308 A73-13655

FORMATION HEAT
U HEAT OF FORMATION

FORMING TECHNIQUES
NT AUSFORMING
NT CASTING
NT COLD ROLLING
NT COLD WORKING
NT ELECTROFORMING
NT ELECTROHYDRAULIC FORMING
NT EXPLOSIVE FORMING
NT EXTRUDING
NT FORGING
NT HOT WORKING
NT INVESTMENT CASTING
NT MAGNETIC FORMING
NT METAL DRAWING
NT METAL SPINNING
NT PRESSING [FORMING]
NT ROLL FORMING
NT STAMPING

Certain results of studies of the accuracy in grinding shaped surfaces by the method of nontemplate shaping of the cutting surface of an abrasive ribbon
02 p0172 A73-11798

An experimental investigation of a rigid-plastic state of deformation with the aid of the Moire method
03 p0306 A73-13148

Titanium powder properties, production, alloying, costs and hardware fabrication by pressing, casting, molding, coining and forging
03 p0322 A73-13263

Metal deformation processes, discussing hot working, fracture, hydrostatic extrusion, superplastic forming, diffusion bonding and powder fabrication
04 p0452 A73-14742

Powder metallurgy production of structural shapes.
04 p0461 A73-15022

Properties of pultruded composites containing high modulus graphite fibers.
06 p0715 A73-18719

Steel wire, boron or carbon filament reinforced Al alloys shaped parts fabrication, discussing sintering, pressure impregnation and filament winding processes
11 p1373 A73-25415

The technology of plasma arc spraying
16 p2017 A73-32698

Forming energy in rigid-plastic materials under steady molding processes, obtaining nonlinear equations system solution by iterative procedure
16 p2037 A73-33237

Flow stress of metals and its application in metal forming analyses.
16 p2019 A73-33534

[ASME PAPER 73-PROD-4] Working of titanium by high energy due to detonation of an explosive charge
19 p2433 A73-37836

Titanium Stresskin panel fabrication and assembly, discussing forming, cutting, thermal processing, welding and applications
19 p2437 A73-38502

FORMULAS [MATHEMATICS]
Contribution to the numerical solution of differential equations by means of Runge-Kutta formulas with Newton-Cotes numbers weights.
09 p1113 A73-22988

Computer checking of rotational line intensity factors for diatomic transitions.
21 p2744 A73-41212

FORSTERITE
Electron paramagnetic resonance of Fe3+/ in forsterite /Mg2SiO4/.
15 p1923 A73-31273

FORTAN
FORTAN subroutine for X-Y plotting and display of two dimensional alphanumeric finite element mesh on line printer
03 p0280 A73-13340

On the number of operations simultaneously executable in Fortran-like programs and their resulting speedup.
05 p0553 A73-16450

Fasp - A student developed application program.
06 p0671 A73-18265

FORTAN sequence with economical computer storage requirement for matrix method application to rigid plastic collapse analysis of frame, considering bounded variable problem
07 p0907 A73-19034

PRADIS - An advanced programming system for 3-D-display.
09 p1059 A73-22225

RC planar distributed networks one and two dimensional analysis techniques and frequency response characterization, noting FORTRAN program use
09 p1067 A73-22309

Direct numerical solution of three-dimensional equations containing elliptic operators.
13 p1647 A73-28080

An algorithm for numerical integration in triangular domains.
14 p1806 A73-30047

Study of methods of computing transition matrices /Computer-program description/.
20 p2532 A73-39129

A computer program SNR-2 for solving an optimal control problem with state constraints.
23 p2956 A73-44126

FORWARD SCATTERING
Statistical theory of light propagation in a turbulent medium /Survey/
02 p0141 A73-12485

Forward scatter chaff system for air-ground long haul communications.
04 p0418 A73-15393

Forward and specular scattering from a rough surface - Theory and experiment.
13 p1659 A73-28490

Forward scattering method for determination of atmospheric aerosols particle size distribution, considering angle-dependent scattering at fixed wave number
17 p2161 A73-34938

Small hypervelocity particle in-flight detection against background noise using forward scattering from laser illuminated particle distribution
17 p2172 A73-35415

Surveyor observations of lunar horizon-glow.
18 p2348 A73-35938

On the use of forward scatter techniques in the study of turbulent stratified layers in the troposphere.
19 p2427 A73-38219

Forward scatter propagation measurements /trans-horizon and line-of-sight/ applied to specific forms of instabilities in layers.
19 p2406 A73-38247

General remarks concerning theories dealing with scattering and diffraction in random media.
20 p2528 A73-38845

Stripping cross sections for production of forward scattered molecular ions in hydrogen and deuterium molecular collisions at kinetic energies below 500 eV, noting isotope effect
23 p3007 A73-44119

Forward scatter CW radar effectiveness for cross path wind velocity profile measurements compared with radiosonde and pilot balloon observations
23 p3004 A73-44261

Successively forward-scattered wave propagating through a random medium.
24 p3110 A73-45028

FOSSIL METEORITE CRATERS
U FOSSILS
U METEORITE CRATERS

FOSSILS
Paleontological evidence on the earth's rotational history since early Precambrian.
02 p0217 A73-12387

Fossil particle tracks in lunar materials, discussing track densities implications, production rates via cosmic ray spallation and interpretation for rock ages and erosion rates
03 p0361 A73-13102

Tracks from extinct radioactivity, ancient cosmic rays, and calibration ions.
10 p1269 A73-24271

Deep sea drilling core sample analysis methods and results relation to sediment age and fossil fauna and flora
11 p1325 A73-25462

Amino acid composition significance in sedimentary fossil skeletal protein calcification, discussing diagenetic temperature effects
11 p1326 A73-25470

Trace fossils from the Nama Group, south-west Africa.
12 p1490 A73-27250

Upper Cretaceous Spumellariina from the Great Valley Sequence, California coast ranges.
13 p1605 A73-28023

Fossil track and thermoluminescence studies of Luna 20 material.
13 p1675 A73-28312

Cenozoic coral and aragonitic fossil age determination by He, U, Th and Ru isotope retentivity consistency checks

13 p1609 A73-29178

Late Precambrian microfossils - A new stromatolitic biota from Boorthanna, South Australia.

14 p1713 A73-29723

17alpha/H/ hopane identified in oil shale of the Green River formation/Eocene/ by carbon-13 NMR.

14 p1746 A73-29734

FOUNDATIONS

Complex resilient-base structure designs incorporating the reaction to an external load

05 p0636 A73-17083

Buckling of a simply-supported beam between two unattached elastic foundations.

09 p1166 A73-23466

Shear stresses and displacements of each layer of elastic plate with multiple layers of varying rigidity resting on elastic Winklerian base

11 p1433 A73-25029

German book - Soil mechanics of retaining structures, roads, and runways.

11 p1344 A73-26255

Buckling of beams supported by Pasternak foundation.

17 p2243 A73-34531

Calculation of a system of two infinite beams on an elastic base

19 p2495 A73-37190

Laying out the foundations for circular-mirror sections of the RATAN-600 radio telescope

21 p2675 A73-41455

FOUR BODY PROBLEM

Periodic perturbation of the libration points of the restricted three-body problem due to presence of a resisting medium and both gravitational and radiative fields of a fourth body.

01 p0103 A73-11018

Four body problem reduction to three body problem via perturbation region, noting Moon-Earth-Sun system

05 p0623 A73-17198

Three dimensional computer plots of zero velocity contours for restricted three and four body problems, discussing motion stability near equilibrium points

24 p3142 A73-45297

FOURIER ANALYSIS

NT FOURIER SERIES

A simple Fourier analysis technique for measuring the dynamic response of manual control systems.

01 p0027 A73-10321

Fourier spectrometer design for high resolution solar optical spectra, emphasizing short scan time

01 p0049 A73-10534

Fourier analysis of laminated anisotropic rectangular plates with strong cross elasticity effects, presenting deflection, bending moments and buckling data

01 p0115 A73-10735

Computation of solutions to the inverse problem of electrocardiography.

01 p0013 A73-11465

Lame equations for stress concentration in half plane with extracted elastic inclusion, solving via Fourier integrals reduced to singular integral equation

07 p0910 A73-19301

Fourier analysis of Mars radar topographic data for magnitude and direction of center of mass/center of figure offset, comparing to earth and moon

11 p1419 A73-25862

Book - Fourier analysis in probability theory.

12 p1517 A73-27051

Fourier decomposition for antenna near field reconstruction from far field pattern data, investigating numerical stability and convergence bounds

14 p1727 A73-30213

High-frequency stellar oscillations - The Cerro Tololo search for luminosity-variable white dwarfs.

15 p1935 A73-31482

A technique for measuring small displacements in digital spectra.

17 p2170 A73-35297

Frequency analysis of spatio-temporal visually evoked cortical potentials during binocular rivalry.

17 p2118 A73-35645

Scattering of electromagnetic waves from rough oscillating surfaces using spectral Fourier method.

22 p2824 A73-41855

Nonlinear development and Fourier analysis of the whistler mode instability.

22 p2893 A73-42391

FOURIER LAW

Heat conductivity dependence on temperature for amorphous and crystalline materials, noting integrodifferential equation for conductive heat transfer and Fourier law

06 p0769 A73-18132

The equations of fast-process hydrodynamics

21 p2676 A73-40205

FOURIER SERIES

Operator remnant power spectral density measurement during compensatory tracking task by serial segments method, noting Fourier coefficient processing

01 p0011 A73-10324

Conditions for localization of Cesaro's rectangular means and of Abel's method means in the limited summing of a multiple trigonometric Fourier series in the Liouville classes

01 p0071 A73-11439

Functions of a generalized restricted variation and the convergence of their Fourier series and conjugate trigonometric series

02 p0188 A73-12551

Sidelobe reduction for linear arrays with elements sampled from equally spaced arrays, using Fourier coefficients of sampling functions

03 p0274 A73-12998

Localization principle for a polyharmonic operator expanded in a Fourier series of a fundamental system of functions

05 p0591 A73-16614

Bending theory of rectangular plates loaded along curve, obtaining solutions by Fourier single and double series

06 p0763 A73-18451

Integrodifferential equation for three dimensional contact problem of elastic half space strengthened by elastic stringer, solving by Fourier series

06 p0766 A73-18876

Book on boundary value problems in physics and engineering covering Fourier series and integrals, heat, wave and potential equations, Laplace transforms and numerical methods

09 p1113 A73-23300

Discrete Wiener-Hopf equations composed of the Fourier coefficients of piecewise Wiener functions

10 p1243 A73-24459

Newton method for calculation of viscous flow around circular cylinder with Fourier series truncation for stream function and vorticity, evaluating numerical error

11 p1345 A73-25115

Linear aperture distribution synthesis by pattern sampling for arbitrary sampling points location and edge exponent alpha choice, using nonharmonic Fourier series theory

11 p1328 A73-25657

Analytical representation of complex signals by expansion in Fourier, Kotelnikov, and Taylor series

12 p1471 A73-27584

Optimal harmonic synthesis of generalized Fourier series and integrals with randomly perturbed coefficients

13 p1650 A73-28893

Approximation of differentiable functions of numerous variables by Fourier sums in an L_2 sub metric

15 p1899 A73-31218

Integrodifferential equation for three dimensional contact problem of elastic half space strengthened by elastic stringer, using Fourier series

15 p1956 A73-32401

Series analysis of cylindrical shells - New look at an old problem.

20 p2622 A73-39550

Truncation error in the solution of integral equations.

24 p3106 A73-45344

FOURIER TRANSFORMATION

NT FAST FOURIER TRANSFORMATIONS

Two-dimensional investigation of absolute instabilities in mirror plasmas.

01 p0083 A73-10458

High resolution apparatus at the focus of large telescopes

01 p0049 A73-10532

Talbot shearing interferometer based on Fourier imaging behind grating illuminated by plane monochromatic wave with spatial filtering, obtaining radial and lateral derivatives

01 p0053 A73-11227

Real-time computer for monitoring a rapid-scanning Fourier spectrometer.

01 p0020 A73-11231

Fourier transformation for stress analysis of anisotropic shells under concentrated forces, solving shallow shell equations via MacDonald functions

01 p0118 A73-11408

Electromagnetic measurement at submillimeter wavelengths for solids and liquids absorption and refraction and atmospheric gases and plasmas emission based on Fourier transform spectrometry

03 p0310 A73-14496

The parameters of an infinite homogeneous elliptical cylinder determined from its gravity effects.

03 p0380 A73-14612

Fourier transformations and Wiener-Hopf equations for stress intensity factor of crack propagation in linearly elastic homogeneous isotropic strip

04 p0512 A73-15238

Optical computer technology based on Fourier transform optics and holography, discussing speed and parallel processing capabilities, image deburring, and applications

04 p0426 A73-15957

Integral Laplace-Fourier transform stability during transient response functions reconstruction from transfer function frequency characteristics in linear circuits

05 p0591 A73-16779

Two dimensional digital Fourier transform applications to picture processing, noting economy in computer storage

05 p0554 A73-17146

A cellular processor for task assignments in polymorphic, multiprocessor computers.

06 p0671 A73-18061

Dipole antenna coaxially mounted on a conducting cylinder.

06 p0666 A73-18189

Coherent and non-coherent optical processing of analog signals.

06 p0667 A73-18313

Display of microwave pulse response via the real-time Fourier transform of the transfer function.

06 p0677 A73-18346

Moiré phenomena theory and applications extension by diffraction and Fourier optics

06 p0696 A73-18696

On the numerical reconstruction of images from a microwave hologram.

06 p0669 A73-18737

Estimate of the probability density and distribution function of a scalar product of vectors with independent, normally distributed components

07 p0845 A73-20050

Lunar and solar geomagnetic tides in declination at Alibab.

07 p0819 A73-20055

Fourier transformations and statistical analysis for spectral content of geomagnetic micropulsations, noting polarization sense preference

07 p0819 A73-20064

Fourier transformation of two-dimensional signals. I

09 p1119 A73-21899

Stellar spectrometry by Fourier transformation from 2 to 5 micron

09 p1150 A73-23142

Images of truncated triangular-wave periodic targets in optical systems in the presence of linear image-motion.

10 p1248 A73-23614

Two dimensional signals Fourier transformations, discussing digital techniques application to linear and optical systems

11 p1397 A73-24993

Method of designing digital devices for bandpass filtration of signals

11 p1333 A73-25023

Lensless Fourier transform holography with mutual coherent reference source close to object, investigating atmospheric turbulence effects on wavefront reconstructed image quality

11 p1370 A73-26539

Image analysis techniques associated with automatic data base generation.

12 p1499 A73-27823

Relationship between pointing precision, spread functions and modulation transfer functions.

12 p1501 A73-27969

Plate theory boundary value problems algorithm from Fourier transformation of ultradistribution functions

13 p1695 A73-28561

Magnetic and gravitational potential anomalies due to uneven nonuniform material layers, using Fourier transforms

13 p1607 A73-28623

Elastostatic invariance in the composite plane.

13 p1696 A73-28747

Point-spread functions, line-spread functions, and edge-response functions associated with MTFs of the form negative exp/n-th power of the ratio of spatial frequency to the MTF frequency constant/.

14 p1768 A73-30158

Rayleigh-fast Fourier transformation techniques for electromagnetic scattering over rough sinusoidal surface, comparing numerical validity with perturbation, physical optics and integral equation methods

14 p1728 A73-30230

A computational scheme used with the epsilon-technique in synthesizing optimal controls.

15 p1853 A73-31625

The stress field near a system of four symmetrically situated line cracks of equal length.

15 p1953 A73-32093

Papers on digital signal processing covering digital filters, fast Fourier transform, finite word length effects, algorithms, and design and programming considerations

15 p1855 A73-32425

The instability due to acoustic radiation striking a vortex sheet on a supersonic stream.

17 p2151 A73-34824

Bipolar LSI building blocks for digital filtering applications.

17 p2138 A73-35228

Wavefront investigation of a Fourier transform lens with the fan trace interferometer.

17 p2172 A73-35427

Numerical methods based on very accurate approximation of partial derivatives.

18 p2330 A73-36828

- Analysis of a method for obtaining near-diffraction-limited information in the presence of atmospheric turbulence. 19 p2461 A73-38485
- The application of constrained least squares estimation to image restoration by digital computer. 20 p2533 A73-39401
- Observation of solar submillimeter-band emission at sea level with the aid of a Fourier spectrometer. 21 p2760 A73-40731
- On numerical reconstruction of the image from a microwave hologram. 21 p2655 A73-41045
- The stress field near a Griffith crack at the interface of two bonded dissimilar elastic half-planes. 21 p2789 A73-41672
- Mathematical model of human pitch perception based on acoustic stimulus Fourier transformation by sense organ into peripheral neural activity pattern recognition. 22 p2811 A73-41816
- Antenna radiation pattern measurement using time-to-frequency transformation (TFT) techniques. 22 p2831 A73-41842
- A high-resolution Fourier-transform infrared spectrometer. 22 p2861 A73-42587
- Probabilistic analysis of random and deterministic phase coding for lowering Fourier transform spectrum dynamic range in digitally generated hologram and kinoform memories. 22 p2864 A73-43149
- Multidimensional Fourier transforms and image processing with finite scanning apertures. 22 p2864 A73-43150
- Cepstrum signal processing with complex algorithm involving Fourier transforms and logarithm for multipath interference distortion reduction in single side-band or multiplexed transmission channels. 23 p2953 A73-43321
- Numerical convective schemes based on accurate computation of space derivatives. 24 p3105 A73-45026
- Computerized simulation of plasma particle collisions, using electric dipole expansion method for grid charge density and electrostatic force determination with Fourier transformation. 24 p3116 A73-45027
- FOVEA**
- Vernier acuity as affected by target length and separation. 03 p0266 A73-13063
- Test field surround effects on onset and offset reaction time to foveal stimulation. 03 p0261 A73-13558
- ERG late photoreceptor potential components time course in macaque monkey cones and rods, noting pure cone foveal response. 03 p0261 A73-13761
- Study of variations of retinal disparities around the fixation point by the binocular vernier method in the foveal region. 03 p0261 A73-13763
- Intrinsic light brightness and intensity estimation tests for foveal and peripheral retina under photopic and scotopic stimuli. 07 p0783 A73-20257
- Foveal contrast sensitivity edge effect dependence on test stimulus size, form and duration. 11 p1321 A73-26716
- The Stiles-Crawford effect - Explanation and consequences. 14 p1717 A73-30396
- Foveal threshold additivity measurements for monochromatic and mixed light, using grating resolution as brightness criterion. 14 p1717 A73-30398
- Applications of a model of the human visual system to pattern recognition problems. 17 p2116 A73-35242
- Eigenvectors of the sensitivity variations across the human central fovea. 22 p2810 A73-42957
- FRACTIONATION**
- Chemical fractionation in iron meteorites and its interpretation. 01 p0108 A73-11474
- FRACTOGRAPHY**
- New morphological element of the microsurface of ductile fracture of hypoeutectoid steel. 01 p0066 A73-11336
- Fractographic observations of fatigue crack tip behavior of age hardened Al-Zn-Mg-Cu alloy during static loading. 04 p0462 A73-15242
- Method for fractographic investigation of high-tensile aluminum alloys. 04 p0466 A73-15674
- Carbon replicas for fracture failure electron fractography by two stage Lucite technique. 05 p0586 A73-16134
- Fractographic aspects of the stress corrosion cracking of titanium in a methanol/HCl mixture. 06 p0705 A73-17800
- Premature and delayed fractures of high strength martensitic steels with graduated carbon contents, including brittle and ductile intercrystalline and transcrystalline cleavage fractures. 06 p0705 A73-17848
- Fractographic investigation of the resistance to fracture of aluminum and titanium alloys. 07 p0840 A73-20505
- Effect of microstructure on measurements of fracture energy of Al₂O₃. [ACS PAPER 44-BN-71P] 08 p0983 A73-21842
- Stress-corrosion cracking of Ti-8Al-1Mo-1V in aqueous environments. I - The kinetics of subcritical crack propagation. II - Plastic zones, crack morphology, and fractography. 13 p1632 A73-28135
- Scanning electron microscopic observation of fracture surfaces of austenitic stainless steels in stress corrosion cracking. 16 p2025 A73-33021
- Fractographic investigation of the ductility of fracture in aluminum and titanium alloys. 19 p2440 A73-37780
- Macrofractographic studies of fatigue fractures in aircraft engine elements. 21 p2754 A73-41593
- Electronic logic device for crack arresting penthrith microcharge pulse initiation, including crack and stress wave propagation measurements. 23 p3047 A73-44286
- FRACTURE MECHANICS**
- Intergrain boundary shape effects on the impact strength and character of brittle fracture. 01 p0064 A73-10606
- Holographic interferometry in materials research and fracture mechanics. 01 p0051 A73-11002
- New morphological element of the microsurface of ductile fracture of hypoeutectoid steel. 01 p0066 A73-11336
- Effect of various surface-active media on the changes taking place in the strength of U8 steel in the high-strength state. 01 p0066 A73-11337
- The fracture energy of carbon-fibre reinforced glass. 01 p0068 A73-11500
- Fracture characteristics of some aluminum alloy sheets in Charpy impact test at super-low temperatures. 02 p0179 A73-11595
- Fracture characteristics of aluminum alloy welds in Charpy impact test at super-low temperatures. 02 p0172 A73-11596
- Application of the theory of linear fracture mechanics to the assessment of turbine rotor strength. 02 p0229 A73-11620
- Fracture resistance curve calculation from fracturing diagram, noting crack propagation in thin plate under tensile deformation. 02 p0232 A73-11930
- The effect of crystallite size on the strength of carbon-graphite materials. 02 p0185 A73-12142
- Engineering method of calculating the parameter of fracture toughness. 02 p0235 A73-12210
- Limiting crack propagation rates during a quasi-brittle failure. 02 p0236 A73-12582
- Fracture mechanics equations for crack propagation braking by elliptic and circular holes at crack tip, noting stress concentration. 02 p0237 A73-12586
- The fracture energy and some mechanical properties of a polyurethane elastomer. 02 p0185 A73-12641
- Physicochemical distinction between separating similar and different materials in terms of cohesive or adhesive fracture energy in continuum mechanics. 03 p0312 A73-13334
- The fracture mechanics of slit-like cracks in anisotropic elastic media. 03 p0394 A73-13979
- The effects of matrix and interface modification on local fractures of carbon fibers in epoxy. 03 p0335 A73-13982
- The dynamic growth of a void in a plastic material and an application to fracture. 03 p0394 A73-13984
- Hold-time effects on the elevated temperature fatigue-crack propagation of type 304 stainless steel. 03 p0328 A73-14448
- Stress intensity factors for surface cracks in bending. 04 p0505 A73-14679
- Fracture mechanics consideration of hydrogen sulfide cracking in high strength steels. 04 p0459 A73-14692
- Crack initiation, acceleration, steady propagation and fatigue growth, considering Griffith criterion on fracture mechanics. 04 p0507 A73-14705
- On the modified Westergaard equations for certain plane crack problems. 04 p0512 A73-15236
- Stress intensity factor for axially stressed thin polymethyl methacrylate plate with cracks, noting fracture angle prediction. 04 p0512 A73-15240
- Structural reliability under cumulative fatigue damage and chance overload interaction, postulating kinetic fracture model based on probabilistic service load histories. 04 p0512 A73-15243
- Fatigue crack propagation in terms of fracture mechanics concepts. 04 p0462 A73-15298
- Method of determining the energy of fracture of aluminum alloys during impact-bead tests with sharp notches. 04 p0466 A73-15675
- The energy of crack propagation in carbon fibre-reinforced resin systems. 04 p0469 A73-15981
- Improvements in the transverse properties of composites. I - Fracture surface energy and mechanism of transverse fracture in glass fibre composites. 04 p0469 A73-15984
- Crack tip stress field variation via elastic pulses for crack path alteration and subsequent fracturing process termination, using photoelastic analysis. 05 p0634 A73-16795
- The probability of fracture as parameter of crack propagation under cyclic stress. 05 p0635 A73-17065
- Fracture mechanism theories based on discrete and continuous models of solids, explaining Griffith brittle crack dynamics. 06 p0760 A73-17776
- Surface effects in solid bodies undergoing deformation and fracture. 06 p0734 A73-17922
- An experimental investigation into the mechanics of deep semielliptical surface cracks in mode I loading. 06 p0763 A73-18478
- Method of analysis and prediction for variable amplitude fatigue crack growth. 06 p0709 A73-18482
- Subcritical crack growth of TRIP steels in air under static loads. 06 p0710 A73-18485
- Fatigue and fracture basic research at the Langley Research Center. 06 p0764 A73-18486
- Borated steel fracture characteristics in the case of cyclic plane bending. 06 p0711 A73-18663
- Durability and fracture mechanics of polymethylmethacrylate under the action of liquid, surface-active media. 06 p0715 A73-18670
- A note on the Cherepanov calculation of viscoelastic fracture. 07 p0908 A73-19090
- Metal surface active properties effects on fracture characteristics and deformation and failure conditions. 07 p0912 A73-19472
- Metal tongues in trailing edge of surface pits near fracture path end in rolling contact fatigue of failed ball bearings. 07 p0831 A73-20158
- Study on fracture mechanism for composite materials based on the concept of the change in Poisson's ratio. 07 p0915 A73-20328
- Creep tests and fracture mechanics for high temperature properties of steels and alloys under static load, noting discrepancies for brittle materials. 07 p0840 A73-20510
- Mixed viscous-brittle fracture model of plastic crack distribution and propagation pattern in bcc polycrystal by electron raster microscope analysis. 09 p1157 A73-21961
- Intercrystalline molybdenum fracture. 09 p1099 A73-21971
- Critical evaluation of Zhurkov theory of metallic material fracture by successive rupture of atomic bonds due to atom thermal motion. 09 p1100 A73-22160
- Using fracture mechanics with aluminum alloy structures. 09 p1103 A73-22494
- Book - Methods of analysis and solutions of crack problems; Recent developments in fracture mechanics; Theory and methods of solving crack problems. 09 p1161 A73-23176
- Alternating method with combined analytical and numerical calculations for two dimensional edge and three dimensional surface crack problems. 09 p1162 A73-23181
- Integral transform solution of mixed boundary value problem for Griffith cracks with complicated geometries and external, star-shaped, cruciform-shaped and circular cracks. 09 p1162 A73-23183

Fracture mechanics of brittle matrix ductile fiber composites. 09 p1111 A73-23251

Research and application problems in fracture of materials and structures in the United States Air Force. 09 p1163 A73-23261

Linear elastic and general yielding fracture mechanics compatibility, investigating crack opening displacement relationship to stress intensity factor. 09 p1109 A73-23263

Ductile fracture strain criteria from known stress-strain relationships, predicting microscopic crack and void nucleation strain. 09 p1164 A73-23322

Stress corrosion cracking characteristics and test data interpretation, considering pitting, brittle fracture, crack propagation, chemical environment and smooth and cracked specimens. 10 p1232 A73-23368

Experimental observations of tensile fracture in unidirectional boron filament reinforced aluminum sheet. 10 p1235 A73-24439

Linearized hydrodynamic instability initiation in polymer melts extrusion, examining Weissenberg number role in melt fracture onset. 10 p1241 A73-24655

Mechanical properties at high temperature of Ni-based unidirectionally solidified eutectic: Ni-Ni₃Ta. 11 p1379 A73-25405

Preliminary design of aircraft structures to meet structural integrity requirements. [AIAA PAPER 73-374] 11 p1439 A73-25506

A statistical theory for failure of brittle materials under combined stresses. [AIAA PAPER 73-381] 11 p1439 A73-25511

Corrosion fatigue: Chemistry, mechanics and microstructure; Proceedings of the International Conference, University of Connecticut, Storrs, Conn., June 14-18, 1971. 11 p1380 A73-25801

The kinetic and dynamic aspects of corrosion fatigue in a gaseous hydrogen environment. 11 p1382 A73-25817

Environment enhanced corrosion fatigue crack growth and fracture mechanics, discussing inspection intervals to maintain structural integrity. 11 p1382 A73-25819

Corrosion fatigue crack propagation behavior in steels above/below stress intensity threshold within framework of linear elastic fracture mechanics. 11 p1382 A73-25821

Corrosive aspects of the fatigue of rubber. 11 p1388 A73-25841

Applications of solid mechanics; Proceedings of the Symposium, University of Waterloo, Waterloo, Ontario, Canada, June 26, 27, 1972. 11 p1442 A73-25842

Service failures and fracture mechanisms under cyclic load at high temperature. 11 p1442 A73-25845

The determination of Mode I stress-intensity factors by holographic interferometry. 12 p1550 A73-27021

Continuum mechanics analysis of local rupture and plastic strains near cracks and fractures, noting elastoplastic applications. 12 p1551 A73-27251

Bending-produced cracks, stresses and fracture of rectangular cross section beam from brittle body homogeneous model. 12 p1552 A73-27255

Elastic-plastic fracture by homogeneous microvoid coalescence tearing along alternating shear planes. 13 p1633 A73-28142

The effect of brittle interfacial compounds on deformation and fracture of molybdenum-aluminum fiber composites. 13 p1636 A73-28794

German monograph - Investigations regarding the strength characteristics of adhesive bonds involving metals in the case of impact stress. 13 p1625 A73-29277

Application of fracture mechanics to the analysis of statically indeterminate structure. 13 p1700 A73-29466

Parametric finite element stress analysis of multiple crack propagation in nonhomogeneous nonisotropic materials, using Griffith criterion. 13 p1701 A73-29472

The interaction of material and geometric aspects in the fracture of aluminum alloys. 13 p1640 A73-29475

Plane strain elastic-plastic state and fracture in cracked blunt notched steel plates under tensile loads. 13 p1701 A73-29477

X-ray investigation of fatigue-crack growth - On critical strain for fracture at the crack tip. 13 p1625 A73-29482

Inelastic strain and hysteresis energy criteria for fatigue fracture of metals. 13 p1641 A73-29499

The micro-structural approach toward a kinetic theory of polymer fracture. 13 p1646 A73-29529

Internal fracture and acoustic emission of fiberglass reinforced plastics. 13 p1647 A73-29544

Stress gradient as one of the causes of the scale effect on the brittle fracture of materials. 13 p1703 A73-29614

Stress distribution about defects such as rigid sharp-angled inclusions. 13 p1703 A73-29619

Experimental and theoretical investigation of the fracture of sheet materials in the presence of cracks. 13 p1703 A73-29625

Finite element method investigation of branch and secondary crack formation and multiple fracture, solving sequences of boundary value problems and strain energy release rates. 14 p1808 A73-30195

Finite element method application to nonlinear, microscopic and ductile fracture mechanics covering crack tip singularity elastoplastic analysis and elastic constants of metal crystals. 14 p1809 A73-30200

Nonlinear thermodynamics of irreversible processes for polymer microfracture process under mechanical, thermal, diffusion and chemical actions. 14 p1766 A73-30479

Investigation of fatigue and brittle failure patterns in 15G2AFDps steel at low temperatures. 14 p1762 A73-30678

Investigation of crack propagation in small samples under conditions of low-cyclic fatigue. 14 p1763 A73-30680

Engineering structures design, discussing stress and strain distributions, mechanical defects, symmetric loading and fracture models. [ASME PAPER 73-DE-19] 14 p1815 A73-30820

Fracture strength of fiber reinforced plastics, investigating crack propagation susceptibility, stress concentration and fracture mechanics. [ASME PAPER 73-DE-20] 14 p1767 A73-30821

Stress and fracture analysis of adhesive joints. [ASME PAPER 73-DE-21] 14 p1755 A73-30822

Fracture mechanics approach to fatigue analysis in design. [ASME PAPER 73-DE-22] 14 p1763 A73-30823

Brittle fracture of a body with a crack under variable shear load. 15 p1945 A73-31040

High strength steel fracture characteristics in vacuum and gaseous medium, noting hydrogen adsorption effect on crack resistance. 15 p1887 A73-31248

Brittle fracture and crack propagation prediction in unidirectionally fiber reinforced composites via Sc theory, comparing with stress intensity factor K_{IC} concept. 15 p1949 A73-31681

Linear elastic fracture mechanics applicability to graphite-epoxy laminated fracture specimens configuration from fractographic studies. 15 p1897 A73-31684

Lattice theory of fracture and crack creep. 15 p1890 A73-31927

Strongly active surfactant effects on metal surface fracture characteristics under various loading conditions. 15 p1952 A73-32071

A numerical and experimental investigation of the use of J-integral. 17 p2246 A73-34880

Classical fracture mechanics concepts, considering Griffith theory and modifications for ductile materials and strain energy density field. 17 p2246 A73-34883

Interdisciplinary communications problems of metal physicists, fracture mechanists, structural designers and reliability analysts for fatigue crack generation and growth. 17 p2246 A73-34886

Welded steel beam fatigue behavior evaluation via stable crack growth concepts, developing fracture mechanics model for cracks originating from pores. 17 p2246 A73-34887

Viscoelastic fracture of solid propellant pressurization condition. [SESA PAPER 2114A] 17 p2220 A73-35449

On the fracture of high-strength metals in the stress fields of various stress-concentration factors. [SESA PAPER 2163A] 17 p2191 A73-35454

Brass matrix composites tensile strain characteristics and fracture mode dependence on fiber volume fraction and properties. 17 p2192 A73-35531

Borsic/Ti-Al-V composite properties, fracture modes and fabrication, discussing tensile strength and temperature dependence of longitudinal strength. 17 p2192 A73-35532

High modulus fiber reinforced metal and plastic matrix composites fracture within linear elastic fracture mechanics framework, reviewing standard notch toughness test. 17 p2192 A73-35536

Borsic-aluminum composites fracture and flexural behavior from Charpy impact and slow bend tests. 17 p2192 A73-35537

Failure mechanisms in impact loaded carbon and glass fiber reinforced plastics, discussing specimen geometry, notch presence, fiber type, fiber orientation and hybridization effects. 17 p2198 A73-35538

Deformation and fracture mechanisms in aluminum reinforced by high strength steel ribbons. 17 p2192 A73-35539

Noncumulative fracture mode of unidirectional boron filament-aluminum matrix composite under axial tension, measuring critical filament stress. 17 p2193 A73-35542

Book - Experimental techniques in fracture mechanics. 17 p2252 A73-35668

Two and three dimensional elasticity theory of linear fracture mechanics covering stress functions, finite element method and crack behavior in solids. 17 p2252 A73-35669

Compliance measurement for determination of crack extension force, specimen dimensions and elastic constants in linear fracture mechanics, discussing instrumentation, precautions and data reduction. 17 p2252 A73-35671

Fracture mechanics testing systems, discussing closed loop assembly, programming, readout and fail-safe units and fully automated computer-controlled technique. 17 p2175 A73-35672

Two dimensional static, dynamic and three dimensional photoelasticity measurement techniques for stress intensity, factors determination in boundary value problems of fracture mechanics. 17 p2252 A73-35673

Dislocation-type mechanism of the influence of solid surface films on the deformation and fracture of metals. 18 p2319 A73-35891

Interfacial, mechanical and fracture properties of fibre reinforced polycaprolactam. 18 p2328 A73-36480

Fracture and flaws; Proceedings of the Thirteenth Annual Symposium, Albuquerque, N. Mex., March 1, 2, 1973. 18 p2363 A73-36482

Fracture mechanics in materials selection and design. 18 p2363 A73-36483

Some applications of spectral analysis in ultrasonic testing. 18 p2316 A73-36485

Brittle fracture mechanics models of structural materials in terms of elastic continuum with crack. 18 p2366 A73-36823

Special features of the fracture of aluminum and titanium alloys at low temperatures. 19 p2439 A73-37267

A simple method for studying slow crack growth. 19 p2497 A73-37588

Fracture types in load-controlled low-cycle fatigue. 19 p2498 A73-37666

Creep tests and fracture mechanics for high temperature properties of steels and alloys under static load, noting discrepancies for brittle materials. 19 p2440 A73-37785

Fracture mechanics of carbon fibers at high temperatures due to fine structure, discussing effects of ribbon unbending during extension. 19 p2444 A73-38089

Mechanical properties of polymeric solids. 19 p2444 A73-38549

Japan Congress on Materials Research, 16th, Osaka, Japan, August 1972, Proceedings. 20 p2575 A73-38636

Brittleness of coated tungsten wire. 20 p2577 A73-39361

Cleavage fracture in alpha phase Ti, considering embrittling species effects on electronic band structure. 20 p2578 A73-39490

Torsional and anti-plane strain delamination of an orthotropic layered composite. 20 p2622 A73-39549

Grain boundary destruction mechanisms in pure nickel polycrystals following plastic deformation, discussing annealing, fault concentration, microscopic techniques and critical loads. 20 p2578 A73-39735

Spallation and fracture resulting from reflected and intersecting stress waves. 21 p2782 A73-39989

Dynamic fracture criteria for a polycarbonate. 21 p2723 A73-40956

Influence of hydrogen on the fracture micromechanism of OT4 and OT4-1 titanium alloys. 21 p2721 A73-41231

Heat resistant materials cracking and fracturing caused by ductility loss at high temperatures, discussing cavitation mechanisms, microcracks, creep tests and time dependence. 21 p2722 A73-41576

Critical evaluation of Zhurkov theory of metallic material fracture by successive rupture of atomic bonds due to atom thermal motion 22 p2874 A73-42108

Progress in flaw growth and fracture toughness testing; Proceedings of the Sixth National Symposium on Fracture Mechanics, Philadelphia, Pa., August 28-30, 1972. 22 p2920 A73-42131

Application of strip model to crack tip resistance and crack closure phenomena. 22 p2875 A73-42132

Some observations on fracture under combined loading. 22 p2920 A73-42133

Effect of a loading sequence on threshold stress intensity determination. 22 p2875 A73-42141

A comparison of the J-integral fracture criterion with the equivalent energy concept. 22 p2920 A73-42145

Applications of the compliance concept in fracture mechanics. 22 p2920 A73-42154

Failure stress levels of flaws in pressurized cylinders. 22 p2921 A73-42156

Matrix methods application to stress in elastic structures, examining Mohr circles, design implications and orthogonality anisotropy 22 p2929 A73-43173

Fracture control - Past, present and future. 23 p3039 A73-43383

Stress-strain state of disk with internal rectilinear cracks under load, solving Fredholm equations 23 p3039 A73-43468

The stress pulses propagated as a result of the rapid growth of brittle fracture. 23 p3042 A73-43805

Molecular rupture mechanism, self reinforcement and failure modes of elastomeric materials dependence on strain, temperature, filler and crosslink density 23 p2997 A73-43808

On Papkovitch-Fadle solutions of crack problems relating to an elastic strip. 23 p3046 A73-44227

Fracture micromechanism characteristics and crack tip plastic zone formation effects on metal embrittlement, using elastoplasticity theory 23 p3047 A73-44277

Surface phenomena in solids during the course of their deformation and failure. 23 p3018 A73-44322

Determination of lifetime characteristics from crack growth kinetics data 24 p3145 A73-44523

FRACTURE RESISTANCE

U FRACTURE STRENGTH

FRACTURE STRENGTH

Equations of the time-dependent strength of solid bodies 01 p0114 A73-10479

Fracture strength of helical-wound composite cylinders. 01 p0117 A73-11121

Application of the theory of linear fracture mechanics to the assessment of turbine rotor strength 02 p0229 A73-11620

Fracture resistance curve calculation from fracturing diagram, noting crack propagation in thin plate under tensile deformation 02 p0232 A73-11930

Statistical evaluation of strength of metals at brittle fracture. 02 p0235 A73-12133

Engineering method of calculating the parameter of fracture toughness. 02 p0235 A73-12210

Impact fracture resistance of Cr-Mn-Si steel, investigating alloying effects on crack initiation and propagation 02 p0181 A73-12211

The effect of reverted austenite on the mechanical properties and toughness of 12 Ni and 18 Ni /200/ maraging steels. 02 p0183 A73-12758

Failure phenomena relationship to kinetic equation for defect buildup from brittle fracture analysis of composite glass fiber reinforced plastic in uniaxial eccentric tension 03 p0394 A73-14008

National Symposium on Fracture Mechanics, 5th, University of Illinois, Urbana, Ill., August 31-September 2, 1971, Proceedings. Part 2 - Fracture toughness. 04 p0506 A73-14693

Rice energy line J integral fracture strength criterion applicability to crack tip elastoplastic testing for steel alloys 04 p0506 A73-14694

Elastoplastic slip line analysis of specimen geometry effects on J fracture strength criterion for

medium strength steel center cracked panel and bend bar 04 p0506 A73-14695

Rice path independent J integral fracture strength criterion estimation as function of crack size and elastoplastically adjusted load point displacement for Ni-Cr-Mo-V steel 04 p0506 A73-14696

Ductile fracture initiation, propagation, and arrest in cylindrical vessels. 04 p0506 A73-14697

Sharp-notch tension testing of thick aluminum alloy plate with cylindrical specimens. 04 p0460 A73-14698

Center cracked tension specimen geometry effects on plane stress fracture toughness of high strength Al, Ti and steel alloy sheets 04 p0460 A73-14699

Fracture toughness of duplex structures. I - Tough fibers in a brittle matrix. 04 p0460 A73-14700

Fracture toughness of duplex structures. II - Laminates in the divider orientation. 04 p0460 A73-14701

Postirradiation notch ductility and fracture strength of pressure vessel steel plate by Charpy V tests 04 p0460 A73-14702

Relationship between material fracture toughness using fracture mechanics and transition temperature tests. 04 p0506 A73-14703

The design and development of fracture resistant structures. 04 p0507 A73-14712

Strength analyses for design with composite materials using metals technology. 04 p0507 A73-14713

Relationships between failure modes and fatigue scatter. 04 p0460 A73-14721

Weibull flaw distribution models for fracture strength and failure analysis of brittle materials and fiber reinforced composites 04 p0468 A73-14726

Critical thickness effect of fatigue notched specimens on stress intensity factor and fracture toughness behavior of Ti-Al-V alloys 04 p0462 A73-15244

The influence of certain experimental factors on the fracture toughness of a high-strength steel 04 p0462 A73-15299

Acoustic model of HF damping and microstructure of dispersed aluminum oxide ceramics systems, using Hugoniot elastic limits for Young modulus and fracture determination 04 p0468 A73-15373

Method of repeatedly determining the fracture roughness with one specimen. 04 p0466 A73-15672

Investigation of the effect of vacuum environment on the fatigue and fracture behavior of 7075-T6. 04 p0466 A73-15764

Evaluation of the compact tension specimen for determining plane strain fracture toughness of high strength materials. 05 p0581 A73-16126

Pressure vessel proof test variables and flaw growth. 05 p0581 A73-16129

Evaluation of fracture toughness in aluminum alloys and welds by the Charpy impact test. 05 p0587 A73-16578

Tensile tests and heat treatment for creep rupture and fracture strengths of heat resistant steel, noting crack initiation and propagation 06 p0706 A73-17884

Susceptibility to brittle fracture of simulated weld seams in Ti-Al-V alloys. 06 p0698 A73-18209

On fracture toughness and its size dependence for steels showing thickness delamination. 06 p0709 A73-18476

Materials cracking resistance characterization by fracture toughness determination as function of crack front speed 06 p0764 A73-18491

A fracture control program for the reusable Space Shuttle booster. 06 p0764 A73-18493

Effects of thermal treatment on the resistance of some steels to crack development and propagation 06 p0711 A73-18664

Decohesive load carrying capacity of elastoplastic bodies based on permissible discontinuities due to strain increase, relating to structural strength determination 07 p0908 A73-19082

Fracture mechanics application to initial notch extension under tension in quasi-isotropic fiberglass reinforced laminates, noting transplanar buckling effects on fracture toughness 07 p0841 A73-19186

Fracture in conditions of creep under complex loading 07 p0910 A73-19302

Fractographic investigation of the resistance to fracture of aluminum and titanium alloys 07 p0840 A73-20505

The fracture toughness and crack propagation properties of polyester resin casts and laminates. 08 p0983 A73-21595

Effect of microstructure on measurements of fracture energy of Al2O3. 08 p0983 A73-21842

[ACS PAPER 44-BN-71P] Effect of surface damage on the strength of Al2O3 ceramics with compressive surface stresses. 08 p0983 A73-21843

[ACS PAPER 37-BN-71P] Comparison of the fracture strength K₁s of aluminum /AK4-1T1, V95T1, and D16T/ and titanium /VT8 and VT9/ alloys under static and cyclic loads. 09 p1105 A73-23054

Yield and fracture of D16T alloy at low temperatures in the presence of a complex stress pattern. 09 p1105 A73-23055

Effect of test temperature on energy of fracture of graphite. 09 p1110 A73-23062

Plasticity and failure of heat-resistant materials at a low number of cycles of simultaneous fluctuations of temperature and load. 09 p1105 A73-23154

Determining the technical cohesive strength of polycrystalline metals from the internal energy. 09 p1106 A73-23158

Resistance to brittle fracture of high-strength steel. 09 p1106 A73-23161

Finite element methods for elastic bodies containing cracks. 09 p1162 A73-23186

Brittle fracture tests of Ti-Cr steels with/without nitrogen hardened layer under shock impact loads 09 p1107 A73-23199

The role of fracture toughness in low-cycle fatigue crack propagation for high-strength alloys. 09 p1108 A73-23254

Void initiation and growth in Al alloys due to inclusions, presenting dislocation model for ductile fracture strength 09 p1109 A73-23256

Improved fracture resistance of 7075 through thermomechanical processing. 09 p1109 A73-23257

Influence of material properties on dynamic fracture toughness of steels. 09 p1109 A73-23259

Tensile, fracture toughness and crack growth properties of a roll-extruded HP 9Ni-4Co-25C steel alloy. 09 p1109 A73-23260

Enhancement of fracture toughness in high strength steel by microstructural control. 09 p1109 A73-23262

Linear elastic and general yielding fracture mechanics compatibility, investigating crack opening displacement relationship to stress intensity factor 09 p1109 A73-23263

Surface crack slow growth onset investigation with near tip strain as ductile fracture criterion, measuring fracture strength 09 p1109 A73-23264

Engineering significance of statistical and temperature-induced fracture mechanics toughness variations on fracture-safe assurance. 09 p1163 A73-23265

[ASME PAPER 72-PVP-15] Brittle fracture of orthogonally reinforced glass-fiber plastics during tension 09 p1111 A73-23349

Energy dissipation sources during reinforced plastic fracture, investigating fiber debonding energetics, toughness and crack propagation resistance 10 p1238 A73-23971

Carbon-carbon composites and bulk graphite fracture toughness and failure modes determination from single-edge-notched specimen responses under three-point bending 10 p1239 A73-24276

The effect of specimen and testing variables on the fracture of some fibre reinforced epoxy resins. 10 p1240 A73-24281

Graphitization of carbon fibre/glassy carbon composites. 10 p1240 A73-24284

Investigation of the fracture of carbon-graphite materials in a complex stress-strain state 10 p1240 A73-24360

The effect of strain rate on the characteristic value of the linear-elastic fracture mechanics determined on large and small specimens 11 p1380 A73-25446

X2048, a high strength, high toughness alloy for aircraft applications. 11 p1380 A73-25514

[AIAA PAPER 73-385] The fracture toughness of beryllium. 11 p1384 A73-26168

Crack toughness evaluation of hot pressed and forged beryllium. 11 p1384 A73-26169

S-200 grade beryllium fracture toughness properties. 11 p1384 A73-26170

Fiber strength, fracture types and material elastic properties relationship to impact resistance in carbon fiber reinforced plastics

12 p1515 A73-26882

Fracture characteristics of thermally strengthened titanium beta-alloys

12 p1510 A73-26914

Fracture mechanism transitions in laminate composites.

12 p1550 A73-26921

The effect of fibre-matrix interface strength on the impact and fracture properties of carbon-fibre-reinforced epoxy resin composites.

12 p1515 A73-26922

Determination of the nominal strength characteristics of fiberglass-strengthened plastics in the stress-concentration zones

13 p1645 A73-29051

Forged or homogenized aged maraging steels, discussing microstructure, tensile strength and fracture toughness dependence on precipitates morphology

13 p1637 A73-29243

Recent developments in precipitation hardenable stainless steels.

13 p1637 A73-29271

Strengthening and fracture of Ta, Nb, Mo and W binary solid solutions with short range order.

13 p1638 A73-29452

Plasticity and fracture of structural metals in complex stress state at low temperatures.

13 p1639 A73-29462

A theoretical study of fracture and yield conditions derived from hypo-elasticity.

13 p1639 A73-29464

Aluminum foils crack propagation observation with electron microscope during tensile tests, noting crystal dislocation role in ductile fracture process

13 p1639 A73-29467

The role of micropores in the fracture of forged sintered steel.

13 p1639 A73-29468

Brittle fracture initiation characteristics of twin notches.

13 p1700 A73-29469

Brittle fracture strength and non-crack propagation.

13 p1639 A73-29470

Fracture toughness-strength relationships in aluminum-zinc-magnesium-copper alloys.

13 p1639 A73-29473

Fracture toughness defined as work required for unit area crack extension, discussing toughness as function of material strength and strain characteristics

13 p1640 A73-29478

Solid fracture theories based on brittle region toughness parameter and absorbed specific fracture work factor above ductile-brittle transition respectively

13 p1640 A73-29479

Thin Al alloy sheet fracture toughness from crack growth resistance curves, discussing failure modes and critical stress intensities

13 p1640 A73-29480

Fatigue crack propagation as successive stochastic processes and fatigue fracture toughness.

13 p1701 A73-29490

Fracture strength of helically wound composite cylinders.

13 p1702 A73-29542

Two dimensional analysis of yielding to fracture process in angle-ply filament wound laminates under biaxial tension and compression

13 p1702 A73-29543

Experimental and theoretical investigation of the fracture of sheet materials in the presence of cracks.

13 p1703 A73-29625

Creep and fracture in OT-4 titanium alloy at temperatures from 400 to 550 C.

13 p1643 A73-29627

Equations for the time-dependent strength of a solid.

14 p1810 A73-30304

Rotors and turbine disks fracture resistance optimization at high temperatures from plane strain toughness criteria

14 p1813 A73-30679

Influence of air pressure on the brittle fracture of graphite

14 p1766 A73-30715

Application of cylindrical specimens with a ring crack for determining the brittle strength in materials

14 p1814 A73-30719

Fracture strength of fiber reinforced plastics, investigating crack propagation susceptibility, stress concentration and fracture mechanics

[ASME PAPER 73-DE-20] 14 p1767 A73-30821

Macromechanic model of notch size effects on tensile fracture strength in angle ply laminated composites

15 p1897 A73-31680

Fracture toughness evaluation by R-curve methods; Proceedings of the Symposium, Hawthorne, Calif., September 29-October 1, 1971.

15 p1950 A73-31982

Crack growth resistance curves /R-curves/ - Literature review.

15 p1950 A73-31983

R-curve determination using a crack-line-wedge-loaded /CLWL/ specimen.

15 p1950 A73-31984

Thin Al alloy sheet plane stress testing with zero K gradient specimen based on tapered double cantilever beam modification, considering fracture toughness and crack propagation

15 p1950 A73-31985

Fracture extension resistance /R-curve/ characteristics for three high-strength steels.

15 p1951 A73-31986

Plane stress fracture testing using center-cracked panels.

15 p1951 A73-31987

Comparison of R-curves determined from different specimen types.

15 p1951 A73-31988

Effect of specimen thickness on the fracture surface energy of 100 axis tungsten single crystals.

15 p1891 A73-32022

Deformation and fracture behaviours of composites of copper and copper-chromium alloys reinforced with tungsten or molybdenum fibres.

16 p2025 A73-33022

Structure, strength, and fracture of electrodeposited nickel and Ni-Co alloys.

16 p2025 A73-33113

Relationship between K_{Ic} and plane-strain tensile ductility and microscopic mode of fracture.

17 p2190 A73-34876

Fracture toughness parameters and elastic-plastic analysis of non-moderate fracture conditions using finite element methods.

17 p2245 A73-34877

The residual strength characteristics of stiffened panels containing fatigue cracks.

17 p2246 A73-34888

High strength Ni-Cr-Mo steel plane-strain fracture toughness measured with circumferentially cracked-notched round bars, discussing heat treatment and test temperature effects

17 p2190 A73-34890

Carbon, boron and glass fiber-epoxy resin composites fracture processes, predicting fracture strength of aligned fibrous composites via linear elastic fracture mechanics concepts

17 p2198 A73-35530

Borsic-Al composites fiber-matrix debonding for toughening mechanism of crack blunting, noting notch insensitivity and delamination

17 p2193 A73-35540

Effect of prestress levels on the long term strength of 1Kh18N9T steel at elevated temperatures

18 p2323 A73-36761

Influence of the structural state of the surface layers on the resistance to crack propagation of steel products

18 p2366 A73-36819

Crack resistance tests of polymethyl methacrylate specimens under tensile stress

18 p2366 A73-36824

Determination of rated strength characteristics of fiberglass in zones of stress concentration.

18 p2328 A73-36883

Fractographic investigation of the ductility of fracture in aluminum and titanium alloys.

19 p2440 A73-37780

Fracture toughness and absorbed energy measurements in impact tests on brittle materials.

19 p2500 A73-38094

Fracture toughness, ductility and cleavage mechanisms of crack extension in structural materials.

19 p2502 A73-38550

Strength of fibrous composite materials.

19 p2502 A73-38551

Temperature dependence of adhesive fracture of epoxy resin.

20 p2580 A73-38642

Tensile deformation and fracture in high-strength Al-Zn-Mg alloys.

20 p2575 A73-39019

Structures and properties of cobalt base-TaC eutectic alloys.

20 p2575 A73-39020

Experimental investigation of changes in the fracture toughness of aluminum alloys

20 p2577 A73-39359

Effect of structural and mechanical factors on the nature of cold shortness curves for steels

20 p2578 A73-39378

Isotropic elastic material fracture and yield criteria in terms of frame-indifferent relation between stress and strain increments

20 p2623 A73-39563

Experimental error equation of stress intensity factor for fracture toughness and crack growth rate testing

21 p2785 A73-40635

Influence of preloading on the sustained load cracking behavior of maraging steels in hydrogen.

21 p2719 A73-40924

Determination of the resistance of VT-14 alloy to brittle fracture

21 p2722 A73-41232

Statistical representation of the strength of fiberglass-reinforced plastic samples

22 p2880 A73-41956

Progress in flaw growth and fracture toughness testing; Proceedings of the Sixth National Symposium on Fracture Mechanics, Philadelphia, Pa., August 28-30, 1972.

22 p2920 A73-42131

Prior to failure extension of flaws in a rate sensitive Tresca solid.

22 p2880 A73-42136

Fatigue crack propagation and fracture toughness of 5Ni and 9Ni steels at cryogenic temperatures.

22 p2875 A73-42143

Some further results of J-integral analysis and estimates.

22 p2920 A73-42144

Experimental verification of lower bound K_{sub Ic} values utilizing the equivalent energy concept.

22 p2875 A73-42147

A method for measuring K_{sub Ic} at very high strain rates.

22 p2866 A73-42148

Influence of stress intensity level during fatigue precracking on results of plane-strain fracture toughness tests.

22 p2876 A73-42149

Influence of sheet thickness upon the fracture resistance of structural aluminum alloys.

22 p2876 A73-42150

Plane-stress fracture toughness and fatigue-crack propagation of aluminum alloy wide panels.

22 p2876 A73-42151

Structure of polymers and fatigue crack propagation.

22 p2880 A73-42152

Effects of strain gradients on the gross strain crack tolerance of A 533-B steel.

22 p2876 A73-42153

Experimentally determined shape factors for deep part-through cracks in a thick-walled pressure vessel.

22 p2866 A73-42157

German monograph on cyclic stress-strain curves and fracture strength of steels with various compositions covering plastic strain energy, S-N diagrams and test equipment

22 p2879 A73-42739

Fracture control - Past, present and future.

23 p3039 A73-43383

Method of determining the susceptibility of metals to brittle fracture under shock loads

23 p2965 A73-43470

Characterization of composites for the purpose of reliability evaluation.

23 p3040 A73-43627

Fracture mechanics and composite materials - A critical analysis.

23 p3040 A73-43628

Fiber reinforced composite crack model performance prediction and tests, noting fiber volume fraction for maximum fracture toughness

23 p3040 A73-43629

Method for estimating fracture strength of specially orthotropic composite laminates.

23 p3040 A73-43630

Fracture behaviour of crystalline Al3Ni intermetallic fibres.

23 p2991 A73-43774

Fracture of thin sections containing surface cracks.

23 p2992 A73-43807

Environmental effects on fracture resistant and biaxial fatigue design of aircraft structures.

23 p3042 A73-43811

Fracture analysis of surface- and through-cracked sheets and plates.

23 p3042 A73-43813

The effect of cold and hot rolling on the microstructure and fracture characteristics of titanium-to-steel explosion welds.

23 p2985 A73-43912

The effect of composition changes on the fracture toughness of an Al-Zn-Mg-Cu-Mn forging alloy.

23 p2993 A73-44025

Resistance to crack propagation in ceramics subjected to thermal shock.

23 p2997 A73-44031

Mathematical model for fracture strength of material undergoing molecular orientation during tensile strain, accounting for anomalous polymer characteristics

24 p3144 A73-44508

Probabilistic molecular contact rupture strength at solid-solid adhesive joint interface

24 p3092 A73-44516

The strength of orthogonally reinforced plastics during uniaxial tension

24 p3145 A73-44522

The mechanism of fracture of reinforced beams during bending. I

24 p3146 A73-44531

- Fracture criteria for a unidirectional glass fiber/plastic material under planar short-term and long-term stress 24 p1303 A73-44884
- The dynamic fracture toughness of carbon-carbon composites. 24 p3105 A73-45147
- FRACTURE TOUGHNESS**
- U FRACTURE STRENGTH**
- FRACTURES [MATERIALS]**
- Stress intensity factor for an elliptical crack approaching the surface of a plate in bending. 04 p0505 A73-14677
- Bending and rolling methods for tensile testing of metals without local necking, considering fracture under reduced axial stress 05 p0581 A73-16130
- Fracture due to damage from projectile impact. 06 p0763 A73-18484
- Evaluation of composite failures through fracture signal analysis. 15 p1879 A73-32250
- Fatigue and fracture of advanced composite materials. [SAE PAPER 730337] 17 p2194 A73-34688
- FRACTURING**
- Compression tests for plastic deformation and fracturing of Al alloy powder at hot working temperatures, noting limiting deformations in forging [ASME PAPER 72-WA/MAT-5] 04 p0456 A73-15808
- Temperature and loading rate effects on yield stress and specific fracture work in tempered carbon steel from notch tests, correlating with linear fracture mechanics 07 p0838 A73-19215
- Gliding, twin formation and fracture of iron-single crystals at 78 K and at 4 K 11 p1386 A73-26571
- An examination of dynamic fracture under biaxial-strain conditions. 12 p1550 A73-27022
- FRAGMENTATION**
- Fog droplet vaporization and fragmentation by a 10.6-micron laser pulse. [AD-758948] 06 p0698 A73-17494
- Approximate analysis of containment/deflection ring responses to engine rotor fragment impact. 07 p0910 A73-19188
- Mass spectrometry in structural and stereochemical problems. CCKVII - Electron impact promoted fragmentation of O-methyl oximes of some alpha, beta-unsaturated ketones and methyl substituted cyclohexanones. 10 p1186 A73-23550
- FRAME PHOTOGRAPHY**
- Photographic observations of Comet Bennett, 1970II. 04 p0495 A73-14766
- Frame photography for temporary creep in cylindrical Al alloy specimen necks under tensile loads, calculating creep diagrams 05 p0634 A73-16748
- Electronics associated with ultrahigh-speed photographic equipment 06 p0679 A73-18855
- Contribution of 1- and 5-nsec frame-type motion-picture photography to the study of dense plasmas 06 p0696 A73-18857
- Block adjustment for color and multispectral high altitude frame photography in photogrammetry, considering terrain caused sun angle effect as discriminant for automatic photointerpretation 12 p1500 A73-27955
- High-speed SFKF photographic camera of the continuous type. 21 p2693 A73-39938
- A multiframe high-speed camera developed to register phase objects with good spatial resolution without parallax. 21 p2696 A73-39980
- High-speed photography of laser damage in solids. 21 p2709 A73-39987
- Picosecond framing photography of a laser-produced plasma. 24 p3090 A73-44920
- FRAMES**
- NT AIRFRAMES**
- NT CHASSIS**
- The analysis of nonlinear three dimensional frames. 03 p0391 A73-13684
- FORTAN sequence with economical computer storage requirement for matrix method application to rigid plastic collapse analysis of frame, considering bounded variable problem 07 p0907 A73-19034
- Deformation of a frame coupled to a fiberglass-plastic shell under the action of local loads 08 p1017 A73-21372
- Dynamic stiffness matrix method for determining natural frequencies of plane frame with axially loaded Timoshenko members of uniform mass distribution 11 p1446 A73-26494
- Line and rectangular plane finite element models for accurate and efficient dynamic vibration frequency analysis of frames and shear walls respectively 13 p1700 A73-29377
- Frame structures dynamic analysis, comparing force method derived from stress and velocities variational principles with displacement method derived from Hamilton principle 14 p1807 A73-30188
- Matrix displacement solution to elastica problems of beams and frames. 16 p2082 A73-33906
- Structural design optimization by iterative analysis using proper stiffness matrix with applications to sandwich plate and frame problems 24 p3150 A73-45236
- FRAMING CAMERAS**
- A 35mm aerial photographic system. 09 p1082 A73-22387
- Dual-beam polariscope and framing camera for dynamic photoelasticity. 12 p1496 A73-27025
- Panoramic and frame cameras for aerial phototopographic survey, noting photo quality and high resolution advantages 12 p1497 A73-27423
- Automatic accurate full-range synchronization of light strobe with shutter opening of fast-framing camera. 21 p2697 A73-39997
- FRAUNHOFER LINES**
- Possible dependence of the differential shifts of Fraunhofer telluric lines on the solar zenith distance 01 p0106 A73-11241
- Photospheric height gradient and solar rotation measurements for Fraunhofer lines by magnetograph, considering telluric lines effect 01 p0107 A73-11376
- The interpretation of absorption-line shifts in the solar spectrum. 03 p0377 A73-14407
- Fraunhofer line depth in daytime airglow 07 p0817 A73-19471
- Possible dependence of differential shifts of telluric Fraunhofer lines on zenith distance of the sun. 10 p1279 A73-24177
- Solar Fraunhofer spectral lines having simple Zeeman triplet splitting with large Lande g-factors tabulated, noting missing lines in identification 11 p1421 A73-25932
- Solar limb Ca I Fraunhofer line polarization rate computation, considering radiation field anisotropy effects and depolarizing collisions in wings 12 p1544 A73-27826
- Fraunhofer line data reduction and wavelengths identification in solar UV spectra recorded during flight of Skylark rocket SL 601 12 p1544 A73-27827
- Influence of a traveling acoustic wave on spectral line profiles. II - Asymmetry of weak Fraunhofer lines 13 p1683 A73-29092
- Depth of the Fraunhofer lines in the spectrum of the daytime sky. 15 p1873 A73-32061
- Concorde-borne astronomical observation for Fraunhofer corona IR and photospheric and chromospheric radiations in lunar shadow during 30 June 1973 solar eclipse 15 p1940 A73-32184
- FRAUNHOFER REGION**
- U FAR FIELDS**
- FREDHOLM EQUATIONS**
- Boundary value problem of Lamé equation in elasticity theory of two dimensional region with angular points, solving by Fredholm integral equation 02 p0237 A73-12591
- Fredholm operator theory application to linear feedback system input-output stability in terms of origin encirclement counting in complex plane 05 p0561 A73-16488
- Iterative methods for best approximate solutions of linear integral equations of the first and second kinds. 06 p0717 A73-18170
- Numerical solution of the integral equations for optimal sequential filtering. 06 p0719 A73-18814
- Laplace equation and elasticity theory problems solution via Fredholm integral equation, noting boundary value problems for discrete points of given curve 07 p0909 A73-19127
- The stress intensity factors of a radial crack in a point loaded disc. 07 p0918 A73-20567
- Solutions of some Fredholm integral equations using fractional integration, with an application to a forced convection problem. 13 p1704 A73-28413
- Solution of the first boundary value problem of statics in the moments theory of elasticity 14 p1810 A73-30382
- A new method for the Lebedev-Ufliand integral equation for contact problems of elasticity. 15 p1946 A73-31103
- Fredholm integral equation singularity method solution for calculating stresses and elastic displacements in bodies of revolution of arbitrary shape under torsional loads 15 p1947 A73-31327
- Numerical solution of the integral equations for optimal sequential filtering. 15 p1844 A73-32039
- First fundamental problem of the theory of elasticity for a bi-periodic system of cuts 15 p1953 A73-32100
- An approach to the analysis of boundary value problems in the theory of functions and two-dimensional problems in the theory of elasticity 15 p1954 A73-32124
- Book - Mathematical programming and the numerical solution of linear equations. 15 p1901 A73-32300
- The Fredholm alternative in the case of linear approximation-regular operators 15 p1901 A73-32371
- Plane stress fields in isotropic disks due to singular and distributed loads, obtaining Fredholm integral equation solution via cubic spline function 16 p2079 A73-33238
- Asymptotic expansions for product integration. 17 p2200 A73-34213
- Fredholm integral equation for solving boundary value problem of heat transfer across contact of two regions bounded by simple closed Jordan curves 20 p2628 A73-39399
- Fredholm-uniformization computation of elastic scattering amplitudes in the presence of arbitrarily many open channels. 21 p2738 A73-40212
- Determination of the limiting equilibrium of a brittle body weakened by a system of cracks whose form on a plane approaches a circular form 22 p2921 A73-42284
- Effect of a Griffith crack on the distribution of stress in a semi-infinite two-dimensional medium. 22 p2922 A73-42470
- Numerical solution of Fredholm integral equation describing incompressible inviscid potential flow past three dimensional bodies 23 p2939 A73-43474
- Thermal stresses in rotationally symmetric semi-infinite elastic body with heat input along hole boundary and on plane bounding surface, reducing to solution of Fredholm equation 24 p3147 A73-44745
- FREDHOLM OPERATORS**
- U FREDHOLM EQUATIONS**
- U OPERATORS [MATHEMATICS]**
- FREE ATMOSPHERE**
- Internal gravity wave-atmospheric wind interaction - A cause of clear air turbulence. 04 p0473 A73-15071
- A numerical study of coupling between the boundary layer and free atmosphere in an accelerated low-latitude flow. 05 p0592 A73-16193
- The relation between temperature and humidity in the free atmosphere under conditions of stable stratification and strong thermal intermittency - A case study. 07 p0847 A73-19041
- Energy transport over turbulence spectrum of free atmosphere, using aircraft experiments 08 p0984 A73-21187
- Direct measurement of water vapor absorption of solar radiation in the free atmosphere. 08 p0985 A73-21389
- Russian monograph on turbulence in free atmosphere covering measurement and statistical techniques, tropospheric and stratospheric disturbances, wind pulsations, effects on aircraft flights, etc 12 p1521 A73-27134
- Basic characteristics of the temperature distribution and air currents in the free atmosphere of the earth 18 p2332 A73-35915
- FREE BOUNDARIES**
- Rigid and free boundaries effects on radiative heat transfer stabilization of fluid layer against Bénard thermal convection 01 p0120 A73-10397
- Continuous methods based on particular solutions for free boundary problems in partial differential equations, considering heat equation Stefan problem and Laplace equation interface 01 p0071 A73-11462
- Existence and uniqueness of heat equation two phase free boundary problem classical solutions 03 p0336 A73-12922
- The treatment of natural boundary conditions in the finite element and finite difference methods. 07 p0907 A73-19033
- Two approximate methods for describing the steady motions of an incompressible viscous fluid with a free boundary 09 p1072 A73-22619
- Free boundary flow invariant solutions of Navier-Stokes equations for optimal S/H subgroup systems, using continuous transformation group operators 10 p1204 A73-23583

- Temperature dependence of the accommodation coefficient of liquid-helium film. 10 p1249 A73-24341
- Plane subsonic jet free boundaries flapping measurements from oppositely placed hot-wire probes 11 p1346 A73-25251
- Finite element method applied to analysis of flow over a spillway crest. 13 p1563 A73-28078
- Vertical submersion of a floating cylindrical solid 15 p1861 A73-31283
- Differential equations with free boundaries in stochastic control problems 16 p2031 A73-32822
- Two dimensional wedge flow singularities for free and fixed boundaries at flow separation points, applying to water entry problem 16 p1999 A73-32928
- Mises variables in problems with a free boundary for the Navier-Stokes equations 19 p2419 A73-37245
- Thin steady two dimensional potential flow with free and/or rigid boundaries in presence of gravity, determining outer and inner expansions characteristics 20 p2546 A73-39085
- Convergence of Huber's method for heat conduction problems with change of phase. 20 p2626 A73-39100
- Rotation of an electrically conducting fluid with a free surface in a rotating field 21 p2747 A73-40885
- Free boundary problem involving elliptic differential equation, discussing iterative method instabilities inhibition of convergence 21 p2727 A73-40998
- Eigenmodes in vibrations of circular cylindrical shells with free boundaries, calculating frequencies from theory of inextensional vibrations 21 p2788 A73-41614
- Classical diffusion of free boundary plasma in plane and cylindrical slab geometries, calculating belt pinch effect and pressure decay rate 21 p2750 A73-41679
- The existence of a minimal surface with a free boundary of a given length 22 p2885 A73-41774
- FREE CONVECTION**
- Natural convective heat transfer in cavities and horizontal circular tubes, considering boundary layer and core flow interaction effects 01 p0120 A73-10290
- Thermal convection in a horizontal fluid layer with uniform volumetric energy sources. 01 p0120 A73-10442
- Variational formulation for hydromagnetic stability 01 p0084 A73-10550
- Heat and mass transfer theory and applications in aerothermoptics, thermoconvective and ferromagnetic fluid studies, chemical engineering, capillary transport and heat pipes 01 p0029 A73-10624
- Developing laminar free convection between vertical flat plates with asymmetric heating. 01 p0122 A73-10811
- Interaction of thermal radiation with laminar free convection from a heated vertical plate. 01 p0123 A73-11141
- Combined forced and free-convection heat transfer from vertical thin needles in a uniform stream. 02 p0238 A73-12052
- Study of the natural convection between two plane, vertical plates parallel and isothermal 02 p0238 A73-12795
- Isothermal vertical plate turbulent thermal boundary layer during free convection, noting temperature pulsations dispersion 03 p0396 A73-13184
- Carbon dioxide turbulent flow heat transfer in single phase near-critical region under forced and free convection 03 p0396 A73-13185
- Unsteady laminar natural and forced convection at transparent medium boundary layer radiating surface, noting turbulence effects on heat exchange 03 p0397 A73-13187
- Synoptic conditions of wave formation above convection streets. 04 p0473 A73-14826
- Resultant value of the inertial emf during thermal convection in a rotating plasma 04 p0481 A73-15604
- Transient free-convection horizontal laminar flow between two parallel plates. 04 p0517 A73-15681
- Study of the laminar free convection wake above an isothermal vertical plate. [ASME PAPER 72-WA/HT-41] 04 p0518 A73-15815
- Free convection along the downward-facing surface of a heated horizontal plate. 04 p0520 A73-15943
- Combined free and forced laminar convection in inclined tubes. 05 p0564 A73-16173
- Free convective heat transfer between vertical parallel plates One plate isothermally heated and the other thermally insulated. 05 p0638 A73-16221
- Stagnation-point free-convection film boiling on a hemisphere. 05 p0638 A73-16353
- Longitudinal rolls and Benard cells in water layer natural convection, predicting wavelength-depth relations and Rayleigh numbers for comparison with experiments [AIAA PAPER 73-42] 06 p0684 A73-17623
- Solid-gas mass transfer in the case of laminar free convection 06 p0768 A73-17919
- Description of the transfer of heat by natural convection in a horizontal porous layer with the help of a solid-fluid transfer coefficient 06 p0769 A73-18538
- * On laminar free convection stagnation heat transfer from an isothermal cylinder with internal sources-sinks. 07 p0918 A73-19101
- A computational method for low Mach number unsteady compressible free convective flows. 07 p0918 A73-19268
- Kinetics and convection in the combustion of alkane droplets. 07 p0919 A73-19391
- Nonlinear thermal convection in electrically conducting Boussinesq fluid subject to temperature gradient and magnetic field, calculating flow stability limit by energy method 07 p0920 A73-19513
- German monograph - Free convection of air in a horizontal circular gap in the case of temperature- and pressure-dependent density. 07 p0920 A73-19579
- Nonlinear Boussinesq convective model for large scale solar circulations. 08 p1001 A73-20751
- Numerical solutions to flow and heat transfer characteristics of free convection micropolar flow with Newtonian solvent substructure 08 p1023 A73-21260
- Natural convection in annular horizontal space 08 p1024 A73-21498
- A theoretical study of natural convection heat transfer from downward-facing horizontal surfaces with uniform heat flux. 08 p1024 A73-21638
- Influence of various surface roughness on the natural convection. 08 p1024 A73-21639
- An experimental study of combined forced- and free-convective heat transfer from flat plates to air at low Reynolds numbers. 10 p1295 A73-23777
- Inertial emf due to thermal convection in a rotating plasma. 10 p1254 A73-24194
- Free convection from a semi-infinite flat plate inclined at a small angle to the horizontal. 10 p1296 A73-24339
- Unsteady three dimensional laminar incompressible boundary layer with free and forced convection, determining flow and temperature fields adjacent to heated body 10 p1208 A73-24810
- Interaction between a sound field and natural convection on a horizontal cylinder. 10 p1296 A73-24846
- A note on the structure of thermal convection in a slightly slanted slot. 10 p1297 A73-24969
- Interaction of free and forced convection in horizontal tubes in the transition regime. 11 p1448 A73-25153
- Convection in a rotating annulus uniformly heated from below. II - Nonlinear results. 11 p1449 A73-25159
- Transpiration and natural convection - The vertical-flat-plate problem. 11 p1449 A73-25219
- Natural convection in a sloping porous layer. 11 p1449 A73-25220
- Periodic solutions of the set of equations governing the nonadiabatic convection of dry isolated thermals. 11 p1393 A73-25690
- A model for investigating eddy viscosity effects on mesoscale cellular convection. 11 p1393 A73-25716
- Heat transfer law for free convection in cylindrical and spherical interlayers 11 p1450 A73-25726
- Investigation of a film boiling crisis in the presence of natural convection 11 p1451 A73-25734
- Laminar free convection flow of an electrically conducting fluid from an inclined isothermal plate. 11 p1452 A73-26369
- Convection near critical Rayleigh numbers in the case of an almost vertical temperature gradient 11 p1453 A73-26435
- Determination of the coefficient alpha real in convection in air with allowance for the Jacq effect 12 p1557 A73-26797
- Classical solutions to the second boundary value problem for the unsteady free convection equations 12 p1559 A73-27421
- MHD free convective flow in a vertical channel. 13 p1663 A73-28164
- On thermal convection between non-uniformly heated planes. 13 p1705 A73-28430
- Experiments in magneto-fluid-mechanic natural and forced heat transfer from horizontal hot-film probes. 13 p1620 A73-29254
- Experimental investigation of the convection inversion process in the viscous sublayer of a turbulent boundary layer during blowing of carbon dioxide through a vertical porous heated surface under conditions of natural convection 13 p1708 A73-29407
- Free convection effects on the oscillatory flow past an infinite, vertical, porous plate with constant suction. I, II. 14 p1816 A73-30049
- Natural convection boundary layer flow over horizontal and slightly inclined surfaces. 14 p1817 A73-30607
- On the stability of natural convection boundary layer flow over horizontal and slightly inclined surfaces. 14 p1817 A73-30608
- Natural convection in a sound field giving large streaming Reynolds numbers. 14 p1817 A73-30613
- Thermal convective instability in uniformly rotating magnetized isothermal stellar atmosphere with constant Alfven speed, discussing heat loss mechanism dependence on temperature 15 p1929 A73-31060
- Heat transfer in the case of free convection of air between vertical surfaces 15 p1958 A73-31908
- Natural convective heat transfer between vertical parallel plates - One plate with a uniform heat flux and the other thermally insulated. 15 p1958 A73-32057
- Measurement using the Doppler effect of small velocities in flows occurring in the free convection of fluids. 15 p1864 A73-32069
- Planar free convection flow over horizontal cylinders with a small Grashof number under the influence of a planar wall 16 p2085 A73-33254
- Heat-transfer regimes during mixed convection in vertical pipes 17 p2253 A73-34133
- Papers on heat transfer covering thermosiphon technology, flowing gas-solid mixtures, condensation, free convection, flow stability and cryogenic insulation 17 p2254 A73-34351
- Thermosiphon technology advances covering open and closed single-phase natural convection and mixed convection systems, two phase systems and turbine blade cooling 17 p2254 A73-34352
- Natural convection flow equations and stability of laminar and transition flows, external and free boundary flows and boundary layer regimes 17 p2254 A73-34354
- Optimum thermal design of electronic packages cooled by free air convection. 17 p2141 A73-35387
- Free convection and thermal explosion in reactive systems. 17 p2255 A73-35662
- Combined forced and free-convection over thin needles. 18 p2371 A73-36697
- Turbulent free convection in a boundary layer with variable wall temperature 18 p2301 A73-36815
- On the stability of the conduction regime of natural convection in a vertical slot. 19 p2505 A73-38476
- A tilted plate interferometer for heat transfer studies. 20 p2564 A73-38879
- Suppression of free convection by a distributed automatic controller 20 p2626 A73-39043
- Heat transfer through free convection of air between vertical plates, obtaining Nusselt and Grashof numbers, and temperature and pressure effects 20 p2628 A73-39407
- Convection in a liquid heated from below in a closed cavity with temperature-dependent viscosity 20 p2628 A73-39612
- Heat release by free convection from horizontal cylinders to CO2 under near-critical conditions 20 p2628 A73-39613

Complex flow in vapour columns over boiling cryogenic liquids. 21 p2740 A73-41102

The method of the false transient for the solution of coupled elliptic equations. 21 p2727 A73-41473

Mathematical model for temperature inversion rise velocity under penetrative free surface convection based on unstable atmospheric boundary layer environment 23 p3002 A73-43595

Thermal convection in a large rotating fluid annulus - Some effects of varying the aspect ratio. 23 p3002 A73-43597

The effect of rotation on nonlinear thermal convection. 24 p3158 A73-45559

FREE ELECTRONS

Interaction between intense optical radiation and free electrons /Nonrelativistic case/ 01 p0061 A73-11248

Thermal free electron constant approximation in space charge current theory, considering I-V characteristics and ionized donor concentrations at injection levels 08 p0951 A73-21484

Effect of shielding on charge carrier mobility in compensated materials 09 p1133 A73-22674

Calculations of electrical transport properties of liquid metals at high pressures. 11 p1399 A73-25899

Facility to determine spectra of light scattered at free plasma electrons during single laser pulse, obtaining electron component profiles with high speed streak camera 12 p1506 A73-27301

A general formula for free-free absorption on highly-polarizable neutral atoms. 16 p2039 A73-33740

Interaction of intense optical radiation with free electrons /nonrelativistic case/. 22 p2892 A73-42346

Stellar radiation Thomson scattering by free electrons compared to atomic processes as mechanism for H II regions continuous emission 23 p3030 A73-43756

FREE ENERGY

NT GIBBS FREE ENERGY

Three dimensional linear theory of thermoelasticity covering homogeneous and isotropic bodies, work, free energy, boundary value problems and variational principles 02 p0233 A73-11978

Assembly for measurement of free surface energy, contact angles, and melt densities by a lying drop technique 09 p1085 A73-23017

Measurement of interfacial free energies and associated temperature coefficients in 304 stainless steel. 13 p1634 A73-28259

Response function class for constitutive equations in nonlinear isothermal theory of elastic-plastic metals, discussing free energy and stress response as measure of deformation [ASME PAPER 73-APMW-30] 22 p2925 A73-42890

Solvable pair potential for the Bogoliubov-de Gennes equations of space-dependent superconductivity. 23 p3018 A73-44275

FREE FALL

Earth vertical gravity field probing by observing body free fall from several hundred kilometers altitude 02 p0159 A73-12167

A comparison of neutral buoyancy and free fall for liquid propellant system zero-G simulations. 03 p0287 A73-13376

Air-space analogies - The velocity limits in aeronautics and astronautics 03 p0374 A73-13765

Close range photogrammetry of objects moving at high speed. 09 p1081 A73-22377

Precipitation patterns effective fall velocity determination from three dimensional radar scan data, discussing interpolation/extrapolation technique to improve coarse sampling time effects 12 p1520 A73-26808

The orientations of ice crystal models during a fall in an electric field 13 p1654 A73-28882

Zero Gravity Facility for space vehicle fluid systems research. 16 p1994 A73-33151

Free fall effects on differential growth and radiation sensitivity of higher plants in space flight and ground based clinostat experiments 22 p2804 A73-42172

FREE FLIGHT

Free flight and re-entry of a missile with a high ballistic coefficient. 09 p1147 A73-22625

Experimental study of wakes produced by hypersonic cones in free flight. 15 p1823 A73-31312

The mechanism of gyroscopic tracking. II. [ASME PAPER 72-MECH-33] 15 p1883 A73-32285

Aerodynamic coefficients determination for non-linear equations of motion solution to fit experimental free flight data, obtaining starting solution by noniterative continuation method 18 p2263 A73-36307

Tetrahedral Mylar plastic balloon drag coefficient measurement as function of Reynolds numbers from experimental free flight test data 23 p3004 A73-44263

FREE FLIGHT TEST APPARATUS

Aeromechanical measurements in free flight on piloted aircraft 09 p1032 A73-22447

A precise position and attitude measurement system for free-flying wind-tunnel models 11 p1362 A73-25443

FREE FLOW

Two-dimensional boundary layers in a free stream which oscillates without reversing. 01 p0032 A73-10446

Numerical calculation of supersonic opposing jet directed upstream against supersonic main stream by the use of time-dependent finite-difference method. 01 p0003 A73-11130

Nonlinear instability of two dimensional unbounded incompressible viscous fluid flows under periodic small perturbation 03 p0296 A73-14049

Analysis of free turbulent mixing flows without a net momentum defect. 03 p0296 A73-14187

CW dye laser with dye solution pumped through simple nozzles to provide unconfined flowing thin streams with optical quality and long term stability 03 p0320 A73-14460

A transformation for the numerical solution of two-dimensional free mixing flow problems. [ASME PAPER 72-WA/FE-3] 04 p0434 A73-15841

Effect of an oscillating free stream on the unsteady pressure on a circular cylinder. [ASME PAPER 72-WA/FE-12] 04 p0434 A73-15843

Free turbulent mixing in axial pressure gradients. [ASME PAPER 72-WA/APM-31] 04 p0435 A73-15888

Influences of free stream turbulence on mean velocities of turbulent boundary layer without pressure gradient. 04 p0435 A73-15972

Numerical solution of laminar jet mixing with and without free stream. 05 p0564 A73-16174

Generalization of J. K. Lunde's method for determining the flow around models in a rectangular-section test tank 08 p0955 A73-21195

Free boundary flow invariant solutions of Navier-Stokes equations for optimal S/H subgroup systems, using continuous transformation group operators 10 p1204 A73-23583

On structure of the laminar boundary layer in the presence of a fluctuating free stream. 10 p1209 A73-24830

Unsteady turbulent boundary layer flow past infinite flat plates with free stream acceleration or deceleration, computing characteristics by finite difference method 10 p1209 A73-24834

Numerical computation for entropy layer on blunt nosed cone in terms of shock layer fraction for given free stream and Mach number 11 p1299 A73-25113

Earliest classic result for the turbulent hydraulic wake behind body of revolution. 11 p1348 A73-25781

Measurements of free stream velocity and ionization relaxation behind a shock in xenon. 12 p1527 A73-27172

Approximate shock-free transonic solution for a symmetric profile at zero incidence. 13 p1564 A73-28823

Effects of free stream velocity profile on turbulent boundary layer, with some reference to the effects of free stream turbulence. 13 p1602 A73-29013

Free stream turbulence and transition in a circular duct. 13 p1602 A73-29014

Free parallel shear flow approximation by velocity discontinuity involving Kelvin-Helmholtz waves longer than shear layer thickness 13 p1605 A73-29448

Heat transfer to a strongly accelerated turbulent boundary layer - Some experimental results, including transpiration. 14 p1818 A73-30615

Investigation of the stability of a hollow vortex bounded by a rigid wall 15 p1861 A73-31156

Harmonic vibrations of inclined plate in separated free surface flow of ideal fluid in terms of weak perturbation flow theory 15 p1946 A73-31157

Statistical models of turbulent free shear mixing layer structure in incompressible air streams 17 p2156 A73-35507

Aircraft turbine engine exhaust emissions under simulated high altitude, supersonic free-stream flight conditions. [AIAA PAPER 73-507] 17 p2223 A73-35625

Calculation of free turbulent mixing by interaction approach. [AIAA PAPER 73-649] 18 p2297 A73-36204

Recombination effects in chemical laser nozzles. [AIAA PAPER 73-643] 18 p2287 A73-36258

Parametric analysis of turbulent wall jets. 19 p2376 A73-37491

Steady separated flow over finite flat plate in linearly decelerated free stream, using numerical solution of two dimensional Navier-Stokes equation 20 p2546 A73-39089

Boundary-layer separation at a free streamline. III - Axisymmetric flow and the flow downstream of separation. 20 p2549 A73-39806

Plume boundary jump of an underexpanded jet exhausting counter to a freestream. 21 p2790 A73-40433

Unsteady stagnation point heat transfer due to unsteady free stream temperature. 22 p2931 A73-42290

The effects of the exit velocity profile on the flow of a circular jet exhausting normal to the free stream. 23 p2969 A73-44125

A theoretical and experimental study of sound attenuation in an annular duct. 24 p3077 A73-44838

On aerodynamic coupling in free-stream turbulence manipulators. [AIAA PAPER 73-1015] 24 p3054 A73-44847

FREE JETS

Density and temperature measurement in laminar boundary layer and free jet of hypersonic nozzles by electron beam probe. [ONERA, TP NO. 1131] 01 p0045 A73-10239

Comparative study of free jets and jets emitted in the wake of a cylinder with axis parallel to a hypersonic flow 01 p0002 A73-10417

Free jet expansion from concentric orifices into vacuum. 02 p0152 A73-11528

Sound generation at an elastic plate acting as an obstruction in a turbulent free jet [DGLR PAPER 72-085] 02 p0152 A73-11667

Acoustic feedback phenomena in the case of a subsonic and supersonic free jet which impinges on an obstacle [DGLR PAPER 72-084] 02 p0127 A73-11683

The ordered structure of free-jet turbulence and its significance for the free-jet noise [DGLR PAPER 72-075] 02 p0128 A73-11701

Experimental investigation of the pressure and velocity fluctuations in a sound-affected free jet 03 p0290 A73-12965

Characteristics of pressure fluctuations in the subsonic free jet 03 p0290 A73-12966

Noise from free jets and airfoils in jets. 03 p0290 A73-12969

Some laws of the propagation of discrete-tone perturbations in a free supersonic jet 03 p0245 A73-13668

German monograph - Axisymmetric free jets and free-jet flames and a numerical procedure for calculating them. 03 p0398 A73-13810

Development of a submerged round laminar jet from an initially parabolic profile. [ASME PAPER 72-WA/FLCS-3] 04 p0408 A73-15861

Study of the specific characteristics of the diffusion method for measuring turbulence characteristics under conditions of a free homogeneous jet 05 p0576 A73-16617

Determination of the shape of jets flowing off the walls of an asymmetrically positioned bucket 07 p0776 A73-20098

IR radiometers for free jets sound emission mechanism probing, describing optical and electronic equipment [ONERA, TP NO. 1212] 07 p0825 A73-20164

Development of a procedure for measuring the degree of turbulence at the axis of a free two-phase jet by a thermal-diffusion method 09 p1167 A73-22847

On the Kutta-condition at the trailing edge of a nozzle in a weakly nonstationary jet flow. 10 p1209 A73-24827

Coanda effect physical explanation and applications to free jet and partially bounded jet, analyzing surface shutter characteristics 13 p1601 A73-28913

- Studies on bounded jets. 13 p1603 A73-29032
- German monograph on laser and schlieren photographic investigation of supersonic free jet flow from nozzle at supercritical pressure ratio into free atmosphere 13 p1567 A73-29286
- Unsteady separated free jet flow of an ideal fluid past a wing 15 p1861 A73-31155
- HF laser flow visualization with an infrared television system. 15 p1874 A73-31357
- Subsonic free jet wind tunnel turbulence damping in settling chamber via screen, yielding uniform velocity profile and low turbulence level in nozzle exit 16 p1996 A73-33266
- A generalized theory for the turbulent mixing of axially symmetric compressible free jets. 17 p2156 A73-35505
- Nonlinear radial wave propagation in low density expanding flows with application to the free jet. 18 p2300 A73-36630
- Linearized MPD jet and channel flows in external magnetic fields with the Hall effect. 19 p2465 A73-37175
- The magnetic channeling of a supersonic axisymmetric plasma jet. 19 p2470 A73-38318
- Condensation in CO₂ free jet expansions. I - Dimer formation. 21 p2743 A73-40937
- Condensation in CO₂ free jet expansions. II - Growth of small clusters. 21 p2743 A73-40938
- Some features of the propagation of a discrete tone perturbation in a free supersonic jet. 21 p2633 A73-41318
- An analog investigation of the gas jet resonance tube. 23 p2967 A73-43401
- Laminar and turbulent mixing of compressible jets at low Reynolds numbers. 23 p2967 A73-43403
- Approximate calculation of dividing streamline of heterogeneous coaxial supersonic jets. 23 p2940 A73-44127
- Comparison of results obtained with various sensors used to measure fluctuating quantities in jets. [AIAA PAPER 73-1043] 24 p3079 A73-44867
- Development of a mathematical model for vortex configuration in jets and flames. 24 p3157 A73-45376
- Vortex model for flames and free jets characteristic velocities based on three dimensional turbulent combustible flow 24 p3158 A73-45387
- FREE MOLECULAR FLOW**
- Asymptotic theory of the Boltzmann equation at large Knudsen number. 07 p0853 A73-20473
- Free molecular flow past a flat plate in the presence of a nontrivial gas-surface interaction. 08 p0926 A73-21401
- Diffusion of a hypersonic flow by a supersonic gas jet in the case of a free-molecular mode of interaction 11 p1304 A73-26446
- Influence of the surface-radiation law on the calculation of the aerodynamic coefficients in the near free molecular flow transient regime 12 p1487 A73-27391
- Photographic studies of the transition between continuum and free molecular flow. 15 p1864 A73-31935
- Electrical network analogy application to thermal energy steady diffusion within Knudsen gas filled enclosure, discussing free molecule limit and transition regime 15 p1959 A73-32283
- An analytical study of hypersonic inlets in free molecule flow. 18 p2264 A73-36325
- Monatomic and diatomic gas supersonic flow field calculation for sharp leading edge by BGK and ordinate models 18 p2265 A73-36631
- An aerodynamic test facility with free molecular flow and high stagnation temperature 20 p2545 A73-39615
- Knudsen free molecular flow explanation of thermomagnetic torque on circular cylinder suspended in axial molecular field, noting apparatus tilt effect 22 p2842 A73-42233
- Expansion of a plane rarefied gas layer into a vacuum 24 p3076 A73-44655
- FREE OSCILLATIONS**
- U FREE VIBRATION**
- FREE RADICALS**
- Changes of the free radical concentration in the cerebral cortex depending on the functional state of the cerebrum 01 p0009 A73-11082
- Vapor deposition of thin films of DFPF and BDPA. 02 p0201 A73-12639
- Kinetics of the sulphur dioxide catalyzed recombination of radicals in hydrogen flames. 03 p0352 A73-14393
- Comet photometry to explain origin of free radicals discovered in cometary spectra, considering clathrate hydrates and possible parent molecules 04 p0494 A73-14756
- Direct measurement of the lifetimes and predissociation probabilities for rotational levels of the OH and OD A-2Sigma+ states. 05 p0601 A73-17341
- The hydroperoxyl radical in atmospheric chemical dynamics - Reaction with carbon monoxide. 06 p0661 A73-18224
- Calculation of probabilities of energy transfer - Application to the vibrational relaxation of the CS radical in the presence of argon 07 p0854 A73-20608
- A shock tube determination of the CN ground state dissociation energy and the CN violet electronic transition moment. 08 p0989 A73-20789
- Mass spectrometric studies of tetrafluorohydrazine and the difluoroamino radical. 08 p0936 A73-21173
- Prohibited autodetachment in OD- formed by collisions of O- with D2. 09 p1048 A73-22075
- An evaluation of molecular constants and transition probabilities for the NH free radical. 11 p1402 A73-26582
- Rate constants for the reactions of hydroxyl and hydroperoxyl radicals with ozone. 14 p1724 A73-30619
- Changes in the quantity of overall sulphydryl groups in the blood of persons coming in contact with microwave radiation sources 15 p1837 A73-31169
- Laser induced fluorescence of CN radicals. 19 p2437 A73-37902
- Circadian rhythms of free radical state concentrations in the organs of mice. 20 p2512 A73-39104
- Photochemical model for homogeneous gas phase radical chain mechanism to remove tropospheric methane, carbon monoxide, molecular hydrogen and formaldehyde 21 p2646 A73-40082
- Some reactions and hydroperoxyl and hydroxyl radicals at high temperatures. 22 p2898 A73-42754
- Atomic oxygen reaction with acetylene in low pressure fast flow system, measuring free radical formation rate by photoionization mass spectrometer 22 p2818 A73-42768
- Inhibition by selenium of the free-radical states of the retina of the eye 24 p3059 A73-44724
- FREE STREAM EFFECTS**
- U FREE FLOW**
- FREE STREAMS**
- U FREE FLOW**
- FREE VIBRATION**
- Bubnov-Galerkin method for natural vibration frequencies of thin elastic circular conical shell under thermal loading 01 p0113 A73-10015
- Linearization method for analytic solution of oscillatory motion differential equations of elastic nonlinear system, studying combinations of free and forced vibrations 01 p0075 A73-10093
- Free vibration of prestressed cylindrical shells having arbitrary homogeneous boundary conditions. 01 p0114 A73-10730
- Phase plane analysis of free vibration of rectangular plate loaded by in-plane compressive load, calculating critical load and amplitude in postbuckling region 01 p0115 A73-10770
- Steel/pig iron friction pair natural vibrations due to starting force and sliding friction force difference, noting starting force dependence on loading rate 01 p0058 A73-11403
- Incompressible elastic circular cylinders quasi-equilibrated motions analysis, obtaining free and forced oscillations periods 02 p0191 A73-11573
- Stress analysis and dynamic investigation of turbine blades from constrained torsion theory, calculating free torsional vibration frequencies 02 p0229 A73-11621
- Free three-dimensional vibration processing of gas-turbine engine blades 02 p0172 A73-11723
- Oscillations of open cylindrical shells of variable curvature 02 p0233 A73-11941
- Determination of attenuation factors from experimental vibrograms of multifrequency attenuating oscillations 02 p0233 A73-11942
- Dynamics of flexible satellites with active attitude control. 02 p0228 A73-11994

Large amplitude oscillations of a hollow spherical dielectric. 02 p0236 A73-12518

Non-linear oscillations of a nonuniform fixed circular plate. 02 p0236 A73-12519

Free vibrations of elastic systems with discrete dynamic systems attached. 03 p0384 A73-12983

Nonlinear responses for a circular plate subjected to a dynamic ring load. 03 p0388 A73-13319

A finite element analogue of the modified Rayleigh-Ritz method for vibration problems. 03 p0390 A73-13336

Resonant frequencies of free vibrating plate via finite difference method, noting difference equations for plate equilibrium 03 p0391 A73-13345

A variational principle for the nonrotational flow of a perfect compressible liquid in a flexible tank [ONERA, TP NO. 1178] 03 p0294 A73-13601

Calculation of the natural oscillations of an ideal liquid in an axisymmetrical container with allowance for surface forces 03 p0294 A73-13607

Small steady free oscillations of liquid in rigid tanks, considering HF modes 03 p0296 A73-14047

Natural vibration frequency spectra of circular cylindrical and spherical shells of revolution, using Bessel function 03 p0395 A73-14052

Beam transverse vibration with nonlinear-spring supported free end and concentrated mass, determining free vibration frequencies 04 p0508 A73-14940

Application of the method of summary representations to problems of cylindrical shell oscillations 04 p0511 A73-15086

Use of Green's function in the study of the natural oscillations of two-dimensional structures 04 p0511 A73-15087

Piezoelectric transducers for the study of short-duration mechanical loads 04 p0448 A73-15374

Velocity corrected theory of laminated plates applied to free plate strip vibrations. 04 p0513 A73-15588

Free vibration of cantilever circular cylindrical shells - A comparative study. 04 p0513 A73-15589

Considerations concerning the orthogonality of the natural oscillation modes in elastic systems with many degrees of freedom 04 p0476 A73-15658

Spectral analysis of the vibrations of mechanical systems with continuous mass which have a finite number of attached concentrated masses 04 p0476 A73-15659

Free vibration of a beam with one end spring-hinged and the other free. 05 p0633 A73-16542

Free vibrations in nonlinear systems with two degrees of freedom 05 p0599 A73-17087

Finite element analysis of nonlinear vibration of beam columns. 05 p0636 A73-17118

Comparison of eigenvalues and characteristic vibration modes of circular ring bars, circular ring disks, and circular ring fibers 06 p0758 A73-17584

Comparison of the characteristic values and characteristic vibration forms of a circular ring beam, a circular ring disk, and a circular ring fiber. II 06 p0759 A73-17586

Containers with isochronous fluid oscillations. 06 p0686 A73-18147

Possibilities of control of radiation emitted by lasers with telescopic resonators. 06 p0702 A73-18588

Second-harmonic conversion of laser radiation generated under free-oscillation conditions. 06 p0702 A73-18594

Nonlinear natural vibrations of rectangular plates and cylindrical panels. 06 p0765 A73-18640

Free vibration analysis of spinning structural systems. 07 p0907 A73-19032

Free vibration of multi-degree-of-freedom nonlinear systems. 07 p0909 A73-19164

Vibration of cylindrically orthotropic circular plates. 07 p0913 A73-19968

Finite element displacement method for large amplitude free flexural vibrations of beams and plates. 07 p0914 A73-20212

Calculation of the natural and forced vibrations of circular plates with allowance for energy dissipation in the material 07 p0917 A73-20501

- Three dimensional analysis in series form for statics and dynamics of simply supported rectangular plates of micropolar elastic material, obtaining free vibration frequencies
07 p0917 A73-20565
- Free vibrations of square plates with stiffened square openings.
08 p1016 A73-20826
- Free vibrations of an infinite strip of variable thickness.
08 p1016 A73-20940
- Vibration of four point-supported plates by a finite element method.
08 p1017 A73-20945
- Velocity ratio in the analysis of linear dynamical systems.
08 p0988 A73-21467
- Natural vibrations of laminated orthotropic spheres.
09 p1160 A73-22890
- Effect of elastic displacements of a cylindrical shell on the vibrations of the free surface of a fluid
09 p1073 A73-23345
- Free particle gravitating cylindrical model for gravitational kinetic instabilities, calculating natural vibration spectrum and parameters for beam instability development
10 p1253 A73-23714
- Complex natural vibrations of space vehicles performing a maneuver
10 p1285 A73-23876
- The methods of time-variable systems analysis based on new trends in theory of these systems.
10 p1200 A73-24047
- Solution of quadratic matrix equations for free vibration analysis of structures.
10 p1290 A73-24299
- Axisymmetric vibrations of circular plates with stepped thickness.
10 p1291 A73-24394
- Three-dimensional problem of the vibrations of a circular plate with initial stresses
10 p1292 A73-24506
- The free vibrations of a thin circular finite rotating cylinder.
11 p1443 A73-26088
- Natural oscillations of density-stratified ideal incompressible liquid in rectangular vessel, solving oscillation equation for various density distributions
11 p1349 A73-26441
- Dynamic stiffness matrix method for determining natural frequencies of plane frame with axially loaded Timoshenko members of uniform mass distribution
11 p1446 A73-26494
- Rayleigh-Ritz method for natural frequencies of transversely vibrating polar orthotropic annular perforated plates, proposing coordinate transformations for asymmetric mode solutions
11 p1446 A73-26495
- Multilocal difference method for free vibration analysis of closed and open orthotropic noncircular cylindrical shells with supported curved edges
12 p1551 A73-27035
- Static, vibration and buckling analysis of axisymmetric circular plates using finite elements.
12 p1555 A73-27738
- Approximate dependences for the vibration frequencies of smooth cylindrical shells and for ones with concentrated inclusions
12 p1555 A73-27789
- Influence of rotational inertia on the frequency spectrum of the natural vibrations of a cylindrical shell
12 p1556 A73-27801
- Free vibration of cantilever beam with/without tip mass and with nonlinear material properties, using perturbation and finite element techniques
12 p1556 A73-27928
- Improvement of damping characteristics of structural members with high damping elastic inserts.
13 p1690 A73-28056
- Free vibrations of a laminated beam by a microstructure theory.
13 p1691 A73-28063
- Reflection of plane heterogeneous and uniform electromagnetic waves and the reflected wave displacement
13 p1658 A73-28072
- Natural vibrations of thin, prismatic flat-walled structures.
13 p1694 A73-28247
- Complementary energy method in elastodynamics.
13 p1694 A73-28249
- Earth axis 14 month variation with latitude /Eulerian nutation/ as free vibration subject to damping, obtaining nonuniform drift rate from seven year interval observations
13 p1678 A73-28382
- Excitation of the Chandler wobble by large earthquakes.
13 p1607 A73-28407
- On the eigenvalue problem for fluid sloshing in a half-space.
13 p1599 A73-28410
- Axisymmetric vibrations of circular plates of linearly varying thickness.
13 p1695 A73-28415
- Free and forced vibration analysis of laminated ring structure with elastic inner, outer layers and core, obtaining natural frequency response by variational method
13 p1695 A73-28486
- Elastic structures nonlinear free vibrations theory based on Hamilton principle and perturbation method, applying to beams and rectangular plates
13 p1696 A73-28751
- Clamped orthotropic triangular plates free nonlinear vibrations, solving equations of motion in first order approximation by von Karman plate theory
13 p1697 A73-28808
- A finite element study of the vibration of trapezoidal plates.
13 p1700 A73-29378
- Book - Theory of vibration with applications.
13 p1703 A73-29676
- Free vibrations of shells of revolution with variable thickness.
14 p1805 A73-29768
- Matrix method analysis of stiffened plates free vibrations, deriving governing equation in stiffness matrix form by combining plane stress theory and lateral vibration equation
14 p1807 A73-30186
- Steel structures analysis based on cubic interpolating functions with parameters of nodal displacements, discussing method extension to natural vibration
14 p1809 A73-30199
- Coupled twist-bending waves and natural frequencies of multispan curved beams.
14 p1815 A73-30914
- Natural oscillations of multilayer shells and plates with fillers
15 p1944 A73-30970
- Stability and free oscillations of conjugate conical shells
15 p1944 A73-30972
- Vertical free vibrations of rectangular vessel partially filled with perfect incompressible liquid analyzed by power series
15 p1860 A73-31045
- Calculation of natural frequencies and modes of steadily rotating systems - A teaching note.
15 p1946 A73-31123
- Computation of upper and lower bounds to the frequencies of elastic systems by the method of Lehmann and Maehly.
15 p1951 A73-32027
- Lower bounds to the frequencies of continuous elastic systems.
15 p1954 A73-32125
- Free vibration of an inflated oblate spheroidal shell.
15 p1955 A73-32155
- On the vibrations of a rotor with rotating inequality and with variable rotating speed.
15 p1883 A73-32216
- Corresponding function solutions of discrete mechanics problems based on difference polynomials, applying to Lagrange problem of string natural vibrations for distributed point masses
16 p2035 A73-32680
- Natural vibrations of variable-thickness shells of revolution with apparent additional masses
16 p2074 A73-32685
- Application of extended variational principles to finite element analysis.
16 p2077 A73-32982
- Nonlinear algebraic equations in continuum mechanics.
17 p2199 A73-34102
- Free vibrations of multilayered composite plates.
17 p2241 A73-34192
- Combined Rayleigh-Ritz and Lagrange multiplier technique for investigation of free vibrations of constrained cylindrical shell, considering axisymmetric mode
17 p2241 A73-34198
- Asymptotic characteristics of the problem involving intrinsic asymmetrical vibrations of circular conical shells
17 p2241 A73-34267
- Approximate method for determining the natural frequencies of flexible rectangular plates
18 p2363 A73-36408
- Free particle gravitating cylindrical model for gravitational kinetic instabilities, calculating natural vibration spectrum and parameters for beam instability development
18 p2340 A73-36739
- Natural transverse vibrations of sandwich beams of unsymmetrical structure.
18 p2367 A73-37141
- Free oscillations of a double layer in a turning rectangular basin of constant depth
19 p2419 A73-37530
- Calculation of forced and free oscillations of round plates taking into account the dissipation of energy in the material.
19 p2499 A73-37776
- A note on the period of oscillation of non-linear systems.
19 p2460 A73-38108
- Free harmonic vibrations of thin pretwisted rectangular plates analyzed in terms of torsional and bending vibration coupling based on shell theory
19 p2500 A73-38115
- Complex self-excited vibrations of space vehicles during maneuver.
20 p2614 A73-38895
- Investigation of the free vibrations of sectorial plates and conical panels by a theoretical-experimental method
20 p2618 A73-39314
- Study of the two-frequency natural oscillation regime of a circular membrane on a nonlinearly elastic base
20 p2593 A73-39501
- Free vibration and buckling loads of anisotropic pressurized thin walled shells of revolution, considering cylinders, barrels and spherical sections
20 p2621 A73-39538
- Modal technique to obtain forced axisymmetric response of elastic spherical shells from free vibration response relations, taking into account transverse shear and rotational inertia
20 p2621 A73-39541
- Dynamic response of laminated composite circular cylindrical shells with freely supported or clamped edges.
20 p2621 A73-39543
- Limiting zero and infinite edge beam stiffness effect on natural vibrational frequencies of reinforced annular plates
20 p2622 A73-39548
- Finite-element formulations for elastic plates by general variational statements with discontinuous fields.
20 p2623 A73-39558
- Free and forced nonlinear oscillations of anisotropic orthotropic annular plate with free inner boundary and fixed immovable outer boundary
20 p2623 A73-39561
- Method for calculation of natural and induced oscillations in elastic shells of revolution which are filled with an ideal incompressible liquid
20 p2624 A73-39647
- Natural oscillations of shells of revolution with an open profile and concentrated inclusions
20 p2625 A73-39654
- Free vibration of arches flexible in shear.
21 p2782 A73-40002
- Comments on the mathematical theory of small oscillations of an inviscid gas
21 p2738 A73-40191
- Application of the method of integrating matrices to the calculation of the natural vibrations of a propeller blade with allowance for deflection in two planes and for torsion
21 p2783 A73-40389
- A natural frequency analogy between spherically curved panels and flat plates.
21 p2785 A73-40754
- Critical pressure and vibration frequencies of cylindrical shells with edges elastically reinforced in the axial direction
21 p2786 A73-40980
- In-plane free vibrations of tapered oval rings, determining normal modes and resonant frequencies from differential force and moment equilibrium equations
22 p2918 A73-41818
- Free flexural vibrations of elliptical thin plate with free edge, calculating mode shapes and frequencies by use of Mathieu function
22 p2918 A73-41822
- Free vibrations of fluid-conveying cylindrical shells. [ASME PAPER 73-DET-96]
22 p2919 A73-42075
- Reduction of the degrees of freedom in solving dynamic problems by the finite element method.
22 p2922 A73-42479
- Vibration and stability of nondivergent elastic systems.
22 p2922 A73-42551
- An exact method for the study of the dynamic stability of supporting structures acted upon by periodical impulses.
22 p2927 A73-43031
- Normal modes of elastically connected circular plates.
22 p2929 A73-43140
- Experiments on free vibration of shells of revolution.
23 p3039 A73-43384
- Monofrequent oscillations in mechanical systems governed by second order hyperbolic differential equations with small non-linearities.
23 p3044 A73-44077
- In-plane vibration of continuous curved beams.
23 p3045 A73-44165
- Large amplitude vibrations of elastically restrained rectangular plates.
23 p3048 A73-44380
- Free vibrational development of laser-induced cracks
24 p3095 A73-44510
- Mixed finite-difference scheme for analysis of simply supported thick plates.
24 p3150 A73-45226

On response of initially stressed structures to random excitations. 24 p3150 A73-45229

Natural, flexural and torsional vibration frequencies and modes for helicopter tail rotor blades 24 p3057 A73-45245

Free vibration of square plates under different boundary conditions, determining opening geometry effects on fundamental frequencies by grid framework model with finite difference operators 24 p3151 A73-45266

The problem of natural oscillations of a thin shell containing an elastoacoustic medium 24 p3152 A73-45359

Boundary value problem concerning the oscillations of a rotating ideal fluid 24 p3081 A73-45531

FREEZE DRYING

Freeze drying - A unique approach to the synthesis of ultrafine powders. 04 p0455 A73-15753

FREEZING

NT VIBRATIONAL FREEZING

NT ZONE MELTING

Diffusion freezeout in gas-loaded heat pipes.

[ASME PAPER 72-WA/HT-33] 04 p0518 A73-15822

Thermoset polymers for freezing and cryogenic temperatures, noting theory, methodology and preparation for science and industry 10 p1241 A73-24675

FREQUENCY POINTS

U MELTING POINTS

FREIGHT COSTS

Air freight handling equipment, techniques and costs in cargo terminals, including forklifts, pallets, containers, conveyor belts and warehouse configurations 19 p2418 A73-37821

FREIGHTERS

Freighter airships economical and technological feasibility study, discussing performance requirements and design concepts [SAWE PAPER 951] 19 p2385 A73-37879

FRENCH SATELLITES

NT EOLE SATELLITES

FRENCH SPACE PROGRAMS

SAGESSE /Analytical System for Managing Space Assemblies and Systems/ - A management system applicable to CNES 01 p0124 A73-11252

Budgeting role in development and implementation of five year plan of operations at French space research center 01 p0124 A73-11253

Physical contents and financial underpinning of future French and European space research programs, noting meteorology, satellite communication and R and D planning 01 p0125 A73-11254

Cs ion bombardment and contact ionization engines in French space program for communication and geostationary satellites electric propulsion 04 p0488 A73-15715

Accurate localization by the Geole Project satellite 05 p0623 A73-17192

French telemetry processing center, discussing data acquisition and reduction systems and application software 05 p0552 A73-17299

French computation center equipment for satellite orbit calculations and attitude corrections, describing links between teleprocessing and data transmission 05 p0555 A73-17300

Book - French space technology. Volumes 1 and 2. 07 p0904 A73-18901

Electro-gilding of coverings and light alloy component parts for satellites D2 and EOLE. 07 p0829 A73-18911

French D2A satellite construction, describing AG5 sheet covering and gold coating fabrication methods 07 p0829 A73-18912

French spacecraft electronic components reliability program, considering failure characteristics, operating limits, environmental conditions and confidence level 07 p0797 A73-18915

Quality control in Concerto reliable space components procurement program for multilayer ceramic capacitors and thermistors manufacture 07 p0829 A73-18920

French Concerto aerospace part procurement program contribution to mass produced electronic component reliability assessment, control and improvement based on tin oxide resistor experience 07 p0829 A73-18923

Pneumatic torque generator subsystem of French D2 satellite, discussing engineering technical difficulties 07 p0778 A73-18925

Work carried out by Societe Bertin under contract to CNES in the field of fluidic control 07 p0904 A73-18938

French Guiana space center facilities for missile tracking, telemetry, data processing and transmission of command instructions, discussing PCM, PAM and PDM links equipment 07 p0807 A73-18942

Tracking radar equipment evolution in connection with French space program development, describing reliability technology 07 p0807 A73-18943

The operational facilities of the French Guyana Space Center. 07 p0807 A73-18946

French Guiana space center Diamant and Europa service towers structure, operational security features and protection against corrosion and contamination 07 p0807 A73-18947

French satellites attitude stabilization and control systems, describing electronic sensor and servocontrol circuitry 07 p0904 A73-18967

French Concerto program for component reliability and quality assurance in manufacturing and procurement controls for Symphonie satellite 07 p0790 A73-18975

Diamant launcher tilting system. 07 p0905 A73-18993

The space environment simulation chamber of Toulouse. 07 p0807 A73-19000

The large space simulation chamber of Toulouse and its evacuations pumps 07 p0808 A73-19003

French CNES and Toulouse space center organization and activities, describing installation history 07 p0808 A73-19006

The space environment simulation chamber of the Toulouse space center 07 p0808 A73-20245

French scientific space research progress assessment, noting ionospheric rocket sounding, plasma wave propagation study and absorption technique for upper atmosphere millimetric radiation measurement. 09 p1168 A73-23275

Eole experiment processing network for data pretreatment, system management aid and accuracy study and feasibility demonstration of fast response time operational system 10 p1187 A73-23619

D-2A /Tournesol/ satellite data processing procedures for technological controls, operation in flight and scientific purposes 10 p1187 A73-23620

The preprocessing of French laser observations from the ISAGEX program 10 p1187 A73-23621

Program objectives and propulsive, equipment case, attitude control, interstage, separation skirt and nose cone subassemblies of French Diamant B-P4 launch vehicle 10 p1285 A73-23654

Recovery objectives - Review of the most interesting aspects of problems related to this technique 14 p1804 A73-30087

The concept of the flight safeguard interferometer for rocket probes of the French Guiana Space Center 14 p1773 A73-30090

A priori evaluation of the position finding system of the Guiana Space Center /CSG/ by the application of Kalman's algorithm 14 p1727 A73-30092

Methods of evaluation of tracking procedures used at the French Guiana Space Center 14 p1727 A73-30093

French launching base real time trajectory photography system for rocket space location information, investigating evolution towards maximum reliability 14 p1773 A73-30094

Definition, philosophy, and development of safety interventions in flight at the Guiana Space Center 14 p1804 A73-30096

Electre nose cones reentry impact safety policy, discussing launcher trajectory, cost and performance indices and ascent optimization 14 p1804 A73-30097

Manufacturing, integration and launching phases of Diamant B launcher inspection, discussing automatic control and testing bench structure and safety 14 p1742 A73-30104

Preparation on the launch base and setting in operation in the launch area of the D2 A scientific satellite 14 p1804 A73-30108

Soviet-French cooperation in space exploration 14 p1818 A73-30250

FRENKEL DEFECTS

Hot-electron concept for Poole-Frenkel conduction in amorphous dielectric solids. 02 p0201 A73-12817

Electric properties of 5,12-6,11-tetraoxotetrasene crystals 07 p0862 A73-20007

Optimal superplasticity model of metallic materials involving interphase surface of new phase fluctuation nuclei in framework of Frenkel theory 09 p1099 A73-21960

FREON

Action of Freon-114B2 on the activity of lactate-dehydrogenase iso-enzymes 06 p0650 A73-17696

Temperature effects on liquid drop evaporation in an air flow 14 p1816 A73-30015

Development of experimental turbine facilities for testing scaled models in air or freon. 17 p2145 A73-34381

Freon-22 circular and flat jet propagation in air cross flow in wind tunnel, examining air-gas dynamic pressure ratio effects 21 p2676 A73-40405

FREQUENCIES

NT AUDIO FREQUENCIES

NT BEAT FREQUENCIES

NT BROADBAND

NT C BAND

NT CARRIER FREQUENCIES

NT CRITICAL FREQUENCIES

NT CYCLOTRON FREQUENCY

NT EXTREMELY HIGH FREQUENCIES

NT EXTREMELY LOW FREQUENCIES

NT EXTREMELY LOW RADIO FREQUENCIES

NT HIGH FREQUENCIES

NT INFRASONIC FREQUENCIES

NT INTERMEDIATE FREQUENCIES

NT IONIZATION FREQUENCIES

NT LOW FREQUENCIES

NT LOW FREQUENCY BANDS

NT MAXIMUM USABLE FREQUENCY

NT MICROWAVE FREQUENCIES

NT NYQUIST FREQUENCIES

NT PLASMA FREQUENCIES

NT RADIO FREQUENCIES

NT RESONANT FREQUENCIES

NT SUPERHIGH FREQUENCIES

NT SWEEP FREQUENCY

NT ULTRAHIGH FREQUENCIES

NT VERY HIGH FREQUENCIES

NT VERY LOW FREQUENCIES

FREQUENCY AMPLIFIERS

U AMPLIFIERS

FREQUENCY ANALYZERS

A hybrid broad-band EEG frequency analyzer for use in long-term experiments. 04 p0411 A73-14847

Texture dependent features recognition in terms of spatial frequencies of remotely sensed multispectral data small sections 05 p0555 A73-17152

Measurement of vibration characteristics by impact testing. 05 p0637 A73-17233

Fasp - A student developed application program. 06 p0671 A73-18265

A spectral analysis method for single radio signals 11 p1331 A73-26101

Frequency synthesizer technology review, discussing direct frequency synthesis and frequency analysis /phase lock/ techniques 14 p1732 A73-29874

The information content of successive RR-interval times in the ECG - Preliminary results using factor analysis and frequency analysis. 14 p1722 A73-30883

Photomixing of the fundamental and reference laser beams during analysis of the frequency spectrum of laser radiation by the method of optical heterodyning 24 p3096 A73-44955

FREQUENCY ASSIGNMENT

A study of frequency sharing between satellite and terrestrial broadcasting systems. 01 p0018 A73-11179

Required carrier-to-interference ratios for frequency sharing between frequency-modulation television signal and amplitude-modulation vestigial sideband television signal. 01 p0018 A73-11181

Satellite charges for a mixed pre-demand-assigned system. 03 p0276 A73-13901

A three channel telemetry system, compatible with the British medical and biological telemetry regulations. 03 p0269 A73-14277

System design, hardware and software of RF interference measurement experiment regarding microwave frequency optimal sharing between ATS-F satellite and terrestrial relay telecommunication 04 p0422 A73-15460

Computerized short- and long term ionospheric propagation forecasting for HF communications, frequency scheduling and broadcasting circuits 09 p1048 A73-21983

Factors affecting the frequency chosen for aircraft to satellite communications. 12 p1472 A73-27667

Satellite communication channels assignment to ships and aircraft, considering automated digital calling method for ship-to-shore communication 12 p1472 A73-27670

Technical factors determining the choice of frequency bands for the links between satellite and coast stations of a maritime communications satellite service. 12 p1473 A73-27674

RF spectrum utilization for optimum communication capacity, considering tradeoff between bandwidth and interference, antenna directivity and wave reflection and scattering effects 13 p1584 A73-29113

A study of frequency sharing between satellite and terrestrial broadcasting systems.

Efficient utilization of orbit/frequency for satellite broadcasting.

Regional and international communication satellite systems, discussing frequencies assignment, power supplies, three axis stabilization trends and military, navigation and TV developments

[DGLR PAPER 73-039]

Effect of double optical resonance on frequency interaction and selection in a gas laser

Interstellar radio communication and the frequency selection problem.

FREQUENCY CONTROL

NT AUTOMATIC FREQUENCY CONTROL
Control of the frequency of Gunn-effect oscillators by a magnetic field

Electromechanical techniques for rapid frequency tuning of lasers.

Four-field parametric frequency selection in stimulated emission lines from nonlinear mirror, noting reflection coefficient

Fast accurate phase lock loop with self calibrating frequency discriminator, showing dynamic response of frequency lock-up

Real time 3-D holographic display, discussing reusable thermoplastic photoconducting recording film and frequency compensation with short laser pulses and acousto-optic modulator

Frequency selection schemes based on combined use of dispersive prism and interferometer in laser resonator

Possibility of smoothly tuning the emission frequency of a mixed-dye laser

Stabilization of relaxation oscillators based on devices with an S-type current-voltage characteristic.

Single mode ion laser tuning over entire emission range via intracavity etalon tilting by piezoelectric drive

Development of cavities for microwave solid state sources.

System for automatic regulation of the constant-absolute-slip mode of an asynchronous electrical actuating element with frequency-modulation control by a thyristor converter

Programmed radiation spectrum control in a ruby laser

Frequency-agile coaxial magnetrons.

Preliminary frequency selection for signal matched filtering.

Selection of the parameters of a rectangular-pulse generator with quartz-crystal controlled frequency

In-flight frequency calibration of IR sensor systems using LEDs.

Frequency distortions of signals in frequency-modulated oscillators with a delayed feedback.

A frequency-tunable mode-locked CW Nd:glass laser.

Near-harmonic integrated oscillators in the 10 MHz to 40 MHz range.

A square-wave generator with digital frequency setting

Information dependent frequency control of an automatic typewriter.

Linear system resonance effects in single loop controlled frequency tank circuit with variable capacitor under variable or constant emf

Gunn diode negative resistance microwave oscillators with simultaneous lower frequency mode and individual tunings of two frequencies

An inverse torsion pendulum with continuous frequency variation for studies of elastic relaxation and fatigue

FREQUENCY CONVERSION

U FREQUENCY CONVERTERS

FREQUENCY CONVERTERS

NT DOWN-CONVERTERS

NT FREQUENCY DIVIDERS

NT FREQUENCY MULTIPLIERS

NT FREQUENCY SYNTHESIZERS

NT PARAMETRIC FREQUENCY CONVERTERS

Design of digital phase meters with intermediate frequency converters

Noise factor and power formula for cooled SHF broadband frequency converters with semiconductor mixer diode

Use of cycloconverters and variable speed alternators as engine starters.

Frequency conversion using the real current-voltage characteristic of a metal-semiconductor contact

Conversion coefficients of optical heterodyne receiver mixer for various amplitude-phase distributions of interfering signal

Self regulated transistorized voltage and frequency converters for multiple motor drives power supply, discussing circuit design, performance characteristics and overload protection

Thermal stability improvement of variable inductance electronic circuits for analog magnitudes conversion to frequencies, noting instrument errors compensation

Equivalent circuits for microwave frequency converter design, noting small and large signal operation and power efficiency of variable capacity diode circuit

Large-signal noise, frequency conversion, and parametric instabilities in IMPATT diode networks.

Deformation of the power spectrum of a random function during frequency translation

Doppler signal detection with negative-resistance diode oscillators.

Combinational noise and interference effects during frequency conversion, noting mathematical methods

Modulation functions and transmission coefficients for static frequency converter representation in form of equivalent multipole networks for reactive loads

Analysis of primary currents in a three-phase/single-phase frequency converter with direct coupling and artificial commutation

Harmonic analysis of voltages and currents at the output of a frequency converter with direct coupling and artificial commutation

Analysis of primary currents and voltages in single-modulation frequency converters

Special features of the suppression of low-frequency modulation in a direct-coupled frequency converter

Digital single sideband mixing circuit for sum or difference frequency conversion in phase quadrature, using exclusive-or logic gates

High-speed frequency count-down circuit using a tunnel diode and a delay line.

Wideband negative resistance by synthesizing parallel tank converter circuit, discussing input and load admittance

Variable speed single- and multi-quadrant drives using thyristor electronic regulating unit with static converter motor and frequency changers

Noise factor and power formula for cooled SHF broadband frequency converters with semiconductor mixer diode

Experimental investigation of a millimeter band frequency converter on n-InSb at 4.2 K.

Josephson junction mixing of monochromatic sources at two microwave frequencies, noting output power dependence on dc bias

Difference frequency generation by optical mixing of two dye lasers in proustite.

Book - Frequency synthesis: Theory, design and applications.

FREQUENCY DISTRIBUTION

Laser mode locking effect on conversion efficiency of beat frequency excitation in multimode emission, using two photon fluorescence method

Influence of inhomogeneities in a nonlinear crystal on the conversion of an image by sum-frequency generation.

AC starter generator featuring variable-to-constant frequency conversion by cycloconverters as switching device for use with aircraft engines

FREQUENCY DISTRIBUTION

Time variable dynamics of plasma beam discharge oscillations frequency spectra

Equipment for determining the amplitude-frequency characteristics of nonlinear elements in the range of low and extra-low frequencies

The fluctuation spectrum of laser radiation in a turbulent atmosphere in the presence of rain

Optimization of input-signal levels during amplification in a TWT

Theory of the electrodiffusion method for measuring the spectral characteristics of turbulent flows

Frequency distribution function for free rotation and uniform angular distribution of molecules, detecting conformations from vibrational spectrum characteristics

Integral Laplace-Fourier transform stability during transient response functions reconstruction from transfer function frequency characteristics in linear circuits

Frequency spectra of the inner and outer structures of wind waves at different stages of wave development

Pulsed CO laser vibrational distribution function time dependent evolution, considering V-V and V-T processes, spontaneous and stimulated emission, electron impact excitation and kinetic heating

Classical theory of spectral distribution of isolated nonlinear oscillations at combined frequencies

Residual geomagnetic field from the satellite Cosmos 49.

Equation of motion derived for laser resonator with frequency dispersion effect on emission kinetics and spectral features, analyzing unsteady /transient/ processes

Construction of the frequency spectrum of a three-degree-of-freedom gyroscope with a flexible rotor shaft and elastic gimbal mountings

Frequency spectrum of cosmic ray intensity and solar activity variations

Optimum operational flow characteristics derivation for control valves based on frequency distribution of relative pressure drop occurring in practical applications

Amplitude predistortion and deemphasis filters, measuring channel noise immunity enhancement by mean square deviation

Steady state lasing stability in ring-type gas laser with symmetrical distribution of three longitudinal modes

Radome insertion phase delay errors due to element impedance, frequency uncertainty, power instability and heat effects

Utilization of human voice for estimation of man's emotional stress and state of attention.

Geomagnetic field polarity reversal mechanism, interpreting frequency distribution by energy exchange between dynamo models and conversion between kinetic and magnetic energies

The frequency dispersion of the transverse electrical conductivity of ionospheric plasma

Asymptotic distribution of the natural frequencies of elastic shells

Harmonic spectral analysis of nystagmus waveform frequency content for clinical vestibular examination via digital computer

High-power broadly tunable difference-frequency generation in proustite.

- The spectrum of fluctuations of laser radiation in a turbulent atmosphere during rain. 13 p1627 A73-28696
- A study of frequency selection and jumping peculiar to some fluidic oscillations. 13 p1603 A73-29034
- Daily variations of the characteristics of beating-type Fe3/Bpc3/pulsations. 13 p1611 A73-29661
- Point-spread functions, line-spread functions, and edge-response functions associated with MTFs of the form negative exp/n-th power of the ratio of spatial frequency to the MTF frequency constant/. 14 p1768 A73-30158
- Investigations of Pi2 micropulsations. I - Frequency spectra and polarisation. II - Relevance of observations to generation theories. 15 p1866 A73-31064
- Optimization of input signal levels in TWT amplifiers. 17 p2134 A73-34319
- Poisson frequency distribution of flare stars in Pleiades, including statistical analysis of photographic amplitudes 17 p2226 A73-34364
- Fatigue strength of materials under a two-frequency load /Review/. 18 p2366 A73-36754
- Theory of two-channel laser action in spectrally inhomogeneous media. I - Noncorrelated frequencies 19 p2437 A73-37958
- Frequency spectra of strong fluctuations of laser radiation in a turbulent atmosphere 19 p2406 A73-38337
- Frequency distribution of the parameters of the diurnal variation of the cosmic ray intensity 21 p2755 A73-40112
- Asymptotic distribution of the eigenfrequencies of elastic shells. 22 p2881 A73-41811
- A meteorological and a geophysical example of the use of the scale autocorrelation coefficient to determine ratios of frequencies present in periodic phenomena. 22 p2883 A73-42542
- Shaping device for frequency analysis of electrical processes in peripheral neural stems and ganglia 22 p2815 A73-42664
- Asymptotic method for approximate elastodynamic plate theories derivation from elasticity equations with application to plate free extensional and forced flexural vibration frequency spectrum [ASME PAPER 73-APMW-44] 22 p2926 A73-42900
- Frequency distribution functions of pulsars, supernovae and sunspot groups relationship to age and lifetime, considering stellar mass and initial luminosity 22 p2915 A73-43033
- Frequency dispersion of transverse electrical conductivity of ionospheric plasma. 23 p2971 A73-43256
- Some physiological mechanisms of alpha-rhythm frequency fluctuations in man under conditions of relative rest 24 p3059 A73-44717
- A mathematical model of real signal spectra 24 p3068 A73-45005

FREQUENCY DIVIDERS

- Quadratically coupled oscillators interaction at semiresonant frequencies, considering time dependent Duffing equation and frequency divider application 13 p1661 A73-29375
- Book - Frequency synthesis: Theory, design and applications. 20 p2542 A73-39143
- CODYMOS frequency dividers achieve low power consumption and high frequency. 21 p2670 A73-41111
- FREQUENCY DIVISION MULTIPLEXING**
- Application of random time and frequency multiplexing to a data collection satellite. 01 p0018 A73-11182
- Deformation of the power spectrum of a random function during frequency translation 06 p0664 A73-17807
- Multiple access analog and digital satellite telecommunication systems, discussing Intelsat /FM/ and Spade /frequency division/ systems 07 p0790 A73-19181
- Optical birefringent multichannel splitting and combining wideband FDM communications filters, considering crosstalk, pulse response, extinction ratio and detuning 08 p0939 A73-21046
- Optical communications links with EDM digital data channels, examining signal optimal reception and noise stability 09 p1048 A73-22043
- Intelsat 4 communications system, discussing radio transponders, earth stations, and multiple access, modulation and multiplexing methods 09 p1051 A73-22700
- Satellite frequency division multiple access communication net, examining channel monitoring and self

- regulating downlink power output for performance improvement 09 p1053 A73-23363
- Convolutional coding for multiple-access satellite communication. 09 p1056 A73-23399
- Modulation distortions during fading in frequency-modulated multichannel radio communication 10 p1187 A73-23740
- Injection-locked IMPATT oscillations applied to F.D.M. microwave transmission. 11 p1338 A73-26285
- Maritime Satellite System with broadband and multibeam dish antennas, assessing FDM communication capability as function of channel quality and ship terminal antenna gain 12 p1473 A73-27679
- Multipath propagation effects on 11, 20 and 37 GHz FM-FDM systems at different path lengths 16 p1284 A73-33711
- Interference into angle-modulated systems carrying multichannel telephony signals. 16 p1983 A73-33742
- Multiple access techniques for the Canadian domestic satellite communications systems. 17 p1214 A73-35305
- Wideband multidrop asynchronous TDM/FDM multichannel data distribution system for space station application, discussing analog and digital buses design 17 p1214 A73-35308
- Increasing the storage density of holographic recording by spatial frequency multiplexing. 20 p2563 A73-38670
- Low pass filter design for FDM and PCM systems, discussing active RC realization techniques and microelectronics model tests 22 p2832 A73-42293
- FREQUENCY MEASUREMENT**
- Output signal-to-noise ratios in frequency measurement system using correlation detector. 01 p0018 A73-11183
- Orbit determination for the scientific satellite in Japan. 01 p0105 A73-11186
- Component errors of digital frequency meter with nonius estimation of measured quantity smaller digits 02 p0167 A73-11863
- Parameter selection scheme for unit measuring frequency deviation as function of voltage, resistance and circuit sensitivity 02 p0149 A73-11864
- Stroboscope-like frequency spectrum examination of short impulses. 03 p0308 A73-13570
- Uncertainties in coherent measurement of the mean frequency and variance of the Doppler spectrum from meteorological echoes. 03 p0279 A73-14525
- Comparative analysis of methods of determination of frequency response in searchless adaptive systems. 04 p0430 A73-15206
- Accurate time and frequency comparisons based on TV frame pulses 06 p0692 A73-17587
- Properties and applications of the iterative synthesizer with a search oscillator 07 p0798 A73-19178
- Far IR molecular lasers evaluation, discussing excitation, line assignment, relaxation, frequency measurement and development predictions 07 p0835 A73-19636
- Determination of the apparatus constant during multifrequency measurements of radio-wave absorption by the A1 method 08 p0939 A73-21303
- Selective amplifier with zero group delay in pass-band phase characteristics for sinusoidal frequency signal measurement 09 p1066 A73-23118
- Digital microwave receiver with passive discriminator for precise and instantaneous pulsed RF signal frequency measurement 10 p1188 A73-24168
- A fast method to determine the noise frequency and minimum group delay of a whistle when the causative spheric is unknown. 11 p1358 A73-26705
- Determining elasticity constants of disc-shaped specimens of material. 13 p1613 A73-28521
- A new zero-beat indicator and its use in frequency measurements 13 p1617 A73-28859
- Equivalence of geoelectric cross sections in the frequency probing method 14 p1750 A73-30835
- Errors in the absolute method of measuring the frequency of difference oscillations 15 p1853 A73-31256
- Determination of the instrument constant in multifrequency measurements of radio wave absorption by the A1 method. 19 p2404 A73-37932

- Lamb-dip-stabilized carbon dioxide laser line frequency separations, discussing beat frequencies, C 12 and O 16 molecular rotation constants and vibration level reduction 21 p2712 A73-40324
- A new technique for designing high-speed frequency counters. 21 p2658 A73-41146
- Diffraction techniques for vibration measurement. [ASME PAPER 73-DET-116] 22 p2859 A73-42081
- Precision comparison of time and frequency by means of TV signals. 22 p2859 A73-42191
- Reconciliation of calculated and measured natural frequencies and normal modes. 22 p2929 A73-43136
- FREQUENCY MODULATION**
- NT FEEDBACK FREQUENCY MODULATION**
- NT FREQUENCY SHIFT KEYING**
- NT PULSE FREQUENCY MODULATION**
- NT PULSE FREQUENCY MODULATION**
- TELEMETRY**
- Transistorized varicap diode frequency modulator circuit with restricted parasitic AM, using phase shift control and frequency multiplication 01 p0022 A73-10031
- Linear response transistorized FM temperature measuring transducer with thermistor, noting low distortion and digital display convenience 01 p0044 A73-10032
- Required carrier-to-interference ratios for frequency sharing between frequency-modulation television signal and amplitude-modulation vestigial sideband television signal. 01 p0018 A73-11181
- Phase switched FM-CW radio altimeter, noting error reduction by controlled switching of phase difference between emitted and echo signals 02 p0165 A73-11526
- Mobile FM-CW radar sounder with scanning capability for high resolution remote sensing in lower troposphere, discussing design and performance 02 p0140 A73-11959
- FM threshold performance of the frequency demodulator with feedback. 03 p0276 A73-13903
- Binary noncoherent FSK communication under influence of bandpass Gaussian noise and linear FM jamming waveform, deriving error probability 03 p0276 A73-13905
- Frequency discriminator use for range measurements with FM radar systems, deriving reflecting target distance relationship to output voltage 03 p0278 A73-14028
- Mathematical expectation of angularly modulated signal in unsteady linear random noise, using Marchenko formula 03 p0278 A73-14074
- Pulse duration-frequency modulation multichannel biotelemetry system for physiological parameter assessment during exercise, noting circuit diagrams of radio transmitter and receiver 03 p0270 A73-14281
- Voltage controlled subcarrier oscillator design and performance for FM/FM multiplex telemetry system for ECG recording during exercise 03 p0271 A73-14293
- FM-CW radar range measurement at 10-micron wavelength. 03 p0278 A73-14459
- The use of tolerance detectors for data protection in the case of FM data transfer 04 p0415 A73-14773
- Phase and frequency tracking accuracy in direct-detection optical-communication systems. 04 p0416 A73-14993
- Influence of external high-frequency modulation of the electron beam on ion heating during beam-plasma interaction 04 p0478 A73-15032
- Multifrequency modulation of electron beam for instability oscillations control and energy transfer to plasma particles 04 p0479 A73-15044
- A compact low-cost electronic time division multiplexer. 04 p0417 A73-15295
- Comparison of coherent and noncoherent detection of phase continuous binary FM signals. 04 p0420 A73-15410
- Single channel per carrier FCM FDMA demand assignment satellite communications system /SPADE/ for INTEL SAT, discussing hardware and software introduction at first terminal 04 p0420 A73-15414
- The nonlinear analysis and design constraints of a multi-filter phase-lock loop. 04 p0421 A73-15434
- Communications technology satellite /CTS/ with transponder and TWT operating into steerable antenna, discussing experiments on TV broadcast, data transmission, FM and transportable terminals 04 p0422 A73-15446

FM Gaussian electromagnetic pulse distortion during reflection from ionospheric model with linear electron density profile and constant collision frequency 04 p0422 A73-15479

Pulsed random process energy spectra methods for spectral distribution of signal power in multichannel AM, FM and PM PCM systems with time division multiplexing 04 p0423 A73-15918

FM noise spectrum measurement in feedback harmonic oscillators with crystal or transmission cavity resonators as discriminator for frequency stability 05 p0556 A73-16164

Discrete frequency modulated signals with frequency shifted identical-envelope pulses, discussing transmission, construction and correlation functions 05 p0550 A73-16778

Frequency modulated laser radiation detection, studying photomultiplier current harmonics, phase/amplitude detector nonlinearities and noise-resonator coupling effects 05 p0585 A73-16782

An IRIG FM-FM telemetry system for the Petrel sounding rocket. 05 p0551 A73-16850

Undistorted short sounding pulse reception at exit from ionosphere obtained by signal carrier frequency modulation 06 p0663 A73-17537

Design of modern semiconductor senders for frequency-modulated directional radio systems. I 06 p0663 A73-17585

Intelligible crosstalk and AM/FM transfer in commercial communications satellites. I 06 p0663 A73-17589

Digitalized or sampled data FM demodulator recursive algorithm synthesis and SNR performance comparison with optimum analog and conventional limiter discriminator demodulators 06 p0664 A73-17712

A sampling FM wide-band demodulator useful for laser Doppler velocimeters. 06 p0673 A73-17786

Modulated laser beam photographic recorder/reproducer system bandwidth and SNR tradeoff alternatives consideration for high dynamic range performance, suggesting FM recording technique superiority 06 p0701 A73-18309

Microwave amplifier with internal negative feedback, using IF output for frequency modulation of mixer oscillator signal 06 p0677 A73-18394

Properties and applications of the iterative synthesizer with a search oscillator 07 p0798 A73-19178

Multiple access analog and digital satellite telecommunication systems, discussing Intelsat /FM/ and Spade /frequency division/ systems 07 p0790 A73-19181

Intrinsic FM noise of Gunn oscillators. 07 p0798 A73-19341

Influence of fluctuations in the tape speed on the accuracy of magnetic recording of measurement signals by the wideband frequency modulation method 07 p0828 A73-20549

Waveguide cavity multistage Gunn reflection amplifiers for FM-CW systems, discussing stabilization techniques, bandwidth, noise, power variation with temperature and group delay distortion 07 p0803 A73-20552

Direct frequency demodulation with CW Gunn and IMPATT oscillators. 07 p0795 A73-20554

Gunn diode characteristics under large and small signal conditions, noting applications for FM oscillators and voltage tuned and magnetically tuned oscillators 08 p0943 A73-20711

Preemphasis for an S-band constant bandwidth FM/FM system. 08 p0939 A73-21085

Oscillator synchronization by FM signal for constant central frequency-sideband phase difference operation 08 p0946 A73-21112

Digital FM signal receiver with postdetector integration, determining error probability as function of input SNR and noise stability 09 p1049 A73-22044

Noiselike FM signals shaping by numerical periodic pseudoeven sequences, analyzing FSK signals 09 p1049 A73-22049

X band Gunn oscillator FM noise spectrum dependence on quality factor of resonant circuit 09 p1062 A73-22322

Digital quartz pressure transducer for FM signal output to interface with digital computer and telemetry, noting insensitivity to temperature and vibration interference effects 09 p1082 A73-22503

Effects of tape flutter on notch noise loading test performance of predetection recording of a frequency modulated carrier. 09 p1087 A73-23367

Digital phase locked loop for FM demodulation in real time, computing SNR for frequency offsets and sinusoidal modulation 09 p1054 A73-23373

Miniature single channel narrow-band differential pulse width modulation-FM crystal controlled transmitter for biomedical telemetry system 09 p1047 A73-23381

A new FM system with a novel modulator design yielding high linearity and thermal stability 09 p1058 A73-23430

Investigation of the mutual ambiguity function of a wideband signal with complex angle modulation 10 p1187 A73-23731

Multichannel wideband FM communication systems, discussing method for channel density increase with reduced linearity requirement and enhanced noise immunity 10 p1187 A73-23732

Modulation distortions during fading in frequency-modulated multichannel radio communication 10 p1187 A73-23740

Influence of signal amplitude changes in systems with phase and frequency modulation 10 p1189 A73-24377

Operational features of an FM rangefinder employing a gas laser 10 p1229 A73-24602

Noise immunity of quasi-coherent reception of phase-shift keyed signals with respect to additive fluctuation noise. 10 p1191 A73-24938

Self excited LC and RC oscillator networks based on FETs, discussing frequency tuning and FM methods 10 p1197 A73-24941

A method for smoothing level fluctuations caused by echoes in the case of FM directional radio links 11 p1328 A73-25344

FM laser noise effects on optical Doppler radar systems. 11 p1333 A73-26639

System for automatic regulation of the constant-absolute-slip mode of an asynchronous electrical actuating element with frequency-modulation control by a thyristor converter 12 p1460 A73-26786

Stabilized two-pulse operation of the phase-modulated, frequency-doubled laser. 12 p1504 A73-26831

Discrete wideband FM signals optimal filter synthesis by coupling two nonlinear servosystems 12 p1467 A73-26869

Certain features of the analysis of a crystal-controlled FM oscillator at high modulating voltage levels 12 p1477 A73-26872

Investigation of the permissible power level of FM radio interference at the input of the frequency converter in an FM-signal receiver 12 p1477 A73-26873

Multiple target CW FM Doppler radar with solid state devices and CRT indicator, noting range resolution advantage over pulse radar 12 p1469 A73-27164

Ranging and data transmission using digital encoded FM-'chirp' surface acoustic wave filters. 12 p1470 A73-27571

Analysis of the distortions of an FM signal in a servo loop with external control 12 p1470 A73-27576

An electrooptical method for storage of weak linear FM signals 12 p1470 A73-27577

Experimental investigation of the AM-FM distortions of a signal passing through a linear filter 12 p1481 A73-27589

The concept of an installation for measuring partial reflections with the aid of the FM-CW procedure and the principle of measurement involved 12 p1486 A73-27764

Correlation and indeterminate functions of signals with discrete frequency-time structure, noting linear frequency modulation of signal element 13 p1583 A73-28669

Low noise temperature measurement converter with electrical oscillation frequency output, presenting computer calculations of sensor components 13 p1617 A73-28860

Echo signal spectral compression in airborne FM Doppler radar measurement, allowing for flight trajectory and target surface characteristics 13 p1584 A73-28889

Influence of the nonlinearity of the phase characteristic of the RF signal path in an FM receiver on the signal distortions 13 p1584 A73-28897

Special features of the suppression of low-frequency modulation in a direct-coupled frequency converter 13 p1593 A73-28943

Some investigations on frequency demodulating systems with fluidic jet deflection amplifiers. 13 p1572 A73-29046

The design and applications of highly dispersive acoustic surface-wave filters. 14 p1732 A73-29933

Ranging and data transmission using digital encoded FM-'chirp' surface acoustic wave filters. 14 p1733 A73-29935

Interaction between a plasma and an electron beam modulated by low-frequency oscillations. 14 p1781 A73-30335

Noise immunity of the optimal noncoherent reception of an FM signal in the presence of fluctuations in the synchronization channel 14 p1729 A73-30558

Undistorted short sounding pulse reception at exit from ionosphere obtained by signal carrier frequency modulation 16 p1978 A73-32761

Hybrid optoelectronics - High frequency modulation and detection of light by semiconductor sources and sensors. 16 p1978 A73-32886

The application of digital techniques to a VOR signal generator. 16 p1979 A73-33405

Multipath propagation effects on 11, 20 and 37 GHz FM-FDM systems at different path lengths 16 p1981 A73-33711

Interference into angle-modulated systems carrying multichannel telephony signals. 16 p1983 A73-33742

Propagation of frequency-modulated pulses in a randomly stratified plasma. 17 p2214 A73-34095

Distortions of signal frequency in FM oscillators. 17 p2136 A73-35154

Frequency deviation equations for FM gas laser with modulation achieved by resonator optical length variations 17 p2184 A73-35168

Digital step transform for airborne radar linear FM signal pulse compression, reducing data memory requirements 17 p2123 A73-35237

Use of pulse compression in mapping-type radars. 17 p2127 A73-35632

Susceptibility measurements at high frequency - A versatile and sensitive apparatus. 17 p2176 A73-35771

FM-CW method application to partial reflection measurements of ionospheric electron density to avoid man-made interference and interpretation difficulties from frequency spectrum broadening 18 p2305 A73-36008

New developments in FM-CW radar sounding. 19 p2405 A73-38210

COS/MOS phase-locked-loop - A versatile building block for micro-power digital and analog applications. 20 p2534 A73-38657

FM distortion of a TV signal and subcarriers due to bandpass filtering and additive Gaussian noise. 20 p2523 A73-38722

Frequency modulation of a gas laser 20 p2574 A73-39730

Thermally induced FM noise in Gunn oscillators and jitter in Gunn-effect digital devices. 21 p2660 A73-40096

Baseband modeling and distortion equalization of the DeLange FM oscillator by functional methods. 21 p2662 A73-40337

Effects of modulation nonlinearity on the range response of FM radars. 21 p2650 A73-40341

A method of reducing the influence of interference on the operation of a correlation interferometer 21 p2667 A73-41511

On the derivation of Zone I spectra for a pulsed finite-amplitude source operating in a nonviscous non-dispersive fluid medium. 22 p2885 A73-41819

Analysis of a frequency-modulated tunnel-diode oscillator. 24 p3072 A73-44941

FREQUENCY MULTIPLIERS

Transistorized varicap diode frequency modulator circuit with restricted parasitic AM, using phase shift control and frequency multiplication 01 p0022 A73-10031

Phase-frequency characteristics of a tunnel-diode regenerative frequency multiplier 01 p0026 A73-11263

Separate generation of odd and even harmonics of a fundamental frequency, with the aid of pulse circuits. 06 p0663 A73-17576

Frequency multipliers for the millimeter wave band employing gallium arsenide diodes. 07 p0802 A73-20146

GaAs diffused diode, ECL-1350. 07 p0804 A73-20570

Narrow band and broad band step-recovery diode frequency multipliers for microwave power generation. 08 p0947 A73-21138

Frequency multiplication due to nonparabolicity of dispersion law in semiconductor structure subbands, noting electromagnetic signal transformation 09 p1133 A73-22665

Multiplex even harmonic frequency multipliers using nonlinear magnetic reactors with bridge rectifiers, considering output signal waveforms 12 p1477 A73-26788

A tunnel diode regenerative frequency multiplier with a high multiplication factor. 13 p1591 A73-28734

Probability of error in selecting the information signal and the synchronization signal by frequency multiplication 13 p1584 A73-28892

Varactor frequency multipliers of the parallel type. I - Spectrum analysis of the voltage on a partially open-circuited varactor. 15 p1849 A73-30991

Burst-mode frequency-doubled YAG:Nd³⁺/ laser for time-sequenced high-speed photography and holography. 15 p1886 A73-32384

Optimal parallel-type varactor frequency multiplier calculation for reverse-biased conditions in terms of nonlinear conductance loss and diffusion capacitance Q factor 16 p1991 A73-33981

Phase-frequency responses of a tunnel diode regenerative frequency multiplier. 17 p2134 A73-34316

Design of nonlinear resistive networks with prescribed input-output behavior. 17 p2145 A73-35378

Book - Frequency synthesis: Theory, design and applications. 20 p2542 A73-39143

Engineering design and optimization of the parameters of frequency doublers for the visible range. 20 p2573 A73-39685

Bias controlled step recovery diode as combined frequency multiplier and analog phase shifter for applications in microwave phased array antenna systems 21 p2663 A73-40668

Limitations for mode-locking enhancement of internal SHG in a laser. 21 p2714 A73-40759

Russian book on semiconductor radio transmitter design covering power amplifiers, frequency multipliers, oscillators and Gunn effect devices for sub-microwave frequencies 21 p2666 A73-41424

Two-loop frequency multipliers employing the barrier capacitance of a p-n junction and exhibiting maximum energetic indices 24 p3071 A73-44592

An analytical solution of the problem of a frequency tripler employing a varactor diode with an arbitrary voltage-charge characteristic 24 p3072 A73-44927

FREQUENCY RANGES

NT OCTAVES

NT RADIO RANGE

Frequency-selective surfaces for multiple-frequency antennas Design data plus experimental results. 14 p1737 A73-30625

Synchronization range of phase control systems 21 p2665 A73-41271

FREQUENCY REGULATION

U FREQUENCY CONTROL

FREQUENCY RESPONSE

Linear rapid frequency settling time solid state voltage controlled oscillators (VCO) for electronic countermeasure and B-scan tracking radar applications 01 p0024 A73-10723

An earphone coupling system for acute physiological studies. 01 p0013 A73-10829

Instrument requirements for eddy correlation measurements. 01 p0052 A73-11057

Phase-frequency characteristics of a tunnel-diode regenerative frequency multiplier 01 p0026 A73-11263

Quasi-steady heat transfer equation for frequency response of wedge shaped hot film sensors for flow temperature, velocity and turbulence measurement 02 p0166 A73-11711

Design and fabrication of helix-like strip meander line delay equalizer in printed circuit technology, noting group delay and insertion loss frequency responses 02 p0145 A73-11823

Electromagnetic near field energy flow characteristics of dipole/monopole receiving rod antenna, investigating frequency dependence of antenna effective area shape 02 p0145 A73-11824

A linear approach to the analysis of a force control system incorporating a hydraulic pressure-ratio valve. 02 p0132 A73-12002

Amplitude-frequency and stability characteristics of parametric amplification by triple-frequency interaction in nonlinear nonautonomous system 02 p0147 A73-12491

Gain and frequency characteristics of a 20 mW C.W. water vapour laser oscillating at 118.6 microns. 02 p0177 A73-12724

Experimental investigation of the frequency response of a planar rigid airfoil 03 p0241 A73-12915

Diurnal and latitudinal variations and frequency dependence of scintillation due to ionospheric irregularities, using rms electron density fluctuation and transverse scale size model 03 p0275 A73-13643

Data analysis criteria and instrumentation requirements for the transient measurement of mechanical impedance. 03 p0343 A73-13837

Time-averaged power stage models transient and frequency responses characterization and circuit component values derivation for switched dc-dc converters design 03 p0282 A73-13927

Parasitic oscillations in external excitation oscillators due to internal feedback in transistor, investigating frequency dependence of stability coefficient in common emitter stage 03 p0284 A73-14032

Silicon violet solar cell energy conversion efficiency improvement through extended spectral response and increased fill factor 03 p0254 A73-14212

The effect of frequency upon the fatigue-crack growth of Type 304 stainless steel at 1000 F. 04 p0459 A73-14689

Low-sensitivity, frequency-selective amplifier circuits for hybrid and bipolar fabrication. 04 p0427 A73-15054

Nonlinear radio-frequency response of a non-uniform plasma slab-condenser system with realistic density and velocity profiles. 04 p0479 A73-15189

Comparative analysis of methods of determination of frequency response in searchless adaptive systems. 04 p0430 A73-15206

Exact frequency dependent complex admittance of the MOS diode including surface states, Shockley-Read-Hall (SRH) impurity effects, and low temperature dopant impurity response. 04 p0427 A73-15347

Wideband microwave device with diode and single component correction circuits Q factors measurement from frequency dependence of input traveling wave coefficients 04 p0429 A73-15927

Class of stepped-reflector antennas with improved frequency response. 05 p0547 A73-16159

Aircraft antisid system technical history and evolution, presenting frequency response of three-way configuration [SAE PAPER 720868] 05 p0534 A73-16651

GaAs Gunn diode LSA operation mode in multiloop circuit to extend high frequency limit 05 p0558 A73-16788

Recursive MTT radar filter design for sharp spectrum rolloff and flat pass band, investigating clutter rejection performance vs spectral spread 05 p0558 A73-16808

The determination of free-body responses of a structure from constrained test data. 05 p0635 A73-16928

Circuit parameters and performance of monolithic IC operational amplifiers, noting data sheets with voltage and temperature ranges and frequency response characteristics 06 p0672 A73-17450

Determination of the transfer function of a digital filter from the real part of the frequency response. 06 p0674 A73-17811

Response characteristics of photodiodes, phototransistors and photoresistors in near IR range, showing output signal levels as function of wavelength and illumination intensity 06 p0692 A73-17837

Mean square error automatic equalizer for synchronous data transmission by gradient projection method for parameter optimization in discrete frequency domain, noting algorithm convergence 06 p0665 A73-18141

Experimental investigations on the impedance behavior of a cylindrical antenna in a collisional magnetoplasma. 06 p0729 A73-18186

High speed, high performance /Hg,Cd/Te photodiode detectors. 06 p0667 A73-18314

Cut-off frequency calculation for TE and TM modes in doubly ridged circular and elliptical microwave waveguides, using Mathieu function and eigenfunctions 06 p0669 A73-18736

Compact YIG bandpass filter with finite-pole frequencies for applications in microwave integrated circuits. 06 p0678 A73-18742

Si varactor diode series resistance resonance measurements in UHF band, noting approximate invariance with frequency 06 p0678 A73-18842

Symphonic satellite radio link equipment design and performance, noting transmission characteristics and frequency response of repeater 07 p0821 A73-18965

Type L linear multivariable systems with state integral feedback control, deriving optimal conditions for zero steady state error compensatory tracking by frequency domain techniques 07 p0805 A73-19133

Precision design of millimeter-wave band-pass filter. 07 p0799 A73-19371

Synthesis of a system with a Pi-shaped amplitude-frequency characteristic and a 'zero' equivalent phase-frequency characteristic 07 p0794 A73-20293

Common emitter/common base cascade amplifier overall gain and frequency response dependence on first transistor parameters 07 p0802 A73-20301

Identification of large structures using data from ambient and low level excitations. 07 p0916 A73-20431

Characteristics of beam- and membrane-type strain-gauge sensors of linear acceleration 07 p0826 A73-20529

Operational tests of the K-115 loop oscillograph 07 p0828 A73-20548

A wide-band low-shape-factor amplifier module using an acoustic surface-wave bandpass filter. 07 p0804 A73-20557

Measurement of the dielectric constant of polyvinyl chloride at very low frequencies, and influence of the superposition of a continuous voltage 08 p0942 A73-20648

Frequency response of a dynamic system with statistical damping. 08 p0950 A73-20715

Improvement of frequency characteristics of digital filters. 08 p0945 A73-20801

Millimeter-wave frequency response of hot electrons in n-type GaAs. 08 p0994 A73-20845

Application of equiangular conical antennas with thick leads 08 p0938 A73-20963

Mathematical description of nonlinear systems with distributed parameter 08 p0938 A73-20964

Low pass symmetrical filters of composite attenuation with infinite and flat points of attenuation around a given frequency 08 p0945 A73-20967

Establishment of a relationship between the frequency and contrast characteristics of objects on aerial photographs and the resolving power 08 p0963 A73-21024

Nonlinear filter with a Pi-shaped amplitude-frequency characteristic 08 p0946 A73-21110

Rytov method to predict random vibration amplitude and phase fluctuations range and frequency dependence in Mintzer region, noting applicability domain 08 p0988 A73-21193

Theory of a generalized Helmholtz resonator. 08 p0952 A73-21471

Resistive MOS-gated diode light sensor. 08 p0948 A73-21477

Application of the numerical study of random time series to the analysis of the electroencephalogram of the normal infant 08 p0935 A73-21540

Frequency criteria for the absolute stability and instability of pulse-width modulated control systems 08 p0951 A73-21544

Phase-amplitude and amplitude characteristics of a regenerative parametric amplifier 08 p0948 A73-21555

Analysis of transient visual sensations above the flicker fusion frequency. 08 p0932 A73-21566

Nozzle-target system geometry and gas dynamics parameters effect on supersonic underexpanded jets interaction with walls, noting frequency response and pressure oscillations 08 p0927 A73-21610

Equivalent circuit of unbent p-PbS point diodes 09 p1061 A73-22022

Lamb dip measurements on low pressure CO laser vibrational-rotational lines, determining line widths, velocity-changing collision rate and saturation intensities with curve fitting 09 p1090 A73-22078

RC planar distributed networks one and two dimensional analysis techniques and frequency response characterization, noting FORTRAN program use 09 p1067 A73-22309

Variation of atmospheric radio noise level with sunspot number. 09 p1051 A73-22493

- Digital pressure transducer based on vibrating cylinder frequency response to pressure changes, discussing operational principles and applications
09 p1082 A73-22502
- Propagation mode deduced from signal strengths in the VHF band on the trans-equatorial path.
09 p1051 A73-22749
- A frequency response analysis of fusomotor-driven muscle spindles.
09 p1041 A73-22934
- Least-squares monotonic lowpass filters with sharp cutoff.
09 p1065 A73-23093
- Moving-target-indicator recursive radar filter using bucket-brigade circuits.
09 p1065 A73-23096
- Microstrip bandpass filters with reduced radiation effects.
09 p1065 A73-23098
- A linear voltage-tunable distributed null device.
09 p1066 A73-23246
- The complex digital filter and its applications in digital signal processing.
09 p1058 A73-23425
- Design and manufacture of delay equalized comb-line filters.
10 p1193 A73-23608
- Acoustic emission studies of large advanced composite rocket motor cases.
10 p1288 A73-23967
- Linear multivariable control systems - A survey.
10 p1201 A73-24058
- Microwave characteristics of ion-implanted bipolar transistors.
10 p1194 A73-24156
- Narrow band microwave active bandpass filter with inverted-common-collector transistor circuit, discussing design algorithm, insertion loss, stability, sensitivity and frequency selectivity
10 p1201 A73-24169
- Study of ionospheric phase distortion at Ahmedabad.
10 p1188 A73-24170
- Determination of eigenvalues in a class of waveguides of doubly connected cross section.
10 p1249 A73-24392
- Synthesis of nonrecurrent digital filters utilizing the knowledge of the spectral characteristics of the input signal
10 p1195 A73-24421
- A numerical algorithm to design multivariable low-pass equiripple filters.
10 p1202 A73-24600
- Iterative computer-aided design of optimum cascaded digital recursive filter, using unconstrained Fletcher-Powell algorithm for frequency domain synthesis
11 p1327 A73-25189
- Determination of the maximum scan-gain contours of a beam-scanning paraboloid and their relation to the Petzval surface.
11 p1328 A73-25651
- Frequency dependence of circular polarization in three compact radio sources.
11 p1419 A73-25777
- Ultrasonic investigation of the nematic-isotropic phase transition in MBBA.
11 p1409 A73-26213
- InSb and Ga-doped Ge bolometers performance tests, discussing detector circuitry and dc, noise and responsivity measurements
11 p1368 A73-26512
- Transversely isotropic /anisotropic/ elastic beam bending and torsion, determining frequency dependent compliances by approximate analytic solution via variational method
11 p1447 A73-26655
- Frequency response of helix and coupled cavity traveling wave tubes and amplifiers power output, discussing electronic countermeasures and space communications
11 p1339 A73-26692
- Direct conversion a.s.b. receivers - A comparison of possible circuit configurations for speech communication.
12 p1467 A73-26800
- Frequency selective coupler with thin film waveguides in periodic medium, discussing bandwidth and coupling factor from Brillouin diagram
12 p1504 A73-26827
- Frequency characteristics of directional loop-type bandpass filters
12 p1477 A73-26870
- Series-fed antennas principal beam direction and grating lobes buildup as function of antenna and feed characteristics, considering frequency dependence
12 p1469 A73-27041
- Considerations about jump effect in microwave power amplifier.
12 p1478 A73-27073
- Design and performance of deflected-beam electron-bombarded semiconductor amplifiers.
12 p1478 A73-27113
- Influence of a SHF field on the inhomogeneities of a nonequilibrium plasma from a low-pressure gas discharge
12 p1528 A73-27304
- Frequency method of synthesis for an active dynamic vibration damper
12 p1525 A73-27948
- Silicon semiconductor resistance strain gage intrinsic thermal noise characteristics at 20 Hz-10 kHz, noting 1/f type as dominant noise component in audio frequency range
13 p1611 A73-28021
- A computer program for filter design having arbitrary magnitude specifications in the frequency domain.
13 p1587 A73-28085
- Stationary multiport networks frequency response and representation by equivalent circuits
13 p1589 A73-28122
- Viscous fluid sloshing in rectangular vessel, studying forced oscillations, ejected flow and frequency equation based on Navier-Stokes equations and boundary conditions
13 p1600 A73-28444
- Flat circular acoustic transducer for pressure spectrum analysis, deriving flow noise response correction factor in terms of polynomial coefficients and frequency-dependent constants
13 p1613 A73-28492
- Synthesis of regenerative amplifiers with isothermal approximation of the amplitude-frequency characteristics
13 p1592 A73-28896
- Response of a jet to a pressure gradient and its relation to edgetones.
13 p1603 A73-29035
- Mean frequency response characteristics of graphical smoothing operator for latitude observations analysis
13 p1683 A73-29099
- Relaxation spectra of niobium irradiated at low temperature.
13 p1638 A73-29455
- Rainfall crosspolarization at microwave frequencies with differential phase shift and attenuation, considering rain models
13 p1587 A73-29670
- On linear parasitic array of dipoles with reactive loading.
14 p1734 A73-30203
- Frequency-domain criteria for stability of a class of nonlinear stochastic systems.
14 p1739 A73-30506
- A comparison of silicon and gallium arsenide large signal IMPATT diode behaviour between 10 and 100 GHz.
15 p1850 A73-31131
- Some properties of the amplitude frequency characteristics of linear automatic control systems and their control quality under random influences
15 p1854 A73-31695
- Response of thermally controlled, vibrating piezoelectric quartz to the deposition of multiple metal layers
15 p1924 A73-31843
- X band oscillators for microwave generation based on silicon avalanche diodes, presenting power and efficiency dependence on frequency and bias current
15 p1851 A73-32160
- Impedance of a short cylindrical dipole antenna in a hot uniaxial plasma.
15 p1845 A73-32237
- Cup anemometer input/output frequency characteristics, determining nonlinear behavior via inertia considerations
15 p1879 A73-32345
- Bucket-brigade shift-register operation-exact correlation between experimental data and a computer model.
16 p1988 A73-33397
- Small-signal modelling and characterization of microwave transistors.
16 p1990 A73-33687
- Application of frequency analysis to ultrasonic non-destructive testing
16 p2016 A73-34014
- Phase-frequency responses of a tunnel diode regenerative frequency multiplier.
17 p12134 A73-34316
- Book - Design of modern transistor circuits.
17 p2134 A73-34458
- The visual cortex as a spatial frequency analyser.
17 p2112 A73-34840
- State-space analysis of a magnetically tuned IMPATT oscillator lumped model.
17 p2136 A73-34973
- A frequency response approach to flying qualities criteria and flight control system design.
17 p2105 A73-35073
- Book - Introduction to servomechanism system design.
17 p2110 A73-35275
- Field penetration through a flush mounted coaxial aperture - Variational calculation.
17 p2127 A73-35630
- Magnitude error bounds for sampled-data frequency response obtained from the truncation of an infinite series.
17 p2145 A73-35640
- Limit cycles resulting from quantization in digital control systems.
17 p2145 A73-35642
- The effects of the microwave structure parameters on the behavior of X-band Gunn oscillator.
17 p2142 A73-35650
- A comparison of time- and frequency-domain measurement techniques in antenna theory.
17 p2129 A73-35702
- Quantitative studies on optokinetic nystagmus in the monkey.
18 p2273 A73-36459
- Method for plotting frequency cutoff measurements for GaAs varactor diodes.
18 p2292 A73-36596
- Synthesis of a system of pi-shaped amplitude-frequency and 'zero' equivalent phase-frequency characteristics.
18 p2291 A73-37130
- Common emitter/common base cascode amplifier overall gain and frequency response dependence on first transistor parameters
18 p2294 A73-37138
- Application of the coherence function to acoustic noise measurements.
19 p2458 A73-37284
- Transient and steady state sound absorption coefficients of fiberglass and polyurethane foam.
19 p2459 A73-37286
- Spatial frequency channels in human vision and the threshold for adaptation.
19 p2394 A73-37416
- Electro-mechano-hydraulic servovalve system, calculating dynamic frequency response in vibrating accelerated field under external disturbance
19 p2388 A73-37670
- Oscillations in nonlinear feedback systems.
19 p2414 A73-38069
- Parallel resonator with a resistance and a frequency dependent negative resistance realized with a single operational amplifier.
19 p2411 A73-38536
- Realization of canonical bandpass filters with frequency-dependent and frequency-independent negative resistances.
19 p2412 A73-38537
- Seismometer compensation for broadband, low-level acceleration measurements.
20 p2563 A73-38773
- [AIAA PAPER 73-828] The selection of test frequencies for system fault diagnosis.
20 p2586 A73-38802
- [AIAA PAPER 73-864] Precision gimbal rate control for single gimbal control moment gyro /CMG/ pointing control systems, designing for high frequency response, bandwidth and output torque dynamic range
20 p2587 A73-38808
- [AIAA PAPER 73-871] Frequency response of short pressure probes.
20 p2564 A73-38872
- Operational temperature and frequency effects on radial driving point mechanical impedance of damped thin walled ring with mass segments attached by viscoelastic material
20 p2616 A73-39051
- Frequency-domain analysis of laser Doppler signals for estimation of turbulence parameters.
20 p2572 A73-39130
- Superconducting Josephson junction power flow relations dependence on harmonically or subharmonically phase locked autonomous frequency
20 p2536 A73-39411
- Optimal matching by using band filters
20 p2537 A73-39452
- Sensitivity and resolution of panoramic analyzers
20 p2537 A73-39455
- Design of MOS-transistor integrated-circuit amplifiers
21 p2660 A73-40021
- Frequency dependence of radiation-pattern orientation in phased-array antennas
21 p2661 A73-40196
- Effects of non-linearity due to large deflections in the derivation of frequency response data from the impulse response of structures.
21 p2783 A73-40287
- Frequency-dependent parasitic modulation component effects on null distortion in spectrometer and temperature measurement accuracy
21 p2700 A73-40541
- The design of a wide band wide scan-angle waveguide radiating element.
21 p2652 A73-40660
- Transient frequency response analysis and far field measurement of linear phased array with tandem series feed network, noting instantaneous bandwidth
21 p2653 A73-40673
- AC conductivities of amorphous Ge-As-Te and Ge-As-Se systems.
21 p2753 A73-41119

Pure-tone equal-loudness contours for standard tones of different frequencies. 21 p2645 A73-41176

Optimization of electronic circuits with characteristics depending on a continuously varying parameter 21 p2666 A73-41311

Method of calculating the amplitude and phase-amplitude characteristics of high-frequency amplifiers 21 p2666 A73-41314

Polynomial approximations of the characteristics of low-sensitivity filters 21 p2666 A73-41315

Specific problems of the dynamics of composite systems 21 p2788 A73-41603

Frequency response of laser scanners and its optimization through apodization. 21 p2717 A73-41610

Electroexplosive device pin-pin firing frequency mathematical modeling and prediction based on RF impedance data obtained nondestructively by automatic network analyzer 22 p2822 A73-41793

Antenna radiation pattern measurement using time-to-frequency transformation/TFT/ techniques. 22 p2831 A73-41842

High loop gain operational amplifiers voltage changes as slewing rates using nonlinear circuit model, discussing equivalent circuits, frequency characteristics and bandwidth 22 p2832 A73-41896

On the design of wave digital filters with low sensitivity properties. 22 p2835 A73-41950

Sinusoidal response of composite-material plates with material damping. 22 p2919 A73-42082

[ASME PAPER 73-DET-120] Structural sensitivity transfer matrix for dynamic multiple link control system response minimization with corrections within frequency range 22 p2836 A73-42613

Identification of damping coefficients in multidimensional linear systems. 22 p2926 A73-42899

[ASME PAPER 73-APMW-43] Applications of digital frequency warping to unequal bandwidth and Vernier spectrum analysis. 23 p2952 A73-43312

Interpolation using finite duration impulse response digital filters. 23 p2952 A73-43313

Dynamic range and frequency response of the vortex rate sensor. 23 p2942 A73-43406

The design of digital fluidic components and systems - A review. 23 p2945 A73-43433

Junction or Schottky gate type FET power gain and high frequency limitations from γ parameters calculation, using analog RC transmission line as equivalent network 23 p2963 A73-43452

Certain problems of frequency settling in ideal filters 23 p2959 A73-43514

Substrates with end effect in shorted slot, measuring normalized inductive reactance dependence on thickness to wavelength ratio 23 p2954 A73-44068

Slot microwave transmission line with thick metal coating on dielectric substrate, calculating phase constant variation with frequency, slot width and coating thickness 23 p2954 A73-44069

TEM-TE coupled transmission line model for microstrip, calculating frequency-dependent wave dispersion curves for comparison with experiment 23 p2964 A73-44073

Dipole antenna with variable capacitance diodes for wideband tuning, calculating and measuring input impedance frequency response 23 p2960 A73-44110

Frequency to time domain sensitivity matrix for equivalent tolerance field and response error evaluation, using Fourier transform 23 p2955 A73-44114

Coupling coefficient/frequency characteristics of rectangular dielectric waveguide channel dropping coupled line filter for millimeter wave 23 p2961 A73-44118

Ac electroconductivity of polycrystalline Co-Fe ferrite as function of temperature, composition and frequency at 1 kHz-200 MHz 24 p3119 A73-44403

Experimental investigation of the frequency dependence of the steady-state noise temperature of reverse-biased tunnel diodes between 0.001 and 30 MHz 24 p3072 A73-44931

Investigation of the input impedance of an emitter-input transistor amplifier at near-cutoff frequencies 24 p3072 A73-44935

Application of the sensitivity theory to an analysis of the high-frequency components of motion 24 p3074 A73-45096

Frequency methods for simulation, analysis and identification of multiply-connected dynamic systems with delay 24 p3074 A73-45097

The determination of whistler nose-frequency and minimum group delay and its implication for the measurement of the east-west electric field and tube content in the magnetosphere. 24 p3087 A73-45210

Darlington composite transistor frequency properties concerning alpha and beta cut-off points and high frequency power gain in common-emitter configuration 24 p3073 A73-45481

FREQUENCY SCANNING

Generation spectra of a ruby laser with frequency scanning 09 p1095 A73-22680

Frequency hopping principle for precision L band DME as complementary aid to microwave landing system 15 p1911 A73-32490

FREQUENCY SHIFT

Some features of the Leiden radial velocity instrument. 01 p0047 A73-10516

Laser Doppler shift velocity correlation meter operation in turbulent flow analyzed by optical mixing theory 02 p0153 A73-12049

Radial and nonradial oscillation modes of gaseous polytrope with toroidal magnetic field, using variational principle 02 p0217 A73-12400

The interpretation of absorption-line shifts in the solar spectrum. 03 p0377 A73-14407

Stationary turbulence of a parametrically unstable plasma. 04 p0480 A73-15474

Phononless lines shift and broadening during electron phonon interaction in lanthanum trifluoride-Nd crystal, obtaining temperature dependence of non-radiative transition probability 04 p0484 A73-15566

Nonlinear interaction between circular coherent light and modulating electromagnetic waves in presence of quadratic electrooptical effect, noting frequency shift 04 p0459 A73-15921

The Doppler frequency shift in ionospheric propagation of radio waves 05 p0548 A73-16260

Discrete frequency modulated signals with frequency shifted identical-envelope pulses, discussing transmission, construction and correlation functions 05 p0550 A73-16778

Electro-optical media for initial light radiation frequency shift maximum, analyzing circular light/modulating wave interactions 05 p0551 A73-16780

Frequency shift in a mode-selected dye laser. 05 p0586 A73-17225

Violet shift of the H alpha absorption line of the hydrogen-depleted star HD 30353 07 p0877 A73-19598

Some problems of statistical estimation of a signal source in a dispersive medium 07 p0792 A73-19912

Time behavior of the internal Q switching in GaAs lasers under electron-beam excitation. 09 p1092 A73-22245

Flow velocity measurement method based on laser light frequency Doppler shift in scattering experiment on particle seeded liquid, presenting velocity profiles 09 p1094 A73-22314

Modification of the phase methods for investigation of non-stationary processes in the ionosphere, magnetosphere and interplanetary space. 09 p1078 A73-22835

Effects of plasma temperature on the frequency shift in resonant cavities. 09 p1131 A73-22907

Spectral shift between components of homogeneous /radiation or shock/ line, using ring laser spatial and frequency burnout effects 10 p1228 A73-24464

New method of increasing the emission frequency of high-power laser pulses. 10 p1229 A73-24769

A dynamic transformation method for modal synthesis. 11 p1440 A73-25525

[AIAA PAPER 73-396] Injection-locked IMPATT oscillations applied to F.D.M. microwave transmission. 11 p1338 A73-26285

Multipaths by diffusion on the ground and application to the transmission of digital messages affected by jumps of the carrier frequency 14 p1725 A73-29732

Experimental study of fluctuations of the difference frequency in a ring laser 16 p2024 A73-32895

Nonlinear frequency shift and damping stabilization mechanisms of unstable plasma waves in hot beam-cold plasma system 16 p2043 A73-34058

Reference radiation frequency shift for holographic interferometry of vibrating objects 17 p2172 A73-35428

Susceptibility measurements at high frequency - A versatile and sensitive apparatus. 17 p2176 A73-35771

On the stabilization of explosive instabilities by nonlinear frequency shifts. 17 p2218 A73-35822

Spectral shift between components of homogeneous /radiation or shock/ line, using ring laser spatial and frequency burnout effects 19 p2438 A73-38136

Light shift and light broadening in the Rb-87 maser. 20 p2572 A73-38861

Laser induced red-blue energy transfer upconversion in Pr³⁺/doped lanthanum fluorides via excitation annihilation involving pairs of ions 21 p2715 A73-40934

Light spectral width and constant frequency shift during spontaneous diffusion in ideal gas for fixed photon wave 22 p2885 A73-41721

On the infrared emission of H II regions due to dust. 22 p2908 A73-42314

Minimum detectable frequency deviations in output of He-Ne laser stabilized by external methane absorption cell 23 p2989 A73-44366

FREQUENCY SHIFT KEYING

Binary noncoherent FSK communication under influence of bandpass Gaussian noise and linear FM jamming waveform, deriving error probability 03 p0276 A73-13905

Partially coherent detection of binary FSK system with adaptive receiver, determining optimum and sub-optimum estimators of channel parameters for phase and bit synchronization 03 p0277 A73-13909

Effects of a finite-width decision threshold on binary CPSK and FSK communication systems. 03 p0277 A73-13911

The performance of a noncoherent FSK receiver preceded by a bandpass limiter. 04 p0416 A73-14992

Detection of multichannel FSK signals using chirp dispersion method. 04 p0419 A73-15407

Programmable, digital, rapidly frequency-shift-keyed, high-frequency generators for driving acoustooptical light deflectors 05 p0586 A73-17239

The effect of impulsive noise on FSK digital communication. 08 p0938 A73-20834

Noiselike FM signals shaping by numerical periodic pseudorandom sequences, analyzing FSK signals 09 p1049 A73-22049

Noise immunity evaluation for noncoherent demodulators or FSK and PSK signals in short wave channels, using minimum a priori information on additive noise properties 13 p1592 A73-28899

Choice of the duration of an elementary signal in the presence of fluctuations in the synchronization channel 24 p3067 A73-44605

FREQUENCY STABILITY

Frequency stabilization of Q factor modulated ruby laser with mode selection, using rotating prism and quartz selecting element 01 p0060 A73-11087

Stable frequency and synchronicity alterations in the discharges of cortical neuron populations in feedback experiments 01 p0010 A73-11445

Standing wave approximation of distributed dual frequency parametric oscillators consisting of semiconductor diodes and transmission line in steady state 02 p0147 A73-12490

Beat conditions during synchronization of an oscillator by an external sinusoidal force 02 p0147 A73-12492

Parasitic oscillations in external excitation oscillators due to internal feedback in transistor, investigating frequency dependence of stability coefficient in common emitter stage 03 p0284 A73-14032

Quartz self-oscillator short term frequency instability lower limit estimation by calculating Q values and nonlinearity and resonator parameter fluctuation effects 03 p0284 A73-14064

Amplitron stability in optimal frequency regime, relating cut-off voltage and plate current as function of magnetic field, input power and geometrical parameters 03 p0284 A73-14068

Laser frequency fluctuations due to mechanical vibrations. 03 p0319 A73-14451

Absolute instability of nonlinear pulse-amplitude control systems - Frequency criteria. 04 p0430 A73-15204

Stabilization bandwidth reduction in microwave parallel tuned tunnel diode amplifier circuits synthesis 04 p0429 A73-15919

Short term instability of frequency standard using AFC of quartz crystal oscillator by phase locking to optically pumped Rb 87 vapor clock 05 p0583 A73-16071

FM noise spectrum measurement in feedback harmonic oscillators with crystal or transmission cavity resonators as discriminator for frequency stability 05 p0556 A73-16164

Feedback networks for RC oscillators with maximum frequency stability 06 p0673 A73-17581

Hydrogen maser frequency stability dependence on signal output, magnetic polarization field and relaxation effects, describing automated relaxation rate measurement and atomic line spectrum registration 06 p0699 A73-17588

Nonreciprocal circulator coupled reflection type microwave amplifier gain and stability characteristics, presenting scattering matrix and signal flow diagram 06 p0673 A73-17590

Frequency stability criterion for a variable-structure automatic control system. 06 p0680 A73-17958

Radio oscillators short term frequency instability, examining relations between time domain and frequency domain sample variance definitions 07 p0798 A73-19176

High level quartz resonators and oscillators 07 p0798 A73-19177

Noise of local oscillators of high capacity radio links 07 p0798 A73-19179

Attainment of a low-noise high-power and highly stable Gunn oscillator by coupling to a superconducting cavity. 07 p0801 A73-20109

Investigation of the fluctuation characteristics of quartz-crystal harmonic generators 07 p0802 A73-20300

Frequency stabilization of a CO₂ or N₂O power laser by a fast sampling method 08 p0976 A73-21444

Periodic regime stability of two channel relay system as function of main channels identicalness and cross coupling symmetry, using Tsypkin method 09 p1063 A73-22340

High-frequency instability of an electromagnetic wave in a nonequilibrium magnetized plasma 09 p1130 A73-22705

A laser amplifier with resonator natural frequencies misaligned with respect to the gain profile of the active medium 09 p1096 A73-22969

A tunable laser based on an organic dye solution and providing highly monochromatic, stable single-frequency emission 09 p1097 A73-23010

Phase locked bit synchronization design tradeoffs between acquisition and noise performance, considering frequency tolerance of decision-directed loop with nonreturn-to-zero input 09 p1056 A73-23403

Noncrystal controlled oscillator with transistor and tunnel diode, noting high frequency stability due to automatic regulation of dc operating conditions 10 p1194 A73-23735

Electron-cyclotron drift instability in high-beta plasmas, developing nonlinear theory based on wave kinetic equation for weak turbulence 10 p1255 A73-24263

Steady state lasing stability in ring-type gas laser with symmetrical distribution of three longitudinal modes 10 p1228 A73-24580

The elimination of tuning-induced burnout and bias-circuit oscillations in IMPATT oscillators. 10 p1196 A73-24622

Dispersion equation of parametric longitudinal LF instability of electromagnetic wave propagation in bounded electron beam in metallic waveguide 10 p1257 A73-24876

Stability of the monochromatic mode of emission in a multimode solid-state laser 11 p1376 A73-25631

Parametron circuit current fluctuations analysis via successive approximation solution of nonlinear differential equation, investigating operational mode stability 11 p1400 A73-26452

Investigation of new elements and equipment configurations in stable-frequency, alternating-current, electrical power supply systems employing primary power plants consisting of engines with varying rotational speed 12 p1460 A73-26785

Development of acoustic and overheat instabilities in a plasma with molecular impurities 12 p1528 A73-27303

Influence of a nonlinear lens on the stability of steady-state laser emission. 12 p1507 A73-27506

Investigation of the stability of the oscillation frequency of a mercury laser emitting at 1.53 microns. 12 p1507 A73-27511

Analysis of the stochastic stability of pulsed control systems in the frequency domain 12 p1485 A73-27622

Frequency stability of millimetre-band reflex klystrons with various cooling techniques. 13 p1589 A73-28049

Short term frequency stability and single sideband phase noise measurements on signal generators, considering frequency deviation and amplitude modulation produced by noise 13 p1582 A73-28570

Use of narrow resonances in methane for frequency stabilization of a 3.39-micron He-Ne laser 13 p1627 A73-28763

Injection phase locked microwave oscillator for FM amplifier, calculating frequency drift caused gain limitation in terms of diode and circuit properties temperature effects 13 p1593 A73-29116

Frequency fluctuations in a gas laser with nonlinear absorption. 13 p1629 A73-29430

Influence of self-focusing on the stability of steady-state laser emission. 13 p1629 A73-29441

Stability condition of an intense two-modes regime in a gas laser 13 p1630 A73-29557

Extension of the theory of frequency noise of oscillating masers 13 p1630 A73-29558

Automatic control of positive feedback depth and its application for stabilization of high Q-factor circuit characteristics 15 p1853 A73-31494

A simple, single-frequency He-Ne laser for practical uses. 15 p1885 A73-32018

Investigation of longitudinal-mode selection and frequency stabilization of the emission from a helium-neon laser with a ring resonator 15 p1886 A73-32335

NMR spectrometer magnetic field strength-HF field frequency ratio instability spectral density in presence of spin stabilizers 16 p2011 A73-32824

Carbon dioxide laser technological advances and applications including frequency stability systems, remote sensing, air pollution detection, optical heterodyning and pumping 16 p2023 A73-32860

Monochromatic field frequency misalignment effect on polarization and population ratio instabilities of single frequency traveling wave laser with broadened active medium 16 p2024 A73-32894

Atmospheric refractivity fluctuation caused transit time variation effects on propagation noise and frequency stability in microwave radio link signal reception at 36 GHz 16 p1982 A73-33714

A self-stabilized 3.5-micron waveguide He-Xe laser. 17 p2183 A73-34206

Temperature effects on modulation sensitivity and vibrational spectra in Gunn diode oscillators, suggesting frequency stability improvement method 17 p2136 A73-35162

Stability, reproducibility, and absolute wavelength of a 633-nm He-Ne laser stabilized to an iodine hyperfine component. 17 p2185 A73-35424

Frequency-time domain stability criterion for nonlinear negative feedback system with linear transfer function, using Zame positive operator theory 17 p2203 A73-35731

Highly stabilized IMPATT oscillators at millimeter wavelengths. 18 p2293 A73-36607

Investigation of the fluctuation characteristics of quartz harmonic oscillators. 18 p2294 A73-37137

Reproducibility of the frequency of a stabilized laser employing a ring cavity 19 p2437 A73-37246

Stability of the monochromatic generation mode in multimode solid-state lasers. 19 p2438 A73-38147

Short-term frequency stability of the Rb-87 maser. 21 p2716 A73-41148

Some characteristics of an operational system for measuring UT 1 using very long baseline interferometry. 21 p2705 A73-41330

Dispersion equation of parametric longitudinal LF instability of electromagnetic wave propagation in bounded electron beam in metallic waveguide 21 p2744 A73-41651

The frequency stabilization of gas lasers. 22 p2868 A73-41698

Short-term frequency stability of an L band oscillator with a superconducting cavity. 23 p2961 A73-44117

The frequency stability and noise of passive Rb standard. 23 p2965 A73-44137

Minimum detectable frequency deviations in output of He-Ne laser stabilized by external methane absorption cell 23 p2989 A73-44366

Utilization of the impedance variation of the plasma of a CO₂ laser for frequency stabilization on the 'Lamb dip' 24 p3096 A73-45223

Limitation of m.t.i. improvement factor due to oscillator instability. 24 p3069 A73-45259

FREQUENCY STANDARDS

Short term instability of frequency standard using AFC of quartz crystal oscillator by phase locking to optically pumped Rb 87 vapor clock 05 p0583 A73-16071

High level quartz resonators and oscillators 07 p0798 A73-19177

Application of ultrastable oscillators to the aerospace field 07 p0798 A73-19180

Investigation of nonstationary processes in the ionosphere and space with quantum frequency standards. 10 p1211 A73-24214

Frequency generators performance with stability associated with atomic/molecular transition, considering rubidium and hydrogen clocks and He-Ne lasers 10 p1219 A73-24396

Tunnel and Gunn diode oscillators coupled to superconducting cavity as S and X band frequency standards 10 p1195 A73-24397

Corrugated horn antenna with high efficiency and monotonic amplitude in microwave pattern ranges applicable as calibrating standard 17 p2143 A73-35693

Ultrastable atomic and molecular oscillators and their applications to navigation 19 p2429 A73-37384

Russian book on design and operational principles of monopause and moving target radar, atomic time and frequency measuring devices, radio navigation and optical processing 21 p2650 A73-40510

Atomic time and frequency standards 21 p2700 A73-40513

NBS radiometric calibration services extended to far UV spectrum with dc high power hydrogen wall stabilized arc as primary standard of spectral radiance 21 p2703 A73-41256

The frequency stability and noise of passive Rb standard. 23 p2965 A73-44137

FREQUENCY SYNCHRONIZATION

Stable frequency and synchronicity alterations in the discharges of cortical neuron populations in feedback experiments 01 p0010 A73-11445

Parallel operation of two Brayton-cycle alternators with parasitic speed controllers. 09 p1035 A73-22773

Ring laser output calculation in the region of capture 12 p1504 A73-26885

Investigation of the synchronization of Gunn diode oscillators having a stripline resonance system 12 p1480 A73-27448

Probability density characteristics of elapsed time interval to synchronization disruption in phase locked AFC systems 13 p1584 A73-28890

Probability of error in selecting the information signal and the synchronization signal by frequency multiplication 13 p1584 A73-28892

Injection frequency locking of the avalanche transit-time oscillator. 13 p1594 A73-29292

Voltage-locked diode oscillators. II - The effect of harmonics on the locking range. 14 p1734 A73-30074

Dependence of the locking zone of a gas ring laser on the emission frequency 15 p1885 A73-32316

Measurement of external Q factor of microwave oscillators using frequency pulling or frequency locking. 15 p1852 A73-32646

Synchronization of the frequency of tunnel-diode, IMPATT-diode, and Gunn-device oscillators 20 p2537 A73-39460

- Frequency-following injection microwave oscillator with bias voltage control for tracking speed to provide amplifier or noise improvement circuit
21 p2664 A73-41091
- Synchronization range of phase control systems
21 p2665 A73-41271
- Noise immunity of quasi-optimal noncoherent reception during resynchronization with respect to time and frequency
24 p3067 A73-44590
- Frequency dependence of locking in a ring laser.
24 p3095 A73-44622

FREQUENCY SYNTHESIZERS

- Properties and applications of the iterative synthesizer with a search oscillator
07 p0798 A73-19178
- Surface elastic wave microwave bandpass filter for miniaturized frequency synthesizer in satellite communications systems, noting insertion loss and sidelobe reduction
12 p1484 A73-27573
- Frequency synthesizer technology review, discussing direct frequency synthesis and frequency analysis/phase lock/ techniques
14 p1732 A73-29874
- Book - Frequency synthesis: Theory, design and applications.
20 p2542 A73-39143
- Spectra of signals with functional phase modulation in digital frequency synthesizers
20 p2537 A73-39461

**FREQUENCY TRANSLATION
U FREQUENCY CONVERTERS**

FRESNEL DIFFRACTION

- Fresnel diffraction by a circular aperture illuminated with partially coherent light. 1.
01 p0078 A73-11004
- Unstable resonators for CO₂ electric-discharge convection lasers.
06 p0703 A73-18747
- Laser beam steering in confocal unstable resonators, interpreting mirror misalignment effects as far field dependence on magnification and Fresnel number from mode solution
09 p1090 A73-22076
- Properties of unstable resonators with large equivalent Fresnel numbers.
12 p1507 A73-27505
- Iterative diffraction calculations of transverse mode distributions in confocal unstable laser resonators.
14 p1756 A73-30156
- An analysis of helicopter rotor modulation interference.
15 p1843 A73-31731
- Electromagnetic theory of Fresnel holograms in the first perturbation theory approximation
22 p2862 A73-42927

FRESNEL INTEGRALS

- E-polarized plane wave diffraction by conducting wedge loaded with thin dielectric slab, obtaining Fresnel integral solution with application to cylindrical wave excitation
07 p0792 A73-19383

FRESNEL REFLECTORS

- Importance of Fresnel reflections in laser surface damage of transparent dielectrics.
01 p0076 A73-10131
- Single reflection Fresnel rhomb for quarter-wave retardation in the infrared.
11 p1400 A73-26251
- Mode selection in GaAs injection lasers resulting from Fresnel reflection.
17 p2186 A73-35797

FRESNEL REGION

- Incident plane wave fluctuations effect on diffraction pattern formed by scattering on reflecting sphere, calculating amplitude distribution in Fresnel and Fraunhofer regions
01 p0016 A73-10211
- Computer aided directivity measurements of large antennas in Fresnel zone
10 p1188 A73-24184
- Method of calculation of radioelectric performances of airborne radomes
11 p1327 A73-25282
- Method of measuring the parameters of axisymmetrical mirror antennas on the basis of the emission of a 'black' disk positioned in the Fresnel region
11 p1332 A73-26162
- Reconstruction of an antenna radiation pattern from field values available within a limited sector of angles in the Fresnel region
12 p1479 A73-27227
- Characteristics of a dual-mirror antenna producing a sum-difference type of radiation pattern
12 p1480 A73-27234
- Waveguide laser mode patterns in the near and far field.
14 p1756 A73-30157
- Properties and fabrication of micro Fresnel zone plates.
17 p2173 A73-35434
- Linear phased array antenna focused in Fresnel region, noting radiation pattern indoor measurement

simplicity advantage over far field observation in performance monitoring
17 p2128 A73-35694

A new method for calculating correction factors for near-field gain measurements.
22 p2830 A73-41829

**FRESNEL-KIRCHHOFF INTEGRALS
U FRESNEL INTEGRALS**

FRETTING

- Wear and energy dissipation of contacts vibrated at high frequencies, analyzing mechanism of fretting wear
[ASME PAPER 72-LUB-20] 03 p0314 A73-14335
- Surface effects during fretting fatigue of Ti-6Al-4V.
04 p0461 A73-14998
- The influence of fretting and geometric stress concentrations on the fatigue strength of clamped joints.
07 p0912 A73-19572
- Fretting fatigue in titanium helicopter components.
11 p1383 A73-25837
- A new fretting fatigue testing machine.
11 p1344 A73-25839
- Fretting fatigue strength of several materials combinations.
11 p1385 A73-26335
- Scanning electron microscope analysis of Ti-Al-V specimens under simultaneous fatigue and fretting loads
15 p1883 A73-32148
- Study of fretting wear in titanium, Monel-400, and cobalt-25 percent molybdenum using scanning electron microscopy.
[ASLE PREPRINT 73AM-8A-3] 17 p2190 A73-34993
- The fretting fatigue of titanium and some titanium alloys in a corrosive environment.
22 p2876 A73-42356

FRETTING CORROSION

- Vibratory loads effect on metal microstructure under sliding friction, noting rheological criteria for fretting corrosion wear resistance
02 p0180 A73-11934
- Fatigue strength of constructional materials and components of GTD-type compressors under conditions of fretting corrosion.
02 p0181 A73-12217
- Fretting-fatigue mechanisms and the effect of direction of fretting motion on fatigue strength.
05 p0581 A73-16128
- The role of electrochemical processes in the fretting corrosion of metals
06 p0710 A73-18660
- The effect of fretting corrosion in fatigue crack initiation.
11 p1383 A73-25835
- Surface damage under fretting fatigue as function of applied normal load and clamping pressure
11 p1383 A73-25836
- Ti alloy coating and surface treatment to prolong fatigue life by eliminating fretting damage, discussing design parameters selection, screening and strength tests and performance evaluation
11 p1383 A73-25838
- Influence of fretting on the endurance of 40KhNMA steel with various thermochemical processing
11 p1386 A73-26735
- Al and Ti alloy corrosion and fretting fatigue in aqueous environment, noting protective oxide surface film effects
13 p1642 A73-29524
- Book on fretting corrosion covering contacting surface theory, damage characteristics, wear variables effect, fatigue, adhesion and electrochemical properties, etc
13 p1643 A73-29575
- Behavior of the electrode potential of a metal under conditions of fretting corrosion
14 p1763 A73-30711

FRICTION

- NT AERODYNAMIC DRAG
NT DRY FRICTION
NT FLOW RESISTANCE
NT FRICTION DRAG
NT INTERNAL FRICTION
NT KINETIC FRICTION
NT SKIN FRICTION
NT SLIDING FRICTION
NT STATIC FRICTION
NT VISCOUS DRAG
- Friction in ultrahigh vacuum, discussing physicochemical problems, self lubricating material advantages and drawbacks, and solid lubricant choice for space applications
07 p0828 A73-18906
- The effect of metal gripping during dynamic loading
08 p0973 A73-21132
- High speed oscillating tests of lubricating composites.
[ASLE PREPRINT 73AM-3C-2] 17 p2179 A73-34987
- Cryptosteady flow energy separation mechanisms, considering bearing friction and rotor torque effects and rotor nozzle proportion equations
[ASME PAPER 73-FE-24] 17 p2153 A73-35019

Experimental study on the interference of inertia and friction forces in turbulent lubrication.
[ASME PAPER 73-LUBS-12] 17 p2181 A73-35393

**FRICTION COEFFICIENT
U COEFFICIENT OF FRICTION**

FRICTION DRAG

NT AERODYNAMIC DRAG
NT VISCOUS DRAG

- Turbulent incompressible boundary layer on porous heat insulated plate with uniform suction, calculating ratio of friction drag coefficients
08 p0954 A73-21178
- Turbulent friction drag of a dusty gas. 1 - Theoretical study.
09 p1072 A73-23325
- Numerical calculation of heat exchange and frictional resistance for a turbulent flow in a tube in the case of a gas with variable physical characteristics
18 p2301 A73-36816

FRICTION FACTOR

- A linearized analysis for frictionally damped systems.
01 p0090 A73-10782
- The technique and results of ground tests of Lunokhod's friction members.
01 p0030 A73-11154
- Steel/pig iron friction pair natural vibrations due to starting force and sliding friction force difference, noting starting force dependence on loading rate
01 p0058 A73-11403
- Effect of friction in suspension bearings on the motion of a gyroscope with a forced rotation of its base
01 p0054 A73-11415
- An estimate of the decrease in friction during vibrations of normal direction
01 p0058 A73-11437
- Problem of the influence of an instantaneous change in normal pressure on the magnitude of contact friction force
02 p0172 A73-11796
- Pulsating vertical load effect on friction force magnitude between two horizontal solid surfaces during initial phase of static to kinetic friction transition
02 p0172 A73-11797
- The effects of viscous friction on axial rotation of celestial bodies.
02 p0216 A73-12376
- The effects of viscous friction on the precession and nutation of celestial bodies.
02 p0217 A73-12396
- Consideration of wall friction in the streamline procedure with the aid of a modified boundary layer calculation for laminar flows according to the momentum method
03 p0291 A73-13126
- Rubber friction effect on vehicle tire force-slip and breaking behavior in terms of peripheral and sideslip components and structural and operational parameters
03 p0251 A73-13242
- Effects of Hall currents and collisions with neutrals on the dynamic stability of a composite hydromagnetic plasma.
03 p0346 A73-13292
- The relative validity of the concepts of coefficient of friction and interface friction shear factor for use in metal deformation studies.
[ASLE PREPRINT 72LC-7A-3] 03 p0316 A73-14368
- Unsteady one-dimensional compressible frictional flow with heat transfer.
03 p0298 A73-14639
- Investigations into film failure /transition point/ of lubricated concentrated contacts.
05 p0580 A73-16103
- Thermal collapse theory of hydrodynamic oil lubrication films failure for slider bearing, noting frictional forces role
05 p0580 A73-16105
- A technical note on the correspondence between Amontons' law and wear-scar data in a 4-ball machine.
05 p0581 A73-16108
- Supersonic boundary layer on a permeable surface
05 p0534 A73-17268
- Solid-solid interface temperature rise during sliding from model with surface topography statistics, frictional conditions, surface hardness and thermal parameters
[ASME PAPER 72-LUB-34] 07 p0832 A73-20483
- An improved method for calculating the spin torque in a fully lubricated ball-race contact.
07 p0833 A73-20485
- Effects of metal grain size on friction and wear characteristics
10 p1223 A73-24067
- Small parameter method, with the parameter proportional to the friction forces, in the case of forced vibrations of complex trusses
11 p1435 A73-25395
- Friction reduction by perpendicular oscillation.
11 p1374 A73-26064
- Fretting fatigue strength of several materials combinations.
11 p1385 A73-26335

Rotating flexible shaft stability criterion development by perturbation method, considering internal and external friction and rotor inertia loading moments effects

11 p1444 A73-26368

Conditions for powder compaction over the deformation zone width during rolling

12 p1503 A73-27554

Investigation of the friction and wear behavior of polytetrafluoroethylene composite materials as compared with that of artificial coal and sintered metal. II

13 p1647 A73-29652

Effect of treatment factors on the properties of friction materials. II - Effect of sintering conditions on the structure and friction and wear properties of friction materials

15 p1892 A73-32244

General solution to the subsonic through-flow problem in a turbomachine including losses.

17 p2092 A73-34385

Pulsatile Newtonian frictional losses in a rigid tube.

17 p2151 A73-34532

Leakage and frictional characteristics of turbulent helical flow in fine clearance.

17 p2152 A73-35001

Corrosion wear mechanism with emphasis on chemical and mechano-chemical reaction products formation and removal from friction surface /tribo-mechanical processes/

18 p2320 A73-36494

Interaction of self-excited vibrations in mechanical vibrational systems

19 p2494 A73-37181

A comparison of the capabilities of continuous drive friction and inertia welding.

19 p2436 A73-38493

Expanding split ring seal types for pistons, discussing straight cut, step, two piece and three piece rings and pressure and friction effects

22 p2865 A73-41777

Study of a dynamic problem in viscoelasticity and ideal plasticity with conditions of friction at the boundary

23 p3044 A73-43973

Solid friction oscillation characteristics of self excited rotational shaft-spring system with sliding contact surfaces

23 p2986 A73-44273

Parametrizing turbulent-friction effects in a planetary boundary layer

24 p3108 A73-45450

FRICION LOSS COEFFICIENT

U FRICTION FACTOR

FRICION MEASUREMENT

Role of the crystalline structure and orientation of single crystals in the formation of the external friction process

01 p0062 A73-10259

Laboratory experience with long-term bearing lubrication.

01 p0057 A73-11278

Investigation of anti wear additives under various loads and at different sliding speeds.

03 p0316 A73-14359

Metallic contact resistance and friction behavior under microdisplacement for lead/gold surfaces with lubricant or oxide film, noting consistency with Greenwood theory

03 p0316 A73-14364

Metallic additions effect on wear and friction behavior of lead monoxide, lead silicate and calcium fluoride solid lubricants coatings for high temperature operations

03 p0317 A73-14374

Continuous measurement of internal friction and modulus with a regenerative feedback loop and composite oscillator.

05 p0559 A73-17255

Friction in ultrahigh vacuum, discussing test program definition and testing machine design taking into account space environment effects

07 p0829 A73-18907

Prototype skin friction measuring instrument for short period or continuous operation at high temperature, considering alternative feasible systems design and experimental data

10 p1217 A73-24013

The effect of deformations in the measurement of the force and the couple of friction

11 p1374 A73-25871

Friction, wear, and noise of slip ring and brush contacts for synchronous satellite use.

11 p1374 A73-26211

Investigation of friction behavior in titanium alloy with 3.8% Al

15 p1894 A73-32535

Influence of hydrodynamics on the performance of radial lip seals.

17 p2179 A73-34998

FRICION PRESSURE DROP

U SKIN FRICTION

FRICION REDUCTION

An estimate of the decrease in friction during vibrations of normal direction

01 p0058 A73-11437

Effects of hardening conditions on the physicochemical and frictional properties of polyvinyl furfural

08 p0982 A73-21591

Influence of thermally stabilizing alloying additions on the antifriction properties of lamellar graphites with a organic silicon binders

09 p1110 A73-22978

Effect of solid lubricants on the physicochemical and friction properties of materials

10 p1225 A73-24686

Friction reduction by perpendicular oscillation.

11 p1374 A73-26064

'Glazes' produced on nickel-base alloys during high temperature wear.

12 p1513 A73-27598

Radial MHD bearing with a floating bush

15 p1881 A73-31412

Investigation of the thermophysical and antifriction characteristics of polyethylene composites. III - The effect of fillers on the heat conductivity of polyethylene

16 p2030 A73-33930

Comparative evaluation of the wear resistance of electrolytic and plasma chromium coatings

18 p2318 A73-35883

Experimental investigation of the antifriction properties of Teflon-base materials at low temperatures

21 p2724 A73-41197

Some results of experimental investigations of turbulent flow in flexible tubes

22 p2841 A73-42120

Antifriction materials employing fibers and liquid-metal lubricants

24 p3101 A73-44413

FRINGE PATTERNS

U DIFFRACTION PATTERNS

FROGS

Two visual systems in the frog.

21 p2640 A73-41302

FRONTAL AREAS (METEOROLOGY)

U FRONTS (METEOROLOGY)

FRONTAL WAVES

Comment on the effect of a vorticity centre on a frontal boundary.

13 p1656 A73-29663

FRONTS (METEOROLOGY)

NT COLD FRONTS

Investigation of planetary high-altitude frontal zones with the aid of natural orthogonal functions

05 p0568 A73-16239

Mode of thickening of a low morning convective layer in clear sky

09 p1115 A73-23036

An experimental investigation of the nature of changes in the intensity of precipitations from stratiform and cumuliiform clouds

12 p1522 A73-27747

Subsynoptic rainbands within precipitation ahead of surface warm front, discussing midtropospheric large-scale dynamic ascent interaction with upper boundary potential instability

13 p1651 A73-28265

Mechanisms influencing the distribution of precipitation within baroclinic disturbances.

13 p1652 A73-28266

Hail growth in cold front, discussing relationship to air flow changes

13 p1652 A73-28267

Observation of Kelvin-Helmholtz billows and their mesoscale environment by radar, instrumented aircraft, and a dense radiosonde network.

13 p1652 A73-28268

Weather forecasting in the recent past, at the present time, and in the near future

13 p1655 A73-29189

Some results of ozone observations by satellite on June 17 and 18, 1966

15 p1868 A73-31607

Relation between turbulence in a clear sky and the evolution of the baric field

17 p2204 A73-34543

On the maintenance of the polar front jet stream.

17 p2205 A73-34854

Evidence of frontal structures in nonblanketing sporadic-E layers.

18 p2304 A73-35990

Comparison and synthesis of the characteristics of long- and short-duration blocking systems over the Euroatlantic region

19 p2447 A73-38124

FROST

Water frost absorptions in IR reflectivities of Jupiter Galilean satellites, discussing surface cover distributions and underlying material reflectivity

04 p0497 A73-15070

Frost and ice column models for analysis of heat and mass transfer and effective thermal conductivity relationship to density in frost layer

05 p0638 A73-16225

Permanent frost formation on steep north-facing Mars surface slopes above 25 deg north latitude, considering explanation by insolation and surface albedo

09 p1145 A73-22274

FROSTBITE

Effect of skin wetting on finger cooling and freezing.

20 p2518 A73-39779

FROUDE NUMBER

Unbounded nondiffusive high Reynolds number stratified flow with lee waves over vertical barrier investigated for Froude number range on basis of Oseen-Boussinesq approximation

15 p1863 A73-31341

Parachute axisymmetric self excited breathing oscillations dependence on descent velocity, Froude number, canopy/line length ratio, drag and line stiffness

15 p1826 A73-31438

FROZEN EQUILIBRIUM FLOW

Quasi-frozen flow of a thermodynamically relaxing gas

03 p0295 A73-13791

On an equilibrium-frozen flow approximation in the analysis of nonequilibrium nozzle flows.

19 p2422 A73-38282

A method of calculating a chemically nonequilibrium flow of gas in a heated tube under conditions close to the equilibrium or frozen state

24 p3081 A73-45527

FROZEN FOODS

Microbiological testing of Skylab foods.

12 p1464 A73-27075

FROZEN LAKES

U LAKES

FROZEN SOILS

U PERMAFROST

FRUSTUMS

Transient axisymmetric response of a conical shell frustum.

04 p0513 A73-15585

Influence coefficients for end-loaded conical frustums.

07 p0913 A73-19983

FUEL CAPSULES

Fuel capsule vent system development for the Viking radioisotope thermoelectric generator.

21 p2737 A73-40766

FUEL CELL CATALYSTS

U ELECTROCATALYSTS

FUEL CELLS

NT HYDROGEN OXYGEN FUEL CELLS

NT REGENERATIVE FUEL CELLS

Electrical evaluation of doped and undoped cobalt chromite as the interconnection material for high-temperature, zirconia-electrolyte, fuel-cell batteries.

01 p0006 A73-10724

Utilization of composite materials for the fabrication of fuel cells

03 p0334 A73-13595

Cell assemblies for a molten carbonate fuel battery. I - The construction of cell assemblies. II - Electrolyte paste discs for molten carbonate fuel cells.

04 p0406 A73-14985

International Symposium on Fuel Cells, 4th, Antwerp, Belgium, October 2, 3, 1972. Proceedings. Volume 1.

04 p0406 A73-15101

Nitrogen-containing active carbon as the cathode catalyst in acid fuel cells.

04 p0407 A73-15107

Cobalt phosphide CoP3 as a catalyst for electrochemical H2 oxidation in acid fuel cells.

04 p0407 A73-15108

Organic compounds catalytic activity comparison for use in fuel cell, noting superiority of dihydrodibenzo-tetraazannulene cobalt complex

04 p0407 A73-15109

Electronically conducting oxides as cathodes or interconnection materials in high-temperature fuel cell batteries.

04 p0407 A73-15111

Fuel cell air cathode for high current densities at low polarization and ambient temperature, noting performance improvement with pure oxygen supply

04 p0407 A73-15112

Bipolar noble-metal free electrodes for fuel cells with acid electrolytes.

04 p0407 A73-15113

Carbon-PTFE fuel cell electrode for hydrogen-KOH-air batteries for operation over long time periods, discussing rolling technique and industrialization possibilities

04 p0407 A73-15114

Raney-Ni catalysts preparation for carbon-PTFE fuel cell electrodes from Ni-Al alloy, discussing rolling technique suitability and electrode characteristics

04 p0407 A73-15115

High temperature zirconium dioxide electrolyte fuel cell systems design and operation with methane or gasoline as fuel, evaluating performance characteristics

04 p0408 A73-15118

- Transition metals nitrides, carbides and silicides applications as electrocatalysts in fuel cells for economic operation, considering hydrogen, formaldehyde and formic acid oxidation 04 p0414 A73-16038
- Fuel cells for improved electrical power supply. [AIAA PAPER 73-82] 06 p0649 A73-17641
- Autonomous hydrogen/air fuel cell for long-life missions. 09 p1033 A73-22752
- Solid polymer electrolyte fuel cell technology application to space shuttle orbiter requirements, noting 2000 hours maintenance free life and thermal stability 09 p1035 A73-22786
- Shuttle Orbiter fuel cell power system simulation, describing data management, programming and computational control 09 p1060 A73-22804
- Thermionic fuel unit cell major component materials selection for life and performance improvements, giving out-of-pile and in-pile results 09 p1036 A73-22816
- The phosphoric acid fuel cell, a long life power source for the low to medium wattage range. 09 p1037 A73-22821
- Calculation and comparison of the economics of electrochemical fuel cells 11 p1410 A73-25346
- Study of fuel cell thermal control systems for advanced missions. 11 p1309 A73-25993
- Space shuttle orbiter power system requirements and design tradeoffs, comparing fuel cells, solar array/battery and radioisotope Brayton cycle and cryogenic fueled turboalternators 11 p1312 A73-26017
- Power Sources Symposium, 25th, Atlantic City, N.J., May 23-25, 1972, Proceedings. 13 p1572 A73-29581
- Long-life light weight reliable fuel cell development for long term space missions power supplies, describing system components and construction materials 13 p1573 A73-29596
- Megawatt fuel cells for aerospace applications. 13 p1573 A73-29597
- Optimizing power efficiency of hydrazine-oxygen fuel cells. 13 p1574 A73-29598
- High power density hydrazine-oxygen fuel cell, discussing cell polarization, critical resistance losses and efficiency 19 p2390 A73-38398
- Studies of a homogeneous copper catalyst for fuel cell cathodes in acid media. 19 p2390 A73-38400
- Molybdenum-oxygen-sulfur fuel cell anode catalysts capable of oxidizing low cost fuels in acid electrolytes 19 p2390 A73-38401
- High energy density silver-hydrogen cells for space and terrestrial applications. 19 p2391 A73-38403
- Hybrid biological power cells for cardiac pacemakers - Materials evaluation. 20 p2520 A73-39823
- Concerning the stability of the triple-phase boundary in gas-diffusion electrodes of fuel cells. 21 p2636 A73-41320
- Hydrazine and methanol fuel cells comparison with hydrogen-air cells in terms of fuel costs and conversion efficiency, considering electric generators and automotive applications 24 p3057 A73-45025
- ### FUEL COMBUSTION
- Turbulent flame velocities in premixed sprays. I - Experimental study. 01 p0121 A73-10635
- On turbulent flows with fast chemical reactions. I - The closure problem. 01 p0032 A73-10637
- A critical discussion of theories of flame spread across solid and liquid fuels. 01 p0121 A73-10643
- Analysis of NO formation in single droplet combustion. 01 p0014 A73-10645
- The investigation of the effect of acoustic oscillations on the combustion process of gaseous fuel 03 p0396 A73-12955
- TF-30-P1 engine mixed flow augmentor test for combustion instability under operation with abnormal fuel zone combination, comparing with predicted pressure oscillations from model 03 p0358 A73-13489
- [AIAA PAPER 72-1206] Combustion of stabilized ethylene within a supersonic flow by a Mach configuration 03 p0352 A73-13578
- The influence of fuel preparation and operating conditions on flame radiation in a gas turbine combustor. [ASME PAPER 72-WA/HT-26] 04 p0519 A73-15828
- Droplets size and velocity distribution in air-kerosene atomized spray flame as function of fuel-air ratio from double image high speed photographic measurements [ASME PAPER 72-WA/HT-25] 04 p0519 A73-15829
- Pollutants from methane fueled gas turbine combustion. [ASME PAPER 72-WA/GT-3] 04 p0485 A73-15867
- Design and development of a high pressure facility for droplet combustion experiments. 05 p0562 A73-16440
- A shocktube study of the combustion of Sheldyne-H with additives. [WSCI PAPER 72-29] 05 p0639 A73-16686
- Characterization and suppression of aircraft and fuel fires. [WSCI PAPER 72-26] 05 p0639 A73-16688
- Modeling radial dilution air injection in axial flow combustors. [WSCI PAPER 72-24] 05 p0639 A73-16689
- Gas temperature, carbon monoxide and nitric oxide axial and radial distribution in J-33 combustor, presenting combustion process model based on measurements [WSCI PAPER 72-22] 05 p0639 A73-16690
- The influence of combustor parameters on the combustion of particle-laden fuels in ducted flows. [AIAA PAPER 73-177] 05 p0640 A73-16919
- Ignition analysis of adiabatic, homogeneous systems including reactant consumption. [AIAA PAPER 73-215] 05 p0640 A73-16945
- Photochemical ignition and combustion enhancement in high speed flows of fuel-air mixtures. [AIAA PAPER 73-216] 05 p0641 A73-16946
- Effect of fuel composition on particulate emissions from gas turbine engines. 06 p0740 A73-17733
- Measurement of nitric oxide formation within a multifueled turbine combustor. 06 p0740 A73-17734
- Extension of combustion in the supersonic flow downstream of a pilot flame stabilized with the help of a Mach configuration 06 p0769 A73-18539
- Flame structure and flame reaction kinetics. VIII - Structure, properties and mechanism of a rich hydrogen + nitrogen + oxygen flame at low pressure. 07 p0918 A73-19154
- Red fuming nitric acid suitability for nonhypergolic rocket fuel ignition in presence of chromate and dichromate catalysts 07 p0865 A73-19986
- Brightness balancing spectrograph method for flame temperature measurement of liquid fuel drop 07 p0826 A73-20423
- Determination of burning velocity by double ignition in a closed vessel. 10 p1294 A73-23559
- Temperature at the surface of a heat-conducting liquid behind a shock wave in the presence of mass transfer and chemical reactions in the boundary layer 10 p1296 A73-24679
- Approximate nomograms for the characteristics of chemical-fuel combustion products 12 p1532 A73-27087
- An approximate estimate of the reaction coefficient during the motion of a vaporizing droplet of fuel in a gas flow 12 p1532 A73-27088
- Gas turbine engine exhaust pollutants consisting of unburned hydrocarbons, nitric oxide, carbon dioxide, nitrogen dioxide and carbon monoxide 12 p1467 A73-27934
- Experimental drag coefficients for evaporating and burning drops at elevated pressures. 13 p1707 A73-28998
- Hydroxyl radical mechanism for autoignition inhibition of alkane fuels for antiknock additives at various concentrations 13 p1707 A73-29000
- Test data obtained with an experimental gas turbine operated with kerosene combustion products artificially contaminated by dust 14 p1785 A73-30650
- Low emissions combustion for the regenerative gas turbine. I - Theoretical and design considerations. [ASME PAPER 73-GT-11] 16 p2086 A73-33489
- Supersonic combustion aid for liquid and gaseous fuels. 17 p2253 A73-34191
- An experimental-analytical method to study steady spray combustion. 17 p2255 A73-35499
- Combustion of droplets of liquid fuels - A review. 18 p2372 A73-37096
- Ignition temperature of liquid fuel-fuel droplets 18 p2342 A73-37115
- Condition for flameout from a burning droplet 18 p2372 A73-37116
- Application of thermal analysis to the determination of the thermophysical properties and combustion characteristics of metallic particle conglomerates in an oxidizer flow 18 p2342 A73-37119
- Formation of a nonstationary diffusive flame front during the ignition of a liquid fuel droplet 19 p2471 A73-37507
- Thermal limit of heterogeneous ignition 19 p2503 A73-37512
- A study on opposing jets in air stream and their flame. I - A structure of two dimensional opposing jets in the state without flames. 19 p2377 A73-37945
- Experimental investigation of premixed swirling jet flames - Combustion characteristics. 19 p2504 A73-37946
- Mechanism of hydrocarbon formation in combustion processes. 19 p2402 A73-38322
- Effects of thermal and mass diffusivities on the burning of fuel droplets. [AICHE PREPRINT 22] 20 p2626 A73-39249
- Unsteady combustion of a confined spray. [AICHE PREPRINT 23] 20 p2626 A73-39250
- Stability of a conical burning surface during solid fuel combustion in a semiclosed volume 20 p2627 A73-39290
- The possibility of crystallization of condensed combustion products in nozzles 21 p2753 A73-40697
- Combustion of a solid fuel in a gaseous oxidizer flow 21 p2754 A73-40701
- Concentration and combination limits of heterogeneous ignition 21 p2791 A73-40704
- Influence of combustion phenomena on the Pogo effect 21 p2754 A73-41551
- Elementary reactions in the combustion of small inorganic molecules. 22 p2818 A73-42752
- Effect of combustion upon precessing vortex cores generated by swirl combustors. 22 p2934 A73-42781
- Experiments on the propagation of mixing and combustion injecting hydrogen transversely into hot supersonic streams. 22 p2934 A73-42785
- Nitric oxide formation weightless in diffusion flame ethanol drop combustion as function of air temperature and diffusion and spray characteristics 22 p2935 A73-42797
- Soot formation by combustion of an atomized liquid fuel. 22 p2936 A73-42800
- Time variation in the reaction-zone structure of two-phase spray detonations. 22 p2936 A73-42811
- High pressure burning rates of liquid alcohol and hydrocarbon fuels with droplet simulation by porous spheres, deriving surface temperature, pressure distribution and critical burning conditions 22 p2937 A73-42817
- Liquid fuel spray burning characteristics in stabilizer disk wake of luminous hollow cone pressure jet flame, using spark photographic technique 22 p2937 A73-42818
- Deviations from the Le Chatelier principle for flame propagation limits 24 p3155 A73-44716
- The theory of free ambient fires - The convectively mixed combustion of fuel reservoirs. 24 p3156 A73-45161
- Burning rate studies of fuel air mixtures at high pressures. 24 p3156 A73-45162
- Chemiluminescence spectra from cool and blue flames - Electronically excited formaldehyde. 24 p3066 A73-45163
- Fuel combustion rate and turbulent diffusion induced self ignition in pulsejet engine combustion chamber from schlieren photography and pressure distribution measurements 24 p3123 A73-45377
- Air-hydrogen-carbon fuel mixtures chemical composition determination by measuring carbon dioxide and moisture content of combustion products, presenting nomogram 24 p3157 A73-45378
- Influence of velocity pulsations on the range of stable combustion of homogeneous mixtures 24 p3157 A73-45382
- Solid fuels combustion stability and shock wave induced detonations propagation stability in aerosols investigation based on one dimensional turbulence, using multistage mathematical models 24 p3157 A73-45383
- Analysis of the process of combustion of a single dose of liquid fuel in a constant-volume chamber 24 p3158 A73-45384
- Gaseous fuel combustion in water flow by introducing fuel-oxygen mixture in stagnation region behind body for flame stabilization 24 p3158 A73-45386
- Investigation of the mechanism of reverse jet flame stabilization for a heterogeneous mixture. 24 p3158 A73-45388
- Analysis of the self-ignition of fuel droplets behind a reflected shock wave 24 p3121 A73-45390

FUEL CONSUMPTION

The development of a device for measuring fuel consumption 02 p0165 A73-11521

Effect of the guidance reserve of the Europa II third stage on the consumption of propellants for stationing 04 p0504 A73-15294

Storable fueled power system for Space Shuttle. [SAE PAPER 720836] 05 p0537 A73-16632

Small turbine advanced gas generator for future propulsion requirements. [SAE PAPER 720831] 05 p0537 A73-16634

Propellant requirements for midcourse velocity corrections. [AIAA PAPER 73-172] 05 p0630 A73-16916

Volvo RM8 turbofan engine for Viggen fighter and ground attack aircraft, emphasizing low fuel consumption for long range cruise and high thrust/weight ratio 05 p0608 A73-17099

Explosive systems with reactant fuel consumption, deriving asymptotic stability, with application to self heating chemical reaction via Liapunov functions 07 p0919 A73-13993

Minimum fuel rocket maneuvers in horizontal flight. 08 p1014 A73-20714

Possibilities of optimal processing of capacitance fuel meter data 09 p1083 A73-22652

Investigation of the dynamics of a rotation scheme of a spacecraft composed of two units 10 p1286 A73-23877

Co-60 kernel modular power and reentry system design for space station and base, noting fuel and launch cost savings over Pu-238 systems 11 p1310 A73-25998

Minimum fuel problem link to Kalman controllability theorem, deriving solution based on state transition and controllability matrices 12 p1517 A73-27152

Air transportation direct and indirect costs analysis, considering cruising speed, flight time, aircraft design and manufacture and fuel expenses 13 p1569 A73-28950

Spacecraft single-turn reorientation optimization with respect to fuel expenditure depending on maneuver duration and reaction control torque constraints 14 p1803 A73-29852

Satellite oscillation in circular orbit plane, determining gravitational stability in minimum time with least fuel consumption 14 p1803 A73-29868

German monograph on bypass turbojet propulsion systems with jet mixing covering engine parts, thrust characteristics and fuel consumption 14 p1785 A73-30671

Time and fuel consumption optimal nutation damping and attitude-angular velocity control of spin-stabilized flight vehicles 16 p2072 A73-33234

Critical behaviour in chemically reacting systems. I - Difficulties with the Semenov theory. II - An exactly soluble model. 16 p1976 A73-33342

Second generation supersonic transport, discussing fuel costs, changing markets, travel patterns, electronic displays and sound suppressor development [SAE PAPER 730349] 17 p2102 A73-34697

Fuel-optimal angular momentum vector control for spinning and dual-spin spacecraft. 17 p2240 A73-35663

Civil aviation environmental and economic aspects, discussing noise and air pollution, fuel consumption and airspace and ground space utilization 18 p2267 A73-36685

Air transportation economic efficiency as function of fuel consumption, cruising flight speed, altitude range and load factor /payload/ 19 p2506 A73-38118

Dynamics of a twisting mode for a two-section space vehicle. 20 p2614 A73-38896

Station acquisition fuel minimization for third stage apogee motor impulse compensation of geostationary transfer orbit dispersions 21 p2781 A73-40618

FUEL CONTAMINATION

The removal of impurities from hydrazine for control of contamination caused by rocket engine exhaust. [AIAA PAPER 72-1046] 03 p0351 A73-13379

Contamination damage avoidance concepts for propulsion feed system components. 07 p0868 A73-20470

Test data obtained with an experimental gas turbine operated with kerosene combustion products artificially contaminated by dust 14 p1785 A73-30650

Method for the determination of impurity particle dispersion in fuels and lubricants 15 p1876 A73-31834

FUEL CONTROL

Selection of a surface tension propellant management system for the Viking 75 Orbiter. [AIAA PAPER 72-1042] 03 p0381 A73-13377

Minimum fuel control solution for linear discrete systems, discussing finite iterative algorithm based on dual problem of functional analysis 07 p0806 A73-20595

A simplified fuel control approach for low cost aircraft gas turbines. 17 p2222 A73-34725

T700 fuel and control system - A modern system today for tomorrow's helicopters. [AHS PREPRINT 771] 17 p2109 A73-35089

Computerized control system for fuel flow into and out of fuel cells and aircraft gravity center optimization during supersonic cruise and takeoff 21 p2634 A73-40939

VAK 191B.

22 p2798 A73-41752

FUEL CORROSION

Corrosion tests for rocket propulsion system components materials for use with nitric acid-nitrogen tetroxide blend oxidizer 03 p0329 A73-13007

Effects of fuel corrosion inhibitors on filter-separator coalescence. [SAE PAPER 720862] 05 p0582 A73-16666

Improved corrosion protection for solid rocket propulsion systems. 13 p1645 A73-29273

High-temperature corrosion in gas turbines and steam boilers by fuel impurities. II - The sodium sulfate-magnesium sulfate-vanadium pentoxide system. 15 p1841 A73-32175

Gas-releasing additives to jet fuels 21 p2754 A73-41070

FUEL ELEMENTS (NUCLEAR REACTORS)

U NUCLEAR FUEL ELEMENTS

FUEL FLOW

NT PROPELLANT TRANSFER

Up-rating the fuel system flow capacity with high rotational speed. 16 p2046 A73-32922

FUEL FLOW REGULATORS

H2/O2-fuel cells supplied with a H2/N2-mixture and air. 04 p0408 A73-15116

Servomechanism design techniques and applications - Aerospace problems. 23 p2945 A73-43450

FUEL GAGES

Possibilities of optimal processing of capacitance fuel meter data 09 p1083 A73-22652

FUEL INJECTION

Effect of injection velocity ratio and combustion chamber pressure on experimental performance of throttleable LO2/GH2-rocket engines with coaxial injectors. [AIAA PAPER 72-1079] 03 p0354 A73-13402

A new experimental method for the investigation of fuel spray evaporation. [AIAA PAPER 72-1148] 03 p0356 A73-13453

Factor of fuel pyrolysis in injector design. 05 p0606 A73-17109

Effects of fuel injection method on gas turbine combustor emissions. 06 p0768 A73-17735

Atomization of cryogenic liquid droplets by shock waves 07 p0811 A73-19656

Fuel-air turbulent mixing process in double concentric jet type burner, measuring average velocity, pressure distribution, turbulence intensity and shear stress 13 p1601 A73-28648

Breakdown of a drop of cryogenic liquid by shock waves. 14 p1745 A73-30322

Analytical modeling of a spherical combustor including recirculation. 22 p2934 A73-42783

Burn-up of the high temperature products of incomplete combustion in a supersonic flow by a second injection of oxidizer 24 p3156 A73-45076

Analysis of the process of combustion of a single dose of liquid fuel in a constant-volume chamber 24 p3158 A73-45384

FUEL OILS

Large payload aircraft for Alaskan and Canadian gas-oil transportation, examining alternative pipeline economic factors and possible new North Canadian island fuel fields 16 p2088 A73-33183

FUEL PUMPS

Some causes for the appearance of the 'extraneous noise' defect in transfer pumps of aircraft fuel systems 12 p1460 A73-27094

FUEL SPRAYS

Turbulent flame velocities in premixed sprays. I - Experimental study. 01 p0121 A73-10635

Turbulent flame velocities in premixed sprays. II - Theoretical analysis. 01 p0121 A73-10636

A new experimental method for the investigation of fuel spray evaporation. [AIAA PAPER 72-1148] 03 p0356 A73-13453

Optical anemometers applicability to steady atomized fuel sprays, obtaining particle velocity profiles and probability density distributions 05 p0565 A73-16761

An experimental-analytical method to study steady spray combustion. 17 p2255 A73-35499

Combustion of droplets of liquid fuels - A review. 18 p2372 A73-37096

Investigation of the mechanism of reverse jet flame stabilization for a heterogeneous mixture. 24 p3158 A73-45388

FUEL SYSTEMS

NT AIRCRAFT FUEL SYSTEMS

Problems in modeling fuel systems for turbine engines 03 p0258 A73-14616

High voltage fuel supplies intended for ion thrusters 04 p0489 A73-15734

Development of propellant loading systems and checkout systems for the TD-1A and AEROS satellite projects 11 p1430 A73-25354

The use of hydrogen for aircraft propulsion in view of the fuel crisis. 17 p2220 A73-35469

FUEL TANK PRESSURIZATION

Vehicle-scale investigation of a fluorine jet-pump liquid hydrogen tank pressurization system. [AIAA PAPER 72-1133] 03 p0355 A73-13440

VAK 191B. 22 p2798 A73-41752

Fuel tank wall response to hydraulic ram during the shock phase. 22 p2843 A73-43114

FUEL TANKS

NT WING TANKS

Analysis of the vibrational characteristics of a liquid contained in a tank [ONERA, TP NO. 1197] 07 p0812 A73-20074

Longitudinal vibration analysis of partially-filled ellipsoidal tanks. 07 p0914 A73-20215

Analysis of gas flow through a multilayer insulation system. 17 p2149 A73-34184

VAK 191B. 22 p2798 A73-41752

New developments in aircraft refuelling vehicles. 22 p2838 A73-41861

FUEL TESTS

Effects of fuel corrosion inhibitors on filter-separator coalescence. [SAE PAPER 720862] 05 p0582 A73-16666

Book - ASTM manual for rating motor, diesel, and aviation fuels. 06 p0740 A73-18402

Vapor pressure of supersonic aircraft fuels 07 p0865 A73-20014

Method for the determination of impurity particle dispersion in fuels and lubricants 15 p1876 A73-31834

JFTOT - A new fuel thermal stability test [A summary of a Coordinating Research Council activity]. [SAE PAPER 730385] 17 p2147 A73-34722

Military and civil jet aircraft fuel specifications, discussing additives types, test procedures and quality control complexity 17 p2220 A73-34848

Burning rate studies of fuel air mixtures at high pressures. 24 p3156 A73-45162

FUEL VALVES

Advanced technology for Space Shuttle Auxiliary Propellant Valves. [AIAA PAPER 72-1157] 03 p0356 A73-13459

FUEL-AIR RATIO

Flammable fuel-air mixture ignition by transient turbulent hot inert gas jet, calculating minimum required jet size 03 p0399 A73-14390

Methane-air mixtures burning velocity as function of equivalence ratio at atmospheric pressure, using bomb/hot-wire and corrected density ratio techniques 03 p0399 A73-14398

Photochemical ignition and combustion enhancement in high speed flows of fuel-air mixtures. [AIAA PAPER 73-216] 05 p0641 A73-16946

Combustion of fuel vapor-drop-air systems. I - Open burner flames. II - Spherical flames in a vessel. 16 p2085 A73-33343

Centrifugal force effects on flame spread and extinction limits of fuel-air mixture combustion with laminar, turbulent and buoyant bubble transport 22 p2933 A73-42776

Formation of nitric oxide in fuel-lean and fuel-rich flames. 22 p2820 A73-42794

The effects of imperfect fuel-air mixing in a burner on NO formation from nitrogen in the air and the fuel. 22 p2820 A73-42795

- Deviations from the Le Chatelier principle for flame propagation limits 24 p3155 A73-44716
- Burning rate studies of fuel air mixtures at high pressures. 24 p3156 A73-45162
- Propane-air flame stabilization via combustion product recirculation due to transverse gas jet injection, increasing fuel-air ratio 24 p3123 A73-45379
- Influence of velocity pulsations on the range of stable combustion of homogeneous mixtures 24 p3157 A73-45382
- Investigation of the mechanism of reverse jet flame stabilization for a heterogeneous mixture. 24 p3158 A73-45388

FUELING

U REFUELING

FUELS

- NT AIRCRAFT FUELS
- NT CRYOGENIC ROCKET PROPELLANTS
- NT DOUBLE BASE ROCKET PROPELLANTS
- NT FUEL OILS
- NT HIGH ENERGY FUELS
- NT HYDROCARBON FUELS
- NT HYDROGEN FUELS
- NT HYPERGOLIC ROCKET PROPELLANTS
- NT JET ENGINE FUELS
- NT JP-5 JET FUEL
- NT LIQUID ROCKET PROPELLANTS
- NT MONOPROPELLANTS
- NT NUCLEAR FUELS
- NT SOLID ROCKET PROPELLANTS

FULL SCALE FATIGUE TESTS

U FATIGUE TESTS

U FULL SCALE TESTS

FULL SCALE TESTS

- Automated test stands for full scale aircraft structure and engine parts fatigue tests, noting equipment for programmed static and dynamic loading 02 p0166 A73-11629
- Full-scale fire tests on a simulated aircraft carrier flight deck. [WSCI PAPER 72-31] 05 p0639 A73-16684
- Full scale reentry vehicle laminar to turbulent wake transition characteristics from electrostatic probe in-flight measurements of charged particle density fluctuations [AIAA PAPER 73-109] 05 p0529 A73-16868
- Engine noise reduction by fan blade tip speed reduction and high lift coefficient operation, presenting full scale test results 06 p0740 A73-17571

- Aircraft noise reduction problems, noting trained personnel and research laboratories shortage and full scale tests requirements [AIAA PAPER 73-5] 06 p0646 A73-17601
- Icing testing in the large Modane wind-tunnel on full-scale and reduced scale models 07 p0808 A73-20244

- Buffeting pressures on a swept wing in transonic flight - Comparison of model and full scale measurements. [AIAA PAPER 73-311] 11 p1305 A73-25542

- Phenomenological approach to low-cycle fatigue fracture of a typical aircraft full scale component static test. [AIAA PAPER 73-324] 11 p1305 A73-25554

- Viking 75 lander deceleration system qualification flight tests at expected Mars conditions, discussing design requirements and full scale vehicle simulation in earth atmosphere [AIAA PAPER 73-457] 15 p1827 A73-31443

- Experimental investigation and correlation of the ground impact acceleration characteristics of a full scale capsule and a 1/4 scale model aircraft emergency crew escape capsule system. [AIAA PAPER 73-480] 15 p1829 A73-31463

- DC 10 airframe structure full scale fatigue tests for crack initiation and growth, residual strength and service life. [AIAA PAPER 73-803] 19 p2379 A73-37463

- Multihundred watt radioisotope thermoelectric generator full scale thermal performance, vibration, shock, acoustic, acceleration and magnetic field tests 19 p2456 A73-38421

- Noise comparisons from full-scale fan tests at NASA Lewis Research Center. [AIAA PAPER 73-1017] 24 p3121 A73-44849

- Low frequency noise generation within aircraft gas turbine engine core portion, discussing sources prediction, model and full scale engine tests, and future technology [AIAA PAPER 73-1027] 24 p3122 A73-44858

- A comparison of the overall and broadband noise characteristics of full-scale and model helicopter rotors. 24 p3057 A73-45264

FUNCTION GENERATORS

- Design of digital force function generator for aircraft tire load testing. 04 p0424 A73-15064

- Accelerated generation of deflecting voltages by the functional beam-control method 08 p0967 A73-21589

- Function generation technique based on variables stochastic representation and clocked random pulses in data processing operations, noting application to closed loop control systems 10 p1242 A73-24016

- Centrosymmetric metric generator of field models of particles, discussing Einstein tensor components representation 22 p2887 A73-42431

- Electronic fringe-follower for interferometer. 23 p2983 A73-44086

FUNCTION SPACE

NT BANACH SPACE

NT HILBERT SPACE

- Imbedding theorem for the spaces of functions whose mixed derivatives satisfy the multiple integral Holder condition 02 p0187 A73-12178

- Polynomial traces and smoothness moduli of functions of many variables 02 p0187 A73-12179

- Phase space structure of neutral-type quasi-linear differential equations 05 p0589 A73-16294

- Existence and conical intersection theorems for extremum conditions of Euclidean space subset function, noting discrete objects optimality conditions 05 p0589 A73-16334

- Control of functional differential equations of retarded and neutral type to target sets in function space. [AD-758569] 05 p0561 A73-16486

- The local form of the entropy inequality in neoclassical thermodynamics. 06 p0768 A73-17897

- Approximative calculation of flutter regions for collision body systems in phase space, noting fluttering duration as function of post-impact velocity recovery factor 06 p0725 A73-18880

- An attainable sets approach to optimal control of functional differential equations with function space terminal conditions. 07 p0846 A73-20497

- Fractional exponents of an elliptic operator and parabolic differential equations in spaces of Holder-continuous functions 08 p0983 A73-21250

- Necessary and sufficient conditions for differentiable nonscalar-valued functions to attain extrema. 10 p1243 A73-24537

- Vectorial topological continuous function spaces bounded parts, constructing tunneled, quasi-tunneled and nontunneled spaces 11 p1390 A73-25865

- Time-related behavior of causal, anticausal, memoryless and crosscausal nonlinear control systems modeled as operator on group-valued function space 11 p1391 A73-26366

- On the mapping associated with the complex representation of functions and processes. 11 p1333 A73-26645

- Regularity of conditional probabilities for random processes 12 p1518 A73-27192

- On the existence of solutions of the nonlinear theory of shallow shells. 12 p1554 A73-27538

- Approximate solution of the Laplace and Poisson equations in weighted Holder spaces 13 p1647 A73-28340

- Control of functional differential equations with function space boundary conditions. 14 p1770 A73-30754

- Koethe spaces topological properties, considering vector functions integration 15 p1899 A73-31566

- Boundary value properties of weighting space functions and applications of the functions in boundary value problems 15 p1900 A73-32101

- Topology of tunneled locally convex spaces, considering Kelley theorem 15 p1900 A73-32206

- A priori estimates for solution operators of diffusion equations. 15 p1901 A73-32368

- Approximative calculation of flutter regions for collision body systems in phase space, noting fluttering duration as function of post-impact velocity recovery factor 15 p1915 A73-32405

- Application of the generalized Galerkin method to the computation of fluid flows. 17 p2154 A73-35133

- Bireductive spaces, Jordanian algebras, and spinor representations of non-Euclidean and quasi-non-Euclidean motions 17 p2212 A73-35566

- Non-singular control problems. II - Integral equation function-space method applied to the solution of optimization problems in the mechanics of deformable bodies. 19 p2498 A73-37649

- Configuration space and phase space of a system with an infinite number of degrees of freedom 20 p2594 A73-39640

- Transformation symmetry of x-space coordinates of geometric transors, tensors and M-objects with constant length dimensionality 20 p2594 A73-39729

- Finite difference approximation of the weak solution of a mildly nonlinear Dirichlet problem. 21 p2725 A73-40379

- Riesz representability, sigma-additivity and Daniell-integral properties of measures on uniform spaces 21 p2726 A73-40945

- The variable metric algorithm for non-definite quadratic functions. 21 p2727 A73-40999

- Optimal control of multiple-link plants with bounded phase coordinates 22 p2887 A73-42607

- Topological modification and bounded length of decomposition series for convergence space 23 p3000 A73-44301

- Function space approach to prestressed nonlinear orthotropic shallow shell theory boundary value problems 24 p3149 A73-45006

- Integral representations of solutions for general parabolic boundary value problems and the correct solution in spaces of increasing functions 24 p3106 A73-45352

- Geometrical properties of normed spaces, associated with the convexity and smoothness moduli of a unit sphere 24 p3106 A73-45353

FUNCTION TESTS

U TESTS

FUNCTIONAL ANALYSIS

NT BANACH SPACE

NT CONVOLUTION INTEGRALS

NT FOURIER TRANSFORMATION

NT FREDHOLM EQUATIONS

NT HARMONIC ANALYSIS

NT HILBERT SPACE

NT HILBERT TRANSFORMATION

NT INTEGRAL EQUATIONS

NT INTEGRAL TRANSFORMATIONS

NT LAPLACE TRANSFORMATION

NT SINGULAR INTEGRAL EQUATIONS

NT TESSERAL HARMONICS

NT VOLTERRA EQUATIONS

NT WIENER HOPF EQUATIONS

NT ZONAL HARMONICS

- Analysis of certain nonstationary processes by using Wiener functionals 01 p0026 A73-10026

- Absorption line shape computerized functional analysis in solar physics, deriving $H/\alpha, v$ function from Faddeyeva-Terentev probability 01 p0107 A73-11377

- Russian book - Study of the theory of differentiable functions of many variables and its applications. IV. 02 p0187 A73-12176

- Imbedding theorem for the spaces of functions whose mixed derivatives satisfy the multiple integral Holder condition 02 p0187 A73-12178

- Polynomial traces and smoothness moduli of functions of many variables 02 p0187 A73-12179

- Boundary value problems with variable boundaries for a special differential equation 03 p0337 A73-14630

- The time optimal control of a class of distributed systems. 04 p0517 A73-15230

- Functional analysis approach of the partial differential equation arising from non-linear filtering theory. 04 p0472 A73-15263

- Coordinate transformation in arbitrarily dimensional spaces 04 p0443 A73-15509

- Russian book - Variational method and the method of monotonic operators in the theory of nonlinear equations. 04 p0472 A73-15963

- Localization principle for a polyharmonic operator expanded in a Fourier series of a fundamental system of functions 05 p0591 A73-16614

- Stress principle relationship to mechanical power additivity, presenting topological, measure theory and functional analysis theorems 06 p0760 A73-17762

- Contribution to the classical theory of solids with statistical structural characteristics 06 p0762 A73-17994

- Optimal control of a class of linear multivariable systems with integral quadratic energy constraint. 06 p0681 A73-18521

- Construction of a set of systems of second-order delayed-argument differential equations having a prescribed integral curve 06 p0718 A73-18687

The calculus of variations and various direct methods in engineering analysis. 06 p0719 A73-18722

Some preliminary notions towards improved stochastic controller synthesis via transformed indices of performance. 06 p0681 A73-18817

Topologies for neutral functional differential equations. 07 p0845 A73-20493

Minimum fuel control solution for linear discrete systems, discussing finite iterative algorithm based on dual problem of functional analysis 07 p0806 A73-20595

Autocorrelation function synthesis from arbitrary function on finite interval for case of random signals 08 p0951 A73-21102

Turbulent dynamo theory based on functional analysis, noting equation with variational derivatives of characteristic functional 08 p0989 A73-21697

The numerical solution of boundary value problems for second order functional differential equations by finite differences. 09 p1113 A73-23021

Scalar sequence spaces theory extension to vectorial sequence spaces based on bounded ensemble concept 10 p1241 A73-23763

On the duality of sequence spaces with vectorial values 10 p1243 A73-24123

Functional analysis and optimal control of linear discrete systems, deriving algorithms for minimum fuel, energy or amplitude from linear equations solution 11 p1390 A73-25188

Optimal control for functional differential systems through Krasovskii generalization for time delay systems and resulting Riccati equations numerical solution 11 p1392 A73-26581

Analytical properties of solutions to linear differential equations and systems 12 p1516 A73-26951

A method for studying the completeness of systems of analytic functions 12 p1516 A73-26960

Symposium on Ordinary Differential Equations, University of Minnesota, Minneapolis, Minn., May 29, 30, 1972, Proceedings. 12 p1519 A73-27919

Extendibility over the entire plane and the functional equation of a scalar product of Hecke L-series of two quadratic fields 13 p1648 A73-28344

Book - Optimal control of differential and functional equations. 13 p1651 A73-29550

A survey of recent results in differential equations. 14 p1769 A73-30411

Delay and functional differential equations and their applications; Proceedings of the Conference, Park City, Utah, March 6-11, 1972. 14 p1770 A73-30753

Numerical methods for functional differential equations. 14 p1770 A73-30755

Oscillations of higher-order retarded differential equations generated by the retarded argument. 14 p1770 A73-30756

Oscillations of nonlinear functional differential equations generated by retarded actions. 14 p1770 A73-30761

Stability in the critical case of purely imaginary roots for neutral functional differential equations. 14 p1771 A73-30773

Approximation of differentiable functions of numerous variables by Fourier sums in an L sub p metric 15 p1899 A73-31218

An approach to the analysis of boundary value problems in the theory of functions and two-dimensional problems in the theory of elasticity 15 p1954 A73-32124

Proof of B-completeness of locally convex spaces in series of quasi-reflective Banach spaces, generalizing Van Dulst theorem 15 p1900 A73-32205

Nonlinear functional minimization under auxiliary constraints, discussing convergence conditions and iterative solution algorithm performance for least squares weighted sum problem 17 p2199 A73-34106

Kantorovich functional analysis algorithms providing rigorous theory for convergence of iterative methods to nonlinear functional equations on Banach spaces, emphasizing Newton method 17 p2163 A73-35268

A note on saddle point behavior for ordinary and functional differential equations. 17 p2204 A73-35733

Duality relationships for a nonlinear version of the generalized Neyman-Pearson problem. 18 p2330 A73-36636

Fractured solutions in the calculus of variations. 18 p2330 A73-36640

Coordinate function construction in solving the boundary value problems of heat conductivity by direct methods 18 p2372 A73-36818

Some consequences of introducing the geometrical-dynamic characteristic ratio in studies of the heat transfer to surfaces with artificial roughnesses or to microwaving surfaces 19 p2504 A73-37655

Some numerical aspects of the solution of functional equations in dynamic programming 19 p2445 A73-38163

Proposal of a new criterion for evaluating the adequacy of models 21 p2669 A73-40499

Thermoelasticity problems and related particular solutions of a nonhomogeneous Bessel equation 21 p2787 A73-41273

An analytical method of designing long turbine blades 22 p2918 A73-41960

On the Volterra series functional evaluation of the response of non-linear discrete-time systems. 22 p2837 A73-43069

Continuous dependence of holomorphic functions on partly given boundary values. 23 p3000 A73-44302

The governing equations and extremum principles of elasticity and plasticity generated from a single functional. I. 24 p3152 A73-45315

FUNCTIONAL INTEGRATION

Operational algorithms for probabilistic digital integrators for Stieltjes integral and nonhypertranscendental functions 09 p1060 A73-22555

Construction of upper and lower functions during approximate integration of a nonlinear system containing a biharmonic operator 13 p1651 A73-29678

Koethe spaces topological properties, considering vector functions integration 15 p1899 A73-31566

Stochastic integrals of cylindrical Brownian movements on Hilbert space 15 p1900 A73-32207

FUNCTIONALS

Variational optimization problems for hyperbolic-type equations 01 p0077 A73-10952

Sufficient conditions for the optimal control problem 01 p0071 A73-11269

Stationary functionals for introducing eigenfunctions in diffraction theory of electrodynamic systems 03 p0337 A73-14080

Calculus of variations for functional conditional extremum, determining minimum drag shape for body of revolution in hypersonic flow 04 p0403 A73-14886

A new method of obtaining Q solutions to extremal problems in certain special classes of analytic functions associated with functions whose real part is positive in a circle 04 p0470 A73-15083

The limiting theorems for certain functionals of multidimensional additive processes 05 p0591 A73-17226

Algorithmic construction of optimal controllers on the basis of incomplete information about the state of the plant 09 p1068 A73-22562

Weak convergence of stepwise random processes 09 p1112 A73-22886

Numerical solution of the optimal control problem by the direct method 10 p1197 A73-23999

Use of the least squares criterion in the finite element formulation. 10 p1243 A73-24295

Two quadratic cost functionals equivalence conditions derivation in terms of system parameters and weighting matrices for optimal control law generation 11 p1341 A73-25196

Calculation of functionals of the eigenfunctions in the boundary value problem of a system of linear ordinary differential equations 11 p1391 A73-26331

Variational method for a generalized class of functionals and its application to aeromechanics problems 11 p1304 A73-26438

Variational optimization problems for equations of hyperbolic type. 12 p1518 A73-27528

On the connection between the elliptic equations of the Navier-Stokes type and the theory of harmonic functionals. 14 p1769 A73-30521

Russian book on inverse problems for hyperbolic differential equations covering functionals, uniqueness theorems, integral geometry and earth interior structure from seismological data 15 p1899 A73-31581

FUNCTIONS [MATHEMATICS]

Optimal control in a finite time interval for discrete systems in the minimization problem of an inhomogeneous quadratic functional /a case of fixed terminals/ 15 p1854 A73-31802

Minimization of quadratic functionals in the presence of quadratic constraints and the necessity of a frequency condition in the quadratic criterion of absolute stability for nonlinear control systems 16 p2034 A73-34071

Book - Variational analysis: Critical extremals and sturmian extensions. 17 p2203 A73-35598

Necessary conditions for Chebyshev-Bolza optimal control problems. 19 p2415 A73-38489

Chebyshev minimax functional solution for optimal control system design, noting flexible rocket and nuclear reactor control applications 20 p2592 A73-38683

Nonnegative additive functionals of Markov processes and certain limit theorems 20 p2582 A73-39389

Lower bounds on the cost functional for systems governed by partial differential equations. 21 p2726 A73-40838

Nonlinear methods for evaluating the informative value of meteorological parameters and for classifying meteorological phenomena /Functional methods and algorithms/ 23 p3001 A73-43464

Optimal control over a finite time-interval for discrete systems in the problem of minimizing an inhomogeneous quadratic functional /The case of fixed end-points/. 23 p2965 A73-44331

FUNCTIONS [MATHEMATICS]

NT ABEL FUNCTION

NT AIRY FUNCTION

NT ANALYTIC FUNCTIONS

NT APERIODIC FUNCTIONS

NT ASYMPTOTES

NT BOOLEAN FUNCTIONS

NT CONFORMAL MAPPING

NT COORDINATE TRANSFORMATIONS

NT DELTA FUNCTION

NT DISCRETE FUNCTIONS

NT DISTRIBUTION FUNCTIONS

NT DISTURBING FUNCTIONS

NT ELLIPTIC FUNCTIONS

NT ENTIRE FUNCTIONS

NT ERROR FUNCTIONS

NT EXPONENTIAL FUNCTIONS

NT FOURIER TRANSFORMATION

NT FRESNEL INTEGRALS

NT GAMMA FUNCTION

NT GREEN FUNCTION

NT HAMILTONIAN FUNCTIONS

NT HANKEL FUNCTIONS

NT HARMONIC FUNCTIONS

NT HYPERBOLIC FUNCTIONS

NT HYPERGEOMETRIC FUNCTIONS

NT KERNEL FUNCTIONS

NT LAGUERRE FUNCTIONS

NT LAME FUNCTIONS

NT LAPLACE TRANSFORMATION

NT LEGENDRE FUNCTIONS

NT LIAPUNOV FUNCTIONS

NT LINEAR TRANSFORMATIONS

NT LOGARITHMS

NT LORENTZ TRANSFORMATIONS

NT MATHIEU FUNCTION

NT MAXWELL-BOLTZMANN DENSITY FUNCTION

NT MELLIN TRANSFORMS

NT MEROMORPHIC FUNCTIONS

NT MONOTONE FUNCTIONS

NT NORMAL DENSITY FUNCTIONS

NT ORTHOGONAL FUNCTIONS

NT ORTHONORMAL FUNCTIONS

NT PERIODIC FUNCTIONS

NT POISSON DENSITY FUNCTIONS

NT PROBABILITY DENSITY FUNCTIONS

NT PROBABILITY DISTRIBUTION FUNCTIONS

NT RATIONAL FUNCTIONS

NT RAYLEIGH DISTRIBUTION

NT RECURSIVE FUNCTIONS

NT SCHWARZ-CHRISTOFFEL TRANSFORMATION

NT SPACE-TIME FUNCTIONS

NT SPHERICAL HARMONICS

NT SPLINE FUNCTIONS

NT STEP FUNCTIONS

NT STRESS FUNCTIONS

NT TIME FUNCTIONS

NT TRANSCENDENTAL FUNCTIONS

NT TRANSFER FUNCTIONS

NT TRIGONOMETRIC FUNCTIONS

NT WALSH FUNCTION

NT WEIBULL DENSITY FUNCTIONS

NT WEIGHTING FUNCTIONS

NT WHITTAKER FUNCTIONS

Steady ergodic Markovian random function construction 01 p0071 A73-11271

- Numerical Laplace transform inversion of a function arising in viscoelasticity. 01 p0119 A73-11469
- Approximation by functions of fewer variables. 02 p0186 A73-11969
- Comparison of the Powell 1, Powell 2, and Zangwill static optimization methods. 06 p0670 A73-17859
- Evaluations of matrix functions by real similarity transformation. 06 p0718 A73-18536
- Mathematical properties of and optimization methods for bandlimited function systems, discussing applications to engineering problems. 09 p1051 A73-22491
- Linear dependence of functions along the solutions of systems of differential equations and of a system with algebraic loci. 10 p1241 A73-23743
- Immittance functions realizability by passive normal bipoles based on poles and zeros dislocations. 10 p1202 A73-24415
- A new method for studying the symmetry reduction of a system by means of a perturbation. 11 p1326 A73-25867
- Modeling irregular surfaces. 13 p1619 A73-29242
- Determining unknown coefficients in a nonlinear heat conduction problem. 14 p1817 A73-30406
- An equivalence theorem on best approximation of continuous functions by algebraic polynomials. 15 p1902 A73-32376
- The choice of step length, a crucial factor in the performance of variable metric algorithms. 16 p2033 A73-33853
- Mathematical functional modular building block implementation in LSI microelectronics for signal and data processing, discussing primitive functions and 8-bit family design example. 17 p2138 A73-35229
- Constrained optimization using a nondifferentiable penalty function. 21 p2725 A73-40384
- FUNGI**
- NT RHIZOPUS
- NT YEAST
- Volatile terpenoids from aeciospores of *Cronartium fusiforme*. 12 p1462 A73-27145
- Space-related research in mycology concurrent with the first decade of manned space exploration. 20 p2513 A73-39478
- Biophysical considerations concerning gravity receptors and effectors including experimental studies on *Phycomyces blakesleeana*. 22 p2804 A73-42171
- Sterols of the fungi - Distribution and biosynthesis. 24 p3059 A73-44699
- FURAN RESINS**
- NT POLYAMIDE RESINS
- FURFURYL ALCOHOL**
- Effects of hardening conditions on the physicochemical and frictional properties of polyvinyl furfural. 08 p0982 A73-21591
- FURLABLE ANTENNAS**
- Critical velocities of the steady motion of a pliable thread in plane homogeneous flow. 22 p2928 A73-43061
- FURNACES**
- NT VACUUM FURNACES
- Equipment for casting directionally solidified parts. 09 p1089 A73-23294
- A computer model for three-dimensional flow in furnaces. 22 p2934 A73-42787
- FUSELAGE MOUNTING**
- U AIRCRAFT PRODUCTION
- FUSELAGES**
- Optimization and design of the rear fuselage of the A 300 B aircraft structure. 10 p1288 A73-23799
- Taylor series algorithms for computerized structural design and reanalysis of modified structures, applying to aircraft fuselage midsection [AIAA PAPER 73-338]. 11 p1436 A73-25478
- Contribution to the theory of the finite element method applied to the overall stress analysis of a fuselage. 12 p1551 A73-27084
- Pressurized fuselage design studies for short haul transport aircraft, discussing sandwich structures and bonding techniques for Al and Ti alloy construction materials. 16 p2018 A73-33069
- Applications and concepts for the incorporation of composites in large military transport aircraft. 17 p2104 A73-34816
- An investigation of the flow field and drag of helicopter fuselage configurations. [AHS PREPRINT 700]. 17 p2095 A73-35051
- Exploratory development of composite missile fuselages. 17 p2181 A73-35354

- Aircraft fuselage structure weight estimation method assuming bending, shear, torque and internal pressurization loading for skin-stringer-shallow frame types [SAWE PAPER 981]. 19 p2385 A73-37887
- A computer-aided design procedure to approximate aircraft area curve shapes. [SAWE PAPER 982]. 19 p2385 A73-37888
- Some results of fuselage calculations on a digital computer by the finite-element method. 21 p2783 A73-40387
- FUSES [ORDNANCE]**
- The utilization of detonating fuses on launchers. 07 p0865 A73-18996
- FUSIFORM SHAPES**
- U CONES
- FUSION [MELTING]**
- Activation energy volume relation to heat of fusion and lattice characteristics for vacancy diffusion along crystal grains in melting metals. 01 p0087 A73-10256
- Titanium nitrides effect on austenite grains formation by high temperature fusion, considering electric arc and vacuum melting of structural steels. 06 p0706 A73-17883
- Correlation between the diffusion activation energy, the heat of fusion, and the bond energy in metals. 06 p0708 A73-18046
- Fused salt techniques for metal diffusion coatings with beryllium, boron, silicon, aluminum, titanium and chromium. 16 p2017 A73-32697
- The emissivities of liquid metals at their fusion temperatures. 22 p2930 A73-41983
- FUSION WELDING**
- NT ARC WELDING
- NT BRAZING
- NT ELECTRON BEAM WELDING
- NT ELECTROSLAG WELDING
- NT GAS TUNGSTEN ARC WELDING
- NT GAS WELDING
- NT PLASMA ARC WELDING
- Reflections on the nature of the bond in welding of metals - The particular case of fusion welding. 06 p0698 A73-18693
- Mechanical behavior of assemblies welded by fusion on steel. 06 p0698 A73-18694
- Laser beam welding technology review, discussing technical and economic aspects of pulse and CW techniques. 11 p1374 A73-25850
- The metallurgical implications of welding processes. 16 p2021 A73-33863
- Scribe line technique detects incomplete fusion in EB welds. 21 p2708 A73-41251
- F4H AIRCRAFT**
- U F-4 AIRCRAFT
- F8U AIRCRAFT**
- U F-8 AIRCRAFT
- G**
- G FORCE**
- U ACCELERATION [PHYSICS]
- GADOLINIUM**
- NT GADOLINIUM ISOTOPES
- The magnetic characteristics of the alloys of palladium with gadolinium, dysprosium, and holmium. 13 p1667 A73-28183
- GADOLINIUM ISOTOPES**
- Apollo 16 neutron stratigraphy. 18 p2354 A73-36514
- GAGES**
- U MEASURING INSTRUMENTS
- GAIN [AMPLIFICATION]**
- U AMPLIFICATION
- GALACTIC CLUSTERS**
- The interaction of primordial gravitational waves with groups of galaxies. 01 p0098 A73-10585
- The n-body problem with variable gravitational constant, and some dynamical consequences for large-scale cosmic systems. 01 p0107 A73-11327
- Intergalactic ionized hydrogen in nearby groups of galaxies. 02 p0225 A73-12803
- Isotropic system development of gravitating point particles in galactic clusters and superclusters in expanding universe from Liouville theorem and BBGKY hierarchy. 03 p0365 A73-12927
- The redshifts of quasi-stellar objects and associated galaxies. 03 p0375 A73-13896
- The redshift-distance relation. II - The Hubble diagram and its scatter for first-ranked cluster galaxies: A formal value for q-sub 0. III Photometry and the Hubble diagram for radio sources and the possible turn-on time for QSOs. 04 p0498 A73-15351
- Astronomical catalogs for galactic superclusters existence including north galactic pole region, noting distance differentiation for structural singularities isolation. 05 p0613 A73-16213
- Central portion of the galactic cluster Coma Berenices. III. 05 p0617 A73-16458
- Sphericity distribution function of galaxy-cluster members. 05 p0617 A73-16459
- Mean radial velocity of Virgo galactic cluster from red shift data, approximating velocity distribution of elliptical-lenticular and spiral galaxies. 05 p0622 A73-17074
- Expansion hypothesis and assumption of invisible intergalactic matter in galactic clusters stability theory, noting IR spectroscopy and radio observation. 05 p0623 A73-17196
- Observations of the extended X-ray sources in the Perseus and Coma clusters from Uhuru. 05 p0625 A73-17327
- Observations of the radio source PKS0123-01 at 5000, 408, and 80 MHz. 06 p0754 A73-18627
- Stability of clusters of galaxies with mass loss to gravitational radiation. 07 p0873 A73-19053
- Rocket-borne measurement of UV background radiation at 1115, 1425 and 1446 Å, setting upper limit to flux from Coma galactic cluster. 07 p0868 A73-19057
- Physics of the X-radiation from clusters of galaxies. 07 p0874 A73-19074
- Determination of the type of motion in spherically symmetric systems of galaxies. 07 p0901 A73-20313
- Clusters of galaxies and the cosmic light. 08 p1002 A73-20876
- Shakhbazian I - A distant cluster of compact galaxies. 08 p1004 A73-20897
- Redshifts of a BSO and galaxies in the vicinity of the radio source RN 8. 08 p1009 A73-21171
- The role of Schmidt telescopes in the study of galactic structure /Photometric methods/. 08 p1011 A73-21355
- The role of Schmidt telescopes in the study of external galaxies. 08 p1011 A73-21361
- Surface colour photometry of galaxies with Schmidt telescopes. 08 p1011 A73-21363
- Nonzero neutrino rest mass to account for virial mass discrepancy in Coma cluster and missing cosmological mass needed to close universe. 09 p1141 A73-22027
- Main results of the investigation of the Sculptor-type dwarf galaxies. 09 p1147 A73-22549
- The observation of relic radiation as a test of the nature of X-ray radiation from the clusters of galaxies. 09 p1138 A73-22953
- The dependence of Compton X-ray emission from clusters of galaxies on the velocity dispersion of the cluster. 10 p1264 A73-23544
- Upper limits on an ionized intracluster medium in the Coma cluster. 10 p1272 A73-23545
- Causes of the rotation of galaxies in terms of the nonlinear theory of gravitational instability. 10 p1274 A73-23712
- Formation of stars in a rotating cloud with magnetic field. 10 p1275 A73-23830
- Primordial random motions and angular momenta of galaxies and galaxy clusters. 11 p1427 A73-26601
- The spectrum of the extranuclear regions of Ton 256. 11 p1428 A73-26624
- List of clusters of galaxies with published redshifts. 11 p1428 A73-26677
- Metagalactic cosmic ray origin models and cosmic ray energy density around Galaxy, considering gamma ray flux, measurement from Magellanic Clouds. 12 p1539 A73-27142
- Determination of the type of motion in spherically symmetric clusters of galaxies. 12 p1539 A73-27285
- Neutral hydrogen clouds gravitational binding of Coma cluster, providing mechanism for heating of diffuse gas between clouds and galaxies. 13 p1684 A73-29352
- Mariner 9 ultraviolet spectrometer experiment - Upper limits on the Lyman-alpha flux from clusters of galaxies. 15 p1936 A73-31551

The properties of extragalactic X-ray sources from visible light observations. 16 p2050 A73-32742

Evidence for the existence of galactic superclusters near the galactic North Pole 16 p2063 A73-33661

On the apparent association of quasi-stellar objects with clusters or groups of galaxies with about the same redshift. 17 p2231 A73-34767

The applications of relativistic kinetic theory to cosmological models - Some observational consequences. 17 p2234 A73-35616

Extragalactic radio sources modeled as bubbles of relativistic plasma rising through hot gas, producing galactic clusters X ray emission 18 p2353 A73-36508

Development of rotation in galaxies in the nonlinear theory of gravitational instability. 18 p2354 A73-36737

Limits to the spectra of the Perseus and Coma clusters above 7 keV from the OSO-7. 18 p2357 A73-37101

Nonuniform model construction for dense intergalactic medium with gravitational binding of all galactic groups and clusters by ionized gas 19 p2484 A73-37608

Soft X-ray flux of the Coma cluster of galaxies. 19 p2475 A73-37626

The redshift-distance relation. VI - The Hubble diagram from S20 photometry for rich clusters and sparse groups - A study of residuals. 19 p2487 A73-38505

The redshift-distance relation. VII - Absolute magnitudes of the first three ranked cluster galaxies as functions of cluster richness and Bautz-Morgan cluster type - The effect on q sub 0. 19 p2487 A73-38506

Study of the redshift structure of the Coma cluster. 20 p2610 A73-39580

Dynamical models of tailed radio sources in clusters of galaxies. 20 p2610 A73-39584

Clusters of galaxies - A possible source of background emission in the X-ray band 21 p2759 A73-40709

Residual velocities of clusters and indications of the existence of a local cluster 21 p2768 A73-40713

Balloon measurement of angular extent of Coma and Virgo clusters hard X ray emission 21 p2762 A73-41393

Model for galactic cluster formation after radiation decoupling from matter in Einstein-De Sitter universe, discussing turbulence in primeval cosmos 21 p2778 A73-41526

Effect of Gaunt factors on analysis of X-ray spectra - Viability of a thermal intergalactic medium in the Coma cluster. 22 p2900 A73-41753

Shakhbazian I compact galactic cluster, discussing red shift, angular size, galactic type, velocity dispersion, mass/light ratio and photographic plates 22 p2909 A73-42586

Concerning the forms of the velocity-distance relation clusters. 22 p2913 A73-43001

Isothermal gas-sphere model with thermal bremsstrahlung for X ray emission from Coma, Perseus and Virgo galactic clusters, noting gas distribution 22 p2904 A73-43120

Galactic protocluster radio emission detection, using adiabatic density perturbation theory of galactic evolution 23 p3037 A73-44256

Radius-parameter and surface brightness as a function of galaxy total magnitude for clusters of galaxies. 24 p3135 A73-44582

Clusters of galaxies with a wide range of X-ray luminosities. 24 p3139 A73-45055

The relation between redshift and surface brightness for normal galaxies in systems of galaxies. 24 p3141 A73-45193

GALACTIC EVOLUTION

Book - Astrometry - Theoretical astrophysics Instrumentation - Spectroscopy - Galactic structure - Galaxies. 01 p0095 A73-10293

Spiral structure and kinematics of the galaxy from a study of the H II regions - Fabry-Perot interference methods applied to ionized hydrogen. 01 p0096 A73-10297

Structure and dynamics of barred spiral galaxies, in particular of the Magellanic type. 01 p0096 A73-10298

Hypothetical process of galaxy or quasar formation by material outflow from singularity, discussing expansion velocity, stellar light concentration, interstellar lines and universe density 01 p0102 A73-10968

Newtonian analysis of cosmological model for galactic accretion from small initial perturbation of central black hole 01 p0104 A73-11048

Stellar gas injection into nucleus of radio galaxy NGC 4486, estimating energy release during gas accretion 01 p0106 A73-11301

Single gaseous object and stellar cluster models of quasars and galactic nuclei stability, noting neutron and collapsing star lifetimes 01 p0106 A73-11302

Pregalactic vortex motion decay calculation from kinetic equation of hot expanding universe model 01 p0106 A73-11307

Direction of winding in spiral galaxies. 01 p0106 A73-11317

Rotational perturbations in anisotropic cosmology. 01 p0107 A73-11328

Generation of the large-scale galactic magnetic field. 01 p0107 A73-11329

II. 01 p0107 A73-11329

The evolution of galaxies - A heretical view. 02 p0211 A73-11592

Biorthogonal function pairs for gravitational field calculations for flat galaxies, deriving algorithms from Hankel-Laguerre functions properties 02 p0216 A73-12380

Changes in the gravitational energy of galaxies during collisions. 02 p0217 A73-12392

21-cm neutral hydrogen line study of early type galaxies. 02 p0222 A73-12716

A numerical hydrodynamic study of coalescence in head-on collisions of identical stars. 02 p0223 A73-12727

A galactic formation model based on post-big bang fragmentation. 02 p0224 A73-12740

Star formation in the galaxy. 02 p0224 A73-12744

Condensation and protostar expansion hypotheses of stellar and galactic evolution in view of discoveries of quasars, central bodies and stellar associations 03 p0365 A73-12902

Tidal generation of narrow intergalactic filaments from computer simulations, discussing alternative models 03 p0372 A73-13353

Epicyclic motion of stars at different regions of the galaxy. 03 p0379 A73-14586

Galaxy formation from amihilation-generated supersonic turbulence in the baryon-symmetric big-bang cosmology and the gamma-ray background spectrum. 04 p0499 A73-15353

Primordial turbulence and the formation of galaxies. 04 p0499 A73-15354

Evidence for elliptical galaxy rotation, considering flattening, orbital statistics and interactions of external and internal forces 05 p0616 A73-16453

Stability conditions for strongly flattened galaxy model with respect to axisymmetric disturbances of gaseous subsystem in finite isothermal layer 05 p0616 A73-16456

Gravitational field effects on processes near stars and galaxies in late evolution phases, describing particle motion and light propagation near rotating sources 05 p0623 A73-17197

Tidal gravity models of interacting pair formation of galactic bridges and tails in terms of orbit geometry, outer shapes and forced spiral waves 05 p0626 A73-17378

Velocity dispersions in galaxies. II - The ellipticals NGC 1889, 3115, 4473, and 4494. 07 p0873 A73-19054

The stability of a self-gravitating, nonrotating gas layer with stellar, magnetic, and cosmic-ray components. II. 07 p0873 A73-19058

Origin of magnetic fields in the early universe. 07 p0877 A73-19607

Preliminary quasar model based on the Yilmaz exponential metric. 07 p0899 A73-20178

Time variation of metal abundance in galaxies - Super-metal-rich stage. 07 p0902 A73-20446

A neutral hydrogen survey of the galaxy M33. II - Distribution and kinematics of the neutral hydrogen. 08 p1005 A73-20913

Nonaxisymmetric kinematics in galaxies with axisymmetric mass distributions. 08 p1008 A73-21154

The history of star formation and the colors of late-type galaxies. 08 p1008 A73-21155

Quasars as events in the nuclei of galaxies - The evidence from direct photographs. 08 p1009 A73-21168

Stellar formation and cloud collision energy dissipations as energy sources for self gravitating shock waves maintenance in Galactic spiral theory 09 p1141 A73-22008

A search for neutral hydrogen remnants of strong tidal disruption of the Small Magellanic Cloud. 09 p1141 A73-22012

Cloud-cloud collision destruction of interstellar clouds in inter-spiral arm regions, discussing observational tests 09 p1141 A73-22028

X ray background emission and behavior of infalling intergalactic gas into Galaxy resulting from shock wave generation and heating in accretion process 10 p1264 A73-23495

Causes of the rotation of galaxies in terms of the nonlinear theory of gravitational instability 10 p1274 A73-23712

An exact solution for a collisionless flat galactic model. 10 p1275 A73-23826

The manifold of galaxies - Galaxies with known dynamical parameters. 10 p1281 A73-24407

Rotating galaxies gravothermal catastrophe via violent relaxation leading to black hole core and halo system 10 p1284 A73-24911

Small perturbations in flat galaxies. I - Equilibrium models and adiabatic perturbations. 10 p1284 A73-24913

Dense stellar systems dynamics, considering gravitation relaxation, star evaporation, antiequipation, growth of dense galactic cores, stellar coalescence, disruption and formation 11 p1414 A73-25065

Primordial random motions and angular momenta of galaxies and galaxy clusters. 11 p1427 A73-26601

Galaxies as local perturbations in homogeneous universe, considering galactic manufacture within Einstein theory context 12 p1539 A73-27141

Condensation of stars and magnetic field formation in protogalaxies 12 p1547 A73-27868

Wave model of Galaxy spiral structure, assuming subsystem mass distribution and old star rotating bar mechanism 12 p1547 A73-27879

Dependence of the integrated background light on cosmology, galactic spectra, and galactic evolution. 13 p1671 A73-28035

Dynamical contraction of rotating gaseous spheroids. 13 p1680 A73-28774

Vortex motions of cosmic matter as cosmological evolution mechanism, considering galactic and solar system kinetics 13 p1681 A73-28780

Turbulence dissipation model for galactic origin, accounting for masses and angular momenta of large galaxies 14 p1796 A73-30002

Hypothesis postulating two types of quasars, considering cosmologically distant quasars /type I/ and type II branch produced by explosions in nearby galaxies 14 p1797 A73-30003

The process of galaxy formation according to the universal turbulence hypothesis. 14 p1798 A73-30142

Young open star clusters. II - Their nature and their significance for galaxy research 14 p1798 A73-30274

Low energy galactic cosmic ray exploration via space mission to Jupiter and Saturn, considering nuclear abundances and galactic evolution theories 14 p1787 A73-30542

Eruptive binary stars evolutionary origin, outburst mechanisms and effects on Galactic evolution 15 p1935 A73-31487

Re-187, recycling r-process elements through stars, and the age of the Galaxy. 15 p1939 A73-32014

The dynamical effects of cosmic rays in the Galaxy and the generation of the galactic magnetic field. 16 p2054 A73-33287

Development of rotation in galaxies in the nonlinear theory of gravitational instability. 18 p2354 A73-36737

Implications of the statistical bootstrap model for cosmology and galaxy formation. 19 p2482 A73-37559

Astronomische Gesellschaft, Scientific Meeting, Vienna, Austria, September 18-23, 1972, Reports 20 p2605 A73-39056

Optical and radio observations of NGC 4258 anomalous arms indicating eruptive processes in galactic nucleus as possible source of spiral structure 20 p2605 A73-39057

Star contraction and magnetic-field generation in protogalaxies. 20 p2608 A73-39242

- Universe evolutionary model construction based on observations of high flux gravitational radiation generated within Milky Way Galaxy
20 p2609 A73-39434
- On galaxy formation from primeval universal turbulence. II.
20 p2609 A73-39572
- Galaxy formation associated with active galaxies and the binding of rich clusters.
20 p2613 A73-39827
- A new estimate of the fluctuation of relic radiation in the universe
21 p2759 A73-40708
- Galactic nucleosynthesis time interval from birth to solar system formation /Galactic age/ from radioactive decay nuclear yield ratios
22 p2916 A73-43049
- Galactic protocluster radio emission detection, using adiabatic density perturbation theory of galactic evolution
23 p3037 A73-44256

GALACTIC MAGNETIC FIELDS

U INTERSTELLAR MAGNETIC FIELDS

GALACTIC NUCLEI

- Absorption line width method for stellar population of galaxies NGC 1052, 2655, 2903 and 4569 nuclei
03 p0371 A73-13221
- Velocity dispersions in galaxies. II - The ellipticals NGC 1889, 3115, 4473, and 4494.
07 p0873 A73-19054
- Lambda-Sco, a possible source of soft X-rays.
07 p0900 A73-20183
- Optical variability of the nuclei of Seyfert galaxies
07 p0901 A73-20306
- Stokes polarization parameters of optical emission scattered in absorbing medium calculated for Galaxy and M 82 galaxy, assuming thermal IR radiation from nucleus
07 p0901 A73-20312
- Virgo A nucleus compact radio source observation from February 1971 to August 1972, noting absence of intensity or size variations
08 p1004 A73-20898
- Quasars as events in the nuclei of galaxies - The evidence from direct photographs.
08 p1009 A73-21168
- A model for peaking of galactic gravitational radiation.
08 p1009 A73-21201
- Application of statistics to results in gamma ray astronomy.
08 p1012 A73-21644
- 327-MHz observations of the galactic center - Possible detection of a deuterium absorption line.
08 p1013 A73-21808
- A discussion of the new variations observed in the nucleus of the Seyfert galaxy NGC 3516.
09 p1140 A73-22004
- H I absorption in the galactic center region and between galactic longitudes 350 deg and 359 deg.
09 p1141 A73-22009
- Preliminary data for the optical variability of the eruption from the NGC 4486 /M87/ nucleus
09 p1145 A73-22287
- A synchrotron radiation model of the infrared radiation from the nucleus of NGC 1068.
09 p1150 A73-23144
- Galactic nuclei and QSO far IR radiation luminosity explanation by nonthermal maser emission due to gas molecules in dense clouds
09 p1150 A73-23145
- Optical and near-infrared observations of the nearby spiral galaxy Maffei 2.
10 p1272 A73-23528
- Gamma-ray emission from the region of the Galactic center.
10 p1264 A73-23530
- Validity of zeta Oph cloud carbon isotope abundance extrapolation to dense dusty regions of Galactic center and Orion Nebula
10 p1275 A73-23824
- Radio pulses from the direction of the galactic centre.
10 p1280 A73-24272
- Rotating galaxies gravothermal catastrophe via violent relaxation leading to black hole core and halo system
10 p1284 A73-24911
- Infrared and radio observations of the nucleus of NGC 253.
11 p1428 A73-26625
- Optical variability of the nuclei of Seyfert galaxies.
12 p1539 A73-27278
- Stokes polarization parameters of optical emission scattered in absorbing medium calculated for Galaxy and M 82 galaxy, assuming thermal IR radiation from nucleus
12 p1539 A73-27284
- Limit to pulses of radiofrequency emission from the galactic centre.
14 p1800 A73-30600
- Search for infrared anomalies associated with gravitational events at the galactic centre.
14 p1800 A73-30601

- Positron-annihilation radiation from neutron stars.
14 p1788 A73-30738
- Gamma-ray observations of the galactic centre.
15 p1933 A73-31354
- Photometry and some characteristics of spiral Seyfert galaxies beyond the nucleus boundary
15 p1938 A73-31951
- Double structure characterization in ideal model by two extended radio emitting regions near nucleus of optical galaxy or quasar
15 p1940 A73-32073
- An upper limit to the angular diameter of the nucleus of NGC 4151.
17 p2231 A73-34751
- Far-infrared observations of galactic nuclei.
17 p2232 A73-34771
- Optical and radio observations of NGC 4258 anomalous arms indicating eruptive processes in galactic nucleus as possible source of spiral structure
20 p2605 A73-39057
- Detection of a gamma-ray spectral line from the galactic-center region.
20 p2602 A73-39438
- Quasar and galactic nuclei energy source models, considering supermassive rotating magnetoplasma body, black hole and compact star cluster with flares and collisions
20 p2609 A73-39570
- Observations of neutral hydrogen near the galactic center. II - The nuclear disc.
20 p2610 A73-39578
- Quantized magnetic bremsstrahlung from white dwarfs surface layer as possible source of Galactic center infrared radiation
20 p2611 A73-39709
- Galaxy formation associated with active galaxies and the binding of rich clusters.
20 p2613 A73-39827
- Infrared maps of the galactic nucleus.
22 p2904 A73-41757
- Pulsar search in Galactic nucleus region at 430 MHz with 140 foot telescope, discussing data reduction and results
22 p2909 A73-42484
- Galactic nuclei, pulsars and supernovae as sources of primary cosmic rays from ground based and satellite observations, relating chemical composition to origin
22 p2904 A73-43116
- Ion-grain collision cooling rate for hot gas above million K, discussing applications to supernova explosions, Seyfert nuclei and intergalactic matter within galactic clusters
22 p2916 A73-43121
- Sensitive search for microwave pulses from the galactic centre.
23 p3033 A73-43961
- Normal galaxy central region dust content /mass/ estimates based on photoelectric measurements
23 p3035 A73-44235
- Photometry and some features of Seyfert spiral galaxies beyond the nuclear region.
24 p3131 A73-44476
- Neutral hydrogen rotational motions near galactic center and 3-kpc arm, using dispersion ring model
24 p3140 A73-45180
- Physical conditions in nuclei of spiral galaxies. I - Study of galaxies with a nuclear radio-component.
24 p3141 A73-45192

GALACTIC RADIATION

NT GALACTIC RADIO WAVES

- Supernova remnants descriptions, distance and hydrodynamic evolution, considering galactic nonthermal radio sources, radio maps, and X ray and radio polarization
01 p0094 A73-10057
- Book - Cosmic rays: Selected readings in physics.
01 p0091 A73-10122
- A survey of linear polarization at 1415 MHz. III - Method of reduction and results for the galactic spurs.
01 p0096 A73-10319
- The image tube nebular spectrograph of the Asiago Observatory.
01 p0050 A73-10543
- Energy distribution in the near infrared from nuclei of galaxies. I - M31, M32, NGC 3115, NGC 4151, NGC 4406.
01 p0098 A73-10552
- Observational data on galaxies with UV continuum, listing objects with emission lines, s-sd classification and quasar spectral energy distribution
01 p0099 A73-10701
- Nature of galaxies with an ultraviolet continuum. I - Basic spectral and color characteristics
01 p0099 A73-10702
- Hydrogen lines in the spectrum of the Markarian 6 galaxy during its activity period
01 p0100 A73-10703
- Space maser with feedback
01 p0060 A73-10934
- Galactic and extragalactic X and gamma ray sources identification from satellite, rocket and high altitude balloon observations, discussing radiation generation theories
01 p0092 A73-10990

- High-energy cosmic gamma-ray observations from the OSO-3 satellite.
01 p0092 A73-11028
- Positive detection of an excess of low-energy diffuse X-rays at high galactic latitude.
01 p0092 A73-11029
- Galactic-latitude dependence of low-energy diffuse X-rays.
01 p0092 A73-11030
- Observations of galactic cosmic-ray intensity at heliocentric radial distances of from 1.0 to 2.0 astronomical units.
01 p0093 A73-11044
- International Conference on Cosmic Rays, 12th, University of Tasmania, Hobart, Tasmania, Australia, August 16-25, 1971, Papers. Volumes 1, 2, 3, 4, 5 & 6.
01 p0093 A73-11375
- Radial gradients and anisotropies due to galactic cosmic rays.
02 p0207 A73-12378
- Extensive cosmic ray shower production by relativistic dust grain accelerated in interstellar space by galactic radiation pressure and subsequent magnetic processes
02 p0207 A73-12388
- Diffuse galactic FUV radiation and interstellar dust grains.
02 p0207 A73-12399
- Cosmic-ray production of deuterium, He3/, lithium, beryllium, and boron in the galaxy.
02 p0208 A73-12412
- Relativistic electron radio emission models, calculating magnetic bremsstrahlung spectra from galactic electron space-energy distributions
02 p0208 A73-12459
- The radio emission of NGC 4258 and the possible origin of spiral structure.
02 p0221 A73-12701
- 21-cm neutral hydrogen line study of early type galaxies.
02 p0222 A73-12716
- Long time optical variability model of quasars and Seyfert galaxies in terms of grain extinction variations in intervening clouds due to thermal and atom impact evaporation
02 p0226 A73-12839
- Variation of emission-line strengths across M31.
03 p0366 A73-12928
- Adiabatic propagation of cosmic rays in the Galaxy.
03 p0360 A73-12929
- Interstellar OH lambda doublet radiation observations at 5 cm from six galactic sources and IR star, observing various transitions
03 p0366 A73-12930
- Polarimeter search for optical circular polarization in eclipsing binaries, magnetic Ap stars, planetary nebula, Hubble and Orion nebulae, M87 and Sirius
03 p0366 A73-12939
- The absorption by the interstellar medium of 80 MHz radio emission from galactic supernova remnants.
03 p0372 A73-13346
- Asymmetry of soft X-ray emission near M87.
03 p0361 A73-13713
- Observations of planets, nebulae, and galaxies at 350 microns.
03 p0374 A73-13716
- Solar cyclic intensity variation of excess radiation with respect to galactic radiation background at low altitudes from satellite data analysis
03 p0365 A73-14575
- Kinematics of H-alpha emission from an abnormal filament of the galaxy NGC 4258
03 p0380 A73-14609
- Molecular clouds in the galactic center region - Carbon monoxide observations at 2.6 millimeters.
04 p0499 A73-15357
- Distances and absolute luminosities of galactic X-ray sources.
04 p0492 A73-15358
- Modulation of low-energy galactic cosmic rays over solar maximum /cycle 20/.
04 p0493 A73-15549
- Cosmological deceleration parameter differences prediction from light evolution correction on diameter-red shift relation of cluster elliptical galaxies
04 p0502 A73-15689
- Disk-shaped diffusion model with inhomogeneous distribution of gas and heavy relativistic nuclei sources for galactic cosmic rays chemical composition
05 p0608 A73-16081
- Diffuse radiation of a two-layer galaxy with carbon-silicate particles
05 p0617 A73-16460
- Spectrophotometric survey of diffuse galactic nebulae
05 p0617 A73-16463
- Galactic cosmic radiation He 3 and deuterium abundances interpretation from production cross sections and reaction kinematics
05 p0609 A73-16741
- Radio galaxies luminosity function from radio power range at 178 MHz with known red shift, using 3C catalog galaxies
05 p0622 A73-17071

- Pulsed galactic nuclei and the origin of cosmic rays. 05 p0611 A73-17308
- Nuclear gamma rays from Li-7 in the galactic cosmic radiation. 05 p0612 A73-17329
- A soft X-ray survey of the galactic plane from Cygnus to Norma. 05 p0612 A73-17389
- The radio continuum of the Large Magellanic Cloud. I - The sources at 6 cm wavelength. 06 p0754 A73-18629
- The radio continuum of the Large Magellanic Cloud. II - Continuum observations at 11 cm wavelength. 06 p0754 A73-18630
- Fokker-Planck equation for solar atmosphere modulation of galactic proton and electron flux at earth, including convection, diffusion and adiabatic deceleration effects 07 p0870 A73-19576
- Radionuclides in lunar rocks from solar and galactic cosmic ray bombardment, examining long and short-lived isotopes activity 07 p0889 A73-19793
- Solar flare and galactic cosmic ray studies of Apollo 14 and 15 samples. 07 p0871 A73-19876
- Gravitational energy conversion into rotational energy in contraction process for pulsars, quasars and galactic radio emission energy sources 07 p0898 A73-19934
- Properties of the radio continuum emission from interacting galaxies. 07 p0900 A73-20280
- Optical variability of the nuclei of Seyfert galaxies 07 p0901 A73-20306
- Stokes polarization parameters of optical emission scattered in absorbing medium calculated for Galaxy and M 82 galaxy, assuming thermal IR radiation from nucleus 07 p0901 A73-20312
- Photometric plane and spherical characteristics of spiral galaxies from statistical analysis of SQ, S and Irr morphological profiles 07 p0901 A73-20314
- Mean path length of high energy galactic cosmic rays in the galactic disk. 07 p0873 A73-20563
- Variations in spectral-energy distributions and absorption-line strengths among elliptical galaxies. 08 p1002 A73-20878
- Observations of spatial structure in the soft X-ray diffuse flux. 08 p0997 A73-20881
- Aperture synthesis study of neutral hydrogen in the galaxies NGC 6946 and IC 342. 08 p1005 A73-20914
- Three-colour photometry of a field in the galactic anticentre section near NGC 1664. 08 p1005 A73-20922
- A search for hard X-rays from extragalactic objects. 08 p0997 A73-21153
- Spectrophotometry of Ton 524a, b. 08 p1009 A73-21170
- Microwave background radiation in terms of isotropy, universe mass density, sky brightness temperature spectra investigations and H distribution in intergalactic space 08 p1010 A73-21229
- Galactic cosmic ray particle intensity decrease relationship to low energy proton flux increase based on interplanetary Zond 3 and Venera probes measurements 08 p0999 A73-21326
- Galactic cosmic ray modulation region evaluation from meteoroid orbit, velocity and radioactive dating data 08 p1000 A73-21342
- Solar active regions effects on galactic cosmic ray distribution and interplanetary magnetic field structure 08 p1000 A73-21344
- Diffusion and stochastic variations of galactic cosmic rays in solar wind 08 p1000 A73-21346
- Application of statistics to results in gamma ray astronomy. 08 p1012 A73-21644
- H beta emitting diffuse nebulae as reflection nebulae illuminated by galactic light, based on photometric observation of H alpha emitting external spiral galaxies 08 p1013 A73-21809
- A possible cosmic ray primary particle energy spectrum above 10 TeV and its astrophysical implications. 08 p1000 A73-21824
- Preliminary data for the optical variability of the eruption from the NGC 4486/M87 nucleus 09 p1145 A73-22287
- UBV photometry of the irregular galaxies NGC 5363 and NGC 5360 09 p1146 A73-22548
- Main results of the investigation of the Sculptor-type dwarf galaxies 09 p1147 A73-22549
- Cosmic gamma ray studies for metagalactic and remote galactic model construction as substitute for radio and X ray emission data 09 p1138 A73-22725
- Cosmic maser generator model with resonance scattering feedback for galactic clouds OH molecule radio emission 09 p1147 A73-22729
- Cosmic gamma ray observations for choice between galactic and metagalactic models of cosmic ray origin, discussing proton nuclear component 09 p1138 A73-22952
- Infrared and microwave emission from nebulae in the galaxy. 09 p1150 A73-23133
- Observational data and interpretation of infrared spectra and microwaves of galaxies and the intergalactic matter 09 p1150 A73-23143
- A synchrotron radiation model of the infrared radiation from the nucleus of NGC 1068. 09 p1150 A73-23144
- An estimate of the energy spectrum of gamma rays from the central region of the Galaxy and some implications. 10 p1263 A73-23486
- Galactic background spectrum at 230-2600 kHz from IMP-6 radio astronomy, discussing ambient plasma effects on synchrotron emission in galactic models 10 p1272 A73-23529
- Gamma-ray emission from the region of the Galactic center. [AD-759042] 10 p1264 A73-23530
- Faraday pulsations and circular polarization of optical radiation from cosmic sources in terms of angle between interstellar dust orientation vector and galactic plane 10 p1273 A73-23709
- All-Union Conference on the Physics of Cosmic Rays, Tiflis, Georgian SSR, October 18-21, 1971, Proceedings 10 p1265 A73-23901
- Solar wind effect on azimuthal and radial galactic cosmic ray currents, noting Forbush decreases relation to current structures 10 p1265 A73-23907
- Particle motion diffusion model for cosmic ray propagation in Galaxy, investigating electron component energy spectra and background radio emission 10 p1265 A73-23908
- Spatial variations of cosmic rays on the basis of data for the radioactivity of meteorites with known orbits 10 p1266 A73-23910
- Problems of linear and nonlinear theory of cosmic ray modulation 10 p1266 A73-23913
- Comparative characteristics of the soft component of solar and galactic cosmic rays on the basis of rocket and stratospheric measurements at Heis Island and Apatite Station 10 p1267 A73-23920
- Energy spectrum of galactic cosmic rays beyond the region of modulation and the anisotropy of cosmic rays in the Galaxy 10 p1267 A73-23925
- Radio pulses from the direction of the galactic centre. 10 p1280 A73-24272
- Solar modulation of the galactic cosmic rays. III - Implications of the Compton-Getting coefficient. 10 p1269 A73-24726
- Remarks on the soft X-ray emission from the galactic radio spurs. 10 p1270 A73-24904
- On the secondary production of galactic cosmic ray electrons. 10 p1270 A73-24910
- X ray ionization and heating of H I regions refuted from energy input rate computations of observed flux in Galactic plane 11 p1415 A73-25118
- Continuum radio emission from NGC 4656/7 and NGC 891 at 408 MHz. 11 p1415 A73-25170
- The distribution of X-ray sources in our galaxy. 11 p1415 A73-25178
- Investigation of the diffuse glow of the clouds of dark absorbing matter in the region of the Aquila constellation 11 p1416 A73-25229
- Luminescence of isolated dark clouds caused by the integral field of stellar galactic radiation 11 p1416 A73-25234
- A phenomenological study of cosmic ray propagation. I - The nuclei component. 11 p1412 A73-25263
- IR sources at 1-5 microns, discussing Betelgeuse, R Doradus, dying stars, new stars and galaxies 11 p1422 A73-25974
- Review of results in infrared space astronomy. 11 p1426 A73-26502
- X ray source identified with galaxy NGC 5128 located at center of radio source Cen A, noting 3.4 keV low energy cutoff in X ray spectrum 11 p1427 A73-26603
- Preliminary Pioneer-10 intensity gradients of galactic cosmic rays. 11 p1414 A73-26622
- Metagalactic cosmic ray origin models and cosmic ray energy density around Galaxy, considering gamma ray flux, measurement from Magellanic Clouds 12 p1539 A73-27142
- Criticism of Galactic cosmic ray production model with rotating magnetic white dwarfs, noting contrary evidence in magnetic field observations and decay theories 12 p1539 A73-27149
- Optical variability of the nuclei of Seyfert galaxies. 12 p1539 A73-27278
- Stokes polarization parameters of optical emission scattered in absorbing medium calculated for Galaxy and M 82 galaxy, assuming thermal IR radiation from nucleus 12 p1539 A73-27284
- Photometric plane and spherical characteristics of spiral galaxies from statistical analysis of SQ, S and Irr morphological profiles 12 p1539 A73-27286
- Modulation of galactic cosmic rays by a solar wind asymmetric with respect to the heliopause 12 p1539 A73-27332
- Convection and diffusion transport equation of galactic cosmic ray electrons with energy loss and absorption allowance for supernova compressed halo models 12 p1535 A73-27635
- IR spectra of quasars and Seyfert galaxies interpreted as thermal radiation from dust envelopes around cores, considering graphite and silica dust particles 12 p1547 A73-27876
- Identification and radio spectra of bright galaxies in the second Bologna Catalogue of radioresources and their radio luminosity function. 13 p1671 A73-28034
- Dependence of the integrated background light on cosmology, galactic spectra, and galactic evolution. 13 p1671 A73-28035
- Galactic continuum loops and the diameter-surface brightness relation for supernova remnants. 13 p1672 A73-28041
- Cometary nuclei chemical composition and molecular structure, suggesting radial-forming organic molecules synthesis by solar and galactic cosmic radiation 14 p1723 A73-29816
- Interplanetary radial gradients of galactic cosmic ray protons and helium nuclei - Pioneer 8 and 9 measurements from 0.75 to 1.10 AU. 14 p1786 A73-29951
- Redshift-magnitude bands, quasi-stellar sources, and systems of redshift. 14 p1797 A73-30004
- Low energy galactic cosmic ray exploration via space mission to Jupiter and Saturn, considering nuclear abundances and galactic evolution theories 14 p1787 A73-30542
- Search for infrared anomalies associated with gravitational events at the galactic centre. 14 p1800 A73-30601
- Surface photometry of galaxies - Comparison of the luminosity profiles and photometric parameters of southern galaxies measured at Cordoba and Mount Stromlo. 14 p1801 A73-30644
- Gamma and cosmic ray astronomy review, covering balloon and rocket measurements, galactic and metagalactic source locations and radio source information 15 p1926 A73-31148
- Composition of galactic cosmic rays with energy ranging between 10 and 30 MeV/nucleon. 15 p1926 A73-31355
- Mariner 9 ultraviolet spectrometer experiment - Upper limits on the Lyman-alpha flux from clusters of galaxies. 15 p1936 A73-31551
- The fluorine abundance in the galactic cosmic radiation. 15 p1926 A73-31552
- Production of astrophysical X-rays by transition radiation. 15 p1926 A73-31553
- The direct and inverse problems of cosmic-ray propagation in interplanetary space 15 p1926 A73-31878
- Energy losses of galactic cosmic rays in the interplanetary medium. 15 p1927 A73-32010
- Relativistic electron radio emission models, calculating magnetic bremsstrahlung spectra from galactic electron space-energy distributions 15 p1927 A73-32609
- X- and gamma-ray astronomy; Proceedings of the Symposium, Madrid, Spain, May 11-13, 1972. 16 p2049 A73-32727

Uhuru observed galactic X ray sources, discussing whole-galaxy X ray emission, Sco X-1 type binary sources and emissions in GX263+2 and Small Magellanic Cloud 16 p2049 A73-32728

Galactic and extragalactic X ray observations at 20-500 keV, considering supernova remnants, Sco-1 and Cyg 1 type sources, M31, Magellanic Clouds and Crab Nebula 16 p2049 A73-32731

Sco X 1, Cygnus and galactic center X ray sources radio observations, discussing identification, properties and variabilities 16 p2050 A73-32733

Galactic X-ray polarimetry and high-resolution X-ray spectroscopy. 16 p2058 A73-32736

Uhuru extragalactic X ray observations including normal galaxies, quasars, giant radio galaxies, Seyferts and galactic clusters 16 p2050 A73-32741

Soft X ray background observations at 0.1-10 keV, considering interstellar absorption effects, galactic radiation and extragalactic components 16 p2051 A73-32745

Absorption and production of soft X-rays in the Galaxy. 16 p2051 A73-32746

Diffuse background X ray origin theories with emphasis on soft flux in galactic plane and at poles 16 p2051 A73-32748

High energy gamma ray discrete source identification in Crab Nebula, pulsar NP 0532 and galactic regions from Apollo and TD-1 satellite measurements 16 p2051 A73-32750

Observation of excess gamma-radiation fluxes from the region of the northern galactic pole. 16 p2054 A73-33078

Cosmic ray trapping region and characteristic exit time from Galaxy, discussing electronic component and chemical composition 16 p2054 A73-33286

The dynamical effects of cosmic rays in the Galaxy and the generation of the galactic magnetic field. 16 p2054 A73-33287

Extragalactic radio phenomena. 16 p2054 A73-33288

Solar electrons, Galactic electron radiation modulation and spectrum of high energy cosmic ray electrons 16 p2055 A73-33293

Galactic sources and the propagation of cosmic rays - A review of the light isotopes and the odd-Z elements. 16 p2055 A73-33295

Calculations of neutron flux spectra induced in the earth's atmosphere by galactic cosmic rays. 16 p2055 A73-33426

Calculated cosmic ray neutron monitor response to solar modulation of galactic cosmic rays. 16 p2056 A73-33444

Absorption of ultrahigh energy photons in the universe 17 p2223 A73-34368

Magneto-gravitational and thermal instability in the Galactic disk. 17 p2231 A73-34752

Transition radiation from interstellar dust grains. 17 p2231 A73-34755

A new test for solar modulation theory - The 1972 May-July low-energy galactic cosmic-ray proton and helium spectra. 17 p2224 A73-34769

Observations at 1415 MHz of radio sources in the field of the double-galaxy system NGC 2798/99. 17 p2234 A73-35614

On the role of plasma effects in the cosmic ray propagation and isotropization in the galaxy. 17 p2225 A73-35779

Properties of cosmic X-ray sources. 18 p2343 A73-35924

Faraday pulsations and circular polarization of optical radiation from cosmic sources in terms of angle between interstellar dust orientation vector and galactic plane 18 p2354 A73-36734

Solar proton and galactic background radiation measurements project Cold Flare at SST cruising altitudes, using high altitude radiation instrument system /HARIS/ 18 p2347 A73-36905

A stochastic model of the galactic magnetic field. 18 p2356 A73-36974

Evidence for the softening of the cosmic-ray electron spectrum at a few hundred GeV and the origin of the galactic-ridge X-radiation. 18 p2348 A73-37102

Cosmic X-ray sources - A progress report. 19 p2474 A73-37149

Outermost low surface brightness regions of interacting galaxies in Stephan Quintet from interference filter, hydrogen spectra and long exposure direct photograph observations 19 p2484 A73-37609

The redshift-distance relation. V - Galaxy colors as functions of galactic latitude and redshift - Observed

colors compared with predicted distributions for various world models. 19 p2487 A73-38504

Radio luminosity function of galaxies. 20 p2606 A73-39062

A search for 21-centimeter absorption in quasars and other sources near to spiral galaxies. 20 p2609 A73-39437

Detection of a gamma-ray spectral line from the galactic-center region. 20 p2602 A73-39438

The cosmological significance of molecular band strengths in the infrared spectra of elliptical galaxies. 20 p2609 A73-39447

Brightness and polarization distributions of head-tail galaxies at 1415 MHz. 20 p2610 A73-39583

Nuclide production rates in stone meteorites and lunar samples by galactic cosmic radiation. 20 p2612 A73-39716

Investigation of primary gamma radiation from the northern polar region of the Galaxy 21 p2756 A73-40578

Role of plasma effects in the propagation and isotropization of cosmic rays in the Galaxy 21 p2756 A73-40579

Flux measurements of galactic cosmic-ray albedo neutrons by the Molnia 1 satellite in 1972. 21 p2758 A73-40605

Variability of high-energy gamma-radiation sources 21 p2759 A73-40707

Galactic positronium annihilation gamma ray spectrum with 476 keV photon peak, indicating possible origin in supernova explosive nucleosynthesis of positrons 21 p2770 A73-40941

Neutral interstellar hydrogen and extraterrestrial Lyman alpha radiation. 21 p2773 A73-41396

Al-26 and Na-22 measurements on Luna 16 samples by non-destructive gamma-gamma coincidence spectrometry. 21 p2774 A73-41405

Origin of cosmic rays, atomic nuclei, and pulsars in explosions of massive stars. 22 p2905 A73-41765

French monograph - Preliminary photometric study in the far ultraviolet of the zodiacal and galactic emission. 22 p2910 A73-42716

The abundances of galactic cosmic-ray carbon, nitrogen, and oxygen and their astrophysical implications. 22 p2914 A73-43012

Modulation of galactic cosmic-rays by solar wind which is unsymmetric in solar latitude. 23 p3020 A73-43230

Sensitive search for microwave pulses from the galactic centre. 23 p3033 A73-43961

Cosmic gamma ray studies for metagalactic and remote galactic model construction as substitute for radio and X ray emission data 23 p3025 A73-44325

Radius-parameter and surface brightness as a function of galaxy total magnitude for clusters of galaxies. 24 p3135 A73-44582

Physical conditions in nuclei of spiral galaxies. I - Study of galaxies with a nuclear radio-component. 24 p3141 A73-45192

The relation between redshift and surface brightness for normal galaxies in systems of galaxies. 24 p3141 A73-45193

GALACTIC RADIO WAVES

Velocity structures in hydrogen profiles. 01 p0096 A73-10315

Brightness temperatures in the southern sky at 408 MHz. 07 p0876 A73-19357

Galactic and extragalactic radio emission and satellite observations of RF cosmic radiation and noise intensity 12 p1544 A73-27783

Galactic radio emission at 38 MHz using steerable reflector telescope with defined beam and small sidelobes 13 p1673 A73-28278

Continuum galactic background radio emission, considering rarefied ionized hydrogen gas with filaments due to dense inhomogeneities 15 p1938 A73-31953

Extragalactic radio phenomena. 16 p2054 A73-33288

Continuum galactic background radio emission, considering rarefied ionized hydrogen gas with filaments due to dense inhomogeneities 24 p3131 A73-44478

GALACTIC ROTATION

Stellar proper motion effects on precession and galactic rotation constants determination, considering star velocity fields in solar neighborhood 01 p0098 A73-10583

Determination of the type of motion in spherically symmetric systems of galaxies 07 p0901 A73-20313

The distribution of neutral hydrogen and the velocity field of the galaxy NGC 3109. 08 p1004 A73-20905

Galactic differential rotation derived from the radial velocities of some population I objects. 08 p1005 A73-20912

Tidal, primordial turbulence and spinning core theories for galactic rotation origin, considering rotational waves, gravitational waves and wave excitations 09 p1143 A73-22123

Causes of the rotation of galaxies in terms of the nonlinear theory of gravitational instability 10 p1274 A73-23712

Rotating galaxies gravothermal catastrophe via violent relaxation leading to black hole core and halo system 10 p1284 A73-24911

Determination of the type of motion in spherically symmetric clusters of galaxies. 12 p1539 A73-27285

Aperture synthesis study of neutral hydrogen in NGC 2403 and NGC 4236. II - Discussion. 15 p1929 A73-31057

A problem in distance-determination for Mira variables with an appendix on OB-star distances. 15 p1932 A73-31306

The dynamics of the Andromeda Nebula. 15 p1941 A73-32400

Development of rotation in galaxies in the nonlinear theory of gravitational instability. 18 p2354 A73-36737

Comparison of rotation curves of different galaxy types /Research note/. 20 p2611 A73-39592

Properties of galactic orbits and motion integrals of high-velocity stars. II - Periodic and nonperiodic orbits in the 2nd Schmidt potential 22 p2907 A73-42303

The angular momentum of spiral galaxies. I - Methods of rotation-curve analysis. II - Detailed methods and correlations for 17 galaxies. 22 p2913 A73-43002

Galactic rotation of the centroids of various objects 23 p3035 A73-44239

Neutral hydrogen rotational motions near galactic center and 3-kpc arm, using dispersion ring model 24 p3140 A73-45180

GALACTIC STRUCTURE

Stability of gravitating systems with a quadratic potential. I - Methods of investigating the stability of systems with a limited phase volume: Vibration spectrum of the Maclaurin stellar disk 12 p1546 A73-27856

High Galactic latitude intermediate-negative velocity neutral hydrogen properties, noting large complexes and systematic velocity pattern 13 p1671 A73-28029

Andromeda galaxy absorbing material distribution obtained with population I cepheids in Baade four variable star fields 13 p1671 A73-28031

A high resolution neutral hydrogen study of the galaxy M 51. 13 p1671 A73-28033

Galactic loops as supernova remnants in the local galactic magnetic field. 13 p1672 A73-28042

The Perseus spiral arm at 21-cm. 13 p1685 A73-29354

A forcing mechanism for spiral density waves in galaxies. 13 p1686 A73-29372

Young open star clusters. II - Their nature and their significance for galaxy research 14 p1798 A73-30274

Patterns of waves in galactic disks. 14 p1801 A73-30728

The number-intensity distribution of X-ray sources observed by Uhuru. 14 p1788 A73-30733

On the kinematical and spatial coincidence of optical and radio spiral arms in our galaxy. 15 p1929 A73-31055

Solar nearby star velocity field variation model for Oort constants derivation with application to faint stars motion analysis and galactic center distance calculation 15 p1933 A73-31397

The absence of formaldehyde radiation toward cold regions of the galactic plane - Further investigation. 15 p1936 A73-31554

Double structure characterization in ideal model by two extended radio emitting regions near nucleus of optical galaxy or quasar 15 p1940 A73-32073

Galactic neutral hydrogen observations along loop III, noting loop effects on gas velocity distribution 16 p2058 A73-32835

Theories of galactic spiral structure comparisons with observations. 16 p2062 A73-33575

The Berkeley low-latitude survey of neutral hydrogen. I - Profiles. 16 p2063 A73-33600

Magneto-gravitational and thermal instability in the Galactic disk. 17 p2231 A73-34752

A discussion of the distribution of interstellar matter close to the sun. 17 p2234 A73-35619

Small perturbations in flat galaxies. II - Time-dependent azimuthal perturbations. 17 p2236 A73-35782

Book - General astrophysics with elements of geophysics. 18 p2356 A73-36968

Optical and radio observations of NGC 4258 anomalous arms indicating eruptive processes in galactic nucleus as possible source of spiral structure. 20 p2605 A73-39057

Stability of gravitating systems with a quadratic potential. I - Systems bounded in phase space - Oscillation spectrum for a Maclaurin stellar disk. 20 p2608 A73-39230

Observations of neutral hydrogen near the galactic center. II - The nuclear disc. 20 p2610 A73-39578

Brightness and polarization distributions of head-tail galaxies at 1415 MHz. 20 p2610 A73-39583

Comparison of rotation curves of different galaxy types /Research note/. 20 p2611 A73-39592

Galactic spiral arm structure mapping by 21 cm data taken at different latitudes, discussing high velocity hydrogen clouds distribution. 21 p2778 A73-41533

Aperture synthesis of interstellar neutral hydrogen in absorption. I - The Perseus arm feature of Casiopeia A. 22 p2904 A73-41756

Infrared maps of the galactic nucleus. 22 p2904 A73-41757

An attempt to interpret the mean properties of the velocity field of young stars in terms of Lin's theory of spiral waves. 22 p2908 A73-42310

Galactic mass distribution models from matter density near sun, discussing halo mass and RR Lyrae effects observation. 22 p2912 A73-42940

Neutral hydrogen spectral line observation for Milky Way Galaxy mapping, discussing role of spiral structure density wave theory in interpretation. 23 p3028 A73-43348

Structural characteristics of galaxies caused by screening of the Newtonian gravitational potential. 23 p3029 A73-43646

Gravitational fields calculation in three dimensional mass distribution galaxies, using biorthogonal functions with ultraspherical polynomials. 23 p3030 A73-43749

The problem of the apparent-flattening characteristic of spiral galaxies. 23 p3035 A73-44234

Neutral hydrogen rotational motions near galactic center and 3-kpc arm, using dispersion ring model. 24 p3140 A73-45180

Bending of the galactic plane and the nature of the high velocity clouds. 24 p3140 A73-45189

Galactic structure in the direction of Cepheus. 24 p3140 A73-45191

GALAXIES

NT ANDROMEDA GALAXIES

NT ELLIPTICAL GALAXIES

NT GALACTIC CLUSTERS

NT MAFFEI GALAXIES

NT MAGELLANIC CLOUDS

NT MILKY WAY GALAXY

NT RADIO GALAXIES

NT SEYFERT GALAXIES

NT SPIRAL GALAXIES

UV astronomy advances from rocket and satellite observations, discussing early stars, interstellar extinction and gas, galaxies and globular clusters. 01 p0094 A73-10059

The spectrum of the compact galaxy IIZw43. 01 p0098 A73-10557

High frequency radio observations of optically interacting galaxies. 01 p0099 A73-10586

Changes in the gravitational energy of galaxies during collisions. 02 p0217 A73-12392

Statistical analysis of galaxy counts in small red shift quasar fields, comparing to number of galaxies around randomly chosen point. 03 p0370 A73-13194

The redshifts of quasi-stellar objects and associated galaxies. 03 p0375 A73-13896

NGC 2992 and the blue stellar object Weedman No. 2. 04 p0502 A73-15690

Turbulent plasma 'piles' in the nuclei of galaxies. 04 p0504 A73-16022

Measurements of diameters of galaxies on the Palomar Observatory Sky Survey. 05 p0613 A73-16211

Surface distribution of interacting and normal galaxies near the galactic north pole. 05 p0613 A73-16212

Extragalactic objects state of knowledge including galaxy definition and classification systems and quasar characteristics. 05 p0614 A73-16307

Russian book - Problems of galactic and extragalactic astronomy. 05 p0616 A73-16451

Integral equations suitability and solution instability of stellar system models, referring to globular cluster densities and mass distribution equations. 05 p0616 A73-16452

Evidence for elliptical galaxy rotation, considering flattening, orbital statistics and interactions of external and internal forces. 05 p0616 A73-16453

Extremely compact galaxy CGCG 1439 + 5344. 07 p0877 A73-19601

The stability of certain model binary stellar systems in galactic gravitational fields. 07 p0898 A73-19935

Observational discrepancies of redshift-distance relationships associated with galaxies and quasars. 07 p0904 A73-20639

The distribution of neutral hydrogen and the velocity field of the galaxy NGC 3109. 08 p1004 A73-20905

Dynamic analysis of tidal effects arising from hyperbolic close encounters of massive body past galaxy, calculating matter velocity field and galactic structure distortion. 08 p1004 A73-20907

Study of the galactic structure from observations of interstellar calcium. I - Analysis of radial velocities. 08 p1004 A73-20909

Surface colour photometry of galaxies with Schmidt telescopes. 08 p1011 A73-21363

Models for extragalactic objects with very high IR and X-ray luminosity. 09 p1141 A73-22007

UBV photometry of the irregular galaxies NGC 5363 and NGC 5360. 09 p1146 A73-22548

Main results of the investigation of the Sculptor-type dwarf galaxies. 09 p1147 A73-22549

IR galaxy model consisting of low energy cosmic or X rays at center of dust shell, discussing physical dimensions of radiating region. 09 p1151 A73-23146

Invalidity of quasar-nearby galaxy angular distance dependence on galaxy red shift from investigation of larger sampling of pairing systems. 10 p1273 A73-23702

Black holes existence and tentative configuration, discussing galaxies great group missing mass mystery and X ray source investigation. 10 p1282 A73-24653

Composite distribution function for absolute magnitudes of uniformly distributed galaxies. 11 p1416 A73-25238

The redshift-distance relation. IV - The composite nature of N galaxies, their Hubble diagram, and the validity of measured redshifts as distance indicators. 11 p1427 A73-26602

The spectrum of the extranuclear regions of Ton 256. 11 p1428 A73-26624

Universe rest energy density, isotropic background radiation energy and galactic kinetic energy. 13 p1686 A73-29654

Redshift-magnitude bands, quasi-stellar sources, and systems of redshift. 14 p1797 A73-30004

Aperture synthesis study of neutral hydrogen in NGC 2403 and NGC 4236. I - Observations. 15 p1929 A73-31056

Aperture synthesis study of neutral hydrogen in NGC 2403 and NGC 4236. II - Discussion. 15 p1929 A73-31057

Determination of the absolute intrinsic motions of stars with respect to galaxies in area 32 of a special Kapteyn map. 15 p1938 A73-31961

Secular parallaxes of stars and the speed of the sun according to absolute intrinsic motions of 14,600 stars with respect to galaxies. 15 p1938 A73-31962

Invalidity of quasar-nearby galaxy angular distance dependence on galaxy red shift from investigation of larger sampling of pairing systems. 18 p2354 A73-36727

Radio luminosity function of galaxies. 20 p2606 A73-39062

Computerized simultaneous numerical integration of motion equations for solar system, star cluster and galaxies, considering radar observations of moon, Mercury, Venus, Mars and Icarus. 21 p2772 A73-41241

An optical Atlas of galactic supernova remnants. 23 p3028 A73-43448

Determination of absolute stellar proper motions relative to galaxies in selected area 32 of the special Kapteyn plan. 24 p3132 A73-44486

Secular parallaxes and space velocity of the sun from absolute proper motions of 14,600 stars relative to galaxies. 24 p3132 A73-44487

Smoothing and filtering of apparent surface distribution of galaxies. 24 p3143 A73-45363

GALAXY AIRCRAFT

U C-5 AIRCRAFT

GALERKIN METHOD

A variant of the solution of problems of fluid oscillations in cylindrical cavities by the Bubnov-Galerkin method. 01 p0031 A73-10101

On a semi-variational method for parabolic equations. I. 02 p0186 A73-11589

The convergence of separation /Galerkin/ formulations in the case of time-dependent equations. 03 p0336 A73-13165

Complex transmission coefficient of waveguide with two arbitrarily spaced infinitely thin plane parallel inhomogeneities, using Galerkin method for single-parameter approximation of electrodynamic problem. 03 p0278 A73-14057

Stability of the Bubnov-Galerkin method for unstable operator equations with variable coefficients. 04 p0470 A73-15085

On the semi-discrete Galerkin method for hyperbolic problems and its application to problems in elastodynamics. 04 p0471 A73-15222

The transmission of sound in an acoustically treated rectangular duct with boundary layer. 04 p0476 A73-15586

Determination of root locus for nonlinear multi-variable system. [ASME PAPER 72-WA/AUT-21] 04 p0472 A73-15879

Galerkin stress functions for non-local theories of elasticity. 05 p0631 A73-16123

Application of general Boussinesq-Galerkin forms of the Navier equation solution to a plane problem. 05 p0632 A73-16328

Discrete Galerkin and related one-step methods for ordinary differential equations. 05 p0590 A73-16375

Vertical electric dipole excited electromagnetic field in earth-ionosphere waveguide, using Galerkin method for VLF electromagnetic wave propagation equation. 05 p0549 A73-16389

Galerkin methods for vibration problems in two space variables. 06 p0717 A73-18408

Galerkin method for approximate solution of differential equation with boundary conditions, considering applicability to nonself-adjoint and nonlinear systems. 06 p0765 A73-18725

On parameter identification for distributed systems using Galerkin's criterion. 07 p0804 A73-19130

Galerkin methods for parabolic equations with non-linear boundary conditions. 07 p0844 A73-19138

A special form of Galerkin's method applied to heat transfer in plane Couette-Poiseuille flows. [AD-757002] 08 p1023 A73-21412

An economical approximation for the coefficients in the development of a function with respect to an orthogonal system. 08 p0984 A73-21413

Numerical computation of forced oscillations in coupled Duffing equations. 09 p1113 A73-23022

A finite element method for non-self-adjoint problems. 10 p1243 A73-24292

Galerkin finite element method for vibration problems. 11 p1445 A73-26389

Galerkin method application to approximation functions selection in development of thrust gas bearing with sloping. 11 p1375 A73-26429

Solvability of the boundary value problem in the theory of shallow shells of revolution and estimation of errors in the approximate solution. 12 p1556 A73-27813

The mathematical foundations of the finite element method with applications to partial differential equations; Proceedings of the Symposium, University of Maryland, Baltimore, Md., June 26-30, 1972. 12 p1519 A73-27921

The stability of Poiseuille flow - An analysis of two- and three-dimensional disturbances. 13 p1600 A73-28418

- Analytical approximation of high order Galerkin solutions to ordinary differential equations describing forced oscillations of systems with polynomial nonlinearities, considering first-order harmonic effects
13 p1648 A73-28440
- The Ritz-Galerkin procedure for nonlinear control problems.
13 p1649 A73-28607
- Bubnov-Galerkin method for mixed boundary value problem solution via sequence of coordinate functions, illustrated by steady state conductive heat transfer problem
14 p1768 A73-30019
- Pseudospectral approximation to two-dimensional turbulence.
14 p1746 A73-30909
- Calculation of radiant energy transfer by the Galerkin method
15 p1956 A73-30963
- Convergence of the Bubnov-Galerkin method for a type of nonlinear operator equation
15 p1898 A73-30966
- Cylindrical panels buckling under nonuniform axial compression with various load distributions, basing analysis on Donnell equations and Galerkin method
15 p1948 A73-31635
- A periodic solution of a singular differential system with a retarded argument - Construction and approximate calculation
15 p1900 A73-32165
- A survey of finite element methods in continuum mechanics.
16 p2036 A73-32988
- Galerkin variational method combination with least squares error distribution technique for application in plate and shell theory
16 p2077 A73-32992
- Application of the generalized Galerkin method to the computation of fluid flows.
17 p2154 A73-35133
- Generalized Galerkin method for approximate solution of eigenvalue self-adjoint boundary value problems in stability analysis of mechanical distributed parameter systems
19 p2458 A73-37189
- The Ritz-Galerkin procedure for parabolic control problems.
19 p2446 A73-38375
- Flow theoretical model for nonstationary creep in metals, using Galerkin method for approximate solution of boundary value problem
20 p2616 A73-39099
- Book - An analysis of the finite element method.
20 p2581 A73-39139
- A numerical realization of the Bubnov-Galerkin method using a computer for the solution of nonlinear problems in the theory of shallow shells
20 p2617 A73-39307
- Successive approximation technique for dynamic-load problems of nonlinear viscoelastic systems
20 p2593 A73-39322
- The numerical solution of nonlinear parabolic problems by variational methods.
21 p2725 A73-40382
- A priori L sub 2 error estimates for Galerkin approximations to parabolic partial differential equations.
21 p2725 A73-40383
- GALLIUM**
Gallium and germanium in the metal and silicates of L- and LL-chondrites.
07 p0789 A73-20621
- Anisotropy of gallium elasticity and thermal expansion
12 p1531 A73-27936
- Distribution of Ni, Ga, Ge and Ir between metal and silicate portions of H-group chondrites.
21 p2771 A73-41009
- GALLIUM ALLOYS**
Superconducting-normal phase boundary as function of applied magnetic field and transition temperature in Nb-Ga alloys
02 p0200 A73-11840
- Electron characteristics of sprayed vanadium-gallium alloys
15 p1922 A73-31178
- Structure and properties of alloys of the V3Si-V3Ga-V3Al system
15 p1922 A73-31179
- Phase diagram of the niobium-gallium system
15 p1922 A73-31182
- Structure and properties of alloys of the V3Si-V3Ga-V3Ge system
15 p1923 A73-31190
- Phase composition of Ni-Al and Ni-Ga alloys hardened from the liquid state
21 p2719 A73-40849
- The influence of testing temperature and thermal history on the intergranular embrittlement and penetration of aluminium by liquid gallium.
23 p2993 A73-44026
- GALLIUM ARSENIDE LASERS**
Hologram reconstruction by incoherent light. II - Experimental results.
01 p0045 A73-10431

- Laser beam self focusing possibility in GaAs, considering nonlinearity mechanism of intervalley carrier transfer due to applied dc field
04 p0458 A73-14874
- Neutron damage in GaAs laser diodes - At and above laser threshold.
05 p0584 A73-16523
- Russian papers on phosphor crystal luminescence and nonlinear optics covering spectral line decomposition, GaAs laser and electromagnetic wave interaction
05 p0584 A73-16551
- Investigation of a gallium arsenide laser pumped by an electron beam
05 p0584 A73-16553
- Transmission of a GaAs laser beam through the atmosphere.
06 p0699 A73-17495
- Optical and electrical properties of proton-bombarded p-type GaAs.
06 p0739 A73-18786
- Doping dependence of photon yield as a function of excitation energy in optically-excited n-type GaAs at 300 K.
06 p0704 A73-18844
- Pulse broadening in multimode fibres excited by GaAs lasers.
07 p0833 A73-19155
- Effect of impurity gradient on the time delays and Q-switching in junction lasers.
07 p0836 A73-20189
- Cavity dimension effect on single mode generation spectrum of GaAs epitaxial CW injection laser at 77 K.
08 p0976 A73-21655
- Variation of spontaneous emission with current in GaAs homostructure and double-heterostructure injection lasers.
09 p1091 A73-22236
- Additional data on the effect of doping on the lasing characteristics of GaAs-Al_xGa_{1-x}As double-heterostructure lasers.
09 p1091 A73-22237
- Investigation of the dielectric waveguide modes in homostructure GaAs laser.
09 p1091 A73-22238
- Gain-current relation for GaAs lasers with n-type and undoped active layers.
09 p1091 A73-22239
- Room temperature pulsed n-type GaAs cleaved platelet lasers bulk optically pumped near band gap by tunable parametric oscillator, noting emission peak at threshold
[AD-758950] 09 p1092 A73-22240
- Gradual degradation of GaAs double-heterostructure lasers.
09 p1092 A73-22241
- /GaAl/As lasers with a heterostructure for optical confinement and additional heterojunctions for extreme carrier confinement.
09 p1092 A73-22243
- Time behavior of the internal Q switching in GaAs lasers under electron-beam excitation.
09 p1092 A73-22245
- Behavior of threshold current and polarization of stimulated emission of GaAs injection lasers under uniaxial stress.
09 p1092 A73-22247
- Mesa-stripe-geometry double-heterostructure injection lasers.
09 p1093 A73-22251
- Spectral behavior and linewidth of /GaAl/As-GaAs double-heterostructure lasers at room temperature with stripe geometry configuration.
09 p1093 A73-22252
- Resonant enhancement of photoexcited nitrogen trap n-type GaAs laser electron-hole recombination probability by crystal composition variation and gamma conduction band degeneration
09 p1093 A73-22255
- Spontaneous emission and stimulated recombination of p-n-n double heterojunction /AlGa/As-GaAs laser diodes above and below threshold currents
09 p1093 A73-22256
- Double heterojunction [GaAl]As laser pulse modulation at 200 Mbits/sec continuous operation at room temperature, considering lasing delay time and damped oscillations problems
09 p1093 A73-22257
- Spectral self modulation and pulsation instabilities of single mode injection GaAs laser with tunable composite cavity
09 p1093 A73-22258
- Pulsed GaAs illuminators for night-vision systems.
10 p1216 A73-23785
- Experimental properties of injection lasers - Modal distribution of laser power.
10 p1228 A73-24530
- Te-doped GaAs injection laser with nonplanar p-n junction for enhanced power output, discussing diode construction and fabrication by Zn diffusion
12 p1505 A73-26890
- A technique of modulating pulsed semiconductor lasers.
12 p1505 A73-27009

- Use of semiconductor lasers in compact communication systems.
12 p1470 A73-27521
- Influence of heat treatment on characteristics of injection lasers.
12 p1507 A73-27522
- Statistical distribution of the failure of injection lasers.
12 p1508 A73-27524
- Electron-beam tube with a semiconductor target - An electron-beam-pumped scanning laser.
12 p1508 A73-27526
- Short-pulse modulation of gallium-arsenide lasers with TRAPATT diodes.
13 p1626 A73-28050
- GaAs and GaAlAs semiconductor injection lasers, discussing system design and applications for ranging, illumination and communication with peak power and repetition rate requirements
16 p2023 A73-32866
- High-pressure chamber for optical studies at low temperatures
17 p2164 A73-34174
- The transversely adjusted gap laser for optical communication systems.
17 p2186 A73-35795
- Mode selection in GaAs injection lasers resulting from Fresnel reflection.
17 p2186 A73-35797
- A new lidar for meteorological application.
18 p2333 A73-36708
- Double heterostructure lasers for optical communications systems
20 p2572 A73-38664
- Modulation of gallium arsenide laser diodes
20 p2572 A73-38665
- Refractive index of n-type gallium arsenide.
20 p2599 A73-38892
- Self-switching in single-heterojunction injection lasers.
20 p2574 A73-39690
- Asymptotic nature of threshold conditions and multimode laser emission.
20 p2574 A73-39691
- Kinetics of recovery of luminescence properties of gallium arsenide single crystals irradiated with high-energy electrons.
20 p2574 A73-39697
- Laser action from optically pumped epitaxial GaAs crystal waveguides with feedback provided by surface corrugation
21 p2713 A73-40455
- Threshold, spectral, and output power characteristics of GaAs/Ga_{1-x}Al_x/GaAs single-heterostructure diode lasers.
21 p2713 A73-40462
- Measurements of refractive index step and of carrier confinement at AlGaAs-GaAs heterojunctions.
21 p2752 A73-40962
- Cw degradation at 300 K of GaAs double-heterostructure junction lasers. I - Emission spectra. II - Electronic gain.
21 p2715 A73-40964
- Red-light-emitting Al_xGa_{1-x}As heterojunction laser diodes.
21 p2716 A73-40971
- Heterojunction injection lasers [Review].
22 p2869 A73-42244
- Divergence of the output radiation of electron-beam-pumped 'radiating mirror' lasers.
22 p2869 A73-42258
- Defect structure introduced during operation of heterojunction GaAs lasers.
24 p3096 A73-44923
- Mode guidance parallel to the junction plane of double-heterostructure GaAs lasers.
24 p3097 A73-45423
- GALLIUM ARSENIDES**
High-efficiency Ga_{1-x}Al_x/As-GaAs solar cells.
01 p0005 A73-10132
- Influence of light on the electron work function of GaAs single crystals at low temperatures
01 p0088 A73-10631
- 50 GHz gallium-arsenide IMPATT oscillator.
02 p0144 A73-11519
- Gunn diodes - Physical principles and simulation calculations
02 p0144 A73-11529
- Limited space charge accumulation oscillations in gallium arsenide
02 p0199 A73-11530
- LF noise in n-type GaAs and its correlation with HF noise of Gunn-diode oscillators
02 p0145 A73-11535
- Determination of the dopant concentration profile in epitaxial GaAs by the method of the differential capacitance of a Schottky diode
02 p0145 A73-11548
- GaAs-GaAlAs heterojunction transistor for high frequency operation.
02 p0147 A73-12046
- A two-dimensional analysis of gallium arsenide junction field effect transistors with long and short channels.
02 p0147 A73-12047

- Spectral characteristics and black body radiation sensitivity of submillimeter band radiometer based on n-type epitaxial GaAs films 02 p0147 A73-12496
- Microwave harmonic generator using the nonlinearity of negative resistance in n-type GaAs. 03 p0281 A73-12997
- X-band GaAs FET. 03 p0281 A73-13173
- Arsenic emitter silicon bipolar transistor and gallium arsenide FET transistor devices for low noise microwave amplification to 10 GHz 04 p0426 A73-14731
- Investigation of the phonon drag effect in n-GaAs. 04 p0482 A73-14866
- Observation of Kohn-type anomalies in the electron-phonon interaction on the Fermi surface of degenerate semiconductors. 04 p0483 A73-15469
- Purity evaluation of n type GaAs LSA diodes from low-field temperature-dependent mobility. 05 p0556 A73-16435
- Electrical properties of electron-irradiated GaAs. 05 p0604 A73-16516
- Experimental study of millimeter-wave characteristics of hot electrons in n-type GaAs by electrodeless method. 05 p0558 A73-16525
- Some optical properties of solid solutions in the 2GaAs-ZnSiAs₂ section 05 p0605 A73-16612
- Transverse magnetic field effects on n-type GaAs Gunn diodes microwave power, coherence and dynamic I-V characteristics 05 p0558 A73-16784
- GaAs Gunn diode LSA operation mode in multiloop circuit to extend high frequency limit 05 p0558 A73-16788
- Electron beam fabrication of submicrometer diameter mixer diodes for millimeter and submillimeter wavelengths. 05 p0559 A73-16811
- GaAs transferred electron /Gunn/ device microwave oscillator with harmonic tuning, noting reactive termination and bias voltage effects on efficiency optimization 05 p0559 A73-16813
- Electrical properties of nickel-low-doped n-type gallium arsenide Schottky-barrier diodes. 05 p0559 A73-17072
- Morphological, structural and electrical nonuniformities correlation in epitaxial GaAs films on planes, noting Miller indices effects on morphological and electrical properties 05 p0605 A73-17290
- Electron diffraction investigations of the short-range order in GaAs and GaP films 05 p0605 A73-17291
- Comparative study of the epitaxial growth in GaAs-I and GaP-I systems over a wide range of crystallization conditions 05 p0605 A73-17292
- The GaAs traveling-wave amplifier as a new kind of microwave transistor. 06 p0673 A73-17788
- Technology and properties of epitaxial GaAs layer grown from liquid phase, considering GaAs solubility in Ga 06 p0734 A73-17798
- Computer simulation model of field independent trapping effects on slow Gunn domains in gallium arsenide, noting double symmetry electron-ion density distributions 06 p0737 A73-18368
- Magnetophotconductivity of semi-insulating GaAs and its behavior upon electron bombardment. 06 p0738 A73-18369
- Theoretical and experimental study of GaAs IMPATT oscillator efficiency. 06 p0678 A73-18789
- Electrical contacts to ion cleaned n-type gallium arsenide. 07 p0797 A73-19136
- Noise performance of gallium-arsenide and indium-phosphide injection-limited diodes. 07 p0798 A73-19158
- Optimum R.F.-power transport in Nd-limited gallium-arsenide travelling-wave amplifiers. 07 p0798 A73-19159
- Current spreading at contacts to planar Gunn devices. 07 p0799 A73-19343
- A scanned light emitting diode display. 07 p0862 A73-19608
- Faraday effect in n-GaAs in the intermediate doping region 07 p0862 A73-20009
- Frequency multipliers for the millimeter wave band employing gallium arsenide diodes. 07 p0802 A73-20146
- X- and Ku-band amplifiers with GaAs Schottky-barriers field-effect transistors. 07 p0803 A73-20555
- GaAs diffused diode, ECL-1350. 07 p0804 A73-20570
- Passivation of gallium arsenide with silicon nitride. 07 p0864 A73-20571
- Gunn diode effect in n-type GaAs, discussing electron drift velocity relationship to electric field, I-V characteristics and fabrication 08 p0943 A73-20709
- GaAs Schottky-barrier diodes for ultrahigh-frequency communication systems. 08 p0945 A73-20808
- Millimeter-wave frequency response of hot electrons in n-type GaAs. 08 p0994 A73-20845
- Characteristics of a gallium-arsenide travelling-wave amplifier with Schottky-barrier contacts. 08 p0946 A73-21118
- On the mechanism for microwave amplification in 'supercritically' doped n-GaAs. 08 p0947 A73-21212
- Computer simulations of the large signal characteristics of supercritical GaAs transferred electron amplifiers. 09 p1063 A73-22492
- Effect of shielding on charge carrier mobility in compensated materials 09 p1133 A73-22674
- Magnetic field influence of the Gunn effect threshold. 10 p1258 A73-23568
- Investigation of the growth surface of GaAs epitaxial films by chemical decoration and small-angle shadowing technique. 10 p1259 A73-23570
- Stability criteria for dipole domains in Gunn diodes 10 p1193 A73-23726
- Photoemission from cesium-oxide-activated In-GaAsP. 10 p1259 A73-23839
- Semiconductor electroluminescent diode displays. 10 p1218 A73-24118
- Experimental observation of Wannier levels in semi-insulating gallium arsenide. 10 p1260 A73-24638
- Current saturation and small-signal characteristics of GaAs field-effect transistors. 10 p1197 A73-24868
- Optical waveguide structures for CO₂ lasers. 11 p1375 A73-25058
- Overlength modes of transferred-electron oscillators. 11 p1337 A73-25359
- Experimental verification of new Gunn-effect reflection-insensitive pulse regenerator. 11 p1337 A73-25361
- Distribution coefficients and solubility curves of certain rare-earth elements in GaAs 12 p1531 A73-27194
- Boltzmann transport equation solution for electron mobility in ellipsoidal valleys of n-type GaAs and GaP, taking into account arbitrary magnetic fields and scattering mechanisms 13 p1668 A73-28217
- A modified GaAs IMPATT structure for high-efficiency operation. 13 p1595 A73-29577
- Efficiencies of Schottky-barrier GaAs and both complementary structures of Si IMPATT diodes. 13 p1595 A73-29579
- High-power high-efficiency operation of Read-type IMPATT-diode oscillators. 14 p1736 A73-30447
- A comparison of silicon and gallium arsenide large signal IMPATT diode behaviour between 10 and 100 GHz. 15 p1850 A73-31131
- Ge-doped p-type epitaxial GaAs for microwave device application. 15 p1923 A73-31399
- Investigation of defects in GaAs on the basis of the photoluminescence 15 p1923 A73-31717
- Low-frequency noise characteristics of commercial silicon and gallium arsenide IMPATT diodes. 15 p1851 A73-32188
- French monograph - Contribution to the study of background noise in Gunn effect diodes. 15 p1852 A73-32589
- Reliability of GaAs/1-x/P/x/ light emitting diodes. 16 p1990 A73-33623
- State of the art of GaAs IMPATT diodes. 16 p1990 A73-33896
- A study of millimeter-wave GaAs IMPATT oscillator and amplifier noise. 17 p1213 A73-34217
- Design considerations of high-efficiency GaAs IMPATT diodes. 17 p1214 A73-34219
- Quenched-domain mode oscillation in waveguide circuits. 17 p1216 A73-34969
- Experimental gain and noise parameters of microwave GaAs FET's in the L and S bands. 17 p1216 A73-34972
- Cryogenic preamplifier with cooled GaAs junction FET in input stage, discussing application to sensor systems using high impedance cryogenically cooled optical detectors 17 p2137 A73-35219
- Method for plotting frequency cutoff measurements for GaAs varactor diodes. 18 p2292 A73-36596
- The role of surface states in the formation of a Schottky barrier at a metal/gallium arsenide contact 18 p2341 A73-36717
- Application of the semiconductor p-n junction to measurements of rapidly varying pressures. 19 p2432 A73-38308
- Degradation studies of diffused GaAs electroluminescent diodes subjected to mechanical stress. 19 p2439 A73-38458
- Observation of zero-degree pulse propagation in a resonant medium. 20 p2570 A73-38602
- Design and application of low noise GaAs FET amplifiers. 20 p2534 A73-38749
- Book - Gallium arsenide microwave bulk and transit-time devices. 20 p2536 A73-39137
- Electroluminescent display device of integrated XY structure utilizing GaAlAs and GaAsP 20 p2536 A73-39202
- A technique for the investigation of deep-level states in diffused p-n junction devices - Application to GaAs electroluminescent diodes. 20 p2536 A73-39412
- GaAs two-photon absorption coefficient obtained from transmission measurements with Q switched Nd-YAG laser, noting thermal self focusing 21 p2713 A73-40459
- Optical waveguides in GaAs-AlGaAs epitaxial layers. 21 p2752 A73-40969
- Accuracy of gallium arsenide diode thermometers in the range 4-300 K. 22 p2856 A73-42019
- High power GaAs double-drift IMPATT devices. 22 p2834 A73-42693
- Properties of a light-modified-breakdown detector in GaAs. 22 p2864 A73-43164
- The rectifying barrier in gallium arsenide Schottky diodes 23 p2959 A73-43618
- Si and Ge doping characteristics and energy levels in vapor phase epitaxially grown GaAs from sample photoluminescence spectra 23 p3018 A73-44370
- Ion-implanted nitrogen in gallium arsenide. 24 p3120 A73-45402
- The relation between the diffusivity-mobility ratio and the linewidth of spontaneous emission in degenerate semiconductors at relatively high temperatures. 24 p3120 A73-45488
- GALLIUM COMPOUNDS**
- NT GALLIUM ARSENIDES
- NT GALLIUM PHOSPHIDES
- NT GALLIUM SELENIDES
- Determination of the parameters of r-type recombination centers in germanium-doped GaTe single crystals 11 p1410 A73-26587
- GALLIUM PHOSPHIDES**
- The growth and electrical characteristics of epitaxial layers of zinc sulphide and of zinc selenide on p-type gallium phosphide. 01 p0088 A73-10683
- Electron diffraction investigations of the short-range order in GaAs and GaP films 05 p0605 A73-17291
- Comparative study of the epitaxial growth in GaAs-I and GaP-I systems over a wide range of crystallization conditions 05 p0605 A73-17292
- A scanned light emitting diode display. 07 p0862 A73-19608
- The effects of device configuration in the degradation of GaP red light-emitting diodes. 08 p0944 A73-20743
- Photoemission from cesium-oxide-activated In-GaAsP. 10 p1259 A73-23839
- Semiconductor electroluminescent diode displays. 10 p1218 A73-24118
- Boltzmann transport equation solution for electron mobility in ellipsoidal valleys of n-type GaAs and GaP, taking into account arbitrary magnetic fields and scattering mechanisms 13 p1668 A73-28217
- The Li donor, and binding of excitons at neutral donors and acceptors in crystals 15 p1924 A73-31722
- Reliability of GaAs/1-x/P/x/ light emitting diodes. 16 p1990 A73-33623
- Gallium phosphide with nitrogen doping from the gas phase 20 p2599 A73-38666

- Electroluminescent display device of integrated XY structure utilizing GaAlAs and GaAsP
20 p2536 A73-39202
- A new vapor growth method for GaP using a single flat temperature zone.
24 p3119 A73-44412
- GALLIUM SELENIDES**
- Influence of an electric field on the laser-induced impurity photoconductivity of gallium selenide
07 p0861 A73-19398
- Photovoltaic and photoconductivity measurements on p- and n-type GaSe, determining light polarization direction effect, photovoltage relaxation times and minority carriers diffusion lengths
10 p1259 A73-23569
- GALVANIC CELLS**
- U ELECTROLYTIC CELLS**
- GALVANIC SKIN RESPONSE**
- Emotional stimulation traces in the spectra of EEG and cutaneo-galvanic reaction of man under normal conditions and in the case of memory impairment
12 p1461 A73-27106
- Physiological nature of the electroencephalographic and vegetative components of human conditioned reactions
12 p1462 A73-27107
- GALVANOMAGNETIC EFFECTS**
- NT NERNST-ETTINGSHAUSEN EFFECT**
- Selective differential broadband precision amplifier for weak signals of galvanomagnetic sensor of magnetic induction indicator based on Hall effect
01 p0022 A73-10083
- Investigation of the phonon drag effect in n-GaAs.
04 p0482 A73-14866
- Galvanomagnetic effects measured in p-type bismuth selenide single crystal within magnetic field for Hall and conductivity mobilities, determining temperature dependences
06 p0733 A73-17741
- Russian book - Physics of carbographite materials.
15 p1897 A73-31583
- Studies of galvanomagnetic and thermomagnetic phenomena in selenium and tellurium doped InSb.
15 p1924 A73-32159
- Anisotropy of galvanomagnetic effects in laminarily inhomogeneous semiconductors
23 p3017 A73-44044
- A galvanomagnetic analog device for extracting square roots
24 p3070 A73-45101
- GALVANOMAGNETISM**
- U GALVANOMAGNETIC EFFECTS**
- GALVANOMETERS**
- Magnetometers using superconducting galvanometers.
07 p0826 A73-20406
- Design and performance of multichannel current ink jet recording instruments with galvanometers, noting mercury lamp light source, sensitivity and temperature effects
07 p0828 A73-20547
- GAME THEORY**
- NT SADDLE POINTS [GAME THEORY]**
- Optimal control problems in differential games of pursuit and evasion involving deterministic, random and controlled motion
01 p0028 A73-11071
- Pursuit-evasion reconnaissance game with evader reconnoitering target from close distance with guaranteed safe escape from pursuer
03 p0336 A73-13523
- Game problem of impulse controlled soft rendezvous of two material points under attraction and control forces
03 p0344 A73-14044
- Nonlinear stochastic optimal control theory application to guidance policies determination of nonmaneuvering target interception or rendezvous and goal-tending game
03 p0286 A73-14478
- Pursuit/evasion game problem with two pursuers to one evader, discussing coalition tactic based on open loop and closed loop conjugate points difference [AIAA PAPER 73-230]
05 p0536 A73-16955
- Decomposition strategies for one on one aerial dog-fight game models with reinforcement learning [AIAA PAPER 73-233]
05 p0536 A73-16958
- Trajectory deviation conditions in second order linear differential escape game
07 p0850 A73-19014
- Approach and evasion games in conflict controlled system with nonlinear control, deriving necessary condition for winning
09 p1068 A73-22355
- Extremal targeting in a nonlinear rendezvous game
09 p1112 A73-22476
- Optimal control problems in differential games of pursuit and evasion involving deterministic, random and controlled motion
09 p1113 A73-22996
- Optimization methods in control systems design, discussing nonlinear and linear programming, variational and maximum principles, dynamic programming and game and graph theories
10 p1242 A73-24032

- Optimal stochastic linear systems with exponential performance criteria and their relation to deterministic differential games.
10 p1202 A73-24536
- Necessary termination conditions for difference-differential rendezvous /pursuit with evasion/ game with functional goal set
12 p1524 A73-27401
- Existence solution to linear differential rendezvous game of dynamic system with pursuit and evasion
12 p1524 A73-27402
- Extremal controls in a nonlinear differential game
13 p1660 A73-29077
- Conditions for evading a point in a second-order differential game
13 p1660 A73-29078
- Differential game estimate of phase point pursuit of evading closed convex set for feedback control in irregular case
13 p1660 A73-29079
- Game problem of the rigid collision of two points with impulsive thrust in a linear central field
13 p1660 A73-29080
- Zero sum differential game theory for two players, discussing strategies, stochastic versions and saddle value and points existence
13 p1651 A73-29650
- Numerical methods for solving some problems in studies of operations
18 p2331 A73-36985
- Differential games applied to some interception models
18 p2268 A73-37080
- Optimum minimax strategy in pursuit game with observation of evading player phase vector at fixed times
21 p2724 A73-40180
- Dynamic programming method for constructing stable bridges based on mixed strategies in differential games of rendezvous-evasion
21 p2669 A73-40856
- Game theory mathematical model for optimal control of glide modes in conflict situation
23 p2999 A73-43263
- Optimal stopping time for stochastic games corresponding to diffusion process, obtaining saddle point characterization via elliptical variational inequality solution
23 p2999 A73-44083
- GAMETOCYTES**
- Space flight factors effects on Drosophila development in terms of dominant, autosomal and sex-linked recessive lethals frequency, noting gametogenesis stage sensitivity
22 p2804 A73-42173
- GAMMA FUNCTION**
- The generalized gamma distribution and the power distribution as element lifetime distributions
02 p0145 A73-11584
- Generalized gamma distribution with a negative shape parameter as a model of the lifetime distribution of electrical elements with a single-maximum failure rate
02 p0145 A73-11585
- Gamma time-dependency in Blaxter's compartmental model.
02 p0187 A73-12550
- Operative determination of the characteristics of polydisperse systems
18 p2338 A73-37114
- GAMMA RADIATION**
- U GAMMA RAYS**
- GAMMA RAYS**
- Influence of gamma-radiation on the electrical properties of a real germanium surface
01 p0087 A73-10039
- A shielding application of perturbation theory to determine changes in neutron and gamma doses due to changes in shield layers.
01 p0075 A73-10244
- Global nitric oxide and gamma emission measurements with Ebert-Fastie scanning spectrometer on-board polar orbiting OGO 4 satellite
01 p0040 A73-10878
- Galactic and extragalactic X and gamma ray sources identification from satellite, rocket and high altitude balloon observations, discussing radiation generation theories
01 p0092 A73-10990
- High-energy cosmic gamma-ray observations from the OSO-3 satellite.
01 p0092 A73-11028
- Effects of chemical impurities, oxygen and dopant, on the gamma and neutron damage of silicon solar cells.
01 p0006 A73-11163
- Rocket stages separation distance measurement by monitoring gamma ray flux variation, noting separation mechanisms and retromotor performances
01 p0052 A73-11166
- Luna 16 rock composition, gamma radiation and natural radioactive element content determination by neutron activation and radiometric analysis
02 p0213 A73-12230
- Solar white light flares induced neutron and gamma ray emission, discussing acceleration mechanism

through high energy proton bombardment induced photospheric heating
02 p0206 A73-12322

- Saturation of stimulated ruby laser radiation under the action of CO-60 gamma rays
02 p0176 A73-12353
- Spectroscopic properties of ruby and neodymium lasers under the action of a Co-60 gamma ray
02 p0176 A73-12355
- The study of biological macromolecules using perturbed angular correlations of gamma radiation.
02 p0136 A73-12648
- Multilayer X ray film chamber for gamma quanta energy spectrum determination by primary photon impact and absorber calorimetric methods
02 p0208 A73-12660
- Study of the effect of cobalt on redistribution of atoms of alloying elements in iron-base alloys by the nuclear gamma resonance method.
02 p0182 A73-12697
- Spectrum of the cosmic X- and gamma ray background in the energy range 1 keV-1 MeV.
02 p0210 A73-12730
- Low energy atmospheric gamma rays near geomagnetic equator.
03 p0360 A73-12890
- Influence of gamma irradiation on the surface properties of metal-dielectric-semiconductor structures
03 p0349 A73-13661
- Response of motoneurons of the spinal cord to gamma radiation - A cytochemical study.
03 p0262 A73-13808
- Detection of 10-100 MeV gamma-rays from the Crab Nebula pulsar NP 0532.
03 p0362 A73-13847
- Laboratory-produced radiation related to the solar flare emission.
03 p0364 A73-13957
- Spectroscopic remote sensing of lunar surface composition.
04 p0448 A73-15181
- Galaxy formation from annihilation-generated supersonic turbulence in the baryon-symmetric big-bang cosmology and the gamma-ray background spectrum.
04 p0499 A73-15353
- High energy /X ray, gamma ray and cosmic ray/ astronomy research impact on astrophysical and cosmological models
05 p0610 A73-16932
- Investigation of the gamma-emission of lunar soil delivered by the automatic station Luna 16
05 p0620 A73-17020
- Analysis of oxygen in aluminum by activation by means of charged particles and gamma photons
05 p0547 A73-17217
- Mechanisms of optical, X-ray and gamma-radiation from Crab pulsar.
05 p0611 A73-17314
- Nuclear gamma rays from Li-7 in the galactic cosmic radiation.
05 p0612 A73-17329
- Gamma ray dose and energy absorption buildup factors approximation based on geometrical progression formula as function of source energy and medium atomic number
06 p0704 A73-17445
- Effect of gamma irradiation on carbon redistribution processes in the martensite lattice
06 p0706 A73-17902
- High energy astronomy research in space, discussing HEAO A and B, UV astronomy, X ray astronomy, gamma rays, cosmic rays, hot stars, stellar energy sources and elementary particles
06 p0743 A73-18016
- Effect of molecular shape and flexibility on gamma-ray directional correlations.
06 p0725 A73-18122
- Satellite-borne vidicon camera and associated control and telemetry electronics for imagery and dimensional parameters of sparks generated by gamma radiation
07 p0822 A73-18987
- Geomagnetic field perturbation by gamma quanta pulsating source, studying accompanying radio emission behavior
07 p0816 A73-19445
- Neutron flux anisotropy from plasma focus measured by gamma spectroscopy of activated Ag target, discussing axial concentration
07 p0857 A73-19529
- Co-60 source gamma irradiation of Mo-Au doped p-type Si MOS transistors, noting threshold voltage increase and current carrier mobility decrease
07 p0862 A73-19541
- Gamma-ray measurements of Apollo 12, 14, and 15 lunar samples.
07 p0888 A73-19789
- A first look at the lunar orbital gamma-ray data.
07 p0871 A73-19824
- Consequences of a universal cosmic-ray theory for gamma-ray astronomy.
07 p0872 A73-20154
- Diffuse cosmic gamma rays - Present status of theory and observations.
07 p0872 A73-20186

- Evaluation of gamma-ray shielding calculations and determination of shielding parameters with bremsstrahlung radiation. 07 p0850 A73-20232
- Analysis procedure of gamma ray astronomy spark chamber data. 07 p0828 A73-20644
- Solar gamma ray lines observed during the solar activity of August 2 to August 11, 1972. 08 p0996 A73-20665
- Morphological changes in the testicles of dogs exposed to chronic and combined gamma-radiation 08 p0929 A73-20981
- Gamma-ray lines from an expanding supernova shell. 08 p1008 A73-21162
- Lunar surface radioactivity - Preliminary results of the Apollo 15 and Apollo 16 gamma-ray spectrometer experiments. 08 p1009 A73-21224
- Atmospheric gamma ray spectra from balloon spectrometer scintillator measured energy loss spectra 08 p0998 A73-21280
- High energy electrons and gamma quantum flux in upper atmospheric layers from high altitude balloon measurements 08 p0999 A73-21337
- Calculations of the transport of neutrons and secondary gamma rays through concrete for incident neutrons in the energy range 15 to 75 MeV. 08 p0987 A73-21528
- Application of statistics to results in gamma ray astronomy. 08 p1012 A73-21644
- Cosmic gamma ray studies for metagalactic and remote galactic model construction as substitute for radio and X ray emission data 09 p1138 A73-22725
- Cosmic gamma ray observations for choice between galactic and metagalactic models of cosmic ray origin, discussing proton nuclear component 09 p1138 A73-22952
- An estimate of the energy spectrum of gamma rays from the central region of the Galaxy and some implications. 10 p1263 A73-23486
- Diffuse cosmic gamma rays observed at an equatorial balloon altitude. 10 p1263 A73-23491
- Gamma-ray emission from the region of the Galactic center. 10 p1264 A73-23530
- [AD-759042] Pulsed gamma ray emission at 5-25 MeV from Crab Nebula pulsar, noting time-averaged energy flux with consideration for telescope efficiency 10 p1272 A73-23535
- Detection of a flux of gamma quanta in the direction of the Cygnus constellation 10 p1265 A73-23906
- A method for determining the polarization and energy spectrum of cosmic-ray gamma quanta 10 p1266 A73-23914
- Investigation of rigid gamma rays in the atmosphere with the aid of a telescope with an acoustic spark chamber 10 p1267 A73-23923
- Color centers in gamma-irradiated ruby with vanadium additions 10 p1259 A73-24069
- Application of gamma-resonance emission spectroscopy to the study of the structure of laminar compounds of graphite with Co-57-labeled cobalt and cobalt chloride 10 p1186 A73-24466
- Nuclear laser realizability for gamma quanta production from population inversion during radiative capture of neutrons, considering constraints imposed on heating of active medium 10 p1229 A73-24754
- LiF albedo dosimeter for fast neutron and gamma irradiation measurement on personnel, using Cf-252 source for calibration 11 p1361 A73-25313
- An integrated radiation physics computer code system. 11 p1334 A73-25997
- Gamma-gamma total hadronic cross section and absorption of extragalactic gamma-rays. 11 p1413 A73-26107
- Simple model for scanning-angle distribution of planetary albedo gamma-rays. 11 p1414 A73-26475
- Spatial-temporal structure of emission from a ruby laser irradiated by gamma rays 11 p1378 A73-26523
- Metagalactic cosmic ray origin models and cosmic ray energy density around Galaxy, considering gamma ray flux, measurement from Magellanic Clouds 12 p1539 A73-27142
- Means of measuring the linear polarization of cosmic gamma quanta by means of the Compton effect 12 p1496 A73-27204
- The BD-9 integral discriminator in the circuit of a scintillation-type fast neutron detector 12 p1497 A73-27207
- Effects of chronic irradiation of dogs with Co-60 gamma rays on the level of auto-antibodies 12 p1462 A73-27706
- Morphological changes in the liver of dogs induced by chronic gamma irradiation 12 p1463 A73-27707
- Proliferative activity of bone marrow cells in dogs exposed to chronic and repeated acute gamma irradiation 12 p1463 A73-27708
- Solar radio bursts of 4 and 7 August 1972, deducing positron synchrotron process effects on radio spectrum from gamma ray measurements 12 p1535 A73-27785
- A telescope for soft gamma ray astronomy. 12 p1499 A73-27892
- UV radiation effects on gamma irradiated Cr ions spin lattice relaxation rate in ruby and on resonant phonon scattering 13 p1668 A73-28219
- Influence of gatemetall on gamma-ray induced defects in MOS structures. 13 p1589 A73-28421
- Neutron emission after muon capture in Ce, Ba and Sn, analyzing delayed gamma ray energies and branching ratios to excited nuclear states 13 p1662 A73-28650
- Gamma-ray emission above 20 MeV from the Crab Nebula and NP 0532. 14 p1785 A73-29737
- Valency transfers of vanadium ions in ruby 14 p1783 A73-30582
- The cosmic gamma-ray spectrum between 0.3 and 27 MeV measured on Apollo 15. 14 p1788 A73-30731
- Nuclear gamma resonance spectra of Sn119 and Te125 and the electron structure of ternary diamond-like semiconductors Cu2SnS3, Cu2SnSe3 and Cu2SnTe3 14 p1784 A73-30851
- Gamma and cosmic ray astronomy review, covering balloon and rocket measurements, galactic and metagalactic source locations and radio source information 15 p1926 A73-31148
- Preparation of CdS single crystals with a radiation-stable sensitivity to ionizing emissions 15 p1923 A73-31208
- Gamma-ray observations of the galactic centre. 15 p1933 A73-31354
- Characteristics of the narcotic action of hexenal in combination with aminothyl-series radioprotective drugs in irradiated animals 15 p1838 A73-31391
- An electronically gated gamma and X-ray calibration scheme. 15 p1879 A73-32222
- X- and gamma-ray astronomy; Proceedings of the Symposium, Madrid, Spain, May 11-13, 1972. 16 p2049 A73-32727
- High energy gamma ray discrete source identification in Crab Nebula, pulsar NP 0532 and galactic regions from Apollo and TD-1 satellite measurements 16 p2051 A73-32750
- Observation of excess gamma-radiation fluxes from the region of the northern galactic pole. 16 p2054 A73-33078
- Gamma ray astronomical state-of-art, discussing cosmic gamma ray sources observation and diffuse radiation measurement 16 p2055 A73-33290
- Apollo 15 and 16 lunar orbital X and gamma ray spectrometer for lunar surface composition and radioisotopes surveys, detailing experimental results 16 p2015 A73-33353
- Recoilless nuclear transition based gamma laser, using resonant gamma rays or thermal neutron beam irradiation and selective photoionization 16 p2024 A73-34055
- The KP303 field transistor in a soft gamma radiation spectrometer 17 p12133 A73-34163
- Morphological and electron-microscopic alterations of the myocardium in dogs subjected to lasting chronic gamma irradiation 17 p2111 A73-34230
- Gamma detectors using mercuric iodide and other heavy metal compounds as semiconductors with charge carriers for current surge in quantum energy resolution 17 p2134 A73-34247
- Observations of gamma-ray bursts of cosmic origin. 17 p2224 A73-34770
- Satellite measurements of interstellar gamma radiation, describing spark chamber and optical recording system 18 p2349 A73-35975
- Gamma ray and neutron measurements and their relation to the solar flare problem. 18 p2345 A73-36126
- Atmospheric gamma ray spectra from balloon spectrometer scintillator measured energy loss spectra 19 p2476 A73-37909
- Periodic analysis of arrival times in delayed cosmic-ray coincidences. 19 p2476 A73-38086
- Cosmic sources of X rays and gamma rays 20 p2601 A73-39061
- Detection of a gamma-ray spectral line from the galactic-center region. 20 p2602 A73-39438
- Progress report on aircraft gamma-ray surveys for soil-moisture detection at a NOAA test site near Phoenix, Arizona. 20 p2558 A73-39871
- Low energy gamma ray spectrum following muon capture by oxygen 16 leading to bound states of nitrogen 16 21 p2743 A73-40475
- Investigation of primary gamma radiation from the northern polar region of the Galaxy 21 p2756 A73-40578
- Acoustical spark chamber in a telescope designed for investigations of primary cosmic gamma radiation 21 p2701 A73-40612
- Monte-Carlo-method based calculation of the linearity and resolving power of a Cerenkov spectrometer for purposes of gamma astronomy 21 p2701 A73-40613
- Variability of high-energy gamma-radiation sources 21 p2759 A73-40707
- A study of the properties of stimulated ruby laser emission during the action of Co-60 gamma rays 21 p2715 A73-40796
- Chemical protection from genetic damages induced by radiation in the period of aftereffect of acceleration. 21 p2643 A73-40815
- Galactic positronium annihilation gamma ray spectrum with 476 keV photon peak, indicating possible origin in supernova explosive nucleosynthesis of positrons 21 p2770 A73-40941
- Diffuse X and gamma radiation at 0.1-100 MeV, discussing nonthermal mechanisms, thermal emission from uniform intergalactic medium, isotropic background, galactic clusters, etc 21 p2760 A73-41246
- Lunar orbital gamma ray measurements from Apollo 15 and Apollo 16. 21 p2762 A73-41397
- Gamma-spectrometric analysis of lunar samples from Luna 16. 21 p2774 A73-41404
- Pulsed high-energy gamma rays from the Crab Nebula. 22 p2901 A73-41760
- Gamma irradiation induced abiogenic radiochemical synthesis of deoxynucleosides from dry mixtures of purine bases with deoxyribose and ribose 22 p2803 A73-42166
- Expected gamma ray emission spectra from the lunar surface as a function of chemical composition. 22 p2903 A73-42494
- Fading of thermoluminescence induced in lunar fines. 22 p2915 A73-43027
- High energy gamma quanta families and multiple generation processes in electron photon cascades detected by nuclear emulsion X ray chamber 23 p3021 A73-43536
- Fluctuations of the total path of charged particles in electron-photon showers caused by gamma-quanta with energies of 40, 60 and 200 m/c-squared/ 23 p3023 A73-43555
- Galactic and extragalactic gamma ray bursts contribution to diffuse cosmic X ray flux, noting superposition of supernovae outbursts 23 p3025 A73-43957
- Structural changes caused in glassy arsenic trisulfide and triselenide by penetrating radiation 23 p3017 A73-44042
- Theoretical possibilities for the creation of a gamma laser /gazer/ using nuclear transitions 23 p2988 A73-44092
- Stimulated gamma emission in long-lived nuclear isomers, proposing gamma lasers based on Mossbauer line broadening effect 23 p2988 A73-44093
- Cosmic gamma ray studies for metagalactic and remote galactic model construction as substitute for radio and X ray emission data 23 p3025 A73-44325
- Are the recently observed soft gamma-ray bursts from stellar superflares. 23 p3124 A73-44989
- Energy spectra of cosmic gamma-ray bursts. 23 p3125 A73-45053
- Production of gamma radiation in dense interstellar clouds by cosmic-ray interactions. 24 p3125 A73-45054
- Absence of cosmic gamma-ray bursts in association with normal stellar flares. 24 p3127 A73-45492

GANGLIA
NT NERVES
NT NEURONS
Retinal S-potential receptive field relationship to light energy and wavelength, considering cone and rod potentials, ganglion cells and vision
09 p1043 A73-23314

- Receptive fields of retinal ganglion cells.
09 p1043 A73-23315
- Effect of light deprivation on the metabolic reaction development in retinal ganglion cells
10 p1178 A73-23681
- The effect of iontophoretically applied acetylcholine upon the cat's retinal ganglion cells.
14 p1715 A73-30061
- Retinal receptive fields - Correlations between psychophysics and electrophysiology.
14 p1717 A73-30397
- Rabbit optokinetic reactions and retinal direction-selective cells /A preliminary model/.
18 p2273 A73-36455
- Protein synthesis in the neurons and glial cells of the stellate ganglia of rats during the adaptation to the effects of high altitude hypoxia
19 p2393 A73-37396
- Investigation of the geometry of the dendritic tree of retinal ganglion cells
19 p2395 A73-37944
- Shaping device for frequency analysis of electrical processes in peripheral neural stems and ganglia
22 p2815 A73-42664

GAPS

- NT SPARK GAPS
Reentry vehicle ablating control surface gap and slot regions flow characteristics prediction based on quasi-one-dimensional compressible flow finite difference solution
[AIAA PAPER 73-742] 18 p2265 A73-36663
- GARNETS
NT YTTRIUM-ALUMINUM GARNET
NT YTTRIUM-IRON GARNET
Shock wave compression of iron-silicate garnet.
09 p1076 A73-22146
- Paramagnetic resonance line broadening in ferrite garnets with small additions of rare-earth elements
10 p1261 A73-24703

GARP

- U GLOBAL ATMOSPHERIC RESEARCH PROGRAM

GAS ANALYSIS

- NT OZONOMETRY
Instrumentation and measurement for determination of emissions from jet engines in altitude test cells.
[AIAA PAPER 72-1068] 04 p0432 A73-14902
- Development and evaluation of materials for vacuum power interrupters.
04 p0456 A73-15763
- Pollutants from methane fueled gas turbine combustion.
[ASME PAPER 72-WA/GT-3] 04 p0485 A73-15867
- Inorganic gas release and thermal analysis study of Apollo 14 and 15 soils.
07 p0890 A73-19814
- Analysis of organogenic compounds in Apollo 11, 12, and 14 lunar samples.
07 p0890 A73-19819
- Laser application for remote analysis of gaseous air pollutants emission based on Raman scattering, resonance fluorescence or absorption measurements
11 p1375 A73-25399
- Determination of the combustion efficiency by continuous analysis of the combustion products
12 p1558 A73-27386
- Quantitative analysis of specific gases by means of a microwave cavity spectrometer.
13 p1612 A73-28224
- Spectroscopic laser methods of automatic gas analysis based on Raman backscattering, resonance fluorescence or absorption measurements for atmospheric pollutant and exhaust gas detection
16 p2023 A73-32876
- Surveillance and correction of gas analysis devices and the analysis evaluation with the aid of a process computer
16 p2014 A73-33223
- A system for automatic end-tidal gas sampling at rest and during exercise.
20 p2519 A73-39794
- Real time nitrogen dioxide and nitric oxide pollution measurement by molecular fluorescence induced by argon laser beam
21 p2671 A73-40135
- A rapid method for determining the CO₂ transport characteristics in man by using a capnograph and a multichannel respirator
22 p2815 A73-42665

GAS BEARINGS

- On the general solution of externally pressurized gas journal bearings.
[ASME PAPER 72-LUB-Q] 01 p0055 A73-10218
- Optimization of hybrid gas lubricated conical bearings.
01 p0057 A73-10698
- Hybrid fluid film and rolling element bearings for long fatigue life and gas bearings for high temperature operation in gas turbine applications
[SAE PAPER 720739] 02 p0173 A73-12005
- The steady state performance of an externally pressurized gas lubricated porous thrust bearing with a uniform film.
03 p0311 A73-13203

Externally pressurized gas bearings development and applications, considering design, control systems and manufacture

- 03 p0311 A73-13205
- Externally pressurized gas-lubricated journal bearings with herringbone grooves - Load capacity and stability analysis.
03 p0311 A73-13208
- A method of analysing the effect of inertia and compressibility in an externally pressurized gas lubricated thrust bearing.
03 p0312 A73-13209
- The effects of wall conductance on torque of the MHD viscous coupler and hydrostatic thrust bearing.
[ASME PAPER 72-LUB-1] 03 p0313 A73-14326
- An application of pneumatic phase shifting to stabilization of externally pressurized journal gas bearings.
[ASME PAPER 72-LUB-4] 03 p0313 A73-14327
- Dynamic stability of gimbaled spiral-grooved thrust bearing.
[ASME PAPER 72-LUB-13] 03 p0313 A73-14329
- A study of the stability of externally pressurized gas bearings with porous wall by Liapunov's direct method.
[ASME PAPER 72-LUB-18] 03 p0314 A73-14333
- Experimental rotor unbalance response using hydrostatic gas lubrication.
[ASME PAPER 72-LUB-31] 03 p0315 A73-14341
- A hero-jet driven porous spherical hydrostatic gas bearing gyro.
[ASME PAPER 72-LUB-41] 03 p0315 A73-14348
- Theoretical and experimental pressure distribution in supersonic domain for an inherently compensated circular thrust bearing.
[ASME PAPER 72-LUB-43] 03 p0315 A73-14349
- German monograph - The calculation of the stability limit of statically operating circular gas bearings, taking into account the effect of the supported mass.
07 p0832 A73-20390
- Isotope Brayton space power systems and their technology.
07 p0850 A73-20467
- A condition for drift invariance with respect to acting accelerations in a two-degree-of-freedom gyroscope having arbitrary gas lubricated bearings on the main axis
09 p1084 A73-22658
- Summary of gas bearing applications in the field of space electric power systems.
09 p1089 A73-22771
- Galerkin method application to approximation functions selection in development of thrust gas bearing with blowing
11 p1375 A73-26429
- Characteristics of supercharge devices in gas bearings
15 p1881 A73-31296
- A pseudo shock theory of pressure depression in externally pressurized circular thrust gas bearings.
15 p1882 A73-31699
- Analysis of externally pressurized gas bearings with journal rotation.
15 p1883 A73-32147
- Experimental investigation of air bearings for gas turbine engines.
[ASLE PREPRINT 73AM-2B-1] 17 p2178 A73-34981
- An economical method of analyzing transient motion of gas-lubricated rotor-bearing systems.
[ASLE PREPRINT 73AM-2B-2] 17 p2178 A73-34982
- Recent test results - A strapdown IMU utilizing hydrodynamic spin bearing rate sensors and pulse rebalance loops.
[AIAA PAPER 73-898] 20 p2564 A73-38833
- Dual spin gas bearing reaction wheel for spacecraft fine pointing applications requiring long component life, describing manufacturing methods, safety factors and testing
[AIAA PAPER 73-907] 20 p2568 A73-38841
- Gas bearing technique for ultrahigh speed rotating mirror mounted on opto-mechanical camera
21 p2693 A73-39936
- The impact of space navigation on the spherical gas bearing gyro.
21 p2697 A73-40025
- GAS CHROMATOGRAPHY**
Viking lander-borne gas chromatograph mass spectrometer for Martian atmosphere sampling and soil analyses
02 p0168 A73-12000
- Methane pyrolysis in a low current DC discharge.
03 p0398 A73-13798
- Gas-chromatography investigation of volatile metabolites in man on reduced food rations and during starvation
06 p0657 A73-17690
- Quantitative gas-liquid chromatography of non-protein amino acids in the presence of the twenty protein amino acids.
06 p0661 A73-18175
- Nanogram level lunar organic compound separation and detection by gas-liquid chromatography
06 p0661 A73-18413

Aromatic and heteroatom-containing organic compounds in the lunar samples.

- 06 p0662 A73-18424
- Resolution by gas-liquid chromatography of diastereomers of five nonprotein amino acids known to occur in the Murchison meteorite.
06 p0662 A73-18468
- Distribution of methane and carbide in Apollo 11 fines.
07 p0900 A73-20188
- Usage of the VNII NP-300A lubricant in gas-liquid chromatography and high-vacuum technology
10 p1239 A73-24250
- Gas-liquid chromatographic resolution of several protein amino acid enantiomers on a packed column.
10 p1186 A73-24658
- Gas-liquid chromatography of trifluoroacetyl derivatives of cyclitols.
11 p1325 A73-25150
- Complex mixture analysis - Geochemical and environmental applications of a compound classifier based on computer analysis of low resolution mass spectra.
11 p1326 A73-25464
- The diagenesis and maturation of phytol - The stereochemistry of 2,6,10,14-tetramethylpentadecane from an ancient sediment.
11 p1326 A73-25466
- Geochemistry of amino acid enantiomers - Gas chromatography of their diastereomeric derivatives.
11 p1326 A73-25469
- An automated gas chromatographic analysis of phenylalanine in serum.
11 p1326 A73-25571
- Measurement of hydrazine gas generator performance by gas chromatography.
11 p1326 A73-26398
- Organic compounds chemical analysis with cold trap to allow materials evaporation according to vapor pressure characteristics for replacing gas chromatograph
17 p2175 A73-35760
- Racemization of amino acids in marine sediments determined by gas chromatography.
23 p2973 A73-43843
- Gas chromatography-mass spectrometry study of sterols from *Pinus eliottii* tissues.
24 p3065 A73-44698
- GAS COMPOSITION**
NT CARBON DIOXIDE CONCENTRATION
Instrumentation and measurement for determination of emissions from jet engines in altitude test cells.
[AIAA PAPER 72-1068] 04 p0432 A73-14902
- O-18/O-16, Si-30/Si-28, C-13/C-12, and D/H studies of Apollo 14 and 15 samples.
07 p0887 A73-19771
- Lunar atmosphere gas concentrations from Apollo 14 and 15 ALSEP cold cathode ionization gage measurements, considering solar wind and contamination sources
07 p0891 A73-19830
- Estimation of the seasonal variation of the gas composition of the atmosphere at the height of the F1 layer from data on the developmental conditions of the layer
08 p0958 A73-21281
- Influence of initial gas conditions in a coaxial accelerator on plasma parameters
13 p1666 A73-28956
- KCl ionization and diffusion in premixed flames with uniform temperature and composition, studying gas velocity and photometry
13 p1707 A73-28995
- Calculation of the electron density in heterogeneous mixtures with allowance for the tunneling effect and for super-barrier reflection
15 p1915 A73-31854
- The interaction of gases and carbon with refractory metals
15 p1890 A73-31925
- Use of fluidic and pneumatic elements to determine the composition of a gas mixture
16 p1970 A73-33025
- Carbon dioxide laser active element design features for service life extension through regenerating working mixture composition while preserving discharge tube seal tightness
17 p2182 A73-34167
- Parametric test results of a swirl-can combustor.
17 p2222 A73-35471
- Estimation of the seasonal variation of the gas composition of the height of the F1-layer from data on the conditions of its development.
19 p2424 A73-37910
- Distribution of gases within Apollo 15 samples - Implications for the incorporation of gases within solid bodies of the solar system.
20 p2612 A73-39715
- On the possibility of measuring gas concentrations by stimulated anti-Stokes scattering.
21 p2699 A73-40458
- Effect of initial gas conditions in a coaxial accelerator on the plasma parameters.
23 p3013 A73-44308
- GAS COOLED REACTORS**
NT HIGH TEMPERATURE NUCLEAR REACTORS

- GAS COOLING**
 Hypersonic turbulent boundary layer flow parameters and heat transfer during blowing of coolant air and He through slot
 03 p0242 A73-13186
 A process for delubrication, presintering, sintering, and rapid cooling in a vacuum induction furnace.
 04 p0455 A73-15751
 Enthalpy driving forces for gas cooling data correlation in convective heat transfer in reacting turbulent boundary layers with mass injection
 [ASME PAPER 72-WA/HT-31] 04 p0519 A73-15824
 Thermodynamic optimization of current leads into low temperature regions.
 13 p1707 A73-29067
 Effectiveness of a gas screen in plasmatrons of axial configuration
 15 p1917 A73-31191
 Porous cooling in a supersonic turbulent boundary layer
 20 p2628 A73-39609
 Emission of infrared molecular hydrogen lines from a cooled-gas laser.
 20 p2574 A73-39694
 The decay of perturbations in an electrically conducting and thermally radiating gas.
 21 p2789 A73-40246
 Unsteady convective heat transfer attending the cooling of gas in tubes.
 21 p2791 A73-41053
 50 kG gas cooled superconducting solenoid operated at 13 K.
 21 p2702 A73-41103
 The rapid cooling of a hot gas discharge by liquid sprays.
 22 p2929 A73-41743
 Ion-grain collision cooling rate for hot gas above million K, discussing applications to supernova explosions, Seyfert nuclei and intergalactic matter within galactic clusters
 22 p2916 A73-43121
 Unsteady convective heat exchange for various hot-gas cooling laws in tubes
 24 p3156 A73-45077
- GAS DENSITY**
 Gas density measurements in a jet using Raman scattering.
 01 p0050 A73-10763
 Cold matter consisting of atomic nuclei submerged in electron-neutron gas, relating subnuclear density relation to existence and binding energy of neutron-rich nuclei
 01 p0081 A73-11310
 Lunar surface observation with cold cathode ionization gage left by Apollo 14, noting low concentration atmospheric particles and gas clouds
 02 p0213 A73-12239
 Density changes in a laser cavity including wall reflections and kinetics of energy release.
 [ALAA PAPER 73-141] 05 p0585 A73-16890
 Statistical mechanics and virial functions for equation of state of dense gas with spherical nonpolar molecules, calculating compressibility factor for methane and Ar
 06 p0726 A73-18555
 Noble gases concentration profiles in lunar fines and minerals, investigating thermal release patterns
 07 p0889 A73-19807
 Shock wave formation in a statistically inhomogeneous gas
 08 p0955 A73-21450
 Equation of state and phase diagram of dense hydrogen.
 11 p1399 A73-25890
 Light scattering from weakly ionized nonhomogeneous plasmas.
 11 p1405 A73-25971
 Explosion in detonating media with a variable initial density
 12 p1487 A73-27419
 Explosion in a variable-density medium in the presence of variable counterpressure.
 12 p1487 A73-27532
 Apparatus and techniques for electron beam fluorescence probe measurements.
 13 p1612 A73-28365
 Investigation of high-temperature gas flow around axisymmetric bodies in the presence of several discontinuity surfaces
 13 p1708 A73-29404
 Shock-wave generation in a randomly inhomogeneous gas.
 15 p1860 A73-31014
 Viscosity coefficients and heat conductivity of dense gases with rotational degrees of freedom
 15 p1915 A73-31022
 Interstellar gas excitation due to supernova explosions using time dependent model based on statistical correlation of gas neutral density, ionization and temperature parameters
 15 p1928 A73-31053
 A microscopic theory of density fluctuations in partially ionized gases.
 15 p1916 A73-31086
- Statistical mechanics and virial functions for equation of state of dense gas with spherical nonpolar molecules, calculating compressibility factor for methane and Ar
 16 p2039 A73-33580
 Superfluidity of the Fermi component in a Fermi-Bose gas and in He3-He4 solutions
 16 p2038 A73-34067
 Interstellar matter observations, discussing densest stages spatial distribution near solar system and dense clouds
 17 p2227 A73-34409
 Gas concentration measurement by coherent Raman antistokes scattering.
 [ALAA PAPER 73-702] 18 p2315 A73-36251
 Determination of local gas states from scattered laser light
 19 p2438 A73-38270
 Galactic shocks as consequence of large amplitude nonlinear density waves in interstellar gas perturbed via steady forcing by spiral gravitational fields
 19 p2488 A73-38511
 Dimensionless pressure method to account for air density variations in gas turbine cooling system design
 21 p2677 A73-41051
 Interaction of a shock wave with blunt bodies in supersonic flow
 21 p2633 A73-41222
 Neutral interstellar hydrogen and extraterrestrial Lyman alpha radiation.
 21 p2773 A73-41396
 A gas density control system for X-ray proportional counters in space.
 22 p2851 A73-41699
 Diurnal and semidiurnal nitrogen density and temperature variations from thermosphere probe measurements.
 22 p2845 A73-41926
 A device for the on-line measurement of nitrogen rotational temperature in low density flows.
 22 p2854 A73-41995
 A reexamination of the mean H I density along the Hubble sequence.
 22 p2913 A73-43003
 Gasdynamic equations for low temperature monatomic gas, showing Wigner distribution function independence of density gradient in agreement with nonequilibrium statistical thermodynamics concepts
 23 p2939 A73-43704
 Density and velocity fluctuations in young nebulae of Orion type
 23 p3035 A73-44232
 Opening time of brittle shock-tube diaphragms for dense fluids.
 24 p3075 A73-44820
 Physical particle description of moderately dense gases. II - Equilibrium properties.
 24 p3111 A73-45397
- GAS DETECTORS**
 Hazardous gas detection system for analysis of gases escaping during cryogenic loading in Apollo-Saturn launch tests, discussing utilization for environmental pollution detection
 05 p0578 A73-17135
 An analytical study of hypersonic inlets in free molecule flow.
 18 p2264 A73-36325
 Compact carbon monoxide sensor utilizing a confocal optical cavity.
 [ASME PAPER 73-ENAS-20] 19 p2400 A73-37976
 Opto-thermal gas concentration detector operation by measuring temperature variations caused by chopped laser beam in sample cell, using pyroelectric material as temperature sensor
 21 p2701 A73-40691
- GAS DISCHARGE COUNTERS**
U COUNTERS
U GAS DISCHARGE TUBES
GAS DISCHARGE TUBES
NT THYRATRONS
 New mechanism for generating coherent emission from ionized oxygen and nitrogen in the visible region of the spectrum
 01 p0059 A73-10630
 Ar and Kr continuous wave ion lasers with electric arc discharge, noting quartz, graphite and beryllium oxide gas discharge tubes
 01 p0059 A73-10714
 Coaxial gas discharge tubes for pulsed lasers
 01 p0059 A73-10796
 Electron-ion collision frequency and electrical conductivity of non-Debye plasma formed in high pressure discharge from Ar, Kr and Xe tubes
 03 p0345 A73-13176
 Reliable starting technique for an ion laser tube with internal gas return bores.
 [AD-758556] 05 p0586 A73-17263
 Intensity and energy spectrum calculation of albedo electrons recorded in cosmic particle showers by gas discharge counters
 07 p0823 A73-19429
 A model for the kinetics of oxygen dissociation in a microwave discharge.
 07 p0789 A73-20643
- Studies of noble-gas lasers for continuous operation
 13 p1627 A73-28790
 Linear Z pinch magnetohydrodynamic instability mode and characteristic wavelength determined by discharge tube radius and current build up rate
 15 p1918 A73-31703
 Carbon dioxide laser active element design features for service life extension through regenerating working mixture composition while preserving discharge tube seal tightness
 17 p2182 A73-34167
 Origin of terrestrial polypeptides - A theory based on data from discharge-tube experiments.
 20 p2513 A73-39484
 Correlation between output power and composition of discharge products in a water vapor laser.
 20 p2574 A73-39698
 Drift tube and mass spectrometric measurement of molecular positive ion drift velocities in carbon dioxide
 21 p2742 A73-40221
 Transition of a low-pressure plasma into a highly ionized state
 23 p3013 A73-44335
- GAS DISCHARGES**
NT TOROIDAL DISCHARGE
 International Conference on Gas Discharges, 2nd, London, England, September 11-15, 1972, Proceedings.
 01 p0081 A73-10111
 Electron density measurements in time varying plasmas with a microwave reflectometer system.
 01 p0044 A73-10120
 Double discharge TEA carbon dioxide laser trigger circuit, using plastic materials with selected dielectric constant and resistivity for trigger current increase
 02 p0175 A73-11958
 Gas discharge efficiency from populations comparison of Ne absorbing levels in hollow cathode and positive column discharges, measuring laser output power peak
 02 p0176 A73-12096
 Uniform low temperature gas discharge plasma diagnostics in shielded volume, noting application of stable plasma generation effect for isotope analysis
 02 p0199 A73-12693
 Methane pyrolysis in a low current DC discharge.
 03 p0398 A73-13798
 Pulse discharge plasma in Ar with gas ionization level near unity, noting plasma cylinder parameters, electron temperature and I-V characteristics
 03 p0347 A73-14091
 Current trapping in toroidal high current discharges.
 03 p0348 A73-14435
 The light emission of the column plasma in current-modulated noble-gas discharges at intermediate pressures
 03 p0348 A73-14621
 Investigation of fluctuation and wave phenomena in argon low-current low-pressure discharges, taking place under the influence of a 'brief' axial magnetic field
 03 p0348 A73-14623
 Supersonic electrical-discharge copper vapor laser.
 04 p0457 A73-14746
 Investigations of a Kr-Hg mixture regaining laser action
 04 p0458 A73-14896
 Characteristics of an argon RF plasma - Active discharge and laminar sonic flow region.
 05 p0602 A73-16559
 Atmospheric pressure CO2 pulsed laser with semiconducting plastic electrodes.
 05 p0585 A73-16567
 The formation of primary gas discharge zones in electrical wire explosions
 06 p0723 A73-17911
 The emission spectrum of the silent electric discharge in ammonia and hydrazine vapor
 06 p0723 A73-17916
 Plasma parameters in gas discharges for positive-column He-Se/+ lasers.
 06 p0701 A73-18360
 Intermittent behavior of a plasma discharge in turbulent gas flow.
 07 p0856 A73-19517
 A possible mechanism for the change in the discharge current in CO2 through the action of laser radiation.
 07 p0836 A73-20137
 The theory of a coaxial gas-discharge oscillator loaded by a helical line.
 07 p0801 A73-20138
 Discharge current dependence of saturation parameter of a He-Ne gas laser.
 08 p0976 A73-21463
 Dynamics of the current sheath in a pulsed electrodynamic plasma accelerator
 09 p1125 A73-21910
 Calculation of the Knudsen-arc ignition potential in a gas-filled diode with cylindrical and spherical electrode geometries
 09 p1061 A73-21912

Development and properties of the halo in pinch plasmas

10 p1253 A73-23673

Electron impact ionization, three body recombination and thermal energy balance effects on gas discharge positive column between plane parallel walls

10 p1255 A73-24265

Electron-optical investigations of discharge in air and carbon dioxide in the nanosecond range

10 p1219 A73-24469

Output power saturation with a discharge current in powerful continuous argon lasers.

11 p1377 A73-26179

Hydrogen fluoride chemical laser with high voltage pulse initiation in simple transverse discharge geometry, measuring maximum energy output and corresponding efficiency

11 p1378 A73-26323

Nitrogen laser with a longitudinal discharge and high power density

12 p1506 A73-27214

Influence of a SHF field on the inhomogeneities of a nonequilibrium plasma from a low-pressure gas discharge

12 p1528 A73-27304

Effects of target-electrode polarity and of the position of the focal plane of the lens on the characteristics of a discharger with laser ignition

13 p1627 A73-28964

Characteristics of a high-pressure carbon dioxide laser with a transverse discharge

13 p1627 A73-28966

A simple theory of breakdown for nonequilibrium gases in fields of any frequencies ranging from low to optical

13 p1663 A73-29165

Gas discharge CW and pulsed CO laser population inversion mechanism, noting high output and efficiency in CW and Q switched modes

13 p1629 A73-29428

Time behavior of hydrogen discharge in ST-Tokamak based on measured radial electron temperature and density profiles and ohmic-heating current and voltage

14 p1778 A73-29691

Self-igniting pulsed optical discharge in an erosion laser plasma.

14 p1757 A73-30334

Current-shell dynamics in a pulsed electrodynamic plasma accelerator.

15 p1922 A73-32635

Ignition potential of a Knudsen arc in a gas-filled diode with cylindrical and spherical electrodes.

15 p1922 A73-32637

Steady state arc discharge physical properties, discussing boundary geometry of plasma column, and stabilities in gas flow and high current and vacuum conditions

16 p2040 A73-32939

Excitation of atomic nitrogen by electron impact.

16 p2038 A73-33099

Pulsed HCN laser output power enhancement with auxiliary dc discharge, noting low gas flow rate and nonmultiple pulsing advantages

17 p2185 A73-35406

Electron-beam irradiated discharges for initiating high-pressure pulsed chemical lasers.

[ALAA PAPER 73-645]

18 p2322 A73-36259

Investigation of the discharge structure in a noble gas alkali MHD generator plasma. I.

18 p2338 A73-36303

Investigation of the discharge structure in a rare gas alkali MHD generator plasma. II.

18 p2339 A73-36304

Generation of energetic ion fluxes from a high temperature electron discharge in an inhomogeneous magnetic field

19 p2466 A73-37358

Nitrogen ionization in an Hg-N₂ discharge.

19 p2463 A73-37903

Excitation of an open resonator by initial emission from a high current discharge

19 p2469 A73-37963

Quasi-periodic noises in a He-Ne laser.

19 p2438 A73-38166

CW CO₂ laser at atmospheric pressure.

19 p2438 A73-38277

Experimental results concerning the time decay of the line emission in luminescent plasmas of medium-pressure inert-gas discharges

20 p2596 A73-39191

The breakdown condition of the electrode layer in an ionized gas flow

20 p2597 A73-39278

Extraction of electrons from a plasma in the presence of a gas in the high-voltage gap

20 p2598 A73-39606

Gas discharge plasma diagnostics based on polarization plane rotation of submillimeter laser radiation

20 p2598 A73-39622

Kerr-cell studies of exploding wires in vacuum.

21 p2738 A73-39996

Plasma stability of electric discharges in molecular gases.

21 p2744 A73-40220

Recombination and negative ion role in high-frequency gas discharges

21 p2743 A73-40366

An argon ion laser with a gas-discharge tube of relatively large diameter

21 p2714 A73-40556

Large aperture atmospheric pressure excited carbon dioxide laser discharges, using weak volumetric gas preionization to obtain high power for plasma production

21 p2714 A73-40762

A parametric study of the performance of a TEA CO₂ laser.

22 p2868 A73-41700

Russian book - Physical bases of thermionic energy conversion.

22 p2890 A73-41876

Current-induced heating of a dense plasma during collective interactions in a high-current gas discharge

23 p3009 A73-43651

Electrical conductivity of a plasma during collective interactions in a high-current gas discharge

23 p3009 A73-43652

Measurement of turbulent HF fields in a high-current rectilinear gas discharge from the intensity of forbidden HeI lines

23 p3011 A73-43669

A kinetic model of population inversion generation in a gas-discharge carbon monoxide laser

23 p2988 A73-44012

Effects of target-electrode polarity and focal-plane position on a laser-triggered gap.

23 p2989 A73-44316

High-pressure CO₂ laser with a transverse discharge.

23 p2989 A73-44318

Longitudinal inhomogeneity of gain in the active element of a helium-neon laser pumped by direct current

24 p3097 A73-45517

Pulsed high output double discharge TEA carbon dioxide laser with multiple electrodes and gas preionization in cavity, noting energy conversion efficiency

24 p3098 A73-45551

GAS DISSOCIATION

Use of light pressure for selective evacuation of gases

01 p0059 A73-10627

A numerical analysis for chemical non-equilibrium boundary layer of dissociated gases over a flat plate with arbitrary catalytic.

03 p0291 A73-13068

Ideal dissociating/nondissociating gas reentry flow fields hydrodynamic stability for various free stream and disturbance conditions

03 p0242 A73-13312

Determination of the value of blood oxygen capacity and of the oxyhemoglobin dissociation curves by polarographic coulombometry

03 p0267 A73-13750

Oxygen 1S production efficiency of photons at 812-1216 Å measured by O I 5577 Å green line detection during carbon dioxide photodissociation

05 p0546 A73-16049

Dissociative excitation of molecular hydrogen by electron impact.

05 p0600 A73-16596

Optimal profiles of a nozzle for axisymmetric supersonic discharge of a Lighthill dissociating gas

05 p0534 A73-17270

Shock tube investigation of bromine dissociation rates in the presence of carbon dioxide.

06 p0661 A73-18123

Temperature dependence of diatomic gases thermal conductivity coefficient from shock tube tests, noting molecular gases above dissociation temperature

06 p0687 A73-18561

Dissociation of carbon monoxide in a pumped CO laser.

06 p0703 A73-18613

Heat exchanging and catalytic dissociation of ammonia flowing through tubes - Application to micropropulsion.

07 p0867 A73-18931

Photoelectron precipitation induced dissociation of atmospheric nitrogen molecules during moderate solar activity

07 p0816 A73-19459

A model for the kinetics of oxygen dissociation in a microwave discharge.

07 p0789 A73-20643

A shock tube determination of the CN ground state dissociation energy and the CN violet electronic transition moment.

08 p0989 A73-20789

Mass spectrometric studies of tetrafluorohydrazine and the difluoroamino radical.

08 p0936 A73-21173

Mass spectroscopic investigation of dissociation and ionization in a simulated re-entry plasma.

09 p1130 A73-22843

Atomic recombination rate determination through heat-transfer measurement.

09 p1048 A73-23449

Proton-impact dissociation and ionization of H₂+ molecular ions.

10 p1250 A73-23671

Doppler broadening of OI 1304 Å multiplet in dissociative excitation of CO₂ and O₂.

10 p1251 A73-24243

Use of translational energy measurements in the evaluation of the energetics for dissociative attachment processes.

10 p1251 A73-24244

Equator-pole temperature difference and the solar oblateness /Research note/.

12 p1544 A73-27831

Laser interaction and related plasma phenomena; Proceedings of the Second Workshop, Rensselaer Polytechnic Institute of Connecticut, Hartford, Conn., August 30-September 3, 1971. Volume 2.

12 p1508 A73-27922

Study by electronic paramagnetic resonance of the molecular dissociation in an oxygen plasma

13 p1664 A73-28566

Collision induced dissociation - A statistical theory.

15 p1915 A73-31275

Ionospheric D region dissociation-recombination reaction constants derived from ion production rate data compiled during polar cap absorption

15 p1872 A73-31887

Decomposition of hydrazine on Shell 405 catalyst at high pressure.

15 p1841 A73-32174

Temperature dependence of diatomic gases thermal conductivity coefficient from shock tube tests, noting molecular gases above dissociation temperature

16 p2086 A73-33586

Thermal dissociation and recombination of hydrogen according to the reversible reactions H₂ + H to H + H + H.

16 p1977 A73-33674

Hypersonic nozzle flow of air with high initial dissociation levels.

16 p2001 A73-33870

Spectrophotometric determination of the rate of dissociation of nitrogen trifluoride behind shock waves.

16 p1977 A73-34017

Atmospheric attenuation effects on nitric oxide dissociation in mesosphere and stratosphere, noting dissociation profile dependence on absorption of discrete oxygen Schumann-Runge bands

17 p2119 A73-34778

Lower thermospheric oxygen photodissociation evaluation for global average and hemispheric imbalance, discussing wind system to compensate for solar thermal input imbalance

17 p2159 A73-34784

Dissociation of carbon dioxide behind reflected shock waves.

17 p2119 A73-35173

Two dimensional half-jet mixing of dissociated air, investigating chemical rate and diffusion processes interaction effects on mixing layer thermodynamics

17 p2156 A73-35503

Correlation between output power and composition of discharge products in a water vapor laser.

20 p2574 A73-39698

Threshold minima in the superhigh-pressure gas breakdown by Q-switched lasers.

20 p2574 A73-39721

Atmospheric CO production from electron impact on carbon dioxide, considering lightning, radioactivity, discharges, photoelectrons, auroral particles, cosmic rays and solar wind

21 p2680 A73-40079

Regular reflection of an oblique shock in a plane flow of ideally dissociating gas in the presence of a transverse magnetic field

21 p2744 A73-40189

Dissociation and bleaching of a multilevel molecular gas under the influence of radiation from a powerful CO₂ laser

21 p2712 A73-40357

Charge collection measurements on a plasma induced by the CO₂ laser.

21 p2748 A73-41021

Hydrogen production rates of comet Bennett /1969/ in the first half of April 1970.

21 p2778 A73-41530

Laser-induced gas breakdown in superhigh pressure region.

22 p2869 A73-42227

Kinetics of gas absorption by refractory metals in dissociated environments - The nitrogen/tantalum system.

22 p2879 A73-42583

Precise measurements of diatomic dissociation rates in shock waves.

22 p2818 A73-42765

Shock tube kinetics of NO decomposition in mixtures with Ar, measuring ground state atomic oxygen formation rate by resonance absorption spectrophotometry

22 p2818 A73-42766

Sulfur hexafluoride pyrolysis and subsequent oxidation in mixtures with oxygen atoms and molecules, measuring decomposition rate at high temperature in shock tube experiment

22 p2818 A73-42767

Ionised molecules in BCA photospheric model.
22 p2915 A73-43039

The production and distribution of nitrogen oxides in the lower stratosphere.
23 p2977 A73-43897

Sealed carbon dioxide laser output anomalous transient pulsive behavior attributed to gas dissociation and recombination from electron density and temperature measurements
24 p3095 A73-44408

An equation for the oxygen hemoglobin dissociation curve.
24 p3064 A73-45070

GAS DYNAMICS

NT AERODYNAMICS
NT AEROTHERMODYNAMICS
NT RAREFIED GAS DYNAMICS
NT ROTOR AERODYNAMICS

Analytical method of gasdynamic semibounded-space parameter computation allowing for velocity profile inhomogeneity and turbulent combustion of condensed systems
01 p0121 A73-10619

Detonation in a medium of variable density with allowance for variable back pressure
01 p0034 A73-10956

Relativistic gas dynamics problems reduction to equivalent Newtonian flow via transformation of governing equations
01 p0034 A73-11138

Quantum kinetics equations for a nonideal gas and a nonideal plasma
01 p0086 A73-11286

A computer program for molecular dynamics of dilute gases.
01 p0081 A73-11472

Two-dimensional, unsteady, self-similar flows in gas dynamics.
02 p0152 A73-11569

Stationary state of the radially symmetrical motion of vapors heated by laser radiation with allowance for thermal and ionizational nonequilibrium
02 p0175 A73-11601

Navier-Stokes approximation for gas dynamics equations of molecular oscillations in diatomic gas, noting relaxation pressure proportionality to energy density equilibrium deviation
02 p0152 A73-11602

Gasdynamics calculations for a pulsating flow in pipelines
02 p0152 A73-11610

Electric discharge CO mixing gas dynamic laser, noting nitrogen molecules vibrational excitation and mixing with cold CO in supersonic expansion with population inversion
02 p0175 A73-12050

Heavy elements depletion on grains in interstellar medium two phase model, noting gas dynamical analysis of discrete clouds evolution
03 p0366 A73-12931

Classical hard-sphere gas in spherical box with coupling between local thermodynamics and gravitation, noting stellar core-halo structure from equilibrium state calculations
03 p0366 A73-12936

Acoustical studies of rotational relaxation in gases.
03 p0342 A73-12986

Investigation of electronic and gasdynamic parameters of hypersonic wakes behind models moving in argon.
03 p0296 A73-14099

Compression shock formation in arbitrary medium described by first order quasi-linear partial differential equations, considering strongly radiating and emission dominated gases
03 p0400 A73-14629

Axial and transverse wave motions of inviscid perfect gas in isothermal solid-body rotation in cylinder
04 p0434 A73-15163

Magnetopause physical properties, location and shape from continuum gas dynamics analogies, noting agreement with experimental results
04 p0441 A73-15328

On the evolution toward equilibrium in the kinetic theory of gases
05 p0599 A73-17229

Gas-dynamic description of a plasma in a corrugated magnetic field.
05 p0603 A73-17360

Use of approximations of thermodynamic functions in gasdynamics calculations
06 p0644 A73-17470

Boundary value problem for subsonic gas flow, proving existence theorem for gas dynamics problem solution
06 p0645 A73-18069

Gasdynamic structure of a plasma flame arising during vaporization of metals by strong optical radiation
06 p0729 A73-18107

One-dimensional electrogasdynamic flow with shock waves in the case of a small parameter of the electrohydraulic interaction
06 p0733 A73-18883

Monte Carlo method applications in the solution of gas kinetics problems
07 p0853 A73-19987

Gas dynamic characteristics of the helium two stage shock tube for MHD power generation experiments.
07 p0808 A73-20117

Investigation of the burnup process structure under spin conditions
07 p0923 A73-20424

Some methodological questions concerning the simulation of turbine blade operation on gasdynamic stands
07 p0809 A73-20509

Electrode and gasdynamic effects in a large nonequilibrium MHD generator.
08 p0928 A73-20713

Plane or axisymmetric inviscid optically gray hot gas jet radiating near optically thin limit, considering thermal radiation-gas dynamics coupling effects
08 p1020 A73-20783

Nozzle-target system geometry and gas dynamics parameters effect on supersonic underexpanded jets interaction with walls, noting frequency response and pressure oscillations
08 p0927 A73-21610

Gasdynamic and thermal processes during giant laser pulse impingement on target material, considering heat wave propagation at supersonic and subsonic velocities
09 p1127 A73-22610

Thermal conductivity approximation for gasdynamic equations describing stellar gravitational collapse, calculating neutrino and antineutrino energy and momentum transport processes
09 p1147 A73-22701

Slip parameter for electrogasdynamic generators with unsteady flow.
09 p1037 A73-22825

An exact solution for a collisionless flat galactic model.
10 p1275 A73-23826

Explosion gas dynamics experimental investigation, noting fast chemical reactions induced exothermic processes and detonation wave structure
10 p1295 A73-23853

Russian book - Fundamentals of the theory of operational processes in solid-propellant rocket systems.
10 p1262 A73-23948

Gas dynamic theory of gas exchange in organisms based on oxygen and carbon dioxide permanent partial pressure gradients in tissues, blood and lungs
10 p1181 A73-24523

On the origin of oscillations appearing in shock profiles calculated by difference methods
11 p1390 A73-25868

The interaction of weak gravitational waves with a gas.
11 p1400 A73-26177

Implicit difference method of temperature determination in problems of radiative gasdynamics
11 p1348 A73-26329

Laser beam evaporation of dense substances, examining luminous flux densities with gasdynamic equations
12 p1506 A73-27137

Powerful laser beam and material interaction, investigating gas dynamics of plasma heating and ejection
12 p1506 A73-27138

Possibility of gasdynamic effects at the critical point of the phase equilibrium
12 p1487 A73-27418

Thermospheric neutral gas dynamics, discussing acoustic, gravity, tidal and planetary waves disturbance spectrum, propagation characteristics, latitude structure and energy sources
12 p1493 A73-27756

Motion of a conducting gas with variable properties between rotating cylinders
12 p1487 A73-27798

Conjugating a Chaplygin operator with a differential operator in gasdynamics
13 p1563 A73-28443

Kinetic equations for the Green functions describing equilibrium states of a gas.
13 p1662 A73-28551

A forcing mechanism for spiral density waves in galaxies.
13 p1686 A73-29372

Ejection of bodies from the solar system in the course of the accumulation of the giant planets and the formation of the cometary cloud.
14 p1793 A73-29825

Nonlinear effects in steady supersonic dissipative gasdynamics. II - Three-dimensional axisymmetric flow.
14 p1711 A73-30167

Acoustic field produced in a gas by arbitrary disturbances on a moving plate
14 p1775 A73-30834

Approximate solution of a stream problem of subsonic gasdynamics
15 p1821 A73-31152

Heat transfer behind a shock wave in a two-phase gasdynamic flow
15 p1862 A73-31294

The local role of the limit line in the well-posing of steady state problems in gas dynamics. I - Problems involving one space dimension.
15 p1862 A73-31328

German book - Theoretical gasdynamics. Volume I - Theory of the flows of compressible media.
15 p1863 A73-31474

Russian book - Thermophysical properties and gasdynamics of high-temperature materials.
15 p1957 A73-31851

Motion of a heated gas layer and the asymptotic characteristics of the gas layer
15 p1958 A73-32107

Relaxation of a partially ionized gas in a nozzle
15 p1824 A73-32327

One-dimensional electro-gasdynamic flow with shock waves and a small electrohydraulic interaction parameter.
15 p1921 A73-32408

Monograph - Development of hotshot wind tunnels for hypersonic aerodynamic studies.
15 p1859 A73-32595

Upper atmosphere pollution and near surface climate due to aerospace operations, discussing dynamics and trace gas distribution
16 p2005 A73-33536

[ALAA PAPER 73-492]
Book - Gasdynamic theory of detonation.
17 p2253 A73-34297

Numerical solution method for Navier-Stokes equations of a compressible gas over a wide range of Reynolds numbers
17 p2151 A73-34632

Reaction of a cylindrical shell to periodic shock waves propagating in its interior
17 p2243 A73-34735

Multiphase underexpanded plume computational technique including turbulent mixing and nonequilibrium chemistry.
18 p2368 A73-36244

[ALAA PAPER 73-695]
Newtonian method of relativistic gas dynamics for steady gas, shock wave, nozzle, Prandtl-Meyer flow and photon gas applications
18 p2300 A73-36632

Elastic and inelastic scattering in orbital clustering.
18 p2357 A73-37109

Russian papers on physical processes in plasma accelerators covering types, diagnostic methods, gas dynamics, control and space studies
19 p2466 A73-37352

Plasma accelerators in gas dynamics, discussing ion propulsion systems, high velocity wind tunnels with electric arc heating and electromagnetic shock tubes
19 p2466 A73-37354

Gas dynamic models of high speed explosive impacts of solid bodies, discussing metal cavity lining, buckling and hypersonic jet phenomena
19 p2433 A73-37514

A note on Beltrami and complex-lamellar flows behind a three-dimensional curved gasdynamic shock wave.
19 p2420 A73-37753

On some problems of the method of simulating the working conditions of turbine blades on gas-dynamic benches.
19 p2418 A73-37784

Rumanian contributions regarding the application of the Coanda effect
19 p2387 A73-38303

Plane unsteady dispersion of gas behind deflagration wave moved by laser radiation with high flux density
20 p2573 A73-39281

The local role of the limit line in the well-posing of steady state problems in gas dynamics. II - Two dimensional plane flow.
20 p2549 A73-39562

Interferograms of high optical quality by double exposure.
21 p2695 A73-39963

Comments on the mathematical theory of small oscillations of an inviscid gas
21 p2738 A73-40191

Numerical solution of nonlinear resonant wave equation of radiating gas between parallel walls by parametric differentiation
21 p2790 A73-40250

Analysis of gas flow in multinozzle jets
21 p2631 A73-40393

Possibility of radiative acceleration of the gas in stellar atmospheres
21 p2767 A73-40534

Photographic instrumentation in Hyperballistic Range /G/ of the von Karman Gas Dynamics Facility.
22 p2864 A73-43189

Quantum kinetic equations for a nonideal gas and a nonideal plasma.
23 p3009 A73-43507

Sound field created in a gas by arbitrary perturbations on a moving plate.
23 p3006 A73-43584

Gasdynamic equations for low temperature monatomic gas, showing Wigner distribution function independence of density gradient in agreement with nonequilibrium statistical thermodynamics concepts
23 p2939 A73-43704

Gas-dynamic structures of a plasma flare produced during the evaporation of metals by high-intensity optical radiation.

24 p3114 A73-44496

A gasdynamic test stand and its use in studying sprayer nozzles for spraying metallic solutions. I

24 p3075 A73-44742

Transonic equation for flow in apertures between compressor and turbine blades, examining gas dynamic and geometric parameter influence on near-sonic flow

24 p3054 A73-45024

GAS EVACUATING

U EVACUATING [VACUUM]

GAS EVOLUTION

Solar outer atmospheric eruption from photographic recording by OSO 7 spacecraft borne coronagraph, noting ejected gas and plasma clouds caused by flare

06 p0753 A73-18374

Chemically bound nitrogen abundances in lunar samples, and active gases released by heating at lower temperatures /250 to 500 C/.

07 p0890 A73-19817

Thermal analysis-mass spectrometer computer system and its application to the evolved gas analysis of Green River shale and lunar soil samples.

08 p0936 A73-20824

Comet nuclei gas liberation, perihelion mass loss and photometric property dependence on water ice evaporation rate and nongravitational effects

14 p1792 A73-29815

Nickel-water heat pipes accelerated life testing, deriving corrosion model based on hydrogen evolution [AIAA PAPER 73-726]

18 p2369 A73-36343

The hydrogen evolution reaction on Ti-6Al-4V in acidic solutions of NaCl-HCl.

19 p2402 A73-37585

GAS EXCHANGE

A system for continuous measurement of gas exchange and respiratory functions.

01 p0011 A73-10172

Simulation of unsteady gas exchange in internal combustion engines

02 p0202 A73-11632

Gas-blood CO₂ equilibration in dog lungs during rebreathing.

03 p0263 A73-14115

Quantitative estimation of the gas metabolism of continuous higher plant cultures as a life support system component

06 p0656 A73-17680

Impurity transport in a cylinder in the case of a time-dependent flow rate and gas exchange with the wall

08 p1022 A73-20998

A model of time-varying gas exchange in the human lung during a respiratory cycle at rest.

08 p0936 A73-21615

Gas dynamic theory of gas exchange in organisms based on oxygen and carbon dioxide permanent partial pressure gradients in tissues, blood and lungs

10 p1181 A73-24523

Computer simulation of gas exchange in human lungs.

15 p1838 A73-31348

The gas exchange of hydrogen-adapted algae as followed by mass spectrometry.

17 p2118 A73-34225

Validation of open-circuit method for the determination of oxygen consumption.

17 p2117 A73-35462

Validity of Haldane calculation for estimating respiratory gas exchange.

17 p2113 A73-35463

Anaerobic threshold and respiratory gas exchange during exercise.

20 p2519 A73-39785

Effect of acceleration on distribution of lung perfusion and on respiratory gas exchange.

21 p2643 A73-40274

Advantage or disadvantage of a decrease of blood oxygen affinity for tissue oxygen supply at hypoxia - A theoretical study comparing man and rat.

21 p2641 A73-41620

The significance of an increased RQ after sucrose ingestion during prolonged aerobic exercise.

21 p2641 A73-41621

Differences between inspired and expired minute volumes of nitrogen in man.

24 p3060 A73-45069

GAS EXPANSION

Measurements on separated supersonic boundary layer flows after an expansion corner.

01 p0003 A73-11135

Free jet expansion from concentric orifices into vacuum.

02 p0152 A73-11528

Computation of the axisymmetrical free expansion of a nonequilibrium hydrogen plasma

02 p0196 A73-11604

Moon flares due to lunar gas eruptions, investigating degassing in former geological epochs

02 p0212 A73-11950

Hypersonic spherical source flow expansion into rarefied atmosphere of same gas, using kinetic model and asymptotic solution of Boltzmann equation

02 p0154 A73-12054

Similarity solutions for spherically and cylindrically symmetric gas expansions in rarefied atmospheres, taking into account ambient pressure effect

02 p0154 A73-12055

Compressible boundary layer formation on shock tube walls after bursting of diaphragm separating gases at different pressures

03 p0293 A73-13527

Initially uniform gas expansion into ambient atmosphere and subsequent flow into perfect vacuum, noting infinite-strength shock separation from gas-vacuum interface

03 p0294 A73-13532

Nonadiabatic temperature change in rapidly expanded or compressed gas, discussing shearing and volume viscosity effects

05 p0597 A73-16350

Application of hot wires to measurements in freely expanding jets.

05 p0578 A73-17117

Book - Coronal expansion and solar wind.

06 p0742 A73-17671

On the solution of the Navier-Stokes equations for a spherically symmetric expanding flow.

06 p0684 A73-17707

Amplification factor of light in a CO₂ + N₂ + He mixture expanding in a supersonic jet.

06 p0723 A73-17964

Spherical and cylindrical gaseous expansions into a vacuum.

07 p0920 A73-19980

Parameter calculations for a supersonic axisymmetric flow near its expansion center

07 p0775 A73-20093

Pressure changes produced by sudden expansion of a two-phase flow

08 p0955 A73-21197

Species separation in swirling expansion jet of gases mixture.

08 p0956 A73-21774

A one-dimensional problem concerning the discharge of a two-phase fluid from a nozzle

09 p1073 A73-23353

The behavior of vapors of soluble binary systems during expansion in supersonic nozzles - Droplet coalescence in a potential vortex flow

10 p1205 A73-24162

Liquid propellant rockets, discussing effective exhaust velocity, nozzle expansion, chamber pressure effects on equilibrium performance and kinetic recombinations

14 p1784 A73-30136

MHD acceleration in the unsteady expansion of a shock tube driver.

15 p1917 A73-31376

Power law recompression of fully developed centered gas expansion, obtaining flow distribution via closed form integral solution based on similarity theory

16 p2000 A73-33317

Free surface shape of MHD flow due to constant mass source expansion into uniform magnetic field as function of time

16 p2041 A73-33329

Early-time model of laser plasma expansion.

16 p2042 A73-33340

Wave-trains in the solar wind. I - General theory and its application to an ideal, isotropic, one-fluid plasma.

17 p2224 A73-34505

Transient flow and expansion of a pinch discharge plasma in self-induced magnetic fields.

18 p2338 A73-36240

Nonlinear radial wave propagation in low density expanding flows with application to the free jet.

18 p2300 A73-36630

Expansion of a plasma from a spherical source into a vacuum.

19 p2465 A73-37176

Corner expansion flow of ionized argon, calculating electron density, plasma density and recombination rate constant for comparison with measurements

19 p2465 A73-37177

Calculation of the generation of inversion and the laser output power for expanding combustion gases /CO₂-N₂-He/

19 p2504 A73-38157

Approximate determination of the inverted population and amplification factor of a gas expanding adiabatically in a nozzle

20 p2572 A73-39280

Comparison of the plane, cylindrical and spherical one-dimensional models of the free expansion of a collisionless plasma.

21 p2748 A73-40929

Condensation in CO₂ free jet expansions. I - Dimer formation.

21 p2743 A73-40937

Condensation in CO₂ free jet expansions. II - Growth of small clusters.

21 p2743 A73-40938

Tungsten target surface contaminants produced fast ion current peak measured by ion collector in expanding laser produced plasma

21 p2716 A73-40972

Ion acceleration upon expansion of a rarefied plasma.

22 p2890 A73-41724

Dynamical evolution of an expanding gas cloud.

22 p2840 A73-41758

Computer model of Ba ion cloud expansion in magnetosphere, taking into account self-consistent electric and magnetic field interactions

22 p2846 A73-41938

Dense argon plasma expansion into vacuum or low density partially ionized hydrogen plasma, examining momentum transfer, electron density and electric field effects

22 p2891 A73-42239

Thermodynamic expansion processes for argon plasma in a convergent-divergent nozzle.

22 p2894 A73-42632

A numerical study of the explosion of a supernova into the interstellar magnetic field.

22 p2914 A73-43007

Shock attenuation dependence on gas specific heat ratio and wall divergence angle and area ratio of expansion section attached to shock tube

23 p2969 A73-43930

Simeiz 59 /Sharpless 104/ nebula radial and expansion velocity indicating type I supernova origin, discussing spectral and interferometric measurements and relativistic electron energy and density

23 p3035 A73-44233

Expansion of a plane rarefied gas layer into a vacuum

24 p3076 A73-44655

Laser supported gaseous detonation wave propagation above solid surface, calculating momentum transfer as functions of laser energy, pulse duration, and beam and target areas

24 p3097 A73-45455

GAS EXPLOSIONS

Temperature changes in hydrogen-oxygen explosions.

01 p0121 A73-10646

Unflanged electrode spark ignition tests for minimum energy to trigger gas mixtures explosion, using spark energy relation for outward propagating quasi-spherical flame

03 p0399 A73-14400

Difference schemes for two dimensional gas flows with detonation in frame of Lagrange variables, comparing point explosion with self similar solution

09 p1070 A73-21923

Explosion in detonating media with a variable initial density

12 p1487 A73-27419

Explosion in a variable-density medium in the presence of variable counterpressure.

12 p1487 A73-27532

Detonation propelled metal particle sprayed coatings adhesion strength relation to particle kinetic energy

18 p2318 A73-35884

Branched-chain mechanism of propane-oxygen-fluorine explosions.

22 p2819 A73-42778

Cold gas noncentral point explosion generated shock wave propagation in interplanetary medium, discussing shock front geometry, earth orbit parameters and gas dynamics

24 p3137 A73-44781

Thermokinetics and combustion phenomena in non-flowing gaseous systems - An invited review.

24 p3157 A73-45165

GAS FLOW

NT AIR CURRENTS

NT AIR FLOW

NT CONTINUUM FLOW

NT EQUILIBRIUM FLOW

NT FREE MOLECULAR FLOW

NT FROZEN EQUILIBRIUM FLOW

NT JET STREAMS [METEOROLOGY]

NT KNUDSEN FLOW

NT MERIDIONAL FLOW

NT MOLECULAR FLOW

NT NONEQUILIBRIUM FLOW

NT SLIP FLOW

NT TRANSITION FLOW

NT VERTICAL AIR CURRENTS

Analysis of face deformation effects on gas film seal performance.

01 p0055 A73-10246

Use of a mirror shearing interferometer for gas dynamics research.

01 p0050 A73-10830

Equations of motion for nonuniformly heated gas past hot bodies, noting gas heating between two parallel flat surfaces with different temperatures

02 p0152 A73-11612

Numerical calculations of the flow field of low Reynolds number viscous flow with or without real-gas-effects in slender-channel-nozzles.

02 p0152 A73-11674

Equations of motion for steady state spherically symmetric flow of polytropic gases into or out of neutron stars, black holes or Schwarzschild singularities

02 p0223 A73-12729

- The oscillations of supersonic gas flows
03 p0289 A73-12953
- Contribution to the study of noise measured by a microphone placed in a gaseous flow
03 p0290 A73-12973
- Ideal dissociating/nondissociating gas reentry flow fields hydrodynamic stability for various free stream and disturbance conditions
03 p0242 A73-13312
- Gas path analysis applied to turbine engine condition monitoring.
[ALAA PAPER 72-1082] 03 p0354 A73-13405
- Gas generator system with continuously burning driver propellant and demand propellant combustion during exposure to driver gas flow, testing performance
[ALAA PAPER 72-1193] 03 p0358 A73-13483
- Determination of the flow past a cylinder and a sphere in the presence of an incident shock wave
03 p0294 A73-13615
- Supersonic nozzle design for prescribed flight trajectory and variable gas flow parameters, solving variational problem of optimal contour for given Mach number
03 p0244 A73-13616
- Magnetogasdynamic characteristics, transonic and compression regions and pressure losses of conducting gas flow in circular tube within axisymmetric magnetic field
03 p0346 A73-13620
- Decoding of thermoanemometer data for a flow with velocity, pressure, and temperature pulsations
03 p0308 A73-13667
- Acoustic and shock waves interaction in axisymmetric gas flow through variable section channel, calculating flow characteristics variations via isentropic theory of steady flow
03 p0295 A73-13673
- Experimental investigation of the base pressure on slender circular cylinders
03 p0245 A73-13674
- Three dimensional flow pattern from two dimensional supersonic inviscid gas flows around wedged body
03 p0245 A73-13675
- Flutter of flat rectangular sandwich type panels in a supersonic, coplanar gas flow, with arbitrary direction.
03 p0392 A73-13768
- Two-dimensional unsteady flow by hydraulic analogy.
03 p0295 A73-13769
- Circular orifice flow of monatomic rarefied gas between two reservoirs, observing pressure ratio effect
03 p0295 A73-13773
- Quasi-frozen flow of a thermodynamically relaxing gas
03 p0295 A73-13791
- Oxidation and nitridation of Cr-W alloy.
03 p0325 A73-13803
- Boltzmann equation model approach for prediction of velocity profiles and gas flow rates through trapezoidal microgaps
[ASME PAPER 72-LUB-15] 03 p0297 A73-14331
- Inertia and energy effects in the developing gas film between two parallel flat plates.
[ASME PAPER 72-LUB-33] 03 p0297 A73-14343
- A theoretical analysis of non-isentropic flow of a compressible, viscous gas in narrow passages.
[ASLE PREPRINT 72LC-3A-1] 03 p0297 A73-14355
- Thermodynamic equilibrium and relaxation models of ideal and real high temperature gas flows for reversible and irreversible processes
[DFVLR-SONDDR-282] 04 p0517 A73-15678
- Particular variation of the velocity of the driver gas in a shock tube with electromagnetic blowing with two gases
05 p0601 A73-16429
- The Green's function of the linearized viscous transonic equation
05 p0527 A73-16446
- Calculation of transonic flow in three-dimensional nozzles
05 p0527 A73-16447
- Calculation of supersonic viscous gas flow past blunt bodies at large Reynolds numbers
05 p0527 A73-16448
- Investigation of high-power quasi-steady arcs in strong axial gas flows
05 p0602 A73-16583
- Equations of motion for two dimensional steady conducting gas flow in transverse magnetic field, deriving flow equations for transcritical region via small perturbation theory
05 p0602 A73-16585
- Solution of some boundary-value problems in the theory of potential flows of a gas and the propagation of weak shock waves.
05 p0565 A73-16790
- Gas flow temperature determination in the presence of radiation heat exchange between the heat sensor and some surrounding structures
05 p0578 A73-16996
- Operation modes simulation of single stage gas turbine at subcritical and supercritical gas flow, noting scale model tests
05 p0532 A73-17024
- Flow of a gas in a flat channel at a diminishing flow rate
05 p0533 A73-17090
- Ion-current distributions around an electrically conductive body in ionized gas flow.
05 p0603 A73-17110
- Supersonic boundary layer on a permeable surface
05 p0534 A73-17268
- Carbon and graphite sublimation in inert gas flow at 2800-3000 K, determining rate dependence on temperature under kinetic and diffusive conditions
06 p0713 A73-17411
- Boundary value problem for subsonic gas flow, proving existence theorem for gas dynamics problem solution
06 p0645 A73-18069
- Investigation of friction drag during gas flow in a tube with wall temperatures up to 2800 K
06 p0686 A73-18126
- Electrohydrodynamic shock wave evolution in steady gas flow with positive space charge in electric field
06 p0733 A73-18881
- Monatomic gas flow around uniformly heated sphere for small Reynolds numbers, noting drag decrease due to thermal stresses
06 p0646 A73-18884
- Variational mixed boundary value problems of subsonic gas flows for plane parallel symmetric Laval nozzle and transonic wedge, using singular integral equation
06 p0646 A73-18888
- Intermittent behavior of a plasma discharge in turbulent gas flow.
07 p0856 A73-19517
- Viscous incompressible gas turbulent flow in axisymmetric channel under preliminary twist conditions at inlet, using computer numerical solution
07 p0774 A73-19621
- Reduction of the thermal flux through a cylindrical pipe containing an ionized gas flow
07 p0860 A73-20617
- Transonic nozzle flow with nonuniform gas properties.
08 p0925 A73-20719
- Experimental determination of the vibrational temperature of a supersonic gas flow.
08 p1021 A73-20854
- Impurity transport in a cylinder in the case of a time-dependent flow rate and gas exchange with the wall
08 p1022 A73-20998
- On the steady flow of a non-equilibrium ionized gas around sharp corners in the presence of a crossed magnetic field.
08 p0992 A73-21009
- Self-similar hypersonic flows of an inviscid gas
08 p0927 A73-21545
- Discrete vortex scheme of a wing of finite span
08 p0927 A73-21611
- Variable properties laminar gas flow heat transfer in the entry region of parallel porous plates.
08 p1024 A73-21640
- Stability of a ferromagnetic plate within a gas flow in the presence of a magnetic field
08 p0989 A73-21723
- Temperature distribution in gas flow about a linear source of heat variable periodically in function of time.
09 p1166 A73-22169
- Solution of the direct problem of mixed subsonic and supersonic gas flow in a nozzle of finite length
09 p1072 A73-22480
- Supersonic flow of a viscous gas about a spherically blunt cooled object
09 p1028 A73-22620
- Turbulent friction drag of a dusty gas. I - Theoretical study.
09 p1072 A73-23325
- Theoretical possibility of converting the kinetic energy of an ionized gas flow into electricity
10 p1177 A73-23473
- Euler, Lagrange and time turbulence scales for Prandtl mixing length, relating with velocity and pressure pulsations in steady turbulent gas flow
10 p1204 A73-23474
- Nonstationary wave propagation in equilibrium liquid-vapor flow, noting pressure jumps due to expansion
10 p1204 A73-23513
- Radiant heat flux distribution on the surface of a sphere in hypersonic flow of an inviscid radiating gas
10 p1171 A73-23581
- An approximate analysis of the diffusing flow in a self-controlled heat pipe.
[ASME PAPER 72-HT-M] 10 p1295 A73-23776
- Liquid and gas flow visualization methods, discussing water tests and hydraulic analogies
[ONERA, TP NO. 1222] 10 p1172 A73-23864
- An evaluation of optical anemometers for volumetric flow measurement of liquids and gases.
10 p1221 A73-24858
- Diffusion aluminizing of Ni and Ni-base alloys by gas circulation method, investigating gas flow velocity effect relationship to specimen weight gain
10 p1226 A73-24957
- Hydrodynamic theory of heat transfer between a stabilized gas suspension flow and channel walls.
10 p1297 A73-24968
- Fabry-Perot interferometer with etalon for studying gas movements and planetary nebulae in Large Magellanic Cloud by spectral analysis from pressure scanning
11 p1361 A73-25176
- Transpiration and natural convection - The vertical-flat-plate problem.
11 p1449 A73-25219
- Velocity and concentration profiles of isothermal laminar boundary layer flow of incompressible multicomponent gas under strong blowing
11 p1347 A73-25728
- Quasi-linear partial differential equations of nonlinear pulse shock wave propagation in two- and three-dimensional steady transonic gas flow near critical point
11 p1302 A73-25854
- Calculation of the relaxed one-dimensional flow of a gas in a convergent-divergent sonic nozzle
11 p1348 A73-25869
- Mathematical description of the turbulent isobaric flow of a chemically reacting gas in a heated pipe
11 p1453 A73-26428
- Study of disturbance reflection from the subsonic section of a Laval nozzle
11 p1411 A73-26437
- Supersonic gas flow past the leeward side of a conical wing
11 p1304 A73-26439
- Diffusion of a hypersonic flow by a supersonic gas jet in the case of a free-molecular mode of interaction
11 p1304 A73-26446
- Kinetics of the degassing of oxygen-containing niobium in flowing acetylene to form carbon monoxide
11 p1375 A73-26565
- Investigation of the flutter of cylindrical panels in a supersonic gas flow
12 p1550 A73-26954
- An analytical solution to the problem of hypersonic gas past a slender wing
12 p1457 A73-27078
- An approximate estimate of the reaction coefficient during the motion of a vaporizing droplet of fuel in a gas flow
12 p1532 A73-27088
- Three dimensional gas flow noncollinear total impulse normal and tangential components calculation leading to pressure force determination
12 p1486 A73-27089
- Temperature calculation for heat emitting surface in transparent gas flow, using linearizing function method for heat transfer problems with nonlinear boundary conditions
12 p1558 A73-27316
- Qualitative analysis of MHD energy conversion efficiency
12 p1460 A73-27321
- Calculation of the moisture content correction in measuring the quantity of gas flowing through an orifice
12 p1498 A73-27595
- Approximate method for solving a boundary value problem describing gas flow during strong blowing
12 p1458 A73-27811
- Transonic similarity solution for aligned field MHD nozzle flow.
13 p1599 A73-28089
- Two-dimensional calculation of revolution of the relaxed flow of a gas in a convergent-divergent sonic nozzle
13 p1563 A73-28563
- Simultaneous comparison of turbulent gas fluctuations by laser Doppler and hot wire.
13 p1616 A73-28821
- Investigation of high-temperature gas flow around axisymmetric bodies in the presence of several discontinuity surfaces
13 p1708 A73-29404
- Measurement of gas quantities by liquid displacement.
14 p1723 A73-30048
- Some relations for the ultrasonic region of flow of a real gas in the presence of heat transfer.
14 p1817 A73-30603
- Some relations for high pressure flows with and without heat transfer.
14 p1817 A73-30604
- An accurate method for solving some theoretical problems of spatial supersonic gas flows
14 p1712 A73-30826
- The conservative method of flows and the calculation of a viscous heat conducting gas flow past a body of finite size
15 p1821 A73-30962
- Calculation of a subsonic radiating gas flow by an adjustment method
15 p1821 A73-30969

Cauchy problem solution for motion of piston generating shock wave after fast impact under influence of one dimensional gas flow 15 p1822 A73-31289

Longitudinal rarefied diatomic and monatomic gas flows past elongated plates 15 p1822 A73-31293

Heat transfer behind a shock wave in a two-phase gasdynamic flow 15 p1862 A73-31294

Characteristics of supercharge devices in gas bearings 15 p1881 A73-31296

Ion current at the forward stagnation region of an electrically conducting body. 15 p1918 A73-31669

Experimental assembly for complex heat transfer studies 15 p1858 A73-31860

A combinational method of calculating the average velocity and the mean-mass temperature of a gas flow from the phase diagram of the substance 15 p1957 A73-31865

Temperature determination in a gas flow with the aid of two thermocouples 15 p1876 A73-31870

Magnetogasdynamic compression of a coaxial plasma accelerator flow for micrometeoroid simulation. 15 p1919 A73-31932

Spectroscopic observations of subsonic and sonic vapor flow inside an open-ended heat pipe. 15 p1958 A73-31936

Solution of the direct problem on mixed subsonic and supersonic flow of a gas in a nozzle of finite length. 15 p1824 A73-32067

Investigation of a gas flow on an aeroballistic track by holographic methods 15 p1879 A73-32328

Electrohydrodynamic shock wave evolution in steady gas flow with positive space charge in electric field 15 p1921 A73-32406

Monatomic gas flow around uniformly heated sphere for small Reynolds numbers, noting drag decrease due to thermal stresses 15 p1824 A73-32409

Variational mixed boundary value problems of subsonic gas flows for plane parallel symmetric Laval nozzle and transonic wedge, using singular integral equation 15 p1824 A73-32412

Stationary isothermal gas flow subject to self gravitation, finding subsonic regime oscillatory solutions for plane parallel, spherical and rotational symmetric cases 16 p2058 A73-32832

Galactic neutral hydrogen observations along loop III, noting loop effects on gas velocity distribution 16 p2058 A73-32835

Steady state arc discharge physical properties, discussing boundary geometry of plasma column, and stabilities in gas flow and high current and vacuum conditions 16 p2040 A73-32939

Gas flow analysis during thermal vacuum test of a spacecraft. 16 p1994 A73-33150

Planar pressure waves propagation across wall with elastically supported and damped edges, considering induced gas flow characteristics behind wall 16 p2000 A73-33257

Analysis of gas flow through a multilayer insulation system. 17 p2149 A73-34184

Continuum gas plasma boundary layer flow over flat plate, obtaining ion sheath characteristics and downstream solutions by asymptotic and characteristics methods 17 p2149 A73-34186

Shock waves in gas flows in close binary dwarf star systems 17 p2226 A73-34366

Implicit finite difference scheme for Eulerian fluid dynamics of time dependent one dimensional polytropic gas flow, noting numerical stability 17 p2151 A73-34894

A dynamic modeling method of unsteady flows in long fluid lines with turbulent bulk velocities. [ASME PAPER 73-FE-18] 17 p2153 A73-35014

A note on compressible flow through a vortex swirl cup. 17 p2154 A73-35120

Nonstationary wave propagation in equilibrium liquid-vapor flow, noting pressure jumps due to expansion 17 p2155 A73-35193

Chemically reacting gas flow numerical calculations from stiff nonlinear ordinary differential equations solution in finite difference form 17 p2119 A73-35609

Fully coupled nongray radiating gas flows with ablation product effects about planetary entry bodies. [AIAA PAPER 73-672] 18 p2368 A73-36223

Geometry of relaxing gas flows. 18 p2299 A73-36330

An approximation for combined heat transfer in a radiatively absorbing and emitting gas. [AIAA PAPER 73-750] 18 p2370 A73-36366

Thermal control coatings for heat shielding of high-temperature high-speed chemically aggressive gas flows, noting turbine blade shielding application 18 p2371 A73-36812

Numerical calculation of heat exchange and frictional resistance for a turbulent flow in a tube in the case of a gas with variable physical characteristics 18 p2301 A73-36816

Calculation of viscous gas flows in flat channels 18 p2265 A73-36990

Gas expelled from a strongly underexpanded nozzle upstream into a hypersonic flow 18 p2265 A73-37010

Turbulent mixing of gas flows in the presence of a pressure gradient 18 p2266 A73-37016

Some characteristics of the disintegration of glassy bodies in hot gas flows 18 p2372 A73-37020

High enthalpy supersonic ionized gas flow in shock tube experiment, investigating pinch effect on flow acceleration and setup performance 19 p2415 A73-37168

On the flow of a nonequilibrium ionized gas past a wall in the presence of a magnetic field. 19 p2465 A73-37178

Investigation of the flutter of cylindrical panels in a supersonic gas flow. 19 p2500 A73-38139

Non-reacting and equilibrium chemically reacting turbulent boundary-layer flows. 19 p2421 A73-38187

The effect of the porous material characteristics on the internal heat and mass transfer. [ASME PAPER 73-HT-49] 20 p2626 A73-38573

The breakdown condition of the electrode layer in an ionized gas flow 20 p2597 A73-39278

Design modeling of external and internal cooling systems for bodies exposed to high temperature gas flow, discussing operation similarity conditions 20 p2628 A73-39419

Stability of parallel flow of a dusty gas in an annulus. 20 p2548 A73-39523

Analysis of rarefied gas flow through an arbitrary cross section by the finite element method. 20 p2549 A73-39528

Aeroballistic gas flow investigation using holographic device to schlieren system. 21 p2696 A73-39981

The Lagrange function for a gas bubble in an inhomogeneous flow 21 p2676 A73-40206

Supersonic gas flow pattern at blunt body of revolution with attached shock wave 21 p2632 A73-40400

Possibility of radiative acceleration of the gas in stellar atmospheres 21 p2767 A73-40554

Sound propagation in gases, liquids and solids, discussing effects of nonlinear terms in wave and state equations and boundary conditions on solution 21 p2739 A73-40621

Interpretation of hot-wire anemometer readings in a flow with velocity, pressure and temperature fluctuations. 21 p2705 A73-41317

Euler, Lagrange and time turbulence scales for Prandtl mixing length, relating with velocity and pressure pulsations in steady turbulent gas flow 21 p2678 A73-41321

Rarefied gas flows based on variational principle. 22 p2840 A73-41741

Flow of a viscous gas at a slot with strong suction 22 p2796 A73-42283

Vapor flow in cylindrical heat pipes. [ASME PAPER 73-HT-P] 22 p2931 A73-42289

Characteristics of a CS₂/O₂ chemical laser with flow transverse to the optical axis. 22 p2870 A73-42764

Turbulence generation by supersonic nozzle gas flow interaction with plasmas, discussing high current electric arc in axis 22 p2895 A73-43166

Papers on heat pipes covering incompressible laminar vapor flow behavior, startup dynamics, wicking material liquid transport properties, high thermal conductance structures, etc 23 p3049 A73-43459

Precise method for solving certain problems of the theory of three-dimensional supersonic gas flows. 23 p2939 A73-43582

Laminar flow of a viscous barotropic gas through a circular pipe 23 p2968 A73-43721

Calculation of a supersonic gas flow about the atmosphere of a spherical body 24 p3053 A73-44658

Poiseuille flow at arbitrary Knudsen numbers and tangential momentum accommodation. 24 p3079 A73-45313

Compressible laminar boundary layer differential equations solution for incident viscous gas flow on flat plate at high flow velocity 24 p3080 A73-45471

A method of calculating a chemically nonequilibrium flow of gas in a heated tube under conditions close to the equilibrium or frozen state 24 p3081 A73-45527

Universal equations for the laminar boundary layer on a body of revolution in oblique flow 24 p3055 A73-45529

Flow field over pointed wedges in isoelectric flow of thermally and calorically perfect gases with nonuniform incident supersonic flow, noting attached shock formation 24 p3056 A73-45547

GAS GENERATOR ENGINES U GAS GENERATORS

GAS GENERATORS

Mono- and multipropellant, storable and cryogenic, liquid rocket propulsion engines developments including gas generators and engines 03 p0355 A73-13422

[AIAA PAPER 72-1104] 03 p0355 A73-13422

Gas generator system with continuously burning driver propellant and demand propellant combustion during exposure to driver gas flow, testing performance [AIAA PAPER 72-1193] 03 p0358 A73-13483

Feasibility of a fluidized powder demand mode gas generator. [AIAA PAPER 72-1194] 03 p0352 A73-13484

Combustion mechanisms of fuel rich propellants in flow fields. [AIAA PAPER 72-1145] 04 p0485 A73-14915

Hydrogen-air electrolytic fuel cell stack and auxiliary systems for use with methanol feedstock hydrogen generator 04 p0408 A73-15117

Hydrogen gas generation in water/stainless-steel heat pipes. [ASME PAPER 72-WA/HT-37] 04 p0518 A73-15818

Small turbine advanced gas generator for future propulsion requirements. [SAE PAPER 720831] 05 p0537 A73-16634

Design and analysis of an APU monopropellant gas generator. [SAE PAPER 720834] 05 p0537 A73-16635

L 17 satellite booster development from Emeraude stage, discussing gas generator, Valois thruster engine and assembly tests, combustion instability and launching results 07 p0905 A73-18990

Experimental investigation of heat transfer using facilities for testing heatproof materials 08 p1022 A73-21094

Liquid or solid fueled gas generators applications to driving rocket fuel turbopumps, ejector pumps, gas turbine engine starters, torpedo propulsion, etc 11 p1307 A73-24991

Measurement of hydrazine gas generator performance by gas chromatography. 11 p1326 A73-26398

Space-flight qualification of solid-propellant units in the example of the cold-gas generator for the booster rocket Europa I/II 16 p2047 A73-33394

GAS HEATING

Heating and cooling mechanisms, ionization processes, time-dependent models and energy requirements of interstellar H I regions 01 p0091 A73-10064

Properties of H I regions heated by X-rays and cosmic rays 01 p0092 A73-10935

Equations of motion for nonuniformly heated gas past hot bodies, noting gas heating between two parallel flat surfaces with different temperatures 02 p0152 A73-11612

Experimental study of the luminous front produced by a coaxial plasma accelerator. 02 p0197 A73-12060

Spontaneous discharge instability in carbon dioxide laser pumping by ionization source and electric field for time difference in heat removal and gas heating 02 p0177 A73-12553

The applicability of an approximate expression for radiative heating. 07 p0921 A73-20222

Cosmic-ray heating and molecular cooling of dense clouds. 08 p0997 A73-20899

Numerical solutions to wave and hydrodynamic equations for thermal blooming of pulsed focused Gaussian laser beams in heated gas medium 08 p0974 A73-21029

Theoretical study of a flow-resistance gas heater. 08 p1023 A73-21436

Study of thermal phenomena in a Hartmann-Sprenger tube 08 p1024 A73-21634

Properties of H I regions heated by X rays and cosmic rays.

09 p1147 A73-22730
Rotating neutron star gas cocoon heating by LF radiation absorption, noting X ray emission
10 p1263 A73-23481
Space discharge instability in carbon dioxide laser pumping by ionization source and electric field for time difference in heat removal and gas heating
10 p1228 A73-24182
Periodic instability induced in semiconductor situated in crossed electric and magnetic fields via electron gas heating, deriving expressions for properties of steady nonlinear waves
10 p1261 A73-24764
X ray ionization and heating of H I regions refuted from energy input rate computations of observed flux in Galactic plane
11 p1415 A73-25118
The stability of a layer of binary gas mixture heated below.
11 p1449 A73-25222
Mathematical description of the turbulent isobaric flow of a chemically reacting gas in a heated pipe
11 p1453 A73-26428
The heating of interstellar clouds by vibrationally excited molecular hydrogen.
13 p1673 A73-28279
High pressure plasma torch to heat air for high temperature chemical reactions and hypersonic wind tunnels for reentry vehicle ablation studies
13 p1597 A73-28479
Generation of acoustic waves during the passage of a shock wave through a heated gaseous element.
13 p1705 A73-28494
Computer simulation of arc heaters for production of flow with high enthalpy.
13 p1707 A73-29023
Neutral hydrogen clouds gravitational binding of Coma cluster, providing mechanism for heating of diffuse gas between clouds and galaxies
13 p1684 A73-29352
Density measurements in high speed arc heated flows.
13 p1622 A73-29640
Motion of a heated gas layer and the asymptotic characteristics of the gas layer
15 p1958 A73-32107
Experimental study of the stability of differentially heated inclined air layers.
17 p2256 A73-35847
Experimental investigation of heat transfer and resistance in crimped tubes
19 p2505 A73-38561
Thermal conductivity of mercury vapors
20 p2595 A73-39607
Unsteady convective heat transfer attending the cooling of gas in tubes.
21 p2791 A73-41053
Flowing gas mixture ignition at heated blunt body stagnation point, examining Van't Hoff criterion
23 p3048 A73-43328
Optimization of compression constants for cumulated plane shock waves in a closed tube.
24 p3117 A73-45428
Transformation of shock compression into isentropic compression in a nonhomogeneous body.
24 p3117 A73-45429

GAS INJECTION

Equivalent solid obstacle for gas injection into a supersonic stream.
01 p0002 A73-10734
Stability of rotating stratified flow produced by tangential injection of high pressure gas into closed cylindrical vessel filled with gas of different density
01 p0033 A73-10752
Heat transfer from a sphere with injection in a slow moving flow
02 p0152 A73-11611
Rise time and pressure measurements in transient flow during quasi-steady gas injection into vacuum with piston valve, using fast ionization gage
02 p0168 A73-11963
A comparison of two prediction methods with experiment for compressible turbulent boundary layers with air injection.
02 p0129 A73-12505
Calculation of an axisymmetric supersonic gas jet injected in a supersonic slipstream past a given body with heat supply
02 p0129 A73-12583
Vehicle-scale investigation of a fluorine jet-pump liquid hydrogen tank pressurization system.
[AIAA PAPER 72-1133]
03 p0355 A73-13440
Tangential slot injection of carbon dioxide and helium into a supersonic air stream.
[ASME PAPER 72-WA/FE-37]
04 p0435 A73-15854
Modeling radial dilution air injection in axial flow combustors.
[WSCI PAPER 72-24]
05 p0639 A73-16689
Experimental investigation of flow stability during intense injection
06 p0643 A73-17462

Experimental investigation of hypersonic helium flow around sharp and blunted cones in the presence of strong injection
06 p0643 A73-17466
Vectorized injection into isobaric laminar boundary layer flows.
06 p0685 A73-17917
Effectiveness of the thermal protection of a plane wall during injection of air through two rows of rectangular holes arranged in a checkered order
06 p0768 A73-18127
Flow characteristics in air injection through porous surface of blunt bodies, noting blowing parameter effect on boundary layer flow
07 p0774 A73-19622
Further results on the stagnation point boundary layer with hydrogen injection.
07 p0921 A73-20358
Steady state hot toroidal Tokamak plasma, calculating seed current density for bootstrap effect produced by neutral particle injection parameters control
08 p0991 A73-20814
Kochin hydrodynamic equation solutions for gas injection through plate for intense blowing at constant and changing rates
08 p0927 A73-21772
Solution of the Cauchy problem for a nonlinear equation describing a gas flow in the presence of strong blowing
09 p1029 A73-23352
Calculation of the gas parameters in the injection region for the flow at an angle of incidence past a porous cone
10 p1172 A73-24505
Hot-wire measurements of gas mixture concentrations in a supersonic flow.
10 p1220 A73-24637
Incompressible turbulent axisymmetrical impulsive air injection at moderate pressure into stagnant surroundings, measuring flow velocity distribution
10 p1210 A73-24849
Inert gas injection for W-Re thermocouple wire corrosion protection during temperature measurement in aggressive media
12 p1497 A73-27319
Air injection from wall slot into turbulent boundary layer of high temperature gas channel flow, calculating film cooling effectiveness in flat plate
13 p1706 A73-28675
Boundary layer about a plate assuming an arbitrary gas injection law
14 p1711 A73-30017
The nature of viscous flow around the forward stagnation point in the presence of strong injection of a gas through the surface of a slender pointed body
15 p1821 A73-31043
Asymptotic solution of the equations for a multicomponent laminar boundary layer in the case of high injection levels
15 p1822 A73-31292
Experimental investigation of longitudinal flow over a flat plate during strong blowing of a foreign gas under isothermal conditions
15 p1957 A73-31856
Effect of intense injection on flow stability and turbulence development
15 p1864 A73-31857
Experimental investigation of a turbulent boundary layer on a porous plate with intense injection
15 p1824 A73-31858
Interferometric and thermoanemometric methods of studying binary boundary layers
15 p1876 A73-31859
Determination of the thickness of a wall layer by an approximate method in the presence of intense injection
15 p1876 A73-31861
Supersonic mixing nozzle for gas-dynamic lasers.
17 p2183 A73-34205
Characteristics of the heat exchange in the region of injection into a supersonic high-temperature flow
17 p2254 A73-34772
Supersonic turbulent boundary-layer flows with tangential slot injection.
[AIAA PAPER 73-696]
18 p2262 A73-36245
Foreign gas injection at windwardmost meridians of yawed sharp cones.
[AIAA PAPER 73-764]
18 p2264 A73-36379
Flow of a mixture consisting of a fluid and gas bubbles past a corner
18 p2301 A73-37007
Study of turbulent transfer with strong injection, longitudinal pressure gradient and nonisothermicity.
20 p2547 A73-39421
Friction, heat transfer and material removal in a turbulent boundary layer of a compressible high-enthalpy gas under conditions of marked nonisothermicity, injection and negative pressure gradient.
20 p2628 A73-39422
The turbulent boundary layer with stepwise varying boundary conditions at a permeable surface.
20 p2628 A73-39423

Experimental investigation of the performance of a porous electrode in an MHD converter during the injection of argon with potassium addition
20 p2511 A73-39619
Investigation of the laminar boundary layer at a permeable surface.
21 p2678 A73-41054
Variable mass flow rate air injection from porous flat plate into uniform incompressible air flow, obtaining laminar flow velocity profile and pressure measurements
23 p2940 A73-43932
Modified poppet valve for quasisteady gas injection into vacuum.
24 p3093 A73-44813
Propane-air flame stabilization via combustion product recirculation due to transverse gas jet injection, increasing fuel-air ratio
24 p3123 A73-45379
Investigation of the mechanism of reverse jet flame stabilization for a heterogeneous mixture.
24 p3158 A73-45388

GAS IONIZATION

NT ATMOSPHERIC IONIZATION
NT AUROREAL IONIZATION
NT FLAME IONIZATION
Heating and cooling mechanisms, ionization processes, time-dependent models and energy requirements of interstellar H I regions
01 p0091 A73-10064
Study of the conditions of the breakdown threshold of argon at high pressure under the effect of laser radiation
01 p0058 A73-10175
Ionization cross sections for H2, N2, and CO2 clusters by electron impact.
01 p0080 A73-10563
Ionizing potential wave analysis for gas breakdown, noting photoionization role in avalanche propagation and velocity, electron densities and temperature as function of electric field
02 p0197 A73-12063
Low-frequency oscillations in a bounded low-density plasma.
02 p0198 A73-12105
Spherical probe measurements of dense weakly ionized plasma parameters, noting ionization, recombination and secondary surface effects on probe characteristics
02 p0198 A73-12109
Experimental measurement of the O2-/I photodetachment cross section.
02 p0195 A73-12433
Space discharge instability in carbon dioxide laser pumping by ionization source and electric field for time difference in heat removal and gas heating
02 p0177 A73-12553
The feasibility of producing laser plasmas via photoionization.
[AD-753308]
02 p0177 A73-12572
The state of ionization in nova shells.
02 p0222 A73-12706
Intergalactic ionized hydrogen in nearby groups of galaxies.
02 p0225 A73-12803
Breakdown thresholds in rare and molecular gases using pulsed 10.6-micron radiation.
02 p0195 A73-12859
A phenomenological study of the steady-state current sheet speed in a magnetically driven shock tube.
03 p0288 A73-13809
Ionization balance for ions of Na, Al, P, Cl, A, K, Ca, Cr, Mn, Fe and Ni.
03 p0345 A73-13949
Pulse discharge plasma in Ar with gas ionization level near unity, noting plasma cylinder parameters, electron temperature and I-V characteristics
03 p0347 A73-14091
Effect of plasma oscillations on the process of ionizational relaxation
04 p0477 A73-14878
Study on ionizing shock waves in argon. I - Precursor phenomena.
04 p0436 A73-15974
Study on ionizing shock waves in argon. II - Ionization relaxation.
04 p0436 A73-15975
Study of the adiabatic curve of an ionizing shock wave in an inclined magnetic field
06 p0727 A73-17460
Ionization-relaxation time measurements upon krypton and xenon in a shock-wave heated plasma
06 p0728 A73-17912
CO2 laser-induced gas breakdown in hydrogen.
06 p0701 A73-18355
Laser-induced gas breakdown initiated by ultraviolet photoionization.
06 p0703 A73-18749
Experimental investigation of the transient formation of a microwave-generated ionized sheath in air.
06 p0732 A73-18781
Electron loss by helium atoms passing through inert gases and molecular hydrogen, nitrogen, and oxygen.
07 p0853 A73-19334

- Intracavity breakdown in CO and CO₂ lasers.
07 p0835 A73-19638
- Measurements of the structure of an ionizing shock wave in a hydrogen-helium mixture.
07 p0813 A73-20475
- Effect of ionization nonequilibrium on the shock wave in the stagnation region
07 p0776 A73-20616
- Ionization loss effects on cosmic ray lifetime in galactic interstellar medium, noting dependence on particle energy
08 p0999 A73-21335
- Interstellar gas role in cosmic ray yearly variations determined from solar short wave radiation induced gas ionization
08 p0999 A73-21338
- Investigation of the azimuthal symmetry of the discharge in a coaxial plasma injector
09 p1125 A73-21911
- Optimal use of double pin ionization gauges for shock wave detection.
09 p1080 A73-22106
- Molecular nitrogen ionization growth characteristics as function of electric field strength and gas pressure, using thin gold film electrodes
09 p1122 A73-22119
- Spatial and temporal ionization growth characteristics in nitrogen at moderate electric field strength, noting dominant secondary emission effect due to cathode bombardment by metastable molecules
09 p1122 A73-22120
- Steady state Lie group solutions to nonlinear partial differential equations of low temperature plasma ionization instability in strong magnetic field
09 p1127 A73-22591
- Experimental investigation of the excitation of Ar II and Kr II during electron-ion collisions
09 p1122 A73-22593
- Problem of the nuclear pumping of molecular gas lasers
09 p1096 A73-22702
- Characteristics of the diffuse /tenous/ interstellar medium determined from radio recombination lines.
09 p1150 A73-23137
- Chemical composition of the interstellar gas - X-ray determinations.
10 p1263 A73-23480
- Flux magnitude and single transition probabilities as function of electron density and temperature in relaxation model ionization and recombination channels
10 p1253 A73-23503
- Self-similar cylindrical magnetogasdynamic and ionizing shock waves.
10 p1204 A73-23564
- Proton-impact dissociation and ionization of H₂⁺ molecular ions.
10 p1250 A73-23671
- Space discharge instability in carbon dioxide laser pumping by ionization source and electric field for time difference in heat removal and gas heating
10 p1228 A73-24182
- Ionization front propagation velocity as function of microwave power density, showing dependence on precursor electron density profiles
10 p1251 A73-24257
- Electron impact ionization, three body recombination and thermal energy balance effects on gas discharge positive column between plane parallel walls
10 p1255 A73-24265
- Energy and angular correlations of the scattered and ejected electrons in the electron-impact ionization of argon.
10 p1252 A73-24340
- X ray ionization and heating of H I regions refuted from energy input rate computations of observed flux in Galactic plane
11 p1415 A73-25118
- Nonequilibrium radiative and inelastic collisional transitions structuring of ionizing shock waves in He and Ar
11 p1449 A73-25253
- Ion and electron distributions in the boundary layer of hypersonic vehicles.
11 p1404 A73-25290
- Thick target X-ray bremsstrahlung from partially ionized targets in solar flares.
11 p1412 A73-25945
- Experimental determination of the ionization rate behind a strong shock wave in air
11 p1304 A73-26444
- Ionization, recombination, and population of excited levels in hydrogen plasmas.
11 p1407 A73-26584
- Application of lasers, radioisotopes, and the correlation method for measuring flow velocity
12 p1495 A73-26847
- Measurements of free stream velocity and ionization relaxation behind a shock in xenon.
12 p1527 A73-27172
- Study on ionizing shock waves in argon. III - Thermodynamic properties of the plasma.
12 p1527 A73-27173
- Photoionization of atomic nitrogen and atomic oxygen.
13 p1662 A73-28190
- Discharge characteristics in cesium-seeded argon.
13 p1665 A73-28807
- A simple theory of breakdown for nonlight gases in fields of any frequencies ranging from low to optical
13 p1663 A73-29165
- Electron-molecule collision ionization in hydrogen and deuterium.
14 p1776 A73-29700
- Processes altering charge state in collisions of hydrogen atoms with H₂ molecules.
14 p1777 A73-30330
- Ionization of the intercloud medium and the central disk regions of spiral galaxies.
14 p1801 A73-30729
- Interstellar gas excitation due to supernova explosions using time dependent model based on statistical correlation of gas neutral density, ionization and temperature parameters
15 p1928 A73-31053
- Ionization instability in CO₂ laser discharges.
15 p1885 A73-32258
- Kinetics of physicochemical processes in a shock wave in mercury vapors. II - The relaxation zone: Region of initial ionization
15 p1916 A73-32314
- Hydrodynamic theory of high-amplitude ionization waves
15 p1921 A73-32326
- Azimuthal symmetry in a coaxial plasma injector.
15 p1922 A73-32636
- Ionization and relative abundance of hydrogen and helium atoms in filaments of the Crab Nebula
16 p2057 A73-32712
- Secondary electrons and energy per ion-pair in a thermal gas for electron, proton and X-ray ionization.
16 p2052 A73-32826
- Pulsed interferometric holography of laser-produced air breakdown.
16 p2014 A73-33175
- Application of the momentum translation method to multiphoton ionization of hydrogen by intense electromagnetic fields.
16 p2039 A73-33864
- Effects of channel size on the ionization instability in MHD generators.
17 p2108 A73-34185
- Gain and energy measurements on an HF/DF electrically pulsed chemical laser.
17 p2183 A73-34203
- Operational aspects of coaxial plasma accelerator with gas preionization by induction electric field introduced into interelectrode gap via longitudinal slits in external electrode
17 p2215 A73-34304
- Book - Low energy electron collisions in gases: Swarm and plasma methods applied to their study.
17 p2213 A73-34461
- Thermal structure and evolution of interstellar gas exposed to a soft X-ray burst.
17 p2231 A73-34757
- Flux magnitude and single transition probabilities as function of electron density and temperature in relaxation model ionization and recombination channels
17 p2217 A73-35183
- Experimental verification of the effective photon theory of laser induced gas ionization.
17 p2186 A73-35832
- Engineering approximations for radiating nonequilibrium shock layers.
18 p2297 A73-36224
- [AIAA PAPER 73-673]
On the ionization of the intercloud medium by ultraviolet stars.
19 p2484 A73-37611
- Nitrogen ionization in an Hg-N₂ discharge.
19 p2463 A73-37903
- A possibility of creating a new type of thermionic converter
19 p2392 A73-38560
- Structural determination of electric field conditions in ionizing shock waves.
20 p2596 A73-38964
- Structural determination of electric field conditions in ionizing shock waves.
20 p2596 A73-38964
- Ionization of a neutral medium by an electron beam
20 p2597 A73-39279
- Extraction of electrons from a plasma in the presence of a gas in the high-voltage gap
20 p2598 A73-39606
- Plasma stability of electric discharges in molecular gases.
21 p2744 A73-40220
- Calculations of state functions behind ionizing shock-waves in potassium and caesium vapour.
21 p2745 A73-40474
- Electron density in a locally ionized plasma afterglow.
21 p2748 A73-40970
- Solar corona plasma temperature estimation from ground observations based on ionization theory, line width, radio and radar measurements and hydrostatic equilibrium assumption
22 p2906 A73-42067
- Structure of ionizing shock waves with radiative energy loss.
22 p2841 A73-42200
- The production of plasma by lasers on targets in the gaseous state
22 p2892 A73-42350
- Weakly-shocked flows of the solar wind plasma through atmospheres of comets and planets.
23 p3024 A73-43682
- An MHD generator with a nonequilibrium plasma produced by VHF ionization
23 p3011 A73-43714
- Backward ionization waves linear evolution to nonlinear saturated state from gaseous plasma self oscillation instability viewpoint, noting electron temperature and density increase
23 p3011 A73-43829
- Hydrodynamic equations for nonlinear stability of plasma ionization wave interactions in absence of magnetic field
23 p3012 A73-44040
- Transition of a low-pressure plasma into a highly ionized state
23 p3013 A73-44335
- Cyclotron resonance breakdown with submillimeter lasers.
24 p3095 A73-44586
- Low-pressure gas breakdown with CO₂ laser radiation.
24 p3095 A73-44589
- The effect of the Gum Nebula on soft X-rays from galactic sources.
24 p3138 A73-45044
- Breakdown potential of potassium-seeded combustion products.
24 p3121 A73-45164
- Pulsed high output double discharge TEA carbon dioxide laser with multiple electrodes and gas preionization in cavity, noting energy conversion efficiency
24 p3098 A73-45551
- GAS JETS**
Experimental satellite for attitude control. II - Measurement of low thrust gas jet performance.
01 p0111 A73-11189
- Calculation of an axisymmetric supersonic gas jet injected in a supersonic slipstream past a given body with heat supply
02 p0129 A73-12583
- Structural and aerodynamic characteristics changes in turbulent propane-butane and air jets interacting with sound
03 p0290 A73-12971
- Flammable fuel-air mixture ignition by transient turbulent hot inert gas jet, calculating minimum required jet size
03 p0399 A73-14390
- Experimental investigation of the electrical conductivity of a coaxial high-temperature jet with dispersed particles of Ti
07 p0858 A73-20010
- Species separation in swirling expansion jet of gases mixture.
08 p0956 A73-21774
- Contactless switch for three stage gas flow using symmetric jet booster based on Coanda effect
09 p1037 A73-22848
- Gas jet flow at high subsonic velocities, determining stream function, contraction coefficient, convergence at critical velocity and pressure above obstacle
11 p302 A73-26215
- Scattering of light by the medium generated by a space vehicle. I - Emission of vapor jets by spacecraft microthrusters.
12 p1549 A73-27641
- Some noise generation mechanisms in transonic gas jets
14 p1712 A73-30947
- Low-density jets behind a sonic nozzle at large pressure gradients
17 p2150 A73-34263
- Near continuum impact of an underexpanded jet plume on a wall.
17 p2096 A73-35137
- Application of laser Raman spectroscopy to the study of factors that influence turbulent gas mixing rates.
17 p2185 A73-35510
- Turbulence measurements with hot-wire anemometry in a non-homogeneous jet.
17 p2174 A73-35512
- Hot gaseous jet noise emission calculation for dependence on turbulent flow characteristics based on Lighthill theory, using computer program
18 p2343 A73-36997
- Small-scale suppressor of the aerodynamic noise of a subsonic gas jet
21 p2754 A73-40404
- Freon-22 circular and flat jet propagation in air cross flow in wind tunnel, examining air-gas dynamic pressure ratio effects
21 p2676 A73-40405
- Condensation in CO₂ free jet expansions. I - Dimer formation.
21 p2743 A73-40937
- Turbulent diffusion flame velocity, concentration, temperature and momentum flux measurements for hydrogen round jet in co-flowing air stream
22 p2935 A73-42788

Analog investigation of the gas jet resonance tube.
23 p2967 A73-43401

GAS LASERS

NT CARBON DIOXIDE LASERS
NT CARBON MONOXIDE LASERS
NT HCN LASERS
NT HELIUM-NEON LASERS
NT TEA LASERS

Computed secondary-electron and electric field distributions in an electron-beam-controlled gas-discharge laser.

01 p0058 A73-10130

New mechanism for generating coherent emission from ionized oxygen and nitrogen in the visible region of the spectrum

01 p0059 A73-10630

Ar and Kr continuous wave ion lasers with electric arc discharge, noting quartz, graphite and beryllium oxide gas discharge tubes

01 p0059 A73-10714

Measuring the spread function of infrared spectrometers by means of gas lasers.

01 p0060 A73-10838

Spontaneous active medium emission effect on amplification characteristics of linear and nonlinear traveling wave IR gas laser amplifier

01 p0060 A73-11084

Effect of a magnetic field on emission fluctuations in a ring gas laser

01 p0060 A73-11089

UV laser parameters calculation for operation on Lyman transition between H atom resonant excited state and ground state

01 p0061 A73-11334

Gas and solid state lasers amplitude and phase fluctuations calculated from Langevin equations, noting spectral line width and ring laser wave coupling

01 p0061 A73-11355

Design and operation of high power pulsed X ray tube with photocathode and nitrogen laser illumination for electron beam generation

02 p0175 A73-11960

Nonlinear interaction between a spontaneous radiation field and the active media of high-gain gas laser amplifiers

02 p0177 A73-12489

The feasibility of producing laser plasmas via photoionization.

02 p0177 A73-12572

Coupling losses in hollow waveguide laser resonators.

02 p0177 A73-12573

Laser oscillation and anisotropic gain in the 1 to 0 vibrational band of optically pumped HF gas.

02 p0177 A73-12747

Gas-temperature measurement in pulsed H₂O laser discharges.

02 p0178 A73-12814

Pumping rate in He-Cd laser from metastable atoms concentration measurement and plasma diagnostics, noting upper level population dependence on Penning effect

03 p0319 A73-13753

Spectral density curves for intensity fluctuations of stimulated emission from low and IR frequency gas lasers as function of thermal oscillation, mode interference and beat effects

03 p0319 A73-14087

Submicrosecond pulses from a hydrogen-fluorine laser with high energy density and quantum efficiency.

03 p0320 A73-14454

New infrared laser line in OCS and new method for C atom lasing.

03 p0320 A73-14465

Time behavior of a TEA xenon laser.

03 p0320 A73-14466

Supersonic electrical-discharge copper vapor laser.

04 p0457 A73-14746

Chemical lasers population inversion mechanism and excitation energy comparison with other molecular gas lasers including carbon dioxide systems, considering efficiency

04 p0458 A73-14749

Investigations of a Kr-Hg mixture regarding laser action

04 p0458 A73-14896

Protoplanet cloud model for cosmic OH and water masers in H II regions to account for anomalous hydrogen deficiency, discussing pumping mechanisms and chemical composition

04 p0497 A73-14974

Time history of laser power pulses from molecular gas lasers.

04 p0459 A73-16041

Laser plasma generation with high electron densities by photoionization from flashlamp or coherent UV source from harmonic generation or gas lasers

05 p0601 A73-16362

The use of a gas laser for sizing single particles of airborne dust.

05 p0584 A73-16444

Cavity detuning and multimode operation of an optically pumped gas laser.

05 p0585 A73-16598

Chemical lasers with molecular gas excitation and population inversion by chemical reactions, discussing lasing conditions, vibrational transition and pumping mechanism

05 p0585 A73-16602

Laser coupling through nonlinear gas filled absorber cell, discussing molecules mean free path

05 p0585 A73-16783

Density changes in a laser cavity including wall reflections and kinetics of energy release.

[AIAA PAPER 73-141] 05 p0585 A73-16890

Reliable starting technique for an ion laser tube with internal gas return bores.

[AD-758556] 05 p0586 A73-17263

Plasma parameters in gas discharges for positive-column He-Se/+/- lasers.

06 p0701 A73-18360

Output power dependence on mode geometry in CW gas dynamic laser resonator within kinetic theory of interaction between radiation field and optically active medium stream

06 p0702 A73-18459

Pulsed nitrogen laser emitting at 3371 Å.

06 p0702 A73-18587

Use of a semiconductor laser diode as a modulator of gas laser radiation.

06 p0702 A73-18592

Nitrous oxide laser optical pumping at high pressures with TEA hydrogen bromide laser, considering application to other linear triatomic molecules

06 p0704 A73-18796

Selective reabsorption leading to multiple oscillations in the 8446-Å atomic-oxygen laser.

07 p0834 A73-19335

Interactions among multiple lines in the 8446-Å atomic-oxygen laser.

07 p0834 A73-19336

Conference on Chemical and Molecular Lasers, 3rd, St. Louis, Mo., May 1-3, 1972, Proceedings.

07 p0834 A73-19626

CW He-Cd and He-Se metal vapor lasers, discussing atomic energy states, energy emission and absorption by electrons He storage levels and Penning ionization

07 p0836 A73-19933

Saturation resonances by magnetic mode crossing in optical pumping with a multimode gas laser.

07 p0837 A73-20606

Dependence of characteristics of a gas laser on the parameters of an intracavity absorber.

08 p0974 A73-20953

Numerical formulation for constant-gain chemical laser calculations.

08 p0975 A73-21411

High-current gas lasers with a mercury cathode

08 p0976 A73-21717

Pulsed and CW water vapor lasers, investigating He addition effects on time-varying gas temperature and power output

[AD-760377] 09 p1091 A73-22082

High gain gas laser oscillators saturation, verifying with 3.51 micron Xe oscillator having unsaturated single pass intensity gain of ten million

09 p1091 A73-22086

Problem of the nuclear pumping of molecular gas lasers

09 p1096 A73-22702

Dielectric modulation of single mode CW gas laser by acoustic wave, solving equations for creation and annihilation operators to obtain quantum number

09 p1096 A73-22973

Optically pumped gas laser steady state solution for population inversion, gain coefficient, radiative intensity and power output, noting Doppler broadening role

09 p1097 A73-23070

Vibrational relaxation theory of diatomic and multiatomic single component and gas mixture systems for molecular laser mechanisms, using oscillator simulation

09 p1097 A73-23331

Probability model of mode interactions, radiation density and output gain of gas laser channels with common lower energy level in active medium

10 p1227 A73-24071

Steady state lasing stability in ring-type gas laser with symmetrical distribution of three longitudinal modes

10 p1228 A73-24580

He-Se laser low order transverse modes self mode locking at six transition wavelengths, attributing effect to oscillating modes reduction due to hole burning and cross relaxation

10 p1229 A73-24616

A hollow cathode device for CW helium-metal vapour laser systems.

10 p1229 A73-24617

Single mode ion laser tuning over entire emission range via intracavity etalon tilting by piezoelectric drive

11 p1376 A73-26104

A plasma-beam discharge laser.

11 p1377 A73-26181

Electro-optical transient sampling analyzer with neon laser and hydrogen thyratron pulse generator and minimum optical and electrical jitter

11 p1377 A73-26244

Feasibility of high-pressure noble-gas lasers.

11 p1378 A73-26360

Hg vapor laser with He, Ne, Kr, H or N additions, investigating population inversion and lasing properties for optimal performance conditions

12 p1504 A73-26887

Vibrational level populations in diatomic molecules during steady pumping

12 p1504 A73-26888

Commutation of spark gaps with the aid of a pulsed gas laser emitting in the ultraviolet range

12 p1506 A73-27211

Nitrogen laser with a longitudinal discharge and high power density

12 p1506 A73-27214

Nitrogen laser with a transverse discharge

12 p1506 A73-27215

Pulsed gas laser employing substances of low volatility

12 p1506 A73-27218

Investigation of the stability of the oscillation frequency of a mercury laser emitting at 1.53 microns.

12 p1507 A73-27511

Reconstruction of the images of transparencies with a semiconductor laser.

12 p1498 A73-27512

Possible utilization of a vapor, formed by the action of a high-power electron beam on a target, as an active medium for stimulated emission of light.

12 p1507 A73-27517

Improved uniform-field electrode profiles for TEA laser and high-voltage applications.

13 p1626 A73-28366

Population inversion calculations using near-resonant charge exchange as a pumping mechanism.

13 p1627 A73-28549

Studies of noble-gas lasers for continuous operation

13 p1627 A73-28790

Frequency fluctuations in a gas laser with nonlinear absorption.

13 p1629 A73-29430

Pulsed laser utilizing a fluorine and hydrogen mixture.

13 p1629 A73-29434

Chlorine trifluoride chemical laser emission, discussing output power dependence on partial pressures and chemical reaction kinetics

13 p1630 A73-29444

Stability condition of an intense two-modes regime in a gas laser

13 p1630 A73-29557

Quantum theory of a high energy gas laser

14 p1757 A73-30363

Theory of diffraction efficiency maximization for thin-layer amplitude holograms

14 p1753 A73-30364

Indoline series spirochromene polymer matrices for holographic recordings with argon and helium-neon lasers in green and UV spectral regions

14 p1753 A73-30365

Calculation of the nonlinear polarizability of a gas at a lasing transition with allowance for capture of resonance emission

14 p1757 A73-30367

Possibility of electron concentration determination in a plasma with the aid of a gas laser with a nonlinearly rotating absorption cell

14 p1781 A73-30465

Contribution to the theory of single-mode laser modulation. II - Conduction modulation.

14 p1758 A73-30769

Theory of the nonlinear power resonances in gas lasers

14 p1758 A73-30803

Dependence of the locking zone of a gas ring laser on the emission frequency

15 p1885 A73-32316

CW metal vapor lasers, discussing discharge conditions, excitation processes, cathaphoretic effect and He-Se and He-Cd lasers output characteristics

16 p2023 A73-32858

Nitrogen pulsed ultraviolet laser.

16 p2023 A73-32861

Effects of mirror reflectivity in a distributed-feedback laser.

16 p2024 A73-33081

Oscillographic registration of the occurrence of off-axis modes in a gas laser

17 p2183 A73-34169

A self-stabilized 3.5-micron waveguide He-Xe laser.

17 p2183 A73-34206

Frequency deviation equations for FM gas laser with modulation achieved by resonator optical length variations

17 p2184 A73-35168

Laser energy absorption by plasma for controlled thermonuclear fusion, comparing uses of electrically pumped gas, chemical and solid state lasers

17 p2185 A73-35379

Repetitively pulsed high power nitrogen laser for UV radiation at room temperature, discussing electrical design and construction

17 p2185 A73-35767

Pressure dependency of the NF₃-H₂ transverse-discharge pulse-initiated HF chemical laser.

17 p2186 A73-35790

Vacuum UV radiation of electron beam excited high pressure Xe laser, measuring optical gain due to diatomic state-repulsive ground state transitions

17 p2186 A73-35794

Electron-beam irradiated discharges for initiating high-pressure pulsed chemical lasers.

[AIAA PAPER 73-645]

18 p2322 A73-36259

Book - Atomic physics and astrophysics, Volume 2.

18 p2356 A73-36969

Laser absorption study of carbon monoxide vibrational relaxation behind incident shock waves, discussing vibration-rotation levels, shock tubes, oscilloscope traces and Boltzmann distributions

19 p2437 A73-37900

A study of the CW 28-micron water-vapor laser.

19 p2438 A73-38278

Dispersion characteristic of a three-mode gas laser during modulation of relative excitation

19 p2406 A73-38335

Non-Gaussian statistics of superradiant radiation from saturated xenon 3.5-micron laser amplifier.

20 p2570 A73-38620

Self-pulsing in laser amplification of broadband noise.

20 p2571 A73-38635

Intensity limitation and energy spreading in an optical field under transient thermal defocusing conditions.

20 p2574 A73-39689

Emission of infrared molecular hydrogen lines from a cooled-gas laser.

20 p2574 A73-39694

Effect of double optical resonance on frequency interaction and selection in a gas laser

21 p2711 A73-40303

The frequency stabilization of gas lasers.

22 p2868 A73-41698

Kinetics of the generation spectrum of a photodissociation iodine laser.

22 p2868 A73-41722

Mode competition in the 3s sub 2-3p sub 4 transition in a neon laser with a methane absorbing cell.

22 p2869 A73-42256

Time constants of spark discharges initiated by a gas-laser beam of 0.3371 micron wavelength.

22 p2869 A73-42257

Measurements of the upper and lower level lifetime in He-Se lasers.

22 p2871 A73-43086

Nonlinear transmission loss in Ge beam splitter in pulsed HF and DF lasers operating at 2.5 to 4 microns

22 p2897 A73-43145

Collisional radiative processes and molecular lasers

23 p2988 A73-44013

Frequency dependence of locking in a ring laser.

24 p3095 A73-44622

Generation of nonunidirectionally polarized modes by a gas laser oscillator with a mode selector.

24 p3096 A73-45031

Excitation mechanisms in He-Cd and He-Zn ion lasers.

24 p3097 A73-45418

GAS LIQUEFACTION

U CONDENSING

GAS LUBRICATED BEARINGS

U GAS BEARINGS

GAS MASERS

Rb87 vapor maser with optical pumping, measuring nitrogen or nitrogen argon mixture buffer gas partial pressure effect on power output

04 p0459 A73-15920

Hydrogen maser frequency stability dependence on signal output, magnetic polarization field and relaxation effects, describing automated relaxation rate measurement and atomic line spectrum registration

06 p0699 A73-17588

Hydrogen maser amplifier performance characteristics, discussing relaxation time measurements, frequency stability and performance enhancement via resonator cavity magnetic shielding improvement

08 p0974 A73-20774

Water masers in a protostellar gas cloud.

19 p2483 A73-37573

Light shift and light broadening in the Rb-87 maser.

20 p2572 A73-38861

GAS MIXTURES

NT AIR

NT DETONABLE GAS MIXTURES

Theoretical treatment of the translational absorption spectrum induced in mixtures of rare gases

01 p0079 A73-10500

French monograph - Contribution to the experimental study of the integrated intensity of the translational absorption bands induced in pressurized rare-gas mixtures.

01 p0080 A73-10601

French monograph - Experimental study of the thermal conductivity of rare gases and helium-argon mixtures as functions of temperature and pressure.

01 p0120 A73-10604

Adsorption equilibria at high pressures in the helium-nitrogen-activated carbon system.

01 p0014 A73-10725

Analysis of the problem of the thermal propagation of a flame by the method of joining asymptotic expansions

01 p0123 A73-10958

Temperatures of aluminum during its combustion in oxygen-argon mixtures, in nitrogen, and in air

01 p0123 A73-11275

Swirling jet of gases mixture into vacuum.

03 p0289 A73-12908

Turbulent gas mixing measurements using a laser schlieren technique.

03 p0296 A73-14202

A nondimensional parameter characterizing mixing processes in a model of thermal gas ignition.

03 p0399 A73-14389

Gas concentration profiles in combustion gas sampling probes, using IR absorption technique

03 p0399 A73-14397

Methane-air mixtures burning velocity as function of equivalence ratio at atmospheric pressure, using bomb/hot-wire and corrected density ratio techniques

03 p0399 A73-14398

Unflanged electrode spark ignition tests for minimum energy to trigger gas mixtures explosion, using spark energy relation for outward propagating quasi-spherical flame

03 p0399 A73-14400

H₂/O₂-fuel cells supplied with a H₂/N₂-mixture and air.

04 p0408 A73-15116

Rb87 vapor maser with optical pumping, measuring nitrogen or nitrogen argon mixture buffer gas partial pressure effect on power output

04 p0459 A73-15920

Ignition analysis of adiabatic, homogeneous systems including reactant consumption.

[AIAA PAPER 73-215]

05 p0640 A73-16945

Hydrodynamics equations for multicomponent mixtures with higher-order approximations of transport coefficients

06 p0684 A73-17467

Effects of contaminants in CO₂ lasers.

[AIAA PAPER 73-52]

06 p0699 A73-17628

Gain correlation with sidelight and plasma impedance properties of a CO₂ laser discharge.

06 p0700 A73-18137

Calculation of the transfer coefficients for planetary atmospheres consisting of CO₂-N₂ mixtures

06 p0754 A73-18568

Dissociative recombination at elevated temperatures. IV - N₂/+ / dominated afterglows.

07 p0853 A73-19149

The effect of higher alkanes on the ignition of methane-oxygen-argon mixtures in shock waves.

[AD-756982]

07 p0918 A73-19389

A CW-CO chemical laser from the reaction of active nitrogen with O₂ + CS₂.

07 p0835 A73-19633

Study of the ignition reaction in an oxygen-hydrogen mixture at relatively high pressures and low temperatures in the shock tube

07 p0920 A73-19993

Upper self-ignition limit of hydrogen in oxygen

07 p0921 A73-19994

Comparison of four simple models of steady flow combustion of pyrolyzed methane and air.

07 p0865 A73-20360

Measurements of the structure of an ionizing shock wave in a hydrogen-helium mixture.

07 p0813 A73-20475

Equation of state of a mixture of nonideal, chemically reacting gases.

08 p0936 A73-20856

On the He-H₂ thermal opacity in planetary atmospheres.

08 p1003 A73-20890

Photoinitiated transversely sustained CO₂ laser.

08 p0975 A73-21208

Possibility of argon-nitrogen gas metal-arc welding of some non-ferrous metals.

08 p0973 A73-21237

Fire retardance of mixtures of inert gases and oxygen.

09 p1045 A73-22532

Vibrational relaxation theory of diatomic and triatomic single component and gas mixture systems for molecular laser mechanisms, using oscillator simulation

09 p1097 A73-23331

A study of the stability of slow combustion of gas mixtures subjected to the action of a magnetic field

09 p1167 A73-23351

Determination of burning velocity by double ignition in a closed vessel.

10 p1294 A73-23559

Kinetic equations for vibrational energy relaxation in a polyatomic gas mixture

10 p1250 A73-23579

Absorption of laser emission by He-CO₂ mixtures, CO₂ and NH₃ gases, and water vapors

10 p1227 A73-24074

Approximate solution of the system of Boltzmann equations for a mixture of reacting gases

10 p1252 A73-24490

Hot-wire measurements of gas mixture concentrations in a supersonic flow.

10 p1220 A73-24637

Methyl nitrite photolysis reaction products under various ambient gas mixture environments, noting irradiation time and gas pressure effects

10 p1186 A73-24656

Electric current in pressurized N₂, O₂, and their mixtures under conditions of strong ionization by an electron beam

10 p1230 A73-24883

IR spectrum line reversal for measurement of CO and gas mixture laser plasma vibrational temperatures as function of discharge current and gas pressure

10 p1230 A73-24884

Design of an R.F. excited helium-neon visible gas laser and study of the optimal conditions for gas mixtures and pressures.

10 p1230 A73-24923

The response of a hot-wire anemometer in flows of gas mixtures.

10 p1222 A73-24971

Heat pipe oven as instrument for laser absorption and fluorescence spectroscopy of metal vapors, vapor-gas, vapor-vapor mixtures and metal vapor plasmas

11 p1361 A73-25148

The stability of a layer of binary gas mixture heated below.

11 p1449 A73-25222

Phase equilibria in fluid mixtures at high pressures - The He-CH₄ system.

11 p1399 A73-25889

Vibrational relaxation in hydrogen-rare-gases mixtures.

11 p1402 A73-25969

Thermodynamics of heterogeneous gas equilibria. VII - Gas phase composition and chemical transport reactions in the tungsten-oxygen-hydrogen system

11 p1386 A73-26568

Determination of the temperature of a methane-fluorine diffusion flame by means of the vibration-rotation spectrum of the HF molecule

11 p1453 A73-26586

Carbon dioxide thermodynamic and transport characteristics calculation, treating gas as multicomponent ideal mixture including carbon monoxide and oxygen and carbon atoms and ions

12 p1526 A73-27308

Experimental investigation of heat and mass transfer in the condensation of vapor from gas-vapor mixtures under viscous and viscous-gravitational flow conditions

12 p1558 A73-27315

Analysis of the problem of thermal flame propagation by the method of matched asymptotic expansions.

12 p1559 A73-27534

On the Aller's admixture radiation effect during the compression process in the solar corona and generation of coronal formations.

12 p1536 A73-27844

Mechanism and kinetics of the formation of intermediate products in an auxiliary mixture and the effect of such products on the combustion of the working mixture

13 p1704 A73-28293

Turbulent transport coefficients for compressible heterogeneous mixing.

13 p1705 A73-28435

Relaxation of the bending vibration of CO₂ in pure CO₂ and in mixtures of CO₂ with noble gases.

13 p1662 A73-28553

Flame quenching, extinction, propagation, convection and ignition limits in premixed gas mixtures

13 p1707 A73-29003

Parametric studies on CO₂ TEA lasers with extracavity and intracavity electrodes.

13 p1628 A73-29187

Procedure for preparing an oxygen-nitrogen gas mixture for respiration in a pressure chamber

13 p1580 A73-29409

Microwave pulse excited argon ion laser.

14 p1758 A73-30472

Slow motions of bodies in gas mixtures

15 p1861 A73-31198

Three-dimensional motion of a reacting gas mixture around a blunt body

15 p1822 A73-31290

Calculation of the composition of 79% N₂ + 21% O₂ and 50% N₂ + 50% O₂ mixtures containing carbon at high temperatures

15 p1840 A73-31853

Potential distribution in a two-gas thermionic converter at current saturation.

15 p1832 A73-32638

Use of fluidic and pneumatic elements to determine the composition of a gas mixture

16 p1970 A73-33025

Mechanism of decay of ammonia in flame gases from an NH₃/O₂ flame.

16 p1976 A73-33345

Calculation of the transfer coefficients of planetary atmospheres formed by mixtures of CO₂ and N₂.

16 p2039 A73-33593

Tunable-laser derivative spectroscopy on spectral lines with combined Doppler and collision broadening.

16 p2039 A73-33741

Gain and energy measurements on an HF/DF electrically pulsed chemical laser.

17 p2183 A73-34203

Effect of temperature and composition of gas mixture on population inversion in pulsed CO₂ laser.

17 p2183 A73-34295

Quantum scattering theory of rotational relaxation and spectral line shapes in H₂-He gas mixtures.

17 p2119 A73-35175

Nitric oxide emissions from tube combustor burning premixed gaseous propane-air mixture, considering inlet conditions for equivalence ratios

17 p2222 A73-35468

An experimental-analytical method to study steady spray combustion.

17 p2255 A73-35499

Experimental investigation of a fast ion-acoustic wave in a multicomponent plasma

18 p2339 A73-36564

Certain patterns of heat transfer in a hypersonic shock layer in the presence of mass entrainment

18 p2266 A73-37014

Shock tube study of the effect of unsymmetric dimethyl hydrazine on the ignition characteristics of hydrogen-air mixtures.

18 p2372 A73-37098

Comparison of electron and electronic temperatures in recombining nozzle flow of ionized nitrogen-hydrogen mixture. I, II.

19 p2462 A73-37441

Modification of the Chapman-Enskog method for a mixture of reactive gases with allowance for fast and slow processes

19 p2462 A73-37845

Integral transport equations for component distribution function of gas mixture with internal degrees of freedom and chemical reactions

19 p2463 A73-37847

Calculation of the generation of inversion and the laser output power for expanding combustion gases /CO₂-N₂-He/

19 p2504 A73-38157

Numerical and analytical prediction methods for time dependent reactions in homogeneous gas mixtures, considering accuracy and computing times

20 p2626 A73-39095

Electrical current in electron-beam ionized N₂ and CO₂.

21 p2749 A73-41658

IR spectrum line reversal for measurement of CO and gas mixture laser plasma vibrational temperatures as function of discharge current and gas pressure

21 p2717 A73-41659

Nonthermal metabolic response of rats to He-O₂, N₂-O₂, and Ar-O₂ at 1 atm.

22 p2805 A73-42201

State variables and transport coefficients of binary gaseous mixtures. I - A simple method for the accurate determination of the second virial coefficient of binary gaseous mixtures

22 p2931 A73-42373

State variables and transport coefficients of binary gaseous mixtures. II - The binary interaction between identical and nonidentical molecules

22 p2931 A73-42374

State variables and transport coefficients of binary gaseous mixtures. III - The calculation of transport coefficients with the aid of consistent potential parameters

22 p2931 A73-42375

Experimental study of the thermal conductivity coefficient of noble gas mixtures at low and moderate densities.

22 p2932 A73-42503

Elementary reaction rates from post-induction-period profiles in shock-initiated combustion.

22 p2933 A73-42755

Reaction rate constants for carbon monoxide-hydrogen-oxygen and hydrogen-nitrogen-oxygen systems at high temperatures, modeling hydrocarbon combustion for product distribution

22 p2933 A73-42758

Laminar combustion of polymethylmethacrylate in O₂/N₂ mixtures.

22 p2898 A73-42805

Combustion of boron particles - Experiment and theory.

22 p2899 A73-42821

Flowing gas mixture ignition at heated blunt body stagnation point, examining Van't Hoff criterion

23 p3048 A73-43328

Effect of an electric field on the ignition of a reacting binary gas mixture

23 p3009 A73-43441

Theory of nonequilibrium phenomena in chemically reacting gas mixtures

23 p2950 A73-43703

Numerical integration of the equations of chemical kinetics

24 p3065 A73-44703

Thermokinetics and combustion phenomena in non-flowing gaseous systems - An invited review.

24 p3157 A73-45165

The behavior of hot-film anemometers in gas mixtures.

24 p3091 A73-45325

Predicted electron transport coefficients and operating characteristics of CO₂-N₂-He laser mixtures.

24 p3097 A73-45420

Heat and mass transfer in a turbulent layer above permeable plates

24 p3081 A73-45528

GAS PHASES

VAPOR PHASES

GAS PIPES

Nonlinear gas oscillations in pipes. I - Theory.

18 p2299 A73-36505

Nonlinear gas vibrations maintained in a closed tube by a heat source

23 p2968 A73-43719

GAS PRESSURE

The light emission of the column plasma in current-modulated noble-gas discharges at intermediate pressures

03 p0348 A73-14621

I-V characteristics and luminescence changes in Cs vapor arc discharge at various spark gap widths, noting pressure effect on gas stratification

04 p0481 A73-15613

Investigation of a coaxial plasma accelerator with a uniform gas pressure distribution in the electrode gap

04 p0481 A73-15616

Shadowgraph photography for electromagnetic excitation of shock waves in normal pressure gas, noting plasma and shock compressed regions in shock tube

04 p0434 A73-15618

Pressure, temperature, current density and potential difference fluctuations in subsonic flow of combustion products plasma, noting steadiness, ergodicity and distribution functions

06 p0732 A73-18616

Effects of a high-pressure gas medium on the mechanical properties of polymethylmethacrylate

06 p0715 A73-18671

Comparison of theory and experiment for a transversely excited high-pressure CO₂ laser.

07 p0835 A73-19637

I-V characteristics and luminescence changes in Cs vapor arc discharge at various spark gap widths, noting pressure effect on gas stratification

10 p1254 A73-24203

Coaxial plasma accelerator with uniform pressure distribution.

10 p1254 A73-24206

Shadowgraph photography for electromagnetic excitation of shock waves in normal pressure gas, noting plasma and shock compressed regions in shock tube

10 p1205 A73-24208

Design of an R.F. excited helium-neon visible gas laser and study of the optimal conditions for gas mixtures and pressures.

10 p1230 A73-24923

Low gas pressure measurement with ionization and extractor gases, discussing methods for suppressing or eliminating disturbance effects

11 p1361 A73-25400

Calculation of the pumping characteristic of a turbomolecular vacuum pump

12 p1461 A73-27475

Parametric studies on CO₂ TEA lasers with extracavity and intracavity electrodes.

13 p1628 A73-29187

High-pressure CO₂-N₂ laser excited by electric discharge controlled by means of electron beam.

14 p1757 A73-30260

Hypersonic wind tunnel MHD accelerator design and operating principles, discussing flux density, I-V characteristics, cooling losses, plasma temperature, gas pressure and velocity, etc

14 p1743 A73-30295

Development and employment of a measurement transformer for a difference in pressure. I

16 p2014 A73-33224

Applicability of an adiabatic compression method to the study of a cesium plasma

17 p2214 A73-34130

Transport coefficients of air at temperatures from 3000 to 25,000 K and at pressures of 0.1, 1, 10, and 100 atm

17 p2253 A73-34264

Correspondence laws of diatomic and adiabatic gas flows referring to similarity between pressure, temperature, sound velocity and Mach numbers

18 p2299 A73-36488

Single axis analog fluoric accelerometer using mercury as solid proof mass, describing differential gas pressure outputs, porous cylindrical configuration and hydrostatic pressure gradients

19 p2389 A73-38076

Gas management system for control, bleeding, evacuating and radiological and pressure monitoring of He atmosphere in multihundred watt heat source

19 p2457 A73-38428

Thermodynamic properties of air and thermal equation of state as function of pressure and temperature from piezometer measurement

20 p2627 A73-39298

Tungsten inert gas arc welding for refractory or active metals working in gas-tight chamber, noting effects of reduced pressure on cathode zone energy density

20 p2569 A73-39666

Lunar specific surface adsorption-desorption processes discussing near-surface atmospheric diurnal variations, nitrogen temperature, sorption capacity, gas concentration from regolith structure

21 p2774 A73-41402

Investigation of conditions for the formation of a beam-plasma discharge without a magnetic field

21 p2748 A73-41516

Peak expiratory flow rate and rate of change of pleural pressure.

21 p2642 A73-41636

The post-eclipse brightening of Io.

24 p3134 A73-44563

Interaction between flows with different velocities in the solar wind

24 p3124 A73-44780

Influence of a discrete component of acoustic vibration on flow in a supersonic jet with a nondesign ratio of active to passive pressure

24 p3055 A73-45538

GAS SPECTROSCOPY

Prolonged luminescence of complex molecules in the gas phase

09 p1123 A73-23334

Microwave rotational spectroscopy - A technique for specific pollutant monitoring.

10 p1221 A73-24891

Vibrational relaxation in hydrogen-rare-gases mixtures.

11 p1402 A73-25969

An improved separability approximation for line radiative transport in nonhomogeneous media.

15 p1959 A73-32391

Measurement of trace gases in the stratosphere using far infra-red spectroscopy.

16 p2006 A73-33553

Spectroscopy of the vapors of weakly volatile compounds, supercooled in a supersonic flow

16 p2038 A73-34054

Interference filter laser Raman spectrometry of gases and volatile liquids, discussing instrument sensitivity and response linearity, signal to noise ratios, and bandwidths

21 p2698 A73-40140

Nonlinear effects in the emission and absorption spectra of gases in resonant optical fields

21 p2712 A73-40443

Spectroscopic studies of low-pressure hydrogen-fluorine flames.

22 p2898 A73-42760

The absorption cross sections of N₂, O₂, CO, NO, CO₂, N₂O, CH₄, C₂H₄, C₂H₆, and C₄H₁₀ from 180 to 700 Å.

22 p2890 A73-42992

A supersynthesis radio telescope for neutral hydrogen spectroscopy at the Dominion Radio Astrophysical Observatory.

23 p2958 A73-43362

GAS STREAMS

Two-stream heterogeneous mixing measurements using laser Doppler velocimeter.

01 p0050 A73-10741

Heat transfer from a circular cylinder in a rarefied gas stream.

01 p0122 A73-10761

Stellar gas injection into nucleus of radio galaxy NGC 4486, estimating energy release during gas accretion

01 p0106 A73-11301

Local emission coefficients fields for ionized gas in arbitrary and rectangular cross section streams

03 p0344 A73-13179

Stabilization of flames formed behind cylinders wetted by liquid fuels in high velocity gas streams

05 p0639 A73-16679

An apparatus for testing components in a high temperature supersonic gas stream containing abrasive particles.

09 p01070 A73-23065

The rapid cooling of a hot gas discharge by liquid sprays.

22 p2929 A73-41743

GAS TEMPERATURE

Stationary state of the radially symmetrical motion of vapors heated by laser radiation with allowance for thermal and ionizational nonequilibrium

02 p0175 A73-11601

Thermocouple circuits for measurement of unsteady temperatures in gases by the two-thermoreceiver method and an analysis of thermocouple circuit errors

02 p0166 A73-11710

Gas-temperature measurement in pulsed H₂O laser discharges. 02 p0178 A73-12814

Enhanced N₂ vibrational temperatures in the thermosphere. 03 p0298 A73-12881

Boundary conditions for temperature perturbations in stability problems of compressible gas flows. 03 p0245 A73-13672

Electron temperature elevation compared to gas temperature in hydrocarbon flames, discussing energy exchange mechanism. 03 p0352 A73-14394

Nonadiabatic temperature change in rapidly expanded or compressed gas, discussing shearing and volume viscosity effects. 05 p0597 A73-16350

Gas temperature, carbon monoxide and nitric oxide axial and radial distribution in J-33 combustor, presenting combustion process model based on measurements [WSCIPAPER 72-22]. 05 p0639 A73-16690

Influence of the thermal effect of the gas on the motion of an electric arc in a transverse magnetic field. 07 p0858 A73-20081

Emissions from and within an Allison J-33 combustor. 07 p0868 A73-20359

Some methodological questions concerning the simulation of turbine blade operation on gasdynamic stands. 07 p0809 A73-20509

Experimental determination of the vibrational temperature of a supersonic gas flow. 08 p1021 A73-20854

Dynamic method for measuring thermal conductivity of liquids and gases at high pressures. 08 p1021 A73-20861

Pulsed and CW water vapor lasers, investigating He addition effects on time-varying gas temperature and power output [AD-760377]. 09 p1091 A73-22082

Temperature distribution in gas flow about a linear source of heat variable periodically in function of time. 09 p1166 A73-22169

Transient functions to estimate thermal inertia of gas temperature sensors with film resistance thermometer mounted on wedge shape insulating base. 09 p1081 A73-22346

Measurement of vibrational temperature of CO and N₂ using the He/2 3S/ Penning ionization technique. 10 p1218 A73-24246

The transport coefficients and material functions of a plasma with different electron and gas temperatures. 11 p1404 A73-25343

A probe system for spectrometric determination of temperature and concentration distributions in combustion gases. 13 p1612 A73-28432

Near-satellite neutral gas temperature determination from measurement of molecular nitrogen velocity distribution. 13 p1687 A73-28630

KCl ionization and diffusion in premixed flames with uniform temperature and composition, studying gas velocity and photometry. 13 p1707 A73-28995

Interstellar gas excitation due to supernova explosions using time dependent model based on statistical correlation of gas neutral density, ionization and temperature parameters. 15 p1928 A73-31053

Mariner 9 ultraviolet spectrometer experiment - Upper limits on the Lyman-alpha flux from clusters of galaxies. 15 p1936 A73-31551

Dynamic gas temperature measurements in a gas turbine transition duct exit. [ASME PAPER 73-GT-7]. 16 p2047 A73-33485

Rotational temperature measurement of gases using laser Raman scattering techniques. 17 p2166 A73-34623

Thermal structure and evolution of interstellar gas exposed to a soft X-ray burst. 17 p2231 A73-34757

Correspondence laws of diabatic and adiabatic gas flows referring to similarity between pressure, temperature, sound velocity and Mach numbers. 18 p2299 A73-36488

Temperature of exhaled air of healthy subjects. 18 p2277 A73-36583

On some problems of the method of simulating the working conditions of turbine blades on gas-dynamic benches. 19 p2418 A73-37784

Cold gas cloud embeddings in interstellar hot gas, determining radiation temperature from absorption line profiles and kinetic temperature from thermal and turbulent energy components. 20 p2606 A73-39066

Thermodynamic properties of air and thermal equation of state as function of pressure and temperature from piezometric measurement. 20 p2627 A73-39298

The effect of comparison source reflectance on gas temperature measurement by Kuribbaum's method and line reversal methods. 21 p2692 A73-39916

The spectral comparison method for temperature measurement in two-phase flames. 22 p2853 A73-41987

Effect of radiometric errors on accuracy of temperature-profile measurement by the spectral-scanning method. 22 p2853 A73-41988

Short duration temperature measurements by infrared emission-absorption. 22 p2853 A73-41990

Use of edge-tone resonators as gas temperature sensing devices. 22 p2853 A73-41991

A device for the on-line measurement of nitrogen rotational temperature in low density flows. 22 p2854 A73-41995

Trends of design in gas turbine temperature sensing equipment. 22 p2858 A73-42043

New measurements of the thermal conductivity of argon and nitrogen to 200 C and 1600 atmospheres. 22 p2932 A73-42502

The temperature dependence of the half widths of some self- and foreign-gas-broadened lines of methane. 22 p2821 A73-42989

The slab thickness of the mid-latitude ionosphere. 23 p2972 A73-43694

Effect of the circumferential nonuniformity of a temperature field in front of a turbine on the vibrational stresses in the turbine blades. 23 p3020 A73-43740

Preparation of liquid fuels by evaporation from a hot wall. 24 p3158 A73-45389

GAS TRANSPORT

Experimental investigation of turbulent flow structure in a circular pipe with delivery through a porous wall. 10 p1204 A73-23512

Transport coefficients of air at temperatures from 3000 to 25,000 K and at pressures of 0.1, 1, 10, and 100 atm. 17 p2253 A73-34264

Experimental investigation of turbulent flow structure in a circular tube with expansion through a porous wall. 17 p2155 A73-35192

Gas transport in the human lung. 22 p2806 A73-42421

A rapid method for determining the CO₂ transport characteristics in man by using a capnograph and a multichannel respirator. 22 p2815 A73-42665

Hemoglobin species diffusion effect on oxygen transport in moving and stationary flat films of hemoglobin solution. 23 p2949 A73-43993

Digital microstress gauge for magneto-thermal gas transport studies. 24 p3089 A73-44815

GAS TUNGSTEN ARC WELDING

Reignition characteristics of low current a.c. TIG welding arcs. 01 p0055 A73-10115

Electron microanalysis of backfilled hot cracks in Inconel 600. 01 p0067 A73-11373

HF dc straight polarity current pulsations effects on quality and mechanical properties of gas tungsten arc welds in Al alloy [SAE PAPER 720874]. 05 p0582 A73-16669

Effects of the initial structures of pressed semi-finished products made of AK-8 alloy on their weldability. 07 p0832 A73-20370

Plasma-MIG arc welding with deposition from automatic reel fed wire via rotating arc, noting suitability for stainless steel sheet. 09 p1089 A73-22693

Effect of welding variables on aluminum alloy weldments. 10 p1230 A73-23627

Microstructural observations of arc welded boron-aluminum composites. 10 p1223 A73-23630

Cape Kennedy Space Center ground support equipment welding machines and techniques, emphasizing propellant storage tanks and mobile launcher transporters. 16 p1995 A73-33195

Tungsten inert gas arc welding for refractory or active metals working in gas-tight chamber, noting effects of reduced pressure on cathode zone energy density. 20 p2569 A73-39666

An investigation of pulsed GTA welding variables. 21 p2708 A73-41254

Research carried out by the Aviation Institute on electric welding in protective atmospheres. 21 p2708 A73-41578

GAS TURBINE ENGINES

NT BRISTOL-SIDDELEY BS 53 ENGINE

NT BRISTOL-SIDDELEY VIPER ENGINE

NT J-33 ENGINE

NT J-85 ENGINE

NT JET ENGINES

NT PULSEJET ENGINES

NT RAMJET ENGINES

NT SUPERSONIC COMBUSTION RAMJET ENGINES

NT TF-30 ENGINE

NT TURBOFAN ENGINES

NT TURBOJET ENGINES

NT TURBOPROP ENGINES

Investigation of the influence of technological factors on the endurance of gas-turbine engine rotor blades. 01 p0114 A73-10477

Manganese additive effects on emissions from a model gas turbine combustor. 01 p0121 A73-10644

The effect of the precooling of the air before compression in the case of air-breathing propulsion systems of boosters for space vehicles [DGLR PAPER 72-060]. 02 p0202 A73-11673

Free three-dimensional vibration processing of gas-turbine engine blades. 02 p0172 A73-11723

Low-cost fluid film bearings for gas turbine engines. [SAE PAPER 720740]. 02 p0174 A73-12006

Flexible rotor balancing of a high-speed gas turbine engine. 02 p0203 A73-12007

Gas turbine engine hot part equivalent accelerated tests duration determination by analytical method based on Larson-Miller parametric description of long term strength. 02 p0236 A73-12216

Experimental verification of a digital computer simulation method for predicting gas turbine dynamic behaviour. 02 p0204 A73-12647

Computer programs for air cooled gas turbine engine design and performance prediction, noting aerodynamic effect of turbine coolant. 02 p0129 A73-12848

Gas path analysis applied to turbine engine condition monitoring. 03 p0354 A73-13405

Gas turbine engine exhaust emissions measurement data scatter, investigating temperature and humidity effects and emission variations in tailpipe plane [AIAA PAPER 72-1199]. 03 p0358 A73-13487

Stoichiometric gas turbines - Development problems. 03 p0359 A73-14146

Supersonic compressor performance for gas turbine engines, discussing cascade, single stage compressor rigs and experimental engine test results. 03 p0360 A73-14152

Aircraft gas turbine mainshaft ball bearings fatigue life estimation via failure distribution [ASME PAPER 72-LUB-10]. 03 p0313 A73-14328

Investigation of air stream from air-entry holes of the high-intensity combustor-liner. 03 p0400 A73-14447

Problems in modeling fuel systems for turbine engines. 03 p0258 A73-14616

Metallic materials developments in aircraft construction and gas turbine engine applications, discussing superalloys, refractory metals, composites and directionally solidified alloys. 04 p0460 A73-14741

Gas turbine engine swirl-can combustor pollution tests of nitrogen oxides, unburned hydrocarbons and carbon monoxide levels for elevated temperature performance. 04 p0485 A73-14921

The influence of fuel preparation and operating conditions on flame radiation in a gas turbine combustor. [ASME PAPER 72-WA/HT-26]. 04 p0519 A73-15828

A proposed method for calculating film-cooled wall temperatures in gas turbine combustion chambers. [ASME PAPER 72-WA/HT-24]. 04 p0519 A73-15830

Modelling of gas turbine combustors - Considerations of combustion efficiency and stability. [ASME PAPER 72-WA/GT-1]. 04 p0489 A73-15865

Pollutants from methane fueled gas turbine combustion. [ASME PAPER 72-WA/GT-3]. 04 p0485 A73-15867

Aircraft turbine engine emissions and the possibilities for control. [ASME PAPER 72-WA/GT-4]. 04 p0490 A73-15868

Assessment of emission control technology for turbine-engine aircraft. [ASME PAPER 72-WA/GT-8]. 04 p0490 A73-15872

A method of early failure detection for gas turbines. 05 p0581 A73-16186

Small turboshaft aircraft engine historical evolution and current state of art, discussing performance, cost, weight, reliability and maintainability interrelationships. [SAE PAPER 720830]. 05 p0606 A73-16626

Small turbine advanced gas generator for future propulsion requirements.
[SAE PAPER 720831] 05 p0537 A73-16634

High temperature gas turbine engines rotor blades cooling, deriving generalized dimensionless relations for heat transfer data extension from static tests to operational conditions
05 p0607 A73-16797

Effect of fuel composition on particulate emissions from gas turbine engines.
06 p0740 A73-17733

Measurement of nitric oxide formation within a multifueled turbine combustor.
06 p0740 A73-17734

Effects of fuel injection method on gas turbine combustor emissions.
06 p0768 A73-17735

Effect of operating variables on pollutant emissions from aircraft turbine engine combustors.
06 p0768 A73-17736

Control and reduction of aircraft turbine engine exhaust emissions.
06 p0768 A73-17737

Development trends in design methods for aircraft engine compressors. II - Centrifugal-flow compressors
06 p0741 A73-17996

Electrochemical machining application to aircraft gas turbine engine components manufacture, discussing removal rate, accuracy and surface finish capability
[SME PAPER MR 72-536] 06 p0697 A73-18093

Lubricants thermophysical properties effects on gas turbine engine design, considering thermal stability, vapor pressure, autoignition, load capacity and bearing life
07 p0843 A73-19563

Turbulent intensity induced by wakes near secondary air jet inlet to gas turbine engine flame tube
07 p0867 A73-19625

Moving radiography for photographic recording and display of transient or cyclic motion, emphasizing application to aircraft gas turbines under dynamic conditions
07 p0832 A73-20451

Space shuttle air breathing gas turbine engine design, modification, weight and test requirements associated with launch, space residence and reentry
07 p0906 A73-20463

Isotope Brayton space power systems and their technology.
07 p0850 A73-20467

Gas turbine engine transient performance presentation for digital computer programs.
[SAE ARP 1257] 08 p0996 A73-20696

Stress concentration and groove design as factors in crack failure of low power single stage gas turbine rotor disk, using optical polarization technique
09 p1157 A73-22166

Influence of a change in the throughput of the power turbine on the parameters of a dual-shaft gas turbine engine
10 p1262 A73-23599

Gas turbine engine turbine blades service life increase by Cr and Al vacuum diffusion metallization, presenting full scale endurance test results
10 p1227 A73-24965

A reappraisal of design methods for inward flow radial gas turbines.
11 p1411 A73-26370

Gas-turbine processes with interrupted expansion and interrupted compression
11 p1452 A73-26371

Turbine blades cooling effectiveness for engines gas temperature energy gain compensation
12 p1532 A73-27090

Influence of the turbine air cooling system on the characteristics of a turbojet engine during regulation of the latter
12 p1532 A73-27091

High energy ignition systems using silicon controlled rectifiers.
12 p1533 A73-27931

Gas turbine engine exhaust pollutants consisting of unburned hydrocarbons, nitric oxide, carbon dioxide, nitrogen dioxide and carbon monoxide
12 p1467 A73-27934

Nitric oxide formation in gas turbine combustors.
13 p1670 A73-28805

Superalloys processing technology for aircraft gas turbine applications, discussing developments in eutectics and powder metallurgy for increased operating temperatures
13 p1636 A73-28931

Protective coating systems for Navy aircraft turbine engines.
[NACE PAPER 113] 13 p1637 A73-29313

Study of the effect of technical factors on the fatigue limit of the working blades of gas turbine motors.
14 p1810 A73-30302

GTD-350 gas turbine engine for Soviet Mi-2 twin engine helicopter, describing compressor, combustion chamber, turbine, reduction gear, exhaust, starting, lubrication, deicing and fuel systems
14 p1785 A73-30450

Ceramics replacement for Ni-Cr superalloys to improve automotive gas turbine performance by increasing inlet temperature, considering material selection
15 p1897 A73-31250

Generalized mathematical model for gas turbine dynamic behavior simulation based on one dimensional flow theory with functional integration for rotor speed time derivative
15 p1925 A73-31629

Standard indoor method of collection and presentation of the bare turboshaft engine noise data for use in helicopter installations.
[SAE ARP 1279] 16 p2046 A73-33020

Dynamic gas temperature measurements in a gas turbine transition duct exit.
[ASME PAPER 73-GT-7] 16 p2047 A73-33485

Low emissions combustion for the regenerative gas turbine. I - Theoretical and design considerations.
[ASME PAPER 73-GT-11] 16 p2086 A73-33489

Low emissions combustion for the regenerative gas turbine. II - Experimental techniques, results, and assessment.
[ASME PAPER 73-GT-12] 16 p2086 A73-33490

Effectiveness and heat transfer with full-coverage film cooling.
[ASME PAPER 73-GT-18] 16 p2086 A73-33495

Remanufacture of jet engine compressor components.
[ASME PAPER 73-GT-43] 16 p2048 A73-33504

Welding techniques for high strength superalloy turbine blades and vanes repair, discussing controlled preheating and cooling methods for crack prevention
[ASME PAPER 73-GT-44] 16 p2019 A73-33505

Effect of 'bulk' heat transfers in aircraft gas turbines on compressor surge margins.
17 p2221 A73-34382

Market trends and technical progress in small gas turbine engines for general aviation and executive aircraft and helicopters
17 p2256 A73-34447

Parameters controlling nitric oxide emissions from gas turbine combustors.
17 p2221 A73-34474

Exhaust emissions analysis system for aircraft gas turbine engines.
17 p2146 A73-34615

Noise reduction modifications in JT3D and JT8D gas turbine engine by single stage fan replacements
[SAE PAPER 730346] 17 p2222 A73-34694

A simplified fuel control approach for low cost aircraft gas turbines.
17 p2222 A73-34725

Experimental investigation of air bearings for gas turbine engines.
[ASLE PREPRINT 73AM-2B-1] 17 p2178 A73-34981

Combustion noise prediction techniques for small gas turbine engines.
19 p2473 A73-37296

High temperature cyclic oxidation resistance tests on Ni-, Co- and Fe-base alloys for aircraft gas turbine engines
19 p2440 A73-37496

Blade synchronous rotation about pitch axis in single stage axial compressor at front of gas turbine engine during fan rotation
20 p2601 A73-39663

Trimming and checking aircraft gas-turbine engines with the aid of the ratio of total pressure behind the turbine to total pressure in front of the compressor
21 p2754 A73-40403

Trends of design in gas turbine temperature sensing equipment.
22 p2858 A73-42043

Stress concentration and groove design as factors in crack failure of low power single stage gas turbine rotor disk, using optical polarization technique
22 p2920 A73-42114

Experimental investigation of a gas-liquid thruster model with a ballasting-reinforced thrust
22 p2841 A73-42127

Utilization of semiautomatic thermocouples in gas-turbine engine tests
23 p2982 A73-43743

Determination of the temperature fields of turbine disks and blades, using irradiated diamond indicators
23 p2987 A73-44294

Low frequency noise generation within aircraft gas turbine engine core portion, discussing sources prediction, model and full scale engine tests, and future technology
[AIAA PAPER 73-1027] 24 p3122 A73-44858

Aircraft gas turbine engines with single crystal blades to avoid conventional casting grain boundary weakness and premature damage
24 p3094 A73-45155

Principal failures of turbines during turbine engine operation
24 p3122 A73-45196

GAS TURBINES

Method of calculation of the three-dimensional turbulent boundary layer up to separation - Application to a simple gas turbine case
[ONERA, TP NO. 1111] 01 p0001 A73-10233

Device signaling unsteady modes of compressor operation
02 p0166 A73-11635

Application of basic research to the study of combustion in turbine combustion chambers
[DGLR PAPER 72-058] 02 p0237 A73-11693

Hybrid fluid film and rolling element bearings for long fatigue life and gas bearings for high temperature operation in gas turbine applications
[SAE PAPER 720739] 02 p0173 A73-12005

Design study for long-lived compact 750 kW industrial gas turbine, discussing optimal aerodynamic proportioning and size determination
[ONERA, TP NO. 1174] 02 p0204 A73-12791

Inlet sound power of axial compressors.
03 p0241 A73-12956

High pressure stage efficiency of the turbines of modern turbojets
03 p0359 A73-14137

Operation modes simulation of single stage gas turbine at subcritical and supercritical gas flow, noting scale model tests
05 p0532 A73-17024

Inspection of fir-tree roots of gas-turbine rotor blades
05 p0578 A73-17025

Some observations on flows described by coupled mixing and kinetics.
06 p0767 A73-17729

Gas turbine combustion rig simulation of pollutant carbon and nitrogen oxide emissions as function of air-fuel mixing, metallic additions and chamber design
06 p0767 A73-17732

Effects of ash deposition on the fatigue strength of the working blade material in gas turbines
06 p0741 A73-18662

Investigation of the heat transfer between the gas and casing in the area of the apertures between the nozzle diaphragm blades and guide vanes of turbines
07 p0868 A73-20086

Calculation of temperature fields in cooled gas-turbine blades on a digital computer
07 p0868 A73-20099

Pressure gage performance tests for air turbine through flow static pressure measurement
07 p0824 A73-20100

Aerodynamic experimental investigation of annular cascade of gas turbine nozzle blade in subsonic and supersonic flow.
08 p0925 A73-20939

Metallurgical principle guidance of alloy design, discussing gas turbine alloys, dispersion hardened and composite alloys, high damping alloys and superalloys
08 p0979 A73-21657

French project for high speed hydrofoil marine vehicle with hydrodynamic lifting surfaces, completely submerged wings, gas turbine propulsion and automatic control
09 p1031 A73-22208

Gas turbine combustor optimization dependence on combustion length and efficiency, cutoff pressure fall, wall cooling and pollution
09 p1135 A73-22213

Computer calculation of the characteristics of multistage gas turbines
09 p1136 A73-22567

Thermal stresses in cooled gas turbine blade foils and roots with allowance for thermoelastic effects
09 p1136 A73-22568

Static tests of the working-channel cascade of a tangential turbine
09 p1028 A73-22571

Advances in directional solidification spur usage in turbine airfoil shapes.
09 p1089 A73-23293

A gas turbine stage with additional blades between the rotor waves
10 p1263 A73-24670

Joint operation of the last gas-turbine stage and a diagonal diffuser
11 p1299 A73-25050

Tests concerning the production of gas turbine blades with directionally solidified structure
11 p1372 A73-25104

Thermodynamic performance analysis of gas turbine power plants with intercooler. II - Performance of intercooling-regeneration-reheat type and precise calculation method.
11 p1411 A73-26343

Effects of prevaporized fuel on exhaust emissions of an experimental gas turbine combustor.
11 p1411 A73-26424

Temperature field in front of or behind gas turbine with additive white noise, deriving optimal filter for dynamic programming technique in random fields analysis
12 p1483 A73-27080

Investigation of the throughput capacity of the longitudinal cooling ducts of gas turbine blades
12 p1532 A73-27093

A modern mechanical laboratory for the support of aircraft engine design
12 p1486 A73-27385

Methods of simulating the thermal and stressed state at the edges of gas turbine blades

13 p1698 A73-29054

Metallurgical and strength studies of heat resisting alloys for gas turbines after long term service.

13 p1625 A73-29519

Gas flow properties in curvilinear turbine ducts, considering pressure gradient, outer flow shear and Coriolis force on boundary layer

14 p1712 A73-30649

Test data obtained with an experimental gas turbine operated with kerosene combustion products artificially contaminated by dust

14 p1785 A73-30650

Mechanism of the formation and control of pollutants due to combustion

15 p1840 A73-31225

High-temperature corrosion in gas turbines and steam boilers by fuel impurities. II - The sodium sulfate-magnesium sulfate-vanadium pentoxide system.

15 p1841 A73-32175

A method for complex design of axial-flow compressor stages at the mean streamline

15 p1925 A73-32203

A method of analytical error identification in the inspection of the working profiles of blades

16 p2019 A73-33300

Evaluation of additives for prevention of high temperature corrosion of superalloys in gas turbines.

[ASME PAPER 73-GT-1] 16 p2047 A73-33479

Reduction of nitrogen oxide emissions from a gas turbine by fuel modifications.

[ASME PAPER 73-GT-5] 16 p2045 A73-33483

Calculation of temperature distribution in multistage axial gas turbine rotor assemblies when blades are uncooled.

[ASME PAPER 73-GT-8] 16 p2047 A73-33486

The use of a finite difference technique to predict cascade, stator, and rotor deviation angles and optimum angles of attack.

[ASME PAPER 73-GT-10] 16 p1963 A73-33488

The use of a hybrid computer in the optimization of gas turbine control parameters.

[ASME PAPER 73-GT-13] 16 p2047 A73-33491

Transient analysis of ceramic vanes for heavy duty gas turbines.

[ASME PAPER 73-GT-46] 16 p2048 A73-33507

Silicon nitride materials for gas turbine components.

[ASME PAPER 73-GT-47] 16 p2048 A73-33508

Gas turbine vibration limits - A fundamental view.

[ASME PAPER 73-GT-48] 16 p2048 A73-33509

Evaluation of machinery characteristics through on-line vibration spectrum monitoring.

[ASME PAPER 73-GT-68] 16 p2048 A73-33520

Conference on Heat and Fluid Flow in Steam and Gas Turbine Plant, University of Warwick, Coventry, England, April 3-5, 1973, Proceedings.

17 p2092 A73-34376

Computerized stream-curve method for calculation velocity distribution and stream surface twist effects for three dimensional flow through gas turbine blade passage

17 p2092 A73-34378

Air/water mist spray coolant for high gas temperature and pressure environment at gas turbine inlet

17 p2221 A73-34388

Flow studies in radial inflow turbines interspace between nozzles and rotors.

17 p2093 A73-34392

Sinusoidal pulse flow through an axial flow gas turbine.

17 p2093 A73-34395

Book - Gas turbine theory /2nd edition/.

17 p2221 A73-34471

Self-acting and hydrodynamic shaft seals.

17 p2179 A73-34999

Methods of modeling thermal and stressed states in the edges of gas turbine blades.

18 p2366 A73-36886

Design for teaching aerospace engineering at Texas A & M University.

[AIAA PAPER 73-786] 19 p2505 A73-37456

Gas turbine blade effusion cooling by air blowing, determining heat transfer coefficients for laminar and turbulent boundary layer

19 p2504 A73-38156

Gas turbine nozzle guide vane trailing edge protection by air films cooling, measuring gas temperatures with chromel-alumel thermocouples

20 p2600 A73-39425

Investigation of different air-cooling methods for the first-stage disk of a two-stage gas turbine

21 p2754 A73-40397

Dimensionless pressure method to account for air density variations in gas turbine cooling system design

21 p2677 A73-41051

Combustion in high speed swirling flow in gas turbine combustion chamber, discussing flame stability, pressure measurements and chamber configuration

22 p2935 A73-42790

The prediction of the performance of variable geometry free gas turbines.

23 p3019 A73-43297

Thermodynamics of an air-cooled gas-turbine stage

23 p3019 A73-43733

GAS VALVES

Advanced technology for Space Shuttle Auxiliary Propellant Valves.

[AIAA PAPER 72-1157] 03 p0356 A73-13459

Modified poppet valve for quasisteady gas injection into vacuum.

24 p3093 A73-44813

GAS VISCOSITY

Heated Fleisch pneumotachometer - A calibration procedure.

08 p0935 A73-21509

Experimental investigation of the viscosity of cesium vapors

10 p1253 A73-23506

Viscosity of atomic hydrogen.

11 p1397 A73-25075

Viscosity coefficients and heat conductivity of dense gases with rotational degrees of freedom

15 p1915 A73-31022

Experimental investigation of the viscosity of cesium vapor.

17 p2217 A73-35186

Absolute viscosity of air down to cryogenic temperatures and up to high pressures.

19 p2422 A73-38296

Comments on the mathematical theory of small oscillations of an inviscid gas

21 p2738 A73-40191

The temperature dependence of viscosity and thermal conductivity of dilute noble gases at moderate and high temperatures.

22 p2932 A73-42504

GAS WELDING

Joining copper and copper alloys.

07 p0831 A73-20269

Book - Welding and welding technology.

17 p2177 A73-34454

Gas metal arc welding of 9% Ni steel using ferritic filler metal.

22 p2866 A73-42226

GAS-GAS INTERACTIONS

Quenching of vibrationally excited N₂ by atomic oxygen.

02 p0139 A73-12085

Book on statistical mechanics, covering thermodynamics, canonical ensembles, quantum statistics, simple gases, ensemble theory, phase transitions, cluster expansions and interacting systems

14 p1775 A73-30360

Modification of the Chapman-Enskog method for a mixture of reactive gases with allowance for fast and slow processes

19 p2462 A73-37845

Theory of nonequilibrium phenomena in chemically reacting gas mixtures

23 p2950 A73-43703

GAS-ION INTERACTIONS

Thermal energy charge transfer reactions of rare-gas ions to methane, ethane, propane, and silane - The importance of Franck-Condon factors.

02 p0195 A73-12084

Effect of ion viscosity on the stability of a finite-pressure plasma.

02 p0198 A73-12104

N₂⁺/Meinel and O₂⁺/second negative bands laser theory.

22 p2871 A73-43144

GAS-LIQUID INTERACTIONS

NT AIR WATER INTERACTIONS

Axisymmetric problem of the equilibrium of a cylindrical film under hydrostatic pressure

01 p0035 A73-11412

Optimum design of space storable gas/liquid coaxial injectors.

03 p0354 A73-13400

[AIAA PAPER 72-1076] Heat and mass transfer during the evaporation of liquids from capillary porous bodies situated in a hot air flow

12 p1559 A73-27474

Mass transfer approximation model in unidirectional swirled two phase flow, considering transfer resistance of liquid phase

14 p1816 A73-30016

Nonlinear stability of a liquid film adjacent to a supersonic stream.

14 p1711 A73-30166

Formation of a nonstationary diffusive flame front during the ignition of a liquid fuel droplet

19 p2471 A73-37507

Second-harmonic resonance in the interaction of an air stream with capillary-gravity waves.

20 p2550 A73-39816

GAS-METAL INTERACTIONS

Nitrogen thermochemistry during the combustion of zirconium droplets in N₂/O₂ mixtures.

01 p0123 A73-10922

Sintering of nonstoichiometric nickel monoxide

02 p0179 A73-11546

Simultaneous manifestation of temper brittleness and hydrogen embrittlement during low-cycle fatigue of high-strength structural steel

02 p0180 A73-11927

Hydrogen reactions and detection by line broadening in beta transformed Ti-Al-V alloy, using X ray diffraction analysis

02 p0183 A73-12759

The rate of vaporization of tungsten in argon.

02 p0183 A73-12767

High-temperature oxidation of a Ti-15Mo-5Zr alloy at low pressure of oxygen /40 microtorr to roughly 0.2 millitorr/.

03 p0321 A73-12918

Covalent bond formation role in Ti strengthening by oxygen from evidence of alpha phase stabilization, ordered structures, abnormal resistivity and high activation energy

03 p0323 A73-13371

Hydrogen self-diffusion in the niobium-zirconium-hydrogen system

03 p0327 A73-13973

Effect of hydrogen on internal friction in molybdenum

03 p0327 A73-13975

Hydrogen/proton adsorption behavior on fuel cell Pt electrode, considering surface roughness factor, Pt sites number and equilibrium data

04 p0407 A73-15104

Mechanisms and kinetics of absorption and desorption reactions in systems of refractory metals with nitrogen, oxygen or carbon.

04 p0462 A73-15302

The diffusivity and solubility of oxygen in liquid tin and solid silver and the diffusivity of oxygen in solid nickel.

04 p0463 A73-15315

The effect of noncondensable gas on laminar film condensation of liquid metals.

[ASME PAPER 72-WA/HT-9] 04 p0520 A73-15836

Cr effect on N solubility increase during Fe alloy nitriding, noting temperature effect on nitrides precipitation

06 p0697 A73-18054

The adsorption and decomposition of CO on Pt(111).

08 p0937 A73-21617

Processes determining the composition of a two-dimensional oxide film on a molybdenum surface

09 p1098 A73-21886

Features of the structure and of plastic deformation in zirconium saturated with nitrogen and oxygen

09 p1099 A73-21967

High strength TRIP /transformation induced plasticity/ steels hydrogen embrittlement susceptibility under cathodic charging, gaseous hydrogen environment and loading conditions

09 p1102 A73-22410

The mechanism responsible for luminescence of polymer films during their formation by ion-beam bombardment of solids

10 p1252 A73-24762

Diffusion aluminizing of Ni and Ni-base alloys by gas circulation method, investigating gas flow velocity effect relationship to specimen weight gain

10 p1226 A73-24957

Decomposition of carbon monoxide on a /110/ nickel surface.

11 p1325 A73-25203

Coadsorption of oxygen and carbon monoxide on tungsten - Desorption spectra, electron stimulated desorption and field emission microscopy.

11 p1325 A73-25204

Hydrogen promoted corrosion of tungsten by oxygen in an electric field A field ion microscope study.

11 p1325 A73-25205

Gaseous environments compatibility with structural alloys under fatigue loading, presenting crack growth rate data

11 p1381 A73-25816

Experimental evaluation of the role of surface reactions in studies of hydrogen penetration through titanium, nickel and copper

13 p1630 A73-28009

The interaction between two hydrogen atoms adsorbed on /100/ tungsten.

13 p1580 A73-28215

States of absorption, velocities of absorption, of desorption of oxygen on rhenium, and mechanisms of atomization and oxidation at high temperature and low pressure

13 p1580 A73-28451

Access to uncombined titanium through an inhibiting film in sublimation pumping of deuterium.

13 p1581 A73-28929

Surface solid solutions and chemical compounds formation due to gas sorption by titanium and barium

13 p1663 A73-28968

Temperature dependence of the cross section of O⁺ ion desorption by electrons from an oxygen layer adsorbed on a tungsten surface

13 p1663 A73-28969

Determination of diffusion characteristics in the boundary and volume components of a diffusing hydrogen stream in a polycrystalline metal

14 p1763 A73-30716

Catalytic effects in corrosion processes with hydrogen depolarization of multiphase magnesium alloys

14 p1764 A73-30827

Investigation of the influence of the method of supplying hydrogen to the furnace on the properties of tungsten metal

14 p1765 A73-30885

Influence of hydrogen on the failure of the VT3-1 titanium alloy in programmed cyclic loading

15 p1886 A73-31035

High strength steel fracture characteristics in vacuum and gaseous medium, noting hydrogen adsorption effect on crack resistance

15 p1887 A73-31248

The interaction of tungsten and molybdenum melts with gaseous oxygen

15 p1890 A73-31924

The interaction of gases and carbon with refractory metals

15 p1890 A73-31925

Study of gas-solid chemical interactions by the molecular beam technique. V - Reactions of oxygen and carbon monoxide with polycrystalline tantalum strips

15 p1841 A73-31970

The reaction of a titanium alloy with hydrogen gas at low temperatures.

15 p1890 A73-31993

Subscale inclusions formation in solid Fe alloys with small amounts of Mn and other elements, noting inward oxygen thermal diffusion role and metallurgical implications

15 p1891 A73-32171

Oxidizability of the IVT1 beta titanium alloy and its protection from gaseous corrosion

15 p1894 A73-32537

Oxidizability of AN-type beta titanium alloys and their protection from gaseous corrosion

15 p1894 A73-32538

Oxidation of OT4 and OT4-1 alloys in the process of prolonged heating in air at temperatures from 200 to 400 deg

15 p1894 A73-32539

Molybdenum evaporation rates in oxygen, air, and water vapor at high temperatures and low pressures

16 p2026 A73-33956

Composition of a two-dimensional oxide film on a molybdenum surface.

17 p2186 A73-34309

Composition and temperature effects on hydrogen solubility in Ni-Al liquid alloys

17 p2187 A73-34553

New methods for studying gas solid reaction kinetics using automated resistance monitoring.

17 p2175 A73-35756

The gas carrier problem during the crystallization of metals from a gas phase

18 p2323 A73-35880

Adsorption of hydrogen, carbon monoxide, and oxygen on vacuum degassed stainless steel 304 at 20 C.

19 p2402 A73-37194

Investigation of the kinetics of high-temperature aluminum/oxygen interaction by the ignition method

19 p2503 A73-37504

Influence of hydrogen and oxygen on the mechanical behavior of unalloyed titanium

19 p2441 A73-37837

Influence of hydrogen on the mechanical properties of zirconium and some of its alloys

21 p2718 A73-40483

Thermodynamics of the Al-O and Al-O-C systems

21 p2718 A73-40847

The partial molar thermodynamic magnitudes of oxygen and the nonstoichiometry of oxides - Model with interactions

21 p2791 A73-40950

Calculation of the heat resistance of metals at variable temperatures

21 p2721 A73-41230

Influence of hydrogen on the fracture micromechanism of OT4 and OT4-1 titanium alloys

21 p2721 A73-41231

Oxygen interaction with tantalum and niobium at high temperatures

21 p2722 A73-41594

Excitation of surface molecular orbitals on the 100/ face of molybdenum

21 p2722 A73-41597

Technique for measuring the diffusivity of hydrogen in titanium alloys.

22 p2878 A73-42505

Kinetics of gas absorption by refractory metals in dissociated environments - The nitrogen/tantalum system.

22 p2879 A73-42583

Microplasticizing mechanism of hydrogen embrittlement due to stress activated chemisorption, noting association with temperature dependent hydrogen-metal atomic interaction

23 p3039 A73-43465

Surface solid solutions and chemical compounds formation due to gas sorption by titanium and barium

23 p3008 A73-44320

Temperature dependence of the cross section for electron-induced O+ desorption from tungsten.

23 p3008 A73-44321

Oxygen-W/100/ surface interactions investigated simultaneously by secondary ion mass spectrometry (SIMS) and electron induced desorption (EID)

24 p3066 A73-45330

GAS-SOLID INTERFACES

Influence of roughness on the process of interaction between a rarefied gas and the surface of a solid

02 p0194 A73-11608

Isotherm data for physical adsorption of Ar on pyrex surface at low pressure, noting correlation in terms of Dubinin-Radushkevich equation

04 p0456 A73-15765

Some problems of gas-solid surface interaction.

05 p0638 A73-16177

Recent results of plasma-wall heat transfer studies in highly ionized, dense plasmas.

05 p0603 A73-16762

Solid-gas mass transfer in the case of laminar free convection

06 p0768 A73-17919

Some surface characteristics and gas interactions of Apollo 14 fines and rock fragments.

07 p0891 A73-19831

Microphysical, microchemical, and adhesive properties of lunar material. III - Gas interaction with lunar material.

07 p0892 A73-19832

Solid/vapour heat transfer in helium at low temperatures.

07 p0922 A73-20412

The kinetics of ulvöspinel reduction - Synthetic study and applications to lunar rocks.

08 p0936 A73-20840

Compound heat exchange between a high temperature gas-fluidized bed and a solid surface.

08 p1022 A73-21251

The experimental determination of wall-fluid mass transfer coefficients using plasticized polymer surface coatings.

08 p1023 A73-21261

Free molecular flow past a flat plate in the presence of a nontrivial gas-surface interaction

08 p0926 A73-21401

Hydrodynamic theory of heat transfer between a stabilized gas suspension flow and channel walls.

10 p1297 A73-24968

Gas molecule-solid surface interactions, considering rainbow scattering, roughness at molecular scale, potential well and statistical analysis procedures

13 p1663 A73-28912

Electromagnetic wave reflection and transmission by slant air/dielectric interface in rectangular waveguide investigated by Green function technique

14 p1724 A73-29706

New methods for studying gas solid reaction kinetics using automated resistance monitoring.

17 p2175 A73-35756

Thermal limit of heterogeneous ignition

19 p2503 A73-37512

Dispersion model of a single-vortex function of structural scattering of atoms by surfaces

19 p2462 A73-37842

Unique solution of boundary value problem of Boltzmann equation for unsteady rarefied gas flow of formless particles past arbitrary surface

19 p2462 A73-37843

The ignition of solid materials in oxygen by electrical sparks.

19 p2504 A73-38275

High-temperature gas-solid reactions.

19 p2403 A73-38552

Role of gas-surface interactions in the reduction of Ogo 6 neutral particle mass spectrometer data.

20 p2551 A73-38941

Law of micro-liquid-layer formation between a growing bubble and a solid surface with a special reference to nucleate boiling.

21 p2792 A73-41144

Elements of a model of oxygen interactions under low pressure with transition metals at high temperature

21 p2648 A73-41562

Reflection of a shock wave from a thermally accommodating wall - Molecular simulation.

22 p2842 A73-42234

GASDYNAMIC LASERS

Carbon dioxide-nitrogen gasdynamic lasers, predicting population inversion from numerical model of vibrational relaxation of anharmonic diatomic oscillators in supersonic expansions

07 p0834 A73-19511

A reliable high efficiency atmospheric pressure CO2 laser.

07 p0836 A73-20194

Low cost nitrogen laser design for dye laser pumping.

08 p0974 A73-21027

Directly excited subsonically flowing CW gas laser with carbon monoxide and dioxide generation as reaction products formed by organic molecule electrochemical oxidation

09 p1091 A73-22084

Lasing characteristics of flat resonator carbon dioxide-nitrogen-helium gasdynamic laser in terms of mirror reflection index, resonator length and gas pressure and composition

09 p1095 A73-22609

A high pressure gas-dynamic laser powered by a slow compression heater

[ONERA, TP NO. 1184] 09 p1096 A73-22712

Filling tests in single and double arm plenum configuration models used in gasdynamic laser systems, noting wave controlled unsteady flow processes

09 p1030 A73-23447

Gasdynamic laser with a high water vapor content.

12 p1507 A73-27510

Relaxation processes in electrically excited discharge pumped gasdynamic lasers with supersonic gas mixture flow

13 p1627 A73-28967

Time-resolved gain of a volume-excited TEA CO2 laser amplifier.

15 p1885 A73-31945

Gas dynamic lasers - A state-of-the-art survey.

16 p2022 A73-32726

Spectroscopy of the vapors of weakly volatile compounds, supercooled in a supersonic flow

16 p2038 A73-34054

Supersonic mixing nozzle for gas-dynamic lasers.

17 p2183 A73-34205

Pulsed HCN laser output power enhancement with auxiliary dc discharge, noting low gas flow rate and nonmultiple pulsing advantages

17 p2185 A73-35406

CW IR laser action in slowly flowing premixed He-air-CO mixture with simultaneous molecular excitation and carbon dioxide generation by discharge-initiated CO oxidation

17 p2186 A73-35799

Two dimensional Mach 5 supersonic nozzle configurations with hot nitrogen expansion for mixing carbon dioxide gasdynamic laser, calculating and measuring gain distribution

18 p2321 A73-36170

Aerodynamic parameters affecting practical gas dynamic laser design.

18 p2321 A73-36173

Density nonuniformities in a gas dynamic laser cavity.

18 p2321 A73-36174

Experimental studies of chemically reactive /F + H2/ flow in supersonic free jet mixing layers.

18 p2321 A73-36198

Output-power-characteristics of a CW-gasdynamic-laser.

20 p2572 A73-39224

Approximate determination of the inverted population and amplification factor of a gas expanding adiabatically in a nozzle

20 p2572 A73-39280

Effect of water vapor on output power of CO2 gasdynamic laser.

20 p2573 A73-39303

Correlation between output power and composition of discharge products in a water vapor laser.

20 p2574 A73-39698

High power carbon dioxide-nitrogen gasdynamic laser vibration kinetics model, suggesting closed cycle photon generator engine for energy conversion to work

21 p2710 A73-40094

Gasdynamic processes in obtaining inversion in shock tubes

21 p2677 A73-40696

Dependence of the output power of CO2 gasdynamic laser on the distance from nozzle throat.

22 p2869 A73-42225

Study of light amplification in a pulsed gas-dynamic laser with burning acetylene-air mixtures

23 p2988 A73-44011

Relaxation processes in electrically excited discharge pumped gasdynamic lasers with supersonic gas mixture flow

23 p2989 A73-44319

Determination of vibrational and translational temperatures in gas-dynamic lasers.

24 p3095 A73-44588

Study of the processes in a gasdynamic laser in a large-diameter shock tube

24 p3095 A73-44701

Calculation of the mode structure in the Fabry-Perot cavity of a laser with a high flow rate

24 p3095 A73-44752

GASEOUS CAVITATION

U CAVITATION FLOW

U GAS FLOW

GASEOUS DIFFUSION

NT GASEOUS SELF-DIFFUSION

A criterion for oxygen supply optimality in tissues and the capillary circulation rate

03 p0268 A73-13821

Indexes of ventilation distribution before/after airway occlusion in dogs, indicating collateral channel inspired gas distribution reduction

03 p0262 A73-14113

Diffusion freezeout in gas-loaded heat pipes. [ASME PAPER 72-WA/HT-33]

04 p0518 A73-15822

- Atmospheric dispersion of aircraft exhaust.
[AIAA PAPER 73-100] 05 p0570 A73-16860
- Theory of steady-state burning of porous propellants by means of a gas-penetrative mechanism.
[AIAA PAPER 73-221] 06 p0767 A73-17663
- Numerical study of a diffusion-type chemical laser.
07 p0836 A73-19959
- Impurity transport in a cylinder in the case of a time-dependent flow rate and gas exchange with the wall.
08 p1022 A73-20998
- Effect of diffusion on the growth and decay of acceleration waves in gases.
08 p0955 A73-21189
- Significance of the Bohr and Haldane effects in the pulmonary capillary.
08 p0935 A73-21614
- Determination of hydrogen permeation parameters in alpha titanium using the mass spectrometer.
09 p1102 A73-22412
- An approximate analysis of the diffusing flow in a self-controlled heat pipe.
[ASME PAPER 72-HT-M] 10 p1295 A73-23776
- Nb nitriding kinetics and external effects observations, noting nitrogen diffusion through crystal lattices.
10 p1236 A73-24955
- Alloy steels supercooled austenite nitriding in ammonia flow, examining diffusion layers by X ray analysis and hardness tests
10 p1236 A73-24956
- Austenitic stainless steels diffusion layer formation and structure by gaseous carburization with FeAl-ammonium chloride powder mixture, describing elements redistribution
10 p1226 A73-24958
- Ionospheric electron-ion gas distribution, allowing for diffusion, recombination and vertical drift
11 p1357 A73-26081
- KCl ionization and diffusion in premixed flames with uniform temperature and composition, studying gas velocity and photometry
13 p1707 A73-28995
- Determination of diffusion characteristics in the boundary and volume components of a diffusing hydrogen stream in a polycrystalline metal
14 p1763 A73-30716
- Determination of diffusive capacity components in lungs and of alveolar oxygen gradients for the estimation of oxygen transport conditions in lungs
14 p1719 A73-30849
- Hypoxic pulmonary steady-state diffusing capacity for CO and cardiac output in rats born at a simulated altitude of 3500 m.
14 p1720 A73-30911
- Slow motions of bodies in gas mixtures
15 p1861 A73-31198
- Correlation and prediction of gaseous diffusion coefficients.
15 p1958 A73-31998
- Certain systematic errors in determining parameters of oxygen diffusion in alpha titanium
15 p1894 A73-32540
- Diffusive motion of initially ellipsoidal plasma irregularities or ion clouds in upper atmosphere, considering space charge electric field effects
17 p2160 A73-34787
- Anelastic studies of hydrogen diffusion in niobium.
17 p2193 A73-35622
- Gas mixing during breath holding studied by intrapulmonary gas sampling.
18 p2277 A73-36651
- Effect of gas diffusion on creep behavior of polycarbonate.
20 p2580 A73-39403
- Effect of acceleration on distribution of lung perfusion and on respiratory gas exchange.
21 p2643 A73-40274
- The partial molar thermodynamic magnitudes of oxygen and the nonstoichiometry of oxides - Model with interactions
21 p2791 A73-40950
- Concerning the stability of the triple-phase boundary in gas-diffusion electrodes of fuel cells.
21 p2636 A73-41320
- A numerical diffusion model for continuous releases.
21 p2732 A73-41568
- A model of diffusion in the respiratory unit.
21 p2645 A73-41638
- Rebreathing and steady state pulmonary diffusing capacity for O₂ in the dog and in inhomogeneous lung models.
21 p2645 A73-41639
- Diffusion parameters of oxygen in alpha and beta titanium modifications
22 p2874 A73-42098
- Absorption of gas bubbles in flowing blood.
22 p2806 A73-42414
- Technique for measuring the diffusivity of hydrogen in titanium alloys.
22 p2878 A73-42505
- Rare gas diffusion studies in individual lunar soil particles and in artificially implanted glasses.
23 p3031 A73-43769

GASEOUS FISSION REACTORS

A model of the dynamic behavior of the coaxial-flow gaseous-core nuclear reactor.
23 p3005 A73-43387

On the emission coefficient of uranium plasmas.
23 p3005 A73-43388

GASEOUS ROCKET PROPELLANTS

Hydrogen-oxygen Space Shuttle ACPS thruster technology review.
[AIAA PAPER 72-1158] 03 p0356 A73-13460

GASEOUS SELF-DIFFUSION

Species separation in swirling expansion jet of gases mixture.
08 p0956 A73-21774

GASES

NT AIR
NT ARGON
NT ARGON ISOTOPES
NT CARBON DIOXIDE
NT CARBON MONOXIDE
NT COLD GAS
NT COMPRESSED GAS
NT COSMIC GASES
NT DETONABLE GAS MIXTURES
NT DEUTERIUM
NT DEUTERIUM PLASMA
NT DIATOMIC GASES
NT EXHAUST GASES
NT FLAMMABLE GASES
NT GAS MIXTURES
NT GAS STREAMS
NT GRAY GAS
NT HELIUM
NT HELIUM ATOMS
NT HELIUM FILM
NT HELIUM ISOTOPES
NT HIGH TEMPERATURE AIR
NT HIGH TEMPERATURE GASES
NT HYDROGEN
NT HYDROGEN ATOMS
NT HYDROGEN IONS
NT HYDROGEN ISOTOPES
NT HYDROGEN PLASMA
NT IDEAL GAS
NT INTERPLANETARY GAS
NT INTERSTELLAR GAS
NT IONIZED GASES
NT LIQUEFIED GASES
NT LIQUID AMMONIA
NT LIQUID HELIUM
NT LIQUID HELIUM 2
NT LIQUID HYDROGEN
NT LIQUID NITROGEN
NT LIQUID OXYGEN
NT LORENTZ GAS
NT MOLECULAR GASES
NT MONATOMIC GASES
NT NATURAL GAS
NT NEON
NT NEON ISOTOPES
NT NITROGEN
NT NONCONDENSABLE GASES
NT NONGRAY GAS
NT NONPOLAR GASES
NT ORTHO HYDROGEN
NT OXYGEN
NT OXYGEN PLASMA
NT PARA HYDROGEN
NT POLAR GASES
NT POLYATOMIC GASES
NT RADON
NT RADON ISOTOPES
NT RARE GASES
NT RAREFIED GASES
NT REAL GASES
NT RESIDUAL GAS
NT SOLIDIFIED GASES
NT TRITIUM
NT XENON
NT XENON ISOTOPES
NT XENON 129

GASKETS

Thermal conductance of gasket materials for spacecraft joints.
[AIAA PAPER 73-119] 05 p0640 A73-16875

Environmental effects on EMI gaskets.
16 p1987 A73-33153

GASP

U GLOBAL AIR SAMPLING PROGRAM

GASTROINTESTINAL SYSTEM

NT INTESTINES
Gamma time-dependency in Blaxter's compartmental model.
02 p0187 A73-12550

Electrogastric data pertinent to exposures in a pressure chamber to moderate hypoxia levels.
06 p0657 A73-17684

Study of intestinal Lactobacillus species composition during a long stay of humans in a closed space
17 p2112 A73-34239

Starch hydrolysis in man - An intraluminal process not requiring membrane digestion.
20 p2519 A73-39789

GATES [CIRCUITS]

NT THRESHOLD GATES

Integrated subnanosecond circuits with low power dissipation and few components
01 p0021 A73-11487

Investigation of surface states in the MOS system by gate controlled diode structure.
05 p0559 A73-17170

Josephson tunneling devices - A new technology with potential for high-performance computers.
06 p0735 A73-18066

The breakdown mechanism and methods for measuring breakdown voltages in insulated-gate MOS field-effect transistors
08 p0946 A73-21081

Resistive MOS-gated diode light sensor.
08 p0948 A73-21477

Complementary MOS/silicon-on-sapphire LSI technology developments, assessing impact of incorporated Al and Si gates applications on high speed and low power capabilities
10 p1259 A73-23791

A method for the assessment of the electrical stability of TTL gates
10 p1194 A73-23995

MOSFET devices with trapezoidal gates - I-V characteristics and magnetic sensitivity.
10 p1194 A73-24157

Monolithic IC digital circuits using Si planar technology with Schottky diodes in DTL and TTL gates for high computational speed
11 p1341 A73-25345

Steady state mathematical theory for the insulated gate field effect transistor.
11 p1338 A73-25789

A time-optimal response inverter.
11 p1308 A73-25981

Range-gated moving target indicator with digital filters.
12 p1469 A73-27161

Influence of gammetal on gamma-ray induced defects in MOS structures.
13 p1589 A73-28421

A two-dimensional mathematical model of the insulated-gate field-effect transistor.
13 p1590 A73-28543

Harmonic analysis of voltages and currents at the output of a frequency converter with direct coupling and artificial commutation
13 p1593 A73-28941

Multiple-fault detection in large logical networks.
13 p1588 A73-29296

The extension of self-registered gate and doped oxide diffusion technology to the fabrication of complementary MOS transistors.
13 p1595 A73-29576

Transient analysis of multiple-input integrated digital structures.
13 p1595 A73-29580

The insulated-gate field-effect transistor - A bipolar transistor in disguise.
15 p1850 A73-31372

Two-phase charge-coupled devices with overlapping polysilicon and aluminum gates.
15 p1850 A73-31373

An electronically gated gamma and X-ray calibration scheme.
15 p1879 A73-32222

Thermal noise behavior of a FET as a function of the doping profile of the gate-channel junction
16 p1988 A73-33274

Charge transfer in overlapping gate charge-coupled devices.
16 p1988 A73-33396

Gated phase locked loop tracking device for maximum likelihood estimation of pulsed sinusoid imbedded in noise, predicting phase noise performance
16 p1980 A73-33408

Fluidic component performance and circuit reliability.
16 p1971 A73-33475

Binary capacitors made with p-channel MOS Si gate technology, discussing threshold voltage effects, structural characteristics, bootstrapping and artificial voltage enhancement
16 p1991 A73-33962

Gunn-effect digital functional devices and their performance evaluation.
17 p2143 A73-35814

Capacitance of a field-effect MOS transistor gate
18 p2293 A73-36721

Versatile logic system for use in nuclear experiments on scientific satellites.
19 p2412 A73-37147

Electrical properties and simplified theory of a particular junction field-effect transistor operating with a forward gate-source bias.
19 p2409 A73-37428

A technique for gating short microwave pulses.
19 p2410 A73-38000

Threshold voltage stability improvement of p- and n-channel SNOS FET by annealing silicon nitride in oxygen or steam prior to gate deposition
19 p2471 A73-38451

Observation of turn-on action in a gate-triggered thyristor using a new microwave technique.
20 p2543 A73-39414

- Digital LC branch filter transformation with direct element /adapter/ connections, considering gate number and passband attenuation distortion
23 p2957 A73-43314
- Fluidic circuits application to stochastic computer with analog to digital converter and logic gates for arithmetic operations
23 p2944 A73-43419
- GAUGE INVARIANCE**
Gauge invariant and covariant description of plasma response to electromagnetic disturbances, deriving waves dispersion properties in arbitrary reference frame
07 p0859 A73-20234
- Quantum mechanical formalism for unitary transformations of wave functions, gauge transformations and current conservation, discussing use of gauge invariant atomic orbitals
10 p1251 A73-24245
- GAUSS EQUATION**
An 'ab initio' Gaussian orbital calculation of the /100/ surface of crystalline lithium hydride.
06 p0737 A73-18252
- Equations of motion for systems with nonlinear, second-order, nonholonomic connections
17 p2211 A73-34147
- Application of the Gauss principle in the dynamics of systems having rigid solids of variable mass as constituent elements
19 p2459 A73-37652
- The approach to thermal equilibrium in systems of coupled quantum oscillators initially in a generalized Gaussian state.
20 p2571 A73-38634
- GAUSS FUNCTION**
U GAUSS EQUATION
- GAUSSIAN DISTRIBUTIONS**
U NORMAL DENSITY FUNCTIONS
- GAUSSIAN NOISE**
U RANDOM NOISE
- GAUSSMETERS**
U MAGNETOMETERS
- GAUZE**
Flow through non-uniform gauze screens.
20 p2508 A73-39811
- GC-130 AIRCRAFT**
U C-130 AIRCRAFT
- GEAR TEETH**
The application of elastohydrodynamic lubrication in gear tooth contacts.
03 p0317 A73-14375
- Experimental investigation of undulatory multiplication gear systems
10 p1222 A73-23597
- The problem of structural analysis of a wave gear
21 p2708 A73-41198
- Helicopter transmission research.
22 p2798 A73-41750
- GEARS**
Geared fan engine systems - Their advantages and potential reliability.
[AIAA PAPER 72-1173] 03 p0357 A73-13469
- Gear and bearing designs with lubricated and reinforced thermoplastics.
10 p1223 A73-23957
- Reliability analysis of helicopter mechanical transmission components and reduction gearboxes
11 p1306 A73-26596
- Choosing the transmission ratio of position servomechanism reduction gears
12 p1460 A73-26792
- Basic principles of variable speed drives.
17 p2182 A73-35472
- GEGENSCHEN**
A photometric model of the zodiacal light.
07 p0876 A73-19359
- Imaging photopolarimeter for measuring orthogonal, sky glow and gegenschein brightness and polarization in sky mapping mode
11 p1415 A73-25177
- A photometric study of the counterglow from space.
18 p2351 A73-36182
- Photometric variability of counterglow radiance as evidence for dust cloud presence in earth-moon system region
18 p2351 A73-36183
- Observations of zodiacal light from the Pioneer 10 Asteroid-Jupiter probe - Preliminary results.
21 p2776 A73-41423
- GEIGER COUNTERS**
Russian book on elementary particle counters covering gas discharge /Geiger-Mueller/, scintillation, Cerenkov and semiconductor counters and matter-radiation interactions
15 p1880 A73-32418
- GEIGER-MUELLER TUBES**
U GEIGER COUNTERS
- GELATINS**
Certain features of sensitive layers containing bifunctional polymers /fixatives/ on a blank film
21 p2646 A73-40257
- Advantages of using polymer bases as fixing agents in hydrotype printing
21 p2646 A73-40258
- Physical nature of gelatin as polymer material, emphasizing low temperature restoration of collagen structure, supermolecular structure formation capability and glassy-elastic state transition temperature
21 p2647 A73-40265
- Silver halogenide bichromatic gelatin chemical and photographic properties, noting decelerating development effect
21 p2647 A73-40266
- Stability of silver bromide dispersions in the presence of gelatin and other surface-active substances
21 p2647 A73-40267
- Physicochemistry of the deposition of gelatinous photographic emulsion layers on a substrate
21 p2647 A73-40268
- Photographic nuclear emulsions with total replacement of gelatin by synthetic polymers
21 p2647 A73-40269
- Physico-mechanical properties and damage mechanism of moving-picture photographic materials as film systems
21 p2699 A73-40270
- GELS**
NT DOUBLE BASE ROCKET PROPELLANTS
- GEMINID METEORIODS**
Radio-echo measurements of the flux of the Quadrantid, Perseid and Geminid meteor streams.
11 p1415 A73-25169
- Positive ion composition in the lower ionosphere during the Geminid meteorshower and the occurrence of a winter anomaly.
18 p2305 A73-36005
- Micrometeoroid flux measurement during the 1970 Geminid meteor shower.
22 p2915 A73-43035
- Parameter behavior in mass distribution analysis of overdense Geminid trail radio echoes
22 p2915 A73-43041
- GENERAL AVIATION AIRCRAFT**
NT CESSNA 172 AIRCRAFT
- In-flight structural failures involving general aviation aircraft.
02 p0131 A73-12566
- Private business aircraft economic aspects, discussing costs vs time savings and indirect advantages
03 p0401 A73-13997
- Realistic pilot training and aircraft handling qualities in pilot error risk minimization for military, commercial and general aviation
05 p0545 A73-16733
- Business aircraft operational costs, considering maintenance, repair and depreciation
06 p0771 A73-17998
- General aviation requirements within National Aviation System, discussing basic services, facilities, federal spending and R and D
12 p1459 A73-27361
- Conference on General Aviation Business Flying, University of Tennessee, Tullahoma, Tenn., August 17-19, 1972, Proceedings.
13 p1570 A73-29344
- General aviation aircraft technology developments based on military and transport aircraft design, considering cost, complexity and reliability
13 p1570 A73-29348
- Multibladed shrouded fan /Q-fan/ with rotary or piston engines as propulsion system for light/medium business aircraft, noting noise and drag reduction
14 p1785 A73-29996
- The lowering of minima of third-level and business aircraft
15 p1831 A73-32476
- Status of international noise certification standards for business aircraft.
17 p2101 A73-34651
- New low-pressure-ratio fans for quiet business aircraft propulsion.
17 p2221 A73-34653
- [SAE PAPER 730288] FAA General Aviation Crashworthiness Program.
17 p2257 A73-34657
- [SAE PAPER 730293] Electric trim systems - Design and certification considerations under FAR 23.677 /CAM 3.337-2/.
17 p2101 A73-34662
- [SAE PAPER 730299] Control-configured general aviation aircraft.
17 p2101 A73-34664
- [SAE PAPER 730303] Stepped aluminum extrusions - Designing for business aircraft.
17 p2177 A73-34668
- [SAE PAPER 730308] Turbo and jet powered general aviation aircraft-borne weathering memory radar system with digital processing technique to eliminate direct view storage tube
17 p2122 A73-34674
- [SAE PAPER 730316] NASA in general aviation research: Past - present - future.
17 p2257 A73-34675
- [SAE PAPER 730317] Stall/spin studies relating to light general-aviation aircraft.
17 p2102 A73-34678
- [SAE PAPER 730320] Application of advanced control system and display technology to general aviation.
17 p2102 A73-34679
- [SAE PAPER 730321]
- The development of reciprocating engine installation data for general aviation aircraft.
[SAE PAPER 730325] 17 p2102 A73-34681
- Feasibility and optimization of variable-geometry wing for jet amphibian business aircraft.
[SAE PAPER 730330] 17 p2102 A73-34683
- Development of a low-cost flight director system for general aviation.
[SAE PAPER 730331] 17 p2167 A73-34684
- Computer aided parametric analysis for general aviation aircraft.
[SAE PAPER 730332] 17 p2130 A73-34685
- General aviation aircraft stall/spin prevention device for limiting tail power near wing stall angle of attack
[SAE PAPER 730333] 17 p2102 A73-34686
- General aviation pilot operational profile study, discussing implications for airman certification standards, flight safety regulations and aircraft design
[SAE PAPER 730334] 17 p2115 A73-34687
- Civil and military aircraft
18 p2268 A73-36689
- Trends in avionics simplification for light utility aircraft.
19 p2450 A73-37801
- An approach to the synthesis of separate surface automatic flight control systems.
[AIAA PAPER 73-834] 20 p2508 A73-38777
- Annual Corporate Aircraft Safety Seminar, 18th, Arlington, Va., April 1-3, 1973, Proceedings.
20 p2509 A73-39210
- Electric powered commercial jet aircraft emergency power supplies, discussing attitude gyros, Ni-Cd batteries, voltmeters, equipment running times, static inverters and transmitters
20 p2510 A73-39213
- Fire hazard reduction in corporate aircraft oxygen system, covering hoses, regulators, manifolds, cylinders, leakage, combustion conditions and servicing procedures
20 p2518 A73-39215
- Corporate aircraft design and operational problems, including supercritical wing and wasp-waist body design, airport private/airline interfaces, noise criteria, flight simulation and ATC
20 p2509 A73-39218
- Corporate aircraft accident analysis to reduce accident rate, examining seasonal and diurnal statistics, aircraft types, runway conditions, crew factors and maintenance defects
20 p2509 A73-39219
- Estimation of general aviation air traffic.
[ASCE PREPRINT 2041] 22 p2839 A73-42866
- GENERAL DYNAMICS AIRCRAFT**
NT CL-84 AIRCRAFT
NT F-111 AIRCRAFT
- GENERAL DYNAMICS MILITARY AIRCRAFT**
U MILITARY AIRCRAFT
- GENETIC CODE**
Russian book - Information macromolecules during radiation injury to cells.
04 p0410 A73-15707
- Genetic code evolution in terms of abiotic polynucleotide synthesis, suggesting alternating sequences of purines and pyrimidines as polypeptide codes
09 p1044 A73-23469
- Experimental models of communication at the molecular and microsystemic levels.
11 p1324 A73-25140
- Chemical protection from genetic damages induced by radiation in the period of aftereffect of acceleration.
21 p2643 A73-40815
- GENETICS**
NT GENETIC CODE
NT MUTATIONS
- Concepts related to the origin of the genetic apparatus.
03 p0265 A73-14317
- Russian book on radiation genetics of microorganisms covering lethal and mutagenic action of radiation on fungi, microscopic algae, bacteria and viruses
04 p0410 A73-15701
- Atomic, molecular, cellular, genetic, multicellular, neural, mental, social and suprasocial levels of evolution, discussing systems constituents, interactions and selective focus
06 p0651 A73-17929
- Correlational inter-relationships between the neuroendocrinal system and the genotype in the formation of protective reactions of the organism
15 p1835 A73-31875
- Gravity, weightlessness and organismic genetic structures.
18 p2269 A73-35923
- Effects of space flight factors on the heredity of higher and lower plants.
22 p2804 A73-42168
- Space flight factors effects on Drosophila development in terms of dominant, autosomal and sex-linked recessive lethals frequency, noting gametogenesis stage sensitivity
22 p2804 A73-42173

Ribonucleic acid (RNA) polymerase and adenylyl cyclase in cardiac hypertrophy and cardiomyopathy. 22 p2808 A73-42687

GENITOURINARY SYSTEM
NT TESTES

EMG from smooth musculature/uterus, ureter, gut in unrestrained animals monitored by telemetry. 03 p0271 A73-14297

GEOASTROPHYSICS
U ASTROPHYSICS
U GEOPHYSICS

GEOCENTRIC COORDINATES

Evolution of a satellite orbit under the influence of light pressure 02 p0211 A73-11777

A method of a determination of earth's motions around its mass center from simultaneous laser and photographic observations of artificial earth satellites made by two stations. 02 p0159 A73-12168

Results concerning the movement of the instantaneous pole of rotation of the earth, using the data published by R. Vicente and S. Yumi 03 p0304 A73-14580

Absolute topocentric directions and geograv coordinate system for satellite triangulation, using photographs against star background from different camera sites 04 p0436 A73-14779

Secor equatorial network evaluation of satellite geodesy program, discussing range data and geocentric coordinate computation and adjustments 04 p0437 A73-14782

Time variation of the geomagnetic main field /on the basis of spherical harmonics analyses of geomagnetic world charts for the period from 1880 to 1960/ 04 p0440 A73-15281

Substorm variations of the magnetotail plasma sheet at geocentric distances measured along the solar magnetospheric x-axis from -6 to -60 earth radii. 07 p0813 A73-19235

Computerized precession and nutation matrix calculations of rectangular equatorial coordinates with longitude and inclination allowance for radar data processing 09 p1142 A73-22092

Algorithm for locating a moving object 11 p1394 A73-26097

Determination of the relative position of points on the earth surface with the aid of satellite observations 11 p1357 A73-26294

The influence of laser ranging on selenodetic control. 21 p2774 A73-41408

GEOCHEMISTRY

NT BIOGEOCHEMISTRY

Atomic and molecular interactions investigation by computer aided mass spectrometry, considering applications in bio-organic chemistry, isotope analysis, geochemistry and cosmochemistry 02 p0139 A73-12425

Trace-element variation of individual plagioclase and hornblende phenocrysts. 04 p0414 A73-14986

The mineralogy, petrology and geochemistry of lunar samples - A review. 04 p0498 A73-15186

The origin and stability of lunar goethite, hematite and magnetite. 05 p0618 A73-16836

An experimental investigation of the significance of zirconium partitioning in lunar ilmenite and ulvöspinel. 05 p0619 A73-16838

Genetic significance of chemical, isotopic, and petrographic features of some peralkaline salic rocks from the island of Pantelleria. 05 p0570 A73-16842

The sources of phosphorus on the primitive earth - An inquiry. 06 p0651 A73-17933

Site preferences of Ni²⁺/ and Co²⁺/ in clinopyroxene and olivine - Limitations of the statistical approach. 06 p0690 A73-18268

Lunar carbon chemistry - Relations to and implications for terrestrial organic geochemistry. 06 p0662 A73-18429

Neutron activation analysis for geochemical origin and trace element compositions of moldavites and source rocks from Ries impact crater 07 p0877 A73-19652

Fra Mauro crystalline rocks - Mineralogy, geochemistry and subsolidus reduction of the opaque minerals. 07 p0880 A73-19698

Pb-204 in Apollo 14 samples and inferences regarding primordial Pb lunar geochemistry. 07 p0888 A73-19786

Allende meteorite carbonaceous phase - Intractable nature and scanning electron morphology. 07 p0900 A73-20283

Chemical composition of some Apollo 14 lunar samples. 08 p0936 A73-20841

Geochemical significance of perylene occurrence in marine sediments, discussing land organism biogenic pigment precursors and polycyclic aromatic hydrocarbon conversion 10 p1211 A73-24105

Mixed valencies and site occupancies of iron in silicate minerals from Moessbauer spectroscopy. 11 p1324 A73-25142

Advances in organic geochemistry 1971; Proceedings of the Fifth International Meeting, Hanover, West Germany, September 7-10, 1971. 11 p1325 A73-25459

C-13 nuclear magnetic resonance in organic geochemistry. 11 p1325 A73-25461

A new approach to the isolation of milligram amounts of significant geochemical compounds. 11 p1325 A73-25463

Complex mixture analysis - Geochemical and environmental applications of a compound classifier based on computer analysis of low resolution mass spectra. 11 p1326 A73-25464

Geochemistry of amino acid enantiomers - Gas chromatography of their diastereomeric derivatives. 11 p1326 A73-25469

Applications of activation analysis to geochemical, meteoritic and lunar studies. 11 p1326 A73-25800

Planetary and lunar surface color as geochemical history indicator in terms of oxidation state, solar wind access to atmosphere and planetary moisture content 12 p1541 A73-27484

Russian book - Geochemistry and cosmochemistry of inert gas isotopes. 15 p1840 A73-31585

Europium anomaly in plagioclase feldspar - Experimental results and semiquantitative model. 16 p1976 A73-32902

Ultraminiature X-ray fluorescence spectrometer for in-situ geochemical analysis on Mars. 21 p2765 A73-40241

Distribution and diagenesis of organic compounds in JOIDES sediment from Gulf of Mexico and western Atlantic. 21 p2683 A73-40562

Russian book - Chemistry of terrestrial and lunar basaltic rocks. 21 p2648 A73-41436

Organic geochemical analysis of lunar samples with emphasis on detecting biologically significant organogenic elements, projecting techniques to Mars soil analysis 22 p2803 A73-42163

Geochemical coherence between trace elements and K, P and rare earth elements in lunar soils evaluated for samples evolutionary history 23 p2951 A73-43767

GEOCHRONOLOGY
Solar system origin and variable gravitational constant theory from earth history viewpoint 01 p0101 A73-10874

The Rb-Sr age of a crystalline rock from Apollo 16. 02 p0220 A73-12483

The Angra dos Reis /stone/ mineral assemblage and the Genesis of stony meteorites. 03 p0374 A73-13797

Apollo 17 lunar surface experiments for lunar composition, structure and chronology investigation, discussing landing site and instrument selection based on prior Apollo flights 04 p0493 A73-14671

U-Th-Pb systematics in lunar highland samples from the Luna 20 and Apollo 16 missions. 05 p0618 A73-16832

Moon geochronology from U-Pb systematics applied to lunar basalt data, discussing two and three stage evolutionary models based on Pb isotope ratios 05 p0618 A73-16834

Lunar craters and exposure ages derived from crater statistics and solar flare tracks. 07 p0896 A73-19869

Trace fossils from the Nama Group, south-west Africa. 12 p1490 A73-27250

The age and petrography of two Luna 20 fragments and inferences for widespread lunar metamorphism. 13 p1675 A73-28319

Cenozoic coral and aragonitic fossil age determination by He, U, Th and Ru isotope reactivity consistency checks 13 p1609 A73-29178

Possible stratotype sequences for the basal Paleozoic in North America. 15 p1865 A73-31025

Whole rock Th-Pb age for the Masuke and Dember Divula complexes, Rhodesia. 17 p2159 A73-34519

Lunar volcanism - Age of the glass in the Apollo 17 orange soil. 17 p2230 A73-34522

North American microtektites from the Caribbean Sea and their fission track age. 18 p2354 A73-36511

Mechanical erasure of particle tracks - A tool for lunar microstratigraphic chronology. 20 p2612 A73-39713

Thermal track fading factor in Georgia tektite stratigraphy and fission track ages, noting agreement with K/Ar ages 20 p2612 A73-39717

GEOCORONAL EMISSIONS

Vela 4 Lyman-alpha observations - Evidence for an aspherical hydrogen geocorona at 18 earth radii. 04 p0492 A73-15528

Interpretation of Ogo 5 Lyman alpha measurements in the upper geocorona. 07 p0813 A73-19233

Low-intensity Balmer emissions from the interstellar medium and geocorona. 08 p1009 A73-21167

Neutral hydrogen distribution in the upper atmosphere of the earth 14 p1747 A73-29871

Investigation of the hydrogen in the upper atmosphere and geocorona from observations of the H-alpha emission line in the nightglow spectrum /Survey/ 15 p1867 A73-31267

Geocorona originated low intensity nighttime H alpha and H beta emission components from high resolution observation, considering Balmer line producing mechanism 20 p2555 A73-39433

Apollo 16 far-ultraviolet camera/spectrograph - Instrument and operations. 22 p2864 A73-43165

GEODESY

NT CELESTIAL GEODESY

Application of ultrastable oscillators to aerospace [ONERA, TP NO. 1114] 01 p0045 A73-10235

Earth satellites in resonance with the moon and the sun as objects of laser ranging - Analytical solution for their motion. 01 p0099 A73-10695

A method of a determination of earth's motions around its mass center from simultaneous laser and photographic observations of artificial earth satellites made by two stations. 02 p0159 A73-12168

The use of artificial satellites for geodesy; Proceedings of the Third International Symposium, Washington, D.C., April 15-17, 1971. 04 p0436 A73-14776

Singularity solutions to critical configurations of geodetic range networks with distributed and in plane ground stations and target satellites 04 p0436 A73-14777

Geometrical adjustment with simultaneous laser and photographic observations on the European datum. 04 p0437 A73-14781

Secor equatorial network evaluation of satellite geodesy program, discussing range data and geocentric coordinate computation and adjustments 04 p0437 A73-14782

Earth gravitational field representation via potential of simple layer in satellite geodesy applied to satellite optical observations and Doppler data 04 p0438 A73-14789

Interior point mass earth potential model for satellite geodesy, considering geoid heights, gravity anomalies and spherical harmonics 04 p0438 A73-14791

Detailed gravimetric geoid computation for U.S. area from satellite spherical harmonic and surface gravity data, comparing with astrogeodetic geoid 04 p0439 A73-14798

Geodesy information and accuracy obtainable by laser ranging from earth onto lunar retroreflector packages 04 p0495 A73-14810

Selenodesy and planetary geodesy progress review, discussing gravitational fields and topography variations, outer planets oblateness and mass determinations, lunar body tides, etc 04 p0496 A73-14813

Analysis of the accuracy of a determination of the reciprocal azimuths of a geodesic line 04 p0443 A73-15510

Determination of the mean square errors of functions of variables in uniquely determinate geodetic constructions 04 p0443 A73-15511

A method for computing the gravitational attraction of three-dimensional bodies in a spherical or ellipsoidal earth. 05 p0569 A73-16379

Spherical analysis of the geomagnetic field during the epoch of 1965 from ground data up to n = 23. I 06 p0689 A73-17545

Orbit determination by range-only data. 08 p1013 A73-21816

Relationship between the coefficients of spherical and ellipsoidal expansion of the gravity force in the case of the biaxial earth ellipsoid 11 p1352 A73-25431

Determination of the relative position of points on the earth surface with the aid of satellite observations. 11 p1357 A73-26294

Worldwide geodetic system construction by using satellites at sufficient altitude, discussing gravity waves avoidance
12 p1493 A73-27691

Earth figure theory and gravimetric measurements using satellite observations and photography
13 p1605 A73-28007

Photographic satellite observations with the Automatic Camera for Astrogeodesy.
13 p1611 A73-28150

Computational algorithm for three dimensional mixed boundary value problem for perturbing potential in earth figure theory
13 p1609 A73-29130

Simultaneous determination of chord length and direction by artificial earth satellite geodetic observations in Arctic and Antarctic regions
13 p1610 A73-29320

Earth shape determination from ellipsoidal model, comparing with spherical functions
15 p1871 A73-31798

Spherical analysis of the geomagnetic field of the 1965 epoch to $n = 23$ from ground-based data. I.
16 p2002 A73-32769

Book - Theory of the earth's gravity field.
17 p2162 A73-35148

Satellite geodesy application to earth internal structure and gravity field relationship to geomagnetism, noting magnetic secular variation correspondence with large scale mass motion
18 p2302 A73-35932

Determination of the shape of the earth's physical surface from the anomalies of the vertical gradient of gravitational acceleration
19 p2427 A73-38554

Results of latitude observations from 1948 to 1954 and analysis of the 1948-1967 latitude series obtained by the ZTF-135 instrument in Pulkovo
21 p2772 A73-41268

Results of the 1959 to 1965 six-year series of latitude observations in Blagoveshchensk
21 p2772 A73-41269

Geoeiver passive Doppler receiver precision capabilities and accuracy experience, noting portability, commercial availability, error sources enumerated and quantified
21 p2705 A73-41329

Geodetic tasks during the construction and alignment of the RATAN-600 radio telescope
21 p2675 A73-41454

Laying out the foundations for circular-mirror sections of the RATAN-600 radio telescope
21 p2675 A73-41455

GEODETTIC COORDINATES

Precision measurement of the sun's gravitational field by means of the twin probe method.
02 p0218 A73-12414

The adjustment of a spatial terrestrial net according to the method of satellite geodesy
03 p0299 A73-13257

Absolute topocentric directions and geograv coordinate system for satellite triangulation, using photographs against star background from different camera sites
04 p0436 A73-14779

Secor range observations on Geos 1 satellite in Pacific tracking network, determining station coordinates, relative positions and geodetic heights
04 p0437 A73-14783

Earth polar motion from revised station coordinates and data from additional Doppler satellite tracking stations
04 p0439 A73-14800

Spectrum of the earth's pole coordinates over the period from 1846 to 1971
10 p1274 A73-23723

Mathematical processing of measurement data in the orbital method of space geodesy
10 p1281 A73-24480

Determination of the coordinates of points in a cosmic geodetic grid by the orbital method
10 p1281 A73-24481

Analysis of the Chandler period of polar coordinates calculated by the Orlov method.
13 p1678 A73-28383

Comparison of the coordinates of the pole as obtained by classical astrometry/IPMS, BIH/ and as obtained by Doppler measurements on artificial satellites/Dahlgren polar monitoring service/.
13 p1679 A73-28390

Experience in constructing analytical planar phototriangulation grids from 1:40,000 and 1:75,000 scale aerial photographs for the preparation of 1:10,000 scale photographic maps
14 p1753 A73-30416

Approximate description of the evolution of a synchronous-satellite orbit
18 p2350 A73-36101

Spectrum of the coordinates of the earth's pole during the period 1846-1971.
18 p2355 A73-36748

Geodetic net optimal design with known configuration matrix, basin, approach on calculus of inverse matrices
22 p2847 A73-42496

GEODETTIC SATELLITES

NT GEOS 1 SATELLITE
NT GEOS 2 SATELLITE
NT GEOS-C SATELLITE
NT PAGEOS SATELLITE

Center of mass coordinates of Baker-Nunn camera tracking stations from Geos 1 and Geos 2 optical flash data
04 p0437 A73-14785

Geodetic satellite timing accuracies with Loran C, portable atomic clocks and long baseline interferometry
04 p0446 A73-14807

Accurate localization by the Geole Project satellite
05 p0623 A73-17192

Mathematical processing of measurement data in the orbital method of space geodesy
10 p1281 A73-24480

GEOS geostationary satellite experiments for dc magnetic fields, dc/ac electric fields and plasma resonances, thermal plasma, electrons and protons
12 p1499 A73-27775

GEODETTIC SURVEYS

Radio interferometry observation of extragalactic radio sources for geodetic survey of baseline between antenna sites in Massachusetts and West Virginia
01 p0039 A73-10405

Survey improvement and calibration analysis for the Air Force Eastern Test Range with Geos C.
04 p0437 A73-14786

Earth geodetic mapping with rotating torsional gravity gradiometers onboard spin stabilized satellite in low polar orbit
04 p0446 A73-14806

Airborne photogrammetric system with mapping and geodetic surveying data acquisition capability, discussing inertial navigation subsystem, terrain profile recorder and electronic distance measuring equipment
09 p1081 A73-22380

Problem of continuous survey of the earth, and kinematically correct satellite systems. II
10 p1276 A73-23882

Mathematical processing of measurement data in the orbital method of space geodesy
10 p1281 A73-24480

Optimum processor accuracy for radar altimetry for geodesy over sea, considering surface reflectivity, height variation additive noise and pointing errors
11 p1371 A73-26631

Space geodetic techniques since 1957 covering photography, radar and laser uses in satellite observations with geodetic applications
13 p1671 A73-28006

Use of a computer to design surveys made by the stereotopographic method
13 p1621 A73-29416

Geodetic control point accurate position determination by Navy navigation Doppler satellite observations with geoeiver and teletype tape
15 p1873 A73-32268

Cartographic products from the Mariner 9 mission.
19 p2480 A73-37231

The problem of continuous earth coverage and kinematically regular satellite networks. II.
20 p2603 A73-38901

Satellite borne diffused pulsed laser with scattered light detection by optical receiver on ground for applications to wide range geodetic survey
21 p2681 A73-40133

The definition of the geotectonic domains of the Southern African crystalline shield by ERTS 1 imagery and its economic importance.
21 p2685 A73-40810

Arctic-Antarctic geodetical survey program, discussing length and direction determination for lines connecting eight principal locations
21 p2685 A73-40813

Analysis of the results of the geometric satellite world network
22 p2849 A73-42589

GEOELECTRICITY

NT TELLURIC CURRENTS

Contribution to the problem of the geoelectric effects on lightning hazard
04 p0473 A73-15283

Effect of the earth's electrical properties on the characteristics of VLF wave propagation in the earth-ionosphere waveguide
05 p0550 A73-16398

Structure of the pulsations of the earth's electromagnetic field as a random function of time
06 p0689 A73-17541

The electromagnetic perturbation fields of conductivity anomalies within the earth.
06 p0690 A73-17925

Distortion corrections in geophysically traced gravitational, magnetic and geoelectric field maps, discussing automation
07 p0816 A73-19442

Charge separation induced vertical electric field calculated for wind motion periodic with height, latitude and longitude at magnetic equator, noting relationship to electrojet
09 p1074 A73-22067

VLF atmospheric measurement and geophysical analysis, discussing meteorological, geoelectric and propagation aspects
13 p1582 A73-28151

Equivalence of geoelectric cross sections in the frequency probing method
14 p1750 A73-30835

Solutions of boundary value problems of multilayer analogs of geoelectrics and hydrology.
15 p1872 A73-32040

Structure of pulsations of the electromagnetic field of the earth as a random function of time.
16 p2001 A73-32765

Distribution of electric conductivity in the mantle of the earth, according to data on secular geomagnetic field variations.
19 p2425 A73-37924

GEOFRACURES

U GEOLOGICAL FAULTS

GEOGRAPHY

NT OROGRAPHY

Russian book on aircraft natural-climatic environmental factors covering geographic region adverse effects on design, performance and maintenance
09 p1031 A73-22349

The hyperelliptical and other new pseudo cylindrical equal area map projections.
13 p1608 A73-28845

GEOIDS

Detailed gravimetric geoid computation for U.S. area from satellite spherical harmonic and surface gravity data, comparing with astrogeodetic geoid
04 p0439 A73-14798

Orbiting altimeter system feasibility for global scale geoidal mapping via satellite altimetry
04 p0439 A73-14803

Geoid equatorial section approximation by zonal spherical harmonics using axially-symmetric features
15 p1940 A73-32050

Physical relations of the asymmetric structure of the earth
24 p3088 A73-45448

GEOLOGICAL FAULTS

Experimental studies on the formation of lunar surface features by fluidization - Discussion.
10 p1280 A73-24349

Crustal movements in tectonic areas.
11 p1352 A73-25564

Ultraviolet, panchromatic, infrared and radar remote sensing of Mesabi Range/Minnesota/, discussing Precambrian rock formations, geological faults, predawn and daytime photography and vegetation patterns
20 p2561 A73-39894

GEOLOGICAL SURVEYS

Radar imagery and aerial photography for geological remote sensing applications in coastal mapping, land-form analysis, engineering and reconnaissance
06 p0667 A73-18282

ERTS-1 satellite-borne multispectral scanner photographic mapping of Israel vegetation, hydrology, geological structure, atmospheric phenomena and oceanography
17 p2162 A73-34947

The cartographic and scientific application of ERTS-1 imagery in polar regions.
18 p2306 A73-36019

An overview of geological results from Mariner 9.
19 p2477 A73-37200

Utilization of thermal infra-red ground measurements for determination of adequate surveying periods in remote sensing.
20 p2558 A73-39868

Remote sensor geological mapping of Rio Grande rift zone/Colorado/ using aerial color infrared photography for compilation of tectonic and geomorphic histories
20 p2560 A73-39893

Geological analysis of aerial thermography of the Canary Islands, Spain.
20 p2561 A73-39896

Small scale Gemini photographs of Indian regions for interpretation of tonal variations, geomorphologic, geologic and structural features and drainage patterns
20 p2561 A73-39898

Experimental design to produce visible-reflective IR ratio image from ERTS data for geological mapping of iron compounds
20 p2561 A73-39899

GEOLOGY

NT GEOCHRONOLOGY
NT GEOMORPHOLOGY
NT GLACIOLOGY
NT HYDROGEOLOGY
NT LITHOLOGY
NT LUNAR GEOLOGY
NT OROGRAPHY
NT PETROGRAPHY
NT PETROLOGY
NT PHOTOGEOLOGY
NT STRUCTURAL PROPERTIES [GEOLOGY]
NT TECTONICS
NT VOLCANOLOGY

Lower boundary of occurrence of magnetically active masses. 19 p2425 A73-37925

Expected results of hydrologic and geologic studies using ERTS imagery of the Atacama Desert, Altiplano, and Puna de Atacama, South America /Southwest Bolivia, Northwest Argentina, and Northern Chile/. 20 p2563 A73-39914

GEOMAGNETIC ANOMALIES
U MAGNETIC ANOMALIES
GEOMAGNETIC CROTCHETS
U SUDDEN IONOSPHERIC DISTURBANCES
GEOMAGNETIC EFFECTS
U MAGNETIC EFFECTS
GEOMAGNETIC EQUATOR
U MAGNETIC EQUATOR
GEOMAGNETIC FIELD
U GEOMAGNETISM
GEOMAGNETIC LATITUDE
 Latitudinal characteristics search in Pc 4 and Pc 5 micropulsations events via generalized three dimensional spectral analysis 02 p0156 A73-11737

Magnetospheric field fluctuations and the penetration of solar protons to low geomagnetic latitude. 03 p0360 A73-12891

Shallow-solar-zenith-angle control to topside ionospheric parameters. 04 p0445 A73-15636

Short period geomagnetic pulsations with gradual amplitude increase and abatement, noting latitudinal variation 07 p0816 A73-19465

Nighttime ionospheric wave propagation curves in the broadcast band 08 p0939 A73-21286

Latitudinal energy distribution of geomagnetic disturbances. 10 p1212 A73-24229

Latitudinal rotation direction daytime characteristics of Pc 5 pulsation polarization based on global magnetic observations 10 p1212 A73-24231

Geomagnetic latitude variation of cosmic radiation rates measured onboard Concorde SST prototypes, investigating solar flares 11 p1324 A73-26588

East-west asymmetry of cosmic rays at sea level at geomagnetic latitudes from 50 N to 20 S. 13 p1670 A73-28702

The values of ionospheric absorption of VLF electromagnetic waves in middle geomagnetic latitudes. 15 p1868 A73-31523

Semi-annual modulation of earth's magnetic field in the equatorial electrojet region. 18 p2311 A73-36187

Propagation curves of an ionospheric wave at night for the broadcasting range. 19 p2404 A73-37915

Latitude distribution of the regularity in F2-region irregularities. 20 p2553 A73-39132

Position of the equatorial boundary of the anomalous ionization occurrence region in relation to the planet's magnetic activity during the solar activity cycle 20 p2554 A73-39175

Determination of the wind field from the pressure field and the latitudinal effect of the geomagnetic field in the ionosphere 21 p2681 A73-40105

A comparison of the latitudinal variation of auroral absorption at different longitudes. 21 p2684 A73-40785

Location in magnetic latitude and local time of the tropical ultraviolet bands seen from Apollo 16. 21 p2684 A73-40788

Latitudinal distributions and composition of the radiation on nonclosed drift shells in the altitude range from 200 to 400 km 21 p2686 A73-40908

Geomagnetic disturbance diurnal variation /DS/ component evolution and equatorial electrojet strength changes observation during magnetic storms by globally located stations at various latitudes 22 p2844 A73-41918

Hydromagnetic gradient waves in the ionosphere 24 p3083 A73-44789

Relationship of the sporadic F2 layer with certain features of the ionosphere and magnetosphere at sub-auroral latitudes 24 p3083 A73-44792

GEOMAGNETIC MICROPULSATIONS
 Latitudinal characteristics search in Pc 4 and Pc 5 micropulsations events via generalized three dimensional spectral analysis 02 p0156 A73-11737

Three-dimensional polarization characteristics of high-latitude Pc 5 geomagnetic micropulsations. 02 p0156 A73-11738

Continuous Pc micropulsations with discrete latitude dependent frequencies in H components,

recording simultaneously at ground based magnetometer stations 02 p0157 A73-11749

A sub-class of pi 1 micropulsations associated with the diurnal transit of the neutral sheet. 02 p0158 A73-11908

Diurnal effects in pc 1 hydromagnetic whistlers - An early afternoon source model. 02 p0158 A73-11909

Spectrographic observation of quasi-periodic pc 1 micropulsation emission after geomagnetic storm associated with geotail plasma bunching in night time magnetosphere 02 p0158 A73-11918

Latitude effects on the amplitude of Pi 2 micropulsations. 02 p0159 A73-12034

The ducted propagation of PP micropulsations in the magnetosphere and PP dotting. 03 p0298 A73-12877

Propagation of Pcl micropulsations in a proton-helium magnetosphere. 03 p0298 A73-12883

Magnetic field variations at micropulsation frequencies. 03 p0303 A73-13881

Analytical study of the evolution of the normal to the wave during the magnetospheric passage of PC 1's 04 p0440 A73-15248

12.5-minute periodicity in solar proton fluxes at balloon altitude and in magnetic micropulsations. 04 p0492 A73-15527

Relation of Pc 1 micropulsations to the ring current and geomagnetic storms. 04 p0444 A73-15536

Feasibility of ground-based generation of artificial micropulsations. 04 p0444 A73-15537

Geomagnetic micropulsations within magnetosphere, investigating MHD waves and particle-wave interactions 05 p0570 A73-17051

Characteristics of spectra of pi2-type geomagnetic pulsations along the meridional profile 06 p0689 A73-17543

Irregular auroral pulsation commencement and termination times from photometric recordings compared with geomagnetic micropulsations 06 p0690 A73-17557

Fourier transformations and statistical analysis for spectral content of geomagnetic micropulsations, noting polarization sense preference 07 p0819 A73-20064

Correlation of ground-based measurements of structured Pc 1 micropulsations withOGO-V plasmopause observations. 08 p0937 A73-20652

Characteristics of hydromagnetic wave propagation in a slowly varying magnetic field /Geometrical optics approximation/ 08 p0959 A73-21294

Physical conditions in the magnetosphere and interplanetary space during the excitation of pc 1 geomagnetic pulsations 08 p0960 A73-21306

Special features of the dynamic spectrum of Pi2 type pulsations 08 p0960 A73-21307

Fine structure of Pc 1 pulsations. I - Experimental evidence. 09 p1074 A73-22068

Latitudinal rotation direction daytime characteristics of Pc 5 pulsation polarization based on global magnetic observations 10 p1212 A73-24231

Pi 2 micropulsation period and frequency correlation coefficients for planetary magnetic activity Kp index and magnitude of accompanying auroral bay 11 p1357 A73-25930

Harmonically unrelated spectral components of Pi 2 micropulsations generated by oscillations in magnetospheric tail cavities 11 p1359 A73-26711

Earth crustal conductivity structure from micropulsation activity cycle using magnetic variometer array 12 p1488 A73-26986

A magnetosonic resonator of Pc2,3 pulsations in the earth's magnetosphere 12 p1491 A73-27351

Method for determining the longitudinal conductivity of the magnetosphere from the pulsations of a Pi-2 type magnetic field 13 p1606 A73-28291

The effect of two periodic conductivity anomalies on geomagnetic micropulsation measurements. 13 p1607 A73-28622

Some results of an analysis of stable geomagnetic Pc4 pulsations at a network of stations. 13 p1608 A73-28719

Investigations of Pi2 micropulsations. I - Frequency spectra and polarisation. II - Relevance of observations to generation theories. 15 p1866 A73-31064

Pi 2 micropulsations occurrence time, morphology change with magnetic activity and source meridian shift from solar wind variations effects 15 p1866 A73-31072

Geomagnetic pulsations and micropulsation research bibliography covering January 1969 through July 1972 with theoretical and observational groupings and Pc and Pi classifications 15 p1869 A73-31759

Zonal nature of some micropulsation disturbances at the geomagnetic pole 15 p1872 A73-31897

Relationship of the Pc 3 and 4 geomagnetic pulsation period with the parameters of the interplanetary medium at the earth orbit 15 p1937 A73-31904

French monograph - Experimental study of conditions of resonance of tubes of forces of the terrestrial magnetic field. 15 p1874 A73-32594

Properties of geomagnetic Pi2 pulsation spectra along a meridional profile. 16 p2001 A73-32767

Irregular auroral pulsation commencement and termination times from photometric recordings compared with geomagnetic micropulsations 16 p2002 A73-32781

Simultaneous observations of Pcl micropulsation polarization at four low latitude sites. 16 p2008 A73-33877

Pi 2 and geomagnetic bay maximum occurrence dependence on geomagnetic time, discussing computation methods for geomagnetic time 16 p2010 A73-33922

Equatorial and auroral zone geomagnetic indices and micropulsations variations relation to 11-18keV protons occurrence in interplanetary space 18 p2345 A73-36120

Interaction between high-frequency turbulence and magnetospheric micropulsations. 18 p2352 A73-36277

Occurrence of IPDP events accompanied by cosmic noise absorption in the course of proton aurora substorms. 18 p2312 A73-36298

Characteristics of hydromagnetic wave propagation in a slowly varying magnetic field /in the approximation of geometric optics/. 19 p2425 A73-37923

Physical conditions in the magnetosphere and in interplanetary space during excitation of type Pcl geomagnetic pulsations. 19 p2425 A73-37935

Characteristics of the dynamic spectrum of Pi2 type pulsations. 19 p2425 A73-37936

Effects of local conductivity anomalies on the magnetic fields of micropulsations. I - Electromagnetic induction in the English Channel. II - Effect of subterranean conductivity anomalies. 19 p2425 A73-38012

Wave guide propagation of micropulsations out of the plane of the geomagnetic meridian. 20 p2529 A73-38937

The nature of the polarization of geomagnetic micropulsations of Pi 2 type 21 p2681 A73-40108

Periodically structured Pc 1 micropulsations during the recovery phase of intense magnetic storms. 22 p2844 A73-41913

Magnetosonic resonator of Pc2,3 pulsations in the earth's magnetosphere. 23 p2970 A73-43248

Correlation between the excitation of pi 1 and pc 1 geomagnetic pulsations and magnetospheric substorms 24 p3084 A73-44811

GEOMAGNETIC PULSATIONS
NT GEOMAGNETIC MICROPULSATIONS
 Pi 2 type geomagnetic pulsation spectra from simultaneous meridional measurements at equatorial, middle and auroral latitudes, noting secondary amplitude maximum and HF augmentation 01 p0039 A73-10414

Auroral X-ray and conjugate ionospheric absorption observations of an electron precipitation event accompanying a sudden impulse in the geomagnetic field. 02 p0157 A73-11759

Spectral analysis of geomagnetic variations to study the tidal and the storm modulation effects. 02 p0158 A73-11906

Effect of the slope of geomagnetic field lines on the field of the magnetosphere-ionosphere current system 02 p0164 A73-12458

Structure of the pulsations of the earth's electromagnetic field as a random function of time 06 p0689 A73-17541

Relationship between pi2 geomagnetic pulsations and processes in the auroral zone 06 p0689 A73-17542

Geomagnetic field perturbation by gamma quanta pulsating source, studying accompanying radio emission behavior 07 p0816 A73-19445

Short period geomagnetic pulsations with gradual amplitude increase and abatement, noting latitudinal variation 07 p0816 A73-19465

Earth electrical conductivity radial distribution effect on solar quiet day geomagnetic field variations 07 p0816 A73-19466

Modulation of auroral electron fluxes and the geomagnetic pulsations during the storm of March 8, 1970 08 p0959 A73-21291

Some statistical characteristics of the spectra of polar magnetic substorms 08 p0959 A73-21293

Energy evaluation of protons responsible for Pc 1 emissions based on sources drift determination 08 p0961 A73-21494

Earth magnetosphere pinch effect related to geomagnetic field pulsations and polar aurora luminosity fluctuations 10 p1212 A73-24228

Earth surface magnetic field intensity variations in terms of magnetospheric resonator excitation, assuming three dimensional Alfvén waves 10 p1212 A73-24230

Secular geomagnetic field variation of the epoch 1965-1970, according to observatory and satellite observations. 10 p1212 A73-24232

OGO 5 observation of ULF geomagnetic fluctuation at polar cus boundaries in terms of ionospheric drift wave and Kelvin-Helmholtz instabilities 10 p1214 A73-24744

Super-Alfvén displacement of hydromagnetic pulses in the earth's radiation belt 12 p1491 A73-27349

Relationship between geomagnetic pulsations of diminishing period and the motion of plasma discontinuities in the magnetosphere 12 p1491 A73-27350

Observation and first evaluation of geomagnetic pulsations near the polar aurora zone in connection with the occurrence of si's and ssc's 12 p1494 A73-27778

Nature of auroral emission intensity pulsations associated with geomagnetic pulsations of the P2 type. 13 p1607 A73-28706

Determination of the density of protons in the magnetosphere on the basis of observations of Pc-3 type geomagnetic pulsations 13 p1610 A73-29560

Long term observations of geomagnetic pulsations activity during various phases of magnetic storm at midlatitudes, noting regular and irregular morphological features 13 p1611 A73-29660

Daily variations of the characteristics of beating-type Pc3/Bpc3/ pulsations. 13 p1611 A73-29661

Geomagnetic pulsations and micropulsation research bibliography covering January 1969 through July 1972 with theoretical and observational groupings and Pc and Pi classifications 15 p1869 A73-31759

Study of ULF geomagnetic variations in connection with the equatorial electrojet /the Chad-Central African Republic magnetic project/ 15 p1869 A73-31760

Influence of the inclination of the geomagnetic lines of force on the field of the magnetospheric-ionospheric current system. 15 p1874 A73-32608

Structure of pulsations of the electromagnetic field of the earth as a random function of time. 16 p2001 A73-32765

Relationship between the parameters of geomagnetic Pi2 pulsations and processes in the auroral zone. 16 p2001 A73-32766

Wave polarizations of geomagnetic pulsations observed in high latitudes on the earth's surface. 16 p2003 A73-33440

Hydromagnetic waves directed by the geomagnetic field 19 p2481 A73-37337

Modulation of auroral electron fluxes and geomagnetic pulsations during the storm of March 8, 1970. 19 p2424 A73-37920

Some statistical characteristics of the spectra of polar magnetic substorms. 19 p2425 A73-37922

Worldwide distribution of geomagnetic tides. 19 p2426 A73-38104

Stratifications in the F region of the ionosphere 20 p2554 A73-39174

Position of the equatorial boundary of the anomalous ionization occurrence region in relation to the planet's magnetic activity during the solar activity cycle 20 p2554 A73-39175

Harmonic frequency content analysis from fluxgate magnetometer recorded Pi 2 pulsation spectral waveform, noting agreement with earth current spectrum 21 p2681 A73-40154

Super-Alfvén displacement of hydromagnetic pulses in the radiation belt of the earth. 23 p2970 A73-43246

Relationship between geomagnetic PDP pulsations and the motion of plasma inhomogeneities in the magnetosphere. 23 p2970 A73-43247

Plasma conductivity model of current structure of MHD waves propagating from electric dipole source in magnetosphere in relation to geomagnetic pulsations 24 p3084 A73-44805

Influence of the conductivity of the ionosphere on the pulsations of DPI and DP2 current systems 24 p3084 A73-44806

GEOMAGNETIC STORMS

U MAGNETIC STORMS

GEOMAGNETIC TAIL

Magnetopause motions at lunar distance determined from the Explorer 35 plasma experiment. 02 p0155 A73-11730

Magnetic field strength change in equatorial plasma-sphere, considering quiet ring current as equatorial sheet current extension of neutral sheet current in magnetospheric tail 02 p0155 A73-11732

On the plasma sheet contribution to the force balance requirements in the geomagnetic tail. 02 p0156 A73-11746

Magnetospheric tail plasma sheet near earth structure explained via tangential magnetic field gradient drift velocity coupling to strong pitch-angle diffusion 02 p0157 A73-11898

Consistency of fields and particle motion in the 'speiser' model of the current sheet. 02 p0157 A73-11901

A sub-class of pi 1 micropulsations associated with the diurnal transit of the neutral sheet. 02 p0158 A73-11908

Spectrographic observation of quasi-periodic pc 1 micropulsation emission after geomagnetic storm associated with geotail plasma bunching in night time magnetosphere 02 p0158 A73-11918

Auroral particle precipitation patterns from satellite observations, discussing electron and proton penetration from magnetosheath plasma and magnetotail 02 p0163 A73-12308

Interplanetary anisotropy measurements of energetic solar proton entry into geomagnetic tail by ESR0 2 satellite 03 p0362 A73-13860

Solar wind interaction with geomagnetic field, discussing magnetosphere polar cusp region and geomagnetic tail neutral sheet structure 03 p0302 A73-13871

A self-consistent theory of the tail of the magnetosphere. 03 p0302 A73-13872

Particle motion and electrostatic instabilities of geomagnetic tail and magnetopause plasma neutral sheets in relation to substorms, using Alfvén and Cowley models 03 p0302 A73-13873

Geomagnetic tail plasma sheet thinning and auroral zone negative bays development during magnetospheric substorms, suggesting auroral particles acceleration along magnetic field lines 03 p0304 A73-13887

Geomagnetic tail quantitative model with validity to beyond moon orbit, noting adequacy of representation under quiet conditions 03 p0304 A73-14590

The self-consistent geomagnetic tail under static conditions. 04 p0440 A73-14957

Magnetosphere configuration models based on open and closed field line hypotheses, discussing solar wind-magnetosphere interactions, magnetotail, sub-storm growth, flux transport, etc 04 p0441 A73-15327

Geomagnetic tail and neutral sheet origin based on geomagnetic flux diffusion through magnetopause, discussing Dungey reconnection mechanism and Kelvin-Helmholtz instability effects 04 p0441 A73-15329

Magnetospheric convection, discussing ionospheric twin vortex pattern, reconnection model for solar wind induced generation, plasmasphere response and magnetotail dynamics 04 p0442 A73-15337

Characteristics of the lunar photoelectron layer in the geomagnetic tail. 04 p0492 A73-15529

Magnetotail plasma leakage into magnetosheath during magnetospheric substorms from Vela satellites proton flux measurements 04 p0443 A73-15530

Anisotropy of low-energy solar protons at the boundary of the magnetotail. 04 p0493 A73-15544

Fluctuations in geomagnetic wake region at 500 earth radii connected with magnetotail Kelvin-Helmholtz instability, using plasma cylinder model 04 p0445 A73-15556

On the equilibrium configuration of the geomagnetic tail. 05 p0568 A73-16140

Stability of a model current sheet with finite transverse field and finite flow velocity. 05 p0568 A73-16141

Demarcation layer between magnetosphere central portion and geomagnetic tail as layer of least resistance to incident solar plasma 05 p0610 A73-17010

Theory of diurnal fluctuations of the earth's magnetic tail 05 p0620 A73-17011

Excitation of natural oscillations in the earth's magnetic tail 06 p0748 A73-17540

Influence of magnetic-field nonuniformity on the fluctuations of the plasma layer in the magnetospheric tail 06 p0690 A73-17559

Substorm variations of the magnetotail plasma sheet at geocentric distances measured along the solar magnetospheric x-axis from -6 to -60 earth radii. 07 p0813 A73-19235

Magnetosphere tail internal plasma boundary layer dynamics during substorms based on aurora data 07 p0816 A73-19463

Penetration of solar protons into the geomagnetic tail 08 p0998 A73-21276

Acceleration of charged particles in the region of the neutral line of the magnetic field 08 p0959 A73-21292

Relationship of magnetospheric substorms on the ground and in the distant magnetotail. 08 p0961 A73-21392

Two dimensional model of solar wind passage past magnetosphere, assuming hot plasma current sheath in geomagnetic tail 09 p1077 A73-22485

Interaction of the interplanetary medium with the earth's magnetosphere 09 p1146 A73-22542

Influence of pressure anisotropy on the fluctuations of the magnetospheric tail 10 p1276 A73-23884

A possible current system associated with the Sap variation. 11 p1356 A73-25910

Magnetotail model for magnetic field strength and particle drift in magnetic equatorial plane earth, using current sheet from satellite observations 11 p1357 A73-25929

Inertial magnetic field reconnection and magnetospheric substorms. 11 p1357 A73-26206

Harmonically unrelated spectral components of Pi 2 micropulsations generated by oscillations in magnetospheric tail cavities 11 p1359 A73-26711

Anisotropic contact discontinuities at magnetospheric boundary and tail from MHD space plasma data analysis, suggesting sector boundary identification in interplanetary magnetic field 12 p1528 A73-27329

Oscillations of the earth's magnetic tail in a quasi-hydrodynamics approximation 12 p1491 A73-27347

Variations of solar-wind parameters, magnetic activity, and the electron tail of the magnetosphere and of the outer radiation zone. 13 p1608 A73-28714

Instability of the current in the neutral sheet of the tail of the earth's magnetosphere. 13 p1608 A73-28715

Zonal nature of some micropulsation disturbances at the geomagnetic pole 15 p1872 A73-31897

Absorption of hydromagnetic waves in the plasma layer of the magnetospheric tail 15 p1872 A73-31902

Excitation of natural oscillations of the geomagnetic tail. 16 p2058 A73-32764

Effect of magnetic field inhomogeneity on oscillations of the plasma sheet of the magnetospheric tail. 16 p2002 A73-32783

Satellite studies of magnetospheric substorms on August 15, 1968. I - State of the magnetosphere. 16 p2004 A73-33449

A self-consistent two-dimensional approach to magnetospheric structures. 17 p2158 A73-34502

Magnetotail response to sudden changes in the interplanetary magnetic field. 17 p2158 A73-34509

The ionospheric electric field during substorms - An interpretation based on non-uniform reconnection in the geomagnetic tail. 17 p2159 A73-34512

Self consistent geomagnetic tail current sheet model described by exact analytic solution of time independent Vlasov-Maxwell equations 18 p2351 A73-36274

Synoptic survey for the neutral line in the magnetotail during the substorm expansion phase.

18 p2352 A73-36275

ULF magnetic fluctuations in the plasma sheet as recorded by the Explorer 34 satellite.

18 p2352 A73-36276

Hydromagnetic eigenoscillations in the magnetospheric tail.

18 p2352 A73-36295

Oscillations of the earth's magnetic tail

19 p2482 A73-37349

Penetration of solar protons into the geomagnetic tail.

19 p2476 A73-37905

Acceleration of charged particles in the region of the neutral line of the magnetic field.

19 p2425 A73-37921

Effect of pressure anisotropy on oscillations of magnetotail.

20 p2603 A73-38903

A mechanism for the growth phase of magnetospheric substorms.

21 p2682 A73-40157

Observational comparison with a self-consistent model of the geomagnetic tail.

21 p2691 A73-41377

Magnetotail plasma flow observation with Vela 4A oriented perpendicular to ecliptic plane, considering plasma sheet recovery relation to auroral electrojet poleward shift

22 p2844 A73-41907

Effects on the geomagnetic tail at 60 earth radii of the geomagnetic storm of April 9, 1971.

22 p2844 A73-41908

Synoptic survey of geomagnetic field neutral line formation in magnetotail during magnetic substorms noting nightside magnetosphere reconnection and associated plasma sheet behavior

22 p2849 A73-42573

Anisotropic contact discontinuities at magnetospheric boundary and tail from MHD space plasma data analysis, suggesting sector boundary identification in interplanetary magnetic field

23 p3008 A73-43227

Oscillations of the earth's magnetic tail in the approximation of quasi-hydrodynamics.

23 p2970 A73-43244

Role of the neutral sheet in the illumination of polar caps by solar protons.

24 p3086 A73-45132

Bow shock position fromOGO-5, Explorer 35 and Heos satellites observation, emphasizing shock in tail for low Mach numbers

24 p3086 A73-45136

Observation of plasma flow in the neutral sheet at lunar distance during two magnetic bays.

24 p3139 A73-45137

Collisionless magnetospheric-solar wind plasmas interactions, noting boundary stability and tail instability

24 p3127 A73-45213

GEOMAGNETICALLY TRAPPED PARTICLES U RADIATION BELTS GEOMAGNETISM

Numerical solution for propagation of longitudinal waves along the geomagnetic field using a three-fluid ionosphere model.

01 p0016 A73-10197

Radio wave propagation effects in a three-dimensionally inhomogeneous magnetoactive ionosphere

01 p0016 A73-10204

Response of the ionosphere to the spectrum of acoustic-ionic waves emitted by a localized impulse source in space - Application to suddenly arising geomagnetic storms

01 p0035 A73-10327

A two-component model of the annual line in the spectrum of the geomagnetic field.

01 p0036 A73-10331

Airglow 6300 A emission predawn enhancement amplitude variation with geomagnetic and solar activity

01 p0037 A73-10347

Observation of low-charge low-energy geomagnetically forbidden particles.

02 p0155 A73-11726

Effects of the secular magnetic variation on the distribution function of inner-zone protons.

02 p0155 A73-11731

Satellite observations of energetic heavy ions during a geomagnetic storm.

02 p0204 A73-11733

Earth atmosphere He isotopes abundance based on calculation of ionization rates and solar wind interaction during geomagnetic dipole reversal

02 p0156 A73-11741

Infinite set of velocity fields to describe geomagnetic field lines and interpret discrepancy in plasma sheet motion observations during substorms

02 p0157 A73-11754

Non-dipole terms in the magnetic fields of Jupiter and the earth.

02 p0212 A73-11897

Relationship between the various indices of geomagnetic activity and the interplanetary plasma parameters.

02 p0159 A73-12033

Geomagnetic control over evolution of F2-layer at sunrise.

02 p0159 A73-12183

Horizontal and vertical drift motions in F 2 region caused by electrostatic and geomagnetic fields

02 p0162 A73-12294

The international magnetospheric study 1975-1977 - Scientific fundamentals and objectives.

02 p0164 A73-12313

Effect of the slope of geomagnetic field lines on the field of the magnetosphere-ionosphere current system

02 p0164 A73-12458

MHD equations for velocity distribution of magnetic field motion in conducting fluid, noting evolution equations of geomagnetic field

02 p0164 A73-12555

Extensive air showers radio emission polarization, spatial distribution and electric field strength, noting geomagnetic mechanism effect

02 p0209 A73-12672

Geomagnetic field variations caused by changes in the quiet-time solar wind pressure.

03 p0298 A73-12885

Magnetic horizontal component variations on quiet days, suggesting effect of electric field reversal at equatorial electrojet ionospheric region

03 p0299 A73-12949

Wavelike structure of magnetic field-aligned irregularities detected by phase interferometry.

03 p0300 A73-13696

Geomagnetic indexes Kp, ap, AE and Dst computation, interpretation, reliability and use in statistical studies of solar-terrestrial interactions

03 p0301 A73-13708

Recent satellite measurements of the morphology and dynamics of the plasmasphere.

03 p0301 A73-13709

Inferring the interplanetary magnetic field by observing the polar geomagnetic field.

[AD-755684] 03 p0373 A73-13712

Mechanisms for the injection of protons into the magnetosphere.

03 p0362 A73-13858

A self-consistent theory of the tail of the magnetosphere.

03 p0302 A73-13872

Solar activity and the variations of the geomagnetic K sub p-index. I.

03 p0378 A73-14422

Nonoriented astronomical satellite attitude determination from onboard measurements of geomagnetic field and stellar luminosity

03 p0379 A73-14560

Observations of ionospheric electron content at medium latitude geomagnetically conjugate stations.

04 p0440 A73-14955

Time variation of the geomagnetic main field /on the basis of spherical harmonics analyses of geomagnetic world charts for the period from 1880 to 1960/

04 p0440 A73-15281

Magnetospheric field distortion relation to ring currents based on satellite-borne magnetometer measurements of magnetic field topology

04 p0442 A73-15338

Two substorm studies of relations between westward electric fields in the outer plasmasphere, auroral activity, and geomagnetic perturbations.

04 p0444 A73-15545

K indices measurements at antipodal earth surface observatories for aa indices, discussing one hundred year series

04 p0444 A73-15547

Line existence in H component magnetic power spectra of geomagnetic field LF components

04 p0445 A73-15552

Magnetically coupled transport of a cold plasma in the outer ionosphere at low latitudes.

05 p0567 A73-16094

Ionospheric double layer theory extended to conditions including gravity and expansion effects in diverging geomagnetic flux tubes

05 p0568 A73-16145

Certain states of rotation of a magnetized spin-stabilized satellite in the geomagnetic field

05 p0627 A73-16291

Equatorial coronal arches and geomagnetic disturbance.

05 p0621 A73-17037

ESRO 1A satellite-borne Langmuir probe measurement for anisotropy in ionospheric thermal electron temperature relative to geomagnetic field

05 p0571 A73-17053

ELF signal generation by solar protons observed via tape recording of north-south horizontal geomagnetic field variations in 3-75 Hz resonance range

05 p0571 A73-17064

Book - Geophysics 3. Part 4.

06 p0688 A73-17501

Radiation belt buildup from particles moving in magnetic field applied to terrestrial inner belt characteristics, considering extraterrestrial belts

06 p0741 A73-17503

Magnetospheric plasma waves propagation effects on rapid geomagnetic field variations, noting magnetic pulsations and ionospheric propagation

06 p0747 A73-17504

Structure of the pulsations of the earth's electromagnetic field as a random function of time

06 p0689 A73-17541

Anomaly configuration maps showing westward drift and positions of residual geomagnetic fields and eccentric dipoles during 1885-1965 period

06 p0689 A73-17544

Spherical analysis of the geomagnetic field during the epoch of 1965 from ground data up to $n = 23$.

06 p0689 A73-17545

Geographic distribution of anomalies of residual geomagnetic field derived from eccentric dipole and observed field comparing with thermal flux fields and geotectonic features

06 p0689 A73-17546

Speed of propagation of shock waves responsible for geomagnetic storms and Forbush decreases

06 p0689 A73-17548

Possibility of experimentally dividing a variable magnetic field into poloidal and toroidal components

06 p0690 A73-17561

The null magnetic field as reference for the study of geomagnetic directional effects in animals and man.

06 p0658 A73-18033

Seasonal variations in the solar and lunar daily geomagnetic variations.

07 p0813 A73-19024

Drift shell splitting and magnetic equator surface topography model based on charged particle adiabatic motion and trapping in presence of internal geomagnetic multipoles

07 p0813 A73-19236

Solar cosmic rays spectrum and geomagnetic cut-off rigidity determination from ion production rates in lower ionosphere

07 p0870 A73-19427

Distortion corrections in geophysically traced gravitational, magnetic and geoelectric field maps, discussing automation

07 p0816 A73-19442

DR ring current belt formation due to electron and proton gradient drift in inhomogeneous geomagnetic field, calculating charged particles trajectories

07 p0816 A73-19446

Harmonic analysis of solar wind geometry and geomagnetic activity levels during even and odd cycles based on cosmic ray intensity variations for 1900-1969 period

07 p0870 A73-19451

Magnetospheric quasi-stationary pinch effect and filamentary structure due to electron streams parallel to geomagnetic field lines

07 p0816 A73-19464

Eccentric geomagnetic dipole drift field as function of time dependent parameters, calculating potential components in spherical coordinates

07 p0817 A73-19467

Intrinsic bandwidth of cyclotron resonance in the geomagnetic field.

07 p0792 A73-19532

Estimation of the precision of presentation of gravimetric, magnetic and other geophysical and experimental data.

07 p0817 A73-19542

Mathematical models of the earth's magnetic field.

07 p0818 A73-20030

Lunar and solar geomagnetic tides in declination at Alibag.

07 p0819 A73-20055

Mid-latitude winter anomalies in radio absorption and stratospheric temperature distribution - Observations concerning the influence of auroral and magnetic activity.

07 p0819 A73-20058

Magnetic irregularities in interplanetary space and geomagnetic activity.

08 p1007 A73-21004

The possibility of disappearance of the earth's magnetic field during inversion

08 p0958 A73-21275

Identification of discontinuities at the magnetosphere boundary

08 p0958 A73-21277

Distribution of electrical conductivity in the earth's mantle from data on the secular variations of the geomagnetic field

08 p0959 A73-21295

Lower boundary of the occurrence of magnetoactive masses

08 p0959 A73-21296

Analytical description of the geomagnetic field of past epochs and the determination of the magnetic-wave spectrum in the earth's core

08 p0959 A73-21297

Earth crust inhomogeneities from high altitude aeromagnetic survey, noting informativeness loss increase with height

08 p0960 A73-21308

Pulsed magnetic system /terrella/ for model of earth radiation belts and geomagnetic field-solar wind interaction

08 p0960 A73-21309

Geomagnetic field optimal model with expansion of spherical harmonic series by least squares method

08 p0960 A73-21353

- Geomagnetic storms and wintertime 300-mb trough development in the North Pacific-North America area. 08 p0961 A73-21384
- Summary of daily observational results of solar phenomena, cosmic ray, geomagnetic variation, ionosphere, radio wave propagation and airglow during October 1969 through December 1971. 08 p0961 A73-21393
- Influence of eddy currents on the rotation and orientation of an asymmetric artificial earth's satellite 08 p1014 A73-21547
- Evening/forenoon asymmetry in the 27-day oscillation of the low-latitude magnetic field. 09 p1076 A73-22140
- Mode coupling importance in midlatitude nonblanketing sporadic E layers from observations of ordinary and extraordinary blanketing frequencies 09 p1076 A73-22142
- Residual geomagnetic field from the satellite Cosmos 49. 09 p1076 A73-22192
- Response to critiques of paper on earth core paradox consisting of stratification inhibition on outer core fluid circulation needed for dynamo theory of geomagnetic field generation 09 p1077 A73-22193
- Oscillation of the earth's inner core and its relation to the generation of geomagnetic field. 09 p1077 A73-22194
- Effect of geomagnetic activity on occurrence of whistler atmospherics. 09 p1077 A73-22373
- Catalog of geomagnetic activity indices for the years 1841-1864 and 1870 09 p1077 A73-22543
- Field-aligned currents between 400 and 3000 km in auroral and polar latitudes. 09 p1078 A73-22834
- Cosmic ray, solar activity, supernova outbursts and geomagnetic field effects on atmospheric C-14 concentration 10 p1266 A73-23911
- Sporadic ionization of the ionospheric E-region at high latitudes as a function of magnetic activity. 10 p1212 A73-24221
- Nature of the drift of the main eccentric geomagnetic dipole. 10 p1212 A73-24233
- Possibility of determining the secular variation of geomagnetic field components from the distribution of variations of the absolute value of the total vector. 10 p1212 A73-24234
- Spherical analyses of the main geomagnetic field in 1550-1800. 10 p1212 A73-24235
- Effects of interplanetary magnetic sector structure on auroral zone and polar cap magnetic activity. 10 p1213 A73-24730
- Field-aligned ionospheric E-region irregularities and sporadic E. 10 p1191 A73-24897
- A diffusion model for the electron density distribution along the earth's magnetic field in an F-region plasma cloud. 11 p1354 A73-25768
- Geomagnetic field polarity reversal mechanism, interpreting frequency distribution by energy exchange between dynamo models and conversion between kinetic and magnetic energies 11 p1355 A73-25792
- Nonlinear resistive boundary layer in rotating hydromagnetic flow related to earth dynamo theory, discussing steady solution uniqueness and numerical temporal stability 11 p1355 A73-25794
- Precise calculation of the magnetosphere surface for a tilted dipole. 11 p1421 A73-25923
- Plasma research in space and in the laboratory. 12 p1526 A73-26849
- Measurement of geomagnetic cutoff rigidities and particle fluxes below geomagnetic cutoff near Palestine, Texas. 12 p1533 A73-26978
- Low energy auroral electron pitch angle diffusion in postbreakup aurora due to injected particle loss in closed magnetic field lines 12 p1488 A73-26987
- Daily variation of geomagnetic field at the Indian stations under the electrojet during the period of the July 1966 proton flare. 12 p1534 A73-26998
- Solar radiation effects on terrestrial electromagnetic environment, considering interplanetary space, earth internal structure, geomagnetism, upper atmosphere, dynamo action, energetic particles and magnetospheric storms 12 p1538 A73-27053
- The growth and decay of the main phase of the September 21-23, 1963 magnetic storm. 12 p1490 A73-27275
- Magnetosphere boundary location relationship to geomagnetic activity level and solar activity cycle during 1963-68 based on theoretical model 12 p1491 A73-27348
- Magnetovariational frequency sounding of the earth, using the ratio of magnetic potentials 12 p1491 A73-27352
- Spherical harmonic analysis of the geomagnetic field during the epoch 1965.0 up to $n = 23$ from ground data. II - Results 12 p1491 A73-27353
- Cosmos 321 geomagnetic measurement data for construction of satellite geomagnetic survey and geomagnetic field models 12 p1491 A73-27359
- Heat flow from earth core to mantle, discussing geomagnetic field generation by adiabatic MHD circulation of outer core and core-mantle interfacial temperature gradients 12 p1492 A73-27482
- On the variation of the coronal lambda-5303 intensity relative to the interplanetary and solar magnetic sector structure, and to geomagnetic activity. 12 p1542 A73-27615
- Space distribution of the intensity of excess radiation at low altitudes. 12 p1535 A73-27637
- Nonadiabatic condition effects on ultrarelativistic electron energy losses in geomagnetic trap in remote magnetosphere regions 12 p1535 A73-27649
- Analogies between substorm phenomena of the visual polar aurora and the radio aurora 12 p1493 A73-27757
- Determination of the effect of electric fields on the ionosphere, based on the behavior of the F2-layer above geomagnetically conjugate points 12 p1493 A73-27760
- Solar-terrestrial relations in the retrospective world interval from July 26 to August 14, 1972 12 p1535 A73-27766
- Geomagnetic disturbance recurrence interval correlation with long term sunspots rotation period 12 p1494 A73-27771
- Earth main magnetic field description by cartography and analytic methods based on dipole or spherical harmonic series representations 13 p1608 A73-28713
- Polar cap E layer conductivity difference effects on ring currents associated with vertical current along lines of force at conjugate points 13 p1608 A73-28717
- Geomagnetic storm families, direction of the interplanetary magnetic field, and solar activity. 13 p1608 A73-28718
- The Ze field, some of its properties, and geophysical information. 13 p1608 A73-28720
- Threshold of appearance of anomalous resistance for field-aligned currents in the magnetosphere. 13 p1608 A73-28726
- Magnetic anomalies in New Guinea-New Zealand region from proton magnetometer measurements, noting effects of andesite-basalt volcanic processes and nuclear precession signal variations 13 p1608 A73-28727
- Cometary brightness variations and conditions in interplanetary space. 14 p1789 A73-29779
- Polar cap magnetic variations and their relationship with the interplanetary magnetic sector structure. 14 p1747 A73-29959
- Correspondence of solar field sector direction and polar cap geomagnetic field changes for 1965. 14 p1747 A73-29960
- Least squares method for geomagnetic potential transformation in spherical offset inclined dipole coordinates with Schmidt coefficients 14 p1749 A73-29982
- Average high latitude magnetic field: Variation with interplanetary sector and with season. I - Disturbed conditions. 15 p1866 A73-31073
- Choice of a zero approximation of the angular position of a satellite on a trajectory segment of oriented motion in the case of a dipolar approximation of the geomagnetic field 15 p1942 A73-31237
- The problem of choosing a zero approximation of the angular position of an oriented satellite in the case of a nondipolar approximation of the geomagnetic field 15 p1942 A73-31238
- Geomagnetically calm intervals and their forecasts. 15 p1868 A73-31521
- Diurnal variations of the vertical component of the magnetic field in high latitude regions as a function of the east-west component of the interplanetary magnetic field 15 p1868 A73-31570
- The field levels near midnight at low and equatorial geomagnetic stations. 15 p1869 A73-31758
- Geomagnetic variations total field confinement described by Parkinson, discussing primary and secondary fields Maxwell equations linear relationship by induction tensor 15 p1871 A73-31777
- The perturbation of alternating geomagnetic fields by discontinuities with high conductivity contrasts. 15 p1871 A73-31780
- Interaction of the geomagnetic field with the antiparallel solar-wind field 15 p1926 A73-31891
- Separation of the variable geomagnetic field into normal and anomalous components 15 p1872 A73-31896
- Influence of the inclination of the geomagnetic lines of force on the field of the magnetospheric-ionospheric current system. 15 p1874 A73-32608
- Structure of pulsations of the electromagnetic field of the earth as a random function of time. 16 p2001 A73-32765
- Anomaly configuration maps showing westward drift and positions of residual geomagnetic fields and eccentric dipoles during 1885-1965 period 16 p2002 A73-32768
- Spherical analysis of the geomagnetic field of the 1965 epoch to $n = 23$ from ground-based data. I. 16 p2002 A73-32769
- Geographic distribution of anomalies of residual geomagnetic field derived from eccentric dipole and observed field, comparing with thermal flux fields and geotectonic features 16 p2002 A73-32770
- Propagation velocity of shock waves causing geomagnetic storms and Forbush decreases. 16 p2002 A73-32772
- Possibility of experimental separation of the variable geomagnetic field into a poloidal and a toroidal part. 16 p2002 A73-32785
- Geomagnetic effects on cosmic ray cut-off daily, seasonal and secular variations, considering north-south symmetry and magnetospheric models 16 p2055 A73-33297
- Electric coil systems for magnetic field simulation, discussing field size and characteristics and coil configurations 16 p1997 A73-33383
- Magnetic field of a horizontal current above a conducting earth. 16 p2004 A73-33448
- Satellite studies of magnetospheric substorms on August 15, 1968. II - Solar wind and outer magnetosphere. 16 p2004 A73-33450
- Quiet time magnetospheric field depression at 2.3-3.6 earth radii. 16 p2005 A73-33464
- Sudden disappearance of Es-q and the reversal of the equatorial electric fields. 16 p2008 A73-33879
- A search for periodic variations in geomagnetic activity and their solar cycle dependence. 17 p2157 A73-34073
- Periodic variations in geomagnetic activity and sector structure of the interplanetary magnetic field. 17 p2157 A73-34075
- Interplanetary magnetic field and geomagnetic Dst variations. 17 p2158 A73-34507
- The compensation method for measuring the components of the earth's magnetic field. 17 p2159 A73-34750
- Dynamo theory of earth magnetic field generation, discussing earth core characteristics, electromagnetic induction processes and magnetic field energy sources 17 p2162 A73-35049
- Digital data acquisition and processing from a remote magnetic observatory. 17 p2175 A73-35667
- Solar energy cycle and its relation to geomagnetic activity. 17 p2236 A73-35777
- Satellite geodesy application to earth internal structure and gravity field relationship to geomagnetism, noting magnetic secular variation correspondence with large scale mass motion 18 p2302 A73-35932
- The southern boundary region of the winter anomaly in ionospheric absorption in winter 1971/72 observed on board the cargo vessel 'Hanau' of Hapag-Lloyd moving between 10 deg and 55 deg N. 18 p2305 A73-36002
- Control laws of magnetic attitude stabilization systems of earth satellites 18 p2359 A73-36103
- Periodic variations of the cosmic radiation. III - The 27-day variation. 18 p2345 A73-36180
- On solar wind interaction with the earth's magnetosphere. 18 p2346 A73-36184
- Solar wind interaction with the earth's magnetic field. I - Magnetosheath. 18 p2346 A73-36270
- Solar wind interaction with the earth's magnetic field. II - Magnetohydrodynamic bow shock. 18 p2346 A73-36271

Solar wind interaction with the earth's magnetic field. III - On the earth's bow shock structure.

18 p2346 A73-36272

Sector boundary geomagnetic activity average Kp elevation relationship to southward component of interplanetary field, suggesting magnetosphere role

18 p2347 A73-36292

Ionospheric magnetic field measurements at auroral latitudes.

18 p2313 A73-36647

The sporadic E layer and the variation of the geomagnetic field

18 p2313 A73-36650

Magnetic measurements in laboratory model tests of solar wind-geomagnetic field interactions

19 p2481 A73-37338

Solar wind-geomagnetic field interaction simulation by plasma flow and magnetic dipole, proving collisionless dissipation presence

19 p2481 A73-37339

Plasma acceleration techniques in space studies, discussing simulation experiments, solar wind-geomagnetic field interaction and astronomical models

19 p2482 A73-37355

Identification of discontinuities at the magnetosphere boundary.

19 p2424 A73-37906

Distribution of electric conductivity in the mantle of the earth, according to data on secular geomagnetic field variations.

19 p2425 A73-37924

Lower boundary of occurrence of magnetically active masses.

19 p2425 A73-37925

Analytical description of the geomagnetic field of past epochs and determination of the spectrum of magnetic waves in the core of the earth.

19 p2425 A73-37926

Earth crust inhomogeneities from high altitude aeromagnetic survey, noting information loss increase with height

19 p2425 A73-37937

Pulsed magnetic system /terrella/ as earth model with dipole magnetic field for laboratory simulation of geophysical phenomena

19 p2425 A73-37938

Observations of ionospheric storms at low latitudes and their correlation with magnetic field changes near the magnetic equator.

19 p2425 A73-38011

Protonospheric columnar electron content determination. I - Analysis.

19 p2426 A73-38017

Effect of the solar wind on geomagnetic activity

19 p2476 A73-38154

Structure of vortical motion systems in the ionosphere that generate Sq variations of the geomagnetic field

20 p2553 A73-39153

Correlation of variations in the horizontal component of the geomagnetic field with drift in the ionosphere

20 p2553 A73-39154

Ionospheric inhomogeneity parameters and geoelectromagnetic field variations

20 p2553 A73-39156

Geomagnetic field effects in Martin theory of radio wave propagation in ionosphere with oblique and vertical signal incidence

20 p2555 A73-39181

A geomagnetic variation anomaly across the northern Gulf of California.

21 p2678 A73-39927

Anomalies in geomagnetic variations across the central Gulf of California.

21 p2679 A73-39928

Dynamo theory for geomagnetic field, emphasizing fluid flow symmetric and asymmetric velocity component relative magnitudes

21 p2679 A73-39930

Cosmic ray albedo neutron decay injection theory for proton belt, considering radial diffusion, atmospheric losses, geomagnetic models, atmospheric density, etc

21 p2755 A73-40071

Atomic oxygen and helium concentrations variation at 120 km in thermospheric composition models, discussing association with geomagnetic activity

21 p2679 A73-40074

Russian book - Certain problems concerning solar-terrestrial links and physics of the atmosphere.

21 p2730 A73-40102

Differences between geomagnetic storms with gradual and sudden commencements

21 p2681 A73-40103

Midlatitude F 2 layer critical frequency fluctuations as ionosphere disturbance criteria during magnetically quiet days

21 p2681 A73-40104

Solar atmosphere and ionosphere phenomena in terms of conducting gas motion at magnetic field neutral points

21 p2681 A73-40106

Counter equatorial electrojet currents in the Indian zone.

21 p2682 A73-40162

Sunspot activity, flare observation, electromagnetic and magnetic disturbances, auroral activity and solar radio bursts in March and April 1973

21 p2767 A73-40567

Geomagnetic field, cosmic rays, and radiocarbon content in the earth's atmosphere

21 p2756 A73-40585

Satellite counting of excess radiation measured as ionospheric electron and proton intensity dependent on geomagnetic activity, discussing proton energy spectra and electron albedo

21 p2758 A73-40604

Limit of the region of low-energy solar proton irruption into the polar ionosphere

21 p2758 A73-40607

Exospheric and thermospheric structure variations with solar activity, diurnal variation, geomagnetic activity, seasonal-latitudinal variations of He, H and density waves

21 p2683 A73-40630

Geomagnetic variation terms neglect in Chapman-Miller method, noting Bartels-Johnston method comparison and possible consequences for lunar tides

21 p2684 A73-40780

The upward propagation of LF waves /electron whistlers/ into the ionosphere and the turning of the Poynting vector towards the earth's magnetic field.

21 p2654 A73-40782

Book on cosmic ray effective cut-off rigidities calculations in dipole and geomagnetic fields, using trajectory calculations of penumbra function

21 p2760 A73-40805

Characteristic features of the solar diurnal variation according to data obtained by magnetic observatories in Kazakhstan

21 p2686 A73-40846

A study of geoelectro corpuscles and photoelectrons on the Cosmos 261 satellite. VI - Epithermal electrons in the energy range from 30 to 150 eV in the region of the dayside and nightside polar cusps

21 p2686 A73-40909

Complex studies of corpuscular radiation in the upper atmosphere at midlatitudes during geomagnetic perturbations

21 p2760 A73-40918

The determination of ionospheric charged particle temperatures from in situ measurements.

21 p2690 A73-41362

Field aligned electron anisotropies observed by the ESRO 1 A /Aurora/ satellite.

21 p2691 A73-41370

Secular geomagnetic variation consequences for steady state inner zone of energetic protons, discussing minimum altitude decrease and mirror point field magnitude increase

21 p2761 A73-41375

Rotation of the earth's magnetic field.

21 p2692 A73-41641

Solar cycle control in the 27-day variation of geomagnetic activity.

22 p2846 A73-41945

Some statistical characteristics of sudden ionospheric disturbances, and the distribution of geoelectrochromospheric flares over the solar disk

22 p2847 A73-42326

Particle streams along the force lines of a magnetic field in a multicomponent ionospheric plasma in the presence of longitudinal currents

22 p2892 A73-42329

A meteorological and a geophysical example of the use of the scale autocorrelation coefficient to determine ratios of frequencies present in periodic phenomena.

22 p2883 A73-42542

Synoptic survey of geomagnetic field neutral line formation in magnetotail during magnetic substorms noting nightside magnetosphere reconnection and associated plasma sheet behavior

22 p2849 A73-42573

Electron precipitation caused auroral zone bremsstrahlung X rays classification with respect to magnetic storm phases

22 p2851 A73-42750

Magnetosphere boundary location relationship to geomagnetic activity level and solar activity cycle during 1963-68 based on theoretical model

23 p2970 A73-43245

Frequency magnetovariational sounding of the earth, using the ratio of potentials.

23 p2970 A73-43249

Spherical harmonic analysis of the geomagnetic field for the 1965 epoch up to $n = 23$ according to ground-based data. II - Results.

23 p2971 A73-43250

Cosmos 321 geomagnetic measurement data for construction of satellite geomagnetic survey and geomagnetic field models

23 p2971 A73-43259

Atmospheric oscillations. V - The propagator matrix and the transmission of an electrostatic potential along the geomagnetic field lines.

23 p2971 A73-43686

A magnetospheric field model incorporating theOGO 3 and 5 magnetic field observations.

23 p2972 A73-43693

Rocket-borne magnetometer measurement of magnetic field changes associated with electron density fluctuations and wind structure, testing wind shear theory of sporadic E formation

23 p3024 A73-43701

An analytical expression for the secular variation of the geomagnetic field and a comparison of the activity of secular variations with some astronomical phenomena

23 p2973 A73-43793

Relativistic electron belt formation mechanism hypothesis based on Cosmos 137 data on electron intensity near geomagnetic shell L equal to 2.8

24 p3124 A73-44808

Spherical harmonic analysis of geomagnetic and gravitational field correlation, showing longitudinal shift in magnetic field pattern over six epochs

24 p3084 A73-44812

Theory of the polarisation of the ordinary wave reflected from the ionosphere in the limit of vertical incidence and vertical magnetic field.

24 p3069 A73-45202

Dispersion characteristics of whistler atmospherics during higher geomagnetic activity.

24 p3088 A73-45365

GEOMETRICAL HYDROMAGNETICS U MAGNETOHYDRODYNAMICS GEOMETRICAL OPTICS U OPTICS GEOMETRODYNAMICS U RELATIVITY GEOMETRY

NT ANALYTIC GEOMETRY
NT ANGLES [GEOMETRY]
NT BRAGG ANGLE
NT CARTESIAN COORDINATES
NT CHORDS [GEOMETRY]
NT CIRCLES [GEOMETRY]
NT COLLINEARITY
NT COPLANARITY
NT CURL [VECTORS]
NT CURVATURE
NT CURVES [GEOMETRY]
NT CUSPS [MATHEMATICS]
NT DIFFERENTIAL GEOMETRY
NT DOUBLE CUSPS
NT EPICYCLOIDS
NT EUCLIDEAN GEOMETRY
NT FIXED POINTS [MATHEMATICS]
NT FLOW GEOMETRY
NT HEXAGONS
NT HOMOTOPY THEORY
NT IMBEDDINGS [MATHEMATICS]
NT INVARIANT IMBEDDINGS
NT LIE GROUPS
NT METRIC SPACE
NT NOZZLE GEOMETRY
NT OBLATE SPHEROIDS
NT PARABOLAS
NT PARALLELEPIPEDS
NT POINTS [MATHEMATICS]
NT POLYGONS
NT POLYHEDRONS
NT PROJECTIVE GEOMETRY
NT PROLATE SPHEROIDS
NT PYRAMIDS
NT QUADRANTS
NT RHOMBOHEDRONS
NT RIEMANN MANIFOLD
NT SPHEROIDS
NT SPINOR GROUPS
NT TANK GEOMETRY
NT TENSOR ANALYSIS
NT TETRAHEDRONS
NT TOPOLOGY
NT TORUSES
NT TRIANGLES
NT VECTOR ANALYSIS
NT VORTICITY

The influence of the reference geometry on the response of elastic shells.

05 p0637 A73-17236

GEOMORPHOLOGY

Preliminary observations of stratified rocks of the Hadley Appennines photographed by the Apollo 15 astronauts

01 p0095 A73-10268

Concentric craters on the moon

01 p0102 A73-10943

Geomorphological analysis of the area of Mare Imbrium explored by the automatic roving vehicle Lunokhod 1.

02 p0213 A73-12240

Apollo 16 exploration of Descartes - A geologic summary.

05 p0614 A73-16320

Interplanet variations in scale of crater morphology - Earth, Mars, Moon.

06 p0745 A73-17442

Terrestrial heat flow determinations in the north central United States.

09 p1076 A73-22148

- Concentric craters on the moon.
09 p1147 A73-22738
- The structure and geological-morphological features of the landing site of the Luna 20 automatic station
10 p1281 A73-24452
- Lunar cinder cone deposits in Taurus-Littrow region of Apollo 17 landing site as counterparts of terrestrial pyroclastic eruptions
11 p1426 A73-26375
- Toros side-looking radar system for sea-ice distribution and geomorphological mapping and agricultural soil studies
12 p1474 A73-27962
- Lunar crater structure geological and morphological interpretations from lunar maria photographs in terms of age, density and stony debris size distribution
13 p1672 A73-28115
- Chemistry and surface morphology of soil particles from Luna 20 LRL sample 22003.
13 p1674 A73-28308
- Long term observations of geomagnetic pulsations activity during various phases of magnetic storm at midlatitudes, noting regular and irregular morphological features
13 p1611 A73-29660
- Lunar core sample structure morphology and composition examined by microanalysis, revealing tenite to martensite transformation
15 p1930 A73-31220
- Morphological characteristics of the moon and convection in its mantle
16 p2065 A73-33784
- Certain problems of the internal structure of the moon/Pyrolytic models of the moon/
16 p2066 A73-33789
- Possible trend of the earth's evolution
19 p2481 A73-37242
- Structure and geologic-morphological features of the region where Luna-20 landed.
19 p2486 A73-38126
- Remote sensor geological mapping of Rio Grande rift zone/Colorado/ using aerial color infrared photography for compilation of tectonic and geomorphic histories
20 p2560 A73-39893
- Two probable astroblemes in Brazil, considering meteorite impact origin by discovery of diagnostic shock-metamorphic effects in rocks from ERTS-1 satellite and aerial photographs
21 p2771 A73-41078
- Ventifact evolution in Wright Valley, Antarctica.
21 p2687 A73-41211
- Reversing barchan dunes in lower Victoria Valley, Antarctica.
21 p2687 A73-41214
- A study of lineaments from a Zond 5 photograph of northern Africa.
21 p2687 A73-41332
- Lunar core sample structure morphology and composition examined by microanalysis, revealing tenite to martensite transformation
22 p2905 A73-41808
- The use of near-infrared photography in the analysis of surface morphology of an Argentine alluvial floodplain.
22 p2850 A73-42728
- Lunar cross hatching lineament patterns at Silver Spur on Apollo 15 landing site, relating to geological, lighting or meteorite impact gas flow effects
23 p3034 A73-43962
- GEON [TRADEMARK]**
U POLYVINYL CHLORIDE
GEOGRAPHICAL OBSERVATORIES
NT POGO
Geophysical data transmission from automatic stations in the antarctic via earth synchronous satellites.
04 p0421 A73-15430
- GEOGRAPHICAL SATELLITES**
NT INTERCOSMOS SATELLITES
NT POGO
The use of radio beacons in geophysics and their applications.
21 p2657 A73-41331
- GEOPHYSICS**
Effect of solar activity delays on the processes in solar-terrestrial space.
02 p0212 A73-12185
- Considerations for an earth physics information-management service.
04 p0439 A73-14814
- Some consequences of the Mach-Einstein doctrine for celestial mechanics and geophysics
04 p0498 A73-15280
- IR satellite photographs in the earth sciences - A comparison of the IR ranges from 3 to 4 micrometers and from 10 to 12 micrometers
06 p0691 A73-18438
- Distortion corrections in geophysically traced gravitational, magnetic and geoelectric field maps, discussing automation
07 p0816 A73-19442
- Report on the NATO Advanced Study Institute on magnetohydrodynamic phenomena in rotating fluids.
11 p1404 A73-25851
- Statistical analysis of Forbush decreases and of cosmic-ray intensity increases preceding them.
13 p1670 A73-28701
- The Ze field, some of its properties, and geophysical information.
13 p1608 A73-28720
- Relation between the tidal-force momentum and atmospheric depressions
13 p1609 A73-28862
- The implications for geophysics of modern cosmologies in which G is variable.
14 p1799 A73-30525
- Correlation of reported gravitational radiation events with terrestrial phenomena.
14 p1749 A73-30554
- EROS Program and ERTS-1 satellite applications to geophysical problems.
18 p2307 A73-36032
- Book - General astrophysics with elements of geophysics.
18 p2356 A73-36968
- Pulsed magnetic system /terrella/ as earth model with dipole magnetic field for laboratory simulation of geophysical phenomena
19 p2425 A73-37938
- Geophysical field cartographic isoline recording via least generalized course representation of observation points, discussing analytic functions and least squares method
22 p2850 A73-42734
- Engineering applications of geophysical phenomena covering earthquakes, volcanology, hydrology, glaciology and wind stress effects during severe storms
23 p2979 A73-44007
- GEOPOTENTIAL**
NT **GEOPOTENTIAL HEIGHT**
Earth vertical gravity field probing by observing body free fall from several hundred kilometers altitude
02 p0159 A73-12167
- Earth normal gravity field spherical harmonics in terms of Stokes constants from satellite orbit dynamics, comparing with Helmert system
03 p0305 A73-14613
- Analysis of methods for computing an earth gravitational model from a combination of terrestrial and satellite data.
04 p0437 A73-14787
- Isostatic reduction potential of earth mass distribution for spherical harmonic solutions of satellite determined gravity anomalies
04 p0437 A73-14788
- Earth gravitational field representation via potential of simple layer in satellite geodesy applied to satellite optical observations and Doppler data
04 p0438 A73-14789
- Propagation of errors in orbits computed from density layer models.
04 p0438 A73-14790
- Interior point mass earth potential model for satellite geodesy, considering geoid heights, gravity anomalies and spherical harmonics
04 p0438 A73-14791
- Geopotential /geoid/ representation with spherical harmonics sampling functions for satellite altimeter applications
04 p0438 A73-14792
- Orbital elements and geopotential coefficients estimation with increased accuracy by satellite-satellite tracking
04 p0438 A73-14794
- Accuracy of potential coefficients obtained from present and future gravity data.
04 p0438 A73-14796
- Geopotential coefficient error model using Geos 2 tracking data and SAO 1969 standard earth
04 p0439 A73-14797
- On the damping of high-frequency motions in four-dimensional assimilation of meteorological data.
05 p0592 A73-16199
- Interrelation between processes occurring along a vertical, and the forecasting of stratospheric wind
05 p0592 A73-16232
- Numerical model for calculation of the geopotential field with a new generalized vertical velocity profile incorporating the influence of orography
05 p0572 A73-17352
- Estimates of the coefficients of a spherical harmonics expansion of the geopotential
09 p1143 A73-22095
- Explicit and implicit weather forecast expressions based on differential hydrodynamics equation relating horizontal and vertical wind velocity, geopotential and temperature gradients
10 p1244 A73-23813
- Satellite observed cloud signatures associated with mature and decaying depressions over high and middle southern latitudes, deriving surface pressure and upper geopotential anomaly patterns
10 p1244 A73-23980
- Earth satellites and the gravitational potential.
12 p1539 A73-27148
- Magnetovariational frequency sounding of the earth, using the ratio of magnetic potentials
12 p1491 A73-27352
- Stratospheric geopotential pressure field numerical prediction based on quasi-geostrophic atmosphere model, considering stratospheric heating period
12 p1521 A73-27742
- The normal gravitational fields of the earth and the moon
12 p1546 A73-27865
- Gaussian curvature of smoothed equipotential surfaces from satellite orbit dynamics.
13 p1611 A73-29659
- Least squares method for geomagnetic potential transformation in spherical offset inclined dipole coordinates with Schmidt coefficients
14 p1749 A73-29982
- A numerical model of the geopotential field with a new profile of the generalized vertical velocity that takes orography into account.
15 p1865 A73-31002
- Vorticity advection and geopotential change due to dynamic causes as two-layer problem
15 p1907 A73-32355
- The permissible scale of spatial averaging of geopotential values in the stratosphere when the impact of wind on the flight of a supersonic aircraft is taken into account
17 p2100 A73-34546
- A synoptic model for evaluation of vertical temperature and geopotential profiles from satellite pictures.
17 p2206 A73-34939
- Book - Theory of the earth's gravity field.
17 p2162 A73-35148
- Zonal gravity harmonics from long satellite arcs by a seminumeric method.
17 p2233 A73-35269
- Density scale height and geopotential coefficients evaluations from analysis of Cosmos 54 rocket orbit perturbations due to drag and odd-zonal harmonics
18 p2351 A73-36176
- Matching the geopotential and wind fields with the aim of improving the accuracy of objective analysis
19 p2449 A73-38544
- Influence of the atmosphere on the gravity force and its potential at points on the earth's physical surface
19 p2428 A73-38555
- Normal gravity fields of the earth and the moon.
20 p2608 A73-39239
- Terrestrial gravitational models derived from satellite tracking and surface gravimetric data, comparing to 1969 Smithsonian Standard Earth II models
21 p2773 A73-41326
- Allowance for the effects of the relief and of the Coriolis force in forecasting meteorological elements
22 p2883 A73-41954
- Frequency magnetovariational sounding of the earth, using the ratio of potentials.
23 p2970 A73-43249
- An exact solution to the system of prognostic equations of a barotropically divergent model of the atmosphere
23 p3001 A73-43461
- Structure of global geopotential fields in view of the quasi-two-year cyclicity in the equatorial stratosphere
23 p3001 A73-43463
- Spectral analysis of traveling planetary scale waves - Vertical structure in middle latitudes of Northern Hemisphere.
23 p2978 A73-43982
- GEOPOTENTIAL HEIGHT**
Utilization of meteorological data from satellites in studies of the general atmospheric circulation
05 p0593 A73-16245
- Analysis of pressure and cloud anomaly fields.
18 p2333 A73-37054
- Calculation of geopotential fields at various atmospheric levels from data on the overall cloudiness and temperature.
18 p2314 A73-37072
- GEORGIA**
Airborne remote sensing of Georgia tidal marshes.
16 p2003 A73-33359
- GEOS SATELLITES [ESRO]**
Effect of some external factors on accuracy of observations of active satellites.
13 p1680 A73-28516
- ESRO Geos geostationary satellite for measurement of magnetospheric plasma electric and magnetic fields and drift rate at various frequency regions via electron injection
17 p2176 A73-35816
- GEOS 1 SATELLITE**
Secor range observations on Geos 1 satellite in Pacific tracking network, determining station coordinates, relative positions and geodetic heights
04 p0437 A73-14783
- Geos 1 and 2 long periodic and secular orbit perturbations, discussing osculating elements transformation with maximum accuracy via minitrack system
11 p1423 A73-26070
- GEOS 2 SATELLITE**
Geopotential coefficient error model using Geos 2 tracking data and SAO 1969 standard earth
04 p0439 A73-14797

Geos 1 and 2 long periodic and secular orbit perturbations, discussing osculating elements transformation with maximum accuracy via minitrack system
11 p1423 A73-26070

GEOS-C SATELLITE

Geos-C mini arc orbit determination from radar altimeter observations under perturbations from gravitational anomalies
04 p0437 A73-14784

Survey improvement and calibration analysis for the Air Force Eastern Test Range with Geos C.
04 p0437 A73-14786

GEOSTATIONARY OPERATIONAL ENVIRON SATS

U GOE SATELLITES

GEOSTATIONARY SATELLITES

U SYNCHRONOUS SATELLITES

GEOSTROPHIC WIND

On the meridional form of baroclinic waves in a two-layer quasi-geostrophic model.
03 p0304 A73-14312

The effect of the baroclinicity of the atmosphere on the structure of the wind field in the steady planetary boundary layer
04 p0441 A73-15289

Adiabatic inviscid quasi-geostrophic planetary scale perturbations forced by stratospheric disturbance, obtaining vertical propagation from layered models representation for zonal wind
05 p0591 A73-16189

The Leipzig wind profile and the boundary layer wind-stress relationship.
07 p0847 A73-19045

Some observations of the influence of geostrophic shear on the cross-isobar angle of the surface wind.
11 p1393 A73-25695

Stratospheric geopotential pressure field numerical prediction based on quasi-geostrophic atmosphere model, considering stratospheric heating period
12 p1521 A73-27742

Stability of a two-layer fluid model to non-geostrophic disturbances.
13 p1610 A73-29334

Four dimensional forecast assimilation of temperature data from Nimbus 4 SIRS radiance measurements, using two level model with geostrophic wind adjustment
15 p1902 A73-31314

The stability of a time-variable surface wind
15 p1906 A73-32353

Considerations concerning the quasi-geostrophic model equations for an energetically open system
15 p1907 A73-32360

Investigations of the 500mb level in relation to the general circulation. I - Transport of relative angular momentum at the 500mb level, by considering daily and monthly eddies that were obtained by applying Fisher's partitioning.
19 p2446 A73-37499

A comparison of geostrophic and rocket winds at stratospheric levels, measured from a small network of rocket sounding stations.
19 p2424 A73-37604

Matching the geopotential and wind fields with the aim of improving the accuracy of objective analysis
19 p2449 A73-38544

Numerical forecasting experiments based on the conservation of potential vorticity on isentropic surfaces.
21 p2728 A73-40053

Objective cross-section analyses by Hermite polynomial interpolation on isentropic surfaces.
21 p2728 A73-40054

Surface wind-geostrophic wind relationship at Salisbury Plain, England, deducing geostrophic drag coefficients for open sea
21 p2732 A73-41571

Dynamics of quasigeostrophic flows and instability theory.
22 p2842 A73-42450

GEOSYNCLINES

The tsunami model of the origin of ring structures concentric with large lunar craters.
11 p1419 A73-25791

GEOTROPISM

The effects of mercury compounds on the growth and orientation of cucumber seedlings.
12 p1462 A73-27274

Biophysical considerations concerning gravity receptors and effectors including experimental studies on *Phycomyces blakesleeanus*.
22 p2804 A73-42171

GEP TELESCOPES

U PARTICLE TELESCOPES

GERDIEN ARC HEATERS

U ARC HEATING

U HEATING EQUIPMENT

GERMANATES

Energetic and structural models of microdefects in germanate glasses
10 p1240 A73-24465

GERMANIDES

Chemical stability of tantalum germanide powders in air and aggressive media, including acids, fluorine ions and perhydrol
09 p1133 A73-22465

Room temperature electrical properties and dopant precipitation for SiGe thermoelectric alloys.
09 p1134 A73-22758

The development of SiGe-PbTe segmented thermoelectric couples involving pressure-contacted junctions.
11 p1409 A73-26035

GERMANIUM

Influence of gamma-radiation on the electrical properties of a real germanium surface
01 p0087 A73-10039

Comparison of data on irradiation of germanium by 1- and 28-MeV electrons
02 p0201 A73-12592

Investigation of hole scattering in surface inversion channels arising on a cleaved germanium surface
03 p0349 A73-13659

Third harmonic generation in Ge induced by conduction nonlinearity during bulk heating of charge carriers by microwave fields
03 p0350 A73-14077

The mechanism of surface mass transfer in the thin-film Ge-Al system
06 p0738 A73-18651

Low-temperature epitaxy of Ge films by sputter deposition.
06 p0739 A73-18777

Residual conductivity in unannealed amorphous germanium.
07 p0864 A73-20455

Gallium and germanium in the metal and silicates of L- and LL-chondrites.
07 p0789 A73-20621

On the procedures of measuring microwave Faraday rotation in semiconductors.
08 p0994 A73-21016

Optical constants measurement for far IR materials of crystalline quartz, sapphire, Ge and Si at room temperature and 1.5 K [AD-760151]
08 p0994 A73-21049

Ionization energy of adhesion levels and heat-generation centers in the microplasma volume in germanium p-n junctions
08 p0995 A73-21274

Sensitivity limits for extrinsic and intrinsic infrared detectors.
08 p0967 A73-21422

Microwave oscillation in germanium avalanche diodes. I, II.
08 p0947 A73-21461

Semiconductor strain transducer
08 p0950 A73-21720

Investigation of the growth of the disperse structure of gold on a germanium surface
11 p1408 A73-25247

Pinch effect in a germanium electron-hole plasma.
11 p1409 A73-26189

Investigation of radiation defects in silicon and germanium single crystals irradiated by 50-MeV electrons
11 p1410 A73-26449

InSb and Ga-doped Ge bolometers performance tests, discussing detector circuitry and dc, noise and responsivity measurements
11 p1368 A73-26512

Determination of the parameters of r-type recombination centers in germanium-doped GaTe single crystals
11 p1410 A73-26587

Weak-beam high-resolution electron micrographs of plastic deformation-generated extended dislocations in Ge single crystals
13 p1668 A73-28222

Cleaved Si and Ge surfaces roughness investigation by low energy electron diffraction, electron microscopy and optical reflection technique
13 p1668 A73-28452

Transition probabilities of neutral and singly ionized germanium.
14 p1783 A73-30243

German monograph - The effect of germanium additions on the superconductor characteristics and the transition processes in technical titanium-niobium alloys.
14 p1762 A73-30666

Electromagnetic wave propagation in p-type Ge and Si semiconductor plasmas, studying dispersion, cyclotron resonance, and kinetic equations
15 p1925 A73-32214

Physical and chemical analysis of germanium tunnel diodes.
17 p2219 A73-34865

Influence of electrically active impurities on the mobility of individual dislocations in germanium
21 p2751 A73-40370

The chemical classification of iron meteorites. VII - A reinvestigation of irons with Ge concentrations between 25 and 80 ppm.
21 p2647 A73-40564

Distribution of Ni, Ga, Ge and Ir between metal and silicate portions of H-group chondrites.
21 p2771 A73-41009

Germanium resistance thermometers for cryogenic temperature precision measurement, discussing design technology, resistance-temperature characteristics types, installation and measurement methods
22 p2854 A73-41999

Germanium resistance thermometers - Resistance vs. temperature and thermal time constant characteristics.
22 p2854 A73-42000

Representation of the temperature-resistance characteristic of germanium thermometers below 30 K.
22 p2854 A73-42001

Nonlinear transmission loss in Ge beam splitter in pulsed HF and DF lasers operating at 2.5 to 4 microns
22 p2897 A73-43145

Interface properties of oxidized germanium-doped silicon.
23 p3016 A73-43778

Si and Ge doping characteristics and energy levels in vapor phase epitaxially grown GaAs from sample photoluminescence spectra
23 p3018 A73-44370

Amplification of magnetostatic surface waves in the YIG-Ge hybrid system.
24 p3120 A73-45431

GERMANIUM ALLOYS

Phase equilibrium diagram of the lanthanum-germanium system
04 p0484 A73-15692

Silicon-germanium technology program of the Jet Propulsion Laboratory.
09 p1117 A73-22759

Vaporization and compatibility of SiGe radioisotope thermoelectric generators.
09 p1117 A73-22761

SiGe alloys thermoelectric properties long term time and temperature dependent behavior, using diffusion limited dopant precipitation model
09 p1136 A73-22762

Radioisotope thermoelectric generator SiGe thermopile power degradation and operating temperature changes, discussing performance prediction model
09 p1117 A73-22763

Metallurgical investigations of phase equilibria in the titanium-niobium-germanium ternary system
10 p1231 A73-23692

The calculated long-term performance characteristics of a typical silicon-germanium RTG.
11 p1312 A73-26030

Structure and properties of alloys of the V3Si-V3Ga-V3Ge system
15 p1923 A73-31190

Oxidation of powdered germanium, tin and lead tellurides under atmospheric conditions
15 p1887 A73-31594

The influence of vacancies on the nucleation of incoherent germanium precipitates in aluminum-germanium alloys. III - The effect of germanium nuclei on precipitation at higher temperatures
16 p2026 A73-33959

The behavior of xenon when used as a fill-gas in a silicon germanium radioisotope thermoelectric generator.
19 p2455 A73-38388

High temperature material interactions of thermoelectric systems using silicon germanium.
19 p2455 A73-38390

Analytical model for long term performance prediction of multihundred watt radioisotope thermoelectric generator with Si-Ge alloy as thermoelectric material, noting degradation mechanisms
19 p2390 A73-38391

GERMANIUM COMPOUNDS

NT GERMANATES

NT GERMANIDES

NT GERMANIUM OXIDES

Cerium-germanium system state diagram based on microstructural, differential thermal, dilatometric and X ray phase analyses, emphasizing intermetallics observation
10 p1260 A73-24684

Crystal growth by vapor transport of GeSe, GeSe₂, and GeTe and transport mechanism and morphology of GeTe.
15 p1842 A73-32652

Investigation of the design parameters and experimental parameters of medium-temperature thermopiles based on lead, germanium and tin tellurides
17 p2108 A73-34282

GERMANIUM DIODES

Mixing properties of germanium thermoelectric indicators of SHF radiation with 'hot' charge carriers
09 p1063 A73-22456

Double-injection negative differential resistance in compensated gold-doped germanium.
10 p1259 A73-23752

GERMANIUM OXIDES

A study of germanium monoxide at high temperatures
06 p0739 A73-18659

Earth mantle rutile-structure germanium dioxide elastic properties as function of pressure and temperature in single crystals
11 p1352 A73-25585

Spatial resolution of an incoherent-to-coherent converter using bismuth germanium oxide.
22 p2863 A73-43098

GERMANIUM RECTIFIERS

U GERMANIUM DIODES

GERMANY

NT ALPS MOUNTAINS [EUROPE]

Long term German observations of auroral activity compared to other midlatitude observations
04 p0445 A73-15551

GERMICIDES

U BACTERICIDES

GERMINATION

Life processes in ammonia - Anomalous germination behavior of onion seed in ammonia and amines.
11 p1321 A73-26491

GERONTOLOGY

Functional aging - Present status of assessments regarding airline pilot retirement.
21 p2645 A73-41161

GESTALT THEORY

Visibility of an afterimage alone and in the presence of one or two additional afterimages.
09 p1039 A73-21894

GETOL AIRCRAFT

Air cushion landing systems; Proceedings of the First Conference, Miami Beach, Fla., December 12-14, 1972.
19 p2380 A73-37676

Air cushion landing systems application to tactical airlift aircraft for personnel, and equipment delivery to dispersed sites under diverse climatic, terrain and combat conditions
19 p2380 A73-37678

Air cushion landing systems for STOL transport aircraft, investigating structural and power requirements, ground and in-flight handling, mission capability, operational life, weight and cost
19 p2381 A73-37682

Air cushion landing system applications and operational considerations.
19 p2381 A73-37684

On the cost benefits of air cushion landing gear to civil aviation.
19 p2381 A73-37685

Ground and flight testing of air cushion landing system /ACLS/ equipped CC-115 Buffalo aircraft for performance and stability/control characteristics
19 p2382 A73-37691

Surface effect take-off and landing system for high performance aircraft.
19 p2382 A73-37695

A multicell air cushion system for landing gear application.
19 p2383 A73-37700

The potential influence of the ACLS on the development of logistical cargo aircraft.
19 p2383 A73-37701

Theory and experiments for air cushion landing system - A ground jet concept.
19 p2383 A73-37704

A digital computer flight simulation of an ACLS vehicle.
19 p2383 A73-37705

Simulation of the ACLS during landing roll.
19 p2383 A73-37706

Ground loads analysis for air cushion landing system /ACLS/ equipped aircraft during landing and taxiing, predicting peak trunk pressures via energy considerations
19 p2383 A73-37707

GETTERS

Electrostatic getter-ion pump performance.
08 p0989 A73-21618

The performance characteristics of modern vacuum pumps.
21 p2707 A73-39915

GIACOBINI-ZINNER COMET

Investigation of the motion of periodic comet Giacobini-Zinner and the origin of the Draconid meteor showers of 1926, 1933 and 1946.
14 p1791 A73-29802

Nongravitational forces and periodic comet Giacobini-Zinner.
14 p1791 A73-29803

GIANT STARS

Photometry and spectroscopy of red variables in Omega Centauri.
01 p0098 A73-10584

Mean absolute magnitudes and color indices of the red-giant concentrations in the color-magnitude diagrams of open clusters.
01 p0106 A73-11319

Hydrodynamic model calculations for supermassive stars. II - The collapse and explosion of a nonrotating 520,000 solar-mass star.
02 p0222 A73-12713

Remarks on the comparison of the Sanduleak and Fehrenbach-Duflo catalog of stars belonging to the Large Magellanic Cloud
02 p0223 A73-12718

Massive stars evolution in hydrogen and helium burning phases, taking into account mass loss from light pressure in optically thick media
02 p0224 A73-12801

Statistical fractions of variable A and F stars, considering main sequence stars, giants, subgiants and open clusters NGC 2548, Praesepe and Coma
02 p0226 A73-12834

Microturbulence in atmospheres of F, G, K, type stars. I - Curve of growth analysis of G, K, type subgiants.
03 p0370 A73-13196

Surface gravities, Doppler broadening velocities, effective temperatures and metal abundances of K giants from narrow band photometry
03 p0371 A73-13224

M giant atmospheric molecular evolution, discussing carbon/oxygen ratios, s-process overabundances and relationships between M, S and C stars
04 p0496 A73-14971

Bright red giants in the globular clusters M3, M5, and M13.
04 p0503 A73-16006

The old open cluster NGC 6819.
05 p0618 A73-16744

Advanced evolution of massive stars. III - Hydrostatic carbon-burning nucleosynthesis and energy generation.
07 p0874 A73-19062

The luminosity function and density distribution of disk population stars.
07 p0876 A73-19358

Hydrodynamic calculations for novae origin and mass ejection from luminous red giants, considering planetary nebulae and plausible models
07 p0903 A73-20628

He red giants models with degenerate C-O cores, He burning shell sources and He-rich envelopes, noting stellar luminosity
08 p1004 A73-20903

Evolution from the main sequence to the helium flash for population II stars.
08 p1005 A73-20915

Three-colour photometry of a field in the galactic anticentre section near NGC 1664.
08 p1005 A73-20922

Three-colour photometry in a field in the direction of the galactic anticentre near M 35.
08 p1005 A73-20923

Stellar evolution at high mass based on the Ledoux criterion for convection.
08 p1008 A73-21159

Luminosity functions for K giant stars derived from the two-micron sky survey.
11 p1414 A73-25066

Spectral types and UVB photometry of G-K giants at the North Galactic Pole.
11 p1429 A73-26678

Metal content in the atmospheres of red giants which are members of dispersed star clusters and dynamical groups
12 p1537 A73-26853

Metal-poor stars. IV - The evolution of red giants.
12 p1540 A73-27328

Late stage nonrotating star evolution, discussing red giant models, planetary nebulae, degenerate carbon cores, supernova explosions and pulsars
12 p1543 A73-27748

Central gravitational field of stars and evolution to red giants.
16 p2058 A73-32837

Stellar masses on the asymptotic branch of red giants in globular clusters
21 p2768 A73-40719

Luminosity and velocity distribution of high-luminosity stars near the sun. II - The young disk giants.
22 p2909 A73-42585

The C-classification of the spectra of carbon stars.
24 p3138 A73-44997

Calibration of luminosity criteria for G and K giants by means of trigonometric parallaxes.
24 p3140 A73-45181

The unstable eclipsing giant system RZ Cancri.
24 p3143 A73-45438

GIBBS FREE ENERGY

Second law of thermodynamics revision to include only spontaneous processes made to yield work, discussing heat flow, solutes diffusion and Gibbs free energy
14 p1816 A73-29735

GIMBALS

Certain problems of dynamics and accuracy of gyroscopes in gimbals.
01 p0053 A73-11197

Vibrational resonance modes of balanced gyroscope on fixed base, determining gimbal vibration amplitude and gyro drift rate as function of perturbation frequency
01 p0054 A73-11401

Effect of friction in suspension bearings on the motion of a gyroscope with a forced rotation of its base
01 p0054 A73-11415

Determination of gimbal errors in an astatic gyroscope with allowance for drift
01 p0054 A73-11416

Equations of motion of composite space pendulum formed by gyroscopes with Cardan suspension, noting equations integrability
02 p0192 A73-11767

Drift rate of the rotor axis in the generalized problem of the gyroscope with a Cardan mounting
02 p0167 A73-11768

Dynamic stability of gimbaled spiral-grooved thrust bearing.
[ASME PAPER 72-LUB-13] 03 p0313 A73-14329

Geometric properties and basic errors of rotating support devices of the gimbal suspension type
04 p0447 A73-14848

Hall effect gimbal angle transducer /HEGAT/ for relative angular orientation measurement between rotor and stator in low cost inertial platform
04 p0447 A73-15066

Stability analysis of gyroscopic systems for parametric resonance case, allowing for viscous friction at gimbal axes
05 p0578 A73-17085

One degree of freedom fluid suspension gyros, direct drive gimbal motors and microelectronic control assemblies review, noting miniature inertial platforms availability
07 p0820 A73-18941

Numerical position deviation and release delay time estimates for gyroscope motion in gimbal suspension during rotor start-up
09 p1081 A73-22345

Ponderous nutational motion of gyroscope in gimbal suspension, calculating precession rate from reduced equations of motion
09 p1081 A73-22351

Construction of the frequency spectrum of a three-degree-of-freedom gyroscope with a flexible rotor shaft and elastic gimbal mountings
09 p1084 A73-22656

Systematic drift of a gyroscope with variable angular momentum in the gimbal suspension during vibrations of the frame
09 p1084 A73-22657

Precession motion stability and drift rates of gimbal gyroscope under angular and translational resonant base vibration
09 p1087 A73-23343

Stable-member mounted instrument environment simulation model development.
11 p1395 A73-26638

Influence of elastic deformations of the gimbal support on the motion of a three-degree-of-freedom astatic gyroscope
13 p1618 A73-29147

Gimbaled electrostatic gyro inertial aircraft navigation system /GEANS/ designs balancing performance against cost of ownership
16 p2034 A73-33086

Influence of clearances on the behavior of a gyroscope on a vibrating base
19 p2428 A73-37188

Failure detection and isolation methods for redundant gimbaled inertial measurement units.
[AIAA PAPER 73-851] 20 p2585 A73-38790

Precision gimbal rate control for single gimbal control moment gyro /CMG/ pointing control systems, designing for high frequency response, bandwidth and output torque dynamic range
[AIAA PAPER 73-871] 20 p2587 A73-38808

2-SPEED, a single-gimbal control moment gyro attitude control system.
[AIAA PAPER 73-895] 20 p2589 A73-38831

Effect of the elastic deformation of a gimbal suspension on the nutation oscillation frequency of a gyroscope
22 p2860 A73-42359

Combinational parametric resonance in a gyro-pendulum mounted on a mobile base
22 p2860 A73-42367

Effect of the gyromotor torque on the dynamics of a gyroscope
24 p3091 A73-45021

GIRDERS

Design optimization of prestressed concrete spans for high speed ground transportation.
12 p1554 A73-27735

GLACIAL DRIFT

Lunar sinuous rilles as inverted eskers formed by volatiles /water and carbon dioxide/ moving in channel between basement surface and permafrost layer
17 p2237 A73-35859

GLACIERS

Icelandic geothermal activity and the mercury of the Greenland icecap.
09 p1079 A73-22949

Applications of ERTS imagery to snow and glacier hydrology.
18 p2306 A73-36022

Solar structure and evolution, calculating neutrino emission for Pleistocene glacial age caused by solar luminosity reduction
21 p2764 A73-41613

GLACIOFLUVIAL DEPOSITS

U GLACIAL DRIFT

GLACIOLOGY

Analog scale model of radio interferometry depth sounding at centimeter wavelengths, examining glacier layer boundaries
24 p3082 A73-44750

GLANDS [ANATOMY]

NT ADRENAL GLAND

NT GONADS

NT PANCREAS

NT PINEAL GLAND

- NT PITUITARY GLAND
NT TESTES
NT THYROID GLAND
Transductal fluxes of Na, K, and water in the human eccrine sweat gland. 15 p1836 A73-31923
- GLARE
Ophthalmological assessment of visual functional impairment due to glare, stimulus motion and aging changes 05 p0540 A73-16485
- GLASS
NT BOROSILICATE GLASS
NT GLASS FIBERS
NT S GLASS
NT SILICA GLASS
Difference of thermal properties between threshold type and memory type chalcogenide glass semiconductors. 01 p0087 A73-10432
Analogies in the laser-induced destruction of the surface and interior of transparent glass. 02 p0176 A73-12115
Glass bead reinforced epoxy and polyester resins mechanical properties as function of volume fraction and interfacial bond strength, discussing beads chemical surface treatment effects 02 p0185 A73-12428
The composition of the lunar highlands - Evidence from modal and normative plagioclase contents in anorthositic lithic fragments and glasses. 02 p0220 A73-12478
Chlorine, bromine, iodine, and uranium in tektites, obsidians, and impact glasses. 02 p0223 A73-12720
Interferometric studies on Apollo 11 and Apollo 12 lunar glass objects. 03 p0369 A73-13096
Surface features on glass spherules from the Luna 16 sample. 04 p0498 A73-15187
Bubbles and operating voltage effects in electrochemical machining of tungsten carbide and discharge machining of glass [ASME PAPER 72-WA/PROD-21] 04 p0456 A73-15804
Major element composition of Luna 20 glasses. 05 p0546 A73-16827
The magnetic properties and morphology of metallic iron produced by subsolidus reduction of synthetic Apollo 11 composition glasses. 05 p0619 A73-16837
Preparation of transmitting coatings for As2S3 glass 05 p0605 A73-17293
Change in sign of thermal lens of glass laser rods with change in thermooptical constant of glass. 06 p0703 A73-18635
The major element compositions of lunar rocks as inferred from glass compositions in the lunar soils. 07 p0880 A73-19700
Chemical classification and composition of Apollo 11, 12, 14 and 15 soil samples glasses, describing breccias and chondrules 07 p0882 A73-19723
Inclusions and interface relationships between glass and breccia in lunar sample 14306, 50. 07 p0883 A73-19731
Chemistry and particle track studies of Apollo 14 glasses. 07 p0884 A73-19736
Structure of lunar glasses by Raman and soft X-ray spectroscopy. 07 p0888 A73-19737
Glassy particles in Apollo 14 soil 14163, 88 - Peculiarities and genetic considerations. 07 p0885 A73-19747
Temperature-dependent magnetic properties of individual glass spherules, Apollo 11, 12, and 14 lunar samples. 07 p0893 A73-19844
Applications to lunar geophysical models of the velocity-density properties of lunar rocks, glasses, and artificial lunar glasses. 07 p0894 A73-19854
Crystallization behavior and glass formation of selected lunar compositions. 07 p0895 A73-19858
Optical properties of lunar glass spherules from Apollo 14 fines. 07 p0898 A73-19893
Tantalum-glass cermet thin-film resistors. 08 p0945 A73-20809
Electronic conduction and switching in chalcogenide glasses. 09 p1133 A73-21985
Reversible thermal breakdown as a switching mechanism in chalcogenide glasses. 09 p1133 A73-21986
Solute rejection by porous glass membranes. II - Pore size distributions and membrane permeabilities. 09 p1048 A73-22525
Accuracy of interferometric plasma investigations involving heating of the optical elements 09 p1131 A73-22883
- Adhesive metal/glass laminate bonding, discussing materials, tests and interlaminar strength effects 10 p1224 A73-24092
Major element chemistry of glasses in Apollo 14 soil 14156. 10 p1278 A73-24111
Facility for studying the strength and deformability of high-strength brittle materials in biaxial compression 10 p1203 A73-24372
Energetic and structural models of microdefects in germanate glasses 10 p1240 A73-24465
Mechanical, thermal and electrical properties of machinable glass ceramics, discussing application as electromagnetic window materials 11 p1387 A73-25293
Rain-erosion resistance and other properties of Schott infrared-transmitting glasses. 11 p1387 A73-25299
Photochromic glass as reversible optical recording storage medium, discussing image resolution, configuration improvements, merits and applications in holography, random access memory and displays 11 p1370 A73-26537
Reversible recording of holograms on chalcogenide glass films 12 p1495 A73-26940
Electrical conductivity of semiconductor glass crystals on an arsenic and lead selenide base 12 p1531 A73-27195
Spectral and boundary effects on coupled conduction-radiation heat transfer through semitransparent solids. 12 p1559 A73-27695
Luna 20 lunar glass particle samples chemical composition, noting aluminum oxide content similarity to Apollo 16 samples 13 p1675 A73-28314
Comparison of the magnetic properties of glass from Luna 20 with similar properties of glass from the Apollo missions. 13 p1677 A73-28332
The polished surface of a telescope mirror as seen in an electron microscope 14 p1752 A73-30060
Low-temperature relaxations in amorphous polymers. 14 p1765 A73-30134
A controlled single-pulse neodymium-glass laser 14 p1757 A73-30369
Cooperative mechanisms during laser excitation of luminescence in Yb-Tb and Yb-Eu ion activated glass. 15 p1884 A73-31713
French monograph - Study of craters formed on glass surfaces by the impact of artificial micrometeoroids. 15 p1898 A73-32591
Mechanism of failure in transparent organic-glass-type dielectrics under the action of laser radiation 16 p2030 A73-33927
Lunar volcanism - Age of the glass in the Apollo 17 orange soil. 17 p2230 A73-34522
Fast differential thermal analysis. 17 p2119 A73-34799
Tektite ablation calculation taking into account transient effects, internal radiation, melting and nonequilibrium vaporization of glass and drag effect of flanges 17 p2233 A73-35272
Investigation of failure of a fiberglass plastic due to differential carbon burnup 18 p2328 A73-36813
Some characteristics of the disintegration of glassy bodies in hot gas flows 18 p2372 A73-37020
The yielding of a two-dimensional void assembly in an organic glass. 19 p2444 A73-38090
Apollo 15 breccia and soils with spheres and fragments of iron-rich green glass originating in Apennine Front materials 19 p2487 A73-38174
Unpaired electrons and charge carriers in oxide semiconductor glasses based on the oxides of titanium, vanadium, and phosphorus 20 p2599 A73-39394
Nature of the damage caused by laser radiation on the surfaces or in the bulk of transparent glasses. 20 p2573 A73-39687
Amorphous material conduction, discussing glass transparency relation to electronic properties, semiconducting glasses and switching behavior 21 p2723 A73-40272
Study of the properties of thick-film chalcogenide glass holograms 21 p2701 A73-40571
Mechanical, chemical and physical characteristics of glass and ceramics with respect to adhesion, friction and wear behavior 21 p2707 A73-40633
Certain properties of semiconductor glasses from the Ge-As-Se-Te system 21 p2752 A73-40749
- Optical waveguide refractive index control process for glass film during deposition by sputtering power density variance 21 p2665 A73-41116
Properties of thin-film holograms on chalcogenide glasses 22 p2860 A73-42409
Rare gas diffusion studies in individual lunar soil particles and in artificially implanted glasses. 23 p3031 A73-43769
Kinetics of shrinkage during the sintering of porous glass/metal composites 24 p3092 A73-44415
- GLASS COATINGS
Channel electron multiplier prepared from shaped glass tubing with inner conductive coating, discussing electron and photon detection characteristics 02 p0146 A73-11954
RF sputtered integral covers of glass coating for thermal protection of Si solar cells, noting intrinsic stress, adhesion, transparency and radiation damage resistance 03 p0256 A73-14227
Evaluation of cerium stabilised microsheet coverslips for higher solar cell outputs. 03 p0256 A73-14229
Protection of certain borides from oxidation in air at 1200 C 18 p2318 A73-35888
Effect of oxides on certain properties of glass-ceramic coatings for titanium 18 p2319 A73-35889
Synthesis of metal-ceramic and other heat-resistant coatings by the electrochemical method 18 p2319 A73-35890
Fabry-Perot etalon with evaporated Schott glass as a spacer-layer. 22 p2863 A73-43143
- GLASS FIBER REINFORCED PLASTICS
Calculation and design of highly stressed fiberglass-reinforced plastic components 13 p1703 A73-29653
Statistical representation of the strength of fiberglass-reinforced plastic samples 22 p2880 A73-41956
Experimental investigation of the strength and deformability of vacuum-prepared fiberglass-reinforced plastic shells 22 p2881 A73-43062
Response of glass-fiber-reinforced epoxy specimens to high rates of tensile loading. 23 p2996 A73-43385
Some important aspects in testing high-modulus fiber composite tubes in axial tension. 23 p2996 A73-43639
Mechanism of surface microcracking of matrix in glass-reinforced polyester by artificial weathering. 23 p2997 A73-44034
Experimental evaluation of the load capacity of smooth fiberglass-reinforced plastic shells under external hydrostatic pressure 23 p2998 A73-44191
A device for durability and creep testing of fiberglass-reinforced plastic pipes and shells in a complex stressed state 23 p2967 A73-44293
Fiberglass reinforced plastic laminate creep rate for ultrasonic vibrational and static tensile loads, showing nonlinear viscoelasticity and stress amplitude effects 24 p3102 A73-44504
Numerical realization of a possible way of determining the tensor of elastic constants in an anisotropic body 24 p3144 A73-44506
Prediction of failure processes in fiberglass-reinforced plastics by a seismoacoustic method. II - Features of damage buildup in woven fiberglass-reinforced plastics in uniaxial tension 24 p3102 A73-44507
Correlation between the static and fatigue strength of reinforced plastics 24 p3102 A73-44509
Process anisotropy of randomly reinforced fiberglass plastics 24 p3102 A73-44515
Conditions of production of high-compressive-strength, orthogonally reinforced fiberglass plastics 24 p3102 A73-44526
Determination of the magnitude and distribution of initial stresses in fiberglass-reinforced plastics. I 24 p3103 A73-44527
Critical stresses of compressed cylindrical shells consisting of orthotropic layers with various orientations 24 p3145 A73-44529
The mechanism of fracture of reinforced beams during bending. I 24 p3146 A73-44531
Analytical relations of physicochemical, strength and geometrical factors in formation of high strength monolithic glass fiber reinforced structures 24 p3103 A73-44533
Arbeitsgemeinschaft Verstaerkte Kunststoffe, Open Meeting, 10th, Freudenstadt, West Germany, October 3-6, 1972, Reports 24 p3103 A73-44876

The effect of impregnation and wetting characteristics on the mechanical parameters of glass-fiber-reinforced plastics 24 p3103 A73-44877

Glass fiber reinforced casting plastics mechanical properties dependence on processing quality fluctuations, considering laminates with unsaturated polyesters and fiber glass mats 24 p3103 A73-44878

Determination of the point at which damage occurs in glass-reinforced laminates - New nondestructive methods and their suitability as production control procedures 24 p3103 A73-44879

The use of glass-fiber-reinforced plastics for containers which are subjected to external pressure 24 p3147 A73-44881

Experimental investigations regarding optimally designed three-layer wound glass fiber/plastic tubes under internal pressure 24 p3147 A73-44882

'Crack boundaries' in the case of unidirectional glass-fiber-reinforced plastic wound laminates under uniaxial and multiaxial stress 24 p3103 A73-44883

Fracture criteria for a unidirectional glass fiber/plastic material under planar short-term and long-term stress 24 p3103 A73-44884

Creep and aging characteristics of glass-fiber-reinforced plastics 24 p3104 A73-44885

Mechanical properties of unidirectionally reinforced polyester and epoxy resin laminates under combined stresses perpendicular or parallel to glass fiber direction 24 p3104 A73-44886

Low-pressure prepreps as structural material for light-construction designs 24 p3104 A73-44887

Hardening with UV radiation in the manufacture of glass-fiber-reinforced unsaturated polyester resin molding materials 24 p3093 A73-44889

Mechanical properties of glass fiber reinforced plastic laminate formed by spraying unsaturated polyester resin on glass rovings 24 p3094 A73-44890

GLASS FIBERS

Investigation of the macroscopic rheonomic properties of a monodirectional fiberglass-reinforced plastic 01 p0067 A73-10002

Highly-stressed centrifuge and rotor drums made of reinforced plastics 01 p0056 A73-10308

Measurement of the angular distribution of light scattered from a glass fiber optical waveguide. 01 p0078 A73-11215

Optical communication systems with glass fiber waveguide, using semiconductor lasers and photodiodes as transmitters and receivers respectively 01 p0019 A73-11486

Physicomechanical properties of a structural cold-hardened fiberglass-reinforced plastic 02 p0184 A73-11719

Crack initiation and propagation in glass fiber reinforced plastic materials, noting rod bending 02 p0231 A73-11810

Glass reinforced epoxy structure for a lightweight superconducting dipole magnet. 02 p0232 A73-11836

Glass laminates and high strength oriented fiberglass reinforced plastics failure mechanism in tension and bending, noting equalizing effect through proper cohesion characteristics between layers 02 p0185 A73-12134

Randomly oriented glass fiber reinforced epoxy composites tensile strength properties as function of fiber volume fraction 02 p0185 A73-12427

Attempts at using fiberglass cloth as skin for aircraft 02 p0185 A73-12450

Effect of vacuum solidification on the porosity of wound fiberglass-reinforced plastics 02 p0174 A73-12577

Advances in glass fiber fabrics for plastic reinforcement. 03 p0330 A73-13014

Fiber strength of S-glass/epoxy composites under biaxial loading. 03 p0330 A73-13017

Glass reinforced structural components for the synchronous meteorological satellite. 03 p0331 A73-13030

Metallized fiberglass antenna meshes for spacecraft deployable reflectors, discussing low mass/area, long term stability and performance characteristics and degradation tests 03 p0333 A73-13045

Mechanical properties and applications of reinforced plastics for cast alloy elements, machine parts and noncorrosive light structures production, emphasizing glass fiber reinforcement 03 p0334 A73-13593

Effect of the glass fiber diameter on the compressive strength of glass fiber reinforced plastics 03 p0335 A73-13738

Compensation, by the layer winding method, for thermal stresses in articles manufactured from reinforced plastics 03 p0313 A73-13740

Creep of wound orthotropic glass fiber reinforced plastic 03 p0335 A73-13745

Stability of fiberglass-reinforced cylindrical shell under the action of axial dynamic loads 03 p0392 A73-13746

High frequency fatigue test assembly for glass fiber reinforced plastics specimens under symmetric tension-compression 03 p0288 A73-13747

Failure phenomena relationship to kinetic equation for defect buildup from brittle fracture analysis of composite glass fiber reinforced plastic in uniaxial eccentric tension 03 p0394 A73-14008

The application of adhesive bonded structures and composite materials on advanced turbofan engines. 03 p0359 A73-14134

Fiberglass reinforced composite material application to light weight ballistic damage tolerant military helicopter flight control components previously vulnerable to small arms fire 04 p0452 A73-14722

Nonlinear physical stress-strain relation for reticular polymers and fiberglass plastics under conditions of microcreep and elastic aftereffect 04 p0468 A73-15508

Improvements in the transverse properties of composites. I - Fracture surface energy and mechanism of transverse fracture in glass fibre composites. 04 p0469 A73-15984

Effect of specimen geometry on fatigue strength of boron and glass epoxy composites. 05 p0588 A73-16139

Bright future forecast for composites in aerospace. 05 p0589 A73-16185

The mechanical properties of thermoplastics strengthened by short discontinuous fibres. 05 p0589 A73-16434

The refractive index profile in a glass-fiber light waveguide 05 p0584 A73-16472

Response of a cylindrical fiberglass-reinforced plastic shell to the action of an explosive load 05 p0635 A73-17079

Glass fiber reinforced thermoplastic molding materials mechanical and thermal-dimensional stability properties, considering time dependent behavior under static and dynamic loads 06 p0714 A73-18450

Crack propagation measurements by surface gage of polymethyl methacrylate, epoxy resin and glass reinforced epoxy composites, conforming with Mott energy balance equation 06 p0714 A73-18499

Viscosity investigation of sintered fiberglass in the region of softening and annealing temperatures 06 p0715 A73-18657

Pulse broadening in multimode fibres excited by GaAs lasers. 07 p0833 A73-19155

Fracture mechanics application to initial notch extension under tension in quasi-isotropic fiberglass reinforced laminates, noting transplanar buckling effects on fracture toughness 07 p0841 A73-19186

Glass fiber reinforced polyester laminates, testing layer base material and molding condition effects on tensile and bending strengths and other mechanical properties 07 p0843 A73-20326

Hybrid composite of carbon and glass fiber reinforced epoxy resin, testing mechanical properties and optimal fibrous modulus ratios and volume fraction 07 p0844 A73-20327

On the torsional strength of composite materials reinforced with glass fabric laminates and the effect of the voids in matrix. 07 p0915 A73-20332

On the compressive strength of composite materials reinforced with glass fabric laminates. 07 p0844 A73-20333

Wave propagation along radially inhomogeneous glass fibres. 08 p0937 A73-20832

Radiative heat transfer in fiberglass insulation. 08 p1021 A73-20866

Large deflections and stability of a long cylindrical panel prepared from an orthotropic fiberglass plastic under the action of piecewise-uniform loading 08 p1017 A73-21370

Deformation of a frame coupled to a fiberglass-plastic shell under the action of local loads 08 p1017 A73-21372

Flammability comparisons of glass-reinforced unsaturated polyester moldings in various laboratory-scale tests. 08 p0983 A73-21820

Izod impact properties of carbon-fibre/glass-fibre sandwich structures. 09 p1110 A73-22517

Random function theory method for estimation of tensile, compressive and shear strength and elastic constants of monodirectional fiberglass reinforced plastics 09 p1110 A73-23056

The thermal expansion coefficients of some glass-reinforced plastics and their components at low and high temperatures. 09 p1111 A73-23063

Brittle fracture of orthogonally reinforced glass-fiber plastics during tension 09 p1111 A73-23349

Evaluation of static test methods for determining the fundamental mechanical properties of fiberglass-reinforced plastics 10 p1237 A73-23663

Fiberglass reinforced plastics dynamic models, discussing stress-strain relationship, Poisson ratio and fatigue 10 p1288 A73-23962

Creep-rupture strength criterion in the case of interlayer shearing of oriented fiberglass plastics 10 p1240 A73-24355

Limiting deformability of lengthwise-crosswise wound fiberglass-reinforced plastics under conditionally instantaneous and prolonged biaxial compression 11 p1386 A73-25034

Effect of heat treatment on the fatigue properties of unwoven fiberglass-reinforced plastics 11 p1386 A73-25047

Glass fiber optical waveguides for laser communication systems. 11 p1376 A73-26119

Glass fiber reinforced polyester laminates mechanical properties evaluation for structural design, considering failure criteria in terms of fiber debonding and resin and gel coat cracking 12 p1515 A73-26877

Reinforcing glass fiber preparation effect on fiber wetting by polyethylene melt, analyzing adhesion strength relationship to residual stresses 12 p1516 A73-27178

Statistical characteristics of the mechanical constants of glass-fiber-reinforced plastics 12 p1516 A73-27184

Probability characteristics of the shear modulus of fiberglass-strengthened plastics 13 p1644 A73-27997

Determination of the mechanical characteristics of fiberglass-strengthened plastics in the winding state 13 p1644 A73-27998

High strength glass fibre-resin composites. 13 p1645 A73-28498

Method for the investigation of the fatigue strength of fiberglass produced by winding and loaded by interlayer shear. 13 p1695 A73-28523

Glass fiber reinforced plastics optimum glass volume fraction for maximum flexural rigidity and strength 13 p1645 A73-28777

Determination of the nominal strength characteristics of fiberglass-strengthened plastics in the stress-concentration zones 13 p1645 A73-29051

Glass fiber for optical communication with existing light source and detector devices, assessing materials and fabrication technology for capacity, attenuation and environmental requirements 13 p1585 A73-29114

German monograph - A contribution to the stability calculation and the test of cylindrical shells of glass-fiber reinforced plastics under uniform external pressure. 13 p1646 A73-29280

German monograph on signal transmission and radiation distribution in optical waveguide consisting of glass fibers with refractive index gradient and optically dense envelope 13 p1628 A73-29282

Heat and mass transfer on the surface of a fiberglass-reinforced plastic in a high-temperature air flow 13 p1708 A73-29403

Internal fracture and acoustic emission of fiberglass reinforced plastics. 13 p1647 A73-29544

On fatigue damage and debonding of glass fiber reinforced plastics. 13 p1647 A73-29546

Bending vibration test of glass-textolites, noting temperature effect on vibration damping properties 13 p1647 A73-29607

Fiberglass-reinforced plastics for glider laminate wing spars, describing elastic properties and strength characteristics 14 p1809 A73-30241

Samarium oxide neodymium oxide activated glass fiber output power under lasing conditions 14 p1766 A73-30468

Application of fiber optics to the observation of fatigue crack development

14 p1754 A73-30691

Conditionally-instantaneous and long term strength of a longitudinally-transversely wound glass-fiber-reinforced plastic under biaxial compression

15 p1896 A73-30975

Effect of lasting high temperatures on the mechanical properties and microstructure of bonded glass mat with an aluminophosphate binder

15 p1896 A73-31213

Critical stress intensity factors applied to glass reinforced polyester resin.

15 p1897 A73-31676

Orthotropic characteristics of glass-fibre-epoxy laminates under plane stress.

15 p1897 A73-31698

Mechanism of breakdown in the interface region of glass reinforced polyester by artificial weathering.

15 p1898 A73-31838

Recent progress in fibres for optical communications.

16 p2023 A73-32863

Void free high temperature resistant bismaleimide/woven fiberglass composite laminates, discussing synthesis, processing and fabrication

16 p2028 A73-33046

Low void polyimide/glass and graphite reinforced composite properties and fabrication, showing improved interlaminar shear and wet strength

16 p2029 A73-33048

Glass fabric structures, properties and designs of reinforced polyester and epoxy laminates for aerospace applications

16 p2030 A73-33064

Nonlinear creep in glassfiber-reinforced plastics in the presence of some types of complex stress conditions

16 p2030 A73-33926

Experimental investigation of the effect of vibrations on the creep of glassfiber-reinforced plastics in the presence of complex stress conditions

16 p2030 A73-33939

Factors affecting the impact strength of glass-fibre-reinforced polyester composites.

16 p2031 A73-33987

The effects of adverse environmental conditions on the resin-glass interface of epoxy composites.

16 p2031 A73-33989

Aircraft structural applications of filamentary composites, discussing fiberglass, boron-epoxy and graphite-epoxy composites

17 p2103 A73-34814

Low cost manufacturing methods for highly reliable ballistic-tolerant composite helicopter flight control components.

[AHS PREPRINT 754]

17 p2180 A73-35082

Performance, structural reliability and fatigue life of glass fiber-epoxy twin beam helicopter rotor blades

[AHS PREPRINT 782]

17 p2106 A73-35095

Non-destructive testing of plastics by means of holographic interferometry.

17 p2181 A73-35355

Carbon, boron and glass fiber-epoxy resin composites fracture processes, predicting fracture strength of aligned fibrous composites via linear elastic fracture mechanics concepts

17 p2198 A73-35530

The strength prediction problem of unidirectional fiberglass-reinforced plastics under transverse tension and shear

18 p2326 A73-36409

Initiator composition and glass content effects on polyester resin hardening in glass laminate fabrication

18 p2327 A73-36467

Rational winding of vessels with nonlinear winding programs

18 p2319 A73-36470

Concepts from the realization of the development of the technology and assembly lines for the fabrication of polyester glass laminates

18 p2320 A73-36472

On stress concentration factors in orthotropic glass-fiber reinforced plastics.

18 p2327 A73-36474

Studies of fiberglass plastic under tensile load with the aid of transparency measurements

18 p2327 A73-36476

Nondestructive testing of fiberglass reinforced plastic plates by means of holographic interferometry

18 p2316 A73-36477

Self extinguishing properties of polyester-glass laminates with reduced flammability due to polyvinyl chloride and antimony trioxide additives

18 p2327 A73-36478

Mechanical characteristics of thermoplastic materials reinforced with short glass fibers, taking into account various degrees of reinforcement

18 p2327 A73-36479

The effect of a fiberglass reinforcement on the properties of laminates with a polyamide binder

18 p2328 A73-36481

Adhesion effect on the tensile properties of fibre reinforced composite materials.

18 p2328 A73-36683

Heat and mass transfer processes during thermal decomposition of resin binders in fiberglass reinforced plastics

18 p2328 A73-36814

Determination of rated strength characteristics of fiberglass in zones of stress concentration.

18 p2328 A73-36883

An improved method of production for high strength fibre-reinforced thermoplastics.

18 p2329 A73-37092

Fatigue of fibre-reinforced plastics - A review.

18 p2329 A73-37094

Transient and steady state sound absorption coefficients of fiberglass and polyurethane foam

19 p2459 A73-37286

Studies on glass-reinforced epoxy resin using either Vulkadur A or a mixture of Vulkadur A and triethanolamine as crosslinking agent.

19 p2444 A73-38092

A critical examination of the impact test for glassy polymers.

19 p2444 A73-38093

Glass fiber reinforced polypropylene composites fabrication technology and physico-mechanical properties

19 p2444 A73-38162

Influence of cycle ratio on the elastic modulus of glassfiber reinforced plastics subjected to repeated tensile load.

20 p2580 A73-38644

The impact resistance of glassfiber reinforced plastics under accumulation of fatigue damage.

20 p2580 A73-38645

Equivalent circuit and transfer function of the multimode glass fiber with random mode conversions.

20 p2521 A73-38658

Multimode glass fiber as transmission medium for digital signals.

20 p2521 A73-38659

Glass fiber transmission characteristics as optical waveguides for communication systems, considering transit time and attenuation

20 p2522 A73-38660

Using the new fundamental system of modified cylindrical functions for designing optical core fiber waveguides with cladding of finite thickness.

20 p2522 A73-38661

Detachable liquid filled capillary waveguide connector for glass fiber multimode optical transmission lines, discussing propagation efficiency as function of dimensional tolerances

20 p2522 A73-38662

Determining the absorption coefficients of low-loss bulk glass materials.

20 p2563 A73-38663

Use of laser amplifiers in a glass-fiber communications system.

20 p2522 A73-38667

Method of studying the resistivity to external effects in fiberglass plastic structural elements with highly dispersed initial-state properties

20 p2580 A73-39380

New developments regarding wide-band communication with waveguide, glass fiber, and superconductivity

21 p2655 A73-41072

Fiber glass reinforced plastics measurement for ratio of elastic modulus to mean thermal conduction for use in cryostat to resist large forces

21 p2723 A73-41106

Thermal contraction of a system of glassfiber and epoxy resin between 300 and 77 K.

21 p2724 A73-41107

Theoretical and experimental investigations of the coupling of two glass-fiber light waveguides

22 p2861 A73-42424

Prediction and control of macroscopic fabrication stresses in hoop wound, fiberglass rings.

23 p3041 A73-43638

High strength filaments for cables and lines, discussing bundle theory and comparing dielectric and tensile properties for glass, graphite and organic fibers

23 p2997 A73-43645

Glass and plastic optical fiber properties, performance, limitations and applications

23 p3007 A73-44211

Investigation of the possibility of obtaining an desite-based alkali-resistant glass compositions for a continuous glass fiber

23 p2998 A73-44298

Deformation of molten glass in the zone where a hollow glass fiber is formed

24 p3102 A73-44520

GLAUBER THEORY

Use of the Glauber approximation in atomic collisions - A progress report.

02 p0195 A73-12649

GLAUCOMA

Ocular tonus measurements for glaucoma detection in flying personnel, discussing subsequent test procedures in case of abnormal findings

02 p0134 A73-12158

Glaucoma development in aging flight personnel.

18 p2285 A73-36926

Patterns of diurnal variation in the intraocular pressure of airline pilots.

20 p2512 A73-39107

Ocular tension in flying personnel

21 p2637 A73-40347

GLAUERT COEFFICIENT

U AERODYNAMIC FORCES

U MACH NUMBER

GLIDE ANGLES

U GLIDE PATHS

GLIDE LANDINGS

Analysis of various automatic homing techniques for gliding airdrop systems with comparative performance in adverse winds.

[AIAA PAPER 73-462]

15 p1827 A73-31448

ILS technology assessment, considering landing glide path determination, interference due to multipath propagation and ground effects, and operating frequency range problem

21 p2737 A73-41075

GLIDE PATHS

Comparison of conventional flight control systems with a modern integrated flight control system

10 p1175 A73-32762

Guidance methods for heat-optimal three-dimensional descent paths of aerodynamic reentry bodies

11 p1430 A73-25350

Display system for monitoring automatically controlled STOL landing glide paths, discussing computer controlled simulation

11 p1362 A73-25440

Evaluation of glide paths for landing a VTOL airplane using linear regulator theory.

12 p1458 A73-27154

Nonimage glidepath antenna design for ILS system within international civil aviation convention specifications

15 p1909 A73-32463

Possibilities for improving conventional ILS systems

17 p2207 A73-34479

Game theory mathematical model for optimal control of glide modes in conflict situation

23 p2999 A73-43263

GLIDE SLOPES

U GLIDE PATHS

GLIDERS

NT HYPERSONIC GLIDERS

NT PARAWINGS

Synoptic conditions of wave formation above convection streets.

04 p0473 A73-14826

Glider soaring flight energy budget analysis, discussing rate of climb indicator error compensation

08 p0968 A73-21656

Electronic systems for time constant and altitude error compensation of rate of climb indicator used in high performance glider flight

10 p1222 A73-24916

Aircraft compass design with magnetic needle free turning capability around two orthogonal axes, noting advantage over conventional devices and suitability for glider navigation

13 p1613 A73-28555

Fiberglass-reinforced plastics for glider laminate wing spars, describing elastic properties and strength characteristics

14 p1809 A73-30241

Computational program for calculating the Re-number-dependent polar of a glider with arbitrary double trapezoidal wing

16 p1967 A73-33024

A fatigue test program for the wing of the Jantar SZD-37 sailplane

20 p2509 A73-39245

Influence of wing flexibility on sailplane loading by individual gusts

21 p2635 A73-41577

Flight tests of load factors for multirecorderequipped gliders of various designs during pullout and looping maneuvers

22 p2799 A73-41866

GLIDING

Gliding, twin formation and fracture of iron-single crystals at 78 K and at 4 K

11 p1386 A73-26571

Electronic differentiator for aircraft flight data on-board calculation in performance gliding, discussing compensation method and vertical air velocity measuring instrument advantage

13 p1569 A73-28556

Performance/stability of midair recovery system with tandem parachute configuration, discussing gliding and nongliding systems

[AIAA PAPER 73-461]

15 p1827 A73-31447

Electronic developments for performance gliding.

III

16 p2014 A73-33023

GLOBAL AIR SAMPLING PROGRAM

Measurement of high-altitude air quality using aircraft.

[AIAA PAPER 73-517]

16 p2006 A73-33554

Remote sensing of the global distribution of total ozone and the inferred upper-tropospheric circulation from Nimbus IRIS experiments. 23 p2975 A73-43876

GLOBAL ATMOSPHERIC RESEARCH PROGRAM
The Meteosat system - Europe space contribution to global atmosphere observation. 03 p0381 A73-13275

A system of four geosynchronous satellites for global observations 15 p1903 A73-31605

Global circulation numerical modeling problems and numerical weather forecasting status as basis for GARP programs, considering tropical experiment on deep convective cloud systems 17 p2205 A73-34927

Role of the meteorological satellites of the earth atmosphere observation system for the first global experiment of the 'Global Atmospheric Research Programme' 17 p2205 A73-34935

Post GARP Global Experiment programs, considering tropical vertical wind structure, satellite temperature measurement accuracy increase, data handling for real time and long term prediction 21 p2732 A73-40819

GLOBAL TRACKING NETWORK
The growing role of standards in the national and international coordination of space programs. 04 p0524 A73-15381

Intelsat communication satellites global network analysis, investigating technical factors affecting design options 09 p1059 A73-23436

GLOBULAR CLUSTERS
UV astronomy advances from rocket and satellite observations, discussing early stars, interstellar extinction and gas, galaxies and globular clusters 01 p0094 A73-10059

Photometry and spectroscopy of red variables in Omega Centauri. 01 p0098 A73-10584

UBV photometry of the metal-rich globular cluster NGC 6171. 04 p0500 A73-15487

Bright red giants in the globular clusters M3, M5, and M13. 04 p0503 A73-16006

Integral equations suitability and solution instability of stellar system models, referring to globular cluster densities and mass distribution equations 05 p0616 A73-16452

The stability of certain model binary stellar systems in galactic gravitational fields. 07 p0898 A73-19935

Axial ratio and position angle of the major axis of the globular cluster M92 07 p0901 A73-20317

Variations in spectral-energy distributions and absorption-line strengths among elliptical galaxies. 08 p1002 A73-20878

On the metal abundance of RR Lyrae stars in the globular cluster M22. 08 p1009 A73-21169

Thermal instability caused primary interstellar dust cloud fragmentation and resulting star formation according to Peebles-Dicke hypothesis for cosmological origin of globular clusters 10 p1274 A73-23713

Axial ratio and position angle of the major axis for the globular cluster M92. 12 p1539 A73-27289

Chemical composition of stars in globular clusters and the morphological characteristics of their horizontal branches 12 p1546 A73-27852

Thermal instability caused primary interstellar dust cloud fragmentation and resulting star formation according to Peebles-Dicke hypothesis for cosmological origin of globular clusters 18 p2355 A73-36738

Chemical composition of globular-cluster stars and the form of the horizontal branch. 20 p2608 A73-39226

Stellar masses on the asymptotic branch of red giants in globular clusters 21 p2768 A73-40719

Photometry of southern globular clusters. I - Bright stars in omega Centauri. II - Bright stars in NGC 6752. 22 p2907 A73-42206

Globular cluster mass determination from analysis of field stars proper motions 23 p3035 A73-44237

GLOBULES
On the presence of H2 molecules inside neutral globules imbedded in H II regions. 09 p1140 A73-22005

The shapes of neutral globules associated with diffuse nebulae. 24 p3141 A73-45194

GLOMERULUS
Morphological changes in the juxtaglomerular apparatus of rat kidneys exposed to the action of diversely directed accelerations for many hours 08 p0929 A73-20978

GLOTRAC [TRACKING NETWORK]
U GLOBAL TRACKING NETWORK
GLOVES
Mercury, Gemini and Apollo space suits, discussing glove development, boot design, portable life support equipment and extravehicular mobility 16 p1976 A73-34025

GLOW
U LUMINESCENCE
GLOW DISCHARGES
Glow discharge electron guns for welding. 01 p0055 A73-10113

The role of CO in CO2 lasers. 04 p0459 A73-16039

A simple bakeable hollow cathode device for the direct study of plasma constituents. 05 p0563 A73-17262

Macroscopic instability and anomalous diffusion in a glow discharge plasma 07 p0854 A73-19047

Measurement of the electron temperature of a quasi-stationary pulsed glow-discharge plasma in highly overcharged gaps 09 p1129 A73-22663

Niobium and tungsten cementation in a glow-discharge plasma 09 p1089 A73-23197

Local transient phenomena induced in an inert gas plasma by a short pulse. 10 p1257 A73-24626

IR spectroscopic study of polydimethylsiloxane thin film structure and polymerization under glow discharge 11 p1400 A73-26144

Microwave spectrometer with internal dc glow discharge for transient paramagnetic molecules observation, discussing design features and operating parameters effects on spectrum 11 p1366 A73-26303

Influence of CO on the population inversion in CO2 lasers. 14 p1756 A73-29921

Contributions to the mechanism and the plasma diagnostics at the negative glow light in the case of the cylindrical hollow cathode discharge 14 p1780 A73-30427

Cylindrical probe in a glowing-discharge nitrogen plasma at medium pressures 17 p2215 A73-34261

Laser gain characterization of near-atmospheric CO2:N2:He glows in a planar electrode geometry. 21 p2715 A73-40965

GLUCOSE
Effect of excessive glucose administration on the lipid level, glycolysis rates, and oxygen uptake in the tissues of the liver, heart, cerebrum and aorta 11 p1314 A73-25042

Studies on the metabolism of glucose-1,6-diphosphate in human erythrocytes. 21 p2639 A73-41139

Diurnal variations of plasma cortisol and glucose and of urinary excretion of free cortisol in man at rest 24 p3061 A73-45158

GLUCOSIDES
Transglucosidase activity of heart-muscle per-glucosylhydrolase 08 p0930 A73-21136

Energy requirements of ouabain-sensitive Na-K positive ion membrane pump during norepinephrine induced thermogenesis of brown adipose tissue in cold-exposed hamsters 09 p1040 A73-22649

GLUES
Glued metal joints polished samples interface corrosion under alternate immersions and withdrawals in baths of different compositions 04 p0468 A73-15991

GLUTAMATES
Effect of the administration of free amino acids and metabolic cofactors on the distribution of regional biogenic amine contents in the brain and blood of animals 09 p1040 A73-22864

GLUTAMIC ACID
Synthesis of glutamic acid via cyanoethylation of n-acetylaminocetonitriles in liquid ammonia. 06 p0661 A73-17936

GLYCERINS
U GLYCEROLS
GLYCEROLS
Phase dependence of positron annihilation in tristearin. 06 p0661 A73-18267

Lactate, alpha-GP, and Krebs cycle in sea-level and high-altitude native guinea pigs. 11 p1318 A73-26122

GLYCOGENS
Diet, exercise, and glycogen changes in human muscle fibers. 01 p0007 A73-10160

Adrenal influence on the supercompensation of cardiac glycogen following exercise. 11 p1318 A73-26121

Glycogen content in the rabbit retina in relation to blood circulation. 22 p2802 A73-41732

GLYCOLYSIS
Evolutionary significance of carbohydrate metabolism alterations in animal brains during adaptation to hypoxia 01 p0007 A73-10153

The use of glycolytic metabolism in the assessment of hypoxia in human hearts. 07 p0781 A73-19929

Effect of excessive glucose administration on the lipid level, glycolysis rates, and oxygen uptake in the tissues of the liver, heart, cerebrum and aorta 11 p1314 A73-25042

Apparent paradoxical patterns of anaerobic glycolysis and hexokinase activity in the red blood cells of acutely bled rats, with evidence that the responses were in part hormone-dependent. 11 p1315 A73-25568

Glycolytic intermediates and adenosine phosphates in rat liver at high altitude /3,800 m/. 20 p2514 A73-39602

GODDARD EXPERIMENT PACKAGE TELESCOPE
U PARTICLE TELESCOPES
GOE SATELLITES
GOES system data collection performance estimates. 20 p2525 A73-38743

GOLD
Influence of structural perturbations applied to platinum and gold on kinetic processes at the electrode. 04 p0407 A73-15105

Gold high temperature thermoelectric properties from electron model based on scattering resulting from d band-Fermi level relative position changes 04 p0463 A73-15313

Intermetallics formation and diffusion of contacting Al-Au thin films dependence on temperature, thickness ratio and contact time 06 p0706 A73-17903

Chemical and electrolytic coatings for satellite surface thermal control, discussing surface anodic oxidation treatment of adhesive Au platings on Al alloys 07 p0829 A73-18910

Study of the channeling of light ions of 0.5 to 2 MeV across gold crystals of some hundreds of angstroms thickness 07 p0864 A73-20609

Double-injection negative differential resistance in compensated gold-doped germanium. 10 p1259 A73-23752

Investigation of the growth of the disperse structure of gold on a germanium surface 11 p1408 A73-25247

Low-energy positrons from metallic moderators in a back scattering mode. 11 p1402 A73-26544

Experimental study of the diffusion of electrons of conduction by superficial defects of thin gold films 13 p1668 A73-28453

Diffusion in thin film couples of platinum-gold. 23 p3015 A73-43528

GOLD ALLOYS
Niobium-gold alloys crystal structure, phase diagrams, peritectic crystallization and microhardness, noting intermetallics formation by solid state reactions 16 p2026 A73-33957

Gold-iron alloys for low temperature thermocouples. 22 p2857 A73-42030

Reference data for thermocouple materials below the ice point. 22 p2857 A73-42031

GOLD COATINGS
Electrical conductivity of very thin gold films. 04 p0484 A73-15948

French D2A satellite construction, describing AG5 sheet covering and gold coating fabrication methods 07 p0829 A73-18912

Molecular nitrogen ionization growth characteristics as function of electric field strength and gas pressure, using thin gold film electrodes 09 p1122 A73-22119

Spatial and temporal ionization growth characteristics in nitrogen at moderate electric field strength, noting dominant secondary emission effect due to cathode bombardment by metastable molecules 09 p1122 A73-22120

Effects of oxygen environment and surface diffused coatings on fatigue crack development in copper single crystals. 11 p1380 A73-25806

Determination of the temperature dependence of the Debye-Waller factor for thin gold films by electron diffraction observations 12 p1532 A73-27944

Bonding degradation in the tantalum nitride-chromium-gold metallization system. 19 p2435 A73-38440

Electrodeposited Au on TO-5 headers, discussing discoloration measurement and ultrasonic test for bondability from correlation between optical reflectivity and bond pull strength 19 p2435 A73-38441

GOLD PLATE
U GOLD COATINGS

GONADS

Relation between the frequency-amplitude characteristics of cerebral electrical activity and gonadotropic hormone excretion levels at various stages of ontogenesis
08 p0930 A73-21319

GONIOMETERS

NT RADIOGONIOMETERS

Some results using the ultrasonic goniometer - The corner reflector method.
04 p0447 A73-14930

A goniometer for use with high-frequency circularly disposed aerial arrays.
21 p2703 A73-41207

GOSS [SUPPORT SYSTEM]

U GROUND OPERATIONAL SUPPORT SYSTEM

GOVERNMENT PROCUREMENT

C-5 program developments and alterations in terms of defense requirements and cost problems, discussing objectives and management policies in F-15 and B-1 projects
01 p0124 A73-11069

Reducing the cost of the R&D proposal process.
02 p0239 A73-12349

GOVERNMENT/INDUSTRY RELATIONS

Technology transfer from aerospace to public sector, discussing JPL experience, problem definition, funding, user concerns and interpersonal communications
04 p0521 A73-14729

Aircraft noise as a continuing national problem.
04 p0521 A73-14894

Communications Satellites and the international communications industry.
07 p0923 A73-19139

Performance control in government R&D projects - The measurable effects of performing required management and engineering techniques.
08 p1025 A73-20971

Book - Civil aviation development - A policy and operations analysis.
08 p1026 A73-21837

Government request to industry to propose product or service for buyer, discussing procurement role and centralized vs decentralized control
09 p1168 A73-21946

USAF experience in lightweight fighter aircraft acquisition as illustration of requests for industrial proposals simplification and source selection process streamlining
09 p1168 A73-21947

Government request to industry to propose product or service to buyer, discussing communications effectiveness, technical and management requirements and procurement
09 p1168 A73-21948

Co-existence of scheduled and charter services in public air transport.
09 p1168 A73-23123

Capital equipment marketing, discussing industry-customer-government interface, marketing and sales techniques and functions, products initiation, etc
10 p1298 A73-24650

Airport design and management for safe aircraft ground handling, discussing FAA rules on pavement and safety areas, marking and lighting, fire fighting, etc
10 p1204 A73-24714

An appraisal of the funding provisions of the Airport and Airways Development Act of 1970 to implement system improvements.
12 p1561 A73-27366

Airport and Airway Development Act trust fund surplus, discussing expenditure policy determination and incentive plan provisions to expedite improvements
12 p1561 A73-27367

Multi-Role Combat Aircraft Program management, discussing international cooperation, industrial arrangements and governmental objectives
13 p1709 A73-29384

Commercial air transportation in France - National administration and aviation enterprises
14 p1818 A73-30294

History, evolution, and role of the Civil Aviation Secretariat General
15 p1960 A73-32554

Toronto airport relocation project, summarizing provincial government planning and decision making process, site choice and community resistance to airport
16 p1995 A73-33181

The financing of aircraft procurement.
17 p2257 A73-34534

The financing of essential communication, navigation and terminal aids.
17 p2257 A73-34535

Management and control of military flight test programs at McDonnell Douglas St. Louis, Missouri.
23 p3050 A73-44059

Air Force Prototype Program management.
23 p3051 A73-44061

The transatlantic charter policy of the United States.
24 p3158 A73-44575

Maplin airport planning history, noise reduction features and government surveys, noting future air traffic trends and planning alternatives
24 p3076 A73-45373

GOVERNORS

U SPEED REGULATORS

GRABBERS

U GEOLOGICAL FAULTS

GRADIENTS

NT ELECTRON DENSITY PROFILES

NT POTENTIAL GRADIENTS

NT PRESSURE GRADIENTS

NT TEMPERATURE GRADIENTS

Automatic search system synthesis for linear programming, using gradient method and logic operations for system optimization
01 p0028 A73-10675

Application of the conditional-gradient method to the solution of an optimum control problem in a Hilbert space
02 p0187 A73-12188

Summary and comparison of gradient-restoration algorithms for optimal control problems.
06 p0715 A73-17567

Analysis of voltage steps with a time resolution of 12 picoseconds
08 p0962 A73-20833

The conjugate gradient method and its application to aerospace vehicle guidance and control. I - Basic results in the conjugate gradient method.
08 p0951 A73-21428

The conjugate gradient method and its application to aerospace vehicle guidance and control. II - Mars entry guidance and control.
08 p0986 A73-21429

Higher-order numerical differentiation of experimental information.
10 p1244 A73-24719

Supermemory gradient-restoration algorithm in flight-path optimization problems
12 p1548 A73-27082

Multistep conjugate gradient search methods with memory, describing convergence of iterative procedure for functional minimization
12 p1485 A73-27617

Gradient methods with penalty functions for solution of optimal control with terminal constraints, noting convergence superiority of conjugate gradient algorithm
16 p2034 A73-33998

Use of weighting functions in conjugate gradient methods
18 p2295 A73-37079

The method of virtual powers in mechanics of continuous media. I - Theory of the second gradient
19 p2495 A73-37424

Gradient method of nonsmooth function minimization on an analog computer
20 p2531 A73-38682

A maximum principle and gradient bounds for linear elliptic equations.
24 p3105 A73-44421

GRADIOMETERS

U MAGNETOMETERS

GRADUATION

U CALIBRATING

GRAIN BOUNDARIES

Grain growth in alloyed molybdenum under conditions of creep
01 p0063 A73-10486

Intergrain boundary shape effects on the impact strength and character of brittle fracture
01 p0064 A73-10606

Boron segregation at austenite grain boundary and matrix sites in steel by autoradiography
02 p0183 A73-12761

An observation of the effect of grain structure on the appearance of Kirkendall porosity.
02 p0184 A73-12772

Accommodation of the stress field at a grain boundary under heterogeneous shear by initiation of microcracks.
02 p0237 A73-12812

Creep rupture under multi-axial states of stress.
03 p0327 A73-13981

Pseudo-subgrain-boundaries in stainless steel.
04 p0461 A73-14872

Grain boundary interface and crystal structure effect on elastic and plastic deformation and mechanical properties of metals at low and high temperatures
04 p0462 A73-15301

Electron microscopic investigation of cold worked and annealed thin V and Mo foils recrystallization characteristics, considering effect of grain boundaries pinning at surface
05 p0588 A73-17245

Effect of recovery on recrystallization of aluminum
99.85
06 p0705 A73-17849

Effect of grain refinement on the microstructure and mechanical properties of 4340M.
06 p0713 A73-18773

Superrefractory Ni-based alloys mechanical properties enhancement through unidirectional solidification, considering grain boundary structure
07 p0838 A73-19116

Determination of some kinetic recrystallization parameters of thin films by mathematical and graphical analysis of crystallite boundary shapes
07 p0861 A73-19329

The effect of grain size on the fatigue of an Al-Mg alloy.
07 p0839 A73-20114

On relationship between stress corrosion resistance and grain shape of extruded Al-Zn-Mg alloys with heavy section.
08 p0977 A73-21140

Mechanism by which hot cracks form during welding aluminium and its alloys.
08 p0977 A73-21236

Creep strength of low alloy ferritic steels at low strain rates as function of grain boundary structure and matrix deformation
08 p0979 A73-21673

The effect of niobium content on the steady-state creep of stabilized 20/25 austenitic stainless steels.
08 p0981 A73-21786

Low stress creep tests of niobium stabilized austenitic steels.
08 p0981 A73-21789

Grain-boundary internal friction of copper-nickel alloys
09 p1099 A73-21965

Correlation between pore formation at grain boundaries and internal friction during creep of nickel
09 p1099 A73-21970

Intercrystalline molybdenum fracture
09 p1099 A73-21971

Observations on the interaction of twins with grain boundaries in Mo-35 at.% Re alloy.
09 p1100 A73-21982

Grain size effects on strength and ductility of two phase Ni-Cr and Ni-Mo alloys at high and low deformation temperatures
09 p1101 A73-22164

Surface fatigue crack morphology comparison to bulk crack developments, considering surface grains constraints by adjoining grains
09 p1103 A73-22441

High temperature mechanical properties measurements verifying metal polycrystal internal friction background origin in diffusion of vacancies formed under grain boundary loading
09 p1105 A73-23060

Ductility of recrystallized molybdenum as a function of oxygen concentration and grain size
09 p1108 A73-23231

Effects of metal grain size on friction and wear characteristics
10 p1223 A73-24067

Grain-boundary corrosion of type 304 stainless steel by cesium oxides.
10 p1234 A73-24427

Flow stress dependence on grain size in microstrain region of Ni strip machined to produce different grain sizes
10 p1235 A73-24444

Determination of alpha plus gamma/gamma phase boundaries in Fe-Cr-Ni, Fe-Cr-Co, and Fe-Cr-Mn systems
11 p1384 A73-26108

Dislocation structure of subgrain boundaries in creep-deformed aluminium.
12 p1511 A73-27028

On the relationship between grainboundary corrosion and stress corrosion cracking of Al-Zn-Mg alloys.
12 p1511 A73-27059

Determination of the boundaries of single-phase edge regions in the Mo-Cu-Ni system in solid state
12 p1513 A73-27559

Precipitation processes in Nb microalloyed converter steel
12 p1514 A73-27685

Al, Sr or Co effects on kinetics of grain boundary ferrite allotriomorph formation relative to iron alloys, noting displacement of TTT curve
13 p1632 A73-28129

Measurement of interfacial free energies and associated temperature coefficients in 304 stainless steel.
13 p1634 A73-28259

Crystal surface topography investigation by scanning electron microscopy for dihedral angle measurements on thermally grooved grain boundaries
13 p1617 A73-28935

Effect of microstructure and environment on stress corrosion of 7075 aluminum alloy.
13 p1637 A73-29312

Interpretation of mechanical behavior of pure aluminium in terms of microstructure.
13 p1639 A73-29459

Some observations on grain boundary sliding in aluminium bicrystals deformed at elevated temperatures.
13 p1641 A73-29508

Mathematical theory of elasticity for stress concentration in homogeneous isotropic perfectly elastic composites with spherical inclusions, noting grain boundary stresses
13 p1702 A73-29535

Investigation of the structure of turbine disc materials after use.
13 p1643 A73-29632

Increase in the boundary strength of cast electron-beam-melted molybdenum by microadditions of vanadium.

13 p1643 A73-29634

Grain growth during creep of alloyed molybdenum.

14 p1759 A73-30311

Kinetics of changes in deformability of a heat-resistant nickel-base alloy

14 p1764 A73-30861

Influence of annealing temperature on the changes in the chemical and phase compositions of the intercrystalline boundaries of weakly-alloyed molybdenum

14 p1764 A73-30865

Grain-boundary sliding and recrystallization of Nimonic 108 during creep.

15 p1887 A73-31352

Grain boundary dislocations in aluminium bicrystals after high-temperature deformation.

15 p1891 A73-32020

Auger spectroscopy usefulness demonstration by determination of impurity segregation in localized regions, reviewing grain boundary segregation role in metal properties deterioration

15 p1892 A73-32248

A quantitative model of hydrogen induced grain boundary cracking.

17 p2191 A73-35124

Grain growth in commercial alpha and alpha + beta/Ti alloys.

18 p2326 A73-37143

Effects of interstitial content and grain size on the strength of titanium at low temperatures.

19 p2440 A73-37542

Diagrams of cumulative damage during tension of polycrystalline metals

20 p2577 A73-39371

Substructure of type 316 stainless steel deformed in slow tension at temperatures between 21 and 816 C.

20 p2578 A73-39491

Grain boundary destruction mechanisms in pure nickel polycrystals following plastic deformation, discussing annealing, fault concentration, microscopic techniques and critical loads

20 p2578 A73-39735

Heat resistance of chromium-nickel and chromium-nickel-molybdenum steels with additions of boron

21 p2718 A73-40734

Influence of grain size on effects of thermal expansion anisotropy in MgTi2O5.

21 p2752 A73-40893

Fractography of stress corrosion cracks in aluminum alloy 7075.

21 p2720 A73-40925

Materials testing via ultrasonic spectroscopy developed from pulse-echo technique, discussing application to metal grain size determination and carbon fiber composite quality control

21 p2707 A73-41136

Grain size effects on strength and ductility of two phase Ni-Cr and Ni-Mo alloys at high and low deformation temperatures

22 p2875 A73-42112

Grain boundary cavitation and sliding in copper/tungsten composites due to thermal stresses.

22 p2876 A73-42339

The influence of testing temperature and thermal history on the intergranular embrittlement and penetration of aluminium by liquid gallium.

23 p2993 A73-44026

Consideration of lattice translations in computer studies of grain-boundary coincidence.

24 p3120 A73-45405

GRAINS

The consequences of grains in the atmospheres of late-type stars. I - Intrinsic polarization, infrared excesses, and emission lines.

01 p0103 A73-11035

GRAINS [FOOD]

NT CORN

GRAMMARS

Syntax specification system for computerized hand-drawn pattern grammar generation with user style description for concurrent inputting and analysis at high recognition speed

06 p0671 A73-18535

GRAND TOURS

Grand Tour missions to the outer solar system with Saturn /Intermediate 20/.

06 p0750 A73-18024

The selection and design of electro-optical instruments for outer planet exploration.

06 p0695 A73-18320

Solar independent power source with radioisotope thermoelectric generator for Grand Tour missions, discussing radiation and thermal interfaces

11 p1313 A73-26042

GRANITE

Whole rock Th-Pb age for the Masuke and Dembe-Divula complexes, Rhodesia.

17 p2159 A73-34519

GRANULAR MATERIALS

Triaxial plastic compression soil theory generalization to three dimensional complex stress fields, discussing yield surface for granular materials

03 p0390 A73-13332

Dispersive granulation by spinning electrode melting in helium atmosphere for steels and Ti, Ni and Mo alloys powder production

03 p0323 A73-13503

Granularity produced by a diffuser illuminated in partially coherent light

03 p0320 A73-14606

Review of theories and experimental results pertaining to the dynamic behavior of porous bodies

07 p0912 A73-19905

Microstructure, microhardness and mechanical strength of ingots and granules of Al alloys with high refractory metal contents

12 p1511 A73-26917

Particle track densities in 100-200 micron crystalline grains from soil column returned from lunar highlands by Luna 20 and 16

12 p1541 A73-27487

Lunar soil models for equipment environmental testing, using vibrationally compacted volcanic granular materials

13 p1606 A73-28119

Small grain aggregates created by equalized grain orbits on Kepler trajectories, with low collisional frequency in early state of solar system planetary evolution

17 p2227 A73-34407

Models comparison for heavy elements segregation mechanism from gaseous hydrogen and helium for terrestrial planets formation from primordial granular matter

17 p2228 A73-34422

Linear structure theory from analysis of structural mechanical models, proposing three dimensional model for behavior of granular materials

17 p2245 A73-34832

GRAPHITE

NT PYROLYTIC GRAPHITE

On the mechanism of particle emission from graphite during pulsed laser heating.

01 p0068 A73-10923

Assessment of the heat resistance of graphites over a wide range of temperatures

02 p0184 A73-11619

The effect of crystallite size on the strength of carbon-graphite materials.

02 p0185 A73-12142

Development and evaluation of graphite and boron polyimide composites.

03 p0329 A73-13003

Graphite-epoxy composite missile adapter design, fabrication, tooling, bonded assembly and costs, comparing with boron-aluminum material

03 p0331 A73-13022

Graphite-epoxy composite properties, fabrication and tests for light weight low distortion spacecraft antenna reflector applications

03 p0331 A73-13023

Properties of pultruded composites containing high modulus graphite fibers.

03 p0332 A73-13032

Light weight graphite-polyimide composite honeycomb core and sandwich panel design, fabrication and tests for shuttle orbiter thermal protection system

03 p0333 A73-13051

Shubnikov-de Haas oscillations in graphite selective scattering by charged impurities.

04 p0468 A73-14871

Bright future forecast for composites in aerospace.

05 p0589 A73-16185

Carbon and graphite sublimation in inert gas flow at 2800-3000 K, determining rate dependence on temperature under kinetic and diffusive conditions

06 p0713 A73-17411

Enthalpy and heat capacity of graphite in the temperature interval between 273 and 3650 K

06 p0714 A73-18557

Si and silicon carbide effects on silicided graphite thermal and electrical conductivities

06 p0714 A73-18558

High strength and low density graphite fiber yarn for reinforcement in structural composite components on heavily loaded flight vehicles

06 p0715 A73-18716

Properties of pultruded composites containing high modulus graphite fibers.

06 p0715 A73-18719

Polyimide composites development for aircraft structures.

06 p0715 A73-18720

Shock wave generation for industrial applications in graphite to diamond conversion and incompatible materials bonding

07 p0850 A73-19048

Self lubricating bearing materials strength, friction, wear, thermal and dimensional stability properties, considering plastic, metal matrix and carbon graphite composites

07 p0842 A73-19555

IR absorption spectra of powdered graphite samples during treatment in laminar propane-butane diffusion flame zones

07 p0921 A73-19996

The plane-wave method in the study of helium atoms physisorbed on graphite

07 p0843 A73-20000

Reaction of graphite with carbon dioxide at temperatures from 1200 to 2400 C

08 p0982 A73-21095

High-energy electron-beam deposition onto a hot graphite surface.

08 p0990 A73-21210

Material design concepts for filament-wound, graphite-graphite heatshields Further analysis.

08 p1020 A73-21819

Influence of thermally stabilizing alloying additions on the antifriction properties of lamellar graphites with a organic silicon binders

09 p1110 A73-22978

Development of special graphites for lithium hydride/fluorine rocket engines

09 p1110 A73-23019

Effect of test temperature on energy of fracture of graphite.

09 p1110 A73-23062

Feasibility evaluation of graphite/epoxy composite materials to helicopter transmission housing.

10 p1238 A73-23969

The effect of long-time thermal exposure on the mechanical properties of graphite/polyimide composites.

10 p1238 A73-23970

Bearing materials from graphite fiber composites.

10 p1238 A73-23974

Carbon-carbon composites and bulk graphite fracture toughness and failure modes determination from single-edge-notched specimen responses under three-point bending

10 p1239 A73-24276

Development and investigation of fine-grain metal ceramic contacts of silver/graphite and silver/nickel/graphite composition for low-voltage device applications

10 p1225 A73-24320

Investigation of the fracture of carbon-graphite materials in a complex stress-strain state

10 p1240 A73-24360

Application of gamma-resonance emission spectroscopy to the study of the structure of laminar compounds of graphite with Co-57-labeled cobalt and cobalt chloride

10 p1186 A73-24466

Temperature change induced material properties variations effects on impact stresses in graphite and stainless steels, considering impact velocity

10 p1220 A73-24575

A statistical investigation on the mechanical properties of metals impregnated graphites.

11 p1388 A73-25416

A theory of an elastic-plastic continuum with special emphasis to artificial graphite.

13 p1644 A73-28168

The isotopic composition of 'graphitic' carbon from iron meteorites and some remarks on the troilite sulfur of iron meteorites.

13 p1684 A73-29180

Graphite content effect on vibration damping properties of Al-Sn and Al-Zn alloys

13 p1643 A73-29608

Influence of air pressure on the brittle fracture of graphite

14 p1766 A73-30715

Russian book - Physics of carbographite materials.

15 p1897 A73-31583

Dynamic mechanical properties of graphite-epoxy and carbon-epoxy composites.

15 p1897 A73-31677

Some mechanical properties of carbon fiber reinforced aluminum.

16 p2025 A73-32849

Low void polyimide/glass and graphite reinforced composite properties and fabrication, showing improved interlaminar shear and wet strength

16 p2029 A73-33048

Graphite-epoxy composite door landing gear assembly for space shuttle orbiter, discussing design, analysis, fabrication and structural testing

16 p2029 A73-33058

Enthalpy and specific heat of graphite in the temperature range 273-3650 K.

16 p2030 A73-33583

Si and silicon carbide effects on silicided graphite thermal and electrical conductivities

16 p2030 A73-33584

Graphite fiber optimization and evaluation efforts for utilization as fiber-epoxy composites reinforcement in tensile-critical applications

17 p2198 A73-35838

High temperature coatings on graphite

18 p2318 A73-35885

Assessment of chemical nonequilibrium for massively ablating graphite.

18 p2368 A73-36322

Graphite oxidation at low temperature in subsonic air.

18 p2326 A73-36352

Surface properties of carbon and graphite fibers

18 p2327 A73-36465

A study on graphite-base high-temperature composite materials. II Graphite-tantalum composite materials.

19 p2443 A73-37375

Composite fabrication and structural design for commercial aircraft, discussing graphite post installation and testing and pultrusion and autoclave molding processes

[SME PAPER EM 73-717] 19 p2436 A73-38497

Study of the effect of stress concentration on the variation of stability characteristics in graphites

20 p2580 A73-39383

Burnout of a graphite surface during the blowing of an inert gas through it

21 p2790 A73-40698

Polarization of rare gas atoms in the successive layers adsorbed on graphite

21 p2724 A73-41599

Measurement of the heat capacity of graphite in the range 1500 to 3000 K by a pulse heating method.

22 p2881 A73-42510

Graphite fiber tensile property evaluation, discussing single filament method and improved dry bundle test including electrical resistivity measurement and stress-strain curve analysis

23 p2996 A73-43644

The influence of flaw density and flaw size distribution on the static and dynamic fatigue behaviour of graphite.

23 p2998 A73-44037

Selection of phosphate impregnants for graphite oxidation inhibition

24 p3104 A73-44954

Influence of porosity on the effective heat conductivity of graphite

24 p3104 A73-45082

GRAPHITIZATION

Graphitization of carbon fibre/glassy carbon composites.

10 p1240 A73-24284

Diffraction spectra and electron density distributions of interatomic graphitizing carbon molecule bonds as polymer combinations, using diffractometer and scintillation counter recording

14 p1767 A73-30839

High modulus graphite fiber preparation from polyacrylonitrile yarn, discussing graphitization, properties and stabilization oxidation treatment

16 p2028 A73-33042

Microstructure and its related properties on carbon fiber composites.

23 p2998 A73-44134

GRAPHS [CHARTS]

Variational methods for linear numerical filtering with operator and transfer function spreads compromise, presenting graphical data

[ONERA, TP NO. 1127] 01 p0070 A73-10236

Numerical Laplace transform inversion of a function arising in viscoelasticity.

01 p0119 A73-11469

A graphical test for checking the stability of a linear time-invariant feedback system.

03 p0285 A73-13519

Analytical investigation of a cylindrical shell embedded in a soft medium.

04 p0511 A73-15172

Observations of extragalactic variable sources at 2.8 and 4.5 cm wavelength.

04 p0500 A73-15515

Book - Electronic properties of composite materials.

06 p0714 A73-17872

VV 281-427, variable stars in a Cepheus-Lacerta field of the Milky Way.

07 p0874 A73-19117

Reliability of sealed reed switches [SRS/]

07 p0801 A73-19423

A graphical method for analyzing pool-boiling systems.

08 p1023 A73-21262

Graphical method of profiling and contouring microcraters on lunar rocks from stereomicrograph pair obtained by scanning electron microscope

09 p1081 A73-22378

Graphoanalytic method of calculating plane potential flows

09 p1029 A73-23106

A chart for the computation of the gravitational attraction of a right rectangular prism.

11 p1351 A73-25160

Book - Thermal radiative properties: Nonmetallic solids.

11 p1387 A73-25275

A high-speed automatic strip-chart recorder

12 p1497 A73-27220

VIEW - A distributed system for graphical analysis of large data bases.

[ALAA PAPER 73-431] 12 p1476 A73-27824

Mean frequency response characteristics of graphical smoothing operator for latitude observations analysis

13 p1683 A73-29099

Graphs, tables and discussion to aid in the design and evaluation of an acceptance sampling procedure based on cumulative sums.

13 p1709 A73-29297

A computer program for plotting exponentially smoothed average control charts.

13 p1588 A73-29299

The effect of groupings of surface couples on flat plates

14 p1814 A73-30703

Problem of the legibility of records produced by strip chart recorders with curvilinear coordinate systems

14 p1754 A73-30875

Graphical distribution in colors adapted to traffic control

15 p1911 A73-32486

Book - Methods for estimating drag polars of subsonic airplanes.

16 p1963 A73-33422

The Berkeley low-latitude survey of neutral hydrogen. I - Profiles.

16 p2063 A73-33600

Mechanical, thermal and electrical properties of polymers as functions of temperature, radiation and frequency for cryogenic environment material and design selection

19 p2443 A73-37525

Arizona-NASA Atlas of the Infrared Solar Spectrum. X.

19 p2483 A73-37576

Tables and graphs for characteristics and pulse profiles of pulsars discovered in low Galactic latitude radio telescope survey

20 p2605 A73-39017

Graphical analysis of traveling-wave-tube oscillator with external feedback loop.

21 p2663 A73-41046

Product reliability management, providing MTBF charts for relationships between part count, laboratory test results and operational performance

22 p2867 A73-42969

A simple graphical solution for rocket wake boundaries.

23 p2939 A73-43680

GRASHOF NUMBER

Heat transfer in horizontal annular air gaps at small Grashof numbers

09 p1167 A73-23108

Planar free convection flow over horizontal cylinders with a small Grashof number under the influence of a planar wall

16 p2085 A73-33254

Heat transfer through free convection of air between vertical plates, obtaining Nusselt and Grashof numbers, and temperature and pressure effects

20 p2628 A73-39407

GRASSES

Plant canopy models for simulating composite scene spectroradiance in the 0.4 to 1.05 micrometer region.

20 p2562 A73-39906

GRASSLANDS

Remote mapping of standing crop biomass for estimation of the productivity of the shortgrass prairie, Pawnee National Grasslands, Colorado.

20 p2562 A73-39907

GRASSMANN ALGEBRA U VECTOR SPACES

GRATINGS

Foveal threshold additivity measurements for monochromatic and mixed light, using grating resolution as brightness criterion

14 p1717 A73-30398

GRATINGS [SPECTRA]

NT ECHELETTE GRATINGS

A new Cassegrain grating spectrograph. I - Optical design.

01 p0047 A73-10513

A new Cassegrain grating spectrograph. II - Mechanical design and operation.

01 p0047 A73-10514

Spectroscopic telescope diffraction gratings, discussing fabrication methods and performance characteristics of echelle and Coude gratings

01 p0047 A73-10518

Holographic gratings application to astronomical spectrograph design for IR to extreme UV and X rays, considering characteristics advantage

01 p0047 A73-10519

Stellar spectroscopy with holographic gratings.

01 p0047 A73-10520

Grating mosaic for use in conjunction with coude focus of 3.6 meter reflecting telescope, discussing optical and optomechanical implementation methods

01 p0047 A73-10521

Organic dye lasers tuning by diffraction gratings and prisms, noting CW, pulsed and mode locking operations

01 p0059 A73-10716

Talbot shearing interferometer based on Fourier imaging behind grating illuminated by plane monochromatic wave with spatial filtering, obtaining radial and lateral derivatives

01 p0053 A73-11227

Applications of conformal mappings to the diffraction of electromagnetic waves by a grating.

06 p0665 A73-18182

Modulation of intensity in multiple images of a luminous source given by a system of two parallel networks

07 p0824 A73-20163

Angular dispersion of diffraction gratings used for tuning organic dye lasers.

08 p0975 A73-21057

Color encoded multispectral image recording on black-and-white photographic film with synthetically generated diffraction gratings, noting color recognition, resolution and contrast ratio

10 p1216 A73-23786

Holographic construction and application of optical elements, discussing hologram lenses, holographic multiple imaging systems and diffraction gratings

12 p1498 A73-27501

The use of surface-elastic-wave reflection gratings in large time-bandwidth pulse-compression filters.

12 p1480 A73-27566

Calculation of the constants of an infinitely narrow beam in spectral devices

13 p1660 A73-28769

Developments in the optical spatial filtering of superposed, crossed gratings.

13 p1620 A73-29302

Polarization cascade matrix describing arbitrary elliptically polarized microwave transmission through inclined grating of parallel wires

13 p1587 A73-29669

Dark field method for phase diffraction grating visualization by microwave holography, using radio lens for object microwave spectrum formation

17 p2168 A73-35165

Restoration of degraded images by composite gratings in a coherent optical processor.

17 p2173 A73-35435

A comparison of the efficiency and focused stray light characteristics of a conventionally ruled- and a holographically produced-concave diffraction grating in the vacuum ultraviolet.

19 p2431 A73-38164

Optical diffraction grating design and production, discussing application of interferometry and electronics to ruling engine control

21 p2698 A73-40136

Double frequency diffraction grating lateral shear interferometer for lens focusing and heterodyne phase detection

21 p2698 A73-40137

Threshold, spectral, and output power characteristics of GaAs/Ga_{1-x}Al_x/As single-heterostructure diode lasers.

21 p2713 A73-40462

Diffraction grating model in terms of amplitude and phase modulation to explain angular spectrum of light reflection from corrugated surface for various incidence angles

21 p2740 A73-40790

An array technique with grating-lobe suppression for limited-scan applications.

22 p2830 A73-41826

Improved point-matching method with application to scattering from a periodic surface.

22 p2824 A73-41833

Self diffraction of coherent wave radiation by absorption from excited levels of Nd laser light induced phase diffraction gratings in thin layer rhodamine

22 p2870 A73-42723

Over-size waveguide polarization duplexers based on metal grating or dielectric plate at Brewster angle, measuring performances in microwave circuit and with HCN IR laser

23 p2960 A73-44071

Far IR grating spectrometer using InSb detector with narrow spectral band responsivity and tunability due to cyclotron resonance absorption in magnetic field

23 p2984 A73-44364

GRAVIMETERS

Low weight thermostat for temperature compensation of Sharpe quartz gravimeters

03 p0311 A73-14614

Vibrating string total field/absolute gravity meter/accelerometer, discussing calibration at single reference point

13 p1617 A73-28849

Capabilities of the GS-12 gravimeter for studying gravitational field variations

13 p1621 A73-29412

Thermal design and testing of the Apollo 17 lunar traverse gravimeter.

18 p2316 A73-36385

GRAVIMETRY

Detailed gravimetric geoid computation for U.S. area from satellite spherical harmonic and surface gravity data, comparing with astrogeodetic geoid

04 p0439 A73-14798

Earth geodetic mapping with rotating torsional gravity gradiometers onboard spin stabilized satellite in low polar orbit

04 p0446 A73-14806

Estimation of the precision of presentation of gravimetric, magnetic and other geophysical and experimental data.

07 p0817 A73-19542

- Earth figure theory and gravimetric measurements using satellite observations and photography 13 p1605 A73-28007
- GRAVIRECEPTORS**
NT OTOLITH ORGANS
Calculation of a Coriolis acceleration acting on semicircular canal receptors of man in rotating systems 15 p1835 A73-31518
- Adequate vestibular stimulants on earth and in space 17 p2110 A73-34122
- Histological studies on the vestibular organ of frog embryos and larvae after the influence of simulated weightlessness. 18 p2270 A73-35979
- Biophysical considerations concerning gravity receptors and effectors including experimental studies on *Phycomyces blakesleeanus*. 22 p2804 A73-42171
- GRAVITATION**
NT ARTIFICIAL GRAVITY
NT GRAVITY ANOMALIES
NT LUNAR GRAVITATION
NT LUNAR GRAVITATIONAL EFFECTS
NT PLANETARY GRAVITATION
NT REDUCED GRAVITY
NT SOLAR GRAVITATION
Computer realization of a method of scaling the gravity force 13 p1609 A73-29128
- German book - The physics of the scientist: Mechanics, relativity, gravitation. 17 p2229 A73-34465
- GRAVITATION THEORY**
Dynamics of gravitating systems against the neutrino background of the universe 01 p0100 A73-10712
- Schwarzschild coordinate system identification with frames of reference within exterior gravitational field of spherical nonrotating star 02 p0211 A73-11896
- Exact cosmological solutions in Brans and Dicke's scalar-tensor theory. II. 02 p0224 A73-12743
- Calculation of the perihelion advance of planets in a field approach to gravitation. 02 p0225 A73-12802
- Design of a space probe for the experimental investigation of Einstein's theory of gravitation 03 p0381 A73-13296
- Gravitational equations derivation identical to electromagnetic Maxwell equations, noting nonviolation of energy conservation 03 p0373 A73-13358
- Gravitation theory - Empirical status from solar system experiments. 04 p0498 A73-15249
- Some consequences of the Mach-Einstein doctrine for celestial mechanics and geophysics. 04 p0498 A73-15280
- Harmonic frames of reference in Einstein's theory of gravitation. 05 p0598 A73-16791
- Gravitational field effects on processes near stars and galaxies in late evolution phases, describing particle motion and light propagation near rotating sources 05 p0623 A73-17197
- Newtonian and relativistic gravitational theories, discussing gravitational waves generating mechanism and black holes formation 06 p0753 A73-18274
- Gravitation finite range evidence presentation of major theoretical problem for general relativity, discussing continuity and invariance 06 p0724 A73-18548
- Gravitation theory harmonic condition equations to separate relativity-valid subclass of extremal manifolds from class of m-dimensional pseudo-Riemannian manifolds 08 p0987 A73-20700
- Description of hydrodynamics in the theory of gravitation on the basis of covariant statistical equations 08 p0989 A73-21522
- Modification of the phase methods for investigation of non-stationary processes in the ionosphere, magnetosphere and interplanetary space. 09 p1078 A73-22835
- Quasi-radial pulsations of rotating white dwarfs and neutron stars in the relativistic theory of gravitation 10 p1274 A73-23711
- Gravitational waves - A progress report. 10 p1280 A73-24324
- Gravitational instability of regular model-universes in a modified theory of general relativity. 11 p1423 A73-26106
- Conservation laws and preferred frames in relativistic gravity. I Preferred-frame theories and an extended PPN formalism. II - Experimental evidence to rule out preferred-frame theories of gravity. 12 p1540 A73-27326
- On Maxwell-type equations in the theory of inertial-gravitational field. 13 p1657 A73-28025

- Rotation effects in stellar and quasi-stellar relativistic objects models required for pulsars and quasars explanation, discussing gravitation theories 14 p1798 A73-30141
- Mach principle incorporation into general relativity, discussing application as selection rule in Einstein field equations solution and other gravitation theories 14 p1798 A73-30238
- Relativistic stellar stability - An empirical approach. 14 p1801 A73-30740
- Dyadic formalism in two dimensional distributions in general relativity theory, discussing gravitational, diffusive, wave, Einstein and preservation equations 14 p1776 A73-30942
- Kinematic invariants and their relation to chronometric invariants in Einstein's theory of gravitation 15 p1913 A73-31246
- Basic trends in the development of modern analytic mechanics 15 p1913 A73-31622
- Evaluation of the directivity of gravitational wave radiators. 15 p1914 A73-31944
- A new theory of gravity. 16 p2036 A73-33123
- Isotropic solution of Einstein gravitational equations for anisotropic homogeneous cosmological models with hydrodynamic energy-momentum tensor 16 p2071 A73-34051
- Quasiradial pulsation of rotating white dwarfs and neutron stars in general relativity. 18 p2354 A73-36736
- A theory of gravitation incorporating the quadratic action principle of relativity. 19 p2459 A73-37446
- Comparison of various gravitational energy tensors 20 p2594 A73-39726
- Gravitational red shift, Mercury perihelion, light deflection and signal delay tests of Einstein relativity vs Jordan-Brans-Dicke theory 20 p2613 A73-39751
- Nonrelativistic effects in phenomenology of gravitation, describing gravitational field as curvature-tensor field within equivalence principle limits 21 p2766 A73-40352
- Gravitational radiation in the scalar-tensor gravitation theory. 22 p2885 A73-41718
- General relativistic gravitation theories based space-time curvature tests near sun from interplanetary probe motion analysis using probe-borne laser light transmission [ONERA, TP NO. 1210] 22 p2907 A73-42216
- The gravitational influence of a beam of light. I. 22 p2886 A73-42320
- Gravitational-wave observations as a tool for testing relativistic gravity. 22 p2887 A73-42709
- On the problem of the initial state in the isotropic scalar-tensor cosmology of Brans-Dicke. 22 p2911 A73-42931
- Interplanetary radar time delays in different theories of gravitation. 23 p3032 A73-43842
- Relativistic gravity in the solar system. III - Experimental disproof of a class of linear theories of gravitation. 24 p3138 A73-45034
- On a possible repulsive interaction in universal gravitation. 24 p3110 A73-45038

GRAVITATIONAL COLLAPSE

NT BLACK HOLES [ASTRONOMY]

- Hydrodynamic model calculations for supermassive stars. II - The collapse and explosion of a nonrotating 520,000 solar-mass star. 02 p0222 A73-12713
- Gaseous star as first limit to nebular matter gravitational collapse, considering equilibrium, neutron stars, black holes, forbidden lines and ionized hydrogen clouds 03 p0365 A73-12913
- Pulsars as rotating magnetic neutron stars created during cataclysmic collapses of old stars, discussing radiation mechanism 06 p0750 A73-18012
- Gravitational contraction and energy dissipation and compensation in stellar nuclear reactions, noting He thermonuclear reactions and nucleosynthesis 06 p0751 A73-18158
- Star formation from interstellar clouds gravitational collapse, discussing protostars evolution based on model calculations 07 p0878 A73-19675
- Gravitational energy conversion into rotational energy in contraction process for pulsars, quasars and galactic radio emission energy sources 07 p0898 A73-19934
- Black hole creation via partial gravitational collapse of matter ejected by explosion within asymptotically Friedmannian space-time 07 p0900 A73-20182

Magnetic field in the plasmasphere of a compact star. 08 p1007 A73-21001

Thermal conductivity approximation for gaseodynamic equations describing stellar gravitational collapse, calculating neutrino and antineutrino energy and momentum transport processes 09 p1147 A73-22701

Black holes existence and tentative configuration, discussing galaxies great group missing mass mystery and X ray source investigation 10 p1282 A73-24653

Gravitational collapse with a physical singularity on an isotropic hypersurface 10 p1283 A73-24751

Probabilistic fragmentation model for collapsing interstellar cloud, predicting stellar mass spectrum 11 p1415 A73-25171

Stellar evolutionary calculation for Jupiter, considering gravitational contraction 11 p1420 A73-25892

General relativistic effects detection experiments for supernova and collapsed objects, noting gravitational radiation transfer of energy equal to entire energy generation during thermonuclear evolution 12 p1542 A73-27550

Relativistic astrophysics. III - Gravitational collapse, singularities, and black holes 12 p1543 A73-27749

Dynamical contraction of rotating gaseous spheroids. 13 p1680 A73-28774

Interstellar cloud collapse into protostellar objects and star formation, discussing young stellar objects observation 13 p1681 A73-28946

Book on variable stars, covering high energy astrophysics, low energy outbursts, extensive convection, galaxies, pulsations, white dwarfs, cepheids, flares and gravitational collapse 14 p1796 A73-29950

Amplification of cylindrical electromagnetic waves reflected from a rotating body. 14 p1728 A73-30333

Painleve metric replacement for Schwarzschild metric in tests of general relativity, considering problem of supermassive celestial body gravitational collapse 15 p1937 A73-31650

Local structure of space-time singularity and gravitational collapse. 15 p1940 A73-32177

Numerical model construction for primitive solar nebula and physical accumulation processes within collapsing interstellar gas cloud 17 p2227 A73-34405

Collapse calculations and their implications for the formation of the solar system. 17 p2227 A73-34411

Mass and angular momentum distribution in primitive solar nebula during rotation and contraction hydrodynamics of collapse 17 p2227 A73-34412

Disk formation by collapsing rotating gas cloud, considering free turbulence and intermittency effects on gravitational instability 17 p2227 A73-34413

Compactness criterion for the formation of averaged trapped surfaces in gravitational collapse. 17 p2234 A73-35734

Massive singlet f-meson gravitational field effects on gravitational collapse in universe model with ten to eightieth power aligned neutrons 20 p2605 A73-39016

Magnetic stars origin from gravitational collapse of ionized hydrogen clouds, discussing implications of interstellar magnetic fields and critical mass according to Chandrasekhar-Fermi virial theorem 20 p2605 A73-39058

Black hole formation conditions in terms of critical masses, spherical symmetry and asymmetrical star collapse 21 p2765 A73-40233

Oscillating spherically symmetric charge-matter fluid for avoidance of singularities in gravitational collapse models 21 p2766 A73-40316

Numerical model for cold gaseous planets /Jupiter, Saturn, Uranus, Neptune/ as remnants of star formation attempts, taking into account density fluctuations in collapse region 21 p2766 A73-40374

Dense cloud formation and gravitational collapse onset, discussing thermal properties and magnetic field presence 21 p2772 A73-41244

Gravitational radiation in the scalar-tensor gravitation theory. 22 p2885 A73-41718

Global coordinate systems for spherical collapsing and expanding Oppenheimer-Snyder dust cloud behavior after critical Schwarzschild radius attainment 22 p2908 A73-42438

Neutrino losses effects on 4-8 solar mass stars leading to collapse of degenerate carbon-oxygen cores, discussing type II supernovae and pulsar formation 22 p2914 A73-43008

Planetary formation processes in primitive solar nebula analyzed from collapse phase for accumulation time 24 p3127 A73-44393

GRAVITATIONAL CONSTANT

Gravitational constant anisotropy effects on planets with orbits close to ecliptic in solar system two body problem 01 p0099 A73-10689

Solar system origin and variable gravitational constant theory from earth history viewpoint 01 p0101 A73-10874

The n-body problem with variable gravitational constant, and some dynamical consequences for large-scale cosmic systems. 01 p0107 A73-11327

Cosmological vacuum solutions in Brans and Dicke's scalar-tensor theory. 03 p0373 A73-13356

Gravitational constant variations from natural satellites and lunar observation, discussing tidal problems solution from lunar orbit tracking 03 p0377 A73-14310

Gravitational constant constancy from 1663-1972 earth rotation and 1943-1972 stellar occultations by moon, discussing various time scales used 09 p1079 A73-22948

The implications for geophysics of modern cosmologies in which G is variable. 14 p1799 A73-30525

Solar mass, earth mass and kilogram re-examined for gravitational constants, discussing geocentric constant 20 p2613 A73-39750

GRAVITATIONAL EFFECTS

NT LAGRANGIAN EQUILIBRIUM POINTS

NT LUNAR GRAVITATIONAL EFFECTS

NT STELLAR GRAVITATION

Gravity thrust Jupiter orbiter trajectories generated by encountering the Galilean satellites. 01 p0095 A73-10103

Gravitational interaction effects between parts of gravity stabilized satellite on attitude dynamics and control 01 p0095 A73-10110

Relative equilibrium of a mass of charged particles /electrons/ subject to its own gravitation and uniformly rotating about an axis 01 p0082 A73-10267

High frequency radio observations of optically interacting galaxies. 01 p0099 A73-10586

Wolf number solar activity and planetary tidal force correlation during 1770-1970, noting 11-year cycle relation 01 p0101 A73-10848

Electromyographic study on human standing posture in experimental hypogravic state. 01 p0013 A73-11211

Newtonian force field effect on gyroscope motion for coordinate axes coincident with inertia tensor axes, solving equations of motion by energy integral 02 p0192 A73-11769

New solutions of the problem of the motion of a gyroscope in a central Newtonian force field 02 p0192 A73-11770

Regular gyrostat precession in a central Newtonian field of forces 02 p0192 A73-11771

Meteoroid activity on the lunar surface from the Surveyor 3 sample examination. 02 p0214 A73-12257

Changes in the gravitational energy of galaxies during collisions. 02 p0217 A73-12392

Isotropic system development of gravitating point particles in galactic clusters and superclusters in expanding universe from Liouville theorem and BBGKY hierarchy 03 p0365 A73-12927

Classical hard-sphere gas in spherical box with coupling between local thermodynamics and gravitation, noting stellar core-halo structure from equilibrium state calculations 03 p0366 A73-12936

On the interaction between tectonic processes of the earth and the moon. 03 p0299 A73-13093

Tidal generation of narrow intergalactic filaments from computer simulations, discussing alternative models 03 p0372 A73-13353

Equilibrium motions of rigid spinning satellite in circular orbit around central body subject to gravitational torque 03 p0376 A73-14268

Sufficient conditions for return in the three-body problem. 03 p0377 A73-14274

Hubble law from constant light velocity in Euclidean space, noting red shift equation and Einstein gravitational shift 03 p0379 A73-14577

The parameters of an infinite homogeneous elliptical cylinder determined from its gravity effects. 03 p0380 A73-14612

The effect of gravity on the thermal and calorimetric measurements for pure fluid substances at the critical point 03 p0400 A73-14634

Experimental test for Mach-Einstein doctrine concerning particle inertial mass variation due to tension or space-time curvature created by interlocking gravitational field 04 p0476 A73-15524

Gravitational origin of high energy interactions and general relativity equivalence principle for unitary symmetry, noting quantum geometrodynamical cosmological model 04 p0501 A73-15632

Effect of hypergravity on the circadian rhythms of white rats. [ASME PAPER 72-WA/BHF-14] 04 p0410 A73-15877

Self similar procedure derived for gas infall to solid surface in constant gravitational field, applying to initial phase of neutron star matter accretion 04 p0503 A73-16003

Expansion of the force function of two homogeneous spheroids with noncoincident symmetry planes. 04 p0503 A73-16021

Ionospheric double layer theory extended to conditions including gravity and expansion effects in diverging geomagnetic flux tubes 05 p0568 A73-16145

Solar luminance via light nuclei fusion into heavier nuclei with temperature gradient maintenance by gravity, relating to H-R diagram of different star clusters 05 p0614 A73-16302

A method for computing the gravitational attraction of three-dimensional bodies in a spherical or ellipsoidal earth. 05 p0569 A73-16379

Investigation of the process of the explosive disintegration and simultaneous collision of n gravitating material points 05 p0619 A73-16844

Heat pipe operation in a gravity field with liquid pool pumping. [AIAA PAPER 73-120] 05 p0640 A73-16876

Alteration of the Laplace spheres of planetary influence during the application of a new intermediate orbit 05 p0620 A73-17022

Gravitational field effects on processes near stars and galaxies in late evolution phases, describing particle motion and light propagation near rotating sources 05 p0623 A73-17197

Internal models of uniformly rotating synchronous close binary systems via modified double approximation scheme, considering gravity darkening effect on primary position in H-R diagram 05 p0624 A73-17306

Gravity-darkening of the secondary component of RW monocerotids. 05 p0624 A73-17315

Nonlinear stability analysis of nonhomogeneous self-gravitating unstable equilibrium stellar systems, using numerical techniques and water bag configurations 05 p0624 A73-17317

Effects of resonant tesseral gravity coefficients on Viking-type orbits. [AIAA PAPER 73-146] 06 p0748 A73-17648

General relativity in the equal proper time formalism. 06 p0724 A73-18626

Space-time transformation for equation of relative motion of two bodies on gravitating matter background of Einstein-de Sitter universe 06 p0724 A73-18689

The stability of a self-gravitating, nonrotating gas layer with stellar, magnetic, and cosmic-ray components. II. 07 p0873 A73-19058

Limits on gravitational radiation from two gravitationally bound black holes. 07 p0876 A73-19346

The stability of certain model binary stellar systems in galactic gravitational fields. 07 p0898 A73-19935

Numerical experiments on probability distribution of random force in stellar gravitational systems, noting agreement with Chandrasekhar and von Neumann theory 08 p1003 A73-20884

Dynamic analysis of tidal effects arising from hyperbolic close encounters of massive body past galaxy, calculating matter velocity field and galactic structure distortion 08 p1004 A73-20907

Combined gravitational and solar radiation pressure effects on the semimajor axis of the earth's satellite. 08 p1010 A73-21314

Viscoelastic strains in a thick-walled cylinder under the long-term effect of a gravitational load 08 p1017 A73-21371

Effects of the sun and the moon on a near-equatorial synchronous satellite. 08 p1011 A73-21430

Dwarf binary component convective shell behavior under gravitational field periodic tidal action, noting conditions for thermal instability 08 p1012 A73-21548

Cometary parent bodies transfer to short period orbits by Jupiter caused gravitational disturbances, noting qualitative analysis of orbits evolution 08 p1012 A73-21576

Nonzero neutrino rest mass to account for virial mass discrepancy in Coma cluster and missing cosmological mass needed to close universe 09 p1141 A73-22027

Satellite-caused energy dissipation via tides in spinning planet leading to orbital decay induced destruction or escape or to stable synchronism 09 p1142 A73-22041

On the accretion mechanism for the formation of a protoplanetary disc. 09 p1143 A73-22110

Effects of collisions and gyroviscosity on gravitational instability in a two-component plasma. 09 p1127 A73-22286

Satellite resonance with longitude-dependent gravity. III - Inclination changes for close satellites. 09 p1154 A73-22837

Exact analytical solutions for orbits of bodies with atmospheric drag. 09 p1152 A73-23454

A numerical-analytical method of calculating stream flow of a heavy liquid around curvilinear obstacles 10 p1205 A73-23585

Causes of the rotation of galaxies in terms of the nonlinear theory of gravitational instability 10 p1274 A73-23712

Free particle gravitating cylindrical model for gravitational kinetic instabilities, calculating natural vibration spectrum and parameters for beam instability development 10 p1253 A73-23714

Stability of a gravitating fluid layer in the presence of a uniform magnetic field perpendicular to its boundary. 10 p1253 A73-23832

Stability of planar oscillations of a satellite in an elliptic orbit. 10 p1287 A73-24663

Singularities and collisions in linear many body problem of Newtonian gravitational systems, noting moment of inertia role 10 p1284 A73-24788

The equilibrium, stability and evolution of a rotating magnetized gaseous disk. 10 p1284 A73-24903

On the origin of the electric field of polarization in a gravitational plasma. 11 p1350 A73-24990

Dense stellar systems dynamics, considering gravitation relaxation, star evaporation, antiequijustion, growth of dense galactic cores, stellar coalescence, disruption and formation 11 p1414 A73-25065

A chart for the computation of the gravitational attraction of a right rectangular prism. 11 p1351 A73-25160

Gravitational effects on biological systems in terms of animal body size, age, sex and posture as factors affecting acceleration tolerance 11 p1315 A73-25573

Critique of theory on monotonic entropy of black hole as linear function of area, considering gravitational energy and compression to singularity 11 p1418 A73-25650

Friedmann expanding cosmological model with superimposed spherically symmetric inhomogeneity for gravitational lens and point light sources dispersion and motion effects on images 11 p1418 A73-25747

Mercury, Venus and Pluto satellite system elimination by tidal friction, discussing possible erosion of earth and Mars small satellites 11 p1419 A73-25778

Explosive disintegration and simultaneous collision of n material gravitating points. 11 p1423 A73-26054

Model of a stationary stellar cluster with a high binding energy. 11 p1425 A73-26176

Equilibrium stability of liquid filled body with closed internal cavity partially filled with ideal homogeneous incompressible fluid under gravitation 11 p1401 A73-26470

Investigation of star orbits in stellar clusters with allowance for the disturbing force of the galaxy 12 p1538 A73-26863

Certain quantum-gravitational effects in central classical fields 12 p1538 A73-26970

General theory of optimal trajectory for rocket flight in a resisting medium. 12 p1538 A73-27119

The limits and the nature of the onset of influence of thermogravitational forces on turbulent flow and heat transfer in vertical tubes 12 p1487 A73-27313

Experimental investigation of heat and mass transfer in the condensation of vapor from gas-vapor mixtures under viscous and viscous-gravitational flow conditions 12 p1558 A73-27315

Determination of the equilibrium positions of mechanisms with two degrees of freedom 12 p1524 A73-27465

Stability of gravitating systems with a quadratic potential. I - Methods of investigating the stability of systems with a limited phase volume: Vibration spectrum of the Maclaurin stellar disk 12 p1546 A73-27856

A measurement of the gravitational deflection of radio waves by the sun during 1972 October. 13 p1673 A73-28281

Instability of surface-stratified incompressible inviscid rotary Couette flow between corotating coaxial vertical cylinders due to gravitational effects 13 p1600 A73-28439

Some aversive characteristics of centrifugally generated gravity. 13 p1575 A73-28506

Relation between the tidal-force momentum and atmospheric depressions 13 p1609 A73-28862

Neutral hydrogen clouds gravitational binding of Coma cluster, providing mechanism for heating of diffuse gas between clouds and galaxies 13 p1684 A73-29352

Gaseous ring mechanism of Titan atmosphere, considering atmospheric particle outgassing and recapture under Saturn gravitational field to form torus at Titan orbit 14 p1788 A73-29719

On the motion of short-period comets in the neighbourhood of Jupiter. 14 p1790 A73-29786

Linkage of seven apparitions of periodic comet Faye 1925-1970 and investigation of the orbital evolution during 1660-2060. 14 p1791 A73-29801

Periodic comet Stephan-Oterma orbit, taking into account perturbations by major planets 14 p1792 A73-29808

Determination of planetary masses from the motions of comets. 14 p1792 A73-29809

Ejection of bodies from the solar system in the course of the accumulation of the giant planets and the formation of the cometary cloud. 14 p1793 A73-29825

Focusing effect of planetary perturbations on meteor stream particles for comet formation 14 p1795 A73-29846

Isochronous derivatives of certain spacecraft-trajectory parameters 14 p1796 A73-29857

Satellite oscillation in circular orbit plane, determining gravitational stability in minimum time with least fuel consumption 14 p1803 A73-29868

On convection and gravitational layering in Jupiter and in stars of low mass. 14 p1797 A73-30009

Features of the influence of hypergravitation on the motor activity of the chicken embryo amnion developing under normal conditions and under conditions of constant rotation 14 p1715 A73-30022

Positron-annihilation radiation from neutron stars. 14 p1788 A73-30738

Existence of a new type of rotating equilibrium ellipsoids in the presence of a toroidal magnetic field 14 p1782 A73-30816

Wolf number solar activity and planetary tidal force correlation during 1770-1970, noting 11-year cycle relation 15 p1928 A73-30984

Basic theory for PROD, a program for computing the development of satellite orbits. 15 p1930 A73-31108

Phenomena of scattering of electromagnetic and gravitational wave packets in the gravitational field of a black hole 15 p1932 A73-31245

Duplicity and its consequences among variable stars in general. 15 p1935 A73-31484

Earth deflections of vertical due to luni-solar gravitation changes determined by astronomical observation with Herstmonceux photographic zenith tube, noting semidiurnal tidal effects 15 p1937 A73-31779

Evolution of satellite resonances by tidal dissipation. 15 p1938 A73-31950

Gradient instabilities in a system of gravitating point masses 15 p1938 A73-31954

Forward precession motion of the moon caused by attraction to the earth and the sun 15 p1939 A73-31966

The possibility of measuring gravitational redshift by means of earth satellites. 15 p1940 A73-32074

X ray power derivation from gravitational energy release during matter accretion onto surface of component of mass transfer binary star 16 p2049 A73-32730

Stationary isothermal gas flow subject to self gravitation, finding subsonic regime oscillatory solutions for plane parallel, spherical and rotational symmetric cases 16 p2058 A73-32832

Scattering of electromagnetic radiation from a black hole. 16 p2060 A73-33120

Stable tumbling motions of a dual-spin satellite subject to gravitational torques. 17 p2237 A73-34177

On the magnetogravitational instability of a plasma which possesses an anisotropic pressure in uniform movement of rotation and under the influence of the Hall current - The equation of dispersion. I 17 p2215 A73-34250

The effect of multiple encounters on short-period comet orbits. 17 p2226 A73-34291

Waves in a plasma amid magnetic and gravitational fields 17 p2226 A73-34373

Book on large scale structure of space-time covering gravity roles, differential geometry, general relativity, gravitational collapse, black holes, spatially homogeneous cosmological models, etc 18 p2336 A73-35901

Large-scale variations in the obliquity of Mars. 18 p2348 A73-35921

Gravity, weightlessness and organismic genetic structures. 18 p2269 A73-35923

Gravitational stress and exercise. 18 p2270 A73-35980

Metabolic responses of monkeys to increased gravitational fields. 18 p2270 A73-35982

Survival and mutability of *Chlorella* under various orientation in the earth's gravitational field. 18 p2270 A73-35997

Technology requirements for ballistic mode Mercury orbiter mission, discussing performance potential with Venus gravity assist and conventional spacecraft propulsion techniques [AIAA PAPER 73-581] 18 p2350 A73-36073

Spatial motion of a two body cluster under the action of gravitational and aerodynamic forces 18 p2351 A73-36119

Development of rotation in galaxies in the nonlinear theory of gravitational instability. 18 p2354 A73-36737

Free particle gravitating cylindrical model for gravitational kinetic instabilities, calculating natural vibration spectrum and parameters for beam instability development 18 p2340 A73-36739

Intracranial hemodynamic changes in pilots to tilting. 18 p2279 A73-36916

Light curves of the gravitational lens-like action for binaries with degenerate stars. 19 p2483 A73-37563

Nonuniform model construction for dense intergalactic medium with gravitational binding of all galactic groups and clusters by ionized gas 19 p2484 A73-37608

Stellar kinetic energy gain in spherical systems by transient external gravitational perturbations, computing dynamic models for compressive shocks 19 p2484 A73-37616

Four-stage planetesimal accretion from solar nebula describing dust particle condensation, disk formation, gas drag, orbital decay and particle collisions 19 p2489 A73-38524

A numerical integration scheme for the N-body gravitational problem. 20 p2604 A73-38973

Massive singlet f-meson gravitational field effects on gravitational collapse in universe model with ten to eightieth power aligned neutrons 20 p2605 A73-39016

Thin steady two dimensional potential flow with free and/or rigid boundaries in presence of gravity, determining outer and inner expansions characteristics 20 p2546 A73-39085

Stability of gravitating systems with a quadratic potential. I - Systems bounded in phase space - Oscillation spectrum for a Maclaurin stellar disk. 20 p2608 A73-39230

Altered susceptibility to motion sickness as a function of subgravity level. 20 p2518 A73-39486

Liquid jet development under gravity, discussing jet surface elastic film, axisymmetric membrane elastic deformations, liquid drop pressure variations and hydrostatic pressure 20 p2548 A73-39517

Effect of coagulation and spatial redistribution of cloud particles on the precipitation spectrum 21 p2730 A73-40120

Comments on the mathematical theory of small oscillations of an inviscid gas 21 p2738 A73-40191

Beacon Explorer C satellite laser tracking for effects of lunar and solar tides on orbit, noting geogravitational field distortion 21 p2765 A73-40275

Statistical dynamics formulation of motion equations for particle system in gravitational interaction with neither gas law nor hydromagnetic effects, applying to solar system evolution 21 p2766 A73-40313

Angular momentum decrease of slowly rotating Kerr black holes due to stationary distribution of outside matter 21 p2766 A73-40314

Gravitational Compton effect and graviton photoproduction by electrons 21 p2742 A73-40351

Rotating cylinder model for plasma gradient-temperature instability in gravitational field, showing heat convection due to Coriolis-caused particle drift 21 p2769 A73-40730

Interaction between radiation effects, gravity and other environmental factors in Tribolium confusum. 21 p2643 A73-40808

Gravitational effects on animal ontogeny from centrifugation studies of acceleration tolerance, considering egg and embryo development, body composition, etc 22 p2804 A73-42174

The gravitational influence of a beam of light. I. 22 p2886 A73-42320

Gravitational analogy of electromagnetic Aharonov-Bohm effect, considering massless Dirac equation for weak gravitational fields arising from mass currents moving between particle beams 22 p2887 A73-42434

Solar pressure induced librations of spinning axisymmetric satellites. 22 p2910 A73-42633

An analytical and experimental investigation of gravity effects upon laminar gas jet-diffusion flames. 22 p2933 A73-42775

Vertical arm reaching movements for various gravitational levels, measuring reach time and angular and lower arm velocities 23 p2948 A73-43218

Gravitational red shift - A simple quantum field-theoretical consideration in a curved space. 23 p3006 A73-43607

Forces acting upon an asteroid moving through a meteoroid stream. 23 p3029 A73-43745

Gravitational perturbations of equatorial orbits. 23 p3032 A73-43839

Nonpotential gravitationally-dissipative instability of a plasma in toroidal systems 23 p3015 A73-44348

Meteoroids impact rate on lunar and earth surfaces for given geocentric and selenocentric velocity distributions, taking into account gravitational effects 24 p1311 A73-44461

Gradient instabilities in a system of gravitating point masses. 24 p1312 A73-44479

Translational-precessional motion of the moon in the gravitational field of the earth and sun. 24 p1312 A73-44491

Tidal generation of magnetic fields in binary celestial systems, calculating growth times 24 p1314 A73-44578

Hydrodynamics in weak gravitational fields - Plane oscillation problems of an ideal liquid in a vessel 24 p3076 A73-44653

Determination of the equilibrium state of a capillary liquid in a vessel 24 p3080 A73-45526

GRAVITATIONAL FIELDS NT STELLAR GRAVITATION

Determination of the dynamic characteristics of a fluid in a moving vessel in the presence of a weak gravitational field by the eigenfunction expansion method 01 p0030 A73-10095

Nonlinear magnetic sound in a gravitational field 01 p0016 A73-10202

The equations of motion of gyroscopes in general relativity 01 p0098 A73-10559

Planetary orbits numerical relationships applied to artificial satellite orbits for earth gravity studies, expressing gravitational potential as latitude dependent spherical harmonics series 01 p0040 A73-10875

Periodic perturbation of the libration points of the restricted three-body problem due to presence of a resisting medium and both gravitational and radiative fields of a fourth body.

01 p0103 A73-11018

Cosmological evolution from initial inhomogeneous and anisotropic universe to present structure, using general relativity for free gravitational field and waves

01 p0106 A73-11242

Gravitational fields of Jupiter and Saturn.

01 p0107 A73-11332

Elliptical orbits of mass point under Newtonian gravitational forces of two fixed centers with different mass in Cartesian coordinates as function of time

02 p0211 A73-11776

Earth vertical gravity field probing by observing body free fall from several hundred kilometers altitude

02 p0159 A73-12167

Time-dependent Yukawa-potentials of a class of weak gravitational fields.

02 p0193 A73-12182

Estimation of gravity field harmonics in the presence of spin-axis direction error using radio tracking data.

02 p0164 A73-12373

Biorthogonal function pairs for gravitational field calculations for flat galaxies, deriving algorithms from Hankel-Laguerre functions properties

02 p0216 A73-12380

Precision measurement of the sun's gravitational field by means of the twin probe method.

02 p0218 A73-12414

Synthesis of optimal control over the motion of a material point in a thin spherical layer of a central gravitational field with noncollinear vectors of the final gross error in the radius vector and velocity vector

02 p0193 A73-12452

Flow stability of ideal compressible and incompressible fluids, solving Navier-Stokes equation for rotating liquid with free boundary in gravitational field

02 p0154 A73-12692

Calculation of the perihelion advance of planets in a field approach to gravitation.

02 p0225 A73-12802

The equilibrium and stability of uniformly rotating gaseous systems in hydromagnetics. I.

02 p0225 A73-12806

Surface gravities, Doppler broadening velocities, effective temperatures and metal abundances of K giants from narrow band photometry

03 p0371 A73-13224

Hydrodynamics in weak gravitational fields - Plane oscillations of an ideal fluid in a rectangular channel

03 p0294 A73-13606

Field dynamics equilibrium equation for particle rotational motion in gravitational field of central body, noting energy spectra of stationary orbits

03 p0374 A73-13751

Motion stability of librational points in gravitational field of rotating triaxial ellipsoid, applying to planets of solar system

03 p0376 A73-14266

About the motion of a heavy flexible string attached to the satellite in the central field of attraction.

03 p0376 A73-14267

Pulsed motion of gravity gradient vehicle in central gravity field, presenting expressions of optimized attitude control

03 p0383 A73-14573

A method of solution of Vlasov's equation - Application to a nonlinear overall theory of the galactic rotation and of the galactic spiral structure

03 p0380 A73-14608

Earth normal gravity field spherical harmonics in terms of Stokes constants from satellite orbit dynamics, comparing with Helmert system

03 p0305 A73-14613

Analysis of methods for computing an earth gravitational model from a combination of terrestrial and satellite data.

04 p0437 A73-14787

Refinement of the gravity field by satellite-to-satellite Doppler tracking.

04 p0438 A73-14793

Accuracy of potential coefficients obtained from present and future gravity data.

04 p0438 A73-14796

An empirically derived lunar gravity field.

04 p0498 A73-15184

Motion of a body of variable mass in a many-body gravitational field near collision

05 p0615 A73-16326

Tidal gravity models of interacting pair formation of galactic bridges and tails in terms of orbit geometry, outer shapes and forced spiral waves

05 p0626 A73-17378

Finite-amplitude convection occurring in a modulated gravitational field

06 p0767 A73-17463

Application of linear feedback control theory techniques to continuum dominated by electrostatic and gravitational fields.

06 p0680 A73-18004

Influence of scalar and vector fields on the nature of a cosmological singularity

06 p0751 A73-18101

Time/T-field/solutions to Einstein equations of test particles and light rays in nonstatic spherically symmetric gravitational field

06 p0724 A73-18646

Electromagnetic current and charge due to interaction between a gravitational and a free electromagnetic field.

06 p0732 A73-18715

Distortion corrections in geophysically traced gravitational, magnetic and geoelectric field maps, discussing automation

07 p0816 A73-19442

Anomalous magnetic and gravitational field models autocorrelation function behavior dependence on circular cylindrical sources depth and spacing

07 p0816 A73-19447

Estimation of the precision of presentation of gravimetric, magnetic and other geophysical and experimental data.

07 p0817 A73-19542

Preliminary quasar model based on the Yilmaz exponential metric.

07 p0899 A73-20178

Electromagnetic radiation from charges in weak gravitational fields.

07 p0852 A73-20179

Small perturbations solution for spatially homogeneous expanding gravitating medium, using Vlasov kinetic equation with self consistent Newtonian field

07 p0901 A73-20315

The hydromagnetic oscillations and stability of self-gravitating masses. III - Magnetic polytropes.

08 p1005 A73-20917

The macroscopic high-frequency quantum generator and detector of the gravitational radiation.

08 p0987 A73-21017

Radiation fields in the Schwarzschild background.

08 p0988 A73-21202

Estimates of the coefficients of a spherical harmonics expansion of the geopotential

09 p1143 A73-22095

Literal theory of the motion of a satellite in the tesseral-harmonic field of the earth's gravitational potential at small eccentricities

09 p1143 A73-22097

Linear perturbations of the coordinates of satellites in the normal gravitational field of the earth

09 p1143 A73-22099

Investigation of the motion of a body of variable mass within a multipole gravitational field with the aid of a regularizing variable

09 p1121 A73-22852

A classification of particle motions in the equatorial plane of a gravitational monopole-quadrupole field in Newtonian mechanics and general relativity.

09 p1148 A73-22910

Martian spin axis wandering resulting from equatorial volcanic convections and gravity field nonhydrostatic low order components

09 p1151 A73-23172

Physical librations due to the third and fourth degree harmonics of the lunar gravity potential.

10 p1277 A73-24083

Cosmological evolution from initial inhomogeneous and anisotropic universe to present structure, using general relativity for free gravitational field and waves

10 p1279 A73-24178

Perturbation function expansion in series of orbital elements for satellite motion in rotating oblate planet gravitational field with two fixed centers

10 p1282 A73-24493

Russian book on analytical theory of optimization in gravitational fields covering orbital transfer trajectories, variational optimization problems, Lagrange multiplier properties, etc

10 p1284 A73-24800

Kinetic equations for gravitating point rotating system model of stellar systems evolution phases, taking into account dissipation-produced motions

11 p1416 A73-25235

Stellar system gravitational field structure in terms of system-mass attraction/regular force/ and force due to random distribution of stars/irregular force/

11 p1416 A73-25236

Sidereal periods in a gravitational field characterized by Schwarzschild's internal solution

11 p1416 A73-25237

Motion of fast particles in a spherically-symmetric gravitational field

11 p1416 A73-25239

Geopause satellite orbit, tracking, environment, gravity and station position properties and applications to earth and oceanographic dynamics studies

11 p1430 A73-25317

Relationship between the coefficients of spherical and ellipsoidal expansion of the gravity force in the case of the biaxial earth ellipsoid

11 p1352 A73-25431

Influence of heating-surface orientation in a gravitational field on the nucleate boiling crisis of liquid

11 p1450 A73-25729

A survey of dynamical data for the major planets and satellites.

11 p1420 A73-25880

Stability of the steady motions of a gyroscope with spring limiters on a revolving platform in a Newtonian central force field

11 p1364 A73-26095

Magneto-viscous effects on the ideal and resistive gravitational instabilities in Cartesian geometry.

11 p1406 A73-26553

Combined electromagnetic and gravitational field equations derivation with explicit interaction term and tensors for curved space-times unrestrained in Einstein-Maxwell equations framework

11 p1401 A73-26658

Earth satellites and the gravitational potential.

12 p1539 A73-27148

Small perturbations solution for spatially homogeneous expanding gravitating medium, using Vlasov kinetic equation with self consistent Newtonian field

12 p1539 A73-27287

Polydynamic equilibrium equation for steady particle motion along stationary orbits in central body attraction field, comparing with Schrodinger wave equation

13 p1657 A73-28001

On Maxwell-type equations in the theory of inertial-gravitational field.

13 p1657 A73-28025

Spherical harmonic representation of the gravitational potential of a point mass, a spherical cap, and a spherical rectangle.

13 p1681 A73-28846

Game problem of the rigid collision of two points with impulsive thrust in a linear central field

13 p1660 A73-29080

Computational algorithm for three dimensional mixed boundary value problem for perturbing potential in earth figure theory

13 p1609 A73-29130

Capabilities of the GS-12 gravimeter for studying gravitational field variations

13 p1621 A73-29412

Major planets gravitational fields models from flyby spacecraft measurements, discussing Red Spot and Jupiter effect on Galilean satellites

14 p1799 A73-30531

Quasar red shift mechanism based on atomic energy levels and particle rest masses variations in scalar gravitational field

15 p1929 A73-31062

Hydrodynamics in weak gravitational fields - Small oscillations of an ideal liquid in a cylindrical vessel

15 p1861 A73-31280

Contribution to the synthesis of optimum control of motion of a point mass in a spherical lamella of a central gravitational field with finite mass vectors noncollinear with respect to radius vector and velocity vector.

15 p1915 A73-32602

Intermediate-thrust arcs and their optimality in a central, time-invariant force field.

16 p2062 A73-33305

Optimization of a vibration generator in the presence of external perturbations

16 p2083 A73-33969

Explicit formulas for the representation of the Green's functions of covariant wave equations in the case of a weak gravitational field. I, II

16 p2038 A73-34021

Magneto-gravitational and thermal instability in the Galactic disk.

17 p2231 A73-34752

Book - Theory of the earth's gravity field.

17 p2162 A73-35148

Superposition of Schwarzschild solutions and metric of a gravitational dipole

17 p2212 A73-35561

Almost projective mapping of gravitational fields - Degenerate case

17 p2212 A73-35564

Nonconformally plane relativistic recurrent-curvature spaces

17 p2212 A73-35567

Satellite geodesy application to earth internal structure and gravity field relationship to geomagnetism, noting magnetic secular variation correspondence with large scale mass motion

18 p2302 A73-35932

Calculation of geopotential fields at various atmospheric levels from data on the overall cloudiness and temperature.

18 p2314 A73-37072

Influence of the atmosphere on the gravity force and its potential at points on the earth's physical surface

19 p2428 A73-38555

Celestial bodies gravitational potential mathematical representation by Lamé functions via series expansion of Laplace differential equation in ellipsoidal coordinates

20 p2606 A73-39080

Elliptical orbit of two coupled material points in Newtonian central gravitation field, discussing flexi-

ble weightless filament coupling, equations of motion and sinusoidal oscillations

20 p2608 A73-39319

Comparison of various gravitational energy tensors

20 p2594 A73-39726

Centrosymmetrical nonstatic pulsating metric development, discussing minipulsar particles, perihelion displacement, gravitational energy, red shift, luminous ray curvature and Schwarzschild metric

20 p2594 A73-39765

Self-similar flows behind shock waves in a gravitational field

21 p2676 A73-40190

Nonrelativistic effects in phenomenology of gravitation, describing gravitational field as curvature-tensor field within equivalence principle limits

21 p2766 A73-40352

Experiments to determine satellite orbit geometry in spherically symmetric gravitational field, discussing aging asymmetry in clock paradox

21 p2739 A73-40623

Condensation of drops in motion through a gravitational field

21 p2731 A73-40743

Terrestrial gravitational models derived from satellite tracking and surface gravimetric data, comparing to 1969 Smithsonian Standard Earth II models

21 p2773 A73-41326

Nonradiative motion in a radiative gravitational field.

21 p2742 A73-41631

A nonstationary model of charged-particle diffusion in a gravitational field

22 p2902 A73-41955

Gravitational energy quantization model of noncharged particle based on proposed centrosymmetric metric with nonzero Einstein matter tensor and without Schwarzschild singularity

22 p2887 A73-42430

Correction to calculation of temperature rise in connection with gravitational energy release accompanying rapid core formation from undifferentiated earth

22 p2848 A73-42499

Determination of the orbital period of a satellite moving in the earth's gravitational field

23 p3027 A73-43268

Structural characteristics of galaxies caused by screening of the Newtonian gravitational potential

23 p3029 A73-43646

Gravitational fields calculation in three dimensional mass distribution galaxies, using biorthogonal functions with ultraspherical polynomials

23 p3030 A73-43749

Oscillatory motion existence in expanding n-body gravitational systems with distance bound and particle escape

23 p3034 A73-44208

Effect of scalar and vector fields on the nature of the cosmological singularity.

24 p3132 A73-44493

Calculation of a supersonic gas flow about the atmosphere of a spherical body

24 p3053 A73-44658

Spherical harmonic analysis of geomagnetic and gravitational field correlation, showing longitudinal shift in magnetic field pattern over six epochs

24 p3084 A73-44812

Physical relations of the asymmetric structure of the earth

24 p3088 A73-45448

GRAVITATIONAL POTENTIAL

U GRAVITATIONAL FIELDS

GRAVITATIONAL RADIATION

U GRAVITATIONAL FIELDS

GRAVITATIONAL WAVES

Gravitational waves astrophysical nature and origin, discussing current theories and possible applications in astronomy

01 p0094 A73-10063

Search for gravitational radiation of extraterrestrial origin.

01 p0097 A73-10424

The interaction of primordial gravitational waves with groups of galaxies.

01 p0098 A73-10585

Cosmological evolution from initial inhomogeneous and anisotropic universe to present structure, using general relativity for free gravitational field and waves

01 p0106 A73-11242

Spinorial solution associated to a radially symmetric radiation field in general relativity.

01 p0079 A73-11257

Propagation of the discontinuities of the covariant derivative of the electromagnetic and of the curvature tensor in an electromagnetic and gravitational wave

01 p0079 A73-11261

Collision between an electromagnetic wave and a gravitational wave packet

01 p0019 A73-11280

Gravitational radiation effects on cosmological time scale and models from matter fractional conversion and mass loss rate profile analysis

02 p0205 A73-11873

Computer analyses of gravitational radiation detector coincidences.

02 p0144 A73-12222

Cosmic gravitational waves detection and measurement, describing Weber experimental apparatus and theoretical foundations based on Einstein relativity theory

03 p0341 A73-12924

Possible sidereal period for the seismic lunar activity.

03 p0367 A73-13057

Search for seismic signals from gravitational radiation of pulsar CP1133.

03 p0367 A73-13058

Gravitation theory - Empirical status from solar system experiments.

04 p0498 A73-15249

A search for isolated radio pulses from the Crab Nebula at 151.5 MHz.

04 p0500 A73-15493

Fermions spin polarization reversal for HF high intensity gravitational waves generation and detection, suggesting superconducting metals for waves receiver

04 p0476 A73-15633

Invariant criterion generalization for pure gravitational waves in tetrad formulation of general relativity theory, noting electromagnetic field energy tensor

04 p0476 A73-15638

Maxwell equations in a spherically symmetric black-hole background and radiation by a radially moving charge.

05 p0597 A73-16470

On the location of the source of Weber's gravitational events.

05 p0625 A73-17330

Newtonian and relativistic gravitational theories, discussing gravitational waves generating mechanism and black holes formation

06 p0753 A73-18274

Macroscopic systems response to gravitational radiation for detector design and calibration, noting accessibility to people unfamiliar with general relativity

06 p0724 A73-18549

Stability of clusters of galaxies with mass loss to gravitational radiation.

07 p0873 A73-19053

Limits on gravitational radiation from two gravitationally bound black holes.

07 p0876 A73-19346

On the detection of gravitational radiation by its interaction with electromagnetic fields.

07 p0852 A73-20227

Earth as gravitational waves detector, discussing pulsar CP 1133 emission

08 p1000 A73-20675

A model for peaking of galactic gravitational radiation.

08 p1009 A73-21201

Event manifold curvature tensor as six dimensional bivector space via dyadic projections, applying to gravitational waves description

08 p0989 A73-21521

Tidal, primordial turbulence and spinning core theories for galactic rotation origin, considering rotational waves, gravitational waves and wave excitations

09 p1143 A73-22123

Modification of the phase methods for investigation of non-stationary processes in the ionosphere, magnetosphere and interplanetary space.

09 p1078 A73-22835

Anisotropic model of gravitational radiation enhancement from relativistic disk located in Galactic nucleus

09 p1149 A73-22946

Ejection of matter and gravitational radiation from orbiting bodies.

09 p1149 A73-22961

Cosmological evolution from initial inhomogeneous and anisotropic universe to present structure, using general relativity for free gravitational field and waves

10 p1279 A73-24178

Gravitational waves - A progress report.

10 p1280 A73-24324

Gravitational radiation from a mass projected into a Schwarzschild black hole.

10 p1280 A73-24343

Vector and tensor radiation from Schwarzschild relativistic circular geodesics.

10 p1249 A73-24346

The interaction of weak gravitational waves with a gas.

11 p1400 A73-26177

General relativistic effects detection experiments for supernova and collapsed objects, noting gravitational radiation transfer of energy equal to entire energy generation during thermonuclear evolution

12 p1542 A73-27550

A characteristic initial value problem in general relativity in the case of a perfect fluid with axial symmetry.

13 p1658 A73-28199

Relativistic stars and gravitational waves - An account for non-relativists.

13 p1683 A73-28991

Correlation of reported gravitational radiation events with terrestrial phenomena.

14 p1749 A73-30554

Search for infrared anomalies associated with gravitational events at the galactic centre.

14 p1800 A73-30601

Phenomena of scattering of electromagnetic and gravitational wave packets in the gravitational field of a black hole

15 p1932 A73-31245

Detection of gravitational waves by the method of light scattering by elastic oscillations

15 p1913 A73-31321

Evaluation of the directivity of gravitational wave radiators.

15 p1914 A73-31944

Dispersion of gravitational waves by a collisionless gas.

16 p2036 A73-33122

Gravitational and electromagnetic shock waves

17 p2212 A73-35048

Gravitational-inertial waves in the general theory of relativity

17 p2212 A73-35563

Flexural vibration frequencies of right circular cylindrical tensor gravitational wave detectors in regime with sound wavelength comparable to diameter

17 p2176 A73-35763

Optimization and data analysis of the Frascati gravitational-wave detector.

20 p2565 A73-39013

Universe evolutionary model construction based on observations of high flux gravitational radiation generated within Milky Way Galaxy

20 p2609 A73-39434

Antenna system design for detection of random gravitational waves with separation from effects of antenna random fluctuations

21 p2662 A73-40315

Nonradiative motion in a radiative gravitational field.

21 p2742 A73-41631

Gravitational radiation in the scalar-tensor gravitation theory.

22 p2885 A73-41718

Gravitational radiation detection via computerized delay-dependent coincidence comparisons of squared time derivatives of output powers of Argonne and Maryland cylindrical antenna detectors

22 p2885 A73-41734

Gravitational waves in a space-time of any dimension.

22 p2885 A73-41773

Gravitational-wave observations as a tool for testing relativistic gravity.

22 p2887 A73-42709

An operational approach to the energy of gravitational waves.

22 p2888 A73-42929

Collision between an electromagnetic wave and a gravitational wave packet.

23 p3006 A73-43501

Role of constraining forces for ultrarelativistic particle motion as a source of gravitational radiation.

23 p3006 A73-43606

Amplification of electromagnetic and gravitational waves during scattering on a rotating black hole

23 p3034 A73-44008

Antenna design for intergalactic gravitational wave detection, discussing binary star and pulsar sources, Weber wave receiver and Zeldovich-Braginsky dumbbell antenna

24 p3071 A73-44900

Gravitational radiation emission by star tidally deformed by black hole, computing energy loss rate

24 p3138 A73-45037

GRAVITONS

Certain quantum-gravitational effects in central classical fields

12 p1538 A73-26970

Gravitational Compton effect and graviton photoproduction by electrons

21 p2742 A73-40351

GRAVITY ANOMALIES

Geos-C mini arc orbit determination from radar altimeter observations under perturbations from gravitational anomalies

04 p0437 A73-14784

Isostatic reduction potential of earth mass distribution for spherical harmonic solutions of satellite determined gravity anomalies

04 p0437 A73-14788

Interior point mass earth potential model for satellite geodesy, considering geoid heights, gravity anomalies and spherical harmonics

04 p0438 A73-14791

Gravity anomalies determination from satellite orbit perturbations, using least squares method

04 p0439 A73-14799

Venus gravity anomalies and physical properties arising from convection currents and topography deduced from geodetic aspects derived from mass, radius and surface temperature

04 p0496 A73-14812

- A method for computing the gravitational attraction of three-dimensional bodies in a spherical or ellipsoidal earth. 05 p0569 A73-16379
- Lunar Sea of Serenity mascon analysis from Lunar Orbiter and Apollo 15 Doppler gravity data, correlating gravity anomalies with surface mass distribution 05 p0615 A73-16384
- Evaluation of gravity anomalies directly from satellite observations. 07 p0813 A73-19025
- Anomalous magnetic and gravitational field models autocorrelation function behavior dependence on circular cylindrical sources depth and spacing 07 p0816 A73-19447
- A direct method of interpreting gravity and magnetic anomalies - The case of a horizontal cylinder. 11 p1351 A73-25162
- ATS-F and Nimbus-E satellites use for range and range rate determination, earth gravity anomaly detection and orbital position determination 13 p1656 A73-28391
- Magnetic and gravitational potential anomalies due to uneven nonuniform material layers, using Fourier transforms 13 p1607 A73-28623
- Capabilities of the GS-12 gravimeter for studying gravitational field variations 13 p1621 A73-29412
- Lunar circular maria morphological features and fill deposits surface evolution, considering high velocity large body impact role based on Doppler gravity anomaly data 18 p2349 A73-35952
- Determination of the shape of the earth's physical surface from the anomalies of the vertical gradient of gravitational acceleration 19 p2427 A73-38554
- Influence of the atmosphere on the gravity force and its potential at points on the earth's physical surface 19 p2428 A73-38555
- Mars equatorial region crustal structure from Bouguer gravity anomalies computed by differencing free air gravity and topographically predicted gravity 20 p2612 A73-39710
- Mare Humorum mascon anomaly characteristics from gravity measurements obtained by Doppler tracking of Apollo 15 subsatellite 23 p3030 A73-43759
- ### GRAVITY GRADIENT SATELLITES
- #### NT APPLICATIONS TECHNOLOGY SATELLITES
- NT ATS 1
- NT ATS 3
- NT ATS 5
- NT ATS 6
- Gravitational interaction effects between parts of gravity stabilized satellite on attitude dynamics and control 01 p0095 A73-10110
- Effects of gravity-gradient torque on the rotational motion of a triaxial satellite in a precessing elliptic orbit. 01 p0099 A73-10685
- Gravitational stabilization systems parameters determination for minimum amplitude of satellite eccentric vibrations 03 p0383 A73-14557
- Pulsed motion of gravity gradient vehicle in central gravity field, presenting expressions of optimized attitude control 03 p0383 A73-14573
- Study of the dynamics of the preliminary-damping system of a gravitationally stable satellite with allowance for constraints on its sensors and on the flexural vibrations of the stabilizer 05 p0628 A73-16406
- Analytical design of optimal nutation dampers. 05 p0630 A73-17206
- Eole satellite gravity gradient stabilized pointing control system, discussing implementation by eddy current, inertia and magnetic hysteresis devices 07 p0904 A73-18936
- Magnetic articulation damping for gravity gradient satellite stabilization, using digital simulation 07 p0904 A73-18937
- Non-linear resonant attitude motions in gravity-stabilized gyrostats satellites. 07 p0905 A73-19162
- Reducing the thermal bending of a gravity-gradient stabilizer with the aid of a protective covering 10 p1286 A73-23894
- Equilibrium attitude transitions of a three-rotor gyrostatt in a circular orbit. 11 p1431 A73-26379
- Small oscillations of gravity gradient satellite in circular near-equatorial orbit, discussing operational efficiency of magnetic damping systems 12 p1549 A73-27648
- Gravity oriented satellite librational damping by solar radiation pressure, comparing WKB method with numerical integration results 15 p1943 A73-31640
- Gravitational stabilization of a two-body satellite. 15 p1943 A73-31916
- Gravity-gradient stabilization of synchronous orbiting satellites - Additional considerations of attitude stability. 15 p1944 A73-32218
- Damping of gravity stabilized satellite small rotary oscillations in circular orbit via stepwise change of moment of inertia 16 p2072 A73-33232
- Control laws of magnetic attitude stabilization systems of earth satellites 18 p2359 A73-36103
- Reduction of thermal deflection of gravitational stabilizer using shielding cover. 20 p2614 A73-38913
- Russian book on satellite attitude stabilization systems design covering gravity gradients, linear and nonlinear control laws, spin stabilization, high torque control moment gyros, etc 23 p3038 A73-43335
- ### GRAVITY WAVES
- #### NT BAROCLINIC WAVES
- Trapped gravity waves velocity oscillations in solar plages under magnetic field, comparing with Bilerberg continuum atmosphere 01 p0108 A73-11386
- Atmospheric gravity waves to be expected from the solar eclipse of June 30, 1973. 02 p0159 A73-12223
- Mesoscale traveling ionospheric disturbances in electron density interpretation in terms of acoustic gravity waves 02 p0162 A73-12295
- Interaction between gravity waves and ionization in the ionospheric F region. 02 p0162 A73-12298
- An analysis of coexistent waves and turbulence near clear air echoes. 03 p0339 A73-14535
- Instabilities resulting from gravity wave perturbation of ionization via neutral-charged particle collisions in nighttime E region 03 p0305 A73-14595
- Constant height sporadic E velocities and heights at night explained via instabilities generated from recombination and photoionization rate variations induced by gravity wave perturbations 03 p0305 A73-14596
- Internal gravity wave-atmospheric wind interaction - A cause of clear air turbulence. 04 p0473 A73-15071
- Asymptotic solution for vertical propagation of equatorial planetary waves in shear, noting gravity-Rossby and Kelvin waves and wind effects on diurnal tides 05 p0591 A73-16190
- Lower F region ionospheric wave dispersion observation for horizontal phase and group velocities relationship to period, considering interpretation by internal gravity wave hypothesis 05 p0552 A73-17056
- Finite-amplitude convection occurring in a modulated gravitational field 06 p0767 A73-17463
- A critique of multilayer analyses in application to the propagation of acoustic-gravity waves. 07 p0814 A73-19248
- Ionospheric winds in the F-region and their effects on the limiting periods of gravity waves. 07 p0818 A73-19673
- Equivalent gravity wave mode approximation for main solar diurnal tide in rotating spherical dissipative atmosphere modeled by Newtonian cooling and Rayleigh friction 08 p0958 A73-20959
- Intermittence effects in the equilibrium range of developing wind waves 08 p0986 A73-21458
- Atmospheric turbulent fluctuations explained via eddy-wind shear and convective rolls-gravity wave interactions, using wind-temperature data from White Sands 09 p1114 A73-22329
- Finite element method for solution of two dimensional flow equations with applications to passive advection and nonlinear gravity wave problems, noting computing time 09 p1113 A73-22955
- Supersonic generation of atmospheric gravity waves, via atmospheric cooling by moon shadows during lunar eclipses, noting analogy to terminator action 10 p1211 A73-23825
- Upper sporadic E layer downward velocity, considering corkscrew mechanism, ionization following gravity wave particular phase and velocity decrease 10 p1215 A73-24750
- Results of an investigation of the ionospheric effect of a sudden commencement of a magnetic storm 11 p1351 A73-25097
- An investigation of internal gravity waves generated by a buoyantly rising fluid in a stratified medium. 11 p1351 A73-25152
- Internal gravity waves in an atmosphere with wind shear - Validity of the WKB approximation at critical layers in the presence of buoyancy forces. 11 p1394 A73-25721
- Ionosphere spatial resonance as result of internal gravity wave phase velocity equal to ionization irregularity drift rate 11 p1356 A73-25908
- On the estimation of the directional spectrum of surface gravity waves from a programmed aircraft altimeter. 11 p1358 A73-26347
- Internal atmospheric gravity wave effect on ionospheric columnar electron content on basis of viscous atmosphere model with isothermal layers 11 p1359 A73-26709
- An existence proof for permanent capillary gravity waves with general vortex distributions 11 p1349 A73-26747
- Turbulence, billows and gravity waves in a high shear region of the upper atmosphere. 12 p1492 A73-27608
- Worldwide geodetic system construction by using satellites at sufficient altitude, discussing gravity waves avoidance 12 p1493 A73-27691
- Thermospheric neutral gas dynamics, discussing acoustic, gravity, tidal and planetary waves disturbance spectrum, propagation characteristics, latitude structure and energy sources 12 p1493 A73-27756
- The heating of the thermosphere by atmospheric gravity waves 12 p1493 A73-27758
- Influence of viscosity, thermal conduction, and ion drag on the propagation of atmospheric gravity waves in the thermosphere. 13 p1606 A73-28154
- The wave patterns produced by a moving body in a compressible, density-stratified fluid. 13 p1606 A73-28273
- Acoustic-gravity modes and large-scale traveling ionospheric disturbances of a realistic, dissipative atmosphere. 14 p1748 A73-29977
- Valve effect of inhomogeneities on anisotropic wave propagation. 14 p1780 A73-30165
- Boundary conditions in primitive equation weather prediction models with special emphasis on the control of gravity wave propagation. 14 p1772 A73-30902
- Large scale equatorial spread F irregularities motion velocity observation in Africa, interpreting quasi-periodic structures in west-east extension by atmospheric gravity waves 15 p1870 A73-31764
- Steady induced capillary-gravitational finite-amplitude waves on the surface of a finite-depth liquid 15 p1865 A73-32116
- Gravity wave magnitudes and horizontal and vertical scales measured and applied to eddy diffusion coefficients in upper stratosphere [AIAA PAPER 73-495] 16 p2005 A73-33538
- On the existence of critical levels, with applications to hydromagnetic waves. 16 p2043 A73-33869
- Ionospheric response to internal gravity waves observed at Delhi. 16 p2010 A73-33919
- The composite scattering model for radar sea return. 17 p2163 A73-35364
- Evidence and characteristics of internal and planetary waves within the D-region plasma. 18 p2304 A73-35967
- Velocity of the reflection points reveals structure and motions in the ionosphere. 18 p2305 A73-36000
- Predicted acoustic gravity wave enhancement during the solar eclipse of June 30, 1973. 18 p2352 A73-36301
- A preliminary study of the transient response of the atmosphere produced by mid-tropospheric heating. 18 p2332 A73-36701
- Optical wave measurement technique and experimental comparison with conventional wave height probes. 19 p2458 A73-37263
- Effect of wind shear on atmospheric wave instabilities revealed by FM/CW radar observations. 19 p2447 A73-38206
- Acoustic echo-sounding techniques and their application to gravity-wave, turbulence, and stability studies. 19 p2405 A73-38207
- Wave-mean flow interactions in the upper atmosphere. 19 p2427 A73-38217
- Occurrence and features of ducted modes of internal gravity waves over Western Europe and their influence on microwave propagation. 19 p2405 A73-38225

- Observed generation of an atmospheric gravity wave by shear instability in the mean flow of the planetary boundary layer. 19 p2448 A73-38229
- Interactions between internal gravity waves and their traumatic effect on a continuous stratification. 19 p2422 A73-38237
- Hydrodynamics of stratified fluids - The applicability of linear theory. 19 p2422 A73-38243
- Book - Gravitational waves in Einstein's theory. 19 p2461 A73-38366
- Flow stabilization by methods of distributed automatic control. 20 p2545 A73-39042
- On the nature and origin of the solar five-minute oscillations. 20 p2606 A73-39071
- Gravity waves in the F region of the ionosphere. 20 p2554 A73-39173
- Second-harmonic resonance in the interaction of an air stream with capillary-gravity waves. 20 p2550 A73-39816
- On the strategy of combining coarse and fine grid meshes in numerical weather prediction. 21 p2728 A73-40055
- Atmospheric gravity waves and the energy of the jet stream. 21 p2729 A73-40091
- Measurement of the dispersion of waves in the ionosphere. 21 p2682 A73-40232
- Interpretation of the results of photometric observations of noctilucent clouds. 21 p2732 A73-40859
- Internal gravity waves and turbulence in simultaneous upper atmosphere temperature and wind measurements. 21 p2732 A73-41342
- Gravity wave nonlinear interactions producing secondary waves of opposite polarization, discussing tide polarization. 21 p2688 A73-41343
- Waves and tides and their observation from ground and space. 21 p2689 A73-41356
- MHD frequency wavelength relation to five-minute period oscillation in solar magnetically active regions. 21 p2777 A73-41483
- Wave-induced eddy diffusion coefficients in the upper atmosphere of Mars. 22 p2906 A73-41903
- Charged black hole collisions as gravitational radiation sources in terms of conservation of mass and surface area. 22 p2908 A73-42428
- Atmospheric gravity wave observations after the solar eclipse of June 30, 1973. 22 p2847 A73-42487
- Resonance conditions for nonlinear interaction of acoustic gravity waves with viscous damping taken into account. 22 p2828 A73-43178
- Internal gravity wave-mean wind interaction. 23 p3000 A73-43339
- Gravity-shear waves in jet flow near tropopause with arbitrary temperature-wind stratification. 23 p3001 A73-43462
- Diurnal harmonic oscillation instability of atmospheric boundary layer as mesoscale internal gravity waves generation mechanism in lower atmosphere, considering unsteady flow equations. 23 p3001 A73-43589
- Anisotropic turbulent distributions for waves with a nondecay-type dispersion law. 23 p3012 A73-44018
- Radiative damping of trapped gravity waves in the solar atmosphere. 24 p3135 A73-44629
- Periodic variations in geostationary satellite polarisation observations. 24 p3082 A73-44735
- Current instability of atmospheric gravitational waves. 24 p3083 A73-44786
- GRAY GAS**
- The propagation of small disturbances in radiative magnetogas dynamics. 03 p0345 A73-12923
- Plane or axisymmetric inviscid optically gray hot gas jet radiating near optically thin limit, considering thermal radiation-gas dynamics coupling effects. 08 p1020 A73-20783
- Radiative heat transfer with no temperature jump at interface of media. 17 p2254 A73-34773
- An approximation for combined heat transfer in a radiatively absorbing and emitting gas. 18 p2370 A73-36366
- [AIAA PAPER 73-750]
- Approximate configuration factors for a gray nonisothermal gas-filled conical enclosure. 18 p2370 A73-36368
- [AIAA PAPER 73-752]
- Radiative equilibrium of a gray medium in a rectangular enclosure. 18 p2371 A73-36800
- Nonlinear acoustics of a radiating gas. II - Weak shock waves. 18 p2337 A73-36989
- Unsteady, combined radiation and conduction in an absorbing, scattering, and emitting medium. 22 p2930 A73-42288
- [ASME PAPER 73-HT-J]
- Effect of the absorbers upon the thermal structure of a LTE atmosphere, hydrogen and helium. 22 p2908 A73-42309
- An exact solution on the propagation of small disturbances in a radiating grey gas with isotropic scattering. 22 p2932 A73-42570
- Titan molecular hydrogen greenhouse effect responsibility for IR temperature disagreement with atmosphereless equilibrium temperature from analysis of nongray radiative and gray convective equilibrium. 24 p3129 A73-44450
- Radiating optically thick gas boundary layer based on approximation of gray gas in LTE, noting similarity to Knudsen layer. 24 p3158 A73-45535
- GRAZING LANDS**
- U GRASSLANDS**
- GREASES**
- Performance tests for steel-steel lubrication capability of dimethyl silicone oils and greases modified by soluble, heat-stable extreme pressure and antiwear additives. 03 p0329 A73-13011
- The assessment of recently developed lubricants for rolling elements. 03 p0316 A73-14361
- [ASLE PREPRINT 72LC-4C-2]
- The evaporation of various lubricant fluids in vacuum. 03 p0335 A73-14366
- [ASLE PREPRINT 72LC-6C-2]
- Lubricating grease technological development trends, discussing petroleum oils, esters, silicones, ethers and fluorocarbons base types and different thickeners. 07 p0842 A73-19556
- New high performance silicone greases and their applications. 07 p0842 A73-19557
- A review of the perfluoroalkyl ether class of greases. 07 p0843 A73-19558
- Polytetrafluoroethylene and fluorinated ethylene-propylene grease lubricants. 17 p2195 A73-34977
- [ASLE PREPRINT 73AM-1A-2]
- Grease lubrication of helicopter transmissions. 17 p2178 A73-34980
- GREAT BRITAIN**
- Atmospheric dust trace elements levels sampled in United Kingdom, considering natural origin. 07 p0820 A73-20279
- GREAT POLAR CAPS**
- U POLAR CAPS**
- GREEN FUNCTION**
- The radiation efficiency of a dipole antenna located above an imperfectly conducting ground. 01 p0015 A73-10185
- Ray optical procedure to obtain scalar Green function for polygonal waveguides by image diagram identification from rectangular guide equivalent combinations. 01 p0024 A73-10684
- Singular solutions of the plane distortion problem of micropolar elasticity. 03 p0392 A73-13776
- Use of Green's function in the study of the natural oscillations of two-dimensional structures. 04 p0511 A73-15087
- The Green's function of the linearized viscous transonic equation. 05 p0527 A73-16446
- Green's function of the Maxwell equations in laminar media. 05 p0598 A73-16819
- A matrix Green's formula and optimal control of linear distributed-parameter systems. 06 p0679 A73-17564
- The 'second' plane distortion problem of the theory of micropolar elasticity. 06 p0761 A73-17891
- Differential operators transformation into integral functions by Green function and distributions theory methods in structural analysis. 06 p0719 A73-18727
- Electromagnetic radiation from charges in weak gravitational fields. 07 p0852 A73-20179
- Green operator evaluation by Fourier transform method for wave propagation in bianisotropic media, obtaining constitutive equations. 09 p1049 A73-22311
- Numerical solution of mixed boundary value problems using numerical Green's functions. 09 p1112 A73-22394
- Nonlinear singular multipoint boundary value problems. 10 p1243 A73-24161
- The asymptotic behavior of Green's function for a heat-conduction equation with a small parameter. 12 p1558 A73-27248
- Kinetic equations for the Green functions describing equilibrium states of a gas. 13 p1662 A73-28551
- Rigorous resolution of the hierarchy of grand-canonical-ensemble Green functions. 13 p1662 A73-28552
- Generalized Green function for infinite plate strip with free edges, noting application to elastic boundary value problems. 13 p1695 A73-28560
- Complex resonant frequencies calculation in external diffraction problems for arbitrary shaped bodies, noting Green function poles correspondence to eigenvalue zeros of integral equation. 13 p1582 A73-28652
- Application of Papkovitch-Neuber potentials to a crack problem. 13 p1635 A73-28756
- Statistical displacement characteristics of random multiphase composite elastic structures in terms of stochastic Green functions and Neumann series. 14 p1811 A73-30482
- On dynamic response of prestressed cylindrical shells - Green's tensor technique. 15 p1947 A73-31367
- Explicit formulas for the representation of the Green's functions of covariant wave equations in the case of a weak gravitational field. I, II. 16 p2038 A73-34021
- Effects of the boundary conditions and of the deformation of a region on the spectrum of operators which are generated by boundary value problems with a spectral parameter contained in the boundary conditions on a boundary section. 18 p2329 A73-36161
- Short-wave asymptotics of the Green's function in the problem of diffraction at a plane layer. 18 p2290 A73-36987
- Green function and Poynting vector calculation of solid angles of radiation outside and inside anisotropic crystal in laser light scattering experiments. 20 p2591 A73-38617
- Green function hydrodynamic asymptotic behavior obtained via closed inhomogeneous linear equations, discussing distribution function kinetic equation, correlation function spectral distribution and adiabatic conditions. 21 p2677 A73-40636
- Integral equation analysis of cylindrical antennas having arbitrary surface impedance. 21 p2655 A73-41093
- Quasi-averages for Green functions construction in solving quantum statistical mechanics problems with degenerate equilibrium states. 21 p2741 A73-41297
- French monograph - On the representation of linear dynamic systems with distributed parameters and its application to the study of intrinsic properties of these systems. 22 p2837 A73-42746
- The use of fundamental Green's functions for the solution of problems of heat conduction in anisotropic media. 22 p2938 A73-42954
- The Laplace and Poisson equations in Schwarzschild's space-time. 23 p3005 A73-43345
- Turbulent mean emf in presence of nonvanishing mean conducting fluid flow, modifying Green tensor of induction equation for constant strain rate velocity fields. 23 p2969 A73-44050
- Analyses of some potential problems in cylindrical coordinates in connection with four-point probe technique. 23 p3018 A73-44368
- GREEN THEOREM**
- U GREEN FUNCTION**
- GREENHOUSE EFFECT**
- The runaway Greenhouse in the Venus atmosphere. 05 p0622 A73-17124
- Venus 4 chemical composition and pressure data for construction of Venus atmospheric model, emphasizing Greenhouse effect. 16 p2068 A73-33826
- Effect of noble gases on an atmospheric greenhouse /Titan/. 19 p2487 A73-38173
- Jupiter radiative greenhouse model overestimation of lower cloud level temperature due to convective heat transport neglect, discussing rejection of water cumulus cloud possibility. 24 p3129 A73-44439
- Titan molecular hydrogen greenhouse effect responsibility for IR temperature disagreement with atmosphereless equilibrium temperature from analysis of nongray radiative and gray convective equilibrium. 24 p3129 A73-44450
- Greenhouse effect for Titanian atmospheric models with different methane, hydrogen, helium and ammonia proportions, deriving brightness temperature spectrum and surface pressure. 24 p3130 A73-44457

GREENLAND

Icelandic geothermal activity and the mercury of the Greenland icecap.

09 p1079 A73-22949

GRIDS

Finite difference method for boundary layer flow, noting truncation errors due to nonuniform grid

01 p0035 A73-11468

Grid model to derive biharmonic difference operators with computer programming application, assessing errors in boundary conditions

02 p0236 A73-12512

Minimum weight rectangular beam grillages and reinforced plates of given strength or stiffness, presenting solutions for various boundary conditions

04 p0508 A73-14937

Monograph - Grid analysis of orthotropic plates.

06 p0761 A73-17873

Nonphysical noises and instabilities in plasma simulation due to a spatial grid.

07 p0854 A73-19267

Averaged boundary conditions for a grid consisting of nonparallel and nonrectilinear conductors placed on a nonplane surface.

07 p0801 A73-20127

Finite difference programs with grid self adjustment for steady or unsteady problems with arbitrary boundaries and without coordinate hierarchy, noting computer time saving

09 p1071 A73-22400

Optimization of finite element grids based on minimum potential energy.

[ASME PAPER 72-PVP-3]

09 p1163 A73-23268

Turbulence intensity and turbulent transfer characteristics behind grids in tubes

11 p1349 A73-26431

Comparison of grids and difference approximations for numerical weather prediction over a sphere.

12 p1519 A73-26803

Performance characteristics of a TEA double-discharge grid amplifier.

12 p1505 A73-27015

Light-weight Al isogrid panel design with triangular reinforcement elements for aerospace structural applications, discussing load response characteristics, fabrication and cost reduction

13 p1624 A73-28906

Sylvester matrix equation analysis of rigidly connected beam gridworks with weak regularity and translational properties, considering iterative and eigenvalue-eigenvector solutions

20 p2621 A73-39534

Turbulent flow velocity pulsations damping in wind tunnel chamber by wire grids, calculating grid turbulence effect

21 p2633 A73-41319

GRIFFITH CRACK

The diffusion of point defects to a propagating crack tip.

01 p0116 A73-11000

Crack initiation, acceleration, steady propagation and fatigue growth, considering Griffith criterion on fracture mechanics

04 p0507 A73-14705

Fracture mechanism theories based on discrete and continuous models of solids, explaining Griffith brittle crack dynamics

06 p0760 A73-17776

Crack problem of transversely isotropic strip.

06 p0762 A73-17986

The stress intensity factor of an edge crack in a finite rotating elastic disc.

07 p0918 A73-20566

The stress intensity factors of a radial crack in a point loaded disc.

07 p0918 A73-20567

A special theory of crack propagation.

09 p1161 A73-23177

Integral transform solution of mixed boundary value problem for Griffith cracks with complicated geometries and external, star-shaped, cruciform-shaped and circular cracks

09 p1162 A73-23183

Body centered cubic lattice transition metals favored cleavage plane prediction for crack propagation

13 p1635 A73-28261

Parametric finite element stress analysis of multiple crack propagation in nonhomogeneous nonisotropic materials, using Griffith criterion

13 p1701 A73-29472

Stress distribution due to a Griffith crack at the interface of an elastic half plane and a rigid foundation.

14 p1815 A73-30917

Classical fracture mechanics concepts, considering Griffith theory and modifications for ductile materials and strain energy density field

17 p2246 A73-34883

The stress field near a Griffith crack at the interface of two bonded dissimilar elastic half-planes.

21 p2789 A73-41672

Effect of a Griffith crack on the distribution of stress in a semi-infinite two-dimensional medium.

22 p2922 A73-42470

The influence of flaw density and flaw size distribution on the static and dynamic fatigue behaviour of graphite.

23 p2998 A73-44037

GRINDING

Composite material production by grinding Ni-Al-Ti alloy powder with other mixed powders, noting alloying elements effects on corrosion resistance and ductility

11 p1372 A73-25406

GRINDING [MATERIAL REMOVAL]

NT METAL GRINDING

Certain results of studies of the accuracy in grinding shaped surfaces by the method of nontemplate shaping of the cutting surface of an abrasive ribbon

02 p0172 A73-11798

GRINDING MACHINES

Transient vibration processes during diamond grinding and their statistical evaluation

24 p3094 A73-44971

GRIT

Accretion and electrostatic interaction of interstellar dust grains - Interstellar grit.

23 p3030 A73-43757

GROOVES

Spiral groove thrust bearing with load carrying lubricating oil film between stationary and rotating surfaces, discussing design, manufacturing and applications

03 p0313 A73-13925

The gas liquid interface and the load capacity of helical grooved journal bearings.

[ASME PAPER 72-LUB-19]

03 p0314 A73-14334

Stress concentration and groove design as factors in crack failure of low power single stage gas turbine rotor disk, using optical polarization technique

09 p1157 A73-22166

Effect of deep annular grooves on the strength of some metals under static tension and torsion

14 p1763 A73-30693

Calculation of stress-concentration factors for grooved shafts in bending using the point-matching technique.

15 p1948 A73-31616

Recent developments on noncontacting face seals.

[ASLE PREPRINT 73AM-8B-3]

17 p2179 A73-34995

Stress concentration and groove design as factors in crack failure of low power single stage gas turbine rotor disk, using optical polarization technique

22 p2920 A73-42114

GROUND BASED CONTROL

NT AIR TRAFFIC CONTROL

NT RADAR APPROACH CONTROL

Lunar surface exploration with Lunokhod 1 roving vehicle, discussing soft landing, ground based control, sensors, scientific equipment and observations

02 p0212 A73-12227

Ground control facilities and organization of Helios space probe mission and flight operations system based on U.S.-German cooperation

03 p0381 A73-13297

French computation center equipment for satellite orbit calculations and attitude corrections, describing links between teleprocessing and data transmission

05 p0555 A73-17300

Ground based and airborne collision avoidance systems comparison, discussing interrogator/transponder concept, pilot warning indicator, and air traffic handling capacity and economics

07 p0848 A73-18900

Operational set up of Europa II launch vehicle control units.

07 p0808 A73-19005

Apollo 15 and 16 ground-commanded television assembly.

07 p0823 A73-19375

Real-time analysis and ground command control to achieve accurate vehicle and payload event functions.

[AIAA PAPER 73-298]

09 p1117 A73-23217

The German telecommand ground station for HELIOS - A new concept.

09 p1070 A73-23418

German command station for Helios solar probe, discussing antenna design, transmitter parameters, back-up operation and compatibility with deep space network

[DFVLR-SONDDER-263]

13 p1598 A73-29275

The contribution of the German Telecommand Station to the overall command safety in the Helios project.

14 p1727 A73-30101

Electronic landing system satisfying IFR requirements for air traffic, noting simulated ILS and ground controlled approach operations

[DGLR PAPER 73-020]

17 p2146 A73-34494

Air based collision avoidance system feasibility appraisal, discussing YG1054 proximity warning indicator, cost analysis and implementation prognosis

19 p2454 A73-38468

Ground based aircraft collision avoidance systems, discussing three dimensional tracking, aircraft velocity vector determination, radar systems and tracking errors

19 p2454 A73-38470

Midair collision avoidance strategies for ATC improvement, discussing relative effectiveness of structural airspace, airborne and ground-based systems based on US statistics

21 p2733 A73-40030

GROUND CREWS

Commercial airline operational control, discussing flight plan approval by pilot and ground personnel, preflight duties, weather information assessment and fuel monitoring

15 p1909 A73-32446

GROUND EFFECT

Ground reflection effects upon radiated and received signals as viewed via image theory.

01 p0015 A73-10181

The radiation efficiency of a dipole antenna located above an imperfectly conducting ground.

01 p0015 A73-10185

Numerical solution for a flat plate experiencing a ground effect

03 p0245 A73-13721

Input impedance of a thin biconical antenna vertically buried near the air-ground interface.

05 p0548 A73-16162

Low-frequency loop antenna arrays - Ground reaction and mutual interaction.

06 p0665 A73-18176

Nonplanar wings in nonplanar ground effect.

15 p1824 A73-31744

Further developments in surface effect takeoff and landing system concepts - Application to high performance aircraft.

17 p2099 A73-34293

Further developments in surface effect takeoff and landing systems concepts - A multicell system.

[CASI PAPER 76/11B]

17 p2099 A73-34294

Antenna gain calibration on a ground reflection range.

17 p2128 A73-35688

Development of an Air Cushion Landing System.

19 p2379 A73-37468

A theoretical note on the lift distribution of a nonplanar ground effect wing.

19 p2376 A73-37493

Air cushion landing systems; Proceedings of the First Conference, Miami Beach, Fla., December 12-14, 1972.

19 p2380 A73-37676

Air cushion landing systems for aircraft mobility on unprepared surfaces, considering refraction, vertical energy absorption, braking, steering and weight and power reduction

19 p2380 A73-37677

Air cushion landing systems application to tactical airlift aircraft for personnel, and equipment delivery to dispersed sites under diverse climatic, terrain and combat conditions

19 p2380 A73-37678

Aircraft with air cushion landing system for off airport transport of goods and passengers

19 p2417 A73-37679

The Navy SETOLS program and its potential applications to Navy aircraft.

19 p2381 A73-37680

Air cushion landing systems for STOL transport aircraft, investigating structural and power requirements, ground and in-flight handling, mission capability, operational life, weight and cost

19 p2381 A73-37682

ACLS trade study for application to STOL tactical aircraft.

19 p2381 A73-37683

Air cushion landing system applications and operational considerations.

19 p2381 A73-37684

On the cost benefits of air cushion landing gear to civil aviation.

19 p2381 A73-37685

ACLS equipped vehicles in inter-city transportation.

19 p2381 A73-37686

CC-115 /Buffalo/ aircraft air cushion landing system design, testing and implementation prognosis, discussing propeller design, power systems, wings and U.S.-Canadian project cooperation

19 p2381 A73-37687

Buffalo aircraft modification for air cushion landing system, considering weight, performance, stability and control, configuration alternatives and ground maneuvering

19 p2382 A73-37688

The aircraft modification phase of the joint U.S./Canadian ACLS program.

19 p2382 A73-37689

LA-4 aircraft air cushion landing system ACLS development tests covering static and mobile ground tests, flight tests and performance from and to various surfaces

19 p2382 A73-37692

Air cushion landing system [ACLS/ application to Jindivik target drone aircraft for recovery improvement, considering flight performance degradation

19 p2383 A73-37698

A multicell air cushion system for landing gear application.

19 p2383 A73-37700

The potential influence of the ACLS on the development of logistical cargo aircraft. 19 p2383 A73-37701

Theory and experiments for air cushion landing system - A ground jet concept. 19 p2383 A73-37704

Simulation of the ACLS during landing roll. 19 p2383 A73-37706

Ground loads analysis for air cushion landing system (ACLS) equipped aircraft during landing and taxiing, predicting peak trunk pressures via energy considerations 19 p2383 A73-37707

ILS technology assessment, considering landing glide path determination, interference due to multipath propagation and ground effects, and operating frequency range problem 21 p2737 A73-41075

Contribution to the rotorcraft ground resonance theory 22 p2800 A73-43056

GROUND EFFECT MACHINES

NT GETOL AIRCRAFT

Heaving and pitching response of a hovercraft moving over regular waves. 01 p0004 A73-10700

High-pressure axial fan for air-cushion vehicles 02 p0203 A73-11713

Analysis of the longitudinal perturbed motion of a ground-effect flight vehicle 02 p0128 A73-11785

An axial-flow compressor for an air-cushion vehicle 03 p0358 A73-13724

Nonlinear modeling and dynamic simulation of vehicle air cushion suspensions. [ASME PAPER 72-WA/AUT-5] 04 p0406 A73-15883

From theory to practical use of air cushions for transport of heavy loads in the factory 05 p0535 A73-16753

Air cushion landing gears for transport aircraft, discussing peripheral jet stream performance prediction and system installation on Buffalo STOL 10 p1174 A73-23659

Power plants, cost estimates, freighter missions, commercial feasibility and technology for nuclear air cushion vehicles 15 p1912 A73-32194

Interaction of an air-cushioned vehicle with an elastic guideway. 17 p2098 A73-34181

Hovercraft propeller and turbine engine fan blades with glass and carbon fiber reinforced plastics respectively, discussing design and constructions 17 p2103 A73-34813

Report on an ST6 powered air supply package for air cushion landing systems. 19 p2382 A73-37690

ACLS CC-115 model simulation, test analysis and correlation. 19 p2382 A73-37693

Preliminary results from dynamic model tests of an air cushion landing system. 19 p2382 A73-37694

Feasibility study of skirt configurations and materials for an ACLS aircraft. 19 p2443 A73-37696

The Jindivik Drone Program to demonstrate air cushion launch and recovery. 19 p2382 A73-37697

Air cushion landing system (ACLS) design and drone flight tests for low cost unmanned military aircraft recovery, comparing with mid air retrieval system (MARS) 19 p2383 A73-37699

Air cushion landing system twin pod (ACLS) configuration design and test installation on A-4 Navy fighter 19 p2383 A73-37702

Static performance of plenum and peripheral jet air cushions. 19 p2377 A73-37703

GROUND HANDLING

Airport internal transportation systems for passengers and baggage, considering time scheduled, continuously moving and individually controlled systems 01 p0029 A73-10306

Airport design and management for safe aircraft ground handling, discussing FAA rules on pavement and safety areas, marking and lighting, fire fighting, etc 10 p1204 A73-24714

Aircraft and ground equipment damage during ground handling operations, discussing repair costs and out-of-service time 10 p1176 A73-24715

Concorde aircraft introduction into airline network, discussing time gain over various routes, operating costs, passenger service, departure and arrival problems, maintenance, etc [SAE PAPER 730351] 17 p2102 A73-34699

GROUND OPERATIONAL SUPPORT SYSTEM

The ground operations system for the AEROS research satellite. 08 p0953 A73-21661

International regional rental system for air transportation ground installations and route services, discussing ICAO recommendations 16 p2087 A73-32971

GROUND RESONANCE

U GROUND EFFECT

U RESONANCE

GROUND RUN-UP

U ENGINE TESTS

U GROUND TESTS

GROUND SPEED

Utilization of the Doppler effect to measure the drift angle and the ground speed of an aircraft 11 p1305 A73-25797

Book - The aerodynamics of high speed ground transportation. 17 p2097 A73-35854

GROUND STATE

Oscillator strengths and ground-state photoionization cross-sections for Mg+ and Ca+. 01 p0104 A73-11043

UV laser parameters calculation for operation on Lyman transition between H atom resonant excited state and ground state 01 p0061 A73-11334

Photoionization of vibrationally excited N2. II - Quenching by CO2 and N2O. 04 p0414 A73-14817

An instrument for the simultaneous detection of the OI ground state /2p4 3P/ and first metastable state /2p4 1D/ populations. 05 p0580 A73-17258

Magnetite absolute zero behavior with restriction to three order parameter theory, showing metallic band resultant from interatomic Coulomb energy ratio to bandwidth 06 p0734 A73-17835

A shock tube determination of the CN ground state dissociation energy and the CN violet electronic transition moment. 08 p0989 A73-20789

Oscillator strength and photoionization cross section computation for Cs ground state during photoabsorption, using semiempirical model potential with adjustable parameters 10 p1250 A73-23672

Ground state energy of solid molecular hydrogen at high pressure. 11 p1401 A73-25891

High-resolution magnetic hyperfine resonance in harmonically bound ground-state Hg-199 ions. 16 p2038 A73-32850

Self consistent field calculations of CO positive ion dipole moment in ground state 17 p2119 A73-35180

Experimental investigation of collisions of He atoms in the ground state and the 2/3S/ metastable state 19 p2462 A73-37248

GROUND STATIONS

NT STADAN [SATELLITE TRACKING NETWORK]

Polar motion from laser tracking of artificial satellites. 01 p0039 A73-10406

Three station interferometric observation of TAC-SAT synchronous communications satellite radio signals for orbit determination, discussing method feasibility for tracking and geodesy applications 01 p0097 A73-10407

A study of frequency sharing between satellite and terrestrial broadcasting systems. 01 p0018 A73-11179

Unified S-band ground system design and management for Apollo program, deep space and manned space flight network tracking and communications requirements 01 p0030 A73-11184

Continuous Pc micropulsations with discrete latitude dependent frequencies in H components, recording simultaneously at ground based magnetometer stations 02 p0157 A73-11749

A description of the lunar ranging station at McDonald Observatory. 02 p0151 A73-12249

High resolution limitations and improvement for earth based visual and photographic planetary observation, considering atmospheric boundary layer and use of elevated stations 02 p0169 A73-12331

Beyond the horizon ionospheric propagation experiment from an equatorial orbiting satellite to a middle latitude station. 03 p0274 A73-12892

An analysis of multi-station ground observations of VLF hiss. 03 p0274 A73-12950

Ground based goniometric observations of medium and high latitude VLF emissions due to transverse resonance instability and auroral oval Cerenkov radiation from magnetosheath 03 p0276 A73-13884

Cost goals for silicon solar arrays for large scale terrestrial applications. 03 p0258 A73-14250

Technological evolution of solar generators for terrestrial applications and sounding balloons, discussing environment caused problems and solutions, energy cost estimate and future prospects 03 p0258 A73-14253

Singularity solutions to critical configurations of geodetic range networks with distributed and in plane ground stations and target satellites 04 p0436 A73-14777

Geometric accuracy obtainable from simultaneous range measurements to satellites. 04 p0436 A73-14778

Status of data reduction and analysis methods for the worldwide geometric satellite triangulation program. 04 p0437 A73-14780

A fixed reflector, steerable beam, earth station antenna. 04 p0428 A73-15415

High capacity, dual antenna earth station. 04 p0432 A73-15416

System design, hardware and software of RF interference measurement experiment regarding microwave frequency optimal sharing between ATS-F satellite and terrestrial relay telecommunication 04 p0422 A73-15460

Feasibility of ground-based generation of artificial micropulsations. 04 p0444 A73-15537

Satellite data concentration, memorization, transmission and processing, discussing central computer control unit, ground stations peripheral links, magnetic tapes and system reliability 07 p0795 A73-18952

Mobile ground station for sounding balloons remote control, telemetry and localization, noting antenna pointing control, tracking receiver and trajectory recording 07 p0790 A73-18972

Calculation of the satellite tracking accuracy for ground stations with medium-diameter parabolic antennas 07 p0791 A73-19373

Economical system design for remote data acquisition. 07 p0824 A73-19948

A new earth-station antenna for domestic satellite communications. 08 p0947 A73-21144

Management of a magnetic tape dubbing and evaluation station. 09 p1087 A73-23408

U.S.S.R. ionospheric stations and observations during IQSY, discussing ionosphere formation, morphology, radio wave absorption, nonuniformity and upper atmosphere motions 11 p1351 A73-25101

Project management and installation of the Arvi satellite communication earth station. 11 p1344 A73-26147

Mobile satellite communication systems constraints imposed by international institution disagreements on management, procurement and operation, considering US and European conflicts on Aerosat project 12 p1471 A73-27653

The provision of ground station facilities for an aeronautical satellite system. 12 p1471 A73-27658

Skyenet satellite communication service for small dish antenna equipped mobile ground stations, emphasizing necessity of rapid central control response to configuration and propagation condition changes 12 p1471 A73-27660

Technical factors determining the choice of frequency bands for the links between satellite and coast stations of a maritime communications satellite service. 12 p1473 A73-27674

Balloon-aircraft ranging, data, and voice experiment. 12 p1473 A73-27680

Some results of an analysis of stable geomagnetic Pc4 pulsations at a network of stations. 13 p1608 A73-28719

German command station for Helios solar probe, discussing antenna design, transmitter parameters, back-up operation and compatibility with deep space network [DFVLR-SONDDR-263] 13 p1598 A73-29275

A study of frequency sharing between satellite and terrestrial broadcasting systems. 14 p1725 A73-29748

Ground communications networks for aeronautical operations. 14 p1740 A73-29885

The German Central-Ground-Station concept motivation and its multipurpose and automation aspects. 14 p1742 A73-30099

Satellite tracking interferometer systems with three steerable directional antennas mounted over azimuth mounts near Lichtenau / German Federal Republic/

14 p1742 A73-30100

PCM mobile ground station design covering telemetry receivers, digital data magnetic recording and computer interface circuitry and software

14 p1742 A73-30112

Correlation of 'satellite estimates' of the equatorial electrojet intensity with ground observations at Addis Ababa.

15 p1870 A73-31771

A procedure for studying the statistical structure of solar radiation fluxes at the ground under clouded conditions

15 p1905 A73-31792

Measuring earth-to-space contrast transmittance from ground stations.

15 p1914 A73-32386

Small earth terminals for satellite communications.

16 p1979 A73-33084

The R.S.R.S. ground stations for receiving 11.6 GHz transmission from the SIRIO satellite.

16 p1982 A73-33717

Italian SIRIO satellite cross polarization signal measurements aided by ground station antenna system using narrow bandwidth

16 p1983 A73-33725

Monitoring interruptions at the satellite earth station.

17 p1222 A73-34870

Satellite operation mode coordination with space program mission, considering orbital position and velocity and time at ground station horizon

17 p1260 A73-34932

Processing of aircraft data.

17 p1232 A73-35583

Digital data acquisition and processing from a remote magnetic observatory.

17 p1215 A73-35667

Satellite measurements of solar X-ray flux and ground observations of sudden ionospheric disturbances.

18 p2347 A73-36389

Domestic communication satellite systems with microwave transmission links and coast-to-coast earth stations and receivers, detailing design and interference problems

18 p2289 A73-36776

A limited steerable dual reflector antenna.

18 p2293 A73-36881

Ducted propagation of low-latitude whistlers deduced from simultaneous observations at multi-stations.

19 p2404 A73-38019

Radio interferometer for the range from 136 to 138 MHz in the central German ground station

19 p2432 A73-38273

Small earth terminal applications for satellite communications.

[AAS PAPER 73-121]

20 p2543 A73-38582

Design features of an unattended earth terminal for satellite communications.

20 p2522 A73-38716

A proposed time division multiple access /TDMA/ satellite system for Anik I.

20 p2523 A73-38719

Ground stations in Intelsat 4 communication satellite radio relay system, discussing all-solid-state equipment design, carrier frequency assignment and antenna installation

20 p2523 A73-38723

A satellite-switched SDMA/TDMA system for a wideband multibeam satellite.

20 p2524 A73-38730

Multiple-beam spherical-reflector antenna systems for satellite communications.

20 p2525 A73-38739

Implementation of fixed multiple beam spherical antenna systems and measured test results.

20 p2525 A73-38740

Optimization in the design of a 12 GHz low cost ground receiving system for broadcast satellites.

20 p2527 A73-38762

TDMA system design for small satellite terminals.

20 p2528 A73-38767

Calculation of structurally compressed satellite radio lines

20 p2531 A73-39469

Ground based microwave landing system for aircraft navigation, guidance and control in terminal area, discussing system requirements for flight safety

21 p2735 A73-40047

Satellite borne diffused pulsed laser with scattered light detection by optical receiver on ground for applications to wide range geodetic survey

21 p2681 A73-40133

Phased array antennas in ground based remote sensor system, assessing technologies of AN/FPS-85, HAPDAR and AP/TPN-19 radar systems

21 p2672 A73-40645

The combined use of satellite differential Doppler and ground-based measurements for ionospheric studies.

22 p2843 A73-41837

Accuracy of photographic artificial earth satellite observations at the observational station in Riga

22 p2910 A73-42644

Telesat Canada-Anik - Canada's domestic satellite communications system

24 p3069 A73-45392

GROUND SUPPORT EQUIPMENT NT GROUND OPERATIONAL SUPPORT SYSTEM

Airlines aircraft, engines and instruments maintenance, overhaul and repair procedures and equipment

06 p0648 A73-18254

French Guiana space center facilities for missile tracking, telemetry, data processing and transmission of command instructions, discussing PCM, PAM and PDM links equipment

07 p0807 A73-18942

The operational facilities of the French Guyana Space Center.

07 p0807 A73-18946

The liquefied ergol supply-trailers for DIAMANT B and EUROPA II launchers.

07 p0807 A73-18948

General requirements for aerospace powered mobile ground support equipment.

[SAE ARP 1247]

08 p0952 A73-20694

Sounding rocket range facilities at Esrange /Sweden/ for auroral studies, discussing telemetry support for simultaneous launchings

14 p1741 A73-30085

Radio navigation and landing aid equipment for major airports and airlines, noting simplified equipment for minor airports

15 p1912 A73-32559

Cape Kennedy Space Center ground support equipment welding machines and techniques, emphasizing propellant storage tanks and mobile launcher transporters

16 p1995 A73-33195

Ground visual aids for civil STOL aircraft steep gradient approach and blind landing, discussing flight trials and simulator experiments

[RAE-TM-AVIONICS-136/BLEU/]

17 p2208 A73-34489

Vehicle and ground support in space shuttle sortie and delivery-retrieval mission profiles

19 p2491 A73-37594

Fixed installation ground electrical power supply system for aircraft service, discussing motor-alternators, plant control cubicles, selector and busbar switchboxes and fault protection devices

24 p3075 A73-45156

GROUND SUPPORT SYSTEMS

Computerized ground support acceptance checkout systems for space shuttle program, discussing capabilities, future goal and unified test equipment

04 p0432 A73-15458

Space shuttle flight operations ground support systems for trajectory control and systems/mission management, discussing payloads data acquisition and transmission to user

[AIAA PAPER 73-36]

06 p0755 A73-17620

German ground operations network design, describing data system and flow with automatic handling of telemetry data, tracking data and operational information

14 p1727 A73-30098

The German Central-Ground-Station concept motivation and its multipurpose and automation aspects.

14 p1742 A73-30099

Transport cargo aircraft design requirements and supporting ground system concepts in view of future market demands with emphasis on economic constraints

[SAE PAPER 730352]

17 p2102 A73-34700

Radio-TV satellite ground support systems, discussing frequency ranges, satellite orbit, transponder signal amplification and ground reception systems

[DGLR PAPER 73-055]

17 p2126 A73-35488

A concept for Space Shuttle payload ground operations.

[AIAA PAPER 73-615]

18 p2359 A73-36093

Some considerations for Space Tug launch site support operations.

[AIAA PAPER 73-620]

18 p2360 A73-36502

The MINFAP system - First phase in the automation of the EUROCONTROL Maastricht Centre.

22 p2884 A73-42323

GROUND TESTS

NT COLD FLOW TESTS

NT PRELAUNCH TESTS

NT STATIC FIRING

The technique and results of ground tests of Lunokhod's friction members.

01 p0030 A73-11154

Experimental satellite for attitude control. I - System design.

01 p0111 A73-11188

Lunokhod 1 vehicle terrestrial mobility tests, simulating lunar gravity, soil and traction on scale and mockup models

02 p0151 A73-12234

Irradiation of solar cell candidates for the ATS-F solar cell flight experiment.

03 p0257 A73-14245

Estimation of engine emissions at altitude through ground testing.

04 p0485 A73-14892

Rocket exhaust plume ground test facilities and scaling for in-flight conditions simulation and separation in supersonic flow

[AIAA PAPER 72-1072]

04 p0414 A73-14903

Experimental studies of a Ludwig tube high Reynolds number transonic tunnel.

[AIAA PAPER 73-212]

06 p0645 A73-17661

Airlines flight safety management, discussing visual systems simulator /VSS/ for Tristar systems environmental and cycling endurance ground tests

10 p1176 A73-24710

Symphonic satellite communication equipment payload, discussing mission requirements, receiving and transmitting antennas, transponder and ground testing methods and arrangements

11 p1417 A73-25356

Space-flight qualification of solid-propellant units in the example of the cold-gas generator for the booster rocket Europa I/II

16 p2047 A73-33394

Ground and flight test results for standard VOR and double parasitic loop counterpoise antennas.

17 p2129 A73-35700

Evaluation of aerodynamic heating uncertainties for Space Shuttle.

[AIAA PAPER 73-737]

18 p2359 A73-36354

Orbiting Astronomical Observatory heat pipe flight performance data.

[AIAA PAPER 73-758]

18 p2370 A73-36373

Ground and flight testing of air cushion landing system /ACLS/ equipped CC-115 Buffalo aircraft for performance and stability/control characteristics

19 p2382 A73-37691

LA-4 aircraft air cushion landing system ACLS development tests covering static and mobile ground tests, flight tests and performance from and to various surfaces

19 p2382 A73-37692

Russian book - Hydraulic ducts of control systems in aviation: The effects of external factors. Shop testing, and reliability.

19 p2389 A73-37766

Navigation and landing aid systems in-flight and ground performance monitoring, discussing safety, legal, operational and economic aspects

19 p2450 A73-37802

Functional tests with hypersonic flight vehicles, using an infrared heating system to simulate the temperature loads in flight

19 p2419 A73-38269

Analysis of ground tests of a microwave, earth-occlusion, pressure-reference-level system.

21 p2729 A73-40065

GROUND TRACKS

NT SATELLITE GROUND TRACKS

Synchronous satellite ground track drift analysis for ecological survey application, discussing zonal, tesseral and sectorial harmonics and perturbation compensation

03 p0370 A73-13150

Lunar soil density estimation from Lunar Orbiter photographic measurements of boulder tracks, determining friction angle

10 p1277 A73-24085

GROUND TRUTH

The use of stress situations in vegetation for detecting ground conditions on aerial photographs.

03 p0301 A73-13844

Automatic digital image processing for remote sensing with ERTS, Skylab and NASA survey aircraft, considering image registration, projective transformation and ground truth information

03 p0309 A73-14487

The utility of a low flying aircraft or helicopter when collecting ground data for regional resource surveys.

08 p0961 A73-21710

The cloud bright spot.

13 p1619 A73-29238

Airborne remote sensing of Georgia tidal marshes.

16 p2003 A73-33359

Earth resources monitoring from satellites, aircraft and ground stations for fast data acquisition and management

17 p2161 A73-34934

Photodensity and the impact of shifting agriculture on subtropical vegetation - A case study in the Bahamas.

20 p2562 A73-39905

Interdisciplinary research on the application of ERTS-1 data to the regional land use planning process.

20 p2563 A73-39910

GROUND WATER

Water and processes of degradation in the Martian landscape.

19 p2477 A73-37202

GROUND WAVE PROPAGATION

Russian book on radio wave propagation covering ground, ionospheric and tropospheric propagation,

ratio attenuation, scattering and ionospheric and tropospheric reflection
02 p0143 A73-12775

Lunar surface SEP transmitter-receiver ground wave experiment, discussing electronic equipment, multifrequency antennas and signal variation
04 p0428 A73-15391

Effect of the earth's electrical properties on the characteristics of VLF wave propagation in the earth-ionosphere waveguide
05 p0550 A73-16398

Height-gain experimental data for groundwave propagation. I - Homogeneous paths.
07 p0791 A73-19377

Height-gain experimental data for groundwave propagation. II - Heterogeneous paths.
07 p0791 A73-19378

A surface-wave antenna integrated with the excitation device
07 p0802 A73-20294

Calculation of the field amplitude and phase velocity of low-frequency waves in the earth's spherical waveguide
08 p0939 A73-21285

Propagation of low-frequency electromagnetic waves in the spherical waveguide formed by the earth and the ionosphere
12 p1469 A73-27340

Ground-wave perturbation over a transition zone between two different sections.
13 p1583 A73-28798

Distortions of UHF pulse signals propagating along the earth at distances below the radio horizon
14 p1729 A73-30559

A surface-wave antenna matched to the exciter.
18 p2291 A73-37131

Computations of the field amplitude and phase velocity of low-frequency waves in a spherical surface waveguide.
19 p2404 A73-37914

Propagation of low-frequency electromagnetic waves in a spherical earth-ionosphere waveguide.
23 p2952 A73-43238

GROUND WIND
Wind shear near the ground and aircraft operations.
03 p0337 A73-13702

Ground wind component calculations from synoptic parameters
13 p1655 A73-29190

GROUND-AIR-GROUND COMMUNICATIONS
Experimental validation and design refinement program for air-ground-air data link based on automatic time division multiplex transmission of air traffic messages
02 p0190 A73-11852

Forward scatter chaff system for air-ground long haul communications.
04 p0418 A73-15393

ATC research - Simulating Arrival/Tower communications.
05 p0595 A73-16620

AEROSAT - An aeronautical communications satellite for oceanic areas.
[AIAA PAPER 73-46]
06 p0771 A73-17624

On the reduction of rainfall outages by space diversity for millimeter-wave earth-satellite communications systems.
06 p0668 A73-18712

Management and cost of European-U.S. Aerosat program based on geostationary satellites for air/ground voice and data messages relay and aircraft position determination
07 p0905 A73-19174

Airborne visible laser optical communication experiment between high altitude aircraft and ground station, discussing tracker-transmitter equipment and atmospheric effects on performance
09 p1055 A73-23395

Satellite communication channels assignment to ships and aircraft, considering automated digital calling method for ship-to-shore communication
12 p1472 A73-27670

Satellite communication systems for long haul air transport operations, discussing political, operational/technical and economic problems
12 p1472 A73-27671

ESRO Aerosat L-band communication techniques experiments with stratospheric balloon-borne transponders relaying ground station signals to aircraft flying over sea
12 p1498 A73-27672

ATC concepts and air/ground data link requirements for U.S. airspace structure in 1980s to support anticipated Los Angeles basin traffic densities in 1995
14 p1772 A73-29879

U.S. civil and military air-ground communications development history and expectations, considering information exchange, radar beacon transponders, digital communication and data links
14 p1725 A73-29880

VOLMET transmission automation with the aid of the "DECLAM" system using a speech synthesizer
15 p1846 A73-32429

Automation of the Yugoslav AFTN network and its future expansion
15 p1855 A73-32482

Procedures and ground methods associated with the exploitation of a system of aeronautical satellites
15 p1911 A73-32488

Problems related to the operation of an air-ground data-link system
18 p2289 A73-36686

Discrete address beacon system /DABS/ data links and digital communication between ground based ATC computer and aircraft for IFR-VFR conflict detection and safety separation
19 p2453 A73-38466

The universal data link system for air/ground communications.
20 p2526 A73-38757

The ARINC plan for implementing air/ground DATALINK.
20 p2527 A73-38758

The utility of data link to military aircraft communication - An operational view.
20 p2527 A73-38760

GROUND-TO-AIR MISSILES
U SURFACE TO AIR MISSILES
GROUP BEHAVIOR
U GROUP DYNAMICS
GROUP DYNAMICS
Studies in interactive communication. I - The effects of four communication modes on the behavior of teams during cooperative problem-solving.
06 p0658 A73-18241

Group performance in a visual signal-detection task.
11 p1322 A73-25182

GROUP THEORY
NT AUTOMORPHISMS
NT HOMOMORPHISMS
NT SUBGROUPS
Series expansion of the perturbation function
01 p0102 A73-10948

Infinite groups with constraints on subgroups, discussing Chernikov theorems, minimality requirements, laminary finite groups and Abelian subgroups
01 p0070 A73-11075

An equation for the product of semigroups defined by the method of bilinear forms and its application to the Schroedinger equation.
01 p0071 A73-11333

Topologic group theory for stress analysis of non-linearly elastic body under complex load, representing loads set by Lie group
01 p0119 A73-11428

Transformation group theory for Poisson equation solutions to boundary value problem of steady heat conduction with generation
03 p0400 A73-14631

Group theory application to in-plane vibrations natural frequencies of nth order polygonal particle elastic system, obtaining analytical solution through eigenvalue problem simplification
05 p0599 A73-17373

On an application of Lie group theory to the optimal control problem for linear dynamic systems with time-varying parameters.
06 p0679 A73-17954

Storage and transmission of sequences of moving images
08 p0941 A73-21559

Free boundary flow invariant solutions of Navier-Stokes equations for optimal S/H subgroup systems, using continuous transformation group operators
10 p1204 A73-23583

Problem of continuous survey of the earth, and kinematically correct satellite systems. II
10 p1276 A73-23882

Matrix eigenvalue search algorithms of Rutishauser-Francis type, showing relationship to linear group decompositions
10 p1243 A73-24124

Topologic group theory for stress analysis of non-linearly elastic body under complex load, representing loads set by Lie group
11 p1443 A73-26057

Group properties and invariant solutions of the Bellman equation in the problem of optimal control synthesis for second-order systems
12 p1483 A73-27079

Group classification of the hydrodynamics equations of an ideal fluid
12 p1487 A73-27409

Maximal finite groups of $n \times n$ integral matrices and complete groups of integral automorphisms of positive quadratic forms /Bravais types/
13 p1648 A73-28342

Space point group theory classification and analysis of antenna array lattices, noting current excitation space symmetries and orthogonal field pattern design
13 p1583 A73-28698

Classification theorem for analytical transformations of second order differential equations of motion at arbitrary resonance based on group theory
13 p1661 A73-29081

Classical mechanics-quantum mechanics relations and analogies, considering symmetry groups, Casimir invariants, energy levels and quantization
14 p1774 A73-30239

Group theory generalization of Dicke quantum theory for spontaneous coherent radiation of multi-level molecules, noting angular distribution of photon echo effects
14 p1757 A73-30332

Description of the $I/\text{sub } 0$ class in a special subgroup of probabilistic measures
15 p1899 A73-31243

Lie group theory of differential equations in continuum mechanics, gas dynamics, heat conduction, biharmonic and second order quasi-linear equations
15 p1914 A73-32109

Type-III Einsteinian void spaces with a $G/2$ Abelian group of motions and solvable $G/3$ groups
17 p2212 A73-35565

Bireductive spaces, Jordanian algebras, and spinor representations of non-Euclidean and quasi-non-Euclidean motions
17 p2212 A73-35566

Geometric interpretation of spinor representations for groups of motions in quasi-elliptic 5-spaces
17 p2213 A73-35568

Classification theorem for analytical transformations of second order differential equations of motion at arbitrary resonance based on group theory
19 p2445 A73-37632

The problem of continuous earth coverage and kinematically regular satellite networks. II.
20 p2603 A73-38901

Group properties of the equations of strain theory of thermoplasticity
20 p2618 A73-39329

Russian book on topological spaces and groups with continuous operations covering rings, Lie group, compact groups, homomorphism, automorphism, isomorphism, etc
21 p2726 A73-40801

Spectral theory and convolution systems of diagonal and nondiagonal discrete transformation filters on Abelian groups, comparing with computational simulations
23 p2957 A73-43311

Automorphism groups of W algebras operating in Hilbert space with application to noncommutative dynamic systems analysis and ergodic theory
23 p2999 A73-44102

Splittability of radically semisimple torsion over local and commutative Noetherian rings
24 p3144 A73-44423

Singular integral equations with a Carleman shift in the case of discrete coefficients and investigation of the Noetherian character of a class of linear operators with involution
24 p3105 A73-44425

Group properties and invariant solutions in the problem of the analytic design of controllers for a process with distributed parameters
24 p3074 A73-44661

Reference image /brightness distribution functions/ existence and normalization under additive and multiplicative groups of transformations in visual field
24 p3064 A73-44908

Topology of linear operators in Banach space generalized to invariant polynomials for minimum Schatten ideals in Hilbert space
24 p3105 A73-45008

Tensorial norms properties with respect to Hilbert spaces, constructing perfect ideals in Banach space
24 p3105 A73-45010

Reduction of systems of nonlinear differential equations to normal form
24 p3107 A73-45511

GROUP VELOCITY
The velocity of a wave packet in an anisotropic absorbing medium.
01 p0079 A73-11494

Determination of exospheric electron content from group delay and Faraday rotation observations of geostationary satellite signals.
03 p0300 A73-13636

Interferometric CW radar for group delay difference measurement of reflected signal components in ionospheric sounding
05 p0548 A73-16253

Investigation of a signal scattered in the lower ionosphere on the basis of a group delay model
05 p0548 A73-16254

Lower F region ionospheric wave dispersion observation for horizontal phase and group velocities relationship to period, considering interpretation by internal gravity wave hypothesis
05 p0552 A73-17056

The rate of motion of weak inhomogeneities in the ionospheric plasma
08 p0959 A73-21302

Group delay equalization in waveguide communications systems for signal regeneration with tapered meander transmission line
09 p1053 A73-23110

Selective amplifier with zero group delay in pass-band phase characteristics for sinusoidal frequency signal measurement

09 p1066 A73-23118

Group velocity and nonlinear dispersive wave propagation.

10 p1249 A73-24775

Nose extension method based on approximate dispersion function for calculating ducted whistler frequency and associated travel time, discussing ionosphere-magnetosphere interactions

11 p1358 A73-26704

A fast method to determine the nose frequency and minimum group delay of a whistler when the causative spheric is unknown.

11 p1358 A73-26705

Super-Alfven displacement of hydromagnetic pulses in the earth's radiation belt

12 p1491 A73-27349

Group delay times of magnetoionic components for horizontal electron density profiles in magnetic meridian plane, noting comparison with ionospheric sounding data

13 p1608 A73-28708

Electrostatic waves in warm random plasmas.

14 p1779 A73-29708

Wave propagation in uniform laminar cylindrical shells, discussing group and phase velocities on wave numbers in sandwich walls

17 p2243 A73-34734

On energy, group velocity and small damping of sound waves in ducts with shear flow.

18 p2302 A73-37031

Velocity of weak inhomogeneities in the ionospheric plasma.

19 p2425 A73-37931

Refraction of plasma waves in the ionosphere /in connection with topside sounding of the ionosphere/

21 p2691 A73-41507

Super-Alfven displacement of hydromagnetic pulses in the radiation belt of the earth.

23 p2970 A73-43246

The determination of whistler nose-frequency and minimum group delay and its implication for the measurement of the east-west electric field and tube content in the magnetosphere.

24 p3087 A73-45210

GROUP 1A COMPOUNDS

U ALKALI METAL COMPOUNDS

GROUP 2A COMPOUNDS

U ALKALINE EARTH COMPOUNDS

GROUP 7A COMPOUNDS

U HALOGEN COMPOUNDS

GROUP 2B COMPOUNDS

Structure diagram, crystal growth, band structure, physical, optical and photoelectric properties of A/II/B/V/ compounds, emphasizing CdSb-ZnSb solid solutions

10 p1258 A73-23566

GROUP 3A COMPOUNDS

Dissociation of semiconductor compounds under the action of a laser beam

11 p1378 A73-26675

GROUP 5A COMPOUNDS

Structure diagram, crystal growth, band structure, physical, optical and photoelectric properties of A/II/B/V/ compounds, emphasizing CdSb-ZnSb solid solutions

10 p1258 A73-23566

Dissociation of semiconductor compounds under the action of a laser beam

11 p1378 A73-26675

GROUP 8 COMPOUNDS

The solubility of hydrogen in rhodium, ruthenium, iridium and nickel.

09 p1047 A73-21981

GROWTH

NT CROP GROWTH

NT CRYSTAL GROWTH

NT EPITAXY

NT HYDROTHERMAL CRYSTAL GROWTH

High energy phosphate deficit-produced myocardial cell genetic apparatus activation as cardiac hypertrophy mechanism, discussing mitochondrial biogenesis and cardiac hyperfunction roles

02 p0134 A73-12511

Sleep and the maturing nervous system; Proceedings of the Symposium on the Maturation of Brain Mechanisms Related to Sleep Behavior, Boiling Springs, Pa., June 21-24, 1970.

03 p0263 A73-14255

Morphological, physiological and pharmacological investigations of rat cerebellar cortex synaptic structure and function maturation and neurotransmitter receptivity development

03 p0264 A73-14256

Maturing neuronal subsystems - The dendrites of spinal motoneurons.

03 p0264 A73-14257

Plant growth response to low temperature and UV treatment, discussing chlorophyll synthesis, carbohydrate levels, ion balance and enzyme characteristics

11 p1320 A73-26486

The effects of mercury compounds on the growth and orientation of cucumber seedlings.

12 p1462 A73-27274

Preliminary results of the action of cosmic heavy ions on development of eggs of *Artemia salina*.

18 p2271 A73-36129

Rotary and fixed wing aircraft growth factors from implicit differentiation of gross weight relative to fixed weight

[SAWE PAPER 952]

19 p2385 A73-37880

GRUMMAN AIRCRAFT

NT F-14 AIRCRAFT

NT F-111 AIRCRAFT

GRUMMAN MILITARY AIRCRAFT

U MILITARY AIRCRAFT

GUIDANCE [MOTION]

NT AIRCRAFT GUIDANCE

NT COMMAND GUIDANCE

NT INERTIAL GUIDANCE

NT INJECTION GUIDANCE

NT MAP MATCHING GUIDANCE

NT MIDCOURSE GUIDANCE

NT REENTRY GUIDANCE

NT RENDEZVOUS GUIDANCE

NT SATELLITE GUIDANCE

NT SPACECRAFT GUIDANCE

NT STRAPDOWN INERTIAL GUIDANCE

NT TERMINAL GUIDANCE

Russian book on remote guidance control systems covering theory, optimization and constraints for steady, unsteady, linear and nonlinear automatic control systems

15 p1853 A73-31374

Interaction of an air-cushioned vehicle with an elastic guideway.

17 p2098 A73-34181

GUIDANCE SENSORS

Experimental satellite for attitude control. V - Attitude control electronics.

01 p0112 A73-11192

A semiinertial homing guidance system

10 p1247 A73-24498

A numerical method in the analytic dynamics of gyrocompasses

20 p2566 A73-39499

GUIDANCE STABILITY

U CONTROL STABILITY

U GUIDANCE [MOTION]

GUIDE VANES

NT JET VANES

An axial-flow compressor for an air-cushion vehicle

03 p0358 A73-13724

Influence of regulated unequal guide-vane spacing on the alternating stress level in the working blades of a compressor

09 p1157 A73-22165

Improvement of the calculation of the guide vanes of centrifugal pumps

09 p1028 A73-22569

Supersonic annular blade cascades starting conditions, presenting static pressure and Mach number distributions

[ONERA, TP NO. 1219]

13 p1565 A73-28837

Transient analysis of ceramic vanes for heavy duty gas turbines.

[ASME PAPER 73-GT-46]

16 p2048 A73-33507

Gas turbine nozzle guide vane trailing edge protection by air films coating, measuring gas temperatures with chromel-alumel thermocouples

20 p2600 A73-39425

Investigation of the influence of the leading-edge configuration on the efficiency of cooled rotor- and guide-vane cascades

21 p2632 A73-40406

Effect of an adjustable nonuniform pitch in the distributor on the alternating stresses in compressor rotor blades.

22 p2919 A73-42113

Transverse deflection of guided projectile tail fins during deployment.

22 p2797 A73-42629

Effectiveness of film cooling in a curvilinear channel formed by guide vanes

23 p3048 A73-43442

GUIDED MISSILES

U MISSILES

GULF OF CALIFORNIA [MEXICO]

A geomagnetic variation anomaly across the northern Gulf of California.

21 p2678 A73-39927

Anomalies in geomagnetic variations across the central Gulf of California.

21 p2679 A73-39928

Oceanographic analysis of orbital photographs of the upper Gulf of California.

21 p2692 A73-41634

GULF OF MEXICO

Paleomagnetic excursion recorded in latest Pleistocene deep-sea sediments, Gulf of Mexico.

18 p2313 A73-36513

Distribution and diagenesis of organic compounds in JOIDES sediment from Gulf of Mexico and western Atlantic.

21 p2683 A73-40562

GULF STREAM

Gulf Stream eddies - Recent observations in the western Sargasso Sea.

18 p2313 A73-36642

GULFS

NT GULF OF CALIFORNIA [MEXICO]

NT GULF OF MEXICO

GUM NEBULA

The effect of the Gum Nebula on soft X-rays from galactic sources.

24 p3138 A73-45044

GUM VULCANIZATES

U VULCANIZED ELASTOMERS

GUMBEL THEORY

U RANGE [EXTREMES]

GUN LAUNCHERS

Appraisal of UTIAS implosion-driven hypervelocity launchers and shock tubes.

[AD-753252]

05 p0562 A73-16180

Gun launched sounding rockets and sabot projectiles for low cost meteorological and geophysical data acquisition, considering cost advantages

06 p0756 A73-18020

GUN PROPELLANTS

Mathematical model for extinguishing gunpowder combustion via pressure variations, assuming gunpowder surface dependence on combustion rates

09 p1167 A73-22617

Oblique reflection of a plane acoustic wave from a burning surface

19 p2503 A73-37513

Burning gunpowder interaction with an acoustic field in the presence of balanced chemical reactions behind the flame

21 p2791 A73-40699

GUNFIRE

JF8 and JP4 aircraft fuel fire and explosion susceptibility from gunfire hits, discussing combat survivability relative to fuel volatility

16 p2045 A73-32670

GUNN DIODES

Stability criteria for dipole domains in Gunn diodes

10 p1193 A73-23726

Narrowband time domain reflectometer uses pulse modulated Gunn-oscillator to measure small reflections in 6 and 7.5 GHz band waveguides.

14 p1733 A73-30057

S-type current-voltage characteristic in Gunn diodes.

15 p1923 A73-31674

Microwave integrated circuit applications at special microwave devices operation.

15 p1851 A73-32274

French monograph - Contribution to the study of background noise in Gunn effect diodes.

15 p1852 A73-32589

Characteristics change of Gunn diodes with uniaxial stress and temperature.

16 p1991 A73-33996

Q band /38 GHz/ varactor-tuned Gunn oscillators.

16 p1991 A73-34018

An X-band Gunn-diode generator with varactor tuning

17 p2126 A73-35550

Gunn diode parameters from a small signal analysis.

17 p2142 A73-35651

Pulse modulation of Gunn-effect oscillator.

17 p2142 A73-35652

Synchronization of the frequency of tunnel-diode, IMPATT-diode, and Gunn-device oscillators

20 p2537 A73-39460

Design of Gunn-diode oscillators on the basis of normalized characteristics

21 p2659 A73-40007

Summation of the output power from two Gunn diodes

21 p2659 A73-40008

Self excited mixer/detector of Gunn diode oscillator, calculating detection characteristics from combined equivalent circuit and computer simulated analysis

21 p2664 A73-41092

Self-resonant LSA oscillator diode of rectangular cross-section.

22 p2832 A73-41895

Observation of doping profiles in Gunn diodes with a scanning electron microscope using the beta-conductivity.

23 p2960 A73-43777

Analysis of microwave circuit for characterization of negative-conductance devices by transients.

23 p2964 A73-44076

Calculation of the energetic characteristics of Gunn diode oscillators in retarded- and quenched-domain modes

24 p3072 A73-44928

Gunn diode negative resistance microwave oscillators with simultaneous lower frequency mode and individual tunings of two frequencies

24 p3073 A73-45483

GUNN EFFECT

Instability nature in Gunn diode type system with negative differential conductivity, presenting expressions for oscillation threshold and gain

01 p0088 A73-10629

- Control of the frequency of Gunn-effect oscillators by a magnetic field 01 p0024 A73-10978
- Microwave-power attenuation in Gunn diodes 01 p0025 A73-10979
- Series-connected operation of Gunn diodes in a coaxial resonator 01 p0025 A73-10980
- Gunn diodes - Physical principles and simulation calculations 02 p0144 A73-11529
- Microwave amplifier design based on negative differential mobility in Gunn diodes 02 p0144 A73-11531
- Microwave Gunn diode oscillators applications, noting use as Doppler radar and synchronized oscillators 02 p0144 A73-11532
- Bidimensional and surface effects in a coplanar-contact Gunn diode 02 p0144 A73-11533
- Pulse communication at microwave bit rates using Gunn domains. 02 p0145 A73-11534
- LF noise in n-type GaAs and its correlation with HF noise of Gunn-diode oscillators 02 p0145 A73-11535
- Indium phosphide as a new material for microwave/transferred electron effect/oscillators. 02 p0199 A73-11536
- Wideband varactor-tuned Gunn effect oscillators. 04 p0426 A73-14732
- Some theoretical and practical considerations in the design of wideband varactor tuned Gunn oscillators. 04 p0426 A73-14733
- Advances in YIG-tuned Gunn effect oscillators. 04 p0426 A73-14734
- Subharmonic generation and its implications in Gunn effect devices. 04 p0427 A73-15055
- Effect of ionizing radiation on Gunn diode amplifiers. 05 p0557 A73-16502
- Transverse magnetic field effects on n-type GaAs Gunn diodes microwave power, coherence and dynamic I-V characteristics 05 p0558 A73-16784
- GaAs Gunn diode LSA operation mode in multiloop circuit to extend high frequency limit 05 p0558 A73-16788
- Gunn diodes oscillating circuit with waveguide cavity in push-pull mode at 42 GHz for high power parametric amplifier pump applications 05 p0558 A73-16807
- GaAs transferred electron /Gunn/ device microwave oscillator with harmonic tuning, noting reactive termination and bias voltage effects on efficiency optimization 05 p0559 A73-16813
- Optimize Gunn circuits for wideband varactor tuning. 06 p0675 A73-17841
- Varactor or YIG tuned Gunn effect microwave oscillators for ECM applications, noting low noise octave tuning and high sweep rates 06 p0675 A73-17842
- Investigation of regularities characterizing impact ionization within a high-field domain in Gunn diodes 06 p0675 A73-18076
- CW Q band Gunn diode microwave oscillator fabricated by integral heat sink technique for high power output and efficiency 06 p0677 A73-18345
- Computer simulation model of field independent trapping effects on slow Gunn domains in gallium arsenide, noting double symmetry electron-ion density distributions 06 p0737 A73-18368
- Intrinsic FM noise of Gunn oscillators. 07 p0798 A73-19341
- Current spreading at contacts to planar Gunn devices. 07 p0799 A73-19343
- Attainment of a low-noise high-power and highly stable Gunn oscillator by coupling to a superconducting cavity. 07 p0801 A73-20109
- Integrated electrically tuned X-band power amplifier utilizing Gunn and IMPATT diodes. 07 p0803 A73-20551
- Waveguide cavity multistage Gunn reflection amplifiers for FM-CW systems, discussing stabilization techniques, bandwidth, noise, power variation with temperature and group delay distortion 07 p0803 A73-20552
- Direct frequency demodulation with CW Gunn and IMPATT oscillators. 07 p0795 A73-20554
- Gunn diode effect in n-type GaAs, discussing electron drift velocity relationship to electric field, I-V characteristics and fabrication 08 p0943 A73-20709
- Finite difference calculation for Gunn effect mathematical model, noting negative slope in electron drift velocity versus electric field characteristics for microwave oscillation 08 p0943 A73-20710
- Gunn diode characteristics under large and small signal conditions, noting applications for FM oscillators and voltage tuned and magnetically tuned oscillators 08 p0943 A73-20711
- Light emission phenomenon in the Gunn effect device. 08 p0994 A73-20846
- Measurement of admittance of Gunn diodes in passive and active regions of bias voltage. 08 p0947 A73-21432
- X band Gunn oscillator FM noise spectrum dependence on quality factor of resonant circuit 09 p1062 A73-22322
- Thermal limitation for CW output power of a Gunn diode. 09 p1064 A73-23043
- Book - Transferred electron devices. 09 p1066 A73-23299
- Magnetic field influence of the Gunn effect threshold. 10 p1258 A73-23568
- Tunnel and Gunn diode oscillators coupled to superconducting cavity as S and X band frequency standards 10 p1195 A73-24397
- J-band transferred-electron oscillators. 10 p1196 A73-24863
- Wide-band varactor-tuned X-band Gunn oscillators in full-height waveguide cavity. 10 p1197 A73-24865
- Overlength modes of transferred-electron oscillators. 11 p1337 A73-25359
- Experimental verification of new Gunn-effect reflection-insensitive pulse regenerator. 11 p1337 A73-25361
- Development of cavities for microwave solid state sources. 11 p1338 A73-26150
- Gunn microwave oscillators electron temperature dependent noise in absence of 1/f type, considering thermal or Johnson noise augmented by carriers hopping 12 p1478 A73-27111
- Investigation of the synchronization of Gunn diode oscillators having a stripline resonance system 12 p1480 A73-27448
- Use of an yttrium-iron garnet sphere as the tuning element in Gunn oscillators 12 p1481 A73-27592
- Effect of donor density and temperature on the performance of stabilized transferred-electron devices. 17 p2134 A73-34220
- An electronically tuned Gunn oscillator circuit. 17 p2134 A73-34222
- Generation-recombination noise and the microwave emission from InSb. 17 p2219 A73-34912
- Quenched-domain mode oscillation in waveguide circuits. 17 p2136 A73-34969
- Temperature effects on modulation sensitivity and vibrational spectra in Gunn diode oscillators, suggesting frequency stability improvement method 17 p2136 A73-35162
- Review of some mathematical models of non-linear domain dynamics in bulk-effect semiconductor. 17 p2219 A73-35516
- The effects of the microwave structure parameters on the behavior of X-band Gunn oscillator. 17 p2142 A73-35650
- Gunn-effect digital functional devices and their performance evaluation. 17 p2143 A73-35814
- Active electronic devices - Microwave diodes 20 p2535 A73-39054
- Book - Gallium arsenide microwave bulk and transit-time devices. 20 p2536 A73-39137
- Thermally induced FM noise in Gunn oscillators and jitter in Gunn-effect digital devices. 21 p2660 A73-40096
- Gunn effect digital functional device. 22 p2829 A73-42204
- Some general observations on the tuning characteristics of 'electromechanically' tuned Gunn oscillators. 23 p2960 A73-44070
- GUNPOWDER**
U GUN PROPELLANTS
GUST ALLEVIATORS
Rotorcraft stability augmentation and gust alleviation by collective and cyclical rotor blade pitch angle changes, discussing nonlinear dynamic effects 18 p2267 A73-36397
- STOL passenger aircraft ride smoothing control system based on vertical and lateral acceleration limits for design flight condition of 7 fps rms gust velocity [ALAA PAPER 73-885] 20 p2509 A73-38821
- A new approach to gust alleviation of a flexible aircraft using an open loop device [ONERA, TP NO. 1236] 22 p2799 A73-42219
- GUST LOADS**
Random gust response statistics for coupled torsion-flapping rotor blade vibrations. 01 p0004 A73-10046
- Light aircraft vertical gust induced structural failures, analyzing 1960-71 accident reports for injuries biomechanics and environmental conditions 16 p1967 A73-32678
- Critical study of the effects of gusts on an aircraft 16 p1961 A73-32808
- Wind tunnel gust simulation for STOL aircraft behavior during low velocity flight in turbulent atmosphere near ground 16 p1962 A73-32813
- Effect of load sequences on crack propagation under random and program loading. 17 p2190 A73-34879
- Response of a rigid aircraft to nonstationary atmospheric turbulence. 18 p2267 A73-36305
- Determination of statistics of turbulence in clear air 18 p2332 A73-36687
- Dynamic gust, landing, and taxi loads determination in the design of the L-1011. 20 p2508 A73-38647
- Analysis of airplane response to nonstationary turbulence including wing bending flexibility. II. 21 p2784 A73-40437
- Influence of wing flexibility on sailplane loading by individual gusts 21 p2635 A73-41577
- GUSTS**
Number of gust series in turbulent velocity pulsations 09 p1115 A73-22992
- Statistical model of gust factor relation to lake and terrain surface roughness and height from wind velocity measurement data 13 p1655 A73-29341
- Three bladed model rotor gust induced impulsive discrete noise characteristics prediction by point dipole and rotational noise theories for comparison with measurement 16 p1967 A73-32917
- Lift and measurements in an aerofoil in unsteady flow. [ASME PAPER 73-GT-41] 16 p1964 A73-33503
- GYMNASTICS**
U EXERCISE [PHYSIOLOGY]
GYRATOR
NT AUTOROTATION
NT EARTH ROTATION
NT LARMOR PRECESSION
NT MOLECULAR ROTATION
NT PRECESSION
NT PROTON PRECESSION
NT ROTATION
NT SATELLITE ROTATION
NT SOLAR ROTATION
NT STELLAR ROTATION
GYRATORS
NT MICROWAVE FILTERS
Synthesis of gyrator RC filters from the cascaded model 10 p1193 A73-23729
- Synthesis of RC gyrator circuits with a constant characteristic resistance 10 p1196 A73-24608
- Active LC, RC and C /gyrator/ filters design, operation, tolerance, cost and noise characteristics 14 p1736 A73-30375
- Electronic integrated HF selective gyrator for TV IF filter development 21 p2661 A73-40230
- GYROCOMPASSES**
Equations for the compass motion of a triaxial gyrostabilizer in gyrocompass operation 05 p0577 A73-16993
- A comparison of the effectiveness of some adaptive optimal filtering techniques applied to the gyrocompassing problem. 10 p1201 A73-24052
- Digital attitude reference system for three-axis-stabilized earth oriented satellites, using gyrocompasses with solar and horizon sensors 17 p2209 A73-34875
- Shop level maintenance of inertial platforms without a surveyed site. 17 p2148 A73-35644
- Effect of the random disturbances in the principal gyro axis on the readings of a ground gyrocompass 18 p2317 A73-36854
- Design and analysis of a practical on-line filter to process gyrocompass data. 20 p2564 A73-38782
- A numerical method in the analytic dynamics of gyrocompasses 20 p2566 A73-39499
- Simultaneous systematic treatment of the readings of a directional gyroscope and a magnetic compass 24 p3089 A73-44547
- GYROFREQUENCY**
Ionospheric resonance signal envelope and waveform observation by rocket-borne RF sounder,

noting electron gyrofrequency third harmonic due to beating waves 02 p0140 A73-11750

Nonlinear frequency correction to plasma instability at half harmonics of electron gyrofrequency as observed by OGO 5 near geomagnetic equator outside plasmapause 09 p1075 A73-22069

Electrostatic waves with frequencies above the gyrofrequency in a plasma with a loss-cone. 17 p2218 A73-35831

Off-resonance microwave-created plasmas. 20 p2597 A73-39196

Electrostatic waves with frequencies exceeding the gyrofrequency in the magnetosphere. 22 p2851 A73-42933

GYROINTERACTION

U MAGNETIC RIGIDITY

GYROMAGNETISM

NT GYROFREQUENCY

Plasma diffusion across a magnetic field due to thermal vortices. 09 p1126 A73-22217

Relativistic effects on gyromagnetic ratio of massive rotating body with uniform charge density and with shell large in comparison to Schwarzschild radius 10 p1252 A73-24345

Solar microwave burst radiation spectrum, explaining burst intensity decreasing phase by gyromagnetic absorption model 11 p1413 A73-25946

GYROPLANES

U HELICOPTERS

GYROS

U GYROSCOPES

GYROSCOPES

NT ATTITUDE GYROS

NT CONTROL MOMENT GYROSCOPES

NT CRYOGENIC GYROSCOPES

NT ELECTROSTATIC GYROSCOPES

NT FLUID ROTOR GYROSCOPES

NT GYROCOMPASSES

NT GYROSCOPIC PENDULUMS

NT GYROSTABILIZERS

NT OPTICAL GYROSCOPES

NT ROTARY GYROSCOPES

The equations of motion of gyroscopes in general relativity 01 p0098 A73-10539

Investigation of a moving angular-velocity hodograph in the symmetrical solution to the problem of the motion of a body having a fixed point 02 p0191 A73-11762

Intersection line of axes cone with sphere and locus of angular velocity vectors for uniform gyroscope rotation with different moments of inertia 02 p0191 A73-11764

Dynamic characteristics of two bodies coupled by common axis, noting equations of motion of Lagrange gyroscopes system 02 p0192 A73-11766

Equations of motion of composite space pendulum formed by gyroscopes with Cardan suspension, noting equations integrability 02 p0192 A73-11767

Newtonian force field effect on gyroscope motion for coordinate axes coincident with inertia tensor axes, solving equations of motion by energy integral 02 p0192 A73-11769

New solutions of the problem of the motion of a gyroscope in a central Newtonian force field 02 p0192 A73-11770

A hero-jet driven porous spherical hydrostatic gas bearing gyro. [ASME PAPER 72-LUB-41] 03 p0315 A73-14348

Logic network design for digital waveform shaping of polypulse voltage generator, noting application for airborne and marine gyroscope power supply 03 p0258 A73-14618

Inertial navigation system based on two schuler gyropendulums and one azimuth gyro. [DFVLR-SONDDR-246] 05 p0595 A73-16765

Air and naval gyroscopic instruments development in Germany during 1927-1945, discussing inertial platforms, antiaircraft fire control, gas bearings and accelerometers 05 p0577 A73-16766

Suboptimal feedback control of linear gyroscopic systems. 06 p0679 A73-17568

Atomic nuclei physical properties for space navigation system gyroscopes, noting nuclear magnetic resonance and nuclei polarization 06 p0692 A73-17774

Cassiopee triaxial gyroscopic aiming device for sounding rocket attitude control, using stellar and inertial sensors and jet micropulsion 07 p0866 A73-18924

Ponderous nutational motion of gyroscope in gimbal suspension, calculating precession rate from reduced equations of motion 09 p1081 A73-22351

Artificial satellites to test general relativity theory 11 p1431 A73-26590

Dynamic characteristics, stability and steady state accuracy for orbital gyroscope with digital control, noting bit density requirements of onboard computer 12 p1523 A73-27632

Pulse rebalance gyro electronic system with hybrid microcircuitry for digitizing sensor inputs to computer 13 p1589 A73-28047

Minimax failure detection and identification in redundant gyro and accelerometer systems. 13 p1616 A73-28832

High-reliability strapdown platforms using two-degree-of-freedom gyros. 13 p1657 A73-29214

Rapid balancing of gyroscopes with TEA CO₂ laser. 15 p1883 A73-30996

Gyroscopic moment effect on rotating shafts lowest critical velocity, plotting convergence characteristics 15 p1949 A73-31668

The mechanism of gyroscopic tracking. I. 15 p1883 A73-32284

[ASME PAPER 72-MECH-32] The mechanism of gyroscopic tracking. II. 15 p1883 A73-32285

[ASME PAPER 72-MECH-33] Periodic solutions of singularly perturbed equations arising from gyroscopic systems. 16 p2032 A73-33310

Precise attitude control of the Stanford relativity satellite. 19 p2494 A73-38080

Short term gyro drift measurements. 19 p2430 A73-38081

Some linear problems in the theory of gyroscopes 20 p2565 A73-38983

Use of gyro technology to measure small random angular motion. 21 p2700 A73-40504

[AIAA PAPER 73-839] Russian book on gyroscope theory covering maritime, aircraft, rocket and spacecraft applications, instrument error, differential equations of motion, rotor precession and degrees of freedom 21 p2705 A73-41437

GYROSCOPIC COUPLING

Periodic Faraday bias and lock-in phenomena in a laser gyro. 17 p2172 A73-35413

Random vibration of distributed systems strongly coupled at discrete points. 22 p2918 A73-41820

Prediction and measurement of the proportionality constant in statistical energy analysis of structures. 22 p2918 A73-41821

Error analysis of a coupled inertial navigation system 22 p2884 A73-42358

On the gyroscopic coupling of a Van der Pol oscillator in the forced regime and of a free linear oscillator 24 p3111 A73-45396

GYROSCOPIC DRIFT

U GYROSCOPES

U GYROSCOPIC STABILITY

GYROSCOPIC PENDULUMS

Energy dissipation and drift angular velocity calculation for horizontal pendulum on vibrating base, using revised differential equation of motion 01 p0079 A73-11417

Equations of motion of composite space pendulum formed by gyroscopes with Cardan suspension, noting equations integrability 02 p0192 A73-11767

Inertial navigation system based on two schuler gyropendulums and one azimuth gyro. 05 p0595 A73-16765

[DFVLR-SONDDR-246] Strap-down inertial guidance systems study. 18 p2335 A73-36955

Investigation of the motion of a gyroscopic pendulum on a randomly vibrating base 20 p2566 A73-39504

Combinational parametric resonance in a gyro-pendulum mounted on a mobile base 22 p2860 A73-42367

GYROSCOPIC STABILITY

Stabilization of the relative equilibrium and steady motion of a mechanical system by partial dissipation forces 01 p0077 A73-10953

Gyrostabilized systems stability analysis with allowance for elasticity, internal friction and electric circuits transient processes, examining steady motion under parametric disturbances 01 p0051 A73-10965

Certain problems of dynamics and accuracy of gyroscopes in gimbals. 01 p0053 A73-11197

Vibrational resonance modes of balanced gyroscope on fixed base, determining gimbal vibration amplitude and gyro drift rate as function of perturbation frequency 01 p0054 A73-11401

Experimental determination of the probability characteristics of perturbations relative to the principal axis of a gyroscope 01 p0054 A73-11414

Determination of gimbal errors in an astatic gyroscope with allowance for drift 01 p0054 A73-11416

Equations of motion for Kovalevskaja gyroscope uniform rotation about axes differing from inertia ellipsoid principal axes, noting sufficient stability conditions 02 p0167 A73-11765

Drift rate of the rotor axis in the generalized problem of the gyroscope with a Cardan mounting 02 p0167 A73-11768

Regular gyrostat precession in a central Newtonian field of forces 02 p0192 A73-11771

Existence conditions of precessional motions of gyroscope with fixed point, assuming constant time function and unit vector coincident with gravity force direction 02 p0192 A73-11772

Flexible satellite with three axisymmetrical bodies spinning at different rates about common axis of symmetry, deriving stability conditions based on Sturm theorem 02 p0228 A73-11997

Stability of the motion of a nonautonomous gyrostat 04 p0475 A73-14932

Russian book on hydrodynamic gyroscope theory and design covering casing angular velocity, cavity fluid motion, induction removal, noise levels and threshold sensitivity 04 p0450 A73-15705

Equations of motion for precession theory of two rotor gyroscopes on earth satellites for orbit plane determination, noting noise spectrum transformation 05 p0628 A73-16407

Stability analysis of gyroscopic systems for parametric resonance case, allowing for viscous friction at gimbal axes 05 p0578 A73-17085

French Monograph - Contribution to the study of the stabilization of gyroscopic satellites - Conception and development of an active nutation damper. 06 p0757 A73-18097

Stability of a gyroscope on a vibrating base under resonance conditions 08 p0972 A73-21763

Errors in measuring the angles of rotation of an object with a triaxial gyrostabilized platform with allowance for its drift 09 p1115 A73-22343

The motion of a dynamically unbalanced gyroscopic linear-acceleration integrator 09 p1081 A73-22344

Numerical position deviation and release delay time estimates for gyroscope motion in gimbal suspension during rotor start-up 09 p1081 A73-22345

Characteristic indices of vanishing solutions to a gyro system with partial dissipation 09 p1081 A73-22352

Construction of the frequency spectrum of a three-degree-of-freedom gyroscope with a flexible rotor shaft and elastic gimbal mountings 09 p1084 A73-22656

Systematic drift of a gyroscope with variable angular momentum in the gimbal suspension during vibrations of the frame 09 p1084 A73-22657

A condition for drift invariance with respect to acting accelerations in a two-degree-of-freedom gyroscope having arbitrary gas lubricated bearings on the main axis 09 p1084 A73-22658

Precession motion stability and drift rates of gimbal gyroscope under angular and translational resonant base vibration 09 p1087 A73-23343

Periodic small parameter solutions of rotary gyroscope motions about axis of ellipsoid of inertia, using Euler-Poisson equations 10 p1220 A73-24678

Stability predictions with the aid of energy expressions in the case of a turborotor with gyroscopic effects 11 p1432 A73-24999

Vertical two axis gyrostabilizer equations of motion analysis by averaging method 11 p1360 A73-25048

The dynamical effect of inertial waves on the gyroscopic motion of a body containing several eccentrically located liquid-filled cylinders. 11 p1346 A73-25224

Reduction of a gyrostat problem to that of a rigid body. [ASME PAPER 72-APM-QQ] 11 p1398 A73-25704

Stability of the steady motions of a gyroscope with spring limiters on a revolving platform in a Newtonian central force field 11 p1364 A73-26095

Calculation of the rotor potential of an electrostatic gyroscope 11 p1364 A73-26098

Drift moments produced by rotor nonsphericity in a suspension system with an axially-symmetric field 11 p1367 A73-26453

Stable-member mounted instrument environment simulation model development. 11 p1395 A73-26638

On the stabilization of relative equilibrium and steady-state motion of a mechanical system by partial dissipation forces. 12 p1524 A73-27529

Gyrostabilized systems stability analysis with allowance for elasticity, internal friction and electric circuits transient processes, examining steady motion under parametric disturbances 12 p1498 A73-27541

Dynamic characteristics, stability and steady state accuracy for orbital gyroscope with digital control, noting bit density requirements of onboard computer 12 p1523 A73-27632

Nonlinear effects of axial load and rigidity changes on ball bearings of gyroscopes with symmetrical gyromotor design 13 p1618 A73-29145

Influence of the rotor weight on the changes in the axial rigidity of gyromotors 13 p1572 A73-29146

Influence of elastic deformations of the gimbal support on the motion of a three-degree-of-freedom astatic gyroscope 13 p1618 A73-29147

Influence of the orthogonal axes of the suspension of an electrostatic gyroscope at zero rotor potential 13 p1618 A73-29148

Analytical description of the three-dimensional distribution of the scattering of a gyromotor magnetic field 13 p1618 A73-29149

Helium superleak metastable persistent current quantum states use to provide nondecaying angular momentum for gyroscopic element 15 p1876 A73-31942

Strapdown electrostatic gyroscope spin axis precession drift rate calibration, using virtual work technique for modeling bearing torques on rotor 17 p2137 A73-35210

Some problems of orientation accuracy for a gyroscopic orbit with nonlinear control laws 18 p2335 A73-36118

The position of the axis of rotation of a free gyroscope ball rotor 18 p2317 A73-36852

Gyroscopic orbit errors caused by random perturbations 18 p2317 A73-36853

Influence of clearances on the behavior of a gyroscope on a vibrating base 19 p2428 A73-37188

A hybrid fluidic directional gyro. 19 p2430 A73-38055

Short term gyro drift measurements. 19 p2430 A73-38081

Precision pointing control thruster design for satellite experiment to test relativistic precession of gyroscope moving through gravitational field, determining gyro orientation via superconducting circuitry [AIAA PAPER 73-858] 20 p2586 A73-38796

Recent test results - A strapdown IMU utilizing hydrodynamic spin bearing rate sensors and pulse rebalance loops. [AIAA PAPER 73-898] 20 p2564 A73-38833

Some linear problems in the theory of gyroscopes 20 p2565 A73-38983

Gyroscopes as prime attitude references for the large space telescope. [AIAA PAPER 73-870] 21 p2700 A73-40506

Combinational parametric resonance in a gyro-pendulum mounted on a mobile base 22 p2860 A73-42367

Stability of an indicator gyrostabilizer during the rotation of a three-stage gyroscope 22 p2860 A73-42368

Stability of a biaxial gyroframe on a vibrating base in resonance conditions 23 p3007 A73-44186

The drifts of a gyroscope mounted on the oscillating housing. 23 p2983 A73-44271

Deflecting moments in magnetic suspensions of gyroscopic devices 24 p3089 A73-44546

Effect of the gyromotor torque on the dynamics of a gyroscope 24 p3091 A73-45021

Calculation of the force characteristics of the external spherical suspension of a cryogenic gyroscope 24 p3091 A73-45023

GYROSTABILIZERS

Gyrostabilized systems stability analysis with allowance for elasticity, internal friction and electric circuits transient processes, examining steady motion under parametric disturbances 01 p0051 A73-10965

Control theory analysis of equilibrium state asymptotic stability of system with dry friction, applying to power driven gyrostabilizer 01 p0054 A73-11402

Precession equations of a triaxial power-driven gyrostabilizer 02 p0167 A73-11775

Equations for the compass motion of a triaxial gyrostabilizer in gyrocompass operation 05 p0577 A73-16993

Autonomous determination of meridian plane with triaxial gyroscopic stabilizer during initial display of inertial system 09 p1116 A73-22659

Gyroscopic device for compensating external moments of sextants or binoculars optical axis due to spontaneous hand movements 09 p1084 A73-22673

Vertical two axis gyrostabilizer equations of motion analysis by averaging method 11 p1360 A73-25048

Equilibrium attitude transitions of a three-rotor gyrostabilizer in a circular orbit. 11 p1431 A73-26379

Constant-Q pulsed feedback electronics for strapped-down gyro systems. 11 p1342 A73-26635

Gyrostabilized systems stability analysis with allowance for elasticity, internal friction and electric circuits transient processes, examining steady motion under parametric disturbances 12 p1498 A73-27541

Errors of the gravitational stabilization system of a satellite with gyrodamping 14 p1803 A73-29869

Russian book - Calculation and designing of gyroscopic stabilizers. 15 p1875 A73-31587

Errors of a single-axis gyrostabilizer as an angular velocity integrator 22 p2860 A73-42366

Stability of an indicator gyrostabilizer during the rotation of a three-stage gyroscope 22 p2860 A73-42368

French paper on satellite attitude stabilization by gyroscopes covering autonomous activator systems, kinetic moment principles and control in roll-yaw for flexible panels 22 p2917 A73-42743

Extremal search method errors in determining azimuthal position of gyrostabilized platform relative to meridian plane, comparing with gyrocompasses 24 p3109 A73-45022

GYROSTATS

U GYROSCOPES

GYROTROPISM

Tikhonov conditions of field excitation for dipole antenna radiation study in stratified gyrotropic medium 02 p0147 A73-12470

Normal-mode analysis of anisotropic and gyrotropic thin-film waveguides for integrated optics. 06 p0702 A73-18365

Gyrotropic flat ionosphere model with elliptical nonuniform conductivity for electrojet generation by magnetosphere current entering and leaving auroral zone 15 p1872 A73-31895

Tikhonov conditions of field excitation for dipole antenna radiation study in stratified gyrotropic medium 15 p1847 A73-32621

Nonlinear expansion of arbitrarily polarized electromagnetic waves in gyrotropic media 18 p2340 A73-36961

H

H ALPHA LINE

Spiral structure and kinematics of the galaxy from a study of the H II regions - Fabry-Perot interference methods applied to ionized hydrogen. 01 p0096 A73-10297

Hydrogen lines in the spectrum of the Markarian 6 galaxy during its activity period 01 p0100 A73-10703

Investigation of the faint nebula identified with radio source HB-21. 01 p0106 A73-11304

Photospheric network properties and transition to sunspot of solar bright points in 3840 Å and H alpha, comparing with Ellerman bomb 01 p0108 A73-11384

Faint H alpha emissions in solar corona prominences photographed through coronagraph and Lyot filter 01 p0108 A73-11388

H alpha subflare associated X-ray burst of 10 October 1970 observed by balloon-borne scintillator and OGO 5 and SOLRAD 9 satellites 01 p0093 A73-11389

Planetary nebulae NGC 7635, 7008, 1514, 650-1, 7139, 3587, 6781 and 6543 monochromatic images, centering filters on H alpha, N II and O III forbidden lines 02 p0221 A73-12703

Rapid changes in the new shell star HR 6000. 03 p0366 A73-12941

Hydrogen recombination line and continuum observations at 5000 MHz of 13 southern HII regions. 03 p0372 A73-13347

Photometric search for H alpha optical emission in Sco X-1 nebulosity region for linking companion radio sources to X ray source 03 p0373 A73-13374

Moustaches in solar H alpha filtergrams and spectra, studying relations to photospheric and chromospheric phenomena 03 p0378 A73-14413

The magnetic structure of arch filament systems. 03 p0378 A73-14415

Kinematics of H-alpha emission from an abnormal filament of the galaxy NGC 4258 03 p0380 A73-14609

Solar flares recognition from H-alpha centered birefringent filtered photographs, determining statistical pattern of filament movements 04 p0491 A73-14842

Recombination radio lines in H I regions. 04 p0504 A73-16026

Absolute intensity of the H-alpha line in the nebulae NGC 2068 and S-57 05 p0617 A73-16464

The absence of flares in 3835 Å and the heating of the chromosphere. 05 p0610 A73-17041

X-radiation /E greater than 10 keV/, H-alpha and microwave emission during the impulsive phase of solar flares. 05 p0610 A73-17041

The magnetic configuration of the November 18, 1968 loop prominence system. 05 p0621 A73-17043

Running waves in quiet sunspots with well developed penumbras, noting intensity fluctuation in H alpha centerline or wing 05 p0626 A73-17347

Violet shift of the H alpha absorption line of the hydrogen-depleted star HD 30353 07 p0877 A73-19598

Detection of relativistic solar particles before the H alpha maximum of a solar flare. 08 p0996 A73-20666

The spectra of near-vertical structures on the solar disk. 08 p1001 A73-20752

On the size of the structure elements in the solar chromosphere. 08 p1001 A73-20754

H alpha observations of vertical velocity distribution periodic oscillations in sunspot, noting transverse waves formation and propagation to penumbral boundary 08 p1001 A73-20757

Flares, magnetic configurations, and magnetic energy release. 08 p0996 A73-20764

Funnel prominences evolution and relation to solar active regions from H alpha filter observations 08 p0999 A73-21311

Stark effect and line broadening in three-dimensional stochastic fields. 09 p1125 A73-21939

Objective prism spectrum surveys for H alpha emission of stars in Chamaleon T association, listing emission line stars 09 p1142 A73-22033

Photospheric and circumstellar H-alpha line profiles in M-supergiant spectra 10 p1273 A73-23706

Sunspots moving magnetic features analysis from longitudinal magnetograms time series and H alpha filtergrams 11 p1422 A73-25938

Solar surges magnetic properties analysis from high resolution H alpha filtergrams, matching surge trajectories by computed magnetic lines of force 11 p1422 A73-25941

Detailed correlation of type III radio bursts with H alpha activity. I - Active region of 22 May 1970. 11 p1413 A73-25950

Optical and radio observations of the Orion Nebula. 11 p1425 A73-26265

Spectral investigation of the chromosphere. II. 12 p1544 A73-27829

Isophotes comparison of quiescent and quasi-quietest solar prominences in D3 and H alpha lines, noting structural similarity from narrow band filter observation 12 p1545 A73-27836

Some comments on the low intensity H alpha emission observed by J.-L. Leroy in the solar corona. 12 p1545 A73-27838

Dynamics and localization of surges in the chromosphere. 12 p1545 A73-27846

Beginning, maximum and ending times uncertainty and maximum areas of H alpha flares, stressing international coordination in solar patrol service 12 p1536 A73-27851

Cavity-like instability observed in quiescent prominence from H alpha slit-yaw pictures shown with Ca ion 8542 Å spectra 13 p1670 A73-29371

A search for H alpha emission from interstellar clouds.

14 p1797 A73-30008

Stark broadening of high-principal-quantum-number n-alpha lines of hydrogen.

14 p1777 A73-30552

Diurnal variations of H-alpha nightglow emission intensity

15 p1867 A73-31261

Spatial distribution of H alpha emission in the earth's upper atmosphere, the variations of the emission during a solar cycle, and the dependence of the emission on geomagnetic perturbations

15 p1867 A73-31262

Investigation of the hydrogen in the upper atmosphere and geocorona from observations of the H-alpha emission line in the nightglow spectrum /Survey/

15 p1867 A73-31267

Multicolor photometry of five SBC galaxies: NGC 925, NGC 1073, NGC 3359, NGC 4088, and NGC 7741

16 p2058 A73-32713

Study of a narrow-band interference filter at various angles of incidence

16 p2012 A73-32844

On some transient H-alpha features associated with metric type III bursts.

16 p2053 A73-32963

19-20 May 1969, an example of type III emission during the impulsive phase of flares.

18 p2344 A73-36013

Satellite observations of strong Balmer alpha atmospheric emissions around the magnetic equator.

18 p2346 A73-36284

Profiles of the photospheric and circumstellar H alpha line in the spectra of type M supergiants.

18 p2354 A73-36731

Interpretation of the H-alpha atmospheric emissions observed by the D-2A Tournesol satellite around the magnetic equator

19 p2423 A73-37538

H alpha line contrast profiles evaluation from solar chromosphere supergranulation observations, obtaining chromospheric fine structure characteristics

20 p2606 A73-39072

Line widths of CaII K2 and H-alpha and the chromospheres of late stars

20 p2606 A73-39073

Geocorona originated low intensity nighttime H alpha and H beta emission components from high resolution observation, considering Balmer line producing mechanism

20 p2555 A73-39433

Shell nebulae and Wolf-Rayet stars - Observations of NGC 2359

21 p2768 A73-40714

Solar spicule morphology, observing diameter, height, expansion and threshold intensity with H alpha filtergrams

21 p2777 A73-41484

Spectroscopic investigation of the chromosphere. III - H-alpha line profile from the interior of supergranular cells.

21 p2777 A73-41485

Optical solar flare kinematic model, relating chromosphere response to downward propagating supersonic disturbance

21 p2762 A73-41490

Stellar chromospheric velocity fields and the width luminosity relations.

21 p2779 A73-41540

The topological association of H alpha structures and magnetic fields.

24 p3136 A73-44639

Spatial relationship between 5303-A and H alpha components of a loop prominence system.

24 p3123 A73-44640

Statistical analysis of transient brightenings in solar chromosphere /Elerman bombs/ from H alpha filtergrams, obtaining histograms for durations near disk center and limb

24 p3136 A73-44641

A radially streaming proton model for the broad component of hydrogen emission in Seyfert galaxies.

24 p3138 A73-45039

H BETA LINE

Southern open star clusters. I - UVB-H beta photometry of 15 clusters between Galactic longitudes 231 and 256 deg.

01 p0096 A73-10318

Hydrogen lines in the spectrum of the Markarian 6 galaxy during its activity period

01 p0100 A73-10703

Rapid variations of Psi Per shell star H beta line, indicating shell and stellar atmosphere activity

05 p0617 A73-16466

HD 215441 and 53 Camelopardalis - Intrinsic polarization of H-beta and the continuum.

07 p0874 A73-19075

Geocorona originated low intensity nighttime H alpha and H beta emission components from high resolution observation, considering Balmer line producing mechanism

20 p2555 A73-39433

H GAMMA LINE

Spectral energy distribution, spectrophotometric gradients and Balmer discontinuities for eclipsing binary RZ Scuti from spectrograms with low dispersion in H gamma line

18 p2354 A73-36732

French monograph - Preparation of a space experiment intended for high resolution study of the far ultraviolet spectrum of the star gamma Gemini.

22 p2910 A73-42714

H LINES

NT H ALPHA LINE

NT H BETA LINE

NT H GAMMA LINE

NT K LINES

NT LYMAN SPECTRA

NT PASCHEN SERIES

NT RYDBERG SERIES

NT TELLURIC LINES

Velocity structures in hydrogen profiles.

01 p0096 A73-10315

Experimental study of the luminous front produced by a coaxial plasma accelerator.

02 p0197 A73-12060

21-cm neutral hydrogen line study of early type galaxies.

02 p0222 A73-12716

Variation of emission-line strengths across M31.

03 p0366 A73-12928

H emission line shape of plasma radiation under anisotropic electric microfields, calculating field distribution function, dispersion and frequency

04 p0480 A73-15601

Supergiant stars with very strong hydrogen lines in the Great Cloud of Magellan

04 p0502 A73-15998

Spectrophotometric survey of diffuse galactic nebulae

05 p0617 A73-16463

Measurements of the structure of an ionizing shock wave in a hydrogen-helium mixture.

07 p0813 A73-20475

H flux density observations for 21 cm absorption spectrum in front of Cyg X-3

07 p0902 A73-20560

The distribution of neutral hydrogen and the velocity field of the galaxy NGC 3109.

08 p1004 A73-20905

Measurements of the electron temperatures in M42 from the profiles of H-alpha, forbidden N II, H-beta, and forbidden O III.

08 p1004 A73-20906

Aperture synthesis study of neutral hydrogen in the galaxies NGC 6946 and IC 342.

08 p1005 A73-20914

Studies in molecular dynamics by collision-induced infrared absorption in H2-rare gas mixtures. I - Profile analysis and the intercollisional interference effect.

08 p0990 A73-21630

H beta emitting diffuse nebulae as reflection nebulae illuminated by galactic light, based on photometric observation of H alpha emitting external spiral galaxies

08 p1013 A73-21809

Properties and nature of shell stars. III - Periodic radial-velocity changes of 4 Herculis.

09 p1140 A73-22003

On the detection of H2 from interstellar clouds in the wavelength range 4.4 to 28.2 microns.

09 p1148 A73-22870

Spectroscopic changes in the suspected X-ray source X Persei.

10 p1275 A73-23846

Cross correlation coefficients for H, K and H beta lines of solar spectrum related to observed peculiarities from microphotometer intensity traces [AD-759889]

10 p1278 A73-24131

Suggested interpretation of the correlations in intensity fluctuations in the lines Ca II H and K, magnesium b, and hydrogen H beta /Research note/.

10 p1278 A73-24132

H emission line shape of plasma radiation under anisotropic electric microfields, calculating field distribution function, dispersion and frequency

10 p1254 A73-24191

Solar disk emission lines in Ca II H and K line wings from high resolution spectral observations

11 p1422 A73-25934

Formation of spectral lines in planetary atmospheres. V - Collision narrowed profiles of quadrupole lines in hydrogen atmospheres.

13 p1680 A73-28456

Determination of magnetic fields in a plasma from the contour of hydrogen spectral lines.

14 p1780 A73-30339

Quantitative analysis of the spectrum of beta Lyr. I - Variation of certain hydrogen and helium emission lines

16 p2057 A73-32710

Changes of the Balmer-series lines of hydrogen in the spectrum of the spectrally variable silicon Ap star CU Vir

16 p2057 A73-32711

Spectral analysis of sunspot flares.

16 p2052 A73-32957

Feature recognition method in small scale structure analyses of neutral hydrogen emissions, applying to surveys at negative intermediate galactic latitudes

19 p2483 A73-37562

Theory of Stark broadening of hydrogen spectral lines in a plasma

21 p2745 A73-40365

A 21-cm radio spectrograph

21 p2705 A73-41462

Computer processing of RF neutral-hydrogen line observations carried out with a fixed antenna

21 p2659 A73-41468

Observation of the star gamma-Cassiopeia of the Be spectral type by Fourier spectrometry from 1 to 2.5 micron

22 p2908 A73-42354

Measurements of hydrogen-helium radiation at shock-layer temperatures appropriate for Jupiter entry.

22 p2938 A73-42993

Neutral hydrogen spectral line observation for Milky Way Galaxy mapping, discussing role of spiral structure density wave theory in interpretation

23 p3028 A73-43348

A supersynthesis radio telescope for neutral hydrogen spectroscopy at the Dominion Radio Astrophysical Observatory.

23 p2958 A73-43362

Spectroscopic polarization analysis of turbulent plasma noise produced by the annihilation of opposite magnetic fields

23 p3012 A73-44016

On the level of H2 quadrupole absorption in the Jovian atmosphere.

24 p3129 A73-44443

Formation of spectral lines in planetary atmosphere. IV - Theoretical evidence for structure of the Jovian clouds from spectroscopic observations of methane and hydrogen quadrupole lines.

24 p3129 A73-44449

H WAVES

Scattering by nonconcentric circular plasma cylinders with axial magnetic fields.

06 p0729 A73-18204

Dispersion equations for E and H waves in multilayer plasma, defining amplitudes correlation for incident, transmitted and reflected waves

07 p0855 A73-19278

Dispersion equations for E and H waves in multilayer plasma, defining amplitudes correlation for incident, transmitted and reflected waves

13 p1665 A73-28678

H-33 HELICOPTER

Sikorsky CH-53D helicopter main rotor head design, considering spherical elastomeric bearing, microstructural analysis, flight and ground fatigue tests and forging techniques

17 p2104 A73-35059

CH-53D titanium main rotor blade, describing spar, fiberglass cover and honeycomb core, fabrication methods, ground and flight tests and vibrational characteristics

17 p2106 A73-35096

H-56 HELICOPTER

AH-56A rigid rotor compound helicopter configuration and handling qualities under autorotation conditions, discussing flight test program, piloting descent performance

09 p1030 A73-22179

HABITABILITY

Mars precession scheme for prolonged equinoctial habitable spring in terms of Sagan model extension

24 p3131 A73-44464

HABITUATION [LEARNING]

Alpha wave peak amplitude dependence on blocking pattern after stimulation during habituation-pseudoconditioning, conditioning and extinction

14 p1714 A73-29992

HADRONS

NT BARYONS

NT MESONS

Hadron number density model to predict fossil quark abundance in big bang cosmology

01 p0104 A73-11098

Ionization calorimeter study of cosmic ray hadrons inelastic collision cross sections and partial K-neutral pion inelasticity factor

02 p0208 A73-12656

Ionization calorimeter measurement of energy transfer to electron photon cascade secondary particles during hadron interaction with lead nuclei

02 p0209 A73-12662

Inelastic pionization cross section of cosmic ray hadrons with carbon nuclei at energies of 100 to 300 GeV

02 p0209 A73-12665

Cosmic radiation high energy hadron component relation to extensive electron-photon showers, comparing sampling events based on multicore structure and total energy

02 p0209 A73-12676

K-neutral pion energy fractions and inelasticity coefficients at primary energies of 100-1500 GeV during cosmic ray hadron-target interaction

02 p0210 A73-12689

Relativistic spheres of hadron gas with zero baryon number constructed from Hagedorn hadronic equation of state, considering sphere stability properties
03 p0370 A73-13211

Multiple production of hadrons at cosmic ray energies - Experimental results and theoretical concepts.
07 p0870 A73-19374

Study of strong interactions between cosmic-ray hadrons and nuclei at 200 to 2000 GeV energies
10 p1264 A73-23816

Gamma-gamma total hadronic cross section and absorption of extragalactic gamma-rays.
11 p1413 A73-26107

Abundance and lateral distribution of muons in inclined showers.
13 p1670 A73-28371

Relativistic cosmology of interacting hadronic matter-radiation models, discussing compatibility with Hagedorn equation of state based on statistical mechanics
15 p1939 A73-32002

Absorption of ultrahigh energy photons in the universe
17 p2223 A73-34368

Implications of the statistical bootstrap model for cosmology and galaxy formation.
19 p2482 A73-37559

High-transverse-momentum secondaries and rising total cross sections in cosmic-ray interactions.
19 p2476 A73-38292

A study of elementary acts of interaction between hadrons with energies of about 10 TeV
23 p3021 A73-43533

Preliminary results of the Pamir-20-71 experiment on interactions at energies of about 1000 TeV
23 p3021 A73-43534

Properties of secondary high-energy particles in hadron interactions
23 p3021 A73-43538

Identification of hadrons with 500 GeV energies in cosmic rays by using transitional emission
23 p2981 A73-43566

HAFNIUM

A comparative study of the thermal diffusivities of stainless steel, hafnium, and Zircaloy.
[ECTP PAPER C-6]
13 p1630 A73-28051

The partitioning of refractory metal elements in hafnium-modified cast nickel-base superalloys.
13 p1633 A73-28138

Rare-earth elements, Co, Sc and Hf in the Steens Mountain basalts.
15 p1874 A73-32389

HAFNIUM ALLOYS

Laves phases in hafnium alloys containing period-IV transition metals
09 p1108 A73-23234

Phase composition of Nb-1% Zr-C and Nb-2% Hf-C alloys
09 p1108 A73-23237

Temperature effects in quadrupole interaction in NbHf alloys
15 p1923 A73-31710

Structure and mechanical properties of internally oxidized Ta-8 pct W-2 pct Hf (T-111) alloy.
20 p2576 A73-39025

HAFNIUM CARBIDES

Synthesis and fabrication of high purity hafnium nitride and hafnium carbide.
04 p0455 A73-15752

Investigations regarding structure, preparation, and hardness properties in the system Ta-Hf-C-N
22 p2873 A73-41949

HAFNIUM COMPOUNDS

NT HAFNIUM CARBIDES

NT HAFNIUM OXIDES

Synthesis and fabrication of high purity hafnium nitride and hafnium carbide.
04 p0455 A73-15752

Investigation of the electrical resistivity of zirconium and hafnium nitrides
06 p0714 A73-18559

HAFNIUM OXIDES

Effect of hafnium dioxide on grain growth and strength characteristics in niobium
09 p1108 A73-23233

Determination of the boundaries of fluorite-type Y2O3 solid solutions in HfO2
13 p1645 A73-28292

Behavior of hafnium dioxide particles in dispersively hardened nickel during isothermal annealing
17 p2188 A73-34560

HAIL

A comparison of precipitation attenuation and radar backscatter along earth-space paths.
01 p0015 A73-10183

Evaluation of a dual-wavelength radar hail detector.
03 p0337 A73-14505

Pulse Doppler radar observations of hailstone maximum diameters as function of time
03 p0337 A73-14506

Time lapse stereo photogrammetry of ring vortex type circulation in cumulonimbus cloud tops of hail bearing storms
07 p0847 A73-19042

The energetic degree of shielding provided by hail-protection screens in the case of certain distribution spectra of hailstone diameters
11 p1394 A73-26373

Hailstones icicle lobe formation growth in wind tunnel, using supercooled or frozen hydrometers
12 p1521 A73-26817

Hail growth in cold front, discussing relationship to air flow changes
13 p1652 A73-28267

Dual wavelength synchronized and slaved radars for hail shaft boundaries detection based on average echo power ratio logarithm range derivative computation
21 p2728 A73-40061

Hailswaths mapping with airborne fixed beam and scanning IR radiometers, noting dimensions, orientation and fine structure
21 p2729 A73-40062

Photographic investigation of hailstone form, size and structure, determining layer growth from air bubble shape and spectrum
21 p2730 A73-40116

The steady-state thickness of a liquid water film on the surface of hailstones of various shapes
21 p2730 A73-40118

Certain results of radar studies of the evolution of convective clouds
21 p2731 A73-40494

HAILSTONES

U HAIL

HALF LIFE

Half life and activity of cosmogenic radionuclides in Haverø (Finland)/ achondrite determined by non-destructive gamma ray spectrometry
09 p1139 A73-21861

HALF PLANES

Stressed state of an isotropic half-plane with a finite number of circular holes situated along the boundary
02 p0230 A73-11782

Diffraction of an arbitrary plane electromagnetic wave by a half-plane.
06 p0667 A73-18203

Lame equations for stress concentration in half plane with extracted elastic inclusion, solving via Fourier integrals reduced to singular integral equation
07 p0910 A73-19301

Extremal stresses in the first basic two-dimensional problem of elasticity theory for a half-plane
07 p0911 A73-19310

Two dynamic contact problems for a half-plane with elastic cover pieces
07 p0911 A73-19314

A problem for a half-plane with a finite vertical cut
08 p1019 A73-21722

Stress-strain state of a piecewise homogeneous plane with thin-walled elastic inclusions of finite length
08 p1019 A73-21765

Stress distribution in a half-plane with a hole strengthened by an elastic insert
11 p1432 A73-25026

Time-dependent electromagnetic field scattering and diffraction by half plane during illumination by impulsive plane cylindrical or spherical wave
11 p1330 A73-25683

Composite solid with two contacting or bonded half planes of different elastic moduli, considering interplane force transmission from stress distribution calculation
11 p1443 A73-26277

Elastic domain similar to half plane with perturbed boundaries, comparing small parameter method accuracy with exact solutions
11 p1446 A73-26467

Elastostatic invariance in the composite plane.
13 p1696 A73-28747

Crack propagation in an elastic solid subjected to general loading. III - Stress wave loading.
13 p1696 A73-28792

Stress distribution due to a Griffith crack at the interface of an elastic half plane and a rigid foundation.
14 p1815 A73-30917

Half plane stress boundary value problems in elastodynamics, obtaining similarity solutions in terms of analytic functions via integral transforms
16 p2082 A73-33903

Problem of an elastic semiinfinite cover plate fastened to a linearly deformable base
20 p2624 A73-39646

Two-dimensional contact problem for a prestressed elastic body
20 p2625 A73-39652

Thermoelastic dilatational deformation in two perfectly bonded orthotropic half-planes, showing linear relations between elastic and homogeneous field
21 p2789 A73-41674

Elastic deformation of isotropic infinite plane with central circular inhomogeneity and elastokinetics of two bonded dissimilar half planes under uniformly moving body force
24 p3152 A73-45343

Plastic relaxation of a shear crack near a planar interface.
24 p3152 A73-45403

HALF SPACES

Singular integral equations analysis of elasticity theory boundary value problem to determine axisymmetric thermoelastic stress-strain state of half space with cylindrical cavity
01 p0112 A73-10012

Solution of the thermoelasticity problem for half-spaces with boundary conditions divided by circular lines
01 p0113 A73-10013

Kinetic theory of electromagnetic fluctuations in an anisotropic plasma half-space
01 p0082 A73-10210

Transition radiation from a plasma boundary.
01 p0085 A73-11063

Stress determination below thin elastic stiffeners partially braced to finite boundary of elastic half space
01 p0117 A73-11091

Impact and contact stress analysis in multilayer media.
02 p0234 A73-12072

Radiation from a magnetic line source in a compressible and anisotropic plasma half-space.
03 p0345 A73-12996

Analysis of wire antennas in the presence of a conducting half-space. II - The horizontal antenna in free space.
03 p0276 A73-13694

Finite element analysis of finite sized plates bonded to an elastic half space.
04 p0510 A73-15012

Distortion of electromagnetic pulses undergoing total internal reflection from a moving dielectric half-space.
06 p0666 A73-18200

Two dimensional indentation of elastic half space by rigid punch under slowly applied normal load for case with finite friction between surfaces
06 p0765 A73-18508

Integrodifferential equation for three dimensional contact problem of elastic half space strengthened by elastic stringer, solving by Fourier series
06 p0766 A73-18876

Initial free-surface motion of an impulsively loaded half-space.
07 p0810 A73-19509

Stress functions for the 'second' plane problem of micropolar elasticity.
07 p0914 A73-20198

A remark on the sloshing frequencies for a half-space.
08 p0953 A73-20788

Impact-deflection by oblique fibers in sparsely reinforced composites.
08 p1018 A73-21408

Ultrarelativistic electrons beam steady injection into plasma filled half space, using weak turbulence theory for assumed beam excited oscillations interaction
08 p0994 A73-21698

Penetration of a solid into a half-space of compressible liquid in the presence of a magnetic field
08 p0994 A73-21724

Steady temperature fields and stresses in a half-space heated by a linear inductive source
08 p1019 A73-21759

One-dimensional finite amplitude wave propagation in a compressible elastic half-space.
09 p1160 A73-22895

A triangular plate bending element for contact problems.
09 p1160 A73-22899

Simultaneous diffusion of photons and particles in a semiinfinite space. I - Distribution of excited atoms in a semiinfinite space
09 p1123 A73-23068

Propagation of one-dimensional disturbances in a linear viscoelastic half-space under thermal shock
10 p1293 A73-24677

Transient temperature distribution of an anisotropic half space.
11 p1453 A73-26401

Shock wave formation in an elastic half-space during one-dimensional nonlinear transient wave processes generated by a continuous force
11 p1445 A73-26456

Antiplane deformation near a cut in a hardening elastoplastic material
11 p1445 A73-26458

Design of an infinite beam with an elastic base in a nonclassical formulation
12 p1555 A73-27796

Application of series to an investigation of a plane electromagnetic wave in a ferromagnetic half-space
12 p1474 A73-27804

On the eigenvalue problem for fluid sloshing in a half-space.
13 p1599 A73-28410

Stress formulation of the 'second' axially symmetric problem of micropolar theory of elasticity.
14 p1809 A73-30253

Thermal stress in an anisotropic elastic half-space
14 p1810 A73-30407

Poisson formula analogs for a class of higher-order elliptic-type differential equations with a singular line in the case of a half-space

15 p1898 A73-31020

Integro-differential equation for three dimensional contact problem of elastic half space strengthened by elastic stringer, using Fourier series

15 p1956 A73-32401

An investigation of the reflection of electromagnetic pulses from moving plasmas.

16 p2041 A73-33199

The mixed boundary value problem for the elastic half space.

16 p2081 A73-33901

Solving some contact problems by electrical modeling

17 p2244 A73-34795

Stresses in an anisotropic half-space.

18 p2362 A73-36319

An integral-equation approach to dispersion relations for guided elastic surface waves.

20 p2592 A73-39048

Dynamics of structural systems subjected to moving loads. II - Half-spaces, plates, and shells under the action of moving loads

20 p2617 A73-39304

Continuous distributions of dislocations in bonded half spaces.

21 p2742 A73-41666

A coupled thermo-elastic problem of a half-space under the action of a thermal shock on the bounding surface.

22 p2922 A73-42467

Reflection and transmission of electromagnetic waves at a moving magnetoplasma half-space.

22 p2896 A73-43179

Multiphase incompressible half-space as simplified earth model for investigating surface displacements due to time- and depth-dependent heat sources

23 p2973 A73-43797

Elastic semispace motion under the action of a shock wave in a magnetic field

23 p3006 A73-43919

Shear crack stress intensity and displacement jump solution for half space under plane strain in form of singular integral equation

24 p3146 A73-44677

HALIDES

NT ALKALI HALIDES
NT ALUMINUM CHLORIDES
NT AMMONIUM CHLORIDES
NT BARIUM FLUORIDES
NT BORON FLUORIDES
NT BROMIDES
NT CADMIUM FLUORIDES
NT CALCIUM CHLORIDES
NT CALCIUM FLUORIDES
NT CESIUM HALIDES
NT CESIUM IODIDES
NT CHLORIDES
NT CHLORINE FLUORIDES
NT COPPER CHLORIDES
NT DIFLUORIDES
NT FLUORIDES
NT HYDROCHLORIC ACID
NT HYDROFLUORIC ACID
NT HYDROGEN CHLORIDES
NT LANTHANUM FLUORIDES
NT LITHIUM FLUORIDES
NT MAGNESIUM CHLORIDES
NT MAGNESIUM FLUORIDES
NT NITROGEN FLUORIDES
NT POTASSIUM CHLORIDES
NT POTASSIUM IODIDES
NT SILVER BROMIDES
NT SILVER CHLORIDES
NT SILVER HALIDES
NT SILVER IODIDES
NT SODIUM CHLORIDES
NT SODIUM IODIDES
NT STRONTIUM FLUORIDES
NT SULFUR CHLORIDES
NT SULFUR FLUORIDES

Some anionic tetrahalo/2,4-pentanedionato/stannate/IV/ complexes.

06 p0661 A73-18271

Vibration-rotation state populations and laser output spectra of CW chemical hydrogen halide lasers under subsonic transverse flow

07 p0835 A73-19640

The effect of halide impurities on the mass production of metal whiskers by reduction.

24 p3098 A73-44401

HALL ACCELERATORS

Experiments on the Polytron, a toroidal Hall accelerator employing cusp containment.

24 p3116 A73-45239

HALL COEFFICIENT

U HALL EFFECT

HALL CURRENTS

U ELECTRIC CURRENT

U HALL EFFECT

HALL EFFECT

Effect of heterogeneity and Hall current on the MHD power generator.

01 p0005 A73-10434

Hall mobility measurements on iron rich nickel ferrites from room temperature to 600 C.

02 p0199 A73-11725

Effects of Hall currents and collisions with neutrals on the dynamic stability of a composite hydromagnetic plasma.

03 p0346 A73-13292

Hall effect gimbal angle transducer /HEGAT/ for relative angular orientation measurement between rotor and stator in low cost inertial platform

04 p0447 A73-15066

Space charge neutralized Hall ion microthrusters, discussing ion exhaust velocity, thrust and efficiency relationships

04 p0489 A73-15729

Electrical properties of evaporated mercury telluride films.

06 p0734 A73-17815

Hall current effects on waves in an electrically conducting rotating fluid.

07 p0854 A73-19104

Effects of collisions with neutrals on the dynamic stability of a finitely conducting hydromagnetic composite plasma in the presence of Hall currents.

07 p0858 A73-19600

Concentration and mobility of electrons in indium-doped zinc oxide crystals

07 p0862 A73-20016

Comparison between a Hall configuration and a Corbino configuration for the amplification of ultrasonic waves

07 p0864 A73-20613

Electrodynamic mathematical model for electroconductivity of nonuniform plasma with Hall effect, calculating current distribution from Riemann problem solution

08 p0992 A73-20863

The bus-probe and multiprobe methods of measuring Hall mobility in semiconductor layers of nonuniform depth

08 p0995 A73-21272

Electrical properties of InAs to very high pressures.

08 p0995 A73-21535

Influence of the Hall effect on current structure in a plasma flow through a spatially periodic magnetic field

09 p1127 A73-22606

Hall current effects in the Lewis magnetohydrodynamic generator.

09 p1130 A73-22823

Magnetic field influence of the Gunn effect threshold.

10 p1258 A73-23568

MOSFET devices with trapezoidal gates - I-V characteristics and magnetic sensitivity.

10 p1194 A73-24157

Second-order solutions for steady magnetohydrodynamic channel flow with anisotropic conductivity.

11 p1404 A73-25746

Longitudinal magnetospheric currents contribution to auroral electrojet from satellite observation data, noting magnetosphere electric field excitation of meridional Pedersen and Hall currents

12 p1493 A73-27650

Bi2Se3 Hall effect magnetometer for reliable low temperature use.

13 p1612 A73-28368

Determination of the basic characteristics of an impurity level by Hall effect measurements

13 p1668 A73-28461

A note on the effect of Hall currents on hydromagnetic flow near an accelerated plate.

13 p1664 A73-28617

Electric field and plasma density oscillations due to the high-frequency Hall current two-stream instability in the auroral E region.

14 p1748 A73-29971

Electrical properties of semiconductors with nonspherical radiation damage regions.

16 p2044 A73-33198

Hall effect and electrical resistance in Ni, Co and Ni-Co alloys

16 p2027 A73-34009

Effect of finite resistivity on the dynamic stability of a composite plasma.

17 p2214 A73-34074

On the magnetogravitational instability of a plasma which possesses an anisotropic pressure in uniform movement of rotation and under the influence of the Hall current - The equation of dispersion. I

17 p2215 A73-34250

OGO-5 observations of the physical processes occurring in the disturbed polar cusp and the cusp-magnetosheath interface.

18 p2303 A73-35943

Charge carrier mobility distribution along the channel of an MDS field transistor

18 p2293 A73-36720

Titanium carbide nitride and zirconium niobium carbide solid solutions electromotive forces, examining

temperature-concentration dependencies, carbide and carbonitride conductivity mechanisms, resistivity and Hall effect

18 p2325 A73-36964

Linearized MPD jet and channel flows in external magnetic fields with the Hall effect.

19 p2465 A73-37175

Closed Hall current accelerators for physical and technological applications involving ion acceleration

19 p2466 A73-37356

MPD annular duct flows in crossed external fields for arbitrary values of the Hall parameter

20 p2599 A73-39675

Electric field in an MHD channel of rectangular cross section in the presence of the Hall effect

21 p2744 A73-40183

Hydromagnetic stability of a composite plasma in the presence of Hall currents.

22 p2894 A73-42439

Experimental investigation of a 'poloidal' current in a plasma flow in an inhomogeneous axially-symmetric magnetic field

23 p3010 A73-43657

Structure of currents in a stationary plasma jet in the presence of the Hall effect

23 p3010 A73-43664

A simple theory of the anomalous Hall effect in semiconductors.

24 p3120 A73-45329

HALL GENERATORS

Nonequilibrium ionization in magnetohydrodynamic conversion generators

13 p1571 A73-28071

Semiconductor carrier mobility measurements with Hall generator, calculating sample geometry and finite dimension electrical contact effects on error

19 p2430 A73-37718

HALO PARACHUTING

U PARACHUTE DESCENT

HALOGEN COMPOUNDS

NT ALKALI HALIDES
NT ALUMINUM CHLORIDES
NT AMMONIUM CHLORIDES
NT AMMONIUM PERCHLORATES
NT BARIUM FLUORIDES
NT BORON FLUORIDES
NT BROMIDES
NT BROMINE COMPOUNDS
NT CADMIUM FLUORIDES
NT CALCIUM CHLORIDES
NT CALCIUM FLUORIDES
NT CARBON TETRAFLUORIDE
NT CESIUM HALIDES
NT CESIUM IODIDES
NT CHLORIDES
NT CHLORINE COMPOUNDS
NT CHLORINE FLUORIDES
NT COPPER CHLORIDES
NT DIFLUORIDES
NT DIFLUORO COMPOUNDS
NT FLUORINE ORGANIC COMPOUNDS
NT FLUORITE
NT FLUORO COMPOUNDS
NT FLUOROCARBONS
NT FLUOROXYDROCARBONS
NT HALIDES
NT HYDROCHLORIC ACID
NT HYDROFLUORIC ACID
NT HYDROGEN CHLORIDES
NT IODIDES
NT IODINE COMPOUNDS
NT LANTHANUM FLUORIDES
NT LITHIUM FLUORIDES
NT MAGNESIUM CHLORIDES
NT MAGNESIUM FLUORIDES
NT NITROGEN FLUORIDES
NT POLYTETRAFLUOROETHYLENE
NT POTASSIUM CHLORIDES
NT POTASSIUM IODIDES
NT SILVER BROMIDES
NT SILVER CHLORIDES
NT SILVER HALIDES
NT SILVER IODIDES
NT SODIUM CHLORIDES
NT SODIUM IODIDES
NT STRONTIUM FLUORIDES
NT SULFUR CHLORIDES
NT SULFUR FLUORIDES

Linear and nonlinear dielectric properties of tetrahedral structure crystals. III - Theory of dielectric properties of tetrahedral structure compounds

08 p0990 A73-20965

Application of activators in contact diffusion saturation processes in metals and powders

18 p2318 A73-35878

Reaction of H atoms with CH2Cl2 - Application to the inhibition of flames.

22 p2819 A73-42779

HALOGENATION

NT CHLORINATION

HALOGENS

NT BROMINE
NT FLUORINE
NT IODINE
NT IODINE ISOTOPES

Classical dynamical investigations of reaction mechanism in three-body hydrogen-halogen systems. 13 p1581 A73-29427

HALOPHILES
Studies of the electron transport chain of extremely halophilic bacteria. VIII - Respiration-dependent detergent dissolution of cell envelopes. 01 p0009 A73-10625
A salt-inhibited cytochrome c reductase obtained from the moderately halophilic bacterium, *Micrococcus halodentificans*. 03 p0261 A73-13598
Studies on acid production during carbohydrate metabolism by extremely halophilic bacteria. 07 p0780 A73-19500
Structure of the lipid phase in cell envelope vesicles from *Halobacterium cutirubrum*. 17 p2112 A73-34599

HALOS
Atmospheric optical phenomena, discussing physical origin of rainbows and halos 04 p0445 A73-15629
Properties of solar halos in the Martian limb zone and at the terminator 07 p0902 A73-20322
Development and properties of the halo in pinch plasmas 10 p1253 A73-23673
Properties of solar halos in the limb zone and at the terminator of Mars. 12 p1540 A73-27294
Convection and diffusion transport equation of galactic cosmic ray electrons with energy loss and absorption allowance for supernova compressed halo models 12 p1535 A73-27635
The color deficiency of the solar halo of 22 deg radius 15 p1873 A73-32358
Manifestations and causes of atmospheric optical phenomena related to solar light dispersion and diffraction by particles, noting halos, polar auroras and mirages 16 p2002 A73-32949
Vector theory of the glory and rainbow 21 p2731 A73-40742

HAMBURGER AIRCRAFT
NT HFB-320 AIRCRAFT
HAMBURGER HFB-320 AIRCRAFT
U HFB-320 AIRCRAFT
HAMILTON-JACOBI EQUATION
Liapunov function for Hamilton-Jacobi equation for motion stability of linear and nonlinear mechanical systems, calculating vibration damping factor 03 p0342 A73-13157
On a quadratic first integral for the charged particle orbits in the charged Kerr solution. 06 p0725 A73-17889
General relativistic time analysis leading to scalar Hamiltonian formalism for particle mass based on Riemannian metric, considering Hamilton-Jacobi equation in particle dynamics 22 p2888 A73-43048
Construction of particular solutions of the restricted plane circular three-body problem 24 p3112 A73-45506

HAMILTONIAN FUNCTIONS
A theory of perturbations in angle-action variables: Application to the motion of a solid about a fixed point - Precession-nutation 01 p0107 A73-11362
Variational aspects of oscillation phenomena for higher order differential equations. [AD-758575] 02 p0188 A73-12823
Momentum constraints as integrability conditions for the Hamiltonian constraint in general relativity. 05 p0599 A73-17350
Relative motion integrals of interacting identical mass particles in terms of Hamiltonian function and momentum relation 06 p0725 A73-18887
On the analytical study of Saturn's satellites, Enceladus-Dione 08 p1005 A73-20921
Monograph on Hamiltonian cosmology, considering cosmological models with Hamiltonian equations of motion, Bianchi universes, superspace concepts and quantum mechanical Hamiltonian construction 08 p0984 A73-21834
Parallel perturbation solution for ideal resonance problem characterized by one degree of freedom Hamiltonian system, considering singularities at separatrix 10 p1283 A73-24666
Group velocity and nonlinear dispersive wave propagation. 10 p1249 A73-24775
Dynamical system of N degrees of freedom reduced to ideal resonance problem involving Hamiltonian function, presenting algorithm for calculating ignorable coordinates 11 p1423 A73-26071
A Hamiltonian theory for weakly interacting vortices. 13 p1609 A73-28917

All order stability of Hamiltonian systems with two degrees of freedom. 14 p1773 A73-29756
Stellar resonant motion in axisymmetric galactic potential, deriving invariant energy mappings from Hamiltonian system of differential equations 14 p1770 A73-30772
Basic trends in the development of modern analytic mechanics 15 p1913 A73-31622
Optimal control solution existence for relaxed linear systems with strictly convex Hamiltonian 16 p2021 A73-33303
Stromgren doubly asymptotic orbits analyzed by Hamiltonian functions with two degrees of freedom, investigating homoclinic and heteroclinic orbits in restricted three body problem 18 p2352 A73-36419
Satellite vibration-rotation motions studied via canonical transformations. 18 p2352 A73-36422
Stability of Lagrange solutions to the three-dimensional elliptic problem of three bodies 24 p3111 A73-45299
A simple theory of the anomalous Hall effect in semiconductors. 24 p3120 A73-45329

HAND [ANATOMY]
Solid state neutron radiation dosimeter for hands of medical and industrial personnel working with spontaneously fissionable fuels, describing Th foil detector and automatic spark counter 11 p1361 A73-25312
Specific features in the activity of the oxygen transport system of the organism during hand-performed working cycles of submaximum intensity 18 p2277 A73-36579

HANDBOOKS
Materials properties data tables on composition, preparation, temperature and field strength parameters of superconducting compounds in Ni alloys 02 p0201 A73-11878
Book - Forging design handbook. 02 p0173 A73-11884
Handbook on mechanical face seals covering applications, operational capabilities, design, environmental control, handling, installation, malfunctions, auxiliary equipment, optical flats, etc 03 p0313 A73-13995
Silicon solar cell design, describing handbook organization and derivation of design curves and data tables 03 p0254 A73-14209
Aircraft maintenance manuals optimization for human errors minimization, discussing DC-10 in-flight and ground maintenance fault isolation philosophy and techniques 10 p1226 A73-24716
German handbook of functions and numerical values in physics, chemistry, astronomy, geophysics and engineering covering thermodynamics, combustion physics and heat transfer 11 p1450 A73-25473

HANDICAPS
Monocular pilot ability in securing and retaining license as compared to controls 21 p2639 A73-41163

HANDLING
U MATERIALS HANDLING
HANDLING EQUIPMENT
French Guiana space center Diamant and Europa service towers structure, operational security features and protection against corrosion and contamination 07 p0807 A73-18947

HANDLING QUALITIES
U CONTROLLABILITY

HANGARS
Fire protection and insurance in airport hangars, discussing governmental safety codes, fire prevention systems, aircraft vs building values and legislative proposals 20 p2544 A73-39214

HANKEL FUNCTIONS
An integral representation of the Dirac delta function for axisymmetric boundary value problems. 16 p2032 A73-33309
The elastic layer with a cylindrical hole subjected to a nonuniform axisymmetric radial displacement. 20 p2624 A73-39566

HARBORS
Remote sensing in a circulatory survey of Boston Harbor. 16 p2003 A73-33356

HARDENING
Phase transformational kinetics and hardenability of low-carbon, boron-treated steels. 09 p1102 A73-22416

HARDENING [MATERIALS]
NT CARBURIZING
NT HOT PRESSING
NT MARAGING
NT NITRIDING
NT PRECIPITATION HARDENING
NT PULSE HEATING
NT SILICONIZING

NT STRAIN HARDENING
NT WORK HARDENING
Physical nature of the processes of formation of the set of mechanical properties of quench-hardened alloyed structural steel during tempering 01 p0055 A73-10263
Some aspects of the instability of superrefractory alloys rich in nickel 01 p0062 A73-10270
Unalloyed and alloyed steels hardening by pulse heating methods, noting hardness and ductility characteristics due to fine-grained structure 01 p0056 A73-10307
Explosive shock hardening effects on roller steel fatigue strength, surface hardness and wear resistance 01 p0056 A73-10493
An analysis of the breaking elongation in high velocity impact of the power law hardening materials. 01 p0117 A73-11123
Russian book on physics of explosive hardening and welding covering high velocity inelastic collisions, shock wave generation, strengthening mechanisms of metals, etc 02 p0173 A73-11892
Structural hardening calculation procedures and thermal strength problems. 02 p0235 A73-12201
Recording of metal hardening during fatigue testing at elevated temperatures. 03 p0307 A73-13287
Predicting the service life of neoprene launch tube liner pads for the Poseidon missile. 04 p0468 A73-14861
Investigation of the temperature dependence of hardening characteristics in an aging nimonic alloy 06 p0707 A73-17908
Stacking faults effect on martensitic phase formation during steel hardening based on X ray diffraction analysis and Paterson theory 06 p0735 A73-18034
Wear resistant coatings deposition by spark discharge alloying of machine part surfaces, examining surface hardening process and assessing state of art 08 p0946 A73-21083
The phenomenon of superplasticity of polymorphous metals and alloys and its use for welding and hardening in the solid state. 08 p0978 A73-21242
Effects of hardening conditions on the physicochemical and frictional properties of polyvinyl furfural 08 p0982 A73-21591
High strength properties and hardening of epoxy resin bonding materials using dicyaninediamides 10 p1239 A73-24094
Study of the effectiveness of various thermomechanical methods of hardening alpha + beta titanium alloys 10 p1234 A73-24425
Wear-resistant surfaces through electrical spark hardening 11 p1371 A73-24992
German monograph - Effect of creep strains at 700 C on the hardening characteristics of the steel X 8 Cr-NiMoNb 16 16 at room temperature. 13 p1637 A73-29281
Strengthening and fracture of Ta, Nb, Mo and W binary solid solutions with short range order. 13 p1638 A73-29452
Explosive shock hardening effects on roller steel fatigue strength, surface hardness and wear resistance 14 p1755 A73-30318
Solid solution strengthening of high purity niobium alloys. 14 p1761 A73-30631
Phase transformations in alloys of the titanium-molybdenum system 15 p1893 A73-32517
Influence of heating rate on the phase composition of the VT3-1 alloy 15 p1894 A73-32525
Relations between the hardening conditions and the degree of hardening of unsaturated polyester resins 18 p2327 A73-36466
Initiator composition and glass content effects on polyester resin hardening in glass laminate fabrication 18 p2327 A73-36467
Study of the hardening and mechanical properties of polyester resins 18 p2327 A73-36468
Theory of hardening applicability to the description of deformation law singleness under various conditions of uniaxial tension 18 p2366 A73-36759
Phase composition of Ni-Al and Ni-Ga alloys hardened from the liquid state 21 p2719 A73-40849
Preparation and properties of materials containing titanium carbide 21 p2719 A73-40851
Static and fatigue strength of the KhN40MDTlu /EP 543/ alloy after various hardening treatments 24 p3098 A73-44475

- Determination of the magnitude and distribution of initial stresses in fiberglass-reinforced plastics. I 24 p3103 A73-44527
- Hardening with UV radiation in the manufacture of glass-fiber-reinforced unsaturated polyester resin molding materials 24 p3093 A73-44889
- ### HARDNESS
- #### NT KNOOP HARDNESS
- #### NT MICROHARDNESS
- Microstructure, hardness, electrical resistivity and thermal properties of Ni alloys with Al and Ta, noting composition of heat resistant alloys 01 p0067 A73-11436
- Ni-Mo-W alloys hardness rating and corrosion resistance to sulfuric and hydrochloric acids, discussing dispersion hardening, quenching and aging treatments 03 p0327 A73-14001
- Resistance to hydroerosion of hard-faced maraging steels 06 p0706 A73-17881
- Concentration dependence of the hardness of non-stoichiometric group IV and V transition metal carbides 06 p0710 A73-18658
- Microstructure, hardness, electrical resistivity and thermal properties of Ni alloys with Al and Ta, noting composition of heat resistant alloys 11 p1384 A73-26063
- Austenitic steel dislocation density, X ray interference width and hardness changes due to intensified crystal fragmentation from biaxial elongation under tension 12 p1512 A73-27246
- Microstructure and hardness investigations of alpha prime, alpha double prime and omega metastable phases formed during quenching of Ti-Ru alloys 17 p2188 A73-34567
- Effect of austenitization temperature on the properties of Kh5Ni2M3Ti steel 21 p2718 A73-40738
- ### HARDNESS TESTS
- Austenite deformation effect on thermal stability and hardness of Ni steels at various C and Ni concentrations 01 p0067 A73-11349
- Alloy hardening and softening in binary molybdenum alloys as related to electron concentration. 03 p0323 A73-13300
- A new criterion for predicting rolling-element fatigue lives of through-hardened steels. [ASME PAPER 72-LUB-32] 03 p0328 A73-14342
- Parametric-graphical method of cumulative creep damage evaluation for Cr-Mo-V steel in terms of postexposure rupture and hardness measurements 04 p0460 A73-14855
- Metallographic investigation and notch, tensile and hardness tests for electrosag welding of austenitic stainless steels 07 p0831 A73-19949
- Investigation of the plastic state of disks by the hardness measurement method 07 p0917 A73-20514
- W-Ta alloys prepared by electron beam melting, testing Ta content effects on oxidation resistance and hardness at high temperatures 09 p1103 A73-22424
- Short time aging characteristics of Inconel X-750. 10 p1230 A73-23631
- Relaxation of diagonal length and indentation depth of Vickers microhardness measurements on plastics 11 p1388 A73-25449
- Temperature dependence of the hardness and estimation of the creep of the Rh-18% Re alloy 12 p1509 A73-26899
- Rhenium solubility determination for deformed and annealed Re-Al alloy at 500 and 600 C by microstructural analysis and hardness and electrical resistance measurements 12 p1510 A73-26907
- Indenter materials for use in high-temperature hardness measurements 12 p1513 A73-27561
- Machine for measuring hardness and microhardness at high temperatures. 13 p1613 A73-28524
- Testing machine with control panel and vacuum chamber for microhardness measurement at high temperatures with precise test point selection and indentation observation capability 13 p1613 A73-28525
- Friction of hard alloys in vacuum at low temperatures 18 p2320 A73-36861
- Plastic state of disks studied from hardness measurements. 19 p2499 A73-37789
- The preparation and anisotropic hardness of tantalum single crystals with principal orientations. 20 p2575 A73-38637
- Effects of hydrogen on tantalum by the cathodic charging. 20 p2575 A73-38638

- The effect of molybdenum on gamma prime coarsening and on elevated-temperature hardness in some experimental nickel-base superalloys. 20 p2576 A73-39029
- Temperature dependence of hardness and creep of alloy Rh 18Re. 21 p2720 A73-41032
- The hardness of titanium-diboride single crystal grown from metal bath. 23 p2994 A73-44154

HARDWARE

- Roundoff and uncertain data error analysis, discussing hasty judgements, double precision, trajectory problems, ill-posed problems, computer software and hardware flaws, etc 01 p0021 A73-11460
- Nonrecursive digital filter hardware design based on analysis of bit level counting operations in convolution, using fixed and floating point representations 12 p1483 A73-27115
- Counting operation based recursive digital filter hardware design in canonic and direct forms, emphasizing low cost, low speed and high flexibility 12 p1483 A73-27116
- ### HARDWOOD FORESTS
- ### U FORESTS
- ### HARMONIC ANALYSIS
- #### NT TESSERAL HARMONICS
- #### NT ZONAL HARMONICS
- A linear harmonic analysis of atmospheric motion with radiative dissipation. 01 p0039 A73-10399
- Annual and sub-annual effects of EUV heating. I - Harmonic analysis. II Comparison with density variations. 02 p0158 A73-11914
- Perturbation and harmonic balance methods for nonlinear panel flutter. 03 p0395 A73-14182
- Nonlinear harmonic analysis of reflex klystrons with high electron conductance, using average method in second approximation 05 p0556 A73-16065
- The problem of the excitation of subharmonics and higher harmonics in circuits, determined by a nonlinear differential equation of second order 06 p0715 A73-17698
- Gravitation theory harmonic condition equations to separate relativity-valid subclass of extremal manifolds from class of m-dimensional pseudo-Riemannian manifolds 08 p0987 A73-20700
- Treatment of harmonic mixed boundary problems by conformal transformation methods. 08 p0983 A73-20785
- Observations of the variation of temperature with latitude in the upper solar photosphere. II - Magnetic-field comparison, implications for solar-oblateness measurements, and harmonic analysis. 08 p1009 A73-21166
- Half-harmonic modes for different frequency ranges and wave vectors from infinite homogeneous plasma model for high frequency electrostatic wave propagation in magnetosphere 10 p1213 A73-24733
- The diurnal and semidiurnal barometric oscillations, global distribution and annual variation. 11 p1351 A73-25167
- Harmonic structure of flare related type 5 burst, suggesting plasma wave emission 11 p1412 A73-25856
- Experimental method for structure identification in nonlinear objects with recycling processes 11 p1342 A73-26082
- Application of the harmonic balance method for studying oscillations of nonlinear systems with distributed parameters 11 p1400 A73-26464
- Comparative analysis of the longitudinal and orthogonal magnetic second-harmonic modulators. 12 p1477 A73-26789
- Spherical harmonic analysis of the geomagnetic field during the epoch 1965.0 up to $n = 23$ from ground data. II - Results 12 p1491 A73-27353
- Harmonic spectral analysis of nystagmus waveform frequency content for clinical vestibular examination via digital computer 13 p1579 A73-28502
- Analysis of primary currents in a three-phase/single-phase frequency converter with direct coupling and artificial commutation 13 p1592 A73-28940
- Harmonic analysis of voltages and currents at the output of a frequency converter with direct coupling and artificial commutation 13 p1593 A73-28941
- Analysis of primary currents and voltages in single-modulation frequency converters 13 p1593 A73-28942
- Special features of the suppression of low-frequency modulation in a direct-coupled frequency converter 13 p1593 A73-28943

- A first-harmonic method for nonlinear distributed-parameter systems subjected to deterministic or stochastic loads 14 p1738 A73-29707
- Harmonic balance method for spectral investigation of periodic and disturbing functions of nonlinear systems in radio engineering, using autofiltration hypothesis 14 p1739 A73-30555
- Meteor trail drift observations in equatorial region /Somalia/ for lower thermosphere wind velocity and direction calculation via harmonic analysis 15 p1902 A73-31223
- Zonal gravity harmonics from long satellite arcs by a seminumeric method. 17 p2233 A73-35269
- FET for AM large signal processing and regulation without distortion in resonant circuits, discussing characteristics and harmonic analysis 19 p2409 A73-37433
- Negative resistance oscillators, predicting fundamental, harmonic and subharmonic locking characteristics by nonlinear models and equivalent circuit 19 p2410 A73-38307
- Conditions, based on the estimation of the sensitivity of a periodic solution, for the application of the harmonic linearization method to higher harmonics and small parameters 20 p2592 A73-38693
- Determination of optimal regimes of a common-emitter transistor cascade which ensure minimal distortions 21 p2659 A73-40012
- Harmonic frequency content analysis from fluxgate magnetometer recorded Pi 2 pulsation spectral waveform, noting agreement with earth current spectrum 21 p2681 A73-40154
- Determination of equations of conditions between harmonics of resonance of the order of 14 starting with observations from the Eole satellite 21 p2781 A73-41327
- Spherical harmonic analysis of the geomagnetic field for the 1965 epoch up to $n = 23$ according to ground-based data. II - Results. 23 p2971 A73-43250
- Application of harmonic analysis to the calculation of stators with variable blade pitch 23 p3019 A73-43734
- On the gyroscopic coupling of a Van der Pol oscillator in the forced regime and of a free linear oscillator 24 p3111 A73-45396
- A numerical conformal transformation method for harmonic mixed boundary value problems in polygonal domains. 24 p3107 A73-45544
- ### HARMONIC EXCITATION
- On the stability of steady-state response of certain nonlinear dynamic systems subjected to harmonic excitations. 03 p0393 A73-13792
- Applications of the theory of impulsive parametric excitation and new treatments of general parametric excitation problems. [ASME PAPER 72-WA/APM-6] 04 p0476 A73-15903
- The problem of the excitation of subharmonics and higher harmonics in circuits, determined by a nonlinear differential equation of second order 06 p0715 A73-17698
- A new measurement device for measuring harmonic forces 06 p0695 A73-18434
- Monofrequent resonance oscillations with external excitation. 07 p0851 A73-19544
- German monograph - Harmonically excited forced oscillations of a spring/mass system with controlled Coulomb damping. 07 p0851 A73-19581
- Estimation of the response of a mechanical structure to arbitrary excitation 17 p2243 A73-34649
- Large amplitude forced vibrations of simply supported thin cylindrical shells. [ASME PAPER 73-APM-Q] 17 p2249 A73-35107
- Calculation of the current of a nonlinear element with inertia in the presence of a biharmonic input 20 p2537 A73-39454
- Dynamic stability of a nonlinear beam subjected to both longitudinal and transverse excitation. 20 p2621 A73-39532
- Analysis of the accuracy of a system for controlling vibration tests with sinusoidal excitation 21 p2674 A73-40996
- A method for selecting a nonlinear clutch in a system undergoing vibration forced by polyharmonic excitation 21 p2708 A73-41583
- Transient heat conduction in laminated composites. [ASME PAPER 73-HT-R] 22 p2930 A73-42286
- ### HARMONIC FUNCTIONS
- Solution of the thermoelasticity problem for half-spaces with boundary conditions divided by circular lines 01 p0113 A73-10013

Localization principle for a polyharmonic operator expanded in a Fourier series of a fundamental system of functions

05 p0591 A73-16614

Possibility of using harmonic functions in the solution of problems in elasticity theory for inhomogeneous media

06 p0766 A73-18885

Alternative algorithmic scheme for spherical harmonics series summation, noting high speed and precision loss at high resolution in comparison with conventional methods

10 p1246 A73-23993

Capacity theory and removable sets for finite energy harmonic functions extended to nonlinear Navier-Stokes equations, using multiple trigonometric series

13 p1648 A73-28539

Optimal harmonic synthesis of generalized Fourier series and integrals with randomly perturbed coefficients

13 p1650 A73-28893

On the possibility of using harmonic functions for solving problems of the theory of elasticity of non-homogeneous media.

15 p1956 A73-32410

Use of Gq functions for the representation of solutions to equations of statics in the theory of elasticity

17 p2251 A73-35586

HARMONIC GENERATIONS

Second harmonic generation in an inhomogeneous laser plasma

01 p0086 A73-11288

Polycrystalline organic compounds effect on second harmonic generation of neodymium laser, noting relation between nonlinear susceptibility and intramolecular charge transport

02 p0176 A73-12097

Third harmonic generation in Ge induced by conduction nonlinearity during bulk heating of charge carriers by microwave fields

03 p0350 A73-14077

Subharmonic generation and its implications in Gunn effect devices.

04 p0427 A73-15055

Separate generation of odd and even harmonics of a fundamental frequency, with the aid of pulse circuits

06 p0663 A73-17576

Second-harmonic conversion of laser radiation generated under free-oscillation conditions.

06 p0702 A73-18594

Maximum permissible pulse duration in second-harmonic generation in a KDP crystal.

06 p0703 A73-18595

Phase matching in second-harmonic generation using artificial periodic structures.

07 p0834 A73-19538

Two-pass-internal second-harmonic generation using a prism coupler.

07 p0834 A73-19539

Combined operations with negative resistance and nonlinear characteristics in an avalanche diode.

07 p0804 A73-20569

Outlet of second harmonic emission for the laser resonant cavity

09 p1097 A73-23011

Generation of the second harmonic of laser emission in organic crystals

10 p1228 A73-24583

Harmonic generation and parametric excitation of waves in a laser-created plasma.

11 p1405 A73-25972

Parametric instabilities and harmonic generation in Tonks-Dattner resonances in inhomogeneous bounded electron plasma layer

13 p1665 A73-28791

Transient processes in second harmonic excitation by ultrashort laser light pulse train related to crystal length and phase matching

13 p1629 A73-29433

Harmonic enhancement for airborne low voltage lightweight TWT amplifier band edge performance improvement to provide bandwidth in excess of two octaves

16 p1988 A73-33298

Book - Frequency synthesis: Theory, design and applications.

20 p2542 A73-39143

Engineering design and optimization of the parameters of frequency doublers for the visible range.

20 p2573 A73-39685

Generation of fifth picosecond laser harmonic.

20 p2574 A73-39700

Limitations for mode-locking enhancement of internal SHG in a laser.

21 p2714 A73-40759

Theory of power rectification and harmonic generation processes at super-high frequencies

22 p2800 A73-42213

Some features of second-harmonic generation in a lithium metaniobate crystal.

22 p2896 A73-42247

Noncollinear second harmonic generation in KDP.

22 p2871 A73-43078

Second-harmonic generation in an inhomogeneous laser plasma.

23 p3009 A73-43509

HARMONIC GENERATORS

Microwave harmonic generator using the nonlinearity of negative resistance in n-type GaAs.

03 p0281 A73-12997

Cascade phase-lock loops for the generation of harmonic and subharmonic components.

04 p0421 A73-15433

Investigation of the fluctuation characteristics of quartz-crystal harmonic generators

07 p0802 A73-20300

Narrow band and broad band step-recovery diode frequency multipliers for microwave power generation.

08 p0947 A73-21138

Multiphase even harmonic frequency multipliers using nonlinear magnetic reactors with bridge rectifiers, considering output signal waveforms

12 p1477 A73-26788

Quasistatic generation of harmonics in a ferroelectric crystal with a second order transition above the Curie point.

15 p1924 A73-32157

Investigation of the fluctuation characteristics of quartz harmonic oscillators.

18 p2294 A73-37137

Generation of high-power light pulses at wavelengths 1.06 and 0.53 microns and their application in plasma heating. II - Neodymium-glass laser with a second-harmonic converter.

22 p2869 A73-42248

HARMONIC MOTION

Jacobi-Hamilton equation of motion of mass point, using elliptic functions for harmonic potential

05 p0597 A73-16467

Propagation of a transverse harmonic wave in a plate with a statistically rough circular hole

08 p1020 A73-21770

A harmonic drive used as an ultrahigh vacuum rotary feedthrough.

21 p2671 A73-39919

HARMONIC OSCILLATION

Flutter analysis method for unsteady aerodynamic forces on wings and rotating blades under harmonic vibrations and uniform flow

[ONERA, TP NO. 1099]

01 p0001 A73-10230

Analog computer study of the effect of initial conditions on the excitation and sustaining of lower harmonic oscillations in a single-phase electroferromagnetic oscillatory circuit

02 p0147 A73-12352

Harmonic oscillations of elastic system with viscous damping, calculating maximum amplitude of third subharmonic

04 p0509 A73-14978

Short-life mode of electrostatic electron cyclotron harmonic waves.

04 p0477 A73-15196

Propagation of harmonic waves in orthotropic circular cylindrical shells.

[ASME PAPER 72-WA/APM-23]

04 p0515 A73-15893

Magnetohydrodynamic viscous flow induced by an oscillating disk.

06 p0728 A73-17792

Electron cyclotron off-resonance heating rate in hot electron plasmas, comparing numerical calculation in terms of harmonic resonance with computerized simulation

07 p0856 A73-19519

Recursive solution for steady forced vibration modes of tensed string under concentrated harmonic forces

09 p1120 A73-22583

Analysis of parametric oscillation characteristics based on the collector-junction capacitance of the transistor.

10 p1193 A73-23666

Calculation of unsteady transonic aerodynamics for oscillating wings with thickness.

[AIAA PAPER 73-316]

11 p1301 A73-25547

Oscillations of a shell partially filled with a liquid and containing sources of the liquid

11 p1446 A73-26462

Waves produced by a source of harmonic oscillations located in a cylindrical layer of liquid

11 p1349 A73-26468

Laser dynamic theory with uniformly broadened and Doppler spectral lines based on nonlinear interactions between harmonic oscillations

12 p1506 A73-27139

Approximate method for solving dynamic problems in thermoviscoelasticity

13 p1690 A73-27993

Transverse vibration of membranes of arbitrary shape by the method of constant-deflection contours.

13 p1690 A73-28058

German monograph - Rapid excitation of quasi-harmonic oscillations in a class of nonlinear oscillators.

13 p1594 A73-29285

Book - Theory of vibration with applications.

13 p1703 A73-29676

Parametric instability in the region of low-frequency hybrid resonances.

14 p1778 A73-29686

Nonlinear two-dimensional oscillations of a satellite in an elliptic orbit

14 p1803 A73-29854

Voltage-locked diode oscillators. II - The effect of harmonics on the locking range.

14 p1734 A73-30074

Harmonic vibrations of inclined plate in separated free surface flow of ideal fluid in terms of weak perturbation flow theory

15 p1946 A73-31157

Two dimensional nonlinear oscillations around center of mass of vehicle moving along circular orbit with magnetic damping under gravitational field and external perturbation

15 p1942 A73-31233

Asymmetric missile subharmonic response to nonlinear aerodynamic moments, considering spin and aerodynamic damping effects

15 p1943 A73-31667

An approximate method for the calculation of the velocities induced by a wing oscillating in subsonic flow

15 p1824 A73-31905

High-frequency oscillation passage through a circuit with modulated damping

17 p2144 A73-34589

Superharmonic resonance in piecewise-linear system - Effect of damping and stability problem.

19 p2459 A73-37669

Free harmonic vibrations of thin pretwisted rectangular plates analyzed in terms of torsional and bending vibration coupling based on shell theory

19 p2500 A73-38115

Transverse oscillations of a beam lying on an elastic base under the action of a perturbation force which has several harmonics with frequencies close to the first natural frequency

20 p2620 A73-39512

Unsteady incompressible fluid flow past a doubly periodic grid

21 p2631 A73-40185

The dynamic stability of a pipe conveying a pulsatile flow.

21 p2678 A73-41671

Impulse analysis of subharmonic oscillations in control systems with thyristor converters.

22 p2835 A73-42299

Diurnal harmonic oscillation instability of atmospheric boundary layer as mesoscale internal gravity waves generation mechanism in lower atmosphere, considering unsteady flow equations

23 p3001 A73-43589

System stability analysis technique for nonlinear oscillation via Van der Pol and Duffing equations, noting ease of approximating higher harmonics

23 p3007 A73-44085

HARMONIC OSCILLATORS

Application of the asymptotic method to third-order oscillatory systems

01 p0021 A73-10030

A simple illustration of the principle of correspondence in quantum mechanics

02 p0193 A73-12542

Parametric subharmonic oscillators - Static behaviour.

04 p0429 A73-15929

FM noise spectrum measurement in feedback harmonic oscillators with crystal or transmission cavity resonators as discriminator for frequency stability

05 p0556 A73-16164

Quasi-linear equivalent circuit for harmonic LC oscillator design with FET transistor, using effective transconductance method

06 p0675 A73-17829

A magnetically controlled tube generator of very-low-frequency sinusoidal oscillations

09 p1063 A73-22337

Generator of rectilinear vibrations for the study of structures at low frequency

[ONERA, TP NO. 1185]

09 p1084 A73-22713

Transistor harmonic oscillator design.

10 p1192 A73-23573

Noncrystal controlled oscillator with transistor and tunnel diode, noting high frequency stability due to automatic regulation of dc operating conditions

10 p1194 A73-23735

A source of nonlinear distortions in acoustic emission

11 p1399 A73-26093

Oscillations of a mathematical pendulum of variable length during rectilinear motion of the suspension point

11 p1401 A73-26466

Two coupled nonlinear oscillators driven by sinusoidal input, calculating fractional harmonic frequency pairs relationship to driving and resonance frequencies

13 p1659 A73-28487

A high-power oscillator triode with zero bias

15 p1850 A73-31259

The effect of a magnetic field on the operation of a dual-base-diode oscillator.

17 p2136 A73-35161

- Negative resistance oscillators, predicting fundamental, harmonic and subharmonic locking characteristics by nonlinear models and equivalent circuit
19 p2410 A73-38307
- Near-harmonic integrated oscillators in the 10 MHz to 40 MHz range.
19 p2412 A73-38538
- The approach to thermal equilibrium in systems of coupled quantum oscillators initially in a generalized Gaussian state.
20 p2571 A73-38634
- Amplitude stability and distortion in thermistor-controlled oscillators.
20 p2535 A73-39131
- Design of Gunn-diode oscillators on the basis of normalized characteristics
21 p2659 A73-40007
- Baseband modeling and distortion equalization of the DeLange FM oscillator by functional methods.
21 p2662 A73-40337
- Dynamical symmetries of the Kepler problem and of the harmonic oscillator in classical mechanics revisited.
22 p2887 A73-42429
- Identification of damping coefficients in multidimensional linear systems.
[ASME PAPER 73-APMW-43]
22 p2926 A73-42899
- Analysis of a frequency-modulated tunnel-diode oscillator.
24 p3072 A73-44941
- Unitary transition probabilities for atom-atomic oscillator collisions.
24 p3113 A73-44982
- Periodic solutions of a spring-pendulum system.
24 p3111 A73-45294
- HARMONIC RADIATION**
- Influence of the degree of uniformity of the magnetic field on the emission of electron cyclotron frequency harmonics from a plasma
04 p0478 A73-15036
- Wave propagation in a micro-isotropic, micro-elastic solid.
06 p0762 A73-17990
- On the reflection of harmonic waves in fiber-reinforced materials.
07 p0909 A73-19096
- Signal level fluctuations line spectra energy characteristics comparison for oblique and oblique-backscatter sounding, noting changes in harmonics intensity and period
07 p0792 A73-19438
- Wave spectrum transformation in an active nonlinear medium
07 p0792 A73-19907
- Nonlinear frequency correction to plasma instability at half harmonics of electron gyrofrequency as observed by OGO 5 near geomagnetic equator outside plasmopause
09 p1075 A73-22069
- A general theory of harmonic wave propagation in linear periodic systems with multiple coupling.
13 p1658 A73-28066
- Ionospheric echoes due to sideland and harmonic radiation from Isis topside sounder transmitters, discussing effects of satellite spread and ion sheath distortions
14 p1752 A73-29974
- The prevalence of second harmonic radiation in type III bursts observed at kilometric wavelengths.
16 p2053 A73-32964
- Harmonic and impulsive acoustic source-produced sound propagation across vortex sheet separating two subsonic fluids, investigating instability waves
17 p2151 A73-34825
- Three-wavelength holographic diagnostics of an optical flare at a potassium target
21 p2700 A73-40529
- Dispersion of a harmonic signal within a turbulent pipe flow.
21 p2678 A73-41687
- Radiatively driven harmonic acoustic waves in vibrational equilibrium in closed cylindrical tube, deriving pressure response, radiative absorption coefficient and spectral detail
22 p2930 A73-42235
- Experiments on radiatively driven harmonic acoustic waves in a confined gas.
22 p2930 A73-42236
- HARMONICS**
- NT HARMONIC EXCITATION
NT HARMONIC GENERATIONS
NT HARMONIC OSCILLATION
NT SPHERICAL HARMONICS
NT SUPERHARMONICS
NT TESSERAL HARMONICS
NT ZONAL HARMONICS
- Harmonic oscillations of elastic system with viscous damping, calculating maximum amplitude of third subharmonic
04 p0509 A73-14978
- Laminated composites displacement equations of motion, obtaining stored kinetic and strain energy and free harmonic waves dispersion normal and along layers
09 p1161 A73-23117

- Excitation of an electron semicyclotron wave and its harmonics during the interaction of high-current excited electron beams
15 p1920 A73-32312
- Two-frequency unsteady forced oscillations of a beam
20 p2593 A73-39502
- Excitation of electron-cyclotron waves by high-current counter-streaming electron beams.
24 p3115 A73-44620
- HARNESSES**
- Single point emergency equipment divestment system for instantaneous parachute harness, lap belt and leg restraint release, describing pyrotechnic actuation system
16 p1966 A73-32666
- Anthropometric dummy design improvements, detailing verisimilitude specifications for harness support in accident tests and design of chest, spine, shoulder and pelvic areas
17 p2114 A73-34617
- Restraint systems /lap belts and shoulder harnesses/ for military, transport and general aviation aircraft, with emphasis on pilot and crew systems
[SAE PAPER 730291]
17 p2114 A73-34656
- HARRIER AIRCRAFT**
- Harrier trial operations onboard Sea Control Ship /SCS/ U.S.S. Guam as model for future V/STOL aircraft-aircraft carrier systems
[SAE PAPER 720853]
05 p0534 A73-16661
- V/STOL aircraft testing for the sea control ship environment.
[AIAA PAPER 73-810]
19 p2379 A73-37466
- HARTMANN FLOW**
- Hartmann flow stability of conducting incompressible viscous fluid between parallel plates at arbitrary Reynolds numbers under transverse magnetic field
06 p0727 A73-17453
- Steady nonlinear Ekman-Hartmann boundary layer on flat surface, evaluating pumping and electric current as functions of Rossby number and magnetic interaction parameter
07 p0856 A73-19512
- Electrically conducting unsteady viscoplastic plane channel Hartmann and Couette MHD flows in presence of uniform transverse magnetic field and time variable electric field
10 p1256 A73-24589
- Turbulent Hartmann flow based on differential equations for steady isothermic turbulent motion of incompressible electrically conducting fluid in magnetic field
10 p1256 A73-24591
- Nonlinear hydrodynamic and hydromagnetic spin-up driven by Ekman-Hartmann boundary layers.
11 p1403 A73-25156
- Shock oscillation associated with Hartmann resonance tubes excited by underexpanded sonic jets, using schlieren streak photography
21 p2677 A73-40616
- A note on the drag due to steady flow of a conducting fluid past a disk at high Hartmann number.
22 p2894 A73-42475
- Viscous laminar Hartmann flow of electrically conducting liquid between parallel walls in transverse magnetic field, assessing thermal radiation effects and temperature distribution
23 p3008 A73-43207
- On laminar two-phase flows in magnetohydrodynamics.
23 p3013 A73-44228
- Effects of thermal conductivity in radiative magnetohydrodynamic channel flow.
24 p3117 A73-45370
- HARTREE APPROXIMATION**
- Renormalized Brueckner-Hartree-Fock theory generalization to calculate intrinsic states of many-body nuclear system with permanent deformation
01 p0079 A73-10243
- Inelastic scattering calculations with projected Hartree-Fock wave functions. II - Coupled-channel treatment.
03 p0345 A73-13806
- Need of LS-dependent energy parameters in the second spectra of the fifth-group elements.
05 p0600 A73-16496
- Simplified Hartree-Fock approximation for complex atom opacity efficient calculation based on homogeneous one-electron orbital equation solution with effective potential optimization
13 p1662 A73-28455
- Theoretical assignments of the low-lying electronic states of carbon dioxide.
19 p2462 A73-37583
- Polarizability of interacting atoms - Relation to collision-induced light scattering and dielectric models.
21 p2742 A73-40211
- Spin contamination in unrestricted Hartree-Fock calculations.
22 p2889 A73-42442
- Hartree-Fock equation with allowance for the correlation
22 p2889 A73-42647

- Hartree-Fock model for metal to insulator transition in vanadium oxide based on electronic band structure at zero and finite temperatures
23 p2961 A73-44163
- HARTREE-APPLETON APPROXIMATION**
- U HARTREE APPROXIMATION
- HARTREE-FOCK APPROXIMATION**
- U HARTREE APPROXIMATION
- HATCHES**
- A photoelastic and finite-element investigation of a nonsymmetrical plug-hatch configuration.
10 p1293 A73-24721
- HAWKER SIDDELEY AIRCRAFT**
- NT HARRIER AIRCRAFT
HS 1182 multipurpose ground attack trainer aircraft describing weapon system, hydraulic flight control, power plant and avionics
14 p1713 A73-30934
- HAZARDS**
- NT AIRCRAFT HAZARDS
NT FLIGHT HAZARDS
NT OPERATIONAL HAZARDS
NT RADIATION HAZARDS
NT TOXIC HAZARDS
- Selected analytic procedures for range safety analysis.
01 p0117 A73-11200
- Contribution to the problem of the geoelectric effects on lightning hazard
04 p0473 A73-15283
- The hazards of transferring loads between phases, sources and ground.
17 p2133 A73-34092
- HAZE**
- Influence of haze layers upon remotely-sensed surface properties.
01 p0037 A73-10360
- Brief history of the Martian 'violet haze' problem.
03 p0373 A73-13707
- A study of tropospheric radar propagation characteristics during an unusual spell of persistent dust haze followed by thunderstorm over Delhi during May 1966.
03 p0280 A73-14547
- Contrast transmittance Monte Carlo computation for atmospheric haze models based on aircraft measurement data from various geographical areas
06 p0694 A73-18302
- A new look at the Martian 'violet haze' problem. II - 'Blue clearing' in 1969.
09 p1145 A73-22275
- Radiative transfer model for simulation of airborne remote sensing scanner data under flight conditions in hazy atmosphere with scattering and absorption effects
09 p1077 A73-22386
- Influence of atmospheric haze on the color of the underlying surface observed from a manned spacecraft
09 p1077 A73-22484
- Atmospheric air characteristics classification as haze, foggy haze, fog and drizzle from light scattering matrix on basis of aerosol condensation
13 p1654 A73-29159
- Matrix operator theory of radiative transfer. II - Scattering from maritime haze.
14 p1749 A73-30163
- Thermal imaging through hazes and fogs in the middle and far infrared windows - Some experimental results.
16 p2016 A73-33997
- Estimation of the absorptive capacity of atmospheric haze from the brightness of clouds
20 p2583 A73-39183
- HC-1 HELICOPTER**
- U CH-47 HELICOPTER
- HCN LASERS**
- Parametric heating of a dense arc plasma with 0.337 mm laser radiation.
09 p1125 A73-21944
- Open resonator operating at 337-micron wavelength.
09 p1097 A73-23094
- Pulsed HCN laser output power enhancement with auxiliary dc discharge, noting low gas flow rate and nonmultiple pulsing advantages
17 p2185 A73-35406
- A 337-micron HCN laser interferometer for plasma diagnostics.
24 p3097 A73-45410
- HEAD [ANATOMY]**
- NT CRANIUM
NT INTRACRANIAL CAVITY
NT SKULL
- Impact on a simple physical model of the head.
10 p1185 A73-24770
- Some effects of cooling and heating areas of the head and neck on body temperature measurement at the ear.
13 p1575 A73-28504
- Cat and rat lung damage due to hyperbaric oxygen exposure and head injury, discussing alveolar surfactants, sympathetic stimulation and monkey injuries [AD-759298]
13 p1576 A73-28507

A comparison and analysis of head sizes of Navy
aircrew to the standard anthropometric data.
16 p1974 A73-32656

HEAD MOVEMENT

Effect of forward head inclination on visual orienta-
tion during lateral body tilt.
03 p0266 A73-13000

Direction-specific adaptation effects acquired in a
slow rotation room.
03 p0268 A73-14154

Apparatus note - A system for detecting and record-
ing movements of the head.
06 p0656 A73-17522

Observations on perceived changes in aircraft atti-
tude attending head movements made in a 2-g bank
and turn.
07 p0785 A73-19485

Adjustment of saccade characteristics during head
movements.
11 p1319 A73-26222

Absolute motion parallax and the specific distance
tendency.
13 p1578 A73-28096

Nystagmic response persistence to Fitzgerald-Hall-
pike caloric tests as function of directional cupular
deflections due to head movement
13 p1576 A73-28510

Binaural acoustic field sampling, head movement
and echo effect in auditory localization of sound
sources position, distance and orientation
14 p1715 A73-30282

Inflated air bag head restraints for prevention of
brain injuries due to whiplash acceleration during
crash landings or ejection
16 p1965 A73-32654

Space-time adaptation of visual position constancy.
17 p2114 A73-34223

Supranuclear structures regulating binocular eye
and head movements.
18 p2272 A73-36451

Central programming and peripheral feedback dur-
ing eye-head coordination in monkeys.
18 p2273 A73-36452

Altered susceptibility to motion sickness as a func-
tion of subgravity level.
20 p2518 A73-39486

HEAD-UP DISPLAYS

Cockpit device with optical head-up display for
visual slope guidance to any runway at any airport
01 p0051 A73-11011

Functional aspects of head-up display operation,
discussing data accumulated by pilot during low vi-
sibility runway approach in executive jet
01 p0013 A73-11012

Head-up displays for flight control information on
velocity vector, angle of attack, glide path slope and
ground reference data, considering VFR and IFR con-
ditions
15 p1831 A73-32507

Aircraft flight control head-up display system
design, equipment installation particulars, per-
formance tests and merits evaluation
15 p1831 A73-32508

VTOL and STOL projects flight simulation trials for
autostabilization, head-up displays and flight controls
effectiveness in handling qualities improvement and
pilot workload reduction
16 p1996 A73-33209

HEADSETS

U EARPHONES

HEALING

NT WOUND HEALING

Physical/electrical sealing mechanisms of myocar-
dial and muscle fiber healing after surface injury, con-
sidering ionic factors, sodium and calcium rates and
contraction relation
11 p1316 A73-25600

HEALTH

NT HEALTH PHYSICS

NT MENTAL HEALTH

The National Aeronautics and Space Administra-
tion-U.S. Public Health Service Health Evaluation and
Enhancement Program - Summary of results.
03 p0260 A73-13545

Cigarette-smoking and coronary atherosclerosis.
18 p2275 A73-36535

HEALTH PHYSICS

Civil aviation medicine functional standardization
and expansion, emphasizing preventive medicine,
health education and operational safety
10 p1185 A73-24718

Book - An introduction to radiation protection.
12 p1464 A73-27048

The effects of fatigue on health and flight safety.
17 p2113 A73-34080

HEAO

Space astronomy-developments in the sixties to
scientific achievements in the seventies.
01 p0112 A73-11203

High energy astronomy research in space,
discussing HEAO A and B, UV astronomy, X ray as-
tronomy, gamma rays, cosmic rays, hot stars, stellar
energy sources and elementary particles
06 p0743 A73-18016

A position-sensitive X-ray detector for the HEAO-
A satellite.
11 p1364 A73-25963

HEARING

NT ACOUSTIC FATIGUE

NT BINAURAL HEARING

Book - Human factor aspects of aircraft noise.
12 p1465 A73-27450

Impairment to hearing from exposure to noise.
16 p1973 A73-33676

Hearing conservation studies covering impulse
noise produced threshold shift, damage risk criteria,
ultrasound hazards and hearing protection
17 p2117 A73-35326

Impulse noise damage risk criteria.
17 p2117 A73-35327

Effect of sonic boom on hearing and vestibular
equilibrium
18 p2284 A73-36910

Voltage controlled attenuator circuit for acoustic
signal duration and repetition control in hearing ex-
aminations
24 p3064 A73-44910

HEARING LOSS

U AUDITORY DEFECTS

HEART

NT CARDIAC AURICLES

NT CARDIAC VENTRICLES

NT MYOCARDIUM

Intensity of exercise and heart tissue catecholamine
content.
03 p0259 A73-13498

Origin, classification, nomenclature and incidence
of the atrial arteries in normal human hearts, with
special reference to their clinical importance.
04 p0409 A73-15522

Book - Understanding electrocardiography:
Physiological and interpretive concepts.
05 p0542 A73-16359

Regression of altitude-produced cardiac hyper-
trophy.
24 p3060 A73-45065

HEART DISEASES

NT ANGINA PECTORIS

On the causes of the changes of the second heart
sound in left bundle branch block.
01 p0009 A73-11008

Fingerprint patterns incidence relation in congenital
vitium cordis patients, using Henry dactyloscopic
classification
01 p0009 A73-11080

Pilot incapacitation as cause of aircraft accidents,
noting age connected cardiovascular disease as leading
cause for loss of pilot license
01 p0013 A73-11238

Non-invasive technique for diagnosing atrial septal
defect and assessing shunt volume using directional
Doppler ultrasound - Correlations with phasic flow
velocity patterns of the shunt.
01 p0014 A73-11505

Atrioventricular block response to exercise and in-
traventricular conduction at rest.
01 p0010 A73-11506

Q waves and coronary arteriography in cardio-
myopathy.
01 p0010 A73-11507

Left ventricular end-diastolic pressures following
selective coronary arteriography.
01 p0010 A73-11508

Echocardiographic analysis of mitral valve motion
in atrial septal defect.
02 p0138 A73-12444

Usefulness of vectorcardiography combined with
His bundle recordings and cardiac pacing in evaluation
of the preexcitation /Wolff-Parkinson-White/ syn-
drome.
02 p0138 A73-12445

Echocardiographic findings in experimental
myocardial infarction of the posterior left ventricular
wall.
02 p0138 A73-12446

High energy phosphate deficit-produced myocardial
cell genetic apparatus activation as cardiac hyper-
trophy mechanism, discussing mitochondrial biogene-
sis and cardiac hyperfunction roles
02 p0134 A73-12511

Relationship of anginal symptoms to lung mechanics
during myocardial ischemia.
02 p0136 A73-12820

Unusual diastolic heart beat in pericardial effusion.
03 p0259 A73-13059

Exercise testing for evaluation of cardiac per-
formance.
03 p0259 A73-13538

Exercise electrocardiography and vasoregulatory
abnormalities.
03 p0260 A73-13541

Exercise testing for detecting changes in cardiac
rhythm and conduction.
03 p0260 A73-13542

Correlation of computer-quantitated treadmill exer-
cise electrocardiogram with arteriographic location of
coronary artery disease.
03 p0260 A73-13543

Diagnostic value of vectorcardiogram in strictly
posterior infarction.
03 p0268 A73-13891

P wave of electrocardiogram in early ischaemic
heart disease.
03 p0268 A73-13892

Computerized ECG interpretation system for heart
and circulatory disorder detection and diagnosis and
health screening
03 p0272 A73-14660

Clinical electrocardiographic and vectorcardio-
graphic diagnosis of left posterior subdivision block,
isolated or associated with RBBB.
04 p0409 A73-15200

An epidemiological survey of risk factors for
ischemic heart disease in 42,804 men. I - Serum
cholesterol value.
04 p0409 A73-15521

Elevated ST segments with exercise in ventricular
aneurysm.
04 p0410 A73-15643

Effects of hypoxemia and acute coronary occlusion
on myocardial metabolism in dogs.
05 p0538 A73-16154

Study of intraventricular conduction times in pa-
tients with left bundle-branch block and left axis
deviation and in patients with left bundle-branch block
and normal QRS axis using His bundle electrograms.
05 p0540 A73-16582

Uses and limitations of stress testing in the evalua-
tion of ischemic heart disease.
05 p0552 A73-17278

Correlation of electrocardiographic studies and ar-
teriographic findings with angina pectoris.
05 p0546 A73-17279

Systolic time intervals in constrictive pericarditis
and severe primary myocardial disease.
06 p0649 A73-17596

Pathological cardiac conduction system lesions
anatomy associated with arrhythmia, discussing
atrioventricular, His bundle and bundle branch blocks
06 p0655 A73-18872

Cardiac arrhythmias generation by impulse initia-
tion and conduction abnormalities, considering
depressed excitability, reentrant excitation, summa-
tion, inhibition and parasystole
06 p0656 A73-18874

Intermittent trifascicular block - Different
mechanisms of conduction disturbances in the bundle
branches.
07 p0780 A73-19152

Assessment of hypoxia in the human heart.
07 p0781 A73-19928

The use of glycolytic metabolism in the assessment
of hypoxia in human hearts.
07 p0781 A73-19929

Sinus venosus atrial septal defect - Analysis of fifty
cases.
07 p0784 A73-20368

Inability of the submaximal treadmill stress test
to predict the location of coronary disease.
08 p0932 A73-21802

Thirty-month follow-up of maximal treadmill stress
test and double Master's test in normal subjects.
08 p0932 A73-21803

Ventriculographic patterns and hemodynamics in
primary myocardial disease.
08 p0933 A73-21804

Relation of electrolyte disturbances to cardiac ar-
rhythmias.
08 p0933 A73-21807

Clinical evidence of cardiac weakness and incoor-
dination secured by simultaneous records of the force
BCG and carotid pulse derivative and interpreted by
an electrical analogue.
09 p1046 A73-23174

Familial syndrome of midsystolic click and late
systolic murmur.
11 p1317 A73-25697

Phonocardiogram and apex cardiogram in systolic
click-late systolic murmur syndrome.
11 p1317 A73-25698

Angina pectoris in men - Prognostic significance of
selected medical factors.
11 p1319 A73-26288

Slow and fast heart rates and syncope and dizzy at-
tacks as manifestations of sick sinus syndrome,
discussing ventricular artificial pacemaker as therapy
11 p1319 A73-26289

Computer analysis of the orthogonal electrocardio-
gram and vectorcardiogram in 939 cases with hyper-
tensive cardiovascular disease.
11 p1324 A73-26361

Maximal oxygen intake and nomographic assess-
ment of functional aerobic impairment in cardiovascu-
lar disease.
11 p1319 A73-26362

Exercise-induced ventricular arrhythmias in pa-
tients with coronary artery disease - Their relation to
angiographic findings.
12 p1464 A73-27890

Relationship between ventricular premature con-
tractions on routine electrocardiography and sub-
sequent sudden death from coronary heart disease.
14 p1715 A73-30051

Echocardiography status, potentialities and requirements in congenital heart disease diagnosis, considering feasibility in left ventricular performance evaluation

14 p1721 A73-30053

Coronary atherosclerosis development and prevention in children, discussing hyperlipidemia, hypertension, cigarette smoking and high risk identification

14 p1715 A73-30065

Predicting coronary heart disease.

14 p1716 A73-30351

Risk factors for developing myocardial infarction and other diseases - The 'Men born in 1913' study.

14 p1716 A73-30352

Book on echocardiography covering examination of mitral, aortic, tricuspid and pulmonary valves, ventricles, atrium, pericardial effusion, coronary artery disease and tumors

14 p1721 A73-30358

Prevention of the atherosclerotic diseases - Opportunities for military medicine.

14 p1718 A73-30518

Intracardiac heart murmurs and sounds influenced by respiration.

15 p1836 A73-32546

A new method for diagnosing myocardial damage in patients with normal electrocardiograms and vector cardiograms.

16 p1973 A73-33375

Book on vectorcardiography covering equipment, techniques, lead systems and abnormalities associated with atrial and ventricular hypertrophy, bundle branch blocks, myocardial infarction and arrhythmia

17 p2114 A73-34452

Electrocardiographic diagnosis of sinus node rhythm variations and SA block.

18 p2274 A73-36520

QRS abnormalities in AV block - Variations and their significance.

18 p2274 A73-36521

Identification of the sites of atrioventricular conduction defects by means of His bundle electrography and atrial pacing.

18 p2282 A73-36522

The differential electrocardiographic manifestations of hemiblocks, bilateral bundle branch block, and trifascicular blocks.

18 p2274 A73-36523

The clinical causes and mechanisms of intraventricular conduction disturbances.

18 p2274 A73-36524

Current status of correlations between vectorcardiogram and hemodynamic data.

18 p2274 A73-36526

Diagnostic power of the Q wave - Critical assay of its significance in both detection and localization of myocardial deficit.

18 p2274 A73-36527

Mid- and late changes in the QRS complex.

18 p2274 A73-36528

The pathogenesis and clinical significance of primary T-wave abnormalities.

18 p2274 A73-36529

Central nervous system influence upon electrocardiographic waveforms.

18 p2275 A73-36530

Book - Atherosclerosis and coronary heart disease.

18 p2275 A73-36531

Hereditary aspects of coronary atherosclerosis.

18 p2275 A73-36532

Cigarette-smoking and coronary atherosclerosis.

18 p2275 A73-36535

Coronary atherosclerosis and ischemic myocardial damage.

18 p2275 A73-36538

Factors influencing coronary blood flow in the presence of coronary obstructive disease.

18 p2275 A73-36539

Experimental myocardial infarction - Hemodynamic evaluation.

18 p2275 A73-36540

Problems in the recognition of angina pectoris.

18 p2275 A73-36541

Electrocardiographic alterations in the presence of angina pectoris.

18 p2282 A73-36542

Clinical manifestations of acute myocardial infarction.

18 p2275 A73-36543

Electrocardiographic diagnosis of myocardial infarction - Pitfalls of a graphic technique.

18 p2282 A73-36544

Drug therapy for treatment of cardiogenic shock syndrome following myocardial infarction, discussing sympathomimetics, alpha-adrenergic blocks and combinations

18 p2276 A73-36546

Evaluation, diagnosis and treatment of common structural complications of acute myocardial infarction.

18 p2276 A73-36548

The prognosis of myocardial infarction.

18 p2276 A73-36549

Responsibility for ischemic cardiopathies in civil aviation flight personnel

18 p2284 A73-36902

The use of simple indicators for detecting potential coronary heart disease susceptibility in the third-class airman population.

18 p2284 A73-36912

Some metric characteristics of myocardial cells under various conditions of cardiac and cardiovascular pathology

18 p2280 A73-36962

Mechanisms of cardiac arrhythmias - From hypothesis to physiologic fact.

19 p2394 A73-37582

Assessing the severity of aortic stenosis by phonocardiography and external carotid pulse recordings.

20 p2516 A73-38867

Echocardiographic evaluation of the hemodynamic effects of chronic aortic insufficiency with observations on left ventricular performance.

20 p2512 A73-38868

Detection of left ventricular asynergy by echocardiography.

20 p2512 A73-38869

Prediction of the outcomes of myocardial infarction from formulas derived by the dynamic programming method

20 p2516 A73-39000

Structural conditions in the hypertrophied and failing heart.

22 p2807 A73-42685

Abnormal biochemistry in myocardial failure.

22 p2808 A73-42686

Ribonucleic acid (RNA) polymerase and adenyl cyclase in cardiac hypertrophy and cardiomyopathy.

22 p2808 A73-42687

Myocardial oxygen consumption in experimental hypertrophy and congestive heart failure due to pressure overload.

22 p2808 A73-42688

Nature and significance of alterations in myocardial compliance.

22 p2808 A73-42689

Alterations of cardiac sympathetic neurotransmitter activity in congestive heart failure.

22 p2808 A73-42690

Early diagnosis of coronary heart disease; Proceedings of the Second Paavo Nurmi Symposium, Porvoo, Finland, September 9-11, 1971.

22 p2808 A73-42826

The early diagnosis of coronary heart disease - Critical review.

22 p2808 A73-42827

Preventive value of early diagnosis of coronary heart disease, noting importance of screening populations for genetic and environmental risk factors

22 p2808 A73-42828

Significance of arterial obstructive lesions in early diagnosis of coronary heart disease.

22 p2808 A73-42829

Indications and value of coronary arteriography.

22 p2808 A73-42830

The value of different angiographic procedures in coronary heart disease.

22 p2808 A73-42831

Myocardial infarction susceptibility correlated with psychosocial factors in life change measurement studies

22 p2809 A73-42833

Ischemic heart disease prediction via exercise ECG tests, discussing work load standardization

22 p2809 A73-42835

Angina pectoris and ECG abnormalities in relation to prognosis of coronary heart disease in population studies in Finland.

22 p2809 A73-42836

Emotionally induced increases in heart rate and plasma catecholamine and free fatty acids, noting relation to coronary heart disease

22 p2809 A73-42837

Coronary heart disease; Proceedings of the Second International Symposium, Frankfurt am Main, West Germany, June 1972.

22 p2809 A73-42856

Prevalence of hyperlipoproteinaemias in a random sample of men and in patients with ischaemic heart disease.

22 p2811 A73-42975

Transient S-T elevation detected by 24-hour ECG monitoring during normal daily activity.

23 p2946 A73-43492

Ischemic polarcardiographic changes induced by exercise - A new criterion.

24 p3060 A73-44946

Doppler echocardiography - The localization of cardiac murmurs.

24 p3064 A73-44947

HEART FUNCTION

NT HEART MINUTE VOLUME

Effects of exercise on activity of heart and muscle mitochondria.

01 p0006 A73-10135

Cardiorespiratory responses to exercise in air and underwater.

01 p0007 A73-10161

On the causes of the changes of the second heart sound in left bundle branch block.

01 p0009 A73-11008

The value of the ultrasonic Doppler method and apexcardiography as reference tracings in phonocardiography.

01 p0014 A73-11509

Usefulness of vectorcardiography combined with His bundle recordings and cardiac pacing in evaluation of the preexcitation /Wolff-Parkinson-White/ syndrome.

02 p0138 A73-12445

Effect of a 5-day space flight on cardiodynamics during physical work of moderate intensity

02 p0138 A73-12467

High energy phosphate deficit-produced myocardial cell genetic apparatus activation as cardiac hypertrophy mechanism, discussing mitochondrial biogenesis and cardiac hyperfunction roles

02 p0134 A73-12511

Unusual diastolic heart beat in pericardial effusion.

03 p0259 A73-13059

Myocardial function and ultrastructure in chronically hypoxic rats.

03 p0259 A73-13369

Exercise testing for evaluation of cardiac performance.

03 p0259 A73-13538

Evaluation of cardiac performance in exercise.

03 p0259 A73-13539

Practical exercise test for physical fitness and cardiac performance.

03 p0259 A73-13540

Exercise testing for detecting changes in cardiac rhythm and conduction.

03 p0260 A73-13542

Cardiac dysrhythmias associated with exercise stress testing.

03 p0260 A73-13544

Electro-rheocardiotelemetric device for complex monitoring of the dynamics and efficiency of cardiac contraction.

03 p0271 A73-14292

Effects of hypoxemia and acute coronary occlusion on myocardial metabolism in dogs.

05 p0538 A73-16154

Effects of physical training on cardiac actomyosin adenosine triphosphatase activity.

05 p0539 A73-16157

Cardiac output and oxygen transport in early ontogenesis

05 p0541 A73-16738

Pathology of angina pectoris.

05 p0542 A73-17276

Ultrasonic Doppler locators for peripheral vessel blood circulation and myocardium and valvular motor activity measurements

06 p0656 A73-17682

Cardiovascular system reactions to alternating transverse accelerations in man

06 p0650 A73-17687

Effects of cardiac output on I/O-18/2 lung diffusion in normal resting man.

06 p0654 A73-18335

The use of a compartmental hypothesis for the estimation of cardiac output from dye-dilution curves and the analysis of radiocardiograms.

07 p0784 A73-19124

Adaptation to high altitude hypoxia as a factor preventing development of myocardial ischemic necrosis.

07 p0780 A73-19151

Search of optimal biological conservation conditions for a heart, using methods of mathematical experiment planning

07 p0781 A73-19648

The contractile function of the myocardium in two types of cardiac adaptation to a chronic load.

07 p0781 A73-19931

Hypoxia, an adjunct in helium-cold hypothermia - Sparing effect on hepatic and cardiac metabolites.

07 p0782 A73-20169

A comparison between the effects of dynamic and isometric exercise as evaluated by the systolic time intervals in normal man.

07 p0784 A73-20369

A model to predict respiration from VCG measurements.

07 p0787 A73-20578

Role of the sympathetic nervous system in supporting cardiac function in essential arterial hypertension.

08 p0930 A73-21015

Transglucosidase activity of heart-muscle per-glucosylase

08 p0930 A73-21136

Morphometric and histochemical investigation on human right atrial and mitral papillary muscle.

08 p0930 A73-21215

Analysis of indicator distribution in the determination of cardiac output by thermal dilution.

08 p0933 A73-21216

Choice of detection site for the determination of cardiac output by thermal dilution - The injection-thermistor-catheter.

08 p0933 A73-21217

Left ventricular performance after myocardial infarction assessed by radioisotope angiocardiology.

08 p0932 A73-21801

Order and disorder in the rhythm of the heart /Fifth Annual George C. Griffith Lecture/.
08 p0933 A73-21806

Neuroendocrine, cardiorespiratory, and performance reactions of hypoxic men during a monitoring task.
09 p1044 A73-22527

Distribution of systemic blood flow during cardiopulmonary bypass.
09 p1041 A73-22930

Myocardial metabolism during exposure to carbon monoxide in the conscious dog.
09 p1042 A73-22935

Organism-machine interactions in hybrid control systems for cardiac stimulation, artificial breathing apparatus and intelligence assignments
09 p1047 A73-23298

Coronary flow and left ventricular function during environmental stress.
09 p1047 A73-23380

Heart activity characteristics in a human operator during a control process
10 p1183 A73-23806

Effect of respiration stabilization on hemodynamic reactions during acute hypoxic hypoxia
10 p1180 A73-23938

Origin of the external electric field detected near animals and men
10 p1184 A73-23942

Controlled tachycardia through voluntary change in exercise regime, investigating relation between heart rate and blood circulation
10 p1185 A73-24521

Regional myocardial dynamics from single-plane coronary cineangiograms.
10 p1185 A73-24771

Cardiac arrhythmias during exercise testing in healthy men.
11 p1315 A73-25336

Morphological and experimental excitation models of cardiac muscle ultrastructure, transmission activity and intercellular contact relationships
11 p1315 A73-25590

Cardiac action potential rising phase and generation mechanism, discussing pacemaker potential and slow depolarization initiating upstroke in spontaneously active cardiac cells
11 p1316 A73-25592

Ionic current mechanisms for cardiac muscle repolarization time course of Purkinje fibers and other heart cells, relating charge transfer data to earlier studies
11 p1316 A73-25593

Electrogenic potassium inward transport involvement in mechanism of enhanced repolarization, correlating cardiac excitation with Na, K and Ca ions transfer and active ion transport
11 p1316 A73-25594

Sinoatrial node pacemaker cell functions, discussing ionic and metabolic principles, electrical activity, membranar effects of neurohormonal control factors and cardioactive drug effects
11 p1316 A73-25595

Cardiac membrane capacitance physiological properties and measurements in Purkinje fibers, ventricular and atrial muscles and heart tissues
11 p1316 A73-25596

Physical/electrical sealing mechanisms of myocardiac and muscle fiber healing after surface injury, considering ionic factors, sodium and calcium rates and contraction relation
11 p1316 A73-25600

Stethoscope- or phonocardiograph-detectable systole-associated left atrial sound in terms of activity recording, sound genesis, hemodynamic correlations and clinical applications
11 p1317 A73-25696

Adrenal influence on the supercompensation of cardiac glycogen following exercise.
11 p1318 A73-26121

Myocardial contraction velocity and acceleration in man measured by ultrasound echocardiography differentiation.
12 p1461 A73-27026

A simplified method for the in vitro calibration of electromagnetic flowmeters.
12 p1464 A73-27027

Heart function mechanism explanation by activation potential stimulation of muscular contraction via calcium ions
12 p1462 A73-27690

High-fidelity left ventricular pressure measurements for the assessment of cardiac contractility in man.
12 p1464 A73-27888

Comparison of isometric exercise and angiotensin infusion as stress test for evaluation of left ventricular function.
12 p1464 A73-27889

Exogenous free fatty acid effects on hypoxic myocardial function in isolated isometric rat papillary muscles
13 p1577 A73-29572

Influence of flow and pressure on wave propagation in the canine aorta.
14 p1715 A73-30066

German monograph - Comparative investigations regarding the phenomenon of force potentiation in the case of the heart muscle of cold-blooded and warm-blooded animals.
14 p1719 A73-30669

Hypoxic pulmonary steady-state diffusing capacity for CO and cardiac output in rats born at a simulated altitude of 3500 m.
14 p1720 A73-30911

The role of carotid sinuses in the regulation of hemodynamics during motor activity
15 p1833 A73-31161

Assessment of left heart function by noninvasive exercise test in normal subjects.
15 p1834 A73-31345

Histochemical investigation of some energy metabolism characteristics in a rat heart after acute fatigue
15 p1834 A73-31393

Changes in cardiac activity and in the latter's phase structure during decompression of the lower half of the body
15 p1835 A73-31513

Assessment of left ventricular performance in man - Instantaneous tension-velocity-length relations obtained with the aid of an electromagnetic velocity catheter in the ascending aorta.
15 p1836 A73-31996

Echocardiographic detection of regional myocardial infarction - An experimental study.
15 p1839 A73-31997

Effect of a 5-day space flight on the cardiac dynamics during moderately severe physical work.
15 p1840 A73-32617

Phase progression of the QRS complexes in electrocardiograms versus the inscribing directions of the QRS loops in vectorcardiograms.
16 p1975 A73-33116

Effect of maximal work load on cardiac function.
16 p1973 A73-33991

Assessment of left ventricular dimensions and function by echocardiography.
16 p1973 A73-34038

Roentgenographic study of relative heart motion during vibration in water-immersed cats.
16 p1973 A73-34039

Heart muscle viability following hypoxia - Protective effect of acidosis.
17 p2110 A73-34097

Influence of lower-body decompression on the state of the human cardiovascular system /according to roentgenokymographic data/
17 p2111 A73-34234

Advances in electrocardiography; Proceedings of the Symposium, Emory University, Atlanta, Ga., May 10-13, 1971.
18 p2274 A73-36516

Limitations of the dipole concept in electrocardiographic interpretation.
18 p2281 A73-36517

Power failure of the heart in acute myocardial infarction.
18 p2276 A73-36547

Molecular diffusion model of cardiogenic gas mixing during inspiration at alveolar boundary in dogs
18 p2277 A73-36652

Cardiorespiratory transients in exercising man. I - Tests of superposition. II - Linear models.
18 p2278 A73-36656

Comparative value of both hypoxic and positive pressure breathing tests for detection of premature beats.
18 p2280 A73-36944

Respiratory changes in the stroke volume of the left ventricle in healthy humans
19 p2393 A73-37397

Use of a video system in the study of ventricular function in man.
19 p2399 A73-37797

The effect of exercise on intrinsic myocardial performance.
19 p2396 A73-38258

Ejection time by ear densitogram and its derivative - Clinical and physiologic applications.
20 p2511 A73-38866

Evaluation of several methods for computing stroke volume from central aortic pressure.
21 p2638 A73-40638

Examination of a multiple dipole inverse cardiac generator, based on accurately determined model data.
22 p2813 A73-41961

P wave analysis in 2464 orthogonal electrocardiograms from normal subjects and patients with atrial overload.
22 p2806 A73-42341

Russian book - Integral topograms of heart potentials.
22 p2807 A73-42489

Measuring characteristics of the displacement cardiograph.
22 p2815 A73-42676

A simple cardiac contractility computer.
22 p2815 A73-42677

Myocardial oxygen consumption in experimental hypertrophy and congestive heart failure due to pressure overload.
22 p2808 A73-42688

Polyparmetric information of the electrocardiogram in injured tissue.
22 p2809 A73-42834

Cardiovascular adjustments to progressive dehydration.
24 p3060 A73-45063

Rebreathing equilibration of CO₂ during exercise.
24 p3060 A73-45068

HEART MINUTE VOLUME

Normal pulmonary pressure-flow relationship during exercise in the sitting position.
03 p0266 A73-13124

Changes in gaseous metabolism and cardiac output per minute during local muscle work in man
10 p1179 A73-23809

Measurement of cardiac output with and organ trapping of radioactive microspheres.
18 p2282 A73-36661

Use of the single-breath method of estimating cardiac output during exercise-stress testing.
18 p2283 A73-36788

A new technique for the study of left ventricular pressure-volume relations in man.
19 p2401 A73-38259

Effects of posture on exercise performance - Measurement by systolic time intervals.
19 p2396 A73-38260

HEART RATE

NT ARRHYTHMIA
NT BRADYCARDIA
NT SYSTOLE
NT TACHYCARDIA

Oxygen uptake, heart rate and pulmonary ventilation during swimming for different speeds and styles, comparing to running and cycling data
01 p0008 A73-10171

The effect of O₂ breathing on maximal aerobic power.
01 p0010 A73-11504

Passive and active warm-up effects on track athletes heart and respiration rates
03 p0266 A73-13123

Perceived exertion, heart rate, oxygen uptake and blood lactate in different work operations.
03 p0267 A73-13698

Acclimatization to severe dry heat by brief exposures to humid heat.
03 p0267 A73-13700

Interdependence of oxygen uptake, heart rate and ventilation during treadmill exercise from regression slope analysis of lag logarithms
03 p0263 A73-14118

Changes in cardiac rhythm during sustained high levels of positive /+Gz/ acceleration.
03 p0269 A73-14157

[AD-754146] A quick and inexpensive method of monitoring on tape the heart rate during exposure of the human head to pulsed magnetic fields.
03 p0270 A73-14289

A new method to measure non-uniformity in the intact heart.
04 p0412 A73-15645

Cardiac arrhythmias generation by impulse initiation and conduction abnormalities, considering depressed excitability, reentrant excitation, summation, inhibition and parasystole
06 p0656 A73-18874

Investigations concerning the coordination of heart rate and respiration rate /pulse-respiration quotient/ during exercise
07 p0782 A73-20034

Method for measuring the contractions of small hearts in organ culture.
08 p0933 A73-21218

Order and disorder in the rhythm of the heart /Fifth Annual George C. Griffith Lecture/.
08 p0933 A73-21806

Predicting heart rate response to work, environment, and clothing.
09 p1046 A73-22931

Isometric effects on treadmill exercise response in healthy young men.
10 p1179 A73-23842

Alternative mechanisms of apparent supranormal atrioventricular conduction.
10 p1184 A73-23843

Temporal sequence of right and left atrial contractions during spontaneous sinus rhythm and paced left atrial rhythm.
11 p1317 A73-25699

Slow and fast heart rates and syncopal and dizzy attacks as manifestations of sick sinus syndrome, discussing ventricular artificial pacemaker as therapy
11 p1319 A73-26289

Physiological nature of the electroencephalographic and vegetative components of human conditioned reactions
12 p1462 A73-27107

Heart rate variability and work-load measurement.
14 p1720 A73-30879

Mental load and the measurement of heart rate variability. 14 p1720 A73-30881

Procedure for recording the rate of pressure changes in heart cavities 15 p1837 A73-31167

Breath to breath cyclical variations in functional residual capacity, oxygen uptake, carbon dioxide release, tidal volume, respiratory period, alveolar gas tension and heart rate 15 p1834 A73-31346

Changes in cardiac activity and in the latter's phase structure during decompression of the lower half of the body 15 p1835 A73-31513

Relationship of physiological strain to change in heart rate during work in the heat. 15 p1836 A73-32548

Cardiovascular responses to sudden strenuous exercise - Heart rate, blood pressure, and ECG. 17 p2112 A73-35461

Electrocardiographic diagnosis of sinus node rhythm variations and SA block. 18 p2274 A73-36520

The use of simple indicators for detecting potential coronary heart disease susceptibility in the third-class airman population. 18 p2284 A73-36912

The effects of the Westinghouse active magnetometer /WD-4/ on implanted cardiac pacemakers. 18 p2286 A73-36936

Study of the heart rate of humans exposed to heat 18 p2280 A73-36942

Serial correlation of physiological time series and its significance for a stress analysis 19 p2401 A73-38159

Inversion of lighting regimen alters acrophase relations of circadian rhythms in body temperature, heart rate and movement of pocket mice. 20 p2513 A73-39480

Variations of heart rate during sleep as a function of the sleep cycle. 20 p2514 A73-39762

Hybrid biological power cells for cardiac pacemakers - Materials evaluation. 20 p2520 A73-39823

Evaluation of effects of the microwave oven /915 and 2450 MHz/ and radar /2810 and 3050 MHz/ electromagnetic radiation on noncompetitive cardiac pacemakers. 20 p2520 A73-39824

Automatic identification of cardiac rhythm and conductivity disturbances with the aid of digital computers 21 p2643 A73-40751

Stress and strain in student helicopter pilots. 21 p2644 A73-41155

The relationship between left ventricular ejection time and stroke volume during passive cardiovascular stress. 21 p2641 A73-41565

Submaximal exercise with increased inspiratory resistance to breathing. 22 p2806 A73-42419

Permanent catheterism of the thoracic aorta - Direct measurement of arterial pressure, injection of substances, and the taking of blood in wake rats 24 p3065 A73-45160

HEART VALVES

Echocardiographic analysis of mitral valve motion in atrial septal defect. 02 p0138 A73-12444

Case histories of valvular cardiopathies in military pilots, determining tolerance to flight 07 p0784 A73-19209

Phonocardiogram and apex cardiogram in systolic click-late systolic murmur syndrome. 11 p1317 A73-25698

Book on echocardiography covering examination of mitral, aortic, tricuspid and pulmonary valves, ventricles, atrium, pericardial effusion, coronary artery disease and tumors 14 p1721 A73-30358

Experimental studies on the mechanisms of closure of cardiac valves with use of roentgen videodensitometry. 19 p2395 A73-37795

Assessing the severity of aortic stenosis by phonocardiography and external carotid pulse recordings. 20 p2516 A73-38867

Echocardiographic evaluation of the hemodynamic effects of chronic aortic insufficiency with observations on left ventricular performance. 20 p2512 A73-38868

Doppler echocardiography - The localization of cardiac murmurs. 24 p3064 A73-44947

HEAT

NT DRY HEAT

NT NUCLEAR HEAT

Thermodynamic heat concept, discussing kinetic and potential particle energy, internal energy, heat absorption and release and thermal energy 20 p2627 A73-39293

HEAT ACCLIMATIZATION

Effect of high-fat diet on thermal acclimation with special reference to thyroid activity. 05 p0541 A73-16800

Heat acclimatization while wearing vapor-barrier clothing. 17 p2115 A73-34742

Cardiovascular adjustments to progressive dehydration. 24 p3060 A73-45063

HEAT BALANCE

Global distributions of thermal energy content and losses in thermosphere, discussing energy sources, continuity equations and transport mechanisms for heat balance 02 p0162 A73-12288

Basic relationships in turbulent lubrication and their extension to include thermal effects. [ASME PAPER 72-LUB-16] 03 p0314 A73-14332

Energy balance and lactic acid production in the exercising rabbit. 05 p0538 A73-16156

Study of thermal phenomena in a Hartmann-Sprenger tube 08 p1024 A73-21634

Calculation of the steady thermal and stress boundary conditions in the Phoebus 2 reactor 10 p1248 A73-24495

Energy balance during moderate exercise at altitude. 15 p1833 A73-31343

Mathematical modeling of combustors based on turbulent mixing, droplet evaporation and chemical kinetics, considering stirred reactor heat balance and combustor performance prediction 22 p2935 A73-42789

An investigation of the numerical properties of the surface heat-balance equation. 23 p3004 A73-44265

HEAT BUDGET

NT ATMOSPHERIC HEAT BUDGET

HEAT CAPACITY

U SPECIFIC HEAT

HEAT CONDUCTION

U CONDUCTIVE HEAT TRANSFER

HEAT CONTENT

U ENTHALPY

HEAT DISSIPATION

U COOLING

HEAT DISSIPATION CHILLING

U COOLING

HEAT EFFECTS

U TEMPERATURE EFFECTS

HEAT EQUATIONS

U THERMODYNAMICS

HEAT EXCHANGERS

NT TUBE HEAT EXCHANGERS

Pipe array design for thermoelectric air conditioners, noting temperature distribution in half-cell and heat conductor junction 01 p0006 A73-10618

Heat exchanger for dissipating heat due to energy losses in enclosed dust-proof electronic equipment 07 p0921 A73-20125

Isotope Brayton space power systems and their technology. 07 p0850 A73-20467

Method for determining the thermal resistance of channel-wall deposits 08 p1022 A73-21198

Calculation of single phase pressure drop in heat exchangers considering the change of fluid properties along the flow path. 12 p1559 A73-27694

B-52 aircraft-borne short range attack missile weapon system air conditioner thermal performance fulfillment with Freon refrigerant and air distribution in heat exchangers [AIAA PAPER 73-723] 18 p2269 A73-36340

Study of a compact counterflow heat-exchanger with mercury at small Peclet numbers. [ASME PAPER 73-HT-54] 20 p2626 A73-38575

Plasma heat source and heat exchanger design for liquid potassium circulation system, using air-kerosene aviation gas turbine combustion chamber 20 p2545 A73-39617

Evaluating the performance of shell-and-tube heat-exchangers. 23 p3048 A73-43299

HEAT FLOW

U HEAT TRANSMISSION

HEAT FLUX

Effect of heat propagation rates on the temperature field and stresses in thin plates 01 p0113 A73-10022

Comparison of solutions to the inverse unsteady heat conduction problem by the successive interval method and by the Sparrow, Hadji Sheikh and Lundgren method 01 p0123 A73-10862

Internal friction and heat release in engineering and tool steels in the presence of intense ultrasonic oscillations 01 p0065 A73-10926

Circular cylindrical shell stability for thermal shock on end face, calculating critical thermal flux 02 p0232 A73-11818

Oscillation effects upon film boiling from a sphere. 03 p0398 A73-13548

Buoyancy forces contribution to heat flux during turbulent mixing in upper atmosphere, noting kinetic turbulence balance components 04 p0473 A73-15573

Peak pool boiling heat flux from finite heater configurations, improving Zuber hydrodynamic theory by combining vapor escape path thickness empirical values with velocity matching hypothesis [ASME PAPER 72-WA/HT-10] 04 p0519 A73-15835

Temperature and heat flux distributions in incompressible turbulent equilibrium boundary layers. 04 p0520 A73-15942

Application of Olfe's modified differential approximation to the radiation-layer problem on a flat plate. [DFVLR-SONDDR-254] 04 p0520 A73-15946

Lunar interior temperature and surface heat flux distribution from numerical calculations for convection cells within self gravitating fluid sphere, comparing with magnetic induction results 05 p0615 A73-16376

Characterization and suppression of aircraft and fuel fires. [WSCIPAPER 72-26] 05 p0639 A73-16688

Laminar film boiling on inclined isothermal flat plates. 05 p0641 A73-17107

Calculation of the thermal fluxes and the temperatures of the surfaces of a plate with heat transfer between fluids flowing around the plate. 06 p0766 A73-17408

Characteristics of a vacuum discharge triggered by an electron beam. 06 p0722 A73-17424

Two-dimensional temperature fields in straight rectangular fins 06 p0768 A73-17921

Adsorption conditions and vapor molecule balance in wall layer at liquid boiling initiation, noting heat flux dependence on underheating effect, pressure and velocity 06 p0769 A73-18564

Influence of the distortion of the temperature field at the point of thermocouple fixation on measurements of the heat conduction coefficient by the steady-state method of radial thermal flux 06 p0770 A73-18566

A modified Monte Carlo model for the ionospheric heating rates. 07 p0815 A73-19380

Ionospheric electrons and neutral particles temperature and concentration profiles explanation by electron gas cooling due to atomic oxygen excitation, calculating heat flow 07 p0815 A73-19441

Correlation of the vaporization onset heat flux for cylinders in saturated liquid helium-II. 07 p0922 A73-20411

One-dimensional line radiative transfer. 08 p1021 A73-20792

Skin friction and heat flux in the impingement region of a low speed air jet upon a normal flat plate. 08 p0925 A73-20941

Application of the regularization principle to the construction of approximate solutions to inverse heat-conduction problems 08 p1022 A73-21097

Short-wave spectral radiant heat influx in the atmosphere 08 p0984 A73-21133

Specular reflection of heat radiation from an arbitrary reflector surface to an arbitrary receiver surface. 08 p1022 A73-21254

Heat flux contours on a plane for parallel radiation specularly reflected from a cone, a hemisphere and a paraboloid. 08 p1022 A73-21255

Laminar flow heat transfer from wedge-shaped bodies with limited heat conductivity. 08 p1023 A73-21257

Thermal fluxometry - Heat well influence on detector response 08 p0967 A73-21500

Gasdynamic and thermal processes during giant laser pulse impingement on target material, considering heat wave propagation at supersonic and subsonic velocities 09 p1127 A73-22610

Atomic recombination rate determination through heat-transfer measurement. 09 p1048 A73-23449

Radiant heat flux distribution on the surface of a sphere in hypersonic flow of an inviscid radiating gas 10 p1171 A73-23581

The effect of an external field on transport phenomena in a Knudsen molecular gas 10 p1252 A73-24453

First order approximation of collisionless protons expansion in quiet solar wind 10 p1269 A73-24651

Recombination coefficient, heat flux, ionization balance and photoelectron kinetic energy from ionospheric electron temperature and density profiles and solar UV absorption data 11 p1350 A73-25081

Interaction of free and forced convection in horizontal tubes in the transition regime. 11 p1448 A73-25153

Modification of the two-flow approximation in radiant-transfer calculations 11 p1450 A73-25623

Regularization schemes for solving inverse heat conduction problems 11 p1451 A73-25743

Heat flow from earth core to mantle, discussing geomagnetic field generation by adiabatic MHD circulation of outer core and core-mantle interfacial temperature gradients 12 p1492 A73-27482

Compressible boundary layer flow at a three-dimensional stagnation point with intensive suction or injection 12 p1458 A73-27699

Comparison of the solutions found for the inverse transient heat-conduction problem by the method of successive intervals and the method of Sparrow, Haji-Sheikh, and Lundgren. 12 p1560 A73-27911

Use of inertial heat sensors for measuring the rate of temperature variation 13 p1617 A73-28865

Comments on the determination of the total heat flux from the sea with a two-wavelength radiometer system as developed by McAlister. 13 p1610 A73-29197

Seasonal and sunspot cycle variations of F region electron temperatures and protonospheric heat fluxes. 14 p1749 A73-29986

Emission instability of thermionic converters. 14 p1713 A73-30474

Study of the effect of heat influxes on the formation of lower and higher baric fields in the Northern Hemisphere 15 p1903 A73-31602

Closure of the equations for heat influx in the atmospheric boundary layer /according to experimental data/ 15 p1905 A73-31789

A procedure for simultaneous measurement of convective and radiant thermal fluxes in permeable walls 15 p1957 A73-31866

Method for boundary condition selection in the heat transfer problem with phase transition 15 p1958 A73-31872

Radiative heat transfer through semitransparent solid plane layer, measuring temperature profile and heat flux for comparison with rectangular multiband model calculation [ASME PAPER 72-WA/HT-6] 15 p1958 A73-32276

Keraug near-ground wind profiles approximation by Monin-Obukhov universal function, obtaining solutions for turbulent heat flux and shear flow velocity 15 p1906 A73-32343

Isotropic bonded thermoelastic laminar bodies calculations for thermal flux and temperature fields, using linear quasi-static thermal elasticity equations 16 p2080 A73-33242

Adsorption conditions and vapor molecule balance in wall layer at liquid boiling initiation noting heat flux dependence on underheating effect, pressure and velocity 16 p2086 A73-33589

Effect of temperature field distortions caused by embedded thermocouples on the measurement of the thermal conductivity coefficient by the steady radial heat flux method. 16 p2086 A73-33591

The thermal regime and convective motions in the lower layers of the Venusian atmosphere 16 p2068 A73-33825

Comparison of the solutions obtained by Tikhonov's and Sparrow's methods for the inverse unsteady-heat-conductivity problem 17 p2253 A73-34134

The effect of large-scale eddies on climatic change. 17 p2160 A73-34851

Transient temperatures in a plate from a Gaussian distribution of normal heat flux and current flow with application to the free arc discharge. 17 p2255 A73-35843

Experimental study of the stability of differentially heated inclined air layers. 17 p2256 A73-35847

View function in generalized curvilinear coordinates for specular reflection of radiation from a curved surface. 17 p2256 A73-35849

Solar wind heat transport in the vicinity of the earth's bow shock. 18 p2346 A73-36269

Computation of heat flux in numerical weather forecasting. 18 p2334 A73-37059

Experiments on incorporating radiative heat influx in numerical forecasting. 18 p2334 A73-37077

Influence of an external field on transport effects in a Knudsen molecular gas. 19 p2463 A73-38134

Shape of porous cooled region for surface heat flux and temperature both specified. 19 p2505 A73-38482

Experimental measurement of heat transfer to a cylinder immersed in a large aviation-fuel fire. [ASME PAPER 73-HT-2] 20 p2625 A73-38565

Unsteady stagnation point heat transfer due to unsteady free stream temperature. 22 p2931 A73-42290

Ammonium perchlorate gasification and combustion at high heating rates and low pressures. 22 p2899 A73-42815

Direct methods for solving inverse linear problems of thermal conductivity 23 p3048 A73-43444

Extrapolation algorithm for inverse thermal conductivity problem solution of body heat flux and temperature gradients, using successive approximations 23 p3048 A73-43445

Thermal response of an unsteady laminar boundary layer on a flat plate due to step changes in wall temperature and in wall heat flux. 23 p3049 A73-43802

Some further studies on the transition to turbulent convection. 23 p3003 A73-43935

A Riemann-Hilbert problem for a heat conduction in a finned surface. 23 p3049 A73-44051

Ions bombarding the cathode of a pulsed plasma accelerator and their participation in the development of thermal fluxes 23 p3014 A73-44343

Thermal stresses in rotationally symmetric semi-finite elastic body with heat input along hole boundary and on plane boundary surface, reducing to solution of Fredholm equation 24 p3147 A73-44745

Critical heat flux for two-phase flow of helium I. 24 p3155 A73-44822

Numerical solution of a nonlinear inverse heat-conduction problem 24 p3156 A73-45084

Heat current and anisotropy-driven instabilities in connection with the solar wind. 24 p3126 A73-45126

A method for studying the radiant flux distribution in the circumfocal area of a concentrator with the aid of an asymptotic calorimeter 24 p3058 A73-45253

Air flow in circular convection chamber, investigating transition to turbulence by simultaneous measurements of heat flux and temperature field at low Rayleigh number 24 p3157 A73-45311

Preparation of liquid fuels by evaporation from a hot wall 24 p3158 A73-45389

HEAT GAIN

U HEATING

HEAT GENERATION

Transformation group theory for Poisson equation solutions to boundary value problem of steady heat conduction with generation 03 p0400 A73-14631

Integral method for nonlinear transient heat transfer in a semi-infinite solid. 07 p0919 A73-19493

Steady-state heat conduction in slabs, cylindrical and spherical shells with non-uniform heat generation. 07 p0921 A73-20181

Thermal limitations of CW and pulsed silicon TRAPATT diodes. 12 p1478 A73-27110

Nonlinear heat flow in anisotropic media with property variations and nonlinear heat generation. 14 p1816 A73-29915

The significance of the climate factor air velocity in environmental simulation 16 p1997 A73-33381

An experimental study of the heat generated in the plastic region of a running crack in different polymeric materials. 17 p2195 A73-34878

Analysis and temperature control of hybrid microcircuits. [ASME PAPER 73-ENAS-6] 19 p2412 A73-37968

HEAT MEASUREMENT

Heat flow meter and calorimeter measurements of heat transfer between human body and environment under various climatic conditions for temperature regulation studies 03 p0268 A73-14123

The effect of gravity on the thermal and calorimetric measurements for pure fluid substances at the critical point 03 p0400 A73-14634

Determination of degradation of nylon 66 using differential scanning calorimetry. 04 p0468 A73-14857

Thermodynamic characteristics of molybdenum silicides in the temperature interval between 400 and 1200 K 06 p0710 A73-18560

Measurement of high-temperature thermal conductivity of Lucalox /Al₂O₃/ using a heat pipe technique. 06 p0715 A73-18778

An improved thin-film gauge for shock-tube thermal studies. 06 p0696 A73-18845

Thermal conductivity of nineteen igneous rocks. I - Application of the needle probe method to the measurement of the thermal conductivity of rock. II - Estimation of the thermal conductivity of rock from the mineral and chemical compositions. 07 p0788 A73-20031

Balanced heat transfer type calorimeter designed and tested for spark energy measurement, comparing performance to conventional calorimeters of transient heat transfer type 07 p0922 A73-20365

Dynamic method for measuring thermal conductivity of liquids and gases at high pressures. 08 p1021 A73-20861

Use of the linear heat flow for poor conductors and its application to the thermal conductivity of nylon. [AD-758307] 09 p1166 A73-22200

Some heat transfer measurements in compressible turbulent boundary layers. 10 p1296 A73-24648

Measurement of plasmod energy in a time-variable magnetic field 10 p1258 A73-24881

Determination of the convective heat transfer coefficient by 'half-space period' method 11 p1451 A73-25741

A method of measuring thermal conductivity in the presence of extraneous heat currents and the thermal conductivity of brass at low temperatures. 11 p1367 A73-26307

A method for calculating the low temperature surface specific heat of a crystal lattice. 13 p1704 A73-28214

Experimental assembly for complex heat transfer studies 15 p1858 A73-31860

A procedure for simultaneous measurement of convective and radiant thermal fluxes in permeable walls 15 p1957 A73-31866

Thermodynamic properties of molybdenum silicides in the temperature range 400-1200 K. 16 p2026 A73-33585

Experimental methods regarding the thermodynamics of metals and alloys. I 16 p2026 A73-33953

Differential calorimetry technique with heat link placement between samples for maintaining near equilibrium state to achieve accuracy in specific heat ratio measurement 17 p2175 A73-35753

Calorimeter measurement of heat transfer at hyper-sonic conditions. [AIAA PAPER 73-760] 18 p2264 A73-36375

Human calorimeter with a new type of gradient layer. 18 p2282 A73-36662

Thermal conductivity measurement for particulate materials in vacuum, comparing line and differential-line source methods in terms of test and data reduction times 20 p2565 A73-38882

Differential method for determining specific heat 20 p2627 A73-39299

Small surface plate calorimeter for convection and radiation heat transfer measurements from heated body in air 21 p2692 A73-39920

Measurement of plasmod energy in a time-varying magnetic field. 21 p2749 A73-41656

Design considerations and applications of gradient layer calorimeters for use in biological heat production measurement. 22 p2813 A73-42054

High temperature thermophysical properties of tungsten. [ECP PAPER D1-5] 22 p2876 A73-42405

Some thermophysical properties of titanium in the neighborhood of the melting point. 22 p2878 A73-42508

HEAT OF COMBUSTION

Study of exothermic processes in shock ignited gases by the use of laser shear interferometry. [AIAA PAPER 73-178] 05 p0640 A73-16920

Chain interaction and heat release near the lower limit for self-ignition of hydrogen with oxygen 12 p1465 A73-26967

HEAT OF FORMATION

Characterization of the mixed oxides of lithium and aluminum. 01 p0089 A73-11113

- Knudsen measurements of the decomposition and the heat of formation of manganese ditelluride.
09 p1048 A73-22442
- A mass spectrometric investigation of reactions involving tungsten and molybdenum with potassium-seeded H₂/O₂ flames.
10 p1186 A73-23554
- A mass spectrometric investigation of reactions involving vanadium and chromium with potassium-seeded H₂/O₂ flames.
10 p1186 A73-23555
- ### HEAT PIPES
- Heat and mass transfer theory and applications in aerothermoptics, thermoconvective and ferromagnetic fluid studies, chemical engineering, capillary transport and heat pipes
01 p0029 A73-10624
- The operational condition of heat pipes.
01 p0111 A73-11153
- Thermal design and tests of transcendent solid state power thyristor, rectifier and transistor devices, using heat pipe-silicon wafer construction
03 p0283 A73-13940
- Thermal development of heat pipe cooled IC packages.
[ASME PAPER 72-WA/HT-44] 04 p0518 A73-15812
- Active control heat pipe performance for long life battery cooling.
[ASME PAPER 72-WA/HT-43] 04 p0518 A73-15813
- The application of heat pipe techniques to electronic component cooling.
[ASME PAPER 72-WA/HT-42] 04 p0518 A73-15814
- Predicting performance of heat pipes with partially saturated wicks.
[ASME PAPER 72-WA/HT-38] 04 p0518 A73-15817
- Hydrogen gas generation in water/stainless-steel heat pipes.
[ASME PAPER 72-WA/HT-37] 04 p0518 A73-15818
- Arterial wick heat pipes self filling capability theoretical and experimental investigation, deriving expressions for mesh size, artery radius and stem height relationships
[ASME PAPER 72-WA/HT-36] 04 p0518 A73-15819
- Electrohydrodynamic heat pipe design based on electrode structure to orient and guide dielectric liquid phase flow, using polarization force in place of capillarity
[ASME PAPER 72-WA/HT-35] 04 p0518 A73-15820
- Steady two-dimensional heat and mass transfer in the vapor-gas region of a gas-loaded heat pipe.
[ASME PAPER 72-WA/HT-34] 04 p0518 A73-15821
- Diffusion freezeout in gas-loaded heat pipes.
[ASME PAPER 72-WA/HT-33] 04 p0518 A73-15822
- Heat pipe operation in a gravity field with liquid pool pumping.
[AIAA PAPER 73-120] 05 p0640 A73-16876
- Preliminary study for the design of a satellite thermal control heat pipe.
07 p0918 A73-18913
- Neutron radiography as a diagnostic tool in the study of corrosion in lithium-filled heat pipes.
09 p1079 A73-21991
- An out-of-core version of a six-cell heat-pipe heated thermionic converter array.
09 p1036 A73-22820
- An approximate analysis of the diffusing flow in a self-controlled heat pipe.
[ASME PAPER 72-HT-M] 10 p1295 A73-23776
- Electronic equipment thermal management for energy dissipation rejection, summarizing heat pipe, phase-change heat transfer and high pressure gas convection techniques
10 p1295 A73-23789
- Heat pipe oven as instrument for laser absorption and fluorescence spectroscopy of metal vapors, vapor-gas, vapor-vapor mixtures and metal vapor plasmas
11 p1361 A73-25148
- Experimental operation of constant temperature heat pipes.
11 p1451 A73-25989
- Heat pipe cooling of electronic components for design requirements of high voltage insulation, small size, low temperature and protection from external heat sources
11 p1451 A73-25990
- Vapor chamber fin radiator study for the potassium Rankine cycle.
11 p1451 A73-25991
- Heat pipe thermal control of spacecraft batteries.
11 p1309 A73-25992
- Study of fuel cell thermal control systems for advanced missions.
11 p1309 A73-25993
- Application of heat pipes to unmanned space power systems.
11 p1452 A73-25994
- Heat pipe substituting polarization electrohydrodynamic force effects for capillarity to collect, guide and pump working fluid condensate liquid phases
13 p1705 A73-28434

- Heat pipe operational principle and liquid metal working fluids, discussing design, construction and experiments
13 p1706 A73-28674
- Physical conditions of heat transfer and design of heat pipes for the evaporation mode of operation at moderate temperatures
14 p1816 A73-30011
- Spectroscopic observations of subsonic and sonic vapor flow inside an open-ended heat pipe.
15 p1958 A73-31936
- Phenomena associated with bench and thermal-vacuum testing of superconductors - Heat pipes.
16 p2084 A73-33131
- Heat pipe operation and characteristics, considering working fluid properties, choice and figure of merit
16 p2086 A73-34043
- An evolutionary approach for a compact-split-core reactor.
17 p2211 A73-35470
- Gas occlusions in arterial heat pipes.
[AIAA PAPER 73-724] 18 p2369 A73-36341
- Nickel-water heat pipes accelerated life testing, deriving corrosion model based on hydrogen evolution
[AIAA PAPER 73-726] 18 p2369 A73-36343
- Construction and testing of a gas-loaded, passive-control, variable-conductance heat pipe.
[AIAA PAPER 73-727] 18 p2369 A73-36344
- Development of a high capacity variable conductance heat pipe.
[AIAA PAPER 73-728] 18 p2369 A73-36345
- Development of a high capacity cryogenic heat pipe.
[AIAA PAPER 73-729] 18 p2369 A73-36346
- A probabilistic approach to the design of heat pipes.
[AIAA PAPER 73-754] 18 p2370 A73-36370
- Baseplate heat pipe system for waste heat dissipation and temperature control of TWT microwaves amplifier in space shuttle communication equipment, discussing design and performance
[AIAA PAPER 73-755] 18 p2370 A73-36371
- Thermal control flight experiment onboard ATS-F to evaluate feedback controlled variable conductance heat pipe performance in space environment
[AIAA PAPER 73-757] 18 p2370 A73-36372
- Orbiting Astronomical Observatory heat pipe flight performance data.
[AIAA PAPER 73-758] 18 p2370 A73-36373
- Heat pipe and phase changing material (PCM)/sounding rocket experiment.
[AIAA PAPER 73-759] 18 p2371 A73-36374
- Mathematical modeling for ATS-F spacecraft louvers and heat pipes thermal control heat rejection capacity, noting correlation with solar environment simulation data
[AIAA PAPER 73-773] 18 p2360 A73-36387
- Application of heat pipes and their thermal transport capability.
19 p2502 A73-37445
- Applications Technology Satellite F aluminum-ammonia heat pipes design, fabrication and life and thermal vacuum testing
[ASME PAPER 73-ENAS-46] 19 p2493 A73-37993
- Development of a cryogenic heat pipe radiator for a detector cooling system.
[ASME PAPER 73-ENAS-47] 19 p2493 A73-37994
- Axial grooved heat pipes - Cryogenic through ambient.
[ASME PAPER 73-ENAS-48] 19 p2434 A73-37995
- Design and test of a self-controlled heat pipe radiator.
[ASME PAPER 73-ENAS-49] 19 p2435 A73-37996
- A cryogenic heat pipe for satellite sensor cooling.
[ASME PAPER 73-ENAS-50] 19 p2494 A73-37997
- Design and testing of a 150 watt SNAP 19 high performance generator.
[IECEC PAPER 739090] 19 p2458 A73-38437
- Nb heat pipe design with Na coolant for high temperature operation, discussing slopes effect on transmitted power
20 p2628 A73-39418
- Thermal design and analysis aspects of advanced communication spacecraft.
20 p2531 A73-39773
- Prediction of long-term heat-pipe performance from accelerated life tests.
21 p2643 A73-40438
- Heat pipe theory and design, discussing typical operating conditions and heat transfer capacity from flow equations solution by finite difference method
21 p2792 A73-41059
- A study of startup regimes of high-temperature heat pipes.
21 p2792 A73-41060
- Vapor flow in cylindrical heat pipes.
[ASME PAPER 73-HT-P] 22 p2931 A73-42289
- Heat pipe applications utilizing, high thermal conductivity, small temperature variations, heat flux transformation and temperature sensitivity for heat transportation and distribution and temperature control
22 p2931 A73-42292
- Papers on heat pipes covering incompressible laminar vapor flow behavior, startup dynamics,

wicking material liquid transport properties, high thermal conductance structures, etc
23 p3049 A73-43459

HEAT RADIATORS

NT SPACECRAFT RADIATORS

Vapor chamber fin radiator study for the potassium Rankine cycle.
11 p1451 A73-25991

Study of fuel cell thermal control systems for advanced missions.
11 p1309 A73-25993

The thermal analysis of a belt type radiator by the method of matched asymptotic expansions.
14 p1817 A73-30609

Development of a direct condensing radiator for use in a spacecraft vapor compression refrigeration system.
[ASME PAPER 73-ENAS-5] 19 p2493 A73-37967

Design and test of a self-controlled heat pipe radiator.
[ASME PAPER 73-ENAS-49] 19 p2435 A73-37996

HEAT REGULATION

U TEMPERATURE CONTROL

HEAT REJECTION DEVICES

U HEAT RADIATORS

HEAT RESISTANCE

U THERMAL RESISTANCE

HEAT RESISTANT ALLOYS

NT MOLYBDENUM ALLOYS

NT NIMONIC ALLOYS

NT NIOBIUM ALLOYS

NT REFRACTORY METAL ALLOYS

NT RENE 41

NT RHENIUM ALLOYS

NT TANTALUM ALLOYS

NT TUNGSTEN ALLOYS

NT UDIMET ALLOYS

NT WASPALOY

Test results of fatigue at elevated temperatures on aeronautical materials.
[ONERA, TP NO. 1098] 01 p0061 A73-10229

Development of IN-100 powder-metallurgy disks for advanced jet engine application.
01 p0063 A73-10283

Hot extrusion and filled billet techniques to process superalloy powder metallurgy products into complex shapes, bars or wire
01 p0056 A73-10284

Processing of high-performance alloys by powder metallurgy.
01 p0063 A73-10286

Properties and uses of UMC-50 and related Co-Cr-Fe alloys.
01 p0066 A73-11051

Mechanical properties anisotropy in heat resistant Ni alloys due to strengthening phase nonmetallic inclusions distribution, suggesting purification by vacuum melting
01 p0066 A73-11346

Microstructure, hardness, electrical resistivity and thermal properties of Ni alloys with Al and Ta, noting composition of heat resistant alloys
01 p0067 A73-11436

Influence of repeated loads on the resistance to relaxation of a heat-resistant nickel-chromium alloy
02 p0180 A73-11624

Correlations between the properties of some heat-resistant alloys
02 p0180 A73-11627

Ultrasonic inspection of nickel-base alloy products.
02 p0174 A73-12150

The influence of test temperature on the fatigue strength of ZhS6K alloy.
02 p0181 A73-12204

Electron-vacancy prediction methods for sigma phase precipitation in residual matrix compositions of austenitic Niand Co-base superalloys
02 p0183 A73-12757

Effects of alloying elements on elevated-temperature mechanical strength of high Cr, Ni-base heat resistant alloy.
03 p0321 A73-12921

Mechanical properties of Fe, Al, Ti and heat resistant alloys consolidated powders, establishing coupling between fundamental concepts and engineering application
03 p0322 A73-13261

Vacuum arc melting for improved heat resistance and mechanical properties of Ni alloy blanks, comparing with electro-beam and plasma arc melting and powder sintering
03 p0323 A73-13502

Means of improving the quality of heat-resistant metals and their alloys
03 p0324 A73-13504

Changes in the fine structure of heat-resistant nickel-chromium alloys during the creep process
03 p0324 A73-13505

New magnesium alloys intended for operation at elevated temperatures
03 p0324 A73-13513

Ways of enhancing the strength characteristics of heat-resistant and high-strength cast aluminum alloys
03 p0324 A73-13514

Liquation-induced microinhomogeneity of heat resistant submerged-arc-smelted steel 4Kh12N8G8MFB /EI481/

03 p0326 A73-13829
Sn alloying effect on heat resistant Ni-Cr alloys plastic strain resistance and strength at room and high temperatures

03 p0327 A73-14003
Metallic materials developments in aircraft construction and gas turbine engine applications, discussing superalloys, refractory metals, composites and directionally solidified alloys

04 p0460 A73-14741
Heat resistant Ni and Cr alloys powder metallurgy, discussing inert and solute gas atomization, rotating electrode and gatorizing processes for powder fabrication

04 p0461 A73-15023
Japan-U.S. Seminar on the Physical Metallurgy of Heat Resisting Alloys, Diamond Point, N.Y., September 13-15, 1972, Proceedings.

04 p0464 A73-15576
Some factors affecting high-temperature strength of matrix in heat resisting alloys.

04 p0464 A73-15577
Characteristics of secondary phases in heat-resisting alloys.

04 p0465 A73-15580
The effect of alloying elements on creep rupture strength and microstructure of 12 percent chromium heat resisting steel.

04 p0465 A73-15581
Effects of rare earth elements on the oxidation resistance of iron and nickel base alloys.

04 p0465 A73-15584
Experience with the application parametric diagrams to the calculation of the heat resistance of construction materials

04 p0466 A73-15665
Importance of arc gap control in vacuum consumable arc remelting of superalloys.

04 p0454 A73-15743
The feasibility of producing superalloy electroslag remelted hollows.

04 p0455 A73-15747
Temperature effects on intragranular sigma phase precipitation in low carbon superrefractory alloys

04 p0467 A73-15956
Strength and microstructure of nickel-base superalloys after long term heating.

05 p0587 A73-16622
Porcelain enamels for heat resistant alloys low temperature fatigue strength and high temperature vibration damping increase
[SAE PAPER 720809]

05 p0633 A73-16629
Properties of a cobalt superalloy resistant to hot corrosion

05 p0588 A73-17247
Tensile tests and heat treatment for creep rupture and fracture strengths of heat resistant steel, noting crack initiation and propagation

06 p0706 A73-17884
Cyclic loads for decrease in relaxation softening of heat resistant Ni-Cr alloys, noting working temperature effects

06 p0706 A73-17885
Influence of rare-earth metals on the grain growth process during recrystallization of heat-resistant steels

06 p0706 A73-17887
Book - The superalloys.

06 p0708 A73-18073
Composite Al- and Ni-base alloys strengthened by B and W/Mo fibers respectively for reduced weight wing spars and high temperature applications

06 p0710 A73-18638
Effect of overheating on creep resistance in metastable alloys.

06 p0710 A73-18639
Saturation of 1Kh18N9T steel with beryllium and corrosion resistance of the coating in a lithium melt

06 p0711 A73-18669
High temperature behavior of superalloys exposed to sodium chloride. I - Mechanical properties. II - Corrosion.

06 p0713 A73-18766
Creep of precipitation-hardened nickel-base alloy single crystals at high temperatures.

06 p0713 A73-18768
Development and properties of cobalt-base alloys with improved hot-corrosion resistance.

07 p0838 A73-19497
The effect of carbon on the hot corrosion of cobalt-base alloys.

07 p0838 A73-19498
Creep tests and fracture mechanics for high temperature properties of steels and alloys under static load, noting discrepancies for brittle materials

07 p0840 A73-20510
Superalloys oxidation behavior under long term exposure to high temperatures for suitability as Co-60 heat sources encapsulation materials

08 p0978 A73-21415
Stress rupture behavior of a dispersion strengthened superalloy.
[ASME PAPER 72-MAT-G]

08 p0978 A73-21570

Metallurgical principle guidance of alloy design, discussing gas turbine alloys, dispersion hardened and composite alloys, high damping alloys and superalloys

08 p0979 A73-21657
The influence of prior fatigue deformation on creep behaviour.

08 p0979 A73-21672
Creep strength in steel and high temperature alloys; Meeting, Sheffield, England, September 20-22, 1972, Preprints.

08 p0980 A73-21776
The influence of some structural factors on the creep strength of wrought precipitation-hardened Ni-Cr alloys.

08 p0982 A73-21793
Dispersion-strengthened ferritic alloys for high-temperature application.

08 p0982 A73-21798
The influence of nickel content on the structure and high temperature properties of a 12% Cr Mo V Nb steel.

08 p0982 A73-21799
Investigation of the failure characteristics of electrically heated samples of heat-resistant steels and alloys in a high-pressure oxidizing flow

09 p1069 A73-21980
Certain regularities in the deformation and rupture of molybdenum-, niobium-, and tantalum-based high-melting-point alloys under programmed temperature changes

09 p1100 A73-22151
Plasticity and failure of heat-resistant materials at a low number of cycles of simultaneous fluctuations of temperature and load.

09 p1105 A73-23154
Heat resistant alloys stress-rupture strength tests for operating temperatures based on equivalent high temperatures damageability

09 p1106 A73-23156
Effect of magnesium additions on the ductility of heat-resistant nickel alloys

09 p1108 A73-23230
Advances in directional solidification spur usage in turbine airfoil shapes.

09 p1089 A73-23293
Hot die forging /gatorizing/ technique for Ti and heat resistant alloys jet engine parts, emphasizing material and cost savings

09 p1089 A73-23295
Protecting metals in corrosive high-temperature environments.

09 p1089 A73-23296
Influence of temperature on the damping characteristics of heat resistant EP452 and EI696 steels in a uniform stress-strain state produced by tension and compression

10 p1233 A73-24358
Fine precipitate within coarse gamma-prime particles in cast Ni-base superalloy during elevated temperature exposure

10 p1235 A73-24446
Heat resistant Ni alloys residual stresses from machining operations, considering cutting rates, temperature, work piece blanks and cutting tools parameter effects

10 p1226 A73-24798
Heat resistant and refractory materials contact eutectic melting for surface coating production

10 p1227 A73-24967
Directionally solidified eutectic high temperature alloys.

11 p1379 A73-25404
Thermal characteristics of constantan, Ni-Cr-Fe, Ni-Mo, Ce-Al-Fe and Ni-Cr alloy filaments for high temperature strain gages

11 p1362 A73-25456
Microstructure, hardness, electrical resistivity and thermal properties of Ni alloys with Al and Ta, noting composition of heat resistant alloys

11 p1384 A73-26063
Consideration of creep probability in a low-alloyed heat-resistant CrMoV steel

11 p1384 A73-26111
Bivariant eutectic alloys located on liquidus surface within Ni-Nb-Cr-Al quaternary, permitting production of aligned delta Ni-Nb lamellae within nichrome matrix containing Ni-Al fcc precipitate

12 p1509 A73-26845
Relaxation stability of iron and nickel alloys at high temperatures

12 p1509 A73-26898
The nature of slated cleavage planes in pressed VAD 23 alloy

12 p1511 A73-26915
Optimal electrical conductivity and mechanical properties of Cu-Mg-Fe-Si-Zr and Be-B containing heat resistant Al alloys, comparing to Cu at room and elevated temperatures

12 p1511 A73-26918
The partitioning of refractory metal elements in hafnium-modified cast nickel-base superalloys.

13 p1633 A73-28138
Superalloys processing technology for aircraft gas turbine applications, discussing developments in eutectics and powder metallurgy for increased operating temperatures

13 p1636 A73-28931
Heat resistant nickel alloys creep rupture strength diagram, determining time to failure as function of loads

13 p1636 A73-29062
Changes in the electrical resistance of heat-resistant EI 826 alloy in the presence of creep

13 p1636 A73-29065
Protective coating systems for Navy aircraft turbine engines.
[NACE PAPER 113]

13 p1637 A73-29313
The relations between superplasticity and high temperature resistance alloys of metallic systems.

13 p1639 A73-29457
Present situation of Japanese research on the long-time creep and creep rupture properties of steels.

13 p1642 A73-29513
Study on material for investment cast turbine wheel.

13 p1642 A73-29518
Metallurgical and strength studies of heat resisting alloys for gas turbines after long term service.

13 p1625 A73-29519
Investigation of the structure of turbine disc materials after use.

13 p1643 A73-29632
Service life determination in heat-resistant alloys under unsteady working conditions with allowance for brief overloading

14 p1763 A73-30690
Kinetics of changes in deformability of a heat-resistant nickel-base alloy

14 p1764 A73-30861
Automated machining and surface finishing of heat resistant stainless steel nozzles for wind tunnel applications

15 p1855 A73-31200
Book - Forging of powder metallurgy preforms.

15 p1891 A73-32195
Eutectic superalloys strengthened by aligned delta, Ni3Cb lamellae, gamma-prime, Ni3Al precipitates and reduced interlamellar spacing.

16 p2026 A73-33425
Evaluation of additives for prevention of high temperature corrosion of superalloys in gas turbines.
[ASME PAPER 73-GT-1]

16 p2047 A73-33479
Welding techniques for high strength superalloy turbine blades and vanes repair, discussing controlled preheating and cooling methods for crack prevention
[ASME PAPER 73-GT-44]

16 p2019 A73-33505
Hot fatigue strength during fluctuating axial tension of PER 7 and IN 100 superalloys

16 p2026 A73-33971
Characteristics of the temperature dependence of the microhardness of a highly heat resistant dispersion-hardened nickel alloy

18 p2324 A73-36765
Effect of temperature on true energy dissipation in heat resistant EI893 nickel alloy

18 p2324 A73-36766
Heat resistant nickel alloys creep rupture strength diagram, determining time to failure as function of loads

18 p2325 A73-36894
The change in the electrical resistance of EI826 refractory alloy with creep.

18 p2325 A73-36897
Effect of temperature on the effectiveness of hardening components made of heat-resistant alloys

19 p2439 A73-37268
Creep tests and fracture mechanics for high temperature properties of steels and alloys under static load, noting discrepancies for brittle materials

19 p2440 A73-37785
The fabrication of fiber-reinforced composites with the aid of high-speed extrusion presses

19 p2435 A73-38272
Borazon compact cutting tools.
[SME PAPER MR 73-143]

19 p2436 A73-38500
Turning high-temperature alloys with Borazon tools.
[SME PAPER MR 73-145]

19 p2437 A73-38501
Aerospace applications of heat resistant alloy diffusion welding techniques, describing mechanical properties, metal bonding, surface cleaning, vacuum levels, temperature effects and microstructure

20 p2569 A73-39246
Statistical characteristics of the fatigue strength of heat-resistant 1Kh18N9T steel under steady and programmed loading conditions at high temperatures

20 p2577 A73-39355
Investigation of the plasticity of coatings on heat-resistant alloys

20 p2566 A73-39367
Some specific features of crack initiation and development in heat-resistant alloys under various loading conditions

20 p2578 A73-39376
Effect of supersonic gas flows on the structure and heat resistance of metal alloys

21 p2717 A73-40481
Influence of magnesium on the structure of heat-resistant nickel-base alloys

21 p2718 A73-40485

A study of the heat resistance of Nb-Mo alloys containing titanium and zirconium 21 p2718 A73-40489

Relaxation resistance of alloys based on iron and nickel at high temperatures. 21 p2720 A73-41031

Ti, Al, W and Mo concentrations effect on heat resistance of precipitation hardened Ni-based alloys 21 p2720 A73-41035

Microstructure of recrystallized alloy Kh20N80. 21 p2721 A73-41042

Heat resistant materials cracking and fracturing caused by ductility loss at high temperatures, discussing cavitation mechanisms, microcracks, creep tests and time dependence 21 p2722 A73-41576

Effect of technological and metallurgical treatment on the properties of electroslag-welded joints in heat resistant steels 22 p2865 A73-41778

The creep characteristics of the heat-resistant ferritic steels X 20 CrMoV 12 1 and X 18 CrMoNi V Nb 12 1 and their welded connections 22 p2872 A73-41780

Some patterns of deformation and failure of refractory alloys of molybdenum, niobium and tantalum during a programmed change of temperature. 22 p2874 A73-42101

Development of methods for long-term prediction of heat-resistance characteristics 24 p3099 A73-44768

Ten years' experience of UMCo-type alloys in a special steel foundry. 24 p3099 A73-45074

HEAT SHIELDING

NT REENTRY SHIELDING

Ceramic film indicator for determining and recording of temperatures on space vehicle heat shield. 01 p0052 A73-11168

Weave geometry effects on pyrolytic infiltration of carbon-carbon /graphite-graphite/ composite structures for nose tip and thermal shield materials 03 p0332 A73-13044

Material evaluation under direct rocket exhaust impingement. [AIAA PAPER 72-1167] 03 p0287 A73-13465

Thermal conductivity measurements of porous materials in several gaseous environments at subatmospheric pressures. [AIAA PAPER 73-95] 05 p0640 A73-16858

Flight evaluation of a quartz-fiberglass heat shield. 05 p0641 A73-17209

Reinforced plastics role in construction and shielding of Diamant B satellite booster main components 07 p0905 A73-18995

Solar radiation absorptivity control by metal film coatings, noting thermal control coatings for heat shielding 07 p0778 A73-19300

Effect of low heat-shield ablation rates on flight test turbulent base pressure. 07 p0920 A73-19975

Reduction of the thermal flux through a cylindrical pipe containing an ionized gas flow 07 p0860 A73-20617

Method of determining the mass removal from heat-shield materials on the basis of strain measurements in loaded shells 08 p1023 A73-21369

Material design concepts for filament-wound, graphite-graphite heatshields Further analysis. 08 p1020 A73-21819

Light weight beaded and tubular structural panels for heat shielded aerodynamic surfaces [AIAA PAPER 73-370] 11 p1438 A73-25504

Evaluation of columbium alloy thermal protection systems for space shuttle. [AIAA PAPER 73-378] 11 p1380 A73-25508

Investigation of heatproof materials under unsteady operating conditions 11 p1450 A73-25730

Determination of the required thickness of thermal insulation casings and evaluation of the weight-based effectiveness of materials 12 p1558 A73-27092

Italian contributions to present aerospace activities; Conference, 2nd, Turin, Italy, June 9, 10, 1972, Proceedings 12 p1548 A73-27376

Europa 3 booster heat shields configuration selection factors and design, considering mechanical and electrical interfaces with vehicle equipment 12 p1548 A73-27378

Thermal and mechanical properties of zirconia cloth, felt and braid for heat shielding of reusable space shuttle 12 p1548 A73-27379

Low-cost fabrication and installation of ablative heat shields for the space shuttle orbiter. 16 p2072 A73-33060

Thermal shielding by subliming volume reflectors in convective and intense radiative environments. 17 p2253 A73-34183

The operational performance of reentry vehicle heatshield thermodynamic instrumentation. 17 p2238 A73-34605

Heat shielding for Venus entry probes. [AIAA PAPER 73-712] 18 p2368 A73-36332

Reflecting heat-shield entry analysis computer program for planetary probes. [AIAA PAPER 73-714] 18 p2368 A73-36333

Radiation heat transfer in multilayer insulation having perforated shields. [AIAA PAPER 73-718] 18 p2369 A73-36337

Initial development of an ablative leading edge for the Space Shuttle orbiter. [AIAA PAPER 73-739] 18 p2369 A73-36356

Thermal control coatings for heat shielding of high-temperature high-speed chemically aggressive gas flows, noting turbine blade shielding application 18 p2371 A73-36812

Europa III heat shields - Aerothermodynamic analysis and design. 18 p2361 A73-36954

Some characteristics of the disintegration of glassy bodies in hot gas flows 18 p2372 A73-37020

Development of a thermistor type temperature probe for use at low absolute pressures. 22 p2856 A73-42016

HEAT SINKS

A design study of thermal louver system. 01 p0111 A73-11152

Thermally conducting alumina and boron nitride filled silicone and polysulfide elastomer sheet materials for electrical insulation and heat sink applications 03 p0331 A73-13028

CW Q band Gunn diode microwave oscillator fabricated by integral heat sink technique for high power output and efficiency 06 p0677 A73-18345

The use of a diamond heat sink for a high reliability IMPATT diode. 08 p0944 A73-20736

Construction and testing of a gas-loaded, passive-control, variable-conductance heat pipe. [AIAA PAPER 73-727] 18 p2369 A73-36344

High power transistor amplifier thermal design with heat sink convective and radiant cooling for low junction temperature and long service life 19 p2411 A73-38474

HEAT SOURCES

Liapunov-Schmidt analysis of convection bifurcation scheme in internally heated viscous fluid layers of infinite horizontal extent 02 p0238 A73-12053

Possible thermal history of the moon. 03 p0369 A73-13106

Thermal stresses due to a moving heat source in a circular disk. 03 p0389 A73-13328

Thermospheric parameters seasonal and latitudinal variations calculation based on atmospheric model with components ionization and molecular oxygen dissociation as main heat sources 03 p0304 A73-14563

Note on the thermal stresses in an elastic semi-circular disc due to an internal source of heat, the curved boundary being exposed to radiation while the straight insulated boundary is in contact with a smooth rigid surface. 04 p0511 A73-15173

Temperature of a duct flow under conditions of unsteady-state heat transfer 06 p0769 A73-18131

Ionosphere heating effects produced by transverse electric field, discussing strong nighttime source 07 p0815 A73-19431

Thermosphere kinetic temperature diurnal variation from heat conduction equation periodic solution, determining heat sources from solar radiation atmospheric absorption 07 p0815 A73-19440

Origin, evolution and present thermal state of the moon. 07 p0899 A73-20032

Characteristics of the calculation of radiant transfer in a system of diathermic bodies separated by an absorbing and scattering medium 07 p0921 A73-20080

Temperature distribution in gas flow about a linear source of heat variable periodically in function of time. 09 p1166 A73-22169

Spacecraft nuclear power source optimization, considering radioisotope and reactor heat sources, cryogenic cooler cycle types and spacecraft design 09 p1118 A73-22799

Development of an actinium fueled thermionic converter. 09 p1038 A73-23282

Five year lifetime space radioisotope thermoelectric generator with lead telluride panels and plutonium 238 dioxide heat source, analyzing reliability, design and performance 09 p1038 A73-23284

Operational safety experience and advances of space nuclear power systems fueled with Pu-238, discussing modular heat sources 09 p1119 A73-23287

Plane strain dynamics on magneto-thermoviscoelastic materials, noting conductivity, heat sources, potential and rotation 11 p1433 A73-25163

Radioisotope heater design and optimization for manned spacecraft thermal control and life support systems and various mission times 11 p1310 A73-25996

An isotope heat source integrated with a 7 kW/e/ to 25 kW/e/ Brayton cycle space power supply. 11 p1312 A73-26019

Development of a plutonium-fueled miniature power supply based on thermionic conversion. 11 p1396 A73-26028

Diffusion of heat from a line source downstream of a turbulence grid. 11 p1453 A73-26399

Energy transfer from a pulsed thermal source to He II below 0.3 K. 13 p1658 A73-28191

Unsteady temperature condition of a conductor with a nonlinear source of heat 13 p1705 A73-28466

Temperature fields in a hollow cylinder in presence of heat source under the boundary conditions of the second kind. 13 p1708 A73-29666

Constant line sources of heat in infinite media, whose thermal resistivities are linear functions of the temperature. 14 p1817 A73-30610

Measurements of temperature fluctuations behind a linear heat source placed in a turbulent boundary layer 17 p2254 A73-34550

Solid state convection role in moon from analysis of models with homogeneous initial distribution of radioactive heat sources 17 p2232 A73-35262

Semiannual effect in thermosphere due to solar heat input associated with subsolar point migration and auroral heating by magnetic storms 18 p2312 A73-36300

Atmospheric entry and impact behavior of modular disk shaped radioisotope heat source for space nuclear power 19 p2454 A73-38387

Cost-effective radioisotope thermoelectric generator designs involving Cm-244 and Pu-238 heat sources. 19 p2455 A73-38389

The multi-hundred watt RTG - Technology background and flight systems program. 19 p2456 A73-38418

Multihundred watt radioisotope thermoelectric generator design for on-pad and orbital conditions, discussing configurations, Pu-238 heat source and operating characteristics 19 p2456 A73-38419

The MHW heat source - An advance in radioisotope heat source technology for space applications. 19 p2456 A73-38420

Multihundred watt power supply with Si-Ge thermoelectric couples for Pu-238 source heat energy conversion into electric power, discussing computer model for performance projection 19 p2456 A73-38422

Multihundred watt radioactive isotope heat source wind tunnel tests to obtain aerodynamic coefficients, heating rate, stability and ablation for reentry protection design 19 p2456 A73-38425

Multihundred watt radioactive isotope heat source assembly for multiple space missions, discussing aerodynamic heating, shield ablation and thermal stress performance during reentry 19 p2456 A73-38426

Multihundred watt radioisotope thermoelectric generator heat source materials compatibility with thermochemical environment, considering maximum operational and reentry temperatures 19 p2457 A73-38427

Gas management system for control, bleeding, evacuating and radiological and pressure monitoring of He atmosphere in multihundred watt heat source 19 p2457 A73-38428

Curium 244 heat source design for multihundred watt radioisotope thermoelectric generator with Si-Ge thermocouples for energy conversion, noting low cost 19 p2457 A73-38429

Design of a nuclear isotope heat source assembly for a spaceborne mini-Brayton power module. 19 p2457 A73-38431

Nuclear safety considerations for the design of a shuttle launched 500 to 2000 watt isotope Brayton power system. 19 p2457 A73-38432

Plasma heat source and heat exchanger design for liquid potassium circulation system, using air-kerosene aviation gas turbine combustion chamber 20 p2545 A73-39617

Two types of instability of steady convective motion caused by internal heat sources
21 p2789 A73-40192

Self-similar solutions of the plasma equations
21 p2747 A73-40553

Convective heat transfer with allowance for three-dimensional heat sources in the fluid for turbulent flow in a plane slit
21 p2792 A73-41196

Thermal stresses due to an internal source of heat in a solid elastic hemisphere with radiating curved surface and the plane base resting on a smooth rigid insulating plane surface.
22 p2932 A73-42469

On the interaction between the zonal mean flow and equatorial waves excited by diabatic heat sources at 20 deg latitude.
23 p3001 A73-43587

Global distribution of thermospheric heat sources - EUV absorption and Joule dissipation.
23 p2971 A73-43681

Nonlinear gas vibrations maintained in a closed tube by a heat source
23 p2968 A73-43719

Multiphase incompressible half-space as simplified earth model for investigating surface displacements due to time- and depth-dependent heat sources
23 p2973 A73-43797

Calculation of the thermal field of an inhomogeneous plate of complex composition with energy sources
24 p3157 A73-45361

HEAT STROKE
Corticosterone level and the binding capacity of blood plasma proteins under thermal effects
03 p0261 A73-13749

HEAT TESTS
U HIGH TEMPERATURE TESTS
HEAT TOLERANCE
Utility of heat stress indices and effect of humidity and temperature on single physiologic strains.
[AD-751735] 01 p0007 A73-10163

A versatile silver oxide-zinc battery for synchronous orbit and planetary missions.
02 p0133 A73-12622

Acclimatization to severe dry heat by brief exposures to humid heat.
03 p0267 A73-13700

Physical work induced hyperthermia effects on detection rate in visual vigilance task performance in hot and humid environment
06 p0659 A73-18469

Central tracking task performance simultaneously with response to peripheral stimulus under high heat stress environments
06 p0659 A73-18473

Work-heat test comparisons of dry and wet heat and exercise programs for heat acclimatization
09 p1041 A73-22932

Portable electronic thermometer for temperature measurement during exercise elevation of body temperature in heat acclimatization experiment
10 p1185 A73-24567

Comparison of the metabolic effects of centrifugation and heat stress in man.
11 p1315 A73-25338

Physiological effect of air nitrogen replacement by inert gases under high and low temperature conditions
12 p1465 A73-27701

High temperature tolerance enhancement in rats by thermal training and medicinal preparations
12 p1462 A73-27705

Motor, thermal and sensory factors in heart rate variation A methodology for indirect estimation of intermittent muscular work and environmental heat loads.
14 p1720 A73-30880

The combined influence of microwave radiation and an adverse climate on the organism
15 p1837 A73-31170

The effects of core temperature elevation and thermal sensation on performance.
15 p1839 A73-32396

Relationship of physiological strain to change in heart rate during work in the heat.
15 p1836 A73-32548

Biological indicators and the effectiveness of sterilization procedures.
16 p1976 A73-33692

Tolerance to heat following cold stress.
18 p2283 A73-36784

Human performance at elevated environmental temperatures.
18 p2283 A73-36787

Study of the heart rate of humans exposed to heat
18 p2280 A73-36942

Study of performances in a warm environment in case of air conditioning breakdown on a supersonic transport
18 p2286 A73-36947

Model of evaporation responses to heat load in
19 p2395 A73-38150

Responses of men and women to two-hour walks in desert heat.
20 p2518 A73-39784

Heat conduction in blackened skin accompanying pulsatile heating with a xenon flash lamp.
20 p2519 A73-39791

Work-heat tolerance derived from interval training.
22 p2806 A73-42416

HEAT TRANSFER
NT AERODYNAMIC HEAT TRANSFER
NT CONDUCTIVE HEAT TRANSFER
NT CONVECTIVE HEAT TRANSFER
NT HYPERSONIC HEAT TRANSFER
NT LAMINAR HEAT TRANSFER
NT RADIATIVE HEAT TRANSFER
NT SUPERSONIC HEAT TRANSFER
NT TURBULENT HEAT TRANSFER
Book on momentum, heat and mass transfer at various interfaces based on Prandtl eddy mixing length concept
01 p0030 A73-10049

Temperature stresses in an elastic infinite strip due to sudden heating and heat transfer at the boundary of the strip
01 p0113 A73-10091

Book - Advances in heat transfer.
01 p0119 A73-10287

Mathematical methods in heat transfer analysis, considering perturbation, matched asymptotic expansions, variational, complex variables, matrix and several specialized methods
01 p0119 A73-10288

Heat transfer and hydraulic resistance of single banks and systems of tubes in cross flow of gases and viscous liquids
01 p0120 A73-10289

Two-dimensional boundary layers in a free stream which oscillates without reversing.
01 p0032 A73-10446

Heat and mass transfer theory and applications in aerothermoptics, thermoconvective and ferromagnetic fluid studies, chemical engineering, capillary transport and heat pipes
01 p0029 A73-10624

Numerical solution of one-dimensional non-steady flow with supersonic and subsonic flows and heat transfer.
01 p0003 A73-10765

Heat transfer as function of temperature on small horizontal wires in water and organic liquids noting application for heater low gravity behavior prediction
01 p0122 A73-10801

Forced convection droplet evaporation with finite vaporization kinetics and liquid heat transfer.
01 p0122 A73-10803

Flow and heat transfer on a flat plate normal to a two-dimensional laminar jet issuing from a nozzle of finite height.
01 p0033 A73-10804

Navier-Stokes equations numerical solution for steady state axisymmetric flow of incompressible Newtonian fluid between two parallel infinite rotating disks
01 p0122 A73-10805

Experimental study of the turbulent flow of a suspension: Trajectories and velocities of particles - Heat transfers between the two phases
01 p0122 A73-10810

Liquid- and wall-temperature calculations for a flow in tubes with allowance for heat losses into the ambient medium and for axial heat conductivity
01 p0122 A73-10860

Temperature characteristics in the wall of an annular channel heated internally at supercritical pressures
01 p0123 A73-10861

Pressure drop, gas content, liquid drop size and nozzle length effects on flow velocity and heat transfer in two phase nozzle flow
01 p0033 A73-10863

Temperature field and heat transfer equation of unsteady conducting fluid motion on porous plate within magnetic field, allowing for Joule dissipation
01 p0085 A73-11079

The operational condition of heat pipes.
01 p0111 A73-11153

Normal flame velocity in aerodisperse systems
01 p0123 A73-11245

Optimum heat transfer characteristics of semi-circular surfaces cooled by air impingement from airjet arrays and row of air jet nozzles.
02 p0237 A73-11692

[DGLR PAPER 72-061] Quasi-steady heat transfer equation for frequency response of wedge shaped hot film sensors for flow temperature, velocity and turbulence measurement
02 p0166 A73-11711

Investigation of a laminar boundary layer on a continuously moving smooth surface with allowance for heat transfer
02 p0153 A73-11786

Russian book on temperature and stress distributions in thin plates covering unsteady heat transfer and thermoelasticity of isotropic and anisotropic plates
02 p0232 A73-11891

Calculation of an axisymmetric supersonic gas jet injected in a supersonic slipstream past a given body with heat supply
02 p0129 A73-12583

Heat flow and magnetic field diffusion in turbulent fluids.
02 p0199 A73-12841

Carbon dioxide turbulent flow heat transfer in single phase near-critical region under forced and free convection
03 p0396 A73-13185

Hypersonic turbulent boundary layer flow parameters and heat transfer during blowing of coolant air and He through slot
03 p0242 A73-13186

Experimental study of heat transfer in the boiling of nitrogen tetroxide.
03 p0397 A73-13188

Laser induced infrared fluorescence - Thermal heating, mass diffusion, and collisional relaxation in SF₆.
03 p0318 A73-13281

Additives for heat transfer reduction in the propellant combinations N2O4-MMH and N2O4-A-50.
03 p0352 A73-13439

[AIAA PAPER 72-1132] Combustion theory of hybrid rocket propellant-oxidizer combinations based on heat transfer limited model, discussing chemical kinetics and temperature effects on regression rate
03 p0397 A73-13449

[AIAA PAPER 72-1143] Hydrodynamics and heat transfer in a fluid with an asymmetrical stress tensor
03 p0398 A73-13722

On a heat transfer problem in the laminar flow in a tube
03 p0398 A73-13772

Simulations of the annual variation of the zonally averaged state of the atmosphere.
03 p0301 A73-13799

Heat flow meter and calorimeter measurements of heat transfer between human body and environment under various climatic conditions for temperature regulation studies
03 p0268 A73-14123

Calculation of compressible turbulent boundary layers with roughness and heat transfer.
03 p0296 A73-14179

Influence of the magnetic field on the heat transfer of a ferromagnetic viscoplastic fluid
03 p0347 A73-14323

Finite element method for calculating temperature distributions in complex structures, taking into account heat transfer by radiation, conduction and convection
03 p0400 A73-14632

Unsteady one-dimensional compressible frictional flow with heat transfer.
03 p0298 A73-14639

Development of a process utilizing heated rolls for hot rolling metals.
04 p0454 A73-15001

Russian book - Heat transfer in liquid films.
04 p0517 A73-15710

Compressible flow characteristic generalizations, considering flow with/without heat transfer and losses in terms of empirical loss coefficient or heat transfer coefficient
04 p0434 A73-15803

[ASME PAPER 72-WA/PWR-1] Survey of heat transfer techniques applied to electronic equipment.
04 p0518 A73-15816

[ASME PAPER 72-WA/HT-39] Steady two-dimensional heat and mass transfer in the vapor-gas region of a gas-loaded heat pipe.
04 p0518 A73-15821

[ASME PAPER 72-WA/HT-34] Heat transfer to film-cooled combustion chamber liners.
04 p0518 A73-15823

[ASME PAPER 72-WA/HT-32] Nonlinear heat transfer systems design optimization based on physical properties cost functionals, presenting geometric programming method
04 p0519 A73-15833

[ASME PAPER 72-WA/HT-15] The effect of noncondensable gas on laminar film condensation of liquid metals.
04 p0520 A73-15836

[ASME PAPER 72-WA/HT-9] Heat transfer in fully developed laminar flow between flat parallel boundary walls, deriving approximations to higher eigenvalues
05 p0563 A73-16101

A study of mist cooling /1st Report - Investigation of mist cooling/.
05 p0638 A73-16222

Frost and ice column models for analysis of heat and mass transfer and effective thermal conductivity relationship to density in frost layer
05 p0638 A73-16225

Recent results of plasma-wall heat transfer studies in highly ionized, dense plasmas.
05 p0603 A73-16762

High temperature gas turbine engines rotor blades cooling, deriving generalized dimensionless relations for heat transfer data extension from static tests to operational conditions
05 p0607 A73-16797

A non-similar solution of heat transfer in external non-Newtonian flow with thermal radiation.
05 p0640 A73-16873

[AIAA PAPER 73-116] Surface roughness effects on bidirectional reflectance.
05 p0598 A73-16900

[AIAA PAPER 73-152]

Aerothermodynamic aspects of shock-interference patterns for shuttle configurations during entry. [AIAA PAPER 73-238] 05 p0532 A73-16963

Transverse and longitudinal heat flow in a laser-heated magnetically confined plasma. 05 p0603 A73-17162

Supersonic boundary layer on a permeable surface. 05 p0534 A73-17268

High performance cryogenic multilayer thermal insulation with plastic films coated by vapor deposited metal, discussing heat transfer mechanism for comparison with microsphere insulation. 05 p0642 A73-17285

Solution of the general heat-transfer problem for flow past cylindrical bodies by the Tolubinskii integral method. 06 p0766 A73-17407

Calculation of the thermal fluxes and the temperatures of the surfaces of a plate with heat transfer between fluids flowing around the plate. 06 p0766 A73-17408

Calculation of the temperature field of the heated zone of a complex shape consisting of a chassis with parts mounted on it. 06 p0766 A73-17412

Transient heat transfer through a thin-walled circular pipe. 06 p0766 A73-17443

Heat transfer in the thermal entrance region of rectangular channels with a circumference only partially heated. 06 p0768 A73-17918

Heat exchange between gas and air cooled porous metal plate prepared from stainless steel powder under induction and resistance heating. 06 p0768 A73-18129

Calculation of heat and mass transfer in devices employing spray nozzles. 06 p0769 A73-18130

Heat transfer in a periodic boundary layer near a two-dimensional stagnation point. 06 p0769 A73-18526

Heat removal in a sectioned channel of an electric-arc plasmatron. 06 p0731 A73-18572

On generalized hydrodynamic equations used in heat transfer theory. 06 p0688 A73-18834

Thermal performance evaluation of REI panel gaps for Space Shuttle Orbiter. 07 p0919 A73-19487

Spatial stability of stagnation water boundary layer with heat transfer. 07 p0919 A73-19503

Sharply defined upper limit existence for lunar ash flow with heat transfer, presenting altitude dependence of pressure, gas density, temperature and velocity distributions. 07 p0895 A73-19864

Application of the integral balance method to the solution of the problem of interrelated heat and mass transfer in an unbounded plate. 07 p0921 A73-20011

Thermal conductivity of nineteen igneous rocks. I - Application of the needle probe method to the measurement of the thermal conductivity of rock. II - Estimation of the thermal conductivity of rock from the mineral and chemical compositions. 07 p0788 A73-20031

The study of disperse regimes with film boiling of liquid nitrogen in tubes. 07 p0922 A73-20409

Solid/vapour heat transfer in helium at low temperatures. 07 p0922 A73-20412

Post impact behavior of mobile reactor core containment systems. 07 p0850 A73-20468

Heat transfer, adiabatic enthalpy /temperature/ of the wall, and hydrodynamic resistance associated with the turbulent and laminar flow of a compressible fluid in a circular tube. 08 p0954 A73-20858

Heat transfer and friction in the turbulent boundary layer of a compressible gas on a permeable surface. 08 p0926 A73-20992

Unsteady heat transfer in dispersion media at small values of time. 08 p1021 A73-20994

Designing electrical analogs for solving a hyperbolic energy equation. 08 p1022 A73-20999

A method of calculating heat and mass transfer between liquid droplets and a gaseous phase in an acoustic wave field. 08 p1022 A73-21196

Compound heat exchange between a high temperature gas-fluidized bed and a solid surface. 08 p1022 A73-21251

Numerical solutions to flow and heat transfer characteristics of free convection micropolar flow with Newtonian solvent substructure. 08 p1023 A73-21260

A graphical method for analyzing pool-boiling systems. 08 p1023 A73-21262

A special form of Galerkin's method applied to heat transfer in plane Couette-Poiseuille flows. [AD-757002] 08 p1023 A73-21412

Film boiling heat transfer feedback control, comparing experimental process dynamics with analytical transfer function. 08 p1024 A73-21526

Numerical solution of mixed boundary value problems using numerical Green's functions. 09 p1112 A73-22394

Sensitive platinum film resistance thermometers for heat transfer measurement. 09 p1083 A73-22509

Particle seeded RF hydrogen plasma opacity, emission spectra, heat transfer and temperature profile at high temperatures [TTU-SR-2] 09 p1128 A73-22636

Atomic recombination rate determination through heat-transfer measurement. 09 p1048 A73-23449

Entrance region heat transfer between parallel plates with uniform wall temperature. 09 p1167 A73-23460

The influence of diameter on the burning velocity of strands of solid propellant. 10 p1261 A73-23560

Closed form solution for heat transfer through Rankine vortex, noting square root dependence of Nusselt number on Peclet number. 10 p1295 A73-23780

Electronic equipment thermal management for energy dissipation rejection, summarizing heat pipe, phase-change heat transfer and high pressure gas convection techniques. 10 p1295 A73-23789

Book - Heat transfer in microelectronic equipment: A practical guide. 10 p1194 A73-23900

Normal flame velocity in aerosol systems. 10 p1295 A73-24185

Dissipation of mechanical energy in a deformable body during thermal diffusion processes. 10 p1291 A73-24351

Unsteady flow of a conducting viscous fluid between parallel porous walls with heat transfer. 10 p1256 A73-24587

Some heat transfer measurements in compressible turbulent boundary layers. 10 p1296 A73-24648

Influence of liquid circulation within a droplet on the vaporization rate and drag in a viscous flow. 10 p1206 A73-24680

Incompressible boundary layer flow over semi-infinite plate with impulsive heat transfer, obtaining numerical solution for time dependent boundary layer growth. 10 p1296 A73-24812

Study of the phase of the wall transfer of heat or mass in incompressible pulsed flow. 10 p1297 A73-24850

Porous layer strongly nonlinear heat transfer curve bounds numerical computation by variational method, using boundary layer analysis. 11 p1448 A73-25055

Asymptotic Nusselt numbers for dissipative non-Newtonian flow through ducts. 11 p1346 A73-25370

German handbook of functions and numerical values in physics, chemistry, astronomy, geophysics and engineering covering thermodynamics, combustion physics and heat transfer. 11 p1450 A73-25473

Analytical investigation of heat transfer in bodies with moving boundaries. 11 p1450 A73-25622

Modification of the two-flow approximation in radiant-transfer calculations. 11 p1450 A73-25623

Influence of heating-surface orientation in a gravitational field on the nucleate boiling crisis of liquid. 11 p1450 A73-25729

A method of measuring thermal conductivity in the presence of extraneous heat currents and the thermal conductivity of brass at low temperatures. 11 p1367 A73-26307

Investigation of heat transfer in a rarefied molecular gas with the aid of the Senftleben effect. 11 p1453 A73-26445

A new conception of modeling the process of heat transfer on a surface with artificial roughnesses and microfins. 12 p1557 A73-26798

Taking into account heat-transfer irreversibility in calculating the total change in entropy of individual substances. 12 p1557 A73-26939

Thermal limitations of CW and pulsed silicon TRAPATT diodes. 12 p1478 A73-27110

The limits and the nature of the onset of influence of thermogravitational forces on turbulent flow and heat transfer in vertical tubes. 12 p1487 A73-27313

Stability of heat transfer during boiling at a nonisothermal surface. 12 p1558 A73-27314

Experimental investigation of heat and mass transfer in the condensation of vapor from gas-vapor mixtures under viscous and viscous-gravitational flow conditions. 12 p1558 A73-27315

Temperature calculation for heat emitting surface in transparent gas flow, using linearizing function method for heat transfer problems with nonlinear boundary conditions. 12 p1558 A73-27316

Investigation of heat and mass transfer for plasma flows in channels of various shape under conditions of intense condensation. 12 p1558 A73-27318

Heat and mass transfer during the evaporation of liquids from capillary porous bodies situated in a hot air flow. 12 p1559 A73-27474

Biased wall heat transfer in electric arc chamber, noting I-V characteristics and electron current saturation in superimposed axial flow. 12 p1560 A73-27700

Russian papers on mathematical physics boundary value problems covering electrodynamics, electromagnetic fields in conducting channels and ferromagnetic cylinders, heat transfer, shell theory, etc. 12 p1525 A73-27803

Liquid and wall temperature during flow in tubes, with heat loss to the surrounding medium and axial heat conduction. 12 p1560 A73-27909

Temperature conditions at the wall of an annular channel with internal heating at supercritical pressures. 12 p1560 A73-27910

Pressure drop, gas content, liquid drop size and nozzle length effects on flow velocity and heat transfer in two phase nozzle flow. 12 p1560 A73-27912

Kinetic phenomena in a Knudsen gas with rotational degrees of freedom. 12 p1530 A73-27982

Numerical solution to transient heat flow problems. 13 p1704 A73-28172

Heat transfer to laminar flow in vertical rounded corner square duct, noting wall shear stress parameter as laminarization criterion. 13 p1704 A73-28428

An integral equation approach to heat and mass transfer problem in an infinite cylinder. 13 p1705 A73-28431

Generalization of the integral balance method in problems of correlated heat and mass transfer. 13 p1705 A73-28464

Increase of boundary-layer heat transfer by mass injection. 13 p1706 A73-28816

Detection of flight vehicle transition from base measurements. 13 p1706 A73-28834

Perfect thermal cycles family definition for heat supply and extraction as function of temperature. 13 p1706 A73-28911

Variational formalism of a quasi-linear compressible fluid flow with heat exchange. 13 p1602 A73-29022

Optical method for studying the heat transfer mechanism in bubble boiling. 13 p1708 A73-29173

Constant current and temperature hot-wire anemometer systems evaluation via ratio of changes in bridge balance to heat transfer changes between sensor and environment. 13 p1620 A73-29257

German monograph on compressible turbulent boundary layer equations solution for heat transfer in divergent nozzle flow based on modified Patankar-Spalding difference method. 13 p1605 A73-29276

Heat and mass transfer on the surface of a fiberglass-reinforced plastic in a high-temperature air flow. 13 p1708 A73-29403

Heat transfer during helium boiling in narrow channels of different orientations. 13 p1661 A73-29405

Similarity properties of shockless axisymmetric flows with heat addition, considering convergent base and divergent duct flows. 13 p1567 A73-29449

Heat transfer by fluctuating flow of an elastico-viscous liquid past an infinite plate with time varying suction. 14 p1816 A73-29999

Physical conditions of heat transfer and design of heat pipes for the evaporation mode of operation at moderate temperatures. 14 p1816 A73-30011

Boundary layer about a plate assuming an arbitrary gas injection law 14 p1711 A73-30017

Compressor or fan location at intake or outflow side of compressible flow plant, considering power and size requirements with and without heat exchange 14 p1711 A73-30297

Approximate solutions and applications of hodograph equations in elliptic diabolic flow 14 p1745 A73-30428

Some relations for the ultrasonic region of flow of a real gas in the presence of heat transfer. 14 p1817 A73-30603

Application of the optimal linearization method to the heat transfer problem. 14 p1817 A73-30605

The thermal analysis of a belt type radiator by the method of matched asymptotic expansions. 14 p1817 A73-30609

Heat transfer to a cylindrical laminar liquid jet ejecting into a gas. 14 p1817 A73-30612

Heat transfer to a strongly accelerated turbulent boundary layer - Some experimental results, including transpiration. 14 p1818 A73-30615

Heat transfer behind a shock wave in a two-phase gasdynamic flow 15 p1862 A73-31294

Russian papers on heat exchange in atmosphere covering stratus and convective cloud effects, clear sky conditions, turbulent transfer, atmospheric boundary layer, etc 15 p1904 A73-31781

Thermal well representation of cloud layer from radiative cooling and weak dependence on thickness, deriving approximate formulas for radiant fluxes 15 p1904 A73-31784

Efficiency of the recovery of high thermal energy densities during porous vaporization of alkali metals 15 p1957 A73-31864

Method for boundary condition selection in the heat transfer problem with phase transition 15 p1958 A73-31872

Experimental study of heat exchange in a chemically reacting laminar boundary layer 15 p1958 A73-31874

The heat loss of hot wires and heat films in steady flow 15 p1879 A73-32349

Development of convection in horizontal layers of a non-Newtonian fluid 16 p2084 A73-32679

Numerical solution for the flow of a fluid in a heated closed cavity. 16 p2084 A73-32929

Investigations regarding the heat exchange integral in turbulent incompressible flows 16 p2085 A73-33256

Electric analogy procedure for simulating heat and mass transfer processes 16 p2085 A73-33380

Some effects of variable surface temperature on heat transfer to a partially porous flat plate. [ASME PAPER 73-GT-4] 16 p2086 A73-33482

Heat removal in the sectionalized channel of an electrode-type plasmatron. 16 p2042 A73-33597

Stability of composite-material cylindrical shells under unsteady heating and axial compression 16 p2083 A73-33934

Heat-transfer regimes during mixed convection in vertical pipes 17 p2253 A73-34133

Approximate method of solution for three-dimensional boundary layers. 17 p2150 A73-34188

A model of a long-term process of heat and moisture transfer in the atmosphere over the ocean 17 p2158 A73-34344

Papers on heat transfer covering thermosiphon technology, flowing gas-solid mixtures, condensation, free convection, flow stability and cryogenic insulation 17 p2254 A73-34351

Heat transfer to flowing gas-solid mixtures. 17 p2254 A73-34353

Cryogenic insulation heat transfer. 17 p2254 A73-34355

Conference on Heat and Fluid Flow in Steam and Gas Turbine Plant, University of Warwick, Coventry, England, April 3-5, 1973, Proceedings 17 p2092 A73-34376

Effect of 'bulk' heat transfers in aircraft gas turbines on compressor surge margins. 17 p2221 A73-34382

The effect of heat transfer on boundary layer stability in axial flow compressors. 17 p2093 A73-34394

Numerical solution procedure for calculating the unsteady, one-dimensional flow of compressible fluid /with allowance for the effects of heat transfer and friction/. [ASME PAPER 73-FE-30] 17 p2153 A73-35022

Magneto-fluid-mechanic heat transfer from hot film probes. 17 p2255 A73-35845

Laminar mixed convection from a horizontal rotating disc. 17 p2256 A73-35848

Russian book - Fundamentals of the dynamics and heat and mass transfer of fluids under conditions of weightlessness. 18 p2297 A73-35868

Computation of hypersonic turbulent boundary layers with heat transfer. [ALAA PAPER 73-699] 18 p2263 A73-36248

An integral procedure for estimating boundary layer parameters and heat transfer in arbitrary pressure gradients. [ALAA PAPER 73-700] 18 p2298 A73-36249

Numerical stability of boundary layers with massive blowing. 18 p2298 A73-36321

Impingement of small, very high pressure solid rocket motor plumes upon nearby surfaces. 18 p2342 A73-36347

Thermal modeling of a plate with coupled heat transfer modes. [ALAA PAPER 73-748] 18 p2370 A73-36364

An approximation for combined heat transfer in a radiatively absorbing and emitting gas. [ALAA PAPER 73-750] 18 p2370 A73-36366

Calorimeter measurement of heat transfer at hypersonic conditions. [ALAA PAPER 73-760] 18 p2264 A73-36375

Heat and mass transfer processes during thermal decomposition of resin binders in fiberglass reinforced plastics 18 p2328 A73-36814

Numerical calculation of heat exchange and frictional resistance for a turbulent flow in a tube in the case of a gas with variable physical characteristics 18 p2301 A73-36816

Experimental study of the heat transfer in the vicinity of the critical point during nonequilibrium physicochemical transformations and determination of the nitrogen recombination rate constant 18 p2287 A73-37013

Plasma channel flow theoretical and experimental review, considering heat transfer studies, turbulent nonequilibrium plasma boundary layers and plasma sheaths 19 p2464 A73-37161

Mach number and Reynolds number effect on orbiter/tank interference heating. 19 p2491 A73-37403

Some consequences of introducing the geometrical-dynamic characteristic ratio in studies of the heat transfer to surfaces with artificial roughnesses or to microwaving surfaces 19 p2504 A73-37655

Heat transfer in rotating cylindrical enclosures with axial inflow and outflow of coolant. 19 p2504 A73-37877

Axial grooved heat pipes - Cryogenic through ambient. [ASME PAPER 73-ENAS-48] 19 p2434 A73-37995

Stability criteria for explicit finite difference solutions of the parabolic diffusion equation with nonlinear boundary conditions. 19 p2445 A73-38189

Heat transfer from a vibrating circular cylinder. 19 p2505 A73-38478

Transonic laminar boundary layers with surface curvature. 19 p2423 A73-38480

Experimental investigation of heat transfer and resistance in crimped tubes 19 p2505 A73-38561

The effect of the porous material characteristics on the internal heat and mass transfer. [ASME PAPER 73-HT-49] 20 p2626 A73-38573

Temperature field calculation for a plate of a complex shape with systems of double-periodic holes, inclusions, and energy sources 20 p2627 A73-39255

Fredholm integral equation for solving boundary value problem of heat transfer across contact of two regions bounded by simple closed Jordan curves 20 p2628 A73-39399

An approach to the determination of conditions impairing heat transfer under supercritical pressure 20 p2628 A73-39614

High-speed cine-photography and oscillography in a boiling simulation. 21 p2697 A73-39994

Burnout of a graphite surface during the blowing of an inert gas through it 21 p2790 A73-40698

An experimental study of strong injection at axisymmetrical bodies of revolution. 21 p2633 A73-41057

Experimental study of heat and mass transfer in chemically reacting laminar boundary layers. 21 p2791 A73-41058

Heat pipe theory and design, discussing typical operating conditions and heat transfer capacity from flow equations solution by finite difference method 21 p2792 A73-41059

A study of startup regimes of high-temperature heat pipes. 21 p2792 A73-41060

Effect of deflector geometry on the heat transfer in the coolant passages of deflector blades. 21 p2754 A73-41322

Fluctuating flow and heat transfer from a vertical surface. 21 p2792 A73-41524

Unique platinum resistance temperature sensors for lunar heat flow measurements. 22 p2855 A73-42013

Irreversible heat transfer in the total entropy change for a pure substance. 22 p2930 A73-42273

Unsteady stagnation point heat transfer due to unsteady free stream temperature. 22 p2931 A73-42290

Heat pipe applications utilizing, high thermal conductivity, small temperature variations, heat flux transformation and temperature sensitivity for heat transportation and distribution and temperature control 22 p2931 A73-42292

Rarefied-gas heat transfer in Knudsen layer using ellipsoidal model. 22 p2932 A73-42471

French monograph - Study of the behavior of the laminar boundary layer in the presence of a positive or negative pressure gradient in hypersonic flow around obstacles. 22 p2797 A73-42744

A computer model for three-dimensional flow in furnaces. 22 p2934 A73-42787

Modes of one-dimensional wave propagation in an infinite thermoelastic medium with finite heat propagation rates 22 p2927 A73-42928

Heat transfer in liquids due to second order boundary layer flows with dissipation. 22 p2938 A73-42996

Heat transfer in plane Couette flow of rarefied gas between parallel plates, determining temperature jumps at plates from transfer equations 23 p3048 A73-43206

A model of heat transfer in a biological tissue perfused by blood of arbitrary temperature. 23 p2948 A73-43292

Cumulus-scale vertical transport of mass, heat and momentum calculated from radar and rain gauge precipitation measurement 23 p3002 A73-43596

The problem of extrapolating test data on the efficiency of turbine-blade cooling to actual conditions 23 p3020 A73-43741

Thermal response of an unsteady laminar boundary layer on a flat plate due to step changes in wall temperature and in wall heat flux. 23 p3049 A73-43802

Heat transfer from a hypersonic turbulent boundary layer on a flat plate. 23 p3049 A73-43933

Calculation of the thermal field of an inhomogeneous plate of complex composition with energy sources 24 p3157 A73-45361

Heat and mass transfer in a turbulent layer above permeable plates 24 p3081 A73-45528

The incompressible boundary layer of higher order at the axisymmetrical stagnation point in the case of strong suction or blowing 24 p3056 A73-45545

HEAT TRANSFER COEFFICIENTS

Measurement of transient heat-transfer coefficients in the contact between solid materials 01 p0120 A73-10413

French monograph - Experimental study of the thermal conductivity of rare gases and helium-argon mixtures as functions of temperature and pressure. 01 p0120 A73-10604

Radiative and convective heating during Venus entry. 01 p0003 A73-10757

Convective heat transfer coefficients at stagnation point of blunt body immersed in flames of fuel gases combustion with pure oxygen 01 p0122 A73-10807

Analytical study of the sensitivity of a sensor for studying pulsations of the heat-transfer coefficient in a boiling high-temperature layer 01 p0051 A73-10864

Study of the natural convection between two plane, vertical plates parallel and isothermal 02 p0238 A73-12795

Practical application of boundary layer theory to flow and heat transfer problems in turbomachines. 03 p0398 A73-14145

Mass transfer technique for investigation of heat transfer by jet-impingement systems. 03 p0400 A73-14642

Shell-and-coil condenser for packed air conditioners, testing heat transfer coefficients relationship to Reynolds number, heat flux and condensed refrigerant level

05 p0638 A73-16220

Heat transfer characteristics of air conditioner finned tube heat exchanger surfaces from steady state heat balance, monitoring fluid temperature response at outlet

05 p0638 A73-16223

Study of local heat transfer coefficients in a tube in the case of a local flow swirling by swirl vanes

05 p0639 A73-16768

Coupled thermoelasticity with a finite heat propagation rate

05 p0634 A73-16770

An experimental investigation of some heat transfer characteristics on an orbiter/HO-tank/SRM Space Shuttle configurations, freestream Mach number equal to 8.0.

05 p0640 A73-16856

Critical flows in open vertical ducts filled with superfluid helium under pressure

05 p0599 A73-17230

Experimental investigation of worsened heat-transfer conditions with the turbulent flow of carbon dioxide at supercritical pressure.

06 p0766 A73-17410

Heat transfer from hypersonic turbulent flow at a wedge compression corner.

06 p0646 A73-18531

Description of the transfer of heat by natural convection in a horizontal porous layer with the help of a solid-fluid transfer coefficient

06 p0769 A73-18538

Heat conductivity and the Lorentz number of tungsten-rhenium alloys within the solid-solution limits from 0 to 27% Re at temperatures between 1200 and 3000 K

06 p0710 A73-18556

Influence of the distortion of the temperature field at the point of thermocouple fixation on measurements of the heat conduction coefficient by the steady-state method of radial thermal flux

06 p0770 A73-18566

Investigation of the heat transfer between the gas and casing in the area of the apertures between the nozzle diaphragm blades and guide vanes of turbines

07 p0868 A73-20086

Application of the solution to an inverse heat conduction problem to the calculation of the heat transfer coefficient from experimentally measured temperatures at internal point of the body

08 p1021 A73-20996

Experimental investigation of heat transfer using facilities for testing heatproof materials

08 p1022 A73-21094

Experiments on a shrouded, parallel disk system with rotation and coolant throughflow.

[AD-759594] 08 p1023 A73-21256

Influence of various surface roughness on the natural convection.

08 p1024 A73-21639

Ablation of large meteor particles

09 p1147 A73-22573

Certain results of an experimental study of local heat transfer under supercritical pressure in a unilaterally heated rectangular channel

10 p1293 A73-23510

Experimental study of the heat transfer in the separation zones in front of cylindrical projections

10 p1294 A73-23587

Hydrodynamic theory of heat transfer between a stabilized gas suspension flow and channel walls.

10 p1297 A73-24968

Heat transfer and friction coefficients for turbulent flow of air in smooth annuli at high temperatures.

10 p1297 A73-24970

Determination of the convective heat transfer coefficient by 'half-space period' method

11 p1451 A73-25741

Heat conduction nonlinear boundary value problems approximate solution via Westphal similarity theorem, considering inhomogeneous media with temperature dependent heat transfer coefficients

11 p1451 A73-25742

Regularization schemes for solving inverse heat conduction problems

11 p1451 A73-25743

Analytical model for radioisotope thermoelectric generator performance prediction in air and vacuum, taking into account modified heat transfer rates

11 p1312 A73-26031

Considerations concerning the inadequacy of the classical concept of equivalent diameter in calculations of heat transfer in elliptical pipes

12 p1557 A73-26796

Determination of the coefficient alpha real in convection in air with allowance for the Jacq effect

12 p1557 A73-26797

Solution of the dynamic problem of thermoelasticity for a circular plate with allowance for the finite velocity of heat propagation

12 p1552 A73-27263

Nonuniform heat transfer coefficient effect on double-pipe heat exchanger analysis with effectiveness method, discussing exchanger sizing

12 p1559 A73-27693

Applied electrical potential effect on heat transfer to tube immersed in highly ionized flow of atmospheric pressure Ar plasma

12 p1529 A73-27696

The influence of the thermal properties of the heating-surface on the heat-transfer of bubble boiling

12 p1559 A73-27698

The heat and mass transfer of a binary laminar boundary layer in the presence of simultaneous convection at a vertical permeable flat surface

13 p1708 A73-29350

On the motion of small spheres in gases. III - Drag and heat transfer.

13 p1567 A73-29425

Rough estimate of the heat transfer coefficient of a liquid in laminar and turbulent flow through plane ducts

14 p1744 A73-30012

Switching effect in amorphous semiconductors at discontinuous changes in the heat transfer from the sample.

14 p1783 A73-30434

Thermal conductivity and Lorenz number of tungsten-rhenium alloys in the solid-solution region 0-27% Re/at temperatures of 1200-3000 K.

16 p2026 A73-33582

Effect of temperature field distortions caused by embedded thermocouples on the measurement of the thermal conductivity coefficient by the steady radial heat flux method.

16 p2086 A73-33591

Infinitesimal canonical transformation for obtaining the thermal conductivity coefficient under the theory of linear response

17 p2253 A73-34126

Calculation of turbulent heat transfer and skin friction.

17 p2150 A73-34196

Characteristics of the heat exchange in the region of injection into a supersonic high-temperature flow

17 p2254 A73-34772

Temperature restitution coefficients for turbulent fluid flow in a circular pipe.

17 p2155 A73-35189

Results of an experimental investigation of local heat transfer at supercritical pressure in a rectangular channel heated from one side.

17 p2255 A73-35190

Turbulent heat transfer and the periodic viscous sublayer.

17 p2255 A73-35844

Convective heating in dust-laden hypersonic flows. [AIAA PAPER 73-761]

18 p2371 A73-36376

A method for computing roughwall heat transfer rates on reentry nosetips.

[AIAA PAPER 73-763] 18 p2264 A73-36378

Determination of the heat transfer coefficient for bodies of arbitrary shape at Re tending to 0

18 p2372 A73-37121

Comparative study of patches for liquid cooled garments.

19 p2398 A73-37404

Gas turbine blade effusion cooling by air blowing, determining heat transfer coefficients for laminar and turbulent boundary layer

19 p2504 A73-38156

Film effectiveness and heat transfer coefficient downstream of a metered injection slot.

[ASME PAPER 73-HT-31] 20 p2625 A73-38570

Flow film boiling heat transfer correlations - Parametric study with data comparisons.

[ASME PAPER 73-HT-50] 20 p2626 A73-38574

Thermoelasticity of coupled bodies in the case of stress-dependent heat transfer

20 p2618 A73-39327

Method for determining the heat conductivity coefficient of high-temperature materials during unsteady heating

20 p2629 A73-39616

A class of heat conduction problems with a time-variable heat transfer coefficient

21 p2790 A73-40396

Improvement to Klineberg's method for the calculation of viscous-inviscid interactions in supersonic flow.

21 p2632 A73-40429

The influence of rotation on the heat transfer from a sphere to an air stream.

22 p2938 A73-42955

The effect of variable environment temperature on heat transfer in extended surfaces.

23 p3048 A73-43296

Heat release from turbine rotor blades

23 p3020 A73-43744

Heat transfer rate and flow field and pressure distribution behind flat plate backward facing step in hypersonic flow

23 p3049 A73-43832

Thermal stresses in heated orthotropic plates with variable heat-transfer coefficients

23 p3046 A73-44195

Effect of modified thermal conductivity on the temperature distribution in the protonosphere.

24 p3082 A73-44727

Pulse method for determining heat-transfer coefficients of coatings

24 p3155 A73-44756

Radiation pyrometric probe /homogeneous thermally insulated rod/ for measuring body surface thermal loads and heat transfer coefficients

24 p3089 A73-44758

Analysis of the heat transfer associated with the evaporation of a fluid film on a rotating disk

24 p3156 A73-45078

Temperature field boundary value problem with variable heat transfer coefficients and specific heat, using Laplace transformation and variation methods

24 p3156 A73-45083

HEAT TRANSMISSION

NT AERODYNAMIC HEAT TRANSFER

NT CONDUCTIVE HEAT TRANSFER

NT CONVECTIVE HEAT TRANSFER

NT HEAT TRANSFER

NT HYPERSONIC HEAT TRANSFER

NT LAMINAR HEAT TRANSFER

NT RADIATIVE HEAT TRANSFER

NT SUPERSONIC HEAT TRANSFER

NT TURBULENT HEAT TRANSFER

Heating of a viscoelastic beam subjected to transverse vibrations

01 p0112 A73-10003

Linear solutions for heat propagation in relativistic fluid dynamics

01 p0076 A73-10266

Geothermal energy extraction from hot rocks via deep dry wells by pressurized water circulation, solving numerically fluid flow, heat transport and rock fracture equations

05 p0569 A73-16382

A method for solving moving boundary problems in heat flow using cubic splines or polynomials.

06 p0768 A73-17979

The linear thermoelastic problem of uniform heat flow disturbed by a two-dimensional crack in a strip.

06 p0762 A73-17985

Electrical components heat dissipation via thermal radiation, determining nonlinear temperature dependence from Stefan-Boltzmann law

08 p1020 A73-20775

Periodic nozzle flow with heat addition. [AD-758555]

08 p1025 A73-21669

Terrestrial heat flow determinations in the north central United States.

09 p1076 A73-22148

Use of the linear heat flow for poor conductors and its application to the thermal conductivity of nylon. [AD-758307]

09 p1166 A73-22200

Gasdynamic and thermal processes during giant laser pulse impingement on target material, considering heat wave propagation at supersonic and subsonic velocities

09 p1127 A73-22610

Second law of thermodynamics revision to include only spontaneous processes made to yield work, discussing heat flow, solutes diffusion and Gibbs free energy

14 p1816 A73-29735

Influence of the diathermancy of an arc-shaped crack on the thermoelastic state of the area about the crack

14 p1814 A73-30720

Determination of the heat flux from the lunar interior for a nonhomogeneous structure of the lunar surface layer

16 p2065 A73-33783

A general expression for the rate of evaporation of a layer of liquid on a solid body.

19 p2505 A73-38483

Determination of heat flow shape factors for hollow, regular polygonal prisms.

23 p3049 A73-44164

HEAT TREATMENT

NT ANNEALING

NT MARAGING

NT NITRIDING

NT PULSE HEATING

NT STRESS RELIEVING

NT TEMPERING

Nickel structure stabilization by multiply alternated thermocyclic treatment and isothermal annealing

01 p0062 A73-10253

Characteristics of the formation of austenite during rapid heating of cold-worked KVK-42 [42Kh2NGSM/steel

01 p0062 A73-10260

Physical fatigue limit of hardened steels

01 p0063 A73-10485

Investigation of structural changes during the heat treatment of carbonized fibers with the aid of a scanning electron microscope

01 p0068 A73-11246

Cast Nb alloys ductility enhancement by heat treatment, discussing solid solution decay kinetics and carbides composition of Nb-Mo-Zr-C system

01 p0066 A73-11344

Conductivity of 2024-T42 aluminum sheet solution heat treated at various temperatures. 02 p0168 A73-11986

Cooling modes effect on heat treated Ti-Nb alloys as function of Nb content, investigating alpha prime and double prime martensites 02 p0181 A73-12500

Effect of heat treatment on filament wound carbon composites. 03 p0332 A73-13043

Effects of hot-salt stress corrosion on titanium alloys. 03 p0323 A73-13268

Warm forging of steels for increased precision and mechanical properties. 03 p0323 A73-13269

Mechanical properties of base and coating metals for explosive plating, noting heat treatment for strain hardening prevention 03 p0312 A73-13584

Comparison and analysis of residual stress measuring techniques and the effect of post-weld heat treatment on residual stresses in Inconel 600, Inconel X-750 and Rene 41 weldments. 03 p0313 A73-13596

The influence of certain experimental factors on the fracture toughness of a high-strength steel 04 p0462 A73-15299

The effect of a hydrogen preheat-treatment on the oxidation behavior of Ni-Cr-Al-ThO2 alloys. 04 p0463 A73-15319

Molybdenum corner in Mo-Ti-B and Mo-Zr-B ternary systems 04 p0464 A73-15494

Effects of heat treatment on the mechanical properties and microstructure of Inconel Alloy 718. 04 p0465 A73-15582

Plastic deformation magnitude and direction /sign/ for maraging steels under heat treatment, noting optimal conditions for maximum hardening 06 p0697 A73-17878

Resistance to hydroerosion of hard-faced maraging steels 06 p0706 A73-17881

Tensile tests and heat treatment for creep rupture and fracture strengths of heat resistant steel, noting crack initiation and propagation 06 p0706 A73-17884

Stability of the dislocation structure in cold-deformed Kh18Ni2T and Kh16Ni9M2 steels during high-temperature aging 06 p0707 A73-17905

Structural and phase transformations in silicon steels during heat treatment 06 p0707 A73-18035

Polymorphous transformation mechanism in thallium 06 p0735 A73-18045

Influence of low-temperature heat treatment on the electrical and recombinational properties of silicon-silicon dioxide systems 06 p0736 A73-18085

The mechanical properties of titanium alloys with isomorphous beta-stabilizing elements. 06 p0708 A73-18206

Magnetostriction of stainless steels in relation to heat treatment. 06 p0709 A73-18212

Effects of thermal treatment on the resistance of some steels to crack development and propagation 06 p0711 A73-18664

Ferritic chromium steels embrittlement under high temperature aging, using hardness measurements, impact tests and electron metallography 06 p0712 A73-18762

Regeneration and recrystallization of austenite in low-carbon stainless steel 18-10 after rolling at room temperature 07 p0837 A73-19113

Effects of heat treatment on the properties of a molybdenum-carbon-nickel alloy and joints in it. 07 p0840 A73-20371

Hole preparation in titanium and high strength steels. [SME PAPER IQ 72-208] 07 p0832 A73-20450

Low stress creep tests of niobium stabilized austenitic steels. 08 p0981 A73-21789

The ageing and creep behaviour of a Cr-Ni-Mn austenitic steel. 08 p0981 A73-21791

The influence of structure upon the notched creep strength of a nickel-base alloy. 08 p0982 A73-21795

Influence of composition and heat treatments on the structure and mechanical characteristics of martensitic stainless steels derived from the 16 percent chrome and 4 percent nickel type 09 p1098 A73-21924

Texture and anisotropy of the thermal emf of sheet titanium 09 p1099 A73-21969

Effect of thermomechanical processing on fatigue crack propagation. 09 p1102 A73-22415

Recrystallization in Ti-15 Mo base beta titanium alloys. 09 p1103 A73-22423

Red cell flexibility and pressure-flow relations in isolated lungs. 09 p1041 A73-22927

Interaction of graphite with titanium and zirconium 09 p1105 A73-22977

Effect of heat treatment on the structure and properties of NV10MST3T alloy 09 p1106 A73-23190

Influence of heat treatment on the mechanical properties of the VT3-1 titanium alloy 09 p1107 A73-23191

Physical characteristics of sponge titanium of a hardness below 100 HB units, obtained by heat treatment with magnesium 09 p1107 A73-23227

Improved fracture resistance of 7075 through thermomechanical processing. 09 p1109 A73-23257

Influence of heat treatment on the high-temperature strength and creep of the NV10M5T3T niobium alloy 10 p1230 A73-23600

Effect of welding variables on aluminum alloy weldments. 10 p1230 A73-23627

Study of the effectiveness of various thermomechanical methods of hardening alpha + beta titanium alloys 10 p1234 A73-24425

Effect of heat treatment on the fatigue properties of unwoven fiberglass-reinforced plastics 11 p1386 A73-25047

Investigation of the heat conductivity of aluminum oxide deposited by plasma spraying 11 p1373 A73-25731

Heat treatment effects on the mechanical properties in Ti-6Al-4V-2Sn. 11 p1385 A73-26172

Property control in reinforced plastics through interface tailoring. 11 p1389 A73-26296

Embrittlement of 2-1/4Cr-1Mo steel weld metal by postweld heat treatment. 11 p1375 A73-26354

Influence of deformation and heat treatment on the structural changes of the OKh12Ni13M alloy 12 p1508 A73-26836

Improving the properties of the MA5 magnesium alloy by high-temperature thermomechanical treatment 12 p1510 A73-26910

Fracture characteristics of thermally strengthened titanium beta-alloys 12 p1510 A73-26914

On the relationship between grainboundary corrosion and stress corrosion cracking of Al-Zn-Mg alloys. 12 p1511 A73-27059

Electrical conductivity of semiconductor glass crystals on an arsenic and lead selenide base 12 p1531 A73-27195

Influence of heat treatment on characteristics of injection lasers. 12 p1507 A73-27522

Tensile properties of high strength Al-Zn-Mg and Al-Zn-Mg-Cu alloy products processed by T-AHA type final thermomechanical treatments 13 p1633 A73-28141

Vanadium galliumide tape preparation and critical temperature and current as function of heat treatment temperature and applied magnetic field, considering pancake current capacity 13 p1669 A73-29069

Creep properties of low alloy steel in relation to microstructure. 13 p1641 A73-29509

Solidification structure and tensile properties of 2014 aluminum alloy welds. 14 p1755 A73-30149

Physical fatigue limit of hardened steels. 14 p1759 A73-30310

German monograph - Effect of the transformation and heat treatment conditions on the mechanical properties and the creep characteristics of the alloy TiAl6V4. 14 p1762 A73-30668

Structure, composition and photoelectrical properties of cadmium sulfide and selenide epitaxial films subjected to heat treatment 14 p1784 A73-30856

Moessbauer effect in Nb3Sn as a function of heat treatment 15 p1922 A73-31180

Influence of heat treatment on the critical currents in binary alloys of niobium with zirconium and titanium 15 p1887 A73-31185

High strength Ti alloy cracking and brittle fracture prevention during aging by high heat rate treatment at 250-500 C 15 p1889 A73-31814

Superplasticity of the Kh18Ni10T steel 15 p1890 A73-31816

Ferritic martensitic stainless steels stress corrosion cracking, emphasizing heat treatment and environment conditions effects on corrosion resistance 15 p1891 A73-32170

Transformations during heat treatment of Ti-Mo system alloys with additions of aluminum, zirconium, and tin 15 p1893 A73-32518

Phase transformations during heat treatment of the VT18 alloy 15 p1894 A73-32524

Influence of heating rate on the phase composition of the VT3-1 alloy 15 p1894 A73-32525

Heat treatment effects upon the properties of PAN base carbon fibers. 16 p2028 A73-33040

Processing and properties of composites based on NR-150 polyimide binders. 16 p2029 A73-33047

The precipitation behavior of a commercial aluminum-copper-lithium alloy. I - The microstructure after isothermal heat treatment 16 p2026 A73-33954

Effect of additional alloying and heat treatment on the strength of steels 17 p2187 A73-34336

Effects of cold deformation and heat treatment on the elastic properties of niobium 17 p2188 A73-34562

Axial alignment of basal planes in polyacrylonitrile base carbon fibers, increasing axial and radial microstructural textures via heat treatment temperature 17 p2198 A73-35837

The effect of very short time-at-temperature on the yield stress of 6061-T651 aluminum. 19 p2440 A73-37590

Microstructural characteristics of the TA6V alloy as a function of thermomechanical treatments in alpha plus beta - Effects on the mechanical characteristics in tension 19 p2441 A73-37831

Principal aspects of thermal treatments of the alloy Ti-11, 5 Mo-6, Zr-4, 5 Sn /Beta III/ 19 p2441 A73-37833

Effect of autoclave heat treatments on the mechanical properties of the prealloyed-powder cobalt-base alloy HS-31. 19 p2443 A73-38248

French monograph - Mechanical behavior of the titanium alloy TA6V6E2 with reference to hydrogen - Influence of heat treatment and oxygen content. 19 p2443 A73-38362

Titanium Stresskin panel fabrication and assembly, discussing forming, cutting, thermal processing, welding and applications [SME PAPER MF 73-158] 19 p2437 A73-38502

The influence of heat treatment on the stress-corrosion susceptibility of a ternary Al-5.3 pct Zn-2.5 pct Mg alloy. 20 p2576 A73-39031

Changes in the physicomechanical properties of structural polymers after heat treatment 20 p2580 A73-39333

The effect of heat treatment on the tensile strength and hardness of a quenched ternary zirconium-base alloy /Zr-0.5 wt. % Nb-1 wt. % Cr/. 21 p2717 A73-40319

Effect of mechanothermal treatment on the heat-resistant properties of 1Kh14Ni18V2B steel with boron additives 21 p2718 A73-40735

Drop forged Ti alpha-beta alloy textures after heat treatment, quenching, aging and surface machining 22 p2866 A73-42089

Elastic properties of alloys of the Ti-Al-Mo system as a function of the composition and heat treatment 22 p2874 A73-42095

Influence of diffusion coating and heat treatment on the wear resistance of VT-8 alloy 23 p2990 A73-43485

Influence of heat treatment and surface quality on the endurance of EI961 steel 23 p2995 A73-44288

Formation of the overheating structure in cast AL9 and VAL5 Silumin alloys 24 p3098 A73-44473

High strength Ti alloy cracking and brittle fracture prevention during aging by high heat rate treatment at 250-500 C 24 p3100 A73-45277

Superplasticity of steel Kh18Ni10T. 24 p3100 A73-45279

Influence of heat treatment on the posistor effect of semiconductive BaTiO3-ceramic. 24 p3120 A73-45367

HEATERS

Peak pool boiling heat flux from finite heater configurations, improving Zuber hydrodynamic theory by combining vapor escape path thickness empirical values with velocity matching hypothesis [ASME PAPER 72-WA/HT-10] 04 p0519 A73-15835

Radioisotope heater design and optimization for manned spacecraft thermal control and life support systems and various mission times
11 p1310 A73-25996

HEATING

NT AERODYNAMIC HEATING
NT ARC HEATING
NT ATMOSPHERIC HEATING
NT BASE HEATING
NT GAS HEATING
NT INDUCTION HEATING
NT IONOSPHERIC HEATING
NT KINETIC HEATING
NT LASER HEATING
NT PLASMA HEATING
NT PULSE HEATING
NT RADIANT HEATING
NT RADIO FREQUENCY HEATING
NT RESISTANCE HEATING
NT SHOCK HEATING
NT SOLAR HEATING
NT SUPERHEATING
NT TRANSIENT HEATING

Characteristics of the fatigue curve of plastics.

Installing the heater cable directly in the redesigned leading edge.
16 p1970 A73-32924

HEATING EQUIPMENT

NT BOILERS
NT FURNACES
NT VACUUM FURNACES
Heat transfer as function of temperature on small horizontal wires in water and organic liquids noting application for heater low gravity behavior prediction
01 p0122 A73-10801
The design of components for an advanced Rankine cycle test facility.
11 p1344 A73-25995
Radioisotope heater design and optimization for manned spacecraft thermal control and life support systems and various mission times
11 p1310 A73-25996
Venturi exhausts for air pumping augmentation in ram air operated aircraft heater or combustor, discussing experimental data on section variation
18 p2343 A73-36396
Improved technology for multiwatt radioisotope heater units.
18 p2336 A73-36681

HEAVING

Heaving and pitching response of a hovercraft moving over regular waves.
01 p0004 A73-10700

HEAVY COSMIC RAY PRIMARIES

U HEAVY NUCLEI
U PRIMARY COSMIC RAYS

HEAVY ELEMENTS

NT CURIUM ISOTOPES
NT CURIUM 244
NT PLUTONIUM ISOTOPES
NT PLUTONIUM 238

Heavy elements depletion on grains in interstellar medium two phase model, noting gas dynamical analysis of discrete clouds evolution
03 p0366 A73-12931

A photometric study of the integrated light of clusters in the Magellanic Clouds and the Fornax dwarf galaxy.
14 p1801 A73-30726

Models comparison for heavy elements segregation mechanism from gaseous hydrogen and helium for terrestrial planets formation from primordial granular matter
17 p2228 A73-34422

The peculiar A stars and the origin of the heaviest chemical elements.
20 p2611 A73-39623

Heavy elements in surface materials - Determination by alpha particle scattering.
23 p2981 A73-43529

HEAVY IONS

Satellite observations of energetic heavy ions during a geomagnetic storm.
02 p0204 A73-11733

Charge assignment to cosmic ray heavy ion tracks in lunar pyroxenes.
07 p0872 A73-19877

Delta ray particle track structure theory for radiation dosimetry and biological cell response to heavy ions, fast neutrons, stopped pions and mixed radiation fields
11 p1323 A73-25423

Solar flare heavy ion damage in Luna 20 soil sample, producing angular amorphous micron-sized grains via accumulated radiation damage
13 p1676 A73-28327

Composition of galactic cosmic rays with energy ranging between 10 and 30 MeV/nucleon.
15 p1926 A73-31355

Experimental methods of correlation between the trajectories of cosmic heavy ions and biological objects: Dosimetric results - Experiment Biostack on Apollo XVI and XVII.
18 p2270 A73-35946

Preliminary results of the action of cosmic heavy ions on development of eggs of *Artemia salina*.
18 p2271 A73-36129

Characteristics of tracks of ions of 14 less than or equal to Z less than or equal to 36 in common rock silicates.
21 p2682 A73-40242

Acceleration of heavy ions by radiation pressure.
22 p2900 A73-41759

Frequency of heavy ions in space and their biologically important characteristics.
22 p2805 A73-42178

The radiobiological effects of heavy ions on mammalian cells and bacteria.
22 p2805 A73-42182

Probability cross sections of heavy ion single hit inactivation paths for human cells using nitrogen ion accelerator experiments
22 p2805 A73-42183

Heavy ion irradiation effects on bacteria mutations in balloon flight and accelerator experiments, comparing with cosmic rays
22 p2805 A73-42184

Apollo 16 Biostack experiment for biological effects of cosmic ray heavy primaries on cell and tissue development and mutations of bacilli, *Artemia* and plant seeds
22 p2805 A73-42185

HEAVY NUCLEI

Observation of low-charge low-energy geomagnetically forbidden particles.
02 p0155 A73-11726

Further evidence for a cosmic ray selection mechanism.
02 p0207 A73-12397

Scintillation and anticoincidence Cerenkov counters for recording heavy nonrelativistic single charge particles in cosmic rays at sea level
02 p0209 A73-12670

The Os-Pt-Hg abundance peak in Ap stars and the problem of very heavy cosmic rays.
02 p0210 A73-12733

Low energy solar nuclear particle irradiation of lunar and meteoritic breccias.
03 p0361 A73-13100

Two stage analytical model for mechanism of heavy nuclei acceleration in solar flares, considering ion Fermi acceleration to higher energies
03 p0362 A73-13720

Disk-shaped diffusion model with inhomogeneous distribution of gas and heavy relativistic nuclei sources for galactic cosmic rays chemical composition
05 p0608 A73-16081

Enrichment of heavy nuclei in the 17 April 1972 solar flare.
05 p0609 A73-16571

Biogenic elemental distribution and isotopic abundance in lunar samples, discussing heavy isotopes enrichment by solar wind irradiation, meteorite impacts and hydrogen stripping
06 p0654 A73-18417

The propagation of the energetic very heavy nuclei in the cosmic radiation.
07 p0870 A73-19340

Energy dependence of primary cosmic ray nuclei abundance ratios.
07 p0873 A73-20564

Solar cosmic ray heavy nuclei acceleration independence from solar activity phenomena, based on Elektron 4 satellite observation
08 p0999 A73-21332

Semiautomatic photometer for determining the charge of heavy cosmic-ray nuclei in photonuclear emulsions
09 p1085 A73-23001

Superheavy element fissionability on r-process path, considering experimental search methods and doubly magic nucleus concept
10 p1272 A73-23536

Measurements of the iron-group abundance in energetic solar particles.
10 p1264 A73-23538

Solar cosmic ray heavy nucleus abundances relation to oxygen nuclei in solar corona and photosphere
10 p1265 A73-23898

Certain data concerning heavy primary nuclei /Z above 33/ obtained outside the earth's magnetosphere
10 p1266 A73-23915

Methods for determining the charges of heavy primary nuclei /Z greater than 26/ in photonuclear emulsions of different sensitivities
10 p1267 A73-23922

Iron energy spectra due to acceleration at neutron star surface vs primary cosmic rays
14 p1787 A73-30618

Composition of low energy cosmic radiation from silicon to nickel.
17 p2225 A73-35787

The charge spectrum of heavy cosmic ray nuclei measured on board of Apollo 16 /Biostack/ using plastic detectors.
18 p2344 A73-35987

Apollo 14 and Apollo 16 heavy-particle dosimetry experiments.
19 p2396 A73-37150

Solar cosmic ray heavy nucleus abundances relation to oxygen nuclei in solar corona and photosphere
20 p2601 A73-38917

Asymptotic electron terms of colliding identical heavy nuclei
21 p2742 A73-40353

Differential energy spectra of low-energy /less than 8.5 MeV per nucleon/ heavy cosmic rays during solar quiet times.
21 p2755 A73-40509

Preferential acceleration of heavy nuclei on the sun
21 p2756 A73-40582

Biological effects due to single accelerated heavy particles and the problems of nervous system exposure in space.
22 p2814 A73-42181

The abundances of galactic cosmic-ray carbon, nitrogen, and oxygen and their astrophysical implications.
22 p2914 A73-43012

Study of low-energy heavy-nucleus track regression in plastic detectors /cellulose triacetate and polyethylene terephthalate/ and in low-sensitivity nuclear photoemulsion
23 p2981 A73-43567

Observation of cosmic-ray particles with Z greater than 35.
23 p3024 A73-43609

Observation of cosmic-ray particles with Z of 50 or greater and interpretation of the charge spectrum.
23 p3024 A73-43610

Primordial abundance values for heavy nuclei related to content of type 1 and 2 carbonaceous chondrites
23 p2950 A73-43752

HEAVY WATER

Rocket-based mass spectrometric measurements of midlatitude and north polar region ionospheric ion composition, discussing ionization of water and heavy water vapors
14 p1747 A73-29864

Dipole moment of water from Stark measurements of H₂O, HDO, and D₂O.
24 p3113 A73-44978

HEF [HIGH ENERGY FUELS]

U HIGH ENERGY FUELS

HEIGHT

On the determination of the height of the Ekman boundary layer.
06 p0720 A73-18326

Solar microwave emission height determination from latitude shift, noting precision comparable with observation based on rate of motion in longitude
12 p1536 A73-27842

HEISENBERG THEORY

Antenna effective area lower limit based on photon limited localizability and Heisenberg uncertainty principle, deriving directivity dependence on area
11 p1338 A73-25672

HELICAL ANTENNAS

Helical antenna for satellite transmission.
16 p1980 A73-33686

Numerical computation of the current distribution and far-field-radiation pattern of the axial-mode helical aerial.
16 p1985 A73-34020

HELICAL FLOW

Influence of dispersion on the nonlinear evolution of quasi-monochromatic spiral waves in a magnetoactive plasma
09 p1130 A73-22708

Spiral flows with multiple circulation in channels of simple shape
15 p1861 A73-31284

Leakage and frictional characteristics of turbulent helical flow in fine clearance.
17 p2152 A73-35001

[ASME PAPER 73-FE-1]
Velocity wave interaction and helical turbulence equilibrium spectra for two dimensional and three dimensional flow with quadratic energy and enstrophy states
20 p2549 A73-39812

On the stability of a class of plasma flows with helical flow and field lines.
22 p2892 A73-42351

Sound interaction with a helical flow contained in an annular duct with radial gradients of flow, density and temperature.
24 p3078 A73-44842

[AIAA PAPER 73-1010]
Investigation of the operation of a coaxial plasma injector employing preionization of the gas
09 p1124 A73-21880

HELICAL INDUCERS

Investigation of the operation of a coaxial plasma injector employing preionization of the gas
09 p1124 A73-21880

HELICAL WINDINGS

Fracture strength of helical-wound composite cylinders.
01 p0117 A73-11121

Magnetic surfaces decay for parametric instability in helical magnetic configuration, noting nonlinear equations of magnetic field lines
08 p0991 A73-20822

Optimal, elliptic and circular windings for superconducting nonferrous magnetic MHD generators, comparing cross sections
10 p1178 A73-24594

Operating properties of a helical microwave plasma source in high density high magnetic field regime. 11 p1407 A73-26562

Fracture strength of helically wound composite cylinders. 13 p1702 A73-29542

Construction techniques for an S-band high-power fluid-cooled TWT helix. 22 p2834 A73-42697

Helical wound composite cylindrical tube under pure bending, determining elastic response from boundary value problem solution 23 p3041 A73-43637

HELICOPTER ATTITUDE INDICATORS
U ATTITUDE INDICATORS
U HELICOPTERS

HELICOPTER CONTROL
A procedure for the barometric altitude control in the case of hovering devices and helicopters 03 p0249 A73-12916

Trends in helicopter guidance and control systems with bad weather capability. 03 p0340 A73-13921

Fiberglass reinforced composite material application to light weight ballistic damage tolerant military helicopter flight control components previously vulnerable to small arms fire 04 p0452 A73-14722

Perceptual considerations for a wide field of view, helicopter night landing system/HENILAS/. 05 p0543 A73-16705

Application of pole-placement theory to helicopter stabilization systems. 06 p0682 A73-18819

Russian book - Control of aircraft and helicopter flight. 07 p0850 A73-20381

Precision hover sensor for heavy-lift helicopter. 10 p1216 A73-23784

Ballistic-tolerant helicopter flight control components from plastic composite materials. 10 p1237 A73-23964

Theoretical and practical aspects of an automatic hover control system for an unmanned tethered rotor-platform. 10 p1175 A73-24009

Computerized adaptive flight control for helicopter dynamic systems based on identification and optimization methods 13 p1569 A73-28829

Helicopter automatic flight control system design, testing and development, noting stability and control augmentation and attitude retention units 13 p1656 A73-28903

Night search and rescue techniques over sea in poor visibility by helicopter, discussing automatic flight control systems, radar, plotting facility and pilot training 15 p1825 A73-31094

Russian book on civil aviation aircraft and helicopter equipment covering navigation, automatic control, electrical and oxygen systems and aircraft instruments 15 p1829 A73-31548

Automatic helicopter approach in poor visibility 15 p1910 A73-32465

Helicopter night and bad weather navigation aids, examining ground-independent navigation, low flight, obstacle warning, terrain detectors, blind landing and optoelectric sensing 17 p2206 A73-34258

Digital control of rotary wing aircraft landing approach based on spatially variable preassigned flight path [MBB-UF-1021] 17 p2207 A73-34486

Helicopter steep angle approach limits during instrument-guided landing comparison with classical ILS method, describing flight performance results [DGLR PAPER 73-026] 17 p2208 A73-34497

Solid state Digital Slip Sync Strobe/Camera Control System design for powered wind tunnel helicopter models testing 17 p2101 A73-34622

Redundant system design and flight test evaluation for the TAGS digital control system. 17 p2131 A73-35062

Integrated image and symbolic display hierarchy with increasing horizontal and vertical information content for superposition as helicopter aid in approach and precision hovering [AHS PREPRINT 724] 17 p2168 A73-35065

Reduction of helicopter control system loads with fixed system damping. [AHS PREPRINT 733] 17 p2105 A73-35069

Handling qualities comparison of two hingeless rotor control system designs. [AHS PREPRINT 741] 17 p2105 A73-35074

ABC helicopter stability, control, and vibration evaluation on the Princeton Dynamic Model Track. [AHS PREPRINT 744] 17 p2105 A73-35077

Control requirements for sling-load stabilization in heavy lift helicopters. 20 p2509 A73-39406

French automatic beam coupler system for V/STOL and helicopter low speed and low altitude instrument approach 21 p2737 A73-40975

Studies of pilot performance. III - Validation of objective performance measures for rotary-wing aircraft. 21 p2644 A73-41154

HELICOPTER DESIGN

The pressure-jet helicopter propulsion system. 02 p0130 A73-11858

A study of environmental degradation of adhesive bonded titanium structures in Army helicopters. 03 p0332 A73-13039

Advantage of reinforced plastics for helicopter blades and hubs 03 p0250 A73-13586

Russian book on aviation fundamentals covering aerodynamics and flight theory, designs, components, engines and instrumentation of aircraft, including helicopters, VTOL and STOL 09 p1032 A73-23224

Noise control modification to HH-43B helicopter for 50 percent reduction in forward flight octave band sound pressure level signature 11 p1304 A73-25383

Sensitivity of rotor blade vibration characteristics to torsional oscillations. [AIAA PAPER 73-404] 11 p1440 A73-25533

Twin-engined Anglo-French Lynx helicopter main rotor head, blade and drive train with conformal gearing, discussing design and material features 11 p1374 A73-25790

Fretting fatigue in titanium helicopter components. 11 p1383 A73-25837

Russian book on airplane and helicopter design and stability covering selection of wing /rotor/ configuration and power plant, subsystem design, strength, reliability, lifetime, etc 11 p1306 A73-26256

Italian contributions to present aerospace activities; Conference, 2nd, Turin, Italy, June 9, 10, 1972, Proceedings 12 p1548 A73-27376

Development program of medium range winged design helicopter, describing wing-fuselage structure, propulsion and power transmission systems and combustion, electrical and hydraulic plants 12 p1459 A73-27383

Helicopter rotor blade passing close to tip vortex, calculating fluctuating lift induced harmonic blade loads and generated cyclic banging noise 13 p1570 A73-29382

Three dimensional flow analysis for helicopter rotor aerodynamic design, considering Mach number, inclination, angle of attack, trajectory, Reynolds number and vortex shedding 16 p1962 A73-32973

Future technology and economy of the VTOL aircraft; International Helicopter Forum, 10th, Bueckeburg, West Germany, June 5-7, 1973, Proceedings 17 p2098 A73-34251

Future technical developments and efficiency of helicopters and their derivatives 17 p2098 A73-34252

An investigation of the flow field and drag of helicopter fuselage configurations. [AHS PREPRINT 700] 17 p2095 A73-35051

Aerodynamic design parameters effects on static performance of short ducted fans for helicopter tail rotor applications, comparing theoretical analysis and experimental results [AHS PREPRINT 701] 17 p2104 A73-35052

Heavy lift helicopter rotor blade design including airfoils, fiberglass skin, titanium spar, fail-safety and aerodynamic and structural features [AHS PREPRINT 710] 17 p2104 A73-35056

Westland Sea Lynx naval variant aircraft design and development for multiservice multirole application, emphasizing high reliability and maintenance ease requirements [AHS PREPRINT 711] 17 p2104 A73-35057

Helicopter design and production cost target and tradeoff considerations based on past programs, supplier quotations, government documents, estimating practices and functional requirements [AHS PREPRINT 712] 17 p2257 A73-35058

Sikorsky CH-53D helicopter main rotor head design, considering spherical elastomeric bearing, microstructural analysis, flight and ground fatigue tests and forging techniques [AHS PREPRINT 713] 17 p2104 A73-35059

Tradeoff studies for feasibility of multiblade ring rotor configuration for helicopter design, discussing ring drag [AHS PREPRINT 714] 17 p2104 A73-35060

The application of system analysis techniques for the solution of complex helicopter crew station design problems. [AHS PREPRINT 723] 17 p2105 A73-35064

An investigation of the vibratory and acoustic benefits obtainable by the elimination of the blade tip vortex. [AHS PREPRINT 735] 17 p2105 A73-35071

Handling qualities comparison of two hingeless rotor control system designs. [AHS PREPRINT 741] 17 p2105 A73-35074

Recognition and control of abusive machining effects on helicopter components. [AHS PREPRINT 750] 17 p2180 A73-35078

Low cost manufacturing methods for highly reliable ballistic-tolerant composite helicopter flight control components. [AHS PREPRINT 754] 17 p2180 A73-35082

Tactical aircraft guidance system for CH-47B helicopter utilizing fly by wire control system, describing design, display devices, flight instruments, computer configuration and crew duties [AHS PREPRINT 761] 17 p2210 A73-35084

Helicopter tail rotor teeter hinge with Teflon conical journal bearing allowing axial and radial preload inservice adjustment, discussing oscillatory loads and temperature effects [AHS PREPRINT 762] 17 p2180 A73-35085

U.S. Army helicopter vibration data for OH-6A, OH-58A, UH-1H and CH-54B models obtained from triaxial accelerometer locations, presenting spectral and statistical analyses [AHS PREPRINT 763] 17 p2106 A73-35086

Plastohydrodynamic principles applied to the design of helicopter components. [AHS PREPRINT 770] 17 p2248 A73-35088

T700 fuel and control system - A modern system today for tomorrow's helicopters. [AHS PREPRINT 771] 17 p2109 A73-35089

Helicopter power transfer systems analysis in terms of weight reduction and reliability improvement [AHS PREPRINT 773] 17 p2106 A73-35091

Helicopter turboshaft engine vibration reduction through engine-airframe interface compatibility design and torsional stability of drive trains with automatic fuel control [AHS PREPRINT 774] 17 p2106 A73-35092

The integration of NASTRAN into helicopter airframe design/analysis. [AHS PREPRINT 780] 17 p2106 A73-35093

A consistent crashworthiness design approach for rotary-wing aircraft. [AHS PREPRINT 781] 17 p2106 A73-35094

Performance, structural reliability and fatigue life of glass fiber-epoxy twin beam helicopter rotor blades [AHS PREPRINT 782] 17 p2106 A73-35095

CH-53D titanium main rotor blade, describing spar, fiberglass cover and honeycomb core, fabrication methods, ground and flight tests and vibrational characteristics [AHS PREPRINT 783] 17 p2106 A73-35096

Heavy lift helicopter rotor hub design and fatigue test technology, using fail-safe criteria, finite element analysis and fracture mechanics [AHS PREPRINT 784] 17 p2180 A73-35097

An advanced composite tailboom for the AH-1G helicopter. [AHS PREPRINT 785] 17 p2107 A73-35098

Helicopter and fixed wing aircraft design consideration comparison, examining maintenance and reliability requirements, rigid, hinged and tilted rotors and load characteristics 21 p2634 A73-40225

Effects of certain flight parameters and of certain structural parameters on helicopter main-rotor blade flutter 21 p2635 A73-41581

Helicopter transmission research. 22 p2798 A73-41750

HELICOPTER ENGINES

GTD-350 gas turbine engine for Soviet Mi-2 twin engine helicopter, describing compressor, combustion chamber, turbine, reduction gear, exhaust, starting, lubrication, deicing and fuel systems 14 p1785 A73-30450

Standard indoor method of collection and presentation of the bare turboshaft engine noise data for use in helicopter installations. [SAE ARP 1279] 16 p2046 A73-33020

Sand erosion tests and protective coatings for aircraft jet and turbojet engines and helicopter compressor airfoils 16 p2046 A73-33029

Turboshaft engine for 5-8 passenger single and twin engine commercial helicopter, discussing cost reduction design emphasis, gearbox module and particle separator 17 p2220 A73-34253

HELICOPTER PERFORMANCE

A probabilistic evaluation of helicopter lift capability. 10 p1175 A73-23775

Reliability analysis of helicopter mechanical transmission components and reduction gearboxes 11 p1306 A73-26596

Solid body on elastic supports as model for helicopter stability and nonlinear oscillations analysis 12 p1459 A73-27791

Pilot operation practices for helicopter noise level reduction, with emphasis on flight altitude increase and routing over noise insensitive areas 17 p2099 A73-34442

Helicopter steep angle approach limits during instrument-guided landing comparison with classical ILS method, describing flight performance results [DGLR PAPER 73-026] 17 p2208 A73-34497
Tail rotor performance in presence of main rotor, ground, and winds. [AHS PREPRINT 764] 17 p2106 A73-35087
Analysis of the use of an auxiliary wing on a helicopter 18 p2268 A73-37021
Management and control of military and commercial flight test programs at Bell Helicopter Company. 23 p3050 A73-44058

HELICOPTER PROPELLER DRIVE

The pressure-jet helicopter propulsion system. 02 p0130 A73-11858
Feasibility evaluation of graphite/epoxy composite materials to helicopter transmission housing. 10 p1238 A73-23969
Grease lubrication of helicopter transmissions. [ASLE PREPRINT 73AM-2A-1] 17 p2178 A73-34980
Elastohydrodynamic principles applied to the design of helicopter components. [AHS PREPRINT 770] 17 p2248 A73-35088
Increasing the critical rotational speed of the tail rotor drive shaft in SM-1 and SM-2 helicopters 24 p3057 A73-45195

HELICOPTER ROTORS

U ROTARY WINGS
HELICOPTER WAKES
Theoretical determination of the characteristics of helicopter rotors 09 p1027 A73-22205

HELICOPTERS

NT CH-46 HELICOPTER
NT CH-47 HELICOPTER
NT COMPOUND HELICOPTERS
NT H-53 HELICOPTER
NT H-56 HELICOPTER
NT HH-43 HELICOPTER
NT MILITARY HELICOPTERS
NT P-531 HELICOPTER
NT RIGID ROTOR HELICOPTERS
NT S-61 HELICOPTER
NT UH-1 HELICOPTER

Helicopter internal and external noise level measurements under various flight conditions, obtaining noise radiation directivity patterns via time measuring trajectory equipment [ONERA, TP NO. 1136] 01 p0004 A73-10241
Review of New York Airways helicopter operations. [AIAA PAPER 73-25] 06 p0647 A73-17614
Russian book - Methods and equipment for in-flight aircraft strength tests. 07 p0777 A73-20376

The utility of a low flying aircraft or helicopter when collecting ground data for regional resource surveys. 08 p0961 A73-21710

Dynamic analysis of helicopter structures 09 p1031 A73-22206

Doppler TACAN navigation system for helicopters obtaining data through computer display method 10 p1247 A73-24475

Prediction for a park of helicopters of the same type 12 p1561 A73-27077

Helicopter use for urban transportation to meet economic growth needs and alleviate traffic congestion, considering IFR equipment and noise reduction 14 p1712 A73-30470

VTOL and helicopter design considerations, including nonsymmetrical rotor flow characteristics, rotor types, airspeed capacities, compound helicopters, tilt wing and tilt rotor aircraft 17 p2099 A73-34259

Helicopters for business executive transport between cities or to isolated locations, police use, ambulance service, etc 17 p2256 A73-34445

Helicopter operations in London area, describing controlled airspace, helicopter routes and heliport approach and takeoff procedures 17 p2206 A73-34446

The application of circulation control aerodynamics to a helicopter rotor model. [AHS PREPRINT 704] 17 p2104 A73-35055

Electronic location finder radio antenna homing system for helicopter search and rescue of downed air crewmen [AHS PREPRINT 720] 17 p2116 A73-35061

Helicopter engineering applications of antiresonance theory, showing eigenvalue nature and matrix iteration determination of antiresonances [AHS PREPRINT 736] 17 p2105 A73-35072

The human side of quality assurance [as viewed from helicopter manufacturing experiences]. [AHS PREPRINT 751] 17 p2180 A73-35079

VTOL applications in civil aviation, discussing safety, noise reduction, fatigue life, industrial applications, economic factors, short haul utilization and wind tunnel tests 19 p2384 A73-37813

On the aerodynamic damping moment in pitch of a rigid helicopter rotor in hovering. I - Experimental phase. 19 p2387 A73-38281

Perceived noise level ratings for helicopter noise, discussing blade slap, tail rotor whine, broadband noise and PNL rating shortcomings 22 p2798 A73-41708

Helicopter noise experiments in an urban environment. 22 p2800 A73-42944

HELIOCENTRIC ORBITS

U SOLAR ORBITS

HELIOGRAPHS

U SPECTROHELIOGRAPHS

HELIOGRAPHY

U SPECTROHELIOGRAPHS

HELIOMAGNETISM

U SOLAR MAGNETIC FIELD

HELIOMETERS

NT PYROHELIOMETERS

Long term heliometric Moestring crater distance measurements applied to moon libration relationship to lunar radius 16 p2064 A73-33775

HELIOMETRY

U HELIOMETERS

U PYROHELIOMETERS

HELIOS PROJECT

Scientific mission and German and U.S. plans/design for Helios cooperative solar probe, stressing advanced technology requirements 01 p0110 A73-11103

The development of the heat control system of the Helios solar probe [DGLR PAPER 72-102] 02 p0227 A73-11652

Solar cell generator design for Helios solar probe, considering thermal stresses at sun proximity and sufficient power generating capacity at orbital apogee [DGLR PAPER 72-091] 02 p0131 A73-11663

Helios solar probe structural adapter design for linking to booster rocket end stage, investigating orthotropic cylindrical shell carrying capacity [DGLR PAPER 72-101] 02 p0227 A73-11685

Helios A and B interplanetary exploration objectives, considering solar plasma, high energy particles and interplanetary dust characteristics [DGLR PAPER 72-068] 02 p0227 A73-11688

The onboard data processing system of the Helios probe [DGLR PAPER 72-092] 02 p0228 A73-11700

German-American cooperative solar probe project Helios, discussing design features, mission objectives and project development status [DGLR PAPER 72-104] 02 p0228 A73-11706

Solar cells and generator technology for the Helios sun probe. 03 p0256 A73-14235

Recent development results on the HELIOS S-band command receiver. 09 p1057 A73-23416

The German telecommand ground station for HELIOS - A new concept. 09 p1070 A73-23418

A telecommunications link model for deep space - With applications to the HELIOS probe. 09 p1058 A73-23419

Micrometeoroid mass, velocity and composition from Heos 2 and Helios satellite experiments, using hypervelocity dust particle impacting plasma emission 10 p1218 A73-24119

The contribution of the German Telecommand Station to the overall command safety in the Helios project. 14 p1727 A73-30101

HELIOS SATELLITES
Ground control facilities and organization of Helios space probe mission and flight operations system based on U.S.-German cooperation 03 p0381 A73-13297

German command station for Helios solar probe, discussing antenna design, transmitter parameters, back-up operation and compatibility with deep space network [DFVLR-SONDDR-263] 13 p1598 A73-29275

Helios probe design for solar wind acceleration mechanism, magnetic and electric fields, interplanetary dust and cosmic radiation 21 p2780 A73-40449

HELIPORTS

AIR-CO-SCAN landing system for STOL and heliports, combining localizer and glide control functions in 20 by 20 deg approach window 15 p1910 A73-32470

Social acceptability of heliports particularly from the standpoint of noise. 17 p2146 A73-34441

Feasibility of downtown heliport facilities in terms of public concerns including fear, noise and economics 17 p2146 A73-34443

City center heliport design and location for scheduled intercity helicopter services, discussing terminal facilities, economic factors, elevated sites, etc 17 p2146 A73-34444

Helicopter operations in London area, describing controlled airspace, helicopter routes and heliport approach and takeoff procedures 17 p2206 A73-34446

HELITRONS

Low pressure plasma equilibrium in helitron device with stellarator confinement system, calculating plasma pressure from MHD equations 04 p0479 A73-15039

HELIUM

NT HELIUM ATOMS

NT HELIUM FILM

NT HELIUM IONS

NT HELIUM ISOTOPES

NT LIQUID HELIUM

NT LIQUID HELIUM 2

Evolutionary sequences for massive stars with various initial chemical compositions, studying semiconvection effects on core helium burning star distribution in H-R diagram 01 p0104 A73-11037

Gas-liquid hydrogen mixture and helium adiabatic model of Jupiter temperature and pressure distribution, estimating planet center temperature 01 p0107 A73-11324

Massive stars evolution in hydrogen and helium burning phases, taking into account mass loss from light pressure in optically thick media 02 p0224 A73-12801

A search for He-weak stars in very young clusters. 03 p0372 A73-13227

Thermal pulses in helium shell-burning stars. 04 p0499 A73-15364

Auroral He 4 precipitation flux measurements by exposed metal foils recovered from rocket flights 04 p0443 A73-15534

Tangential slot injection of carbon dioxide and helium into a supersonic air stream. [ASME PAPER 72-WA/FE-37] 04 p0435 A73-15854

He odd parity states computed via Hylleraas trial wave function with nonlinear parameters, considering mass-polarization correction and electron transitions 05 p0600 A73-16599

On the location of pulsational blue edges and estimates of the luminosity and helium content of RR Lyrae stars. 05 p0625 A73-17335

Experimental investigation of hypersonic helium flow around sharp and blunted cones in the presence of strong injection 06 p0643 A73-17466

Thermoregulatory reactions of animals in a helium-oxygen medium 06 p0650 A73-17695

Solid/vapour heat transfer in helium at low temperatures. 07 p0922 A73-20412

Spectrophotometric observation of He-rich subluminescent subdwarf peculiar O-type star CPD-31 1701, noting spectrum dominance by extremely stark-broadened He lines 08 p1003 A73-20894

He red giants models with degenerate C-O cores, He burning shell sources and He-rich envelopes, noting stellar luminosity 08 p1004 A73-20903

Thermoregulatory reactions of rats in a nitrogen and helium-diluted hypoxic atmosphere 08 p0929 A73-20979

Pulsed and CW water vapor lasers, investigating He addition effects on time-varying gas temperature and power output [AD-760377] 09 p1091 A73-22082

Chemical composition of classical Cepheids in the Galaxy and Magellanic Clouds 10 p1273 A73-23705

Electron impact excitation rates calculation for He I and II transitions, comparing measured, theoretical and semiempirical impact cross sections 10 p1251 A73-24133

Observations of the Helium II 304-A and Helium I 584-A atmospheric dayglow radiation. 10 p1213 A73-24735

Solar He abundance from neutrino flux, He lines intensity in prominences and chromosphere spectra, solar cosmic rays and solar wind He/H ratio 10 p1284 A73-24780

Auroral He precipitation flux and charge state measurements for auroral ions source location by comparison with ionospheric and solar wind ion abundances 10 p1215 A73-24783

Nonequilibrium radiative and inelastic collisional transitions structuring of ionizing shock waves in He and Ar 11 p1449 A73-25253

Thermodynamic parameters for metallic hydrogen-helium alloy of Saturn and Jupiter interiors, using Monte Carlo chains and dielectric function theory 11 p1420 A73-25888

Phase equilibria in fluid mixtures at high pressures - The He-CH4 system. 11 p1399 A73-25889

Helium-cold induced hypothermia in the white rat. 12 p1461 A73-26975

Chemical composition of stars in globular clusters and the morphological characteristics of their horizontal branches 12 p1546 A73-27852

Secular stability of an 8 solar mass star during central helium burning. 13 p1685 A73-29355

Determination of van der Waals broadening of Fe I emission lines induced by neutral He 13 p1685 A73-29360

On convection and gravitational layering in Jupiter and in stars of low mass. 14 p1797 A73-30009

Jupiter He abundance determination methods, considering mean density, spectral line broadening and stellar occultations with emphasis on far IR emission 14 p1799 A73-30533

Scanner observations of hot helium-carbon stars. 15 p1932 A73-31269

Thermal instability of the helium-burning shell in massive stars. 15 p1936 A73-31557

Quantitative analysis of the spectrum of beta Lyr. I. Variation of certain hydrogen and helium emission lines 16 p2057 A73-32710

Thermospheric wind effects on the distribution of helium and argon in the earth's upper atmosphere. 16 p2004 A73-34441

Figures and internal structure of hydrogen-helium planets 16 p2069 A73-33838

Models comparison for heavy elements segregation mechanism from gaseous hydrogen and helium for terrestrial planets formation from primordial granular matter 17 p2228 A73-34422

Quantum scattering theory of rotational relaxation and spectral line shapes in H₂-He gas mixtures. 17 p2119 A73-35175

Velocity distribution in hypersonic helium flow near the leading edge of a flat plate. 18 p2262 A73-36242

[AIAA PAPER 73-691] A unique method of leak-rate measurements. 18 p2316 A73-36714

Chemical composition of the classical Cepheids in the Galaxy and the Magellanic Clouds. 18 p2354 A73-36730

The He I lambda 5876 line in O-star spectra. 18 p2356 A73-36973

Structure of helium burning regions in stars - Dependence on molecular weight and burning rates. 19 p2483 A73-37560

Evidence for an interstellar or interplanetary source of diffuse He I 584 A radiation. 19 p2475 A73-37629

Gas management system for control, bleeding, evacuating and radiological and pressure monitoring of He atmosphere in multihundred watt heat source 19 p2457 A73-38428

Venus topside ionosphere He content estimated from ionization profiles and discovery of radioactive materials in crust 20 p2604 A73-38942

Chemical composition of globular-cluster stars and the form of the horizontal branch. 20 p2608 A73-39226

Complete hydrogen and helium particle spectra from 30- to 60-MeV proton bombardment of nuclei with A = 12 to 209 and comparison with the intranuclear cascade model. 21 p2744 A73-41019

Design of a piston-driven shock tube 21 p2675 A73-41552

Liquid helium cryopump extension to gaseous hydrogen and helium pumping via adsorption on argon cryodeposit, obtaining gases partial pressures evolution 22 p2886 A73-41871

Observation of the star gamma-Cassiopeia of the Be spectral type by Fourier spectrometry from 1 to 2.5 micron 22 p2908 A73-42354

Estimate of extreme ultraviolet dayglow of helium in the Martian atmosphere. 22 p2909 A73-42485

Measurements of hydrogen-helium radiation at shock-layer temperatures appropriate for Jupiter entry. 22 p2938 A73-42993

Measurements of the upper and lower level lifetime in He-Ne lasers. 22 p2871 A73-43086

Low-pressure gas breakdown with CO₂ laser radiation. 24 p3095 A73-44589

Critical two phase He flow rates prediction based on homogeneous thermal equilibrium model, Henry-Fauske data and empirical correction factor curve 24 p3077 A73-44823

The effect of the Gum Nebula on soft X-rays from galactic sources. 24 p3138 A73-45044

Resonance scattering from interstellar and interplanetary helium. 24 p3140 A73-45188

HELIUM AFTERGLOW

Electron-ion recombination in cryogenic helium plasmas. 01 p0084 A73-10565

Recombination of electrons with positive ions of the H₃O⁺/H₂O⁺ series. 01 p0014 A73-10901

Velocity distribution of plasma electrons in the negative H₂- and He-glow with superimposed longitudinal magnetic field. 04 p0477 A73-14897

Study of excitation transfer in a flowing helium afterglow pumped with a tuneable dye laser. I - Measurement of the rate coefficient for selected quenching reactions involving He(5-3P). 05 p0600 A73-16044

Study of excitation transfer in a flowing helium afterglow pumped with a tuneable dye laser. II - Measurement of the rate coefficient for the rotational relaxation of He(2/3p 3Pi-g). 05 p0600 A73-16045

HELIUM ATOMS

Two new He I lines in the spectra of B-type supergiants. 03 p0371 A73-13218

Investigation of molybdenum after exposure to single-charge helium atom radiation 06 p0707 A73-17909

The plane-wave method in the study of helium atoms physisorbed on graphite 07 p0843 A73-20000

Optical orientation of metastable He-3 atoms and its influence on the electron density and on the emission of helium atoms in a plasma 10 p1257 A73-24755

Interplanetary radial gradients of galactic cosmic ray protons and helium nuclei - Pioneer 8 and 9 measurements from 0.75 to 1.10 AU. 14 p1786 A73-29951

Ionization and relative abundance of hydrogen and helium atoms in filaments of the Crab Nebula 16 p2057 A73-32712

Experimental investigation of collisions of He atoms in the ground state and the 2/3S/ metastable state 19 p2462 A73-37248

HELIUM FILM

Temperature dependence of the accommodation coefficient of liquid-helium film. 10 p1249 A73-24341

Heat transfer during helium boiling in narrow channels of different orientations 13 p1661 A73-29405

HELIUM IONS

Propagation of Pcl micropulsations in a proton-helium magnetosphere. 03 p0298 A73-12883

On the 4686-A He II line intensity in H II regions and the cosmic ray flux. 03 p0361 A73-13220

Observations of the He II 304-A radiation in the night sky. 07 p0869 A73-19232

Interaction of singly charged interstellar helium ions with the solar wind. 07 p0870 A73-19253

Electron loss by helium atoms passing through inert gases and molecular hydrogen, nitrogen, and oxygen. 07 p0853 A73-19334

Calculated distributions of hydrogen and helium ions in the low-latitude ionosphere. 07 p0818 A73-20052

Intermolecular potential energy curve crossing probabilities and associated phases determination for low energy elastic scattering cross section of He cations by Ne, noting rainbow effect 10 p1250 A73-23670

Low-energy elastic differential scattering of He⁺/++ by He. 15 p1916 A73-32290

Optical study of charge exchange collisions between He⁺ and CO₂. 16 p2039 A73-33675

Cavity perturbation technique for determining the presence of molecular ions of helium in a dc discharge plasma. 19 p2469 A73-37901

On the backscatter of solar He II, 304 A radiation from interplanetary He⁺/+. 23 p3024 A73-43695

Detection of phosphorus in heavily diffused silicon by He⁺/+ backscattering. 24 p3120 A73-45262

HELIUM ISOTOPES

Earth atmosphere He isotopes abundance based on calculation of ionization rates and solar wind interaction during geomagnetic dipole reversal 02 p0156 A73-11741

Galactic cosmic radiation He 3 and deuterium abundances interpretation from production cross sections and reaction kinematics 05 p0609 A73-16741

He 3 burning burst complication of mixing in solar core for solar luminosity variations resulting from central temperature decrease 05 p0611 A73-17187

The nuclear resonance in liquid helium three at very low temperatures 08 p0987 A73-20647

The nuclear resonance in a hypothetical superfluid phase of helium three 08 p0989 A73-21491

Solar neutrino problem - No low energy He-3 + He-3 resonance. 08 p1000 A73-21530

Isotopic composition of helium in solar corpuscular fluxes 10 p1266 A73-23912

Spallation production of He-3, Ne-21, and Ar-38 from target elements in the Bruderheim chondrite. 10 p1277 A73-24103

Hydrogen and helium isotopes differential energy spectra during solar flare particle acceleration related to nuclear interaction processes 11 p1414 A73-26610

Liquid He 3 superfluidity near absolute zero, noting two solid and four liquid phases within millidegrees 14 p1775 A73-30617

Role of laser radiation self-focusing during breakdown in liquid He4 15 p1884 A73-31701

Superfluidity of the Fermi component in a Fermi-Bose gas and in He-3-He4 solutions 16 p2038 A73-34067

The A, B, C's of trapped helium, neon, and argon in meteorites and lunar samples. 17 p2228 A73-34417

He, Ne and Ar in chondritic Ni-Fe as irradiation hardness sensors. 17 p2120 A73-35801

Isotopes of helium and hydrogen in solar corpuscular fluxes 21 p2757 A73-40593

Variability of the He-3 and Ne-21 production rates in ordinary chondrites. 21 p2771 A73-41008

Some experiments on the influence of surface treatment on the Kapitza conductance between copper and He4 at temperatures from 1.2 to 2.0 K. 21 p2741 A73-41105

Energy spectra of localized elementary excitations for dilute solutions of He 3 atoms in superfluid He 4 using Feynman type wave function, considering Raman scattering 23 p3007 A73-44173

Investigation of anomalously fast stars of early spectral class. III - Search for the He-3 isotope 23 p3036 A73-44244

Helium in the terrestrial atmosphere. 24 p3107 A73-44948

HELIUM PLASMA

Electron-ion recombination in cryogenic helium plasmas. 01 p0084 A73-10565

Spatial plasma echoes of ion acoustic waves in low pressure He and Ne discharges in anode direction 03 p0348 A73-14622

Propagation of ion acoustic waves in a weakly ionized plasma 03 p0348 A73-14625

Plasma parameters in gas discharges for positive-column He-Ne/+ lasers. 06 p0701 A73-18360

Charged-particle lifetime measurements in a helium plasma 07 p0855 A73-19284

Gas dynamic characteristics of the helium two stage shock tube for MHD power generation experiments. 07 p0808 A73-20117

Temperature determination of rare gas plasmas seeded with alkali, considering oscillator forces of K excited states in He plasma 08 p0990 A73-20649

Heating of laser-induced plasmas in helium. 09 p1125 A73-21998

Local transient phenomena induced in an inert gas plasma by a short pulse. 10 p1257 A73-24626

Lifetime of charged particles in a helium plasma. 13 p1665 A73-28684

Experimental study of a conical theta-pinch plasma gun. 14 p1779 A73-29928

Measurements of the electronic recombination coefficient in a helium plasma jet. 14 p1780 A73-30245

Recombination of doubly ionized atoms in the afterglow of a helium plasma produced by laser. 15 p1915 A73-31675

Influence of atom-atom collisions on electron density decay in laser-produced helium plasmas. 16 p2041 A73-32944

Decay of a high temperature helium plasma - Validity of local thermodynamic equilibrium and estimation of recombination coefficients for He⁺/+, He⁺/+, and He²⁺/+. 16 p2043 A73-33867

- Investigation of plasma inhomogeneities between coaxial electrodes in a magnetic field
17 p2214 A73-34128
- Electron temperature and density in the He-Cd12 positive column used for an I/+ laser.
17 p2186 A73-35798
- Streaming plasma interaction with variable longitudinal magnetic fields.
19 p2465 A73-37171
- Afterglow studies in helium-cesium mixtures.
21 p2745 A73-40223
- Measurement of turbulent HF fields in a high-current rectilinear gas discharge from the intensity of forbidden HeI lines
23 p3011 A73-43669
- Some electric and spectroscopic properties of the radiofrequency plasma in a steady magnetic field.
23 p3012 A73-43831

HELIUM 2

U HELIUM ISOTOPES

U LIQUID HELIUM

HELIUM 3

U HELIUM ISOTOPES

HELIUM 4

U HELIUM ISOTOPES

HELIUM-NEON LASERS

- Laser frequency fluctuations due to mechanical vibrations.
03 p0319 A73-14451
- Light speed determination methods, considering He-Ne laser modulation at microwave frequency via intracavity electro-optic KDP crystal
05 p0575 A73-16341
- He-Ne laser beam intrinsic third order intensity statistical correlation function measurement by digital technique for comparison with calculations
06 p0699 A73-17520
- Emission risetime fluctuations in a gas laser with nonlinear resonant absorption
06 p0700 A73-18104
- Pressed cathodes made from barium scandate and refractory metals mixture, investigating operation in plasma discharge of He-Ne lasers
06 p0703 A73-18601
- Comparative study of reflectivity measurements performed in the visible and infrared wavelengths.
07 p0824 A73-19945
- Analysis of He-Ne laser surface reflections from an off-axis parabolic mirror.
08 p0974 A73-21032
- Dependence of He-Ne laser output power on discharge current, gas pressure and tube radius.
08 p0976 A73-21462
- Discharge current dependence of saturation parameter of a He-Ne gas laser.
08 p0976 A73-21463
- Holographic method of controlling the spatial-angular characteristics of laser emission
09 p1090 A73-21951
- Demonstration of the transmission and reception of modulated oscillations with a helium-neon laser beam
09 p1097 A73-23328
- Some characteristics of transition processes in He-Ne lasers operating at the 0.63-micron wavelength
10 p1227 A73-24073
- Frequency generators performance with stability associated with atomic/molecular transition, considering rubidium and hydrogen clocks and He-Ne lasers
10 p1219 A73-24396
- Spectroscopic study of the vibrational-energy dissipation of the I2 molecule excited by a He-Ne laser
10 p1228 A73-24577
- Operational features of an FM rangefinder employing a gas laser
10 p1229 A73-24602
- Design of an R.F. excited helium-neon visible gas laser and study of the optimal conditions for gas mixtures and pressures.
10 p1230 A73-24923
- Influence of elastic collisions on the intensity of natural oscillations in a He-Ne laser
11 p1376 A73-25432
- Influence of laser field polarization on nonlinear interference effects.
11 p1377 A73-26180
- Application of longitudinal multimode laser coherence properties to increase the holographic depth of field.
12 p1504 A73-26830
- Coherent optical signal supergenerative amplification in Q switched gas laser, calculating sensitivity of He-Ne laser light amplifier
13 p1627 A73-28663
- Use of narrow resonances in methane for frequency stabilization of a 3.39-micron He-Ne laser
13 p1627 A73-28763
- Absorption of He-Ne laser radiation by an iodine molecule beam
13 p1627 A73-28773
- Spatially filtered helium-neon laser link operation parallel to IR radiometer for real time atmospheric propagation monitoring over short path
13 p1661 A73-29328

- Amplitude characteristics of a helium-neon laser at the 0.63-micron wavelength in the region of strong interaction between two modes.
13 p1630 A73-29446
- Influence of atmospheric parameters on the wavelength of single-frequency laser radiation
14 p1756 A73-30023
- Method for measuring the collision-induced broadening of spectral lines
15 p1884 A73-31702
- A simple, single-frequency He-Ne laser for practical uses.
15 p1885 A73-32018
- Investigation of longitudinal-mode selection and frequency stabilization of the emission from a helium-neon laser with a ring resonator
15 p1886 A73-32335
- Stability, reproducibility, and absolute wavelength of a 633-nm He-Ne laser stabilized to an iodine hyperfine component.
17 p2185 A73-35424
- Quasi-periodic noises in a He-Ne laser.
19 p2438 A73-38166
- Measurements of the log-irradiance distribution of a laser wave propagated through the turbulent atmosphere.
19 p2405 A73-38222
- Two-photon time distributions in mixed light beams.
20 p2570 A73-38615
- Third- and higher-order intensity correlations in laser light.
20 p2571 A73-38630
- Frequency modulation of a gas laser
20 p2574 A73-39730
- Photoelastic investigation of dynamic stress conditions involving rapidly varying principal stress directions
21 p2695 A73-39965
- Statistical effects in the transient response of a He-Ne laser with a given initial photon distribution
21 p2714 A73-40568
- A study of the effect of the number of axial modes of a laser on its degree of coherence
21 p2714 A73-40748
- Nonstationarity of the three-mode regime in a gas laser in the case of mode-frequency symmetry
22 p2870 A73-42388
- Measurement of the natural linewidth of a traveling wave neon-helium laser in the 0.63-micron range
22 p2870 A73-42411
- Longitudinal alignment of working levels in a helium-neon laser
22 p2870 A73-42412
- On the thermomdiffusion effect in the CW He-Ne lasers.
22 p2871 A73-43080
- High order nonlinear effects in a gas laser - Saturation anomaly observable on a J equals 1 - J equals 2 transition
22 p2871 A73-43084
- CW single mode He-Ne laser intensity fine structure fluctuations correlation measurement near threshold by digital correlator, obtaining higher order relaxation rates
22 p2871 A73-43085
- Low power He-Ne laser beam intensity modulation in thermal medium, applying to temperature fluctuation detection in transparent materials
22 p2872 A73-43154
- Investigation of the influence of a nonuniform high-frequency electric field on the parameters of a helium-neon laser
23 p2987 A73-43575
- Minimum detectable frequency deviations in output of He-Ne laser stabilized by external methane absorption cell
23 p2989 A73-44366
- Measurement of optically induced refractive-index changes with sharp edged illumination pattern.
23 p2984 A73-44371
- Fluctuations of the radiation rise time in a gas laser with nonlinear resonant absorption.
24 p3095 A73-44494
- Measurement of the gain distribution in a helium-neon laser /0.63-micron wavelength/ cell during high-frequency pumping
24 p3096 A73-44956
- Laser interferometer for displaying small rapid motions
24 p3092 A73-45468
- Longitudinal inhomogeneity of gain in the active element of a helium-neon laser pumped by direct current
24 p3097 A73-45517

HELIX TUBES

U TRAVELING WAVE TUBES

HELIXES

U CURVES [GEOMETRY]

HELMETS

- Protective helmets performance evaluation for design optimization, considering failure analysis from aircraft accident reports
16 p1973 A73-32655

- A comparison and analysis of head sizes of Navy aircrew to the standard anthropometric data.
16 p1974 A73-32656
- Light weight impact protective helmet shell materials and designs, noting E- or S-glass and polyimide resin for oxygen rich space station/shuttle applications
16 p2027 A73-32677
- Helmets effectiveness evaluation from acceleration and impact tests, discussing test criteria and civilian and military standards
16 p1975 A73-33132
- Technique for extemporaneously obtaining an electroencephalogram
18 p2286 A73-36937

HELMHOLTZ EQUATIONS

- The Kelvin-Helmholtz instability in type-I cometary tails
01 p0102 A73-10946
- Approximate reduction of the equations of elasticity theory and electrodynamics for inhomogeneous media to Helmholtz equations
01 p0077 A73-10959
- Axisymmetric triangular finite elements for the scalar Helmholtz equation.
09 p1120 A73-22392
- Kelvin-Helmholtz instability in type I comet tails.
09 p1148 A73-22741
- Approximate reduction of the equations of the theory of elasticity and electrodynamics for inhomogeneous media to the Helmholtz equations.
12 p1524 A73-27535
- Point matching /collocation/ computation of transverse resonances by complex valued solutions of Helmholtz equation with Neumann or Dirichlet problems, applying to electromagnetic waveguides
13 p1581 A73-28076
- Resonant scattering from inhomogeneous nonspherical targets.
14 p1775 A73-30906
- Theory of mountain lee waves for an arbitrary-profile elevation
15 p1905 A73-31818
- A note on the use of the finite difference method for predicting steady state sound fields.
16 p2036 A73-33217
- Calculation of reflection and transmission coefficients for a class of one-dimensional wave propagation problems in inhomogeneous media.
19 p2459 A73-37587
- Scalar waves in the mixmaster universe. I - The Helmholtz equation in a fixed background.
21 p2766 A73-40317
- Integral representations for solution of mixed boundary value problems for generalized axisymmetric Helmholtz equation, considering Sommerfeld half plane and transonic flow problems
21 p2727 A73-41017
- Relation between the fundamental solutions in cylindrical and spherical coordinates /with identical coordinate origins/ for certain equations of mathematical physics
21 p2753 A73-41025
- The exterior Neumann problem for the Helmholtz equation.
24 p3112 A73-45470

HELMHOLTZ VORTICITY EQUATION

- Helmholtz-Rayleigh instability of nondivergent horizontal flows in a barotropic atmosphere
04 p0441 A73-15287

HEMATITE

- The origin and stability of lunar goethite, hematite and magnetite.
05 p0618 A73-16836
- Atmospheric moisture effects on hematitic sandstone, pyrite and galena electrical resistivity, noting comparison with semiconductors and insulators
13 p1609 A73-28847
- Electron transitions in interstellar dust 4430 A line, indicating ferric oxide /alpha-hematite/ in type I super-novae
24 p3138 A73-44990

HEMATOCRIT

- Investigation of some blood characteristics in albino rats subjected to 60-day hypokinesia
15 p1834 A73-31502
- Model experiments on apparent blood viscosity and hematocrit in pulmonary alveoli.
24 p3064 A73-45064

HEMATOCRIT RATIO

- Red cell volume with changes in plasma osmolality during maximal exercise.
18 p2277 A73-36654
- Erythropoietin production in dogs exposed to high altitude and carbon monoxide.
20 p2513 A73-39599
- The specific resistance of blood at body temperature.
22 p2807 A73-42670
- Erythrocyte volume in acidified venous blood from exercising limbs.
24 p3062 A73-45557

HEMATOLOGY

- Peripheral blood composition changes in cosmonauts during 18- and 24-day space flights
12 p1463 A73-27710

A method for calculating the sedimentation characteristics of particles in linear dextrane-density gradients and its application to the separation of red blood cells according to the sedimentation rate
13 p1578 A73-28476

Human hematologic responses to 4 hr of isobaric hyperoxic exposure /100% oxygen at 760 mm Hg/.
14 p1714 A73-29751

Hematological, biochemical, and immunological studies during a 14-day continuous exposure to 5.2% O₂ in N₂ at pressure equivalent to 100 FSW /4 ata/.
18 p2278 A73-36794

Changes in the peripheral blood of the rat exposed to microwave radiation /2400 MHz/ in conditions of chronic exposure.
21 p2645 A73-41159

Erythrocyte volume in acidified venous blood from exercising limbs.
24 p3062 A73-45557

HEMATOPOIESIS
Erythropoietin production in dogs exposed to high altitude and carbon monoxide.
20 p2513 A73-39599

HEMATOPOIETIC SYSTEM
Differentiations and maturations in red and white blood cells construction in red bone marrow, noting hematopoietic system formation from single source cell
06 p0649 A73-17473

Role of adrenalin and alpha-receptor deactivation in reactions of hemopoietic organs to stress
07 p0781 A73-19644

Proliferative activity of bone marrow cells in dogs exposed to chronic and repeated acute gamma irradiation
12 p1463 A73-27708

Peripheral blood composition changes in cosmonauts during 18- and 24-day space flights
12 p1463 A73-27710

HEMISPHERE CYLINDER BODIES
Stagnation-point free-convection film boiling on a hemisphere.
05 p0638 A73-16353

Nose pressure distribution and separation on an inclined axisymmetric body.
05 p0533 A73-17123

HEMISPHERES
Natural frequencies of a hemispherical shell.
03 p0395 A73-14474

Hemispherical reflectivity and transmissivity of an absorbing, isotropically scattering slab with a reflecting boundary.
08 p1025 A73-21643

The geometrical factor of large aperture hemispherical electrostatic analyzers.
20 p2564 A73-38877

HEMISPHERICAL SHELLS
Axisymmetric buckling of rigidly clamped hemispherical shells.
11 p1447 A73-26648

Thin clamped hemispherical shell nonlinear dynamic response to suddenly applied pressure, deriving finite difference formulation of fourth order coupled nonlinear equations
18 p2362 A73-36310

Axisymmetrical bending of circular plates and shallow spherical cupolas with allowance for physical and geometrical nonlinearities
20 p2618 A73-39310

Exact hydroelastic solution for an ideal fluid in a hemispherical container.
22 p2843 A73-42631

HEMODYNAMIC RESPONSES
Effect of interstitial edema on distribution of ventilation and perfusion in isolated lung.
01 p0008 A73-10167

Renal vascular response to saline infusion from radioactive Xe washout and sodium excretion concentration data
01 p0008 A73-10170

High altitude adaptation in mountain inhabitants of Tian Shan and Pamir, discussing effects on hemodynamic and pulmonary functions
02 p0133 A73-11922

Cardiocirculatory adaptation to chronic hypoxia. III - Comparative study of cardiac output, pulmonary and systemic circulation between sea level and high altitude residents.
04 p0410 A73-15523

Cerebral circulation alteration during hypothermia
05 p0541 A73-16698

Cardiovascular system reactions to alternating transverse accelerations in man
06 p0650 A73-17687

Application of multichannel rheography to physiological studies on a centrifuge
06 p0657 A73-17693

The contractile function of the myocardium in two types of cardiac adaptation to a chronic load.
07 p0781 A73-19931

Time course of pulmonary vascular response to hypoxia in dogs.
07 p0782 A73-20168

A comparison between the effects of dynamic and isometric exercise as evaluated by the systolic time intervals in normal man.
07 p0784 A73-20369

Analysis of some mechanisms of human stability to decompression of the lower portion of the body
08 p0930 A73-20987

Role of the sympathetic nervous system in supporting cardiac function in essential arterial hypertension.
08 p0930 A73-21015

Cardiovascular changes in middle-aged men during two years of training.
08 p0934 A73-21504

Changes in hemodynamics and efferent sympathetic pulsation during pressor cardiovascular reflexes under conditions of acute hypoxic hypoxia
09 p1039 A73-22365

Red cell flexibility and pressure-flow relations in isolated lungs.
09 p1041 A73-22927

Immediate hemodynamic effects of cardiac angiography in man.
10 p1179 A73-23841

Isometric effects on treadmill exercise response in healthy young men.
10 p1179 A73-23842

Effect of respiration stabilization on hemodynamic reactions during acute hypoxic hypoxia
10 p1180 A73-23938

Effect of electrostimulation on hemodynamic shifts during prolonged hypokinesia
10 p1180 A73-23940

Vestibular stresses effects on systemic and cerebral hemodynamics, considering human acceleration adaptation and compensation mechanisms
12 p1463 A73-27714

Hemodynamics alteration caused by acute hypoxia in animals with denervated carotid sinuses
13 p1574 A73-28350

Changes in blood-flow distribution during acute emotional stress in dogs.
13 p1576 A73-28533

Effect of the Valsalva maneuver on tolerance to +Gz acceleration.
14 p1714 A73-29754

Some compensatory adjustment reactions of the blood circulation system in pulmonary pathology
15 p1835 A73-31623

Nutritional circulation in the heart. IV - Effect of calcium chloride and potassium chloride on myocardial hemodynamics and clearance of rubidium-86.
16 p1973 A73-33990

Effectiveness of some hemodynamic indices in the detection of vestibulo-vegetative disorders under ordinary conditions and those of hypoxia
17 p2110 A73-34121

Influence of lower-body decompression on the state of the human cardiovascular system /according to roentgenokymographic data/
17 p2111 A73-34234

Certain features of hemodynamics during orthostatic tests with persons of different vestibulo-vegetative tolerance levels
17 p2111 A73-34236

Cardiovascular responses to sudden strenuous exercise - Heart rate, blood pressure, and ECG.
17 p2112 A73-35461

Normalisation of haemodynamic changes caused by action of prolonged accelerations in rats.
18 p2270 A73-35985

Experimental myocardial infarction - Hemodynamic evaluation.
18 p2275 A73-36540

The effects of training on some parameters of hemodynamics and of the oxygen transportation function of the blood during static strains
18 p2277 A73-36581

Cardiovascular reactions of a healthy man exposed to sonic booms
18 p2284 A73-36909

Intracranial hemodynamic changes in pilots to tilting.
18 p2279 A73-36916

Respiratory changes in the stroke volume of the left ventricle in healthy humans
19 p2393 A73-37397

The effect of exercise on intrinsic myocardial performance.
19 p2396 A73-38258

Echocardiographic evaluation of the hemodynamic effects of chronic aortic insufficiency with observations on left ventricular performance.
20 p2512 A73-38868

Ventilatory and hemodynamic responses to acute hypoxia and hypercapnia in Hereford calf, comparing with man
20 p2515 A73-39782

Effects of tilting on pulmonary capillary blood flow in normal man.
20 p2519 A73-39786

Effect of stimulation of certain hypothalamic structures on systemic and pulmonary circulation
21 p2637 A73-40282

Cardiopulmonary responses of male and female swine to simulated high altitude.
24 p3060 A73-45058

HEMODYNAMICS
Hemodynamic effects of physical maneuvers /Valsalva, effort, respiration/ and of pharmacodynamic tests - Their clinical application
02 p0138 A73-12159

Effect of a 5-day space flight on cardiodynamics during physical work of moderate intensity
02 p0138 A73-12467

Maximal treadmill exercise electrocardiography - Correlations with coronary arteriography and cardiac hemodynamics.
02 p0136 A73-12821

Electro-rheocardiotelemetric device for complex monitoring of the dynamics and efficiency of cardiac contraction.
03 p0271 A73-14292

An implantable blood pressure and flow transmitter.
04 p0447 A73-14845

Spline function interpolation in interactive hemodynamic simulation.
06 p0660 A73-18889

Devices for dynamic recording of volumetric blood flow rates lower than 1 ml per minute
08 p0934 A73-21325

Ventriculographic patterns and hemodynamics in primary myocardial disease.
08 p0933 A73-21804

Modification of the electroencephalograph EEG-I for polygraphy
09 p1044 A73-22370

Influence of flow and pressure on wave propagation in the canine aorta.
14 p1715 A73-30066

The role of carotid sinuses in the regulation of hemodynamics during motor activity
15 p1833 A73-31161

Effect of a 5-day space flight on the cardiac dynamics during moderately severe physical work.
15 p1840 A73-32617

Current status of correlations between vectorcardiogram and hemodynamic data.
18 p2274 A73-36526

Nonlinear analysis of aortic flow in living dogs.
21 p2638 A73-40640

Flow patterns and velocity and shear stress distribution downstream of steady and pulsatile flow models for fluid dynamics of blood vessel branches
22 p2816 A73-43103

HEMOGLOBIN
NT CARBOXYHEMOGLOBIN
NT OXYHEMOGLOBIN

Stochastic model application to divergence of horse-pig lineage from common ancestor in terms of hemoglobin and fibrinopeptides alpha and beta chains.
07 p0780 A73-19218

Investigation of some blood characteristics in albino rats subjected to 60-day hypokinesia
15 p1834 A73-31502

A new method for determining the degree of oxygenation of hemoglobin spectra in the case of inhomogeneous light paths, explained in an analysis of spectra of the human skin
20 p2517 A73-39145

Erythropoietin production in dogs exposed to high altitude and carbon monoxide.
20 p2513 A73-39599

Oxygen transport augmentation mechanism for human hemoglobin, considering hemoglobin translational mobility absence effects
20 p2515 A73-39795

Hemoglobin molecule oxygenation mechanism in various animals, discussing erythrocytes as hemoglobin carriers, ecological factors and physicochemical conditions
23 p2947 A73-43929

Hemoglobin species diffusion effect on oxygen transport in moving and stationary flat films of hemoglobin solution
23 p2949 A73-43993

Prospects for studying mechanisms responsible for the nonthermal effects of millimeter- and submillimeter-band electromagnetic radiation on biologically active compounds
23 p2949 A73-44096

Response of coronary blood flow to pH-induced changes in hemoglobin-O₂ affinity.
24 p3060 A73-45061

HEMORRHAGES
Digestive hemorrhages in aircrew - Individual and collective safety
18 p2280 A73-36952

HEMOSTASIS
U HEMOSTATICS
HEMOSTATICS

Hemotherapy of coagulation system disturbances of hepatolienal origin
23 p2947 A73-44299

HENRY LAW
Solubilities of noble gases in magnetite - Implications for planetary gases in meteorites.
13 p1684 A73-29182

HEOS A SATELLITE

Directional measurements of the solar wind by the ESRO HEOS 1 probe, S 58-73

06 p0749 A73-17863
Spinning HEOS-A2 satellite active deconing with pulse sequence from attitude reorientation system, discussing optimal control pulse number and timing
18 p2361 A73-36957

HEOS B SATELLITE

Heos 2 satellite instrumentation and space exploration objectives, considering earth and interplanetary magnetic fields, electron and proton energies, solar radiation and wind, cosmic dust and micrometeoroids
02 p0228 A73-11949

Electromagnetic interference caused by a solar array.
18 p2269 A73-36958

HEOS SATELLITES

NT HEOS A SATELLITE

NT HEOS B SATELLITE

Micrometeoroid mass, velocity and composition from Heos 2 and Helios satellite experiments, using hypervelocity dust particle impacting plasma emission
10 p1218 A73-24119

HEPARINS

Effect of heparin on blood platelet aggregation and thrombosis under the action of direct electric current
08 p0931 A73-21321

Experimental studies on the production of pulmonary infarction. IV - Effects of UK, heparin, t-AMCHA or ellagic acid.
22 p2805 A73-42319

HEPTANES

The cool-flame oxidation of n-heptane. I - The kinetic features of the reaction.
07 p0918 A73-19385

HERCULES AIRCRAFT

U C-130 AIRCRAFT

HERCULES NOVA

Spectrophotometry of i Hercules
23 p3037 A73-44356

HEREDITY

Russian papers on human adaptability covering altitude and temperature acclimatization, work capacity and anthropogegetic and medicogenetic factors
02 p0133 A73-11921

Correlational inter-relationships between the neuroendocrinal system and the genotype in the formation of protective reactions of the organism
15 p1835 A73-31875

Hereditary aspects of coronary atherosclerosis.
18 p2275 A73-36532

Human intrapair twin differences, examining age, height, weight, heart volume, metabolism, respiratory rate and monozygous/dizygous differences
20 p2519 A73-39792

Effects of space flight factors on the heredity of higher and lower plants.
22 p2804 A73-42168

HERMETIC SEALS

Recent research results in the field of hermetically sealed miniature silver-zinc storage batteries.
02 p0133 A73-12513

Development and evaluation of materials for vacuum power interrupters.
04 p0456 A73-15763

Mechanical energy storage by flywheel with magnetic fluid hermetic seal and bearing, using anisotropic and whisker materials
11 p1399 A73-25979

High-reliability plastic package for integrated circuits.
19 p2411 A73-38455

HERMITIAN POLYNOMIAL

Simple iterative method for determining the eigenvalues of a Hermitian /real-symmetrical/ pair of matrices
09 p1111 A73-22107

A finite element collocation method for quasilinear parabolic equations.
10 p1241 A73-23638

Gaussian quadrature formula derivation by integration of linear interpolation operator replacing Hermite polynomial with vanishing derivative for error minimization
13 p1647 A73-28194

Quantizer functions and their use in the analyses of digital beamformer performance.
13 p1582 A73-28496

Objective cross-section analyses by Hermite polynomial interpolation on isentropic surfaces.
21 p2728 A73-40054

The recursive generation, differentiation, and integration of Hermite interpolation polynomials together with an example concerning the application of the method
23 p3044 A73-44048

HERTZSPRUNG-RUSSELL DIAGRAM

Photometry and spectroscopy of red variables in Omega Centauri.
01 p0098 A73-10584

Evolutionary sequences for massive stars with various initial chemical compositions, studying semicon-

vection effects on core helium burning star distribution in H-R diagram
01 p0104 A73-11037

Solar luminance via light nuclei fusion into heavier nuclei with temperature gradient maintenance by gravity, relating to H-R diagram of different star clusters
05 p0614 A73-16302

Internal models of uniformly rotating synchronous close binary systems via modified double approximation scheme, considering gravity darkening effect on primary position in H-R diagram
05 p0624 A73-17306

Evolution of single stars. VII - Evolution of massive stars.
08 p1002 A73-20848

Stellar structure and evolution models in conformity with observational luminosity, mass and size from H-R diagram
13 p1682 A73-28977

Close binaries structure and evolution, discussing model computations for H-R diagram and mass-luminosity relations
13 p1682 A73-28983

Photometry of field horizontal-branch stars.
13 p1682 A73-28986

On the use of UVB photometric diagrams for inferring the existence of an open star cluster.
16 p2058 A73-32833

Mass-luminosity relations for unevolved stars in high mass eclipsing binaries and low mass visual binary systems for hydrogen and metal abundances of Population I stars
20 p2609 A73-39439

Multiple solutions of the equations of stellar structure. II - E model sequences.
24 p3140 A73-45179

HERZBERG BANDS

Excitation of the Herzberg bands of O₂ in laboratory afterglow and night airglow.
02 p0156 A73-11743

HETEROCYCLIC COMPOUNDS

NT ADENOSINE DIPHOSPHATE [ADP]

NT ADENOSINE TRIPHOSPHATE [ATP]

NT ADENOSINES

NT AZINES

NT BIOTIN

NT HYOSCINE

NT INDOLES

NT PYRIDOXINE

NT PYRROLES

NT THIAMINE

NT TRYPTOPHAN

Thermogravimetry of thermally stable aromatic and heterocyclic polymers.
01 p0015 A73-11447

Thermally stable heterocyclic ladder polymer films preparation techniques in manufacture of solar cells with CdS or CdTe thin films for space applications
07 p0841 A73-18903

Heterocyclic compounds extraction and identification from carbonaceous meteorites by gas chromatography and mass spectrometry, noting pyrimidine distribution and absence of biological heterocycles
10 p1277 A73-24101

Indoline series spirochromene polymer matrices for holographic recordings with argon and helium-neon lasers in green and UV spectral regions
14 p1753 A73-30365

New improved laser dye for the blue-green spectral region.
17 p2186 A73-35800

Hyperfine structure of furan.
22 p2818 A73-42712

HETERODYNING

NT OPTICAL HETERODYNING

Electromagnetic measurement of frequency and amplitude of mechanical vibration, based on echo signal phase modulation, explaining heterodyne detection system
07 p0827 A73-20532

Heterodyne detection of frequency sweeping in the output of transverse-excitation CO₂ lasers.
13 p1628 A73-29186

A low temperature bolometer heterodyne receiver for millimeter wave astronomy.
20 p2564 A73-38878

Heterodyne detection of Arcturus at 10.6 microns.
24 p3143 A73-45493

HETEROGENEITY

Effect of heterogeneity and Hall current on the MHD power generator.
01 p0005 A73-10434

Compression and elastic moduli of heterogeneous viscoelastic materials consisting of mechanical mixture of homogeneous phases, using elastic-viscoelastic analogy
03 p0385 A73-13139

HEURISTIC METHODS

Validity of averaging methods for certain systems with periodic solutions.
01 p0070 A73-10273

Reasoning by analogy as an aid to heuristic theorem proving.
01 p0020 A73-11453

Features selection by heuristic method with figure of merit in pattern recognition
01 p0021 A73-11488

Heuristic response strategies and operator performance errors as function of practice in cross coupled pursuit tracking control tasks
07 p0785 A73-19548

Some delinearization problems in the dynamics of complex vibrational systems
08 p0989 A73-21768

Ergatic modeling as dynamic goal-oriented physical process based on heuristic autonomous information-structured organization system with regulated model-human operator interaction
13 p1580 A73-29418

Digital processing of stereoscopic image pairs.
19 p2432 A73-38534

Structure of self-organizing automated design systems and the processes of their functioning
20 p2569 A73-39391

HEXAGONAL CELLS

Sn suppression of Al-Cu-Sn alloy aging at low temperatures, relating to Cu solubility decrease in alpha phase
02 p0179 A73-11599

Stacking faults in alpha titanium alloys
03 p0327 A73-13977

Environmental hydrogen embrittlement of an alpha-beta titanium alloy - Effect of hydrogen pressure.
06 p0713 A73-18769

Thermal-activation parameters of plastic deformation in alpha-titanium single crystals
09 p0199 A73-21964

Determination of hydrogen permeation parameters in alpha titanium using the mass spectrometer.
09 p1102 A73-22412

Cast, annealed and hardened zirconium binary alloys cubic to hexagonal phase transitions from X ray and differential thermal analysis
10 p1233 A73-24318

Importance of slip mode for dispersion-hardened beta-titanium alloys.
10 p1235 A73-24441

Alpha phase lattice constant curves and composition effects of Cr-Ni-Co-Mo steels on microstress rate reduction during age hardening
12 p1509 A73-26840

The nature of the nonuniformity of the structure and properties of semiproducts pressed from titanium and its alpha-alloys
12 p1502 A73-26909

Crystallographic analysis of hexagonal vacancy type Al-Mg alloy cube plane dislocation loops produced by specimen deformation before quenching
13 p1634 A73-28260

Influence of alloying on the phase composition and properties of maraging stainless steels
13 p1644 A73-29647

Anomalous creep behavior of crystal bar alpha-Zr during dynamic strain aging at 723-823 K as function of temperature, stress and oxygen content
14 p1760 A73-30626

Alpha phase decomposition and precipitation measurement in titanium rich Ti-Al alloys by electrical resistivity and microscopic methods
14 p1761 A73-30638

Influence of alpha- and beta-stabilizers on the plastic deformation mechanism of titanium
14 p1765 A73-30888

Al addition effect on strength of Ti via short range order, considering strengthening by alpha stabilizing solutes
15 p1893 A73-32273

Diffusional and nondiffusional metastable-phase transformations in titanium alpha + beta alloys
15 p1893 A73-32520

Failure retardation mechanism in plastic titanium alloys
15 p1894 A73-32529

Characteristics of failure in alpha-titanium alloys at high temperatures
15 p1894 A73-32536

Certain systematic errors in determining parameters of oxygen diffusion in alpha titanium
15 p1894 A73-32540

Passive alpha structure Ti base alloys with Al, Mn, Sn, Nb, Cr or Mo, investigating dissolution characteristics by chronoamperometric measurement using sulfuric acid
15 p1895 A73-32568

Low temperature deformation of commercial Ti alloys.
16 p2024 A73-32848

Metallurgical investigations of atomic ordering and transformation behavior of close packed ordered nine-layered hexagonal structure /kappa phase/ in V-Co-Ni ternary alloys
17 p2190 A73-34646

Atmospheric vorticity effects on hexagonal convection cells formation, considering temperature profiles nonlinearity, turbulent viscosity and perturbation scale
18 p2333 A73-37052

Grain growth in commercial alpha and /alpha + beta/ Ti alloys.
18 p2326 A73-37143

Cleavage fracture in alpha phase Ti, considering embrittling species effects on electronic band structure
20 p2578 A73-39490

Effect of alloying and phase composition on the properties of maraging stainless steels.
21 p2720 A73-41040

Influence of Co, Ni, Mo, and W on the solubility of Fe16N2 in alpha-iron.
23 p2994 A73-44156

Investigation of the kinetics of the redistribution of alloying elements between the alpha solid solution and cementite in cobalt and nickel steels
24 p3100 A73-45362

HEXAGONS
On the transverse strength of fiber-reinforced materials.
[ASME PAPER 72-APM-BEE] 17 p2249 A73-35111

HEXOGENES (TRADEMARK)
Investigation of the detonation characteristics of hexogen-filler systems
13 p1706 A73-28970

Spectroscopic investigations of the combustion zone of flame jets of compacted systems
19 p2402 A73-37508

HEXOKINASE
Apparent paradoxical patterns of anaerobic glycolysis and hexokinase activity in the red blood cells of acutely bled rats, with evidence that the responses were in part hormone-dependent.
11 p1315 A73-25568

HFB-320 AIRCRAFT
Flight mechanics problems associated with landing approaches using direct lift control, as exemplified by the HFB 320 Hansa aircraft
[DGLR PAPER 73-024] 17 p2100 A73-34496

HH-43B HELICOPTER
U HH-43 HELICOPTER
HH-43 HELICOPTER
Noise control modification to HH-43B helicopter for 50 percent reduction in forward flight octave band sound pressure level signature
11 p1304 A73-25383

HHX HELICOPTER
U H-53 HELICOPTER

HIbernATION
Hibernation applications in manned space flight, considering feasibility and advantages
03 p0269 A73-14170

Low body temperature effects on learned behavior retention under hibernation conditions in squirrels
05 p0539 A73-16324

Ventilation measured by body plethysmography in hibernating mammals and in poikilotherms.
08 p0932 A73-21612

Pulmonary respiration and acid-base state in hibernating marmots and hamsters.
08 p0932 A73-21613

Circadian rhythms in catecholamines in organs of the golden hamster.
11 p1318 A73-26120

Serotonin content in various parts of the brain during hibernation and awakening
15 p1834 A73-31390

Serotonin content variations in the fore-brain during hibernation
18 p2276 A73-36567

The inhibiting action of 5-oxytryptophan on thermal regulation during the awakening from hibernation
19 p2393 A73-37252

Contraction kinetics of ventricular muscle from hibernating and nonhibernating mammals.
20 p2514 A73-39603

Book on comparative physiology of thermoregulation covering primitive and aquatic mammals, torpidity aspects, evolution and newborns
22 p2809 A73-42859

Torpor and hibernation physiology in mammals covering evolution, hypothermia, energy conservation, cell and organ adaptations, nervous and cardiovascular system changes, etc
22 p2809 A73-42862

HICAT [RADAR TECHNIQUE]
U HIGH RESOLUTION COVERAGE ANTENNAS

HICAT PROJECT
U HIGH RESOLUTION COVERAGE ANTENNAS

HIERARCHIES
NT BBGKY HIERARCHY
On turbulent flows with fast chemical reactions. I - The closure problem.
01 p0032 A73-10637

Programmed control of a two-level hierarchical system
01 p0027 A73-10665

Calculation of the reliability of hierarchical systems with quorum redundancy
09 p1088 A73-22552

Probability characteristics of complex systems with a hierarchical control
09 p1068 A73-22559

Rigorous resolution of the hierarchy of grand-canonical-ensemble Green functions.
13 p1662 A73-28552

French monograph - Study and preparation of algorithms of coordination in the structures of hierarchized control systems.
15 p1855 A73-32592

HIGH ACCELERATION
Positive / + Gz/ acceleration tolerances of the miniature swine - Application as a human analog.
11 p1315 A73-25337

HIGH ALTITUDE
Airborne laser-beam scintillation measurements at high altitudes.
03 p0305 A73-14657

High altitude remote spectroscopy of the ocean.
04 p0451 A73-15779

Upper atmosphere thermodynamic and circulation characteristics for high altitude aircraft flights, including geomagnetic disturbance factors
07 p0847 A73-19298

Solar energy outside the earth's atmosphere.
08 p1010 A73-21265

Physiological studies of human organism adaptation to high altitudes in temporary and permanent mountain inhabitants, discussing oxygen uptake, lung ventilation and cardiac ventricle hypertrophy
10 p1181 A73-24514

Dynamic parachute inflation model for dimensionless time and maximum force predictions at high altitudes
15 p1826 A73-31436

[AIAA PAPER 73-450] Earth crust inhomogeneities from high altitude aeromagnetic survey, noting information loss increase with height
19 p2425 A73-37937

HIGH ALTITUDE BALLOONS
NT SKYHOOK BALLOONS
Atmospheric tidal measurements at 50 km from a constant-altitude balloon.
01 p0043 A73-11061

High angular resolution solar observation from balloon borne instruments.
02 p0169 A73-12334

Observed effects of earth-reflected radiation and hydrogen drag on the orbital accelerations of balloon satellites.
04 p0439 A73-14802

Long-duration flight performance of medium large unpressurized stratospheric balloons.
04 p0406 A73-15099

Industrial manufacturing of stratospheric balloons.
07 p0829 A73-18998

An apparatus for the orientation of stratospheric-balloon payloads
11 p1304 A73-25355

Skyhook plastic balloons for transporting scientific instruments to high altitudes for long durations
11 p1306 A73-26348

ESRO Aerosat L-band communication techniques experiments with stratospheric balloon-borne transponders relaying ground station signals to aircraft flying over sea
12 p1498 A73-27672

Measurements and interpretation of the polarization of radiation emerging from the atmosphere at an altitude of 28 km over south-western New Mexico /USA/.
13 p1652 A73-28269

Participation of the Air Force Weather Service in the Eole experiment
17 p2206 A73-34940

Teledetection experiments using balloons
17 p2176 A73-35815

Remote sensing experiments with balloons
19 p2431 A73-38180

HIGH ALTITUDE BREATHING
The diluter-demand oxygen system used during the international Himalayan expedition to Mount Everest.
11 p1322 A73-25145

Mechanics of breathing in high altitude and sea level subjects.
11 p1318 A73-26217

Erythropoietin production in dogs exposed to high altitude and carbon monoxide.
20 p2513 A73-39599

Phase IV volume of the single-breath nitrogen washout curve on exposure to altitude.
20 p2518 A73-39783

HIGH ALTITUDE ENVIRONMENTS
Hawaii's Mauna Kea Observatory today.
03 p0287 A73-13549

High altitude acclimatization and mountain climbing effects on human organism, considering oculomotor, cardiovascular and respiratory responses and endurance
08 p0930 A73-20991

High altitude chamber effect on thyroid stimulating hormone and thyroxine concentrations, noting shift from extra to intravascular
09 p1041 A73-22926

Lactate, alpha-GP, and Krebs cycle in sea-level and high-altitude native guinea pigs.
11 p1318 A73-26122

Hemocoagulation and trombocyte state during hypokinesia after highland adaptation
12 p1463 A73-27713

Russian book on passenger aircraft high altitude equipment covering cabin pressurization, air conditioning and temperature and pressure control, human tolerances, reliability factors, etc
14 p1712 A73-30355

Aircraft cabin altitude hypoxia effects on mother, embryo and fetus during first trimester of pregnancy in air hostesses and women passengers
14 p1718 A73-30519

Myoglobin distribution in the heart of growing rats exposed to a simulated altitude of 3500 m in their youth or born in the low pressure chamber.
14 p1720 A73-30910

Stratospheric mixing estimated from high altitude turbulence measurements.
16 p2005 A73-33539

[AIAA PAPER 73-497] Some characteristics of the muon component of extensive air showers at mountain level
23 p3023 A73-43562

HIGH ALTITUDE FLIGHT
U HIGH ALTITUDE

HIGH ALTITUDE NUCLEAR DETECTION
WB-57F aircraft with instrument package for nuclear test detection and upper atmosphere research, discussing range, altitude, speed, payload capacity and onboard equipment
16 p1969 A73-33548

HIGH ALTITUDE PRESSURE
High altitude aircraft cabin pressurization for crews and passengers, discussing altitude tolerance, reaction times, decompression and oxygen equipment
14 p1723 A73-30937

HIGH ALTITUDE TESTS
Turbulence variations during the high altitude clear air turbulence /HICAT/ program.
07 p0847 A73-19190

Earth crust inhomogeneities from high altitude aeromagnetic survey, noting informativeness loss increase with height
08 p0960 A73-21308

Effects of some antimotion sickness drugs and secobarbital on postural equilibrium functions at sea level and at 12,000 feet /simulated/.
09 p1045 A73-22529

Viking 75 Mars lander parachute high altitude qualification flight tests for camera, telemetry and radar performance, using ground based computer-aided monitoring system
15 p1826 A73-31442

[AIAA PAPER 73-456] Influence of stimulation of the vestibular analyzer under conditions of hypoxia on certain functions of the visual analyzer
15 p1835 A73-31516

Measured thermal response to the MIL-STD 210B cold atmosphere.
16 p2034 A73-33140

High altitude aircraft water vapor measurements using aluminum oxide hygrometer, noting comparison with remote sounders
16 p2006 A73-33549

Aircraft turbine engine exhaust emissions under simulated high altitude, supersonic free-stream flight conditions.
17 p2223 A73-35625

[AIAA PAPER 73-507] Simulation of the flow past a high-altitude ion-concentration sensor
21 p2633 A73-41223

HIGH ASPECT RATIO
Analysis of high aspect ratio jet flap wings of arbitrary geometry.
05 p0530 A73-16880

[AIAA PAPER 73-125] Finite chord effects on vortex induced large aspect ratio wing loads, noting rolling moment magnitude overestimate from lifting line solution
15 p1823 A73-31670

HIGH ASPECT RATIO WINGS
U SLENDER WINGS

HIGH CURRENT
Radial anode current density distribution measurement in high current pulsed arcs in air on copper split anode, using Rogowski coils
06 p0723 A73-18357

Investigation of the structure of a high-current discharge in a lithium plasma.
08 p0992 A73-20853

Relationship between adsorption processes on the cathode surface and processes in the region near the electrode in a high-current plasma discharge
09 p1127 A73-22608

Electrical explosion of wires at high energy input rates
12 p1523 A73-26936

Exploding wires with high energy input.
22 p2886 A73-42270

Possible causes of failures in pulse-switched thyristors
24 p3072 A73-44933

HIGH ENERGY ASTRONOMY OBSERVATORIES
U HEAO

HIGH ENERGY ELECTRONS
Solar coronal plasma cyclotron radiation, taking into account temperature effects
01 p0096 A73-10309

The infrared spectrum of nitrogen excited by fast electrons.

01 p0036 A73-10338

Heating of plasma by high-energy electrons, and nonthermal X-ray emission in solar flares.

01 p0093 A73-11313

The nature of the first Cygnus X-3 radio outburst.

02 p0204 A73-11551

Radio emission source picture from observed Cygnus X-3 outburst, suggesting expanding cloud with traveling relativistic electrons and protons

02 p0211 A73-11870

Energy distribution of relativistic electrons generated within radio sources with constant magnetic field and diffusion coefficient, discussing simplified model representation for Crab nebula

02 p0207 A73-12379

Linear synchrotron instability theory results via quantum method with Einstein coefficients, obtaining synchrotron radiation growth rate in relativistic electrons with anisotropic momentum distribution

02 p0223 A73-12726

Trapped and precipitated electron energy spectra in relativistic electron precipitation events [REP], discussing bremsstrahlung measurements deductions

03 p0304 A73-14591

Instability of a relativistically strong electromagnetic wave of circular polarization.

[AD-759478]

04 p0482 A73-15960

Incoherent radiation from relativistic electrons with power energetic spectrum.

05 p0611 A73-17313

Collective processes in the passage of high-current relativistic beams through a gas and a plasma.

06 p0732 A73-18714

The stopping power of atomic matter for relativistic ions, mesons, electrons and positrons.

07 p0852 A73-19036

Cosmic ray electrons of E greater than 1 GeV - Some new measurements and interpretations.

07 p0869 A73-19226

Differential light scattering cross section derivation for photon interaction with relativistic electrons, comparing with quantum electrodynamical calculation and Thomson scattering experiment

07 p0851 A73-19516

Parametric radiation of relativistic electron bundles in a waveguide with a stratified dielectric filling.

07 p0802 A73-20145

German monograph - Investigations of the behavior of high energetic protons and electrons in the inner magnetosphere.

07 p0872 A73-20385

High-energy electron-beam deposition onto a hot graphite surface.

08 p0990 A73-21210

Rapid injection of energetic particles into the gap between the inner and outer radiation belts

08 p0998 A73-21300

Hypotheses for excess background radiation at 200-500 km, suggesting single high energy electrons or electron clusters

08 p0999 A73-21336

High energy electrons and gamma quantum flux in upper atmospheric layers from high altitude balloon measurements

08 p0999 A73-21337

Ultrarelativistic electrons beam steady injection into plasma filled half space, using weak turbulence theory for assumed beam excited oscillations interaction

08 p0994 A73-21698

Nonlinear theory of a relativistic monotron

09 p1065 A73-23086

Diffraction study of fast electrons of the adsorption layer of oxygen on the surface of a film of epitaxial copper

10 p1259 A73-23767

Fluxes of electrons with energies above 80 MeV at the equator on the basis of measurements by the Cosmos 490 satellite

10 p1265 A73-23897

Jovian decametric emission origin in cyclotron instability of weakly relativistic electrons trapped in magnetic field, considering group velocity in magnetospheric plasma

11 p1424 A73-26129

The possibility of microfission explosions by laser or relativistic electron-beam high-density compression.

11 p1378 A73-26657

Stability of a magneto-active plasma with a relativistic electron beam, situated in a high-frequency electric field

12 p1527 A73-26927

Nonadiabatic condition effects on ultrarelativistic electron energy losses in geomagnetic trap in remote magnetosphere regions

12 p1535 A73-27649

Two-stream instability heating of plasmas by relativistic electron beams.

13 p1663 A73-28186

Relativistic electron beam focusing by neutral gas filled conical guide tube, comparing efficiency,

fluence gain, energy loss and pressure variation predictions with experiments

14 p1777 A73-30658

Effect of induced axial electric field on a relativistic electron beam pulse propagating through a plasma.

14 p1777 A73-30661

Transition radiation production by relativistic electrons traversing cosmic grains as source of celestial X rays, discussing formation zone effect

14 p1787 A73-30730

Universality of the power spectra of relativistic electrons generated in a turbulent plasma

14 p1782 A73-30808

Ultrahigh energy photons, electrons, and neutrinos, the microwave background, and the universal cosmic-ray hypothesis.

15 p1927 A73-32004

On a possible mechanism responsible for the differential energy spectrum of relativistic electrons and non-linear low-frequency spectra of cosmic radio sources.

15 p1927 A73-32005

Formation of fast electrons in a plasma under the influence of SHF power near harmonics of the electron cyclotron frequency

15 p1920 A73-32309

Quasilinear relaxation of a monoenergetic relativistic electron beam in an external magnetic field.

15 p1922 A73-32628

Crab Nebula pulsar electromagnetic radiation emission model based on high energy electron circular motion around magnetic field lines

15 p1942 A73-32649

Study of high energy electrons at upper layers of atmosphere during magnetic perturbations.

16 p2054 A73-33282

Axial compression of the astron E-layer during neutralization.

16 p2042 A73-33337

Satellite studies of magnetospheric substorms on August 15, 1968. V - Energetic electrons, spatial boundaries, and wave-particle interactions at Ogo 5.

16 p2056 A73-33453

Satellite studies of magnetospheric substorms on August 15, 1968. VI - Ogo 5 energetic electron observations - Pitch angle distributions in the nighttime magnetosphere.

16 p2056 A73-33454

Generation of intense infrared radiation from an electron beam propagating through a rippled magnetic field.

17 p2214 A73-34204

Transition radiation from interstellar dust grains.

17 p2231 A73-34755

An investigation on the spatial distribution of the quasi-trapped energetic electrons observed on board the satellite 'Shinsei.'

18 p2344 A73-35929

Electron calibration on a high-energy cosmic ray detector.

18 p2317 A73-36979

Generation of energetic ion fluxes from a high temperature electron discharge in an inhomogeneous magnetic field

19 p2466 A73-37358

Statistical acceleration of ultrarelativistic electrons by random electromagnetic waves.

19 p2462 A73-37558

On the energy spectrum of relativistic electrons in the Crab Nebula.

19 p2475 A73-37619

Fast injection of energetic particles into the gap between the inner and outer radiation belts.

19 p2476 A73-37929

Generation and decay of a narrow belt of energetic electrons in the earth's magnetosphere.

19 p2476 A73-37934

Electron fluxes with energies greater than 80 MeV at the equator based on measurement data from the Cosmos-490 satellite.

20 p2601 A73-38916

ULF geomagnetic power near $L = 4$. II - Temporal variation of the radial diffusion coefficient for relativistic electrons.

20 p2551 A73-38936

Collisionless damping of hydromagnetic waves in relativistic plasma. I - Weak Landau damping - Heating of the Crab Nebula.

20 p2609 A73-39442

Kinetics of recovery of luminescence properties of gallium arsenide single crystals irradiated with high-energy electrons.

20 p2574 A73-39697

Fluxes of electrons with energies greater than 10 MeV at heights from 200 to 500 km

21 p2758 A73-40603

Dependence of high-energy electron fluxes at an altitude of 200 to 300 km on threshold rigidity

21 p2686 A73-40917

Electron calibration of a high-energy cosmic ray detector.

21 p2703 A73-41150

High energy electrons at the magnetopause above the north pole - Preliminary results from the HEOS 2 satellite.

21 p2761 A73-41376

Stability of a magnetoactive plasma with a relativistic electron beam in an RF electric field.

22 p2891 A73-42261

Spatial electron distribution in extensive air showers at energies of one thousand to one billion TeV

23 p3022 A73-43552

Calculated characteristics of the electron and muon components of extensive air showers at the 690 g/sq cm level

23 p3022 A73-43553

Distribution function of relativistic electrons in a strong magnetic field.

23 p3011 A73-43753

Pair production near energy threshold by electron oscillation and acceleration to relativistic velocities at laser beam focus with plasma wave excitation

23 p2989 A73-44121

Production of fast plasma electrons by microwave power at harmonics of the electron cyclotron frequency.

24 p3114 A73-44617

A device for recording the energy spectrum and fluxes of electrons with energies greater than 100 MeV in cosmic rays

24 p3124 A73-44782

Relativistic electron belt formation mechanism hypothesis based on Cosmos 137 data on electron intensity near geomagnetic shell L equal to 2.8

24 p3124 A73-44808

Parametric instability of strong circularly polarized electromagnetic wave in plasma producing relativistic electrons and backscattered light

24 p3117 A73-45459

HIGH ENERGY FUELS

A shocktube study of the combustion of Sheldyne-H with additives.

[WSCI PAPER 72-29]

05 p0639 A73-16686

HIGH ENERGY INTERACTIONS

Multiple scattering of cosmic ray muons in the range 10-70 GeV/c.

01 p0091 A73-10787

High energy muons /not less than 150 GeV/ in extensive air showers.

01 p0092 A73-10788

All-Union Conference on the Physics of Cosmic Rays, Moscow, USSR, October 26-November 2, 1970, Transactions.

02 p0208 A73-12651

Inelastic nuclear interactions between 200-GeV cosmic ray particles and polyethylene targets, correlating similarity property, momentum spectra and secondary particle pairs

02 p0208 A73-12652

Particle multiplicity and momentum spectra for high energy inelastic nuclear interactions in Wilson chamber with polyethylene target

02 p0208 A73-12655

Multiple production processes hydrodynamic-type models validated by high energy particle collision collective interactions

02 p0208 A73-12659

High energy cosmic ray pions and nucleons interactions with atomic nuclei, using ionization calorimeter and spark chambers system

02 p0209 A73-12661

Cosmic ray particle high energy inelastic interactions, discussing pion and nucleon interaction angular and energy characteristics and muon production mechanism

02 p0209 A73-12664

Inelastic pionization cross section of cosmic ray hadrons with carbon nuclei at energies of 100 to 300 GeV

02 p0209 A73-12665

Nuclear photoemulsions under bombardment by pion beam of 60 GeV/c momentum, investigating pion-nucleon interactions involving recoil protons

02 p0195 A73-12667

Pion-nucleon high energy interactions, determining inelasticity coefficient distribution

02 p0195 A73-12668

High energy cosmic ray interactions at one TeV, including X process, horizontal showers and muon poor showers

02 p0209 A73-12679

Muon densities in penetrating high energy particles, comparing with extensive air showers

02 p0210 A73-12683

K-neutral pion energy fractions and inelasticity coefficients at primary energies of 100-1500 GeV during cosmic ray hadron-target interaction

02 p0210 A73-12689

Gravitational origin of high energy interactions and general relativity equivalence principle for unitary symmetry, noting quantum geometrodynamical cosmological model

04 p0501 A73-15632

Description of a device for studying inelastic nuclear processes with nucleons at energies from .1 to

10 TeV and analysis of its operation at an altitude of 3250 m above sea level

05 p0577 A73-16823

Multiplicity link to transverse momenta in ultrahigh energy nucleon-nucleon interaction processes, considering resonance formation and expected average elasticity

06 p0743 A73-17830

Cosmic ray electrons of E greater than 1 GeV - Some new measurements and interpretations.

07 p0869 A73-19226

Secondary particles multiplicity law validity in cosmic ray showers highest energy interactions

09 p1138 A73-23035

Study of strong interactions between cosmic-ray hadrons and nuclei at 200 to 2000 GeV energies

10 p1264 A73-23816

Effect of rapidly rising proton-proton total cross sections on idealized extensive air showers.

11 p1412 A73-25745

Bounds on mean excitation energies-Lamb shift, stopping power, straggling, and grazing collision of high-energy charged particle.

12 p1526 A73-27128

Asymptotic form for the cross section for the Coulomb interacting rearrangement collisions.

14 p1777 A73-30551

Null correlation method for estimation of the primary energies of cosmic ray jets.

15 p1927 A73-32149

Evidence for the possible existence of a charged particle with large mass.

16 p2016 A73-33700

High-energy pulsed CO₂-laser-target interactions in air.

17 p2184 A73-34914

Large underground showers and multiple muons in association with E.A.S.

19 p2475 A73-37574

Low-energy cosmic ray protons from nuclear interactions of cosmic rays with the interstellar medium.

22 p2902 A73-41927

Estimation of the biological danger of the very high energy component of space radiation.

22 p2805 A73-42180

Particle number fluctuations and transient effects in electron-photon showers in lead at energies above 20 GeV

23 p3021 A73-43531

Study of nucleon interactions with carbon, iron and lead nuclei in the energy range 600 to 10,000 GeV

23 p3008 A73-43532

A study of elementary acts of interaction between hadrons with energies of about 10 TeV

23 p3021 A73-43533

Preliminary results of the Pamir-20-71 experiment on interactions at energies of about 1000 TeV

23 p3021 A73-43534

High energy gamma quanta families and multiple generation processes in electron photon cascades detected by nuclear emulsion X ray chamber

23 p3021 A73-43536

Pion-nucleon interaction structure based on negative pion beam data from Serpukhov accelerator, showing secondary particle energy distribution asymmetry

23 p3021 A73-43537

Properties of secondary high-energy particles in hadron interactions

23 p3021 A73-43538

Measurement of the effective cross section of inelastic interaction between protons and carbon nuclei in the energy range 0.1 TeV to 1.0 TeV, on the Proton-4 space station

23 p3021 A73-43539

Inelastic interaction between pions and emulsion nuclei at an energy of 60 GeV

23 p3021 A73-43541

High energy nucleon inelastic interaction characteristics calculated from artificial event model based on covariant statistical theory of multiple generation of particles

23 p3022 A73-43542

Extensive air showers and nuclear interaction characteristics at superhigh energies

23 p3022 A73-43551

Energy spectrum and angular distribution of outer space muons and the processes of their production in the 1 TeV energy range

23 p3024 A73-43564

Identification of hadrons with 500 GeV energies in cosmic rays by using transitional emission

23 p2981 A73-43566

HIGH EXPLOSIVES

U EXPLOSIVES

HIGH FREQUENCIES

Theoretical and experimental study of the H.F. current associated with a plasma wave.

01 p0081 A73-10118

Geometrical theory to approximate HF electromagnetic wave diffraction from moving conducting strip under incident field

01 p0016 A73-10192

GaAs-GaAlAs heterojunction transistor for high frequency operation.

02 p0147 A73-12046

Accuracy limitation in measurements of HF field intensities for protection against radiation hazards.

03 p0310 A73-14491

Method of calculating high-frequency parameters of m.o.s. transistors in the nonpinchoff region

05 p0556 A73-16163

High-frequency physical equivalent circuit of junction transistors in common collector configuration.

06 p0682 A73-18843

Superconductors HF properties and losses measurement and separation techniques, discussing applications to filters, oscillators, mixers, transmission lines and radiation detection

07 p0863 A73-20106

High-frequency radio-wave propagation through plane-stratified ionospheric models.

09 p1077 A73-22430

Some effects of the equatorial ionosphere on terrestrial HF radiocommunication.

09 p1051 A73-22500

Transmission loss at high frequencies on 3260 km temperate-latitude path.

09 p1052 A73-22958

Computer simulation of HF frequency-selective fading and performance of the mode-averaging diversity combiner.

10 p1190 A73-24894

Output characteristics of high frequency transistor power amplifiers.

12 p1479 A73-27169

Relative transit time measurements of high-frequency signals using an FM-CW technique

12 p1474 A73-27763

A bipolar transistor model for high frequencies

13 p1589 A73-28124

Theory of surface wave dispersion in an inhomogeneous plasma situated in a strong HF field

13 p1667 A73-29161

Equivalent circuit HF model of MOS transistor active region based on transient response equation, voltage and structural parameters

15 p1850 A73-31492

Wide-band power amplifier for studying the high-frequency properties of plasmas

15 p1850 A73-31497

High-frequency current states in small-size superconductors

16 p2044 A73-34066

Plasma hydrodynamics in high frequency electromagnetic field, discussing hydrodynamic equations, small perturbations, plasma equilibrium and movement in field

17 p2216 A73-34341

High frequency vibration of aircraft structures.

17 p2250 A73-35329

Entry of a high-frequency longitudinal field into a nonequilibrium plasma

18 p2339 A73-36554

Investigation of the high-frequency oscillations in the flow of a pulsed coaxial plasma accelerator - One mechanism of inhomogeneity

19 p2467 A73-37364

Emission of longitudinal waves from a charge in an external high-frequency electric field in a magnetoactive plasma

19 p2470 A73-38331

The susceptibility of modern aircraft instrument systems to interference in the HF band.

22 p2851 A73-41694

Measurement of attenuation of 9.303 MHz waves from ISIS-II through the ionosphere.

22 p2825 A73-42193

Investigation of the influence of a nonuniform high-frequency electric field on the parameters of a helium-neon laser

23 p2987 A73-43575

German book on HF technology, Volume 1, covering coupling filters, transmission lines, antennas, Lecher waves, waveguides, etc

24 p3073 A73-44999

HIGH GRAVITY (ACCELERATION)

U HIGH GRAVITY ENVIRONMENTS

HIGH GRAVITY ENVIRONMENTS

Changes in functional construction of bone in rats under conditions of simulated increased gravity.

17 p2113 A73-35863

HIGH LATITUDES

U POLAR REGIONS

HIGH LIFT DEVICES

U LIFT DEVICES

HIGH MELTING COMPOUNDS

U REFRACTORY MATERIALS

HIGH PASS FILTERS

Semircircular waveguide-type, band-splitting filter for millimeter waves.

08 p0945 A73-20807

Materials suitable for making far infrared high-pass transmission filters.

21 p2701 A73-40692

HIGH POLYMERS

Extended chain crystals of linear high polymers.

02 p0139 A73-12650

Nonclassical flow theory for continuum mechanics with asymmetrical stress concentration, noting rheological problems in laminar high polymers flow, hydrodynamic instability and turbulent flow

03 p0291 A73-13152

Linear viscoelasticity theory application to high polymers mechanical properties determination via relaxation spectrum with emphasis on polymethyl methacrylate

22 p2881 A73-43170

A two-layer slab method for measuring thermal diffusivity of polymer by irradiated light heat-wave. I. II - Transient response of temperature sensor attached on a polymer substrate. III - Quantitative evaluation of the effect of edge losses in a parallelepiped.

23 p3049 A73-44363

HIGH PRESSURE

Adsorption equilibria at high pressures in the helium-nitrogen-activated carbon system.

01 p0014 A73-10725

Polychromatic X-ray diffraction - A rapid and versatile technique for the study of solids under high pressure and high temperature.

01 p0054 A73-11482

Possibility of obtaining mullite at high dynamic pressures

02 p0178 A73-11542

Influence of the bending radius on the strength, volume deformation, and bending rigidity of high-pressure hoses

03 p0318 A73-14599

Theoretical-experimental studies and research concerning the technical safety of the casing of a high-pressure cylindrical tank. I

04 p0454 A73-15657

Feasibility study of a slanted 'O-ring' as a high-pressure rotary seal.

[ASME PAPER 72-WA/DE-14] 04 p0457 A73-15873

Design and development of a high pressure facility for droplet combustion experiments.

05 p0562 A73-16440

Piston motion in semiclosed tube under high initial pressure, using gas-to-piston mass ratio as perturbation parameter in analysis based on Lagrange solution [DFVLR-SONDDR-255] 06 p0685 A73-17739

Effects of a high-pressure gas medium on the mechanical properties of polymethylmethacrylate

06 p0715 A73-18671

Dynamic method for measuring thermal conductivity of liquids and gases at high pressures.

08 p1021 A73-20861

Mechanical behaviour of molybdenum and tantalum under high pressures at elevated temperatures.

09 p1105 A73-23018

Reflex excitability of spinal motor neurons in man under high atmospheric pressure

10 p1182 A73-24525

Thick walled multilayer wideband radomes for supporting high hydrostatic pressures and protecting weakly directional submarine antennas with circular polarization

11 p1336 A73-25305

High pressure physics and planetary interiors; Proceedings of the Conference, Houston, Tex., March 1-3, 1972.

11 p1419 A73-25876

High pressure physical model of hydrogen planets Jupiter, Saturn, Uranus and Neptune

11 p1419 A73-25877

Ground state energy of solid molecular hydrogen at high pressure.

11 p1401 A73-25891

Feasibility of high-pressure noble gas lasers.

11 p1378 A73-26360

An equation for thermal expansion coefficient at high pressures.

13 p1673 A73-28206

Design and development of Manganin and other wire sensors together with a resistance strain gauge transducer for use at pressures up to 200 000 lbf/sq in /1.38 GN/sq m/.

14 p1750 A73-29702

Influence of air pressure on the brittle fracture of graphite

14 p1766 A73-30715

Utilization of hydrostatic compression at high pressures as a means of improving the properties of acoustic nickel ferrite

14 p1765 A73-30890

Some observations of the relationship between film thickness and load in high Hertz pressure sliding elastohydrodynamic contacts.

[ASME PAPER 73-LUB-D] 19 p2433 A73-37450

Absolute viscosity of air down to cryogenic temperatures and up to high pressures.

19 p2422 A73-38296

Laser-induced gas breakdown in superhigh pressure region.

22 p2869 A73-42227

New measurements of the thermal conductivity of argon and nitrogen to 200 C and 1600 atmospheres.

22 p2932 A73-42502

High pressure burning rates of liquid alcohol and hydrocarbon fuels with droplet simulation by porous

- spheres, deriving surface temperature, pressure distribution and critical burning conditions 22 p2937 A73-42817
- Kinetics of chemical high-pressure lasers 23 p2987 A73-43716
- Optically pumped 33-atm CO₂ laser. 24 p3095 A73-44587
- HIGH PRESSURE OXYGEN**
- Computed total radiation properties of compressed oxygen between 100 and 1000 K. 01 p0122 A73-10809
- Sensitivity of the brain to repeated exposures of hyperbaric oxygen. 11 p1314 A73-25328
- Results of electron microscopic studies in the rat brain under oxygen at high pressure. 11 p1314 A73-25330
- NASA use of liquid and gaseous oxygen under extreme pressure, temperature and flow rate conditions, discussing safety requirements in terms of structural and chemical compatibility 11 p1410 A73-26525
- Cat and rat lung damage due to hyperbaric oxygen exposure and head injury, discussing alveolar surfactants, sympathetic stimulation and monkey injuries [AD-759298] 13 p1576 A73-28507
- A survey of compatibility of materials with high pressure oxygen service. 23 p2991 A73-43525
- HIGH Q**
- U Q FACTORS**
- HIGH RESOLUTION**
- Instrumental considerations in high dispersion requirements of stellar spectroscopy and interstellar absorption and emission line studies, emphasizing spectral resolution and SNR optima determination 01 p0046 A73-10503
- Comparison of high-resolution photographic emulsions for recording three-dimensional holograms. 01 p0051 A73-10839
- Rocket-borne instrumentation to measure ionospheric electron temperature with good spatial resolution. 02 p0167 A73-11953
- Mobile FM-CW radar sounder with scanning capability for high resolution remote sensing in lower troposphere, discussing design and performance 02 p0140 A73-11959
- Ground based solar astronomy potential for obtaining photographs with factor of two in resolution and time series, discussing optical performance of vacuum solar telescope 02 p0216 A73-12329
- Planetary observation by earth based photography, discussing resolution limitation and improvement in terms of modulation transfer function 02 p0216 A73-12330
- High resolution limitations and improvement for earth based visual and photographic planetary observation, considering atmospheric boundary layer and use of elevated stations 02 p0169 A73-12331
- Linear photoelectric scanning techniques for achieving high resolution, comparing with two dimensional scanning at telescope or of electronographic images 02 p0169 A73-12332
- Solar IR imaging techniques for providing high resolution data with short exposure time 02 p0169 A73-12333
- High angular resolution observations from rockets - Solar XUV observations. 02 p0216 A73-12336
- Spaceborne high resolution solar telescopes optical systems, discussing construction, alignment and thermal control problems 02 p0169 A73-12338
- High resolution marker transport sintering study. 02 p0175 A73-12771
- Importance of high time resolution in flare star observations. 03 p0373 A73-13373
- Scanning and transmission type electron microscopes, discussing operating principles, image quality, resolution and applications 05 p0575 A73-16311
- Reversible high speed high resolution imaging in amorphous semiconductors. 07 p0862 A73-19609
- High resolution spectra of the stratosphere between 30 and 200/cm. 08 p0961 A73-21533
- Photographic process based on ultrathin photosensitive molecular dispersion layer of benzenediazophenyl and autocatalytic Ag deposition during development process 09 p1084 A73-22691
- A position sensitive proportional counter with high spatial resolution. 13 p1622 A73-29643
- High resolution spectroscopy with lasers. 14 p1756 A73-29925
- Wolter-Schwarzschild telescopes for X-ray astronomy. 14 p1752 A73-30159

- Comparison of the resolutions of two projective holography methods by comparing their line scattering functions corresponding to holographic images 14 p1753 A73-30376
- Culgoora-1 list of radio source measurements at 80 MHz. 15 p1940 A73-32182
- A high-resolution photoelectric spectrophotometer at the coude focus of a 2.6-m telescope 16 p2011 A73-32714
- High resolution radio observation of sun at 3.71 and 11.1 cm with three-element interferometer, noting flare near east limb 16 p2060 A73-33097
- Ultra high resolution electronic imaging and storage with the return beam vidicon. 17 p2136 A73-34904
- Image-converter camera with subpicosecond temporal resolution. 21 p2694 A73-39947
- The microchannel picroscope - A high temporal resolution scanning tube for study of luminous phenomena in the subnanosecond range 21 p2694 A73-39949
- A multiframe high-speed camera developed to register phase objects with good spatial resolution without parallax. 21 p2696 A73-39980
- Technique of an ultrahigh-speed sampling camera based on the use of a unique photomultiplier 21 p2697 A73-39995
- Phase contrast transfer damping functions for various beam apertures in high resolution electron microscopy 21 p2702 A73-40949
- Ultrahigh resolution holographic spectroscopy by double exposure of light scattering medium interferogram recording and reconstruction, noting equivalence to use of narrower laser line width 22 p2861 A73-42413
- Extragalactic radio sources identification with galaxies and quasars by high sensitivity and resolution astronomical telescopes, obtaining angular structure maps and radio spectra 23 p3028 A73-43347
- Long baseline interferometry with high angular resolution widely separated radio telescopes and video signal magnetic recording tapes, discussing coherence and timing requirements and calibration 23 p2980 A73-43349
- High angular resolution very long baseline interferometry for emission spectra and angular size determination and structure mapping of galactic and extragalactic radio sources 23 p2980 A73-43355
- Tracking the Apollo Lunar Rover with interferometry techniques. 23 p2953 A73-43356
- Electrooptical radio spectrograph design for high resolution in time and frequency based on photographic film recording density and coherent optical processing data rate 23 p2980 A73-43374
- High resolution analysis of the sun's radiation received at the ground from 9 to 11.6 microns. 23 p3003 A73-43888
- Holographic technique for coherent optical imaging system superresolution via storage of image amplitude 23 p2983 A73-44088
- HIGH RESOLUTION COVERAGE ANTENNAS**
- Possibility of obtaining radio images of celestial bodies with a resolution greater than .01 arc sec 21 p2667 A73-41466
- HIGH SENSITIVITY**
- U SENSITIVITY**
- HIGH SPEED**
- The biodynamic aspects of low altitude, high speed flight. 06 p0659 A73-18471
- High data rate hard decision digital IC sequential decoder for earth-orbiting satellite space missions, discussing computational efficiency of modified Fano algorithm 09 p1056 A73-23398
- Monolithic IC digital circuits using Si planar technology with Schottky diodes in DTL and TTL gates for high computational speed 11 p1341 A73-25345
- High feed rate electrochemical machining Fe in aqueous NaCl, using high supply voltage, electrolyte pressures and flow velocities [ASME PAPER 73-PROD-3] 16 p1971 A73-33533
- Book - The aerodynamics of high speed ground transportation. 17 p2097 A73-35854
- A new technique for designing high-speed frequency counters. 21 p2658 A73-41146
- HIGH SPEED CAMERAS**
- NT FRAMING CAMERAS**
- A diode-type shutter tube for ultrahigh-speed photography 06 p0679 A73-18854
- Electronics associated with ultrahigh-speed photographic equipment 06 p0679 A73-18855

- Ultrahigh-speed electronic camera - CELER 2-500 06 p0696 A73-18856
- Some applications of a tube with proximity focusing in ultrahigh-speed motion-picture photography 06 p0696 A73-18858
- Photometric measurements with the aid of image converter tubes 06 p0696 A73-18859
- Microchannel image intensifiers - Applications to ultrahigh-speed photography 06 p0697 A73-18860
- The microchannel Picroscope - A tube with high-temporal-resolution scanning for studying luminous phenomena in the subnanosecond range 06 p0679 A73-18862
- Close range photogrammetry of objects moving at high speed. 09 p1081 A73-22377
- High speed cinetheodolite for missile tracking incorporating LED/light emitting diode/ system for metric data recording 10 p1222 A73-24950
- Advances in high-speed photography 1957-1972. 11 p1359 A73-24995
- Multistage image converter tubes for studying high-speed phenomena. 13 p1611 A73-28175
- Investigation of the characteristics of a mode-locked Nd:glass laser with the aid of a picosecond streak camera. 17 p2186 A73-35796
- International Conference on Ultrahigh-Speed Cinematography, 10th, Nice, France, September 25-30, 1972, Transactions 21 p2693 A73-39933
- Literature survey on high speed photography and cinematography, discussing gas discharge tube and open spark equipment, Kerr cells, image dissection and holographic interferometry 21 p2693 A73-39934
- Mechano-optical camera giving ten million images per second 21 p2693 A73-39935
- Gas bearing technique for ultrahigh speed rotating mirror mounted on opto-mechanical camera 21 p2693 A73-39936
- Ultrahigh speed cinematography with rotating Ti drums bound by monocrySTALLINE boron fibers, noting prototype performance 21 p2693 A73-39937
- High-speed SFKF photographic camera of the continuous type. 21 p2693 A73-39938
- Ultrahigh-speed high-frequency motion picture camera type W.K.2 21 p2693 A73-39939
- Application of image-converter technique in quantum radiophysics and nonlinear optics [Survey paper]. 21 p2709 A73-39940
- Image converter intensification for ultrahigh speed photography, discussing photographic film sensitivity, optical fiber output, slit analysis and camera types 21 p2694 A73-39941
- Slit electronic camera with scanned memory used in high speed cineradiography 21 p2694 A73-39942
- Characteristics and limitation of microchannel plates used in shutters for ultrahigh-speed photography 21 p2694 A73-39943
- High speed camera with locked mode laser activated Kerr cell shutter to obtain picoseconds exposure duration 21 p2709 A73-39945
- Flashlamp pumped CW mode-locked dye laser picosecond light pulse duration measurement by electro-optical streak camera 21 p2694 A73-39946
- Image-converter camera with subpicosecond temporal resolution. 21 p2694 A73-39947
- Ultrafast streaking camera for picosecond laser diagnostics. 21 p2694 A73-39948
- The microchannel picroscope - A high temporal resolution scanning tube for study of luminous phenomena in the subnanosecond range 21 p2694 A73-39949
- Subpicosecond time-resolution image converter - The picrochro. 21 p2694 A73-39950
- Why exact metrology in an ultrahigh-speed cinematographic system - An application example: Calibration of image converters with a view to photometric measurements 21 p2694 A73-39951
- Resetting in time of recordings in ultrahigh-speed cinematography 21 p2694 A73-39952
- Ultrashort laser pulse generators for dynamic marking of 'chronodiode' and 'chronolas' slit cameras 21 p2709 A73-39953
- Utilization for high speed cinematography of phased-locked CW lasers 21 p2709 A73-39954

- A method for the calibration of a quantitative high-speed schlieren procedure involving photographic recording
21 p2694 A73-39955
- Measurement of change in a cross section and position of small particles by diffraction techniques.
21 p2695 A73-39959
- The use of holographic techniques for recording high-speed events.
21 p2695 A73-39962
- High-speed interferometry of expanding and collapsing laser produced plasma.
21 p2744 A73-39964
- High-speed photography of laser-induced cavities in liquids
21 p2709 A73-39968
- Repetitive recording of stress waves in a photoelastic material using a multi-pulsed laser and an inexpensive streak camera.
21 p2695 A73-39970
- Utilization of the laser as a source in ultrahigh-speed cinematography
21 p2709 A73-39972
- Visualization of gas flows by means of high-speed holography
21 p2696 A73-39978
- A multiframe high-speed camera developed to register phase objects with good spatial resolution without parallax.
21 p2696 A73-39980
- High-speed photographic observation of the propagation of a shockwave in a branched-tunnel system
21 p2676 A73-39983
- High-speed photography of laser damage in solids.
21 p2709 A73-39987
- High-speed photographic study of failure processes in composite materials.
21 p2723 A73-39988
- Visualization of the shape and symmetry of detonation waves by a slit camera - Application to hollow charges
21 p2697 A73-39992
- High-speed camera study of the shock wave propagation.
21 p2697 A73-39993
- High-speed cine-photography and oscillography in a boiling simulation.
21 p2697 A73-39994
- Technique of an ultrahigh-speed sampling camera based on the use of a unique photomultiplier
21 p2697 A73-39995
- Automatic accurate full-range synchronization of light strobe with shutter opening of fast-framing camera.
21 p2697 A73-39997
- The application of high-speed photography and spectrography for investigations of erosive pulsed plasma streams.
21 p2744 A73-39999
- Photographic laboratory studies of explosions.
21 p2706 A73-41553
- An electronically synchronized drum-type film camera
21 p2706 A73-41580
- HIGH SPEED FLIGHT**
U HIGH SPEED
- HIGH SPEED TRANSPORTATION**
U RAPID TRANSIT SYSTEMS
- HIGH STRENGTH**
Possibilities regarding the development and the employment of fiber-reinforced composites in comparison with conventional materials
11 p1454 A73-25419
- An improved method of production for high strength fibre-reinforced thermoplastics.
18 p2329 A73-37092
- Analysis of the test methods for high modulus fibers and composites; Proceedings of the Symposium, San Antonio, Tex., April 12, 13, 1972.
23 p2996 A73-43626
- Some important aspects in testing high-modulus fiber composite tubes in axial tension.
23 p2996 A73-43639
- HIGH STRENGTH ALLOYS**
NT HIGH STRENGTH STEELS
NT MARAGING STEELS
- Powder metallurgy for high-performance applications; Proceedings of the Eighteenth Sagamore Army Materials Research Conference, Raquette Lake, N.Y., August 3-September 3, 1971.
01 p0062 A73-10276
- Hot isostatic pressing of high-performance materials.
01 p0056 A73-10280
- Fabrication of high-strength aluminum products from powder.
01 p0063 A73-10281
- Processing of high-performance alloys by powder metallurgy.
01 p0063 A73-10286
- Microstructural, mechanical and thermal properties of Nb-W-Ti-Zr alloys, noting cold rolled sheet products
02 p0182 A73-12580
- Ways of enhancing the strength characteristics of heat-resistant and high-strength cast aluminum alloys
03 p0324 A73-13514
- High modulus Be-Al alloy strengthening and aging as function of Cu, Mg and Zn additions
03 p0325 A73-13517
- High strength alloys hydrogen embrittlement mechanisms and effects and preventive measures, considering steel decarburization, stress corrosion cracking, hydride sheath formation and failure modes
03 p0328 A73-14425
- Center cracked tension specimen geometry effects on plane stress fracture toughness of high strength Al, Ti and steel alloy sheets
04 p0460 A73-14699
- Characterization of age-hardenable and stress-rupture properties of some cobalt-base alloys.
04 p0465 A73-15579
- Evaluation of the compact tension specimen for determining plane strain fracture toughness of high strength materials.
05 p0581 A73-16126
- Stress-corrosion cracking of high-strength aluminum alloys.
06 p0704 A73-17509
- Lattice dilatation and hydrogen embrittlement cracking.
07 p0840 A73-20353
- High strength and plastic properties of two phase austenitic-martensitic Fe alloys after aging in alpha and gamma states
07 p0841 A73-20522
- Metallurgical principle guidance of alloy design, discussing gas turbine alloys, dispersion hardened and composite alloys, high damping alloys and superalloys
08 p0979 A73-21657
- Stress corrosion cracking of commercial Al-Mg alloys and its prevention.
09 p1102 A73-22422
- Dependence on the cobalt content of the strength of a WC-Co cutting alloy in tension
09 p1159 A73-22473
- Using fracture mechanics with aluminum alloy structures.
09 p1103 A73-22494
- Ti based beta alloy strain hardening and failure characteristics, emphasizing initial deformation phase and microdefect onset and development
09 p1105 A73-23064
- The role of fracture toughness in low-cycle fatigue crack propagation for high-strength alloys.
09 p1108 A73-23254
- Stress corrosion cracking of metals - A state of the art; Proceedings of the Symposium, Detroit, Mich., October 18, 1971.
10 p1231 A73-23867
- Tests concerning the production of gas turbine blades with directionally solidified structure
11 p1372 A73-25104
- X2048, a high strength, high toughness alloy for aircraft applications.
11 p1380 A73-25514
- Cast microstructure and fatigue behavior of a high strength aluminum alloy /KO-1/.
13 p1633 A73-28137
- Tensile properties of high strength Al-Zn-Mg and Al-Zn-Mg-Cu alloy products processed by T-AHA type final thermomechanical treatments
13 p1633 A73-28141
- Mechanical behavior of high-strength beta-titanium alloys.
13 p1638 A73-29456
- Fracture toughness-strength relationships in aluminum-zinc-magnesium-copper alloys.
13 p1639 A73-29473
- A study of fatigue crack propagation in high strength aluminum alloys at high stresses.
13 p1640 A73-29488
- Significance of intergranular corrosion in high-strength aluminum alloy products.
15 p1889 A73-31740
- High strength Ti alloy cracking and brittle fracture prevention during aging by high heat rate treatment at 250-500 C
15 p1889 A73-31814
- R-curve determination using a crack-line-wedge-loaded /CLWL/ specimen.
15 p1950 A73-31984
- Corrosion-fatigue crack growth in high-strength aluminum alloys with and without susceptibility to stress-corrosion cracking.
15 p1895 A73-32571
- Flaw detection and characterization using acoustic emission.
16 p2022 A73-34013
- Tensile deformation and fracture in high-strength Al-Zn-Mg alloys.
20 p2575 A73-39019
- The effect of heat treatment on the tensile strength and hardness of a quenched ternary zirconium-base alloy /Zr-0.5 wt. % Nb-1 wt. % Cr/.
21 p2717 A73-40319
- A titanium-base composite material
21 p2724 A73-41276
- A review of fatigue crack growth in high strength aluminum alloys and the relevant metallurgical factors.
23 p2991 A73-43806
- The effect of composition changes on the fracture toughness of an Al-Zn-Mg-Cu-Mn forging alloy.
23 p2993 A73-44025
- High strength Ti alloy cracking and brittle fracture prevention during aging by high heat rate treatment at 250-500 C
24 p3100 A73-45277
- HIGH STRENGTH STEELS**
NT MARAGING STEELS
- Strength and ductility of chromium-nickel-manganese steel as a function of the carbon and nitrogen content in the range from 20 to 253 C
01 p0064 A73-10490
- Cr, Ti, Ce, V and Nb carbide-forming additives effects on crystal dislocations growth and movement during strain hardening of Mn rich steel
01 p0066 A73-11345
- Cr and V additions effects on Mn steels mechanical properties and wear resistance, noting strength limit increase
01 p0067 A73-11351
- Simultaneous manifestation of temper brittleness and hydrogen embrittlement during low-cycle fatigue of high-strength structural steel
02 p0180 A73-11927
- Certain regularities in the influence of preliminary loading by alternating tensile stress on the long-term strength of Kh18N10T steel
02 p0180 A73-11928
- Stress history effect on incubation time for stress corrosion crack growth in AISI 4340 steel.
02 p0183 A73-12763
- Corrosion fatigue of type 4140 high strength steel.
02 p0183 A73-12764
- Reinforcement of aluminum alloys by high strength steel ribbons
03 p0312 A73-13581
- The dynamic growth of a void in a plastic material and an application to fracture.
03 p0394 A73-13984
- Fracture mechanics consideration of hydrogen sulfide cracking in high strength steels.
04 p0459 A73-14692
- High speed tool steel, Ti alloys and vanadium carbide products manufacturing by powder metallurgy, using vacuum and high pressure techniques
04 p0460 A73-14745
- The influence of certain experimental factors on the fracture toughness of a high-strength steel
04 p0462 A73-15299
- On the production of fatigue cracks for determining the work of rupture in bending tests.
04 p0450 A73-15670
- Premature and delayed fractures of high strength martensitic steels with graduated carbon contents, including brittle and ductile intercrystalline and trans-crystalline cleavage fractures
06 p0705 A73-17848
- A comparison of hydrogen embrittlement and stress corrosion cracking in high-strength steels.
06 p0709 A73-18479
- Borated steel fracture characteristics in the case of cyclic plane bending
06 p0711 A73-18663
- Effects of thermal treatment on the resistance of some steels to crack development and propagation
06 p0711 A73-18664
- Evaluation of protective coatings for prevention of corrosion of high strength steels when subjected to extreme environments.
06 p0711 A73-18717
- Effect of grain refinement on the microstructure and mechanical properties of 4340M.
06 p0713 A73-18773
- Temper embrittlement of pressure vessel steels.
07 p0839 A73-20271
- Hole preparation in titanium and high strength steels.
07 p0832 A73-20450
- [SME PAPER IQ 72-208]
An analysis of plastic instability in pure shear in high strength AISI 4340 steel.
09 p1101 A73-22405
- High strength TRIP /transformation induced plasticity/ steels hydrogen embrittlement susceptibility under cathodic charging, gaseous hydrogen environment and loading conditions
09 p1102 A73-22410
- Loading mode effects on high strength steel hydrogen embrittlement, considering stress tensor invariants and interstitial diffusion relationships
09 p1102 A73-22414
- Resistance to brittle fracture of high-strength steel.
09 p1106 A73-23161
- Enhancement of fracture toughness in high strength steel by microstructural control.
09 p1109 A73-23262
- Stress corrosion cracking of metals - A state of the art; Proceedings of the Symposium, Detroit, Mich., October 18, 1971.
10 p1231 A73-23867

- Stress corrosion cracking of a high strength steel.
10 p1232 A73-23869
- The resistance of wrought high strength aluminum alloys to stress corrosion cracking.
10 p1232 A73-23872
- Stress corrosion crack protection from coatings on high strength H-11 steel aerospace bolts.
10 p1232 A73-23874
- Resistance of high strength structural steel to environmental stress corrosion cracking.
10 p1232 A73-23875
- Influence of temperature on the damping characteristics of heat resistant EP452 and EL696 steels in a uniform stress-strain state produced by tension and compression
10 p1233 A73-24358
- Failure of high-strength welded structures with initial cracks
10 p1225 A73-24368
- Effect of cyclic stress form on corrosion fatigue crack propagation below K_{Isc} in a high yield strength steel.
11 p1382 A73-25822
- The strength differential of steel and Ti alloys as influenced by test temperature and microstructure.
12 p1513 A73-27681
- TRIP steel embrittlement and notch sensitivity in high pressure hydrogen environment resulting from interaction between hydrogen and stress-assisted martensite during deformation
13 p1633 A73-28144
- Rotating bending fatigue tests on Al coated steels, investigating electroplating, hot dip and spraying production methods effects on fatigue strength
13 p1635 A73-28645
- Brittle fracture initiation characteristics of twin notches.
13 p1700 A73-29469
- Statistical definition of fatigue behavior of strength of low alloy steels.
13 p1641 A73-29492
- Creep properties of low alloy steel in relation to microstructure.
13 p1641 A73-29509
- Development of austenitic heat-resistant steel containing a high concentration of nitrogen.
13 p1642 A73-29516
- The strength of welded joints in high strength stainless steels at cryogenic temperatures.
13 p1625 A73-29615
- Strength and ductility of chromium-nickel-manganese steel as a function of carbon and nitrogen contents over the range 20-253 C.
14 p1759 A73-30315
- Effect of tensile deformation in the austenite range on transformation kinetics of a high-strength low-alloy/HSLA/ steel.
14 p1762 A73-30641
- High strength steel fracture characteristics in vacuum and gaseous medium, noting hydrogen adsorption effect on crack resistance
15 p1887 A73-31248
- High strength steel developments, discussing chemical compositions, mechanical properties, production technology and applications
15 p1888 A73-31624
- Strengthening of chromium-nickel steels with unstable austenite
15 p1889 A73-31809
- Influence of vanadium, niobium, carbon, and silicon on the properties of low-pearlite steel
15 p1889 A73-31810
- Properties of low-alloy steels with small niobium additions
15 p1889 A73-31811
- Fracture extension resistance (R-curve) characteristics for three high-strength steels.
15 p1951 A73-31986
- Properties of HSLA steels, with and without molybdenum.
15 p1891 A73-32169
- Book - Forging of powder metallurgy preforms.
15 p1891 A73-32195
- Study of multiple surface compound precipitation during passivation of D6AC-steel.
15 p1895 A73-32566
- Some physicochemical characteristics of failure in tempered high strength steels
17 p2189 A73-34580
- High strength Ni-Cr-Mo steel plane-strain fracture toughness measured with circumferentially cracked-notched round bars, discussing heat treatment and test temperature effects
17 p2190 A73-34890
- Recognition and control of abusive machining effects on helicopter components.
[AHS PREPRINT 750] 17 p2180 A73-35078
- On the fracture of high-strength metals in the stress fields of various stress-concentration factors.
[SESA PAPER 2163A] 17 p2191 A73-35454
- Deformation and fracture mechanisms in aluminum reinforced by high strength steel ribbons.
17 p2192 A73-35539
- High strength steel strain hardening residual stresses, discussing rolling treatment, complex strengthening, fatigue strength, asymmetric stress cycles and torsional stress
18 p2323 A73-36762
- Influence of relief annealing on the mechanical properties of high-strength hydrogenized steel
21 p2721 A73-41228
- Effect of technological and metallurgical treatment on the properties of electroslog-welded joints in heat resistant steels
22 p2865 A73-41778
- Cadmium embrittlement of high strength, low alloy steels at elevated temperatures.
22 p2873 A73-41968
- Microstructural features of Cr12NiWMoVTi /T60/ steel after electroslog remelting
24 p3100 A73-45170
- Strengthening of Cr-Ni steels with unstable austenite.
24 p3100 A73-45272
- Effect of vanadium, niobium, and silicon on the properties of low-pearlite steel.
24 p3100 A73-45273
- Properties of low-alloy steels with small niobium additions.
24 p3100 A73-45274
- HIGH TEMPERATURE**
Analytical study of the sensitivity of a sensor for studying pulsations of the heat-transfer coefficient in a boiling high-temperature layer
01 p0051 A73-10864
- A study of startup regimes of high-temperature heat pipes.
21 p2792 A73-41060
- HIGH TEMPERATURE AIR**
Electrical conductivity and total radiant power of air plasma.
01 p0081 A73-10121
- Random stresses effect on dynamic creep properties of Ti alloy in high temperature air flow
02 p0180 A73-11625
- Further results on the stagnation point boundary layer with hydrogen injection.
07 p0921 A73-20358
- Determination of the electron concentration in the boundary layer of air mixed with ablation products of an asbestos plastic
09 p1128 A73-22622
- Heat and mass transfer during the evaporation of liquids from capillary porous bodies situated in a hot air flow
12 p1559 A73-27474
- High pressure plasma torch to heat air for high-temperature chemical reactions and hypersonic wind tunnels for reentry vehicle ablation studies
13 p1597 A73-28479
- Heat and mass transfer on the surface of a fiberglass-reinforced plastic in a high-temperature air flow
13 p1708 A73-29403
- Electrical conductivity and total emission coefficient of air plasma.
15 p1918 A73-31657
- Effect of H₂O, SF₆ and CCl₃F additions on the electron concentration in highly heated air
15 p1840 A73-31852
- Cooling of the heated region formed during breakdown of air by laser radiation
17 p2183 A73-34262
- Transport coefficients of air at temperatures from 3000 to 25,000 K and at pressures of 0.1, 1, 10, and 100 atm
17 p2253 A73-34264
- Protection of certain borides from oxidation in air at 1200 C
18 p2318 A73-35888
- Particle combustion mechanism in aluminum-magnesium alloys
19 p2472 A73-37511
- Thermodynamic properties of air and thermal equation of state as function of pressure and temperature from piezometer measurement
20 p2627 A73-39298
- Radiative-convective heat transfer in flows of hot air past a flat plate.
21 p2791 A73-41056
- HIGH TEMPERATURE ALLOYS**
U HEAT RESISTANT ALLOYS
HIGH TEMPERATURE ENVIRONMENTS
Russian papers on human adaptability covering altitude and temperature acclimatization, work capacity and anthropogenetic and medicogenetic factors
02 p0133 A73-11921
- Simple mathematical model of shift of threshold voltage induced in an m.o.s. transistor by testing at elevated temperatures.
05 p0560 A73-17324
- Graphite fiber reinforced polyimide resin composites for structural applications in long duration high temperature environments, discussing fabrication with match-metal die
[SME PAPER EM 72-107] 07 p0832 A73-20448
- Unidirectional filament reinforced metal matrix composites compositional changes due to temperature induced interatomic diffusion, using diffusion equation finite difference solutions superposition technique
09 p1101 A73-22404
- High temperature fatigue sensor based on conductive composite device irreversible resistance increase resulting from cumulative strain damage
09 p1083 A73-22504
- High temperature tolerance enhancement in rats by thermal training and medicinal preparations
12 p1462 A73-27705
- Changes in the gas content of blood in man during exposure to high ambient temperatures
12 p1463 A73-27711
- Study of crystalline transformations at high temperature above 2000 K; International Colloquium, Odello, Pyrenes-Orientales, France, September 27-30, 1971, Proceedings
12 p1514 A73-27918
- Survival of common bacteria in liquid culture under carbon dioxide at high temperatures.
15 p1837 A73-32650
- Certain mechanisms of the solid-phase interaction arising during the formation and operation of high-temperature coatings
18 p2322 A73-35877
- Hyperfiltration technique applied to wash water reclamation at elevated temperatures.
[ASME PAPER 73-ENAS-27] 19 p2400 A73-37982
- Acoustic fatigue resistance of aircraft structures at elevated temperatures.
[ALAA PAPER 73-994] 24 p3056 A73-44829
- HIGH TEMPERATURE FLUIDS**
NT HIGH TEMPERATURE AIR
NT HIGH TEMPERATURE GASES
High-temperature low pressure hose assembly, convoluted, tetrafluoroethylene-, for aerospace.
[SAE ARP 1227] 16 p1970 A73-33017
- A comparison of hydraulic fluid characterizations in two evaluation systems.
[ASLE PREPRINT 73AM-9A-2] 17 p2196 A73-34997
- HIGH TEMPERATURE GASES**
NT HIGH TEMPERATURE AIR
Book - Emission, absorption, and transfer of radiation in heated atmospheres.
01 p0119 A73-10125
- Flammable fuel-air mixture ignition by transient turbulent hot inert gas jet, calculating minimum required jet size
03 p0399 A73-14390
- High temperature zirconium dioxide electrolyte fuel cell systems design and operation with methane or gasoline as fuel, evaluating performance characteristics
04 p0408 A73-15118
- Thermodynamic equilibrium and relaxation models of ideal and real high temperature gas flows for reversible and irreversible processes
[DFVLR-SONDDR-282] 04 p0517 A73-15678
- Electron density reduction in high temperature air via boron powder aerosol, presenting shock tube data for temperature range 2800-4200 K and pressure range 1-2 atm
[ALAA PAPER 73-261] 05 p0603 A73-16982
- Gas shell surrounding Galaxy with temperatures intermediate between corona and disk due to hot gas accretion from intergalactic space of Local Group
05 p0622 A73-17179
- Investigation of the vapor pressure of cesium by the boiling-point method.
06 p0722 A73-17404
- Two chamber adiabatic test compression system design with controlled throttle for high temperature nitrogen- and nitrous oxide-type gases with exothermal reactions
06 p0683 A73-17413
- Heat and mass transfer at the surfaces of glass-graphite materials in a high-temperature gas flow
06 p0766 A73-17457
- High temperature compressed gas heat conductivity calculation by least squares and basis isotherm methods
06 p0770 A73-18569
- Use of oblique shock waves in high-temperature shock-tube studies.
06 p0683 A73-18793
- Experimental investigation of the electrical conductivity of a coaxial high-temperature jet with dispersed particles of Ti
07 p0858 A73-20010
- Effects of Compton scattering in a moving gas
07 p0853 A73-20308
- Plane or axisymmetric inviscid optically gray hot gas jet radiating near optically thin limit, considering thermal radiation-gas dynamics coupling effects
08 p1020 A73-20783
- Compound heat exchange between a high-temperature gas-fluidized bed and a solid surface.
08 p1022 A73-21251
- An effective cross section method of accounting for the selectivity of emission and absorption in a hot gas
09 p1123 A73-22613

Induction flowmeter theory in a T-tube of circular section. 10 p1220 A73-24619

Transpiration and natural convection - The vertical-plate problem. 11 p1449 A73-25219

Hot gas environment fatigue analysis from corrosion viewpoint, considering gas-alloy reactions 11 p1383 A73-25833

Compton-scattering effects in a moving gas. 12 p1526 A73-27280

Air injection from wall slot into turbulent boundary layer of high temperature gas channel flow, calculating film cooling effectiveness in flat plate 13 p1706 A73-28675

Investigation of high-temperature gas flow around axisymmetric bodies in the presence of several discontinuity surfaces 13 p1708 A73-29404

Russian book - Thermophysical properties and gasdynamics of high-temperature materials. 15 p1957 A73-31851

Calculation of the composition of 79% N₂ + 21% O₂ and 50% N₂ + 50% O₂ mixtures containing carbon at high temperatures 15 p1840 A73-31853

Calculation of the parameters of a chemically reacting gas behind an incident and reflected shock wave 15 p1840 A73-31855

Experimental assembly for complex heat transfer studies 15 p1858 A73-31860

A combinational method of calculating the average velocity and the mean-mass temperature of a gas flow from the phase diagram of the substance 15 p1957 A73-31865

Temperature determination in a gas flow with the aid of two thermocouples 15 p1876 A73-31870

High temperature compressed gas heat conductivity calculation by least squares and isotherm methods 16 p2086 A73-33594

Time-dependent radiative cooling of a hot low-density cosmic gas. 17 p2231 A73-34756

Characteristics of the heat exchange in the region of injection into a supersonic high-temperature flow 17 p2254 A73-34772

Approximate configuration factors for a gray nonisothermal gas-filled conical enclosure. [AIAA PAPER 73-752] 18 p2370 A73-36368

Extragalactic radio sources modeled as bubbles of relativistic plasma rising through hot gas, producing galactic clusters X ray emission 18 p2353 A73-36508

Thermal control coatings for heat shielding of high-temperature high-speed chemically aggressive gas flows, noting turbine blade shielding application 18 p2371 A73-36812

Some characteristics of the disintegration of glassy bodies in hot gas flows 18 p2372 A73-37020

High-temperature gas-solid reactions. 19 p2403 A73-38552

Carbon deposition and the role of reducing agents in hot-corrosion processes. 20 p2576 A73-39027

Cold gas cloud embeddings in interstellar hot gas, determining radiation temperature from absorption line profiles and kinetic temperature from thermal and turbulent energy components 20 p2606 A73-39066

Design modeling of external and internal cooling systems for bodies exposed to high temperature gas flow, discussing operation similarity conditions 20 p2628 A73-39419

High temperature jet noise dependence on velocity and temperature, discussing Lighthill source term, Reynolds stresses, entropy fluctuations and velocity critical threshold 22 p2795 A73-41703

The rapid cooling of a hot gas discharge by liquid sprays. 22 p2929 A73-41743

New measurements of the thermal conductivity of argon and nitrogen to 200 C and 1600 atmospheres. 22 p2932 A73-42502

The temperature dependence of viscosity and thermal conductivity of dilute noble gases at moderate and high temperatures. 22 p2932 A73-42504

Some reactions and hydroperoxyl and hydroxyl radicals at high temperatures. 22 p2898 A73-42754

A hot gas actuator for missile control. 23 p2942 A73-43398

Ignition of metal particles in the case of a logarithmic oxidation law 24 p3154 A73-44704

Burn-up of the high temperature products of incomplete combustion in a supersonic flow by a second injection of oxidizer 24 p3156 A73-45076

Unsteady convective heat exchange for various hot-gas cooling laws in tubes 24 p3156 A73-45077

HIGH TEMPERATURE LUBRICANTS

High temperature solid lubrication technology developments, discussing bonded films, plastic and metal bonded composites and temperature ranges 03 p0330 A73-13013

Review of recent advances in bonded solid film lubrication at high temperatures. 07 p0842 A73-19552

A review of the perfluoroalkyl ether class of greases. 07 p0843 A73-19558

Silicone oil lubricants technology for steel-steel lubrication over wide temperature and load ranges. 07 p0843 A73-19560

Usage of the VNII NP-300A lubricant in gas-liquid chromatography and high-vacuum technology 10 p1239 A73-24250

High temperature solid lubricants lubricating and environmental stability characteristics, discussing ball and journal bearings wear test results [ASME PAPER 73-DE-9] 14 p1767 A73-30818

Antifricition materials employing fibers and liquid-metal lubricants 24 p3101 A73-44413

HIGH TEMPERATURE MATERIALS

U REFRACTORY MATERIALS

ZrH space power reactors design, discussing long life fuel elements, high temperature hard vacuum irradiation environment control drive components and shield fabrication 11 p1395 A73-26011

HIGH TEMPERATURE PLASMAS

Electrical conductivity and total radiant power of air plasma. 01 p0081 A73-10121

Solution of the Boltzmann equation for a fully ionized plasma in an oscillatory electric field and a steady magnetic field. VI - The first velocity moments of distribution function for a homogeneous plasma in a high-frequency electric field. 03 p0349 A73-14650

The thickness of perpendicular collisionless shocks in a hot plasma. 04 p0479 A73-15191

The measurement of plasma transport properties in a free-burning electric arc. 05 p0603 A73-16763

Temperature dependence of the ion recombination coefficient in a hydrocarbon flame plasma 06 p0731 A73-18553

Steady-state charged and neutral particle densities in a bounded turbulent high-temperature plasma. 06 p0732 A73-18607

Production of hot plasmas of solid-state density by ultrashort laser pulses. 06 p0733 A73-18783

Self trapping modulational instability of electron cyclotron wave whistler in cold and hot dense plasmas, discussing relevance to phenomena in magnetosphere 07 p0814 A73-19239

Electron energy loss effect on cross-field electron streaming instability in low density high temperature plasmas, using high voltage theta pinch 07 p0859 A73-20192

German monograph on collective dissipation processes in collisionless shock waves in high ion temperature plasma, using laser beam scattering technique 07 p0837 A73-20387

Waves in a hot uniaxial plasma excited by a current source. 07 p0860 A73-20477

Steady state hot toroidal Tokamaks plasma, calculating seed current density for bootstrap effect produced by neutral particle injection parameters control 08 p0991 A73-20814

Investigation of the structure of a high-current discharge in a lithium plasma. 08 p0992 A73-20853

Solar cosmic rays propagation between shock front and solar flare hot plasma, examining fine structure from Explorer 34 and Venera 6 data 08 p0999 A73-21328

Excitation of low-frequency oscillations by an electron beam in a hot plasma confined in a magnetic mirror 09 p1125 A73-21907

Propagation of electronic longitudinal modes in a non-Maxwellian plasma. 09 p1126 A73-22278

Two dimensional model of solar wind passage past magnetosphere, assuming hot plasma current sheath in geomagnetic tail 09 p1077 A73-22485

Cyclotron heating of plasmas with finite amplitude waves. 09 p1128 A73-22630

Fast wave propagation and damping at the second harmonic of the ion cyclotron frequency. 09 p1128 A73-22631

Particle seeded RF hydrogen plasma opacity, emission spectra, heat transfer and temperature profile at high temperatures 09 p1128 A73-22636

HIGH TEMPERATURE RESEARCH

Measurement of the current distribution at the surface of a doublet immersed in an isotropic hot plasma 09 p1131 A73-23034

Electrostatic probe theories and measurements in flame plasmas. 10 p1220 A73-24621

Superthermal plasma nodules and their relation to solar flares. 11 p1413 A73-25949

Influence of electric drift on the cone instability of a plasma in adiabatic traps 12 p1527 A73-26930

Application of the collisionless absorption of an extraordinary wave to the determination of plasma electron temperatures 12 p1528 A73-27302

Laser light pulse absorption in transient dense hot plasma generated around metallic anode tip by fast capacitive discharge in vacuum 13 p1664 A73-28460

Investigation of the feasibility of the injection of electrons into heliotron-type closed magnetic mirror configurations 13 p1666 A73-28957

Temporal development of longitudinal plasma current radial profile, obtaining effective collision frequency estimation for electron heating, hot plasma production conditions and stability restoration force 14 p1777 A73-29685

Comprehensive theory of r.f. energy absorption by a hot ion-electron plasma cylinder excited by an arbitrary electromagnetic field. 15 p1916 A73-31080

Transport phenomena in a fully ionized ultrarelativistic plasma 15 p1919 A73-31709

Impedance of a short cylindrical dipole antenna in a hot uniaxial plasma. 15 p1845 A73-32237

Dispersion equation for nonpotential oscillations and hydrodynamic instabilities in hot ion plasma with transverse current in magnetic field 15 p1920 A73-32304

Electron-beam excitation of low-frequency waves in a hot plasma confined in a mirror machine. 15 p1922 A73-32632

Axial distribution for a hot electron plasma. 16 p2041 A73-33325

Effect of a sheath on the fields of a probe in a hot magnetized plasma. 16 p2041 A73-33330

Temperature dependence of the ion recombination coefficient for a hydrocarbon flame. 16 p2042 A73-33578

Decay of a high temperature helium plasma - Validity of local thermodynamic equilibrium and estimation of recombination coefficients for He⁺ + ν , He⁺ + ν , and He²⁺ + ν . 16 p2043 A73-33867

A high-temperature plasma state in a high-power microwave discharge 17 p2214 A73-34136

Recent developments in strong shock wave research. 19 p2415 A73-37155

High temperature relativistic plasmas, calculating post-shock properties for steady hydromagnetic shock wave production 19 p2464 A73-37156

Investigation of the performance of a coaxial accelerator in the production of a dense high-energy plasma 19 p2467 A73-37367

Effect of electric drift on the loss-cone plasma instability. 22 p2891 A73-42264

German monograph - Model of a parallel shock wave with turbulent dissipation in a hot plasma. 22 p2895 A73-42718

Large amplitude electromagnetic waves in hot relativistic plasmas. 22 p2895 A73-43024

Some diagnostic methods for dense plasmas from high-pressure pulse discharges 23 p3011 A73-43667

Electron injection through the diverter in a heliotron. 23 p3013 A73-44309

Dispersion equation for nonpotential oscillations and hydrodynamic instabilities in hot ion plasma with transverse current in magnetic field 24 p3114 A73-44612

Hot plasma in contact with cold wall, calculating dynamic behavior in magnetic field from numerical solution of one-fluid two-temperature equations 24 p3117 A73-45456

HIGH TEMPERATURE RESEARCH

Ignition of systems having refractory reaction products 07 p0920 A73-19988

Investigation of the enthalpy and heat capacity of niobium carbide based materials at high temperatures 12 p1513 A73-27310

Book - Progress in high temperature physics and chemistry. Volume 5. 17 p2255 A73-35592

A high-speed /subsecond/ system for accurate thermophysical measurements at high temperatures.
[AIAA PAPER 73-743] 03 p2316 A73-36359

Investigation of the kinetics of high-temperature aluminum/oxygen interaction by the ignition method
19 p2503 A73-37504

High temperature thermophysical properties of tungsten.
[ECTP PAPER D1-5] 22 p2876 A73-42405

High reliability protective coatings for high temperature technology.
22 p2879 A73-42596

Reaction rate constants for carbon monoxide-hydrogen-oxygen and hydrogen-nitrogen-oxygen systems at high temperatures, modeling hydrocarbon combustion for product distribution
22 p2933 A73-42758

HIGH TEMPERATURE TESTS

Experimental investigation of the magnetic properties and magnetization conditions of magnetically solid materials at elevated temperatures
01 p0044 A73-10084

Test results of fatigue at elevated temperatures on aeronautical materials.
[ONERA, TP NO. 1098] 01 p0061 A73-10229

High temperature effects on near order transformations in TiC-WC solid solutions during heat treatment and cooling, using X ray diffraction scattering measurements
01 p0064 A73-10615

Fatigue crack propagation in stainless steel weldments at high temperature.
01 p0067 A73-11372

Electron microanalysis of backfilled hot cracks in Inconel 600.
01 p0067 A73-11373

Thermogravimetry system designed for use in dispersion strengthening studies.
01 p0015 A73-11449

High-temperature thermal analysis of high boron alloys using automatic optical pyrometry.
01 p0015 A73-11450

Polychromatic X-ray diffraction - A rapid and versatile technique for the study of solids under high pressure and high temperature.
01 p0054 A73-11482

Thermophysical properties of arc-cast tungsten using the TPRC multi-property apparatus /direct heating method/.
01 p0067 A73-11483

Influence of high-temperature annealing on the rupture characteristics of zirconium carbide
02 p0178 A73-11541

Assessment of the heat resistance of graphites over a wide range of temperatures
02 p0184 A73-11619

Generalized and modified parametric methods for extrapolating results of long term high temperature strength tests for service life determination
02 p0181 A73-12205

Apparatus for investigations into long-term strength and creep of coated materials at temperatures above 1400 C in air.
02 p0150 A73-12219

Electron beam heating test arrangement for high temperature testing of refractory materials in vacuum, describing temperature control systems
02 p0150 A73-12220

Performance of an inhibitor-protector of steel against corrosion-fatigue failure at elevated temperatures and pressures.
02 p0182 A73-12700

The high temperature thermodynamic properties of Ni-Ti alloys.
02 p0182 A73-12753

High-temperature oxidation of a Ti-15Mo-5Zr alloy at low pressure of oxygen /40 microtorr to roughly 0.2 millitorr/.
03 p0321 A73-12918

Preparation and high-temperature properties of carbon fiber-Ni composites.
03 p0321 A73-12919

Effects of alloying elements on elevated-temperature mechanical strength of high Cr, Ni-base heat resistant alloy.
03 p0321 A73-12921

Effect of heat treatment on filament wound carbon composites.
03 p0332 A73-13043

The thermal and electrical conductivities of tantalum at high temperatures.
03 p0322 A73-13182

Pyrometric obturation devices effect on sample temperature level during high temperature tests with radiant heating
03 p0306 A73-13189

Thermal properties of tantalum-tungsten alloys at high temperatures.
03 p0322 A73-13192

Recording of metal hardening during fatigue testing at elevated temperatures.
03 p0307 A73-13287

Supersonic mixing and combustion of a hydrogen jet in a coaxial high-temperature test gas.
[AIAA PAPER 72-1179] 03 p0397 A73-13474

The effect of small magnesium additions on microstructure and high-temperature properties of nickel-2 1/2 vol. % alumina.
03 p0326 A73-13966

Stresses governing the high-temperature creep rate in single crystals with a bcc lattice
03 p0326 A73-13971

Phase transformations in the VT9 quenched titanium alloy during heating
03 p0327 A73-13974

Refractory alloys fatigue life up to 950 C under non-stationary loading, noting log-normal law distribution
03 p0327 A73-14010

Zirconium carbide creep characteristics and limit at 2450-2810 K, examining test conditions effects on parameters
03 p0328 A73-14017

Thin film CdS solar cell stability improvement by etching, noting cuprous sulfide oxidation effects on degradation from short term tests at high temperature
03 p0255 A73-14221

Solar cells and generator technology for the Helios sun probe.
03 p0256 A73-14235

Evaluation of materials for sliding at 600F-1800F in air.
[ASLE PREPRINT 72LC-7C-2] 03 p0317 A73-14371

Metallic additions effect on wear and friction behavior of lead monoxide, lead silicate and calcium fluoride solid lubricants coatings for high temperature operations
[ASLE PREPRINT 72LC-7C-5] 03 p0317 A73-14374

Performance of liquid jet pumps at elevated temperatures.
03 p0317 A73-14502

Elevated temperature toughness and a dimensionless parameter involving the zero-ductility temperature.
04 p0459 A73-14670

Predictive testing in elevated temperature fatigue and creep - Status and problems.
04 p0453 A73-14853

The high-temperature oxidation of nickel-20 wt. % chromium alloys containing dispersed oxide phases.
04 p0461 A73-14923

The functional form of rate curves for the high-temperature oxidation of dispersion-containing alloys forming Cr₂O₃ scales.
04 p0461 A73-14924

The high-temperature oxidation of cobalt-21 wt % chromium-3 vol. % Y₂O₃ alloys.
04 p0461 A73-14925

An inelastic stress-strain law for elevated temperature and slowly time varying loads.
04 p0512 A73-15235

High temperature tests for chemical vapor deposited W ring and tensile specimens mechanical properties, investigating slip traces and fracture surfaces
04 p0462 A73-15305

High temperature creep properties of recrystallized W-thoria alloy wires, noting dependence on temperature, grain structure and stress
04 p0463 A73-15306

A study of precipitation at elevated temperatures in a Mg-8.7 pct Y alloy.
04 p0463 A73-15318

Some factors affecting high-temperature strength of matrix in heat resisting alloys.
04 p0464 A73-15577

High temperature strength and microstructure of nickel-base heat resisting No. 64BC alloy.
04 p0465 A73-15583

Some experiments on dynamic and quasi-static forging of aluminum at elevated temperatures.
[ASME PAPER 72-WA/MAT-1] 04 p0457 A73-15811

Internal stress and dislocation structure of aluminum in high-temperature creep.
04 p0467 A73-15930

High temperature steady state creep determination in Al by dip test technique interpreted in terms of slip and recovery activation energy due to effective and internal stress
04 p0467 A73-15933

A technical note on the correspondence between Amontons' law and wear-scar data in a 4-ball machine.
05 p0581 A73-16108

Earth crust materials high temperature lattice and radiative thermal conductivity from laser IR measurements, discussing single crystal and polycrystal forsterite-rich olivines and enstatite
05 p0569 A73-16378

Torsional fatigue fixture for high temperature investigation of high strength steels crack growth rate in tensile mode
05 p0563 A73-17254

Directional dependence of the thermal conductivity of crystal-oriented pyrolytic graphite at high temperatures.
06 p0713 A73-17405

Carbon and graphite sublimation in inert gas flow at 2800-3000 K, determining rate dependence on temperature under kinetic and diffusive conditions
06 p0713 A73-17411

New method for determining the total radiating power of partially transparent materials at high temperatures.
06 p0722 A73-17414

Enthalpy and heat capacity of boron carbide in the temperature range 273-2600 K.
06 p0714 A73-17415

The VDTA-3 apparatus for high-temperature differential thermal analysis
06 p0693 A73-18043

Structural changes in molybdenum single crystals during high temperature creep
06 p0708 A73-18048

High temperature and metallographic investigation of Nd-Y alloys, measuring heat and electrical conductivity, thermal expansion and emf, magnetic susceptibility and Hall coefficient
06 p0735 A73-18050

Postirradiation mechanical properties of Types 304 and 304 + 0.15% titanium stainless steel.
06 p0710 A73-18545

Enthalpy and heat capacity of graphite in the temperature interval between 273 and 3650 K
06 p0714 A73-18557

Investigation of high-temperature evaporation of heat-resistant ceramic coatings on metals
06 p0714 A73-18656

A study of germanium monoxide at high temperatures
06 p0739 A73-18659

Nickel-base alloys hot corrosion mechanism due to sodium sulfate induced accelerated or catastrophic oxidation as result of protective oxide scale dissolution
06 p0712 A73-18763

High temperature behavior of superalloys exposed to sodium chloride. I - Mechanical properties. II - Corrosion.
06 p0713 A73-18766

Creep of precipitation-hardened nickel-base alloy single crystals at high temperatures.
06 p0713 A73-18768

Measurement of high-temperature thermal conductivity of Eucalox /Al₂O₃/ using a heat pipe technique.
06 p0715 A73-18778

Development and properties of cobalt-base alloys with improved hot-corrosion resistance.
07 p0838 A73-19497

The effect of carbon on the hot corrosion of cobalt-base alloys.
07 p0838 A73-19498

Passivation of chrome steels under isothermal oxidation at 1020 deg C
07 p0839 A73-19660

Russian book - Heat resistance of welded joints.
07 p0831 A73-20230

Creep tests and fracture mechanics for high temperature properties of steels and alloys under static load, noting discrepancies for brittle materials
07 p0840 A73-20510

Creep-rupture strength of OT4 alloy
07 p0840 A73-20511

Damping properties of 1Kh13 and 2Kh13 high-chromium steels in a uniform stress-strain state in tension and compression at room and high temperatures
07 p0841 A73-20513

Enthalpy and specific heat of tantalum carbide in the range 273-3600 K.
08 p0977 A73-20865

Reaction of graphite with carbon dioxide at temperatures from 1200 to 2400 C
08 p0982 A73-21095

High frequency equipment for studying fatigue in sheet materials in conditions of plane stress and elevated temperatures.
08 p0952 A73-21149

Superalloys oxidation behavior under long term exposure to high temperatures for suitability as Co-60 heat sources encapsulation materials
08 p0978 A73-21415

The dependence of the notch sensitivity of Waspaloy at 1000-1400 deg F on the gamma prime phase.
[ASME PAPER 72-MAT-J] 08 p0979 A73-21571

Some problems in the assessment of high temperature properties for engineering purposes.
08 p0981 A73-21782

Phase separation analysis of ternary Co-W-Ti alloy during high temperature aging by X ray and electron microscopy method
09 p1099 A73-21963

Investigation of the failure characteristics of electrically heated samples of heat-resistant steels and alloys in a high-pressure oxidizing flow
09 p1069 A73-21980

Certain regularities in the deformation and rupture of molybdenum-, niobium-, and tantalum-based high-melting-point alloys under programmed temperature changes
09 p1100 A73-22151

High temperature creep resistance enhancement by stress relaxation or removal of unstable surface layers, increasing activation energy for different alloys

09 p1101 A73-22403
Fine grained ingot source Be ductility at 700 C as function of strain rate, noting superplastic behavior with grain boundary sliding at low strain rates
09 p1102 A73-22413
Effects of hold time on low-cycle fatigue behavior of AISI Type 304 stainless steel at 593 C.

09 p1102 A73-22417
W-Ta alloys prepared by electron beam melting, testing Ta content effects on oxidation resistance and hardness at high temperatures

09 p1103 A73-22424
Matthiessen's rule and the electric resistance of solid solutions of silicon in iron at high temperatures
09 p1104 A73-22602

Mechanical behaviour of molybdenum and tantalum under high pressures at elevated temperatures.

09 p1105 A73-23018
High temperature mechanical properties measurements verifying metal polycrystal internal friction background origin in diffusion of vacancies formed under grain boundary loading

09 p1105 A73-23060
Effect of test temperature on energy of fracture of graphite.

09 p1110 A73-23062
An apparatus for testing components in a high temperature supersonic gas stream containing abrasive particles.

09 p1070 A73-23065
High temperature creep in nickel and its alloys

09 p1108 A73-23229
Influence of the combined effect of plastic deformation and high temperatures on the diffusion mobility of carbon

09 p1108 A73-23241
Electrical resistance and emissivity of certain transition metals and alloys in the high-temperature range

10 p1230 A73-23520
Influence of heat treatment on the high-temperature strength and creep of the NV10M5T3's niobium alloy
10 p1230 A73-23600

Mineral filler reinforcement value in polyolefins, stressing composite properties at high temperatures

10 p1237 A73-23963
High temperature creep properties of P10P polyimide - HMS graphite composites.

10 p1239 A73-23975
Prototype skin friction measurement instrument for short period or continuous operation at high temperature, considering alternative feasible systems design and experimental data

10 p1217 A73-24013
Fatigue properties of sandwich material with a honeycomb filler

10 p1289 A73-24097
Temperature dependence of the adhesive strength and elasticity of some high-melting coatings

10 p1225 A73-24371
Thermophysical and electrical properties of powdered boron carbonitride as high temperature insulating and refractory material at 1800-2020 C

10 p1241 A73-24687
Manifestation of the defect structure of cadmium telluride through high-temperature electrical conductivity

10 p1261 A73-24776
Machine for life testing materials under varying tension in working media with high temperatures and pressures.

10 p1204 A73-24946
New arrangement for testing materials in the volume stressed state and at elevated temperatures [Exchange of experience].

10 p1222 A73-24947
Solid body contact interaction devices at high temperatures in vacuum, gas and air for evaluation of surface coatings, adhesion, diffusion, mechanical properties, etc

10 p1222 A73-24966
Tests concerning the production of gas turbine blades with directionally solidified structure

11 p1372 A73-25104
Fatigue-crack growth in Type 304 stainless steel weldments at elevated temperatures.

11 p1379 A73-25131
Russian book on thermal stability of refractory ceramics covering strength and thermophysical characteristics, high temperature thermal fracture and facilities for normal and cyclic load tests

11 p1386 A73-25174
Mechanical properties at high temperature of Ni-based unidirectionally solidified eutectic: Ni-Ni₃Ta.

11 p1379 A73-25405
Measurement of a set of thermal properties of metals at high temperatures by the periodic-heating method

11 p1379 A73-25426
Investigation of the preparation of high-temperature strain gauges based on heat-resistant oxides

11 p1362 A73-25455

Thermal characteristics of constantan, Ni-Cr-Fe, Ni-Mo, Ce-Al-Fe and Ni-Cr alloy filaments for high temperature strain gages

11 p1362 A73-25456
Udimet 700 creep behavior under cyclic tensile stresses at 925 C from hodograph of monotonic stress-strain relations, taking into account strain rate effects [ALAA PAPER 73-387]

11 p1439 A73-25516
Thermal diffusivity and thermal conductivity of pyrolytic titanium and niobium carbides and of titanium nitride at high temperatures

11 p1380 A73-25740
The effect of vacuum on the high temperature, low cycle fatigue behavior of structural metals.

11 p1383 A73-25834
A new fretting fatigue testing machine.

11 p1344 A73-25839
Service failures and fracture mechanisms under cyclic load at high temperature.

11 p1442 A73-25845
Recent materials compatibility studies in refractory metal-alkali metal systems for space power applications.

11 p1310 A73-26005
Stability of nickel coated sapphire whiskers.

11 p1389 A73-26044
Elevated temperature stability of carbon-fibre, nickel-matrix composites Morphological and mechanical property degradation.

11 p1384 A73-26047
High temperature density measuring apparatus using the photon attenuation technique.

11 p1367 A73-26309
Crack propagation behavior in type 304 stainless steel weldments at elevated temperature.

11 p1375 A73-26357
Deterioration of impermeable alumina tubes in inert atmospheres at elevated temperatures.

12 p1513 A73-27032
Kinetic strain criteria of cyclic failure at high temperatures

12 p1552 A73-27252
Nickel base alloys high temperature steady creep rate and stress relations

12 p1512 A73-27256
Experimental investigation of the enthalpy of titanium oxides at temperatures ranging from 500 to 2000 K

12 p1513 A73-27325
Indenter materials for use in high-temperature hardness measurements

12 p1513 A73-27561
Thermal expansion of tungsten from 293 to 1800 K. [ECTP PAPER E-1]

13 p1631 A73-28052
Ditantal carbide thermodynamic stability determination from measurement of carbon monoxide pressure in equilibrium with ditantalum carbide-tantalum oxide-tantalum mixture at 1470-1620 C

13 p1632 A73-28128
On the electrical properties of nonstoichiometric oxides alpha-Nb₂O₅, MnO, and CoO at high temperature

13 p1634 A73-28202
Measurement of interfacial free energies and associated temperature coefficients in 304 stainless steel.

13 p1634 A73-28259
Investigation at the Moscow University of the thermal characteristics of material

13 p1704 A73-28426
Machine for measuring hardness and microhardness at high temperatures.

13 p1613 A73-28524
Testing machine with control panel and vacuum chamber for microhardness measurement at high temperatures with precise test point selection and indentation observation capability

13 p1613 A73-28525
NiO-CoO solid solutions defect structure from high temperature measurements of integrated Bragg peak intensities

13 p1645 A73-28934
The relations between superplasticity and high temperature resistance alloys of metallic systems.

13 p1639 A73-29457
Effects of small amounts of carbide-forming elements on the elevated temperature strength of austenitic stainless steel.

13 p1642 A73-29517
High temperature tests of microalloying effect on creep and stress rupture characteristics of hot rolled and annealed Mo alloys

13 p1643 A73-29605
Mechanical strength of titanium alloys AT-2 and AT-3 and of their welded seams at extreme temperatures.

13 p1643 A73-29633
The electrical resistivity of transition metals at high temperatures.

14 p1759 A73-29746
The thermal conductivity of a number of alloys at elevated temperatures.

14 p1760 A73-30435
High-speed/subsecond/ simultaneous measurement of specific heat, electrical resistivity, and hemispherical total emittance of Ta-10/wt.%W alloy in the range 1500 to 3200 K.

14 p1760 A73-30437
[ECTP PAPER D2-4]

High speed pyrometer for high temperature measurement of thermophysical properties, presenting experiment computer program outline

14 p1753 A73-30438
Thoria particle dispersion TD-nickel creep and tensile deformation at elevated temperature dependence on grain size and L/D ratio

14 p1761 A73-30635
A theoretical model for the elevated temperature deformation of dispersion hardened metals.

14 p1761 A73-30636
Rotors and turbine disks fracture resistance optimization at high temperatures from plane strain toughness criteria

14 p1813 A73-30679
Bakelite lacquer and epoxy and phenol-formaldehyde solidified resin binders strength at high temperatures

14 p1766 A73-30687
A high temperature vacuum assembly for precision creep tests

14 p1743 A73-30694
Hot environment lubrication failures of sleeve bearing diester lubricant system in small electric motors, using reliability-temperature accelerated tests

14 p1767 A73-30819
High-temperature electrical conductivity relaxations induced in CdTe crystals by variations in cadmium vapor pressure

15 p1923 A73-31201
Nitrides and oxides formed on a niobium surface at high temperatures in vacuum

15 p1887 A73-31203
Physicochemical properties of metal silicides under vacuum at high temperatures, assessing suitability as antineutron materials on Mo grids in high power vacuum electron tubes

15 p1898 A73-31842
High temperature specific heats of iron-rich iron-titanium alloys between 600 and 1150 K.

15 p1891 A73-31994
Grain boundary dislocations in aluminium bicrystals after high-temperature deformation.

15 p1891 A73-32020
High-temperature corrosion in gas turbines and steam boilers by fuel impurities. II - The sodium sulfate-magnesium sulfate-vanadium pentoxide system.

15 p1841 A73-32175
Mach 1 oxidation of thoriated nickel chromium at 1204 C /2200 F/.

15 p1892 A73-32271
Properties of the 4201 alloy at elevated temperatures

15 p1894 A73-32528
Characteristics of failure in alpha-titanium alloys at high temperatures

15 p1894 A73-32536
Investigation of titanium alloys at high temperatures in vacuum

15 p1894 A73-32541
X-ray diffraction at high temperatures for a study of thermal expansion of MnSe and MnSe₂

15 p1925 A73-32651
Oxidation resistant carbon-carbon composite for Space Shuttle application.

16 p2028 A73-33043
Evaluation of additives for prevention of high temperature corrosion of superalloys in gas turbines.

16 p2047 A73-33479
Enthalpy and specific heat of graphite in the temperature range 273-3650 K.

16 p2030 A73-33583
Molybdenum evaporation rates in oxygen, air, and water vapor at high temperatures and low pressures

16 p2026 A73-33956
The influence of vacancies on the nucleation of incoherent germanium precipitates in aluminum-germanium alloys. III - The effect of germanium nuclei on precipitation at higher temperatures

16 p2026 A73-33971
Hot fatigue strength during fluctuating axial tension of PER 7 and IN 100 superalloys

16 p2026 A73-33971
X-ray investigation of the fine crystalline structure of aluminum with creep

17 p2186 A73-34117
Special features of high-temperature creep in metals with an fcc lattice

17 p2188 A73-34563
Electrical resistivity and emissivity of some transition metals and alloys in the high-temperature range.

17 p1291 A73-35200
Dynamic yield strength determination at elevated temperatures after nanosecond pulse heating.

17 p2148 A73-35450
High temperature tensile and stress rupture tests of tungsten (Nichrome laminar composites and tungsten alloy/ Inconel sheet and foil specimens

17 p2193 A73-35545
High temperature thermal cavity system with vitreous carbon tube and end plugs for material and thermochemical environment investigations, discussing mass spectroscopic measurement

17 p2149 A73-35752

Thermoplastic temperature range extended up to 260 C by polysulphones. 18 p2326 A73-36068

Effect of prestress levels on the long term strength of 1Kh18N9T steel at elevated temperatures 18 p2323 A73-36761

Book - Elevated temperature properties as influenced by nitrogen additions to types 304 and 316 austenitic stainless steels. 18 p2325 A73-36971

A study on graphite-base high-temperature composite materials. II Graphite-tantalum composite materials. 19 p2443 A73-37375

Specific characteristics of the high-temperature decomposition of ammonium perchlorate and of ammonium perchlorate-based heterogeneous systems 19 p2471 A73-37503

Creep tests and fracture mechanics for high-temperature properties of steels and alloys under static load, noting discrepancies for brittle materials 19 p2440 A73-37785

The damping properties of high-chrome steels 1Kh13 and 2Kh13 in a homogeneous stress state of tension-compression under the conditions of normal and elevated temperatures. 19 p2440 A73-37788

A model of strain hardening during high-temperature creep. 19 p2442 A73-38168

Analysis of integrated circuit failure modes and failure mechanisms derived from high temperature operating life tests. 19 p2411 A73-38449

System for measuring the thermal diffusivity of electrically conducting materials at high temperatures 19 p2432 A73-38543

Yield surfaces of metals at elevated temperatures. 20 p2615 A73-38640

The effect of molybdenum on gamma prime coarsening and on elevated-temperature hardness in some experimental nickel-base superalloys. 20 p2576 A73-39029

Damping of glass-like materials at high temperatures. 20 p2580 A73-39272

System of experimentally verified equations for calculating the thermodynamic characteristics of some technologically important gases at temperatures ranging from the normal boiling point to 1300 K at pressures up to 1000 bar 20 p2627 A73-39297

Nb heat pipe design with Na coolant for high-temperature operation, discussing losses effect on transmitted power 20 p2628 A73-39418

Liquid anorthite viscosity and thermal expansion at 1450-1620 C and 820-950 C, noting agreement with Bottinga-Weill model predictions 20 p2555 A73-39718

Russian book - High-temperature strain gauges based on heat-resistant oxides. 21 p2704 A73-41286

Oxygen interaction with tantalum and niobium at high temperatures 21 p2722 A73-41594

High-temperature internal friction in boron fibers 22 p2880 A73-41957

Basic method for realization of temperature scale at 10,000 K by photometric comparison between vacuum-UV-blackbody radiation of a plasma and synchrotron radiation. 22 p2852 A73-41978

Measuring transient high temperatures by optical pyrometry. 22 p2853 A73-41989

High temperature platinum resistance thermometry. 22 p2855 A73-42005

Stability of 25 ohm platinum thermometer up to 1100 C. 22 p2855 A73-42007

The high temperature stability of platinum resistance thermometers. 22 p2855 A73-42008

Thermal properties of tungsten-rhenium alloys used in high temperature thermocouples. 22 p2858 A73-42038

Studies of the performance of W-Re type thermocouples. 22 p2858 A73-42039

On the stability of metal sheathed noble metal thermocouples. 22 p2858 A73-42044

Some patterns of deformation and failure of refractory alloys of molybdenum, niobium and tantalum during a programmed change of temperature. 22 p2874 A73-42101

European Conference on Thermophysical Properties, 3rd, Turin, Italy, June 20-23, 1972, Proceedings. 22 p2876 A73-42401

Investigation of the thermal expansion of molybdenum and tungsten at high temperatures. [ECTP PAPER E-5] 22 p2876 A73-42406

Some thermophysical properties of titanium in the neighborhood of the melting point. 22 p2878 A73-42508

Measurement of the heat capacity of graphite in the range 1500 to 3000 K by a pulse heating method. 22 p2881 A73-42510

Revision of high temperature and critical properties of cesium. 22 p2932 A73-42513

The activation energy for creep of columbium/niobium/. 22 p2879 A73-42580

High-temperature oxidation of hydrogen by nitrous oxide in shock waves. 22 p2933 A73-42756

High temperature creep of lithium zinc silicate glass-ceramics. I - General behaviour and creep mechanisms. II - Compression creep and recovery. 23 p2997 A73-44030

Changes in surface structure during high-temperature creep flow. 23 p2994 A73-44159

Influence of the type of loading on high-temperature creeping of zirconium carbide 23 p2998 A73-44287

Thermal diffusivity and conductivity of titanium and zirconium carbides at high temperatures 24 p3099 A73-44760

HIGH THRUST

High and low thrust systems for primary and auxiliary spacecraft propulsion, noting electron bombardment electrostatic thruster for north-south station-keeping [AIAA PAPER 72-1123] 03 p0355 A73-13435

HIGH VACUUM

Device for studying the effect of ultrasonic oscillations on contact interaction in high vacuum 07 p0822 A73-19295

Usage of the VNII NP-300A lubricant in gas-liquid chromatography and high-vacuum technology 10 p1239 A73-24250

Icy cometary nuclei laboratory simulation by sublimation of dust particle containing ice and frozen electrolyte mixtures in high vacuum at low temperature 14 p1793 A73-29823

HIGH VOLTAGES

The performance of recently developed high voltage high current power transistors. 03 p0283 A73-13944

Pulse width amplitude converter design and performance for ion engine high voltage power supply, noting oscillator, modulator and circuit protection 04 p0489 A73-15733

High voltage fuel supplies intended for ion thrusters 04 p0489 A73-15734

Breakdown criteria for streamer formation, electrostatic field analysis and laboratory high voltage experiments on aircraft initiation of lightning strikes 10 p1175 A73-24558

Concept for a high voltage solar array with integral power conditioning. 11 p1310 A73-26001

High voltage phase meter with electrostatic logometer for loss angle measurements in capacitors and power cables during operation 12 p1495 A73-26790

Certain features of the analysis of a crystal-controlled FM oscillator at high modulating voltage levels 12 p1477 A73-26872

Improved uniform-field electrode profiles for TEA laser and high-voltage applications. 13 p1626 A73-28366

A generator of rectangular voltage pulses with 50 kV amplitude 17 p2120 A73-34153

Features of a high voltage airborne superconducting generator. 17 p2109 A73-35254

HIGHLY ECCENTRIC ORBIT SATELLITES U HEOS SATELLITES

HIGHWAYS

The reliability of the interpretation of soils from aerial photographs in highway planning practice. 20 p2558 A73-39872

The role ground transportation can play in the airport site selection process. [ASME PAPER 73-ICT-70] 23 p2966 A73-43497

HIJACKING

U AIR PIRACY

HILBERT SPACE

NT BANACH SPACE

Existence and stability of the secondary periodic solution figuring in Navier-Stokes type evolution problems [ONERA, TP NO. 1172] 01 p0033 A73-10780

An equation for the product of semigroups defined by the method of bilinear forms and its application to the Schrodinger equation. 01 p0071 A73-11333

A selfadjoint formulation of overdamped systems. 02 p0193 A73-12090

Application of the conditional-gradient method to the solution of an optimum control problem in a Hilbert space 02 p0187 A73-12188

Hilbert space and calculus of variations for eigenvalue bounds of integral equations of elasticity and potential theories 03 p0387 A73-13162

Spectrum of the self-adjoint extensions of a minimal operator generated by the Sturm-Liouville equation with an operator potential 04 p0470 A73-14931

Stability of the Bubnov-Galerkin method for unstable operator equations with variable coefficients 04 p0470 A73-15085

Arithmetic of probability laws defined on a separable Hilbert space 07 p0845 A73-20148

Energy-like Liapunov functionals for linear elastic systems on a Hilbert space. 07 p0852 A73-20336

An approximate method for the synthesis of optimal control of distributed systems. 07 p0806 A73-20596

Dual characterizations of optimal control systems governed by linear and nonlinear differential equations with dynamic constraints, using complementary variational principle in Hilbert space 07 p0846 A73-20598

Optimal binary quantum signal detection in two dimensional Hilbert space by a priori probability vector projection method, using randomized decision strategy 09 p1049 A73-22230

An optimal control problem for a class of distributed parameter systems. 10 p1202 A73-24549

The initial value problem for the free-space Schrodinger equation. 10 p1244 A73-24787

Potential operator theory in Hilbert spaces applied to rigorous definition of conservative loading, examining pressure loading case 11 p1434 A73-25212

Stability of the solutions of differential equations with a nonlinear potential operator in a Hilbert space 12 p1516 A73-26959

Some general questions in the theory of probability measures in linear spaces 12 p1517 A73-27187

Canonical representations of random processes with multiplicities of one and two 12 p1518 A73-27193

Application of mathematical programming methods to determine the optimal control for systems described by heat conduction equations 13 p1704 A73-28016

Linear distributed parameter system minimum time control, considering Hilbert space final value and Banach space inequality solutions 13 p1596 A73-28700

Existence of generalized tensorial fields in linear asymmetric elastodynamics. 14 p1809 A73-30256

Kalman-Bucy method for optimal filtering of time and space dependent random fields in Hilbert space in presence of additive white noise 15 p1854 A73-31689

Hilbert space of states, considering variational principles, linear elasticity pointwise bounds for homogeneous/inhomogeneous problems and potential theory 15 p1954 A73-32112

Stochastic integrals of cylindrical Brownian movements on Hilbert space 15 p1900 A73-32207

Regularity theorems for the solution of a second-order abstract linear differential equation 16 p2032 A73-33373

Complementary variational principle existence condition and duality in linear and quadratic programming in Hilbert space setting, considering relationship to Kuhn-Tucker saddle point theory 21 p2724 A73-40296

Concentration functions of finite-dimensional and infinite-dimensional random vectors 22 p2882 A73-42649

German monograph on regularization and penalty function methods of numerical analysis in Hilbert or Banach space covering minimax technique and optimal control theory application 22 p2882 A73-42847

Automorphism groups of W algebras operating in Hilbert space with application to noncommutative dynamic systems analysis and ergodic theory 23 p2999 A73-44102

Convergence of the Bazley-Fox method in the problem of eigenvalues of a bilinear form relative to another bilinear form 24 p3109 A73-44649

Topology of linear operators in Banach space generalized to invariant polynomials for minimum Schatten ideals in Hilbert space 24 p3105 A73-45008

Topological analysis of integral operators with Agmon kernel in Sobolev spaces within Hilbert space framework 24 p3105 A73-45009

Tensorial norms properties with respect to Hilbert spaces, constructing perfect ideals in Banach space
24 p3105 A73-45010

HILBERT TRANSFORMATION

Hilbert transform for single and narrow band signal analysis with 90 deg spectral component phase shift in frequency region
01 p0015 A73-10076

Vortex lattice discretization for finite Hilbert transform of two dimensional incompressible thin wing flow integral equation with singularities, noting numerical solution accuracy
04 p0403 A73-15004

Hilbert boundary value problem solution for piecewise holomorphic vector in singly connected region with Liapunov contour bound
15 p1900 A73-32086

HILLER MILITARY AIRCRAFT

U MILITARY AIRCRAFT

HILSCH TUBES

Influence of geometrical parameters on the energetic separation of superheated water vapor in a conical vortex tube
02 p0153 A73-11789

The Ranque-Hilsch vortex tube and its application to spacecraft environmental control systems.
03 p0287 A73-13313

HINDRANCE

U CONSTRAINTS

HINGE MOMENTS

U TORQUE

HINGED ROTOR BLADES

U HINGES

U ROTARY WINGS

HINGLESS ROTORS

U RIGID ROTORS

HINGES

Free vibration of a beam with one end spring-hinged and the other free.
05 p0633 A73-16542

HIPPOCAMPUS

Participation of the hippocampal structures in the formation of external inhibition
06 p0653 A73-18162

Rabbit hippocampal neuron activity relation to theta-wave phases from cell potential and extracellular recording analyses
07 p0782 A73-20005

Biopotential alpha and theta rhythms of neocortex and hippocampus of milk drinking cats after food and water deprivation
09 p1040 A73-28262

Hippocampus contribution to conditioned reflexes, memory, voluntary motions, orientation and emotional reactions, noting theta rhythm in stimuli response
10 p1180 A73-24326

Sinusoidal stimuli induced electrical activity of hippocampus in waking rhesus monkeys and baboons
10 p1180 A73-24330

Nature and significance of periodic electrical activity variations in the neocortex and the hippocampus during the paradoxical phase of sleep
11 p1317 A73-26083

Effect of stimulation of the mesencephalic reticular formation on the convulsive electrical activity of the brain
14 p1716 A73-30381

Serotonin content variations in the fore-brain during hibernation
18 p2276 A73-36567

Diminution of uncertainty in the firing of hippocampal units in response to a stimulus
20 p2516 A73-39803

The nature and significance of the dynamics of electrical activity in the neocortex and hippocampus during the paradoxical phase of sleep
24 p3059 A73-44718

HIS BUNDLE

Study of intraventricular conduction times in patients with left bundle-branch block and left axis deviation and in patients with left bundle-branch block and normal QRS axis using His bundle electrograms.
05 p0540 A73-16582

Immediate and remote prognostic significance of fascicular block during acute myocardial infarction.
14 p1715 A73-30052

Book on vectorcardiography covering equipment, techniques, lead systems and abnormalities associated with atrial and ventricular hypertrophy, bundle branch blocks, myocardial infarction and arrhythmia
17 p2114 A73-34452

QRS abnormalities in AV block - Variations and their significance.
18 p2274 A73-36521

Identification of the sites of atrioventricular conduction defects by means of His bundle electrography and atrial pacing.
18 p2282 A73-36522

The differential electrocardiographic manifestations of hemiblocks, bilateral bundle branch block, and trifascicular blocks.
18 p2274 A73-36523

The clinical causes and mechanisms of intraventricular conduction disturbances.
18 p2274 A73-36524

Effects of beta-blocking agents on atrio-ventricular and intraventricular conduction in man.
21 p2641 A73-41564

HISS

Ionospheric VLF and ELF electric field observation by Alouette 2 satellite, obtaining ion mass distribution from lower hybrid resonance hiss during geomagnetic storm
02 p0164 A73-12623

An analysis of multi-station ground observations of VLF Hiss.
03 p0274 A73-12950

Study of VLF and ELF noises observed by Alouette 2.
05 p0552 A73-17163

Incoherent Cerenkov radiation in the magnetosphere and the ground observations of VLF hiss.
07 p0814 A73-19240

Steady ELF plasmaspheric hiss, studying whistler mode turbulence, band limitation, power spectra and peak intensities
12 p1488 A73-26984

Space probe observed VLF hiss powers disparity with theoretical prediction for incoherent Cerenkov radiation, considering Landau instability generated wave amplification
17 p2160 A73-34788

An attempt to explain satellite observations of high latitude VLF hiss in terms of generation by incoherent Cerenkov radiation.
21 p2685 A73-40828

HISTAMINES

Daily rhythm of biogenic amine /histamine and serotonin/ contents in human blood during usual and shifted work schedules
06 p0650 A73-17688

Influence of histamine on cutaneous capillary circulation and on the oxygen tension of subcutaneous cellular tissue in various age periods
10 p1178 A73-23676

HISTOGRAMS

Operative visibility limits over the airports of Milan Linate and Malpensa in the 1960-1969 decade
19 p2447 A73-38125

Selection of analogs to composite kinematic charts of natural synaptic periods
19 p2449 A73-38545

Analysis of the results of the geometric satellite world network
22 p2849 A73-42589

HISTOLOGY

Myocardial function and ultrastructure in chronically hypoxic rats.
03 p0259 A73-13369

Pathomorphological and histochemical analysis of Luna 16 fine lunar soil fraction biological effect on mice
03 p0272 A73-14569

Myosin ATPase and fiber composition from trained and untrained rat skeletal muscle.
05 p0538 A73-16155

Morphological changes in the testicles of dogs exposed to chronic and combined gamma-radiation
08 p0929 A73-20981

Morphometric and histochemical investigation on human right atrial and mitral papillary muscle.
08 p0930 A73-21215

Inhibitory interaction in the retina of Limulus.
09 p1043 A73-23311

Study of the possibilities of histone-RNA complex formation in experiments in vitro
10 p1181 A73-24513

Incidence of Lucke renal adenocarcinoma in Rana pipiens as determined by histological examination.
11 p1314 A73-25136

Morphological changes in the liver of dogs induced by chronic gamma irradiation
12 p1463 A73-27707

Neurophysiological characteristics of isolated structures of the cerebral cortex
14 p1718 A73-30570

Histochemical investigation of some energy metabolism characteristics in a rat heart after acute fatigue
15 p1834 A73-31393

Histochemical correlates of changes in the primate brain associated with varying environmental light conditions.
15 p1837 A73-32600

Histological studies on the vestibular organ of frog embryos and larvae after the influence of simulated weightlessness.
18 p2270 A73-35979

Histopathological and histochemical studies of one year isolation and six months immobilization effects on rhesus monkeys internal organs and tissues
18 p2270 A73-35983

Retinal change induced in the primate /Macaca mulatta/ by oxygen nuclei radiation.
18 p2271 A73-36125

Cell viability in acute myocardial infarction, discussing pathogenesis, histological, histochemical and biochemical responses to ischemia, homeostasis maintenance and treatment methods
18 p2276 A73-36545

Power failure of the heart in acute myocardial infarction.
18 p2276 A73-36547

Structural changes in the adrenal nerve apparatus during experimental subtotal pancreatectomy
20 p2513 A73-39400

Effect of hind-limb immobilization on contractile and histochemical properties of skeletal muscle.
21 p2642 A73-41624

The effect of low X-ray doses on the central nervous system
23 p2947 A73-44179

HISTORIES

NT CASE HISTORIES

HODOGRAPHS

Investigation of a moving angular-velocity hodograph in the symmetrical solution to the problem of the motion of a body having a fixed point
02 p0191 A73-11762

Russian book - Fundamentals of the general theory for the root loci of automatic control systems.
02 p0149 A73-12750

Two dimensional steady nonrotational flow of perfect compressible fluid around symmetric convex profile, reducing to variational inequality in hodograph plane
07 p0776 A73-20147

Features of the application of the root-locus method to the study of sampled-data automatic systems on the basis of the w-transform
09 p1068 A73-22341

Udimet 700 creep behavior under cyclic tensile stresses at 925 C from hodograph of monotonic stress-strain relations, taking into account strain rate effects [AIAA PAPER 73-387]
11 p1439 A73-25516

Extension of the hodograph method for the one-dimensional elastic-plastic wave propagation.
13 p1696 A73-28646

Automation of plotting root-locus curves for automatic control systems
13 p1596 A73-29142

Approximate solutions and applications of hodograph equations in elliptic diabatic flow.
14 p1745 A73-30428

Hodograph construction by root trajectory method to provide maximum information on linear feedback systems dynamics
14 p1740 A73-30945

Velocity hodograph solvability and univalence problems in hydrodynamics for profiles in duct, bounded flow and cascades
15 p1861 A73-31151

Calculation of plane blade cascades in isentropic flow
18 p2266 A73-37085

On the interaction of shocks and simple waves of the same family. II.
20 p2545 A73-39011

HODOSCOPES

Description of a device for studying inelastic nuclear processes with nucleons at energies from .1 to 10 TeV and analysis of its operation at an altitude of 3250 m above sea level
05 p0577 A73-16823

An arrangement for studying horizontal air showers - Initial results
23 p2966 A73-43549

HOHMANN TRAJECTORIES

U ELLIPTICAL ORBITS

U TRANSFER ORBITS

HOHMANN TRANSFER ORBITS

U ELLIPTICAL ORBITS

U TRANSFER ORBITS

HOLDERS

NT FLAME HOLDERS

HOLDING

Effects of hold time on low-cycle fatigue behavior of AISI Type 304 stainless steel at 593 C.
09 p1102 A73-22417

HOLE DISTRIBUTION [ELECTRONICS]

Space-time distribution of excess carriers and their space charge in doped semiconductors.
06 p0734 A73-17814

Impurity concentration relationship to electrons and holes density and potential fluctuations in completely compensated crystalline semiconductors with randomly distributed donors and acceptors
06 p0735 A73-17976

Electron-hole processes in CaF₂ crystals doped with rare-earth ions
07 p0837 A73-20208

Iterative method for calculating hot carrier distributions in semiconductors.
08 p0994 A73-21221

Numerical analysis of the properties of an avalanche diode in the avalanche multiplication range
11 p1337 A73-25321

Injection and field processes in thin semiconductor films in the current jump region
18 p2341 A73-36723

A two-dimensional numerical analysis of a silicon n-p-n transistor. 20 p2536 A73-39413

Concentration effect in semiconductors with bipolar conductivity in an alternating external magnetic field 23 p3017 A73-44046

Determination of hole and electron traps from capacitance measurements. 24 p3119 A73-44405

Calculation of the nonstationary electric field, carrier concentration, and current distribution in semiconductor integrated circuits 24 p3119 A73-45177

HOLE DISTRIBUTION [MECHANICS]

Doubly-periodic problem in elasticity theory for an isotropic medium weakened by congruent groups of arbitrary holes 01 p0116 A73-10961

Microstructural changes that drilling and reaming can cause in the bore holes in DTD 5014 /RR58 extrusions/. 03 p0325 A73-13573

Antenna-aperture distributions from holographic type of radiation-pattern measurement. 06 p0668 A73-18443

Theoretical calculation of the compressibility of porous media. 09 p1157 A73-22144

Effects of circular holes on the fatigue resistance of AlMg6BM aluminum-alloy sheet in symmetrical bending. 09 p1105 A73-23053

Experimental investigation of oscillation damping in shells with holes 11 p1435 A73-25398

Plane strain plastic yielding due to bending of end-loaded cantilevers containing circular, triangular or diamond-shaped holes. 11 p1443 A73-26091

Doubly-periodic problem of the theory of elasticity for an isotropic medium weakened by congruent groups of arbitrary holes. 12 p1554 A73-27537

Measurement of residual stresses in a cylinder. III - On the effect of eccentricity of holes bored out in Sachs method. 19 p2501 A73-38345

Improvement of damping capacity of structural members by introduced stress concentration. [ASME PAPER 73-DET-76] 22 p2919 A73-42072

Determination of the temperature field in a perforated plate with convective heat transfer 24 p3157 A73-45171

Stress concentration in infinite strip with periodically spaced circular holes under uniformly distributed bending loads 24 p3149 A73-45176

HOLE MOBILITY

Drift mobilities of holes and electrons in naphthalene single crystals. 11 p1407 A73-24988

Drift mobility of holes and electrons in perdeuterated anthracene single crystals. 12 p1531 A73-27688

Russian book - Electrons and holes in semiconductors: Energy spectrum and dynamics. 15 p1852 A73-32298

HOLES

Stressed state of an isotropic half-plane with a finite number of circular holes situated along the boundary 02 p0230 A73-11782

Time taken for a laser pulse to make a hole in a metal film. 02 p0176 A73-12114

Machining precision in deep-hole boring by a feed-division technique 02 p0174 A73-12578

Fracture mechanics equations for crack propagation braking by elliptic and circular holes at crack tip, noting stress concentration 02 p0237 A73-12586

Coronal holes during 12 November 1966 eclipse, comparing distribution to calculated current-free coronal magnetic field 05 p0621 A73-17035

Dynamic stress concentration at an elliptic hole due to plane SH-waves 15 p1947 A73-31331

The effect of couple-stresses on the stress concentration around an elliptic hole. 15 p1947 A73-31335

The elastic layer with a cylindrical hole subjected to a nonuniform axisymmetric radial displacement. 20 p2624 A73-39566

Thermal stresses in rotationally symmetric semi-infinite elastic body with heat input along hole boundary and on plane bounding surface, reducing to solution of Fredholm equation 24 p3147 A73-44745

Load concentration factors for circular holes in composite laminates. 24 p3149 A73-45151

HOLES [ELECTRON DEFICIENCIES]

Electron-vacancy prediction methods for sigma phase precipitation in residual matrix compositions of austenitic Niand Co-base superalloys 02 p0183 A73-12757

Investigation of hole scattering in surface inversion channels arising on a cleaved germanium surface 03 p0349 A73-13659

Kadomtsev-Nedospasov helical instability during a strong pinch effect in an electron-hole plasma 06 p0729 A73-18119

A transport equation treatment of tunnelling in semiconductors. 13 p1668 A73-28218

Thermal noise measurements on space-charge-limited hole current in silicon. 13 p1668 A73-28542

Quantization effects in semiconductor inversion and accumulation layers. 13 p1669 A73-29291

Oxidation of organic molecules by photoproducts of ZnO. 15 p1841 A73-31969

Current carriers and electron impurity centers in ferrimagnetic semiconductors - The case of weak interaction 19 p2471 A73-37959

Surface wave propagation parallel to applied magnetic field in electron hole plasma, explaining observed resonances in InSb by LF mode 21 p2751 A73-40325

Electron and hole ionization rates in epitaxial silicon at high electric fields. 21 p2668 A73-41561

Illumination aftereffects due to semiconducting ferrite electron and ion motion, discussing dielectric properties and electron hole deficiencies 22 p2833 A73-42514

Kadomtsev-Nedospasov helical instability in a strong pinch effect in an electron-hole plasma. 24 p3114 A73-44503

HOLLOW

The feasibility of producing superalloy electrosag remelted hollows. 04 p0455 A73-15747

HOLLOW CATHODES

Gas discharge efficiency from populations comparison of Ne absorbing levels in hollow cathode and positive column discharges, measuring laser output power peak 02 p0176 A73-12096

High current low voltage magnetically confined hollow cathode discharge for vacuum evaporation and ionization, noting vacuum deposition of quartz and copper 04 p0455 A73-15755

A simple bakeable hollow cathode device for the direct study of plasma constituents. 05 p0563 A73-17262

Ion thruster thermal characteristics and performance. 07 p0867 A73-19488

Performance of a modified downstream-cathode MPD thruster. 07 p0867 A73-19492

Evidence of fireball phenomena in hollow cathode of electron bombardment ion thrusters. 09 p1136 A73-23462

A hollow cathode device for CW helium-metal vapour laser systems. 10 p1229 A73-24617

Contributions to the mechanism and the plasma diagnostics at the negative glow light in the case of the cylindrical hollow cathode discharge 14 p1780 A73-30427

Low-frequency flute instabilities of a hollow cathode arc discharge - Theory and experiment. 19 p2468 A73-37858

HOLMIUM

The magnetic characteristics of the alloys of palladium with gadolinium, dysprosium, and holmium 13 p1667 A73-28183

HOLOGRAPHIC INTERFEROMETRY

The application of dual hologram interferometry to wind tunnel testing. [AIAA PAPER 73-210] 05 p0577 A73-16941

Holographic nondestructive evaluation of interference fit fasteners. 11 p1366 A73-26247

Phase characteristic function of holographic images of objects in parabolic motion. 11 p1366 A73-26248

Wave front reconstruction principle application to side-looking radar, diffused holograms, holographic interferometry and computer storage 11 p1369 A73-26527

Volume holograms reconstruction differences due to interferences, noting color and directional selectivity effects 11 p1369 A73-26528

Interference fringes and surface displacement interrelationship in holographic interferometry, discussing fringe localization, visibility and interpretation and postrecording techniques 11 p1369 A73-26530

Live fringes time averaging, fringe spoiling, stroboscopic and speckle pattern real time recording techniques in holographic interferometry for surface vibration modes analysis 11 p1369 A73-26531

Hologram interferometry and laser speckle methods - Further applications. 11 p1370 A73-26532

Reference fringes in holographic interferometry. 13 p1616 A73-28599

Sensitivity and resolution in holographic interferometry of focused images 13 p1616 A73-28766

Application of holographic interferometry to predict long time torsional relaxation. 13 p1620 A73-29301

Measuring accuracy of three-dimensional displacements in holographic interferometry. 14 p1752 A73-30154

A kinematically designed mount for the precise location of specimens for holographic interferometry. 14 p1753 A73-30414

Pulsed holographic interferometry at 10.6 microns. 15 p1875 A73-31400

Thermal expansion coefficient measurement of diffusely reflecting samples by holographic interferometry. 15 p1877 A73-31980

Investigation of a gas flow on an aeroballistic track by holographic methods 15 p1879 A73-32328

Speckle reference beam /by retro reflection/ holography for the real time visualisation of vibration patterns. 16 p2012 A73-32847

A hologram interferometer with a retro-reflected speckle reference beam for the real time visualization of vibration patterns. 16 p2013 A73-32880

Pulsed interferometric holography of laser-produced air breakdown. 16 p2014 A73-33175

Investigation of thermal deformations by methods of holographic interferometry 17 p2164 A73-34172

Dark field method for phase diffraction grating visualization by microwave holography, using radio lens for object microwave spectrum formation 17 p2168 A73-35165

Non-destructive testing of plastics by means of holographic interferometry. 17 p2181 A73-35355

Reference radiation frequency shift for holographic interferometry of vibrating objects 17 p2172 A73-35428

Distortionless recording in double-exposure holographic interferometry. 17 p2173 A73-35430

Diffraction versus holography - A stress analyst's comparison. 17 p2173 A73-35440

On the limitations of interferometric methods in three-dimensional photoelasticity. [SESA PAPER 2165] 17 p2251 A73-35455

Determination of slope and strain contours by double-exposure shearing interferometry. [SESA PAPER 2215A] 17 p2174 A73-35459

Turbulent boundary layer flow separation measurements using holographic interferometry. [AIAA PAPER 73-664] 18 p2261 A73-36215

Nondestructive testing of fiberglass reinforced plastic plates by means of holographic interferometry 18 p2316 A73-36477

Quantitative study of an aerodynamic flow by holographic interferometry 18 p2317 A73-37082

Application of a holographic technique to the determination of the dispersity of a two-phase gas/liquid flow 18 p2318 A73-37122

Strain analysis of a disk subjected to diametral compression by means of holographic interferometry. 19 p2429 A73-37264

A direct approach to reduce recording time in stroboscopic holographic interferometry. 19 p2429 A73-37541

Study of a linear noncylindrical discharge by holographic interferometry 20 p2597 A73-39198

Rapid in situ processing for real-time holographic interferometry. 21 p2692 A73-39918

Relaxation of coherence requirements in holography. 21 p2695 A73-39961

The use of holographic techniques for recording high-speed events. 21 p2695 A73-39962

Practical lasers for photographic and holographic recording. 21 p2709 A73-39973

Aeroballistic gas flow investigation using holographic device to schlieren system. 21 p2696 A73-39981

Holographic interferometry applied to aerodynamics 21 p2696 A73-39984

Double frequency diffraction grating lateral shear interferometer for lens focusing and heterodyne phase detection 21 p2698 A73-40137

Degree of coherence mapping of single ruby laser pulses using holographic interferometry, discussing self-coherence, length and photographic recording 21 p2710 A73-40146

Coherent imaging system suppression of noise / extraneous non-image light/ through multiple-wave illumination, periodic phase modulation and diffuse wave illumination 21 p2698 A73-40148

Three-wavelength holographic diagnostics of an optical flare at a potassium target 21 p2700 A73-40529

Vibration analysis of circular cylinders by holographic interferometry. 21 p2701 A73-40756

Multiple-beam holographic spectroscopy. 22 p2852 A73-41812

Ultrahigh resolution holographic spectroscopy by double exposure of light scattering medium interferogram recording and reconstruction, noting equivalence to use of narrower laser line width 22 p2861 A73-42413

German monograph on holographic interferometry for displacement and deformation determination of diffusely reflecting bodies covering wave front reconstruction methods and diffraction pattern characteristics 22 p2862 A73-42719

Holographic thin-beam reconstruction technique for the study of 3-D refractive-index field. 22 p2862 A73-43087

Time-average holography of objects vibrating sinusoidally and moving with constant acceleration. 22 p2863 A73-43092

Fringe localization and visibility in hologram and classical broad source interferometry. 22 p2863 A73-43094

Effective application of double exposure holographic interferometry to the study of deformations of ceramics due to the impact of a projectile 22 p2863 A73-43096

Application of holographic subtraction to time-average hologram interferometry of vibrating objects. 22 p2863 A73-43141

Automated data reduction of holographic interferometry translational measurement of diffusely reflecting rigid body by reconstructed virtual image processing on CDC 6600 computer 22 p2863 A73-43147

Holographic shearing interferometer using two linearly polarized reference light beams with application to refractivity and density gradient measurements in aqueous solutions 24 p3088 A73-44406

Elastomechanical model measurements conducted with the aid of holographic approaches in the case of a mirror cell 24 p3090 A73-44897

Radon transform application in holographic interferometry for reconstructing two and three dimensional spatial distribution of refractivity in object 24 p3091 A73-44944

Holographic photo-elasticity - Independent observation of the isochromatic and isopachic fringes for a single model subjected to only one process. 24 p3091 A73-45335

HOLOGRAPHY

NT ACOUSTICAL HOLOGRAPHY

NT HOLOGRAPHIC INTERFEROMETRY

NT MICROWAVE HOLOGRAPHY

Hologram reconstruction by incoherent light. II - Experimental results. 01 p0045 A73-10431

Holographic gratings application to astronomical spectrograph design for IR to extreme UV and X rays, considering characteristics advantage 01 p0047 A73-10519

Stellar spectroscopy with holographic gratings. 01 p0047 A73-10520

Interferometric measurements of the vibrostability of a holographic stand 01 p0050 A73-10798

Holographic inspection of shapes of unpolished surfaces. 01 p0051 A73-10835

Comparison of high-resolution photographic emulsions for recording three-dimensional holograms. 01 p0051 A73-10839

Piezoelectric matrices for reception of acoustic images and holograms 01 p0051 A73-10930

Holographic interferometry in materials research and fracture mechanics. 01 p0051 A73-11002

Diffraction and nonlinearity characteristics of amplitude holograms for reconstructed nonlinear images on photosensitive layer 01 p0052 A73-11085

Holographic image polarization recording and sum wave simulation on photoanisotropic materials, using Weigert effect 01 p0052 A73-11086

Bell Laboratories laser optics development and technology applications, discussing CW lasers, light deflectors, holography, optical memories, pattern generator, remote blackboard and micrographics 01 p0060 A73-11213

Holo-diagram coherent optics device for studying interference patterns of object near focal points representing illumination and/or observation points 01 p0053 A73-11220

Interferometric testing of large optical components with circular computer holograms. 01 p0053 A73-11225

Double exposure holographic interferometry for comparison of object of two points in time evolution, discussing space division multiplexing of exposures onto photographic plate 01 p0054 A73-11234

Coding technique to record computer generated binary hologram on numerically controlled CRT with resolution cell of two beam spots 01 p0019 A73-11235

Incoherent optical correlation with a hologram - An example of identifying fingerprints 01 p0054 A73-11489

Optical modeling of antenna radiation patterns by radio holograms of aperture fields 02 p0146 A73-12020

Coherent laser radiation and holography in an optically inhomogeneous medium. 02 p0176 A73-12111

Vibrational analysis with the aid of holographic interferometry vibrational analysis of acoustic radiators with the aid of holographic interferometry 03 p0306 A73-12985

Limiting resolution of reconstructed image of focused hologram in electron microscopes as function of aberration and spatial coherence 03 p0309 A73-14088

Holograms of spark discharges produced by nanosecond electrical pulses. 03 p0309 A73-14100

Book - Holography: State of the art review 1971-72. 03 p0309 A73-14440

Imaging radar techniques for remote sensing applications. 03 p0278 A73-14486

Ultrasonic holography application to NDT, discussing small angle approximation to spherical beam, hologram formation, image reproduction and wavelength change effect 04 p0446 A73-14674

Holographic correlation offers new possibilities for acoustical NDT. 04 p0446 A73-14675

A dynamic holographic grating for a mode of operation with peaks 04 p0447 A73-14884

NDT applications of acoustic or stress wave, ultrasonic spectroscopy, imaging, critical angle reflectivity and holography 04 p0447 A73-14927

Holography without fringes in the electron microscope. 04 p0447 A73-15049

Special features of recording 'pure' phase /binary/ acoustic holograms 04 p0450 A73-15619

A model of a memory device based on neuron-like elements which realizes the holographic principles of data recording and readout 04 p0413 A73-15792

Mathematical description of frequency difference hologram obtained by superposition of two holograms of same object produced with light of different frequencies 04 p0451 A73-15924

Optical computer technology based on Fourier transform optics and holography, discussing speed and parallel processing capabilities, image deblurring, and applications 04 p0426 A73-15957

Computer development of holographic mass memory plans 05 p0553 A73-16168

Semiconductor photodetection matrices for holographic memory reading 05 p0553 A73-16170

Acoustic holographic scanning techniques for imaging flaws in thick metal sections. 05 p0574 A73-16284

Display of HF acoustic holograms utilizing liquid crystals. 05 p0574 A73-16285

Holographic interferometry techniques and applications, discussing gas and ruby lasers in imaging, measurements and NDT of materials and mechanical components 05 p0574 A73-16286

Velocity measurements made holographically of diffusely reflecting objects. 05 p0574 A73-16287

Finite fringe holographic interferometry applied to a right circular cone at angle of attack. 05 p0527 A73-16528

[ASME PAPER 72-APM-PP] A triple-exposure technique to reduce recording time in stroboscopic holographic interferometry. 05 p0576 A73-16557

Airborne synthetic aperture hologram/ radar maximum ambiguity range extension by using additional receive-only antenna ahead of transmit-receive unit. 05 p0577 A73-16817

Noise magnitude calculation for intensity quantized hologram based on Laplace transform for nonlinear device analysis and Gaussian random process 05 p0579 A73-17220

Wavefront sampling in holographic interferometry. 05 p0579 A73-17223

Application of holographic subtraction to time-average hologram interferometry of vibrating objects. 06 p0691 A73-17499

Coherent optical processing and display techniques for microwave imagery generation from synthetic aperture radar system data, discussing hologram and side-looking radar 06 p0667 A73-18279

Acousto-optical profilometer system with two diffracted laser beams for surface topography holographic measurements 06 p0694 A73-18290

High data rate holographic recorder with six-channel acousto-optical modulator array as input composer and mode locked Ar laser as light source 06 p0694 A73-18311

Antenna-aperture distributions from holographic type of radiation-pattern measurement. 06 p0668 A73-18443

Electron-beam tube with semiconducting laser screen. 06 p0677 A73-18636

On the numerical reconstruction of images from a microwave hologram. 06 p0669 A73-18737

Use of nonstationary holography to improve the directivity of laser radiation. 07 p0834 A73-19275

Holographic visualization of elastic waves 07 p0822 A73-19287

Microwave or acoustic holographic synthetic aperture interferometry with pulsed techniques, noting single scan, resolution and fringe number advantages 07 p0824 A73-20110

Three dimensional models images information content increase in coherent light by interference shadow marking, noting automatic systems for distant objects recognition 07 p0824 A73-20140

Some new developments in nondestructive testing. 08 p0963 A73-20869

Wavefront tilter for double-exposure holographic interferometry. 08 p0963 A73-20874

Evaluation of the wavefront aberration in holography. 08 p0963 A73-21013

Holographic optical element for visual display applications. 08 p0963 A73-21034

Diffuser box for holography spatial and temporal coherence requirements relaxation, explaining speckling and SNR reduction by time and frequency domain analysis 08 p0963 A73-21035

Auto- and cross-correlations of diffuse objects for coherent optical data processing, using single lensless Fresnel hologram 08 p0963 A73-21036

Speckle reduction by simulation of partially coherent object illumination in holography. 08 p0964 A73-21037

Relation between object position and autocorrelation spots in the Vander Lugt filtering process. II - Influence of the volume nature of the photographic emulsion. 08 p0964 A73-21044

Pulsed laser produced holograms with iron doped lithium niobate, noting application in high capacity information storage 08 p0964 A73-21051

Recording and reconstruction method for image plane hologram multiplexed tenfold in small area, using He-Cd laser 08 p0964 A73-21052

Image contrast increase in holographic interferometry, using double exposure technique with reference beam half-wavelength phase shift 08 p0964 A73-21053

Amplitudes of mth order holographic images recorded on film with power law characteristics. 08 p0964 A73-21054

Three-dimensional holograms by rotational multiplexing of two-dimensional films. 08 p0964 A73-21055

Time variable field recording and reconstruction theory and wave equations of holography and holo-

graphic interferometry, including double exposure and time averaged techniques

08 p0965 A73-21137

Noise reduction in acousto-optic /Bragg/ imaging systems by holographic recording.

08 p0965 A73-21209

Real time 3-D holographic display, discussing reusable thermoplastic photoconducting recording film and frequency compensation with short laser pulses and acousto-optic modulator

08 p0965 A73-21246

Holographic interferometry applied to aerodynamics

[ONERA, TP NO. 1161F]

08 p0968 A73-21677

Holographic system parameter relations from wave phase analysis of undistorted reconstructed image

09 p1079 A73-21915

Application of lens-raster optics for recording holograms with discrete information

09 p1079 A73-21916

Self-enhancement of LiNbO₃ holograms.

09 p1079 A73-21943

Holographic method of controlling the spatial-angular characteristics of laser emission

09 p1090 A73-21951

Vibration measurement by vibrating-plate holograms.

09 p1079 A73-21997

Multielement scanning system for acoustic holography application in nondestructive testing, combining multiple mechanical sensors with simultaneous electronic commutation

09 p1080 A73-22297

A temperature interferometer using laser holography.

09 p1083 A73-22510

Holographic laboratory practice for NDT, discussing data reduction, display and pulse laser development

09 p1083 A73-22513

Acoustical holography applications in nondestructive testing.

09 p1083 A73-22514

Possibility of holographic observation of the interference of independent weakly degenerate fields

09 p1084 A73-22670

Holographic recording of focused images in multimode laser radiation

09 p1084 A73-22879

Optimum holographic recording of complex light fields generated by diffusive objects in presence of point sources, maximizing SNR or distortion-free diffraction level

09 p1084 A73-22880

Recording of parasequence-coded binary information on phase holograms

09 p1085 A73-22881

Simple method of obtaining high-sensitivity interferograms

09 p1085 A73-22882

Optical wavelengths and microwaves operated holographic refractometers and reflectometers based on dielectric microwaveguides

09 p1085 A73-23013

Holographic photography of high-speed processes with the aid of paired radiation pulses

09 p1085 A73-23014

Application of lateral illumination in holography of small objects

09 p1085 A73-23015

Vibration resistant holographic table consisting of polished iron plate resting on four elastic dampers mounted on two concrete supports

09 p1085 A73-23016

Photodetector matrix circuit for holographic memory converting optical bits into electrical signals

09 p1086 A73-23074

Study of antenna cross-polarization characteristics by using microwave holography

09 p1065 A73-23087

Defect detection in solid materials with the aid of holographic vibration analysis

09 p1089 A73-23115

Some investigations on the methods of measuring 3-dimensional plastic deformations by laser.

09 p1086 A73-23321

Holographic recording and reproduction of wave polarization information by correlation matrix and Stokes parameter method

09 p1087 A73-23333

Investigation of the electrical explosion of conductors by holographic methods

10 p1248 A73-23507

Holographic recording of moving objects.

10 p1215 A73-23613

Ultrasonic holography by one-dimensional moving of the source or the object.

10 p1216 A73-23664

Book - RCA advanced technology.

10 p1216 A73-23781

Holographic read-only memory with high speed and density optical storage on low-cost changeable media, discussing feasibility model design, construction and test

10 p1216 A73-23796

Multicolor documentation type information holographic storage, recording, indexing, registration and reconstruction technology assessment and application, emphasizing displays and automatic test equipment systems

10 p1216 A73-23797

Holographic interferometry as nondestructive testing method, discussing applications to defects detection in tires, metal-rubber vibration isolators and glass fiber reinforced plastic tubing

10 p1218 A73-24173

Piezoelectric matrices for the reception of acoustic images and holograms.

10 p1218 A73-24190

Nonlinear /binary/ transformation effects on acoustic hologram spatial signal amplitude noting multiple images and reconstructed image distortion

10 p1218 A73-24209

A new interpretation of interferometric fringe patterns.

10 p1220 A73-24661

Holographic contour mapping using a dye laser.

10 p1221 A73-24874

Comment on: Holographic interferometry applied to measurements of small static displacements of diffusely reflecting surfaces.

11 p1360 A73-25064

Image holography through convective fog.

11 p1361 A73-25365

Holographic interferograms for demonstration of acoustic field near supersonic air, nitrogen and helium jets, noting generated Mach wave convection velocity

11 p1346 A73-25382

Holographic motion picture camera allows front surface detail to be recorded in real time using a continuous wave laser.

11 p1366 A73-26249

Huygens principle, power spectrum and photon and photographic noise intensities effects in holography, discussing optical information transmission by eigen-solutions

11 p1369 A73-26529

Coherent light optical filtering, holographically produced complex filters, imaging systems and pattern recognition multiplex arrangement for optical data processing, discussing image reconstruction

11 p1370 A73-26533

Computer generated binary synthetic holograms, discussing information coding and processing, detour phase effect and kinoforms

11 p1370 A73-26534

Holographic approach to real time correction of optical instruments images, discussing restoration by spatial frequency filtering

11 p1370 A73-26535

The wave length dependence of the transfer properties of photographic materials for holography.

11 p1370 A73-26536

Holographic optical memory superiority over conventional localized computer storage devices, considering capacity, access time, immunity to local imperfections, and crosstalk problem

11 p1370 A73-26538

Lensless Fourier transform holography with mutual coherent reference source close to object, investigating atmospheric turbulence effects on wavefront reconstructed image quality

11 p1370 A73-26539

Hologram interferometry adaptation to industrial conditions for dimensions, deformation, vibration and refractivity measurements, noting advantages over ordinary interferometry

11 p1370 A73-26540

Fringe control in real time and double exposure holography for nondestructive testing of multilaminated and thin laminated structures and vibration analysis

11 p1370 A73-26541

Acoustic wave propagation, scanning and liquid surface techniques in acoustical holography, noting applications in geophysics, oceanography, medicine and nondestructive testing

11 p1371 A73-26542

Mathematical principles of optical image deblurring by holography for photographic and electron micrographic applications

11 p1371 A73-26543

Nondestructive flaw detection by holographic interferometry, discussing methods, equipment and applications for materials testing and vibrational analysis

11 p1371 A73-26551

The application of holography to sonic boom investigations.

11 p1371 A73-26633

Tomosynthesis - A holographic method for variable depth display.

12 p1495 A73-26829

Application of longitudinal multimode laser coherence properties to increase the holographic depth of field.

12 p1504 A73-26830

Reversible recording of holograms on chalcogenide glass films

12 p1495 A73-26940

The determination of Mode I stress-intensity factors by holographic interferometry.

12 p1550 A73-27021

Temperature sensitivity of cfrp honey-comb structures under holographic adt.

12 p1496 A73-27036

Book - An introduction to acoustical holography.

12 p1496 A73-27052

Holographic focused image recording and reconstruction in white light, considering source size, shape and spectral composition effects and interferometry

12 p1497 A73-27424

Multibeam holographic spectroscopy

12 p1497 A73-27453

Holographic construction and application of optical elements, discussing hologram lenses, holographic multiple imaging systems and diffraction gratings

12 p1498 A73-27501

Reconstruction of the images of transparencies with a semiconductor laser.

12 p1498 A73-27512

Controllable liquid-crystal transparency for recording of holograms.

12 p1498 A73-27513

Investigation of coherence with the aid of the diffraction shearing interferometer.

12 p1507 A73-27515

Determination of the height of ionospheric irregularities with the holographic method.

13 p1606 A73-28155

Conditions of anastigmatization for Rowland assemblies fitted with concave holographic networks

13 p1613 A73-28567

International Symposium on Acoustical Holography, 4th, Santa Barbara, Calif., April 10-12, 1972, Proceedings.

13 p1614 A73-28576

A progress report on the laser scanned acoustic camera.

13 p1614 A73-28577

Real-time reconstruction of images from hydroacoustic holograms.

13 p1614 A73-28578

Real time high resolution 100 MHz acoustic image or hologram microscope using optical measurement of boundary displacement by incident angular sound wave

13 p1614 A73-28579

Foil-electret transducer arrays for real-time acoustical holography.

13 p1614 A73-28583

Acoustical hologram recording by electrostatic transducers using rigid backplate electrode insulated with thin dielectric film transparent to ultrasonic radiation

13 p1614 A73-28584

Diffraction theory treatment of long wave holography to demonstrate spiral scan and other circular sampling formats in microwave or acoustic hologram recording

13 p1615 A73-28585

Acoustic hologram irradiation with sound waves to yield image as acoustic intensity pattern, noting parallels in optical holography

13 p1615 A73-28587

Cylindrical scan acoustical holographic transmitter/sensor system for ultrasonic under ocean surveillance and NDT applications

13 p1615 A73-28588

Analysis of various ultrasonic holographic imaging methods for medical diagnosis.

13 p1615 A73-28589

The effects of scanning position and motion errors on hologram resolution.

13 p1615 A73-28590

Ray optics model analysis for spherical aberration effects on acoustic hologram resolution in image reconstruction, discussing computer generated correction for quality improvement

13 p1615 A73-28591

Phase and amplitude only scanned acoustical holograms, noting Fraunhofer diffraction region reconstructed images

13 p1615 A73-28592

A comparison of holographic versus lens type acoustic image systems by computer simulation.

13 p1616 A73-28595

Longitudinal and lateral magnification distortion correction in three dimensional long wavelength holography from standpoint of observer visual perception

13 p1616 A73-28596

Ultrasonic acoustic holography for wave source and object in relative motion, predicting reconstructed image aberration elimination performance in point-by-point mapping technique

13 p1616 A73-28597

Reference wave elimination in acoustic holographic experiments via boundary surface of medium having sound wave propagation used as hologram

13 p1616 A73-28687

The recording of three-dimensional holograms on photochromic glass with the use of an optical bleaching process. I

13 p1616 A73-28765

Holographic recording of three-dimensional ensembles of rapidly moving particles

13 p1616 A73-28767

Establishment of hologram memory system with capacity as high as 10,000,000 bits.

13 p1588 A73-29236

A Fabry-Perot acoustic surface vibration detector-application to acoustic holography.

13 p1622 A73-29422

Some problems in the optimization of holographic memories.

13 p1622 A73-29435

Sensitometric tests on plane-parallel organic photochromic bulk material film samples of styrene, methylmethacrylate and inoline spiropyrans, evaluating photosensitivity suitability for holography.

13 p1622 A73-29436

Holographic visualization of large amplitude vibration using reference beam phase modulation.

13 p1622 A73-29642

High-resolution microwave holographic technique - Application to the imaging of objects obscured by dielectric media.

13 p1622 A73-29668

Geometrical projection for holographic image reconstruction, assuming configuration and wavelength differences from reference wave

14 p1752 A73-30024

Effect of laser pulse shape on the form of holographic velocity fringes.

14 p1752 A73-30153

Theory of diffraction efficiency maximization for thin-layer amplitude holograms

14 p1753 A73-30364

Indoline series spirochromene polymer matrices for holographic recordings with argon and helium-neon lasers in green and UV spectral regions

14 p1753 A73-30365

Investigation of the dependence of the quality of a reconstructed holographic image on the parameters of the photoemulsion layer. I - Diffractive efficiency of the hologram

14 p1753 A73-30370

Comparison of the resolutions of two projective holography methods by comparing their line scattering functions corresponding to holographic images

14 p1753 A73-30376

Holographic imaging and aberrations due to an incorrectly repositioned hologram in a system with lenses having aberrations.

15 p1915 A73-31015

A technique to retain the hologram reconstruction efficiency in elimination of the intense reference beam by the method of pre- or postexposure.

15 p1874 A73-31137

Diffraction gratings manufacture by holographic recording of laser beam generated interference fringes on photosensitized surfaces, describing etching and metallization process

15 p1875 A73-31417

High-density image-storage holograms by sampling and random phase shifter method.

15 p1876 A73-31946

Limiting information capacity of a holographic system

15 p1879 A73-32317

Optical model of a holographic television system

15 p1879 A73-32331

Holographic method for measuring spatial coherence functions

15 p1879 A73-32339

Three-dimensional hologram recordings on photochrome glass with the application of an optical discoloration process. II

15 p1879 A73-32340

Burst-mode frequency-doubled YAG:Nd³⁺/ laser for time-sequenced high-speed photography and holography.

15 p1886 A73-32384

Microwave holography application to landing without visibility

15 p1911 A73-32497

Holographic system parameter relations from wave phase analysis of undistorted reconstructed image

15 p1880 A73-32641

Lens raster optics for holograms with digital information.

15 p1880 A73-32642

Diffraction of an electromagnetic wave on a plane hologram

16 p2011 A73-32823

A fast access holographic memory.

16 p2012 A73-32868

Block organized holographic read only optical memory /ROOM/ model for random access large storage capacities with electro-optical or acousto-optical light deflection system

16 p2012 A73-32869

Fast random access permanent storage read only optical memory, using light emitting diode matrix addressing, semiconductor laser and holographic lens system

16 p2012 A73-32870

Holographic read-write memory, optical organisation and capacity enhancement by three-dimensional storage.

16 p2013 A73-32871

High speed serial multiplexed holographic recording for large capacity random access memories, using piezoelectric deflector and ferroelectric ceramic array modulators

16 p2013 A73-32872

Holographic document data recording and storage for single- and multiterminal information processing system, emphasizing Fourier and carrier frequency photography techniques

16 p2013 A73-32873

Reflected light holographic microscopy of moving objects.

16 p2014 A73-33174

An introduction to holography by shadow casting.

16 p2016 A73-33950

Holography, radar data and interpreter performance.

17 p2165 A73-34286

Holography of large objects in a turbulent atmosphere with a CW laser.

17 p2167 A73-34896

Holographic image enhancement using deblurring filters, discussing application to Polaroid photographs, electron micrographs and X ray photos

17 p2168 A73-34908

Holographic methods of laser radiation divergence control

17 p2184 A73-34919

Role of cooperative effects in hologram generation and in the formation of reconstructed images

17 p2168 A73-34921

Holographic investigation of electrical explosions of conductors.

17 p2212 A73-35187

Optical data storage and data processing, and holography in aerospace and electronic instrumentation.

17 p2131 A73-35382

On-axis computer generated hologram with multiemulsion color film for retaining kinoform advantages and effective control over amplitude and phase transmittance

17 p2171 A73-35401

Speckle reduction in holography by means of random spatial sampling.

17 p2172 A73-35429

Holographic coding plate - A new application of holographic memory.

17 p2173 A73-35431

Block oriented random access and read-only archival holographic memories design, considering relationships between lens geometric parameters, laser power and packing density requirements

17 p2173 A73-35432

Vibration analysis of plates by real-time stroboscopic holography.

[SESA PAPER 2111]

17 p2173 A73-35448

A survey of nondestructive testing techniques.

18 p2320 A73-36484

Hologram matrix and its application to a novel radar.

19 p2428 A73-37145

Reconstruction of surface-wave fields in liquids with the aid of holographic methods

19 p2431 A73-38158

A comparison of the efficiency and focused stray light characteristics of a conventionally ruled- and a holographically produced-concave diffraction grating in the vacuum ultraviolet.

19 p2431 A73-38164

Method of holography in nondestructive testing.

19 p2432 A73-38359

Increasing the storage density of holographic recording by spatial frequency multiplexing.

20 p2563 A73-38670

Angular distribution patterns of thick-film holograms.

20 p2567 A73-39701

Angular distribution patterns of thick-film holograms obtained by rigorous solution of the diffraction problem.

20 p2567 A73-39702

Observation of the surface of hypersonic projectiles by holography

21 p2694 A73-39956

Hypervelocity projectile holography for application to bullets and shells, calculating rotational velocity and flight direction from fringe on wave front reconstruction

21 p2694 A73-39957

Holographic method of recording temporal characteristics of optical signals.

21 p2695 A73-39958

Short interval double-pulsed holography of reflecting objects.

21 p2695 A73-39960

Visualization of gas flows by means of high-speed holography

21 p2696 A73-39978

Holographic investigations and measurements in a cloud of moving microparticles

21 p2696 A73-39979

Color holographic technique through wave front coding of colored object, discussing He-Ne, He-Cd and argon laser irradiation, coding masks and image reconstruction

21 p2697 A73-40128

Resiliently mounted objects holographic system sensitivity threshold control by proper selection of support stiffness and vibration damping

21 p2698 A73-40132

Perturbation analysis of holographic grating couplers in thin film waveguides, discussing coupling efficiency dependence on evanescent tail length, refractive index and gelatin film thickness

21 p2699 A73-40149

Automatic surface mapping via holographic system, describing Q switched ruby laser holograms, image dissector, computer video signal analysis and scan signals

21 p2699 A73-40150

Rear projection holographic and interferometric viewing screens using deflected and scattered light, discussing microfilm reading applications, dichromated gelatin film and laser exposures

21 p2699 A73-40151

Optical processing of radar signals

21 p2651 A73-40515

Elimination of a fundamental defect of two-dimensional holograms

21 p2700 A73-40570

Study of the properties of thick-film chalcogenide glass holograms

21 p2701 A73-40571

Image contrast and efficiency of nonlinearly recorded holograms of diffusely reflecting objects

21 p2703 A73-41133

Application of transverse reference beams in holographic investigations of small particles.

22 p2860 A73-42253

Properties of thin-film holograms on chalcogenide glasses

22 p2860 A73-42409

Holographic image nonlinear distortion analysis based on photographic film material characteristic curve representation by Taylor series

22 p2861 A73-42410

Computer techniques for scatterer shape from far field data /inverse scattering/ via remote sensing, with application to antenna radiation pattern synthesis and holography

22 p2828 A73-42845

Electromagnetic theory of Fresnel holograms in the first perturbation theory approximation

22 p2862 A73-42927

Redundant speckle free hologram production without spurious background patterns, blocking intensity by cutting of lower order frequencies

22 p2862 A73-43089

Optimization of exposure time in linear hologram recording by pre-exposure or post-exposure.

22 p2862 A73-43090

Interference patterns from spatially separate holograms and holograms superimposed on same region of recording medium, comparing to double exposure holography performance

22 p2862 A73-43091

Speckle noise reduction by the composition of diffused Fraunhofer holograms.

22 p2863 A73-43093

Probabilistic analysis of random and deterministic phase coding for lowering Fourier transform spectrum dynamic range in digitally generated hologram and kinoform memories

22 p2864 A73-43149

The imaging properties and aberrations of thick transmission holograms.

22 p2864 A73-43185

The nature of quasi-axial reconstructed pictures generated by 'nonreferenced' focused-image holograms

23 p2982 A73-43705

Study of the parameters of three-dimensional holographic gratings in LiNbO₃ crystals

23 p2987 A73-43717

Holographic technique for coherent optical imaging system superresolution via storage of image amplitude

23 p2983 A73-44088

Maximum information capacity of a holograph system.

24 p3089 A73-44623

Vector wave field hologram generation via polarization contrast method, described by correlation matrix formalism

24 p3091 A73-44957

Chromatic photosensitization of a variable-index material for the recording of high-efficiency phase holograms

24 p3091 A73-45011

Angular selectivity of lithium niobate volume holograms.

24 p3092 A73-45424

HOLOMORPHISM U ANALYTIC FUNCTIONS HOMEOSTASIS

Stability criteria in manifestations of the activity of the central nervous system in humans

01 p0006 A73-10152

- Ergatic organism defined as multipurpose nonautonomous control system with homeostasis with respect to functional operations conservation
07 p0786 A73-20048
- Water-salt homeostasis mathematical model, solving equations with analog and digital computers
10 p1184 A73-23941
- Formalization of an arterial pressure stabilization system
10 p1181 A73-24467
- Book - Principles of biological regulation: An introduction to feedback systems.
15 p1840 A73-32576
- Cell viability in acute myocardial infarction, discussing pathogenesis, histological, histochemical and biochemical responses to ischemia, homeostasis maintenance and treatment methods
18 p2276 A73-36545

HOMEOTHERMS

- Chronic acceleration effects on homeotherm physiological adaptation in terms of body weight, tolerable field intensity, growth and fat deposition inhibition, etc
22 p2804 A73-42177
- Primitive mammals phylogeny relationship to homeothermic abilities, discussing body temperature, thermoregulation, basal metabolism rates, hibernation, nycthemeral rhythms and responses to heat and cold
22 p2809 A73-42860

HOMING DEVICES

- Russian book on aircraft control systems covering radio communication and navigation, automatic guidance and landing and homing and radar tracking
04 p0474 A73-15964
- A semiinertial homing guidance system
10 p1247 A73-24498
- Analysis of various automatic homing techniques for gliding airdrop systems with comparative performance in adverse winds.
[AIAA PAPER 73-462] 15 p1827 A73-31448
- Book - Recommended basic characteristics for airborne radio homing and alerting equipment for use with emergency locator transmitters (ELT).
17 p2207 A73-34475
- Electronic location finder radio antenna homing system for helicopter search and rescue of downed air crewmen
[AHS PREPRINT 720] 17 p2116 A73-35061
- Real-time hybrid hardware-in-the-loop simulation of a terminal homing missile.
18 p2291 A73-36834
- Noise processes in a homing radar secker.
18 p2290 A73-37088
- GDC/EOSS - Real-time visual and motion simulators for evaluation of fire control and electro-optical guidance systems.
[AIAA PAPER 73-919] 21 p2673 A73-40867

HOMODYNE RECEPTION

- Josephson junction millimeter microwave source and homodyne detector.
07 p0863 A73-20104
- Measurement of the temperature of an optically thick luminous gas layer in the upper atmosphere by the homodyne detection method
08 p0960 A73-21304
- Temperature determination of the upper atmosphere by the low-level detection of artificial luminous cloud radiation.
18 p2311 A73-36149
- Measurement of the temperature of an optically dense layer of luminous gas in the upper atmosphere by the homodyne detection method.
19 p2425 A73-37933

HOMOGENEITY

- Closed form exact solution to quasi-static problem in linear viscoelasticity for homogeneous anisotropic material with time invariant properties
01 p0116 A73-10967
- Closed form exact solution to quasi-static problem in linear viscoelasticity for homogeneous anisotropic material with time invariant properties
12 p1554 A73-27543
- A study of the real structure of titanium mononitride in its homogeneity region
21 p2721 A73-41225

HOMOGENEOUS TURBULENCE

- The Reynolds tensor in a homogeneous turbulence associated with a mean shearing flow
04 p0436 A73-15995
- The correlations of the vortex in a homogeneous turbulence associated with a mean shearing flow
05 p0567 A73-17227
- Repeated cascade structure and kinetic description for homogeneous turbulence spectrum, considering coupled hierarchies origin from transfer function and eddy viscosity development
07 p0812 A73-20472
- Experimental determination of the turbulent transfer coefficient in the case of homogeneous isotropic turbulence.
10 p1205 A73-24176
- Spectral energy transfer models of turbulence decay compared with numerical simulation of three dimensional homogeneous isotropic turbulence, considering eddy viscosity and diffusion models
10 p1246 A73-24252

On the application of Cramer's theorem to axisymmetric, incompressible turbulence.
10 p1284 A73-24909

- Intermittency in fully developed turbulence as a consequence of the Navier-Stokes equations.
15 p1860 A73-31092
- Theory of turbulence with a vortex-type anisotropy
15 p1864 A73-32084
- Multipoint distribution calculation of the isotropic turbulent energy spectrum.
19 p2421 A73-37854

- Homogeneous anisotropic to isotropic turbulence convergence based on shear flow component measurements of turbulence energy distribution in axisymmetric flow
20 p2546 A73-39097

HOMOGENIZATION

- U HOMOGENIZING
HOMOGENIZING
Delta-ferrite alteration in steel 1Kh16N4B during homogenization
03 p0326 A73-13828

HOMOMORPHISMS

- NT AUTOMORPHISMS
NT SUBGROUPS
State minimization of incompletely defined deterministic automaton by imbedding one-to-one mapping into homomorphism
24 p3074 A73-44664

HOMOTOPY THEORY

- Nonlinear homotopies for obtaining initial solutions for iteration procedures
01 p0069 A73-10069

HONEYCOMB CORES

- Light weight graphite-polyimide composite honeycomb core and sandwich panel design, fabrication and tests for shuttle orbiter thermal protection system
03 p0333 A73-13051
- Plastic behavior of two-layer sandwich structures.
[ASME PAPER 72-WA/APM-11] 04 p0516 A73-15901
- Technology of production of bonded sandwich structures
10 p1224 A73-24096
- Fatigue properties of sandwich material with a honeycomb filler
10 p1289 A73-24097
- Rigid lightweight honeycomb core radome development from materials and processes standpoint, discussing cost reduction and fabrication
[SAE PAPER 730310] 17 p2177 A73-34670
- Calculation of three-layer minimum-weight panels as a problem of mathematical programming
20 p2625 A73-39651

HONEYCOMB STRUCTURES

- NT HONEYCOMB CORES
Tensile, compressive and shear strength and absolute modulus of PRD fibers from reinforced plastic honeycomb and filament wound strand tests
03 p0330 A73-13015
- The influence of adhesive components on the corrosion of aluminum honeycomb.
03 p0321 A73-13038
- Organization and management for adhesive bonding aircraft structures.
03 p0333 A73-13048
- The application of adhesive bonded structures and composite materials on advanced turbofan engines.
03 p0359 A73-14134
- Airship design for short-medium distance heavy payload transport, describing honeycomb skin construction, power plant installation and hovering loading/unloading operations
04 p0405 A73-14825
- Nondestructive eddy current tests of Al braise alloy fillet size and flatwise distribution in Ti honeycomb sandwich panels
05 p0581 A73-16131
- Dynamic properties of graphite fiber honeycomb panels.
[AIAA PAPER 73-326] 11 p1388 A73-25556
- Structural failures in light weight solar cell arrays under thermal cycling.
11 p1310 A73-25999
- Temperature sensitivity of cfrp honeycomb structures under holographic ndt.
12 p1496 A73-27036
- Epoxy resin adhesive for metal-to-metal and honeycomb sandwich bonding, featuring high flow during cure for high structural strength
16 p2029 A73-33054
- Brazed honeycomb structure design, fabrication and aerospace applications covering brazing methods, filler metal selection, nondestructive testing, sandwich designs, aircraft and spacecraft structures, etc
17 p2177 A73-34100
- Use of honeycomb and bonded structures in light aircraft.
[SAE PAPER 730307] 17 p2101 A73-34667

The successful use of composites in the L-1011 TriStar commercial transport.
17 p2103 A73-34815

- An advanced composite tailboom for the AH-1G helicopter.
[AHS PREPRINT 785] 17 p2107 A73-35098
- British X4 spacecraft mechanical design configuration with honeycomb sandwich panels, on yo-yo principle based despin system and flexible solar array
20 p2615 A73-39774
- Aluminum brazed titanium honeycomb sandwich structure - A new system.
23 p2985 A73-44000
- Procedure development for brazing Inconel 718 honeycomb sandwich structures.
23 p2985 A73-44001

HOOKES LAW

- Mathematical model for plastic deformation of polycrystalline materials with Hookes Law elastic strains
06 p0765 A73-18641
- Stress field singularities due to cracks in isotropic elastic bodies, assuming Hookes law stress-strain relationship in integral equation representations
09 p1162 A73-23182
- Maxwell kinetic theory of gases with elasticity of shape /modulus of rigidity/ and obeying Hookes law, deriving expressions for simple shear and relaxation time
14 p1745 A73-30477
- Thin shell elastoplastic deformation theory development for small strains, using Hooke's law to analyze hardening, stress and unloading
16 p2084 A73-34033
- Unique relations between equilibrium and Galimov-Novozhilov stability equations of geometrically nonlinear elasticity theory based on Hookes law
20 p2617 A73-39305

HORIZON

- NT RADIO HORIZONS
Test of horizon sensor for the ionosphere sounding satellite.
01 p0053 A73-11172
- Variation with altitude of the scatter coefficient in the stratosphere, based on measurements from the Soiuz-3 spacecraft
07 p0817 A73-19585
- Near horizon anomalies in astronomical refraction due to ground air layer effects on tropospheric processes
13 p1610 A73-29322
- Slope angle determination with respect to photograph surface from visible horizon line configuration
16 p2017 A73-34049

HORIZON SCANNERS

- Thermopile IR static horizon sensor for Symphonie satellite three axis attitude stabilization in geostationary orbit
07 p0821 A73-18985
- Image formation radiometers for blind landing, aerial reconnaissance over land and sea, horizon detection and detection of obstacles at sea
08 p0986 A73-21087

HORIZON SENSING

- U HORIZON SCANNERS
HORIZONTAL FINS
U FINS
HORIZONTAL FLIGHT
Minimum fuel rocket maneuvers in horizontal flight.
08 p1014 A73-20714

HORIZONTAL STABILIZERS

- U STABILIZERS (FLUID DYNAMICS)
HORIZONTAL TAILS
U TAIL ASSEMBLIES
HORMONE METABOLISMS
Corticosterone level and the binding capacity of blood plasma proteins under thermal effects
03 p0261 A73-13749
- Multiple hormonal responses to graded exercise in relation to physical training.
03 p0263 A73-14116
- Multiple hormonal responses to prolonged exercise in relation to physical training.
03 p0263 A73-14117
- Thyroid and adrenal cortical rhythmicity during bed rest.
03 p0263 A73-14122
- Human endocrine-metabolic responses to graded oxygen pressures.
07 p0785 A73-19479
- Catecholamine exchange in the hormonal and mediator links of the sympathoadrenal system under stress
07 p0784 A73-20367
- Renal component of the antigravitation function of the organism
08 p0929 A73-20976
- Relation between the frequency-amplitude characteristics of cerebral electrical activity and gonadotropic hormone excretion levels at various stages of ontogenesis
08 p0930 A73-21319
- Effects of an hyperoxic hypobaric environment on renin-aldosterone in normal man.
08 p0934 A73-21503

Comparison of the metabolic effects of centrifugation and heat stress in man.

11 p1315 A73-25338
Sinoatrial node pacemaker cell functions, discussing ionic and metabolic principles, electrical activity, membranar effects of neurohormonal control factors and cardioactive drug effects

11 p1316 A73-25595
Mechanisms of secretion of neurohypophysial hormones - Cellular and subcellular aspects

15 p1836 A73-32286
Effects of the hypodynamics and other factors of a spaceflight on the excretion of 17-oxycorticosteroids and aldosterone

17 p2111 A73-34233
Metabolic responses of monkeys to increased gravitational fields.

18 p2270 A73-35982
Endocrine studies during a 14-day continuous exposure to 5.2% O₂ in N₂ at pressure equivalent to 100 FSW /4 ata/.

18 p2279 A73-36795
Reaction of neurocytes of the paraventricular hypothalamic nucleus to unilateral thyroidectomy

21 p2637 A73-40283
Participation of the hypophysis and adrenal glands in intra-ocular pressure regulation

22 p2807 A73-42661
The presence in the heart of compounds which participate in the neurohumoral regulation of coronary circulation

24 p3059 A73-44769

HORMONES

NT ALDOSTERONE
NT CORTICOSTEROIDS
NT CORTISONE
NT HYDROXYCORTICOSTEROID
NT PITUITARY HORMONES
NT THYROXINE

Adaptive hormone action and nonspecific adaptive function of steroid hormones, discussing stress resistance mechanisms of steroids pharmacologically classified as syntoxic and catatonic

09 p1045 A73-22536

HORN ANTENNAS

Comparing ECM antennas - Horns vs spirals.

02 p0147 A73-12568
Computation of element patterns of an E plane sectoral-horn planar phased array.

04 p0415 A73-14987
Two channel multimode feed for circular horn tracking antenna applications, discussing channel patterns, coupling, isolation and frequency response

04 p0428 A73-15417
Parabolic, Cassegrain, spherical and horn-parabolic axisymmetric mirror antennas, calculating primary radiating element orientation effects on radiation polarization characteristics

05 p0547 A73-16052
Calculation of input-voltage standing-wave ratio for a reflector antenna.

05 p0547 A73-16161
Errors in the predicted gain of pyramidal horns.

06 p0676 A73-18180
Propagation and radiation characteristics of corrugated horns.

07 p0798 A73-19156
Influence of horn length on radiation pattern of oblique-flare-angle corrugated horn.

07 p0798 A73-19160
Corrugated horn antenna for constant bandwidth and circularly symmetric radiation pattern free of primary sidelobes, noting VSWR reduction

07 p0803 A73-20492
Horizontal-polarization biconical horn antenna excited by TE/sub-11/ mode in circular waveguide.

08 p0945 A73-20805
Selectively faded nondiversity and space diversity narrowband microwave radio channels.

08 p0939 A73-21086
Rectangular horn with dielectric-slab insert.

08 p0946 A73-21117
Horn antennas dephasing based on quadrupole with circular guides, cones of revolution and air space

11 p1327 A73-25279
Design of multiple-edge blinders for large horn reflector antennas.

11 p1337 A73-25653
Active electromagnetic horn antenna with tunnel diode.

11 p1331 A73-26124
Horn-element antenna phase center position calculation for directivity characteristics by power series of radiation patterns

12 p1480 A73-27236
Corrugated circular waveguide horn as monopulse antenna feed for optimal tracking performance, using difference-sum patterns with hybrid modes

14 p1731 A73-29705
Radiation characteristics of corrugated E-plane sectoral horns.

14 p1734 A73-30209
Radiation patterns of dielectric loaded rectangular horns.

14 p1735 A73-30220

A simplification in the analysis of four- and five-horn fed Cassegrainian reflectors when the horns have nearly symmetric patterns.

14 p1735 A73-30224
Radiation characteristics of a waveguide excited dielectric sphere backed by a metallic hemisphere.

14 p1728 A73-30225
Radiation patterns and structural design of two mirror millimeter wave Cassegrain antennas with horn radiator

16 p1991 A73-33985
Time domain current interaction coefficients for sheet antenna structures.

17 p2142 A73-35647
Corrugated horn antenna with high efficiency and monotonic amplitude in microwave pattern ranges applicable as calibrating standard

17 p2143 A73-35693
Directional properties of horn-parabolic antennas

21 p2661 A73-40193
Design of coincident dual-frequency mirror antennas

21 p2661 A73-40194
Advances in the theory and technology of horn antennas and reflector antennas

21 p2664 A73-41073
A new method for calculating correction factors for near-field gain measurements.

22 p2830 A73-41829
Short axial length broad-band horns.

22 p2831 A73-41846
Corrugated conical horn antenna feed design, discussing Newton-Raphson iterative solution and computer program for spherical hybrid mode eigenvalues

22 p2832 A73-42296
Experimental determination of the field parameters in a sectorial horn aperture with the aid of a passive probe

22 p2826 A73-42337
Radiation characteristics of a corrugated conical horn.

24 p3069 A73-45029

HOSES

Influence of the bending radius on the strength, volume deformation, and bending rigidity of high-pressure hoses

03 p0318 A73-14599
High-temperature low pressure hose assembly, convoluted-, tetrafluoroethylene-, for aerospace. (SAE ARP 1227)

16 p1970 A73-33017

HOT AIR

U HIGH TEMPERATURE AIR

HOT CATHODES

Rotation of the ion component of a plasma from a hot-cathode Penning discharge

09 p1125 A73-21955
Plasma diagnostics in overcompensation operated Knudsen thermionic converter with Cs-Ba filler, noting W cathode surface properties

10 p1177 A73-24204
Rotational instability of a plasma from a hot-cathode Penning discharge

11 p1403 A73-25243

HOT CYCLE PROPULSION SYSTEM

U TIP DRIVEN ROTORS

HOT ELECTRONS

Hot-electron concept for Poole-Frenkel conduction in amorphous dielectric solids.

02 p0201 A73-12817
Experimental study of millimeter-wave characteristics of hot electrons in n-type GaAs by electrodeless method.

05 p0558 A73-16525
Diffusion of hot electrons in n indium phosphide.

07 p0861 A73-19157
Electron cyclotron off-resonance heating rate in hot electron plasmas, comparing numerical calculation in terms of harmonic resonance with computerized simulation

07 p0856 A73-19519
Measurement of the attenuation of an electromagnetic wave in a bounded hot electron plasma.

07 p0860 A73-20478
Millimeter-wave frequency response of hot electrons in n-type GaAs.

08 p0994 A73-20845
Earth radiation belts energetic electrons quiet equilibrium structure based on balance between pitch angle scattering loss and inward radial diffusion

14 p1786 A73-29965
Comparison of the hot-electron plasmas produced using two different plasma sources in a magnetic mirror compression experiment.

14 p1781 A73-30657
Electromagnetic instabilities of finite pressure anisotropic plasma with hot electrons.

15 p1916 A73-31084
Hot-electron production and anomalous microwave absorption near the plasma frequency.

19 p2469 A73-38289

HOT EXTRUDING

U EXTRUDING

HOT FORMING

U HOT WORKING

HOT GAS SYSTEMS

U HIGH TEMPERATURE GASES

HOT GASES

U HIGH TEMPERATURE GASES

HOT JET EXHAUST

U HIGH TEMPERATURE GASES

HOT JET EXHAUST

HOT JETS

U JET FLOW

HOT MACHINING

Hot fluomachining of Ti alloy tubes and turbine casings, noting dimensional accuracy dependence on temperature

19 p2441 A73-37835
German monograph - Materials removal in the case of the drilling of holes with the aid of solid-state lasers.

22 p2866 A73-42699

HOT PLASMAS

U HIGH TEMPERATURE PLASMAS

HOT PRESSING

Processing and properties of powder forgings.

01 p0056 A73-10279
Hot isostatic pressing of high-performance materials.

01 p0056 A73-10280
Aluminum-stainless steel and Ni-Mo composites prepared by dynamic hot pressing, determining bond strength between fibers and reinforced metal matrix

03 p0328 A73-14013
Measurements of the emissivity of materials fabricated by powder- and plasma-metallurgy techniques

09 p1103 A73-22472
Creep associated with hot pressing titanium carbide powders

10 p1224 A73-24315
Hot deformation of metal ceramic titanium preforms

10 p1225 A73-24321

The fracture toughness of beryllium.

11 p1384 A73-26168

Crack toughness evaluation of hot pressed and forged beryllium.

11 p1384 A73-26169

S-200 grade beryllium fracture toughness properties.

11 p1384 A73-26170

The nature of the nonuniformity of the structure and properties of semiproducts pressed from titanium and its alpha-alloys

12 p1502 A73-26909
Analysis of the energy losses during dynamic hot pressing of reinforced metals

12 p1503 A73-27557

The pressing of profiles of aluminum casting alloys from granules and the study of their mechanical properties

12 p1503 A73-27560

The effect of processing on the microstructure of CFRP.

13 p1645 A73-28779
Characteristics of dynamic hot pressing with high deformation rates

15 p1881 A73-31589

Book - Forging of powder metallurgy preforms.

15 p1891 A73-32195

Hot isostatic pressing of titanium alloys for turbine engine components.

16 p2019 A73-33516
[ASME PAPER 73-GT-63]

Sintering and hot pressing of Fra Mauro composition glass and the lithification of lunar breccias.

16 p2070 A73-33875

Hot-pressed eutectics of oxides and metal fibers.

21 p2723 A73-40895

Additive distribution and formation of internal stress in fired magnesias.

23 p2998 A73-44133

Shrinkage of reinforced sandwich-type materials during hot pressing

24 p3092 A73-44416

Hot closed-die forging of powder titanium

24 p3093 A73-44739

Creep during the hot compression of titanium diboride powder

24 p3093 A73-44740

HOT STARS

NT A STARS

NT B STARS

NT O STARS

NT WHITE DWARF STARS

Infrared excesses in early-type stars - Free-free emission.

02 p0225 A73-12826

A search for density and pressure inversions in high-temperature, low-gravity model atmospheres.

03 p0366 A73-12935

Chromospheric heating of very hot stars by radiation driven sound waves.

03 p0371 A73-13222

Stratification of the emission in the envelope of the eclipsing-binary WOLF-Rayet star V444 Cygni.

04 p0503 A73-16009

Rapid variations of Psi Per shell star H beta line, indicating shell and stellar atmosphere activity

05 p0617 A73-16466

Stellar winds and mass loss of a rotating star.

05 p0624 A73-17312

Mass transfer during evolution of close binaries within zero velocity surfaces related to nova outbursts and Wolf-Rayet star composition

06 p0753 A73-18246

SkyLab experiment for measuring color indices of extended sources and of spectral types O, B and A hot stars at various galactic latitudes

07 p0822 A73-18989

Optically thin stellar winds in early-type stars

07 p0873 A73-19061

Spectrum of a dust-embedded Wolf-Rayet star in Cygnus OB2.

07 p0900 A73-20241

Chromospheric heating of very hot stars by radiation driven sound waves. II.

09 p1148 A73-22868

Statistical significance of some optical evidence for the bending of the galactic plane.

10 p1271 A73-23492

An abundance analysis of the delta Scuti variable delta Delphini.

10 p1275 A73-23831

LTE and hydrogen and ionized He lines approximations for model atmosphere computations of hot early stars, discussing UV line blanketing

13 p1686 A73-29367

A new age indicator for Galactic clusters.

14 p1799 A73-30449

Scanner observations of hot helium-carbon stars.

15 p1932 A73-31269

The dynamics of the Andromeda Nebula.

15 p1941 A73-32400

The effect of hot white dwarfs on the interstellar medium. II - The changes in its structure with height above the galactic plane and some consequences of the finite lifetimes and velocities of the white dwarfs.

19 p2483 A73-37561

Possibility of radiative acceleration of the gas in stellar atmospheres

21 p2767 A73-40554

Shell nebulae and Wolf-Rayet stars - Observations of NGC 2359

21 p2768 A73-40714

Narrow-band photoelectric observations of the Wolf-Rayet type eclipsing binary star V444 Cyg in the continuum [4244 - 7512A]

21 p2768 A73-40717

Wolf-Rayet and high temperature stars; Proceedings of the Symposium, Buenos Aires, Argentina, August 9-14, 1971.

23 p3025 A73-43191

The Wolf-Rayet stars - The general problems of extended atmospheres and non-classical atmospheric models.

23 p3025 A73-43192

Classification and distribution of WR stars and an interpretation of the WN sequence.

23 p3025 A73-43193

Wolf-Rayet stars UV spectra from OAO-2 satellite-borne spectrometer measurements, considering radio spectra of W stars with symmetrical nebulae from ground based observations

23 p3025 A73-43194

Wolf-Rayet stars effective temperature estimation from UVB photometry of surrounding ring nebulae with optically thick H II region excited by stellar Lyman radiation

23 p3025 A73-43195

Line identification and profiles in emission spectra of Wolf-Rayet stars from microphotometer tracings at high dispersion, noting effects of companion stars

23 p3026 A73-43196

O, Of, Oe and Wolf-Rayet star comparison in terms of emission and absorption line spectra, noting relationship to evolutionary status on H-R diagram

23 p3026 A73-43197

P Cyg type O and B supergiant stars relationship to Wolf-Rayet stars in terms of spectra, absolute magnitudes, mass and variability

23 p3026 A73-43198

Planetary nebulae nuclei emission line spectral features similarity to spectra of Population I Wolf-Rayet and O-type stars

23 p3026 A73-43199

Wolf-Rayet stars luminosity to mass ratios, internal structure, mass loss to companion or interstellar space and spectral peculiarities related to evolutionary status

23 p3026 A73-43200

Wolf-Rayet stars continuous and line spectral features interpretation by model involving wide emission lines due to Doppler effect in rapidly expanding envelope

23 p3026 A73-43201

Wolf-Rayet binary stars detection and use in WR stellar mass, evolutionary status and luminosity estimation, noting atmospheric stratification relationship to temperature

23 p3026 A73-43202

Summary of problems and conclusions on the nature and physical structure of Wolf-Rayet stars.

23 p3026 A73-43204

Single component wind model for stellar rotation dependent mass loss from hot corona with application to T Tauri star observations

24 p3140 A73-45186

HOT SURFACES

Indentation of the semi-infinite elastic solid by a hot sphere.

22 p2929 A73-43174

HOT WORKING

Hot extrusion and filled billet techniques to process superalloy powder metallurgy products into complex shapes, bars or wire

01 p0056 A73-10284

Hot extrusion and properties of rods from sintered molybdenum and tungsten blanks.

01 p0065 A73-10817

Cracking of Zircaloy as a result of unusual localized texturing.

02 p0183 A73-12756

Hot worked Al alloy machine elements mechanical properties scattering, discussing quality control procedures

03 p0327 A73-14004

Metal deformation processes, discussing hot working, fracture, hydrostatic extrusion, superplastic forming, diffusion bonding and powder fabrication

04 p0452 A73-14742

Development of a process utilizing heated rolls for hot rolling metals.

04 p0454 A73-15001

Influence of hydrogen on the technological plasticity of the alloy Ti + 9% Al

04 p0464 A73-15499

Heated rolls application in hot rolling of metals, estimating residual thermal stresses and heat transfer [ASME PAPER 72-WA/MAT-2]

04 p0457 A73-15810

Effect of overheating on creep resistance in metastable alloys.

06 p0710 A73-18639

Influence of hot rolling on the mechanical properties of unstable austenitic chromium-manganese steels

09 p1098 A73-21848

Recrystallization of the IVT-1 beta titanium alloy

09 p1107 A73-23192

The effect of carbon and titanium on the hot workability of 25Cr-6Ni stainless steels.

10 p1235 A73-24440

German monograph - Investigations concerning the hot working of heterogeneous iron-molybdenum alloys with differing precipitation distribution.

14 p1762 A73-30670

Fabrication techniques for Ti alloys in aerospace applications, discussing hot forming, electron beam and diffusion welding under vacuum and stress relaxation annealing

23 p2985 A73-43911

The effect of cold and hot rolling on the microstructure and fracture characteristics of titanium-to-steel explosion welds.

23 p2985 A73-43912

Influence of deformation on the strength and ductility of low-alloy chromium

23 p2996 A73-44290

Recrystallization and precipitation induced by high temperature deformation - Case of a weldable construction steel containing niobium

24 p3101 A73-45524

HOT-FILM ANEMOMETERS

Quasi-steady heat transfer equation for frequency response of wedge shaped hot film sensors for flow temperature, velocity and turbulence measurement

02 p0166 A73-11711

Application of constant temperature anemometry in measurement of intra-arterial blood flow velocity.

05 p0545 A73-17274

The development of a hot-foil probe for measurements in turbulent flows

08 p0962 A73-20748

Turbulence measurements with the split-film anemometer probe.

13 p1619 A73-29253

Experiments in magneto-fluid-mechanic natural and forced heat transfer from horizontal hot-film probes.

13 p1620 A73-29254

The comparison of a new constant temperature anemometer with several laser anemometer configurations.

13 p1620 A73-29268

The heat loss of hot wires and heat films in steady flow

15 p1879 A73-32349

Magneto-fluid-mechanic heat transfer from hot film probes.

17 p2255 A73-35845

Temperature compensation in a thermoanemometer

24 p3089 A73-44548

The behavior of hot-film anemometers in gas mixtures.

24 p3091 A73-45325

HOT-WIRE ANEMOMETERS

Free and forced convection from fine hot wires.

01 p0120 A73-10447

Low Reynolds number flow past a transverse cylinder at Mach two.

01 p0003 A73-10758

Thermoanemometer with automatically stabilized temperature of its sensitive element and output signal linearization

02 p0170 A73-12344

Rotor unsteady wakes three dimensional flow analysis by wave front averaging technique, using constant temperature hot-wire anemometer

02 p0129 A73-12504

Hot-wire anemometers calibration characteristics for steady channel turbulent air flow measurement, noting linearization error analysis

03 p0306 A73-13166

Subsonic wind tunnel tests for laminar boundary layer investigation in low level turbulence flow, noting turbulence measurement with hot-wire anemometers

03 p0308 A73-13666

Decoding of thermoanemometer data for a flow with velocity, pressure, and temperature pulsations

03 p0308 A73-13667

Hot wire measurement of velocity gradients in a fluid flow.

[ALAA PAPER 73-50]

06 p0692 A73-17626

Copper resistance thermoanemometer for channel unsteady air flow rate measurement, discussing design, operation principles and maximum error

07 p0823 A73-19623

An evaluation of the heat pulse anemometer for velocity measurement in inhomogeneous turbulent flow.

[AD-758460]

09 p1071 A73-22102

Calibration of a hot-wire anemometer for velocity perturbation measurement.

10 p1218 A73-24121

Hot-wire anemometer probe operation in constant current in continuous high-temperature hypersonic turbulent boundary layer, computing velocity and temperature fluctuations

10 p1205 A73-24254

Hot-wire measurements of gas mixture concentrations in a supersonic flow.

10 p1220 A73-24637

Spatial amplitude distribution of vibrating ribbon two dimensional wake mean, periodic and random velocity components measured in uniform flow by hot-wire anemometry

10 p1173 A73-24828

The response of a hot-wire anemometer in flows of gas mixtures.

10 p1222 A73-24971

Conditional sampling and other measurements in a plane turbulent wake.

11 p1299 A73-25056

A low-velocity hot-wire anemometer.

12 p1496 A73-27055

Some remarks on the thermal equilibrium equation of hot-wire probes.

13 p1613 A73-28528

Simultaneous comparison of turbulent gas fluctuations by laser Doppler and hot wire.

13 p1616 A73-28821

Turbulent interface detector using a multiple array of single hot wires.

13 p1619 A73-29252

Hot-wire anemometric velocity measurements in nonisothermal turbulent flows, compensating for local temperature effects on downstream wire

13 p1620 A73-29255

Interpretation of hot-film anemometer response in a non-isothermal field.

13 p1620 A73-29256

Constant current and temperature hot-wire anemometer systems evaluation via ratio of changes in bridge balance to heat transfer changes between sensor and environment

13 p1620 A73-29257

Interferometric and thermoanemometric methods of studying binary boundary layers

15 p1876 A73-31859

The heat loss of hot wires and heat films in steady flow

15 p1879 A73-32349

Isolation and sampling of random signals transmitted by several hot-wire anemometers

16 p2017 A73-34016

Turbulence measurements with hot-wire anemometry in a non-homogeneous jet.

17 p2174 A73-35512

Rapid scanning, three-dimensional, hot-wire anemometer surveys for wing tip vortices in the Ames 40- by 80-foot wind tunnel.

[ALAA PAPER 73-681]

18 p2315 A73-36232

Turbulent correlation measurements in a two-stream mixing layer.

18 p2298 A73-36311

On the correction of anemometric measurements in air flows of slowly varying temperature

19 p2429 A73-37529

A universal static calibration procedure for yawed hot wires.

21 p2693 A73-39926

Hot-wire anemometer investigation of turbulent boundary layers at a permeable plate with injection.

21 p2678 A73-41055

Hot-wire investigation of the steady laminar wake behind a circular cylinder.

21 p2703 A73-41117

Hot-wire investigation of the steady laminar wake behind a thin flat plate placed perpendicularly to a uniform flow.

21 p2703 A73-41118

Subsonic wind tunnel tests for laminar boundary layer investigation in low level turbulence flow, noting turbulence measurement with hot-wire anemometers 21 p2704 A73-41316

Interpretation of hot-wire anemometer readings in a flow with velocity, pressure and temperature fluctuations. 21 p2705 A73-41317

Aerodynamic effects due to configuration of X-wire anemometers. [ASME PAPER 73-APM-P] 23 p2984 A73-44375

Modal analysis of turbulent correlations in compressible flow. 23 p2970 A73-44382

Temperature compensation in a thermocouple anemometer. 24 p3089 A73-44548

On the correction of hot wire turbulence measurements for spatial resolution errors. 24 p3089 A73-44691

Measurement of turbulence transport properties in a supersonic boundary-layer flow using laser velocimeter and hot-wire anemometer techniques. [AIAA PAPER 73-1045] 24 p3090 A73-44869

HOT-WIRE FLOWMETERS

Measurement of longitudinal and normal velocity fluctuations by sensing the temperature downstream of a hot wire. 05 p0576 A73-16438

Application of hot wires to measurements in freely expanding jets. 05 p0578 A73-17117

Hot wire probe applications to radiation, fluid flow, vacuum and temperature measurements, deriving mathematical expressions for physical laws 08 p0962 A73-20750

Using a single hot-wire probe in three-dimensional turbulent flow fields. 13 p1600 A73-28526

Influence of wall proximity on hot-wire velocity measurements. 13 p1613 A73-28527

A study of systematic errors in measurements with the constant-temperature anemometer in high-turbulence flows with and without hot-wire signal linearization. 13 p1613 A73-28529

Constant line sources of heat in infinite media, whose thermal resistivities are linear functions of the temperature. 14 p1817 A73-30610

Measurements of temperature fluctuations behind a linear heat source placed in a turbulent boundary layer 17 p2254 A73-34550

Mean flow and turbulence measurements in a Mach 5 shear layer. 17 p2097 A73-35506

Observation and calculation of a steady, laminar separated flow. 17 p2157 A73-35866

HOT-WIRE TURBULENCE METERS

U HOT-WIRE FLOWMETERS

U TURBULENCE METERS

HOTSHOT WIND TUNNELS

Monograph - Development of hotshot wind tunnels for hypersonic aerodynamic studies. 15 p1859 A73-32595

HOURLASS VALLEYS

U VALLEYS

HOUSINGS

NT RADOMES

Russian book on aircraft onboard instruments and equipment arrangement and housing for weight reduction covering electric, radar, navigation, control, display and auxiliary devices 21 p2635 A73-41425

HOVERCRAFT

U GROUND EFFECT MACHINES

HOVERING

Optimum performance of static propellers and rotors. 03 p0242 A73-13308

A summary of wind tunnel research on tilt-rotors from hover to cruise flight. [ONERA, TP NO. 1133] 08 p0928 A73-21683

Theoretical and practical aspects of an automatic hover control system for an unmanned tethered rotor-platform. 10 p1175 A73-24009

Aerodyne flight vehicle testing for hover flight characteristics during remote control by radio with pilot commands, noting reliability and attitude control. 13 p1569 A73-28785

Integrated image and symbolic display hierarchy with increasing horizontal and vertical information content for superposition as helicopter aid in approach and precision hovering [AHS PREPRINT 724] 17 p2168 A73-35065

Non-linear flap-lag dynamics of hingeless helicopter blades in hover and in forward flight. 22 p2800 A73-43134

HOVERING STABILITY

Precision hover sensor for heavy-lift helicopter. 10 p1216 A73-23784

Stability of elastic bending and torsion of uniform cantilevered rotor blades in hover. [AIAA PAPER 73-405] 11 p1440 A73-25534

Anthropotechnical investigation of an above-ground indication and of an artificial horizon with preindication in connection with the manual control of VTOL aircraft 15 p1839 A73-32044

Experimental investigation of model variable-geometry and ogee tip rotors. [AHS PREPRINT 703] 17 p2104 A73-35054

A study of stall-induced flap-lag instability of hingeless rotors. 17 p2095 A73-35066

On the aerodynamic damping moment in pitch of a rigid helicopter rotor in hovering. II - Analytical phase. 21 p2631 A73-40087

HRB-1 HELICOPTER

U CH-46 HELICOPTER

HU-1 HELICOPTER

U UH-1 HELICOPTER

HUBBLE DIAGRAM

Hubble law from constant light velocity in Euclidean space, noting red shift equation and Einstein gravitational shift 03 p0379 A73-14577

Hubble law correspondence in invariant mechanical theory of universe expansion to direct consequence of impulse conservation in inertially moving many body system 03 p0380 A73-14603

The redshift-distance relation. II - The Hubble diagram and its scatter for first-ranked cluster galaxies: A formal value for q-sub 0. III Photometry and the Hubble diagram for radio sources and the possible turn-on time for QSOs. 04 p0498 A73-15351

A comparative study of Brans-Dicke and general relativistic cosmologies in terms of observationally measurable quantities. 05 p0624 A73-17303

Observational discrepancies of redshift-distance relationships associated with galaxies and quasars 07 p0904 A73-20639

Hubble diagram construction for optically luminous quasars, noting relation between red shift and apparent magnitude 08 p1002 A73-20877

The redshift-distance relation. IV - The composite nature of N galaxies, their Hubble diagram, and the validity of measured redshifts as distance indicators. 11 p1427 A73-26602

The redshift-distance relation. VI - The Hubble diagram from S20 photometry for rich clusters and sparse groups - A study of residuals. 19 p2487 A73-38505

The redshift-distance relation. VII - Absolute magnitudes of the first three ranked cluster galaxies as functions of cluster richness and Bautz-Morgan cluster type - The effect on q sub 0. 19 p2487 A73-38506

Concerning the forms of the velocity-distance relation clusters. 22 p2913 A73-43001

A reexamination of the mean H I density along the Hubble sequence. 22 p2913 A73-43003

Relativistic torque detection on freely spinning rotor, obtaining phenomenological expression by incremental Hubble law 24 p3142 A73-45342

HUBS

Rotatory inertia and hub radius effects on transverse vibrational characteristics of clamped Rayleigh beam, using Galerkin method 03 p0388 A73-13316

Disks with inclined face, investigating effects of joint between hub and disk face on stress-strain state in elastic deformation range 03 p0394 A73-14012

Heavy lift helicopter rotor hub design and fatigue test technology, using fail-safe criteria, finite element analysis and fracture mechanics [AHS PREPRINT 784] 17 p2180 A73-35097

HUGHES MILITARY AIRCRAFT

U MILITARY AIRCRAFT

HUGONIOT ADIABAT

U HUGONIOT EQUATION OF STATE

HUGONIOT EQUATION OF STATE

Shock waves existence and behavior in elastic non-conductors, investigating Hugoniot stress-strain curve properties 01 p0033 A73-10778

Upper and lower stability limits criterion for plane shock waves, based on Hugoniot curve positive slope 15 p1860 A73-31090

Interacting continuum theory concerning steady shock wave in composite materials, discussing energy interaction terms error correction effects on Hugoniot relations 15 p1949 A73-31685

HULLS (STRUCTURES)

Aircraft accident statistics for passenger fatalities, worldwide jet hull losses and estimated costs to suggest proposals for approach, landing and takeoff accident reduction 18 p2268 A73-36846

HUMAN BEHAVIOR

Conjoint-measurement framework for the study of probabilistic information processing. 02 p0138 A73-12545

Reflex act structural components interaction in terms of reflection, creativity and organism-environment relations, noting subjective and objective perception and attitude formation 04 p0410 A73-15798

Studies in interactive communication. I - The effects of four communication modes on the behavior of teams during cooperative problem-solving. 06 p0658 A73-18241

A vecto-oculographic approach to fast sleep eye movements in man. 14 p1715 A73-29994

Behavioral stress response related to passenger briefings and emergency warning systems on commercial airlines. 16 p1965 A73-32660

Self destructive behavior of aircraft pilot due to stress accumulation, discussing man machine relationship, coping mechanisms, competence and invulnerability myth 17 p2115 A73-34746

The problem of spiritual requirements and the theory of human higher nervous activity 20 p2515 A73-39796

Experimental analysis of conditions for onset of emotional stress 20 p2516 A73-39800

HUMAN BODY

Interrelation between hardness, viscosity, strength, and bioelectric activity of human muscles 01 p0007 A73-10155

Reduced dimensionality for minimization of degrees of freedom of skeletal activity models for anthropomorphic locomotion system synthesis 01 p0013 A73-11052

Perspiration secretion distribution over human body based on extended Kerslake cylinder model, comparing with predicted 4 hr sweat rate 03 p0259 A73-13122

Human body mathematical model described by kinematic and dynamic equations of joined rigid bodies for investigation of self-controlled movements in specified goal attainment 04 p0411 A73-15207

Biophysical properties of vibration energy transfer to human body structure, noting harmful effects dependence on frequency range 06 p0657 A73-17748

Human tendon stress recovery after load removal as function of time, sex, age and side differences 07 p0782 A73-20033

Quaternary structure /subunit composition/ of human ceruloplasmin 11 p1316 A73-25638

Moire topography for full size living human body contour stereophotographic pictures with high contrast, discussing instrument construction, performance and accuracy 17 p2114 A73-34617

A distributed parameter model of the inertially loaded human spine. 18 p2281 A73-36429

Intracellular-extracellular action potentials - Considerations for the formation of wavefronts and their detection on the body surface. 18 p2282 A73-36518

Physiologic correlates and clinical comparisons of isopotential pressure maps with other electrocardiographic methods. 18 p2282 A73-36519

Electrical field distribution in the human body. 23 p2950 A73-44216

HUMAN CENTRIFUGES

Positive-pressure breathing as a protective technique during +Gz acceleration. 20 p2519 A73-39793

HUMAN ENGINEERING

U HUMAN FACTORS ENGINEERING

HUMAN FACTORS ENGINEERING

Angular measurements of foot motion for application to the design of foot-pedals. 01 p0013 A73-10773

Aircraft fault isolation based on pattern of cockpit indications - A human factors approach. 02 p0136 A73-11857

Book - Applied maintainability engineering. 02 p0238 A73-11883

The effects of various seat surface inclinations on posture and subjective feeling of comfort 03 p0266 A73-13121

German monograph - Investigations concerning perception levels and transferred vibrational forces in the

case of a vertical action of periodic vibrational mixtures on man. 03 p0268 A73-13818

Human factors evaluation of labelled radar displays. 03 p0268 A73-14155

Multidimensional coding for telemetric transmission of work load factors in ergonomics research. 03 p0272 A73-14307

Telemetric transmission of ergonomic and time study data to describe work load of radar controllers. 03 p0272 A73-14308

The problem of human efficiency in automated control systems 05 p0542 A73-16410

Technology for man 72; Proceedings of the Sixteenth Annual Meeting, Los Angeles, Calif., October 17-19, 1972. 05 p0542 A73-16701

Human factors analysis of forward looking infrared (FLIR) imagery in air-to-ground target detection/recognition. 05 p0550 A73-16712

An evaluation of sinus arrhythmia as a measure of mental load. 05 p0543 A73-16718

Computer programs for operator performance time prediction and workspace design 05 p0544 A73-16721

A human factors approach to lighting recommendations and standards. 05 p0545 A73-16730

Transinformation and real time identification applied to the study of pilot workload 05 p0545 A73-17195

Human factor role in flying personnel errors, noting man machine system performance and medical service engagement 06 p0659 A73-18258

Outline of a new approach to the analysis of complex systems and decision processes. 06 p0671 A73-18622

Implications of psychoanalytic factors for Air Force operations. 11 p1323 A73-25340

Ergonomic endurance limits, physiological strains and fatigue assessment in video coding information task performance as function of work shift time length 11 p1323 A73-25649

Human factors aspects in aircraft electronic display systems, discussing cathode ray tubes (CRT) and light emitting diodes (LED) applications and characteristics 11 p1324 A73-26500

Radio Technical Commission for Aeronautics, Annual Assembly Meeting, Washington, D.C., November 9, 10, 1972, Proceedings. 12 p1522 A73-27360

Book - Human factor aspects of aircraft noise. 12 p1465 A73-27450

Aircraft accident prevention problems, considering pilot judgement errors, factory skill degradation, training, lightning and structure factors and air bag use 13 p1570 A73-29349

Application of human engineering principles and techniques in the design of electronic production equipment. 14 p1722 A73-30497

Heart rate variability analysis for ergonomics purposes, discussing interpolations, algorithms and physiological effects and spectral analysis methods 14 p1720 A73-30882

Avionics and human factors in flight simulator economics, interrelating aircraft design to simulation system 16 p1995 A73-33206

System engineering aspects of the man-machine interface. 16 p1975 A73-33645

Aircraft crash injury reduction through seat and restraint design, discussing dummy size considerations, seat belts, aircraft acceleration and injury types [SAE PAPER 730290] 17 p2114 A73-34655

Nonadjectival rating scales in human response experiments. 17 p2117 A73-35400

Teleoperator system incorporating touch feedback and sequenced automatic control for experimental investigation of human touch sensing relation to manipulative skills 19 p2397 A73-37328

Symposium on Flight Deck Environment and Pilot Workload, London, England, March 15, 1973, Proceedings. 19 p2383 A73-37726

Cockpit layout effects on pilot and flight crew activities, using in-flight observation, photography and pilot eye movement evaluation 19 p2384 A73-37733

Waste Management System overview for future spacecraft. [ASME PAPER 73-ENAS-18] 19 p2400 A73-37974

Zero-gravity and ground testing of a waste collection subsystem for the Space Shuttle. [ASME PAPER 73-ENAS-42] 19 p2401 A73-37989

Laundering in space - A summary of recent developments. 19 p2401 A73-37990

Cockpit evolution, considering pilot visual problems in approach final stage during poor visibility, instrument number and placement, supersonic aircraft, digital computer-CRT interfaces, etc 20 p2510 A73-39662

A visual display system approach for an advanced spaceflight simulator. [AIAA PAPER 73-923] 21 p2673 A73-40871

Human motion perception in motion drive logic design for flight simulation discussing feedback control, angular velocity and degrees of freedom [AIAA PAPER 73-931] 21 p2674 A73-40878

Russian book - Psychological problems of activity regulation. 22 p2812 A73-41884

Effect of the information panel structure on operator activity 22 p2812 A73-41889

Effect of a subjective ambiguity estimate concerning the duration of work on activity regulation 22 p2812 A73-41892

Some psychological and engineering aspects of the extravehicular activity of astronauts. 22 p2814 A73-42167

Biodynamic applications regarding isolation of humans from shock and vibration. 22 p2816 A73-42926

Techniques for decreasing power and increasing legibility of electronic watches. 22 p2863 A73-43101

Development of pilot-in-the-loop analysis. [AIAA PAPER 72-898] 22 p2817 A73-43110

Eye function and the illumination of instrument dials in aircraft 22 p2817 A73-43133

Keeping track of sequential events - Implications for the design of displays. 23 p2948 A73-43215

Optimal work-rest schedules under prolonged vibration. 23 p2948 A73-43217

Use of the conditioned reflex method to study the motor analyzer during hygienic evaluation of working conditions in the presence of vibrations 24 p3062 A73-44673

HUMAN PATHOLOGY

Favorable effect of flight on pilots exhibiting degenerative arteriopathy of the lower limbs 02 p0137 A73-12151

Idiopathic central serous retinopathy /choioidopathy/ in flying personnel. [AD-754147] 03 p0269 A73-14164

Solar activity effects on tree growth, farm crop yield, fish availability and human sickness trends, discussing indirect effects via meteorological factors 05 p0622 A73-17171

Pathology of angina pectoris. 05 p0542 A73-17276

Book - Peripheral vascular diseases: Diagnosis and management. 06 p0651 A73-17871

Physiological effects of microwave electromagnetic fields on human and animal organisms, considering etiology, diagnostics and prophylaxis 06 p0659 A73-18256

Pathological cardiac conduction system lesions anatomy associated with arrhythmia, discussing atrioventricular, His bundle and bundle branch blocks 06 p0655 A73-18872

Pathophysiological and clinical aspects of atherosclerosis and frontal sinus neomatoma formation due to barometric pressure changes from pilot case history studies 09 p1039 A73-22538

Method of PaCO₂ determination in men with functional disorders of external respiration 13 p1579 A73-29075

Characteristics of spontaneous oxygen tension variations in human brain structures 14 p1719 A73-30844

Some compensatory adjustment reactions of the blood circulation system in pulmonary pathology 15 p1835 A73-31623

The pathogenesis and clinical significance of primary T-wave abnormalities. 18 p2274 A73-36529

Cell viability in acute myocardial infarction, discussing pathogenesis, histological, histochemical and biochemical responses to ischemia, homeostasis maintenance and treatment methods 18 p2276 A73-36545

The prognosis of myocardial infarction. 18 p2276 A73-36549

The role of the sympathetic section of the vegetative nervous system in the training of the organism for the influence of statokinetic irritants. 18 p2279 A73-36903

The use of simple indicators for detecting potential coronary heart disease susceptibility in the third-class airman population. 18 p2284 A73-36912

The significance of retinal pathology in ageing aircrew. 18 p2285 A73-36925

Hepatic lesions observed among flight crews following aviation accidents 18 p2279 A73-36933

Ribes Nigrum anthocyanosides in ophthalmology 18 p2280 A73-36935

Annex 13 and the work of the aviation pathologist - Practical problems. 19 p2398 A73-37739

Management of the treatment of illnesses as a problem of modern control theory 20 p2518 A73-39348

Symmetry of the visual evoked potential in normal subjects. 21 p2638 A73-41012

Probability cross sections of heavy ion single hit inactivation paths for human cells using nitrogen ion accelerator experiments 22 p2805 A73-42183

Radiological assessment of the vertebral column from the point of view of aviation medicine 22 p2817 A73-43131

The frequency of barotraumas as determined by nasal findings and X-rays of the paranasal sinuses 22 p2817 A73-43132

HUMAN PERFORMANCE

NT ASTRONAUT PERFORMANCE

NT OPERATOR PERFORMANCE

NT PILOT PERFORMANCE

A method for aiding human operator performance in a noncompensatory tracking task. 01 p0011 A73-10323

Observers detecting a signal in two multiple observation tasks. 01 p0011 A73-10350

Influence of observing strategies and stimulus variables on watchkeeping performances. 01 p0012 A73-10771

Target detection during picture transmission through a TV system [DGLR PAPER 72-099] 02 p0166 A73-11682

Effects of intermittent and continuous noise on serial search performance. 03 p0267 A73-13560

Human factors evaluation of labelled radar displays. 03 p0268 A73-14155

Prediction of flight safety hazards from drug induced performance decrements with alcohol as reference substance. 03 p0269 A73-14158

DFVLR-SONDDR-268] Motion sickness symptomatology and performance decrements occasioned by hurricane penetrations in C-121, C-130 and P-3 Navy aircraft. 03 p0269 A73-14161

Identification and adjustment of psychological factors to improve solar patrol observing. 04 p0411 A73-14841

Energy cost of muscle work in a state of fatigue 05 p0541 A73-16697

Observer target acquisition performance dependence on target position within restricted visual field 05 p0543 A73-16711

Visual time compression. II - Detecting moving targets in dense radar ground clutter. [AD-753746] 05 p0550 A73-16715

Crew performance in extended operation under vibrational stress. 05 p0543 A73-16717

Double cross-validation of video cartographic symbol location performance. 05 p0543 A73-16719

Psychological and physiological components of biorhythm cycles governing periodic variations in physical, emotional and intellectual performance 05 p0544 A73-16720

A human factors approach to lighting recommendations and standards. 05 p0545 A73-16730

Estimation of the passing of four consecutive hours. 06 p0656 A73-17524

Psychological and psychophysiological factors of human performance in manned space missions, considering environmental effects of space flight and man-machine system 06 p0650 A73-17775

Sensory, learned, and cognitive mechanisms of size perception. 06 p0657 A73-18031

Statistical correlation between human mental activity and EEG beta rhythm wave energy and frequency characteristics 06 p0653 A73-18159

Visual performance with high-contrast cathode-ray tubes at high levels of ambient illumination. 06 p0658 A73-18243

Human performance measures relationship determination across sense modes under visual, auditory and combined stimulus conditions by controlling for task difficulty on individual basis 06 p0658 A73-18244

Physical work induced hyperthermia effects on detection rate in visual vigilance task performance in hot and humid environment

06 p0659 A73-18469

Central tracking task performance simultaneously with response to peripheral stimulus under high heat stress environments

06 p0659 A73-18473

A method for the investigation of interpolated information and time effects in short term retention.

06 p0659 A73-18475

German monograph - The objectivity of the effect of load and stress on an information-reception process of man with the aid of acoustically evoked potentials.

07 p0786 A73-20389

German monograph - Vigilance prognosis with the aid of a computer analysis of the spontaneous electroencephalogram.

07 p0786 A73-20391

High altitude acclimatization and mountain climbing effects on human organism, considering oculomotor, cardiovascular and respiratory responses and endurance

08 p0930 A73-20991

Meridional amblyopia - Evidence for modification of the human visual system by early visual experience.

08 p0931 A73-21562

Influence of high ambient temperatures on the performance and some physiological parameters in a tracking problem and an optical vigilance problem

08 p0935 A73-21575

Simultaneous motor and verbal processing of visual information in a modified Stroop test.

09 p1044 A73-21896

Neuroendocrine, cardiorespiratory, and performance reactions of hypoxic men during a monitoring task.

09 p1044 A73-22527

Effects of some antinotion sickness drugs and secobarbital on postural equilibrium functions at sea level and at 12,000 feet/simulated/.

09 p1045 A73-22529

Fatigue levels of cerebral hemispheres in response to visual task and test stimuli, noting left hander reduced performance capacity

09 p1040 A73-22925

Hedging, proper and improper skill scoring rules for meteorological probability forecasts

10 p1246 A73-23992

Independence of the recognition of an object's orientation and position in the field of vision

10 p1180 A73-24331

Aircraft maintenance manuals optimization for human errors minimization, discussing DC-10 in-flight and ground maintenance fault isolation philosophy and techniques

10 p1226 A73-24716

Field of view and target uncertainty in visual search and inspection.

11 p1322 A73-25181

Group performance in a visual signal-detection task.

11 p1322 A73-25182

Utilization of human voice for estimation of man's emotional stress and state of attention.

11 p1322 A73-25329

Combined effects of noise and vibration on human tracking performance and response time.

11 p1323 A73-25334

Kinetics of oxygen uptake and recovery for supramaximal work of short duration.

11 p1323 A73-25648

Ergonomic endurance limits, physiological strains and fatigue assessment in video coding information task performance as function of work shift time length

11 p1323 A73-25649

Effects of prolonged dark adaptation on autokinetic movement.

11 p1324 A73-26322

Flashblindness recovery following exposure to constant energy adaptive flashes.

13 p1579 A73-28505

Effects of flying and of time changes on menstrual cycle length and on performance in airline stewardesses.

13 p1576 A73-28509

A simple approach to post-evaluation of research.

13 p1708 A73-28926

Oxygen consumption alteration effects on human endurance capacity as function of relative work, muscle blood flow and anaerobic metabolism

14 p1714 A73-29753

Psychoacoustic theory of signal detectability based on mathematical input-output mapping model and memory role in human auditory system

14 p1721 A73-30278

Vector correlation theory and neural mechanisms of binaural signal detection in human auditory system

14 p1716 A73-30283

Optimal lighting for visual tasks, discussing color, type, transillumination, crossed polarization, brightness patterns, diffuse reflection and surface shadowgraphing

14 p1722 A73-30498

Towards an objective assessment of cockpit workload. I - Physiological variables during different flight phases.

14 p1718 A73-30515

Electrical activity of the external ear muscles in man /at rest and during identification of acoustic signals/

14 p1719 A73-30843

The effects of core temperature elevation and thermal sensation on performance.

15 p1839 A73-32396

Optimal duration of endurance performance on the cycle ergometer in relation to maximal oxygen intake.

15 p1836 A73-32397

A standard psychophysiological preparation for the study of environmental stress.

16 p1975 A73-33130

Book - Biological rhythms and human performance.

16 p1972 A73-33155

The explanation and investigation of biological rhythms.

16 p1972 A73-33156

Circadian rhythms in human mental performance from waking day, round of clock and simulated shift-work studies

16 p1972 A73-33157

Daytime human performance and temperament rhythms as function of individual introversion-extroversion rating

16 p1975 A73-33160

Industrial work rhythm and between-day fluctuation studies 1920-1969, emphasizing industrial record and between-day fluctuations

16 p2020 A73-33647

System effectiveness and the one error per man per day expectation.

17 p2097 A73-34077

Safety in operation and human error.

17 p2113 A73-34078

Man machine systems for flight safety, studying accidents, human factors in system design and implementation of personnel

17 p2113 A73-34149

Motivation in vigilance - A test of the goal-setting hypothesis of the effectiveness of knowledge of results.

17 p2257 A73-34657

FAA General Aviation Crashworthiness Program. [SAE PAPER 730293]

17 p2180 A73-35079

The human side of quality assurance /as viewed from helicopter manufacturing experiences/.

17 p2257 A73-35216

A survey of behavioral science contributions to laboratory management.

17 p2116 A73-35240

Spatial information coding in the human visual system - Psychophysical data.

18 p2283 A73-36787

Human performance at elevated environmental temperatures.

18 p2283 A73-36793

Physical energy expenditure in long-haul cabin crew.

18 p2279 A73-36920

The mechanisms of the occurrence of emotional stress in man.

18 p2280 A73-36942

Study of the heart rate of humans exposed to heat.

19 p2393 A73-37251

Study of performances in a warm environment in case of air conditioning breakdown on a supersonic transport

19 p2393 A73-37395

Reinforcement of unconscious traces of stimuli in the human being during ontogenesis

19 p2396 A73-38258

Interaction between contours in visual masking

19 p2396 A73-38260

The effect of exercise on intrinsic myocardial performance.

19 p2396 A73-38360

Effects of posture on exercise performance - Measurement by systolic time intervals.

19 p2402 A73-38378

Aerobic capacity of relatively sedentary males.

19 p2517 A73-39109

Effects of prestimulus cuing and target load variability on maintenance of response strategies in a visual search task.

20 p2509 A73-39216

Air traffic controller responsibilities and performance evaluation criteria development, discussing manager/monitor functions, field evaluation tests and training criteria

20 p2513 A73-39479

Contingent negative variation expectancy waveform relation to human psychic state in response to visual and imperative acoustic stimuli

20 p2516 A73-39804

Effect of carbon monoxide on time perception.

21 p2642 A73-40000

A flight evaluation of pilotage error in area navigation with vertical guidance.

21 p2733 A73-40029

Sleep deprivation effects on accuracy and speed of response selection and execution.

21 p2644 A73-40853

Effects of repeated simulated sonic booms of 1.0 PSF on the sleep behavior of young and old subjects.

21 p2644 A73-41151

Interactive effects of intense noise and low-level vibration on tracking performance and response time.

21 p2644 A73-41153

The psychophysical inquiry into binocular summation.

21 p2640 A73-41187

Russian book - Psychological problems of activity regulation.

22 p2812 A73-41884

Human recognition of dynamic pattern changes in numerical series displayed on spatiotemporal panels, discussing learning times and reactions to pattern disruptions

22 p2812 A73-41887

Visual perception of relative object dimension during monocular and binocular rod equalization experiment in various visual field restriction conditions, recording eye movements and focusing characteristics

22 p2812 A73-41890

Effect of exercise on the response time in an identification problem

22 p2813 A73-41894

A model of the human in a cognitive prediction task.

22 p2814 A73-42223

Eye movements of trained inspectors recorded during visual inspection of colored slides of IC chips, determining performance with emphasis on speed

23 p2947 A73-43212

Noise blurred image recognition probability characteristics from experimental investigation, showing difference from statistical decision theory data

24 p3062 A73-44667

Response surface /descriptive function/ methodology design for human performance research, discussing central composite design, observations at experimental points and orthogonal blocking

24 p3062 A73-44773

Response surface methodology analysis of training transfer in pursuit rotor tracking task, relating three independent variables through multiple-regression prediction equations

24 p3063 A73-44774

Decrements in tracking and visual performance during vibration.

24 p3063 A73-44777

Visual and verbal coding in the interhemispheric transfer of information.

24 p3065 A73-45337

Asymmetry in perception - Attention versus other determinants.

24 p3065 A73-45338

Two components and two stages in search performance - A case study in visual search.

24 p3065 A73-45339

HUMAN REACTIONS

Annoyance reactions from aircraft noise exposure.

01 p0005 A73-10781

Electromyographic study on human standing posture in experimental hypogravic state.

01 p0013 A73-11211

Color effects in visual discrimination, measuring response times in letter matching task

02 p0135 A73-12525

Behavioural awakening and subjective reactions to indoor sonic booms.

04 p0412 A73-15592

Mathematical description of some visual inertia effects

04 p0413 A73-15786

Effect of hypoxia on free fatty acid metabolism during exercise.

05 p0540 A73-16609

Augmentation of chemosensitivity during mild exercise in normal man.

05 p0540 A73-16610

The interaction of auditory noise and subjective noise annoyance sensitivity with peripheral visual sensitivity.

05 p0543 A73-16703

The prediction of team monitoring performance under conditions of varied team size and decision rules.

05 p0543 A73-16710

Step input tracking experiment for testing human psychological refractory period, noting directional error correcting reaction time similarities with keyboard tasks

06 p0659 A73-18470

German monograph - Work-physiological investigations for the objectivization of the tracking behavior, the mental load, and its psychopharmacological modularity.

07 p0786 A73-20388

Perceived level calculation methods for aircraft flyover noise scaling, rating jets, turboprops, piston aircraft and helicopters with frequency weighting functions, duration and tone corrections

10 p1175 A73-24391

Community response to aircraft noise.

10 p1298 A73-24562

Cardiac arrhythmias during exercise testing in healthy men.

11 p1315 A73-25336

Interindividual differences in homomodal and heteromodal scaling of auditory and vibrotactile stimulation intensity and duration, using magnitude estimation method

12 p1464 A73-26750

Emotional stimulation traces in the spectra of EEG and cutaneo-galvanic reaction of man under normal conditions and in the case of memory impairment

12 p1461 A73-27106

Physiological nature of the electroencephalographic and vegetative components of human conditioned reactions

12 p1462 A73-27107

Bactericide activity of the integument of man at different times of the day

12 p1463 A73-27716

Stimulus luminance-duration relationship of adapting light effect in human electroretinography, referring to Bunsen-Roscoe and Bloch constant law

13 p1575 A73-28363

Human hematologic responses to 4 hr of isobaric hyperoxic exposure /100% oxygen at 760 mm Hg.

14 p1714 A73-29751

Oscillations in oxygen consumption of man at rest.

14 p1714 A73-29755

Manipulating the response criterion in visual monitoring.

14 p1722 A73-30499

Influence of increased air atmosphere pressure on the excitability of the neuro-motor apparatus in man

14 p1719 A73-30845

Mental load and the measurement of heart rate variability.

14 p1720 A73-30881

Ventilatory responses to transient hypoxia and hypocapnia in man.

15 p1832 A73-31126

Evoked negative electrical potentials due to auditory zone stimulation by local cooling, mechanical trauma and potential recording, observing reaction regeneration variations

15 p1833 A73-31159

Definitions and procedures for computing the effective perceived noise level for flyover aircraft noise. [SAE ARP 1071]

16 p1967 A73-33015

Polarcardiographic responses to maximal exercise and to changes in posture in healthy middle-aged men.

16 p1972 A73-33114

Human response to transportation noise and vibration.

17 p2117 A73-35328

Modeling, instrumentation and data evaluation in clinical electroretinography, discussing Fourier analysis of sinusoidal light stimulation response in normal and abnormal humans

17 p2117 A73-35359

A model of psychological annoyance of noise.

17 p2118 A73-35627

Cardiovascular reactions of a healthy man exposed to sonic booms

18 p2284 A73-36909

Motor unit reactions of man to spinal and supraspinal inhibitory stimuli

19 p2395 A73-37943

Inverted posture illusion phenomenon in astronauts during weightless space flight, discussing vestibular organ function, acceleration effects and body gravitation sensing system

20 p2513 A73-39149

Circadian variations in presumably healthy men under conditions of peace-time army reserve unit training.

20 p2513 A73-39482

Participation of cholinergic mechanisms in negative human emotions

20 p2515 A73-39799

Pulmonary function in man after short-term exposure to ozone.

21 p2642 A73-40001

Effect of acceleration on distribution of lung perfusion and on respiratory gas exchange.

21 p2643 A73-40274

A descriptive model of multi-sensor human spatial orientation with applications to visually induced sensations of motion.

[AIAA PAPER 73-915]

21 p2644 A73-40863

Oxygen uptake, muscle high-energy phosphates, and lactate in exercise under acute hypoxic conditions in man.

21 p2638 A73-41131

Colored aftereffects after prolonged inspection of convex lines of one color and concave lines of another color

21 p2640 A73-41303

Spatial frequency selectivity of a visual tilt illusion.

21 p2642 A73-41642

Methods for quantifying the effect of noise on people.

22 p2811 A73-41707

The effect of aircraft noise on the countryside.

22 p2798 A73-41709

Mathematics of interaction between blood and electromagnetic fields.

22 p2802 A73-41788

Human perception of moderate strength low frequency magnetic fields tested by whole body immersion in large Helmholtz coil field under acoustic isolation

22 p2811 A73-41789

Operator response to sinusoidally varying normal and emergency cycles in dynamic control task, testing anticipatory aversion response ability and error response

22 p2812 A73-41885

Individual physiological differences in evoked potential reactions to light sources, discussing latent periods, potential amplitude distribution and EEG measurement techniques

22 p2812 A73-41888

Operator reaction functional readiness manifestation in evoked potential characteristics of stimulus-response situations, obtaining response amplitude distribution

22 p2812 A73-41891

Reaction time to changes in the tempo of acoustic pulse trains.

22 p2816 A73-42705

Eigenvectors of the sensitivity variations across the human central fovea.

22 p2810 A73-42957

Individual personality variability difficulties in measurement of human psychophysiological reactions to flight stress, emphasizing psychological interview and evaluation methods

22 p2817 A73-43130

Human reactions to whole-body transverse angular vibrations compared to linear vertical vibrations.

23 p2948 A73-43216

Influence of physical stress on the state of human higher nervous activity under conditions of underwater labor

24 p3059 A73-44672

Human noise sensitivity, discussing personality effects, Maplin airport planning and population separation into sensitive and imperturbable groups

24 p3062 A73-44770

HUMAN TOLERANCES

The second noise and social survey around Heathrow, London airport.

03 p0266 A73-12980

Acclimatization to severe dry heat by brief exposures to humid heat.

03 p0267 A73-13700

Direction-specific adaptation effects acquired in a slow rotation room.

03 p0268 A73-14154

Crew performance in extended operation under vibrational stress.

05 p0543 A73-16717

Human perception of humidity under four controlled conditions.

06 p0657 A73-17864

Case histories of valvular cardiopathies in military pilots, determining tolerance to flight

07 p0784 A73-19209

Mountain inhabitants physiological characteristics due to altitude effects, investigating human tolerance and adaptation to ambient environment

07 p0784 A73-19212

Analysis of some mechanisms of human stability to decompression of the lower portion of the body

08 p0930 A73-20987

Influence of an oxygen and carbon dioxide rich gas mixture on the human orthostatic stability

08 p0933 A73-20988

Reflex excitability of spinal motor neurons in man under high atmospheric pressure

10 p1182 A73-24525

Positive $\pm G_z$ acceleration tolerances of the miniature swine - Application as a human analog.

11 p1315 A73-25337

Comparison of the metabolic effects of centrifugation and heat stress in man.

11 p1315 A73-25338

Vestibular stresses effects on systemic and cerebral hemodynamics, considering human acceleration adaptation and compensation mechanisms

12 p1463 A73-27714

Effects of ethyl alcohol on pilot performance.

13 p1579 A73-28501

Effect of the Valsalva maneuver on tolerance to $\pm G_z$ acceleration.

14 p1714 A73-29754

Russian book on passenger aircraft high altitude equipment covering cabin pressurization, air condi-

tioning and temperature and pressure control, human tolerances, reliability factors, etc

14 p1712 A73-30355

High altitude aircraft cabin pressurization for crews and passengers, discussing altitude tolerance, reaction times, decompression and oxygen equipment

14 p1723 A73-30937

Effect of antiradiation drugs on the functional condition of the vestibular analyzer

15 p1838 A73-31509

Parachutist biomedical effects during 110-175 knot towing by aircraft, establishing maximum feasible airspeed

16 p1974 A73-32675

Impairment to hearing from exposure to noise.

16 p1973 A73-33676

Certain features of hemodynamics during orthostatic tests with persons of different vestibulo-vegetative tolerance levels

17 p2111 A73-34236

Heat acclimatization while wearing vapor-barrier clothing.

17 p2115 A73-34742

Tolerance to heat following cold stress.

18 p2283 A73-36784

Thermal comfort - New directions and standards.

18 p2283 A73-36785

Human statokinetic stability as component of non-specific resistance, discussing revolving, altitude, hypoxic and orthostatic stress dependence tests

18 p2279 A73-36904

Human physiological responses to high speed aerial tow.

18 p2286 A73-36939

Tolerance to immersion in cold water

18 p2280 A73-36943

Estimation of hypoxia tolerance in a decompression chamber

18 p2280 A73-36945

The capacity for muscular work in acute hypoxia

18 p2286 A73-36946

Aircraft noise disruption in public schools - A definition of an impasse.

19 p2505 A73-37282

Serial correlation of physiological time series and its significance for a stress analysis

19 p2401 A73-38159

Laser hazards and safety performance standards, discussing ocular and skin damage and exposure limits and operational regulation

20 p2517 A73-39205

Responses of men and women to two-hour walks in desert heat.

20 p2518 A73-39784

Heat conduction in blackened skin accompanying pulsatile heating with a xenon flash lamp.

20 p2519 A73-39791

Influence of small electromagnetic-field fluctuations on the bioelectric activity of the human brain

22 p2813 A73-41964

Work-heat tolerance derived from interval training.

22 p2806 A73-42416

Climbing and cycling with additional weights on the extremities.

22 p2806 A73-42418

Human reactions to whole-body transverse angular vibrations compared to linear vertical vibrations.

23 p2948 A73-43216

HUMAN WASTES

NT SWEAT

NT URINE

Radiation-induced oxidation of impurities in the water obtained from human moisture-containing bioactivity products

08 p0933 A73-20984

Study of intestinal Lactobacillus species composition during a long stay of humans in a closed space

17 p2112 A73-34239

Waste Management System overview for future spacecraft. [ASME PAPER 73-ENAS-18]

19 p2400 A73-37974

HUMIDITY

Utility of heat stress indices and effect of humidity and temperature on single physiologic strains.

[AD-751735]

01 p0007 A73-10163

Gas turbine engine exhaust emissions measurement data scatter, investigating temperature and humidity effects and emission variations in tailpipe plane

[AIAA PAPER 72-1199]

03 p0358 A73-13487

Human perception of humidity under four controlled conditions.

06 p0657 A73-17864

The relation between temperature and humidity in the free atmosphere under conditions of stable stratification and strong thermal intermittency - A case study.

07 p0847 A73-19041

Work-heat test comparisons of dry and wet heat and exercise programs for heat acclimatization

09 p1041 A73-22932

Temperature and humidity spectra in the atmospheric surface layer.

11 p1393 A73-25693

The effect of environmental relative humidity upon the ultrasonic fatigue endurance of an age hardening aluminum alloy. 11 p1382 A73-25825

Some specific features of the near-ground temperature field mesostructure and air humidity and their influence on convective processes 13 p1654 A73-28886

Simultaneous control of temperature and humidity in a confined space. III Feedback control synthesis via optimal control theory. 15 p1855 A73-32549

Simultaneous control of temperature and humidity in a confined space. I - Mathematical modeling of the dynamic behavior of temperature and humidity in a confined space. 15 p1959 A73-32597

Simultaneous control of temperature and humidity in a confined space. II - Feedback control synthesis via classical control theory. 15 p1855 A73-32598

Artificial inducement of drizzling rain in an uncloudy atmosphere at relatively high humidity 16 p2034 A73-33109

Heat acclimatization while wearing vapor-barrier clothing. 17 p2115 A73-34742

Hydrolytic stability of electrical insulation materials. 17 p2197 A73-35348

Hydrolytic degradation of polymer electrical insulating materials in warm humid environments, noting relation to ester and ether linkage presence 17 p2197 A73-35349

Thermal comfort - New directions and standards. 18 p2283 A73-36785

Some characteristics of the vertical structure of the humidity field over the North Atlantic. 18 p2334 A73-37076

Temperature-humidity acceleration of metal-electrolysis failure in semiconductor devices. 19 p2411 A73-38450

On the mechanism of adaptation of micro-organisms to conditions of extreme low humidity. 22 p2803 A73-42164

HUMIDITY MEASUREMENT

Tethered balloon measurements of turbulent wind, temperature and humidity fluctuations up to 200 meters over open sea, allowing for wave induced ship motion 01 p0072 A73-10142

Radar and Nimbus 4 infrared measurements of the Oklahoma City tornados, 30 April 1970. 03 p0338 A73-14512

Utilization of vacuum ultraviolet radiation for measurement of humidity pulsations 12 p1521 A73-26966

Use of cellulose crystallite structures with solid state strain gages for humidity and moisture measurement. 17 p2166 A73-34621

Low-inertia ultraviolet hygrometer 21 p2701 A73-40744

The Marsta micro-meteorological field project - Profile measurement system and some preliminary data. 21 p2732 A73-41567

Estimation of atmospheric moisture profiles from satellite measurements by a combination of linear and non-linear methods. 23 p3001 A73-43526

HURRICANES

An asymmetrically rotating fluid disc with applications. [AD-751727] 02 p0217 A73-12393

Use of airborne radar to evaluate hurricane modification experiments. 03 p0338 A73-14513

Radiosonde soundings for typhoons and hurricanes isobaric surface heights, temperatures and humidities, calculating correlation coefficients between sea level pressure and other parameters 10 p1245 A73-23985

A model of a Martian Great dust storm. 11 p1418 A73-25715

Hurricane prediction - Progress and problem areas. 21 p2731 A73-40641

Analysis of hurricane data using the variational optimization approach with a dynamic constraint. 23 p3004 A73-44258

Motion of a tropical hurricane in the field of the North Atlantic trade wind 24 p3107 A73-44428

HUSKIE HELICOPTER

U HH-43 HELICOPTER

HUYGENS PRINCIPLE

Huygens principle, power spectrum and photon and photographic noise intensities effects in holography, discussing optical information transmission by eigen-solutions 11 p1369 A73-26529

Book - Applications of the electromagnetic reciprocity principle. 15 p1915 A73-32577

Mutual coherence function of a finite optical beam and application to coherent detection. 21 p2710 A73-40147

HYBRID COMBUSTION

U HYBRID PROPELLANT ROCKET ENGINES

HYBRID COMPUTERS

Automation of solutions to mathematical physics problems described by partial differential equations 01 p0019 A73-10100

Solution of navigation problems with a hybrid analog computer 01 p0075 A73-11400

Analysis of noncircular cylindrical shells. 06 p0758 A73-17446

A hybrid analog computer for schooling in control technology 07 p0796 A73-20302

Systems analysis applied to a hybrid computer simulation of a missile reentering the atmosphere. 08 p0941 A73-20825

The evaluation of the domain of attraction of non-linear control systems with hybrid computing systems. 10 p1192 A73-24040

Hybrid computer systems of high speed and accuracy 10 p1192 A73-24674

Application of analog and digital computers to fatigue testing. 13 p1622 A73-29547

Construction principles of a controlled universal functional converter for a hybrid computer 15 p1848 A73-31805

The use of a hybrid computer in the optimization of gas turbine control parameters. [ASME PAPER 73-GT-13] 16 p2047 A73-33491

A serial CSDT predictor-corrector technique for the hybrid computer solution of partial differential equations. 18 p2291 A73-36425

Hybrid computer technique for desensitized optimal design of system with uncertain plant parameters, with application to Saturn 5 Apollo attitude control system design 18 p2291 A73-36426

Hidden-line removal at 20 pictures/second through hybrid techniques. 18 p2291 A73-36830

Real-time hybrid hardware-in-the-loop simulation of a terminal homing missile. 18 p2291 A73-36834

Computation of launch vehicle system requirements using hybrid computer. 18 p2360 A73-36838

Development of a program basis for statistical data processing on an analog-digital complex 20 p2532 A73-39392

Hybrid computer laboratory construction, organization and operation principles, including computer selection and personnel requirements 23 p2956 A73-43950

The 'multiplexing' CTDS method of solving certain second-order partial differential equations on a hybrid computer system 23 p2956 A73-43951

Design of a controlled general-purpose functional converter for a hybrid computer system. 24 p3071 A73-45349

HYBRID NAVIGATION SYSTEMS

Circular, hyperbolic, hybrid and angular measurement procedures of satellite navigation, describing Transit system 10 p1246 A73-23660

Hybrid-inertial navigation with range updates in a relative grid. [AIAA PAPER 73-873] 20 p2587 A73-38810

Digital computer simulation program for North Atlantic hybrid navigation systems configurations, using covariance matrix error analysis for planned increase of commercial air traffic capacity 21 p2733 A73-40028

HYBRID PROPELLANT ROCKET ENGINES

NT LITHERGOL ROCKET ENGINES

Investigations in connection with the preliminary development of a FLOX-polyethylene hybrid propulsion system [DGLR PAPER 72-086] 02 p0202 A73-11676

Combustion theory of hybrid rocket propellant-oxidizer combinations based on heat transfer limited model, discussing chemical kinetics and temperature effects on regression rate 03 p0397 A73-13449

[AIAA PAPER 72-1143] 03 p0397 A73-13449

Transport phenomena of reactive fluid flow in heterogeneous combustion processes. [ASME PAPER 72-WA/HT-30] 04 p0519 A73-15825

German book - Hybrid rocket propulsion systems: An introduction to theoretical and technical problems. 06 p0741 A73-17669

Development of special graphites for lithium hydride/fluorine rocket engines 09 p1110 A73-23019

Restart transients of hybrid rocket engines. 11 p1411 A73-26669

Temperature and velocity profiles measurement in hybrid rocket engine combustion, using optical method based on Na line reversal technique 15 p1957 A73-31636

Effect of secondary oxidizer supply through a porous solid fuel on the hybrid combustion process 23 p3019 A73-43783

HYDRATES

Reaction mechanisms and bonding energies for ion-hydrates /ion-water clusters/ of ionospheric interest. 01 p0014 A73-10899

Shock layer measurements of decomposition reactions of water cluster ions. 01 p0014 A73-10900

Recombination of electrons with positive ions of the H3O+ /H2O/n series. 01 p0014 A73-10901

D and E ionospheric regions behavior, emphasizing water cluster ions formation, minor neutral constituents measurement and daytime ionization sources 01 p0043 A73-10912

Titan atmosphere composition of methane hydrate with ammonia impurity, discussing hydrogen and hydrocarbon production, liquid water existence and greenhouse effects 04 p0497 A73-14973

HYDRATION

Cardiovascular and temperature regulatory changes during progressive dehydration and euhydration. 01 p0008 A73-10165

Rates of clustering of oxygen negative ions with water vapor. 01 p0014 A73-10902

Effects of rehydration on +Gz tolerance after 14-days' bed rest. 23 p2946 A73-43524

HYDRAULIC ACTUATORS

U ACTUATORS

U HYDRAULIC EQUIPMENT

HYDRAULIC ANALOGIES

Two-dimensional unsteady flow by hydraulic analogy. 03 p0295 A73-13769

Optimal stabilization conditions of turboreactor combustor initial recirculation zone determined by hydraulic analogy technique, describing vorticity generation and mass flow rates [ONERA, TP NO. 1105] 03 p0359 A73-14126

Mathematical analogy between the bending of a plate and the circulating motion of a liquid in a geometrically similar region 10 p1205 A73-23598

Liquid and gas flow visualization methods, discussing water tests and hydraulic analogies [ONERA, TP NO. 1222] 10 p1172 A73-23864

Base pressures in flow expansions by hydraulic analogy. 13 p1564 A73-28811

An analog investigation of the gas jet resonance tube. 23 p2967 A73-43401

HYDRAULIC CONTROL

A linear approach to the analysis of a force control system incorporating a hydraulic pressure-ratio valve. 02 p0132 A73-12002

Hydrostatic journal bearings design review covering pad coefficients, flow control, optimization, dynamic behavior, thermal effects, turbulence and tolerances 03 p0311 A73-13207

Model studies of an electrohydraulic amplifier 03 p0258 A73-14617

An analytical and empirical basis for the design of turbulence amplifiers. II - Empirical relationships and design procedure. [ASME PAPER 72-WA/FLCS-2] 04 p0408 A73-15860

Maximum safety hydraulic systems for A300B airbus powered flight controls for normal flying and auto land operations 04 p0409 A73-16031

Hydraulic and flight control system for Space Shuttle Orbiter. [SAE PAPER 720838] 05 p0537 A73-16630

Control of electro-hydraulic shaker by digital iteration techniques. [SAE PAPER 720823] 05 p0562 A73-16636

Some incompressible jet flow and reattachment effects in fluid control elements. 06 p0687 A73-18513

Hydraulic drive and control systems used for landing gear retraction and extension on Piper Cherokee Arrow and for main wheel braking on F-111 07 p0779 A73-19604

Fluidics terminology and vocabulary development and practical use, describing control functions and symbols 11 p1307 A73-25378

French book - Hydraulic and electrohydraulic automatic control. Volume 1 - Theory and technique. Volume 2 - Supplementary techniques and technologies 11 p1313 A73-26253

Book on fluid power control covering servovalve orifices discharge characteristics, flow forces, hydraulic

lic and pneumatic servomechanisms, fluid logic and sequential circuits

11 p1313 A73-26258

Hydraulic powered integrated actuator package /IAP/ for V/STOL aircraft flight control, noting advantages in system weight, mechanical complexity and power loss reduction

11 p1313 A73-26271

A servo-controlled axial fatigue machine with strain rate feedback for testing polymers and composites.

11 p1344 A73-26311

Problems in constructing aerodynamically active elements - Converters of input and output signals in automatic control systems

12 p1459 A73-26769

Hydrofluidic component and system reliability.

16 p1971 A73-33478

V/STOL hydraulic controls including internal and external blown jet flap and augmentor wing, describing integrated flight control actuator packages and aircraft configuration

17 p2108 A73-35851

Electro-mechano-hydraulic servovalve system, calculating dynamic frequency response in vibrating accelerated field under external disturbance

19 p2388 A73-37670

Integrated hydraulic flight control actuator packages replacing mechanical linkages for aerodynamic surface control during V/STOL operation

20 p2510 A73-39015

Synthesis of optimal control with allowance for the real characteristics of the executive mechanism

22 p2835 A73-42363

Use of fluidics in explosive component fabrication.

23 p2941 A73-43391

Pneumatic fluidic operational amplifier application to proportional position servocontrol with hydraulic actuator for high force output, considering working fluid and Reynolds number effects

23 p2941 A73-43397

Oil hydraulic button vortex valve optimization experiment for power consumption reduction, noting Reynolds number effects on turn down and pressure ratios

23 p2942 A73-43404

Periodic oscillations of a closed hydraulic throttle servomechanism with inertial and positional loads

23 p2945 A73-43739

Ram air turbine with hydraulic pitch change servo regulated speed as emergency power source for aircraft control in event of main engine failure

24 p3058 A73-45475

HYDRAULIC EQUIPMENT

NT AIRCRAFT HYDRAULIC SYSTEMS

A standard format for mathematical models of fluid power systems.

02 p0132 A73-12001

A linear approach to the analysis of a force control system incorporating a hydraulic pressure-ratio valve.

02 p0132 A73-12002

Design of digital force function generator for aircraft tire load testing.

04 p0424 A73-15064

Thermodynamic determination of power loss in hydraulic components.

[ASME PAPER 72-WA/FE-22] 04 p0435 A73-15848

The effects of compressibility in multi-element hydraulic lines.

[ASME PAPER 72-WA/FE-43] 04 p0435 A73-15857

Prevention of pollution in hydraulic circuits.

06 p0649 A73-17845

A modified sensor of linear accelerations, velocities, and displacements over a path of 0 to 1500 mm

07 p0826 A73-20527

Packaged servosystem drives mobile missile launcher.

08 p0929 A73-21844

Electric resistance of hydraulically extruded and annealed beryllium

09 p1098 A73-21847

State of art of water flow measurement by weirs and flumes in artificial channels

10 p1221 A73-24854

State of art of flowmetering, discussing acceptability factors, weirs, laser Doppler velocity method, ultrasonic time, pressure difference technique and turbine and electromagnetic devices

10 p1221 A73-24862

Stress corrosion cracking and corrosion fatigue for hydraulic aluminum pressure cylinders used for landing gear, stabilizers and aircraft systems

11 p1383 A73-25827

Testing machine for thermal fatigue with variable constraint ratio.

13 p1611 A73-28195

The tolerance of fluid machinery to contaminant wear.

13 p1571 A73-29031

Automatic machine test equipment and procedures for hydraulic systems, tractor shafts and automobile wheels

13 p1625 A73-29135

Standard Hydraulic Impulse Machine design for testing hose assemblies, tubing, coils and fittings, including circuit diagrams and component identifications

[SAE AIR 1228] 16 p1970 A73-33018

Hydraulic system noise measurements and control, discussing source, vibrating parts isolation, transmission path and acoustic barriers and enclosures

16 p1971 A73-33993

Analysis of some functional parameters of rotary hydrostatic engines under dynamic conditions by modeling on a computer

19 p2388 A73-37557

Quality requirements for Ti-3Al-2.5V annealed and cold worked hydraulic tubing.

[SAE SP-378] 19 p2434 A73-37868

Production of extruded tube hollows for titanium 3Al-2.5V hydraulic tubing.

[SAE SP-378] 19 p2434 A73-37869

The development and control of crystallographic texture in 3Al-2.5V titanium alloy tubing.

[SAE SP-378] 19 p2434 A73-37870

The effects of crystallographic texture on the mechanical and fracture properties of Ti-3Al-2.5V hydraulic tubing.

[SAE SP-378] 19 p2434 A73-37871

Surface conditioning of titanium alloy tubing.

[SAE SP-378] 19 p2434 A73-37872

Application of the hydrostatic extrusion process toward production of 3Al-2.5V titanium alloy hydraulic tubing.

[SAE SP-378] 19 p2434 A73-37873

Book - Hydraulic systems and maintenance.

20 p2510 A73-39142

The characteristics of hydraulic tensile-test machines of the pendulum type and their effect on the tensile test

20 p2545 A73-39629

The effect of valve area gain on the performance of the hydraulic servomechanism.

20 p2511 A73-39755

German monograph - Theoretical and experimental investigation of digital hydraulic positioning devices.

22 p2801 A73-42848

Fuel tank wall response to hydraulic ram during the shock phase.

22 p2843 A73-43114

Oil hydraulic fluidic amplifier mathematical model and computerized design for power consumption optimization at high pressures, testing performance dependence on viscosity

23 p2942 A73-43405

HYDRAULIC FLUIDS

The analysis of particulate contaminants in hydraulic fluids.

02 p0132 A73-12004

Hydrolysis of a disiloxane/ester fluid in a simulated hydraulic system at 275 F.

[ASLE PREPRINT 72LC-6C-1] 03 p0335 A73-14365

A comparison of hydraulic fluid characterizations in two evaluation systems.

[ASLE PREPRINT 73AM-9A-2] 17 p2196 A73-34997

Book - Hydraulic systems and maintenance.

20 p2510 A73-39142

Gas solubility in hydraulic liquids from measurements of air in mineral oils, noting oil molecular weight effect

21 p2724 A73-41579

Damping of mechanical systems with the aid of viscoelastic liquids

24 p3109 A73-44915

HYDRAULIC HEATING SOURCES

U HEAT SOURCES

U HYDRAULIC EQUIPMENT

HYDRAULIC JETS

Earliest classic result for the turbulent hydraulic wake behind body of revolution.

11 p1348 A73-25781

A feed nozzle for hydraulic amplifiers

16 p1971 A73-33671

Hydraulic jet amplifier design, considering selector static and dynamic characteristics, membrane attached plate, piston with feedback control and self oscillation elimination

16 p1971 A73-33672

Some results in the erosion of prestressed materials due to water-jet impact.

19 p2443 A73-38299

Transient stress distribution caused by water-jet impact.

19 p2435 A73-38300

Experimental investigation of a gas-augmented water-jet engine model

22 p2841 A73-42126

HYDRAULIC PUMPS

U HYDRAULIC EQUIPMENT

U PUMPS

HYDRAULIC SHOCK

Hydraulic impact in coaxial cylindrical tubes

15 p1860 A73-31046

Hydraulic impact in a circular cylindrical shell

15 p1860 A73-31047

HYDRAULIC SYSTEMS

U HYDRAULIC EQUIPMENT

HYDRAULIC TEST TUNNELS

Perforated water tunnel to decrease wall effect on deflected cavitation flow, studying suction coefficient, pressure losses and blowing parameters

13 p1597 A73-28450

Water towing tank facility for studies of boundary layers, aircraft ground effects, wakes and unsteady and stratified fluid flows

15 p1858 A73-32041

HYDRAULIC VALVES

U HYDRAULIC EQUIPMENT

U VALVES

HYDRAULICS

Studies on the hydraulic loss in pipe bends - Results for 90-deg screw type elbows.

19 p2420 A73-37672

Relationship between the hydraulic losses of a centrifugal wheel and the energy imparted by the wheel to the fluid by circulation in the relative motion

21 p2676 A73-40407

HYDRAZINE BORANE

Spectroscopic study and molecular structure of 1,1-dimethylhydrazine-monomorane.

02 p0139 A73-12628

HYDRAZINE ENGINES

Development and qualification results of the monergolic propulsion system for the aeronomy satellite Aeros

[DGLR PAPER 72-079] 02 p0228 A73-11696

Propulsion system performance for satellite attitude and orbit correction, discussing hydrogen, ammonia and hydrazine resistojets

[DGLR PAPER 72-078] 02 p0203 A73-11697

Experimental evolution of an earth-storable bimodal rocket engine.

[AIAA PAPER 72-1128] 04 p0486 A73-14913

Experimental evaluation of a 600 lbf spacecraft rocket engine.

[AIAA PAPER 72-1129] 04 p0486 A73-14914

An operational satellite propulsion system providing for vernier velocity, high and low level attitude control and spin trim.

[AIAA PAPER 72-1130] 04 p0486 A73-14916

Electrothermal hydrazine thruster analyses and performance evaluation.

[AIAA PAPER 72-1152] 04 p0486 A73-14917

Storable fueled power system for Space Shuttle.

[SAE PAPER 720836] 05 p0537 A73-16632

Design and analysis of an APU monopropellant gas generator.

[SAE PAPER 720834] 05 p0537 A73-16635

Propulsion system for space applications, based on the catalytic decomposition of hydrazine

07 p0866 A73-18929

Performance of an auxiliary power unit on anhydrous hydrazine.

11 p1308 A73-25980

HYDRAZINES

NT DIMETHYLHYDRAZINES

NT HYDRAZINE BORANE

NT TETRAFLUOROHYDRAZINE

Long-life firings of a catalytic reactor for monopropellant hydrazine.

[AIAA PAPER 72-1045] 03 p0350 A73-13378

The removal of impurities from hydrazine for control of contamination caused by rocket engine exhaust.

[AIAA PAPER 72-1046] 03 p0351 A73-13379

Decomposition and hybrid combustion of hydrazine, MMH and UDMH as droplets in a combustion gas environment.

03 p0352 A73-14392

Studies of the anodic oxidation of hydrazine in an alkali electrolyte and of the side reaction of ammonia formation during the decomposition of hydrazine

04 p0407 A73-15103

Vibrational spectra and structure of tetrakis(trifluoromethyl)hydrazine in the crystalline and fluid states.

04 p0414 A73-16036

The emission spectrum of the silent electric discharge in ammonia and hydrazine vapor

06 p0723 A73-17916

Ir catalysts for high performance hydrazine decomposition, discussing preparation by coprecipitation of active metallic element with support in chloroiridic acid solution

07 p0865 A73-18928

Energetically and financially economical hydrazine synthesis method based on ammonia oxidation by water solution of hydrogen peroxide

07 p0787 A73-19325

Organic and species-related differences in the action of certain hydrazine derivatives and of aminopropylhydroacridine on the oxidative deamination of serotonin

10 p1183 A73-23679

Hydrazine derivative poisoning in industry and clinical medicine treatments, noting causes of vitamin B6 deficiency

10 p1183 A73-23819

Development of propellant loading systems and checkout systems for the TD-1A and AEROS satellite projects 11 p1430 A73-25354

Measurement of hydrazine gas generator performance by gas chromatography. 11 p1326 A73-26398

Monopropellant hydrazine system for satellite attitude control, reporting catalysts properties, decomposition mechanisms and activities 12 p1532 A73-27064

Optimizing power efficiency of hydrazine-oxygen fuel cells. 13 p1574 A73-29598

Decomposition of hydrazine on Shell 405 catalyst at high pressure. 15 p1841 A73-32174

Vibrational spectra of substituted hydrazines. IV - Raman and far-infrared spectra and structure of tetramethylhydrazine. 15 p1841 A73-32220

Study of the dependence of the properties of radicals on the characteristics of the initial hydrazine structure 17 p2220 A73-34638

High power density hydrazine-oxygen fuel cell, discussing cell polarization, critical resistance losses and efficiency 19 p2390 A73-38398

HYDRIDES

NT BERYLLIUM BOROHYDRIDES

NT HYDRAZINE BORANE

NT LITHIUM ALUMINUM HYDRIDES

NT LITHIUM HYDRIDES

NT METAL HYDRIDES

NT NITROGEN HYDRIDES

NT PHOSPHINES

NT SILANES

NT ZIRCONIUM HYDRIDES

Gas-phase acidities of binary hydrides. 02 p0139 A73-12632

The spectrum of FeH - Laboratory and solar identification. 03 p0374 A73-13718

Nondestructive detection of hydrides and alpha-case in titanium alloys. 04 p0461 A73-15217

Effect of high pressure on the superconducting transition temperature of Pd-H. 21 p2753 A73-41126

HYDROACOUSTICS

U UNDERWATER ACOUSTICS

HYDROAEROMECHANICS

U AERODYNAMICS

HYDROCARBON COMBUSTION

Hydrocarbon fuels diffusion flame ignition characteristics in hypersonic ramjet engines, testing additives effect for thermal self-ignition improvement 03 p0398 A73-14132

Electron temperature elevation compared to gas temperature in hydrocarbon flames, discussing energy exchange mechanism 03 p0352 A73-14394

Soot particles oxidation by oxygen diffusion in laminar hydrocarbon flames, deriving kinetic expression from observed time dependent particle concentration variations 03 p0399 A73-14395

Methane-air mixtures burning velocity as function of equivalence ratio at atmospheric pressure, using bomb/hot-wire and corrected density ratio techniques 03 p0399 A73-14398

Multistage ignition behind second and third cool flames of hydrocarbon combustion, presenting graphs of propane mixtures ignition limits 03 p0400 A73-14401

Cool flame oxidation studies of acyclic and cyclic hydrocarbons. 05 p0606 A73-16691

Current kinetic modeling techniques for continuous flow combustors. 06 p0767 A73-17728

Investigation of NO formation kinetics in combustion processes - The methane-oxygen-nitrogen reaction. 06 p0767 A73-17731

Measurement of nitric oxide formation within a multi-fueled turbine combustor. 06 p0740 A73-17734

Effects of fuel injection method on gas turbine combustor emissions. 06 p0768 A73-17735

Temperature dependence of the ion recombination coefficient in a hydrocarbon flame plasma 06 p0731 A73-18553

The effect of higher alkanes on the ignition of methane-oxygen-argon mixtures in shock waves. [AD-756982] 07 p0918 A73-19389

Kinetics and convection in the combustion of alkane droplets. 07 p0919 A73-19391

The role of mixing in burner-generated carbon monoxide and nitric oxide. 07 p0919 A73-19392

Slow combustion of n-pentane in single pulse chemical shock tube, discussing yields of oxygenated products 07 p0788 A73-20356

Quasi-stationary theory of hydrocarbon droplet ignition. I - Moment and limit of ignition 07 p0923 A73-20422

Experimental study of influence of an electric field on a laminar flame. 08 p1021 A73-20864

The transfer of radiation from a flame to its fuel. 08 p1025 A73-21822

Mechanism and kinetics of the formation of intermediate products in an auxiliary mixture and the effect of such products on the combustion of the working mixture 13 p1704 A73-28293

German monograph - Determination of the OH-concentration distribution in a axisymmetric methane/oxygen flame. 13 p1708 A73-29279

Homogeneous turbulent forward and inverted flame front structure during hydrocarbon combustion, investigating gas flow velocity distribution, activation energy levels and burning zone boundaries 14 p1818 A73-30871

Flame propagation in a transverse electric field 15 p1957 A73-31869

Experimental study of heat exchange in a chemically reacting laminar boundary layer 15 p1958 A73-31874

The combustion of the n-pentenes in the cool flame region. 16 p2085 A73-33341

Combustion of fuel vapor-drop-air systems. I - Open burner flames. II - Spherical flames in a vessel. 16 p2085 A73-33343

Shock-tube measurements of soot oxidation rates. 16 p2085 A73-33344

Temperature dependence of the ion recombination coefficient for a hydrocarbon flame. 16 p2042 A73-33578

Quasi-stationary theory of hydrocarbon droplet ignition. II - Ignition limits of cold and hot droplets 18 p2372 A73-37117

Experimental study of heat and mass transfer in chemically reacting laminar boundary layers. 21 p2791 A73-41058

Elementary reactions in the combustion of small inorganic molecules. 22 p2818 A73-42752

Organic compounds oxidation and combustion reactions, discussing hydrogen dioxide radical role and reaction rate 22 p2933 A73-42753

Reaction rate constants for carbon monoxide-hydrogen-oxygen and hydrogen-nitrogen-oxygen systems at high temperatures, modeling hydrocarbon combustion for product distribution 22 p2933 A73-42758

High temperature ionic and charged species reactions in hydrocarbon and cyanogen flames and additive combustion systems 22 p2819 A73-42770

Relation between ion creation and C₂, CH, and OH formation in the combustion of hydrocarbons. 22 p2819 A73-42771

Ambipolar diffusion generator based on self generated electric fields in premixed ionized methane-air flame, comparing with opposite caloelectric effects 22 p2895 A73-42773

Centrifugal force effects on flame spread and extinction limits of fuel-air mixture combustion with laminar, turbulent and buoyant bubble transport 22 p2933 A73-42776

Reaction of H atoms with CH₂C₂ - Application to the inhibition of flames. 22 p2819 A73-42779

Influence of aerodynamic field on shock-induced combustion of hydrogen and ethylene in supersonic flow. 22 p2934 A73-42786

Kinetics of nitric oxide formation in premixed laminar flames. 22 p2820 A73-42792

Formation of nitric oxide in fuel-lean and fuel-rich flames. 22 p2820 A73-42794

Carbon particles size distribution and charged fraction in acetylene-oxygen flame using molecular beam system and electron microscopy, noting particle interaction formation mechanism 22 p2936 A73-42801

Pressure waves generated by constant velocity deflagration flame in explosive hydrocarbon-air mixture for self-similar flow field 22 p2936 A73-42808

Experimental studies on the flame structure in the wake of a burning droplet. 22 p2937 A73-42816

Study of light amplification in a pulsed gas-dynamic laser with burning acetylene-air mixtures 23 p2988 A73-44011

Deviations from the Le Chatelier principle for flame propagation limits 24 p3155 A73-44716

Combustion noise radiation by open turbulent flames. 24 p3156 A73-44856

[AIAA PAPER 73-1025]

Propane-air flame stabilization via combustion product recirculation due to transverse gas jet injection, increasing fuel-air ratio 24 p3123 A73-45379

Preparation of liquid fuels by evaporation from a hot wall 24 p3158 A73-45389

HYDROCARBON FUELS

NT JET ENGINE FUELS

NT JP-5 JET FUEL

Hydrocarbon fuels diffusion flame ignition characteristics in hypersonic ramjet engines, testing additives effect for thermal self-ignition improvement 03 p0398 A73-14132

High temperature zirconium dioxide electrolyte fuel cell systems design and operation with methane or gasoline as fuel, evaluating performance characteristics 04 p0408 A73-15118

Pyrolysis of kerosene and mechanism of formation of carbon deposits [ONERA, TP NO. 1157] 04 p0485 A73-15989

Physicochemical parameters associated with surfactants, investigating effects on hydrocarbon fuels coalescence [SAE PAPER 720863] 05 p0582 A73-16674

Stabilization of flames formed behind cylinders wetted by liquid fuels in high velocity gas streams [WSCI PAPER 72-38] 05 p0639 A73-16679

A shocktube study of the combustion of Sheldlyne-H with additives. [WSCI PAPER 72-29] 05 p0639 A73-16686

Suppression of evaporation of hydrocarbon liquids and fuels by aqueous films. [WSCI PAPER 72-27] 05 p0639 A73-16687

Effect of fuel composition on particulate emissions from gas turbine engines. 06 p0740 A73-17733

Hydroxyl radical mechanism for autoignition inhibition of alkane fuels for antiknock additives at various concentrations 13 p1707 A73-29000

Supersonic combustion aid for liquid and gaseous fuels. 17 p2253 A73-34191

The role of physicochemical processes in surface wear under rolling friction in low-molecular hydrocarbon media 18 p2343 A73-36821

The ignition of hydrocarbon-air mixtures with laser radiation 22 p2938 A73-43190

HYDROCARBONS

NT ACETYLENE

NT ALKANES

NT ALKENES

NT ANTHRACENE

NT BUTANES

NT CYCLIC HYDROCARBONS

NT ETHANE

NT ETHYLENE

NT HEPTANES

NT METHANE

NT NAPHTHALENE

NT NATURAL GAS

NT OXYACETYLENE

NT PENTANES

NT PROPANE

NT PROPYLENE

NT TRIPHENYLS

Gas turbine engine swirl-can combustor pollution tests of nitrogen oxides, unburned hydrocarbons and carbon monoxide levels for elevated temperature performance [AIAA PAPER 72-1201] 04 p0485 A73-14921

Life origin on earth, considering hydrocarbon molecules and macromolecular synthesis under earth atmospheric evolutionary conditions 06 p0651 A73-17928

Pyrolysis system with high sensitivity medium-resolution mass spectroscopy to quantify ions pyrolyzed in lunar fines, confirming presence of indigenous lower hydrocarbons 06 p0662 A73-18431

Synthetic hydrocarbon lubricants performance characteristics under extreme temperature service conditions, considering viscosity, antiwear, oxidation stability, demulsibility and corrosion protection properties 07 p0843 A73-19562

Removal of hydrocarbon contaminant film from spacecraft optical surfaces using a radiofrequency-excited oxygen plasma. [AIAA PAPER 72-263] 08 p0989 A73-21835

Usage of the VNII NP-300A lubricant in gas-liquid chromatography and high-vacuum technology 10 p1239 A73-24250

The origin and incorporation of organic molecules in sediments as elucidated by studies of the sedimentary sequence from a residual Pleistocene lake.

11 p1326 A73-25468

Carbon compounds in pyrolysates and amino acids in extracts of Apollo 14 lunar samples.

11 p1426 A73-26471

Photo-decarbonylation of beta-styryl isocyanates.

12 p1466 A73-27225

17 α /H/ hopane identified in oil shale of the Green River formation/Eocene/ by carbon-13 NMR.

14 p1746 A73-29734

The photochemistry of hydrocarbons in the Jovian atmosphere.

14 p1802 A73-30766

Friction induced surface activity of some simple organic chlorides and hydrocarbons with iron. [ASLE PREPRINT 73AM-8A-1]

17 p2179 A73-34991

Mechanism of hydrocarbon formation in combustion processes.

19 p2402 A73-38322

Instrumentation and techniques for measuring emissions.

19 p2432 A73-38324

Nonurban nonmethane low molecular weight hydrocarbon concentrations related to air mass identification.

21 p2680 A73-40084

Photochemical model with vertical transport for CO and hydrocarbons profiles in stratosphere and mesosphere, discussing boundary conditions and water vapor

21 p2681 A73-40086

Protection of mineral oils from microbiological damage by compounds of the quinone group

21 p2723 A73-41069

Change in the hyperfine state of the hydrogen atom during its collisions with unsaturated hydrocarbon molecules in the gaseous state.

22 p2889 A73-41719

The absorption cross sections of N₂, O₂, CO, NO, CO₂, N₂O, CH₄, C₂H₄, C₂H₆, and C₄H₁₀ from 180 to 700 Å.

22 p2890 A73-42992

HYDROCHLORIC ACID

Effect of reagent vibrational excitation on reaction rate and product energy distribution in F + HCl yields HF + Cl.

03 p0273 A73-13290

An anomalous reaction of aceto-4-/or 6-/ nitro-2,5-xylidines with hydrochloric acid.

03 p0273 A73-13900

Electrical properties of MOS capacitors with oxide grown in the presence of HCl.

09 p1062 A73-22308

Investigation of the structure and corrosion behavior of alloys of the Ti-Ta-Cr system

15 p1895 A73-32542

Studies of a homogeneous copper catalyst for fuel cell air cathodes in acid media.

19 p2390 A73-38400

HYDROCYANIC ACID

Accurate relative acidities in the gas phase - Hydrogen sulfide and hydrogen cyanide.

02 p0139 A73-12634

Origin of terrestrial polypeptides - A theory based on data from discharge-tube experiments.

20 p2513 A73-39484

HYDRODYNAMIC EQUATIONS

HELMHOLTZ VORTICITY EQUATION

Application of the averaging method to the problem of plane wave propagation in a dissipative heat conducting medium

01 p0075 A73-10086

Hydrodynamic motions and the vacuum stage in an anisotropic cosmological model

01 p0108 A73-11432

Model development of supersonic trough wind with shocks.

03 p0298 A73-12887

Hydrodynamics in weak gravitational fields - Plane oscillations of an ideal fluid in a rectangular channel

03 p0294 A73-13606

'Barycentric' averaging of the hydro-dynamical equations with respect to coordinate systems with arbitrary vertical coordinate

04 p0473 A73-15697

Peak pool boiling heat flux from finite heater configurations, improving Zuber hydrodynamic theory by combining vapor escape path thickness empirical values with velocity matching hypothesis [ASME PAPER 72-WA/HT-10]

04 p0519 A73-15835

Hydrodynamic phenomena during high-speed collision between liquid droplet and rigid plane.

04 p0435 A73-15850

Investigation of the characteristics of atmospheric motion at low latitudes

05 p0592 A73-16227

Numerical analysis of far turbulent wakes in ideal gas, determining hydrodynamic field moments, turbulence levels and mean square enthalpy fluctuations

06 p0643 A73-17454

Hydrodynamics equations for multicomponent mixtures with higher-order approximations of transport coefficients

06 p0684 A73-17467

Quasi-hydrodynamic equations for transverse quanta in inhomogeneous plasma, using geometric optics approximation

06 p0728 A73-17969

Approximate calculations of the hydrodynamic characteristics of a turbulent flow of liquid in annular channels

06 p0688 A73-18562

Present state and further developments in short-range hydrodynamic weather forecasting

07 p0848 A73-20624

Description of hydrodynamics in the theory of gravitation on the basis of covariant statistical equations

08 p0989 A73-21522

Kochin hydrodynamic equation solutions for gas injection through plate for intense blowing at constant and changing rates

08 p0927 A73-21772

Small perturbations analysis of hydrodynamic relations of shock front propagation in inhomogeneous medium

09 p1070 A73-21888

Calculation of one-dimensional hydrodynamic in Eulerian coordinates

09 p1070 A73-21922

Explicit and implicit weather forecast expressions based on differential hydrodynamics equation relating horizontal and vertical wind velocity, geopotential and temperature gradients

10 p1244 A73-23813

Fluid turbulence equations for large molecular drift velocity gradients in rarefied gas, near surface and stellar system motions, using Predvoditelev hydrodynamic equations

11 p1347 A73-25733

Hydrodynamic motions and the vacuum stage in an anisotropic cosmological model.

11 p1423 A73-26052

Group classification of the hydrodynamics equations of an ideal fluid

12 p1487 A73-27409

Stellar evolution as succession of quasi-equilibrium states, investigating dynamic stability via hydrodynamic and state equations

13 p1682 A73-28980

A discretization method for atmospheric dynamics equations and for the construction of numerical weather forecast schemes

13 p1654 A73-29151

A basis for four-dimensional /continuous/ processing of meteorological observation data, using a dynamic statistical approach

15 p1904 A73-31608

Determination of the thickness of a wall layer by an approximate method in the presence of intense injection

15 p1876 A73-31861

Approximate calculations of the hydrodynamic characteristics of turbulent fluid flow in annular ducts.

16 p2000 A73-33587

Hydrodynamic equilibrium structure of plane shock waves in arbitrary liquid or gas at large distance behind shock front

16 p2001 A73-34059

Small perturbations analysis of hydrodynamic relations of shock front propagation in inhomogeneous medium

17 p2150 A73-34311

Plasma hydrodynamics in high frequency electromagnetic field, discussing hydrodynamic equations, small perturbations, plasma equilibrium and movement in field

17 p2216 A73-34341

Flux-corrected transport - A minimum-error finite-difference technique designed for vector solution of fluid equations.

17 p2202 A73-35145

Numerical techniques in two- and three-dimensional radiation hydrodynamics.

17 p2255 A73-35596

Numerical weather prediction models based on hydrothermodynamic equations and nonadiabatic factors for short term regional, hemispheric and global forecasting

18 p2331 A73-35909

Three to five day numerical forecasting making use of the complete hydrodynamics equations, and problems of correlating the original fields of meteorological elements

18 p2331 A73-35911

Ellipsoidal coordinates - A natural coordinate system for calculations of laser irradiations of slabs.

20 p2572 A73-38972

Numerical solution of hydrothermodynamics equations for atmospheric processes on a flat earth

20 p2584 A73-39471

The equations of fast-process hydrodynamics

21 p2676 A73-40205

Bilinear hydrodynamics and the Stokes-Einstein law.

21 p2676 A73-40218

A scheme for synoptic-hydrodynamic-statistical weather forecasting for 3 to 10 days

21 p2730 A73-40491

Permissible hydrodynamic and hydrostatic stellar atmosphere models described by system of equations dependent on initial level conditions

21 p2767 A73-40532

Dynamics of quasigeostrophic flows and instability theory.

22 p2842 A73-42450

Hydrodynamic equations for nonlinear propagation of plasma ionization wave interactions in absence of magnetic field

23 p3012 A73-44040

HYDRODYNAMIC STABILITY

U FLOW STABILITY

HYDRODYNAMIC TUNNELS

U PLASMA JET WIND TUNNELS

HYDRODYNAMICS

NT ELASTOHYDRODYNAMICS

NT ELECTROHYDRODYNAMICS

NT MAGNETOHYDRODYNAMICS

Multiple production processes hydrodynamic-type models validated by high energy particle collision collective interactions

02 p0208 A73-12659

Theorems on general fluid particle vorticity acquisition by nonanalytic process

03 p0292 A73-13309

Hydrodynamics of the convective zone of the sun

03 p0373 A73-13608

Hydrodynamics and heat transfer in a fluid with an asymmetrical stress tensor

03 p0398 A73-13722

Monograph on hydrodynamics of nonisothermal laminar duct flows of real fluids with temperature dependent properties

03 p0295 A73-13998

Reversible instantaneous deformations and internal energy in viscoelastic incompressible fluids, using Oldroyd and De Witt hydrodynamic models

03 p0296 A73-14053

On the influence of the contact pattern on the sealing capacity and the power loss of hydrodynamic lip seals.

[ASLE PREPRINT 72LC-7A-1]

03 p0316 A73-14367

Time dependent hydrodynamic models of solar wind, considering coronal electron density and temperature distribution and magnetic field

04 p0491 A73-14835

Russian book on hydrodynamic gyroscope theory and design covering casing angular velocity, cavity fluid motion, induction removal, noise levels and threshold sensitivity

04 p0450 A73-15705

On generalized hydrodynamic equations used in heat transfer theory.

06 p0688 A73-18834

Turbulent hydrodynamics and heat transfer in rotating flows of incompressible fluid

08 p0954 A73-21184

Boundary layer theory approximation for hydrodynamic parameters of unsteady laminar boundary layer on body moving in incompressible fluid

08 p0956 A73-21546

Hydrodynamics, hydroelasticity, technology and automatic control of H 890 hydrofoil craft

09 p0131 A73-22209

A hydrodynamic theory of radial-face mechanical seals.

10 p1223 A73-23698

Approximate determination of the hydrodynamic coefficients for the sloshing of a liquid in moving cylindrical cavities

10 p1206 A73-24309

Hydrodynamic theory of heat transfer between a stabilized gas suspension flow and channel walls.

10 p1297 A73-24968

Frequencies and virtual masses of a liquid in a cavity formed by eccentric cylinders

11 p1347 A73-25391

Rectangular channel mixed boundary layer flow patterns dependence on inlet edge configurations, channel geometry and hydrodynamic flow core parameters

13 p1601 A73-28737

Hydrodynamic tilting pad thrust bearings performance estimation in turbulent region based on laminar flow operation data

14 p1755 A73-30062

Calculation of the resultant moment of the hydrodynamic forces on jet profiles

15 p1824 A73-32000

Magnetohydrodynamics, hydrodynamics and dynamics of solar system model as contracting rotating cloud, discussing effects of turbulence

17 p2226 A73-34403

Book - Foundations of fluid flow theory.

17 p2151 A73-34466

Approximate method based on the application of hydrodynamic analogy

17 p2244 A73-34794

An economical method of analyzing transient motion of gas-lubricated rotor-bearing systems. [ASLE PREPRINT 73AM-2B-2] 17 p2178 A73-34982

Influence of hydrodynamics on the performance of radial lip seals. [ASLE PREPRINT 73AM-9B-2] 17 p2179 A73-34999

Self-acting and hydrodynamic shaft seals. 17 p2179 A73-34999

Current status and immediate problems of hydrodynamic short-term weather forecasting. 18 p2331 A73-35908

Contribution to the hydrodynamic lubrication theory of the bearing with a floating bushing. 18 p2319 A73-36411

Hydrodynamics of stratified fluids - The applicability of linear theory. 19 p2422 A73-38243

Hydrodynamic bearing damping in infinitely broad gap between oppositely oscillating parallel boundary surfaces, discussing inertia, Reynolds number and coefficient of friction. 20 p2547 A73-39409

Experimental investigation of hydrodynamic stability for flows past simple membrane surfaces. 22 p2840 A73-42117

The hydrodynamic analogy and its application to a two-dimensional problem in elasticity theory. 22 p2921 A73-42282

Multiperipherism and Landau hydrodynamic models of multiple particle collision processes with inhomogeneous and homogeneous energy liberation spaces. 23 p3008 A73-43543

Free point method finite difference solution for two dimensional nonstationary hydrodynamic problem of continuous media, demonstrating feasibility by plasma pinch effect calculation. 23 p2968 A73-43799

Hydrodynamics in weak gravitational fields - Plane oscillation problems of an ideal liquid in a vessel. 24 p3076 A73-44653

HYDROELASTICITY

Axisymmetric hydroelastic sloshing in a circular cylindrical container. 08 p0956 A73-21690

Hydrodynamics, hydroelasticity, technology and automatic control of H 890 hydrofoil craft. 09 p1031 A73-22209

The task of constructing transition functions in problems involving interaction of weak shock waves with cylindrical and spherical surfaces. 12 p1486 A73-27241

Hydroelastic oscillations in a rigid circular cylinder in the presence of an elastic fluid surface covering. 18 p2297 A73-36065

Exact hydroelastic solution for an ideal fluid in a hemispherical container. 22 p2843 A73-42631

HYDROFLUORIC ACID

Flame-sheet analysis of C.W. diffusion-type chemical lasers. II - Coupled radiation. 01 p0059 A73-10727

Laser oscillation and anisotropic gain in the 1 to 0 vibrational band of optically pumped HF gas. 02 p0177 A73-12747

Monte Carlo classical trajectory calculation of the rates of F-atom vibrational relaxation of HF and DF. 03 p0318 A73-13279

Monte Carlo classical trajectory calculation of the rates of Hand D-atom vibrational relaxation of HF and DF. 03 p0318 A73-13280

Atmospheric windows for HF laser radiation between 2.7 and 3.2 microns. 03 p0319 A73-14431

Direct overtone excitation of hydrogen fluoride second vibrational level, measuring global deactivation rate by temperature tuned Nd-YAG laser excited fluorescence technique. 06 p0703 A73-18750

Laser-excited vibrational energy transfer studies of HF, CO, and NO. 07 p0834 A73-19627

Measurement of the temperature dependence of the vibrational relaxation rate of HF and the effect of SF₆, N₂, and F₂ as diluents. 07 p0853 A73-19628

Parametric studies of pulsed HF lasers using transverse excitation. 07 p0835 A73-19641

Chemical laser device bibliography. 07 p0836 A73-19642

Numerical study of a diffusion-type chemical laser. 07 p0836 A73-19959

Energy and threshold characteristics of chemical lasers. 08 p0975 A73-21213

HF chemical lasers kinetics, radiative interactions and gas dynamics, deriving closed form solutions for excited states populations. 08 p0976 A73-21671

Hydrogen fluoride chemical laser with high voltage pulse initiation in simple transverse discharge

geometry, measuring maximum energy output and corresponding efficiency. 11 p1378 A73-26323

Design and performance characteristics of a small subsonic flow HF chemical laser. 15 p1885 A73-31978

Vibrational relaxation in the HF-HCl, HF-HBr, HF-HI, and HF-DF systems. 17 p2119 A73-35176

Pressure dependency of the NF₃-H₂ transverse-discharge pulse-initiated HF chemical laser. 17 p2186 A73-35790

Monte Carlo calculations of reaction rates and energy distributions among reaction products. IV - F + HF/nu/ yields HF/nu-prime/ + F and F + DF/nu/ yields DF/nu-prime/ + F. 19 p2463 A73-37898

HF and DF molecules vibrational relaxation investigation by recording IR radiation behind incident shock wave at 1500-5000 K. 21 p2743 A73-40360

Relative performance of a variety of NF₃+/- hydrogen-donor transverse-discharge HF chemical-laser systems. 21 p2714 A73-40757

Catalytic efficiencies of atoms in the vibrational relaxation of HF and DF. 22 p2818 A73-42763

HF and molecular fluorine refractive indices in visible spectral region computed from interferometer fringe shift vs pressure measurements. 24 p3113 A73-44983

HYDROFOIL BOATS

U HYDROFOIL CRAFT

HYDROFOIL CRAFT

French project for high speed hydrofoil marine vehicle with hydrodynamic lifting surfaces, completely submerged wings, gas turbine propulsion and automatic control. 09 p1031 A73-22208

Hydrodynamics, hydroelasticity, technology and automatic control of H 890 hydrofoil craft. 09 p1031 A73-22209

HYDROGEN

NT DEUTERIUM

NT DEUTERIUM PLASMA

NT HYDROGEN ATOMS

NT HYDROGEN IONS

NT HYDROGEN ISOTOPES

NT HYDROGEN PLASMA

NT LIQUID HYDROGEN

NT METALLIC HYDROGEN

NT ORTHO HYDROGEN

NT PARA HYDROGEN

NT TRITIUM

Ionization cross sections for H₂, N₂, and CO₂ clusters by electron impact. 01 p0080 A73-10563

Temperature changes in hydrogen-oxygen explosions. 01 p0121 A73-10646

Evolutionary models for helium white dwarves with uniformly accreting hydrogen shell, noting thermally unstable laminar energy source formation in shell lower layers. 01 p0100 A73-10709

Laser power density calculation with complete rotational analysis for molecular hydrogen Lyman and Werner bands vibrational-rotational transitions. 01 p0061 A73-11224

The diurnal variations of hydrogen and oxygen constituents in the mesosphere and lower thermosphere. 02 p0158 A73-12026

21-cm neutral hydrogen line study of early type galaxies. 02 p0222 A73-12716

Hydrogen reactions and detection by line broadening in beta transformed Ti-Al-V alloy, using X ray diffraction analysis. 02 p0183 A73-12759

Massive stars evolution in hydrogen and helium burning phases, taking into account mass loss from light pressure in optically thick media. 02 p0224 A73-12801

Effects of alloying elements on the solubility of hydrogen in beta titanium. 03 p0321 A73-12920

Thermal instability of the hydrogen-burning shell in nondegenerate stars. 03 p0366 A73-12937

Supersonic mixing and combustion of a hydrogen jet in a coaxial high-temperature test gas. 03 p0397 A73-13474

Hydrogen distribution between the phases in metals [AIAA PAPER 72-1179]. 03 p0324 A73-13507

Hydrogen self-diffusion in the niobium-zirconium-hydrogen system. 03 p0327 A73-13973

Effect of hydrogen on internal friction in molybdenum. 03 p0327 A73-13975

High strength alloys hydrogen embrittlement mechanisms and effects and preventive measures,

considering steel decarburization, stress corrosion cracking, hydride sheath formation and failure modes. 03 p0328 A73-14425

Submicrosecond pulses from a hydrogen-fluorine laser with high energy density and quantum efficiency. 03 p0320 A73-14454

Study by autoradiography at high resolution power of the role of hydrogen in the mechanism of cracking of TA6V titanium alloy in salt water. 04 p0461 A73-15097

Hydrogen/proton adsorption behavior on fuel cell Pt electrode, considering surface roughness factor, Pt sites number and equilibrium data. 04 p0407 A73-15104

Possibility of generating ultrashort laser pulses on combination vibrational-rotational transitions of molecular hydrogen. 04 p0458 A73-15472

Influence of hydrogen on the technological plasticity of the alloy Ti + 9% Al. 04 p0464 A73-15499

Vela 4 Lyman-alpha observations - Evidence for an aspherical hydrogen geocorona at 18 earth radii. 04 p0492 A73-15528

Hydrogen gas generation in water/stainless-steel heat pipes. 04 p0518 A73-15818

Effect of H₂ pressure on pulsed H₂ + F₂ laser - Experiment and theory. 05 p0583 A73-16043

Solidification pressure effect on hydrogen in Al ingots, noting blister formation correlation to pressure. 05 p0587 A73-16579

Dissociative excitation of molecular hydrogen by electron impact. 05 p0600 A73-16596

Deuterium-hydrogen ratio in Jupiter. 05 p0623 A73-17182

Absolute Raman scattering cross-section of molecular hydrogen. 05 p0601 A73-17340

Chemisorption and catalysis of hydrogen on polycrystalline wires of tungsten and nickel. 06 p0661 A73-18253

A comparison of hydrogen embrittlement and stress corrosion cracking in high-strength steels. 06 p0709 A73-18479

Diffusion of hydrogen in titanium alloys due to composition, temperature, and stress gradients. 06 p0712 A73-18764

Interstellar molecular hydrogen observed in the ultraviolet spectrum of delta Scorpii. 07 p0874 A73-19071

The gas-phase reaction of perchloric acid with hydrogen. 07 p0787 A73-19387

Study of the ignition reaction in an oxygen-hydrogen mixture at relatively high pressures and low temperatures in the shock tube. 07 p0920 A73-19993

Upper self-ignition limit of hydrogen in oxygen. 07 p0921 A73-19994

Line broadening of Lyman alpha wings due to protons calculated via positive molecular hydrogen ion wave functions. 08 p0997 A73-20892

The distribution of neutral hydrogen and the velocity field of the galaxy NGC 3109. 08 p1004 A73-20905

A neutral hydrogen survey of the galaxy M33. II - Distribution and kinematics of the neutral hydrogen. 08 p1005 A73-20913

Neutral hydrogen in Markarian galaxies. 08 p1006 A73-20933

Problems of mixing and supersonic combustion of hydrogen in a hypersonic ramjet [ONERA, TP NO. 973]. 08 p1025 A73-21684

Variable photosynthetic units, energy transfer and light-induced evolution of hydrogen in algae and bacteria. 08 p0932 A73-21685

The solubility of hydrogen in rhodium, ruthenium, iridium and nickel. 09 p1047 A73-21981

Calculation of the magnetic properties of a hydrogen molecule with the aid of the method of varying the vector potential and the method of varying the induced current. 09 p1122 A73-22017

Valence-bond study of the H₂, D₂/ exchange reaction mechanism. 09 p1047 A73-22074

Evolution of a white dwarf during accretion of hydrogen-rich matter. II. 09 p1145 A73-22291

High strength TRIP /transformation induced plasticity/ steels hydrogen embrittlement susceptibility under cathodic charging, gaseous hydrogen environment and loading conditions. 09 p1102 A73-22410

Determination of hydrogen permeation parameters in alpha titanium using the mass spectrometer. 09 p1102 A73-22412

On ultraviolet absorption by molecular hydrogen in stellar atmospheres.

09 p1148 A73-22867

Statistical significance of some optical evidence for the bending of the galactic plane.

10 p1271 A73-23492

Nitric oxide formation and radical overshoot in premixed hydrogen flames.

10 p1294 A73-23558

Thermodynamic properties of the nickel-tungsten system as determined from its hydrogen solubility

10 p1231 A73-23689

Solar Lyman alpha changes and related hydrogen density distribution at the earth's exobase /1969-1970/.

10 p1269 A73-24736

X ray ionization and heating of H I regions refuted from energy input rate computations of observed flux in Galactic plane

11 p1415 A73-25118

Search for neutral hydrogen in the galactic cluster NGC 2287.

11 p1415 A73-25119

Hydrogen promoted corrosion of tungsten by oxygen in an electric field A field ion microscope study.

11 p1325 A73-25205

High pressure physical model of hydrogen planets Jupiter, Saturn, Uranus and Neptune

11 p1419 A73-25877

Electrical conductivity of condensed molecular hydrogen in the giant planets.

11 p1420 A73-25885

Correlation of theory and experiment for high-pressure hydrogen.

11 p1398 A73-25887

Equation of state and phase diagram of dense hydrogen.

11 p1399 A73-25890

Ground state energy of solid molecular hydrogen at high pressure.

11 p1401 A73-25891

Vibrational relaxation in hydrogen-rare-gases mixtures.

11 p1402 A73-25969

Effect of high dislocation density on stress corrosion cracking and hydrogen embrittlement of type 304L stainless steel.

11 p1385 A73-26174

Localized hydrogen in titanium welds.

11 p1375 A73-26358

Chain interaction and heat release near the lower limit for self-ignition of hydrogen with oxygen

12 p1465 A73-26967

Experimental evaluation of the role of surface reactions in studies of hydrogen penetration through titanium, nickel and copper

13 p1630 A73-28009

Theory of the thermal explosion in the hydrogen shell of a white dwarf

13 p1683 A73-29091

Solubility of nitrogen and hydrogen in cobalt and cobalt alloys - A review.

13 p1637 A73-29245

The Perseus spiral arm at 21-cm.

13 p1685 A73-29354

Pulsational instability of a star of 0.5 solar mass during core hydrogen burning.

13 p1685 A73-29362

On the kinematics of a local component of the interstellar hydrogen gas possibly related to Gould's Belt.

13 p1686 A73-29369

Classical dynamical investigations of reaction mechanism in three-body hydrogen-halogen systems.

13 p1581 A73-29427

Pulsed laser utilizing a fluorine and hydrogen mixture.

13 p1629 A73-29434

Autoionizing transitions in N2 and H2 produced by electron impact.

14 p1776 A73-29695

Neutral hydrogen distribution in the upper atmosphere of the earth

14 p1747 A73-29871

Determination of diffusion characteristics in the boundary and volume components of a diffusing hydrogen stream in a polycrystalline metal

14 p1763 A73-30716

Spectrophotometric results from the Copernicus satellite. IV - Molecular hydrogen in interstellar space.

14 p1802 A73-30747

Catalytic effects in corrosion processes with hydrogen depolarization of multiphase magnesium alloys

14 p1764 A73-30827

Investigation of the influence of the method of supplying hydrogen to the furnace on the properties of tungsten metal

14 p1765 A73-30885

Vibrational excitation of H2 by proton impact.

14 p1777 A73-30957

Influence of hydrogen on the failure of the VT3-1 titanium alloy in programmed cyclic loading

15 p1886 A73-31035

Stellar nuclear hydrogen burning shell thermal stability to radial perturbations, discussing growth rate, energy generation and temperature increases

15 p1929 A73-31058

Absorption and production of soft X-rays in the Galaxy.

16 p2051 A73-32746

Galactic neutral hydrogen observations along loop III, noting loop effects on gas velocity distribution

16 p2058 A73-32835

Vertical profiles of molecular H2 and CH4 in the stratosphere.

[AIAA PAPER 73-518]

16 p2006 A73-33555

The Berkeley low-latitude survey of neutral hydrogen. I - Profiles.

16 p2063 A73-33600

Figures and internal structure of hydrogen-helium planets

16 p2069 A73-33838

Models comparison for heavy elements segregation mechanism from gaseous hydrogen and helium for terrestrial planets formation from primordial granular matter

17 p2228 A73-34422

Composition and temperature effects on hydrogen solubility in Ni-Al liquid alloys

17 p2187 A73-34553

The escape of H2 from Titan.

17 p2232 A73-34861

Application of the hydrogen-bubble technique for velocity measurements in thin liquid films.

[ASME PAPER 73-APM-8]

17 p2153 A73-35033

Quantum scattering theory of rotational relaxation and spectral line shapes in H2-He gas mixtures.

17 p2119 A73-35175

Evaluation of the intermolecular energy between two hydrogen molecules near the van der Waals minimum, from a perturbative procedure.

17 p2213 A73-35179

Thermodynamics of b.c.c. solid solutions of hydrogen in niobium, vanadium and tantalum.

17 p2193 A73-35623

Experimental studies of chemically reactive /F + H2/ flow in supersonic free jet mixing layers.

[AIAA PAPER 73-640]

18 p2321 A73-36198

The hydrogen evolution reaction on Ti-6Al-4V in acidic solutions of NaCl-HCl.

19 p2402 A73-37585

Spatial distributions of H2 desorbed from Fe, Pt, Cu, Nb, and stainless steel surfaces.

19 p2402 A73-37951

Adsorption of spacecraft contaminants on Bosch carbon.

[ASME PAPER 73-ENAS-15]

19 p2399 A73-37972

High energy density silver-hydrogen cells for space and terrestrial applications.

19 p2391 A73-38403

Diffusion of hydrogen and deuterium in Ta, Nb, and V.

20 p2576 A73-39134

Emission of infrared molecular hydrogen lines from a cooled-gas laser.

20 p2574 A73-39694

Resonant nuclear measurement of hydrogen concentration vs depth in Apollo 11, 15 and 16 lunar soil fragments and platinum foil exposed to solar event

21 p2765 A73-40237

Detailed balance as check on impact parameter calculations, discussing proton-hydrogen collisions with small transition amplitudes and interpolation errors

21 p2743 A73-40467

Complete hydrogen and helium particle spectra from 30- to 60-MeV proton bombardment of nuclei with A = 12 to 209 and comparison with the intranuclear cascade model.

21 p2744 A73-41019

Influence of hydrogen on the fracture micromechanism of OT4 and OT4-1 titanium alloys

21 p2721 A73-41231

Prediction of weld metal hydrogen levels obtained under test conditions.

21 p2708 A73-41252

Neutral interstellar hydrogen and extraterrestrial Lyman alpha radiation.

21 p2773 A73-41396

Measurements of neutral-hydrogen absorption in the spectra of eight pulsars.

21 p2779 A73-41538

Aperture synthesis of interstellar neutral hydrogen in absorption. I - The Perseus arm feature of Cassiopeia A.

22 p2904 A73-41756

Liquid helium cryopump extension to gaseous hydrogen and helium pumping via adsorption on argon cryodeposit, obtaining gases partial pressures evolution

22 p2886 A73-41871

Temperature dependent chemisorption effects on hydrogen embrittlement of steel, showing strength-ductility correlation

22 p2874 A73-42106

Chemisorption of H2 on W/211/.

22 p2817 A73-42444

Technique for measuring the diffusivity of hydrogen in titanium alloys.

22 p2878 A73-42505

High-temperature oxidation of hydrogen by nitrous oxide in shock waves.

22 p2933 A73-42756

Studies of the relaxation of internal energy of molecular hydrogen.

22 p2898 A73-42762

Inhibition of the first limit of the hydrogen-oxygen reaction by ethyl bromide.

22 p2898 A73-42777

Turbulent diffusion flame velocity, concentration, temperature and momentum flux measurements for hydrogen round jet in co-flowing air stream

22 p2935 A73-42788

Thermodynamics of transition metal-hydrogen solid solutions.

22 p2880 A73-43076

A supersynthesis radio telescope for neutral hydrogen spectroscopy at the Dominion Radio Astrophysical Observatory.

23 p2958 A73-43362

The concentration of molecular H2 and CH4 in the stratosphere.

23 p2976 A73-43891

Reorientation /collision/ cross sections for hydrogen intermolecular potentials, taking into account quadrupole-quadrupole interaction effects

24 p3113 A73-44980

Neutral hydrogen rotational motions near galactic center and 3-kpc arm, using dispersion ring model

24 p3140 A73-45180

HYDROGEN ATOMS

Heating and cooling mechanisms, ionization processes, time-dependent models and energy requirements of interstellar H I regions

01 p0091 A73-10064

Dependence of the D-region positive-ion composition on the atomic oxygen and atomic hydrogen concentrations.

01 p0041 A73-10891

Second-level population of a hydrogen atom in a plasma medium

01 p0085 A73-10950

Two quantum induced photon-plasmon transition probability for hydrogen atom in processes of nebulas and stellar chromospheres

01 p0080 A73-11308

UV laser parameters calculation for operation on Lyman transition between H atom resonant excited state and ground state

01 p0061 A73-11334

Radio spectrum analysis of loop prominence development, temperature and H atom density on May 13, 1971, noting consistency with Jefferies-Orrall model

01 p0108 A73-11387

Observations of Cygnus X-3 at the Mullard Radio Astronomy Observatory.

02 p0210 A73-11561

Use of the Glauber approximation in atomic collisions - A progress report.

02 p0195 A73-12649

Monte Carlo classical trajectory calculation of the rates of Hand D-atom vibrational relaxation of HF and DF.

03 p0318 A73-13280

Hydrogen atomic structure in magnetic field, using Bohr model, Schroedinger equation and energy eigenvalues

03 p0299 A73-13352

Close coupled calculations of electron-hydrogen atom scattering using a noniterative integral equation technique.

04 p0477 A73-14818

A neutral hydrogen survey of the galaxy M 33. I.

05 p0618 A73-16740

The damping of the NaD lines in the solar spectrum by atomic hydrogen.

06 p0753 A73-18239

Observations of the neutral-hydrogen absorption spectrum of Cygnus X-3.

07 p0874 A73-19073

Interpretation of Ogo 5 Lyman alpha measurements in the upper geocorona.

07 p0813 A73-19233

Atomic hydrogen concentrations in the mesosphere and the hydroxyl emissions.

07 p0815 A73-19257

Cross sections for emission of Lyman-alpha radiation in collisions of 1-25 keV protons and hydrogen atoms with constituents of planetary atmospheres.

08 p0957 A73-20660

Spiral arm structure as standing wave, of magnetically controlled star creation, considering various hydromagnetic models, dust and H I distributions

08 p1002 A73-20879

Aperture synthesis study of neutral hydrogen in the galaxies NGC 6946 and IC 342.

08 p1005 A73-20914

Stark effect and line broadening in three-dimensional stochastic fields.

09 p1125 A73-21939

- Population of the second level of the hydrogen atom in a plasma medium. 09 p1130 A73-22744
- Inelastic collision of fast charged particles with arbitrary levelled hydrogen-like atoms. 10 p1250 A73-23575
- Lyman-alpha radiation in the hydrogen atmospheres of comets - A model with multiple scattering. 10 p1281 A73-24408
- Viscosity of atomic hydrogen. 11 p1397 A73-25075
- Rotational and vibrational hydroxyl excitation in the laboratory and in the night airglow. 11 p1354 A73-25761
- Spatial and temporal variations of the Lyman-alpha airglow and related atomic hydrogen distributions. 11 p1356 A73-25909
- Diurnal atomic hydrogen variation at exospheric temperatures as function of thermal ion and proton charge exchange with plasmasphere. 12 p1492 A73-27612
- The interaction between two hydrogen atoms adsorbed on 100/ tungsten. 13 p1580 A73-28215
- Reaction $H + C_2H_4$ - Investigation into the effects of pressure, stoichiometry, and the nature of the third body species. 13 p1581 A73-29426
- Solar Lyman alpha radiation scattering analysis to determine neutral hydrogen atom distribution in upper atmosphere. 14 p1747 A73-29865
- Charge changing processes in hydrogen beams. 14 p1776 A73-30125
- Processes altering charge state in collisions of hydrogen atoms with H_2 molecules. 14 p1777 A73-30330
- Ionization and relative abundance of hydrogen and helium atoms in filaments of the Crab Nebula. 16 p2057 A73-32712
- Atomic hydrogen and water vapour in the lower arctic thermosphere during geomagnetic storm and PCA event. 18 p2310 A73-36141
- Satellite observations of strong Balmer alpha atmospheric emissions around the magnetic equator. 18 p2346 A73-36284
- Extraterrestrial ultraviolet radiation and the parameter of the H I medium near the sun. 20 p2601 A73-39074
- Laboratory studies of collisions of energetic H^+ and hydrogen with atmospheric constituents. 21 p2679 A73-40072
- Hydrogen production rates of comet Bennett /1969/ in the first half of April 1970. 21 p2778 A73-41530
- Change in the hyperfine state of the hydrogen atom during its collisions with unsaturated hydrocarbon molecules in the gaseous state. 22 p2889 A73-41719
- Reaction of H atoms with CH_2Cl_2 - Application to the inhibition of flames. 22 p2819 A73-42779
- A reexamination of the mean H I density along the Hubble sequence. 22 p2913 A73-43003
- Singlet s-wave electron-hydrogen scatter below first excitation threshold, computing phase shift in Feshbach operator and static exchange approximation. 22 p2890 A73-43127
- Pulsars radio observations of magnetic field, electron density and neutral hydrogen atoms in interstellar space. 23 p3028 A73-43369
- Electrostatic Hellmann-Feynman theorem applied to long-range interatomic forces - The hydrogen molecule. 24 p3113 A73-44981
- Lyman alpha 1216 A intensity behavior for atomic hydrogen density distribution below 200 km on Mars, calculating radiative transfer. 24 p3139 A73-45108
- The shapes of neutral globules associated with diffuse nebulae. 24 p3141 A73-45194
- Magnetic resonance spectrometer measurements of atomic hydrogen surface recombination. 24 p3113 A73-45425
- HYDROGEN BONDS**
- Structure of beryllium boron hydrides $BeBH_5$ and BeB_2H_8 . 12 p1466 A73-27045
- HYDROGEN CHLORIDES**
- NT HYDROCHLORIC ACID**
- Stress corrosion cracking of titanium alloys in hydrogen chloride. 15 p1896 A73-32573
- The hydrogen evolution reaction on Ti-6Al-4V in acidic solutions of NaCl-HCl. 19 p2402 A73-37585
- HYDROGEN CLOUDS**
- Spiral structure and kinematics of the galaxy from a study of the H II regions - Fabry-Perot interference methods applied to ionized hydrogen. 01 p0096 A73-10297
- An upper limit on the OH abundance in the intercloud medium. 01 p0096 A73-10314
- Physical conditions in interstellar hydroxyl and formaldehyde clouds. 01 p0100 A73-10790
- Properties of H I regions heated by X-rays and cosmic rays. 01 p0092 A73-10935
- Rocket infrared observations of H II regions. 01 p0103 A73-11026
- 21-micron observations of H II regions. 01 p0104 A73-11045
- A simple analytic approximation for dusty Stromgren spheres. 01 p0104 A73-11047
- The state of ionization in nova shells. 02 p0222 A73-12706
- Separate star groups in Sco OB 1 association coinciding with previously established gaseous subgroups. 02 p0222 A73-12711
- Polarimeter search for optical circular polarization in eclipsing binaries, magnetic Ap stars, planetary nebula, Hubble and Orion nebulae, M87 and Sirius. 03 p0366 A73-12939
- On the 4686-A He II line intensity in H II regions and the cosmic ray flux. 03 p0361 A73-13220
- Protoplanet cloud model for cosmic OH and water masers in H II regions to account for anomalous hydrogen deficiency, discussing pumping mechanisms and chemical composition. 04 p0497 A73-14974
- Infra-red sources in the H II region W3. 04 p0499 A73-15485
- H I clouds with spin temperatures less than 25 K. II - Physical properties of two neutral hydrogen clouds. 04 p0500 A73-15517
- Astrophysical CO isotopic constituents from H II regions line emissions, determining relative abundances. 04 p0502 A73-15688
- Recombination radio lines in H I regions. 04 p0504 A73-16026
- Neutral hydrogen cloud rotation and recurrent eflux from central region of Galaxy, considering material and energy resources limitation. 05 p0616 A73-16457
- The formation of diatomic molecules in interstellar clouds. 05 p0625 A73-17333
- Interstellar molecular hydrogen cloud size and optical extinction by interstellar Na D and Ca lines, estimating molecular lifetime within dark cloud. 06 p0752 A73-18230
- On the differing molecular line widths in dense interstellar clouds. 07 p0874 A73-19072
- 5 GHz observations of the infrared star MWC 349, and the H II condensation W3/OH. 07 p0899 A73-20121
- H flux density observations for 21 cm absorption spectrum in front of Cyg X-3. 07 p0902 A73-20560
- Cosmic-ray heating and molecular cooling of dense clouds. 08 p0997 A73-20899
- High velocity clouds as part of Galactic spiral arms, obtaining spiral structure maps from observations of Galactic plane. 08 p1005 A73-20918
- Nebular Fabry-Perot, Pepsios, and Sisam monochromators. 08 p0964 A73-21039
- On the presence of H_2 molecules inside neutral globules imbedded in H II regions. 09 p1140 A73-22005
- H I absorption in the galactic center region and between galactic longitudes 350 deg and 359 deg. 09 p1141 A73-22009
- A search for neutral hydrogen remnants of strong tidal disruption of the Small Magellanic Cloud. 09 p1141 A73-22012
- Cloud-cloud collision destruction of interstellar clouds in inter-spiral arm regions, discussing observational tests. 09 p1141 A73-22028
- Galactic interstellar molecules, discussing physical, chemical and spectral characteristics, hydroxyl emission, occurrence regions, hydrogen clouds, isotope ratios, interstellar masers and probes. 09 p1146 A73-22446
- Properties of H I regions heated by X rays and cosmic rays. 09 p1147 A73-22730
- On the detection of H_2 from interstellar clouds in the wavelength range 4.4 to 28.2 microns. 09 p1148 A73-22870
- Observations of the outer spiral structure of the Milky Way and its relation to the high velocity clouds. 09 p1151 A73-23292
- Some limits on cosmic-ray heating of H I clouds by magnetic stars. 10 p1263 A73-23487
- The evolution of interstellar clouds. II - Hydrodynamic treatment of the phase change. III - Cloud collisions and statistical theory. 10 p1272 A73-23531
- The manifold of galaxies - Galaxies with known dynamical parameters. 10 p1281 A73-24407
- Probabilistic fragmentation model for collapsing interstellar cloud, predicting stellar mass spectrum. 11 p1415 A73-25171
- Molecule formation. I - In normal H I clouds. II - In interstellar shock waves. 12 p1547 A73-27973
- The large-scale distribution of low-velocity hydrogen gas at high galactic latitudes. 13 p1671 A73-28028
- High Galactic latitude intermediate-negative velocity neutral hydrogen properties, noting large complexes and systematic velocity pattern. 13 p1671 A73-28029
- A high resolution neutral hydrogen study of the galaxy M 51. 13 p1671 A73-28033
- The heating of interstellar clouds by vibrationally excited molecular hydrogen. 13 p1673 A73-28279
- Interpretation of hydrogen quadrupole and methane observations of Jupiter and the radiative properties of the visible clouds. 13 p1673 A73-28280
- Interstellar cloud collapse into protostellar objects and star formation, discussing young stellar objects observation. 13 p1681 A73-28946
- Neutral hydrogen clouds gravitational binding of Coma cluster, providing mechanism for heating of diffuse gas between clouds and galaxies. 13 p1684 A73-29352
- Lyman alpha radiation transfer in spherically symmetric hydrogen nebula from Monte Carlo techniques, computing for different optical depths. 13 p1685 A73-29358
- A search for H alpha emission from interstellar clouds. 14 p1797 A73-30008
- Ionization of the intercloud medium and the central disk regions of spiral galaxies. 14 p1801 A73-30729
- Spectrophotometric results from the Copernicus satellite. II - Composition of interstellar clouds. 14 p1801 A73-30745
- Deuterium in interstellar molecules. 14 p1802 A73-30749
- On the kinematical and spatial coincidence of optical and radio spiral arms in our galaxy. 15 p1929 A73-31055
- Aperture synthesis study of neutral hydrogen in NGC 2403 and NGC 4236. I - Observations. 15 p1929 A73-31056
- Aperture synthesis study of neutral hydrogen in NGC 2403 and NGC 4236. II - Discussion. 15 p1929 A73-31057
- A preliminary classification scheme for interstellar absorbing clouds. 15 p1933 A73-31309
- Two-component equilibrium model of the H I regions of the interstellar medium satisfying a set of radio observations. 15 p1938 A73-31965
- The dynamics of the Andromeda Nebula. 15 p1941 A73-32400
- Fabry-Perot interferometric studies on H II regions. 16 p2058 A73-32831
- Thermal and ionization equilibrium in a dense hydrogen cloud. 16 p2059 A73-32841
- IR and molecular radio emissions from interstellar clouds representing formation stage of normal stars, discussing dust screening effects. 17 p2229 A73-34433
- A discussion of the distribution of interstellar matter close to the sun. 17 p2234 A73-35619
- Feature recognition method in small scale structure analyses of neutral hydrogen emissions, applying to surveys at negative intermediate galactic latitudes. 19 p2483 A73-37562
- Dynamics of step heat waves in gases and plasmas. 20 p2592 A73-38863
- Magnetic stars origin from gravitational collapse of ionized hydrogen clouds, discussing implications of interstellar magnetic fields and critical mass according to Chandrasekhar-Fermi virial theorem. 20 p2605 A73-39058
- IR astronomical objects, methods and instruments, discussing galactic and extragalactic sources, early and late stars, planetary nebulae, interstellar dust and hydrogen ion clouds. 20 p2605 A73-39060
- Observations of neutral hydrogen near the galactic center. II - The nuclear disc. 20 p2610 A73-39578

H II region OH maser source pumping by far IR radiation-induced population inversions between Lambda doublet levels

21 p2759 A73-40712

Galactic spiral arm structure mapping by 21 cm data taken at different latitudes, discussing high velocity hydrogen clouds distribution

21 p2778 A73-41533

Neutral hydrogen spectral line observation for Milky Way Galaxy mapping, discussing role of spiral structure density wave theory in interpretation

23 p3028 A73-43348

Stellar radiation Thomson scattering by free electrons compared to atomic processes as mechanism for H II regions continuous emission

23 p3030 A73-43756

Two-component equilibrium model of interstellar HI regions that satisfy the overall radio observations.

24 p3132 A73-44490

Bending of the galactic plane and the nature of the high velocity clouds.

24 p3140 A73-45189

HYDROGEN COMPOUNDS

NT BERYLLIUM BOROHYDRIDES

NT DEUTERIUM COMPOUNDS

NT HEAVY WATER

NT HYDRAZINE BORANE

NT HYDRIDES

NT HYDROCYANIC ACID

NT HYDROGEN SULFIDE

NT LITHIUM ALUMINUM HYDRIDES

NT LITHIUM HYDRIDES

NT METAL HYDRIDES

NT NITROGEN HYDRIDES

NT PHOSPHINES

NT SILANES

NT ZIRCONIUM HYDRIDES

Measurements of some hydrogen-oxygen-nitrogen compounds in the stratosphere from Concorde 002.

09 p1079 A73-22947

Reactions of HO₂ with carbon monoxide and nitric oxide and of O(1D) with water.

14 p1723 A73-30069

Photochemistry of the ozone in the stratosphere

18 p2287 A73-36938

Reaction of HO₂ with O₃.

19 p2402 A73-37674

Spectroscopic studies of low-pressure hydrogen-fluorine flames.

22 p2898 A73-42760

HYDROGEN CYANIDES

U HYDROCYANIC ACID

HYDROGEN DEUTERIUM OXIDE

U HEAVY WATER

HYDROGEN EMBRITTLEMENT

Temperature dependent chemisorption effects on hydrogen embrittlement of steel, showing strength-ductility correlation

09 p1100 A73-22158

TRIP steel embrittlement and notch sensitivity in high pressure hydrogen environment resulting from interaction between hydrogen and stress-assisted martensite during deformation

13 p1633 A73-28144

An X-ray study of hydrogen induced phenomena affecting mechanical behaviours of austenitic stainless steels.

13 p1625 A73-29522

The low-temperature embrittlement of niobium and vanadium by both dissolved and precipitated hydrogen.

14 p1761 A73-30630

High strength steel fracture characteristics in vacuum and gaseous medium, noting hydrogen adsorption effect on crack resistance

15 p1887 A73-31248

An electrochemical model for hot-salt stress-corrosion of titanium alloys.

17 p2189 A73-34643

Hydrogen embrittlement and stress corrosion cracking in Ti-Al binary alloys.

17 p2191 A73-35099

A quantitative model of hydrogen induced grain boundary cracking.

17 p2191 A73-35124

Acoustic emission instrumentation and application for plastic deformation, flaw detection monitoring of fatigue crack growth, stress corrosion and hydrogen embrittlement

17 p2175 A73-35670

A simple method for studying slow crack growth.

19 p2497 A73-37588

Influence of hydrogen and oxygen on the mechanical behavior of unalloyed titanium

19 p2441 A73-37837

French monograph - Mechanical behavior of the titanium alloy TA6V6E2 with reference to hydrogen - Influence of heat treatment and oxygen content.

19 p2443 A73-38362

Effects of hydrogen on tantalum by the cathodic charging.

20 p2575 A73-38638

Influence of hydrogen on the mechanical properties of zirconium and some of its alloys

21 p2718 A73-40483

Influence of preloading on the sustained load cracking behavior of maraging steels in hydrogen.

21 p2719 A73-40924

Influence of relief annealing on the mechanical properties of high-strength hydrogenized steel

21 p2721 A73-41228

Cadmium embrittlement of high strength, low alloy steels at elevated temperatures.

22 p2873 A73-41968

Microplasticizing mechanism of hydrogen embrittlement due to stress activated chemisorption, noting association with temperature dependent hydrogen-metal atomic interaction

23 p3039 A73-43465

Hydrogen-induced transformation and embrittlement in 18-8 stainless steel.

23 p2994 A73-44158

HYDROGEN FLUORIDES

U HYDROFLUORIC ACID

HYDROGEN FUELS

Extraterrestrial propellant resupply for advanced manned missions.

02 p0221 A73-12599

Supersonic mixing and combustion of confined coaxial hydrogen-air streams.

[AIAA PAPER 72-1178] 03 p0397 A73-13473

Air breathing hypersonic aircraft technology developments in propulsion systems and structures with emphasis on use of hydrogen fuel

[AIAA PAPER 73-58] 06 p0647 A73-17631

Flame structure and flame reaction kinetics. VIII - Structure, properties and mechanism of a rich hydrogen + nitrogen + oxygen flame at low pressure.

07 p0918 A73-19154

Potentials and problems of hydrogen fueled supersonic and hypersonic aircraft.

09 p1032 A73-22830

Laminar flame propagation in hydrogen, oxygen, nitrogen mixtures.

13 p1707 A73-29001

Condition of the medium before the flame front during the initial phase of a combustion process

15 p1957 A73-31867

Deflagration in the combustion of hydrogen-fluorine mixtures.

16 p2045 A73-33349

The use of hydrogen for aircraft propulsion in view of the fuel crisis.

17 p2220 A73-35469

Shock tube study of the effect of unsymmetric dimethyl hydrazine on the ignition characteristics of hydrogen-air mixtures.

18 p2372 A73-37098

Nitrogen oxide turbojet emissions minimization with hydrogen compared to kerosene (JP) fuels due to flammability limits, burning velocity and introduction in combustor as gas

19 p2473 A73-37498

Electrolytic hydrogen fuel production with solid polymer electrolyte technology.

19 p2391 A73-38413

Experiments on the propagation of mixing and combustion injecting hydrogen transversely into hot supersonic streams.

22 p2934 A73-42785

Influence of aerodynamic field on shock-induced combustion of hydrogen and ethylene in supersonic flow.

22 p2934 A73-42786

Potential of hydrogen fuel for future air transportation systems.

[ASME PAPER 73-ICT-104] 23 p3019 A73-43499

HYDROGEN IONS

Semicalculation theory for low-energy molecular collisions - H⁺/H₂ vibrational excitation.

01 p0080 A73-10564

Hydrogen ion concentration in the blood of man under high mountain conditions with physical loads

02 p0133 A73-11924

Intergalactic ionized hydrogen in nearby groups of galaxies.

02 p0225 A73-12803

Theoretical models of photoionized intergalactic hydrogen.

03 p0365 A73-12926

Magnetospheric thermal plasma and hydrogen cation density profile characteristics in different local time regions explained by time-varying convection model

03 p0303 A73-13879

Kinematics of H-alpha emission from an abnormal filament of the galaxy NGC 4258

03 p0380 A73-14609

Calculated distributions of hydrogen and helium ions in the low-latitude ionosphere.

07 p0818 A73-20052

5 GHz observations of the infrared star MWC 349, and the H II condensation W3/OH.

07 p0899 A73-20121

Validity criteria for local thermodynamic equilibrium and coronal equilibrium.

08 p0992 A73-21007

Proton-impact dissociation and ionization of H₂+ molecular ions.

10 p1250 A73-23671

Independent effects of changes in H⁺ and CO₂ concentrations on hypoxic pulmonary vasoconstriction.

10 p1182 A73-24565

Thermochemical calculation for high temperature and pressure formation of interstellar molecules in compact H II regions, considering prestellar and late stellar atmospheres

11 p1423 A73-26105

Charge changing processes in hydrogen beams.

14 p1776 A73-30125

Stark broadening of high-principal-quantum-number n-alpha lines of hydrogen.

14 p1777 A73-30552

Continuum galactic background radio emission, considering reified ionized hydrogen gas with filaments due to dense inhomogeneities

15 p1938 A73-31951

Fabry-Perot interferometric studies on H II regions.

16 p2058 A73-32831

Excitation of highly excited hydrogenic ions and atoms by charged particles. IV.

16 p2039 A73-33865

Estimation of H⁺/H₂ fluxes at the polar regions.

18 p2304 A73-35969

Penetration and crossing of transverse magnetic field barrier by a purely ionic plasma.

19 p2465 A73-37170

Height distribution of O⁺ and H⁺ ions in the ionosphere F2 region. I

19 p2427 A73-38333

Laboratory studies of collisions of energetic H⁺/H₂ and hydrogen with atmospheric constituents.

21 p2679 A73-40072

On the infrared emission of H II regions due to dust.

22 p2908 A73-42314

The H II region G333.6-0.2, a very powerful 1-20 micron source.

23 p3028 A73-43527

Continuum galactic background radio emission, considering rarefied ionized hydrogen gas with filaments due to dense inhomogeneities

24 p3131 A73-44478

Accretion onto black holes - The emergent radiation spectrum. II Magnetic effects.

24 p3138 A73-45036

HYDROGEN ISOTOPES

NT DEUTERIUM

NT METALLIC HYDROGEN

NT TRITIUM

Hydrogen and helium isotopes differential energy spectra during solar flare particle acceleration related to nuclear interaction processes

11 p1414 A73-26610

Carbon isotope abundance ratios in comets and Jupiter atmosphere, discussing hydrogen isotope ratio determination for Saturn and Jupiter atmospheres

17 p2228 A73-34418

Isotopes of helium and hydrogen in solar corpuscular fluxes

21 p2757 A73-40593

Ultrafiltration by a compacted clay membrane. I - Oxygen and hydrogen isotopic fractionation. II - Sodium ion exclusion at various ionic strengths.

23 p2973 A73-43845

HYDROGEN OXYGEN ENGINES

Development of pulsed hydrogen/oxygen attitude-control engines

[DGLR PAPER 72-077] 02 p0202 A73-11689

Effect of injection velocity ratio and combustion chamber pressure on experimental performance of throttleable LO₂/GH₂-rocket engines with coaxial injectors.

[AIAA PAPER 72-1079] 03 p0354 A73-13402

Cryogenic liquid O₂/H₂ reaction control systems for Space Shuttle.

[AIAA PAPER 72-1155] 03 p0382 A73-13458

Advanced technology for Space Shuttle Auxiliary Propellant Valves.

[AIAA PAPER 72-1157] 03 p0356 A73-13459

Hydrogen oxygen propulsion component design and hot firing tests for space shuttle auxiliary systems and upper stage applications

[AIAA PAPER 72-1156] 04 p0486 A73-14918

Space Shuttle Orbiter main engine design.

[SAE PAPER 720807] 05 p0607 A73-16644

Technology applied to the Space Shuttle Main Engine.

[AIAA PAPER 73-60] 06 p0741 A73-17633

Cryogenic problems involved in the development of the structure of a hydrogen/oxygen rocket stage.

07 p0905 A73-18991

Open cycle hydrogen-oxygen turbine driven generator system for space shuttle auxiliary power supply, discussing components, control mode and performance potential

09 p1153 A73-22779

High pressure dual fuel chemical LOX/hydrocarbon rocket vehicle concepts for reusable one stage to orbit shuttles

16 p2072 A73-33085

Application of digital computer APU modeling techniques to control system design.

19 p2392 A73-38416

H2-O2 auxiliary power unit for Space Shuttle vehicles - A progress report. (IECEC PAPER 739028) 19 p2392 A73-38436

HYDROGEN OXYGEN FUEL CELLS

H2/O2-fuel cells supplied with a H2/N2-mixture and air. 04 p0408 A73-15116

Hydrogen-air electrolytic fuel cell stack and auxiliary systems for use with methanol feedstock hydrogen generator 04 p0408 A73-15117

Stratospheric airship propulsion system using electric engine, hydrogen-air fuel cells and liquid hydrogen 04 p0408 A73-15119

Dynamics of moisture diffusion through a partially liquid filled porous matrix. 06 p0649 A73-18259

Fuel cell for Apollo command and service module power supply, discussing voltage-power requirements and operating temperature control 09 p1035 A73-22774

Space shuttle orbiter electrical power system requirements and constraints, considering hydrogen/oxygen fuel cell for compact energy storage and turbine driven generators 09 p1153 A73-22776

Hydrogen-oxygen fuel cell as reliable electric power supply for space shuttle mission requirements, assessing technological developments 09 p1035 A73-22777

Analysis of external mass transfer and choice of its parameters for convective removal of reaction-product vapors in a hydrogen-oxygen fuel cell with a capillary membrane 11 p1308 A73-25727

Experimental evaluation of the single-cell concept for a lightweight, rechargeable hydrogen-oxygen fuel cell. 11 p1309 A73-25987

Performance studies on a rechargeable hydrogen-oxygen fuel cell. 11 p1309 A73-25988

Hydrazine and methanol fuel cells comparison with hydrogen-air cells in terms of fuel costs and conversion efficiency, considering electric generators and automotive applications 24 p3057 A73-45025

HYDROGEN PLASMA

NT DEUTERIUM PLASMA

A simple method for calculating nongray radiation. 01 p0119 A73-10109

Nature of the emission of UV Ceti-type stars 01 p0100 A73-10708

Computation of the axisymmetrical free expansion of a nonequilibrium hydrogen plasma 02 p0196 A73-11604

Purification of hydrogen plasmoids by the magnetic field in an injector-diverter. 02 p0198 A73-12113

Collisional-radiative coefficients and population coefficients of hydrogen plasma. 02 p0198 A73-12347

Current trapping in toroidal high current discharges. 03 p0348 A73-14435

Velocity distribution of plasma electrons in the negative H2- and He-glow with superimposed longitudinal magnetic field. 04 p0477 A73-14897

Continuum radiation from nonisothermal hydrogen plasmas. 05 p0602 A73-16558

Experimental observation of heating of a hydrogen plasma by a relativistic electron beam. 05 p0603 A73-17161

CO2 laser-induced gas breakdown in hydrogen. 06 p0701 A73-18355

Radiation effects on state of gas behind strong shock wave, representing power density of non-relativistic fully ionized hydrogen plasma 07 p0920 A73-19508

Comparison of exact and mean beam length results for a radiating hydrogen plasma. 07 p0859 A73-20221

Electrical and thermal conductivities of a relativistic degenerate plasma. 08 p0992 A73-21161

CO2 laser induced Compton effect in underdense hydrogen plasma. 09 p1125 A73-22025

Enhanced energy transfer to a cylindrical plasma by an Alfvén wave. 09 p1128 A73-22629

Fast wave propagation and damping at the second harmonic of the ion cyclotron frequency. [TTU-SR-2] 09 p1128 A73-22631

Particle seeded RF hydrogen plasma opacity, emission spectra, heat transfer and temperature profile at high temperatures 09 p1128 A73-22636

Kinetic equations for time behavior of electron concentration and proton, electron and H I atom temperatures in ionized hydrogen medium 10 p1282 A73-24492

Measurement of the ion energy distribution resulting from the turbulent heating of a plasma. 11 p1404 A73-25269

Quantum statistical mechanics of dense partially ionized hydrogen. 11 p1405 A73-25886

On the evolution of turbulent magnetic fields in a collision dominated plasma. 11 p1406 A73-26559

Ionization, recombination, and population of excited levels in hydrogen plasmas. 11 p1407 A73-26584

Dissipation of hydromagnetic waves with application to the outer solar corona. III - Transition from collisional to collisionless protons. 11 p1428 A73-26619

Determination of the parameters of a fluctuating plasma from the modulation of microwave signals 13 p1666 A73-28961

Electron-molecule collision ionization in hydrogen and deuterium. 14 p1776 A73-29700

Determination of magnetic fields in a plasma from the contour of hydrogen spectral lines. 14 p1780 A73-30339

Electron density characteristics in magnetized hydrogen arcs in the case of a deviation of the ion temperature from the electron temperature 14 p1780 A73-30419

Ion Mach number of ion shock embedded in collisional shock wave propagating in electron proton gas plasma 14 p1777 A73-30660

The turbulent heating of ions and related efficiencies in a current carrying plasma. 15 p1916 A73-31081

Measurement of density and temperature of a hydrogen plasma using an argon laser. 15 p1920 A73-32257

Secondary electrons and energy per ion-pair in a thermal gas for electron, proton and X-ray ionization. 16 p2052 A73-32826

Arc plasmas as radiation standards in the vacuum ultraviolet. 16 p2036 A73-32942

Lineshape of stable electrostatic fluctuations in a beam plasma system. 16 p2042 A73-33338

Book - Equilibrium compositions and thermodynamic properties of mixed plasmas. III - Argon-hydrogen plasmas at .01 to 1000 atmospheres between 2,000 and 35,000 K. 16 p2042 A73-33420

Heat conductivity measurements for a hydrogen plasma in a stabilized electric arc 17 p2214 A73-34129

A high-temperature plasma state in a high-power microwave discharge 17 p2214 A73-34136

VUV radiometry with hydrogen arcs. I - Principle of the method and comparisons with blackbody calibrations from 1650 A to 3600 A. 17 p2212 A73-35425

Penetration and crossing of transverse magnetic field barrier by a purely ionic plasma. 19 p2465 A73-37170

Coaxial hydrogen and erosion pulsed plasma accelerators in vacuum, discussing experiment design, discharge characteristics and practical applications. 19 p2466 A73-37361

Hydrogen plasma compression producing collisionless shock waves, measuring turbulence intensity as function of cut-off angle and anisotropy 20 p2596 A73-38966

High-speed camera study of the shock wave propagation. 21 p2697 A73-39993

Studies of collisional preionization in large pinch vessels. 21 p2748 A73-40927

Cyclotron resonance in a weakly ionized hydrogen plasma with nitrogen, oxygen and air impurities 22 p2890 A73-41864

Electron concentrations calculated from the lower hybrid resonance noise band observed by Ogo 3. 22 p2901 A73-41912

Saha's equation under deviation from thermodynamic equilibrium. 22 p2915 A73-43040

On the determination of electron temperature in diffusion-dominated non-L.T.E. plasmas. 22 p2896 A73-43167

Motion of a plasma in curvilinear magnetic fields of constant and alternating curvature 23 p3010 A73-43661

Determination of the parameters of a fluctuating plasma from modulation of a microwave signal. 23 p3013 A73-44313

Intensity of charged particle recombination on the surface of certain borides of high-melting-point metals in a weakly ionized hydrogen plasma 24 p3098 A73-44418

Calculation of the Lyman-alpha asymmetry in a dense, partially-ionized hydrogen plasma. 24 p3116 A73-45323

HYDROGEN RECOMBINATIONS

Hydrogen recombination line and continuum observations at 5000 MHz of 13 southern HII regions. 03 p0372 A73-13347

Kinetics of the sulphur dioxide catalyzed recombination of radicals in hydrogen flames. 03 p3352 A73-13493

Recombination of H/+ and H/- ions in slow collisions. 07 p0852 A73-19146

Ionization, recombination, and population of excited levels in hydrogen plasmas. 11 p1407 A73-26584

Thermal dissociation and recombination of hydrogen according to the reversible reactions H2 + H to H + H + H. 16 p1977 A73-33674

Interstellar grain temperature fluctuations due to interstellar radiation field, discussing H atom recombination problem 23 p3029 A73-43747

Magnetic resonance spectrometer measurements of atomic hydrogen surface recombination. 24 p3113 A73-45425

HYDROGEN SULFIDE

Accurate relative acidities in the gas phase - Hydrogen sulfide and hydrogen cyanide. 02 p0139 A73-12634

Fracture mechanics consideration of hydrogen sulfide cracking in high strength steels. 04 p0459 A73-14692

HYDROGEN 2

U DEUTERIUM

HYDROGEN 3

U TRITIUM

HYDROGENATION

Hydrogenation as a means of utilization of industrial titanium scrap. 01 p0065 A73-10821

The reaction of a titanium alloy with hydrogen gas at low temperatures. 15 p1890 A73-31993

HYDROGENOLYSIS

Sterically controlled syntheses of optically active organic compounds. XVI - Temperature dependence of hydrogenolytic asymmetric transamination. 12 p1467 A73-27974

HYDROGEOLOGY

Applications of the ERTS-1 satellite in remote sensing of water resource data in Canada. 18 p2307 A73-36026

Geological analysis of aerial thermography of the Canary Islands, Spain. 20 p2561 A73-39896

HYDROGRAPHY

Experiments in the determination of turbulent layer thickness in monochromatic-type waves 13 p1655 A73-29160

HYDROKINETICS

U HYDROMECHANICS

HYDROLOGY

NT HYDROGEOLOGY

Satellite data and estimates of precipitation for hydrologic applications. 04 p0473 A73-15774

The determination of the evaporation from a class-A pan by means of empirical evaporation formulas 13 p1653 A73-28746

Solutions of boundary value problems of multilayer analogs of geoelectrics and hydrology. 15 p1872 A73-32040

Airborne and satellite remote sensing of Anacapa Island for hydrology and aquatic biology. 17 p2161 A73-34944

Applications of ERTS imagery to snow and glacier hydrology. 18 p2306 A73-36022

Hydrological phenomena teledetection based on multispectral band scanners for IR and visible frequency ranges 18 p2307 A73-36027

Use of continuous simulation models in application of remote sensing to hydrology. 18 p2292 A73-36840

The role of applications satellites in the management of the human environment. 19 p2424 A73-37713

Statistical uniformity of hydrological data from series of river drainage pattern observations 19 p2446 A73-38546

Expected results of hydrologic and geologic studies using ERTS imagery of the Atacama Desert, Altiplano, and Puna de Atacama, South America /Southwest Bolivia, Northwest Argentina, and Northern Chile/. 20 p2563 A73-39914

Assessment of applications of space-borne remote sensing to hydrology and water resources - An overview. 21 p2686 A73-40832

Engineering applications of geophysical phenomena covering earthquakes, volcanology, hydrology, glaciology and wind stress effects during severe storms 23 p2979 A73-44007

HYDROLYSIS

Russian book on titanium chemistry covering physicochemical and electrochemical properties, hydrolysis and production of metal-organic and complex titanium compounds

02 p0139 A73-11890

An anomalous reaction of aceto-4-/or 6-/ nitro-2,5-xyldides with hydrochloric acid.

03 p0273 A73-13900

Hydrolysis of a disiloxane/ester fluid in a simulated hydraulic system at 275 F.
[ASLE PREPRINT 72LC-6C-1]

03 p0335 A73-14365

Hydrolysis of aqueous extract of lunar dust samples for identification and quantitation of amino acid precursors in extraterrestrial sources, considering prebiotic evolutionary pathways termination

06 p0655 A73-18421

The non-equilibrium ortho/para spin state ratio for molecular H₂ formed in the hydrolysis of lithium aluminum hydride.

07 p0787 A73-19144

Transglucosidase activity of heart-muscle per-glucosylase

08 p0930 A73-21136

Hydrolytic reversion of elastomeric potting compounds.

13 p1646 A73-29274

Hydrolytic stability of electrical insulation materials.

17 p2197 A73-35348

Hydrolytic degradation of polymer electrical insulating materials in warm humid environments, noting relation to ester and ether linkage presence

17 p2197 A73-35349

Starch hydrolysis in man - An intraluminal process not requiring membrane digestion.

20 p2519 A73-39789

Microchemical urinalysis. IX - Determination of hydroxyproline in urine.

21 p2648 A73-41213

HYDROMAGNETIC FLOW

U MAGNETOHYDRODYNAMIC FLOW

HYDROMAGNETIC STABILITY

U MAGNETOHYDRODYNAMIC STABILITY

HYDROMAGNETIC WAVES

U MAGNETOHYDRODYNAMIC WAVES

HYDROMAGNETICS

U MAGNETOHYDRODYNAMICS

HYDROMAGNETISM

U MAGNETOHYDRODYNAMICS

HYDROMECHANICS

NT ELASTOHYDRODYNAMICS

NT ELECTROHYDRODYNAMICS

NT HYDRODYNAMICS

NT HYDROSTATICS

NT MAGNETOHYDRODYNAMICS

NT MAGNETOHYDROSTATICS

Autoscillations in the directional hydromechanical servocontrol with play in the reaction linkage

03 p0252 A73-13771

Airfoil profile determination in inverse hydromechanics problem for given flow velocity distribution, discussing univalent solvability conditions

06 p0686 A73-18067

Velocity hodograph solvability and univalence problems in hydromechanics for profiles in duct, bounded flow and cascades

15 p1861 A73-31151

HYDROMETEOROLOGY

Principal trends of investigations in the field of theoretical meteorology performed in Hungary

04 p0473 A73-15284

Prospects of developing an automated hydrometeorological system

10 p1203 A73-24375

Russian book - Scattering and attenuation of electromagnetic radiation by atmospheric particles.

15 p1843 A73-31586

Rational distribution of meteorological stations as a problem of operation studies

15 p1903 A73-31604

Computer experiments in selective distribution of hydrometeorological bibliographic information

15 p1904 A73-31611

The global distribution of the maximum 24-hour totals of precipitation

15 p1906 A73-32346

Hydrometeorological data processing and dissemination techniques and equipment, with emphasis on computerized regional centers and space-based systems

18 p2295 A73-35907

Problems associated with automation of the checking and processing of meteorological and climatological data

18 p2332 A73-35916

The investigation of the periodicity of hydrometeorological phenomena according to the autocorrelation method of Fuhrich

22 p2883 A73-42449

HYDRONIUM IONS

Recombination of electrons with positive ions of the H₃O⁺/H₂O/n series.

01 p0014 A73-10901

HYDROSPHERE [EARTH]

U EARTH HYDROSPHERE

HYDROSTATIC PRESSURE

Time characteristics of rupture and creep in metals during tension under hydrostatic pressure conditions

01 p0064 A73-10605

Initial postbuckling of circular rings under pressure loads.

01 p0115 A73-10744

Axisymmetric problem of the equilibrium of a cylindrical film under hydrostatic pressure

01 p0035 A73-11412

A method of analysing the effect of inertia and compressibility in an externally pressurized gas lubricated thrust bearing.

03 p0312 A73-13209

Algorithm for stress tensor and stability analysis of glass fiber reinforced plastic shells under hydrostatic pressure

03 p0392 A73-13741

New method of measuring rapidly varying pressures in the range below 500 atm

07 p0827 A73-20541

Mechanical behaviour of molybdenum and tantalum under high pressures at elevated temperatures.

09 p1105 A73-23018

Martian spin axis wandering resulting from equatorial volcanic convections and gravity field non-hydrostatic low order components

09 p1151 A73-23172

Thick walled multilayer wideband radomes for supporting high hydrostatic pressures and protecting weakly directional submarine antennas with circular polarization

11 p1336 A73-25305

Buckling analysis of elastically constrained conical shells under hydrostatic pressure by the collocation method.

11 p1438 A73-25499

Study of plasticity laws of polycrystalline metals at elevated temperatures - Specifically the influence of hydrostatic stress on creep.

13 p1641 A73-29506

The influence of back pressure on the point of instability of axisymmetric shells deformed by fluid pressure.

14 p1813 A73-30662

On the influence of inertia forces in hydrostatic turbulent lubrication.

14 p1755 A73-30705

Utilization of hydrostatic compression at high pressures as a means of improving the properties of acoustic nickel ferrite

14 p1765 A73-30890

Temperature dependence of the electrical resistance of superconducting Ti-Nb and Ti-Nb-Zr alloys subjected to working by hydrostatic pressure

15 p1887 A73-31186

Buckling analysis of elastically constrained stiffened conical shells under hydrostatic pressure by the collocation method.

15 p1948 A73-31642

Assembly for optical studies of semiconductors under pressures up to 10 kbar at 77 K

17 p2145 A73-34175

A reliable Teflon cell with many electrical leads for pressures up to 40 kilobars.

17 p2175 A73-35761

The effect of hydrostatic pressure environment on the low cycle fatigue properties of a maraging steel.

[ASME PAPER 73-MAT-K] 18 p2323 A73-36616

Application of the hydrostatic extrusion process toward production of 3Al-2.5V titanium alloy hydraulic tubing.

[SAE SP-378] 19 p2434 A73-37873

Single axis analog flueric accelerometer using mercury as solid proof mass, describing differential gas pressure outputs, porous cylindrical configuration and hydrostatic pressure gradients

19 p2389 A73-38076

Effect of high pressure on the superconducting transition temperature of Pd-H.

21 p2753 A73-41126

Unified plastic yield criterion for ductile solids.

22 p2923 A73-42555

Buckling of toroidal shells under hydrostatic pressure.

22 p2923 A73-42560

Mechanism of ordered dislocation structure formation in metals deformed under high hydrostatic pressure

23 p2993 A73-44043

Influence of high hydrostatic pressure on the flow stress of 18-8 stainless steel.

23 p2994 A73-44161

Experimental evaluation of the load capacity of smooth fiberglass-reinforced plastic shells under external hydrostatic pressure

23 p2998 A73-44191

HYDROSTATICS

NT MAGNETOHYDROSTATICS

Evaluation of a two-pocket hydrostatic journal bearing suitable for use over a wide range of temperature.

03 p0311 A73-13204

The performance of a four-pocket conical hydrostatic bearing.

03 p0311 A73-13206

Hydrostatic journal bearings design review covering pad coefficients, flow control, optimization, dynamic behavior, thermal effects, turbulence and tolerances

03 p0311 A73-13207

Static and dynamic behavior of spherical hydrostatic bearings - Theory and experiments.

[ASME PAPER 72-LUB-35] 03 p0315 A73-14344

A hero-jet driven porous spherical hydrostatic gas bearing gyro.

[ASME PAPER 72-LUB-41] 03 p0315 A73-14348

Hydrostatic equilibrium conditions for hydromagnetic field, discussing topology of wrapping pattern of lines of force

14 p1782 A73-30741

The lower atmosphere in hydrostatically stable conditions.

19 p2449 A73-38245

Permissible hydrodynamic and hydrostatic stellar atmosphere models described by system of equations dependent on initial level conditions

21 p2767 A73-40532

HYDROTHERMAL CRYSTAL GROWTH

Organic inclusions within hydrothermal minerals from S.W. Africa and elsewhere.

11 p1352 A73-25472

HYDROX ENGINES

U HYDROGEN OXYGEN ENGINES

HYDROXIDES

NT SODIUM HYDROXIDES

German monograph - The tribology of solid lubricants of the type of the alkaline-earth hydroxides in the system Fe-Me/OH/2.

22 p2881 A73-42846

HYDROXYCORTICOSTEROID

NT CORTISONE

Microchemical urinalysis. VIII - Determination of urinary 17-hydroxycorticosteroids.

11 p1324 A73-25138

Effects of the hypodynamics and other factors of a spaceflight on the excretion of 17-oxycorticosteroids and aldosterone

17 p2111 A73-34233

HYDROXYL COMPOUNDS

NT ALCOHOLS

NT ETHYL ALCOHOL

NT METHYL ALCOHOLS

NT POLYVINYL ALCOHOL

Rate constants for the reactions of hydroxyl and hydroperoxyl radicals with ozone.

14 p1724 A73-30619

Influence of certain hydroxyl- and nitrogen-containing low-molecular-weight substances on the structural viscosity of cellulose acetate solutions

21 p2647 A73-40263

Some reactions and hydroperoxyl and hydroxyl radicals at high temperatures.

22 p2898 A73-42754

HYDROXYL EMISSION

An upper limit on the OH abundance in the intercloud medium.

01 p0096 A73-10314

Physical conditions in interstellar hydroxyl and formaldehyde clouds.

01 p0100 A73-10790

A vertical profile of OH in the mesosphere.

01 p0041 A73-10883

Space maser with feedback

01 p0060 A73-10934

Infrared stars with strong 1665/1667-MHz OH microwave emission.

01 p0104 A73-11040

Radiant flux densities of Cygnus X-3, observing OH and formaldehyde absorption

02 p0210 A73-11560

Search for OH-IR stars with emission concentrated in main lines, considering water vapor line emission or absorption band in near IR

02 p0222 A73-12717

Gas-temperature measurement in pulsed H₂O laser discharges.

[AD-755012] 02 p0178 A73-12814

Interstellar OH lambda doublet radiation observations at 5 cm from six galactic sources and IR star, observing various transitions

03 p0366 A73-12930

Hydrogen recombination line and continuum observations at 5000 MHz of 13 southern HII regions.

03 p0372 A73-13347

Correcting the OH contribution in emission line measurements in the night airglow filter photometry.

04 p0440 A73-14969

Protoplanet cloud model for cosmic OH and water masers in H II regions to account for anomalous hydrogen deficiency, discussing pumping mechanisms and chemical composition

04 p0497 A73-14974

Possible cause of the variations of the intensity of an interstellar maser.

04 p0493 A73-16023

Direct measurement of the lifetimes and predissociation probabilities for rotational levels of the OH and OD A-2Sigma+ states. 05 p0601 A73-17341

Class I OH emission sources structure and variability, considering variable gain maser models. 06 p0751 A73-18227

Atomic hydrogen concentrations in the mesosphere and the hydroxyl emissions. 07 p0815 A73-19257

H I absorption in the galactic center region and between galactic longitudes 350 deg and 359 deg. 09 p1141 A73-22009

Galactic interstellar molecules, discussing physical, chemical and spectral characteristics, hydroxyl emission, occurrence regions, hydrogen clouds, isotope ratios, interstellar masers and probes. 09 p1146 A73-22446

Cosmic maser generator model with resonance scattering feedback for galactic clouds OH molecule radio emission. 09 p1147 A73-22729

Analytic approximation for the saturation behavior of OH emission regions. 10 p1272 A73-23542

Probabilities of infrared and RF transitions in OH and CH molecules. 10 p1250 A73-23710

Restrictions on the intensity of cosmic masers and the possibility of detecting new OH and H₂O sources in a rapid sky survey. 10 p1275 A73-23725

Balloon-borne spectroscopic observation of the infrared hydroxyl airglow. 11 p1350 A73-25061

Rotational and vibrational hydroxyl excitation in the laboratory and in the night airglow. 11 p1354 A73-25761

An interference filter radiometer with cooled optics and a cooled PbS detector for rocket application. 11 p1368 A73-26507

High angular resolution photography of complex OH airglow structures in IR night sky. 11 p1358 A73-26666

German monograph - Determination of the OH-concentration distribution in a axisymmetric methane/oxygen flame. 13 p1708 A73-29279

Hydroxyl emission intensity and rotational and vibrational temperatures, discussing statistical properties of geomagnetic storm effects and diurnal, seasonal and latitudinal variations. 15 p1867 A73-31260

A balloon study of the OH airglow emission from evening twilight to sunrise. 15 p1867 A73-31311

Concentration of OH and NO in Y93-GE-3 engine exhausts measured in situ by narrow-line UV absorption. 16 p2045 A73-33546

[AIAA PAPER 73-506] OH emission band, studying effect of adiabatic infrasonic oscillations on upper atmospheric temperature and intensity. 16 p2008 A73-33883

Compact radio source associated with the OH source ON-1/OH69.5-1.0/. 16 p2071 A73-34037

New rate measurements on the reaction of O(3P), O(3), and OH. 16 p1977 A73-34045

[AIAA PAPER 73-501] Diurnal, annual and solar cycle variations of hydroxyl and sodium nightglow intensities in the Europe-Africa sector. 17 p2160 A73-34785

Infrared and radio transition probabilities of OH and CH. 18 p2338 A73-36735

Constraints on cosmic maser intensity, and the possibility of detecting new OH and H₂O radio sources by a rapid sky survey. 18 p2355 A73-36750

Hydroxyl emission band high resolution spectra in airglow, examining doublet state ratio and rotational temperatures, vibration-rotation levels, temperature sensitivity and Boltzmann equilibrium. 20 p2551 A73-38946

OH observations of sixteen interstellar dust clouds. 20 p2607 A73-39118

18-cm OH absorption of W 49 A and W 49 B. 20 p2610 A73-39575

H II region OH maser source pumping by far IR radiation-induced population inversions between Lambda doublet levels. 21 p2759 A73-40712

Relation between ion creation and C₂, CH, and OH formation in the combustion of hydrocarbons. 22 p2819 A73-42771

Airglow hydroxyl emission IR spectral bands intensity measurements with allowance for atmospheric extinction, deriving vibrational level excitation rates from spontaneous emission transition probabilities. 23 p2972 A73-43690

Ozone and airglow in the mesosphere region. 23 p2976 A73-43886

OH radical concentration in the stratosphere. 23 p2976 A73-43895

Distribution of interstellar hydroxyl in the Cyg X region. 23 p3035 A73-44231

Bandpass filter IR observations of hydroxyl airglow, mapping mean nightly level spatial and temporal fluctuations in brightness. 24 p3087 A73-45208

Nature of the peculiar emission object V1016 Cygni. 24 p3143 A73-45490

HYGIENE

Soaps, detergents and surfactants dermatological hazards in personal hygiene use by spacecrews during long term space flight/Skylab/[ASME PAPER 73-ENAS-26] 19 p2400 A73-37981

HYGROMETERS

High altitude aircraft water vapor measurements using aluminum oxide hygrometer, noting comparison with remote sounders [AIAA PAPER 73-511] 16 p2006 A73-33549

Low-inertia ultraviolet hygrometer. 21 p2701 A73-40744

HYGROSCOPICITY

Moisture absorption characteristics of solid lubricant coatings. 10 p1239 A73-24247

Growth rate calculation for hygroscopic condensation nuclei in the presence and absence of a monolayer of a surface-active substance. 13 p1654 A73-28880

Study of the conditions defining the passivating action of surface-active substances on hygroscopic condensation nuclei. 18 p2332 A73-35918

HYOSCINE

Effect of some pharmacological preparations on the fall-out nystagmus and Bechterew nystagmus. 08 p0929 A73-20982

HYPERBARIC CHAMBERS

Cat and rat lung damage due to hyperbaric oxygen exposure and head injury, discussing alveolar surfactants, sympathetic stimulation and monkey injuries [AD-759298] 13 p1576 A73-28507

Influence of increased air atmosphere pressure on the excitability of the neuro-motor apparatus in man. 14 p1719 A73-30845

Exercise during hyperoxia and hyperbaric oxygenation. 19 p2396 A73-38160

Intracellular measurements in a closed hyperbaric chamber. 24 p3065 A73-45072

HYPERBOLIC DIFFERENTIAL EQUATIONS

An explicit second order method of characteristics for the initial value problem in the case of quasi-linear hyperbolic differential-equations systems of the first order with two independent variables. 15 p1899 A73-31361

Russian book on inverse problems for hyperbolic differential equations covering functionals, uniqueness theorems, integral geometry and earth interior structure from seismological data. 15 p1899 A73-31581

The Dirichlet boundary and initial value problem for hyperbolic differential equations. 15 p1901 A73-32369

On the construction of accurate difference schemes for hyperbolic partial differential equations. 23 p3000 A73-43208

Technically oriented algorithms for unsteady pipe flow. 23 p2968 A73-43800

Monofrequent oscillations in mechanical systems governed by second order hyperbolic differential equations with small non-linearities. 23 p3044 A73-44077

The entropy rate admissibility criterion for solutions of hyperbolic conservation laws. 23 p3000 A73-44203

Solution of the Riemann problem for a class of hyperbolic systems of conservation laws by the viscosity method. 24 p3112 A73-45469

HYPERBOLIC FUNCTIONS

Some numerical experiments with Dafermos's method for nonlinear hyperbolic equations. 01 p0069 A73-10071

Variational optimization problems for hyperbolic-type equations. 01 p0077 A73-10952

Analog-analytic construction of supercritical flows past profiles [DGLR PAPER 72-129] 03 p0248 A73-14384

On the semi-discrete Galerkin method for hyperbolic problems and its application to problems in elastodynamics. 04 p0471 A73-15222

Hyperbolic equations and systems with multiple characteristics. 04 p0471 A73-15224

Boundary techniques for the multistep formulation of the optimized Lax-Wendroff method for non-linear hyperbolic systems in two space dimensions. 04 p0471 A73-15227

A method of perturbation for a weakly nonlinear hyperbolic equation with two small parameters - Study of a mathematical model. 04 p0471 A73-15246

Estimate of the time of occurrence of discontinuities in the solution of a boundary value problem for a second order quasilinear hyperbolic system. 07 p0844 A73-19023

Elastic waves induced fluctuating stresses in turbulent parallel mean flow, deriving hyperbolic relations consistent with Taylor frozen field hypothesis. 07 p0810 A73-19109

Existence of optimal controls for processes described by a system of hyperbolic equations. 18 p2331 A73-36986

HYPERBOLIC NAVIGATION

NT DECCA NAVIGATION

NT LORAN

NT LORAN C

Application of ultrastable oscillators to aerospace [ONERA, TP NO. 1114] 01 p0045 A73-10235

Circular, hyperbolic, hybrid and angular measurement procedures of satellite navigation, describing Transit system. 10 p1246 A73-23660

HYPERBOLIC REENTRY

Analytical estimate of the landing range of a spacecraft for hyperbolic return-flight paths. 05 p0627 A73-16078

Investigation of the range interval of the landing phase for hyperbolic velocities of re-entry into the earth's atmosphere. 05 p0627 A73-16079

Impulsive deboost analysis for maximum and minimum atmospheric entry angles for hyperbolically orbiting rocket vehicles. 07 p0875 A73-19207

Ablation and radiation coupled viscous hypersonic shock layers. 18 p2264 A73-36315

HYPERBOLIC SYSTEMS

A second-order accurate difference method for systems of hyperbolic partial differential equations. 04 p0470 A73-15007

Stress analysis of hyperbolic paraboloid membrane shells for applications in architecture. 06 p0757 A73-17395

A unified boundary controllability theory for hyperbolic and parabolic distributed parameter systems. 07 p0846 A73-20591

Periodic method of characteristics for solution of hyperbolic partial differential equations of physical system specified by two boundary conditions at single spatial location. 10 p1241 A73-23604

A note on the stability of an iterative finite-difference method for hyperbolic systems. 10 p1241 A73-23639

A boundary value problem for higher-order hyperbolic equations. 12 p1516 A73-26961

Variational optimization problems for equations of hyperbolic type. 12 p1518 A73-27528

Construction of doubly branched fundamental solutions of the Cauchy problem for homogeneous rotationally invariant hyperbolic operators with constant coefficients. 12 p1518 A73-27817

Global solutions to a class of nonlinear hyperbolic systems of equations. 13 p1647 A73-28024

Quasi-conformal mapping theory of two- and multidimensional regions, considering superposition, hyperbolic and mixed systems and Chebyshev problem. 13 p1647 A73-28339

Improperly posed initial value problems for self-adjoint hyperbolic and elliptic equations. 13 p1648 A73-28424

Minimum-energy terminal state control of first order linear hyperbolic systems in one spatial variable using the method of characteristics. 14 p1769 A73-30453

Hyperbolic equation initial-boundary problem in finite cylinder solved via elliptic boundary problem with parameter. 14 p1770 A73-30545

Investigation of a weakly generalized solution to the mixed self-conjugate problem of a class of quasi-linear second-order hyperbolic systems with a nonlinear right-hand operator member. 14 p1771 A73-30791

Convergence, accuracy and stability of finite element approximations of a class of non-linear hyperbolic equations. 15 p1899 A73-32030

Spectral resolution of differential operators associated with symmetric hyperbolic systems. 15 p1901 A73-32373

Russian book - Linear and nonlinear boundary value problems. 17 p2201 A73-34640

Boundary value problems with a normal derivative for a mixed-type equation with discontinuous coefficients

17 p2203 A73-35584

An integration algorithm for hyperbolic systems having non-zero, non-analytic steady-state solutions.

17 p2203 A73-35610

The effect of nonlinear transformations on the computation of weak solutions.

18 p2330 A73-36610

Discontinuous solutions of hyperbolic optimum problems

20 p2581 A73-38675

Book - Hyperbolic systems of conservation laws and the mathematical theory of shock waves.

20 p2581 A73-39140

Book on oscillation theory covering classical, abstract and complex theories, nonselfadjoint differential equations, hyperbolic and elliptic equations, Sturm-Picone theorem, etc

20 p2582 A73-39141

A method of solving a slightly disturbed mixed problem for a hyperbolic equation with a small delay of the argument

22 p2881 A73-42277

Higher order accuracy finite difference algorithms for quasi-linear, conservation law hyperbolic systems.

22 p2882 A73-42518

HYPERBOLIC TRAJECTORIES

Analytical expressions for postmaneuver velocity and transfer impulse optimizing elliptic-to-hyperbolic orbital transfer

02 p0219 A73-12453

Complex variable analysis for exact solution to Kepler equation for elliptical and hyperbolic orbits based on canonical solutions to Riemann problem

03 p0376 A73-14269

The transition from elliptic to hyperbolic orbits in the two-body problem by slow loss of mass.

03 p0377 A73-14273

Interplanetary spacecraft transfer maneuver for hyperbolic trajectory change into eccentric orbit, using aerodynamic drag to obtain nearly circular orbit

03 p0379 A73-14571

Dynamic analysis of tidal effects arising from hyperbolic close encounters of massive body past galaxy, calculating matter velocity field and galactic structure distortion

08 p1004 A73-20907

On the motion of short-period comets in the neighbourhood of Jupiter.

14 p1790 A73-29786

Comet motion and hyperbolic orbital statistics, discussing secular accelerations, decelerations and nongravitational effects

14 p1794 A73-29830

Analytical expressions for postmaneuver velocity and transfer impulse optimizing elliptic-to-hyperbolic orbital transfer

15 p1941 A73-32603

HYPERCAPNIA

The role of the carotid chemoreceptors in the CO₂-hyperpnea under hyperoxia.

01 p0010 A73-11502

Augmentation of chemosensitivity during mild exercise in normal man.

05 p0540 A73-16610

Effect of hypercapnia on the electrical discharges of the bulbar respiratory neurons and motor neuron ganglia of respiratory muscles

05 p0541 A73-16735

The effects of hypoxia, hypercapnia, and asphyxia on the baroreceptor-cardiac reflex at rest and during exercise in man.

06 p0654 A73-18348

Influence of an oxygen and carbon dioxide rich gas mixture on the human orthostatic stability

08 p0933 A73-20988

Mathematical analysis of the responses of the human respiratory system to hypoxia and hypercapnia

08 p0931 A73-21322

Quantitative influence of CO₂ inhalation on thermal sweating in man.

11 p1314 A73-25331

Method of PaCO₂ determination in men with functional disorders of external respiration

13 p1579 A73-29075

Ventilatory responses to transient hypoxia and hypercapnia in man.

15 p1832 A73-31126

Plasma electrolytes, pH, and ECG during and after exhaustive exercise.

15 p1834 A73-31347

Correlation of ventilatory responses to hypoxia and hypercapnia.

20 p2514 A73-39776

Ventilatory and hemodynamic responses to acute hypoxia and hypercapnia in Hereford calf, comparing with man

20 p2515 A73-39782

HYPERFINE STRUCTURE

Stellar spectroscopy with holographic gratings.

01 p0047 A73-10520

A search for the solar Sr-87 content and the solar Rb/Sr ratio.

05 p0620 A73-17027

Temperature-dependent hyperfine interactions in Fe2B.

06 p0734 A73-17833

327-MHz observations of the galactic center - Possible detection of a deuterium absorption line.

08 p1013 A73-21808

E resonance line broadening due to superhyperfine interactions in ruby, noting angular dependence of mosaic structure mechanism

09 p1132 A73-21954

Solar Mn abundance derivation based on center-limb absorption line profiles, taking into account hyperfine structure broadening

10 p1278 A73-24130

Some aspects of the exchange-interaction and dipole-dipole broadening of the individual hyperfine components of the EPR spectrum

14 p1775 A73-30580

Observations of formamide at 6 cm in Sagittarius B2.

15 p1933 A73-31377

High-resolution magnetic hyperfine resonance in harmonically bound ground-state Hg-199 ions.

16 p2038 A73-32850

Stability, reproducibility, and absolute wavelength of a 633-nm He-Ne laser stabilized to an iodine hyperfine component.

17 p2185 A73-35424

Change in the hyperfine state of the hydrogen atom during its collisions with unsaturated hydrocarbon molecules in the gaseous state.

22 p2889 A73-41719

Comment on 'Anomalous hyperfine lines in formaldehyde in a dust cloud.'

22 p2904 A73-41755

Hyperfine structure of furan.

22 p2818 A73-42712

Nitrogen quadrupole coupling constants in cis-propyleneimine.

23 p2950 A73-43272

HYPERGEOMETRIC FUNCTIONS

Applications of Jacobi polynomials to non-linear differential equation associated with generalized hypergeometric function.

06 p0716 A73-17791

Symmetries of differential equations - The hypergeometric and Euler-Darboux equations.

13 p1648 A73-28538

Radiating near-field power density and directivity reduction of tapered circular apertures.

22 p2829 A73-43181

HYPERGEOMETRY

U HYPERSPACES

HYPERGOLIC ROCKET PROPELLANTS

Hypergol rocket engines restart difficulties investigation via cold flow and hot firing tests, simulating worst case environmental conditions

[AIAA PAPER 72-1160] 03 p0357 A73-13461

HYPEROXIA

Studies of blood gas analysis at abnormal environment.

01 p0013 A73-11210

The role of the vagus nerves in the respiratory response to CO₂ under hyperoxic conditions.

01 p0010 A73-11501

The role of the carotid chemoreceptors in the CO₂-hyperpnea under hyperoxia.

01 p0010 A73-11502

Effect of sleep-wake reversal and sleep deprivation on the circadian rhythm of oxygen toxicity seizure susceptibility.

02 p0135 A73-12561

CNS epinephrine tone, a possible etiology for the threshold in susceptibility to oxygen toxicity seizures.

03 p0263 A73-14156

Effect of a 30-day stay in a medium with increased oxygen content on the discharge of some gaseous bioactivity products in rats

06 p0650 A73-17676

Sensitivity to oxygen at high pressure of radioreistant and radiosensitive strains of bacteria.

07 p0780 A73-19483

Influence of an oxygen and carbon dioxide rich gas mixture on the human orthostatic stability

08 p0933 A73-20988

Effects of an hyperoxic hypobaric environment on renin-aldosterone in normal man.

08 p0934 A73-21503

Sensitivity of the brain to repeated exposures of hyperbaric oxygen.

11 p1314 A73-25328

Results of electron microscopic studies in the rat brain under oxygen at high pressure.

11 p1314 A73-25330

Effect of antioxidants on the blood deoxygenation rate in animals exposed to altered atmospheres

12 p1465 A73-27702

Effect of lithium on acute oxygen toxicity and associated changes in brain gamma-aminobutyric acid.

13 p1575 A73-28503

Procedure for preparing an oxygen-nitrogen gas mixture for respiration in a pressure chamber

13 p1580 A73-29409

Human hematologic responses to 4 hr of isobaric hyperoxic exposure /100% oxygen at 760 mm Hg/.

14 p1714 A73-29751

Development and reversibility of pulmonary oxygen poisoning in the rat.

14 p1718 A73-30516

Physiological criteria of early toxic normobaric hyperoxia manifestations

17 p2110 A73-34123

Protein synthesis in lung - Recovery from exposure to hyperoxia.

18 p2277 A73-36653

Exercise during hyperoxia and hyperbaric oxygenation.

19 p2396 A73-38160

Oxygen uptake during maximal work at lowered and raised ambient air pressures.

21 p2638 A73-41132

HYPERPLANES

Matrix transformation in hyperplanes method for successive solution of boundary value problems of multidimensional differential equations, using space-time functions

06 p0715 A73-17718

First derivative discontinuities of space-time metric tensor in Einstein equations solution for nonisotropic and isotropic hypersurfaces, proving coordinate system existence for continuity

14 p1774 A73-30328

A constraining hyperplane technique for state variable constrained optimal control techniques.

19 p2413 A73-38036

HYPERPNEA

The role of the carotid chemoreceptors in the CO₂-hyperpnea under hyperoxia.

01 p0010 A73-11502

Control of exercise hyperpnea under varying durations of exposure to moderate hypoxia.

03 p0259 A73-13499

HYPERSONIC AIRCRAFT

NT HYPERSONIC GLIDERS

Nongray atmospheric model to assess radiative effects of water vapor and carbon dioxide layer injected into lower stratosphere by SST and HST exhaust gases

01 p0038 A73-10388

Performance and stability of hypervelocity aircraft flying on a minor circle.

05 p0534 A73-16179

Some structure synthesis problems for systems controlling the three-dimensional motion of orbital-aircraft in the earth's atmosphere

05 p0594 A73-16418

Choices for the future - An industry viewpoint on prototyping.

[SAE PAPER 720848] 05 p0534 A73-16659

Air breathing hypersonic aircraft technology developments in propulsion systems and structures with emphasis on use of hydrogen fuel

[AIAA PAPER 73-58] 06 p0647 A73-17631

Potentials and problems of hydrogen fueled supersonic and hypersonic aircraft.

09 p1032 A73-22830

Mixing controlled supersonic combustion for air breathing engine equipped hypersonic aircraft, discussing chemical and fluid dynamic interaction effects

10 p1295 A73-23862

Hypersonic transports - Economics and environmental effects.

17 p2099 A73-34435

HYPERSONIC BOUNDARY LAYER

Boundary layer transition on cones in hypersonic He wind tunnel tests, obtaining turbulent spot geometry and propagation velocity by spark schlieren photography

01 p0003 A73-10762

Hypersonic turbulent boundary layer flow parameters and heat transfer during blowing of coolant air and He through slot

03 p0242 A73-13186

Turbulent properties of a compressible boundary layer.

03 p0296 A73-14177

Plateau pressure in hypersonic turbulent boundary-layer interactions.

03 p0296 A73-14200

Effects of a fully catalytic wall on a non-equilibrium boundary layer including ablation products.

[ASME PAPER 72-WA/HT-28] 04 p0519 A73-15826

Initial conditions for the hypersonic shock/boundary layer interaction problem.

[AIAA PAPER 73-201] 05 p0532 A73-16935

Measurements in a transitional/turbulent Mach 10 boundary layer at high-Reynolds numbers.

[AIAA PAPER 73-165] 06 p0645 A73-17649

The influence of the accommodation coefficients on the flow variables in the viscous interaction region of a hypersonic slip-flow boundary layer.

[DFVLR-SONDDR-267] 07 p0773 A73-19206

An extension of the vector potential concept to the case of a three-dimensional unsteady boundary layer. 07 p0776 A73-20287

Hot-wire anemometer probe operation in constant current in continuous high-temperature hypersonic turbulent boundary layer, computing velocity and temperature fluctuations 10 p1205 A73-24254

Viscous flow over a cone at moderate incidence. I - Hypersonic tip region. 11 p1300 A73-25114

Ion and electron distributions in the boundary layer of hypersonic vehicles. 11 p1404 A73-25290

Initial conditions for the hypersonic-shock/boundary-layer interaction problem. 11 p1303 A73-26384

Calculation of transitional boundary-layer flows. 11 p1348 A73-26394

Effects of upstream wall temperatures on hypersonic tunnel wall boundary-layer profile measurements. 11 p1344 A73-26395

Effect of surface catalytic activity on stagnation heat-transfer rates. 13 p1706 A73-28804

Entropy layer effects in constant pressure hypersonic boundary layers. 13 p1564 A73-28812

Three-dimensional hypersonic transitional/turbulent mean flow profiles. [AIAA PAPER 73-635] 18 p2260 A73-36194

Computation of hypersonic turbulent boundary layers with heat transfer. [AIAA PAPER 73-699] 18 p2263 A73-36248

Continuum thick sheath probe studies in hypersonic ionized boundary layers. 19 p2375 A73-37164

Recent progress in boundary layer research. [AIAA PAPER 73-780] 19 p2419 A73-37451

Heat transfer from a hypersonic turbulent boundary layer on a flat plate. 23 p3049 A73-43933

Surface pressure fluctuations in hypersonic turbulent boundary layers. [AIAA PAPER 73-997] 24 p3053 A73-44832

HYPERSONIC COMBUSTION

Hydrocarbon fuels diffusion flame ignition characteristics in hypersonic ramjet engines, testing additives effect for thermal self-ignition improvement 03 p0398 A73-14132

HYPERSONIC FLIGHT

Experimental investigation of hypersonic buzz on a high cross-range shuttle configuration. [AIAA PAPER 73-157] 05 p0531 A73-16904

A rocket system for hypersonic, high Reynolds number aerothermodynamic research. [AIAA PAPER 73-304] 09 p1156 A73-23223

Compact gas transpiration cooling system for thermal protection of hypersonic flight leading edges, discussing computer program 11 p1452 A73-26212

Calorimeter measurement of heat transfer at hypersonic conditions. [AIAA PAPER 73-760] 18 p2264 A73-36375

Computation of the nonlinear dynamic stability functions of a reentry body in hypersonic flight 18 p2361 A73-37081

Study of turbulent wakes behind cones in hypersonic flight using Schlieren photograph correlation 21 p2696 A73-39985

Correlation of hypersonic zero-lift drag data. 22 p2797 A73-42635

HYPERSONIC FLOW

Three-dimensional effects on electron density in a blunt body laminar boundary layer. 01 p0002 A73-10731

Shear layer extent caused by slip surface in inviscid flow with shock interactions, noting viscous effect in hypersonic flow 01 p0033 A73-10747

Cryoprobe with truncated circular cross sectioned Cu cone with copper slug heat sink for momentum flow rate measurement in hypersonic low density flow 01 p0003 A73-10755

Aerodynamics of blunt bodies in hypersonic stream at the angle of attack. 01 p0003 A73-11133

Least-squares solution for the blunt body hypersonic flow problem. 01 p0004 A73-11473

Hypersonic spherical source flow expansion into rarefied atmosphere of same gas, using kinetic model and asymptotic solution of Boltzmann equation 02 p0154 A73-12054

Hypersonic and supersonic flow over caret wings at off-design conditions with attached bow shock at leading edges 02 p0128 A73-12502

Far field steady inviscid flow behavior of hypersonic blunt axisymmetric slender body, obtaining unsteady two dimensional solution with cylindrical symmetry 03 p0242 A73-13310

Radiative and convective heat transfer occurring in the hypersonic flow past a blunt body 03 p0244 A73-13617

Lee-side vortices on delta wings at hypersonic speeds. 03 p0247 A73-14180

A new algorithm for three-dimensional method of characteristics. 03 p0337 A73-14201

Calculus of variations for functional conditional extremum, determining minimum drag shape for body of revolution in hypersonic flow 04 p0403 A73-14886

Hypersonic rarefied flow past an insulated flat plate with suction/injection. 04 p0520 A73-15939

Viscous shock layer flow in the windward plane of cones at angle of attack. [AIAA PAPER 73-134] 05 p0530 A73-16886

Measured axial and normal force coefficients for 9-deg cones in rarefied, hypersonic flow. [AIAA PAPER 73-154] 05 p0531 A73-16902

Numerical computation of the hypersonic rarefied flow near the sharp leading edge of a flat plate. [AIAA PAPER 73-200] 05 p0531 A73-16934

Numerical solution of viscous reacting blunt body flows of a multicomponent mixture. [AIAA PAPER 73-202] 05 p0532 A73-16936

A study of fin-induced laminar interactions on sharp and spherically blunt cones. [AIAA PAPER 73-235] 05 p0532 A73-16960

Transformation of the hypersonic compressible Navier-Stokes equations. 05 p0567 A73-17120

Experimental investigation of hypersonic helium flow around sharp and blunt cones in the presence of strong injection 06 p0643 A73-17466

Use of approximations of thermodynamic functions in gasdynamics calculations 06 p0644 A73-17470

A study of the rarefaction of the interaction between an exhaust plume and a hypersonic external flow. [AIAA PAPER 73-199] 06 p0645 A73-17657

Heat transfer from hypersonic turbulent flow at a wedge compression corner. 06 p0646 A73-18531

Hypersonic flows in large-scale inlet models. 07 p0773 A73-19189

Experimental and numerical studies of flush electrostatic probes in hypersonic ionized flows. II - Theory. 07 p0858 A73-19961

Multiple-orifice liquid injection into hypersonic air streams. 07 p0775 A73-19976

Detachment of the outer shock from underexpanded rocket plumes. 07 p0920 A73-19977

Oblique shock-sound interaction at a freestream Mach number of about 20 in helium. 07 p0775 A73-19984

Rotational temperature measurements in nitrogen at hypersonic flow using an electron beam technique [ONERA, TP NO. 1206] 07 p0853 A73-20605

Locally similar solutions of equations of a turbulent boundary layer on a circular cone 08 p0925 A73-20646

Self-similar hypersonic flows of an inviscid gas 08 p0927 A73-21545

Mass spectroscopic investigation of dissociation and ionization in a simulated re-entry plasma. 09 p1130 A73-22843

Laminar boundary layer on a cone near a plane of symmetry. 09 p1029 A73-23442

Numerical analysis of the viscous, hypersonic, MHD blunt-body problem. 09 p1132 A73-23455

Radiant heat flux distribution on the surface of a sphere in hypersonic flow of an inviscid radiating gas 10 p1171 A73-23581

Dynamic viscous pressure interaction on a cone. 10 p1173 A73-24821

Aerodynamical and acromechanical investigations involving pin-equipped models in hypersonic flow 11 p1300 A73-25441

Asymptotic solution of shock-layer equations in the vicinity of the stagnation point of a sphere in the case of strong blowing 11 p1304 A73-26442

Diffusion of a hypersonic flow by a supersonic gas jet in the case of a free-molecular mode of interaction 11 p1304 A73-26446

A method for the calculation of the aerodynamic coefficients of a body of any form. 12 p1457 A73-27067

An analytical solution to the problem of hypersonic gas flow past a slender wing 12 p1457 A73-27078

The thin shock layer in the hypersonic flow problem 15 p1821 A73-31194

Three-dimensional motion of a reacting gas mixture around a blunt body 15 p1822 A73-31290

Linear problem for delta and V-shaped wings 15 p1823 A73-31301

Unsteady shock wave interaction with plane hypersonic flow about a blunt body investigated by second order difference method 15 p1862 A73-31326

Ion current at the forward stagnation region of an electrically conducting body. 15 p1918 A73-31669

Method for the interpretation of surface pressure measurements under rarefied hypersonic conditions. 16 p1963 A73-33316

Applications of a ray reflection model in the problem of highly rarefied gas flow past bodies. 17 p2094 A73-34549

Supersonic and hypersonic two-dimensional laminar flow over a compression corner. 17 p2096 A73-35134

Mean flow and turbulence measurements in a Mach 5 shear layer. 17 p2097 A73-35506

Velocity distribution in hypersonic helium flow near the leading edge of a flat plate. [AIAA PAPER 73-691] 18 p2262 A73-36242

Effect of adverse pressure gradient on film cooling effectiveness. [AIAA PAPER 73-697] 18 p2368 A73-36246

Ablation and radiation coupled viscous hypersonic shock layers. 18 p2264 A73-36315

Convective heating in dust-laden hypersonic flows. [AIAA PAPER 73-761] 18 p2371 A73-36376

Three-dimensional nosetip shape changes in hypersonic flow. I - Illustration of a mathematical model-characteristic method. [AIAA PAPER 73-762] 18 p2264 A73-36377

Mass transfer effects on turbulent heating in the vicinity of slots. [AIAA PAPER 73-766] 18 p2371 A73-36381

Monatomic and diatomic gas supersonic flow field calculation for sharp leading edge by BGK and ordinate models 18 p2265 A73-36631

Gas expelled from a strongly underexpanded nozzle upstream into a hypersonic flow 18 p2265 A73-37010

Supersonic-hypersonic motion past a permeable cone at zero angle of attack 19 p2376 A73-37544

Hypersonic polytropic transformations of an ideal fluid. II 19 p2420 A73-37645

A modulation technique for measuring small disturbances in the upstream flow field of a sharp leading edge in a rarefied hypersonic flow. 19 p2377 A73-37714

Effect of yaw on supersonic and hypersonic flow over delta wings. 19 p2377 A73-38008

Approximation for hypersonic flow past circular cone with angle of attack, discussing density asymptotic expansion, flow velocity and density distribution 21 p2632 A73-40428

Methods for calculating nonlinear flows with attached shock waves over conical wings. 22 p2796 A73-42562

French monograph - Study of the behavior of the laminar boundary layer in the presence of a positive or negative pressure gradient in hypersonic flow around obstacles. 22 p2797 A73-42744

A theoretical and experimental study of sound attenuation in an annular duct. [AIAA PAPER 73-1005] 24 p3077 A73-44838

Hypersonic flow velocity measurements using laser velocimeter. [AIAA PAPER 73-1046] 24 p3090 A73-44870

Hypersonic flow about a spatial body with an attached shock wave 24 p3054 A73-45172

Relationships between forces acting on bodies moving in a rarefied gas, in a light flux, and in hypersonic Newtonian flow 24 p3055 A73-45532

HYPERSONIC GLIDERS

Optimal lift control by Miele's method for the atmospheric entry of a hypersonic glider. I - Simple type problems. 03 p0245 A73-13766

Optimal lift control by Miele's method for the atmospheric entry of a hypersonic glider. II - Isoperimetric type problems. 04 p0404 A73-15168

Some design aspects of Space Shuttle orbiters. 05 p0627 A73-16178

Similarity relationship for wing-like bodies at high Mach numbers. [AIAA PAPER 73-203] 05 p0532 A73-16937

Optimal lift control by Miele's method for the atmospheric entry of a hypersonic glider. III. 10 p1285 A73-23616

HYPERSONIC HEAT TRANSFER

Heat and mass transfer at the surfaces of glass-graphite materials in a high-temperature gas flow 06 p0766 A73-17457

- Investigation of heatproof materials under unsteady operating conditions 11 p1450 A73-25730
- Effect of surface catalytic activity on stagnation heat-transfer rates. 13 p1706 A73-28804
- Certain patterns of heat transfer in a hypersonic shock layer in the presence of mass entrainment 18 p2266 A73-37014
- Heat transfer rate and flow field and pressure distribution behind flat plate backward facing step in hypersonic flow 23 p3049 A73-43832

HYPERSONIC INLETS

- An analytical study of hypersonic inlets in free molecule flow. 18 p2264 A73-36325

HYPERSONIC NOZZLES

- Density and temperature measurement in laminar boundary layer and free jet of hypersonic nozzles by electron beam probe. [ONERA, TP NO. 1131] 01 p0045 A73-10239
- Investigation of the effect of the nozzle cone angle on the parameters of a rarefied gas flow 03 p0245 A73-13624
- Relaxation of a partially ionized gas in a nozzle 15 p1824 A73-32327
- Hypersonic nozzle flow of air with high initial dissociation levels. 16 p2001 A73-33870
- Calculation of hypersonic nonequilibrium nozzle flows with excited vibrational degrees of freedom 18 p2266 A73-37018

HYPERSONIC REENTRY

- Aerothermodynamic aspects of shock-interference patterns for shuttle configurations during entry. [AIAA PAPER 73-238] 05 p0532 A73-16963
- Investigation of convective and radiative heating of blunt bodies in hypersonic flow 06 p0644 A73-17469
- Transition effects on slender vehicle stability and trim characteristics. [AIAA PAPER 73-126] 06 p0756 A73-17646
- Russian book - Mechanics of optimal spatial motion of flight vehicles in the atmosphere. 07 p0777 A73-20380
- Russian book - Nonequilibrium physicochemical processes in aerodynamics. 09 p1029 A73-23225
- Unsteady three-dimensional motion of a flight vehicle during hypersonic reentry in the atmosphere 10 p1286 A73-24304
- Engineering analysis of hypersonic lifting body windward surface inviscid and viscous flow fields at high angles of incidence. [AIAA PAPER 73-637] 18 p2263 A73-36257
- Boundary-layer plasma of a re-entry vehicle - A comparison of prediction models and flight measurements. 21 p2632 A73-40420

HYPERSONIC SHOCK

- Hypersonic, viscous shock layer with chemical nonequilibrium for spherically blunt cones. 01 p0002 A73-10746
- Initial conditions for the hypersonic shock/boundary layer interaction problem. [AIAA PAPER 73-201] 05 p0532 A73-16935
- Closed form solutions for dust density and temperature distributions in shock layer of hypersonic wedge flow 05 p0533 A73-17115
- An effective cross section method of accounting for the selectivity of emission and absorption in a hot gas 09 p1123 A73-22613
- Initial conditions for the hypersonic-shock/boundary-layer interaction problem. 11 p1303 A73-26384
- Spherical concentric shock wave excitation in elastic medium by hypersonic thermal wave in terms of displacements, particle velocity and stresses 14 p1817 A73-30252
- Hypersonic merged stagnation shock layers. [AIAA PAPER 73-639] 18 p2260 A73-36197
- Certain patterns of heat transfer in a hypersonic shock layer in the presence of mass entrainment 18 p2266 A73-37014
- Pressure fields over hypersonic wing-bodies at moderate incidence. 20 p2508 A73-39808
- Total shock-tube working time in the investigation of the discharge through holes in the end face 24 p3076 A73-44755

HYPERSONIC SPEED

- Some averaged properties of wave solutions for a hypersonic thermal wave. 06 p0728 A73-17890
- Radiating-conducting thick-transparent normal shock solution. 07 p0919 A73-19507
- Effect of ionization nonequilibrium on the shock wave in the stagnation region 07 p0776 A73-20616
- Liquid film cooling on hypersonic slender bodies. 10 p1172 A73-24540

Book - Experimental methods of hypersonics.

- 17 p2097 A73-35338
- Observation of the surface of hypersonic projectiles by holography 21 p2694 A73-39956

HYPERSONIC VEHICLES

- NT HYPERSONIC AIRCRAFT
- NT HYPERSONIC GLIDERS
- NT LIFTING REENTRY VEHICLES
- Hypersonic flight vehicles aerodynamic heating, structural design and materials and propulsion problems, discussing research work and facilities 03 p0242 A73-13055
- A rocket system for hypersonic, high Reynolds number aerothermodynamic research. [AIAA PAPER 73-304] 09 p1156 A73-23223
- Ion and electron distributions in the boundary layer of hypersonic vehicles. 11 p1404 A73-25290

- Viscous effects in massively-ablating planetary entry body flow fields. [AIAA PAPER 73-716] 18 p2264 A73-36335
- Lifting body configurations for sustained hypersonic flight. 19 p2377 A73-37710

- Functional tests with hypersonic flight vehicles, using an infrared heating system to simulate the temperature loads in flight 19 p2419 A73-38269

- An aerodynamic entry control technique utilizing the yaw flap concept. [AIAA PAPER 73-888] 20 p2588 A73-38824

HYPERSONIC WAKES

- Comparative study of free jets and jets emitted in the wake of a cylinder with axis parallel to a hypersonic flow 01 p0002 A73-10417

- Investigation of electronic and gasdynamic parameters of hypersonic wakes behind models moving in argon. 03 p0296 A73-14099

- Structure of turbulent wakes of hypersonic spheres as inferred with ion probes. 05 p0527 A73-16568

- Full scale reentry vehicle laminar to turbulent wake transition characteristics from electrostatic probe in-flight measurements of charged particle density fluctuations [AIAA PAPER 73-109] 05 p0529 A73-16868

- Ion density and current distribution measurements in hypersonic turbulent wakes behind sphere flown in ballistic range, using cylindrical electrostatic probes 06 p0645 A73-18135

- Band position predictions in schlieren visualization of hypersonic entropy wake behind blunt bodies, assuming bow shock geometry 07 p0775 A73-19970

- Russian book - Nonequilibrium physicochemical processes in aerodynamics. 09 p1029 A73-23225

- Experimental study of wakes produced by hypersonic cones in free flight. 15 p1823 A73-31312

- Density and temperature distributions in hypersonic sphere wakes. 15 p1824 A73-32150

- Aeroballistic range facilities development and application to reentry physics, discussing program for turbulent wake properties of hypersonic projectiles 24 p3054 A73-44993

HYPERSONIC WIND TUNNELS

- NT CASCADE WIND TUNNELS
- NT HOTSHOT WIND TUNNELS
- NT PLASMA JET WIND TUNNELS
- NT SHOCK TUNNELS
- High pressure plasma torch to heat air for high temperature chemical reactions and hypersonic wind tunnels for reentry vehicle ablation studies 13 p1597 A73-28479

- Hypersonic wind tunnel MHD accelerator design and operating principles, discussing fluid density, I-V characteristics, cooling losses, plasma temperature, gas pressure and velocity, etc 14 p1743 A73-30295

- Hypersonic flow velocity measurements using laser velocimeter. [AIAA PAPER 73-1046] 24 p3090 A73-44870

HYPERSPACES

- Event manifold curvature tensor as six dimensional bivector space via dyadic projections, applying to gravitational waves description 08 p0989 A73-21521
- Gravitational collapse with a physical singularity on an isotropic hypersurface 10 p1283 A73-24751

- Extension of the principle of variable structure systems to the case where the slip hypersurface is nonlinear - Application to suboptimal control 11 p1341 A73-25574

- Quasi-conformal mapping theory of two- and multidimensional regions, considering superposition, hyperbolic and mixed systems and Chebyshev problem 13 p1647 A73-28339

Rigid motion of relativistic surfaces

- 15 p1914 A73-32095
- Analytic and computer solutions for Schwarzschild black hole geometry slicing into asymptotically flat and static maximal spacelike hypersurfaces 16 p2060 A73-33121
- Geometric interpretation of spinor representations for groups of motions in quasi-elliptic 5-spaces 17 p2213 A73-35568

- Correlations among the parameters of the spherical model for eclipsing binaries. 17 p2236 A73-35778

- Nonholonomic generalization of the Stokes theorem 19 p2462 A73-38542

- Multidimensional linear extrapolation in problems of optimal design and control 20 p2539 A73-38687

- Comparison of a suggested polynomial method with the method of F. M. Perelman in the calculation of the solidus surface of the W-Ta-Mo-Nb system 22 p2877 A73-42456

- Pseudo-umbilical manifolds of codimension 2 and of constant mean curvature in an n plus 2 dimensional elliptic space and generalizations 23 p3000 A73-44300

- Weak invariance conditions and synthesis algorithms for control systems with discontinuities on hypersurfaces in phase space 24 p3074 A73-44666

HYPERTENSION

- Role of the sympathetic nervous system in supporting cardiac function in essential arterial hypertension. 08 p0930 A73-21015

- Electrocardiographic evidence of left atrial hypertension in acute myocardial infarction. 11 p1319 A73-26287

- Angina pectoris in men - Prognostic significance of selected medical factors. 11 p1319 A73-26288

- Computer analysis of the orthogonal electrocardiogram and vectorcardiogram in 939 cases with hypertensive cardiovascular disease. 11 p1324 A73-26361

- Coronary atherosclerosis development and prevention in children, discussing hyperlipidemia, hypertension, cigarette smoking and high risk identification 14 p1715 A73-30065

- Prevention of the atherosclerotic diseases - Opportunities for military medicine. 14 p1718 A73-30518

- Some metric characteristics of myocardial cells under various conditions of cardiac and cardiovascular pathology 18 p2280 A73-36962

- Quantitative evoked-potential analyses for the neurophysiological characterization of faulty learning processes in the experimental arterial hypertoniopathogenesis 19 p2394 A73-37756

- Management of the treatment of illnesses as a problem of modern control theory 20 p2518 A73-39348

- Mechanism of 'readjustment' of aorta baroreceptors during hypertension 22 p2807 A73-42655

HYPERTHERMIA

- Effect of controlled elevation of body temperature on human tolerance to +Gz acceleration. 01 p0007 A73-10159

- Physical work induced hyperthermia effects on detection rate in visual vigilance task performance in hot and humid environment 06 p0659 A73-18469

- Portable electronic thermometer for temperature measurement during exercise elevation of body temperature in heat acclimatization experiment 10 p1185 A73-24567

- Changes in the gas content of blood in man during exposure to high ambient temperatures 12 p1463 A73-27711

- Hypothalamo-adenohypophysis-adrenal neurosecretory system under hyperthermia 14 p1719 A73-30847

- Heat conduction in blackened skin accompanying pulsatile heating with a xenon flash lamp. 20 p2519 A73-39791

- Russian book - Mutual relationship of water and salt secretion functions in digestive and excretory organs under conditions of high temperature. 21 p2641 A73-41438

HYPERTONIA

U OSMOSIS

HYPERVELOCITY

- Small hypervelocity particle in-flight detection against background noise using forward scattering from laser illuminated particle distribution 17 p2172 A73-35415

HYPERVELOCITY CRATERING

U HYPERVELOCITY PROJECTILES

U PROJECTILE CRATERING

HYPERVELOCITY FLOW

- Book - Progress in aerospace sciences. 05 p0627 A73-16176

Photochemical ignition and combustion enhancement in high speed flows of fuel-air mixtures.
[AIAA PAPER 73-216] 05 p0641 A73-16946

Correlation and statistical characteristics of turbulence fronts in the wakes of hypervelocity bodies.
13 p1567 A73-29269

Engineering approximations for radiating nonequilibrium shock layers.
[AIAA PAPER 73-673] 18 p2297 A73-36224

Flow field measurements in an asymmetric axial corner at $M = 12.5$.
[AIAA PAPER 73-676] 18 p2297 A73-36227

Slightly ionized low density hypersonic flow about a sharp plate and its diagnostics.
[AIAA PAPER 73-690] 18 p2262 A73-36241

Investigation of multiple slot film cooling to a blunt nose cone.
[AIAA PAPER 73-698] 18 p2368 A73-36247

HYPERVELOCITY IMPACT

Complex phenomena in metal surface layers after high velocity impact loading in Ar atmosphere
02 p0182 A73-12698

Simulated microscale erosion on the lunar surface by hypervelocity impact, solar wind sputtering, and thermal cycling.
07 p0896 A73-19867

Metal barrier maximum puncturable thickness dependence on high velocity meteorite particle impact parameters
12 p1554 A73-27642

Studies of plasma production at hypervelocity microparticle impact.
13 p1667 A73-29424

Planetary accretion from grains in intersecting solar orbits, investigating velocity impact behavior of silicate particles
17 p2228 A73-34423

Angular dependence of the impulse of recoil in the case of high-speed impact
18 p2362 A73-36123

X radiation arising during collisions between metal bodies
19 p2458 A73-37249

Gas dynamic models of high speed explosive impacts of solid bodies, discussing metal cavity lining, buckling and hypersonic jet phenomena
19 p2433 A73-37514

Effect of simulated lunar impact on the survival of bacterial spores.
20 p2513 A73-39485

Spallation and fracture resulting from reflected and intersecting stress waves.
21 p2782 A73-39989

Investigation of the hypervelocity impact on thin plastics and metal foils
21 p2696 A73-39990

Effective application of double exposure holographic interferometry to the study of deformations of ceramics due to the impact of a projectile
22 p2863 A73-43096

Lunar asymmetries in crustal thickness, maria distribution and gamma radioactivity due to intense early bombardment by interplanetary meteoroid flux
23 p3031 A73-43762

Damping of a plane shock wave during high-velocity impact
24 p3076 A73-44712

HYPERVELOCITY LAUNCHERS

Appraisal of UTIAS implosion-driven hypervelocity launchers and shock tubes.
[AD-753252] 05 p0562 A73-16180

HYPERVELOCITY PROJECTILES

Terrestrial, Martian and lunar doublet craters origin from simultaneous multiple meteorite impacts, using Lexan plastic projectiles against sand targets in ballistic range tests
10 p1277 A73-24079

Observation of the surface of hypersonic projectiles by holography
21 p2694 A73-39956

Hypervelocity projectile holography for application to bullets and shells, calculating rotational velocity and flight direction from fringe on wave front reconstruction
21 p2694 A73-39957

HYPERVELOCITY WIND TUNNELS

NT CASCADE WIND TUNNELS

NT HOTSHOT WIND TUNNELS

NT PLASMA JET WIND TUNNELS

NT SHOCK TUNNELS

Some development of hypersonic flow experiment by the gun tunnel.
01 p0003 A73-11129

Three-degree-of-freedom motions of a slender asymmetric cone in a hypersonic wind tunnel.
03 p0287 A73-13494

The S4-Modane hypersonic wind-tunnel - Its use for air breathing engine tests
[ONERA, TP NO. 1103] 03 p0288 A73-14140

The laser heated wind tunnel - A new approach to hypersonic laboratory simulation.
[AIAA PAPER 73-211] 05 p0563 A73-16942

Fluid undercutting in the successive channel flow of two gases.
[AIAA PAPER 73-214] 05 p0566 A73-16944

Mach numbers up to 30 obtained in a continuous operating wind tunnel
05 p0533 A73-17194

Hypersonic flows in large-scale inlet models.
07 p0773 A73-19189

A precise position and attitude measurement system for free-flying wind-tunnel models
11 p1362 A73-25443

Laser activated, model surface recession compensation system for testing ablative materials.
[AIAA PAPER 73-380] 11 p1343 A73-25510

Effects of upstream wall temperatures on hypersonic tunnel wall boundary-layer profile measurements.
11 p1344 A73-26395

Monograph - Development of hotshot wind tunnels for hypersonic aerodynamic studies.
15 p1859 A73-32595

HYPERVENTILATION

Dynamic aspects of regulation of ventilation in man during acclimatization to high altitude.
03 p0259 A73-13500

Characteristics of vasomotor alterations during brief arbitrary hyperventilation according to data from rheographic and plethysmographic studies
11 p1314 A73-25041

Role of the arterial chemoreceptors in ventilatory adaptation to hypoxia of awake dogs and rabbits.
11 p1318 A73-26220

Posthyperventilation breathing - Different effects of active and passive hyperventilation.
14 p1714 A73-29752

Pulmonary volume, respiration rate and alveolar air carbon dioxide content measurements in pilots during flight, noting hyperventilation occurrence
19 p2392 A73-37197

Effects of hyperinflation of the thorax on the mechanics of breathing.
22 p2806 A73-42415

Rebreathing equilibration of CO₂ during exercise.
24 p3060 A73-45068

Ventilation at transition from rest to exercise.
24 p3061 A73-45375

HYPOBARIC ATMOSPHERES

Hypobaric hypoxia - Within-subject transition effects in albino rats.
06 p0649 A73-17525

Electrogastric data pertinent to exposures in a pressure chamber to moderate hypoxia levels
06 p0657 A73-17684

Effects of an hypoxic hypobaric environment on renin-aldosterone in normal man.
08 p0934 A73-21503

Central, femoral, and brachial circulation during exercise in hypoxia.
08 p0934 A73-21506

A study of Halon 1301 /CBrF₃/ toxicity under simulated flight conditions.
09 p1045 A73-22537

HYPODYNAMIA

Biological effects of lasting hypodynamia on young albino rats in 62 day confinement, considering weight, growth and sexual behavior
08 p0929 A73-20983

Investigation of certain indices of higher nervous activity in man during prolonged stay in a water environment
09 p1039 A73-22364

Effects of the hypodynamia and other factors of a spaceflight on the excretion of 17-oxycorticosteroids and aldosterone
17 p2111 A73-34233

HYPOELASTICITY

Tresca type plastic material shear, considering hypoelastic yield interrelation to Tresca yields
06 p0763 A73-18457

Tresca-type plastic materials in the theory of hypoelasticity. I Mechanical constitutive equations and simple shear deformation.
07 p0909 A73-19161

Tresca-type plastic materials in the theory of hypoelasticity. II Optical constitutive equations and birefringence in simple shear.
11 p1447 A73-26649

A theoretical study of fracture and yield conditions derived from hypo-elasticity.
13 p1639 A73-29464

HYPOGLYCEMIA

Antidiabetic medications and aircrew
08 p0935 A73-21541

Hypoglycemia in airline pilots.
18 p2278 A73-36790

HYPOKINESIA

Topochemical differences in RNA content in spinal cord motoneurons during hypoxia and hypokinesia
02 p0135 A73-12558

Circadian rhythm asynchrony in man during hypokinesia.
03 p0263 A73-14121

Research on the displacement of blood-plasma proteins and on the nerve conduction velocity in rats subjected to accelerations and hypokinesia
06 p0650 A73-17769

Vertical posture control after Soiz 6, 7 and 8 flights and 120-day hypokinesia
08 p0933 A73-20985

Effect of electrostimulation on hemodynamic shifts during prolonged hypokinesia
10 p1180 A73-23940

Water and salt metabolism in hypokinesia-subjected animals
12 p1462 A73-27704

Hemocoagulation and trombocyte state during hypokinesia after highland adaptation
12 p1463 A73-27713

Circadian rhythm of urinary calcium excretion during immobilization.
14 p1717 A73-30512

Investigation of some blood characteristics in albino rats subjected to 60-day hypokinesia
15 p1834 A73-31502

Protein and nucleic acid contents in animal tissues under hypokinesia
15 p1834 A73-31503

Functional condition of skeletal muscles in rats under lasting movement constraints /up to 120 days/
15 p1834 A73-31504

Effect of prolonged hypokinesia on certain energy transfer characteristics in skeletal muscles and some internal organs
15 p1834 A73-31505

Retinal vessel reactions and intraocular tension in humans staying in a horizontal position for 120 days
15 p1835 A73-31514

Influence of restricted motor activity on the resistance of animals to acute action of carbon monoxide
15 p1835 A73-31519

Histopathological and histochemical studies of one year isolation and six months immobilization effects on rhesus monkeys internal organs and tissues
18 p2270 A73-35983

Prolonged space flight and hypokinesia.
18 p2278 A73-36789

Functional state of the auditory analyzer under conditions of prolonged cinostatic hypokinesia
23 p2946 A73-43789

Effect of prolonged hypokinesia on the higher nervous activity of humans
24 p3058 A73-44668

HYPOTENSION

Airline flight and ground personnel fatigue and orthostatic hypotension syndrome manifested by variations in retinal arterial pressure and brain circulation
02 p0134 A73-12156

Mechanisms of certain functional shifts during change in the blood of the content level of external pancreatic-gland secretion components
05 p0541 A73-16700

HYPOTHALAMUS

Comparative physiological characteristics of functional relations among the hypothalamus and the olfactory and limbic systems of the brain
01 p0006 A73-10151

Structural organization and electrophysiological properties of the intercentral functional systems of the hypothalamic region of the brain
01 p0009 A73-11024

Structural change in the paradoxical phase of sleep due to the stimulation of the reticular formation and hypothalamus on a background of deep slow sleep
01 p0009 A73-11081

Hypothalamic norepinephrine - Circadian rhythms and the control of feeding behavior.
02 p0134 A73-12417

Response of single units of the posterior hypothalamus to thermal stimulation.
03 p0262 A73-14111

Physiological tests for hypothalamic regions stimulation effects on coronary circulation, noting hypoxia and emotional stress effects
06 p0650 A73-17770

The effects of bilateral destruction of certain medial-hypothalamus structures on the formation of complement-binding antibodies
07 p0781 A73-19647

Statistical investigation of the impulse activity of neurons in various hypothalamic regions
10 p1179 A73-23802

Thermosensitive interoreceptors and their interaction with thermosensitive structures of the hypothalamus
10 p1179 A73-23803

Neurochemical aspects of the formation of electrographical and behavioral reactions
10 p1184 A73-24327

Acetylcholinesterase activity of hypothalamic and cortical structures under pharmacological effects
10 p1182 A73-24597

On the functional significance of subcortical single unit activity during sleep.
14 p1714 A73-29993

Hypothalamo-adenohypophysis-adrenal neurosecretory system under hyperthermia
14 p1719 A73-30847

Evoked potentials in the hypothalamus in response to stimulation of the vagus and sciatic nerves
19 p2395 A73-37941

Brain calcium - Role in temperature regulation.
19 p2396 A73-38294

- Determinants of hypothalamic neuronal thermosensitivity in ground squirrels and rats. 20 p2513 A73-39600
- Changes in thermosensitive characteristics of hypothalamic units over time. 20 p2514 A73-39601
- Russian book - Role of the hypothalamus and the limbic system of the brain in regulating vegetative functions. 21 p2636 A73-40276
- The role of the amygdaloid nuclei in the regulation of water intake. 21 p2636 A73-40278
- The nature of chemoreception in posterior hypothalamic structures. 21 p2636 A73-40279
- Effect of stimulation of the hypothalamus on the pH of arterial and venous blood. 21 p2637 A73-40281
- Effect of stimulation of certain hypothalamic structures on systemic and pulmonary circulation. 21 p2637 A73-40282
- Reaction of neurocytes of the paraventricular hypothalamic nucleus to unilateral thyroidectomy. 21 p2637 A73-40283
- Influence of electric stimulation of the hypothalamus on catecholamine, phosphorylated compound, and cholesterol levels. 21 p2637 A73-40284
- Evoked potentials in the hypothalamus and mesencephalic reticular formation upon stimulation of the vagus nerve. 21 p2640 A73-41263
- The presence in the heart of compounds which participate in the neurohumoral regulation of coronary circulation. 24 p3059 A73-44769

HYPOTHERMIA

- Electron-microscopic investigations regarding the protective effect of hypothermia on cell organelles in the case of whole-body X-irradiation. 03 p0262 A73-13824
- Deep hypothermia induced in the golden hamster by altering cerebral calcium levels. 05 p0538 A73-16151
- Cerebral circulation alteration during hypothermia. 05 p0541 A73-16698
- Some physiological reactions to acceleration in albino rats in a state of hypothermia. 05 p0541 A73-16737
- Hypoxia, an adjunct in helium-cold hypothermia - Sparing effect on hepatic and cardiac metabolites. 07 p0782 A73-20169
- Effect of low temperature on metabolism of rat liver slices and epididymal fat pads. 07 p0782 A73-20170
- Helium-cold induced hypothermia in the white rat. 12 p1461 A73-26975
- Nitrogen metabolite dynamics in the brain during repeated hypothermia and subsequent spontaneous warming. 12 p1462 A73-27703
- Torpor and hibernation physiology in mammals covering evolution, hypothermia, energy conservation, cell and organ adaptations, nervous and cardiovascular system changes, etc. 22 p2809 A73-42862

HYPOTHESES

- NT EXPECTANCY HYPOTHESIS
- NT INTERMITTENCY HYPOTHESIS
- NT LAGRANGE SIMILARITY HYPOTHESIS
- NT NULL HYPOTHESIS
- NT VORTICITY TRANSPORT HYPOTHESIS

HYPOVENTILATION

- Human respiration under increased pressures. 12 p1461 A73-26924
- External airway resistance effects on ventilation and carbon dioxide response during human steady state exercise. 22 p2806 A73-42417
- Submaximal exercise with increased inspiratory resistance to breathing. 22 p2806 A73-42419

HYPOVOLEMIA

- Effects of rehydration on +Gz tolerance after 14-days' bed rest. 23 p2946 A73-43524

HYPOXEMIA

- Effects of hypoxemia and acute coronary occlusion on myocardial metabolism in dogs. 05 p0538 A73-16154
- Oxygen consumption and its 'critical' tension for the cerebral cortex in situ. 10 p1179 A73-23801
- Evaluation of positive end-expiratory pressure in hypoxemic dogs. 20 p2515 A73-39781

HYPOXIA

- Insensitivity of the alveolar septum to local hypoxia. 01 p0006 A73-10134
- Evolutionary significance of carbohydrate metabolism alterations in animal brains during adaptation to hypoxia. 01 p0007 A73-10153

- Topochemical differences in RNA content in spinal cord motoneurons during hypoxia and hypokinesia. 02 p0135 A73-12558
- Effect of altitude acclimatization and simultaneous acclimatization to altitude and cold on critical flicker frequency at 11,000 ft. altitude in man. 02 p0135 A73-12562
- Myocardial function and ultrastructure in chronically hypoxic rats. 03 p0259 A73-13369
- Control of exercise hyperpnea under varying durations of exposure to moderate hypoxia. 03 p0259 A73-13499
- Dynamic aspects of regulation of ventilation in man during acclimatization to high altitude. 03 p0259 A73-13500
- Cardiocirculatory adaptation to chronic hypoxia. III - Comparative study of cardiac output, pulmonary and systemic circulation between sea level and high altitude residents. 04 p0410 A73-15523
- Effect of hypoxia on free fatty acid metabolism during exercise. 05 p0540 A73-16609
- Augmentation of chemosensitivity during mild exercise in normal man. 05 p0540 A73-16610
- Hypobaric hypoxia - Within-subject transition effects in albino rats. 06 p0649 A73-17525
- Electrogastrographic data pertinent to exposures in a pressure chamber to moderate hypoxia levels. 06 p0657 A73-17684
- Vestibular reactions to Coriolis accelerations under hypoxia conditions. 06 p0650 A73-17691
- Physiological tests for hypothalamus regions stimulation effects on coronary circulation, noting hypoxia and emotional stress effects. 06 p0650 A73-17770
- The effects of hypoxia, hypercapnia, and asphyxia on the baroreceptor-cardiac reflex at rest and during exercise in man. 06 p0654 A73-18348
- Learning ability of rats to regulate hypoxic ambient atmosphere by instrumental response, discussing motivation and reinforcement factors. 06 p0655 A73-18439
- Adaptation to high altitude hypoxia as a factor preventing development of myocardial ischemic necrosis. 07 p0780 A73-19151
- Russian book - Tissue, oxygen in the presence of extremal flight factors. 07 p0780 A73-19425
- Inhibition of the adrenocortical response to hypoxia by dexamethasone. 07 p0780 A73-19476
- Assessment of hypoxia in the human heart. 07 p0781 A73-19928
- The use of glycolytic metabolism in the assessment of hypoxia in human hearts. 07 p0781 A73-19929
- Time course of pulmonary vascular response to hypoxia in dogs. 07 p0782 A73-20168
- Hypoxia, an adjunct in helium-cold hypothermia - Sparing effect on hepatic and cardiac metabolites. 07 p0782 A73-20169
- Thermoregulatory reactions of rats in a nitrogen and helium-diluted hypoxic atmosphere. 08 p0929 A73-20979
- Mathematical analysis of the responses of the human respiratory system to hypoxia and hypercapnia. 08 p0931 A73-21322
- Central, femoral, and brachial circulation during exercise in hypoxia. 08 p0934 A73-21506
- Changes in hemodynamics and efferent sympathetic pulsation during pressor cardiovascular reflexes under conditions of acute hypoxic hypoxia. 09 p1039 A73-22365
- Neuroendocrine, cardiorespiratory, and performance reactions of hypoxic men during a monitoring task. 09 p1044 A73-22527
- Reflex bradycardia elicited from left ventricular receptors during acute severe hypoxia in cats. 09 p1042 A73-23244
- Changes in the cardiac rhythm during a hypoxic functional test. 10 p1179 A73-23820
- Effect of respiration stabilization on hemodynamic reactions during acute hypoxic hypoxia. 10 p1180 A73-23938
- Age-related characteristics of pulmonary edema development during acute hypoxic hypoxia. 10 p1180 A73-23939
- Physiological responses of rats to intermittent high-altitude stress - Effects of age. 10 p1182 A73-24564
- Independent effects of changes in H+ and CO2 concentrations on hypoxic pulmonary vasoconstriction. 10 p1182 A73-24565

- Role of the arterial chemoreceptors in ventilatory adaptation to hypoxia of awake dogs and rabbits. 11 p1318 A73-26220

- Effect of antioxidants on the blood deoxygenation rate in animals exposed to altered atmospheres. 12 p1465 A73-27702

- Dynamics of certain characteristics of the evoked potential of the optic cortex in rabbits under conditions of increasing hypoxia. 12 p1463 A73-27709

- Hemodynamics alteration caused by acute hypoxia in animals with denervated carotid sinuses. 13 p1574 A73-28350

- Threshold Pco2 as a chemical stimulus for ventilation during acute hypoxia in dogs. 13 p1576 A73-28534

- Procedure for preparing an oxygen-nitrogen gas mixture for respiration in a pressure chamber. 13 p1580 A73-29409

- Exogenous free fatty acid effects on hypoxic myocardial function in isolated isometric rat papillary muscles. 13 p1577 A73-29572

- Effects of altitude stress on mitochondrial function. 14 p1717 A73-30430

- Effect of mild acute hypoxia on a decision-making task. 14 p1717 A73-30514

- Aircraft cabin altitude hypoxia effects on mother, embryo and fetus during first trimester of pregnancy in air hostesses and women passengers. 14 p1718 A73-30519

- Role of peripheral chemoreceptors in reactions of rats to short and lasting hypoxia. 14 p1719 A73-30840

- Hypoxic pulmonary steady-state diffusing capacity for CO and cardiac output in rats born at a simulated altitude of 3500 m. 14 p1720 A73-30911

- Ventilatory responses to transient hypoxia and hypercapnia in man. 15 p1832 A73-31126

- Energy balance during moderate exercise at altitude. 15 p1833 A73-31343

- Effect of protein quality in the diet of rats on their tolerance to severe hypoxia. 15 p1835 A73-31511

- Influence of stimulation of the vestibular analyzer under conditions of hypoxia on certain functions of the visual analyzer. 15 p1835 A73-31516

- Influence of restricted motor activity on the resistance of animals to acute action of carbon monoxide. 15 p1835 A73-31519

- Relative rates of arterial lactate and oxygen-deficit accumulation in hypoxic dogs. 15 p1836 A73-31922

- Heart muscle viability following hypoxia - Protective effect of acidosis. 17 p2110 A73-34097

- Effectiveness of some hemodynamic indices in the detection of vestibulo-vegetative disorders under ordinary conditions and those of hypoxia. 17 p2110 A73-34121

- Influence of hypoxia on the release of certain gaseous wastes in white rats. 17 p2111 A73-34228

- Cobalt compound administration effects on hypoxic stress control, testing polycythemic response and cobalt retention in rats. 17 p2115 A73-34744

- Responses to graded hypoxia at high and low 2,3-diphosphoglycerate concentrations. 17 p2112 A73-35460

- Activity variations of some renal enzymes during stepwise increased hypoxia. 18 p2277 A73-36582

- Intellectual performance during prolonged exposure to noise and mild hypoxia. 18 p2283 A73-36783

- Human statokinetic stability as component of non-specific resistance, discussing revolving, altitude, hypoxic and orthostatic stress dependence tests. 18 p2279 A73-36904

- Comparative value of both hypoxic and positive pressure breathing tests for detection of premature beats. 18 p2280 A73-36944

- Estimation of hypoxia tolerance in a decompression chamber. 18 p2280 A73-36945

- The capacity for muscular work in acute hypoxia. 18 p2286 A73-36946

- Protein synthesis in the neurons and glial cells of the stellate ganglia of rats during the adaptation to the effects of high altitude hypoxia. 19 p2393 A73-37396

- Sudden incapacitation in flight - 1 Jan. 1966-30 Nov. 1971. 20 p2512 A73-39112

- Correlation of ventilatory responses to hypoxia and hypercapnia. 20 p2514 A73-39776

Transient ventilatory response to hypoxia with and without controlled alveolar PCO₂.
20 p2515 A73-39777

Ventilatory and hemodynamic responses to acute hypoxia and hypercapnia in Hereford calf, comparing with man
20 p2515 A73-39782

Changes in respiration accompanying a diencephalic vegetative-vascular syndrome under the action of a hypoxic mixture
21 p2636 A73-40280

Effect of certain flight factors on crew efficiency
21 p2643 A73-40350

Oxygen uptake, muscle high-energy phosphates, and lactate in exercise under acute hypoxic conditions in man.
21 p2638 A73-41131

Advantage or disadvantage of a decrease of blood oxygen affinity for tissue oxygen supply at hypoxia - A theoretical study comparing man and rat.
21 p2641 A73-41620

Nonthermal metabolic response of rats to He-O₂, N₂-O₂, and Ar-O₂ at 1 atm.
22 p2805 A73-42201

Cerebral tolerance to asphyxial hypoxia in the dog.
22 p2805 A73-42202

The frequency of barotraumas as determined by nasal findings and X-rays of the paranasal sinuses
22 p2817 A73-43132

Influence of histotoxic hypoxia on the activity of lactic dehydrogenase isoenzymes in neurons and neuroglia of various sections of the central nervous system
24 p3058 A73-44429

Effect of adaptation to altitude hypoxia on the behavior of animals in a conflict situation
24 p3058 A73-44549

HYSTERESIS
Thermochromic cuprous mercuric iodide for IR recording applications, observing phase transition hysteresis from reflectance-vs-temperature, specific heat and sensitivity measurements
01 p0054 A73-11230

The effect of a preliminary plastic strain on the form of a mechanical hysteresis loop.
02 p0235 A73-12208

A procedure for the determination of hysteresis losses at a point of a body in the case of variable stresses
03 p0306 A73-13149

Plane film elements demagnetizing factor measurement from material-element hysteresis loop comparison
09 p1084 A73-22655

Consideration of the hysteresis behavior of a solid medium in a complex stress state under the conditions of simple cyclic loading.
09 p1161 A73-23059

A generalization of equations of the outline of a hysteresis loop for the case of an asymmetrical cycle.
09 p1161 A73-23152

Magnetic reversal mechanisms of obliquely deposited permalloy films possessing perpendicular anisotropy
12 p1530 A73-26833

Thermal stresses arising in high-frequency fatigue tests
12 p1512 A73-27259

Inelastic strain and hysteresis energy criteria for fatigue fracture of metals.
13 p1641 A73-29499

Hysteresis loop equation for calculation of elastoplastic deformations caused by forced vibrations, taking into account medium compressibility and inertial forces
13 p1703 A73-29609

Titanium and zirconium alpha-omega transformation hysteresis at room temperature from dilatometry, X ray phase analysis and electrical resistance and shear measurements
14 p1764 A73-30863

Fast differential thermal analysis.
17 p2119 A73-34799

Method of studying thermal fatigue from the parameters of the hysteresis loop in temperature-force coordinates
20 p2619 A73-39362

Estimation of the effect of the internal properties of the material on the characteristics of string sensors
22 p2860 A73-42370

Nonlinear stress-strain hysteresis equation of cyclic straining for vibrating imperfectly elastic systems, using Masing principle
23 p3047 A73-44276

Compensation method for non-linear systems having jump and hysteresis properties.
24 p3075 A73-45555

I

I BEAMS
Interaction curves for bending and axial forces of perfectly plastic curved I-beams.
06 p0762 A73-18339

Effect of major axis curvature on I-beam stability.
07 p0916 A73-20437

Lateral buckling of cantilevered I beam columns.
08 p1017 A73-20942

Maximum stress calculation for I beam and thin walled sphere redundant structures under stationary creep by perturbation method
14 p1811 A73-30487

IAPETUS
Radii, albedos, and 20-micron brightness temperatures of Iapetus and Rhea.
01 p0104 A73-11050

Iapetus UVB light curve minima depths difference explained by two-hemisphere model
11 p1425 A73-26134

IBM COMPUTERS
NT IBM 1130 COMPUTER
IBM 1130 COMPUTER
Software design and implementation for real time power spectral analysis on IBM-1130 8K-core computer, discussing coherence and cross spectra estimation and arithmetic errors
15 p1848 A73-32032

ICBM [MISSILES]
U INTERCONTINENTAL BALLISTIC MISSILES
ICE
NT GLACIERS
NT ICE FLOES
NT LAND ICE
NT SEA ICE
Backscatter from snow and ice surfaces at near incident angles.
01 p0016 A73-10191

The deformations and stresses in floating ice plates.
01 p0118 A73-11366

Icy conglomerate cometary nucleus models, discussing clathrates role in comet condensation from solar nebula
04 p0494 A73-14752

Spectroscopic sounding of cloud; snow and ice covers from below /earth surface/ and above /space or planet/
04 p0473 A73-15570

Electrodynamic models for radio attenuation in ice by electromagnetic absorption and reflection from ice sheet interfaces, noting radar sounding
04 p0445 A73-15572

Nongravitational effects on comets - The current status.
14 p1791 A73-29797

Encke comet icy nucleus core-mantle evolutionary model, investigating mantle sublimation, fading and capture time approximation for nongravitational forces effect in terms of mass output
14 p1793 A73-29822

New estimates of cometary disintegration times and the implications for diffusion theory.
14 p1794 A73-29829

Determination of the radius of a cometary nucleus from photometric data
15 p1928 A73-31024

Oil spread over Arctic ice, considering spread rate and oil slick size attainment for pollution potential during spills on tundra or pack ice [AIAA PAPER 73-701]
18 p2312 A73-36250

Liquid droplet and ice particle distribution in spatially homogeneous mixed clouds, solving kinetic coagulation equations via distribution function moments
21 p2730 A73-40119

ICE FLOES
Statistical comparison of airborne laser and stereophotogrammetric sea ice profiles.
22 p2850 A73-42731

ICE FORMATION
NT CLOUD GLACIATION
Meteorological parameters conducive to ice formation on aircraft, analyzing data statistics on atmospheric moisture content, temperature and drop size [DGLR PAPER 72-109]
02 p0130 A73-11660

Contrail ice budget measurements with optical array particle size spectrometer onboard Sabreliner, noting water abundance reduction at subtropopause jet traffic levels
02 p0189 A73-12785

Icing testing in the large Modane wind-tunnel on full-scale and reduced scale models
07 p0808 A73-20244

Airliner radomes erosion by atmospheric precipitation, water penetration, icing, bird and stone impact and lightning
11 p1335 A73-25297

A technique for measuring relative threshold nucleation temperatures for active nucleation catalysts.
12 p1521 A73-26816

Hailstones icicle lobe formation growth in wind tunnel, using supercooled or frozen hydrometeors
12 p1521 A73-26817

Icing conditions of modern transport aircraft according to cruise flight data
17 p2100 A73-34545

Polar albedo changes and its climatic consequences.
18 p2307 A73-36028

The effect of ice formation on the stability and maneuverability characteristics of aircraft
19 p2387 A73-38117

Photographic investigation of hailstone form, size and structure, determining layer growth from air bubble shape and spectrum
21 p2730 A73-40116

Growth mechanism of charged ice crystals in water vapor
21 p2742 A73-40123

Venus atmosphere water vapor phase transformation possibilities, discussing ice crystal and supercooled water drop formation
22 p2911 A73-42736

Martian W cloud diurnal brightening observation by Mariners 6 and 7 flyby missions, considering probable water ice formation
24 p3128 A73-44398

ICE MAPPING
Aircraft measurements of microwave emission from Arctic Sea ice.
02 p0171 A73-12773

Analysis and interpretation of air-borne multifrequency side-looking radar sea ice imagery.
09 p1080 A73-22150

Sea ice observation by means of satellite.
11 p1358 A73-26346

Toros side-looking radar system for sea-ice distribution and geomorphological mapping and agricultural soil studies
12 p1474 A73-27962

Aerial cameras functional testing and calibration, discussing film plane flatness measurement methods and camera applications to ice surface photography
12 p1502 A73-27971

Millimeter wave backscatter measurements for snow, ice and sea ice, discussing penetration into snow and ice
16 p1983 A73-33728

Satellite detection of melting snow and ice by simultaneous visible and near-IR measurements.
20 p2556 A73-39840

Two-dimensional statistic analysis of radar imagery of sea ice.
20 p2556 A73-39843

Statistical comparison of airborne laser and stereophotogrammetric sea ice profiles.
22 p2850 A73-42731

ICE NUCLEI
Radiative properties of terrestrial clouds at visible and infra-red thermal window wavelengths.
13 p1652 A73-28274

Calculation of the growth and melting of ice particles and the radar signal reflection profiles in cumulonimbus clouds
13 p1653 A73-28878

The orientations of ice crystal models during a fall in an electric field
13 p1654 A73-28882

Heavy precipitation from mixed phase composition cloud systems vs light precipitation from droplet and crystal containing clouds
13 p1654 A73-28887

On nongravitational effects in two classes of models for cometary nuclei.
14 p1793 A73-29820

Icy cometary nuclei laboratory simulation by sublimation of dust particle containing ice and frozen electrolyte mixtures in high vacuum at low temperature
14 p1793 A73-29823

Comets and cometesimals formation from icy material during solar system evolution from collapsing dust and gas cloud
14 p1794 A73-29835

Criteria for the existence of H₂O crystals on Mars
16 p2069 A73-33836

Cirrus-contrail cloud spectra studies with the Sabreliner.
17 p2206 A73-35579

Aerosol ice nuclei concentration measurements in remote regions of Southern Hemisphere near Australia by shipborne membrane filters, noting land or stratospheric sources
23 p3002 A73-43598

ICE OBSERVATION
U ICE REPORTING
ICE PACKS
U SEA ICE
ICE PREVENTION
Installing the heater cable directly in the redesigned leading edge.
16 p1970 A73-32924

ICE REPORTING
Earth satellite measurements as applied to sea ice problems.
18 p2310 A73-36134

Locating large masses of ground ice with an impulse radar system.
20 p2556 A73-39841

Satellite measurements of microwave and infrared radiobrightness temperature of the earth's cover and clouds.
20 p2556 A73-39844

ICE SHELVES
U LAND ICE

ICING
U ICE FORMATION
IDEAL FLUIDS

A variant of the solution of problems of fluid oscillations in cylindrical cavities by the Bubnov-Galerkin method

01 p0031 A73-10101

On the integration of Einstein's equation for energy density inside a perfect fluid sphere.

01 p0076 A73-10250

Shear waves and perturbations in linearized steady plane flows of a thermally nonconducting compressible ideal fluid

[ONERA, TP NO. 1169] 01 p0034 A73-11359

Ideal fluid flow past a body with an upstream jet

01 p0035 A73-11427

Stability of a nonstationary circular jet of ideal incompressible fluid

02 p0152 A73-11609

Flow stability of ideal compressible and incompressible fluids, solving Navier-Stokes equation for rotating liquid with free boundary in gravitational field

02 p0154 A73-12692

A variational principle for the nonrotational flow of a perfect compressible liquid in a flexible tank

[ONERA, TP NO. 1178] 03 p0294 A73-13601

Hydrodynamics in weak gravitational fields - Plane oscillations of an ideal fluid in a rectangular channel

03 p0294 A73-13606

Calculation of the natural oscillations of an ideal liquid in an axisymmetrical container with allowance for surface forces

03 p0294 A73-13607

Three dimensional ideal incompressible fluid flows under small velocity perturbation, using Euler equations linearized with respect to steady flow

03 p0296 A73-14048

Schwarzschild interior metric singularity for ideal fluid sphere radius relation to Schwarzschild radius, noting conditions for emitted light red shift

03 p0380 A73-14588

High-frequency vibrations of a circular wing in the flow of an ideal fluid

05 p0636 A73-17089

Velocity distribution of quasi-steady and steady flow of ideal incompressible fluids with congruent streamlines, investigating conditions for vortex and irrotational flow

07 p0809 A73-19017

Flow of an ideal incompressible ponderable fluid around a thin profile placed under a free line. I, II

07 p0811 A73-19998

Analysis of the vibrational characteristics of a liquid contained in a tank

[ONERA, TP NO. 1197] 07 p0812 A73-20074

Two dimensional steady nonrotational flow of perfect compressible fluid around symmetric convex profile, reducing to variational inequality in hodograph plane

07 p0776 A73-20147

Equations of motion of ideally conducting medium in MHD approximation, solving under constant magnetic field and magnetic-hydrodynamic pressure equilibrium

09 p1126 A73-22280

One parameter family of axisymmetric vortex rings propagating steadily through unbounded ideal fluid at rest at infinity

11 p1345 A73-25051

Flow of an ideal fluid past a body with a reverse-stream.

11 p1348 A73-26056

Conformal mapping method application to unsteady motion of arbitrary deformable contour in potential flow of ideal incompressible fluid

11 p1348 A73-26426

Equilibrium stability of liquid filled body with closed internal cavity partially filled with ideal homogeneous incompressible fluid under gravitation

11 p1401 A73-26470

High velocity moving body in ideal incompressible fluid flow, determining lift coefficient from acceleration potential algorithm

12 p1486 A73-27239

Nonvortical axisymmetric flow of inviscid ideal incompressible fluid from partial differential equations solution

12 p1486 A73-27242

Group classification of the hydrodynamics equations of an ideal fluid

12 p1487 A73-27409

Solid profile wing motion in ideal incompressible fluid at variable distance from screen in terms of small perturbation theory

12 p1488 A73-27815

Thermodynamics of relativistic rotating perfect fluids.

12 p1525 A73-27886

Flows with wakes about a zero-incidence symmetric profile

13 p1599 A73-28069

A direct integral equation method for the potential flow about arbitrary bodies.

13 p1563 A73-28083

A characteristic initial value problem in general relativity in the case of a perfect fluid with axial symmetry.

13 p1658 A73-28199

Existence of a corner-type steady flow for an ideal fluid with a free surface

13 p1605 A73-29554

Kerr metric properties and astrophysical implications, presenting perfect fluid boundaries family in weak field approximation and photon orbits behavior in equatorial plane

14 p1798 A73-30143

Motions of perfect incompressible homogeneous fluid planets surrounded by rigid oscillating rings, noting application to two-satellite planets

15 p1860 A73-31049

Unsteady separated free jet flow of an ideal fluid past a wing

15 p1861 A73-31155

Hydrodynamics in weak gravitational fields - Small oscillations of an ideal liquid in a cylindrical vessel

15 p1861 A73-31280

Hydromagnetic stability of parallel flow of an ideal heterogeneous fluid.

16 p2043 A73-33872

Plane unsteady irrotational flow of ideal incompressible fluid through turbomachine stage due to interaction between stationary and moving grids

16 p2001 A73-34015

Hypersonic polytropic transformations of an ideal fluid. II

19 p2420 A73-37645

Nonlinear model for plane unsteady flow resulting from collapse of homogeneous density region in heavy ideal density-stratified fluid

20 p2547 A73-39287

Thermodynamic conditions of conservation of irrotational or oligotropic motions across a shock wave

21 p2677 A73-40948

Acceleration waves in ideal fluid mixtures with several temperatures.

22 p2929 A73-41772

Equations of the boundary perturbations of a cavity moving near a solid wall

22 p2841 A73-42124

Exact hydroelastic solution for an ideal fluid in a hemispherical container.

22 p2843 A73-42631

Hydrodynamics in weak gravitational fields - Plane oscillation problems of an ideal liquid in a vessel

24 p3076 A73-44653

Stability of a flow bounded by elastic walls

24 p3079 A73-44898

On a criterion for the occurrence of a Dedekind-like point of bifurcation along a sequence of axisymmetric systems. I - Relativistic theory of uniformly rotating configurations.

24 p3110 A73-45032

On a criterion for the occurrence of a Dedekind-like point of bifurcation along a sequence of axisymmetric systems. II - Newtonian theory for differentially rotating configurations.

24 p3110 A73-45033

Boundary value problem concerning the oscillations of a rotating ideal fluid

24 p3081 A73-45531

IDEAL GAS

On self-similar blast waves headed by the Chapman-Jouguet detonation.

01 p0120 A73-10441

A note on the flow regimes in the unsteady, rectilinear flow of a perfect gas.

01 p0034 A73-11005

Gasdynamics calculations for a pulsating flow in pipelines

02 p0152 A73-11610

Self-similar flows with increasing energy. II - Isothermal flow.

02 p0238 A73-12091

Ideal dissociating/nondissociating gas reentry flow fields hydrodynamic stability for various free stream and disturbance conditions

03 p0242 A73-13312

Axial and transverse wave motions of inviscid perfect gas in isothermal solid-body rotation in cylinder

04 p0434 A73-15163

Thermodynamic equilibrium and relaxation models of ideal and real high temperature gas flows for reversible and irreversible processes

[DFVLR-SONDDR-282] 04 p0517 A73-15678

Numerical analysis of far turbulent wakes in ideal gas, determining hydrodynamic field moments, turbulence levels and mean square enthalpy fluctuations

06 p0643 A73-17454

Use of approximations of thermodynamic functions in gasdynamics calculations

06 p0644 A73-17470

Instability of shock waves in inhomogeneous gases.

07 p0812 A73-20445

Special relativity theory for steady irrotational ideal gas flow, noting subsonic, supersonic and transonic flow calculations based on small perturbation theory

08 p0926 A73-21128

Two phase channel flow behavior from three dimensional phase diagram for one dimensional steady flow of ideal gas carrying solid particles

09 p1072 A73-22621

Carbon dioxide thermodynamic and transport characteristics calculation, treating gas as multicomponent ideal mixture including carbon monoxide and oxygen and carbon atoms and ions

12 p1526 A73-27308

Variational equations of unsteady near-similar perfect gas flow at strong shock front in terms of mass, energy and momentum in perturbed region

12 p1487 A73-27408

Explosion in detonating media with a variable initial density

12 p1487 A73-27419

Linearized theory of finite conductivity steady ideal MGD flow past thin wedge in aligned magnetic field, using Fourier integral transform

15 p1917 A73-31338

Special relativity theory for steady irrotational ideal gas flow, noting subsonic, supersonic and transonic flow calculations based on small perturbation theory

15 p1864 A73-32060

Wave-trains in the solar wind. I - General theory and its application to an ideal, isotropic, one-fluid plasma.

17 p2224 A73-34505

On the mass transfer produced by oscillations in a compressible, dissipative, and inhomogeneous medium

19 p2503 A73-37528

Existence and uniqueness conditions for solid surface vaporization products dispersion into vacuum formulated for equations of motion of ideal gas under variable energy release

20 p2573 A73-39282

Light spectral width and constant frequency shift during spontaneous diffusion in ideal gas for fixed photon wave

22 p2885 A73-41721

Magnetogasdynamics shock polar - Exact solution in aligned fields.

22 p2893 A73-42393

Real gas turbocompressor calculations based on equations of state for fundamental thermodynamic processes in ideal gas

22 p2797 A73-42645

Unsteady transonic flows with shock waves in two-dimensional channels.

23 p2969 A73-43938

Flows past exponential bodies in the presence of strong compression in the shock layer

24 p3055 A73-45534

IDENTIFYING

NT CROP IDENTIFICATION

Engineering systems structure and parameter identification using transfer function, learning model and nonlinear filtering

07 p0796 A73-20427

Dynamic system model identification computational considerations, discussing equation error methods based on regression analysis, maximum likelihood estimates and gradient dependent algorithms for optimization

07 p0845 A73-20428

Methods and application of system identification in shock and vibration.

07 p0916 A73-20429

Shock and vibration disturbance identification based on structural system response, discussing linear programming, curve fitting, constraints, objective functions and applications

07 p0916 A73-20430

Identification of large structures using data from ambient and low level excitations.

07 p0916 A73-20431

The state of the art of system identification of aerospace structures.

07 p0916 A73-20432

On the application of parameter identification to high-speed ground transportation systems.

07 p0808 A73-20433

Adaptive control and identification via Liapunov's direct method.

09 p1067 A73-22232

Convergent iterative smoothing algorithm for aircraft stability parameter identification from measurement, using variational optimization procedure

09 p1067 A73-22233

State-of-art review in identification, state estimation and decision processes for time variant systems, discussing parametric, nonparametric, static and dynamic models

10 p1197 A73-23635

Order determination and parameter identification of time-invariant state variable models.

10 p1201 A73-24054

Suboptimal input signal synthesis for linear control system identification based on output SNR maximization, bandwidth matching and pseudorandom binary noise nature

11 p1327 A73-25197

Modelling and identification theory - A flight control application.

14 p1739 A73-30777

Mixed autoregressive moving average models parameters recursive joint identification and order determination extended for Kalman-Bucy filter transition and covariance parameters estimation 15 p1853 A73-31630

Identification and coding of fluid and electrical piping system functions. [SAE AIR 1273] 16 p1970 A73-33019

Secondary Surveillance Radar application to aircraft identification in upper airspace of Eurocontrol member states, emphasizing code assignment 22 p2884 A73-42322

Real-time identification using adaptive discrete model. 23 p2962 A73-43286

Asymptotically stable adaptive observer and identification scheme for linear system, using Liapunov canonical state representation 23 p2954 A73-43825

IFR (RULES)

U INSTRUMENT FLIGHT RULES

IGNEOUS ROCKS

NT ANORTHOSITE

NT BASALT

NT DUNITE

NT GRANITE

NT MOLDAVITE

NT OBSIDIAN

NT PERIDOTITE

Comparison of the linear polarization and albedo of volcanic rocks in the spectral region between 0.75 and 3.0 microns with the values of these parameters for the moon 01 p0101 A73-10841

Russian book - Fundamentals of lunar soil science: Physicochemical properties of lunar soils. 02 p0211 A73-11893

Maria lavas, mascons, layered complexes, achondrites and the lunar mantle. 03 p0368 A73-13088

Lunar gabbroic rock internal origin hypothesis support by petrologic data, giving temperature interval of crystallization from dry silicate melt 03 p0369 A73-13095

Comparative petrology of Apollo 16 sample 68415 and Apollo 14 samples 14276 and 14310. 03 p0375 A73-14103

Trace-element variation of individual plagioclase and hornblende phenocrysts. 04 p0414 A73-14986

Some textures in Apollo 12 lunar igneous rocks and in terrestrial analogs. 07 p0879 A73-19688

Electron petrography of Apollo sample 14310. 07 p0880 A73-19692

Petrographic features and petrologic significance of melt inclusions in Apollo 14 and 15 rocks. 07 p0880 A73-19694

Fra Mauro crystalline rocks - Mineralogy, geochemistry and subsolidus reduction of the opaque minerals. 07 p0880 A73-19698

Electron petrography of Apollo 14 and 15 rocks. 07 p0881 A73-19702

On the amount of ferric iron in plagioclases from lunar igneous rocks. 07 p0882 A73-19716

Rock 14068 - An unusual lunar breccia. 07 p0883 A73-19732

Compositions and mineralogy of lithic fragments in 1-2 mm soil samples 14002,7 and 14258,33. 07 p0884 A73-19739

Mineralogy, petrology, and surface features of some fragmental material from the Fra Mauro site. 07 p0885 A73-19748

Compositional data for twenty-one Fra Mauro lunar materials. 07 p0885 A73-19756

Composition of the lunar uplands - Chemistry of Apollo 14 samples from Fra Mauro. 07 p0886 A73-19757

Rare earths and other trace elements in Apollo 14 samples. 07 p0886 A73-19760

U-Th-Pb and Rb-Sr measurements on some Apollo 14 lunar samples. 07 p0888 A73-19779

Apollo 14 and 15 igneous rock, fines and breccia intrinsic and structure-sensitive magnetic parameters 07 p0893 A73-19842

Magnetic phases in lunar material and their electron magnetic resonance spectra - Apollo 14. 07 p0894 A73-19847

Ultrasonic P and S waves velocity of Apollo 14 and 15 lunar igneous and breccia rocks for elastic properties determination, noting cracks distribution function 07 p0894 A73-19853

Cosmic ray track densities of Apollo 14 breccias, igneous rock and soils from Fra Mauro, indicating surface residence times 07 p0871 A73-19871

Luminescence of Apollo 14 and Apollo 15 lunar samples. 07 p0897 A73-19882

Thermal conductivity of nineteen igneous rocks. I - Application of the needle probe method to the measurement of the thermal conductivity of rock. II - Estimation of the thermal conductivity of rock from the mineral and chemical compositions. 07 p0788 A73-20031

Indium abundances in cosmos, meteorites, tektites, rock-forming and ore minerals and igneous rocks, considering behavior in magmatogenic processes and rock weathering and alteration 12 p1490 A73-27125

Mineralogy, petrology and chemistry of lithic fragments from Luna 20 fines - Origin of the cumulate ANT suite and its relationship to high-alumina and mare basalts. 13 p1676 A73-28328

Comparison of linear polarization and albedo of igneous rocks in the spectral region 0.75-3.0 mu and lunar values of those parameters. 15 p1928 A73-30977

Darkening of silicate rock powders by solar wind sputtering. 17 p2235 A73-35740

Major and trace elements in igneous rocks from Apollo 15. 23 p2950 A73-43765

A survey of the selenochemistry of major, minor and trace elements. 23 p2951 A73-43768

IGNIMBRITE

U IGNEOUS ROCKS

IGNITEES

NT DETONATORS

NT INITIATORS [EXPLOSIVES]

Physical and chemical properties of solid propellant igniter materials, determining averaged heat of reaction and burning rate values [AIAA PAPER 72-1195] 03 p0352 A73-13485

Hot particle igniter for end-burning solid propellant rocket motors, noting ignition capability at 219 K and 110,000 ft simulated altitude [AIAA PAPER 72-1196] 04 p0485 A73-14919

Loading configurations with large combustion surface and reduced thickness for solid propellant rocket ignition [ONERA, TP NO. 1211] 10 p1262 A73-23658

Pyrotechnic explosive power devices and systems for aerospace applications. 16 p2045 A73-33106

IGNITION

NT ELECTRIC IGNITION

NT SOLID PROPELLANT IGNITION

NT SPARK IGNITION

Reignition characteristics of low current a.c. TIG welding arcs. 01 p0055 A73-10115

Ignition of nonhypergolic rocket fuels with fuming nitric acid under suitable conditions. 01 p0089 A73-10736

Hydrocarbon fuels diffusion flame ignition characteristics in hypersonic ramjet engines, testing additives effect for thermal self-ignition improvement 03 p0398 A73-14132

A nondimensional parameter characterizing mixing processes in a model of thermal gas ignition. 03 p0399 A73-14389

Flammable fuel-air mixture ignition by transient turbulent hot inert gas jet, calculating minimum required jet size 03 p0399 A73-14390

Study of exothermic processes in shock ignited gases by the use of laser shear interferometry. [AIAA PAPER 73-178] 05 p0640 A73-16920

Photochemical ignition and combustion enhancement in high speed flows of fuel-air mixtures. [AIAA PAPER 73-216] 05 p0641 A73-16946

The effect of higher alkanes on the ignition of methane-oxygen-argon mixtures in shock waves. [AD-756982] 07 p0918 A73-19389

Ignition of systems having refractory reaction products 07 p0920 A73-19988

Propane-oxygen pilot flame ignition of steady flowing Al powder stream in oxygen 07 p0865 A73-20362

Critical mass of cryogenic rocket propellants. 07 p0866 A73-20415

Effects of target-electrode polarity and of the position of the focal plane of the lens on the characteristics of a discharger with laser ignition 13 p1627 A73-28964

Ignition of nonhypergolic bipropellants in presence of suitable catalysts. 14 p1784 A73-30044

Supersonic combustion aid for liquid and gaseous fuels. 17 p2253 A73-34191

Shock tube study of the effect of unsymmetric dimethyl hydrazine on the ignition characteristics of hydrogen-air mixtures. 18 p2372 A73-37098

Investigation of the kinetics of high-temperature aluminum/oxygen interaction by the ignition method 19 p2503 A73-37504

Effects of target-electrode polarity and focal-plane position on a laser-triggered gap. 23 p2989 A73-44316

Ignition of metal particles in the case of a logarithmic oxidation law 24 p3154 A73-44704

Fuel combustion rate and turbulent diffusion induced self ignition in pulsejet engine combustion chamber from schlieren photography and pressure distribution measurements 24 p3123 A73-45377

Analysis of the self-ignition of fuel droplets behind a reflected shock wave 24 p3121 A73-45390

IGNITION LIMITS

Multistage ignition behind second and third cool flames of hydrocarbon combustion, presenting graphs of propane mixtures ignition limits 03 p0400 A73-14401

Ignition analysis of adiabatic, homogeneous systems including reactant consumption. [AIAA PAPER 73-215] 05 p0640 A73-16945

Upper self-ignition limit of hydrogen in oxygen 07 p0921 A73-19994

Quasi-stationary theory of hydrocarbon droplet ignition. I - Moment and limit of ignition 07 p0923 A73-20422

Chain interaction and heat release near the lower limit for self-ignition of hydrogen with oxygen 12 p1465 A73-26967

Modeling the ignition and cool-flame limits of acetaldehyde oxidation. 13 p1581 A73-28999

Flame quenching, extinction, propagation, convection and ignition limits in premixed gas mixtures 13 p1707 A73-29003

Quasi-stationary theory of hydrocarbon droplet ignition. II - Ignition limits of cold and hot droplets 18 p3272 A73-37117

Formation of a nonstationary diffusive flame front during the ignition of a liquid fuel droplet 19 p2471 A73-37507

Thermal limit of heterogeneous ignition 19 p2503 A73-37512

Ignition limit of metallic particles in a mixture of two oxidizers 19 p2503 A73-37517

The ignition of solid materials in oxygen by electrical sparks. 19 p2504 A73-38275

Concentration and combination limits of heterogeneous ignition 21 p2791 A73-40704

Dynamic effects on ignitability limits of solid propellants subjected to radiative heating. 22 p2899 A73-42813

Combustion of boron particles - Experiment and theory. 22 p2899 A73-42821

Boron particle ignition limit dependence on particle size and oxygen content, taking into account kinetic and diffusion resistance 24 p3155 A73-44708

IGNITION SYSTEMS

Ignition system development for end-burning solid propellant rocket motor, describing tubular, orifice and perforated type igniter configurations experiments [AIAA PAPER 72-1137] 03 p0355 A73-13444

Fluidic ignition system with two-component aerodynamic resonance heating /pneumatic match/ and hand pump for solid propellant sounding rocket engine [AIAA PAPER 72-1197] 03 p0252 A73-13486

Red fuming nitric acid suitability for nonhypergolic rocket fuel ignition in presence of chromate and dichromate catalysts 07 p0865 A73-19986

Reduced scale experimental study of propogol propulsion system ignition phases, defining pressure buildup curve shape and ignition limits [ONERA, TP NO. 1182] 09 p1135 A73-22711

High energy ignition systems using silicon controlled rectifiers. 12 p1533 A73-27931

Research on ignition and combustion in oxygen systems. 13 p1708 A73-29402

IGNITION TEMPERATURE

NT FLASH POINT

The cool-flame oxidation of n-heptane. I - The kinetic features of the reaction. 07 p0918 A73-19385

Study of the ignition reaction in an oxygen-hydrogen mixture at relatively high pressures and low temperatures in the shock tube 07 p0920 A73-19993

Magnesium particle ignition in various media 07 p0923 A73-20419

Al filament ignition temperature in carbon dioxide flow at various current values, noting relation to surface oxide film melting temperature 14 p1764 A73-30872

The combustibility of aluminum-nickel powders 18 p2325 A73-36862

- Ignition temperature of liquid fuel-fuel droplets
18 p2342 A73-37115
- Ignition temperature of conglomerates which form by burnout of the binder in a suspension of aluminum powder in kerosene
18 p2372 A73-37118
- Flowing gas mixture ignition at heated blunt body stagnation point, examining Van't Hoff criterion
23 p3048 A73-43328
- Experimental study of the critical conditions of powder ignition and combustion
24 p3155 A73-44707

IGY [GEOPHYSICAL YEAR]
U INTERNATIONAL GEOPHYSICAL YEAR
IL-62 AIRCRAFT

- Iliushin 62 aircraft horizontal stabilizer structural design and control, discussing mounting hardware and electrically driven servomechanism
11 p1305 A73-25795

ILLUMINANCE

- Extended border enhancement during intermittent illumination - Binocular effects.
17 p2112 A73-34842
- Illuminance and albedo variations /whiteness constancy/ category judgments for stimuli with unpatterned and patterned surfaces
21 p2639 A73-41183

ILLUMINATING

- A human factors approach to lighting recommendations and standards.
05 p0545 A73-16730

ILLUMINATION

- Effect of illumination on the form of current-voltage characteristics of SbSI in the paraelectric region
03 p0350 A73-13756
- The effect of illumination level, stroke width and figure ground on legibility of NAMEL numbers.
05 p0544 A73-16729
- Influence of changes in the contact region on the basic characteristics of a semiconductor in the illuminated mode
09 p1134 A73-22685
- Application of lateral illumination in holography of small objects
09 p1085 A73-23015
- Limulus photoreceptor response to single photon stimulation, discussing flash intensity, dim lights, discrete waves and subliminal responses
09 p1042 A73-23308
- Influence of the illumination law on the radioelectric performance of radomes - Contribution to the determination of apparent illumination of the antenna
11 p1328 A73-25284
- Cockpit instrument display systems visibility and reliability requirements, discussing various illumination methods in terms of power consumption, cost and human factors engineering
12 p1495 A73-26825
- Influence of illumination on the temporal resolution of photomultipliers
16 p1988 A73-33273
- Eye function and the illumination of instrument dials in aircraft
22 p2817 A73-43133

ILLUMINATORS

- Lidar illuminator/sensor system for range and/or angle spatial resolution enhancement, discussing pulse shape, optical characteristics and atmospheric effects on performance
06 p0667 A73-18303
- Pulsed GaAs illuminators for night-vision systems.
10 p1216 A73-23785
- A cooled illuminator for studying ruby lasers
12 p1506 A73-27219
- Investigation of a planar analyzing system employing laser illumination for facsimile transmitters
13 p1627 A73-28857

ILLUSIONS

- NT MOON ILLUSION
NT OCULOGRAVIC ILLUSIONS

ILMENITE

- X-ray study and Moessbauer spectroscopy on lunar ilmenites /Apollo 11/.
02 p0220 A73-12480
- Stability relations of ilmenite and ulvöspinel in the Fe-Ti-O system and application of these data to lunar mineral assemblages.
02 p0220 A73-12482
- An experimental investigation of the significance of zirconium partitioning in lunar ilmenite and ulvöspinel.
05 p0619 A73-16838
- Electron microprobe investigations of the oxidation states of Fe and Ti in ilmenite in Apollo 11, Apollo 12, and Apollo 14 crystalline rocks.
07 p0880 A73-19696
- Luna 20 - Mineral chemistry of spinel, pleonaste, chromite, ulvöspinel, ilmenite and rutile.
13 p1675 A73-28316

ILS [LANDING SYSTEMS]

U INSTRUMENT LANDING SYSTEMS

ILYUSHIN AIRCRAFT

NT IL-62 AIRCRAFT

- Russian book on Il-18 aircraft practical aerodynamics covering aerodynamic characteristics, performance, controllability, stability and flight safety
04 p0406 A73-15968

ILYUSHIN IL-62 AIRCRAFT

U IL-62 AIRCRAFT

IMAGE CONTRAST

- Some differences among figural aftereffects, apparent motion, and paracontrast.
01 p0011 A73-10435
- Investigation of the edge vision contrast phenomenon using the null method
01 p0009 A73-10654
- Influence of border and background on perception of straightness.
02 p0137 A73-12081
- Resolution of a solid-state image amplifier
03 p0282 A73-13664
- Psychophysical effects of night vision perceptual contrast in terms of central visual receptive field organization
03 p0261 A73-13759
- Stereoscopic depth magnitude in viewing background-contrasted superimposed half-fields, noting relation to binocular disparity detection
03 p0261 A73-13762
- Cortical area of neural loci involved in monoptic and dichoptic metacontrast occurring for target and masking stimuli imaged on different retinal regions
03 p0261 A73-13764
- Limiting resolution of reconstructed image of focused hologram in electron microscopes as function of aberration and spatial coherence
03 p0309 A73-14088
- The contrast and the visibility of noctilucous clouds in the twilight sky
04 p0441 A73-15293
- Axiomatic mathematical model for human visual edge contrast based on additivity, one-dimensionality and contrast continuity parameters
04 p0413 A73-15788
- Differential interference contrast microscope with continuously variable wavefront shear and pupilar compensation.
05 p0573 A73-16150
- Scanning and transmission type electron microscopes, discussing operating principles, image quality, resolution and applications
05 p0575 A73-16311
- Visual performance with high-contrast cathode-ray tubes at high levels of ambient illumination.
06 p0658 A73-18243
- Contrast transmittance Monte Carlo computation for atmospheric haze models based on aircraft measurement data from various geographical areas
06 p0694 A73-18302
- Electro-optic contrast observations in single-domain epitaxial films of bismuth titanate.
06 p0739 A73-18748
- Computer calculation of spectral brightness coefficients on aerial photographs, determining contrast features density gradients
07 p0824 A73-20044
- Vernier alignment acuity task accuracy related to retinal image line position location, noting effect of high contrast grating background
07 p0782 A73-20159
- Random dot pattern luminance and contrast effects on limiting inter-stimulus interval for visual apparent motion masking by bright field
07 p0783 A73-20256
- Contrast and assimilation effects analysis based on receptive field models of vertebrate retinal function
08 p0929 A73-20812
- Establishment of a relationship between the frequency and contrast characteristics of objects on aerial photographs and the resolving power
08 p0963 A73-21024
- Image contrast increase in holographic interferometry, using double exposure technique with reference beam half-wavelength phase shift
08 p0964 A73-21053
- Results of contrast measurements of some Martian maria in July-August 1971
08 p1007 A73-21062
- Eye dominance measurement relationship to image sharpness or visual acuity from binocular and monocular tests, obtaining dominance normal distribution
09 p1039 A73-21893
- Peripheral threshold of perceived contrast of the human eye.
09 p1046 A73-22964
- Optical fiber element image microcontrast dependence on fiber lightguide output and light-tight shell illuminance difference
10 p1228 A73-24584
- On neural inhibition, contrast effects and visual sensitivity.
11 p1318 A73-26197
- Moire topography for full size living human body contour stereophotographic pictures with high contrast, discussing instrument construction, performance and accuracy
11 p1365 A73-26239

- Foveal contrast sensitivity edge effect dependence on test stimulus size, form and duration
11 p1321 A73-26716

- The effects of edge sharpness and exposure duration on detection threshold.
11 p1321 A73-26718

- Investigation of the influence of temperature and velocity fields on the quality of an astronomical image
12 p1546 A73-27864

- Brightness functions for a complex field with changing illumination and background.
13 p1578 A73-28100

- Evoked potentials to changes in the chromatic contrast and luminance contrast of checkerboard stimulus patterns.
13 p1575 A73-28355

- Moire techniques of incoherent and coherent light filtering, line multiplication and contrast amelioration in framework of physical optics and diffraction theory for stress analysis
13 p1612 A73-28470

- Image contrast in a microscope with synchronous scanning of the object by point or raster field diaphragms
13 p1616 A73-28771

- Atmospheric effects in multispectral photographs.
13 p1619 A73-29239

- Some aspects of the design and performance of a small high-contrast channel image intensifier.
14 p1751 A73-29909

- Comparison of the resolutions of two projective holography methods by comparing their line scattering functions corresponding to holographic images
14 p1753 A73-30376

- Subjective brightness contrast lack of correlation with steady state evoked potential amplitude in suprathreshold stimuli range
15 p1837 A73-31017

- Modulation-transfer functions of scattering media, derived from observations in direct light.
15 p1914 A73-32189

- Visible solar disk contrasts in radiation controlled line, noting role of lateral differences in local shapes of line absorption profile
16 p2059 A73-32951

- Statistical brightness distributions for photometric planetary image improvement, considering telescope resolution, diaphragm diffraction and atmospheric turbulence
16 p2069 A73-33832

- Choice of optimal light characteristics for marks in optical sighting devices
17 p2114 A73-34241

- Visual acuity dependence on background brightness, object contrast, pupil diameter and visual time lag
17 p2114 A73-34639

- Evidence for non-linear response processes in the human visual system from measurements on the thresholds of spatial beat frequencies.
17 p2112 A73-34839

- Stabilized target visibility as a function of contrast and flicker frequency.
17 p2112 A73-34846

- Contrast measurement data of Martian maria in July-August, 1971.
18 p2355 A73-36863

- Spatial characteristics of chromatic induction - The segregation of lateral effects from straightly artefacts.
19 p2394 A73-37419

- Effects of temperature and velocity fields on the quality of astronomical images.
20 p2608 A73-39238

- ERTS-1 satellite return beam vidicon and multispectral scanner comparative evaluation for image quality, considering response functions, resolution, measurability, detectability and image motion effects
20 p2563 A73-39909

- New tubes and techniques for flash X-ray diffraction and high contrast radiography.
21 p2696 A73-39974

- Chromatic aberration effects on inelastic image resolution for high voltage electron microscopes
21 p2702 A73-40789

- The possibility of using information theory in optics
21 p2740 A73-41100

- Image contrast and efficiency of nonlinearly recorded holograms of diffusely reflecting objects.
21 p2703 A73-41133

- Application of transverse reference beams in holographic investigations of small particles.
22 p2860 A73-42253

- Stimulus specificity in the human visual system.
22 p2810 A73-42960

- Polarization - A key to an airborne optical system for the detection of oil on water.
23 p2979 A73-43225

- Mars seasonal effects from observations of contrast changes in blue light, discussing diurnal variations and UV contrast reversal
24 p3134 A73-44567

- Noise blurred image recognition probability characteristics from experimental investigation, showing difference from statistical decision theory data
24 p3062 A73-44667

A mathematical model for controlled image contour sharpness enhancement 24 p3064 A73-44907

Vector wave field hologram generation via polarization contrast method, described by correlation matrix formalism 24 p3091 A73-44957

IMAGE CONVERTERS

NT CELESCOPIES

NT IMAGE TUBES

Semiconductor thin film image amplifiers and converters based on electroluminescent and photoconducting films 01 p0022 A73-10037

Low energetic efficiency of semiconductor microwave scanning converters for radio images of fog obscured objects 05 p0556 A73-16072

Improvements in solid state radiographic converter screens. 05 p0574 A73-16280

A model of image-shape analysis based on fiber-optics elements and on the principle of photoelectric conversion 06 p0671 A73-18084

Photometric measurements with the aid of image converter tubes 06 p0696 A73-18859

TV vidicon image converter with arbitrary scanning format and computer-compatible output signals, using power spectrum redistribution functions 09 p1060 A73-22945

Multistage image converter tubes for studying high-speed phenomena. 13 p1611 A73-28175

Theory of image conversion in nonlinear optical systems 13 p1660 A73-28772

Comparison of an aluminum-coated phosphor layer and a Channeltron Electron Multiplier Array as extreme ultraviolet-to-visible image converters for use in space applications. 14 p1752 A73-30155

Ultraviolet proximity focussed converters for use in a satellite SEC-TV system. 17 p2170 A73-35296

Pulse time of flight measurements using mode locked laser ranging systems consisting of image converter tubes with deflection plates 17 p2185 A73-35411

The oblique electron lens. 18 p2316 A73-36597

Application of image-converter technique in quantum radiophysics and nonlinear optics [Survey paper]. 21 p2709 A73-39940

Image converter intensification for ultrahigh speed photography, discussing photographic film sensitivity, optical fiber output, slit analysis and camera types 21 p2694 A73-39941

Image-converter camera with subpicosecond temporal resolution. 21 p2694 A73-39947

Subpicosecond time-resolution image converter - The picochron. 21 p2694 A73-39950

Why exact metrology in an ultrahigh-speed cinematographic system - An application example: Calibration of image converters with a view to photometric measurements 21 p2694 A73-39951

High-speed interferometry of expanding and collapsing laser produced plasma. 21 p2744 A73-39964

Schlieren-optic and interferometric methods using TEA-CO₂ lasers and thermal liquid crystal IR image converters in the diagnostics of fast processes 21 p2744 A73-39998

Influence of inhomogeneities in a nonlinear crystal on the conversion of an image by sum-frequency generation. 22 p2869 A73-42245

Spatial resolution of an incoherent-to-coherent converter using bismuth germanium oxide. 22 p2863 A73-43098

Investigation of some characteristics of UM-92 image converters with oxygen-caesium photocathodes 23 p2983 A73-44361

IMAGE CORRELATORS

Image quality and energy distribution for mirror cone and toroidal annular mirror optical coordinators in wide angle measuring instruments 05 p0575 A73-16318

Radar correlation navigation map matching systems for civilian and military application, noting preprocessing aspects 06 p0721 A73-18280

IMAGE DISSECTOR TUBES

Working prototype image dissector photoelectron beam scanning by crossed electric and magnetic fields to measure beam density distribution in proton synchrotron 01 p0048 A73-10528

Astronomical position detector with image dissector tube at Cassegrain telescope focus for automatic guiding by illumination distribution analysis 01 p0029 A73-10544

High-speed stereoscopic investigation of paths of luminous objects 08 p0969 A73-21719

Photoelectron detection ability increase of image dissector by buffer intensifier tube, noting application for photon counting spectroscopy 08 p0971 A73-21745

IMAGE ENHANCEMENT

On the dependence of quietness and sharpness of solar image on local and large scale atmospheric circulation. 01 p0098 A73-10561

Planetary observation by earth based photography, discussing resolution limitation and improvement in terms of modulation transfer function 02 p0216 A73-12330

Real time linear and nonlinear motion desmeasuring of imagery telemetered from airborne platform, discussing inverse filter error analysis and analog simulation 03 p0276 A73-13907

Apollo 17 spacecraft telemetered IR scanner remote sensing data, reduction, discussing use of interpolating and smoothing splines for restored image resolution improvement 06 p0696 A73-18807

Schmidt telescopes for quasars and blue stars radio astronomy in southern sky survey, considering UV filtering-out for image quality improvement 08 p1011 A73-21362

Self-enhancement of LiNbO₃ holograms. 09 p1079 A73-21943

Remote sensing of lunar color differences using isoluminous enhancement techniques. 09 p1082 A73-22384

Backward masking and enhancement of multisegmented visual targets. 11 p1321 A73-25133

Mathematical principles of optical image deblurring by holography for photographic and electron micrographic applications 11 p1371 A73-26543

Digitally scanned spectral convolution by computerized filtering for noise spectra quality improvement with instrument signature removal 11 p1334 A73-26679

Image analysis techniques associated with automatic data base generation. 12 p1499 A73-27823

Piston engine or turboprop aircraft photography, measuring camera vibration components in roll, pitch and yaw by flashing light technique for image quality improvement 12 p1500 A73-27954

Electronic image enhancement in remote sensing by information content reduction before computer read-in, discussing electronic image transformations 12 p1501 A73-27961

Controlled-quality images from synthetic-aperture radar data. 16 p2015 A73-33358

Digital computer processing for automatic feature classification of ERTS-borne MSS and RBV imagery data, emphasizing interactive man-machine analysis for image enhancement 16 p1985 A73-33366

Holographic image enhancement using deblurring filters, discussing application to Polaroid photographs, electron micrographs and X ray photos 17 p2168 A73-34908

Exploration of Mars by Mariner 9 - Television sensors and image processing. 17 p2170 A73-35298

Restoration of degraded images by composite gratings in a coherent optical processor. 17 p2173 A73-35435

Advanced radiographic imaging techniques. 18 p2316 A73-36680

The application of constrained least squares estimation to image restoration by digital computer. 20 p2533 A73-39401

Thermal IR image recording, processing and enhancement, discussing prevention of defects or irregularities caused by aircraft motion, weather and electronic noise 20 p2566 A73-39670

Enhancement of Earth Resources Technology Satellite [ERTS/] and aircraft imagery using atmospheric corrections. 20 p2567 A73-39835

Image restoration filter with preprocessing to minimize distortion due to truncation errors and edge effects 21 p2697 A73-40131

The use of Skylab and ERTS data in an integrated natural resources development programme. 23 p2973 A73-43785

The Saturn rings in 1969: Morphological and photometric study. II - Deconvolution of the raw photometric curves 24 p3128 A73-44435

A mathematical model for controlled image contour sharpness enhancement 24 p3064 A73-44907

IMAGE FILTERS

Real time linear and nonlinear motion desmeasuring of imagery telemetered from airborne platform, discussing inverse filter error analysis and analog simulation 03 p0276 A73-13907

Holographic image enhancement using deblurring filters, discussing application to Polaroid photographs, electron micrographs and X ray photos 17 p2168 A73-34908

Image restoration filter with preprocessing to minimize distortion due to truncation errors and edge effects 21 p2697 A73-40131

IMAGE INTENSIFIERS

NT IMAGE ORTHICONS

Semiconductor thin film image amplifiers and converters based on electroluminescent and photoconducting films 01 p0022 A73-10037

Fast spectrograph and image slicers for avoidance of light transmission loss caused by central obscuration in astronomical telescope and image intensifier tubes 01 p0048 A73-10526

Resolution of a solid-state image amplifier 03 p0282 A73-13664

Noise figures, detection probabilities and scintillation energy distributions in second generation image intensifier tubes 06 p0676 A73-18299

Miniaturized second generation night vision image intensifier system operation and performance based on secondary photoelectron emission 06 p0694 A73-18300

Microchannel image intensifiers - Applications to ultrahigh-speed photography 06 p0697 A73-18860

An image intensifier spectrometer for remote sensing applications. 07 p0824 A73-19943

German monograph - Properties and dimensions of storage image intensifiers with lens raster storage, magnetic guiding field and microlens cathode. 07 p0803 A73-20392

Instrumentation in astronomy; Proceedings of the Seminar-in-Depth, Tucson, Ariz., March 13-15, 1972. 08 p0969 A73-21726

Image intensifier systems and their applications to astronomy. 08 p0971 A73-21743

Photoelectron detection ability increase of image dissector by buffer intensifier tube, noting application for photon counting spectroscopy 08 p0971 A73-21745

Image integration and display system for guiding on stars beyond the visual detection limit. 08 p0987 A73-21748

Some aspects of the design and performance of a small high-contrast channel image intensifier. 14 p1751 A73-29909

Design considerations for night-vision system optics. 16 p2012 A73-32865

A moderately-priced modern cathode-ray tube without intensifier electrode 16 p1987 A73-33166

The University College London image photon counting system - Performance and observing configuration. 17 p2169 A73-35279

Digital pulse counting astronomical spectrograph system with TV camera tube, image intensifier and minicomputer for camera scan control and video data processing 17 p2169 A73-35282

Photon counting with a self-scanned diode array. 17 p2169 A73-35283

The effect of system blocking in an intensifier dissector scanner. 17 p2169 A73-35284

A rapid-scanning image intensifier spectrometer for astronomy. 17 p2169 A73-35286

Spatially forbidden regions in the aurora. 18 p2313 A73-36648

Sensor development - An overview of recent Canadian experience. 20 p2533 A73-38578

[AAS PAPER 73-114] 20 p2533 A73-38578

Image converter intensification for ultrahigh speed photography, discussing photographic film sensitivity, optical fiber output, slit analysis and camera types 21 p2694 A73-39941

Characteristics and limitation of microchannel plates used in shutters for ultrahigh-speed photography 21 p2694 A73-39943

Coherent imaging system suppression of noise /extraneous non-image light/ through multiple-wave illumination, periodic phase modulation and diffuse wave illumination 21 p2698 A73-40148

Technical and economic problems in use of military passive night vision systems including image intensifiers, IR detectors and thermographic imaging devices 23 p2979 A73-43219

Design and performance of light-intensification night vision telescopes 23 p2979 A73-43220

Performances and physical limitations of image intensifiers 23 p2979 A73-43221

Microchannel image intensifiers for detection at low light levels 23 p2979 A73-43222

Image formation by light intensification and thermographic imagery compared from energy viewpoint, considering effect of parasitic light sources in visual field 23 p2979 A73-43223

Improvement of the electron optics of X-ray image-intensifiers. 23 p2982 A73-43678

Multichannel secondary electron image intensifier design, using dynode and separate channel transmission 23 p2961 A73-44386

Study of the spatial development of oxidation and combustion reactions by means of image photoelectric receivers, and of a thermometric method 24 p3091 A73-45398

IMAGE MOTION COMPENSATION

Image quality in telescopes with image motion compensation by secondary mirror control. 03 p0309 A73-14429

Automatic control for aircraft photographic camera pitch compensation via optical space filters and frequency methods, noting flight velocity to altitude relation 06 p0693 A73-18154

A method for the analysis of optical tracking systems. 07 p0822 A73-19194

The use of image quality criteria in designing a diffraction limited large space telescope. 08 p0969 A73-21730

Balloon-borne telescope-UV spectrometer for stellar spectrophotometric measurement with high spectral resolution, discussing system design and operation, image motion compensation and data acquisition 08 p0971 A73-21751

An electronically synchronized drum-type film camera 21 p2706 A73-41580

IMAGE ORTHICONS

Limiting magnitude techniques with the Corralitas 24 inch Cassegrain image orthicon system. 17 p2169 A73-35290

IMAGE TRANSDUCERS

Small view field high resolution all-reflective optical image scanner capable of straight line production for space applications 02 p0170 A73-12374

High resolution image data sensors and recorders characteristics and performance limits, describing transmission system 04 p0449 A73-15385

Charged coupled IC image sensors based on MOS capacitors for low light level TV, considering operation, performance and production technologies 06 p0676 A73-18301

IMAGE TUBES

Fast spectrograph and image slicers for avoidance of light transmission loss caused by central obscuration in astronomical telescope and image intensifier tubes 01 p0048 A73-10526

Electronography application to telescope and auxiliary instrumentation designs for astronomical photometry, considering spectracon and suitable image tubes 01 p0049 A73-10537

Electronographic image tubes for stellar field photometry. 01 p0049 A73-10539

The image tube nebular spectrograph of the Asiago Observatory. 01 p0050 A73-10543

Electro-optical multiband cameras for spaceborne remote sensing, discussing optical multiplexing, return beam vidicon, intensifier vidicon storage tube, image spectrophotometer and dissector 04 p0450 A73-15770

Radiation sensitivity of silicon imaging sensors on missions to the outer planets. 05 p0557 A73-16512

Ruby laser radiation removal of glowing spot from Kron electronographic image tube 05 p0580 A73-17260

A diode-type shutter tube for ultrahigh-speed photography 06 p0679 A73-18854

Some applications of a tube with proximity focusing in ultrahigh-speed motion-picture photography 06 p0696 A73-18858

Pyroelectric tubes for thermal imaging system, discussing materials, electron beam read-out, SNR and performance limit compared with scanned photon detectors 07 p0798 A73-19224

An instrument panel on an image tube in color 08 p0935 A73-21543

Accelerated generation of deflecting voltages by the functional beam-control method 08 p0967 A73-21589

Digicon multichannel image tube photoelectron counter for astronomical spectroscopy, discussing design information density and accuracy, noise and quantum efficiency 08 p0971 A73-21747

Image tube spectra of planetary nebulae for relative line intensities and radial velocities, considering nebulae properties 09 p1141 A73-22015

Properties of magnetic focusing systems for picture tubes 10 p1194 A73-23850

Photo-electronic image devices; Proceedings of the Fifth Symposium, Imperial College of Science and Technology, London, England, September 13-17, 1971. 14 p1751 A73-29903

Spectracon camera for astronomical telescope prime focus operation, discussing image tube extended area photocathode and mica window 14 p1751 A73-29906

Sources of spurious background in the Spectracon. 14 p1732 A73-29907

Electronographic image tube development at the Royal Greenwich Observatory. 14 p1732 A73-29908

Pick-up storage tube having an electronic shutter, automatic exposure control, wobbling correction, and slow scanning. 14 p1751 A73-29911

Electron-optical image transfer using opaque photocathodes with electromagnetic lens in image tubes 17 p2136 A73-34905

Preliminary progress with digital image-tubes at Cerro Tololo. 17 p2169 A73-35281

Characteristics of the U.B.C. television systems. 17 p2169 A73-35288

Image tube systems for ground based and spaceborne astronomical observations, considering self scanning diode array, phosphor screen output devices, electronography, etc 21 p2703 A73-41239

IMAGERY

NT AERIAL PHOTOGRAPHY
NT ALL SKY PHOTOGRAPHY
NT ASTRONOMICAL PHOTOGRAPHY
NT AUTORADIOGRAPHY
NT BLACK AND WHITE PHOTOGRAPHY
NT CHRONOPHOTOGRAPHY
NT CINEMATOGRAPHY
NT CLOUD PHOTOGRAPHY
NT COLOR PHOTOGRAPHY
NT ELECTRO-OPTICAL PHOTOGRAPHY
NT ELECTRON PHOTOGRAPHY
NT HOLOGRAPHY
NT INFRARED IMAGERY
NT INFRARED PHOTOGRAPHY
NT KINOFORM
NT LUNAR PHOTOGRAPHY
NT MICROWAVE IMAGERY
NT MICROWAVE PHOTOGRAPHY
NT PHOTOMICROGRAPHY
NT PHOTORECONNAISSANCE
NT RADAR IMAGERY
NT RADAR PHOTOGRAPHY
NT RADIOGRAPHY
NT REPRODUCTION (COPYING)
NT ROCKET-BORNE PHOTOGRAPHY
NT SATELLITE-BORNE PHOTOGRAPHY
NT SCHLIENEN PHOTOGRAPHY
NT SHADOWGRAPH PHOTOGRAPHY
NT SPACEBORNE PHOTOGRAPHY
NT SPECTROHELIOGRAPHS
NT SPECTROPHOTOGRAPHY
NT STEREOPHOTOGRAPHY
NT ULTRAVIOLET PHOTOMETRY
NT XEROGRAPHY

IMAGES

NT AFTERIMAGES
NT RETINAL IMAGES
Ground reflection effects upon radiated and received signals as viewed via image theory. 01 p0015 A73-10181

Atmospheric turbulence vs residual surface inaccuracy refracting and reflecting telescopic image degradation for solar observations 16 p2014 A73-32969

Optimum detection of an optical image on a photoelectric surface. 21 p2650 A73-40338

IMAGING TECHNIQUES

NT IMAGE ENHANCEMENT
NT RADAR IMAGERY

Electronographic image receptor advantages in spectrography, noting linearity, efficiency and detection threshold and receiver noise absence 01 p0049 A73-10540

Image transformation in visual condition simulators of aircraft training equipment 01 p0029 A73-10666

Comparison of high-resolution photographic emulsions for recording three-dimensional holograms. 01 p0051 A73-10839

Diffraction and nonlinearity characteristics of amplitude holograms for reconstructed nonlinear images on photosensitive layer 01 p0052 A73-11085

Holographic image polarization recording and sum wave simulation on photoanisotropic materials, using Weigert effect 01 p0052 A73-11086

Some new techniques for processing remotely obtained images by self-generated spectral masks. 01 p0078 A73-11219

Holo-diagram coherent optics device for studying interference patterns of object near focal points representing illumination and/or observation points 01 p0053 A73-11220

Talbot shearing interferometer based on Fourier imaging behind grating illuminated by plane monochromatic wave with spatial filtering, obtaining radial and lateral derivatives 01 p0053 A73-11227

Digital image processing for the earth resources technology satellite data. 01 p0020 A73-11457

Digital image-processing activities in remote sensing for earth resources. 01 p0021 A73-11476

A near-infrared view of the Uranus system. 01 p0109 A73-11491

Coherent laser radiation and holography in an optically inhomogeneous medium. 02 p0176 A73-12111

Linear photoelectric scanning techniques for achieving high resolution, comparing with two dimensional scanning at telescope or of electronographic images 02 p0169 A73-12332

Solar IR imaging techniques for providing high resolution data with short exposure time 02 p0169 A73-12333

Spin-scan imaging devices for various space missions, describing monochromatic and multicolor cameras, IR radiometer, multispectral scanner and imaging photopolarimeter 02 p0170 A73-12339

Planetary nebulae NGC 7635, 7008, 1514, 650-1, 7139, 3587, 6781 and 6543 monochromatic images, centering filters on H alpha, N II and O III forbidden lines 02 p0221 A73-12703

German monograph - Effect of spatial partial coherence on the measurement of optical transfer functions. 03 p0343 A73-13813

German monograph - Spatial oscillations of light in the refraction and image field of rough objects. 03 p0319 A73-13817

Ultrasonic holography application to NDT, discussing small angle approximation to spherical beam, hologram formation, image reproduction and wavelength change effect 04 p0446 A73-14674

Photographic observations of Comet Bennett, 1970II. 04 p0495 A73-14766

NDT applications of acoustic or stress wave, ultrasonic spectroscopy, imaging, critical angle reflectivity and holography 04 p0447 A73-14927

Digital image registration by correlation techniques. 04 p0449 A73-15413

Color image quantization error assessment from noninferior bit assignment determination for several coordinate systems by color shift comparison, using computer simulation 04 p0449 A73-15444

Mathematical description of frequency difference hologram obtained by superposition of two holograms of same object produced with light of different frequencies 04 p0451 A73-15924

Charged particle beams focusing in combined dual spiral system with uniform magnetic field along axis, applying to imaging of flat object 05 p0556 A73-16067

Imaging techniques for testing and inspection; Proceedings of the Seminar-in-Depth, Los Angeles, Calif., February 14, 15, 1972. 05 p0573 A73-16276

An overview - Advantages of imaging techniques for nondestructive testing. 05 p0573 A73-16277

Dynamic radiography - A new imaging technique using penetrating radiation. 05 p0573 A73-16278

- Imaging techniques for low-flux neutron radiography. 05 p0573 A73-16279
- Bragg-diffraction imaging and its application for non destructive testing. 05 p0574 A73-16281
- Ultrasonic isometric imaging. 05 p0574 A73-16283
- Acoustic holographic scanning techniques for imaging flaws in thick metal sections. 05 p0574 A73-16284
- Display of HF acoustic holograms utilizing liquid crystals. 05 p0574 A73-16285
- Holographic interferometry techniques and applications, discussing gas and ruby lasers in imaging, measurements and NDT of materials and mechanical components 05 p0574 A73-16286
- Quantitative materials evaluation and inspection with the image analysing computer. 05 p0575 A73-16288
- Human factors analysis of forward looking infrared (FLIR) imagery in air-to-ground target detection/recognition. 05 p0550 A73-16712
- Considerations and techniques for incorporating remotely sensed imagery into the land resource management process. 05 p0642 A73-17127
- Automatic analysis and classification methods based on statistical characteristics of aerial photometric and TV photographs, noting contour related interval distribution 05 p0579 A73-17143
- Wavefront sampling in holographic interferometry. 05 p0579 A73-17223
- Electronic creation of still and animated complex images, discussing techniques for supplying computer with object description 06 p0669 A73-17474
- Picture information acquisition, storage and transmission characteristics of film and vidicon systems for photographic reconnaissance of planets 06 p0750 A73-18010
- Complex images application of target isolation algorithms based on brightness distributions, discussing allocation of target classification parameters 06 p0694 A73-18289
- Recent advances in low light level field sequential color television. 06 p0694 A73-18298
- High bandwidth and resolution laser scanners and recorders for imagery transmission, discussing component constraints and integrated optics utilization in modulator and scanner development 06 p0701 A73-18310
- Pyroelectric IR detector materials thermal and electric properties, discussing applications in thermographs, focal plane reticle scanners, linear array thermal imaging, radiometers and laser detectors 06 p0694 A73-18317
- Launching base telelinter apparatus with image superposition on TV screen for controlling missile or rocket from going beyond security limits during initial flight 07 p0789 A73-18950
- Satellite-borne vidicon camera and associated control and telemetry electronics for imagery and dimensional parameters of sparks generated by gamma radiation 07 p0822 A73-18987
- Optics, image scanning mechanism and response characteristics of visible/IR radiometer onboard stationary satellite for earth imagery 07 p0822 A73-18988
- Holographic visualization of elastic waves 07 p0822 A73-19287
- Kinetics of electrostatic image formation during exposure of electrophotographic layers 07 p0823 A73-19331
- Reversible high speed high resolution imaging in amorphous semiconductors. 07 p0862 A73-19609
- Three dimensional models images information content increase in coherent light by interference shadow marking, noting automatic systems for distant objects recognition 07 p0824 A73-20140
- Modulation of intensity in multiple images of a luminous source given by a system of two parallel networks 07 p0824 A73-20163
- Holographic optical element for visual display applications. 08 p0963 A73-21034
- Speckle reduction by simulation of partially coherent object illumination in holography. 08 p0964 A73-21037
- Amplitudes of mth order holographic images recorded on film with power law characteristics. 08 p0964 A73-21054
- Three-dimensional holograms by rotational multiplexing of two-dimensional films. 08 p0964 A73-21055
- Noise reduction in acousto-optic /Bragg/ imaging systems by holographic recording. 08 p0965 A73-21209
- Analysis of thermal spread in a pyroelectric imaging system. 08 p0967 A73-21420
- Natural resources information system. 08 p0961 A73-21707
- A study of optical image sensors for the large space telescope. 08 p0971 A73-21742
- Electronic imaging systems with TV vidicon competition with film photography for spaceborne solar astronomy, comparing resolution, sensitivity and SNR 08 p0971 A73-21749
- Holographic system parameter relations from wave phase analysis of undistorted reconstructed image 09 p1079 A73-21915
- Two direct methods for reconstructing pictures from their projections - A comparative study. 09 p1080 A73-22224
- Ground based photometric observations of Mars during 1971 opposition, using conventional photography, multichannel spot photometry and dual channel area scanning 09 p1145 A73-22272
- New optical measurements of planetary diameters. IV - Size of the North polar cap of Mars. 09 p1145 A73-22273
- Acoustical holography applications in nondestructive testing. 09 p1083 A73-22514
- Characteristics of interference pattern formation during a self-reproduction process 09 p1096 A73-22858
- Holographic recording of focused images in multimode laser radiation 09 p1084 A73-22879
- The image-readout system of the combination photographic and television scanners of the Mars-2 and Mars-3 automatic interplanetary space probes. 09 p1086 A73-23050
- Optical properties of vertebrate eyes. 09 p1043 A73-23312
- Adaptive algorithm with error control for line by line encoder for image transmission, noting reconstructed image quality improvement 09 p1055 A73-23392
- Images of truncated triangular-wave periodic targets in optical systems in the presence of linear image-motion. 10 p1248 A73-23614
- Ultrasonic holography by one-dimensional moving of the source or the object. 10 p1216 A73-23664
- Visible and infrared sensor arrays for imaging systems. 10 p1216 A73-23787
- Nonlinear /binary/ transformation effects on acoustic hologram spatial signal amplitude noting multiple images and reconstructed image distortion 10 p1218 A73-24209
- Projective properties of an anamorphic bundle of projecting beams 10 p1219 A73-24484
- New techniques of acoustic image detection. 11 p1360 A73-25073
- Imaging photopolarimeter for measuring orthogonal, sky glow and gegenschein brightness and polarization in sky mapping mode 11 p1415 A73-25177
- Image holography through convective fog. 11 p1361 A73-25365
- A light and compact X-ray image read-out system for space applications. 11 p1364 A73-26050
- Solar chromatograph for monochromatic image production with variable bandwidth and simple shift to visible spectrum, discussing design and applications 11 p1365 A73-26235
- Image plane or optical system focal point location based on grain size variations from laser speckle patterns 11 p1378 A73-26245
- Sea ice observation by means of satellite. 11 p1358 A73-26346
- Coherent light optical filtering, holographically produced complex filters, imaging systems and pattern recognition multiplex arrangement for optical data processing, discussing image reconstruction 11 p1370 A73-26533
- Lensless Fourier transform holography with mutual coherent reference source close to object, investigating atmospheric turbulence effects on wavefront reconstructed image quality 11 p1370 A73-26539
- Application of an electronic image analyzer to dimensional measurements from neutron radiographs. 11 p1371 A73-26743
- Tomosynthesis - A holographic method for variable depth display. 12 p1495 A73-26829
- Application of longitudinal multimode laser coherence properties to increase the holographic depth of field. 12 p1504 A73-26830
- Circular carrier-frequency photography for observing phase objects. 12 p1495 A73-26832
- The facsimile camera - Its potential as a planetary lander imaging system. 12 p1495 A73-26875
- Book - An introduction to acoustical holography. 12 p1496 A73-27052
- A numerical algorithm for identifying spread functions of shift-invariant imaging systems. 12 p1475 A73-27114
- Holographic focused image recording and reconstruction in white light, considering source size, shape and spectral composition effects and interferometry 12 p1497 A73-27424
- Holographic construction and application of optical elements, discussing hologram lenses, holographic multiple imaging systems and diffraction gratings 12 p1498 A73-27501
- Reconstruction of the images of transparencies with a semiconductor laser. 12 p1498 A73-27512
- Image analysis techniques associated with automatic data base generation. 12 p1499 A73-27823
- [AIAA PAPER 73-430] 12 p1499 A73-27823
- Remote sensor dynamic imageries produced by stereo systems, discussing line-by-line and section-by-section orientation methods and triple channel recording scheme 12 p1500 A73-27956
- Spaceborne imaging sensors planimetric resolution characteristics, describing Apollo, Mariner, ERTS, Jupiter Pioneer, Skylab and Viking imaging systems 12 p1500 A73-27957
- Instruments and techniques for cartographic processing of space photographs. 12 p1500 A73-27959
- The resolving power and the modulation transfer function of terrestrial and aerial cameras in working conditions. 12 p1501 A73-27963
- Relationship between pointing precision, spread functions and modulation transfer functions. 12 p1501 A73-27969
- Aerial radar photograph restitution for photogrammetric application, discussing geometric qualities and methods and instruments for partial removal of distortion 12 p1502 A73-27972
- IR thermographic scanners and viewers operational principles, equipment performance specifications and thermal radiation distribution 13 p1611 A73-28020
- Confined optical and radio source image reconstruction from spatial frequency components of source not passed by imaging system 13 p1671 A73-28030
- Conditions of anastigmatization for Rowland assemblies fitted with concave holographic networks 13 p1613 A73-28567
- International Symposium on Acoustical Holography, 4th, Santa Barbara, Calif., April 10-12, 1972, Proceedings. 13 p1614 A73-28576
- A progress report on the laser scanned acoustic camera. 13 p1614 A73-28577
- Real-time reconstruction of images from hydroacoustic holograms. 13 p1614 A73-28578
- Real time high resolution 100 MHz acoustic image or hologram microscope using optical measurement of boundary displacement by incident angular sound wave 13 p1614 A73-28579
- Bragg-diffraction imaging - A potential technique for medical diagnosis and material inspection. 13 p1614 A73-28582
- Acoustical hologram recording by electrostatic transducers using rigid backplate electrode insulated with thin dielectric film transparent to ultrasonic radiation 13 p1614 A73-28584
- Analysis of various ultrasonic holographic imaging methods for medical diagnosis. 13 p1615 A73-28589
- The effects of scanning position and motion errors on hologram resolution. 13 p1615 A73-28590
- Spatial filtering considerations in Bragg diffraction imaging. 13 p1615 A73-28593
- Acoustic imaging by Bragg diffraction using point sources and spherical optics 13 p1616 A73-28594
- A comparison of holographic versus lens type acoustic image systems by computer simulation. 13 p1616 A73-28595
- Longitudinal and lateral magnification distortion correction in three dimensional long wavelength holography from standpoint of observer visual perception 13 p1616 A73-28596
- Ultrasonic acoustic holography for wave source and object in relative motion, predicting reconstructed

image aberration elimination performance in point-by-point mapping technique 13 p1616 A73-28597

Experimental investigation of the direct quasi-optical radio-wave imaging of small objects. 13 p1583 A73-28673

Reference wave elimination in acoustic holographic experiments via boundary surface of medium having sound wave propagation used as hologram 13 p1616 A73-28687

The recording of three-dimensional holograms on photochromic glass with the use of an optical bleaching process. I 13 p1616 A73-28765

Sensitivity and resolution in holographic interferometry of focused images 13 p1616 A73-28766

Video-to-film color-image recorder. 13 p1619 A73-29240

On the results of observations of occultations of stars by the moon according to the double image principle 13 p1686 A73-29559

High-resolution microwave holographic technique - Application to the imaging of objects obscured by dielectric media. 13 p1622 A73-29668

A non-stroboscopic system for examining high speed rotating objects. 14 p1750 A73-29704

Geometrical projection for holographic image reconstruction, assuming configuration and wavelength differences from reference wave 14 p1752 A73-30024

Photosensor aperture shaping to reduce aliasing in optical-mechanical line-scan imaging systems. 14 p1753 A73-30161

Theory of diffraction efficiency maximization for thin-layer amplitude holograms 14 p1753 A73-30364

Investigation of the dependence of the quality of a reconstructed holographic image on the parameters of the photoemulsion layer. I - Diffraction efficiency of the hologram 14 p1753 A73-30370

Imaging as primary exploration tool for outer planets and satellites, considering flyby and orbital imaging for planetary atmospheres 14 p1800 A73-30536

Holographic imaging and aberrations due to an incorrectly repositioned hologram in a system with lenses having aberrations. 15 p1915 A73-31015

A technique to retain the hologram reconstruction efficiency in elimination of the intense reference beam by the method of pre- or postexposure. 15 p1874 A73-31137

Russian book on ionizing radiation introspective methods for nondestructive flaw detection in non-transparent objects covering imaging techniques and quality control equipment 15 p1875 A73-31580

Digital image processing for information extraction. 15 p1875 A73-31800

High-density image-storage holograms by sampling and random phase shifter method. 15 p1876 A73-31946

Polarimetric observation of moon and planets via imaging system consisting of slot scanner, telescope, condenser lens, rotating disk analyzer and photomultiplier tube 15 p1876 A73-31960

Limiting information capacity of a holographic system 15 p1879 A73-32317

Optical model of a holographic television system 15 p1879 A73-32331

Radar data digital relay from outlying stations to ATC centers for air traffic image integration, discussing computerized plotting and alphanumeric display techniques 15 p1847 A73-32435

Holographic system parameter relations from wave phase analysis of undistorted reconstructed image 15 p1880 A73-32641

A hologram interferometer with a retro-reflected speckle reference beam for the real time visualization of vibration patterns. 16 p2013 A73-32880

Electrooptical-phase imaging device using nematic liquid crystals 16 p2013 A73-32881

Reflected light holographic microscopy of moving objects. 16 p2014 A73-33174

Utility of remote-sensing data for urban land use planning. 16 p2003 A73-33363

Applications of high-altitude remote sensing to coastal zone ecological studies. 16 p2003 A73-33364

Hybrid techniques for automatic imagery interpretation. 16 p2016 A73-33367

An introduction to holography by shadow casting. 16 p2016 A73-33950

Simulated ERTS data for coastal management. 17 p2157 A73-34285

Developments in electronic imaging techniques; Proceedings of the Seminar-in-Depth, San Mateo, Calif., October 16, 17, 1972. 17 p2167 A73-34901

Capabilities and limitations of infrared imaging systems. 17 p2167 A73-34902

A real-time simulator for image data systems. 17 p2147 A73-34903

Ultra high resolution electronic imaging and storage with the return beam vidicon. 17 p2136 A73-34904

Electron-optical image transfer using opaque photocathodes with electromagnetic lens in image tubes 17 p2136 A73-34905

Digital processing of Mariner 9 television data. 17 p2168 A73-34907

Role of cooperative effects in hologram generation and in the formation of reconstructed images 17 p2168 A73-34921

Satellite imagery of land resources, discussing synoptic views, spatial dependence, closed loop information and sequential sampling 17 p2161 A73-34945

Image quality of binary and multigradation microwave holograms, noting HF components and background noise 17 p2168 A73-35164

The use of television type sensors in astronomy. 17 p2169 A73-35278

Digital hardware and computer system for a digital image recorder. 17 p2131 A73-35280

Imaging techniques in spaceborne X ray astronomy, discussing ray focusing, data processing and observational requirements of single photon detection and high time resolution 17 p2170 A73-35294

The optical design of the 40-in. telescope and of the Irene Dupont telescope at Las Campanas Observatory, Chile. 17 p2171 A73-35408

Reference radiation frequency shift for holographic interferometry of vibrating objects 17 p2172 A73-35428

Single step detection of blurred images in a coherent optical processor. 17 p2173 A73-35436

Vibration analysis of plates by real-time stroboscopic holography. [SESA PAPER 2111] 17 p2173 A73-35448

Extraterrestrial life detection from imaging observations on lunar samples and meteorites, discussing application to Mars surface 17 p2113 A73-35804

Satellite imagery in national resource surveys and vegetation growth monitoring on mine dumps from ERTS-1 data 18 p2311 A73-36151

Advanced radiographic imaging techniques. 18 p2316 A73-36680

Hidden-line removal at 20 pictures/second through hybrid techniques. 18 p2291 A73-36830

Noise source distribution in subsonic jets. 19 p2472 A73-37290

Recent developments in digital image processing at the Image Processing Laboratory of JPL. 19 p2429 A73-37324

Image reconstruction from the modulus of the correlation function - A practical approach to the phase problem of coherence theory. 20 p2570 A73-38616

German book - Practical photoelasticity/3rd revised and enlarged edition/. 20 p2566 A73-39273

Imaging system pointing precisions, deriving ground target size relationships to spread function and modulation transfer function respectively 20 p2567 A73-39672

Ground based and airborne microwave radiometer imaging techniques for surface mapping and atmospheric investigations, discussing self calibration, antennas, waveforms and aircraft nose instrumentation 20 p2567 A73-39838

Structure of dust storms from ITOS-1 T.V. images obtained over Iraq and the Gulf of Persia. 20 p2584 A73-39854

The interpretation of multispectral imagery - An analysis of automated versus human interpretation techniques. 20 p2558 A73-39875

Spacecraft television image comparison between earth and Mars surface features and geology, discussing mountain chains, deserts and tectonic mapping techniques 20 p2613 A73-39897

ERTS-1 multispectral scanner analysis of Kansas reservoirs color and water content, discussing turbidity, gray coloration levels, water management possibilities and water sample data 20 p2563 A73-39912

Expected results of hydrologic and geologic studies using ERTS imagery of the Atacama Desert, Atiplano, and Puna de Atacama, South America /Southwest Bolivia, Northwest Argentina, and Northern Chile/. 20 p2563 A73-39914

International Conference on Ultrahigh-Speed Cinematography, 10th, Nice, France, September 25-30, 1972, Transactions 21 p2693 A73-39933

Ultrahigh speed cinematography with rotating Ti drums bound by monocrystalline boron fibers, noting prototype performance 21 p2693 A73-39937

High-speed SFKF photographic camera of the continuous type. 21 p2693 A73-39938

Observation of the surface of hypersonic projectiles by holography 21 p2694 A73-39956

Short interval double-pulsed holography of reflecting objects. 21 p2695 A73-39960

Rainfall estimation from satellite visible and IR imagery, discussing calibration and accuracy requirements 21 p2730 A73-40093

Color holographic technique through wave front coding of colored object, discussing He-Ne, He-Cd and argon laser irradiation, coding masks and image reconstruction 21 p2697 A73-40128

Double frequency diffraction grating lateral shear interferometer for lens focusing and heterodyne phase detection 21 p2698 A73-40137

Coherent imaging system suppression of noise/ extraneous non-image light/ through multiple-wave illumination, periodic phase modulation and diffuse wave illumination 21 p2698 A73-40148

Automatic surface mapping via holographic system, describing Q switched ruby laser holograms, image dissector, computer video signal analysis and scan signals 21 p2699 A73-40150

A study of the statistical patterns of visual perception of a black and white raster image 21 p2644 A73-40861

An approach to computer image generator for visual simulation. [AIAA PAPER 73-928] 21 p2673 A73-40875

Electrofluoroplanigraphy for human body layer single-plane sections synchronization, using X ray tomography and TV imaging followed by roentgenogram electronic summation 21 p2645 A73-41216

Space-variant system analysis of image motion. 21 p2706 A73-41609

Quantitative analysis of sonic fields during their visualization by holographic methods 22 p2852 A73-41899

A laser raster setup with programmed control for image lithoplate synthesis 22 p2869 A73-42362

Time-average holography of objects vibrating sinusoidally and moving with constant acceleration. 22 p2863 A73-43092

Speckle noise reduction by the composition of diffused Fraunhofer holograms. 22 p2863 A73-43093

Geostationary meteorological satellite network development for static and cinematographic image transmission based on international cooperation 22 p2884 A73-43118

Automated data reduction of holographic interferometry translational measurement of diffusely reflecting rigid body by reconstructed virtual image processing on CDC 6600 computer 22 p2863 A73-43147

Numerical method for computer generated kinoform image reconstruction error minimization, comparing with random phase method 22 p2863 A73-43148

Multidimensional Fourier transforms and image processing with finite scanning apertures. 22 p2864 A73-43150

The imaging properties and aberrations of thick transmission holograms. 22 p2864 A73-43185

Optical system imaging in partially coherent light, noting Rayleigh criterion insensitivity to aberration as characteristic of two-point resolution criteria 22 p2889 A73-43187

Image formation by light intensification and thermographic imagery compared from energy viewpoint, considering effect of parasitic light sources in visual field 23 p2979 A73-43223

- Role of the outer scale of turbulence in atmospheric degradation of optical images. 23 p3005 A73-43341
- The nature of quasi-axial reconstructed pictures generated by 'nonreferenced' focused-image holograms 23 p2982 A73-43705
- Holographic technique for coherent optical imaging system superresolution via storage of image amplitude 23 p2983 A73-44088
- Polarimetric instrument of moon and planets via imaging system consisting of slot scanner, telescope, condenser lens, rotating disk analyzer and photomultiplier tube 24 p3089 A73-44485
- Maximum information capacity of a holograph system. 24 p3089 A73-44623
- A double image chopping polarimeter. 24 p3091 A73-45185

IMBEDDINGS [MATHEMATICS]

- NT INVARIANT IMBEDDINGS**
- Conformal transformation of semiordered linear space via inclusion statement, considering second order differential operators 01 p0069 A73-10068
- Nonlinear homotopies for obtaining initial solutions for iteration procedures 01 p0069 A73-10069
- Russian book - Study of the theory of differentiable functions of many variables and its applications. IV. 02 p0187 A73-12176
- Imbedding theorem for the spaces of functions whose mixed derivatives satisfy the multiple integral Holder condition 02 p0187 A73-12178
- Integral bounds of generalized derivative solutions of second-order equations of elliptic type in the L_p metric and certain related embedding theorems 02 p0187 A73-12181
- Construction of the spinor field equations in cosmological space 08 p1010 A73-21271
- Pseudo-umbilical manifolds of codimension 2 and of constant mean curvature in an n plus 2 dimensional elliptic space and generalizations 23 p3000 A73-44300
- State minimization of incompletely defined deterministic automaton by imbedding one-to-one mapping into homomorphism 24 p3074 A73-44664

IMDES

- Vibration-rotation bands of NH in the spectrum of alpha Orionis. 01 p0104 A73-11041
- Influence of excitation power on the energetic characteristics of phthalimide solutions 11 p1376 A73-26143
- Synthesis and characterization of isomeric cis- and trans-pyrone model compounds. 21 p2648 A73-41215

IMINES

- An evaluation of molecular constants and transition probabilities for the NH free radical. 11 p1402 A73-26582
- Nitrogen quadrupole coupling constants in cis-propyleneimine. 23 p2950 A73-43272

IMMERSION

U SUBMERGING

IMMISCIBILITY

U SOLUBILITY

IMMITTANCE

U ELECTRICAL IMPEDANCE

IMMOBILIZATION

- Organ and body mass changes in restrained and fasted domestic fowl. 04 p0409 A73-14975
- The effect of prolonged immobilization on diuresis and water intake in rats. 11 p1320 A73-26489
- The effect of immobilization on body fluid volume in the rat. 20 p2513 A73-39487
- Effect of hind-limb immobilization on contractile and histochemical properties of skeletal muscle. 21 p2642 A73-41624

IMMUNITY

- Correlational inter-relationships between the neuroendocrinal system and the genotype in the formation of protective reactions of the organism 15 p1835 A73-31875

IMMUNOLOGY

- Effects of the space flight environment on man's immune system. II - Lymphocyte counts and reactivity. 02 p0135 A73-12565
- Russian book on auto-antibodies of X ray irradiated animal and human blood and organisms covering cell formation, isolation, preparations, sickness treatment and auto-immune reactions 04 p0410 A73-15711

Possible role of antitissular autoantibodies in the protective mechanism of local shielding during total radiation exposure 06 p0657 A73-17685

The effects of bilateral destruction of certain medial-hypothalamus structures on the formation of complement-binding antibodies 07 p0781 A73-19647

Reactivity and certain metabolic indices during prolonged sustenance of animals in artificial nutrient conditions 15 p1833 A73-31162

Study of myocardial antigen localization using the immunofluorescence method 15 p1834 A73-31392

Effects of oxygen-augmented atmosphere on the immune response. 17 p2115 A73-34743

Hematological, biochemical, and immunological studies during a 14-day continuous exposure to 5.2% O₂ in N₂ at pressure equivalent to 100 FSW /4 ata/. 18 p2278 A73-36794

Ocular antigens. IV - A comparative study of the localisation of immunogenic determinants of ocular structural glycoproteins in connective tissues of various organs. 22 p2802 A73-41729

IMP-E

U EXPLORER 35 SATELLITE

IMP-I

U EXPLORER 43 SATELLITE

IMP-6

U EXPLORER 43 SATELLITE

IMPACT

NT ELECTRON IMPACT

NT HYPERVELOCITY IMPACT

NT ION IMPACT

NT POINT IMPACT

NT PROTON IMPACT

Impact interaction of an absolutely hard body and an elastic two-mass system 11 p1400 A73-26455

IMPACT ACCELERATION

Cylindrical metal projectile impact induced elastoplastic deformation, determining dynamic yield point by computer simulation of Taylor stress wave propagation model 10 p1292 A73-24529

Experimental investigation and correlation of the ground impact acceleration characteristics of a full scale capsule and a 1/4 scale model aircraft emergency crew escape capsule system. 15 p1829 A73-31463

Leading edge effects on displacement thickness and skin friction variations of unsteady boundary layer on flat plate under impulsive motion in viscous fluid 16 p1962 A73-32927

Impact acceleration effects on rabbit central nervous system, noting changes in nerve tissue elements and cerebral vessels 17 p2111 A73-34227

Atmospheric entry and impact behavior of modular disk shaped radioactive isotope heat source for space nuclear power 19 p2454 A73-38387

IMPACT DAMAGE

NT METEORITIC DAMAGE

NT RAIN IMPACT DAMAGE

Successive solidification origin of central peaks and terrace ring wall in lunar crater formations filled with melt after impacts, using freezing water experiments 03 p0369 A73-13094

Fiberglass reinforced composite material application to light weight ballistic damage tolerant military helicopter flight control components previously vulnerable to small arms fire 04 p0452 A73-14722

Hydrodynamic phenomena during high-speed collision between liquid droplet and rigid plane. [ASME PAPER 72-WA/FE-30] 04 p0435 A73-15850

Theoretical low-speed particles collision with symmetrical and cambered aerofoils. [ASME PAPER 72-WA/FE-35] 04 p0404 A73-15852

Large deflexion elastic-plastic response of certain structures to impulsive load - Numerical solutions and experimental results. 06 p0761 A73-17818

Fracture due to damage from projectile impact. 06 p0763 A73-18484

Approximate analysis of containment/deflection ring responses to engine rotor fragment impact. 07 p0910 A73-19188

Apollo 14 regolith and fragmental rocks, their compositions and origin by impacts. 07 p0883 A73-19725

Lunar micrometeoroid flux, calculating rocks survival time before impact damage and mass wasting rate by single particle abrasion 07 p0895 A73-19865

Scanning electron microscope and energy dispersive X-ray analysis of the surface features of Surveyor III television mirror. 07 p0872 A73-19899

The erosion of carbon fibre reinforced plastic by repeated liquid impact. 07 p0843 A73-20224

Photographic and metallographic evidence of two stage ductile materials erosion mechanism under particle impact, describing impact velocity, particle size and angle effects 07 p0839 A73-20225

Damage produced by high-speed liquid-drop impacts. 09 p1109 A73-21932

Cometary collision energy triggering of catastrophic changes in climate, geological period terminations and lava flow initiation, noting tektite-geologic period ages correlation 10 p1275 A73-23823

Ballistic-tolerant helicopter flight control components from plastic composite materials. 10 p1237 A73-23964

Displaced mass, depth, diameter, and effects of oblique trajectories for impact craters formed in dense crystalline rocks. 10 p1276 A73-24077

Sheet, tecto-, ortho- and chain silicates crystal lattice breakdown under shock from ballistic range experiments, using Debye-Scherrer method for X ray diffraction studies 10 p1277 A73-24078

Terrestrial, Martian and lunar doublet crater origins from simultaneous multiple meteorite impacts, using Lexan plastic projectiles against sand targets in ballistic range tests 10 p1277 A73-24079

Temperature change induced material properties variations effects on impact stresses in graphite and stainless steels, considering impact velocity 10 p1220 A73-24575

Raindrop impact erosion damage on ceramic radome materials, discussing Rayleigh wave mathematical model comparison with sled test data, and laboratory simulation 11 p1336 A73-25306

A contribution to Hertz's theory of elastic impact. 13 p1696 A73-28748

Impact body or medium damage prediction and modification technology, discussing test facilities and applications 13 p1699 A73-29310

A consistent crashworthiness design approach for rotary-wing aircraft. [AHS PREPRINT 781] 17 p2106 A73-35094

Effect of simulated lunar impact on the survival of bacterial spores. 20 p2513 A73-39485

Mechanical erasure of particle tracks - A tool for lunar microstratigraphic chronology. 20 p2612 A73-39713

Dynamic fracture criteria for a polycarbonate. 21 p2723 A73-40956

IMPACT DECELERATION

U DECELERATION

U IMPACT ACCELERATION

IMPACT LOADS

Long-wave approximation in problems of stability loss by impact 01 p0118 A73-11410

Complex phenomena in metal surface layers after high velocity impact loading in Ar atmosphere 02 p0182 A73-12698

High speed testing of materials mechanical behavior over range of impact loading rates 03 p0394 A73-14023

Impact loading on structures with random properties. 04 p0510 A73-15028

Effect of the cross sectional shape of specimens on their strength under transverse-bending impact loads 05 p0632 A73-16327

Short-term longitudinal dynamic stability of rods with allowance for clamping methods and for previous transverse deflection 05 p0632 A73-16329

Impact of a cylindrical shell against the surface of a compressible fluid. 06 p0758 A73-17451

The critical rate of tensile stress application and its significance for characterizing the behavior of materials under impact loads 07 p0838 A73-19213

Initial free-surface motion of an impulsively loaded half-space. 07 p0810 A73-19509

Impact-deflection by oblique fibers in sparsely reinforced composites. 08 p1018 A73-21408

Dynamic behaviour of thin cylindrical shells collided with dampers. 08 p1019 A73-21527

Longitudinal impact of a rigid body against a clamped rod 09 p1158 A73-22361

Impact on a simple physical model of the head. 10 p1185 A73-24770

- Elastic impact against a beam with allowance for internal energy absorption 11 p1433 A73-25032
- Stress waves in finite longitudinally layered shells. 11 p1442 A73-25712
- Vibrations of an Euler beam with a system of discrete masses, springs, and dashpots. 11 p1442 A73-25788
- Elastic and elastoviscoplastic unloading waves propagation in semiinfinite bar under axial impact stress, considering bilinear stress-strain curve 11 p1447 A73-26646
- Influence of impact deformation on the strengthening and aging kinetics of austenitic steel 4Kh12N8G8MFB 12 p1510 A73-26901
- Substructure alteration in manganese and nickel austenitic alloys under the action of microimpacts 13 p1630 A73-28013
- Normal impact of a cone against an elastoplastic membrane 14 p1815 A73-30789
- Numerical solution to the problem of elastic ring impact at a rigid obstacle 14 p1815 A73-30798
- Impact interaction between a soft shell and a hard obstacle 15 p1947 A73-31276
- Further developments in surface effect takeoff and landing systems concepts - A multicell system. [CASI PAPER 76/11B] 17 p2099 A73-34294
- The dynamic response of columns under short duration axial loads. 17 p2248 A73-35040
- Anisotropic laminated fiber composite plates under short duration impact line forces, calculating one dimensional transient stress and displacement waves by fast Fourier transform [ASME PAPER 73-APM-L] 17 p2249 A73-35108
- A necessary condition for the nonoccurrence of von Mises yielding in impulsively loaded plates. 17 p2250 A73-35118
- Failure mechanisms in impact loaded carbon and glass fiber reinforced plastics, discussing specimen geometry, notch presence, fiber type, fiber orientation and hybridization effects 17 p2198 A73-35538
- A distributed parameter model of the inertially loaded human spine. 18 p2281 A73-36429
- Special features of the fracture of aluminum and titanium alloys at low temperatures 19 p2439 A73-37267
- Front-end collision of a partially liquid-filled cylindrical shell with a solid body 20 p2616 A73-39261
- Experimental study of the stressed state of an elastic beam undergoing transverse impact 20 p2620 A73-39385
- Short interval double-pulsed holography of reflecting objects. 21 p2695 A73-39960
- Effect of explosive impact on hardening and kinetics of aging of austenitic steel 4Kh12N8G8MFB. 21 p2720 A73-41034
- A higher order theory for extensional motion of laminated composites. 22 p2929 A73-43139
- A survey of compatibility of materials with high pressure oxygen service. 23 p2991 A73-43525
- The stress pulses propagated as a result of the rapid growth of brittle fracture. 23 p3042 A73-43805
- Propagation of shock waves in anisotropic composite plates. 24 p3149 A73-45149
- Shock wave propagation in colliding elastic bars under axial end-on impact, deriving closed form solution for curvilinear stress-strain characteristics 24 p3112 A73-45430

IMPACT PREDICTION

- Prediction of the landing point of a balloon payload. 01 p0005 A73-11208
- Correction for angle of incidence of meteoric particle with penetration and piezoelectric sensors in estimates of spatial density of meteoric matter. 12 p1554 A73-27644
- Impact body or medium damage prediction and modification technology, discussing test facilities and applications 13 p1699 A73-29310
- Planetary quarantine constraints for outer planet satellite encounter missions, determining spacecraft impact probability in terms of trajectory analysis and navigation error numerical integration 18 p2349 A73-35976
- IMPACT PRESSURES
- U IMPACT LOADS
- IMPACT RESISTANCE
- Rain-erosion resistance and other properties of Schott infrared-transmitting glasses. 11 p1387 A73-25299

- Fiber strength, fracture types and material elastic properties relationship to impact resistance in carbon fiber reinforced plastics 12 p1515 A73-26882
- Recent developments in precipitation hardenable stainless steels. 13 p1637 A73-29271
- Light weight impact protective helmet shell materials and designs, noting E- or S-glass and polyimide resin for oxygen rich space station/shuttle applications 16 p2027 A73-32677
- Low cost manufacturing methods for highly reliable ballistic-tolerant composite helicopter flight control components. [AHS PREPRINT 754] 17 p2180 A73-35082
- The impact resistance of glassfiber reinforced plastics under accumulation of fatigue damage. 20 p2580 A73-38645
- Method of observing processes in the interior of explosives 21 p2695 A73-39966
- The dynamic fracture toughness of carbon-carbon composites. 24 p3105 A73-45147

IMPACT SENSITIVITY

U IMPACT RESISTANCE

IMPACT STRENGTH

- Intergrain boundary shape effects on the impact strength and character of brittle fracture 01 p0064 A73-10606
- Impact and contact stress analysis in multilayer media. 02 p0234 A73-12072
- Low-temperature mechanical properties of the alloys AT3 and AT6. 02 p0180 A73-12136
- Impact fracture resistance of Cr-Mn-Si steel, investigating alloying effects on crack initiation and propagation 02 p0181 A73-12211
- Temper embrittlement response and toughness of a rare earth treated Ni-Cr-Mo steel. 02 p0183 A73-12762
- Significance of the sequence of treatment for the notch impact strength of cold-worked steel samples 02 p0175 A73-12850
- The properties of 18Ni 350 maraging steel produced from elemental and prealloyed powders. 04 p0466 A73-15800
- The significance of impact data for brittle non-metallic materials. 04 p0469 A73-15985
- Structure and properties of the weld metal in maraging N18K9M5T steel 06 p0697 A73-17879
- Alloy composition and temperature effects on nitrogen solubility in austenitic Cr-Ni steels, noting nitride precipitation effect on impact strength reduction 07 p0839 A73-19950
- Fiber reinforced plastics with adhesive bonded elements, investigating ply number and adhesive pressure effects on shear, bending and impact strengths 07 p0844 A73-20330
- Flat laminated FRP-FRTP and carbon FRP-FRTP composites, testing lamination effects on bending and impact strengths 07 p0844 A73-20331
- Izod impact properties of carbon-fibre/glass-fibre sandwich structures. 09 p1110 A73-22517
- Impact strength and fracture of carbon fiber composite beams. 10 p1238 A73-23972
- Izod impact tests of carbon fiber composites strength, measuring residual compressive strength 10 p1238 A73-23973
- Impact response of curved box beam-columns with large global and local deformations. 11 p1440 A73-25530
- [AIAA PAPER 73-401] The impact toughness of discontinuous boron-reinforced epoxy composites. 11 p1389 A73-26046
- The effect of fibre-matrix interface strength on the impact and fracture properties of carbon-fibre-reinforced epoxy resin composites. 12 p1515 A73-26922
- German monograph - Investigations regarding the strength characteristics of adhesive bonds involving metals in the case of impact stress. 13 p1625 A73-29277
- Deformation mechanism and strength of metals under impulsive loading. 13 p1639 A73-29463
- Effect of cooling /to -269 C/ on failure in Kh18N10T and Kh16N6 steels under impact bending 14 p1763 A73-30692
- Properties of HSLA steels, with and without molybdenum. 15 p1891 A73-32169
- Factors affecting the impact strength of glass-fibre-reinforced polyester composites. 16 p2031 A73-33987

- Effect of oxides on certain properties of glass-ceramic coatings for titanium 18 p2319 A73-35889
- Investigation of the impact toughness of construction materials at temperatures of 20 and 4.2 K 18 p2324 A73-36767
- Studies on the impact resistance of composite plates. 18 p2367 A73-37093
- A photographic method for testing the impact strength of metals 21 p2696 A73-39991
- Physico-mechanical properties and damage mechanism of moving-picture photographic materials as film systems 21 p2699 A73-40270
- Ceramic component strength degradation by projectile impacts in terms of momentum and elasticity relation 21 p2723 A73-40892
- Effect of technological and metallurgical treatment on the properties of electrosag-welded joints in heat resistant steels 22 p2865 A73-41778
- Al-aluminum nickelide eutectic fiber composite impact strength dependence on crystallization rate, examining crack propagation rate relation to fiber spacing 23 p2996 A73-43437
- Gamma to alpha transformation and notch depth effects on metastable austenitic steel impact strength at cryogenic temperatures 23 p2995 A73-44282

IMPACT TESTING MACHINES

- Photo-optic instrumentation of magnetic flyer plate facility for pressure-time response measurement of impact loaded test specimens, using streak and high speed framing cameras 09 p1083 A73-22512

IMPACT TESTS

NT CHARTY IMPACT TEST

- An analysis of the breaking elongation in high velocity impact of the power law hardening materials. 01 p0117 A73-11123
- Complex phenomena in metal surface layers after high velocity impact loading in Ar atmosphere 02 p0182 A73-12698
- On the production of fatigue cracks for determining the work of rupture in bending tests. 04 p0450 A73-15670
- Method of determining the energy of fracture of aluminum alloys during impact-bend tests with sharp notches. 04 p0466 A73-15675
- Some experiments on dynamic and quasi-static forging of aluminum at elevated temperatures. [ASME PAPER 72-WA/MAT-1] 04 p0457 A73-15811
- Axial impact response of semiinfinite cylindrical membrane shell of helically oriented linearly elastic orthotropic fiber reinforced material, solving motion equations 05 p0631 A73-16112
- Measurement of vibration characteristics by impact testing. 05 p0637 A73-17233
- Rocket sled facility for impact tests with friable balloon platforms, describing braking and accelerating jet configurations, vibration damping measures and telemetry system 07 p0808 A73-19004
- Post impact behavior of mobile reactor core containment systems. 07 p0850 A73-20468
- An examination of the perforation of a mild steel plate by a flat-ended cylindrical projectile. 08 p1016 A73-20828
- Low-temperature impact bending with recording of the stress-strain diagrams 09 p1100 A73-22157
- Brittle fracture tests of Ti-Cr steels with/without nitrogen hardened layer under shock impact loads 09 p1107 A73-23199
- Effects of composition on embrittlement of austenitic stainless steels. 10 p1230 A73-23628
- Izod impact tests of carbon fiber composites strength, measuring residual compressive strength 10 p1238 A73-23973
- Interlaminar shear strength of a carbon fiber reinforced composite material under impact conditions. 10 p1240 A73-24286
- Fatigue and impact tests on composite propeller blades made of glass- and carbon fiber reinforced plastics, noting comparison with measured vibratory strains 12 p1458 A73-26881
- Metal barrier maximum puncturable thickness dependence on high velocity meteorite particle impact parameters 12 p1554 A73-27642
- Impact tests for aid in data interpretation of measured meteor particles impact on spacecraft structures, noting transducer response dependence on impact angle 12 p1554 A73-27643

Experimental investigation and correlation of the ground impact acceleration characteristics of a full scale capsule and a 1/4 scale model aircraft emergency crew escape capsule system.
[AIAA PAPER 73-480] 15 p1829 A73-31463

French monograph - Study of craters formed on glass surfaces by the impact of artificial micrometeoroids.
15 p1898 A73-32591

Intensity of mechanical influences and mechanical degradation of hard polymers
16 p2030 A73-33940

Impact gages for detecting meteoroid and other orbital debris impacts on space vehicles.
17 p2238 A73-34606

Development of airframe design technology for crashworthiness.
[SAE PAPER 730319] 17 p2101 A73-34677

Angular dependence of the impulse of recoil in the case of high-speed impact
18 p2362 A73-36123

A critical examination of the impact test for glassy polymers.
19 p2444 A73-38093

Some results in the erosion of prestressed materials due to water-jet impact.
19 p2443 A73-38299

Recording strain diagrams in low-temperature impact bending tests.
22 p2874 A73-42105

Experimental determination of the transient uniaxial stress in a bar by dynamic photoplasticity.
[ASME PAPER 73-APMW-37] 22 p2926 A73-42894

IMPACTORS

Relative efficiencies of filters and impactors for collecting stratospheric particulate matter.
17 p2167 A73-34863

Theory of a two-mass model of a vibrational impactor
20 p2592 A73-38981

IMPATT DIODES

U AVALANCHE DIODES

IMPEDANCE

NT ACOUSTIC IMPEDANCE
NT CONTACT RESISTANCE
NT ELECTRICAL IMPEDANCE
NT ELECTRICAL RESISTANCE
NT MECHANICAL IMPEDANCE
NT REACTANCE
NT RESPIRATORY IMPEDANCE
NT SKIN RESISTANCE

Spectral characteristics of the scatter field from a rotating impedance cylinder in uniform motion.
17 p2129 A73-35707

IMPEDANCE MATCHING

Aperture matching of wideband phased array radar antennas, using digital ferrite phase shifters and dielectric transformer with magnetic resonance limiting
01 p0022 A73-10178

Resonant feedback loops and impedance matching network analysis of pulsed and CW transistor microwave power oscillators
01 p0024 A73-10722

Synthesis of active RC circuits by means of equivalent circuits of impedance converters
02 p0148 A73-11549

A decoupling supply network for small antenna arrays
02 p0145 A73-11825

Calculation of input-voltage standing-wave ratio for a reflector antenna.
05 p0547 A73-16161

GaAs transferred electron /Gunn/ device microwave oscillator with harmonic tuning, noting reactive termination and bias voltage effects on efficiency optimization
05 p0559 A73-16813

Lambda/4 directional coupler in an inhomogeneous medium with deviations of even and odd mode parameters from the ideal value
05 p0559 A73-17000

Matching of capacitive sensors to low-noise amplifiers based on field effect transistors
07 p0802 A73-20296

Evaluation of the norm of the wave-impedance distribution function in the synthesis of an inhomogeneous line for wide-band matching
08 p0946 A73-21105

Conditions derived for reactive two-terminal-pair matching transformer networks operation at maximum power transfer efficiency
09 p1061 A73-22046

Active RC filter synthesis with decoupling stage and third order element for minimizing impedance mismatching and overall capacitance
10 p1193 A73-23734

Microwave transistor power amplifier.
11 p1338 A73-26149

Book - Microwave power measurement.
12 p1480 A73-27425

Inductive flow meter sensor design for optimal electrode diameter to ensure signal quality and impedance matching, proposing circuit diagram
13 p1611 A73-28019

Resonant bipolar linear networks representation by matched equivalent circuits
13 p1589 A73-28121

IMEKO Symposium on Microwave Measurement, Budapest, Hungary, May 10-13, 1972, Proceedings.
14 p1733 A73-30054

Broad-band impedance matching of rectangular waveguide phased arrays.
14 p1734 A73-30205

Self complementary wire element phased array antennas, discussing matching, operating bandwidth, structural design and isolation
15 p1850 A73-31255

Astronomic follow-up systems with mismatch signal buildup
15 p1877 A73-32134

Digital photoelectric tracking systems with accumulation of the mismatch signal
16 p1977 A73-32716

Matching of capacitive pickups to low-noise junction-gate field-effect transistor amplifiers.
18 p2294 A73-37133

Enhancement of the sensitivity of microwave admittance measurements through the use of 'matching' two-ports
19 p2409 A73-37717

Optimal matching by using band filters
20 p2537 A73-39452

Microstrip junction circulators with fixed ferrite disks, achieving broadband impedance matching between center conductor and transmission line by transformer on alumina substrate
20 p2538 A73-39668

A new procedure for the design of a waveguide element for a phased-array antenna.
21 p2652 A73-40658

Wide-angle impedance matching of phased-array antennas - A survey of theory and practice.
21 p2652 A73-40659

Multimode phased array element for wide scan angle impedance matching.
21 p2652 A73-40661

Design of a phased array radiating face for prevention of performance degradation in the presence of rain.
21 p2663 A73-40663

Low-noise microwave down-converter with optimum matching at idle frequencies.
21 p2666 A73-41428

Modification of antenna radiating characteristics with multi-impedance loading.
22 p2831 A73-41848

A digital system for receiving binary phase-coded signals
23 p2952 A73-43319

IMPEDANCE MEASUREMENTS

Negative resistance in metal-semiconductor-metal /MSM/ diodes.
01 p0023 A73-10579

On the measurement of the local impedance of acoustical duct liners in the presence of grazing mean air flow.
03 p0342 A73-12989

An accurate bridge method for impedance measurements of impatt diodes.
03 p0281 A73-13175

Data analysis criteria and instrumentation requirements for the transient measurement of mechanical impedance.
03 p0343 A73-13837

Measurement of admittances of microwave oscillators with injection locking.
03 p0310 A73-14497

Experimental investigations on the impedance behavior of a cylindrical antenna in a collisional magnetoplasma.
06 p0729 A73-18186

Plasma sheath capacitance and resistance in double inverse pinch device from I-V measurements with Langmuir probe, noting relationship to plasma temperature and density
06 p0696 A73-18784

Si varactor diode series resistance resonance measurements in UHF band, noting approximate invariance with frequency
06 p0678 A73-18842

Measurement of admittance of Gunn diodes in passive and active regions of bias voltage
08 p0947 A73-21432

Inductance and Q factor measurements of inductive p-n-p transistor element in IC circuit as function of frequency, temperature and junction capacitance
10 p1196 A73-24613

AC impedance of silicon solar cells.
11 p1310 A73-26000

Panoramic measurement of the coupling impedance of delay systems by the heterodyne method
12 p1479 A73-27210

Magnetovariational frequency sounding of the earth, using the ratio of magnetic potentials
12 p1491 A73-27352

Measurement of semiconductor junction parameters using lock-in amplifiers.
13 p1595 A73-29578

Description of the measurement design and the measurement principle in the measurement of the chip impedance of coaxially mounted semiconductor diodes in the microwave range
14 p1733 A73-30058

An impedance tube for precision measurement of acoustic impedance and insertion loss at high sound pressure levels.
16 p2013 A73-32916

Fluctuation theory of the two-dimensional mixed state of superconductors of the first kind
16 p2044 A73-34068

Electron depletion in the wake of ionospheric spacecraft - A comparison between results from Langmuir probes and antennas.
17 p2159 A73-34783

Measurement techniques for antennas in dissipative media.
17 p2143 A73-35685

Measurement of impedance transformation on practical dipoles.
17 p2128 A73-35690

The generalized multiprobe reflectometer and its application to automated transmission line measurements.
17 p2143 A73-35691

Antenna impedance measurement with Weissfloch transformer between terminals and point in input transmission line for achieving high precision
17 p2129 A73-35704

Wideband VHF whip antenna impedance simulation using AI cylindrical chamber to simplify impedance-controlling network tuning and power testing
17 p2148 A73-35705

The acoustic impedance of perforates at medium and high sound pressure levels.
18 p2337 A73-37030

Measurement technique for large-signal admittance of IMPATT diodes.
19 p2409 A73-37427

Enhancement of the sensitivity of microwave admittance measurements through the use of 'matching' two-ports
19 p2409 A73-37717

Surface strip coplanar waveguide characteristic impedance measurement as function of aspect ratio and substrate thickness
20 p2538 A73-39595

Small arrays - Their analysis and their use for the design of array elements.
21 p2652 A73-40656

A new flush mounted antenna element for phased array application.
21 p2663 A73-40662

Electromagnetic interference and compatibility control in aircraft communication, discussing RF current, voltage, impedance and SNR measurement techniques
22 p2821 A73-41692

Use of magnetic materials for improvement of screening properties of different types of cables.
22 p2830 A73-41805

On input impedance of an arbitrarily oriented small loop antenna in a cold collisionless magnetoplasma.
22 p2824 A73-41858

Input admittance or impedance and effective height measurement for small metal antennas of prolate and oblate spheroidal and spherical shape, noting transient response
22 p2829 A73-43180

A theoretical and experimental study of the insulated loop antenna in a dissipative medium.
22 p2829 A73-43184

Frequency magnetovariational sounding of the earth, using the ratio of potentials.
23 p2970 A73-43249

Determination of hole and electron traps from capacitance measurements.
24 p3119 A73-44405

IMPEDANCE PROBES

NT RADIO FREQUENCY IMPEDANCE PROBES

The plasma diagnostics experiments of the Aeros satellite
[DGLR PAPER 72-070] 02 p0166 A73-11669

Satellite-borne swept frequency impedance probe /gyroplasma probe/ for ionospheric plasma parameters including electron density and ion composition, noting PCM telemetry system
22 p2917 A73-42571

IMPELLER BLADES

U ROTOR BLADES [TURBOMACHINERY]

IMPELLERS

NT PUMP IMPELLERS

Predicting method of the change in stage performance of axial flow machinery for the variation of cascade geometry.
07 p0867 A73-19225

The computation and utilization of Busemann's analysis of potential flow in an impeller.
16 p1964 A73-33506

[ASME PAPER 73-GT-45]

Design method of the axial-flow blade row on modified isolated aerofoil theory with interference coefficient. II - The influence of the aerodynamic parameter on the fan performance at low flow rate.
19 p2377 A73-37671

- Blade tip clearance loss between centrifugal impellers and shrouds during two dimensional viscous laminar flow, discussing energy dissipation and pressure and temperature distribution 19 p2474 A73-38417
- The use of analytic surfaces for the design of centrifugal impellers by computer graphics. 22 p2900 A73-42477
- Evaluation of slip factor of centrifugal impellers. 22 p2796 A73-42625

IMPERFECTIONS**U DEFECTS****IMPERMEABILITY****U PERMEABILITY****IMPINGEMENT****NT JET IMPINGEMENT**

Numerical solution to kinetic equations of rarefied supersonic steady gas flow normal to plate by method of characteristics 06 p0643 A73-17461

IMPLANTATION**NT ION IMPLANTATION**

Hazard and interference avoidance in implant telemetry, discussing leakage currents, muscle interference, magnetic influence, high frequency noise, electrode and respiratory artifacts, etc 03 p0271 A73-14295

Surgically implanted single and multichannel telemetry systems for monitoring single and multiple physiological parameters, discussing size and power requirements 03 p0271 A73-14302

A remotely operated ECG telemeter for chronic implantation in rats. 03 p0272 A73-14303

An implantable blood pressure and flow transmitter. 04 p0447 A73-14845

An implantable glass electrode used for pH measurement in working skeletal muscle. 08 p0935 A73-21510

Technique for the implantation of long-term diagnostic electrodes in the amygdaloid complex of the human brain 09 p1046 A73-22857

Implantable transducer for in vivo measurement of bone strain. 12 p1464 A73-27443

Ionic machine tools for microelectronic manufacture, discussing ion jets properties, optics and construction and implantation, micromachining and deposition technologies 16 p1987 A73-33088

IMPLOSIONS

Appraisal of UTIAS implosion-driven hypervelocity launchers and shock tubes. [AD-753252] 05 p0562 A73-16180

Laser-initiated fusion - Key experiments looming. 06 p0727 A73-17570

Simplified averaged equations of concentric laser compression of plasma. 24 p3117 A73-45427

IMPREGNATING

Elastic behavior of polymer-impregnated porous ceramics. 07 p0842 A73-19198

A statistical investigation on the mechanical properties of metals impregnated graphites. 11 p1388 A73-25416

The effect of impregnation and wetting characteristics on the mechanical parameters of glass-fiber-reinforced plastics 24 p3103 A73-44877

IMPROVED TIROS OPERATIONAL SATELLITES**NT ITOS I****IMPULSE NOISE****U ELECTROMAGNETIC NOISE****IMPULSE TRANSFER ORBITS****U TRANSFER ORBITS****IMPULSES**

The behavior of a self-excited system acted upon by a sequence of random impulses. 04 p0469 A73-14664

Three dimensional gas flow noncollinear total impulse normal and tangential components calculation leading to pressure force determination 12 p1486 A73-27089

Impulse reaction resulting from the in-air irradiation of aluminum by a pulsed CO₂ laser. 21 p2715 A73-40960

IMPURITIES

The role of impurity particles in the combustion of double-base propellants. 01 p0089 A73-10639

Cold shortness of W and related refractory metals, noting oxide phases and impurities effects on mechanical properties temperature dependence 01 p0066 A73-11341

Impurities effect on Mo plastic properties and toughness, suggesting lower vacuum arc welding rates and increased electron beam zone refining runs 01 p0066 A73-11343

Doping additions dissociation effect on impurities distribution in grown semiconductor crystals of melts, calculating atomic and molecular concentration 02 p0201 A73-12356

Impurities effect on platinum resistance thermometers temperature reading accuracy, presenting empirical formula for approximate error estimate as function of operational conditions 03 p0307 A73-13193

Minority carrier lifetime and diffusion constant as function of impurity concentration in double junction vertical solar cell, determining power efficiency 03 p0254 A73-14213

Temperature dependence of impurity resistivity in dilute Al-based Ti, V, Fe, Cu, Zn alloys between 78 and 930 K. 04 p0461 A73-14875

Impurity centers effect on I-V characteristics of double injection level semiconductors, noting negative resistance region 04 p0482 A73-14877

Trace phase analysis as an aid in the study of heterogeneous raw material impurities in powder metallurgy 04 p0464 A73-15370

Impurities and cooling rate effects on cast W structure during crystallization from optical metallurgy 04 p0466 A73-15668

Purity evaluation of n type GaAs LSA diodes from low-field temperature-dependent mobility. 05 p0556 A73-16435

Influence of the degree of purity on the kinetics of the recrystallization of deformed magnesium 05 p0587 A73-17216

Investigation of dislocation locking by interstitial impurities in bcc-lattice metals 06 p0708 A73-18055

The concentration-dependent diffusion of chromium in nickel oxide. 06 p0712 A73-18760

Effect of impurity gradient on the time delays and Q-switching in junction lasers. 07 p0836 A73-20189

Investigation of the lasing and luminescent properties of fluorite and strontium fluoride crystals containing bivalent dysprosium impurities 07 p0837 A73-20207

Impurity transport in a cylinder in the case of a time-dependent flow rate and gas exchange with the wall 08 p1022 A73-20998

Fabrication, electrical properties and reliability of thin film capacitors, noting surface irregularity and impurity effects on reliability 08 p0946 A73-21082

Computer optimisation of double-drift-region IMPATT diodes. 08 p0947 A73-21433

Comparison of the efficiency of photocells with stepwise and exponential distributions of the impurities in the doped layer 09 p1033 A73-22721

Multistage diffusion model of IC transistor electrical characteristics and impurity distributions as function of surface concentrations and junction depths during fabrication 10 p1196 A73-24606

The photometric determination of aluminum in steel after separation on a cation-exchanger 11 p1380 A73-25447

Variation in the kinetics of the natural aging process for Mg-Li-Al alloys as a function of the presence of impurities and small additions of rare-earth elements 12 p1510 A73-26911

Distribution coefficients and solubility curves of certain rare-earth elements in GaAs 12 p1531 A73-27194

Influence of the impurity compensation effect on the magnitude of the negative reluctance of alloys of the $\text{In}_2\text{Te}_3/\text{x}-\text{Hg}_3\text{Te}_3/1-\text{x}$ system 12 p1532 A73-27940

Influence of the chrome content and the interstitial impurities content /carbon and nitrogen/ on the volumetric and intergranular diffusion of iron 59' in iron-chrome alloys with from 0 to 15 per cent chrome - Relations with alpha to alpha plus gamma reversible transformations 12 p1514 A73-27985

Effect of impurities on the substructure and dislocation formation in metal crystals grown from melts 13 p1631 A73-28103

Properties of iron impurity in aluminium matrix studied by Mossbauer spectroscopy. 13 p1634 A73-28220

Determination of the basic characteristics of an impurity level by Hall effect measurements 13 p1668 A73-28461

Light scattering in coherent systems for Stokes and anti-Stokes impurity centers in terms of classical and quantum mechanical theories 13 p1660 A73-28770

Characteristics of the decomposition of an interstitial-impurities solid solution in molybdenum during recrystallization 14 p1760 A73-30589

Influence of interstitial impurities on the formation of a cellular structure and on the properties of chromium 14 p1764 A73-30858

Method for the determination of impurity particle dispersion in fuels and lubricants 15 p1876 A73-31834

Auger spectroscopy usefulness demonstration by determination of impurity segregation in localized regions, reviewing grain boundary segregation role in metal properties deterioration 15 p1892 A73-32248

Thermal conductivity and temperature dependence of energy gaps in niobium samples containing large amounts of impurity atoms 16 p2027 A73-34061

Theory for the inelastic tunneling effect in normal metals 16 p2027 A73-34063

Injection currents in semiconductors with deep polarizable impurity centers 18 p2341 A73-37046

Some details concerning plastic deformation mechanism of commercial titanium between -100 and 400 C 19 p2441 A73-37839

Dynamic scattering of oscillating charged centers in semiconductors 19 p2471 A73-38541

Calculation of the base layer conductivity of a transistor structure 20 p2535 A73-38859

Effect of impurities on the temperature of the superconducting transition in W₃Si type compounds 20 p2600 A73-39731

Influence of electrically active impurities on the mobility of individual dislocations in germanium 21 p2751 A73-40370

CAD for realization of an impurity distribution in a semiconductor. 21 p2753 A73-41095

Cyclotron resonance in a weakly ionized hydrogen plasma with nitrogen, oxygen and air impurities 22 p2890 A73-41864

Interaction of interstitial impurities with iron-subgroup metals in as-cast molybdenum-based dilute solid solutions 22 p2873 A73-42090

Impurity diffusion of iron in molybdenum. 23 p2994 A73-44157

The effect of halide impurities on the mass production of metal whiskers by reduction. 24 p3098 A73-44401

IN-FLIGHT MONITORING

Real-time computer for monitoring a rapid-scanning Fourier spectrometer. 01 p0020 A73-11231

Integrated engine diagnostics and displays for Navy aircraft of the 1980's. [AIAA PAPER 72-1084] 03 p0354 A73-13406

System monitoring techniques: Practical applications and experience at Eastern - Jet engines. [SAE PAPER 720818] 05 p0606 A73-16639

Russian book - Methods and equipment for in-flight aircraft strength tests. 07 p0777 A73-20376

System for in-flight recording of the rotational speed of the turbine of a jet engine 07 p0828 A73-20546

Display system for monitoring automatically controlled STOL landing glide paths, discussing computer controlled simulation 11 p1362 A73-25440

In-flight flutter testing methods for determining aircraft structure natural frequencies and vibration damping ratios with air flow [ONERA, TP NO. 1224] 11 p1306 A73-26593

A-300 B airbus active and passive operational monitoring systems, considering visual and aural routine functional indicators, emergency warning devices and flight data recorders 15 p1830 A73-32458

Minicomputer application to in-flight control of A300-B airbus engines, describing computational procedure for low pressure compressor stage RPM limit /N 1 limit/ 15 p1831 A73-32477

Data sample analysis of anomalous in-flight behavior incidents for spacecraft reliability covering incident causes and occurrence time, effects on mission and corrective actions 16 p2073 A73-33625

In-flight frequency calibration of IR sensor systems using LEDs. 17 p2165 A73-34275

Jet engine malfunction diagnosis - The sensing problem, candidate solutions and experimental results. 17 p2222 A73-35243

YF-12 aircraft flight loads measurement program with strain gage bridges in fuselage, fuel tanks, control surfaces and left wing 17 p2107 A73-35444

Inflight electrostatic probe measurements of the effect of chemical injection on the properties of the re-entry flow field. [AIAA PAPER 73-692] 18 p2338 A73-36243

Determination of statistics of turbulence in clear air 18 p2332 A73-36687

Cockpit layout effects on pilot and flight crew activities, using in-flight observation, photography and pilot eye movement evaluation 19 p2384 A73-37733

Navigation and landing aid systems in-flight and ground performance monitoring, discussing safety, legal, operational and economic aspects 19 p2450 A73-37802

Environment effects on tape recorder design for in-flight data collection in military aircraft 19 p2431 A73-38197

Drive logic computation for variable stability aircraft in-flight simulators with six independent controllers providing dynamic motion and ground, crosswind and special effects [AIAA PAPER 73-933] 22 p2799 A73-41971

Total In-Flight Simulator for X-22A aircraft based on variable stability-and-control system concept for reliability design 24 p3057 A73-45153

IN-FLIGHT THRUST MEASUREMENT

U IN-FLIGHT MONITORING

U THRUST MEASUREMENT

INACTIVATION

U DEACTIVATION

INCENTIVES

Statistical expectation application to risk density functions and fee/incentive-element relationships for contract incentive structuring, considering C-5A procurement 08 p1025 A73-20958

INCIDENCE

Separated flow past a slender delta wing at incidence. 15 p1821 A73-31121

INCIDENT RADIATION

Incidence of a plane electromagnetic wave on a moving shock wave in an ionized gas 01 p0016 A73-10205

Average monostatic scattering cross section for plane electromagnetic wave incident on ideally conducting convex body, considering wavelength relation to body dimensions 03 p0278 A73-14072

Absorption of light at oblique incidence on a plasma layer. 07 p0854 A73-19262

Inverse problem of diffraction for a reactance plane 07 p0793 A73-19919

Numerical study of a diffusion-type chemical laser. 07 p0836 A73-19959

Analytic ray trajectory model of radio wave lateral incidence on traveling large scale ionospheric inhomogeneities as function of location and departure angle 13 p1583 A73-28724

Solution of a boundary value problem for the oblique incidence of a plane E-polarized wave on a metallic strip array with an optically active medium 13 p1623 A73-29682

Zone of Poynting vector rotation toward the direction of an applied magnetic field for a wave incident on an inhomogeneous plasma 15 p1919 A73-31707

Calculation of the parameters of a chemically reacting gas behind an incident and reflected shock wave 15 p1840 A73-31855

Average intensity of the normal wave during super-refraction 16 p1978 A73-32897

Nonlinear transformation of an electromagnetic wave at the boundary of a magnetoactive plasma 18 p2289 A73-36562

A generalized extinction theorem and its role in scattering theory. 20 p2591 A73-38613

Geomagnetic field effects in Martin theory of radio wave propagation in ionosphere with oblique and vertical signal incidence 20 p2555 A73-39181

Laser beam incidence in active nonlinear medium, considering Kerr effect, beam generation, Green function and intensity calculations for wave scattering 21 p2710 A73-40153

Use of the backscattering method to measure the atmospheric transparency in oblique directions 21 p2731 A73-40495

Evanescent fields produced by totally reflected beams. 22 p2824 A73-41853

Observations of the ionospheric absorption at oblique incidence during the IASY. 22 p2847 A73-42195

Incident electromagnetic wave reflection in inhomogeneous plasma with local nonlinearity, discussing reflection point shift and dielectric permittivity effect 22 p2892 A73-42328

The wall condition of the specific density of a radiation field 22 p2888 A73-43046

Angstrom pyroheliometer scale correction for ratio of incident circumsolar radiation to electric current

heating power derived from nonuniform painted surface strip illumination 23 p3025 A73-43985

Theory of the polarisation of the ordinary wave reflected from the ionosphere in the limit of vertical incidence and vertical magnetic field. 24 p3069 A73-45202

INCLINATION

Satellite resonance with longitude-dependent gravity. III - Inclination changes for close satellites. 09 p1154 A73-22837

Slope angle determination with respect to photograph surface from visible horizon line configuration 16 p2017 A73-34049

Pallas evolution on basis of orbital eccentricity and inclination, discussing accumulation in asteroid belt in quiescent solar nebula, collisions and planetary gravitational encounters 17 p2229 A73-34428

INCLUSIONS

On some relation between the mechanical properties and the bond strength of elastomer to solid inclusion in solid propellant. 01 p0090 A73-11117

Role of absorbing inclusions in the fracture mechanism of transparent dielectrics by laser emission 01 p0026 A73-11291

Mechanical properties anisotropy in heat resistant Ni alloys due to strengthening phase nonmetallic inclusions distribution, suggesting purification by vacuum melting 01 p0066 A73-11346

Study of the composition of inclusions in synthetic diamond crystals by microanalysis. 02 p0185 A73-12691

Oxygen and nonmetallic inclusions in chromium and aluminothermic ferrochrome 04 p0465 A73-15662

On the effective moduli of composite materials - Slender rigid inclusions at dilute concentrations. 05 p0630 A73-16099

Stress-strain state of a spheroidal inclusion/measuring device/ embedded in a thermoelastic medium. 05 p0633 A73-16616

Mathematical model for electric current in granulated media, establishing temperature dependence of tunneling conductivity for tunnel junction with metallic inclusions in oxide layer 06 p0736 A73-18117

Notch induced stress concentrations at elastic rectangular core /inclusion/ in extended rectangular plate with rigidly supported edges, using finite element method 07 p0910 A73-19196

Lame equations for stress concentration in half plane with extracted elastic inclusion, solving via Fourier integrals reduced to singular integral equation 07 p0910 A73-19301

Inclusions and interface relationships between glass and breccia in lunar sample 14306.50. 07 p0883 A73-19731

Stress-strain state of a piecewise homogeneous plane with thin-walled elastic inclusions of finite length 08 p1019 A73-21765

Influence of inclusion content on fatigue crack propagation in aluminum alloys. 09 p1101 A73-22409

Computerized two dimensional boundary value problem solutions for bounded multiply connected structural regions with periodic inclusions, using three step R-functions and Rvachev method 09 p1120 A73-22586

Void initiation and growth in Al alloys due to inclusions, presenting dislocation model for ductile fracture strength 09 p1109 A73-23256

Influence of the shape of inclusions on the initial stage of failure of two-component composite materials 11 p1389 A73-26738

Approximate dependences for the vibration frequencies of smooth cylindrical shells and for ones with concentrated inclusions 12 p1555 A73-27789

Elastic circular inclusion in an infinite plane containing two cracks. 13 p1696 A73-28749

Allende carbonaceous chondrite Ca-Al rich inclusion refractory trace metals condensation temperature calculation, indicating high temperature primitive solar nebula condensates 13 p1684 A73-29176

Couple-stresses effects in vicinity of interface for infinite elastic plane with a rigid inclusion. 13 p1702 A73-29533

Mathematical theory of elasticity for stress concentration in homogeneous isotropic perfectly elastic composites with spherical inclusions, noting grain boundary stresses 13 p1702 A73-29535

Stress distribution about defects such as rigid sharp-angled inclusions. 13 p1703 A73-29619

INCOHERENT SCATTERING

Observation of dislocations and inclusions in neodymium-doped yttrium aluminium garnet by transmission electron microscopy. 14 p1782 A73-29744

Effect on the stresses around a crack due to the presence of circular inclusion. 14 p1806 A73-30042

Note on volume integrals of the elastic field around an ellipsoidal inclusion. 15 p1946 A73-31104

Propagation of stress gradient through an inclusion. I. [ASME PAPER 73-APM-15] 17 p2247 A73-35038

Propagation of stress gradient through an inclusion. II. [ASME PAPER 73-APM-16] 17 p2247 A73-35039

The use of a high modulus inclusion gauge in non-linear viscoelastic materials. 17 p2173 A73-35457

Nitride inclusions in titanium ingots - A study of possible sources in the production of magnesium-reduced sponge. 20 p2576 A73-39026

Coefficients of stress intensity near rigid acute-angled inclusions 20 p2619 A73-39370

Natural oscillations of shells of revolution with an open profile and concentrated inclusions 20 p2625 A73-39654

Interaction of cracks with rigid inclusions in longitudinal shear deformation. II - Further results. 22 p2920 A73-42134

Equations of an elastic medium with a large number of absolutely solid inclusions 22 p2921 A73-42278

On the integral equations of three-dimensional multiple inclusion problems. 22 p2924 A73-42682

The role of absorbing impurities in laser-induced damage of transparent dielectrics. 23 p2959 A73-43512

Torsion of a cylindrical shell with a lateral surface containing an elastic circular inclusion 23 p3042 A73-43727

INCOHERENCE

Hologram reconstruction by incoherent light. II - Experimental results. 01 p0045 A73-10431

Incoherent optical correlation with a hologram - An example of identifying fingerprints 01 p0054 A73-11489

Chaotic photon bunching effect interpretation by theoretical incoherent source model with atomic excitation and emission at stochastically independent times without interaction 07 p0837 A73-20610

INCOHERENT SCATTERING

Radiation transfer within spectral line in symmetric isothermal medium, assuming spherical incoherent scattering characteristic and scattering angle-independent redistribution law 01 p0100 A73-10705

Structure of the thermosphere as inferred from incoherent scatter measurements. 02 p0161 A73-12282

Incoherent scatter observations of meridional winds in the 150-225 km region. 02 p0161 A73-12283

E region electromagnetic east-west drift velocity measurement at magnetic equator by incoherent scatter radar 02 p0161 A73-12285

A noncoherent model for microwave emissions and backscattering from the sea surface. 02 p0164 A73-12362

Radar measurement of ionosphere motion in the presence of current-induced spectral asymmetries. 02 p0143 A73-12532

Isotropic and incoherent light scattering by atomic slab, calculating Doppler effect induced diffuse radiation energy partial redistribution by Monte Carlo method 05 p0597 A73-16562

Comparison of Te and Ti from Ogo 6 and from various incoherent scatter radars. 07 p0790 A73-19241

Comparison of the correlation of incoherent scatter and ionosonde measurements of temperature with calcium phase and 2800-Megahertz intensities. 07 p0815 A73-19250

Noncoherent reflection of electromagnetic waves from a plasma layer 07 p0855 A73-19281

Incoherent ionospheric scatter sounding facility for ionospheric energy balance, neutral atmospheric structure and upper atmosphere dynamics studies 07 p0817 A73-19550

Modulation Langmuir probe and incoherent scatter radar measurements of ionospheric electron temperature. 09 p1075 A73-22128

Theory of incoherent-scatter measurements using compressed pulses. 09 p1050 A73-22429

Combined-operations method for diffuse reflection by an isotropic, non-coherent scattering homogeneous sphere. 10 p1271 A73-23484

Multistatic incoherent scatter measurements of ionospheric drift velocity. 10 p1188 A73-24274

Possibilities and some results of studying the ionosphere by the method of 'incoherent' scattering of radio waves 11 p1350 A73-25088

Line source functions with variable Doppler width and noncoherent scattering. 11 p1415 A73-25135

The causes of storm-time increases of the F-layer at mid-latitudes. 11 p1353 A73-25751

Structure at the poleward edge of a mid-latitude F-region trough. 11 p1353 A73-25756

Forward and specular scattering from a rough surface - Theory and experiment. 13 p1659 A73-28490

Incoherent reflection of electromagnetic waves from a plasma layer. 13 p1665 A73-28681

Faraday effect of incoherently scattered radar signals. 13 p1583 A73-28712

Magnetic dip equator region ionospheric drifts and electric fields measurements and experimental techniques 15 p1868 A73-31752

Incoherent scatter observations of the ionosphere over Chatanika, Alaska. 16 p2004 A73-33442

Non-coherent scattering in transfer problems in spherical shell media. I - Frequency-independent source function. 17 p2236 A73-35780

Probabilistic model for radiative transfer problems in cylindrical shell media with complete redistribution in frequency. 17 p2236 A73-35781

Non-coherent scattering in transfer problems in spherical shell media. II - Frequency-dependent source function. 17 p2237 A73-35789

Tentative E-region electron density profiles. 18 p2309 A73-36099

Incoherent radar target extraction in clutter of unknown level by recursive integration for signal and threshold. 18 p2290 A73-37089

Theory of radio wave incoherent scattering by a plasma and the application of the theory in ionospheric studies 20 p2554 A73-39164

Angle and Doppler measurements of the quasi-coherent and incoherent components of microwave transhorizon signals. 22 p2824 A73-41859

Incompatibility of solar EUV fluxes and incoherent scatter measurements at Arecibo. 22 p2902 A73-41923

INCOMPRESSIBILITY

Incompressible elastic circular cylinders quasi-equilibrated motions analysis, obtaining free and forced oscillations periods 02 p0191 A73-11573

Calculus of variations for minimum energy method in elasticity theory of incompressible elastic body, calculating elastic deformations 04 p0509 A73-14980

Inflation-extension and eversion of a tube of incompressible isotropic elastic material. 04 p0512 A73-15234

Dynamically possible finite deformations of isotropic, incompressible, elastic-inelastic solids with temperature independent response. 13 p1695 A73-28416

Conditions for stability of incompressible elastic material obtained from small-amplitude plane sinusoidal waves superposed on finitely deformed state of material 13 p1696 A73-28753

Solution of the plane problem in elasticity theory for an incompressible material by the fractional step method 17 p2211 A73-34299

INCOMPRESSIBLE BOUNDARY LAYER

Separation of turbulent boundary layer - Wall pressure distribution near separation. 02 p0154 A73-12523

Dimension-theory determination of the separation parameter for an incompressible magnetohydrodynamic boundary layer. 06 p0726 A73-17406

Mean velocity profiles in three-dimensional incompressible turbulent boundary layers. 09 p1029 A73-23445

An extended boundary-layer analysis of the impulsive motion of a flat plate in a viscous fluid. 10 p1208 A73-24809

Unsteady three dimensional laminar incompressible boundary layer with free and forced convection, determining flow and temperature fields adjacent to heated body 10 p1208 A73-24810

Incompressible boundary layer flow over semi-infinite plate with impulsive heat transfer, obtaining numerical solution for time dependent boundary layer growth 10 p1296 A73-24812

Incompressible laminar boundary layer separation, displacing separation point by adjusting flow surface velocity 13 p1600 A73-28445

Approximate calculation of the incompressible laminar boundary layer on a plate with suction 13 p1600 A73-28446

Two dimensional incompressible turbulent boundary layer flow theory, considering Bradshaw turbulence field and Felsch integral methods 14 p1745 A73-30298

Free stream vorticity effect on incompressible boundary layer stability via Orr-Sommerfeld equation, considering self-similar flows with pressure gradients 14 p1712 A73-30651

The principle of spatial variations - Application to the boundary layer theory. 16 p1999 A73-32978

Laminar-turbulent transition in incompressible laminar boundary layer flow from stability theoretical viewpoint, considering pressure gradient, free stream turbulence and wall roughness effects 16 p1999 A73-33229

A finite difference solution of the two and three-dimensional incompressible turbulent boundary layer equations. [ASME PAPER 73-FE-20] 17 p2153 A73-35016

Finite-difference solution of the incompressible three-dimensional boundary layer equations for a blunt body. 18 p2259 A73-36156

Aerodynamic sound and the low-wavenumber wall-pressure spectrum of nearly incompressible boundary-layer turbulence. 20 p2545 A73-39053

A biparametric method for laminar boundary layer calculations 24 p3079 A73-45173

The incompressible boundary layer of higher order at the axisymmetrical stagnation point in the case of strong suction or blowing 24 p3056 A73-45545

INCOMPRESSIBLE FLOW

NT STOKES FLOW

An experimental study of the dynamic lift on a cylinder subjected to a high Reynolds number flow perpendicular to its axis. [ONERA, TP NO. 1073] 01 p0001 A73-10226

Free and forced convection from fine hot wires. 01 p0120 A73-10447

Exact vorticity solutions of the incompressible Navier-Stokes equations. 01 p0034 A73-11358

Confined laminar jet mixing in a circular channel with arbitrary entrance velocity distribution. [AD-758578] 01 p0034 A73-11363

Incompressible flow characteristics and temperature transverse behavior in completely turbulent wall boundary layer 03 p0292 A73-13172

Computer methods for simulation of multidimensional, nonlinear, subsonic, incompressible flow. [ASME PAPER 72-HT-61] 03 p0294 A73-13546

Flow parameter iterative formulas for laminar incompressible viscous fluid flow between two parallel disks rotating at same angular velocity 03 p0295 A73-13625

Nonlinear instability of two dimensional unbounded incompressible viscous fluid flows under periodic small perturbation 03 p0296 A73-14049

Quasi-stable energy spectrum of isotropic turbulence. 03 p0297 A73-14444

Performance of truncated conical diffusers with compressible flow. 03 p0249 A73-14641

On the uniformly valid approximate solutions of Laplace equation for an inviscid fluid flow past a three-dimensional thin body. [ONERA, TP NO. 1145] 04 p0433 A73-15094

Finite difference technique for numerical calculation of two dimensional stratified incompressible fluid flows 04 p0433 A73-15162

Statistical transfer theory in non-homogeneous turbulence. 04 p0520 A73-15937

Temperature and heat flux distributions in incompressible turbulent equilibrium boundary layers. 04 p0520 A73-15942

Experimental analysis of lift on a fixed cylinder subjected to a flow perpendicular to its axis at high Reynolds numbers 04 p0405 A73-15990

Incompressible plane flow subject to infinitely small vibrations, expressing complex potential as Abelian integral [ONERA, TP NO. 1191] 04 p0472 A73-15993

Navier-Stokes equation solutions for steady laminar viscous flow of incompressible fluid with mixed no-slip and no-shear conditions 05 p0563 A73-16097

A class of airfoils designed for high lift in incompressible flow. 05 p0528 A73-16851

Linearized theory for infinite span wing small unsteady motions in curved flight in inviscid incompressible fluid, obtaining time dependent forces, pressure and velocity fields [AIAA PAPER 73-90] 05 p0529 A73-16854

Finite element analysis of unsteady incompressible flow around an oscillating obstacle of arbitrary shape. [AIAA PAPER 73-91] 05 p0529 A73-16855

Negative Magnus forces in the critical Reynolds number regime. 05 p0533 A73-17212

Small perturbation stability of two dimensional incompressible viscous fluid flow with periodic velocity function, reduced to undulating surface boundary layer problem 06 p0684 A73-17452

Steady rectilinear universal motions of a Navier-Stokes fluid. 06 p0685 A73-17861

Some incompressible jet flow and reattachment effects in fluid control elements. 06 p0687 A73-18513

Mass-transfer effects on higher-order boundary layer solutions - The leading edge of a swept cylinder. 06 p0688 A73-18833

Magnetohydrodynamic laminar source flow between two parallel disks. 07 p0854 A73-19102

Development of flow in the entrance region of a converging channel. 07 p0810 A73-19103

Energy conserving finite difference approximation for solution of unaveraged Navier-Stokes equations of three dimensional incompressible turbulent flow in square duct 07 p0810 A73-19263

The prediction of the optimum performance of ejectors. 07 p0810 A73-19571

Analysis of flow of viscous fluids by the finite-element method. 07 p0811 A73-19953

A correction to 'lifting-line theory as a singular perturbation problem.' 07 p0775 A73-19964

Stationary vortices behind a flat plate normal to the freestream in incompressible flow. 07 p0775 A73-19974

Flow of a viscous incompressible fluid between a fixed porous disk and a rotating nonporous disk, with radial discharge 07 p0811 A73-20069

The Stokes problems for a suspension of particles. 08 p0955 A73-21426

Some remarks on the behaviour of surface source distributions near the edge of a body. 08 p0926 A73-21437

Cylinder surface roughness and transverse curvature effects on turbulent boundary layer in incompressible and compressible flows, deriving formula for skin friction coefficient 08 p0956 A73-21603

Flow through moving cascades of lifting lines with fluctuating lift. 10 p1171 A73-23697

Flow near an accelerated plate in the presence of a magnetic field. 10 p1206 A73-24528

Prandtl boundary layer equations for unsteady three dimensional axisymmetrical and two dimensional symmetrical incompressible flows about solid bodies, considering approximate solution convergence 10 p1208 A73-24808

Incompressible turbulent axisymmetrical impulsive air injection at moderate pressure into stagnant surroundings, measuring flow velocity distribution 10 p1210 A73-24849

Study of the phase of the wall transfer of heat or mass in incompressible pulsed flow 10 p1297 A73-24850

Laminar incompressible fluid steady secondary flow in circular cross section curved tube at various Reynolds numbers 11 p1346 A73-25225

Parametric excitation of Tollmein-Schlichting waves in a boundary layer 11 p1347 A73-25430

Dynamic stability of cable in incompressible flow at angle of incidence, calculating characteristic lengths and vibration frequencies by singular perturbation theory [AIAA PAPER 73-395] 11 p1440 A73-25524

On MHD flow along an infinite flat wall with constant suction. 11 p1405 A73-25975

High velocity moving body in ideal incompressible fluid flow, determining lift coefficient from acceleration potential algorithm
12 p1486 A73-27239

Propagation of electrohydrodynamic surface waves in a conducting fluid.
13 p1663 A73-28160

Instability of density-stratified incompressible inviscid rotary Couette flow between corotating coaxial vertical cylinders due to gravitational effects
13 p1600 A73-28439

Two dimensional incompressible steady potential electrohydrodynamic flows past flat dielectric plate, using quasi one dimensional and boundary layer approximation
13 p1664 A73-28442

Lifting-surface theory for a wing oscillating in yaw and sideslip with an angle of attack.
13 p1564 A73-28802

Two dimensional opposing incompressible viscous fluid jets impingement, investigating stagnation surface stability characteristics
13 p1603 A73-29036

Book - Computer fluid dynamics: Recent advances.
14 p1744 A73-29743

Study of a new family of solutions of Navier-Stokes equations
14 p1744 A73-29758

Free convection effects on the oscillatory flow past an infinite, vertical, porous plate with constant suction, I, II.
14 p1816 A73-30049

Radiation from line vortex filaments exhausting from a two-dimensional semi-infinite duct.
14 p1744 A73-30168

Book - Computational fluid dynamics.
14 p1745 A73-30359

On the connection between the elliptic equations of the Navier-Stokes type and the theory of harmonic functionals.
14 p1769 A73-30521

Pseudospectral approximation to two-dimensional turbulence.
14 p1746 A73-30909

Pressure distribution on multicomponent airfoils in two dimensional incompressible potential flow, using Martensen-Jacob vorticity distribution method to derive Fredholm type circulation equation
15 p1823 A73-31637

A high order finite element for completely incompressible creeping flow.
15 p1951 A73-32026

Boundary layer separation in a steady plane-parallel incompressible fluid flow
15 p1864 A73-32110

Steady solutions of a nonlinear problem for the Navier-Stokes equations
16 p2031 A73-32933

The solutions of the boundary layer equations in the case of extremely intensive blowing or suction
16 p1963 A73-33250

Integration of an extended Orr-Sommerfeld equation in connection with a stability investigation of laminar boundary-layer flows
16 p1963 A73-33252

The computation of the flow in the gap between two concentrically rotating spherical surfaces
16 p2000 A73-33255

Investigations regarding the heat exchange integral in turbulent incompressible flows
16 p2085 A73-33256

The numerical integration of the Navier-Stokes equations for the two-dimensional incompressible flow along a planar plate
16 p2000 A73-33261

On the solution of magnetohydrodynamic elastico-viscous flow past a plane porous plate.
16 p2042 A73-33370

Inviscid flow through a cascade of thick, cambered airfoils. I - Incompressible flow.
[ASME PAPER 73-GT-84] 16 p1964 A73-33527

Theoretical investigation of the incompressible, turbulent, and axisymmetric internal flow with vanishing wall friction
16 p1964 A73-33749

Calculation of flows past wings without thickness in the presence of developing vortex sheets
16 p1965 A73-33963

Jet-induced external flows of an incompressible viscous liquid
17 p2149 A73-34138

On unsteady Stokes, Ekman and Rayleigh layers in a rotating fluid.
17 p2150 A73-34322

Viscous flow in radial turbomachine blade passages.
17 p2093 A73-34389

The finite element method in fluid mechanics.
17 p2151 A73-34830

Boundary-layer separation from downstream moving boundaries.
[ASME PAPER 73-APM-11] 17 p2153 A73-35036

Numerical solution of the three-dimensional Navier-Stokes equations in integro-differential form - Flow about a finite body.
17 p2155 A73-35139

Linearized implicit schemes for the computation of viscous incompressible flow - with applications.
17 p2155 A73-35141

Statistical models of turbulent free shear mixing layer structure in incompressible air streams
17 p2156 A73-35507

Numerical studies of viscous, incompressible flow through an orifice for arbitrary Reynolds number.
17 p2157 A73-35602

Numerical solutions of time-dependent incompressible Navier-Stokes equations using an integro-differential formulation.
18 p2297 A73-36159

Unsteady turbulent boundary layers in two-dimensional, incompressible flow.
[AIAA PAPER 73-650] 18 p2260 A73-36205

Forces acting on a small body in an arbitrary incompressible fluid flow and equations of motion of a two-phase medium
18 p2302 A73-37008

Incompressible potential flow past axisymmetric bodies in cylindrical pipes.
19 p2376 A73-37489

Theoretical and experimental study, for different electrical conditions, of the laminar motion of an incompressible and electrically conducting fluid drawn along in a confined medium, and in the presence of an axial magnetic field, by the uniform rotation of a disk
19 p2468 A73-37531

Incompressible potential flow past sphere parallel to contact plane tangent as model to determine critical velocity for dissipation onset in superfluid liquid He II
19 p2421 A73-37853

The balance of turbulence energy and its components in incompressible turbulent boundary layers
20 p2546 A73-39096

The effect of the wedge angle on the similarity parameter of the turbulent mixing region in the case of an incompressible flow
20 p2547 A73-39408

Non-steady, stratified Couette flow between concentric rotating spheres.
20 p2548 A73-39521

Incompressible turbulent boundary layer separation from a curved axisymmetric body.
20 p2548 A73-39525

Incompressible flow planar-nozzle discharge coefficient computations for one dimensional inviscid flow, considering nozzle geometry, flow cross sections and turbulence
20 p2548 A73-39526

Variational analysis of the flow development in the entrance region of circular tubes and parallel-plate channels.
20 p2548 A73-39527

Unsteady incompressible fluid flow past a doubly periodic grid
21 p2631 A73-40185

Turbulent incompressible plane wall jet flow in still air, examining maximum velocity, total thickness and inner length scale with parametric analysis
21 p2678 A73-41191

Spatial stability of incompressible two-dimensional Gaussian wake in steady viscous flow.
22 p2796 A73-42243

Numerical analysis of magnetic field lines of force reconnection along transition layers or at flow stagnation point of incompressible conducting viscous fluid
22 p2894 A73-42396

Some investigation on base flow behind cylindrical bodies in incompressible flow.
22 p2797 A73-42997

Papers on heat pipes covering incompressible laminar vapor flow behavior, startup dynamics, wicking material liquid transport properties, high thermal conductance structures, etc
23 p3049 A73-43459

Numerical solution of Fredholm integral equation describing incompressible inviscid potential flow past three dimensional bodies
23 p2939 A73-43474

Variable mass flow rate air injection from porous flat plate into uniform incompressible air flow, obtaining laminar flow velocity profile and pressure measurements
23 p2940 A73-43932

Study of the steady flow of an incompressible viscous fluid around a cylinder in rotation
24 p3079 A73-45219

INCOMPRESSIBLE FLUIDS
NT MICROPOLAR FLUIDS

Nonlinear waves on interface of two incompressible inviscid fluids of different densities and arbitrary surface tension analyzed by multiple scales method
01 p0032 A73-10445

Stability criteria for unsteady motion of incompressible Cosserat fluid in arbitrary time dependent domain, using Liapunov function
01 p0033 A73-10776

Existence and stability of the secondary periodic solution figuring in Navier-Stokes type evolution problems
[ONERA, TP NO. 1172] 01 p0033 A73-10780

Navier-Stokes equations numerical solution for steady state axisymmetric flow of incompressible Newtonian fluid between two parallel infinite rotating disks
01 p0122 A73-10805

Magnetohydrodynamic flow around a hollow sphere
01 p0085 A73-11259

Electrohydrodynamic stability of insulating fluids subjected to a unipolar injection
01 p0086 A73-11361

Stability of a nonstationary circular jet of ideal incompressible fluid
02 p0152 A73-11609

Theory of the electrodiffusion method for measuring the spectral characteristics of turbulent flows
02 p0165 A73-11614

Three linear invariant relations in the problem of motion of a heavy solid body with a liquid filler
02 p0153 A73-11773

Integral method of calculating a semibounded laminar jet
02 p0153 A73-11784

Flow stability of ideal compressible and incompressible fluids, solving Navier-Stokes equation for rotating liquid with free boundary in gravitational field
02 p0154 A73-12692

On the uniqueness of solutions of the Falkner-Skan equation.
02 p0154 A73-12798

Incompressible fluid turbulent boundary layer flow stability, considering effect of high polymer additives
03 p0291 A73-13168

Incompressible viscous fluid creep flow past deforming sphere for small Reynolds numbers, considering cases of different Strouhal numbers
03 p0244 A73-13529

Boundary-layer development at a two-dimensional rear stagnation point.
03 p0294 A73-13536

Solution of the wedge entry problem by numerical conformal mapping.
03 p0244 A73-13537

Calculation of the natural oscillations of an ideal liquid in an axisymmetrical container with allowance for surface forces
03 p0294 A73-13607

Lagrange equations of motion for ideal incompressible fluid flow under asymmetric deformation of expanding circular cylinders and spheres, calculating resistance forces
03 p0294 A73-13613

Heat transfer in the turbulent boundary layer of an incompressible fluid flow past a surface when the pressure gradient and temperature on the surface are variable
03 p0295 A73-13622

Numerical solution for a flat plate experiencing a ground effect
03 p0245 A73-13721

Reversible instantaneous deformations and internal energy in viscoelastic incompressible fluids, using Oldroyd and De Witt hydrodynamic models
03 p0296 A73-14053

Oscillatory point force generated motion in inviscid incompressible rotating stratified fluid, obtaining closed form solutions via Fourier transforms
03 p0296 A73-14313

The motion of a plate in a rotating fluid at an arbitrary angle of attack.
04 p0404 A73-15161

Study of plane flows of viscous fluid around a body
04 p0404 A73-15652

Flow in the entrance region at low Reynolds numbers.
[ASME PAPER 72-WA/FE-21] 04 p0435 A73-15847

Numerical solution of laminar jet mixing with and without free stream.
05 p0564 A73-16174

Numerical solution of a boundary value problem for the Navier-Stokes equations
05 p0564 A73-16449

Effect of the asymmetry of an external magnetic field on a viscous fluid flow in an annular MHD channel
05 p0603 A73-16589

On unsteady forced flow against a rotating disk.
06 p0643 A73-17394

Physical principles in incompressible fluid and plasma turbulence comparison, noting quasi-linear approximation for nonlinear particle diffusion in turbulent oscillations
06 p0728 A73-17924

Small amplitude viscous similarity solution for vertical two dimensional internal wave production by circular cylinder resonant oscillation in incompressible stratified fluid
06 p0646 A73-18527

Equations of disturbed motion and equilibrium for solid body with incompressible fluid filled cavity, noting equilibrium position stability conditions
06 p0688 A73-18878

Velocity distribution of quasi-steady and steady flow of ideal incompressible fluids with congruent

streamlines, investigating conditions for vortex and irrotational flow

07 p0809 A73-19017

On the plane-parallel symmetric boundary layer generated by sudden motion.

07 p0809 A73-19020

Viscous incompressible gas turbulent flow in axisymmetric channel under preliminary twist conditions at inlet, using computer numerical solution

07 p0774 A73-19621

Flow of an ideal incompressible ponderable fluid around a thin profile placed under a free line. I, II

07 p0811 A73-19998

The laws of reflection and refraction of incompressible magnetohydrodynamic waves at a fluid-solid interface.

07 p0858 A73-20028

On the transmission of the energy in an incompressible magnetohydrodynamic wave into a conducting solid.

07 p0858 A73-20029

Flow of a conductive fluid through a cylindrical duct with periodic deformations in the presence of an azimuthal magnetic field

07 p0858 A73-20073

Analysis of the vibrational characteristics of a liquid contained in a tank

[ONERA, TP NO. 1197]

07 p0812 A73-20074

Determination of the shape of jets flowing off the walls of an asymmetrically positioned bucket

07 p0776 A73-20098

Cylindrical pores in viscous incompressible liquid film, considering existence duration and pore wall motion under surface tension forces

07 p0923 A73-20420

A remark on the sloshing frequencies for a half-space.

08 p0953 A73-20788

Numerical studies of two-dimensional vortex motion by a system of point vortices.

08 p0954 A73-21010

Unsteady laminar boundary layers calculation for arbitrary velocity distributions at inner boundary in presence of suction/blowing through porous surface

08 p0954 A73-21176

Turbulent incompressible boundary layer on porous heat insulated plate with uniform suction, calculating ratio of friction drag coefficients

08 p0954 A73-21178

Turbulent hydrodynamics and heat transfer in rotating flows of incompressible fluid

08 p0954 A73-21184

Three dimensional steady flow of incompressible viscid fluid near thin wing trailing edge, using Stewartson-Williams triple layer method

08 p0926 A73-21495

Boundary layer theory approximation for hydrodynamic parameters of unsteady laminar boundary layer on body moving in incompressible fluid

08 p0956 A73-21546

Discrete vortex scheme of a wing of finite span

08 p0927 A73-21611

Two approximate methods for describing the steady motions of an incompressible viscous fluid with a free boundary

09 p1072 A73-22619

Analysis of the shrouded Rayleigh step pad for an incompressible fluid film with the centrifugal inertia effect included.

09 p1089 A73-23103

Numerical study of the flow of a viscous incompressible fluid around a circular cylinder

10 p1171 A73-23766

Putting an electrically conducting fluid in rotation by a rotating magnetic field

10 p1254 A73-24125

Finite element solution algorithm for viscous incompressible fluid dynamics.

10 p1243 A73-24296

Turbulent Hartmann flow based on differential equations for steady isothermic turbulent motion of incompressible electrically conducting fluid in magnetic field

10 p1256 A73-24591

Unsteady boundary layer over a flat plate started from rest.

10 p1209 A73-24829

Unsteady flow between a fixed porous disk and a rotating disk

10 p1209 A73-24837

Transient Ekman and Stewartson layers in a rotating tank with a spinning cover.

10 p1210 A73-24840

The motion of a viscous, stratified fluid subjected to forced oscillations.

10 p1210 A73-24844

Acoustic streaming and forces generated on circular cylinder in radially oscillatory incompressible fluid, considering steady and unsteady flow

10 p1174 A73-24847

Unsteady uniform-length turbulent flow of incompressible fluid in circular pipe studied via Reynolds and turbulence energy balance equations

10 p1210 A73-24851

On the application of Cramer's theorem to axisymmetric, incompressible turbulence.

10 p1284 A73-24909

Axisymmetric flow model of rotating inviscid incompressible fluid into point sink at low Rossby numbers, discussing selective withdrawal and blocking wave

11 p1345 A73-25053

An investigation of internal gravity waves generated by a buoyantly rising fluid in a stratified medium.

11 p1351 A73-25152

Viscous incompressible Jeffery-Hamel fluid flow in divergent channel, discussing secondary supercritical flow, winding and vortex formation

11 p1346 A73-25223

Conformal mapping method application to unsteady motion of arbitrary deformable contour in potential flow of ideal incompressible fluid

11 p1348 A73-26426

Equilibrium stability of liquid filled body with closed internal cavity partially filled with ideal homogeneous incompressible fluid under gravitation

11 p1401 A73-26470

An existence proof for permanent capillary gravity waves with general vortex distributions

11 p1349 A73-26747

Movement of viscous incompressible fluids through annular interstices with walls in relative alternating translational motion

12 p1486 A73-26795

Nonvortical axisymmetric flow of inviscid ideal incompressible fluid from partial differential equations solution

12 p1486 A73-27242

Potential flow of an inviscid incompressible liquid around a profile in the presence of solid rectilinear boundaries

12 p1487 A73-27797

Solid profile wing motion in ideal incompressible fluid at variable distance from screen in terms of small perturbation theory

12 p1488 A73-27815

Flows with wakes about a zero-incidence symmetric profile

13 p1599 A73-28069

On the numerical treatment of the Navier-Stokes equations for an incompressible fluid.

13 p1599 A73-28090

Pulsation energy calculations in axisymmetric turbulent jet flows of incompressible fluids with a zero excess impulse

13 p1600 A73-28448

Parameter calculation for laminar incompressible fluid jet expanding in gradient streamline along moving surface, determining velocity distribution in jet axis

13 p1601 A73-28736

Potential flow about arbitrary thick blades of large camber in cascade.

13 p1565 A73-29009

Two dimensional flow of viscous incompressible fluid, discussing formulation in analytic functions with applications to flows past elliptic cylinder and flat plates

13 p1603 A73-29048

Stability of elliptical cylinder consisting of perfect incompressible gravitating fluid subject to arbitrary perturbations

15 p1860 A73-31048

Motions of perfect incompressible homogeneous fluid planets surrounded by rigid oscillating rings, noting application to two-satellite planets

15 p1860 A73-31049

Apparent added masses of a plate array in an incompressible liquid

15 p1861 A73-31281

Spiral flows with multiple circulation in channels of simple shape

15 p1861 A73-31284

Reynolds equation solutions for transverse velocity and pressure variations in incompressible fluids within journal bearings and between rotating eccentric cylinders

15 p1882 A73-31639

Plane boundary layer equations of asymmetric MHD incompressible fluid motion for case of high and low electroconductivity

15 p1919 A73-31829

Calculation of the resultant moment of the hydrodynamic forces on jet profiles

15 p1824 A73-32000

Equations of disturbed motion and equilibrium for solid body with incompressible fluid filled cavity, noting equilibrium position stability conditions

15 p1915 A73-32403

Plane unsteady irrotational flow of ideal incompressible fluid through turbomachine stage due to interaction between stationary and moving grids

16 p2001 A73-34015

Re-connexion of magnetic lines of force - Evolution in incompressible MHD fluids.

18 p2338 A73-36181

Rheology of steady turbulent flows of an incompressible fluid

18 p2301 A73-37001

Pulsation-energy balance equation in turbulent boundary layer theory

18 p2301 A73-37002

Incompressible conducting fluid flows in an arbitrary region in the presence of a strong magnetic field

18 p2340 A73-37015

Steady-state solutions to the problem of viscous incompressible fluid flow past a body

19 p2419 A73-37244

Mises variables in problems with a free boundary for the Navier-Stokes equations

19 p2419 A73-37245

On the torsional oscillations of a sphere placed at the axis of a rotating viscous incompressible fluid.

19 p2419 A73-37422

Numerical study of viscous flow in a cavity.

20 p2545 A73-38971

Linear wave motion analysis of viscous incompressible fluid of infinite depth at small and large times by asymptotic quadrature method

21 p2676 A73-40207

Russian book - Convective stability of an incompressible fluid.

21 p2790 A73-40417

Russian book on turbomachinery using compressible and incompressible working fluids covering gas and fluid flow equations, energy losses in axial and radial flow stages, etc

21 p2633 A73-40807

A three-dimensional MHD boundary layer in an incompressible fluid

21 p2747 A73-40882

Study of MHD effects in a viscous conducting fluid flow in a traveling magnetic field

21 p2747 A73-40884

Steady-state heat transfer between fluids divided by a thin wall

21 p2792 A73-41224

The integrals of the system of Navier-Stokes equations for axisymmetric motion of an incompressible fluid

22 p2841 A73-42123

Equations of the boundary perturbations of a cavity moving near a solid wall

22 p2841 A73-42124

Cylindrical circular shell vibrational frequencies, examining free surface or solid plane influence on shell natural vibrations in incompressible fluids

22 p2920 A73-42130

Flow stability of viscous homogeneous incompressible electrically conducting fluid between nonconducting walls at large magnetic Reynolds numbers

22 p2894 A73-42639

Rayleigh-Taylor problem of thermal instability of density-stratified layer of incompressible fluid heated from above, considering oscillatory and nonoscillatory modes stability

23 p3048 A73-43346

Plane boundary layer equations for viscous incompressible fluid with asymmetric stress tensor produced by moment stresses and mass moments

23 p2968 A73-43922

Analytic solutions for potential flow over a class of semi-infinite two-dimensional bodies having circular-arc noses.

23 p2940 A73-43931

Physical principles in incompressible fluid and plasma turbulence comparison, noting quasi-linear approximation for nonlinear particle diffusion in turbulent oscillations

23 p3013 A73-44326

Acoustic velocity and sound propagation differences in incompressible and compressible fluids related to Mach cone formation and sonic boom effects

24 p3054 A73-45269

Boundary value problem concerning the oscillations of a rotating ideal fluid

24 p3081 A73-45531

INCONEL [TRADEMARK]

Electron microanalysis of backfilled hot cracks in Inconel 600.

01 p0067 A73-11373

Comparison and analysis of residual stress measuring techniques and the effect of post-weld heat treatment on residual stresses in Inconel 600, Inconel X-750 and Rene 41 weldments.

03 p0313 A73-13596

Effects of heat treatment on the mechanical properties and microstructure of Inconel Alloy 718.

04 p0465 A73-15582

Morphology of gamma prime and gamma double prime precipitates and thermal stability of Inconel 718 type alloys.

06 p0711 A73-18755

Scanning electron microscope for heat transfer surfaces characterization, noting Inconel surface roughness change in convective heat transfer experiment

08 p1025 A73-21642

Short time aging characteristics of Inconel X-750.

10 p1230 A73-23631

Relationship of mechanical characteristics and microstructural features to the time-dependent edge-notch sensitivity of Inconel 718 sheet.

[ASME PAPER 73-MAT-G]

13 p1637 A73-29200

Effect of heat input on properties of Inconel filler metal 82 weld deposits. 19 p2435 A73-38002

Procedure development for brazing Inconel 718 honeycomb sandwich structures. 23 p2985 A73-44001

INDENTATION

Dislocation density in Mo single crystals subject to uniaxial tensile stress or sphere-produced indentation, evaluating plastic strain level 01 p0063 A73-10484

Relaxation of diagonal length and indentation depth of Vickers microhardness measurements on plastics 11 p1388 A73-25449

Assessment of the degree of plastic deformation in a crater with ball imprint. 14 p1810 A73-30309

Indentation of the semi-infinite elastic solid by a hot sphere. 22 p2929 A73-43174

INDEPENDENT VARIABLES

NT LATTICE PARAMETERS

Approximation by functions of fewer variables. 02 p0186 A73-11969

Elliptic partial differential equations may be related by a change of independent variables. 02 p0186 A73-11975

Measuring hybrid parameters of composite transistors. 02 p0148 A73-12855

Operational methods for analysis of discontinuous systems with multiple lumped parameter attachments and concentrated forces, obtaining steady state closed form solutions 09 p1159 A73-22648

Optimization problems with large parameters. 11 p1391 A73-26365

Elastic domain similar to half plane with perturbed boundaries, comparing small parameter method accuracy with exact solutions 11 p1446 A73-26467

Practical quadratic optimal control for systems with large parameter variations. 12 p1483 A73-27166

Modeling irregular surfaces. 13 p1619 A73-29242

Estimated solutions for the second and third boundary value problems of a second-order parabolic equation in regions with unbounded spatial variables 14 p1771 A73-30836

Differential and pseudodifferential operators with an infinite number of independent variables, and their applications 15 p1900 A73-32081

Examination of the parameters in solutions to systems of two-dimensional nonlinear Volterra-type integral equations 17 p2203 A73-35590

Simplex method for linear programming for computerized design global optimization problems involving large numbers of equations and variables 19 p2407 A73-37406

Approximate solution of second-order nonlinear systems with heredity of a single independent variable 19 p2445 A73-37642

INDEXES (DOCUMENTATION)

Book - Holography: State of the art review 1971-72. 03 p0309 A73-14440

Russian book - Biomedical problems of space flights: Index of domestic and foreign literature. 04 p0410 A73-16034

Determination of the information-forecasting indices of biometeorological phenomena 13 p1579 A73-28861

INDEXES (RATIOS)

NT KP INDEX

Geomagnetic indexes Kp, ap, AE and Dst computation, interpretation, reliability and use in statistical studies of solar-terrestrial interactions 03 p0301 A73-13708

K indices measurements at antipodal earth surface observatories for aa indices, discussing one hundred year series 04 p0444 A73-15547

Some preliminary notions towards improved stochastic controller synthesis via transformed indices of performance. 06 p0681 A73-18817

INDIA

Small scale Gemini photographs of Indian regions for interpretation of tonal variations, geomorphologic, geologic and structural features and drainage patterns 20 p2561 A73-39898

INDIAN OCEAN

Characteristics of the development of the quasi-biennial cycle above the Indian Ocean 09 p1115 A73-22991

INDICATING INSTRUMENTS

NT ANEMOMETERS

NT APPROACH INDICATORS

NT ATTITUDE INDICATORS

NT CLOUD HEIGHT INDICATORS

NT GYROCOMPASSES

NT HOT-FILM ANEMOMETERS

NT HOT-WIRE ANEMOMETERS

NT MICROBALANCES

NT MICROWAVE SENSORS

NT PLAN POSITION INDICATORS

NT POSITION INDICATORS

NT RADIO DIRECTION FINDERS

NT SONIC ANEMOMETERS

NT SPACECRAFT POSITION INDICATORS

NT SPEED INDICATORS

NT STRAIN GAGE BALANCES

NT TACHOMETERS

NT WEIGHT INDICATORS

Quadrature phase splitter with indications of the quadrature and equality of output voltage amplitudes 01 p0022 A73-10081

Ceramic film indicator for determining and recording of temperatures on space vehicle heat shield. 01 p0052 A73-11168

Indicating instrument for angle of attack and sideslip on subsonic flight vehicles via static pressure sensing, noting wind tunnel tests 02 p0166 A73-11724

Aircraft fault isolation based on pattern of cockpit indications - A human factors approach. 02 p0136 A73-11857

A semiautomatic tracking device for satellites 02 p0190 A73-12013

Predicting failures with conducting-polymer fatigue-damage indicators. 06 p0759 A73-17598

Mixing properties of germanium thermoelectric indicators of SHF radiation with 'hot' charge carriers 09 p1063 A73-22456

Magnetic coil type electrical measurement indicating instruments accuracy dependence on manufacturing tolerances, discussing error reducing design methods 12 p1499 A73-27873

Direct-reading measurement of receiver-noise parameters. 13 p1590 A73-28531

An automatic reflectometer for the upper shortwave range 13 p1590 A73-28569

A new zero-beat indicator and its use in frequency measurements 13 p1617 A73-28859

Biological indicators and the effectiveness of sterilization procedures. 16 p1976 A73-33692

INDIUM

Investigation of the temporal-spatial distribution of optical density in a plasma of high-current Li and In discharges 01 p0085 A73-10853

Conversion of electromagnetic into acoustic energy via indium films. 06 p0734 A73-17834

Thin In film sealing techniques at temperatures below 300 C for binding Pyrex to various materials, using Au layer as alloy flux 09 p1085 A73-22950

Indium abundances in cosmos, meteorites, tekites, rock-forming and ore minerals and igneous rocks, considering behavior in magmatogenic processes and rock weathering and alteration 12 p1490 A73-27125

Investigation of the space-time distribution of the optical density of the plasma in high-current Li-In discharges. 12 p1529 A73-27903

INDIUM ALLOYS

Microstructure alignment in Ni-In system eutectic alloys due to directional solidification 04 p0463 A73-15312

Crystallization of nickel-based alloys and indium-lithium system alloys at ultrahigh cooling rates 13 p1632 A73-28112

Thermodynamic properties and phase composition of the In-Ni system 23 p2991 A73-43706

INDIUM ANTIMONIDES

Experimental investigation of millimeter-band electromagnetic wave propagation in a waveguide filled with n-type InSb under a magnetic field 01 p0017 A73-10977

Spin saturation and pump depletion in continuous spin-flip Raman oscillation. 03 p0319 A73-14452

Power output of a pulsed Raman laser with saturable excitation. 03 p0319 A73-14453

Oscillations of injected carriers in p-type indium antimonide. 04 p0482 A73-14869

Electron impulse interactions of heat in semiconductors 04 p0483 A73-15470

Non-ohmic transport and phonon amplification in polar semiconductors. 04 p0484 A73-16035

Thermal emf of indium antimonide of a p- and-n type of conductivity at room temperature 06 p0738 A73-18652

Microwave properties of n-type InSb in a magnetic field between 4 and 300 K. 06 p0739 A73-18792

Comparison between a Hall configuration and a Corbino configuration for the amplification of ultrasonic waves 07 p0864 A73-20613

Alternating spectral oscillations of nonequilibrium photoelectron current in p-InSb in the presence of a quantizing magnetic field 10 p1261 A73-24763

InSb and Ga-doped Ge bolometers performance tests, discussing detector circuitry and dc, noise and responsivity measurements 11 p1368 A73-26512

Nonlinear mechanisms for self-focusing of microwaves in semiconductors. 14 p1732 A73-29920

Studies of galvanomagnetic and thermomagnetic phenomena in selenium and tellurium doped InSb. 15 p1924 A73-32159

Generation-recombination noise and the microwave emission from InSb. 17 p2219 A73-34912

Experimental investigation of a millimeter band frequency converter on n-InSb at 4.2 K. 17 p1316 A73-35158

An experimental investigation of the propagation of electromagnetic waves in a rectangular waveguide, partially filled with n-InSb in a transverse magnetic field. 17 p1213 A73-35166

Bandpass filter with cooled InSb detector for measurement of far IR radiation and temperature-vs-wavelength characteristics of Hg arc lamp 17 p1716 A73-35774

Semiconductor laser beam self focusing action due to combined effects of linear and nonlinear dielectric constant and absorption coefficients, considering n-InSb sample 21 p2711 A73-40226

Surface wave propagation parallel to applied magnetic field in electron hole plasma, explaining observed resonances in InSb by LF mode 21 p2751 A73-40325

Far IR grating spectrometer using InSb detector with narrow spectral band responsivity and tunability due to cyclotron resonance absorption in magnetic field 23 p2984 A73-44364

INDIUM ARSENIDES

Electrical properties of InAs to very high pressures. 08 p0995 A73-21535

Photoemission from cesium-oxide-activated In-GaAsP. 10 p1259 A73-23839

INDIUM COMPOUNDS

NT INDIUM ANTIMONIDES

NT INDIUM ARSENIDES

NT INDIUM PHOSPHIDES

NT INDIUM SULFIDES

NT INDIUM TELLURIDES

Electron emission of In₂Se crystals in strong electric fields 17 p2219 A73-35555

INDIUM PHOSPHIDES

Influence of the polarization of phonons on the thermal conductivity of single crystals of indium phosphide between 300 and 800 K 01 p0087 A73-10430

Indium phosphide as a new material for microwave /transferred electron effect/ oscillators. 02 p0199 A73-11536

Diffusion of hot electrons in n indium phosphide. 07 p0861 A73-19157

Noise performance of gallium-arsenide and indium-phosphide injection-limited diodes. 07 p0798 A73-19158

Photoemission from cesium-oxide-activated In-GaAsP. 10 p1259 A73-23839

INDIUM SULFIDES

Nonlinear optical susceptibility measurements for zinc silver indium sulfide quaternary compounds, noting agreement with bond charge theory 09 p1120 A73-22090

INDIUM TELLURIDES

Influence of the impurity compensation effect on the magnitude of the negative reluctance of alloys of the [In₂Te₃/x-/Hg₃Te₃/1-x system 12 p1532 A73-27940

INDOLES

NT TRYPTOPHAN

Hydroxyindole-O-methyl transferases in rat pineal, retina and Harderian gland. 02 p0136 A73-12644

Control of pineal indole biosynthesis by changes in sympathetic tone caused by factors other than environmental lighting. 19 p2393 A73-37300

INDUCED FLUID FLOW

U FLUID FLOW

INDUCERS

U INTAKE SYSTEMS

INDUCTANCE

Experimental investigation of the coupling impedance in resonator chains with a positive mutual inductance coefficient

01 p0025 A73-10987

Thermal stability improvement of variable inductance electronic circuits for analog magnitudes conversion to frequencies, noting instrument errors compensation

05 p0577 A73-16987

Inductance and magnetic reversal losses in pulse operated communication, describing bridge circuit for comparing test sample current with capacitor voltage/time characteristics

05 p0559 A73-17241

Inductance and Q factor measurements of inductive p-n-p transistor element in IC circuit as function of frequency, temperature and junction capacitance

10 p1196 A73-24613

Transient processes in an inductive energy storage element for a plasma injector

12 p1460 A73-26931

Formation of current pulses in an inductive load by reactive two-terminal networks

12 p1481 A73-27586

Certain problems in controlling phase of microwave electromagnetic oscillations using an inductive transistor.

13 p1591 A73-28670

Some operational aspects of an inductively loaded transistorized pulse amplifier at short time intervals

15 p1851 A73-31831

Transients in inductive energy-storage devices for plasma injectors.

22 p2891 A73-42265

Equivalent circuits for differential bridge quartz filter inductance evaluation in mass production

24 p3071 A73-44600

Investigation of the input impedance of an emitter-input transistor amplifier at near-cutoff frequencies

24 p3072 A73-44935

INDUCTION HEATING

A process for delubrication, presintering, sintering, and rapid cooling in a vacuum induction furnace.

04 p0455 A73-15751

Heat exchange between gas and air cooled porous metal plate prepared from stainless steel powder under induction and resistance heating

06 p0768 A73-18129

Time optimal heating of thin plates with constraints placed on the thermal stresses

07 p0923 A73-20634

Steady temperature fields and stresses in a half-space heated by a linear inductive source

08 p1019 A73-21759

Response-optimal heating of thin plates with constraints on the temperature stresses.

15 p1957 A73-31688

Temperature and stress fields in a cylindrical shell subjected to induction heat treatment

21 p2787 A73-41233

Determination of the temperature fields and thermal stresses in a bimetallic layer subjected to induction heating

23 p3046 A73-44194

INDUCTION SYSTEMS

U INTAKE SYSTEMS

INDUCTORS

Computer-aided design and graphics applied to the study of inductor-energy-storage dc-to-dc electronic power converters.

03 p0252 A73-13931

Three phase alternators with two/four poles superconducting inductors and with outer/inner induction winding, determining magnetic field radial distribution

10 p1177 A73-24411

Effect of linear load graduation in the end zones of an inductor on the longitudinal side effect in induction machines

15 p1832 A73-31410

Computer-aided design and graphics applied to the study of inductor-energy-storage dc-to-dc electronic power converters.

21 p2635 A73-40340

Results of the application of the physical modeling method to a study of the tangential component of the magnetic field of a linear inductor on the surface of a massive ferromagnetic body

22 p2800 A73-42214

INDUSTRIAL MANAGEMENT

NT ENGINEERING MANAGEMENT

NT INVENTORY MANAGEMENT

NT PERSONNEL MANAGEMENT

Charter air fleet maintenance economic management, discussing budget, manpower, time and materials control

09 p1168 A73-23243

Industrial material management, considering departments requirements, identification effort, costs and benefit, numbering and standardization systems, and uniform commodity description problem

13 p1624 A73-28788

Industrial work rhythm and between-day fluctuation studies 1920-1969, emphasizing industrial record and between-day fluctuations

16 p1975 A73-33160

Developing country industrial product reliability from buying and manufacturing viewpoints, considering local methods, customs, attitudes and working conditions effects on management techniques

16 p2089 A73-33646

Aerospace industry project managers and support personnel authority perceptions based on assessment of situational factors surrounding decision making, tabulating empirical investigation statistics

17 p2257 A73-35214

Computer data base use by industrial management for product design, development, manufacturing, testing and documentation coordination to achieve system communication and control improvement

17 p2257 A73-35215

Managerial implications of computerized aircraft design synthesis.

19 p2379 A73-37462

Product reliability management, providing MTBF charts for relationships between part count, laboratory test results and operational performance

22 p2867 A73-42969

INDUSTRIAL PLANTS

Russian book - Organization and planning of production at aircraft-construction plants.

04 p0524 A73-15965

Thermal effects of urbanization and industrialization in the boundary layer A numerical study.

06 p0720 A73-18330

Dynamic prediction model and optimal control of a commercial plant

12 p1561 A73-27081

Selection of an optimal structure for a tabular model of a control plant

21 p2670 A73-40995

INDUSTRIAL SAFETY

Hydrazine derivative poisoning in industry and clinical medicine treatments, noting causes of vitamin B6 deficiency

10 p1183 A73-23819

Russian book - safety measures in aviation industry.

18 p2281 A73-35869

INDUSTRIES

NT AEROSPACE INDUSTRY

NT AIRCRAFT INDUSTRY

INELASTIC BODIES

U RIGID STRUCTURES

INELASTIC COLLISIONS

Transfer of electronic excitation by atomic collision between highly excited cesium atoms

01 p0079 A73-10174

Cosmic ray particle high energy inelastic interactions, discussing pion and nucleon interaction angular and energy characteristics and muon production mechanism

02 p0209 A73-12664

Inelastic pionization cross section of cosmic ray hadrons with carbon nuclei at energies of 100 to 300 GeV

02 p0209 A73-12665

Pion-nucleon high energy interactions, determining inelasticity coefficient distribution

02 p0195 A73-12668

K-neutral pion energy fractions and inelasticity coefficients at primary energies of 100-1500 GeV during cosmic ray hadron-target interaction

02 p0210 A73-12689

Molecular gas presence effect on electron energy balance in atomic gases, noting inelastic collisions loss factor in heated Ar plasma containing nitrogen molecules

03 p0347 A73-14098

Strong electromagnetic waves in semiconductors under conditions of inelastic scattering of current carriers by optical phonons.

04 p0484 A73-15568

Description of a device for studying inelastic nuclear processes with nucleons at energies from .1 to 10 TeV and analysis of its operation at an altitude of 3250 m above sea level

05 p0577 A73-16823

Collision matrix elements near a pseudocrossing of potential energy curves.

06 p0726 A73-18249

Semiclassical theory of inelastic collisions. II - Momentum-space formulation.

06 p0726 A73-18262

Semiclassical theory of inelastic collisions. I - Classical picture and semiclassical formulation.

06 p0726 A73-18264

Influence of inelastic energy losses by electrons on the development of ionization instability in a plasma.

08 p0992 A73-20852

Inelastic collision of fast charged particles with arbitrary levelled hydrogen-like atoms.

10 p1250 A73-23575

Nonequilibrium radiative and inelastic collisional transitions structuring of ionizing shock waves in He and Ar

11 p1449 A73-25253

The kinetic reflection coefficient in a formula for the current at a plasma/semiconductor interface in the case of an inelastic mechanism of electron energy relaxation

12 p1527 A73-26928

Asymptotic form for the cross section for the Coulomb interacting rearrangement collisions.

14 p1777 A73-30551

Optical study of charge exchange collisions between He+ and CO2.

16 p2039 A73-33675

Elastic and inelastic scattering in orbital clustering.

18 p2357 A73-37109

Kinetic reflection coefficient at a plasma-semiconductor boundary for inelastic electron energy relaxation.

22 p2891 A73-42262

On the theoretical possibility of the libration cloud.

22 p2911 A73-42936

Inelastic interaction between pions and emulsion nuclei at an energy of 60 GeV

23 p3021 A73-43541

High energy nucleon inelastic interaction characteristics calculated from artificial event model based on covariant statistical theory of multiple generation of particles

23 p3022 A73-43542

Two level atomic inelastic transitions in plasma with damping for static, Weisskopf, adiabatic, exponential and Purcell/Born particle regions

23 p3008 A73-44014

INELASTIC SCATTERING

Semiclassical theory for low-energy molecular collisions - H/+/-H2 vibrational excitation.

01 p0080 A73-10564

Inelastic nuclear interactions between 200-GeV cosmic ray particles and polyethylene targets, correlating similarity property, momentum spectra and secondary particle pairs

02 p0208 A73-12652

Particle multiplicity and momentum spectra for high energy inelastic nuclear interactions in Wilson chamber with polyethylene target

02 p0208 A73-12655

Ionization calorimeter study of cosmic ray hadrons inelastic collision cross sections and partial K-neutral pion inelasticity factor

02 p0208 A73-12656

Inelasticity factor dependence on particle energy spectra to explain nucleon flux calculations and Proton satellite data, considering scattering cross sections

02 p0208 A73-12658

K-neutral pion inelasticity factor measurement for nucleon interactions in carbon corresponding to primary neutron energy transferred to pions

02 p0209 A73-12663

Inelastic scattering calculations with projected Hartree-Fock wave functions. II - Coupled-channel treatment.

03 p0345 A73-13806

Theory for the inelastic tunneling effect in normal metals

16 p2027 A73-34063

Measurement of the effective cross section of inelastic interaction between protons and carbon nuclei in the energy range 0.1 TeV to 1.0 TeV, on the Proton-4 space station

23 p3021 A73-43539

INELASTICITY

U ELASTIC PROPERTIES

INEQUALITIES

On the regularity of solutions of two-dimensional variational problems with obstructions.

01 p0069 A73-10044

Existence theorems for boundary value problems of elasticity defined by unilateral constraints, developing abstract theory of functional inequalities

02 p0233 A73-11979

The local form of the entropy inequality in neoclassical thermodynamics.

06 p0768 A73-17897

On the solution of linear inequalities with applications to threshold logic.

10 p1191 A73-23746

Positive solutions of infinite equation and inequality systems and Lagrange multipliers for infinite differentiable optimization problems

10 p1243 A73-24163

Certain finitely converging algorithms for the solution of infinite systems of inequalities and their application in the theory of adaptive systems

10 p1192 A73-24486

Inequalities for the large deviation probabilities of sums of independent random quantities in the case of a limiting stable law

12 p1518 A73-27221

Generalization of an exact method for solving equality constrained problems to deal with inequality constraints.

16 p2033 A73-33858

Nonlinear boundary value problems and several Lyapunov functions.

17 p2203 A73-35730

Improvable estimates in some non-well-posed problems for a system of elliptic equations. 20 p2581 A73-38975

Unboundedness of solutions and comparison theorems for time-dependent quasilinear differential matrix inequalities. 23 p3000 A73-44202

INERT ATMOSPHERE

The synthesis and characterization of tin complexes using inert atmosphere techniques - An advanced laboratory experiment. 06 p0661 A73-18272

INERT GASES

U RARE GASES

INERTIA

NT INERTIA PRINCIPLE

NT MACH INERTIA PRINCIPLE

A method of analysing the effect of inertia and compressibility in an externally pressurized gas lubricated thrust bearing. 03 p0312 A73-13209

Impulsive loading of liquid squeeze film plane circular bounding surfaces, showing fluid inertia effect on bonding strength and cavitation relationship to viscosity. 03 p0292 A73-13305

Inertia and energy effects in the developing gas film between two parallel flat plates. [ASME PAPER 72-LUB-33] 03 p0297 A73-14343

A method for including the effects of transverse shear and rotatory inertia on flexural motion of elastic plates. 04 p0510 A73-15074

Analysis of the shrouded Rayleigh step pad for an incompressible fluid film with the centrifugal inertia effect included. 09 p1089 A73-23103

The dynamical effect of inertial waves on the gyroscopic motion of a body containing several eccentrically located liquid-filled cylinders. 11 p1346 A73-25224

Rotating flexible shaft stability criterion development by perturbation method, considering internal and external friction and rotor inertia loading moments effects. 11 p1444 A73-26368

Influence of rotational inertia on the frequency spectrum of the natural vibrations of a cylindrical shell. 12 p1556 A73-27801

Use of inertial heat sensors for measuring the rate of temperature variation. 13 p1617 A73-28865

Hysteresis loop equation for calculation of elastoplastic deformations caused by forced vibrations, taking into account medium compressibility and inertial forces. 13 p1703 A73-29609

Irreversible thermodynamics with internal inertia - Principle of stationary total dissipation. 14 p1817 A73-30484

Impact interaction between a soft shell and a hard obstacle. 15 p1947 A73-31276

The inertia tensor of the atmosphere, annual variations in its components, and variations in the earth's rotation. 17 p2158 A73-34343

Inertial motion of a plastic ring under the action of a pulsed load. 17 p2244 A73-34797

An analytical and experimental investigation of turbulent flow in bearing films including convective fluid inertia forces. [ASME PAPER 73-LUBS-1] 17 p2181 A73-35388

On the possibilities of improving the accuracy of the evaluation of inertia forces in laminar and turbulent films. [ASME PAPER 73-LUBS-3] 17 p2181 A73-35389

Experimental study on the interference of inertia and friction forces in turbulent lubrication. [ASME PAPER 73-LUBS-12] 17 p2181 A73-35393

Gravitational-inertial waves in the general theory of relativity. 17 p2212 A73-35563

A quantitative estimate of the effect of the parameters of oscillatory systems on the natural frequencies. 19 p2498 A73-37653

Inertial force field patterns due to nutational motion of spinning satellites. 19 p2492 A73-37709

On the behavior of a numerical approximation to the rotatory inertia and transverse shear plate. [ASME PAPER 73-APMW-7] 22 p2924 A73-42880

Motion of the inertia pole of the earth over a hundred years. 23 p3037 A73-44255

INERTIA MOMENTS

U MOMENTS OF INERTIA

INERTIA PRINCIPLE

NT MACH INERTIA PRINCIPLE

On the influence of inertia forces in hydrostatic turbulent lubrication. 14 p1755 A73-30705

Curved twisted space beam elements, expressing displacement function and inertia property by rotation and mass matrices. 20 p2621 A73-39533

INERTIA WHEELS

U REACTION WHEELS

INERTIAL ACCELEROMETERS

U ACCELEROMETERS

INERTIAL COORDINATES

Automatic impulse frequency stabilization of space vehicle rotation angle with respect to inertial coordinates by Liapunov discrete method. 01 p0110 A73-10595

Algorithm for locating a moving object. 11 p1394 A73-26097

Algorithms for calculating Euler angles of moving objects. 20 p2590 A73-39044

INERTIAL FORCES

U INERTIA

INERTIAL GUIDANCE

NT STRAPDOWN INERTIAL GUIDANCE

Lateral velocity measurement error analysis in inertial guidance system, noting automatic compensation of mass imbalance effects. 05 p0596 A73-16992

Titan III-C guidance with the Carousel VB inertial guidance system. 06 p0721 A73-18826

The use of automatic test equipment for performing screening and production reliability verification testing. 08 p0942 A73-20681

Powered-flight trajectory optimization for an inertial-guidance ballistic vehicle. 08 p1011 A73-21427

A semiinertial homing guidance system. 10 p1247 A73-24498

UV photography of star field by Eridan rocket-borne wide angle camera, noting inertial guidance system pointing errors data reduction problems. 18 p2315 A73-35994

The P-star technique and its application to inertial guidance. [AIAA PAPER 73-837] 20 p2584 A73-38780

Europa 2 Inertial Guidance System technology assessment covering design features, sensor, computer and interface units, first launch failure causes and need for improvements. 24 p3108 A73-44694

INERTIAL MEASURING UNITS

U INERTIAL PLATFORMS

INERTIAL NAVIGATION

Mathematical model and error equations of inertial navigation system with two leveled accelerometers, comparing with three component and pendulum gyroscopic systems. 02 p0190 A73-11778

Determination of the location of a moving object with the aid of navigation systems using information on the cruising speed of the object. 02 p0190 A73-11779

German book - Deutsche Gesellschaft fur Luft- und Raumfahrt, 1971 Yearbook. 05 p0528 A73-16755

Inertial navigation system based on two schuler gyropendulums and one azimuth gyro. 05 p0595 A73-16765

Application of a mathematical filter in the design of a spacecraft inertial stabilization system without a platform. 05 p0630 A73-17005

An all-earth inertial navigation scheme. 06 p0721 A73-18255

The pre-flight handling of inertial navigation systems. 07 p0849 A73-19347

Instrument axes trihedron orientation relative to reference, deriving expressions for angular misalignment statistical estimation. 09 p1115 A73-22353

Radio navigation review, discussing Decca, Loran, Omega, VOR/DME, satellite, inertial, integrated, area, approach and landing, collision avoidance and space navigation systems. 10 p1246 A73-23636

Algorithm for locating a moving object. 11 p1394 A73-26097

Inertial air navigation system error minimization, using discrete-sampled position fixing and star sighting data in computerized calculations. 12 p1522 A73-26821

A new approach to Doppler-inertial navigation /Doppler Beam Sampling/. 12 p1522 A73-27162

Kalman filter design considerations for space-stable inertial navigation systems. 13 p1657 A73-29220

MGC 30 inertial navigation system for civil aviation, emphasizing economics and ease of maintenance. 15 p1909 A73-32457

Gimbaled electrostatic gyro inertial aircraft navigation system /GEANS/ designs balancing performance against cost of ownership. 16 p2034 A73-33086

INERTIAL PLATFORMS

Altitude damping of space-stable inertial navigation systems. 16 p2034 A73-33403

Prospects of automation of air traffic control systems using satellites for radio navigation. 17 p2209 A73-34961

LN-33 airborne inertial navigation system with low cost precision instruments and miniaturized digital computer, noting built-in calibration and test capability for minimizing maintenance. 17 p2210 A73-35212

Stardrift - A navigational system for relativistic interstellar flight. 17 p2210 A73-35659

Strapped down inertial navigation systems. 19 p2452 A73-37876

Ships inertial navigation system automated degradation detection and isolation, specifying decision error probabilities as function of degradation magnitude and observation time. [AIAA PAPER 73-849] 20 p2585 A73-38788

Optimum inertial sensor orientation for earth inertial navigation systems allowing for azimuth error and g-sensitive instrument error effects. [AIAA PAPER 73-850] 20 p2585 A73-38789

Optimal filtering and smoothing simulation results for CIRIS inertial and precision ranging data. [AIAA PAPER 73-872] 20 p2587 A73-38809

Hybrid-inertial navigation with range updates in a relative grid. [AIAA PAPER 73-873] 20 p2587 A73-38810

The evaluation of autonomous navigation systems for cruise vehicles. [AIAA PAPER 73-874] 20 p2587 A73-38811

Data compression in recursive estimation with applications to navigation systems. [AIAA PAPER 73-901] 20 p2589 A73-38835

Equations for the instrumental errors of a type of inertial navigation system. 20 p2590 A73-39045

Strapdown inertial navigation with high speed digital computer, discussing attitude propagation algorithms and life cycle system cost advantages. 21 p2734 A73-40036

Low cost strapdown inertial navigator with miniature electrostatically suspended gyros, discussing system performance goal in terms of position, velocity and attitude errors. 21 p2734 A73-40037

Failure detection and isolation techniques for gimbaled and strapdown inertial systems examining redundant system reliability relationship to MTBF. [AIAA PAPER 73-852] 22 p2884 A73-41969

Error analysis of a coupled inertial navigation system. 22 p2884 A73-42358

INERTIAL PLATFORMS

Hall effect gimbal angle transducer /HEGAT/ for relative angular orientation measurement between rotor and stator in low cost inertial platform. 04 p0447 A73-15066

One degree of freedom fluid suspension gyros, direct drive gimbal motors and microelectronic control assemblies review, noting miniature inertial platforms availability. 07 p0820 A73-18941

An attitude control system for a stellar X-ray source mapping payload. [AIAA PAPER 73-291] 09 p1116 A73-23210

A digital attitude control system for orientation of rocket launched scientific payloads. [AIAA PAPER 73-292] 09 p1116 A73-23211

Tilt-table alignment for inertial-platform maintenance without a surveyed site. 15 p1858 A73-31728

Shop level maintenance of inertial platforms without a surveyed site. 17 p2148 A73-35644

Inertial symmetrization of large spin-stabilized spacecraft. [SAWE PAPER 965] 19 p2493 A73-37883

Seismometer compensation for broadband, low-level acceleration measurements. [AIAA PAPER 73-828] 20 p2563 A73-38773

Digital control of a pneumatic isolation system for inertial instrument testing. [AIAA PAPER 73-830] 20 p2543 A73-38775

Failure detection and isolation methods for redundant gimbaled inertial measurement units. [AIAA PAPER 73-851] 20 p2585 A73-38790

Continuous calibration and alignment techniques for an all-attitude inertial platform. [AIAA PAPER 73-865] 20 p2586 A73-38803

Navigation of the Titan IIIC space launch vehicle using the Carousel VB IMU. [AIAA PAPER 73-905] 20 p2589 A73-38839

Stability of a biaxial gyroframe on a vibrating base in resonance conditions. 23 p3007 A73-44186

Extremal search method errors in determining azimuthal position of gyro-stabilized platform relative to meridian plane, comparing with gyrocompasses. 24 p3109 A73-45022

INERTIAL REFERENCE SYSTEMS

Spacecraft control hardware for use with digital processors.

04 p0424 A73-14737

A quasi-inertial attitude mode for orbiting spacecraft.

05 p0630 A73-17203

Autonomous determination of meridian plane with triaxial gyroscopic stabilizer during initial display of inertial system

09 p1116 A73-22659

Precession, nutation and the choice of reference system for close earth satellite orbits.

11 p1423 A73-26067

Analytical estimates of the accuracy of spacecraft autonomous navigation based on measurements of flight altitude and zenith-distance inertial-space reference point.

12 p1523 A73-27647

Lorentz contraction and transformation of equilibrium forces and moments in inertial reference systems transition, discussing special relativity theory

12 p1525 A73-27733

Lagrange function based Poincare mechanics of inertial relativity, using Mach-Einstein inertia principle for gravitational potential

16 p2036 A73-33072

Y-covariant formulation of the relativistic electrodynamics of material media

17 p2213 A73-35569

Local Y-transformations in the electrodynamics of inhomogeneous accelerated media

17 p2213 A73-35570

Airborne IRP alignment using acceleration and angular rate matching.

19 p2386 A73-38048

Competitive evaluation of failure detection algorithms for strapdown redundant inertial instruments.

[AIAA PAPER 73-853] 20 p2585 A73-38791

Optimal filtering and smoothing simulation results for CRIS inertial and precision ranging data.

[AIAA PAPER 73-872] 20 p2587 A73-38809

Gyroscopes as prime attitude references for the large space telescope.

[AIAA PAPER 73-870] 21 p2700 A73-40506

INFARCTION

NT MYOCARDIAL INFARCTION

Diagnostic value of vectorcardiogram in strictly posterior infarction.

03 p0268 A73-13891

Experimental studies on the production of pulmonary infarction. IV - Effects of UK, heparin, t-AMCHA or ellagic acid.

22 p2805 A73-42319

INFECTIONS

U INFECTIOUS DISEASES

INFECTIOUS DISEASES

NT SMALLPOX

NT TUBERCULOSIS

Remote sensing application to habitat of mosquito vectors of disease, considering St. Louis and Venezuelan encephalitis strains and human filariasis

20 p2520 A73-39866

INFLATABLE DEVICES

U INFLATABLE STRUCTURES

INFLATABLE SPACECRAFT

NT BEACON SATELLITES

INFLATABLE STRUCTURES

NT BALLOONS

NT BALLUTES

NT BEACON SATELLITES

NT HIGH ALTITUDE BALLOONS

NT METEOROLOGICAL BALLOONS

NT SKYHOOK BALLOONS

NT TETHERED BALLOONS

Bending rigidity of an inflated circular cylindrical membrane of rubbery materials.

03 p0395 A73-14183

A linearised theory of parachute opening dynamics.

08 p0928 A73-21692

Nonlinear toroidal curved elastic sheet inflated by fluid at constant pressure, discussing existence, uniqueness and asymptotic behavior

14 p1812 A73-30520

Analysis of the static deformations of flexible extensible gas-filled shells

15 p1947 A73-31279

Stress measurement on cloth of inflated solid circular parachute model, noting sensor interference with canopy shape and stress pattern

[AIAA PAPER 73-445] 15 p1825 A73-31431

High strength fiber woven cloth materials for inflatable structure, discussing characteristics assembly methods and tests

[AIAA PAPER 73-448] 15 p1826 A73-31434

Two dimensional unsteady vortex flow of ideal fluid past inflating decelerating wedge, obtaining pressure distribution on wedge surface

[AIAA PAPER 73-449] 15 p1823 A73-31435

Aircraft recovery by inflatable wing canopy with steel cable or fiber suspension lines, discussing aerodynamic characteristics, suspension system and centrifugal compressor performance

[AIAA PAPER 73-470] 15 p1828 A73-31454

Inflated air bag head restraints for prevention of brain injuries due to whiplash acceleration during crash landings or ejection

16 p1965 A73-32654

Finite element analysis of inflatable shells.

17 p2242 A73-34528

Effects of axisymmetric loads on inflated non-linear membranes.

23 p3045 A73-44081

INFLATING

Dynamic parachute inflation model for dimensionless time and maximum force predictions at high altitudes

[AIAA PAPER 73-450] 15 p1826 A73-31436

Analysis of deployment and inflation of large ribbon parachutes.

[AIAA PAPER 73-451] 15 p1826 A73-31437

A model and calculation procedure for predicting parachute inflation.

[AIAA PAPER 73-453] 15 p1826 A73-31439

INFLUENCE COEFFICIENT

NT STRUCTURAL INFLUENCE COEFFICIENTS

Flexible rotor balancing of a high-speed gas turbine engine.

[SAE PAPER 720741] 02 p0203 A73-12007

Evaluation of the coefficients of the effect of errors in the original information and in the model of optimization results.

02 p0149 A73-12122

Slowly oscillating lifting surfaces at subsonic and supersonic speeds.

03 p0245 A73-13704

Influence areas for some cross sectional parameters of shallow double-curvature shells

04 p0513 A73-15507

Indirect structural analysis by finite element method.

06 p0758 A73-17447

Aerodynamic influence coefficient method using singularity splines.

[AIAA PAPER 73-123] 06 p0644 A73-17645

Development and applications of supersonic unsteady consistent aerodynamics for interfering parallel wings.

[AIAA PAPER 73-317] 11 p1301 A73-25548

Influence function of a nonheated region and the relationship between the method of superposition and the method of expanding solutions in series of form parameters

12 p1558 A73-27312

An approximate method for the calculation of the velocities induced by a wing oscillating in subsonic flow

15 p1824 A73-31905

Book - Computer methods in structural analysis.

17 p2251 A73-35473

INFORMATION DISSEMINATION

NT SELECTIVE DISSEMINATION OF INFORMATION

Effective development, documentation, and distribution of computer programs.

03 p0392 A73-13691

SPACEWARN - An international mechanism for rapid distribution of information on satellites and space probes.

11 p1454 A73-25569

Determination of the information-forecasting indices of biometeorological phenomena

13 p1579 A73-28861

Apollo Experience Reports contents and development, detailing engineering, life sciences, flight crew operations, flight control safety and applications

17 p2256 A73-34300

Sabreliner Airborne Data Acquisition and Recording System /ADARS/ for communication with flight observers to evaluate research missions

17 p2174 A73-35582

Hydrometeorological data processing and dissemination techniques and equipment, with emphasis on computerized regional centers and space-based systems

18 p2295 A73-35907

Indian national educational communications program for information dissemination on health, family planning, hygiene and agriculture, discussing satellite TV development project

[AAS PAPER 73-106] 20 p2629 A73-38576

INFORMATION FLOW

Information transfer system of digital avionics system, examining signal reduction by baseband time division multiplexing and video distribution systems

17 p2138 A73-35230

Information dependent frequency control of an automatic typewriter.

23 p2944 A73-43423

INFORMATION MANAGEMENT

Considerations for an earth physics information-management service.

04 p0439 A73-14814

Information management system breadboard data acquisition and control system.

04 p0425 A73-15461

Statistical diagnostics and information synthesis relating to the reliability and maintenance of an equipment

07 p0830 A73-19414

Eole project data processing organization and operations management, describing information acquisition and reduction

09 p1060 A73-23377

Design considerations for shuttle information management.

14 p1818 A73-29945

Environmental data - From sensors to users.

[AAS PAPER 73-138] 20 p2521 A73-38592

Information seeking with multiple sources of conflicting and unreliable information.

24 p3063 A73-44778

INFORMATION RETRIEVAL

Mathematical model for information search and retrieval under Poisson process requests, discussing data processing time minimization sorting algorithms

06 p0670 A73-17856

The limiting advantage derived from the compounding of information-extracting devices in the presence of wideband Gaussian noise

12 p1482 A73-26867

Parachutes computer aided design and performance analysis system development and operation, presenting information storage and retrieval tasks mechanics

[AIAA PAPER 73-484] 15 p1829 A73-31466

Computer experiments in selective distribution of hydrometeorological bibliographic information

15 p1904 A73-31611

Design concepts for an earth resources data management system.

[AAS PAPER 73-151] 20 p2521 A73-38597

INFORMATION SYSTEMS

NT MANAGEMENT INFORMATION SYSTEMS

Information processing 71: Proceedings of the Congress, Ljubljana, Yugoslavia, August 23-28, 1971. Volume 1 - Foundation and Systems. Volume 2 Applications.

01 p0020 A73-11451

Simulation aids for designing integrated information systems - The ECSS language.

02 p0144 A73-12600

Data acquisition, processing and retrieval in information system for product design and development, noting storage system for spring material data

03 p0400 A73-13238

NASA's Technology Utilization Program.

04 p0521 A73-14730

Problems of the synthesis of spacecraft onboard data computation units

05 p0553 A73-16417

Natural resources information system.

08 p0961 A73-21707

Educational radio and television satellite networks, considering computer networks, cable TV and NASA Applications Technology Satellites /ATS/ utilization

09 p1056 A73-23397

Multicolor documentation type information holographic storage, recording, indexing, registration and reconstruction technology assessment and application, emphasizing displays and automatic test equipment systems

10 p1216 A73-23797

Prospects of developing an automated hydrometeorological system

10 p1203 A73-24375

SPACEWARN - An international mechanism for rapid distribution of information on satellites and space probes.

11 p1454 A73-25569

The data processing architecture on the launch bases of the Directorate of Research and Test Methods

14 p1742 A73-30091

ATC radar information processing systems optimization, discussing hard- and software selection criteria

15 p1847 A73-32440

Information systems enabling pilots to report incidents involving safety, including human fallibility and system errors in construction, operation and regulation

17 p2256 A73-34087

Military aircraft onboard Digital Avionics Information System for computerized integration of navigation, guidance, weapon delivery, cockpit display, communication, flight control and energy management

17 p1316 A73-35202

Aircraft onboard computerized avionics and electrical systems architecture for information flow and control with maximum efficiency, flexibility, modularity and minimum maintenance

17 p2137 A73-35204

Computer data base use by industrial management for product design, development, manufacturing, testing and documentation coordination to achieve system communication and control improvement

17 p2257 A73-35215

Sorcerer Apprentice head mounted display with wand for interaction with computer generated

synthetic objects, describing creation of illusory three dimensional environment

19 p2397 A73-37323

Digital information management system of navigational and flight data for post-1975 fighter aircraft. [AIAA PAPER 73-897]

20 p2589 A73-38832

Integration of remote sensing data into spatial information systems, discussing data specification, acquisition, storage, retrieval, processing, etc

21 p2658 A73-40820

Russian book on reliability optimization in complex automatic control system information transfer and processing covering performance criteria, noise immunity, error sources and types, etc

21 p2670 A73-41293

Russian book on radio telemetry systems analysis and theory covering analog and digital data, signal processing, algebraic and trigonometric polynomials and discrete representations

22 p2824 A73-41879

Philosophical approaches of technological forecasting and assessment, discussing Dialectical and Singerian inquiring /information/ systems for ill structured problems

23 p3051 A73-44218

INFORMATION THEORY

Evaluation of the coefficients of the effect of errors in the original information and in the model of optimization results.

02 p0149 A73-12122

Information theory mathematical models applied to different visual function activity phases, covering Shannon and Fisher probability models, Shreider semantic theory and Kolmogorov algorithm

04 p0412 A73-15784

Information-loss and risk-increase estimation during observational data reduction in successive estimation problems

05 p0589 A73-16299

Transinformation and real time identification applied to the study of pilot workload

05 p0545 A73-17195

Cosmological aspects of order, relevance, and information theory.

06 p0749 A73-18002

Thermodynamics and morphological orders - A generalized concept of information transfer.

06 p0749 A73-18003

Thermodynamic probability and statistical interpretations of entropy, with particular attention to information theory, negentropy and Boltzmann-Gibbs theory

08 p1022 A73-21234

Most convenient intervals of amplitude quantization in direction finding

08 p0939 A73-21394

Random coding bound of information theory providing upper bound to decoding error probability for best code of given rate and block length

09 p1111 A73-22117

Linear decision rule for probabilistic signal estimation in image recognition problems with sampling

09 p1060 A73-22556

Information in the time of arrival of a photon packet - Capacity of PPM channels.

10 p1188 A73-23836

Huygens principle, power spectrum and photon and photographic noise intensities effects in holography, discussing optical information transmission by eigen-solutions

11 p1369 A73-26529

Problems involving efficient transmission of informative parameters in the adaptive discretization of an analog signal

13 p1583 A73-28852

Maximum information compression and minimum entropy of random process, using Karhunen-Loeve basis

13 p1596 A73-28869

Logic and computational complexity of decoders for BCH codes, discussing channel capacity, error correction and information theory

13 p1587 A73-29672

Book - Topics in intersystem electromagnetic compatibility.

14 p1729 A73-30596

Spatial information coding in the human visual system - Psychophysical data.

17 p2116 A73-35240

Institute of Electrical and Electronics Engineers, International Convention and Exposition, New York, N.Y., March 26-30, 1973, Technical Papers.

17 p2140 A73-35299

The problem of applying information theory to efficient image transmission.

17 p2124 A73-35302

Electrical engineering - Service to mankind; Proceedings of the Southeast Region 3 Conference, Louisville, Ky., April 30-May 2, 1973.

17 p2142 A73-35626

Mean square and reflectivity variance decrease due to radar beam smoothing and post-detection integration in terms of reflectivity fields autocorrelation function

18 p2333 A73-36706

The mechanisms of the occurrence of emotional stress in man.

18 p2279 A73-36920

The most advantageous amplitude quantization intervals for direction finding.

19 p2407 A73-38352

Information processes in control systems, discussing stability, state reproduction, invariance, entropy balance and statistical physics analogies

20 p2539 A73-38698

Information content subsetting of highly correlated error sources.

[AIAA PAPER 73-867]

20 p2586 A73-38805

A method of processing a priori information about a controlled plant with the aim of reducing the number of changing parameters of the dynamic characteristics

20 p2541 A73-38993

Analysis of methods for selecting significant attributes in the classification of patterns

20 p2532 A73-38999

Application of information theory to the study of mechanical systems

20 p2592 A73-39260

Noise immunity of digital methods for the transmission of analog messages with an enhanced information content

20 p2531 A73-39463

The filtering of random sequences with gaps by optimal discrete filters with a constant memory volume

21 p2658 A73-40857

The quantity of initial-parameter information contained in trajectory measurements

21 p2726 A73-40916

The possibility of using information theory in optics

21 p2740 A73-41100

Continuous information theory and modulation methods.

22 p2826 A73-42463

Signal theory problems of discrete signal representation decomposition and characterization by Walsh and orthogonal functions, noting voiced speech analysis

23 p2952 A73-43309

Visual and verbal coding in the interhemispheric transfer of information.

24 p3065 A73-45337

INFORMATION TRANSFER

U COMMUNICATING

INFORMATION TRANSMISSION

U DATA TRANSMISSION

INFRARED ASTRONOMY

Photometry and spectroscopy of red variables in Omega Centauri.

01 p0098 A73-10584

Rocket infrared observations of H II regions.

01 p0103 A73-11026

Photometry of supernova 1972 in NGC 5253.

01 p0104 A73-11046

Discovery of infrared emission from the radio source near Cygnus X-3.

02 p0210 A73-11558

Observations of planets, nebulae, and galaxies at 350 microns.

03 p0374 A73-13716

IR observations of comets Bennett and Tago-Sato-Kosaka, noting thermal origin of flux, source structure and material temperature, emissivity and composition

04 p0494 A73-14754

Infrared observations of Comets Ikeya-Seki /1965I/ and Bennett /1969I/.

04 p0494 A73-14755

Infra-red sources in the H II region W3.

04 p0499 A73-15485

3C 120, BL Lacertae, and OJ 287 - Coordinated optical, infrared, and radio observations of intraday variability.

05 p0625 A73-17342

Infrared measurements of R. Coroneae Borealis through its 1972 March-June minimum.

05 p0627 A73-17391

Matter heating based IR astronomy, describing liquid helium cooled Ge bolometer and IR telescope

07 p0875 A73-19324

IR interferometry with heterodyne detection and tuned laser focusing for stellar envelopes, interstellar dust, planetary surfaces and low temperature sources observation

07 p0825 A73-20242

Optical variability of the nuclei of Seyfert galaxies

07 p0901 A73-20306

The role of Schmidt telescopes in the study of external galaxies.

08 p1011 A73-21361

Considerations about far infrared detectors for astronomical purposes.

08 p0967 A73-21421

RCW 117 and DR 15 observed in the far infrared.

08 p1012 A73-21531

Hadamard transform spectrometer designed for airborne IR astronomical observations of Mars, using binary orthogonal pseudonoise codes in multiplexing scheme

08 p0972 A73-21753

Models for extragalactic objects with very high IR and X-ray luminosity.

09 p1141 A73-22007

Infra-red observations of young stars. I - Stars in young clusters. II - T Tauri stars and the Orion population. III - Nebulous emission-line stars.

09 p1143 A73-22112

Recent progress in infrared and microwave techniques of astronomical interest.

09 p1086 A73-23128

Optical and near-infrared observations of the nearby spiral galaxy Maffei 2.

10 p1272 A73-23528

IR sources at 1-5 microns, discussing Betelgeuse, R Doradus, dying stars, new stars and galaxies

11 p1422 A73-25974

Infrared detection techniques for space research; Proceedings of the Fifth ESLAB-ESRIN Symposium, Noordwijk, Netherlands, June 8-11, 1971.

11 p1367 A73-26501

Review of results in infrared space astronomy.

11 p1426 A73-26502

Airborne IR 32 cm observatory, discussing atmospheric transmission and guiding methods to overcome aircraft instability effects

11 p1368 A73-26503

Balloon-borne Newtonian telescope with parabolic pyrex primary mirror for far IR observation of celestial sources

11 p1368 A73-26504

Infrared detectors - Survey of the present state of the art.

11 p1368 A73-26509

Astronomical polarimeter design, polarization sensitivity and 5 and 10 micron analyzers efficiency

11 p1369 A73-26513

Cooling systems for spaceborne infrared experiments.

11 p1453 A73-26515

Interferometric spectrometry for infrared astronomy.

11 p1369 A73-26517

Far infrared broad band interferometry.

11 p1369 A73-26518

Dust emission nebulae around Orion O and B stars.

11 p1427 A73-26606

Optical variability of the nuclei of Seyfert galaxies.

12 p1539 A73-27278

Optical space astronomy and goals of the large space telescope.

12 p1497 A73-27436

HTS spectrometer for airborne infrared astronomy.

15 p1880 A73-32379

Far-infrared observations of galactic nuclei.

17 p2232 A73-34771

2.2- and 3.5-micron polarization measurements of the Becklin-Neugebauer object in the Orion Nebula.

19 p2489 A73-38528

Ground based photometry of planets, stars and galactic nebulae at 34 microns

19 p2489 A73-38529

Astronomische Gesellschaft, Scientific Meeting, Vienna, Austria, September 18-23, 1972, Reports

20 p2605 A73-39056

IR astronomical objects, methods and instruments, discussing galactic and extragalactic sources, early and late stars, planetary nebulae, interstellar dust and hydrogen ion clouds

20 p2605 A73-39060

Considerations about the atmospheric background and the technique of differential modulation in infrared astronomy.

21 p2740 A73-40690

Observations of far infrared atmospheric windows at 44/cm and 50/cm from Pikes Peak.

21 p2780 A73-41647

Infrared maps of the galactic nucleus.

22 p2904 A73-41757

Jupiter Red Spot photographic, IR image, spectral, photometric, polarimetric and chemical studies, comparing with earth and Mars atmospheric data

23 p3032 A73-43940

Jupiter zone and Red Spot latitude measurements and visual color evaluation in near IR methane band

23 p3032 A73-43943

Absolute measurements and computed values for Martian irradiance between 10.5 and 12.5 microns.

24 p3127 A73-44394

Determination of radii of satellites and asteroids from radiometry and photometry.

24 p3130 A73-44453

Infrared and X-ray variability of Cyg X-3.

24 p3143 A73-45347

Heterodyne detection of Arcturus at 10.6 microns.

24 p3143 A73-45493

INFRARED DETECTORS

Doped CdSb single crystal production and physical properties for IR detectors and thermocouple use

01 p0087 A73-10040

Atmospheric moisture and wind field synoptic analysis based on Nimbus 4 temperature-humidity IR radiometer /THIR/ measurements

01 p0073 A73-10379

Heterojunction photocell, sensitive in the near infrared.

01 p0051 A73-10834

Spacecraft-borne IR optical remote sensor for detection, identification and distribution measurement of asteroid and meteoroid particles

01 p0105 A73-11205

Spectral characteristics and black body radiation sensitivity of submillimeter band radiometer based on n-type epitaxial GaAs films

02 p0147 A73-12496

Fabrication of a lightweight circular orbit passive radiative cooler.

03 p0329 A73-13010

Book on passive IR sensing devices design and use in industrial and manufacturing problems solution covering detector types, display devices and reliability analysis

03 p0283 A73-13994

Infrared detection by reconfiguration of high field domains in CDS:Ag, Al.

06 p0733 A73-17500

Pyroelectric IR detector materials thermal and electric properties, discussing applications in thermographs, focal plane reticle scanners, linear array thermal imaging, radiometers and laser detectors

06 p0694 A73-18317

Fast solid state IR detection photodiodes design, properties and utilization, investigating high speed response conditions and quantum efficiency

06 p0678 A73-18853

The performance of a satellite-borne infrared target acquisition system.

07 p0824 A73-19946

IR radiometers for free jets sound emission mechanism probing, describing optical and electronic equipment

[ONERA, TP NO. 1212]

07 p0825 A73-20164

IR interferometry with heterodyne detection and tuned laser focusing for stellar envelopes, interstellar dust, planetary surfaces and low temperature sources observation

07 p0825 A73-20242

Experimental verification and assessment of an infra-red radiation modulator based on a Fabry-Perot etalon.

07 p0825 A73-20373

Optimum spectral band of an infrared detection system for use against forest background radiation.

08 p0962 A73-20811

Considerations about far infrared detectors for astronomical purposes.

08 p0967 A73-21421

Sensitivity limits for extrinsic and intrinsic infrared detectors.

08 p0967 A73-21422

Vacuum system for an infrared calibration facility.

08 p0968 A73-21622

An infrared pneumatic transducer with capacitive detection.

[ONERA, TP NO. 1150]

08 p0968 A73-21682

Characteristics of infrared photodetectors produced by radiation doping.

09 p1079 A73-21934

Improved responsivity and sensitivity characteristics of the thin-film bismuth bolometer.

09 p1080 A73-22087

Visible and infrared sensor arrays for imaging systems.

10 p1216 A73-23787

Thermal reference system with linear temperature profile down fin axis for thermography, using scanning IR camera as image detector

11 p1366 A73-26305

Infrared detection techniques for space research; Proceedings of the Fifth ESLAB-ESRIN Symposium, Noordwijk, Netherlands, June 8-11, 1971.

11 p1367 A73-26501

Infrared detectors - Survey of the present state of the art.

11 p1368 A73-26509

High responsivity large surface liquid helium cooled IR bolometers based on carbon resistors and Ge and Si elements

11 p1368 A73-26510

A new type of helium-cooled bolometer.

11 p1368 A73-26511

Problems and design of black-body references.

11 p1401 A73-26514

Application of Nimbus 4 THIR 6.7-micron observations to regional and global moisture and wind field analyses.

12 p1520 A73-26812

Thermal IR radiation receiver with ferroceramic capacitor for amplification and transformation of signals from RF oscillator

13 p1618 A73-29133

Infra-red detection for satellite attitude sensing - The ANS horizon sensor.

16 p2012 A73-32853

Air quality monitoring instruments involving atmospheric pollution chemiluminescent reactions and CO IR, optical absorption and laser detectors

16 p2016 A73-33402

In-flight frequency calibration of IR sensor systems using LEDs.

17 p2165 A73-34275

Bandpass filter with cooled InSb detector for measurement of far IR radiation and temperature-vs-wavelength characteristics of Hg arc lamp

17 p2176 A73-35774

Detection of optical and infrared radiation with dc-biased electron-tunneling metal-barrier-metal diodes.

17 p2143 A73-35792

Theoretical analysis of improvements in remote sensing of atmospheric and pollutant gases through high resolution detection of individual infrared emission lines.

[ALAA PAPER 73-703]

18 p2315 A73-36252

Probing the structure and composition of the Jupiter atmosphere from Pioneer 10/11.

[ALAA PAPER 73-561]

18 p2353 A73-36498

Preliminary report on infrared radiometric measurements from the Mariner 9 spacecraft.

19 p2479 A73-37221

Survey of clear air turbulence detection methods.

19 p2430 A73-37822

Compact carbon monoxide sensor utilizing a confocal optical cavity.

[ASME PAPER 73-ENAS-20]

19 p2400 A73-37976

IR test data evaluation for printed circuits using computer techniques, discussing testing time reduction and efficiency optimization, programming language and error analysis

20 p2567 A73-39769

Improvements brought to the measurement of the ocean surface temperature by utilization of a polarizing infrared radiometer

21 p2698 A73-40142

Technical and economic problems in use of military passive night vision systems including image intensifiers, IR detectors and thermographic imaging devices

23 p2979 A73-43219

INFRARED FILTERS

Report on results of research conducted by the Thin Film Department of SEAVOM, under CNES contract.

07 p0821 A73-18980

Low pass wide and medium band IR filter obtained by cooling crystalline material to liquid He or nitrogen temperatures, tabulating transmission characteristics

21 p2697 A73-40127

Materials suitable for making far infrared high-pass transmission filters.

21 p2701 A73-40692

INFRARED HORIZON SCANNERS

U HORIZON SCANNERS

U INFRARED SCANNERS

INFRARED IMAGERY

The requirements on the parameters of a mechanical modulator for an IR scanning radiometer.

01 p0050 A73-10833

Infrared maps of Jupiter.

01 p0109 A73-11490

Solar IR imaging techniques for providing high resolution data with short exposure time

02 p0169 A73-12333

Human factors analysis of forward looking infrared /FLIR/ imagery in air-to-ground target detection/recognition.

05 p0550 A73-16712

Interpretation of numerical observations of meteorological satellites with infrared and monochromatic vision by means of high resolution satellites - The case of storm cloud systems

05 p0594 A73-17232

Quantitative temperature data from Direct-Readout Infrared /DRIR/ pictures.

[AD-759891]

06 p0696 A73-18711

Pyroelectric tubes for thermal imaging system, discussing materials, electron beam read-out, SNR and performance limit compared with scanned photon detectors

07 p0798 A73-19224

Flight planning and navigation for thermal-IR surveys.

07 p0849 A73-20019

Recent progress in infrared and microwave techniques of astronomical interest.

09 p1086 A73-23128

Visible and infrared sensor arrays for imaging systems.

10 p1216 A73-23787

Far IR mapping of lunar surface during 19 December 1964 eclipse, discussing thermal contours and Apollo observed regions

10 p1282 A73-24644

Lunar surface thermal response from IR atlas charts of eclipsed moon, noting thermal enhancements in maria

12 p1541 A73-27483

Laser illumination for infrared nondestructive testing.

15 p1874 A73-31050

HF laser flow visualization with an infrared television system.

15 p1874 A73-31357

The impact of silicon technology on near-infrared and low-light-level imaging.

16 p2012 A73-32867

Thermal imaging through hazes and fogs in the middle and far infrared windows - Some experimental results.

16 p2016 A73-33997

Capabilities and limitations of infrared imaging systems.

17 p2167 A73-34902

Some problems associated with wind drag and infrared images of the sea surface.

18 p2313 A73-36643

Optimum parameters of an infrared imaging system for aerial scanning of earth resources.

18 p2317 A73-36874

IR quasi-synoptic global sensing of ocean surface temperature, covering IR theory, airborne radiation thermometry and single band satellite data analysis techniques

[AAS PAPER 73-146]

20 p2550 A73-38595

Thermal IR image recording, processing and enhancement, discussing prevention of defects or irregularities caused by aircraft motion, weather and electronic noise

20 p2566 A73-39670

Satellite detection of melting snow and ice by simultaneous visible and near-IR measurements.

20 p2556 A73-39840

Utilizing remote sensing data for land use decisions for Indian lands in South Dakota.

20 p2557 A73-39850

Ultraviolet, panchromatic, infrared and radar remote sensing of Mesabi Range /Minnesota/, discussing Precambrian rock formations, geological faults, pre-dawn and daytime photography and vegetation patterns

20 p2561 A73-39894

Experimental design to produce visible-reflective IR ratio image from ERTS data for geological mapping of iron compounds

20 p2561 A73-39899

A comparison of four remote sensing media for assessing salt marsh primary productivity.

20 p2562 A73-39903

Detection of small fires and mapping of large forest fires by infrared imagery.

20 p2562 A73-39904

Polar region soil moisture content remote sensing based on electromagnetic backscattering and depolarization by ice and terrain, considering radar, microwave and IR sensors

21 p2654 A73-40814

Earth surveys by remote sensing in Israel.

21 p2685 A73-40816

Remote sensing of estuarine circulation dynamics.

22 p2851 A73-42823

Technical and economic problems in use of military passive night vision systems including image intensifiers, IR detectors and thermographic imaging devices

23 p2979 A73-43219

Image formation by light intensification and thermographic imagery compared from energy viewpoint, considering effect of parasitic light sources in visual field

23 p2979 A73-43223

INFRARED INSPECTION

Reversing the trend - Infrared testing is simplicity itself.

08 p0952 A73-20685

INFRARED INSTRUMENTS

NT INFRARED DETECTORS

NT INFRARED SCANNERS

NT INFRARED SPECTROMETERS

NT INFRARED SPECTROPHOTOMETERS

Synchronously pulsed high repetition rate IR up converter based on Nd-YAG pump laser and proustite nonlinear crystal, describing experimental arrangement and operation

01 p0044 A73-10133

Radar and Nimbus 4 infrared measurements of the Oklahoma City tornados, 30 April 1970.

03 p0338 A73-14512

Spaceborne IR systems cryogenic cooling, considering passive radiators and open or closed cycle cryogenic fluid systems

06 p0683 A73-18315

Determination of the sensitivity of an infrared pyrometer with a thermocouple

06 p0695 A73-18567

Cryostats with and without radiation passage through window into vacuum space in balloon-borne far IR instruments requiring cooling to liquid He temperature

11 p1453 A73-26516

A SISAM interferometer and a simple Michelson-interferometer with spherical mirrors for space application.

11 p1369 A73-26519

Spacecraft local vertical estimation and error limits in meridional and equatorial planes based on terrestrial IR radiation measuring instruments

12 p1543 A73-27630

Determination of sensitivity of infrared pyrometer with a thermopile.

16 p2016 A73-33592

Temperature measurements with an infrared television system. 22 p2853 A73-41984

Short duration temperature measurements by infrared emission-absorption. 22 p2853 A73-41990

INFRARED INTERFEROMETERS

Plasma self radiation and absorption, schlieren signals and lasing levels recording methods based on dioxide lasers, using Mach-Zehnder IR interferometer 10 p1253 A73-23517

Interferometric spectrometry for infrared astronomy. 11 p1369 A73-26517

Far infrared broad band interferometry. 11 p1369 A73-26518

Plasma self radiation and absorption, schlieren signals and lasing levels recording methods based on carbon dioxide lasers, using Mach-Zehnder IR interferometer 17 p2217 A73-35197

INFRARED LASERS

Spontaneous active medium emission effect on amplification characteristics of linear and nonlinear traveling wave IR gas laser amplifier 01 p0060 A73-11084

Gain and frequency characteristics of a 20 mW C.W. water vapour laser oscillating at 118.6 microns. 02 p0177 A73-12724

The generation of tunable near IR radiation using a nitrogen laser pumped dye laser. 03 p0318 A73-12869

Spectral density curves for intensity fluctuations of stimulated emission from low and IR frequency gas lasers as function of thermal oscillation, mode interference and beat effects 03 p0319 A73-14087

Atmospheric windows for HF laser radiation between 2.7 and 3.2 microns. 03 p0319 A73-14431

FM-CW radar range measurement at 10-micron wavelength. 03 p0278 A73-14459

New infrared laser line in OCS and new method for Cation lasing. 03 p0320 A73-14465

Response of edge- and face-electroded pyroelectric detectors to infrared laser signals. 06 p0704 A73-18798

Steady state dense arc plasma heating by inverse bremsstrahlung process with IR carbon dioxide laser, calculating maximum attainable temperature 07 p0857 A73-19531

Far IR molecular lasers evaluation, discussing excitation, line assignment, relaxation, frequency measurement and development predictions 07 p0835 A73-19636

Pressure-induced optical distortion in laser windows. 09 p1090 A73-21937

Excitation mechanism of the far-infrared sulfur dioxide molecular laser. 09 p1090 A73-21938

[AD-760378]

Megawatt power IR output of Nd-YAG 50 micron pulse laser, using antireflection coated lithium niobate crystal for Q switch with high polarization contrast ratio 09 p1091 A73-22088

Kinetics of the excitation of molecular vibrations by infrared laser radiation 09 p1094 A73-22597

Sealed off 9.4 micron 15 W output power carbon dioxide laser with barium difluoride windows, noting long service life 09 p1096 A73-23009

Decimicrometer band laser operated communication system to link earth observation satellites with geosynchronous satellites, discussing key technologies 09 p1055 A73-23393

IR laser terrestrial communication system with 5 Mbit/sec digital data capacity, using intracavity optical frequency modulation or frequency shift keying modulation 09 p1055 A73-23394

Some characteristics of transition processes in He-Ne lasers operating at the 0.63-micron wavelength 10 p1227 A73-24073

Absorption of laser emission by He-CO₂ mixtures, CO₂ and NH₃ gases, and water vapors 10 p1227 A73-24074

Lasing characteristics of neodymium glasses at the 0.92-micron wavelength 10 p1260 A73-24581

Broadly tunable, narrow linewidth dye laser emission in the near infrared. 11 p1375 A73-25366

Confirmation of an electron avalanche causing laser-induced bulk damage at 1.06 micron. 11 p1377 A73-26227

Dynamics and energetics of the explosive vaporization of fog droplets by a 10.6-micron laser pulse. 11 p1377 A73-26231

Investigation of the stability of the oscillation frequency of a mercury laser emitting at 1.53 microns. 12 p1507 A73-27511

CO₂ laser communication through an urban atmosphere. 13 p1582 A73-28481

Theory of an infrared high-pressure chemical laser 13 p1627 A73-28762

Pulsed holographic interferometry at 10.6 microns. 15 p1875 A73-31400

A review of near-infrared optically pumped solid-state lasers. 16 p2023 A73-32856

Optical parametric oscillators. 16 p2023 A73-32857

Pb-salt tunable diode lasers. 16 p2023 A73-32859

Detection of short CO₂ laser pulses using the optical Kerr effect. 16 p2024 A73-34027

Visual observation of the picture of a CO₂-laser radiation field 17 p2182 A73-34166

A self-stabilized 3.5-micron waveguide He-Xe laser. 17 p2183 A73-34206

IR laser induced change in atmospheric temperature as function of time, using kinetic model with input molecular energy transfer rates for thermal blooming 17 p2163 A73-35414

CW IR laser action in slowly flowing premixed He-air-CO mixture with simultaneous molecular excitation and carbon dioxide generation by discharge-initiated CO oxidation 17 p2186 A73-35799

Propulsion by absorption of laser radiation. 18 p2342 A73-36172

[AIAA PAPER 73-624]

Difference frequency generation by optical mixing of two dye lasers in proustite. 19 p2438 A73-38165

A study of the CW 28-micron water-vapor laser. 19 p2438 A73-38278

Generation of high-power light pulses at wavelengths 1.06 and 0.53 micron and their application in plasma heating. I - Experimental investigations of reflection of light of two wavelengths in laser heating of plasma. 20 p2573 A73-39684

Emission of infrared molecular hydrogen lines from a cooled-gas laser. 20 p2574 A73-39694

Thermal defocusing avoidance by short pulse duration reduction to permit IR laser window operation before temperature rise, considering changes in index of refraction 21 p2710 A73-40134

Carbon dioxide laser pumped dielectric and metallic far IR waveguide, discussing size, mirror coupling and gas medium 21 p2713 A73-40461

High quantum efficiency IR up-conversion into visible photons through three wave interactions in nonlinear medium, using laser pump light feedback technique 21 p2699 A73-40464

Far IR laser lines measurements in carbon dioxide laser pumped ethylene glycol, dimethyl ether, formic acid, and monomethyl amine, using grating spectrometer and Golay-cell detector 21 p2715 A73-40765

Tunable Pb-Sn-Te junction laser characteristics and fabrication by impurity diffusion for IR CW operation at liquid helium temperatures 21 p2716 A73-40967

Performance and characteristics of smectic liquid crystal storage displays. 22 p2861 A73-42525

Nonlinear transmission loss in Ge beam splitter in pulsed HF and DF lasers operating at 2.5 to 4 microns 22 p2897 A73-43145

Collisional radiative processes and molecular lasers 23 p2988 A73-44013

Fast linear detection system for TE CO₂ lasers. 24 p3096 A73-44922

A 337-micron HCN laser interferometer for plasma diagnostics. 24 p3097 A73-45410

INFRARED MASERS

U INFRARED LASERS

INFRARED PHOTOGRAPHY

Measurement of surface temperatures by means of an infrared camera - Application in non-destructive testing 01 p0050 A73-10590

A near-infrared view of the Uranus system. 01 p0109 A73-11491

IR satellite photographs in the earth sciences - A comparison of the IR ranges from 3 to 4 micrometers and from 10 to 12 micrometers 06 p0691 A73-18438

Dual channel high resolution radiometer of French synchronous meteorological satellite Meteosat for full time cloud coverage of earth in visible and IR ranges 11 p1368 A73-26508

High angular resolution photography of complex OH airglow structures in IR night sky 11 p1358 A73-26666

Remote sensing and photointerpretation, discussing black and white, color and IR photography, microwave imagery, atmospheric attenuation, reflectance and potential application for ERTS satellites 16 p2014 A73-33100

Cartographic applications of high-altitude aircraft photographs. 16 p2016 A73-33362

Remote sensing with VHRR satellite imagery. 18 p2308 A73-36041

Photographic parallax heights of infrared airflow structures. 18 p2313 A73-36510

Automatic analysis of cloud cover by infrared photography of the earth from meteor satellites. 18 p2334 A73-37068

Equipment for checking of terrestrial resources 19 p2431 A73-38177

Computer processing of earth resources data from mono- and multispectral band scanners and IR photography 19 p2431 A73-38178

A new method for evaluating and mapping colours in aerial photographs. 20 p2568 A73-39884

NOAA environmental satellites with IR remote sensors for detection of upwelling off Mexican Pacific Coast and cold water eddies in Sargasso Sea 20 p2560 A73-39890

Thermal activity of the Uson Caldera based on infrared and photographic aerial survey. 20 p2561 A73-39895

Hailswaths mapping with airborne fixed beam and scanning IR radiometers, noting dimensions, orientation and fine structure 21 p2729 A73-40062

The use of near-infrared photography in the analysis of surface morphology of an Argentine alluvial floodplain. 22 p2850 A73-42728

An analysis of the earth's resources satellite /ERTS-1/ data. 22 p2850 A73-42732

Narrow band IR vidicon Jupiter and Saturn photography, showing limb darkening and surface details 23 p3032 A73-43942

Picture of the month - NOAA 2 scanning radiometer visual and infrared imagery received real-time over a 50,000-mile transmission link. 24 p3085 A73-45020

INFRARED RADIATION

NT FAR INFRARED RADIATION

NT NEAR INFRARED RADIATION

IR radiative energy transfer in gases, applying spectroscopic band absorption information 01 p0120 A73-10291

Radiative calculation models for infrared transfer through cloud, aerosol and the continuum. 01 p0073 A73-10358

Electromagnetic wave transmission through 8-12 micron atmospheric window, investigating particulate matter effects on radiation energy extinction 01 p0037 A73-10372

IR absorption and refraction index of atmospheric aerosol, using KBr disk transmittance and specular reflection measurements 01 p0038 A73-10373

Computed total radiation properties of compressed oxygen between 100 and 1000 K. 01 p0122 A73-10809

21-micron observations of H II regions. 01 p0104 A73-11045

Long wavelength spectrometry and photometry of M, S and C-stars. 02 p0222 A73-12708

Infrared excesses in early-type stars - Free-free emission. 02 p0225 A73-12826

Infrared excesses in supergiant stars - Evidence for silicates. 02 p0225 A73-12827

Circumstellar infrared emission. 02 p0226 A73-12829

Breakdown thresholds in rare and molecular gases using pulsed 10.6-micron radiation. 02 p0195 A73-12859

Morphic effects. V - Time reversal symmetry and the mode properties of long wavelength optical phonons. 03 p0349 A73-12901

Laser induced infrared fluorescence - Thermal heating, mass diffusion, and collisional relaxation in SF₆. 03 p0318 A73-13281

Two beam optical recording instrument for atmospheric IR transmissivity, discussing spectrophotometers with changeable NaCl, KBr and LiF prisms 04 p0450 A73-15575

Turbulent plasma 'piles' in the nuclei of galaxies. 04 p0504 A73-16022

Infrared radiative heating and cooling in the Venusian mesosphere. I - Global mean radiative equilibrium.

05 p0613 A73-16197

IR radiation source shape and size effects on aerial IR surveys at various flight altitudes, noting spectral composition change with height

05 p0578 A73-17140

The infrared variability of a dust model for Seyfert galaxies.

05 p0624 A73-17311

Effect of humidity on infrared and visual atmospheric transmission.

06 p0694 A73-18304

High speed, high performance /Hg,Cd/Te photodiode detectors.

06 p0667 A73-18314

Comparative study of reflectivity measurements performed in the visible and infrared wavelengths.

07 p0824 A73-19945

The applicability of an approximate expression for radiative heating.

07 p0921 A73-20222

Measurement of the vertical transparency of the atmosphere in the infrared using an artificial source.

07 p0848 A73-20349

Light emission phenomenon in the Gunn effect device.

08 p0994 A73-20846

Spectral energy distribution and IR radiation source size of M8 star cluster, determining stellar dust temperature

08 p1003 A73-20893

Infrared circular polarization of NML Cygni and VY Canis Majoris.

08 p1009 A73-21172

Generation of vibrationally excited O₂ and nonthermal infrared emission in the upper atmosphere

08 p0959 A73-21289

A numerical model of thermal radiation in a dusty atmosphere.

08 p0960 A73-21383

A magnetically controlled tube generator of very-low-frequency sinusoidal oscillations

09 p1063 A73-22337

Infrared and microwave emission from nebulae in the galaxy.

09 p1150 A73-23133

A synchrotron radiation model of the infrared radiation from the nucleus of NGC 1068.

09 p1150 A73-23144

IR galaxy model consisting of low energy cosmic or X rays at center of dust shell, discussing physical dimensions of radiating region

09 p1151 A73-23146

Modulation of infrared and sub-mm waves with crossed forward-biased junction diodes.

10 p1194 A73-24171

20-micron fluxes of bright stellar standards.

10 p1282 A73-24639

Radiative heat transport models for evacuated powder to specify IR radiation environment on lunar surface

10 p1282 A73-24645

Balloon-borne spectroscopic observation of the infrared hydroxyl airglow.

11 p1350 A73-25061

The spatial distribution of the 11.7 micron radiation of NGC 7027.

11 p1415 A73-25071

Rain-erosion resistance and other properties of Schott infrared-transmitting glasses.

11 p1387 A73-25299

Preliminary results of measurements of the infrared temperature of the Mars surface by the Mars 3 interplanetary spacecraft

11 p1418 A73-25629

Infrared radiative heating and cooling in the Venusian mesosphere. II - Day-to-night variation.

11 p1418 A73-25719

Stratospheric aerosol properties and their effects on infrared radiation.

11 p1357 A73-26344

The moon as a proposed radiometric standard for microwave and infrared observations of extended sources.

11 p1426 A73-26545

Spectrophotometry of the supernova in NGC 5253 from 0.33 to 2.2 microns.

11 p1427 A73-26613

Infrared and radio observations of the nucleus of NGC 253.

11 p1428 A73-26625

Role of exchange in shifted scattering of light for a double hole

13 p1660 A73-28760

Radio star MWC 349 observations at 10.52 and 6.63 GHz, obtaining angular size from flux density and IR temperature

13 p1681 A73-28924

Radiation temperatures of the earth's blankets in the microwave and infrared ranges according to experiment data on the Cosmos-384 artificial earth satellite

13 p1609 A73-29154

Measurement of the temperature coefficient of the refractive index of infrared materials with the aid of a carbon dioxide laser

14 p1757 A73-30371

Search for infrared anomalies associated with gravitational events at the galactic centre.

14 p1800 A73-30601

IR seeing disks/blurred interference patterns of corrugated wave fronts/ speckles and intensity profiles from atmospheric turbulence models

15 p1929 A73-31061

Visible luminescence of Yb³⁺ and Er³⁺ during IR excitation

15 p1884 A73-31712

Concorde-borne astronomical observation for Fraunhofer corona IR and photospheric and chromospheric radiations in lunar shadow during 30 June 1973 solar eclipse

15 p1940 A73-32184

Infrared emission from the OH/H₂O sources in W49.

15 p1940 A73-32196

The abnormal stratosphere studied with the aid of satellite radiation measurements.

[AIAA PAPER 73-493]

16 p2005 A73-33537

Generation of intense infrared radiation from an electron beam propagating through a rippled magnetic field.

17 p2214 A73-34204

Polarization plane rotation under magnetic field for IR waves in nonmagnetic semiconductors with cubic crystal lattices, explained by magneto-optical Faraday effect

17 p2219 A73-34342

IR and molecular radio emissions from interstellar clouds representing formation stage of normal stars, discussing dust screening effects

17 p2229 A73-34433

Rapid interferometric technique for MTF measurements in the visible or infrared region.

17 p2171 A73-35404

Density of the radiation of the earth/atmosphere system into space

18 p2309 A73-36112

Infrared absorption and local symmetry of negative ClO₄ and ReO₄ impurity ions in KI and CsI crystals

18 p2340 A73-36673

Some results of determining cloud top heights from satellite infrared measurements.

18 p2334 A73-37060

Effect of cloud cover on the variability of outgoing radiation.

18 p2314 A73-37069

Production of vibrationally excited O₂ and nonthermal infrared emission in the upper atmosphere.

19 p2424 A73-37918

Preliminary results of infrared temperature measurements of the surface of Mars by the Mars-3 automatic interplanetary station.

19 p2486 A73-38141

Jupiter atmosphere discrete source maps of 5 micron radiation distribution, correlating brightness temperature and photographically recorded colors

19 p2489 A73-38525

Quantized magnetic bremsstrahlung from white dwarfs surface layer as possible source of Galactic center infrared radiation

20 p2611 A73-39709

Utilization of thermal infra-red ground measurements for determination of adequate surveying periods in remote sensing.

20 p2558 A73-39868

Dissociation and bleaching of a multilevel molecular gas under the influence of radiation from a powerful CO₂ laser

21 p2712 A73-40357

HF and DF molecules vibrational relaxation investigation by recording IR radiation behind incident shock wave at 1500-5000 K

21 p2743 A73-40360

Photon retinue and infra-red divergence problem in quantum electrodynamics.

22 p2889 A73-42426

Measurements of the energy exchange between earth and space from satellites during the 1960's.

22 p2851 A73-42858

The H II region G333.6-0.2, a very powerful 1-20 micron source.

23 p3028 A73-43527

Combined lidar and radiometric measurements of cirrus clouds for IR emissivity, optical thickness and albedo

23 p3003 A73-43600

Spectral emissivity of skin and pericardium.

23 p2950 A73-44213

Bandpass filter IR observations of hydroxyl airglow, mapping mean nightly level spatial and temporal fluctuations in brightness

24 p3087 A73-45208

INFRARED REFLECTION

The effect of solar radiation reflected from water surfaces on airborne and surface measurements in the thermal infrared.

01 p0038 A73-10385

Water frost absorptions in IR reflectivities of Jupiter Galilean satellites, discussing surface cover distributions and underlying material reflectivity

04 p0497 A73-15070

Single reflection Fresnel rhomb for quarter-wave retardation in the infrared.

11 p1400 A73-26251

Optical effects of cryodeposits on low scatter mirrors.

[AIAA PAPER 73-732]

18 p2336 A73-36349

Statistical structure of the brightness field of reflected radiation in the 0.6-0.8 micron spectral interval.

18 p2314 A73-37063

Infrared reflection characteristics of lunar mare regolith.

21 p2774 A73-41400

INFRARED SCANNERS

The requirements on the parameters of a mechanical modulator for an IR scanning radiometer.

01 p0050 A73-10833

Remote CAT detection by IR scanning of atmospheric temperature profiles, discussing flight tests design and results

04 p0450 A73-15767

Infrared scanning radiometer for temperature mapping of the lunar surface on the Apollo 17 flight.

06 p0695 A73-18319

Apollo 17 spacecraft telemetered IR scanner remote sensing data, reduction, discussing use of interpolating and smoothing splines for restored image resolution improvement

06 p0696 A73-18807

Solar, stellar and IR sensors, discussing structural, optical and electronic design features, operational requirements and performance specifications

07 p0821 A73-18984

Thermopile IR static horizon sensor for Symphonie satellite three axis attitude stabilization in geostationary orbit

07 p0821 A73-18985

IR thermographic scanners and viewers operational principles, equipment performance specifications and thermal radiation distribution

13 p1611 A73-28020

Spatially filtered helium-neon laser link operation parallel to IR radiometer for real time atmospheric propagation monitoring over short path

13 p1661 A73-29328

Infra-red detection for satellite attitude sensing - The ANS horizon sensor.

16 p2012 A73-32853

Scanning IR spectrometer combination with optical telescope for 0.8-2.2 microns reflected IR light measurement during full moon phases in lunar surface composition determination

16 p2064 A73-33763

The design, construction and calibration of an infrared temperature profile radiometer /ITPR/ for Nimbus E.

17 p2328 A73-34602

Capabilities and limitations of infrared imaging systems.

17 p2167 A73-34902

Infrared sensing of the surface temperature of certain lakes of Northern Italy

17 p2206 A73-34942

Radiometric measurements of temperature of the ocean surface - Improvement brought by use of a polarizing radiometer

17 p2161 A73-34946

IR line scanners using stereoscopic techniques for aerial remote sensing of topography, discussing pivoting mechanism, scanner cameras and scan planes

17 p2168 A73-34957

Airborne passive IR line scanner, noting spectral resolution and thermal sensitivity for land and water surfaces energy

17 p2174 A73-35577

Gulf Stream eddies - Recent observations in the western Sargasso Sea.

18 p2313 A73-36642

Optimum parameters of an infrared imaging system for aerial scanning of earth resources.

18 p2317 A73-36874

Accuracy and coverage of temperature data derived from the IR radiometer on the NOAA 2 satellite.

19 p2424 A73-37665

IR scanner for aerial stereoscopic photography, discussing use of computer controlled orthophoto printer for image distortion reduction by rectification

20 p2566 A73-39671

Salinity surveys using an airborne microwave radiometer.

20 p2558 A73-39865

Thermal structure of the sand desert from the data of IR aerophotography.

20 p2558 A73-39869

Southern California coastal processes as analyzed from multi-sensor data.

20 p2560 A73-39886

Geological analysis of aerial thermography of the Canary Islands, Spain.

20 p2561 A73-39896

- Detection of small fires and mapping of large forest fires by infrared imagery. 20 p2562 A73-39904
- Hailswaths mapping with airborne fixed beam and scanning IR radiometers, noting dimensions, orientation and fine structure 21 p2729 A73-40062
- A fast IR spectral transform imager. 21 p2699 A73-40273
- Development of an infrared scanning system for the empirical evaluation of aerodynamic heating. 22 p2853 A73-1985
- A direct comparison of satellite and aircraft infrared /10 to 12 microns/ remote measurements of surface temperature. 22 p2850 A73-42729
- A procedure for estimating cloud amount and height from satellite infrared radiation data. 24 p3084 A73-44925
- ### INFRARED SPECTRA
- Preliminary report on the infrared spectrum of Nova Serpentis 1970. 01 p0095 A73-10269
- The IR emission spectrum of N₂ excited under auroral conditions. 01 p0036 A73-10337
- The infrared spectrum of nitrogen excited by fast electrons. 01 p0036 A73-10338
- Line-by-line computations of transmittance for non-homogeneous paths in designing application-oriented representations for water vapor and carbon dioxide channels IR spectral responses 01 p0037 A73-10365
- The infrared spectrum of Jupiter - Structure and radiative properties of the clouds. 01 p0097 A73-10370
- Radiometric techniques for observing the atmosphere from aircraft. 01 p0073 A73-10404
- Polarimetric investigations of the giant planets. II - Phase variation of the polarization of selected regions on the Saturn disk 01 p0102 A73-10941
- The consequences of grains in the atmospheres of late-type stars. I - Intrinsic polarization, infrared excesses, and emission lines. 01 p0103 A73-11035
- Thermochromic cuprous mercuric iodide for IR recording applications, observing phase transition hysteresis from reflectance-vs-temperature, specific heat and sensitivity measurements 01 p0054 A73-11230
- The infrared reflection, emission and absorption spectra of regolith from the Sea of Fertility and its scattering coefficient. 02 p0213 A73-12237
- Cation determinative curves for Mg-Fe-Mn olivines from vibrational spectra. 02 p0139 A73-12636
- Continuous near-infrared spectrum of two Be stars - HD 50138 and HD 51585 02 p0224 A73-12735
- Spectra of several Be stars between 7000 and 9600 Å 02 p0224 A73-12736
- Distribution of nitric acid vapor in the stratosphere as determined from infrared atmospheric emission data. 02 p0189 A73-12786
- Energy flux intensity in IR bands of selectively radiating molecular gas nonisothermal layer from radiative transfer equation and mathematical model 03 p0396 A73-13183
- Two new He I lines in the spectra of B-type supergiants. 03 p0371 A73-13218
- Laser Raman spectrum of crystalline cyclopentane-d/sub 0/ and -d/sub 10/. 03 p0318 A73-13282
- Foreign gas collision broadening effects on 15 micron carbon dioxide bands radiation absorption lines 03 p0345 A73-13697
- Observations of carbon monoxide in cool stars at 4.7 microns. 03 p0374 A73-13717
- Jovian spectrum at 8-13 microns from 60 inch IR telescope, discussing surface brightness of central disk and brightness temperature spectrum 03 p0374 A73-13850
- Gas concentration profiles in combustion gas sampling probes, using IR absorption technique 03 p0399 A73-14397
- Calculation of pressure-broadened linewidths of SO₂ and NO₂. 04 p0414 A73-14815
- Atmospheric transmittance calculation from 0.7-micron oxygen band fine structure parameters 04 p0473 A73-15571
- Stratospheric nitrogen dioxide from infrared absorption spectra. 04 p0445 A73-15626
- Study of the dispersion curve of polaritons excited by Raman diffusion in the presence of damping 04 p0476 A73-15997
- Vertical distribution of minor atmospheric constituents as derived from air-borne measurements of atmospheric emission and absorption infrared spectra. [AIAA PAPER 73-103] 05 p0570 A73-16863
- Venus atmosphere water vapor content from IR spectra observed by airborne Fourier interferometric spectrometer, discussing different models for abundance 06 p0744 A73-17434
- Mariner 9 IR spectral features due to carbon dioxide, water vapor and silicate dust suspended in Mars atmosphere before/after planet-wide dust storm 06 p0746 A73-17482
- The synthesis and characterization of tin complexes using inert atmosphere techniques - An advanced laboratory experiment. 06 p0661 A73-18272
- Connection of the linear polarization level of atmosphere-air scattered light with the light reduction in the infrared spectral region 06 p0691 A73-18733
- Pressure broadening of magnetically-tuned infrared absorption spectrum of NO using a CO laser. 07 p0833 A73-19145
- Crystal-field effects of iron and titanium in selected grains of Apollo 12, 14, and 15 rocks, glasses, and fine fractions. 07 p0881 A73-19710
- Midinfrared emission spectra of Apollo 14 and 15 soils and remote compositional mapping of the moon. 07 p0897 A73-19888
- IR absorption spectra of powdered graphite samples during treatment in laminar propane-butane diffusion flame zones 07 p0921 A73-19996
- Measurements on the infrared lines of planetary gases at low temperatures. I - Nu-3 fundamental of methane. 08 p1003 A73-20891
- Jupiter upper atmosphere temperature inversion to explain brightness temperature variation in 7.9 micron methane band, observing limb brightening 08 p1004 A73-20900
- Infrared spectra of the Galilean satellites of Jupiter. 08 p1004 A73-20901
- The investigation of the middle infrared absorption spectrum of DyVO₄ at low temperatures. 08 p0994 A73-21219
- Studies in molecular dynamics by collision-induced infrared absorption in H₂-rare gas mixtures. I - Profile analysis and the intercollisional interference effect. 08 p0990 A73-21630
- Spectroscopic investigation of the interaction of oxides with a metallic surface. III - Systems Al₂O₃-Me/Al, Cu, Ti, Kh18N9T steel, Ni, Co, Mo, W, Si/ 09 p1103 A73-22470
- Polarimetric observations of the major planets. II - Phase dependence of the polarization for selected areas on the disk of Saturn. 09 p1147 A73-22736
- On the detection of H₂ from interstellar clouds in the wavelength range 4.4 to 28.2 microns. 09 p1148 A73-22870
- Measurements of some hydrogen-oxygen-nitrogen compounds in the stratosphere from Concorde 002. 09 p1079 A73-22947
- The infrared and microwave spectra of stars; International Colloquium on Astrophysics, 17th, Universite de Liege, Liege, Belgium, June 28-30, 1971, Proceedings 09 p1149 A73-23126
- Recent experimental and theoretical investigations of infrared and microwave molecular spectra of astronomical interest /Introductory report/. 09 p1123 A73-23127
- Carbon stars molecular band strength variations in two-micron spectral region due to thermal emission from circumstellar dust shell 09 p1149 A73-23129
- Molecular absorption spectra of S-type stars in the one-micron region. 09 p1123 A73-23130
- Observational, theoretical, and predicted data on the infrared and microwave spectra of interstellar matter /Introductory report/. 09 p1150 A73-23135
- Spectroscopy of tetraenzoporphin molecules and possible astrophysical implications. 09 p1048 A73-23136
- Observational data and interpretation of infrared spectra and microwaves of galaxies and the intergalactic matter 09 p1150 A73-23143
- Spectrophotometric measurements of noctulicent clouds. 09 p1079 A73-23339
- Probabilities of infrared and RF transitions in OH and CH molecules 10 p1250 A73-23710
- Determination of emission spectra of the sky in the infrared between 45 and 500 micrometer using an interferometer aboard an airplane 10 p1210 A73-23749
- Infrared observations of southern RV Tauri stars. 10 p1275 A73-23844
- IR spectrum line reversal for measurement of CO and gas mixture laser plasma vibrational temperatures as function of discharge current and gas pressure 10 p1230 A73-24884
- OJ 287 and BL Lacertae with rapid radio, IR and optical variability, high IR luminosity, line free optical spectra and varying polarization 11 p1416 A73-25179
- Brightness and polarization of the sky in the solar aluminant in the near infrared region of the spectrum 11 p1353 A73-25604
- Equipment and procedures for measurement of atmospheric spectral transmittance in the infrared region of the spectrum 11 p1363 A73-25643
- The absorption spectrum of atmospheric water vapor in the vicinity of the He 10830 Å triplet. 11 p1421 A73-25933
- Sunspot umbral intensity measurements at IR and visual wavelengths, discussing correction methods for earth atmosphere and instrument induced stray light 11 p1422 A73-25937
- Galilean satellites surface thermal properties from radiometry of 20-micron band during eclipses of Jupiter 11 p1424 A73-26132
- IR spectroscopic study of polydimethylsiloxane thin film structure and polymerization under glow discharge 11 p1400 A73-26144
- The spectral albedo of water clouds in the 1-6 micron band. 11 p1357 A73-26195
- IR spectra of quasars and Seyfert galaxies interpreted as thermal radiation from dust envelopes around cores, considering graphite and silica dust particles 12 p1547 A73-27876
- On the observability of far infrared line emission originating from the interstellar medium. 13 p1686 A73-29368
- Distribution of water vapor in the stratosphere as determined from balloon measurements of atmospheric emission spectra in the 24- to 29-micron region. 14 p1749 A73-30160
- Comparison of linear polarization and albedo of igneous rocks in the spectral region 0.75-3.0 μ and lunar values of those parameters. 15 p1928 A73-30977
- Probability distribution function of cloud spectral brightness for IR range based on 1966-1969 observations 15 p1905 A73-31821
- Reflection-absorption infrared spectrum of alpha-CH₃ chemisorbed on polycrystalline tungsten. 15 p1841 A73-31971
- The infrared spectrum and angular size of Eta Carinae. 15 p1940 A73-32197
- Vibrational spectra of substituted hydrazines. IV - Raman and far-infrared spectra and structure of tetramethylhydrazine. 15 p1841 A73-32220
- Vibrational spectrum of bis(trifluoromethyl) trioxide. 15 p1841 A73-32221
- Long-path infrared spectra of CO, NO₂, NO, SO₂ and N₂O observed in a simulated atmosphere in trace amounts. 16 p1976 A73-32700
- Aerological investigation of the volcanic beds of Kamchatka by polarizational and spectral methods 16 p1977 A73-33760
- Infrared radiation of the moon at 3.5 to 3.9 microns 16 p2064 A73-33764
- Solar absorption in the CO fundamental region. 17 p2231 A73-34761
- Preliminary data on the optical properties of solid ammonia and scattering parameters for ammonia cloud particles. 17 p2211 A73-34858
- New infrared spectra of the Jovian planets from 12,000 to 4000/cm by Fourier transform spectroscopy. I - Study of Jupiter in the 3 nu-sub 3 CH₄ band. 17 p2234 A73-35617
- Hydrological phenomena teledetection based on multispectral band scanners for IR and visible frequency ranges 18 p2307 A73-36027
- Infrared transmittances for indirect soundings of the atmosphere from satellite-based measurements. 18 p2308 A73-36043
- IR spectral measurements of reusable surface insulations via radiative four flux model [AIAA PAPER 73-745] 18 p2370 A73-36361
- Infrared and radio transition probabilities of OH and CH. 18 p2338 A73-36735
- Spatial frequencies of clear sky radiance in the range 4.5 to 5.2 microns 18 p2314 A73-36899
- 8-13-micron spectra of NGC 7027, BD +30.3639 deg, and NGC 6572. 18 p2357 A73-37104

An upper limit on the 4.9-micron flux from Titan.
18 p2357 A73-37112

Observation of stratospheric nitric oxide by infrared absorption spectrometry from a balloon
19 p2423 A73-37533

Arizona-NASA Atlas of the Infrared Solar Spectrum. X.
19 p2483 A73-37576

Spectral albedos of the Galilean satellites.
19 p2483 A73-37578

Observations of carbon monoxide at 4.7 microns in IRC + 10216, VY Canis Majoris, and NML Cygni.
19 p2484 A73-37612

Multicolor observations of stars in the vicinity of the Orion Nebula.
19 p2484 A73-37613

Infrared spectrum of the Orion Nebula between 55 and 200 microns.
19 p2484 A73-37614

Sulfur dioxide infrared-active vibration-rotation combination spectral band, examining quantum numbers, infrared absorption, centrifugal distortion effects and dipole moments
19 p2402 A73-37896

Infrared spectrum and geometry of ozone isolated in inert gas matrices at 20.4 K.
19 p2463 A73-37904

Atmospheric temperature and humidity vertical profiles from satellite-borne IR spectral radiance measurements, using linear extrapolation and statistical regression techniques
[AAS PAPER 73-124] 20 p2521 A73-38584

Minor planets and related objects. X - Spectrophotometric study of the composition of /1685/ Toro.
20 p2607 A73-39120

The cosmological significance of molecular band strengths in the infrared spectra of elliptical galaxies.
20 p2609 A73-39447

Remote sensing of stratospheric gases using submillimetre radiation.
20 p2557 A73-39856

CO atmospheric vertical distribution from balloon-borne IR grating spectrometer observations, noting concentration decrease with altitude
21 p2680 A73-40078

Possibilities of calculating the spectral albedo of Venus in the near infrared
21 p2770 A73-40914

Far infrared and Raman spectra of gaseous carbon suboxide and the potential function for the low frequency bending mode.
21 p2740 A73-40935

Chromium-ytterbium energy transfer in silicate glass.
21 p2752 A73-40963

IR spectrum line reversal for measurement of CO and gas mixture laser plasma vibrational temperatures as function of discharge current and gas pressure
21 p2717 A73-41659

Observations of silicon monoxide in cool stars at 4.05 microns.
22 p2905 A73-41768

Titan narrow band observations at 8-13 microns, noting temperature inversion and spectroscopically active component
22 p2905 A73-41770

Design and test of a photometer with nine wavelength bands for the measurement of astronomical objects
22 p2852 A73-41784

The inference of temperature from the infrared spectra of planets.
22 p2906 A73-42065

Observation of the star gamma-Cassiopeia of the Be spectral type by Fourier spectrometry from 1 to 2.5 micron
22 p2908 A73-42354

Observation of 9.0-micron line emission from Ar III in NGC 7027 and NGC 6572.
22 p2910 A73-42704

Radiative transfer within the atmospheres of the major planets.
22 p2913 A73-42991

Airglow hydroxyl emission IR spectral bands intensity measurements with allowance for atmospheric extinction, deriving vibrational level excitation rates from spontaneous emission transition probabilities
23 p2972 A73-43690

Ozone and airglow in the mesosphere region.
23 p2976 A73-43886

Stratospheric methane and nitrogen dioxide from infrared spectra.
23 p2976 A73-43887

High resolution analysis of the sun's radiation received at the ground from 9 to 11.6 microns.
23 p3003 A73-43888

Atmospheric water vapor concentration in upper stratosphere above tropopause from balloon observations of solar IR absorption spectra
23 p2976 A73-43890

Sulfuric acid solution composition to account for Venus cloud temperature, stratosphere dryness and IR spectrum
24 p3129 A73-44441

Solar coronal Fe XIII 10747 A emission line resonance polarization observations during 12 November 1966 eclipse, discussing magnetic field effects
24 p3135 A73-44633

Laser Doppler interferometry for measuring small absorption coefficients.
24 p3090 A73-44924

Absorption at about 4.3 microns by /N2-N2/ and /N2-O2/ complexes in the terrestrial atmosphere
24 p3084 A73-44964

Bending potential of an H2O molecule.
24 p3113 A73-44977

INFRARED SPECTROMETERS

Precipitable water vapor temperature-geopotential height profiles from satellite IR spectrometer /SIRS/ measurements, using stepwise regression technique
01 p0073 A73-10380

Atmospheric ozone distribution from remote sensing with spaceborne IR interferometer spectrometer, estimating error due to cloud cover
01 p0038 A73-10384

The global distribution of outgoing long-wave radiation derived from SIRS radiance measurements.
01 p0038 A73-10391

Measuring the spread function of infrared spectrometers by means of gas lasers.
01 p0060 A73-10838

Real-time computer for monitoring a rapid-scanning Fourier spectrometer.
01 p0020 A73-11231

High resolution infrared spectrometer with multiplex advantage.
06 p0695 A73-18318

Hadamard transform spectrometer designed for airborne IR astronomical observations of Mars, using binary orthogonal pseudonoise codes in multiplexing scheme
08 p0972 A73-21753

Interferometric spectrometry for infrared astronomy.
11 p1369 A73-26517

Worldwide variations in atmospheric transmission. I - Baseline results from Smithsonian observations.
15 p1904 A73-31724

HTS spectrometer for airborne infrared astronomy.
15 p1880 A73-32379

Nitric oxide detection in stratosphere from characteristic absorption line spectrum via airborne IR spectrometer, obtaining molecular concentration
[ONERA, TP NO. 1256] 17 p2159 A73-34552

Critical analysis of the results obtained by SIRS-A in remote sensing of the temperature field over the Mediterranean
17 p2205 A73-34936

Vacuum IR spectrometer measurement of C 12 methane absorption band at 1.1 microns, describing technique for extending standards to photomultiplier region of spectra
21 p2743 A73-40936

Mariner Mars 1969 infrared spectrometer - Gas delivery system and Joule-Thomson cryostat.
21 p2702 A73-41101

Airborne IR spectrometer with solar sensor for stratospheric minor molecular constituents vertical distribution, indicating spectral resolution for vibrational-rotational absorption bands
[ONERA, TP NO. 1216] 22 p2847 A73-42221

A high-resolution Fourier-transform infrared spectrometer.
22 p2861 A73-42587

Remote sensing of the global distribution of total ozone and the inferred upper-tropospheric circulation from Nimbus IRIS experiments.
23 p2975 A73-43876

Far IR grating spectrometer using InSb detector with narrow spectral band responsivity and tunability due to cyclotron resonance absorption in magnetic field
23 p2984 A73-44364

INFRARED SPECTROPHOTOMETERS

Spectroelectrophotometer for atmospheric optical measurements in the near infrared region of the spectrum
11 p1362 A73-25610

An infrared photometer for the balloon-borne telescope Thisbe.
11 p1368 A73-26505

Equipment for infrared photometric and polarimetric observations
15 p1878 A73-32138

Lower atmospheric intensity-calibrated thermal emission spectra with digital recording near IR spectrometer, discussing applications to pollutant detection
21 p2692 A73-41574

INFRARED SPECTROSCOPY

Atmospheric solid and liquid water particles IR spectral properties, interpreting Nimbus 4 IR spectroscopic cloud observations
01 p0037 A73-10371

Spectroscopic remote sensing of lunar surface composition.
[AD-756154] 04 p0448 A73-15181

Infrared spectroscopy of regolith /Luna-16 interplanetary probe/.

05 p0612 A73-16088

Expansion hypothesis and assumption of invisible intergalactic matter in galactic clusters stability theory, noting IR spectroscopy and radio observation
05 p0623 A73-17196

Quantitative evaluation of superficial organic contaminants, soluble in halogenated solvents, discussing sampled surface solvent extraction method and subsequent IR absorption spectrographic analysis
06 p0660 A73-18547

Infrared and Raman spectroscopic studies of structural variations in minerals from Apollo 11, 12, 14, and 15 samples.
07 p0897 A73-19887

Far infrared and Raman spectroscopic investigations of lunar materials from Apollo 11, 12, 14, and 15.
07 p0897 A73-19889

Investigation of long-chain molecule dynamics in condensed state by the IR-spectroscopy and Rayleigh-scattering methods
09 p1122 A73-21956

The earth resources experiment package on Skylab and proposed resource investigations.
09 p1082 A73-22389

IR-spectroscopic investigation of the thermal stability of albumin at different levels of its ionization
10 p1182 A73-24685

Measurement of trace gases in the stratosphere using far infra-red spectroscopy.
[AIAA PAPER 73-516] 16 p2006 A73-33553

Atmospheric and surface properties of Mars obtained by infrared spectroscopy on Mariner 9.
19 p2479 A73-37219

Submillimeter wave spectroscopy with a vacuum Fabry-Perot interferometer
22 p2852 A73-41782

IR absorption spectrometry to determine vertical distribution of nitric oxide abundance in stratosphere
23 p2978 A73-43959

High altitude infrared spectroscopic evidence for bound water on Mars.
24 p3127 A73-44395

INFRARED STARS

Infrared stars with strong 1665/1667-MHz OH microwave emission.
01 p0104 A73-11040

Search for OH-IR stars with emission concentrated in main lines, considering water vapor line emission or absorption band in near IR
02 p0222 A73-12717

Interstellar OH lambda doublet radiation observations at 5 cm from six galactic sources and IR star, observing various transitions
03 p0366 A73-12930

5 GHz observations of the infrared star MWC 349, and the H II condensation W3/OH.
07 p0899 A73-20121

Spectra of the Becklin-Neugebauer point source and the Kleinmann-Low nebula from 2.8 to 13.5 microns.
08 p1008 A73-21157

Infrared circular polarization of NML Cygni and VY Canis Majoris.
08 p1009 A73-21172

Observations of circumstellar circular polarization in four more infrared stars.
08 p1013 A73-21813

Balloon observations of galactic and extragalactic objects at 100 microns.
09 p1150 A73-23134

Infrared observations of southern RV Tauri stars.
10 p1275 A73-23844

Review of results in infrared space astronomy.
11 p1426 A73-26502

IR objects in Orion Nebula, discussing temperature range and pre T Tauri evolutionary stage
15 p1934 A73-31419

On the nature of the infrared point source in the Orion Nebula.
18 p2356 A73-36975

Cygnids and Taurids - Two classes of infrared objects.
18 p2357 A73-37111

Observations of carbon monoxide at 4.7 microns in IRC + 10216, VY Canis Majoris, and NML Cygni.
19 p2484 A73-37612

Spectrographic observations of the peculiar Be star with infrared excess HD 45677.
20 p2611 A73-39586

Detection of radio emission from V1016 Cygni.
21 p2780 A73-41644

Radio emission from HD167362 and V y2-2.
21 p2780 A73-41645

Detection of radio emission from M1-11 and HD37806.
21 p2780 A73-41646

Observations of silicon monoxide in cool stars at 4.05 microns.
22 p2905 A73-41768

INFRARED TRACKING

IR tracking system for automatic target acquisition, discussing analyzer operation principles, closed loop

characteristics, spectral field and equipment specifications 07 p0789 A73-18945

INFRASONIC FREQUENCIES
NT MICROSONICS
Infrasound in the ionosphere generated by severe thunderstorms. 01 p0040 A73-10826
OH emission band, studying effect of adiabatic infrasonic oscillations on upper atmospheric temperature and intensity 16 p2008 A73-33883
Infrasound from convective storms - Examining the evidence. 21 p2679 A73-40070

INGESTION (BIOLOGY)
NT DRINKING
INGESTION (ENGINES)
Contribution to the problem of suction of foreign bodies into engine intakes [DGLR PAPER 72-107] 02 p0202 A73-11687

INGOTS
Characteristics of the ingot crystallization process under conditions of melting in vacuum furnaces with a consumable electrode, and the stability of the cast structure in alloys of the Nb-Ti system 04 p0464 A73-15496
Ferrous and nonferrous metal alloys melting and remelting in plasma induction and beam furnaces, noting cost reduction and ingots homogeneity 04 p0455 A73-15748
Solidification pressure effect on hydrogen in Al ingots, noting blister formation correlation to pressure 05 p0587 A73-16579
Microstructure, microhardness and mechanical strength of ingots and granules of Al alloys with high refractory metal contents 12 p1511 A73-26917
Precipitation in EB welded beryllium ingot sheet. 14 p1759 A73-30146
Nitride inclusions in titanium ingots - A study of possible sources in the production of magnesium-reduced sponge. 20 p2576 A73-39026
Application of the method of straight lines to the solution of a modified Stefan problem 20 p2626 A73-39253

INHABITANTS
NT MOUNTAIN INHABITANTS
INHAILATION
U RESPIRATION
INHIBITION
Time course of lateral inhibition in the human visual system. 12 p1462 A73-27124

INHIBITION (PSYCHOLOGY)
Inhibitive mechanisms activity in behavior control by neostriatum, discussing suppressive reactions, evoked sleep, conditioned and instrumental reflexes and neurophysiological aspects 01 p0009 A73-11025
Participation of the hippocampal structures in the formation of external inhibition 06 p0653 A73-18162
The effect of accessory auditory stimulation upon detection of visual signals. 06 p0660 A73-18625

INHIBITORS
NT WEAR INHIBITORS
Investigation of the possibility for ultrasonic dispersion of certain corrosion inhibitors introduced in easily removable film coatings 02 p0184 A73-11643
Effects of inhibitors PB-5 and of dialkyl-dimethyl ammonium chloride on the corrosion resistance and mechanical strength of structural materials during the cleaning of heat exchangers from scale by the hydrochloric acid method 02 p0174 A73-12537
Performance of an inhibitor-protector of steel against corrosion-fatigue failure at elevated temperatures and pressures. 02 p0182 A73-12700
The inhibition of the dendritic electrocrystallization of zinc from doped alkaline zincate solutions. 03 p0273 A73-13727
Effects of fuel corrosion inhibitors on filter-separator coalescence. 05 p0582 A73-16666 [SAE PAPER 720862]
Photosensitized inhibitor formation in isolated, aging chloroplasts. 07 p0784 A73-20453
Grain growth inhibition by carbide additives in hard metal alloys of the ISO-K 10 type 10 p1231 A73-23688
Investigation of flame expansion inhibition in air-dispersed systems 19 p2503 A73-37506
Protection of mineral oils from microbiological damage by compounds of the quinone group 21 p2723 A73-41069

INHOMOGENEITY
Light scattering from an inhomogeneous fluid. 01 p0077 A73-10971

Elastic waves originating at the surface of a spherical opening in nonhomogeneous isotropic media. 01 p0116 A73-11065
Higher conservation laws for coherent optical pulse propagation in an inhomogeneously broadened medium. 01 p0078 A73-11221
General analysis and synthesis of alloys and materials with inhomogeneous physical properties, noting thermal physicochemical methods for laminates and metal powders 01 p0066 A73-11340
Coherent laser radiation and holography in an optically inhomogeneous medium. 02 p0176 A73-12111
Complex transmission coefficient of waveguide with two arbitrarily spaced infinitely thin plane parallel inhomogeneities, using Galerkin method for single-parameter approximation of electrodynamic problem. 03 p0278 A73-14057
Solar atmosphere inhomogeneities from observations, discussing theoretical analysis via two dimensional model atmosphere 03 p0377 A73-14406
Parameter optimization technique for remote radio probing and diagnostics of inhomogeneous media with properties variation along single dimension 04 p0422 A73-15478
Macroscopic inhomogeneities in amorphous semiconductors - Contactless conductivity. 05 p0605 A73-16570
Lambda/4 directional coupler in an inhomogeneous medium with deviations of even and odd mode parameters from the ideal value 05 p0559 A73-17000
Integral representations for a nonhomogeneous region in couple stress theory of elasticity. 07 p0909 A73-19105
Dielectric gradient waveguides inhomogeneous core layer, solving differential equation by perturbation method 09 p1065 A73-23113
Two dimensional statics for isotropic elastic body with inhomogeneous mechanical properties, discussing two-step solutions for differential equilibrium equation and boundary value problem 10 p1293 A73-24676
Focused laser irradiance fluctuations in a turbulent medium. 11 p1376 A73-25874
Possibility of correlating the field of a wide wave beam in a smoothly nonhomogeneous medium with the field of a beam in vacuum 11 p1331 A73-26161
Influence of field inhomogeneity on the intrinsic spectral linewidth of a laser 11 p1332 A73-26166
Intensity and displacement fields of microinhomogeneous medium with random permittivity tensor field described by step functions, using renormalization method 12 p1530 A73-26929
Influence of the inversion inhomogeneity on the transverse structure of oscillations in solid-state lasers. 12 p1507 A73-27518
Short-term average optical-beam spread in a turbulent medium. 15 p1913 A73-31016
Dispersion of electromagnetic waves on a weak isolated inhomogeneity. 15 p1843 A73-31522
A study of electrical conductivity inhomogeneities in CdS single crystals 18 p2341 A73-36963
Amplification of backscattering by bodies placed in a medium with random inhomogeneities 21 p2657 A73-41513
Bounds on effective dielectric constant of inhomogeneous material. 22 p2896 A73-42263

INITIAL VALUE PROBLEMS
U BOUNDARY VALUE PROBLEMS
INITIATORS
Initiator composition and glass content effects on polyester resin hardening in glass laminate fabrication 18 p2327 A73-36467

INITIATORS (EXPLOSIVES)
NT DETONATORS
Hot particle igniter for end-burning solid propellant rocket motors, noting ignition capability at 219 K and 100,000 ft simulated altitude 04 p0485 A73-14919 [AIAA PAPER 72-1196]
Nondestructive and impulsive testing of electroexplosive devices. 05 p0606 A73-17207
Microelectronic circuitry for monitoring stray electromagnetic energy coupled into electroexplosive device, using fiber optic transmission with photovoltaic energy conversion to eliminate wiring caused interference 22 p2822 A73-41794

Electronic logic device for crack arresting penthrite microcharge pulse initiation, including crack and stress wave propagation measurements 23 p3047 A73-44286

INJECTION
NT CARRIER INJECTION
NT FLUID INJECTION
NT FUEL INJECTION
NT GAS INJECTION
NT ION INJECTION
NT LIQUID INJECTION
NT SECONDARY INJECTION
NT WATER INJECTION
Variational analysis of high mass transfer rates from spherical particles - Boundary-layer injection suction considerations at low particle Reynolds numbers and high Peclet numbers. 01 p0122 A73-10802
Techniques for microinjection of biologically active substances into subcellular structures of the brain 18 p2282 A73-36574

INJECTION CARBURETORS
U FUEL INJECTION
INJECTION GUIDANCE
Differential transformation for satellite injection. 16 p2070 A73-33999

INJECTION LASERS
Coherence of the radiation of a pulsed single-mode injection semiconductor laser. 01 p0061 A73-11335
Heterojunction injection lasers with high efficiency and low threshold currents, discussing amplification, emission, epitaxial layers, and performance superiority over homostructures 05 p0586 A73-17266
Influence of waveguide properties of heterojunction layers on the principal characteristics of injection lasers. 06 p0702 A73-18585
Cavity dimension effect on single mode generation spectrum of GaAs epitaxial CW injection laser at 77 K 08 p0976 A73-21655
Variation of spontaneous emission with current in GaAs homostructure and double-heterostructure injection lasers. 09 p1091 A73-22236
Additional data on the effect of doping on the lasing characteristics of GaAs-Al_x/Ga_{1-x}/As double-heterostructure lasers. 09 p1091 A73-22237
Gradual degradation of GaAs double-heterostructure lasers. 09 p1092 A73-22241
/GaAl/As lasers with a heterostructure for optical confinement and additional heterojunctions for extreme carrier confinement. 09 p1092 A73-22243
Time delays and Q switching in homostructure and heterostructure injection lasers. 09 p1092 A73-22246
Behavior of threshold current and polarization of stimulated emission of GaAs injection lasers under uniaxial stress. 09 p1092 A73-22247
Mesa-stripe-geometry double-heterostructure injection lasers. 09 p1093 A73-22251
Spectral self modulation and pulsation instabilities of single mode injection GaAs laser with tunable composite cavity 09 p1093 A73-22258
The directivities and spectral contents of radiation of multidiode injection lasers. 09 p1097 A73-23049
Experimental properties of injection lasers - Modal distribution of laser power. 10 p1228 A73-24530
Te-doped GaAs injection laser with nonplanar p-n junction for enhanced power output, discussing diode construction and fabrication by Zn diffusion 12 p1505 A73-26890
Soviet papers on quantum radio physics covering injection lasers, high intensity beam and material interactions, laser dynamics and masers 12 p1505 A73-27135
Semiconductor injection lasers, discussing optical transitions threshold effects, radiative recombination, coherent emission, etc 12 p1506 A73-27136
Use of semiconductor lasers in compact communication systems. 12 p1470 A73-27521
Influence of heat treatment on characteristics of injection lasers. 12 p1507 A73-27522
Empirical estimation of the service life of injection lasers from short-term tests. 12 p1507 A73-27523
Statistical distribution of the failure of injection lasers. 12 p1508 A73-27524
Output radiation influence on catastrophic and slow degradation process in heterojunction injection lasers, noting service life dependence on current density 12 p1508 A73-27525

- Thermal deformation of an injection laser crystal during the passage of pumping current pulses. 13 p1630 A73-29443
- Direct modulation of a double heterostructure laser at a rate of 2.3 Gbit/s 14 p1758 A73-30700
- Pb-salt tunable diode lasers. 16 p2023 A73-32859
- GaAs and GaAlAs semiconductor injection lasers, discussing system design and applications for ranging, illumination and communication with peak power and repetition rate requirements 16 p2023 A73-32866
- Hybrid optoelectronics - High frequency modulation and detection of light by semiconductor sources and sensors. 16 p1978 A73-32886
- Inexpensive fast solid state current drive circuit for injection lasers, using parallel conventional transistor switches operated at avalanche breakdown for pulse generation 16 p2024 A73-33400
- High peak power from /GaAl/As-GaAs double-heterostructure injection lasers. 17 p2183 A73-34202
- Theory of the threshold of an injection laser operating at the experimental band tails 17 p2184 A73-34922
- The transversely adjusted gap laser for optical communication systems. 17 p2186 A73-35795
- Mode selection in GaAs injection lasers resulting from Fresnel reflection. 17 p2186 A73-35797
- Self-switching in single-heterojunction injection lasers. 20 p2574 A73-39690
- Asymptotic nature of threshold conditions and multimode laser emission. 20 p2574 A73-39691
- Influence of semiconductor laser heating on the parameters of the output pulses 21 p2710 A73-40006
- Heterojunction injection lasers (Review). 22 p2869 A73-42244
- Mode guidance parallel to the junction plane of double-heterostructure GaAs lasers. 24 p3097 A73-45423

INJECTORS

- NT VORTEX INJECTORS**
- Influence of the parameters of the accelerating circuit of an injector with inductive energy storage on the process of plasma-cluster acceleration 02 p0196 A73-11633
- Plasma jet acceleration by plasma injectors with capacitive and inductive energy storage for instantaneous breaking of charging circuit, noting energy conversion efficiency 02 p0196 A73-11712
- Optimum design of space storable gas/liquid coaxial injectors. [AIAA PAPER 72-1076] 03 p0354 A73-13400
- Factor of fuel pyrolysis in injector design. 05 p0606 A73-17109
- Aerodynamic rig and wind tunnel developments of compound ejector thrust augments for V/STOL aircraft with combined Coanda and center injection flows [ASME PAPER 73-GT-67] 16 p2048 A73-33519
- INJURIES**
- NT BACK INJURIES
- NT BAROTRAUMA
- NT BRAIN DAMAGE
- NT BURNS (INJURIES)
- NT CRASH INJURIES
- NT EJECTION INJURIES
- NT FROSTBITE
- NT LESIONS
- NT NOISE INJURIES
- NT PARALYSIS
- NT PULMONARY LESIONS
- NT RADIATION INJURIES

INLET FLOW

- An empirical flowfield analysis technique for preliminary evaluation of inlet systems operating in a vehicle generated flowfield. 01 p0003 A73-11132
- Method for increasing wind tunnel Mach number for large-scale inlet testing. [AIAA PAPER 72-1096] 03 p0287 A73-13416
- A method of testing full-scale inlet/engine systems at high angles of attack and yaw at transonic velocities. [AIAA PAPER 72-1097] 03 p0287 A73-13417
- A feasibility study for definition of inlet flow quality and development criteria. [AIAA PAPER 72-1098] 03 p0243 A73-13418
- Inlet produced flow distortion effect on compressor stability and engine stall, presenting unified theoretical analysis technique for compatible inlet/engine design [AIAA PAPER 72-1115] 03 p0355 A73-13430
- Inlet flow distortion induced axial flow compressor stall, converting stagnation pressure and temperature maps into vorticity maps via Crocco theorem [AIAA PAPER 72-1116] 03 p0243 A73-13431

- Oblique shock wave interaction with approach boundary layer at combustor entrance in supersonic scramjet engines, observing wall pressure distribution [AIAA PAPER 72-1181] 03 p0357 A73-13476
- Inlet-combustor interface problems in scramjet engines. 03 p0360 A73-14153
- Inlet shear heating in elastohydrodynamic lubrication. [ASME PAPER 72-LUB-21] 03 p0314 A73-14336
- A procedure for estimating maximum time-variant distortion levels with limited instrumentation. [AIAA PAPER 72-1099] 04 p0432 A73-14908
- Flow in the entrance region at low Reynolds numbers. [ASME PAPER 72-WA/FE-21] 04 p0435 A73-15847
- An experimental investigation of naturally developing turbulent flow and flow with fixed transition in a parallel pipe. [ASME PAPER 72-WA/FE-38] 04 p0435 A73-15855
- Numerical solutions of the Navier-Stokes equations in inlet regions. [ASME PAPER 72-APM-DD] 05 p0564 A73-16526
- An analytical fluid dynamic model of turbulent inlet flow. [AIAA PAPER 73-138] 06 p0644 A73-17647
- Heat transfer in the thermal entrance region of rectangular channels with a circumference only partially heated 06 p0768 A73-17918
- Development of flow in the entrance region of a converging channel. 07 p0810 A73-19103
- Hypersonic flows in large-scale inlet models. 07 p0773 A73-19189
- Highly uniform inlet velocity profile influence on conical diffuser characteristics 07 p0774 A73-19615
- Circular conical diffuser inlet velocity profile effect on efficiency, presenting experimental results for different cone angles and expansion ratios 07 p0774 A73-19616
- Viscous incompressible gas turbulent flow in axisymmetric channel under preliminary twist conditions at inlet, using computer numerical solution 07 p0774 A73-19621
- Turbulent intensity induced by wakes near secondary air jet inlet to gas turbine engine flame tube 07 p0867 A73-19625
- The effect of nozzle inlet shape, lip thickness, and exit shape and size on subsonic jet noise. [AIAA PAPER 73-187] 07 p0776 A73-20465
- Inlet air flow distortion in high hub/tip ratio mixed flow turbomachines, using modified actuator disc theory 08 p0925 A73-20784
- Numerical calculation of the laminar inlet flow. I. 08 p0954 A73-21011
- Entrance region heat transfer between parallel plates with uniform wall temperature. 09 p1167 A73-23460
- Turbulence in a conical diffuser with fully developed flow at entry. 11 p1345 A73-25057
- Interaction of free and forced convection in horizontal tubes in the transition regime. 11 p1448 A73-25153
- Performance characteristics of a model VTOL lift fan in crossflow. 11 p1301 A73-25782
- Researches on the two-dimensional retarded cascade. III - Cascade performances at high inlet angles. 11 p1302 A73-26338
- Flow of liquid metals with a transversely applied magnetic field. I - Laminar flow in the entrance region. 11 p1406 A73-26341
- Emissions from and within an Allison J-33 combustor. II - The effect of inlet air temperature. 11 p1411 A73-26423
- Diffuser static pressure recovery coefficient for varying turbulence intensity at inlet, considering performance correlation with geometrical and/or velocity profile parameters 12 p1488 A73-27930
- Rectangular channel mixed boundary layer flow patterns dependence on inlet edge configurations, channel geometry and hydrodynamic flow core parameters 13 p1601 A73-28737
- Numerical solution of the viscous flow in the entrance region of parallel plates. 14 p1746 A73-30907
- Upstream attenuation and quasi-steady rotor lift fluctuations in asymmetric flows in axial compressors. [ASME PAPER 73-GT-30] 16 p2048 A73-33501
- Numerical representation of inlet and exit boundary conditions in transient cascade flow. [ASME PAPER 73-GT-55] 16 p2048 A73-33511
- The unsteady response of a blade row from measurements of the time-mean total pressure. [ASME PAPER 73-GT-94] 16 p1964 A73-33531
- Theoretical and experimental work on losses in 2-D turbine cascades with supersonic outlet flow. 17 p2092 A73-34377

- Secondary loss measurements in a cascade of turbine blades. 17 p2092 A73-34380
- Further data on the pressure recovery performance of straight-channel, plane-divergence diffusers at high subsonic Mach numbers. [ASME PAPER 73-FE-5] 17 p2152 A73-35005
- Performance of low-aspect-ratio diffusers with fully developed turbulent inlet flows. I - Some experimental results. [ASME PAPER 73-FE-12] 17 p2152 A73-35009
- Performance of low-aspect-ratio diffusers with fully developed turbulent inlet flows. II - Development and application of a performance prediction method. [ASME PAPER 73-FE-13] 17 p2152 A73-35010
- A note on compressible flow through a vortex swirl cup. 17 p2154 A73-35120
- Inlet state limitations and flow characteristics equations for supersonic ejector jet mixing duct 17 p2156 A73-35504
- Theoretical analysis of forced laminar convection heat transfer in the entrance region of an elliptic duct. 17 p2256 A73-35850
- Application of compressibility correction to calculation of flow in inlets. 18 p2265 A73-36395
- Evaluation of F-15 inlet dynamic distortion. [AIAA PAPER 73-784] 19 p2379 A73-37454
- Turbulent flow development characteristics in channel inlets. 19 p2421 A73-38184
- A new method of solving one-dimensional unsteady flow equations and its application to shock wave stability in sonic inlets. 20 p2548 A73-39522
- Some effects of pipe flow generated entry conditions on the performance of straight walled conical diffusers with high sub-sonic entry Mach number. 23 p2939 A73-43294
- Emissions from and within an Allison J-33 combustor. II - The effect of inlet air temperature. 23 p3019 A73-43327
- The vapour core pump vortex inlet valve. 23 p2941 A73-43393
- Effect of the circumferential nonuniformity of a temperature field in front of a turbine on the vibrational stresses in the turbine blades 23 p3020 A73-43740
- INLET NOZZLES**
- Calculation of the potential flow about axisymmetrical fuselages, annular profiles, and propulsion system inlets [DFVLR-SONDDR-265] 07 p0773 A73-19205
- Improvement of the calculation of the guide vanes of centrifugal pumps 09 p1028 A73-22569
- INLET PRESSURE**
- Minimum pressure zone determination for pressure field at axial plunger pump inlet during cavitation onset, discussing working fluid temperature and composition 02 p0172 A73-11800
- Prediction of inlet duct overpressures resulting from engine surge. [AIAA PAPER 72-1142] 03 p0243 A73-13448
- INLETS (DEVICES)**
- U INTAKE SYSTEMS**
- INNER RADIATION BELT**
- High energy proton model for the inner radiation belt. 03 p0363 A73-13880
- Radiation belt buildup from particles moving in magnetic field applied to terrestrial inner belt characteristics, considering extraterrestrial belts 06 p0741 A73-17503
- Existence of geomagnetically trapped electrons at altitudes below the inner radiation belt. 14 p1749 A73-29985
- Differential energy spectrum of low-energy protons in the inner regions of the radiation belt. 18 p2345 A73-36110
- Energetic neutrons leaking from the top of the atmosphere. 19 p2474 A73-37299
- Dynamic variations in intensity and energy spectra of electrons in the inner radiation belt. 20 p2601 A73-38934
- Inner belt equilibrium equatorial proton flux computation from albedo neutron measurements, including effects of atmospheric collisions, radial diffusion and geomagnetic secular decrease 20 p2601 A73-38943
- Inner zone population of trapped 2.14-9.0 MeV alpha particles, noting strong peak in pitch angle and intensity decrease with L value decrease 22 p2901 A73-41910
- INOCULATION**
- Automatic surface inoculation of agar trays. 09 p1045 A73-22550
- INORGANIC COATINGS**
- NT ANODIC COATINGS
- NT CERAMIC COATINGS

The destruction of reflecting dielectric coatings by laser radiation.

01 p0059 A73-10836

The deposition of multicomponent phases by ion plating.

04 p0456 A73-15758

Utilization of the detonation phenomenon for the deposition of coatings/Survey/

09 p1088 A73-22468

Metallic, nonmetallic, inorganic and organic protective coatings for metals against mechanical and chemical damage, discussing processing methods and applications

11 p1374 A73-25847

INORGANIC COMPOUNDS

NT AMMONIA

NT LIQUID AMMONIA

Inorganic flame retardants, considering antimony, phosphorus, boron, aluminum, nitrogen, iron and sulfur compounds

18 p2287 A73-37124

Inorganic flame retardants and their mode of action.

18 p2288 A73-37125

Elementary reactions in the combustion of small inorganic molecules.

22 p2818 A73-42752

INORGANIC MATERIALS

Fabrication and physical, mechanical and electrical properties of inorganic composite material for aircraft radomes

11 p1387 A73-25288

INORGANIC NITRATES

NT AMMONIUM NITRATES

NT POTASSIUM NITRATES

INORGANIC PEROXIDES

Plasma chemical synthesis of higher oxides of cesium and rubidium.

13 p1581 A73-29599

INORGANIC SULFIDES

NT CADMIUM SULFIDES

NT COPPER SULFIDES

NT HYDROGEN SULFIDE

NT INDIUM SULFIDES

NT LEAD SULFIDES

NT MOLYBDENUM DISULFIDES

NT MOLYBDENUM SULFIDES

NT POLYSULFIDES

NT WURTZITE

NT ZINC SULFIDES

NT ZINCBLLENDE

The evolution of ferredoxins from primitive life to higher organisms.

03 p0265 A73-14318

Some properties of synthesized stephanite /Ag₅SbS₄/ specimens

17 p2219 A73-35551

Preparation of lanthanum sulfides using carbon disulfide as a sulfurizing agent and the change of these sulfides on heating in air.

23 p3018 A73-44130

INOSITOLS

Gas-liquid chromatography of trifluoroacetyl derivatives of cyclitols.

11 p1325 A73-25150

INPUT/OUTPUT ROUTINES

Iterative scheme for identifying linear systems from input/output samples or construction of rational z-transform approximations to sample data sequences

06 p0718 A73-18534

Automated generation and condensation of large mass- and rigidity-matrices

07 p0909 A73-19175

Oakland airport oceanic ATC with input-output display device, describing minicomputer, CRT displays and data link system

19 p2454 A73-38471

PEARL middle level programming language for process control, discussing algorithms, structure, time behavior and input/output of real time operation

23 p2956 A73-44388

INSECTICIDES

NT URETHANES

INSECTS

NT BEES

NT DROSOPHILA

NT TRIBOLIA

The structural organization of the compound eye in insects.

09 p1042 A73-23302

INSENSITIVITY

U SENSITIVITY

INSEQUENT STREAMS

U STREAMS

INSTRUCTION LOSS

Design and fabrication of helix-like strip meander line delay equalizer in printed circuit technology, noting group delay and insertion loss frequency responses

02 p0145 A73-11823

Microstrip bandpass filters with reduced radiation effects.

09 p1065 A73-23098

Narrow band microwave active bandpass filter with inverted-common-collector transistor circuit,

discussing design algorithm, insertion loss, stability, sensitivity and frequency selectivity

10 p1201 A73-24169

A numerical algorithm to design multivariable low-pass equiripple filters.

10 p1202 A73-24600

The design and applications of highly dispersive acoustic surface-wave filters.

12 p1484 A73-27564

An impedance tube for precision measurement of acoustic impedance and insertion loss at high sound pressure levels.

16 p2013 A73-32916

The present state of the microwave filter art.

19 p2415 A73-38533

Synthesis of reactive ladder filters with uniform losses, discussing iterative solution for nonlinear equations and low, high and band pass filters loss compensation

21 p2662 A73-40498

A goniometer for use with high-frequency circularly disposed aerial arrays.

21 p2703 A73-41207

Noise reduction by enclosures to block airborne and structure-borne acoustic paths, developing models for insertion loss in different frequency ranges

22 p2888 A73-42924

Approximation of transfer functions for filters with equalized group-delay characteristics.

23 p2960 A73-43676

INSERTS

NT NOZZLE INSERTS

Thermoelastic problem for plate with an elliptic insert in the case of nonideal thermal contact

07 p0911 A73-19316

Thermoelastic boundary value problem for heat conduction in elastic bodies with linear and three dimensional inserts

10 p1290 A73-24305

Stress distribution in a half-plane with a hole strengthened by an elastic insert

11 p1432 A73-25026

Stress concentration in an anisotropic plate with an insert in pure bending

11 p1433 A73-25031

Stress-strain state of a thermoelastic spheroidal insert in a thermal viscoelastic medium

11 p1434 A73-25388

Improvement of damping characteristics of structural members with high damping elastic inserts.

13 p1690 A73-28056

Contact problem of the elastic interaction between a plate and an elliptic insert

19 p2499 A73-37762

INSOLATION

Effects of changes in the atmosphere on solar insolation.

08 p0958 A73-21269

Permanent frost formation on steep north-facing Mars surface slopes above 25 deg north latitude, considering explanation by insolation and surface albedo

09 p1145 A73-22274

Mars polar regions layered deposits annual solar insolation variations due to eccentricity

13 p1687 A73-29674

INSPECTION

NT INFRARED INSPECTION

NT X RAY INSPECTION

Imaging techniques for testing and inspection; Proceedings of the Seminar-in-Depth, Los Angeles, Calif., February 14, 15, 1972.

05 p0573 A73-16276

Field of view and target uncertainty in visual search and inspection.

11 p1322 A73-25181

Calculation of redundant equipment recovery time when only failures of entire systems are detected by inspection

14 p1754 A73-30036

Maintenance of public transportation aircraft - Evolution of methods

15 p1925 A73-32556

Selection, application, and inspection of electric overcurrent protective devices.

16 p1987 A73-33016

Defects in high quality aircraft tubing and inspection methods.

19 p2434 A73-37867

Sequential determination of inspection epochs for reliability systems with general lifetime distributions.

24 p3093 A73-44576

INSTABILITY

U STABILITY

INSTRUCTION SETS [COMPUTERS]

Complementary MOS LSI microprogrammed digital computer design, for Space Ultrareliable Modular Computer Demonstration Vehicle, discussing instruction operation codes, I/O peripherals and software support

10 p1191 A73-23795

Automaton external and internal languages linking by computer programming languages discussing structure and operation relation to language structure and realization

12 p1485 A73-27893

INSTRUCTIONS

U EDUCATION

INSTRUCTORS

Flight personnel training meetings, covering decision making, cockpit personnel selection and instructor role analysis

03 p0266 A73-13073

Airline flight simulator programs for aircraft type conversion training, outlining flight instructor training, certification and instructional aids

16 p1995 A73-33203

INSTRUMENT APPROACH

Extension of a portable tactical instrument approach and landing system.

03 p0340 A73-13574

An instrument approach system for Hong-Kong International Airport.

15 p1910 A73-32464

French automatic beam coupler system for V/STOL and helicopter low speed and low altitude instrument approach

21 p2737 A73-40975

INSTRUMENT COMPENSATION

NT TEMPERATURE COMPENSATION

Self-compensating digital phase meter with discrete phase shifters

01 p0044 A73-10078

Differential interference contrast microscope with continuously variable wavefront shear and pupilar compensation.

05 p0573 A73-16150

Thermal stability improvement of variable inductance electronic circuits for analog magnitudes conversion to frequencies, noting instrument errors compensation

05 p0577 A73-16987

Thermomagnetic shunt for compensation of instrument errors due to temperature effects on magnetoelectric transducers material, calculating magnetic circuit

05 p0577 A73-16988

Lateral velocity measurement error analysis in inertial guidance system, noting automatic compensation of mass imbalance effects

05 p0596 A73-16992

Heated Fleisch pneumotachometer - A calibration procedure.

08 p0935 A73-21509

Gyroscopic device for compensating external moments of sextants or binoculars optical axis due to spontaneous hand movements

09 p1084 A73-22673

Radio direction finders error compensation in air navigation, considering flight speed, polarization, near field and ground effects and great circle deviation

10 p1246 A73-23686

Instrumental polarization concerning magnetographic measurements.

10 p1218 A73-24148

Plasma diagnostics in overcompensation operated Knudsen thermionic converter with Cs-Ba filter, noting W cathode surface properties

10 p1177 A73-24204

Electronic systems for time constant and altitude error compensation of rate of climb indicator used in high performance glider flight

10 p1222 A73-24916

Error in the interferometric measurement of length by the rotational movement of a mirror and multipass corner cube arrangement.

11 p1365 A73-26240

Electronic differentiator for aircraft flight data on-board calculation in performance gliding, discussing compensation method and vertical air velocity measuring instrument advantage

13 p1569 A73-28556

Hot-wire anemometric velocity measurements in nonisothermal turbulent flows, compensating for local temperature effects on downstream wire

13 p1620 A73-29255

Use of spectral characteristics for the determination of the parameters of a corrector for thermal pickups

19 p2430 A73-37844

Seismometer compensation for broadband, low-level acceleration measurements.

20 p2563 A73-38773

Determination of the centering conditions of two-mirror systems with the aid of Hartmann photographs

20 p2565 A73-39067

Compensation of the longitudinal-trim and altitude control systems of an aircraft

22 p2800 A73-42949

Angstrom pyroheliometer scale correction for ratio of incident circumsolar radiation to electric current heating power derived from nonuniform painted surface strip illumination

23 p3025 A73-43985

A method for accurately compensating for the effects of the error beam of the NRAO 300-ft radio telescope at 21-cm wavelength.

24 p3067 A73-44581

INSTRUMENT DRIFT

U DRIFT [INSTRUMENTATION]

INSTRUMENT ERRORS

Effect of inhomogeneity of normal specimens on measurement error estimation in devices with an incompletely closed magnetic system
01 p0044 A73-10085

Inexpensive solar radiation measuring instruments comparison to standard solarimeter for mean and weekly errors
01 p0044 A73-10146

A high-precision computer-controlled dual-channel polarizing radiometer.
01 p0045 A73-10383

The accuracy of measurements of star transits
01 p0098 A73-10553

Instrument requirements for eddy correlation measurements.
01 p0052 A73-11057

Digital attitude sun sensor for ionosphere sounding satellite.
01 p0053 A73-11171

Determination of gimbal errors in an astatic gyroscope with allowance for drift
01 p0054 A73-11416

Instrument errors of film type thermocouple pyrometers for surface temperature measurement, discussing effects of shunting and junction geometry
02 p0166 A73-11636

Thermocouple circuits for measurement of unsteady temperatures in gases by the two-thermoelement method and an analysis of thermocouple circuit errors
02 p0166 A73-11710

Component errors of digital frequency meter with nonius estimation of measured quantity smaller digits
02 p0167 A73-11863

Intermediate resistance standards for low resistivity resistance thermometer calibration, discussing accuracy requirements and error analysis
02 p0167 A73-11866

Automated system with CW signal and feedback to measure delay line group delay and transfer function frequency responses, detailing operation and errors
02 p0146 A73-11952

Ultrahigh vacuum quartz spring microbalance for determination of evaporation rate and vapor pressure.
02 p0168 A73-11965

Molecular fluorine concentration and pressure change monitor based on UV absorption spectrum during chemical reactants mixing, noting measurement accuracy
02 p0168 A73-11967

Iteration method for statistical treatment of measurements when information on measurement error characteristics is incomplete
02 p0219 A73-12455

Dynamic errors in force measuring transducers, simulating unsteady processes by analog model with varying step function input signals
02 p0170 A73-12540

A criterion for establishing the principal dimensions of metallic standard measures of volume
03 p0306 A73-12897

Impurities effect on platinum resistance thermometers temperature reading accuracy, presenting empirical formula for approximate error estimate as function of operational conditions
03 p0307 A73-13193

Determination of directional corrections and the time required for passage through the meridian on the basis of 'pivot irregularities' obtained with the aid of 'pivot deviations'
03 p0307 A73-13244

A small model of the Nussli-Fric diazenithal and position determination
03 p0307 A73-13245

Determination of systematic errors in time determinations with the passage instrument
03 p0307 A73-13251

Radio aurora aspect sensitivity from radar VHF measurement error analysis
03 p0300 A73-13692

A very accurate X-band rotary attenuator with an absolute digital angular measuring system.
03 p0310 A73-14498

Radar measurement errors due to rain attenuation compensation and improper system calibration, discussing error reduction procedures
03 p0279 A73-14518

Satellite borne Ku-band pulsed radar altimeter for altitude measurement above ocean surface, evaluating random and bias errors due to instrument, propagation and geometry
04 p0446 A73-14805

Geometric properties and basic errors of rotating support devices of the gimbal suspension type
04 p0447 A73-14848

Design and field tests of astronomical optical theodolite, noting latitude, longitude and azimuth determination and objective aberration
04 p0447 A73-14849

Optical transfer function /OTF/ measurement standards and specification for high quality aerial photographic mapping lens, discussing error sources
05 p0573 A73-16147

Statistical multifactor analysis of the accuracy of continuously recorded cosmic-ray data
05 p0573 A73-16271

Effects of proton irradiation on several spacecraft science components.
05 p0596 A73-16513

Inertial navigation system based on two schuler gyropendulums and one azimuth gyro.
[DFVLR-SONDDR-246] 05 p0595 A73-16765

Thermomagnetic shunt for compensation of instrument errors due to temperature effects on magnetolectric transducers material, calculating magnetic circuit
05 p0577 A73-16988

Instrument circuitry, calibration and errors in p-n junction capacitance measurement
06 p0691 A73-17399

Turbine blade radiation pyrometer system.
06 p0692 A73-17844

Determination of the sensitivity of an infrared pyrometer with a thermocouple
06 p0695 A73-18567

Digital simulation of the Lunar Roving Vehicle navigation system.
06 p0722 A73-18828

Sun sensors for D-2B scientific satellite spin axis alignment and attitude stabilization with pointing control accuracy, discussing tests, compensatory tracking and solar simulation
07 p0821 A73-18986

Calculation of the satellite tracking accuracy for ground stations with medium-diameter parabolic antennas
07 p0791 A73-19373

Transverse sensitivity effect on measurement errors and rig calibrating of strain gages
07 p0823 A73-19568

Russian book on onboard distance measuring systems for flight vehicles covering design of cw and pulsed devices, modulators, error analysis, noise, logic elements, etc
07 p0825 A73-20378

Connecting measured objects with sensors measuring the parameters of vibrational motion
07 p0826 A73-20531

Differentiators and integrators with RC circuits for piezoelectric transducer signals, noting instrument errors and SNR
07 p0827 A73-20534

Optical pyrometers with dual spectral ratios to eliminate instrument error due to selective radiation
08 p0962 A73-20862

Technique for measuring time-base errors of magnetic instrumentation recorders/reproducers.
08 p0965 A73-21084

Pyranometer calibration by substandard and working instrument comparison on X-Y recorder, using computerized statistical analysis
08 p0966 A73-21264

Jupiter astrolabe observations analysis, investigating corrections for defective illumination, instrumental comparisons and systematic errors
09 p1140 A73-22002

Stress miscalculation due to resistance strain gage errors, deriving expressions for stress-strain error relationships
09 p1083 A73-22505

Possibilities of optimal processing of capacitance fuel meter data
09 p1083 A73-22652

Microwave noise measurement with Dicke type radiometers, discussing measurement error reduction
09 p1052 A73-23109

Drift phenomena in shaken measurement systems prone to torsional vibrations. III
09 p1086 A73-23116

Range instrumentation system timing error sources classification and uncertainty reduction for comparison of telemetry inertial guidance data with radar and optical data
09 p1057 A73-23413

Radio direction finders error compensation in air navigation, considering flight speed, polarization, near field and ground effects and great circle deviation
10 p1246 A73-23686

Airborne atmospheric temperature measurements correction for sensor response lag, deriving numerical scheme based on sensing systems wind tunnel calibration
10 p1217 A73-23991

Instrumental polarization concerning magnetographic measurements.
10 p1218 A73-24148

Strain gage measurement errors under long term installation conditions, considering drift, temperature and moisture effects, connection wires impedance and selector switch contact resistance
10 p1219 A73-24568

Piezoresistive semiconductor strain gage optimum applications and practical merits comparison with wire or foil resistance types, considering stability, accuracy and temperature compensation
10 p1195 A73-24571

Equipment for highly accurate and repeatable strain gauge factor determination.
10 p1220 A73-24574

Variable area, positive displacement, turbine type, electromagnetic and pressure difference flowmeters, noting reliability, repeatability and accuracy
10 p1221 A73-24853

Effect of measuring-device error on the accuracy of the determination of the mathematical expectation and dispersion of a stationary random process
11 p1360 A73-25016

Photometric error of the NA-MK-25 camera field
11 p1361 A73-25250

Navier-Stokes equation solution for steady state, tandem and Rankine capillary viscometer precision measurements, including compressibility correction
11 p1361 A73-25367

Low gas pressure measurement with ionization and extractor gages, discussing methods for suppressing or eliminating disturbance effects
11 p1361 A73-25400

Determination of the instrumental profile of the DFS-13 diffraction spectrograph
11 p1363 A73-25615

Reduction of ILS errors caused by building reflections.
11 p1330 A73-25784

Active cavity radiometer as pyroheliotometer for accurate radiation scale definition, determining measurement uncertainty through error analysis on quasi-equilibrium of power balance
11 p1365 A73-26236

Calibrations of the airglow photometers and spectrometers.
11 p1365 A73-26237

Moire topography for full size living human body contour stereophotographic pictures with high contrast, discussing instrument construction, performance and accuracy
11 p1365 A73-26233

Error in the interferometric measurement of length by the rotational movement of a mirror and multipass corner cube arrangement.
11 p1365 A73-26240

Automatic sensor with parabola null test and ray intercept error measurement for optical system wave front error determination, noting interferometric sensitivity
11 p1365 A73-26242

Thermoanemometer errors in turbulent wind velocity pulsations measurement
11 p1367 A73-26436

Digital measuring devices with a constant range of relative error variations
12 p1495 A73-26777

Modified X band microwave calorimeter design for precision power and attenuation measurements in GHz and MHz ranges
12 p1498 A73-27752

Piezoelectric gages for fluid dynamic multicomponent force measurements, discussing quartz transducers, measurement accuracy and capability for rapidly fluctuating forces measurement
12 p1499 A73-27871

Magnetic coil type electrical measurement indicating instruments accuracy dependence on manufacturing tolerances, discussing error reducing design methods
12 p1499 A73-27873

Radioactive spallation induced scintillator errors in satellite measurements of diffuse cosmic X ray spectrum, considering astrophysical implications
12 p1537 A73-27882

Apparatus and techniques for electron beam fluorescence probe measurements.
13 p1612 A73-28365

Quantization and roundoff errors in a digital MTI filter.
13 p1590 A73-28478

Some remarks on the thermal equilibrium equation of hot-wire probes.
13 p1613 A73-28528

An automatic reflectometer for the upper shortwave range
13 p1590 A73-28569

Minimax failure detection and identification in redundant gyro and accelerometer systems.
13 p1616 A73-28832

Geometric dilution of position /GDOP/ in spherical or hyperbolic system determination, noting position error relationship to collinearity between platform and radio sources pair
13 p1585 A73-29121

Capabilities of the GS-12 gravimeter for studying gravitational field variations
13 p1621 A73-29412

Electrical model for calculation of resistance strain gage errors due to grid-grid and grid-body shunt currents
13 p1622 A73-29617

Errors of the gravitational stabilization system of a satellite with gyro damping
14 p1803 A73-29869

Determination of the collimation error of a radio telescope 15 p1849 A73-31021

Errors due to electrode-instrument wear during the electric-erosion treatment of cavities 15 p1881 A73-31146

Errors in the absolute method of measuring the frequency of difference oscillations 15 p1853 A73-31256

Stress measurement on cloth of inflated solid circular parachute model, noting sensor interference with canopy shape and stress pattern [AIAA PAPER 73-445] 15 p1825 A73-31431

Instrumental theory in absolute radiometry 15 p1875 A73-31500

Russian book - Calculation and designing of gyroscopic stabilizers. 15 p1875 A73-31587

A modified interferometer for vibration amplitude measurement. 16 p2013 A73-32878

Radiation pattern of a low-frequency beacon antenna in the presence of a semi-elliptic terrain irregularity. 16 p1979 A73-32913

An impedance tube for precision measurement of acoustic impedance and insertion loss at high sound pressure levels. 16 p2013 A73-32916

A sequential programmer for rocket payloads. 16 p1992 A73-33105

Errors in ion and electron temperature measurements due to grid plane potential nonuniformities in retarding potential analyzers. 16 p2016 A73-33436

Determination of sensitivity of infrared pyrometer with a thermopile. 16 p2016 A73-33592

Possibilities for improving conventional ILS systems 17 p2207 A73-34479

Venus and Jupiter telescopic observation aiming errors using Wanschaff verticle circle, suggesting error sources and correction procedures 17 p2230 A73-34593

Accuracy of type K thermocouple wire below 500 F - A statistical analysis. 17 p2167 A73-34624

Data processing for earth resources survey including data handling, preprocessing for instrument errors, decision making and data bank 17 p2161 A73-34941

Improvement of absolute accuracy for a multiple bounce reflectometer through a detailed effort to reduce systematic errors. 17 p2172 A73-35420

Single beam spectrophotometer for transmittance measurement constructed from off-axis parabolic mirrors and plane grating monochromator, considering systematic errors 17 p2172 A73-35426

Testing and calibration of aircraft sensors and systems. 17 p2174 A73-35580

Large antennas and radomes boresight measurement with angular accuracy by laser mirror system incorporated into pattern range for antenna tower alignment 17 p2143 A73-35696

Differential calorimetry technique with heat link placement between samples for maintaining near equilibrium state to achieve accuracy in specific heat ratio measurement 17 p2175 A73-35753

Burnett cell design and fabrication for error reduction in high precision P-V-T data generation without volume or mass measurements 17 p2182 A73-35772

Precise and rapid measurements of small currents from high impedance sources. 17 p2143 A73-35775

Range and range-rate measuring equipments for communication satellites. 17 p2130 A73-35813

Thermal control of the large space telescope /LST/. [AIAA PAPER 73-720] 18 p2359 A73-36338

Corrections for response errors in a three-component propeller anemometer. 18 p2316 A73-36710

Gyroscopic orbit errors caused by random perturbations 18 p2317 A73-36853

Effect of the random disturbances in the principal gyro axis on the readings of a ground gyrocompass 18 p2317 A73-36854

Strap-down inertial guidance systems study. 18 p2335 A73-36955

Noise processes in a homing radar seeker. 18 p2290 A73-37088

On the correction of anemometric measurements in air flows of slowly varying temperature 19 p2429 A73-37529

Semiconductor carrier mobility measurements with Hall generator, calculating sample geometry and finite dimension electrical contact effects on error 19 p2430 A73-37718

Computer program for aircraft navigation error synthesis with evaluation of component error distribution on traffic control system effectiveness to provide cost effective guidance 19 p2452 A73-37875

Combined determination of the turn value and screw errors of the position micrometer of an astronomical universal instrument 19 p2432 A73-38553

Non-critical Rayleigh scattering from pure liquids. 20 p2570 A73-38618

Selected applications of a biaxial tiltmeter in the ground motion environment. 20 p2564 A73-38781

Ships inertial navigation system automated degradation detection and isolation, specifying decision error probabilities as function of degradation magnitude and observation time [AIAA PAPER 73-849] 20 p2585 A73-38788

Optimum inertial sensor orientation for earth inertial navigation systems allowing for azimuth error and g-sensitive instrument error effects [AIAA PAPER 73-850] 20 p2585 A73-38789

Competitive evaluation of failure detection algorithms for strapdown redundant inertial instruments. [AIAA PAPER 73-853] 20 p2585 A73-38791

Continuous calibration and alignment techniques for an all-attitude inertial platform. [AIAA PAPER 73-865] 20 p2586 A73-38803

Frequency response of short pressure probes. 20 p2564 A73-38872

Selenographic coordinates determination of ALSEP 12 and 14 telemetry transmitters via differential interferometric signal reception at two tracking stations, discussing instrument error reduction 20 p2603 A73-38894

Comments on paper by N. F. Ness, K. W. Behannon, R. P. Lepping, and K. H. Shatten, 'Use of two magnetometers for magnetic field measurements on a spacecraft.' 20 p2615 A73-38963

Equations for the instrumental errors of a type of inertial navigation system 20 p2590 A73-39045

Determination of the centering conditions of two-mirror systems with the aid of Hartmann photographs 20 p2565 A73-39067

Detuning of Wheatstone-bridge circuit during the measurement with wire strain gages - Influence and elimination of undesired effects on detuning 20 p2566 A73-39630

A universal static calibration procedure for yawed hot wires. 21 p2693 A73-39926

Low cost strapdown inertial navigator with miniature electrostatically suspended gyros, discussing system performance goal in terms of position, velocity and attitude errors 21 p2734 A73-40037

Navy Transit Navigation System precision improvements for stationary and nonstationary users, considering uncertainties due to satellite position and instrumentation errors and user motion 21 p2734 A73-40039

Satellite based ATC system with radar range and rate measurements, analyzing errors due to ground station position, transponder delay time and atmospheric refraction uncertainties 21 p2735 A73-40042

Redundant independent guidance, navigation and control system application to space shuttle, estimating channel output divergence due to sensor bias and scale factor errors 21 p2735 A73-40043

CIE interlaboratory comparison of measurements of photocell spectral sensitivity. 21 p2698 A73-40141

Frequency-dependent parasitic modulation component effects on null distortion in spectrometer and temperature measurement accuracy 21 p2700 A73-40541

Computerized simulation of radio telescope control for minimum rms error and system parameter optimization 21 p2672 A73-40551

Total power filter spectrometer for radio astronomy, featuring local oscillators with commutation for removing output instabilities to reduce instrument errors 21 p2703 A73-41149

Russian book - The laser gyroscope. 21 p2704 A73-41295

Lunar laser telemetry technological developments, discussing light beam generation and detection, SNR and ranging accuracy improvements, and receiver-optics diameter reduction 21 p2774 A73-41407

Errors arising in the RATAN-600 radio telescope due to temperature effects 21 p2675 A73-41453

Effect of radiometric errors on accuracy of temperature-profile measurement by the spectral-scanning method. 22 p2853 A73-41988

Reproducibility, stability and linearization of thermistor resistance thermometers. 22 p2855 A73-42012

Accuracy of gallium arsenide diode thermometers in the range 4-300 K. 22 p2856 A73-42019

Instrumentation errors in nuclear resonance thermometry. 22 p2856 A73-42023

Equivalent circuit modeling of insulator shunting errors in high temperature sheathed thermocouples. 22 p2858 A73-42045

The travelling gradient approach to thermocouple research. 22 p2859 A73-42049

Error accumulation in thermocouple thermometry. 22 p2859 A73-42052

Precision comparison of time and frequency by means of TV signals. 22 p2859 A73-42191

Errors of a single-axis gyrostabilizer as an angular velocity integrator 22 p2860 A73-42366

Estimation of the effect of the internal properties of the material on the characteristics of string sensors 22 p2860 A73-42370

Accuracy of photographic artificial earth satellite observations at the observational station in Riga 22 p2910 A73-42644

On separating aberrant effects from random scattering effects in radio telescopes. 23 p2958 A73-43379

Uses of tunnel diodes for zero-transition discrimination in phasometric devices 23 p2959 A73-43477

Spectrophotometer design for total ozone measurement for Dobson instrument replacement, describing spectrophotograph, reeds, electronic control, photon counter, readout system and accuracy 23 p2982 A73-43852

Errors produced by the influence of unsteady heating in strain measurement by wire-type resistance strain gages 23 p2983 A73-44292

Aerodynamic effects due to configuration of X-wire anemometers. [ASME PAPER 73-APM-P] 23 p2984 A73-44375

Simultaneous statistical treatment of the readings of a directional gyroscope and a magnetic compass 24 p3089 A73-44547

Laser range measurement to lunar surface retroreflector, discussing initial Apollo 11 observations and achieved lunar orbit and selenophysical information accuracy improvement 24 p3137 A73-44686

On the correction of hot wire turbulence measurements for spatial resolution errors. 24 p3089 A73-44691

Satellite laser ranging instruments operated at Tokyo Astronomical Observatory. 24 p3068 A73-44998

INSTRUMENT FLIGHT RULES

S-61N helicopter all-weather IFR operation for North Sea oil rigs supply and harbor pilots transportation, describing onboard instrumentation, navigation and communication systems 05 p0535 A73-16847

Curved landing approaches under visual and instrument flight conditions, investigating steep glide slope display configurations and flight control modes 13 p1569 A73-28901

Electronic landing system satisfying IFR requirements for air traffic, noting simulated ILS and ground controlled approach operations [DGLR PAPER 73-020] 17 p2146 A73-34494

Air traffic control and the prevention of collisions 19 p2450 A73-37386

INSTRUMENT LANDING SYSTEMS

NT AUTOMATIC LANDING CONTROL

Onboard ILS equipment reliability in integrated airborne all-weather landing system 02 p0190 A73-11855

Extension of a portable tactical instrument approach and landing system. 03 p0340 A73-13574

A system for the precise calibration of air navigational receivers. 03 p0310 A73-14501

A model of signal detection for the instrument landing system. 04 p0474 A73-15441

Reduction of ILS errors caused by building reflections. 11 p1330 A73-25784

Meteorological radar and the WILM landing aid 14 p1772 A73-29731

Microwave Landing System under U.S. national development plan for replacing ILS, discussing system requirements and design, precision DME and flare-out guidance 14 p1773 A73-29884

Automatic runway and aircraft approach path surveillance system /CORAIL/ consisting of Doppler

radar, signal extractor and data processing, alarm, display and control equipment

14 p1773 A73-30444

PRS-system for determination of position of flight inspection aircraft for control of ILS and VOR facilities.

15 p1909 A73-32449

A VOR sensor of advanced design - The Bendix RVA-33A.

15 p1909 A73-32454

An ILS sensor for fail operative autoland systems - The Bendix RIA-32A.

15 p1880 A73-32461

Nonimage glidepath antenna design for ILS system within international civil aviation convention specifications

15 p1909 A73-32463

Automatic helicopter approach in poor visibility

15 p1910 A73-32465

French civil aviation inexpensive C band landing system with ILS angular coding and simplified on-board equipment for STOL and Alpine airports

15 p1910 A73-32467

Microwave guidance system for aircraft landing, discussing civil and military requirements, position measurement capability, shadowing in propagation, and ground reflection induced signal fading

15 p1910 A73-32468

Pulse coded scanning beam microwave landing system technology assessment for civil aviation application, describing ground equipment and procedures

15 p1910 A73-32469

AIL-CO-SCAN landing system for STOL and heliports, combining localizer and glide control functions in 20 by 20 deg approach window

15 p1910 A73-32470

Multiple path induced position errors in microwave landing systems, considering beating beam and Doppler systems based on time and frequency division multiplexing respectively

15 p1910 A73-32471

Frequency hopping principle for precision L band DME as complementary aid to microwave landing system

15 p1911 A73-32490

Runway VHF localizer antenna array for Norwegian airports ILS, taking into account difficulties due to course bends and snow

15 p1859 A73-32498

Doppler scanning landing guidance system based on linear array of equally spaced radiators with RF source commutation

15 p1912 A73-32502

The multipath challenge for the microwave landing system.

15 p1912 A73-32503

M.A.D.G.E. - Microwave Aircraft Digital Guidance Equipment: Description of the system

15 p1912 A73-32504

FAA air traffic control systems projected improvements, including microwave landing system, aeronautical satellites, electronic voice switching and discrete address radar beacon

16 p2087 A73-33179

Air traffic control, discussing man machine systems, multipath with ILS, target indicator radars and flight progress strip preparation

17 p2206 A73-34086

Possibilities for improving conventional ILS systems

17 p2207 A73-34479

Compatible ILS involving pilot signal from microwave oscillator and precision ILS involving linear antenna array of emitter elements

17 p2207 A73-34484

Mixed CTOL-QTOL traffic effects on air traffic controller tasks, microwave landing and radio navigation systems, airport operation and ground equipment [MBB-UH-05-73]

17 p2207 A73-34487

Flight-path control device for generating curvilinear flight path profiles using microwave landing systems [DGLR PAPER 73-016]

17 p2208 A73-34492

Electronic landing system satisfying IFR requirements for air traffic, noting simulated ILS and ground controlled approach operations

17 p2146 A73-34494

Helicopter steep angle approach limits during instrument-guided landing comparison with classical ILS method, describing flight performance results

17 p2208 A73-34497

Aircraft microwave landing system development, including conventional system history and shortcomings, program objectives and implementation schedule for ATC

17 p2208 A73-34611

Doppler landing system based on standard DME for ILS replacement, describing development history and operational principles

19 p2450 A73-37385

U.S. instrument landing system performance improvements, considering terrain and weather effects, installation requirements, airport limitations, accuracy, reliability and maintainability

19 p2450 A73-37805

United States Microwave Landing System development program.

19 p2451 A73-37815

Simulated flight tests of a digitally autopiloted STOL-craft on a curved approach with scanning microwave guidance.

19 p2386 A73-38049

Nonlinear trajectory following in the terminal area - Guidance, control and flight mechanics concepts using the microwave landing system.

[AIAA PAPER 73-903] 20 p2589 A73-38837
Annual Corporate Aircraft Safety Seminar, 18th, Arlington, Va., April 1-3, 1973, Proceedings.

20 p2509 A73-39210

Instrument landing monitor (ILM) evaluation program for potential and actual capability to restore poor and/or missing visibility

20 p2590 A73-39211

Nonlinear trajectory-following and control techniques in the terminal area using the Microwave Landing System Navigation Sensor.

21 p2734 A73-40038

Microwave Landing System with air-derived sample data and scanning narrow beam antennas for signal-in-space generation, discussing design requirements and performance test

21 p2735 A73-40046

Ground based microwave landing system for aircraft navigation, guidance and control in terminal area, discussing system requirements for flight safety

21 p2735 A73-40047

ILS capability improvements on localizer and glide-slope antenna arrays and monitors, considering effects of reflecting objects on or near aerodrome and terrain

21 p2736 A73-40049

Microwave landing system elevation data or altimeter information for flare-out guidance, considering airport, aircraft autopilot and ground equipment and cost factors

21 p2736 A73-40050

ILS technology assessment, considering landing glide path determination, interference due to multipath propagation and ground effects, and operating frequency range problem

21 p2737 A73-41075

Evolution of blind landing systems

22 p2885 A73-43032

INSTRUMENT ORIENTATION

The pre-flight handling of inertial navigation systems.

07 p0849 A73-19347

Camera orientation with peripheral image coordinates of oblique circles.

08 p0968 A73-21704

Instrument axes trihedron orientation relative to reference, deriving expressions for angular misalignment statistical estimation

09 p1115 A73-22353

STRAP IV - High accuracy, low drift attitude control system.

09 p1116 A73-23208

Two concepts for the reduction of payload attitude slewing times.

09 p1155 A73-23209

Strapdown inertial system alignment using statistical filters - A simplified formulation.

11 p1395 A73-26377

Orientation dependence of certain RF impedance probes in the ionosphere.

18 p2288 A73-36188

Airborne IRP alignment using acceleration and angular rate matching.

19 p2386 A73-38048

Optimum inertial sensor orientation for earth inertial navigation systems allowing for azimuth error and g-sensitive instrument error effects

[AIAA PAPER 73-850] 20 p2585 A73-38789

Geodetic tasks during the construction and alignment of the RATAN-600 radio telescope

21 p2675 A73-41454

Laying out the foundations for circular-mirror sections of the RATAN-600 radio telescope

21 p2675 A73-41455

Experimental study of an autocollimation method for alignment of a variable-profile antenna

21 p2675 A73-41457

Television guidance for astronomical telescopes

23 p2984 A73-44362

INSTRUMENT PACKAGES

NT APOLLO LUNAR SURFACE EXPERIMENTS PACKAGE

Skyhook plastic balloons for transporting scientific instruments to high altitudes for long durations

11 p1306 A73-26348

WB-57F aircraft with instrument package for nuclear test detection and upper atmosphere research, discussing range, altitude, speed, payload capacity and onboard equipment

[AIAA PAPER 73-510] 16 p1969 A73-33548

Measurement of high-altitude air quality using aircraft.

[AIAA PAPER 73-517] 16 p2006 A73-33554

INSTRUMENT RECEIVERS

Radio astronomy interferometer receiver IF control for centimeter wave polarized signal processing and parabolic antenna instrumentation

23 p2980 A73-43377

INSTRUMENTAL ANALYSIS

U AUTOMATION

INSTRUMENTATION

U INSTRUMENTS

INSTRUMENTS

Conference on Auxiliary Instrumentation for Large Telescopes, 2nd, Geneva, Switzerland, May 2-5, 1972, Proceedings.

01 p0046 A73-10501

Instrumentation and some principal programs of the McDonald Observatory 2.75-meter /107-inch/ reflector.

01 p0046 A73-10505

Basic instrumentation components for prime, Cassegrain and coude focal positions of Anglo-Australian telescope, discussing acquisition and guiding, photography, photometry and spectrography

01 p0046 A73-10506

Telescopes for northern and southern hemisphere astronomical observatories, discussing auxiliary instrumentation and construction state on Calar Alto mountain

01 p0046 A73-10507

Electronography application to telescope and auxiliary instrumentation designs for astronomical photometry, considering spectrocon and suitable image tubes

01 p0049 A73-10537

INSULATED STRUCTURES

Insulating houses against aircraft noise.

14 p1743 A73-30913

INSULATION

NT ELECTRICAL INSULATION

NT MULTILAYER INSULATION

NT THERMAL INSULATION

INSULATORS

Current near the insulator wall in plasma accelerators.

03 p0348 A73-14437

Electronic transport in insulating films.

05 p0604 A73-16503

On the origin of strongly conducting states in thin insulator films.

06 p0734 A73-17812

Concentrations of carriers and electric field along an insulating or semiconducting sample: Developments of steady solutions up to the second order Case of weak potentials

08 p0995 A73-21445

Diffusion effects in the double injection negative-resistance problem.

08 p0948 A73-21483

Transient photocurrent pulse shapes and transit times in insulators with uniform and exponential trapped space charge in excitation layer or insulator surface

09 p1119 A73-21945

A relationship between photoemission-determined valence band gaps in semiconductors and insulators and ionicity parameters.

09 p1134 A73-22903

Semiconductor and semi-insulator resistivity measurements using a direct current four point probe apparatus with non-penetrating tips.

10 p1194 A73-24158

Determination of the dispersion relation in tunnel structures - Influence of the barrier shape and validity of the WKB approximation.

17 p2220 A73-35655

INSULIN

Antidiabetic medications and aircrew

08 p0935 A73-21541

Plasma insulin and carbohydrate metabolism after sucrose ingestion during rest and prolonged aerobic exercise.

21 p2641 A73-41622

INTAKE SYSTEMS

NT AIR INTAKES

NT ENGINE INLETS

NT HELICAL INDUCERS

NT HYPERSONIC INLETS

NT SUPERSONIC INLETS

An empirical flowfield analysis technique for preliminary evaluation of inlet systems operating in a vehicle generated flowfield.

01 p0003 A73-11132

Boundary layer bleed system design for supersonic inlets, discussing bleed hole geometry effects on boundary layer velocity profile and inlet efficiency

[AIAA PAPER 72-1138] 03 p0243 A73-13445

Development of aft inlets for a ramjet powered missile.

03 p0246 A73-14133

Visualization study of flow in axial flow inducer. [ASME PAPER 72-FE-33]

05 p0565 A73-16547

Magnetic intake limitations on interstellar ramjets.

10 p1262 A73-24539

Effect of solidity on rocket pump inducer performance.

13 p1624 A73-29011

Inlet system design procedures and wind tunnel facility modifications allowing for verification on large scale models at Mach 4.5

15 p1824 A73-31743

Three-dimensional flow field in rocket pump inducers. I - Measured flow field inside the rotating blade passage and at the exit.

[ASME PAPER 73-FE-33] 17 p2095 A73-35024

Theoretical studies of sound emission from aircraft ducts.

[AIAA PAPER 73-1012] 24 p3078 A73-44844

INTEGRAL CALCULUS

Relations between the first integrals of a non-holonomic mechanical system and of the corresponding system freed of constraints.

07 p0850 A73-19013

Use of Olver's algorithm to evaluate certain definite integrals of plasma physics involving Chebyshev polynomials.

07 p0854 A73-19270

The stationary-phase method for a double integral with an arbitrarily located stationary point

09 p1048 A73-21918

Rockafellar duality theorem generalization to integrands over locally convex sublinear topological vector spaces, permitting Banach space transcendence

11 p1390 A73-25866

Remark on the behavior of an approximated process related to singular integrals near the terminals of an integration segment

11 p1391 A73-26077

Solutions of some Fredholm integral equations using fractional integration, with an application to a forced convection problem.

13 p1704 A73-28413

Arrangement of integral surfaces in weakly-nonlinear systems of differential equations

13 p1650 A73-29137

Matrix calculus operations and Taylor expansions.

14 p1769 A73-30410

The three-dimensional turbulent boundary layer - Theoretical and experimental analysis

16 p1961 A73-32810

A numerical and experimental investigation of the use of J-integral.

17 p2246 A73-34880

Fundamental integral representation of x-analytical functions and its application to the solution of some integral equations

20 p2583 A73-39497

Integral representations for solution of mixed boundary value problems for generalized axisymmetric Helmholtz equation, considering Sommerfeld half plane and transonic flow problems

21 p2727 A73-41017

The asymptotic analysis of canonical problems in high-frequency scattering theory. I - Stratified media above a plane boundary. II - The circular and parabolic cylinders.

22 p2886 A73-42347

Integrals for optimal flight over a spherical earth.

22 p2884 A73-42561

Prediction of satellite motion by a combined method of recurrent relations

23 p3027 A73-43267

An application of integral invariants to the n-body problem

23 p3034 A73-44100

Velocity field determination in meridional plane of potential field using third isolating integral of motion

23 p3035 A73-44238

INTEGRAL EQUATIONS

NT FREDHOLM EQUATIONS

NT SINGULAR INTEGRAL EQUATIONS

NT VOLTERRA EQUATIONS

NT WIENER HOPF EQUATIONS

Numerical solution of nonlinear partial differential and integrodifferential equations; Meeting, Oberwolfach, West Germany, November 28-December 4, 1971, Reports

01 p0069 A73-10066

A comparison of geometrical theory of diffraction and integral equation formulation for analysis of reflector antennas.

01 p0022 A73-10179

Integral equations for current distribution and input impedances of curved thin symmetrical dipole antenna, noting Q factor of fourth wave antennas

01 p0017 A73-10216

Construction of finite-difference schemes in engineering theory of elasticity on the basis integral representations of the resolvent functions

01 p0114 A73-10483

Reduction of integral equations in elasticity theory to infinite systems

01 p0116 A73-10960

Stress analysis for two stamps impression into linearly deformable base, solving integral stress equation by orthogonal polynomials method

01 p0118 A73-11411

Ordinary integrodifferential equations for dynamic and quasi-static problems of nonlinear viscoelasticity theory

01 p0119 A73-11431

Spectral analysis of integro-differential forms in spatial dynamic problems of the theory of elasticity

02 p0232 A73-11820

Determination of elastic stresses at notches and corners by integral equations.

02 p0234 A73-12075

Dual integral equations and diffraction of electromagnetic waves by a thin conducting strip.

02 p0141 A73-12101

Local transport equations for turbulent shear flow.

02 p0154 A73-12825

Hilbert space and calculus of variations for eigenvalue bounds of integral equations of elasticity and potential theories

03 p0387 A73-13162

Numerical integration of nonlinear integrodifferential equations of thin viscoelastic beams deflection, considering cantilever beam under uniformly distributed loads

03 p0390 A73-13343

Vortex sheath formalism based on coupled integral equations for rectangular wing-slipstream aerodynamic interference

03 p0244 A73-13562

Analysis of wire antennas in the presence of a conducting half-space. II - The horizontal antenna in free space.

03 p0276 A73-13694

Linear integral equation, wave function and parameter optimization for numerical analysis of remote sensing problem

03 p0337 A73-14488

Rice energy line J integral fracture strength criterion applicability to crack tip elastoplastic testing for steel alloys

04 p0506 A73-14694

Rice path independent J integral fracture strength criterion estimation as function of crack size and elastoplastically adjusted load point displacement for Ni-Cr-Mo-V steel

04 p0506 A73-14696

Integral representation of positive solutions of linear elliptic and parabolic differential equations with constant coefficients

04 p0470 A73-14898

Vortex lattice discretization for finite Hilbert transform of two dimensional incompressible thin wing flow integral equation with singularities, noting numerical solution accuracy

04 p0403 A73-15004

Certain analytical solutions of the Cauchy problem for a disturbed loaded linear integrodifferential equation

04 p0470 A73-15080

The solvability of integral equations of shell theory

04 p0511 A73-15082

State and integral equations formulations for signal design problem of channels with known time dispersion and additive white Gaussian noise

04 p0419 A73-15405

The integral equation and boundary conditions for a cylindrical antenna in a warm plasma.

[AD-760102] 04 p0429 A73-15482

Proof of the eigenvalues 0 and -1 in the spectra of integral operators of two-dimensional elasticity theory

04 p0514 A73-15677

Singular solutions for shallow cylindrical shells.

[ASME PAPER 72-WA/JP-27] 04 p0515 A73-15891

Orthogonalization method application to problems of wave diffraction from several bodies through reduction to integral equations

05 p0547 A73-16053

Implications of a quadratic stream definition in radiative transfer theory.

05 p0592 A73-16196

Integral equations suitability and solution instability of stellar system models, referring to globular cluster densities and mass distribution equations

05 p0616 A73-16452

Numerical solution of integral equations of the first kind using a priori information on the function to be determined.

05 p0591 A73-16789

Variational principle application to nonself adjacent lifting surface integral equation from finite element viewpoint, considering two dimensional flat plate

[AIAA PAPER 73-87] 05 p0529 A73-16852

A momentum integral solution for pulsatile flow in a rigid tube with and without longitudinal vibration.

05 p0567 A73-17273

On a quadratic first integral for the charged particle orbits in the charged Kerr solution.

06 p0725 A73-17889

Integral equations for temperature distribution in radiative and conductive heat transfer in semitransparent medium, noting temperature oscillation propagation

06 p0769 A73-18565

Differential operators transformation into integral functions by Green function and distributions theory methods in structural analysis

06 p0719 A73-18727

Relative motion integrals of interacting identical mass particles in terms of Hamiltonian function and momentum relation

06 p0725 A73-18887

Singular integrodifferential and linear integral equations for load transfer from stringer to wedge under concentrated force and for stringer-coupled wedge shaped regions

07 p0910 A73-19306

Solution of a contact problem for an infinite elastic cylinder with two contact areas by the method of triple integral equations

07 p0910 A73-19307

Resonances and certain cases of integrability of the motion of a heavy solid about a fixed point

07 p0851 A73-19469

Preliminary quasar model based on the Yilmaz exponential metric.

07 p0899 A73-20178

A proposal for the calculation of characteristic functions for certain differential and integral operators via initial-value methods.

07 p0845 A73-20490

On the third integral of motion in stellar dynamics. I.

08 p1002 A73-20849

Axisymmetric Stefan problem with boundary conditions of the third kind

08 p1022 A73-21100

An iteration procedure for the solution of special nonlinear boundary-value problems

09 p1112 A73-22448

Quantum mechanical operator for photon flux density passing through spatial point over infinite time, interpreting photon wave functions

09 p1094 A73-22598

Method of integral equations in the statistical theory of fluids

09 p1121 A73-22724

Probabilistic model for the resolvent kernel in diffusion problems in spherical-shell media.

09 p1121 A73-23071

Stress field singularities due to cracks in isotropic elastic bodies, assuming Hooke's law stress-strain relationship in integral equation representations

09 p1162 A73-23182

Combined-operations method for diffuse reflection by an isotropic, non-coherent scattering homogeneous sphere.

10 p1271 A73-23484

Construction of the solution to a nonlinear boundary value problem for a heat-radiating body of complex shape

10 p1296 A73-24510

Unsteady creep in a symmetrical cylindrical shell

10 p1293 A73-24793

Ambipolar drift, deformation, and diffusion of a plasma in a magnetic field.

11 p1402 A73-24989

Higher order numerical solution of the integral equation for the two-dimensional Neumann problem.

11 p1300 A73-25434

Direct time numerical integration of spatially discretized linear elastodynamics integral equations, comparing one-step algorithms for stability and accuracy in terms of frequency spectrum

11 p1435 A73-25439

Interdisciplinary computer analyses of three-dimensional solids defined by polyhedral surfaces.

11 p1437 A73-25491

Solution of fundamental three-dimensional problems in the theory of elasticity for arbitrarily shaped bodies by way of a numerical realization of the method of integral equations

11 p1441 A73-25627

Integral equation numerical solution by minimum mean-squared estimator for atmospheric electromagnetic refractivity profile from satellite radio tracking data, noting iterative procedure convergence

11 p1330 A73-25686

Ordinary integrodifferential equations for dynamic and quasi-static problems of nonlinear viscoelasticity theory

11 p1443 A73-26066

Application of the harmonic balance method for studying oscillations of nonlinear systems with distributed parameters

11 p1400 A73-26464

Several estimates in the theory of stochastic integrals

12 p1517 A73-27186

Construction of asymptotic solutions to the Cauchy problem with an initial jump for nonlinear systems of integrodifferential equations containing a small parameter at the higher derivative

12 p1518 A73-27298

On the reduction of integral equations of the theory of elasticity to infinite systems.

12 p1554 A73-27536

Inverse problems of a logarithmic potential with analytic closeness

12 p1518 A73-27729

Nonlinear integral equations for the electrodynamics of conducting media

12 p1525 A73-27805

Some error estimates for approximate solutions of nonlinear integral Hammerstein-type equations
12 p1519 A73-27818

Iterative-zonal method for studying and calculating the local characteristics of radiative heat transfer.
12 p1560 A73-27913

Symposium on Ordinary Differential Equations, University of Minnesota, Minneapolis, Minn., May 29, 30, 1972, Proceedings.
12 p1519 A73-27919

A method for obtaining bounds on eigenvalues and eigenfunctions by solving non-homogeneous integral equations.
13 p1647 A73-28192

An integral equation approach to heat and mass transfer problem in an infinite cylinder.
13 p1705 A73-28431

Complex resonant frequencies calculation in external diffraction problems for arbitrary shaped bodies, noting Green function poles correspondence to eigenvalue zeros of integral equation
13 p1582 A73-28652

Integral relations for an equilibrium toroidal plasma filament with a noncircular cross section
13 p1665 A73-28951

Application of paired integral equations to the problem of the torsion of an elastic space weakened by a conical slot of finite dimensions
13 p1698 A73-29090

Book - Optimal control of differential and functional equations.
13 p1651 A73-29550

A quadrature-iterative method of solving linear and nonlinear integral equations
13 p1651 A73-29679

Secondary source method solutions for media interface integral equations of electrostatic fields in piecewise homogeneous anisotropic media
14 p1774 A73-30027

Integral equation formulation for electromagnetic scattering by conducting cylinders, investigating coupling between complementary boundary value problem and nonuniqueness consequences on numerical resolution
14 p1727 A73-30215

Construction of finite difference diagrams of the engineering theory of elasticity, on the basis of integral representations of the resolvent functions.
14 p1810 A73-30308

Radiant heat transfer on circular-finned cylinders.
14 p1817 A73-30574

Effect of nonlinearity in a coherent pulse integrator on signal-to-noise gain.
15 p1842 A73-30988

The transonic aerofoil problem with embedded shocks.
15 p1821 A73-31122

Error investigations regarding the solution of the inhomogeneous natural boundary value problem by means of a Ritz approach with standardized coordinate functions
15 p1899 A73-31364

Integral equations for nondestructive determination of buckling loads for elastic plates and bars.
15 p1948 A73-31634

Integral equations for piecewise-homogeneous media in the solution of boundary value problems of electrodynamics
15 p1913 A73-31693

Resonances and some cases of integrability of the motion of a heavy rigid body about a fixed point.
15 p1914 A73-32068

The global aspect of the complex analysis in the theory of the morphic functions
15 p1900 A73-32106

Integral operators and the first initial boundary value problem for pseudoparabolic equations with analytic coefficients.
15 p1902 A73-32399

Three-dimensional turbulent boundary layer - Calculations and experiments
16 p1961 A73-32806

The analysis of three dimensional problems of elasticity by integral representation of displacement.
16 p2078 A73-33003

Solution of equations of Reissner's theory of plates by application of Hajdin's method.
16 p2078 A73-33004

New problems pertaining to nonlinear integro-differential equations with several independent variables. I - Search for solutions in the case of initial integral boundary conditions
16 p2032 A73-33172

The derivation of the mechanical balance equations of the Cosserat continuum on the basis of the energy equation and its behavior at the transition to rotating systems
16 p2080 A73-33240

An integral representation of the Dirac delta function for axisymmetric boundary value problems.
16 p2032 A73-33309

Integral equations for temperature distribution in radiative and conductive heat transfer in semitrans-

parent medium, noting temperature oscillation propagation
16 p2086 A73-33590

A difference method of solving boundary value problem for a parabolic-type quasi-linear integro-differential equation
16 p2034 A73-34070

An integro-differential equation technique for the time-domain analysis of thin wire structures. I - The numerical method.
17 p2246 A73-34892

Numerical solution of the three-dimensional Navier-Stokes equations in integro-differential form - Flow about a finite body.
17 p2155 A73-35139

Symmetric integral equations of the theory of elasticity
17 p2251 A73-35585

Numerical solutions of time-dependent incompressible Navier-Stokes equations using an integro-differential formulation.
18 p2297 A73-36159

A new form of the integral equations of a boundary value problem in the theory of simply supported shallow spherical shells
19 p2495 A73-37198

Application of dual integral equations to the problem of torsion of an elastic space, weakened by a conical crack of finite dimensions.
19 p2498 A73-37640

Non-singular control problems. II - Integral equation function-space method applied to the solution of optimization problems in the mechanics of deformable bodies.
19 p2498 A73-37649

Integral equation in the theory of lifting surfaces
19 p2377 A73-37846

Integral transport equations for component distribution function of gas mixture with internal degrees of freedom and chemical reactions
19 p2463 A73-37847

Third integral of motion and the velocity field for a quasi-Newtonian potential. I
19 p2486 A73-37848

A path-independent integral for transient crack problems.
19 p2500 A73-38114

Numerical solutions of basic three-dimensional elasticity theory problems for bodies of arbitrary shape.
19 p2500 A73-38149

An integral-equation approach to dispersion relations for guided elastic surface waves.
20 p2592 A73-39048

Boundary value problems for linear generalized differential equations and their adjoints.
20 p2582 A73-39402

Fundamental integral representation of x-analytical functions and its application to the solution of some integral equations
20 p2583 A73-39497

Study of shock wave and turbulent boundary layer interaction using the energy integral equation.
20 p2548 A73-39524

Small oscillations of a heavy solid body about a stationary point and certain cases of the existence of 'linear integrals'
21 p2738 A73-40188

Initial-value problems for pseudo-parabolic partial differential equations.
21 p2726 A73-40694

Regularization of solutions of inverse problems of heat conduction.
21 p2792 A73-41061

Integral equation analysis of cylindrical antennas having arbitrary surface impedance.
21 p2655 A73-41093

The integrals of the system of Navier-Stokes equations for axisymmetric motion of an incompressible fluid
22 p2841 A73-42123

Maxwell integral equations in problems of wave scattering by moving media
22 p2826 A73-42376

On the integral equations of three-dimensional multiple inclusion problems.
22 p2924 A73-42682

Monograph - Generation of acoustic waves in piezoelectric devices.
22 p2861 A73-42700

Papers on computer techniques for electromagnetic radiation and scattering problems via integral equation formulation covering iterative and variational methods and antenna patterns
22 p2827 A73-42839

Numerical solution of wire antenna boundary value problems based on integral equations formulation, considering Yagi-Uda array, antenna design and radiation patterns
22 p2827 A73-42840

Integral equation solutions of three-dimensional scattering problems.
22 p2827 A73-42842

Variational and iterative methods for waveguides and arrays.
22 p2834 A73-42843

On an integral equation governing the reflection of electromagnetic waves by a random surface
22 p2888 A73-42948

A method for solving ill-posed integral equations of the first kind.
23 p2999 A73-43803

An existence and uniqueness theorem for the solution of a stochastic integrodifferential equation
23 p2999 A73-44101

The eigenvalue solution of asymmetric-ridge waveguides using the mode-matching method.
23 p2955 A73-44146

Equilibrium of a toroidal plasma with noncircular cross section.
23 p3013 A73-44303

Method of integral equations in statistical theory of liquids.
23 p3007 A73-44324

Topological analysis of integral operators with Agmon kernel in Sobolev spaces within Hilbert space framework
24 p3105 A73-45009

Differential and integral formulations of variational principles in mechanics, discussing Hoelder-Voss, d'Alembert-Lagrange, Gauss and Jourdain principles
24 p3110 A73-45246

Truncation error in the solution of integral equations.
24 p3106 A73-45344

Integral representations of solutions for general parabolic boundary value problems and the correct solution in spaces of increasing functions
24 p3106 A73-45352

On the existence, uniqueness, and stability of solutions of a new boundary layer problem concerning certain nonlinear integral-differential polyvibratory systems. I
24 p3106 A73-45395

Simplified averaged equations of concentric laser compression of plasma.
24 p3117 A73-45427

The exterior Neumann problem for the Helmholtz equation.
24 p3112 A73-45470

INTEGRAL FUNCTIONS
U ENTIRE FUNCTIONS
INTEGRAL TRANSFORMATIONS
NT CONVOLUTION INTEGRALS
NT FAST FOURIER TRANSFORMATIONS
NT FOURIER TRANSFORMATION
NT HILBERT TRANSFORMATION
NT LAPLACE TRANSFORMATION
Application of the Meler-Fok complex conversion formulas in the solution of certain problems of heat conductivity
01 p0119 A73-10017

Analysis of certain nonstationary processes by using Wiener functionals
01 p0026 A73-10026

Integral transformations and conformal mapping for velocity distribution of steady two dimensional potential flow along given profile curve
03 p0241 A73-12904

Solution of the asymmetric steady-state heat conduction problem for a two-layer hollow cylinder of finite length
08 p1021 A73-20995

A note on Eulerian-Lagrangian time scale transformation for large-scale atmospheric turbulence.
08 p0985 A73-21424

Integral transform solution of mixed boundary value problem for Griffith cracks with complicated geometries and external, star-shaped, cruciform-shaped and circular cracks
09 p1162 A73-23183

Integral transform and heat conduction in a hollow cone with radiation.
10 p1297 A73-24920

Statistically orthogonal functions for finite intervals of a random process
11 p1390 A73-25642

Optimal harmonic synthesis of generalized Fourier series and integrals with randomly perturbed coefficients
13 p1650 A73-28893

Integral transform theory for derivation of compound binomial beta, uniform, and gamma distributions with applications to series-parallel systems reliability determination in manufacturing
16 p2020 A73-33604

An integral equation approach to the semi-infinite strip problem.
[ASME PAPER 73-APMW-5] 22 p2924 A73-42878

Application of finite integral transformations to optimal control problems
23 p2963 A73-43576

Microphone radiated acoustic power directivity measurement enhancement by integral transform, matrix inversion and relaxation techniques, considering application limits, resolution, noise sensitivity and computation
[AIAA PAPER 73-1040] 24 p3090 A73-44865

Radon transform application in holographic interferometry for reconstructing two and three dimensional spatial distribution of refractivity in object
24 p3091 A73-44944

INTEGRATED CIRCUITS

NT LARGE SCALE INTEGRATION

Integrated subnanosecond circuits with low power dissipation and few components
01 p0021 A73-11487

Low cost monolithic range gated radar moving target indicator using bucket brigade delay line circuits
02 p0141 A73-12360

Designing limiter/detectors for ECM receivers.
02 p0143 A73-12569

Circuit variants of dynamically operated MIS /metal-insulator-semiconductor/ structures
03 p0281 A73-13241

Microelectronic metal-dielectric-semiconductor devices for physical properties of multilayer multiphase systems, noting field effect transistors, integrated circuits and electro-optical elements
03 p0349 A73-13656

The IHTS - A new building block for power conditions.
03 p0282 A73-13934

A universal digital autopilot and integrated avionics system.
04 p0474 A73-14735

Probability model and causal approach to failure mechanisms and reliability of control system elements applied to IC
04 p0424 A73-15208

Thermal development of heat pipe cooled IC packages.
[ASME PAPER 72-WA/HT-44] 04 p0518 A73-15812

Programmable digital pulse generator for NMR applications based on master clock, several counters and inexpensive ICs
05 p0559 A73-17256

Simple mathematical model of shift of threshold voltage induced in an m.o.s. transistor by testing at elevated temperatures.
05 p0560 A73-17324

Circuit parameters and performance of monolithic IC operational amplifiers, noting data sheets with voltage and temperature ranges and frequency response characteristics
06 p0672 A73-17450

Separate generation of odd and even harmonics of a fundamental frequency, with the aid of pulse circuits
06 p0663 A73-17576

Book - Transistor circuit design.
06 p0673 A73-17672

The design of electronic equipment for biotelemetry using microcircuit techniques.
06 p0673 A73-17674

Charged coupled IC image sensors based on MOS capacitors for low light level TV, considering operation, performance and production technologies
06 p0676 A73-18301

Compact YIG bandpass filter with finite-pole frequencies for applications in microwave integrated circuits.
06 p0678 A73-18742

Effects of ionizing radiations on MOS components
07 p0860 A73-18914

MOS field effect components integration on Si operation, performance and application to logic circuits
07 p0797 A73-18916

Improving the performance of M.I.S. circuits under radiation.
07 p0797 A73-18918

Tantalum thin film capacitors fabrication procedure for hybrid ICs, presenting temperature and frequency responses and I-V characteristics of test samples
07 p0801 A73-19535

Antennas have it tough - when forced to ride on spacecraft.
07 p0803 A73-20491

Microstrip transmission line microwave IC, discussing electrical characteristics, dielectric and conductor materials, photo-etching processes, connection fabrication and circuit encapsulation
08 p0942 A73-20702

Microwave integrated circuits on a ferrite substrate.
08 p0942 A73-20704

A laser scanner for integrated circuit testing.
08 p0974 A73-20731

Prediction of IC and LSI performance by specialized vibration/detection test for presence of conductive particles.
08 p0943 A73-20732

IC reliability enhancement by molded dual in-line packaging /DIP/ technique, considering mold shrinkage effects on failure rates during temperature cycling tests
08 p0944 A73-20737

IC plastic package performance prediction, discussing procedure to estimate degradation rate due to moisture effects
08 p0944 A73-20738

Reliability aspects of plastic encapsulated integrated circuits.
08 p0944 A73-20739

Thin film nickel-chromium resistor failures in integrated circuits.
08 p0944 A73-20746

Optical modulator based on coupled waveguides for integrated optical circuits, presenting design and dynamic characteristics
08 p0974 A73-20810

Effect of engineering-design factors on the parameters of microstrip transmission lines
08 p0951 A73-21109

1-2 GHz high-power linear transistor amplifier.
08 p0947 A73-21146

Measurement of admittance of Gunn diodes in passive and active regions of bias voltage.
08 p0947 A73-21432

Integrated circuits fabrication and technology development, discussing digital and analog circuit capabilities, cost reduction and diffusion techniques
08 p0949 A73-21647

Two stage microwave monolithic integrated circuit power amplifier design with matched transistors, calculating distributed matching network
08 p0950 A73-21826

Miniature pressure transducers with a silicon diaphragm.
09 p1084 A73-22692

Photoresist technology for passive ICs production with optical waveguides, describing vaporization deposition and processing for glass films
09 p1086 A73-23075

An IC piezoresistive pressure sensor for biomedical instrumentation.
10 p1183 A73-23649

Integrated neuristor lines based on p-n-p-n structures with diffused resistors
10 p1193 A73-23727

Experimental investigation of the effective permittivity and of the resonator Q of slot lines on ceramic substrates in the frequency range from 1 to 18 GHz
10 p1194 A73-23994

A method for the assessment of the electrical stability of TTL gates
10 p1194 A73-23995

The application of integrated magnetic devices for circuit checking and error correcting.
10 p1198 A73-24021

Multistage diffusion model of IC transistor electrical characteristics and impurity distributions as function of surface concentrations and junction depths during fabrication
10 p1196 A73-24606

Inductance and Q factor measurements of inductive p-n-p transistor element in IC circuit as function of frequency, temperature and junction capacitance
10 p1196 A73-24613

A quick accurate method to measure the dielectric constant of microwave integrated-circuit substrates.
10 p1197 A73-24866

Optical waveguide structures for CO2 lasers.
11 p1375 A73-25058

Monolithic IC digital circuits using Si planar technology with Schottky diodes in DTL and TTL gates for high computational speed
11 p1341 A73-25345

Calculation of the y-parameters of an integrated-circuit amplifier by reducing the matrix of an n-terminal network to the matrix of a two terminal pair network
11 p1338 A73-26102

Microwave electronic packaging with integrated multifunction assemblies, considering stripline choice for transmission line
11 p1338 A73-26113

Integrated microoptical circuit technology with lenses, prisms, reflectors, mixers, detectors, gratings, filters, lasers, amplifiers and modulators fabricated around waveguides, assessing advantages and potentials
11 p1399 A73-26117

Low loss fiber optics communication technology with almost infinite bandwidth potential, discussing transmission lines, light sources, detectors, integrated circuits, systems and applications
11 p1399 A73-26118

Book - Introduction to semiconductor devices: Diodes, bipolar transistors, JFETs, IGFETs, SCRs and integrated circuits.
12 p1478 A73-27050

Binary counters design based on TTL, DTL and ECL integrated circuits, giving circuit diagrams for 70 MHz 24 stage and 20 MHz dual 16 stage counters
12 p1497 A73-27208

Microelectronics developments and limitations, considering bipolar IC, metal-dielectric-semiconductor structures and optoelectronic communication links
12 p1480 A73-27267

A programmable surface acoustic wave matched filter for phase-coded spread spectrum waveforms.
12 p1484 A73-27574

Review of microwave-integrated-circuit technology.
13 p1588 A73-28043

Cooling of IC chips by heat conduction.
13 p1590 A73-28480

High power latching ferrite phase shifters for AEGIS.
13 p1591 A73-28620

A new concept for the realization of data modems with integrated digital filters and modulators.
13 p1594 A73-29293

Suppressing spurious signals in saturated switching systems.
13 p1595 A73-29394

Thick film multilayer IC for electro-optical applications, discussing package techniques, sealing materials, ultrathick printing cold cathode panel and liquid crystal displays
13 p1669 A73-29395

Transient analysis of multiple-input integrated digital structures.
13 p1595 A73-29580

An integrated random access memory with full-current recording and readout
14 p1730 A73-30290

Microwave integrated circuit applications at special microwave devices operation.
15 p1851 A73-32274

Secondary radar interrogator based on IC technology, discussing video processing and monitoring
15 p1847 A73-32436

A monolithic pair of dielectrically isolated high-sensitivity photodiodes operating in the visible spectrum.
16 p2012 A73-32854

An integrated-circuit solar aspect sensor for spacecraft use.
16 p2013 A73-32884

Hybrid optoelectronics - High frequency modulation and detection of light by semiconductor sources and sensors.
16 p1978 A73-32886

Noise properties of a transistor in an integrated circuit
16 p1987 A73-33089

International Microelectronic Symposium, Washington, D.C., October 30-November 1, 1972, Proceedings.
16 p1989 A73-33466

Mechanical design of microwave integrated circuit enclosures.
16 p1989 A73-33469

Ceramic waveguide microwave integrated circuits.
16 p1989 A73-33470

An integrated, modular approach to automatic testing and data monitoring.
16 p1986 A73-33632

System effectiveness and the one error per man per day expectation.
16 p2020 A73-33647

Synthesis of a universal cell with increased reliability for the realization of an iterative automatic system
16 p1986 A73-33667

Transient analysis of complementary MOS IC inverter.
16 p1990 A73-33688

Integrated semiconductor storage devices, discussing bipolar transistor, Schottky diode and MOS memories and RAM, ROM and PROM types with circuit compatibility considerations
16 p1991 A73-33960

Book - Compatibility and testing of electronic components.
17 p2134 A73-34573

Determination of the geometrical dimensions of a bandpass filter for a microwave hybrid integrated circuit
17 p2134 A73-34584

A solid state bonding and packaging technique for integrated sensor transducers.
17 p2166 A73-34618

Electronic Components Conference, 23rd, Washington, D.C., May 14-16, 1973, Proceedings.
17 p2135 A73-34726

C band low noise IC microwave amplifier for phased array module in multiple access communication links, discussing photofabrication for low cost batch processing
17 p2135 A73-34727

Detection of random chip defects in monolithic microcircuits.
17 p2135 A73-34732

High speed parallel multiplier design based on threshold logic adder using integrated logic circuits
17 p2139 A73-35238

150 KVA integrated drive generator for aircraft electrical systems.
17 p2109 A73-35253

Thin film hybrid microwave integrated circuit.
17 p2141 A73-35323

Papers on integrated optics covering waveguides, mode launching, radiation losses, lasers, parametric devices, light deflectors and thin film deposition
17 p2185 A73-35599

Book - Low-noise electronic design.
17 p2143 A73-35825

Book - MOS integrated circuit design.
18 p2294 A73-36966

Reliability estimation for integral logical elements from intermittent failures under noise effects
18 p2292 A73-37045

Reliability physics 1973; Proceedings of the Eleventh Annual Symposium, Las Vegas, Nev., April 3-5, 1973.
19 p2410 A73-38438

A bonding-wire failure mode in plastic encapsulated integrated circuits.

19 p2410 A73-38442

Torque and thermal cycling as methods of testing reliability of reflow-soldered chip-to-substrate joints.

19 p2436 A73-38445

Analysis of integrated circuit failure modes and failure mechanisms derived from high temperature operating life tests.

19 p2411 A73-38449

Temperature-humidity acceleration of metal-electrolysis failure in semiconductor devices.

19 p2411 A73-38450

Process control stress test of MOS IC circuit susceptibility to charge spreading with channel formation

19 p2436 A73-38452

Improve reliability of electron devices through optimized coverage of surface topography.

19 p2411 A73-38453

High-reliability plastic package for integrated circuits.

19 p2411 A73-38455

Screening of metallization step coverage on integrated circuits.

19 p2411 A73-38456

Microwave integrated circuit technology.

19 p2411 A73-38535

Near-harmonic integrated oscillators in the 10 MHz to 40 MHz range.

19 p2412 A73-38538

Book - RCA COS/MOS technology.

20 p2533 A73-38653

Fundamentals of COS/MOS integrated circuits.

20 p2534 A73-38655

High reliability manufacturing technology for COS/MOS IC devices, discussing failure mechanisms and MIL-STD-883 and MIL-M-38510 tests for quality control

20 p2534 A73-38656

Statistical analysis of the influence of various factors on the quality of photolithographic operations in the production of integrated circuits

20 p2534 A73-38851

Injection-modulation devices as elements of integrated circuits

20 p2534 A73-38855

Application of distributed p-n and p-i-n structures in the development of integrated circuits for electrically controlled SHF devices

20 p2535 A73-38856

Selection of conditions for the fabrication of planar n-p-n silicon transistors with the application of the ion-beam alloying method

20 p2535 A73-38858

Mobile IC coherent radar with computerized display and calibration, incorporating cold cathode crossed field amplifier tube in transmitter amplifier stage

20 p2528 A73-38871

Ion implanted megohm silicon monolithic IC resistors with buried n-guard layer protection against slice-to-slice variations of fixed surface charge

20 p2537 A73-39416

Mathematical equipment of a system of automatic designing of components of logic-type semiconductor integrated circuits

21 p2660 A73-40015

Morphological indices of digital microelectronic structures

21 p2660 A73-40016

Synthesis of combination circuits in a universal basis and its use in estimating the complexity of digital structures containing integrated circuits

21 p2668 A73-40017

Microwave IC devices covering circulators, directional couplers, frequency multipliers, phase shifters, power amplifiers and reference oscillators, discussing technological development and applications

21 p2668 A73-40019

Physical modeling of active microcircuits for the SHF range

21 p2668 A73-40020

Design of MOS-transistor integrated-circuit amplifiers

21 p2660 A73-40021

Electronic integrated HF selective gyrator for TV IF filter development

21 p2661 A73-40230

A bilevel thin film hybrid circuit containing crossovers, resistors, capacitors, and integrated circuits.

21 p2669 A73-40773

Operation, design and applications of inductorless digital IC selective N-path filters

21 p2664 A73-41099

CODYMOS frequency dividers achieve low power consumption and high frequency.

21 p2670 A73-41111

An automated system for designing integrated circuits

21 p2666 A73-41305

An effective algorithm for optimizing electronic circuits

21 p2671 A73-41312

Eye movements of trained inspectors recorded during visual inspection of colored slides of IC chips, determining performance with emphasis on speed

23 p2947 A73-43212

Hybrid fluid logic systems for integrated circuits using static and dynamic logical elements, considering fluidic circuits design with redundancy

23 p2943 A73-43411

Malfunction diagnostics in digital integrated-circuit devices

23 p2956 A73-43581

V groove MOS transistor fabrication by preferential silicon etching and masking process with noncritical alignment tolerances

23 p2960 A73-44115

Designing with microprocessors instead of wired logic asks more of designers.

23 p2956 A73-44122

Calculation of the nonstationary electric field, carrier concentration, and current distribution in semiconductor integrated circuits

24 p3119 A73-45177

Four-quadrant analog multiplier synthesis for IC implementation based on logarithmic addition in all n-p-n bipolar transistor configuration for algebraic product derivation

24 p3074 A73-45260

INTEGRATION [REAL VARIABLES]

U MEASURE AND INTEGRATION

INTEGRATORS

NT DIGITAL INTEGRATORS

Automation of solutions to mathematical physics problems described by partial differential equations

01 p0019 A73-10100

Differentiators and integrators with RC circuits for piezoelectric transducer signals, noting instrument errors and SNR

07 p0827 A73-20534

Electronic six-channel phase shifter

08 p0950 A73-21715

The motion of a dynamically unbalanced gyroscopic linear-acceleration integrator

09 p1081 A73-22344

Optimal control of n-order system with transport delay by variational calculation, comparing with proportional integrator /PI/ controller

09 p1069 A73-22974

A new FM system with a novel modulator design yielding high linearity and thermal stability.

09 p1058 A73-23430

Operational amplifier integrator for storage element in track-hold circuit, discussing drift rate reduction with large equal-value resistors from input terminal to ground

16 p1988 A73-33398

Single-loop delay line integrator SNR enhancement properties in additive zero mean correlated noise channels for finite signal observation times

16 p1979 A73-33406

Low cost beam current integrator for use with dc accelerators in ion implantation experiments

17 p2175 A73-35759

Considerations concerning the evaluation of the detection probability in radar systems

21 p2650 A73-40500

Errors of a single-axis gyrostabilizer as an angular velocity integrator

22 p2860 A73-42366

INTEGRODIFFERENTIAL EQUATIONS

U DIFFERENTIAL EQUATIONS

U INTEGRAL EQUATIONS

INTELLECT

Intellectual ability and performance on a non-verbal problem-solving task.

03 p0260 A73-13553

INTELLIGENCE

NT ARTIFICIAL INTELLIGENCE

NT INTELLECT

Organism-machine interactions in hybrid control systems for cardiac stimulation, artificial breathing apparatus and intelligence assignments

09 p1047 A73-23298

Extraterrestrial intelligent life existence possibility in terms of hypothesis involving earth as wilderness area or zoo with failure of interaction with other civilization

24 p3058 A73-44554

Communication possibilities between earth and technologically advanced galactic civilizations, discussing radio astronomy requirements, technology differences and communication distance estimates

24 p3133 A73-44555

Project Cyclops investigation of extraterrestrial civilization signal detection, discussing microwave apparatus, frequency bands, antenna arrays and research implementation proposals

24 p3134 A73-44561

INTELLIGIBILITY

NT SPEECH RECOGNITION

Speech scrambling by the matrixing of amplitude samples.

21 p2657 A73-41206

INTELSAT SATELLITES

Progress in commercial satellite communications.

03 p0381 A73-13200

Current and near future data transmission via satellites of the Intelsat network.

03 p0280 A73-14659

Permanent arrangements for the global commercial communications satellite system of INTELSAT.

04 p0523 A73-15148

Single channel per carrier FCM FDMA demand assignment satellite communications system /SPADE/ for INTELSAT, discussing hardware and software introduction at first terminal

04 p0420 A73-15414

High capacity, dual antenna earth station.

04 p0432 A73-15416

Communications, despin control, electrical power telemetry and command, positioning and orientation subsystems of Intelsat 4 satellite

09 p1152 A73-22696

Launch and orbital injection of Intelsat IV satellites.

09 p1152 A73-22699

Intelsat 4 communications system, discussing radio transponders, earth stations, and multiple access, modulation and multiplexing methods

09 p1051 A73-22700

Intelsat 3 power system design and orbital performance, discussing solar arrays, cell bypass, output, conversion efficiency, regulation, reliability and testing

09 p1153 A73-22787

Intelsat 4 power subsystem with solar panels, Ni-Cd batteries, controller and relays for bus paralleling, discussing spacecraft and system configurations and performance

09 p1154 A73-22788

Intelsat communication satellites global network analysis, investigating technical factors affecting design options

09 p1059 A73-23436

A shipboard satellite communication experiment.

12 p1473 A73-27675

Transmission characteristics of PSK wave in nonlinear system - Application to INTELSAT IV satellite systems.

13 p1586 A73-29234

Evaluation of Intelsat IV nickel-cadmium cells.

13 p1572 A73-29582

Book - The politics and technology of satellite communications.

14 p1818 A73-29949

Space radiation environment effects on Intelsat 4 design, emphasizing trapped electrons and protons influences on solar cell shielding requirements

17 p2108 A73-34864

Investigations of the Intelsat IV bearing and power transfer assembly.

17 p2238 A73-34867

Prototype TDMA system design for Intelsat 4 satellite, discussing separate synchronization and data bursts transmission feature for service quality and reliability improvement

17 p2122 A73-34967

Time division multiple access in the INTELSAT system.

17 p2124 A73-35306

Technological trends in commercial satellite communications.

18 p2290 A73-37034

Design features of an unattended earth terminal for satellite communications.

20 p2522 A73-38716

Error rate of a 4-phase coherent PSK satellite channel with non-Gaussian interference.

20 p2523 A73-38721

Ground stations in Intelsat 4 communication satellite radio relay system, discussing all-solid-state equipment design, carrier frequency assignment and antenna installation

20 p2523 A73-38723

A satellite-switched SDMA/TDMA system for a wideband multibeam satellite.

20 p2524 A73-38730

Communication satellite history and present developments, discussing Intelsat and ATS programs and TDMA techniques

20 p2526 A73-38747

Applications of error-correcting codes to TDMA satellite communications.

20 p2526 A73-38751

INTENSIFICATION

U AMPLIFICATION

INTENSIFIER TUBES

U IMAGE INTENSIFIERS

INTENSIFIERS

NT IMAGE INTENSIFIERS

NT IMAGE ORTHONICS

INTERACTIONS

NT AIR WATER INTERACTIONS

INTERATOMIC FORCES

Magnetic absolute zero behavior with restriction to three order parameter theory, showing metallic band resultant from interatomic Coulomb energy ratio to bandwidth

06 p0734 A73-17835

Correlation between the diffusion activation energy, the heat of fusion, and the bond energy in metals

06 p0708 A73-18046

On the analysis of glory scattering data for the extraction of information on the interatomic potential well. 09 p1122 A73-22072

Brittle cleavage crack propagation in crystals in terms of bonds acting between pairs of atoms, considering stress distribution around crack tip 11 p1409 A73-25812

Diffraction spectra and electron density distributions of interatomic graphitizing carbon molecule bonds as polymer combinations, using diffractometer and scintillation counter recording 14 p1767 A73-30839

Short-acting repulsive forces between atoms and molecules of atmospheric gases 19 p2462 A73-37350

Polarizability of interacting atoms - Relation to collision-induced light scattering and dielectric models. 21 p2742 A73-40211

Calculation of the physicochemical constants of metals associated with the strength of interatomic bonds 22 p2874 A73-42097

Electrostatic Hellmann-Feynman theorem applied to long-range interatomic forces - The hydrogen molecule. 24 p3113 A73-44981

Dependence of electrical erosion on the interatomic bond strength in binary titanium alloys 24 p3101 A73-45514

INTERCEPTION

Differential games applied to some interception models 18 p2268 A73-37080

New missile guidance concepts as applied to command guidance control system. [AIAA PAPER 73-855] 20 p2584 A73-38778

INTERCEPTOR AIRCRAFT

U FIGHTER AIRCRAFT

INTERCONTINENTAL BALLISTIC MISSILES

NT MINUTEMAN ICBM

The application of digital filters using observers to the design of an ICBM flight control system. [AIAA PAPER 73-845] 20 p2541 A73-38784

INTERCOSMOS SATELLITES

Apparatus PG-1 for the study of the radiation characteristics in the neighbourhood of the earth by satellite Interkosmos 3. 01 p0051 A73-11021

Investigations of high-energy charged particles and VLF radiation with the Interkosmos 3 satellite. 05 p0608 A73-16085

Interkosmos 2 satellite design, construction, on-board scientific instrumentation, ionospheric experiments and data processing equipment 10 p1217 A73-23886

Interkosmos 5 investigation of VLF electromagnetic signals and emissions, discussing onboard instruments to measure particle fluxes 13 p1622 A73-29662

Interkosmos satellite-borne X ray polarimeter measurements of solar flares 18 p2345 A73-36144

Localization of sources of two-hop whistlers observed aboard the Interkosmos 3 satellite over Europe. 19 p2404 A73-38021

Interkosmos 2 satellite design, construction, on-board scientific instrumentation, ionospheric experiments and data processing equipment 20 p2565 A73-38905

Interkosmos 6 cosmic ray shower experiment using emulsion stack, spark chamber and scintillation counter to measure particle energy, angular distribution and production multiplicity 23 p2981 A73-43540

INTRACRANIAL CIRCULATION

Xenon 133 measurement of cerebral volumetric circulation rates during papaverin and intensin vasodilation of canine and feline intracranial vessels, showing vessel resistance reduction 13 p1576 A73-29074

Intracranial hemodynamic changes in pilots to tilting. 18 p2279 A73-36916

INTERFACE STABILITY

Wave motion of low-tension interfaces with electrical double layers. 02 p0196 A73-12038

Growth of ternary composites from the melt. I, II. 04 p0463 A73-15310

Stresses in laminated composites containing a broken layer. [ASME PAPER 72-WA/APM-14] 04 p0516 A73-15899

Optimal stabilization of the Rayleigh-Taylor instability in the multiarm fluid pendulum. 09 p1119 A73-21942

Parallel magnetic field effect upon plane interface stability between two conducting viscous fluids in uniform relative motion, obtaining neutral shear flow stability curves 11 p1402 A73-25054

Microscopic, kinetic and microhardness observations of Ti-W metal matrix composite solid state interface reactions, showing enhanced shear resistance 11 p1384 A73-26049

The effect of fibre-matrix interface strength on the impact and fracture properties of carbon-fibre-reinforced epoxy resin composites. 12 p1515 A73-26922

Nonlinear stability of a liquid film adjacent to a supersonic stream. 14 p1711 A73-30166

Investigation of the bond strength between layers of textolite materials 17 p2194 A73-34333

Instability of the interface between colliding metal surfaces 21 p2707 A73-40706

Electrohydrodynamic Rayleigh-Taylor instabilities of a plane circular interface. 21 p2749 A73-41626

INTERFACES

NT FLUID BOUNDARIES

NT GAS-SOLID INTERFACES

NT JET BOUNDARIES

NT LIQUID-LIQUID INTERFACES

NT LIQUID-SOLID INTERFACES

NT LIQUID-VAPOR INTERFACES

NT SOLID-SOLID INTERFACES

INTERFACIAL ENERGY

Carbon fibre adhesion to organic matrices. [ONERA, TP NO. 1173] 01 p0068 A73-11499

Square well fluid liquid-vapor interface density profiles from perturbation expansion in chemical potential, comparing to BGYB and excess free energy minimization approaches 03 p0342 A73-13277

Effects of alloying on structural stability and cohesion between phases in oxide/metal composites. 03 p0326 A73-13964

Effect of microstructure on measurements of fracture energy of Al2O3. [ACS PAPER 44-BN-71P] 08 p0983 A73-21842

Measurement of interfacial free energies and associated temperature coefficients in 304 stainless steel. 13 p1634 A73-28259

INTERFACIAL STRAIN

U INTERFACIAL TENSION

INTERFACIAL TENSION

Wave motion of low-tension interfaces with electrical double layers. 02 p0196 A73-12038

Selection of a surface tension propellant management system for the Viking 75 Orbiter. [AIAA PAPER 72-1042] 03 p0381 A73-13377

Calculation of the natural oscillations of an ideal liquid in an axisymmetrical container with allowance for surface forces 03 p0294 A73-13607

Cylindrical pores in viscous incompressible liquid film, considering existence duration and pore wall motion under surface tension forces 07 p0923 A73-20420

On the influence of deformation rate on intergranular crack propagation in Type 304 stainless steel. 09 p1100 A73-22000

Certain two-dimensional problems with discontinuous displacements in the theory of elasticity and their application to problems of dislocation-surface propagation 09 p1158 A73-22358

Application of the fluctuation model of superplasticity to calculate the surface tension of metals during phase transformations 10 p1235 A73-24455

Solid sphere meandering trajectory in viscous liquid filled cylinder, postulating oscillating molecular surface tension layer at interface 10 p1206 A73-24701

The free surface on a liquid between cylinders rotating at different speeds. II. 10 p1207 A73-24790

Generalized van der Waals theories for surface tension and interfacial width. 11 p1400 A73-26214

An existence proof for permanent capillary gravity waves with general vortex distributions 11 p1349 A73-26747

The employment of an extended theorem of corresponding conditions in the computation of the surface tension of pure substances 14 p1776 A73-30124

Two-dimensional bubbles in slow viscous flows. II. 14 p1744 A73-30170

Hydrodynamics in weak gravitational fields - Small oscillations of an ideal liquid in a cylindrical vessel 15 p1861 A73-31280

Fluctuation model of superplasticity and surface tension of a metal at a phase transition. 19 p2442 A73-38137

A note on residual drop and single drop formation. 22 p2840 A73-41748

Transmission of anti-plane shear waves past an interface crack in dissimilar media. 23 p3043 A73-43815

Wettability and interfacial tension of magnesia single crystals by molten magnesium oxide-aluminum trioxide-silicon dioxide glasses, discussing contact angle relationship to temperature 23 p2998 A73-44132

Surface tension and interfacial density profile of fluids near the critical point. 24 p3110 A73-44986

INTERFERENCE

Characteristics of interference pattern formation during a self-reproduction process 09 p1096 A73-22858

Electrical interference /noise/ effects on measurements of high accuracy low-level differential data signals, discussing noise reduction, capacitive coupling problem and design principles 10 p1189 A73-24570

Study of a narrow-band interference filter at various angles of incidence 16 p2012 A73-32844

Quantum interference effects due to singlet-spin pairing in superconductors, considering normal metal, electron correlations, single particle excitations, thermodynamic properties and ideal superconductors 21 p2752 A73-40642

Interference structure of oscillating point charge near resonance cone in warm magnetized collisionless plasma, relating structure location to cyclotron frequency and plasma parameters 22 p2891 A73-42242

INTERFERENCE FACTOR TABLE

Performance of M-ary PSK systems in Gaussian noise and intersymbol interference. 06 p0665 A73-18140

INTERFERENCE GRATING

Interference grating production for viscoelasticity investigation by moire method, noting tensile tests of viscoelastic plates 03 p0306 A73-13159

A dynamic holographic grating for a mode of operation with peaks 04 p0447 A73-14884

Three dimensional models images information content increase in coherent light by interference shadow marking, noting automatic systems for distant objects recognition 07 p0824 A73-20140

The use of solid etalon devices as narrow band interference filters. 08 p0970 A73-21736

Moire gauging by projected interference fringes. 13 p1616 A73-28600

Diffraction gratings manufacture by holographic recording of laser beam generated interference fringes on photosensitized surfaces, describing etching and metallization process 15 p1875 A73-31417

Josephson junction interference grating. 17 p2219 A73-34915

Nondestructive optical contour mapping for non-contact testing of reflecting surface deformations from interference pattern due to monochromatic illumination of grating 17 p2172 A73-35419

Non-linearity of visual signals in relation to shape-sensitive adaptation responses. 19 p2394 A73-37418

Perturbation analysis of holographic grating couplers in thin film waveguides, discussing coupling efficiency dependence on evanescent tail length, refractive index and gelatin film thickness 21 p2699 A73-40149

Interference filters for the VUV /1200-1900 A/. 22 p2863 A73-43142

Multiple-beam lateral-shear interferometer. 22 p2863 A73-43146

INTERFERENCE LIFT

Simplification of the wing-body interference problem. 01 p0001 A73-10048

The significance of the aerodynamic jet interference for the development and the testing of the V/STOL transport DO 31. [DGLR PAPER 72-106] 02 p0127 A73-11651

Aerodynamic interference between jet propulsion system and airframe for supersonic transport with wing-mounted nacelles, noting wing performance role in lift effectiveness 03 p0243 A73-13428

A general solution for lift interference in rectangular ventilated wind tunnels. [AIAA PAPER 73-209] 05 p0563 A73-16940

INTERFERENCE MONOCHROMATIZATION

U DIFFRACTION

INTERFEROGRAMS

U INTERFEROMETRY

INTERFEROMETERS

NT FABRY-PEROT INTERFEROMETERS

NT INFRARED INTERFEROMETERS

NT MACH-ZEHNDER INTERFEROMETERS

NT MICHELSON INTERFEROMETERS

NT MICROWAVE INTERFEROMETERS

NT PHASE SWITCHING INTERFEROMETERS

NT RADIO INTERFEROMETERS

Diffraction limited astronomical telescope resolution retrieval by speckle interferometer, noting information extraction via Fourier analysis

01 p0049 A73-10536

Measurement of particle size, number density, and velocity using a laser interferometer.

01 p0053 A73-11226

Talbot shearing interferometer based on Fourier imaging behind grating illuminated by plane monochromatic wave with spatial filtering, obtaining radial and lateral derivatives

01 p0053 A73-11227

Earth based and spaceborne stellar interferometer with optical balanced mixer system for coherent detection, discussing principles, construction, SNR and sensitivity

02 p0170 A73-12341

Laser interferometer for measuring high velocities of any reflecting surface.

02 p0171 A73-12818

Wavelength dependence of moire patterns

05 p0577 A73-16822

An antiresonant ring interferometer for coupled laser cavities, laser output coupling, mode locking, and cavity dumping.

09 p1091 A73-22085

A temperature interferometer using laser holography.

09 p1083 A73-22510

Frequency selection schemes based on combined use of dispersive prism and interferometer in laser resonator

09 p1097 A73-23012

Displacement comparator based on laser interferometer with photoelectric counter for monitoring inside and outside dimensions of cylinder bores, shafts, spheres, etc

11 p1364 A73-26103

Reflection plate interferometer with thin glass shearing plate replacing knife edge in Schlieren system, noting optimum operating range and fringe spacing

11 p1365 A73-26238

Error in the interferometric measurement of length by the rotational movement of a mirror and multipass corner cube arrangement.

11 p1365 A73-26240

A SISAM interferometer and a simple Michelson-interferometer with spherical mirrors for space application.

11 p1369 A73-26519

Investigation of coherence with the aid of the diffraction shearing interferometer.

12 p1507 A73-27515

Satellite tracking interferometer systems with three steerable directional antennas mounted over azimuth mounts near Lichtenau/German Federal Republic/

14 p1742 A73-30100

The Budrio station of the meteoric radar system of the CNR for the systematic study of the upper atmosphere

17 p2147 A73-34959

Rapid interferometric technique for MTF measurements in the visible or infrared region.

17 p2171 A73-35404

Wavefront investigation of a Fourier transform lens with the fan trace interferometer.

17 p2172 A73-35427

A tilted plate interferometer for heat transfer studies.

20 p2564 A73-38879

Inexpensive portable vibration-insensitive wave front shearing interferometer developed at NBS for lens testing

21 p2704 A73-41259

Interference patterns and operation of four unit interferometer consisting of beam splitter, mirrors and analyzer

21 p2704 A73-41261

Holographic shearing interferometer using two linearly polarized reference light beams with application to refractivity and density gradient measurements in aqueous solutions

24 p3088 A73-44406

A 337-micron HCN laser interferometer for plasma diagnostics.

24 p3097 A73-45410

INTERFEROMETRY

NT DIFFERENTIAL INTERFEROMETRY

Interferometric measurements of the vibrostability of a holographic stand

01 p0050 A73-10798

Holographic interferometry in materials research and fracture mechanics.

01 p0051 A73-11002

Holo-diagram coherent optics device for studying interference patterns of object near focal points representing illumination and/or observation points

01 p0053 A73-11220

Interferometric testing of large optical components with circular computer holograms.

01 p0053 A73-11225

Double exposure holographic interferometry for comparison of object of two points in time evolution,

discussing space division multiplexing of exposures onto photographic plate

01 p0054 A73-11234

Observations at 408 MHz of the Cyg X-3 radio outburst.

02 p0204 A73-11552

Very long baseline interferometry observations of radio emissions from geostationary satellites.

02 p0215 A73-12270

Vibrational analysis with the aid of holographic interferometry vibrational analysis of acoustic radiators with the aid of holographic interferometry

03 p0306 A73-12985

Interferometric studies on Apollo 11 and Apollo 12 lunar glass objects.

03 p0369 A73-13096

Geodetic satellite timing accuracies with Loran C, portable atomic clocks and long baseline interferometry

04 p0446 A73-14807

Properties of photons determined by interferometric spectroscopy.

04 p0475 A73-15046

Interferometric CW radar for group delay difference measurement of reflected signal components in ionospheric sounding

05 p0548 A73-16253

Holographic interferometry techniques and applications, discussing gas and ruby lasers in imaging, measurements and NDT of materials and mechanical components

05 p0574 A73-16286

Velocity measurements made holographically of diffusely reflecting objects.

05 p0574 A73-16287

Finite fringe holographic interferometry applied to a right circular cone at angle of attack.

[ASME PAPER 72-APM-PP] 05 p0527 A73-16528

A triple-exposure technique to reduce recording time in stroboscopic holographic interferometry.

05 p0576 A73-16557

Wavefront sampling in holographic interferometry.

05 p0579 A73-17223

Electro-optical fiducial system for shock wave interferometry relating impact time to free surface motion

05 p0580 A73-17261

Some applications of interferometry in coherent light

05 p0586 A73-17321

Interferometric observations of Mars at 21-cm wavelength.

06 p0747 A73-17491

Application of holographic subtraction to time-average hologram interferometry of vibrating objects.

06 p0691 A73-17499

Microwave or acoustic holographic synthetic aperture interferometry with pulsed techniques, noting single scan, resolution and fringe number advantages

07 p0824 A73-20110

IR interferometry with heterodyne detection and tuned laser focusing for stellar envelopes, interstellar dust, planetary surfaces and low temperature sources observation

07 p0825 A73-20242

Wavefront tilter for double-exposure holographic interferometry.

08 p0963 A73-20874

Image contrast increase in holographic interferometry, using double exposure technique with reference beam half-wavelength phase shift

08 p0964 A73-21053

Time variable field recording and reconstruction theory and wave equations of holography and holographic interferometry, including double exposure and time averaged techniques

08 p0965 A73-21137

Holographic interferometry applied to aerodynamics [ONERA, TP NO. 1161F] 08 p0968 A73-21677

Length measurement interferometry principles and limitations imposed by available coherent sources, discussing laser source techniques and fringe counting method

09 p1093 A73-22313

Holographic laboratory practice for NDT, discussing data reduction, display and pulse laser development

09 p1083 A73-22513

Simple method of obtaining high-sensitivity interferograms

09 p1085 A73-22882

Accuracy of interferometric plasma investigations involving heating of the optical elements

09 p1131 A73-22883

Defect detection in solid materials with the aid of holographic vibration analysis

09 p1089 A73-23115

Some investigations on the methods of measuring 3-dimensional plastic deformations by laser.

09 p1086 A73-23321

Holographic interferometry as nondestructive testing method, discussing applications to defects detec-

tion in tires, metal-rubber vibration isolators and glass fiber reinforced plastic tubing

10 p1218 A73-24173

A new interpretation of interferometric fringe patterns.

10 p1220 A73-24661

Holographic contour mapping using a dye laser.

10 p1221 A73-24874

Interference measurement techniques for small phase difference changes, noting diffraction and noise effects as limiting factors

10 p1222 A73-24945

Accuracy of statistical measurements of random field characteristics in interferometric systems

11 p1360 A73-25020

Self-consistent and direct reading laser homodyne measurement technique.

11 p1360 A73-25063

Comment on: Holographic interferometry applied to measurements of small static displacements of diffusely reflecting surfaces.

11 p1360 A73-25064

Holographic interferograms for demonstration of acoustic field near supersonic air, nitrogen and helium jets, noting generated Mach wave convection velocity

11 p1346 A73-25382

Hologram interferometry adaptation to industrial conditions for dimensions, deformation, vibration and refractivity measurements, noting advantages over ordinary interferometry

11 p1370 A73-26540

Nondestructive flaw detection by holographic interferometry, discussing methods, equipment and applications for materials testing and vibrational analysis

11 p1371 A73-26551

Interferometric studies of interstellar CH₄/molecules.

11 p1427 A73-26617

The determination of Mode I stress-intensity factors by holographic interferometry.

12 p1550 A73-27021

Multibeam holographic spectroscopy

12 p1497 A73-27453

Optical interferometry for ultrasonic surface wave detection, using two coherent light beams focusing for recording standing wave ratio, attenuation, transmission and harmonic content

13 p1613 A73-28497

Conditions of anastigmatization for Rowland assemblies fitted with concave holographic networks

13 p1613 A73-28567

Optical method for studying the heat transfer mechanism in bubble boiling

13 p1708 A73-29173

Measurement of the radius of curvature of a laser beam by an interferometric method.

13 p1629 A73-29442

Influence of atmospheric parameters on the wavelength of single-frequency laser radiation

14 p1756 A73-30023

The concept of the flight safeguard interferometer for rocket probes of the French Guiana Space Center

14 p1773 A73-30096

Interferometric and thermoanemometric methods of studying binary boundary layers

15 p1876 A73-31859

Correlation interferometric measurement of trace species in the atmosphere.

[AIAA PAPER 73-515] 16 p2006 A73-33552

Angle-of-arrival difference spectrum of a simple interferometer in turbulent air.

16 p2037 A73-33683

Interferometric surface strain measurement with optical strain gage using laser-generated interference pattern with linear fringe motion-intensity relation [SESA PAPER 2158A] 17 p2173 A73-35453

Analysis of a method for obtaining near-diffraction-limited information in the presence of atmospheric turbulence.

19 p2461 A73-38485

Image reconstruction from the modulus of the correlation function - A practical approach to the phase problem of coherence theory.

20 p2570 A73-38616

High-speed interferometry of expanding and collapsing laser produced plasma.

21 p2744 A73-39964

Optical diffraction grating design and production, discussing application of interferometry and electronics to ruling engine control

21 p2698 A73-40136

Two wavelength variable sensitivity interferometry, extending static technique to real time dynamic testing

21 p2698 A73-40138

Phase measurement microscopy consisting of phase modulation optical system using interferometry and optical heterodyning, and phase detection system using digital processing

21 p2698 A73-40144

Rear projection holographic and interferometric viewing screens using deflected and scattered light, discussing microfilm reading applications, dichromated gelatin film and laser exposures

21 p2699 A73-40151

Direct determination of universal time based on east-west interferometer observations of radio sources using 5 km radio telescope

21 p2739 A73-40373

Temperature distribution measurement for air about hot object by double exposure interferometry, using beam from He-Ne laser

21 p2701 A73-40625

Interferometric test of an f/8, 24-inch /60.96 cm/ diameter paraboloidal mirror in the atmosphere.

21 p2704 A73-41260

Possible scientific utilization of long laser bases

21 p2716 A73-41328

Some characteristics of an operational system for measuring UT 1 using very long baseline interferometry.

21 p2705 A73-41330

Two frequency radar interferometry applied to the measurement of ocean wave height.

22 p2843 A73-41832

Interferometric measurements of apparent stellar diameters

22 p2863 A73-43102

Tracking the Apollo Lunar Rover with interferometry techniques.

23 p2953 A73-43356

Laser Doppler interferometry for measuring small absorption coefficients.

24 p3090 A73-44924

INTERGALACTIC MEDIA

Intergalactic matter existence experiments, discussing critical cosmological energy and matter density, neutral and ionized gas, clustering and hot media

01 p0094 A73-10060

Intergalactic ionized hydrogen in nearby groups of galaxies.

02 p0225 A73-12803

Long time optical variability model of quasars and Seyfert galaxies in terms of grain extinction variations in intervening clouds due to thermal and atom impact evaporation

02 p0226 A73-12839

Theoretical models of photoionized intergalactic hydrogen.

03 p0365 A73-12926

Tidal generation of narrow intergalactic filaments from computer simulations, discussing alternative models

03 p0372 A73-13353

Expansion hypothesis and assumption of invisible intergalactic matter in galactic clusters stability theory, noting IR spectroscopy and radio observation

05 p0623 A73-17196

The possibility that nongaseous hydrogen supplies the missing cosmological mass.

05 p0625 A73-17328

Physics of the X-radiation from clusters of galaxies.

07 p0874 A73-19074

Nonprimordial hypothesis for cosmic microwave background radiation generation by ordinary astronomical processes and subsequent thermalization by interaction with dust grains

08 p1008 A73-21152

The observation of relic radiation as a test of the nature of X-ray radiation from the clusters of galaxies.

09 p1138 A73-22953

Observational data and interpretation of infrared spectra and microwaves of galaxies and the intergalactic matter

09 p1150 A73-23143

X ray background emission and behavior of infalling intergalactic gas into Galaxy resulting from shock wave generation and heating in accretion process

10 p1264 A73-23495

Upper limits on an ionized intracluster medium in the Coma cluster.

10 p1272 A73-23545

Neutral hydrogen clouds gravitational binding of Coma cluster, providing mechanism for heating of diffuse gas between clouds and galaxies

13 p1684 A73-29352

Mariner 9 ultraviolet spectrometer experiment - Upper limits on the Lyman-alpha flux from clusters of galaxies.

15 p1936 A73-31551

Nonuniform model construction for dense intergalactic medium with gravitational binding of all galactic groups and clusters by ionized gas

19 p2484 A73-37608

Soft X-ray flux of the Coma cluster of galaxies.

19 p2475 A73-37626

Galaxy formation associated with active galaxies and the binding of rich clusters.

20 p2613 A73-39827

X ray background radiation intensity fluctuations from random discrete point sources, indicating extragalactic origin

21 p2759 A73-40710

Model for gas bridge and magnetic field connecting Magellanic Clouds from optical and radio polarization measurements

21 p2779 A73-41535

Effect of Gaunt factors on analysis of X-ray spectra - Viability of a thermal intergalactic medium in the Coma cluster.

22 p2900 A73-41753

Isothermal gas-sphere model with thermal bremsstrahlung for X ray emission from Coma, Perseus and Virgo galactic clusters, noting gas distribution

22 p2904 A73-43120

Ion-grain collision cooling rate for hot gas above million K, discussing applications to supernova explosions, Seyfert nuclei and intergalactic matter within galactic clusters

22 p2916 A73-43121

Magnitude-redshift and count-magnitude relations in presence of a uniform intergalactic absorption.

24 p3143 A73-45436

INTERGRANULAR CORROSION

Microstructure and microsegregation effects in the intergranular corrosion of austenitic stainless steel.

02 p0183 A73-12765

Influence of microstructure on the mechanical properties and stress corrosion susceptibility of 7075 aluminum alloy.

04 p0463 A73-15314

Surface layer grain boundary corrosion damage of Ti alloys during vacuum annealing, reducing rupture strength, vibration resistance and bending fatigue limit

06 p0698 A73-18205

On the influence of deformation rate on intergranular crack propagation in Type 304 stainless steel.

09 p1100 A73-22000

Grain-boundary corrosion of type 304 stainless steel by cesium oxides.

10 p1234 A73-24427

Study on the superposition of intergranular corrosion and pitting corrosion by fatigue cracking of stainless steels.

11 p1383 A73-25831

Service failures and fracture mechanisms under cyclic load at high temperature.

11 p1442 A73-25845

Dynamic potential method of estimating the susceptibility of corrosion-resistant steels to intercrystalline corrosion

11 p1364 A73-26112

On the study of the intergranular corrosion of a stainless steel with the help of twin crystals

11 p1385 A73-26297

On the relationship between grainboundary corrosion and stress corrosion cracking of Al-Zn-Mg alloys.

12 p1511 A73-27059

Corrosion properties and structural transformations of the N70M27 alloy containing vanadium and niobium

13 p1644 A73-29645

Mo and W alloying effects on low carbon chromium nickel steels intergranular corrosion resistance

13 p1644 A73-29648

Intergranular corrosion in iron and nickel base alloys.

15 p1888 A73-31739

Significance of intergranular corrosion in high-strength aluminum alloy products.

15 p1889 A73-31740

Scanning electron microscopic observation of fracture surfaces of austenitic stainless steels in stress corrosion cracking.

16 p2025 A73-33021

Fractography of stress corrosion cracks in aluminum alloy 7075.

21 p2720 A73-40925

Corrosion characteristics and structural transformations in alloy N70M27 with vanadium and niobium.

21 p2720 A73-41038

Mo and W alloying effects on low carbon chromium nickel steels intergranular corrosion resistance

21 p2721 A73-41041

Intergranular corrosion of iron-nickel-chromium alloys.

23 p2990 A73-43458

The stress corrosion of titanium materials - The present status of research

23 p2992 A73-43910

INTERIOR BALLISTICS

Russian book - Fundamentals of the theory of operational processes in solid-propellant rocket systems.

10 p1262 A73-23948

Design criteria for inert or consumable polymer cartridge materials.

15 p1925 A73-31919

INTERLACING DRAINAGE

U DRAINAGE PATTERNS

INTERLAYERS

NT MULTILAYER INSULATION

Heat transfer in horizontal annular air gaps at small Grashof numbers

09 p1167 A73-23108

Heat transfer law for free convection in cylindrical and spherical interlayers

11 p1450 A73-25726

Thin ferrosilicon intermediate cylindrical layer tensile strength, microhardness and yield point determination at 20-1000 C

13 p1624 A73-29064

Thin ferrosilicon intermediate cylindrical layer tensile strength, microhardness and yield point determination at 20-1000 C

18 p2320 A73-36896

INTERMEDIATE FREQUENCIES

Daily altitude variations of medium frequency radio waves reflection in ionosphere over Tsunemb, SW Africa, examining attenuation correlation with solar zenith angle

12 p1494 A73-27767

Spatial extent of the winter anomaly in absorption.

18 p2305 A73-36003

Degradation of probability of error due to IF filtering.

21 p2649 A73-40335

A computing digital phase meter

21 p2664 A73-41083

INTERMEDIATE FREQUENCY AMPLIFIERS

Microwave amplifier with internal negative feedback, using IF output for frequency modulation of mixer oscillator signal

06 p0677 A73-18394

Distribution of equivalent attenuations and generalized detunings in a stagger single-tuned IF amplifier with critical staggering.

10 p1197 A73-24936

Spread of transistor parameters as a factor in the design of IF amplifiers with pairs of staggered stages

10 p1197 A73-24937

INTERMEDIATE RANGE BALLISTIC MISSILES

NT POLARIS MISSILES

INTERMETALLICS

Structural studies of Laves intermetallic phase precipitation in Fe-Ta alloys by microscopic, X ray diffraction and electron probe techniques

02 p0182 A73-12754

Interdentritic structures of a directionally solidified cobalt-base alloy.

02 p0184 A73-12770

Intermetallics formation and diffusion of contacting Al-Au thin films dependence on temperature, thickness ratio and contact time

06 p0706 A73-17903

Interaction between the ZrCr2 intermetallic compound and some zirconium compounds with iron, cobalt, and nickel

06 p0708 A73-18056

Diffusion in the titanium-aluminum system. I - Interdiffusion between solid Al and Ti or Ti-Al alloys.

06 p0709 A73-18332

Diffusion in the titanium-aluminum system. II - Interdiffusion in the composition range between 25 and 100 at.% Ti.

06 p0709 A73-18333

Dynamic yield, compressional, and elastic parameters for several lightweight intermetallic compounds.

09 p1099 A73-21926

Thermal stability of the microstructure in the eutectic composition Al-Al3Ni

09 p1099 A73-21966

Crystalline structure of the Cr3AlB4 compound

10 p1259 A73-24066

Formation of continuous solid solutions of intermetallic compounds

10 p1260 A73-24512

Cerium-germanium system state diagram based on microstructural, differential thermal, dilatometric and X ray phase analyses, emphasizing intermetallics observation

10 p1260 A73-24684

The effect of brittle interfacial compounds on deformation and fracture of molybdenum-aluminum fiber composites.

13 p1636 A73-28794

Dislocation structure of Ni3Al intermetallic compound during various stages of deformation

14 p1760 A73-30591

Nickel niobide tested along crystal growth direction for twinning mode of intermetallic phase in tensile deformation, projecting crystallographic structure upon crystal plane

14 p1762 A73-30640

Saturation of Kh18N10T steel by molybdenum from the vapor phase

15 p1889 A73-31807

Investigation of the influence of certain elements on the heat resistance of titanium aluminide Ti3Al

15 p1894 A73-32530

Electric contact materials technology, discussing intermetallics, ordered alloys, metal matrix composites and silver, gold and platinum based dispersion hardened alloys manufacture and properties

16 p2027 A73-32946

Niobium-gold alloys crystal structure, phase diagrams, peritectic crystallization and microhardness, noting intermetallics formation by solid state reactions

16 p2026 A73-33957

Ti rich corner of Ti-Al alloys phase diagrams investigated by differential thermal analysis and radiography for thermal resistance and intermetallic compounds existence

19 p2441 A73-37838

- The nature of the interaction between scandium and aluminum in the aluminum-rich part of the Al-Sc system 21 p2718 A73-40486
- The influence of phase size on the creep of lamellar and particulate Al-CuAl₂ eutectic composites. 21 p2719 A73-40896
- AC conductivities of amorphous Ge-As-Te and Ge-As-Sc systems. 21 p2753 A73-41119
- Ternary systems: Rare earth metal - iron family metal - silicon /Component interaction and crystal structures of compounds/ 22 p2873 A73-42084
- Specific structural features of the phase diagrams of the Ti-Cr-V, Ti-Cr-Nb and Ti-Cr-Ta ternary systems 22 p2873 A73-42087
- Specific structural features of the binary phase diagrams of some transition metals in a region containing Laves phases 22 p2877 A73-42453
- Isothermal cross sections of the phase diagram of the nickel-molybdenum-tungsten system at 1200 and 700 C 22 p2877 A73-42459
- Al-aluminum nickelide eutectic fiber composite impact strength dependence on crystallization rate, examining crack propagation rate relation to fiber spacing 23 p2996 A73-43437
- Fracture behaviour of crystalline Al₃Ni intermetallic fibres. 23 p2991 A73-43774
- Saturation of steel Kh18N10T with molybdenum from the vapor phase. 24 p3100 A73-45270
- INTERMITTENCY**
- Thermal intermittency coefficient distribution across turbulent boundary layer as function of free stream turbulence level 01 p0031 A73-10412
- Dynamic loads intermittency effects on structural fatigue strength, discussing conditions for materials structural recovery during load pauses 03 p0385 A73-13137
- Statistical properties of intermittency in large scale turbulent flows, considering boundary layer, shear and convective flows 10 p1205 A73-23855
- Intermittency in fully developed turbulence as a consequence of the Navier-Stokes equations. 15 p1860 A73-31092
- Probability distribution of the concentration and intermittency in turbulent jets 15 p1862 A73-31286
- INTERMITTENCY HYPOTHESIS**
- The structure of internal intermittency in turbulent flows at large Reynolds number - Experiments on scale similarity. 20 p2546 A73-39090
- INTERMODULATION**
- Intermodulation noise and system analysis in SSB-FM multiple access system. 05 p0552 A73-17169
- Circuit model for characterizing the nearly linear behavior of avalanche diodes in amplifier circuits. [AD-757849] 06 p0677 A73-18738
- The effect of a nonlinearity upon signals in the presence of noise. 07 p0795 A73-20499
- Intelligible crosstalk and AM-FM transfer in commercial communication satellites. II 08 p0937 A73-20773
- Doppler effect intermodulation distortion derivation by perturbation method for loudspeaker modeled with pulsating sphere, considering boundary condition and nonlinear effect in wave propagation 08 p0987 A73-21123
- Interference protection of regenerative parametric amplifiers. 09 p1061 A73-22042
- Disturbances of directional radio due to echoes caused by high buildings 12 p1473 A73-27753
- Time-domain analysis of intermodulation effects caused by nonlinear amplifiers. 17 p2136 A73-34868
- Communication system with self limiting multiple access repeaters, calculating critical intermodulation power levels resulting from N equal amplitude carriers for comparison with measurements 20 p2526 A73-38750
- An investigation of the combined amplification of monochromatic and noise signals in a TWT. 20 p2529 A73-38930
- Equipment for measuring cross-modulation distortions in high-frequency power transistors 21 p2660 A73-40014
- Baseband modeling and distortion equalization of the DeLange FM oscillator by functional methods. 21 p2662 A73-40337
- Noise loading analysis of a memoryless nonlinearity characterized by a Taylor series of finite order. 21 p2656 A73-41147

- Radio receiver intermodulation characteristics description by generic model, discussing frequency/distance separation criteria to avoid interference, signal measurement procedure and application to equipment standards 22 p2823 A73-41801
- INTERMOLECULAR FORCES**
- Intermolecular potential energy curve crossing probabilities and associated phases determination for low energy elastic scattering cross section of He cations by Ne, noting rainbow effect 10 p1250 A73-23670
- Empirical intermolecular potentials for N₂ and CO₂ from crystal data. 15 p1915 A73-31272
- Evaluation of the intermolecular energy between two hydrogen molecules near the van der Waals minimum, from a perturbative procedure. 17 p2213 A73-35179
- Short-acting repulsive forces between atoms and molecules of atmospheric gases 19 p2462 A73-37350
- State variables and transport coefficients of binary gaseous mixtures. III - The calculation of transport coefficients with the aid of consistent potential parameters [DFVLR-SONDDER-280] 22 p2931 A73-42375
- Light scattering intermolecular and Raman spectra in liquid and solid hydrogen, showing short wave collective excitations in relation to phonon processes 23 p3007 A73-44171
- Reorientation /collision/ cross sections for hydrogen intermolecular potentials, taking into account quadrupole-quadrupole interaction effects 24 p3113 A73-44980
- INTERMONTANE FLOORS**
- U VALLEYS**
- INTERNAL COMBUSTION ENGINES**
- NT BRISTOL-SIDDELEY BS 53 ENGINE
- NT BRISTOL-SIDDELEY VIPER ENGINE
- NT DIESEL ENGINES
- NT GAS TURBINE ENGINES
- NT HELICOPTER ENGINES
- NT J-33 ENGINE
- NT J-85 ENGINE
- NT JET ENGINES
- NT PULSEJET ENGINES
- NT RAMJET ENGINES
- NT SUPERSONIC COMBUSTION RAMJET ENGINES
- NT TF-30 ENGINE
- NT TURBOFAN ENGINES
- NT TURBOJET ENGINES
- NT TURBOPROP ENGINES
- NT WANKEL ENGINES
- Simulation of unsteady gas exchange in internal combustion engines 02 p0202 A73-11632
- Comparison of modern aircraft engines with other power plants used in transportation 03 p0352 A73-13072
- Exhaust emission reduction through two-stage combustion. 07 p0921 A73-20361
- Piston engine turbocharging system based on split low and high pressure exhaust gas discharge porting, discussing different turbine staging arrangements 10 p1263 A73-24925
- Mechanism of the formation and control of pollutants due to combustion 15 p1840 A73-31225
- Analysis of the process of combustion of a single dose of liquid fuel in a constant-volume chamber 24 p3158 A73-45384
- INTERNAL ENERGY**
- Nonequilibrium thermodynamics description of convective motion, using internal energy and absolute mass flows as generalized convective flow 01 p0123 A73-10867
- Nuclear energy sources in superdense celestial bodies. 01 p0106 A73-11311
- Reversible instantaneous deformations and internal energy in viscoelastic incompressible fluids, using Oldroyd and De Witt hydrodynamic models 03 p0296 A73-14053
- The effect of gravity on the thermal and caloric measurements for pure fluid substances at the critical point 03 p0400 A73-14634
- Determining the technical cohesive strength of polycrystalline metals from the internal energy. 09 p1106 A73-23158
- Elastic impact against a beam with allowance for internal energy absorption 11 p1433 A73-25032
- Asymmetric mechanics of turbulent flows - Energy and entropy 12 p1487 A73-27411
- Nonequilibrium thermodynamics description of convective motion, using internal energy and absolute mass flows as generalized convective flow 12 p1560 A73-27917

- Turbulent flow energy transfer paths and irreversible dissipation as internal thermal energy analyzed by Reynolds convention for turbulent velocity 13 p1605 A73-29267
- Irreversible thermodynamics with internal inertia - Principle of stationary total dissipation. 14 p1817 A73-30484
- Charge-storage diodes with an internal field in the base 15 p1851 A73-31774
- Critical slope of the vapor pressure curve of a pure substance. 22 p2932 A73-42506
- Studies of the relaxation of internal energy of molecular hydrogen. 22 p2898 A73-42762
- INTERNAL FRICTION**
- Internal friction study of intercrystalline phosphorus adsorption during temper brittleness development in iron alloys 01 p0064 A73-10608
- Internal friction and heat release in engineering and tool steels in the presence of intense ultrasonic oscillations 01 p0065 A73-10926
- The effects of viscous friction on axial rotation of celestial bodies. 02 p0216 A73-12376
- Effect of hydrogen on internal friction in molybdenum 03 p0327 A73-13975
- Frequency dependence of the damping of mechanical vibrations in some commercially pure metals 03 p0327 A73-13976
- Internal friction in polycrystalline copper foils after alpha-irradiation at 78 K 03 p0328 A73-14653
- Dislocation-point defect interactions in fatigued pure aluminum 05 p0588 A73-17231
- Continuous measurement of internal friction and modulus with a regenerative feedback loop and composite oscillator. 05 p0559 A73-17255
- Influence of the dose of neutron irradiation on the anelastic behavior of an aluminum deformed at 80 K 06 p0710 A73-18542
- Mechanical properties of lunar soil - Density, porosity, cohesion, and angle of internal friction. 07 p0898 A73-19902
- Grain-boundary internal friction of copper-nickel alloys 09 p1099 A73-21965
- Correlation between pore formation at grain boundaries and internal friction during creep of nickel 09 p1099 A73-21970
- Austenitic alloys internal friction and strain aging under quenching, cold working and electron irradiation, considering carbon vacancies stress induced reorientation effects 09 p1101 A73-22407
- High temperature mechanical properties measurements verifying metal polycrystal internal friction background origin in diffusion of vacancies formed under grain boundary loading 09 p1105 A73-23060
- Small parameter method, with the parameter proportional to the friction forces, in the case of forced vibrations of complex trusses 11 p1435 A73-25395
- Relaxation processes in metastable beta titanium alloys. 11 p1385 A73-26498
- The heating of the thermosphere by atmospheric gravity waves 12 p1493 A73-27758
- Vibrations of a system with memory, non-linear elasticity, friction and relaxation. 13 p1690 A73-28055
- Relaxation spectra of niobium irradiated at low temperature. 13 p1638 A73-29455
- Mechanical behavior of high-strength beta-titanium alloys. 13 p1638 A73-29456
- Low-temperature internal friction in boron fibers 14 p1766 A73-30380
- Atomic modeling of internal friction in solids, considering paraelastic point defects relaxation time 16 p2037 A73-33227
- Anelastic studies of hydrogen diffusion in niobium. 17 p2193 A73-35622
- Internal low-frequency friction in niobium in a normal and superconducting state 18 p2323 A73-36676
- Internal friction in niobium quenched from premelting temperatures 18 p2324 A73-36772
- Material damping - An introductory review of mathematical models, measures and experimental techniques. 19 p2500 A73-38105
- High-temperature internal friction in boron fibers 22 p2880 A73-41957

INTERNAL PRESSURE

- Fracture strength of helical-wound composite cylinders. 01 p0117 A73-11121
- Finite axisymmetric deformations of elastic membranes. 02 p0234 A73-12089
- Variable thickness orthotropic shell of revolution with bending suppressed. 05 p0633 A73-16537
- Two types of loss of stability and strength in cylindrical shells 05 p0634 A73-16747
- Time variable stress-strain state of viscoelastoplastic hollow sphere under internal pressure, using piecewise linear differential law 05 p0635 A73-17080
- Dynamic behaviour of thin cylindrical shells subjected to high-speed travelling inner pressures. 06 p0758 A73-17518
- Effects of shearing force and rotary inertia to dynamical behaviours of thin cylindrical shells subjected to impulsive inner pressures. 07 p0915 A73-20286
- Calculation of the stress concentration produced by an internal pressure in the region where a cylindrical shell is connected to a branch pipe. 09 p1161 A73-23058
- Time evolution of rotating incoherent matter with vanishing internal pressure by Einstein field equations 09 p1151 A73-23342
- Conformal mapping technique for stress concentration around elliptical hole in shallow spherical shell under internal pressure 14 p1806 A73-30045
- Stresses in a pressurized ribbed cylindrical shell with a reinforced hole. 15 p1948 A73-31621
- Experimental evaluation of the strength of elements of thin-walled pressure vessels during severe cooling 17 p2177 A73-34331
- Creep relaxation approximations and exact solutions, discussing rectangular beam pure bending, spherical shell internal pressure loading and thin circular tube bending 20 p2616 A73-39115
- Limit pressures for cylindrical shells with two adjacent circular cut outs. 22 p2929 A73-43175
- Effects of axisymmetric loads on inflated non-linear membranes. 23 p3045 A73-44081

INTERNAL STRESS

U RESIDUAL STRESS

INTERNATIONAL COOPERATION

- German-NASA joint Aeros aeronomy satellite project, discussing mission objectives and related instrumentation 01 p0109 A73-10470
- Scientific mission and German and U.S. plans/design for Helios cooperative solar probe, stressing advanced technology requirements 01 p0110 A73-11103
- Some of the more important problems of international space rescue. 01 p0110 A73-11106
- The Earth Resources Program - International benefits from space. 01 p0043 A73-11107
- Astronomical determination of pole motions by procedures employed at international latitude stations 02 p0155 A73-11650
- Space experience and ethics impact on world development, considering knowledge advancement, regional applications, economy stimulation, environment improvement and international cooperation 02 p0239 A73-11998
- The international magnetospheric study 1975-1977 - Scientific fundaments and objectives. 02 p0164 A73-12313
- Polish space research and prospects, discussing Intercosmos and Intersputnik participation and studies in space physics, communications, meteorology, geodesy, biology, radiology and medicine 04 p0521 A73-15021
- The legal status of Orbital Laboratories as the next step to the development of the collaboration between the cosmic powers on earth. 04 p0522 A73-15131
- Soviet Union-proposed draft International Treaty governing lunar exploration and use 04 p0522 A73-15135
- Space law provisions concerning terrestrial and celestial bodies environmental contamination, advocating establishment of international code of conduct and control authority 04 p0522 A73-15138
- Space and terrestrial pollution definitions, discussing control and preventive measures by national and international public and private organizations 04 p0522 A73-15139

- Earth environment damage potential of space program side effects, discussing environmental protection from international responsibility viewpoint 04 p0522 A73-15142
- The evaluation, conservation, and international development of terrestrial resources from outer space 04 p0523 A73-15143
- Legal problems relating to the evaluation, conservation and development of earth resources by means of space objects. 04 p0523 A73-15144
- Legal regulation of investigation of natural environment from outer space. 04 p0523 A73-15145
- CERS/ESRO role, nonmember states participation and experimental systems in European telecommunication satellites program 04 p0523 A73-15147
- Permanent arrangements for the global commercial communications satellite system of INTELSTAT. 04 p0523 A73-15148
- The future of international space cooperation in treaty-making. 04 p0524 A73-15154
- Satellite orbits allocation by international conventions to prevent interference with existing vehicles, noting international cooperation in communication frequencies allocation 04 p0524 A73-15157
- UN space treaty proposals relating to moon and other celestial bodies natural resources utilization 04 p0524 A73-15158
- The growing role of standards in the national and international coordination of space programs. 04 p0524 A73-15381
- Extending lunar nomenclature to the far side of the moon. 05 p0612 A73-16089
- International space station program for global resources and ecological monitoring and management, reviewing US Skylab and Space Shuttle and USSR Soyuz projects 06 p0757 A73-18026
- Management and cost of European-U.S. Aerosat program based on geostationary satellites for air/ground voice and data messages relay and aircraft position determination 07 p0905 A73-19174
- U.S.S.R. sponsored international space communication system, discussing technological, organizational and legal aspects 07 p0923 A73-19202
- Apollo-Soyuz docking project for flight testing systems compatibility for safe and reliable crew transfer, discussing program objectives, technical requirements and solutions 09 p1152 A73-22187
- Eole project data processing organization and operations management, describing information acquisition and reduction 09 p1060 A73-23377
- Recent development results on the HELIOS S-band command receiver. 09 p1057 A73-23416
- Book - The law of outer space. 10 p1297 A73-23944
- Aeritalia-Boeing passenger aircraft design features in short, medium and long haul versions 10 p1175 A73-24474
- German book - International air traffic conventions: Air piracy - Concept, facts, protective measures. 11 p1454 A73-25570
- ELDO and ESRO space research activities review, stressing increased European cooperation, negotiations with U.S. and project budgeting vs national priorities 11 p1455 A73-26420
- Mobile satellite communication systems constraints imposed by international institution disagreements on management, procurement and operation, considering US and European conflicts on Aerosat project 12 p1471 A73-27653
- The Canadian/U.S. High-Power Communications Technology Satellite. 12 p1472 A73-27669
- Beginning, maximum and ending times uncertainty and maximum areas of H alpha flares, stressing international coordination in solar patrol service 12 p1536 A73-27851
- Remote sensing capability development program planning, discussing world participation in ERTS and alternatives 12 p1500 A73-27951
- Multi-Role Combat Aircraft Program management, discussing international cooperation, industrial arrangements and governmental objectives 13 p1709 A73-29384
- Space shuttle missions relationship to post-Apollo, European and joint European-U.S. space exploration programs 13 p1690 A73-29387
- Soviet-French cooperation in space exploration 14 p1818 A73-30250

- Extraatmospheric space utilization and exploration concepts, discussing international agreements and space law 14 p1819 A73-30899
 - European telecommunication satellite program implementation and preoperational phase regulation, stressing international constraints 14 p1819 A73-30900
 - Role of the Juridical Committee of the International Civil Aviation Organization in the elaboration of air law 15 p1960 A73-32551
 - Book - Satellite broadcasting. 17 p2121 A73-34473
 - The Concorde manufacturing consortium - An exercise in international engineering collaboration. [SAE PAPER 730350] 17 p2257 A73-34698
 - Organization, administration and technological aspects of ERTS system on international scale 17 p2162 A73-34952
 - Space shuttle implementation prognosis, discussing spacecraft configurations, international cooperation, research possibilities in TR telescopes, space physics laboratories and exobiology 18 p2348 A73-35937
 - Some results obtained from the European Cooperation concerning studies of the winter anomaly in ionospheric absorption. 18 p2305 A73-36004
 - Easing international language difficulties via an accommodating software design. [ALAA PAPER 73-614] 18 p2288 A73-36092
 - International cooperation in the field of spatial meteorology 18 p2373 A73-36391
 - Russian book on Soviet news agency space exploration articles for 1971 covering Soyuz, Salyut, Molniya, Luna, Meteor and Lunokhod programs, agricultural satellites and lunar exploration 19 p2486 A73-37771
 - Book - Aircraft hijacking and international law. 20 p2629 A73-39138
 - Book - Twelfth report by the International Telecommunication Union on telecommunication and the peaceful uses of outer space. 20 p2607 A73-39151
 - Remote sensor role in international environmental management, considering monitoring of biosphere, atmosphere and oceans and UN action plan for natural resources 20 p2629 A73-39837
 - International cooperation in weapons systems development, discussing military R and D technology interdependence within NATO, duplication and security 21 p2793 A73-41173
 - Air traffic control in the EUROCONTROL area. 22 p2884 A73-42321
 - Secondary Surveillance Radar application to aircraft identification in upper airspace of Eurocontrol member states, emphasizing code assignment 22 p2884 A73-42322
 - The MINFAP system - First phase in the automation of the EUROCONTROL Maastricht Centre. 22 p2884 A73-42323
 - The International Planetary Patrol Program - An assessment of the first three years. 22 p2912 A73-42978
 - Geostationary meteorological satellite network development for static and cinematographic image transmission based on international cooperation 22 p2884 A73-43118
 - Program plan to develop airworthiness standards for STOL aircraft. 24 p3056 A73-44994
 - 'Air piracy' and the latest work of ICAO on this subject 24 p3159 A73-45345
 - The development of civil air navigation in the People's Republic of China - Agreements with other states as well as the tasks and the position of the China Civil Aviation Corporation (CAAC) 24 p3159 A73-45346
 - Liability and insurance in international air traffic 24 p3159 A73-45443
- INTERNATIONAL GEOPHYSICAL YEAR**
- Equatorial anomaly in the F2 layer during local noon and the IGY and IQSY periods 11 p1350 A73-25089
 - Effective altitudes of the F region in the IGY and IQSY periods 20 p2554 A73-39167
- INTERNATIONAL LAW**
- International convention on damage caused by aircraft concluded 1952 in Rome, proposing revision to include damages before takeoff, after landing and during flight 01 p0124 A73-10566
 - Liability under international law for damages caused by space objects 01 p0124 A73-10567
 - Illegal seizure of aircraft 01 p0124 A73-10650

- International legal problems concerning earth environmental survey system composed of ERT satellites, survey aircraft and ground data handling systems
04 p0521 A73-15129
- International law aspects of catastrophic disaster prohibition in terms of endangering earth environment /resources/
04 p0522 A73-15137
- Earth environment pollution protection in space exploration, noting international law principles application
04 p0522 A73-15140
- International law for earth environment protection against pollution by activities in outer space, noting International Court of Justice Advisory Opinion procedure
04 p0522 A73-15141
- Some international legal issues on the direct television broadcast satellites.
04 p0523 A73-15149
- Spaceflight and the problem of vertical limit of state sovereignty.
04 p0524 A73-15153
- The influence of space law on the development of public international law
04 p0524 A73-15155
- International law principles application to space liability codification, noting United Nations role in Draft Convention on space liability
04 p0524 A73-15159
- Financing of route installations and services to aircraft in flight, suggesting international rules for rental collection
06 p0771 A73-17862
- Book - Aviation law: Cases and materials.
06 p0771 A73-17870
- The legal position of earth orbiting stations
07 p0923 A73-19201
- German book - International air traffic conventions: Air piracy - Concept, facts, protective measures.
11 p1454 A73-25570
- German book on national airspace protection against foreign aircraft intrusion in peacetime covering sovereign rights according to international law, conventions and treaties
11 p1454 A73-26257
- Study of terrestrial resources by space objects and international law
11 p1454 A73-26295
- Regularization of the legal status of international air charter services.
11 p1454 A73-26349
- Legal definition of space objects for international space law purposes regarding damage liabilities
14 p1818 A73-30292
- Book - International bibliography of air law 1900-1971.
14 p1818 A73-30362
- Role of the Juridical Committee of the International Civil Aviation Organization in the elaboration of air law
15 p1960 A73-32551
- Air piracy suppression measures adopted 23 September 1971 at Montreal international convention, discussing prevention and punishment provisions
16 p2087 A73-32972
- Teledetection of terrestrial resources by satellites
18 p2373 A73-36390
- International law aspects of direct broadcasting communication satellites, discussing United Nations, UNESCO and International Telecommunications Union contributions
18 p2373 A73-36392
- Symposium on International Aircraft Accidents Investigation, London, England, January 15, 1973, Proceedings.
19 p2505 A73-37736
- International Civil Aviation standards concerning rights and duties of appointed observers at inquiry by state of aircraft accident occurrence
19 p2505 A73-37737
- ICAO meeting reports on international aircraft accident investigation, onboard data recording, inquiry process and low-safety interface
19 p2506 A73-37738
- Book - Aircraft hijacking and international law.
20 p2629 A73-39138
- Book - Twelfth report by the International Telecommunication Union on telecommunication and the peaceful uses of outer space.
20 p2607 A73-39151
- INTERNATIONAL PRACTICAL TEMPERATURE**
U TEMPERATURE SCALES
INTERNATIONAL QUIET SUN YEAR
D region HF radio wave noontime absorption correlation to winds and temperature in Northern Hemisphere during IQSY
03 p0304 A73-14593
- Diurnal and seasonal variations in conditions for the occurrence of the F1 layer over Middle Asia during the IQSY period
05 p0569 A73-16615
- Analysis of the meteor wind data.
05 p0622 A73-17167
- Latitudinal and longitudinal auroral radio wave absorption in Arctic during IQSY, noting comparison with geomagnetic field disturbances
11 p1350 A73-25086
- Anomalous absorption of cosmic radio emission in the auroral zone during the IQSY
11 p1411 A73-25087
- Equatorial anomaly in the F2 layer during local noon and the IGY and IQSY periods
11 p1350 A73-25089
- Disturbances observation in E-F region and sporadic E layer by vertical ionospheric sounding during IQSY
11 p1351 A73-25098
- U.S.S.R. ionospheric stations and observations during IQSY, discussing ionosphere formation, morphology, radio wave absorption, nonuniformity and upper atmosphere motions
11 p1351 A73-25101
- Earth outer radiation belt and unstable radiation zone dynamics during IQSY magnetically quiet and disturbed period based on Elektron-series satellite data
12 p1535 A73-27636
- Electron-density profiles obtained from MF sounding at Tsumeb.
18 p2306 A73-36012
- Effective altitudes of the F region in the IGY and IQSY periods
20 p2554 A73-39167
- INTERNATIONAL RELATIONS**
NT INTERNATIONAL COOPERATION
Charters, the new mode - Setting a new course for international air transportation.
16 p2087 A73-33101
- Book - The law of international spaces.
19 p2506 A73-38365
- INTERNATIONAL SATS FOR IONOSPHERIC STUDY**
U ISIS SATELLITES
INTERNATIONAL SYSTEM OF UNITS
International Symposium on Metrology, Bratislava, Czechoslovakia, September 5-8, 1972, Proceedings
03 p0305 A73-12893
- International system of units applicability to constitutive equations of four dimensional relativistic electrodynamics
03 p0341 A73-12896
- Aircraft performance calculations in SI units, considering conversion factors for forces, pressures and specific fuel consumption
06 p0648 A73-18511
- Metric technical, Imperial /British/ and SI dimensional systems, discussing conversion rules for mass, force, length, area, volume, density, moment of inertia and stress relationships
19 p2499 A73-37881
- [SAWE PAPER 963]
- INTERNATIONAL TRADE**
World Bank support for airports.
22 p2938 A73-42317
- INTERNATIONAL ULTRAVIOLET EXPLORER**
U IUUE
INTERPLANETARY COMMUNICATION
Concatenated coding for deep space interplanetary communication with low data rate and SNR, comparing performance of three binary codes
09 p1058 A73-23424
- INTERPLANETARY DUST**
NT METEOROID DUST CLOUDS
NT ZODIACAL DUST
Meteor dust motion in the upper atmosphere and in the vicinity of the earth's orbit.
02 p0214 A73-12255
- Interplanetary dust particle flux curves, number densities and size distributions from zodiacal light investigations
02 p0215 A73-12262
- The zodiacal light as seen from the Pioneer F/G and Helios probes.
02 p0215 A73-12263
- Spall/pit diameter ratio decrease in lunar microcraters with decreasing size, considering origin from interplanetary dust particles impact
07 p0896 A73-19866
- Interstellar and interplanetary dust grains orientation distribution function in anisotropic corpuscular or radiation fluxes
10 p1271 A73-23482
- Results of optical observations of dust in upper atmosphere and interplanetary space.
13 p1680 A73-28520
- On the rate of ejection of dust by long-period comets.
14 p1795 A73-29841
- Observations of the inner F and K coronas below 2220-A wavelength.
16 p2060 A73-32954
- Pioneer 10 space probe measurement of interplanetary particulates and aggregates via reflected and scattered sunlight, with emphasis on distribution in asteroid belt
18 p2350 A73-36095
- [ALAA PAPER 73-546]
- Photometric variability of counter glow radiance as evidence for dust cloud presence in earth-moon system region
18 p2351 A73-36183
- Optical and mechanical models of interplanetary dust.
21 p2776 A73-41420
- Asteroidal dust population model coinciding with spatial density demonstrating distribution below astrodynamical mass limit and larger time for distribution function extrapolation
21 p2776 A73-41422
- On the theoretical possibility of the liberation cloud.
22 p2911 A73-42936
- INTERPLANETARY FLIGHT**
NT GRAND TOURS
Helios A and B interplanetary exploration objectives, considering solar plasma, high energy particles and interplanetary dust characteristics
[DGLR PAPER 72-068] 02 p0227 A73-11688
- Comparison of advanced propulsion concepts for deep space exploration.
05 p0608 A73-17201
- Orbit determination capability analysis for the Mariner-Jupiter-Saturn 1977 mission.
06 p0748 A73-17650
- [ALAA PAPER 73-171]
- Nuclear pulse propulsion system for interplanetary space flight, describing operational principles and design concepts
06 p0722 A73-18022
- Mars 2 and 3 - Technology and investigation results
11 p1432 A73-26741
- Sealed silver oxide zinc cells for orbiting and planetary missions.
13 p1572 A73-29586
- INTERPLANETARY GAS**
Interplanetary gas. XVII - An astrometric determination of solar-wind velocities from orientations of ionic comet tails.
03 p0361 A73-12947
- Interplanetary plasma shock event of 8 March 1970 from Heos 1 data, noting magnetospheric compression and solar wind velocity at geosynchronous orbit
10 p1270 A73-24742
- Interplanetary gas dynamics, discussing solar atmospheric structure, plasma kinetics, continuous flows, collective particle behavior, hydrodynamic coronal and free expansions
15 p1939 A73-31975
- Evidence for an interstellar or interplanetary source of diffuse He I 584 A radiation.
19 p2475 A73-37629
- Ionosphere, magnetosphere and interplanetary plasma instabilities effects on magnetosphere dynamics
19 p2476 A73-37758
- Interplanetary gas. XVIII - Models and the mean free path of protons at 1 astronomical unit.
19 p2489 A73-38523
- Extraterrestrial ultraviolet radiation and the parameter of the HI medium near the sun
20 p2601 A73-39074
- Interplanetary gas. XIX - Observational evidence for a meridional solar wind flow diverging from the plane of the solar equator.
20 p2602 A73-39431
- Annual review of astronomy and astrophysics. Volume 11.
21 p2771 A73-41234
- Turbulence and scintillations in the interplanetary plasma.
21 p2748 A73-41235
- Phase method of investigation of short time scale disturbances and motions in space plasma.
21 p2748 A73-41373
- On the backscatter of solar He II, 304 A radiation from interplanetary He/+/.
23 p3024 A73-43695
- Resonance scattering from interstellar and interplanetary helium.
24 p3140 A73-45188
- INTERPLANETARY MAGNETIC FIELDS**
Long-lived sectors of enhanced density irregularities in the solar wind.
02 p0205 A73-11911
- Inferring the interplanetary magnetic field by observing the polar geomagnetic field.
[AD-755684] 03 p0373 A73-13712
- Excitation of polar substorms by northward interplanetary magnetic field.
03 p0304 A73-13890
- Precipitation of low-energy electrons at high latitudes - Effects of interplanetary magnetic field and dipole tilt angle.
04 p0493 A73-15531
- Study of the effect of the east-west component of the interplanetary magnetic field on the currents equivalent to the magnetic perturbations of high latitude regions
04 p0502 A73-16000
- Dayside magnetopause distance calculation at subsolar point for various solar wind parameters, allowing for southward interplanetary field component diffusion
05 p0610 A73-17008
- Solar wind magnetic field and particle concentration disturbances near moon, noting electric field effect on ion motion
05 p0620 A73-17009

Equatorial coronal arches and geomagnetic disturbance.

05 p0621 A73-17037

Cosmic ray number density modulation by off-ecliptic phenomena to explain interplanetary magnetic field measurements onboard Heos 1 and 2

05 p0611 A73-17186

Electrostatic ion cyclotron waves in an anisotropic plasma.

05 p0611 A73-17305

Dependence of the position of the magnetopause on the orientation of the interplanetary magnetic field

06 p0690 A73-17560

Further study of the theta component of the interplanetary magnetic field.

07 p0875 A73-19230

On the relation between solar wind structure and solar wind rotational and tangential discontinuities.

07 p0869 A73-19231

Geomagnetic activity semiannual and diurnal variations due to interplanetary field southward component interaction with magnetosphere based on model ordered in solar equatorial coordinates

07 p0813 A73-19234

Numerical studies of the transport of solar protons in interplanetary space.

07 p0870 A73-19664

The heliocentric radial gradient in cosmic ray density and the 'Swinson' sidereal time variation.

07 p0870 A73-19671

Magnetic irregularities in interplanetary space and geomagnetic activity.

08 p1007 A73-21004

Characteristics of cosmic ray variations near the solar equator plane

08 p0998 A73-21299

Solar and magnetic fields characteristics relative to 11 year cosmic ray modulation in interplanetary space

08 p0999 A73-21340

Solar active regions effects on galactic cosmic ray distribution and interplanetary magnetic field structure

08 p1000 A73-21344

Forbush predecrease observation by supernutron monitors, interpreting cosmic ray depletion and rigidity dependence by model of interplanetary magnetic field propagating disturbance from sun

09 p1073 A73-22051

Cross-correlation analysis of the AE index and the interplanetary magnetic field Bz component.

09 p1142 A73-22055

Observation of the entrance of solar protons in the magnetosphere at very high latitudes

10 p1211 A73-23769

Sector structure of the interplanetary magnetic field, and magnetic disturbances in the circumpolar region

10 p1276 A73-23896

Investigation of cosmic-ray propagation in the interplanetary magnetic field on the basis of the kinetic equation

10 p1265 A73-23904

Problems of linear and nonlinear theory of cosmic ray modulation

10 p1266 A73-23913

Solar quiet long-term modulation of cosmic ray intensity diurnal variation explained via interplanetary sector pattern changes

10 p1269 A73-24448

Effects of interplanetary magnetic sector structure on auroral zone and polar cap magnetic activity.

10 p1213 A73-24730

Magnetospheric substorms correlation with interplanetary magnetic field, discussing balloon and satellite electric field measurements

10 p1215 A73-24784

Anisotropic contact discontinuities at magnetospheric boundary and tail from MHD space plasma data analysis, suggesting sector boundary identification in interplanetary magnetic field

12 p1528 A73-27329

Day-to-day variability of the quiet-day solar-diurnal variations and the orientation of the interplanetary magnetic field

12 p1540 A73-27358

Solar magnetic sector structure - Relation to circulation of the earth's atmosphere.

12 p1491 A73-27441

On the variation of the coronal lambda-5303 intensity relative to the interplanetary and solar magnetic sector structure, and to geomagnetic activity.

12 p1542 A73-27615

Variations of solar-wind parameters, magnetic activity, and the electron tail of the magnetosphere and of the outer radiation zone.

13 p1608 A73-28714

Geomagnetic storm families, direction of the interplanetary magnetic field, and solar activity.

13 p1608 A73-28718

Influence of the interplanetary magnetic field on the magnetic perturbations of high latitude regions - Demonstration of an asymmetry in relation to the earth-sun direction

13 p1611 A73-29563

Identification of interplanetary tangential and rotational discontinuities.

14 p1796 A73-29958

Polar cap magnetic variations and their relationship with the interplanetary magnetic sector structure.

14 p1747 A73-29959

Interplanetary medium rotational discontinuities polarization, vorticity transport and angular momentum properties, implying solar wind velocity jump from magnetic field transverse perturbation

14 p1796 A73-29961

Induced lunar magnetosphere and solar wind formed downstream cylindrical cavity for interplanetary magnetic fields arbitrary orientation, assuming lunar core and shell electrical conductivity model

14 p1796 A73-29962

Earth nonuniform bow shock oblique structure and pulsation, obtaining statistical occurrences from three dimensional distribution of interplanetary field directions for solar wind sector

14 p1749 A73-29983

Stability of solar wind against electromagnetic streaming instability.

14 p1788 A73-30743

Interplanetary scintillations of cosmic rays.

14 p1788 A73-30752

Average high latitude magnetic field: Variation with interplanetary sector and with season. 1 - Disturbed conditions.

15 p1866 A73-31073

Recurrent magnetic storms in relation to the structure of solar and interplanetary magnetic fields.

15 p1868 A73-31384

Diurnal variations of the vertical component of the magnetic field in high latitude regions as a function of the east-west component of the interplanetary magnetic field

15 p1868 A73-31570

The direct and inverse problems of cosmic-ray propagation in interplanetary space

15 p1926 A73-31878

Solar wind flow in interplanetary space, discussing comets, cometary tail, interplanetary magnetic field and Alfvén waves characteristics

15 p1940 A73-32183

Dependence of the position of the magnetopause on the orientation of the interplanetary magnetic field.

16 p2002 A73-32784

On the role of fluctuations in the interplanetary magnetic field on heat conduction in the solar wind.

16 p2056 A73-33461

The magnetic field in the vicinity of Venus

16 p2067 A73-33805

Periodic variations in geomagnetic activity and sector structure of the interplanetary magnetic field.

17 p2157 A73-34075

The propagation of Alfvén waves and their directional anisotropy in the solar wind.

17 p2223 A73-34501

Interplanetary magnetic field and geomagnetic Dst variations.

17 p2158 A73-34507

Magnetotail response to sudden changes in the interplanetary magnetic field.

17 p2158 A73-34509

Radial variation of magnetic fluctuations and the cosmic-ray diffusion tensor in the solar wind.

17 p2224 A73-34762

Topology of induced lunar magnetic fields.

17 p2235 A73-35736

Russian book - Magnetic properties of meteorites: Meteorites in the laboratory.

18 p2348 A73-35871

Observations of the entry of solar protons into the magnetosphere by use of riometers.

18 p2344 A73-35930

On solar wind interaction with the earth's magnetosphere.

18 p2346 A73-36184

Observation and analysis of abrupt changes in the interplanetary plasma velocity and magnetic field.

18 p2351 A73-36265

Night side electromagnetic response of the moon.

18 p2351 A73-36268

Dependence of the polar cusp on the north-south component of the interplanetary magnetic field.

18 p2351 A73-36273

Sector boundary geomagnetic activity average Kp elevation relationship to southward component of interplanetary field, suggesting magnetosphere role

18 p2347 A73-36292

Imp-3 satellite measurement-based investigation of variability of interplanetary magnetic field component normal to plane of ecliptic during passage across sector field boundary

19 p2480 A73-37241

Interplanetary shock waves and cosmic rays.

19 p2476 A73-37759

Characteristics of cosmic-ray variations near the solar equatorial plane.

19 p2476 A73-37928

The rate of separation of magnetic lines of force in a random magnetic field.

19 p2489 A73-38522

Sector-patterned structure of interplanetary magnetic field and magnetic disturbances in the circumpolar region.

20 p2603 A73-38915

Comments on paper by N. F. Ness, K. W. Behannon, R. P. Lepping, and K. H. Shatten, 'Use of two magnetometers for magnetic field measurements on a spacecraft.'

20 p2615 A73-38963

Helios probe design for solar wind acceleration mechanism, magnetic and electric fields, interplanetary dust and cosmic radiation

21 p2780 A73-40449

Cosmic ray intensity variation observation during August 2-8, 1972, suggesting complex interactions with interplanetary shock waves and magnetic field and magnetosphere

21 p2757 A73-40590

Nonlinear and nonstationary effects in the solar wind

21 p2757 A73-40594

Influence of the polarity of the interplanetary magnetic field on magnetic activity at high latitudes.

21 p2773 A73-41378

Analysis and synthesis of coronal and interplanetary energetic particle, plasma, and magnetic field observations over three solar rotations.

22 p2901 A73-41901

Effects of electrostatic instabilities on planetary and interstellar ions in the solar wind.

22 p2902 A73-41940

Comparison of the sectorial structure of the interplanetary magnetic field and the occurrence of SC and SI events.

22 p2908 A73-42447

Anisotropic contact discontinuities at magnetospheric boundary and tail from MHD space plasma data analysis, suggesting sector boundary identification in interplanetary magnetic field

23 p3008 A73-43227

Day-to-day variability of quiet-day solar daily variations and the direction of the interplanetary magnetic field.

23 p3027 A73-43258

Small amplitude Alfvén waves propagation in solar wind under interplanetary magnetic field, relating wave and wind velocity

23 p3029 A73-43612

Short-period interplanetary and polar magnetic field variations.

23 p3029 A73-43691

North-south asymmetry of the interplanetary magnetic field

23 p3025 A73-44250

Large-scale inhomogeneities in the sector structure of the solar wind

24 p3124 A73-44779

Correlation length for interplanetary magnetic field fluctuations.

24 p3139 A73-45125

Polar cap electric field measurements by balloons indicating ionospheric convection control by interplanetary magnetic field

24 p3086 A73-45135

INTERPLANETARY MEDIUM

NT INTERPLANETARY DUST

NT INTERPLANETARY GAS

NT METEOROID DUST CLOUDS

NT ZODIACAL DUST

The Kelvin-Helmholtz instability in type-I cometary tails

01 p0102 A73-10946

Characteristics of the quiet solar wind beyond the earth's orbit.

01 p0092 A73-11042

Relationship between the various indices of geomagnetic activity and the interplanetary plasma parameters.

02 p0159 A73-12033

Satellite-borne radio telescope observation of traveling solar radio bursts for energetic solar particle propagation in interplanetary space, discussing wind density and magnetic field

02 p0208 A73-12419

Electromagnetic wave observation in interplanetary medium and in magnetosphere, emphasizing magnetic and electric field measurements

03 p0374 A73-13855

Interplanetary anisotropy measurements of energetic solar proton entry into geomagnetic tail by ESRO 2 satellite

03 p0362 A73-13860

Intensity and polarization of the solar light scattered by an isolated volume of interplanetary matter

03 p0380 A73-14611

Characteristics of interplanetary electron irregularities according to observations in 1967-1969.

04 p0503 A73-16015

Anomalous recurrent diurnal anisotropy in cosmic ray intensity with maximum along the garden hose direction.

05 p0608 A73-16142

Resonance and propagation theory for all electromagnetic wave types in plasmas of ionosphere and

interplanetary space, discussing stability and oscillations 06 p0689 A73-17505

Spectrum of small-scale inhomogeneities in the interplanetary plasma 06 p0747 A73-17529

The recurrent solar wind streams observed by interplanetary scintillation of 3C 48. 07 p0870 A73-19595

The extralunar component in lunar soils and breccias. 07 p0887 A73-19767

Photography of the zodiacal light outside the ecliptic in quadrature and in opposition with the sun 09 p1073 A73-22001

Cosmic rays in a random magnetic field - Breakdown of the quasilinear derivation of the kinetic equation. 09 p1137 A73-22036

Interaction of the interplanetary medium with the earth's magnetosphere 09 p1146 A73-22542

Kelvin-Helmholtz instability in type I comet tails. 09 p1148 A73-22741

Direct measurements of solar-wind fluctuations between 0.0048 and 13.3 Hz. 10 p1264 A73-23539

Particle scattering in interplanetary space and the properties of solar corpuscular streams 10 p1265 A73-23902

Solar cosmic ray diffusion, convection, accumulation and acceleration as function of interplanetary medium perturbation and flare coordinates 10 p1266 A73-23909

Spatial variations of cosmic rays on the basis of data for the radioactivity of meteorites with known orbits 10 p1266 A73-23910

Forbush decreases and their relation to solar activity and the parameters of the interplanetary medium 10 p1267 A73-23921

Polar coupling coefficients and generalization of the spectrographic method for studying cosmic-ray variations of magnetospheric and interplanetary origin 10 p1267 A73-23927

Determination of the velocity of shock waves in the interplanetary medium. 10 p1279 A73-24236

Energetic solar proton observations by Explorer 33 and 35 [interplanetary medium] and Injun 5 [polar caps], comparing proton fluxes in space and poles 10 p1269 A73-24729

Interplanetary scintillations observations from solar wind plasma density fluctuations power spectrum 12 p1533 A73-26980

Analysis of the non-Gaussian spectra of interplanetary scintillations. 12 p1547 A73-27877

Interplanetary radial gradients of galactic cosmic ray protons and helium nuclei - Pioneer 8 and 9 measurements from 0.75 to 1.10 AU. 14 p1786 A73-29951

Solar wind proton temperature anomalies relation to interplanetary shock waves, considering solar flare induced material ejection and magnetic bottle formation 14 p1786 A73-29952

Solar wind interpenetrating ion streams from Imp 6 electrostatic analyzer measurements, considering origin due to interplanetary high velocity filaments merging into rarefied plasma regions 14 p1786 A73-29954

Solar wind velocity and proton temperature time dependent relations, considering interplanetary medium nonlinear unsteady processes effects 14 p1786 A73-29955

Solar wind velocity fluctuations with heliocentric distance beyond one AU via nonlinear fluid dynamic equations numerical solution, considering interplanetary plasma turbulence effects 14 p1786 A73-29956

Interplanetary plasma inhomogeneities effect on Alfvén wave propagation direction from Pioneer 6 magnetic measurements 14 p1796 A73-29957

Interplanetary medium rotational discontinuities polarization, vorticity transport and angular momentum properties, implying solar wind velocity jump from magnetic field transverse perturbation 14 p1796 A73-29961

Remote sensing of LF nonthermal radio emission for composition and dynamic processes of interplanetary and interstellar media and planetary magnetospheres 14 p1800 A73-30539

Interplanetary scintillations of cosmic rays. 14 p1788 A73-30752

Relationship of the Pc 3 and 4 geomagnetic pulsation period with the parameters of the interplanetary medium at the earth orbit 15 p1937 A73-31904

Plasma fine velocity structure and dynamics from diffraction pattern of interplanetary radio sources scintillation 15 p1919 A73-31959

Energy losses of galactic cosmic rays in the interplanetary medium. 15 p1927 A73-32010

Test for detection of fine structure of the solar wind velocity. 15 p1927 A73-32015

Interplanetary shock fronts thickness, calculating magnetosonic Mach number and Larmor radius 15 p1942 A73-32620

Spectrum of small-scale interplanetary plasma inhomogeneities. 16 p2058 A73-32753

A test for revealing the fine-scale velocity structure of the solar wind 16 p2059 A73-32888

Interplanetary-scintillation observations of 203 sources identified as radio galaxies or quasars. 17 p2225 A73-34289

Wave-trains in the solar wind. I - General theory and its application to an ideal, isotropic, one-fluid plasma. 17 p2224 A73-34505

Close connexion between flare-generated coronal and interplanetary shock waves. 17 p2232 A73-35147

Observation and analysis of abrupt changes in the interplanetary plasma velocity and magnetic field. 18 p2351 A73-36265

A density scale for the interplanetary medium from observations of a type II solar radio burst out to 1 astronomical unit. 18 p2348 A73-37113

Russian book - Interplanetary medium and the physics of the magnetosphere. 19 p2481 A73-37336

Structural formations in the interplanetary medium 19 p2481 A73-37342

Low-energy protons of solar origin and interplanetary medium studies 19 p2474 A73-37345

Pioneer 8 observations and interpretations of sixteen interplanetary shock waves observed in 1968. 20 p2603 A73-38931

Configuration of interplanetary shock waves from powerful chromospheric flares [from space probe measurements]. 20 p2602 A73-39233

Meridional flow and the validity of the two-dimensional approximation in stellar-wind modeling. 20 p2602 A73-39430

Interaction of the lower thermosphere with the solid component of the interplanetary medium. 21 p2682 A73-40158

Russian book - Stellar atmospheres and interplanetary plasma. 21 p2671 A73-40531

Solar wind velocity investigation based on solar corona and interplanetary plasma data, analyzing possible acceleration mechanisms 21 p2755 A73-40533

Inhomogeneous structure of plasma near sun due to drift, slipping and anisotropic temperature distribution instabilities, noting association with radio astronomy observed fine structure 21 p2767 A73-40537

Propagation of protons injected near 1 AU in a medium with a constant transport length 21 p2756 A73-40583

Certain characteristics of the August 1972 solar flares which generated cosmic radiation, plasma clouds, and interplanetary shock waves 21 p2757 A73-40587

Evidence for confinement of low-energy cosmic rays ahead of interplanetary shock waves. 21 p2763 A73-41504

On the relation between the pattern and wind velocities in interplanetary scintillations. 22 p2903 A73-42702

The observational evidence for mass distribution in the meteoritic complex. 23 p3031 A73-43770

Plasma fine velocity structure and dynamics from diffraction pattern of interplanetary radio sources scintillation 24 p3132 A73-44484

Cold gas noncentral point explosion generated shock wave propagation in interplanetary medium, discussing shock front geometry, earth orbit parameters and gas dynamics 24 p3137 A73-44781

Solar wind fluctuations mapping procedure applied to Explorer 35 wind data for solar wind structure to Mars orbit 24 p3125 A73-45104

Power spectra of solar wind parameters at 20 solar radii derived from Mariner 5 data. 24 p3126 A73-45133

MilliHertz plasma oscillations associated with strong gradients in density and temperature 24 p3087 A73-45139

INTERPLANETARY NAVIGATION

Propellant requirements for midcourse velocity corrections. [AIAA PAPER 73-172] 05 p0630 A73-16916

Orbit determination capability analysis for the Mariner-Jupiter-Saturn 1977 mission. 06 p0748 A73-17650

[AIAA PAPER 73-171] Planetary quarantine constraints for outer planet satellite encounter missions, determining spacecraft impact probability in terms of trajectory analysis and navigation error numerical integration 18 p2349 A73-35976

Navigation system design for the Mariner Jupiter/Saturn Mission. [AIAA PAPER 73-838] 21 p2736 A73-40503

A linear method of autonomous space navigation and guidance 21 p2737 A73-40906

INTERPLANETARY PROPULSION

U INTERPLANETARY SPACECRAFT

U ROCKET ENGINES

INTERPLANETARY SPACE

Propagation through the solar corona of the shock waves responsible for type II radio bursts. 01 p0093 A73-11314

Russian book on physicochemical basis of space research covering near earth and interplanetary environmental factors and effects on spacecraft designs and materials 02 p0211 A73-11886

Use of an electron beam for low-temperature plasma measurement in the magnetosphere and interplanetary space. 04 p0450 A73-15553

Evidence for the existence of adiabatic energy loss in interplanetary space from observations of the decay of the February 25-March 2, 1969 series of solar cosmic ray events. 05 p0611 A73-17048

Propagation anisotropies of solar flare protons and electrons at low energies in interplanetary space. 07 p0869 A73-19227

Pitch angle distribution of solar flare particles in interplanetary space. 07 p0869 A73-19228

Physical conditions in the magnetosphere and interplanetary space during the excitation of pc 1 geomagnetic pulsations 08 p0960 A73-21306

Three dimensional cosmic ray anisotropy and density distribution at earth orbit and in interplanetary space with allowance for primary particle and nucleon energy spectrum 08 p1000 A73-21343

Chromospheric flares and shock waves in interplanetary space 09 p1137 A73-22540

Cosmic ray electrons from 0.2 to 8 MeV - Pioneer 8 and 9 measurements of their spectrum, time variations, and interplanetary radial gradient. 12 p1533 A73-26976

Solar radiation effects on terrestrial electromagnetic environment, considering interplanetary space, earth internal structure, geomagnetism, upper atmosphere, dynamo action, energetic particles and magnetospheric storms 12 p1538 A73-27053

Theory of cosmic ray transfer by anisotropically scattered particles 12 p1534 A73-27331

Cometary brightness variations and conditions in interplanetary space. 14 p1789 A73-29779

Time dependent diffusion equation for solar flare cosmic ray propagation through interplanetary space, specifying continuous emission curve shape and period 16 p2053 A73-32966

Equatorial and auroral zone geomagnetic indices and micropulsations variations relation to 11-18keV protons occurrence in interplanetary space 18 p2345 A73-36120

Use of charged particle beams for low temperature plasma measurement in magnetosphere and interplanetary space. 19 p2429 A73-37381

Physical conditions in the magnetosphere and in interplanetary space during excitation of type Pc1 geomagnetic pulsations. 19 p2425 A73-37935

A kinetic description of the interaction between cosmic rays and shock waves 21 p2758 A73-40596

Investigation of isotropic and anisotropic effects of cosmic rays during October through November 1968. 21 p2758 A73-40600

Diurnal, semidiurnal, and the eight-hour components of cosmic-ray anisotropy 21 p2758 A73-40601

Energy losses of solar cosmic rays in interplanetary space. 21 p2763 A73-41503

Contribution to the theory of cosmic-ray propagation with anisotropic particle scattering. 23 p3020 A73-43229

Interplanetary radar time delays in different theories of gravitation. 23 p3032 A73-43842

INTERPLANETARY SPACECRAFT

NT JUPITER PROBES
NT MARINER SPACE PROBES
NT MARINER SPACECRAFT
NT MARINER VENUS-MERCURY 1973
NT MARINER 3 SPACE PROBE
NT MARINER 5 SPACE PROBE
NT MARINER 7 SPACE PROBE
NT MARINER 9 SPACE PROBE
NT MARS PROBES
NT MARS 2 SPACECRAFT
NT MARS 3 SPACECRAFT
NT PIONEER SPACE PROBES
NT PIONEER 6 SPACE PROBE
NT PIONEER 8 SPACE PROBE
NT PIONEER 9 SPACE PROBE
NT PIONEER 10 SPACE PROBE
NT TOPS [SPACECRAFT]
NT VENERA SATELLITES
NT VENERA SATELLITES
NT VIKING LANDER SPACECRAFT
NT VIKING ORBITER SPACECRAFT
NT VIKING 75 ENTRY VEHICLE
NT ZOND SPACE PROBES

Interplanetary spacecraft transfer maneuver for hyperbolic trajectory change into eccentric orbit, using aerodynamic drag to obtain nearly circular orbit
03 p0379 A73-14571

The determination and treatment of temperature coefficients of silicon solar cells for interplanetary spacecraft application.
09 p1036 A73-22810

Unmanned interplanetary spacecraft power systems with nickel-cadmium batteries, solar panels or radioisotope thermoelectric generators
11 p1312 A73-26022

Multi-mission nuclear electric propulsion stage design.
19 p2457 A73-38433

General relativistic gravitation theories based space-time curvature tests near sun from interplanetary probe motion analysis using probe-borne laser light transmission
[ONERA, TP NO. 1210]
22 p2907 A73-42216

INTERPLANETARY TRAJECTORIES

Gravity thrust Jupiter orbiter trajectories generated by encountering the Galilean satellites.
01 p0095 A73-10103

Three parameter boundary value problem for trajectory optimization of maximum weight station injection from earth orbit into interplanetary flight trajectory
02 p0219 A73-12454

Error sources in numerical integration of spacecraft equations of motion in solar and planetary gravitational fields, suggesting methods for improving accuracy
03 p0379 A73-14553

Nonlinear estimation theory applied to the interplanetary orbit determination problem.
04 p0498 A73-15271

Application of the graphic flight path design program /FPDP/ for fast interactive trajectory design.
[AIAA PAPER 73-113]
05 p0619 A73-16871

Alteration of the Laplace spheres of planetary influence during the application of a new intermediate orbit
05 p0620 A73-17022

Estimating trajectory correction requirements for multiple outer planet missions.
05 p0623 A73-17205

The effects of trajectory characteristics on scientific objectives for major planetary orbiters.
06 p0757 A73-18376

Performance of recoverable single and multiple Space Tugs for missions beyond earth escape.
07 p0906 A73-20471

Nonlinear estimation theory applied to the interplanetary orbit determination problem.
07 p0805 A73-20582

Russian book on earth satellite, lunar, interplanetary and reentry trajectory analysis and optimal control covering motions under low thrust, aerodynamic heating and ablation
10 p1286 A73-23949

The selection of measurable parameters in the determination of the trajectory of a space vehicle.
12 p1543 A73-27626

Isochronous derivatives of certain spacecraft-trajectory parameters
14 p1796 A73-29857

Three parameter boundary value problem for trajectory optimization of maximum weight station injection from earth orbit into interplanetary flight trajectory
15 p1941 A73-32604

Interference parameters in the problem of estimating the accuracy of prediction of spacecraft motion
21 p2781 A73-40904

Trajectory of a solar-electric propelled vehicle passing through the shadow cone of a celestial body
21 p2779 A73-41556

INTERPLANETARY TRANSFER ORBITS

Three parameter boundary value problem for trajectory optimization of maximum weight station injection from earth orbit into interplanetary flight trajectory
02 p0219 A73-12454

Method of solving the interplanetary orbit optimization problem with an invariant nomographic scale.
05 p0613 A73-16093

Optimal correction of a planetary-approach trajectory for transfer to an artificial-satellite orbit
05 p0616 A73-16428

Optimization of multiple target electric propulsion trajectories.
[AIAA PAPER 73-205]
06 p0748 A73-17658

Hohmann trajectories efficiency for interplanetary transfers of spacecraft between circular coplanar orbits, considering earth-Mars-earth flight and transition to parabolic trajectory
12 p1538 A73-27065

Three parameter boundary value problem for trajectory optimization of maximum weight station injection from earth orbit into interplanetary flight trajectory
15 p1941 A73-32604

INTERPOLATION

Signal interpolation errors in adaptive-discretization systems
01 p0015 A73-10029

Detonation in a medium of variable density with allowance for variable back pressure
01 p0034 A73-10956

The role of interpolation and approximation theory in variational and projection methods for solving partial differential equations.
01 p0071 A73-11458

Interpolation theory over curved elements, with applications to finite element methods.
04 p0470 A73-15010

Interpolation methods in aeroclastic analysis, comparing wing structural influence coefficients derived by surface splines and interpolation-in-the-small techniques with static test data
05 p0637 A73-17215

A simple interpolation algorithm for improvement of the numerical solution of a differential equation.
06 p0717 A73-18407

A method for the investigation of interpolated information and time effects in short term retention.
06 p0659 A73-18475

Estimating the accuracy of longitudinal interpolation of f0F2 from shipboard observations
08 p0959 A73-21301

Asymptotic approximation to crack problems with emphasis on stress intensity factor, discussing interpolation procedure based on simplified problem form.
09 p1162 A73-23180

Degrees of freedom elimination method shown equivalent to interpolation by splining by means of actual structure in curve connection for given points
09 p1166 A73-23465

Book - Digital simulation of physical systems.
10 p1191 A73-23946

Spline representation by finite functions
12 p1518 A73-27238

Explosion in a variable-density medium in the presence of variable counterpressure.
12 p1487 A73-27532

Gaussian quadrature formula derivation by integration of linear interpolation operator replacing Hermitian polynomial with vanishing derivative for error minimization
13 p1647 A73-28194

Discrete element development for anisotropic plates via bicubic Hermite interpolation functions, considering patch generation from boundary geometry data
15 p1951 A73-32033

The effects of the observational system and the method of interpolation on the computation of spectra.
17 p2201 A73-34852

Evaluation of the accuracy of longitudinal interpolation of f0F2 based on ship observations.
19 p2425 A73-37930

Objective cross-section analyses by Hermite polynomial interpolation on isentropic surfaces.
21 p2728 A73-40054

Platinum resistance thermometer as standard instrument for interpolation on International Practical Temperature Scale, discussing design development, operational characteristics and errors
22 p2855 A73-42010

German monograph on display unit nonlinear interpolation approach based on higher order curve for reduced computer storage requirements covering Chebyshev approximation and coordinate transformations
22 p2830 A73-42738

Interpolation using finite duration impulse response digital filters.
23 p2952 A73-43313

The formation of resonance lines in multidimensional media. III Interpolation functions, accuracy, and stability.
24 p3138 A73-45042

Curve fitting by application of splines under tension, discussing polynomial interpolation drawbacks and linear system solution for unknown second derivatives
24 p3070 A73-45090

Interpretation
Linear programming for optimization, discussing definitions, practical examples, simplex algorithm,

duality theory, heuristic interpretations and integer solutions
21 p2726 A73-40836

INTERROGATION

Bit synchronized discrete address radar beacon system with ground based U.S. civil interrogator complex for compatibility with ATC and aircraft operator services
14 p1772 A73-29882

Secondary radar interrogator based on IC technology, discussing video processing and monitoring
15 p1847 A73-32436

Three dimensional transponders array for exact solution to positioning problem, discussing large measurements sequential interrogation effects on accuracy
21 p2734 A73-40034

INTERSTELLAR COMMUNICATION

Optimal search strategy to investigate probability of habitable systems with civilization transmitting detectable signals
08 p1013 A73-21645

The interpretation of signals from space.
11 p1428 A73-26661

Communication possibilities between earth and technologically advanced galactic civilizations, discussing radio astronomy requirements, technology differences and communication distance estimates
24 p3133 A73-44555

Project Cyclops investigation of extraterrestrial civilization signal detection, discussing microwave apparatus, frequency bands, antenna arrays and research implementation proposals
24 p3134 A73-44561

Interstellar radio communication and the frequency selection problem.
24 p3068 A73-44992

INTERSTELLAR EXTINCTION

UV astronomy advances from rocket and satellite observations, discussing early stars, interstellar extinction and gas, galaxies and globular clusters
01 p0094 A73-10059

Instrumental considerations in high dispersion requirements of stellar spectroscopy and interstellar absorption and emission line studies, emphasizing spectral resolution and SNR optima determination
01 p0046 A73-10503

A simple analytic approximation for dusty stromgren spheres.
01 p0104 A73-11047

Stellar sources UV photography from sounding rocket, obtaining mean interstellar absorption, stars magnitudes and distribution and UVB spectrum
02 p0216 A73-12326

Cosmic diffuse soft X rays intensity distribution, taking interstellar absorption into account
02 p0207 A73-12402

Diffuse interstellar lines and bands interpreted as extinction structure due to impurities in cosmic dust grains, comparing theory with observation
02 p0225 A73-12807

Light variation and extinction of the variable WW Vulpeculae
02 p0226 A73-12836

Long time optical variability model of quasars and Seyfert galaxies in terms of grain extinction variations in intervening clouds due to thermal and atom impact evaporation
02 p0226 A73-12839

The absorption by the interstellar medium of 80 MHz radio emission from galactic supernova remnants.
03 p0372 A73-13346

GX 17 + 2 X ray source optical counterpart identification, noting interstellar absorption role in magnitude estimation
03 p0374 A73-13795

Interstellar extinction curve structure via photographic techniques, considering optical observation extension into UV with OAO-C telescope
06 p0751 A73-18228

Interstellar molecular hydrogen cloud size and optical extinction by interstellar Na D and Ca lines, estimating molecular lifetime within dark cloud
06 p0752 A73-18230

Observational aspects of RR Lyrae and W Virginis stars - Some conundrums of stellar populations and galactic distribution.
07 p0903 A73-20629

The interstellar reddening law in the ultraviolet deduced from filter photometry obtained by the OAO-2 satellite.
09 p1141 A73-22029

Cosmic absorption of stellar light in the belt of a local system
09 p1148 A73-22861

The extinction curve for Cygnus OB2 no. 12.
11 p1414 A73-25068

Investigation of the diffuse glow of the clouds of dark absorbing matter in the region of the Aquila constellation
11 p1416 A73-25229

Optical and radio observations of the Orion Nebula.
11 p1425 A73-26265

Interstellar light absorption and distribution of stars about the star cluster NGC 6834 12 p1537 A73-26854

Interstellar light absorption and distribution of stars about the star cluster NGC 7654 12 p1537 A73-26855

Interstellar light absorption in the Orion constellation area 12 p1537 A73-26856

Andromeda galaxy absorbing material distribution obtained with population I cepheids in Baade four variable star fields 13 p1671 A73-28031

A preliminary classification scheme for interstellar absorbing clouds. 15 p1933 A73-31309

Relationship between T-associations and the interstellar medium in the northern region of the Monoceros complex 15 p1934 A73-31421

Mariner 9 ultraviolet spectrometer experiment - Interstellar absorption at Lyman alpha in OB stars. 15 p1936 A73-31556

Spectrophotometric results from the Copernicus satellite. VI - Extinction by grains at wavelengths between 1200 and 1000 Å. 15 p1936 A73-31561

Extinction and scattering by several types of silicate sphere of radius 0.05-1.0 micron, for the wavelength range 0.21-50 microns. 15 p1939 A73-32012

Southern Milky Way early type star interstellar extinction curves, considering position with regard to galactic plane and local dust cloud conditions 15 p1939 A73-32046

Soft X ray background observations at 0.1-10 keV, considering interstellar absorption effects, galactic radiation and extragalactic components 16 p2051 A73-32745

Intrinsic ultraviolet colors from OAO-2 Telescope observations for stars on the main sequence. 17 p2225 A73-34290

Interstellar absorption lines observed with the orbiting spectrophotometer S59. 18 p2349 A73-35993

X-ray absorption and optical extinction in interstellar space. 19 p2475 A73-37567

Interstellar extinction, relation to spatial dust distribution, light scattering by grains, diffuse absorption lines and polarization 21 p2772 A73-41247

On the infrared emission of H II regions due to dust. 22 p2908 A73-42314

Scattered-light phenomena in interstellar space 24 p3137 A73-44824

Interstellar reddening calculation with respect to U-B/V diagram for hot and main sequence stars as function of luminosity based on model stellar atmospheres 24 p3138 A73-45012

INTERSTELLAR GAS

UV astronomy advances from rocket and satellite observations, discussing early stars, interstellar extinction and gas, galaxies and globular clusters 01 p0094 A73-10059

Heating and cooling mechanisms, ionization processes, time-dependent models and energy requirements of interstellar H I regions 01 p0091 A73-10064

Cool giant star-ejected high velocity dust grains interaction with interstellar clouds, discussing solid state defect accumulation, sputtering and grain and cloud heating 01 p0098 A73-10582

Physical conditions in interstellar hydroxyl and formaldehyde clouds. 01 p0100 A73-10790

Properties of H I regions heated by X-rays and cosmic rays 01 p0092 A73-10935

Stellar gas injection into nucleus of radio galaxy NGC 4486, estimating energy release during gas accretion 01 p0106 A73-11301

Radial and nonradial oscillation modes of gaseous polytrope with toroidal magnetic field, using variational principle 02 p0217 A73-12400

The mass spectrum of interstellar clouds and the assumption of total coalescence. 04 p0500 A73-15489

H I clouds with spin temperatures less than 25 K. II - Physical properties of two neutral hydrogen clouds. 04 p0500 A73-15517

Radio spectroscopy superiority for interstellar cloud chemical composition studies, detecting formaldehyde, X-ogen, HNC and other exotic molecular species 05 p0546 A73-16305

Nuclear gamma rays from Li-7 in the galactic cosmic radiation. 05 p0612 A73-17329

Radio telescope identification of interstellar isocyanic acid, methylacetylene and hydrogen isocyanide molecules from pure rotational transitions 06 p0751 A73-18229

Interstellar molecular hydrogen observed in the ultraviolet spectrum of delta Scorpii. 07 p0874 A73-19071

Observations of the neutral-hydrogen absorption spectrum of Cygnus X-3. 07 p0874 A73-19073

Interaction of singly charged interstellar helium ions with the solar wind. 07 p0870 A73-19253

Star formation from interstellar clouds gravitational collapse, discussing protostars evolution based on model calculations 07 p0878 A73-19675

5 GHz observations of the infrared star MWC 349, and the H II condensation W3/OH/. 07 p0899 A73-20121

The disc model of gaseous accretion on a relativistic star in a close binary system 07 p0901 A73-20305

Time variation of metal abundance in galaxies - Super-metal-rich stage. 07 p0902 A73-20446

Cosmic-ray heating and molecular cooling of dense clouds. 08 p0997 A73-20899

Ionization loss effects on cosmic ray lifetime in galactic interstellar medium, noting dependence on particle energy 08 p0999 A73-21335

Interstellar gas role in cosmic ray yearly variations determined from solar short wave radiation induced gas ionization 08 p0999 A73-21338

Cloud-cloud collision destruction of interstellar clouds in inter-spiral arm regions, discussing observational tests 09 p1141 A73-22028

The influence of dust upon the dynamics and thermal stability of planetary nebulae. 09 p1142 A73-22032

Properties of H I regions heated by X rays and cosmic rays. 09 p1147 A73-22730

Characteristics of the diffuse /tenous/ interstellar medium determined from radio recombination lines. 09 p1150 A73-23137

Chemical composition of the interstellar gas - X-ray determinations. 10 p1263 A73-23480

Statistical significance of some optical evidence for the bending of the galactic plane. 10 p1271 A73-23492

Luminosity and frequency spectrum of radiation from spherically symmetric steady state accretion of interstellar gas onto nonrotating black hole at rest 10 p1272 A73-23534

Formation of stars in a rotating cloud with magnetic field. 10 p1275 A73-23830

Isotopic combination identification in interstellar clouds through radio spectral line observations, discussing millimeter wave astronomy, molecular clouds, excitation mechanisms, galactic structure, etc 10 p1280 A73-24323

X ray ionization and heating of H I regions refuted from energy input rate computations of observed flux in Galactic plane 11 p1415 A73-25118

Search for neutral hydrogen in the galactic cluster NGC 2287. 11 p1415 A73-25119

Particle injection in the Cygnus X-3 radio outburst. 11 p1419 A73-25859

Disk model of gas accretion on a relativistic star in a close binary system. 12 p1539 A73-27277

High Galactic latitude intermediate-negative velocity neutral hydrogen properties, noting large complexes and systematic velocity pattern 13 p1671 A73-28029

The heating of interstellar clouds by vibrationally excited molecular hydrogen. 13 p1673 A73-28279

Interstellar cloud collapse into protostellar objects and star formation, discussing young stellar objects observation 13 p1681 A73-28946

On the kinematics of a local component of the interstellar hydrogen gas possibly related to Gould's Belt. 13 p1686 A73-29369

A search for H alpha emission from interstellar clouds. 14 p1797 A73-30008

Stark broadening of high-principal-quantum-number n-alpha lines of hydrogen. 14 p1777 A73-30552

Interstellar gas abundances from rocket observations of ultraviolet absorption lines. 14 p1801 A73-30734

Search for interstellar absorption in 4250 Å line of singly ionized CO in direction of different stars 14 p1801 A73-30736

Spectrophotometric results from the Copernicus satellite. IV - Molecular hydrogen in interstellar space. 14 p1802 A73-30747

Deuterium in interstellar molecules. 14 p1802 A73-30749

Time-dependent models of the interstellar gas. 14 p1802 A73-30960

Interstellar gas excitation due to supernova explosions using time dependent model based on statistical correlation of gas neutral density, ionization and temperature parameters 15 p1928 A73-31053

Aperture synthesis study of neutral hydrogen in NGC 2403 and NGC 4236. I - Observations. 15 p1929 A73-31056

Primordial cosmic ray abundance from rotating magnetic A stars with accelerating ionized interstellar gas particles 15 p1925 A73-31059

Small perturbation method study of nonlinear weak D-type unsteady ionization front geometry with radiation source in interstellar incompressible gas medium 15 p1932 A73-31295

Interaction of solar wind with interstellar neutral gas at the heliospheric boundary. 15 p1926 A73-31380

Two-component equilibrium model of the HI regions of the interstellar medium satisfying a set of radio observations 15 p1938 A73-31965

Interaction between the interstellar medium and solar wind plasma. 15 p1927 A73-32001

Absorption and production of soft X-rays in the Galaxy. 16 p2051 A73-32746

Fabry-Perot interferometric studies on H II regions. 16 p2058 A73-32831

Galactic neutral hydrogen observations along loop III, noting loop effects on gas velocity distribution 16 p2058 A73-32835

Thermal and ionization equilibrium in a dense hydrogen cloud. 16 p2059 A73-32841

Single-fluid model of the distant solar wind. 16 p2056 A73-33459

Cosmic antiproton production in interstellar pp collisions. 17 p2223 A73-34099

Cosmic ray pulses conduction to interstellar gas by magnetic field, describing effects on sound vibration 17 p2223 A73-34369

Numerical model construction for primitive solar nebula and physical accumulation processes within collapsing interstellar gas cloud 17 p2227 A73-34405

IR and molecular radio emissions from interstellar clouds representing formation stage of normal stars, discussing dust screening effects 17 p2229 A73-34433

Time-dependent radiative cooling of a hot low-density cosmic gas. 17 p2231 A73-34756

Thermal structure and evolution of interstellar gas exposed to a soft X-ray burst. 17 p2231 A73-34757

A discussion of the distribution of interstellar matter close to the sun. 17 p2234 A73-35619

On the role of plasma effects in the cosmic ray propagation and isotropization in the galaxy. 17 p2225 A73-35779

A survey of interstellar formaldehyde in dust clouds. 19 p2475 A73-37610

On the ionization of the intercloud medium by ultraviolet stars. 19 p2484 A73-37611

Galactic shocks as consequence of large amplitude nonlinear density waves in interstellar gas perturbed via steady forcing by spiral gravitational fields 19 p2488 A73-38511

A low temperature bolometer heterodyne receiver for millimeter wave astronomy. 20 p2564 A73-38878

Cold gas cloud embeddings in interstellar hot gas, determining radiation temperature from absorption line profiles and kinetic temperature from thermal and turbulent energy components 20 p2606 A73-39066

Quasar scintillations at an inhomogeneous interstellar plasma 21 p2767 A73-40535

Variations of pulsar intensity as a result of scintillations at an inhomogeneous plasma 21 p2767 A73-40536

Role of plasma effects in the propagation and isotropization of cosmic rays in the Galaxy 21 p2756 A73-40579

Neutral interstellar hydrogen and extraterrestrial Lyman alpha radiation. 21 p2773 A73-41396

- A 21-cm radio spectrograph 21 p2705 A73-41462
- Comment on 'Anomalous hyperfine lines in formaldehyde in a dust cloud.' 22 p2904 A73-41755
- Aperture synthesis of interstellar neutral hydrogen in absorption. I - The Perseus arm feature of Cassiopeia A. 22 p2904 A73-41756
- Dynamical evolution of an expanding gas cloud. 22 p2840 A73-41758
- On the E sub 1-E sub 2 labeling of energy levels and the anomalous excitation of interstellar methanol. 22 p2914 A73-43005
- Measurements of recombination of electrons with HCO⁺ ions. 23 p3007 A73-43530
- Distribution of interstellar hydroxyl in the Cyg X region 23 p3035 A73-44231
- Two-component equilibrium model of interstellar HI regions that satisfy the overall radio observations. 24 p3132 A73-44490
- Resonance scattering from interstellar and interplanetary helium. 24 p3140 A73-45188
- ### INTERSTELLAR MAGNETIC FIELDS
- Generation of the large-scale galactic magnetic field. II. 01 p0107 A73-11329
- The stability of a self-gravitating, nonrotating gas layer with stellar, magnetic, and cosmic-ray components. II. 07 p0873 A73-19058
- Cellular or filamentary structure of galactic magnetic fields, noting correlations between rotations of radio sources and angular separation 08 p1002 A73-20880
- Realization of a zero-force magnetic field configuration in the case of axisymmetric magnetohydrodynamic flows 09 p1146 A73-22541
- Turbulent plasma dynamo mechanisms of magnetic field origin in astrophysics, noting Steenbeck and Parker theories 10 p1285 A73-24942
- Photon rest mass limit determination from Galactic magnetic field measurements, utilizing maximum current density capability of plasmas 11 p1415 A73-25121
- Condensation of stars and magnetic field formation in protogalaxies 12 p1547 A73-27868
- Galactic loops as supernova remnants in the local galactic magnetic field. 13 p1672 A73-28042
- Crab Nebula magnetic field origin and internal electron acceleration mechanism nature 13 p1673 A73-28225
- The effect of interstellar medium parameters on the accretion by neutron stars. 13 p1687 A73-29658
- Magnetic stars formation from interstellar matter in presence of interstellar magnetic field, considering critical mass based on Chandrasekhar-Fermi virial theorem 14 p1799 A73-30426
- Cosmic ray pulses conduction to interstellar gas by magnetic field, describing effects on sound vibration 17 p2223 A73-34369
- Magneto-gravitational and thermal instability in the Galactic disk. 17 p2231 A73-34752
- A stochastic model of the galactic magnetic field. 18 p2356 A73-36974
- The rate of separation of magnetic lines of force in a random magnetic field. 19 p2489 A73-38522
- Magnetic stars origin from gravitational collapse of ionized hydrogen clouds, discussing implications of interstellar magnetic fields and critical mass according to Chandrasekhar-Fermi virial theorem 20 p2605 A73-39058
- Polarization of stellar light between the two Magellanic clouds 20 p2606 A73-39063
- Star contraction and magnetic-field generation in protogalaxies. 20 p2608 A73-39242
- Model for gas bridge and magnetic field connecting Magellanic Clouds from optical and radio polarization measurements 21 p2779 A73-41535
- The generation and dissipation of solar and galactic magnetic fields. 22 p2911 A73-42934
- A numerical study of the explosion of a supernova into the interstellar magnetic field. 22 p2914 A73-43007
- Pulsar radio observations of magnetic field, electron density and neutral hydrogen atoms in interstellar space 23 p3028 A73-43369
- Accretion onto black holes - The emergent radiation spectrum. II Magnetic effects. 24 p3138 A73-45036
- ### INTERSTELLAR MATTER
- Cool giant star-ejected high velocity dust grains interaction with interstellar clouds, discussing solid state defect accumulation, sputtering and grain and cloud heating 01 p0098 A73-10582
- New interpretations of extraterrestrial Lyman-alpha observations. 02 p0206 A73-12323
- Further evidence for a cosmic ray selection mechanism. 02 p0207 A73-12397
- Diffuse galactic FUV radiation and interstellar dust grains. 02 p0207 A73-12399
- Cosmic-ray production of deuterium, He/3, lithium, beryllium, and boron in the galaxy. 02 p0208 A73-12412
- Solar neighborhood dynamically determined mass discrepancy with observed stars and interstellar matter, proposing low mass invisible stars existence 02 p0218 A73-12413
- Heavy elements depletion on grains in interstellar medium two phase model, noting gas dynamical analysis of discrete clouds evolution 03 p0366 A73-12931
- 4830 MHz observations of the formaldehyde molecule in the direction of discrete radio sources. 03 p0371 A73-13214
- Molecular clouds and stellar origin in interstellar space 03 p0376 A73-14175
- Interstellar molecules detection, sources and destruction observed via visible, UV and radio wave spectra 04 p0501 A73-15627
- Interstellar magnesium abundances and electron density in the direction of Orion and Cassiopeia. 04 p0502 A73-15976
- Physical significance of interstellar matter accretion on rotating magnetized star with emphasis on implications for X ray sources 04 p0493 A73-15979
- Interaction of stars with local dust formations. 04 p0503 A73-16008
- Diffuse radiation of a two-layer galaxy with carbon-silicate particles 05 p0617 A73-16460
- The formation of diatomic molecules in interstellar clouds. 05 p0625 A73-17333
- A study of the unidentified interstellar diffuse features. 05 p0626 A73-17379
- Interstellar matter. II - Diffuse interstellar lines and porphyrins. 06 p0750 A73-18013
- Interstellar molecules and cosmochemistry; Proceedings of the Conference, New York, N.Y., June 16-18, 1971. 06 p0751 A73-18226
- Interstellar elemental abundance table from carbonaceous chondrites and solar abundances, considering solar Fe composition 06 p0752 A73-18232
- Interstellar medium chemical composition, considering emission line spectra, density fluctuations, He/H ratio in different galaxies and H II regions 06 p0752 A73-18233
- Cosmochemical evolution of large organic molecules - Illustrative laboratory simulations for porphyrins. 06 p0752 A73-18235
- Photochemistry chemical kinetics in the interstellar medium. 06 p0752 A73-18236
- Nonlinear mode-mode coupling of Alfvén waves in the interstellar medium. 06 p0730 A73-18465
- Study of the galactic structure from observations of interstellar calcium. I - Analysis of radial velocities 08 p1004 A73-20909
- Low-intensity Balmer emissions from the interstellar medium and geocorona. 08 p1009 A73-21167
- Galactic dust region molecular cloud effects on cloud chemical evolution, star and planetary formation and life development on planets 09 p1140 A73-21975
- On the presence of H₂ molecules inside neutral globules imbedded in H II regions. 09 p1140 A73-22005
- Galactic interstellar molecules, discussing physical, chemical and spectral characteristics, hydroxyl emission, occurrence regions, hydrogen clouds, isotope ratios, interstellar masers and probes 09 p1146 A73-22446
- Galactic absorbing material effects on quasar apparent distribution, noting brightness decrease with red shift 09 p1147 A73-22572
- On the detection of H₂ from interstellar clouds in the wavelength range 4.4 to 28.2 microns. 09 p1148 A73-22870
- Radio halos around old pulsars - Ghost supernova remnants. 09 p1148 A73-22871
- Observational, theoretical, and predicted data on the infrared and microwave spectra of interstellar matter [Introductory report]. 09 p1150 A73-23135
- Spectroscopy of tetrabenzoporphin molecules and possible astrophysical implications. 09 p1048 A73-23136
- Ultraviolet effects on the chemical composition and optical properties of interstellar grains. 09 p1150 A73-23138
- Interferometric observations of formaldehyde absorption in front of strong galactic sources. 09 p1150 A73-23139
- Formamide rotational transition microwave emission detection in interstellar medium in Sgr B2 and Sgr A direction 09 p1150 A73-23140
- Interstellar organic molecules millimeter wave line spectra and transition rotational quantum numbers 09 p1150 A73-23141
- Stellar spectrometry by Fourier transformation from 2 to 5 micron 09 p1150 A73-23142
- Observations of the outer spiral structure of the Milky Way and its relation to the high velocity clouds. 09 p1151 A73-23292
- Interstellar and interplanetary dust grains orientation distribution function in anisotropic corpuscular or radiation fluxes 10 p1271 A73-23482
- The evolution of interstellar clouds. II - Hydrodynamic treatment of the phase change. III - Cloud collisions and statistical theory. 10 p1272 A73-23531
- Faraday pulsations and circular polarization of optical radiation from cosmic sources in terms of angle between interstellar dust orientation vector and galactic plane 10 p1273 A73-23709
- Thermal instability caused primary interstellar dust cloud fragmentation and resulting star formation according to Peebles-Dicke hypothesis for cosmological origin of globular clusters 10 p1274 A73-23713
- Validity of zeta Oph cloud carbon isotope abundance extrapolation to dense dusty regions of Galactic center and Orion Nebula 10 p1275 A73-23824
- The extinction curve for Cygnus OB2 no. 12. 11 p1414 A73-25068
- Russian book - Physics of stars and nebulae. 11 p1416 A73-25226
- Investigation of the diffuse glow of the clouds of dark absorbing matter in the region of the Aquila constellation 11 p1416 A73-25229
- Luminescence of isolated dark clouds caused by the integral field of stellar galactic radiation 11 p1416 A73-25234
- Thermochemical calculation for high temperature and pressure formation of interstellar molecules in compact H II regions, considering prestellar and late stellar atmospheres 11 p1423 A73-26105
- Interferometric studies of interstellar CH₄+/molecules. 11 p1427 A73-26617
- Atoms and molecules in astrophysics; Proceedings of the Twelfth Session of the Scottish Universities Summer School in Physics, University of Stirling, Stirling, Scotland, August 1971. 12 p1538 A73-26920
- Universe evolution explanation via interstellar deuterium investigation, discussing galactic gas chemical composition history 12 p1543 A73-27692
- Annual solar activity changes due to interstellar matter capture by sun, noting uneven sunspots distribution 12 p1535 A73-27770
- Interstellar molecules and radio spectroscopy in the cm- and mm-wave range 12 p1544 A73-27779
- Molecule formation. I - In normal H I clouds. II - In interstellar shock waves. 12 p1547 A73-27973
- On a correlation between the magnitude and the radial velocity of hot stars. 13 p1672 A73-28036
- On the observability of far infrared line emission originating from the interstellar medium. 13 p1686 A73-29368
- Interaction of the interstellar medium with the solar wind. 14 p1787 A73-30543
- Ionization of the intercloud medium and the central disk regions of spiral galaxies. 14 p1801 A73-30729
- Interferometric observations of formaldehyde absorption in front of strong galactic sources. 14 p1801 A73-30735

Spectrophotometric results from the Copernicus satellite. II - Composition of interstellar clouds.

14 p1801 A73-30745

Spectrophotometric results from the Copernicus satellite. III - Ionization and composition of the intercloud medium.

14 p1801 A73-30746

Spectrophotometric results from the Copernicus satellite. V - Abundances of molecules in interstellar clouds.

14 p1802 A73-30748

Observations of formamide at 6 cm in Sagittarius B2.

15 p1933 A73-31377

Detection of interstellar thioformaldehyde.

15 p1933 A73-31378

Relationship between T-associations and the interstellar medium in the northern region of the Monoceros complex

15 p1934 A73-31421

The fluorine abundance in the galactic cosmic radiation.

15 p1926 A73-31552

Production of astrophysical X-rays by transition radiation.

15 p1926 A73-31553

The absence of formaldehyde radiation toward cold regions of the galactic plane - Further investigation.

15 p1936 A73-31554

Cosmic abundance of boron.

15 p1942 A73-32648

Methylacetylene and isocyanic acid data from April 1972 and February 1973 observation of interstellar media in direction of Galactic center source Sgr B2

16 p2060 A73-33095

Interstellar matter observations, discussing densest stages spatial distribution near solar system and dense clouds

17 p2227 A73-34409

Silicates and water identification in interstellar grains, considering possibility of iron and carbon components

17 p2227 A73-34410

Transition radiation from interstellar dust grains.

17 p2231 A73-34755

Faraday pulsations and circular polarization of optical radiation from cosmic sources in terms of angle between interstellar dust orientation vector and galactic plane

18 p2354 A73-36734

Thermal instability caused primary interstellar dust cloud fragmentation and resulting star formation according to Peebles-Dicke hypothesis for cosmological origin of globular clusters

18 p2355 A73-36738

Book - General astrophysics with elements of geophysics.

18 p2356 A73-36968

The effect of hot white dwarfs on the interstellar medium. II - The changes in its structure with height above the galactic plane and some consequences of the finite lifetimes and velocities of the white dwarfs.

19 p2483 A73-37561

Feature recognition method in small scale structure analyses of neutral hydrogen emissions, applying to surveys at negative intermediate galactic latitudes

19 p2483 A73-37562

X-ray absorption and optical extinction in interstellar space.

19 p2475 A73-37567

Oscillator strength calculations for vibrational transitions of X-A electronic system of interstellar CH positive ion, noting agreement with astrophysical observations of line spectra

19 p2488 A73-38512

Dissociative recombination rate for CH positive ions in interstellar clouds

19 p2490 A73-38531

OH observations of sixteen interstellar dust clouds.

20 p2607 A73-39118

Life origin hypothesis based on interstellar molecular concentration in gas clouds, examining radical types and molecular Doppler spectra

21 p2638 A73-41080

Measurements of neutral-hydrogen absorption in the spectra of eight pulsars.

21 p2779 A73-41538

Doublet ratio method for abundance determination application to interstellar multiple clouds, considering column density error due to velocity distribution simplification

22 p2910 A73-42703

A search for interstellar acrylonitrile, pyrimidine, and pyridine.

22 p2821 A73-43004

Theory of interstellar abundances of the isotopes of carbon, nitrogen and oxygen.

22 p2914 A73-43006

Cosmic deuterium abundance derived from measured HD/H₂ ratio, noting derivation sensitivity to ionizing flux and to oxygen and carbon depletion

22 p2904 A73-43119

Ion-grain collision cooling rate for hot gas above million K, discussing applications to supernova explo-

sions, Seyfert nuclei and intergalactic matter within galactic clusters

22 p2916 A73-43121

Spectral line radio astronomy observations of interstellar molecular clouds in Galaxy, relating to stellar and life evolution

23 p3028 A73-43350

Interstellar grain temperature fluctuations due to interstellar radiation field, discussing H atom recombination problem

23 p3029 A73-43747

Accretion and electrostatic interaction of interstellar dust grains - Interstellar grit.

23 p3030 A73-43757

Many body model for comet nucleus formation from solid materials and interstellar gas consistent with Whipple icy conglomerate model

24 p3131 A73-44466

Scattered-light phenomena in interstellar space

24 p3137 A73-44824

Production of gamma radiation in dense interstellar clouds by cosmic-ray interactions.

24 p3125 A73-45054

Interstellar trace element ionization predictions by cosmic ray, X-ray and UV star models with hydrogen allowance, showing disagreement with satellite observation

24 p3125 A73-45056

INTERSTELLAR MICROWAVE SPECTRA

U INTERSTELLAR RADIATION

U MICROWAVE SPECTRA

INTERSTELLAR RADIATION

The short-wavelength spectrum of the microwave background.

01 p0015 A73-10062

Instrumental considerations in high dispersion requirements of stellar spectroscopy and interstellar absorption and emission line studies, emphasizing spectral resolution and SNR optimum determination

01 p0046 A73-10503

Diffuse interstellar lines and bands interpreted as extinction structure due to impurities in cosmic dust grains, comparing theory with observation

02 p0225 A73-12807

Interstellar OH lambda doublet radiation observations at 5 cm from six galactic sources and IR star, observing various transitions

03 p0366 A73-12930

Possible cause of the variations of the intensity of an interstellar maser.

04 p0493 A73-16023

Interstellar matter. II - Diffuse interstellar lines and porphyrins.

06 p0750 A73-18013

Interstellar extinction curve structure via photographic techniques, considering optical observation extension into UV with OAO-C telescope

06 p0751 A73-18228

Stellar and interstellar K lines - Gamma Pegasi and iota Herculis.

08 p1003 A73-20882

Interstellar Na I, K I, Ca II, and CH⁺ line profiles toward zeta Ophiuchi.

10 p1273 A73-23549

Energy spectrum of galactic cosmic rays beyond the region of modulation and the anisotropy of cosmic rays in the Galaxy

10 p1267 A73-23925

Contribution of pion production by primary cosmic-ray nucleons to the interstellar electron-positron flux.

10 p1269 A73-24348

Interstellar microwave radiation measured by spectroscopic analysis of chemical composition, distribution, excitation and emission data

16 p2058 A73-32722

Satellite measurements of interstellar gamma radiation, describing spark chamber and optical recording system

18 p2349 A73-35975

Evidence for an interstellar or interplanetary source of diffuse He I 584 A radiation.

19 p2475 A73-37629

Interstellar grain temperature fluctuations due to interstellar radiation field, discussing H atom recombination problem

23 p3029 A73-43747

INTERSTELLAR REDDENING

U INTERSTELLAR EXTINCTION

INTERSTELLAR SPACE

Theoretical structure and spectrum of a shock wave in the interstellar medium - The Cygnus Loop.

04 p0499 A73-15359

Diatom molecule formation in interstellar medium via two body collision, calculating rate coefficients for radiative association

06 p0752 A73-18231

Comets origin in interstellar space or solar system evaluated with-reference to comet streaming from perihelions statistical analysis, assuming Oort cloud accretion

14 p1794 A73-29838

Remote sensing of LF nonthermal radio emission for composition and dynamic processes of interplane-

tary and interstellar media and planetary magnetospheres

14 p1800 A73-30539

INTERSTELLAR TRAVEL

The effects of drag on relativistic spaceflight.

01 p0095 A73-10274

Interstellar flight and intelligence in the Universe.

03 p0370 A73-13198

Magnetic intake limitations on interstellar ramjets.

10 p1262 A73-24539

Reaction equilibrium and energy balance in thermonuclear fusion propulsion for interstellar space flight, discussing nuclear fuel and ion temperature effects

10 p1262 A73-24544

Propulsion system optimization for interstellar probes.

15 p1943 A73-32217

Superrelativistic interstellar flight or cracks in the light barrier.

17 p2234 A73-35658

Stardrift - A navigational system for relativistic interstellar flight.

17 p2210 A73-35659

Propulsion system optimisation for a single-stage constant-thrust relativistic rocket.

18 p2361 A73-37037

Decelerator sail erosion during interstellar vessel deceleration, using drag screens to improve vehicle mass ratio via propellant requirement reduction

18 p2361 A73-37039

Long range post-Apollo space exploration goals, considering earth orbital station, moon base, manned Mars landing and interstellar flights

23 p3038 A73-43990

INTERSTITIALS

Effect of interstitial edema on distribution of ventilation and perfusion in isolated lung.

01 p0008 A73-10167

Thermal properties of tantalum-tungsten alloys at high temperatures.

03 p0322 A73-13192

Tensile strength dependence on temperature and interstitial oxygen and nitrogen concentration in powdered Nb, noting microhardness and yield point

03 p0326 A73-13968

Symposium on Capillary Exchange and the Interstitial Space, Bad Duerkheim, West Germany, May 3-6, 1972, Proceedings.

03 p0265 A73-14649

Dislocation dynamics in niobium-oxygen solid solutions.

04 p0462 A73-15303

Dislocation interstitial impurities interactions in high purity Mo, using dislocation damping techniques

04 p0462 A73-15304

Zone refining of chromium alloys with rare-earth metals

06 p0707 A73-18042

Investigation of dislocation locking by interstitial impurities in bcc-lattice metals

06 p0708 A73-18055

Diffusion of hydrogen in titanium alloys due to composition, temperature, and stress gradients.

06 p0712 A73-18764

Mechanical properties of interstitial alloys of niobium.

07 p0838 A73-19123

Some further comments on Stage III recovery in Group VA body-centered cubic transition metals.

07 p0839 A73-20113

Nature of chemical bonds in metal-like compounds based on transition metals

07 p0841 A73-20519

Effects of composition and structure on the creep strength of molybdenum bearing ferritic steels.

08 p0982 A73-21796

Loading mode effects on high strength steel hydrogen embrittlement, considering stress tensor invariants and interstitial diffusion relationships

09 p1102 A73-22414

Phase equilibria in three-component alloys containing an interstitial element, and the stability of composite materials

10 p1233 A73-24317

Stability of micromorphology of carbon fibres and their interstitial compounds.

11 p1389 A73-25858

Influence of the chrome content and the interstitial impurities content /carbon and nitrogen/ on the volumetric and intergranular diffusion of iron 59' in iron-chrome alloys with from 0 to 15 per cent chrome - Relations with alpha to alpha plus gamma reversible transformations

12 p1514 A73-27985

Characteristics of the decomposition of an interstitial-impurities solid solution in molybdenum during recrystallization

14 p1760 A73-30589

German monograph - The effect of interstitial elements and recrystallization on the defined yield point of titanium.

14 p1762 A73-30665

Influence of interstitial impurities on the formation of a cellular structure and on the properties of chromium 14 p1764 A73-30858

Influence of interstitials on the behavior in tension of niobium between 20 and 1000 C 17 p2193 A73-35624

Effects of interstitial content and grain size on the strength of titanium at low temperatures. 19 p2440 A73-37542

Field-ion-microscopic study of interstitial plasticity of tungsten microcrystals. 22 p2872 A73-41726

Interaction of interstitial impurities with iron-subgroup metals in as-cast molybdenum-based dilute solid solutions 22 p2873 A73-42090

Patterns of the structure of transition metal/interstitial element diagrams /Me - B, C, N, O, H/ 22 p2877 A73-42452

Dislocation locking by interstitial oxygen atoms and the temperature dependence of the yield point in niobium 24 p3099 A73-44574

INTERVALS

Admissible step sizes for Adams-Bashforth, Adams-Moulton, Nystrom and Milne-Simpson difference methods for initial value problems solution 11 p1392 A73-26729

INTESTINES

EMG from smooth musculature /uterus, ureter, gut/ in unrestrained animals monitored by telemetry. 03 p0271 A73-14297

Relationship between cyclic AMP, phosphodiesterase activity, calcium and contraction in intestinal smooth muscle. 21 p2638 A73-41130

INTOXICATION

Effects of ethyl alcohol on pilot performance. 13 p1579 A73-28501

INTRACRANIAL CAVITY

The role of the elastic properties of brain and spine cavities in hyperemia compensation 18 p2276 A73-36572

INTRACRANIAL PRESSURE

The use of telemetry to study the physiological and clinical variations of intracranial pressure in man. 03 p0271 A73-14300

INTRAMOLECULAR STRUCTURES

On the dimensions of intramolecularly crosslinked polymer molecules. I - The synthesis and chemical characterization of intramolecularly crosslinked polystyrene molecules having a narrow distribution of molecular weight. II - The theoretical prediction of the dimensions in solution of intramolecularly crosslinked polystyrene molecules. III - The measurement of the dimensions of intramolecularly crosslinked polystyrene. 23 p3008 A73-43795

INTRAOCULAR PRESSURE

Ocular tonus measurements for glaucoma detection in flying personnel, discussing subsequent test procedures in case of abnormal findings 02 p0134 A73-12158

Functional dependence of the ciliary epithelium ATPase activity and intraocular pressure on the autonomic nervous system. 05 p0539 A73-16248

Retinal vessel reactions and intraocular tension in humans staying in a horizontal position for 120 days 15 p1835 A73-31514

Patterns of diurnal variation in the intraocular pressure of airline pilots. 20 p2512 A73-39107

Ocular tension in flying personnel 21 p2637 A73-40347

Participation of the hypophysis and adrenal glands in intra-ocular pressure regulation 22 p2807 A73-42661

INTRAVASCULAR SYSTEM

Intravascular changes associated with hyperbaric decompression - Theoretical considerations using ultrasound. 09 p1045 A73-22534

INTRAVEHICULAR ACTIVITY

Description of the docking module ECS for the Apollo-Soyuz Test Project. [ASME PAPER 73-ENAS-21] 19 p2493 A73-37977

INTRAVENOUS PROCEDURES

External field electromagnetic measurement of blood flow - An alternative approach to the solution of the baseline problem. 04 p0414 A73-15992

Analysis of indicator distribution in the determination of cardiac output by thermal dilution. 08 p0933 A73-21216

Choice of detection site for the determination of cardiac output by thermal dilution - The injection-thermistor-catheter. 08 p0933 A73-21217

Permanent catheterism of the thoracic aorta - Direct measurement of arterial pressure, injection of substances, and the taking of blood in wake rats 24 p3065 A73-45160

INVARIANCE

NT GAUGE INVARIANCE

Variational method in the invariance problem for controlled systems. 02 p0149 A73-12117

Invariant criterion generalization for pure gravitational waves in tetrad formulation of general relativity theory, noting electromagnetic field energy tensor 04 p0476 A73-15638

Invariance principle extended to bounded uncertain time-varying systems, deriving asymptotic Liapunov stability criteria with application to guaranteed cost control problems 05 p0590 A73-16492

Harmonic frames of reference in Einstein's theory of gravitation. 05 p0598 A73-16791

Scaling invariance hypothesis for local structure of turbulence, using quantum field theory methods 06 p0686 A73-17977

Gravitation finite range evidence presentation of major theoretical problem for general relativity, discussing continuity and invariance 06 p0724 A73-18548

Invariance conditions and controllability relation of linear and nonlinear dynamic systems, including composite systems and systems with deviating argument 06 p0724 A73-18678

Conformally invariant cosmological and physical models in terms of Einstein, Maxwell and Dirac equations 08 p1009 A73-21228

Conformal invariance of the equations of motion in curved spaces. 10 p1241 A73-23637

Vehicle coordinate-parametric control problems and some solution methods. 10 p1198 A73-24007

A structural model of random processes and its invariant properties 11 p1340 A73-25007

Accuracy of conserving the third adiabatic invariant of the motion of a charged particle in axially symmetrical fields. II. 12 p1535 A73-27634

Elastostatic invariance in the composite plane. 13 p1696 A73-28747

Matrix invariant subspace computation via LU, QR, treppen and bi-iterations, comparing to power method 14 p1768 A73-29940

Kinematic invariants and their relation to chromometric invariants in Einstein's theory of gravitation 15 p1913 A73-31246

Optimal invariant solution for compensating circuit of nonlinear control system under disturbances, using unperturbed motion prediction 20 p2538 A73-38676

Dynamical symmetries of the Kepler problem and of the harmonic oscillator in classical mechanics revisited. 22 p2887 A73-42429

Experimental study of the adiabatic invariant of self-oscillating processes 23 p3006 A73-43850

Group properties and invariant solutions in the problem of the analytic design of controllers for a process with distributed parameters. 24 p3074 A73-44661

Weak invariance conditions and synthesis algorithms for control systems with discontinuities on hypersurfaces in phase space 24 p3074 A73-44666

INVARIANT IMBEDDINGS

Invariant imbedding and Chandrasekhar's planetary problem of radiative transfer. 02 p0207 A73-12389

Mathematical algorithm using invariant imbedding method for accurate range and range rate estimates in terms of pulse Doppler radar ambiguity resolution 03 p0276 A73-13902

Application of invariant imbedding techniques to flow instability problems. [AD-756824] 05 p0591 A73-16608

An analysis of optimal control system algorithms. 06 p0670 A73-18059

Invariant imbedding and a transformation procedure for reducing classes of boundary value problems into equivalent initial value systems. 06 p0719 A73-18804

Application of the principle of invariant imbedding in the solution of optimal control problems 09 p1069 A73-22722

Use of the principle of invariant imbedding in solving an optimal control problem. 14 p1740 A73-30955

Book - Methods of nonlinear analysis, Volume 2. 17 p2200 A73-34453

INVENTORIES

NT TIMBER INVENTORY

Regional land inventory systems development in the Houston area. 20 p2629 A73-39832

INVESTMENT CASTING

A comprehensive remote sensing legend system for the ecological characterization and annotation of natural and altered landscapes. 20 p2557 A73-39851

INVENTORY CONTROLS

Optimal control in a finite time interval for discrete systems in the minimization problem of an inhomogeneous quadratic functional /a case of fixed terminals/ 15 p1854 A73-31802

Optimal control over a finite time-interval for discrete systems in the problem of minimizing an inhomogeneous quadratic functional /The case of fixed end-points/. 23 p2965 A73-44331

INVENTORY MANAGEMENT

NT INVENTORY CONTROLS

The use of model building in a production environment. 06 p0698 A73-18514

INVERSIONS

NT CENTRIFUGING STRESS

NT POPULATION INVERSION

NT TEMPERATURE INVERSIONS

Pivoting for size and sparsity in linear programming inversion routes. 06 p0716 A73-17978

Inversion of Prony series characterization for viscoelastic stress analysis. 09 p1158 A73-22393

Inversion illusion in the so-called zero-gravity conditions of parabolic flight. 14 p1722 A73-30511

INVERTEBRATES

NT ARTHROPODS

NT BEES

NT CRABS

NT DROSOPHILA

NT INSECTS

NT PROTOZOA

NT TRIBOLIA

Light evoked responses in invertebrate photoreceptor cells, considering cell organization, microvilli, lateral eye of Limulus, generator potentials, visual responses, etc 09 p1042 A73-23307

INVERTED CONVERTERS [DC TO AC]

Analysis of commutator inverters with allowance for capacitive coupling to an ac amplifier 13 p1591 A73-28854

Voltage-to-frequency converters with an avalanche-recombination discharge diode 22 p2832 A73-42357

Analysis of starting circuits for a class of hard oscillators - Two-transistor saturable-core parallel inverters. 22 p2834 A73-42909

System oscillations from negative input resistance at power input port of switching-mode regulator, amplifier, dc/dc converter, or dc/ac inverter. 22 p2802 A73-42911

Sequence amplitude modulated inverters. 22 p2802 A73-42917

INVERTERS

NT STATIC INVERTERS

Circuit variants of dynamically operated MIS /metal-insulator-semiconductor/ structures 03 p0281 A73-13241

Analysis of limit cycles in a two-transistor saturable-core parallel inverter. 03 p0252 A73-13929

High power inverter with commutator of single LC network and steering SCR capable of multiple high voltage dc bridge operation 03 p0253 A73-13936

Statistical approach to the prediction of M.O.S.-device performance. 08 p0946 A73-21116

Methods of calculating high-power rectifier and inverter circuits 15 p1832 A73-31696

An analog computer study of a thyristor inverter with opposite-parallel diodes under load switched-on between input throttles 15 p1851 A73-31697

Transient analysis of complementary MOS IC inverter. 16 p1990 A73-33688

Analysis of limit cycles in a two-transistor saturable-core parallel inverter. 21 p2662 A73-40339

Complementary MOS transistor inverter application to quartz oscillator in terms of frequency, temperature and supply voltage 23 p2960 A73-44112

INVESTIGATION

NT ACCIDENT INVESTIGATION

NT AIRCRAFT ACCIDENT INVESTIGATION

INVESTMENT CASTING

Lost-model method of precision casting - Its possibilities, limitations and present trends 07 p0831 A73-20160

The casting of titanium and its alloys by the lost-model method 07 p0831 A73-20161

- Advances in directional solidification spur usage in turbine airfoil shapes. 09 p1089 A73-23293
- Equipment for casting directionally solidified parts. 09 p1089 A73-23294
- Study on material for investment cast turbine wheel. 13 p1642 A73-29518

INVESTMENTS

- World Bank support for airports. 22 p2938 A73-42317

INVISCID FLOW

NT STAGNATION FLOW

- An extremum principle for three-dimensional compressible inviscid flows. 01 p0031 A73-10427

- Nonlinear waves on interface of two incompressible inviscid fluids of different densities and arbitrary surface tension analyzed by multiple scales method. 01 p0032 A73-10445

- Three-dimensional effects on electron density in a blunt body laminar boundary layer. 01 p0002 A73-10731

- Shear layer extent caused by slip surface in inviscid flow with shock interactions, noting viscous effect in hypersonic flow. 01 p0033 A73-10747

- Two-dimensional, unsteady, self-similar flows in gas dynamics. 02 p0152 A73-11569

- Solution of the wedge entry problem by numerical conformal mapping. 03 p0244 A73-13537

- Three dimensional flow pattern from two dimensional supersonic inviscid gas flows around wedged body. 03 p0245 A73-13675

- Asymptotic solution for inviscid conducting fluid flow past arbitrary wing profile in magnetic field. 03 p0347 A73-14045

- Small disturbance theory of rotating subsonic and transonic cascades. 03 p0246 A73-14136

- Flow conditions at inlet and exit of a flat plate cascade at supersonic velocities. 03 p0246 A73-14139

- Calculation of metric coefficients for streamline coordinates. 03 p0247 A73-14196

- Oscillatory point force generated motion in inviscid incompressible rotating stratified fluid, obtaining closed form solutions via Fourier transforms. 03 p0296 A73-14313

- The prediction of airfoil pressure distributions for subcritical viscous flow and for supercritical inviscid flow. 03 p0247 A73-14378

- Stability of nonrotationally symmetric disturbances for inviscid flow between rotating cylinders in the presence of an axial magnetic field. 04 p0433 A73-14899

- On the uniformly valid approximate solutions of Laplace equation for an inviscid fluid flow past a three-dimensional thin body. [ONERA, TP NO. 1145] 04 p0433 A73-15094

- Mathematical prediction for pressure distribution over arbitrary thin airfoil in inviscid potential and real fluid flows, determining velocity increment at leading edge. 05 p0527 A73-16593

- Linearized theory for infinite span wing small unsteady motions in curved flight in inviscid incompressible fluid, obtaining time dependent forces, pressure and velocity fields. [AIAA PAPER 73-90] 05 p0529 A73-16854

- A correction to 'lifting-line theory as a singular perturbation problem.' 07 p0775 A73-19964

- Stability of clamped rectangular plates in uniform subsonic flow. 07 p0913 A73-19982

- A remark on the sloshing frequencies for a half-space. 08 p0953 A73-20788

- Numerical studies of two-dimensional vortex motion by a system of point vortices. 08 p0954 A73-21010

- Quasi isothermal, transonic flow of radiating gases. 08 p1024 A73-21497

- Self-similar hypersonic flows of an inviscid gas. 08 p0927 A73-21545

- Discrete vortex scheme of a wing of finite span. 08 p0927 A73-21611

- Remarks on variational principle for an inviscid, perfect, magnetized plasma. 09 p1126 A73-22122

- Steady nonviscous nonheat-conducting plane flow of compressible fluid, calculating entropy, speed and pressure under assumption of variable pressure along streamlines. 09 p1071 A73-22419

- Intrinsic coordinate method of characteristics application to supersonic steady two dimensional nonisotropic inviscid flow, noting shock wave interaction. [ONERA, TP NO. 1186] 09 p1072 A73-22714

- Axisymmetric flow model of rotating inviscid incompressible fluid into point sink at low Rossby numbers, discussing selective withdrawal and blocking wave. 11 p1345 A73-25053

- Two dimensional inviscid flow model of shear layer motion and vortex shedding in near wake of bluff-based body, using Schwarz-Christoffel transformation. 11 p1300 A73-25155

- Calculation of unsteady transonic aerodynamics for oscillating wings with thickness. [AIAA PAPER 73-316] 11 p1301 A73-25547

- The stability of simply supported rectangular surfaces in uniform subsonic flow. [ASME PAPER 72-APM-ZZ] 11 p1441 A73-25702

- Finite core model of self induced motions and stability of filament vortex rings in inviscid fluid under small sinusoidal perturbation. 11 p1348 A73-26202

- Nonvortical axisymmetric flow of inviscid ideal incompressible fluid from partial differential equations solution. 12 p1486 A73-27242

- Explosion in detonating media with a variable initial density. 12 p1487 A73-27419

- Potential flow of an inviscid incompressible liquid around a profile in the presence of solid rectilinear boundaries. 12 p1487 A73-27797

- Propagation of electrohydrodynamic surface waves in a conducting fluid. 13 p1663 A73-28160

- Approximate shock-free transonic solution for a symmetric profile at zero incidence. 13 p1564 A73-28823

- Stability of a two-layer fluid model to non-geostrophic disturbances. 13 p1610 A73-29334

- Further investigations on the nonlinear behavior of a system of parallel line vortices. 14 p1746 A73-30652

- The thin shock layer in the hypersonic flow problem. 15 p1821 A73-31194

- The local role of the limit line in the well-posing of steady state problems in gas dynamics. I - Two dimensional involving one space dimension. 15 p1862 A73-31328

- Noncirculative MHD inviscid conducting fluid flow past circular cylinder and plane profile in magnetic field, using Fredholm equation. 15 p1918 A73-31414

- Nonlinear acoustics of inviscid fluid in duct with varying cross section, obtaining propagation velocity potential as power series for reduction to Neumann problem. 15 p1865 A73-32154

- Inviscid flow through a cascade of thick, cambered airfoils. I - Incompressible flow. [ASME PAPER 73-GT-84] 16 p1964 A73-33527

- Inviscid flow through a cascade of thick, cambered airfoils. II - Compressible flow. [ASME PAPER 73-GT-85] 16 p1964 A73-33528

- Spatially growing wave trails of an inviscid fluid discontinuity. 16 p2001 A73-33868

- Hypersonic nozzle flow of air with high initial dissociation levels. 16 p2001 A73-33870

- Some aspects of 'sound' attenuation in lined ducts containing inviscid mean flows with boundary layers. 16 p2049 A73-33946

- Mathematical formulation of viscous-inviscid interaction problems in supersonic flow. 17 p2091 A73-34178

- Book - Foundations of fluid flow theory. 17 p2151 A73-34466

- Foppl vortices stability for two dimensional inviscid irrotational steady flow past circular cylinder. 17 p2154 A73-35117

- Relaxation solutions for inviscid axisymmetric transonic flow over blunt or pointed bodies. 17 p2095 A73-35128

- Boundary condition calculation procedures for inviscid supersonic flow fields. 17 p2155 A73-35143

- Computation of three dimensional flows about aircraft configurations. 18 p2259 A73-36158

- Transonic inviscid flows over lifting airfoils with embedded shock wave using method of integral relations. [AIAA PAPER 73-658] 18 p2261 A73-36212

- Theory of supersonic laminar non-adiabatic boundary layer flow past small rearward-facing steps including viscous-inviscid interaction. [AIAA PAPER 73-668] 18 p2261 A73-36219

- Inviscid supersonic far wake flow past pointed bodies using the method of integral relations. [AIAA PAPER 73-671] 18 p2262 A73-36222

- Numerical solution for the inviscid supersonic flow in the corner formed by two intersecting wedges. [AIAA PAPER 73-675] 18 p2262 A73-36226

- The response of unsteady boundary-layer separation to impulsive changes of outer flow. [AIAA PAPER 73-684] 18 p2298 A73-36235

- Boundary conditions and stability of inviscid plane-parallel flows. 19 p2420 A73-37751

- Stability of stratified shear flows. 19 p2421 A73-38226

- On a stagnation condition for combining or branching inviscid flows. 20 p2546 A73-39091

- Incompressible flow planar-nozzle discharge coefficient computations for one dimensional inviscid flow, considering nozzle geometry, flow cross sections and turbulence. 20 p2548 A73-39526

- The local role of the limit line in the well-posing of steady state problems in gas dynamics. II - Two dimensional plane flow. 20 p2549 A73-39562

- Two dimensional flow theory of Weis-Fogh lift generation in inviscid motions of insect wings involving viscous effects. 21 p2631 A73-40244

- Numerical solution of Fredholm integral equation describing incompressible inviscid potential flow past three dimensional bodies. 23 p2939 A73-43474

- Flows past exponential bodies in the presence of strong compression in the shock layer. 24 p3055 A73-45534

INVISIBILITY

U VISIBILITY

INVOLUNTARINESS

U INVOLUNTARY ACTIONS

INVOLUNTARY ACTIONS

- Ability of a human operator to estimate the probability characteristics of alternative stimuli. 22 p2813 A73-41893

IO

- Major planets nonthermal radio emission observations, noting powerful decametric sources related to Jupiter rotation and Io orbital motion. 11 p1420 A73-25879

- Jupiter radiation reception at decametric wavelengths by Yagi antenna and radiometer, taking into account Io modulation effect. 11 p1424 A73-26131

- Ten-micron eclipse observations of Io, Europa, and Ganymede. 11 p1424 A73-26133

- Light velocity from Io eclipse times observation by Picard and Roemer, noting rms deviation with present value. 11 p1429 A73-26685

- The geometry and dynamic spectra of Io-modulated Jovian decametric radio emissions. 12 p1540 A73-27327

- Jupiter magnetospheric interaction with innermost satellite Io, noting magnetic field annihilation enhancement in neutral point by LF MHD waves. 21 p2764 A73-40166

- The propagation of Alfvén waves along Io's flux tube. 21 p2764 A73-40167

- Jupiter satellite Io controlled decametric Alfvén wave emission pattern, considering relationship to coherent cyclotron radiation growth rate. 21 p2764 A73-40168

- Jupiter satellite Europa polar cap from photoelectric observation of occultations by satellite Io. 21 p2687 A73-41077

- The post-eclipse brightening of Io. 24 p3134 A73-44563

- Posteclipse brightening of Io observed at 3500 and 4000 Å suggested as transient partial covering of high-albedo material. 24 p3134 A73-44564

IODIDES

NT CESIUM IODIDES

NT POTASSIUM IODIDES

NT SILVER IODIDES

NT SODIUM IODIDES

- Demonstration of the inhibiting action of certain mineral iodides on the stress corrosion of type 18-10 low-carbon stainless steel. 02 p0178 A73-11524

- Molecular beam study of the K+CH3I reaction - Energy dependence of the detailed differential reactive cross section. 05 p0546 A73-16047

- The photochemical oxidation of iodide to iodine in the presence of oxygen. 07 p0788 A73-20398

- Electrophysical properties of BiTeI thin films. 10 p1259 A73-24154

- Fabrication procedures, structure, and mechanical properties of BiTeI thin films. 10 p1260 A73-24470

- Surface effects on trapping and recombination processes in BiI3 single crystals. 12 p1531 A73-27938

- Exciton absorption band splitting in the PbI2 spectrum. 12 p1532 A73-27945

Magneto-oscillatory absorption effect in SbI3
13 p1667 A73-28004

IODINE
NT IODINE ISOTOPES
Molecular iodine photolysis in photodissociative laser due to selective pumping, noting recombination-like storage mechanism
04 p0458 A73-15561
Comparative study of the epitaxial growth in GaAs-I and GaP-I systems over a wide range of crystallization conditions
05 p0605 A73-17292
Spectroscopic study of the vibrational-energy dissipation of the I2 molecule excited by a He-Ne laser
10 p1228 A73-24577
New method of increasing the emission frequency of high-power laser pulses.
10 p1229 A73-24769
Absorption of He-Ne laser radiation by an iodine molecule beam
13 p1627 A73-28773
Kinetics of the generation spectrum of a photodissociation iodine laser.
22 p2868 A73-41722

IODINE COMPOUNDS
NT CESIUM IODIDES
NT IODIDES
NT POTASSIUM IODIDES
NT SILVER IODIDES
NT SODIUM IODIDES
Determination of iodo amino acids in plasma by gel chromatography
10 p1178 A73-23760

IODINE ISOTOPES
Orgueil chondrite magnetite age via I 129/Xe 129 method compared to Karoonda magnetite age
13 p1684 A73-29250

ION ACCELERATORS
Structure of the current front in an unsteady plasma accelerator, and turbulent acceleration of the ions. I
09 p1124 A73-21881
Structure of the current front in an unsteady plasma accelerator, and turbulent acceleration of the ions. II
09 p1124 A73-21882
Acceleration of ions during the formation of an electron beam from a stationary vacuum-arc plasma
09 p1125 A73-21909
A computational study of the non-linear stage of the development of radiation instability in relativistic electron rings.
09 p1131 A73-22909
Observation of stationary acceleration of ions to energies of 2 to 20 keV in a nonisothermal plasma
10 p1258 A73-24888
Access to uncombined titanium through an inhibiting film in sublimation pumping of deuterium.
13 p1581 A73-28929
Ion acceleration in the formation of an electron beam in a vacuum arc.
15 p1922 A73-32634
Structure of the current front and turbulent acceleration of ions in a pulsed plasma accelerator. I.
17 p2215 A73-34305
Structure of current front and turbulent acceleration of ions in a plasma accelerator. II.
17 p2215 A73-34306
Closed Hall current accelerators for physical and technological applications involving ion acceleration
19 p2466 A73-37356
Dynamics of plasma column constriction and electromagnetic acceleration of ions
21 p2745 A73-40362
Steady-state acceleration of ions to 2-20 keV in a nonisothermal plasma.
21 p2749 A73-41663
Acceleration of heavy ions by radiation pressure.
22 p2900 A73-41759
Ion acceleration by relativistic electron beam extracted from discharge plasma, discussing proton acceleration and beam composition and energy distribution
23 p3014 A73-44339

ION ACOUSTIC WAVES
Propagation of ion acoustic waves in a weakly ionized plasma
03 p0348 A73-14625
Multiple soliton excitation by ion acoustic square pulse wave in double plasma device in frame of Korteweg-de Vries equation
04 p0477 A73-14771
Ion sound turbulence in dense plasma within magnetic fields, representing global equilibrium spectrum
04 p0480 A73-15563
Stationary nonlinear ion acoustic oscillations in dense weakly ionized current carrying plasma, considering wave propagation velocity and instability process
06 p0728 A73-17971
Ion-acoustic oscillations effect on turbulent plasma electric conductivity within weak external electric field
06 p0729 A73-17973
Current-induced nonlinear ion oscillations in a plasma
06 p0729 A73-18112

Damping of an ion acoustic wave in a weakly ionized plasma
06 p0730 A73-18460

Two dimensional simulation of nonlinear ion-sound instability in current carrying collisionless plasma due to modification of electron distribution function
06 p0730 A73-18464

High-frequency instabilities in a plasma with a nonlinear ion-acoustic wave.
06 p0731 A73-18603
Stochastic ion heating by ion-acoustic turbulence.
06 p0733 A73-18850
Propagation of a nonlinear wave in a weakly turbulent plasma
07 p0854 A73-19276
Theory of parametric resonance in an inhomogeneous plasma
07 p0855 A73-19279
Instability of surface ion-acoustic waves of finite amplitude
07 p0855 A73-19291
Mode-coupling and wave-particle interactions for unstable ion-acoustic waves.
07 p0856 A73-19521
Simultaneous suppression of an electron plasma wave and an ion acoustic wave by beam modulation.
08 p0992 A73-21006
Quasi-static ion acoustic surface wave propagation along warm plasma layer-dielectric boundary
08 p0993 A73-21460
Structure of the current front in an unsteady plasma accelerator, and turbulent acceleration of the ions. II
09 p1124 A73-21882
Excitation of low-frequency oscillations by an electron beam in a hot plasma confined in a magnetic mirror
09 p1125 A73-21907
Characteristics of the electric field far from and close to a radiating antenna around the lower hybrid resonance in the ionospheric plasma.
09 p1049 A73-22277
Measurement of ion-rich sheath thickness by ion acoustic wave.
09 p1126 A73-22279
One-dimensional numerical experiment on anomalous plasma resistivity
09 p1127 A73-22482
Wave-wave interactions in turbulent plasma and ion sound turbulence enhancement of three wave interaction processes, considering plasma heating experiments
09 p1131 A73-22901
Negative energy mode loss to positive energy mode in positive-negative energy wave interactions within magnetized plasma, considering ion acoustic waves
11 p1402 A73-25123
Unstable Langmuir or ion acoustic wave saturation in collisionless plasma due to electron trapping, estimating amplitude via adiabatic and sudden approximation
11 p1404 A73-25258
Nonlinear ion sound in a fully ionized current-carrying plasma.
11 p1406 A73-26186
Collective interactions and electrical conductivity of plasma in strong electric fields.
11 p1406 A73-26554
Small amplitude hydromagnetic waves for a plasma with a generalized polytrope law.
11 p1406 A73-26555
Parametric instability in an inhomogeneous plasma containing hot ions
12 p1526 A73-26926
Nonlinear ion sound waves in a plasma with three-dimensional random inhomogeneities
12 p1530 A73-27980
Nonlinear theory of parametric wave instability in a plasma
12 p1530 A73-27981
Propagation of a nonlinear wave in a weakly turbulent plasma.
13 p1665 A73-28676
Parametric resonance in an inhomogeneous plasma.
13 p1665 A73-28679
Instability of ion-acoustic surface waves of finite amplitude.
13 p1665 A73-28691
Threshold of appearance of anomalous resistance for field-aligned currents in the magnetosphere.
13 p1608 A73-28726
Parametric instabilities and anomalous absorption and heating of plasmas.
14 p1779 A73-30118
Investigation of the heating of a plasma ion component by a collisionless shock wave.
14 p1780 A73-30336
Ion acoustic wave scattering effects on stochastic ion heating in turbulent plasma
14 p1780 A73-30340
The effect of temperature perturbations on ion-acoustic and drift waves in a weakly collisional plasma.
15 p1916 A73-31087

ION ATOM INTERACTIONS
Ion-acoustic turbulence as MHD wave damping mechanism in weakly turbulent magnetosphere plasma at high and low frequencies
15 p1919 A73-31893
Earth magnetosphere ion acoustic turbulence generation by longitudinal currents and electric fields, relating turbulence induced current dissipation to plasma heating
15 p1872 A73-31894
Nonlinear ion-acoustic and electron-acoustic waves of a plasma in a magnetic field
15 p1921 A73-32324
Electron-beam excitation of low-frequency waves in a hot plasma confined in a mirror machine.
15 p1922 A73-32632
On electron trapping in ion sound waves in turbulent plasma.
16 p2040 A73-32800
Remote feedback stabilization of ion acoustic type instability in plasma with L.F density modulation, noting Van der Pol approach agreement and crossed field diffusion decrease
16 p2041 A73-33327
Observations of two-stream ion wave instability.
16 p2041 A73-33335
Parametric instabilities in a plasma containing two types of ions
16 p2043 A73-34057
Structure of current front and turbulent acceleration of ions in a plasma accelerator. II.
17 p2215 A73-34306
Anomalous heating of dense plasma by laser radiation.
17 p2218 A73-35823
One-dimensional model for nonlinear reflection of laser radiation by an inhomogeneous plasma layer.
17 p2218 A73-35824
Radar aurora type III spectra with phase velocities exceeding ion acoustic velocity, discussing relation to current-excited ionospheric electrostatic ion cyclotron oscillations
18 p2312 A73-36299
Experimental investigation of a fast ion-acoustic wave in a multicomponent plasma
18 p2339 A73-36564
Nonlinear excitation of an ion-acoustic wave in a bounded plasma
18 p2340 A73-36675
Structure of almost collisionless shocks in a magnetoplasma and the ion-acoustic instability.
19 p2464 A73-37158
Parametric decay of obliquely incident electromagnetic waves into ion acoustic and electron plasma waves in vicinity of resonance
20 p2595 A73-38874
Convective amplification of type I irregularities in the equatorial electrojet.
20 p2551 A73-38938
Current driven ion wave instability in a weakly ionized collisional magnetoplasma.
20 p2599 A73-39725
Nonlinear ion surface oscillations in a semibounded current-carrying plasma
21 p2745 A73-40361
Parametric excitation of ion-acoustic oscillations in a plasma situated in an alternating electric field and a constant magnetic field
21 p2746 A73-40519
Rocket experiments on nonlinear wave-wave interaction in the ionospheric plasma.
21 p2685 A73-40823
Parametric instability in an inhomogeneous plasma with hot ions.
22 p2891 A73-42260
Contribution to the theory of parametric instability of a bounded homogeneous plasma
22 p2892 A73-42380
Experimental observation of the decay of high-frequency waves in a plasma
22 p2826 A73-42389
Nonlinear plasma ion oscillations excited by a current.
24 p3114 A73-44501
The ion-sound instability and its associated multimode phenomena.
24 p3115 A73-44874
Transfer of energy to light ions from the ion-acoustic-wave instability developed in a heavy-ion plasma.
24 p3117 A73-45406
Current driven ion acoustic plasma instability based on ion orbit perturbation by turbulent waves, calculating angular spectrum for comparison with computerized simulation
24 p3118 A73-45463

ION ATOM INTERACTIONS
Rate coefficient calculation for near resonant charge transfer reaction between oxygen cations and hydrogen atoms as function of temperature at thermal energies
02 p0217 A73-12391
One-electron model for charge exchange in ion-atom collisions.
03 p0344 A73-13283

- Low-energy elastic differential scattering of He^{++}/He . 15 p1916 A73-32290
- Decay of the magnetic storm ring current by the charge-exchange mechanism. 17 p2159 A73-34782
- Detailed balance as check on impact parameter calculations, discussing proton-hydrogen collisions with small transition amplitudes and interpolation errors 21 p2743 A73-40467
- Calculation of the Lyman-alpha asymmetry in a dense, partially-ionized hydrogen plasma. 24 p3116 A73-45323
- ION BEAMS**
- Capture of plasma electrons by the field of a wave that is excited by an ion beam 01 p0084 A73-10632
- A large double plasma device for plasma beam and wave studies. 02 p0168 A73-11964
- Electromagnetic dispersion relation for two equisense counterstreaming ion beams in warm electron background oscillating plasma, considering ion instability criteria 02 p0197 A73-12066
- Ion beam lifetimes measurement by temporal correlation of photons emitted in cascades 03 p0341 A73-12912
- Ion-cyclotron instability of a plasma produced by a fast-ion beam. 03 p0347 A73-14101
- Projectile structure effects on neon K X-ray production by fast, highly ionized argon beams. 04 p0476 A73-14769
- Physical phenomena of controlled experiments in earth magnetosphere using test particles, radio emission and electron and ion beams 04 p0443 A73-15342
- Relaxation of ion beam injected into a plasma transversely to a magnetic field. 05 p0602 A73-16550
- Mode-coupling and wave-particle interactions for unstable ion-acoustic waves. 07 p0856 A73-19521
- A nonlinear, nonconvex optimization problem 08 p0983 A73-20778
- Ion gun sputter cleaning of thin film metal substrate for in situ corrosion studies by UHV transmission electron microscopy 08 p0990 A73-21616
- Plasma-ion beam nonlinear interaction for beam velocity exceeding electrons thermal velocity, noting plasma heating and beam energy dissipation 08 p0994 A73-21696
- Experimental investigation of the excitation of Ar II and Kr II during electron-ion collisions 09 p1122 A73-22593
- Excitation of long-wave oscillations by a secondary electron stream in a plasma generated by an ion beam 09 p1129 A73-22684
- Contributions to the kinematics of type I tails of comets. 10 p1271 A73-23477
- Obtaining beams of singly charged metal ions with the aid of giant ruby laser pulses 10 p1227 A73-23815
- Two-flow instability of interpenetrating ion beams propagating in the same direction along an external magnetic field 12 p1529 A73-27941
- Charge changing processes in hydrogen beams. 14 p1776 A73-30125
- Third-order treatment of combined effects of space charge and external fields on cylindrical ion and electron beams. 15 p1915 A73-31933
- Ionic machine tools for microelectronic manufacture, discussing ion jets properties, optics and construction and implantation, micromachining and deposition technologies 16 p1987 A73-33088
- Experimental observation of the high-density plasma-beam formation by continuous-flow Z-pinch. 17 p2217 A73-35523
- Interaction between an ion beam and a turbulent low-pressure theta-pinch plasma 18 p2340 A73-36667
- Penetration and crossing of transverse magnetic field barrier by a purely ionic plasma. 19 p2465 A73-37170
- Instability of an azimuthal ion beam in a dense plasma 21 p2746 A73-40522
- Biological effects due to single accelerated heavy particles and the problems of nervous system exposure in space. 22 p2814 A73-42181
- Correlation of ion and beam current densities in Kaufman thrusters. 22 p2900 A73-42636
- Exponential projectile charge dependence of Ar K and Ne K X-ray production by fast, highly ionized argon beams in thin neon targets. 22 p2890 A73-42710
- Quantum-beat g-value measurements on transitions from levels of aligned fast ions. 22 p2890 A73-42974
- Influence of Langmuir electron oscillations on the degree of neutralization of an ion beam 23 p3014 A73-44342
- Transient ion neutralization by electrons. 24 p3111 A73-45411
- ION CHAMBERS**
- U IONIZATION CHAMBERS**
- ION CHARGE**
- Differential dielectric equations for probability of water droplet electrification in weakly ionized medium during cloud and fog formation 13 p1654 A73-28883
- High temperature electron transfer and Bi and Sb ion valency pair predictions in ordered perovskite-type oxides, using lattice constants 23 p3017 A73-44129
- ION CONCENTRATION**
- Hydrogen ion concentration in the blood of man under high mountain conditions with physical loads 02 p0133 A73-11924
- Ion density and electron temperature calculations for metallic plasma population inversion possibility by near resonant charge exchange with inert gas ions 02 p0194 A73-12847
- Pyrolysis system with high sensitivity medium-resolution mass spectroscopy to quantify ions pyrolyzed in lunar fines, confirming presence of indigenous lower hydrocarbons 06 p0662 A73-18431
- Independent effects of changes in H^+ and CO_2 concentrations on hypoxic pulmonary vasoconstriction. 10 p1182 A73-24565
- Photoionization and charge exchange reaction kinetics inadequacy for explanation of observed positive nitrogen dioxide ion concentration in lower ionosphere, considering alternative mechanism 10 p1214 A73-24749
- Ion and electron distributions in the boundary layer of hypersonic vehicles. 11 p1404 A73-25290
- Diffusion spreading of weak plasma inhomogeneities in the presence of two kinds of positive ions. 13 p1608 A73-28710
- Ionization instability in CO_2 laser discharges. 15 p1885 A73-32258
- Mesospheric positive ion observation via measurement of polar electrical conductivities by subsonic parachute-borne blunt probe system launched on meteorological rockets 18 p2305 A73-36006
- Simultaneous measurements of some ionospheric parameters at altitudes 100-170 km. 18 p2310 A73-36131
- Thermoelectric effects and power calculation of solid electrolyte silver-silver iodide-silver thermocell as function of impurity ion concentration and temperature 21 p2636 A73-40842
- Simulation of the flow past a high-altitude ion-concentration sensor 21 p2633 A73-41223
- ION CURRENTS**
- Ion acceleration in a plasma boundary layer formed by two electron groups 03 p0347 A73-13755
- Ion-current distributions around an electrically conductive body in ionized gas flow. 05 p0603 A73-17110
- Steady state hot toroidal Tokamaks plasma, calculating seed current density for bootstrap effect produced by neutral particle injection parameters control 08 p0991 A73-20814
- A comparative experimental study of electron and positive-ion current collection by a cylindrical Langmuir probe under orbital-limited conditions. 08 p0967 A73-21598
- Ionic current mechanisms for cardiac muscle repolarization time course of Purkinje fibers and other heart cells, relating charge transfer data to earlier studies 11 p1316 A73-25593
- Electrogenic potassium inward transport involvement in mechanism of enhanced repolarization, correlating cardiac excitation with Na, K and Ca ions transfer and active ion transport 11 p1316 A73-25594
- Charged particle production and plasma electron/ion current discharges from W targets under laser beam, noting dependence on electric field strength, pressure and operation mode 11 p1378 A73-26522
- Direct measurements of ion drift velocity in the upper ionosphere during a magnetic storm. I - Methodological aspects and some results of measurements in magnetically quiet periods. II - Results of measurements during the magnetic storm of November 3, 1967 14 p1746 A73-29863
- Ion current at the forward stagnation region of an electrically conducting body. 15 p1918 A73-31669
- Ruby laser light spark ion-electron currents in gap between copper plates under electric field 18 p2322 A73-37047
- Generation of energetic ion fluxes from a high temperature electron discharge in an inhomogeneous magnetic field 19 p2466 A73-37358
- Low-frequency vibrations of a high-frequency E-discharge plasma in a magnetic field 20 p2598 A73-39398
- An appraisal of the mass spectrometer diagnostic technique in the study of afterglow plasmas. 21 p2702 A73-40792
- Tungsten target surface contaminants produced fast ion current peak measured by ion collector in expanding laser produced plasma 21 p2716 A73-40972
- An experimental investigation of the induced turbulence in laminar channel flow due to a transverse ion current and its applications to fluidic turbulence amplifiers. 23 p2942 A73-43402
- ION CYCLOTRON RADIATION**
- Ion-cyclotron instability of a plasma produced by a fast-ion beam. 03 p0347 A73-14101
- Numerical and analytic solutions for dispersion equation for flute-like ion cyclotron instabilities in high beta plasma, noting magnetic field inhomogeneity effect 03 p0348 A73-14436
- Electrostatic ion cyclotron waves in an anisotropic plasma. 05 p0611 A73-17305
- Combined plasma heating by an electron beam and an intense ion-cyclotron wave 06 p0729 A73-18106
- Spectra of potential ion-cyclotron plasma oscillations 07 p0855 A73-19289
- R and L modes of ion cyclotron whistler propagation in ionosphere, noting refractive indexes and wave polarization for multicompound plasma 07 p0819 A73-20060
- VLF ion cyclotron whistler propagation in upper ionosphere, noting polarization reversal and mode coupling from satellite observation 08 p0937 A73-20653
- Ion cyclotron wave generation in a two-ion plasma. 08 p0991 A73-20817
- Fast wave propagation and damping at the second harmonic of the ion cyclotron frequency. [TTU-SR-2] 09 p1128 A73-22631
- Operating features of an ion-cyclotron-wave plasma apparatus running in the RF-sustained mode. [TTU-SR-2] 09 p1128 A73-22632
- The ion cyclotron drift loss-cone instability with a coexisting cold plasma. 11 p1404 A73-25271
- Electrostatic ion-cyclotron plasma oscillations. 13 p1665 A73-28689
- Ion cyclotron waves observed in the polar cusp. 16 p2003 A73-33437
- Parametric instabilities in a plasma containing two types of ions 16 p2043 A73-34057
- Radar aurora type III spectra with phase velocities exceeding ion acoustic velocity, discussing relation to current-excited ionospheric electrostatic ion cyclotron oscillations 18 p2312 A73-36299
- Ion cyclotron instability of a rotating plasma 18 p2340 A73-36671
- Electron-acoustic and ion-cyclotron parametric instabilities of a plasma in an alternating electric field. I, II 21 p2746 A73-40520
- Growth rates of the ion cyclotron instability in the earth's magnetosphere. 21 p2685 A73-40824
- Investigation of the waveguide properties of a plasma cylinder for axially asymmetric waves 22 p2892 A73-42379
- Combined heating of a plasma by an electron beam and an intense ion-cyclotron wave. 24 p3114 A73-44495
- A new ion and electron detector for ion cyclotron resonance spectroscopy. 24 p3089 A73-44816
- ION DENSITY [CONCENTRATION]**
- NT IONOSPHERIC ION DENSITY**
- NT MAGNETOSPHERIC ION DENSITY**
- NT MAGNETOSPHERIC PROTON DENSITY**
- NT PROTON DENSITY [CONCENTRATION]**
- Electron temperature measurement in collisional plasma with double probe, noting electron and ion density distribution near isolated electrode under floating potential 01 p0085 A73-10866
- Electron-ion density fluctuations in turbulent weakly ionized Ar plasma, comparing experimental results with theory based on quasi-static formulation of Boltzmann equation 04 p0479 A73-15192

Study on ionizing shock waves in argon. I - Precursor phenomena. 04 p0436 A73-15974

Ion density and current distribution measurements in hypersonic turbulent wakes behind sphere flown in ballistic range, using cylindrical electrostatic probes 06 p0645 A73-18135

Computer simulation model of field independent trapping effects on slow Gunn domains in gallium arsenide, noting double symmetry electron-ion density distributions 06 p0737 A73-18368

IR-spectroscopic investigation of the thermal stability of albumin at different levels of its ionization 10 p1182 A73-24685

Formation of the density profile of charged particles at heights from 10 to 90 km 11 p1411 A73-25082

Electron temperature measurement in recombination collisional plasma with double probe, noting electron and ion density distribution near isolated electrode under floating potential 12 p1499 A73-27916

Metal ion density measurement in sporadic E layer during beta Taurids shower by rocket-borne mass spectrometer, noting origin in cosmic debris ablation 13 p1673 A73-28277

Planar retarding potential analyzer onboard Explorer satellite for ion temperature and ion/electron concentration investigation 13 p1688 A73-28635

Ar laser output characteristics variation due to mutual influence of 4880 and 5145 A transitions, solving ion density formation rate equations 13 p1628 A73-29184

Sources of spurious background in the Spectrocon. 14 p1732 A73-29907

Current extension from a quasi-steady MPD arcjet. 15 p1918 A73-31550

Ionization oscillations in a plasma in the presence of negative ions 15 p1920 A73-32319

The electric field and structure of a weakly ionized plasma in the vicinity of a small charged body 15 p1921 A73-32322

Probe design for orbit-limited current collection. 16 p2041 A73-33320

Simultaneous measurements of ion concentration and corpuscular stream intensity at altitudes ranging from 10 to 79 km 18 p2345 A73-36121

Afterglow studies in helium-cesium mixtures. 21 p2745 A73-40223

Mass-spectrometric investigation of the ion composition of potassium and cesium discharge plasmas 21 p2746 A73-40526

Correlation of ion and beam current densities in Kaufman thrusters. 22 p2900 A73-42636

Observations of water vapor ions at the lunar surface. 23 p3031 A73-43764

Transition of a low-pressure plasma into a highly ionized state 23 p3013 A73-44335

Volt-ampere characteristics of double electrical plasma probe measuring ionization level in low temperature dense plasma under interelectrode gap near-breakdown conditions 23 p2983 A73-44344

High-latitude proton precipitation and light ion density profiles during the magnetic storm initial phase. 24 p3126 A73-45114

Nonlinear saturation of the relativistic beam-plasma instability in the presence of ion density fluctuations. 24 p3118 A73-45465

ION DISTRIBUTION

Plasmasphere hydrogen, helium, oxygen and nitrogen ions inbound and outbound profiles from OGO 5 mass spectrometric measurements 02 p0164 A73-12320

Ionoapheric VLF and ELF electric field observation by Alouette 2 satellite, obtaining ion mass distribution from lower hybrid resonance hiss during geomagnetic storm 02 p0164 A73-12623

Diffusion approximation for kinetic equation of repeatedly ionized plasma, calculating direct transitions between excited ion states 03 p0344 A73-13180

Stability of a plasma with ineqilibrium ions with respect to the generation of magneto-sonic waves 04 p0481 A73-15603

Contribution of Coulomb collisions to plasma relaxation in the DECA mirror machine. 05 p0604 A73-17367

Diffusion of weak inhomogeneities in a magnetoactive two-ion plasma 06 p0727 A73-17536

Sporadic E relation to ionized particle redistribution in E layer during solar eclipse 07 p0815 A73-19256

Fe2+/-Mg site distribution in Apollo 12021 clinopyroxenes - Evidence for bias in Moessbauer measurements, and relation of ordering to exsolution. 07 p0881 A73-19706

Calculated distributions of hydrogen and helium ions in the low-latitude ionosphere. 07 p0818 A73-20052

Theoretical vertical profiles of minor ions at the Equator. 07 p0819 A73-20053

Stability of a plasma with nonequilibrium ions with respect to magnetosonic waves. 10 p1254 A73-24193

Ionospheric electron-ion gas distribution, allowing for diffusion, recombination and vertical drift 11 p1357 A73-26081

Ion distribution in the crystal structure of complex spinel phases of the Mn-Fe-Ti-O system 11 p1386 A73-26674

Influence of electric drift on the cone instability of a plasma in adiabatic traps 12 p1527 A73-26930

Metal ions role in sporadic E layer formation in terms of magnesium ions profile redistribution by vertical gradient in neutral particle wind 13 p1608 A73-28723

Spectrophotometric results from the Copernicus satellite. III - Ionization and composition of the intercloud medium. 14 p1801 A73-30746

Diffusion of weak inhomogeneities in a magnetically active plasma consisting of two ions. 16 p2039 A73-32760

Auroral ion velocity distributions using a relaxation model. 18 p2311 A73-36178

Instrumentation and techniques for measuring emissions. 19 p2432 A73-38324

Yield and ion distribution for the barium cloud at 31,000 kilometers, September 21, 1971. 22 p2845 A73-41935

Preliminary analysis of NASA optical data obtained in barium ion cloud experiment of September 21, 1971. 22 p2846 A73-41937

Effect of electric drift on the loss-cone plasma instability. 22 p2891 A73-42264

Perturbation of ion density by a body moving through the ionosphere. 23 p3008 A73-43254

Regularities in the behavior of semiconductors and dielectrics in connection with deviation from stoichiometry 23 p2959 A73-43479

ION EMISSION

Local emission coefficients fields for ionized gas in arbitrary and rectangular cross section streams 03 p0344 A73-13179

Ion acceleration in a plasma boundary layer formed by two electron groups 03 p0347 A73-13755

Ion engines with ion emission from liquid metal drops under electric field, noting emitter I-V characteristics and engine design 04 p0488 A73-15726

Lunar water vapor spectra during Apollo 14 ALSEP suprathermal ion detector experiment (SIDE) and total ion detector (TID) observations 07 p0891 A73-19829

Contributions to the kinematics of type I tails of comets. 10 p1271 A73-23477

Chemical analysis of surfaces by mass spectrography with secondary ion emission 21 p2648 A73-41595

A dynamic mass spectrometer for the study of laser-produced plasmas. 24 p3090 A73-44817

ION ENGINES

NT CESIUM ENGINES

Diode behaviour in an electron-bombardment ion engine. 01 p0090 A73-10112

Control of electron bombardment ion engine for stationary satellite. 01 p0090 A73-11110

Durability tests of a five-centimeter diameter ion thruster system. 03 p0356 A73-13455

[AIAA PAPER 72-1151] Integration of an ion engine on the Communications Technology Satellite. 04 p0487 A73-15448

Electric propulsion and its space applications; Workshop, 2nd, Toulouse, France, June 21-23, 1972, Proceedings 04 p0487 A73-15712

Cs ion bombardment and contact ionization engines in French space program for communication and geostationary satellites electric propulsion 04 p0488 A73-15715

The RIT engine family. - From microthruster to main propulsion units. 04 p0488 A73-15716

ION EXCHANGING

Electrostatic ion thrusters of the DFVLR Braunschweig for primary propulsion. 04 p0488 A73-15717

Cs ion bombardment engines for communication satellites stationkeeping and attitude control, noting mission life and test facilities 04 p0488 A73-15718

Research at O.N.E.R.A. on ion thrusters suitable for satellite station-keeping 04 p0505 A73-15719

Long life contact-ionized cesium low thrust engine design, considering ionizer working temperatures and neutralizer ion current densities 04 p0488 A73-15720

Conformal mapping for Cs ion engine beam optical system with laminar flux, calculating design parameters for current limitation by Cs flow 04 p0488 A73-15722

Ion engines with ion emission from liquid metal drops under electric field, noting emitter I-V characteristics and engine design 04 p0488 A73-15726

Space charge neutralized Hall ion microthrusters, discussing ion exhaust velocity, thrust and efficiency relationships 04 p0489 A73-15729

Description of power conditioning systems intended for satellite stabilization thrusters 04 p0489 A73-15732

Pulse width amplitude converter design and performance for ion engine high voltage power supply, noting oscillator, modulator and circuit protection 04 p0489 A73-15733

High voltage fuel supplies intended for ion thrusters 04 p0489 A73-15734

ESKA ion thrusters - Development and application for geocentric missions. 04 p0489 A73-15739

Planetary exploration with electrically propelled vehicles. 06 p0750 A73-18021

Ion thruster thermal characteristics and performance. 07 p0867 A73-19488

Electron bombardment ion rocket engine with large diameter and divergent magnetic field for efficiency improvement, considering application as source in plasma wind tunnel 07 p0868 A73-20486

Thermionic reactor power systems design for spacecraft auxiliary power supply and electrical propulsion, discussing performance and design guidelines for various applications 09 p1118 A73-22798

Evidence of fireball phenomena in hollow cathode of electron bombardment ion thrusters. 09 p1136 A73-23462

Certain results of flight tests of a model ion thruster employing contact ionization of cesium on tungsten 10 p1262 A73-23892

Development costs for a nuclear electric propulsion stage. 19 p2458 A73-38434

Some results of flight tests of an ion-engine model using surface ionization of cesium on tungsten. 20 p2600 A73-38911

ION EXCHANGE MEMBRANE ELECTROLYTES

Relation of electrolyte disturbances to cardiac arrhythmias. 08 p0933 A73-21807

Solute rejection by porous glass membranes. II - Pore size distributions and membrane permeabilities. 09 p1048 A73-22525

Energy requirements of ouabain-sensitive Na-K positive ion membrane pump during norepinephrine induced thermogenesis of brown adipose tissue in cold-exposed hamsters 09 p1040 A73-22649

Autonomous composite power system with electrochemical generator, ion exchange membrane and storage battery 11 p1308 A73-25625

ION EXCHANGE RESINS

Effectiveness of the application of tightly bonded sulfo-cation exchange resins in water recycling by the sorption method 06 p0656 A73-17677

ION EXCHANGING

Cation exchange binding of rubidium and cesium by rat liver cell microsomes. 02 p0135 A73-12549

Ion-exchange chromatography in lunar organic analysis. 06 p0662 A73-18414

Chromatographic separation of niobium from titanium, tungsten, molybdenum, and vanadium on the fluorosorb of the AV-16 anion exchanger 20 p2520 A73-39820

Effective interchange effects between the ions in metals 21 p2721 A73-41141

Ultrafiltration by a compacted clay membrane. I - Oxygen and hydrogen isotopic fractionation. II - Sodium ion exclusion at various ionic strengths. 23 p2973 A73-43845

ION GAGES

U IONIZATION GAGES

ION IMPACT

Investigation of regularities characterizing impact ionization within a high-field domain in Gunn diodes

06 p0675 A73-18076

Diatomic molecules dissociation investigation from effective cross section measurement of slow atomic negative ions formation by molecules collisions with fast ions and atoms

08 p0990 A73-21694

Power-generation potential of various IMPATT structures from a scaling approximation.

21 p2668 A73-41591

ION IMPLANTATION

The electrical properties of phosphorus doped silicon layers obtained by ion implantation through a passivating oxide.

17 p2220 A73-35654

Low cost beam current integrator for use with dc accelerators in ion implantation experiments

17 p2175 A73-35759

Ion implanted X-band IMPATT/TRAPATT back-to-back diodes.

19 p2408 A73-37146

Selection of conditions for the fabrication of planar n-p-n silicon transistors with the application of the ion-beam alloying method

20 p2535 A73-38858

Ion implanted megohm silicon monolithic IC resistors with buried n-guard layer protection against slice-to-slice variations of fixed surface charge

20 p2537 A73-39416

Bi implant CdS studies, discussing sputtering, surface concentration, p-type behavior and light emission characteristics

21 p2752 A73-40951

Ion-implanted varicaps with a steep capacitance-voltage characteristic

21 p2664 A73-41096

New device techniques for microwave bipolar power transistors.

22 p2833 A73-42692

German monograph - Doping profiles of boron-implanted silicon layers.

22 p2897 A73-42717

German monograph - The back-scattering method as a procedure for the determination of the radiation damage profile in silicon doped by ion implantation.

22 p2897 A73-42852

Ion-implanted nitrogen in gallium arsenide.

24 p3120 A73-45402

ION INJECTION

Precipitation of auroral and ring current particles by artificial plasma injection.

03 p0301 A73-13711

Metal ions implantation to produce alloy or semiconductor, discussing transmission electron microscopy use for viewing target material defect clusters

03 p0350 A73-13794

Methods of plasma injection into closed magnetic confinement systems

04 p0479 A73-15041

Threshold voltage shift for low voltage operation of transistor circuits with boron ion implanted MOS

04 p0427 A73-15322

On the distinction between the auroral electrojet and partial ring current systems.

04 p0444 A73-15550

Use of ion implantation in the fabrication of semiconductor devices

06 p0672 A73-17449

Quartz optical waveguide by ion implantation.

06 p0703 A73-18745

Silicon planar diodes produced by the ion implantation process

08 p0946 A73-21080

Investigation of the operation of a coaxial plasma injector employing preionization of the gas

09 p1124 A73-21880

Investigation of the azimuthal symmetry of the discharge in a coaxial plasma injector

09 p1125 A73-21911

Properties of silicon implanted with boron ions through thermal silicon dioxide.

09 p1064 A73-23040

Ion-implanted bipolar transistor carrier concentration profiles.

10 p1194 A73-24155

Microwave characteristics of ion-implanted bipolar transistors.

10 p1194 A73-24156

Ion implantation method and diffusion process for microelectronics semiconductor components manufacture

13 p1590 A73-28573

Azimuthal symmetry in a coaxial plasma injector.

15 p1922 A73-32636

ION IRRADIATION

NT DEUTERON IRRADIATION

NT PROTON IRRADIATION

Low energy solar nuclear particle irradiation of lunar and meteoritic breccias.

03 p0361 A73-13100

The influence of ion bombardment on the microstructure of thick deposits produced by high rate physical vapor deposition processes.

04 p0456 A73-15760

Nitriding by ion bombardment of 18-10 stainless steels

04 p0457 A73-15954

Study of nitriding by ion bombardment of titanium and titanium alloys

04 p0457 A73-15955

Absolute cross section for producing C-11 from carbon by 270-MeV/nucleon N-14 ions.

06 p0725 A73-17519

Semiconductor radiation detectors fabrication methods, discussing p-n junctions diffusion and ion implantation techniques and surface barrier, dE/dx, chessboard and rod type counters

07 p0822 A73-19172

A target design for irradiation of NaI at high beam current.

07 p0853 A73-20469

Annealing of effects arising during ion-bombardment alloying of metals at energies up to 10 keV

10 p1223 A73-23817

The mechanism responsible for luminescence of polymer films during their formation by ion-beam bombardment of solids

10 p1252 A73-24762

Changes in the optical properties of minerals and their atomization caused by ion bombardment

16 p1977 A73-33756

Probability cross sections of heavy ion single hit inactivation paths for human cells using nitrogen ion accelerator experiments

22 p2805 A73-42183

Heavy ion irradiation effects on bacteria mutations in balloon flight and accelerator experiments, comparing with cosmic rays

22 p2805 A73-42184

Ions bombarding the cathode of a pulsed plasma accelerator and their participation in the development of thermal fluxes

23 p3014 A73-44343

ION MICROSCOPES

Use of LEED, Auger emission spectroscopy and field ion microscopy in microstructural studies.

02 p0171 A73-12843

Field-ion microscopic study of the high-speed deformation of tungsten

12 p1509 A73-26838

Field-ion-microscopic study of interstitial plasticity of tungsten microcrystals.

22 p2872 A73-41726

ION MOTION

Reductive perturbation theory application to non-linear Schrodinger equation for plasma of cold ions and isothermal electrons, investigating ion oscillation mode automodulation

01 p0082 A73-10420

Polar ionospheric ion escape /polar wind/ hydrodynamic model equations, discussing singularities and critical points in terms of reduced Mach number

04 p0444 A73-15546

Non-linear damping of longitudinal ion oscillations in a collisionless non-isothermal plasma.

04 p0482 A73-16042

Solar wind magnetic field and particle concentration disturbances near moon, noting electric field effect on ion motion

05 p0620 A73-17009

Effect of ion viscosity and thermal conductivity on the drift instability in an inhomogeneous high-pressure collisional plasma.

05 p0604 A73-17362

Theoretical analysis of a time-of-flight mass spectrometer with spherical electrodes and radial ion paths.

06 p0693 A73-18270

Instability of a magnetoactive plasma with a transverse ion beam.

06 p0731 A73-18602

Rotation of the ion component of a plasma from a hot-cathode Penning discharge

09 p1125 A73-21955

Structure of a collisionless boundary layer and the turbulent braking of ions

09 p1127 A73-22607

Excitation of magnetosonic waves in a plasma with nonequilibrium ions

09 p1131 A73-23076

Direct measurements of plasma convection in the upper ionosphere

10 p1211 A73-23885

Ambipolar diffusion in the FI-region of the ionosphere.

11 p1357 A73-25928

Two-flow instability of interpenetrating ion beams propagating in the same direction along an external magnetic field

12 p1529 A73-27941

Measurement of rarefied gas flow rates from the drift of an ion mark produced by an electron beam

13 p1619 A73-29167

Solar wind interpenetrating ion streams from Imp 6 electrostatic analyzer measurements, considering origin due to interplanetary high velocity filaments merging into rarefied plasma regions

14 p1786 A73-29954

Self-consistent calculation of the motion of a sheet of ions in the magnetosphere.

16 p2003 A73-33433

Ion trajectories in plasma focusing devices based on numerical integration of three dimensional equations of motion

19 p2468 A73-37856

Direct measurements of plasma convection in the upper ionosphere.

20 p2550 A73-38904

Non-turbulent electric fields in soliton and shock-like structures in magnetized plasmas.

20 p2596 A73-38967

Potential created by a test particle in one-, two- and three-dimensions in a flowing ion-electron plasma.

20 p2596 A73-38969

Energy distribution functions of kilovolt ions in a modified Penning discharge.

20 p2597 A73-39197

Anomalous transport due to the dissipative trapped-ion instability.

21 p2750 A73-41682

Illumination aftereffects due to semiconducting ferrite electron and ion motion, discussing dielectric properties and electron hole deficiencies

22 p2833 A73-42514

Non-linear propagation of VLF waves in a magnetoplasma including the effect of ions.

23 p3012 A73-44143

Plasma instabilities in the region in front of a body moving rapidly in the ionosphere

24 p3115 A73-44790

Electric field observations by incoherent scatter radar in the auroral zone.

24 p3085 A73-45117

Nighttime meridional neutral winds near 350 km at low to mid-latitudes.

24 p3087 A73-45209

ION OSCILLATION

U PLASMA OSCILLATIONS

ION PROBES

Structure of turbulent wakes of hypersonic spheres as inferred with ion probes.

05 p0527 A73-16568

Ion microprobe mass analyzer for solid materials science research, discussing instrument potential and limitations

05 p0576 A73-16675

Ion microprobe analyzers for solid surfaces high resolution mass spectrometric chemical analysis, using focused ion beam sputtering technique

07 p0822 A73-19171

Concentration profiles through thin oxide scales by ion-probe microanalysis.

09 p1101 A73-22402

Lunar 20 lunar soil samples Pb-207/Pb-206 age determination by ion microprobe mass analysis, determining U, Th and radiogenic Pb concentrations

13 p1674 A73-28304

ION PRODUCTION RATES

Two X-ray bursts /1 August 1967 and 30 January 1968/ and some associated VLF disturbances.

01 p0091 A73-10556

High current low voltage magnetically confined hollow cathode discharge for vacuum evaporation and ionization, noting vacuum deposition of quartz and copper

04 p0455 A73-15755

Solar cosmic rays spectrum and geomagnetic cut-off rigidity determination from ion production rates in lower ionosphere

07 p0870 A73-19427

Use of translational energy measurements in the evaluation of the energetics for dissociative attachment processes.

10 p1251 A73-24244

Solar 1.9 A X ray spectral line effects on SOLRAD satellite-borne photometer sensitivity and lower ionospheric ion production rate

11 p1354 A73-25771

Experimental determination of the ionization rate behind a strong shock wave in air

11 p1304 A73-26444

Ionospheric production and loss processes of atomic sulfur ions, considering dissociative ionization sources

12 p1489 A73-26999

S-type current-voltage characteristic in Gunn diodes.

15 p1923 A73-31674

Ionospheric D region dissociation-recombination reaction constants derived from ion production rate data compiled during polar cap absorption

15 p1872 A73-31887

Experimental verification of the effective photon theory of laser induced gas ionization.

17 p1286 A73-35832

Cosmic ray total ionization - 1970-1972.

18 p2347 A73-36293

Estimates of thermospheric neutral constituents from ion composition measurements.

21 p2688 A73-41350

D region electron density profiles at geomagnetic equator by rocket sounding, showing ionization production by Lyman alpha radiation and cosmic rays

21 p2690 A73-41361

Rocket measurements of production and ionization during a PCA event.

21 p2760 A73-41371

Steady state coefficients in the D region during solar particle events.

21 p2760 A73-41372

Electron and hole ionization rates in epitaxial silicon at high electric fields.

21 p2668 A73-41561

Incompatibility of solar EUV fluxes and incoherent scatter measurements at Arecibo.

22 p2902 A73-41923

Relation between ion creation and C₂, CH, and OH formation in the combustion of hydrocarbons.

22 p2819 A73-42771

Helium in the terrestrial atmosphere.

24 p3107 A73-44948

Kinetics of formation of chloride ions in atmospheric pressure flames by way of the reversible reaction HCl + e⁻ yields H + Cl⁻.

24 p3085 A73-44991

ION PROPULSION

The construction of an operational model of the high-frequency ionic propulsion system RIT 10 M [DGLR PAPER 72-088]

02 p0202 A73-11672

Investigation of the fitness for space travel of the electric propulsion plant ESKA 18 [DGLR PAPER 72-087]

02 p0131 A73-11694

Thermionic reactor ion propulsion system (TRIPS) - Its multi-mission capability.

03 p0381 A73-13389

Optimization of ion propulsion for north-south stationkeeping of communications satellites.

03 p0356 A73-13454

Contribution to the analysis and conception of satellite stabilization systems based on ion propulsion

04 p0505 A73-15737

Considerations on transfer into geostationary orbit using ion propulsion - Application to the Europa III booster

04 p0505 A73-15742

Ion thrusters with cesium contact ionization - Study of the main elements.

07 p0867 A73-18933

French technology assessment on satellite stabilization by ion propulsion, stressing geostationary satellites orbit correction

07 p0904 A73-18934

French research on cesium contact ion sources. [AIAA PAPER 72-495]

08 p0996 A73-21815

Plasma accelerators in gas dynamics, discussing ion propulsion systems, high velocity wind tunnels with electric arc heating and electromagnetic shock tubes

19 p2466 A73-37354

ION PUMPS

Electrostatic getter-ion pump performance.

08 p0989 A73-21618

Vacuum system for an infrared calibration facility.

08 p0968 A73-21622

The performance characteristics of modern vacuum pumps.

21 p2707 A73-39915

ION RECOMBINATION

Ion composition dependent recombination coefficient loss rate changes in D region during solar flares, using electron density and X ray flux measurements

01 p0042 A73-10903

Ionization balance for ions of Na, Al, P, Cl, A, K, Ca, Cr, Mn, Fe and Ni.

03 p0345 A73-13949

Investigation of regularities characterizing impact ionization within a high-field domain in Gunn diodes

06 p0675 A73-18076

Recombination of H⁺ and H⁻ ions in slow collisions.

07 p0852 A73-19146

Electron temperature measurement in recombination collisional plasma with double probe, noting electron and ion density distribution near isolated electrode under floating potential

12 p1499 A73-27916

Recombination of doubly ionized atoms in the afterglow of a helium plasma produced by laser.

15 p1915 A73-31675

Thermal and ionization equilibrium in a dense hydrogen cloud.

16 p2059 A73-32841

Radiative and dielectronic recombination coefficients for complex ions.

16 p2038 A73-32842

Dissociative recombination rate for CH⁺ positive ions in interstellar clouds

19 p2490 A73-38531

Violet and UV laser transitions in Ca II and Sr II resulting from impact radiation recombination of doubly charged metal ions

21 p2712 A73-40358

Temperature dependence for dissociative recombination of NO⁺ in E- and F-region models.

21 p2684 A73-40787

Excitation of the CO fourth positive system by the dissociative recombination of CO₂⁺ ions.

22 p2843 A73-41904

ION SCATTERING

Helicon/whistler/turbulence spectra in collisionless plasma, noting ion scattering relation to self trapping and concentration along magnetic field with Landau absorption decay

04 p0480 A73-15564

Energy spectra of Ca⁺ ions scattered from the surface of a tungsten single crystal.

06 p0726 A73-18615

Study of the channeling of light ions of 0.5 to 2 MeV across gold crystals of some hundreds of angstroms thickness

07 p0864 A73-20609

Partially ionized nonideal plasma model electron-ion interactions, equilibrium, equations of state and thermodynamic quantities

10 p1252 A73-23501

Low-energy elastic differential scattering of He⁺ by He.

15 p1916 A73-32290

Partially ionized nonideal plasma model electron-ion interactions, equilibrium equations of state and thermodynamic quantities

17 p2216 A73-35181

ION SHEATHS

The excitation of resonances by a dipole antenna inside a hollow cylindrical plasma.

03 p0346 A73-13695

Measurement of ion-rich sheath thickness by ion acoustic wave.

09 p1126 A73-22279

Impedance of an ion-sheathed spherical probe in a warm, isotropic plasma.

09 p1127 A73-22431

Wave propagation in the ion sheath of an antenna immersed in a plasma

14 p1731 A73-29730

Continuum gas plasma boundary layer flow over flat plate, obtaining ion sheath characteristics and downstream solutions by asymptotic and characteristics methods

17 p2149 A73-34186

ION SOURCES

NT DUOPLASMATRONS

NT PLASMATRONS

Ionization sources of the ionospheric D and E regions.

01 p0041 A73-10886

D and E ionospheric regions behavior, emphasizing water cluster ions formation, minor neutral constituents measurement and daytime ionization sources

01 p0043 A73-10912

Atmospheric atomic oxygen density vertical distribution measurement by rocket-borne cryocooled mass spectrometer ion source

02 p0157 A73-11756

Neutral composition measurements in the lower thermosphere by means of a mass spectrometer with helium cooled ion source.

02 p0160 A73-12276

Space discharge instability in carbon dioxide laser pumping by ionization source and electric field for time difference in heat removal and gas heating

02 p0177 A73-12553

Collision effects on electromagnetic wave propagation in a plasma generated by a moving ionization source

07 p0858 A73-19906

Solid material ion source discharge chamber with cathode sputtering-introduced metal vapor, based on conventional ion source with electrons oscillating in magnetic field

08 p0993 A73-21515

French research on cesium contact ion sources. [AIAA PAPER 72-495]

08 p0996 A73-21815

Thermal fragmentation of quinoline and isquinoline N-oxides in the ion source of a mass spectrometer.

09 p1048 A73-23470

Space discharge instability in carbon dioxide laser pumping by ionization source and electric field for time difference in heat removal and gas heating

10 p1228 A73-24182

Atomic oxygen loss in ion source of sounding rocket-borne mass spectrometer for determining lower thermosphere neutral composition

12 p1489 A73-26991

Population inversion calculations using near-resonant charge exchange as a pumping mechanism.

13 p1627 A73-28549

A thermosphere composition measurement using a quadrupole mass spectrometer with a side energy focusing quasi-open ion source.

14 p1748 A73-29976

Satellite measurements of atmospheric composition in the altitude range 150 to 450 km.

18 p2303 A73-35957

Generation of energetic ion fluxes from a high temperature electron discharge in an inhomogeneous magnetic field

19 p2466 A73-37358

Investigation of the possibility of developing a wide-aperture injector of fast neutral atoms

23 p3010 A73-43665

ION TEMPERATURE

Probe measurements of positive ions and electron temperatures in high latitude rocket flights.

02 p0159 A73-12032

Oblique shock waves heating of high beta plasma ions, suggesting Landau damping of wave energy

02 p0197 A73-12059

Ionospheric electron and ion temperature profile measurements with satellite- and rocket-borne probes, comparing merits and discrepancies

02 p0163 A73-12303

Transverse ion temperature measurements in plasma stream wind tunnel simulating ionospheric conditions, using cylindrical Langmuir probe and collimator-collection device [ONERA, TP NO. 1180]

02 p0151 A73-12813

Influence of external high-frequency modulation of the electron beam on ion heating during beam-plasma interaction

04 p0478 A73-15032

Anomalous ion heating in a laser heated plasma.

06 p0730 A73-18461

Stochastic ion heating by ion-acoustic turbulence.

06 p0733 A73-18850

Comparison of Te and Ti from Ogo 6 and from various incoherent scatter radars.

07 p0790 A73-19241

Energy distribution functions of kilovolt ions in a modified Penning discharge.

07 p0808 A73-20459

Anomalous plasma ion heating by parametric excitation of lower hybrid instabilities, using long wavelength oscillating electric field [AD-759477]

07 p0860 A73-20482

The heating of the solar corona. I - Observation of ion energies in the transition zone.

08 p1005 A73-20919

Heating of charged particles by electric waves.

08 p0993 A73-21233

Ogo 6 measurements of supercooled plasma in the equatorial exosphere.

09 p1074 A73-22066

Ion velocity temperature observation at Mars surface boundary, suggesting solar plasma interaction with outer atmosphere from ion flux disturbance ahead of shock wave

09 p1126 A73-22264

Ion cyclotron instability in current-carrying plasmas with anisotropic temperatures.

09 p1127 A73-22284

Computer simulation of ion heating by pulsed microwaves. [TTU-SR-2]

09 p1129 A73-22642

Development and properties of the halo in pinch plasmas

10 p1253 A73-23673

Improved Hanle effect measurement technique for fast ions.

10 p1251 A73-24117

Electrostatic turbulence and ion thermalization in modified Penning discharge, investigating ion heating processes

10 p1251 A73-24259

Electron-cyclotron drift instability in high-beta plasmas, developing nonlinear theory based on wave kinetic equation for weak turbulence

10 p1255 A73-24263

Solar wind He nuclei kinetic temperature, considering resonant heating and proton temperature

10 p1269 A73-24723

Measurement of the ion energy distribution resulting from the turbulent heating of a plasma.

11 p1404 A73-25269

Parametric instability in an inhomogeneous plasma containing hot ions

12 p1526 A73-26926

Correspondence of main trough ion temperatures with horizontal drift speed.

12 p1489 A73-27006

Planar retarding potential analyzer onboard Explorer satellite for ion temperature and ion/electron concentration investigation

13 p1688 A73-28635

A nonlinear theory for the parametric instability with comparable electron and ion temperatures.

14 p1779 A73-30119

Instabilities in a system of a plasma and an intense relativistic electron beam.

14 p1780 A73-30122

Energy partitioning of gaseous ions in an electric field.

14 p1776 A73-30246

Investigation of the heating of a plasma ion component by a collisionless shock wave.

14 p1780 A73-30336

Ion acoustic wave scattering effects on stochastic ion heating in turbulent plasma

14 p1780 A73-30340

- Electron density characteristics in magnetized hydrogen arcs in the case of a deviation of the ion temperature from the electron temperature
14 p1780 A73-30419
- The turbulent heating of ions and related efficiencies in a current carrying plasma.
15 p1916 A73-31081
- Wake past an obstacle in a magnetized plasma flow.
15 p1916 A73-31089
- Current extension from a quasi-steady MPD arcjet.
15 p1918 A73-31550
- Probe design for orbit-limited current collection.
16 p2041 A73-33320
- Nonlinear evolution of the decay instability in a plasma with comparable electron and ion temperatures.
16 p2041 A73-33324
- Errors in ion and electron temperature measurements due to grid plane potential nonuniformities in retarding potential analyzers.
16 p2016 A73-33436
- Ion heating in thermal plasma flows.
16 p2042 A73-33465
- Satellite retarding potential trap contamination relationship to electron and ion temperatures evaluation, discussing Langmuir probes, sweep frequency and plasma density
19 p2429 A73-37373
- Model experiment on solar flares and the neutral sheet. III.
19 p2475 A73-37383
- Energy distribution functions of kilovolt ions in a modified Penning discharge.
20 p2597 A73-39197
- A search for high-ionization redshift systems in the absorption spectra of five quasars.
20 p2609 A73-39435
- Theory of a steady-state nonisothermal positive column in a magnetic field.
21 p2748 A73-40954
- The determination of ionospheric charged particle temperatures from in situ measurements.
21 p2690 A73-41362
- Non-thermal solar wind heating by supra-thermal ions.
21 p2763 A73-41499
- Ionospheric slab thickness relationship to electron density profile shape, plasma and neutral constituents scale heights and electron to ion temperature ratio
22 p2846 A73-41947
- Temperature measurements in the thermosphere and ionosphere.
22 p2847 A73-42063
- Theoretical and experimental investigations of the electron temperature in laser-produced plasmas.
22 p2891 A73-42249
- Parametric instability in an inhomogeneous plasma with hot ions.
22 p2891 A73-42260
- Ion temperature in the case of ohmic heating of the plasma in the 'Uragan' stellarator
22 p2893 A73-42382
- Temperature and ion energy spectra of laser plasma produced by giant-pulse ruby laser heating metallic targets
23 p3012 A73-43849
- ION TRAPS [INSTRUMENTATION]**
On the calibration system of the amplifying tract of spherical ion trappers.
02 p0169 A73-12186
- Studies of the equatorial anomaly in the F region and outer ionosphere with the aid of spherical ion traps
14 p1746 A73-29860
- Some characteristics of charged particle flux studies using traps and analyzers. II - Modulation trap utilization for investigating the solar wind
18 p2345 A73-36113
- Satellite retarding potential trap contamination relationship to electron and ion temperatures evaluation, discussing Langmuir probes, sweep frequency and plasma density
19 p2429 A73-37373
- Interpretation of measurement results with ion traps in a bicomponent medium.
22 p2911 A73-42735
- A new ion and electron detector for ion cyclotron resonance spectroscopy.
24 p3089 A73-44816
- ION-GAS INTERACTIONS**
U GAS-ION INTERACTIONS
IONIC COLLISIONS
The relation between momentum transfer and capture and total scattering cross sections for ion-dipole collisions.
02 p0195 A73-12842
- Electron-ion collision frequency and electrical conductivity of non-Debye plasma formed in high pressure discharge from Ar, Kr and Xe tubes
03 p0345 A73-13176
- One-electron model for charge exchange in ion-atom collisions.
03 p0344 A73-13283
- Absolute cross section for producing C-II from carbon by 270-MeV/nucleon N-14 ions.
06 p0725 A73-17519

- Density and electric field oscillations of plasma in stellarator, considering magnetic field strength effect, stabilization by ionic collisions and energy pumping mechanism
06 p0728 A73-17968
- Intensity calculation of X-ray scattering by the atom and ion of aluminum
06 p0725 A73-18216
- Recombination of H⁺ and H⁻ ions in slow collisions.
07 p0852 A73-19146
- Collision absorption of a rapid hydromagnetic wave in a plasma of two kinds of ions - Experiment
07 p0859 A73-20149
- Possibilities of using a quadrupole probe in the 0 to 1000-Hz range to measure the collision frequencies of charged particles in the ionosphere
08 p0957 A73-20654
- Ion saturation currents to planar Langmuir probes in a collision-dominated flowing plasma.
08 p0993 A73-21597
- Diatomic molecules dissociation investigation from effective cross section measurement of slow atomic negative ions formation by molecules collisions with fast ions and atoms
08 p0990 A73-21694
- Experimental investigation of the excitation of Ar II and Kr II during electron-ion collisions
09 p1122 A73-22593
- Collisional absorption of the fast hydromagnetic wave in a plasma with two ion species - Theory
09 p1131 A73-23029
- Approximation to the collisional-radiative recombination coefficient in a partially ionized gas.
17 p2213 A73-34197
- Momentum transfer and total scattering cross sections for ions with polar molecules.
17 p2213 A73-35178
- Exponential projectile charge dependence of Ar K and Ne K X-ray production by fast, highly ionized argon beams in thin neon targets.
22 p2890 A73-42710

IONIC CONDUCTIVITY**U ION CURRENTS****IONIC CRYSTALS**

- An 'ab initio' Gaussian orbital calculation of the /100/ surface of crystalline lithium hydride.
06 p0737 A73-18252
- Russian book - Spectroscopy of laser crystals with ionic structure.
07 p0836 A73-20201
- Certain problems of spectroscopy of laser crystals with ionic structure
07 p0836 A73-20202
- Spectroscopy of optical centers of Nd³⁺ in CaF₂ and SrF₂ crystals
07 p0836 A73-20203
- Static and kinetic strength estimation of ionic and metal single crystals, discussing microcracks in brittle materials and surface quality and pore distribution effects
09 p1160 A73-22900
- Effect of impurities and X-ray irradiation on the motion of pores in ionic crystals under the action of an external electric field
11 p1401 A73-25242
- Some comments on the importance of third order contributions to the screening of the ionic potential and to the structural energy of metals.
14 p1783 A73-30432
- Valency transfers of vanadium ions in ruby
14 p1783 A73-30582
- Application of a cluster component technique in the interpretation of concentration dependences of the properties of binary metal alloys and anion-substituted spinel solid solutions
15 p1923 A73-31205
- Role of electron processes in the vaporization mechanism and in the formation of binary semiconductor alloy compositions with ion bonds
23 p3016 A73-43711
- Influence of ion ordering on the induced anisotropy in Li-Fe ferrites
23 p3018 A73-44175
- Thermodynamics of white dwarf matter in crystalline phase.
24 p3143 A73-45435

IONIC DIFFUSION

- Calcium stabilized zirconia electrolyte with appreciable oxygen ionic diffusivity used as permeation membrane for oxygen leak source
02 p0167 A73-11955
- Wave motion of low-tension interfaces with electrical double layers.
02 p0196 A73-12038
- Ambipolar diffusion in the F1-region of the ionosphere.
11 p1357 A73-25928
- Titanium monoxide system cation self-diffusion coefficients, and quenched in vacancy concentrations as function of stoichiometry, tabulating Arrhenius parameters
13 p1633 A73-28145

- Magnesium oxide crystal dislocation loop shrinkage rate measurement, suggesting oxygen ion diffusion as rate controlling process for dislocation climb
13 p1634 A73-28257
- Ion implantation method and diffusion process for microelectronics semiconductor components manufacture
13 p1590 A73-28573
- Diffusion spreading of weak plasma inhomogeneities in the presence of two kinds of positive ions.
13 p1608 A73-28710
- Ion and electron diffusion in nonisothermal ionospheric F layer, analyzing ionization balance equations
15 p1871 A73-31882

IONIC MOBILITY

- Plasmasphere hydrogen, helium, oxygen and nitrogen ions inbound and outbound profiles fromOGO 5 mass spectrometric measurements
02 p0164 A73-12320
- Ion velocity distributions in the auroral ionosphere.
04 p0440 A73-14966
- Investigation of the influence of biologically active substances on the permeability of the skin
15 p1838 A73-31174
- Sodium chloride electrolyte data at high temperatures and pressures.
16 p1971 A73-33532
- Selection and preliminary evaluation of three structures as potential solid conductors of alkali ions - Two hollandites, a titanate, and a tungstate.
17 p2219 A73-35325
- Drift tube and mass spectrometric measurement of molecular positive ion drift velocities in carbon dioxide
21 p2742 A73-40221
- Diurnal thermospheric and ionospheric variations from time dependent continuity equations for O⁺, H⁺, O₂⁺, and NO⁺ ions, motion and heat conduction equations
22 p2849 A73-42572

IONIC PROPELLANTS**U ION ENGINES****IONIC REACTIONS**

- Review of laboratory measurements of aeronomical-neutral reactions.
01 p0014 A73-10335
- Symposium on D- and E-Region Ion Chemistry, University of Illinois, Urbana, Ill., July 6-8, 1971, Informal Record.
01 p0040 A73-10876
- Dependence of the D-region positive-ion composition on the atomic oxygen and atomic hydrogen concentrations.
01 p0041 A73-10891
- Ionic reaction mechanism for F region nitrogen vibrational temperature, using positive ion composition
01 p0042 A73-10894
- Reaction mechanisms and bonding energies for ion-hydrates /ion-water clusters/ of ionospheric interest.
01 p0014 A73-10899
- Shock layer measurements of decomposition reactions of water cluster ions.
01 p0014 A73-10900
- Thermal energy charge transfer reactions of rare-gas ions to methane, ethane, propane, and silane - The importance of Franck-Condon factors.
02 p0195 A73-12084
- Gas-phase acidities of binary hydrides.
02 p0139 A73-12632
- Multiphoton transitions. III - Rates of multiphotodetachment of negative ions.
07 p0852 A73-19147
- Disturbed ionospheric electron and ion kinetics, detailing dissociative recombination as regulating process for temporal evolution
07 p0816 A73-19454
- Magnesium and associated ionospheric processes in Es-layer formation.
08 p0957 A73-20655
- Prohibited autodetachment in OD⁻ formed by collisions of O⁻ with D₂.
09 p1048 A73-22075
- Kinetics of stimulated scattering of Langmuir waves by plasma ions
15 p1919 A73-31708
- Effect of chloride ions on the dissolution behavior of Fe-Ni alloys.
15 p1895 A73-32565
- Ionic dissociation energy in polymeric electrical conductivity behavior, taking into account conductivity, viscosity, dissociation energy, dielectric constant, gas constant and absolute temperature
20 p2581 A73-39667
- High temperature ionic and charged species reactions in hydrocarbon and cyanogen flames and additive combustion systems
22 p2819 A73-42770
- Estimate of the effect of photoionization and ion-molecule reactions on the diffusion coefficient in the ionosphere.
23 p2971 A73-43257

IONIC WAVES

Response of the ionosphere to the spectrum of acoustic-ionic waves emitted by a localized impulse source in space - Application to suddenly arising geomagnetic storms

Life-time of ion waves in unstable and turbulent plasmas.

Ring current proton injection instability for ion loss cone and electromagnetic ion cyclotron waves in high beta low density region outside magnetopause

A large double plasma device for plasma beam and wave studies.

Nonrelativistic collisionless plasma ion acoustic waves modulation by hf electromagnetic oscillation, calculating wave complex frequency

Resonances of an antenna associated with the excitation of ion Bernstein modes.

Spatial plasma echoes of ion acoustic waves in low pressure He and Ne discharges in anode direction

Confined plasma diffusion due to growing or nonlinearly saturated LF ion waves causing energy transfer from electrons to ions in slabs

Instability of a magnetoactive plasma with a transverse ion beam.

Waves in magnetoactive plasma in the presence of a distinct transverse ion velocity

Parametric excitation of circularly polarized and ion waves in a magnetized plasma.

Shock wave large particle model of ion density discontinuity decay in nonisothermal plasma, assuming high electron temperature and Boltzmann distribution

Waves in a magnetoplasma with an isolated transverse ion velocity component.

Current driven ion wave instability in a weakly ionized collisional magnetoplasma.

Role of nonlinear effects in the problem of the anomalous resistance of plasma.

Ion acceleration upon expansion of a rarefied plasma.

Magnetic pulsation spectra in a nonisothermal plasma.

Experimental investigation of current-driven ion wave turbulence in plasma.

IONIZATION

NT ATMOSPHERIC IONIZATION

NT AURORAL IONIZATION

NT AUTOIONIZATION

NT FLAME IONIZATION

NT GAS IONIZATION

NT ION PRODUCTION RATES

NT NONEQUILIBRIUM IONIZATION

NT PHOTOIONIZATION

NT SURFACE IONIZATION

Energetic solar particles and their relation to optical flares.

11 p1413 A73-25952

IONIZATION CHAMBERS

NT BUBBLE CHAMBERS

NT CLOUD CHAMBERS

NT GEIGER COUNTERS

NT PROPORTIONAL COUNTERS

NT SPARK CHAMBERS

Nuclear-electron cascades longitudinal evolution calculation in ionization calorimeter for primary nucleons and pions, using Monte Carlo method

Ionization calorimeter study of cosmic ray hadrons inelastic collision cross sections and partial K-neutral pion inelasticity factor

High energy cosmic ray pions and nucleons interactions with atomic nuclei, using ionization calorimeter and spark chambers system

Ionization calorimeter measurement of energy transfer to electron photon cascade secondary particles during hadron interaction with lead nuclei

Muon generated cascade showers in iron, using ionization calorimeter and hodoscopic detectors

Electron photon shower particle flux transition effect on ionization chamber and scintillation counter readings

02 p0210 A73-12685

Description of a device for studying inelastic nuclear processes with nucleons at energies from .1 to 10 TeV and analysis of its operation at an altitude of 3250 m above sea level

Ultraviolet ion chamber measurements of the solar minimum brightness temperature.

Ionization vacuum chambers for radiation measurement, discussing secondary emission, Greening theory and dosimeters, electron beam monitors, pulse measurement, energy spectrometers and interface dosimetry applications

Continuum analysis of the photoionization chamber in the transition from low to high rates of ionization.

Particle number fluctuations and transient effects in electron-photon showers in lead at energies above 20 GeV

Preliminary results of the Pamir-20-71 experiment on interactions at energies of about 1000 TeV

High energy gamma quanta families and multiple generation processes in electron photon cascades detected by nuclear emulsion X ray chamber

Properties of secondary high-energy particles in hadron interactions

Generation of high-energy muons in cosmic rays

Identification of hadrons with 500 GeV energies in cosmic rays by using transitional emission

IONIZATION COEFFICIENTS

Characteristics of ionization-recombination processes in a plasma discharge diode

Molecular nitrogen ionization growth characteristics as function of electric field strength and gas pressure, using thin gold film electrodes

Experimental determination of the ionization rate behind a strong shock wave in air

Nickel single crystal target ionization by high voltage electron beam bombardment, using time of flight mass spectroscopic analysis

Non-thermal ionization and recombination processes during solar flares.

Ionization and recombination in a plasma diode.

Application of mathematical methods for the description of the planetary distribution of ionosphere parameters

Ten years Antarctic region ionosphere investigation during IGY-ISQY period considering ionization maxima, inhomogeneity drifts, electron density and short wave propagation

Interstellar trace element ionization predictions by cosmic ray, X-ray and UV star models with hydrogen allowance, showing disagreement with satellite observation

24 p3125 A73-45056

IONIZATION COUNTERS

U IONIZATION CHAMBERS

U RADIATION COUNTERS

IONIZATION CROSS SECTIONS

Ionization cross sections for H2, N2, and CO2 clusters by electron impact.

Oscillator strengths and ground-state photoionization cross-sections for Mg+ and Ca+.

Cross sections for the production of excited products in the photoionization of N2, O2, CO, and N2O by 58.4-nm radiation.

Further evidence for a cosmic ray selection mechanism.

Experimental measurement of the O2-/ photodetachment cross section.

Inelastic pionization cross section of cosmic ray hadrons with carbon nuclei at energies of 100 to 300 GeV

Influence of ionization losses on the conditions of cosmic ray generation on the sun

Measurement of the cross section for photodetachment of O3/-.

Ionization of 6s- and 5p-electrons of the cesium atom by electron impact

Excitation of autoionization states of the cesium atom by electron impact

Proton-impact dissociation and ionization of H2+ molecular ions.

Oscillator strength and photoionization cross section computation for Cs ground state during photodetachment, using semiempirical model potential with adjustable parameters

Threshold energies of K-shell photoionization cross sections for various cosmic ionic species

Inhomogeneous plasma density distribution relation to ambipolar diffusion and ionization balance processes of electron cooling, particle recombination and ground state, step wise and Penning ionization

Nitrogen and oxygen molecules, photodissociation continuums from absorption and ionization cross sections, calculating upper atmosphere emission rates

Photoionization of atomic nitrogen and atomic oxygen.

The photoionization cross section of magnesium near threshold.

Electron-molecule collision ionization in hydrogen and deuterium.

Processes altering charge state in collisions of hydrogen atoms with H2 molecules.

Ionization transitions from the 8/2P11/2 level of a cesium atom in a low-temperature plasma

Effect of ionization losses on cosmic-ray generation conditions on the sun.

High-resolution photodetachment study of Se-/ ions.

Polarization phenomena in multiphoton ionization of atoms.

Inhomogeneous plasma density distribution relation to ambipolar diffusion and ionization balance processes of electron cooling, particle recombination and ground state, step wise and Penning ionization

Stripping cross sections for production of forward scattered molecular ions in hydrogen and deuterium molecular collisions at kinetic energies below 500 eV, noting isotope effect

Solar Fe 13 coronal lines relative intensity calculation as function of electron density from cross sections for collisional excitation by protons

IONIZATION FREQUENCIES

Diffusion time of charged particles in a plasma with volume ionization.

A simple theory of breakdown for nonlign gases in fields of any frequencies ranging from low to optical

Recombination and negative ion role in high-frequency gas discharges

IONIZATION GAGES

NT PHILIPS IONIZATION GAGES

Rise time and pressure measurements in transient flow during quasi-steady gas injection into vacuum with piston valve, using fast ionization gage

Lunar atmosphere gas concentrations from Apollo 14 and 15 ALSEP cold cathode ionization gage measurements, considering solar wind and contamination sources

Optimal use of double pin ionization gauges for shock wave detection.

Low gas pressure measurement with ionization and extractor gages, discussing methods for suppressing or eliminating disturbance effects

A noise-immune ionizational manometer for pressures between 1 millitorr and 1 nanotorr

Atmosphere Explorer pressure measurements - Ion gauge and capacitance manometer.

Gas flow analysis during thermal vacuum test of a spacecraft.

Vacuum Technology Workshop, Versailles, France, May 30-June 3, 1972, Proceedings

Influence of the wall temperatures of gauges on the measurement of limit pressures

IONIZATION POTENTIALS

- Secondary ionisation and its possible bearing on the performance of a solar cell.
02 p0132 A73-12048
- Ionizing potential wave analysis for gas breakdown, noting photoionization role in avalanche propagation and velocity, electron densities and temperature as function of electric field
02 p0197 A73-12063
- Radial velocity and microturbulence dependence on excitation potential and time in A type supergiants at atmosphere, deriving chemical composition
03 p0371 A73-13215
- Search for 3C 191 ionization potential-red shift correlations to other quasar absorption lines
07 p0900 A73-20237
- Mass spectrometric studies of tetrafluorohydrazine and the difluoroamino radical.
08 p0936 A73-21173
- Ionization energy of adhesion levels and heat-generation centers in the microplasma volume in germanium p-n junctions
08 p0995 A73-21274
- Formation of continuous solid solutions of intermetallic compounds
10 p1260 A73-24512
- Effect of Debye shielding on the ionization energy of air plasma components
13 p1667 A73-29164
- Temperature distribution and ionization characteristics of sodium and rubidium chlorides, silicon dioxide and atomized carbon jets generated by plasmatron
14 p1781 A73-30464
- The kinetic characteristics of the electrons of the anisothermal homogeneous steady neon plasma in the ionization level range from 10 to the minus 9th power to 0.01
16 p2043 A73-34022
- An electrostatic suspension method for determining photoionization energies of solids.
23 p3015 A73-43447
- Breakdown potential of potassium-seeded combustion products.
24 p3121 A73-45164
- IONIZED GASES**
NT CATIONS
NT CESIUM PLASMA
NT CHARGED PARTICLES
NT COLD PLASMAS
NT COLLISIONLESS PLASMAS
NT COSMIC PLASMA
NT ELECTRON PLASMA
NT PLASMA CLOUDS
NT PLASMA JETS
NT PLASMA LAYERS
NT PLASMA SHEATHS
NT PLASMA SLABS
NT RELATIVISTIC PLASMAS
NT SOLAR WIND
NT STELLAR WINDS
NT THERMAL PLASMAS
NT TOROIDAL PLASMAS
- Measurement of the macroscopic velocity of the neutral component of weakly ionized gas in the crossed fields.
01 p0081 A73-10116
- Incidence of a plane electromagnetic wave on a moving shock wave in an ionized gas
01 p0016 A73-10205
- Local emission coefficients fields for ionized gas in arbitrary and rectangular cross section streams
03 p0344 A73-13179
- Ionization balance for ions of Na, Al, P, Cl, A, K, Ca, Cr, Mn, Fe and Ni.
03 p0345 A73-13949
- Laboratory-produced radiation related to the solar flare emission.
[AD-758606] 03 p0364 A73-13957
- Solar corona X-ray emission from O VII and Ne IX ions by rocket-borne Bragg spectrometers observations, determining electron temperature from resonance lines intensity
03 p0364 A73-14418
- Recent results of plasma-wall heat transfer studies in highly ionized, dense plasmas.
05 p0603 A73-16762
- Ion-current distributions around an electrically conductive body in ionized gas flow.
05 p0603 A73-17110
- Experimental study of argon ion laser discharge at high current.
[AD-754727] 06 p0701 A73-18361
- Experimental and numerical studies of flush electrostatic probes in hypersonic ionized flows. II - Theory.
07 p0858 A73-19961
- Departure from thermodynamic equilibrium of an ionized cesium vapor - Experimental study and comparison with a statistical model
07 p0854 A73-20607
- Reduction of the thermal flux through a cylindrical pipe containing an ionized gas flow
07 p0860 A73-20617

- On the steady flow of a non-equilibrium ionized gas around sharp corners in the presence of a crossed magnetic field.
08 p0992 A73-21009
- Calculation of the boundary layers of a fully ionized two-temperature plasma for given temperatures of components at the electrodes
09 p1127 A73-22605
- Nonequilibrium transport process calculation by theoretical microscopic model for interaction between ionized gas and solid particles in suspension, noting free electron concentration change
09 p1130 A73-22826
- Self-mode-locking in an argon ion laser with a nonlinear absorber
09 p1096 A73-22878
- Theoretical possibility of converting the kinetic energy of an ionized gas flow into electricity
10 p1177 A73-23473
- Investigation of the motion of artificially ionized clouds in the upper atmosphere.
10 p1212 A73-24225
- Nonstationary distribution of the electron-ion gas in the ionosphere.
10 p1212 A73-24239
- Kinetic equations for time behavior of electron concentration and proton, electron and H I atom temperatures in ionized hydrogen medium
10 p1282 A73-24492
- Electric current in pressurized N₂, CO₂, and their mixtures under conditions of strong ionization by an electron beam
10 p1230 A73-24883
- Single mode ion laser tuning over entire emission range via intracavity etalon tilting by piezoelectric drive
11 p1376 A73-26104
- Electron-beam ionized pulsed CO₂ laser
12 p1506 A73-27216
- A microscopic theory of density fluctuations in partially ionized gases.
15 p1916 A73-31086
- Numerical study of the interaction of a shock-wave caused, supersonic, ionized-argon flow with electric and magnetic fields, using the method of characteristics
15 p1918 A73-31571
- Dwell times of thin exploding wires.
15 p1913 A73-31934
- Relaxation of a partially ionized gas in a nozzle
15 p1824 A73-32327
- Physics of ionized gases 1972; Proceedings of the Sixth Yugoslav Symposium and Summer School, Miljevac, Yugoslavia, July 16-21, 1972.
16 p2040 A73-32938
- Arc discharge properties in ionized gases, discussing interruption and reignition in terms of instabilities, decay processes, and circuit breaker problem
16 p2040 A73-32940
- Influence of diffusion on plasma parameters - A qualitative estimate and a physical interpretation.
16 p2040 A73-32941
- Transport coefficients of ionized argon.
16 p2039 A73-33318
- Approximation to the collisional-radiative recombination coefficient in a partially ionized gas.
17 p2213 A73-34197
- Book - Plasma engineering.
17 p2217 A73-35475
- Slightly ionized low density hypersonic flow about a sharp plate and its diagnostics.
[AIAA PAPER 73-690] 18 p2262 A73-36241
- Dynamics of ionized gases; Proceedings of the International Symposium, Tokyo, Japan, September 13-17, 1971.
19 p2463 A73-37151
- A review of electrostatic probe response in a flowing, low density plasma.
19 p2465 A73-37165
- High enthalpy supersonic ionized gas flow in shock tube experiment, investigating pinch effect on flow acceleration and setup performance
19 p2415 A73-37168
- Expansion of a plasma from a spherical source into vacuum.
19 p2465 A73-37176
- On the flow of a nonequilibrium ionized gas past a wall in the presence of a magnetic field.
19 p2465 A73-37178
- Comparison of electron and electronic temperatures in recombining nozzle flow of ionized nitrogen-hydrogen mixture. I, II.
19 p2462 A73-37441
- Boltzmann equation with Gross-Krook type model for investigation of steady plane shock wave structure in fully ionized gas
20 p2596 A73-38968
- A tensor surface harmonic expansion of the collision integral for a weakly ionized plasma. I
20 p2596 A73-39193
- The breakdown condition of the electrode layer in an ionized gas flow
20 p2597 A73-39278

- Electrical current in electron-beam ionized N₂ and CO₂.
21 p2749 A73-41658
- Theoretical studies and experimental verifications of thermal and electrical conductivity, molecular diffusivity and viscosity of a partially ionized suspension in an electric field.
22 p2894 A73-42512
- Effects of translational disequilibrium on the structure of a shock wave in an ionized monatomic gas
22 p2895 A73-43045
- IONIZED PLASMAS**
U PLASMAS (PHYSICS)
IONIZERS
Fabrication of porous tungsten foils for contact ionization of cesium
[ONERA, TP NO. 1113] 01 p0055 A73-10234
- French research on cesium contact ion sources.
[AIAA PAPER 72-495] 08 p0996 A73-21815
- IONIZING RADIATION**
NT ALPHA PARTICLES
NT BETA PARTICLES
NT COSMIC RAY SHOWERS
NT COSMIC RAYS
NT FAR ULTRAVIOLET RADIATION
NT GAMMA RAYS
NT LYMAN ALPHA RADIATION
NT NEAR ULTRAVIOLET RADIATION
NT PRIMARY COSMIC RAYS
NT SECONDARY COSMIC RAYS
NT SOLAR COSMIC RAYS
NT SOLAR X-RAYS
NT ULTRAVIOLET RADIATION
NT X RAYS
- Influence of strong external factors on the characteristics of semiconductor devices sensitive to the state of the surface [Review/
01 p0022 A73-10036
- Highlights of the COSPAR Symposium on the solar eclipse of 7 March 1970.
01 p0101 A73-10911
- Ionizing potential wave analysis for gas breakdown, noting photoionization role in avalanche propagation and velocity, electron densities and temperature as function of electric field
02 p0197 A73-12063
- Cytochemical-luminescence study of adrenal cortex proteins under the influence of ionizing radiation
02 p0134 A73-12354
- A short description of the ESRO-IV satellite.
03 p0381 A73-13274
- Effect of ionizing radiation on Gunn diode amplifiers.
05 p0557 A73-16502
- Transient ionizing radiation effects on IMPATT diode oscillators.
05 p0558 A73-16519
- Effects of ionizing radiation on dielectrically isolated junction field effect transistors.
[AD-757969] 05 p0558 A73-16524
- De Gaston decharger with ionizing radiation for temporary jet fuel conductivity increase and charge density reduction, discussing theory, design and tests
[SAE PAPER 720864] 05 p0537 A73-16673
- Effects of ionizing radiations on MOS components
07 p0860 A73-18914
- Improving the performance of M.I.S. circuits under radiation.
07 p0797 A73-18918
- Ionization front propagation velocity as function of microwave power density, showing dependence on precursor electron density profiles
10 p1251 A73-24257
- Carbon dioxide laser active medium excitation by ionizing radiation from external source during electric current passage, discussing gain dependence on pressure and mixture
10 p1229 A73-24756
- Mechanism of the action of radiation protecting agents - A biochemical shock hypothesis
12 p1465 A73-27499
- A simple theory of breakdown for nonlinear gases in fields of any frequencies ranging from low to optical
13 p1663 A73-29165
- Small perturbation method study of nonlinear weak D-type unsteady ionization front geometry with radiation source in interstellar incompressible gas medium
15 p1932 A73-31295
- Russian book on ionizing radiation microscopic methods for nondestructive flaw detection in non-transparent objects covering imaging techniques and quality control equipment
15 p1875 A73-31580
- Aftereffects in IMPATT oscillators with transient ionizing radiation.
15 p1851 A73-32187
- The synergistic inactivation of biological systems by thermoradiation.
16 p1976 A73-33696
- Russian book on ionizing radiation protection covering shielding design, radiation source characteristics, maximum permissible levels, neutron, alpha, beta and gamma radiation, albedo, etc
18 p2336 A73-35872

Russian book - Primary and initial processes of the biological action of radiation. 18 p2269 A73-35896

Retinal change induced in the primate /Macaca mulatta/ by oxygen nuclei radiation. 18 p2271 A73-36125

Photoeffect applications in MDS systems with a nonstationary depletion layer in ionizing radiation detectors 18 p2316 A73-36716

Effect of ionizing radiation on second breakdown. 20 p2599 A73-39007

A catalog of data on optically visible H II regions. 20 p2607 A73-39084

IONOGRAMS

Ionospheric electron density profiles calculation from ionograms via nomogram relating gradients of possible and actual height in given frequency interval of integration 02 p0159 A73-12184

Conjugate ducted echoes observed on Alouette II ionograms. 02 p0143 A73-12624

The production and analysis of transmission ionograms. 04 p0440 A73-14953

Conjugate ducted echoes observed on Alouette II ionograms. 05 p0572 A73-17164

Ionograms for slant sporadic E layer under continuous sunlight inside polar cap, noting occurrence probability and auroral activity 07 p0819 A73-20065

Ionogram traces production by mode coupling process in thin sporadic E layers, using calculated reflection and transmission coefficients for radio waves incidence 09 p1076 A73-22139

Correct statement of the problem of computing the N/h/ profiles of the lower ionosphere. 10 p1212 A73-24241

Small scale loop structuring of F region ionogram traces due to HF ray propagation through irregularities 11 p1354 A73-25766

Calculation of ionospheric N/z/ profiles with the use of radio-wave absorption data 15 p1871 A73-31883

Ionospheric electron density profiles calculation method based on oblique backscatter ionograms, presenting virtual height vs frequency 15 p1873 A73-32229

Three dimensional ionograms synthesis method, considering quasi-parabolic layer ionospheric model application and ray path parameters 15 p1845 A73-32232

Evidence of frontal structures in nonblanketing sporadic-E layers. 18 p2304 A73-35990

Electron density profiles from ionograms - Comparisons with rocket profiles. 18 p2306 A73-36017

F region disturbances in wake of burnt-out Black Brant rocket body, discussing electron depletion from ground based Gisonde 21 p2690 A73-41363

IONOSONDES

Automatic N/h, t/ profiles of the ionosphere with a digital ionosonde. 02 p0143 A73-12530

Minimized calculation errors in phase ionosonde true height reduction technique for electron density profile, noting lowest observable radio frequency 02 p0143 A73-12531

Further ionosonde observations of ionospheric modification by a high-powered HF transmitter. 04 p0444 A73-15540

Transition region response of the symmetric double probe and its application in the lower ionosphere. 09 p1080 A73-22101

Empirical formula suitability for analysis of ionosonde data on blanketing sporadic E, noting time variation effects of limiting frequency and layer intensities 17 p2159 A73-34776

Evidence of frontal structures in nonblanketing sporadic-E layers. 18 p2304 A73-35990

Electron density profiles from ionograms - Comparisons with rocket profiles. 18 p2306 A73-36017

The combined use of satellite differential Doppler and ground-based measurements for ionospheric studies. 22 p2843 A73-41837

Kinesonde observations of ionosphere modification by intense electromagnetic fields from Platteville, Colorado. 22 p2844 A73-41921

IONOSPHERE

NT D REGION

NT E REGION

NT F REGION

NT F1 REGION

NT F2 REGION

NT LOWER IONOSPHERE

NT SPORADIC E LAYER

NT UPPER IONOSPHERE

Response of the ionosphere to the spectrum of acoustic-ionic waves emitted by a localized impulse source in space - Application to suddenly arising geomagnetic storms 01 p0035 A73-10327

Highlights of the COSPAR Symposium on the solar eclipse of 7 March 1970. 01 p0101 A73-10911

Neutral wind measurement during daytime in the thermosphere. 02 p0159 A73-12224

Tropospheric and ionospheric refraction errors in satellite tracking over the Indian sub-continent. 02 p0141 A73-12299

Ion velocity distributions in the auroral ionosphere. 04 p0440 A73-14966

Time dependent and independent electric coupling between magnetosphere and ionosphere, discussing auroral arcs formation and magnetospheric plasma convection 04 p0442 A73-15335

Magnetically coupled transport of a cold plasma in the outer ionosphere at low latitudes. 05 p0567 A73-16094

Double layer formation in homogeneous plasma with constant current, considering occurrence in ionosphere and solar atmosphere 05 p0601 A73-16146

Reaction kinetics of nitric oxide positive ion with ozone yielding nitrogen dioxide positive ion and oxygen, noting impact on ionospheric chemistry 07 p0787 A73-19258

Magnetospheric and ionospheric potential electric fields, using variational process based on transverse/longitudinal conductivity ratios in plasma 07 p0815 A73-19433

Possibilities of using a quadrupole probe in the 0 to 1000-Hz range to measure the collision frequencies of charged particles in the ionosphere 08 p0957 A73-20654

Penetration of solar protons into the geomagnetic tail 08 p0998 A73-21276

Summary of daily observational results of solar phenomena, cosmic ray, geomagnetic variation, ionosphere, radio wave propagation and airglow during October 1969 through December 1971. 08 p0961 A73-21393

Deformation and striation of plasma clouds in the ionosphere. I, II. 09 p1074 A73-22062

Monte Carlo simulation of a model ionosphere. II - Energy flow and energy dissipation. 09 p1075 A73-22129

Ionospheric and plasma sheet particle densities, fluxes and bulk velocities along auroral magnetic field line for collisionless ion-exosphere model. 09 p1079 A73-22842

On what ionospheric workers should know about the plasmapause-plasmasphere. 10 p1215 A73-24781

U.S.S.R. ionospheric stations and observations during IQSY, discussing ionosphere formation, morphology, radio wave absorption, nonuniformity and upper atmosphere motions 11 p1351 A73-25101

The effect of a uniform external pressure on the ionospheric boundary of a non-magnetic planet in a steady solar wind. 11 p1421 A73-25925

Atmosphere Explorer mission of lower thermosphere and ionosphere physics investigation, discussing orbit selection 13 p1687 A73-28626

Jupiter, Saturn, Uranus and Neptune upper atmospheric ionization equilibrium distribution, emphasizing ionosphere 14 p1799 A73-30535

Numerical simulation of equatorial electric fields and magnetic variations based on global ionospheric dynamo and equatorial electrojet models 15 p1869 A73-31753

Additional results from an Ogo 6 experiment concerning ionospheric electric and electromagnetic fields in the range 20 Hz to 540 kHz. 16 p2003 A73-33438

On the extent of the Martian ionosphere. 16 p2062 A73-33462

Atmosphere and ionosphere of Venus on the basis of data obtained by Mariner 5 in the S band during radio occultation 16 p2067 A73-33801

Ionospheric electron thermal conductivity obtained for power law dependence of electron-neutral collision frequency dependence on velocity 16 p2010 A73-33923

The ionospheric electric field during substorms - An interpretation based on non-uniform reconnection in the geomagnetic tail. 17 p2159 A73-34512

Book - Space physics and space astronomy. 17 p2230 A73-34575

Meteor radar study of tides in the 80 to 100 km altitude range. 18 p2305 A73-35999

Penetration of solar protons into the geomagnetic tail. 19 p2476 A73-37905

Lunar thermal ionosphere acceleration and detection within lunar electric field for electric potential of moon in solar wind or magnetosheath 20 p2604 A73-38933

Jovian ionospheric and magnetospheric ionization and temperature distributions from solutions of momentum and chemical equations for electrons, ions and neutrals, and heat transport equation 21 p2764 A73-40165

COSPAR mean international reference atmosphere for 25-500 km region, considering 25-75, 75-120 and regions above 120 km 21 p2683 A73-40627

Atmospheric structure and its variations in the region from 25 to 120 km. 21 p2683 A73-40628

Atmospheric models for 110-2000 km region, considering composition, temperature profiles, thermosphere and exosphere variations, density and boundary condition computation, etc 21 p2683 A73-40629

Variations in density and chemical composition at 120 km from chemical and dynamical processes. 21 p2689 A73-41355

Development of a vacuum chamber for ionospheric plasma simulation - Utilization of liquid helium cryopumping 22 p2838 A73-41869

ESRO I /Aurora/ satellite observations of aurora, magnetosphere-ionosphere interaction at high latitudes and auroral particle flux density 24 p3087 A73-45207

IONOSPHERIC ABSORPTION

U ELECTROMAGNETIC ABSORPTION

U IONOSPHERIC PROPAGATION

IONOSPHERIC BLACKOUT

U BLACKOUT (PROPAGATION)

IONOSPHERIC COMPOSITION

Review of laboratory measurements of aeronomical ion-neutral reactions. 01 p0014 A73-10335

D and E region aeronomy, discussing ionization sources, ion composition, water cluster ion formation and ratio of molecular oxygen and nitric oxide ions 01 p0040 A73-10877

Mass spectrometric measurements of minor constituents in the lower thermosphere. 01 p0041 A73-10880

Mesospheric nitric oxide concentrations during a PCA. 01 p0041 A73-10881

Estimation of nitric oxide concentration in the lower E region from rocket and satellite measurements of electron densities and X-ray fluxes. 01 p0041 A73-10882

Atomic oxygen profiles in the lower thermosphere. 01 p0041 A73-10884

Lower ionosphere variability due to atmospheric dynamics, considering temperature variations, minor constituent transport and eddy diffusion 01 p0041 A73-10885

Positive ion composition measurements in the D and E regions of the equatorial ionosphere. 01 p0041 A73-10889

Positive ion composition measurements in disturbed D region, noting positive molecular oxygen ions as major source of water cluster ions 01 p0041 A73-10890

Dependence of the D-region positive-ion composition on the atomic oxygen and atomic hydrogen concentrations. 01 p0041 A73-10891

Ion composition and photochemistry of the E-region. 01 p0042 A73-10892

D-region negative-ion chemistry. 01 p0042 A73-10895

Negative-ion composition measurements in the D and lower E regions. 01 p0042 A73-10896

Equilibrium composite negative ion density profiles in nighttime D region from mass spectrometer measurements 01 p0042 A73-10897

Reaction mechanisms and bonding energies for ion-hydrates /ion-water clusters/ of ionospheric interest. 01 p0014 A73-10899

Shock layer measurements of decomposition reactions of water cluster ions. 01 p0014 A73-10900

Ion composition dependent recombination coefficient loss rate changes in D region during solar flares, using electron density and X ray flux measurements 01 p0042 A73-10903

D and E ionospheric regions behavior, emphasizing water cluster ions formation, minor neutral constituents measurement and daytime ionization sources 01 p0043 A73-10912

Rocket payload designs simulated by Monte Carlo method for aerodynamic properties during D region composition measurements

02 p0156 A73-11740

Energetic metastable molecular oxygen as a source of ionization in the D region.

02 p0157 A73-11757

Diurnal latitudinal composition variations in light ion trough from OGO mass spectrometric observations, noting magnetic storm effects

02 p0157 A73-11904

A technique for recovering the vertical number density profile of atmospheric gases from planetary occultation data.

02 p0158 A73-11913

Atomic oxygen concentration from the forbidden OI 5577 A line emission at the auroral zone latitude.

02 p0158 A73-11916

Molecular oxygen densities in atmosphere near 100 km from solar hydrogen Lyman alpha absorption measurements by Intercosmos 4 satellite and Vertical 1 rocket

02 p0160 A73-12275

Neutral composition measurements in the lower thermosphere by means of a mass spectrometer with helium cooled ion source.

02 p0160 A73-12276

E and F regions ion composition measurement with rockets, noting nitric oxide variation with molecular/atomic oxygen cations ratios at different solar activity phases

02 p0206 A73-12305

The light-ion trough, the main trough, and the plasmapause.

04 p0493 A73-15533

Auroral He 4 precipitation flux measurements by exposed metal foils recovered from rocket flights

04 p0443 A73-15534

Airglow height profiles of forbidden O I 6300 and 5577 A line emissions in morning ionosphere from rocket photometric measurement

04 p0444 A73-15542

Midlatitude sporadic E layer vertical electron and ion distributions from rocket experimental wind velocity profile, assuming molecular and metallic ions in ionosphere

06 p0742 A73-17535

Parametric description of thermospheric ion composition results.

07 p0815 A73-19255

Sunrise changes in concentrations of minor neutral constituents in the mesosphere.

07 p0819 A73-20062

Estimation of the seasonal variation of the gas composition of the atmosphere at the height of the F1 layer from data on the developmental conditions of the layer

08 p0958 A73-21281

Ion composition and photochemistry of the E region

08 p0958 A73-21282

Metallic ion composition and electron density measurements in equatorial E region, considering three body reaction kinetics with dissociative ion-electron recombination

09 p1074 A73-22064

Investigation of geoeactive corpuscular particles and photoelectrons on board the Cosmos 261 satellite. V - Spectra of ionospheric photoelectrons and migration of the latter from the conjugate ionosphere

10 p1211 A73-23887

Investigation of charged-particle fluxes at altitudes of 200 to 300 km with the aid of the Saliut orbital station

10 p1267 A73-23930

A two-component model of the diurnal variations in the thermospheric composition.

11 p1354 A73-25758

Lower thermosphere density and composition model from satellite drag and accommodation coefficients

12 p1488 A73-26990

Atomic oxygen loss in ion source of sounding rocket-borne mass spectrometer for determining lower thermosphere neutral composition

12 p1489 A73-26991

Time dependent studies of the aurora. I - Ion density and composition.

12 p1492 A73-27601

Auroral heating and the composition of the neutral atmosphere.

12 p1492 A73-27602

Photochemistry of minor constituents in the troposphere.

12 p1466 A73-27603

Rocket-based mass spectrometric measurements of midlatitude and north polar region ionospheric ion composition, discussing ionization of water and heavy water vapors

14 p1747 A73-29864

A thermosphere composition measurement using a quadrupole mass spectrometer with a side energy focusing quasi-open ion source.

14 p1748 A73-29976

Midlatitude sporadic E layer vertical electron and ion distributions from rocket experimental wind

velocity profile, assuming molecular and metallic ions in ionosphere

16 p2052 A73-32759

Satellite measurements of atmospheric composition in the altitude range 150 to 450 km.

18 p2303 A73-35957

ALADDIN II ionospheric composition measurements, obtaining ion and neutral vertical density profiles and dynamic parameters for E region nighttime ion layering prediction model

18 p2303 A73-35958

Ion and neutral composition measurements in the lower ionosphere.

18 p2303 A73-35960

Positive ion composition in the lower ionosphere during the Geminid meteorshower and the occurrence of a winter anomaly.

18 p2305 A73-36005

Ion composition measurements at altitudes 100-180 km in 1972.

18 p2310 A73-36143

Mass spectrometric investigations of the night polar ionospheric structure.

18 p2310 A73-36145

System for calibrating on-board instruments and for laboratory simulation of low-density plasma flows past models

19 p2417 A73-37351

Estimation of the seasonal variation of the gas composition of the height of the F1-layer from data on the conditions of its development.

19 p2424 A73-37910

Ion composition and photochemistry of the E-region.

19 p2424 A73-37911

Investigation of geoeactive corpuscles and photoelectrons with the Cosmos 261 satellite. V - Spectra of ionospheric photoelectrons and their transfer from the conjugate ionosphere.

20 p2550 A73-38906

Satellite-borne swept frequency impedance probe /gyroplasma probe/ for ionospheric plasma parameters including electron density and ion composition, noting PCM telemetry system

22 p2917 A73-42571

Estimate of the effect of photoionization and ion-molecule reactions on the diffusion coefficient in the ionosphere.

23 p2971 A73-43257

Ionospheric aeronomy problems with emphasis on photochemical processes of neutral and ionized components, discussing nighttime ionizing agents, ion recombination, water vapor and nitrogen oxide behavior, etc

23 p2978 A73-43977

Ionospheric metastable particle production and annihilation during photochemical reactions, determining neutral and ionized particle abundance profiles

23 p2978 A73-43979

Layering of the neutral metals of meteoric origin in the lower ionosphere.

24 p3066 A73-44733

Calculation of a model of the neutral atmosphere of Mars above 140 km from ionospheric data

24 p3137 A73-44785

Diurnal ion composition variations in E region under quiet and perturbed solar conditions, using continuity equations for positive ions and electroneutrality equations

24 p3083 A73-44793

Atomic nitrogen and nitrogen oxide in the perturbed ionosphere at heights ranging from 100 to 200 km

24 p3066 A73-44802

IONOSPHERIC CONDUCTIVITY

On the types of current patterns of weak geomagnetic disturbances at the polar caps.

02 p0158 A73-11915

Electric fields and conductivities derived from wake measurements on a rocket.

02 p0164 A73-12311

Effect of the slope of geomagnetic field lines on the field of the magnetosphere-ionosphere current system

02 p0164 A73-12458

Characteristic functions of potential distribution on sphere with longitude dependent conductivity for application to ionosphere electrodynamics

07 p0816 A73-19444

Low latitude equatorial electrojet analysis based on three dimensional electric field equation for ionosphere and magnetosphere

10 p1211 A73-24215

The frequency dispersion of the transverse electrical conductivity of ionospheric plasma

12 p1491 A73-27357

Polar cap E layer conductivity difference effects on ring currents associated with vertical current along lines of force at conjugate points

13 p1608 A73-28717

Gyrotropic flat ionosphere model with elliptical nonuniform conductivity for electrojet generation by magnetosphere current entering and leaving auroral zone

15 p1872 A73-31895

Influence of the inclination of the geomagnetic lines of force on the field of the magnetospheric-ionospheric current system.

15 p1874 A73-32608

Frequency dispersion of transverse electrical conductivity of ionospheric plasma.

23 p2971 A73-43256

Magnetospheric plasma motion during a sudden commencement.

23 p2972 A73-43689

Influence of the conductivity of the ionosphere on the pulsations of DP1 and DP2 current systems

24 p3084 A73-44806

Simultaneous growth of high-latitude positive bay and DR-field in the course of proton aurora substorm.

24 p3127 A73-45215

IONOSPHERIC CURRENTS

NT AUROREAL ELECTROJETS

NT ELECTROJETS

NT EQUATORIAL ELECTROJET

Effect of the slope of geomagnetic field lines on the field of the magnetosphere-ionosphere current system

02 p0164 A73-12458

Radar measurement of ionosphere motion in the presence of current-induced spectral asymmetries.

02 p0143 A73-12532

Study of the effect of the east-west component of the interplanetary magnetic field on the currents equivalent to the magnetic perturbations of high latitude regions

04 p0502 A73-16000

Earth magnetosphere essential processes, discussing outermost atmosphere, solar wind theory and sector structure, models, plasmapause, polar cusps, tail theory and ionospheric currents

06 p0688 A73-17502

A semiempirical model of large-scale magnetospheric electric fields.

07 p0814 A73-19238

Moment equations of temperature and high latitude spread F instability in presence of north-south electric field, relating to maximum Pedersen current and barium cloud deformation

07 p0814 A73-19243

Three layer atmospheric model for neutral gas motion-produced ionosphere and magnetosphere currents, electromagnetic field and charged particle concentration perturbations

07 p0815 A73-19432

Geomagnetic variations with the period of a sidereal day.

07 p0818 A73-19672

A possible current system associated with the Ssp variation.

11 p1356 A73-25910

Ionospheric currents induced by solar wind interaction with planetary atmospheres.

11 p1412 A73-25921

Auroral atmosphere temperature variations relation to nightly auroral streamer length variations, assuming ionospheric current dissipation as heat source

12 p1491 A73-27344

Polar cap E layer conductivity difference effects on ring currents associated with vertical current along lines of force at conjugate points

13 p1608 A73-28717

Polar cap magnetic variations and their relationship with the interplanetary magnetic sector structure.

14 p1747 A73-29959

Electric field and plasma density oscillations due to the high-frequency Hall current two-stream instability in the auroral E region.

14 p1748 A73-29971

Seasonal movement of the Sq current foci and related effects in the equatorial electrojet.

15 p1869 A73-31754

Equatorial electrojet. I - Development of a model including winds and instabilities. II - Use of the model to study the equatorial ionosphere.

15 p1904 A73-31756

Equatorial Esq disappearance relationship to daily magnetic Sr variation inverted latitudinal profiles during magnetical quiet periods, considering counter electrojet current belt hypothesis

15 p1869 A73-31757

POGO satellite observed electrojet current data comparison with ground measurement at Ibadan, discussing data ratios variation by upper earth mantle conductivity structure

15 p1870 A73-31772

Influence of the inclination of the geomagnetic lines of force on the field of the magnetospheric-ionospheric current system.

15 p1874 A73-32608

Model of dayside magnetopause displacement relation to convection currents feeding polar cap ionosphere to estimate electric field and flux return as function of displacement

16 p2003 A73-33432

Magnetic field of a horizontal current above a conducting earth.

16 p2004 A73-33448

An instrument for real-time determination of polar electrojet position and current parameters.

17 p2176 A73-35768

OGO-5 observations of the physical processes occurring in the disturbed polar cusp and the cusp-magnetosheath interface.

18 p2303 A73-35943

Ground and synchronous orbit magnetic observations of magnetospheric and ionospheric wave propagation to model substorm current system variations

18 p2303 A73-35945

Joule heating effect due to currents in the equatorial electrojet as observed by rocket borne probes.

18 p2310 A73-36128

Thermospheric observations combining chemical seeding and ground-based techniques. II - Ionospheric drifts and the Sq current system.

18 p2311 A73-36186

Semi-annual modulation of earth's magnetic field in the equatorial electrojet region.

18 p2311 A73-36187

Radar aurora type III spectra with phase velocities exceeding ion acoustic velocity, discussing relation to current-excited ionospheric electrostatic ion cyclotron oscillations

18 p2312 A73-36299

Ionospheric magnetic field measurements at auroral latitudes.

18 p2313 A73-36647

Structure of vortical motion systems in the ionosphere that generate Sq variations of the geomagnetic field

20 p2553 A73-39153

Correlation of variations in the horizontal component of the geomagnetic field with drift in the ionosphere

20 p2553 A73-39154

The relation between cosmic ray intensity variations and effects due to the electromagnetic complex

21 p2755 A73-40110

Numerical calculation for polar ionospheric current under realistic electric field and conductivity distributions, considering solar wind effect on charged particles in magnetosphere

21 p2681 A73-40155

Solar quiet dynamo region electric fields and currents diurnal and semidiurnal field components variations with latitude

21 p2689 A73-41357

Investigation of mid-latitude ionospheric currents by combined rocket techniques.

21 p2689 A73-41359

A current mechanism for the formation of inhomogeneities resulting in the ionospheric spread F region at high latitudes

21 p2692 A73-41508

Particle streams along the force lines of a magnetic field in a multicomponent ionospheric plasma in the presence of longitudinal currents

22 p2892 A73-42329

Auroral atmosphere temperature variations relation to nightly auroral streamer length variations, assuming ionospheric current dissipation as heat source

23 p2970 A73-43241

Current instability of atmospheric gravitational waves

24 p3083 A73-44786

Influence of the conductivity of the ionosphere on the pulsations of DP1 and DP2 current systems

24 p3084 A73-44806

IONOSPHERIC DISTURBANCES

NT IONOSPHERIC STORMS

NT SUDDEN IONOSPHERIC DISTURBANCES

NT TRAVELING IONOSPHERIC

DISTURBANCES

Off-path transequatorial propagation in decametric waves. II - Application to the study by diffusion of ionospheric irregularities

01 p0017 A73-10334

Precipitation patterns in the Arctic ionosphere determined from airborne observations.

01 p0036 A73-10341

Infrasound in the ionosphere generated by severe thunderstorms.

01 p0040 A73-10826

Positive ion composition measurements in disturbed D region, noting positive molecular oxygen ions as major source of water cluster ions

01 p0041 A73-10890

E region irregularities investigation via phase path measurements and radio wave ionospheric soundings, using model for undulatory variation of reflection height

02 p0158 A73-12028

Effect of solar activity delays on the processes in solar-terrestrial space.

02 p0212 A73-12185

Scintillation phenomenon due to radio wave propagation through ionospheric and tropospheric regions with irregularities in refractive index

02 p0162 A73-12300

Electron density fluctuations during periods of scattered reflections at the ionospheric F-region maximum ionization level

02 p0164 A73-12359

Magnetic horizontal component variations on quiet days, suggesting effect of electric field reversal at equatorial electrojet ionospheric region

03 p0299 A73-12949

Atmospheric wave perturbations of total electron content.

03 p0299 A73-13633

Some results about the satellite scintillation on 150/400 MHz and the horizontal gradient of the total electron content in the polar ionosphere.

03 p0300 A73-13648

A proposed ionospheric disturbance index.

03 p0300 A73-13651

Characteristics of large scale ionospheric irregularities.

03 p0300 A73-13652

Instabilities resulting from gravity wave perturbation of ionization via neutral-charged particle collisions in nighttime E region

03 p0305 A73-14595

Constant height sporadic E velocities and heights at night explained via instabilities generated from recombination and photoionization rate variations induced by gravity wave perturbations

03 p0305 A73-14596

VLF wave propagation properties in waveguide formed by ground and ionospheric shell, noting diurnal phase and amplitude anomalies due to ionospheric disturbances

04 p0416 A73-15060

Estimation of the cumulative amplitude probability distribution function of ionospheric scintillations.

04 p0443 A73-15477

Equatorward shift of the polar F layer irregularity zone as a function of the Kp index.

04 p0445 A73-15557

Lower ionosphere at medium latitudes during geomagnetic disturbances.

05 p0568 A73-16214

Geomagnetic storm effects in the nighttime E layer during increasing and maximal solar activities

05 p0568 A73-16215

Electron density increase in the F region after proton bursts

05 p0609 A73-16257

Spatial variations in F2 layer critical frequencies

05 p0568 A73-16258

Latitude, longitude and hemisphere effects on Appleton E layer seasonal anomaly from statistical analysis of critical frequency

05 p0571 A73-17059

Disturbed ionospheric electron and ion kinetics, detailing dissociative recombination as regulating process for temporal evolution

07 p0816 A73-19454

Equatorial sporadic E and cross-field instability.

08 p0958 A73-21150

Some problems in methods for determining the parameters of scattering inhomogeneities

08 p0959 A73-21284

Magnetic storm of March 8-10, 1970 from Cosmos-321 and ground observations. I - Morphology of the disturbance

08 p0959 A73-21290

The rate of motion of weak inhomogeneities in the ionospheric plasma

08 p0959 A73-21302

Cross correlation functions skewness of fading records, noting dispersion correlation with ionospheric irregularities horizontal drift

09 p1076 A73-22143

Investigation of nonstationary processes in the ionosphere and space with quantum frequency standards.

10 p1211 A73-24214

Ionospheric magnetic disturbances during March 1970 related to solar flare corpuscular and proton fluxes, generating ring current and PCA absorption

10 p1211 A73-24218

Results of an investigation of the ionospheric effect of a sudden commencement of a magnetic storm

11 p1351 A73-25097

Disturbances observation in E-F region and sporadic E layer by vertical ionospheric sounding during IQSY

11 p1351 A73-25098

Time dependent geophysical effects associated with chromospheric and coronal flares, tabulating for 1957-1961

11 p1411 A73-25099

Effect of the May 20, 1966 solar eclipse in the ionosphere on the basis of observations at Rostov on the Don and at Adler

11 p1351 A73-25100

Small scale loop structuring of F region ionogram traces due to HF ray propagation through irregularities

11 p1354 A73-25766

Ionosphere spatial resonance as result of internal gravity wave phase velocity equal to ionization irregularity drift rate

11 p1356 A73-25908

A study of the relationship between geomagnetic storms and ionospheric disturbances at mid-latitudes.

11 p1356 A73-25912

HF radio wave enhanced electron cyclotron frequency lines and ion plasma fluctuations due to artificial ionospheric excitation

12 p1490 A73-27008

Complex studies of the disturbance of March 8, 1970 from observations in the midnight sector

12 p1490 A73-27342

Solar-terrestrial relations in the retrospective world interval from July 26 to August 14, 1972

12 p1535 A73-27766

Determination of the height of ionospheric irregularities with the holographic method.

13 p1606 A73-28155

Asymmetrical model for F 2 critical frequency variability analysis to determine dimensions and effective number of large scale ionospheric electron density inhomogeneities

13 p1608 A73-28707

Ionospheric plasma waves instabilities induced by energetic electron beam fired perpendicular to magnetic field

14 p1747 A73-29967

Anisotropy parameters of the ionospheric irregularities at Thumba during high solar activity period.

14 p1750 A73-30905

Mars 3 solar wind probe of upper Mars atmosphere, showing plasma interaction with ionosphere measured by energy spectra

15 p1930 A73-31150

Equatorial spread-F irregularities observed at Nairobi and on the transequatorial path Lindau-Tsumeb.

15 p1870 A73-31765

Some characteristics of the ionospheric irregularities associated with Esq layers.

16 p2004 A73-33443

Simplified space/earth signal scintillation parameters as auxiliary reference for measurements concerning ionospheric irregularities.

17 p2162 A73-34949

The use of VLF propagation measurements for studies of magnetospheric and meteorological influences on the lower ionosphere.

18 p2303 A73-35953

A rocket observation of the disturbed mid-latitude nighttime ionosphere.

18 p2308 A73-36048

Ionosphere, magnetosphere and interplanetary plasma instabilities effects on magnetosphere dynamics

19 p2476 A73-37758

Magnetic storm of March 8-10, 1970, according to ground-based and Kosmos-321 observations.

19 p2424 A73-37919

Analysis of VHF/UHF frequency dependence, space, and polarization properties of ionospheric scintillation in the equatorial region.

20 p2525 A73-38741

Spread E occurrence relationship to blanketing frequency from cross field plasma instability mechanism

20 p2552 A73-38948

Midlatitude ionospheric disturbances

20 p2554 A73-39172

Method of studying magnetic-ionospheric disturbances and solar flare effects on long-upset periods.

20 p2555 A73-39767

Interpretation of the results of drift measurements by the space diversity reception method

20 p2555 A73-39819

Infrasound from convective storms - Examining the evidence.

21 p2679 A73-40070

Midlatitude F 2 layer critical frequency fluctuations as ionosphere disturbance criteria during magnetically quiet days

21 p2681 A73-40104

Determination of the wind field from the pressure field and the latitudinal effect of the geomagnetic field in the ionosphere

21 p2681 A73-40105

Limit of the region of low-energy solar proton irruption into the polar ionosphere

21 p2758 A73-40607

Ionospheric research by rocket, satellite and ground based methods, discussing ion and neutral chemistry, stratospheric-ionospheric coupling, ionospheric thermal structure, etc

21 p2689 A73-41358

F region disturbances in wake of burnt-out Black Brant rocket body, discussing electron depletion from ground based Digisonde

21 p2690 A73-41363

Tropospheric and stratospheric response to solar influence during geomagnetic disturbances.

21 p2690 A73-41364

A current mechanism for the formation of inhomogeneities resulting in the ionospheric spread F region at high latitudes

21 p2692 A73-41508

Radio source signal scintillation correlation with high power HF transmitter caused F region electron density fluctuations

22 p2825 A73-41920

Kinesonde observations of ionosphere modification by intense electromagnetic fields from Platteville, Colorado. 22 p2844 A73-41921

Short wave radio signal fadeout due to ionospheric disturbances, obtaining experimental equation on magnitude relationship with solar zenith angle and operating frequency 22 p2825 A73-42194

Hydromagnetic gradient waves in the ionosphere 24 p3083 A73-44789

Determination of the vertical parameters of wavelike ionospheric disturbances 24 p3083 A73-44797

Two types of radio emission from the auroral ionosphere and ionospheric disturbances 24 p3083 A73-44798

Atomic nitrogen and nitrogen oxide in the perturbed ionosphere at heights ranging from 100 to 200 km 24 p3066 A73-44802

Enhancement of the equatorial anomaly in the topside ionosphere during magnetic storms. 24 p3088 A73-45216

IONOSPHERIC DRIFT

Full correlation ionospheric drift analysis for a general observing triangle. 01 p0036 A73-10330

Incoherent scatter observations of meridional winds in the 150-225 km region. 02 p0161 A73-12283

Observation and interpretation of ionization drift measurements in the F region at St-Santin-Nancy. 02 p0161 A73-12284

E region electromagnetic east-west drift velocity measurement at magnetic equator by incoherent scatter radar 02 p0161 A73-12285

A modernized technique for ionospheric drifts with spectral analysis. 02 p0161 A73-12286

Features of the ionospheric drift over the magnetic equator. 02 p0162 A73-12287

Horizontal and vertical drift motions in F 2 region caused by electrostatic and geomagnetic fields 02 p0162 A73-12294

Rocket sounding of ionospheric electron density and temperature profiles during moderate auroral event, noting field-aligned motion of irregularities in F region 02 p0163 A73-12309

Time-dependent characteristics of radio waves passing through the irregular ionosphere. 03 p0275 A73-13645

Plasma drifts in the auroral ionosphere derived from barium releases. 03 p0303 A73-13876

On the effect of the vertical drift in the equatorial F region. 04 p0443 A73-15476

Nonuniformities of the ion density at an altitude of 600 km in the ionosphere. 05 p0567 A73-16083

Lunisolar tidal effects and motions in the F region 05 p0568 A73-16255

Electron drift instabilities in turbulent equatorial electrojet from radar echo observations at 50 MHz 07 p0814 A73-19244

Generation of small-scale irregularities in the equatorial electrojet. 07 p0814 A73-19245

Two-beam observations of ionospheric irregularity structure and velocity at Arecibo. 07 p0791 A73-19379

6300 A night airglow enhancements in low latitudes. 07 p0818 A73-20051

Ionospheric plasma interaction with neutral meridional wind, noting effects of east-west gradients in electron concentration 07 p0819 A73-20057

Some characteristics of the ionospheric irregularities over the magnetic equator derived from spaced fading records. 08 p0957 A73-20656

An indirect method for measuring equatorial electrojet currents and its relation to nonlinear saturation of type I instabilities. 09 p1075 A73-22070

Cross correlation functions skewness of fading records, noting dispersion correlation with ionospheric irregularities horizontal drift 09 p1076 A73-22143

Es-q layer at Huancayo during the March 1970 geomagnetic storm. 09 p1078 A73-22836

Direct measurements of plasma convection in the upper ionosphere 10 p1211 A73-23885

Structure of ionospheric inhomogeneities, according to simultaneous observations on two magnetoeionic components. 10 p1211 A73-24217

Multistatic incoherent scatter measurements of ionospheric drift velocity. 10 p1188 A73-24274

OGO 5 observation of ULF geomagnetic fluctuation at polar cusp boundaries in terms of ionospheric drift wave and Kelvin-Helmholtz instabilities 10 p1214 A73-24744

The causes of storm-time increases of the F-layer at mid-latitudes. 11 p1353 A73-25751

The effects of thermospheric winds on the ionosphere at low and middle latitudes during magnetic disturbances. 11 p1353 A73-25752

Ionospheric electron-ion gas distribution, allowing for diffusion, recombination and vertical drift 11 p1357 A73-26081

The measurement of winds in the D-region of the ionosphere by the use of partially reflected radio waves. 11 p1358 A73-26707

Correspondence of main trough ion temperatures with horizontal drift speed. 12 p1489 A73-27006

Effective 'radius of operation' of a system for measuring ionospheric drifts 12 p1490 A73-27341

Equatorial ionospheric electron drift rate measurement over Thumba, deriving north-south component 13 p1609 A73-28921

Direct measurements of ion drift velocity in the upper ionosphere during a magnetic storm. I - Methodological aspects and some results of measurements in magnetically quiet periods. II - Results of measurements during the magnetic storm of November 3, 1967 14 p1746 A73-29863

Magnetospheric collisionless drift waves from ATS-5 electron and proton velocity distribution measurements, comparing with predicted perturbation distribution function 14 p1750 A73-30659

Solar and lunar effects on neutral atmospheric tidal winds and induced electrostatic and geomagnetic fields effects on low latitude F2 and sporadic E layers 15 p1868 A73-31751

Magnetic dip equator region ionospheric drifts and electric fields measurements and experimental techniques 15 p1868 A73-31752

Large scale equatorial spread F irregularities motion velocity observation in Africa, interpreting quasi-periodic structures in west-east extension by atmospheric gravity waves 15 p1870 A73-31764

Drift measurement with spectral analysis during period of chemical releases into the ionosphere. 18 p2314 A73-35955

Ionospheric drift measurements. I - A new method for ionospheric drift measurements. II - The effect of random drift velocities upon the determination of ionospheric drift velocities. 18 p2304 A73-35989

Cross-field instability as a mechanism for equatorial E region irregularities. 18 p2304 A73-35998

Velocity of the reflection points reveals structure and motions in the ionosphere. 18 p2305 A73-36000

Tromsø /Norway/ Auroral Observatory partial reflection experiment, considering data processing techniques, height resolution, phase detection, antenna arrays and D region drift measurements 18 p2315 A73-36009

Lunar tidal oscillations in the horizontal ionospheric drift at the Equator. 18 p2311 A73-36177

Thermospheric observations combining chemical seeding and ground-based techniques. II - Ionospheric drifts and the Sq current system. 18 p2311 A73-36186

Some problems concerning the method of determining the parameters of scattering inhomogeneities. 19 p2424 A73-37913

Velocity of weak inhomogeneities in the ionospheric plasma. 19 p2425 A73-37931

Direct measurements of plasma convection in the upper ionosphere. 20 p2550 A73-38904

Dynamics of ionization inhomogeneities in the ionosphere 20 p2553 A73-39152

Correlation of variations in the horizontal component of the geomagnetic field with drift in the ionosphere 20 p2553 A73-39154

Vertical sounding investigation of ionospheric ionization inhomogeneity sizes, orientation, elongation degree and drift rate, determining F region electron density fluctuations 20 p2553 A73-39155

Ionospheric inhomogeneity parameters and geoelectromagnetic field variations 20 p2553 A73-39156

Drift velocity measurements for small-scale inhomogeneities at various levels of the F2 layer 20 p2553 A73-39158

Investigation of the inhomogeneous structure of the ionosphere using observations of discrete cosmic radio emission sources and vertical soundings 20 p2553 A73-39159

Statistical characteristics of the diurnal drift velocity variations in the F2 layer 20 p2554 A73-39160

Diurnal variations in the drift velocity and direction of the ionization inhomogeneities in the F layer 20 p2554 A73-39161

Altitude distribution of the drift velocity and direction of ionosphere inhomogeneities over Ashkhabad in years of maximum and minimum solar activity 20 p2554 A73-39162

Investigation of the fine-structure inhomogeneities of the Es layer at oblique radio wave incidence 20 p2554 A73-39163

B-2 installation for radio wave absorption measurements in the ionosphere at two frequencies simultaneously by the /A1/ pulse method 20 p2566 A73-39165

Ten years Antarctic region ionosphere investigation during IGY-ISQY period considering ionization maxima, inhomogeneity drifts, electron density and short wave propagation 20 p2554 A73-39171

Interpretation of the results of drift measurements by the space diversity reception method 20 p2555 A73-39819

One dimensional computer simulation model of spaced-receiver drift experiment with radio fading produced by reflections from perfectly reflecting ionosphere 21 p2684 A73-40783

Latitudinal distributions and composition of the radiation on nonclosed drift shells in the altitude range from 200 to 400 km 21 p2686 A73-40908

Effective 'radius of action' of a device for measuring ionospheric drifts. 23 p2970 A73-43239

Ionosphere dynamic process investigations, describing wind models, E region drift velocity curves and energy distribution chart 23 p2978 A73-43978

Effect of neutral winds on ionospheric F-region at a pair of conjugate stations in low latitude. 24 p3082 A73-44729

Diurnal and semidiurnal variations in amplitude and phase of midlatitude ionosphere tidal motions, using sodium cloud drift rate 24 p3082 A73-44732

Formation of the sporadic E layer and the nighttime E region of the ionosphere at midlatitudes 24 p3083 A73-44794

Polar cap electric field measurements by balloons indicating ionospheric convection control by interplanetary magnetic field 24 p3086 A73-45135

IONOSPHERIC ELECTRON DENSITY

Refraction of whistler-mode waves by large-scale gradients in the middle-latitude ionosphere. 01 p0017 A73-10328

D-region parameters from the extraordinary component of partial reflections. 01 p0036 A73-10329

Two X-ray bursts /1 August 1967 and 30 January 1968/ and some associated VLF disturbances. 01 p0091 A73-10556

Estimation of nitric oxide concentration in the lower E region from rocket and satellite measurements of electron densities and X-ray fluxes. 01 p0041 A73-10882

Rocket measurements of electron fluxes in the upper atmosphere at midlatitudes. 01 p0041 A73-10887

Electron-density and energetic-electron measurements of the midlatitude lower ionosphere during winter. 01 p0041 A73-10888

A nighttime ionospheric E-region model. 01 p0042 A73-10893

Synoptic studies of D-region ionization changes and electron densities by the partial reflection differential absorption experiment. 01 p0042 A73-10904

A comparison of two ground-based techniques for measuring D-region electron densities. I. 01 p0042 A73-10905

A comparison of two ground-based techniques for measuring D-region electron densities. II. 01 p0042 A73-10906

Changes of electron density with zenith angle, with the sunspot cycle, and during eclipses. 01 p0043 A73-10907

Electron density profiles in the equatorial lower ionosphere at Thumba. 01 p0043 A73-10908

Observations of simultaneous auroral D and E layers with incoherent scatter radar. 01 p0043 A73-10909

Isis I observations of the high-latitude ionosphere during a geomagnetic storm. [AD-759885] 02 p0155 A73-11735

Revised calculations of F region ambient electron heating by photoelectrons. 02 p0157 A73-11751

Changes of lower ionosphere electron concentrations with solar activity. 02 p0159 A73-12029

Radioastronomical measurements of ionospheric electron content. 02 p0159 A73-12031

Ionospheric electron density profiles calculation from ionograms via nomograph relating gradients of possible and actual height in given frequency interval of integration 02 p0159 A73-12184

Neutral wind measurement during daytime in the thermosphere. 02 p0159 A73-12224

Effects of vertical mass motions on the composition structure in the thermosphere. 02 p0162 A73-12291

Mesoscale traveling ionospheric disturbances in electron density interpretation in terms of acoustic gravity waves 02 p0162 A73-12295

The standard profile of the mid-latitude F region of the ionosphere as deduced from bottomside and topside ionograms. 02 p0163 A73-12301

Ionospheric bottom side electron density profiles from measured monthly median values, using CCIR and ITS computer programs for critical frequencies 02 p0163 A73-12302

Electron production rates and density profiles in D region during solar flares, presenting ionization vertical distribution model 02 p0206 A73-12304

Simultaneous measurements of height wind profiles and electron concentration for verifying theory of sporadic E layer formation in midlatitudes under wind shear action 02 p0163 A73-12306

Electron density and wind structure observations in lower ionosphere by rocket, noting sporadic E layer due to wind shear 02 p0163 A73-12307

Rocket sounding of ionospheric electron density and temperature profiles during moderate auroral event, noting field-aligned motion of irregularities in F region 02 p0163 A73-12309

Preliminary findings of a petrel rocket experiment to investigate the VLF emission 'chorus' in the ionosphere. 02 p0141 A73-12319

Electron density fluctuations during periods of scattered reflections at the ionospheric F-region maximum ionization level 02 p0164 A73-12359

Latitude-time variations of the total number of electrons and of its gradients in the ionosphere at high latitudes 02 p0164 A73-12474

Automatic N/h, t/ profiles of the ionosphere with a digital ionosonde. 02 p0143 A73-12530

Minimized calculation errors in phase ionosonde true height reduction technique for electron density profile, noting lowest observable radio frequency 02 p0143 A73-12531

On investigation of the electron concentration and inhomogeneous structure of the outer ionosphere by means of coherent radiowaves emitted from artificial earth satellites. 03 p0299 A73-13631

Ionospheric total electron content measurements from the Australian zone. 03 p0299 A73-13632

Atmospheric wave perturbations of total electron content. 03 p0299 A73-13633

Traveling ionospheric disturbance analysis based on quasi-periodic perturbations in satellite transmitted VHF signal Faraday rotation, obtaining wave-like variations in electron content 03 p0300 A73-13634

The use of Faraday rotation measurements on geostationary satellites. 03 p0300 A73-13635

A comparison of total electron content determined by the differential Doppler and the Faraday effects using radio signals from a geostationary satellite. 03 p0300 A73-13637

Problems in estimating the total electron content from Faraday rotation observations on geostationary satellites. 03 p0300 A73-13638

Computed effects of the ionosphere/protonosphere distribution on VHF signals from ATS-F/G. 03 p0275 A73-13641

Diurnal and latitudinal variations and frequency dependence of scintillation due to ionospheric irregularities, using rms electron density fluctuation and transverse scale size model 03 p0275 A73-13643

Some results about the satellite scintillation on 150/400 MHz and the horizontal gradient of the total electron content in the polar ionosphere. 03 p0300 A73-13648

A simple apparatus for signal reception of transit system satellites and principal results. 03 p0308 A73-13649

Ionospheric electron density vertical distribution time dependence for ionospheric storms morphology, noting relationship to geomagnetic storms 03 p0300 A73-13650

A proposed ionospheric disturbance index. 03 p0300 A73-13651

Standard format for reporting electron content data using magnetic tape. 03 p0308 A73-13655

Wavelike structure of magnetic field-aligned irregularities detected by phase interferometry. 03 p0300 A73-13696

E region electron collision frequency vertical distribution from ground and rocket measurements of radio wave absorption and electron density respectively 03 p0304 A73-14562

Equatorial scintillation diurnal and seasonal variations and F region electron density irregularities, noting unusual post sunset behavior of Faraday rotation angle [AD-757291] 04 p0440 A73-14951

Ionospheric scale height from the refraction of satellite signals. 04 p0415 A73-14952

Observations of ionospheric electron content at medium latitude geomagnetically conjugate stations. 04 p0440 A73-14955

Longitudinal variation of the equatorial anomaly. 04 p0440 A73-14960

Electron density and temperature measurements in the lower ionosphere as deduced from the warm plasma theory of the H.F. quadrupole probe. 04 p0480 A73-15199

Solar cycle control of the ionospheric E-region. 04 p0441 A73-15291

On the effect of the vertical drift in the equatorial F region. 04 p0443 A73-15476

The light-ion trough, the main trough, and the plasmopause. 04 p0493 A73-15533

Comparison of theory with experiment for electron density distribution in the near wake of an ionospheric satellite. 04 p0444 A73-15541

Shallow-solar-zenith-angle control to topside ionospheric parameters. 04 p0445 A73-15636

Electron concentration variation in E layer after sunrise, noting critical frequency deviations from Chapman law 05 p0568 A73-16216

Electron velocity distribution function in the ionosphere 05 p0568 A73-16252

Electron density increase in the F region after proton bursts 05 p0609 A73-16257

Temporal variations of the recombination coefficient and electron density profile in the lower ionosphere 05 p0568 A73-16261

A satellite study of the mid-latitude trough in electron density and VLF radio emissions during the magnetic storm of 25-27 May 1967. 05 p0571 A73-17060

Ionospheric electron density profiles model evaluation, considering E region height and thickness seasonal variation 05 p0571 A73-17063

Correlations between X-rays and UV ionizing radiation in the E region from data obtained during the solar eclipse of 25 February 1971 06 p0742 A73-17534

Midlatitude sporadic E layer vertical electron and ion distributions from rocket experimental wind velocity profile, assuming molecular and metallic ions in ionosphere 06 p0742 A73-17535

Vertical profiles of the effective collision number in the E and F regions of the ionosphere 06 p0689 A73-17552

Three dimensional summer time sporadic E layer structure and electron concentration during 1966-1969 by ionospheric space diversity sounding 06 p0689 A73-17553

Vertical distribution of electron concentration in the Northern Hemisphere at the geomagnetic pole /from top-side and ground-based ionospheric sounding data/ 06 p0689 A73-17554

D region electron density profiles analytical determination from pulsed wave interaction measurements 07 p0791 A73-19242

Electron drift instabilities in turbulent equatorial electrojet from radar echo observations at 50 MHz 07 p0814 A73-19244

Two-beam observations of ionospheric irregularity structure and velocity at Arecibo. 07 p0791 A73-19379

Global electron concentration disturbances in low and middle latitude F 2 during magnetic storm 07 p0815 A73-19435

Ionospheric electrons and neutral particles temperature and concentration profiles explanation by electron gas cooling due to atomic oxygen excitation, calculating heat flow 07 p0815 A73-19441

Lower ionospheric seasonal anomaly in electron density levels, noting diurnal and latitudinal characteristics at various heights 07 p0816 A73-19453

Ionospheric electron density changes caused by strong radio waves induced plasma heating 07 p0816 A73-19457

Lower ionosphere electron densities from rocket measurements employing LF radio propagation and DC probe techniques. 07 p0818 A73-19670

Ionospheric winds in the F-region and their effects on the limiting periods of gravity waves. 07 p0818 A73-19673

Global electron density distributions from the Ariel 3 satellite at mid-latitudes during quiet magnetic periods. 07 p0819 A73-20054

Ionospheric plasma interaction with neutral meridional wind, noting effects of east-west gradients in electron concentration 07 p0819 A73-20057

Study on the solar activity dependence of the E region peak electron density and some atmospheric parameters. 08 p0961 A73-21652

Study on the electron density profile in the F1 region. 08 p0961 A73-21653

Aurora and the poleward edge of the main ionospheric trough. 09 p1073 A73-22058

Metallic ion composition and electron density measurements in equatorial E region, considering three body reaction kinetics with dissociative ion-electron recombination 09 p1074 A73-22064

The influence of negative-ion changes in the D-region during sudden ionospheric disturbances. 09 p1075 A73-22126

Storms and the seasonal anomaly in the topside ionosphere. 09 p1075 A73-22132

Preliminary results of studies of the Martian atmosphere with the aid of the Mars-2 satellite 09 p1146 A73-22486

The standard electron density profile of the F2-layer at noon. 09 p1078 A73-22746

Nighttime electron density in the E region at auroral latitudes in sunspot maximum. 09 p1078 A73-22747

On the use of running means in the power spectrum analysis of ionospheric data. 09 p1078 A73-22831

Enhanced energetic electron intensities at 100 km altitude and a whistler propagating through the plasmasphere. 09 p1079 A73-22839

The electron density experiment on-board the Ariel 4 satellite. 09 p1085 A73-22916

Fluxes of electrons with energies above 80 MeV at the equator on the basis of measurements by the Cosmos 490 satellite 10 p1265 A73-23897

Properties of plane asymmetric plasma waveguides as applied to short-wave propagation along inhomogeneities of the topside ionosphere. 10 p1188 A73-24216

Nonstationary distribution of the electron-ion gas in the ionosphere. 10 p1212 A73-24239

Electron content measurements - A method for resolving the n-pi ambiguity. 10 p1214 A73-24746

Empirical model for F layer electron density irregularities responsible for VHF/UHF amplitude scintillation, considering geomagnetic latitude, local time, season and sunspot effects 10 p1190 A73-24895

Some results of ionospheric measurements based on observations of geophysical rocket signals from spaced points and observations of signals reflected by space objects 11 p1350 A73-25077

Vertical electron density and temperature data from geophysical rocket borne Langmuir probes and electrode traps 11 p1350 A73-25078

Ionospheric vertical electron density profiles from geophysical rocket-borne microwave dispersing interferometer 11 p1350 A73-25079

Recombination coefficient, heat flux, ionization balance and photoelectron kinetic energy from ionospheric electron temperature and density profiles and solar UV absorption data

11 p1350 A73-25081

Vertical distribution of absorption of cosmic radio emission and radio waves in ionosphere and lower ionosphere based on electron density profiles

11 p1327 A73-25084

Precursor anomaly of ionization in the F region at the transition latitudes

11 p1350 A73-25090

Statistical characteristics of E and F regions maximum electron density and ionization height, discussing electron content in vertical unit column in upper and lower ionosphere

11 p1351 A73-25092

Autocorrelation and cross correlation coefficients for maximum electron densities and total electron content in E and F regions and upper and lower ionosphere

11 p1351 A73-25093

Diurnal variations in electron density at heights of 160 to 200 km and electron temperature variations

11 p1351 A73-25095

Calculation of the N(h) profiles in the ionosphere from two magnetoionic components

11 p1351 A73-25096

Optimum bandlimited signal synthesis with pulse compression for transionospheric propagation along vertical path, considering statistical effects of total ionospheric electron content variations

11 p1330 A73-25689

Ariel 3 satellite observations of the ionosphere at high southern latitudes.

11 p1353 A73-25754

Structure at the poleward edge of a mid-latitude F-region trough.

11 p1353 A73-25756

The topside ionosphere at mid-latitudes during local sunrise.

11 p1353 A73-25757

A theoretical study of lunar variations in foF2 at low latitude.

11 p1354 A73-25764

A diffusion model for the electron density distribution along the earth's magnetic field in an F-region plasma cloud.

11 p1354 A73-25768

A theoretical study of the ionospheric F region equatorial anomaly. I - Theory. II - Results in the American and Asian sectors.

11 p1356 A73-25919

Ionospheric electron-ion gas distribution, allowing for diffusion, recombination and vertical drift

11 p1357 A73-26081

The nature of seasonal changes in the effects of magnetic storms on mid-latitude F-layer electron concentration.

11 p1358 A73-26708

Internal atmospheric gravity wave effect on ionospheric columnar electron content on basis of viscous atmosphere model with isothermal layers

11 p1359 A73-26709

Diurnal, seasonal and solar cycle changes in southern midlatitude ionosphere electron content from June 1965-August 1971

11 p1359 A73-26712

Total electron content measurements during visible auroras.

11 p1359 A73-26714

Enhancements of ionospheric total electron content in the southern auroral zone associated with magnetospheric substorms.

11 p1359 A73-26715

Three-dimensional analytical model of the electron density distribution in a quiet ionosphere

12 p1490 A73-27334

Influence of a variable ionospheric-protonospheric plasma flow on the nighttime F region of the ionosphere

12 p1490 A73-27336

Midlatitudinal standard ionospheric profile to construct F-region noon electron density profiles and thermal response to solar activity changes

12 p1493 A73-27761

The concept of an installation for measuring partial reflections with the aid of the FM-CW procedure and the principle of measurement involved

12 p1486 A73-27764

D layer electron density long term continuous monitoring, comparing FM-CW method application to partial reflection technique with conventional pulse method

12 p1474 A73-27765

An inversion method for the determination of the electron density profile of the ionosphere on the basis of satellite tracking data

12 p1494 A73-27772

Consideration of the different wave paths of the ordinary and extraordinary component in the calculation of electron density and collision frequency with the aid of the Faraday experiment

12 p1494 A73-27773

Negative horizontal gradients of the integral electron content of the ionosphere - A comparison of satellite and ionosonde data

12 p1494 A73-27774

An analysis of seasonal changes in electron densities at middle latitudes in the lower D-region.

13 p1606 A73-28207

Planar retarding potential analyzer onboard Explorer satellite for ion temperature and ion/electron concentration investigation

13 p1688 A73-28635

Asymmetrical model for F 2 critical frequency variability analysis to determine dimensions and effective number of large scale ionospheric electron density inhomogeneities

13 p1608 A73-28707

Group delay times of magnetoionic components for horizontal electron density profiles in magnetic meridian plane, noting comparison with ionospheric sounding data

13 p1608 A73-28708

Diffusion spreading of weak plasma inhomogeneities in the presence of two kinds of positive ions.

13 p1608 A73-28710

High power radio transmitter for structural investigation and electron concentration profiles of ionospheric D and E regions

13 p1583 A73-28725

Equatorial ionospheric electron drift rate measurement over Thumba, deriving north-south component

13 p1609 A73-28921

Ionospheric electron density and temperature measurement by cylindrical Langmuir probes onboard Interkosmos 2 satellite

14 p1746 A73-29862

Polar ionospheric electron density distribution near closed field line boundaries for ISIS 1 dayside passes, discussing geomagnetic storm effects

14 p1748 A73-29980

Ionospheric model impulse response transfer functions phase and amplitude dependence on profile parameters and TE C, using ray tracing technique

14 p1728 A73-30231

Preliminary results of Martian-atmosphere research with the Mars-2 satellite.

14 p1798 A73-30321

French monograph - Analysis of the functioning of the differential probe for measurement of electronic temperature in the ionosphere.

14 p1753 A73-30672

Anisotropy parameters of the ionospheric irregularities at Thumba during high solar activity period.

14 p1750 A73-30905

Total electron content of the equatorial ionosphere.

15 p1865 A73-31063

Millstone Hill Thomson scatter results for 1966 and 1967.

15 p1866 A73-31067

Numerical study of the seasonal variations of the ionosphere.

15 p1867 A73-31381

Dispersion of electromagnetic waves on a weak isolated inhomogeneity.

15 p1843 A73-31522

Type I and II electron density irregularities due to two-stream and cross field instabilities in E region equatorial electrojet, considering wind shear role

15 p1869 A73-31755

Signal fading and topside electron density profile observation over VHF transequatorial path between Europe and Southern Africa, noting great circle F transmission role

15 p1844 A73-31766

The low-latitude and equatorial outer ionosphere during the magnetic storm of January 2-4, 1964

15 p1871 A73-31881

Ion and electron diffusion in nonisothermal ionospheric F layer, analyzing ionization balance equations

15 p1871 A73-31882

Sporadic E random electron concentration due to wind shift spectral composition, determining empirical autocorrelation functions for frequency parameters

15 p1871 A73-31885

Electron concentrations increase observed at 60-90 km altitudes during anomalous winter radio wave absorption, noting association with upward aerosol transport decrease

15 p1844 A73-31889

Anomalous winter time absorption of radio waves in the middle latitude ionosphere

15 p1844 A73-31900

Ionospheric electron density profiles calculation method based on oblique backscatter ionograms, presenting virtual height vs frequency

15 p1873 A73-32229

D region partial reflection mechanism model based on multiple reflector concept, presenting electron density vertical distribution

15 p1845 A73-32233

Latitudinal and time variations of total electron number and its gradients in the ionosphere at high latitudes.

15 p1874 A73-32625

Correlations between X-rays and ionizing ultraviolet radiation in the E-region, according to data from the solar eclipse of February 25, 1971.

16 p2052 A73-32758

Midlatitude sporadic E layer vertical electron and ion distributions from rocket experimental wind velocity profile, assuming molecular and metallic ions in ionosphere

16 p2052 A73-32759

Vertical profiles of the effective collision frequency in the E- and F-regions of the ionosphere.

16 p2002 A73-32776

Three dimensional summer time sporadic E layer structure and electron concentration during 1966-1969 by ionospheric space diversity sounding

16 p2002 A73-32777

Vertical electron density distribution at the geomagnetic pole in the Northern Hemisphere /from data of topside and ground-based soundings of the ionosphere/.

16 p2002 A73-32778

Faraday rotation based total ionospheric electron content information for correction of near real time satellite position determination errors, using spherically stratified ionospheric model

16 p2035 A73-33414

F region neutral wind profiles and electron densities measured at midlatitude station during equinox months for medium sunspot year

16 p2009 A73-33888

The behaviour of the topside ionosphere during magnetically disturbed conditions.

16 p2010 A73-33912

The latitudinal variation of the electron concentration in the topside ionosphere in winter.

16 p2010 A73-33913

Enhancements of the electron concentration in the F2-layer at magnetic noon.

16 p2010 A73-33914

Multiring probe in a flowing ionospheric plasma.

17 p2214 A73-34199

Electron depletion in the wake of ionospheric spacecraft - A comparison between results from Langmuir probes and antennas.

17 p2159 A73-34783

An evaluation of ionospheric probe performance. I - Evidence of contamination and clean-up of probe surfaces. II - The influence of vehicle wake effects on electron density and temperature measurements.

17 p2160 A73-34786

Physics and chemistry of the ionosphere.

17 p2162 A73-35050

Downward transport of nighttime Es layers into the lower E-region at Arecibo.

18 p2302 A73-35941

The use of the LF A3 absorption measurements in studying the winter anomaly.

18 p2303 A73-35947

Some features of the equatorial D-region as revealed from the Langmuir probe experiments conducted at Thumba.

18 p2303 A73-35954

D region electron density profiles from radio broadcast field strength measurements by rocket-borne passive RF spectrometers, using ray theory for wave propagation

18 p2303 A73-35956

Accuracy of rocket measurements of lower ionosphere electron concentrations.

18 p2304 A73-35965

Ionospheric electron content and its horizontal gradients at high and middle latitudes from radiowave propagation from satellites.

18 p2304 A73-35972

Cross-field instability as a mechanism for equatorial E region irregularities.

18 p2304 A73-35998

Results of simultaneous in-situ-observations in Spain of electron concentration, neutral wind and air pressure in the D-region in different seasons and during an SID-event and their relevance to the winter-anomalous state of the atmosphere.

18 p2305 A73-36001

Comparison of electron density profiles in the lower ionosphere at Equator and midlatitudes.

18 p2305 A73-36007

FM-CW method application to partial reflection measurements of ionospheric electron density to avoid man-made interference and interpretation difficulties from frequency spectrum broadening

18 p2305 A73-36008

Trial of existing models of the lower ionosphere by experimental data on Schumann resonances.

18 p2306 A73-36011

Electron-density profiles obtained from MF sounding at Tsumeb.

18 p2306 A73-36012

Construction of D-region electron-density profiles by combined use of ground-based reflection and satellite-based transmission measurements.

18 p2306 A73-36016

Electron density profiles from ionograms - Comparisons with rocket profiles.

18 p2306 A73-36017

- A rocket-borne riometer for the study of lower ionosphere. 18 p2315 A73-36046
- Tentative E-region electron density profiles. 18 p2309 A73-36099
- D region electron and ion density profiles, recombination coefficient and electron detachment rate changes during solar eclipse 18 p2310 A73-36127
- Simultaneous measurements of some ionospheric parameters at altitudes 100-170 km. 18 p2310 A73-36131
- Rocket measurements of electron density and electron temperature at sunset. 18 p2311 A73-36148
- Neutral wind velocities calculated from temperature measurements during a magnetic storm and the observed ionospheric effects. 18 p2311 A73-36150
- Analysis and interpretation of aspect-dependent ionospheric radar scatter. 18 p2289 A73-36283
- Splitting of an ionospheric layer by ambipolar diffusion. 18 p2313 A73-36388
- Measurement of the ionospheric electron density by using S-210-6 rocket. 19 p2423 A73-37380
- Russian book on electromagnetic wave propagation in ionosphere, covering atmospheric structure, electron concentration, waveguides and earth surface effects 19 p2424 A73-37773
- A phenomenological model of global ionospheric electron densities in the E-, F1- and F2-regions. 19 p2425 A73-38014
- Protonospheric columnar electron content determination. I - Analysis. 19 p2426 A73-38017
- Fine-scale inhomogeneities of the mid-latitude sporadic E layer 19 p2427 A73-38332
- Electron fluxes with energies greater than 80 MeV at the equator based on measurement data from the Cosmos-490 satellite. 20 p2601 A73-38916
- Whistler-mode hiss at low and medium frequencies in the dayside-cusp ionosphere. 20 p2529 A73-38935
- Asymmetrical global O I airglow emission pattern with respect to magnetic equator from Ogo 4 observations, noting poor correlation with ionospheric electron density 20 p2551 A73-38939
- Latitude distribution of the regularity in F2-region irregularities. 20 p2553 A73-39132
- Vertical sounding investigation of ionospheric ionization inhomogeneity sizes, orientation, elongation degree and drift rate, determining F region electron density fluctuations 20 p2553 A73-39155
- Theory of radio wave incoherent scattering by a plasma and the application of the theory in ionospheric studies 20 p2554 A73-39164
- Some results and accuracy of satellite measurements of the electron content in the ionosphere 20 p2554 A73-39166
- Ten years Antarctic region ionosphere investigation during IGY-ISQY period considering ionization maxima, inhomogeneity drifts, electron density and short wave propagation 20 p2554 A73-39171
- Altitude dependence of F 2 layer electron density annual anomaly, discussing summer-winter density discrepancies and noontime critical frequencies 20 p2555 A73-39177
- Thermal electron energy distribution measurements in the ionosphere. 21 p2681 A73-40156
- Topside ionospheric winter and summer diurnal electron density variations in Arctic regions as function of universal time, showing Ariel 3 measurements graphically 21 p2682 A73-40171
- Maintenance of the F-region at night - Incoherent scatter measurements at a mid-latitude station. 21 p2683 A73-40776
- Phase integral corrections to radio wave absorption and virtual height for model ionospheric layers. 21 p2654 A73-40777
- Ground based and rocket techniques for vertical ionospheric electron density distribution measurement, considering incoherent scatter, partial reflection, wave interaction, and Faraday rotation 21 p2685 A73-40809
- Mean D-region electron density profiles derived by combination of rocket and radio wave propagation data. 21 p2686 A73-40831
- The total electron content of the ionosphere and its horizontal gradients, measured on the basis of recordings of satellite signals at scattered points 21 p2686 A73-40910
- Seasonal variation of atmospheric composition in the F region as a function of solar activity. 21 p2690 A73-41360
- D region electron density profiles at geomagnetic equator by rocket sounding, showing ionization production by Lyman alpha radiation and cosmic rays 21 p2690 A73-41361
- F region disturbances in wake of burnt-out Black Brant rocket body, discussing electron depletion from ground based Digisonde 21 p2690 A73-41363
- Rocket measurements of electron concentration and electron temperature in the polar ionosphere. 21 p2690 A73-41367
- Observations of electron fluxes and related variations of ionospheric plasma parameters in the south polar cusp. 21 p2690 A73-41369
- Rocket measurements of production and ionization during a PCA event. 21 p2760 A73-41371
- Steady state coefficients in the D region during solar particle events. 21 p2760 A73-41372
- On the detection of X-rays from celestial sources through their ionization of the terrestrial atmosphere. 21 p2762 A73-41394
- The combined use of satellite differential Doppler and ground-based measurements for ionospheric studies. 22 p2843 A73-41837
- Periodically structured Pc 1 micropulsations during the recovery phase of intense magnetic storms. 22 p2844 A73-41913
- Radio source signal scintillation correlation with high power HF transmitter caused F region electron density fluctuations 22 p2825 A73-41920
- Radio frequency heating effects on electron density in the lower E region. 22 p2845 A73-41930
- Ionospheric slab thickness relationship: to electron density profile shape, plasma and neutral constituents scale heights and electron to ion temperature ratio 22 p2846 A73-41947
- Characteristics of the redistribution of charged particles in the nighttime E region at mid-latitudes 22 p2847 A73-42331
- Atmospheric gravity wave observations after the solar eclipse of June 30, 1973. 22 p2847 A73-42487
- Satellite-borne swept frequency impedance probe /gyroplasma probe/ for ionospheric plasma parameters including electron density and ion composition, noting PCM telemetry system 22 p2917 A73-42571
- Ionospheric electron density profiles and contour plots above F layer maximum from vertical sounding and Faraday rotation techniques 22 p2851 A73-42984
- An iterative mathematical technique for deriving electron-density profiles from multifrequency riometer data. 22 p2828 A73-43177
- Three-dimensional analytical model of electron density distribution of the quiet ionosphere. 23 p2970 A73-43232
- Effect of changing ionospheric-protonospheric plasma flow on the nighttime F-region of the ionosphere. 23 p2970 A73-43234
- A computational study of the diffusion of meteor trains using a self-consistent model for the space-charge electric field. 23 p3029 A73-43684
- The slab thickness of the mid-latitude ionosphere. 23 p2972 A73-43694
- Low latitude whistler activity during geomagnetic storms related to spread F conditions and magnetospheric and ionospheric electron density 23 p2972 A73-43696
- Ionospheric sounding by ATS-3 emitted signal polarization measurement during partial solar eclipse of 10 July 1972, noting electron content decrease and diffusion rate 23 p2972 A73-43697
- On the large scale vertical movements of the F-layer and its effects on the total electron content over low latitude during the magnetic storm of 25 May 1967. 23 p2972 A73-43699
- Rocket-borne magnetometer measurement of magnetic field changes associated with electron density fluctuations and wind structure, testing wind shear theory of sporadic E formation 23 p3024 A73-43701
- Appleton seasonal anomaly in E region maximum electron density investigated by critical frequency data statistical analysis, showing solar activity effects 23 p2979 A73-44006
- Effect of neutral winds on ionospheric F-region at a pair of conjugate stations in low latitude. 24 p3082 A73-44729
- Periodic variations in geostationary satellite polarisation observations. 24 p3082 A73-44735
- Determination of the rate coefficients of ionospheric reactions from experimental data for electron concentration 24 p3083 A73-44787
- Vertical and latitudinal development of a seasonal anomaly in the daytime F2 region. I 24 p3083 A73-44791
- Formation of the sporadic E layer and the nighttime E region of the ionosphere at midlatitudes 24 p3083 A73-44794
- Comparative analysis of rocket measurements of n sub e /h/ and of ground-based vertical sounding data 24 p3083 A73-44795
- Penetration of thundercloud electric fields into the ionosphere and magnetosphere. I - Middle and subauroral latitudes. 24 p3085 A73-45118
- Thermalization and transport of photoelectrons - A comparison of theoretical approaches. 24 p3086 A73-45124
- Nighttime sporadic E layer measurements and integrated content measurements at Arecibo Observatory, using Barker coded incoherent scatter radar pulses 24 p3087 A73-45142
- The behaviour of the upper ionosphere over North America at sunset. 24 p3087 A73-45203
- Enhancement of the equatorial anomaly in the topside ionosphere during magnetic storms. 24 p3088 A73-45216
- IONOSPHERIC F-SCATTER PROPAGATION**
- Electron density fluctuations during periods of scattered reflections at the ionospheric F-region maximum ionization level 02 p0164 A73-12359
- Vertical ionospheric sounding station observation for spread F layer effect on scattered signal fading, using oscillograph display and camera 02 p0142 A73-12498
- Application of satellite radio beacons for measurement of small-scale ionospheric irregularities. 03 p0300 A73-13642
- Mapping of foF2 by means of topside sounder satellites. 19 p2427 A73-38285
- The determination of foF2 and hmF2 from satellite-borne probe data. 19 p2427 A73-38286
- IONOSPHERIC HEATING**
- Revised calculations of F region ambient electron heating by photoelectrons. 02 p0157 A73-11751
- On D-region electron heating by a low-frequency terrestrial line current with ground return. 02 p0143 A73-12533
- Stable electron density fluctuations in a plasma in the presence of a high-frequency electric field. 04 p0444 A73-15539
- Further ionosonde observations of ionospheric modification by a high-powered HF transmitter. 04 p0444 A73-15540
- Induced enhancement of the plasma line in the backscatter spectrum by ionospheric heating. 04 p0445 A73-15555
- A modified Monte Carlo model for the ionospheric heating rates. 07 p0815 A73-19380
- Ionosphere heating effects produced by transverse electric field, discussing strong nighttime source 07 p0815 A73-19431
- Ionospheric electron density changes caused by strong radio waves induced plasma heating 07 p0816 A73-19457
- Joule heating effect due to currents in the equatorial electrojet as observed by rocket borne probes. 18 p2310 A73-36128
- Energy transport by photoelectrons in the early morning ionosphere. 18 p2348 A73-37027
- IONOSPHERIC ION DENSITY**
- Mesospheric nitric oxide concentrations during a PCA. 01 p0041 A73-10881
- Ion composition and photochemistry of the E-region. 01 p0042 A73-10892
- D-region negative-ion chemistry. 01 p0042 A73-10895
- Negative-ion composition measurements in the D and lower E regions. 01 p0042 A73-10896
- Equilibrium composite negative ion density profiles in nighttime D region from mass spectrometer measurements 01 p0042 A73-10897
- Diurnal latitudinal composition variations in light ion trough from OGO mass spectrometric observations, noting magnetic storm effects 02 p0157 A73-11904
- Ion concentration measurements in the earth's ionosphere at altitudes from 200 to 6000 km 02 p0164 A73-12462
- Bombardment of the polar-cap ionosphere by solar cosmic rays. 03 p0301 A73-13710

Ionospheric plasma flow past a semi-infinite cylinder.

04 p0440 A73-14967

Auroral He 4 precipitation flux measurements by exposed metal foils recovered from rocket flights

04 p0443 A73-15534

Polar ionospheric ion escape /polar wind/ hydrodynamic model equations, discussing singularities and critical points in terms of reduced Mach number

04 p0444 A73-15546

Nonuniformities of the ion density at an altitude of 600 km in the ionosphere.

05 p0567 A73-16083

Fluctuations of the ion concentration level in the terrestrial ionosphere at altitudes from 200 to 1300 km

05 p0570 A73-17012

Midlatitude sporadic E layer vertical electron and ion distributions from rocket experimental wind velocity profile, assuming molecular and metallic ions in ionosphere

06 p0742 A73-17535

Critical frequency gradients-geometric parameters equivalence coefficients for ionospheric layer with parabolic vertical ionization distribution for radio wave path determination

06 p0690 A73-17555

Calculated distributions of hydrogen and helium ions in the low-latitude ionosphere.

07 p0818 A73-20052

Theoretical vertical profiles of minor ions at the Equator.

07 p0819 A73-20053

Ion composition and photochemistry of the E region

08 p0958 A73-21282

Metallic ion composition and electron density measurements in equatorial E region, considering three body reaction kinetics with dissociative ion-electron recombination

09 p1074 A73-22064

The negative-ion composition of the daytime D-region.

09 p1048 A73-22127

Nighttime midionosphere dynamical perturbations on ionizations from solutions of time dependent continuity equation with charge transport effects, considering semidiurnal atmospheric tide propagation mode

09 p1075 A73-22130

The gradient instability in Gaussian sporadic E-layers.

09 p1075 A73-22133

Ion angular distribution around Explorer 31, discussing observed ion flux relation to ionospheric parameters derived from ambient ion and electron measurements

09 p1075 A73-22136

Ion composition in the E- and lower F-region above Kiruna during sunset and sunrise.

09 p1078 A73-22838

Nonstationary distribution of the electron-ion gas in the ionosphere.

10 p1212 A73-24239

Correct statement of the problem of computing the N/h profiles of the lower ionosphere.

10 p1212 A73-24241

Ogo 6 retarding potential analyzer observation of vertical and longitudinal gradients in ion concentrations below F region peak near magnetic equator

10 p1214 A73-24738

Photoionization and charge exchange reaction kinetics inadequacy for explanation of observed positive nitrogen dioxide ion concentration in lower ionosphere, considering alternative mechanism

10 p1214 A73-24749

Statistical characteristics of E and F regions maximum electron density and ionization height, discussing electron content in vertical unit column in upper and lower ionosphere

11 p1351 A73-25092

Ionospheric production and loss processes of atomic sulfur ions, considering dissociative ionization sources

12 p1489 A73-26999

Time dependent studies of the aurora. I - Ion density and composition.

12 p1492 A73-27601

Influence of viscosity, thermal conduction, and ion drag on the propagation of atmospheric gravity waves in the thermosphere.

13 p1606 A73-28154

Dayglow nitrogen ion 3914 A emission profiles for average solar activity at 110-240 km heights from Cosmos 224 observations

13 p1607 A73-28704

Metal ions role in sporadic E layer formation in terms of magnesium ions profile redistribution by vertical gradient in neutral particle wind

13 p1608 A73-28723

Damping of a discharge in crossed fields - Application to the ionosphere in the auroral zone

13 p1611 A73-29562

Studies of the equatorial anomaly in the F region and outer ionosphere with the aid of spherical ion traps

14 p1746 A73-29860

Rocket-based mass spectrometric measurements of midlatitude and north polar region ionospheric ion composition, discussing ionization of water and heavy water vapors

14 p1747 A73-29864

Ionospheric nitrogen ion density from rocket-borne dayglow spectrometry, considering charge exchange with metastable oxygen ions and solar EUV photoionization as ionizing mechanisms

14 p1723 A73-29953

Equatorial spread F formation convective electric fields generation by neutral winds and conductivity caused by metallic ion concentrations

14 p1749 A73-29988

Calculation of ionospheric N/z profiles with the use of radio-wave absorption data

15 p1871 A73-31883

Measurement of the ion density in the earth's ionosphere at altitudes from 200 to 6000 km.

15 p1874 A73-32612

Midlatitude sporadic E layer vertical electron and ion distributions from rocket experimental wind velocity profile, assuming molecular and metallic ions in ionosphere

16 p2052 A73-32759

Critical frequency gradients-geometric parameters equivalence coefficients for ionospheric layer with parabolic vertical ionization distribution for radio wave path determination

16 p2002 A73-32779

Incoherent scatter observations of the ionosphere over Chatanika, Alaska.

16 p2004 A73-33442

Atomic nitrogen ion density measurements for loss rate coefficient of N + reaction with oxygen at 150-220 km

16 p2009 A73-33892

ALADDIN II ionospheric composition measurements, obtaining ion and neutral vertical density profiles and dynamic parameters for E region nighttime ion layering prediction model

18 p2303 A73-35958

Positive ion composition in the lower ionosphere during the Geminid meteorshower and the occurrence of a winter anomaly.

18 p2305 A73-36005

Trial of existing models of the lower ionosphere by experimental data on Schumann resonances.

18 p2306 A73-36011

D region electron and ion density profiles, recombination coefficient and electron detachment rate changes during solar eclipse

18 p2310 A73-36127

Meteoric ions in the D and E-regions.

18 p2310 A73-36132

Ion composition measurements at altitudes 100-180 km in 1972.

18 p2310 A73-36143

Meteor ions in the polar ionosphere according to the rocket mass-spectrometric measurements and theoretical calculations.

18 p2311 A73-36146

Auroral ion velocity distributions using a relaxation model.

18 p2311 A73-36178

Ion composition and photochemistry of the E-region.

19 p2424 A73-37911

Height distribution of O+ and H+ ions in the ionosphere F2 region. I

19 p2427 A73-38333

Dynamics of ionization inhomogeneities in the ionosphere

20 p2553 A73-39152

Vertical sounding investigation of ionospheric ionization inhomogeneity sizes, orientation, elongation degree and drift rate, determining F region electron density fluctuations

20 p2553 A73-39155

Diurnal variations in the drift velocity and direction of the ionization inhomogeneities in the F layer

20 p2554 A73-39161

Maintenance of the F-region at night - Incoherent scatter measurements at a mid-latitude station.

21 p2683 A73-40776

Thermal positive ions in the dayside polar cusp measured on the ISIS 1 satellite.

21 p2690 A73-41368

Effects of interhemisphere transport on plasma temperatures at low latitudes.

22 p2844 A73-41919

Incompatibility of solar EUV fluxes and incoherent scatter measurements at Arecibo.

22 p2902 A73-41923

Perturbation of ion density by a body moving through the ionosphere.

23 p3008 A73-43254

Plasma instabilities in the region in front of a body moving rapidly in the ionosphere

24 p3115 A73-44790

Relationship of the sporadic F2 layer with certain features of the ionosphere and magnetosphere at sub-auroral latitudes

24 p3083 A73-44792

Diurnal ion composition variations in E region under quiet and perturbed solar conditions, using continuity equations for positive ions and electroneutrality equations

24 p3083 A73-44793

IONOSPHERIC NOISE

NT WHISTLERS

A sub-class of pi 1 micropulsations associated with the diurnal transit of the neutral sheet.

02 p0158 A73-11908

Ionospheric VLF and ELF electric field observation by Alouette 2 satellite, obtaining ion mass distribution from lower hybrid resonance hiss during geomagnetic storm

02 p0164 A73-12623

Hypotheses for excess background radiation at 200-500 km, suggesting single high energy electrons or electron clusters

08 p0999 A73-21336

Nonducted whistlers observed in the plasmasphere.

09 p1078 A73-22748

Characteristics of the VLF-noise spectrum during excitation of the earth-ionosphere resonator by cosmic sources.

10 p1188 A73-24222

IONOSPHERIC PROPAGATION

NT IONOSPHERIC F-SCATTER PROPAGATION

The influence of chordal paths on signals propagating to the near antipode of an HF radio transmitter.

01 p0015 A73-10182

Numerical solution for propagation of longitudinal waves along the geomagnetic field using a three-fluid ionosphere model.

01 p0016 A73-10197

Influence of an important region of the ionospheric layer on ELF propagation characteristics

01 p0016 A73-10203

Radio wave propagation effects in a three-dimensionally inhomogeneous magnetoactive ionosphere

01 p0016 A73-10204

The EM field of a dipole transmitter in the two-layer medium air space-magnetoactive ionosphere

01 p0035 A73-10299

Refraction of whistler-mode waves by large-scale gradients in the middle-latitude ionosphere.

01 p0017 A73-10328

D-region parameters from the extraordinary component of partial reflections.

01 p0036 A73-10329

Geomagnetic activity effects on D layer absorption from vertical soundings during solar flare induced sudden magnetic storms

01 p0039 A73-10415

Ionospheric propagation indexes prediction based on computer filtered values obtained during solar activity cycles ascending and descending parts

01 p0017 A73-10416

Synoptic studies of D-region ionization changes and electron densities by the partial reflection differential absorption experiment.

01 p0042 A73-10904

Winter anomaly in ionospheric absorption of radio waves on 1.725 MHz during sunspot minimum.

01 p0043 A73-10910

Studies of the lower ionosphere by means of VLF propagation over long distances

01 p0044 A73-11515

Ionospheric effects on the transmission of ultralow-frequency plasma waves.

02 p0155 A73-11520

Ionospheric resonance signal envelope and waveform observation by rocket-borne RF sounder, noting electron gyrofrequency third harmonic due to beating waves

02 p0140 A73-11750

Auroral X-ray and conjugate ionospheric absorption observations of an electron precipitation event accompanying a sudden impulse in the geomagnetic field.

02 p0157 A73-11759

Quasimonochromatic whistler mode packets of slowly varying amplitude.

02 p0140 A73-11920

The theory of coupling of characteristic radio waves in the ionosphere.

02 p0141 A73-12030

Quasi-linear interaction of whistler-mode waves and nonthermal electrons.

02 p0141 A73-12390

Self focusing of two dimensional cylindrical waves propagating in inhomogeneous natural duct, noting tropospheric communications and ionospheric and sound propagation applications

02 p0142 A73-12527

Conjugate ducted echoes observed on Alouette II ionograms.

02 p0143 A73-12624

The effects of ions of VLF and ELF propagation in an abnormally ionized atmosphere.

02 p0143 A73-12851

Transmission and reflection of magnetospheric whistlers in the ionosphere and lower exosphere at high latitudes.

03 p0298 A73-12884

Beyond the horizon ionospheric propagation experiment from an equatorial orbiting satellite to a middle latitude station.

Coupled wave equations for propagation in generally inhomogeneous compressible magnetoplasma.

Multifrequency radio beacon on polar orbiting satellite for wideband transmission through ionosphere without significant signal distortion

A technique for synoptic measurement of ionospheric propagation delays by ranging from geostationary satellites to a network of unmanned transponders.

Satellite transmitted impulse response transfer function evaluation by ray tracing technique for ionospheric model with Chapman ionization vertical profile.

ATS-F satellite borne radio beacon transmitter experiment for obtaining ionospheric electron content, discussing design, in-orbit performance, calibration information dissemination and propagation measurement

Estimation of the cumulative amplitude probability distribution function of ionospheric scintillations.

Time-dependent characteristics of radio waves passing through the irregular ionosphere.

UHF airborne measurement of equatorial ionospheric scintillation fading.

A simple apparatus for signal reception of transit system satellites and principal results.

Characteristics of large scale ionospheric irregularities.

Bombardment of the polar-cap ionosphere by solar cosmic rays.

Fraunhofer zone distribution functions for azimuth and elevation angles of radio waves reflected from inhomogeneous ionospheric scattering layer

Cosmic radio wave anomalous absorption height dependence on zenith distance in midlatitude ionosphere during solar flare emission from polarization study

E region electron collision frequency vertical distribution from ground and rocket measurements of radio wave absorption and electron density respectively

Sporadic E cloud focusing of radio waves as interpretation of observed short duration bursts accompanied by rapid phase variation

D region HF radio wave nighttime absorption correlation to winds and temperature in Northern Hemisphere during IQSY

Absorption measurements at Calcutta compared with current D region models for atomic oxygen production and loss processes

Ionospheric scale height from the refraction of satellite signals.

The production and analysis of transmission ionograms.

VLF wave propagation properties in waveguide formed by ground and ionospheric shell, noting diurnal phase and amplitude anomalies due to ionospheric disturbances

Nonsolar related D region semilunar variation effects on Omega navigation systems signal phase shift from harmonic analysis of VLF propagation data periodicities

The role of atmospheric pressure variations above the mesopause in the phenomena of winter anomaly and variability of the lower ionosphere.

Multipath fading and ionospheric scintillation modes of propagation anomalies measurement to formulate models of propagation media

Estimation of the cumulative amplitude probability distribution function of ionospheric scintillations.

FM Gaussian electromagnetic pulse distortion during reflection from ionospheric model with linear electron density profile and constant collision frequency

Feasibility of ground-based generation of artificial micropulsations.

Further ionosonde observations of ionospheric modification by a high-powered HF transmitter.

Error analysis of ionospheric parameter measurement by satellite transmitted or reflected multiple frequency pulsed radiation signal, using perturbation method

Russian papers on solar radiation effects on ionospheric propagation covering proton flares, thermal fluxes, lunisolar tides, radio propagation and cosmic radio emission

Investigation of a signal scattered in the lower ionosphere on the basis of a group delay model

The Doppler frequency shift in ionospheric propagation of radio waves

Vertical motion of the lower ionosphere during a solar eclipse

Probability of short-wave signal transmission over a medium-range path

Role of the sporadic E layer in short radio wave propagation at frequencies exceeding the maximum usable frequencies of the F2 layer

Radio-wave absorption in the lower ionosphere and stratospheric effects

Ionospheric propagation effects on riometer recorded cosmic radio emission spectra, noting temporal and frequency spectra dependence on ionospheric plasma turbulence scale

Variational method of moments and some iteration procedures for determining the characteristics of VLF wave propagation in the earth-anisotropic ionosphere waveguide channel. I

Vertical electric dipole excited electromagnetic field in earth-ionosphere waveguide, using Galerkin method for VLF electromagnetic wave propagation equation

A model of VLF band radio wave propagation in the earth-ionosphere waveguide channel

VLF field diurnal variations and terminator crossing effect on signal path during transmission in earth-ionosphere waveguide

Passage of medium-frequency radio waves through the ionosphere

Effect of the earth's electrical properties on the characteristics of VLF wave propagation in the earth-ionosphere waveguide

Pulse and monochromatic short wave signals phase/amplitude autocorrelation functions and probability distributions during oblique incidence reflection from ionosphere

Possibility of radar observation of nonlinear wave interaction in ionospheric plasma

The theory of the reflection of low frequency radio waves in the ionosphere near critical coupling conditions.

Lower F region ionospheric wave dispersion observation for horizontal phase and group velocities relationship to period, considering interpretation by internal gravity wave hypothesis

Conjugate ducted echoes observed on Alouette II ionograms.

Nonducted whistlers observed in the plasmasphere.

Magnetospheric plasma waves propagation effects on rapid geomagnetic field variations, noting magnetic pulsations and ionospheric propagation

Resonance and propagation theory for all electromagnetic wave types in plasmas of ionosphere and interplanetary space, discussing stability and oscillations

Vertical profiles of the effective collision number in the E and F regions of the ionosphere

Critical frequency gradients-geometric parameters equivalence coefficients for ionospheric layer with parabolic vertical ionization distribution for radio wave path determination

Generation of small-scale irregularities in the equatorial electrojet.

Ionospheric radio signal reflection fields verified via quantitative statistical reliability criterion

Radio wave reflection from ionosphere, determining polarization and fluctuation characteristics via Stokes parameters

HF radio signal reception behavior near maximum usable frequency during evening and at midnight, noting SNR

Ionospheric attenuation of 3-100 MHz radio waves, interpreting scatter mode propagation mechanism as total reflection from lower ionizational irregularities

Ionospheric anomalies in the night mesosphere after geomagnetic storms.

Lower ionosphere electron densities from rocket measurements employing LF radio propagation and DC probe techniques.

R and L modes of ion cyclotron whistler propagation in ionosphere, noting refractive indexes and wave polarization for multicomponent plasma

Differential phase experiment on signal reflections from D region, noting systematic error in phase jitter calculation with pulse nonoverlap explanation

VLF ion cyclotron whistler propagation in upper ionosphere, noting polarization reversal and mode coupling from satellite observation

Some problems in methods for determining the parameters of scattering inhomogeneities

Calculation of the field amplitude and phase velocity of low-frequency waves in the earth's spherical waveguide

Nighttime ionospheric wave propagation curves in the broadcast band

Second-order corrections for ionospheric radio-wave propagation

Estimating the accuracy of longitudinal interpolation of fOF2 from shipboard observations

Determination of the apparatus constant during multifrequency measurements of radio-wave absorption by the A1 method

Low dispersion whistlers observed simultaneously at two low latitude stations.

Book - Theory of ionospheric waves.

Computerized short- and long term ionospheric propagation forecasting for HF communications, frequency scheduling and broadcasting circuits

Midlatitude signal fading during sunrise and sunset transitions, noting amplitude ratio independence of propagation direction in earth-ionosphere waveguide

Phase and amplitude variations of 40-kHz radio waves propagating over a 7.1-Mm path.

Characteristics of the electric field far from and close to a radiating antenna around the lower hybrid resonance in the ionospheric plasma.

High-frequency radio-wave propagation through plane-stratified ionospheric models

Some effects of the equatorial ionosphere on terrestrial HF radiocommunication.

Propagation through a slab of irregularities in a magneto-ionic medium.

Propagational mode deducted from signal strengths in the VHF band on the trans-equatorial path.

Transmission loss at high frequencies on 3260 km temperate-latitude path.

Coefficients of hydromagnetic wave reflection from conjugate ionospheres

Study of ionospheric phase distortion at Ahmedabad.

Properties of plane asymmetric plasma waveguides as applied to short-wave propagation along inhomogeneities of the topside ionosphere.

Measurement of the integral parameters of the nighttime ionosphere from observations of Intercoms-2 signals.

Frequency correlation of fluctuations of radio waves reflected from the ionosphere.

Signal reflection height seasonal variations effect on radio waves absorption estimation from vertical ionospheric sounding

10 p1188 A73-24242

Computer simulation of HF frequency-selective fading and performance of the mode-averaging diversity combiner.

10 p1190 A73-24894

Empirical model for F layer electron density irregularities responsible for VHF/UHF amplitude scintillation, considering geomagnetic latitude, local time, season and sunspot effects

10 p1190 A73-24895

Ionospherically diffracted monochromatic VHF/UHF plane wave statistics characterization, noting Gaussian and log-normal distributions from ATS-3 satellite data recording

10 p1190 A73-24896

Field-aligned ionospheric E-region irregularities and sporadic E.

10 p1191 A73-24897

Some results of ionospheric measurements based on observations of geophysical rocket signals from spaced points and observations of signals reflected by space objects

11 p1350 A73-25077

Ionospheric radio wave absorption coefficient correlation with solar activity Wolf number in IGY, IGC and IQSY

11 p1327 A73-25083

Vertical distribution of absorption of cosmic radio emission and radio waves in ionosphere and lower ionosphere based on electron density profiles

11 p1327 A73-25084

Relationship of the sporadic Es layer parameters with the absorption of radio waves in the ionosphere

11 p1350 A73-25085

Anomalous absorption of cosmic radio emission in the auroral zone during the IQSY

11 p1411 A73-25087

Possibilities and some results of studying the ionosphere by the method of 'incoherent' scattering of radio waves

11 p1350 A73-25088

Effect of the May 20, 1966 solar eclipse in the ionosphere on the basis of observations at Rostov on the Don and at Adler

11 p1351 A73-25100

Optimum bandlimited signal synthesis with pulse compression for transionospheric propagation along vertical path, considering statistical effects of total ionospheric electron content variations

11 p1330 A73-25689

VLF radio signals propagational effects relationship to ionospheric polar substorm different phases

11 p1330 A73-25765

On the solar Lyman alpha control of the ionospheric absorption at 2775 kHz.

11 p1412 A73-25770

Physical interpretation of the diurnal behavior of the TM and TE components of VLF fields in the far zone

11 p1331 A73-26152

Parametric excitation of Langmuir oscillations in the ionosphere in a field of powerful radio waves

11 p1331 A73-26153

Tunneling transmission through the equatorial lower ionosphere of ELF and VLF electromagnetic waves.

11 p1358 A73-26702

Nose extension method based on approximate dispersion function for calculating ducted whistler frequency and associated travel time, discussing ionosphere-magnetosphere interactions

11 p1358 A73-26704

Results of ship-borne ionospheric absorption measurements on the North Atlantic during winter.

11 p1359 A73-26713

Polarization of radio waves reflected from an inhomogeneous ionosphere

12 p1468 A73-26971

A study of ionospheric absorption in conjugate regions produced by storm sudden commencements and sudden impulses in the geomagnetic field.

12 p1489 A73-26994

F 2 layer characteristics forecasts by extrapolation of critical F 2 frequency data from Moscow, Sverdlovsk, Irkutsk, Alma-Ata and Salehard

12 p1490 A73-27338

Propagation of low-frequency electromagnetic waves in the spherical waveguide formed by the earth and the ionosphere

12 p1469 A73-27340

Measurements of wave normal direction of whistler mode signals in the ionosphere by means of the rocket-Doppler technique.

12 p1492 A73-27610

Arbeitsgemeinschaft Ionosphäre, URSI, and Nachrichtentechnische Gesellschaft, General Session, Kleinheubach, West Germany, October 9-14, 1972, Reports

12 p1493 A73-27750

Long-periodicity fading of short-wave signals

12 p1473 A73-27759

Shimazaki formula corrected for F 2 layer altitude estimation for 2-30 MHz field intensity and transmission losses calculations

12 p1493 A73-27762

Solar-terrestrial relations in the retrospective world interval from July 26 to August 14, 1972

12 p1535 A73-27766

Daily altitude variations of medium frequency radio waves reflection in ionosphere over Tsamab, SW Africa, examining attenuation correlation with solar zenith angle

12 p1494 A73-27767

Employment of mode theory and ray theory for the interpretation of very-long-wave measurements at medium distances

12 p1474 A73-27769

An inversion method for the determination of the electron density profile of the ionosphere on the basis of satellite tracking data

12 p1494 A73-27772

Numerical solution of the problem of transmission of ELF waves through the lower ionosphere.

13 p1582 A73-28651

Effective recombination coefficient in the ionospheric D-region.

13 p1608 A73-28711

Analytic ray trajectory model of radio wave lateral incidence on traveling large scale ionospheric inhomogeneities as function of location and departure angle

13 p1583 A73-28724

Ionospheric echoes due to sideland and harmonic radiation from Isis topside sounder transmitters, discussing effects of satellite spread and ion sheath distortions

14 p1752 A73-29974

Ionospheric and pulse compression induced distortions in chirped Gaussian electromagnetic pulses

14 p1728 A73-30232

On the effect of electron-neutral particle collisions upon the refraction of high-frequency radio waves by the lower atmosphere and ionosphere of Mars.

15 p1929 A73-31078

Dispersion of electromagnetic waves on a weak isolated inhomogeneity.

15 p1843 A73-31522

The values of ionospheric absorption of VLF electromagnetic waves in middle geomagnetic latitudes.

15 p1868 A73-31523

Scintillations of satellite signals and their observation.

15 p1843 A73-31524

Ionospheric tilts and long-range short-wave communications.

15 p1843 A73-31525

Short-wave skip distance for various models of the ionosphere

15 p1843 A73-31575

Equatorial spread-F irregularities observed at Nairobi and on the transequatorial path Lindau-Tsumeb.

15 p1870 A73-31765

Signal fading and topside electron density profile observation over VHF transequatorial path between Europe and Southern Africa, noting great circle F transmission role

15 p1844 A73-31766

Calculation of ionospheric N/z profiles with the use of radio-wave absorption data

15 p1871 A73-31883

Frequency dependence of radio-wave absorption in a reflecting layer

15 p1844 A73-31884

Theory of short radio wave propagation over very great distances

15 p1844 A73-31888

Electron concentrations increase observed at 60-90 km altitudes during anomalous winter radio wave absorption, noting association with upward aerosol transport decrease

15 p1844 A73-31889

Investigation of the signal-to-noise ratio of ionospheric reflection by the method of coherent reception

15 p1844 A73-31890

Anomalous winter time absorption of radio waves in the middle latitude ionosphere

15 p1844 A73-31900

Angular diameter calculation of Ellis atmospheric window via ionospheric wave ray tracing technique

15 p1844 A73-32048

Ionospherically propagated backscatter from Pacific Ocean via swept frequency continuous wave recordings, noting sky wave polarization rotation modulation of received signal

15 p1845 A73-32228

Turbulent scattering phenomenological model for D region partial coherent reflection experiments with measurement noise, presenting amplitude and phase statistics

15 p1845 A73-32230

Phase-difference distributions in a D-region partial-reflection experiment.

15 p1845 A73-32231

D region partial reflection mechanism model based on multiple reflector concept, presenting electron density vertical distribution

15 p1845 A73-32233

Vertical profiles of the effective collision frequency in the E- and F-regions of the ionosphere.

16 p2002 A73-32776

Critical frequency gradients-geometric parameters equivalence coefficients for ionospheric layer with parabolic vertical ionization distribution for radio wave path determination

16 p2002 A73-32779

Relationship between stratospheric warming and ionospheric absorption.

16 p2009 A73-33887

Earth-flattening approximations in the theory of radio wave propagation near the surface of the earth.

16 p1984 A73-33916

Frequency analysis of calculated ionospheric reflection coefficients.

16 p1984 A73-33920

Penetration and reflection of VLF waves through the ionosphere - Full wave calculations with ground effect.

16 p1984 A73-33921

Ionospheric scintillation at 4 and 6 GHz.

17 p2122 A73-34869

Physics and chemistry of the ionosphere.

17 p2162 A73-35050

Propagation of VLF waves in the earth-ionosphere waveguide under nighttime ionospheres.

17 p2126 A73-35629

Methods of measurements and some results of lower ionosphere by using VLF and LF radio waves.

18 p2302 A73-35926

Observations of the entry of solar protons into the magnetosphere by use of riometers.

18 p2344 A73-35930

Experimental results of radio wave absorption measurements in Southwest Europe.

18 p2288 A73-35940

Ground and synchronous orbit magnetic observations of magnetospheric and ionospheric wave propagation to model substorm current system variations

18 p2303 A73-35945

The use of the LF A3 absorption measurements in studying the winter anomaly.

18 p2303 A73-35947

Solar Lyman alpha control of the A3 ionospheric absorption on 2775 kHz.

18 p2288 A73-35948

The use of VLF propagation measurements for studies of magnetospheric and meteorological influences on the lower ionosphere.

18 p2303 A73-35953

Velocity of the reflection points reveals structure and motions in the ionosphere.

18 p2305 A73-36000

The southern boundary region of the winter anomaly in ionospheric absorption in winter 1971/72 observed on board the cargo vessel 'Hanau' of Hapag-Lloyd moving between 10 deg and 55 deg N.

18 p2305 A73-36002

Spatial extent of the winter anomaly in absorption.

18 p2305 A73-36003

Some results obtained from the European Cooperation concerning studies of the winter anomaly in ionospheric absorption.

18 p2305 A73-36004

Analysis and interpretation of aspect-dependent ionospheric radar scatter.

18 p2289 A73-36283

Arbitrary propagation of HM waves along the F region.

18 p2312 A73-36285

Measurements of ionospheric reflectivity from 6 to 35 kHz.

18 p2289 A73-36286

Measurement of the attenuation of 9.303 MHz waves from ISIS-II through the ionosphere.

18 p2289 A73-36876

Russian book on electromagnetic wave propagation in ionosphere, covering atmospheric structure, electron concentration, waveguides and earth surface effects

19 p2424 A73-37773

Some problems concerning the method of determining the parameters of scattering inhomogeneities.

19 p2424 A73-37913

Computations of the field amplitude and phase velocity of low-frequency waves in a spherical surface waveguide.

19 p2404 A73-37914

Propagation curves of an ionospheric wave at night for the broadcasting range.

19 p2404 A73-37915

Second-order corrections for radio-wave propagation through the ionosphere.

19 p2404 A73-37916

Evaluation of the accuracy of longitudinal interpolation of f0F2 based on ship observations.

19 p2425 A73-37930

- Determination of the instrument constant in multifrequency measurements of radio wave absorption by the A1 method. 19 p2404 A73-37932
- On the propagation of ionospheric whistlers at low latitude. 19 p2404 A73-38018
- Relationship between anomalous radio absorption and the solar zenith angle during periods of sudden ionospheric disturbances 19 p2406 A73-38327
- Fine-scale inhomogeneities of the mid-latitude sporadic E layer 19 p2427 A73-38332
- Reflection of powerful radio waves from the lower ionosphere 19 p2406 A73-38334
- Measurements of artificial satellite signal Doppler spectrum. 19 p2407 A73-38351
- Excitation of the earth-ionosphere waveguide by point dipoles at satellite heights. 20 p2528 A73-38846
- Reflection coefficients of hydromagnetic waves from conjugate ionospheres. 20 p2551 A73-38914
- Wave guide propagation of micropulsations out of the plane of the geomagnetic meridian. 20 p2529 A73-38937
- Whistlers association with sudden changes in amplitude of long distance nighttime subionospheric VLF transmission 20 p2530 A73-38944
- Sampled aperture antenna array measurement of RF phase characteristics of diffraction pattern formed on ground by radio waves obliquely reflected from ionosphere 20 p2530 A73-39018
- Ionospheric inhomogeneity parameters and geoelectromagnetic field variations 20 p2553 A73-39156
- Statistics of a pulse signal reflected from an inhomogeneous ionosphere 20 p2530 A73-39157
- Investigation of the fine-structure inhomogeneities of the Es layer at oblique radio wave incidence 20 p2554 A73-39163
- Theory of radio wave incoherent scattering by a plasma and the application of the theory in ionospheric studies 20 p2554 A73-39164
- B-2 installation for radio wave absorption measurements in the ionosphere at two frequencies simultaneously by the |A1| pulse method 20 p2566 A73-39165
- Effective altitudes of the F region in the IGY and IQSY periods 20 p2554 A73-39167
- Ten years Antarctic region ionosphere investigation during IGY-ISQY period considering ionization maxima, inhomogeneity drifts, electron density and short wave propagation 20 p2554 A73-39171
- Gravity waves in the F region of the ionosphere 20 p2554 A73-39173
- Variations in the M/3000/F2 coefficient as a function of the solar energy entering the earth's atmosphere 20 p2555 A73-39179
- Method for the computation of radio paths up to 4000 km long 20 p2530 A73-39180
- Geomagnetic field effects in Martin theory of radio wave propagation in ionosphere with oblique and vertical signal incidence 20 p2555 A73-39181
- Effects of collisions on whistler-mode ray tracing. 20 p2531 A73-39404
- Correlation of random phases spaced over oscillation frequencies 20 p2531 A73-39457
- The propagation of Alfvén waves along I_0 's flux tube. 21 p2764 A73-40167
- The upward propagation of LF waves (electron whistlers) into the ionosphere and the turning of the Poynting vector towards the earth's magnetic field. 21 p2654 A73-40782
- One dimensional computer simulation model of spaced-receiver drift experiment with radio fading produced by reflections from perfectly reflecting ionosphere 21 p2684 A73-40783
- Mean D-region electron density profiles derived by combination of rocket and radio wave propagation data. 21 p2686 A73-40831
- The total electron content of the ionosphere and its horizontal gradients, measured on the basis of recordings of satellite signals at scattered points 21 p2686 A73-40910
- Russian book on statistical properties of ionosphere reflected signals covering statistical modeling, random processes, perturbation method and wave reflection problems 21 p2657 A73-41284
- Refraction of plasma waves in the ionosphere /in connection with topside sounding of the ionosphere/ 21 p2691 A73-41507
- Impedance and large signal excitation of satellite-borne antennas in the ionosphere. 22 p2831 A73-41835
- Sudden commencement and sudden impulse absorption events at high latitudes. 22 p2845 A73-41928
- Fading characteristics and drift and anisotropy parameters of the ground diffraction pattern of the radio waves reflected from the equatorial ionosphere during spread F conditions. 22 p2825 A73-41929
- Sudden ionospheric disturbance effects on L.F. radio pulse train amplitude during reception from Loran-C transmitters, comparing with VLF sudden phase anomaly 22 p2825 A73-42188
- Measurement of attenuation of 9.303 MHz waves from ISIS-II through the ionosphere. 22 p2825 A73-42193
- Short wave radio signal fadeout due to ionospheric disturbances, obtaining experimental equation on magnitude relationship with solar zenith angle and operating frequency 22 p2825 A73-42194
- Observations of the ionospheric absorption at oblique incidence during the IASV. 22 p2847 A73-42195
- A modified composite wave technique for OMEGA. 22 p2884 A73-42325
- Absorption of vlf and elf waves in whistler mode - Sunrise and sunset effects. 22 p2849 A73-42622
- Absorption of whistler waves during night. 22 p2850 A73-42623
- F 2 layer characteristics forecasts by extrapolation of critical F 2 frequency data from Moscow, Sverdlovsk, Irkutsk, Alma-Ata and Salehard 23 p2970 A73-43236
- Propagation of low-frequency electromagnetic waves in a spherical earth-ionosphere waveguide. 23 p2952 A73-43238
- Atmospheric oscillations. V - The propagator matrix and the transmission of an electrostatic potential along the geomagnetic field lines. 23 p2971 A73-43686
- Particle precipitation in Brazilian geomagnetic anomaly during magnetic storms. 23 p2971 A73-43687
- Variations of the total amount of ozone and the behaviour of some ionospheric parameters in the winter time upper atmosphere. 23 p2976 A73-43885
- Generation of VLF waves in the ionosphere near the low-frequency plasma resonance. I 24 p3115 A73-44788
- Determination of the difference in group paths by the method of frequency-diversity reception 24 p3068 A73-44810
- Enhanced scattering and decay of electromagnetic waves in the ionosphere. 24 p3086 A73-45130
- Theory of the polarisation of the ordinary wave reflected from the ionosphere in the limit of vertical incidence and vertical magnetic field. 24 p3069 A73-45202
- IONOSPHERIC REFLECTION
- U IONOSPHERIC PROPAGATION
- IONOSPHERIC SOUNDING
- Prototype solid state radio sounder with digitization concept of multipulse integration for LF sounding of lower ionosphere, noting performance 01 p0043 A73-10909
- Digital attitude sun sensor for ionosphere sounding satellite. 01 p0053 A73-11171
- Test of horizon sensor for the ionosphere sounding satellite. 01 p0053 A73-11172
- The plasma diagnostics experiments of the Aeros satellite [DGLR PAPER 72-070] 02 p0166 A73-11669
- Rocket-borne instrumentation to measure ionospheric electron temperature with good spatial resolution. 02 p0167 A73-11953
- E region irregularities investigation via phase path measurements and radio wave ionospheric soundings, using model for undulatory variation of reflection height 02 p0158 A73-12028
- Ionospheric bottom side electron density profiles from measured monthly median values, using CCIR and ITS computer programs for critical frequencies 02 p0163 A73-12302
- Ionospheric electron and ion temperature profile measurements with satellite- and rocket-borne probes, comparing merits and discrepancies 02 p0163 A73-12303
- Simultaneous measurements of height wind profiles and electron concentration for verifying theory of sporadic E layer formation in midlatitudes under wind shear action 02 p0163 A73-12306
- Preliminary findings of a petrel rocket experiment to investigate the VLF emission 'chorus' in the ionosphere. 02 p0141 A73-12319
- Vertical ionospheric sounding station observation for spread F layer effect on scattered signal fading, using oscillograph display and camera 02 p0142 A73-12498
- Symposium on the Future Application of Satellite Beacon Measurements, Graz, Austria, May 29-June 2, 1972, Proceedings. 03 p0299 A73-13626
- Application of satellite radio beacons for measurement of small-scale ionospheric irregularities. 03 p0300 A73-13642
- Results from barium cloud releases in the ionosphere and magnetosphere. 03 p0301 A73-13805
- De electric field measurement with rocket-borne double probes and by satellite and balloon observation, noting ionospheric fields, magnetospheric plasma and auroras 03 p0302 A73-13874
- Cosmos 381 onboard ionospheric station signals received from magnetically conjugate region by ground wideband antennas 03 p0280 A73-14576
- Electron density and temperature measurements in the lower ionosphere as deduced from the warm plasma theory of the H.F. quadrupole probe. 04 p0480 A73-15199
- Interferometric CW radar for group delay difference measurement of reflected signal components in ionospheric sounding 05 p0548 A73-16253
- Determination of the effective angular distance between the reflection points of an ordinary ray and an extraordinary ray by the interference method 05 p0548 A73-16259
- ESRO 1A satellite-borne Langmuir probe measurement for anisotropy in ionospheric thermal electron temperature relative to geomagnetic field 05 p0571 A73-17053
- The ionospheric effects of geomagnetic sudden commencements as measured with an HF Doppler sounder at Hawaii. 05 p0571 A73-17062
- Assessment of ISS topside sounder system by computer simulation. 05 p0579 A73-17168
- Possibility of detecting weak solar cosmic ray fluxes by ground-based radio engineering methods 06 p0742 A73-17532
- Polarization characteristics of partially scattered radio waves for turbulent ionosphere vertical sounding applications 06 p0662 A73-17533
- Undistorted short sounding pulse reception at exit from ionosphere obtained by signal carrier frequency modulation 06 p0663 A73-17537
- Electric probe performance in weakly ionized dense plasma flow for lower ionosphere measurements, considering stagnation point and particle distribution-potential effects 06 p0689 A73-17538
- Possibility of observing the decay interaction of plasma waves in top-side sounding experiments 06 p0689 A73-17551
- Three dimensional summer time sporadic E layer structure and electron concentration during 1966-1969 by ionospheric space diversity sounding 06 p0689 A73-17553
- Vertical distribution of electron concentration in the Northern Hemisphere at the geomagnetic pole /from top-side and ground-based ionospheric sounding data/ 06 p0689 A73-17554
- Signal level fluctuations line spectra energy characteristics comparison for oblique and oblique-backscatter sounding, noting changes in harmonics intensity and period 07 p0792 A73-19438
- Incoherent ionospheric scatter sounding facility for ionospheric energy balance, neutral atmospheric structure and upper atmosphere dynamics studies 07 p0817 A73-19550
- Magnesium and associated ionospheric processes in Es-layer formation. 08 p0957 A73-20655
- Some characteristics of the ionospheric irregularities over the magnetic equator derived from spaced fading records. 08 p0957 A73-20656
- Relations between ionospheric electric fields and energetic trapped and precipitating electrons. 09 p1073 A73-22056
- Aurora and the poleward edge of the main ionospheric trough. 09 p1073 A73-22058

Ionospheric electron density profile observation by partial reflection experiment, discussing radio signal amplitude and phase data recording sensitivity requirement

09 p1075 A73-22071

Intercoms 2 satellite design, construction, on-board scientific instrumentation, ionospheric experiments and data processing equipment

10 p1217 A73-23886

Structure of ionospheric inhomogeneities, according to simultaneous observations on two magnetoionic components.

10 p1211 A73-24217

Frequency correlation of fluctuations of radio waves reflected from the ionosphere.

10 p1188 A73-24240

Signal reflection height seasonal variations effect on radio waves absorption estimation from vertical ionospheric sounding

10 p1188 A73-24242

ISIS-1 satellite observations of the ionosphere at high southern latitudes.

11 p1353 A73-25753

Satellite-borne electrostatic wave topside ionosphere sounder for electron plasma resonance measurement, discussing data spectra preservation, frequency synthesizer and gain-change mechanism features

11 p1339 A73-26629

Effective 'radius of operation' of a system for measuring ionospheric drifts

12 p1490 A73-27341

Temperature variations in the upper atmosphere during a period of minimum solar activity from topside ionospheric sounding data

12 p1491 A73-27346

Determination of the effect of electric fields on the ionosphere, based on the behavior of the F2-layer above geomagnetically conjugate points

12 p1493 A73-27760

Relative transit time measurements of high-frequency signals using an FM-CW technique

12 p1474 A73-27763

Negative horizontal gradients of the integral electron content of the ionosphere - A comparison of satellite and ionosonde data

12 p1494 A73-27774

Perpendicular and parallel electric fields in the ionosphere during a magnetospheric substorm

12 p1494 A73-27776

Group delay times of magnetoionic components for horizontal electron density profiles in magnetic meridian plane, noting comparison with ionospheric sounding data

13 p1608 A73-28708

Faraday effect of incoherently scattered radar signals.

13 p1583 A73-28712

High power radio transmitter for structural investigation and electron concentration profiles of ionospheric D and E regions

13 p1583 A73-28725

Rocket-borne scientific experiment program Sun-Atmosphere 1971, using meteorological rockets for meteor trail, atmospheric and ionospheric observations during geomagnetic disturbances

13 p1609 A73-29188

Computerized simulation of Ionosphere Sounding Satellite topside sounder system techniques for observation of critical frequencies and apparent distance-frequency characteristic relation

13 p1586 A73-29248

Measurement of electron temperature in the ionosphere by the high-frequency probe method

14 p1746 A73-29861

Ionospheric echoes due to sideland and harmonic radiation from Isis topside sounder transmitters, discussing effects of satellite spread and ion sheath distortions

14 p1752 A73-29974

A satellite-borne positive ion mass spectrometer.

14 p1753 A73-30415

Correlation of 'satellite estimates' of the equatorial electrojet intensity with ground observations at Addis Ababa.

15 p1870 A73-31771

Sporadic E layer pulsed ultrashort oblique wave sounding, analyzing reflected signal distortion

15 p1872 A73-31886

Comparison of true and effective altitudes of the sporadic E layer

15 p1872 A73-31899

Study of traveling ionospheric perturbations

15 p1872 A73-31901

Possibility of detecting weak solar-cosmic-ray fluxes by ground-based radio methods.

16 p2052 A73-32756

Polarization characteristics of partially scattered radio waves for turbulent ionosphere vertical sounding applications

16 p1978 A73-32757

Undistorted short sounding pulse reception at exit from ionosphere obtained by signal carrier frequency modulation

16 p1978 A73-32761

Electric probe performance in weakly ionized dense plasma flow for lower ionosphere measurements, considering stagnation point and particle distribution-potential effects

16 p2001 A73-32762

Possibility of observing the decay interaction of plasma waves in topside sounding experiments.

16 p2002 A73-32775

Three dimensional summer time sporadic E layer structure and electron concentration during 1966-1969 by ionospheric space diversity sounding

16 p2002 A73-32777

Vertical electron density distribution at the geomagnetic pole in the Northern Hemisphere /from data of topside and ground-based soundings of the ionosphere/.

16 p2002 A73-32778

Coaxial cable fed dipole antenna array for observation of coherent backscatter radar signal from ionospheric electron density irregularities in electrojet region

16 p1987 A73-33117

Multiring probe in a flowing ionospheric plasma.

17 p2214 A73-34199

Skylark rocket measurement of earth atmosphere and ionosphere, examining payload capacity, camera image quality, cost, use of smaller rockets and practical applications

17 p2239 A73-34953

On the relative response and absolute gain toward the zenith of HF field-expedient antennas - measured with an ionospheric sounder.

17 p2129 A73-35698

Kinesonde studies of cesium ion clouds in the E-region.

18 p2304 A73-35988

VLF pulse ionosounder measurements of the reflection properties of the lower ionosphere.

18 p2305 A73-36010

Electron-density profiles obtained from MF sounding at Tsunab.

18 p2306 A73-36012

A rocket-borne riometer for the study of lower ionosphere.

18 p2315 A73-36046

Oriental dependence of certain RF impedance probes in the ionosphere.

18 p2288 A73-36188

Satellite measurements of solar X-ray flux and ground observations of sudden ionospheric disturbances.

18 p2347 A73-36389

Ionospheric magnetic field measurements at auroral latitudes.

18 p2313 A73-36647

Probe measurement of the electrostatic field in the ionosphere and magnetosphere

18 p2314 A73-37026

HF radar observations of cesium plasma cloud released from the rocket K-9 M-39.

19 p2423 A73-37378

Rocket measurement of photoelectrons in the ionosphere by K-9 M-40.

19 p2474 A73-37379

Measurement of the ionospheric electron density by using S-210-6 rocket.

19 p2423 A73-37380

Skylark rocket magnetometer measurement of sporadic E layer magnetic fields, testing wind shear theory of ionization redistribution at midlatitudes

19 p2426 A73-38022

Intercoms 2 satellite design, construction, on-board scientific instrumentation, ionospheric experiments and data processing equipment

20 p2565 A73-38905

Vertical sounding investigation of ionospheric ionization inhomogeneity sizes, orientation, elongation degree and drift rate, determining F region electron density fluctuations

20 p2553 A73-39155

Investigation of the inhomogeneous structure of the ionosphere using observations of discrete cosmic radio emission sources and vertical soundings

20 p2553 A73-39159

Electron flux variation measurements in the upper atmosphere at altitudes of 200 to 500 km

20 p2554 A73-39168

Ten years Antarctic region ionosphere investigation during IGY-ISQY period considering ionization maxima, inhomogeneity drifts, electron density and short wave propagation

20 p2554 A73-39171

Thermal electron energy distribution measurements in the ionosphere.

21 p2681 A73-40156

Fluxes of electrons with energies greater than 10 MeV at heights from 200 to 500 km

21 p2758 A73-40603

Satellite counting of excess radiation measured as ionospheric electron and proton intensity dependent on geomagnetic activity, discussing proton energy spectra and electron albedo

21 p2758 A73-40604

Rocket experiments on nonlinear wave-wave interaction in the ionospheric plasma.

21 p2685 A73-40823

Mean D-region electron density profiles derived by combination of rocket and radio wave propagation data.

21 p2686 A73-40831

The optimal number of soundings for a complete investigation of the ionization-neutralization and dynamic characteristics of the middle ionosphere

21 p2686 A73-40911

Dependence of high-energy electron fluxes at an altitude of 200 to 300 km on threshold rigidity

21 p2686 A73-40917

Refraction of plasma waves in the ionosphere /in connection with topside sounding of the ionosphere/

21 p2691 A73-41507

Ionospheric electron density profiles and contour plots above F layer maximum from vertical sounding and Faraday rotation techniques

22 p2851 A73-42984

Effective 'radius of action' of a device for measuring ionospheric drifts.

23 p2970 A73-43239

Temperature variations in the upper atmosphere during the solar activity minimum based on data of topside sounding of the ionosphere.

23 p2970 A73-43243

Ionospheric sounding by ATS-3 emitted signal polarization measurement during partial solar eclipse of 10 July 1972, noting electron content decrease and diffusion rate

23 p2972 A73-43697

Experimental test of the wind-shear theory: A reply - Rocket-borne magnetometers do measure B.

23 p3024 A73-43702

Comparative analysis of rocket measurements of a sub c /h/ and of ground-based vertical sounding data

24 p3083 A73-44795

Determination of the vertical parameters of wavelike ionospheric disturbances

24 p3083 A73-44797

Ionospheric electric field measurements with a spin stabilized detector.

24 p3090 A73-44818

Simultaneous in situ electron temperature comparison of Alouette 2 probe and plasma resonance data.

24 p3086 A73-45129

IONOSPHERIC STORMS

NT SUDDEN IONOSPHERIC DISTURBANCES

Ionospheric electron density vertical distribution time dependence for ionospheric storms morphology, noting relationship to geomagnetic storms

03 p0300 A73-13650

Storms and the seasonal anomaly in the topside ionosphere.

09 p1075 A73-22132

Observations of ionospheric storms at low latitudes and their correlation with magnetic field changes near the magnetic equator.

19 p2425 A73-38011

F 2 region critical frequency variations during geomagnetic storms, noting correlation with main phase onset

24 p3082 A73-44728

Critical frequency evolution during F 2 region storms at middle and low latitudes, showing random global patterns and relation to neutral wind flow

24 p3087 A73-45205

IONOSPHERIC TEMPERATURE

Lower ionosphere variability due to atmospheric dynamics, considering temperature variations, minor constituent transport and eddy diffusion

01 p0041 A73-10885

Ionic reaction mechanism for F region nitrogen vibrational temperature, using positive ion composition

01 p0042 A73-10894

The application of Langmuir probes to the measurement of very low electron temperatures.

02 p0158 A73-11912

Rocket-borne instrumentation to measure ionospheric electron temperature with good spatial resolution.

02 p0167 A73-11953

The global morphology of electron temperature in the topside ionosphere, as measured by an a.c. Langmuir probe.

02 p0158 A73-12027

Probe measurements of positive ions and electron temperatures in high latitude rocket flights.

02 p0159 A73-12032

Molecular nitrogen vibrational temperature in E and F regions, using positive ion data and model for ionic reaction rate and continuity equation numerical solution

02 p0161 A73-12279

Determination of the ionospheric density and temperature using a double probe electric field detector.

02 p0164 A73-12310

Transverse ion temperature measurements in plasma stream wind tunnel simulating ionospheric conditions, using cylindrical Langmuir probe and collimator-collection device

02 p0151 A73-12813

Temperature fluctuations in the ionospheric F region

05 p0568 A73-16256

Planetary-scale fluctuations of pressure in the E-layer, f-min, and pressure in the stratosphere.
05 p0571 A73-17057

Modulation Langmuir probe and incoherent scatter radar measurements of ionospheric electron temperature.
09 p1075 A73-22128

Diurnal variations in electron density at heights of 160 to 200 km and electron temperature variations
11 p1351 A73-25095

Description of the photoelectron interaction with ambient electrons in the ionosphere.
11 p1357 A73-25927

Temperature variations in the upper atmosphere during a period of minimum solar activity from topside ionospheric sounding data
12 p1491 A73-27346

Variations of the global values of F2-layer thickness and the parameters of the neutral atmosphere.
13 p1608 A73-28722

Measurement of electron temperature in the ionosphere by the high-frequency probe method
14 p1746 A73-29861

Ionospheric electron density and temperature measurement by cylindrical Langmuir probes onboard Intercosmos 2 satellite
14 p1746 A73-29862

Millstone Hill Thomson scatter results for 1966 and 1967.
15 p1866 A73-31067

A critical study on the reliability of electron temperature measurements with a Langmuir probe.
15 p1871 A73-31835

An evaluation of ionospheric probe performance. I - Evidence of contamination and clean-up of probe surfaces. II - The influence of vehicle wake effects on electron density and temperature measurements.
17 p2160 A73-34786

Latitudinal and temporal variability of temperature in the lower thermosphere.
18 p2304 A73-35991

Electron temperature profile and its solar activity dependence in the middle latitude region.
18 p2308 A73-36047

Results of air temperature, density and pressure measurements obtained with the aid of foil cloud sensors in the height region between 80 and 95 km.
18 p2311 A73-36179

Effect of an isotropic nonequilibrium plasma on electron temperature measurements.
20 p2552 A73-38947

Maintenance of the F-region at night - Incoherent scatter measurements at a mid-latitude station.
21 p2683 A73-40776

The determination of ionospheric charged particle temperatures from in situ measurements.
21 p2690 A73-41362

Rocket measurements of electron concentration and electron temperature in the polar ionosphere.
21 p2690 A73-41367

Diurnal and semidiurnal nitrogen density and temperature variations from thermosphere probe measurements.
22 p2845 A73-41926

Temperature measurements in the thermosphere and ionosphere.
22 p2847 A73-42063

Temperature variations in the upper atmosphere during the solar activity minimum based on data of topside sounding of the ionosphere.
23 p2970 A73-43243

Global distribution of thermospheric heat sources - EUV absorption and Joule dissipation.
23 p2971 A73-43681

The slab thickness of the mid-latitude ionosphere.
23 p2972 A73-43694

IONOSPHERICS

NT DAWN CHORUS
NT HISS
Satellite-borne HF ionospheric noise receiver system with narrow band monolithic crystal filters, comparing with Ariel 3
01 p0026 A73-11175

IONS

NT ANIONS
NT ANTIPROTONS
NT CATIONS
NT CESIUM ION
NT DEUTERONS
NT FERRIC IONS
NT HEAVY IONS
NT HELIUM IONS
NT HYDROGEN IONS
NT HYDRONIUM IONS
NT MANGANESE IONS
NT METAL IONS
NT MOLECULAR IONS
NT NITROGEN IONS
NT PROTONS
NT SOLAR PROTONS
IP [IMPACT PREDICTION]
U COMPUTERIZED SIMULATION
IQSY [INTERNATIONAL YEAR]
U INTERNATIONAL QUIET SUN YEAR

IRAQ

Structure of dust storms from ITOS-I T.V. images obtained over Iraq and the Gulf of Persia.
20 p2584 A73-39854

IRASERS

U INFRARED LASERS

IRIDIUM

Ir catalysts for high performance hydrazine decomposition, discussing preparation by coprecipitation of active metallic element with support in chloroiridic acid solution
07 p0865 A73-18928

Phase composition of Cu-Ni-O alloys with Ir additions, examining oxygen content influence on Ir distribution and solid solution formation
23 p2990 A73-43483

IRISES [MECHANICAL APERTURES]

Diffraction by double circular irises and scattering by two elliptical reflectors.
06 p0666 A73-18196

IRON

NT FERRIC IONS

NT IRON 57

Diffusive thermal bonding of cermet elements on steel and iron substrates in vacuum
02 p0172 A73-11537

Muon generated cascade showers in iron, using ionization calorimeter and hodoscopic detectors
02 p0210 A73-12684

Depth profiles of Fe I 5250 A line for three sunspot models, noting line-to-continuous absorption ratio relation to emergent intensity location
03 p0377 A73-14410

The dependence of the lower yield strength in iron and steel on grain size and temperature.
04 p0463 A73-15308

Dielectric satellite spectra for highly-charged helium-like ion lines.
04 p0500 A73-15490

The magnetic properties and morphology of metallic iron produced by subsolidus reduction of synthetic Apollo 11 composition glasses.
05 p0619 A73-16837

Electromagnetic interactions of cosmic ray muons in iron. I - Search for a charge asymmetry.
06 p0743 A73-18386

A new relationship between pre-strain and yield stress drop due to Bauschinger effect.
06 p0713 A73-18772

Metallic Fe-Ni-S lunar core as source of remanent magnetism in lunar rocks, consistent with thermal models
07 p0877 A73-19654

Crystal-field effects of iron and titanium in selected grains of Apollo 12, 14, and 15 rocks, glasses, and fine fractions.
07 p0881 A73-19710

Study of excess Fe metal in the lunar fines by magnetic separation, Moessbauer spectroscopy, and microscopic examination.
07 p0788 A73-19745

X-ray electronic studies of metallic iron in the lunar regolith
08 p1008 A73-21134

Interaction lengths of energetic pions and protons in iron.
08 p0990 A73-21523

The extreme-ultraviolet spectrum of Fe XV in a solar flare.
09 p1137 A73-22039

Influence of the combined effect of plastic deformation and high temperatures on the diffusion mobility of carbon
09 p1108 A73-23241

Measurements of the iron-group abundance in energetic solar particles.
10 p1264 A73-23538

Intermediate-coupling line strengths in the iron spectrum and the solar abundance of iron.
10 p1272 A73-23540

Investigation of iron content of lubricating oil using a ferrograph and an emission spectrometer.
10 p1218 A73-24165

Difference of the plastic deformation of the surface and internal layers of polycrystalline iron under fatigue loading.
10 p1233 A73-24183

Boridosilicide and boridoaluminide diffusion coatings on iron and steel, investigating formation kinetics structure and properties
10 p1227 A73-24963

Partition function derived for liquid Fe from Eyring method of significant structures, describing solid at high temperature via Einstein approximation
11 p1355 A73-25904

Gliding, twin formation and fracture of iron-single crystals at 78 K and at 4 K
11 p1386 A73-26571

Polarization measurements in the green coronal line.
11 p1428 A73-26623

Metal content in the atmospheres of red giants which are members of dispersed star clusters and dynamical groups
12 p1537 A73-26853

Highly disperse Fe powder electrodeposition on cathode, examining electrolyte concentration, acidity, current density and bath temperature effects on current efficiency for optimal deposition conditions
12 p1503 A73-27552

Obtaining of carbide and nitride dispersions in iron
13 p1633 A73-28182

Optical and chemical analysis of iron in Luna 20 placoclase.
13 p1674 A73-28305

Luna 20 and Apollo 16 lunar soil samples rare earth, iron and other trace elements contents from neutron activation analysis, noting Eu anomaly
13 p1675 A73-28317

Excitation of the Fe XIII spectrum in the solar corona.
13 p1684 A73-29353

Fe XVII emission from the solar corona.
13 p1685 A73-29356

New observations of Fe XVII in the solar X-ray spectrum.
13 p1685 A73-29357

Determination of van der Waals broadening of Fe I emission lines induced by neutral He
13 p1685 A73-29360

Photometric analysis of monochromatic photographs of the solar corona taken in the green line /5303 A/ and the red line /6374 A/.
13 p1685 A73-29363

Plasticity and fracture of structural metals in complex stress state at low temperatures.
13 p1639 A73-29462

Iron energy spectra due to acceleration at neutron star surface vs primary cosmic rays
14 p1787 A73-30618

High feed rate electrochemical machining Fe in aqueous NaCl, using high supply voltage, electrolyte pressures and flow velocities
16 p1971 A73-33533

[ASME PAPER 73-PROD-3]
Effect of iron and salt on prodigiosin synthesis in *Serratia marcescens*.
17 p2112 A73-34399

Friction induced surface activity of some simple organic chlorides and hydrocarbons with iron.
17 p2179 A73-34991

Iron core age end in terrestrial planets via Ramsey phase change onset producing metallic state core with growth via radioactive heating
17 p2236 A73-35745

Lines of Fe XVII and Fe XVIII during a solar flare.
19 p2476 A73-38170

X-ray spectrum of Cassiopeia A - Evidence for iron line emission.
20 p2603 A73-39446

Vapor-liquid-solid type growth in lunar glass covered breccia 15015, noting metallic iron stalks with bulbous tips of iron and sulfur mixture.
21 p2766 A73-40412

Microturbulence and the effect of departures from LTE on photospheric iron lines.
21 p2777 A73-41481

Impurity diffusion of iron in molybdenum.
23 p2994 A73-44157

Study of aluminum-oxygen equilibrium in liquid iron at 1600 deg C with the aid of a solid ThO₂-Y₂O₃ electrolyte cell
23 p2995 A73-44178

Kinetics of the development of structural changes in iron in the presence of adsorption fatigue
23 p2995 A73-44224

Neutral Fe line profiles for low-lying transitions measured from solar disk center to limb by double pass spectrometer, considering limb darkening effect
24 p3135 A73-44626

Proton collisional excitation in the ground configuration of Fe⁺/+12/.
24 p3123 A73-44634

Solar Fe 13 coronal lines relative intensity calculation as function of electron density from cross sections for collisional excitation by protons
24 p3136 A73-44635

Creep during the hot compression of titanium diboride powder
24 p3093 A73-44740

IRON ALLOYS

NT AUSTENITIC STAINLESS STEELS
NT CARBON STEELS
NT CHROMIUM STEELS
NT FERRITIC STAINLESS STEELS
NT HIGH STRENGTH STEELS
NT MARAGING STEELS
NT MARTENSITIC STAINLESS STEELS
NT NICKEL STEELS
NT STAINLESS STEELS
NT STEELS

Temperature dependence of magnetic susceptibility in nickel-film-coated iron-silicon alloy specimens
01 p0062 A73-10254

Low-temperature induced changes in the martensite crystalline structure of iron-aluminum-carbon alloys
01 p0064 A73-10607

Internal friction study of intercrystalline phosphorus adsorption during temper brittleness development in iron alloys

01 p0064 A73-10608

Properties and uses of UMoCo-50 and related Co-Cr-Fe alloys.

01 p0066 A73-11051

Metallographic investigation of electrodeposited iron-nickel-chromium alloys

02 p0174 A73-12535

Study of the effect of cobalt on redistribution of atoms of alloying elements in iron-base alloys by the nuclear gamma resonance method.

02 p0182 A73-12697

Structural studies of Laves intermetallic phase precipitation in Fe-Ta alloys by microscopic, X ray diffraction and electron probe techniques

02 p0182 A73-12754

Activity of carbon and solubility of carbides in the fcc Fe-Mo-C, Fe-Cr-C, and Fe-V-C alloys.

02 p0183 A73-12755

Mechanical properties of Fe, Al, Ti and heat resistant alloys consolidated powders, establishing coupling between fundamental concepts and engineering application

03 p0322 A73-13261

Hydrogen distribution between the phases in metals

03 p0324 A73-13507

Martensitic transformation kinetics and martensite morphology in the N25KhT2 alloy after aging

03 p0325 A73-13826

Secondary maximum grain size and even-grained texture in the region of low and moderate deformations during recrystallization of certain nickel- and iron-based alloys

03 p0326 A73-13967

A correlation between static adhesion data and the dynamic friction coefficients for two cobalt alloys and iron under vacuum conditions.

[ASLE PREPRINT 72LC-5B-2]

03 p0328 A73-14362

Microstructures and transformation kinetics of continuously cooled carbon free Fe-Mo-Ni alloys.

04 p0463 A73-15311

Effects of rare earth elements on the oxidation resistance of iron and nickel base alloys.

04 p0465 A73-15584

Oxygen and nonmetallic inclusions in chromium and aluminothermic ferrochrome

04 p0465 A73-15662

Influence of cobalt on the maraging of Fe-Ni-Mo alloys

06 p0705 A73-17876

X ray K absorption spectra shifts /Bégard additivity rule deviations/ in Fe-Cr, Fe-V, Fe-Ni and Fe-Co systems due to lattice characteristics and electron structure changes

06 p0707 A73-18039

Structure of the borated layer after diffusion saturation with other elements

06 p0707 A73-18040

Martensite transformation in an aged Fe-Ni-Ti alloy

06 p0708 A73-18052

Cr effect on N solubility increase during Fe alloy nitriding, noting temperature effect on nitrides precipitation

06 p0697 A73-18054

Structure and composition of certain Laves phases and identification of chi phases in Fe-Mn-Ti alloys

06 p0708 A73-18100

The distribution of chromium between ferrite and austenite and the thermodynamics of the alpha/gamma equilibrium in the Fe-Cr and Fe-Mn systems.

06 p0712 A73-18759

Grain size effects on iron substitutional alloys yield stress, investigating Hall-Petch relation

06 p0713 A73-18770

The application of magnetic after-effects in research on the real structure and migrational properties of metals and alloys

07 p0837 A73-19049

Successive diffusion in a ternary system of the iron-metal-carbon type

07 p0841 A73-20520

High strength and plastic properties of two phase austenitic-martensitic Fe alloys after aging in alpha and gamma states

07 p0841 A73-20522

Young modulus anomaly in precipitation-hardening subjected Invars

09 p1099 A73-21562

Dependence of martensite morphology on the isothermal transformation temperature of the Fe-24Ni-3Mn alloy

09 p1100 A73-21974

Austenitic alloys internal friction and strain aging under quenching, cold working and electron irradiation, considering carbon vacancies stress induced reorientation effects

09 p1101 A73-22407

Matthiessen's rule and the electric resistance of solid solutions of silicon in iron at high temperatures

09 p1104 A73-22602

Application of the Moessbauer effect to the study of the mechanism of iron diffusion in beta-titanium

09 p1108 A73-23240

Mechanical behavior of solid solutions of centered cubic symmetry obtained by limited addition of titanium to the iron

10 p1231 A73-23770

Development of a production technology for high-density metal-ceramic materials by the method of impregnating porous preforms with low-melting iron boride alloys

10 p1224 A73-24316

Correlation of coercive force to microstructure in cyclic martensite/austenite transformations in an Fe-Ni-Co alloy.

10 p1234 A73-24438

Stabilization of the austenitic phase of iron-nickel base alloys by cumulative thermal cycling

11 p1379 A73-25323

Determination of alpha plus gamma/gamma phase boundaries in Fe-Cr-Ni, Fe-Cr-Co, and Fe-Cr-Mn systems

11 p1384 A73-26108

'Invar' and 'Elinvar' - Alloys with controllable thermal expansion and elastic properties

11 p1385 A73-26564

Influence of deformation and heat treatment on the structural changes of the OKh12N13M alloy

12 p1508 A73-26836

New mechanism of slowing down screw dislocations in ordered alloys with a bcc lattice

12 p1508 A73-26837

Temperature dependence of the Moessbauer spectra of iron-cobalt-vanadium alloys

12 p1509 A73-26839

Relaxation stability of iron and nickel alloys at high temperatures

12 p1509 A73-26898

X-ray structural investigations of Dy-Fe-Al system alloys in the region of 0 to 33 at. % dysprosium

12 p1512 A73-27243

Solubility of vanadium and tungsten in alpha and gamma phases in the Fe-V and Fe-W binary systems

12 p1513 A73-27683

Equilibrium of vanadium carbide with an alpha or gamma solid solution in the iron-rich Fe-Cr-V-C system at temperatures from 700 to 1150 C and at a carbon concentration of 0.30%

12 p1513 A73-27684

Influence of the chrome content and the interstitial impurities content /carbon and nitrogen/ on the volumetric and intergranular diffusion of iron 59' in iron-chrome alloys with from 0 to 15 per cent chrome - Relations with alpha to alpha plus gamma reversible transformations

12 p1514 A73-27985

Hardening by tempering of Fe-Ni-Mo and Fe-Ni-Co-Mo martensites

12 p1514 A73-27987

Investigation of the ferroniobium oxidation process

13 p1630 A73-28010

Dendritic liquation of hypoeutectic binary, ternary and complex Fe- and Ni-base alloys dependence on phase diagram

13 p1631 A73-28102

Striated, cellular and dendritic substructure formation during growth of Fe-Ni alloy single crystals

13 p1631 A73-28107

Stereometric microanalysis of conglomerate, colony and dispersed structures of binary eutectic Fe, Al, Cu and low melting alloys

13 p1631 A73-28109

Al, Sr or Co effects on kinetics of grain boundary ferrite allotriomorph formation relative to iron alloys, noting displacement of TTT curve

13 p1632 A73-28129

Experimental and thermodynamic study of the equilibria between ferrite, austenite and intermediate phases in the Fe-Mo, Fe-W, and Fe-Mo-W systems.

13 p1633 A73-28136

Plastically deformed Fe-Si and Al alloys surface layer crystal dislocation density and plastic flow onset determination as function of depth

13 p1635 A73-28264

Thin ferrosilicon intermediate cylindrical layer tensile strength, microhardness and yield point determination at 20-1000 C

13 p1624 A73-29064

Strength and ductility of two-phase iron alloy composed of austenite and martensite.

13 p1638 A73-29453

The effect of neutron irradiation damage on the low temperature deformation characteristics of b.c.c. metals and their alloys.

13 p1638 A73-29454

Effects of deformation on diffusion in iron-nickel and iron-chrome systems

14 p1760 A73-30379

Precipitation of iron in rapidly solidified aluminum-iron alloys

14 p1760 A73-30439

Calculation of the binary phase diagrams of iron, chromium, nickel and cobalt.

14 p1760 A73-30440

Influence of recovery and recrystallization on the Young's modulus and its temperature dependence in Invar-type iron-nickel alloys

14 p1760 A73-30586

German monograph - Investigations concerning the hot working of heterogeneous iron-molybdenum alloys with differing precipitation distribution.

14 p1762 A73-30670

Some characteristics of the failure by fatigue of mild steel in vacuum

14 p1763 A73-30681

Martensitic transformation in iron-nickel alloys in a pulsed magnetic field

14 p1764 A73-30860

Temperature dependence of the single-crystal elastic constants of Co-rich Co-Fe alloys.

15 p1890 A73-31926

High temperature specific heats of iron-rich iron-titanium alloys between 600 and 1150 K.

15 p1891 A73-31994

Subscale inclusions formation in solid Fe alloys with small amounts of Mn and other elements, noting inward oxygen thermal diffusion role and metallurgical implications

15 p1891 A73-32171

Russian book - Precision alloys with specific thermal-expansion and elastic properties

15 p1893 A73-32293

Effect of chloride ions on the dissolution behavior of Fe-Ni alloys.

15 p1895 A73-32565

Highly permeable nickel-iron-molybdenum alloys containing 33 to 37% nickel

16 p2026 A73-33958

Temperature dependent crystallization and density of Fe-Mn-C alloys with niobium at 1200-1500 C from gamma ray measurements

16 p2027 A73-34012

Young modulus of elasticity measurement in alloys of Fe with Cr, W and Mo, examining concentration dependence at 20 to 500 C

17 p2187 A73-34334

Tracer diffusion of Ni-63 in Fe-17 wt pct Cr-12 wt pct Ni.

17 p2189 A73-34641

Effect of atom ordering on the martensite decomposition mechanism and kinetics in iron-aluminum-carbon alloys

18 p2324 A73-36769

Certain law controlling the temperature dependence of the microdeformation of Fe-Cu-Ti, W, and W-Re bcc alloys

18 p2324 A73-36803

Thin ferrosilicon intermediate cylindrical layer tensile strength, microhardness and yield point determination at 20-1000 C

18 p2320 A73-36896

High temperature cyclic oxidation resistance tests on Ni-, Co- and Fe-base alloys for aircraft gas turbine engines

19 p2440 A73-37496

Influence of coherency strains on precipitate shape in a Fe-Ni-Ta alloy.

20 p2577 A73-39223

Continuous decomposition of gamma solid solution in iron-nickel-titanium alloys

20 p2579 A73-39736

Effect of iron on the phase composition and mechanism of plastic deformation of titanium

20 p2579 A73-39737

Dislocation structure of Ni3Fe and Ni3FeCr alloys in various stages of strain hardening

20 p2579 A73-39742

Relaxation resistance of alloys based on iron and nickel at high temperatures.

21 p2720 A73-41031

Possible reinforcement of the tungsten-nickel-iron composite with tungsten fibers.

21 p2722 A73-41586

A rhodium-iron resistance thermometer for use below 20 K.

22 p2855 A73-42004

Gold-iron alloys for low temperature thermocouples.

22 p2857 A73-42030

Reference data for thermocouple materials below the ice point.

22 p2857 A73-42031

Investigation of the phase composition of alloys in the Ti-Al-Fe ternary system

22 p2873 A73-42086

Thermodynamic properties and Cr activity measurements in solid Cr-Ni-Fe alloys by solid oxide electrolyte technique

22 p2878 A73-42577

X ray and electron diffraction studies of Ni-containing etched brown rims in meteoritic taenite /Ni-Fe alloy/ associated with kamacite, noting Widmanstätten pattern

23 p2951 A73-43844

A thermodynamic calculation of the iron-chromium-vanadium equilibrium diagram.

23 p2993 A73-43918

The metallurgy of Remendur - Effects of processing variations. 23 p2993 A73-43987

Development of corrosion resistant filler metals for brazing molybdenum. 23 p2986 A73-44004

On the age-hardening of Fe-Pt-Mn ternary alloys. 23 p2994 A73-44139

Effects of additions of Al and Ti on electrical resistivities of oxide films of Fe-18 Cr sealing alloy. 23 p2986 A73-44152

Steady-state creep characteristics of an Fe alloy containing 3.5 at.% Mo. 23 p2994 A73-44153

Influence of Co, Ni, Mo, and W on the solubility of Fe16N2 in alpha-iron. 23 p2994 A73-44156

IRON COMPOUNDS

NT CHROMITES

NT FERRITES

NT HEMATITE

NT ILMENITE

NT IRON OXIDES

NT MAGNETITE

NT PYRITES

NT SIDERITES

NT TROILITE

The spectrum of FeH - Laboratory and solar identification. 03 p0374 A73-13718

The evolution of ferredoxins from primitive life to higher organisms. 03 p0265 A73-14318

Temperature-dependent hyperfine interactions in Fe2B. 06 p0734 A73-17833

Shock wave compression of iron-silicate garnet. 09 p1076 A73-22146

Apollo 15 breccia and soils with spheres and fragments of iron-rich green glass originating in Apennine Front materials 19 p2487 A73-38174

Study of the electronic structure of iron, cobalt, and nickel monosilicides by X-ray photoelectron spectroscopy and X-ray spectroscopy 20 p2578 A73-39734

Experimental design to produce visible-reflective IR ratio image from ERTS data for geological mapping of iron compounds 20 p2561 A73-39899

Charge transport bands in the electronic spectra of Fe/III/ complexes with certain oxygen-containing ligands 21 p2751 A73-40310

Formation of lunar carbide from lunar iron silicates. 21 p2780 A73-41643

IRON ISOTOPES

NT IRON 57

IRON METEORITES

NT SIKHOTE-ALIN METEORITE

Chemical fractionation in iron meteorites and its interpretation. 01 p0108 A73-11474

Iron and stony-iron meteorites kamacite hardness and shock histories, hypothesizing preterrestrial collisions between asteroid sized objects 05 p0615 A73-16377

Siberian iron meteorites and chondrites characteristics and histories during 1965-1971 06 p0753 A73-18247

Nuclear particle fluxes and radioactive isotopes production rate distribution from cosmic rays data along orbits, calculating iron meteorite dimensions prior to atmosphere entry 08 p1012 A73-21582

The Gosnells iron - A fragment of the Mount Dooling octahedrite. 09 p1139 A73-21855

Potentiostatic study of iron meteorite corrosion. 09 p1139 A73-21857

Morphologies of iron crystals from the Haverro meteorite. 09 p1140 A73-21862

Investigation of the Canyon Diablo metallic spheroids and their relationship to the breakup of the Canyon Diablo meteorite. 09 p1144 A73-22145

Stony-iron meteorite shock histories, determining crystallographic character of kamacite in samples via back reflection X ray diffraction technique 11 p1419 A73-25780

X ray and microanalysis of Luna 16 recovered Fe-Ni fragment structure and composition, showing alpha solid solution octahedrite 12 p1538 A73-26893

The isotopic composition of 'graphitic' carbon from iron meteorites and some remarks on the troilite sulfur from meteorites. 13 p1684 A73-29180

The chemical classification of iron meteorites, VII - A reinvestigation of irons with Ge concentrations between 25 and 80 ppm. 21 p2647 A73-40564

Distribution of Ni, Ga, Ge and Ir between metal and silicate portions of H-group chondrites. 21 p2771 A73-41009

X ray and microanalysis of Luna 16 recovered Fe-Ni fragment structure and composition, showing alpha solid solution octahedrite 21 p2771 A73-41026

Fireball spectral data reduction for self absorption, Fe abundance, excitation temperatures, relaxation time and optical thickness effects 22 p2915 A73-43043

The Canyon Diablo meteorite. 24 p3137 A73-44949

IRON ORES

NT HEMATITE

IRON OXIDES

NT CHROMITES

NT HEMATITE

NT ILMENITE

NT MAGNETITE

Electron microprobe investigations of the oxidation states of Fe and Ti in ilmenite in Apollo 11, Apollo 12, and Apollo 14 crystalline rocks. 07 p0880 A73-19696

Phase transformations in the bismuth ferrites BiFeO3 and Bi2Fe4O9 12 p1531 A73-27199

Terrestrial planetary core model concerning mantle-core iron oxide composition to avoid phase transition theory difficulties 15 p1867 A73-31100

Effects of copper chromite and iron oxide catalysts on AP/CTPB sandwiches. 22 p2899 A73-42812

Electron transitions in interstellar dust 4430 A line, indicating ferric oxide [alpha-hematite/ in type I super-nova 24 p3138 A73-44990

IRON 57

Mossbauer spectroscopy of lunar regolith returned by the automatic station Luna 16. 07 p0879 A73-19683

On the amount of ferric iron in plagioclases from lunar igneous rocks. 07 p0882 A73-19716

Properties of iron impurity in aluminium matrix studied by Mossbauer spectroscopy. 13 p1634 A73-28220

The vibrational frequency of Fe-57 atoms in Pt-Fe solid solution from measurements of the second-order Moessbauer Doppler shift. 13 p1634 A73-28258

IROQUOIS HELICOPTER

U UH-1 HELICOPTER

IRRADIANCE

NT ILLUMINANCE

NT SOLAR CONSTANT

Light scattering from an inhomogeneous fluid. 01 p0077 A73-10971

Design and performance of solar simulator with water cooled Xe lamp, calculating irradiance distribution by ray tracing method 01 p0030 A73-11149

Helical gas lenses for guiding optical beam over long distances, calculating irradiance patterns for various propagation mode numbers and temperatures 01 p0053 A73-11218

Atmospheric microthermal turbulence vertical distribution from balloon flights compared with stellar scintillation data, predicting irradiance spectra from turbulence and wind velocity measurement 03 p0305 A73-14656

Measurement of log-irradiance fluctuation of He-Ne laser in the atmosphere. 09 p1096 A73-22750

Focused laser irradiance fluctuations in a turbulent medium. 11 p1376 A73-25874

Total irradiance calibrations using electrically calibrated radiometer, discussing lamp detector alignment procedures 11 p1366 A73-26252

Measurements of the log-irradiance distribution of a laser wave propagated through the turbulent atmosphere. 19 p2405 A73-38222

Bezold-Bruecke effect and visual nonlinearity. 23 p2946 A73-43342

Absolute measurements and computed values for Martian irradiance between 10.5 and 12.5 microns. 24 p3127 A73-44394

IRRADIATION

NT AURORAL IRRADIATION

NT DEUTERON IRRADIATION

NT ELECTRON IRRADIATION

NT ION IRRADIATION

NT NEUTRON IRRADIATION

NT PROTON IRRADIATION

NT X RAY IRRADIATION

IRREVERSIBLE PROCESSES

Liapunov function relation to entropy production in irreversible processes, noting thermodynamic constraints on kinetic equation functions 02 p0191 A73-11613

Irreversible thermodynamics and losses in energy conversion, discussing N-port storage representation, flux rate, power flow and electro-caloric and state space relations 07 p0779 A73-20396

High temperature fatigue sensor based on conductive composite device irreversible resistance increase resulting from cumulative strain damage 09 p1083 A73-22504

Taking into account heat-transfer irreversibility in calculating the total change in entropy of individual substances 12 p1557 A73-26939

Turbulent flow energy transfer paths and irreversible dissipation as internal thermal energy analyzed by Reynolds convention for turbulent velocity 13 p1605 A73-29267

Quantum irreversible statistical thermodynamics with allowance for occurrence of many temperatures based on principle of isentropic motion, applying to laser action 14 p1756 A73-30150

Nonlinear thermodynamics of irreversible processes for polymer microfracture process under mechanical, thermal, diffusion and chemical actions 14 p1766 A73-30479

Irreversible thermodynamics with internal inertia - Principle of stationary total dissipation. 14 p1817 A73-30484

Numerical study on the effects controlling the low-level jet. 18 p2335 A73-37100

Nonequilibrium statistical operators and quasimeans in the theory of irreversible processes 21 p2741 A73-41298

Irreversible heat transfer in the total entropy change for a pure substance. 22 p2930 A73-42273

Transfer phenomena in nonreactive binary fluid mixtures analyzed by nonlinear continuum thermodynamics of irreversible processes 24 p3156 A73-45081

IRRITATION

NT TOXICITY AND SAFETY HAZARD

IRROTATIONAL FLOW

U POTENTIAL FLOW

ISCHEMIA

Q waves and coronary arteriography in cardiomyopathy. 01 p0010 A73-11507

Relationship of anginal symptoms to lung mechanics during myocardial ischemia. 02 p0136 A73-12820

Exercise electrocardiography and vasoregulatory abnormalities. 03 p0260 A73-13541

P wave of electrocardiogram in early ischaemic heart disease. 03 p0268 A73-13892

An epidemiological survey of risk factors for ischemic heart disease in 42,804 men. I - Serum cholesterol value. 04 p0409 A73-15521

Uses and limitations of stress testing in the evaluation of ischemic heart disease. 05 p0552 A73-17278

Correlation of electrocardiographic studies and arteriographic findings with angina pectoris. 05 p0546 A73-17279

Adaptation to high altitude hypoxia as a factor preventing development of myocardial ischemic necrosis. 07 p0780 A73-19151

Intermittent trifascicular block - Different mechanisms of conduction disturbances in the bundle branches. 07 p0780 A73-19152

Assessment of hypoxia in the human heart. 07 p0781 A73-19928

The use of glycolytic metabolism in the assessment of hypoxia in human hearts. 07 p0781 A73-19929

Coronary atherosclerosis and ischemic myocardial damage. 18 p2275 A73-36538

Cell viability in acute myocardial infarction, discussing pathogenesis, histological, histochemical and biochemical responses to ischemia, homeostasis maintenance and treatment methods 18 p2276 A73-36545

Responsibility for ischemic cardiopathies in civil aviation flight personnel 18 p2284 A73-36902

Preventive value of early diagnosis of coronary heart disease, noting importance of screening populations for genetic and environmental risk factors 22 p2808 A73-42828

Ischemic heart disease prediction via exercise ECG tests, discussing work load standardization 22 p2809 A73-42835

Ischemic polarcardiographic changes induced by exercise - A new criterion. 24 p3060 A73-44946

ISENTROPIC PROCESSES

Shock wave and isentropic compression/expansion in plasma with anomalous thermodynamic properties due to strong particle interactions, discussing phase transitions types

03 p0346 A73-13190

Equilibrium equation for weightless flexible two dimensional sail in inviscid supersonic airstream, noting centred isentropic compression

03 p0246 A73-13789

Small disturbance theory of rotating subsonic and transonic cascades.

03 p0246 A73-14136

Isentropic compression of fused quartz and liquid hydrogen to several Mbar.

11 p1398 A73-25884

Isentropic/isopycnic mountain waves tracing from superpressure balloon flights synchronous radar, temperature and pressure data

12 p1520 A73-26809

Method for calculating the steady irrotational isentropic flow in a two-dimensional supercritical turbine cascade.

17 p2093 A73-34390

Calculation of plane blade cascades in isentropic flow

18 p2266 A73-37085

Transformation of shock compression into isentropic compression in a nonhomogeneous body.

24 p3117 A73-45429

ISING MODEL

U FERROMAGNETISM

U MATHEMATICAL MODELS

ISIS SATELLITES

NT ALOUETTE 2 SATELLITE

Mathematical model for ISIS satellite attitude and spin rate computerized predictions during electromagnetic torque control operation

21 p2781 A73-40615

ISLANDS

NT GREAT BRITAIN

NT GREENLAND

NT PUERTO RICO

NT WALLOPS ISLAND

Cloud eddy formation in wakes of single mountain islands similar to Karman vortex streets, noting application to wind field forecasting

18 p2334 A73-37075

Machinery to be developed for an offshore airport constructed by reclamation.

19 p2418 A73-37746

ISOBARS [PRESSURE]

Diurnal variability of temperature and of isobaric surface heights in the troposphere and lower stratosphere

05 p0593 A73-16241

Radiosonde soundings for typhoons and hurricanes isobaric surfaces heights, temperatures and humidities, calculating correlation coefficients between sea level pressure and other parameters

10 p1245 A73-23985

Some observations of the influence of geostrophic shear on the cross-isobar angle of the surface wind.

11 p1393 A73-25695

Vorticity equation advection, divergence and curl terms effects on vorticity changes over isobaric surfaces and on weather and cyclonic development in synoptic meteorology

13 p1653 A73-28745

Study of the effect of heat influxes on the formation of lower and higher baric fields in the Northern Hemisphere

15 p1903 A73-31602

Selection of analogs to composite kinematic charts of natural synoptic periods

19 p2449 A73-38545

Use of meteorological rocketsonde and satellite radiation data for constant-pressure analyses at levels between 5 and 0.4 mb.

21 p2732 A73-41336

ISOBUTANE

U BUTANES

ISOCORIC PROCESSES

The specific isochoric heat capacity of pure fluids on the dew curve and the boiling curve

03 p0400 A73-14633

ISOCROMATICS

Isochromatic curves modeling for stress-strain state of doubly connected regions by optical polarization and photoelastic analysis, using isopach field method

05 p0578 A73-17092

Isochromatic and isoclinic parameters for fiber reinforced birefringent composite materials, discussing mechanical and optical characterization

19 p2495 A73-37195

Dichromatic convergence points obtained by subtractive colour matching.

19 p2398 A73-37420

Measurement accuracy achievable in photographed isochromatic pictures

21 p2706 A73-41605

Holographic photo-elasticity - Independent observation of the isochromatic and isopachic fringes for a single model subjected to only one process.

24 p3091 A73-45335

ISOCYANATES

Photo-decarbonylation of beta-styryl isocyanates.

12 p1466 A73-27225

Methylacetylene and isocyanic acid data from April 1972 and February 1973 observation of interstellar media in direction of Galactic center source Sgr B2

16 p2060 A73-33095

ISOLATION

NT SOCIAL ISOLATION

A new approach to the isolation of milligram amounts of significant geochemical compounds.

11 p1325 A73-25463

Sensory versus perceptual isolation - A comparison of their electrophysiological effects.

14 p1722 A73-30517

ISOLATORS

NT VIBRATION ISOLATORS

Digital control of a pneumatic isolation system for inertial instrument testing.

20 p2543 A73-38775

ISOMERIZATION

NT ORTHO PARA CONVERSION

An investigation of the possible differential radiolysis of amino acid optical isomers by C-14 betas.

06 p0660 A73-17935

Photochemical reactions in condensed phase relevant to biology, discussing molecular energy states, isomerization reactions and bond making/breaking processes

09 p1121 A73-23305

Geochemistry of amino acid enantiomers - Gas chromatography of their diastereomeric derivatives.

11 p1326 A73-25469

Photoisomerization of 2-isocyano- and 2,x'-diisocyanobiphenyls in cyclohexane.

12 p1466 A73-27600

Photo-induced isomerization of aryl isocyanides into cyanides.

13 p1580 A73-28200

ISOMERS

Glyoxal cis form as source of microwave spectra from rotational spectrum investigations of B-type transitions

03 p0273 A73-13286

Stereo-enriched poly-alpha-amino acids - Synthesis under postulated prebiotic conditions.

06 p0661 A73-17940

Syntheses and conformational studies of polyacidic amino acids containing optical active side chains.

06 p0661 A73-17942

Resolution by gas-liquid chromatography of diastereomers of five nonprotein amino acids known to occur in the Murchison meteorite.

06 p0662 A73-18468

Synthesis and characterization of isomeric cis- and trans-pyrone model compounds.

21 p2648 A73-41215

Stimulated gamma emission in long-lived nuclear isomers, proposing gamma lasers based on Mossbauer line broadening effect

23 p2988 A73-44093

ISOMORPHISM

Structural comparison of articulated plane kinematic chains [PKC] with the aid of graph theory

04 p0476 A73-15656

The mechanical properties of titanium alloys with isomorphous beta-stabilizing elements.

06 p0708 A73-18206

Theorems concerning isomorphisms for elliptic boundary value problems with nonnormal boundary conditions

18 p2329 A73-36164

Effect of the information panel structure on operator activity

22 p2812 A73-41889

ISOPERIMETRIC PROBLEM

Optimum configurations for bangless sonic booms.

01 p0031 A73-10302

Optimal lift control by Miele's method for the atmospheric entry of a hypersonic glider. II - Isoperimetric type problems.

04 p0404 A73-15168

ISOPHOTES

Properties of the Red Spot of Jupiter in 1971.

03 p0371 A73-13216

Analysis of some aspects of 25 chromospheric events. I - Reduction of the optical data. II - Discussion on the optical data.

03 p0364 A73-14414

Isophotes comparison of quiescent and quiescent solar prominences in D3 and H alpha lines, noting structural similarity from narrow band filter observation

12 p1545 A73-27836

Airglow green cells diameter, speed and brightness measurements from isophote patterns in diagrams of UT versus distance

16 p2008 A73-33881

On the motion of the tropical red arc north boundary.

16 p2008 A73-33882

The occultation of the star SAO 93826 by Saturn's ring

20 p2606 A73-39076

The problem of the apparent-flattening characteristic of spiral galaxies

23 p3035 A73-44234

ISOPLETHS

U NOMOGRAPHS

ISOPYCNIC PROCESSES

Isentropic/isopycnic mountain waves tracing from superpressure balloon flights synchronous radar, temperature and pressure data

12 p1520 A73-26809

Purification of *Synechococcus lividus* by equilibrium centrifugation and its synchronization by differential centrifugation.

18 p2274 A73-36503

ISOSTASY

Isostatic reduction potential of earth mass distribution for spherical harmonic solutions of satellite determined gravity anomalies

04 p0437 A73-14788

Isostasy and relief of the Earth, the Moon and Mars

07 p0878 A73-19661

ISOSTATIC PRESSURE

Hot isostatic pressing of high-performance materials.

01 p0056 A73-10280

Effect of high isostatic pressures on the compressibility and sinterability of tungsten powders.

01 p0065 A73-10819

Hot isostatic pressing of titanium alloys for turbine engine components.

16 p2019 A73-33516

ISOSTERIC PROCESSES

U ISOPYCNIC PROCESSES

ISOTHERMAL FLOW

Theory of turbulent heating of an isothermal plasma with a transverse current.

01 p0083 A73-10456

Self-similar flows with increasing energy. II - Isothermal flow.

02 p0238 A73-12091

Quasi isothermal, transonic flow of radiating gases

08 p1024 A73-21497

Self-similar cylindrical magnetogasdynamic and ionizing shock waves.

10 p1204 A73-23564

Velocity and concentration profiles of isothermal laminar boundary layer flow of incompressible multicomponent gas under strong blowing

11 p1347 A73-25728

Stationary isothermal gas flow subject to self gravitation, finding subsonic regime oscillatory solutions for plane parallel, spherical and rotational symmetric cases

16 p2058 A73-32832

ISOTHERMAL LAYERS

Isothermal vertical plate turbulent thermal boundary layer during free convection, noting temperature pulsations dispersion

03 p0396 A73-13184

Stability conditions for strongly flattened galaxy model with respect to axisymmetric disturbances of gaseous subsystem in finite isothermal layer

05 p0616 A73-16456

Laminar film boiling on inclined isothermal flat plates.

05 p0641 A73-17107

On calculating the radiation from two plane isothermal layers of carbon dioxide and/or water vapor.

08 p1021 A73-20859

The emissivity of a system consisting of a semitransparent isothermal coating and a flat opaque substrate

10 p1294 A73-23514

Instability of free shear layers adjacent to a vibrating flame surface.

10 p1296 A73-24804

Internal atmospheric gravity wave effect on ionospheric columnar electron content on basis of viscous atmosphere model with isothermal layers

11 p1359 A73-26709

Radiating power of a system consisting of a semitransparent isothermal coating and a flat non-transparent substrate.

17 p2212 A73-35194

Polarization of rare gas atoms in the successive layers adsorbed on graphite

21 p2724 A73-41599

Self-similar flows with increasing energy. III - Radiation-driven shock wave.

21 p2793 A73-41673

Precision measurements of temperature differences with thermistors by a simple technique.

22 p2855 A73-42014

Effect of line or band shape on the radiative flux of an isothermal spherical layer.

22 p2938 A73-42990

ISOTHERMAL PROCESSES

Potential titanium airframe applications.

01 p0063 A73-10285

Axial and transverse wave motions of inviscid perfect gas in isothermal solid-body rotation in cylinder

04 p0434 A73-15163

Study of transformations of TA6V6E2 titanium alloy with 6.4 per cent zirconium, in isothermal conditions after putting in solution in the beta domain
04 p0466 A73-15691

Free convective heat transfer between vertical parallel plates One plate isothermally heated and the other thermally insulated.
05 p0638 A73-16221

An estimate of radiative emission from an isothermal xenon plasma at temperatures up to 50,000 K.
05 p0602 A73-16561

Passivation of chrome steels under isothermal oxidation at 1020 deg C
07 p0839 A73-19660

The complete isothermalization by collective electromagnetic interactions of strongly anisotropic magnetized collisionless plasmas.
07 p0859 A73-20235

Nonisothermal instability of flows of viscoelastic media
09 p1072 A73-22481

Influence of heat treatment on the mechanical properties of the VT3-1 titanium alloy
09 p1107 A73-23191

Criteria for oscillations in closed isothermal reacting systems.
10 p1294 A73-23561

Isothermal wall conical cavity radiant energy streaming, determining annular baffle effects by Monte Carlo method
10 p1295 A73-23835

Isothermal ionization of the lower ionosphere under the effect of radio waves.
13 p1608 A73-28709

Nonisothermal creep of chrome-nickel steel
15 p1890 A73-31830

Study of a niobium-aluminum-silicon system. I - Partial isothermal sections at 1500 and 1300 deg C, and the behavior of the Nb/Si, Al/2 phase
15 p1890 A73-31991

Study of the isothermal transformations of the titanium alloy beta sub III
15 p1892 A73-32212

The precipitation behavior of a commercial aluminum-copper-lithium alloy. I - The microstructure after isothermal heat treatment
16 p2026 A73-33954

Behavior of hafnium dioxide particles in dispersively hardened nickel during isothermal annealing
17 p2188 A73-34560

Emittance of an isothermal, isotropically scattering medium.
18 p2336 A73-36324

On the mass transfer produced by oscillations in a compressible, dissipative, and inhomogeneous medium
19 p2503 A73-37528

Transformations of TA6V6E2Zr alloy in isothermal conditions
19 p2441 A73-37832

ISOTHERMS
Visualization of thermal fields in saturated porous media by the Christiansen effect.
08 p0963 A73-21030

Isothermal mapping of temperature patterns from thermal discharges in Italian coastal waters.
20 p2560 A73-39888

ISOTOPE EFFECT
Possibility of using a laser flame as a source of light in the isotope spectral method
02 p0176 A73-12094

Solar Rb isotopic ratio from Rb I resonance lines at 7800 and 7947 A in photospheric spectrum
05 p0620 A73-17026

Biogenic elemental distribution and isotopic abundance in lunar samples, discussing heavy isotopes enrichment by solar wind irradiation, meteorite impacts and hydrogen stripping
06 p0654 A73-18417

O-18/O-16, Si-30/Si-28, C-13/C-12, and D/H studies of Apollo 14 and 15 samples.
07 p0887 A73-19771

Sulphur concentrations and isotope ratios in lunar samples.
07 p0887 A73-19775

U-Th-Pb and Rb-Sr measurements on some Apollo 14 lunar samples.
07 p0888 A73-19779

Cosmic ray exposure ages from Apollo 14 lunar rocks isotopic anomalies due to neutron capture effect in Gd, Br and Ba
07 p0871 A73-19803

Classification and source of lunar soils; clastic rocks; and individual mineral, rock, and glass fragments from Apollo 12 and 14 samples as determined by the concentration gradients of the helium, neon, and argon isotopes.
07 p0889 A73-19804

Extinct lunar radio activities - Xenon from Pu-244 and I-129 in Apollo 14 breccias.
08 p0936 A73-20843

Solar nebula Lu 176-Hf 176 pair and Zr abundance determinations, using chondrite fraction and s-process model
08 p1006 A73-20937

Isotopic combination identification in interstellar clouds through radio spectral line observations, discussing millimeter wave astronomy, molecular clouds, excitation mechanisms, galactic structure, etc
10 p1280 A73-24323

Radioactivities and He, Ne and Ar stable isotopes measured in meteorites for cosmic ray exposure ages
17 p2233 A73-35267

Effect of high pressure on the superconducting transition temperature of Pd-H.
21 p2753 A73-41126

Stripping cross sections for production of forward scattered molecular ions in hydrogen and deuterium molecular collisions at kinetic energies below 500 eV, noting isotope effect
23 p3007 A73-44119

Investigation of anomalously fast stars of early spectral class. III - Search for the He-3 isotope
23 p3036 A73-44244

ISOTOPE SEPARATION
Classification and source of lunar soils; clastic rocks; and individual mineral, rock, and glass fragments from Apollo 12 and 14 samples as determined by the concentration gradients of the helium, neon, and argon isotopes.
07 p0889 A73-19804

Luna 20 lunar soil elemental and oxygen isotopic composition compared to Apollo 11, 12, 14 and 15 abundances
13 p1675 A73-28310

Isotope separation factor of carbon dioxide-water system and isotopic composition of atmospheric oxygen.
15 p1873 A73-32252

Experiment and observation of isotope and element separation in a plasma with cosmical applications.
17 p2216 A73-34420

Whole rock Tb-Pb age for the Masuke and Dembe-Divula complexes, Rhodesia.
17 p2159 A73-34519

Ultrafiltration by a compacted clay membrane. I - Oxygen and hydrogen isotopic fractionation. II - Sodium ion exclusion at various ionic strengths.
23 p2973 A73-43845

ISOTOPE SHIFT
U ISOTOPE EFFECT
ISOTOPES
NT ALUMINIUM 26
NT ARGON ISOTOPES
NT CARBON ISOTOPES
NT CARBON 12
NT CARBON 13
NT CARBON 14
NT CESIUM VAPOR
NT COBALT ISOTOPES
NT COBALT 60
NT CURIUM ISOTOPES
NT CURIUM 244
NT DEUTERIUM
NT EUROPIUM ISOTOPES
NT GADOLINIUM ISOTOPES
NT HELIUM ISOTOPES
NT HYDROGEN ISOTOPES
NT IODINE ISOTOPES
NT IRON 57
NT KRYPTON ISOTOPES
NT LEAD ISOTOPES
NT LITHIUM ISOTOPES
NT MANGANESE ISOTOPES
NT MERCURY ISOTOPES
NT METALLIC HYDROGEN
NT NEON ISOTOPES
NT NEPTUNIUM ISOTOPES
NT NITROGEN ISOTOPES
NT OXYGEN ISOTOPES
NT OXYGEN 18
NT PLUTONIUM ISOTOPES
NT PLUTONIUM 238
NT POLONIUM 210
NT POTASSIUM ISOTOPES
NT RADIOACTIVE ISOTOPES
NT RADON ISOTOPES
NT RUBIDIUM ISOTOPES
NT SAMARIUM ISOTOPES
NT SILICON ISOTOPES
NT SODIUM ISOTOPES
NT SODIUM 22
NT SODIUM 24
NT STRONTIUM ISOTOPES
NT STRONTIUM 90
NT TELLURIUM
NT TELLURIUM ISOTOPES
NT THALLIUM ISOTOPES
NT THORIUM ISOTOPES
NT TRITIUM
NT URANIUM ISOTOPES
NT URANIUM 238
NT VANADIUM ISOTOPES
NT XENON ISOTOPES
NT XENON 129

Measurements of the isotopic composition of particle fluxes carried out on spacecrafts Soyuz, Zond 8 and Luna 16.
02 p0206 A73-12317

He 4, C 12, O 16, Ne 20, Mg 24, Si 28 and Fe 56 abundance computed as function of time for neutron star atmospheres with strong magnetic fields
02 p0223 A73-12728

Analysis of the isotopic composition of low-energy cosmic ray particles in plastic detectors, taking into account the elements boron, carbon, nitrogen, and oxygen
05 p0611 A73-17275

Isotope Brayton space power systems and their technology.
07 p0850 A73-20467

Russian book - Geochemistry and cosmochemistry of inert gas isotopes.
15 p1840 A73-31585

Study on the charge and isotope composition of medium cosmic ray particles.
16 p2054 A73-33278

Galactic sources and the propagation of cosmic rays - A review of the light isotopes and the odd-Z elements.
16 p2055 A73-33295

Noble gas isotopes abundances for solar wind and outer convective zone of sun, emphasizing isotopic abundance of deuterium
17 p2228 A73-34416

Isotopic composition measurements of cosmic-ray nuclei with Z greater than or equal to 10 made using a new technique.
19 p2475 A73-37628

ISOTOPIC LABELING
Atomic and molecular interactions investigation by computer aided mass spectrometry, considering applications in bio-organic chemistry, isotope analysis, geochemistry and cosmochemistry
02 p0139 A73-12425

The study of biological macromolecules using perturbed angular correlations of gamma radiation.
02 p0136 A73-12648

An implantable radiotelemetric measuring device for simultaneous long term measurements of body temperature and turnover of rabbit serum albumin/I-125 in unrestrained rabbits.
03 p0271 A73-14301

Carbon-13 nuclear magnetic resonance in biosynthetic studies of lipids.
03 p0274 A73-14550

Quantitative radionuclide angiocardiology for determination of chamber to chamber cardiac transit times.
04 p0409 A73-14767

Oxidation effects on rate of C 14-labeled leucine incorporation into rat skeletal muscle protein
05 p0538 A73-16152

An investigation of the possible differential radiolysis of amino acid optical isomers by C-14 betas.
06 p0660 A73-17935

Effect of accelerations on the thiamine-S/35/ distribution in the organism of white mice
08 p0929 A73-20977

Role of nerve structures in the action of low-frequency sinusoidally modulated currents on synovial membrane permeability in the knee joint
10 p1180 A73-23943

Lunar Rb-Sr age correction according to stable isotope tracer /spike/ recalibration, using stoichiometric salts
10 p1278 A73-24112

Investigation of the exchange between the blood and the intraocular fluid with the aid of radioactive phosphorus
10 p1185 A73-24520

Binding of Melatonin to human and rat plasma proteins.
10 p1182 A73-24657

Xenon 133 measurement of cerebral volumetric circulation rates during papaverin and intensin vasodilation of canine and feline intracranial vessels, showing vessel resistance reduction
13 p1576 A73-29074

Tracer diffusion of Ni-63 in Fe-17 wt pct Cr-12 wt pct Ni.
17 p2189 A73-34641

Protein synthesis in lung - Recovery from exposure to hyperoxia.
18 p2277 A73-36653

Measurement of cardiac output with and organ trapping of radioactive microspheres.
18 p2282 A73-36661

Sodium Na-24 and potassium K-42 availability for sweat production after intravenous injection and their handling by sweat glands.
19 p2395 A73-37757

Video instrumentation for radionuclide angiocardiology.
19 p2399 A73-37796

Biosynthesis of RNA in the brain cortex during various functional states
21 p2640 A73-41262

Measurement of coronary blood flow by radiocardiography - Study of 116 cases.
22 p2809 A73-42838

ISOTROPIC MEDIA

- Interaction of opposed beams of electromagnetic waves in a transparent nonlinear medium
01 p0016 A73-10208
- On the integration of Einstein's equation for energy density inside a perfect fluid sphere.
01 p0076 A73-10250
- Mathematical model for the buildup of imperfections in plastic isotropic materials
01 p0114 A73-10476
- Rectangular plates with unidirectional variable rigidity
01 p0114 A73-10572
- Approximate reduction of the equations of elasticity theory and electrodynamics for inhomogeneous media to Helmholtz equations
01 p0077 A73-10959
- Doubly-periodic problem in elasticity theory for an isotropic medium weakened by congruent groups of arbitrary holes
01 p0116 A73-10961
- Elastic waves originating at the surface of a spherical opening in nonhomogeneous isotropic media.
01 p0116 A73-11065
- Stressed state of an isotropic half-plane with a finite number of circular holes situated along the boundary
02 p0230 A73-11782
- Three dimensional linear theory of thermoelasticity covering homogeneous and isotropic bodies, work, free energy, boundary value problems and variational principles
02 p0233 A73-11978
- On two coplanar cracks in an infinite transversely isotropic medium.
02 p0234 A73-12087
- Finite axisymmetric deformations of elastic membranes.
02 p0234 A73-12089
- Curvilinear holes biperiodic array in isotropic plane, determining hole shape for constant shear stress around contours
02 p0235 A73-12193
- Uniqueness theorem for linear thermoelasticity theory allowing for second sound, discussing acceleration waves propagation in isotropic material
02 p0237 A73-12796
- Experimental determination of shear moduli in a compact bone tissue
03 p0267 A73-13742
- Static boundary value problem of asymmetric elasticity for elastic isotropic media with small energy contribution to potential due to moment effects
03 p0394 A73-14050
- Radially symmetrical thermoelastic disturbances in generalized dynamical theory of thermoelasticity.
03 p0395 A73-14311
- Empirical strength criteria for anisotropic and isotropic composite materials with unequal tensile and compressive strength
04 p0508 A73-14860
- Stability of a transversely isotropic solid under large elastic deformation.
04 p0511 A73-15171
- Inflation-extension and eversion of a tube of incompressible isotropic elastic material.
04 p0512 A73-15234
- Propagation of electromagnetic waves in media which vary slowly with position and time.
04 p0423 A73-15483
- Thermoelastic wave propagation in a transversely isotropic circular cylinder
04 p0512 A73-15501
- Application of the method of least squares to the determination of optical constants of uniaxial isotropic and anisotropic substances, and of the rate of polarization of monochromators in the far UV
05 p0597 A73-16148
- Minimum principles in the dynamics of isotropic rigid-plastic and rigid-viscoplastic continuous media.
06 p0757 A73-17396
- Small vibrations of isotropic elastic medium under finite strain and with time proportional elongations in three mutually perpendicular directions
06 p0759 A73-17759
- Note on the wave propagation problems in isotropic discretized bodies.
06 p0723 A73-17893
- Crack problem of transversely isotropic strip.
06 p0762 A73-17986
- Wave propagation in a micro-isotropic, micro-elastic solid.
06 p0762 A73-17990
- Tensor-linear approach to the stability problem of nonlinearly elastic isotropic plates
06 p0765 A73-18690
- Possibility of using harmonic functions in the solution of problems in elasticity theory for inhomogeneous media
06 p0766 A73-18885
- Approximate method of studying the symmetrical deformation of orthotropic bodies
07 p0911 A73-19311
- Thermoelastic problem for plate with an elliptic insert in the case of nonideal thermal contact
07 p0911 A73-19316
- Complex wave existence in some two-layer isotropic structures
07 p0793 A73-19921
- Nonstationary radiation diffusion in a semiinfinite isotropically scattering medium
08 p0985 A73-21453
- Stress-strain state of transversely isotropic shells under concentrated loads
08 p1019 A73-21760
- Measurement of the current distribution at the surface of a doublet immersed in an isotropic hot plasma
09 p1131 A73-23034
- Isotropic homogeneous elastic medium internal crack analysis based on Laurent series expansions of complex potentials consistent with displacements and stress-strain single valuedness
09 p1162 A73-23179
- Universe isotropic state evolution from initial chaotic conditions, considering attractive and repulsive cosmological constants
10 p1271 A73-23526
- Nonstationary equations of the nonlinear theory of elasticity in Euler coordinates
10 p1287 A73-23590
- Yield criteria derivation for laminated media with isotropic and anisotropic layers based on strength constants characterization as tensors
10 p1289 A73-24277
- Combined axial and torsional shear of a tube of incompressible isotropic elastic material.
10 p1291 A73-24336
- Method of variable directions for solving the equations of an isotropic cylindrical shell
10 p1292 A73-24501
- Three-dimensional problem of the vibrations of a circular plate with initial stresses
10 p1292 A73-24506
- Two dimensional statics for isotropic elastic body with inhomogeneous mechanical properties, discussing two-step solutions for differential equilibrium equation and boundary value problem
10 p1293 A73-24676
- Solution of fundamental three-dimensional problems in the theory of elasticity for arbitrarily shaped bodies by way of a numerical realization of the method of integral equations
11 p1441 A73-25627
- Tangential electric field near base driven cylindrical antenna surrounded by free space or by homogeneous isotropic dissipative medium from charge distribution measurement
11 p1329 A73-25665
- Sommerfeld type radiation conditions for asymmetric theory of linear homogeneous and isotropic micropolar elasticity, applying to regular solution to infinite domain field equations
11 p1444 A73-26279
- Universal solutions for fiber-reinforced incompressible isotropic elastic materials.
11 p1447 A73-26656
- The thermal expansion of composites based on polymers.
12 p1515 A73-27030
- Photon conductivity analysis for homogeneous isotropic solid body based on convective-radiant transfer equations, determining molten quartz thermal conductivity and diffusivity
12 p1516 A73-27311
- Ideal plasticity theory for solid bodies of isotropic materials with different yield points in extension and compression
12 p1553 A73-27374
- Approximate reduction of the equations of the theory of elasticity and electrodynamics for inhomogeneous media to the Helmholtz equations.
12 p1524 A73-27535
- Doubly-periodic problem of the theory of elasticity for an isotropic medium weakened by congruent groups of arbitrary holes.
12 p1554 A73-27537
- Response functions for mathematical double membrane model of isotropic elastic shell in form of orientable two dimensional differentiable manifold
13 p1694 A73-28284
- Determining elasticity constants of disc-shaped specimens of material.
13 p1613 A73-28521
- Equilibrium of an anisotropic plane reinforced by an isotropic circular ring
13 p1698 A73-29131
- Receiving characteristics of antennas in an isotropic compressible plasma.
13 p1594 A73-29230
- Creep analysis of transversely isotropic bodies subjected to time-dependent loading.
14 p1805 A73-29769
- A mathematical model of damage accumulation in plastic isotropic materials.
14 p1810 A73-30301
- Some basic solutions in strain gradient elasticity theory of an arbitrary order.
14 p1812 A73-30546
- Thin flexible inextensible fiber reinforced compressible isotropic elastic materials under large elastic deformations, obtaining solutions to equilibrium and constitutive equations
15 p1946 A73-31101
- Infinite elastically isotropic solid under external tensile stress, deriving condition for complete fracture from wedge crack
15 p1951 A73-32023
- Finite deflections of transversely-isotropic plates and shallow shells
15 p1953 A73-32089
- An invariant treatment of interfacial discontinuities in elastic composites.
15 p1954 A73-32121
- Antiplane elasticity boundary value problem solution for isotropic bars under tangential loads, considering twisting and bending
15 p1955 A73-32127
- On the possibility of using harmonic functions for solving problems of the theory of elasticity of non-homogeneous media.
15 p1956 A73-32410
- Some considerations regarding the dynamics problem for an elastic space and the use of its solution
15 p1956 A73-32545
- Resolvent equations, in complex form, of the theory of transversely isotropic shells of revolution
16 p2074 A73-32686
- Rectangular cross section isotropic elastoplastic material behavior under combined compressive and bending stresses with allowance for work hardening
16 p2076 A73-32931
- A stress-strain relation for homogeneous and isotropic continua
16 p2035 A73-32934
- Plane stress fields in isotropic disks due to singular and distributed loads, obtaining Fredholm integral equation solution via cubic spline function
16 p2079 A73-33238
- Propagation of thermoelastic waves in an undefined isotropic soil
16 p2081 A73-33369
- Propagation of frequency-modulated pulses in a randomly stratified plasma.
17 p2214 A73-34095
- Correlation functions of the elastic field of quasi-isotropic composite materials under nonisotropic deformation
17 p2240 A73-34146
- Elastic isotropic infinite body with interior tunneling crack under dynamic shear force perpendicular to crack propagation direction, obtaining solution via Mathieu functions
17 p2241 A73-34329
- Modes and frequencies of transversely isotropic slightly curved Timoshenko beams.
17 p2248 A73-35043
- [ASME PAPER 73-APM-27]
- Russian book on elastic equilibrium boundary value problems for isotropic and anisotropic bodies under load or temperature field induced plane deformation
18 p2361 A73-35874
- Emissance of an isothermal, isotropically scattering medium.
18 p2336 A73-36324
- A contact problem for a transversely isotropic cylindrical shell of finite length
18 p2363 A73-36404
- Homogeneous isotropic body thermoelasticity boundary value problems solved by quadrature series using Green function of Laplace equation, determining circular cylinder stress concentration
18 p2366 A73-36753
- Calculation of the radiation field in a semiinfinite medium in the presence of isotropic scattering
19 p2460 A73-37850
- Numerical solutions of basic three-dimensional elasticity theory problems for bodies of arbitrary shape.
19 p2500 A73-38149
- Equations of motion for ideal isotropic viscoplastic medium in axisymmetric space, determining conditions for flow core existence
20 p2619 A73-39336
- Some three-dimensional boundary value problems for an elastic medium bounded by cylindrical surfaces
20 p2620 A73-39508
- Stability criteria for incompressible elastic isotropic materials subject to shearing displacement superimposed on homogeneous elastic deformation, discussing Cauchy stress and shear modulus
20 p2620 A73-39530
- Isotropic elastic material fracture and yield criteria in terms of frame-indifferent relation between stress and strain increments
20 p2623 A73-39563
- Reflection of a laser beam from an interface between isotropic dielectrics
21 p2714 A73-40569
- Wave amplitude calculation for propagation in inhomogeneous isotropic media by optical ray tracing consisting of integration of first and second order differential equations
22 p2885 A73-41817
- Wave potentials for an elastic transversely isotropic medium
22 p2921 A73-42285

- Possible emission of transverse electromagnetic waves in an isotropic plasma 22 p2893 A73-42390
- Shielding of moving test particles in warm, isotropic plasma. 22 p2893 A73-42392
- Reflection function for an isotropically scattering finite medium. 22 p2887 A73-42565
- Mixed boundary value problem of thin isotropic plate under edge loading, examining bending moment applied to plate with intermittent edge clamping. 22 p2928 A73-43065
- Reflection and transmission of electromagnetic waves at a moving magnetoplasma half-space. 22 p2896 A73-43179
- Insulated electrically thin dipole antenna with surrounding large wave number isotropic medium, discussing transmission line properties and current and charge distribution 22 p2829 A73-43183
- Determination of the stressed state near a curvilinear hole in a transversely isotropic spherical shell 23 p3043 A73-43924
- Papkovich-Neiber solution for stress-strain state of initially isotropic mixture of two elastic bodies 23 p3007 A73-44183
- Bending of transversely isotropic plates with a reinforced edge 24 p3149 A73-45174
- Elastic deformation of isotropic infinite plane with central circular inhomogeneity and elastokinetics of two bonded dissimilar half planes under uniformly moving body force 24 p3152 A73-45343
- Determination of shape for apertures of equal strength in thin isotropic plates 24 p3152 A73-45356
- Variation of amplitudes of thermo-acoustical waves of arbitrary form in isotropic linear thermo-elastic materials. 24 p3157 A73-45372
- Reduced equilibrium equations solution for plane deformations of isotropic incompressible elastic media, using stress-strain relations 24 p3153 A73-45549
- ISOTROPIC TURBULENCE**
- A note on the angular dispersion of a fluid line element in isotropic turbulence. 01 p0032 A73-10443
- Quasi-stable energy spectrum of isotropic turbulence. 03 p0297 A73-14444
- Transverse particle diffusion across external homogeneous magnetic field under random isotropic large scale hydromagnetic turbulence 07 p0856 A73-19450
- Effects of contraction geometry on non-isotropic free-stream turbulence. 08 p0955 A73-21438
- Number of gust series in turbulent velocity pulsations 09 p1115 A73-22992
- Experimental determination of the turbulent transfer coefficient in the case of homogeneous isotropic turbulence. 10 p1205 A73-24176
- Spectral energy transfer models of turbulence decay compared with numerical simulation of three dimensional homogeneous isotropic turbulence, considering eddy viscosity and diffusion models 10 p1246 A73-24252
- Low speed wind tunnel test section anisotropic turbulence decay rates representation by power type laws, comparing with grid and nearly isotropic turbulence 11 p1348 A73-26390
- Diffusion of heat from a line source downstream of a turbulence grid. 11 p1453 A73-26399
- Thermoanemometer errors in turbulent wind velocity pulsations measurement 11 p1367 A73-26436
- Intermittency in fully developed turbulence as a consequence of the Navier-Stokes equations. 15 p1860 A73-31092
- Magnetic field induced energy dissipation in conducting fluid isotropic turbulent flow velocity pulsations, noting Joule dissipation effect on damping 15 p1917 A73-31403
- Multipoint distribution calculation of the isotropic turbulent energy spectrum. 19 p2421 A73-37854
- Turbulence spectra at scales smaller than 1 meter. 19 p2449 A73-38241
- Homogeneous anisotropic to isotropic turbulence convergence based on shear flow component measurements of turbulence energy distribution in axisymmetric flow 20 p2546 A73-39097
- Computerized simulation of isotropic three dimensional turbulence velocity field growth and energy decay based on Navier-Stokes equation numerical integration 23 p3001 A73-43588
- On the correction of hot wire turbulence measurements for spatial resolution errors. 24 p3089 A73-44691
- ISOTROPISM**
- Einstein equations reduction to friction systems in homogeneous cosmological models, investigating Bianchi models solutions isotropization 14 p1798 A73-30327
- ISOTROPY**
- NT ISOTROPIC MEDIA**
- Isotropy postulate verification for strain vectors measurement in annealed steel tubular specimens, showing coincidence of tension-internal pressure and tension-torsion test values 02 p0235 A73-12206
- Isotropic cosmological models of X ray background radiation, presenting observational constraints on source distribution and radiation mechanisms 09 p1138 A73-22869
- Anisotropic and isotropic descriptions of physical process speeds in special relativity theory space-time metric 10 p1250 A73-24944
- Role of plasma effects in the propagation and isotropization of cosmic rays in the Galaxy 21 p2756 A73-40579
- ITALY**
- NT ALPS MOUNTAINS [EUROPE]**
- Infrared sensing of the surface temperature of certain lakes of Northern Italy 17 p2206 A73-34942
- ITERATION**
- NT ITERATIVE SOLUTION**
- Solution to certain boundary value problems of a generalized axisymmetric theory of potential 01 p0070 A73-10092
- Multistep conjugate gradient search methods with memory, describing convergence of iterative procedure for functional minimization 12 p1485 A73-27617
- ITERATIVE SOLUTION**
- Nonlinear homotopies for obtaining initial solutions for iteration procedures 01 p0069 A73-10069
- Iteration approach for elliptic /nonlinear/ difference operators in divergence form 01 p0069 A73-10075
- An improved algorithm for the inversion of limb radiance measurements. 01 p0072 A73-10355
- Iteration accuracy effect on optimal discrete control system synthesis and stability, applying to Zubov damping problem 01 p0027 A73-10591
- Explicit alternating-direction methods of solving the boundary value problem for a fourth-order self-conjugate elliptical differential equation with variable coefficients 01 p0070 A73-10915
- Continuous methods based on particular solutions for free boundary problems in partial differential equations, considering heat equation Stefan problem and Laplace equation interface 01 p0071 A73-11462
- The method of variable directions for solving a boundary-value problem for a self-conjugate elliptic fourth-order differential equation with variable coefficients 02 p0187 A73-12190
- Structural hardening calculation procedures and thermal strength problems. 02 p0235 A73-12201
- Iteration method for statistical treatment of measurements when information on measurement error characteristics is incomplete 02 p0219 A73-12455
- A note on modified optimal linear multistep methods. 02 p0188 A73-12614
- Dynamic structural analysis large eigenvalue problems, presenting subspace iteration algorithm for arbitrary system size and bandwidth 04 p0509 A73-14944
- A system-synthesis approach to the inverse problem of scattering by smooth, convex-shaped scatterers for the high-frequency case. 04 p0423 A73-15484
- Iterative technique for the calculation of double-impulse spacecraft rendezvous maneuvers. 05 p0627 A73-16092
- Modification methods for inverting matrices and solving systems of linear algebraic equations. 05 p0590 A73-16373
- Monotonicity and iterative approximations involving rectangular matrices. 05 p0590 A73-16374
- Variational method of moments and some iteration procedures for determining the characteristics of VLF wave propagation in the earth-anisotropic ionosphere waveguide channel. I 05 p0549 A73-16387
- The application of Newton's method to the problem of elastic stability. [ASME PAPER 72-APM-P] 05 p0632 A73-16531
- Quadratic termination properties of minimization algorithms. I - Statement and discussion of results. II - Proofs of theorems. 06 p0716 A73-17983
- An iterative approach to nonlinear dynamic stability problems. 06 p0717 A73-18145
- Iterative methods for best approximate solutions of linear integral equations of the first and second kinds. 06 p0717 A73-18170
- Iterative least-squares synthesis of nonuniformly spaced linear arrays. 06 p0666 A73-18194
- Iterative scheme for identifying linear systems from input/output samples or construction of rational z-transform approximations to sample data sequences 06 p0718 A73-18534
- Convergence of the small parameter method in deriving periodic solutions to ordinary neutral-type differential equations with small delay 06 p0718 A73-18680
- Iterative formula for wave functions related to sources situated on prism symmetry plane with application to electromagnetically polarized wave diffraction by dielectric wedge 06 p0669 A73-18841
- An iterative procedure for the oscillatory laminar boundary layer. 07 p0809 A73-19035
- A general scheme for solving ordinary differential equations under two-point boundary conditions. 07 p0845 A73-19546
- German monograph - An iteration procedure for the calculation of planar compressible flows around circular profiles. 07 p0774 A73-19580
- Adaptive algorithms for reducing a random field to a prescribed set of states with constraints on the elements of the approximating sequences 07 p0796 A73-20079
- Minimum fuel control solution for linear discrete systems, discussing finite iterative algorithm based on dual problem of functional analysis 07 p0806 A73-20595
- Elastoplastic analysis by matrix displacement or finite element method, presenting various direct and iterative solution techniques 08 p1016 A73-20776
- Iterative method for calculating hot carrier distributions in semiconductors. 08 p0994 A73-21221
- The conjugate gradient method and its application to aerospace vehicle guidance and control. I - Basic results in the conjugate gradient method. 08 p0951 A73-21428
- The conjugate gradient method and its application to aerospace vehicle guidance and control. II - Mars entry guidance and control. 08 p0986 A73-21429
- Diffusion of charged particles in a random magnetic field. 09 p1137 A73-22035
- Simple iterative method for determining the eigenvalues of a Hermitian /real-symmetrical/ pair of matrices 09 p1111 A73-22107
- Convergent iterative smoothing algorithm for aircraft stability parameter identification from measurement, using variational optimization procedure 09 p1067 A73-22233
- Recursive methods in on-line computer photogrammetric data reduction deriving algorithms for fixed and variable parameter numbers cases with matrix partitioning 09 p1059 A73-22381
- An iteration procedure for the solution of special nonlinear boundary-value problems 09 p1112 A73-22448
- Difference iterative solution for two dimensional boundary value problem for rectangular elastic plate with rectangular cutout 09 p1159 A73-22584
- Rank-one and rank-two corrections to positive definite matrices expressed in product form. 09 p1113 A73-22956
- A note on the stability of an iterative finite-difference method for hyperbolic systems. 10 p1241 A73-23639
- Book - Iterative methods for nonlinear optimization problems. 10 p1242 A73-23947
- Iterative optimum control function determination without directly solving the system dynamical equations. 10 p1242 A73-24033
- A numerical method for the solution of an elliptic fourth-order differential equation with variable coefficients 10 p1243 A73-24059
- Numerical solution of some boundary value problems for an isotropic cylindrical shell 10 p1288 A73-24060
- Method of variable directions for solving the equations of an isotropic cylindrical shell 10 p1292 A73-24501

Iterative method for solving some boundary value problems for the equations of an orthotropic shell of revolution 10 p1292 A73-24503

Solution of the stochastic control problem in unbounded domains. 10 p1203 A73-24705

Integral equation numerical solution by minimum mean-squared estimator for atmospheric electromagnetic refractivity profile from satellite radio tracking data, noting iterative procedure convergence 11 p1330 A73-25686

An analytical iterative algorithm for the prediction of special satellite orbit points with the Brouwer orbit theory. 11 p1423 A73-26075

On a solution of an optimization problem in linear control systems with quadratic performance index. 11 p1342 A73-26224

An iterative method for generalized nonlinear complementarity problems. 11 p1391 A73-26577

Calculation of eigenvalues and eigenvectors of normal matrix couples with the aid of Ritz iteration 11 p1392 A73-26726

Superlinear convergent multistep procedure of the regula falsi and the Newton type 11 p1392 A73-26728

Iterative-zonal method for studying and calculating the local characteristics of radiative heat transfer. 12 p1560 A73-27913

Finite element method applied to analysis of flow over a spillway crest. 13 p1563 A73-28078

Effective use of the incremental stiffness matrices in nonlinear geometric analysis. 13 p1694 A73-28252

The splitting-up method and its application to elasticity problems. 13 p1694 A73-28254

Analytical approximation of high order Galerkin solutions to ordinary differential equations describing forced oscillations of systems with polynomial nonlinearities, considering first-order harmonic effects 13 p1648 A73-28440

Automation of a solution to the general boundary value problem of a plane self-conjugate elliptic equation 13 p1650 A73-29129

A quadrature-iterative method of solving linear and nonlinear integral equations 13 p1651 A73-29679

Application of the regularization method to the solution of the inverse problem in potential theory for electron-optical systems 13 p1662 A73-29681

Stability of difference equations and convergence of iterative processes. 14 p1767 A73-29937

Some efficient algorithms for solving systems of nonlinear equations. 14 p1768 A73-29939

Matrix invariant subspace computation via LU, QR, treppen and bi-iterations, comparing to power method 14 p1768 A73-29940

Haralick-Dinstein iterative clustering procedure limitation and explanation as T transformation linear structure effect in matrix theory 14 p1768 A73-30040

Iterative diffraction calculations of transverse mode distributions in confocal unstable laser resonators. 14 p1756 A73-30156

A simple integration method for the momentum and energy theorem of boundary layer theory 14 p1745 A73-30300

Solution of a dual problem in optimal control theory. 14 p1738 A73-30405

Two coplanar cracks in an infinitely long elastic strip bonded to semi-infinite elastic planes. 14 p1815 A73-30918

Calculation of a subsonic radiating gas flow by an adjustment method 15 p1821 A73-30969

An iteration method of solving the three-dimensional problem for equations of the theory of elasticity in displacements 15 p1945 A73-31027

Single point solutions of Dirichlet boundary value problems by Monte Carlo and successive over-relaxation. 15 p1899 A73-32037

Solution of the three-parameter Weibull equations by constrained modified quasilinearization /progressively censored samples/. 15 p1901 A73-32263

Iterative method for the statistical processing of measurements with incomplete information on the measurement error characteristics. 15 p1902 A73-32605

Implementation of simultaneous iteration for vibration analysis. 16 p2075 A73-32788

The iterative solution of two-point linear differential eigenvalue problems. 16 p2031 A73-32930

Forming energy in rigid-plastic materials unsteady molding processes, obtaining nonlinear equations system solution by iterative procedure 16 p2037 A73-33237

The choice of step length, a crucial factor in the performance of variable metric algorithms. 16 p2033 A73-33853

Iterative finite element method for minimum weight structural design with respect to buckling constraints applied to beam and orthogonal frame design 16 p2082 A73-33908

On the solution of large systems of linear algebraic equations with sparse, positive definite matrices. 17 p2199 A73-34104

Some computational techniques for the nonlinear least squares problem. 17 p2199 A73-34105

Nonlinear functional minimization under auxiliary constraints, discussing convergence conditions and iterative solution algorithm performance for least squares weighted sum problem 17 p2199 A73-34106

Computer oriented algorithms for solving systems of simultaneous nonlinear algebraic equations. 17 p2199 A73-34107

On the choice of relaxation parameters for nonlinear problems. 17 p2199 A73-34108

A modified Butcher formula for integration of stiff systems of ordinary differential equations. 17 p2199 A73-34212

Iteration methods for finding all zeros of a polynomial simultaneously. 17 p2200 A73-34215

Book - Methods of nonlinear analysis. Volume 2. 17 p2200 A73-34453

Solution of incorrect problems by methods of successive approximations 17 p2201 A73-34630

An approximate method for the solution of a class nonlinear equations in fluid mechanics and magnetohydrodynamics. 17 p2216 A73-35018

[ASME PAPER 73-FE-22] Perturbation theory for field moments in an inhomogeneous medium. 17 p2123 A73-35151

Kantorovich functional analysis algorithms providing rigorous theory for convergence of iterative methods to nonlinear functional equations on Banach spaces, emphasizing Newton method 17 p2163 A73-35268

Design of nonlinear resistive networks with prescribed input-output behavior. 17 p2145 A73-35378

Experimental force data reduction equations solved by iterative method for multicomponent force transducers used in load tests, discussing wind tunnel balances 17 p2148 A73-35437

Inconsistencies and S.O.R. convergence for the discrete Neumann problem. 17 p2202 A73-35519

Quasi-Newton methods for discretized non-linear boundary problems. 17 p2202 A73-35520

Mass condensation and simultaneous iteration for vibration problems. 17 p2252 A73-35605

Planar aperture antenna synthesis for main beam and complex sidelobe patterns by iterative correction with convergence, using computer program 17 p2142 A73-35648

On the convergence of two-stage iterative processes for solving linear equations. 17 p2203 A73-35726

Convergence of matrix iterations subject to diagonal dominance. 17 p2203 A73-35727

A generalization of the additive correction methods for the iterative solution of matrix equations. 17 p2203 A73-35729

Finite-difference solution of the incompressible three-dimensional boundary layer equations for a blunt body. 18 p2259 A73-36156

Three dimensional jet flap potential flow theory based on vortex lattice method, comparing iterative solution with slatted unswept blown flapped wing experimental results [AIAA PAPER 73-653] 18 p2263 A73-36260

An iterative solution to the second order eigenvalue equation with periodic boundary conditions. 18 p2330 A73-36609

New contributions to the iterative method for aerodynamic calculations of wings in subsonic flows 19 p2376 A73-37545

Calculation of structures by superrelaxation iterations over moments 19 p2497 A73-37549

An approximation method for calculating the attenuation characteristic of dielectric-lined circular waveguides. 19 p2404 A73-37723

On the iterative solution of Dirichlet problem for some mildly non-linear elliptic equations. 19 p2445 A73-38027

A computational algorithm for design of regulators for linear jump parameter systems. 19 p2408 A73-38066

Some numerical aspects of the solution of functional equations in dynamic programming 19 p2445 A73-38163

Eigenproblem solution by a combined Sturm sequence and inverse iteration technique. 19 p2408 A73-38188

Numerical solution of quasi-static problems in viscoelasticity theory 20 p2619 A73-39332

Solution of a boundary-value problem for a second-order differential equation with a lagging argument by the method of spline functions - A scheme of increased accuracy 20 p2582 A73-39472

Application of the Peaceman-Rochford method to the solution of the deflection problem for a plate strengthened by a square grid 20 p2620 A73-39496

Sylvester matrix equation analysis of rigidly connected beam gridworks with weak regularity and translational properties, considering iterative and eigenvalue-eigenvector solutions 20 p2621 A73-39534

Application of simultaneous iteration method to torsional vibration problems. 21 p2783 A73-40289

Strong and weak convergence of the sequence of successive approximations for quasi-nonexpansive mappings. 21 p2724 A73-40297

Synthesis of reactive ladder filters with uniform losses, discussing iterative solution for nonlinear equations and low, high and band pass filters loss compensation 21 p2662 A73-40498

Self-similar solutions of the plasma equations 21 p2747 A73-40553

Free boundary problem involving elliptic differential equation, discussing iterative method instabilities inhibition of convergence 21 p2727 A73-40998

The variable metric algorithm for non-definite quadratic functions. 21 p2727 A73-40999

Electronic circuit optimization via Powell iterative method, describing search techniques, matrix methods and transistor hybrid equivalent circuit application 21 p2671 A73-41313

The method of the false transient for the solution of coupled elliptic equations. 21 p2727 A73-41473

Iterative and matrix inversion techniques for antenna electromagnetic radiation and scattering prediction compared for computer storage and execution time 22 p2823 A73-41799

Inversion techniques for remote sensing of atmospheric temperature profiles. 22 p2883 A73-42056

Gradient control laws in stabilization problems of multidimensional control systems 22 p2887 A73-42605

Iteration methods for identification of multiple-link controlled plants for self-adaptation purposes 22 p2836 A73-42617

Planetary flybys resulting in heliocentric orbits normal to the ecliptic with fixed perihelia. 22 p2909 A73-42628

Calculation of the maximum attainable efficiency of a moving compressor blade cascade 22 p2797 A73-42646

Papers on computer techniques for electromagnetic radiation and scattering problems via integral equation formulation covering iterative and variational methods and antenna patterns 22 p2827 A73-42839

Variational and iterative methods for waveguides and arrays. 22 p2834 A73-42843

An iterative mathematical technique for deriving electron-density profiles from multifrequency interferometer data. 22 p2828 A73-43177

A new approach to optimal design of elastic structures. 23 p3042 A73-43798

On the computation of natural modes of an unsupported vibrating structure by simultaneous iteration. 23 p3042 A73-43801

An iteration method of alternating directions for the Poisson difference equation in curvilinear orthogonal coordinates 24 p3105 A73-44650

Numerical analysis of pre- and post-critical response of elastic continua at finite strains. 24 p3150 A73-45227

Representation of the computer-aided design process by a network of decision tables. 24 p3070 A73-45230

Structural design optimization by iterative analysis using proper stiffness matrix with applications to sandwich plate and frame problems
24 p3150 A73-45236

Optimal convergence of iterative solution for system of linear equations with real roots based on matrix method
24 p3106 A73-45441

Convergence rate of two-real-parameter iterative solution of linear equations system based on matrix eigenvalues relationship
24 p3106 A73-45442

The exterior Neumann problem for the Helmholtz equation.
24 p3112 A73-45470

The problem of an iteration method for solving a nonlinear system of partial differential equations given in implicit form with time lag
24 p3106 A73-45507

ITOS 1
Current trends in the refinement of scientific equipment for meteorological satellites
15 p1875 A73-31606

IUE
The detector system of the International Ultraviolet Explorer satellite.
17 p2170 A73-35295

Ultraviolet proximity focussed converters for use in a satellite SEC-TV system.
17 p2170 A73-35296

IZSAK ELLIPSOID
U ELLIPSOIDS
U GEODESY

J

J-33 ENGINE
Gas temperature, carbon monoxide and nitric oxide axial and radial distribution in J-33 combustor, presenting combustion process model based on measurements
[WSCIPAPER 72-22] 05 p0639 A73-16690

Emissions from and within an Allison J-33 combustor.
07 p0868 A73-20359

Analytical predictions of emissions from and within an Allison J-33 combustor.
08 p1025 A73-21670

Emissions from and within an Allison J-33 combustor. II - The effect of inlet air temperature.
23 p3019 A73-43327

J-85 ENGINE
Diagnostic instrumentation on J-85 engines for gas path and vibration analysis, noting flight test program and installation of remote pressure transducers and signal conditioners
[AIAA PAPER 72-1081] 03 p0308 A73-13404

JACKS [ELECTRICAL]
U ELECTRIC CONNECTORS

JACOBI INTEGRAL
Out-of-plane motion about libration points - Non-linearity and eccentricity effects.
11 p1423 A73-26069

Cometary and asteroidal orbits discrimination using Jacobi integral in three body system with sun and Jupiter
14 p1795 A73-29849

JACOBI MATRIX METHOD
Isoparametric element forms in finite element analysis.
17 p2245 A73-34834

Quasi-Newton methods for discretized non-linear boundary problems.
17 p2202 A73-35520

JACOBI POLYNOMIALS
U HYPERGEOMETRIC FUNCTIONS

JAGUAR AIRCRAFT
Optimisation in construction of the Jaguar and other military aircraft.
08 p0928 A73-20947

JAMMERS
Application of adaptive arrays to suppress strong jammers in the presence of weak signals.
13 p1593 A73-29215

JAMMING
Binary noncoherent FSK communication under influence of bandpass Gaussian noise and linear FM jamming waveform, deriving error probability
03 p0276 A73-13905

Octave-bandwidth, acoustic M/W frequency-memory loop.
22 p2834 A73-42873

JARRING
U MECHANICAL SHOCK

JC-130 AIRCRAFT
U C-130 AIRCRAFT

JEANS THEORY
Dissipation of the Venusian atmosphere
21 p2769 A73-40733

JEES
U AUTOMOBILES

JET AIRCRAFT
NT A-4 AIRCRAFT

NT A-7 AIRCRAFT

NT A-300 AIRCRAFT

NT AN-24 AIRCRAFT

NT B-52 AIRCRAFT

NT B-57 AIRCRAFT

NT B-70 AIRCRAFT

NT BOEING 727 AIRCRAFT

NT BOEING 737 AIRCRAFT

NT BOEING 747 AIRCRAFT

NT C-5 AIRCRAFT

NT C-141 AIRCRAFT

NT CL-84 AIRCRAFT

NT CONCORDE AIRCRAFT

NT DC 9 AIRCRAFT

NT DC 10 AIRCRAFT

NT DHC 5 AIRCRAFT

NT DO-31 AIRCRAFT

NT F-4 AIRCRAFT

NT F-8 AIRCRAFT

NT F-14 AIRCRAFT

NT F-15 AIRCRAFT

NT F-111 AIRCRAFT

NT HFB-320 AIRCRAFT

NT IL-62 AIRCRAFT

NT JINDIVIK TARGET AIRCRAFT

NT L-1011 AIRCRAFT

NT P-3 AIRCRAFT

NT T-33 AIRCRAFT

NT T-39 AIRCRAFT

NT TU-134 AIRCRAFT

NT TURBOFAN AIRCRAFT

NT TURBOPROP AIRCRAFT

Short haul twin jet passenger aircraft Iak-40 for small airfields, noting flight characteristics and cost analysis
03 p0249 A73-13070

Assessment of emission control technology for turbine-engine aircraft.
[ASME PAPER 72-WA/GT-8] 04 p0490 A73-15872

Subsonic jet airframe fatigue cracking as function of load, geometry, material, joint performance and environment
05 p0636 A73-17200

M-15 agricultural turbojet aircraft design for slow low level flight, tabulating dimensions, weights and performance data
13 p1568 A73-28026

Jet procedures trainer for pilot transition from straight wing propeller plane to swept wing jets, discussing pilot instruction and selection
15 p1837 A73-31095

VFW 614 twin-jet short haul aircraft, discussing layout, auxiliary power supply system for ground handling independence, surface movements maneuverability and low noise characteristics
15 p1830 A73-32365

Composite airframe structure effects on jet aircraft maintenance, discussing fire safety, fatigue resistance, environmental durability and quality assurance
16 p1967 A73-33027

Technology developments effect on jet aircraft design, discussing flight controls, engine noise suppression, supercritical aerodynamics and composite structures
16 p1968 A73-33188

STOL jet aircraft with variable pitch fan, discussing engine handling, noise reduction and efficiency
16 p2046 A73-33189

Book - Methods for estimating stability and control derivatives of conventional subsonic airplanes.
16 p1969 A73-33423

V/STOL airframe/propulsion integration problem areas.
[ASME PAPER 73-GT-76] 16 p2048 A73-33522

Performance of jet V/STOL tactical aircraft nozzles.
[ASME PAPER 73-GT-77] 16 p1969 A73-33523

Subsonic jet aircraft contribution to NOx in the stratospheric ozone layer - 1968 to 1990.
[AIAA PAPER 73-534] 16 p2046 A73-33566

Safety in the accident prone flight phases of take-off, approach and landing.
17 p2098 A73-34085

VTOL jet transport aircraft commercial applications, describing lift engine system, hover flight control, engine failure problems and operating cost analysis
17 p2099 A73-34257

Status of international noise certification standards for business aircraft.
[SAE PAPER 730286] 17 p2101 A73-34651

Dynamic behavior of light aircraft interaction with jet transport vortex on basis of accident records and computer simulation
[SAE PAPER 730296] 17 p2094 A73-34660

Feasibility and optimization of variable-geometry wing for jet amphibian business aircraft.
[SAE PAPER 730330] 17 p2102 A73-34683

Key factors in developing a future wide-bodied twin-jet transport.
[SAE PAPER 730354] 17 p2103 A73-34702

Russian book - Aerodynamics and flight dynamics of turbojet aircraft /2nd revised and enlarged edition/.
17 p2104 A73-34900

Future technology and economy of jet-supported VTOL transport aircraft
21 p2793 A73-40448

A look at Soviet ATC and nav facilities and avionics.
21 p2737 A73-41522

JET AIRCRAFT NOISE
Analysis of internally generated sound in continuous materials. II - A critical review of the conceptual adequacy and physical scope of existing theories of aerodynamic noise, with special reference to supersonic jet noise.
03 p0246 A73-13840

Jet noise suppression for commercial CTOL, STOL and SST aircraft, discussing various devices effectiveness
03 p0251 A73-14130

Directional devices for noise reduction of high speed jets
03 p0359 A73-14142

Study of the influence of the volumetric mass of a jet on acoustic sound emission
03 p0359 A73-14143

Attenuation of spiral modes in a circular and annular lined duct.
04 p0487 A73-15591

Disturbance of the environment by jet aircraft noise
05 p0535 A73-16760

Flyover and static tests to investigate external flow effect on jet noise for nonsuppressor and suppressor exhaust nozzles.
[AIAA PAPER 73-190] 05 p0531 A73-16927

Long range air transportation technical and economic future prospects, discussing passenger and cargo developments, noise reduction and SST technology
[AIAA PAPER 73-14] 06 p0646 A73-17607

Phillips aerodynamic noise theory application to directional patterns of high speed hot jets, discussing convection laws and sound field-turbulence correspondence
[AIAA PAPER 73-185] 06 p0684 A73-17654

Sound field generated by spatial instabilities interaction on shear layer shed from duct with nozzle lip, discussing excess noise of subsonic jets
06 p0687 A73-18529

Effects of aircraft noise on human sleep.
06 p0659 A73-18546

Analysis of internally generated sound in continuous materials. III - The momentum potential field description of fluctuating fluid motion as a basis for a unified theory of internally generated sound.
07 p0909 A73-19097

Acoustic results obtained with upper-surface-blowing lift-augmentation systems.
07 p0776 A73-20458

Sound pressure level spectra measurements for four- and three-engine jet transport during concrete and grassy surface runup and flyover
[SAE AIR 1216] 08 p0927 A73-20693

Aircraft turboengine noise, discussing noise level/power output relations
10 p1262 A73-23861

Jet aircraft engine noise reduction.
10 p1263 A73-24555

Acoustic and fluid dynamic tests of multilobed discharge silencers scale models, noting optimum jet noise attenuation configuration
12 p1486 A73-27390

Turbulent jet noise generation theory relationship between flow and acoustic characteristics, obtaining intensity expression with velocity space-time derivatives for moving and stationary coordinates
13 p1603 A73-29138

Reduction of aircraft noise during stationary runs
13 p1570 A73-29651

Concorde engine noise reduction at takeoff, initial climb and landing, discussing noise sources research and exhaust system nozzle modifications
14 p1785 A73-30930

Jet noise suppression technology progress review, discussing Lighthill theory of aerodynamic noise, machinery noise and quiet aircraft future
15 p1830 A73-32186

Spectral moving frame representation of jet noise by far field acoustic pressure autocorrelation and density function
16 p2000 A73-33681

'Quiet' aspects of the Pratt & Whitney Aircraft JT15D turbofan.
[SAE PAPER 730289] 17 p2101 A73-34654

Engine cycle considerations for future transport aircraft.
[SAE PAPER 730345] 17 p2222 A73-34693

Noise reduction modifications in JT3D and JT8D gas turbine engine by single stage fan replacements
[SAE PAPER 730346] 17 p2222 A73-34694

Monograph - Two causality correlation techniques applied to jet noise.
17 p2155 A73-35150

Jet aircraft noise research, emphasizing pure jet mixing noise, shock wave associated noise, and tail-pipe noise produced in engine or nozzle exit plane
17 p2096 A73-35332

- Engine-over-the-wing noise research.
[AIAA PAPER 73-631] 18 p2267 A73-36190
Velocity decay and acoustic characteristics of various nozzle geometries with forward velocity.
[AIAA PAPER 73-629] 18 p2263 A73-36256
SST environment impact aspects in areas of fuel and oxygen consumption, noise, sonic boom, stratospheric pollution and climate modification
18 p2268 A73-36906
Hot gaseous jet noise emission calculation for dependence on turbulent flow characteristics based on Lighthill theory, using computer program
18 p2343 A73-36997
Jet engine noise reduction technology and design, discussing sonic pressure probes, high bypass turbofan engines, noise source fluctuations and far field measurements
19 p2472 A73-37287
Noise source distribution in subsonic jets.
19 p2472 A73-37290
Noise of jets discharging from a duct containing bluff bodies.
19 p2472 A73-37291
Recent studies of fan noise generation and reduction.
19 p2473 A73-37293
Noise reducing choked /sonic/ inlet design for V/STOL jet aircraft, discussing aerodynamic theoretical and experimental studies
19 p2375 A73-37295
Noise from turbomachinery.
[AIAA PAPER 73-815] 19 p2473 A73-37469
Consequences of aircraft noise reduction alternatives on communities around airports.
[AIAA PAPER 73-818] 19 p2380 A73-37471
Jet aircraft noise abatement near airports during takeoff, approach and landing, discussing noise measurement standards and regulatory and noise reduction design efforts
19 p2385 A73-37825
Subsonic jet noise measurements on model jet rig in anechoic chamber, discussing correlation and prediction
19 p2473 A73-38106
Testing noise-reducing approach techniques with the HFB 320 research aircraft of the DFVLR
19 p2387 A73-38265
Maximum air transportation service with minimum community noise.
[AIAA PAPER 73-796] 19 p2388 A73-38369
A status report on jet noise suppression as seen by an aircraft manufacturer.
[AIAA PAPER 73-816] 19 p2388 A73-38374
Overall sound pressure levels of STOL thrust reverse noise as function of jet velocity at touchdown
20 p2600 A73-38650
Geophysical effects of Concorde sonic boom.
20 p2509 A73-39624
On the effect of swirling motion of sources of subsonic jet noise.
21 p2676 A73-40286
Small-scale suppressor of the aerodynamic noise of a subsonic gas jet
21 p2754 A73-40404
Peak subsonic noise level reduction by jet refraction, showing directivity patterns as function of jet velocities and temperature ratios
21 p2754 A73-40753
Technical progress on new vibration and acoustic tests for proposed MIL-STD-810C, 'environmental test methods.'
21 p2674 A73-41200
Rolls-Royce RB-211 jet engine noise reduction program, considering fan, compressor, turbine and tailpipe noise and acoustic linings and powerplant configurations
22 p2900 A73-41717
Aircraft flyover noise - Spectral analysis of sounds and sound intensity fluctuations.
22 p2800 A73-42946
Subsonic and supersonic jets and supersonic supersonic characteristics.
[AIAA PAPER 73-999] 24 p3077 A73-44834
The influence of aerodynamic flow noise in turbofan engines.
[AIAA PAPER 73-1016] 24 p3121 A73-44848
Acoustic investigation of the engine-over-the-wing concept using a D-shaped nozzle.
[AIAA PAPER 73-1030] 24 p3122 A73-44860
- JET AIRSTREAMS**
U JET STREAMS [METEOROLOGY]
JET AMPLIFIERS
Jet deviation fluidic analog amplifiers, noting industrial application to pressure, flow rate and dimensional measurements
11 p1308 A73-25379
Optimization of energy transfer in cascaded fluid jet deflection amplifiers.
13 p1571 A73-29045
Some investigations on frequency demodulating systems with fluidic jet deflection amplifiers.
13 p1572 A73-29046
A feed nozzle for hydraulic amplifiers
16 p1971 A73-33671
- Hydraulic jet amplifier design, considering selector static and dynamic characteristics, membrane attached plate, piston with feedback control and self oscillation elimination
16 p1971 A73-33672
Investigations on fluidic jet deflection amplifiers in dc- and ac networks.
23 p2942 A73-43400
Information dependent frequency control of an automatic typewriter.
23 p2944 A73-43423
- JET AUGMENTED WING FLAPS**
U JET FLAPS
U WING FLAPS
JET BLAST EFFECTS
Gas dynamic models of high speed explosive impacts of solid bodies, discussing metal cavity lining, buckling and hypersonic jet phenomena
19 p2433 A73-37514
- JET BOUNDARIES**
Plane subsonic jet free boundaries flapping measurements from oppositely placed hot-wire probes
11 p1346 A73-25251
Studies on bounded jets.
13 p1603 A73-29032
Jet boundary and a free surface behind a body of revolution in the presence of a longitudinal pressure gradient
17 p2094 A73-34774
Parametric analysis of turbulent wall jets.
19 p2376 A73-37491
The investigation on the secondary flow induced by jets. I.
19 p2422 A73-38349
- JET CONTROL**
The switching of wall-reattachment fluidic devices.
13 p1571 A73-29041
Study of the static and dynamic characteristics of a family of discrete pneumatic jet modules
16 p1971 A73-33670
- JET DAMPING**
U DAMPING
U SPIN REDUCTION
JET DRIVE
U JET PROPULSION
JET ENGINE FUELS
NT JP-5 JET FUEL
Vibrational and chemical nonequilibrium in a stoichiometric turbojet engine using kerosene-type fuel.
[AIAA PAPER 72-1208] 03 p0273 A73-13491
The electrostatic charging tendencies of jet fuel filtration equipment.
[SAE PAPER 720866] 05 p0582 A73-16672
De Gaston decharger with ionizing radiation for temporary jet fuel conductivity increase and charge density reduction, discussing theory, design and tests
[SAE PAPER 720864] 05 p0537 A73-16673
Vapor pressure of supersonic aircraft fuels
07 p0865 A73-20014
Influence of air oxygen concentration on the thermochemical stability of jet fuels
15 p1925 A73-31833
JP8 and JP4 aircraft fuel fire and explosion susceptibility from gunfire hits, discussing combat survivability relative to fuel volatility
16 p2045 A73-32670
JFTOT - A new fuel thermal stability test /A summary of a Coordinating Research Council activity/.
[SAE PAPER 730385] 17 p2147 A73-34722
Military and civil jet aircraft fuel specifications, discussing additives types, test procedures and quality control complexity
17 p2220 A73-34848
Gas-releasing additives to jet fuels
21 p2754 A73-41070
- JET ENGINES**
NT BRISTOL-SIDDELEY BS 53 ENGINE
NT BRISTOL-SIDDELEY VIPER ENGINE
NT J-33 ENGINE
NT J-85 ENGINE
NT PULSEJET ENGINES
NT RAMJET ENGINES
NT SUPERSONIC COMBUSTION RAMJET ENGINES
NT TF-30 ENGINE
NT TURBOFAN ENGINES
NT TURBOJET ENGINES
NT TURBOPROP ENGINES
Development of IN-100 powder-metallurgy disks for advanced jet engine application.
01 p0063 A73-10283
Combustion chamber pressure calculation for a pulsed air jet engine in the process of filling
02 p0203 A73-11708
Applying surface integrity principles in jet engine production.
03 p0312 A73-13272
An automated jet-engine-blade inspection system.
03 p0312 A73-13524
Russian book on jet engines testing covering tests in research and development, design, production and maintenance, test laboratories and stands and automation
04 p0487 A73-15708
- System monitoring techniques: Practical applications and experience at Eastern - Jet engines.
[SAE PAPER 720818] 05 p0606 A73-16639
Jet engine condition monitoring without aids.
[SAE PAPER 720815] 05 p0606 A73-16640
Digital control mounts on jet engine.
05 p0608 A73-17249
System for in-flight recording of the rotational speed of the turbine of a jet engine
07 p0828 A73-20546
Aviation and atmospheric pollution - The real dimension of the problem and its solutions
09 p1136 A73-22216
Hot die forging /gatorizing/ technique for Ti and heat resistant alloys jet engine parts, emphasizing material and cost savings
09 p1089 A73-23295
Compressibility effects on unsteady forces generated by jet engine blade rows aerodynamic interference, considering potential flow and viscous wake interactions
09 p1029 A73-23443
Precision and economy estimates for manual control of spacecraft orientation
10 p1286 A73-23893
Aerodynamic characteristics of torus shaped cascades involved in flame stabilization process of reheat devices for jet engines
11 p1453 A73-26595
An-2R aircraft conversion to flying test bed for feasibility studies of jet engine use in agricultural aircraft, describing structural design modifications
12 p1458 A73-26823
Balancing equipment for jet engine components, compressors, and turbine - Rotating type for measuring unbalance in one or more than one transverse planes.
[SAE ARP 587A] 16 p1993 A73-33013
Turbulence downstream of stationary and rotating cascades.
[ASME PAPER 73-GT-80] 16 p1964 A73-33525
Nondestructive inspection method for jet engine turbine blades.
[ASME PAPER 73-GT-92] 16 p2019 A73-33530
Concentration of OH and NO in YJ93-GE-3 engine exhausts measured in situ by narrow-line UV absorption.
[AIAA PAPER 73-506] 16 p2045 A73-33546
Review of engine maintenance concepts applied to wide body jets.
[SAE PAPER 730375] 17 p2178 A73-34714
Jet engine malfunction diagnosis - The sensing problem, candidate solutions and experimental results.
17 p2222 A73-35243
Film effectiveness and heat transfer coefficient downstream of a metered injection slot.
[ASME PAPER 73-HT-31] 20 p2625 A73-38570
Evaluation of precision and economy of systems of manual spacecraft orientation.
20 p2614 A73-38912
Some comments to mathematical interpretation of performance characteristics of jet engine combustion chambers.
24 p3123 A73-45381
- JET EXHAUST**
The significance of the aerodynamic jet interference for the development and the testing of the V/STOL transport DO 31
[DGLR PAPER 72-106] 02 p0127 A73-11651
Instrumentation and measurement for determination of emissions from jet engines in altitude test cells.
[AIAA PAPER 72-1068] 04 p0432 A73-14902
Turbojet exhaust reactions in stratospheric flight.
[AIAA PAPER 73-99] 05 p0608 A73-16859
B-1 airplane model support and jet plume effects on aerodynamic characteristics.
[AIAA PAPER 73-153] 05 p0563 A73-16901
Phillips aerodynamic noise theory application to directional patterns of high speed hot jets, discussing convection laws and sound field-turbulence correspondence
[AIAA PAPER 73-185] 06 p0684 A73-17654
Wind tunnel simulation of jet exhaust in low speed testing of Franco-German Alpha-Jet trainer and fire support aircraft
16 p1993 A73-32802
Preliminary estimates of the fate of SST exhaust materials using a coupled diffusion/chemistry model.
[AIAA PAPER 73-535] 16 p2046 A73-33567
Velocity decay and acoustic characteristics of various nozzle geometries with forward velocity.
[AIAA PAPER 73-629] 18 p2263 A73-36256
Noise of jets discharging from a duct containing bluff bodies.
19 p2472 A73-37291
A status report on jet noise suppression as seen by an aircraft manufacturer.
[AIAA PAPER 73-816] 19 p2388 A73-38374
- JET FLAMES**
U FLAMES
U JET FLOW
JET FLAPS
NT EXTERNALLY BLOWN FLAPS
Thrust coefficient of artificially excited vortex trail behind a jet flap aerofoil.
03 p0247 A73-14186

Lifting characteristics and spanwise aerodynamic load distribution of an external flow jet flap. 04 p0404 A73-15513

Analysis of high aspect ratio jet flap wings of arbitrary geometry. 05 p0530 A73-16880

Externally blown flap trailing edge noise reduction by slot blowing - A preliminary study. [AIAA PAPER 73-245] 05 p0532 A73-16969

A comparative study of augmentor wing, ejector nozzle and power jet flap low noise STOL concepts. 11 p1300 A73-25385

A note on the lift coefficient of a thin jet-flapped airfoil. 12 p1457 A73-27171

Discrete vortex method of two-dimensional jet flaps. 17 p2091 A73-34179

V/STOL hydraulic controls including internal and external blown jet flap and augmentor wing, describing integrated flight control actuator packages and aircraft configuration. 17 p2108 A73-35851

A jet-wing lifting-surface theory using elementary vortex distributions. [AIAA PAPER 73-652] 18 p2260 A73-36207

Three dimensional jet flap potential flow theory based on vortex lattice method, comparing iterative solution with slatted unswept blown flapped wing experimental results. [AIAA PAPER 73-653] 18 p2263 A73-36260

Investigation of multi-element airfoils with external flow jet flap. 21 p2633 A73-41087

JET FLIGHT

U JET AIRCRAFT

JET FLOW

NT AIR JETS

NT PERIPHERAL JET FLOW

NT SUPERSONIC JET FLOW

Equivalent solid obstacle for gas injection into a supersonic stream. 01 p0002 A73-10734

Gas density measurements in a jet using Raman scattering. 01 p0050 A73-10763

Ideal fluid flow past a body with an upstream jet. 01 p0035 A73-11427

Numerical method for describing turbulent, compressible, subsonic separated jet flows. 01 p0035 A73-11467

Stability of a nonstationary circular jet of ideal incompressible fluid. 02 p0152 A73-11609

Integral method of calculating a semibounded laminar jet. 02 p0153 A73-11784

Jet element output impedance for pneumatic circuits transients determination considering load dynamic properties influence. 02 p0133 A73-12120

Three dimensional jet stream dynamics based on particle population evolution numerical simulation, interpreting solar system evolution. 02 p0218 A73-12415

The oscillations of supersonic gas flows. 03 p0289 A73-12953

Secondary jet interaction with emphasis on outflow and jet location. 03 p0243 A73-13496

Power spectrum due to point source convection at uniform subsonic speed along round jet flow axis. 03 p0246 A73-13841

Cross correlations between turbulent jet flow and noise from hot-film and acoustic signal measurement, using Proudman form of Lighthill integral. 03 p0246 A73-13842

Acoustic power spectrum of a subsonic jet. 03 p0295 A73-14040

Some experiments on the noise emission of coaxial jets. 03 p0360 A73-14148

Closed form linearized solutions of plane laminar jets boundary layer equations based on Legendre functions. 03 p0297 A73-14628

Turbulent flow characteristics of swirling jets with opposite rotation, discussing lateral spreading into potential ambient fluid. [ASME PAPER 72-WA/FE-17] 04 p0435 A73-15844

An explicit numerical method for the solution of jet flows. [ASME PAPER 72-WA/FE-20] 04 p0435 A73-15846

Development of a submerged round laminar jet from an initially parabolic profile. [ASME PAPER 72-WA/FLCS-3] 04 p0408 A73-15861

Jet-driven cylindrical cavity oscillators. [ASME PAPER 72-WA/FLCS-4] 04 p0409 A73-15862

Jet interaction in a simplified model of a bistable fluid amplifier. [ASME PAPER 72-WA/FLCS-6] 04 p0409 A73-15863

Planar jet vortex growth control by excitation through transverse periodic disturbances, studying jet flow field by visualization via hydrogen bubble technique. [ASME PAPER 72-WA/APM-21] 04 p0435 A73-15895

Laminar liquid jets thrust measurement apparatus for dilute polymer solutions rheological characteristics determination, using air bearing suspended rotor with discharge capillary. 05 p0562 A73-16441

Pollutant formation in reacting turbulent jet flow field with recirculation, presenting methane-air system pointwise properties determination by numerical analysis. [WSCI PAPER 72-21] 05 p0638 A73-16676

Application of hot wires to measurements in freely expanding jets. 05 p0578 A73-17117

Noise characteristics of combustion augmented high speed jets. [AIAA PAPER 73-189] 06 p0767 A73-17655

Some incompressible jet flow and reattachment effects in fluid control elements. 06 p0687 A73-18513

Two dimensional semibounded jets in laminar and turbulent flows, discussing boundary layers skin and stream regions, step flow velocities, temperatures and self similar problems. 07 p0811 A73-19612

Determination of the shape of jets flowing off the walls of an asymmetrically positioned bucket. 07 p0776 A73-20098

Refraction of acoustic duct waveguide modes by exhaust jets. 07 p0812 A73-20338

Some studies on opposed-jet diffusion flame considering general Lewis numbers. 07 p0921 A73-20357

Plane or axisymmetric inviscid optically gray hot gas jet radiating near optically thin limit, considering thermal radiation-gas dynamics coupling effects. 08 p1020 A73-20783

An experimental investigation of three-dimensionality of wall jet flows. 08 p0956 A73-21831

Contactless switch for three stage gas flow using symmetric jet booster based on Coanda effect. 09 p1037 A73-22848

Breakup length maximum and decrease achievement in laminar viscous jet with velocity increase, discussing effects of ambient gas. 10 p1206 A73-24255

On the Kutta-condition at the trailing edge of a nozzle in a weakly nonstationary jet flow. 10 p1209 A73-24827

Unsteady viscous jet flow into stationary surroundings. 11 p1345 A73-25117

Pneumatic sensors without contact. 11 p1308 A73-25381

Flow of an ideal fluid past a body with a reverse-stream. 11 p1348 A73-26056

Gas jet flow at high subsonic velocities, determining stream function, contraction coefficient, convergence at critical velocity and pressure above obstacle. 11 p1302 A73-26215

Propagation of unipolarly charged jets in hydrodynamic flows. 12 p1528 A73-27407

The pressure and velocity fields of convected vortices. 13 p1599 A73-28067

Pulsation energy calculations in axisymmetric turbulent jet flows of incompressible fluids with a zero excess impulse. 13 p1600 A73-28448

Parameter calculation for laminar incompressible fluid jet expanding in gradient slipstream along moving surface, determining velocity distribution in jet axis. 13 p1601 A73-28736

Base pressures in flow expansions by hydraulic analogy. 13 p1564 A73-28811

Studies on bounded jets. 13 p1603 A73-29032

Flow analysis of three-dimensional diffuser for fluid amplifier. 13 p1603 A73-29033

A study of frequency selection and jumping peculiar to some fluidic oscillations. 13 p1603 A73-29034

Response of a jet to a pressure gradient and its relation to edgetones. 13 p1603 A73-29035

The input characteristic due to the interaction of jets of beam-deflection amplifier. 13 p1571 A73-29037

Study of the effects of geometrical parameters on the characteristics of air jet flow by some optical methods. 13 p1618 A73-29039

Wall effects on the motion of a two-dimensional jet switching between two parallel flat plates. 13 p1571 A73-29043

Translational temperature and atomic velocity distribution functions in rarefied binary gas jets by electron beam excited Doppler line measurement. 13 p1618 A73-29163

Heat transfer to a cylindrical laminar liquid jet ejecting into a gas. 14 p1817 A73-30612

Unsteady separated free jet flow of an ideal fluid past a wing. 15 p1861 A73-31155

Application of the energy equation for turbulence in the theory of jet flows. 15 p1862 A73-31288

Influence of viscosity on the flow of an underexpanded jet propagating in a supersonic slipstream. 15 p1822 A73-31299

Calculation of the resultant moment of the hydrodynamic forces on jet profiles. 15 p1824 A73-32000

Mean flow and turbulence measurements in a Mach 5 shear layer. 17 p2097 A73-35506

Transmission of upstream sound through a subsonic jet. [AIAA PAPER 73-630] 18 p2259 A73-36175

A three-dimensional wing/jet interaction analysis including jet distortion influences. [AIAA PAPER 73-655] 18 p2261 A73-36209

The role of jet stability in edgetone generation. [AIAA PAPER 73-628] 18 p2263 A73-36255

Investigation of the flow in regions of turbulent boundary layer separation in front of a subsonic jet blown from a circular nozzle. 18 p2265 A73-37003

Gas expelled from a strongly underexpanded nozzle upstream into a hypersonic flow. 18 p2265 A73-37010

Detonation shock wave against metal surface with hemispherical notch, investigating expelled metal jet dimensions relation to notch radius and Reynolds number. 19 p2433 A73-37515

Diffusion of a vertical jet into a fluid medium of arbitrary density. 19 p2420 A73-37547

Jet engine exhaust plume effects on solid bodies, examining nozzle drag effects, nozzle geometry, plume entrainment and shape, wind tunnel tests and pressure effects. 20 p2626 A73-38651

On a stagnation condition for combining or branching inviscid flows. 20 p2546 A73-39091

Wave dispersion equation for large eccentric elliptic jet stability calculations for noise suppression, using approximate Mathieu functions. 20 p2549 A73-39807

Shock oscillation associated with Hartmann resonance tubes excited by underexpanded sonic jets, using schlieren streak photography. 21 p2677 A73-40616

Contribution to the study of the development of a jet issuing from a nozzle of small elongation and confined between two lateral walls. 21 p2677 A73-40620

Conducting fluid jets in a transverse magnetic field. 21 p2747 A73-40888

Turbulent incompressible plane wall jet flow in still air, examining maximum velocity, total thickness and inner length scale with parametric analysis. 21 p2678 A73-41191

High temperature jet noise dependence on velocity and temperature, discussing Lighthill source term, Reynolds stresses, entropy fluctuations and velocity critical threshold. 22 p2795 A73-41703

Interaction of sound with jets. 22 p2795 A73-41704

An experimental investigation of a jet issuing from a wing in crossflow. 22 p2798 A73-43111

Gravity-shear waves in jet flow near tropopause with arbitrary temperature-wind stratification. 23 p3001 A73-43462

The effects of the exit velocity profile on the flow of a circular jet exhausting normal to the free stream. 23 p2969 A73-44125

Swirling flow effect on jet noise suppression based on acoustic field and engine thrust measurements with and without stationary swirl vanes in exhaust nozzle. [AIAA PAPER 73-1003] 24 p3077 A73-44836

Acoustic wave propagation in axisymmetric swirling subsonic jet flow, obtaining directivity patterns for spinning and nonspinning modes from wave equation numerical integration. [AIAA PAPER 73-1004] 24 p3077 A73-44837

A new device for measuring local acoustic power output of subsonic jets. [AIAA PAPER 73-1042] 24 p3090 A73-44866

Stability of a potential vortex with a non-rotating and rigid-body rotating top-hat jet core. 24 p3055 A73-45309

Nonlinear stability of cylindrical vortex enclosing a central jet of light or dense fluid.

24 p3080 A73-45452

JET FUELS

U JET ENGINE FUELS

JET IMPINGEMENT

Sound generation at an elastic plate acting as an obstruction in a turbulent free jet

[DGLR PAPER 72-085] 02 p0152 A73-11667

Acoustic feedback phenomena in the case of a subsonic and supersonic free jet which impinges on an obstacle

[DGLR PAPER 72-084] 02 p0127 A73-11683

Optimum heat transfer characteristics of semi-circular surfaces cooled by air impingement from airjet arrays and row of air jet nozzles.

[DGLR PAPER 72-061] 02 p0237 A73-11692

Material evaluation under direct rocket exhaust impingement.

[AIAA PAPER 72-1167] 03 p0287 A73-13465

A study of the plume impingement environment experienced by the booster during the space shuttle nominal staging maneuver.

[AIAA PAPER 72-1171] 03 p0273 A73-13468

Breakup and penetration of transverse liquid jets in supersonic air cross flow

[AIAA PAPER 72-1180] 03 p0293 A73-13475

An analytical investigation of the impingement of jets on curved deflectors.

03 p0296 A73-14178

Mass transfer technique for investigation of heat transfer by jet-impingement systems.

03 p0400 A73-14642

A momentum integral solution of a three-dimensional turbulent boundary layer.

[ASME PAPER 72-FE-1] 05 p0565 A73-16548

Experimental relations determining the position of shock waves in a jet impinging against an obstacle perpendicular to the jet axis

05 p0528 A73-16769

Turbulent flow characteristics of an impinging jet.

07 p0810 A73-19569

The erosion of carbon fibre reinforced plastic by repeated liquid impact.

07 p0843 A73-20224

Experimental investigation of two-dimensional, supersonic flow impingement on a normal surface.

08 p0925 A73-20720

Skin friction and heat flux in the impingement region of a low speed air jet upon a normal flat plate.

08 p0925 A73-20941

Central shock position in supersonic jet impinging on wall, noting flow velocity dependence on pressure

08 p0927 A73-21605

Diagram of the shock wave processes in the unsteady interaction between a jet and an obstacle

08 p0927 A73-21607

Diffusion of a hypersonic flow by a supersonic gas jet in the case of a free-molecular mode of interaction

11 p1304 A73-26446

Convective heat transfer in the region of interaction between a supersonic overexpanded jet and an oblique obstacle

12 p1458 A73-27324

Two dimensional opposing incompressible viscous fluid jets impingement, investigating stagnation surface stability characteristics

13 p1603 A73-29036

Interaction position and static pressure measurements of two opposing plane turbulent wall jets in still air in terms of frozen flow

15 p1863 A73-31342

Jet-induced external flows of an incompressible viscous liquid

17 p2149 A73-34138

Turbulent jet deflection and impingement in confined cross flow occurring in gas turbine blade impingement cooling schemes

[ASME PAPER 73-FE-15] 17 p2152 A73-35012

Near continuum impact of an underexpanded jet plume on a wall.

17 p2096 A73-35137

Experiments on confined turbulent jets in cross flow.

[AIAA PAPER 73-647] 18 p2260 A73-36202

Impingement of small, very high pressure solid rocket motor plumes upon nearby surfaces.

[AIAA PAPER 73-730] 18 p2342 A73-36347

Transient stress distribution caused by water-jet impact.

19 p2435 A73-38300

Carbon dioxide jet laser cutting technology and rate calculations for metals and dielectrics as function of laser power and material thermal properties

20 p2569 A73-39677

Dynamic and temperature boundary layers of a submerged jet of viscous fluid spreading over the bottom

24 p3080 A73-45503

JET MIXING FLOW

Confined laminar jet mixing in a circular channel with arbitrary entrance velocity distribution.

[AD-758578] 01 p0034 A73-11363

Further studies of the aeroacoustics of jets perturbed by screens.

02 p0154 A73-12200

Supersonic mixing and combustion of confined coaxial hydrogen-air streams.

[AIAA PAPER 72-1178] 03 p0397 A73-13473

Supersonic mixing and combustion of a hydrogen jet in a coaxial high-temperature test gas.

[AIAA PAPER 72-1179] 03 p0397 A73-13474

Analysis of free turbulent mixing flows without a net momentum defect.

03 p0296 A73-14187

Investigation of air stream from air-entry holes of the high-intensity combustor-liner.

03 p0400 A73-14447

Numerical solution of laminar jet mixing with and without free stream.

05 p0564 A73-16174

Solid particle transport effect on structure and axial speed characteristics of two phase submerged turbulent jet

06 p0684 A73-17455

Three-dimensional interaction of jets propagating in a supersonic slipstream

06 p0643 A73-17458

Turbulent mixing at homogeneous wakes boundary, using heat conduction equivalence

07 p0810 A73-19610

Minimum mixing losses of axisymmetric turbulent wakes in profiled wall channels

07 p0811 A73-19611

Prandtl eddy viscosity model for incompressible coaxial jet far field velocity decay prediction with non-dimensional term inclusion

[AD-758488] 07 p0811 A73-19965

Problems of mixing and supersonic combustion of hydrogen in a hypersonic ramjet

[ONERA, TP NO. 973] 08 p1025 A73-21684

Viscous energy transfer from elliptical orifice originated laminar three dimensional jet, using boundary layer assumptions in jet mixing region

09 p1072 A73-22827

Fuel-air turbulent mixing process in double concentric jet type burner, measuring average velocity, pressure distribution, turbulence intensity and shear stress

13 p1601 A73-28648

Diffusion processes in the mixing zone of a low-density supersonic jet

13 p1567 A73-29170

German monograph on bypass turbojet propulsion systems with jet mixing covering engine parts, thrust characteristics and fuel consumption

14 p1785 A73-30671

Mean flow data analysis of supersonic combustion ramjet turbulent jet mixing at high free stream Mach number

16 p2000 A73-33268

Turbulent mixing in the developing region of coaxial jets.

[ASME PAPER 73-FE-19] 17 p2153 A73-35015

Jet aircraft noise research, emphasizing pure jet mixing noise, shock wave associated noise, and tail-pipe noise produced in engine or nozzle exit plane

17 p2096 A73-35332

Fluid mechanics of mixing; Proceedings of the Joint Meeting, Georgia Institute of Technology, Atlanta, Ga., June 20-22, 1973.

17 p2156 A73-35501

Two dimensional half-jet mixing of dissociated air, investigating chemical rate and diffusion processes interaction effects on mixing layer thermodynamics

17 p2156 A73-35503

Inlet state limitations and flow characteristics equations for supersonic ejector jet mixing duct

17 p2156 A73-35504

A generalized theory for the turbulent mixing of axially symmetric compressible free jets.

17 p2156 A73-35505

Application of laser Raman spectroscopy to the study of factors that influence turbulent gas mixing rates.

17 p2185 A73-35510

Kinetic energy transfer during multiple jet mixing from primary jet array to secondary stream for various velocity ratios

17 p2156 A73-35511

Turbulence measurements with hot-wire anemometry in a non-homogeneous jet.

17 p2174 A73-35512

Mixing and structural characteristics of turbulent pulsating jets based on hot-wire anemometer velocity measurement data

17 p2157 A73-35513

Turbulent mixing of cylindrical jet with parallel stream in terms of mixing length concepts and velocity profiles

17 p2157 A73-35515

Two dimensional Mach 5 supersonic nozzle configurations with hot nitrogen expansion for mixing carbon dioxide gasdynamic laser, calculating and measuring gain distribution

[AIAA PAPER 73-622] 18 p2321 A73-36170

Experimental studies of chemically reactive $F_2 + H_2$ flow in supersonic free jet mixing layers.

[AIAA PAPER 73-640] 18 p2321 A73-36198

An evaluation of hypermixing for VSTOL aircraft augmentors.

[AIAA PAPER 73-654] 18 p2267 A73-36208

An investigation of supersonic swirling jets.

19 p2376 A73-37488

A study on opposing jets in air stream and their flame. I - A structure of two dimensional opposing jets in the state without flames.

19 p2377 A73-37945

Coaxial jet mixing in confined tube simulating combustion chamber, considering Reynolds number, stream functions, recirculation, lip condition, vorticity and inlet conditions

20 p2548 A73-39518

The initial development of a submerged laminar round jet.

20 p2550 A73-39815

Recirculation and mixing characteristics prediction for enclosed turbulent jet flames in flow regions, using similarity parameters

22 p2934 A73-42782

Stirring factors in combustion chambers - A finite-element model of mixing along an 'information flow path.'

22 p2934 A73-42784

Experimental and theoretical studies of NO_x formation in a jet-stirred combustor.

22 p2820 A73-42793

Effects of turbulent mixing and chemical kinetics on nitric oxide production in a jet-stirred reactor.

22 p2820 A73-42796

German monograph - A method for the calculation of mixing and combustion processes in a rocket propulsion system with air-augmentation.

22 p2900 A73-42851

Experimental study on optimization parameters of a supersonic jet ejector thrust augmentor.

22 p2798 A73-43113

Laminar and turbulent mixing of compressible jets at low Reynolds numbers.

23 p2967 A73-43403

A study of the interaction between two compressible fluid flows in a flat channel at low Mach numbers.

23 p2968 A73-43731

Introduction of the viscous force sensing fluctuating probe technique, with measurement in the mixing zone of a circular jet.

[AIAA PAPER 73-1044] 24 p3090 A73-44868

JET NOISE

U JET AIRCRAFT NOISE

JET NOZZLES

Acoustic results obtained with upper-surface-blowing lift-augmentation systems.

07 p0776 A73-20458

Thrust measurement bench for afterbody and hot and cold jet nozzle simulated tests in Sigma 4 wind tunnel

16 p1993 A73-32820

A feed nozzle for hydraulic amplifiers

16 p1971 A73-33671

Analysis of gas flow in multinozzle jets

21 p2631 A73-40393

Influence of a discrete component of acoustic vibration on flow in a supersonic jet with a nondesign ratio of active to passive pressure

24 p3055 A73-45538

JET PILOTS

U AIRCRAFT PILOTS

JET PLUMES

U PLUMES

JET PROPULSION

The pressure-jet helicopter propulsion system.

02 p0130 A73-11858

Aircraft aftbody/propulsion system integration for low drag.

[AIAA PAPER 72-1101] 03 p0243 A73-13420

Aerodynamic interference between jet propulsion system and airframe for supersonic transport with wing-mounted nacelles, noting wing performance role in lift effectiveness

[AIAA PAPER 72-1113] 03 p0243 A73-13428

Mass variation laws in light of Tsolokovskii hypothesis, considering particle separation rates and thermal energy losses for actual jet engines

08 p1014 A73-21182

Recent developments in digital image processing at the Image Processing Laboratory of JPL.

19 p2429 A73-37324

Experimental investigation of a gas-augmented water-jet engine model

22 p2841 A73-42126

Russian book on rocketry principles covering jet propulsion, jet engine combustion chambers, rocket propellants, design, aerodynamics, flight control and anti-aircraft rockets

23 p3038 A73-43334

JET PUMPS

Vehicle-scale investigation of a fluorine jet-pump liquid hydrogen tank pressurization system.

[AIAA PAPER 72-1133] 03 p0355 A73-13440

Performance of liquid jet pumps at elevated temperatures.

03 p0317 A73-14502

Venturi exhausts for air pumping augmentation in ram air operated aircraft heater or combustor, discussing experimental data on suction variation

18 p2343 A73-36396

Synchronized operation of a positive-displacement gear pump and a vane pump within the lubricant oil delivery system of a jet engine

23 p3020 A73-43742

JET STREAMS [METEOROLOGY]

Russian book on atmospheric circulation covering temperature distribution, tropospheric and stratospheric winds, jet streams and Southern Hemisphere meteorological features

04 p0474 A73-15961

Two dimensional jet stream dynamics from simulation particle population evolution in different collision models

05 p0623 A73-17301

Jet model of cloud convection - A numerical experiment

05 p0594 A73-17353

Turbulence and tropopause evolution in northeast jet stream over Treviso airport, noting Richardson criterion value as diagnostic and short range prognosis tool

08 p0986 A73-21487

A jet-stream model of cloud convection and a numerical experiment.

15 p1902 A73-31003

Vortex conservation mechanism of earth atmosphere jet stream formation in terms of Hadley cell in meridional divergence/convergence velocity region

15 p1903 A73-31603

Coordinated measurements of atmospheric parameters at stratospheric levels.

[ALAA PAPER 73-526]

16 p2007 A73-33560

On the maintenance of the polar front jet stream.

17 p2205 A73-34854

Irreversible processes in the atmosphere. I

18 p2335 A73-37099

The large-scale displacement of subtropical jet stream over Western Europe in winter.

19 p2446 A73-37431

Numerical investigation of internal waves in jet streams including nonlinear effects.

19 p2449 A73-38233

Atmospheric gravity waves and the energy of the jet stream.

21 p2729 A73-40091

Studies of the vertical distribution of atmospheric ozone in association with western disturbances over India.

23 p2975 A73-43872

JET THRUST

Experimental satellite for attitude control. II - Measurement of low thrust gas jet performance.

01 p0111 A73-11189

Ideal fluid flow past a body with an upstream jet

01 p0035 A73-11427

Thrust coefficient of artificially excited vortex trail behind a jet flap aerofoil.

03 p0247 A73-14186

Potential operating advantages of a variable area turbine turbojet.

[ASME PAPER 72-WA/AERO-4]

04 p0490 A73-15906

Satellite attitude control by reaction jet frequency modulation.

07 p0906 A73-19489

Flow of an ideal fluid past a body with a reverse-stream.

11 p1348 A73-26056

JET VANES

Influence of the effectiveness of jet vanes on the characteristics of VTOL aircraft

21 p2634 A73-40401

JETAVATORS

U GUIDE VANES

JETS

Hybrid type discrete jet-membrane relay system technology and design for discrete signals transformations

12 p1460 A73-26770

JINDIVIK TARGET AIRCRAFT

The Jindivik Drone Program to demonstrate air cushion launch and recovery.

19 p2382 A73-37697

Air cushion landing system (ACLS) application to Jindivik target drone aircraft for recovery improvement, considering flight performance degradation

19 p2383 A73-37698

JITTER

U VIBRATION

JOINING

Continuous ultrasonic joining of thin plastic films

07 p0828 A73-18902

Joining copper and copper alloys.

07 p0831 A73-20269

The joining of fiber-reinforced composite-material components with similar or different components

11 p1373 A73-25418

JOINTS [ANATOMY]

NT ELBOW [ANATOMY]

NT KNEE [ANATOMY]

German monograph - Experimental investigation of the structure of joint movements in the range of motions of the arms and of the entire body, giving attention to a presentation in a man-related basic system.

03 p0267 A73-13812

Muscle control models of joint angle spatial motions, including circle, ellipse and straight line trajectories and orientations in space

06 p0680 A73-17960

Role of visual and articular afferentation in the implementation of motor reactions involving complex coordination and precision

06 p0653 A73-18164

Electromyographic alterations in articular muscles during emotional shifts

10 p1180 A73-24328

JOINTS [JUNCTIONS]

NT BUTT JOINTS

NT LAP JOINTS

NT METAL JOINTS

NT RIVETED JOINTS

NT SEAMS [JOINTS]

NT SOLDERED JOINTS

NT SPOT WELDS

NT WELDED JOINTS

Airfield pavement full scale performance tests under simulated C-SA load conditions, evaluating construction joint systems

01 p0029 A73-10823

Disks with inclined face, investigating effects of joint between hub and disk face on stress-strain state in elastic deformation range

03 p0394 A73-14012

Linear analytical procedure for adhesively bonded flat joints design with minimized shear stress concentration, presenting finite element and automated iterative procedure

[ASME PAPER 72-WA/DE-13]

04 p0514 A73-15874

Thermal conductance of gasket materials for spacecraft joints.

05 p0640 A73-16875

Probabilistic minimum weight limit design of one dimensional pin jointed structures with random continuous variables, using stochastic programming

06 p0757 A73-17397

Geometric nonlinearity effects on rigid joint deformation of three dimensional skeletal structures, including roofing, cable and shallow dome systems

06 p0762 A73-18342

The status of engineering knowledge concerning the damping of built-up structures.

07 p0909 A73-19099

The influence of fretting and geometric stress concentrations on the fatigue strength of clamped joints.

07 p0912 A73-19572

Strain boundary conditions and complex representations of joining conditions in the theory of shells with finite shear rigidity

09 p1159 A73-22588

Fatigue life prediction and design optimization for solar cell interconnectors based on elastoplastic material stress distribution calculation by finite element methods

09 p1036 A73-22809

Calculation of the stress concentration produced by an internal pressure in the region where a cylindrical shell is connected to a branch pipe.

09 p1161 A73-23058

Analysis of load distribution in multiple-row bolt joints

10 p1222 A73-23595

Bonded joints under long-term dynamic load and their resistance to climatic effects

10 p1224 A73-24089

Concentration of thermal stresses at joints between heterogeneous materials

11 p1435 A73-25458

A synthesis procedure for mechanically fastened joints in advanced composite materials.

11 p1437 A73-25486

Stresses in bonded joints of circular cylindrical shells and panels

12 p1551 A73-27182

Formulation of time variant stiffness matrices due to changing joint properties.

12 p1555 A73-27737

Stress and fracture analysis of adhesive joints.

14 p1755 A73-30822

Bonded structural connections analysis by finite element method, presenting stress distribution in adhesive

15 p1952 A73-32038

Joining and assembly by welding.

16 p2021 A73-33860

Mechanical faster types, design considerations and economic factors, detailing nut and bolt joint assembly design, static and dynamic loads and production engineering

16 p2021 A73-33862

The properties of bond graph junction structure matrices.

19 p2460 A73-38083

Comment on 'Film reinforced multifastened mechanical joints in fibrous composites.'

22 p2928 A73-43115

Plane shock wave propagation, reflection and transmission in subsonic flow regime through T-junctions, predicting pressure variation upstream and downstream for comparison with experiment

23 p2967 A73-43295

JORDAN FORM

Bireductive spaces, Jordanian algebras, and spinor representations of non-Euclidean and quasi-non-Euclidean motions

17 p2212 A73-35566

Program of computation of spectral and modal matrices associated with a linear elastic system

18 p2364 A73-36493

JOSEPHSON JUNCTIONS

Josephson tunnel junction fabrication technology evaluation in terms of electrode materials, native oxide and artificial barriers, noting factors affecting stability and I-V characteristics

02 p0200 A73-11846

Effect of alternating current on the steady-state characteristics of a Josephson junction.

03 p0344 A73-14097

Superconducting tunnel junctions as phonon sources and detectors.

04 p0428 A73-15466

Superconductivity theory and applications, considering cryogenic problems low-loss and magnetic properties and Josephson junction effect on low power technology

04 p0484 A73-15958

Parametric regeneration in Josephson superconducting point contacts for combination frequency signal amplification and conversion in microwave application

05 p0556 A73-16073

Book - Superconductive tunnelling and applications.

05 p0556 A73-16357

Influence of fluctuations on the electromagnetic properties of the Josephson tunnel junction.

06 p0733 A73-17425

Josephson tunneling devices - A new technology with potential for high-performance computers.

06 p0735 A73-18066

Sensitivity of Josephson junctions in video detection of microwave and millimeter-wave radiation.

06 p0677 A73-18371

Tunneling observation of bound states in a normal metal-superconductor sandwich.

07 p0862 A73-19606

Low-frequency applications of superconducting quantum interference devices.

07 p0863 A73-20101

Millimeter and submillimeter wave detection and mixing with superconducting weak links.

07 p0863 A73-20102

Analog-computer studies on microwave mixing in superconducting weak links.

07 p0863 A73-20103

Josephson junction millimeter microwave source and homodyne detector.

07 p0863 A73-20104

Effect of paramagnetic impurities on Josephson currents through junctions with normal-metal barriers.

07 p0864 A73-20574

Conversion losses of a point contact presenting the Josephson effect used in a microwave mixer

08 p0938 A73-20968

Study of the geometrical resonances of superconducting tunnel junctions.

08 p0994 A73-21207

Dynamic behavior of Josephson tunnel junctions in the subnanosecond range.

09 p1132 A73-21941

A search for stimulated emission of radiation from superconducting tunnel junctions.

09 p1135 A73-23341

Infrared detectors - Survey of the present state of the art.

11 p1368 A73-26509

The problem of electron-pair tunneling in a sound field in superconductors

16 p2045 A73-34069

Applications of superconductivity.

17 p2218 A73-34111

Josephson junction interference grating.

17 p2219 A73-34915

Properties of a superconducting point contact connected to a resonator.

17 p2220 A73-35725

Josephson junction mixing of monochromatic sources at two microwave frequencies, noting output power dependence on dc bias

18 p2340 A73-36624

Superconducting Josephson junction power flow relations dependence on harmonically or subharmonically phase locked autonomous frequency

20 p2536 A73-39411

Magnetic properties of layered superconductors with a weak layer interaction

21 p2751 A73-40371

Josephson junction I-V characteristics and measurements of phase modulated quasi-particle current in superconducting weak links, taking into account thermal noise

23 p3018 A73-44174

Josephson junction principles for superconducting metals at cryogenic temperatures, considering ultrasensitive electronic measuring instruments and computer components

24 p3073 A73-45224

JOULE HEATING

U OHMIC DISSIPATION
U RESISTANCE HEATING
JOURNAL BEARINGS

On the general solution of externally pressurized gas journal bearings.

[ASME PAPER 72-LUB-Q] 01 p0055 A73-10218

Pressure distribution vs porosity and load variation with permeability for squeeze fluid films in porous metal journal bearings

[ASME PAPER 72-LUB-P] 01 p0055 A73-10219

Low-cost fluid film bearings for gas turbine engines.

[SAE PAPER 720740] 02 p0174 A73-12006

Computer-aided design of externally pressurized bearings.

03 p0311 A73-13202

Evaluation of a two-pocket hydrostatic journal bearing suitable for use over a wide range of temperature.

03 p0311 A73-13204

Hydrostatic journal bearings design review covering pad coefficients, flow control, optimization, dynamic behavior, thermal effects, turbulence and tolerances

03 p0311 A73-13207

Externally pressurized gas-lubricated journal bearings with herringbone grooves - Load capacity and stability analysis.

03 p0311 A73-13208

An application of pneumatic phase shifting to stabilization of externally pressurized journal gas bearings.

[ASME PAPER 72-LUB-4] 03 p0313 A73-14327

The gas liquid interface and the load capacity of helical grooved journal bearings.

[ASME PAPER 72-LUB-19] 03 p0314 A73-14334

Experimental rotor unbalance response using hydrostatic gas lubrication.

[ASME PAPER 72-LUB-31] 03 p0315 A73-14341

Experiments on the stability of various water-lubricated fixed geometry hydrodynamic journal bearings at zero load.

[ASME PAPER 72-LUB-46] 03 p0315 A73-14350

Summary of gas bearing applications in the field of space electric power systems.

09 p1089 A73-22771

Accelerated testing of solid film lubricants.

10 p1225 A73-24635

Unbalance vibration of a rotor-bearing system supported by floating-ring journal bearings.

13 p1623 A73-28647

Turbulence in journal bearings, considering Taylor vortices development beyond laminar range and theoretical models based on mixing length flow theory

13 p1625 A73-29261

Reynolds equation solutions for transverse velocity and pressure variations in incompressible fluids within journal bearings and between rotating eccentric cylinders

15 p1882 A73-31639

Analysis of externally pressurized gas bearings with journal rotation.

15 p1883 A73-32147

Self induced vibration of friction bearing mounted rigid rotor, considering oscillation damping or enhancing effect of oil film

16 p1968 A73-33236

Experimental investigation of air bearings for gas turbine engines.

[ASLE PREPRINT 73AM-2B-1]

Helicopter tail rotor teeter hinge with Teflon conical journal bearing allowing axial and radial preload inservice adjustment, discussing oscillatory loads and temperature effects

17 p2178 A73-34981

An analytical and experimental investigation of turbulent flow in bearing films including convective fluid inertia forces.

[ASME PAPER 73-LUBS-1] 17 p2181 A73-35388

Development and effects of super-critical Taylor-vortex flow in a lightly-loaded journal bearing.

[ASME PAPER 73-LUBS-4] 17 p2181 A73-35390

Thermohydrodynamic lubrication in laminar and turbulent regimes.

[ASME PAPER 73-LUBS-15] 17 p2181 A73-35395

Turbulent lubrication - Its genesis and role in modern design.

[ASME PAPER 73-LUBS-19] 17 p2181 A73-35398

Calculation of pressure, shear, and flow in lubricating films for high speed bearings.

[ASME PAPER 73-LUBS-21] 17 p2182 A73-35399

Journal bearings computerized design optimization by geometric programming with volume, dimensions, torque and horsepower absorption, shaft strength, speed, load, pressure and Sommerfeld number as constraints

21 p2708 A73-41668

Helicopter transmission research.

22 p2798 A73-41750

Finite journal bearings with stepwise discontinuity in hydrodynamic film shape, predicting optimal performance as function of step height, eccentricity and L/D ratios

23 p2984 A73-43293

JOURNALS [SHAFTS]

U SHAFTS [MACHINE ELEMENTS]

JP-5 JET FUEL

Characterization and suppression of aircraft and fuel fires.

[WSCIPAPER 72-26] 05 p0639 A73-16688

Experimental measurement of heat transfer to a cylinder immersed in a large aviation-fuel fire.

[ASME PAPER 73-HT-2] 20 p2625 A73-38565

JUNCTION DIODES

Determination of the complete set of physical parameters of Schottky-barrier diodes

01 p0022 A73-10041

Comments on the conduction mechanism in Schottky diodes.

01 p0088 A73-10474

Recent advances in diode and ferrite phaser technology for phased-array radars. II.

01 p0024 A73-10720

Study of the ac small-signal dynamic characteristic of p-i-n silicon diodes

01 p0024 A73-10921

Determination of the dopant concentration profile in epitaxial GaAs by the method of the differential capacitance of a Schottky diode

02 p0145 A73-11548

A simple method for determining static parameters of large signal semiconductor diode and transistor models.

02 p0147 A73-12044

Structure and electrical characteristics of epitaxial palladium silicide contacts on single crystal silicon and diffused P-N diodes.

02 p0147 A73-12045

Photovoltaic and I-V characteristics of integral diode solar cells as function of temperature and radiation exposure

03 p0256 A73-14231

Calculation of the diffusion current of a finite-base semiconductor diode

03 p0284 A73-14322

CW microwave oscillations of reach-through p-n-p barrier injection transit time /BARITT/ diodes, calculating small signal impedance and noise measure for comparison with experiment

04 p0427 A73-15346

Series diode SP4T switch for satellite applications.

04 p0428 A73-15455

Nondestructive screening and pulse damage mechanism for thermal second breakdown of semiconductor junction diodes

05 p0557 A73-16504

Electron beam fabrication of submicrometer diameter mixer diodes for millimeter and submillimeter wavelengths.

05 p0559 A73-16811

Solar cells with Si Schottky function diode, discussing fabrication and barrier metal and thickness effects on output power and energy conversion efficiency

05 p0538 A73-16816

Electrical properties of nickel-low-doped n-type gallium arsenide Schottky-barrier diodes.

05 p0559 A73-17072

The noise of microwave Schottky diodes at 70 MHz

06 p0673 A73-17579

P-n junction size effect on thermal resistance of reverse biased Si mesa-type diode, considering junction area, mesa height and power dissipation

06 p0674 A73-17795

Shot noise in a Schottky barrier diode in the presence of surface electronic states at the contact

06 p0675 A73-18077

Shot noise in diodes with a Schottky barrier in the case of a disturbed carrier distribution function

06 p0676 A73-18090

Nonlinear analysis for local microwave oscillator voltage waveform across nonlinear junction of Schottky barrier mixer diode, comparing results with analog simulation

06 p0677 A73-18740

Frequency multipliers for the millimeter wave band employing gallium arsenide diodes.

07 p0802 A73-20146

Low-frequency current oscillations in high-resistivity, Au-doped silicon junctions with two Schottky contacts.

07 p0864 A73-20190

Waveguide millimeter wave diode, ECL-2173.

07 p0804 A73-20568

GaAs diffused diode, ECL-1350.

07 p0804 A73-20570

Point contact and Schottky barrier microwave mixer diodes reliability under X band RF pulse operating conditions, considering burnout alleviating fabrication techniques

08 p0943 A73-20735

Microwave baritt /barrier-injection-transit-time/ diodes large signal performance, noting phase delay between injected and total current densities

08 p0945 A73-21074

Silicon planar diodes produced by the ion implantation process

08 p0946 A73-21080

Narrow band and broad band step-recovery device frequency multipliers for microwave power generation.

08 p0947 A73-21138

Investigation of a high-level power switch based on p-i-n diodes

08 p0948 A73-21560

PbTe-SnTe stripe junction diode lasers, discussing fabrication, electrical properties, and mode characteristics from emission spectra, polarization, mirror illumination and far field pattern measurements

[AD-759093] 09 p1092 A73-22250

A limitation on repetition rate of pulsations of junction lasers due to the repetitively Q-switched mechanism.

09 p1093 A73-22253

Spontaneous emission and stimulated recombination of p-n-n double heterojunction /AlGaAs-GaAs laser diodes above and below threshold currents

09 p1093 A73-22256

Design curves for PIN diode transmitter receiver switch based on lumped circuit filter suited to high frequency bands

09 p1063 A73-22496

The directivities and spectral contents of radiation of multidiode injection lasers.

09 p1097 A73-23049

Semiconductor diode mixer for millimeter-wave frequencies.

10 p1193 A73-23665

Equivalent circuits of diodes in millimeter and sub-millimeter wave frequencies.

10 p1193 A73-23667

Modulation of infrared and sub-mm waves with crossed forward-biased junction diodes.

10 p1194 A73-24171

Monolithic IC digital circuits using Si planar technology with Schottky diodes in DTL and TTL gates for high computational speed

11 p1341 A73-25345

Pressure effects on contact potential in diode p-n junction, discussing potential barrier height variation, minority carrier concentration changes and relative position of energy bands

11 p1338 A73-26520

Equivalent noise temperature equation relating HF noise in mm wave Schottky barrier diodes to barrier transport mechanism

11 p1339 A73-26697

Te-doped GaAs injection laser with nonplanar p-n junction for enhanced power output, discussing diode construction and fabrication by Zn diffusion

12 p1505 A73-26890

Semiconductor diodes for controlling microwave power.

12 p1480 A73-27266

Electrical fluctuations in ideal forward-biased non-degenerate diodes.

12 p1480 A73-27272

Influence of heat treatment on characteristics of injection lasers.

12 p1507 A73-27522

The measurement of the lifetime in psn diodes at high injection levels

13 p1589 A73-28477

On the existence in Schottky diodes of correlation laws between the parameters of the direct characteristic and the amplitude of low frequency background noise

13 p1590 A73-28565

An electronically switched microwave radiometer.

13 p1622 A73-29423

A modified GaAs IMPATT structure for high-efficiency operation.

13 p1595 A73-29577

Measurement of semiconductor junction parameters using lock-in amplifiers.

13 p1595 A73-29578

Microwave signal source amplitude stabilization, analyzing circuit with doubly balanced electronically regulated attenuator with p-i-n diodes

14 p1733 A73-30055

Heterojunction laser diode fabrication procedures operation and details, considering peak power levels, wavelengths and operating temperatures for CW and pulsed operations

14 p1736 A73-30575

Pb-salt tunable diode lasers.

16 p2023 A73-32859

The Schottky-barrier silicon photodetector in perspective with other detection devices in the 200 nm to 1100 nm range.

16 p2013 A73-32885

Reliability of GaAs/1-x/P/x/ light emitting diodes.

16 p1990 A73-33623

The effect of a magnetic field on the operation of a dual-base-diode oscillator.

17 p2136 A73-35161

Detection of optical and infrared radiation with dc-biased electron-tunneling metal-barrier-metal diodes.

17 p2143 A73-35792

Group 3-5 compound light emitting diode degradation modes and mechanisms, discussing epoxy lenses, light transmission characteristics, time and temperature functions and surface passivation

19 p2439 A73-38457

Degradation studies of diffused GaAs electroluminescent diodes subjected to mechanical stress.

19 p2439 A73-38458

- Double heterostructure lasers for optical communications systems
20 p2572 A73-38664
- Modulation of gallium arsenide laser diodes
20 p2572 A73-38665
- Effect of ionizing radiation on second breakdown.
20 p2599 A73-39007
- A technique for the investigation of deep-level states in diffused p-n junction devices - Application to GaAs electroluminescent diodes.
20 p2536 A73-39412
- Silicon-on-sapphire thin film junction diodes, investigating second breakdown onset delay time and minimum energy dependence on high resistivity side heating
20 p2536 A73-39415
- Storage tube with silicon target captures very fast transients.
21 p2661 A73-40228
- Determination of the bulk carrier lifetime in the low-doped region of a silicon power diode, by the method of open circuit voltage decay.
21 p2665 A73-41123
- An analytical solution of the problem of a frequency tripler employing a varactor diode with an arbitrary charge-charge characteristic
24 p3072 A73-44927
- ### JUNCTION TRANSISTORS
- The degradation of MOS transistors resulting from junction avalanche breakdown.
01 p0023 A73-10648
- Effects of transverse diffusion and transverse stored charge in alloy transistor base.
01 p0023 A73-10681
- On the measurement of the specific 'emitter efficiency factor in bipolar transistors.'
02 p0147 A73-12043
- A simple method for determining static parameters of large signal semiconductor diode and transistor models.
02 p0147 A73-12044
- GaAs-GaAlAs heterojunction transistor for high frequency operation.
02 p0147 A73-12046
- A two-dimensional analysis of gallium arsenide junction field effect transistors with long and short channels.
02 p0147 A73-12047
- Uniform junction microwave transistor fabrication by automatically controlled diffusion technique, using low temperature phosphosilicate glass films on silicon wafers
02 p0147 A73-12164
- Metal-dielectric-semiconductor junction transistor HF response analysis by digital computer, deriving switching time as function of impurity concentration and electrode voltage
05 p0556 A73-16069
- Current saturation mechanisms in junction field-effect transistors.
05 p0558 A73-16605
- Optimal currents, voltages and frequencies for noise measurement in HF transistors for reliability prediction and failure analysis, noting diffusion alloyed and planar transistors
06 p0675 A73-18078
- Dependence of the current-voltage characteristic of a p-n-p drift triode on the donor concentration in the n-type base
06 p0675 A73-18081
- Temperature dependent small signal operation of junction transistors at low supply voltage
06 p0677 A73-18395
- Distributed base resistance effect on stripline geometry transistor input characteristic, using equivalent circuit with pseudo-junction having high saturation current
06 p0677 A73-18396
- High-frequency physical equivalent circuit of junction transistors in common collector configuration.
06 p0682 A73-18843
- Effect of carrier multiplication in the collector junction of an alloyed transistor on the behavior of the transistor at high current densities
07 p0798 A73-19292
- Temperature effects on transistor input and output static characteristics, proposing thermal stabilization by collector circuit resistance decrease and heat dissipation increase
07 p0798 A73-19294
- Investigation of the influence of the emitter current on the collector junction capacitance of transistors
07 p0799 A73-19399
- Book - Introduction to quantum electronics.
08 p0994 A73-20951
- Surface oxide transistor with MIS and base contacts, investigating I-V characteristics as function of oxide thickness and contact separation distance
08 p0948 A73-21480
- Interdigitated power junction transistor technology assessment for power gain, bandwidth and frequency performance, noting packaging effect and thin film module advantage
08 p0949 A73-21648
- Two dimensional analysis of minority carriers in drift p-n-p junction transistor base for low level injection and constant mobility and diffusivity
09 p1062 A73-22310
- Drift of the breakdown voltage in highly doped planar junctions.
09 p1064 A73-23047
- Analysis of parametron oscillation characteristics based on the collector-junction capacitance of the transistor.
10 p1193 A73-23666
- Multistage diffusion model of IC transistor electrical characteristics and impurity distributions as function of surface concentrations and junction depths during fabrication
10 p1196 A73-24606
- Avalanche mode I-V characteristics of diffused and alloyed junction transistors at large collector currents
10 p1196 A73-24609
- Book - Introduction to semiconductor devices: Diodes, bipolar transistors, JFETs, IGFETs, SCRs and integrated circuits.
12 p1478 A73-27050
- Book - The physics and circuit properties of transistors.
15 p1850 A73-31574
- Book - MOS integrated circuits: Theory, fabrication, design and systems applications of MOS LSI.
15 p1852 A73-32579
- Small-signal modelling and characterization of microwave transistors.
16 p1990 A73-33687
- Transient temperature response of semiconductor devices under pulsed power operation.
17 p2135 A73-34728
- Book - Solid state electronic circuits: For engineering technology.
18 p2292 A73-35899
- An integral transistor model using the quality parameters of a technological process
19 p2409 A73-37400
- Electrical properties and simplified theory of a particular junction field-effect transistor operating with a forward gate-source bias.
19 p2409 A73-37428
- Pulsed RF life of an L-band power transistor.
19 p2411 A73-38460
- High power transistor amplifier thermal design with heat sink convective and radiant cooling for low junction temperature and long service life
19 p2411 A73-38474
- Selection of conditions for the fabrication of planar n-p-n silicon transistors with the application of the ion-beam alloying method
20 p2535 A73-38858
- Calculation of the base layer conductivity of a transistor structure
20 p2535 A73-38859
- On the validity of the gradual channel approximation for junction field effect transistors with drift velocity saturation.
20 p2535 A73-39006
- A study of the effect of the emitter current on the barrier capacitance of a transistor collector junction.
20 p2536 A73-39395
- A two-dimensional numerical analysis of a silicon n-p-n transistor.
20 p2536 A73-39413
- The Ebers-Moll effect transistor used as a low-value controlled resistor in ACC and other variable-gain applications.
21 p2661 A73-40229
- Thermal response of microwave transistors under pulsed power operation.
21 p2663 A73-40774
- Planar conductance transistor based on charge carrier accumulation due to n-n junction, featuring steep negative resistance characteristics and low sustaining voltage
21 p2655 A73-41048
- Diffusion profile measurements in the base of a microwave transistor.
21 p2668 A73-41560
- Junction or Schottky gate type FET power gain and high frequency limitations from γ parameters calculation, using analog RC transmission line as equivalent network
23 p2963 A73-43452
- Two-terminal current-fed negative admittance incorporating field effect transistors.
23 p2961 A73-44145
- Influence of emitter current concentration effects on the temperature distribution in power transistors
24 p3072 A73-44930
- ### JUNCTIONS
- Liquid helium temperature range thermometry using superconducting tunnel junction devices with temperature dependent I-V characteristics
22 p2856 A73-42018
- ### JUPITER (PLANET)
- Time variations of the ultraviolet absorption in the continuous spectrum of Jupiter and Saturn
01 p0101 A73-10843
- Brightness temperature measurement of Callisto satellite thermal radio emission, using ice layer model
01 p0101 A73-10845
- Synoptic Jupiter visual observation during 1966-1968, noting band activity and Red Spot longitude change
01 p0101 A73-10849
- Gas-liquid hydrogen mixture and helium adiabatic model of Jupiter temperature and pressure distribution, estimating planet center temperature
01 p0107 A73-11324
- Measurement of Jupiter's radio emission at 2.94 m.
01 p0107 A73-11330
- Gravitational fields of Jupiter and Saturn.
01 p0107 A73-11332
- Non-dipole terms in the magnetic fields of Jupiter and the earth.
02 p0212 A73-11897
- Jupiter exploration current status, discussing orbital and physical data, mass, density, rotation, atmosphere, band structure, red spot, radio emission, magnetic field, internal structure, etc
02 p0212 A73-11948
- Nonstellar origin of Jupiter from tidal instability considerations, discussing binary star formation
02 p0216 A73-12377
- The transmission of mass and angular momentum from a satellite or planetary system to its primary.
02 p0225 A73-12810
- Jovian spectrum at 8-13 microns from 60 inch IR telescope, discussing surface brightness of central disk and brightness temperature spectrum
03 p0374 A73-13850
- Trajectory analysis for swingly technique using Jovian gravitational field for leaving plane of ecliptic along heliocentric orbit and for solar flyby at specified distance
03 p0378 A73-14552
- Decametre-wave radiation from Jupiter and solar activity.
04 p0491 A73-14956
- Water frost absorptions in IR reflectivities of Jupiter Galilean satellites, discussing surface cover distributions and underlying material reflectivity
04 p0497 A73-15070
- Color structure in Jupiter observations, discussing use of binoculars and graphical representation methods
05 p0578 A73-17097
- Deuterium-hydrogen ratio in Jupiter.
05 p0623 A73-17182
- Far IR brightness temperature, opacity and emissivity of Jupiter, Venus, Mars and Saturn
05 p0626 A73-17348
- Mutual phenomena of Jupiter's satellites in 1973-74.
07 p0875 A73-19260
- Analytical theory of the motion of the fifth Jupiter satellite
07 p0876 A73-19395
- Structure and evolution of the asteroid ring
07 p0902 A73-20324
- Infrared spectra of the Galilean satellites of Jupiter.
08 p1004 A73-20901
- Observations of Jupiter with Danjon astrolabes in 1965, 1966, and 1967
08 p1005 A73-20911
- The beta Scorpii occultation by Jupiter. I - The Jovian diameter.
08 p1006 A73-20934
- Jupiter southern equatorial band eruptive centers and decametric radio sources interrelationship, discussing reconnections responsible for Red Spot displacement sense
08 p1012 A73-21474
- Cometary parent bodies transfer to short period orbits by Jupiter caused gravitational disturbances, noting qualitative analysis of orbits evolution
08 p1012 A73-21576
- Photometric characteristics of Jupiter and Saturn in the 0.48-0.33-micron range.
08 p1012 A73-21578
- Jupiter surface maps for 1965-70 from drawings obtained with astrophot, noting high activity and eruptive changes after 1961-63 outburst
08 p1012 A73-21583
- Jupiter surface maps from synoptic observations with refracting telescope, considering white cloud formations and atmosphere motions
08 p1012 A73-21584
- Fine structure of the Jupiter radio bursts.
08 p1013 A73-21646
- Jupiter astrolabe observations analysis, investigating corrections for defective illumination, instrumental comparisons and systematic errors
09 p1140 A73-22002
- Survey of the outer planets Jupiter, Saturn, Uranus, Neptune, Pluto, and their satellites.
11 p1417 A73-25315
- Major planets nonthermal radio emission observations, noting powerful decametric sources related to Jupiter rotation and Io orbital motion
11 p1420 A73-25879
- Jupiter's decametric rotation period and the Source-A emission beam.
11 p1420 A73-25881

- Thermal radio emission from Jupiter and Saturn.
11 p1420 A73-25883
- Electrical conductivity of condensed molecular hydrogen in the giant planets.
11 p1420 A73-25885
- Thermodynamic parameters for metallic hydrogen-helium alloy of Saturn and Jupiter interiors, using Monte Carlo chains and dielectric function theory
11 p1420 A73-25888
- Stellar evolutionary calculation for Jupiter, considering gravitational contraction
11 p1420 A73-25892
- Jupiter radio observations at 13 cm during 1969 and 1971 oppositions for circular polarization and flux density
11 p1424 A73-26128
- Jovian decametric emission origin in cyclotron instability of weakly relativistic electrons trapped in magnetic field, considering group velocity in magnetospheric plasma
11 p1424 A73-26129
- Energetic electron production and loss model for Jupiter radiation belt, considering drive mechanisms for electron diffusion from solar wind
11 p1424 A73-26130
- Jupiter radiation reception at decametric wavelengths by Yagi antenna and radiometer, taking into account Io modulation effect
11 p1424 A73-26131
- Galilean satellites surface thermal properties from radiometry of 20-micron band during eclipses of Jupiter
11 p1424 A73-26132
- Position and velocity components for Jupiter VIII-XII.
11 p1429 A73-26684
- Observations of the satellites Jupiter VI and VII.
12 p1540 A73-27429
- Preliminary results of observations at the 2-cm wavelength of discrete sources and Jupiter at Pulkovo
12 p1546 A73-27855
- Polarimetric studies of the giant planets. III - Jupiter
12 p1546 A73-27861
- Orbital characteristics of comets passing through the 1:1 commensurability with Jupiter.
14 p1790 A73-29785
- On the motion of short-period comets in the neighbourhood of Jupiter.
14 p1790 A73-29786
- The determination of Jupiter's mass from large perturbations on cometary orbits in Jupiter's sphere of action.
14 p1792 A73-29810
- Determination of the mass of Jupiter from observations of 10 Hygiea during 1932-1969.
14 p1792 A73-29811
- The effect of the ellipticity of Jupiter's orbit on the capture of comets to short-period orbits.
14 p1794 A73-29831
- Evolution of short-period cometary orbits due to close approaches to Jupiter.
14 p1794 A73-29832
- The major planets as powerful transformers of cometary orbits.
14 p1794 A73-29834
- Deformation of a meteor stream caused by an approach to Jupiter.
14 p1795 A73-29843
- Orbital evolution of the alpha Virginid and alpha Capricornid meteor streams.
14 p1795 A73-29844
- On convection and gravitational layering in Jupiter and in stars of low mass.
14 p1797 A73-30009
- Jupiter He abundance determination methods, considering mean density, spectral line broadening and stellar occultations with emphasis on far IR emission
14 p1799 A73-30533
- Long wave measurements of brightness temperature for thermal structure of major planet atmospheres at great depths, discussing Jupiter and Saturn microwave spectra
14 p1800 A73-30537
- Solar wind properties near and beyond Jupiter orbit, considering steady state wind extrapolation to large distances, cosmic ray modulation and interactions with planetary bodies
14 p1787 A73-30541
- Temporal variation of ultraviolet absorption in continuous spectra of Jupiter and Saturn.
15 p1928 A73-30979
- Brightness temperature measurement of Callisto thermal radio emission, using ice layer model
15 p1928 A73-30981
- Synoptic Jupiter visual observation during 1966-1968, noting band activity and Red Spot longitude change
15 p1928 A73-30985
- Observational constraint on the structure of hydrogen planets.
15 p1936 A73-31565
- Horseshoe and Trojan orbits associated with Jupiter and Saturn.
15 p1937 A73-31948
- Pioneer 10 spacecraft spin-scan imaging photopolarimetric optical system for Jupiter mapping
15 p1880 A73-32385
- Contribution to the dynamic study of the Galilean system of Jupiter. I - The intermediate solution in the nonresonant case
16 p2059 A73-32839
- Jupiter's radiation belts and the sweeping effect of its satellites.
16 p2062 A73-33429
- Radio emission from the moon and sun at the 2.25-mm wavelength and from Jupiter at the 2.1-mm wavelength
16 p2064 A73-33768
- Radio emission from Venus and Jupiter at 2 and 8 mm wavelengths
16 p2068 A73-33817
- Jupiter and Saturn optical observations, discussing atmospheric composition, cloud layers and temperature distribution
16 p2069 A73-33837
- Results of observations of methane /6190 A/ and ammonia /6441 and 6478 A/ absorption bands on the Jovian disk over a period of three years
16 p2070 A73-33840
- Continuing activity of Jupiter and comparison of the 1871-1880 and 1961-1965 flare-ups
16 p2057 A73-33842
- Results of Jupiter observations in the centimeter wavelength range
16 p2070 A73-33844
- An experiment in photographic equidensitometry of the moon and planets
16 p2070 A73-33848
- Interior of Jupiter and Saturn.
17 p2226 A73-34357
- Venus and Jupiter telescopic observation aiming errors using Wanschaff verticle circle, suggesting error sources and correction procedures
17 p2230 A73-34593
- Ammonia absorption relevant to the albedo of Jupiter. I - Experimental results.
17 p2231 A73-34764
- New infrared spectra of the Jovian planets from 12,000 to 4000/cm by Fourier transform spectroscopy. I - Study of Jupiter in the 3 nu-sub 3 CH4 band.
17 p2234 A73-35617
- Plasma physics phenomena in the outer planet magnetospheres.
18 p2345 A73-36097
- [AIAA PAPER 73-566] Jupiter and Saturn interior structure models based on state equations and transport properties of hydrogen and helium at high pressures and temperatures
18 p2354 A73-36644
- Fine structure of Jupiter's decametric source B.
19 p2482 A73-37389
- Narrow-band photometry of the Galilean satellites.
19 p2483 A73-37577
- Spectral albedos of the Galilean satellites.
19 p2483 A73-37578
- The electron energy and number densities of the Jovian radiation belt. I.
19 p2475 A73-37621
- Analysis of the Jovian electron radiation belts. II - Observations of the decimetric radiation.
19 p2475 A73-37622
- The occultations and the mutual eclipses of the Galilean satellites of Jupiter
20 p2604 A73-39009
- Preliminary results of observations of discrete sources and of Jupiter with 2-cm wavelength at Pulkovo.
20 p2608 A73-39229
- Polarimetric observations of the giant planets. III.
20 p2608 A73-39235
- Evolution of the orbits and radiants of meteor swarms of the Jupiter family
21 p2768 A73-40724
- On the 3-7 commensurability between Jupiter's outer two Galilean satellites.
21 p2778 A73-41531
- Occultation of beta Scorpio by Jupiter on May 13, 1971.
21 p2779 A73-41544
- A possible connection between variation in the rotational period of Jupiter's central zone and variation in its equatorial diameter.
21 p2779 A73-41545
- The far-ultraviolet spectrum of Jupiter.
22 p2905 A73-41769
- Pioneer 10 flyby trajectory relationship to analogy between earth and Jupiter bow shocks with emphasis on oblique shock structure
22 p2906 A73-41942
- The source and structure of the Jovian radiation belt.
22 p2903 A73-42986
- An atmosphere on Ganymede from its occultation of SAO 186800 on 7 June 1972.
23 p3027 A73-43337
- Narrow band IR vidicon Jupiter and Saturn photography, showing limb darkening and surface details
23 p3032 A73-43942
- Rotation period for a subsurface source in the NNTeB of Jupiter.
23 p3033 A73-43947
- Exploring Jupiter, Saturn and their satellites.
23 p3034 A73-44221
- Mars and Jupiter - Radio emission at 1.35 cm.
24 p3128 A73-44399
- Mutual Jupiter satellite-satellite eclipses and occultation observations for improved ephemerides, albedo maps, radii and limb darkening estimation
24 p3130 A73-44454
- Area-scanning photometric observations of Galilean satellite surface color variations due to orbital phase and Jupiter environment
24 p3130 A73-44455
- Jupiter magnetic dipole offset along rotation axis from 11 cm radio centroid measurements with Parkes telescope
24 p3130 A73-44459

JUPITER ATMOSPHERE

Jovian atmosphere absorption line and spectroscopic data interpretation based on model for structure, composition and radiative properties of visible cloud layers
01 p0097 A73-10359

The infrared spectrum of Jupiter - Structure and radiative properties of the clouds.
01 p0097 A73-10370

Extensive air showers on Jupiter, and its sporadic decametric radio emission.
01 p0106 A73-11323

Infrared maps of Jupiter.
01 p0109 A73-11490

Jupiter atmosphere density fluctuations as cause of time symmetric light flash occurrence during Beta Scorpil occultation
04 p0496 A73-14926

The abundance of NH3 on Jupiter inferred from UHF radiometry data.
05 p0619 A73-16881

[AIAA PAPER 73-128] Engineering models for Jupiter's troposphere and the NH3-H2O cloud systems.
05 p0619 A73-16882

[AIAA PAPER 73-129] An earlier generation of long-enduring south temperate ovals on Jupiter.
06 p0745 A73-17441

Jovian atmosphere upper layers high temperature evidenced during star Beta Scorpion occultation by Jupiter
06 p0745 A73-17475

The abundance of CH3D and the D/H ratio in Jupiter.
07 p0874 A73-19066

Jupiter upper atmosphere temperature inversion to explain brightness temperature variation in 7.9 micron methane band, observing limb brightening
08 p1004 A73-20900

Some results of spectrophotometry of the methane absorption band /7250 A/ on the Jovian disk
08 p1007 A73-21063

Investigation of molecular absorption in the atmospheres of the giant planets
08 p1007 A73-21064

Optical characteristics and structure of the Jovian atmosphere. V - Probable structure of the ammonia aerosol layer.
08 p1012 A73-21577

Summary of Jovian latitude and rotation period observations from 1898 to 1970.
11 p1415 A73-25134

Spectroscopy of Jupiter - 3200 to 11,200 A.
11 p1418 A73-25720

Estimate of the mean size of cloud layer particles in the Jovian atmosphere
11 p1423 A73-26080

Electric discharge and microbiological experiments in simulated Jovian atmosphere for investigation of Jupiter life prospects
11 p1319 A73-26478

The geometry and dynamic spectra of Io-modulated Jovian decametric radio emissions.
12 p1540 A73-27327

Jupiter atmosphere fluid dynamic models, considering cloud spot markers and wave motions from ground and spacecraft observations
12 p1542 A73-27606

Interpretation of hydrogen quadrupole and methane observations of Jupiter and the radiative properties of the visible clouds.
13 p1673 A73-28280

Photometric investigation of the atmospheric activity of Jupiter during 1962-1969
13 p1673 A73-28297

The significance of atmospheric measurements for interior models of the major planets.
14 p1799 A73-30532

The dynamics of the atmospheres of the major planets.
14 p1799 A73-30534

The photochemistry of hydrocarbons in the Jovian atmosphere.
14 p1802 A73-30766

Structure and time variations of the Jovian ionosphere.
15 p1929 A73-31066

K

Photoelectron excitation of the Jupiter dayglow.
16 p2062 A73-33430

Investigation of molecular absorption features in the spectrum of Jupiter
16 p2070 A73-33839

Photometric studies of the Jovian atmospheric activity
16 p2070 A73-33841

Red Spot interaction with small Jupiter dark spots moving along northern edge of south temperate zone
16 p2070 A73-33843

Carbon isotope abundance ratios in comets and Jupiter atmosphere, discussing hydrogen isotope ratio determination for Saturn and Jupiter atmospheres
17 p2228 A73-34418

Atomic collision processes applied to earth atmospheric physics and chemistry, Jovian ionospheric composition and terrestrial tropical UV dayglow
17 p2213 A73-34450

Wave propagation in the magnetosphere of Jupiter.
17 p2229 A73-34506

On limits to Jupiter's magnetospheric diffusion rates.
17 p2224 A73-34511

Jupiter atmospheric circulation as manifestation of large scale convective instability generated by internal heat sources, considering Red Spot production
17 p2232 A73-34859

On the temperature of the Jovian thermosphere.
17 p2232 A73-34860

Photochemical reactions in the Jovian atmosphere.
17 p2237 A73-35835

Spacecraft microbial burden reduction due to atmospheric entry heating - Jupiter.
18 p2281 A73-36100

Effect of downstream massive blowing on Jovian entry heating.
[AIAA PAPER 73-717] 18 p2264 A73-36336

Probing the structure and composition of the Jupiter atmosphere from Pioneer 10/11.
[AIAA PAPER 73-561] 18 p2353 A73-36498

Spectrophotometry of the 7250-A methane absorption band over the disk of Jupiter.
18 p2355 A73-36864

Molecular absorption in the atmospheres of the giant planets.
18 p2355 A73-36865

Jupiter atmosphere discrete source maps of 5 micron radiation distribution, correlating brightness temperature and photographically recorded colors
19 p2489 A73-38525

Jovian ionospheric and magnetospheric ionization and temperature distributions from solutions of momentum and chemical equations for electrons, ions and neutrals, and heat transport equation
21 p2764 A73-40165

Jupiter magnetospheric interaction with innermost satellite Io, noting magnetic field annihilation enhancement in neutral point by LF MHD waves
21 p2764 A73-40166

The propagation of Alfvén waves along Io's flux tube.
21 p2764 A73-40167

Photometric studies of atmospheric activity of Jupiter during 1962-1969.
21 p2779 A73-41541

The International Planetary Patrol Program - An assessment of the first three years.
22 p2912 A73-42978

Jupiter and terrestrial upper atmospheres comparison, discussing solar wind interactions with planetary magnetic fields, Jovian Van Allen belt and cold plasma distribution
22 p2913 A73-42985

Measurements of hydrogen-helium radiation at shock-layer temperatures appropriate for Jupiter entry.
22 p2938 A73-42993

The temperature and ammonia profiles in the Jovian atmosphere from inversion of the Jovian emission spectrum.
22 p2915 A73-43017

Jupiter HD absorption line measurement for model-independent number ratio D/H
22 p2916 A73-43125

Ammonia density profiles and photochemical destruction above Jovian tropopause as function of eddy diffusion coefficient, considering background atmosphere scale height
23 p3028 A73-43601

Multicolor astronomical photography of Jupiter using wideband filters, emphasizing Red Spot, atmospheric bright belts and methane absorption variations above clouds
23 p3032 A73-43941

Jupiter zone and Red Spot latitude measurements and visual color evaluation in near IR methane band
23 p3032 A73-43943

Photographic observations of the occultation of Beta Scorpii by Jupiter.
23 p3033 A73-43944

Initial development of the June 1971 South Equatorial Belt disturbance on Jupiter.
23 p3033 A73-43945

Observations of the South Equatorial Belt disturbance on Jupiter in 1971.
23 p3033 A73-43946

A correlation between colors of Jovian clouds and their 5-micron temperatures.
23 p3033 A73-43948

Recent observations of Jupiter's North North Temperate Belt Current B.
23 p3033 A73-43949

Jupiter radiative greenhouse model overestimation of lower cloud level temperature due to convective heat transport neglect, discussing rejection of water cumulus cloud possibility
24 p3129 A73-44439

The optical properties of Venus and the Jovian planets. I - The atmosphere of Jupiter according to polarimetric observations.
24 p3129 A73-44442

On the level of H₂ quadrupole absorption in the Jovian atmosphere.
24 p3129 A73-44443

Formation of spectral lines in planetary atmosphere. IV - Theoretical evidence for structure of the Jovian clouds from spectroscopic observations of methane and hydrogen quadrupole lines.
24 p3129 A73-44449

Radiative instability model of cloud cover on equatorial beta plane to explain Jupiter bands zonal symmetry and meridional wavelength
24 p3132 A73-44535

Jovian ammonia photolysis to nitrogen, explaining ammonia observations by deep and hot atmosphere and/or electrical discharge phenomena
24 p3065 A73-44536

Methane absorption in the Jovian atmosphere. I - The Lorentz half-width in the 3nu/sub 3/ band at 1.1 micron.
24 p3132 A73-44537

Methane absorption in the Jovian atmosphere. II - Absorption line formation.
24 p3133 A73-44559

Short-term Jovian rotation profiles, 1970-1972.
24 p3134 A73-44562

Spectral data for the nu sub 2 bands of ammonia with applications to radiative transfer in the atmosphere of Jupiter.
24 p3142 A73-45324

JUPITER PROBES

Data return maximization for unpredictable channel capacity, considering planetary entry probe to Venus or Jupiter with unknown atmospheric transmission characteristics
04 p0420 A73-15425

The effects of trajectory characteristics on scientific objectives for major planetary orbiters.
06 p0757 A73-18376

Pioneer Jupiter spacecraft magnetic field control with periodically updated magnetic model for tradeoffs in subsystem moments within allowed magnetic budget
[IEEE PAPER 41,4] 07 p0905 A73-19364

Navigation system design for the Mariner Jupiter/Saturn Mission.
[AIAA PAPER 73-838] 21 p2736 A73-40503

Planetary flybys resulting in heliocentric orbits normal to the ecliptic with fixed perihelia.
22 p2909 A73-42628

JUPITER PROJECT

Mariner Jupiter/Saturn 1977 - The mission frame.
02 p0221 A73-12597

Orbit determination capability analysis for the Mariner-Jupiter-Saturn 1977 mission.
[AIAA PAPER 73-171] 06 p0748 A73-17650

JUPITER RED SPOT

Synoptic Jupiter visual observation during 1966-1968, noting band activity and Red Spot longitude change
01 p0101 A73-10849

Properties of the Red Spot of Jupiter in 1971.
03 p0371 A73-13216

High pressure physics and planetary interiors; Proceedings of the Conference, Houston, Tex., March 1-3, 1972.
11 p1419 A73-25876

Synoptic Jupiter visual observation during 1966-1968, noting band activity and Red Spot longitude change
15 p1928 A73-30985

Red Spot interaction with small Jupiter dark spots moving along northern edge of south temperate zone
16 p2070 A73-33843

Jupiter Red Spot photographic, IR image, spectral, photometric, polarimetric and chemical studies, comparing with earth and Mars atmospheric data
23 p3032 A73-43940

Multicolor astronomical photography of Jupiter using wideband filters, emphasizing Red Spot, atmospheric bright belts and methane absorption variations above clouds
23 p3032 A73-43941

Jupiter zone and Red Spot latitude measurements and visual color evaluation in near IR methane band
23 p3032 A73-43943

**K BAND
U EXTREMELY HIGH FREQUENCIES
K LINES**

L-beta /2/ and K-alpha X ray spectra of niobium and carbon in NbC compound, assuming collectivized valence electrons
02 p0180 A73-12174

X ray K absorption spectra shifts /Bergard additivity rule deviations/ in Fe-Cr, Fe-V, Fe-Ni and Fe-Co systems due to lattice characteristics and electron structure changes
06 p0707 A73-18039

The spectra of near-vertical structures on the solar disk.
08 p1001 A73-20752

Stellar and interstellar K lines - Gamma Pegasi and iota Herculis.
08 p1003 A73-20882

Cross correlation coefficients for H, K and H beta lines of solar spectrum related to observed peculiarities from microphotometer intensity traces
[AD-759889] 10 p1278 A73-24131

Suggested interpretation of the correlations in intensity fluctuations in the lines Ca II H and K, magnesium b, and hydrogen H beta /Research note/.
10 p1278 A73-24132

Solar disk emission lines in Ca II H and K line wings from high resolution spectral observations
11 p1422 A73-25934

Temporal intensity fluctuation measurements in K line wing near solar disk center, noting power spectrum peaks and brightness relationship to Fe I line displacement
12 p1544 A73-27830

X-ray spectral study of the K state in a nickel-chromium alloy
12 p1514 A73-27943

Spectral analysis of sunspot flares.
16 p2052 A73-32957

X-ray absorption K-spectra of zirconium and its compounds with elements of the second period in the periodic table
18 p2325 A73-36811

An X-ray spectral study of the electronic structure of nonstoichiometric titanium carbide
21 p2721 A73-41226

**KA BAND
U EXTREMELY HIGH FREQUENCIES
KALMAN FILTERS**

Comparison of Kalman filter and stepwise methods for real time orbit determination.
01 p0105 A73-11187

Linearized Kalman filtering for turbopump rotating assembly inertial and bearing parameter identification and state estimation, noting state-space model feasibility
03 p0313 A73-13904

A new filter for optimal tracking in dense multitarget environments.
03 p0286 A73-14477

Position and rate aided tracking for conventional pointing systems.
04 p0430 A73-15256

System identification using approximate nonlinear filters.
04 p0430 A73-15257

An adaptive Kalman filter using decomposition of the innovations sequence.
04 p0431 A73-15258

Estimation of the statistical parameters of the Kalman-Bucy filter.
04 p0431 A73-15261

A higher measurement space filter for passive tracking.
04 p0431 A73-15262

Minimum variance linear filter with partial state elimination by linear transformation for reduction of computational burden and storage requirements in Kalman filter
04 p0431 A73-15268

On-line parameter estimation of nonlinear dynamic system with unknown impulsive inputs by Kalman filter with application to maneuvering spacecraft tracking
04 p0431 A73-15270

Stability analysis of Riccati covariance equations of Kalman filter.
04 p0472 A73-15273

Application of adaptive tuning of filters to exoatmospheric target tracking.
04 p0498 A73-15275

Pseudo state measurements applied to recursive nonlinear filtering.
04 p0431 A73-15277

Analytical approach to orbit determination in the presence of model errors.
[AIAA PAPER 73-170] 05 p0619 A73-16915

Sequentially best estimators for linear systems with non-linear noise-free sensors.
06 p0681 A73-18522

Demodulation of pulse modulated signals using Kalman filtering techniques.
06 p0669 A73-18809

Adaptive control of linear stochastic systems.
07 p0804 A73-19132

Nearest neighbor approximation for Kalman-Bucy filtering noisy data generated by multidimensional processes via dimensionality reduction for linear steady state problems
07 p0805 A73-20579

Reduced-order observers for linear discrete-time systems.
07 p0805 A73-20581

A discrete separation principle with a stochastic terminal constraint.
07 p0806 A73-20599

On the adaptive control of linear systems using the open-loop-feedback-optimal approach.
07 p0806 A73-20602

Wiener and Kalman-Bucy filters design with error covariance bound for performance divergence prevention under stochastic processes with unknown signal and noise densities
07 p0806 A73-20603

Comparison of theoretical and simulated performance of optimal and suboptimal filters in a dense multitarget environment.
07 p0806 A73-20604

Kalman-Bucy method solution to time-space dependent random fields optimal filtration under additive white noise
07 p0804 A73-20635

Recurrent orbit estimation biases by filtering, using method representing motion by finite difference equations
09 p1143 A73-22098

Kalman filtering theory application to optimal causal demodulator for pulse amplitude modulated signals in white Gaussian noise
09 p1067 A73-22116

Performance comparison of suboptimal Kalman filters modeled for a continuous nonlinear system.
09 p1067 A73-22228

Wiener and Kalman filters theory for stochastic processes in communication, demonstrating optimum demodulator derivation by Kalman-Bucy theory application to double sideband amplitude modulation
09 p1065 A73-23112

Trajectory optimization for the nonlinear combined estimation and control problem.
10 p1200 A73-24044

Optimal filtering for systems described by linear partial differential equations.
10 p1200 A73-24050

A comparison of the effectiveness of some adaptive optimal filtering techniques applied to the gyrocompassing problem.
10 p1201 A73-24052

Estimation of noise covariance matrices for a linear time-varying stochastic process.
10 p1201 A73-24053

Discrete-time fixed-lag smoothing algorithms.
10 p1243 A73-24547

Strapdown inertial system alignment using statistical filters - A simplified formulation.
11 p1395 A73-26377

Modified Kalman filter for digital communication channel equalization with tap gains and initial state variable estimated by decision feedback and prediction process respectively
13 p1593 A73-29118

Speech data rate reduction. I - Applicability of modern estimation theory. II - Applicability of sensitivity and error analysis.
13 p1585 A73-29201

Kalman filter adaptive tracker for ATC applications, modeling aircraft maneuvers by linear system with random noise accelerations based on statistical decision theory
13 p1593 A73-29212

Kalman filter design considerations for space-stable inertial navigation systems.
13 p1657 A73-29220

Kalman filtering of systems with parameter uncertainties - A survey.
13 p1597 A73-29569

A proposal on automatic tracking of an aircraft for the radar.
14 p1728 A73-30471

Mixed autoregressive moving average models parameters recursive joint identification and order determination extended for Kalman-Bucy filter transition and covariance parameters estimation
15 p1853 A73-31630

Kalman-Bucy method for optimal filtering of time and space dependent random fields in Hilbert space in presence of additive white noise
15 p1854 A73-31689

The application of Kalman filtering to the attitude determination of spinning space vehicles.
15 p1944 A73-32219

Memorization and model change, alpha-beta, adaptive model and Kalman type radar pursuit tracking techniques efficiency comparison
15 p1908 A73-32443

Computational efficiency comparison for discrete linear filtering Kalman algorithms and information

matrix methods, noting Householder square-root implementation identity with Potter technique
16 p2032 A73-33404

Nonlinear filter evaluation for estimating vehicle position and velocity using satellites.
16 p1988 A73-33410

Rapid estimation and detection of impulse inputs under continuity constraints for space vehicles.
17 p2144 A73-35375

Optimal feedback control and Kalman filter design via an interactive computing and visual display system.
18 p2295 A73-36839

Kalman filter for rapid detection and adaptive estimation of state and covariance, deriving Bayes decision rule and algorithm for spacecraft tracking
19 p2410 A73-38030

Suboptimal filter design for dynamic measurement systems, deriving bias and Kalman covariance formulae for error analysis and model sensitivity
19 p2410 A73-38031

Parallel algorithms for optimum nonlinear state estimation.
19 p2413 A73-38041

Polynomial estimators for systems with polynomial nonlinearities.
19 p2445 A73-38042

A comparative evaluation of the application of several aircraft parameter identification methods to flight data - with emphasis on the development of rational evaluation criteria.
19 p2386 A73-38044

Autonomous satellite navigation - An historical summary and current status.
19 p2452 A73-38056

Recursive ideal observer detection of known M-ary signals in multiplicative and additive Gaussian noise.
19 p2407 A73-38385

Correctness of the solution of signal filtration and reconstruction problems by an analog computer
20 p2522 A73-38702

Data compression in recursive estimation with applications to navigation systems.
20 p2589 A73-38835

[ALAA PAPER 73-901]

Computerized trajectory estimation for maneuvering reentry vehicles, obtaining minimum variance trajectory parameters by Kalman filtering of radar, optical and inertial reference measurements
20 p2589 A73-38836

[ALAA PAPER 73-902]

Optimum cross-coupled tracker for pulse-Doppler radar.
21 p2649 A73-40328

Maneuvering target motion modeling with binary random variable in state equation, obtaining optimal tracking solution as weighted combination of two Kalman filter estimates
21 p2649 A73-40331

Linear Kalman filter triangular square root formulation guaranteeing positive covariance matrix, computation and time savings and core storage requirement standardization
21 p2736 A73-40422

Aircraft and spacecraft radio navigation systems, discussing Doppler, inertial and VHF omnirange techniques, Apollo spacecraft guidance systems, TACAN, Harrier and Swedish SAAB37 aircraft navigation
21 p2736 A73-40514

Unsupervised learning of the Kalman filter.
21 p2664 A73-41109

Laguerre transform of a continuous signal - Application to the study of the asymptotic regime of a Kalman filter
22 p2832 A73-42352

Model reference adaptive control system design using Kalman-Yacubovich lemma in connection with Lure problem
23 p2964 A73-43827

Simultaneous statistical treatment of the readings of a directional gyroscope and a magnetic compass
24 p3089 A73-44547

KALMAN-SCHMIDT FILTERING

Linear filtering of ballistic-entry-probe data for atmospheric reconstruction.
20 p2589 A73-38838

[ALAA PAPER 73-904]

KAMACITE

Iron and stony-iron meteorites kamacite hardness and shock histories, hypothesizing preterrestrial collisions between asteroid sized objects
05 p0615 A73-16377

Stony-iron meteorite shock histories, determining crystallographic character of kamacite in samples via back reflection X ray diffraction technique
11 p1419 A73-25780

X ray and electron diffraction studies of Ni-containing etched brown rims in meteoritic taenite [Ni-Fe alloy] associated with kamacite, noting Widmanstatten pattern
23 p2951 A73-43844

KAMIN

KALMAN

KALMAN AIRCRAFT

NT HH-43 HELICOPTER

U GLACIAL DRIFT

KANSAS

ERTS-1 multispectral scanner analysis of Kansas reservoirs color and water content, discussing turbidity, gray coloration levels, water management possibilities and water sample data
20 p2563 A73-39912

KAOLINITE

On the asymmetric adsorption of phenylalanine enantiomers by kaolin.
24 p3066 A73-44772

KAPITZA RESISTANCE

Theory of Kapitza's jump in temperature at the interface between a solid body and liquid helium
01 p0079 A73-11281

Some experiments on the influence of surface treatment on the Kapitza conductance between copper and He4 at temperatures from 1.2 to 2.0 K.
21 p2741 A73-41105

Theory of the Kapitza temperature discontinuity at a solid body-liquid helium boundary.
23 p3006 A73-43502

KARHUNEN-LOEVE EXPANSION

Maximum information compression and minimum entropy of random process, using Karhunen-Loeve basis
13 p1596 A73-28869

KARMAN VORTEX STREET

Karman vortex street characteristics of single circular cylinders and heat exchanger tube bundles, presenting drag, lift and Strouhal number as function of Reynolds number
11 p1299 A73-25108

Cloud eddy formation in wakes of single mountain islands similar to Karman vortex streets, noting application to wind field forecasting
18 p2334 A73-37075

Development of a mathematical model for vortex configuration in jets and flames.
24 p3157 A73-45376

KC-130 AIRCRAFT

U C-130 AIRCRAFT

KELVIN TEMPERATURE SCALE

U TEMPERATURE SCALES

KELVIN-HELMHOLTZ INSTABILITY

Kelvin-Helmholtz instability in a high-beta collisionless plasma.
07 p0856 A73-19520

Observation of Kelvin-Helmholtz billows and their mesoscale environment by radar, instrumented aircraft, and a dense radiosonde network.
13 p1652 A73-28268

Free parallel shear flow approximation by velocity discontinuity involving Kelvin-Helmholtz waves longer than shear layer thickness
13 p1605 A73-29448

Effect of wind shear on atmospheric wave instabilities revealed by FM/CW radar observations.
19 p2447 A73-38206

Finite amplitude Kelvin-Helmholtz billows, describing periodic solutions of nonlinear Boussinesq equation
19 p2448 A73-38230

Turbulence in stably stratified fluids - A review of laboratory experiments.
19 p2449 A73-38234

Thermal structure and stability study of internal and Kelvin-Helmholtz waves in low Reynolds number flows by sampling and stratified wind tunnel methods
19 p2422 A73-38235

The formation and breakdown of Kelvin-Helmholtz billows.
19 p2422 A73-38244

Rayleigh-Taylor instability in octyl alcohol-water interface, observing bubble and spike formation with flattening and curling of spike due to Kelvin-Helmholtz instability
22 p2842 A73-42232

Internal gravity wave-mean wind interaction.
23 p3000 A73-43339

KEPLER LAWS

Universal dimensionless formulas for physical property and trajectory computation in cosmic spherical media, applying to Kepler orbits, particle motions and radio wave paths
01 p1013 A73-11019

Evolution of a satellite orbit under the influence of light pressure
02 p0211 A73-11777

Processing of results of observations of the satellite 65-011-04 carried out within the framework of INT-EROBS program 1966.
02 p0159 A73-12170

Short term bounds for the effect of oblateness on ballistic trajectories.
03 p0373 A73-13495

Complex variable analysis for exact solution to Kepler equation for elliptical and hyperbolic orbits based on canonical solutions to Riemann problem
03 p0376 A73-14269

Newtonian differential equations of Kepler motion, analyzing stability by numerical integration based on Floquet theorem and Runge-Kutta method
04 p0497 A73-15013

Interaction of stars with local dust formations.
04 p0503 A73-16008

Calculus of variations for equations of relative motion of two satellites with unperturbed Kepler orbits of arbitrary eccentricity 05 p0620 A73-17006

The anisotropic Kepler problem in two dimensions. 08 p0988 A73-21204

Transcendental equations solution for satellite Kepler orbit determination from coordinates, velocity and time components, using Lambert-Euler relation 12 p1543 A73-27629

Isochronous derivatives of certain spacecraft-trajectory parameters 14 p1796 A73-29857

A note on the relations between true and eccentric anomalies in the two-body problem. 15 p1930 A73-31116

Contribution to the dynamic study of the Galilean system of Jupiter. I - The intermediate solution in the nonresonant case 16 p2059 A73-32839

Numerical integration errors due to differential equations instability for Kepler orbits, discussing error reduction procedure by substituting for time as independent variable 16 p2061 A73-33231

Third Kepler law application to quanta hypothesis of two body systems of physical nature involving centers of attraction 16 p2071 A73-34004

Small grain aggregates created by equalized grain orbits on Kepler trajectories, with low collisional frequency in early state of solar system planetary evolution 17 p2227 A73-34407

Symmetry transformations of the classical Kepler problem. 19 p2446 A73-38382

Dynamical symmetries of the Kepler problem and of the harmonic oscillator in classical mechanics revisited. 22 p2887 A73-42429

Kustaanheimo-Stiefel transformation in Kepler motion perturbation theory derived from general solution of two body problem, noting application to collision orbits and Lagrange solutions 24 p3142 A73-45298

KERNEL FUNCTIONS

Reduction of integral equations in elasticity theory to infinite systems 01 p0116 A73-10960

Invariant imbedding and Chandrasekhar's planetary problem of radiative transfer. 02 p0207 A73-12389

An improved kernel function formulation for unsteady subsonic flow. 05 p0567 A73-17122

Approximation of experimental rheological curves by distribution functions 08 p1019 A73-21592

Probabilistic model for the resolvent kernel in diffusion problems in spherical-shell media. 09 p1121 A73-23071

Mixed boundary value problems in solid contact and crack mechanics, discussing numerical solution of singular integral equations with simple and generalized Cauchy kernels 09 p1162 A73-23184

Combined-operations method for diffuse reflection by an isotropic, non-coherent scattering homogeneous sphere. 10 p1271 A73-23484

The use of operators with degenerated kernel for nonlinear system investigation. 10 p1242 A73-24043

Coherent state systems for groups of motions of Hermitian bounded homogeneous regions in terms of Bergman kernels 10 p1249 A73-24463

Statistically orthogonal functions for finite intervals of a random process 11 p1390 A73-25642

On the reduction of integral equations of the theory of elasticity to infinite systems. 12 p1554 A73-27536

Equivalence of one type of a Riemann boundary value problem for a system of n pairs of functions relative to a complete singular integral equation with a Cauchy kernel 12 p1518 A73-27730

Some error estimates for approximate solutions of nonlinear integral Hammerstein-type equations 12 p1519 A73-27818

A method for obtaining bounds on eigenvalues and eigenfunctions by solving non-homogeneous integral equations. 13 p1647 A73-28192

Modified separable kernel method for heat conduction with a nonlinear boundary condition. 13 p1706 A73-28819

Radiant heat transfer on circular-finned cylinders. 14 p1817 A73-30574

Optimal grid arrangement in vortex lattice method of lifting surface aerodynamic analysis, comparing numerical with kernel function results for simple wing planforms 15 p1824 A73-31746

Symmetric integral equations of the theory of elasticity 17 p2251 A73-35585

A kernel function method for computing steady and oscillatory supersonic aerodynamics with interference. 18 p2262 A73-36221

[AIAA PAPER 73-670] On the Volterra series functional evaluation of the response of non-linear discrete-time systems. 22 p2837 A73-43069

Truncation error in the solution of integral equations. 24 p3106 A73-45344

KEROSENE

Vibrational and chemical nonequilibrium in a stoichiometric turbojet engine using kerosene-type fuel. 03 p0273 A73-13491

[AIAA PAPER 72-1208] Pyrolysis of kerosene and mechanism of formation of carbon deposits [ONERA, TP NO. 1157] 04 p0485 A73-15989

Test data obtained with an experimental gas turbine operated with kerosene combustion products artificially contaminated by dust 14 p1785 A73-30650

Ignition temperature of conglomerates which form by burnout of the binder in a suspension of aluminum powder in kerosene 18 p2372 A73-37118

KERR CELLS

Measurement on a polarization interferometer of absolute and relative light wave delay in liquid dielectrics under the action of an electric field 07 p0823 A73-19332

Electrooptical Q-switching /EQQS/ in solid-state laser resonators 17 p2184 A73-34917

High speed camera with locked mode laser activated Kerr cell shutter to obtain picoseconds exposure duration 21 p2709 A73-39945

Kerr-cell studies of exploding wires in vacuum. 21 p2738 A73-39996

KERR EFFECTS

Electro-optical, magneto-optical, absorptional and acousto-optical light modulation, noting Kerr effect, Faraday rotation and light absorption 04 p0458 A73-15348

Magneto-optic investigation of MnBi films. 15 p1924 A73-31943

Detection of short CO₂ laser pulses using the optical Kerr effect. 16 p2024 A73-34027

Damage produced by laser radiation in optical materials. II 22 p2868 A73-41824

KERR ELECTROOPTICAL EFFECT

Mode-locking of high power lasers by a combination of intensity and time dependent Q-switching. 09 p1090 A73-21999

Kerr response of nematic liquids. 18 p2340 A73-36620

Propagation velocity of picosecond pulse from mode locked Nd-glass laser investigated by optically induced birefringence, self phase modulation and self focused light 23 p2988 A73-44120

KETONES

Some anionic tetrahalo/2,4-pentanedionato/stannate/IV complexes. 06 p0661 A73-18271

Mass spectrometry in structural and stereochemical problems. CCXVII - Electron impact promoted fragmentation of O-methyl oximes of some alpha, beta-unsaturated ketones and methyl substituted cyclohexanones. 10 p1186 A73-23550

KEYING

NT FREQUENCY SHIFT KEYING

NT PHASE SHIFT KEYING

KIDNEY DISEASES

Incidence of Lucke renal adenocarcinoma in Rana pipiens as determined by histological examination. 11 p1314 A73-25136

Effects of altitude stress on mitochondrial function. 14 p1717 A73-30430

KIDNEYS

Morphological changes in the juxtaglomerular apparatus of rat kidneys exposed to the action of diversely directed accelerations for many hours 08 p0929 A73-20978

Fibrinolytic activity of urine in healthy persons 15 p1833 A73-31165

Morphological changes in kidneys during exposure to variously oriented accelerations at a level of 4 g for many hours 17 p2111 A73-34226

An analogue-computer simulation of the facultative water-reabsorption process in the human kidney - A vascular role for a.d.h. 22 p2815 A73-42668

KIMBERLITE

U PERIDOTITE

KINEMATIC EQUATIONS

Theory of the motion of a rigid model of an aircraft with a vertical landing-gear strut on a runway 01 p0005 A73-10917

Solution of kinematical differential equations for a rigid body. [ASME PAPER 72-APM-AAA] 11 p1398 A73-25705

Gradient decomposition and kinematic constitutive equations for elastoplastic material behavior under large strains 11 p1445 A73-26410

Errors associated with Rodrigues-Hamilton parameters /vector space basis quaternions/ calculation by numerical integration of kinematic equations of moving body orientation 11 p1400 A73-26454

Allowance for the influence of the space charge in the kinematic theory of microwave devices 15 p1850 A73-31491

Kinematic theory of magnetic field reconnection rate for analysis of turbulent flows in solar photosphere, flare phenomena and galaxy 19 p2467 A73-37439

Geometry, kinematics and dynamics of dislocations in non-linear continuum mechanics. 23 p3045 A73-44082

KINEMATICS

NT BODY KINEMATICS

A universal three-angle basis for rotational kinematic analysis, simulation and control. 01 p1019 A73-10108

Problem of continuous survey of the earth, and kinematically correct satellite systems. II 10 p1276 A73-23882

Anisotropic and isotropic descriptions of physical process speeds in special relativity theory space-time metric 10 p1250 A73-24944

The correlation between the kinematic structure of the flow and the energy transfer in the rotors of fluid flow machines 18 p2299 A73-36487

Numerical solutions of the kinematic dynamo problem. 19 p2460 A73-38102

The problem of continuous earth coverage and kinematically regular satellite networks. II. 20 p2603 A73-38901

Optical solar flare kinematic model, relating chromosphere response to downward propagating supersonic disturbance 21 p2762 A73-41490

Some kinematic considerations of tone generation in axial turbomachinery. 22 p2899 A73-41710

KINESCOPES

U PICTURE TUBES

KINETHESIS

U PROPRIOCEPTION

KINETIC ENERGY

Troposphere turbulence kinetic energy dependence on height and scales of motions, presenting vertical energy profiles 01 p0074 A73-10869

Reynolds stresses and turbulent kinetic energy production in wall jets on flat and concave walls 01 p0034 A73-11357

Approximate conditions to account for spring mass redistribution with kinetic energy conversion into strain energy over small critical time interval 02 p0230 A73-11795

Local transport equations for turbulent shear flow. 02 p0154 A73-12825

A relation between the energy distribution of the main flow and the corresponding fluctuating quantities in boundary layers 03 p0292 A73-13171

Energy conversion in the atmospheric boundary layer 04 p0441 A73-15286

Certain problems and results of theoretical and experimental research on the energetics of general atmospheric circulation 05 p0593 A73-16237

Modal damping predictions using substructure testing. [SAE PAPER 720810] 05 p0634 A73-16643

Time spectra and cross-spectra of kinetic energy in the planetary boundary layer. 07 p0847 A73-19044

Quasi two dimensional turbulence model of energy spectra and potential enstrophy transfer in synoptic large scale quasi-horizontal atmospheric motions 07 p0820 A73-20342

Experimental verification of the energy dissipation mechanism in acoustic dampers. 08 p1024 A73-21472

Energy evaluation of protons responsible for Pc 1 emissions based on sources drift determination 08 p0961 A73-21494

Laminated composites displacement equations of motion, obtaining stored kinetic and strain energy and free harmonic waves dispersion normal and along layers 09 p1161 A73-23117

- Tensor theory of perturbations in atmospheric dynamics 09 p1115 A73-23150
- Theoretical possibility of converting the kinetic energy of an ionized gas flow into electricity 10 p1177 A73-23473
- Particle kinetic energy vs number density in equilibrium E layer under external and self magnetic fields related to plasma confinement in astron device 11 p1404 A73-25259
- Effect of polymer additions on some energy balance components in a turbulent flow 11 p1349 A73-26433
- Precipitation drops initial growth and final size limits due to collision mechanism, investigating drop interactions by wind tunnel experiments 12 p1520 A73-26807
- A general theory of harmonic wave propagation in linear periodic systems with multiple coupling. 13 p1658 A73-28066
- Troposphere turbulence kinetic energy dependence on height and scales of motions, presenting vertical energy profiles 13 p1653 A73-28693
- Barotropic and baroclinic contribution to eddy kinetic energy increase in disturbance amplification using quasi-geostrophic equations of motion and omega equation 13 p1610 A73-29335
- Universe rest energy density, isotropic background radiation energy and galactic kinetic energy 13 p1686 A73-29654
- On the atmospheric kinetic energy spectrum and its estimation at some selected stations. 14 p1750 A73-30763
- Superexchange potential and kinetic energy theory in molecular orbital and configurational interaction approximation for three center four electron model of ferromagnetic materials 15 p1924 A73-32156
- Kinetic energy conversions by horizontal and vertical eddy processes from 5 years of hemispheric data. 15 p1873 A73-32253
- Laboratory methods for study of aeronautical reactions of excited ions. 16 p2009 A73-33894
- The kinetic characteristics of the electrons of the anisothermal homogeneous steady neon plasma in the ionization level range from 10 to the minus 9th power to 0.01 16 p2043 A73-34022
- Application of energy model of turbulence to calculation of lubricant flows. [ASME PAPER 73-LUBS-18] 17 p2181 A73-35397
- Kinetic energy transfer during multiple jet mixing from primary jet array to secondary stream for various velocity ratios 17 p2156 A73-35511
- Detonation propelled metal particle sprayed coatings adhesion strength relation to particle kinetic energy 18 p2318 A73-35884
- Upper atmospheric turbulence kinetic energy spectrum from radio meteor trails observations, noting relationship to structure function for isotropic turbulence 18 p2312 A73-36288
- Ratio of Reynolds shear stress to turbulence kinetic energy in a boundary layer. 18 p2300 A73-36633
- Objective analysis method tested via comparison to known function at radiosonde observation stations, considering description of spectral analyses of wind field kinetic energy 18 p2332 A73-36702
- Pulsation-energy balance equation in turbulent boundary layer theory 18 p2301 A73-37002
- Stellar kinetic energy gain in spherical systems by transient external gravitational perturbations, computing dynamic models for compressive shocks 19 p2484 A73-37616
- Thermodynamic heat concept, discussing kinetic and potential particle energy, internal energy, heat absorption and release and thermal energy 20 p2627 A73-39293
- Decay of the kinetic energy of compressible micropolar fluids. 20 p2547 A73-39341
- Atmospheric gravity waves and the energy of the jet stream. 21 p2729 A73-40091
- Observation of cosmic-ray particles with Z greater than 35. 23 p3024 A73-43609
- Numerical simulation of three dimensional atmospheric turbulence with emphasis on kinetic energy transfer from large to small scales of motion with heat conversion 24 p3108 A73-45092

KINETIC EQUATIONS

NT HELMHOLTZ VORTICITY EQUATION
NT HYDRODYNAMIC EQUATIONS
NT KINEMATIC EQUATIONS

- Equations of the time-dependent strength of solid bodies 01 p0114 A73-10479
- Method for deriving normal solutions to kinetic equations by using boundary conditions 01 p0076 A73-10623
- Quantum kinetics equations for a nonideal gas and a nonideal plasma 01 p0086 A73-11286
- Liapunov function relation to entropy production in irreversible processes, noting thermodynamic constraints on kinetic equation functions 02 p0191 A73-11613
- Kinetic theory of surface waves in a cylindrical plasma waveguide. 02 p0198 A73-12106
- Diffusion approximation for kinetic equation of repeatedly ionized plasma, calculating direct transitions between excited ion states 03 p0344 A73-13180
- Failure phenomena relationship to kinetic equation for defect buildup from brittle fracture analysis of composite glass fiber reinforced plastic in uniaxial eccentric tension 03 p0394 A73-14008
- Kinetic and dispersion equations for collisionless plasma interaction with HF magnetic and electric fields, noting conical, drift and cyclotron instabilities prevention 04 p0478 A73-15019
- Quantum kinetic equation for monatomic and molecular gases optical characteristics calculation, considering spontaneous emission spectrum of atoms 04 p0459 A73-15565
- Experience with the application parametric diagrams to the calculation of the heat resistance of construction materials 04 p0466 A73-15665
- Solutions of the chemical kinetic equations for initially inhomogeneous mixtures. [AIAA PAPER 73-101] 05 p0546 A73-16861
- Stochastic kinetic theory of strong wave-plasma interaction. I - Kinetic equations. 05 p0603 A73-17323
- Numerical solution to kinetic equations of rarefied supersonic steady gas flow normal to plate by method of characteristics 06 p0643 A73-17461
- Small perturbations solution for spatially homogeneous expanding gravitating medium, using Vlasov kinetic equation with self consistent Newtonian field 07 p0901 A73-20315
- Investigation of the applicability of some statistical models to the shock-wave structure problem 08 p0956 A73-21606
- Electron energy distribution function in CO laser discharge for elastic collisions, noting kinetic equation solution 09 p1089 A73-21914
- Cosmic rays in a random magnetic field - Breakdown of the quasilinear derivation of the kinetic equation. 09 p1137 A73-22036
- A differential method for the prediction of the effects of atmospheric boundary layer turbulence using the turbulence kinetic energy equation. 09 p1071 A73-22334
- Kinetic equation derived for collective linear fluid oscillations development, applying to longitudinal and transverse wave propagation in fluids 09 p1072 A73-22574
- Kinetic equations for vibrational energy relaxation in a polyatomic gas mixture 10 p1250 A73-23579
- Investigation of cosmic-ray propagation in the interplanetary magnetic field on the basis of the kinetic equation 10 p1265 A73-23904
- Approximate solution of the system of Boltzmann equations for a mixture of reacting gases 10 p1252 A73-24490
- Kinetic equations for time behavior of electron concentration and proton, electron and H I atom temperatures in ionized hydrogen medium 10 p1282 A73-24492
- Some solutions of the unsteady two-dimensional turbulent boundary layer equations. 10 p1209 A73-24835
- Kinetic equations describing thermalization of anisotropic solar wind plasma via linear and nonlinear wave-particle interaction 10 p1270 A73-24912
- Kinetic equations for gravitating point rotating system model of stellar systems evolution phases, taking into account dissipation-produced motions 11 p1416 A73-25235
- Uniform isotropic Brownian motion in a linear-cubic approximation 11 p1397 A73-25428
- Boltzmann kinetic equation for nonideal plasma with allowance for polarization effects, noting collision integral convergence 11 p1406 A73-26187

Small perturbations solution for spatially homogeneous expanding gravitating medium, using Vlasov kinetic equation with self consistent Newtonian field 12 p1539 A73-27287

Kinetic equations solved for population of different molecular quantum states via quasi-steady state approximation 12 p1526 A73-27307

Kinetic equations for the Green functions describing equilibrium states of a gas. 13 p1662 A73-28551

Equations for the time-dependent strength of a solid. 14 p1810 A73-30304

A microscopic theory of density fluctuations in partially ionized gases. 15 p1916 A73-31086

Solution of the plane problem of rarefied-gas aerodynamics on the basis of the Boltzmann kinetic equation 15 p1822 A73-31244

Electron energy distribution function in CO laser discharge for elastic collisions, noting kinetic equation solution 15 p1886 A73-32640

Theory of light scattering from dense plasmas. 16 p2041 A73-33323

Kinetic equations for time behavior of solid photochromic film in photocoloration, photobleaching and thermal bleaching, evaluating absorption cross sections and quantum yields 17 p2172 A73-35422

On the kinetic theory of wave propagation in random media. 19 p2460 A73-38103

Liquid droplet and ice particle distribution in spatially homogeneous mixed clouds, solving kinetic coagulation equations via distribution function moments 21 p2730 A73-40119

A kinetic description of the interaction between cosmic rays and shock waves 21 p2758 A73-40596

Green function hydrodynamic asymptotic behavior obtained via closed inhomogeneous linear equations, discussing distribution function kinetic equation, correlation function spectral distribution and adiabatic conditions 21 p2677 A73-40636

Condensation of drops in motion through a gravitation field 21 p2731 A73-40743

Quantum kinetic equations for a nonideal gas and a nonideal plasma. 23 p3009 A73-43507

Numerical integration of the equations of chemical kinetics 24 p3065 A73-44703

Numerical solution of linearized kinetic equations for coagulation of cloud particles by the Monte-Carlo method 24 p3107 A73-44965

Kinetic models and the problem of shock-wave structure 24 p3081 A73-45537

KINETIC FRICTION

NT SLIDING FRICTION

Role of the crystalline structure and orientation of single crystals in the formation of the external friction process 01 p0062 A73-10259

Pulsating vertical load effect on friction force magnitude between two horizontal solid surfaces during initial phase of static to kinetic friction transition 02 p0172 A73-11797

Influence of pressure on VT14 alloy wear and friction against 30KhGSA steel 10 p1226 A73-24797

The reason for noncorrespondence of the values of the static and kinematic coefficients of sliding friction 12 p1502 A73-27445

Static-kinetic dichotomy in friction theory, examining atmospheric contaminants effects on surfaces, theoretical basis of static friction postulation and sliding velocity effect on theory [ASLE PREPRINT 73AM-8A-2] 17 p2179 A73-34992

KINETIC HEATING

NT AERODYNAMIC HEATING

NT SHOCK HEATING

Kinetic heating in structures with a nonuniform surface temperature 03 p0398 A73-13723

Theoretical study of a flow-resistance gas heater. 08 p1023 A73-21436

Carrier heating or cooling in semiconductor devices. 13 p1590 A73-28540

Two fluid models for solar wind heating under boundary conditions, considering enhanced energy transfer between electrons and protons in kinetic theory calculations 17 p2224 A73-34515

Europa III heat shields - Aerothermodynamic analysis and design. 18 p2361 A73-36954

KINETIC THEORY

NT CHAPMAN-ENSKOG THEORY
NT MIXING LENGTH FLOW THEORY
NT TRANSPORT THEORY

Kinetic theory of scattering by a plasma cylinder. 01 p0081 A73-10136

Kinetic theory of electromagnetic fluctuations in an anisotropic plasma half-space 01 p0082 A73-10210

A method for nonlinear plasma wave kinetics. 01 p0082 A73-10419

Kinetic theory for calculation of low temperature homogeneous plasma electric conductivity in magnetic field, noting monotonic decrease 03 p0346 A73-13177

Kinetic model considering cumulative fatigue damage interaction with chance overload on component or structure under probabilistic service load, discussing crack growth in composites 04 p0508 A73-14717

On the evolution toward equilibrium in the kinetic theory of gases 05 p0599 A73-17229

Relativistic thermodynamics of simple heat conducting fluids. 05 p0641 A73-17235

Boundary conditions for penetration of an electromagnetic wave into a plasma. 06 p0727 A73-17418

Kinetic theory of longitudinal wave dispersion in nonuniform plasma layer in HF electromagnetic field, noting plasma instability for electron parametric resonance 06 p0729 A73-18109

Output power dependence on mode geometry in CW gas dynamic laser resonator within kinetic theory of interaction between radiation field and optically active medium stream 06 p0702 A73-18459

Monte Carlo method applications in the solution of gas kinetics problems 07 p0853 A73-19987

Repeated cascade structure and kinetic description for homogeneous turbulence spectrum, considering coupled hierarchies origin from transfer function and eddy viscosity development 07 p0812 A73-20472

Kinetic theory of suction flow, discussing slip coefficient determination for perturbation boundary conditions in Chapman-Enskog-Hilbert method and pressure gradient effects 07 p0812 A73-20474

Kinetic theory of a two-dimensional magnetized plasma. II - Balescu-Lenard limit. 09 p1126 A73-22282

Kinetic theory of a two-dimensional magnetized plasma. III - Limit of very large magnetic field. 09 p1127 A73-22283

Phase transformational kinetics and hardenability of low-carbon, boron-treated steels. 09 p1102 A73-22416

Kinetic theory for the reflection of waves obliquely incident on the boundary of a magnetoactive plasma 09 p1052 A73-23078

Kinetic phenomena in a Knudsen gas with rotational degrees of freedom 12 p1530 A73-27982

Kinetic cooling with CW carbon dioxide laser, observing time constant as function of atmospheric water pressure with three-beam interferometer 13 p1659 A73-28546

Fundamental equations of a mixture of gas and small spherical solid particles from simple kinetic theory. 13 p1600 A73-28616

The micro-structural approach toward a kinetic theory of polymer fracture. 13 p1646 A73-29529

Book - Statistical mechanics, kinetic theory, and stochastic processes. 14 p1774 A73-29947

Maxwell kinetic theory of gases with elasticity of shape/modulus of rigidity/ and obeying Hooke's law, deriving expressions for simple shear and relaxation time 14 p1745 A73-30477

Kinetic models of the solar and polar winds. 15 p1926 A73-31847

Rigid motion of relativistic surfaces 15 p1914 A73-32095

Dispersion of gravitational waves by a collisionless gas. 16 p2036 A73-33122

Radiative transfer considerations for kinetic modeling and sensitivity studies. 16 p2005 A73-33545

[AIAA PAPER 73-505] Transport coefficients of air at temperatures from 3000 to 25,000 K and at pressures of 0.1, 1, 10, and 100 atm 17 p2253 A73-34264

Viscous fluid dynamic problem solution method implementation in Eulerian code AZTEC within continuum mechanics-kinetic theory union, preserving conservation properties throughout time integration 17 p2155 A73-35142

The applications of relativistic kinetic theory to cosmological models - Some observational consequences. 17 p2234 A73-35616

On an eigenvalue problem in the kinematic approach to dynamo theories of cosmic magnetism. 20 p2609 A73-39571

Contribution to the theory of electromagnetic fluctuations of a plasma situated in a weak SHF electric field 21 p2746 A73-40517

Electromagnetic absorption in magnetized cold plasma, discussing definition and use of velocity-dependent collision frequencies with Legendre polynomials as weighting functions 21 p2654 A73-40818

A shock tube study on condensation kinetics. 21 p2792 A73-41143

Kinetic theory of a collision-dominated plasma. 21 p2749 A73-41618

Kinetic theory of electromagnetic waves in an electron plasma characterized by slowly changing parameters 22 p2892 A73-42327

Gaskinetic treatment of the Rayleigh problem in the case of moderately to greatly diluted gases 22 p2843 A73-42529

A kinetic model of population inversion generation in a gas-discharge carbon monoxide laser 23 p2988 A73-44012

Theory of parametric resonance in a spatially modulated plasma 23 p3013 A73-44334

Kinetic theory of longitudinal wave dispersion in nonuniform plasma layer in HF electromagnetic field, noting plasma instability for electron parametric resonance 24 p3114 A73-44498

Determination of lifetime characteristics from crack growth kinetics data 24 p3145 A73-44523

KINETICS

NT ELECTROKINETICS
NT KINETIC ENERGY
NT NEWTON THEORY
NT REACTION KINETICS
NT VARIABLE MASS SYSTEMS

Kinetics of heating a light-scattering field by radiant heat transfer 02 p0238 A73-12098

KINFOFORM

Computer generated binary synthetic holograms, discussing information coding and processing, detour phase effect and kinoforms 11 p1370 A73-26534

On-axis computer generated hologram with multiemulsion color film for retaining kinoform advantages and effective control over amplitude and phase transmittance 17 p2171 A73-35401

Kinoform production method combining pen-drum plotter with low pass spatial filter converting binary transmittance of precursory mask 22 p2862 A73-43088

KIRCHHOFF LAW OF NETWORKS

Kirchhoff mode theory application to electrical network analysis with arbitrary branch couplings including ideal transformers and controlled sources 16 p1992 A73-32909

Approximate procedure for synthesis of interdigital bandpass filters with lumped capacitance loaded bar ends, deriving transmission response from Kirchhoff nodal law 16 p1986 A73-32911

Extension of Kirchhoff's theory to coupled strip lines - Application to the calculation of band line couplers 24 p3068 A73-44975

KIRCHHOFF LAW OF RADIATION

A comparison of mode match, geometrical theory of diffraction, and Kirchhoff radiation. 06 p0666 A73-18192

Approximate near field parameters computation from Kirchhoff boundary values of antenna aperture field intensity 14 p1733 A73-30072

KIRCHHOFF-HELMHOLTZ FLOW

U PIPE FLOW

KIRCHHOFF-HUYGENS PRINCIPLE

U DIFFRACTION

U WAVE PROPAGATION

KITE BALLOONS

U TETHERED BALLOONS

KJELDAHL METHOD

An atomic absorption method for cation measurements in Kjeldahl digests of biological materials. 02 p0139 A73-12424

KLEIN-GORDON EQUATION

'Farfield' behavior of solutions to partial differential equations asymptotic expansions and maximal rates of decay along a ray. 10 p1241 A73-23700

Klein-Gordon equation for a charged particle interacting with an electromagnetic wave. 16 p1979 A73-33164

Plane transient electromagnetic wave propagation in a generalized conducting medium. 22 p2886 A73-41965

KLYSTRONS

Nonlinear harmonic analysis of reflex klystrons with high electron conductance, using average method in second approximation 05 p0556 A73-16065

High-Q toroidal cavities for high frequency klystrons. 07 p0803 A73-20550

Electron admittance and efficiency of the output cavity of a klystron 08 p0948 A73-21557

High power linear beam microwave klystrons, coupled cavity TWTs and hybrid tubes design and operation, considering electron gun and focusing system 11 p1339 A73-26693

Laddertron oscillator/klystron/ cavity dispersion characteristics via electrodynamic analysis of dispersion equation for surface wave operation and coupled modes 12 p1477 A73-26948

Frequency stability of millimetre-band reflex klystrons with various cooling techniques. 13 p1589 A73-28049

Optimal electron grouping arrangements in multi-resonator klystrons 14 p1736 A73-30565

Generalized representation of electric fields in interaction gaps of klystrons and traveling-wave tubes. 18 p2292 A73-36595

Boost klystron efficiency with three-cavity design. 22 p2833 A73-42400

KNEE [ANATOMY]

Role of nerve structures in the action of low-frequency sinusoidally modulated currents on synovial membrane permeability in the knee joint 10 p1180 A73-23943

KNOOP HARDNESS

Determination of yield locus curves for copper and aluminum crystals with the aid of Knoop hardness measurements 02 p0181 A73-12364

Exceptional hardness and corrosion resistance of Mo5Ru3 and W3Ru2 films. 22 p2866 A73-42581

The hardness of titanium-diboride single crystal grown from metal bath. 23 p2994 A73-44154

KNUDSEN CELLS

U KNUDSEN GAGES

KNUDSEN FLOW

Molecular transmission probability through duct connecting two large vessels calculated from data on cylindrical tubes, comparing with Monte Carlo data for error correction 03 p0341 A73-12905

Plasma diagnostics in overcompensation operated Knudsen thermionic converter with Cs-Ba filler, noting W cathode surface properties 04 p0481 A73-15614

Knudsen flow in a rectangular duct of finite length. 06 p0684 A73-17426

Asymptotic theory of the Boltzmann equation at large Knudsen number. 07 p0853 A73-20473

Application of the method of Bhatnagar-Gross-Krook-Morse to the Knudsen layer of a polyatomic gas which is solidified or in equilibrium - Expression of discontinuities of wall temperatures 09 p1072 A73-23033

The Knudsen layer in a flow with two-temperature relaxation 10 p1250 A73-23580

Molecular gas dynamics, considering molecules internal degrees of freedom, Navier-Stokes and Knudsen layer boundary conditions, heterogeneous reactions, evaporation, condensation and surface shocks 10 p1251 A73-23865

Plasma diagnostics in overcompensation operated Knudsen thermionic converter with Cs-Ba filler, noting W cathode surface properties 10 p1177 A73-24204

The effect of an external field on transport phenomena in a Knudsen molecular gas 10 p1252 A73-24453

Kinetic phenomena in a Knudsen gas with rotational degrees of freedom 12 p1530 A73-27982

Photographic studies of the transition between continuum and free molecular flow. 15 p1864 A73-31935

Electrical network analogy application to thermal energy steady diffusion within Knudsen gas filled en-

closure, discussing free molecule limit and transition regime
15 p1959 A73-32283
Influence of an external field on transport effects in a Knudsen molecular gas.

19 p2463 A73-38134
Knudsen free molecular flow explanation of thermomagnetic torque on circular cylinder suspended in axial molecular field, noting apparatus tilt effect
22 p2842 A73-42233
Rarefied-gas heat transfer in Knudsen layer using ellipsoidal model.

22 p2932 A73-42471
Rarefied gas flow through an orifice at low pressure gradients

23 p2969 A73-44347
Expansion of a plane rarefied gas layer into a vacuum

24 p3076 A73-44655
Poiseuille flow at arbitrary Knudsen numbers and tangential momentum accommodation.

24 p3079 A73-45313
Radiating optically thick gas boundary layer based on approximation of gray gas in LTE, noting similarity to Knudsen layer

24 p3158 A73-45535

KNUDSEN GAGES
A new variant of the Knudsen vacuumometer as a measurement standard for low pressures

03 p0306 A73-12898
Knudsen measurements of the decomposition and the heat of formation of manganese ditelluride.

09 p1048 A73-22442

KNUDSEN NUMBER
U KNUDSEN FLOW

KOLMOGOROFF THEORY
Wiener-Kolmogoroff optimal filtration theory for synthesis of linear stabilization systems under steady random external perturbations, noting control optimality conditions

01 p0028 A73-10670
Kolmogorov's differential equations for non-stationary, countable state Markov processes with uniformly continuous transition probabilities.

06 p0718 A73-18501
On weak convergence of empirical processes for random number of independent stochastic vectors.

06 p0718 A73-18502
Flow velocity fluctuation intensity relationship to turbulent energy dissipation based on Kolmogoroff similarity hypothesis

07 p0811 A73-19624
Solution of the Fokker-Planck-Kolmogorov equation for a dynamic system with analytical characteristics

09 p1068 A73-22563
Experimental determination of the turbulent transfer coefficient in the case of homogeneous isotropic turbulence.

10 p1205 A73-24176
The observed relation between the Kolmogorov and von Karman constants in the surface boundary layer.

11 p1393 A73-25694
Intermittency of the small-scale structure of atmospheric turbulence. II.

19 p2448 A73-38213
Inertial range differences between Kolmogoroff energy spectrum formula for turbulence and modified Navier-Stokes equation, considering mu value deductibility

22 p2840 A73-41733

KOLMOGOROFF-SMIRNOFF TEST
Gaussian channel model for long tropospheric scatter link verification by time varying bandpass impulse response measurements, using Kolmogoroff-Smirnoff tests

04 p0418 A73-15392
The Kolmogorov-Smirnov test modified for censored data.

16 p2033 A73-33619

KP INDEX
Latitude effects on the amplitude of Pi 2 micropulsations.

02 p0159 A73-12034
Solar activity and the variations of the geomagnetic K sub p-index. I.

03 p0378 A73-14422
Equatorward shift of the polar F layer irregularity zone as a function of the Kp index.

04 p0445 A73-15557
Auroral sporadic E layer diurnal distribution correlation to charged particle integral flux diurnal variations observed by satellite in winter, noting Kp index effect

07 p0816 A73-19455
Magnetic irregularities in interplanetary space and geomagnetic activity.

08 p1007 A73-21004
Pi 2 micropulsation period and frequency correlation coefficients for planetary magnetic activity Kp index and magnitude of accompanying auroral bay

11 p1357 A73-25930
Distance to the subsolar point of the magnetosphere boundary for various magnetic activity indices

15 p1932 A73-31266

Periodic variations in geomagnetic activity and sector structure of the interplanetary magnetic field.

17 p2157 A73-34075
Sector boundary geomagnetic activity average Kp elevation relationship to southward component of interplanetary field, suggesting magnetosphere role

18 p2347 A73-36292
Effect of the solar wind on geomagnetic activity

19 p2476 A73-38154
Position of the equatorial boundary of the anomalous ionization occurrence region in relation to the planet's magnetic activity during the solar activity cycle

20 p2554 A73-39175
Wind profiles over Heiss Island.

21 p2685 A73-40812
KREBS CYCLE
Lactate, alpha-GP, and Krebs cycle in sea-level and high-altitude native guinea pigs.

11 p1318 A73-26122

KRONECKER PRODUCT
U ORTHOGONALITY

KRYPTON
NT KRYPTON ISOTOPES

Ar and Kr continuous wave ion lasers with electric arc discharge, noting quartz, graphite and beryllium oxide gas discharge tubes

01 p0059 A73-10714

KRYPTON ISOTOPES
Cosmic ray intensity over the past 100,000 to 1,000,000 years and the Kr-81 isotope content in the atmosphere

21 p2756 A73-40586

KU BAND
U SUPERHIGH FREQUENCIES

KUTTA-JOUKOWSKI CONDITION
The Joukowski condition in three-dimensional flow

04 p0405 A73-15988

L

L BAND
U ULTRAHIGH FREQUENCIES

L-1011 AIRCRAFT
Selection process for a structural adhesive system for application of the L-1011 aircraft.

03 p0333 A73-13050
L-1011 TriStar - Design development.

08 p0928 A73-21574
L-1011 aircraft hydraulic system layout and installation techniques with modular design and plug-in cartridges for Murphy law error reduction during servicing

17 p2108 A73-34523
The successful use of composites in the L-1011 TriStar commercial transport.

17 p2103 A73-34815
Noise certification of a transport airplane.

19 p2378 A73-37279
Automatic flight control and navigation systems on the L-1011 Capabilities and experiences.

19 p2452 A73-37824
Early operational experience with the L-1011 On-Board Weight and Balance System.

19 p2386 A73-37890
[SAWE PAPER 986]
Dynamic gust, landing, and taxi loads determination in the design of the L-1011.

20 p2508 A73-38647
L-1011 Tristar production, sales and airline service experience, discussing RB-211 turbofan engine and fleet performance

20 p2510 A73-39659

LABELING [MARKING]
U MARKING

LABORATORIES
NT ENGINE TESTING LABORATORIES

NT ENVIRONMENTAL LABORATORIES
NT MANNED ORBITAL LABORATORIES

NT MANNED ORBITAL RESEARCH LABORATORIES
NT SPACE LABORATORIES

LABORATORY EQUIPMENT
French CNES and Toulouse space center organization and activities, describing installation history

07 p0808 A73-19006
A modern mechanical laboratory for the support of aircraft engine design

12 p1486 A73-27385
Hybrid computer laboratory construction, organization and operation principles, including computer selection and personnel requirements

23 p2956 A73-43950

LABYRINTH
NT COCHLEA

NT VESTIBULES
The neuronal mechanism of nystagmus.

18 p2271 A73-36437
Effects of round window stimulation on unit discharges in the visual cortex and superior colliculus.

20 p2513 A73-39146

LABYRINTHECTOMY
Effect of some pharmacological preparations on the fall-out nystagmus and Bechterew nystagmus

08 p0929 A73-20982

LACQUERS
Investigation of the antistatic properties of lacquer coatings based on quaternary polyvinylpyridine salts

21 p2647 A73-40261

LACTATES
Perceived exertion, heart rate, oxygen uptake and blood lactate in different work operations.

03 p0267 A73-13698
Muscle metabolites with exhaustive static exercise of different duration.

05 p0539 A73-16247
Sterically controlled syntheses of optically active organic compounds. XV - Syntheses of optically active aspartic acid through beta-lactam.

07 p0787 A73-19204
Lactate, alpha-GP, and Krebs cycle in sea-level and high-altitude native guinea pigs.

11 p1318 A73-26122
Relative rates of arterial lactate and oxygen-deficit accumulation in hypoxic dogs.

15 p1836 A73-31922
Oxygen uptake, muscle high-energy phosphates, and lactate in exercise under acute hypoxic conditions in man.

21 p2638 A73-41131
Lactate origins and renewal in blood plasma, considering metabolism, enzymatic resynthesis and final excretion in urine

24 p3061 A73-45157

LACTIC ACID
The effect of O2 breathing on maximal aerobic power.

01 p0010 A73-11504
Energy balance and lactic acid production in the exercising rabbit.

05 p0538 A73-16156

LADDERS
Laddermil and ergometry - A comparative summary.

11 p1322 A73-25183

LAGRANGE COORDINATES
The Lagrange function for a gas bubble in an inhomogeneous flow

21 p2676 A73-40206
A note on relative motion in the general three-body problem.

23 p3031 A73-43834

LAGRANGE EQUATIONS OF MOTION
U EULER-LAGRANGE EQUATION

LAGRANGE MULTIPLIERS
An optimum settling problem for time lag systems.

06 p0717 A73-18172
Vibration theory optimization problems for rectilinear rods, noting Lagrange multipliers continuity in linear hyperbolic equations

06 p0766 A73-18886
The finite element method with Lagrangian multipliers.

07 p0844 A73-19137
Necessary condition of optimality for some problems of optimal control theory

07 p0844 A73-19296
Positive solutions of infinite equation and inequality systems and Lagrange multipliers for infinite differentiable optimization problems

10 p1243 A73-24163
Russian book on analytical theory of optimization in gravitational fields covering orbital transfer trajectories, variational optimization problems, Lagrange multiplier properties, etc

10 p1284 A73-24800
Kron's method - A consequence of the minimization of the primitive Lagrangian in the presence of displacement constraints.

13 p1700 A73-29381
Vibration theory optimization problems for rectilinear rods, noting Lagrange multipliers continuity in linear hyperbolic equations

15 p1956 A73-32411
Lagrange function based Poincare mechanics of inertial relativity, using Mach-Einstein inertia principle for gravitational potential

16 p2036 A73-33072
An approach to nonlinear programming.

16 p2032 A73-33301
Extensions of Newton's method and Simplex methods for solving quadratic programs.

16 p2033 A73-33856
A survey of methods for solving constrained minimization problems via unconstrained minimization.

16 p2033 A73-33857
Combined Rayleigh-Ritz and Lagrange multiplier technique for investigation of free vibrations of constrained cylindrical shell, considering axisymmetric mode

17 p2241 A73-34198
A variational principle for the laminar boundary layer theory.

19 p2421 A73-38026

LAGRANGE SIMILARITY HYPOTHESIS
Similarity theory of diffusion and the observed vertical spread in the diabatic surface layer.

13 p1655 A73-29339

LAGRANGIAN EQUILIBRIUM POINTS

On the stability of triangular points of equilibrium in the restricted elliptic problem

03 p0376 A73-14270
22 p2911 A73-42936

Parameter distribution of small periodic librations about the equilateral points of the elliptic restricted problem.

24 p3141 A73-45283

Three dimensional computer plots of zero velocity contours for restricted three and four body problems, discussing motion stability near equilibrium points

24 p3142 A73-45297

LAGUERRE FUNCTIONS

On the identifiability of finite mixtures of Laguerre distributions.

18 p2330 A73-36984

LAKE ICE

NT ICE FLOES

LAKES

Carbon dioxide concentration, pH and nutrient concentration effects on blue-green algae relative abundance to green algae in lakes

06 p0655 A73-18577

Statistical model of gust factor relation to lake and terrain surface roughness and height from wind velocity measurement data

13 p1655 A73-29341

Infrared sensing of the surface temperature of certain lakes of Northern Italy

17 p2206 A73-34942

Shallow lake or sea with large class of bottom topographies, obtaining wind-driven current analytic solution with conformal mapping technique

21 p2686 A73-41015

The investigation of the periodicity of hydrometeorological phenomena according to the autocorrelation method of Fuhrich

22 p2883 A73-42449

LALLEMAND CAMERAS

High resolution apparatus at the focus of large telescopes

01 p0049 A73-10532

A Lallemand electronic camera focused by a superconducting magnetic coil.

14 p1751 A73-29904

Development of a new kind of Lallemand camera.

14 p1751 A73-29905

LAMB WAVES

Lamb solution analog for dynamic problem of homogeneous isotropic elastic body with impulsive force applied to semi-infinite plane incision

13 p1698 A73-29088

Propagation of elastic Lamb waves in an initially stressed body

15 p1945 A73-31030

Lamb solution analog for dynamic problem of homogeneous isotropic elastic body with impulsive force applied to semiinfinite plane incision

19 p2498 A73-37638

Contactless on-line NDT of metal plates for concealed defects by Lamb wave excitation through wave generation from air

21 p2708 A73-41138

LAMBDA ROCKET VEHICLES

Lambda-4S solid propellant four-stage sounding rocket and scientific satellite launcher, describing design, operational and performance features

01 p0091 A73-11157

LAMBERT LAW

U BOUGUER LAW

LAME FUNCTIONS

Lie operators admitted by Lame equations in three dimensional dynamic elasticity theory for arbitrary particle velocity and displacement and linear stress-strain tensor relation

09 p1159 A73-22585

Lame problems in theory of elasticity, discussing reduction to Dirichlet sequence for Laplace equation

11 p1446 A73-26597

The normal gravitational fields of the earth and the moon

12 p1546 A73-27865

Celestial bodies gravitational potential mathematical representation by Lame functions via series expansion of Laplace differential equation in ellipsoidal coordinates

20 p2606 A73-39080

Normal gravity fields of the earth and the moon.

20 p2608 A73-39239

LAME WAVE EQUATIONS

Operators tolerated by the dynamics equations in the three-dimensional problem of elasticity theory

02 p0230 A73-11781

Boundary value problem of Lame equation in elasticity theory of two dimensional region with angular points, solving by Fredholm integral equation

02 p0237 A73-12591

Lame equations for stress concentration in half plane with extracted elastic inclusion, solving via Fourier integrals reduced to singular integral equation

07 p0910 A73-19301

LAMINAR BOUNDARY LAYER

Density and temperature measurement in laminar boundary layer and free jet of hypersonic nozzles by electron beam probe.

[ONERA, TP NO. 1131] 01 p0045 A73-10239

Two-dimensional boundary layers in a free stream which oscillates without reversing.

01 p0032 A73-10446

Radiation in the reacting boundary layer.

01 p0121 A73-10642

Three-dimensional effects on electron density in a blunt body laminar boundary layer.

01 p0002 A73-10731

Hydrodynamic stability of boundary layers with surface suction.

01 p0033 A73-10749

Velocity, temperature and component concentration distributions in laminar boundary layer at blown surface for binary mixture flow

01 p0034 A73-10957

A solution of the three-dimensional unsteady compressible boundary layer equations.

01 p0004 A73-11356

Investigation of a laminar boundary layer on a continuously moving smooth surface with allowance for heat transfer

02 p0153 A73-11786

The boundary layer of particulate gas flow.

03 p0289 A73-12914

An analysis of the chemically reacting boundary layer during hybrid combustion.

03 p0273 A73-13450

Existence in the laminar boundary layer of a natural instability not predicted by theory and connected to a wall deformation

03 p0294 A73-13576

Subsonic wind tunnel tests for laminar boundary layer investigation in low level turbulence flow, noting turbulence measurement with hot-wire anemometers

03 p0308 A73-13666

On similarity solution of an unsteady laminar boundary layer along a flat plate.

03 p0297 A73-14314

Observation and spectral analysis of instantaneous signals of velocity fluctuation in the laminar boundary layer

03 p0297 A73-14602

Study of the effect of surface roughness on the laminar boundary layer transition in a turbulent boundary layer

04 p0404 A73-15653

Analysis of unsteady laminar boundary layer flow by an integral method.

04 p0434 A73-15839

Application of Olfe's modified differential approximation to the radiation-layer problem on a flat plate.

04 p0520 A73-15946

Hydromagnetic stability of a laminary boundary layer in a flow past a planar plate

05 p0601 A73-16096

Boundary layer characteristics with radiant energy transfer under adverse pressure gradient.

05 p0530 A73-16874

Shock wave-boundary layer interactions in laminar transonic flow.

05 p0532 A73-16964

Laminar film boiling on inclined isothermal flat plates.

05 p0641 A73-17107

Nonsimilar flows between the solution branches of the Falkner-Skan equation.

05 p0567 A73-17116

Vectored injection into isobaric laminar boundary layer flows.

06 p0685 A73-17917

Thermal boundary layer thickness for laminar forced convection to flat plates with uniform heating and uniform wall temperature.

06 p0769 A73-18260

On the series solution to the laminar boundary layer with stationary origin on a continuous, moving porous surface.

06 p0687 A73-18505

Heat transfer in a periodic boundary layer near a two-dimensional stagnation point.

06 p0769 A73-18526

On the plane-parallel symmetric boundary layer generated by sudden motion.

07 p0809 A73-19020

An iterative procedure for the oscillatory laminar boundary layer.

07 p0809 A73-19035

Characteristics of the unsteady shock-induced laminar boundary layer on a flat plate.

07 p0810 A73-19505

Boundary-layer separation on rotating blades in forward flight.

07 p0774 A73-19955

An extension of the vector potential concept to the case of a three-dimensional unsteady boundary layer.

07 p0776 A73-20287

Unsteady laminar boundary layers calculation for arbitrary velocity distributions at inner boundary in presence of suction/blowing through porous surface

08 p0954 A73-21176

Method of approximate calculation of the laminar boundary layer outside of vibrational equilibrium

08 p1023 A73-21259

Linearized solutions to supersonic laminar boundary layer structure near flat plate with slot injection, using triple deck separation theory

08 p0956 A73-21524

Boundary layer theory approximation for hydrodynamic parameters of unsteady laminar boundary layer on body moving in incompressible fluid

08 p0956 A73-21546

Heat transfer through the unsteady laminar boundary layer on a semi-infinite flat plate. I - Theoretical considerations. II - Experimental results from an oscillating plate.

08 p1024 A73-21635

A theoretical study of natural convection heat transfer from downward-facing horizontal surfaces with uniform heat flux.

08 p1024 A73-21638

Numerical study of the stability of a supersonic laminar boundary layer

09 p1028 A73-22624

Laminar boundary layer on a cone near a plane of symmetry.

09 p1029 A73-23442

Temperature at the surface of a heat-conducting liquid behind a shock wave in the presence of mass transfer and chemical reactions in the boundary layer

10 p1296 A73-24679

On the response of laminar boundary layers to periodic changes in free-stream speed.

10 p1207 A73-24803

The universalization of unsteady boundary layer equations

10 p1207 A73-24805

Similarity solutions of unsteady, compressible plane and axisymmetric laminar boundary layer equations.

10 p1208 A73-24807

Unsteady three dimensional laminar incompressible boundary layer with free and forced convection, determining flow and temperature fields adjacent to heated body

10 p1208 A73-24810

Two dimensional laminar boundary layer separation for unsteady flow or flow past moving walls, considering singularity due to bifurcating wake bubble

10 p1208 A73-24813

Universal equations of the three-dimensional laminar boundary layer in the unsteady state and their treatment

10 p1209 A73-24820

On structure of the laminar boundary layer in the presence of a fluctuating free stream.

10 p1209 A73-24830

Development of unsteady boundary layers under variable suction.

10 p1209 A73-24831

Recent studies in the field of unsteady boundary layers

10 p1173 A73-24833

Study of the phase of the wall transfer of heat or mass in incompressible pulsed flow

10 p1297 A73-24850

Parametric excitation of Tollmein-Schlichting waves in a boundary layer

11 p1347 A73-25430

Flow near the stagnation point of a body which undergoes a sudden change in a steady stream.

11 p1347 A73-25701

Velocity and concentration profiles of isothermal laminar boundary layer flow of incompressible multicomponent gas under strong blowing

11 p1347 A73-25728

Investigation of the transition of a turbulent boundary layer into a laminar boundary layer in the presence of deep negative pressure gradients

11 p1347 A73-25737

Perturbation solutions to laminar boundary layer flow over flat plate with small hump downstream of leading edge, using Blasius equation

11 p1302 A73-25855

Forced convection heat transfer in laminar boundary layer at low Prandtl numbers.

11 p1452 A73-26123

Nonlinear problem of a shock-tube interaction-region boundary layer.

11 p1348 A73-26391

Laminar symmetry-plane boundary layer on a sharp spinning body at incidence.

11 p1303 A73-26397

Enthalpy restoration coefficient in a three-dimensional laminar boundary layer

11 p1303 A73-26434

Experimental investigation of hydrodynamic stability at rigid and elastic-damping surfaces

11 p1349 A73-26440

Velocity, temperature and component concentration distributions in laminar boundary layer at blown surface for binary mixture flow

12 p1487 A73-27533

Compressible boundary layer flow at a three-dimensional stagnation point with intensive suction or injection

12 p1458 A73-27699

Incompressible laminar boundary layer separation, displacing separation point by adjusting flow surface velocity

13 p1600 A73-28445

Approximate calculation of the incompressible laminar boundary layer on a plate with suction

13 p1600 A73-28446

A numerical method for highly accelerated laminar boundary-layer flows.

13 p1600 A73-28608

Entropy layer effects in constant pressure hypersonic boundary layers.

13 p1564 A73-28812

Increase of boundary-layer heat transfer by mass injection.

13 p1706 A73-28816

The heat and mass transfer of a binary laminar boundary layer in the presence of simultaneous convection at a vertical permeable flat surface

13 p1708 A73-29350

Construction of solutions for the equations of a compressible laminar boundary layer on a plate with abruptly changing boundary conditions

13 p1567 A73-29408

Boundary layer about a plate assuming an arbitrary gas injection law

14 p1711 A73-30017

Plate-injection into a separated supersonic boundary layer.

14 p1711 A73-30172

Experimental investigations regarding the behavior of turbulent boundary layers in the case of small periodic pressure changes

14 p1745 A73-30299

Natural convection boundary layer flow over horizontal and slightly inclined surfaces.

14 p1817 A73-30607

Theoretical investigation on laminar boundary layer with combustion on a flat plate.

14 p1817 A73-30611

Asymptotic solution of the equations for a multicomponent laminar boundary layer in the case of high injection levels

15 p1822 A73-31292

Application of the method of characteristics in solving the universal equation of the plane boundary layer of a conducting fluid

15 p1918 A73-31407

On the propagation of disturbances in a laminar boundary layer. I, II.

15 p1863 A73-31725

Investigation of boundary layer flow on a flat porous plate with a regulated pressure gradient in the outer flow

15 p1864 A73-31873

Experimental study of heat exchange in a chemically reacting laminar boundary layer

15 p1958 A73-31874

On the polarographic measurement of the wall gradient of velocity in the upstream stagnation zone or of detachment from the cylinder

15 p1878 A73-32209

The principle of spatial variations - Application to the boundary layer theory.

16 p1999 A73-32978

Experimental investigation of secondary instabilities in the unstable laminar boundary layer of a concave wall in parallel flow

16 p1999 A73-33247

Integration of an extended Orr-Sommerfeld equation in connection with a stability investigation of laminar boundary-layer flows

16 p1963 A73-33252

Correlation of the mass flow rate in the laminar boundary layer on a sphere-cone.

17 p2091 A73-34195

Book - Physical fluid dynamics.

17 p2151 A73-34472

An initial value method for the study of shock-induced laminar compressible boundary layers.

[ASME PAPER 73-FE-4]

17 p2152 A73-35004

Oscillatory flow phenomena in diffusers at low Reynolds numbers.

[ASME PAPER 73-FE-14]

17 p2152 A73-35011

Boundary-layer separation from downstream moving boundaries.

[ASME PAPER 73-APM-11]

17 p2153 A73-35036

Study of the similarity solution in three dimensional compressible laminar boundary layer.

17 p2157 A73-35862

Interference heating due to shock wave impingement on laminar boundary layers.

[AIAA PAPER 73-678]

18 p2368 A73-36229

Foreign gas injection at windwardmost meridians of yawed sharp cones.

[AIAA PAPER 73-764]

18 p2264 A73-36379

Laminar boundary layers in low pressure argon plasma.

19 p2420 A73-37646

Laminar boundary layers along an infinite flat plate with oblique suction.

19 p2420 A73-37852

A variational principle for the laminar boundary layer theory.

19 p2421 A73-38026

Transonic laminar boundary layers with surface curvature.

19 p2423 A73-38480

Numerical experiment in a study of the separation of a laminar boundary layer in an MHD channel

20 p2598 A73-39611

Flow measurements over compression corner in supersonic separated laminar boundary layers with hot-wire probes

21 p2631 A73-40247

Improvement to Klineberg's method for the calculation of viscous-inviscid interactions in supersonic flow.

21 p2632 A73-40429

Investigation of the laminar boundary layer at a permeable surface.

21 p2678 A73-41054

Radiative-convective heat transfer in flows of hot air past a flat plate.

21 p2791 A73-41056

Experimental study of heat and mass transfer in chemically reacting laminar boundary layers.

21 p2791 A73-41058

Subsonic wind tunnel tests for laminar boundary layer investigation in low level turbulence flow, noting turbulence measurement with hot-wire anemometers

21 p2704 A73-41316

Fluctuating flow and heat transfer from a vertical surface.

21 p2792 A73-41524

French monograph - Study of the behavior of the laminar boundary layer in the presence of a positive or negative pressure gradient in hypersonic flow around obstacles.

22 p2797 A73-42744

Aerodynamic and thermal structures of the laminar boundary layer over a flat plate with a diffusion flame.

22 p2933 A73-42774

Thermal response of an unsteady laminar boundary layer on a flat plate due to step changes in wall temperature and in wall heat flux.

23 p3049 A73-43802

Effect of wall conduction on convective heat transfer with laminar boundary layer.

23 p3049 A73-43833

A numerical study of separating supersonic laminar boundary layers.

[ASME PAPER 73-APM-H]

23 p2969 A73-44376

A biparametric method for laminar boundary layer calculations

24 p3079 A73-45173

Extremum principles and error bound for a nonlinear boundary value problem in the theory of laminar boundary layers.

24 p3080 A73-45340

Compressible laminar boundary layer differential equations solution for incident viscous gas flow on flat plate at high flow velocity

24 p3080 A73-45471

Universal equations for the laminar boundary layer on a body of revolution in oblique flow

24 p3055 A73-45529

The incompressible boundary layer of higher order at the axisymmetrical stagnation point in the case of strong suction or blowing

24 p3056 A73-45545

LAMINAR BOUNDARY LAYER SEPARATION

U BOUNDARY LAYER SEPARATION

U LAMINAR BOUNDARY LAYER

LAMINAR FLAMES

U FLAMES

U LAMINAR FLOW

LAMINAR FLOW

NT BLASIUS FLOW

NT HARTMANN FLOW

NT STRATIFIED FLOW

Skin friction on porous surfaces calculated by a simple integral method.

01 p0057 A73-10726

Flow and heat transfer on a flat plate normal to a two-dimensional laminar jet issuing from a nozzle of finite height.

01 p0033 A73-10804

Effects of forced flow, noncondensables, and variable properties on film condensation of pure and binary vapors at the forward stagnation point of a horizontal cylinder.

01 p0122 A73-10806

Developing laminar free convection between vertical flat plates with asymmetric heating.

01 p0122 A73-10811

Liquid- and wall-temperature calculations for a flow in tubes with allowance for heat losses into the ambient medium and for axial heat conductivity

01 p0122 A73-10860

Confined laminar jet mixing in a circular channel with arbitrary entrance velocity distribution.

[AD-758578]

01 p0034 A73-11363

Approximate solutions of laminar flow between two rotating coaxial disks.

02 p0151 A73-11527

Integral method of calculating a semibounded laminar jet

02 p0153 A73-11784

Line and continuous excitation sources for measuring wavelength dependence, angular distribution and polarization of scattered light intensity in turbulent and laminar flames

03 p0396 A73-12925

Consideration of wall friction in the streamline procedure with the aid of a modified boundary layer calculation for laminar flows according to the momentum method

03 p0291 A73-13126

Unsteady laminar natural and forced convection at transparent medium boundary layer radiating surface, noting turbulence effects on heat exchange

03 p0397 A73-13187

Applying quasilinearization to the steady laminar flow between two parallel porous plates.

03 p0292 A73-13307

Infinite Prandtl number fluids with constraint characterized by Taylor number heated from below, choosing boundary conditions for laminar convection

03 p0293 A73-13329

Plane Poiseuille flow with small amplitude modulated pressure gradient, noting disturbance shear wave and stability from energy transfer calculation

03 p0293 A73-13530

Boundary-layer development at a two-dimensional rear stagnation point.

03 p0294 A73-13536

Flow parameter iterative formulas for laminar incompressible viscous fluid flow between two parallel disks rotating at same angular velocity

03 p0295 A73-13625

On a heat transfer problem in the laminar flow in a tube

03 p0398 A73-13772

Monograph on hydrodynamics of nonisothermal laminar duct flows of real fluids with temperature dependent properties

03 p0295 A73-13998

Influence of the magnetic field on the heat transfer of a ferromagnetic viscoplastic fluid

03 p0347 A73-14323

Soot particles oxidation by oxygen diffusion in laminar hydrocarbon flames, deriving kinetic expression from observed time dependent particle concentration variations

03 p0399 A73-14395

Fuel-rich and stoichiometric carbon monoxide-nitrous oxide premixed laminar flames with varying water contents, determining flame temperature by line reversal method

03 p0399 A73-14396

Closed form linearized solutions of plane laminar jets boundary layer equations based on Legendre functions

03 p0297 A73-14628

Convective transport terms effect on laminar flow-field of Newtonian fluid between rotating cylinders, using adapted finite difference solution technique

03 p0298 A73-14643

Transient free-convection horizontal laminar flow between two parallel plates.

04 p0517 A73-15681

A transformation for the numerical solution of two-dimensional free mixing flow problems.

[ASME PAPER 72-WA/FE-3]

04 p0434 A73-15841

Flow in the entrance region at low Reynolds numbers.

[ASME PAPER 72-WA/FE-21]

04 p0435 A73-15847

The effects of compressibility in multi-element hydraulic lines.

[ASME PAPER 72-WA/FE-43]

04 p0435 A73-15857

Development of a submerged round laminar jet from an initially parabolic profile.

[ASME PAPER 72-WA/FLCS-3]

04 p0408 A73-15861

Navier-Stokes equation solutions for steady laminar viscous flow of incompressible fluid with mixed no-slip and no-shear conditions

05 p0563 A73-16097

Heat transfer in fully developed laminar flow between flat parallel boundary walls, deriving approximations to higher eigenvalues

05 p0563 A73-16101

Combined free and forced laminar convection in inclined tubes.

05 p0564 A73-16173

Laminar liquid jets thrust measurement apparatus for dilute polymer solutions rheological characteristics determination, using air bearing suspended rotor with discharge capillary

05 p0562 A73-16441

On the numerical solution of two-dimensional, laminar compressible flows with imbedded shock waves.

[ASME PAPER 72-FE-7]

05 p0564 A73-16545

An engineering approach to the design of laminarizing nozzle flows.

[ASME PAPER 72-FE-19]

05 p0565 A73-16549

Characteristics of an argon RF plasma - Active discharge and laminar sonic flow region.

05 p0602 A73-16559

Magnus force and moment coefficients for spinning ogive and cone cylinders and conical bodies in laminar

- compressible flow, including boundary layer and radial pressure gradient effects
[AIAA PAPER 73-124] 05 p0530 A73-16879
- A study of fin-induced laminar interactions on sharp and spherically blunted cones.
[AIAA PAPER 73-235] 05 p0532 A73-16960
- A force field theory. I - Laminar flow instability.
05 p0567 A73-17103
- Calculation of the thermal fluxes and the temperatures of the surfaces of a plate with heat transfer between fluids flowing around the plate.
06 p0766 A73-17408
- Radial concentration profiles of NO and combustion products formation in laminar diffusion flames, using vertical coaxial burner and quartz microprobe
06 p0740 A73-17730
- Solid-gas mass transfer in the case of laminar free convection
06 p0768 A73-17919
- Critical conditions for steady/unsteady laminar shear flow breakdown into HF oscillations, using kinematic wave theory
[AD-758579] 06 p0687 A73-18533
- Instability of a two-layer geostrophic flow with an antisymmetric velocity profile in the upper layer
06 p0691 A73-18728
- An extension of the modified Oseen solution for laminar viscous flow past a semi-infinite flat plate.
06 p0688 A73-18849
- Magnetohydrodynamic laminar source flow between two parallel disks.
07 p0854 A73-19102
- Development of flow in the entrance region of a converging channel.
07 p0810 A73-19103
- Two dimensional semibounded jets in laminar and turbulent flows, discussing boundary layers skin and stream regions, step flow velocities, temperatures and self similar problems
07 p0811 A73-19612
- IR absorption spectra of powdered graphite samples during treatment in laminar propane-butane diffusion flame zones
07 p0921 A73-19996
- Steady almost parallel flows linear stability, using multiple scales method for perturbation waves analysis
[ONERA, TP NO. 1235] 07 p0811 A73-20072
- Comparison of exact and mean beam length results for a radiating hydrogen plasma.
07 p0859 A73-20221
- Streamline deflection by diffusion flame stabilized on Parker-Wolfhard burner, discussing flow visualization and Burke-Schumann flame sheet in Oseen flow
07 p0921 A73-20355
- Spiral flows in finite rotating annular tubes.
07 p0812 A73-20435
- Heat transfer, adiabatic enthalpy /temperature/ of the wall, and hydrodynamic resistance associated with the turbulent and laminar flow of a compressible fluid in a circular tube.
08 p0954 A73-20858
- Experimental study of influence of an electric field on a laminar flame.
08 p1021 A73-20864
- Unsteady laminar flow in a pipe with arbitrarily changing flow rate.
08 p0954 A73-20867
- Numerical calculation of the laminar inlet flow. I.
08 p0954 A73-21011
- A special form of Galerkin's method applied to heat transfer in plane Couette-Poiseuille flows.
[AD-757002] 08 p1023 A73-21412
- Approximate method for calculating heat transfer to yawed cylinders in laminar flow.
08 p1025 A73-21818
- Experimental study of the laminar-turbulent transition on a concave wall in a parallel flow
09 p1071 A73-22450
- Viscous energy transfer from elliptical orifice originated laminar three dimensional jet, using boundary layer assumptions in jet mixing region
09 p1072 A73-22827
- Computation of time-dependent laminar flame structure.
10 p1294 A73-23552
- Breakup length maximum and decrease achievement in laminar viscous jet with velocity increase, discussing effects of ambient gas
10 p1206 A73-24255
- Finite element solution algorithm for viscous incompressible fluid dynamics.
10 p1243 A73-24296
- Inertia effects in laminar radial flow of power law fluids.
10 p1206 A73-24660
- Instability of free shear layers adjacent to a vibrating flame surface.
10 p1296 A73-24804
- Transient viscous laminar incompressible flow pattern after sudden vanishing of semiinfinite flat plate based on two dimensional unsteady boundary layer equations with boundary conditions
10 p1208 A73-24811
- Unsteady detachment in the three-dimensional laminar regime
10 p1208 A73-24819
- Unsteady flow between a fixed porous disk and a rotating disk
10 p1209 A73-24837
- A numerical study of unsteady laminar combined convective flow over vertical plates.
10 p1296 A73-24848
- Unsteady viscous jet flow into stationary surroundings.
11 p1345 A73-25117
- Unsteady laminar convection in uniformly heated vertical pipes.
11 p1449 A73-25221
- Laminar incompressible fluid steady secondary flow in circular cross section curved tube at various Reynolds numbers
11 p1346 A73-25225
- Steady plane flow of viscous fluid in symmetrical channels with curved walls, considering approximate series for stream function
11 p1347 A73-25646
- Flow of liquid metals with a transversely applied magnetic field. I - Laminar flow in the entrance region.
11 p1406 A73-26341
- Laminar free convection flow of an electrically conducting fluid from an inclined isothermal plate.
11 p1452 A73-26369
- Linear stability theory applied to stability characteristics of laminar condensate film flow along inclined wall, noting critical Reynolds number for disturbance amplification
12 p1559 A73-27697
- Liquid and wall temperature during flow in tubes with heat loss to the surrounding medium and axial heat conduction.
12 p1560 A73-27909
- Boundary layer due to sphere rotation in a medium at rest
13 p1599 A73-28068
- On the numerical treatment of the Navier-Stokes equations for an incompressible fluid.
13 p1599 A73-28090
- The stability of Poiseuille flow - An analysis of two- and three-dimensional disturbances.
13 p1600 A73-28418
- Heat transfer to laminar flow in vertical rounded corner square duct, noting wall shear stress parameter as laminarization criterion
13 p1704 A73-28428
- Parameter calculation for laminar incompressible fluid jet expanding in gradient slipstream along moving surface, determining velocity distribution in jet axis
13 p1601 A73-28736
- Laminar flame propagation in hydrogen, oxygen, nitrogen mixtures.
13 p1707 A73-29001
- Free stream turbulence and transition in a circular duct.
13 p1602 A73-29014
- The unpolarized electrode in a pulsating Poiseuille pipe flow.
13 p1620 A73-29258
- Greenstadt binary index criterion for laminar and pulsating bow shock crossings separation in terms of angle, solar wind velocity and Galilean invariance
14 p1748 A73-29979
- Rough estimate of the heat transfer coefficient of a liquid in laminar and turbulent flow through plane ducts
14 p1744 A73-30012
- Solution of the problem of unsteady heat transfer for a body and the liquid flow around it
14 p1744 A73-30018
- Asymptotic solution of initial value problem for weakly nonlinear wave system including dispersive and diffusive effects related to plane Poiseuille flow instability
14 p1744 A73-30171
- Rotating flow evolution in long circular tubes, deriving mathematical formulation for laminar and turbulent flow
14 p1745 A73-30296
- Heat transfer to a cylindrical laminar liquid jet ejecting into a gas.
14 p1817 A73-30612
- Experimental investigation of the laminar flow along a straight 135-deg corner.
15 p1861 A73-31124
- Electromagnetic wave propagation through a gas lens.
15 p1913 A73-31136
- Nonlinear development of disturbances in a plane-parallel Poiseuille flow
15 p1861 A73-31285
- Influence of viscosity on the flow of an underexpanded jet propagating in a supersonic slipstream
15 p1822 A73-31299
- Stability, solvability and adjoint conditions for time periodic perturbation solutions to subcritical bifurcating plane Poiseuille flow
15 p1863 A73-31340
- Transient forced convection heat transfer from an isothermal flat plate.
15 p1957 A73-31664
- Effect of intense injection on flow stability and turbulence development
15 p1864 A73-31857
- Hagen-Poiseuille flow stability with superimposed rigid rotation, deriving perturbed differential flow equations from Navier-Stokes and continuity equations
16 p1999 A73-33253
- The computation of the flow in the gap between two concentrically rotating spherical surfaces
16 p2000 A73-33255
- Poiseuille flow and thermal creep of a rarefied gas between parallel plates.
16 p2085 A73-33315
- Criteria regarding the predetermination of the laminar-turbulent boundary layer transition in the case of flows about body contours
16 p1965 A73-33750
- Natural convection flow equations and stability of laminar and transition flows, external and free boundary flows and boundary layer regimes
17 p2254 A73-34354
- Book on energy equations for small and large scale atmospheric motion covering laminar and turbulent flow and space-time scales for atmospheric energy balance
17 p2158 A73-34463
- Analysis of flow separation in an annular expansion - Contraction with inner cylinder rotating.
[ASME PAPER 73-FE-7] 17 p2152 A73-35006
- Viscous flow over spinning cones at angle of attack.
17 p2096 A73-35132
- Supersonic and hypersonic two-dimensional laminar flow over a compression corner.
17 p2096 A73-35134
- Finite difference solution of Prandtl boundary layer equations for steady incompressible laminar and turbulent boundary layer flows
17 p2154 A73-35136
- On the possibilities of improving the accuracy of the evaluation of inertia forces in laminar and turbulent films.
[ASME PAPER 73-LUBS-3] 17 p2181 A73-35389
- Development and effects of super-critical Taylor-vortex flow in a lightly-loaded journal bearing.
[ASME PAPER 73-LUBS-4] 17 p2181 A73-35390
- Thermohydrodynamic lubrication in laminar and turbulent regimes.
[ASME PAPER 73-LUBS-15] 17 p2181 A73-35395
- Laminar mixed convection from a horizontal rotating disc.
17 p2256 A73-35848
- Observation and calculation of a steady, laminar separated flow.
17 p2157 A73-35866
- Calculation of the flow on a cone at high angle of attack.
[AIAA PAPER 73-636] 18 p2260 A73-36195
- Rearward-facing steps in laminar supersonic flows with and without suction.
[AIAA PAPER 73-667] 18 p2261 A73-36218
- Theory of supersonic laminar non-adiabatic boundary layer flow past small rearward-facing steps including viscous-inviscid interaction.
[AIAA PAPER 73-668] 18 p2261 A73-36219
- Investigation of laminar flow in a porous pipe with variable wall suction.
[AIAA PAPER 73-725] 18 p2299 A73-36342
- Cylindrical Poiseuille flow and thermal creep of a rarefied gas.
18 p2300 A73-36635
- Theoretical and experimental study, for different electrical conditions, of the laminar motion of an incompressible and electrically conducting fluid drawn along in a confined medium, and in the presence of an axial magnetic field, by the uniform rotation of a disk
19 p2468 A73-37531
- Acceleration of the convergence of functions related to the orientation of a Brownian particle in a laminar flow
19 p2419 A73-37536
- A note on Beltrami and complex-lamellar flows behind a three-dimensional curved gaseodynamic shock wave.
19 p2420 A73-37753
- Numerical simulation of counterstreaming high Mach number plasma laminar interactions, using one dimensional model based on Vlasov equation
19 p2469 A73-37861
- The investigation on the secondary flow induced by jets. I.
19 p2422 A73-38349
- Practical calculations of transitional boundary layers.
19 p2423 A73-38479
- Use of turning ring electrodes for study of the transport of matter in fluid in a laminar or turbulent hydrodynamic regime
19 p2432 A73-38481
- Herschel-type venturimeter discharge coefficients at low Reynolds number.
20 p2566 A73-39116

- Non-steady, stratified Couette flow between concentric rotating spheres. 20 p2548 A73-39521
- Stability of parallel flow of a dusty gas in an annulus. 20 p2548 A73-39523
- Stationary water flow stability through 90-deg bend with rectangular cross section, noting preserved laminar structure of flow along convex wall 20 p2549 A73-39565
- Laminar steady state flow resistor design featuring temperature independence achieved with flattened core capillary tube 20 p2511 A73-39754
- Hankel transforms and boundary layer solutions for pulsating laminar flow in curved circular tube under sinusoidal pressure gradients 20 p2549 A73-39809
- On the coexistence of laminar and turbulent flow in a narrow triangular duct. 20 p2549 A73-39813
- Investigation of secondary flows between coaxial rotating cylinders 21 p2676 A73-40574
- The method of the false transient for the solution of coupled elliptic equations. 21 p2727 A73-41473
- Application of a general finite-difference method to boundary layer flows. 21 p2678 A73-41686
- Vapor flow in cylindrical heat pipes. [ASME PAPER 73-HT-1] 22 p2931 A73-42289
- An analytical and experimental investigation of gravity effects upon laminar gas jet-diffusion flames. 22 p2933 A73-42775
- Kinetics of nitric oxide formation in premixed laminar flames. 22 p2820 A73-42792
- Laminar combustion of polymethylmethacrylate in O₂/N₂ mixtures. 22 p2898 A73-42805
- An experimental investigation of the induced turbulence in laminar channel flow due to a transverse ion current and its applications to fluidic turbulence amplifiers. 23 p2942 A73-43402
- Fluid pad resistor for linear laminar flow resistance between parallel plates with emphasis on fluidic circuits application 23 p2945 A73-43425
- Papers on heat pipes covering incompressible laminar vapor flow behavior, startup dynamics, wicking material liquid transport properties, high thermal conductance structures, etc 23 p3049 A73-43459
- Laminar flow of a viscous barotropic gas through a circular pipe 23 p2968 A73-43721
- Variable mass flow rate air injection from porous flat plate into uniform incompressible air flow, obtaining laminar flow velocity profile and pressure measurements 23 p2940 A73-43932
- The laser-Doppler velocimeter and its application to the measurement of turbulence. 23 p2982 A73-43937
- Introduction of the viscous force sensing fluctuating probe technique, with measurement in the mixing zone of a circular jet. [AIAA PAPER 73-1044] 24 p3090 A73-44868
- Poiseuille flow at arbitrary Knudsen numbers and tangential momentum accommodation. 24 p3079 A73-45313
- Supersonic laminar flow over wedge or backward-facing step for large Reynolds number and small base or step height, predicting pressure distribution at reattachment 24 p3055 A73-45314
- Laser Doppler velocimeter measurement of laminar velocity profiles for developing MHD flow in rectangular duct, noting inlet effects on flow development 24 p3118 A73-45464
- Moment equation solutions for plane nonisothermal Poiseuille gas flow slip rate and temperature and pressure gradients in terms of molecular models 24 p3081 A73-45541
- Experimental investigation of the viscosity of lubricating oil containing air 24 p3094 A73-45548
- LAMINAR FLOW CONTROL**
U BOUNDARY LAYER CONTROL
U LAMINAR BOUNDARY LAYER
LAMINAR HEAT TRANSFER
- Interaction of thermal radiation with laminar free convection from a heated vertical plate. 01 p0123 A73-11141
- Combined forced and free-convection heat transfer from vertical thin needles in a uniform stream. 02 p0238 A73-12052
- Infinite Prandtl number fluids with constraint characterized by Taylor number heated from below, choosing boundary conditions for laminar convection 03 p0293 A73-13329
- Calculation of metric coefficients for streamline coordinates. 03 p0247 A73-14196
- On laminar free convection stagnation heat transfer from an isothermal cylinder with internal sources-sinks. 07 p0918 A73-19101
- Laminar flow heat transfer from wedge-shaped bodies with limited heat conductivity. 08 p1023 A73-21257
- Heat transfer through the unsteady laminar boundary layer on a semi-infinite flat plate. I - Theoretical considerations. II - Experimental results from an oscillating plate. 08 p1024 A73-21635
- Variable properties laminar gas flow heat transfer in the entry region of parallel porous plates. [AD-759455] 08 p1024 A73-21640
- Convective heat transfer in the region of interaction between a supersonic overexpanded jet and an oblique obstacle 12 p1458 A73-27324
- Theoretical analysis of forced laminar convection heat transfer in the entrance region of an elliptic duct. 17 p2256 A73-35850
- Combined forced and free-convection over thin needles. 18 p2371 A73-36697
- Heat transfer in the case of turbulent and laminar trickle films 19 p2505 A73-38477
- Unsteady heat transfer characteristics of a two dimensional laminar wall jet. 20 p2628 A73-39339
- Investigation of the laminar boundary layer at a permeable surface. 21 p2678 A73-41054
- Heat transfer from an enclosed rotating disk with uniform suction and injection. 22 p2938 A73-42998
- LAMINAR JETS**
U JET FLOW
U LAMINAR FLOW
LAMINAR MIXING
- Numerical solution of laminar jet mixing with and without free stream. 05 p0564 A73-16174
- Fluid mechanics of mixing; Proceedings of the Joint Meeting, Georgia Institute of Technology, Atlanta, Ga., June 20-22, 1973. 17 p2156 A73-35501
- Microscopic aspects of turbulent and laminar mixing in terms of molecular, eddy and bulk diffusional operations 17 p2156 A73-35502
- Approximate solution of the problem of local heat transfer at a vertical plate under conditions of laminar mixed convection 18 p2371 A73-36649
- The initial development of a submerged laminar round jet. 20 p2550 A73-39815
- Laminar and turbulent mixing of compressible jets at low Reynolds numbers. 23 p2967 A73-43403
- LAMINAR WAKES**
- Study of the laminar free convection wake above an isothermal vertical plate. [ASME PAPER 72-WA/HT-41] 04 p0518 A73-15815
- Supersonic laminar wakes past wedge, determining pressure distribution, velocity profiles and stream line patterns in recirculation region 16 p1962 A73-32905
- Magnetohydrodynamic wake behind a body placed in a homogeneous flow in the presence of a longitudinal magnetic field 21 p2747 A73-40890
- Hot-wire investigation of the steady laminar wake behind a circular cylinder. 21 p2703 A73-41117
- Hot-wire investigation of the steady laminar wake behind a thin flat plate placed perpendicularly to a uniform flow. 21 p2703 A73-41118
- Spatial and temporal stability of laminar axisymmetric jet and wake shear layers in viscous and inviscid flow 24 p3079 A73-45308
- LAMINATED MATERIALS**
U LAMINATES
LAMINATES
NT PLYWOOD
- Fourier analysis of laminated anisotropic rectangular plates with strong cross elasticity effects, presenting deflection, bending moments and buckling data 01 p0115 A73-10735
- Solution of stresses and strains for laminated monoclinic cylinders. 01 p0115 A73-10748
- Radiation heat transfer in isothermal adjoin plate system with directionally emitting and nondiffuse reflecting surfaces, considering surface roughness effects 01 p0123 A73-11140
- General analysis and synthesis of alloys and materials with inhomogeneous physical properties, noting thermal physicochemical methods for laminates and metal powders 01 p0066 A73-11340
- Wave propagation in elastic laminates using a multi-continuum theory. 01 p0117 A73-11364
- Impact and contact stress analysis in multilayer media. 02 p0234 A73-12072
- Analysis of unbalanced angle-ply rectangular plates. 02 p0234 A73-12073
- Glass laminates and high strength oriented fiberglass reinforced plastics failure mechanism in tension and bending, noting equalizing effect through proper cohesion characteristics between layers 02 p0185 A73-12134
- Three-dimensional problem of the deformation instability of incompressible layered materials in the case of highly elastic strains 02 p0235 A73-12191
- Metal-metal laminar composites for high-temperature applications. 02 p0182 A73-12620
- General purpose autoclave processable polyimide laminating resin selection, evaluating molding process techniques 03 p0329 A73-13004
- Stress redistribution model for anisotropic fiber reinforced laminates with internal cracks, assuming preferred directions to bonding planes and fiber orientation 03 p0334 A73-13333
- Influence of aging on the mechanical properties of polyester glass-resin laminated fabrics 03 p0334 A73-13591
- Three-dimensional finite-element analysis of laminated composites. 03 p0392 A73-13687
- Antifriction bearing with lubricated rubber and metal laminations for wear elimination in limited rotation applications, discussing design guidelines and advantages 03 p0317 A73-14424
- Fracture toughness of duplex structures. II - Laminates in the divider orientation. 04 p0460 A73-14701
- The relationship between design allowances and load induced micromechanical damage in composite materials. 04 p0508 A73-14719
- Velocity corrected theory of laminated plates applied to free plate strip vibrations. 04 p0513 A73-15588
- Russian book on orthotropic laminated cylindrical shells strength and optimal design covering glass ribbon reinforced zero moment shells and interlayer shear theory 04 p0514 A73-15702
- A continuum theory for wave propagation in laminated composites. I - Propagation normal to the laminates. [ASME PAPER 72-WA/APM-20] 04 p0516 A73-15896
- Stresses in laminated composites containing a broken layer. [ASME PAPER 72-WA/APM-14] 04 p0516 A73-15899
- Stress analysis of thick laminated composite and sandwich plates. 05 p0631 A73-16110
- Some remarks concerning heterogeneous anisotropic plates. 05 p0631 A73-16117
- A simple procedure for experimental determination of the longitudinal shear modulus of unidirectional composites. 05 p0588 A73-16119
- Equations for the oscillations of multilayer shells with allowance for shear deformation and for fiber pressing in the filler 05 p0634 A73-16749
- Nonsteady heat conduction of multilayer cylindrical and conical shells in periodic radiation flux, calculating temperature distribution 05 p0640 A73-16798
- Green's function of the Maxwell equations in laminar media 05 p0598 A73-16819
- Book - Electronic properties of composite materials. 06 p0714 A73-17872
- Adhesively bonded multilayer Al and Ti alloy sheet metals for complex airframe components, discussing design, fabrication, tests and performance comparison with monolithic structures [SME PAPER MF 72-513] 06 p0698 A73-18094
- Collocated interfacial stress intensity factors for finite bi-material plates. 06 p0763 A73-18477
- Stress wave propagation in a laminated plate under impulsive loads. 07 p0908 A73-19089
- Fracture mechanics application to initial notch extension under tension in quasi-isotropic fiberglass reinforced laminates, noting transplanar buckling effects on fracture toughness 07 p0841 A73-19186
- Numerical analysis of anisotropic rotational shells subjected to nonsymmetric loads. 07 p0914 A73-20210

Glass fiber reinforced polyester laminates, testing layer base material and molding condition effects on tensile and bending strengths and other mechanical properties 07 p0843 A73-20326

Flat laminated FRP-FRTP and carbon FRP-FRTP composites, testing lamination effects on bending and impact strengths 07 p0844 A73-20331

On the torsional strength of composite materials reinforced with glass fabric laminates and the effect of the voids in matrix. 07 p0915 A73-20332

On the compressive strength of composite materials reinforced with glass fabric laminates. 07 p0844 A73-20333

Solution of the asymmetric steady-state heat conduction problem for a two-layer hollow cylinder of finite length 08 p1021 A73-20995

Axisymmetric deformation of a laminar, orthotropic, cylindrical shell 08 p1017 A73-21368

Thermoelastic bending theory based on structural analysis of multilayer reinforced shells and plates 08 p1017 A73-21373

Stability of the state of moment stress of a three-layer orthotropic cylindrical shell under uniform and nonuniform external pressure 08 p1018 A73-21374

The influence of orthotropy on the stability of some multi-plate structures in compression. 08 p1018 A73-21435

Effects of thermal loading on foil and sheet composites with constituents of differing thermal expansivities. [ASME PAPER 72-MAT-E] 08 p0979 A73-21572

The fracture toughness and crack propagation properties of polyester resin casts and laminates. 08 p0983 A73-21595

Weight optimization for multilayered plates and shells with given load, end conditions and middle surface shape and dimension 08 p1019 A73-21762

Secondary terms of thin multilayer plate equations, involving edge and stress-strain state fluctuation effects on boundary condition formulation 08 p1019 A73-21766

Stability of a shallow three-layer shell with a linearly viscoelastic filler 09 p1157 A73-21994

Natural vibrations of laminated orthotropic spheres. 09 p1160 A73-22890

Laminated composites displacement equations of motion, obtaining stored kinetic and strain energy and free harmonic waves dispersion normal and along layers 09 p1161 A73-23117

Continuum theory of wave propagation in laminated composites. 10 p1287 A73-23565

Attenuation of 15 MeV neutrons in multilayer shields composed of steel, polyethylene and borated materials. 10 p1248 A73-23571

Low void composites based on NR-150 polyimide binders. 10 p1237 A73-23953

Polyester fiber/glass fiber composite sandwich structural design, considering thickness loss during abrasion test, physical properties and flexural strength 10 p1237 A73-23954

On the elastic properties of fiber composite laminates with statistically dispersed fiber and ply orientations. 10 p1288 A73-23959

Analysis, test, and comparison of composite material laminates configured for isotropic low thermal expansion. 10 p1237 A73-23960

Adhesive metal/glass laminate bonding, discussing materials, tests and interlaminar strength effects 10 p1224 A73-24092

Yield criteria derivation for laminated media with isotropic and anisotropic layers based on strength constants characterization as tensors 10 p1289 A73-24277

Nonlinear elastic behavior of unidirectional composite laminae. 10 p1289 A73-24283

Design stability of composite samples with a soft interlayer in static tension 10 p1291 A73-24352

Application of gamma-resonance emission spectroscopy to the study of the structure of laminar compounds of graphite with Co-57-labeled cobalt and cobalt chloride 10 p1186 A73-24466

Shear stresses and displacements of each layer of elastic plate with multiple layers of varying rigidity resting on elastic Winklerian base 11 p1433 A73-25029

Linear elastic behavior of laminated plate with ribs reinforced by continuous unidirectional fibers under

surface distributed loads orthogonal and parallel to plane 11 p1435 A73-25403

Buckling of partially debonded layered cylindrical shells. [AIAA PAPER 73-366] 11 p1438 A73-25501

Elastic stability of biaxially loaded longitudinally stiffened composite structures. [AIAA PAPER 73-367] 11 p1438 A73-25502

Buckling and vibration of unsymmetrically laminated cross-ply rectangular plates. [AIAA PAPER 73-368] 11 p1438 A73-25503

Incremental deformations in orthotropic laminated plates under initial stress. [ASME PAPER 72-APM-VV] 11 p1441 A73-25707

On the vibration of shear deformable curved anisotropic composite plates. 11 p1442 A73-25711

Stress waves in finite longitudinally layered shells. 11 p1442 A73-25712

Shear correction factors for orthotropic laminates under static load. 11 p1442 A73-25713

Bending stresses and strains in anisotropic semi-infinite plates with arbitrary edge and surface loadings. 11 p1445 A73-26404

Theoretical and experimental investigation of the nonlinear behavior of angleplyed boron/aluminum composites. 11 p1385 A73-26524

Fringe control in real time and double exposure holography for nondestructive testing of multilaminated and thin laminated structures and vibration analysis 11 p1370 A73-26541

Glass fiber reinforced polyester laminates mechanical properties evaluation for structural design, considering failure criteria in terms of fiber debonding and resin and gel coat cracking 12 p1515 A73-26877

Fracture mechanism transitions in laminate composites. 12 p1550 A73-26921

Two dimensional elasticity theory boundary value problem, for inhomogeneous laminar elastic medium, using Airy stress functions and power series expansion of inhomogeneity parameter 12 p1553 A73-27412

Compressive buckling analysis and design of stiffened flat plates with multilayered composite reinforcement. 12 p1554 A73-27736

Stressed state of multilayer spherical vessels, cylindrical tubes and circular disks consisting of a linear viscoelastic material 13 p1690 A73-27994

Free vibrations of a laminated beam by a microstructure theory. 13 p1691 A73-28063

Free and forced vibration analysis of laminated ring structure with elastic inner, outer layers and core, obtaining natural frequency response by variational method 13 p1695 A73-28486

Planar shear wave motions polarized in plane of bonded elastic orthotropic layered plates with each layer having distinct mechanical and inertial properties and thickness 13 p1697 A73-28820

Two dimensional analysis of yielding to fracture process in angle-ply filament wound laminates under biaxial tension and compression 13 p1702 A73-29543

Bending vibration test of glass-textolites, noting temperature effect on vibration damping properties 13 p1647 A73-29607

Calculation and design of highly stressed fiberglass-reinforced plastic components 13 p1703 A73-29653

Stress hybrid model extension to stiffness matrix of element with discontinuous stress distribution, considering transverse shear strains in laminated plate layers 14 p1807 A73-30181

Bleustein-Gulyaev shear surface waves in piezoelectric-dielectric-perfect conductor layered system, applying theoretical results to lithium iodate crystals 14 p1783 A73-30259

Supersonic flutter of truncated multilayered orthotropic conical thin shells. 14 p1814 A73-30702

Natural oscillations of multilayer shells and plates with fillers 15 p1944 A73-30970

The large deflection and post-buckling behaviour of some laminated plates. 15 p1946 A73-31117

Photoelastic analysis of an orthotropic ring under diametral compression. 15 p1949 A73-31653

Theoretical post-yielding behavior of composite laminates. I - Inelastic micromechanics. 15 p1897 A73-31678

Macromechanic model of notch size effects on tensile fracture strength in angle ply laminated composites 15 p1897 A73-31680

Nonlinear tension and buckling stress behavior of angle ply unidirectional laminated composites 15 p1949 A73-31683

Linear elastic fracture mechanics applicability to graphite-epoxy laminated fracture specimens configuration from fractographic studies 15 p1897 A73-31684

Orthotropic characteristics of glass-fibre-epoxy laminates under plane stress. 15 p1897 A73-31698

Techniques for fabrication of composite materials. 16 p2017 A73-32699

Optimal design of layered structures under dynamic loading. 16 p2075 A73-32790

Void free high temperature resistant bismaleimide/woven fiberglass composite laminates, discussing synthesis, processing and fabrication 16 p2028 A73-33046

Processing and properties of composites based on NR-150 polyimide binders. 16 p2029 A73-33047

Effect of prepregging solvent on high-temperature stability of KERIMID 601 composites. 16 p2029 A73-33049

Polyphenylquinoxaline/graphite composite laminates tests for flexure, shear and tensile strength at 316 C 16 p2029 A73-33050

Glass fabric structures, properties and designs of reinforced polyester and epoxy laminates for aerospace applications 16 p2030 A73-33064

Isotropic bonded thermoelastic laminar bodies calculations for thermal flux and temperature fields, using linear quasi-static thermal elasticity equations 16 p2080 A73-33242

Equilibrium conditions for multilayer anisotropic viscoelastic plates in a complex stressed state 16 p2083 A73-33933

Matrix analysis of multilayered and sandwich shells by the finite element method 16 p2083 A73-33968

Stresses in a symmetrically-laminar plate weakened by a central crack 17 p2240 A73-34145

Free vibrations of multilayered composite plates. 17 p2241 A73-34192

Investigation of the bond strength between layers of textolite materials 17 p2194 A73-34333

Fatigue and fracture of advanced composite materials. [SAE PAPER 730337] 17 p2194 A73-34688

The processability of unidirectional prepregs in aerospace applications. 17 p2195 A73-34808

The successful use of composites in the L-1011 TriStar commercial transport. 17 p2103 A73-34815

Nonlinear vibration of a rectangular plate arbitrarily laminated of anisotropic material. [ASME PAPER 73-APM-F] 17 p2249 A73-35105

Anisotropic laminated fiber composite plates under short duration impact line forces, calculating one dimensional transient stress and displacement waves by fast Fourier transform [ASME PAPER 73-APM-L] 17 p2249 A73-35108

Continuum theory for elastic laminates in terms of effective stiffness, deriving displacement and stress interface boundary conditions with illustrative wave propagation examples [ASME PAPER 72-WA/APM-13] 17 p2249 A73-35112

Layered composite plate theory with interlaminar transverse shear stress as unknown variables, demonstrating agreement with elasticity solutions 17 p2250 A73-35116

On the opening of a finite crack normal to an interface. 17 p2250 A73-35122

An improved epoxy resin formulation for multilayer circuit boards. 17 p2196 A73-35341

High temperature tensile and stress rupture tests of tungsten/Nichrome laminar composites and tungsten alloy/Inconel sheet and foil specimens 17 p2193 A73-35545

Buffalo aircraft fiberglass laminated polyester nose boom for mounting horizontal and vertical wind sensing probes, describing instruments and measurement procedures 17 p2174 A73-35576

Dynamically-induced large deformations of multilayer, variable thickness shells. 18 p2362 A73-36317

Reinforced plastics; Conference, Karlovy Vary, Czechoslovakia, May 15-17, 1973, Lectures 18 p2326 A73-36464

Initiator composition and glass content effects on polyester resin hardening in glass laminate fabrication 18 p2327 A73-36467

Optimal cutting conditions for working of reinforced plastic laminates, comparing with metals 18 p2319 A73-36471

Concepts from the realization of the development of the technology and assembly lines for the fabrication of polyester glass laminates 18 p2320 A73-36472

Self extinguishing properties of polyester-glass laminates with reduced flammability due to polyvinyl chloride and antimony trioxide additives 18 p2327 A73-36478

The effect of a fiberglass reinforcement on the properties of laminates with a polyamide binder 18 p2328 A73-36481

Vibration of layered shells. 18 p2367 A73-37029

Influence of the structure of the material of a three-layered cylindrical shell on the natural frequencies 19 p2494 A73-37184

Magnetodynamic and magnetostatic surface waves in a ferrite layered structure 19 p2470 A73-37724

Linear dispersive shear waves in two-layer elastic medium. 19 p2461 A73-38185

Electromagnetic wave propagation in inhomogeneous multilayered structures of arbitrarily varying thickness - Generalized field transforms. 19 p2461 A73-38379

Electromagnetic wave propagation in inhomogeneous multilayered structures of arbitrary thickness - Full wave solutions. 19 p2461 A73-38380

A fatigue test program for the wing of the Jantar SZD-37 sailplane 20 p2509 A73-39245

Solution of a nonlinear problem of heat conductivity concerning a multilayer cylindrical wall with a nonideal thermal contact 20 p2627 A73-39257

Inverse bending problems for two-layer orthotropic shallow shells 20 p2618 A73-39313

Large deformations of cord-reinforced multilayered axisymmetric shells. 20 p2621 A73-39542

Dynamic response of laminated composite circular cylindrical shells with freely supported or clamped edges. 20 p2621 A73-39543

Torsional and anti-plane strain delamination of an orthotropic layered composite. 20 p2622 A73-39549

On stress-concentration analysis of laminated composite plates. 20 p2622 A73-39551

An approximate solution for bending of anisotropic laminated plates. 20 p2623 A73-39554

Rotary inertia and energy dissipation effects on dynamic response of three layered symmetrical laminate beam with viscoelastic core vibrating in flexural mode, using variational calculus 20 p2623 A73-39555

Study of elastoplastic deformations in a two-layer shell under dynamic loads 20 p2625 A73-39653

Russian book on elasticity theory for multilayer media covering plate compression and bending under boundary contact conditions, Algol programming, tensile stress, functional equations, etc 21 p2782 A73-40175

Vibration and noise damping of steel structures by prebonded laminates or viscoelastic layer additions, discussing steel sheets 21 p2717 A73-40236

A mixture theory of the response of a laminated plate to impulsive loads. 21 p2783 A73-40291

Magnetic properties of layered superconductors with a weak layer interaction 21 p2751 A73-40371

Mindlin theory extension to transverse shear effects in laminate plates, taking into account continuous stress across thickness and discontinuous shear strain 21 p2784 A73-40432

Parametric study of multiple-layer damping treatments on beams. 21 p2785 A73-40752

The influence of phase size on the creep of lamellar and particulate Al-CuAl₂ eutectic composites. 21 p2719 A73-40896

Water damage in polyester/glass laminates. II - Microscopic evidence. 21 p2723 A73-40921

Pure torsion of prismatic rods composed of different materials 21 p2787 A73-40990

Extraction of Tschebysheff design data for the low-pass dielectric multilayer. 21 p2665 A73-41135

Sinusoidal response of composite-material plates with material damping. 22 p2919 A73-42082

[ASME PAPER 73-DET-120] 22 p2930 A73-42286

Transient heat conduction in laminated composites. [ASME PAPER 73-HT-R] 22 p2923 A73-42566

Vibration analysis of laminated plates and shells by a hybrid stress element. 22 p2924 A73-42881

Experimental verification of dispersion relations for layered composites. [ASME PAPER 73-APMW-14] 22 p2928 A73-43115

Comment on 'Film reinforced multifastened mechanical joints in fibrous composites.' 22 p2928 A73-43135

High frequency vibrations and waves in laminated orthotropic plates. 22 p2929 A73-43139

A higher order theory for extensional motion of laminated composites. 23 p3040 A73-43630

Method for estimating fracture strength of specially orthotropic composite laminates. 23 p3041 A73-43635

Influence of the free edge upon the strength of angle-ply laminates. 23 p3043 A73-43921

Certain methods in the physically nonlinear theory of three-layer plates 23 p3043 A73-43925

Postcritical deformations in a multilayer plate under edge pressure 23 p2999 A73-44097

Study of the existence of compact laminar for certain complex analytical laminated structures 23 p3145 A73-44525

Surface buckling of a laminated medium 23 p3102 A73-44526

Conditions of production of high-compressive-strength, orthogonally reinforced fiberglass plastics 24 p3146 A73-44531

The mechanism of fracture of reinforced beams during bending. I 24 p3103 A73-44878

Glass fiber reinforced casting plastics mechanical properties dependence on processing quality fluctuations, considering laminates with unsaturated polyesters and fiber glass mats 24 p3103 A73-44879

Determination of the point at which damage occurs in glass-reinforced laminates - New nondestructive methods and their suitability as production control procedures 24 p3103 A73-44883

'Crack boundaries' in the case of unidirectional glass-fiber-reinforced plastic wound laminates under uniaxial and multiaxial stress 24 p3104 A73-44885

Creep and aging characteristics of glass-fiber-reinforced plastics 24 p3104 A73-44886

Mechanical properties of unidirectionally reinforced polyester and epoxy resin laminates under combined stresses perpendicular or parallel to glass fiber direction 24 p3104 A73-44890

Mechanical properties of glass fiber reinforced plastic laminate formed by spraying unsaturated polyester resin on fiber rovings 24 p3104 A73-45143

Improved mechanical properties of composites reinforced with neutron-irradiated carbon fibers. 24 p3104 A73-45145

Theoretical post-yielding behavior of composite laminates. II - Inelastic macromechanics. 24 p3149 A73-45149

Propagation of shock waves in anisotropic composite plates. 24 p3149 A73-45150

A note on determination of the shear stress-strain response of unidirectional composites. 24 p3149 A73-45151

Load concentration factors for circular holes in composite laminates. 24 p3149 A73-45152

Three dimensional elasticity solution for layer interaction and shear coupling and deflection effects of laminated anisotropic composite cylinders under bending 24 p3150 A73-45232

Stress wave calculations in composite plates using the fast Fourier transform. 24 p3151 A73-45301

A layered composite with a broken laminate.

LAMINATIONS

U LAMINATES

LAND

NT FARMLANDS

NT GRASSLANDS

NT RANGELANDS

LAND ICE

Locating large masses of ground ice with an impulse radar system. 20 p2556 A73-39841

LAND MANAGEMENT

Considerations and techniques for incorporating remotely sensed imagery into the land resource management process. 05 p0642 A73-17127

Utility of remote-sensing data for urban land use planning. 16 p2003 A73-33363

Applications of high-altitude remote sensing to coastal zone ecological studies. 16 p2003 A73-33364

Multipurpose properties and conflict situations in automatic control systems 16 p1992 A73-33666

Regional land inventory systems development in the Houston area. 20 p2629 A73-39832

LAND USE

Geology, hydrology, land use and transportation net of Dallas-Fort Worth area from Apollo 6 photographs, comparing with ground based data 01 p0035 A73-10139

The use of stress situations in vegetation for detecting ground conditions on aerial photographs. 03 p0301 A73-13844

Dallas/Fort Worth regional airport land use planning for airport-community compatibility assurance via airspace distribution 13 p1598 A73-29107

Cost effective land use mapping and resources inventory for Mississippi via high altitude color IR aerial photography and ERTS-1 multispectral imagery [AIAA PAPER 73-3] 13 p1610 A73-29300

Airport layout and planning standards, considering dimensions, height restrictions, noise exposure, land use compatibility, and long term community and aeronautical requirements 13 p1598 A73-29347

Aircraft noise, exposure factor, land use priorities, public environmental concern and jurisdictional considerations impact on offshore airport planning 15 p1959 A73-31530

Land construction and cost studies for Chicago offshore airport site development in Lake Michigan using rock and sandfill dikes for protection against waves 15 p1857 A73-31536

London third airport planning, discussing site selection, large scale urbanization, land use and reclamation, operational aspects and environmental factors 15 p1857 A73-31539

Utility of remote-sensing data for urban land use planning. 16 p2003 A73-33363

Remote sensing applications in agriculture and forestry including land inventories, soil classification and water resources detection 17 p2162 A73-34948

Remote sensing techniques for support of coastal zone resource management. 18 p2306 A73-36020

Contributions of the EROS Program to the Department of the Interior's resources and management responsibilities. 20 p2550 A73-38588

[AAS PAPER 73-130] 20 p2556 A73-39845

Urban land use from RB-57 photography - Computer graphics of the Boston area. 20 p2557 A73-39846

Remote sensing to detect regional change in land use characteristics, using aerial photo mosaics and high altitude photography 20 p2557 A73-39847

The use of small-scale multi-band photography for detecting land-use change. 20 p2557 A73-39848

NASA environmental applications demonstrations in southeastern United States. 20 p2557 A73-39849

Land use classification in the southeastern forest region by multispectral scanning and computerized mapping. 20 p2557 A73-39850

Utilizing remote sensing data for land use decisions for Indian lands in South Dakota. 20 p2558 A73-39875

The interpretation of multispectral imagery - An analysis of automated versus human interpretation techniques. 20 p2562 A73-39908

Monitoring levels of existing environmental impact utilizing remote sensing techniques. 20 p2563 A73-39910

Interdisciplinary research on the application of ERTS-1 data to the regional land use planning process. 22 p2798 A73-41709

The effect of aircraft noise on the countryside.

LANDAU DAMPING

Neoclassical theory of Landau damping and ion and electron transit-time magnetic pumping /TTMP/ in toroidal geometry. 01 p0083 A73-10459

Oblique shock waves heating of high beta plasma ions, suggesting Landau damping of wave energy 02 p0197 A73-12059

Resonance, particle trapping, and Landau damping in finite amplitude obliquely propagating waves.
02 p0197 A73-12068

Plasma heating and acceleration due to Landau damping of hydromagnetic waves.
04 p0480 A73-15197

One dimensional analysis of saturation spectral lines for energy transfer in plasma waves interaction, noting Landau damping effect on parametric instability
04 p0482 A73-15650

Landau attenuation in a plasma excited by a monochromatic electron beam
05 p0601 A73-16394

Large-amplitude stabilization of the drift instability.
07 p0860 A73-20481

Landau damping of type III solar radiobursts.
08 p0997 A73-20902

Effect of the plasma inhomogeneity on the non-linear damping of monochromatic waves.
09 p1126 A73-22281

A nonlinear theory for the parametric instability with comparable electron and ion temperatures.
14 p1779 A73-30119

Influence of transverse magnetic field on Landau damping.
17 p2217 A73-35812

Modification of weak turbulence theory due to perturbed orbit effects. II - Nonlinear Landau damping of electron plasma waves.
20 p2598 A73-39302

Collisionless damping of hydromagnetic waves in relativistic plasma. I - Weak Landau damping - Heating of the Crab Nebula.
20 p2609 A73-39442

LANDAU FACTOR
Instability of plasma waves with nonlinear Landau effect.
17 p2215 A73-34296

Space probe observed VLF hiss powers disparity with theoretical prediction for incoherent Cerenkov radiation, considering Landau instability generated wave amplification
17 p2160 A73-34788

Temperature aspects of Landau orbital ferromagnetism in white dwarfs and neutron stars.
20 p2610 A73-39573

LANDFORMS
NT CANALS
NT DUNES
NT ISLANDS
NT MOUNTAINS
NT RIDGES
NT STRUCTURAL BASINS
NT TERRACES [LANDFORMS]
Water and processes of degradation in the Martian landscape.
19 p2477 A73-37202

The definition of the geotectonic domains of the Southern African crystalline shield by ERTS 1 imagery and its economic importance.
21 p2685 A73-40810

LANDING
NT AIRCRAFT LANDING
NT BLIND LANDING
NT CRASH LANDING
NT DITCHING [LANDING]
NT GLIDE LANDINGS
NT LUNAR LANDING
NT MARS LANDING
NT PLANETARY LANDING
NT SKID LANDINGS
NT SOFT LANDING
NT SPACECRAFT LANDING
NT TOUCHDOWN
NT VERTICAL LANDING
NT WATER LANDING

LANDING AIDS
NT AIRPORT LIGHTS
NT APPROACH INDICATORS
NT ARRESTING GEAR
NT AUTOMATIC LANDING CONTROL
NT INSTRUMENT LANDING SYSTEMS
NT LANDING INSTRUMENTS
NT RUNWAY LIGHTS

Airborne radar set for weather surveillance, independent landing monitoring, ground visualization and collision avoidance
02 p0190 A73-11854

Perceptual considerations for a wide field of view, helicopter night landing system /HENILAS/.
05 p0543 A73-16705

Airfield requirements for flight safety enhancement, considering approach and takeoff path obstructions, runway conditioning, glide slope information and radio aids
10 p1203 A73-24713

Air navigation evolution and current state of art, discussing MF four axis and nondirectional beacons, VOR, DECCA, DME, TACAN, VOR-Doppler, terminal and landing systems
14 p1773 A73-30445

Microwave holography application to landing without visibility
15 p1911 A73-32497

Runway VHF localizer antenna array for Norwegian airports ILS, taking into account difficulties due to course bends and snow
15 p1859 A73-32498

The multipath challenge for the microwave landing system.
15 p1912 A73-32503

The MADGE system - Operational results and stretch potential.
15 p1912 A73-32505

Radio navigation and landing aid equipment for major airports and airlines, noting simplified equipment for minor airports
15 p1912 A73-32559

Airport lighting systems as visual landing aids, discussing runway disposition, brightness levels, beam orientation, visibility factors and flashing lights
16 p1993 A73-32974

Considerations concerning the design of an electronic landing display for STOL aircraft
17 p2146 A73-34478

TACAN based SETAC and L band DME based DLS approach and landing systems for military aircraft, discussing time division multiplexing and antenna array
17 p2208 A73-34493

[DGLR PAPER 73-019]
Aircraft microwave landing system development, including conventional system history and shortcomings, program objectives and implementation schedule for ATC
17 p2208 A73-34611

C band microwave landing system for increased guidance signal accuracy and reliability in azimuth, elevation and range relative to touchdown point
19 p2450 A73-37494

Modular building block microwave landing system for automatic flight in CAT, discussing ICAO and NIAG missions
19 p2450 A73-37495

Navigation and landing aid systems in-flight and ground performance monitoring, discussing safety, legal, operational and economic aspects
19 p2450 A73-37802

On-board navigation and landing systems for local airlines in the USSR
19 p2452 A73-37819

Studies on the time-to-go indexing control scheme for an automatic aircraft landing system.
19 p2453 A73-38280

Reducing approach and landing accidents.
22 p2799 A73-42523

Evolution of blind landing systems
22 p2885 A73-43032

LANDING GEAR
Theory of the motion of a rigid model of an aircraft with a vertical landing-gear strut on a runway
01 p0005 A73-10917

Test facility for determination of S-3A aircraft landing gear behavior during critical pulse loads while rolling over carrier deck, discussing moving platform components
02 p0150 A73-11999

Hydraulic drive and control systems used for landing gear retraction and extension on Piper Cherokee Arrow and for main wheel braking on F-111
07 p0779 A73-19604

Air cushion landing gears for transport aircraft, discussing peripheral jet stream performance prediction and system installation on Buffalo STOL
10 p1174 A73-23659

A mechanized eddy current scanning system for aircraft struts.
10 p1225 A73-24631

Kneeling landing gear - The C5 variable geometry development.
13 p1568 A73-28158

Mathematical model for shimmy auto-oscillations of aircraft landing gear nose wheel with pneumatic tire under velocity changes
15 p1825 A73-31044

A technological development scenario for offshore jetports.
15 p1857 A73-31534

Graphite-epoxy composite door landing gear assembly for space shuttle orbiter, discussing design, analysis, fabrication and structural testing
16 p2029 A73-33058

Further developments in surface effect takeoff and landing system concepts - Application to high performance aircraft.
17 p2099 A73-34293

Further developments in surface effect takeoff and landing systems concepts - A multicell system.
17 p2099 A73-34294

[CASI PAPER 76/11B]
Development of an Air Cushion Landing System.
19 p2379 A73-37468

[AIAA PAPER 73-812]
Air cushion landing systems; Proceedings of the First Conference, Miami Beach, Fla., December 12-14, 1972.
19 p2380 A73-37676

Air cushion landing systems for aircraft mobility on unprepared surfaces, considering refraction, vertical energy absorption, braking, steering and weight and power reduction
19 p2380 A73-37677

Air cushion landing systems application to tactical airlift aircraft for personnel, and equipment delivery to dispersed sites under diverse climatic, terrain and combat conditions
19 p2380 A73-37678

Aircraft with air cushion landing system for off airport transport of goods and passengers
19 p2417 A73-37679

Air cushion landing systems for STOL transport aircraft, investigating structural and power requirements, ground and in-flight handling, mission capability, operational life, weight and cost
19 p2381 A73-37682

ACLS trade study for application to STOL tactical aircraft.
19 p2381 A73-37683

Air cushion landing system applications and operational considerations.
19 p2381 A73-37684

On the cost benefits of air cushion landing gear to civil aviation.
19 p2381 A73-37685

ACLS equipped vehicles in inter-city transportation.
19 p2381 A73-37686

CC-115 /Buffalo/ aircraft air cushion landing system design, testing and implementation prognosis, discussing propeller design, power systems, wings and U.S.-Canadian project cooperation
19 p2381 A73-37687

Buffalo aircraft modification for air cushion landing system, considering weight, performance, stability and control, configuration alternatives and ground maneuvering
19 p2382 A73-37688

The aircraft modification phase of the joint U.S./Canadian ACLS program.
19 p2382 A73-37689

Report on an ST6 powered air supply package for air cushion landing systems.
19 p2382 A73-37690

Ground and flight testing of air cushion landing system /ACLS/ equipped CC-115 Buffalo aircraft for performance and stability/control characteristics
19 p2382 A73-37691

LA-4 aircraft air cushion landing system ACLS development tests covering static and mobile ground tests, flight tests and performance from and to various surfaces
19 p2382 A73-37692

ACLS CC-115 model simulation, test analysis and correlation.
19 p2382 A73-37693

Air cushion landing system /ACLS/ application to Jindivik target drone aircraft for recovery improvement, considering flight performance degradation
19 p2383 A73-37698

Air cushion landing system /ACLS/ design and drone flight tests for low cost unmanned military aircraft recovery, comparing with mid air retrieval system /MARS/
19 p2383 A73-37699

A multicell air cushion system for landing gear application.
19 p2383 A73-37700

The potential influence of the ACLS on the development of logistical cargo aircraft.
19 p2383 A73-37701

Air cushion landing system twin pod /ACLS/ configuration design and test installation on A-4 Navy fighter
19 p2383 A73-37702

Theory and experiments for air cushion landing system - A ground jet concept.
19 p2383 A73-37704

Simulation of the ACLS during landing roll.
19 p2383 A73-37706

Russian book - Aircraft wheel and braking system designs.
19 p2384 A73-37768

LANDING INSTRUMENTS
NT APPROACH INDICATORS
Independent Landing Monitor for economic Category 3 operation with fail-operational autoland, fog dissipation or fail-passive autoland plus visibility augmentation
15 p1911 A73-32499

Effects of new landing approach procedures on cockpit design and possibilities of taking them into account
17 p2100 A73-34485

Doppler landing system based on standard DME for ILS replacement, describing development history and operational principles
19 p2450 A73-37385

LANDING LOADS
Decelerator parachute systems for heavy loads recovery, discussing stress, stability and reliability assessment
03 p0251 A73-14638

[AIAA PAPER 72-798]
A multicell air cushion system for landing gear application.
19 p2383 A73-37700

Ground loads analysis for air cushion landing system /ACLS/ equipped aircraft during landing and

- taxiing, predicting peak trunk pressures via energy considerations 19 p2383 A73-37707
- Dynamic gust, landing, and taxi loads determination in the design of the L-1011. 20 p2508 A73-38647
- Airport runway and taxiing surfaces modifications for heavy and supersonic aircraft demonstrated by aircraft static and dynamic landing loads and physical dimensions 24 p3075 A73-45199

LANDING MODULES

NT LUNAR MODULE

LANDING SIMULATION

- A computer-generated display to isolate essential visual cues in landing. 05 p0595 A73-16704
- Simulated flight tests of a digitally autopiloted STOL-craft on a curved approach with scanning microwave guidance. 19 p2386 A73-38049
- Carrier landing simulation for pilot visual perception, describing Fresnel lens optical landing system, periscopes, cockpit equipment and glide paths [AIAA PAPER 73-917] 21 p2634 A73-40865
- An optimized video output from a wide angle optical probe. [AIAA PAPER 73-918] 21 p2673 A73-40866
- Touchdown performance with a computer graphics night visual attachment. [AIAA PAPER 73-927] 21 p2673 A73-40874

LANDING SITES

NT LUNAR LANDING SITES

- Prediction of the landing point of a balloon payload. 01 p0005 A73-11208
- Space shuttle abort - Downrange basing and cross-range capability requirements. 02 p0228 A73-12371

LANDING SPEED

- Flight tests of approach path angles and airspeed effects on landing of spoiler equipped light aircraft 13 p1569 A73-28830

LANDING SYSTEMS

U LANDING AIDS

LANDMARKS

- Autonomous satellite navigation from strapdown landmark measurements. 04 p0474 A73-15266
- An autonomous navigation technology system. 04 p0474 A73-15274
- Landmark navigational and topographical mapping techniques for planetary surface exploration using unmanned vehicles and earth based computers 17 p2210 A73-35383

LANDSCAPE

U TERRAIN

U TOPOGRAPHY

LANGMUIR PROBES

U ELECTROSTATIC PROBES

LANGUAGE PROGRAMMING

- Book - Minicomputers for engineers and scientists. 17 p2130 A73-34455

LANGUAGES

NT ALGOL

NT FORTRAN

NT MACHINE ORIENTED LANGUAGES

NT PROGRAMMING LANGUAGES

NT WORDS (LANGUAGE)

LANTHANIDE SERIES METALS

U RARE EARTH ELEMENTS

LANTHANUM

- Theoretical consideration of soft X-ray absorption by the metallic films of lanthanum and cerium 06 p0737 A73-18220
- Variation of chemical composition on the surface of cobalt-base alloys by oxidation in air. 15 p1891 A73-32016

LANTHANUM ALLOYS

- Phase equilibrium diagram of the lanthanum-germanium system 04 p0484 A73-15692

- Cast and annealed chromium-yttrium and chromium-lanthanum alloys peak solubility from metallographic, durometric and differential thermal analyses 12 p1512 A73-27245

LANTHANUM COMPOUNDS

NT LANTHANUM FLUORIDES

NT LANTHANUM OXIDES

- Enthalpy and specific heat of the orthophosphates of lanthanum, neodymium, and yttrium at high temperatures 06 p0738 A73-18654

- Optical properties of Nd³⁺/ in lanthanum oxyfluoride single crystals 07 p0837 A73-20205

- Preparation of lanthanum sulfides using carbon disulfide as a sulfurizing agent and the change of these sulfides on heating in air. 23 p3018 A73-44130

LANTHANUM FLUORIDES

- Phononless lines shift and broadening during electron phonon interaction in lanthanum trifluoride-Nd crystal, obtaining temperature dependence of non-radiative transition probability 04 p0484 A73-15566

- Laser induced red-blue energy transfer upconversion in Pr³⁺/doped lanthanum fluorides via excitation annihilation involving pairs of ions 21 p2715 A73-40934

LANTHANUM OXIDES

- Temperature-induced changes of the electron-vibration spectrum of LaAlO₃-Cr³⁺/ crystals 10 p1260 A73-24578

LAP JOINTS

- Diffusion welding of beryllium. I - Basic studies. 04 p0451 A73-14669
- An investigation of fatigue life performance in lap-type solder joints. 04 p0452 A73-14852

- Circular cylindrical tube lap joints elastic strain relations based on plane contact problem reduction to Prandtl type equation in finite-span wing theory 10 p1225 A73-24363

- Linear elastic finite element stress analysis of lap and tapered adhesive joint bonding of composite to metal substrate [AIAA PAPER 73-371] 11 p1438 A73-25505
- Effect of Poisson's ratio strains in adherends on stresses of an idealized lap joint. 15 p1948 A73-31620

- Stress distribution in a bonded anisotropic lap joint. [ASME PAPER 73-MAT-M] 18 p2365 A73-36618

LAPLACE EQUATION

- Moments of inertia for fluid-filled rotating bodies, solving Laplace and Navier-Stokes equations for cylinder and sphere 01 p0030 A73-10089

- Continuous methods based on particular solutions for free boundary problems in partial differential equations, considering heat equation Stefan problem and Laplace equation interface 01 p0071 A73-11462

- Russian book - Study of the theory of differentiable functions of many variables and its applications. IV. 02 p0187 A73-12176

- Weighted estimates of the error in the grid method of solving the Laplace and Poisson equations 02 p0187 A73-12177

- Boundary value problems of the Laplace equation in a circle 04 p0470 A73-14933

- On the uniformly valid approximate solutions of Laplace equation for an inviscid fluid flow past a three-dimensional thin body. [ONERA, TP NO. 1145] 04 p0433 A73-15094

- Alteration of the Laplace spheres of planetary influence during the application of a new intermediate orbit 05 p0620 A73-17022

- Laplace equation and elasticity theory problems solution via Fredholm integral equation, noting boundary value problems for discrete points of given curve 07 p0909 A73-19127

- Axisymmetric triangular finite elements for the scalar Helmholtz equation. 09 p1120 A73-22392

- Lame problems in theory of elasticity, discussing reduction to Dirichlet sequence for Laplace equation 11 p1446 A73-26597

- Finite element method for solution of Laplace or wave equation in cylindrical coordinates through base matrices, applying to electromagnetic wave propagation in waveguides 13 p1581 A73-28077

- Approximate solution of the Laplace and Poisson equations in weighted Hoelder spaces 13 p1647 A73-28340

- Celestial bodies gravitational potential mathematical representation by Lame functions via series expansion of Laplace differential equation in ellipsoidal coordinates 20 p2606 A73-39080

- Finite difference approximation of the weak solution of a mildly nonlinear Dirichlet problem. 21 p2725 A73-40379

- The Laplace and Poisson equations in Schwarzschild's space-time. 23 p3005 A73-43345

- Determination of heat flow shape factors for hollow, regular polygonal prisms. 23 p3049 A73-44164

LAPLACE OPERATORS

U LAPLACE TRANSFORMATION

LAPLACE TRANSFORMATION

- Two-dimensional investigation of absolute instabilities in mirror plasmas. 01 p0083 A73-10458

- Numerical Laplace transform inversion of a function arising in viscoelasticity. 01 p0119 A73-11469

- A new numerical method for the inversion of the Laplace transform. 04 p0471 A73-15229

- Integral Laplace-Fourier transform stability during transient response functions reconstruction from transfer function frequency characteristics in linear circuits 05 p0591 A73-16779

- Numerical calculation of cumulative probability from the moment-generating function. 05 p0591 A73-16815

- Noise magnitude calculation for intensity quantized hologram based on Laplace transform for nonlinear device analysis and Gaussian random process 05 p0579 A73-17220

- A note on a general linear initial-boundary value problem. 06 p0716 A73-17980

- Iterative scheme for identifying linear systems from input/output samples or construction of rational z-transform approximations to sample data sequences 06 p0718 A73-18534

- Thermal stresses in an anisotropic plate with a circular hole. 07 p0914 A73-20199

- Book on boundary value problems in physics and engineering covering Fourier series and integrals, heat, wave and potential equations, Laplace transforms and numerical methods 09 p1113 A73-23300

- The methods of time-variable systems analysis based on new trends in theory of these systems. 10 p1200 A73-24047

- Single input n-th order linear constant discrete-time adaptive control systems, deriving phase canonical form sensitivity functions by z-transform 11 p1342 A73-26636

- On identifying transfer functions and state equations for linear systems. 11 p1342 A73-26641

- Book - Fourier analysis in probability theory. 12 p1517 A73-27051

- The asymptotic behavior of Green's function for a heat-conduction equation with a small parameter 12 p1558 A73-27248

- Fundamental solution to a single-parameter family of Laplace-parameter difference approximations on a plane 15 p1898 A73-30961

- The solution of heat conduction problems with the aid of the Laplace transformation. II - Numerical evaluation and graphical representation of two specific boundary value problems 15 p1958 A73-31907

- On the generation of rational function approximations for Laplace transform inversion with an application to viscoelasticity. 16 p2032 A73-33307

- Book - Introduction to servomechanism system design. 17 p2110 A73-35275

- Mixed boundary value problem solution for dynamic thermoelasticity, using Laplace transforms in cylindrical coordinates 22 p2918 A73-41952

- Unsteady state coupled thermoelasticity problem solution based on reducing order of Laplace transform equation, using coupling coefficient as small parameter in series expansion 22 p2921 A73-42279

LARGE SCALE INTEGRATION

- Flying-spot scanned or computer controlled electron beam fabrication system for generating high packing density pattern of LSI microelectronic circuit components 01 p0023 A73-10548

- Materials processing technology for LSI electronics, considering wafers, doping, diffusion, ion implantation, photomasking and film deposition 04 p0426 A73-14743

- Enhancing testability of large-scale integrated circuits via test points and additional logic. 06 p0674 A73-17802

- Coherent intensity spatial filtering applied to inspection of photolithography masks for LSI. 06 p0694 A73-18288

- Help derivable from failure analyses for the definition of a reliability evaluation model applicable to large-scale integrated circuits 07 p0800 A73-19411

- Prediction of IC and LSI performance by specialized vibration/detection test for presence of conductive particles. 08 p0943 A73-20732

- Design and fabrication of MOS/LSI circuits for reliability, discussing layout rules and protective circuitry 08 p0943 A73-20733

- Book - MOS/LSI design and application. 08 p0950 A73-21840

- Method of calculating yield for LSI arrays considering radial distribution of defects on wafers. 10 p1193 A73-23668

- Book - RCA advanced technology. 10 p1216 A73-23781

- Complementary MOS/silicon-on-sapphire LSI technology developments, assessing impact of incorporated Al and Si gates applications on high speed and low power capabilities 10 p1259 A73-23791

- Digital simulation methodology for LSI computer design and technology assessment to assure competitive cost, schedule and implementation cycles in manufacturing 10 p1191 A73-23793

LSI computer design and fabrication for Space Ultra-reliable Modular Computer Demonstration Vehicle, discussing assembly, physical and electrical characteristics and electronic testing procedures 10 p1191 A73-23794

Complementary MOS LSI microprogrammed digital computer design, for Space Ultra-reliable Modular Computer Demonstration Vehicle, discussing instruction operation codes, I/O peripherals and software support 10 p1191 A73-23795

Standard flexible LSI logic cell arrays with uniform interconnections as fourth generation computer components, discussing microprograms and algorithms for arithmetic operations 10 p1198 A73-24017

Determination of the proper integration level of the unified functional units of a complex of statistical-measurement methods 11 p1340 A73-25002

Use of Sirtl etch for silicon-slice evaluation. 12 p1530 A73-27044

New structure of on-board microcomputers using large-scale integrated logic circuits 15 p1852 A73-32478

Book - MOS integrated circuits: Theory, fabrication, design and systems applications of MOS LSI. 15 p1852 A73-32579

Technological forecasting for microcomputer architecture and fabrication on LSI chip, considering cost effectiveness, pins number, packing density, power and speed factors 17 p2131 A73-35226

Custom LSI technology utilization in low volume avionics systems, discussing handcrafted chip design, full wafer, array logic and MOS cell approaches and costs 17 p2138 A73-35227

Bipolar LSI building blocks for digital filtering applications. 17 p2138 A73-35228

Mathematical functional modular building block implementation in LSI microelectronics for signal and data processing, discussing primitive functions and 8-bit family design example 17 p2138 A73-35229

Modular MOS LSI digital data bus system design for integrated avionics and remote sensors interconnection in aerospace vehicles 17 p2139 A73-35232

Complementary MOS/silicon on sapphire LSI technology for high speed digital multiplier and correlator logical building blocks design, fabrication and subsystem array implementations 17 p2140 A73-35318

Hierarchical hybrid control of manipulators - Artificial intelligence in LSI. 19 p2407 A73-37334

Metal oxide semiconductor/large scale integration circuit failure analysis and diagnosis, discussing short circuits, cholesteric liquid crystal coloring and aluminum anodization 19 p2411 A73-38448

Present state and future prospects of the design of large-scale integrated circuits using MIS transistors 21 p2660 A73-40018

A design approach for LSI using chip selection and circuit modification techniques. 21 p2670 A73-41049

A laser raster setup with programmed control for image lithoplate synthesis 22 p2869 A73-42362

LARGE SPACE TELESCOPE

General analysis of aplanatic Cassegrain, Gregorian, and Schwarzschild telescopes. 03 p0309 A73-14426

System considerations for a large astronomical space telescope. 08 p0969 A73-21728

Modal control applied to the real-time figure control of a spaceborne telescope mirror. 08 p0969 A73-21729

The use of image quality criteria in designing a diffraction limited large space telescope. 08 p0969 A73-21730

Offset guiding through large space telescopes. 08 p0970 A73-21731

Laser interferometric alignment sensor for the large space telescope /LST/. 08 p0970 A73-21732

A study of optical image sensors for the large space telescope. 08 p0971 A73-21742

Optimization studies in the support design for the Large Space Telescope. 11 p1437 A73-25488

Thermal control of the large space telescope /LST/. [AIAA PAPER 73-350] 18 p2359 A73-36338

Large scale telescope pointing stability augmentation system, using control moment gyro gimbal servo error signal to command momentum augmentation system [AIAA PAPER 73-868] 20 p2587 A73-38806

Assessment of fine stabilization problems for the LST. [AIAA PAPER 73-881] 20 p2587 A73-38817

Large orbiting telescopes fine guidance system for ultrahigh pointing stability based on disturbance accommodation standard deviation optimal controller design [AIAA PAPER 73-882] 20 p2588 A73-38818

Achieving ultrahigh accuracy with a body pointing CMG/RW control system. [AIAA PAPER 73-883] 20 p2588 A73-38819

A high-performance test facility for laboratory simulation of the Large Space Telescope orbiting vehicle in a single-degree-of-freedom mode of rotation. [AIAA PAPER 73-884] 20 p2544 A73-38820

Gyroscopes as prime attitude references for the large space telescope. [AIAA PAPER 73-870] 21 p2700 A73-40506

Large telescope design, discussing optical telescope efficiency as function of aperture, exposure time auxiliary instrumental parameters 21 p2703 A73-41245

LARMOR PRECESSION

Effects of collisions and gyroviscosity on gravitational instability in a two-component plasma. 09 p1127 A73-22286

LASER ALTIMETERS

Lunar shape parameter extraction from Apollo 15 and 16 laser altimeter measurements of CSM to surface distance 06 p0751 A73-18223

Analysis and interpretation of lunar laser altimetry. 07 p0823 A73-19827

On the estimation of the directional spectrum of surface gravity waves from a programmed aircraft altimeter. 11 p1358 A73-26347

Al-Khwarizmi - A new-found basin on the lunar far side. 16 p2060 A73-33125

Statistical comparison of airborne laser and stereophotogrammetric sea ice profiles. 22 p2850 A73-42731

LASER BEAM DEFOCUSING

U THERMAL BLOOMING

LASER COMMUNICATION

U OPTICAL COMMUNICATION

LASER HEATING

Importance of Fresnel reflections in laser surface damage of transparent dielectrics. 01 p0076 A73-10131

Study of the conditions of the breakdown threshold of argon at high pressure under the effect of laser radiation 01 p0058 A73-10175

The destruction of reflecting dielectric coatings by laser radiation. 01 p0059 A73-10836

On the mechanism of particle emission from graphite during pulsed laser heating. 01 p0068 A73-10923

Stimulated Brillouin scattering for hypersound speed measurement as function of temperature in polystyrene, observing pulsed laser induced damage 01 p0068 A73-11232

Interaction between intense optical radiation and free electrons /Nonrelativistic case/ 01 p0061 A73-11248

Role of absorbing inclusions in the fracture mechanism of transparent dielectrics by laser emission 01 p0026 A73-11291

Stationary state of the radially symmetrical motion of vapors heated by laser radiation with allowance for thermal and ionizational nonequilibrium 02 p0175 A73-11601

Development of internal damage in silicate glasses and polymers under the action of laser radiation 02 p0184 A73-11616

Effect of laser working on the wear of machine parts in an abrasive-lubricant medium 02 p0173 A73-11935

Momentum transfer interaction of a laser-produced plasma with a low-pressure background. [AD-755558] 02 p0197 A73-12062

Time taken for a laser pulse to make a hole in a metal film. 02 p0176 A73-12114

Spectral characteristics in visible and UV regions of laser plasma-air interaction, using focused beams on metal targets at atmospheric pressure and vacuum 02 p0176 A73-12351

Laser-induced stress-wave and impulse augmentation. 02 p0177 A73-12746

Cutting thin metal sheets with the CW CO₂ laser. 02 p0175 A73-12819

Prospects for rocket propulsion with laser-induced fusion microexplosions. [AIAA PAPER 72-1063] 03 p0353 A73-13392

Averaged equations of cumulative-laser heating of plasma in Z-pinch with consideration of the recovery of the energy of nuclear fusion. 03 p0347 A73-13782

Averaged equations of cumulative-laser heating of two-temperature plasma in Z-pinch taking into account the nuclear fusion energy. 03 p0347 A73-13783

Equations of laser heating of plasma in a system of the 'focus' type, the recovered energy of nuclear fusion being taken into consideration. 04 p0480 A73-15593

Averaged equations of laser heating of two-temperature plasma in Z-pinch, the thermonuclear fusion energy being taken into consideration. 04 p0480 A73-15594

Cumulation-laser heating of two-temperature plasma, the recovered energy of nuclear fusion being taken into consideration. 04 p0480 A73-15596

Radiation energy distribution in laser pulse heating of moving plasma without reflection, noting thermal wave propagation 04 p0481 A73-15605

Possible mechanisms of turbulent heating of a plasma by ultrashort pulses of laser radiation. 05 p0603 A73-16792

The laser heated wind tunnel - A new approach to hypersonic laboratory simulation. [AIAA PAPER 73-211] 05 p0563 A73-16942

Transverse and longitudinal heat flow in a laser-heated magnetically confined plasma. 05 p0603 A73-17162

Ruby laser radiation removal of glowing spot from Kron electronograph image tube 05 p0580 A73-17260

Cutting and welding using a CO₂ laser. 05 p0582 A73-17264

Fog droplet vaporization and fragmentation by a 10.6-micron laser pulse. [AD-758948] 06 p0698 A73-17494

Laser-initiated fusion - Key experiments looming. 06 p0727 A73-17570

Review of controlled fusion research using laser heating. [AIAA PAPER 73-258] 06 p0728 A73-17667

Controlled nuclear fusion process based on laser heating of deuterium-tritium pellets, considering laser energy reduction by pulse induced plasma compression 06 p0699 A73-17752

Some averaged properties of wave solutions for a hypersonic thermal wave. 06 p0728 A73-17890

Laser-induced fast thermal desorption from solid surfaces 06 p0699 A73-17914

Gasdynamic structure of a plasma flame arising during vaporization of metals by strong optical radiation 06 p0729 A73-18107

Design and characteristics of a single pass normal mode ruby oscillator-amplifier laser for hole drilling in metals. 06 p0700 A73-18277

CO₂ laser-induced gas breakdown in hydrogen. 06 p0701 A73-18355

Optimum thickness for thermomagnetic laser writing on Fe doped EuO films on quartz substrate 06 p0702 A73-18372

Anomalous ion heating in a laser heated plasma. 06 p0730 A73-18461

Thermal processes in metals exposed to high power laser pulses 06 p0702 A73-18571

Thermal tagging for laminar and turbulent liquid flow shadowgraph visualization by ND glass laser beam 06 p0696 A73-18573

Heating of a plasma in stimulated scattering of laser radiation /Review/. 06 p0731 A73-18578

Plasma generation by nanosecond and picosecond laser pulses, discussing Raman scattering from solid hydrogen and deuterium targets 06 p0731 A73-18581

High power laser generation and heating of plasma in solid targets due to radiation damage, discussing liquid lasers as light amplifiers 06 p0731 A73-18582

Measurement of the polarization of the radiation reflected backward from a laser-heated plasma. 06 p0731 A73-18589

Laser-radiation-induced damage to the surface of lithium niobate and tantalate single crystals. 06 p0738 A73-18591

Production of hot plasmas of solid-state density by ultrashort laser pulses. 06 p0733 A73-18783

Microchannel electron multipliers application to X ray cinematography of laser generated plasma 06 p0697 A73-18861

Steady state dense arc plasma heating by inverse bremsstrahlung process with IR carbon dioxide laser, calculating maximum attainable temperature 07 p0857 A73-19531

Lateral expansion of a laser-supported detonation wave in a gas. 07 p0920 A73-19979

A possible mechanism for the change in the discharge current in CO₂ through the action of laser radiation.

07 p0836 A73-20137

Some questions on the evidence of laser X-ray emission from CuSO₄ doped gelatin.

08 p0975 A73-21061

Parametric heating of a dense arc plasma with 0.337 m laser radiation.

09 p1125 A73-21944

Heating of laser-induced plasmas in helium.

09 p1125 A73-21998

Plasma production by laser, discussing basic equations, dimensional analysis, heating, focusing lens and targets

09 p1125 A73-22050

Momentum method extension to thermal conduction laser heating of nonhomogeneous plasma, obtaining closed form solutions for plane waves

09 p1126 A73-22171

Gasdynamic and thermal processes during giant laser pulse impingement on target material, considering heat wave propagation at supersonic and subsonic velocities

09 p1127 A73-22610

Surface and body vaporization mechanisms during intense energy flux interaction with substance, relating flux density to mean depth of surface-to-bulk vaporization shift

09 p1095 A73-22611

Thermodynamic and optical properties of elements vaporized by monochromatic laser light, considering carbon and aluminum vapor stream characteristics

09 p1095 A73-22612

Radiation energy distribution in laser pulse heating of moving plasma without reflection, noting thermal wave propagation

10 p1254 A73-24195

Heating of theta-pinch plasmas by pulsed CO₂ lasers.

10 p1256 A73-24527

Heating of a substance by short laser pulses

10 p1230 A73-24885

Numerical modeling of laser produced plasmas - The dynamics and neutron production in dense spherically symmetric plasmas.

11 p1404 A73-25272

Nd laser radiation thermochemical effects on oxide formation on thin Cr films, Fe-Ni-Co and Cr-SiO alloys and MgO-MnO ferrites, noting resistance and etching rates

11 p1376 A73-25636

Laser beam welding technology review, discussing technical and economic aspects of pulse and CW techniques

11 p1374 A73-25850

Iron silicate disproportionation by ruby laser and static heating in resistance furnace, discussing X ray diffraction patterns

11 p1409 A73-25901

Harmonic generation and parametric excitation of waves in a laser-created plasma.

11 p1405 A73-25972

Photoluminescence of ZnTe during laser stimulation

11 p1376 A73-26145

Direct measurement of the fluorescence energy yield of a rhodamine 6G solution with the aid of an Ar⁺ laser

11 p1377 A73-26146

Dynamics and energetics of the explosive vaporization of fog droplets by a 10.6-micron laser pulse.

11 p1377 A73-26231

High speed welding of sheet steel with a CO₂ laser.

11 p1375 A73-26351

Thermal cumulation equations for concentric conductive laser heating of two temperature D-T plasma with nuclear fusion energy recovery

11 p1406 A73-26411

Laser concentric conduction heating of two-temperature D-T plasma.

11 p1406 A73-26412

Charged particle production and plasma electron/ion current discharges from W targets under laser beam, noting dependence on electric field strength, pressure and operation mode

11 p1378 A73-26522

The possibility of microfission explosions by laser or relativistic electron-beam high-density compression.

11 p1378 A73-26657

Dissociation of semiconductor compounds under the action of a laser beam

11 p1378 A73-26675

Ultraviolet spectrum emitted from a laser-produced uranium plasma.

12 p1527 A73-27123

Laser beam evaporation of dense substances, examining luminous flux densities with gasdynamic equations

12 p1506 A73-27137

Powerful laser beam and material interaction, investigating gas dynamics of plasma heating and ejection

12 p1506 A73-27138

Chemical reaction stimulation by laser radiation

12 p1467 A73-27978

Possibility of atom displacements in solids under the action of laser light pulses

13 p1626 A73-28003

Nonlinear behavior of stimulated Brillouin and Raman scattering in laser-irradiated plasmas.

13 p1664 A73-28187

Role of stimulated Compton scattering in the interaction of laser radiation with a superdense plasma.

13 p1664 A73-28615

Effects of target-electrode polarity and of the position of the focal plane of the lens on the characteristics of a discharger with laser ignition

13 p1627 A73-28964

Averaged equations of cumulative laser heating of a plasma focus with consideration of the heat of nuclear fusion.

13 p1667 A73-29389

Concentric laser cumulation of plasma with consideration of the heat of nuclear fusion.

13 p1667 A73-29393

Mechanism of damage of the surface of a transparent dielectric during illumination with short light pulses.

13 p1629 A73-29429

Possibility of a superconducting transition in a semiconductor subjected to high-power laser radiation.

13 p1629 A73-29439

Focused high power CW carbon dioxide laser sustained Xe, Kr and Ar continuous plasmas, investigating plasma radiative properties by calorimetric techniques

14 p1779 A73-29922

Plasma produced by lasers on solid targets

14 p1779 A73-30025

Experiments on CO₂-laser heating of magnetically confined underdense plasmas.

14 p1780 A73-30123

Concentric, uniform elastic spherical wave excited by thermal explosion of the envelope.

14 p1816 A73-30251

Formation of oriented structures by action of a laser beam on metals.

14 p1760 A73-30325

Self-igniting pulsed optical discharge in an erosion laser plasma.

14 p1757 A73-30334

Particle acceleration by a moving laser focus, focusing front or ultrashort laser pulse front.

14 p1757 A73-30338

Mechanical deformation and failure of metals under the action of a 0.01-sec laser light pulse

14 p1758 A73-30714

Spectral diagnostics of a plasma flare during well-developed vaporization of metals by laser radiation

14 p1782 A73-30804

Rapid balancing of gyroscopes with TEA CO₂ laser.

15 p1883 A73-30996

Laser illumination for infrared nondestructive testing.

15 p1874 A73-31050

Experimental study of the interaction of a plasma with a magnetic field in the case of a plasma generated by laser irradiation of solids

15 p1917 A73-31249

The laser - A unique tool for /for the time being/ unique applications

15 p1884 A73-31325

Ignition and maintenance of a CW plasma in atmospheric-pressure air with CO₂ laser radiation.

15 p1884 A73-31398

Pulsed laser irradiation effects on solid deuterium slab, deriving two-temperature electron-ion model

15 p1884 A73-31660

Recombination of doubly ionized atoms in the afterglow of a helium plasma produced by laser.

15 p1915 A73-31675

Effect of laser pulse rise time on heating of a magnetically confined plasma.

15 p1919 A73-31929

Thermal analysis of thin-film micromachining with lasers.

15 p1882 A73-31938

Laser-induced shock effects in Plexiglas and 6061-T6 aluminum.

15 p1956 A73-32259

Investigation of the absorption of laser radiation in a laser spark in air

15 p1885 A73-32313

Influence of atom-atom collisions on electron density decay in laser-produced helium plasmas.

16 p2041 A73-32944

Influence of saturation effects on stimulating scattering in laser heating of a plasma.

16 p2041 A73-33079

The drilling of a metal plate by a laser beam.

16 p2019 A73-33535

Thermal processes in metals irradiated by powerful laser pulses.

16 p2086 A73-33596

Thermal tagging for laminar and turbulent liquid flow shadowgraph visualization by Nd glass laser beam

16 p2016 A73-33598

Mechanism of failure in transparent organic-glass-type dielectrics under the action of laser radiation

16 p2030 A73-33927

Dependence of laser-induced breakdown field strength on pulse duration.

17 p2183 A73-34201

Cooling of the heated region formed during breakdown of air by laser radiation

17 p2183 A73-34262

Numerical analysis of the averaged equations of concentric laser cumulation of plasma with consideration of nuclear fusion energy.

17 p2216 A73-34323

Heating of an oxidizing metal by CO₂ laser radiation

17 p2184 A73-34634

Anomalous heating of dense plasma by laser radiation.

17 p2218 A73-35823

One-dimensional model for nonlinear reflection of laser radiation by an inhomogeneous plasma layer.

17 p2218 A73-35824

Nearly spherical constant-power detonation waves as driven by focused radiation.

[AIAA PAPER 73-674]

Investigation of the molecular composition of the vapors and the structure of the condensate during the evaporation of arsenic chalcogenides by laser radiation

19 p2437 A73-37957

Shock and compression by TEA-CO₂-laser pulses drastically enhanced by liquid layers spread on surfaces of solids.

19 p2438 A73-38024

Formation of a periodic wave structure on the dry surface of a solid by TEA-CO₂-laser pulses.

19 p2438 A73-38025

Nd laser radiation thermochemical effects on oxide formation on thin Cr films, noting resistance and etching rates

19 p2438 A73-38148

X-ray emission in laser-produced plasmas.

20 p2595 A73-38890

Ellipsoidal coordinates - A natural coordinate system for calculations of laser irradiations of slabs.

20 p2572 A73-38972

Plane unsteady dispersion of gas behind deflagration wave moved by laser radiation with high flux density

20 p2573 A73-39281

Carbon dioxide jet laser cutting technology and rate calculations for metals and dielectrics as function of laser power and material thermal properties

20 p2569 A73-39677

Generation of high-power light pulses at wavelengths 1.06 and 0.53 micron and their application in plasma heating. I - Experimental investigations of reflection of light of two wavelengths in laser heating of plasma.

20 p2573 A73-39684

Nature of the damage caused by laser radiation on the surfaces or in the bulk of transparent glasses.

20 p2573 A73-39687

High-speed interferometry of expanding and collapsing laser produced plasma.

21 p2744 A73-39964

High-speed photography of laser-induced cavities in liquids

21 p2709 A73-39968

Influence of semiconductor laser heating on the parameters of the output pulses

21 p2710 A73-40006

High power carbon dioxide-nitrogen gasdynamic laser vibration kinetics model, suggesting closed cycle photon generator engine for energy conversion to work

21 p2710 A73-40094

Spectral discharge plasma emission analysis with controlled electrical synchronization of laser vaporized microsamples of steel and wolframite

21 p2711 A73-40302

Nonlinear effects in the emission and absorption spectra of gases in resonant optical fields

21 p2712 A73-40443

Stress and temperature analysis for surface cooling or heating of laser window materials.

21 p2716 A73-40966

Kinetic effects in drilling with the CO₂ laser.

21 p2707 A73-40974

Heating with short laser pulses.

21 p2717 A73-41660

Evaporation of metallic targets caused by intense optical radiation.

22 p2868 A73-41727

Experiment involving the application of the LMA-1 laser microanalyzer to the investigation of metallic materials

22 p2868 A73-42100

Laser-induced gas breakdown in superhigh pressure region.

22 p2869 A73-42227

Generation of high-power light pulses at wavelengths 1.06 and 0.53 microns and their application in plasma heating. II - Neodymium-glass laser with a second-harmonic converter.

Changes in the characteristics of giant laser radiation pulses and of luminous plasma during formation of damage regions on the surface or in the bulk of transparent dielectrics.

Characteristics of thin-film metal arrays for laser-beam information storage.

Interaction of intense optical radiation with free electrons /nonrelativistic case/.

The production of plasma by lasers on targets in the gaseous state

Metastable phases produced by laser melt quenching.

German monograph - Materials removal in the case of the drilling of holes with the aid of solid-state lasers.

Dynamic effects on ignitability limits of solid propellants subjected to radiative heating.

Ammonium perchlorate gasification and combustion at high heating rates and low pressures.

The ignition of hydrocarbon-air mixtures with laser radiation

The role of absorbing impurities in laser-induced damage of transparent dielectrics.

Distribution of hot phonons generated by laser radiation

Thermonuclear laser synthesis and parametric instabilities

Effects of target-electrode polarity and focal-plane position on a laser-triggered gap.

Gas-dynamic structures of a plasma flare produced during the evaporation of metals by high-intensity optical radiation.

Free vibrational development of laser-induced cracks

Cyclotron resonance breakdown with submillimeter lasers.

Absorption of laser radiation in a laser spark in air.

Pulse method for determining heat-transfer coefficients of coatings

Neutron emission from laser produced plasmas and collisionless electrostatic shock waves.

Simplified averaged equations of concentric laser compression of plasma.

Optimization of compression constants for cumulated plane shock waves in a closed tube.

Transformation of shock compression into isentropic compression in a nonhomogeneous body.

Laser supported gaseous detonation wave propagation above solid surface, calculating momentum transfer as functions of laser energy, pulse duration, and beam and target areas

Computerized simulation of electrostatic instabilities development in underdense plasmas during heating by high output lasers with frequencies above electron plasma frequency

LASER MATERIALS

The feasibility of producing laser plasmas via photoionization.

Nonlinear aspects of cooling of a strongly anisotropic optical element of a laser.

Nonlinear polarization coefficients of proustite and tellurium.

Change in sign of thermal lens of glass laser rods with change in thermo-optical constant of glass.

Russian book - Spectroscopy of laser crystals with ionic structure.

Certain problems of spectroscopy of laser crystals with ionic structure

Optical centers of Nd³⁺/J in calcium and strontium fluorophosphate crystals

Investigation of the lasing and luminescent properties of fluoride and strontium fluoride crystals containing bivalent dysprosium impurities

Thin film YAG-Nd laser light sources, discussing material selection, incoherent pumping sources, geometrical configuration, heat dissipation, gain saturation and feedback methods

High-current gas lasers with a mercury cathode

Pressure-induced optical distortion in laser windows.

The problem of laser sources of radiation in the far-ultraviolet and X-ray regions of the spectrum

Spectral properties of laser crystal materials, noting deactivation energy storage in nonuniformly widened luminescence band

Spectroscopic and lasing studies of a new laser crystal, KY(WO₄)₂-Nd³⁺/J

Microinhomogeneous active medium effects on laser monopause duration and energy, noting luminescence band random shift and directional diversity in dipole moments

Density homogeneity in a laser cavity due to energy release.

Immersion liquids for a homogeneous optically mixed laser

Theory of spontaneous and stimulated electroluminescence of ZnS-Mn layers

Influence of thionyl chloride on the lasing characteristics of the liquid phosphor POCl₃-SnCl₄-Nd³⁺/J

Pulsed gas laser employing substances of low volatility

Graphs for the design of laser mirrors at normal incidence.

Detection of transient absorption in YAG laser crystals using combined laser.

An approximate solution of the nonstationary heat conduction problem for laser elements with sharply expressed anisotropy

Concentration dependence of the lasing parameters of a laser based on CaF₂:Dy²⁺ crystals

Thin dielectric films as protective coatings for metallic mirrors and antireflective coatings for semiconductors and active laser materials

Laser mode locking using saturable absorbers.

Single crystals for optical applications - Problem of index homogeneity of double niobates Ba_x/Sr_{1-x}/Nb₂O₆ and Ba₂Nb₅O₁₅.

Influence of magnetic spin resonance in optically transparent magnetic materials on the nature of laser radiation

Carbon dioxide laser active element design features for service life extension through regenerating working mixture composition while preserving discharge tube seal tightness

Gain and energy measurements on an HF/DF electrically pulsed chemical laser.

Continuous uniform excitation of medium-pressure CO₂ laser plasmas by means of controlled avalanche ionization.

Laser emission spectral theory, calculating cross relaxation in three and four level systems, monochromatic radiation effects on matter and laser action in inhomogeneous media

New improved laser dye for the blue-green spectral region.

Russian book on solid state pulsed laser design and construction covering optical, electronic and cooling elements, amplifiers, energy storage, illuminators and semiconductor instruments

Thermal lensing of laser beams in optically transmitting materials. I.

Laser cutting of aerospace materials.

Methods for alignment of lasers with unstable resonators.

Nd doped YAG laser crystal relaxation time, describing population inversion, beam gain time dependence and phonon spectra

Acoustooptic materials evaluation based on figures of merits and acoustic attenuation for laser beam deflection device design and fabrication

Emission of aqueous solutions of rhodamine 6G with detergent additives in the presence of flash lamp excitation

Laser resonator mode structure during interaction with active medium, considering combined effects of gain and refractivity variations for arbitrary mirror configurations

Triply ionized Pm in lithium yttrium fluoride laser, calculating crystal field split energy levels and radiative transition probabilities

Far IR laser lines measurements in carbon dioxide laser pumped ethylene glycol, dimethyl ether, formic acid, and monomethyl amine, using grating spectrometer and Golay-cell detector

Chromium-rare-earth energy transfer in YAlO₃.

Absorption of CO₂ laser radiation by carbonyl fluoride.

Stress and temperature analysis for surface cooling or heating of laser window materials.

Damage produced by laser radiation in optical materials. II

Evaluation of a high accuracy reflectometer for specular materials.

Properties of laser mirrors at non-normal incidence.

Bulk and surface damage mechanisms of laser crystalline and nonlinear optical materials and thin films, noting plasma thresholds and surface polishing

Calculation of the mode structure in the Fabry-Perot cavity of a laser with a high flow rate

Laser Doppler interferometry for measuring small absorption coefficients.

Nd-doped Yttralox ceramic lasing performance and interrelationship between ceramic processing, microstructure and optical quality of sintered product

Passive mode locking of the cw dye laser.

An optical bridge for the assessment of mode-locked CO₂ lasers.

Nd glass and ruby lasers in mode locking operation for picosecond light pulses emission, noting pulse duration measurement

Investigation of the statistical properties of ultra-short light pulses with the aid of two-photon absorption in semiconductors

Fiber-dispersion measurements using a mode-locked krypton laser.

Mode-locked high-pressure waveguide CO₂ laser.

Combined nonlinear amplification and absorption role in ultrashort pulse generation of mode locked quasi-continuous dye laser in absence of short relaxation time

Active terminal devices for wide band time multiplexed laser PCM communication systems.

Frequency and time description of mode locked laser system, discussing active and passive phase locking of longitudinal standing wave modes in laser cavity

Mode locked laser system generated picosecond pulses envelope and phase structure measurement methods

Direct measurement of pulse broadening in the second harmonic of mode-locked Nd:glass laser.

Picosecond pulses from a passively mode-locked cw dye laser.

Motional effects in retardation plates and mode locking in ring lasers.

Acoustic-optic modulator design for a high power mode-locked CO₂ laser.

Mode locking picosecond pulse Nd glass laser design for reliable and reproducible operation as function of pump power, mirror alignment and saturable absorber

06 p0700 A73-18293

Ultrafast photodiode for mode locked laser pulses detection, estimating rise time

06 p0678 A73-18851

A stabilized mode-locked Nd:YAlG laser using electronic feedback.

07 p0834 A73-19537

Frequency stabilization of a CO₂ or N₂O power laser by a fast sampling method

08 p0976 A73-21444

Mode-locking of high power lasers by a combination of intensity and time dependent Q-switching.

09 p1090 A73-21999

A new approach to picosecond laser pulse analysis shaping and coding.

09 p1090 A73-22077

Efficient parametric conversion in cesium vapor irradiated by 3470-A mode-locked pulses.

09 p1090 A73-22079

Characteristics of acoustooptic cavity dumping in a mode-locked laser.

09 p1091 A73-22089

Theory of second-order mode locking in semiconductor lasers.

09 p1092 A73-22244

A picosecond single-pulse laser

09 p1095 A73-22661

Self-mode-locking in an argon ion laser with a nonlinear absorber

09 p1096 A73-22878

Powerful nanosecond pulses by stable passive mode-locking of TEA CO₂ lasers.

09 p1098 A73-23340

Internally modulating and multiplexing mode locked Nd-YAG laser techniques for one gigabit optical communication, noting system efficiency improvement over conventional approaches

10 p1227 A73-23783

He-Se laser low order transverse modes self mode locking at six transition wavelengths, attributing effect to oscillating modes reduction due to hole burning and cross relaxation

10 p1229 A73-24616

High data rate YAG laser communication experimental systems with partial cavity dumping, orthogonal setup or harmonic mode locking, investigating internal modulation feasibility

11 p1378 A73-26246

Influence of saturable-absorber transmission and optical pumping on the reproducibility of passive mode locking.

12 p1505 A73-27013

Mode locking in quantum optics.

12 p1506 A73-27442

Time characteristics of a ring laser with a bleachable filter.

12 p1507 A73-27509

Oscillating laser transverse modes locking into off-centered pure Gaussian beam

13 p1626 A73-28347

Mode locking in quantum optics.

13 p1627 A73-28928

Rhodamine laser frequency locking using Faraday filter for tuning to sodium D lines

13 p1628 A73-29249

Investigation of the shape of radiation pulses emitted by a self-mode-locked laser.

14 p1757 A73-30329

Laser mode locking using saturable absorbers.

15 p1885 A73-31941

Papers on laser theory covering historical evolution, optical resonators, oscillators, amplifiers, pulse propagation, gain saturation effects, internal modulation, mode locking and noise problems

15 p1886 A73-32424

Monochromatic field frequency misalignment effect on polarization and population ratio instabilities of single frequency traveling wave laser with broadened active medium

16 p2024 A73-32894

Experimental study of fluctuations of the difference frequency in a ring laser

16 p2024 A73-32895

High speed bit synchronizer for mode-locked laser communications.

17 p2138 A73-35220

Pulse time of flight measurements using mode locked laser ranging systems consisting of image converter tubes with deflection plates

17 p2185 A73-35411

Kinetics of bleaching in polymethine cyanine dyes.

17 p2186 A73-35793

Investigation of the characteristics of a mode-locked Nd:glass laser with the aid of a picosecond streak camera.

17 p2186 A73-35796

A frequency-tunable mode-locked CW Nd:glass laser.

19 p2438 A73-38276

Spatially locked laser mode formation of coherent wave fields with improved angular divergence by degenerate oscillation superposition in laser resonator

20 p2573 A73-39681

Generation of fifth picosecond laser harmonic.

20 p2574 A73-39700

Application of image-converter technique in quantum radiophysics and nonlinear optics [Survey paper].

21 p2709 A73-39940

High speed camera with locked mode laser activated Kerr cell shutter to obtain picoseconds exposure duration

21 p2709 A73-39945

Utilization for high speed cinematography of phased-locked CW lasers

21 p2709 A73-39954

Laser mode locking effect on conversion efficiency of beat frequency excitation in multimode emission, using two photon fluorescence method

21 p2712 A73-40308

Dependence of the induced phase-locking of modes in relationships among laser parameters

21 p2714 A73-40557

Limitations for mode-locking enhancement of internal SHG in a laser.

21 p2714 A73-40759

Frequency-locking band of a traveling-wave laser.

22 p2869 A73-42255

Ultrashort pulses from mode-locked cw dye lasers.

22 p2871 A73-43079

Matched-filter detection of mode-locked laser signals.

22 p2872 A73-43152

Investigation of the statistical properties of ultrashort light pulses by two-photon absorption in semiconductors.

23 p2987 A73-43503

Propagation velocity of picosecond pulse from mode locked Nd-glass laser investigated by optically induced birefringence, self phase modulation and self focused light

23 p2988 A73-44120

Frequency dependence of locking in a ring laser.

24 p3095 A73-44622

Fast linear detection system for TE CO₂ lasers.

24 p3096 A73-44922

LASER MODES

Organic dye lasers tuning by diffraction gratings and prisms, noting CW, pulsed and mode locking operations

01 p0059 A73-10716

Frequency stabilization of Q factor modulated ruby laser with mode selection, using rotating prism and quartz selecting element

01 p0060 A73-11087

Variable reflectivity unstable laser resonator mode selectivity solution by perturbation analysis for mirror misalignment effects, obtaining Fresnel number and output coupling conditions

01 p0060 A73-11223

Coherence of the radiation of a pulsed single-mode injection semiconductor laser.

01 p0061 A73-11335

Ultrashort light pulse generation in lasers with bleachable filters, covering mode formation, secondary effects and two photon recording of emission time structures

01 p0061 A73-11354

Coupling losses in hollow waveguide laser resonators.

02 p0177 A73-12573

Electromagnetic field, polarization and population inversion equations for spiked emission operation analysis in single mode laser

02 p0177 A73-12694

Spectrum of stimulated radiation in a flat-mirror resonator.

02 p0177 A73-12695

High power carbon dioxide electric discharge convection laser operation in closed cycle mode with combined dc and RF excitation and aerodynamic stabilization techniques

02 p0178 A73-12749

Optical sweep generator using single frequency He-Ne lasers with Michelson interferometer for mode selection to provide smooth tuning throughout Doppler width

03 p0319 A73-14065

Diffraction losses and corrections for lower order transverse modes and resonance conditions in optical resonators with cylindrical mirrors

03 p0319 A73-14079

An experimental study of unstable confocal CO₂ resonators.

03 p0320 A73-14456

Pulse pumped Q switched Nd-YAG and ruby lasers single longitudinal mode selection by providing intracavity resonator with active medium

03 p0320 A73-14464

Mode losses in hollow-waveguide lasers.

04 p0457 A73-14747

Cavity detuning and multimode operation of an optically pumped gas laser.

[AD-758495]

05 p0585 A73-16598

Frequency shift in a mode-selected dye laser.

05 p0586 A73-17225

Waveguide properties, modes and optical pumping effects on thin film organic dye lasers, noting temperature effects on refractivity and laser modes

06 p0699 A73-17808

Laser diodes cavity radiative efficiency loss due to sidewall induced internally circulating modes, considering cavity length, width and reflectivity relations

06 p0701 A73-18358

Output power dependence on mode geometry in CW gas dynamic laser resonator within kinetic theory of interaction between radiation field and optically active medium stream

06 p0702 A73-18459

Cylindrical laser resonators with partial radial radiation and strong axial energy focusing, relating low-loss cavity modes to Gaussian beam modes

07 p0833 A73-19273

Laser microspectral analyzer operation in Q switched mode, discussing microplasma generation under inert gas at variable pressure

07 p0836 A73-20162

Saturation resonances by magnetic mode crossing in optical pumping with a multimode gas laser.

07 p0837 A73-20606

Dependence of characteristics of a gas laser on the parameters of an intracavity absorber.

08 p0974 A73-20953

Laser oscillation modes in corrugated optical waveguides with passive core, calculating wavelengths for hybrid modes

08 p0975 A73-21060

Direct modulation of double-heterostructure lasers at rates up to 1 Gbit/s.

08 p0975 A73-21120

Study and development of a dye laser with coupled modes excited by a flash tube and emitting in the near infrared

08 p0976 A73-21493

Cavity dimension effect on single mode generation spectrum of GaAs epitaxial CW injection laser at 77 K

08 p0976 A73-21655

An antiresonant ring interferometer for coupled laser cavities, laser output coupling, mode locking, and cavity dumping.

09 p1091 A73-22085

Variation of spontaneous emission with current in GaAs homostructure and double-heterostructure injection lasers.

09 p1091 A73-22236

Transverse mode control in semiconductor lasers.

09 p1092 A73-22242

PbTe-SnTe stripe junction diode lasers, discussing fabrication, electrical properties, and mode characteristics from emission spectra, polarization, mirror illumination and far field pattern measurements [AD-759093]

09 p1092 A73-22250

Mesa-stripe-geometry double-heterostructure injection lasers.

09 p1093 A73-22251

Feasibility analysis of MIS sandwich structure for pulsed laser based on calculation for field distribution and TE and TM modes in optical cavity

09 p1093 A73-22254

Spectral self modulation and pulsation instabilities of single mode injection GaAs laser with tunable composite cavity

09 p1093 A73-22258

Peak-mode operation and self-Q-switching in a solid state laser

09 p1094 A73-22487

Influence of combinational coupling on the spectral and statistical properties of multimode fluctuations in a traveling-wave laser

09 p1094 A73-22599

The effect of an external signal on a ruby laser in the free-emission mode

09 p1095 A73-22667

Holographic recording of focused images in multimode laser radiation

09 p1084 A73-22879

Dielectric modulation of single mode CW gas laser by acoustic wave, solving equations for creation and annihilation operators to obtain quantum number

09 p1096 A73-22973

Performance of an unstable repetitive pulsed CO₂ laser oscillator.

09 p1098 A73-23338

Probability model of mode interactions, radiation density and output gain of gas laser channels with common lower energy level in active medium

10 p1227 A73-24071

Steady state lasing stability in ring-type gas laser with symmetrical distribution of three longitudinal modes

10 p1228 A73-24580

Stability of the monochromatic mode of emission in a multimode solid-state laser

11 p1376 A73-25631

Single mode ion laser tuning over entire emission range via intracavity etalon tilting by piezoelectric drive

11 p1376 A73-26104

Influence of external self-focusing on the performance of laser amplifiers 11 p1364 A73-26156

Superradiant waveguide dye laser pumped by flash lamps, noting power output and stable mode pattern insensitivity to disturbance and thermal effects 11 p1378 A73-26324

Lowest-order mode selection in a laser interferometer. 12 p1504 A73-26842

Emission of a ruby laser with a moving mirror in the presence of a selector in the resonator 12 p1505 A73-26955

Properties of a radial mode CO₂ laser. 12 p1505 A73-27016

Properties of unstable resonators with large equivalent Fresnel numbers. 12 p1507 A73-27505

Operation of a laser with a planar resonator at high pumping levels. 12 p1507 A73-27507

Competition between longitudinal modes in a ring laser with an anisotropic resonator. 12 p1507 A73-27508

Investigation of the stability of the oscillation frequency of a mercury laser emitting at 1.53 microns. 12 p1507 A73-27511

Separation of rotational lines of a CO₂ laser with a film selector in the resonator. 12 p1508 A73-27527

Emission field structure during transverse mode synchronization in a laser 13 p1626 A73-28005

Amplitude characteristics of a helium-neon laser at the 0.63-micron wavelength in the region of strong interaction between two modes. 13 p1630 A73-29446

Stability condition of an intense two-modes regime in a gas laser 13 p1630 A73-29557

Influence of atmospheric parameters on the wavelength of single-frequency laser radiation 14 p1756 A73-30023

Iterative diffraction calculations of transverse mode distributions in confocal unstable laser resonators. 14 p1756 A73-30156

Waveguide laser mode patterns in the near and far field. 14 p1756 A73-30157

Spike operation and self Q-switching in a solid-state laser. 14 p1757 A73-30323

Maxwell equations for lasing modes of bounded region in laser beam with finite spectral width in form of Fourier integrals 14 p1757 A73-30461

Temperature stability of the disperse phase component of the output emission of an optical quantum amplifier 14 p1758 A73-30576

Kinetics of high-pressure chemical lasers 14 p1758 A73-30577

Contribution to the theory of single-mode laser modulation. II - Conduction modulation. 14 p1758 A73-30769

Unsteady processes in multimode lasers with a nonuniformly widening line of lasing 15 p1886 A73-32329

Investigation of longitudinal-mode selection and frequency stabilization of the emission from a helium-neon laser with a ring resonator 15 p1886 A73-32335

Phase correlations of longitudinal modes in a laser under free emission conditions 15 p1886 A73-32336

Solutions of certain difference equations describing transformation of the temporal characteristics of radiation in a laser 16 p2024 A73-32891

Spatial correlation functions of the field and intensity of laser radiation 16 p2024 A73-34053

Oscillographic registration of the occurrence of off-axis modes in a gas laser 17 p2183 A73-34169

An investigation of the statistical properties of the radiation of a laser, operating in several axial modes, by the photon counting method. 17 p2184 A73-35156

Light pulse structure and bandwidth bounds in ruby laser with delay line inside variable effective length resonator 17 p2185 A73-35169

Single mode operation of flashlamp pumped dye laser achieved after emission spectrum line narrowing by interference filter and successive quartz Fabry-Perot etalons 17 p2185 A73-35769

Mode selection in GaAs injection lasers resulting from Fresnel reflection. 17 p2186 A73-35797

Unstable cavities with a central coupling hole in lasers and amplifiers 18 p2322 A73-36559

Generation in a ruby laser with moving mirror and a selector in the resonator. 19 p2438 A73-38132

Stability of the monochromatic generation mode in multimode solid-state lasers. 19 p2438 A73-38147

Dispersion characteristic of a three-mode gas laser during modulation of relative excitation 19 p2406 A73-38335

Optimal pumping focusing in parametric single-resonator lasers 19 p2439 A73-38336

Two-photon time distributions in mixed light beams. 20 p2570 A73-38615

Detuned single mode laser detailed balance and line width factor in threshold region expressed by Fokker-Planck equation and nonhermitian eigenvalue 20 p2571 A73-38622

Tuning and bandwidth control of laser pumped continuous dye lasers for obtaining stable single axial mode operation 20 p2571 A73-38624

Third- and higher-order intensity correlations in laser light. 20 p2571 A73-38630

General method for the calculation of the frequency of beats in a single-mode ring laser. 20 p2573 A73-39678

Asymptotic nature of threshold conditions and multimode laser emission. 20 p2574 A73-39691

Diffuse parasitics gain thresholds of laser modes for rectangular geometries, discussing radiation field and boundary conditions 21 p2710 A73-40145

Laser transient behavior analysis by quantum theory, obtaining density matrix equation solution in terms of exponentially decaying eigenmodes by truncation method 21 p2711 A73-40214

Effect of double optical resonance on frequency interaction and selection in a gas laser 21 p2711 A73-40303

Lasing mode generation during normal competition in channels with common upper level, assuming line broadening and atomic diffusion 21 p2712 A73-40307

Dye laser operation at independently tunable wavelengths via utilization of holographic wavelength selectors in succession, discussing limitations on multiple frequency tuning range 21 p2713 A73-40460

Generation of internal modes and its influence on the operation of a tunable ruby laser 21 p2714 A73-40558

A study of the effect of the number of axial modes of a laser on its degree of coherence 21 p2714 A73-40748

Finite aperture waveguide laser resonators with external reflectors by matrices coupling linearly polarized modes, calculating power efficiency, resonant frequencies and radiation patterns 21 p2714 A73-40760

Laser resonator mode structure during interaction with active medium, considering combined effects of gain and refractivity variations for arbitrary mirror configurations 21 p2714 A73-40761

The frequency stabilization of gas lasers. 22 p2868 A73-41698

Phase fluctuations in a parametric light source operating inside a laser resonator. 22 p2869 A73-42246

Mode competition in the 3s sub 2-3p sub 4 transition in a neon laser with a methane absorbing cell. 22 p2869 A73-42256

Nonstationarity of the three-mode regime in a gas laser in the case of mode-frequency symmetry 22 p2870 A73-42388

Ideal laser amplifier as a phase measuring system of a microscopic radiation field. 22 p2870 A73-42516

Maximum inversion measurement above threshold as function of pump power for Nd glass laser operating in transverse mode 22 p2871 A73-43081

CW single mode He-Ne laser intensity fine structure fluctuations correlation measurement near threshold by digital correlator, obtaining higher order relaxation rates 22 p2871 A73-43085

Three-dimensional diffraction calculations of laser resonator modes. 22 p2872 A73-43151

Scaled carbon dioxide laser design for transverse mode output power in terms of beam, transmission loss, Fresnel number and cavity parameters 22 p2872 A73-43155

Real laser cavity with nonideal reflecting mirrors, showing Q factor increase relation to mode order for plane monochromatic linearly polarized waves 23 p2987 A73-43650

A method for the study of the gain and the oscillating modes of a CO₂ laser. 23 p2989 A73-44176

Calculation of the mode structure in the Fabry-Perot cavity of a laser with a high flow rate 24 p3095 A73-44752

Photomixing of the fundamental and reference laser beams during analysis of the frequency spectrum of laser radiation by the method of optical heterodyning 24 p3096 A73-44955

Generation of nonunidirectionally polarized modes by a gas laser oscillator with a mode selector. 24 p3096 A73-45031

Mode guidance parallel to the junction plane of double-heterostructure GaAs lasers. 24 p3097 A73-45423

LASER OUTPUTS

Time dependence of carbon monoxide TEA laser emission at 77 K, presenting time resolved transitions spectral data 01 p0058 A73-10128

Subsonic plasma motion in continuous laser light. 01 p0084 A73-10472

Use of light pressure for selective evacuation of gases 01 p0059 A73-10627

The fluctuation spectrum of laser radiation in a turbulent atmosphere in the presence of rain 01 p0060 A73-10872

A study of basilar membrane vibrations. I - Fuzziness-detection: A new method for the analysis of microvibrations with laser light. 01 p0013 A73-10973

Beam spread of laser light propagating through the atmosphere. 01 p0060 A73-11056

Future optical communication systems problems, potentialities and development prospects, considering bandwidth, laser modulation, directionality, fiber transmission, reception, detection, power and efficiency 01 p0018 A73-11066

The laser's impact on crystal technology. 01 p0088 A73-11067

Spontaneous active medium emission effect on amplification characteristics of linear and nonlinear traveling wave IR gas laser amplifier 01 p0060 A73-11084

Accumulation of the light sum in alkali halide crystals under the action of laser emission 01 p0060 A73-11088

Effect of a magnetic field on emission fluctuations in a ring gas laser 01 p0060 A73-11089

Laser power density calculation with complete rotational analysis for molecular hydrogen Lyman and Werner bands vibrational-rotational transitions 01 p0061 A73-11224

Investigation of the statistical properties of ultrashort light pulses with the aid of two-photon absorption in semiconductors 01 p0061 A73-11282

Second harmonic generation in an inhomogeneous laser plasma 01 p0086 A73-11288

Role of absorbing inclusions in the fracture mechanism of transparent dielectrics by laser emission 01 p0026 A73-11291

Ultrashort light pulse generation in lasers with bleachable filters, covering mode formation, secondary effects and two photon recording of emission time structures 01 p0061 A73-11354

Gas and solid state lasers amplitude and phase fluctuations calculated from Langevin equations, noting spectral line width and ring laser wave coupling 01 p0061 A73-11355

Investigation of laser radiation self-focusing by alkali halide single crystals according to data on the damage-focus displacement effect 01 p0061 A73-11443

An 11 megawatt 6.8 joule flashlamp pumped coaxial liquid dye laser. 02 p0175 A73-11956

Laser Doppler shift velocity correlation meter operation in turbulent flow analyzed by optical mixing theory 02 p0153 A73-12049

Possibility of using a laser flame as a source of light in the isotope spectral method 02 p0176 A73-12094

Gas discharge efficiency from populations comparison of Ne absorbing levels in hollow cathode and positive column discharges, measuring laser output power peak 02 p0176 A73-12096

Coherent laser radiation and holography in an optically inhomogeneous medium. 02 p0176 A73-12111

Fracture of nonlinear crystals /KDP and LiNbO₃/ by radiation from a ruby laser. 02 p0176 A73-12112

Time taken for a laser pulse to make a hole in a metal film. 02 p0176 A73-12114

Analogies in the laser-induced destruction of the surface and interior of transparent glass. 02 p0176 A73-12115

Saturation of stimulated ruby laser radiation under the action of CO-60 gamma rays

02 p0176 A73-12353

Dynamics of the CO₂ atmospheric pressure laser with transverse pulse excitation.

[AD-760231]

02 p0177 A73-12435

Nonlinear interaction between a spontaneous radiation field and the active media of high-gain gas laser amplifiers

02 p0177 A73-12489

Electromagnetic field, polarization and population inversion equations for spiked emission operation analysis in single mode laser

02 p0177 A73-12694

Gain and frequency characteristics of a 20 mW C.W. water vapour laser oscillating at 118.6 microns.

02 p0177 A73-12724

Performance characteristics of a helical TEA CO₂ laser.

02 p0177 A73-12745

Laser oscillation and anisotropic gain in the 1 to 0 vibrational band of optically pumped HF gas.

02 p0177 A73-12747

High power carbon dioxide electric discharge convection laser operation in closed cycle mode with combined dc and RF excitation and aerodynamic stabilization techniques

02 p0178 A73-12749

Gas-temperature measurement in pulsed H₂O laser discharges.

[AD-755012]

02 p0178 A73-12814

The generation of tunable near IR radiation using a nitrogen laser pumped dye laser.

03 p0318 A73-12869

Correlation analysis as applied to the observation of fluctuations of laser light diffracted on an ultrasonic wave in an inhomogeneous medium.

03 p0318 A73-12994

Approximate formulas for calculating intensity distributions of intense laser light diffracted on an ultrasonic wave.

03 p0318 A73-12995

Laser Raman spectrum of crystalline cyclopentane-d/sub 0/ and -d/sub 10/.

03 p0318 A73-13282

High performance reactorless nuclear propulsion of reusable orbital space tug by laser rocket engine [AIAA PAPER 72-1095]

03 p0341 A73-13415

Laser measurement of turbulence in exhaust jets.

03 p0308 A73-13568

Investigation of the disintegration of semiconductors exposed to laser radiation

03 p0349 A73-13660

Electro-optical multiple transit laser beam deflection system using KDP crystals and quadrupolar electrode arrangements

03 p0319 A73-14066

Single band optical mixer heterodyne spectrum analyzer for laser radiation image spectrum suppression

03 p0319 A73-14083

Reciprocity theorem for antenna directivity pattern measurement of optical superheterodyne receiver for carbon dioxide laser radiation

03 p0284 A73-14084

Spectral density curves for intensity fluctuations of stimulated emission from low and IR frequency gas lasers as function of thermal oscillation, mode interference and beat effects

03 p0319 A73-14087

A new dimension in front-light laser photography.

03 p0309 A73-14199

Laser energy conversion into electrical energy with photovoltaic cells, noting Si and GaAs cells power efficiencies improvement compared to operation in sunlight

03 p0254 A73-14210

Beam diverging lens system for high power laser transmitters.

03 p0319 A73-14432

Power output of a pulsed Raman laser with saturable excitation.

03 p0319 A73-14453

Submicrosecond pulses from a hydrogen-fluorine laser with high energy density and quantum efficiency.

03 p0320 A73-14454

Carbon dioxide laser output signature calculation as function of cavity length based on homogeneously broadened line with dispersion

03 p0320 A73-14455

An experimental study of unstable confocal CO₂ resonators.

03 p0320 A73-14456

Internal upconversion and doubling of an optical parametric oscillator to extend the tuning range.

03 p0320 A73-14463

Time behavior of a TEA xenon laser.

03 p0320 A73-14466

Calorimetric measurement of optical power from pulsed lasers.

03 p0310 A73-14494

A calorimeter for high-power CW lasers.

03 p0310 A73-14495

Airborne laser-beam scintillation measurements at high altitudes.

03 p0305 A73-14657

Tunable polarized violet light pulse emission from anthracene doped organic molecular fluorene crystal laser pumped with nitrogen laser, noting pulse amplitude and duration

04 p0458 A73-14873

Distortion of laser pulses in resonant media

04 p0458 A73-14883

Laser irradiation testing - A new method for the nondestructive study of plastic material

04 p0458 A73-15324

Proton beam effect on carbon dioxide laser discharge I-V characteristics and emission power

04 p0458 A73-15559

Q switched ruby laser emission absorption by diatomic Rb vapor, noting molecular fluorescence intensity changes

04 p0458 A73-15560

Thermal defocusing of high intensity continuous Ar laser radiation in absorbing medium with allowance for spherical aberrations

04 p0458 A73-15562

Confinement in a magnetic mirror of a plasma generated by laser radiation

04 p0482 A73-15620

Time history of laser power pulses from molecular gas lasers.

04 p0459 A73-16041

Organic dye lasers use as continuously tunable sources of coherent light, discussing molecular energy level systems and transitions

05 p0583 A73-16337

Frequency and time description of mode locked laser system, discussing active and passive phase locking of longitudinal standing wave modes in laser cavity

05 p0583 A73-16338

Mode locked laser system generated picosecond pulses envelope and phase structure measurement methods

05 p0583 A73-16339

Electro-optical and acousto-optical methods of laser beam modulation and deflection with emphasis on various modulator and deflector types

05 p0583 A73-16340

Laser beams for precision alignment and detection using methods based on maximum and minimum principles

05 p0583 A73-16344

Operational characteristics of a volume excited TEA CO₂ laser.

05 p0584 A73-16436

The use of a gas laser for sizing single particles of airborne dust.

05 p0584 A73-16444

Neutron damage in GaAs laser diodes - At and above laser threshold.

05 p0584 A73-16523

Investigation of a gallium arsenide laser pumped by an electron beam

05 p0584 A73-16553

Population inversion by mixing in a shock tube flow.

05 p0600 A73-16556

Atmospheric pressure CO₂ pulsed laser with semiconducting plastic electrodes.

05 p0585 A73-16567

Frequency modulated laser radiation detection, studying photomultiplier current harmonics, phase/amplitude detector nonlinearities and noise-resonator coupling effects

05 p0585 A73-16782

Laser coupling through nonlinear gas filled absorber cell, discussing molecules mean free path

05 p0585 A73-16783

CO₂ laser radiation absorption in SF₆-air boundary layers.

[AIAA PAPER 73-262]

05 p0585 A73-16983

Luminescence signatures induced by lasers with enhanced specificity for remote active sensing.

05 p0585 A73-17157

Propulsion by impinging laser beams.

05 p0585 A73-17211

High intensity CO₂ laser-plasma interaction.

05 p0603 A73-17224

He-Ne laser beam intrinsic third order intensity

statistical correlation function measurement by digital technique for comparison with calculations

06 p0699 A73-17520

Effects of contaminants in CO₂ lasers.

[AIAA PAPER 73-52]

06 p0699 A73-17628

Controlled nuclear fusion process based on laser heating of deuterium-tritium pellets, considering laser energy reduction by pulse induced plasma compression

06 p0699 A73-17752

Visible light flash emission due to strong shock wave of laser spark, investigating strong external magnetic field effect and time variation of luminous intensity

06 p0700 A73-17966

Stimulated Compton scattering of laser radiation by electron plasma, determining electrons diffusion coefficient and velocity distribution function

06 p0700 A73-17970

Emission risetime fluctuations in a gas laser with nonlinear resonant absorption

06 p0700 A73-18104

Laser diodes cavity radiative efficiency loss due to sidewall induced internally circulating modes, considering cavity length, width and reflectivity relations

06 p0701 A73-18358

Experimental study of argon ion laser discharge at high current.

[AD-754727]

06 p0701 A73-18361

Five temperature model of pumping and output power pulse shape predictions for carbon dioxide-nitrogen-helium TEA lasers

06 p0701 A73-18362

Output power dependence on mode geometry in CW gas dynamic laser resonator within kinetic theory of interaction between radiation field and optically active medium stream

06 p0702 A73-18459

CW laser beams steady state thermal self focusing stability, deriving nonlinear absorbing medium geometrical optics ray equation and aberration pattern

06 p0702 A73-18583

Influence of waveguide properties of heterojunction layers on the principal characteristics of injection lasers.

06 p0702 A73-18585

Pulsed nitrogen laser emitting at 3371 A.

06 p0702 A73-18587

Possibilities of control of radiation emitted by lasers with telescopic resonators.

06 p0702 A73-18588

Use of a semiconductor laser diode as a modulator of gas laser radiation.

06 p0702 A73-18592

Second-harmonic conversion of laser radiation generated under free-oscillation conditions.

06 p0702 A73-18594

Maximum permissible pulse duration in second-harmonic generation in a KDP crystal.

06 p0703 A73-18595

High-power Y₃Al₅O₁₂:Nd³⁺/laser with an explosion-type lamp.

06 p0703 A73-18597

Time dependence of the gain of an optically pumped solution of rhodamine 6G.

06 p0703 A73-18598

Optimization of the parameters of a quasi-CW YAG:Nd³⁺/laser with a nonlinear element in the resonator.

06 p0703 A73-18599

Efficient pumping of a CW garnet laser by water-cooled metal-halide lamps.

06 p0703 A73-18600

Pressed cathodes made from barium scandate and refractory metals mixture, investigating operation in plasma discharge of He-Ne lasers

06 p0703 A73-18601

Polarization properties of a traveling-wave laser.

06 p0703 A73-18611

110-J pulsed laser using a solution of rhodamine 6G in ethyl alcohol.

06 p0703 A73-18612

Electrical characteristics of the plasma in a CO laser.

06 p0703 A73-18614

Observation of laser oscillation in a 1-atm CO₂-N₂-He laser pumped by an electrically heated plasma generated via photoionization.

[AD-759094]

06 p0703 A73-18649

Unstable resonators for CO₂ electric-discharge convection lasers.

06 p0703 A73-18747

Light emitting diode pumped Nd-YAG laser analysis for pumping rate and output dependence on temperature, using circular and transverse intensity distribution

06 p0704 A73-18787

Large-aperture Nd-glass laser amplifier for high-peak-power application.

06 p0704 A73-18791

Doping dependence of photon yield as a function of excitation energy in optically-excited n-type GaAs at 300 K.

06 p0704 A73-18844

Use of nonstationary holography to improve the directivity of laser radiation.

07 p0834 A73-19275

Selective reabsorption leading to multiple oscillations in the 8446-A atomic-oxygen laser.

07 p0834 A73-19335

Influence of an electric field on the laser-induced impurity photoconductivity of gallium selenide

07 p0861 A73-19398

Two-pass-internal second-harmonic generation using a prism coupler.

07 p0834 A73-19539

The effect of an electric field on the active medium in a dye laser.

07 p0834 A73-19540

CW and pulsed deuterium fluoride-carbon dioxide transfer chemical laser with molecular vibrational energy transfer for population inversion to obtain high power output

07 p0834 A73-19630

Exothermic deuterium-fluorine chain reaction pumping of high pressure pulsed carbon dioxide chemical transfer laser

07 p0835 A73-19631

Gain measurements on CO P-branch transitions in a C2H2-O2 flame.

07 p0788 A73-19634

Comparison of theory and experiment for a transversely excited high-pressure CO2 laser.

[AD-756053] 07 p0835 A73-19637

Electron-beam-controlled CO2 laser amplifiers.

07 p0835 A73-19639

Vibration-rotation state populations and laser output spectra of CW chemical hydrogen halide lasers under subsonic transverse flow

07 p0835 A73-19640

Parametric studies of pulsed HF lasers using transverse excitation.

[AD-760268] 07 p0835 A73-19641

Occurrence of oriented structures under the action of a laser beam in metals

07 p0839 A73-19658

CW He-Cd and He-Se metal vapor lasers, discussing atomic energy states, energy emission and absorption by electrons He storage levels and Penning ionization

07 p0836 A73-19933

Numerical study of a diffusion-type chemical laser.

07 p0836 A73-19959

Calorimetric measurements of laser energy and power.

08 p0963 A73-20872

Severe self-induced beam distortion in laboratory simulated laser propagation at 10.6 microns.

08 p0974 A73-21031

Statistics of laser beam fade induced by pointing jitter.

08 p0975 A73-21058

Direct modulation of double-heterostructure lasers at rates up to 1 Gbit/s.

08 p0975 A73-21120

Laser oscillation in leaky corrugated optical waveguides.

08 p0975 A73-21206

Photoinitiated transversely sustained CO2 laser.

08 p0975 A73-21208

Energy and threshold characteristics of chemical lasers.

08 p0975 A73-21213

Effects of multiple scattering on laser pulses transmitted through clouds.

08 p0976 A73-21423

Frequency stabilization of a CO2 or N2O power laser by a fast sampling method

08 p0976 A73-21444

Dependence of He-Ne laser output power on discharge current, gas pressure and tube radius.

08 p0976 A73-21462

Discharge current dependence of saturation parameter of a He-Ne gas laser.

08 p0976 A73-21463

Study and development of a dye laser with coupled modes excited by a flash tube and emitting in the near infrared

08 p0976 A73-21493

Submillimeter-band gas laser pumped by a CO2 laser.

08 p0976 A73-21654

Change of vibrational temperature due to laser action in CO2 lasers.

09 p1089 A73-21933

Proposal of periodic layered waveguide structures for distributed lasers.

09 p1090 A73-21935

Pressure-induced optical distortion in laser windows.

09 p1090 A73-21937

Holographic method of controlling the spatial-angular characteristics of laser emission

09 p1090 A73-21951

Collisional effect on the saturation amplitude of nonlinearly excited plasma waves.

09 p1125 A73-22023

X-ray temperature measurements of laser produced plasmas in large radiation fields.

09 p1125 A73-22024

Laser beam steering in confocal unstable resonators, interpreting mirror misalignment effects as far field dependence on magnification and Fresnel number from mode solution

09 p1090 A73-22076

Lamb dip measurements on low pressure CO laser vibrational-rotational lines, determining line widths, velocity-changing collision rate and saturation intensities with curve fitting

[AD-758943] 09 p1090 A73-22078

Loss analysis and design improvement for a continuous dye laser.

09 p1090 A73-22080

High energy and power carbon dioxide laser with nitrogen and He mixtures, transverse electric discharge excitation and modular construction, noting efficiency and gain

09 p1090 A73-22081

Pulsed and CW water vapor lasers, investigating He addition effects on time-varying gas temperature and power output

[AD-760377] 09 p1091 A73-22082

High gain gas laser oscillators saturation, verifying with 3.51 micron Xe oscillator having unsaturated single pass intensity gain of ten million

09 p1091 A73-22086

Megawatt power IR output of Nd:YAG 50 micron pulse laser, using antireflection coated lithium niobate crystal for Q switch with high polarization contrast ratio

09 p1091 A73-22088

Gradual degradation of GaAs double-heterostructure lasers.

09 p1092 A73-22241

Theory of second-order mode locking in semiconductor lasers.

09 p1092 A73-22244

Semiconductor electron-beam-pumped lasers of the radiating mirror type.

09 p1092 A73-22248

Spectral behavior and linewidth of /GaAl/As-GaAs double-heterostructure lasers at room temperature with stripe geometry configuration.

09 p1093 A73-22252

Spontaneous emission and stimulated recombination of p-n-n double heterojunction /AlGa/As-GaAs laser diodes above and below threshold currents

09 p1093 A73-22256

Flow velocity measurement method based on laser light frequency Doppler shift in scattering experiment on particle seeded liquid, presenting velocity profiles

09 p1094 A73-22314

Mandelstam-Brillouin laser light scattering theory and application to atmospheric parameters remote sensing

09 p1094 A73-22327

Laser system output mirrors alignment for beam quality and power performance optimization and external optical component premature degradation prevention, using autocollimator

09 p1094 A73-22445

Optical breakdown of compressed gases by carbon dioxide laser emission

09 p1094 A73-22594

Luminescence of a molecular gas under the action of a carbon dioxide laser pulse

09 p1094 A73-22595

Equation of motion derived for laser resonator with frequency dispersion effect on emission kinetics and spectral features, analyzing unsteady /transient/ processes

09 p1094 A73-22596

The problem of laser sources of radiation in the far-ultraviolet and X-ray regions of the spectrum

09 p1094 A73-22600

Lasing characteristics of flat resonator carbon dioxide-nitrogen-helium gasdynamic laser in terms of mirror reflection index, resonator length and gas pressure and composition

09 p1095 A73-22609

Magnetic field effect on laser radiation intensity and polarization, noting Zeeman component change

09 p1095 A73-22666

High power laser light beam stratification with self induced effects in cubic medium, noting amplitude distribution dependence

09 p1095 A73-22669

Generation spectra of a ruby laser with frequency scanning

09 p1095 A73-22680

Measurement of log-irradiance fluctuation of He-Ne laser in the atmosphere.

09 p1096 A73-22750

Laser energy transfer - An analytic survey of high power applications.

09 p1096 A73-22822

Study of the time correlation of multifrequency-laser emission by the photon coincidence method

09 p1096 A73-22877

Effect of a laser field on the gain line profile of an adjacent transition in an argon laser

09 p1096 A73-22968

A laser amplifier with resonator natural frequencies misaligned with respect to the gain profile of the active medium

09 p1096 A73-22969

Influence of thermo-optical distortions on the emission spectrum of a rhodamine 6G laser with incoherent pumping

09 p1096 A73-22972

Sealed off 9.4 micron 15 W output power carbon dioxide laser with barium difluoride windows, noting long service life

09 p1096 A73-23009

A tunable laser based on an organic dye solution and providing highly monochromatic, stable single-frequency emission

09 p1097 A73-23010

Outlet of second harmonic emission for the laser resonant cavity

09 p1097 A73-23011

Holographic photography of high-speed processes with the aid of paired radiation pulses

09 p1085 A73-23014

Application of lateral illumination in holography of small objects

09 p1085 A73-23015

Optically pumped gas laser steady state solution for population inversion, gain coefficient, radiative intensity and power output, noting Doppler broadening role

09 p1097 A73-23070

Microinhomogeneous active medium effects on laser monopulse duration and energy, noting luminescence band random shift and directional diversity in dipole moments

09 p1097 A73-23083

Some investigations on the methods of measuring 3-dimensional plastic deformations by laser.

09 p1086 A73-23321

Laser spectroscopy of stimulated Raman scattering of weakly interacting molecules, and its applications

09 p1097 A73-23326

Demonstration of the transmission and reception of modulated oscillations with a helium-neon laser beam

09 p1097 A73-23328

Density homogeneity in a laser cavity due to energy release.

09 p1098 A73-23450

The preprocessing of French laser observations from the ISAGEX program

10 p1187 A73-23621

Obtaining beams of singly charged metal ions with the aid of giant ruby laser pulses

10 p1227 A73-23815

Transverse discharge pulsed CO2 chemical transfer laser.

10 p1227 A73-23840

Use of lasers for local measurement of velocity components, species densities, and temperatures.

10 p1217 A73-23852

Resonator parameters effect on stability characteristics of ultrashort pulse produced by ruby laser, using mirror and thin reflector

10 p1227 A73-24070

Absorption of laser emission by He-CO2 mixtures, CO2 and NH3 gases, and water vapors

10 p1227 A73-24074

Injection of a laser-produced plasma into a magnetic trap.

10 p1254 A73-24210

A plasma laser operating on molecular electronic transitions

10 p1228 A73-24454

Experimental properties of injection lasers - Modal distribution of laser power.

10 p1228 A73-24530

Deficits in visual function associated with laser irradiation.

10 p1182 A73-24563

Lasing characteristics of neodymium glasses at the 0.92-micron wavelength

10 p1260 A73-24581

Possibility of smoothly tuning the emission frequency of a mixed-dye laser

10 p1228 A73-24582

Generation of the second harmonic of laser emission in organic crystals

10 p1228 A73-24583

Depolarization of laser radiation in an optical channel

10 p1229 A73-24612

Method of increasing the noise immunity of optical communications lines

10 p1190 A73-24615

Research and technology assessment of high power short wavelength molecular lasers, emphasizing carbon dioxide laser efficiency

10 p1229 A73-24654

New method of increasing the emission frequency of high-power laser pulses.

10 p1229 A73-24769

Laser Doppler velocimeter configuration and operation, discussing applications and test results

10 p1229 A73-24856

Flow measurement in the presence of strong swirl using a laser Doppler anemometer.

10 p1221 A73-24857

Design of an R.F. excited helium-neon visible gas laser and study of the optimal conditions for gas mixtures and pressures.

10 p1230 A73-24923

Self-consistent and direct reading laser homodyne measurement technique.

11 p1360 A73-25063

Characteristics of the vibrational spectrum of laminar As2S3 semiconductors

11 p1408 A73-25244

Broadly tunable, narrow linewidth dye laser emission in the near infrared.

11 p1375 A73-25366

Influence of elastic collisions on the intensity of natural oscillations in a He-Ne laser

11 p1376 A73-25432

- Neodymium-glass laser with tunable pulse width
11 p1376 A73-25433
- Enhanced laser-light absorption by optical resonance in inhomogeneous plasma.
11 p1405 A73-25970
- Investigation of self-focusing of laser radiation with alkali halide single crystals from data concerning the displacement of the focus of damage.
11 p1376 A73-26065
- Relationship between macroinhomogeneity of the field and the kinetics of free regular emission from a ruby laser
11 p1376 A73-26140
- Influence of elastic deformations on the lasing-threshold characteristics of a ruby laser
11 p1376 A73-26141
- Stationary emission of monochromatic spatially bounded laser beams from active medium with thin lens type inhomogeneity due to flat wave converter /resonator/ structure
11 p1376 A73-26142
- Influence of field inhomogeneity on the intrinsic spectral linewidth of a laser
11 p1332 A73-26166
- Output power saturation with a discharge current in powerful continuous argon lasers.
11 p1377 A73-26179
- Influence of laser field polarization on nonlinear interference effects.
11 p1377 A73-26180
- Ruby and Nd-YAG pulsed laser induced surface damage probability comparison at 1.06 and 0.69 micron wavelengths by breakdown starting time distribution measurement
11 p1377 A73-26226
- Confirmation of an electron avalanche causing laser-induced bulk damage at 1.06 micron.
11 p1377 A73-26227
- Thermally induced nonlinear propagation of a laser beam in an absorbing fluid medium.
11 p1377 A73-26229
- Laser speckle for determining ametropia and accommodation response of the eye.
11 p1377 A73-26232
- Limitations of the use of vacuum photodiodes in instruments for the measurement of laser power and energy.
11 p1377 A73-26233
- Coated laser windows characterized by strong surface absorption, calculating absorptivity, transmittance and reflectivity under assumption of insignificant interference effects within substrate
11 p1377 A73-26243
- Image plane or optical system focal point location based on grain size variations from laser speckle patterns
11 p1378 A73-26245
- Hydrogen fluoride chemical laser with high voltage pulse initiation in simple transverse discharge geometry, measuring maximum energy output and corresponding efficiency
11 p1378 A73-26323
- Superradiant waveguide dye laser pumped by flash lamps, noting power output and stable mode pattern insensitivity to disturbance and thermal effects
11 p1378 A73-26324
- Feasibility of high-pressure noble-gas lasers.
11 p1378 A73-26360
- Spatial-temporal structure of emission from a ruby laser irradiated by gamma rays
11 p1378 A73-26523
- Hologram interferometry and laser speckle methods - Further applications.
11 p1370 A73-26532
- FM laser noise effects on optical Doppler radar systems.
11 p1333 A73-26639
- The generation of tunable coherent radiation in the wavelength range 2300-3000 A using lithium formate monohydride.
12 p1504 A73-26826
- Theory of thermally-induced interference and lensing in transparent materials.
12 p1523 A73-26828
- Application of lasers, radioisotopes, and the correlation method for measuring flow velocity
12 p1495 A73-26847
- Programmed radiation spectrum control in a ruby laser
12 p1504 A73-26883
- Mechanism of passive negative feedback in the cavity of a solid-state laser
12 p1504 A73-26884
- Ring laser output calculation in the region of capture
12 p1504 A73-26885
- Single-frequency ruby laser with electrooptical Q switching and smooth frequency tuning
12 p1504 A73-26886
- Te-doped GaAs injection laser with nonplanar p-n junction for enhanced power output, discussing diode construction and fabrication by Zn diffusion
12 p1505 A73-26890
- Influence of the spectral characteristics of liquid filters on the thermal regime and efficiency of a neodymium-glass laser
12 p1505 A73-26891
- Improving the angular divergence of the emission from a neodymium-glass laser with a high pulse energy level
12 p1505 A73-26963
- Gain and saturation intensity measurements in a waveguide CO₂ laser.
12 p1505 A73-27017
- Influence of thionyl chloride on the lasing characteristics of the liquid phosphor POC13-SnCl₄-Nd/3+/
12 p1506 A73-27197
- Commutation of spark gaps with the aid of a pulsed gas laser emitting in the ultraviolet range
12 p1506 A73-27211
- Nitrogen laser with a longitudinal discharge and high power density
12 p1506 A73-27214
- Ring cavity for analyzing the spectral composition of CO₂-laser radiation
12 p1506 A73-27217
- Facility to determine spectra of light scattered at free plasma electrons during single laser pulse, obtaining electron component profiles with high speed streak camera
12 p1506 A73-27301
- Single-frequency neodymium-glass lasers under nonspiking free-oscillation and Q-switched conditions.
12 p1506 A73-27502
- Continuous-wave laser with a vortex-stabilized lamp.
12 p1506 A73-27503
- Investigation of a pulsed laser utilizing an exploding-film Q switch.
12 p1507 A73-27504
- Influence of a nonlinear lens on the stability of steady-state laser emission.
12 p1507 A73-27506
- Operation of a laser with a planar resonator at high pumping levels.
12 p1507 A73-27507
- Influence of the inversion inhomogeneity on the transverse structure of oscillations in solid-state lasers.
12 p1507 A73-27518
- Use of semiconductor lasers in compact communication systems.
12 p1470 A73-27521
- Influence of heat treatment on characteristics of injection lasers.
12 p1507 A73-27522
- Statistical distribution of the failure of injection lasers.
12 p1508 A73-27524
- Output radiation influence on catastrophic and slow degradation process in heterojunction injection lasers, noting service life dependence on current density
12 p1508 A73-27525
- Effect of a magnetic field on the soft X-ray radiation of a laser plasma
12 p1530 A73-27977
- Electron kinetics and stationary emission from semiconductor lasers
12 p1508 A73-27983
- The position of the emission lines of some lasers in the absorption spectrum of the earth's atmosphere.
13 p1626 A73-28174
- An absolute method of measuring energy outputs from CO₂ lasers.
13 p1626 A73-28369
- Laser light pulse absorption in transient dense hot plasma generated around metallic anode tip by fast capacitive discharge in vacuum
13 p1664 A73-28460
- Measurement by double resonance of Landé factors of the 3 s/2l and 2 p/4l of neon pumped optically by a laser beam
13 p1627 A73-28568
- Adjustment of thick-film resistors by laser and new pastes for the thick-film technology
13 p1627 A73-28574
- The possibility of storing laser radiation scattered by an electron beam.
13 p1627 A73-28662
- The spectrum of fluctuations of laser radiation in a turbulent atmosphere during rain.
13 p1627 A73-28696
- Absorption of He-Ne laser radiation by an iodine molecule beam
13 p1627 A73-28773
- Entropy layer effects in constant pressure hypersonic boundary layers.
13 p1564 A73-28812
- Investigation of a planar analyzing system employing laser illumination for facsimile transmitters
13 p1627 A73-28857
- Parallel optical channel communications system with separate laser sources for suppressing mode competition noise due to beam intensity fluctuations /beats/
13 p1584 A73-28898
- Characteristics of a high-pressure carbon dioxide laser with a transverse discharge
13 p1627 A73-28966
- Measurement of Coanda flow in fluidic elements by a laser Doppler velocimeter method and a quantitative tracer method.
13 p1618 A73-29040
- Specific characteristics of interband luminescence in crystals in the presence of intense laser radiation
13 p1628 A73-29049
- Investigation by the laser photolysis method of the spectral and time characteristics of tetrapyrrole molecules in a triplet state
13 p1628 A73-29050
- Investigation of the inversion medium of a quasi-stationary CO₂ laser with 'pulsed' excitation
13 p1628 A73-29162
- Ar laser output characteristics variation due to mutual influence of 4880 and 5145 A transitions, solving ion density formation rate equations
13 p1628 A73-29184
- Parametric studies on CO₂ TEA lasers with extracavity and intracavity electrodes.
13 p1628 A73-29187
- Experimental studies of a method of detecting microwave-modulated laser radiation in a photosensitive detector
13 p1628 A73-29415
- The problem of the deformation of the photoemulsion layer during artificial marking of points on aerial photos
13 p1621 A73-29417
- Gas discharge CW and pulsed CO laser population inversion mechanism, noting high output and efficiency in CW and Q switched modes
13 p1629 A73-29428
- Frequency fluctuations in a gas laser with nonlinear absorption.
13 p1629 A73-29430
- Investigation of the delay of stimulated emission from a CaF₂:Dy²⁺/laser relative to pumping pulses.
13 p1629 A73-29431
- Pulsed laser utilizing a fluorine and hydrogen mixture.
13 p1629 A73-29434
- Influence of self-focusing on the stability of steady-state laser emission.
13 p1629 A73-29441
- Measurement of the radius of curvature of a laser beam by an interferometric method.
13 p1629 A73-29442
- Chlorine trifluoride chemical laser emission, discussing output power dependence on partial pressures and chemical reaction kinetics
13 p1630 A73-29444
- Damping time of a ruby laser with flat mirrors
13 p1630 A73-29556
- Observations of stimulated anti-Stokes radiation in barium vapour.
14 p1776 A73-29697
- Laser photons multiple absorption by atoms, determining transition probabilities from Schrodinger equation solution via space translation operation
14 p1776 A73-29698
- High resolution spectroscopy with lasers.
14 p1756 A73-29925
- Source altitude for experiments to simulate space-to-earth laser propagation.
14 p1756 A73-30151
- Log-intensity correlations of a laser beam in a turbulent medium.
14 p1757 A73-30162
- High-pressure CO₂-N₂ laser excited by electric discharge controlled by means of electron beam.
14 p1757 A73-30260
- Formation of an ultrashort pulse of light in a ruby laser with resonant modulation of losses
14 p1757 A73-30265
- Spectral width of stationary emission from a laser with a spectrally inhomogeneous solid active element
14 p1757 A73-30266
- Investigation of the shape of radiation pulses emitted by a self-mode-locked laser.
14 p1757 A73-30329
- Self-igniting pulsed optical discharge in an erosion laser plasma.
14 p1757 A73-30334
- Quenching of lasing and the short wave fluorescence in a 3,3 diethylthiatricarbocyanine dye laser
14 p1757 A73-30462
- Laser beam transformation into light filament in inhomogeneous weakly absorbing media from Gaussian beam propagation analysis
14 p1758 A73-30466
- Samarium oxide neodymium oxide activated glass fiber output power under lasing conditions
14 p1766 A73-30468
- Microwave pulse excited argon ion laser.
14 p1758 A73-30472
- Temperature stability of the disperse phase component of the output emission of an optical quantum amplifier
14 p1758 A73-30576

Theory of the nonlinear power resonances in gas lasers 14 p1758 A73-30803

Concentration dependence of the lasing parameters of a laser based on $\text{CaF}_2:\text{Dy}^{2+}$ crystals 15 p1884 A73-31221

Injection of a short light pulse into a laser with extensive length of the resonator 15 p1884 A73-31247

Method for measuring the collision-induced broadening of spectral lines 15 p1884 A73-31702

Cooperative mechanisms during laser excitation of luminescence in Yb-Tb and Yb-Eu ion activated glass 15 p1884 A73-31713

Amplified laser absorption - Detection of nitric oxide. 15 p1885 A73-31844

Emission characteristics of a tube-shaped laser oscillator. 15 p1885 A73-31940

Laser mode locking using saturable absorbers. 15 p1885 A73-31941

Design and performance characteristics of a small subsonic flow HF chemical laser. 15 p1885 A73-31978

Triggering characteristics of TEA CO₂ laser. 15 p1885 A73-32019

Dependence of the locking zone of a gas ring laser on the emission frequency 15 p1885 A73-32316

Holographic method for measuring spatial coherence functions 15 p1879 A73-32339

Geometric magnification and collimation of traveling wave unidirectional unstable ring lasers, comparing with standing wave resonators 15 p1886 A73-32382

Burst-mode frequency-doubled YAG:Nd³⁺/ laser for time-sequenced high-speed photography and holography. 15 p1886 A73-32384

Papers on laser theory covering historical evolution, optical resonators, oscillators, amplifiers, pulse propagation, gain saturation effects, internal modulation, mode locking and noise problems 15 p1886 A73-32424

Current status of Nd:YAG lasers. 16 p2022 A73-32855

Optical parametric oscillators. 16 p2023 A73-32857

CW metal vapor lasers, discussing discharge conditions, excitation processes, cathaporetic effect and He-Se and He-Cd lasers output characteristics 16 p2023 A73-32858

Pb-salt tunable diode lasers. 16 p2023 A73-32859

Nitrogen pulsed ultraviolet laser. 16 p2023 A73-32861

Influence of a reflected signal on the operation of a laser 16 p1978 A73-32892

Transient oscillator analysis of a high-pressure electrically excited CO laser. 16 p2024 A73-33082

Pulsed interferometric holography of laser-produced air breakdown. 16 p2014 A73-33175

Laser spectrometer for combination scattering, recording polarized spectra with thermoelectrically cooled photomultiplier by photon count 17 p2164 A73-34164

Visual observation of the picture of a CO₂-laser radiation field 17 p2182 A73-34166

Laser pulse shape measurement by successive oscillographing of pulse front areas and concurrent signal amplitude variation 17 p2183 A73-34168

Lamp pumping system for lasers based on organic compound solutions 17 p2183 A73-34170

High-pressure chamber for optical studies at low temperatures 17 p2164 A73-34174

Chemical laser power output prediction by laminar analysis modification with conventional gross mixing concept of turbulent flow in population inversion 17 p2183 A73-34193

High peak power from /GaAl/As-GaAs double-heterostructure injection lasers. 17 p2183 A73-34202

Momentum transfer to laser-irradiated targets, indicating the nonlinear interaction force. 17 p2184 A73-34897

Thermal blooming of pulsed laser radiation. 17 p2184 A73-34898

Perfectly stirred reactor - New concept for a CW chemical laser. 17 p2184 A73-34911

Experimental studies of pulse lasers using organic-dye solutions covering the spectral range from 7,100 to 11,000 Å - Analysis of optimal generation conditions 17 p2184 A73-34918

Holographic methods of laser radiation divergence control 17 p2184 A73-34919

Investigation of the characteristics of organic compound lasers with dispersive resonators 17 p2184 A73-34920

Laser emission spectral theory, calculating cross relaxation in three and four level systems, monochromatic radiation effects on matter and laser action in inhomogeneous media 17 p2184 A73-34923

Frequency deviation equations for FM gas laser with modulation achieved by resonator optical length variations 17 p2184 A73-35168

Laser power and vibrational energy transfer in CO₂ lasers. 17 p2185 A73-35177

Pulsed HCN laser output power enhancement with auxiliary dc discharge, noting low gas flow rate and nonmultiple pulsing advantages 17 p2185 A73-35406

New algae mapping technique by the use of an airborne laser fluorosensor. 17 p2163 A73-35412

Small hypervelocity particle in-flight detection against background noise using forward scattering from laser illuminated particle distribution 17 p2172 A73-35415

Slant-path scintillation in the planetary boundary layer. 17 p2185 A73-35417

Analysis of multiwavelength observations of optical scintillation. 17 p2212 A73-35418

Reflection coefficients for wires, cables, ropes and chains from scanning laser radar, discussing wire avoidance system for airplanes and helicopters 17 p2210 A73-35421

Stability, reproducibility, and absolute wavelength of a 633-nm He-Ne laser stabilized to an iodine hyperfine component. 17 p2185 A73-35424

Interferometric surface strain measurement with optical strain gage using laser-generated interference pattern with linear fringe motion-intensity relation [SESA PAPER 2158A] 17 p2173 A73-35453

Application of laser Raman spectroscopy to the study of factors that influence turbulent gas mixing rates. 17 p2185 A73-35510

Papers on integrated optics covering waveguides, mode launching, radiation losses, lasers, parametric devices, light deflectors and thin film deposition 17 p2185 A73-35599

Repetitively pulsed high power nitrogen laser for UV radiation at room temperature, discussing electrical design and construction 17 p2185 A73-35767

Pressure dependency of the NF₃-H₂ transverse-discharge pulse-initiated HF chemical laser. 17 p2186 A73-35790

Vacuum UV radiation of electron beam excited high pressure Xe laser, measuring optical gain due to diatomic state-repulsive ground state transitions 17 p2186 A73-35794

Experimental verification of the effective photon theory of laser induced gas ionization. 17 p2186 A73-35832

Aerodynamic parameters affecting practical gas dynamic laser design. 18 p2321 A73-36173

[AIAA PAPER 73-626] Laser measurement of high-altitude aircraft emissions. 18 p2315 A73-36253

[AIAA PAPER 73-704] Control of laser-pulse shape with the aid of an organic dye switch 18 p2322 A73-36558

Dynamics of the emission of semiconductor lasers whose refractive index depends on the emission intensity 18 p2322 A73-36560

Perturbation of a plasma by a focused CO₂ laser beam. 18 p2339 A73-36623

Explicit solution for the photocount statistics with application to atmospheric turbulence. 18 p2337 A73-36625

Stability of the output oscillation amplitude in a linear laser amplifier 18 p2322 A73-36665

Investigation of 'external' self-focusing of ruby laser emission in CdS crystals 18 p2322 A73-36674

An electrooptical modulator based on a coaxial step-shaped resonator 18 p2322 A73-36856

Reproducibility of the frequency of a stabilized laser employing a ring cavity 19 p2437 A73-37246

Cryogenically cooled CO-He TEA laser. 19 p2437 A73-37253

A search for laser-amplified cosmic ray tracks. 19 p2437 A73-37254

Theory of two-channel laser action in spectrally inhomogeneous media. I - Noncorrelated frequencies 19 p2437 A73-37958

Excitation of an open resonator by initial emission from a high current discharge 19 p2469 A73-37963

Parametric measurements on a CO₂ TEA laser with electrodes which have a Rogowsky profile 19 p2438 A73-37999

Electron transitions of molecules in a plasma laser. 19 p2438 A73-38135

Improving the angular divergence of a neodymium-glass laser beam having a high radiation energy per pulse. 19 p2438 A73-38146

Calculation of the generation of inversion and the laser output power for expanding combustion gases /CO₂-N₂-He/ 19 p2504 A73-38157

Quasi-periodic noises in a He-Ne laser. 19 p2438 A73-38166

A frequency-tunable mode-locked CW Nd:glass laser. 19 p2438 A73-38276

CW CO₂ laser at atmospheric pressure. 19 p2438 A73-38277

Magnetically induced collisionless coupling between counterstreaming laser-produced plasmas. 19 p2469 A73-38290

Frequency spectra of strong fluctuations of laser radiation in a turbulent atmosphere 19 p2406 A73-38337

Single-line operation of a 2-W longitudinal cw CO chemical laser with no frequency-selective element in the optical cavity. 19 p2439 A73-38475

Observation of zero-degree pulse propagation in a resonant medium. 20 p2570 A73-38602

A test of Jaynes' neoclassical theory - Incoherent resonance fluorescence from a coherently excited state. 20 p2570 A73-38605

Amplified spontaneous emission comparison with laser stimulated emission during He-Ne transitions, noting threshold condition relation to population inversion density 20 p2570 A73-38619

Laser-pumped tunable spin-flip InSb Raman lasers in terms of low field operation, linewidth measurement technique, power output and applications 20 p2571 A73-38623

Correlation function of a laser beam near threshold. 20 p2571 A73-38631

Adiabatic following and the self-defocusing of light in rubidium vapor. 20 p2571 A73-38632

Cross focusing possibility between two coaxial laser beams in dielectrics with optical inhomogeneities and oscillatory waveguide characteristics, noting critical power role 20 p2572 A73-38848

Peak height measurement system for pulsed laser experiments. 20 p2572 A73-38876

Relative Raman cross section of O₃ for four Ar⁺ laser frequencies. 20 p2595 A73-38893

Intensity modulated laser with expansion and contraction of absorbing medium for thermoacoustic broadside array with highly directional acoustic propagation 20 p2572 A73-39052

Output-power-characteristics of a CW-gasdynamics laser. 20 p2572 A73-39224

Approximate determination of the inverted population and amplification factor of a gas expanding adiabatically in a nozzle 20 p2572 A73-39280

Effect of water vapor on output power of CO₂ gasdynamic laser. 20 p2573 A73-39303

Argon laser application in a study of velocity in flames 20 p2573 A73-39620

Gas discharge plasma diagnostics based on polarization plane rotation of submillimeter laser radiation 20 p2598 A73-39622

CW laser action from acetylene oxidation, noting sensitivity to total pressure and helium, oxygen and acetylene partial pressure changes 20 p2573 A73-39676

Engineering design and optimization of the parameters of frequency doublers for the visible range. 20 p2573 A73-39685

Pulsed lead vapor laser with high peak and average output powers. 20 p2574 A73-39693

Correlation between output power and composition of discharge products in a water vapor laser. 20 p2574 A73-39698

Generation of fifth picosecond laser harmonic. 20 p2574 A73-39700

- Frequency modulation of a gas laser
20 p2574 A73-39730
- Flashlamp pumped CW mode-locked dye laser
picosecond light pulse duration measurement by electro-optical streak camera
21 p2694 A73-39946
- Relaxation of coherence requirements in holography.
21 p2695 A73-39961
- Practical lasers for photographic and holographic recording.
21 p2709 A73-39973
- High-speed photography of laser damage in solids.
21 p2709 A73-39987
- Coherent X ray emission from plasma generated by laser irradiation of copper sulfate doped thin gelatin layer
21 p2710 A73-40126
- Degree of coherence mapping of single ruby laser pulses using holographic interferometry, discussing self-coherence, length and photographic recording
21 p2710 A73-40146
- Mutual coherence function of a finite optical beam and application to coherent detection.
21 p2710 A73-40147
- High-resolution photodetachment study of Se^- ions.
21 p2710 A73-40213
- Quantum mechanics /semiclassical/ theory investigation of shot and thermal noise effects on laser behavior, deriving Fokker-Planck equations for field probability distribution
21 p2711 A73-40215
- Emission spectrum of a Q-switched ruby laser and its dependence on the density of the bleachable filter
21 p2711 A73-40304
- Calculation of the power of polarized emission from a laser with an anisotropic resonator
21 p2712 A73-40312
- Lamb-dip-stabilized carbon dioxide laser line frequency separations, discussing beat frequencies, C 12 and O 16 molecular rotation constants and vibration level reduction
21 p2712 A73-40324
- Slow electron scattering near focused beam of Q-switched ruby laser, investigating scattering probability dependence on electron impact parameter
21 p2712 A73-40354
- Excitation of ultrashort light pulses in a ruby ring laser with resonant Q-switching
21 p2712 A73-40356
- Dissociation and bleaching of a multilevel molecular gas under the influence of radiation from a powerful CO₂ laser
21 p2712 A73-40357
- Violet and UV laser transitions in Ca II and Sr II resulting from impact radiation recombination of doubly charged metal ions
21 p2712 A73-40358
- Laser action from optically pumped epitaxial GaAs crystal waveguides with feedback provided by surface corrugation
21 p2713 A73-40455
- Stimulated emission in multiple-photon-pumped xenon and argon excimers.
21 p2713 A73-40456
- Threshold, spectral, and output power characteristics of GaAs/Ga_{1-x}Al_x/As single-heterostructure diode lasers.
21 p2713 A73-40462
- High quantum efficiency IR up-conversion into visible photons through three wave interactions in nonlinear medium, using laser pump light feedback technique
21 p2699 A73-40464
- Generation of microsecond pulses with controllable pulse width in a ruby laser
21 p2713 A73-40527
- Characteristics of a laser using a grid as the resonator output mirror
21 p2713 A73-40528
- Three-wavelength holographic diagnostics of an optical flare at a potassium target
21 p2700 A73-40529
- Statistical effects in the transient response of a He-Ne laser with a given initial photon distribution
21 p2714 A73-40568
- Reflection of a laser beam from an interface between isotropic dielectrics
21 p2714 A73-40569
- Q switched carbon dioxide laser pulse forms and spectrum, covering mirror and prism configurations, sodium chloride plate irradiation, laser wavelengths and pressure effects
21 p2714 A73-40572
- Opto-thermal gas concentration detector operation by measuring temperature variations caused by chopped laser beam in sample cell, using pyroelectric material as temperature sensor
21 p2701 A73-40691
- Gasdynamic processes in obtaining inversion in shock tubes
21 p2677 A73-40696
- Relative performance of a variety of NF₃/+ hydrogen-donor transverse-discharge HF chemical-laser systems.
21 p2714 A73-40757
- Finite aperture waveguide laser resonators with external reflectors by matrices coupling linearly polarized modes, calculating power efficiency, resonant frequencies and radiation patterns
21 p2714 A73-40760
- Large aperture atmospheric pressure excited carbon dioxide laser discharges, using weak volumetric gas preionization to obtain high power for plasma production
21 p2714 A73-40762
- Sealed-off waveguide carbon dioxide laser, investigating gas mixture and pressure effects on power gain and output and optical properties effects on losses
21 p2715 A73-40763
- A study of the properties of stimulated ruby laser emission during the action of Co-60 gamma rays
21 p2715 A73-40796
- Metal oxide absorption coefficients for use in intense laser interaction with solids.
21 p2715 A73-40961
- Laser gain characterization of near-atmospheric CO₂:N₂:He glows in a planar electrode geometry.
21 p2716 A73-40965
- Variable pulse-length electron beam CO₂ laser.
21 p2716 A73-40973
- Parametric study of a helical TEA CO₂ laser.
21 p2716 A73-41050
- Surface wave radiation pattern determination for solid state lasers, taking into account dielectric interface presence
21 p2716 A73-41113
- Dynamics of a laser with regulated cavity Q
21 p2716 A73-41510
- A parametric study of the performance of a TEA CO₂ laser.
22 p2868 A73-41700
- Kinetics of the generation spectrum of a photodissociation iodine laser.
22 p2868 A73-41722
- Low-noise instrumentation for Raman and luminescence spectrometry with ruby and argon laser excitation.
22 p2868 A73-41783
- Damage produced by laser radiation in optical materials. II
22 p2868 A73-41824
- Dependence of the output power of CO₂ gasdynamic laser on the distance from nozzle throat.
22 p2869 A73-42225
- Heterojunction injection lasers /Review/.
22 p2869 A73-42244
- Some features of second-harmonic generation in a lithium metaniobate crystal.
22 p2896 A73-42247
- Self-termination of free oscillations in ruby at low temperatures.
22 p2896 A73-42251
- Frequency-locking band of a traveling-wave laser.
22 p2869 A73-42255
- Time constants of spark discharges initiated by a gas-laser beam of 0.3371 micron wavelength.
22 p2869 A73-42257
- Divergence of the output radiation of electron-beam-pumped 'radiating mirror' lasers.
22 p2869 A73-42258
- Influence of mechanical treatment of the resonator on the parameters of an electron-beam-pumped cadmium sulfide laser.
22 p2869 A73-42259
- A laser raster setup with programmed control for image lithoplate synthesis
22 p2869 A73-42362
- Measurement of the natural linewidth of a traveling wave neon-helium laser in the 0.63-micron range
22 p2870 A73-42411
- Thermal lensing of laser beams in optically transmitting materials. II - Numerical computations.
22 p2870 A73-42515
- Dye laser tuning with pellicles.
22 p2870 A73-42707
- Polarization characteristics of a regenerative laser with a Faraday cell and a partial polarizer
22 p2870 A73-42721
- Radiation pulse development time instability in electrooptically Q switched lasers due to flash lamp output fluctuations
22 p2870 A73-42722
- Stimulation of two-valent rare earth ion luminescence in CaF₂ crystals by ruby and neodymium lasers
22 p2870 A73-42725
- Characteristics of a CS₂/O₂ chemical laser with flow transverse to the optical axis.
22 p2870 A73-42764
- Investigation of the radiation properties of a laser without external feedback
22 p2871 A73-42971
- On the thermodiffusion effect in the CW He-Ne lasers.
22 p2871 A73-43080
- Quenching effects in flashlamp-excited polymethine dye lasers.
22 p2871 A73-43083
- Optimization of exposure time in linear hologram recording by pre-exposure or post-exposure.
22 p2862 A73-43090
- The effect of change of polarisation of the illuminating beam on the microstructure of speckles produced by a random diffuser.
22 p2871 A73-43095
- N₂/+ Meinel and O₂/+ second negative bands laser theory.
22 p2871 A73-43144
- Low power He-Ne laser beam intensity modulation in thermal medium, applying to temperature fluctuation detection in transparent materials
22 p2872 A73-43154
- Laser cross-beam intensity-correlation spectrum for a turbulent flow.
22 p2872 A73-43158
- Propagation of laser radiation in a turbulent atmosphere.
22 p2828 A73-43159
- Confocal backscatter laser velocimeter with on-axis sensitivity.
22 p2864 A73-43162
- First-order probability densities of laser speckle patterns observed through finite-size scanning apertures.
22 p2872 A73-43188
- Investigation of the statistical properties of ultrashort light pulses by two-photon absorption in semiconductors.
23 p2987 A73-43503
- The role of absorbing impurities in laser-induced damage of transparent dielectrics.
23 p2959 A73-43512
- Study of laser radiation propagation and the diagnostics of a randomly inhomogeneous troposphere
23 p2954 A73-43572
- Investigation of the influence of a nonuniform high-frequency electric field on the parameters of a helium-neon laser
23 p2987 A73-43575
- Problem of increasing the effectiveness of laser usage in experiments on light scattering in a plasma
23 p2987 A73-43670
- Speckle effect use in laser photography for vibration and displacement measurement of mechanical systems, discussing diffraction patterns and measurement methods
23 p2982 A73-43675
- Theory of wide-band laser radiation in a spectrally-inhomogeneous medium
23 p2987 A73-43708
- Kinetics of chemical high-pressure lasers
23 p2987 A73-43716
- Study of the parameters of three-dimensional holographic gratings in LiNbO₃ crystals
23 p2987 A73-43717
- Study of induced four-photon parametric scattering of laser light in alkali metal vapor
23 p2988 A73-44009
- Pair production near energy threshold by electron oscillation and acceleration to relativistic velocities at laser beam focus with plasma wave excitation
23 p2989 A73-44121
- High-pressure CO₂ laser with a transverse discharge.
23 p2989 A73-44318
- Minimum detectable frequency deviations in output of He-Ne laser stabilized by external methane absorption cell
23 p2989 A73-44366
- Q switched Nd-YAG laser third harmonic for pumping dye laser, extending tunable output range to blue region
23 p2989 A73-44373
- Sealed carbon dioxide laser output anomalous transient pulsed behavior attributed to gas dissociation and recombination from electron density and temperature measurements
24 p3095 A73-44408
- Fluctuations of the radiation rise time in a gas laser with nonlinear resonant absorption.
24 p3095 A73-44494
- Frequency dependence of locking in a ring laser.
24 p3095 A73-44622
- Study of the processes in a gasdynamic laser in a large-diameter shock tube
24 p3095 A73-44701
- Determination of the transmittance of an optically not dense plasma by an intracavity method
24 p3115 A73-44762
- Maximum SNR performance calculation for heterodyne laser detection system with parameters optimization under assumed total cost
24 p3096 A73-44875
- Defect structure introduced during operation of heterojunction GaAs lasers.
24 p3096 A73-44923
- Measurement of the gain distribution in a helium-neon laser /0.63-micron wavelength/ cell during high-frequency pumping
24 p3096 A73-44956

Reducing the level of additive noise in the output signal of a laser velocimeter 24 p3096 A73-44958

Laser-induced deformation modes in thin metal targets. 24 p3097 A73-45417

Performance of a large-bore high-power argon ion laser. 24 p3097 A73-45422

Pulsed argon laser discharge oscillographic electron temperature and time variations measurement, obtaining short and long pulse regime emission characteristics 24 p3097 A73-45516

Longitudinal inhomogeneity of gain in the active element of a helium-neon laser pumped by direct current 24 p3097 A73-45517

Influence of photodecomposition on the emission of a lamp-pumped dye laser 24 p3098 A73-45518

Pulsed Nd-YAG laser output spiking for control of materials machining parameters 24 p3098 A73-45552

LASER PLASMAS

Schlieren-optic and interferometric methods using TEA-CO₂ lasers and thermal liquid crystal IR image converters in the diagnostics of fast processes 21 p2744 A73-39998

Electron temperature and ionization state in laser produced plasmas. 21 p2745 A73-40470

Stark broadening of high quantum number delta n = 1 transitions of carbon V and VI in a laser-produced plasma. 21 p2745 A73-40471

Tungsten target surface contaminants produced fast ion current peak measured by ion collector in expanding laser produced plasma 21 p2716 A73-40972

Charge collection measurements on a plasma induced by the CO₂ laser. 21 p2748 A73-41021

Theoretical and experimental investigations of the electron temperature in laser-produced plasmas. 22 p2891 A73-42249

The production of plasma by lasers on targets in the gaseous state 22 p2892 A73-42350

Vacuum-UV radiation of laser-produced plasmas. 23 p3008 A73-43340

Second-harmonic generation in an inhomogeneous laser plasma. 23 p3009 A73-43509

Problem of increasing the effectiveness of laser usage in experiments on light scattering in a plasma 23 p2987 A73-43670

Temperature and ion energy spectra of laser plasma produced by giant-pulse ruby laser heating metallic targets 23 p3012 A73-43849

Nonlinear dissipation of electromagnetic waves in a plasma 23 p3012 A73-44017

Investigation of the efficiency of laser-plasma trapping by a magnetic field 23 p3014 A73-44341

A dynamic mass spectrometer for the study of laser-produced plasmas. 24 p3090 A73-44817

Picosecond framing photography of a laser-produced plasma. 24 p3090 A73-44920

Electron beam concentration enhanced by a laser-produced plasma. 24 p3115 A73-44921

Utilization of the impedance variation of the plasma of a CO₂ laser for frequency stabilization on the 'Lamb dip' 24 p3096 A73-45223

LASER RADAR

U OPTICAL RADAR

LASER RANGE FINDERS

Earth satellites in resonance with the moon and the sun as objects of laser ranging - Analytical solution for their motion. 01 p0099 A73-10695

Lunar laser ranging system for experimental data acquisition, discussing preliminary design, SNR, photodetection method and data processing 02 p0141 A73-12245

Astronomical observatory lunar ranging system with high radiance neodymium-glass laser and transmitting telescope, noting tracking accuracy 02 p0151 A73-12246

Ruby laser ranging experiment for lunar returned signal from Apollo 11 retroreflector package, using multichannel pulse height counter and CRT 02 p0141 A73-12248

A description of the lunar ranging station at McDonald Observatory. 02 p0151 A73-12249

Optical properties of the Apollo laser ranging retroreflector arrays. 02 p0141 A73-12250

Structural and thermal design and fabrication of Lunokhod retroreflecting panel mounted on lunar surface for earth-moon distance determination by laser telemetry 02 p0176 A73-12251

FM-CW radar range measurement at 10-micron wavelength. 03 p0278 A73-14459

Geometric accuracy obtainable from simultaneous range measurements to satellites. 04 p0436 A73-14778

Geometrical adjustment with simultaneous laser and photographic observations on the European datum. 04 p0437 A73-14781

Geodesy information and accuracy obtainable by laser ranging from earth onto lunar retroreflector packages 04 p0495 A73-14810

Distance measurement by means of modulated light. 05 p0575 A73-16342

Telemetry with modulated beams short range high resolution systems. 05 p0576 A73-16343

Lidar illuminator/sensor system for range and/or angle spatial resolution enhancement, discussing pulse shape, optical characteristics and atmospheric effects on performance 06 p0667 A73-18303

Laser reflector for earth/moon laser telemetry. 07 p0833 A73-18983

Determination of lunar libration by earth-moon laser ranging 08 p1004 A73-20910

Retroflecting satellite with laser range finder for Martian roving vehicle navigation, discussing error analysis and minimization by measurement geometry choice through nonlinear programming 10 p1247 A73-24005

Distance measurement by laser based on reflected pulse time measurement, discussing operating principle and military applications 10 p1228 A73-24174

Operational features of an FM rangefinder employing a gas laser 10 p1229 A73-24602

Influence of ephemerides errors on various determinations using laser lunar ranging 11 p1417 A73-25266

Earth rotation axis motion determination through satellite tracking via laser range observation, estimating orbit computation error sources 13 p1656 A73-28392

Pole position studied with artificial earth satellites. 13 p1656 A73-28393

Lunar range measurements with a high-radiance frequency-doubled neodymium-glass laser system. 14 p1756 A73-30152

Potentialities of lunar laser ranging for measuring tectonic motions. 15 p1873 A73-32201

GaAs and GaAlAs semiconductor injection lasers, discussing system design and applications for ranging, illumination and communication with peak power and repetition rate requirements 16 p2023 A73-32866

Pulse time of flight measurements using mode locked laser ranging systems consisting of image converter tubes with deflection plates 17 p2185 A73-35411

Possible scientific utilization of long laser bases 21 p2716 A73-41328

Lunar laser telemetry technological developments, discussing light beam generation and detection, SNR and ranging accuracy improvements, and receiver-optics diameter reduction 21 p2774 A73-41407

The influence of laser ranging on selenodetic control. 21 p2774 A73-41408

Laser range measurement to lunar surface retroreflector, discussing initial Apollo 11 observations and achieved lunar orbit and selenophysical information accuracy improvement 24 p3137 A73-44686

Satellite laser ranging instruments operated at Tokyo Astronomical Observatory. 24 p3068 A73-44998

Measurement of short distances with optical pulse radars 24 p3069 A73-45467

LASER RANGER/TRACKER

Polar motion from laser tracking of artificial satellites. 01 p0039 A73-10406

Tracking stations interdistances and solid-earth tidal perturbations determination by laser ranging to satellites 04 p0439 A73-14801

Method and equipment for localizing satellites by laser range and direction finding. 04 p0417 A73-15096

[ONERA, TP NO. 1149]

Airborne visible laser optical communication experiment between high altitude aircraft and ground station, discussing tracker-transmitter equipment and atmospheric effects on performance 09 p1055 A73-23395

Space geodetic techniques since 1957 covering photography, radar and laser uses in satellite observations with geodetic applications 13 p1671 A73-28006

Measuring the positions of satellites with the aid of laser pulses. 13 p1582 A73-28149

Beacon Explorer C satellite laser tracking for effects of lunar and solar tides on orbit, noting geogravitational field distortion 21 p2765 A73-40275

LASERS

NT ARGON LASERS

NT CARBON DIOXIDE LASERS

NT CARBON MONOXIDE LASERS

NT CHEMICAL LASERS

NT CONTINUOUS WAVE LASERS

NT GALLIUM ARSENIDE LASERS

NT GAS LASERS

NT GASDYNAMIC LASERS

NT HCN LASERS

NT HELIUM-NEON LASERS

NT INFRARED LASERS

NT INJECTION LASERS

NT LIQUID LASERS

NT OPTICAL RESONATORS

NT ORGANIC LASERS

NT PULSED LASERS

NT Q SWITCHED LASERS

NT RAMAN LASERS

NT RING LASERS

NT RUBY LASERS

NT SEMICONDUCTOR LASERS

NT SOLID STATE LASERS

NT TEA LASERS

NT YAG LASERS

Bell Laboratories optical communications research and development on lasers, transmission media, principles, methods and components for systems 01 p0060 A73-11212

Bell Laboratories laser optics development and technology applications, discussing CW lasers, light detectors, holography, optical memories, pattern generator, remote blackboard and micrographics 01 p0060 A73-11213

Laser related Bell Laboratories research on light scattering, solid state physics, nonlinear optics, materials science, quantum electronics and ultrashort light pulses 01 p0060 A73-11214

Russian papers on nonlinear optics and hyperacoustics covering laser use in ultrasound propagation study and thermal and stimulated molecular light scattering effects 02 p0194 A73-11944

Remotely sensing strain-rate meter based on the Doppler shift of laser light. 02 p0168 A73-11961

Lunar laser observatory equipment modifications, noting change of Cassegrain primary mirror from spherical metal alloy to hyperboloid glass construction 02 p0176 A73-12244

Laser Doppler anemometer theory and application to radial flow velocity measurement in oscillating boundary layer in front of blunt body 02 p0171 A73-12559

Laser applications to spectroscopic analysis, Raman, maximum resolution and excited state spectroscopies, and spectral instruments manufacture 02 p0177 A73-12725

Laser interferometer for measuring high velocities of any reflecting surface. 02 p0171 A73-12818

Laser anemometry in an unseeded supersonic wind tunnel by means of photon correlation spectroscopy of backscattered light. 02 p0172 A73-12860

Laser anemometry developments review covering reference-beam, fringe and single-beam modes optical arrangements, signal processing systems and light scattering particles 03 p0308 A73-13535

Sensitivity of optical autodyne quantum receiver in presence of output noise, using photomultiplier signal model 03 p0319 A73-14076

Coupling losses between cylindrical multimode fibers and laser diodes 04 p0458 A73-15321

Course on Physical and Technical Measurements with Lasers, Erice, Italy, May 8-21, 1971, Proceedings. 05 p0583 A73-16336

Laser Doppler velocity measurements in a supersonic flow without artificial seeding. 05 p0576 A73-16361

A signal simulator for testing laser-Doppler fluid-flow velocimeter systems. 05 p0562 A73-16442

Edge diffraction cone detection by illuminating razor blade edge with laser beam, noting agreement with geometrical theory prediction [AD-758568] 05 p0585 A73-16812

A study of vortex rings using a laser Doppler velocimeter. [AIAA PAPER 73-105] 05 p0565 A73-16865

- Laser velocity meters - A comparative study.
05 p0580 A73-17265
- Laser system for fire detection based on heat induced air refractive index changes and smoke induced light transmission loss, using photocell detectors
06 p0699 A73-17751
- A sampling FM wide-band demodulator useful for laser Doppler velocimeters.
06 p0673 A73-17786
- Acousto-optical profilometer system with two diffracted laser beams for surface topography holographic measurements
06 p0694 A73-18290
- Modulated laser system application categories in tabular and pictorial summaries, considering ranging, reconnaissance, tracking, guidance, weapons, navigation, data processing, display and controlled fusion
06 p0700 A73-18292
- Computer output microfilm system technology assessment, discussing two dimensional acousto-optic laser scanner to write on dry process film
06 p0700 A73-18294
- Electro-optical laser beam deflector with lithium niobate for low resolution and high speed operation, discussing system design, construction and tests
06 p0700 A73-18296
- High speed wideband laser scanning technology for extremely small focal points
06 p0701 A73-18307
- Modulated laser beam photographic recorder/reproducer system bandwidth and SNR tradeoff alternatives consideration for high dynamic range performance, suggesting FM recording technique superiority
06 p0701 A73-18309
- High bandwidth and resolution laser scanners and recorders for imagery transmission, discussing component constraints and integrated optics utilization in modulator and scanner development
06 p0701 A73-18310
- Experimental results on the application of an x-y acousto-optic deflection system to wide band laser recorders.
06 p0701 A73-18312
- Comparison between a double and triple monochromator in Raman laser spectrometry
07 p0836 A73-20166
- Book - Introduction to quantum electronics.
08 p0994 A73-20951
- Laser beam spreading, deflection and collimation under atmospheric effects on long high path
08 p0938 A73-21028
- Power reduction and fluctuations caused by narrow laser beam motion in the far field.
08 p0975 A73-21059
- Television rate laser raster scanner, discussing deflectors, beam-shaping and image-forming optics, electronic system and scanning beam frequency response
08 p0975 A73-21141
- Television rate laser scanner with anisotropic Bragg device of paratellurite as acousto-optic horizontal deflector, noting operation efficiency and limiting resolution
08 p0975 A73-21142
- Effect of Doppler ambiguity on the measurement of turbulence spectra by laser Doppler velocimeter.
[AD-756047] 08 p0965 A73-21211
- Broadening of the measured frequency spectrum in a differential laser anemometer due to interference plane gradients.
08 p0967 A73-21596
- Laser interferometric alignment sensor for the large space telescope /LST/.
08 p0970 A73-21732
- Length measurement interferometry principles and limitations imposed by available coherent sources, discussing laser source techniques and fringe counting method
09 p1093 A73-22313
- A temperature interferometer using laser holography.
09 p1083 A73-22510
- Frequency selection schemes based on combined use of dispersive prism and interferometer in laser resonator
09 p1097 A73-23012
- Book - RCA advanced technology.
10 p1216 A73-23781
- Wide view field laser target designation seeker system with photodetector for multiple returns discrimination, discussing sensor breadboard model, signal processing and design feasibility
10 p1216 A73-23788
- Statistical analysis and computer simulation of laser Doppler velocimeter systems.
10 p1217 A73-23997
- Nuclear laser realizability for gamma quanta production from population inversion during radiative capture of neutrons, considering constraints imposed on heating of active medium
10 p1229 A73-24754
- Laser application for remote analysis of gaseous air pollutants emission based on Raman scattering, resonance fluorescence or absorption measurements
11 p1375 A73-25399
- Focused laser irradiance fluctuations in a turbulent medium.
11 p1376 A73-25874
- Displacement comparator based on laser interferometer with photoelectric counter for monitoring inside and outside dimensions of cylinder bores, shafts, spheres, etc
11 p1364 A73-26103
- Laser dynamic theory with uniformly broadened and Doppler spectral lines based on nonlinear interactions between harmonic oscillations
12 p1506 A73-27139
- Laser interaction and related plasma phenomena; Proceedings of the Second Workshop, Rensselaer Polytechnic Institute of Connecticut, Hartford, Conn., August 30-September 3, 1971. Volume 2.
12 p1508 A73-27922
- A progress report on the laser scanned acoustic camera.
13 p1614 A73-28577
- Simultaneous comparison of turbulent gas fluctuations by laser Doppler and hot wire.
13 p1616 A73-28821
- Estimates of possible detection limits for combustion intermediates and products with line-center absorption and derivative spectroscopy using tunable lasers.
13 p1618 A73-28996
- Problems of theory and practical application of Doppler-laser rate measuring devices in turbulent flow studies
13 p1628 A73-29169
- The comparison of a new constant temperature anemometer with several laser anemometer configurations.
13 p1620 A73-29268
- Experimental measurement of ambiguity noise in a laser anemometer.
13 p1622 A73-29641
- Spectral analysis of the signal from the Laser Doppler Velocimeter - Turbulent flows.
14 p1752 A73-29919
- Diffraction gratings manufacture by holographic recording of laser beam generated interference fringes on photosensitized surfaces, describing etching and metallization process
15 p1875 A73-31417
- Insensitivity of single particle time domain measurements to laser velocimeter 'Doppler ambiguity'.
15 p1875 A73-31671
- Thermal expansion coefficient measurements of specularly reflecting samples.
15 p1877 A73-31981
- Application of the perturbation method in a polarization analysis of anisotropic laser resonators
15 p1886 A73-32334
- High-resolution atmospheric-transmission measurement using a laser heterodyne radiometer.
15 p1886 A73-32378
- Two-component dual-scatter laser Doppler velocimeter with frequency burst signal readout.
15 p1880 A73-32383
- German monograph on data transmission by laser covering analysis of electromagnetic wave diffraction by narrow slits via Mathieu function solution of boundary value problem
15 p1847 A73-32585
- Remote measurement of the thickness, distance and velocity of objects by means of a piezoelectric laser beam deflector.
16 p2023 A73-32877
- Measurement of small movements and vibrations by laser photography.
16 p2013 A73-32879
- Air quality monitoring instruments involving atmospheric pollution chemiluminescent reactions and CO IR, optical absorption and laser detectors
16 p2016 A73-33402
- Recoilless nuclear transition based gamma laser, using resonant gamma rays or thermal neutron beam irradiation and selective photoionization
16 p2024 A73-34055
- Laser anemometer for the measurement of air flow velocities
17 p2167 A73-34775
- Laser guided weapon system optical countermeasures /OCM/ vulnerability evaluation, discussing use of LED laser in computerized simulation at low cost
17 p2147 A73-35208
- Large antennas and radomes bore-sight measurement with angular accuracy by laser mirror system incorporated into pattern range for antenna tower alignment
17 p2143 A73-35696
- The application of a scanning laser Doppler velocimeter to trailing vortex definition and alleviation.
[AIAA PAPER 73-680] 18 p2315 A73-36231
- Measurements of aerosol size distributions with a laser Doppler velocimeter /LDVI/.
[AIAA PAPER 73-705] 18 p2315 A73-36254
- Hyperballistics range erosion tests, describing dust, rain and ice simulation, dust and water fixed grid screens and shadowgraph and laser photography
[AIAA PAPER 73-765] 18 p2295 A73-36380
- Determination of local gas states from scattered laser light
19 p2438 A73-38270
- Laser threshold behavior analogy with thermodynamic ferromagnetic order-disorder phase transition, using self consistent field theory
20 p2571 A73-38628
- Use of laser amplifiers in a glass-fiber communications system.
20 p2522 A73-38667
- Comparison of Langmuir double probe and laser scattering measurements of plasma parameters.
20 p2595 A73-38880
- Frequency-domain analysis of laser Doppler signals for estimation of turbulence parameters.
20 p2572 A73-39130
- Laser hazards and safety performance standards, discussing ocular and skin damage and exposure limits and operational regulation
20 p2517 A73-39205
- Ultrashort laser pulse generators for dynamic marking of 'chronodiode' and 'chronolas' slit cameras
21 p2709 A73-39953
- Laser beam incidence in active nonlinear medium, considering Kerr effect, beam generation, Green function and intensity calculations for wave scattering
21 p2710 A73-40153
- Frequency response of laser scanners and its optimization through apodization.
21 p2717 A73-41610
- Laser Doppler instrument for measurement of vibration of moving turbine blades.
22 p2869 A73-42297
- Laser Doppler velocity measuring system parameters and SNR analysis, comparing photomultiplier, p-i-n and avalanche photodiode detectors for performance
22 p2825 A73-42298
- The laser-Doppler velocimeter and its application to the measurement of turbulence.
23 p2982 A73-43937
- Signal conditioning electronics for a laser vector velocimeter.
24 p3090 A73-44819
- LASV**
U F-111 AIRCRAFT
- LATE STARS**
Late B6 stars line spectra, atmospheric electron density, microturbulence velocity, excitation temperature, flux envelopes and energy distributions
17 p2233 A73-35612
- An adaptation of the Stromgren four-color system to photographic photometry.
19 p2430 A73-37568
- CN red system line opacity codes for late star model atmosphere calculation
19 p2488 A73-38513
- IR astronomical objects, methods and instruments, discussing galactic and extragalactic sources, early and late stars, planetary nebulae, interstellar dust and hydrogen ion clouds
20 p2605 A73-39060
- Line widths of CaII K2 and H-alpha and the chromospheres of late stars
20 p2606 A73-39073
- LATENCY**
U REACTION TIME
- LATERAL CONTROL**
Atmospheric reentry optimal lateral guidance for low lift/drag ratio space shuttle vehicle, presenting formulation as optimal stochastic control problem
[AIAA PAPER 71-914] 01 p0074 A73-10106
- Handling characteristics in roll of two light airplanes for steep approach landings.
03 p0250 A73-13701
- Application of geometric decoupling theory to synthesis of aircraft lateral control systems.
03 p0250 A73-13703
- Theory of a single-rotor gyro orbit of a satellite stabilized with respect to roll angle
05 p0628 A73-16408
- Reentry vehicle finned roll rate control - Aerodynamic and flight dynamic analysis.
[AIAA PAPER 73-183] 05 p0531 A73-16923
- An omnidirectional gliding ribbon parachute and control system.
[AIAA PAPER 73-486] 15 p1829 A73-31468
- Experimental evaluation of a roll control system for a shrouded cone.
17 p2239 A73-35500
- Direct side force control for STOL crosswind landings.
[AIAA PAPER 73-811] 19 p2379 A73-37467
- Automatic control of adverse yaw in the landing environment using optimal control theory.
[AIAA PAPER 73-861] 20 p2586 A73-38799
- Closed loop preflight qualification testing of a reentry vehicle roll rate control system.
[AIAA PAPER 73-878] 20 p2587 A73-38815
- Application of direct side force control to commercial transport.
[AIAA PAPER 73-886] 20 p2588 A73-38822
- Direct side-force control for STOL transport aircraft.
[AIAA PAPER 73-887] 20 p2588 A73-38823

LATERAL OSCILLATION

- Damped lateral vibration in an axially creeping beam with random material parameters. 16 p2082 A73-33902
- Lateral bending-torsion vibrations of a thin beam under parametric excitation. [ASME PAPER 73-APM-13] 17 p2247 A73-35037

LATERALIZATION

U LATERAL CONTROL

LATHES

- Correlation analysis of the accuracy of the machining of micromachine components 09 p1088 A73-22660

LATITUDE

NT GEOMAGNETIC LATITUDE

- Continuous Pc micropulsations with discrete latitude dependent frequencies in H components, recording simultaneously at ground based magnetometer stations 02 p0157 A73-11749

- Latitude effects on the amplitude of Pi 2 micropulsations. 02 p0159 A73-12034

- Satellite drag data for analysis of semiannual atmospheric density variations, showing latitudinal dependence of amplitude 02 p0161 A73-12281

- Theoretical model for the latitude dependence of the thermospheric annual and semiannual variations. 04 p0444 A73-15538

- Heliographic latitudinal zonality of periodic sunspot and flare distributions during 1957-1964 and 1923-1962. 21 p2759 A73-40722

- Structure of the neutral atmosphere between 150 and 500 km. 21 p2689 A73-41352

- Latitude and local time dependence of precipitated low-energy electrons at high latitudes. 22 p2901 A73-41914

- Enhanced scintillation sectors outside the plane of the ecliptic. 23 p3029 A73-43679

- A theoretical investigation of tropospheric ozone and stratospheric-tropospheric exchange processes. 23 p2974 A73-43861

- The latitudinal motion of sunspots and solar meridional circulations. 24 p3136 A73-44647

LATITUDE MEASUREMENT

- Polar motion from laser tracking of artificial satellites. 01 p0039 A73-10406

- Time and latitude observations of star groups with photographic zenith tube, including random, layer distortion and coordinate errors 03 p0307 A73-13249

- Summary of Jovian latitude and rotation period observations from 1898 to 1970. 11 p1415 A73-25134

- Dynamical latitude correction requiring changes in ephemeris and time determination, discussing applicability to nutation of pole of earth figure 11 p1429 A73-26689

- General considerations about the revision of all the calculations of the International Latitude Service. 13 p1678 A73-28379

- Power spectral analysis of Chandler wobble latitude variations over 70 year period, showing doubtfulness of two-peak resonance pattern in wobble 13 p1678 A73-28381

- Earth axis 14 month variation with latitude/Eulerian nutation/ as free vibration subject to damping, obtaining nonuniform drift rate from seven year interval observations 13 p1678 A73-28382

- An interpretation of the ambiguity between annual terms obtained by time and latitude observations. 13 p1678 A73-28384

- Non-periodic latitude variations and the secular motion of the earth's pole. 13 p1678 A73-28387

- Washington observatory latitude variations observations compared with earth rotation pole secular variations from International Polar Motion Service data, suggesting seismic influences 13 p1678 A73-28388

- Earth pole secular motion analyzed by latitude observations, suggesting northward drift of major continents 13 p1679 A73-28389

- Earth liquid core effect on axis annual nutation, deriving Z term for correction of International Latitude Service latitude variation data 13 p1606 A73-28400

- On the comparison of diurnal nutation derived from separate series of latitude and time observations. 13 p1679 A73-28402

- Mean frequency response characteristics of graphical smoothing operator for latitude observations analysis 13 p1683 A73-29099

- Circumzenithal instrument for latitude and longitude determination and star transits observation, through almicantar 16 p2017 A73-34048

- Conditional equations of astronomical latitudes, longitudes, and azimuths 19 p2490 A73-38559

- Results of latitude observations from 1948 to 1954 and analysis of the 1948-1967 latitude series obtained by the ZTF-135 instrument in Pulkovo 21 p2772 A73-41268

- Results of the 1959 to 1965 six-year series of latitude observations in Blagoveshchensk 21 p2772 A73-41269

- Jupiter zone and Red Spot latitude measurements and visual color evaluation in near IR methane band 23 p3032 A73-43943

LATTICE DRAINAGE PATTERNS

U DRAINAGE PATTERNS

LATTICE IMPERFECTIONS

U CRYSTAL DEFECTS

LATTICE PARAMETERS

- Structural changes during the deformation of molybdenum alloys 01 p0061 A73-10252

- Van Vleck paramagnetism and bonding parameters in semiconductors. 02 p0201 A73-11900

- Quadrilateral packet structure and lattice atom positions in single crystal ternary Re-Co-B alloy by X ray analysis 02 p0181 A73-12198

- The mechanisms of growth of gamma prime particles and tensile yield in Udimet 520. 04 p0464 A73-15578

- X-ray elastic constants of titanium and TiAl6V4 05 p0588 A73-17242

- A method for performing high precision lattice parameter change measurements on quenched aluminum. 05 p0580 A73-17257

- Influence of lattice defects on EPR line-shapes in ruby. 06 p0734 A73-17794

- Effect of gamma irradiation on carbon redistribution processes in the martensite lattice 06 p0706 A73-17902

- Lattice dynamics, third-order elastic constants, and thermal expansion of titanium. 07 p0839 A73-20173

- Lattice dilatation and hydrogen embrittlement cracking. 07 p0840 A73-20353

- A technique for measuring relative threshold nucleation temperatures for active nucleation catalysts. 12 p1521 A73-26816

- Effect of neutron irradiation on the structure and properties of zirconium carbide 12 p1512 A73-27200

- V and Cr thin film lattice parameter decrease with thickness, discussing vacuum effects and surface energies estimation 12 p1531 A73-27935

- The effect of lattice disorder on the thermodynamic properties of the f.c. tetragonal beta-one NiZn alloys. 13 p1635 A73-28262

- Some problems in measuring the electrical properties of semiconductors 14 p1784 A73-30924

- Long period superlattice in an aged beta titanium alloy. 20 p2577 A73-39222

- Lattice constants vs compositions of body centered tetragonal solid solutions of mixed rare earth dicarbides according to Vegard law 21 p2751 A73-40322

- Investigations regarding structure, preparation, and hardness properties in the system Ta-Hf-C-N 22 p2873 A73-41949

- Recrystallization and X-ray fine structure studies of the age-hardening characteristics of the metastable titanium alloy Ti-13V-11Cr-3Al 23 p2992 A73-43913

- High temperature electron transfer and Bi and Sb ion valency pair predictions in ordered perovskite-type oxides, using lattice constants 23 p3017 A73-44129

- Phase relations and diagram investigation for zirconium silicate-titanium dioxide system by quenching method, obtaining solid solution formation conditions and lattice constants 23 p2998 A73-44131

- Consideration of lattice translations in computer studies of grain-boundary coincidence. 24 p3120 A73-45405

- Martensitic transformations in Fe-Cr-Ni austenitic stainless steels - Relation between the parameters of the epsilon phase and the transformation mechanisms 24 p3101 A73-45522

- Method of calculating the temperature dependence of the integral intensity of light absorption by local vibrations in crystals 12 p1525 A73-27937

- On the quadrupole interaction in the diamond structure. 13 p1667 A73-28213

LATTICE VIBRATIONS

- Dynamic properties of surface layers in semiconductors 21 p2752 A73-40845

- Distribution of hot phonons generated by laser radiation 23 p2988 A73-44020

- Dynamic properties of surface layers in semiconductors 21 p2752 A73-40845

- Distribution of hot phonons generated by laser radiation 23 p2988 A73-44020

LATTICES

- Optimum design of lattice structures in creep conditions with consideration of the Kempner-Hoff theory of buckling. 24 p3148 A73-45002

LATTICES [MATHEMATICS]

NT BOOLEAN ALGEBRA

NT BOOLEAN FUNCTIONS

- Vortex lattice discretization for finite Hilbert transform of two dimensional incompressible thin wing flow integral equation with singularities, noting numerical solution accuracy 04 p0403 A73-15004

- Space point group theory classification and analysis of antenna array lattices, noting current excitation space symmetries and orthogonal field pattern design 13 p1583 A73-28698

- Optimal grid arrangement in vortex lattice method of lifting surface aerodynamic analysis, comparing numerical with kernel function results for simple wing planforms 15 p1824 A73-31746

- Russian book on conformal mapping of plane multiply connected singly periodic regions covering Laurent series, lattice regions, trigonometric interpolation and boundary differential characteristics 21 p2726 A73-40806

- Optimal grid arrangement in vortex lattice method of lifting surface aerodynamic analysis, comparing numerical with kernel function results for simple wing planforms 15 p1824 A73-31746

- Russian book on conformal mapping of plane multiply connected singly periodic regions covering Laurent series, lattice regions, trigonometric interpolation and boundary differential characteristics 21 p2726 A73-40806

LAUNCH COMPLEXES

U LAUNCHING BASES

LAUNCH TIME

U LAUNCH WINDOWS

LAUNCH VEHICLE CONFIGURATIONS

- The Delta launch vehicle for scientific and applications satellites. 01 p0111 A73-11159

LAUNCH VEHICLES

NT ATLAS CENTAUR LAUNCH VEHICLE

NT CENTAUR LAUNCH VEHICLE

NT DELTA LAUNCH VEHICLE

NT DIAMANT LAUNCH VEHICLE

NT ELDORADO LAUNCH VEHICLE

NT EUROPA LAUNCH VEHICLES

NT EUROPA 2 LAUNCH VEHICLE

NT EUROPA 3 LAUNCH VEHICLE

NT RECOVERABLE LAUNCH VEHICLES

NT REUSABLE LAUNCH VEHICLES

NT SATURN LAUNCH VEHICLES

NT SATURN 5 LAUNCH VEHICLES

NT TITAN 3 LAUNCH VEHICLE

- Lambda-4S solid propellant four-stage sounding rocket and scientific satellite launcher, describing design, operational and performance features 01 p0091 A73-11157

- M-4 S four-stage solid propellant rocket launch vehicle for scientific satellites, detailing design and performance characteristics 01 p0111 A73-11158

- Selected analytic procedures for range safety analysis. 01 p0117 A73-11200

- Aerodynamic noise field associated with pressure distributions generated by local protuberance on launch vehicle during atmospheric flight 11 p1300 A73-25384

- Launch vehicle response to inflight winds during ascent, modeling wind velocity as nonstationary random process 11 p1392 A73-25527

- Relative magnitudes of stresses caused by static and dynamic launch vehicle loads. 13 p1697 A73-28833

- Problems related to the development and firing of launchers 14 p1742 A73-30102

- PCM multiplexing system for incorporation into telemetry systems of large ballistic missiles or spacecraft launch vehicles 14 p1727 A73-30110

- Design, capability, and cost of a Versatile Upper Stage [VUS/ family of vehicles. 18 p2357 A73-36078

- Computation of launch vehicle system requirements using hybrid computer. 18 p2360 A73-36838

- Kennedy Space Center Space Shuttle facilities. 19 p2417 A73-37601

- Manned and unmanned aerospace launch vehicle liquid and solid rocket propulsion system effectiveness survey questionnaire response data concerning various tests 21 p2781 A73-41202

- Launch and orbital injection of Intelsat IV satellites. 09 p1152 A73-22699

- Computer program for extraterrestrial physics barium ion cloud project determining daily release launch window for sky target experiments 09 p1116 A73-23216

LAUNCH WINDOWS

- Computer program for extraterrestrial physics barium ion cloud project determining daily release launch window for sky target experiments 09 p1116 A73-23216

LAUNCHERS

- NT AIRCRAFT LAUNCHING DEVICES
 NT CATAPULTS
 NT GUN LAUNCHERS
 NT HYPERVELOCITY LAUNCHERS
 NT MISSILE LAUNCHERS
 NT MOBILE MISSILE LAUNCHERS
 NT ROCKET CATAPULTS
 NT ROCKET LAUNCHERS
 The utilization of detonating fuses on launchers.
 07 p0865 A73-18996
 Payload/launcher radio compatibility, discussing RF link parameters choice, terminal devices quality and test schedule
 14 p1742 A73-30113

LAUNCHING

- NT AIR LAUNCHING
 NT ORBITAL LAUNCHING
 NT ROCKET LAUNCHING
 NT SPACECRAFT LAUNCHING

LAUNCHING BASES

- NT CAPE KENNEDY LAUNCH COMPLEX
 Launching base telelinter apparatus with image superposition on TV screen for controlling missile or rocket from going beyond security limits during initial flight
 07 p0789 A73-18950
 The balloon launch stations of the EOLE program.
 07 p0807 A73-18951
 Launching bases; International Conference, Kourou, French Guiana, November 22-28, 1972, Proceedings
 14 p1741 A73-30076

- ELDO equatorial launching base for Europa 2 vehicle, discussing launch site and telemetry facilities and logistics management/organizational aspects
 14 p1741 A73-30077

- Organization and operations at National Aeronautics and Space Administration Wallops Station.
 14 p1741 A73-30078

- Sounding rocket and satellite launcher facilities at Kagoshima Space Center, considering physical plant for assembling, launching, tracking and data acquisition
 14 p1741 A73-30079

- Launching base creation process and economic factors, considering rocket firing safety, scientific requirements and financial investments criteria
 14 p1741 A73-30080

- Present and future plans for the development of Sriharikota satellite launching range.
 14 p1741 A73-30081

- Andoya Rocket Range facilities in northern Norway, discussing rocket launching for auroral research
 14 p1741 A73-30082

- DFVLR Mobile Rocket Base use of foreign ranges to launch sounding rockets
 14 p1741 A73-30084

- Sounding rocket range facilities at Esrange /Sweden/ for auroral studies, discussing telemetry support for simultaneous launchings
 14 p1741 A73-30085

- Launching operations organization and optimization and information supply, discussing vehicle reliability impact
 14 p1741 A73-30086

- The data processing architecture on the launch bases of the Directorate of Research and Test Methods
 14 p1742 A73-30091

- French launching base real time trajectory system for rocket space location information, investigating evolution towards maximum reliability
 14 p1773 A73-30094

- The influence of the concept of a launcher on the layout of a launch base, and on the organization of test flights and operational launchings
 14 p1804 A73-30103

- Preparation on the launch base and setting in operation in the launch area of the D2 A scientific satellite
 14 p1804 A73-30108

- Scientific and applications satellite launch site facilities, discussing payload preparation
 14 p1742 A73-30109

- Definition and radar measurement of the parameters characterizing the cloud environment of a launch base
 14 p1743 A73-30114

- Meteorological lidar for determining aerological data above launching base prior to rocket firing
 14 p1771 A73-30115

- The problem of launching bases in the meteorological rocket network.
 14 p1743 A73-30116

LAUNCHING DEVICES

U LAUNCHERS

LAUNCHING PADS

- French Guiana space center Diamant and Europa service towers structure, operational security features and protection against corrosion and contamination
 07 p0807 A73-18947
 The concept of the flight safeguard interferometer for rocket probes of the French Guiana Space Center
 14 p1773 A73-30090

- Deleterious vibrations development in support structure of launch pad during initial firing of launch vehicle, noting frequency spectrum dependence on soil characteristics and structural design
 14 p1742 A73-30105

LAUNCHING SITES

NT LAUNCHING PADS

- ELDO equatorial launching base for Europa 2 vehicle, discussing launch site and telemetry facilities and logistics management/organizational aspects
 14 p1741 A73-30077

- Some considerations for Space Tug launch site support operations.
 [ALAA PAPER 73-620]
 18 p2360 A73-36502

LAVA

- Water, alkalis and oxygen selective volatilization losses from hot silicate liquids erupted into high vacuum at lunar surface
 02 p0219 A73-1238

- Maria lavas, mascons, layered complexes, achondrites and the lunar mantle.
 03 p0368 A73-13088

- A point of phase equilibria interpretation in connection with lavas from the Apollo 12 site.
 03 p0375 A73-14106

- Genetic significance of chemical, isotopic, and petrographic features of some peralkaline salic rocks from the island of Pantelleria.
 05 p0570 A73-16842

- Rare-earth elements, Co, Sc and Hf in the Steens Mountain basalts.
 15 p1874 A73-32389

- Apollo 17 'orange soil' and meteorite impact on liquid lava.
 19 p2482 A73-37390

LAW [JURISPRUDENCE]

NT INTERNATIONAL LAW

NT LEGAL LIABILITY

NT PENALTIES

NT SPACE LAW

- Monopoly, concentration, and competition in the air transportation industry of the United States
 01 p0124 A73-10568

- An acceptable exposure level for aircraft noise in residential communities.
 03 p0250 A73-13838

- Legal aspects of water pollution detection through remote sensing.
 05 p0642 A73-17138

- Choice of law - Mass disaster cases involving diversity of citizenship.
 06 p0770 A73-17510

- Discovery procedures in aircraft accident litigations, considering questions of privileged material, relevancy and attorneys work product
 06 p0770 A73-17511

- Counterclaims, cross-claims and impleader in federal aviation litigation.
 06 p0770 A73-17512

- Class action rule application in damage liability litigation, considering various case histories
 06 p0771 A73-17513

- Air piracy as grounds for passenger damage claims, discussing legal liability status under Warsaw and Montreal agreements
 07 p0923 A73-19203

- Civil aircraft commander and crew duties and rights in air piracy cases, discussing international agreements and national legal provisions
 10 p1297 A73-23683

- Book - International bibliography of air law 1900-1971.
 14 p1818 A73-30362

- Aircraft noise, exposure factor, land use priorities, public environmental concern and jurisdictional considerations impact on offshore airport planning
 15 p1959 A73-31530

- Aircraft noise consideration for environmental compatibility, airport development, short haul and supersonic air transport and legislation and regulation problems
 [ALAA PAPER 73-795]
 19 p2387 A73-38368

- Aviation law development regarding ATC influence on legal liability for aircraft accidents, analyzing controller error influence on liability determination
 24 p3159 A73-45444

LAWS

NT CONSERVATION LAWS

NT FOURIER LAW

NT HOOKES LAW

NT KEPLER LAWS

NT KIRCHHOFF LAW OF RADIATION

NT NEWTON PRESSURE LAW

NT OHMS LAW

NT RADIATION LAWS

NT SCALING LAWS

NT SIMILITUDE LAW

NT SNELLS LAW

NT STEFAN-BOLTZMANN LAW

LAYERS

- Free oscillations of a double layer in a turning rectangular basin of constant depth
 19 p2419 A73-37530

LC CIRCUITS

- High power inverter with commutator of single LC network and steering SCR capable of multiple high voltage dc bridge operation
 03 p0253 A73-13936

- The problem of the excitation of subharmonics and higher harmonics in circuits, determined by a nonlinear differential equation of second order
 06 p0715 A73-17698

- Quasi-linear equivalent circuit for harmonic LC oscillator design with FET transistor, using effective transconductance method
 06 p0675 A73-17829

- Analysis of an inhomogeneous bulk 'S-shaped' negative differential conductivity element in a circuit containing reactive elements.
 09 p1061 A73-21989

- Application of similarity theory to the calculation of certain characteristics of an electrical explosion of wires
 12 p1523 A73-26937

- Active analog bandpass RC and LC filters design calculation by wave parameters
 13 p1592 A73-28875

- Active LC, RC and C/gyrator/ filters design, operation, tolerance, cost and noise characteristics
 14 p1736 A73-30375

- High-frequency oscillation passage through a circuit with modulated damping
 17 p2144 A73-34589

- Application of similitude theory to exploding wire experiments.
 22 p2886 A73-42271

- Digital LC branch filter transformation with direct element /adapter/ connections, considering gate number and passband attenuation distortion
 23 p2957 A73-43314

- Oscillation amplitude curve determination of negative resistance oscillator connected to LC circuit, obtaining device I-V characteristics
 23 p2961 A73-44147

LEAD [METAL]

NT LEAD ISOTOPES

- Ionization calorimeter measurement of energy transfer to electron photon cascade secondary particles during hadron interaction with lead nuclei
 02 p0209 A73-12662

- Volatilized lead from Apollo 12 and 14 soils.
 07 p0890 A73-19809

- Microwave energy absorbing elements based on Pd/Ag
 17 p2141 A73-35549

- Pulsed lead vapor laser with high peak and average output powers.
 20 p2574 A73-39693

- Instability of the interface between colliding metal surfaces
 21 p2707 A73-40706

- Particle number fluctuations and transient effects in electron-photon showers in lead at energies above 20 GeV
 23 p3021 A73-43531

- LEAD ALLOYS
 Low temperature tests for magnetic field and temperature effects on differential resistance of lead alloy superconductors, calculating viscous friction coefficient
 06 p0736 A73-18116

- LEAD COMPOUNDS
 NT LEAD OXIDES
 NT LEAD SELENIDES
 NT LEAD SULFIDES
 NT LEAD TELLURIDES
 NT LEAD TITANATES

- Exciton absorption band splitting in the PbI₂ spectrum
 12 p1532 A73-27945

- Raman spectrum of PbZrO₃.
 21 p2752 A73-40894

LEAD ISOTOPES

- Thallium isotope analysis of terrestrial chondrites and achondrite and lunar soil, noting lunar chronology information from lead isotope extinct radioactivity
 03 p0375 A73-14109

- U-Th-Pb systematics in lunar highland samples from the Luna 20 and Apollo 16 missions.
 05 p0618 A73-16832

- Moon geochronology from U-Pb systematics applied to lunar basalt data, discussing two and three stage evolutionary models based on Pb isotope ratios
 05 p0618 A73-16834

- Pb-204 in Apollo 14 samples and inferences regarding primordial Pb lunar geochemistry.
 07 p0888 A73-19786

- Alpha spectrometry of a surface exposed lunar rock.
 07 p0870 A73-19796

- Lunar 20 lunar soil samples Pb-207/Pb-206 age determination by ion microprobe mass analysis, determining U, Th and radiogenic Pb concentrations
 13 p1674 A73-28304

- U-Th-Pb measurements of Luna 20 soil.
 13 p1677 A73-28335

Pb 205 as chronometer for s-process nucleosynthesis is mechanism, discussing cosmochronology implications and abundance at solidification 13 p1657 A73-28923

Time differences in the formation of meteorites as determined from the ratio of lead-207 to lead-206. 17 p2225 A73-34096

Pb isotopic composition measurement in chondrites and achondrite for model ages, noting 50 My variations 17 p2233 A73-35265

A response to a comment on U-Pb systematics in lunar basalts. 18 p2354 A73-36512

Lead isotopic composition ages of carbonaceous chondritic meteorites with correction for terrestrial lead contamination 21 p2765 A73-40239

Solar abundance of Th and Pb based on photospheric line spectrum analysis for comparison with chondritic composition data 24 p3135 A73-44627

LEAD OXIDES

Metallic additions effect on wear and friction behavior of lead monoxide, lead silicate and calcium fluoride solid lubricants coatings for high temperature operations [ASLE PREPRINT 72LC-7C-5] 03 p0317 A73-14374

LEAD SELENIDES

X-ray investigation of textures in thin films 01 p0050 A73-10800

Broad-band laser emission from optically pumped PbS(1-x)Se(x). [AD-759091] 09 p1092 A73-22249

Roentgenographic investigations of thin films of lead chalcogenide based alloys 10 p1260 A73-24472

LEAD SULFIDES

Equivalent circuit of unbent p-PbS point diodes 09 p1061 A73-22022

Broad-band laser emission from optically pumped PbS(1-x)Se(x). [AD-759091] 09 p1092 A73-22249

Roentgenographic investigations of thin films of lead chalcogenide based alloys 10 p1260 A73-24472

An interference filter radiometer with cooled optics and a cooled PbS detector for rocket application. 11 p1368 A73-26507

Atmospheric moisture effects on hematitic sandstone, pyrite and galena electrical resistivity, noting comparison with semiconductors and insulators 13 p1609 A73-28847

LEAD TELLURIDES

PbTe-SnTe stripe junction diode lasers, discussing fabrication, electrical properties, and mode characteristics from emission spectra, polarization, mirror illumination and far field pattern measurements [AD-759093] 09 p1092 A73-22250

Five year lifetime space radioisotope thermoelectric generator with lead telluride panels and plutonium 238 dioxide heat source, analyzing reliability, design and performance 09 p1038 A73-23284

Roentgenographic investigations of thin films of lead chalcogenide based alloys 10 p1260 A73-24472

The development of SiGe-PbTe segmented thermoelectric couples involving pressure-contacted junctions. 11 p1409 A73-26035

Oxidation of powdered germanium, tin and lead tellurides under atmospheric conditions 15 p1887 A73-31594

Investigation of the design parameters and experimental parameters of medium-temperature thermopiles based on lead, germanium and tin tellurides 17 p2108 A73-34282

Electrical properties of single-crystal films of p-type PbTe 17 p2219 A73-35556

Tunable Pb-Sn-Te junction laser characteristics and fabrication by impurity diffusion for IR CW operation at liquid helium temperatures 21 p2716 A73-40967

Compressive strength and plastic deformation of monocrystalline bismuth telluride, polycrystalline lead telluride, Cu-Te compounds and Pb-Sn-Te solid solution 23 p3015 A73-43480

LEAD TITANATES

Static electric quadrupole interaction of Ta- and Hf-ions in barium and lead titanate. 07 p0862 A73-20018

Dielectric breakdown of shock-loaded PZT 65/35. 09 p1132 A73-21927

LEADING EDGE SLATS

Fighter aircraft maneuverability improvement at high subsonic speeds by slotted and unslotted leading- and trailing-edge flaps on delta wing [DGLR PAPER 72-126] 03 p0248 A73-14386

Mechanisms of externally blown flap noise. [AIAA PAPER 73-1029] 24 p3056 A73-44859

LEADING EDGE SWEEP

The prediction of turbulent heat transfer and pressure on a swept leading edge near its intersection with a vehicle. [AIAA PAPER 73-677] 18 p2368 A73-36228

LEADING EDGES

NT SHARP LEADING EDGES

On the mechanism of dynamic stall. 01 p0003 A73-11015

Higher-order delta wings with flow separation at subsonic leading edges 02 p0127 A73-11581

Hypersonic and supersonic flow over caret wings at off-design conditions with attached bow shock at leading edges 02 p0128 A73-12502

Application of an improved transpiration cooling concept to space shuttle type vehicles. 03 p0397 A73-13492

The effects of leading-edge serrations on reducing flow unsteadiness about airfoils. [AIAA PAPER 73-89] 05 p0529 A73-16853

Leading-edge force features of the aerodynamic finite element method. 05 p0533 A73-17213

Nonstationary flow downwash behind a delta wing during supersonic motion 11 p1299 A73-25046

Structural testing of ceramic nose cap and leading edge components for a reusable entry vehicle. [AIAA PAPER 73-376] 11 p1388 A73-25507

Vibration and local edge buckling of thermally stressed, wedge airfoil cantilever wings. [AIAA PAPER 73-327] 11 p1441 A73-25557

Perturbation solutions to laminar boundary layer flow over flat plate with small hump downstream of leading edge, using Blasius equation 11 p1302 A73-25855

Compact gas transpiration cooling system for thermal protection of hypersonic flight leading edges, discussing computer program 11 p1452 A73-26212

Turbulent heat transfer to a fin leading edge - Flight test results. 11 p1303 A73-26405

Supersonic flow around a delta wing, taking into account flow separation at the leading edges 12 p1457 A73-27098

Installing the heater cable directly in the redesigned leading edge. 16 p1970 A73-32924

Leading edge effects on displacement thickness and skin friction variations of unsteady boundary layer on flat plate under impulsive motion in viscous fluid 16 p1962 A73-32927

Method for the interpretation of surface pressure measurements under rarefied hypersonic conditions. 16 p1963 A73-33316

On the unsteady supersonic cascade with a subsonic leading edge - An exact first order theory. [ASME PAPER 73-GT-15] 16 p1963 A73-33492

On the unsteady supersonic cascade with a subsonic leading edge - An exact first order theory. II. [ASME PAPER 73-GT-16] 16 p1964 A73-33493

Experimental evaluation of the effects of a blunt leading edge on the performance of a transonic rotor. [ASME PAPER 73-GT-60] 16 p1964 A73-33515

Successive approximations for calculating supersonic flow past wings with subsonic leading edges 17 p2091 A73-34347

Calculated leading-edge bluntness effect on transonic compressor noise. [AIAA PAPER 73-633] 18 p2260 A73-36192

A conceptual study of leading-edge-vortex enhancement by blowing. [AIAA PAPER 73-656] 18 p2261 A73-36210

Velocity distribution in hypersonic helium flow near the leading edge of a flat plate. [AIAA PAPER 73-691] 18 p2262 A73-36242

Equivalence rule and transonic flow theory involving lift. 18 p2264 A73-36328

Four Space Shuttle wing leading edge concepts. [AIAA PAPER 73-738] 18 p2359 A73-36355

Initial development of an ablative leading edge for the Space Shuttle orbiter. [AIAA PAPER 73-739] 18 p2369 A73-36356

Monatomic and diatomic gas supersonic flow field calculation for sharp leading edge by BGK and ordinate models 18 p2265 A73-36631

Solution of the problem of the flow past a V-shaped wing with a strong shock wave at the leading edge 18 p2265 A73-37011

Influence of the shape of the leading edge on the transition process in the boundary layer on a plate in longitudinal flow 21 p2676 A73-40399

Investigation of the influence of the leading-edge configuration on the efficiency of cooled rotor- and guide-vane cascades 21 p2632 A73-40406

Monograph - Quasi homogeneous approximations for the calculation of wings with curved subsonic leading edges flying at supersonic speeds. 22 p2797 A73-42675

Heat release from turbine rotor blades 23 p3020 A73-43744

Boundary layer on flat plate in shear flow, calculating induced pressure gradients near leading edge and far downstream 24 p3080 A73-45369

LEAKAGE

Laser oscillation in leaky corrugated optical waveguides. 08 p0975 A73-21206

Nonleaking battery terminals design for polyphenylene oxide plastic cased Ag-Zn battery for synchronous satellite applications, describing life tests under thermal and electrical cycling 09 p1034 A73-22757

Leak testing of tritium fuelled experimental batteries. 09 p1038 A73-23288

Leakable gases and water vapor loss rates and service life predictions for sealed alkaline cells in vacuum or aerospace environments, using mass transfer equations [ECS PAPER 32] 11 p1307 A73-24973

HF CW ultrasonics, discussing elimination of electromagnetic leakage or crosstalk between transmitter and receiver by sampling technique 13 p1612 A73-28483

Study of incidence loss models in radial and mixed-flow turbomachinery. 17 p2092 A73-34384

Leakage and frictional characteristics of turbulent helical flow in fine clearance. [ASME PAPER 73-FE-1] 17 p2152 A73-35001

A unique method of leak-rate measurements. 18 p2316 A73-36714

LEARNING

NT ASTRONAUT TRAINING

NT CONDITIONING [LEARNING]

NT HABITUATION [LEARNING]

NT TRANSFER OF TRAINING

Low body temperature effects on learned behavior retention under hibernation conditions in squirrels 05 p0539 A73-16324

Motivation in vigilance - A test of the goal-setting hypothesis of the effectiveness of knowledge of results. 17 p2113 A73-34149

Interference of 'attend to and learn' tasks with tracking. 19 p2401 A73-38377

LEARNING MACHINES

Theoretical foundations for synthesis of learning-type recognition algorithms by the method of R-functions in the complex-plant control problem 05 p0560 A73-16275

Interactive aspects of man/learning system control teams. 05 p0543 A73-16708

An integrated feature selection and supervised learning scheme for fast computer classification of multi-spectral data. 05 p0555 A73-17153

Automaton synthesis and perceptron learning for controlled objects classification according to unknown features, noting adaptive relationships between retina and associative elements 07 p0786 A73-20047

State of the art and survey of learning control applications. 07 p0806 A73-20590

Optimal self learning classification of point in set for image recognition systems, using proximity functions. 09 p1060 A73-22944

Unsupervised learning of the optimal linear signal estimator in the presence of unknown multiplicative, additive, and message generating noise. 17 p2144 A73-35374

Performance improvement in remote manipulation with time delay by means of a learning system. 19 p2417 A73-37331

The control of a manipulator by a computer model of the cerebellum. 19 p2398 A73-37333

Learning control in remote manipulator and robot systems. 19 p2412 A73-37754

Adaptive /learning/ intelligent system design and simulation for control with stochastic goal and environment conditions 20 p2532 A73-38685

Minimum risk classification algorithms in automatic learning system design, applying to learning pulse signal receiver 20 p2532 A73-38686

Convergence of learning and adaptation algorithms. 20 p2532 A73-38711

Pattern recognition learning machine design heuristics, discussing analysis, synthesis and convergence of algorithms 21 p2659 A73-41290

- A recognition learning program based on selecting statistically useful attributes 21 p2659 A73-41291
- LEARNING THEORY**
Book - Introduction to mathematical techniques in pattern recognition. 01 p0019 A73-10050
Image recognition learning algorithm for expanding neural nets composed of active inputs, receptors, associative elements and recognizers 04 p0426 A73-15794
Adaptive trackers based on continuous learning theory. 06 p0682 A73-18821
Adaptation algorithms in multilayer pattern-recognition systems 10 p1192 A73-24502
Pattern recognition based on visual perception relation to transformations and identification by coded sentences 11 p1334 A73-25621
A probabilistic algorithm for grouped handling of arguments with sequential discrimination of input features 21 p2658 A73-40994
Unsupervised learning of the Kalman filter. 21 p2664 A73-41109
- LEAST SQUARES METHOD**
Least-squares solution for the blunt body hypersonic flow problem. 01 p0004 A73-11473
Semidiscrete-least squares methods for a parabolic boundary value problem. 02 p0188 A73-12615
German monograph - Application of estimation procedures for the characteristic parameters of controlled systems on the basis of measurements on the closed control loop. 03 p0285 A73-13811
Solutions of the light curves of eclipsing binaries by the generalized method of least squares. 04 p0503 A73-16010
Application of the method of least squares to the determination of optical constants of uniaxial isotropic and anisotropic substances, and of the rate of polarization of monochromators in the far UV 05 p0597 A73-16148
Need of LS-dependent energy parameters in the second spectra of the fifth-group elements. 05 p0600 A73-16496
Iterative methods for best approximate solutions of linear integral equations of the first and second kinds. 06 p0717 A73-18170
Iterative least-squares synthesis of nonuniformly spaced linear arrays. 06 p0666 A73-18194
Least square approach for system reliability optimization. 06 p0681 A73-18524
Constrained least-squares analysis of petrologic problems with an application to lunar sample 12040. 08 p0936 A73-20842
Least squares method for eclipsing binary stars minimum epoch, noting application to artificial and observed light curves 08 p1006 A73-20928
Geomagnetic field optimal model with expansion of spherical harmonic series by least squares method 08 p0960 A73-21353
Least-squares monotonic lowpass filters with sharp cutoff. 09 p1065 A73-23093
Use of the least squares criterion in the finite element formulation. 10 p1243 A73-24295
Least squares method for satellite motion parameters determination in orbital plane, using altimeter distance to planet surface measurements 12 p1543 A73-27627
Nonlinear least squares - An aid to thermal property determination. 13 p1706 A73-28806
Least squares and non-linear functions. 13 p1619 A73-29241
Least squares method for geomagnetic potential transformation in spherical offset inclined dipole coordinates with Schmidt coefficients 14 p1749 A73-29982
Construction of a uniformly converging sequence of algebraic polynomials by the generalized method of least squares for a class of continuous functions 14 p1768 A73-30249
Standard algorithms application to modified matrix and least squares eigenvalues, determining quadratic forms and Gauss-Radau and Gauss-Lobatto quadrature rules coefficients 14 p1769 A73-30409
Computerized stellar spectrogram processing using semiautomatic diagram-code converters, least squares method and reference spectral lines 15 p1878 A73-32141
Galerkin variational method combination with least squares error distribution technique for application in plate and shell theory 16 p2077 A73-32992

- Nonlinear least squares calculations by Gauss-Newton and Levenberg, Marquardt and Morrison methods, discussing algorithm convergence rate and numerical computational scheme 16 p2033 A73-33854
Some computational techniques for the nonlinear least squares problem. 17 p2199 A73-34105
Nonlinear functional minimization under auxiliary constraints, discussing convergence conditions and iterative solution algorithm performance for least squares weighted sum problem 17 p2199 A73-34106
Simplified proof of error estimates for the least squares method for Dirichlet's problem. 17 p2199 A73-34210
The application of constrained least squares estimation to image restoration by digital computer. 20 p2533 A73-39401
Oxygen and nitrogen thermodynamic state equation determination by least squares fitting to experimental PVT, isochoric heat capacity and saturation density data 21 p2740 A73-41104
On an asymptotic property of the least-mean-square-error design criterion in pattern recognition. 22 p2835 A73-42274
Geophysical field cartographic isoline recording via least generalized course representation of observation points, discussing analytic functions and least squares method 22 p2850 A73-42734
An optimality condition for assessing systematic errors 23 p2999 A73-43264
An innovations approach to least-squares estimation. V - Innovations representations and recursive estimation in colored noise. 23 p2954 A73-43819
Synthesis of a transverse digital filter defined in the complex plane 24 p3072 A73-44973
- LEAVES**
Effects of leaf age for four growth stages of cotton and corn plants on leaf reflectance, structure, thickness, water and chlorophyll concentrations and selection of wavelengths for crop discrimination. 05 p0571 A73-17128
Reflectance and internal structure of leaves from several crops during a growing season. 11 p1352 A73-25566
Physiological factors and optical parameters as bases of vegetation discrimination and stress analysis. 16 p2003 A73-33355
- LEBESGUE THEOREM**
Sufficient optimality conditions for control system described by ordinary differential equations in Banach space with Lebesgue measure of material quantity set 22 p2882 A73-42604
- LED (DIODES)**
U LIGHT EMITTING DIODES
Sierra Nevada mountain lee waves atmospheric structure from lidar, rawinsonde and aircraft observations, delineating atmospheric flow patterns from particulate matter concentrations induced echoes 10 p1245 A73-23988
Mountain waves and CAT encountered by the XB-70 in the stratosphere. 11 p1394 A73-25785
Isentropic/isopycnic mountain waves tracing from superpressure balloon flights synchronous radar, temperature and pressure data 12 p1520 A73-26809
Unbounded nondiffusive high Reynolds number stratified flow with lee waves over vertical barrier investigated for Froude number range on basis of Oseen-Boussinesq approximation 15 p1863 A73-31341
Theory of mountain lee waves for an arbitrary-profile elevation 15 p1905 A73-31818
Mountain range effects on tropopausal turbulence with mountain waves, examining tropopause layer inversions, vertical wind vectors, temperature distribution and buffeting intensity 17 p2204 A73-34542
- LEG [ANATOMY]**
NT KNEE [ANATOMY]
Angular measurements of foot motion for application to the design of foot-pedals. 01 p0013 A73-10773
Telemetry of venous blood pressure at rest and at muscle activity during running. 03 p0271 A73-14290
The interaction between muscle groups in a complex motor act in humans 08 p0930 A73-21320
Effect of chronic pyramid insufficiency on the function of spinal centers of shin and foot muscles in man 22 p2807 A73-42658
- LEGAL LIABILITY**
International convention on damage caused by aircraft concluded 1952 in Rome, proposing revision to

- include damages before takeoff, after landing and during flight 01 p0124 A73-10566
Liability under international law for damages caused by space objects 01 p0124 A73-10567
The future of international space cooperation in treaty-making. 04 p0524 A73-15154
International law principles application to space liability codification, noting United Nations role in Draft Convention on space liability 04 p0524 A73-15159
Choice of law - Mass disaster cases involving diversity of citizenship. 06 p0770 A73-17510
Counterclaims, cross-claims and impleader in federal aviation litigation. 06 p0770 A73-17512
Class action rule application in damage liability litigation, considering various case histories 06 p0771 A73-17513
Air piracy as grounds for passenger damage claims, discussing legal liability status under Warsaw and Montreal agreements 07 p0923 A73-19203
Legal definition of space objects for international space law purposes regarding damage liabilities 14 p1818 A73-30292
Legal consequences resulting from transportation in airline traffic in the case of missing, deficient or not coverage-equivalent contractual basis 14 p1818 A73-30293
Skyjacking - Its domestic civil and criminal ramifications. 16 p2087 A73-33102
Product liability prevention via a controlled system. 16 p2088 A73-33617
Survey of the civil responsibility for damages caused by aircraft noise in American and French law 19 p2506 A73-37998
Book - The law of international spaces. 19 p2506 A73-38365
Liability and insurance in international air traffic 24 p3159 A73-45443
Aviation law development regarding ATC influence on legal liability for aircraft accidents, analyzing controller error influence on liability determination 24 p3159 A73-45444
- LEGENRE CODE**
U COMPUTER PROGRAMMING
U NEUTRON SCATTERING
LEGENRE FUNCTIONS
Series expansion of the perturbation function 01 p0102 A73-10948
Iterative method for calculating hot carrier distributions in semiconductors. 08 p0994 A73-21221
Ritz method extension to mechanics problems by introducing artificial spring parameters at boundary and using Legendre functions as coordinate functions 12 p1555 A73-27740
Solution of axisymmetrical thermoelasticity problems for an infinite region with several spherical cavities 15 p1945 A73-31039
Electromagnetic absorption in magnetized cold plasma, discussing definition and use of velocity-dependent collision frequencies with Legendre polynomials as weighting functions 21 p2654 A73-40818
The Laplace and Poisson equations in Schwarzschild's space-time. 23 p3005 A73-43345
- LEGENRE POLYNOMIALS**
U LEGENRE FUNCTIONS
LEGENRE TRANSFORMATION
U LEGENRE FUNCTIONS
LEGIBILITY
The effect of illumination level, stroke width and figure ground on legibility of NAMEL numbers. 05 p0544 A73-16729
Problem of the legibility of records produced by strip chart recorders with curvilinear coordinate systems 14 p1754 A73-30875
Techniques for decreasing power and increasing legibility of electronic watches. 22 p2863 A73-43101
- LEIDENFROST PHENOMENON**
Leidenfrost temperature - Its correlation for liquid metals, cryogenics, hydrocarbons, and water. [ASME PAPER 73-HT-F] 19 p2504 A73-37641
- LEM [LUNAR MODULE]**
U LUNAR MODULE
LEMMAS
U THEOREMS
LENGTH
A non-contacting length comparator with 10 nanometer precision. 21 p2704 A73-41257
- LENS ANTENNAS**
Axisymmetric lens design for prescribed radiation amplitude patterns 08 p0946 A73-21101

Multifed multifrequency broadband constant index lens antenna with high power and variable polarization handling capabilities and low manufacturing cost advantage 17 p2137 A73-35206

Geometric deformation of spherical dielectric lens antennas 19 p2409 A73-37715

Comparative focusing properties of spherical and plane microwave zone plate antennas. 24 p3069 A73-45480

LENS DESIGN

Helical gas lenses for guiding optical beam over long distances, calculating irradiance patterns for various propagation mode numbers and temperatures 01 p0053 A73-11218

Beam diverging lens system for high power laser transmitters. 03 p0319 A73-14432

Optical transfer function (OTF) measurement standards and specification for high quality aerial photographic mapping lens, discussing error sources 05 p0573 A73-16147

Lens projection system for a solar simulator providing irradiance of 100 solar constants. 08 p0952 A73-21042

The use of image quality criteria in designing a diffraction limited large space telescope. 08 p0969 A73-21730

Application of lens-raster optics for recording holograms with discrete information 09 p1079 A73-21916

Optical beam hybrid lens waveguide with central aperture and surrounding lens, comparing transmission loss and bending effects with iris guides 11 p1365 A73-26230

Influence of a nonlinear lens on the stability of steady-state laser emission. 12 p1507 A73-27506

Solid ultrasonic cylindrical lens design for off-axis aberration minimization for focusing properties improvement, using method analogous to chromatic aberration correction in optics 13 p1612 A73-28491

Eikonal properties for real rays chromatic aberration formulas in terms of path length, image space and lens parameters 13 p1660 A73-28768

Holographic imaging and aberrations due to an incorrectly repositioned hologram in a system with lenses having aberrations. 15 p1915 A73-31015

Electromagnetic wave propagation through a gas lens. 15 p1913 A73-31136

Lens raster optics for holograms with digital information. 15 p1880 A73-32642

Design considerations for night-vision system optics. 16 p2012 A73-32865

A fast access holographic memory. 16 p2012 A73-32868

Electron-optical image transfer using opaque photocathodes with electromagnetic lens in image tubes 17 p2136 A73-34905

Grazing incidence X ray telescope lens design for radio and optical identifications of radiation sources by satellites 17 p2171 A73-35409

Wavefront investigation of a Fourier transform lens with the fan trace interferometer. 17 p2172 A73-35427

Block oriented random access and read-only archival holographic memories design, considering relationships between lens geometric parameters, laser power and packing density requirements 17 p2173 A73-35432

The oblique electron lens. 18 p2316 A73-36597

Study of plasma systems with a closed electron drift and a distributed electric field 19 p2466 A73-37357

Chromatic aberration effects on inelastic image resolution for high voltage electron microscopes 21 p2702 A73-40789

LENSES

NT CONTACT LENSES

NT MAGNETIC LENSES

NT WIDE ANGLE LENSES

Converging lens effect of air jet for upstream moving waves, describing experimental procedure 03 p0290 A73-12968

Lunar metric camera used during Apollo landings, discussing lenses and test and calibration work for inner orientation 07 p0824 A73-20020

An analytic expression for the radial photogrammetric distortion of aerial photo cameras 10 p1219 A73-24479

Electrical characteristics of hardenable metallic lens or radome with near unity refractive index at out-of-band frequencies 11 p1338 A73-25670

Stationary emission of monochromatic spatially bounded laser beams from active medium with thin lens type inhomogeneity due to flat wave converter /resonator/ structure 11 p1376 A73-26142

Holographic construction and application of optical elements, discussing hologram lenses, holographic multiple imaging systems and diffraction gratings 12 p1498 A73-27501

Superposition method for potential distribution in plane tetrod field with unipotential and bipotential grids, noting electro-optical effect in cylindrical lenses 13 p1591 A73-28667

Group 3-5 compound light emitting diode degradation modes and mechanisms, discussing epoxy lenses, light transmission characteristics, time and temperature functions and surface passivation 19 p2439 A73-38457

Inexpensive portable vibration-insensitive wave front shearing interferometer developed at NBS for lens testing 21 p2704 A73-41259

LENTICULAR BODIES

Application of the Meler-Fok complex conversion formulas in the solution of certain problems of heat conductivity 01 p0119 A73-10011

LEONID METEOROIDS

Conditions of Leonid meteor shower encounters with the earth in occurrences of the years 1898-2000 09 p1146 A73-22546

Periodic comest Tempel-Tuttle orbital elements relation to Leonid meteor shower, using computer program for numerical integration 14 p1791 A73-29807

LEPTONS

NT ANTINEUTRINOS

NT ELECTRONS

NT MUONS

NT NEUTRINOS

NT POSITRONS

Conical liquid hydrogen target with large exit aperture and multilayer insulation between inner vessel and vacuum jacket for experiments on leptonic decays 05 p0538 A73-17288

Sea level search for leptonic quarks in cosmic rays. 11 p1414 A73-26660

Big Bang model of universe, discussing 3 K background radiation, thermal history of early universe, lepton number conservation and different eras 21 p2772 A73-41242

LESIONS

NT PULMONARY LESIONS

Cerebral localization of speech, discussing cortical lesions, aphasia and mental activity correlation theories 08 p0931 A73-21425

Residual visual function after brain wounds involving the central visual pathways in man. 16 p1975 A73-33218

Frontal eye-field lesions in monkeys. 18 p2272 A73-36446

Hepatic lesions observed among flight crews following aviation accidents 18 p2279 A73-36933

Significance of arterial obstructive lesions in early diagnosis of coronary heart disease. 22 p2808 A73-42829

LETHALITY

Microorganism heat sterilization process design and control based on logarithmic thermal destruction and Bigelow temperature coefficient models, determining lethality by statistical procedure 16 p1976 A73-33695

LETHARGY

Torpor and hibernation physiology in mammals covering evolution, hypothermia, energy conservation, cell and organ adaptations, nervous and cardiovascular system changes, etc 22 p2809 A73-42862

LETTERS (SYMBOLS)

U SYMBOLS

LEUCINE

Oxidation effects on rate of C 14-labeled leucine incorporation into rat skeletal muscle protein 05 p0538 A73-16152

Protein synthesis in lung - Recovery from exposure to hyperoxia. 18 p2277 A73-36653

LEUKOCYTES

NT EOSINOPHILS

NT LYMPHOCYTES

LEVEL (QUANTITY)

NT ATOMIC ENERGY LEVELS

NT EFFECTIVE PERCEIVED NOISE LEVELS

NT ELECTRON STATES

NT ENERGY LEVELS

NT GROUND STATE

NT INTERMOLECULAR FORCES

NT MOLECULAR ENERGY LEVELS

LEWIS NUMBERS

Some studies on opposed-jet diffusion flame considering general Lewis numbers. 07 p0921 A73-20357

LIABILITIES

NT LEGAL LIABILITY

LIAPUNOV FUNCTIONS

Equations of motion integral properties-based construction of Liapunov functions used to derive sufficient conditions for perturbed nonlinear system solution stability 01 p0075 A73-10090

R-function numerical analysis method for motion stability criteria, developing algorithms for Liapunov function construction and controller design for conservative control system stability 01 p0076 A73-10096

Liapunov function for complex system motion stability analysis, noting stability criteria for subsystems satisfying Routh-Hurwitz conditions 01 p0076 A73-10668

Stability of a spinning body containing an elastic membrane via Liapunov's direct method. 01 p0077 A73-10728

Liapunov vector functions in stability analysis of nonlinear dynamic distributed parameter, interconnected and multivariable systems 01 p0078 A73-11073

Liapunov function relation to entropy production in irreversible processes, noting thermodynamic constraints on kinetic equation functions 02 p0191 A73-11613

A Liapunov function for an autonomous second-order ordinary differential equation. 02 p0186 A73-11974

Construction of Lyapunov functions for nonstationary systems containing memoryless nonlinearities. 02 p0193 A73-12123

Construction of solutions and the application of the joining method to the solution of the Liapunov stability problem for a system of linear homogeneous differential equations with pi-periodic coefficients 02 p0193 A73-12189

Liapunov function for Hamilton-Jacobi equation for motion stability of linear and nonlinear mechanical systems, calculating vibration damping factor 03 p0342 A73-13157

Liapunov functions for quadratic differential equations with applications to adaptive control. 03 p0336 A73-13520

On the almost-sure sample stability of systems with randomly time-varying delays. 03 p0285 A73-13898

Damping perturbation of high order nonlinear autonomous Liapunov system, reducing system equations integration to quadratures via transformation to lower order quasi-linear nonautonomous system 03 p0344 A73-14054

Liapunov function application to stability of unperturbed motion of system of differential equations with respect to part of variables 03 p0344 A73-14056

A study of the stability of externally pressurized gas bearings with porous wall by Liapunov's direct method. [ASME PAPER 72-LUB-18] 03 p0314 A73-14333

An improved design technique for parameter adaptive control systems. 03 p0286 A73-14481

Liapunov stability, boundedness and attraction conditions, using modified quantification theory 04 p0469 A73-14668

A stability theory for perturbed difference equations. 05 p0590 A73-16491

Invariance principle extended to bounded uncertain time-varying systems, deriving asymptotic Liapunov stability criteria with application to quaranteed cost control problems 05 p0590 A73-16492

Couplings effect on Liapunov stability estimation of higher order linear nonstationary systems, using aggregation method 05 p0599 A73-17084

The method of Lyapunov functions in control problems for distributed-parameter systems [A survey]. 06 p0723 A73-17953

Global asymptotic stability of two classes of control systems with pulse duration and pulse frequency modulations. 06 p0680 A73-17957

Synthesis of adaptive systems by Lyapunov's direct method. 06 p0723 A73-17959

Boundedness of infinitely extendable solutions to a system of two equations with quadratic right members, and the manifold of Liapunov's characteristic exponents of solutions to this system 06 p0718 A73-18679

Asymptotic motion stability analysis with respect to part of variables, using Liapunov functions for solution boundedness conditions 07 p0850 A73-19012

Explosive systems with reactant fuel consumption, deriving asymptotic stability, with application to self heating chemical reaction via Liapunov functions 07 p0919 A73-19393

Liapunov method for LF and HF instability of liquid propellant rocket engines

07 p0867 A73-20078

Energy-like Liapunov functionals for linear elastic systems on a Hilbert space.

07 p0852 A73-20336

Conditional stability and separation of solutions to differential equations.

07 p0845 A73-20496

An approximate method for the synthesis of optimal control of distributed systems.

07 p0806 A73-20596

Treatment of dynamic snap-through problems by the direct Liapunov method

08 p1018 A73-21410

Global asymptotic stability estimation for large scale systems of interconnected exponentially stable subsystems, using aggregated comparison and Liapunov function description

09 p1120 A73-22227

Adaptive control and identification via Liapunov's direct method.

09 p1067 A73-22232

Liapunov vector functions in stability analysis of nonlinear dynamic distributed parameter, interconnected and multivariable systems

09 p1121 A73-22998

Stability theory of dynamic large scale system under structural perturbations based on comparison principle and vector Liapunov functions

10 p1248 A73-24039

Study of recurrence relationships and their applications by the Laboratoire d'Automatique et de ses Applications Spatiales.

10 p1200 A73-24042

Liapunov stability analysis and attitude response of a passively stabilized space system.

10 p1286 A73-24541

Converse theorems for Liapunov stability and boundedness of nonlinear discrete-time systems described by difference equations

11 p1389 A73-25186

Nonlinear delay-differential control systems described by periodic functional differential equations with small real parameter, investigating asymptotic stability in Liapunov sense

11 p1390 A73-25190

Method of Liapunov vector functions in the analysis of complex systems with distributed parameters /Survey/

11 p1398 A73-25617

Synthesis, with the aid of Liapunov functions, of optimal and suboptimal discrete systems for controlling determinate and stochastic plants

11 p1341 A73-25619

Synthesis of time-optimal control for linear systems and the minimal-time Lyapunoff function.

11 p1342 A73-26225

Liapunov stability analysis of spinning flexible spacecraft.

11 p1431 A73-26378

Strengthening of Liapunov-type estimates /case where the distributions of members are close to the normal distribution/

12 p1517 A73-27190

Methods of quadratic Liapunov vector-function construction for linear systems

12 p1525 A73-27895

Application of Liapunov functions for studying the convergence of unconstrained minimization methods

13 p1657 A73-28018

Numerical stability criteria for fourth order nonlinear difference equations, using discrete form of Liapunov direct method

13 p1649 A73-28699

Periodic solutions of piecewise-continuous systems with a small parameter

13 p1661 A73-29084

Zero-solution stability in systems of partial differential equations

14 p1768 A73-30248

Multi-parameter sensitivity analysis of linear dynamic systems through the second method of Liapunov.

15 p1854 A73-31632

Spin stability of torque-free elastic dissipative systems with finite number of degrees of freedom, deriving Liapunov function via energy considerations

15 p1943 A73-31663

Hilbert boundary value problem solution for piecewise holomorphic vector in singly connected region with Liapunov contour bound

15 p1900 A73-32086

General linear boundary value problem with measurable coefficients for numerous analytical functions of class E sub p

15 p1900 A73-32092

Liapunov functions and boundedness and global existence of solutions.

15 p1901 A73-32375

Liapunov direct method extended to stability of nonlinear parabolic systems, noting application to Burgers equation

17 p2200 A73-34398

A procedure for investigating the Liapunov stability of nonautonomous linear second-order systems.

[ASME PAPER 73-APM-31] 17 p2201 A73-35044

Stability of the general plane membrane adjacent to a supersonic airstream.

[ASME PAPER 72-APM-UUU] 17 p2248 A73-35103

Nonlinear boundary value problems and several Liapunov functions.

17 p2203 A73-35730

Dual and triple spin-stabilized deformable spacecraft attitude stability, comparing results based on Sturm theorem with Liapunov analysis

18 p2359 A73-36306

Methods of constructing quadratic Liapunov vector functions for linear systems.

18 p2330 A73-36600

Instability of feedback systems containing several time-varying nonlinear amplifiers.

19 p2414 A73-38078

Nonlinear control systems analysis, discussing phase space method, Taylor-Cauchy transform, Volterra functions, Liapunov stability, Popov-Kalman-Yakubovich theorems and limit cycle oscillations

20 p2592 A73-38691

Liapunov theory and perturbations of differential equations.

20 p2581 A73-38974

Study of hydromagnetic stability of a hot rotating layer of fluid by Liapunov method.

22 p2894 A73-42474

Liapunov vector functions for solving stability problems of complex multidimensional dynamic control systems with nonlinear interactions and delay

22 p2887 A73-42606

Liapunov-like theorems of quantitative stability information on trajectory bounds in state space subset form

22 p2888 A73-43020

Comparative studies of model reference adaptive control systems.

23 p2963 A73-43817

An adaptive observer for single-input single-output linear systems.

23 p2963 A73-43818

Asymptotically stable adaptive observer and identification scheme for linear system, using Liapunov canonical state representation

23 p2954 A73-43825

Discrete time composite system stability with non-periodic sampling in terms of vector Liapunov functions and real symmetric matrix test

23 p2964 A73-43826

Asymptotic mean value method for differential equations solution under given Lipschitz condition generalized via Liapunov procedure elimination

23 p2999 A73-44079

Liapunov-like behavior and separation of solutions to nonlinear and linear differential equations

23 p3000 A73-44204

Liapunov functions application to stability analysis of dynamic systems and elastic bodies, considering eigenfunction method, maximum principle and energy criterion

24 p3153 A73-45497

LIBRATION

Catalog of selenographic coordinates for libration-zone and far-side points.

04 p0503 A73-16017

Out-of-plane motion about libration points - Nonlinearity and eccentricity effects.

11 p1423 A73-26069

Lunar orbit and mapping coordinates, discussing libration effects due to motion and surface features

13 p1681 A73-28947

Systematic elevation errors in maps of the lunar edge zone

17 p2230 A73-34594

Quasi-periodic orbits about the translunar libration point.

18 p2352 A73-36420

Ideal resonance problem for dynamic system of N degrees of freedom, obtaining global solution covering libration and circulation regimes under normality condition

24 p3141 A73-45287

Stability of Lagrange solutions to the three-dimensional elliptic problem of three bodies

24 p3111 A73-45299

LIBRATIONAL MOTION

Possibility of determining the lunar rotation elements with a narrow-angle television camera

01 p0051 A73-10944

Periodic perturbation of the libration points of the restricted three-body problem due to presence of a resisting medium and both gravitational and radiative fields of a fourth body.

01 p0103 A73-11018

Lunar librations results of Koziel reevaluated, noting elasticity effects and elastic strain perturbation on satellite

03 p0367 A73-13077

Motion stability of librational points in gravitational field of rotating triaxial ellipsoid, applying to planets of solar system

03 p0376 A73-14266

A variation-of-parameters perturbation theory for the restricted three-body problem.

[AIAA PAPER 73-144] 05 p0619 A73-16893

Determination of lunar libration by earth-moon laser ranging

08 p1004 A73-20910

Stability of the libration points of a triaxial ellipsoid under constantly acting disturbances in the first approximation

09 p1143 A73-22093

Application of a narrow-angle television camera for determining the rotation elements of the moon.

09 p1084 A73-22739

Physical librations due to the third and fourth degree harmonics of the lunar gravity potential.

10 p1277 A73-24083

Resonances and librations of some Apollo and Amor asteroids with the Earth.

11 p1429 A73-26688

On the regularity of fluctuations in annual and secular polar motions.

13 p1678 A73-28385

Gravity oriented satellite librational damping by solar radiation pressure, comparing WKB method with numerical integration results

15 p1943 A73-31640

Existence of stable relative equilibria of an artificial satellite in a model magnetic field

15 p1872 A73-31956

Long term heliometric Moestring crater distance measurements applied to moon libration relationship to lunar radius

16 p2064 A73-33775

A study of planar deployment control and libration damping of a tethered orbiting interferometer satellite.

21 p2781 A73-40900

Solar pressure induced librations of spinning axisymmetric satellites.

22 p2910 A73-42633

On the theoretical possibility of the libration cloud.

22 p2911 A73-42936

About the stability of the libration points of a rotating triaxial ellipsoid in a degenerate case.

23 p3032 A73-43838

Effects of physical librations of the moon on the orbital elements of a lunar satellite.

23 p3032 A73-43841

Existence of stable relative equilibria for an artificial satellite in a model magnetic field.

24 p3081 A73-44481

Parameter distribution of small periodic librations about the equilateral points of the elliptic restricted problem.

24 p3141 A73-45283

Elliptic restricted three body problem equations derived from linear variational equations with periodic coefficients describing motion near libration centers

24 p3141 A73-45284

LIDAR

U OPTICAL RADAR

LIE GROUPS

NT SPINOR GROUPS

Topologic group theory for stress analysis of nonlinearly elastic body under complex load, representing loads set by Lie group

01 p0119 A73-11428

On an application of Lie group theory to the optimal control problem for linear dynamic systems with time-varying parameters.

06 p0679 A73-17954

Lie operators admitted by Lamé equations in three dimensional dynamic elasticity theory for arbitrary particle velocity and displacement and linear stress-strain tensor relation

09 p1159 A73-22585

Steady state Lie group solutions to nonlinear partial differential equations of low temperature plasma ionization instability in strong magnetic field

09 p1127 A73-22591

Topologic group theory for stress analysis of nonlinearly elastic body under complex load, representing loads set by Lie group

11 p1443 A73-26057

Algebraic Lie structure theory of bilinear systems in terms of controllability, observability and equivalent realization

14 p1771 A73-30783

Lie group theory of differential equations in continuum mechanics, gas dynamics, heat conduction, biharmonic and second order quasi-linear equations

15 p1914 A73-32109

A Lie algebra of visual piloting

20 p2590 A73-39038

Dynamical symmetries of the Kepler problem and of the harmonic oscillator in classical mechanics revisited.

22 p2887 A73-42429

Reduction of systems of nonlinear differential equations to normal form

24 p3107 A73-45511

LIFE [BIOLOGY]

U LIFE SCIENCES

LIFE [DURABILITY]

NT FATIGUE LIFE

NT HALF LIFE

NT PLASMA LIFETIME

NT SATELLITE LIFETIME
 NT SERVICE LIFE
 NT STORAGE STABILITY
 Concentration distribution and effective lifetimes of excited atoms at small optical thicknesses of the plasma 01 p0085 A73-11083
 Survival probability of a system with a Poisson flow of losses in life-sustaining elements 01 p0028 A73-11422
 Processes leading to 6300 A radiation during determinations of O/ID/ quenching by nitrogen and oxygen molecules in F region, using model of neutral atmosphere composition 02 p0156 A73-11742
 Ion beam lifetimes measurement by temporal correlation of photons emitted in cascades 03 p0341 A73-12912
 Minority carrier lifetime and diffusion constant as function of impurity concentration in double junction vertical solar cell, determining power efficiency 03 p0254 A73-14213
 Layout of a thermodynamical theory of the life time scattering in materials testing 05 p0635 A73-17066
 Changes in the durability and lifetime of polymer films under simultaneous exposures to an electric field and mechanical loading 07 p0842 A73-19394
 Ionization loss effects on cosmic ray lifetime in galactic interstellar medium, noting dependence on particle energy 08 p0999 A73-21335
 Improved Hanle effect measurement technique for fast ions. 10 p1251 A73-24117
 Lifetime of solar flare particles in coronal storage regions. 10 p1268 A73-24144
 The measurement of the lifetime in p-n diodes at high injection levels 13 p1589 A73-28477
 Stellar evolution lifetime shortening due to thermal instability of nuclear energy generation shell, discussing relaxation oscillations and S-process nucleosynthesis 13 p1683 A73-28990
 A mathematical model of damage accumulation in plastic isotropic materials. 14 p1810 A73-30301
 Interpretation of the results of simulation tests, taking into account scatter effects 16 p2019 A73-33378
 Censored sample size selection for life tests. [AD-758315] 16 p2033 A73-33630
 Determination of the bulk carrier lifetime in the low-doped region of a silicon power diode, by the method of open circuit voltage decay. 21 p2665 A73-41123
 Eigenfunction calculation of injected carrier density in doped semiconductor filaments, relating negative eigenvalues to Suhl effect and lifetime dependence to bulk and surface recombination 23 p3016 A73-43674

LIFE DETECTORS
 Biological, chemical and cytological methods of microorganism detection integrated into single instrument 03 p0272 A73-14320
 Extrasolar life in light of stars, planets, and living systems nuclear, gravitational, electromagnetic and weak interactions 05 p0539 A73-16306
 Historical treatment and inconclusiveness of evidence of extraterrestrial life traces and organic matter in carbonaceous and other meteorites 09 p1146 A73-22545
 Chemical volatilization as a technique for the detection of extraterrestrial biopolymers and possible metabolic products. 11 p1319 A73-26479
 Extraterrestrial life detection from imaging observations on lunar samples and meteorites, discussing application to Mars surface 17 p2113 A73-35804

LIFE RAFTS
 Multiple occupant flotation devices for commercial transport aircraft survivors sea ditching, discussing slide/raft design improvement for high density loading 16 p1974 A73-32658
 DC-10 aircraft slide/raft system for emergency personnel evacuation, discussing certification test program for performance, reliability, seaworthiness and compliance with regulations 16 p1965 A73-32659
 Certification program for the DC-10 slide/raft. 17 p2108 A73-35807

LIFE SCIENCES
 NT MOLECULAR BIOLOGY
 The origin of life problem - A brief critique. 06 p0651 A73-17927
 Life origin on earth, considering hydrocarbon molecules and macromolecular synthesis under earth atmospheric evolutionary conditions 06 p0651 A73-17928

Life sciences and space research XI; Proceedings of the Fifteenth Plenary Meeting, Madrid, Spain, May 10-24, 1972. 22 p2803 A73-42158
 Extraterrestrial intelligent life existence possibility in terms of hypothesis involving earth as wilderness area or zoo with failure of interaction with other civilization 24 p3058 A73-44554

LIFE SUPPORT SYSTEMS
 NT CLOSED ECOLOGICAL SYSTEMS
 NT EMERGENCY LIFE SUSTAINING SYSTEMS
 Progress in the development of the reverse osmosis process for spacecraft wash water recovery. 02 p0137 A73-11993
 Radiation-induced oxidation of impurities in the water obtained from human moisture-containing bioactivity products 08 p0933 A73-20984
 Russian book on mathematical models of biological systems covering biogeocenosis, optimal crop, chemostat cultivation, predator-victim society, trophic control, and life support systems 09 p1044 A73-22347
 An integrated system for space station power, life support, and propulsion. 11 p1311 A73-26009
 Survival and Flight Equipment Association, Annual Symposium, 10th, Phoenix, Ariz., October 2-5, 1972, Proceedings. 16 p1965 A73-32653
 Investigation of the disinfecting properties of sorbents which are used in a spacecraft life support system 17 p2114 A73-34240
 Advanced methods of recovery for space life support systems. 19 p2398 A73-37711
 Nuclear submarine atmospheric constituent monitoring, covering mass spectrometers, IR carbon monoxide sensors, system development, requirements testing and spacecraft applications [ASME PAPER 73-ENAS-9] 19 p2399 A73-37970
 Waste Management System overview for future spacecraft. [ASME PAPER 73-ENAS-18] 19 p2400 A73-37974
 Reverse osmosis for recovering and recycling water in Space Station Prototype Environmental Thermal Control/Life Support System Integrated Water and Waste Management [ASME PAPER 73-ENAS-22] 19 p2400 A73-37978
 Space Shuttle Orbiter Environmental Control and Life Support System for atmosphere revitalization, crew life support, thermal conditioning and airlock support [ASME PAPER 73-ENAS-23] 19 p2400 A73-37979
 Apollo command and service module environmental control system - Mission performance and experience. [ASME PAPER 73-ENAS-29] 19 p2493 A73-37984
 Space science terrestrial applications in biomedical data exchange and telediagnosis, propellant technology, life support atmospheres without fire hazard, industrial mixers and nozzle materials [AAS PAPER 73-133] 20 p2629 A73-38589
 Nutrition systems for pressure suits. 20 p2517 A73-39105

LIFETIME [DURABILITY]
 U LIFE [DURABILITY]

LIFT
 NT INTERFERENCE LIFT
 NT ROTOR LIFT
 An experimental study of the dynamic lift on a cylinder subjected to a high Reynolds number flow perpendicular to its axis. [ONERA, TP NO. 1073] 01 p0001 A73-10226
 Reentry trajectory optimization at superorbital velocities by aerodynamic lift control, using Pontryagin maximum principle 01 p0105 A73-11127
 Nonlinear characteristics of a slender triangular wing near an interface 02 p0127 A73-11630
 Buoyancy distribution of slender axisymmetric bodies of higher order in the case of compressible subsonic flow [DGLR PAPER 72-067] 02 p0127 A73-11681
 Slowly oscillating lifting surfaces at subsonic and supersonic speeds. 03 p0245 A73-13704
 Optimal lift control by Miele's method for the atmospheric entry of a hypersonic glider. I - Simple type problems. 03 p0245 A73-13766
 Lift of wing-body combination. 03 p0247 A73-14194
 Induced drag of finite wing with antisymmetric incidence distribution due to rolling, deriving relations between wing lift distribution and induced downwash. 03 p0248 A73-14472
 Optimal lift control by Miele's method for the atmospheric entry of a hypersonic glider. II - Isoperimetric type problems. 04 p0404 A73-15168

Lifting characteristics and spanwise aerodynamic load distribution of an external flow jet flap. 04 p0404 A73-15513
 Thermodynamic considerations for the design of a sonic-boom reducing powerplant. [ASME PAPER 72-WA/AERO-3] 04 p0404 A73-15907
 Experimental analysis of lift on a fixed cylinder subjected to a flow perpendicular to its axis at high Reynolds numbers 04 p0405 A73-15990
 The tricuspid hypocycloid as envelope of the force of lift, calculated in a first compressible approximation, in the case of a symmetrical profile in a flow of variable direction and a given Mach number 05 p0528 A73-17674
 A class of airfoils designed for high lift in incompressible flow. [AIAA PAPER 73-86] 05 p0528 A73-16851
 Equivalence rule and transonic flows involving lift. [AIAA PAPER 73-88] 06 p0644 A73-17642
 Multiple element airfoils optimized for maximum lift coefficient. 07 p0775 A73-19956
 A correction to 'lifting-line theory as a singular perturbation problem.' 07 p0775 A73-19964
 Fluctuating lift and moment coefficients for cascaded airfoils in a nonuniform compressible flow. 09 p1028 A73-22432
 Correlation of wing-body combination lift data. 09 p1028 A73-22435
 Optimal lift control by Miele's method for the atmospheric entry of a hypersonic glider. III. 10 p1285 A73-23616
 Flow through moving cascades of lifting lines with fluctuating lift. 10 p1171 A73-23697
 A probabilistic evaluation of helicopter lift capability. 10 p1175 A73-23775
 Lift forces on an oscillating cylinder at low Reynolds number. 10 p1173 A73-24822
 Synthesis of superconducting suspensions with a maximum lifting force 11 p1372 A73-25049
 A linearized potential flow theory for airfoils with spoilers. 11 p1301 A73-25853
 Correction for change in fluid flow curvature about a lift-generating airfoil in a two-dimensional test section with perforated walls 11 p1302 A73-25864
 A note on the lift coefficient of a thin jet-flapped airfoil. 12 p1457 A73-27171
 High velocity moving body in ideal incompressible fluid flow, determining lift coefficient from acceleration potential algorithm 12 p1486 A73-27239
 Lift and drag at off-design Mach numbers of conically cambered wings with subsonic leading edges and supersonic trailing edge 12 p1458 A73-27927
 Semiempirical method for flutter prediction of unsteady lift and aerodynamic forces acting on oscillating airfoil in stall regime, using separation function 13 p1566 A73-29029
 A theory for rectangular wings with small tip clearance in a channel. 15 p1821 A73-31120
 Thin rectangular lifting wing investigation at small angle of attack in parallel flow based on Prandtl acceleration potential theory 15 p1955 A73-32126
 German monograph - The flow around wings of arbitrary planform in the case of supersonic flow - A computational method. 15 p1824 A73-32581
 Critical study of the effects of gusts on an aircraft 16 p1961 A73-32808
 Test techniques for high lift, two-dimensional airfoils with boundary layer and circulation control for application to rotary wing aircraft. 17 p2091 A73-34292
 Vortex-lift prediction for complex wing planforms. 17 p2094 A73-34438
 Some effects of camber on swept-back wings. [SAE PAPER 730298] 17 p2094 A73-34661
 A kernel function method for computing steady and oscillatory supersonic aerodynamics with interference. [AIAA PAPER 73-670] 18 p2262 A73-36221
 Equivalence rule and transonic flow theory involving lift. 18 p2264 A73-36328
 The lift on a wing in a turbulent flow. 19 p2376 A73-37487
 A theoretical note on the lift distribution of a non-planar ground effect wing. 19 p2376 A73-37493
 Prediction of the lift and moment on a slender cylinder-segment wing-body combination. 19 p2377 A73-38007

- Two dimensional flow theory of Weis-Fogh lift generation in inviscid motions of insect wings involving viscous effects 21 p2631 A73-40244
- Closed-form lift and moment for Osborne's unsteady thin-airfoil theory. 21 p2632 A73-40442
- On the application of a new version of lifting surface theory to nonlender and kinked wings. 23 p2939 A73-43210
- Airfoil theory calculation of bent thin foil lift coefficient and longitudinal moment characteristics at arbitrary flow separation point location 23 p2940 A73-43720
- The effect of walls on the lifting force of a solid-foil wing 23 p2940 A73-43722
- LIFT AUGMENTATION**
- Externally blown flap trailing edge noise reduction by slot blowing - A preliminary study. [AIAA PAPER 73-245] 05 p0532 A73-16969
- Acoustic results obtained with upper-surface-blowing lift-augmentation systems. 07 p0776 A73-20458
- A comparative study of augmentor wing, ejector nozzle and power jet flap low noise STOL concepts. 11 p1300 A73-25385
- Analysis of the aerodynamic characteristics of wing-lift augmentation devices. II 11 p1301 A73-25796
- Analysis of the aerodynamic characteristics of wing lift augmentation devices 12 p1457 A73-26824
- Augmentor wing design and performance tests for multimission XFV-12 V/STOL prototype aircraft 12 p1459 A73-27731
- A jet-wing lifting-surface theory using elementary vortex distributions. [AIAA PAPER 73-652] 18 p2260 A73-36207
- A three-dimensional wing/jet interaction analysis including jet distortion influences. [AIAA PAPER 73-655] 18 p2261 A73-36209
- On problems of flight over an extended angle-of-attack range. 24 p3056 A73-44692
- LIFT COEFFICIENTS**
- U AERODYNAMIC COEFFICIENTS
- U LIFT
- LIFT DEVICES**
- STOL aircraft technology, operation and markets in view of future European air traffic development, discussing various lift devices, noise aspects and economic factors [DGLR PAPER 72-054] 02 p0130 A73-11662
- STOL aircraft with mechanical high-lift systems in comparison to STOL aircraft with wings having blown flaps [DGLR PAPER 72-057] 02 p0130 A73-11665
- The theoretical and experimental methods used in France for flutter prediction. [AIAA PAPER 73-329] 11 p1305 A73-25558
- Analysis of the aerodynamic characteristics of wing lift augmentation devices 12 p1457 A73-26824
- An improved nonlinear lifting-line theory. 13 p1564 A73-28817
- Lift engine bleed flow management for a V/STOL fighter reaction control system. [ASME PAPER 73-GT-70] 16 p2048 A73-33521
- Fundamental aspects of noise reduction from powered-lift devices. [SAE PAPER 730376] 17 p2103 A73-34715
- Investigation of multi-element airfoils with external flow jet flap. 21 p2633 A73-41087
- Short takeoff and landing/STOL aircraft technology developments for high density air transport, discussing lift system, handling, airfoil design, acoustics and operating economics 23 p2940 A73-43520
- LIFT DISTRIBUTION**
- U FORCE DISTRIBUTION
- U LIFT
- LIFT DRAG RATIO**
- Birds and aircraft aerodynamics, considering thermal and wind induced updrafts, lift-drag ratio, fuel consumption and maneuverability 06 p0648 A73-18148
- Improved aircraft capability through variable camber. 19 p2378 A73-37275
- A new approach to performance optimization of the 1975 Mars Viking lander. [AIAA PAPER 73-889] 20 p2614 A73-38825
- Correlation of hypersonic zero-lift drag data. 22 p2797 A73-42635
- LIFT FANS**
- Installation effects on performance of multiple model V/STOL lift fans. [AIAA PAPER 72-1175] 03 p0250 A73-13471
- Light combat aircraft with hover capability. 03 p0251 A73-13923
- NASA lift fan V/STOL transport technology status. [SAE PAPER 720856] 05 p0535 A73-16663

Performance characteristics of a model VTOL lift fan in crossflow. 11 p1301 A73-25782

- Effect of rotor design tip speed on aerodynamic performance of a model VTOL lift fan under static and crossflow conditions. 16 p1963 A73-33480
- Control of turbofan lift engines for VTOL aircraft. [ASME PAPER 73-GT-20] 16 p2047 A73-33496
- NASA research commercial VTOL transport propulsion system specifications and components development, discussing lift fan propulsion method for aircraft attitude control [ASME PAPER 73-GT-24] 16 p2047 A73-33498

LIFT FORCES

U LIFT

LIFTING BODIES

NT LIFTING REENTRY VEHICLES

Plane flow past vortex of inviscid incompressible fluid jets bound by free surface and horizontal wall, considering complex potential function and submerged lifting airfoils 01 p0031 A73-10304

Calculation of supercritical flow past airfoils by the Murman-Krupp difference method [DGLR PAPER 72-128] 03 p0248 A73-14387

Variational principle application to nonself adjoint lifting surface integral equation from finite element viewpoint, considering two dimensional flat plate [AIAA PAPER 73-87] 05 p0529 A73-16852

Multivortex model for bodies of arbitrary cross-sectional shapes. [AIAA PAPER 73-104] 05 p0529 A73-16864

Unsteady compressible potential flow around lifting bodies - General theory. [AIAA PAPER 73-196] 05 p0531 A73-16931

Similarity relationship for wing-like bodies at high Mach numbers. [AIAA PAPER 73-203] 05 p0532 A73-16937

High-frequency vibrations of a circular wing in the flow of an ideal fluid 05 p0636 A73-17089

French project for high speed hydrofoil marine vehicle with hydrodynamic lifting surfaces, completely submerged wings, gas turbine propulsion and automatic control 09 p1031 A73-22208

Aerodynamic forces and moments estimation for slender bodies of circular and noncircular cross section without and with lifting surfaces at 0-90 degree angles of attack 09 p1030 A73-23468

The theoretical and experimental methods used in France for flutter prediction. [AIAA PAPER 73-329] 11 p1305 A73-25558

Newtonian aerodynamic forces from Poisson's equation. 11 p1303 A73-26382

Transonic flow past lifting wings. 13 p1564 A73-28824

Transonic flow about lifting configurations. 13 p1564 A73-28828

Optimal grid arrangement in vortex lattice method of lifting surface aerodynamic analysis, comparing numerical with kernel function results for simple wing planforms 15 p1824 A73-31746

Aerodyne unmanned wireless reconnaissance aircraft, covering hovering capacity, internal flow duct for conventional flight, flight test results and stability characteristics 17 p2098 A73-34255

Analysis of the aerodynamic characteristics of devices for increasing wing lift. III - Influence of ground proximity on the aerodynamic characteristics of the flaps 18 p2266 A73-37022

Lifting body configurations for sustained hypersonic flight. 19 p2377 A73-37710

Integral equation in the theory of lifting surfaces 19 p2377 A73-37846

An aerodynamic entry control technique utilizing the yaw flap concept. [AIAA PAPER 73-888] 20 p2588 A73-38824

Simplified aerodynamic theory of oscillating thin surfaces in subsonic flow. 21 p2632 A73-40427

LIFTING REENTRY VEHICLES

The optimum reentry trajectory of a lifting vehicle. 01 p0105 A73-11126

Stability characteristics of re-entry wing shapes and their measurement. 03 p0244 A73-13567

Some design aspects of Space Shuttle orbiters. 05 p0627 A73-16178

Aerodynamic entry vehicle autopilots. 06 p0721 A73-18515

Structural testing of ceramic nose cap and leading edge components for a reusable entry vehicle. [AIAA PAPER 73-376] 11 p1388 A73-25507

Experimental study of a high lift re-entry vehicle configuration. 13 p1564 A73-28822

Aerodynamic studies of spacecraft in the freestream Mach number range of 3 to 10 at high Reynolds numbers [DFVLR-SONDDR-286] 13 p1567 A73-29447

Engineering analysis of hypersonic lifting body windward surface inviscid and viscous flow fields at high angles of incidence. [AIAA PAPER 73-637] 18 p2263 A73-36257

Approximation for maximum centerline heating on lifting entry vehicles. 22 p2796 A73-42627

LIFTING ROTORS

Improving reliability and eliminating maintenance with elastomeric dampers for rotor systems. 10 p1175 A73-23950

Rotorcraft design concepts, considering economics, propulsion, control, trim devices, advancing blade concept, materials and rotor aerodynamics 21 p2635 A73-41189

LIFTING SURFACES

U LIFT DEVICES

U LIFTING BODIES

U SURFACES

LIFTS

Lift and measurements in an aerofoil in unsteady flow. [ASME PAPER 73-GT-41] 16 p1964 A73-33503

LIGANDS

Charge transport bands in the electronic spectra of Fe(III) complexes with certain oxygen-containing ligands 21 p2751 A73-40310

LIGHT [VISIBLE RADIATION]

NT AIRGLOW

NT COHERENT LIGHT

NT DAYGLOW

NT GEGENSCHEIN

NT GEOCORONAL EMISSIONS

NT LIGHT BEAMS

NT NIGHTGLOW

NT POLARIZED LIGHT

NT SKY RADIATION

NT SUNLIGHT

NT TWILIGHT GLOW

NT ZODIACAL LIGHT

Flare spectrum in region accessible to ground based optical solar spectrographs, considering Balmer line broadening, electron density, optical thickness, LTE, electron temperature, etc 01 p0091 A73-10052

Optical, far UV and radio spectra observations and results for solar spicules, considering morphology, spectroscopic properties and dynamic models 01 p0094 A73-10055

Effect of visible light on exoelectron emission 01 p0045 A73-10264

Design features and observational feasibility of high resolution Michelson interferometer for use in visible spectral range at coude focus of astronomical telescope 01 p0049 A73-10533

Photoelectric light-curves of TW Cas. 01 p0098 A73-10555

Use of light pressure for selective evacuation of gases 01 p0059 A73-10627

Influence of light on the electron work function of GaAs single crystals at low temperatures 01 p0088 A73-10631

Evolution of a satellite orbit under the influence of light pressure 02 p0211 A73-11777

Re-calculation of efficiency factors for radiation pressure. 02 p0225 A73-12804

Long time optical variability model of quasars and Seyfert galaxies in terms of grain extinction variations in intervening clouds due to thermal and atom impact evaporation 02 p0226 A73-12839

Photometric search for H alpha optical emission in Sco X-1 nebulosity region for linking companion radio sources to X ray source 03 p0373 A73-13374

Brief history of the Martian 'violet haze' problem. 03 p0373 A73-13707

GX 17 + 2 X ray source optical counterpart identification, noting interstellar absorption role in magnitude estimation 03 p0374 A73-13795

I Zw 1727 + 50 energy distribution relationship to lacertid spectra, noting featureless optical spectrum, flat or inverted radio spectrum and fast irregular variations 03 p0380 A73-14636

Cometary heads observations indicating precursor decay lengths from 100-10,000 km, considering visible and UV molecular and atomic emissions 04 p0495 A73-14764

Circular polarization of Saturn. 04 p0499 A73-15368

Electro-optical media for initial light radiation frequency shift maximum, analyzing circular light/modulating wave interactions 05 p0551 A73-16780

- Correction of solar observations for stray light by numerical integration, with application to Mercury's drop. 05 p0621 A73-17032
- Mechanisms of optical, X-ray and gamma-radiation from Crab pulsar. 05 p0611 A73-17314
- Amplification factor of light in a CO₂ + N₂ + He mixture expanding in a supersonic jet. 06 p0723 A73-17964
- VV 281-427, variable stars in a Cepheus-Lacerta field of the Milky Way. 07 p0874 A73-19117
- Yale Observatory photographic monitoring program for quasar observation, presenting light curves and magnitudes for 25 objects 07 p0876 A73-19356
- Comparative study of reflectivity measurements performed in the visible and infrared wavelengths. 07 p0824 A73-19945
- Clusters of galaxies and the cosmic light. 08 p1002 A73-20876
- Optical emission of a ball-lightning 09 p1113 A73-21913
- The structure and reactions of visual pigments. 09 p1042 A73-23306
- Scio X-1 hard X rays and optical emission time variations from simultaneous observations, using balloon-borne counter telescopes 10 p1263 A73-23493
- Visual acuity as a function of exposure duration. 10 p1184 A73-23838
- Effect of heating water droplets by optical radiation. 10 p1246 A73-24181
- Giant polaritons and selfinduced transparency of Frinkel-excitons. 10 p1249 A73-24694
- OJ 287 and BL Lacertae with rapid radio, IR and optical variability, high IR luminosity, line free optical spectra and varying polarization 11 p1416 A73-25179
- Enhanced laser-light absorption by optical resonance in inhomogeneous plasma. 11 p1405 A73-25970
- Interstellar light absorption in the Orion constellation area 12 p1537 A73-26856
- Experimental determination of two-dimensional spatiotemporal power spectra of stellar light scintillation - Evidence for a multilayer structure of the air turbulence in the upper troposphere. 12 p1521 A73-27120
- Holographic focused image recording and reconstruction in white light, considering source size, shape and spectral composition effects and interferometry 12 p1497 A73-27424
- Method of calculating the temperature dependence of the integral intensity of light absorption by local vibrations in crystals 12 p1525 A73-27937
- Optical study of BL Lacertae. II - Brightness variation from March 1969 to January 1971 15 p1928 A73-31052
- A monolithic pair of dielectrically isolated high-sensitivity photodiodes operating in the visible spectrum. 16 p2012 A73-32854
- Ultraviolet proximity focussed converters for use in a satellite SEC-TV system. 17 p2170 A73-35296
- Rapid interferometric technique for MTF measurements in the visible or infrared region. 17 p2171 A73-35404
- Hydrological phenomena teledetection based on multispectral band scanners for IR and visible frequency ranges 18 p2307 A73-36027
- The redshift-distance relation. V - Galaxy colors as functions of galactic latitude and redshift - Observed colors compared with predicted distributions for various world models. 19 p2487 A73-38504
- Optical and near IR absorption line spectra of quasar 1331+170, discussing red shift and line locking process 19 p2487 A73-38508
- Optical pulses interaction with two level atom spins, determining sub-cooperation limit in resonant absorbers 20 p2591 A73-38625
- Orthogonal operators and phase space distributions in quantum optics. 20 p2591 A73-38629
- Minor planets and related objects. X - Spectrophotometric study of the composition of /1685/ Toro. 20 p2607 A73-39120
- Minor planets and related objects. XI - 0.4-0.8 micron spectrophotometry of /1685/ Toro. 20 p2607 A73-39121
- Statistical spectral attenuation characteristics of transmittance windows for visible and near IR under various optical weather conditions 21 p2731 A73-40746
- Light curve for eclipsing binary systems with an extensive atmosphere. 22 p2916 A73-43044
- Relationships between forces acting on bodies moving in a rarefied gas, in a light flux, and in hypersonic Newtonian flow 24 p3055 A73-45532
- LIGHT ABSORPTION**
- U ELECTROMAGNETIC ABSORPTION**
- LIGHT ADAPTATION**
- Axiomatic formulation of a mathematical model for visual adaptation 01 p0012 A73-10655
- Scotopic vision - An unexpected threshold elevation produced by dark annuli. 02 p0137 A73-12080
- Intrinsic light brightness and intensity estimation tests for foveal and peripheral retina under photopic and scotopic stimuli 07 p0783 A73-20257
- Neural channel mechanism for real light and equivalent background coding, using test flashes under bleaching and field adaptation 07 p0783 A73-20258
- Mitotic activity in dorsal epidermis of Rana pipiens. 07 p0784 A73-20456
- Duplex vision theory of photoreceptor rods and cones/ light and dark adaptation, discussing rhodopsin regeneration, bleaching and desensitization mechanisms 09 p1043 A73-23317
- Frog retinal metabolism in photoreceptors during dark and light adaptation, using ERG, radiospirometry, oxygen uptake polarography and pyridine spectrophotometric assay 09 p1044 A73-23319
- Electroretinogram recovery cycle during light adaptation and after dark adaptation 10 p1181 A73-24518
- Single unit and evoked potential responses in cat optic tract to paired light flashes. 11 p1317 A73-25647
- Light adaptation of the late receptor potential in the cat retina. 13 p1574 A73-28352
- Stimulus luminance-duration relationship of adapting light effect in human electroretinography, referring to Bunsen-Roscoe and Bloch constant law 13 p1575 A73-28363
- Flashblindness recovery following exposure to constant energy adaptive flashes. 13 p1579 A73-28505
- Influence of the dazzling of an eye on the state of adaptation of the congenic eye in a normal subject 14 p1716 A73-30388
- Slowed decay of the monkey's cone receptor potential by intense stimuli, and protection from this effect by light adaptation. 19 p2394 A73-37413
- Eigenvectors of the sensitivity variations across the human central fovea. 22 p2810 A73-42957
- LIGHT AIRCRAFT**
- NT CESSNA 172 AIRCRAFT**
- Handling characteristics in roll of two light airplanes for steep approach landings. 03 p0250 A73-13701
- Basic specification research for the main instruments of light aircraft 07 p0825 A73-20248
- Light motorized glider-type aircraft design, development and flight testing, discussing aerodynamic configuration, structural design and performance characteristics 12 p1459 A73-27732
- The state of the art in light aircraft design. 13 p1568 A73-28179
- Flight tests of approach path angles and airspeed effects on landing of spoiler equipped light aircraft 13 p1569 A73-28830
- The lowering of minima of third-level and business aircraft 15 p1831 A73-32476
- Light aircraft vertical gust induced structural failures, analyzing 1960-71 accident reports for injuries biomechanics and environmental conditions 16 p1967 A73-32678
- Some aerodynamic problems applicable to the light aircraft 16 p1961 A73-32809
- Automated prediction of light aircraft performance and riding and handling qualities. 17 p2101 A73-34666
- [SAE PAPER 730305]
- Use of honeycomb and bonded structures in light aircraft. 17 p2101 A73-34667
- [SAE PAPER 730307]
- Applications of advanced aerodynamic technology to light aircraft. 17 p2101 A73-34676
- [SAE PAPER 730318]
- Stall/spin studies relating to light general-aviation aircraft. 17 p2102 A73-34678
- [SAE PAPER 730320]
- Shrouded Q-FAN propulsor for light aircraft, discussing propulsion system performance, weight, noise and cost trends 17 p2221 A73-34680
- [SAE PAPER 730323]
- STOL light aircraft wing with circulation control through blowing around trailing edge, boundary layer control through suction, leading edge modification and increase in chord length 17 p2094 A73-34682
- [SAE PAPER 730328]
- An inexpensive, full-scale aircraft fatigue test system. 17 p2102 A73-34692
- [SAE PAPER 730341]
- Trends in avionics simplification for light utility aircraft. 19 p2450 A73-37801
- Design and analysis of an energy absorbing restraint system for light aircraft crash-impact. 22 p2799 A73-42080
- [ASME PAPER 73-DET-111]
- LIGHT ALLOYS**
- NT ALUMINUM ALLOYS**
- NT BERYLLIUM ALLOYS**
- NT MAGNESIUM ALLOYS**
- Electro-gilding of coverings and light alloy component parts for satellites D2 and EOLE. 07 p0829 A73-18911
- Effects of the initial structures of pressed semi-finished products made of AK-8 alloy on their weldability. 07 p0832 A73-20370
- Investigation of the low-cycle fatigue of light-alloy welds 07 p0833 A73-20506
- Russian book on extra light engineering alloys covering Mg-Li alloys structure and mechanical properties, aging and strain hardening characteristics, corrosion resistance, etc 08 p0979 A73-21600
- Corrosion and corrosion prevention of light metal alloys. 13 p1637 A73-29314
- [NACE PAPER 114]
- Some findings from a preliminary fatigue experiment with model light-alloy specimens 15 p1955 A73-32191
- Investigation of low-cycle fatigue of welded joints in light alloys. 19 p2433 A73-37781
- LIGHT AMPLIFIERS**
- Gain distribution in a CO₂ TEA laser. 02 p0177 A73-12434
- High power laser generation and heating of plasma in solid targets due to radiation damage, discussing liquid lasers as light amplifiers 06 p0731 A73-18582
- Large-aperture Nd-glass laser amplifier for high-peak-power application. 06 p0704 A73-18791
- Electron-beam-controlled CO₂ laser amplifiers. 07 p0835 A73-19639
- A laser amplifier with resonator natural frequencies misaligned with respect to the gain profile of the active medium 09 p1096 A73-22969
- Nanosecond pulse amplification in electron-beam-pumped CO₂ amplifiers. 09 p1097 A73-23336
- Theory of spontaneous and stimulated electroluminescence of ZnS-Mn layers 10 p1261 A73-24766
- Influence of external self-focusing on the performance of laser amplifiers 11 p1364 A73-26156
- Performance characteristics of a TEA double-discharge grid amplifier. 12 p1505 A73-27015
- Coherent optical signal superregenerative amplification in Q switched gas laser, calculating sensitivity of He-Ne laser light amplifier 13 p1627 A73-28663
- Theory of an infrared high-pressure chemical laser 13 p1627 A73-28762
- Temperature stability of the disperse phase component of the output emission of an optical quantum amplifier 14 p1758 A73-30576
- Time-resolved gain of a volume-excited TEA CO₂ laser amplifier. 15 p1885 A73-31945
- Papers on laser theory covering historical evolution, optical resonators, oscillators, amplifiers, pulse propagation, gain saturation effects, internal modulation, mode locking and noise problems 15 p1886 A73-32424
- A light amplifier display device. 16 p2013 A73-32882
- Fiber laser amplifier properties and light dispersion due to fiber structure and materials in optical communication 16 p2024 A73-32883
- Optical communication channel optimization with binary signals preamplified in optical parametric amplifier, noting amplifier gain and SNR 17 p2123 A73-35155
- Effect of rotational level coupling on pulse sharpening in CO₂ amplifiers. 17 p2143 A73-35791
- The transversely adjusted gap laser for optical communication systems. 17 p2186 A73-35795

Chemical laser and molecular amplifiers characteristics covering population inversion and vibrational energy generation, storage, distribution and transfer
18 p2321 A73-35902

Unstable cavities with a central coupling hole in lasers and amplifiers
18 p2322 A73-36559

Amplified spontaneous emission comparison with laser stimulated emission during He-Ne transitions, noting threshold condition relation to population inversion density
20 p2570 A73-38619

Non-Gaussian statistics of superradiant radiation from saturated xenon 3.5-micron laser amplifier.
20 p2570 A73-38620

Self-pulsing in laser amplification of broadband noise.
20 p2571 A73-38635

Use of laser amplifiers in a glass-fiber communications system.
20 p2522 A73-38667

A neodymium-doped yttrium-aluminum-garnet laser amplifier with an integrated design
20 p2572 A73-38669

Technique for gain determinations in pulsed CO₂ TEA lasers.
20 p2572 A73-38885

Amplification of stimulated Raman scattering of light in various nonlinear amplifier pumping circuits
21 p2711 A73-40306

Effect of saturation on light amplification in stimulated Mandelstam-Brillouin scattering
21 p2739 A73-40359

Ideal laser amplifier as a phase measuring system of a microscopic radiation field.
22 p2870 A73-42516

Rotational relaxation effects in short-pulse CO₂ amplifiers.
22 p2870 A73-42520

Comparison of theory and experiment for nanosecond-pulse amplification in high-gain CO₂ amplifier systems.
22 p2870 A73-42521

Polarization characteristics of a regenerative laser with a Faraday cell and a partial polarizer
22 p2870 A73-42721

Amplification of short pulses in CO₂ laser amplifiers.
22 p2871 A73-43025

Study of light amplification in a pulsed gas-dynamic laser with burning acetylene-air mixtures
23 p2988 A73-44011

LIGHT BEAMS

Displacements of spatially bounded light beams in a turbulent medium using the approximation of a random Markov process
01 p0076 A73-10214

Light polarization measurement with multichannel polarimeters, considering achromatic modulators to convert polarization information into intensity modulation before light beam split into constituent wavelengths
01 p0050 A73-10542

Beam spread of laser light propagating through the atmosphere.
01 p0060 A73-11056

Quantum mechanical interpretation for low intensity optical interference experiments with independent light sources and modulated light beams
01 p0078 A73-11250

Theory for the propagation of partially coherent light beams in a turbulent atmosphere
02 p0142 A73-12494

Approximate formulas for calculating intensity distributions of intense laser light diffracted on an ultrasonic wave.
03 p0318 A73-12995

Laser measurement of turbulence in exhaust jets.
03 p0308 A73-13568

Electro-optical multiple transit laser beam deflection system using KDP crystals and quadrupolar electrode arrangements
03 p0319 A73-14066

Beam diverging lens system for high power laser transmitters.
03 p0319 A73-14432

Electro-optical and acousto-optical methods of laser beam modulation and deflection with emphasis on various modulator and deflector types
05 p0583 A73-16340

Laser beams for precision alignment and detection using methods based on maximum and minimum principles
05 p0583 A73-16344

Electromechanical techniques for rapid frequency tuning of lasers.
05 p0584 A73-16443

Outer-scale effects in turbulence-degraded light-beam spectra.
05 p0597 A73-16498

Beam trajectory distortions due to turbulent air refractive index fluctuations in optical waveguides
05 p0551 A73-16785

Edge diffraction cone detection by illuminating razor blade edge with laser beam, noting agreement with geometrical theory prediction
05 p0585 A73-16812

Propagation by impinging laser beams.
05 p0585 A73-17211

Programmable, digital, rapidly frequency-shift-keyed, high-frequency generators for driving acoustooptical light deflectors
05 p0586 A73-17239

Two-dimensional optical phased-array beam steering.
06 p0694 A73-18287

Thermal tagging for laminar and turbulent liquid flow shadowgraph visualization by ND glass laser beam
06 p0696 A73-18573

CW laser beams steady state thermal self focusing stability, deriving nonlinear absorbing medium geometrical optics ray equation and aberration pattern
06 p0702 A73-18583

External self focusing of converging short duration pulsed light beams, analyzing resultant focal points trebling, nonlinear focus motion and intensity distribution
06 p0702 A73-18590

Time /T-field/ solutions to Einstein equations of test particles and light rays in nonstatic spherically symmetric gravitational field
06 p0724 A73-18646

Optical beam spread in a turbulent medium - Effect of the outer scale of turbulence.
07 p0851 A73-19274

Occurrence of oriented structures under the action of a laser beam in metals
07 p0839 A73-19658

Intensity fluctuations of a light beam propagating through a wave guide channel with random refraction-index inhomogeneities
07 p0792 A73-19915

Laser beam spreading, deflection and collimation under atmospheric effects on long high path
08 p0938 A73-21028

Numerical solutions to wave and hydrodynamic equations for thermal blooming of pulsed focused Gaussian laser beams in heated gas medium
08 p0974 A73-21029

Statistics of laser beam fade induced by pointing jitter.
08 p0975 A73-21058

Power reduction and fluctuations caused by narrow laser beam motion in the far field.
08 p0975 A73-21059

High power laser light beam stratification with self induced effects in cubic medium, noting amplitude distribution dependence
09 p1095 A73-22669

Possibility of holographic observation of the interference of independent weakly degenerate fields
09 p1084 A73-22670

Temperature fluctuations in the turbulent wake behind an optically heated sphere.
10 p1296 A73-24251

Stationary emission of monochromatic spatially bounded laser beams from active medium with thin lens type inhomogeneity due to flat wave converter /resonator/ structure
11 p1376 A73-26142

Influence of external self-focusing on the performance of laser amplifiers
11 p1364 A73-26156

Correlation of the shift in the center of gravity of a focused light beam in a turbulent atmosphere
11 p1331 A73-26160

Theory of thermally-induced interference and lensing in transparent materials.
12 p1523 A73-26828

Laser beam evaporation of dense substances, examining luminous flux densities with gasdynamic equations
12 p1506 A73-27137

Powerful laser beam and material interaction, investigating gas dynamics of plasma heating and ejection
12 p1506 A73-27138

Oscillating laser transverse modes locking into off-centered pure Gaussian beam
13 p1626 A73-28347

Calculation of the constants of an infinitely narrow beam in spectral devices
13 p1660 A73-28769

Image contrast in a microscope with synchronous scanning of the object by point or raster field diaphragms
13 p1616 A73-28771

Investigation of a planar analyzing system employing laser illumination for facsimile transmitters
13 p1627 A73-28857

Parallel optical channel communications system with separate laser sources for suppressing mode competition noise due to beam intensity fluctuations /beats/
13 p1584 A73-28898

Photoresistor synchronous detector circuits with rectangular light pulse switching elements for capacitive and resistive loads
13 p1592 A73-28900

Reflection and transmission of a narrow beam of light in a thick turbid medium layer with isotropic scattering and absorption
13 p1609 A73-29158

Video-to-film color-image recorder.
13 p1619 A73-29240

Mechanism of damage of the surface of a transparent dielectric during illumination with short light pulses.
13 p1629 A73-29429

Some problems in the optimization of holographic memories.
13 p1622 A73-29435

Measurement of the radius of curvature of a laser beam by an interferometric method.
13 p1629 A73-29442

Particle acceleration by a moving laser focus, focusing front or ultrashort laser pulse front.
14 p1757 A73-30338

Maxwell equations for lasing modes of bounded region in laser beam with finite spectral width in form of Fourier integrals
14 p1757 A73-30461

Laser beam transformation into light filament in inhomogeneous weakly absorbing media from Gaussian beam propagation analysis
14 p1758 A73-30466

Short-term average optical-beam spread in a turbulent medium.
15 p1913 A73-31016

Polarization-dependent intensity transmittance of optical systems.
15 p1913 A73-31125

Fluctuations of light fluxes propagating in a scattering medium
15 p1903 A73-31323

Propagation laws of a spatially bounded radiation flow in a scattering medium
15 p1903 A73-31324

Role of laser radiation self-focusing during breakdown in liquid He₄
15 p1884 A73-31701

Stimulation of nonradiating transitions during intense excitation by light
15 p1885 A73-31720

Investigation of the absorption of laser radiation in a laser spark in air
15 p1885 A73-32313

Block organized holographic read only optical memory /ROOM/ model for random access large storage capacities with electro-optical or acousto-optical light deflection system
16 p2012 A73-32869

Holographic read-write memory, optical organization and capacity enhancement by three-dimensional storage.
16 p2013 A73-32871

Experimental studies on the scattering pattern from a ruby laser rod.
16 p2023 A73-32875

Remote measurement of the thickness, distance and velocity of objects by means of a piezoelectric laser beam deflector.
16 p2023 A73-32877

A hologram interferometer with a retro-reflected speckle reference beam for the real time visualization of vibration patterns.
16 p2013 A73-32880

Thermal tagging for laminar and turbulent liquid flow shadowgraph visualization by Nd glass laser beam
16 p2016 A73-33598

Holographic methods of laser radiation divergence control
17 p2184 A73-34919

Light pulse structure and bandwidth bounds in ruby laser with delay line inside variable effective length resonator
17 p2185 A73-35169

Light beam absorption correlation with axial dispersion of ink injected into turbulent water flow in pipe
17 p2156 A73-35509

Light beam dispersal of fog with various drop sizes based on energy equation, considering cloud water content, cross wind effects and front velocity
18 p2337 A73-36561

Ruby laser light spark ion-electron currents in gap between copper plates under electric field
18 p2322 A73-37047

Thermal lensing of laser beams in optically transmitting materials. I.
19 p2438 A73-38023

Refraction of light beams in an atmosphere with arbitrary parameters
19 p2449 A73-38558

A test of Jaynes' neoclassical theory - Incoherent resonance fluorescence from a coherently excited state.
20 p2570 A73-38605

- Time delay statistics of photoelectric emissions - An experimental test of classical radiation theory. 20 p2570 A73-38606
- Two-photon time distributions in mixed light beams. 20 p2570 A73-38615
- Correlation function of a laser beam near threshold. 20 p2571 A73-38631
- Cross focusing possibility between two coaxial laser beams in dielectrics with optical inhomogeneities and oscillatory waveguide characteristics, noting critical power role 20 p2572 A73-38848
- Average intensity of a nonsymmetric optical radiation beam in a turbulent atmosphere 20 p2555 A73-39187
- Metal-insulator-semiconductor-insulator-metal information storage system with optical write and read operations. 20 p2533 A73-39683
- Generation of high-power light pulses at wavelengths 1.06 and 0.53 micron and their application in plasma heating. I - Experimental investigations of reflection of light of two wavelengths in laser heating of plasma. 20 p2573 A73-39684
- Acoustooptic materials evaluation based on figures of merits and acoustic attenuation for laser beam deflection device design and fabrication 21 p2710 A73-40095
- Mutual coherence function of a finite optical beam and application to coherent detection. 21 p2710 A73-40147
- Absorption saturation effects on high-power CO₂ laser beam transmission. 21 p2710 A73-40152
- Laser beam incidence in active nonlinear medium, considering Kerr effect, beam generation, Green function and intensity calculations for wave scattering 21 p2710 A73-40153
- Semiconductor laser beam self focusing action due to combined effects of linear and nonlinear dielectric constant and absorption coefficients, considering n-InSb sample 21 p2711 A73-40226
- Reflection of a laser beam from an interface between isotropic dielectrics 21 p2714 A73-40569
- A study of the effect of the number of axial modes of a laser on its degree of coherence 21 p2714 A73-40748
- Impulse reaction resulting from the in-air irradiation of aluminum by a pulsed CO₂ laser. 21 p2715 A73-40960
- Frequency response of laser scanners and its optimization through apodization. 21 p2717 A73-41610
- Evaporation of metallic targets caused by intense optical radiation. 22 p2868 A73-41727
- Application of transverse reference beams in holographic investigations of small particles. 22 p2860 A73-42253
- Divergence of the output radiation of electron-beam-pumped 'radiating mirror' lasers. 22 p2869 A73-42258
- The gravitational influence of a beam of light. I. 22 p2886 A73-42320
- Performance and characteristics of smectic liquid crystal storage displays. 22 p2861 A73-42525
- Self-focusing and self-trapping of light beams in a non-linear medium. 22 p2888 A73-43050
- On the thermodiffusion effect in the CW He-Ne lasers. 22 p2871 A73-43080
- The effect of change of polarisation of the illuminating beam on the microstructure of speckles produced by a random diffuser. 22 p2871 A73-43095
- Multiple-beam lateral-shear interferometer. 22 p2863 A73-43146
- Sealed carbon dioxide laser design for transverse mode output power in terms of beam, transmission loss, Fresnel number and cavity parameters 22 p2872 A73-43155
- Nonlinear dissipation of electromagnetic waves in a plasma 23 p3012 A73-44017
- Absorption of laser radiation in a laser spark in air. 24 p3095 A73-44621
- Photomixing of the fundamental and reference laser beams during analysis of the frequency spectrum of laser radiation by the method of optical heterodyning 24 p3096 A73-44955
- Successively forward-scattered wave propagating through a random medium. 24 p3110 A73-45028
- Multiphotonic absorption spectroscopy without Doppler effect 24 p3096 A73-45327
- U PULSE DURATION**
- LIGHT ELEMENTS**
- Cosmic-ray production of deuterium, He³/lithium, beryllium, and boron in the galaxy. 02 p0208 A73-12412
- Analyses of light-ion spectra in stellar atmospheres. I - Magnesium II in B and O stars. 03 p0366 A73-12934
- Light elements D 2, He 3-4, Li 6-7, He 9 and B 10-11 origin and history in universe, considering nucleosynthesis sites 08 p0997 A73-20885
- Characterization of boron carbide with an electronic microprobe 13 p1645 A73-28346
- Galactic sources and the propagation of cosmic rays - A review of the light isotopes and the odd-Z elements. 16 p2055 A73-33295
- Patterns of the structure of transition metal/interstitial element diagrams [Me - B, C, N, O, H] 22 p2877 A73-42452
- High-latitude proton precipitation and light ion density profiles during the magnetic storm initial phase. 24 p3126 A73-45114
- Transfer of energy to light ions from the ion-acoustic-wave instability developed in a heavy-ion plasma. 24 p3117 A73-45406
- LIGHT EMISSION**
- NT BIOLUMINESCENCE**
- NT CHEMILUMINESCENCE**
- NT ELECTROLUMINESCENCE**
- NT FLUORESCENCE**
- NT LUMINESCENCE**
- NT LUNAR LUMINESCENCE**
- NT OPTICAL RESONANCE**
- NT PHOTOLUMINESCENCE**
- NT SHOCK WAVE LUMINESCENCE**
- NT THERMOLUMINESCENCE**
- NT X RAY FLUORESCENCE**
- Oxygen emission volume rate in auroras due to direct electron impact excitation, obtaining integral cross sections and quenching rates 01 p0036 A73-10336
- The IR emission spectrum of N₂ excited under auroral conditions. 01 p0036 A73-10337
- 6300 A night airglow emission over the magnetic equator. 01 p0036 A73-10344
- Rocket measurements of low energy electrons and optical emissions in the dayglow and aurora. 01 p0036 A73-10346
- Airglow 6300 A emission predawn enhancement amplitude variation with geomagnetic and solar activity 01 p0037 A73-10347
- Nd glass and ruby lasers in mode locking operation for picosecond light pulses emission, noting pulse duration measurement 01 p0059 A73-10713
- Accumulation of the light sum in alkali halide crystals under the action of laser emission 01 p0060 A73-11088
- GaAs-GaAlAs heterojunction transistor for high frequency operation. 02 p0147 A73-12046
- Light-emitting diode and liquid crystal applications to displays, discussing gas discharge plasma, electrophoretic, fluorescent and incandescent devices, electronic wristwatches and calculators 02 p0168 A73-12082
- Airborne photometric measurements of auroral emissions, indicating soft zone and superimposed energetic electron precipitation 03 p0363 A73-13870
- Schwarzschild interior metric singularity for ideal fluid sphere radius relation to Schwarzschild radius, noting conditions for emitted light red shift 03 p0380 A73-14588
- The light emission of the column plasma in current-modulated noble-gas discharges at intermediate pressures 03 p0348 A73-14621
- Solar flare development particle acceleration phase model, noting association with white light emission, hard X-rays and PCA 04 p0490 A73-14833
- Electron excitation and auroral emission parameters. 04 p0440 A73-14959
- Search for weak white-light flares by time-wise photographic cancellation. 05 p0610 A73-17042
- Irregular auroral pulsation commencement and termination times from photometric recordings compared with geomagnetic micropulsations 06 p0690 A73-17557
- Visible light flash emission due to strong shock wave of laser spark, investigating strong external magnetic field effect and time variation of luminous intensity 06 p0700 A73-17966
- Electron-beam tube with semiconducting laser screen. 06 p0677 A73-18636

Light emitting diode pumped Nd-YAG laser analysis for pumping rate and output dependence on temperature, using circular and transverse intensity distribution 06 p0704 A73-18787

A scanned light emitting diode display. 07 p0862 A73-19608

Chaotic photon bunching effect interpretation by theoretical incoherent source model with atomic excitation and emission at stochastically independent times without interaction 07 p0837 A73-20610

The effects of device configuration in the degradation of GaP red light-emitting diodes. 08 p0944 A73-20743

Light emission phenomenon in the Gunn effect device. 08 p0994 A73-20846

Spatial-temporal distribution of E₁/s formations associated with visible forms of polar aurorae 08 p0958 A73-21283

Quasi-stationary emission from ruby and neodymium-glass lasers 08 p0976 A73-21718

Optical anomalies due to scattered disperse cosmic matter in upper atmosphere from Tungusk meteorite fall 10 p1213 A73-24681

The light variation and orbital elements of VW Bootis. 11 p1429 A73-26680

Correlation between pulsations in auroral luminosity variations and X-rays. 11 p1359 A73-26710

Emission of a ruby laser with a moving mirror in the presence of a selector in the resonator 12 p1505 A73-26955

Optoelectronic step-up voltage transformer with optical coupling electrical isolation, using light emitting diode and semiconductor film with high photovoltage levels 12 p1496 A73-26964

Distributions and characteristics of high-latitude field-aligned electron precipitation. 12 p1534 A73-26988

Influence of the shape of radiators on the energy resolution of Cerenkov shower spectrometers 12 p1496 A73-27205

Dependence of the light yield of a plastic scintillator on the energy of protons and electrons 12 p1496 A73-27206

Possible utilization of a vapor, formed by the action of a high-power electron beam on a target, as an active medium for stimulated emission of light. 12 p1507 A73-27517

Stimulated emission of light from solid solutions of tin and lead chalcogenides in the region of 10 microns. 12 p1507 A73-27519

O I 4368 airglow tropical emission excitation due to conjugate photoelectron escape flux, discussing radiative recombination contribution to intensity 14 p1749 A73-29981

Spatial separation of 3914- and 3160-A emissions of nitrogen in an aurora. 14 p1749 A73-29987

Optoelectronic semiconductor components under the influence of ionizing radiation 14 p1733 A73-30070

A uniform belt of diffuse auroral emission seen by the ISIS-2 scanning photometer. 15 p1866 A73-31069

Phase correlations of longitudinal modes in a laser under free emission conditions 15 p1886 A73-32336

Optical emission from ball lightning. 15 p1915 A73-32639

Irregular auroral pulsation commencement and termination times from photometric recordings compared with geomagnetic micropulsations 16 p2002 A73-32781

Fast random access permanent storage read only optical memory, using light emitting diode matrix addressing, semiconductor laser and holographic lens system 16 p2012 A73-32870

Millisecond time scale atmospheric light pulses associated with solar and magnetospheric activity. 16 p2004 A73-33447

Reliability of GaAs/1-x/P/x/ light emitting diodes. 16 p1990 A73-33623

Prolonged monitoring of experimental equipment with the aid of semiconductor emitters 17 p2133 A73-34152

An investigation of the statistical properties of the radiation of a laser, operating in several axial modes, by the photon counting method. 17 p2184 A73-35156

Spatially forbidden regions in the aurora. 18 p2313 A73-36648

ISIS-2 red line photometer for global distribution mapping of atomic oxygen 6300 A emission in airglow and auroras, discussing atomic excitation processes in upper atmosphere 19 p2428 A73-37257

LIGHT COMMUNICATION
U OPTICAL COMMUNICATION
LIGHT RADIATION
U FLASH

Space-time distribution of Es formations associated with visible auroral forms. 19 p2424 A73-37912

Generation in a ruby laser with moving mirror and a selector in the resonator. 19 p2438 A73-38132

Collective spontaneous emission of polyatomic systems 23 p2988 A73-44010

LIGHT EMITTING DIODES

In-flight frequency calibration of IR sensor systems using LEDs. 17 p2165 A73-34275

Miniaturized Nd-YAG laser end pumped by single incoherent gallium-arsenide-phosphide light emitting diode to achieve threshold at room temperature 21 p2713 A73-40457

Bi implant CdS studies, discussing sputtering, surface concentration, p-type behavior and light emission characteristics 21 p2752 A73-40951

LIGHT INTENSITY

U LUMINOUS INTENSITY

LIGHT MODULATION

NT ULTRASONIC LIGHT MODULATION
High-repetition-rate optical pulse generator using a Fabry-Perot electro-optic modulator. 01 p0058 A73-10127

Light polarization measurement with multichannel polarimeters, considering achromatic modulators to convert polarization information into intensity modulation before light beam split into constituent wavelengths 01 p0050 A73-10542

Astronomical seeing and microthermal fluctuations of the atmosphere 01 p0050 A73-10562

Stable optico-mechanical Q-factor modulator for a laser resonator 01 p0059 A73-10797

Antennas for measurement of microwave electromagnetic field by a light-modulated scattering technique. 01 p0025 A73-11055

Electro-optical, magneto-optical, absorptional and acousto-optical light modulation, noting Kerr effect, Faraday rotation and light absorption 04 p0458 A73-15348

Nonlinear interaction between circular coherent light and modulating electromagnetic waves in presence of quadratic electrooptical effect, noting frequency shift 04 p0459 A73-15921

Muller matrix derivation for microwave light modulation studies in quasi-homogeneous magneto-optical and electrooptical media, taking into account finite light speed 04 p0459 A73-15923

Electro-optical and acousto-optical methods of laser beam modulation and deflection with emphasis on various modulator and deflector types 05 p0583 A73-16340

Light speed determination methods, considering He-Ne laser modulation at microwave frequency via intracavity electro-optic KDP crystal 05 p0575 A73-16341

Distance measurement by means of modulated light. 05 p0575 A73-16342

Telemetry with modulated beams short range high resolution systems. 05 p0576 A73-16343

Light signal modulation by traveling wave in circular waveguide with coaxial KDP crystal 05 p0558 A73-16781

Frequency modulated laser radiation detection, studying photomultiplier current harmonics, phase/amplitude detector nonlinearities and noise-resonator coupling effects 05 p0585 A73-16782

Crystal transverse modulators for laser Q-switching, discussing electro-optical properties of various materials 06 p0699 A73-17753

Real time coherent electro-optic two dimensional on-line spatial light modulator role in optical data processing system 06 p0693 A73-18286

Two-dimensional optical phased-array beam steering. 06 p0694 A73-18287

Acoustic-optic modulator design for a high power mode-locked CO2 laser. 06 p0700 A73-18291

Modulated laser system application categories in tabular and pictorial summaries, considering ranging, reconnaissance, tracking, guidance, weapons, navigation, data processing, display and controlled fusion 06 p0700 A73-18292

Acousto-optical modulator for carbon dioxide lasers based on Bragg scattering concept, discussing design parameters and application to lidar system 06 p0700 A73-18295

High-frequency electro-optic prism deflector with application to optical demultiplexing and multiplexing. 06 p0701 A73-18363

Use of a semiconductor laser diode as a modulator of gas laser radiation. 06 p0702 A73-18592

Multichannel television coupling modulation experiments using a CO2 laser. 07 p0833 A73-19195

Polarization dependence of a photoelectric current during the modulated illumination of a system composed of an electrolyte, a porous pigment film, and a metal 07 p0851 A73-19473

Modulation of intensity in multiple images of a luminous source given by a system of two parallel networks 07 p0824 A73-20163

On the approximation of the optical modulation transfer function/MTF/ by analytical functions. 07 p0786 A73-20264

Optical modulator based on coupled waveguides for integrated optical circuits, presenting design and dynamic characteristics 08 p0974 A73-20810

Direct modulation of double-heterostructure lasers at rates up to 1 Gbit/s. 08 p0975 A73-21120

Mode-locking of high power lasers by a combination of intensity and time dependent Q-switching. 09 p1090 A73-21999

Characteristics of acoustooptic cavity dumping in a mode-locked laser. 09 p1091 A73-22089

Precision spectropolarimetry of starlight - Development of a wide-band version of the Dollfus polarization modulator. 09 p1084 A73-22866

Dielectric modulation of single mode CW gas laser by acoustic wave, solving equations for creation and annihilation operators to obtain quantum number 09 p1096 A73-22973

Demonstration of the transmission and reception of modulated oscillations with a helium-neon laser beam 09 p1097 A73-23328

Internally modulating and multiplexing mode locked Nd-YAG laser techniques for one gigabit optical communication, noting system efficiency improvement over conventional approaches 10 p1227 A73-23783

High data rate YAG laser communication experimental systems with partial cavity dumping, orthogonal setup or harmonic mode locking, investigating internal modulation feasibility 11 p1378 A73-26246

Prototype distance measuring instrument for modulated light beam transit time determination 11 p1367 A73-26308

The wave length dependence of the transfer properties of photographic materials for holography. 11 p1370 A73-26536

Experimental studies of a method of detecting microwave-modulated laser radiation in a photosensitive detector 13 p1628 A73-29415

Formation of an ultrashort pulse of light in a ruby laser with resonant modulation of losses 14 p1757 A73-30265

Utilization of optical-frequency carriers for low- and moderate-bandwidth channels. 14 p1728 A73-30418

Direct modulation of a double heterostructure laser at a rate of 2.3 Gbit/s 14 p1758 A73-30700

Contribution to the theory of single-mode laser modulation. II - Conduction modulation. 14 p1758 A73-30769

Modulation-transfer functions of scattering media, derived from observations in direct light. 15 p1914 A73-32189

Phase correlations of longitudinal modes in a laser under free emission conditions 15 p1886 A73-32336

Papers on laser theory covering historical evolution, optical resonators, oscillators, amplifiers, pulse propagation, gain saturation effects, internal modulation, mode locking and noise problems 15 p1886 A73-32424

Hybrid optoelectronics - High frequency modulation and detection of light by semiconductor sources and sensors. 16 p1978 A73-32886

Influence of magnetic spin resonance in optically transparent magnetic materials on the nature of laser radiation 16 p2024 A73-34001

Frequency deviation equations for FM gas laser with modulation achieved by resonator optical length variations 17 p2184 A73-35168

Use of a stable polarization modulator in a scanning spectrophotometer and ellipsometer. 17 p2175 A73-35751

Magnetic modulation of the optical emission intensity of a plasma from a high-frequency H-discharge 18 p2339 A73-36565

An electrooptical modulator based on a coaxial step-shaped resonator 18 p2322 A73-36856

Modulation of gallium arsenide laser diodes 20 p2572 A73-38665

Crosstalk compensation in optical beam transmission. 20 p2528 A73-38769

Considerations about the atmospheric background and the technique of differential modulation in infrared astronomy. 21 p2740 A73-40690

Diffraction grating model in terms of amplitude and phase modulation to explain angular spectrum of light reflection from corrugated surface for various incidence angles 21 p2740 A73-40790

Frequency response of laser scanners and its optimization through apodization. 21 p2717 A73-41610

Low power He-Ne laser beam intensity modulation in thermal medium, applying to temperature fluctuation detection in transparent materials 22 p2872 A73-43154

Electrooptical modulator employing a barium titanate single crystal. I - Estimates of critical control voltages 23 p2987 A73-43571

LIGHT PRESSURE

U ILLUMINANCE

LIGHT PROBES

U LIGHT BEAMS

LIGHT SCATTERING

NT HALOS

Light scattering by cirrus cloud layers. 01 p0038 A73-10376

Theoretical calculation of light scattering and measurements with grating UV double monochromator for anomalous atmospheric transparency 01 p0039 A73-10402

Homogeneous gas sphere model light scattering for different energy source distributions in planetary and stellar atmospheres 01 p0100 A73-10704

Gas density measurements in a jet using Raman scattering. 01 p0050 A73-10763

Light scattering from an inhomogeneous fluid. 01 p0077 A73-10971

Observation of upper atmospheric constituents by laser radar systems. 01 p0018 A73-11202

Laser related Bell Laboratories research on light scattering, solid state physics, nonlinear optics, materials science, quantum electronics and ultrashort light pulses 01 p0060 A73-11214

Measurement of the angular distribution of light scattered from a glass fiber optical waveguide. 01 p0078 A73-11215

Optical power handling capacity of low loss optical fibers as determined by stimulated Raman and Brillouin scattering. 01 p0078 A73-11216

Double-reverse-scatter interference in optical fiber communication systems. 01 p0018 A73-11217

Russian papers on nonlinear optics and hyperacoustics covering laser use in ultrasound propagation study and thermal and stimulated molecular light scattering effects 02 p0194 A73-11944

Spectral composition of thermal and stimulated light scattering in the wing of the Rayleigh line 02 p0194 A73-11945

Stimulated molecular light scattering in gases 02 p0195 A73-11946

Experimental investigation of thermal and induced molecular scattering of light in solutions within a wide spectral range 02 p0195 A73-11947

Kinetics of heating a light-scattering field by radiant heat transfer 02 p0238 A73-12098

Coherent laser radiation and holography in an optically inhomogeneous medium. 02 p0176 A73-12111

Optical measurements of lunar albedo, angular illumination, diffuse and specular reflectance and scattering coefficients on Mare Foecunditatis regolith powder of various sizes 02 p0213 A73-12238

Statistical theory of light propagation in a turbulent medium /Survey/ 02 p0141 A73-12485

Tago-Sato-Kosaka and Bennett comets Lyman alpha radiation explanation via resonant scattering on neutral hydrogen formed by water vaporized from ice core 02 p0224 A73-12742

Line and continuous excitation sources for measuring wavelength dependence, angular distribution and polarization of scattered light intensity in turbulent and laminar flames 03 p0396 A73-12925

Light scattering from systems with chemical oscillations and dissipative structures. 03 p0273 A73-13285

Laser anemometry developments review covering reference-beam, fringe and single-beam modes optical arrangements, signal processing systems and light scattering particles

03 p0308 A73-13535

Scattering of a light pulse by a spherical particle

03 p0343 A73-13752

German monograph - Spatial oscillations of light in the refraction and image field of rough objects.

03 p0319 A73-13817

Degree and direction of polarization of multiple scattered light. I - Homogeneous cloud layers.

03 p0344 A73-14427

Degree and direction of polarization of multiple scattered light. II - Earth's atmosphere with aerosols.

03 p0344 A73-14428

Intensity and polarization of the solar light scattered by an isolated volume of interplanetary matter

03 p0380 A73-14611

Photometry of the lunar surface.

04 p0497 A73-15177

Laser irradiation testing - A new method for the nondestructive study of plastic material

04 p0458 A73-15324

Rayleigh and Brillouin scattering from fluids in thermal equilibrium and light scattering from macromolecules in solution, discussing light and medium properties interrelationship

05 p0583 A73-16345

An optical system for measurement of mean and fluctuating concentrations in a turbulent air stream.

05 p0576 A73-16437

Possibility of emission-line polarization in diffuse nebulae with a C + E spectrum

05 p0617 A73-16462

Isotropic and incoherent light scattering by atomic slab, calculating Doppler effect induced diffuse radiation energy partial redistribution by Monte Carlo method

05 p0597 A73-16562

Radiation field in a scattering medium after a long time interval following exposure to a light pulse

05 p0599 A73-17354

Study of the scattering properties of the atmosphere by light polarization measurements in a twilight sky

05 p0572 A73-17355

Calculation of light scattering in planetary atmospheres with allowance for refraction

05 p0599 A73-17358

Angular distribution of first Stokes component for stimulated combinational Raman scattering investigated under various excitation conditions

06 p0700 A73-17965

Stimulated Compton scattering of laser radiation by electron plasma, determining electrons diffusion coefficient and velocity distribution function

06 p0700 A73-17970

A dual polarization laser backscatter system for water quality studies.

06 p0700 A73-18306

Heating of a plasma in stimulated scattering of laser radiation /Review/.

06 p0731 A73-18578

Anisotropy of piezoelectrical scattering in semiconductors with a wurtzite structure

06 p0738 A73-18648

Connection of the linear polarization level of atmosphere-air scattered light with the light reduction in the infrared spectral region

06 p0691 A73-18733

Investigation of the scattered-light-flux magnitude dependence on the drop size in the aerosol photoelectric counter

06 p0691 A73-18734

Variation of dc domain threshold in a nematic liquid crystal under continual dynamic scattering.

06 p0739 A73-18794

Electrooptic liquid crystal devices - Principles and applications.

07 p0861 A73-19135

Differential light scattering cross section derivation for photon interaction with relativistic electrons, comparing with quantum electrodynamics calculation and Thomson scattering experiment

07 p0851 A73-19516

Scattered twilight light variations at 5500 to 6600-A wavelengths according to spectral observations in 1962 through 1968 at Abastumani

07 p0817 A73-19587

Analysis of light polarization variations in a twilight sky in terms of upper atmosphere effects

07 p0817 A73-19588

Polarization measurement of clear sky light and comparison with theoretical data

07 p0818 A73-19590

A photometric investigation of the packing state of Apollo 11 lunar regolith samples.

07 p0878 A73-19669

Sunlight scattering by dust along lunar horizon at sunset, presenting atmospheric model for dust cloud production

07 p0895 A73-19862

Far infrared and Raman spectroscopic investigations of lunar materials from Apollo 11, 12, 14, and 15.

07 p0897 A73-19889

Remote probing by laser radar.

07 p0793 A73-19947

Stokes polarization parameters of optical emission scattered in absorbing medium calculated for Galaxy and M 82 galaxy, assuming thermal IR radiation from nucleus

07 p0901 A73-20312

German monograph on collective dissipation processes in collisionless shock waves in high ion temperature plasma, using laser beam scattering technique

07 p0837 A73-20387

Turbulent transport measurements with a laser Doppler velocimeter.

07 p0826 A73-20462

Diffuser box for holography spatial and temporal coherence requirements relaxation, explaining speckling and SNR reduction by time and frequency domain analysis

08 p0963 A73-21035

Effects of multiple scattering on laser pulses transmitted through clouds.

08 p0976 A73-21423

Influence of the geometrical parameters of a lidar on the applicability of single-scattering approximation

08 p0986 A73-21457

CO2 laser induced Compton effect in underdense hydrogen plasma.

09 p1125 A73-22025

Flow velocity measurement method based on laser light frequency Doppler shift in scattering experiment on particle seeded liquid, presenting velocity profiles

09 p1094 A73-22314

Mandelsham-Brillouin laser light scattering theory and application to atmospheric parameters remote sensing

09 p1094 A73-22327

Equivalence relationships between diffuse radiation fields for finite slabs bounded by a perfect specular reflector and a perfect absorber.

09 p1121 A73-23072

Image holography through convective fog.

11 p1361 A73-25365

Russian book - Scattering and absorption of light in the atmosphere.

11 p1392 A73-25602

Daytime sky brightness from atmospheric transmittance, noting single and multiple scattering calculations

11 p1352 A73-25603

Optical properties of polydisperse media with different size distributions of particles

11 p1398 A73-25611

Light scattering functions in the atmospheric ground layer for a range of large scattering angles

11 p1393 A73-25616

Light scattering from weakly ionized nonhomogeneous plasmas.

11 p1405 A73-25971

Image plane or optical system focal point location based on grain size variations from laser speckle patterns

11 p1378 A73-26245

Hologram interferometry and laser speckle methods - Further applications.

11 p1370 A73-26532

Optical scattering properties of Saturn's ring.

11 p1429 A73-26683

Radiative transfer theory model of isotropic monochromatic scattering of light in plane layer of finite optical thickness

12 p1538 A73-26862

Angular distribution of induced combinational light scattering in liquid nitrogen

12 p1505 A73-26889

Stokes polarization parameters of optical emission scattered in absorbing medium calculated for Galaxy and M 82 galaxy, assuming thermal IR radiation from nucleus

12 p1539 A73-27284

Facility to determine spectra of light scattered at free plasma electrons during single laser pulse, obtaining electron component profiles with high speed streak camera

12 p1506 A73-27301

Reduction of the switching time of a liquid-crystal optical transparency.

12 p1498 A73-27514

Analysis of the information capacity of optical matched filters.

12 p1498 A73-27516

Determination of the characteristics of light-scattering particles in the atmosphere of Venus from photometric measurements.

12 p1543 A73-27640

Scattering of light by the medium generated by a space vehicle. I - Emission of vapor jets by spacecraft microthrusters.

12 p1549 A73-27641

Light scattering from independent particles - Non-gaussian correction to the clipped intensity correlation function.

13 p1658 A73-28208

Memory effects associated with bulk viscosity on the spectrum of stimulated Brillouin scattering.

13 p1626 A73-28372

Venus atmospheric model based on spectroscopic evidence of carbon dioxide spectral lines phase variation due to two scattering layers

13 p1680 A73-28459

Light scattering by atmospheric aerosols.

13 p1653 A73-28517

Attenuation of monochromatic light in bottom layer of atmosphere and some properties of aerosols.

13 p1653 A73-28518

The possibility of storing laser radiation scattered by an electron beam.

13 p1627 A73-28662

Role of exchange in shifted scattering of light for a double hole

13 p1660 A73-28760

Light scattering in coherent systems for Stokes and anti-Stokes impurity centers in terms of classical and quantum mechanical theories

13 p1660 A73-28770

Atmospheric air characteristics classification as haze, foggy haze, fog and drizzle from light scattering matrix on basis of aerosol condensation

13 p1654 A73-29159

Atmospheric effects in multispectral photographs.

13 p1619 A73-29239

Three-dimensional scattered-light stress analyses of discontinuous fiber reinforced composites. [SESA PAPER 2033]

13 p1699 A73-29306

The application of photon correlation spectroscopy to the measurement of turbulent flows.

13 p1622 A73-29421

Investigation of scattered ultraviolet radiation in the upper Martian atmosphere from the Mars-3 automatic interplanetary station

14 p1796 A73-29866

Matrix operator theory of radiative transfer. II - Scattering from maritime haze.

14 p1749 A73-30163

A nephelometric method for transparency determination in scattering media

14 p1771 A73-30463

Investigation of rough surfaces by a method based on the scattering of coherent light by the sound reflected from such surfaces

14 p1753 A73-30583

The light field existing in a scattering medium long after its illumination by a light pulse.

15 p1912 A73-31004

Derivation of scattering properties of the atmosphere from polarization measurements on the light of the twilight sky.

15 p1865 A73-31005

Calculation of light scattering in planetary atmospheres with allowance for refraction.

15 p1912 A73-31008

The effect of the size distribution of the rain drops on the standard visibility

15 p1902 A73-31139

Detection of gravitational waves by the method of light scattering by elastic oscillations

15 p1913 A73-31321

Fluctuations of light fluxes propagating in a scattering medium

15 p1903 A73-31323

Propagation laws of a spatially bounded radiation flow in a scattering medium

15 p1903 A73-31324

Redistribution of resonance radiation. II - The effect of magnetic fields.

15 p1913 A73-31559

Atmosphere optical thickness determination from satellite and ground measurements of scattered light in solar vertical

15 p1905 A73-31820

Method for the determination of impurity particle dispersion in fuels and lubricants

15 p1876 A73-31834

Extinction and scattering by several types of silicate sphere of radius 0.05-1.0 micron, for the wavelength range 0.21-50 microns.

15 p1939 A73-32012

Modulation-transfer functions of scattering media, derived from observations in direct light.

15 p1914 A73-32189

Bragg diffraction of light by two orthogonal ultrasonic waves in water.

15 p1914 A73-32256

The color deficiency of the solar halo of 22 deg radius

15 p1873 A73-32358

Manifestations and causes of atmospheric optical phenomena related to solar light dispersion and diffraction by particles, noting halos, polar auroras and mirages

16 p2002 A73-32949

Influence of saturation effects on stimulating scattering in laser heating of a plasma.

16 p2041 A73-33079

Theory of light scattering from dense plasmas.

16 p2041 A73-33323

Radiation transport theory for anisotropic light scattering in planetary atmospheres, formulating transmission and reflection coefficients

16 p2066 A73-33790

Optical properties of the Venus atmosphere
16 p2069 A73-33827

Coherent light propagation and scattering in vaporized alkali metal atmosphere as function of refractive index and coherent to incoherent transformation
16 p2086 A73-34002

Laser spectrometer for combination scattering, recording polarized spectra with thermoelectrically cooled photomultiplier by photon count
17 p2164 A73-34164

Localized electroretinography capable of maintaining constant light scattering with small angular dimensions by employing Ulbricht principle of uniformly illuminated sphere
17 p2116 A73-34963

Optical effects of cryodeposits on low scatter mirrors.
[ALAA PAPER 73-732] 18 p2336 A73-36349

Apparent reflectance from a semi-infinite absorbing-scattering medium.
[ALAA PAPER 73-753] 18 p2337 A73-36369

Measurements of F₂, NO, and ONF Raman cross sections and depolarization ratios for diagnostics in chemical lasers.
18 p2322 A73-36978

Time dependent radiative transfer. III - Development of the formalism.
19 p2503 A73-37565

Determination of local gas states from scattered laser light
19 p2438 A73-38270

Nonlinear light scattering in crystals
19 p2462 A73-38539

Comparison of the Beckmann model with bidirectional reflectance measurements.
[ASME PAPER 73-HT-11] 20 p2563 A73-38567

Study of laser remote sensing techniques from space platforms.
[AAS PAPER 73-136] 20 p2521 A73-38591

Coherence and quantum optics; Proceedings of the Third Rochester Conference, University of Rochester, Rochester, N.Y., June 21-23, 1972.
20 p2569 A73-38601

Theory of resonant light scattering processes in solids.
20 p2570 A73-38612

Green function and Poynting vector calculation of solid angles of radiation outside and inside anisotropic crystal in laser light scattering experiments
20 p2591 A73-38617

Comparison of Langmuir double probe and laser scattering measurements of plasma parameters.
20 p2595 A73-38880

Extraterrestrial ultraviolet radiation and the parameter of the H I medium near the sun
20 p2601 A73-39074

Application of G. V. Rozenberg's asymptotic formulas in the interpretation of cloud brightness measurements
20 p2584 A73-39189

Switching of the resonator Q factor by stimulated Mandel'shtam-Brillouin scattering.
20 p2574 A73-39703

Relaxation of coherence requirements in holography.
21 p2695 A73-39961

Derivative light scattering photometer, using angular modulation with photomultiplier entrance slit vibration to obtain gain improvement over conventional technique
21 p2697 A73-40130

Rear projection holographic and interferometric viewing screens using deflected and scattered light, discussing microfilm reading applications, dichromated gelatin film and laser exposures
21 p2699 A73-40151

Polarizability of interacting atoms - Relation to collision-induced light scattering and dielectric models.
21 p2742 A73-40211

Self consistent microscopic theory of Rayleigh light scattering by molecular aggregates based on random phase modulation and stochastic theories
21 p2739 A73-40219

The mechanism responsible for shortening of the stimulated Mandelstam-Brillouin scattering light-pulse duration and for generation of nanosecond-duration pulses
21 p2739 A73-40355

Effect of saturation on light amplification in stimulated Mandelstam-Brillouin scattering
21 p2739 A73-40359

Angular dependence of optical scattering in mixed nematic-cholesteric liquid crystals.
21 p2751 A73-40453

On the possibility of measuring gas concentrations by stimulated anti-Stokes scattering.
21 p2699 A73-40458

Absorption line contours in homogeneous plane-parallel semfinite aerosol layers and planetary atmosphere overcloud gas layers for nonspherical scattering
21 p2768 A73-40723

Circular polarization of light reflected from the planets
21 p2769 A73-40732

Vector theory of the glory and rainbow
21 p2731 A73-40742

Indices of backscattering and attenuation of light by a water aerosol
21 p2731 A73-40747

Light scattering from electrohydrodynamic turbulence in liquid crystals.
21 p2744 A73-41020

Dielectric anisotropy of new liquid-crystal mixtures and its effect on dynamic scattering.
21 p2665 A73-41115

Interstellar extinction, relation to spatial dust distribution, light scattering by grains, diffuse absorption lines and polarization
21 p2772 A73-41247

Russian book - Scattered daytime sky light.
21 p2691 A73-41439

Stimulated entropy /temperature/ scattering and its effect on stimulated Mandel'shtam-Brillouin scattering.
22 p2868 A73-41720

Light spectral width and constant frequency shift during spontaneous diffusion in ideal gas for fixed photon wave
22 p2885 A73-41721

Russian book - Light scattering in planetary atmospheres.
22 p2906 A73-41877

Ultrahigh resolution holographic spectroscopy by double exposure of light scattering medium interferogram recording and reconstruction, noting equivalence to use of narrower laser line width
22 p2861 A73-42413

Computer simulation of light pulse propagation for communication through thick clouds.
22 p2828 A73-43156

Experiments on light pulse communication and propagation through atmospheric clouds.
22 p2828 A73-43157

Laser cross-beam intensity-correlation spectrum for a turbulent flow.
22 p2872 A73-43158

Confocal backscatter laser velocimeter with on-axis sensitivity.
22 p2864 A73-43162

Certain problems in measuring Cerenkov light on the Yakutsk extensive air shower device
23 p3022 A73-43546

Problem of increasing the effectiveness of laser usage in experiments on light scattering in a plasma
23 p2987 A73-43670

Study of induced four-photon parametric scattering of laser light in alkali metal vapor
23 p2988 A73-44009

Light scattering intermolecular and Raman spectra in liquid and solid hydrogen, showing short wave collective excitations in relation to phonon processes
23 p3007 A73-44171

Radiation transfer in a multilayer plane-parallel system with nonisotropic scattering
23 p3154 A73-44659

Extinction coefficient /point source light loss due to atmospheric scattering/ significance in reduction of night airglow data
24 p3082 A73-44734

Radiant-conductive heat transfer in a plane layer of an absorbing and scattering medium
24 p3155 A73-44754

Scattered-light phenomena in interstellar space
24 p3137 A73-44824

Influence of the microstructure of water aerosol on the phase function, its asymmetry, and polarization of scattered light
24 p3084 A73-44963

Numerical experiments in laser sounding of aerosol stratification in the atmosphere
24 p3085 A73-44966

Interior radiances in optically deep absorbing media. II - Rayleigh scattering.
24 p3111 A73-45319

Parametric instability of strong circularly polarized electromagnetic wave in plasma producing relativistic electrons and backscattered light
24 p3117 A73-45459

Determination of the parameters of particle density and size distribution functions from measurements of attenuation and backscattering coefficients
24 p3112 A73-45519

LIGHT SOURCES

NT ILLUMINATORS

Electron beam pumped super radiant light source.
01 p0058 A73-10311

Astronomical telescope research programs, emphasizing spectrographic instrumentation to detect and record extragalactic light sources spectra
01 p0046 A73-10502

Possibility of using a laser flame as a source of light in the isotope spectral method
02 p0176 A73-12094

Line and continuous excitation sources for measuring wavelength dependence, angular distribution and

polarization of scattered light intensity in turbulent and laminar flames
03 p0396 A73-12925

Mathematical description of frequency difference hologram obtained by superposition of two holograms of same object produced with light of different frequencies
04 p0451 A73-15924

Daytime and nighttime stereophotogrammetric photography of moving object using stereoscopic effect, noting pulsed light sources for fast moving near objects
05 p0575 A73-16314

Organic dye lasers use as continuously tunable sources of coherent light, discussing molecular energy level systems and transitions
05 p0583 A73-16337

Source limited gray scale and color selection capabilities for direct and reflected light scanners.
06 p0701 A73-18308

Thin film YAG-Nd laser light sources, discussing material selection, incoherent pumping sources, geometrical configuration, heat dissipation, gain saturation and feedback methods
08 p0975 A73-21143

Length measurement interferometry principles and limitations imposed by available coherent sources, discussing laser source techniques and fringe counting method
09 p1093 A73-22313

Determination of the instrumental profile of the DFS-13 diffraction spectrograph
11 p1363 A73-25615

Friedmann expanding cosmological model with superimposed spherically symmetric inhomogeneity for gravitational lens and point light sources dispersion and motion effects on images
11 p1418 A73-25747

Low loss fiber optics communication technology with almost infinite bandwidth potential, discussing transmission lines, light sources, detectors, integrated circuits, systems and applications
11 p1399 A73-26118

Maximum loads on pulse-discharge light sources producing short flashes.
13 p1629 A73-29437

Theory of the shape of pulses produced by transient parametric generation of light.
13 p1629 A73-29438

Theoretical study of the mechanism of the population inversion and of the efficiency in an ionized argon laser operating in the continuous mode
14 p1755 A73-29729

An optical parametric generator with a large length of nonlinear interaction and weak feedback
14 p1754 A73-30853

Digital photoelectric tracking systems with accumulation of the mismatch signal
16 p1977 A73-32716

Lamp pumping system for lasers based on organic compound solutions
17 p2183 A73-34170

Photodetection volume of coherence for thermal optical source with given intensity and spectral density, defining photon phase space cell concept
20 p2570 A73-38610

A multichannel-discharge of high light intensity and short duration
21 p2695 A73-39971

Utilization of the laser as a source in ultrahigh-speed cinematography
21 p2709 A73-39972

Automatic accurate full-range synchronization of light strobe with shutter opening of fast-framing camera.
21 p2697 A73-39997

Phase fluctuations in a parametric light source operating inside a laser resonator.
22 p2869 A73-42246

Image formation by light intensification and thermographic imagery compared from energy viewpoint, considering effect of parasitic light sources in visual field
23 p2979 A73-43223

Resolution of point sources of light as analyzed by quantum detection theory.
23 p2987 A73-43523

LIGHT SPEED

The deflection of light at the sun and the change of its velocity and wavelength
02 p0225 A73-12809

Hubble law from constant light velocity in Euclidean space, noting red shift equation and Einstein gravitational shift
03 p0379 A73-14577

Muller matrix derivation for microwave light modulation studies in quasi-homogeneous magneto-optical and electro-optical media, taking into account finite light speed
04 p0459 A73-15923

Light speed determination methods, considering He-Ne laser modulation at microwave frequency via intracavity electro-optic KDP crystal
05 p0575 A73-16341

Radiation source motion at supreluminal speed in vacuum, defining conditions for Vavilov-Cerenkov and Doppler effects

10 p1250 A73-24943

Light velocity from Io eclipse times observation by Picard and Roemer, noting rms deviation with present value

11 p1429 A73-26685

On the impossibility of the first-order relativity test

21 p2742 A73-41632

LIGHT TRANSMISSION

NT LIGHT SCATTERING

Correlation and structure functions for pulse propagation in a turbulent atmosphere.

01 p0016 A73-10195

Light scattering by cirrus cloud layers.

01 p0038 A73-10376

General solution for polarized radiation in a homogeneous-slab atmosphere.

01 p0078 A73-11033

Beam spread of laser light propagating through the atmosphere.

01 p0060 A73-11056

Bell Laboratories optical communications research and development on lasers, transmission media, principles, methods and components for systems

01 p0060 A73-11212

Higher conservation laws for coherent optical pulse propagation in an inhomogeneously broadened medium.

01 p0078 A73-11221

Book - Light transmission optics.

02 p0192 A73-11881

Theory for the propagation of partially coherent light beams in a turbulent atmosphere

02 p0142 A73-12494

Beam diverging lens system for high power laser transmitters.

03 p0319 A73-14432

Gravitational field effects on processes near stars and galaxies in late evolution phases, describing particle motion and light propagation near rotating sources

05 p0623 A73-17197

Transmission of a GaAs laser beam through the atmosphere.

06 p0699 A73-17495

Criterion for the choice of exposure time in atmospheric turbulence investigation with an optical wave.

06 p0691 A73-17497

Effect of humidity on infrared and visual atmospheric transmission.

06 p0694 A73-18304

High bandwidth and resolution laser scanners and recorders for imagery transmission, discussing component constraints and integrated optics utilization in modulator and scanner development

06 p0701 A73-18310

Experimental results on the application of an x-y acousto-optic deflection system to wide band laser recorders.

06 p0701 A73-18312

Optical and electrical properties of proton-bombarded p-type GaAs.

06 p0739 A73-18786

Absorption of light at oblique incidence on a plasma layer.

07 p0854 A73-19262

Propagation characteristics of collimated, pulsed laser beams through an absorbing atmosphere.

07 p0833 A73-19272

Measurement on a polarization interferometer of absolute and relative light wave delay in liquid dielectrics under the action of an electric field

07 p0823 A73-19332

Service life estimation of electro-optic devices and degradation kinetics, noting reliability of light transmitters and receivers

07 p0800 A73-19407

Investigation of the time characteristics of the phase fluctuations of optical waves propagating through the earth atmosphere boundary layer

07 p0792 A73-19914

Intensity fluctuations of a light beam propagating through a wave guide channel with random refraction-index inhomogeneities

07 p0792 A73-19915

Wave propagation along radially inhomogeneous glass fibres.

08 p0937 A73-20832

Photon counting statistics of the superposition of coherent and chaotic light of arbitrary spectrum passed through the turbulent atmosphere or a Gaussian medium.

08 p0987 A73-20952

Severe self-induced beam distortion in laboratory simulated laser propagation at 10.6 microns.

08 p0974 A73-21031

Solution of equations for one-dimensional propagation of a monochromatic light pulse in absorbing media

09 p1095 A73-22623

Demonstration of the transmission and reception of modulated oscillations with a helium-neon laser beam

09 p1097 A73-23328

Airborne visible laser optical communication experiment between high altitude aircraft and ground station, discussing tracker-transmitter equipment and atmospheric effects on performance

09 p1055 A73-23395

Analysis of electromagnetic-wave modes in lens-like media.

10 p1248 A73-23834

Information in the time of arrival of a photon packet - Capacity of PPM channels.

10 p1188 A73-23836

The three-ring effect in flexible bunches of optical fibres

10 p1228 A73-24585

Experimental observation of Wannier levels in semi-insulating gallium arsenide.

10 p1260 A73-24638

Twisted nematic liquid-crystal electro-optic devices with areas of reverse twist.

11 p1337 A73-25357

Theory of light deviation by sheets of circular cone geometry

11 p1397 A73-25565

Gaussian light beam transmitted intensity derivation for thermal lensing in solids by vector Kirchhoff approach, obtaining time dependent shift in diffraction focus

11 p1377 A73-26228

Thermally induced nonlinear propagation of a laser beam in an absorbing fluid medium.

11 p1377 A73-26229

Optical beam hybrid lens waveguide with central aperture and surrounding lens, comparing transmission loss and bending effects with iris guides

11 p1365 A73-26230

Indirect transitions in thin quantized semiconductor films

11 p1410 A73-26450

Theory of thermally-induced interference and lensing in transparent materials.

12 p1523 A73-26828

Time characteristics of a ring laser with a bleachable filter.

12 p1507 A73-27509

Visible and near-infra-red transmission and reflectance measurements of the Luna 20 soil.

13 p1674 A73-28303

Scintillation and vibration of stars and structure of a turbulent atmosphere.

13 p1680 A73-28514

Distribution law of light-ray direction fluctuations in telescopes

13 p1618 A73-29098

Reflection and transmission of a narrow beam of light in a thick turbid medium layer with isotropic scattering and absorption

13 p1609 A73-29158

Calculation of phase difference power spectrum for slant-path propagation.

13 p1661 A73-29327

Spatially filtered helium-neon laser link operation parallel to IR radiometer for real time atmospheric propagation monitoring over short path

13 p1661 A73-29328

Absorption saturation effects on high-power CO2 laser beam transmission.

13 p1628 A73-29329

Propagation of ultrashort light pulses in a semiconductor under two-photon resonance conditions.

13 p1630 A73-29445

Source altitude for experiments to simulate space-to-earth laser propagation.

14 p1756 A73-30151

Log-intensity correlations of a laser beam in a turbulent medium.

14 p1757 A73-30162

Statistics of photoelectric sensor readings during propagation of light in a turbulent medium

14 p1753 A73-30270

Gas absorption lines detection based on multiple light passage through absorbing medium during generation process, noting radiation spectra of neodymium glass laser

14 p1757 A73-30331

Laser beam transformation into light filament in inhomogeneous weakly absorbing media from Gaussian beam propagation analysis

14 p1758 A73-30466

Two descriptions for the photocounting detection of radiation passed through a random medium - A comparison for the turbulent atmosphere.

15 p1914 A73-32291

High-resolution atmospheric-transmission measurement using a laser heterodyne radiometer.

15 p1886 A73-32378

Fully automatic assessment of RVR, and comparison with observers.

15 p1910 A73-32466

Recent progress in fibres for optical communications.

16 p2023 A73-32863

Fiber laser amplifier properties and light dispersion due to fiber structure and materials in optical communication

16 p2024 A73-32883

Optical transceiver system requirements for local communications, discussing GaAs light emitting and lasing modes, transmission links, installation, maintenance and environmental error factors

16 p1978 A73-32887

Transmission of isotropic light across a dielectric surface in two and three dimensions.

16 p2037 A73-33685

Calculation of the diffuse reflection and transmission of light by a semifinite atmosphere

16 p2066 A73-33791

Coherent light propagation and scattering in vaporized alkali metal atmosphere as function of refractive index and coherent to incoherent transformation

16 p2086 A73-34002

Explicit solution for the photocount statistics with application to atmospheric turbulence.

18 p2337 A73-36625

Optical coupling system for photon-photon coincidence experiments.

19 p2462 A73-37255

Atmospheric turbulence effects on CW carbon dioxide laser propagation, investigating thermal blooming via theoretical diffusion model and experiment

19 p2437 A73-37260

Thermal lensing of laser beams in optically transmitting materials. I.

19 p2438 A73-38023

A comparison of the efficiency and focused stray light characteristics of a conventionally ruled- and a holographically produced-concave diffraction grating in the vacuum ultraviolet.

19 p2431 A73-38164

Optical and millimeter line-of-sight propagation effects in the turbulent atmosphere.

19 p2405 A73-38220

Measurements of the log-irradiance distribution of a laser wave propagated through the turbulent atmosphere.

19 p2405 A73-38222

Experimental test of optical antenna-gain reciprocity.

19 p2439 A73-38487

Observation of zero-degree pulse propagation in a resonant medium.

20 p2570 A73-38602

Higher conservation laws and coherent pulse propagation.

20 p2570 A73-38603

First order theory of steady state single optical pulses /solitons/ phase modulation during propagation in nonlinear absorbers, predicting nonchirped and chirped pulse trains

20 p2591 A73-38626

Glass fiber transmission characteristics as optical waveguides for communication systems, considering transit time and attenuation

20 p2522 A73-38660

Detachable liquid filled capillary waveguide connector for glass fiber multimode optical transmission lines, discussing propagation efficiency as function of dimensional tolerances

20 p2522 A73-38662

A tilted plate interferometer for heat transfer studies.

20 p2564 A73-38879

Aircraft measurements of effective photon paths in cloud-reflected and transmitted light in the 0.76-micron oxygen band

20 p2583 A73-39184

Mutual coherence function of a finite optical beam and application to coherent detection.

21 p2710 A73-40147

Absorption saturation effects on high-power CO2 laser beam transmission.

21 p2710 A73-40152

Materials suitable for making far infrared high-pass transmission filters.

21 p2701 A73-40692

Optical waveguides in GaAs-AlGaAs epitaxial layers.

21 p2752 A73-40969

Extraction of Tschebysheff design data for the low-pass dielectric multilayer.

21 p2665 A73-41135

On the impossibility of the first-order relativity test.

21 p2742 A73-41632

General relativistic gravitation theories based spacetime curvature tests near sun from interplanetary probe motion analysis using probe-borne laser light transmission

[ONERA, TP NO. 1210] 22 p2907 A73-42216

Theoretical and experimental investigations of the coupling of two glass-fiber light waveguides

22 p2861 A73-42424

Thermal lensing of laser beams in optically transmitting materials. II - Numerical computations.

22 p2870 A73-42515

Propagation of laser radiation in a turbulent atmosphere.

22 p2828 A73-43159

Propagation of optical pulses through clad fibers - Modified theory.

22 p2828 A73-43163

- Study of laser radiation propagation and the diagnostics of a randomly inhomogeneous troposphere
23 p2954 A73-43572
- Leaky rays cause failure of geometric optics on optical fibres.
23 p2955 A73-44105
- Optical information transmission over rectangular waveguide communication channels in terms of geometry-wavelength ratio, transparency and repeater functions
23 p2955 A73-44296
- LIGHTHILL GAS MODEL**
Optimal profiles of a nozzle for axisymmetric supersonic discharge of a Lighthill dissociating gas
05 p0534 A73-17270
- Hot gaseous jet noise emission calculation for dependence on turbulent flow characteristics based on Lighthill theory, using computer program
18 p2343 A73-36997
- LIGHTHILL METHOD**
Aerodynamic sound generation, discussing Lighthill theory, multipole sonic sources, wave equation, power and turbulence models and sound radiating flows
03 p0242 A73-13167
- A perturbation method for obtaining approximate solutions of an equation with two small parameters
17 p2201 A73-35046
- LIGHTING**
U ILLUMINATING
LIGHTING EQUIPMENT
NT AIRCRAFT LIGHTS
NT AIRPORT LIGHTS
NT FLASH LAMPS
NT ILLUMINATORS
NT RUNWAY LIGHTS
NT XENON LAMPS
Crew station lighting - Commercial aircraft.
[SAE ARP 1161] 08 p0925 A73-20692
- Optimal lighting for visual tasks, discussing color, type, transillumination, crossed polarization, brightness patterns, diffuse reflection and surface shadowgraphing
14 p1722 A73-30498
- Illumination and television considerations in teleoperator systems.
19 p2416 A73-37318
- LIGHTNING**
NT BALL LIGHTNING
Poisson model of atmospheric noise from lightning discharges as function of thunderstorm distribution and propagation conditions, calculating statistics for narrow band receiver
02 p0142 A73-12528
- Response of boron/epoxy composite materials to simulated lightning current.
03 p0331 A73-13025
- Contribution to the problem of the geoelectric effects on lightning hazard
04 p0473 A73-15283
- Ball lightning events appearing with cloud to ground lightning discharge, discussing possible explanations
05 p0594 A73-16399
- Contribution to the protection of flight vehicles against lightning effects
06 p0648 A73-18436
- Breakdown criteria for streamer formation, electrostatic field analysis and laboratory high voltage experiments on aircraft initiation of lightning strikes
10 p1175 A73-24558
- Study on the limit efficiency of lightning conductors on aircraft radomes.
11 p1336 A73-25303
- Electrostatic charge induction on aircraft due to charged atmosphere and friction effects, noting lightning protection, fuel container shielding and charge removal methods
11 p1307 A73-26722
- Thunderstorm activity determination on lightning discharge number recorders
14 p1754 A73-30792
- Lightning protection for boron and graphite fibers in epoxy resins for aircraft composite structures
16 p1967 A73-33032
- Lightweight coatings for protecting boron filament and graphite fiber reinforced plastic composites from structural damage by lightning
16 p2028 A73-33033
- Lightning protection for boron and graphite reinforced plastic composite aircraft structures, discussing zonal design concept and channel intermittent contact with protrusions on surface
16 p1968 A73-33034
- F-14 aircraft boron-epoxy and graphite-epoxy composite structure production protection against degradation by lightning discharges, discussing design, processing and tests
16 p2028 A73-33035
- Lightning protection for aircraft canopy, discussing simulation tests, safety margins, side puncture, corona streamer and pilot physiological reactions
16 p1968 A73-33036
- Lightning simulation testing in aerospace.
16 p1994 A73-33145

- Electric field intensity of the lightning return stroke.
17 p2163 A73-35464
- Currents in Florida lightning return strokes.
17 p2163 A73-35465
- High current lightning simulation testing of composite materials.
18 p2296 A73-36713
- The lightning arrester-connector concept - Description and data.
19 p2408 A73-37270
- LIGNIN**
The evolution of lignin - Experiments and observations.
13 p1577 A73-29649
- LINE DARKENING**
Gravity-darkening of the secondary component of RW monerocrotis.
05 p0624 A73-17315
- Venus - New microwave measurements show no atmospheric water vapor.
09 p1151 A73-23171
- Russian book on eclipsing binary stars covering limb darkening law, photometric eclipsing phases, computer applications and models
22 p2911 A73-42747
- Neutral Fe line profiles for low-lying transitions measured from solar disk center to limb by double pass spectrometer, considering limb darkening effect
24 p3135 A73-44626
- LIMBS**
Limb scanning as a method for measuring the temperature structure of a planetary atmosphere.
22 p2883 A73-42058
- LIMBS [ANATOMY]**
NT ARM [ANATOMY]
NT ELBOW [ANATOMY]
NT FOREARM
NT HAND [ANATOMY]
NT KNEE [ANATOMY]
NT LEG [ANATOMY]
Favorable effect of flight on pilots exhibiting degenerative arteriopathy of the lower limbs
02 p0137 A73-12151
- Redintegrated somatotyping technique for physique measurement and classification based on limb and torso photographic diameter integration with height, using photoelectric cell and electronics
06 p0659 A73-18474
- Modification of a ballisto-oscillograph for extremities
09 p1046 A73-22865
- Posture responses of upper limb muscles during electric stimulation of the vestibular apparatus
11 p1317 A73-26087
- Role of arterial and venous vessels of limbs in the process of cardiovascular reflex responses
18 p2277 A73-36578
- Human sensorimotor coordination following space flights.
22 p2814 A73-42170
- Climbing and cycling with additional weights on the extremities.
22 p2806 A73-42418
- LINE**
U CALCIUM OXIDES
LIMITATIONS
U CONSTRAINTS
LIMITER AMPLIFIERS
Phase-amplitude and amplitude characteristics of a regenerative parametric amplifier
08 p0948 A73-21555
- Computation of nonlinear distortions of a wideband amplifier in the vicinity of the overload point
14 p1737 A73-30896
- Output signal-to-noise ratio for a random-access repeater link with an ideal hard limiter.
15 p1844 A73-31733
- Uses of tunnel diodes for zero-transition discrimination in phasometric devices
23 p2959 A73-43477
- Zero-transition discrimination in phase-measuring devices with amplifier-limiters and tunnel diodes
23 p2959 A73-43478
- LIMITER CIRCUITS**
NT CLIPPER CIRCUITS
Application of the variational method in the analysis of a limiter based on a symmetrical strip line
01 p0026 A73-11264
- Designing limiter/detectors for ECM receivers.
02 p0143 A73-12569
- The performance of a noncoherent FSK receiver preceded by a bandpass limiter.
04 p0416 A73-14992
- Acquisition detectability parameter/output SNR/for unrestricted random access through ideal hard-limiter in multiple access communication systems
09 p1053 A73-23365
- Operating conditions of a triggered pulse generator with a limiter diode
10 p1195 A73-24380
- Book - Design performance and applications of microwave semiconductor control components.
20 p2535 A73-39136
- Protection of radiometers from pulse interference
21 p2705 A73-41463

- Suppression of equichannel interference in the case of binary phase shift keying employing a limiter
23 p2953 A73-43324
- LIMITS [MATHEMATICS]**
Reduction of a three-dimensional quasi-static problem of thermoelasticity for plates to a two-dimensional problem by a symbolic method and by the method of passing to the limit
02 p0235 A73-12194
- Limit analysis of structures with stochastic strength variations.
04 p0510 A73-15027
- The limiting theorems for certain functionals of multidimensional additive processes
05 p0591 A73-17226
- Evaluation of the convergence rate in an integral limit theorem
09 p1112 A73-22885
- Uniform estimate of the residual term in the multidimensional limiting theorem for homogeneous Markov chains on the basis of a class of all measured convex sets. II
10 p1242 A73-23814
- Field of attraction of a singularity of a nonlinear recurrence of the second order - Method of determination of the boundary
11 p1389 A73-25137
- Vectorial topological continuous function spaces bounded parts, constructing tunneled, quasi-tunneled and nontunneled spaces
11 p1390 A73-25865
- An algorithm for the computation of the higher order G-transformation.
13 p1649 A73-28601
- Duality of limit theorems for a structure of a standard rigid-plastic material
14 p1812 A73-30491
- Central limiting theorem in the 'noncommutative' probability theory
15 p1899 A73-31215
- Note on error bounds for numerical integration.
17 p2200 A73-34214
- Some nonoscillation theorems for a second order nonlinear differential equation.
20 p2581 A73-38976
- Rate of convergence of the distribution of the maximum of successive sums of independent variously distributed random vectors toward the limiting law
20 p2583 A73-39476
- LIMNOLOGY**
Carbon dioxide concentration, pH and nutrient concentration effects on blue-green algae relative abundance to green algae in lakes
06 p0655 A73-18577
- LINE SHAPE**
Synthetic spectra production via solution of radiative transfer equation at frequencies across absorption line for homogeneous and inhomogeneous atmospheres
01 p0097 A73-10362
- Neutral Mg line at 4571 Å in solar atmosphere, computing line profiles from Harvard-Smithsonian Reference Atmosphere and Bilderberg Continuum Atmosphere
03 p0377 A73-14405
- Carbon dioxide laser output signature calculation as function of cavity length based on homogeneously broadened line with dispersion
03 p0320 A73-14455
- Spectral line shape for interband light absorption with excitons formation in incompletely ordered semiconductor, taking into account interaction with random electrostatic field
04 p0483 A73-14879
- The influence of spatial temperature distribution and measuring configuration on line-reversal temperature.
05 p0602 A73-16563
- New laser technique for the identification of molecular transitions.
05 p0585 A73-16597
- Influence of lattice defects on EPR line-shapes in ruby.
06 p0734 A73-17794
- Solar Mn abundance derivation based on center-limb absorption line profiles, taking into account hyperfine structure broadening
10 p1278 A73-24130
- H emission line shape of plasma radiation under anisotropic electric microfields, calculating field distribution function, dispersion and frequency
10 p1254 A73-24191
- The Coude spectrum scanner at the Lowell Observatory.
11 p1360 A73-25069
- Formation of spectral lines in planetary atmospheres. V - Collision narrowed profiles of quadrupole lines in hydrogen atmospheres.
13 p1680 A73-28456
- Influence of a traveling acoustic wave on spectral line profiles. II - Asymmetry of weak Fraunhofer lines
13 p1683 A73-29092
- Apollo lunar fines ferromagnetic resonance spectral line shape anomaly and anisotropy energy attributed to Fe particles with body centered cubic structure
13 p1684 A73-29177

Determination of magnetic fields in a plasma from the contour of hydrogen spectral lines.

14 p1780 A73-30339

NMR measurements of the speed of vortices in flux flow in a type II superconductor.

14 p1783 A73-30433

Theory of satellite structures on spectral-line profiles.

15 p1915 A73-32289

Visible solar disk contrasts in radiation controlled line, noting role of lateral differences in local shapes of line absorption profile

16 p2059 A73-32951

Application of the Kubo-Mori theory to the line shape of plasma oscillations.

16 p2041 A73-33332

Lineshape of stable electrostatic fluctuations in a beam plasma system.

16 p2042 A73-33338

Quantum scattering theory of rotational relaxation and spectral line shapes in H₂-He gas mixtures.

17 p2119 A73-35175

Profiles of emission lines in Be stars. II - Interpretation of the long-period V/R variation.

19 p2484 A73-37615

H alpha line contrast profiles evaluation from solar chromosphere supergranulation observations, obtaining chromospheric fine structure characteristics

20 p2606 A73-39072

The inversion of the mean and spatially resolved sodium D2 line profiles from the sun.

22 p2908 A73-42311

Effect of line or band shape on the radiative flux of an isothermal spherical layer.

22 p2938 A73-42990

Line identification and profiles in emission spectra of Wolf-Rayet stars from microphotometer tracings at high dispersion, noting effects of companion stars

23 p3026 A73-43196

The shape of the cyclotron absorption line in a weakly ionized plasma

23 p3011 A73-43794

Neutral Fe line profiles for low-lying transitions measured from solar disk center to limb by double pass spectrometer, considering limb darkening effect

24 p3135 A73-44626

LINE SPECTRA

NT BALMER SERIES

NT D LINES

NT ELECTRONIC SPECTRA

NT FRAUNHOFER LINES

NT H ALPHA LINE

NT H BETA LINE

NT H GAMMA LINE

NT H LINES

NT K LINES

NT LYMAN SPECTRA

NT PASCHEN SERIES

NT RYDBERG SERIES

NT TELLURIC LINES

Flare spectrum in region accessible to ground based optical solar spectrographs, considering Balmer line broadening, electron density, optical thickness, LTE, electron temperature, etc

01 p0091 A73-10052

Preliminary report on the infrared spectrum of Nova Serpentes 1970.

01 p0095 A73-10269

The infrared spectrum of nitrogen excited by fast electrons.

01 p0036 A73-10338

Atmospheric windows in different spectral bands due to various gases, comparing continuum and line absorption spectra properties

01 p0037 A73-10364

Line-by-line computations of transmittance for non-homogeneous paths in designing application-oriented representations for water vapor and carbon dioxide channels IR spectral responses

01 p0037 A73-10365

Some features of the Leiden radial velocity instrument.

01 p0047 A73-10516

The spectrum of the compact galaxy IIZw43.

01 p0098 A73-10557

Spontaneous luminescence of ZnTe single crystals and mixed zinc cadmium telluride crystals at low temperatures, describing spectral lines

01 p0088 A73-10628

New mechanism for generating coherent emission from ionized oxygen and nitrogen in the visible region of the spectrum

01 p0059 A73-10630

Radiation transfer within spectral line in symmetric isothermal medium, assuming spherical incoherent scattering characteristic and scattering angle-independent redistribution law

01 p0100 A73-10705

Possibility of accelerating the matter of hot stars by absorption in spectral lines

01 p0100 A73-10706

CO₂ plasma emissivity at temperatures from 7000 to 9000 K in the spectral range of 2100 to 10,000 Å

01 p0085 A73-10854

A study of the spectrum-variable silicon Ap star 56 Ari.

01 p0106 A73-11305

Absorption line profile and equivalent line width derivation for planetary atmosphere with low and high optical thicknesses, assuming arbitrary scattering coefficients

01 p0106 A73-11321

Absorption line shape computerized functional analysis in solar physics, deriving H α /v function from Faddeyeva-Terentev probability

01 p0107 A73-11377

The empirical determination of line source functions, beta-L-values, and the microturbulent and convective velocity components as functions of depth in the photosphere-chromosphere transition region.

01 p0107 A73-11378

Temperature structure and conductive flux in the chromosphere-corona transition region.

01 p0107 A73-11380

Physical properties of solar chromospheric plages. I - Line profiles of the CaII H, K, and infrared triplet lines.

01 p0108 A73-11385

Evidence for two maxima of activity in the 20th solar cycle.

01 p0108 A73-11396

Radiant flux densities of Cygnus X-3, observing OH and formaldehyde absorption

02 p0210 A73-11560

Possibility of O III 304-Å emissions in the extreme ultraviolet airglow.

02 p0157 A73-11755

Book - Radiation transport in spectral lines.

02 p0194 A73-11876

Search for OH-IR stars with emission concentrated in main lines, considering water vapor line emission or absorption band in near IR

02 p0222 A73-12717

Diffuse interstellar lines and bands interpreted as extinction structure due to impurities in cosmic dust grains, comparing theory with observation

02 p0225 A73-12807

New ultraviolet line identifications for early-type stars.

02 p0226 A73-12831

Rocket-ultraviolet spectra of eight stars in Ophiuchus and Scorpius.

03 p0366 A73-12942

Fe ions optical transition lines in solar flares soft X ray spectra, noting continuum emission near 8 Å

03 p0367 A73-12945

4830 MHz observations of the formaldehyde molecule in the direction of discrete radio sources.

03 p0371 A73-13214

Two new He I lines in the spectra of B-type supergiants.

03 p0371 A73-13218

On the 4686-Å He II line intensity in H II regions and the cosmic ray flux.

03 p0361 A73-13220

Statistics on the solar spectrum suitable for the study of the blanketing effect in stars of spectral types F, G and K.

03 p0373 A73-13360

A-type supergiants - A list of line intensities and radial velocity measurements.

03 p0375 A73-13950

Mapping the solar corona in X-ray lines of O VII and Ne IX.

03 p0375 A73-13956

Laboratory-produced radiation related to the solar flare emission.

[AD-758606] 03 p0364 A73-13957

Solar rotation as measured in EUV chromospheric and coronal lines.

[AD-759854] 03 p0377 A73-14403

Neutral Mg line at 4571 Å in solar atmosphere, computing line profiles from Harvard-Smithsonian Reference Atmosphere and Bilderberg Continuum Atmosphere

03 p0377 A73-14405

Depth profiles of Fe I 5250 Å line for three sunspot models, noting line-to-continuous absorption ratio relation to emergent intensity location

03 p0377 A73-14410

Solar spectral line intensities in band 201 of visible and near IR regions, noting water vapor bands presence in sunspot spectra

03 p0377 A73-14412

Measurement of temperature by recording the absolute line intensity with apparent increase of plasma optical thickness.

03 p0348 A73-14439

CW neutral Ar laser line competition effect observation, establishing correct transition assignment

03 p0320 A73-14461

New infrared laser line in OCS and new method for C atom lasing.

03 p0320 A73-14465

Investigations of a Kr-Hg mixture regarding laser action

04 p0458 A73-14896

Correcting the OH contribution in emission line measurements in the night airglow filter photometry.

04 p0440 A73-14969

Molecular clouds in the galactic center region - Carbon monoxide observations at 2.6 millimeters.

04 p0499 A73-15357

Electron scattering effect on spectral line profiles from characteristic electron density estimates for astronomical objects with rapid radial matter outflow, using Monte Carlo method

04 p0499 A73-15362

Ultraviolet photometry from the orbiting astronomical observatory. V - The helium-weak stars.

04 p0499 A73-15363

H I clouds with spin temperatures less than 25 K. II - Physical properties of two neutral hydrogen clouds.

04 p0500 A73-15517

Line existence in H component magnetic power spectra of geomagnetic field LF components

04 p0445 A73-15552

Interstellar molecules detection, sources and destruction observed via visible, UV and radio wave spectra

04 p0501 A73-15627

One dimensional analysis of saturation spectral lines for energy transfer in plasma waves interaction, noting Landau damping effect on parametric instability

04 p0482 A73-15650

Astrophysical CO isotopic constituents from H II regions line emissions, determining relative abundances

04 p0502 A73-15688

Influence of a random magnetic field on the properties of stellar absorption lines.

04 p0503 A73-16011

Oxygen IS production efficiency of photons at 812-1216 Å measured by O I 5577 Å green line detection during carbon dioxide photodissociation

05 p0546 A73-16049

Possibility of emission-line polarization in diffuse nebulae with a C + E spectrum

05 p0617 A73-16462

Need of LS-dependent energy parameters in the second spectra of the fifth-group elements.

05 p0600 A73-16496

P II Zeeman effect spectral line observation for J-value assignments with check on wave functions obtained from energy level least squares fitting

05 p0600 A73-16497

Russian papers on phosphor crystal luminescence and nonlinear optics covering spectral line decomposition, GaAs laser and electromagnetic wave interaction

05 p0584 A73-16551

Four-field parametric frequency selection in stimulated emission lines from nonlinear mirror, noting reflection coefficient

05 p0584 A73-16554

O stars line spectra from high dispersion photographic spectrograms at 3059-6683 Å, tabulating absorption and emission lines identifications, equivalent widths and profiles

05 p0618 A73-16742

Solar Rb isotopic ratio from Rb I resonance lines at 7800 and 7947 Å in photospheric spectrum

05 p0620 A73-17026

On emission lines of hydrogen, helium and ionized calcium seen on a coronal spectrogram of the March 7, 1970 eclipse.

05 p0621 A73-17036

Solution of the transfer equation for interlocked multiplets by probabilistic method.

05 p0599 A73-17320

Ultraviolet photometry from the Orbiting Astronomical Observatory. VI - Magnesium II 2800 Å emission in cool stars.

05 p0625 A73-17336

Absorption lines in the spectrum of the quasar Ton 1530.

05 p0626 A73-17377

Search for coronal line emission from the Cygnus Loop.

05 p0626 A73-17380

Carbon monoxide Cameron bands limb intensity profile in Martian airglow from Mariner 9 UV spectrum observations

06 p0746 A73-17485

Hydrogen maser frequency stability dependence on signal output, magnetic polarization field and relaxation effects, describing automated relaxation rate measurement and atomic line spectrum registration

06 p0699 A73-17588

Absorption-line profiles in the quasi-stellar object PHL 957.

06 p0751 A73-18125

Interstellar medium chemical composition, considering emission line spectra, density fluctuations, He/H ratio in different galaxies and H II regions

06 p0752 A73-18233

General relativity in the equal proper time formalism.

06 p0724 A73-18626

Long-term variations of total and polarized fluxes, absolute energy distribution, and line strength of BL Lacertae and four quasi-stellar sources.

07 p0873 A73-19051

Interactions among multiple lines in the 8446-A atomic-oxygen laser. 07 p0834 A73-19336

Signal level fluctuations line spectra energy characteristics comparison for oblique and oblique-backscatter sounding, noting changes in harmonics intensity and period 07 p0792 A73-19438

Evidence of lunar surface oxidation processes - Electron spin resonance spectra of lunar materials and simulated lunar materials. 07 p0893 A73-19840

Limiting factors of plasma temperature measurement by spectral line reversal method 07 p0859 A73-20152

Population II variable stars shock waves detection via Balmer lines emission and metal line doubling, discussing model for numerical calculations of radiating shock structures 07 p0903 A73-20631

Solar gamma ray lines observed during the solar activity of August 2 to August 11, 1972. 08 p0996 A73-20665

Solar two-component atmospheric model for prediction of Ca II emission arches in spectrogram of strong lines near limb from kinetic equilibrium calculation 08 p1001 A73-20753

Measurements of the solar spectrum between 30 and 128 Å. [AD-757958] 08 p1002 A73-20760

The radial amplification profile of the 4880-Å ionic laser line and the distribution of the charge carriers in the wall-stabilized Ar low-pressure arc column 08 p0989 A73-20786

Variations in spectral-energy distributions and absorption-line strengths among elliptical galaxies. 08 p1002 A73-20878

Measurements on the infrared lines of planetary gases at low temperatures. I - Nu-3 fundamental of methane. 08 p1003 A73-20891

Spectroscopic observations of the Cygnus X-1 optical candidate. 08 p1003 A73-20895

Spectral variations of 53 Cam /AX Cam/. 08 p1006 A73-20931

Atmospheric abundances in the carbon star HD 156074. 08 p1006 A73-20935

Spectroscopic measurement of the source function as a test for deviations from local thermodynamic equilibrium /L.T.E./ in arc plasmas. 08 p0992 A73-21018

Temperature variations in coronal regions in the proximity of a prominence 08 p1007 A73-21067

X-ray electronic studies of metallic iron in the lunar regolith 08 p1008 A73-21134

Gamma-ray lines from an expanding supernova shell. 08 p1008 A73-21162

On the source of the 3840 Å persistent emission by meteors. 08 p1010 A73-21318

Discharge current dependence of saturation parameter of a He-Ne gas laser. 08 p0976 A73-21463

Problem of the selective mechanism for the excitation of the C III 5696-Å line in the spectra of certain stars. I 08 p1012 A73-21549

327-MHz observations of the galactic center - Possible detection of a deuterium absorption line. 08 p1013 A73-21808

A discussion of the new variations observed in the nucleus of the Seyfert galaxy NGC 3516. 09 p1140 A73-22004

The metallic-line star 15 UMa and the F 5 V star 5 And. 09 p1141 A73-22015

Image tube spectra of planetary nebulae for relative line intensities and radial velocities, considering nebulae properties 09 p1095 A73-22680

Fine structure of Pc 1 pulsations. I - Experimental evidence. 09 p1074 A73-22068

Effect of plasma inhomogeneity on the spectral-line profile and the reversal temperature 09 p1129 A73-22662

Generation spectra of a ruby laser with frequency scanning 09 p1095 A73-22680

Effect of a laser field on the gain line profile of an adjacent transition in an argon laser 09 p1096 A73-22968

Cerenkov shower spectrometer with a conical radiator made of TF-5 glass 09 p1085 A73-23002

Simultaneous diffusion of photons and particles in a semiinfinite space. I - Distribution of excited atoms in a semiinfinite space 09 p1123 A73-23068

Infrared and microwave emission from nebulae in the galaxy. 09 p1150 A73-23133

Spectroscopy of tetrabenzoporphin molecules and possible astrophysical implications. 09 p1048 A73-23136

Characteristics of the diffuse /tenuous/ interstellar medium determined from radio recombination lines. 09 p1150 A73-23137

Interstellar organic molecules millimeter wave line spectra and transition rotational quantum numbers 09 p1150 A73-23141

A non-LTE study of silicon line formation in early-type main-sequence atmospheres. 10 p1272 A73-23532

Intermediate-coupling line strengths in the iron spectrum and the solar abundance of iron. 10 p1272 A73-23540

Interstellar Na I, K I, Ca II, and CH⁺/ line profiles toward zeta Ophiuchi. 10 p1273 A73-23549

Quasi-periodic /wave/ motions in the solar photosphere. I - Preliminary results 10 p1274 A73-23718

On the nature of X Persei - Evidence from the 1957 outburst. 10 p1275 A73-23845

Further observations of the solar limb spectrum in the region 550-2000 Å. 10 p1278 A73-24128

High resolution spectroscopic analysis for photospheric Eu II lines with spectrum synthesis techniques, determining solar isotopic composition and abundance 10 p1278 A73-24129

Suggested interpretation of the correlations in intensity fluctuations in the lines Ca II H and K, magnesium b, and hydrogen H beta /Research note/. 10 p1278 A73-24132

Isotopic combination identification in interstellar clouds through radio spectral line observations, discussing millimeter wave astronomy, molecular clouds, excitation mechanisms, galactic structure, etc 10 p1280 A73-24323

Experimental study of the relaxation of excited states in a decaying alkaline plasma 10 p1256 A73-24576

Ultraviolet luminescence and nonlinear extinction in ruby 10 p1260 A73-24579

Paramagnetic resonance line broadening in ferrite garnets with small additions of rare-earth elements 10 p1261 A73-24703

Excitation of oxygen permitted line emissions in the tropical nightglow. 10 p1214 A73-24739

Spectral observations of southern planetary nebulae. I. 11 p1415 A73-25070

Spectrophotometric investigation of the star alpha-2 CVn. II 11 p1416 A73-25232

Investigation of the relationship between 'edge' and exciton emission in CdS single crystals 11 p1408 A73-25246

Water vapor lines controlled atmospheric absorption spectrum in 220 GHz window region, discussing approximate calculation for submillimeter lines residual effect 11 p1330 A73-25688

Extreme ultraviolet line intensities from the sun. 11 p1425 A73-26201

Kinematics of the Huyghenian region of the Orion Nebula. 11 p1427 A73-26605

Polarization measurements in the green coronal line. 11 p1428 A73-26623

Polarization of the emission from the solar corona in the 5303 Å line 12 p1538 A73-26859

Seasonal and diurnal variations of forbidden oxygen and sodium lines emission, stressing nightglow zenith intensity fluctuations connection to F layer electric fields 12 p1489 A73-26992

Single-frequency neodymium-glass lasers under nonspiking free-oscillation and Q-switched conditions. 12 p1506 A73-27502

Separation of rotational lines of a CO₂ laser with a film selector in the resonator. 12 p1508 A73-27527

Solar pole-equator temperature distribution in high photosphere layers from Mg spectral line observations 12 p1544 A73-27832

Fine bright umbral spot structures from photographic line spectra observation of sunspot, noting magnetic field strength, outflow velocity and photospheric temperature 12 p1545 A73-27834

The radiative capacity of a CO₂ plasma at temperatures 7000-9000 K in the spectral interval 2100-10,000 Å. 12 p1529 A73-27904

Large sunspot high dispersion line spectrum at 6610-6770 Å, noting umbral/photospheric contrast and drift curves across limb from photographic recording 12 p1547 A73-27925

The position of the emission lines of some lasers in the absorption spectrum of the earth's atmosphere. 13 p1626 A73-28174

Formation of spectral lines and study of growth curves in a semiinfinite scattering atmosphere 13 p1680 A73-28458

Conditions of Cr IX and Fe XI luminescence in the corona 13 p1683 A73-29094

Spectrophotometry of prominences in the decay-preceding phase 13 p1670 A73-29095

Fe XVII emission from the solar corona. 13 p1685 A73-29356

Coronal densities and temperatures derived from monochromatic images in the red and green lines. 13 p1685 A73-29364

LTE and hydrogen and ionized He lines approximations for model atmosphere computations of hot early stars, discussing UV line blanketing 13 p1686 A73-29367

On the observability of far infrared line emission originating from the interstellar medium. 13 p1686 A73-29368

Ground-based measurement of millimeter-wavelength emission by upper stratospheric O₂. 14 p1751 A73-29718

Neutral hydrogen distribution in the upper atmosphere of the earth 14 p1747 A73-29871

Transition probabilities of neutral and singly ionized germanium. 14 p1783 A73-30243

Gas absorption lines detection based on multiple light passage through absorbing medium during generation process, noting radiation spectra of neodymium glass laser 14 p1757 A73-30331

Spectrophotometric results from the Copernicus satellite. III - Ionization and composition of the intercloud medium. 14 p1801 A73-30746

Aperture synthesis study of neutral hydrogen in NGC 2403 and NGC 4236. I - Observations. 15 p1929 A73-31056

The extreme-ultraviolet spectrum of a solar active region. 15 p1936 A73-31560

Metallic lines in the solar flare of July 12, 1961 and properties of the corresponding emission regions 15 p1938 A73-31957

Determination of damping constants and turbulent speed in the solar photosphere by the Voigt method 15 p1938 A73-31958

Device for spectral line interspace measurements 15 p1878 A73-32145

Quasi-monochromatic measurements of homogeneous arc plasmas. 15 p1841 A73-32393

The large-scale velocity field, the magnetic fields, and the brightness of the solar atmosphere 16 p2057 A73-32701

Velocity field in the active regions of the sun 16 p2057 A73-32702

Spectrographic investigation of the flare star YZ CMi in January 1969 16 p2057 A73-32709

Line blanketing theory tested via G-I index, discussing underestimation of extreme subward effective temperatures 16 p2058 A73-32834

Application of the Kubo-Mori theory to the line shape of plasma oscillations. 16 p2041 A73-33332

Concentration of OH and NO in YJ93-GE-3 engine exhausts measured in situ by narrow-line UV absorption. [AIAA PAPER 73-506] 16 p2045 A73-33546

Tunable-laser derivative spectroscopy on spectral lines with combined Doppler and collision broadening. 16 p2039 A73-33741

Equivalent widths of the oxygen A-band absorption lines at different pressures 16 p2039 A73-33815

Photometric investigation of the 4278 Å and 5577 Å emissions in aurora. 16 p2010 A73-33918

Theory of optical polarization measurements of the turbulence spectrum in a plasma 17 p2216 A73-34627

CO laser emission lines attenuation measurements in atmosphere, attributing inconsistencies in previous experiments to model 17 p2185 A73-35405

Stability, reproducibility, and absolute wavelength of a 633-nm He-Ne laser stabilized to an iodine hyperfine component. 17 p2185 A73-35424

Interstellar absorption lines observed with the orbiting spectrophotometer S59. 18 p2349 A73-35993

- Investigation of the solar X-ray flare spectra by the 'Intercoms-4' and 'Intercoms-7' satellites. 18 p2345 A73-36015
- Quasiperiodic/wavelike/ motions in the solar photosphere. I - Preliminary results. 18 p2355 A73-36743
- The spectrum of eta canis majoris, B5 Ia. 18 p2355 A73-36779
- Temperature variations of coronal regions near a solar prominence. 18 p2355 A73-36868
- Early type stellar line spectra, discussing LTE, hydrogen and helium lines, stellar element abundance and O and B stars 18 p2356 A73-36875
- The He I lambda 5876 line in O-star spectra. 18 p2356 A73-36973
- Studies of beta Coronae Borealis. I - Identification of the Actinides. 18 p2357 A73-37105
- Bragg spectroscopy of Scorpius X-1 in search of the Fe XXV emission lines. 19 p2485 A73-37627
- Theory of two-channel laser action in spectrally inhomogeneous media. I - Noncorrelated frequencies 19 p2437 A73-37958
- Lines of Fe XVII and Fe XVIII during a solar flare. 19 p2476 A73-38170
- Single-line operation of a 2-W longitudinal cw CO chemical laser with no frequency-selective element in the optical cavity. 19 p2439 A73-38475
- Optical and near IR absorption line spectra of quasar 1331+170, discussing red shift and line locking process 19 p2487 A73-38508
- Oscillator strength calculations for vibrational transitions of X-A electronic system of interstellar CH positive ion, noting agreement with astrophysical observations of line spectra 19 p2488 A73-38512
- Search for solar recombination lines in the frequency range 110-115 GHz. 19 p2488 A73-38521
- Solar magnetic field spatial structure in relation to solar activity phenomena, discussing measurements based on Zeeman effect in absorption line spectra formation 20 p2605 A73-39059
- OH observations of sixteen interstellar dust clouds. 20 p2607 A73-39118
- Experimental results concerning the time decay of the line emission in luminescent plasmas of medium-pressure inert-gas discharges 20 p2596 A73-39191
- Coude spectroscopy for quasar Markarian 132 absorption lines wavelengths and profiles and red shift systems 20 p2609 A73-39436
- Detection of a gamma-ray spectral line from the galactic-center region. 20 p2602 A73-39438
- X-ray spectrum of Cassiopeia A - Evidence for iron line emission. 20 p2603 A73-39446
- Photoelectric plasma arc measurements of Si I oscillator line intensities in 2500-8000 A range, relating with transition probabilities 20 p2595 A73-39590
- Stark broadening of high quantum number delta n = 1 transitions of carbon V and VI in a laser-produced plasma. 21 p2745 A73-40471
- Absorption line contours in homogeneous plane-parallel semiinfinite aerosol layers and planetary atmosphere overcloud gas layers for nonspherical scattering 21 p2768 A73-40723
- Far IR laser lines measurements in carbon dioxide laser pumped ethylene glycol, dimethyl ether, formic acid, and monomethyl amine, using grating spectrometer and Golyay-cell detector 21 p2715 A73-40765
- Observations of ultraviolet stellar spectra by the Utrecht Orbiting Stellar Spectrophotometer S59. 21 p2769 A73-40811
- Line identifications in the near ultraviolet spectrum of the peculiar A star epsilon Ursae Majoris. 21 p2769 A73-40829
- Computer checking of rotational line intensity factors for diatomic transitions. 21 p2744 A73-41212
- Ultraviolet stellar spectra obtained with the Utrecht orbiting stellar spectrophotometer S 59 aboard the ESO TD-1 A satellite. 21 p2773 A73-41395
- The formation of Mg I 4571 A in the solar atmosphere. III - The Holweger solar model/Research note/. 21 p2777 A73-41480
- Microturbulence and the effect of departures from LTE on photospheric iron lines. 21 p2777 A73-41481
- Carbon, CN, CH, MgH, NH and OH line behavior in solar photospheric spectra 21 p2778 A73-41528
- Stellar chromospheric velocity fields and the width luminosity relations. 21 p2779 A73-41540
- Comment on 'Anomalous hyperfine lines in formaldehyde in a dust cloud.' 22 p2904 A73-41755
- Chromospheric hydrogen and helium spectral lines investigation in solar flares determining plasma and ionization temperatures, energy spectra and electron density 22 p2903 A73-42066
- Accurate wavelengths of stellar and telluric absorption lines near lambda 7000 A. 22 p2907 A73-42208
- Pitfalls of configuration interaction - Transition probabilities in Fe XIII. 22 p2908 A73-42312
- Measurement of the natural linewidth of a traveling wave neon-helium laser in the 0.63-micron range 22 p2870 A73-42411
- Doublet ratio method for abundance determination application to interstellar multiple clouds, considering column density error due to velocity distribution simplification 22 p2910 A73-42703
- Observation of 9.0-micron line emission from Ar III in NGC 7027 and NGC 6572. 22 p2910 A73-42704
- Line intensities of CO2 in the 2.0 micron region. 22 p2890 A73-42708
- Effect of line or band shape on the radiative flux of an isothermal spherical layer. 22 p2938 A73-42990
- Some statistical characteristics of active regions with the yellow coronal line. 22 p2915 A73-43037
- Line identification and profiles in emission spectra of Wolf-Rayet stars from microphotometer tracings at high dispersion, noting effects of companion stars 23 p3026 A73-43196
- O, Of, Oe and Wolf-Rayet star comparison in terms of emission and absorption line spectra, noting relationship to evolutionary status on H-R diagram 23 p3026 A73-43197
- Planetary nebulae nuclei emission line spectral features similarity to spectra of Population I Wolf-Rayet and O-type stars 23 p3026 A73-43199
- Spectral line radio astronomy observations of interstellar molecular clouds in Galaxy, relating to stellar and life evolution 23 p3028 A73-43350
- Spectral-line analysis of very-long-baseline interferometric data. 23 p2980 A73-43357
- FORTH computer program for National Radio Astronomy Observatory telescope observed millimeter wave spectral line data reduction, summarizing language capabilities 23 p2956 A73-43380
- Measurement of turbulent HF fields in a high-current rectilinear gas discharge from the intensity of forbidden HeI lines 23 p3011 A73-43669
- The solar coronal green line as an index of cosmic ray modulation. 23 p3024 A73-43683
- Radiation transfer equations for atomic spectra lines in stellar magnetic field, allowing for nonequilibrium population of atomic ground state and excited atom-particle collisions 23 p3036 A73-44242
- Temperature and oxygen abundance determination in the sun from the oxygen lines 23 p3037 A73-44257
- Optical characteristics of phononless lines 24 p3109 A73-44427
- Metal lines in the solar flare of July 12, 1961, and the properties of the emission region. 24 p3132 A73-44482
- Damping constants and turbulence velocities in the solar photosphere determined by the Voigt method. 24 p3132 A73-44483
- Methane absorption in the Jovian atmosphere. II - Absorption line formation. 24 p3133 A73-44559
- Solar abundance of Th and Pb based on photospheric line spectrum analysis for comparison with chondritic composition data 24 p3135 A73-44627
- Solar coronal Fe XIII 10747 A emission line resonance polarization observations during 12 November 1966 eclipse, discussing magnetic field effects 24 p3135 A73-44633
- Solar Fe 13 coronal lines relative intensity calculation as function of electron density from cross sections for collisional excitation by protons 24 p3136 A73-44635
- Spatial relationship between 5303-A and H alpha components of a loop prominence system. 24 p3123 A73-44640
- Plasma temperature measurement by a spectroscopic technique with continuous automatic recording 24 p3115 A73-44757
- Electron transitions in interstellar dust 4430 A line, indicating ferric oxide /alpha-hematite/ in type I supernovae 24 p3138 A73-44990
- The formation of resonance lines in multidimensional media. II - Radiation operators and their numerical representation. 24 p3113 A73-45041
- The formation of resonance lines in multidimensional media. III Interpolation functions, accuracy, and stability. 24 p3138 A73-45042
- Type I and II supernovae spectra, identifying different lines and obtaining energy distributions 24 p3138 A73-45043
- H2 pressure-induced lines in the spectra of the major planets. 24 p3138 A73-45050
- An expanded theoretical interpretation of the Venus 1.05-micron CO2 line and the Venus 0.8226-micron H2O line. 24 p3139 A73-45052
- Secular variations in H alpha, H beta and metal line spectra of Be star 88 Hercules from intensity decrease observations, noting envelope hydrogen absorption lines visibility 24 p3140 A73-45187
- Line strength measurements of the 2 nu sub 3 band of methane. 24 p3066 A73-45320
- Strengths and air-broadened widths of H2O lines in the 2950 to 3400 per cm region. 24 p3066 A73-45322
- Spectral data for the nu sub 2 bands of ammonia with applications to radiative transfer in the atmosphere of Jupiter. 24 p3142 A73-45324
- LINEAMENT**
- U STRUCTURAL PROPERTIES [GEOLOGY]**
- LINEAR ACCELERATORS**
- A linear accelerator for simulated micrometers. 17 p2145 A73-34274
- Slit electronic camera with scanned memory used in high speed cineradiography 21 p2694 A73-39942
- LINEAR AMPLIFIERS**
- Calculation of the y-parameters of an integrated-circuit amplifier by reducing the matrix of an n-terminal network to the matrix of a two terminal pair network 11 p1338 A73-26102
- LINEAR ARRAYS**
- NT YAGI ANTENNAS**
- Effects of cross-coupling and of the edge effect on the characteristics of linear phased antenna arrays 02 p0146 A73-12021
- Sidelobe reduction for linear arrays with elements sampled from equally spaced arrays, using Fourier coefficients of sampling functions 03 p0274 A73-12998
- Linear array antenna radiation pattern synthesis for minimum sidelobe level outside of given intervals, calculating current distribution 03 p0278 A73-14060
- Satellite-borne solid state multispectral image remote sensors with photodiode linear arrays for data acquisition, noting system performance and reliability advantages 04 p0451 A73-15781
- Threshold value of the input impedance of a propagating-wave fed, long radiator series 05 p0559 A73-17240
- Iterative least-squares synthesis of nonuniformly spaced linear arrays. 06 p0666 A73-18194
- Radiation patterns of linear equidistant fishbone-type dipole antenna array fed by long symmetrical transmission line 06 p0677 A73-18392
- Pattern synthesis for rectangular and hexagonal planar arrays with triangular elements arrangement 08 p0945 A73-20806
- Synthesis of a traveling wave antenna 08 p0946 A73-21103
- Wideband squintless linear arrays. 10 p1192 A73-23605
- Adaptive control for correction of flexible linear array phase error with resistance strain gages and ferrite phase shifter, noting radiation pattern performance 11 p1332 A73-26283
- The significance of the elementary radiator directivity for the determination of the directive gain of linear arrays 12 p1468 A73-27039
- Reconstruction of an antenna radiation pattern from field values available within a limited sector of angles in the Fresnel region 12 p1479 A73-27227
- Algorithm for choosing the optimal disposition of radiating elements in a linear antenna array by the method of coordinate trials 12 p1479 A73-27232
- Analysis of correlation functions of space-time wideband signals received by linear antennas. 13 p1591 A73-28657

The application of Gegenbauer polynomials to antenna array synthesis. 14 p1725 A73-29747

Mutual coupling effects in semi-infinite arrays. 14 p1734 A73-30202

On linear parasitic array of dipoles with reactive loading. 14 p1734 A73-30203

Matrix analysis of linear antenna arrays of equally spaced elements. 14 p1735 A73-30226

On the scattering cross section of passive linear arrays. 14 p1735 A73-30229

Experimental investigations of coupling phenomena in a periodic linear antenna array 14 p1729 A73-30697

Concept of phase centre of an array applied to elevation-angle measurements. 15 p1842 A73-31098

Compatible ILS involving pilot signal from microwave oscillator and precision ILS involving linear antenna array of emitter elements 17 p2207 A73-34484

Coherent optical processing of linear phased array radar signals. 17 p2132 A73-35649

Linear phased array antenna focused in Fresnel region, noting radiation pattern indoor measurement simplicity advantage over far field observation in performance monitoring 17 p2128 A73-35694

Dependence of sidelobe level on random phase error in a linear array antenna. 17 p2129 A73-35697

Analysis of the characteristics of radiating elements in antenna arrays on the basis of laws describing cross-coupling variations 21 p2661 A73-40195

Frequency dependence of radiation-pattern orientation in phased-array antennas 21 p2661 A73-40196

Numerical solution of edge effects of external coupling between elements in linear phased array of slots covered by dielectric slab, using scattering matrix 21 p2651 A73-40654

Transient frequency response analysis and far field measurement of linear phased array with tandem series feed network, noting instantaneous bandwidth 21 p2653 A73-40673

Near fields of wire antennas by matrix methods. 22 p2830 A73-41827

Circularly polarized linear waveguide array. 22 p2831 A73-41843

Modification of antenna radiating characteristics with multi-impedance loading. 22 p2831 A73-41848

Calculation of the early time radiated electric field from a linear antenna with a finite source gap. 22 p2832 A73-41856

Linear array radio telescope for large aperture synthesis by using earth rotation to change relative orientation to radio source, discussing design and performance 23 p3028 A73-43352

The effect of interaction of array elements with arbitrary amplitude distribution on the radiation pattern. 24 p3068 A73-44942

LINEAR CIRCUITS

Integral Laplace-Fourier transform stability during transient response functions reconstruction from transfer function frequency characteristics in linear circuits 05 p0591 A73-16779

Time optimal control for vibrationless starting of electromechanical devices with moving parts, noting linear magnetic circuit 06 p0649 A73-18383

Construction of analytical formulas for functions of linear circuits by means of engineering-application digital computers 08 p0941 A73-21552

Initial circuit equation transformation into equation of variable states, noting linear and nonlinear circuits in static and dynamic regimes 09 p1068 A73-22452

A linear voltage-tunable distributed null device. 09 p1066 A73-23246

Canonical form of hybrid matrix for linear multipole network circuit, discussing synthesis and analysis 10 p1195 A73-24378

Resonant bipolar linear networks representation by matched equivalent circuits 13 p1589 A73-28121

Spectral analysis of a physical system which can be represented by a stationary linear active electronic network 13 p1589 A73-28474

Differential equations for digital model of linear quadrupole, discussing digital simulation of analog radio equipment circuits 13 p1591 A73-28659

Shaping circuit for complex RF pulse consisting of simultaneous equilength square pulses with different frequencies, discussing carrier frequencies selection 13 p1583 A73-28730

Signal interference and improvement of signal-to-noise ratios in a half-wave linear detector. 15 p1843 A73-31729

Linear theory of an IMPATT diode distributed microwave amplifier. 16 p1991 A73-33983

LINEAR EQUATIONS

Electronic computer design and programming for solving high order linear equations, using matrix determinants and graph trees in letter symbols 01 p0019 A73-10033

Asymptotic properties of solutions of certain linear systems of differential equations with random coefficients 01 p0070 A73-10913

Solutions and stability of a system of two first-order linear differential equations with variable coefficients 01 p0070 A73-10914

Doubly relaxed matrix inverse for linear equations system solution with inadequately conditioned coefficient matrices, noting algorithm for improved conditioning 01 p0071 A73-11279

Second-order abstract and Schroedinger linear differential equations in Beurling spaces 02 p0186 A73-11570

Linear MHD equations for inviscid medium under external forces, discussing magnetoacoustic wave generation by radially pulsating cylinder and sphere 02 p0196 A73-11605

Linear equations for steady wave diffraction and propagation in deformable bodies in multiply connected regions, considering circular cylinders, spherical cavities and fibrous media 02 p0232 A73-11889

Construction of solutions and the application of the joining method to the solution of the Liapunov stability problem for a system of linear homogeneous differential equations with pi-periodic coefficients 02 p0193 A73-12189

Asymptotic estimates for solutions of linear systems of ordinary differential equations having multiple characteristic roots. 02 p0188 A73-12625

Linear integral equation, wave function and parameter optimization for numerical analysis of remote sensing problem 03 p0337 A73-14488

Integral representation of positive solutions of linear elliptic and parabolic differential equations with constant coefficients 04 p0470 A73-14898

The solution of linear, constant-coefficient, ordinary differential equations with APL. 04 p0470 A73-15008

Hypermatrix solution of large sets of symmetric positive-definite linear equations. 04 p0470 A73-15009

Quasi-linear equations for uniform plasma instabilities connected with potential oscillations, noting non-relativistic electron beam relaxation and abnormal plasma resistance 04 p0477 A73-15017

Certain analytical solutions of the Cauchy problem for a disturbed loaded linear integrodifferential equation 04 p0470 A73-15080

Asymptotic waves and Cauchy problem with singular data for a system of linear equations with a double characteristic 04 p0471 A73-15245

On the stability of linear stochastic differential equations. [ASME PAPER 72-WA/APM-16] 04 p0472 A73-15898

Instability of the exponential discreteness characteristic of solutions to a system of differential equations, and the asymmetry of the near-reducibility ratio of a system of differential equations with an integral discreteness of solutions 05 p0590 A73-16335

Modification methods for inverting matrices and solving systems of linear algebraic equations. 05 p0590 A73-16373

Monotonicity and iterative approximations involving rectangular matrices. 05 p0590 A73-16374

Elimination on sparse symmetric systems of a special structure. 05 p0590 A73-16500

A solution of the bilinear matrix equation $AY + YB$ equals -Q. [DFVLR-SONDDR-274] 05 p0591 A73-16607

On forced vibrations in the linear theory of micropolar elasticity. 06 p0762 A73-17987

Iterative methods for best approximate solutions of linear integral equations of the first and second kinds. 06 p0717 A73-18170

High-frequency sound waves to eliminate a horizon in the mixmaster universe. 06 p0724 A73-18550

Topological equivalence of linear systems of Pfaff equations in the neighborhoods of their one-dimensional closed characteristics 06 p0718 A73-18677

Discontinuities propagation in quasi-linear hyperbolic partial differential equation systems, noting MHD flow and crystal optics equations 07 p0850 A73-19016

Construction of exact solutions to certain systems of linear and nonlinear Volterra integral equations by using a power series 07 p0844 A73-19129

Singular integrodifferential and linear integral equations for load transfer from stringer to wedge under concentrated force and for stringer-coupled wedge shaped regions 07 p0910 A73-19306

A direct method for solving Poisson's equation. 07 p0845 A73-19574

Lower bound estimates of solutions to a second boundary-value problem for a second-order parabolic equation in regions with unrestricted spatial variables. 07 p0845 A73-19655

An efficient parallel algorithm for the solution of a tridiagonal linear system of equations. 08 p0983 A73-20960

Application of the regularization principle to the construction of approximate solutions to inverse heat-conduction problems 08 p1022 A73-21097

Investigation of the motion of the medium near the point of contact of shock waves in linear and nonlinear formulations 09 p1070 A73-21921

Nonoscillation of second-order, linear differential equations with retarded argument. 09 p1112 A73-22420

Linear dependence of functions along the solutions of systems of differential equations and of a system with algebraic loci 10 p1241 A73-23743

Solution of fundamental three-dimensional problems in the theory of elasticity for arbitrarily shaped bodies by way of a numerical realization of the method of integral equations 11 p1441 A73-25627

Calculation of functionals of the eigenfunctions in the boundary value problem of a system of linear ordinary differential equations 11 p1391 A73-26331

Analytical properties of solutions to linear differential equations and systems 12 p1516 A73-26951

Solution in Dirichlet series to a system of linear partial differential equations 12 p1518 A73-27223

Spline representation by finite functions 12 p1518 A73-27238

Integral estimates of the derivatives of solutions of elliptic homogeneous linear equations of arbitrary order with variable coefficients in the metric L_p , p ranging between 1 and infinity, and some of their applications 12 p1519 A73-27819

A method for obtaining bounds on eigenvalues and eigenfunctions by solving non-homogeneous integral equations. 13 p1647 A73-28192

Two-sided difference methods of solving linear boundary value problems for ordinary differential equations 13 p1647 A73-28341

Nonoscillation and disconjugacy of systems of linear differential equations. 13 p1648 A73-28441

Linear aerodynamic model incorporating torsional oscillations about two dimensional airfoil midchord for stall flutter description 13 p1697 A73-28814

A quadrature-iterative method of solving linear and nonlinear integral equations 13 p1651 A73-29679

Solution of linear equations in remote sensing and picture reconstruction. 14 p1767 A73-29767

A posteriori estimates of error distribution laws in the solution of linear algebraic equations by analog techniques 14 p1768 A73-30032

Accuracy estimates for analog computer solutions to systems of ordinary linear equations and some algebraic equations 14 p1768 A73-30033

Method of reducing the order of a differential equation when studying transient processes in mechanical systems 14 p1774 A73-30286

Stress determination approximation in structural mechanics problems by linear first order differential equations reduction to linear algebraic equations 14 p1810 A73-30378

An existence theorem for linear boundary value problems. 14 p1770 A73-30524

Asymptotic stability and perturbations for linear Volterra integrodifferential systems. 14 p1770 A73-30757

Extension of the Favard theory to the case of a system of linear differential equations with unbounded coefficients which are nearly periodic according to Levin. 14 p1771 A73-30837

Asymptotic solution of a system of linear differential equations with slowly varying coefficients in a complex domain. 15 p1898 A73-31028

Asymptotic solution of a system of linear differential equations with slowly varying coefficients of the neutral type. 15 p1898 A73-31036

Synthesis of optimal discrete control systems with persisting perturbations. 15 p1854 A73-31803

Book - Two-point boundary value problems: Shooting methods. 15 p1901 A73-32299

Book - Mathematical programming and the numerical solution of linear equations. 15 p1901 A73-32300

Singularities of solutions to linear, second order, analytic elliptic equations in two independent variables. II - The piecewise regular boundary. 15 p1901 A73-32374

Sturm comparison and separation theorems for linear, second order, self-adjoint, ordinary, differential equations and for first order systems. 15 p1902 A73-32377

Solutions of a class of random differential equations. 16 p2032 A73-33308

Regularity theorems for the solution of a second-order abstract linear differential equation. 16 p2032 A73-33373

On the solution of large systems of linear algebraic equations with sparse, positive definite matrices. 17 p2199 A73-34104

An error analysis of a method for solving matrix equations. 17 p2200 A73-34216

Uniqueness theorems for infinite systems of linear equations. 17 p2201 A73-34631

Russian book - Linear and nonlinear boundary value problems. 17 p2201 A73-34640

Inconsistencies and S.O.R. convergence for the discrete Neumann problem. 17 p2202 A73-35519

Computer program for solution of large, sparse, unsymmetric systems of linear equations. 17 p2132 A73-35603

A computer program to find analytical solutions of second order linear differential equations. 17 p2132 A73-35611

On the convergence of two-stage iterative processes for solving linear equations. 17 p2203 A73-35726

Convergence of matrix iterations subject to diagonal dominance. 17 p2203 A73-35727

Russian book on linear differential delay equations covering solvability theorems, solution properties, stable and unstable equations, first and second order equations, periodic equations, etc. 18 p2329 A73-35897

Russian book - Linear differential equations with periodic coefficients and their applications. 18 p2329 A73-35903

A note on uniqueness in the linear theory of heat conduction with finite wave speeds. 18 p2371 A73-36692

Yielding and failure of metals in a complex state of stress. 18 p2366 A73-36756

Numerical solutions of basic three-dimensional elasticity theory problems for bodies of arbitrary shape. 19 p2500 A73-38149

Investigation of the stability of solutions to a quasi-stationary system of linear differential equations with quasi-periodic coefficients. 20 p2581 A73-38987

Nonoscillation and oscillation of a linear differential equation of the n-th order. 20 p2582 A73-39318

Boundary value problems for linear generalized differential equations and their adjoints. 20 p2582 A73-39402

A geometric solvability characteristic for some boundary value problems of linear elliptic-type equations and strongly elliptic second-order systems. 20 p2583 A73-39498

Mixed finite-difference scheme for a class of linear and nonlinear structural mechanics problems. 20 p2621 A73-39544

Deviation of the solution of a quasi-linear wave equation from the solution of the linear equation in the region of continuous first derivatives. 21 p2724 A73-40181

Small oscillations of a heavy solid body about a stationary point and certain cases of the existence of 'linear integrals'. 21 p2738 A73-40188

A finite algorithm for the minimum l-infinity solution to a system of consistent linear equations. 21 p2725 A73-40376

A finite step algorithm for determining the 'strict' Chebyshev solution to $Ax = b$. 21 p2725 A73-40381

Integration of certain ordinary differential equations based on the approximation of continuous functions by linear functions. 21 p2727 A73-41063

The solution and stability of a system of two first-order linear ordinary differential equations with variable coefficients. 21 p2727 A73-41066

Asymptotic properties of solutions to single-point and two-point problems with singular perturbations for systems of ordinary linear differential equations. 22 p2882 A73-42473

Computerized analysis using sparse matrices/matrices with large number of zero elements/describing sorting, reordering and inverse computing techniques and linear equations solution methods. 22 p2922 A73-42480

A method for numerically solving second-order non-homogeneous linear differential equations with variable coefficients. 22 p2882 A73-42482

Solving linear boundary value problems by approximating the coefficients. 22 p2882 A73-42519

An optimality condition for assessing systematic errors. 23 p2999 A73-43264

Piecewise linear law of the relation between stresses and strains for large deformations. 23 p3043 A73-43920

Liapunov-like behavior and separation of solutions to nonlinear and linear differential equations. 23 p3000 A73-44204

Synthesis of optimal sampled-data control systems in the presence of continuous disturbances. 23 p2965 A73-44332

A maximum principle and gradient bounds for linear elliptic equations. 24 p3105 A73-44421

Asymptotic solutions of second-order linear homogeneous differential equations in a Banach space in the case of a higher derivative having a small parameter. 24 p3105 A73-44603

Nonlinear difference schemes for linear partial differential equations. 24 p3106 A73-45332

Stability and small parameter perturbations of a critical neutral functional differential equation. 24 p3106 A73-45336

Solutions of boundary value problems with integral conditions for linear ordinary differential equations by the method of decomposition. 24 p3106 A73-45351

Optimal convergence of iterative solution for system of linear equations with real roots based on matrix method. 24 p3106 A73-45441

LINEAR FILTERS

NT KALMAN FILTERS

Variational methods for linear numerical filtering with operator and transfer function spreads compromise, presenting graphical data [ONERA, TP NO. 1127]. 01 p0070 A73-10236

Pontryagin maximum principle application to optimal linear filtration for multivariable systems with signal processing. 03 p0286 A73-14082

Minimum variance linear filter with partial state elimination by linear transformation for reduction of computational burden and storage requirements in Kalman filter. 04 p0431 A73-15268

Nonlinear estimation theory applied to the interplanetary orbit determination problem. 04 p0498 A73-15271

Narrow band linear filter output SNR relationship to orthogonal radiating elements system directional gain and radiation patterns. 05 p0555 A73-16056

Noisy data filtering of linear steady state control problems based on nearest neighbor interaction, discussing dimensionality reduction model for saving computer time. 06 p0682 A73-18868

Limits of suitability of pseudorandom signals for statistical tests. 08 p0938 A73-20835

Theoretical fundamentals of constructing parametric filters equivalent to linear filters. 09 p1063 A73-22451

Best approximation in digital filtering. 10 p1242 A73-23764

Estimation theory and system state and parameter identification, developing algorithms for optimum linear sequential and nonlinear filters. 10 p1200 A73-24051

A representation of uncorrelated random processes by stochastic integrals. 11 p1340 A73-25010

Construction of discrete shaping filters for the digital simulation of linear Markov processes. 11 p1340 A73-25011

Linear regression filtering and prediction for tracking maneuvering aircraft targets. 11 p1333 A73-26640

Amplitude-modulated pulse code sequence demodulation using physically realizable linear filter for reconstruction of discrete sample message at optimum mean-square error level. 12 p1467 A73-26943

Video-signal improvement using comb filtering techniques. 12 p1468 A73-27012

Experimental investigation of the AM-FM distortions of a signal passing through a linear filter. 12 p1481 A73-27589

Calculation of the amplitude of pulse signals at the output of linear filters in optical communications systems. 13 p1583 A73-28671

A minimax filter for systems with large plant uncertainties using measurements corrupted by colored noise. 13 p1593 A73-29205

The design and applications of highly dispersive acoustic surface-wave filters. 14 p1732 A73-29933

Computational efficiency comparison for discrete linear filtering Kalman algorithms and information matrix methods, noting Householder square-root implementation identity with Potter technique. 16 p2032 A73-33404

Linear and nonlinear filtering techniques for estimating the state of reentry vehicles from optical tracking data. 17 p2125 A73-35371

Linear filtering of random signals according to the criterion of maximum signal-to-noise ratio. 17 p2145 A73-35719

Application of the dynamic filtration method to spacecraft orientation control problems. 18 p2359 A73-36104

Correctness of the solution of signal filtration and reconstruction problems by an analog computer. 20 p2522 A73-38702

Transformation of random signals by circuits containing a majoritarian element. 20 p2542 A73-39046

The filtering of random sequences with gaps by optimal discrete filters with a constant memory volume. 21 p2658 A73-40857

Laguerre transform of a continuous signal - Application to the study of the asymptotic regime of a Kalman filter. 22 p2832 A73-42352

A digital system for receiving binary phase-coded signals. 23 p2952 A73-43319

An innovations approach to least-squares estimation. V - Innovations representations and recursive estimation in colored noise. 23 p2954 A73-43819

LINEAR PREDICTION

Linear regression filtering and prediction for tracking maneuvering aircraft targets. 11 p1333 A73-26640

Unsupervised learning of the optimal linear signal estimator in the presence of unknown multiplicative, additive, and message generating noise. 17 p2144 A73-35374

Application of some data compression systems to ESRO satellite data. 20 p2524 A73-38735

Linear fire control predictor with non-Gaussian inputs, calculating on-target probability lower bounds for verification by digital simulation. 21 p2649 A73-40332

LINEAR PROGRAMMING

Automatic search system synthesis for linear programming, using gradient method and logic operations for system optimization. 01 p0028 A73-10675

The optimum allocation of redundancy - An application of mathematical programming to system design. 01 p0071 A73-11199

Investigation of the effectiveness of the variable-step simplex optimization method in a noise environment. 01 p0028 A73-11420

Application of the device of linear programming to solve certain optimal problems of reliability theory. 02 p0187 A73-12121

Mathematical formulation of linear programming problem, reducing vector valued optimal management plan determination to quadratic programming problem. 02 p0144 A73-12126

Application of mathematical programming to the solution of extremal problems in two-dimensional elasticity theory 02 p0235 A73-12197

Finite element limit analysis using linear programming. 05 p0631 A73-16124

Pivoting for size and sparsity in linear programming inversion routes. 06 p0716 A73-17978

Quadratic termination properties of minimization algorithms. I - Statement and discussion of results. II - Proofs of theorems. 06 p0716 A73-17983

Limit design in the absence of a given layout - A finite element, zero-one programming approach. 06 p0762 A73-18340

A finite element, linear programming method for the limit analysis of thin plates. 07 p0906 A73-19026

Bayes criteria and previous test data for industrial equipment test optimization, using linear and quadratic programming 07 p0831 A73-20076

Shock and vibration disturbance identification based on structural system response, discussing linear programming, curve fitting, constraints, objective functions and applications 07 p0916 A73-20430

A dynamic model of some multistage aspects of research and development portfolios. 08 p1025 A73-20972

Optimum design of stressed skin structures using a sequence of linear programs method. 11 p1436 A73-25481

Linear programming and gradient search algorithms for minimum weight design of finite element structures, applying to bar truss problems [ALAA PAPER 73-343] 11 p1436 A73-25482

Book - Mathematical programming and the numerical solution of linear equations. 15 p1901 A73-32300

Book - Optimum structural design: Theory and applications. 17 p2242 A73-34350

Simplex method for linear programming for computerized design global optimization problems involving large numbers of equations and variables 19 p2407 A73-37406

Feedback controller design for multivariable systems by linear programming. 19 p2454 A73-38052

Calculation of three-layer minimum-weight panels as a problem of mathematical programming 20 p2625 A73-39651

Application of linear programming in the statistical theory of antennas 21 p2661 A73-40201

Complementary variational principle existence condition and duality in linear and quadratic programming in Hilbert space setting, considering relationship to Kuhn-Tucker saddle point theory 21 p2724 A73-40296

A finite algorithm for the minimum L-infinity solution to a system of consistent linear equations. 21 p2725 A73-40376

Linear programming for optimization, discussing definitions, practical examples, simplex algorithm, duality theory, heuristic interpretations and integer solutions 21 p2726 A73-40836

Linear optimization theory, discussing duality theory, matrix calculations, simplex methods, base points, classical transport problems and industrial production applications 21 p2727 A73-41071

Prestressing force and tendon configuration optimization for indeterminate structure with prescribed cross sectional dimensions, using linear programming and design variable transformation 22 p2922 A73-42476

LINEAR RECEIVERS

Linear scan receiver for electronic beam steering of the north-south array of the DKR-1000 radio telescope 21 p2662 A73-40543

LINEAR SYSTEMS

Stability of large-scale systems under structural perturbations. 01 p0070 A73-10322

Abstract theory of systems - Current state and development trends 01 p0027 A73-10664

Wiener-Kolmogoroff optimal filtration theory for synthesis of linear stabilization systems under steady random external perturbations, noting control optimality conditions 01 p0028 A73-10670

On the diffusion function of a stochastic transmission system 01 p0017 A73-10975

Reaction of a damped system to the simultaneous action of an isolated semisinusoidal impact pulse and of vibrational oscillations 01 p0054 A73-11418

Construction of Lyapunov functions for nonstationary systems containing memoryless nonlinearities. 02 p0193 A73-12123

Linear dynamic control system synthesis methods based on aggregation and suboptimal control by decomposition, minimizing quadratic performance criterion 02 p0149 A73-12124

Variational aspects of oscillation phenomena for higher order differential equations. 02 p0188 A73-12823

General optimization criteria with allowance for economic factors and their use in measurement technology 03 p0305 A73-12894

Liapunov function for Hamilton-Jacobi equation for motion stability of linear and nonlinear mechanical systems, calculating vibration damping factor 03 p0342 A73-13157

A graphical test for checking the stability of a linear time-invariant feedback system. 03 p0285 A73-13519

Book on modal control theory and applications covering continuous and discrete time lumped parameter linear dynamic systems controllability and observability characteristics 03 p0285 A73-13989

Book on linear optimal control theory covering systems analysis, state reconstruction, stochastic nature and feedback control 03 p0286 A73-13992

Computerized design and algorithm for linear and nonlinear regulators by mathematical programming approach involving vector determination for objective function minimization 03 p0286 A73-14480

Large scale systems with linear and nonlinear subsystems and coupling connections, investigating connective stability under perturbations due to subsystem on-off participation 03 p0337 A73-14484

The optimal control of merging aircraft-derivation of the hybrid air traffic controller. 03 p0340 A73-14489

Topological analysis of mechanical vibrating linear systems by the method of structural numbers 03 p0396 A73-14598

Analysis of the forced vibrations of composite linear systems by the stiff finite elements method 03 p0396 A73-14600

Linear and nonlinear systems dynamic stability conditions for incomplete coefficients data, determining worst disturbance from Pontryagin principle 04 p0475 A73-14887

Necessary and sufficient conditions of pointwise completeness of linear time-invariant delay-differential systems. 04 p0430 A73-15213

System identification using approximate nonlinear filters. 04 p0430 A73-15257

A higher measurement space filter for passive tracking. 04 p0431 A73-15262

Automatic control system synthesis for optimal correction, maximum accuracy and stability of linear unsteady final action systems under deterministic and random actions 05 p0561 A73-16420

Fredholm operator theory application to linear feedback system input-output stability in terms of origin encirclement counting in complex plane 05 p0561 A73-16488

Linear time-invariant feedback systems with multiple inputs and outputs, deriving necessary and sufficient conditions for stable closed loop impulse response 05 p0561 A73-16493

The calculation of the natural vibration parameters of a damped system on the basis of the results of a vibration test in an exciter configuration 05 p0634 A73-16758

Estimation of the state vector of a plant by minimization of a distance in metric space when using discrete sampling 05 p0561 A73-17281

A matrix Green's formula and optimal control of linear distributed-parameter systems. 06 p0679 A73-17564

Suboptimal feedback control of linear gyroscopic systems. 06 p0679 A73-17568

On the controllability conditions for systems with distributed delays in state and control. 06 p0716 A73-17852

Note on the wave propagation problems in isotropic discretized bodies. 06 p0723 A73-17893

On an application of Lie group theory to the optimal control problem for linear dynamic systems with time-varying parameters. 06 p0679 A73-17954

Frequency stability criterion for a variable-structure automatic control system. 06 p0680 A73-17958

Application of linear feedback control theory techniques to continuum dominated by electrostatic and gravitational fields. 06 p0680 A73-18004

Representation of oscillations in piecewise-linear systems by the phase-shift-averaging method. 06 p0717 A73-18146

An optimum settling problem for time lag systems. 06 p0717 A73-18172

Dc servomotor transfer function equalization, noting stability conditions for linear system design 06 p0680 A73-18380

Design of dynamic programming feedback controllers for multivariable time-invariant linear systems. 06 p0680 A73-18517

Optimal control of a class of linear multivariable systems with integral quadratic energy constraint. 06 p0681 A73-18521

Sequentially best estimators for linear systems with non-linear noise-free sensors. 06 p0681 A73-18522

Iterative scheme for identifying linear systems from input/output samples or construction of rational z-transform approximations to sample data sequences 06 p0718 A73-18534

Invariance conditions and controllability relation of linear and nonlinear dynamic systems, including composite systems and systems with deviating argument 06 p0724 A73-18678

An identification of time varying linear system without a priori information on variation of system parameters. 06 p0681 A73-18812

Disturbance accommodation in linear systems with chattering controllers. 06 p0681 A73-18818

Matrices, polynomials, and linear time-invariant systems. 06 p0719 A73-18863

Properties of linear time-invariant multivariable systems subject to arbitrary output and state feedback. 06 p0682 A73-18865

Frequency domain synthesis algorithm for linear multivariable system via state variable feedback combined with input dynamics compensation, applying to decoupling and model matching 06 p0682 A73-18866

Modeling of linear time-varying systems by linear time-invariant systems of lower order. 06 p0682 A73-18867

An algorithm for the assignment of closed-loop poles using output feedback in large linear multivariable systems. 06 p0672 A73-18869

Digital-computer analysis of linear electronic circuits by the method of structural numbers 07 p0804 A73-18894

The determination of state-space representations for linear multivariable systems. 07 p0804 A73-19131

Adaptive control of linear stochastic systems. 07 p0804 A73-19132

Type L linear multivariable systems with state integral feedback control, deriving optimal conditions for zero steady state error compensatory tracking by frequency domain techniques 07 p0805 A73-19133

Determination of the frequency and amplitude of an external force that induces resonance in a linear system with variable parameters 07 p0792 A73-19908

Stochastic linear system observer eigenvalue optimal placement with respect to quadratic error criterion for adaptation to digital computation and applicability to higher order system 07 p0849 A73-19966

Optimal control of stochastic systems with continuous and discontinuous random disturbances, obtaining problem solution conditions for linear system via dynamic programming 07 p0805 A73-20038

Energy-like Liapunov functionals for linear elastic systems on a Hilbert space. 07 p0852 A73-20336

The state of the art of system identification of aerospace structures. 07 p0916 A73-20432

Conditional stability and separation of solutions to differential equations. 07 p0845 A73-20496

Nearest neighbor approximation for Kalman-Bucy filtering noisy data generated by multidimensional processes via dimensionality reduction for linear steady state problems 07 p0805 A73-20579

Reduced-order observers for linear discrete-time systems. 07 p0805 A73-20581

Minimum fuel control solution for linear discrete systems, discussing finite iterative algorithm based on dual problem of functional analysis 07 p0806 A73-20595

An actively adaptive control for linear systems with random parameters via the dual control approach. [AD-751587] 07 p0806 A73-20601

On the adaptive control of linear systems using the open-loop-feedback-optimal approach.

07 p0806 A73-20602
Fault isolation in complex systems via Bode diagram technique.

08 p0941 A73-20684
Stability of incompletely damped mechanical systems

08 p1014 A73-20780
Mathematical model selection rules for stability studies of linear mechanical or passive electrical network systems with arbitrary degrees of freedom

08 p0987 A73-20787
Scalar and block decoupling of time varying and invariant linear multivariable control systems, discussing sufficiency conditions, state estimation and order reduction possibility

08 p0950 A73-21089
Near-optimal control of high-order systems using low-order models.

08 p0950 A73-21090
Necessary condition for complete controllability with respect to arbitrary function for linear time-invariant differential equation system with time lag

08 p0950 A73-21092
Correlation techniques in the analysis of transient processes.

08 p0988 A73-21466
Velocity ratio in the analysis of linear dynamical systems.

08 p0988 A73-21467
An algebraic algorithm for the design and analysis of linear dynamical systems.

08 p0984 A73-21468
On the control of linear systems using two level periodic output feedback.

09 p1067 A73-22231
Vector-valued optimization of linear systems

09 p1112 A73-22478
Equivalence of systems that follow a stochastic principle of computation

09 p1059 A73-22554
Optimal control system design with respect to vector quality criterion, noting linear system described by differential equations

09 p1068 A73-22560
Signal processing in a randomly time varying system.

10 p1197 A73-23800
Book - Digital simulation of physical systems.

10 p1191 A73-23946
Contraction-mapping algorithm with guaranteed convergence.

10 p1242 A73-24034
Stabilization of linear dynamical systems with output feedback.

10 p1199 A73-24037
An adaptive convex feedback method for linear control systems with quadratic performance index.

10 p1199 A73-24038
Linear stochastic, multivariable, optimal control, realization and time-varying systems theory developments covering external and internal representations and variance computation problems

10 p1200 A73-24045
The algorithms of accuracy research of nonstationary linear systems with continuous and discrete elements.

10 p1200 A73-24048
Estimation of noise covariance matrices for a linear time-varying stochastic process.

10 p1201 A73-24053
Order determination and parameter identification of time-invariant state variable models.

10 p1201 A73-24054
Linear multivariable control systems - A survey.

10 p1201 A73-24058
Unsteady discrete linear systems semisteady realizations existence conditions and matrices elements determination methods

10 p1202 A73-24414
An actively adaptive control for linear systems with random parameters via the dual control approach.

10 p1202 A73-24534
Optimal stochastic linear systems with exponential performance criteria and their relation to deterministic differential games.

10 p1202 A73-24536
A survey of data smoothing for linear and nonlinear dynamic systems.

10 p1243 A73-24546
An optimal control problem for a class of distributed parameter systems.

10 p1202 A73-24549
Two dimensional signals Fourier transformations, discussing digital techniques application to linear and optical systems

11 p1397 A73-24993
Linear system unperturbed motion stability in finite time interval, formulating first approximation vector matrix equation

11 p1397 A73-25045
Linear or nonlinear dynamic systems response to arbitrary input functions, describing numerical computation method with provision for discontinuities

11 p1389 A73-25110

Functional analysis and optimal control of linear discrete systems, deriving algorithms for minimum fuel, energy or amplitude from linear equations solution

11 p1390 A73-25188
Irreducible canonical realizations from external data sequences.

11 p1390 A73-25191
Multiinput multioutput linear time invariant discrete system optimal approximation, noting algorithms and weighting matrices computational difficulties

11 p1390 A73-25192
Signal flow graph methods for four and three degree of freedom linear conservative mechanical vibration systems solution, noting Chan-Mai method superiority

11 p1434 A73-25193
Suboptimal input signal synthesis for linear control system identification based on output SNR maximization, bandwidth matching and pseudorandom binary noise nature

11 p1327 A73-25197
Extension of the principle of variable structure systems to the case where the slip hypersurface is nonlinear - Application to suboptimal control

11 p1341 A73-25574
Memory included linear stochastic system optimum control over finite time, using Liapunov-Krasovskii functionals

11 p1398 A73-25618
Essentially incomplete model construction by non-search method in linear plant parametric control

11 p1341 A73-25620
Normalization of stochastic system analog of linear determinate system with combined normal distribution of input/output signal, noting theorems for random variable distributions

11 p1341 A73-25632
Russian book on linear truss systems potential strain energy and displacements covering matrix and graph-analytic methods, influence functions, simple and complex strains, etc

11 p1442 A73-25775
On a solution of an optimization problem in linear control systems with quadratic performance index.

11 p1342 A73-26224
Synthesis of time-optimal control for linear systems and the minimal-time Lyapunoff function.

11 p1342 A73-26225
Asynchronous linear automatic binary control systems, using interpolation theory of Taylor operators for mathematical modeling

11 p1342 A73-26418
Linear system modeling via optimal finite dimensional approximation based on Sard generalized spline, giving error bounds

11 p1391 A73-26580
Single input n-th order linear constant discrete-time adaptive control systems, deriving phase canonical form sensitivity functions by z-transform

11 p1342 A73-26636
On identifying transfer functions and state equations for linear systems.

11 p1342 A73-26641
Unified approach to the performance analysis of linear modulation systems with coherent detection.

12 p1469 A73-27072
Application of the finite-element method to the study of heat problems

12 p1558 A73-27397
Fourth order linear differential equations solution for time optimal control synthesis with phase limitations

12 p1483 A73-27403
Stability of nonlinear systems with a transformed argument

12 p1524 A73-27416
Synthesis of an approximately optimal control for one class of controlled systems.

12 p1484 A73-27457
Correlation analysis of systems with stochastic inertialess elements.

12 p1484 A73-27458
Estimation of the state vector of a linear plant by the method of distance minimization in metric space on the basis of continuous measurement of plant inputs and outputs

12 p1485 A73-27894
Methods of quadratic Liapunov vector-function construction for linear systems

12 p1525 A73-27895
Optimal estimation of the phase coordinates for a linear dynamic system

12 p1485 A73-27898
Nonsearch self-adapting identification systems

12 p1483 A73-27900
Linear systems with aftereffects of delayed feedback described by differential equations, obtaining optimal control solution in terms of parameters and boundary value problem

12 p1486 A73-27950
Thermo-acoustical waves in linear thermo-elastic materials.

13 p1691 A73-28088
Elastic unipolar discretized linear bodies, considering motion and constitutive equations, conservation

laws, virtual work principle and uniqueness and reciprocity theorems

13 p1659 A73-28559
Linear distributed parameter system minimum time control, considering Hilbert space final value and Banach space inequality solutions

13 p1596 A73-28700
Computer plotted dynamic stability and transient response of linear continuous systems described by high order differential equations of motion

13 p1661 A73-29144
General treatment of the evaluation of tri-diagonal secular determinants.

13 p1700 A73-29379
Routh-Hurwitz method for optimal algebraic stability of ordinary differential equations of fourth order systems with linear control law

13 p1597 A73-29419
Zeros determination in large-scale multivariable systems.

13 p1651 A73-29568
Kalman filtering of systems with parameter uncertainties - A survey.

13 p1597 A73-29569
State space approach to mixed boundary value problems.

13 p1651 A73-29571
Zero-solution stability in systems of partial differential equations

14 p1768 A73-30248
Solution of a dual problem in optimal control theory.

14 p1738 A73-30405
Inverse problem of linear optimal control.

14 p1738 A73-30451
Minimum-energy terminal state control of first order linear hyperbolic systems in one spatial variable using the method of characteristics.

14 p1769 A73-30453
A minimization algorithm for the design of linear multivariable systems.

14 p1769 A73-30504
An efficient algorithm for calculation of the Luenberger canonical form.

14 p1769 A73-30508
Necessary and sufficient conditions for stability for n-input, n-output convolution feedback systems with a finite number of unstable poles.

14 p1739 A73-30509
Controllability of discrete bilinear systems with bounded control.

14 p1739 A73-30510
Theory and applications of variable structure systems; Proceedings of the Seminar, Sorrento, Italy, April 4-7, 1972.

14 p1739 A73-30776
Modelling and identification theory - A flight control application.

14 p1739 A73-30777
Time varying linear and constant bilinear dynamic systems state space structure, obtaining canonical decomposition by suitable choice of input/output interaction properties

14 p1739 A73-30778
Some results on the abstract realization theory of multilinear systems.

14 p1740 A73-30781
Mathematical models and identification of bilinear systems.

14 p1740 A73-30782
Algebraic Lie structure theory of bilinear systems in terms of controllability, observability and equivalent realization

14 p1771 A73-30783
Hodograph construction by root trajectory method to provide maximum information on linear feedback systems dynamics

14 p1740 A73-30945
Linear transformations of variable in system of normal equation in differential correction processes, reducing process to algorithm

15 p1930 A73-31115
The period of nonlinear vibrations of autonomous dynamical systems of the order n

15 p1947 A73-31366
Integral action in the optimal control of linear systems with some inaccessible state variables.

15 p1854 A73-31631
Multi-parameter sensitivity analysis of linear dynamic systems through the second method of Liapunov.

15 p1854 A73-31632
Study of the smoothness properties of the Bellman function in time-optimal problems, based on the equation of motion of the system. I - The linear case.

15 p1854 A73-31687
Some properties of the amplitude frequency characteristics of linear automatic control systems and their control quality under random influences

15 p1854 A73-31695
Multivariable linear passive systems

15 p1900 A73-32087
Lower bounds to the frequencies of continuous elastic systems.

15 p1954 A73-32125

Distribution of the response of linear systems to Poisson distributed random pulses. 16 p2035 A73-32918

An algebraic method for linear dynamical systems with stationary excitations. 16 p2076 A73-32919

Minimum-norm control of linear systems with partially known initial conditions. 16 p1992 A73-33163

A geometrical proof of the maximum principle for systems represented by difference-differential equations. 16 p2032 A73-33302

Optimal control solution existence for relaxed linear systems with strictly convex Hamiltonian 16 p1992 A73-33303

Russian book - Lectures on the theory of stability of the solutions of systems with an aftereffect. 17 p2211 A73-34224

Linear open signal scanning system distortion of stationary stochastic signals, examining transfer characteristic improvement by optimal filter 17 p2121 A73-34245

Papers on optimal control and dynamic systems theory covering linear discrete systems observers, quasi-linearization, national economic policy, decision theory and closed loop formulation 17 p2143 A73-34360

Optimal observer techniques for linear discrete time systems. 17 p2144 A73-34361

Nonstationary response of linear time-varying dynamical systems to random excitation. 17 p2247 A73-35031

A procedure for investigating the Liapunov stability of nonautonomous linear second-order systems. [ASME PAPER 73-APM-31] 17 p2201 A73-35044

Book - Vibration of linear mechanical systems. 18 p2361 A73-35900

Optimal control of linear systems in the case of continuous and discrete controls 18 p2337 A73-36410

Program of computation of spectral and modal matrices associated with a linear elastic system 18 p2364 A73-36493

Methods of constructing quadratic Lyapunov vector functions for linear systems. 18 p2330 A73-36600

Optimal estimation of the phase coordinates of a linear dynamic system. 18 p2294 A73-36603

Searchless self-adjusting identification systems. 18 p2294 A73-36752

Superharmonic resonance in piecewise-linear system - Effect of damping and stability problem. 19 p2459 A73-37669

Poincare-Lighthill and linear-time-scales methods for linear perturbation problems. 19 p2445 A73-37752

Discrete stochastic linear servomechanism with observation costs, deriving optimal control solution with extension to nonlinear systems suggested by dynamic population models 19 p2412 A73-38029

Design of decoupled multivariable control systems. 19 p2412 A73-38032

Decoupling longitudinal motions of an aircraft. 19 p2386 A73-38033

A sensitivity approach to the decoupling of linear systems with parameter disturbances. 19 p2412 A73-38034

Controllability and stabilizability of decentralized dynamic systems. 19 p2413 A73-38045

Stabilization of multivariable systems with constant-gain output feedback. 19 p2413 A73-38046

Derivation of aggregation matrices for simplified models of linear dynamic systems and their applications for optimal control. 19 p2413 A73-38053

A comparison of errors in linear digital models. 19 p2413 A73-38059

An optimal feedback control law for regulator problems with linear state inequality constraints. 19 p2413 A73-38060

Output feedback for linear multivariable systems with parameter uncertainty. 19 p2413 A73-38061

Performance of LQG control systems using optimal k-step-ahead control laws. 19 p2413 A73-38062

A new approach to the 'inverse problem of optimal control theory' by use of a generalized performance index/GPI/. 19 p2414 A73-38063

A computational algorithm for design of regulators for linear jump parameter systems. 19 p2408 A73-38066

Controllability of discrete bilinear systems with bounded control. 19 p2414 A73-38067

Oscillations in nonlinear feedback systems. 19 p2414 A73-38069

Control configuration optimization of linear engineering systems. 19 p2414 A73-38082

Normalization of stochastic system analog of linear determinate system with combined normal distribution of input/output signal, noting theorems for random variable distributions 19 p2414 A73-38143

Approximate synthesis theory in problems of optimization of automatic control systems 20 p2591 A73-38674

Computerized analytical methods for optimal control synthesis of linear and nonlinear systems with constraints, using integral quadratic weighting function estimates 20 p2539 A73-38679

Some problems in the analysis and synthesis of statistically optimal constrained control 20 p2539 A73-38681

Spectral analysis and a synthesis of linear systems with variable and random parameters in finite time intervals 20 p2540 A73-38704

Reproduction of a useful signal by linear feedback systems 20 p2543 A73-39506

Approximate solution of Bellman's equation for a class of problems involving optimal terminal control 21 p2668 A73-40179

Conditions of existence of steady representations for discrete linear systems given in terms of unsteady representations 21 p2669 A73-40497

Russian monograph on linear signal system models covering steady state, variance and transducers of continuous and discrete signals and random and nonstationary estimates 21 p2669 A73-40798

Possibilities of suboptimal control in a linear-quadratic problem 21 p2671 A73-41606

Time-optimal control of a linear plant with time lag 21 p2671 A73-41607

A model of the human in a cognitive prediction task. 22 p2814 A73-42223

Stability of the De Vogelaere method for timewise numerical integration. 22 p2882 A73-42557

Multicircuit structural analysis of linear multiple link control systems with dynamic interchannel cross couplings 22 p2836 A73-42608

Synthesis of optimal discrete controls for a continuous plant over a fixed time interval 22 p2837 A73-42619

French monograph - On the representation of linear dynamic systems with distributed parameters and its application to the study of intrinsic properties of these systems. 22 p2837 A73-42746

Identification of damping coefficients in multidimensional linear systems. [ASME PAPER 73-APMW-43] 22 p2926 A73-42899

Optimal discrete-time feedback control of mixed distributed and lumped parameter systems. 22 p2837 A73-43072

The state space and transfer function approaches in practical linear multivariable systems design. 23 p2962 A73-43281

Reduction of the sensitivity of optimal control systems by using two degrees of freedom. 23 p2962 A73-43285

Synthesis of two-level controller for a class of linear plants in an unknown environment. 23 p2963 A73-43289

An adaptive observer for single-input single-output linear systems. 23 p2963 A73-43818

Linear time variant multivariable decentralized system stabilization by feedback control laws with dynamic compensation 23 p2964 A73-43821

L2-stability and L2-instability of linear time-invariant distributed feedback systems perturbed by a small delay in the loop. 23 p2964 A73-43822

On the adaptive control of linear systems using the open-loop-feedback-optimal approach. 23 p2964 A73-43824

Asymptotically stable adaptive observer and identification scheme for linear system, using Liapunov canonical state representation 23 p2954 A73-43825

State-space matrix rank test in locating zeros of linear multivariable systems, noting application to feedforward regulators 23 p2964 A73-43828

Closed loop linear control system synthesis possibility under condition of incomplete information on state vector with application to aircraft longitudinal motion 23 p2965 A73-44329

Discrete time invariant bilinear systems analysis for controllability, using decomposition by multiplicative feedback and linear compensation loops 24 p3073 A73-44585

Linear system resonance effects in single loop controlled frequency tank circuit with variable capacitor under variable or constant emf 24 p3074 A73-44591

Certain problems of the correctness of the minimum-impulse linear optimal control problem. I - Dependence of the optimal control on the initial state and parameters 24 p3105 A73-44602

German book on digital systems for signal processing covering discrete linear systems characteristics and design, fast Fourier transformation, digital filters, multiplexing, etc 24 p3074 A73-45000

Effect of unity-rank feedback on the transfer-function matrix of a multivariable system. 24 p3075 A73-45263

LINEAR TRANSFORMATIONS

Minimum variance linear filter with partial state elimination by linear transformation for reduction of computational burden and storage requirements in Kalman filter 04 p0431 A73-15268

Simulation of random processes with the aid of piecewise linear transformations of unit interval 11 p1340 A73-25012

Measurement of impedance transformation on practical dipoles. 17 p2128 A73-35690

Transformation, transmission, and reflection of plasma waves in the presence of a tangential velocity discontinuity 18 p2339 A73-36551

Conditions of existence of steady representations for discrete linear systems given in terms of unsteady representations 21 p2669 A73-40497

Digital codings of multi-dimensional information sources and applications to image coding. 21 p2655 A73-41043

LINEAR VIBRATION

Randomly separated ends scattering effect on linear and nonlinear coherent oscillations of elastic string by perturbation technique 06 p0723 A73-17900

The iterative solution of two-point linear differential eigenvalue problems. 16 p2031 A73-32930

LINEARITY

NT COLLINEARITY Theory and application of the optimal linear approximation of linear processes 08 p0983 A73-20645

Cast thermosetting epoxy resin linear elastic stress-strain characteristics under tension, compression, torsional and bending loads 15 p1897 A73-31619

LINEARIZATION

Linearization method for analytic solution of oscillatory motion differential equations of elastic nonlinear system, studying combinations of free and forced vibrations 01 p0075 A73-10093

Some exact solutions in the design of technically orthotropic axisymmetric plates. 01 p0118 A73-11365

Statistical linearization of nonlinear single-mass mechanical system for given distribution function of random disturbances, noting amplitude frequency distribution 04 p0475 A73-14977

Linearization limits for optimal pulse controller adjustments, using comparison with continuous controller and extrapolation 10 p1198 A73-24000

Three-dimensional theory of elastic stability in the presence of finite subcritical strains 10 p1290 A73-24302

Cutting planes for programs with disjunctive constraints. 11 p1391 A73-26578

Application of a modified quasilinearization technique to totally singular optimal control problems. 13 p1597 A73-29570

Application of the optimal linearization method to the heat transfer problem. 14 p1817 A73-30605

Linearization of the relaxation time control of a transistor multivibrator. 15 p1849 A73-30992

A modified quasilinearization technique for optimal control problems with unspecified final time. 15 p1853 A73-31627

Modified quasilinearization method for mathematical programming problems and optimal control problems. 17 p2200 A73-34362

A generalization of the concept of equivalent linearization. 19 p2445 A73-38257

Conditions, based on the estimation of the sensitivity of a periodic solution, for the application of the harmonic linearization method to higher harmonics and small parameters
20 p2592 A73-38693

Linearization of Cauchy's problem for quadratic semilinear partial differential equations.
20 p2581 A73-38865

Use of piecewise linearization for suboptimal control of nonlinear systems.
21 p2669 A73-40451

Linearization technique for synthesis of nonlinear two dimensional automatic control systems with cross disturbances, imposing constraints on motion coordinate deviations
22 p2836 A73-42615

LINERS
U LININGS

LINES [GEOMETRY]
NT CHORDS [GEOMETRY]

LINES OF FORCE
Infinite set of velocity fields to describe geomagnetic field lines and interpret discrepancy in plasma sheet motion observations during substorms
02 p0157 A73-11754

Self consistent model of closed field lines of pulsar magnetosphere valid for oblique rotators and unipolar inductors
02 p0216 A73-12382

Effect of the slope of geomagnetic field lines on the field of the magnetosphere-ionosphere current system
02 p0164 A73-12458

Electrostatic autopilot using atmosphere electric field lines for stabilization and guidance, applying to remotely piloted vehicles
02 p0191 A73-12595

Mechanisms for the injection of protons into the magnetosphere.
03 p0362 A73-13858

Geomagnetic tail plasma sheet thinning and auroral zone negative bays development during magnetospheric substorms, suggesting auroral particles acceleration along magnetic field lines
03 p0304 A73-13887

Magnetosphere configuration models based on open and closed field line hypotheses, discussing solar wind-magnetosphere interactions, magnetotail, substorm growth, flux transport, etc
04 p0441 A73-15327

The magnetic configuration of the November 18, 1968 loop prominence system.
05 p0621 A73-17043

A force field theory. I - Laminar flow instability.
05 p0567 A73-17103

Method for experimental determination of the magnetic well depth in stellarator-type systems
07 p0855 A73-19285

Magnetic surfaces decay for parametric instability in helical magnetic configuration, noting nonlinear equations of magnetic field lines
08 p0991 A73-20822

Acceleration of charged particles in the region of the neutral line of the magnetic field
08 p0959 A73-21292

Special features of the dynamic spectrum of Pi2 type pulsations
08 p0960 A73-21307

Electron heat conductivity along a magnetic field in a decaying plasma
09 p1124 A73-21887

Influence of magnetic field curvature on the stability of a plasma confined by a dense shell of neutral gas
09 p1124 A73-21902

Oppositely directed magnetic fields reconnection rate role in solar flares and small scale turbulent field reduction in photosphere
09 p1142 A73-22037

Ion cyclotron instability in current-carrying plasmas with anisotropic temperatures.
09 p1127 A73-22284

Ultrarelativistic pulsar plasmas with one dimensional distribution functions in strong magnetic fields, considering dispersion ratios of plasma waves along magnetic lines
09 p1145 A73-22294

Ionospheric and plasma sheet particle densities, fluxes and bulk velocities along auroral magnetic field line for collisionless ion-exosphere model
09 p1079 A73-22842

Solar particle measurements interpretation for closed vs open magnetospheric model determination, considering electron-proton polar cap differences, magnetotail flux asymmetries, etc
09 p1149 A73-22951

Quantum theory of line formation in a magnetic field.
10 p1249 A73-24134

On the small-scale structure of solar magnetic fields.
10 p1279 A73-24135

Solar surges magnetic properties analysis from high resolution H alpha filtergrams, matching surge trajectories by computed magnetic lines of force
11 p1422 A73-25941

Equations derived for magnetic field line configuration and plasma flow about rotating object having axisymmetric field with emphasis on pulsar magnetosphere
11 p1427 A73-26614

Magnetic field signatures of substorms on high-latitude field lines in the nighttime magnetosphere.
12 p1488 A73-26981

Low energy auroral electron pitch angle diffusion in postbreakup aurora due to injected particle loss in closed magnetic field lines
12 p1488 A73-26987

Magnetic field line velocity associated with Euler potentials set, considering flux preservation properties of particle motion
12 p1489 A73-27000

Experimental determination of magnetic well depth in stellarators.
13 p1665 A73-28685

Equilibrium equations for vortex lines with allowance for interaction with boundary of ideal superconductor, calculating extremum values of magnetic field
14 p1774 A73-30342

Hydrostatic equilibrium conditions for hydromagnetic field, discussing topology of wrapping pattern of lines of force
14 p1782 A73-30741

Electron current estimation along auroral zone-plasma neutral sheet field line from steady state one dimensional model
15 p1866 A73-31065

Center of forces existence and related configurations for given law of force, rejecting Wintner conjecture
15 p1913 A73-31109

Diurnal variations of the vertical component of the magnetic field in high latitude regions as a function of the east-west component of the interplanetary magnetic field
15 p1868 A73-31570

French monograph - Experimental study of conditions of resonance of tubes of forces of the terrestrial magnetic field.
15 p1874 A73-32594

Influence of the inclination of the geomagnetic lines of force on the field of the magnetospheric-ionospheric current system.
15 p1874 A73-32608

Effect of magnetic field curvature on the stability of a plasma confined by a dense neutral gas.
15 p1921 A73-32627

Electron thermal conductivity along the magnetic field in an afterglow.
17 p2215 A73-34310

Topology of induced lunar magnetic fields.
17 p2235 A73-35736

Re-connexion of magnetic lines of force - Evolution in incompressible MHD fluids.
18 p2338 A73-36181

Current distribution at the zero line of the magnetic field and the turbulent resistance of a plasma
18 p2339 A73-36550

Hydromagnetic waves directed by the geomagnetic field
19 p2481 A73-37337

Acceleration of charged particles in the region of the neutral line of the magnetic field.
19 p2425 A73-37921

Characteristics of the dynamic spectrum of Pi2 type pulsations.
19 p2425 A73-37936

The rate of separation of magnetic lines of force in a random magnetic field.
19 p2489 A73-38522

The effect of magnetic mass on Alfvén waves.
21 p2701 A73-40624

Field aligned electron anisotropies observed by the ESRO 1 A /Aurora/ satellite.
21 p2691 A73-41370

Particle streams along the force lines of a magnetic field in a multicomponent ionospheric plasma in the presence of longitudinal currents
22 p2892 A73-42329

On the stability of a class of plasma flows with helical flow and field lines.
22 p2892 A73-42351

Numerical analysis of magnetic field lines of force reconnection along transition layers or at flow stagnation point of incompressible conducting viscous fluid
22 p2894 A73-42396

Synoptic survey of geomagnetic field neutral line formation in magnetotail during magnetic substorms noting nighttime magnetosphere reconnection and associated plasma sheet behavior
22 p2849 A73-42573

Atmospheric oscillations. V - The propagator matrix and the transmission of an electrostatic potential along the geomagnetic field lines.
23 p2971 A73-43686

The topological association of H alpha structures and magnetic fields.
24 p3136 A73-44639

On self-consistent models for the pulsar magnetosphere.
24 p3140 A73-45190

LING-TEMCO-VOUGHT AIRCRAFT
NT A-7 AIRCRAFT
NT F-8 AIRCRAFT

LING-TEMCO-VOUGHT MILITARY AIRCRAFT
U MILITARY AIRCRAFT

LINGUISTICS
NT PHONEMES
NT SYNTAX
NT WORDS [LANGUAGE]
Outline of a new approach to the analysis of complex systems and decision processes.
06 p0671 A73-18622

LININGS
NT ROCKET LININGS
Heat transfer to film-cooled combustion chamber liners.
[ASME PAPER 72-WA/HT-32] 04 p0518 A73-15823

Effect of bulk-reacting liners on wave propagation in ducts.
[AIAA PAPER 73-227] 05 p0566 A73-16952

Nonlinearity of Helmholtz resonators
05 p0599 A73-17269

Hydromagnetic instabilities of current carrying pinch in magnetic field, noting thin walled resistive liner effect on nonlocal modes stabilization
08 p0991 A73-20821

LINKING
U JOINING

LIOUVILLE EQUATIONS
A nonlinear, nonconvex optimization problem
08 p0983 A73-20778

Overall existence of a solution of the Cauchy problem for the system of equations with Liouville-Newton partial derivatives
17 p2201 A73-35045

Nonequilibrium statistical operators and quasi-means in the theory of irreversible processes
21 p2741 A73-41298

LIOUVILLE THEOREM
Isotropic system development of gravitating point particles in galactic clusters and superclusters in expanding universe from Liouville theorem and BBGKY hierarchy
03 p0365 A73-12927

LIPID METABOLISM
Hepatic lipogenesis in fasted, re-fed rats and mice - Response to dietary fats of differing fatty acid composition.
03 p0258 A73-13054

Effect of cultural conditions on the fatty acid composition of *Thiobacillus novellus*.
03 p0261 A73-13599

An epidemiological survey of risk factors for ischemic heart disease in 42,804 men. I - Serum cholesterol value.
04 p0409 A73-15521

Effect of hypoxia on free fatty acid metabolism during exercise.
05 p0540 A73-16609

Diurnal rhythm oscillations of fat metabolism indices in healthy young men
07 p0781 A73-19646

Thermal factor and dehydration influences on proteic and lipidic catabolisms of young men with partial food deprivation in hot climate, discussing metabolic balances
08 p0934 A73-21248

Effect of excessive glucose administration on the lipid level, glycolysis rates, and oxygen uptake in the tissues of the liver, heart, cerebrum and aorta
11 p1314 A73-25042

Cell membrane molecular structure and lipid composition, discussing phospholipid role in membrane potential maintenance in myocardial cells
11 p1315 A73-25591

Influence of electron transport on the interaction between membrane lipids and Triton X-100 in *Halobacterium cutirubrum*.
15 p1841 A73-32024

Total lipid and sterol components of *Rhizopus arrhizus* - Identification and metabolism.
16 p1973 A73-33900

Metabolic responses of monkeys to increased gravitational fields.
18 p2270 A73-35982

Serum cholesterol and plasma lipid elevation separation of hypercholesterolemic patients for atherosclerosis therapy
18 p2275 A73-36533

Energy supply in acute cold-exposed dogs.
18 p2278 A73-36655

FFA metabolism in thyroidectomized and normal dogs during rest and acute cold exposure.
20 p2515 A73-39787

Mechanisms of hyperlipidaemias in different clinical conditions.
22 p2809 A73-42832

Changes in indices of the carbohydrate and fat metabolism, the state of the sympathoadrenal system, and oxidative processes under varying-intensity cold effects
24 p3059 A73-44671

LIPIDS

LIPIDS

- NT LIPOPROTEINS
- NT OLEIC ACID
 - Carbon-13 nuclear magnetic resonance in biosynthetic studies of lipids. 03 p0274 A73-14550
 - Protein-lipid films as prototypes of biological membranes. 06 p0652 A73-17949
 - UV-induced lipid peroxidation in human epidermis, dermis, and hypodermis in vitro 09 p1038 A73-21873
 - Laboratory simulation of organic geochemical processes. 11 p1325 A73-25460
 - Structure of the lipid phase in cell envelope vesicles from *Halobacterium cutirubrum*. 17 p2112 A73-34599
 - Lipids in arteriosclerotic arterial tissues of man. 18 p2275 A73-36534

LIPOPROTEINS

- Prevalence of hyperlipoproteinaemias in a random sample of men and in patients with ischaemic heart disease. 22 p2811 A73-42975

LIPSCHITZ CONDITION

- The method of penalty functions and necessary conditions of optimality for generalized solutions of the optimal control problem 15 p1901 A73-32367
- Asymptotic mean value method for differential equations solution under given Lipschitz condition generalized via Liapunov procedure elimination 23 p2999 A73-44079

LIQUEFIED GASES

- NT LIQUID AMMONIA
- NT LIQUID HELIUM
- NT LIQUID HELIUM 2
- NT LIQUID HYDROGEN
- NT LIQUID NITROGEN
- NT LIQUID OXYGEN
 - Densities of compressed liquid methane, and the equation of state. 02 p0238 A73-12630
 - H₂/O₂-fuel cells supplied with a H₂/N₂-mixture and air. 04 p0408 A73-15116
 - Dielectric constant and molar polarizability of compressed gaseous and liquid fluorine. 06 p0661 A73-18124
 - Thermal stresses in a spherical vessel filled with liquefied gas 07 p0917 A73-20507
 - Martian polar stacked laminae interpreted in terms of conditions for carbon dioxide liquefaction, considering atmosphere history 19 p2478 A73-37217
 - Thermal stresses in spherical reservoirs while filling with liquefied gas. 19 p2499 A73-37782

LIQUID ALLOYS

- Nucleation during solidification and melting of metals and alloys 02 p0181 A73-12363
- The high temperature thermodynamic properties of Ni-Ti alloys. 02 p0182 A73-12753
- Stable or metastable phase crystallization rate of Cd-Sb liquid alloys as function of time, composition and temperature above liquidus line 05 p0605 A73-17294
- Liquid Ni-Si alloy short range order structure analyzed by X ray scattering, revealing Ni atoms position relation to Si atoms 14 p1764 A73-30870
- Composition and temperature effects on hydrogen solubility in Ni-Al liquid alloys 17 p2187 A73-34553

LIQUID AMMONIA

- Synthesis of glutamic acid via cyanoethylation of n-acylaminoacetnitriles in liquid ammonia. 06 p0661 A73-17936

LIQUID ATOMIZATION

- Atomization of cryogenic liquid droplets by shock waves 07 p0811 A73-19656
- Breakdown of a drop of cryogenic liquid by shock waves. 14 p1745 A73-30322
- Air/water mist spray coolant for high gas temperature and pressure environment at gas turbine inlet 17 p2221 A73-34388

LIQUID BEARINGS

- Application of finite element methods to lubrication - An engineering approach. [ASME PAPER 72-LUB-N] 01 p0055 A73-10221
- Hirs turbulent lubrication theory, discussing plane inclined slider thrust bearing applications and performance predictions 24 p3094 A73-44891

LIQUID COOLED REACTORS

- NT LIQUID METAL COOLED REACTORS
- NT ORGANIC COOLED REACTORS

LIQUID COOLING

- NT FILM COOLING

- Design and performance of solar simulator with water cooled Xe lamp, calculating irradiance distribution by ray tracing method 01 p0030 A73-11149
- A study of mist cooling /1st Report - Investigation of mist cooling/. 05 p0638 A73-16222
- The study of disperse regimes with film boiling of liquid nitrogen in tubes. 07 p0922 A73-20409
- Immersion liquids for a homogeneous optically mixed laser 10 p1227 A73-23768
- Frequency stability of millimetre-band reflex klystrons with various cooling techniques. 13 p1589 A73-28049
- AEGIS Demineralizer/Water Cooler - Design for availability. 16 p1989 A73-33608
- Comparative study of patches for liquid cooled garments. 19 p2398 A73-37404
- The rapid cooling of a hot gas discharge by liquid sprays. 22 p2929 A73-41743

LIQUID CRYSTALS

- Dielectric properties of cholesteric liquid crystals. 02 p0199 A73-11577
- Light-emitting diode and liquid crystal applications to displays, discussing gas discharge plasma, electrophoretic, fluorescent and incandescent devices, electronic wristwatches and calculators 02 p0168 A73-12082
- Liquid crystal optical and physical characteristics and applications to display design, emphasizing field effect and twisted nematic devices 02 p0201 A73-12083
- Liquid crystals for nondestructive testing of composite structures. 03 p0349 A73-13041
- Display of HF acoustic holograms utilizing liquid crystals. 05 p0574 A73-16285
- Cholesteric liquid crystals thermophysical properties application in aerospace sciences and engineering, noting temperature measurement and nondestructive tests 06 p0733 A73-17767
- Variation of dc domain threshold in a nematic liquid crystal under continual dynamic scattering. 06 p0739 A73-18794
- Electrooptic liquid crystal devices - Principles and applications. 07 p0861 A73-19135
- New techniques of acoustic image detection. 11 p1360 A73-25073
- Twisted nematic liquid-crystal electro-optic devices with areas of reverse twist. 11 p1337 A73-25357
- Ultrasonic investigation of the nematic-isotropic phase transition in MBBA. 11 p1409 A73-26213
- Controllable liquid-crystal transparency for recording of holograms. 12 p1498 A73-27513
- Reduction of the switching time of a liquid-crystal optical transparency. 12 p1498 A73-27514
- Dendritic liquefaction of hypoeutectic binary, ternary and complex Fe- and Ni-base alloys dependence on phase diagram 13 p1631 A73-28102
- Investigation of some electrooptical properties of liquid crystals 14 p1784 A73-30854
- Electrooptical-phase imaging device using nematic liquid crystals 16 p2013 A73-32881
- Liquid crystal approach to integrated programmable digital displays and aircraft control, considering flat panel digital-matrix display 17 p2139 A73-35234
- Kerr response of nematic liquids. 18 p2340 A73-36620
- Schlieren-optic and interferometric methods using TEA-CO₂ lasers and thermal liquid crystal IR image converters in the diagnostics of fast processes 21 p2744 A73-39998
- Angular dependence of optical scattering in mixed nematic-cholesteric liquid crystals. 21 p2751 A73-40453
- Light scattering from electrohydrodynamic turbulence in liquid crystals. 21 p2744 A73-41020
- Dielectric anisotropy of new liquid-crystal mixtures and its effect on dynamic scattering. 21 p2665 A73-41115
- Applications of liquid crystals to information display, fault detection, and medical thermography. 22 p2897 A73-42524
- Performance and characteristics of smectic liquid crystal storage displays. 22 p2861 A73-42525

- Electron paramagnetic resonance studies of a viscous nematic liquid crystal. II - Evidence counter to a second-order phase change. 22 p2897 A73-42711

- The behavior of nematic liquid crystals in the electric field 23 p3019 A73-44387

LIQUID DROPS

U DROPS [LIQUIDS]

LIQUID DYNAMICS

U FLUID DYNAMICS

U LIQUID FLOW

LIQUID FILLED SHELLS

- Moments of inertia for fluid-filled rotating bodies, solving Laplace and Navier-Stokes equations for cylinder and sphere 01 p0030 A73-10089
- Determination of the dynamic characteristics of a fluid in a moving vessel in the presence of a weak gravitational field by the eigenfunction expansion method 01 p0030 A73-10095
- Stress field and deformed shapes of liquid filled axisymmetric sessile neo-Hookean membrane during submergence to various depths 03 p0292 A73-13303
- Law governing the oscillations of a circular cylindrical shell of finite length containing a liquid with a variable level 04 p0434 A73-15505
- Spinning satellite with partially filled viscous ring damper, solving equations of motion for nutation-synchronous and spin-synchronous modes [AIAA PAPER 73-143] 05 p0629 A73-16892
- Equations of disturbed motion and equilibrium for solid body with incompressible fluid filled cavity, noting equilibrium position stability conditions 06 p0688 A73-18878
- Longitudinal vibration analysis of partially-filled ellipsoidal tanks. 07 p0914 A73-20215
- Thermal stresses in a spherical vessel filled with liquefied gas 07 p0917 A73-20507
- Some delinearization problems in the dynamics of complex vibrational systems 08 p0989 A73-21768
- Characteristics of the motion of a system composed of a shell and fluid within the limits of hydraulic approximation 09 p1072 A73-22587
- Effect of elastic displacements of a cylindrical shell on the vibrations of the free surface of a fluid 09 p1073 A73-23345
- Approximate determination of the hydrodynamic coefficients for the sloshing of a liquid in moving cylindrical cavities 10 p1206 A73-24309
- Solid sphere meandering trajectory in viscous liquid filled cylinder, postulating oscillating molecular surface tension layer at interface 10 p1206 A73-24701
- Impact on a simple physical model of the head. 10 p1185 A73-24770
- The dynamical effect of inertial waves on the gyroscopic motion of a body containing several eccentrically located liquid-filled cylinders. 11 p1346 A73-25224
- Frequencies and virtual masses of a liquid in a cavity formed by eccentric cylinders 11 p1347 A73-25391
- A finite element method for nonaxisymmetric vibrations of pressurized shells of revolution partially filled with liquid. [AIAA PAPER 73-399] 11 p1440 A73-25528
- Natural oscillations of density-stratified ideal incompressible liquid in rectangular vessel, solving oscillation equation for various density distributions 11 p1349 A73-26441
- Oscillations of a shell partially filled with a liquid and containing sources of the liquid 11 p1446 A73-26462
- Stability of the regular precession of a symmetrical solid with an ellipsoidal cavity 11 p1401 A73-26469
- Equilibrium stability of liquid filled body with closed internal cavity partially filled with ideal homogeneous incompressible fluid under gravitation 11 p1401 A73-26470
- Hydraulic impact in coaxial cylindrical tubes 15 p1860 A73-31046
- Hydraulic impact in a circular cylindrical shell 15 p1860 A73-31047
- Hydrodynamics in weak gravitational fields - Small oscillations of an ideal liquid in a cylindrical vessel 15 p1861 A73-31280
- Equations of disturbed motion and equilibrium for solid body with incompressible fluid filled cavity, noting equilibrium position stability conditions 15 p1915 A73-32403
- Forced vibrations of elastic shells of revolution filled with liquid 16 p2074 A73-32687

Stability of motion in a controlled system consisting of two elastically butted bodies one of which has cavities partially filled with a liquid

17 p2243 A73-34733

Thermal stresses in spherical reservoirs while filling with liquefied gas.

19 p2499 A73-37782

Front-end collision of a partially liquid-filled cylindrical shell with a solid body

20 p2616 A73-39261

Motion of a solid body having a cavity completely filled with two immiscible liquids

20 p2547 A73-39507

Equations of perturbed motion of a body with a liquid-containing cavity when the normal to the free liquid surface deviates sizably from the axis of the cavity

20 p2547 A73-39510

Method for calculation of natural and induced oscillations in elastic shells of revolution which are filled with an ideal incompressible liquid

20 p2624 A73-39647

Vibrations of a rotating solid body with a cavity partly filled with an arbitrary viscous fluid

21 p2677 A73-40988

Free vibrations of fluid-conveying cylindrical shells. [ASME PAPER 73-DET-96]

22 p2919 A73-42075

Exact hydroelastic solution for an ideal fluid in a hemispherical container.

22 p2843 A73-42631

Vibrations of a rotating solid body containing a cavity partially filled with a viscous fluid

22 p2843 A73-43058

Synthesis of optimal control of the longitudinal motion of an elastic tank containing liquid

22 p2843 A73-43059

Analysis of the perturbed motion of a solid with cavities partially filled with liquid

23 p2969 A73-44198

Hydrodynamics in weak gravitational fields - Plane oscillation problems of an ideal liquid in a vessel

24 p3076 A73-44653

The motion of a body containing a liquid-filled cavity with elastic radial ribs and exhibiting perturbations relative to the longitudinal axis

24 p3112 A73-45513

Determination of the equilibrium state of a capillary liquid in a vessel

24 p3080 A73-45526

Boundary value problem concerning the oscillations of a rotating ideal fluid

24 p3081 A73-45531

LIQUID FLOW

NT WATER FLOW

Synthesis of a magnetoelastic control medium for stabilization of hydrodynamic flows

01 p0084 A73-10669

A variational principle for the nonrotational flow of a perfect compressible liquid in a flexible tank [ONERA, TP NO. 1178]

03 p0294 A73-13601

On the influence of the contact pattern on the sealing capacity and the power loss of hydrodynamic lip seals.

[ASLE PREPRINT 72LC-7A-1]

03 p0316 A73-14367

Electrohydrodynamic heat pipe design based on electrode structure to orient and guide dielectric liquid phase flow, using polarization force in place of capillarity

[ASME PAPER 72-WA/HT-35]

04 p0518 A73-15820

Turbulence in the annular flow of a conducting-fluid in a magnetic field

05 p0603 A73-16587

Viscoelastic liquid flow in wake past two dimensional grid, investigating vorticity increase with time for double array of vortices

05 p0565 A73-16592

Heat pipe operation in a gravity field with liquid pool pumping.

[AIAA PAPER 73-120]

05 p0640 A73-16876

A method for measuring the sublayer velocity profile of a liquid with polymer additive.

[AIAA PAPER 73-39]

06 p0692 A73-17621

The study of film boiling crises and transient boiling of cryogenic liquids.

07 p0922 A73-20410

Influence of various surface roughness on the natural convection.

08 p1024 A73-21639

Nonstationary wave propagation in equilibrium liquid-vapor flow, noting pressure jumps due to expansion

10 p1204 A73-23513

A numerical-analytical method of calculating stream flow of a heavy liquid around curvilinear obstacles

10 p1205 A73-23585

Influence of liquid circulation within a droplet on the vaporization rate and drag in a viscous flow

10 p1206 A73-24680

An evaluation of optical anemometers for volumetric flow measurement of liquids and gases.

10 p1221 A73-24858

The force acting from the direction of a flow of liquid on a thin curved body of circular cross section

11 p1348 A73-26427

Oscillations arising when parallel flows of a viscous liquid lose stability relative to periodic long-wave disturbances

11 p1349 A73-26430

Anomalous lower dynamic pressure in piezometer of pitot tube in liquid flow containing solid particles, using seeds in aqueous solution of calcium chloride

11 p1367 A73-26476

Potential flow of an inviscid incompressible liquid around a profile in the presence of solid rectilinear boundaries

12 p1487 A73-27797

Turbulence in liquids; Proceedings of the Symposium, University of Missouri, Rolla, Mo., October 4-6, 1971.

13 p1604 A73-29251

Heat transfer by fluctuating flow of an elastico-viscous liquid past an infinite plate with time varying suction.

14 p1816 A73-29999

Solution of the problem of unsteady heat transfer for a body and the liquid flow around it

14 p1744 A73-30018

Measurement of gas quantities by liquid displacement.

14 p1723 A73-30048

Heat transfer to a cylindrical laminar liquid jet ejecting into a gas.

14 p1817 A73-30612

Flow deceleration as mechanism of vortex ring formation, showing liquid mass variability and vortex clusters of spheroid and hemisphere shapes

15 p1861 A73-31282

Thermal tagging for laminar and turbulent liquid flow shadowgraph visualization by Nd glass laser beam

16 p2016 A73-33598

Development of a turbulent mixing region in a liquid

17 p2150 A73-34265

Nonstationary wave propagation in equilibrium liquid-vapor flow, noting pressure jumps due to expansion

17 p2155 A73-35193

Liquid anorthite viscosity and thermal expansion at 1450-1620 C and 820-950 C, noting agreement with Bottinga-Weill model predictions

20 p2555 A73-39718

Sound propagation in gases, liquids and solids, discussing effects of nonlinear terms in wave and state equations and boundary conditions on solution

21 p2739 A73-40621

Approximate estimation of the possibility of using the viscoelasticity hypothesis for the formulation of an equation of motion for a liquid with polymer additions

22 p2841 A73-42122

Heat transfer in liquids due to second order boundary layer flows with dissipation.

22 p2938 A73-42996

Capillary breakup length and stability of Newtonian and viscoelastic cylindrical liquid jets in terms of dimensionless viscosity and relaxation time

23 p2967 A73-43307

Applicability of difference methods for solving Navier-Stokes equations at large Reynolds numbers

24 p3076 A73-44426

The flow of a viscous liquid down a variable incline.

24 p3080 A73-45368

LIQUID HELIUM

NT LIQUID HELIUM 2

Forced flow, single-phase helium cooling systems.

01 p0123 A73-11099

Theory of Kapitza's jump in temperature at the interface between a solid body and liquid helium

01 p0079 A73-11281

Effect of counterflows of normal and superfluidic fluid on the second-sound velocity in helium II

02 p0154 A73-12543

Critical flows in open vertical ducts filled with superfluid helium under pressure

05 p0599 A73-17230

A cryogenic ultrahigh-vacuum pump with a small liquid-helium flow rate

07 p0830 A73-19288

The nuclear resonance in liquid helium three at very low temperatures

08 p0987 A73-20647

Influence of heating-surface orientation in a gravitational field on the nucleate boiling crisis of liquid

11 p1450 A73-25729

High responsivity large surface liquid helium cooled IR bolometers based on carbon resistors and Ge and Si elements

11 p1368 A73-26510

A new type of helium-cooled bolometer.

11 p1368 A73-26511

Cryostats with and without radiation passage through window into vacuum space in balloon-borne far IR instruments requiring cooling to liquid He temperature

11 p1453 A73-26516

Energy transfer from a pulsed thermal source to He II below 0.3 K.

13 p1658 A73-28191

Cryogenic ultrahigh-vacuum pump with low liquid-helium consumption.

13 p1659 A73-28688

Heat transfer during helium boiling in narrow channels of different orientations

13 p1661 A73-29405

Liquid He 3 superfluidity near absolute zero, noting two solid and four liquid phases within millidegrees

14 p1775 A73-30617

Role of laser radiation self-focusing during breakdown in liquid He4

15 p1884 A73-31701

Some experiments on the influence of surface treatment on the Kapitza conductance between copper and He4 at temperatures from 1.2 to 2.0 K.

21 p2741 A73-41105

Development of a vacuum chamber for ionospheric plasma simulation - Utilization of liquid helium cryopumping

22 p2838 A73-41869

Theory of the Kapitza temperature discontinuity at a solid body-liquid helium boundary.

23 p3006 A73-43502

Critical heat flux for two-phase flow of helium I.

24 p3155 A73-44822

LIQUID HELIUM 2

Discontinuity conditions for two fluid model of liquid helium 2 from total energy and superfluid linear momentum balance and entropy production inequality postulations

07 p0850 A73-19106

Correlation of the vaporization onset heat flux for cylinders in saturated liquid helium-II.

07 p0922 A73-20411

Temperature dependence of the accommodation coefficient of liquid-helium film.

10 p1249 A73-24341

Further investigations on the nonlinear behavior of a system of parallel line vortices.

14 p1746 A73-30652

Helium superleak metastable persistent current quantum states use to provide nondecaying angular momentum for gyroscopic element

15 p1876 A73-31942

Measurement of relaxation time during acceleration of rotation of vessels containing helium II, and superfluidity in pulsars

16 p2038 A73-34065

Incompressible potential flow past sphere parallel to contact plane tangent as model to determine critical velocity for dissipation onset in superfluid liquid He II

19 p2421 A73-37853

LIQUID HYDROGEN

Influence of an ultrasonic field on the behavior of a vapor bubble in liquid hydrogen

01 p0077 A73-10929

Gas-liquid hydrogen mixture and helium adiabatic model of Jupiter temperature and pressure distribution, estimating planet center temperature

01 p0107 A73-11324

Vehicle-scale investigation of a fluorine jet-pump liquid hydrogen tank pressurization system.

[AIAA PAPER 72-1133]

03 p0355 A73-13440

German monograph - Propagation of ion acoustic waves in a weakly ionized plasma.

03 p0398 A73-13814

Conical liquid hydrogen target with large exit aperture and multilayer insulation between inner vessel and vacuum jacket for experiments on leptonic decays

05 p0538 A73-17288

Three meter liquid hydrogen target for K meson production with Serpukhov accelerator, discussing design, operation control and emergency conditions

05 p0538 A73-17289

Potentials and problems of hydrogen fueled supersonic and hypersonic aircraft.

09 p1032 A73-22830

Effect of an ultrasonic field on the behavior of a vapor bubble in liquid hydrogen.

10 p1249 A73-24189

Isentropic compression of fused quartz and liquid hydrogen to several Mbar.

11 p1398 A73-25884

The use of hydrogen for aircraft propulsion in view of the fuel crisis.

17 p2220 A73-35469

Energy supply and its effect on aircraft of the future. II - Liquid-hydrogen-fueled aircraft: Prospects and design issues.

[AIAA PAPER 73-809]

19 p2388 A73-38373

Potential of hydrogen fuel for future air transportation systems.

[ASME PAPER 73-ICT-104]

23 p3019 A73-43499

Light scattering intermolecular and Raman spectra in liquid and solid hydrogen, showing short wave collective excitations in relation to phonon processes

23 p3007 A73-44171

LIQUID INJECTION

NT WATER INJECTION

Breakup and penetration of transverse liquid jets in supersonic air cross flow

[AIAA PAPER 72-1180]

03 p0293 A73-13475

Multiple-orifice liquid injection into hypersonic air streams.

07 p0775 A73-19976

Liquid film cooling on hypersonic slender bodies.

10 p1172 A73-24540

Nonlinear behavior of capillary liquid jets ejected from nonsymmetric nozzles, showing effect on flow stability 11 p1349 A73-26432

Drop size distribution resulting from liquid jet injection across a supersonic stream. 15 p1863 A73-31659

Inflight electrostatic probe measurements of the effect of chemical injection on the properties of the re-entry flow field. [AIAA PAPER 73-692] 18 p2338 A73-36243

LIQUID LASERS

An 11 megawatt 6.8 joule flashlamp pumped coaxial liquid dye laser. 02 p0175 A73-11956

Threshold pump energy value of liquid lasers in quasi-steady-state operation 06 p0699 A73-17915

High power laser generation and heating of plasma in solid targets due to radiation damage, discussing liquid lasers as light amplifiers 06 p0731 A73-18582

110-J pulsed laser using a solution of rhodamine 6G in ethyl alcohol. 06 p0703 A73-18612

Influence of thionyl chloride on the lasing characteristics of the liquid phosphor $\text{POCl}_3\text{-SnCl}_4\text{-N}_2\text{H}_4\text{H}^+/\text{I}^-$ 12 p1506 A73-27197

LIQUID LEVELS

Level and density sensors using pneumatic repeaters 11 p1364 A73-26099

LIQUID MERCURY

U MERCURY [METAL]

LIQUID METAL COOLED REACTORS

Investigation of a liquid-metal magnetohydrodynamic power system. 11 p1308 A73-25978

LIQUID METALS

NT LIQUID POTASSIUM

NT LIQUID SODIUM

NT MERCURY [METAL]

NT MERCURY VAPOR

Equations of state and dissociation equilibrium for CsCl plasma, noting thermodynamic model for phase transitions of liquid metal into nonideal ion plasma 01 p0084 A73-10851

Nitrogen thermochemistry during the combustion of zirconium droplets in N_2/O_2 mixtures. 01 p0123 A73-10922

Mechanism of transformation of a low-carbon 18-10 stainless steel by reaction in liquid tin 02 p0178 A73-11525

Flooded rotor, direct current acyclic motor, with superconducting field winding. 02 p0132 A73-11829

Disilicides solubility in silver and tin melts, discussing ternary phase formation 02 p0181 A73-12367

Practical protective atmospheres for molten magnesium. 03 p0323 A73-13267

The liquid metal slip ring experiment for the Communications Technology Satellite. 04 p0408 A73-15449

Ion engines with ion emission from liquid metal drops under electric field, noting emitter I-V characteristics and engine design 04 p0488 A73-15726

The effect of noncondensable gas on laminar film condensation of liquid metals. [ASME PAPER 72-WA/HT-9] 04 p0520 A73-15836

Turbulence in the annular flow of a conducting-fluid in a magnetic field 05 p0603 A73-16587

Scale factors of adsorptive reduction in the strength of metals in the presence of melts 06 p0711 A73-18667

Inert-gas transport in liquid metals during boiling experiments. 08 p1023 A73-21263

Neutron radiography as a diagnostic tool in the study of corrosion in lithium-filled heat pipes. 09 p1079 A73-21991

Magnetic duct field and induction distributions for liquid metal pump design, using Tozoni integral equations 10 p1177 A73-23475

Investigation of metal droplet shaping during atomization 10 p1225 A73-24688

Calculations of electrical transport properties of liquid metals at high pressures. 11 p1399 A73-25899

Partition function derived for liquid Fe from Eyring method of significant structures, describing solid at high temperature via Einstein approximation 11 p1355 A73-25904

Transport properties of liquid metal hydrogen under high pressures. 11 p1401 A73-25907

Review of liquid-metal magnetohydrodynamic spacecraft energy conversion cycles. 11 p1308 A73-25977

Flow of liquid metals with a transversely applied magnetic field. I - Laminar flow in the entrance region. 11 p1406 A73-26341

Influence of the physical properties of metal melts on the spheroidization of droplets in the process of their crystallization 12 p1503 A73-27551

Equations of state and dissociation equilibrium for CsCe plasma, noting thermodynamic model for phase transitions of liquid metal into nonideal ion plasma 12 p1529 A73-27901

Application of similarity criteria in calculations of a mobile magnetic field to be used for growth stimulation in single crystals of metals 13 p1667 A73-28108

Heat pipe operational principle and liquid metal working fluids, discussing design, construction and experiments 13 p1706 A73-28674

Ostwald ripening of transition-metal carbides in liquid nickel and cobalt 14 p1760 A73-30441

Efficiency of the recovery of high thermal energy densities during porous vaporization of alkali metals 15 p1957 A73-31864

The interaction of tungsten and molybdenum melts with gaseous oxygen 15 p1890 A73-31924

Thermodynamic analysis of liquid metal systems by using a cluster model 17 p2188 A73-34555

Leidenfrost temperature - Its correlation for liquid metals, cryogenics, hydrocarbons, and water. [ASME PAPER 73-HT-F] 19 p2504 A73-37641

Procedure for preparation of metallic titanium by direct reduction of oxides under flux 19 p2441 A73-37829

NaK-nitrogen liquid metal MHD converter tests at 30 kW. 19 p2389 A73-38311

Apparatus for creep and long-term strength testing of materials in aggressive media under irradiation 20 p2544 A73-39368

Conducting fluid jets in a transverse magnetic field 21 p2747 A73-40888

The emissivities of liquid metals at their fusion temperatures. 22 p2930 A73-41983

The melting point of molybdenum as a secondary fixed point on the International Practical Temperature Scale. [ECTP PAPER G-5] 22 p2877 A73-42407

Phase equilibrium technique to measure oxygen solubility in liquid Co at 1510 to 1700 C, determining thermodynamic characteristics and deoxidation curves 23 p2990 A73-43482

The influence of testing temperature and thermal history on the intergranular embrittlement and penetration of aluminium by liquid gallium. 23 p2993 A73-44026

Study of aluminum-oxygen equilibrium in liquid iron at 1600 deg C with the aid of a solid $\text{ThO}_2\text{-Y}_2\text{O}_3$ electrolyte cell 23 p2995 A73-44178

Antifriction materials employing fibers and liquid-metal lubricants 24 p3101 A73-44413

LIQUID NITROGEN

The study of disperse regimes with film boiling of liquid nitrogen in tubes. 07 p0922 A73-20409

The study of film boiling crises and transient boiling of cryogenic liquids. 07 p0922 A73-20410

Investigation of the hardening process of alloy D16 in liquid nitrogen. 10 p1226 A73-24929

Angular distribution of induced combinational light scattering in liquid nitrogen 12 p1505 A73-26889

Effect of temperature on titanium plasticity 15 p1894 A73-32527

High speed cinematographic study of mass flow rate of pressurized subcooled liquid nitrogen inward choked flow through radial gap at various stagnation pressures 21 p2740 A73-40634

Vapour pressures of liquid oxygen and nitrogen. 22 p2930 A73-41979

LIQUID OXYGEN

NASA use of liquid and gaseous oxygen under extreme pressure, temperature and flow rate conditions, discussing safety requirements in terms of structural and chemical compatibility 11 p1410 A73-26525

Vapour pressures of liquid oxygen and nitrogen. 22 p2930 A73-41979

Servomechanism design techniques and applications - Aerospace problems. 23 p2945 A73-43450

Velocity of hypersonic waves in liquid oxygen. 24 p3110 A73-44984

LIQUID PHASES

Forced convection droplet evaporation with finite vaporization kinetics and liquid heat transfer. 01 p0122 A73-10803

Phase dependence of positron annihilation in tristearin. 06 p0661 A73-18267

Investigation of the crystallization of metallic powders obtained by liquid-phase atomization 10 p1224 A73-24313

Mass transfer approximation model in unidirectional swirled two phase flow, considering transfer resistance of liquid phase 14 p1816 A73-30016

LIQUID POTASSIUM

Plasma heat source and heat exchanger design for liquid potassium circulation system, using air-kerosene aviation gas turbine combustion chamber 20 p2545 A73-39617

LIQUID PROPELLANT ROCKET ENGINES

NT HYDRAZINE ENGINES

NT HYDROGEN OXYGEN ENGINES

Corrosion tests for rocket propulsion system components materials for use with nitric acid-nitrogen tetroxide blend oxidizer 03 p0329 A73-13007

Verification of a comprehensive thrust chamber compatibility model for liquid rocket engines. [AIAA PAPER 72-1078] 03 p0354 A73-13401

P propulsion unit, components, environmental tests and development problems of Swedish air to ground missile rocket engine operating on liquid propellants [AIAA PAPER 72-1102] 03 p0355 A73-13421

Mono- and multipropellant, storable and cryogenic, liquid rocket propulsion engines developments including gas generators and engines 03 p0355 A73-13422

A nonlinear model of combustion instability in liquid propellant rocket engines. [AIAA PAPER 72-1146] 03 p0356 A73-13451

Evaluation of acoustic cavities for combustion stabilization. [AIAA PAPER 72-1147] 03 p0356 A73-13452

Cryogenic liquid O_2/H_2 reaction control systems for Space Shuttle. [AIAA PAPER 72-1155] 03 p0382 A73-13458

Experimental evaluation of a 600 lbf spacecraft rocket engine. [AIAA PAPER 72-1129] 04 p0486 A73-14914

Space Shuttle Orbiter main engine design. [SAE PAPER 720807] 05 p0607 A73-16644

Space shuttle bipropellant reaction control system /RCS/ engine design, characteristics and tests, emphasizing reusability and minimum servicing [SAE PAPER 720839] 05 p0607 A73-16668

Cryogenic problems involved in the development of the structure of a hydrogen/oxygen rocket stage. 07 p0905 A73-18991

Liapunov method for LF and HF instability of liquid propellant rocket engines 07 p0867 A73-20078

Longitudinal vibration analysis of partially-filled ellipsoidal tanks. 07 p0914 A73-20215

Pitch amplitude stabilization in a spacecraft carrier body 09 p1155 A73-23107

Experimental determination of three-dimensional liquid rocket nozzle admittances. 09 p1167 A73-23438

Thermodynamic cycle processes in liquid propellant rocket engines, taking into account combustion products chemical dissociation, wall and nozzle heat losses, friction effects, etc 10 p1263 A73-24700

An analytical model for the prediction of liquid rocket plume contamination effects on sensitive surfaces. [AIAA PAPER 72-1172] 12 p1532 A73-27099

A mechanistic model for analysis of pulse-mode engine operation. [AIAA PAPER 72-1184] 12 p1533 A73-27100

Russian book - Physical principles of rocket weaponry. 15 p1944 A73-32419

Cryogenic propellants in rocket engines. 16 p2045 A73-33118

The dynamic behavior and compliance of a stream of cavitating bubbles. [ASME PAPER 73-FE-34] 17 p2153 A73-35025

Space shuttle liquid propellant reusable rocket engine design, discussing regenerative cooling, fuel pump, oxidizer turbopumps and electronic control systems 19 p2492 A73-37597

Rocket power, Redstone to Saturn V, now Space Shuttle, 20 years of development. [SAWE PAPER 971] 19 p2493 A73-37886

Determination of the thermodynamic characteristics of a liquid-propellant rocket engine with nonisobaric combustion 21 p2754 A73-40402

LIQUID ROCKET PROPELLANTS

NT CRYOGENIC ROCKET PROPELLANTS

NT HYPERGOLIC ROCKET PROPELLANTS

NT MONOPROPELLANTS

Ignition of nonhypergolic rocket fuels with fuming nitric acid under suitable conditions.

01 p0089 A73-10736

Multi-droplet combustion of liquid propellants.

01 p0089 A73-11114

A comparison of neutral buoyancy and free fall for liquid propellant system zero-G simulations.

[AIAA PAPER 72-1041]

03 p0287 A73-13376

Selection of a surface tension propellant management system for the Viking 75 Orbiter.

[AIAA PAPER 72-1042]

03 p0381 A73-13377

Monopropellant and bipropellant thruster systems with afterburning for geostationary satellite orbital control, evaluating performance and reliability based on calculation and test data

07 p0866 A73-18930

The liquefied ergol supply-trailers for DIAMANT B and EUROPA II launchers.

07 p0807 A73-18948

Algorithm for calculating unsteady heat transfer in liquid-propellant rocket-engine chambers with regenerative cooling

07 p0868 A73-20087

Influence of the flexibility of the walls on the oscillations of the liquid masses of storage tanks

12 p1487 A73-27395

Ignition of nonhypergolic bipropellants in presence of suitable catalysts.

14 p1784 A73-30044

Liquid propellant rockets, discussing effective exhaust velocity, nozzle expansion, chamber pressure effects on equilibrium performance and kinetic recombinations

14 p1784 A73-30136

LIQUID ROTATION

U ROTATING LIQUIDS

LIQUID SLOSHING

Natural frequencies, forces and moments for liquid propellant sloshing in tilted cylindrical tank as function of tilt angle and liquid depth

03 p0293 A73-13314

Small steady free oscillations of liquid in rigid tanks, considering HF modes

03 p0296 A73-14047

Containers with isochronous fluid oscillations.

06 p0686 A73-18147

A remark on the sloshing frequencies for a half-space.

08 p0953 A73-20788

Axisymmetric hydroelastic sloshing in a circular cylindrical container.

08 p0956 A73-21690

Approximate determination of the hydrodynamic coefficients for the sloshing of a liquid in moving cylindrical cavities

10 p1206 A73-24309

Natural oscillations of density-stratified ideal incompressible liquid in rectangular vessel, solving oscillation equation for various density distributions

11 p1349 A73-26441

Oscillations of a shell partially filled with a liquid and containing sources of the liquid

11 p1446 A73-26462

Influence of the flexibility of the walls on the oscillations of the liquid masses of storage tanks

12 p1487 A73-27395

On the eigenvalue problem for fluid sloshing in a half-space.

13 p1599 A73-28410

Viscous fluid sloshing in rectangular vessel, studying forced oscillations, ejected flow and frequency equation based on Navier-Stokes equations and boundary conditions

13 p1600 A73-28444

Vertical free vibrations of rectangular vessel partially filled with perfect incompressible liquid analyzed by power series

15 p1860 A73-31045

Analysis of the perturbed motion of a solid with cavities partially filled with liquid

23 p2969 A73-44198

LIQUID SODIUM

Corrosion and deposition of steels and nickel-base alloys in liquid sodium.

23 p2990 A73-43456

LIQUID SURFACES

NT MENISCI

The effect of solar radiation reflected from water surfaces on airborne and surface measurements in the thermal infrared.

01 p0038 A73-10385

Laboratory determinations of water surface emissivity.

06 p0691 A73-18713

The free surface on a liquid between cylinders rotating at different speeds. I.

10 p1207 A73-24789

The free surface on a liquid between cylinders rotating at different speeds. II.

10 p1207 A73-24790

Waves produced by a source of harmonic oscillations located in a cylindrical layer of liquid

11 p1349 A73-26468

Acoustic wave propagation, scanning and liquid surface techniques in acoustical holography, noting applications in geophysics, oceanography, medicine and nondestructive testing

11 p1371 A73-26542

Measurement of pulsating pressure with a piezometer

13 p1612 A73-28449

Hydrodynamics in weak gravitational fields - Small oscillations of an ideal liquid in a cylindrical vessel

15 p1861 A73-31280

Steady induced capillary-gravitational finite-amplitude waves on the surface of a finite-depth liquid

15 p1865 A73-32116

Hydroelastic oscillations in a rigid circular cylinder in the presence of an elastic fluid surface covering

18 p2297 A73-36065

Determination of the equilibrium state of a capillary liquid in a vessel

24 p3080 A73-45526

LIQUID-GAS MIXTURES

NT AEROSOLS

NT FOG

Long wave disturbance propagation analysis via equations of motion from mathematical model of liquid-gas mixture, determining velocity, pressure and density perturbation propagation

03 p0294 A73-13612

The structure of a weak shock wave in a gas/liquid medium

08 p0954 A73-21129

Structure of a weak shock wave in a gas-liquid medium.

15 p1864 A73-32064

Application of a holographic technique to the determination of the dispersity of a two-phase gas/liquid flow

18 p2318 A73-37122

Shock wave structure in liquid/gas bubble medium from theoretical two-phase model and experimental piezoelectric pressure profile measurements

20 p2547 A73-39283

Gas solubility in hydraulic liquids from measurements of air in mineral oils, noting oil molecular weight effect

21 p2724 A73-41579

LIQUID-LIQUID INTERFACES

On turbulent flows with fast chemical reactions. II - The distribution of reactants and products near a reacting surface.

[AD-753565]

01 p0032 A73-10638

Turbulent interface structure from eddy viscosity models, discussing equations of motion and Nee-Kovaszny and Prandtl models

10 p1205 A73-24253

A note on residual drop and single drop formation.

22 p2840 A73-41748

Rayleigh-Taylor instability in octyl alcohol-water interface, observing bubble and spike formation with flattening and curling of spike due to Kelvin-Helmholtz instability

22 p2842 A73-42232

LIQUID-SOLID INTERFACES

Theory of Kapitza's jump in temperature at the interface between a solid body and liquid helium

01 p0079 A73-11281

A problem of coupling between the vibration of a thin plate and an acoustic field in a fluid

03 p0383 A73-12982

Some results using the ultrasonic goniometer - The corner reflector method.

04 p0447 A73-14930

Growth of ternary composites from the melt. I, II.

04 p0463 A73-15310

Interaction of TEA-CO₂-laser pulses with metals enhanced by liquid layers.

07 p0836 A73-20195

Solid sphere meandering trajectory in viscous liquid filled cylinder, postulating oscillating molecular surface tension layer at interface

10 p1206 A73-24701

Newtonian and non-Newtonian liquids rotating adjacent to a stationary surface.

11 p1346 A73-25369

Potential flow of an inviscid incompressible liquid around a profile in the presence of solid rectilinear boundaries

12 p1487 A73-27797

Solution of the problem of unsteady heat transfer for a body and the liquid flow around it

14 p1744 A73-30018

Apparent added masses of a plate array in an incompressible liquid

15 p1861 A73-31281

Vertical submersion of a floating cylindrical solid

15 p1861 A73-31283

Hydroelastic oscillations in a rigid circular cylinder in the presence of an elastic fluid surface covering

18 p2297 A73-36065

Shock and compression by TEA-CO₂-laser pulses drastically enhanced by liquid layers spread on surfaces of solids.

19 p2438 A73-38024

The steady-state thickness of a liquid water film on the surface of hailstones of various shapes

21 p2730 A73-40118

Observations of solid/liquid interfaces in dilute binary and ternary Al-rich alloys.

21 p2721 A73-41120

Book - Advances in corrosion science and technology. Volume 3.

23 p2990 A73-43455

Corrosion and deposition of steels and nickel-base alloys in liquid sodium.

23 p2990 A73-43456

Theory of the Kapitza temperature discontinuity at a solid body-liquid helium boundary.

23 p3006 A73-43502

Wettability and interfacial tension of magnesium oxide-silicon dioxide glasses, discussing contact angle relationship to temperature

23 p2998 A73-44132

Quasi-steady Stefan problem solutions for nonlinear heat conduction in two phase /liquid-solid/ state crystallizer

24 p3158 A73-45501

LIQUID-VAPOR EQUILIBRIUM

Influence of an ultrasonic field on the behavior of a vapor bubble in liquid hydrogen

01 p0077 A73-10929

Effect of an ultrasonic field on the behavior of a vapor bubble in liquid hydrogen.

10 p1249 A73-24189

Nonstationary wave propagation in equilibrium liquid-vapor flow, noting pressure jumps due to expansion

17 p2155 A73-35193

Law of micro-liquid-layer formation between a growing bubble and a solid surface with a special reference to nucleate boiling.

21 p2792 A73-41144

Evaporation of metallic targets caused by intense optical radiation.

22 p2868 A73-41727

Liquid-vapour equilibria research on systems of interest in cryogenics - A survey.

24 p3155 A73-44821

LIQUID-VAPOR INTERFACES

Square well fluid liquid-vapor interface density profiles from perturbation expansion in chemical potential, comparing to BGYB and excess free energy minimization approaches

03 p0342 A73-13277

The gas liquid interface and the load capacity of helical grooved journal bearings.

[ASME PAPER 72-LUB-19]

03 p0314 A73-14334

Void fraction measurement based on gas-liquid volume ratio by local void velocity measurement with single probe

05 p0638 A73-16224

Adsorption conditions and vapor molecule balance in wall layer at liquid boiling initiation, noting heat flux dependence on underheating effect, pressure and velocity

06 p0769 A73-18564

A method of calculating heat and mass transfer between liquid droplets and a gaseous phase in an acoustic wave field

08 p1022 A73-21196

Inert-gas transport in liquid metals during boiling experiments.

08 p1023 A73-21263

Destabilization of vapor film boiling around spheres.

08 p1024 A73-21641

Generalized van der Waals theories for surface tension and interfacial width.

11 p1400 A73-26214

Forced convective heat transfer of a gas with condensing vapor around a flat plate.

15 p1958 A73-32058

Adsorption conditions and vapor molecule balance in wall layer at liquid boiling initiation noting heat flux dependence on underheating effect, pressure and velocity

16 p2086 A73-33589

High-speed photography of laser-induced cavities in liquids

21 p2709 A73-39968

Complex flow in vapour columns over boiling cryogenic liquids.

21 p2740 A73-41102

Comparison of experimental microlayer thickness results.

21 p2793 A73-41690

Surface tension and interfacial density profile of fluids near the critical point.

24 p3110 A73-44986

LIQUIDS

NT CRYOGENIC FLUIDS

NT CRYOGENIC ROCKET PROPELLANTS

NT FERMI LIQUIDS

NT FLOX

NT HYDRAULIC FLUIDS

NT HYPERGOLIC ROCKET PROPELLANTS

NT LIQUEFIED GASES

NT LIQUID AMMONIA

NT LIQUID HELIUM
 NT LIQUID HYDROGEN
 NT LIQUID METALS
 NT LIQUID NITROGEN
 NT LIQUID OXYGEN
 NT LIQUID POTASSIUM
 NT LIQUID ROCKET PROPELLANTS
 NT LIQUID SODIUM
 NT MERCURY [METAL]
 NT MERCURY VAPOR
 NT MONOPROPELLANTS
 NT ORGANIC LIQUIDS
 NT ROTATING LIQUIDS
 Dynamic method for measuring thermal conductivity of liquids and gases at high pressures.

08 p1021 A73-20861
 Non-critical Rayleigh scattering from pure liquids.
 20 p2570 A73-38618

LIQUIDUS

Lunar rocks petrogenesis, determining liquidus and solidus temperatures and crystalline phases sequence in lunar samples and synthesized oxides and silicates
 07 p0879 A73-19689

Analytical approach to estimating the source rock of basaltic magmas - Major elements.

09 p1076 A73-22147

Bivariant eutectic alloys located on liquidus surface within Ni-Nb-Cr-Al quaternary, permitting production of aligned delta Ni-Nb lamellae within nichrome matrix containing Ni-Al fcc precipitate
 12 p1509 A73-26845

LITERATURE

NT DOCUMENTATION

LITHERGOL ROCKET ENGINES

German book - Hybrid rocket propulsion systems: An introduction to theoretical and technical problems.
 06 p0741 A73-17669

LITHIASIS

Renal lithiasis among civil operating aircrew

08 p0931 A73-21536

Renal lithiasis among military operating aircrew

08 p0931 A73-21537

LITHIUM

NT LITHIUM ISOTOPES

Investigation of the temporal-spatial distribution of optical density in a plasma of high-current Li and In discharges
 01 p0085 A73-10853

Summary of results of JPL lithium-doped solar cell development program.
 03 p0257 A73-14240

Voltage and power relationships in lithium-containing solar cells.
 03 p0257 A73-14241

Fabrication criteria, mission design factors and I-V characteristics of Li solar cells
 03 p0257 A73-14242

Li and Si p-n solar cells performance comparison for simulated earth orbit environment by real time irradiation with Sr 90 beta particles
 03 p0257 A73-14243

Features of voltage-capacitance relationships in Si/Li/p-n detectors
 06 p0675 A73-18080

Saturation of 1Kh18N9T steel with beryllium and corrosion resistance of the coating in a lithium melt
 06 p0711 A73-18669

Photography of a lithium vapor trail during the daytime.
 07 p0820 A73-20068

Investigation of the structure of a high-current discharge in a lithium plasma.
 08 p0992 A73-20853

Neutron radiography as a diagnostic tool in the study of corrosion in lithium-filled heat pipes.
 09 p1079 A73-21991

Investigation of a liquid-metal magnetohydrodynamic power system.
 11 p1308 A73-25978

Investigation of the space-time distribution of the optical density of the plasma in high-current Li-In discharges.
 12 p1529 A73-27903

Effect of lithium on acute oxygen toxicity and associated changes in brain gamma-aminobutyric acid.
 13 p1575 A73-28503

The Li donor, and binding of excitons at neutral donors and acceptors in crystals
 15 p1924 A73-31722

Stable high energy nonaqueous lithium-organic electrolyte batteries, discussing discharge rates, temperature effects, energy density and voltage regulation
 19 p2390 A73-38396

Reaction Li-6/p, pt/ at 590 MeV.
 21 p2743 A73-41018

LITHIUM ALLOYS

Russian book on extra light engineering alloys covering Mg-Li alloys structure and mechanical properties, aging and strain hardening characteristics, corrosion resistance, etc
 08 p0979 A73-21600

Peritectic solid phase transformations in cast homogenized Al-Cu-Li-Mn-Cd alloy, noting Li strengthening effect
 10 p1236 A73-24927

Crystallization of nickel-based alloys and indium-lithium system alloys at ultrahigh cooling rates
 13 p1632 A73-28112

LITHIUM ALUMINUM HYDRIDES

The non-equilibrium ortho/para spin state ratio for molecular H₂ formed in the hydrolysis of lithium aluminum hydride.
 07 p0787 A73-19144

LITHIUM COMPOUNDS

NT LITHIUM ALUMINUM HYDRIDES

NT LITHIUM FLUORIDES

NT LITHIUM HYDRIDES

NT LITHIUM NIOBATES

NT LITHIUM OXIDES

Fracture of nonlinear crystals /KDP and LiNbO₃/ by radiation from a ruby laser.
 02 p0176 A73-12112

Laser-radiation-induced damage to the surface of lithium niobate and tantalate single crystals.
 06 p0738 A73-18591

Features of the domain structure of cobalt-doped lithium ferrite when changing the direction of easy magnetization
 10 p1260 A73-24508

The generation of tunable coherent radiation in the wavelength range 2300-3000 Å using lithium formate monohydrate.
 12 p1504 A73-26826

High temperature creep of lithium zinc silicate glass-ceramics. I - General behaviour and creep mechanisms. II - Compression creep and recovery.
 23 p2997 A73-44030

Influence of ion ordering on the induced anisotropy in Li-Fe ferrites
 23 p3018 A73-44175

LITHIUM FLUORIDES

Use of MgF₂ and LiF photocathodes in the extreme ultraviolet.
 08 p0964 A73-21048

LiF albedo dosimeter for fast neutron and gamma irradiation measurement on personnel, using Cf-252 source for calibration
 11 p1361 A73-25313

Thermoluminescence and activation energies in Al₂O₃, MgO and LiF /TLD-100/.
 12 p1530 A73-27031

Changes in the microhardness of lithium fluoride crystals subjected to cyclic elastic compression
 19 p2470 A73-37954

Triply ionized Pm in lithium yttrium fluoride laser, calculating crystal field split energy levels and radiative transition probabilities
 21 p2715 A73-40764

LITHIUM HYDRIDES

NT LITHIUM ALUMINUM HYDRIDES

Multiple meson production in 250 GeV nucleon-nucleon collisions in LiH targets, noting 40 per cent formation of heavy meson cluster fireballs
 02 p0208 A73-12653

An 'ab initio' Gaussian orbital calculation of the /100/ surface of crystalline lithium hydride.
 06 p0737 A73-18252

Development of special graphites for lithium hydride/fluorine rocket engines
 09 p1110 A73-23019

LITHIUM ISOTOPES

Nuclear gamma rays from Li-7 in the galactic cosmic radiation.
 05 p0612 A73-17329

Analysis of lunar samples 14163, 14259, and 14321 with isotopic data for Li-7/Li-6.
 07 p0887 A73-19766

LITHIUM NIOBATES

Pulsed laser produced holograms with iron doped lithium niobate, noting application in high capacity information storage
 08 p0964 A73-21051

Self-enhancement of LiNbO₃ holograms.
 09 p1079 A73-21943

Optical damage and internal fields in pyroelectrics.
 10 p1260 A73-24531

Experimental studies of a method of detecting microwave-modulated laser radiation in a photosensitive detector
 13 p1628 A73-29415

Some features of second-harmonic generation in a lithium metaniobate crystal.
 22 p2896 A73-42247

Study of the parameters of three-dimensional holographic gratings in LiNbO₃ crystals
 23 p2987 A73-43717

Measurement of optically induced refractive-index changes with sharp edged illumination pattern.
 23 p2984 A73-44371

Some experiments on a voltage-induced optical waveguide in LiNbO₃.
 23 p3019 A73-44374

Angular selectivity of lithium niobate volume holograms.
 24 p3092 A73-45424

LITHIUM OXIDES

Characterization of the mixed oxides of lithium and aluminum.
 01 p0089 A73-11113

Oxystearate-based multipurpose lithium lubricants
 07 p0843 A73-20013

LITHIUM 4

U LITHIUM ISOTOPES

LITHIUM 6

U LITHIUM ISOTOPES

LITHOGRAPHY

Coherent intensity spatial filtering applied to inspection of photolithography masks for LSI.
 06 p0694 A73-18288

Statistical analysis of the influence of various factors on the quality of photolithographic operations in the production of integrated circuits
 20 p2534 A73-38851

A laser raster setup with programmed control for image lithoplate synthesis
 22 p2869 A73-42362

LITHOLOGY

Sedimentology of clastic rocks returned from the moon by Apollo 15.
 01 p0103 A73-11016

Terrestrial heat flow determinations in the north central United States.
 09 p1076 A73-22148

LITHOSPHERE

NT EARTH CORE

NT EARTH CRUST

NT EARTH MANTLE

NT EARTH SURFACE

The Luna 20 lithic fragments, and the composition and origin of the lunar highlands.
 13 p1677 A73-28336

Russian book - Geochemistry and cosmochemistry of inert gas isotopes.
 15 p1840 A73-31585

Certain features of interaction between the atmosphere and lithosphere on the moon
 16 p2065 A73-33787

LITTORAL CURRENTS

U COASTAL CURRENTS

LIVER

Activated oxygen ashing of biological specimens for the microdetermination of Na, K, Mg, and Ca by atomic absorption spectrophotometry.
 02 p0139 A73-12546

Cation exchange binding of rubidium and cesium by rat liver cell microsomes.
 02 p0135 A73-12549

Hepatic lipogenesis in fasted, re-fed rats and mice - Response to dietary fats of differing fatty acid composition.
 03 p0258 A73-13054

Hypoxia, an adjunct in helium-cold hypothermia - Sparring effect on hepatic and cardiac metabolites.
 07 p0782 A73-20169

Effect of low temperature on metabolism of rat liver slices and epididymal fat pads.
 07 p0782 A73-20170

Study of the possibilities of histone-RNA complex formation in experiments in vitro
 10 p1181 A73-24513

Morphological changes in the liver of dogs induced by chronic gamma irradiation
 12 p1463 A73-27707

Effects of altitude stress on mitochondrial function.
 14 p1717 A73-30430

Effect of prolonged hypokinesia on certain energy transfer characteristics in skeletal muscles and some internal organs
 15 p1834 A73-31505

Hepatic lesions observed among flight crews following aviation accidents
 18 p2279 A73-36933

Hemotherapy of coagulation system disturbances of hepatolitical origin
 23 p2947 A73-44299

LMCR [REACTORS]

U LIQUID METAL COOLED REACTORS

LOAD DISTRIBUTION [FORCES]

Use of a plastic deformation design model of polycrystalline material in the analysis of loading surface transformation
 01 p0112 A73-10008

Bending of a uniformly loaded clamped sector plate.
 01 p0116 A73-11006

Statistical method of determining the load or stress distribution from the failure characteristics of mechanical systems
 01 p0118 A73-11370

Oscillations of nonshallow cylindrical shells loaded by distributed and concentrated masses
 01 p0118 A73-11407

Topologic group theory for stress analysis of nonlinearly elastic body under complex load, representing loads set by Lie group
 01 p0119 A73-11428

Rectangular plate stability under compression by uniformly distributed loads applied to two opposite simply supported edges with mixed boundary conditions at other edges
 02 p0230 A73-11640

Analysis of unbalanced angle-ply rectangular plates.
 02 p0234 A73-12073

Stress-strain state of shallow spherical shell with variable wall thickness under uniformly distributed load, using Vlasov shell theory

02 p0235 A73-12192

Bending of a physically nonlinear viscoelastic rectangular plate under the action of a transversely distributed load

02 p0237 A73-12587

Numerical integration of nonlinear integrodifferential equations of thin viscoelastic beams deflection, considering cantilever beam under uniformly distributed loads

03 p0390 A73-13343

A finite element analysis of an axisymmetrically loaded orthotropic shell of revolution.

03 p0391 A73-13677

Delay effects in fatigue crack propagation.

04 p0459 A73-14690

Lifting characteristics and spanwise aerodynamic load distribution of an external flow jet flap.

04 p0404 A73-15513

Bifurcation of rings under concentrated centrally directed loads.

[ASME PAPER 72-WA/APM-37]

04 p0515 A73-15885

Effect of the cross sectional shape of specimens on their strength under transverse-bending impact loads

05 p0632 A73-16327

Optimal and stiffened simply supported circular plates comparison under uniform pressure and uniform compression loads

05 p0635 A73-16976

Complex resilient-base structure designs incorporating the reaction to an external load

05 p0636 A73-17083

Stress analysis for homogeneous elastic disk under continuous and concentrated load distribution

06 p0760 A73-17783

Stress distribution on astronomical telescope mirror outer surface, calculating deflection and relief load

06 p0693 A73-18157

Bending theory of rectangular plates loaded along curve, obtaining solutions by Fourier single and double series

06 p0763 A73-18451

Fracture in conditions of creep under complex loading

07 p0910 A73-19302

Singular integrodifferential and linear integral equations for load transfer from stringer to wedge under concentrated force and for stringer-coupled wedge shaped regions

07 p0910 A73-19306

Extremal stresses in the first basic two-dimensional problem of elasticity theory for a half-plane

07 p0911 A73-19310

Nonuniformly heated anisotropic rods with variable elastic parameters

07 p0911 A73-19317

Transmission of the load from an annular cover piece to a plane with a circular hole

07 p0911 A73-19321

Axisymmetric buckling of uniformly loaded spherical caps undergoing plastic deformation.

07 p0913 A73-19971

Numerical analysis of anisotropic rotational shells subjected to nonsymmetric loads.

07 p0914 A73-20210

Durability of foil-type tensometric sensors under varying load conditions

07 p0827 A73-20536

Large deflections and stability of a long cylindrical panel prepared from an orthotropic fiberglass plastic under the action of piecewise-uniform loading

08 p1017 A73-21370

Load and support configurations associated with aspherical dioptr of revolution with variable thickness profile generating dioptrics deformed by elasticity

08 p0967 A73-21492

Nonstationary load distribution on an arbitrary-planform wing in supersonic motion

08 p0927 A73-21725

Stress-strain state of transversely isotropic shells under concentrated loads

08 p1019 A73-21760

Determination of the optimal physical load in the local heating of a cylindrical shell

09 p1159 A73-22589

An elastic ribbon under the action of a nonuniform load

09 p1165 A73-23348

Analysis of load distribution in multiple-row bolt joints

10 p1222 A73-23595

Dependence of the coefficient of external friction on a normal load during elastic saturated contact

10 p1222 A73-23596

Stress-strain state in the filler of a three-layer strip under local loading

10 p1291 A73-24354

A modification of the moire fringes technique for the analysis of moments and deflections in a laterally loaded plate.

10 p1220 A73-24573

Elastic deformation of an orthotropic semi-infinite plate with straight boundary asymmetric with respect to the elastic axes of the material under uniform partial loading.

10 p1293 A73-24922

Stress distribution in a half-plane with a hole strengthened by an elastic insert

11 p1432 A73-25026

Structural design errors resulting from conventional treatment of distribution law for local radial and torque loads

11 p1433 A73-25028

Linear elastic behavior of laminated plate with ribs reinforced by continuous unidirectional fibers under surface distributed loads orthogonal and parallel to plane

11 p1435 A73-25403

Surface damage under fretting fatigue as function of applied normal load and clamping pressure

11 p1383 A73-25836

Topologic group theory for stress analysis of non-linearly elastic body under complex load, representing loads set by Lie group

11 p1443 A73-26057

Transient creep of shells of revolution.

11 p1444 A73-26336

Clamped orthotropic skew plates under uniformly distributed transverse load, considering nonlinear analysis based on numerical technique of dynamic relaxation involving critically damped vibration

11 p1444 A73-26381

Bending problem for shell of revolution with finite displacements, axisymmetric loading and nonlinear strain functions

11 p1445 A73-26460

Procedure for studying fatigue failure features in metals under harmonic and complex loading at low temperatures

12 p1486 A73-27254

Stability of a cylindrical anisotropic shell under the action of a ring load with allowance for subcritical deflection

12 p1553 A73-27373

Deformation of a nonshallow spherical shell under local loads

12 p1553 A73-27469

Soft shell strength analysis for contact and static loads

12 p1554 A73-27470

Elastoplastic bending of a cylindrical shell according to the Prandtl-Reuss theory

12 p1554 A73-27472

Shallow conical closed shell stability under axisymmetric loads, using variational difference method

12 p1556 A73-27799

Shallow spherical shell dynamic stability under axisymmetric loads, noting small HF vibrations effect on static stability

12 p1556 A73-27814

Branched solution of integro-power equation for nonlinear bending of shallow spherical shells with clamped edge under uniform radial compression load

12 p1556 A73-27816

Stress-singularities due to uniformly distributed loads along straight boundaries.

13 p1696 A73-28757

Lamb solution analog for dynamic problem of homogeneous isotropic elastic body with impulsive force applied to semi-infinite plane incision

13 p1698 A73-29088

Effects of specimen geometry and loading conditions on the crack tip plastic zone.

13 p1701 A73-29474

The effect of groupings of surface couples on flat plates

14 p1814 A73-30703

Engineering structures design, discussing stress and strain distributions, mechanical defects, symmetric loading and fracture models

[ASME PAPER 73-DE-19]

14 p1815 A73-30820

Fracture mechanics approach to fatigue analysis in design.

[ASME PAPER 73-DE-22]

14 p1763 A73-30823

Use of the surface of influence of the clamping couple on a circular plate for design calculation under an asymmetrical load

15 p1944 A73-30974

Dependence of the closeness of two contacting bodies on the load under a high contour-applied pressure with a plastic contact

15 p1880 A73-31143

Stability of a stochastically excited nonlinear cylindrical shell.

15 p1949 A73-31654

Mixed boundary value problem solution for strip under elastic deformation due to external loads based on reduction to system of integrodifferential equations

15 p1952 A73-32088

Theorem concerning possible bendings in zero-moment shell theory

15 p1953 A73-32090

Antiplane elasticity boundary value problem solution for isotropic bars under tangential loads, considering twisting and bending

15 p1955 A73-32127

Russian book - Plane bending and tension of curvilinear thin-walled beams.

15 p1956 A73-32296

Poisson's Ratio and the deflection of a viscoelastic plate.

15 p1956 A73-32342

Stresses in plastics reinforced by anisotropic fibers in the presence of transversal normal loads

16 p2030 A73-33928

Chernin type second order equation for complex stress function for elastic shells of revolution under lateral load and tilting moment

16 p2084 A73-34034

Inelastic buckling of eccentrically loaded columns.

17 p2240 A73-34180

Elastic equilibrium of an ellipsoid under the action of concentrated loads

17 p2244 A73-34790

Forced plane strain motion of cylindrical shells - A comparison of shell theory with elasticity theory.

[ASME PAPER 73-APM-9] 17 p2247 A73-35034

Dynamic buckling of shallow spherical shells.

[ASME PAPER 73-APM-A] 17 p2249 A73-35104

Shells of revolution belonging to a spherical class subjected to local loads at the pole

18 p2362 A73-36402

Limiting equilibrium of a circular plate with allowance for the shearing stress

18 p2363 A73-36405

Contact problem for infinite elastic isotropic plane weakened by rectilinear cut with free, slipping and adhesive segments and uniformly distributed load at infinity

18 p2363 A73-36415

Axisymmetric deformation of soft spherical shells

18 p2367 A73-37139

Calculation of a system of two infinite beams on an elastic base

19 p2495 A73-37190

Compatibility of maneuver load control and relaxed static stability.

[ALAA PAPER 73-791] 19 p2379 A73-37458

Lamb solution analog for dynamic problem of homogeneous isotropic elastic body with impulsive force applied to semiinfinite plane incision

19 p2498 A73-37638

Postbuckling behavior of circular rings with two or four concentrated loads.

19 p2501 A73-38251

The vibrations of a circular plate with uniformly distributed load around the outer periphery.

19 p2502 A73-38348

Dynamic stability of a nonlinear beam subjected to both longitudinal and transverse excitation.

20 p2621 A73-39532

An approximate solution for bending of anisotropic laminated plates.

20 p2623 A73-39554

Flutter-divergence transition criteria in certain viscoelastic polygenic systems.

20 p2623 A73-39556

Some mathematically equivalent problems in the statics of shells of revolution

20 p2624 A73-39649

Frame of a cylindrical shell under the action of a concentrated radial force

21 p2783 A73-40388

Experimental investigation of a cylindrical shell loaded by a concentrated tangential force and a bending moment

21 p2787 A73-41193

Determination of the limiting equilibrium of a brittle body weakened by a system of cracks whose form on a plane approaches a circular form

22 p2921 A73-42284

The load transfer problem in shafts coupled through a sleeve.

[ASME PAPER 73-APMW-3] 22 p2867 A73-42877

The Morley-Koiter equations for thin-walled circular cylindrical shells. II - Solution for a line loaded cylinder with close-spaced circumferential grooves.

[ASME PAPER 73-APMW-23] 22 p2925 A73-42885

Analytic treatment of minimum weight design of cantilevers.

[ASME PAPER 73-APMW-29] 22 p2925 A73-42889

The elliptical crack subjected to nonuniform shear loading.

[ASME PAPER 73-APMW-42] 22 p2926 A73-42898

Equilibrium of an elastic paraboloid of revolution under a concentrated load applied to its apex

22 p2927 A73-43052

Arbitrarily variable thickness cylindrical shell behavior under radial concentrated load calculated using Fourier series, differential equations and matrices

22 p2928 A73-43063

Normalized stresses around an elliptic hole in a finite plate of linear material subjected to large uniform in-plane loading.

23 p3039 A73-43386

Cylindrical shell design with a frame-connected bottom and a system of concentrated forces applied to the bottom

23 p3042 A73-43726

- Effects of axisymmetric loads on inflated non-linear membranes. 23 p3045 A73-44081
- Numerical calculation of simply supported cylindrical shells of arbitrary cross section 23 p3046 A73-44192
- Influence of neutron bombardment on the mechanical properties of titanium and the magnitude of the programmed-hardening effect 23 p2995 A73-44284
- Plastic plate bending under concentrated forces, defining stress and strain principles at yield limit 24 p3148 A73-44919
- Semicircular plate uniformly loaded over diameter and with concentrated force at arc top, determining stress distribution by complex variable and conformal mapping 24 p3148 A73-45001
- Displacements and rotations in micropolar elastic body with external loading and permanent distortions 24 p3149 A73-45004
- Load concentration factors for circular holes in composite laminates. 24 p3149 A73-45151
- Stress concentration in infinite strip with periodically spaced circular holes under uniformly distributed bending loads 24 p3149 A73-45176
- Three-dimensional axisymmetric problem of a normal load concentrated on an elastic free-underface plate of constant thickness - Expression for the stresses in the vicinity of the load 24 p3149 A73-45218

LOAD FACTORS

U LOADS [FORCES]

LOAD TESTING MACHINES

- Assembly for studying the characteristics of materials under cyclic loads at elevated temperatures 01 p0029 A73-10024
- Facility for studying the strength and rigidity of circular plates prepared from an anisotropic material 07 p0809 A73-20517
- Test assembly for structural component members under different climatic conditions 14 p1743 A73-30689
- Device for studying the strength and rigidity of round plates of anisotropic material. 19 p2418 A73-37793
- Testing set-up for cyclic torsion with tension on a small number of loading cycles. 22 p2861 A73-42530
- A device for durability and creep testing of fiberglass-reinforced plastic pipes and shells in a complex stressed state 23 p2967 A73-44293

LOAD TESTS

- Load carrying capacity of ceramic spherical shells under external pressure 01 p0114 A73-10481
- Plastic strain anisotropy changes in single crystals of beryllium following programmed load application 01 p0064 A73-10610
- Airfield pavement full scale performance tests under simulated C-5A load conditions, evaluating construction joint systems 01 p0029 A73-10823
- The creep of materials being weakly strengthened in nonsteady temperature and force conditions. 02 p0180 A73-12138
- Design, development, fabrication and qualification load testing of high modulus graphite-epoxy reflector support truss for ATS F and G 03 p0330 A73-13021
- Design of digital force function generator for aircraft tire load testing. 04 p0424 A73-15064
- An inelastic stress-strain law for elevated temperature and slowly time varying loads. 04 p0512 A73-15235
- Influence of annealing under load on the structure and properties of a self-ordering Ni₃Mn alloy 09 p1099 A73-21957
- The load life characteristics of thick-film resistors. 09 p1065 A73-23048
- Effect of loading frequency on fatigue strength of metals. 09 p1106 A73-23159
- Studies on fatigue damage caused by stresses below the endurance limit - The effect of program period and fatigue failure by stresses below the endurance limit. 13 p1692 A73-28197
- Thermally activated low temperature creep of solids at constant load, considering creep curve stages and plastic deformation mechanism 13 p1635 A73-28263
- Use of blowing during tests of blade cascades 13 p1623 A73-28469
- Machine for investigating the fatigue and inelasticity of metals with programmed load changes both at room and at elevated temperatures. 13 p1599 A73-29636
- Load-bearing capacity of ceramic spherical shells under external pressure. 14 p1810 A73-30306

- Cast thermosetting epoxy resin linear elastic stress-strain characteristics under tension, compression, torsional and bending loads 15 p1897 A73-31619
- Plane stress fracture testing using center-cracked panels. 15 p1951 A73-31987
- Military specifications provisions regarding load transfer. 17 p2133 A73-34093
- A method of programmed fatigue tests with short-time overloads. 17 p2165 A73-34277
- Experimental force data reduction equations solved by iterative method for multicomponent force transducers used in load tests, discussing wind tunnel balances 17 p2148 A73-35437
- Quantitative estimation of the fatigue crack propagation under varying load conditions. 19 p2501 A73-38346
- Statistical characteristics of the fatigue strength of heat-resistant 1Kh18N9T steel under steady and programmed loading conditions at high temperatures 20 p2577 A73-39355
- Some specific features of crack initiation and development in heat-resistant alloys under various loading conditions 20 p2578 A73-39376
- Study of the effect of stress concentration on the variation of stability characteristics in graphites 20 p2580 A73-39383
- Determination of the resistance of VT-14 alloy to brittle fracture 21 p2722 A73-41232
- Experimental verification of lower bound K sub Ic values utilizing the equivalent energy concept. 22 p2875 A73-42147
- Monograph - Fatigue and stochastic loadings. 22 p2923 A73-42673
- Influence of the type of loading on high-temperature creeping of zirconium carbide 23 p2998 A73-44287
- Improved turbine blade attachment profiles with shoulder locks 23 p2986 A73-44291
- Evaluating structural adhesives under sustained load in a hostile environment. 24 p3093 A73-44767
- LOADING FORCES**
U LOADS [FORCES]
- LOADING MOMENTS**
Structural design errors resulting from conventional treatment of distribution law for local radial and torque loads 11 p1433 A73-25028
- Rotating flexible shaft stability criterion development by perturbation method, considering internal and external friction and rotor inertia loading moments effects 11 p1444 A73-26368
- Incremental servomechanism design and application as substitute for step motor, discussing servomotor properties, mechanical torsional vibration and loading moment effects 12 p1483 A73-27422
- Lorentz contraction and transformation of equilibrium forces and moments in inertial reference systems transition, discussing special relativity theory 12 p1525 A73-27733
- LOADING OPERATIONS**
From theory to practical use of air cushions for transport of heavy loads in the factory 05 p0535 A73-16753
- Airport computerized departure control for check-in, load control, cargo and catering operations, discussing load optimization and passenger acceptance control /LOPAC/ system 11 p1343 A73-25210
- Floating superport. 19 p2418 A73-37748
- DC-10 Twin design, discussing balance characteristics, loading limits and sample forms [SAWE PAPER 987] 19 p2386 A73-37891
- LOADING RATE**
Steel/pig iron friction pair natural vibrations due to starting force and sliding friction force difference, noting starting force dependence on loading rate 01 p0058 A73-11403
- Loading-rate dependence of the deformation mechanism in a Zn-22% Al superplastic alloy 03 p0326 A73-13970
- High speed testing of materials mechanical behavior over range of impact loading rates 03 p0394 A73-14023
- Temperature and loading rate effects on yield stress and specific fracture work in tempered carbon steel from notch tests, correlating with linear fracture mechanics 07 p0838 A73-19215
- Epoxy resins thermal mechanical properties, considering difference between toughness and flexibility in terms of temperature and loading rate insensitivities 10 p1237 A73-23952

- Loading time to failure and creep rupture strength from interatomic stochastic bond fracture 11 p1448 A73-26739
- Conditions of brittle strength of weld joints at different temperatures and applied loading rates. 13 p1626 A73-29628
- Steady state solution for moving point force on solid-solid interface for supersonic load velocities, using DeHoop modification of Cagniard technique 14 p1812 A73-30493
- Threshold for fatigue crack propagation and the effects of load ratio and frequency. 22 p2875 A73-42137
- Influence of initial transients on stress relaxation and creep measurements on visco-elastic materials. 22 p2868 A73-43172
- Response of glass-fiber-reinforced epoxy specimens to high rates of tensile loading. 23 p2996 A73-43385

LOADING WAVES

U ELASTIC WAVES

U LOADS [FORCES]

LOADS [FORCES]

- NT AERODYNAMIC LOADS
- NT AXIAL COMPRESSION LOADS
- NT AXIAL LOADS
- NT BLAST LOADS
- NT COMPRESSION LOADS
- NT CRITICAL LOADING
- NT CYCLIC LOADS
- NT DYNAMIC LOADS
- NT EDGE LOADING
- NT GUST LOADS
- NT IMPACT LOADS
- NT LANDING LOADS
- NT RANDOM LOADS
- NT ROLLING CONTACT LOADS
- NT SHOCK LOADS
- NT STATIC LOADS
- NT THRUST LOADS
- NT TRANSIENT LOADS
- NT VIBRATORY LOADS
- NT WING LOADING
- Development of dynamic modes of the loss of stability in elastic systems during intense loading over a finite interval of time 02 p0229 A73-11615
- Finite elements for axisymmetric solids under arbitrary loadings with nodes on origin. 03 p0395 A73-14192
- Changes in the durability and lifetime of polymer films under simultaneous exposures to an electric field and mechanical loading 07 p0842 A73-19394
- Loading mode effects on high strength steel hydrogen embrittlement, considering stress tensor invariants and interstitial diffusion relationships 09 p1102 A73-22414
- Orthotropic almost cylindrical beams - Bending by a transverse load. 09 p1160 A73-23023
- Deformation of shells of revolution with attached rings under different local loads, deriving approximate expressions for stressed state 10 p1287 A73-23592
- Experimental investigation of undulatory multiplication gear systems 10 p1222 A73-23597
- Electrical measurement of mechanical forces and displacements, discussing transducers design and measurement standards and units 10 p1215 A73-23633
- Potential operator theory in Hilbert spaces applied to rigorous definition of conservative loading, examining pressure loading case 11 p1434 A73-25212
- Piezoelectric gages for fluid dynamic multicomponent force measurements, discussing quartz transducers, measurement accuracy and capability for rapidly fluctuating forces measurement 12 p1499 A73-27871
- Heat resistant nickel alloys creep rupture strength diagram, determining time to failure as function of loads 13 p1636 A73-29062
- On the optimal design of statically indeterminate elastic structures subjected to multiple loading systems and multiple constraints. 14 p1805 A73-29760
- Creep analysis of transversely isotropic bodies subjected to time-dependent loading. 14 p1805 A73-29769
- Influence of in-plane displacements at the boundaries of rigid-plastic beams and plates. 16 p2083 A73-33973
- Analytical study of pressure balancing in gas film seals. 17 p2180 A73-35000
- Failure mode multiplicity in Al-stainless steel and Al-W metal matrix composites under various loading conditions 17 p2191 A73-35527
- The effect of load interaction and sequence on the fatigue behavior of notched coupons. 18 p2364 A73-36589

- Heat resistant nickel alloys creep rupture strength diagram, determining time to failure as function of loads
18 p2325 A73-36894
- A practical load relief control system designed with modern control techniques.
[AIAA PAPER 73-863] 20 p2508 A73-38801
- Motion of a rigid-plastic beam in a resistant medium under the action of a local load
20 p2620 A73-39470
- Il'yushin linear theory for defect accumulation generalized for endurance limit of materials under noncyclic loads, examining time to failure under creep and relaxation conditions
20 p2624 A73-39644
- Helicopter and fixed wing aircraft design consideration comparison, examining maintenance and reliability requirements, rigid, hinged and tilted rotors and load characteristics
21 p2634 A73-40225
- State-change equations relating generalized load increment to response of constraint connected bars, deriving compatibility and equilibrium equations and matrix coefficients
21 p2788 A73-41604
- The method of forces for thermoviscoelastic rod systems
24 p3148 A73-44918
- LOBES**
Radiation patterns of directional end-on antennas, deriving formulas for side lobe levels and main lobe energy distribution
21 p2661 A73-40198
- LOCALIZATION**
U POSITION [LOCATION]
LOCATION
U POSITION [LOCATION]
LOCKHEED AIRCRAFT
NT C-5 AIRCRAFT
NT C-130 AIRCRAFT
NT C-141 AIRCRAFT
NT L-1011 AIRCRAFT
NT P-3 AIRCRAFT
NT T-33 AIRCRAFT
YF-12 aircraft flight loads measurement program with strain gage bridges in fuselage, fuel tanks, control surfaces and left wing
17 p2107 A73-35444
- The F-12 series aircraft aerodynamic and thermodynamic design in retrospect.
[AIAA PAPER 73-820] 19 p2380 A73-37472
- F-12 series aircraft propulsion system performance and development.
[AIAA PAPER 73-821] 19 p2380 A73-37473
- The development of the F-12 series aircraft manual and automatic flight control system.
[AIAA PAPER 73-822] 19 p2380 A73-37474
- Flight testing the F-12 series aircraft.
[AIAA PAPER 73-823] 19 p2380 A73-37475
- LOCKHEED C-5 AIRCRAFT**
U C-5 AIRCRAFT
LOCKHEED MILITARY AIRCRAFT
U LOCKHEED AIRCRAFT
U MILITARY AIRCRAFT
LOCKING
NT LASER MODE LOCKING
Measurement of admittances of microwave oscillators with injection locking.
03 p0310 A73-14497
- Negative resistance oscillators, predicting fundamental, harmonic and subharmonic locking characteristics by nonlinear models and equivalent circuit
19 p2410 A73-38307
- LOCKS [FASTENERS]**
Improved turbine blade attachment profiles with shoulder locks
23 p2986 A73-44291
- LOCOMOTION**
NT ASTRONAUT LOCOMOTION
NT WALKING
Reduced dimensionality for minimization of degrees of freedom of skeletal activity models for anthropomorphic locomotion system synthesis
01 p0013 A73-11052
- The role of muscle stiffness in meeting the changing postural and locomotor requirements for force development by the ankle extensors.
02 p0138 A73-12166
- Some aspects of the inverted pendulum problem for modelling of locomotion systems.
19 p2460 A73-38035
- LOFTING**
The evolution and application of lofting techniques at Hawker Siddeley Aviation.
13 p1623 A73-28054
- LOG PERIODIC ANTENNAS**
A new log-periodic structure with asymmetric dipole elements.
10 p1194 A73-24172
- Optimization of the loop-coupled log-periodic antenna.
11 p1337 A73-25652
- A broadband antenna and multiplexer system in the decimeter-wave range for solar radio astronomy
12 p1481 A73-27782
- Log periodic triangular dipole antenna design and electrical properties, noting improved frequency transition, gain and axial length reduction
14 p1731 A73-29714
- Log periodic dipole antenna design procedure, discussing gain as function of transmission line characteristic impedance, half length/dipole radius ratio and geometric parameters
14 p1734 A73-30206
- Size-reduced log-periodic dipole array antenna.
16 p1988 A73-33299
- Log-periodic dipole arrays - A numerical analysis.
17 p2141 A73-35367
- Time domain current interaction coefficients for sheet antenna structures.
17 p2142 A73-35647
- Antenna gain calibration on a ground reflection range.
17 p2128 A73-35688
- Broad-band antenna array with application to radio astronomy.
22 p2831 A73-41840
- LOG SPIRAL ANTENNAS**
German monograph on logarithmic spiral antennas radiation field theory, extending boundary value solution for cylindrical linear antenna to curved structure by segmentwise linearization
07 p0801 A73-19577
- The dual-aperture counterwound log-spiral antenna direction-finder system.
11 p1338 A73-25669
- Computer controlled steerable array of multiple conical log spiral antennas for solar and discrete radio source studies
23 p2965 A73-43363
- LOGARITHMIC RECEIVERS**
Cell averaging constant-false-alarm-rate radar receiver with noise estimated from logarithmic detector output, determining performance in Gaussian noise by Monte Carlo simulation
03 p0277 A73-13910
- Characteristics of the adaptive optimal detection of Gaussian signals on a pulse-noise background in receivers with a logarithmic amplifier
08 p0940 A73-21554
- LOGARITHMS**
Nonlinear differential equations with logarithmically small perturbations.
01 p0071 A73-11268
- Complex parameter B of Perseids meteors from photographic observations at Dushanbe, giving logarithms
02 p0216 A73-12358
- Convergence to logarithmic distribution laws
09 p1112 A73-22884
- Inverse problems of a logarithmic potential with analytic closeness
12 p1518 A73-27729
- Analog to digital converters with logarithmic input-output law, comparing performance and complexity of various realizations
21 p2658 A73-41145
- LOGIC CIRCUITS**
NT THRESHOLD GATES
Analytical method for diagnostic and checkout testing of logic element faults in complex combinational circuits
01 p0026 A73-10035
- Russian book on nanosecond multiphase multivibrators covering transistorized single- and dual-stage amplifiers and wave shaping circuits for digital control and computer logic applications
02 p0146 A73-11887
- Logic network design for digital waveform shaping of polyphase voltage generator, noting application for airborne and marine gyroscope power supply
03 p0258 A73-14618
- A digital echo suppressor for satellite circuits.
04 p0416 A73-14995
- Optimal control of extraatmospheric spacecraft motion stability by variable structure system with logic circuits
05 p0628 A73-16421
- Terminal modeling and photocompensation of complex microcircuits.
05 p0557 A73-16508
- Enhancing testability of large-scale integrated circuits via test points and additional logic.
06 p0674 A73-17802
- Time difference measuring instrument for asynchronous and synchronized positive pulses in automatic control system, noting pulse generator and switching, trigger and logic circuits
06 p0677 A73-18384
- MOS field effect components integration on Si operation, performance and application to logic circuits
07 p0797 A73-18916
- Flawless operation probability for information transmission reliability of electronic logic circuits with binary data inputs
07 p0801 A73-20040
- Stability behavior of adapting and untrained random logic nets, enabling intelligent interaction with environment
07 p0786 A73-20400
- Thin film nickel-chromium resistor failures in integrated circuits.
08 p0944 A73-20746
- Standard flexible LSI logic cell arrays with uniform interconnections as fourth generation computer components, discussing microprograms and algorithms for arithmetic operations
10 p1198 A73-24017
- Improved analysis of the steady-state operation of a resistive parametron
10 p1189 A73-24381
- Quantization circuit for radio astronomical signals conversion into binary code and bit blocks recording on magnetic tape via Razdan-3 computer
10 p1220 A73-24698
- Monolithic IC digital circuits using Si planar technology with Schottky diodes in DTL and TTL gates for high computational speed
11 p1341 A73-25345
- Sequential pneumatic distribution system [Biselector] with logic control by leakage obstruction, describing industrial pressure perforated card programmer
11 p1307 A73-25377
- Book - Engineering means in automatic control.
12 p1481 A73-26751
- Diagnostic tests and failure checkout for interconnected combinational micrologic circuit components in manufacturing process, tabulating individual failure functions
12 p1474 A73-26755
- Methods of constructing control and diagnosis tests for homogeneous microelectronic circuits
12 p1476 A73-26757
- Microprogrammed digital filters for strapdown guidance application.
12 p1483 A73-27168
- Binary counters design based on TTL, DTL and ECL integrated circuits, giving circuit diagrams for 70 MHz 24 stage and 20 MHz dual 16 stage counters
12 p1497 A73-27208
- A simple method for converting a pulse code into a phase code by using parametrons
12 p1481 A73-27590
- Microwave tunnel diode ring counter with displaced nonlinear load line in multistage transistor driver and current switching configuration
13 p1593 A73-29120
- Multiple-fault detection in large logical networks.
13 p1588 A73-29296
- Transient analysis of multiple-input integrated digital structures.
13 p1595 A73-29580
- Operational modes of the feedback circuit of an asynchronous logical network
14 p1731 A73-30939
- Logic circuit distribution algorithms for asynchronous finite automata synthesis on basis of universal homogeneous medium
15 p1848 A73-31911
- Construction of a diagnostic sequence of tests of a combination automaton
15 p1848 A73-31913
- New structure of on-board microcomputers using large-scale integrated logic circuits
15 p1852 A73-32478
- High speed parallel multiplier design based on threshold logic adder using integrated logic circuits
17 p2139 A73-35238
- Expanded built-in-test for advanced electrical systems for aircraft.
17 p2109 A73-35248
- Complementary MOS/silicon on sapphire LSI technology for high speed digital multiplier and correlator logical building blocks design, fabrication and subsystem array implementations
17 p2140 A73-35318
- Third generation Aircraft Recording Instrumentation System /ARIS III/, consisting of digitizer and logic, analog interface and hybrid instrumentation recorder
17 p2174 A73-35581
- Versatile logic system for use in nuclear experiments on scientific satellites.
19 p2412 A73-37147
- Modes of operation of the feedback loop in an asynchronous logical network.
19 p2414 A73-38193
- Fundamentals of COS/MOS integrated circuits.
20 p2534 A73-38655
- Papers on adaptive electronic devices, circuits and systems covering logic nets, solid state and ferroelectric devices and memory devices and artificial intelligence
20 p2535 A73-39135
- Mathematical equipment of a system of automatic designing of components of logic-type semiconductor integrated circuits
21 p2660 A73-40015

Synthesis of combination circuits in a universal basis and its use in estimating the complexity of digital structures containing integrated circuits

21 p2668 A73-40017

Computerized synthesis of optimal fault-diagnosable logical circuits capable of detecting and repairing faulty modules for circuit reliability and availability improvements

21 p2669 A73-40687

Washout circuit design for multi-degrees-of-freedom moving base simulators.

[AIAA PAPER 73-929]

21 p2674 A73-40876

The use of logic simulation in the design of a large computer system.

21 p2658 A73-41210

The development of the quartz resonator as a digital temperature sensor with a precision of .0001.

22 p2854 A73-41992

Logic-controlled solid-state switchgear for 270 volt dc.

22 p2802 A73-42915

Fluidic logic circuits applications under adverse environmental conditions, considering sequential control devices and rocket engine roll axis numerical control

23 p2941 A73-43394

Fluidic logic circuit universal block with turbulence amplifiers for control of servomechanisms, comparing with use of conventional fluid logical elements

23 p2943 A73-43414

Bayes theorem for probabilistic analysis of logic circuits applied to reliability estimation of switching circuits

23 p2965 A73-44107

LOGIC DESIGN

Systematic method of designing fluidic-pneumatic control circuits.

02 p0133 A73-12646

Spacecraft digital attitude control.

04 p0504 A73-14736

An analytical and empirical basis for the design of turbulence amplifiers. I - Analysis and experimental confirmation.

[ASME PAPER 72-WA/FLCS-1]

04 p0408 A73-15859

Fault insertion techniques and models for digital logic simulation.

06 p0671 A73-18062

Book - MOS integrated circuits: Theory, fabrication, design and systems applications of MOS LSI.

15 p1852 A73-32579

Book - MOS integrated circuit design.

18 p2294 A73-36966

Electromagnetic core storage and switching elements design for Setun threshold ternary logic computer

19 p2408 A73-38562

Multivalued models of computer electronic circuits

20 p2532 A73-39001

Synthesis of combination circuits in a universal basis and its use in estimating the complexity of digital structures containing integrated circuits

21 p2668 A73-40017

Human motion perception in motion drive logic design for flight simulation discussing feedback control, angular velocity and degrees of freedom

[AIAA PAPER 73-931]

21 p2674 A73-40878

A new technique for designing high-speed frequency counters.

21 p2658 A73-41146

The use of logic simulation in the design of a large computer system.

21 p2658 A73-41210

Drive logic computation for variable stability aircraft in-flight simulators with six independent controllers providing dynamic motion and ground, crosswind and special effects

[AIAA PAPER 73-933]

22 p2799 A73-41971

Application of fluidic shift-register modules for sequential control of pneumatic sequential circuits.

23 p2943 A73-43412

Some practical methods for development of modular fluidic devices.

23 p2943 A73-43415

Fluidic circuits application to stochastic computer with analog to digital converter and logic gates for arithmetic operations

23 p2944 A73-43419

Designing with microprocessors instead of wired logic asks more of designers.

23 p2956 A73-44122

Synthesis of minimized formal neurons by means of magnetic current switches

24 p3063 A73-44902

LOGIC NETWORKS

U LOGIC CIRCUITS

LOGICAL ELEMENTS

Checkup and failure diagnostics of an incompletely homogeneous two-dimensional structure

12 p1482 A73-26754

Diagnosis of switching devices in the case where faults are represented by tests of individual elements

12 p1476 A73-26756

External static and dynamic characteristics of input-output sequences of logic elements

12 p1475 A73-26764

Random failure process similarity in redundant schemes for systems with binary elements, noting statistical modeling on specialized Monte Carlo machines

12 p1485 A73-27620

A data display device for switching and logic elements constructed from single-crystal ferromagnetic materials

14 p1731 A73-30941

Reliability testing functions for memory elements

15 p1848 A73-31914

Gunn-effect digital functional devices and their performance evaluation.

17 p2143 A73-35814

Reliability estimation for integral logical elements from intermittent failures under noise effects

18 p2292 A73-37045

Ultrahigh-speed unsaturated diode-transistor logic elements with a small logic differential

21 p2660 A73-40013

Mathematical equipment of a system of automatic designing of components of logic-type semiconductor integrated circuits

21 p2660 A73-40015

Hybrid fluid logic systems for integrated circuits using static and dynamic logical elements, considering fluidic circuits design with redundancy

23 p2943 A73-43411

Systems engineering approach to pneumatic hybrid automatic/manual control system with fluid logical elements and reduced air consumption

23 p2943 A73-43413

Fluidic logic circuit universal block with turbulence amplifiers for control of servomechanisms, comparing with use of conventional fluid logical elements

23 p2943 A73-43414

Structural complexity and technical realization of formal neurons by means of magnetic current switches

24 p3063 A73-44901

Synthesis of minimized formal neurons by means of magnetic current switches

24 p3063 A73-44902

LOGISTICS

Prototype development for Army personnel and equipment airborne mobility, considering various aircraft conceptual designs feasibility relative to logistics requirements

[SAE PAPER 720846]

05 p0534 A73-16658

Naval air weaponry logistics support, discussing criteria for management effectiveness evaluation

13 p1709 A73-29573

Resources management logistics support of research and development laboratories.

13 p1709 A73-29574

The potential influence of the ACLS on the development of logistical cargo aircraft.

19 p2383 A73-37701

LOGISTICS MANAGEMENT

NT INVENTORY MANAGEMENT

Principles of organization and logistical support for systems of automating scientific investigations

04 p0424 A73-14823

Logistics planning with cost reduction for NASA phased programs in conducting R and D and real time inventory control, discussing major activities and objectives

11 p1454 A73-25450

Los Angeles offshore airport planning case study covering design, logistics problems and costs with allowance for airspace and environmental considerations peculiar to Southern California area

15 p1857 A73-31540

Air Force Increase Reliability of Operational Systems computer program and mathematical models for economic logistic resource allocations and cost effective system modification

16 p2088 A73-33627

Computerized approach for aerospace electronic components standardization for procurement cost, logistics and warehousing problems reduction and reliability improvement

17 p2140 A73-35260

Discourse on comparisons between commercial and military aircraft logistics.

20 p2629 A73-39274

The capabilities of army test facilities.

23 p2966 A73-44064

LONG RANGE NAVIGATION

U LORAN

LONG RANGE WEATHER FORECASTING

Upper bounds for long range numerical weather forecasts errors due to inadequate knowledge of frictional constants, heating and initial conditions

02 p0189 A73-12777

Attempt at the application of the theory for linear extrapolation of probabilistic processes in long-range temperature forecasts

05 p0593 A73-16235

Utilization of the convergence of atmospheric processes during construction of long-range weather forecasts

05 p0593 A73-16236

Investigation of planetary high-altitude frontal zones with the aid of natural orthogonal functions

05 p0568 A73-16239

Ultralong atmospheric waves and a long-range forecasting.

10 p1244 A73-23644

A 4-year experiment in long-range weather forecasting, using circulation analogues.

13 p1653 A73-28740

The numerical models of general circulation and their employment for medium-term and long-term weather prediction

13 p1653 A73-28741

International polar experiment /POLEX/ program for global circulation research and long range weather forecasting improvement

13 p1654 A73-28933

A first experiment in constructing a weather forecast for a month by the synoptic method on a computer

13 p1655 A73-29193

On the existence of extended range predictability.

15 p1903 A73-31320

German book - Long-term weather forecaster: Fundamentals of a new experiment with monthly predictions.

15 p1903 A73-31473

Role of the meteorological satellites of the earth-atmosphere observation system for the first global experiment of the 'Global Atmospheric Research Programme'

17 p2205 A73-34935

Long term weather forecasting techniques, criteria and implementation, discussing statistical weather analysis, cloud types, air masses, sunspot activity, precipitation and pressure systems

20 p2584 A73-39628

Climatic means finite time average estimation standard error calculation by stochastic model with application to long range forecasting

23 p3004 A73-44264

LONG TERM EFFECTS

Effects of gravity-gradient torque on the rotational motion of a triaxial satellite in a precessing elliptic orbit.

01 p0099 A73-10685

Effects of the secular magnetic variation on the distribution function of inner-zone protons.

02 p0155 A73-11731

Fatigue in flight personnel during long flights

02 p0137 A73-12153

Generalized and modified parametric methods for extrapolating results of long term high temperature strength tests for service life determination

02 p0181 A73-12205

Gas turbine engine hot part equivalent accelerated tests duration determination by analytical method based on Larson-Miller parametric description of long term strength

02 p0236 A73-12216

Apparatus for investigations into long-term strength and creep of coated materials at temperatures above 1400 C in air.

02 p0150 A73-12219

Circular orbit stability in restricted two body problem with secular variations, giving disturbing function secular terms to eighth order

02 p0222 A73-12710

Evaluation of materials for underground exposure in extreme environments.

03 p0329 A73-13006

Spacecraft lubrication systems design for long mission lifetimes, discussing mechanical design parameters and liquid and solid lubricant characteristics

03 p0330 A73-13012

The role of occultations in the improvement of the lunar ephemeris.

03 p0369 A73-13107

Giant envelopes structure triple solutions yielding bottom pressure-radius curves, discussing stellar evolution, Cepheid variables and secular instability

03 p0371 A73-13226

A numerical investigation of secular terms of the planetary disturbing function.

03 p0372 A73-13351

Development and use of relaxation tests for study of the long-term creep of metals [ONERA, TP NO. 1146]

04 p0511 A73-15095

The secular accelerations of the moon's orbital motion and the earth's rotation.

04 p0497 A73-15176

Stability of the solar system - Evidence from the asteroids.

04 p0497 A73-15179

Time variation of the geomagnetic main field on the basis of spherical harmonics analyses of geomagnetic world charts for the period from 1880 to 1960

04 p0440 A73-15281

Long term German observations of auroral activity compared to other midlatitude observations

04 p0445 A73-15551

Mathematical model for long term creep strength from creep tests, noting crack initiation and microstructural changes

04 p0517 A73-15952

Secular inequalities in the motion of earth satellites.

04 p0503 A73-16020

Prolonged control of cardiac bioelectrical activity in man in ground experiments and during spaceflight
06 p0657 A73-17694

Characteristics, design and performance of power sources in auxiliary systems for spacecraft applications, noting long term standby under environmental conditions
[SAE AIR 744 A] 08 p0928 A73-20690

On the long-term behaviour of the circular polarization from coronal condensation radio emission at 4.3 cm wavelength.
08 p0997 A73-20769

Superalloys oxidation behavior under long term exposure to high temperatures for suitability as Co-60 heat sources encapsulation materials
08 p0978 A73-21415

Thermoelectric generators long term tests, discussing SNAP 11, 19 and 27, TEM-10 and SiGe/PbTe cascaded generator performance characteristics
09 p1136 A73-22760

SNAP 19 thermoelectric generator long term performance tests, attributing output degradation to sublimation and hot junction bond loss due to internal gas cover depletion
09 p1118 A73-22765

Nature of the drift of the main eccentric geomagnetic dipole.
10 p1212 A73-24233

Spherical analyses of the main geomagnetic field in 1550-1800.
10 p1212 A73-24235

Solar radiation climate correlation with long term sunshine records, comparing radiation measurements with predictions based on regression equations for Brisbane area
10 p1269 A73-24450

Alpha particles in solar cosmic rays over the last 80,000 years.
11 p1412 A73-25375

The calculated long-term performance characteristics of a typical silicon-germanium RTG.
11 p1312 A73-26030

The long term performance characteristics of a SNAP-19 generator operating under vacuum conditions.
11 p1396 A73-26038

The earth's rotation and atmospheric circulation. I - Seasonal variations.
13 p1606 A73-28282

On approximate calculation of the principal part of disturbances in an interior bounded three-body problem.
14 p1802 A73-30953

Earth-space slant path radio attenuation measurements above 10 GHz over four year period, noting caution in use of long term statistics
16 p1982 A73-33721

A model of a long-term process of heat and moisture transfer in the atmosphere over the ocean
17 p2158 A73-34344

Characteristics of the future orbital evolution of the comet Churiumov-Gerasimenko, 1969h
17 p2230 A73-34597

Prolonged space flight and hypokinesia.
18 p2278 A73-36789

Trash management during Skylab and long duration missions with compactors, autoclaves, biocides and isotope powered water recovery/waste management systems
[ASME PAPER 73-ENAS-31] 19 p2401 A73-37986

Secular perturbations of the motion of artificial satellites, caused by atmospheric drag
21 p2768 A73-40725

Physiologic cost of prolonged double-crew flights in C-5 aircraft.
21 p2644 A73-41152

Long-term drift of some noble- and refractory-metal thermocouples at 1600 K in air, argon, and vacuum.
22 p2857 A73-42033

Apollo 16 flight program for investigating physiological effects of prolonged weightlessness on central nervous system, vestibular, neuromuscular and cardiovascular functions, metabolism, radiation sensitivity and body weight
22 p2814 A73-42176

Development of methods for long-term prediction of heat-resistance characteristics
24 p3099 A73-44768

LONG WAVE RADIATION

The global distribution of outgoing long-wave radiation derived from SIRS radiance measurements.
01 p0038 A73-10391

Long wavelength spectrometry and photometry of M, S and C-stars.
02 p0222 A73-12708

Magnitude estimate for long wave radiative cooling effects for isolated buoyant thermal rising in uniform ambient atmosphere
[AD-755500] 02 p0224 A73-12779

Mathematical treatment of long wave sound propagation in curved ducts and junctions, obtaining principal mode from linearized equation of motion solved for eigenvalues
03 p0343 A73-13832

Lower ionosphere at medium latitudes during geomagnetic disturbances.
05 p0568 A73-16214

Calculation of averaged values for short- and long-wave fluxes and influxes in a real atmosphere
05 p0593 A73-16243

Measurement of short- and longwave radiant fluxes from the Kosmos-320 satellite.
08 p0961 A73-21586

Study of the radiative properties of the atmosphere between cloud layers
09 p1114 A73-22371

Excitation of long-wave oscillations by a secondary electron stream in a plasma generated by an ion beam
09 p1129 A73-22684

Ring arrays as medium- and long-wave broadcast antennas
11 p1336 A73-25318

Influence of radiation on the conditions in the atmospheric boundary layer
11 p1393 A73-25641

Longitudinal and lateral magnification distortion correction in three dimensional long wavelength holography from standpoint of observer visual perception
13 p1616 A73-28596

Features of the long-wave radiant influx in the presence of stratified cloudiness /A numerical experiment/
15 p1904 A73-31783

Comparison of methods for calculating long-wave radiation fields
15 p1904 A73-31785

Spatial distribution of outgoing long wave radiation fluxes according to Cosmos-320 satellite data
20 p2555 A73-39188

Long wave radiation flux, water content and temperature measurements in stratus and cumulostratus clouds by aircraft radiometry
21 p2731 A73-40496

Cloud destabilization due to long wave radiative cooling resulting from IR radiative heat transfer in cloudy atmosphere, considering temperature inversion effects and cyclogenesis mechanism
24 p3108 A73-45016

LONGERONS

Boron-stiffened longerons on the B-1.
[SME PAPER EM 73-719] 19 p2436 A73-38499

LONGITUDE

Satellite resonance with longitude-dependent gravity. III - Inclination changes for close satellites.
09 p1154 A73-22837

Evaluation of the accuracy of longitudinal interpolation of f0F2 based on ship observations.
19 p2425 A73-37930

Meridional distribution of tropospheric ozone from measurements aboard commercial airliners.
23 p2974 A73-43859

Meridional tropospheric ozone distribution north of 50 deg from airplane measurements.
23 p2974 A73-43860

LONGITUDE MEASUREMENT

Longitudinal variation of the equatorial anomaly.
04 p0440 A73-14960

Estimating the accuracy of longitudinal interpolation of f0F2 from shipboard observations
08 p0959 A73-21301

Autonomous determination of meridian plane with triaxial gyroscopic stabilizer during initial display of inertial system
09 p1116 A73-22659

Circumzenithal instrument for latitude and longitude determination and star transits observation, through almucantar
16 p2017 A73-34048

Conditional equations of astronomical latitudes, longitudes, and azimuths
19 p2490 A73-38559

LONGITUDINAL CONTROL

Heaving and pitching response of a hovercraft moving over regular waves.
01 p0004 A73-10700

Synthesis of nonsearching self-adjusting systems by the root-locus method. II
07 p0807 A73-20637

Analytical design of manual control systems for flight bodies
12 p1549 A73-27896

Synthesis of searchless selfadjusting systems on the basis of the root-locus method. II.
15 p1854 A73-31691

Analytical design of aircraft manual control systems.
18 p2267 A73-36601

Decoupling longitudinal motions of an aircraft.
19 p2386 A73-38033

Digital flight control design using implicit model following.
[AIAA PAPER 73-844] 20 p2508 A73-38783

Compensation of the longitudinal-trim and altitude control systems of an aircraft
22 p2800 A73-42949

LONGITUDINAL STABILITY

Stable longitudes for 12-hr eccentric orbit satellites.
01 p0095 A73-10104

Analysis of the longitudinal perturbed motion of a ground-effect flight vehicle
02 p0128 A73-11785

Experimental and theoretical investigations regarding the unsteady aerodynamic derivatives of the longitudinal motion in the case of slender flight bodies at moderate velocity
[DEVL-R-SONDDR-206] 05 p0528 A73-16757

Nonlinear longitudinal combustion instability in rocket motors.
[AIAA PAPER 73-217] 05 p0641 A73-16947

The instability of hydrodynamic longitudinal oscillations in a non-uniform magnetoactive plasma.
09 p1127 A73-22285

Longitudinal motion of a transport aircraft during steep landing approaches
17 p2100 A73-34482

Synthesis of optimal control of the longitudinal motion of an elastic tank containing liquid
22 p2843 A73-43059

Airfoil theory calculation of bent thin foil lift coefficient and longitudinal moment characteristics at arbitrary flow separation point location
23 p2940 A73-43720

The motion of a body containing a liquid-filled cavity with elastic radial ribs and exhibiting perturbations relative to the longitudinal axis
24 p3112 A73-45513

LONGITUDINAL WAVES

NT PLANE WAVES

Numerical solution for propagation of longitudinal waves along the geomagnetic field using a three-fluid ionosphere model.
01 p0016 A73-10197

Momentum formulae derived for quasi-monochromatic wave packets of transverse and longitudinal waves in plasma without magnetic field
02 p0195 A73-11522

Electromagnetic self induced vibrations in homogeneous unbounded electron beam moving with time dependent velocity, noting longitudinal and transverse wave generation
02 p0198 A73-12102

Forced motion of elastic cylindrical rods - A comparison of two theories.
07 p0915 A73-20284

On the instability of longitudinal oscillations in an inhomogeneous isotropic plasma.
08 p0992 A73-20956

Kinetic equation derived for collective linear fluid oscillations development, applying to longitudinal and transverse wave propagation in fluids
09 p1072 A73-22574

Direct current and voltage effects on plasma longitudinal oscillations, discussing frequency dependence and waves in semiconductors with ionic lattices.
09 p1129 A73-22681

Damping of plasma waves in the lower hybrid frequency range.
09 p1131 A73-22908

A numerical method for the analysis of longitudinal elastic-plastic stress wave propagation.
10 p1290 A73-24297

Spontaneous Cerenkov emission of longitudinal waves produced by single particle and cylindrical electron beam moving inside magnetosphere along magnetic field
10 p1269 A73-24722

A photon rest mass and the propagation of longitudinal electric waves in interstellar and intergalactic space.
11 p1417 A73-25562

Amplification of a travelling wave in a non-homogeneous elastic medium.
11 p1400 A73-26407

Extension of the hodograph method for the one-dimensional elastic-plastic wave propagation.
13 p1696 A73-28646

Existence conditions for magnetoactive plasma longitudinal waves with phase velocity near light velocity, investigating increments during synchrotron instability due to relativistic particles
14 p1780 A73-30337

An investigation of the statistical properties of the radiation of a laser, operating in several axial modes, by the photon counting method.
17 p2184 A73-35156

Wave transformation due to oblique incidence on the boundary of a magnetoactive plasma
18 p2289 A73-36553

Entry of a high-frequency longitudinal field into a nonequilibrium plasma
18 p2339 A73-36554

Traveling longitudinal electrostatic waves excitation in warm nonuniform plasma by external HF electric fields, using kinetic theory
19 p2468 A73-37857

Longitudinal shear waves in a fiber-reinforced composite.
19 p2500 A73-38113

Emission of longitudinal waves from a charge in an external high-frequency electric field in a magnetoactive plasma
19 p2470 A73-38331

Longitudinal-torsional vibrations of rotors
20 p2569 A73-39374

Nonlinear conversion of electromagnetic waves at the boundary of a magnetoactive plasma
21 p2658 A73-41517

Wave spectrum analysis of electron beam-plasma longitudinal electrostatic fluctuations, finding triplet wave line shape and intensity and dispersion relations
22 p2891 A73-42240

Weak longitudinal waves in a nonlinear viscoelastic medium
23 p3045 A73-44182

Energy conversion between longitudinal and transverse waves by mode-mode coupling in a relativistic plasma.
24 p3116 A73-45240

Boundaries of natural frequency variations during the longitudinal oscillations of rods
24 p3152 A73-45360

Far-field analysis of nonlinear shock waves in a lattice.
24 p3112 A73-45412

Longitudinal and transverse shock and acceleration waves propagation and decay in anisotropic and isotropic elastic bodies based on theory of singular surfaces
24 p3153 A73-45498

LONGSHORE CURRENTS
U COASTAL CURRENTS

LOOK ANGLES
U AZIMUTH
U ELEVATION ANGLE

LOOP ANTENNAS
Radiation resistance of small electric and magnetic antennas in a cold uniaxial plasma.
01 p0081 A73-10194

Some aspects of radiation from a circular loop antenna.
02 p0148 A73-12854

Study of the steady motion of a ballistic antenna in a plane homogeneous flow
05 p0528 A73-16750

Low-frequency loop antenna arrays - Ground reaction and mutual interaction.
06 p0665 A73-18176

Theory of double parasitic loop counterpoise antenna radiation patterns.
06 p0666 A73-18190

Determination of the influence of the earth on the active component of the input impedance of loop antennas
08 p0947 A73-21400

Imperfectly conducting circular loop antenna driving-point impedance derivation for uniform resistive loading, comparing differential and integral equation methods for current distribution calculation
10 p1191 A73-24899

Field pattern of two identical nonstaggered parallel circular loop antennas.
11 p1337 A73-25667

Dispersion characteristics of multiloop cylindrical spiral antennas with opposite winding
12 p1480 A73-27237

Receiving characteristics of antennas in an isotropic compressible plasma.
13 p1594 A73-29230

Radiation from travelling wave circular loop antenna in compressible electron plasma.
14 p1731 A73-29709

Concept of phase centre of an array applied to elevation-angle measurements.
15 p1842 A73-31098

General theoretical analysis of impedance loaded rectangular loop antennas.
17 p2141 A73-35368

A concentric ring transverse electromagnetic line antenna array.
17 p2127 A73-35638

General theoretical analysis of loop and folded dipole antennas.
17 p2142 A73-35646

Measurement techniques for antennas in dissipative media.
17 p2143 A73-35685

Ground and flight test results for standard VOR and double parasitic loop counterpoise antennas.
17 p2129 A73-35700

Proximity effects for parallel rectangular conductors in nontransmission-line mode.
17 p2129 A73-35703

Prediction of RS01 design requirements for MIL-STD-461A.
22 p2823 A73-41803

Near fields of wire antennas by matrix methods.
22 p2830 A73-41827

On input impedance of an arbitrarily oriented small loop antenna in a cold collisionless magnetoplasma.
22 p2824 A73-41858

A theoretical and experimental study of the insulated loop antenna in a dissipative medium.
22 p2829 A73-43184

VLF input impedance of a loop antenna embedded in the magnetosphere.
23 p2954 A73-43700

Tuned loop antenna for radio observation of electrostatic spark and corona discharges generated during oil tanker cleaning operations
23 p2945 A73-43960

Theory of a corner-driven loop antenna immersed in a warm plasma.
24 p3070 A73-45486

LORAN
Comparison of medium-distance navigation systems. II
02 p0191 A73-12014

LORAN range difference location system, deriving exact straight line of position on plane or spherical surface with computer-generated error maps
11 p1333 A73-26642

Low cost data processor and display for ICNI, DME/TACAN, LORAN or range/range difference radio navigation systems in aerospace applications
17 p2210 A73-35213

LORAN C
Clock comparisons by short wave, ULF and VLF signals, Loran C and Omega methods, onboard aircraft atomic clocks and TV synchronizing pulses
03 p0307 A73-13246

Geodetic satellite timing accuracies with Loran C, portable atomic clocks and long baseline interferometry
04 p0446 A73-14807

A precision position and time service for the air traffic of the future.
07 p0849 A73-19350

Computer evaluation of large low-frequency antennas.
14 p1735 A73-30227

Sudden ionospheric disturbance effects on LF radio pulse train amplitude during reception from Loran-C transmitters, comparing with VLF sudden phase anomaly
22 p2825 A73-42188

LORENTZ CONTRACTION
Lorentz contraction and transformation of equilibrium forces and moments in inertial reference systems transition, discussing special relativity theory
12 p1525 A73-27733

LORENTZ FORCE
Book on electromagnetic field theory covering free space Maxwell equations, Lorentz force law, vector analysis, Laplace equation, lossless transmission lines and dipole antennas
03 p0343 A73-13988

Longitudinal force exerted by circularly polarized high-powered laser radiation in a dense electron plasma.
15 p1917 A73-31091

Investigation of the possibility of developing a wide-aperture injector of fast neutral atoms
23 p3010 A73-43665

LORENTZ GAS
Screened potential Lorentz model for electrical conductivity of non-Debye plasma, investigating electron energy distribution function
17 p2214 A73-34127

The electron kinetics of a weakly ionized Lorentz plasma in arbitrarily oriented external electric and magnetic fields
20 p2596 A73-39192

A tensor surface harmonic expansion of the collision integral for a weakly ionized plasma. I
20 p2596 A73-39193

LORENTZ TRANSFORMATIONS
How to measure the earth's velocity with respect to absolute space.
05 p0615 A73-16363

The rod contraction-clock retardation ether theory and the special theory of relativity.
21 p2739 A73-40622

The asynchronous formulation of relativistic statics and thermodynamics.
22 p2931 A73-42436

LOS ALAMOS TURRET REACTOR
U HIGH TEMPERATURE NUCLEAR REACTORS

LOST WAX PROCESS
U INVESTMENT CASTING

LOTS CARGO SHIPS
U CARGO SHIPS

LOUDNESS
Loudness enhancement following contralateral stimulation.
01 p0013 A73-10827

Some modeling problems of loudness transformations by the auditory system
04 p0413 A73-15790

Pure-tone equal-loudness contours for standard tones of different frequencies.
21 p2645 A73-41176

Loudness changes resulting from an electrically induced middle-ear reflex.
22 p2811 A73-41815

LOUDSPEAKERS
A linear motion generator for physiological research.
01 p0011 A73-10173

Doppler effect intermodulation distortion derivation by perturbation method for loudspeaker modeled with pulsating sphere, considering boundary condition and nonlinear effect in wave propagation
08 p0987 A73-21123

LOUVERS
Space simulation chamber tests of thermal louver model for spacecraft temperature control
01 p0110 A73-11150

A design study of thermal louver system.
01 p0111 A73-11152

Preventing the shut-off punkah louver from jamming.
16 p1970 A73-32925

Mathematical modeling for ATS-F spacecraft louvers and heat pipes thermal control heat rejection capacity, noting correlation with solar environment simulation data
18 p2360 A73-36387

LOVE WAVES
Bluestein-Gulyaev shear surface waves in piezoelectric-dielectric-perfect conductor layered system, applying theoretical results to lithium iodate crystals
14 p1783 A73-30259

LOW ALLOY STEELS
U HIGH STRENGTH STEELS

LOW ALTITUDE
The biodynamic aspects of low altitude, high speed flight.
06 p0659 A73-18471

Psychophysiological characteristic of the activity of military-transport-aviation flight crews during low-altitude flights
19 p2397 A73-37196

The design of a two wheel momentum bias system for the attitude control of spacecraft in low altitude orbits.
20 p2585 A73-38793

LOW ALTITUDE SUPERSONIC VEHICLES
U F-111 AIRCRAFT

LOW ASPECT RATIO
Performance of low-aspect-ratio diffusers with fully developed turbulent inlet flows. I - Some experimental results.
17 p2152 A73-35009

Performance of low-aspect-ratio diffusers with fully developed turbulent inlet flows. II - Development and application of a performance prediction method.
17 p2152 A73-35010

LOW ASPECT RATIO WINGS
NT DELTA WINGS
NT TRAPEZOIDAL WINGS

Influence of the boundaries of wind-tunnel flow on the flow past a small-aspect-ratio wing
02 p0128 A73-11707

Unsteady transonic flow analysis for low aspect ratio, pointed wings.
05 p0530 A73-16878

A theory for rectangular wings with small tip clearance in a channel.
15 p1821 A73-31120

Russian book - Matrix methods of calculating the strength of low-aspect-ratio wings.
21 p2785 A73-40799

Determination of the deflections and stresses in a small-aspect-ratio wing by the displacement method
23 p3041 A73-43723

Approximate calculation of the cavitation flow past low-aspect-ratio wings
24 p3055 A73-45540

LOW DENSITY FLOW
Cryoprobe with truncated circular cross sectioned Cu cone with copper slug heat sink for momentum flow rate measurement in hypersonic low density flow
01 p0003 A73-10755

Drag coefficient for particles in rarefied, low Mach-number flows.
05 p0564 A73-16354

A study of the rarefaction of the interaction between an exhaust plume and a hypersonic external flow.
06 p0645 A73-17657

Slightly ionized low density hypersonic flow about a sharp plate and its diagnostics.
18 p2262 A73-36241

Nonlinear radial wave propagation in low density expanding flows with application to the free jet.
18 p2300 A73-36630

Interferograms of high optical quality by double exposure.
21 p2695 A73-39963

A device for the on-line measurement of nitrogen rotational temperature in low density flows.
22 p2854 A73-41995

Rarefied gas flow through an orifice at low pressure gradients
23 p2969 A73-44347

LOW DENSITY GASES
U RAREFIED GASES

LOW DENSITY MATERIALS
An appreciation of the design of carbon fibre rigid solar panels for spacecraft.
17 p2238 A73-34812

Thermal conductivity of low density carbon.
[EJCTP PAPER C-5] 22 p2881 A73-42404

LOW DENSITY WIND TUNNELS
Simulation of the flow past a high-altitude ion-concentration sensor 21 p2633 A73-41223

LOW FREQUENCIES
NT VERY LOW FREQUENCIES
Low frequency, high resolution observations of Virgo A. 01 p0100 A73-10791

Prototype solid state radio sounder with digitization concept of multiplex integration for LF sounding of lower ionosphere, noting performance 01 p0043 A73-10909

The theory of the reflection of low frequency radio waves in the ionosphere near critical coupling conditions. 05 p0551 A73-17052

Calculation of the field amplitude and phase velocity of low-frequency waves in the earth's spherical waveguide 08 p0939 A73-21285

Generator of rectilinear vibrations for the study of structures at low frequency [ONERA, TP NO. 1185] 09 p1084 A73-22713

Propagation of low-frequency electromagnetic waves in the spherical waveguide formed by the earth and the ionosphere 12 p1469 A73-27340

LF series expansion for acoustic scattering from soft and hard rotationally symmetric bodies, discussing relevance of magnetic polarizability tensor and electrostatic capacity 13 p1659 A73-28485

Investigation of low-frequency instabilities in a linear plasma betatron 14 p1782 A73-30805

The prevalence of second harmonic radiation in type III bursts observed at kilometric wavelengths. 16 p2053 A73-32964

Unusual LF radio absorption events during a major meteor shower. 18 p2289 A73-36302

SID effects as observed in intensities of LF radio waves. 18 p2290 A73-36879

Computations of the field amplitude and phase velocity of low-frequency waves in a spherical surface waveguide. 19 p2404 A73-37914

Sudden ionospheric disturbance effects on LF radio pulse train amplitude during reception from Loran-C transmitters, comparing with VLF sudden phase anomaly 22 p2825 A73-42188

Propagation of low-frequency electromagnetic waves in a spherical earth-ionosphere waveguide. 23 p2952 A73-43238

Investigation of low-frequency noise in MOS transistors 24 p3071 A73-44593

Experimental investigation of the low-frequency capacitive response of a plasma sheath. 24 p3117 A73-45408

LOW FREQUENCY BANDS
NT VERY LOW FREQUENCIES
Spectral density curves for intensity fluctuations of stimulated emission from low and IR frequency gas lasers as function of thermal oscillation, mode interference and beat effects 03 p0319 A73-14087

The transmission of low frequency medical data using delta modulation techniques. 04 p0412 A73-15408

Determination of the root-mean-square and mean intensity of the atmospheric radio noise field 21 p2648 A73-40208

Decay time of type III solar bursts observed at kilometric wavelengths. 21 p2762 A73-41497

LOW GRAVITY
U REDUCED GRAVITY
LOW LATITUDES
U TROPICAL REGIONS
LOW LEVEL TURBULENCE
Subsonic wind tunnel tests for laminar boundary layer investigation in low level turbulence flow, noting turbulence measurement with hot-wire anemometers 03 p0308 A73-13666

Low level wind measurement error as it affects sounding rocket dispersion. 09 p1116 A73-23215

Statistical turbulence model of meteorological and topographical aircraft flight conditions for low altitude critical air turbulence /LO-LOCAT/ environment 13 p1569 A73-28831

Spatial correlation functions of velocity and temperature components in the atmospheric boundary layer 13 p1654 A73-29153

Subsonic wind tunnel tests for laminar boundary layer investigation in low level turbulence flow, noting turbulence measurement with hot-wire anemometers 21 p2704 A73-41316

LOW MASS
U MASS
LOW MOLECULAR WEIGHTS
Influence of certain hydroxyl- and nitrogen-containing low-molecular-weight substances on the structural viscosity of cellulose acetate solutions 21 p2647 A73-40263

LOW NOISE
Noise considerations in space communication antennas. 07 p0794 A73-20228

A low noise, very low power charge sensitive amplifier for space applications. 17 p2134 A73-34272

C band low noise IC microwave amplifier for phased array module in multiple access communication links, discussing photofabrication for low cost batch processing 17 p2135 A73-34727

Low-frequency 1/f noise in MOSFET's. 19 p2409 A73-37581

Design and application of low noise GaAs FET amplifiers. 20 p2534 A73-38749

Evaluation of the noise immunity of pulse systems for continuous message transmission allowing for quantization and interpolation errors. II 20 p2531 A73-39462

Noise immunity of digital methods for the transmission of analog messages with an enhanced information content 20 p2531 A73-39463

Low-noise microwave down-converter with optimum matching at idle frequencies. 21 p2666 A73-41428

Low noise Si multijunction IMPATT diode measurements for large signal FM X band oscillator performance 21 p2668 A73-41588

LOW PASS FILTERS
Low pass Butterworth and Chebyshev filters design with Sallen-Key network for fabrication of microelectronic circuits 01 p0024 A73-10682

Synthesis of active RC circuits by means of equivalent circuits of impedance converters 02 p0148 A73-11549

The nonlinear analysis and design constraints of a multi-filter phase-lock loop. 04 p0421 A73-15434

Low-pass filters and their realization by means of active circuits with operational amplifiers 06 p0673 A73-17723

The probability density function for the output of a cross-correlator with bandpass inputs. 06 p0665 A73-18139

Low pass symmetrical filters of composite attenuation with infinite and flat points of attenuation around a given frequency 08 p0945 A73-20967

Least-squares monotonic lowpass filters with sharp cutoff. 09 p1065 A73-23093

Speed active multipole filter design with a flexible computer program that calculates the component values for optimum performance. 10 p1191 A73-23755

A numerical algorithm to design multivariable low-pass equiripple filters. 10 p1202 A73-24600

Possibility of independent control of frequency characteristic and coverage band in a PAFC system. 15 p1842 A73-30987

Low pass wide and medium band far IR filter obtained by cooling crystalline material to liquid He or nitrogen temperatures, tabulating transmission characteristics 21 p2697 A73-40127

A rational approach to the synthesis of one-dimensional acoustic filters. 21 p2739 A73-40285

Amplifier with distributed gain for use in radiometry 21 p2700 A73-40540

Extraction of Tschebysheff design data for the low-pass dielectric multilayer. 21 p2665 A73-41135

Tapered corrugated waveguide low-pass filters. 21 p2666 A73-41427

Low pass filter design for FDM and PCM systems, discussing active RC realization techniques and microelectronics model tests 22 p2832 A73-42293

Theoretical and experimental investigation of fluidic signal and noise filters with application to DC and AC fluidic systems. 23 p2944 A73-43418

LOW PRESSURE
NT CYCLOGENESIS
NT HIGH ALTITUDE PRESSURE
Dynamic study of a very-low-pressure sensor 02 p0165 A73-11591

A new variant of the Knudsen vacuumometer as a measurement standard for low pressures 03 p0306 A73-12898

High-temperature oxidation of a Ti-15Mo-5Zr alloy at low pressure of oxygen /40 microtorr to roughly 0.2 millitorr/. 03 p0321 A73-12918

Extinguishment of composite propellants at low pressures. 05 p0640 A73-16918

[AIAA PAPER 73-175] Low gas pressure measurement with ionization and extractor gages, discussing methods for suppressing or eliminating disturbance effects 11 p1361 A73-25400

Investigation of a low-pressure arc erosion plasma 14 p1781 A73-30459

An experimental study of the low pressure limit for steady deflagration of ammonium perchlorate. 16 p2045 A73-33347

Molybdenum evaporation rates in oxygen, air, and water vapor at high temperatures and low pressures 16 p2026 A73-33956

Double-probe measurements of electron temperatures on low pressure diffusion flames - Criticism of the methods for determining the electron temperature from the double-probe current voltage characteristic. 18 p2317 A73-37097

Development of a thermistor type temperature probe for use at low absolute pressures. 22 p2856 A73-42016

LOW PRESSURE CHAMBERS
U VACUUM CHAMBERS
LOW SPEED
Theoretical and experimental study of a swept-back wing at low velocity over a wide range of angles of attack 16 p1962 A73-32814

LOW SPEED HANDLING
U CONTROLLABILITY
U LOW SPEED
LOW SPEED WIND TUNNELS
NT SUBSONIC WIND TUNNELS
Low velocity wind tunnel design with adjustable pressure gradient, determining contraction section wall contour to avoid boundary layer separation via velocity distribution improvement 11 p1347 A73-25714

Low speed wind tunnel test section anisotropic turbulence decay rates representation by power type laws, comparing with grid and nearly isotropic turbulence 11 p1348 A73-26390

The RAE 5m low-speed wind tunnel. 11 p1344 A73-26499

LOW TEMPERATURE
Noise factor and power formula for cooled SHF broadband frequency converters with semiconductor mixer diode 01 p0026 A73-11265

Noise factor and power formula for cooled SHF broadband frequency converters with semiconductor mixer diode 17 p2134 A73-34317

Self balancing ac resistance bridge design with digital readout for low temperature carbon resistance thermometers 21 p2659 A73-39921

LOW TEMPERATURE ENVIRONMENTS
Spontaneous luminescence of ZnTe single crystals and mixed zinc cadmium telluride crystals at low temperatures, describing spectral lines 01 p0088 A73-10628

Relative rate measurements for oxygen atom addition to simple olefins in liquid Ar at 87.5 K, noting activation energies during reactions 02 p0139 A73-12086

Material variability as measured by low temperature electrical resistivity. 05 p0588 A73-17287

Thermoluminescence of Apollo 14 lunar samples following irradiation at -196 C. 07 p0897 A73-19879

Prediction of the low-temperature stability of type 304 stainless steel from a room temperature deformation test. 07 p0840 A73-20414

Plant growth response to low temperature and UV treatment, discussing chlorophyll synthesis, carbohydrate levels, ion balance and enzyme characteristics 11 p1320 A73-26486

Helium-cold induced hypothermia in the white rat. 12 p1461 A73-26975

Ultrasonic attenuation measurements in metals at low temperatures. 13 p1662 A73-29639

Anomalous low-frequency noise in MOS transistors at low temperatures. 14 p1731 A73-29749

Icy cometary nuclei laboratory simulation by sublimation of dust particle containing ice and frozen electrolyte mixtures in high vacuum at low temperature 14 p1793 A73-29823

Structure stability of austenitic chromium-nickel steels at the temperature of liquid helium 14 p1760 A73-30420

Measured thermal response to the MIL-STD 210B cold atmosphere. 16 p2034 A73-33140

Assembly for optical studies of semiconductors under pressures up to 10 kbar at 77 K. 17 p2145 A73-34175

Stability of waves and shock structure in generalized thermoelasticity at low temperatures. 20 p2624 A73-39564

LOW TEMPERATURE PHYSICS

Influence of light on the electron work function of GaAs single crystals at low temperatures. 01 p0088 A73-10631

Kinetic theory for calculation of low temperature homogeneous plasma electric conductivity in magnetic field, noting monotonic decrease. 03 p0346 A73-13177

Electron spin resonance of manganese ions in frozen methanol solution. 04 p0414 A73-15025

Radiation of phonons by metallic films. 04 p0483 A73-15465

The nuclear resonance in liquid helium three at very low temperatures. 08 p0987 A73-20647

The investigation of the middle infrared absorption spectrum of DyVO₄ at low temperatures. 08 p0994 A73-21219

The nuclear resonance in a hypothetical superfluid phase of helium three. 08 p0989 A73-21491

Thermoelectricity in tungsten at low temperatures. 09 p1135 A73-23335

Thermostable polymers for freezing and cryogenic temperatures, noting theory, methodology and preparation for science and industry. 10 p1241 A73-24675

A method for calculating the low temperature surface specific heat of a crystal lattice. 13 p1704 A73-28214

Liquid He 3 superfluidity near absolute zero, noting two solid and four liquid phases within millidegrees. 14 p1775 A73-30617

High-pressure chamber for optical studies at low temperatures. 17 p2164 A73-34174

Electron-electron collisions and the electrical conductivity of metals at low temperatures. 23 p3016 A73-44021

LOW TEMPERATURE PLASMAS

U COLD PLASMAS

Facility for investigating low-cycle fatigue of alloys at cryogenic temperatures. 01 p0029 A73-10491

Nitrided layer effects on austenitic steels mechanical properties at low temperatures, noting improved tensile strength. 01 p0067 A73-11347

Ti-V and Ti-Nb alloys mechanical strength and stress concentration resistance at low temperatures. 01 p0067 A73-11348

Fracture characteristics of some aluminum alloy sheets in Charpy impact test at super-low temperatures. 02 p0179 A73-11595

Fracture characteristics of aluminum alloy welds in Charpy impact test at super-low temperatures. 02 p0172 A73-11596

Crossed-coil nuclear magnetic resonance probe for high sensitivity low temperature measurements. 02 p0168 A73-11962

Low-temperature mechanical properties of the alloys AT3 and AT6. 02 p0180 A73-12136

The effect of tin on the strength and plasticity of titanium at low temperatures. 02 p0181 A73-12212

The influence of stress concentrators on the properties of steel in cryogenic technology. 02 p0181 A73-12213

Alloying effects on Ta binary alloy tensile strength brittleness and yield point at low temperatures. 04 p0466 A73-15669

Thermophysical properties of thermally insulating materials in the cryogenic temperature region. 04 p0520 A73-15938

Experimental analysis of the low-temperature strength of notched bars. 06 p0705 A73-17779

Heat capacity of the TV-10 tantalum-tungsten alloy at low temperatures. 06 p0708 A73-18051

Low temperature tests for magnetic field and temperature effects on differential resistance of lead alloy superconductors, calculating viscous friction coefficient. 06 p0736 A73-18116

Proton irradiation at 30 K and isochronal annealing of reactively sputtered Ta thin-film resistors. 06 p0737 A73-18352

Microwave properties of n-type InSb in a magnetic field between 4 and 300 K. 06 p0739 A73-18792

Influence of low temperatures on the fatigue life of welds. 07 p0833 A73-20508

The low temperature strain sensitivity of MOS transistors. 08 p0948 A73-21476

Parametrization of low-temperature deformation characteristics in single crystals of molybdenum. 09 p1099 A73-21928

Twinning deformation of mild steel at low temperatures as function of stress-strain state. 09 p1100 A73-22154

Investigation of the strength and deformability of thin composite materials used as magnetic recording media. II - Strength and deformability at low temperatures. 09 p1110 A73-22156

Low-temperature impact bending with recording of the stress-strain diagrams. 09 p1100 A73-22157

Device for endurance testing of materials at low temperatures. 09 p1070 A73-22168

Electrical and structural properties of low-temperature bismuth films. 09 p1133 A73-22603

Yield and fracture of D16T alloy at low temperatures in the presence of a complex stress pattern. 09 p1105 A73-23055

Four-section equipment for studying creep and long-term strength in deep cooling conditions. 09 p1086 A73-23067

Investigation of the effect of surface finish and method of surface treatment on the endurance of the steels Kh18N10T and Kh16N6 and of alloy AMG6 at normal and low temperatures. 09 p1106 A73-23163

Low temperature vacuum fatigue testing facility for materials testing under space environment conditions. 11 p1343 A73-25445

A method of measuring thermal conductivity in the presence of extraneous heat currents and the thermal conductivity of brass at low temperatures. 11 p1367 A73-26307

A nanovolt-level MOSFET reversing switch for low temperature applications. 11 p1367 A73-26310

Gliding, twin formation and fracture of iron-single crystals at 78 K and at 4 K. 11 p1386 A73-26571

Procedure for studying fatigue failure features in metals under harmonic and complex loading at low temperatures. 12 p1486 A73-27254

A modernized device for testing metal sheet and welded joints under conditions of planar tension. 12 p1486 A73-27464

Conditional margin of plastic strength for shaft-type elements subjected to torsion at low temperatures. 12 p1554 A73-27478

The strength differential of steel and Ti alloys as influenced by test temperature and microstructure. 12 p1513 A73-27681

Thermally activated low temperature creep of solids at constant load, considering creep curve stages and plastic deformation mechanism. 13 p1635 A73-28263

Bi2Se3 Hall effect magnetometer for reliable low temperature use. 13 p1612 A73-28368

Austenitic stainless steels at cryogenic temperatures. I - Structural stability and magnetic properties. 13 p1636 A73-29070

An empirical function between the resistance and the temperature of a carbon thermometer for 0.3 to 4.2 K. 13 p1618 A73-29071

Plasticity and fracture of structural metals in complex stress state at low temperatures. 13 p1639 A73-29462

The strength of welded joints in high strength stainless steels at cryogenic temperatures. 13 p1625 A73-29615

Mechanical strength of titanium alloys AT-2 and AT-3 and of their welded seams at extreme temperatures. 13 p1643 A73-29633

Low-temperature relaxations in amorphous polymers. 14 p1765 A73-30134

A unit for investigating the low-cycle fatigue of alloys at cryogenic temperatures. 14 p1743 A73-30316

Low-temperature internal friction in boron fibers. 14 p1766 A73-30380

The low-temperature embrittlement of niobium and vanadium by both dissolved and precipitated hydrogen. 14 p1761 A73-30630

Investigation of fatigue and brittle failure patterns in 15G2AFDps steel at low temperatures. 14 p1762 A73-30678

Effect of cooling /to -269 C/ on failure in Kh18N10T and Kh16N6 steels under impact bending. 14 p1763 A73-30692

Mechanism of plastic deformation and low-temperature brittleness of a Cr alloy containing 45 at.% Fe. 14 p1764 A73-30866

Testing assembly for sheet metals and welded joints under static and low-cycle biaxial tension under low temperature conditions. 15 p1855 A73-31147

Influence of plastic deformation and of phase transformations at negative temperatures on the properties of titanium alloys. 15 p1894 A73-32531

Low temperature deformation of commercial Ti alloys. 16 p2024 A73-32848

Determination of the diffusivity-mobility ratio in highly degenerate semiconductors at low temperatures from linewidth measurements in junction lasers. 16 p1990 A73-33689

Temperature dependence of low-temperature strength in aluminum single crystals. 17 p2189 A73-34581

Investigation of the impact toughness of construction materials at temperatures of 20 and 4.2 K. 18 p2324 A73-36767

Low temperature tensile tests for strength and plasticity of pure bcc, hcp and fcc polycrystalline metals, indicating stacking fault energy role. 18 p2324 A73-36804

Low temperature specific heat of neodymium magnesium nitrate. 18 p2341 A73-36977

Special features of the fracture of aluminum and titanium alloys at low temperatures. 19 p2439 A73-37267

Effect of low temperature on the fatigue limit of welded joints. 19 p2433 A73-37783

Infrared spectrum and geometry of ozone isolated in inert gas matrices at 20.4 K. 19 p2463 A73-37904

High-frequency fatigue tests at low temperatures. 20 p2619 A73-39363

Study of low-cycle fatigue of titanium-base alloys at a temperature of -196 C. 20 p2577 A73-39375

Faulty structure in niobium single crystals deformed by rolling at 77 K. 20 p2579 A73-39743

A high vacuum, low temperature specimen transfer device for use in measuring optical properties of thin films. 21 p2693 A73-39925

Experimental investigation of the antifurcation properties of Teflon-base materials at low temperatures. 21 p2724 A73-41197

Application of precise heat-capacity data to the analysis of the temperature intervals of the International Practical Temperature Scale of 1968 in the region of 90 K. 22 p2852 A73-41977

Representation of the temperature-resistance characteristic of germanium thermometers below 30 K. 22 p2854 A73-42001

Platinum resistance thermometry below 13.81 K. 22 p2854 A73-42002

Intercomparison of standard platinum thermometers calibrated on IPTS-68 between 13.81 and 273.15 K. 22 p2854 A73-42003

Low temperature thermometry in high magnetic fields. 22 p2856 A73-42017

A low-temperature, glass-ceramic capacitance thermometer. 22 p2856 A73-42020

High field NMR thermometry below 1 K using HD. 22 p2856 A73-42024

Gold-iron alloys for low temperature thermocouples. 22 p2857 A73-42030

Recording strain diagrams in low-temperature impact bending tests. 22 p2874 A73-42105

A unit for fatigue testing of materials at low temperatures. 22 p2838 A73-42116

Fatigue crack propagation and fracture toughness of 5Ni and 9Ni steels at cryogenic temperatures. 22 p2875 A73-42143

Self-termination of free oscillations in ruby at low temperatures. 22 p2896 A73-42251

Silicon Zener diodes used as temperature sensors. 24 p3090 A73-44937

LOW THRUST

NT MICROTHRUST

The fastest transfer from one circular orbit to another under the action of a small thrust. 20 p2604 A73-38990

LOW THRUST PROPULSION

NT ELECTROMAGNETIC PROPULSION

NT ELECTROSTATIC PROPULSION

NT ION PROPULSION

NT MAN OPERATED PROPULSION SYSTEMS

NT PHOTONIC PROPULSION

NT PLASMA PROPULSION

NT SOLAR PROPULSION

Secondary low thrust propulsion systems technology requirements and parameters, covering electrothermal, radioisotope and ion bombardment thrusters

01 p0090 A73-11109

Guidance of spacecraft controlled by low-thrust rocket engines and evolving in the plane of the initial trajectory

02 p0227 A73-11580

High and low thrust systems for primary and auxiliary spacecraft propulsion, noting electron bombardment electrostatic thruster for north-south station-keeping

[AIAA PAPER 72-1123] 03 p0355 A73-13435

Durability tests of a five-centimeter diameter ion thruster system.

[AIAA PAPER 72-1151] 03 p0356 A73-13455

Spacecraft low thrust propulsion systems applications to earth orbital and planetary missions, discussing payload capabilities vs flight time

[AIAA PAPER 72-1125] 04 p0486 A73-14911

Electrothermal hydrazine thruster analyses and performance evaluation.

[AIAA PAPER 72-1152] 04 p0486 A73-14917

Long life contact-ionized cesium low thrust engine design, considering ionizer working temperatures and neutralizer ion current densities

04 p0488 A73-15720

Low power pulsed ablation plasma thruster design for satellite attitude control and stationkeeping, describing operating principle and performance measurements

04 p0489 A73-15731

Constrained low thrust guidance algorithms for three axis and spin stabilized constant power solar electric propelled spacecraft on fixed time rendezvous missions

[AIAA PAPER 73-173] 05 p0595 A73-16917

Optimization of multiple target electric propulsion trajectories.

[AIAA PAPER 73-205] 06 p0748 A73-17658

A low-power MPD thruster of Duoplasmatron type.

18 p2342 A73-36154

LOW TURBULENCE

LF boundary of inertial range in lowest atmospheric layer, comparing turbulence scale and wind velocity components

08 p0954 A73-21185

LOW VELOCITY

U LOW SPEED

LOW VISIBILITY

Functional aspects of head-up display operation, discussing data accumulated by pilot during low visibility runway approach in executive jet

01 p0013 A73-11012

Low visibility/bad weather aircraft landing systems design, discussing developmental stages for all weather landing implementation, automatic landing control and pilot visual discrimination problems

17 p2207 A73-34481

Analysis of visibility conditions during aircraft landing in radiation fog

17 p2204 A73-34540

Passive low light level television for military and civilian ground surveillance under poor visibility conditions

17 p2168 A73-34906

Operative visibility limits over the airports of Milan Linate and Malpensa in the 1960-1969 decade

19 p2447 A73-38125

LOW VOLTAGE

Processing power for a low voltage source-pulse load system.

03 p0253 A73-13939

Threshold voltage shift for low voltage operation of transistor circuits with boron ion implanted MOS

04 p0427 A73-15322

Temperature dependent small signal operation of junction transistors at low supply voltage

06 p0677 A73-18395

Dynamic characteristics of a plasma diode under conditions of a low-voltage arc discharge. I- Theory of the dynamic characteristics

18 p2339 A73-36557

Approaches to the design of low-voltage pulse generators using avalanche semiconductor devices

20 p2538 A73-39467

LOW WING AIRCRAFT

SOKO Galeb 3 cantilever low wing trainer-fighter monoplane with Bristol-Siddeley Viper 20 turbojet engine, describing flight control, loading gear, fuel system and avionics

14 p1712 A73-30240

LOWER ATMOSPHERE

NT OZONOSPHERE

NT TROPOSPHERE

Measurement of small-scale turbulence and thermal stability in the lower atmosphere by radar.

03 p0279 A73-14536

Two layer model for diurnal temperature variations analysis of radiative heat transfer between planetary lower atmosphere and underlying

04 p0473 A73-15574

Instrument suspended from tethered balloon for oceanic measurement of average lower atmosphere vertical electric field profile

05 p0579 A73-17251

Mars 3 onboard optical measurements of Mars surface and lower atmosphere, considering temperatures, water vapor content, dust cloud and particle characteristics

06 p0746 A73-17481

Certain feedbacks generated during turbulent cellular convection in the atmosphere

08 p0986 A73-21456

Study of average and turbulent characteristics of boundary layers stratified in temperature - Comparison with the corresponding characteristics in low layers of the atmosphere

09 p1072 A73-23028

Mode of thickening of a low morning convective layer in clear sky

09 p1115 A73-23036

Measurement of the horizontal component of the electrostatic field intensity in the lower atmosphere

10 p1219 A73-24400

Statistical aspects of lower atmospheric disturbances delineated from conventional and satellite data over the tropical Pacific.

11 p1394 A73-25724

Dropsonde for continuous temperature measurement during descent through lower atmospheric level, discussing receiving unit and data conversion unit

12 p1495 A73-26815

Space distribution of the intensity of excess radiation at low altitudes.

12 p1535 A73-27637

A comparison of turbulence measurements by different instruments - Tsingyansk field experiment 1970.

13 p1656 A73-29343

Measurement of high-altitude air quality using aircraft.

[AIAA PAPER 73-517] 16 p2006 A73-33554

Thermodynamic characteristics of the lower atmosphere of Venus on the basis of the results of an experiment conducted with the descent vehicle of the Venus 4 interplanetary probe

16 p2067 A73-33800

Electrical balance in the lower atmosphere.

17 p2158 A73-34359

Simultaneous measurements of ion concentration and corpuscular stream intensity at altitudes ranging from 10 to 79 km

18 p2345 A73-36121

Occurrence and features of ducted modes of internal gravity waves over Western Europe and their influence on microwave propagation.

19 p2405 A73-38225

Optical properties of the lower atmosphere of Venus /for interpreting measurements of the Venera 8 planetary probe/

21 p2686 A73-40913

Lower atmospheric intensity-calibrated thermal emission spectra with digital recording near IR spectrometer, discussing applications to pollutant detection

21 p2692 A73-41574

Diurnal harmonic oscillation instability of atmospheric boundary layer as mesoscale internal gravity waves generation mechanism in lower atmosphere, considering unsteady flow equations

23 p3001 A73-43589

LOWER BODY NEGATIVE PRESSURE (LBNP)

U ACCELERATION STRESSES (PHYSIOLOGY)

LOWER IONOSPHERE

NT D REGION

Influence of an important region of the ionospheric layer on ELF propagation characteristics

01 p0016 A73-10203

Lower ionosphere variability due to atmospheric dynamics, considering temperature variations, minor constituent transport and eddy diffusion

01 p0041 A73-10885

Electron-density and energetic-electron measurements of the midlatitude lower ionosphere during winter.

01 p0041 A73-10888

Changes of electron density with zenith angle, with the sunspot cycle, and during eclipses.

01 p0043 A73-10907

Electron density profiles in the equatorial lower ionosphere at Thumba.

01 p0043 A73-10908

Prototype solid state radio sounder with digitization concept of multipulse integration for LF sounding of lower ionosphere, noting performance

01 p0043 A73-10909

Studies of the lower ionosphere by means of VLF propagation over long distances

01 p0044 A73-11515

Changes of lower ionosphere electron concentrations with solar activity.

02 p0159 A73-12029

Electron density and wind structure observations in lower ionosphere by rocket, noting sporadic E layer due to wind shear

02 p0163 A73-12307

The effects of ions of VLF and ELF propagation in an abnormally ionized atmosphere.

02 p0143 A73-12851

Statistical analysis of atmospheric sudden changes in VLF bands, suggesting lower ionosphere ionization increase due to meteors incidence

03 p0299 A73-12948

Electron density and temperature measurements in the lower ionosphere as deduced from the warm plasma theory of the H.F. quadrupole probe.

04 p0480 A73-15199

The role of atmospheric pressure variations above the mesopause in the phenomena of winter anomaly and variability of the lower ionosphere.

04 p0441 A73-15290

Lower ionosphere at medium latitudes during geomagnetic disturbances.

05 p0568 A73-16214

Investigation of a signal scattered in the lower ionosphere on the basis of a group delay model

05 p0548 A73-16254

Temporal variations of the recombination coefficient and electron density profile in the lower ionosphere

05 p0568 A73-16261

Vertical motion of the lower ionosphere during a solar eclipse

05 p0569 A73-16262

Radio-wave absorption in the lower ionosphere and stratospheric effects

05 p0569 A73-16265

Chemical kinetics equations of lower ionosphere and D region particle interactions for aeronomic problems

05 p0569 A73-16396

Electric probe performance in weakly ionized dense plasma flow for lower ionosphere measurements, considering stagnation point and particle distribution-potential effects

06 p0689 A73-17538

Solar cosmic rays spectrum and geomagnetic cut-off rigidity determination from ion production rates in lower ionosphere

07 p0870 A73-19427

Lower ionospheric seasonal anomaly in electron density levels, noting diurnal and latitudinal characteristics at various heights

07 p0816 A73-19453

Impact and bremsstrahlung photoionization due to precipitating electrons in the lower ionosphere.

08 p0957 A73-20657

Solar cosmic ray flare of 11-18 April 1969, investigating effect on polar cap absorption in lower ionosphere

08 p1000 A73-21348

Correct statement of the problem of computing the N/h profiles of the lower ionosphere.

10 p1212 A73-24241

Photoionization and charge exchange reaction kinetics inadequacy for explanation of observed positive nitrogen dioxide ion concentration in lower ionosphere, considering alternative mechanism

10 p1214 A73-24749

Vertical distribution of absorption of cosmic radio emission and radio waves in ionosphere and lower ionosphere based on electron density profiles

11 p1327 A73-25084

Autocorrelation and cross correlation coefficients for maximum electron densities and total electron content in E and F regions and upper and lower ionosphere

11 p1351 A73-25093

Solar 1.9 A X ray spectral line effects on SOLRAD satellite-borne photometer sensitivity and lower ionospheric ion production rate

11 p1354 A73-25771

Tunneling transmission through the equatorial lower ionosphere of ELF and VLF electromagnetic waves.

11 p1358 A73-26702

The concept of an installation for measuring partial reflections with the aid of the FM-CW procedure and the principle of measurement involved

12 p1486 A73-27764

Numerical solution of the problem of transmission of ELF waves through the lower ionosphere.

13 p1582 A73-28651

Isothermal ionization of the lower ionosphere under the effect of radio waves.

13 p1608 A73-28709

On the effect of electron-neutral particle collisions upon the refraction of high-frequency radio waves by the lower atmosphere and ionosphere of Mars.

15 p1929 A73-31078

Electric probe performance in weakly ionized dense plasma flow for lower ionosphere measurements, considering stagnation point and particle distribution-potential effects

16 p2001 A73-32762

A rocket-borne instrument for the measurement of nighttime atmospheric densities.

17 p2164 A73-34270

Methods of measurements and some results of lower ionosphere by using VLF and LF radio waves.

18 p2302 A73-35926

Ion and neutral composition measurements in the lower ionosphere. 18 p2303 A73-35960

Accuracy of rocket measurements of lower ionosphere electron concentrations. 18 p2304 A73-35965

Positive ion composition in the lower ionosphere during the Geminid meteorshower and the occurrence of a winter anomaly. 18 p2305 A73-36005

VLF pulse ionosounder measurements of the reflection properties of the lower ionosphere. 18 p2305 A73-36010

Trial of existing models of the lower ionosphere by experimental data on Schumann resonances. 18 p2306 A73-36011

Electron density profiles from ionograms - Comparisons with rocket profiles. 18 p2306 A73-36017

Dynamic processes as derived from the mean circulation in the upper mesosphere and lower thermosphere. 18 p2307 A73-36036

A rocket-borne riometer for the study of lower ionosphere. 18 p2315 A73-36046

Measurement of the ionospheric electron density by using S-210-6 rocket. 19 p2423 A73-37380

Reflection of powerful radio waves from the lower ionosphere 19 p2406 A73-38334

Analytical approach to the direct and inverse problems of cosmic ray action on the lower ionosphere 21 p2759 A73-40609

Ground based and rocket techniques for vertical ionospheric electron density distribution measurement, considering incoherent scatter, partial reflection, wave interaction, and Faraday rotation 21 p2685 A73-40809

Metastable oxygen atoms radiative lifetime quenching rate as function of altitude in lower ionosphere based on auroral observations and atmospheric model 23 p2972 A73-43692

LOX [OXYGEN]

U LIQUID OXYGEN

LOX-HYDROGEN ENGINES

U HYDROGEN OXYGEN ENGINES

LR CIRCUITS

U RL CIRCUITS

LRC CIRCUITS

U RLC CIRCUITS

LRV [VEHICLE]

U LUNAR ROVING VEHICLES

LSI

U LARGE SCALE INTEGRATION

LST

U LARGE SPACE TELESCOPE

LUBRICANT TESTS

Thermohydrodynamic phenomena in fluid film lubrication. [ASME PAPER 72-LUB-25] 03 p0314 A73-14338

Molybdenum disulfide in oils and greases under boundary conditions. [ASME PAPER 72-LUB-37] 03 p0335 A73-14345

Elastohydrodynamic traction characteristics of 5P4E polyphenyl ether. [ASME PAPER 72-LUB-40] 03 p0335 A73-14347

Fatigue scoring - A new form of lubricant failure. [ASLE PREPRINT 72LC-3B-1] 03 p0316 A73-14356

The additive action of some organic chlorides and sulfides in the four-ball lubricant test. [ASLE PREPRINT 72LC-3C-2] 03 p0316 A73-14357

Investigation of anti wear additives under various loads and at different sliding speeds. [ASLE PREPRINT 72LC-3C-4] 03 p0316 A73-14359

The assessment of recently developed lubricants for rolling elements. [ASLE PREPRINT 72LC-4C-2] 03 p0316 A73-14361

The evaporation of various lubricant fluids in vacuum. [ASLE PREPRINT 72LC-6C-2] 03 p0335 A73-14366

Development of solid lubricant compact bearings for the supersonic transport. [ASLE PREPRINT 72LC-7C-1] 03 p0316 A73-14370

Lubricating characteristics of polyimide bonded graphite fluoride and polyimide thin films. [ASLE PREPRINT 72LC-7C-3] 03 p0317 A73-14372

Metallic additions effect on wear and friction behavior of lead monoxide, lead silicate and calcium fluoride solid lubricants coatings for high temperature operations [ASLE PREPRINT 72LC-7C-5] 03 p0317 A73-14374

The application of elastohydrodynamic lubrication in gear tooth contacts. 03 p0317 A73-14375

Cu and Cu-Sn base self lubricating composites, testing solid lubricants effects on friction coefficient, wear, electrical resistance, hardness, porosity and structure 04 p0454 A73-14996

Frictional behaviour of molybdenum disulfide in high vacuum. 04 p0454 A73-14997

Critical failure conditions in thin film lubrication - Preliminary results. 05 p0581 A73-16109

New high performance silicone greases and their applications. 07 p0842 A73-19557

Influence of pressure on VT14 alloy wear and friction against 30KhGSA steel 10 p1226 A73-24797

High temperature solid lubricants lubricating and environmental stability characteristics, discussing ball and journal bearings wear test results [ASME PAPER 73-DE-9] 14 p1767 A73-30818

Hot environment lubrication failures of sleeve bearing diester lubricant system in small electric motors, using reliability-temperature accelerated tests [ASME PAPER 73-DE-13] 14 p1767 A73-30819

Method for the determination of impurity particle dispersion in fuels and lubricants 15 p1876 A73-31834

Polytetrafluoroethylene and fluorinated ethylene-propylene grease lubricants. [ASLE PREPRINT 73AM-1A-2] 17 p2195 A73-34977

Lubricant testing as an aid to bearing damage analysis. [ASLE PREPRINT 73AM-3B-1] 17 p2178 A73-34983

An analytical and experimental investigation of turbulent flow in bearing films including convective fluid inertia forces. [ASME PAPER 73-LUBS-1] 17 p2181 A73-35388

LUBRICANTS

NT HIGH TEMPERATURE LUBRICANTS

NT LUBRICATING OILS

NT SOLID LUBRICANTS

Effect of laser working on the wear of machine parts in an abrasive-lubricant medium 02 p0173 A73-11935

Preferential adsorption in the lubrication process of zinc dialkyldithiophosphate. [ASLE PREPRINT 72LC-3C-3] 03 p0274 A73-14358

Metallic contact resistance and friction behavior under microdisplacement for lead/gold surfaces with lubricant or oxide film, noting consistency with Greenwood theory [ASLE PREPRINT 72LC-6B-1] 03 p0316 A73-14364

A process for delubrication, presintering, sintering, and rapid cooling in a vacuum induction furnace. 04 p0455 A73-15751

Assessment of lubricant technology; Proceedings of the Annual Spring Lubrication Symposium, Boston, Mass., June 6-8, 1972. 07 p0842 A73-19551

Lubricating grease technological development trends, discussing petroleum oils, esters, silicones, ethers and fluorocarbons base types and different thickeners 07 p0842 A73-19556

Synthetic hydrocarbon lubricants performance characteristics under extreme temperature service conditions, considering viscosity, antiwear, oxidation stability, demulsibility and corrosion protection properties 07 p0843 A73-19562

Lubricants thermophysical properties effects on gas turbine engine design, considering thermal stability, vapor pressure, autoignition, load capacity and bearing life 07 p0843 A73-19563

Oxystearate-based multipurpose lithium lubricants 07 p0843 A73-20013

Influence of liquid lubricant properties on their performance. 07 p0844 A73-20464

Motion of a magnetizable fluid in the lubrication film of a cylindrical bearing 10 p1225 A73-24586

The shear strength of thin lubricant films. 14 p1754 A73-30050

An analysis and prediction of lubricant film starvation in rolling contact systems. [ASLE PREPRINT 73AM-3B-4] 17 p2179 A73-34985

Amine phosphates as antiwear additives in neopentyl polyol esters. [ASLE PREPRINT 73AM-9A-1] 17 p2196 A73-34996

Application of energy model of turbulence to calculation of lubricant flows. [ASME PAPER 73-LUBS-18] 17 p2181 A73-35397

Calculation of pressure, shear, and flow in lubricating films for high speed bearings. [ASME PAPER 73-LUBS-21] 17 p2182 A73-35399

Russian book - Fuels and lubricants for flight vehicles. 19 p2472 A73-37769

LUBRICATING OILS

Performance tests for steel-steel lubrication capability of dimethyl silicone oils and greases modified by soluble, heat-stable extreme pressure and antiwear additives 03 p0329 A73-13011

Spiral groove thrust bearing with load carrying lubricating oil film between stationary and rotating surfaces, discussing design, manufacturing and applications 03 p0313 A73-13925

Inlet shear heating in elastohydrodynamic lubrication. [ASME PAPER 72-LUB-21] 03 p0314 A73-14336

Thermohydrodynamic phenomena in fluid film lubrication. [ASME PAPER 72-LUB-25] 03 p0314 A73-14338

Molybdenum disulfide in oils and greases under boundary conditions. [ASME PAPER 72-LUB-37] 03 p0335 A73-14345

Fatigue scoring - A new form of lubricant failure. [ASLE PREPRINT 72LC-3B-1] 03 p0316 A73-14356

The additive action of some organic chlorides and sulfides in the four-ball lubricant test. [ASLE PREPRINT 72LC-3C-2] 03 p0316 A73-14357

Microcorrosion studies with functional fluids. [ASLE PREPRINT 72LC-4C-1] 03 p0335 A73-14360

The assessment of recently developed lubricants for rolling elements. [ASLE PREPRINT 72LC-4C-2] 03 p0316 A73-14361

Thermal collapse theory of hydrodynamic oil lubrication films failure for slider bearing, noting frictional forces role 05 p0580 A73-16105

A technical note on the correspondence between Amontons' law and wear-scar data in a 4-ball machine. 05 p0581 A73-16108

Critical failure conditions in thin film lubrication - Preliminary results. 05 p0581 A73-16109

An extension of the Grubin theory of elastohydrodynamic lubrication. 05 p0581 A73-16433

Early diagnosis of machine damage on the basis of the determination of rubbed-off materials in highly stressed lubricating oils - Employment of spectrographic methods for the analysis of the oil 05 p0582 A73-16998

Nonhydrocarbon liquid lubricants based on phosphate and neopentyl esters, perfluoroalkyl and polyphenyl ethers, silicone and perfluorotriazines, discussing performance testing techniques 07 p0843 A73-19559

Silicone oil lubricants technology for steel-steel lubrication over wide temperature and load ranges 07 p0843 A73-19560

Optimization of the rheological properties of s-triazine derivatives. 07 p0787 A73-19561

Emission spectrographic analysis of used aero engine oil - A tool of maintenance. 09 p1136 A73-23242

Investigation of iron content of lubricating oil using a ferrograph and an emission spectrometer. 10 p1218 A73-24165

Usage of the VNII NP-300A lubricant in gas-liquid chromatography and high-vacuum technology. 10 p1239 A73-24250

Frictional traction in elastohydrodynamic lubrication. 13 p1623 A73-28198

German monograph - Investigations regarding the elastohydrodynamic lubricant film thickness in the case of elliptical Hertzian contact surfaces. 13 p1625 A73-29287

Self induced vibration of friction bearing mounted rigid rotor, considering oscillation damping or enhancing effect of oil film 16 p1968 A73-33236

Aircraft engine fuel and oil differential temperature measurement via platinum probes, specifying sensor sensitivity, calibration, circuit operation and data reduction 17 p2165 A73-34607

Evaporation rate and vapor pressure of selected polymeric lubricating oils. [ASLE PREPRINT 73AM-1A-3] 17 p2195 A73-34978

Turbulent lubrication - Its genesis and role in modern design. [ASME PAPER 73-LUBS-19] 17 p2181 A73-35398

Differential temperature measurements in engine fluids. 18 p2315 A73-36071

Modeling the effect of air and oil upon the thermal resistance of a sphere-flat contact. [AIAA PAPER 73-746] 18 p2370 A73-36362

Determination of the proneness of aviation oils to carbon deposition 19 p2472 A73-38491

Experimental investigation of a simple squeeze film damper. [ASME PAPER 73-DET-101] 22 p2865 A73-42078
Experimental investigation of the viscosity of lubricating oil containing air 24 p3094 A73-45548

LUBRICATION

NT BOUNDARY LUBRICATION
NT SELF LUBRICATION
NT SPACECRAFT LUBRICATION

The role of compressional viscoelasticity in the lubrication of rolling contacts. [ASME PAPER 72-LUB-O] 01 p0055 A73-10220
Application of finite element methods to lubrication - An engineering approach. [ASME PAPER 72-LUB-N] 01 p0055 A73-10221
Elastohydrodynamic lubrication in rolling and sliding contacts. [ASME PAPER 72-LUB-K] 01 p0055 A73-10222

Basic relationships in turbulent lubrication and their extension to include thermal effects. [ASME PAPER 72-LUB-16] 03 p0314 A73-14332
Elastohydrodynamic lubrication in rolling and sliding contacts. [ASME PAPER 72-LUB-K] 03 p0315 A73-14351

Application of finite-element methods to lubrication - An engineering approach. [ASME PAPER 72-LUB-N] 03 p0315 A73-14353
The role of compressional viscoelasticity in the lubrication of rolling contacts. [ASME PAPER 72-LUB-O] 03 p0315 A73-14354

A review of thermoelastohydrodynamic lubrication in rolling and sliding contacts. 07 p0831 A73-20223
An improved method for calculating the spin torque in a fully lubricated ball-race contact. 07 p0833 A73-20485

A hydrodynamic theory of radial-face mechanical seals. 10 p1223 A73-23698
Fluid film lubrication fluid mechanical theory, considering non-Newtonian fluids, turbulence, inertia and elastohydrodynamic effects in various bearing types. 10 p1223 A73-23698

Gear and bearing designs with lubricated and reinforced thermoplastics. 10 p1223 A73-23957
On the influence of inertia forces in hydrostatic turbulent lubrication. 14 p1755 A73-30705

Radial MHD bearing with a floating bush. 15 p1881 A73-31412
German monograph - Model wear investigations concerning the effect of the intermediate medium on the sliding characteristics in the case of a contact between different materials. 15 p1883 A73-32593

Grease lubrication of helicopter transmissions. [ASLE PREPRINT 73AM-2A-1] 17 p2178 A73-34980
Elastohydrodynamic principles applied to the design of helicopter components. [AHS PREPRINT 770] 17 p2248 A73-35088

Turbulent lubrication theory - Application to design. [ASME PAPER 73-LUBS-10] 17 p2181 A73-35392
Experimental study on the interference of inertia and friction forces in turbulent lubrication. [ASME PAPER 73-LUBS-12] 17 p2181 A73-35393

Thermohydrodynamic lubrication in laminar and turbulent regimes. [ASME PAPER 73-LUBS-15] 17 p2181 A73-35395
Contribution to the hydrodynamic lubrication theory of the bearing with a floating bushing. 18 p2319 A73-36411

Lubricating properties of micropolar fluids in composite and step slider bearings, obtaining analytic expressions for load carrying capacity and skin friction. 24 p3092 A73-44410

Inertia effects in MHD lubricated hydrostatic thrust bearing under axial magnetic field investigated by energy integral method, obtaining flow velocity and load carrying capacity. 24 p3092 A73-44410

LUBRICATION SYSTEMS

Laboratory experience with long-term bearing lubrication. 01 p0057 A73-11278
Spacecraft lubrication systems design for long mission lifetimes, discussing mechanical design parameters and liquid and solid lubricant characteristics. 03 p0330 A73-13012

The application of elastohydrodynamic lubrication in gear tooth contacts. 03 p0317 A73-14375
Synchronized operation of a positive-displacement gear pump and a vane pump within the lubricant oil delivery system of a jet engine. 23 p3020 A73-43742

Hirs turbulent lubrication theory, discussing plane inclined slider thrust bearing applications and performance predictions. 24 p3094 A73-44891

LUCITE (TRADEMARK)

U POLYMETHYL METHACRYLATE

LUDER BANDS

U PLASTIC DEFORMATION

U YIELD POINT

LUMBERING AREAS

U FORESTS

LUMINAIRES

NT AIRCRAFT LIGHTS

NT AIRPORT LIGHTS

NT FLASH LAMPS

NT RUNWAY LIGHTS

NT XENON LAMPS

LUMINANCE

Two stage mathematical model of brightness perception operation for stimuli having luminance field with asymmetric discontinuity. 02 p0137 A73-12078
A human factors approach to lighting recommendations and standards. 05 p0545 A73-16730

Probability estimate for visual target detection in terms of luminance threshold and target size and duration. 06 p0658 A73-18242
Random dot pattern luminance and contrast effects on limiting inter-stimulus interval for visual apparent motion masking by bright field. 07 p0783 A73-20256

The brightness of coloured flashes on backgrounds of various colours and luminances. 08 p0935 A73-21565
Visual sensitivity in the presence of alternating monochromatic fields of light. 08 p0932 A73-21567

Visual discrimination of motion - Stimulus relationships at threshold and the question of luminance-time reciprocity. 09 p1044 A73-21897
Quantitative studies on optokinetic nystagmus in the monkey. 18 p2273 A73-36459

Bezold-Bruecke effect and visual nonlinearity. 23 p2946 A73-43342

LUMINESCENCE

NT BIOLUMINESCENCE

NT CHEMILUMINESCENCE

NT ELECTROLUMINESCENCE

NT FLUORESCENCE

NT LUNAR LUMINESCENCE

NT OPTICAL RESONANCE

NT PHOTOLUMINESCENCE

NT SHOCK WAVE LUMINESCENCE

NT THERMOLUMINESCENCE

NT X RAY FLUORESCENCE

Spontaneous luminescence of ZnTe single crystals and mixed zinc cadmium telluride crystals at low temperatures, describing spectral lines. 01 p0088 A73-10628
I-V characteristics and luminescence changes in Cs vapor arc discharge at various spark gap widths, noting pressure effect on gas stratification. 04 p0481 A73-15613

Russian papers on phosphor crystal luminescence and nonlinear optics covering spectral line decomposition, GaAs laser and electromagnetic wave interaction. 05 p0584 A73-16551
Luminescence signatures induced by lasers with enhanced specificity for remote active sensing. 05 p0585 A73-17157

Cooperative luminescence in trivalent ytterbium and erbium ions in cadmium fluoride crystals. 06 p0738 A73-18543
IR and thermal extinction spectra of luminescence and photoconductivity of zinc cadmium sulfide solid solution films doped with Cu and Cl. 06 p0738 A73-18643

Luminescence of Apollo 14 and Apollo 15 lunar samples. 07 p0897 A73-19882
Investigation of the lasing and luminescent properties of fluorite and strontium fluoride crystals containing bivalent dysprosium impurities. 07 p0837 A73-20207

Luminescence of a molecular gas under the action of a carbon dioxide laser pulse. 09 p1094 A73-22595
Spectral properties of laser crystal materials, noting deactivation energy storage in nonuniformly widened luminescence band. 09 p1095 A73-22671

Microinhomogeneous active medium effects on laser monopulse duration and energy, noting luminescence band random shift and directional diversity in dipole moments. 09 p1097 A73-23083
Two-photon excitation of luminescence in CaF₂:Er³⁺/ crystals by a frequency-scanning laser employing organic dye solutions. 10 p1227 A73-24075

I-V characteristics and luminescence changes in Cs vapor arc discharge at various spark gap widths, noting pressure effect on gas stratification. 10 p1254 A73-24203

Ultraviolet luminescence and nonlinear extinction in ruby. 10 p1260 A73-24579

The mechanism responsible for luminescence of polymer films during their formation by ion-beam bombardment of solids. 10 p1252 A73-24762

Luminescence of isolated dark clouds caused by the integral field of stellar galactic radiation. 11 p1416 A73-25234

Luminescence line width in ruby crystals of a laser resonator. 12 p1505 A73-26892
Scattering of light by the medium generated by a space vehicle. I - Emission of vapor jets by spacecraft microthrusters. 12 p1549 A73-27641

Specific characteristics of interband luminescence in crystals in the presence of intense laser radiation. 13 p1628 A73-29049
International Conference on Luminescence, Leningrad, USSR, August 17-22, 1972, Proceedings. 15 p1884 A73-31711

Visible luminescence of Yb³⁺/ and Er³⁺/ during IR excitation. 15 p1884 A73-31712
Cooperative mechanisms during laser excitation of luminescence in Yb-Tb and Yb-Eu ion activated glass. 15 p1884 A73-31713

Quantum oscillators employing the luminescence of self-localized excitons in condensed inert gases. 15 p1885 A73-31714
Effects of electron-phonon interaction in the luminescence spectra of transition and rare-earth impurity ions in crystals. 15 p1885 A73-31715

Investigation of the structure of electron bands in In_{1-x}Ga_x/As_{1-y}P_y/ on the basis of luminescence. 15 p1923 A73-31716
Quantum losses during excitation of ruby luminescence. 15 p1924 A73-31721

Pb-salt tunable diode lasers. 16 p2023 A73-32859
Optical and luminescent properties of CdBr₂-Sn and CdCl₂-Sn single crystals. 17 p2219 A73-35553

Measurement of the temperature of an optically dense layer of luminous gas in the upper atmosphere by the homodyne detection method. 19 p2425 A73-37933
Cathodoluminescence of ruby /0.05 wt %/ at high temperatures. 21 p2752 A73-40797

Low-noise instrumentation for Raman and luminescence spectrometry with ruby and argon laser excitation. 22 p2868 A73-41783

LUMINESCENT INTENSITY

U LUMINOUS INTENSITY

LUMINOSITY

NT STELLAR LUMINOSITY

Luminosity and efficiency of spectrographs with a slit. 01 p0046 A73-10508
Rocket infrared observations of H II regions. 01 p0103 A73-11026

Photopic luminous efficiency measured by critical flicker frequency method, noting dependence on intermittence frequency of light stimulus or overall radiance level. 02 p0137 A73-12076
Correlation between pulsations in auroral luminosity variations and X-rays. 11 p1359 A73-26710

Conditions of Cr IX and Fe XI luminescence in the corona. 13 p1683 A73-29094
The illumination distribution in the image plane from the radiation of a plane-parallel plate with the actual ray paths taken into consideration. 13 p1621 A73-29325

Radio luminosity function of galaxies. 20 p2606 A73-39062

LUMINOUS FLUX DENSITY

U LUMINOUS INTENSITY

LUMINOUS INTENSITY

NT ILLUMINANCE

NT LUMINANCE

The fluctuation spectrum of laser radiation in a turbulent atmosphere in the presence of rain. 01 p0060 A73-10872
Experimental study of the luminous front produced by a coaxial plasma accelerator. 02 p0197 A73-12060

Closed time as an explanation of the black body background radiation. 02 p0193 A73-12440
Measurements of the ultraweak bioluminescence phenomena as a new biotelemetric method. 03 p0272 A73-14304

The light-curve for the minor planet 4/ Vesta. 03 p0379 A73-14578

Intensity and polarization of the solar light scattered by an isolated volume of interplanetary matter

03 p0380 A73-14611

Distances and absolute luminosities of galactic X-ray sources.

04 p0492 A73-15358

A possible new interpretation of power spectra of solar-granulation brightness fluctuations.

04 p0499 A73-15367

Radio galaxies luminosity function from radio power range at 178 MHz with known red shift, using 3C catalog galaxies

05 p0622 A73-17071

Transmission of a GaAs laser beam through the atmosphere.

06 p0699 A73-17495

Visible light flash emission due to strong shock wave of laser spark, investigating strong external magnetic field effect and time variation of luminous intensity

06 p0700 A73-17966

Charged coupled IC image sensors based on MOS capacitors for low light level TV, considering operation, performance and production technologies

06 p0676 A73-18301

The radio continuum of the Large Magellanic Cloud. II - Continuum observations at 11 cm wavelength.

06 p0754 A73-18630

Yale Observatory photographic monitoring program for quasar observation, presenting light curves and magnitudes for 25 objects

07 p0876 A73-19356

Intensity fluctuations of a light beam propagating through a wave guide channel with random refraction-index inhomogeneities

07 p0792 A73-19915

The interpretation of the X-ray emission detected from some nearby radio galaxies.

07 p0872 A73-19940

Modulation of intensity in multiple images of a luminous source given by a system of two parallel networks

07 p0824 A73-20163

Hubble diagram construction for optically luminous quasars, noting relation between red shift and apparent magnitude

08 p1002 A73-20877

Lunar eclipse brightness dependence on eleven year sunspot activity cycle

08 p1007 A73-21068

Evoked potential correlates of expected stimulus intensity.

08 p0930 A73-21225

Theoretical performance figures for low light level TV cameras.

08 p0972 A73-21757

Mode-locking of high power lasers by a combination of intensity and time dependent Q-switching.

09 p1090 A73-21999

Models for extragalactic objects with very high IR and X-ray luminosity.

09 p1141 A73-22007

Numerical computation of photosphere temperature-associated equatorial brightening in red and green bands used in solar oblateness measurements

[AD-758969] 09 p1142 A73-22040

Mandelstam-Brillouin laser light scattering theory and application to atmospheric parameters remote sensing

09 p1094 A73-22327

UBV photometry of the irregular galaxies NGC 5363 and NGC 5360

09 p1146 A73-22548

Galactic absorbing material effects on quasar apparent distribution, noting brightness decrease with red shift

09 p1147 A73-22572

Autocorrelation function for the 'rapid' light variations of the quasar 3C 273.

09 p1147 A73-22727

Galactic nuclei and QSO far IR radiation luminosity explanation by nonthermal maser emission due to gas molecules in dense clouds

09 p1150 A73-23145

Light flux vertical distribution in spherical multilayer cloud and gas scattering planetary atmosphere, calculating radiation intensity

10 p1276 A73-23891

Earth magnetosphere pinch effect related to geomagnetic field pulsations and polar aurora luminosity fluctuations

10 p1212 A73-24228

A statistical investigation of the properties of quasars.

10 p1280 A73-24401

A first 1415 MHz survey with the Westerbork Synthesis Radio Telescope. An attempt to detect radio emission from quasi stellar objects.

10 p1280 A73-24402

The manifold of galaxies - Galaxies with known dynamical parameters.

10 p1281 A73-24407

Composite distribution function for absolute magnitudes of uniformly distributed galaxies

11 p1416 A73-25238

Single unit reactions in the visual cortex of the unanesthetized rabbit to the light flashes of different intensities.

11 p1321 A73-26719

Solar corona streamers polarization, intensity and electron density and temperature during 22 September 1968 total eclipse

12 p1533 A73-26861

Comparison of methods of photomultiplier photocurrent recording in measurements of weak luminous fluxes

12 p1495 A73-26866

Seasonal and diurnal variations of forbidden oxygen and sodium lines emission, stressing nightglow zenith intensity fluctuations connection to F layer electric fields

12 p1489 A73-26992

Gain and saturation intensity measurements in a waveguide CO₂ laser.

12 p1505 A73-27017

Method of calculating the temperature dependence of the integral intensity of light absorption by local vibrations in crystals

12 p1525 A73-27937

Identification and radio spectra of bright galaxies in the second Bologna Catalogue of radio sources and their radio luminosity function.

13 p1671 A73-28034

The spectrum of fluctuations of laser radiation in a turbulent atmosphere during rain.

13 p1627 A73-28696

Nature of auroral emission intensity pulsations associated with geomagnetic pulsations of the P₂ type.

13 p1607 A73-28706

Holographic visualization of large amplitude vibration using reference beam phase modulation.

13 p1622 A73-29642

Quasar optical luminosities compared to Seyfert galaxies and radio-quiet objects showing broad emission lines of permitted transitions and sharp lines of forbidden transitions

13 p1687 A73-29656

Cometary observations and variations in cometary brightness.

14 p1789 A73-29778

Cometary brightness variations and conditions in interplanetary space.

14 p1789 A73-29779

Quantum theory of a high energy gas laser

14 p1757 A73-30363

Surface photometry of galaxies - Comparison of the luminosity profiles and photometric parameters of southern galaxies measured at Cordoba and Mount Stromlo.

14 p1801 A73-30644

Meteoritic ablation coefficient and brightness dependence on velocity and atmospheric density, considering molecular screen effect

15 p1928 A73-30983

Triggering characteristics of TEA CO₂ laser.

15 p1885 A73-32019

Determination of atmospheric water-vapor densities from measurements of the 6943.8-A absorption line strength.

15 p1845 A73-32227

Compact X ray source models from statistical analysis of Uhuru catalog sources with respect to luminosities, lifetimes and stellar populations

16 p2050 A73-32737

Black holes in binary systems - Observational appearances.

16 p2058 A73-32739

Evidence for luminosity evolution of quasars.

17 p2225 A73-34287

Passive low light level television for military and civilian ground surveillance under poor visibility conditions

17 p2168 A73-34906

Magnetic modulation of the optical emission intensity of a plasma from a high-frequency H-discharge

18 p2339 A73-36565

Lunar eclipse brightness dependence on eleven year sunspot activity cycle

18 p2355 A73-36869

Meteor lifetime and the position of the maximum brightness point

19 p2480 A73-37238

Monkey rod receptor potential suppression at photopic stimulus intensities by neurophysiological inhibitory mechanism for clearing cone initiated visual pathway

19 p2393 A73-37412

The luminosity function of quasars and its evolution - A comparison of optically selected quasars and quasars found in radio catalogs.

19 p2484 A73-37606

Outermost low surface brightness regions of interacting galaxies in Stephan Quintet from interference filter, hydrogen spectra and long exposure direct photograph observations

19 p2484 A73-37609

The redshift-distance relation. VII - Absolute magnitudes of the first three ranked cluster galaxies as functions of cluster richness and Bautz-Morgan cluster type - The effect on q sub 0.

19 p2487 A73-38506

The redshift-magnitude relation for quasi-stellar objects.

19 p2487 A73-38507

Third- and higher-order intensity correlations in laser light.

20 p2571 A73-38630

Light flux vertical distribution in spherical multilayer cloud and gas scattering planetary atmosphere, calculating radiation intensity

20 p2603 A73-38910

Relation between coronal 5303-A intensity, recurrent geomagnetic storms, and solar sector structure.

20 p2553 A73-38960

Average intensity of a nonsymmetric optical radiation beam in a turbulent atmosphere

20 p2555 A73-39187

Brightness and polarization distributions of head-tail galaxies at 1415 MHz.

20 p2610 A73-39583

A multichannel-discharge of high light intensity and short duration

21 p2695 A73-39971

Hole-type confocal active optical cavity resonator loss distribution, discussing Fresnel zone oscillation type intensity within resonator and diffraction at cavity

21 p2714 A73-40559

Rocket observations of electron precipitation in a westward-traveling surge.

22 p2902 A73-41915

Concerning the forms of the velocity-distance relation clusters.

22 p2913 A73-43001

On the thermodiffusion effect in the CW He-Ne lasers.

22 p2871 A73-43080

CW single mode He-Ne laser intensity fine structure fluctuations correlation measurement near threshold by digital correlator, obtaining higher order relaxation rates

22 p2871 A73-43085

Low power He-Ne laser beam intensity modulation in thermal medium, applying to temperature fluctuation detection in transparent materials

22 p2872 A73-43154

Laser cross-beam intensity-correlation spectrum for a turbulent flow.

22 p2872 A73-43158

Burner dimension and flame size effects on relative contributions of luminous soot and nonluminous molecular band radiations from combustion fires

23 p3048 A73-43329

Certain problems in measuring Cerenkov light on the lakutsk extensive air shower device

23 p3022 A73-43546

Theory of wide-band laser radiation in a spectrally-inhomogeneous medium

23 p2987 A73-43708

The post-eclipse brightening of Io.

24 p3134 A73-44563

Radius-parameter and surface brightness as a function of galaxy total magnitude for clusters of galaxies.

24 p3135 A73-44582

Statistical analysis of transient brightenings in solar chromosphere /Ellerman bombs/ from H alpha filtergrams, obtaining histograms for durations near disk center and limb

24 p3136 A73-44641

A self-similar regime of powder combustion with variable optical constants

24 p3154 A73-44706

The relation between redshift and surface brightness for normal galaxies in systems of galaxies.

24 p3141 A73-45193

Magnitude-redshift and count-magnitude relations in presence of a uniform intergalactic absorption.

24 p3143 A73-45436

LUNAR ATMOSPHERES

Upper limits on the lunar atmosphere determined from solar-wind measurements.

02 p0211 A73-11727

Lunar surface observation with cold cathode ionization gage left by Apollo 14, noting low concentration atmospheric particles and gas clouds

02 p0213 A73-12239

Response of lunar atmosphere to volcanic gas releases.

03 p0365 A73-12880

Solar wind, meteoritic, and cometary carbon sources for moon, discussing lunar atmospheric steady state carbon component sustained by meteoritic and cometary carbon vaporization

06 p0754 A73-18427

Atmospheric Ar-40 in lunar fines.

07 p0890 A73-19808

Lunar orbital mass spectrometer experiment.

07 p0891 A73-19828

Lunar atmosphere gas concentrations from Apollo 14 and 15 ALSEP cold cathode ionization gage measurements, considering solar wind and contamination sources

07 p0891 A73-19830

Far UV scanning spectrometer aboard Apollo 17 CSM to measure lunar atmospheric composition, ob-

- serving spectral albedo, LEM atmosphere, and galactic and solar system atmospheres
 12 p1497 A73-27485
- Water sources in lunar atmosphere, calculating minimum depth for existence from water density values
 13 p1681 A73-28844
- Induced lunar magnetosphere and solar wind formed downstream cylindrical cavity for interplanetary magnetic fields arbitrary orientation, assuming lunar core and shell electrical conductivity model
 14 p1796 A73-29962
- Certain features of interaction between the atmosphere and lithosphere on the moon
 16 p2065 A73-33787
- Apollo 17 mass spectrometer indication of rare gases and molecular hydrogen in lunar atmosphere, confirming noncondensable gas model
 18 p2349 A73-35973
- Lunar thermal ionosphere acceleration and detection within lunar electric field for electric potential of moon in solar wind or magnetosheath
 20 p2604 A73-38933
- Lunar specific surface adsorption-desorption processes discussing near-surface atmospheric diurnal variations, nitrogen temperature, sorption capacity, gas concentration from regolith structure
 21 p2774 A73-41402
- Induced magnetosphere of the moon. II - Experimental results from Apollo 12 and Explorer 35.
 22 p2906 A73-41905
- LUNAR BASES**
- Space Treaty legislative provisions for freedom of movement of orbital and lunar laboratories
 04 p0521 A73-15127
- Terrestrial law adaption to lunar surface or orbital space laboratories requirements
 04 p0521 A73-15130
- Legal aspects of laboratories on the moon.
 04 p0522 A73-15132
- Lunar laboratories space law aspects, emphasizing need for prohibition of military activities and right of international community to information
 04 p0522 A73-15133
- Long range post-Apollo space exploration goals, considering earth orbital station, moon base, manned Mars landing and interstellar flights
 23 p3038 A73-43990
- LUNAR CINEMATOGRAPHY**
- U LUNAR PHOTOGRAPHY**
- LUNAR COMMUNICATION**
- Post-occultation reception of lunar ship America radio transmission.
 14 p1725 A73-29733
- LUNAR COMPOSITION**
- NT LUNAR CORE**
- Evolution from amino acids - Lunar occurrence of their precursors.
 01 p0008 A73-10249
- Investigation of the chemical composition of lunar surface along the route of Lunokhod 1.
 02 p0212 A73-12228
- Rare gases in the regolith from the Sea of Fertility.
 02 p0212 A73-12229
- Luna 16 rock composition, gamma radiation and natural radioactive element content determination by neutron activation and radiometric analysis
 02 p0213 A73-12230
- Mossbauer spectroscopic analysis of Sea of Fertility regolith core samples, noting olivine content increase with depth
 02 p0214 A73-12242
- The origin of the moon - Theories involving joint formation with the earth.
 02 p0217 A73-12386
- Water, alkalis and oxygen selective volatilization losses from hot silicate liquids erupted into high vacuum at lunar surface
 02 p0219 A73-12438
- Trace elements profiles, notably Hg, from a preliminary study of the Apollo 15 deep-drill core.
 02 p0220 A73-12477
- The composition of the lunar highlands - Evidence from modal and normative plagioclase contents in anorthositic lithic fragments and glasses.
 02 p0220 A73-12478
- Lunar interior density constraints from moon moment of inertia and mean density calculations and seismometer data on lunar crust mass and density
 02 p0220 A73-12484
- On the possible differences in the bulk chemical composition of the earth and the moon forming in the circumterrestrial swarm.
 03 p0370 A73-13110
- Evolution of the moon - Recent modification of previous ideas.
 03 p0370 A73-13112
- Cosmic ray produced neutron flux equilibrium for lunar surface compositions, calculating isotopic production rates as function of depth
 03 p0364 A73-14105
- Apollo 17 lunar surface experiments for lunar composition, structure and chronology investigation, discussing landing site and instrument selection based on prior Apollo flights
 04 p0493 A73-14671
- Nature of the density reversal beneath the lunar maria.
 04 p0496 A73-14821
- Spectroscopic remote sensing of lunar surface composition.
 04 p0448 A73-15181
- [AD-756154]
 Spacecraft techniques for lunar research.
 04 p0448 A73-15182
- Comparison of the analytical results from the Surveyor, Apollo, and Luna missions.
 04 p0498 A73-15185
- The Apollo 17 landing site.
 04 p0501 A73-15622
- Lunar thermal model with hot interior and cool lithosphere, considering strength and conductivity profiles, volcanic activity absence and composition and origin implications
 05 p0613 A73-16158
- The chemical composition of soil from the Apollo 16 and Luna 20 sites.
 05 p0546 A73-16831
- U-Th-Pb systematics in lunar highland samples from the Luna 20 and Apollo 16 missions.
 05 p0618 A73-16832
- The organic analysis and carbon chemistry of lunar samples: Their significance for exobiology: Proceedings of the Conference, University of Maryland, College Park, Md., October 26-28, 1971.
 06 p0753 A73-18410
- Review of methods used in lunar organic analysis - Extraction and hydrolysis techniques.
 06 p0661 A73-18412
- Nanogram level lunar organic compound separation and detection by gas-liquid chromatography
 06 p0661 A73-18413
- Ion-exchange chromatography in lunar organic analysis.
 06 p0662 A73-18414
- Biogenic elemental distribution and isotopic abundance in lunar samples, discussing heavy isotopes enrichment by solar wind irradiation, meteorite impacts and hydrogen stripping
 06 p0654 A73-18417
- Apollo 11, 12 and 14 surface fines analysis by fluorescent technique for porphyrins content
 06 p0753 A73-18419
- Porphyrins analysis in Apollo 11, 12 and 14 soils via analytical demetallation followed by recovery and complexing with divalent cations
 06 p0753 A73-18420
- Amino acid search in lunar fines, considering terrestrial source contamination, bound and free amino acids, processing and analysis contamination
 06 p0754 A73-18422
- Apollo 14 fines examination for indigenous amino acids or amino acid convertible materials, optimizing gas-liquid chromatographic systems for separation and flame ionization
 06 p0662 A73-18423
- Aromatic and heteroatom-containing organic compounds in the lunar samples.
 06 p0662 A73-18424
- Solar wind, meteoritic, and cometary carbon sources for moon, discussing lunar atmospheric steady state carbon component sustained by meteoritic and cometary carbon vaporization
 06 p0754 A73-18427
- Indigenous lunar organic compound search, considering prebiological chemistry and composition possibility in deeper region under surface
 06 p0655 A73-18428
- Lunar carbon chemistry - Relations to and implications for terrestrial organic geochemistry.
 06 p0662 A73-18429
- Difference between the principal element concentrations on the surface and in the volume of lunar regolith particles
 07 p0876 A73-19474
- Lunar composition and evolution studies results from Apollo and Luna collected soil and rocks radiometric analysis, noting surface materials contamination with solar wind particles
 07 p0878 A73-19674
- Lunar Science Conference, 3rd, Houston, Tex., January 10-13, 1972, Proceedings. Volume 1 - Mineralogy and petrology. Volume 2 - Chemical and isotope analyses, organic chemistry. Volume 3 - Physical properties.
 07 p0878 A73-19676
- Petrology of Apollo 14 high-alumina basalt.
 07 p0879 A73-19684
- Mineral-chemical variations in Apollo 14 and Apollo 15 basalts and granitic fractions.
 07 p0879 A73-19686
- Experimental petrology and petrogenesis of Apollo 14 basalts.
 07 p0880 A73-19690
- Apollo 14 - Subsolidus reduction and compositional variations of spinels.
 07 p0880 A73-19697
- The major element compositions of lunar rocks as inferred from glass compositions in the lunar soils.
 07 p0880 A73-19700
- Microstructure and mineral compositions of impact produced lunar chondrules from Apollo 14 breccia by electron microprobe X ray analyzer
 07 p0882 A73-19722
- Mineralogy and origin of Fra Mauro fines and breccias.
 07 p0883 A73-19726
- Inclusions and interface relationships between glass and breccia in lunar sample 14306.50.
 07 p0883 A73-19731
- Chemistry and particle track studies of Apollo 14 glasses.
 07 p0884 A73-19736
- Metallic mounds produced by reduction of material of simulated lunar composition and implications on the origin of metallic mounds on lunar glasses.
 07 p0884 A73-19738
- Compositions and mineralogy of lithic fragments in 1-2 mm soil samples 14002.7 and 14258.33.
 07 p0884 A73-19739
- Chemical and petrographic characterization of Fra Mauro soils.
 07 p0884 A73-19742
- On lunar metallic particles and their contribution to the trace element content of Apollo 14 and 15 soils.
 07 p0884 A73-19746
- A new titanium and zirconium oxide from the Apollo 14 samples.
 07 p0885 A73-19749
- Composition of the lunar uplands - Chemistry of Apollo 14 samples from Fra Mauro.
 07 p0886 A73-19757
- Major, minor, and trace element data for some Apollo 11, 12, 14, and 15 samples.
 07 p0886 A73-19759
- Rare earths and other trace elements in Apollo 14 samples.
 07 p0886 A73-19760
- Chondrite normalized major and trace element concentrations of Apollo 14 lunar samples, including basalt, breccia and regolith fines
 07 p0886 A73-19761
- Precise determination of rare-earth elements in the Apollo 14 and 15 samples.
 07 p0886 A73-19762
- Beryllium and chromium abundances in Fra Mauro and Hadley-Apennine lunar samples.
 07 p0886 A73-19764
- Chemical analyses of lunar samples 14003, 14311, and 14321.
 07 p0886 A73-19765
- Major impacts on the moon - Characterization from trace elements in Apollo 12 and 14 samples.
 07 p0887 A73-19768
- ESCA-investigation of lunar regolith from the Seas of Fertility and Tranquility.
 07 p0887 A73-19770
- O-18/O-16, Si-30/Si-28, C-13/C-12, and D/H studies of Apollo 14 and 15 samples.
 07 p0887 A73-19771
- Oxygen isotopic compositions and oxygen concentrations of Apollo 14 and Apollo 15 rocks and soils.
 07 p0887 A73-19772
- Deuterium content of lunar material.
 07 p0887 A73-19774
- Sulphur concentrations and isotope ratios in lunar samples.
 07 p0887 A73-19775
- U-Th-Pb and Rb-Sr measurements on some Apollo 14 lunar samples.
 07 p0888 A73-19779
- Pb-204 in Apollo 14 samples and inferences regarding primordial Pb lunar geochemistry.
 07 p0888 A73-19786
- Isotopic anomalies in lunar rhenium.
 07 p0889 A73-19805
- Total nitrogen contents of some Apollo 14 lunar samples by neutron activation analysis.
 07 p0890 A73-19815
- Total carbon, nitrogen, and sulfur in Apollo 14 lunar samples.
 07 p0890 A73-19816
- Amino acid precursors in lunar fines from Apollo 14 and earlier missions.
 07 p0891 A73-19820
- Spectrofluorometric search for porphyrins in Apollo 14 surface fines.
 07 p0891 A73-19823
- Lunar surface chemical composition mapping with onboard Apollo 15 X ray fluorescence spectrometer, showing Al, Mg and Si ratios
 07 p0871 A73-19825
- Lunar water vapor spectra during Apollo 14 ALSEP suprathermal ion detector experiment /SIDE/ and total ion detector /TID/ observations
 07 p0891 A73-19829
- P and S waves propagation velocity distribution for lunar mantle and crust composition, noting petrological models with differentiated mantle
 07 p0894 A73-19849

Viscous flow behavior of lunar compositions 14259 and 14310. 07 p0895 A73-19857

Midinfrared emission spectra of Apollo 14 and 15 soils and remote compositional mapping of the moon. 07 p0897 A73-19888

Chemical composition of some Apollo 14 lunar samples. 08 p0936 A73-20841

Constrained least-squares analysis of petrologic problems with an application to lunar sample 12040. 08 p0936 A73-20842

On the model of the accumulation of the moon compatible with the data on the composition and the age of lunar rocks. 10 p1277 A73-24086

Major element chemistry of glasses in Apollo 14 soil 14156. 10 p1278 A73-24111

Lunar permafrost - Dielectric identification. 10 p1282 A73-24629

Applications of activation analysis to geochemical, meteoritic and lunar studies. 11 p1326 A73-25800

Lunar composition from Apollo orbital measurements. 11 p1422 A73-25956

X ray and microanalysis of Luna 16 recovered Fe-Ni fragment structure and composition, showing alpha solid solution octahedrite 12 p1538 A73-26893

Planetary and lunar surface color as geochemical history indicator in terms of oxidation state, solar wind access to atmosphere and planetary moisture content 12 p1541 A73-27484

Lunar highland soils and breccias chemistry representation by model for mixing during intense cratering period, discussing chemical composition 12 p1466 A73-27493

Apollo 15 soil samples structure and phase equilibrium data noting metal particles of high cobalt content 12 p1466 A73-27544

Lunar composition and origin model based on early condensation processes in solar nebula 12 p1542 A73-27546

Preliminary data on lunar soil recovered by the Luna 16 automatic station 13 p1672 A73-28114

Preliminary data on lunar soil collected by the Luna 20 unmanned spacecraft. 13 p1674 A73-28302

Chemistry and surface morphology of soil particles from Luna 20 LRL sample 22003. 13 p1674 A73-28308

An unusual basalt fragment in Luna 20 sample L2010. 13 p1675 A73-28309

Luna 20 lunar soil elemental and oxygen isotopic composition compared to Apollo 11, 12, 14 and 15 abundances 13 p1675 A73-28310

Inert gases in a terra sample - Measurements in six grain-size fractions and two single particles from Luna 20. 13 p1675 A73-28318

Luna 20 highland soil samples mineralogical and petrological analysis, comparing chemical composition with Apollo 16 soil samples 13 p1676 A73-28322

Luna 20 metaigneous rocks, breccia and soil and Apollo 16 soils chemical composition by neutron activation analysis, tabulating major, minor and trace elements 13 p1676 A73-28323

Mineralogy, petrology and chemistry of lithic fragments from Luna 20 fines - Origin of the cumulate ANT suite and its relationship to high-alumina and mare basalts. 13 p1676 A73-28328

Lunar 16 and 20 soil halogens, uranium and lithium contents, noting chlorine and phosphorus pentoxide noncorrelation with Apollo sites 13 p1676 A73-28329

Luna 20 soil - Abundance and composition of phases in the 45-125 micron fraction. 13 p1677 A73-28330

Petrology of some lithic fragments from Luna 20. 13 p1677 A73-28331

Compositional and X-ray data for Luna 20 feldspar. 13 p1677 A73-28334

U-Th-Pb measurements of Luna 20 soil. 13 p1677 A73-28335

The Luna 20 lithic fragments, and the composition and origin of the lunar highlands. 13 p1677 A73-28336

Oxygen and silicon isotope ratios of the Luna 20 soil. 13 p1677 A73-28337

Composition of metal in type III carbonaceous chondrites and its relevance to the source-assignment of lunar metal. 13 p1686 A73-29564

Zinc, lead, chlorine and FeOOH-bearing assemblages in the Apollo 16 sample 66095 - Origin by impact of a comet or a carbonaceous chondrite. 13 p1686 A73-29565

Lunar origin and composition relationship to solar system evolution, discussing various theories and evidence from Apollo flights 13 p1687 A73-29665

Role of pressure transients in the detection and identification of lunar surface gas sources. 14 p1752 A73-29963

Lunar core sample structure morphology and composition examined by microanalysis, revealing tenite to martensite transformation 15 p1930 A73-31220

Lunar interior composition, structure and thermal evolution models to fit surface igneous activity chronology and lithosphere stress history implied by mascons presence 15 p1937 A73-31778

Detection of a nonuniform distribution of polonium-210 on the moon with the Apollo 16 alpha particle spectrometer. 15 p1941 A73-32266

Fluorine in lunar samples - Implications concerning lunar fluorapatite. 15 p1941 A73-32388

Apollo 15 and 16 lunar orbital X and gamma ray spectrometer for lunar surface composition and radioisotopes surveys, detailing experimental results 16 p2015 A73-33353

Lunar surface investigations by the Luna-9 through Luna-13 lunar landers 16 p2063 A73-33753

Scanning IR spectrometer combination with optical telescope for 0.8-2.2 microns reflected IR light measurement during full moon phases in lunar surface composition determination 16 p2064 A73-33763

The A, B, C's of trapped helium, neon, and argon in meteorites and lunar samples. 17 p2228 A73-34417

Significance of a primitive lunar basaltic composition present in Apollo 15 soils and breccias. 17 p2230 A73-34516

Calcium oxide and aluminum oxide constraints removal for lunar interior composition models 17 p2232 A73-35264

Progress in remote optical analysis of lunar surface composition. 17 p2119 A73-35747

Apollo 15 and 16 results of the integrated geochemical experiment. 17 p2236 A73-35750

Radon emanation from the moon - Spatial and temporal variability. 18 p2349 A73-36033

Physical nature of the lunar surface albedo 19 p2480 A73-37234

Apollo 17 'orange soil' and meteorite impact on liquid lava. 19 p2482 A73-37390

Apollo 15 breccia and soils with spheres and fragments of iron-rich green glass originating in Apennine Front materials 19 p2487 A73-38174

Reports of fourth Lunar Science Conference covering lunar rock chemical composition assessment as information source on early solar system, lunar early geologic history, etc 19 p2487 A73-38293

Distribution of gases within Apollo 15 samples - Implications for the incorporation of gases within solid bodies of the solar system. 20 p2612 A73-39715

Nuclide production rates in stone meteorites and lunar samples by galactic cosmic radiation. 20 p2612 A73-39716

Resonant nuclear measurement of hydrogen concentration vs depth in Apollo 11, 15 and 16 lunar soil fragments and platinum foil exposed to solar event 21 p2765 A73-40237

Characteristics of tracks of ions of 14 less than or equal to Z less than or equal to 36 in common rock silicates. 21 p2682 A73-40242

Helium, neon and argon in Level C of Luna 16 fines. 21 p2770 A73-41004

X ray and microanalysis of Luna 16 recovered Fe-Ni fragment structure and composition, showing alpha solid solution octahedrite 21 p2771 A73-41026

Experimental data on the investigation of lunar surface chemical composition. 21 p2774 A73-41403

Gamma-spectrometric analysis of lunar samples from Luna 16. 21 p2774 A73-41404

Russian book - Chemistry of terrestrial and lunar basaltic rocks. 21 p2648 A73-41436

Lunar core sample structure morphology and composition examined by microanalysis, revealing tenite to martensite transformation 22 p2905 A73-41808

Organic geochemical analysis of lunar samples with emphasis on detecting biologically significant organic elements, projecting techniques to Mars soil analysis 22 p2803 A73-42163

Lunar surface meteoritic material composition, distribution and amounts from trace element studies, discussing micrometeorites, ancient planetesimal debris and recent crater-forming projectiles 23 p3030 A73-43758

Lunar and planetary chemical composition dependence on condensation temperature in solar nebula 23 p3030 A73-43760

Lunar asymmetries in crustal thickness, maria distribution and gamma radioactivity due to intense early bombardment by interplanetary meteoroid flux 23 p3031 A73-43762

Crater Copernicus age determination using mass spectrometric Ar isotope ratio dating of KREEP glasses from lunar soil 23 p3031 A73-43763

Observations of water vapor ions at the lunar surface. 23 p3031 A73-43764

Major and trace elements in igneous rocks from Apollo 15. 23 p2950 A73-43765

Geochemical coherence between trace elements and K, P and rare earth elements in lunar soils evaluated for samples evolutionary history 23 p2951 A73-43767

A survey of the selenochemistry of major, minor and trace elements. 23 p2951 A73-43768

On Pu-244 in lunar rocks from Fra Mauro and implications regarding their origin. 23 p2951 A73-43771

Radiochemical neutron activation analysis for extralunar trace elements in Apollo 14 lunar soil 14141, comparing with mature samples and Fra Mauro subregolith materials 23 p2951 A73-43846

High concentration of refractory elements in lunar crust explained by melting and differentiation model 23 p3033 A73-43958

LUNAR CORE

Lunar interior density constraints from moon moment of inertia and mean density calculations and seismometer data on lunar crust mass and density 02 p0220 A73-12484

Evolution of the moon - Recent modification of previous ideas. 03 p0370 A73-13112

Lunar interior temperature and surface heat flux distribution from numerical calculations for convection cells within self gravitating fluid sphere, comparing with magnetic induction results 05 p0615 A73-16376

Metallic Fe-Ni-S lunar core as source of remanent magnetism in lunar rocks, consistent with thermal models 07 p0877 A73-19654

Surface magnetometer experiments - Internal lunar properties and lunar field interactions with the solar plasma. 07 p0892 A73-19834

Depth relationships for Apollo 14 and 15 core tubes and Apollo 15 drill core, noting sample recovery ratio 07 p0898 A73-19900

Lunar interior temperature profiles from olivine and pyroxene electrical conductivity data, indicating high temperature accretion from hydrogen depleted material 09 p1148 A73-22874

Viscosity of the moon. I - After mare formation. II - During mare formation. 10 p1277 A73-24081

Lunar interior materials seismic compressional velocities, indicating differentiated structure consistent with solidus thermal history 11 p1421 A73-25895

Liquid core model with precessionally driven magnetoturbulence applied to moon, discussing tidal effects in outer solid and liquid shells 12 p1541 A73-27489

Lunar interior composition, structure and thermal evolution models to fit surface igneous activity chronology and lithosphere stress history implied by mascons presence 15 p1937 A73-31778

Lunar evolution theory review covering separation from earth, capture by earth, formation by particle accumulation and core iron content approximation 16 p2065 A73-33781

Certain features of interaction between the atmosphere and lithosphere on the moon 16 p2065 A73-33787

New seismic data on the state of the deep lunar interior. 17 p2237 A73-35805

LUNAR CRATERS

Concentric craters on the moon 01 p0102 A73-10943

Geomorphological analysis of the area of Mare Imbrium explored by the automatic roving vehicle Lunokhod 1. 02 p0213 A73-12240

Micrometeoroid particle flux impacting on lunar surface measured by observation of Surveyor 3 glass surfaces craters 02 p0214 A73-12256

Lunar surface cratering history from Apollo rock age data, implying earth-moon and solar system evolution mechanism 02 p0217 A73-12406

Successive solidification origin of central peaks and terrace ring wall in lunar crater formations filled with melt after impacts, using freezing water experiments 03 p0369 A73-13094

Surface features on glass spherules from the Luna 16 sample. 04 p0498 A73-15187

Distributions of lunar and Martian craters in relation to their origin 05 p0613 A73-16202

Extralunar materials in Apollo 16 soils and the decay rate of the extralunar flux 4.0 Gy ago. 05 p0618 A73-16835

Lunar crater Copernicus - Search for debris of impacting body at Apollo 12 site. 07 p0877 A73-19653

Chemical and petrographic characterization of Fra Mauro soils. 07 p0884 A73-19742

Composition of the lunar uplands - Chemistry of Apollo 14 samples from Fra Mauro. 07 p0886 A73-19757

Spall/pit diameter ratio decrease in lunar microcraters with decreasing size, considering origin from interplanetary dust particles impact 07 p0896 A73-19866

Microcrater size frequency distribution and exposure age for Apollo 12 and 14 rocks 07 p0896 A73-19868

Lunar craters and exposure ages derived from crater statistics and solar flare tracks. 07 p0896 A73-19869

Endogenic craters count and measurement for Hyginus Rille floor, establishing size distributions by Lunar Orbiter 5 photographs processing 07 p0900 A73-20278

Lunokhod 2 exploration of Le Monnier crater during lunar night, noting laser probings from earth 08 p1007 A73-20975

Detection of radon emanation from the crater Aristarchus by the Apollo 15 alpha particle spectrometer. 08 p1009 A73-21222

Graphical method of profiling and contouring microcraters on lunar rocks from stereomicrograph pair obtained by scanning electron microscope 09 p1081 A73-22378

Concentric craters on the moon. 09 p1147 A73-22738

Crater frequency age determinations for the proposed Apollo 17 site at Taurus-Littrow. 09 p1148 A73-22873

Displaced mass, depth, diameter, and effects of oblique trajectories for impact craters formed in dense crystalline rocks. 10 p1276 A73-24077

Terrestrial, Martian and lunar doublet craters origin from simultaneous multiple meteorite impacts, using Lexan plastic projectiles against sand targets in ballistic range tests 10 p1277 A73-24079

The tsunami model of the origin of ring structures concentric with large lunar craters. 11 p1419 A73-25791

Photomicrographic investigation of plutonic and metamorphic equilibration in polished thin sections of Apollo 16 feldspathic microbreccia samples from North Ray crater rim 11 p1326 A73-25863

Lunar crater structure geological and morphological interpretations from lunar maria photographs in terms of age, density and stony debris size distribution 13 p1672 A73-28115

Orange colored lunar soil from Shorty crater associated with volcanic fumarolic activity of water vapors reacting with lava 14 p1789 A73-29721

Al-Khwarizmi - A new-found basin on the lunar far side. 16 p2060 A73-33125

Long term heliometric Moesting crater distance measurements applied to moon libration relationship to lunar radius 16 p2064 A73-33775

Certain conclusions concerning the morphometry of sections of the moon photographed by the Luna 12 probe 16 p2065 A73-33779

General features of lunar volcanism 16 p2065 A73-33785

The origin of large lunar craters and circular seas 16 p2065 A73-33786

Moon - 'Ghost' craters formed during Mare filling. 17 p2236 A73-35746

Lunar and terrestrial impact crater spherules. 17 p2236 A73-35749

Distribution density of small lunar craters - Models and actual distribution 21 p2770 A73-40915

Geometric interpretation of the ratio of overall diameter to rim crest diameter for lunar and terrestrial craters. 22 p2909 A73-42498

Crater Copernicus age determination using mass spectrometric Ar isotope ratio dating of KREEP glasses from lunar soil 23 p3031 A73-43763

LUNAR CRUST

Mossbauer spectroscopic analysis of Sea of Fertility regolith core samples, noting olivine content increase with depth 02 p0214 A73-12242

Lunar interior density constraints from moon moment of inertia and mean density calculations and seismometer data on lunar crust mass and density 02 p0220 A73-12484

Thermal gradients in the outer lunar layers. 03 p0369 A73-13104

Infrared spectroscopy of regolith /Luna-16 interplanetary probe/. 05 p0612 A73-16088

K, Rb, Sr, Ba contents and rare earths in specimens from the Apollonius /lunar mountains/ crater region brought back by the Soviet probe Luna 20 05 p0546 A73-16829

Lunar highlands soil analysis from Luna 20 and Apollo 16 samples, estimating lunar crust differentiation process age from Rb-Sr concentrations 05 p0618 A73-16833

Role of water in the evolution of the lunar crust: An experimental study of sample 14310 - An indication of lunar calc-alkaline volcanism. 07 p0880 A73-19691

Uranium and potassium fractionation in pre-Imbrian lunar crustal rocks. 07 p0880 A73-19695

P and S waves propagation velocity distribution for lunar mantle and crust composition, noting petrological models with differentiated mantle 07 p0894 A73-19849

Lunar surface radioactivity - Preliminary results of the Apollo 15 and Apollo 16 gamma-ray spectrometer experiments. 08 p1009 A73-21224

Stress differences in the moon as an evidence for a cold moon. 10 p1277 A73-24084

Compressional wave velocity profile of lunar near-surface and crust derived from seismic refraction data at Apollo 14 and 16 sites 12 p1541 A73-27486

Meteoritic vs lunar origin of Luna 20 lunar soil samples metal particles and metallic inclusions discussing meteoritic microstructural obliteration due to shock reheating of crust 13 p1675 A73-28315

Bibliography on the measurement of electrical parameters of layered lunar/earth surfaces. 13 p1619 A73-29221

Role of pressure transients in the detection and identification of lunar surface gas sources. 14 p1752 A73-29963

Detection of a nonuniform distribution of polonium-210 on the moon with the Apollo 16 alpha particle spectrometer. 15 p1941 A73-32266

Apollo 17 seismic profiling - Probing the lunar crust. 16 p2059 A73-32903

Determination of the heat flux from the lunar interior for a nonhomogeneous structure of the lunar surface layer 16 p2065 A73-33783

Morphological characteristics of the moon and convection in its mantle 16 p2065 A73-33784

Certain problems of the internal structure of the moon /Pyrolyte models of the moon/ 16 p2066 A73-33789

Thermal history and evolution of the moon. 17 p2235 A73-35735

Lunar asymmetries in crustal thickness, maria distribution and gamma radioactivity due to intense early bombardment by interplanetary meteoroid flux 23 p3031 A73-43762

High concentration of refractory elements in lunar crust explained by melting and differentiation model 23 p3033 A73-43958

Ancient lunar mega-regolith and subsurface structure. 24 p3129 A73-44448

Monte Carlo computer simulation of lunar regolith evolution, considering buffering regolith effect via computation for debris produced by crater 24 p3130 A73-44460

Lunar 25 km discontinuity seismically examined, discussing hypotheses with shock metamorphism lack and annealing of shock induced microcracks 24 p3131 A73-44470

LUNAR DUST

Optical measurements of lunar albedo, angular illumination, diffuse and specular reflectance and scattering coefficients on Mare Foecunditatis regolith powder of various sizes 02 p0213 A73-12238

Cosmic black glassy spherules composition, mineralogy and physical properties compared to lunar fines, considering possible common origin 02 p0214 A73-12254

Dynamical model for evolution of melted spherical drop of homogeneous glassy material to explain observed glassy spherules in lunar dust 03 p0368 A73-13090

Solar corpuscular irradiation induced latent and etched nuclear particle tracks in lunar dust grains, presenting electron microscopic studies of Apollo 11/12 lunar soil samples 03 p0361 A73-13099

Lunar seismic wave velocity change at 25 km interpreted in terms of fine rock powder undergoing final densification 05 p0622 A73-17181

Hydrolysis of aqueous extract of lunar dust samples for identification and quantitation of amino acid precursors in extraterrestrial sources, considering pre-biotic evolutionary pathways termination 06 p0655 A73-18421

Pyrolysis system with high sensitivity medium-resolution mass spectroscopy to quantify ions pyrolyzed in lunar fines, confirming presence of indigenous lower hydrocarbons 06 p0662 A73-18431

Reflection spectra of lunar dust grains with amorphous coatings. 07 p0876 A73-19583

Chromatographic and mineralogical study of Apollo 14 fines. 07 p0884 A73-19743

Study of excess Fe metal in the lunar fines by magnetic separation, Moessbauer spectroscopy, and microscopic examination. 07 p0788 A73-19745

Compositional data for twenty-one Fra Mauro lunar materials. 07 p0885 A73-19756

Analysis of single particles of lunar dust for dissolved gases. 07 p0890 A73-19813

Temperature-dependent magnetic properties of individual glass spherules, Apollo 11, 12, and 14 lunar samples. 07 p0893 A73-19844

Photoemission from lunar surface fines and the lunar photoelectron sheath. 07 p0895 A73-19860

Secondary electron emission characteristics of lunar surface fines. 07 p0871 A73-19861

Sunlight scattering by dust along lunar horizon at sunset, presenting atmospheric model for dust cloud production 07 p0895 A73-19862

An explanation of transient lunar phenomena from studies of static and fluidized lunar dust layers. 07 p0895 A73-19863

Infrared and Raman spectroscopic studies of structural variations in minerals from Apollo 11, 12, 14, and 15 samples. 07 p0897 A73-19887

Dielectric properties of Apollo 14 lunar samples at microwave and millimeter wavelengths. 07 p0898 A73-19894

A search for porphyrin biomarkers in Nonesuch Shale and extraterrestrial samples. 11 p1319 A73-26481

Response of tobacco tissue cultures growing in contact with lunar fines. 11 p1320 A73-26483

Mammalian tissue response to subcutaneous and intraperitoneal injection of aqueous suspensions of lunar fine material, noting insolubility in tissue and irritant action 11 p1320 A73-26484

Apollo lunar fines ferromagnetic resonance spectral line shape anomaly and anisotropy energy attributed to Fe particles with body centered cubic structure 13 p1684 A73-29177

Far ultraviolet reflectivity of lunar dust samples - Apollo 11, 12, and 14. 15 p1932 A73-31270

Electrostatic charging of the lunar surface and possible consequences. 16 p2062 A73-33463

Surveyor observations of lunar horizon-glow. 18 p2348 A73-35938

Lunar surface fine rock powders seismic measurements in terms of Q factor and acoustic propagation velocity under various temperatures and pressures 20 p2612 A73-39712

- Trapped solar wind noble gases and exposure age of Luna 16 lunar fines. 21 p2770 A73-41001
- O-18/O-16 ratios in Luna 16 fines. 21 p2770 A73-41003
- Preliminary measurements of spherules of the Pontina Plain and of micrometeorites of Apollo 12 and related impact studies. 21 p2775 A73-41412

LUNAR ECHOES

NT LUNAR RADAR ECHOES

- Astronomical observatory lunar ranging system with high radiance neodymium-glass laser and transmitting telescope, noting tracking accuracy 02 p0151 A73-12246
- Ruby laser ranging experiment for lunar returned signal from Apollo 11 retroreflector package, using multichannel pulse height counter and CRT 02 p0141 A73-12248
- A description of the lunar ranging station at McDonald Observatory. 02 p0151 A73-12249
- Analysis of the first laser echoes obtained on the reflector of Luna 21 13 p1686 A73-29561
- Determination of the lunar albedo at the 6-m wavelength 16 p2064 A73-33772
- Lunar electromagnetic scattering. I - Propagation parallel to the diamagnetic cavity axis. 24 p3139 A73-45109

LUNAR ECLIPSES

- Eclipse calculations of lunar features. 01 p0095 A73-10294
- Photometry of the lunar surface. 04 p0497 A73-15177
- Lunar eclipse brightness dependence on eleven year sunspot activity cycle 08 p1007 A73-21068
- Observations during total lunar eclipse on 6 August, 1971, noting low visibility of lunar features and earth shadow reddish hue 08 p1007 A73-21071
- Book - Advances in astronomy and astrophysics. Volume 9. 10 p1282 A73-24641

Lunar eclipses in astronomical history, discussing deviations from geometrical theory, earth atmospheric effects, photometric observations, lunar luminescence, etc 10 p1282 A73-24643

Far IR mapping of lunar surface during 19 December 1964 eclipse, discussing thermal contours and Apollo observed regions 10 p1282 A73-24644

Solar and lunar eclipses, orbits and perturbations prediction from Saros /recurring time periods/ 12 p1540 A73-27481

Lunar surface thermal response from IR atlas charts of eclipsed moon, noting thermal enhancements in maria 12 p1541 A73-27483

Results of optical observations of dust in upper atmosphere and interplanetary space. 13 p1680 A73-28520

Determination of the density of the surface covering of the moon from given surface temperatures during eclipse and lunar-night periods 16 p2063 A73-33754

Lunar eclipse brightness dependence on eleven year sunspot activity cycle 18 p2355 A73-36869

Observations during total lunar eclipse on 6 August 1971, noting low visibility of lunar features and earth shadow reddish hue 18 p2356 A73-36872

Photoelectric and visual observation of the total eclipse of the moon of August 6, 1971. 24 p3134 A73-44568

LUNAR EFFECTS

NT LUNAR GRAVITATIONAL EFFECTS

NT LUNAR TIDES

Nonsolar related D region semilunar variation effects on Omega navigation systems signal phase shift from harmonic analysis of VLF propagation data periodicities 04 p0416 A73-15062

Solar and lunar eclipses, orbits and perturbations prediction from Saros /recurring time periods/ 12 p1540 A73-27481

Solar and lunar effects on neutral atmospheric tidal winds and induced electrostatic and geomagnetic fields effects on low latitude F 2 and sporadic E layers 15 p1868 A73-31751

Night side electromagnetic response of the moon. 18 p2351 A73-36268

Effect of simulated lunar impact on the survival of bacterial spores. 20 p2513 A73-39485

Effects of physical librations of the moon on the orbital elements of a lunar satellite. 23 p3032 A73-43841

LUNAR ENVIRONMENT

NT LUNAR ATMOSPHERES

Survival of micro-organisms on the moon. 07 p0780 A73-19111

Photoelectron layer detection above sunlit lunar surface with ion-electron spectrometer in Apollo 14 charged particle lunar environment experiment, noting energy spectra 07 p0895 A73-19859

Laboratory modeling of 'vaporization-condensation and spilling' type processes taking place on the lunar surface 13 p1672 A73-28118

Preliminary results obtained with astrophotometer installed on Lunokhod II. 18 p2315 A73-35992

Investigation of cosmic radiation about the moon aboard the Luna 10, 11, and 12 artificial lunar satellites 19 p2474 A73-37344

Emission measurement of Surveyor 3 spacecraft aluminum support tubing returned from moon by Apollo 12, noting lunar environment effects from control sample data 24 p3139 A73-45110

LUNAR EVOLUTION

Moon flares due to lunar gas eruptions, investigating degassing in former geological epochs 02 p0212 A73-11950

Radioactive crystallization ages of Apollo 14 basaltic rocks from Fra Mauro formation, comparing with Apollo 11 samples 02 p0213 A73-12231

The origin of the moon - Theories involving joint formation with the earth. 02 p0217 A73-12386

Evidence for objects of lunar mass in the early solar system and for capture as a general process for the origin of satellites. 02 p0217 A73-12394

Model for meteorite impact generated gas flow on moon as function of mass, velocity and composition, noting wind effects on lunar erosion 02 p0223 A73-12719

Large disks as representations for the lunar mascons with implications regarding theories of formation. 03 p0367 A73-13081

The geomorphic evolution of the lunar surface. 03 p0367 A73-13082

Dynamical model for evolution of melted spherical drop of homogeneous glassy material to explain observed glassy spherules in lunar dust 03 p0368 A73-13090

Successive solidification origin of central peaks and terrace ring wall in lunar crater formations filled with melt after impacts, using freezing water experiments 03 p0369 A73-13094

Possible thermal history of the moon. 03 p0369 A73-13106

On the initial distance of the moon forming in the circumterrestrial swarm. 03 p0369 A73-13108

Lunar and planetary topography formation by exogenous and endogenous mechanisms, considering fluidization by volcanism 03 p0369 A73-13109

On the possible differences in the bulk chemical composition of the earth and the moon forming in the circumterrestrial swarm. 03 p0370 A73-13110

Moon and solar system origin in view of chemical evidence and Apollo lunar rock Rb-87/Sr-87 ages and remelting conditions 03 p0370 A73-13111

Evolution of the moon - Recent modification of previous ideas. 03 p0370 A73-13112

Lunar thermal model with hot interior and cool lithosphere, considering strength and conductivity profiles, volcanic activity absence and composition and origin implications 05 p0613 A73-16158

Lunar evolution, age and surface composition data obtained from Apollo missions 05 p0616 A73-16400

K, Rb, Sr, Ba contents and rare earths in specimens from the Apollonius /lunar mountains/ crater region brought back by the Soviet probe Luna 20 05 p0546 A73-16829

Rb-87/Sr-87 'ages' of the soil and rock fragments brought back from the lunar mountains by the automatic probe Luna 20 /Apollonius crater region/ 05 p0546 A73-16830

Moon geochronology from U-Pb systematics applied to lunar basalt data, discussing two and three stage evolutionary models based on Pb isotope ratios 05 p0618 A73-16834

Extralunar materials in Apollo 16 soils and the decay rate of the extralunar flux 4.0 Gy ago. 05 p0618 A73-16835

Lunar composition and evolution studies results from Apollo and Luna collected soil and rocks radiometric analysis, noting surface materials contamination with solar wind particles 07 p0878 A73-19674

Role of water in the evolution of the lunar crust: An experimental study of sample 14310 - An indication of lunar calc-alkaline volcanism. 07 p0880 A73-19691

Analysis of Fra Mauro samples and the origin of the Imbrium Basin. 07 p0880 A73-19701

Pyroxenes as recorders of lunar basalt petrogenesis - Chemical trends due to crystal-liquid interaction. 07 p0881 A73-19704

Clinopyroxenes from Apollo 12 and 14 - Exsolution, domain structure, and cation order. 07 p0881 A73-19708

Apollo 14 regolith and fragmental rocks, their compositions and origin by impacts. 07 p0883 A73-19725

Thermal and mechanical history of breccias 14306, 14063, 14270, and 14321. 07 p0883 A73-19729

The extralunar component in lunar soils and breccias. 07 p0887 A73-19767

Apollo 14 mineral ages and the thermal history of the Fra Mauro formation. 07 p0887 A73-19776

Apollo 14 and 15 samples - Rb-Sr ages, trace elements, and lunar evolution. 07 p0887 A73-19777

Uranium and extinct Pu-244 effects in Apollo 14 materials. 07 p0888 A73-19784

Pb-204 in Apollo 14 samples and inferences regarding primordial Pb lunar geochemistry. 07 p0888 A73-19786

Abundances of primordial and cosmogenic radionuclides in Apollo 14 rocks and fines. 07 p0888 A73-19787

Lunar surface processes and cosmic ray characterization from Apollo 12-15 lunar sample analyses. 07 p0870 A73-19790

Cosmic ray exposure ages from Apollo 14 lunar rocks isotopic anomalies due to neutron capture effect in Gd, Br and Ba 07 p0871 A73-19803

Atmospheric Ar-40 in lunar fines. 07 p0890 A73-19808

Microcrater size frequency distribution and exposure age for Apollo 12 and 14 rocks 07 p0896 A73-19868

Lunar craters and exposure ages derived from crater statistics and solar flare tracks. 07 p0896 A73-19869

Collision controlled radiation history of the lunar regolith. 07 p0871 A73-19870

Radiation and shock effects on Apollo 14 and 15 breccias substructure history, reporting optical microscope observations of solar flares and cosmic ray tracks 07 p0896 A73-19872

Temperature scaling of heat metamorphism evolved during lunar and meteoritic brecciation, evaluating dust sintering degree 07 p0896 A73-19874

Origin, evolution and present thermal state of the moon. 07 p0899 A73-20032

Rb-Sr ages and initial strontium in basalts from Apollo 15. 08 p0936 A73-20839

The role of the satellite swarm in the origin of the earth's rotation. 08 p1012 A73-21579

Lunar interior temperature profiles from olivine and pyroxene electrical conductivity data, indicating high temperature accretion from hydrogen depleted material 09 p1148 A73-22874

On the model of the accumulation of the moon compatible with the data on the composition and the age of lunar rocks. 10 p1277 A73-24086

Lunar Rb-Sr age correction according to stable isotope tracer /spike/ recalibration, using stoichiometric salts 10 p1278 A73-24112

Lunar interior materials seismic compressional velocities, indicating differentiated structure consistent with solidus thermal history 11 p1421 A73-25895

Critique of Anderson hypothesis of moon origin by condensation of material off median plane of initial solar nebula 11 p1428 A73-26664

Astronomical, geochemical and geophysical data and constraints for lunar evolution, considering remanent magnetization, electrical conductivity and early evolution model 12 p1541 A73-27491

Lunar maria basins fast and slow filling implications to moon history, considering meteorite bombardment, maria cooling and mascons 12 p1542 A73-27496

Lunar composition and origin model based on early condensation processes in solar nebula
12 p1542 A73-27546

Lunar differentiation model based on chemical data from Luna 20 soil and Apollo 16 core samples analysis by combined semimicro atomic absorption spectrophotometric and colorimetric method
13 p1676 A73-28326

Lunar origin and composition relationship to solar system evolution, discussing various theories and evidence from Apollo flights
13 p1687 A73-29665

Permanent magnetization of lunar deep interior due to formation as gas sphere in solar magnetic field
13 p1687 A73-29673

Lunar origin dynamics, discussing earth-moon tidal evolution, capture probability, fragmentary collisions, precession and auxiliary models
14 p1800 A73-30550

Lunar interior composition, structure and thermal evolution models to fit surface igneous activity chronology and lithosphere stress history implied by mascons presence
15 p1937 A73-31778

Lunar evolution theory review covering separation from earth, capture by earth, formation by particle accumulation and core iron content approximation
16 p2065 A73-33781

The origin of large lunar craters and circular seas
16 p2065 A73-33786

Lunar volcanism - Age of the glass in the Apollo 17 orange soil
17 p2230 A73-34522

Thermal history and evolution of the moon.
17 p2235 A73-35735

Conjectures about the evolution of the moon.
17 p2235 A73-35737

Electrical conductivity, internal temperatures and thermal evolution of the moon.
17 p2235 A73-35741

Properties of the solar nebula and the origin of the moon.
17 p2235 A73-35742

Lunar circular maria morphological features and fill deposits surface evolution, considering high velocity large body impact role based on Doppler gravity anomaly data
18 p2349 A73-35952

A response to a comment on U-Pb systematics in lunar basalts.
18 p2354 A73-36512

Reports of fourth Lunar Science Conference covering lunar rock chemical composition assessment as information source on early solar system, lunar early geologic history, etc
19 p2487 A73-38293

Inclination of the moon's orbit - The early history.
20 p2605 A73-39055

Distribution density of small lunar craters - Models and actual distribution
21 p2770 A73-40915

Lunar and planetary chemical composition dependence on condensation temperature in solar nebula
23 p3030 A73-43760

Lunar asymmetries in crustal thickness, maria distribution and gamma radioactivity due to intense early bombardment by interplanetary meteoroid flux
23 p3031 A73-43762

Geochemical coherence between trace elements and K, P and rare earth elements in lunar soils evaluated for samples evolutionary history
23 p2951 A73-43767

High concentration of refractory elements in lunar crust explained by melting and differentiation model
23 p3033 A73-43958

Ancient lunar mega-regolith and subsurface structure.
24 p3129 A73-44448

Monte Carlo computer simulation of lunar regolith evolution, considering buffering regolith effect via computation for debris produced by crater
24 p3130 A73-44460

Lunar 25 km discontinuity seismically examined, discussing hypotheses with shock metamorphism lack and annealing of shock induced microcracks
24 p3131 A73-44470

LUNAR EXPLORATION

Possibility of determining the lunar rotation elements with a narrow-angle television camera
01 p0051 A73-10944

Lunar surface exploration with Lunokhod 1 roving vehicle, discussing soft landing, ground based control, sensors, scientific equipment and observations
02 p0212 A73-12227

Lunar surface observation with cold cathode ionization gage left by Apollo 14, noting low concentration atmospheric particles and gas clouds
02 p0213 A73-12239

Engineering potential for lunar missions after Apollo.
03 p0380 A73-13087

Apollo 17 lunar surface experiments for lunar composition, structure and chronology investigation,

discussing landing site and instrument selection based on prior Apollo flights
04 p0493 A73-14671

Soviet Union-proposed draft International Treaty governing lunar exploration and use
04 p0522 A73-15135

Spacecraft techniques for lunar research.
04 p0448 A73-15182

Engineering support activities for the Apollo 17 Surface Electrical Properties Experiment.
04 p0428 A73-15390

Lunar surface SEP transmitter-receiver ground wave experiment, discussing electronic equipment, multifrequency antennas and signal variation
04 p0428 A73-15391

Indigenous lunar organic compound search, considering prebiological chemistry and composition possibility in deeper region under surface
06 p0655 A73-18428

Apollo 16 lunar mission results, discussing lunar geology, spacecraft operational procedures and hardware
09 p1152 A73-22186

Application of a narrow-angle television camera for determining the rotation elements of the moon.
09 p1084 A73-22739

Solar array concept for a portable retractable oriented power system.
11 p1310 A73-26007

Absolute calibration of Apollo lunar orbital mass spectrometer.
13 p1617 A73-28930

Soviet Lunokhod 2 lunar rover design, guidance systems, mineralogical analyses by X ray fluoroscopic spectroscopy, magnetic field measurements and operations site
16 p1996 A73-33225

Apollo program contributions to lunar cosmology and composition, discussing core-mantle structure, earth-moon gravitational system, mineral types and cosmological hypotheses
18 p2356 A73-37044

Russian book on lunar study by telescopes and unmanned and manned spacecraft covering Luna Zond and Lunokhod probes, Apollo flights, topography, structure and magnetic field
19 p2485 A73-37770

LUNAR FAR SIDE

Catalog of selenographic coordinates for libration-zone and far-side points.
04 p0503 A73-16017

A new unified system for designating objects on the moon.
04 p0504 A73-16030

Extending lunar nomenclature to the far side of the moon.
05 p0612 A73-16089

Photogeologic interpretations of Apollo 14 orbital photographs of far side craters and lunar surface formations
07 p0879 A73-19681

Al-Khwarizmi - A new-found basin on the lunar far side.
16 p2060 A73-33125

Electrostatic charging of the lunar surface and possible consequences.
16 p2064 A73-33766

Photometric relief of the lunar continent cover
16 p2064 A73-33766

General features of lunar volcanism
16 p2065 A73-33785

Surface and orbital magnetic results from Apollo 15.
21 p2691 A73-41398

LUNAR FIGURE

Lunar maria and uplands global shape as triaxial ellipsoids with long axes in earth direction
03 p0367 A73-13079

Some differences between geometrical and dynamical figures of the moon.
03 p0367 A73-13080

Lunar shape parameter extraction from Apollo 15 and 16 laser altimeter measurements of CSM to surface distance
06 p0751 A73-18223

Dynamic figure of the moon and the density distribution in the lunar interior
12 p1546 A73-27866

Apollo 15 photogrammetric measurements of lunar figure, describing system characteristics and analytical triangulation techniques
12 p1501 A73-27967

Monochromatic phase curves and albedos for the lunar disk.
15 p1932 A73-31271

Systematic elevation errors in maps of the lunar edge zone
17 p2230 A73-34594

Approximation of the geometric figure of the moon by using spherical functions
17 p2230 A73-34596

Dynamical figure of the moon and the density distribution of the lunar interior.
20 p2608 A73-39240

LUNAR GEOLOGY

NT LUNAR CORE

Preliminary observations of stratified rocks of the Hadley Appennines photographed by the Apollo 15 astronauts
01 p0095 A73-10268

Lunar breccias lithification and metamorphism model construction from experimental and analytical data, discussing scale of lunar metamorphic temperatures
02 p0220 A73-12476

Response of lunar atmosphere to volcanic gas releases.
03 p0365 A73-12880

Lunar 'dunite', 'pyroxenite' and 'anorthosite'.
03 p0375 A73-14108

Spacecraft techniques for lunar research.
04 p0448 A73-15182

Apollo 16 exploration of Descartes - A geologic summary.
05 p0614 A73-16320

Luna 20 landing site geologic setting from Apollo 16 panoramic photographs, discussing complexly faulted terrain
05 p0618 A73-16826

Spectrophotofluorometers for returned lunar samples and geological materials organic analyses, discussing optical component performance and calibration to avoid instrumental artifacts effect on spectra
06 p0662 A73-18415

Lunar geology developments by remotely sensed earth-based, moon satellite and unmanned and manned lunar lander observations, discussing moon structure and evolution
07 p0875 A73-19223

Lunar Science Conference, 3rd, Houston, Tex., January 10-13, 1972, Proceedings. Volume 1 - Mineralogy and petrology. Volume 2 - Chemical and isotope analyses, organic chemistry. Volume 3 - Physical properties.
07 p0878 A73-19676

Hadley Rille geologic and morphologic investigation from Apollo 15 data, supporting collapsed lava tube concept
07 p0878 A73-19677

Geology of the Apollo 14 landing site.
07 p0878 A73-19679

New geological findings in Apollo 15 lunar orbital photography.
07 p0878 A73-19680

Astronaut observations from lunar orbit and their geologic significance.
07 p0879 A73-19682

Petrography and crystallization history of basalts 14310 and 14072.
07 p0879 A73-19685

Petrology of Fra Mauro basalt 14310.
07 p0879 A73-19687

Metamorphism of Apollo 14 breccias.
07 p0882 A73-19717

Apollo 14 breccias - General characteristics and classification.
07 p0882 A73-19718

Apollo 12 lunar KREEP samples possible origin, considering mixture of ejecta from Copernicus, Reinhold and local highlands and Fra Mauro deposits
07 p0886 A73-19763

The nature and effect of the volatile cloud produced by volcanic and impact events on the moon as derived from a terrestrial volcanic model.
07 p0890 A73-19812

Moonquakes and lunar tectonism results from the Apollo passive seismic experiment.
07 p0894 A73-19848

Applications to lunar geophysical models of the velocity-density properties of lunar rocks, glasses, and artificial lunar glasses.
07 p0894 A73-19854

Apollo 16 lunar mission results, discussing lunar geology, spacecraft operational procedures and hardware
09 p1152 A73-22186

Crater frequency age determinations for the proposed Apollo 17 site at Taurus-Littrow.
09 p1148 A73-22873

Identification, distribution and significance of lunar volcanic domes.
10 p1276 A73-24076

Experimental studies on the formation of lunar surface features by fluidization - Discussion.
10 p1280 A73-24349

The structure and geological-morphological features of the landing site of the Luna 20 automatic station
10 p1281 A73-24452

Lunar cinder cone deposits in Taurus-Littrow region of Apollo 17 landing site as counterparts of terrestrial pyroclastic eruptions
11 p1426 A73-26375

Astronomical, geochemical and geophysical data and constraints for lunar evolution, considering remanent magnetization, electrical conductivity and early evolution model
12 p1541 A73-27491

Lunar crater structure geological and morphological interpretations from lunar maria photographs in terms of age, density and stony debris size distribution
13 p1672 A73-28115

Oxide minerals in lithic fragments from Luna 20 fines.

13 p1674 A73-28306

Mineralogy, petrology and chemistry of lithic fragments from Luna 20 fines - Origin of the cumulate ANT suite and its relationship to high-alumina and mare basalts.

13 p1676 A73-28328

Development of soil on the lunar surface.

15 p1941 A73-32226

Avalanche mode of motion - Implications from lunar examples.

16 p2059 A73-32901

Investigation of the dielectric properties of terrestrial rocks at super-high frequencies for the purpose of improving accuracy for the composition of lunar material

16 p2064 A73-33771

General features of lunar volcanism

16 p2065 A73-33785

Petrology of the 2-4 mm soil fragments from the Hadley-Apennine region of the moon.

17 p2230 A73-34517

Lunar sinuous rilles as inverted eskers formed by volatiles /water and carbon dioxide/ moving in channel between basement surface and permafrost layer

17 p2237 A73-35859

Structure and geologic-morphological features of the region where Luna-20 landed.

19 p2486 A73-38126

Reports of fourth Lunar Science Conference covering lunar rock chemical composition assessment as information source on early solar system, lunar early geologic history, etc

19 p2487 A73-38293

Photogrammetry in Apollo lunar roving vehicle conducted geometry and geology exploration, using horizontal stereophotography with special gnomon for sun-line and vertical control

20 p2611 A73-39669

Lunar cross hatching lineament patterns at Silver Spur on Apollo 15 landing site, relating to geological, lighting or meteorite impact gas flow effects

23 p3034 A73-43962

LUNAR GRAVITATION

A method of determining the center of mass of the moon from ground observations

01 p0100 A73-10840

Large disks as representations for the lunar mascons with implications regarding theories of formation.

03 p0367 A73-13081

Lunar gravity model obtained by using spherical harmonics with mascon terms.

04 p0495 A73-14811

An empirically derived lunar gravity field.

04 p0498 A73-15184

Lunar Sea of Serenity mascon analysis from Lunar Orbiter and Apollo 15 Doppler gravity data, correlating gravity anomalies with surface mass distribution

05 p0615 A73-16384

Accuracy of the moon potential computation based on integral formulae

06 p0751 A73-18151

Viscosity of the moon. I - After mare formation. II - During mare formation.

10 p1277 A73-24081

Physical librations due to the third and fourth degree harmonics of the lunar gravity potential.

10 p1277 A73-24083

Lunar gravity derived from long-period satellite motion - A proposed method.

10 p1283 A73-24664

Model for lateral variations of lunar density minimizing total shear strain energy of moon, noting gravitational potential equal to observed potential at surface

12 p1541 A73-27488

The normal gravitational fields of the earth and the moon

12 p1546 A73-27865

Dynamic figure of the moon and the density distribution in the lunar interior

12 p1546 A73-27866

Thermal design and testing of the Apollo 17 lunar traverse gravimeter.

[AIAA PAPER 73-771]

18 p2316 A73-36385

Normal gravity fields of the earth and the moon.

20 p2608 A73-39239

Dynamical figure of the moon and the density distribution of the lunar interior.

20 p2608 A73-39240

Mare Humorum mascon anomaly characteristics from gravity measurements obtained by Doppler tracking of Apollo 15 subsatellite

23 p3030 A73-43759

Effects of physical librations of the moon on the orbital elements of a lunar satellite.

23 p3032 A73-43841

LUNAR GRAVITATIONAL EFFECTS

Effects of the sun and the moon on a near-equatorial synchronous satellite.

08 p1011 A73-21430

Lunar and solar perturbation effects on communication satellite orbits, considering Kozai luni-solar theories

09 p1149 A73-22913

Lunar circular maria morphological features and fill deposits surface evolution, considering high velocity large body impact role based on Doppler gravity anomaly data

18 p2349 A73-35952

Biomechanics of locomotion via jumping on lunar surface, discussing subgravity effects on energy requirements, body potential and kinetic energy, muscular work, etc

22 p2804 A73-42175

Meteoroids impact rate on lunar and earth surfaces for given geocentric and selenocentric velocity distributions, taking into account gravitational effects

24 p3131 A73-44461

LUNAR GRAVITY SIMULATOR

Lunokhod 1 vehicle terrestrial mobility tests, simulating lunar gravity, soil and traction on scale and mockup models

02 p0151 A73-12234

LUNAR IONOSPHERE

U LUNAR ATMOSPHERES

LUNAR LANDING

NT APOLLO LUNAR EXPERIMENT MODULE

Visibility of lunar surface features - Apollo 14 orbital observations and lunar landing.

05 p0617 A73-16713

Lunar geology developments by remotely sensed earth-based, moon satellite and unmanned and manned lunar lander observations, discussing moon structure and evolution

07 p0875 A73-19223

Lunar metric camera used during Apollo landings, discussing lenses and test and calibration work for inner orientation

07 p0824 A73-20020

Translunar flight plan of Luna 21 probe, describing Lunokhod structure and lunar descent procedure

08 p1007 A73-20974

Apollo LM guidance computer software for the final lunar descent.

10 p1247 A73-24548

LUNAR LANDING MODULES

NT LUNAR MODULE

LUNAR LANDING SITES

Characteristics of radio wave scattering by the lunar surface at the landing sites of the Luna 16 and Luna 17 automatic stations

02 p0220 A73-12473

Erosion, transportation and the nature of the maria.

03 p0368 A73-13083

Plans and objectives of the remaining Apollo missions.

03 p0368 A73-13086

A point of phase equilibria interpretation in connection with lavas from the Apollo 12 site.

03 p0375 A73-14106

Apollo 17 lunar surface experiments for lunar composition, structure and chronology investigation, discussing landing site and instrument selection based on prior Apollo flights

04 p0493 A73-14671

The Apollo 17 landing site.

04 p0501 A73-15622

Apollo 16 exploration of Descartes - A geologic summary.

05 p0614 A73-16320

A control system for soft landings on the lunar surface

05 p0595 A73-16424

Luna 20 landing site geologic setting from Apollo 16 panoramic photographs, discussing complexly faulted terrain

05 p0618 A73-16826

Apennine Front lineaments origin at Apollo 15 landing site, interpreting topographic irregularities in terms of obliquely incident sunlight illusions

07 p0878 A73-19678

Geology of the Apollo 14 landing site.

07 p0878 A73-19679

Chemical characteristics of trace element rich KREEP basaltic rocks from Apollo 12 landing site

07 p0885 A73-19753

The abundances of components of the lunar soils by a least-squares mixing model and the formation age of KREEP.

07 p0887 A73-19769

Crater frequency age determinations for the proposed Apollo 17 site at Taurus-Littrow.

09 p1148 A73-22873

The structure and geological-morphological features of the landing site of the Luna 20 automatic station

10 p1281 A73-24452

Lunar cinder cone deposits in Taurus-Littrow region of Apollo 17 landing site as counterparts of terrestrial pyroclastic eruptions

11 p1426 A73-26375

Compressional wave velocity profile of lunar near-surface and crust derived from seismic refraction data at Apollo 14 and 16 sites

12 p1541 A73-27486

Lunar 16 and 20 soil halogens, uranium and lithium contents, noting chlorine and phosphorus pentoxide noncorrelation with Apollo sites

13 p1676 A73-28329

Radio-wave scattering characteristics of the moon's surface at the landing sites of Luna 16 and Luna 17.

15 p1942 A73-32624

Avalanche mode of motion - Implications from lunar examples.

16 p2059 A73-32901

Distribution and origin of rocks in the landing area of the Luna 13 automatic lunar station

16 p2065 A73-33778

A study of the topography of the landing sites of the Luna 9 and Luna 13 lunar probes

16 p2065 A73-33780

Urey meteoritic chondrule impact theory confirmation from Apollo sites and Lunar Crater /India/ impact generated silicate spherules

17 p2236 A73-35748

Structure and geologic-morphological features of the region where Luna-20 landed.

19 p2486 A73-38126

Results of radar experiments performed on automatic stations Luna 16 and Luna 17.

21 p2774 A73-41401

Low albedo lunar areas, discussing spectral reflectivity, radar backscatter characteristics and Apollo 17 landing site

22 p2909 A73-42495

LUNAR LIMB

Lunar magnetic field measurements with Apollo 15 subsatellite, discussing surface remanent magnetization, solar wind interactions and limb shocks

07 p0892 A73-19833

Solar wind-lunar limb interaction from viscous MHD approach including continuum fluids, kinetic plasma and magnetic boundary layer

12 p1534 A73-27003

Photoelectrons and solar wind/lunar limb interaction.

12 p1534 A73-27495

Systematic elevation errors in maps of the lunar edge zone

17 p2230 A73-34594

LUNAR LUMINESCENCE

On the interaction between tectonic processes of the earth and the moon.

03 p0299 A73-13093

Luminescence excitation by protons and electrons, applied to Apollo lunar samples.

03 p0369 A73-13098

Lunar tidal phenomena and the lunar Rille system.

03 p0370 A73-13113

Photometry of the lunar surface.

04 p0497 A73-15177

A photometric and polarimetric study of the moon's surface.

04 p0497 A73-15183

On surface photometry of the moon.

04 p0448 A73-15188

Lunar surface chemical composition mapping with onboard Apollo 15 X ray fluorescence spectrometer, showing Al, Mg and Si ratios

07 p0871 A73-19825

An explanation of transient lunar phenomena from studies of static and fluidized lunar dust layers.

07 p0895 A73-19863

Luminescence of lunar material excited by electrons.

07 p0897 A73-19881

On a possible relation between lunar transient phenomena and the earth-shine /Research note/.

10 p1277 A73-24082

Lunar eclipses in astronomical history, discussing deviations from geometrical theory, earth atmospheric effects, photometric observations, lunar luminescence, etc

10 p1282 A73-24643

Some results of lunar surface luminescence studies at the Kharkov Astronomical Observatory

16 p2063 A73-33762

Experimental results on combined ultraviolet-proton excitation of moon rock luminescence.

17 p2233 A73-35273

Surveyor observations of lunar horizon-glow.

18 p2348 A73-35938

LUNAR MAGNETIC FIELDS

Lunar magnetic field measurements, electrical conductivity calculations and thermal profile inferences.

03 p0369 A73-13103

Evolution of the moon - Recent modification of previous ideas.

03 p0370 A73-13112

Metallic Fe-Ni-S lunar core as source of remanent magnetism in lunar rocks, consistent with thermal models

07 p0877 A73-19654

Lunar magnetic field measurements with Apollo 15 subsatellite, discussing surface remanent magnetization, solar wind interactions and limb shocks

07 p0892 A73-19833

Surface magnetometer experiments - Internal lunar properties and lunar field interactions with the solar plasma.

07 p0892 A73-19834

The induced magnetic field of the moon - Conductivity profiles and inferred temperature.

07 p0892 A73-19835

Remanent magnetization of Apollo 14 rocks and fines, discussing iron contribution and early internal magnetic field

07 p0892 A73-19837

On the remanent magnetism of lunar samples with special reference to 10048, 55 and 14053, 48.

07 p0892 A73-19838

Deep planetary interior models and internal structure evidence from lunar magnetism, considering planetary magnetic field studies from flyby and orbiting satellite measurements

11 p1420 A73-25893

Preliminary mapping of the lunar magnetic field.

11 p1421 A73-25903

Liquid core model with precessionally driven magnetoturbulence applied to moon, discussing tidal effects in outer solid and liquid shells

12 p1541 A73-27489

A determination of the intensity of the ancient lunar magnetic field.

12 p1542 A73-27494

Permanent magnetization of lunar deep interior due to formation as gas sphere in solar magnetic field

13 p1687 A73-29673

Lunar magnetic field model with primeval liquid shell dynamo driven by thermal convection or earth tidal motions

14 p1789 A73-29722

Explorer 35 lunar studies, discussing orbit characteristics, circumlunar magnetic field, surface electromagnetic properties and solar wind model

16 p2065 A73-33782

Topology of induced lunar magnetic fields.

17 p2235 A73-35736

Orbital mapping of the lunar magnetic field.

17 p2235 A73-35739

Apollo 15 and 16 subsatellite magnetometer measurements of the lunar magnetic field.

18 p2349 A73-35944

Surface and orbital magnetic results from Apollo 15.

21 p2691 A73-41398

Induced magnetosphere of the moon. II - Experimental results from Apollo 12 and Explorer 35.

22 p2906 A73-41905

Lunar electromagnetic scattering. I - Propagation parallel to the diamagnetic cavity axis.

24 p3139 A73-45109

Solar wind interaction modes with lunar magnetic fields, discussing moon surface charging, magnetic field compression and wind deflection

24 p3126 A73-45127

LUNAR MAPS

Lunar radar mapping at 162.4 MHz from Jodrell Bank observations in January and February 1970, discussing depolarized returns

03 p0368 A73-13084

Lunar topography - Global determination by radar.

03 p0378 A73-14445

Lunar maps from CW radar imagery by aperture synthesis method at long wavelengths, noting depolarized return from highland regions

04 p0417 A73-15178

Catalog of selenographic coordinates for libration-zone and far-side points.

04 p0503 A73-16017

Hypsometric properties of the near side of the moon.

04 p0503 A73-16018

A new unified system for designating objects on the moon.

04 p0504 A73-16030

A first look at the lunar orbital gamma-ray data.

07 p0871 A73-19824

Lunar surface radioactivity - Preliminary results of the Apollo 15 and Apollo 16 gamma-ray spectrometer experiments.

08 p1009 A73-21224

Far IR mapping of lunar surface during 19 December 1964 eclipse, discussing thermal contours and Apollo observed regions

10 p1282 A73-24644

Book - Maps of lunar hemispheres: Giving the views of the lunar globe from six cardinal directions in space.

11 p1429 A73-26742

Lunar surface thermal response from IR atlas charts of eclipsed moon, noting thermal enhancements in maria

12 p1541 A73-27483

Classification, scale sequence, and nomenclature of lunar maps

13 p1672 A73-28117

Lunar orbit and mapping coordinates, discussing libration effects due to motion and surface features

13 p1681 A73-28947

Mathematical lunar cartography based on networks of reference points and absolute elevation heights,

considering progress since Luna orbiters launchings in 1959

16 p2064 A73-33774

Problems of morphometric studies of the lunar surface

16 p2064 A73-33776

Lunar surface hypsographic curve plotting from point absolute height measurements

16 p2065 A73-33777

Orbital mapping of the lunar magnetic field.

17 p2235 A73-35739

Apollo 15 and 16 results of the integrated geochemical experiment.

17 p2236 A73-35750

LUNAR MARIA

Geomorphological analysis of the area of Mare Imbrium explored by the automatic roving vehicle Lunokhod 1.

02 p0213 A73-12240

The geomorphic evolution of the lunar surface.

03 p0367 A73-13082

Erosion, transportation and the nature of the maria.

03 p0368 A73-13083

Maria lavas, mascons, layered complexes, achondrites and the lunar mantle.

03 p0368 A73-13088

Lunar mare ridge formation with broad gentle arch overlaid by sharper contorted ridge, discussing ring structures and volcanic ring complexes

03 p0368 A73-13091

A possible mechanism of the generating of the unusually long lunar seismic oscillations.

03 p0368 A73-13092

Nature of the density reversal beneath the lunar maria.

04 p0496 A73-14821

Hypsometric properties of the near side of the moon.

04 p0503 A73-16018

Investigation of the gamma-emission of lunar soil delivered by the automatic station Luna 16

05 p0620 A73-17020

Neutron activation analysis of lunar soil brought by 'Luna-16' from Mare Foecunditatis

05 p0620 A73-17021

Structure of lunar maria from their albedo data

07 p0902 A73-20323

Viscosity of the moon. I - After mare formation. II - During mare formation.

10 p1277 A73-24081

Albedo distribution in lunar maria.

12 p1540 A73-27295

Lunar maria basins fast and slow filling implications to moon history, considering meteorite bombardment, maria cooling and mascons

12 p1542 A73-27496

Lunar crater structure geological and morphological interpretations from lunar maria photographs in terms of age, density and stony debris size distribution

13 p1672 A73-28115

Problems of morphometric studies of the lunar surface

16 p2064 A73-33776

The origin of large lunar craters and circular seas

16 p2065 A73-33786

Discreteness of the dimensions of lunar circular maria and thalassoids

16 p2065 A73-33788

Moon - 'Ghost' craters formed during Mare filling.

17 p2236 A73-35746

Lunar circular maria morphological features and fill deposits surface evolution, considering high velocity large body impact role based on Doppler gravity anomaly data

18 p2349 A73-35952

Comparison of Apollo and earth-based observations - Definition of surface units in Mare Serenitatis.

21 p2769 A73-40821

Study by the method of nuclear tracking of the soil of Mare Foecunditatis / Luna 16/

21 p2770 A73-41002

Infrared reflection characteristics of lunar mare regolith.

21 p2774 A73-41400

Mare Humorum mascon anomaly characteristics from gravity measurements obtained by Doppler tracking of Apollo 15 subsatellite

23 p3030 A73-43759

Lunar asymmetries in crustal thickness, maria distribution and gamma radioactivity due to intense early bombardment by interplanetary meteoroid flux

23 p3031 A73-43762

Spectral reflectivity of Humorum basin region, comparing to Apollo 11 site and Mare Serenitatis

24 p3129 A73-44436

LUNAR MODULE

NT APOLLO LUNAR EXPERIMENT MODULE

Apollo LM guidance computer software for the final lunar descent.

10 p1247 A73-24548

LUNAR OBSERVATORIES

The lunar regolith as a site for an astronomical observatory.

01 p0105 A73-11204

Lunar laser observatory equipment modifications, noting change of Cassegrain primary mirror from spherical metal alloy to hyperboloid glass construction

02 p0176 A73-12244

On automatic angle measurements and a proposition of their application into zenith distance measurements on the surface of the moon.

03 p0307 A73-13258

Lunar Surface Ultraviolet Spectrographic Camera for location and extent determination of gaseous material, describing capability for acquisition of direct imagery and spectroscopy

05 p0576 A73-16746

Selection of stars for observations from the lunar surface by the method of equal altitudes

15 p1938 A73-31963

The Lunar and Planetary Laboratory and its telescopes.

19 p2417 A73-37580

Selection of stars for observation from the lunar surface by the method of equal altitudes.

24 p3132 A73-44488

LUNAR OCCULTATION

NT SOLAR ECLIPSES

Study of the angular structure of radio sources from their lunar occultations. II

01 p0102 A73-10951

Lunar occultation of stars to determine moon diameter and orbital elements, noting time measurement difficulties due to scintillation effects

01 p0102 A73-10994

The angular diameter of X Cancri.

04 p0500 A73-15518

Occultation of the Pleiades by the moon on March 19, 1972

06 p0753 A73-18375

Lunar occultations of radio sources as a technique for investigating their angular structure. II.

09 p1148 A73-22745

Gravitational constant constancy from 1663-1972 earth rotation and 1943-1972 stellar occultations by moon, discussing various time scales used

09 p1079 A73-22948

Out-of-plane motion about libration points - Non-linearity and eccentricity effects.

11 p1423 A73-26069

The angular diameter of upsilon Capricorni and an occultation of SAO 118655.

12 p1540 A73-27427

On the results of observations of occultations of stars by the moon according to the double image principle

13 p1686 A73-29559

GX5-1 X ray source position determination from lunar occultation observations by Copernicus satellite, noting error bounds

20 p2605 A73-39014

Detection of a gamma-ray spectral line from the galactic-center region.

20 p2602 A73-39438

X-ray studies of the Crab nebula occultations, 1974-75.

21 p2765 A73-40300

LUNAR ORBITER

Concentric craters on the moon

01 p0102 A73-10943

Lunar gravity model obtained by using spherical harmonics with mascon terms.

04 p0495 A73-14811

An empirically derived lunar gravity field.

04 p0498 A73-15184

Concentric craters on the moon.

09 p1147 A73-22738

LUNAR ORBITS

Determination of lunar orbital elements by the method of equal altitudes.

03 p0372 A73-13247

Resonance rotation of celestial bodies and Cassini's laws.

03 p0377 A73-14275

Gravitational constant variations from natural satellites and lunar observation, discussing tidal problems solution from lunar orbit tracking

03 p0377 A73-14310

A control system for soft landings on the lunar surface

05 p0595 A73-16424

Possibility for observational verification of the relativistic motion of the periselenuum of artificial satellites of the moon

06 p0748 A73-17765

Lunar gravity derived from long-period satellite motion - A proposed method.

10 p1283 A73-24664

Solar and lunar eclipses, orbits and perturbations prediction from Saros / recurring time periods/

12 p1540 A73-27481

Apollo 15 and 16 lunar orbital X and gamma ray spectrometer for lunar surface composition and radioisotopes surveys, detailing experimental results

16 p2015 A73-33553

Explorer 35 lunar studies, discussing orbit characteristics, circumlunar magnetic field, surface electromagnetic properties and solar wind model

16 p2065 A73-33782

- Selection of a trajectory for the return to earth from lunar orbit of an artificial satellite 18 p2351 A73-36106
- Quasi-periodic orbits about the translunar libration point. 18 p2352 A73-36420
- Cost reductions in transportation to geosynchronous and lunar orbits by a swing station. 19 p2490 A73-37193
- LUNAR PERTURBATION**
- U LUNAR EFFECTS**
- LUNAR PHASES**
- On a possible relation between lunar transient phenomena and the earth-shine /Research note/. 10 p1277 A73-20482
- LUNAR PHOTOGRAPHS**
- Catalog of selenographic coordinates for libration-zone and far-side points. 04 p0503 A73-16017
- Luna 20 landing site geologic setting from Apollo 16 panoramic photographs, discussing complexly faulted terrain 05 p0618 A73-16826
- Photogeologic interpretations of Apollo 14 orbital photographs of far side craters and lunar surface formations 07 p0879 A73-19681
- Astronaut observations from lunar orbit and their geologic significance. 07 p0879 A73-19682
- Lunar surface properties as determined from earthshine and near-terminator photography. 07 p0897 A73-19892
- Endogenic craters count and measurement for Hyginus Rille floor, establishing size distributions by Lunar Orbiter 5 photographs processing 07 p0900 A73-20278
- Apollo 15 optical bar panoramic lunar surface photography, considering luminance, exposure time, resolution and camera performance 08 p0970 A73-21735
- Lunar crater structure geological and morphological interpretations from lunar maria photographs in terms of age, density and stony debris size distribution 13 p1672 A73-28115
- LUNAR PHOTOGRAPHY**
- Concentric craters on the moon 01 p0102 A73-10943
- New geological findings in Apollo 15 lunar orbital photography. 07 p0878 A73-19680
- Lunar control densification with panoramic space photography. 08 p0968 A73-21702
- Reduction of lunar panoramic photography on the analytical stereoplotter. 09 p1081 A73-22379
- Remote sensing of lunar color differences using isoluminous enhancement techniques. 09 p1082 A73-22384
- Concentric craters on the moon. 09 p1147 A73-22738
- Investigation of the lunar surface with the aid of a polarivisor-discriminator 16 p2063 A73-33759
- Ultraviolet measurements of the moon in the 1950- to 2750-A band 16 p2064 A73-33765
- Mathematical lunar cartography based on networks of reference points and absolute elevation heights, considering progress since Luna orbiters launchings in 1959 16 p2064 A73-33774
- LUNAR PROBES**
- NT LUNIK LUNAR PROBES
- NT LUNIK 9 LUNAR PROBE
- NT LUNIK 13 LUNAR PROBE
- NT LUNIK 16 LUNAR PROBE
- NT LUNIK 17 LUNAR PROBE
- NT LUNIK 20 LUNAR PROBE
- NT SURVEYOR LUNAR PROBES
- NT SURVEYOR 3 LUNAR PROBE
- Russian book on lunar study by telescopes and un-manned and manned spacecraft covering Luna Zond and Lunokhod probes, Apollo flights, topography, structure and magnetic field 19 p2485 A73-37770
- LUNAR PROGRAMS**
- NT APOLLO PROJECT
- Engineering potential for lunar missions after Apollo. 03 p0380 A73-13087
- LUNAR RADAR ECHOES**
- Lunar radar mapping at 162.4 MHz from Jodrell Bank observation: in January and February 1970, discussing depolarized returns 03 p0368 A73-13084
- Lunar topography - First radar-interferometer measurements of the Alphonso-Ptolemaeus-Arzachel region. 03 p0378 A73-14446
- Moon and Venus relief from backscattering diagrams based on radar echoes, calculating root-mean-square angles of surface inclination 03 p0379 A73-14568

- Lunar maps from CW radar imagery by aperture synthesis method at long wavelengths, noting depolarized return from highland regions 04 p0417 A73-15178
- Specific effective scattering area of the surface of the moon, Mars, and Venus in the radio-frequency range. 12 p1543 A73-27639
- Dual frequency bistatic radar lunar investigations from Apollo 14 and 15 echo spectra 20 p2612 A73-39714

LUNAR RADIATION

- Characteristics of the lunar photoelectron layer in the geomagnetic tail. 04 p0492 A73-15529
- Lunar polarized 1420 MHz thermal radio emission aperture synthesis maps evaluation 06 p0752 A73-18237
- Observation of lunar radon emanation with the Apollo 15 alpha particle spectrometer. 07 p0891 A73-19826
- An explanation of transient lunar phenomena from studies of static and fluidized lunar dust layers. 07 p0895 A73-19863
- Structure of lunar maria from their albedo data 07 p0902 A73-20323
- Extinct lunar radio activities - Xenon from Pu-244 and I-129 in Apollo 14 breccias. 08 p0936 A73-20843
- Detection of radon emanation from the crater Aristarchus by the Apollo 15 alpha particle spectrometer. 08 p1009 A73-21222
- Lunar surface radioactivity - Preliminary results of the Apollo 15 and Apollo 16 gamma-ray spectrometer experiments. 08 p1009 A73-21224
- Radiative heat transport models for evacuated powder to specify IR radiation environment on lunar surface 10 p1282 A73-24645
- The moon as a proposed radiometric standard for microwave and infrared observations of extended sources. 11 p1426 A73-26545
- Albedo distribution in lunar maria. 12 p1540 A73-27295
- A recalibration of the quiet sun millimeter spectrum based on the moon as an absolute radiometric standard. 12 p1545 A73-27840
- Results of lunar surface investigations based on its intrinsic radiation 13 p1672 A73-28116
- Moonlight polarization study and the nature of the lunar surface 16 p2063 A73-33758
- Some results of lunar surface luminescence studies at the Kharkov Astronomical Observatory 16 p2063 A73-33762
- Infrared radiation of the moon at 3.5 to 3.9 microns 16 p2064 A73-33764
- Lunar radio emission in the 1.25- to 2.5-cm band 16 p2064 A73-33767
- Radio emission from the moon and sun at the 2.25-mm wavelength and from Jupiter at the 2.1-mm wavelength 16 p2064 A73-33768
- Radio emission of the moon at millimeter and sub-millimeter wavelengths 16 p2064 A73-33769
- Some results of a theoretical study of radio emission polarization on a rough moon 16 p2064 A73-33770
- Physical nature of the lunar surface albedo 19 p2480 A73-37234
- Lunar orbital gamma ray measurements from Apollo 15 and Apollo 16. 21 p2762 A73-41397
- Expected gamma ray emission spectra from the lunar surface as a function of chemical composition. 22 p2903 A73-42494
- The effects of scattering and conduction upon radiative transfer in lunar and Mercurian surfaces. 24 p3133 A73-44541

LUNAR RANGEFINDING

- Laser reflector for earth/moon laser telemetry. 07 p0833 A73-18983
- Analysis and interpretation of lunar laser altimetry. 07 p0823 A73-19827
- Influence of ephemerides errors on various determinations using laser lunar ranging 11 p1417 A73-25266
- Lunar range measurements with a high-radiance frequency-doubled neodymium-glass laser system. 14 p1756 A73-30152
- Potentialities of lunar laser ranging for measuring tectonic motions. 15 p1873 A73-32201
- Lunar laser telemetry technological developments, discussing light beam generation and detection, SNR and ranging accuracy improvements, and receiver-optics diameter reduction 21 p2774 A73-41407

- Laser range measurement to lunar surface retroreflector, discussing initial Apollo 11 observations and achieved lunar orbit and selenophysical information accuracy improvement 24 p3137 A73-44686

LUNAR RETROREFLECTORS

- Geodesy information and accuracy obtainable by laser ranging from earth onto lunar retroreflector packages 04 p0495 A73-14810
- Optical instrumentation for satellite attitude control, solar direction and earth magnetic field sensors, thermal detection, star tracking and Lunokhod 1 laser reflector 07 p0821 A73-18979
- Laser reflector for earth/moon laser telemetry. 07 p0833 A73-18983
- Determination of lunar libration by earth-moon laser ranging 08 p1004 A73-20910
- Analysis of the first laser echoes obtained on the reflector of Luna 21 13 p1686 A73-29561
- Lunar range measurements with a high-radiance frequency-doubled neodymium-glass laser system. 14 p1756 A73-30152
- Laser transit-time measurements between the earth and the moon with a transportable system. 15 p1873 A73-32265
- The influence of laser ranging on selenodetic control. 21 p2774 A73-41408

LUNAR ROCKS

- Preliminary observations of stratified rocks of the Hadley Appennines photographed by the Apollo 15 astronauts 01 p0095 A73-10268
- Comparison of the linear polarization and albedo of volcanic rocks in the spectral region between 0.75 and 3.0 microns with the values of these parameters for the moon 01 p0101 A73-10841
- Sedimentology of clastic rocks returned from the moon by Apollo 15. 01 p0103 A73-11016
- Major, minor and trace elements, specific gravities and refraction indices of Ivory Coast tektites, comparing composition to Bosumtwi crater glasses and Apollo lunar materials 01 p0109 A73-11475
- Russian book - Fundamentals of lunar soil science: Physicochemical properties of lunar soils. 02 p0211 A73-11893
- Investigation of the chemical composition of lunar surface along the route of Lunokhod 1. 02 p0212 A73-12228
- Rare gases in the regolith from the Sea of Fertility. 02 p0212 A73-12229
- Luna 16 rock composition, gamma radiation and natural radioactive element content determination by neutron activation and radiometric analysis 02 p0213 A73-12230
- Radioactive crystallization ages of Apollo 14 basaltic rocks from Fra Mauro formation, comparing with Apollo 11 samples 02 p0213 A73-12231
- Luna 16 powdery regolith specimens magnetic properties, giving specific susceptibility, remanent magnetization and structure related recession 02 p0213 A73-12236
- The infrared reflection, emission and absorption spectra of regolith from the Sea of Fertility and its scattering coefficient. 02 p0213 A73-12237
- Geomorphological analysis of the area of Mare Imbrium explored by the automatic roving vehicle Lunokhod 1. 02 p0213 A73-12240
- The composition and crystalline structure of the minerals of regolith from the Sea of Fertility. 02 p0214 A73-12243
- Lunar surface cratering history from Apollo rock age data, implying earth-moon and solar system evolution mechanism 02 p0217 A73-12406
- Apollo 14 lunar rock ultrabasic fragments chemical analysis, noting pyroxene and olivine compositions 02 p0219 A73-12441
- Comparative analysis of the magnetic properties of lunar rocks and meteorites 02 p0220 A73-12464
- Lunar breccias lithification and metamorphism model construction from experimental and analytical data, discussing scale of lunar metamorphic temperatures 02 p0220 A73-12476
- The composition of the lunar highlands - Evidence from modal and normative plagioclase contents in anorthositic lithic fragments and glasses. 02 p0220 A73-12478
- Lunar rock C 14 production rate as function of depth, discussing solar and galactic cosmic radiation induced nuclear reactions 02 p0220 A73-12479

Stability relations of ilmenite and ulvoespinel in the Fe-TiO system and application of these data to lunar mineral assemblages.

02 p0220 A73-12482

The Rb-Sr age of a crystalline rock from Apollo 16.

02 p0220 A73-12483

Lunar gabbroic rock internal origin hypothesis supported by petrologic data, giving temperature interval of crystallization from dry silicate melt

03 p0369 A73-13095

The valence states of 3d - Transition elements in Apollo 11 and 12 rocks.

03 p0369 A73-13097

Luminescence excitation by protons and electrons, applied to Apollo lunar samples.

03 p0369 A73-13098

Low energy solar nuclear particle irradiation of lunar and meteoritic breccias.

03 p0361 A73-13100

Trapped electrons decay to ground state via nonthermal process in lunar samples during thermoluminescence emission at lunar day temperatures, proposing quantitative model

03 p0369 A73-13101

Fossil particle tracks in lunar materials, discussing track densities implications, production rates via cosmic ray spallation and interpretation for rock ages and erosion rates

03 p0361 A73-13102

Moon and solar system origin in view of chemical evidence and Apollo lunar rock RB-87/SR-87 ages and remelting conditions

03 p0370 A73-13111

Comparative petrology of Apollo 16 sample 68415 and Apollo 14 samples 14276 and 14310.

03 p0375 A73-14103

A point of phase equilibria interpretation in connection with lavas from the Apollo 12 site.

03 p0375 A73-14106

Lunar 'dunite', 'pyroxenite' and 'anorthosite.'

03 p0375 A73-14108

Phase diagrams, microstructure and interface composition of two phase metallic particles from lunar soils and rocks, determining equilibrium temperature and equilibration time

03 p0376 A73-14110

Oxygen from electrolyzed lunar rocks - A discussion of the energetics.

03 p0253 A73-14169

Microfracture effects on seismic wave propagation velocity and Q factor in lunar rocks by Rayleigh ultrasonic surface wave technique

04 p0497 A73-15125

Comparison of the analytical results from the Surveyor, Apollo, and Luna missions.

04 p0498 A73-15185

The mineralogy, petrology and geochemistry of lunar samples - A review.

04 p0498 A73-15186

Infrared spectroscopy of regolith /Luna-16 interplanetary probe/.

05 p0612 A73-16088

The Apollo 16 lunar samples - Petrographic and chemical description.

05 p0614 A73-16319

Apollo 16 exploration of Descartes - A geologic summary.

05 p0614 A73-16320

Breccias from the lunar highlands - Preliminary petrographic report on Apollo 16 samples 60017 and 63335.

05 p0615 A73-16322

Spinel troctolite and anorthosite in Apollo 16 samples.

05 p0615 A73-16323

K, Rb, Sr, Ba contents and rare earths in specimens from the Apollonius lunar mountains/ crater region brought back by the Soviet probe Luna 20

05 p0546 A73-16829

Rb-87/Sr-87 'ages' of the soil and rock fragments brought back from the lunar mountains by the automatic probe Luna 20 /Apollonius crater region/

05 p0546 A73-16830

Moon geochronology from U-Pb systematics applied to lunar basalt data, discussing two and three stage evolutionary models based on Pb isotope ratios

05 p0618 A73-16834

The origin and stability of lunar goethite, hematite and magnetite.

05 p0618 A73-16836

The magnetic properties and morphology of metallic iron produced by subsolidus reduction of synthetic Apollo 11 composition glasses.

05 p0619 A73-16837

An experimental investigation of the significance of zirconium partitioning in lunar ilmenite and ulvoespinel.

05 p0619 A73-16838

The determination of iron, titanium, and nickel in Apollo 14 samples by cathode ray polarography.

06 p0660 A73-17899

Low molecular weight compounds of organogenic elements on Apollo 11 and 12 fines and breccias obtained by vacuum pyrolysis, acid hydrolysis and crushing

06 p0654 A73-18418

Terrestrial contamination in Apollo lunar samples.

06 p0754 A73-18425

Metallic Fe-Ni-S lunar core as source of remanent magnetism in lunar rocks, consistent with thermal models

07 p0877 A73-19654

Petrography and crystallization history of basalts 14310 and 14072.

07 p0879 A73-19685

Petrology of Fra Mauro basalt 14310.

07 p0879 A73-19687

Some textures in Apollo 12 lunar igneous rocks and in terrestrial analogs.

07 p0879 A73-19688

Lunar rocks petrogenesis, determining liquidus and solidus temperatures and crystalline phases sequence in lunar samples and synthesized oxides and silicates

07 p0879 A73-19689

Role of water in the evolution of the lunar crust: An experimental study of sample 14310 - An indication of lunar calc-alkaline volcanism.

07 p0880 A73-19691

Electron petrography of Apollo sample 14310.

07 p0880 A73-19692

Mineralogical evidence for subsolidus vapor-phase transport of alkalis in lunar basalts.

07 p0880 A73-19693

Petrographic features and petrologic significance of melt inclusions in Apollo 14 and 15 rocks.

07 p0880 A73-19694

Uranium and potassium fractionation in pre-Imbrian lunar crustal rocks.

07 p0880 A73-19695

Electron microprobe investigations of the oxidation states of Fe and Ti in ilmenite in Apollo 11, Apollo 12, and Apollo 14 crystalline rocks.

07 p0880 A73-19696

Fra Mauro crystalline rocks - Mineralogy, geochemistry and subsolidus reduction of the opaque minerals.

07 p0880 A73-19698

Mineralogical and petrographic features of two Apollo 14 rocks.

07 p0880 A73-19699

The major element compositions of lunar rocks as inferred from glass compositions in the lunar soils.

07 p0880 A73-19700

Analysis of Fra Mauro samples and the origin of the Imbrium Basin.

07 p0880 A73-19701

Electron petrography of Apollo 14 and 15 rocks.

07 p0881 A73-19702

Crystallography and chemical trends of orthopyroxene-pigeonite from rock 14310 and coarse fine 12033.

07 p0881 A73-19703

Pyroxenes as recorders of lunar basalt petrogenesis - Chemical trends due to crystal-liquid interaction.

07 p0881 A73-19704

Pyroxenes from breccia 14303.

07 p0881 A73-19705

Fe/2+/-Mg site distribution in Apollo 12021 clinopyroxenes - Evidence for bias in Moessbauer measurements, and relation of ordering to exsolution.

07 p0881 A73-19706

Distinct subsolidus cooling histories of Apollo 14 basalts.

07 p0881 A73-19707

Clinopyroxenes from Apollo 12 and 14 - Exsolution, domain structure, and cation order.

07 p0881 A73-19708

Crystal field spectra of lunar pyroxenes.

07 p0881 A73-19709

Crystal-field effects of iron and titanium in selected grains of Apollo 12, 14, and 15 rocks, glasses, and fine fractions.

07 p0881 A73-19710

Lunar plagioclase and pyroxene observation for lamella thicknesses by X ray diffraction, noting twinning, exsolution and crystal disorder effects

07 p0788 A73-19711

Lunar plagioclase - A mineralogical study.

07 p0881 A73-19712

Twin laws, optic orientation, and composition of plagioclases from rocks 12051, 14053, and 14310.

07 p0881 A73-19713

Plagioclase and Ba-K phases from Apollo samples 12063 and 14310.

07 p0881 A73-19714

Crystallographic studies of lunar plagioclases from samples 14053, 14163, 14301, and 14310.

07 p0882 A73-19715

On the amount of ferric iron in plagioclases from lunar igneous rocks.

07 p0882 A73-19716

Metamorphism of Apollo 14 breccias.

07 p0882 A73-19717

Apollo 14 breccias - General characteristics and classification.

07 p0882 A73-19718

Apollo 14 breccia 14313 - A mineralogic and petrologic report.

07 p0882 A73-19719

Chondrules in Apollo 14 samples and size analyses of Apollo 14 and 15 fines.

07 p0882 A73-19720

Chemical classification and composition of Apollo 11, 12, 14 and 15 soil samples glasses, describing breccias and chondrules

07 p0882 A73-19723

Vapor phase crystallization in Apollo 14 breccia.

07 p0882 A73-19724

Apollo 14 regolith and fragmental rocks, their compositions and origin by impacts.

07 p0883 A73-19725

Mineralogy, petrology, and chemical composition of lunar samples 15085, 15256, 15271, 15471, 15475, 15476, 15535, 15555, and 15556.

07 p0883 A73-19727

Experimental petrology and origin of Fra Mauro rocks and soil.

07 p0883 A73-19728

Thermal and mechanical history of breccias 14306, 14063, 14270, and 14321.

07 p0883 A73-19729

Rock 14068 - An unusual lunar breccia.

07 p0883 A73-19732

The magnesian spinel-bearing rocks from the Fra Mauro formation.

07 p0883 A73-19733

Deformation of silicates in some Fra Mauro breccias.

07 p0883 A73-19734

Apollo 14 glasses of impact origin and their parent rock types.

07 p0883 A73-19735

Compositions and mineralogy of lithic fragments in 1-2 mm soil samples 14002, 7 and 14258, 33.

07 p0884 A73-19739

Noritic fragments in the Apollo 14 and 12 soils and the origin of Oceanus Procellarum.

07 p0884 A73-19741

Glassy particles in Apollo 14 soil 14163, 88 - Peculiarities and genetic considerations.

07 p0885 A73-19747

Mineralogy, petrology, and surface features of some fragmental material from the Fra Mauro site.

07 p0885 A73-19748

Electron microscopy of some experimentally shocked counterparts of lunar minerals.

07 p0885 A73-19750

Distribution of elements between different phases of Apollo 14 rocks and soils.

07 p0885 A73-19751

Oxygen and bulk element composition studies of Apollo 14 and other lunar rocks and soils.

07 p0885 A73-19752

Chemical characteristics of trace element rich KREEP basaltic rocks from Apollo 12 landing site

07 p0885 A73-19753

Bulk, rare earth, and other trace elements in Apollo 14 and 15 and Luna 16 samples.

07 p0885 A73-19754

Apollo 14 regolith fractions and soil breccia compositional characteristics by neutron activation analysis

07 p0885 A73-19755

Compositional data for twenty-one Fra Mauro lunar materials.

07 p0885 A73-19756

Elements abundances in Apollo 14 and 15 soils and breccias and in eucrite Juvinas and howardite Kapoeta, suggesting initial chemical layering of moon

07 p0886 A73-19758

Major, minor, and trace element data for some Apollo 11, 12, 14, and 15 samples.

07 p0886 A73-19759

Precise determination of rare-earth elements in the Apollo 14 and 15 samples.

07 p0886 A73-19762

Analysis of lunar samples 14163, 14259, and 14321 with isotopic data for Li-7/Li-6.

07 p0887 A73-19766

The abundances of components of the lunar soils by a least-squares mixing model and the formation age of KREEP.

07 p0887 A73-19769

O-18/O-16, Si-30/Si-28, C-13/C-12, and D/H studies of Apollo 14 and 15 samples.

07 p0887 A73-19771

Oxygen isotopic compositions and oxygen concentrations of Apollo 14 and Apollo 15 rocks and soils.

07 p0887 A73-19772

Apollo 14 mineral ages and the thermal history of the Fra Mauro formation.

07 p0887 A73-19776

Rb-Sr systematics for chemically defined Apollo 14 breccias.

07 p0888 A73-19778

The ages of lunar material from Fra Mauro, Hadley Rille, and Spur Crater.

07 p0888 A73-19780

Lunar rocks age determination by Ar isotopes technique, noting plagioclase gas retention and cosmic ray exposure characteristics

07 p0888 A73-19782

Ar-40/Ar-39 ages of Apollo 14 and 15 samples.

07 p0888 A73-19783

Uranium and extinct Pu-244 effects in Apollo 14 materials.

07 p0888 A73-19784

Abundances of primordial and cosmogenic radionuclides in Apollo 14 rocks and fines.

07 p0888 A73-19787

Primordial radioelements and cosmogenic radionuclides in lunar samples from Apollo 15.

07 p0888 A73-19788

Gamma-ray measurements of Apollo 12, 14, and 15 lunar samples.

07 p0888 A73-19789

Cosmic-ray produced radioisotopes in Apollo 12 and Apollo 14 samples.

07 p0870 A73-19791

Argon, radon, and tritium radioactivities in the sample return container and the lunar surface.

07 p0870 A73-19792

Radionuclides in lunar rocks from solar and galactic cosmic ray bombardment, examining long and short-lived isotopes activity

07 p0889 A73-19793

Solar flare intensity estimation based on measurements for Ar 37 radioactivities and depth dependence of tritium in Apollo 11 and 12 lunar rock samples

07 p0889 A73-19794

Alpha spectrometry of a surface exposed lunar rock.

07 p0870 A73-19796

Vanadium isotopic composition and the concentrations of it and ferromagnesian elements in lunar material.

07 p0889 A73-19797

Rare-gas analyses on neutron irradiated Apollo 12 samples.

07 p0889 A73-19798

Noble gas studies on regolith materials from Apollo 14 and 15.

07 p0889 A73-19799

Trapped solar wind noble gases in Apollo 12 lunar fines 12001 and Apollo 11 breccia 10046.

07 p0871 A73-19800

Inert gases from Apollo 12, 14, and 15 fines.

07 p0889 A73-19801

Apollo 14 and 15 lunar rocks and soils rare gas content via fast neutron irradiation, noting radioactive age determination

07 p0889 A73-19802

Cosmic ray exposure ages from Apollo 14 lunar rocks isotopic anomalies due to neutron capture effect in Gd, Br and Ba

07 p0871 A73-19803

Classification and source of lunar soils; elastic rocks; and individual mineral, rock, and glass fragments from Apollo 12 and 14 samples as determined by the concentration gradients of the helium, neon, and argon isotopes.

07 p0889 A73-19804

Trace element relations between Apollo 14 and 15 and other lunar samples, and the implications of a moon-wide Cl-KREEP coherence and Pt-metal non-coherence.

07 p0890 A73-19810

Thermal volatilization studies on lunar samples.

07 p0890 A73-19811

Total nitrogen contents of some Apollo 14 lunar samples by neutron activation analysis.

07 p0890 A73-19815

Chemically bound nitrogen abundances in lunar samples, and active gases released by heating at lower temperatures /250 to 500 C/.

07 p0890 A73-19817

Analysis of organogenic compounds in Apollo 11, 12, and 14 lunar samples.

07 p0890 A73-19819

Compounds of carbon and other volatile elements in Apollo 14 and 15 samples.

07 p0891 A73-19822

Some surface characteristics and gas interactions of Apollo 14 fines and rock fragments.

07 p0891 A73-19831

Iron-titanium-chromite, a possible new carrier of remanent magnetization in lunar rocks.

07 p0892 A73-19836

Remanent magnetization of Apollo 14 rocks and fines, discussing iron contribution and early internal magnetic field

07 p0892 A73-19837

On the remanent magnetism of lunar samples with special reference to 10048,55 and 14053,48.

07 p0892 A73-19838

Lunar breccia 14321 natural remanent magnetization characteristics from alternating field and thermal demagnetization tests, describing magnetic measurement procedures

07 p0893 A73-19841

Apollo 14 and 15 igneous rock, fines and breccia intrinsic and structure-sensitive magnetic parameters

07 p0893 A73-19842

Lunar surface rock remanent magnetization, considering breccia, igneous samples, thermal demagnetization and Apollo landing sites

07 p0893 A73-19843

Apollo 14 samples with Fe-bearing minerals examined by Mossbauer spectroscopy, noting parallelism with Apollo 11 and 12 samples

07 p0893 A73-19845

Nuclear magnetic resonance properties of lunar samples.

07 p0893 A73-19846

Magnetic phases in lunar material and their electron magnetic resonance spectra - Apollo 14.

07 p0894 A73-19847

Elastic wave velocities and thermal diffusivities of Apollo 14 rocks.

07 p0894 A73-19851

Elastic velocity and Q factor measurements on Apollo 12, 14, and 15 rocks.

07 p0894 A73-19852

Ultrasonic P and S waves velocity of Apollo 14 and 15 lunar igneous and breccia rocks for elastic properties determination, noting cracks distribution function

07 p0894 A73-19853

Applications to lunar geophysical models of the velocity-density properties of lunar rocks, glasses, and artificial lunar glasses.

07 p0894 A73-19854

Thermal expansion of Apollo lunar samples and Fairfax diabase.

07 p0895 A73-19855

Apollo 14 returned lunar rock fine thermal conductivity measurement as function of temperature under vacuum conditions, using least squares curve fitting method

07 p0895 A73-19856

Lunar micrometeoroid flux, calculating rocks survival time before impact damage and mass wasting rate by single particle abrasion

07 p0895 A73-19865

Microcrater size frequency distribution and exposure age for Apollo 12 and 14 rocks

07 p0896 A73-19868

Collision controlled radiation history of the lunar regolith.

07 p0871 A73-19870

Radiation and shock effects on Apollo 14 and 15 breccias substructure history, reporting optical microscope observations of solar flares and cosmic ray tracks

07 p0896 A73-19872

Track studies of Apollo 14 rocks, and Apollo 14, Apollo 15, and Luna 16 soils.

07 p0896 A73-19873

Solar flare and galactic cosmic ray studies of Apollo 14 and 15 samples.

07 p0871 A73-19876

Interlaboratory comparison for solar flare track density data on feldspars in individual sections of lunar rock 14310, noting depth dependence and irradiation history

07 p0896 A73-19878

Thermoluminescence of Apollo 14 lunar samples following irradiation at -196 C.

07 p0897 A73-19879

Thermoluminescence of Apollo 12 samples - Implications for lunar temperature and radiation histories.

07 p0897 A73-19880

Luminescence of Apollo 14 and Apollo 15 lunar samples.

07 p0897 A73-19882

Thermoluminescence of individual grains and bulk samples of lunar fines.

07 p0897 A73-19883

Electronic spectra of pyroxenes and interpretation of telescopic spectral reflectivity curves of the moon.

07 p0897 A73-19885

Far infrared properties of lunar rock.

07 p0897 A73-19886

Infrared and Raman spectroscopic studies of structural variations in minerals from Apollo 11, 12, 14, and 15 samples.

07 p0897 A73-19887

Far infrared and Raman spectroscopic investigations of lunar materials from Apollo 11, 12, 14, and 15.

07 p0897 A73-19889

Reflectance and absorption spectra of Apollo 11 and Apollo 12 samples.

07 p0897 A73-19890

Dielectric properties of Apollo 14 lunar samples at microwave and millimeter wavelengths.

07 p0898 A73-19894

Dielectric properties of Apollo 14 lunar samples.

07 p0898 A73-19895

Electrical conductivity and Moessbauer study of Apollo lunar samples.

07 p0898 A73-19896

Grain size analysis, optical reflectivity measurements, and determination of high-frequency electrical properties for Apollo 14 lunar samples.

07 p0898 A73-19897

The kinetics of ulvöspinel reduction - Synthetic study and applications to lunar rocks.

08 p0936 A73-20840

Constrained least-squares analysis of petrologic problems with an application to lunar sample 12040

08 p0936 A73-20842

Extinct lunar radio activities - Xenon from Pu-244 and I-129 in Apollo 14 breccias.

08 p0936 A73-20843

Electron microprobe chemical analysis and structural formula of niobian rutile in Apollo 14 microbreccia sample KREEP fragment

09 p1139 A73-21856

Graphical method of profiling and contouring microcraters on lunar rocks from stereomicrograph pair obtained by scanning electron microscope

09 p1081 A73-22378

Thermal diffusivity of lunar rocks under atmospheric and vacuum conditions.

09 p1148 A73-22872

Lunar interior temperature profiles from olivine and pyroxene electrical conductivity data, indicating high temperature accretion from hydrogen depleted material

09 p1148 A73-22874

Isotopic and crystalline structure changes in lunar rock and meteorite constituents for cosmic ray nuclei intensity and energy spectrum

09 p1138 A73-23169

Volatilization studies on a terrestrial basalt and their applicability to volatilization from the lunar surface.

10 p1275 A73-23738

Displaced mass, depth, diameter, and effects of oblique trajectories for impact craters formed in dense crystalline rocks.

10 p1276 A73-24077

Lunar soil density estimation from Lunar Orbiter photographic measurements of boulder tracks, determining friction angle

10 p1277 A73-24085

On the model of the accumulation of the moon compatible with the data on the composition and the age of lunar rocks.

10 p1277 A73-24086

Tracks from extinct radioactivity, ancient cosmic rays, and calibration ions.

10 p1269 A73-24271

Photomicrographic investigation of plutonic and metamorphic equilibration in polished thin sections of Apollo 16 feldspathic microbreccia samples from North Ray crater rim

11 p1326 A73-25863

Apollo 15 mare olivine and quartz basalts major and trace element composition and petrogenesis, deriving model of magma genesis

12 p1466 A73-27545

Apollo 15 soil and rock particle tracks density and stability and uranium content

12 p1542 A73-27547

Luna 20: A study of samples from the lunar highlands returned by the unmanned Luna 20 spacecraft.

13 p1674 A73-28301

Oxide minerals in lithic fragments from Luna 20 fines.

13 p1674 A73-28306

Petrology of fine-grained rock fragments and petrologic implications of single crystal from the Luna 20 soil.

13 p1674 A73-28307

Petrology of Luna 20 regolith from the lunar highlands.

13 p1675 A73-28311

Fossil track and thermoluminescence studies of Luna 20 material.

13 p1675 A73-28312

The age and petrography of two Luna 20 fragments and inferences for widespread lunar metamorphism.

13 p1675 A73-28319

Luna 20 soil and rock fragments chemical composition from neutron activation analysis, noting low rare earth content and contamination with W and Mo

13 p1676 A73-28321

Luna 20 metaigneous rocks, breccia and soil and Apollo 16 soils chemical composition by neutron activation analysis, tabulating major, minor and trace elements

13 p1676 A73-28323

Siderophile and volatile elements in Luna 20 fine soil and breccia samples from radiochemical neutron activation analysis, noting comparing with Apollo 16 results

13 p1676 A73-28325

Mineralogy, petrology and chemistry of lithic fragments from Luna 20 fines - Origin of the cumulate ANT suite and its relationship to high-alumina and mare basalts.

13 p1676 A73-28328

Compositional and X-ray data for Luna 20 feldspar.

13 p1677 A73-28334

The Luna 20 lithic fragments, and the composition and origin of the lunar highlands.

13 p1677 A73-28336

Xenoliths in maars and diatremes with inferences for the moon, Mars, and Venus.

13 p1681 A73-28848

Zinc, lead, chlorine and FeOOH-bearing assemblages in the Apollo 16 sample 66095 - Origin by impact of a comet or a carbonaceous chondrite.

13 p1686 A73-29565

Apollo 17 landing site crystalline rock age determinations for coarse grained basalt and anorthositic gabbro samples via Ar isotope ratios

14 p1788 A73-29720

Apollo 17 basalt ortho- and para-armalcolite, noting differences in optical properties, crystal habit and distribution between coarse and fine grained rocks
14 p1789 A73-29739

Natural exoelectron emission from anorthositic rocks supplied by the Luna-20 automatic interplanetary station
14 p1802 A73-30833

Comparison of linear polarization and albedo of igneous rocks in the spectral region 0.75-3.0 μ m and lunar values of those parameters.
15 p1928 A73-30977

Volatile elements in Apollo 16 samples - Possible evidence for outgassing of the moon.
15 p1933 A73-31370

Apollo 16 rocks - Petrology and classification.
15 p1937 A73-31850

Comparative analysis of the magnetic properties of lunar rocks and meteorites.
15 p1942 A73-32614

Water vapor from a lunar breccia - Implications for evolving planetary atmospheres.
16 p2060 A73-33124

Lunar surface investigations by the Luna-9 through Luna-13 lunar landers
16 p2063 A73-33753

Distribution and origin of rocks in the landing area of the Luna 13 automatic lunar station
16 p2065 A73-33778

Sintering and hot pressing of Fra Mauro composition glass and the lithification of lunar breccias.
16 p2070 A73-33875

Apollo 15 sample 15597 vitrophyric nature, pyroxenes segregation and textural appearance as evidence for arrival on lunar surface in entirely liquid state
17 p2230 A73-34518

Laser probe mass spectrometric in situ measurements of stable and radioactive Ar isotopes in lunar breccia
17 p2232 A73-35263

Experimental results on combined ultraviolet-proton excitation of moon rock luminescence.
17 p2233 A73-35273

Anisotropy of absorption bands in some lunar, meteoritic, and terrestrial pyroxenes.
17 p2235 A73-35738

Darkening of silicate rock powders by solar wind sputtering.
17 p2235 A73-35740

Lunar sample quarantine procedures - Interaction with non-quarantine experiments.
18 p2281 A73-35978

A response to a comment on U-Pb systematics in lunar basalts.
18 p2354 A73-36512

Chemistry of lunar basalts with very high alumina contents.
18 p2354 A73-36598

Reports of fourth Lunar Science Conference covering lunar rock chemical composition assessment as information source on early solar system, lunar early geologic history, etc
19 p2487 A73-38293

Co-60 concentration measurement for lunar soil and rock samples, determining lunar neutron production rate
21 p2765 A73-40238

Vapor-liquid-solid type growth in lunar glass covered breccia 15015, noting metallic iron stalks with bulbous tips of iron and sulfur mixture.
21 p2766 A73-40412

Rb-87 - Sr-87 age of fragments and soils from the lunar Sea of Fertility.
21 p2770 A73-41005

Experimental data on the investigation of lunar surface chemical composition.
21 p2774 A73-41403

Absorption spectra of lunar sections from different lunar areas.
21 p2774 A73-41406

Russian book - Chemistry of terrestrial and lunar basaltic rocks.
21 p2648 A73-41436

Natural exoelectron emission of anorthositic rocks returned by the automatic interplanetary station Luna-20.
23 p3028 A73-43583

Major and trace elements in igneous rocks from Apollo 15.
23 p2950 A73-43765

Track density gradient and light noble gas isotope analysis of lunar breccia, postulating higher solar flux densities during early brecciation history
23 p2950 A73-43766

A survey of the selenochemistry of major, minor and trace elements.
23 p2951 A73-43768

On Pu-244 in lunar rocks from Fra Mauro and implications regarding their origin.
23 p2951 A73-43771

Production of lunar fragmental material by meteoroid impact.
24 p3129 A73-44447

Ancient lunar mega-regolith and subsurface structure.
24 p3129 A73-44448

LUNAR ROTATION

Rotation of the moon and lunar coordinate systems.
04 p0497 A73-15180

Determination of lunar libration by earth-moon laser ranging
08 p1004 A73-20910

Lunar rotation secular acceleration and tidal friction related to earth rotational velocity and creep properties
13 p1677 A73-28378

Forward precession motion of the moon caused by attraction to the earth and the sun
15 p1939 A73-31966

Deformation of a selenodetic reference system due to errors in lunar rotation constants
17 p2230 A73-34595

Translational-precessional motion of the moon in the gravitational field of the earth and sun.
24 p3132 A73-44491

LUNAR ROVING VEHICLES

NT LUNOKHOD LUNAR ROVING VEHICLES
Digital simulation of the Lunar Roving Vehicle navigation system.
06 p0722 A73-18828

Equations of motion of the lunar roving vehicle.
07 p0808 A73-19490

The development of light tracked vehicles for lunar and planetary exploration
08 p0952 A73-20781

Thermal design and testing of the Apollo 17 lunar traverse gravimeter.
18 p2316 A73-36385

[AIAA PAPER 73-771]
Planetary surface rover/remotely manned system concepts and applications from lunar and Mars mission studies
19 p2416 A73-37312

A study of remote guidance and control for planetary surface vehicles.
19 p2403 A73-37313

Photogrammetry in Apollo lunar roving vehicle conducted geometry and geology exploration, using horizontal stereophotography with special gnomon for sun-line and vertical control
20 p2611 A73-39669

Tracking the Apollo Lunar Rover with interferometry techniques.
23 p2953 A73-43356

LUNAR SATELLITES

NT LUNAR ORBITER
Possibility for observational verification of the relativistic motion of the periselenium of artificial satellites of the moon
06 p0748 A73-17765

Preliminary orbit determination for lunar satellites.
11 p1426 A73-26396

Investigation of the lunar surface by the method of the scattering of radio waves emitted by lunar satellites
16 p2064 A73-33773

Effects of physical librations of the moon on the orbital elements of a lunar satellite.
23 p3032 A73-43841

LUNAR SCATTERING

U DIFFUSE RADIATION

U LUNAR RADAR ECHOES

LUNAR SEISMOGRAPHS

Lunar seismicity interpretation in terms of warm moon based on lunar-therm placement in stable sliding field of rock failure
02 p0219 A73-12437

Lunar interior density constraints from moon moment of inertia and mean density calculations and seismometer data on lunar crust mass and density
02 p0220 A73-12484

Possible sidereal period for the seismic lunar activity.
03 p0367 A73-13057

A possible mechanism of the generating of the unusually long lunar seismic oscillations.
03 p0368 A73-13092

On the interaction between tectonic processes of the earth and the moon.
03 p0299 A73-13093

Lunar tidal phenomena and the lunar Rille system.
03 p0370 A73-13113

Lunar seismic wave velocity change at 25 km interpreted in terms of fine rock powder undergoing final densification
05 p0622 A73-17181

Measurements of the acoustical parameters of rock powders and the Gold-Soter lunar model.
07 p0894 A73-19850

Apollo 17 seismic profiling - Probing the lunar crust.
16 p2059 A73-32903

Lunar structure and dynamics - Results from the Apollo passive seismic experiment.
17 p2236 A73-35744

New seismic data on the state of the deep lunar interior.
17 p2237 A73-35805

Lunar surface fine rock powders seismic measurements in terms of Q factor and acoustic propagation velocity under various temperatures and pressures
20 p2612 A73-39712

LUNAR SHADOW

Supersonic generation of atmospheric gravity waves, via atmospheric cooling by moon shadows during lunar eclipses, noting analogy to terminator action
10 p1211 A73-23825

Concorde-borne astronomical observation for Fraunhofer corona IR and photospheric and chromospheric radiations in lunar shadow during 30 June 1973 solar eclipse
15 p1940 A73-32184

LUNAR SOIL

NT LUNAR DUST

Investigations of mechanical properties of lunar soil by self-propelled vehicle Lunokhod-1.
01 p0104 A73-11104

Investigations of physical and mechanical properties of lunar soil delivered by Luna-16.
01 p0105 A73-11105

The lunar regolith as a site for an astronomical observatory.
01 p0105 A73-11204

Russian book - Fundamentals of lunar soil science: Physicomechanical properties of lunar soils.
02 p0211 A73-11893

Luna 16 direct measurements for soil mechanical properties, determining bulk density, failure characteristics, compressibility and shear and bearing strength
02 p0213 A73-12232

Lunar soil bearing strength, shear and cohesion properties in natural state along Lunokhod 1 self propelled vehicle route
02 p0213 A73-12233

Lunokhod 1 vehicle terrestrial mobility tests, simulating lunar gravity, soil and traction on scale and mockup models
02 p0151 A73-12234

The morphology, types and distribution of sizes of regolith particles in the Sea of Fertility.
02 p0214 A73-12241

Refrigeration of lunar samples destined for thermoluminescence studies.
02 p0219 A73-12439

X-ray study and MOESSBAUER spectroscopy on lunar ilmenites/Apollo 11/.
02 p0220 A73-12480

Thermal cycling and frequency tests for lunar soil dielectric constant, loss tangent and dc conductivity, noting moisture effects
02 p0220 A73-12481

Petrochemistry and chemical features of lunar glassy spherules.
03 p0273 A73-13089

Interferometric studies on Apollo 11 and Apollo 12 lunar glass objects.
03 p0369 A73-13096

Fossil particle tracks in lunar materials, discussing track densities implications, production rates via cosmic ray spallation and interpretation for rock ages and erosion rates
03 p0361 A73-13102

Thallium isotope analysis of terrestrial chondrites and achondrite and lunar soil, noting lunar chronology information from lead isotope extinct radioactivity
03 p0375 A73-14109

Phase diagrams, microstructure and interface composition of two phase metallic particles from lunar soils and rocks, determining equilibrium temperature and equilibration time
03 p0376 A73-14110

Pathomorphological and histochemical analysis of Luna 16 fine lunar soil fraction biological effect on mice
03 p0272 A73-14569

The mineralogy, petrology and geochemistry of lunar samples - A review.
04 p0498 A73-15186

Effect of lunar soil on radiation injuries in mice.
05 p0538 A73-16090

Volatile-rich lunar soil - Evidence of possible cometary impact.
05 p0615 A73-16321

Lunar evolution, age and surface composition data obtained from Apollo missions
05 p0616 A73-16400

Major element composition of Luna 20 glasses.
05 p0546 A73-16827

Luna 20 and Apollo 16 core fines - Large-ion lithophile trace-element abundances.
05 p0546 A73-16828

Rb-87/Sr-87 'ages' of the soil and rock fragments brought back from the lunar mountains by the automatic probe Luna 20/Apollonius crater region/
05 p0546 A73-16830

The chemical composition of soil from the Apollo 16 and Luna 20 sites.
05 p0546 A73-16831

U-Th-Pb systematics in lunar highland samples from the Luna 20 and Apollo 16 missions.
05 p0618 A73-16832

Lunar highlands soil analysis from Luna 20 and Apollo 16 samples, estimating lunar crust differentiation process age from Rb-Sr concentrations
05 p0618 A73-16833

Extralunar materials in Apollo 16 soils and the decay rate of the extralunar flux 4.0 Gy ago.

05 p0618 A73-16835

Dispersion-free X-ray-fluorescent analysis in studies of space and terrestrial objects

05 p0546 A73-17019

Investigation of the gamma-emission of lunar soil delivered by the automatic station Luna 16

05 p0620 A73-17020

Neutron activation analysis of lunar soil brought by 'Luna-16' from Marc Focunditatis

05 p0620 A73-17021

Lunar fines thermal diffusivity measurement, calculating lunar surface temperature distribution

[ALAA PAPER 73-40]

06 p0767 A73-17622

The determination of iron, titanium, and nickel in Apollo 14 samples by cathode ray polarography.

06 p0660 A73-17899

An evaluation of pyrolytic techniques with regard to the Apollo 11, 12 and 14 lunar samples analyses.

06 p0753 A73-18411

Low molecular weight compounds of organogenic elements on Apollo 11 and 12 fines and breccias obtained by vacuum pyrolysis, acid hydrolysis and crushing

06 p0654 A73-18418

Porphyryns analysis in Apollo 11, 12 and 14 soils via analytical demetallation followed by recovery and recomplexing with divalent cations

06 p0753 A73-18420

Terrestrial contamination in Apollo lunar samples.

06 p0754 A73-18425

Lunar samples organic analysis avoiding organic molecules synthesis from indigenous constituents, considering pyrosynthetic and ionic reactions in solution

06 p0662 A73-18426

Difference between the principal element concentrations on the surface and in the volume of lunar regolith particles

07 p0876 A73-19474

Lunar crater Copernicus - Search for debris of impacting body at Apollo 12 site.

07 p0877 A73-19653

A photometric investigation of the packing state of Apollo 11 lunar regolith samples.

07 p0878 A73-19669

Moessbauer spectroscopy of lunar regolith returned by the automatic station Luna 16.

07 p0879 A73-19683

Petrographic features and petrologic significance of melt inclusions in Apollo 14 and 15 rocks.

07 p0880 A73-19694

The major element compositions of lunar rocks as inferred from glass compositions in the lunar soils.

07 p0880 A73-19700

Analysis of Fra Mauro samples and the origin of the Imbrium Basin.

07 p0880 A73-19701

Crystallographic studies of lunar plagioclases from samples 14053, 14163, 14301, and 14310.

07 p0882 A73-19715

Chondrules in Apollo 14 samples and size analyses of Apollo 14 and 15 fines.

07 p0882 A73-19720

Petrology and chemistry of some Apollo 14 lunar samples.

07 p0882 A73-19721

Chemical classification and composition of Apollo 11, 12, 14 and 15 soil samples glasses, describing breccias and chondrules

07 p0882 A73-19723

Mineralogy and origin of Fra Mauro fines and breccias.

07 p0883 A73-19726

Mineralogy, petrology, and chemical composition of lunar samples 15085, 15256, 15271, 15471, 15475, 15476, 15535, 15555, and 15556.

07 p0883 A73-19727

Experimental petrology and origin of Fra Mauro rocks and soil.

07 p0883 A73-19728

Petrology and origin of lithic fragments in the Apollo 14 regolith.

07 p0883 A73-19730

Inclusions and interface relationships between glass and breccia in lunar sample 14306,50.

07 p0883 A73-19731

Chemistry and particle track studies of Apollo 14 glasses.

07 p0884 A73-19736

Structure of lunar glasses by Raman and soft X-ray spectroscopy.

07 p0788 A73-19737

Compositions and mineralogy of lithic fragments in 1-2 mm soil samples 14002,7 and 14258,33.

07 p0884 A73-19739

Apollo 14 soils - Size distribution and particle types.

07 p0884 A73-19740

Noritic fragments in the Apollo 14 and 12 soils and the origin of Oceanus Procellarum.

07 p0884 A73-19741

Chemical and petrographic characterization of Fra Mauro soils.

07 p0884 A73-19742

Metallic particles in the Apollo 14 lunar soil.

07 p0884 A73-19744

On lunar metallic particles and their contribution to the trace element content of Apollo 14 and 15 soils.

07 p0884 A73-19746

Glassy particles in Apollo 14 soil 14163,88 - Peculiarities and genetic considerations.

07 p0885 A73-19747

Distribution of elements between different phases of Apollo 14 rocks and soils.

07 p0885 A73-19751

Oxygen and bulk element composition studies of Apollo 14 and other lunar rocks and soils.

07 p0885 A73-19752

Bulk, rare earth, and other trace elements in Apollo 14 and 15 and Luna 16 samples.

07 p0885 A73-19754

Apollo 14 regolith fractions and soil breccia compositional characteristics by neutron activation analysis

07 p0885 A73-19755

Elements abundances in Apollo 14 and 15 soils and breccias and in eucrite Juvinas and howardite Kapoeta, suggesting initial chemical layering of moon

07 p0886 A73-19758

Apollo 12 lunar KREEP samples possible origin, considering mixture of ejecta from Copernicus, Reinhold and local highlands and Fra Mauro deposits

07 p0886 A73-19763

Analysis of lunar samples 14163, 14259, and 14321 with isotopic data for Li-7/Li-6.

07 p0887 A73-19766

The extralunar component in lunar soils and breccias.

07 p0887 A73-19767

Major impacts on the moon - Characterization from trace elements in Apollo 12 and 14 samples.

07 p0887 A73-19768

The abundances of components of the lunar soils by a least-squares mixing model and the formation age of KREEP.

07 p0887 A73-19769

ESCA-investigation of lunar regolith from the Seas of Fertility and Tranquility.

07 p0887 A73-19770

Oxygen isotopic compositions and oxygen concentrations of Apollo 14 and Apollo 15 rocks and soils.

07 p0887 A73-19772

Isotopic abundance ratios and concentrations of selected elements in Apollo 14 samples.

07 p0887 A73-19773

Apollo 14 and 15 samples - Rb-Sr ages, trace elements, and lunar evolution.

07 p0887 A73-19777

Rb-Sr systematics for chemically defined Apollo 14 breccias.

07 p0888 A73-19778

U-Th-Pb and Rb-Sr measurements on some Apollo 14 lunar samples.

07 p0888 A73-19779

K-Ar dating of lunar fines - Apollo 12, Apollo 14, and Luna 16.

07 p0888 A73-19781

Np-237, U-236, and other actinides on the moon.

07 p0888 A73-19785

Abundances of primordial and cosmogenic radionuclides in Apollo 14 rocks and fines.

07 p0888 A73-19787

Primordial radioelements and cosmogenic radionuclides in lunar samples from Apollo 15.

07 p0888 A73-19788

Lunar surface processes and cosmic ray characterization from Apollo 12-15 lunar sample analyses.

07 p0870 A73-19790

Cosmic-ray produced radioisotopes in Apollo 12 and Apollo 14 samples.

07 p0870 A73-19791

Argon, radon, and tritium radioactivities in the sample return container and the lunar surface.

07 p0870 A73-19792

Study on the cosmic ray produced long-lived Mn-53 in Apollo 14 samples.

07 p0870 A73-19795

Noble gas studies on regolith materials from Apollo 14 and 15.

07 p0889 A73-19799

Inert gases from Apollo 12, 14, and 15 fines.

07 p0889 A73-19801

Apollo 14 and 15 lunar rocks and soils rare gas content via fast neutron irradiation, noting radioactive age determination

07 p0889 A73-19802

Classification and source of lunar soils; clastic rocks; and individual mineral, rock, and glass fragments from Apollo 12 and 14 samples as determined by the concentration gradients of the helium, neon, and argon isotopes.

07 p0889 A73-19804

Isotopic anomalies in lunar rhodium.

07 p0889 A73-19805

A comparison of noble gases released from lunar fines /no. 15601.64/ with noble gases in meteorites and in the earth.

07 p0889 A73-19806

Noble gases concentration profiles in lunar fines and minerals, investigating thermal release patterns

07 p0889 A73-19807

Atmospheric Ar-40 in lunar fines.

07 p0890 A73-19808

Volatilized lead from Apollo 12 and 14 soils.

07 p0890 A73-19809

Trace element relations between Apollo 14 and 15 and other lunar samples, and the implications of a moon-wide Cl-KREEP coherence and Pt-metal non-coherence.

07 p0890 A73-19810

Thermal volatilization studies on lunar samples.

07 p0890 A73-19811

Inorganic gas release and thermal analysis study of Apollo 14 and 15 soils.

07 p0890 A73-19814

Total carbon, nitrogen, and sulfur in Apollo 14 lunar samples.

07 p0890 A73-19816

Survey of lunar carbon compounds. II - The carbon chemistry of Apollo 11, 12, 14, and 15 samples.

07 p0890 A73-19818

Analysis of organogenic compounds in Apollo 11, 12, and 14 lunar samples.

07 p0890 A73-19819

Amino acid precursors in lunar fines from Apollo 14 and earlier missions.

07 p0891 A73-19820

Amino acid analyses of Apollo 14 samples.

07 p0891 A73-19821

Compounds of carbon and other volatile elements in Apollo 14 and 15 samples.

07 p0891 A73-19822

Microphysical, microchemical, and adhesive properties of lunar material. III - Gas interaction with lunar material.

07 p0892 A73-19832

Evidence of lunar surface oxidation processes - Electron spin resonance spectra of lunar materials and simulated lunar materials.

07 p0893 A73-19840

Magnetic phases in lunar material and their electron magnetic resonance spectra - Apollo 14.

07 p0894 A73-19847

Measurements of the acoustical parameters of rock powders and the Gold-Soter lunar model.

07 p0894 A73-19850

Crystallization behavior and glass formation of selected lunar compositions.

07 p0895 A73-19858

Sharply defined upper limit existence for lunar ash flow with heat transfer, presenting altitude dependence of pressure, gas density, temperature and velocity distributions

07 p0895 A73-19864

Collision controlled radiation history of the lunar regolith.

07 p0871 A73-19870

Cosmic ray track densities of Apollo 14 breccias, igneous rock and soils from Fra Mauro, indicating surface residence times

07 p0871 A73-19871

Track studies of Apollo 14 rocks, and Apollo 14, Apollo 15, and Luna 16 soils.

07 p0896 A73-19873

Radiation effects in soils from five lunar missions.

07 p0896 A73-19875

Charge assignment to cosmic ray heavy ion tracks in lunar pyroxenes.

07 p0872 A73-19877

Luminescence of lunar material excited by electrons.

07 p0897 A73-19881

Thermoluminescence of individual grains and bulk samples of lunar fines.

07 p0897 A73-19883

Spectral emission of natural and artificially induced thermoluminescence in Apollo 14 lunar sample 14163,147.

07 p0897 A73-19884

Electronic spectra of pyroxenes and interpretation of telescopic spectral reflectivity curves of the moon.

07 p0897 A73-19885

Midinfrared emission spectra of Apollo 14 and 15 soils and remote compositional mapping of the moon.

07 p0897 A73-19888

Far infrared and Raman spectroscopic investigations of lunar materials from Apollo 11, 12, 14, and 15.

07 p0897 A73-19889

Polarimetric properties of the lunar surface and its interpretation. V - Apollo 14 and Luna 16 lunar samples.

07 p0897 A73-19891

Optical properties of lunar glass spherules from Apollo 14 fines.

07 p0898 A73-19893

Grain size analysis, optical reflectivity measurements, and determination of high-frequency electrical properties for Apollo 14 lunar samples.

07 p0898 A73-19897

Quantitative size and shape analyses of Apollo 14 and 15 fines by computer evaluation of scanning electron microscope images

07 p0898 A73-19898

- Apollo 12 soil sample strength, compressibility, bulk density, porosity and shear wave velocity
07 p0898 A73-19901
- Mechanical properties of lunar soil - Density, porosity, cohesion, and angle of internal friction.
07 p0898 A73-19902
- Lunar soil porosity and its variation as estimated from footprints and boulder tracks.
07 p0898 A73-19903
- On-surface and laboratory size measurements of fine lunar particles.
07 p0900 A73-20184
- Distribution of methane and carbide in Apollo 11 fines.
07 p0900 A73-20188
- Thermal analysis-mass spectrometer computer system and its application to the evolved gas analysis of Green River shale and lunar soil samples.
08 p0936 A73-20824
- X-ray electronic studies of metallic iron in the lunar regolith
08 p1008 A73-21134
- Optical properties of Apollo 12 moon samples.
09 p1144 A73-22191
- Apollo 14 lunar fines thermal radiation properties as function of bulk density, illumination angle and wavelength, calculating solar albedo and total emittance
10 p1277 A73-24080
- Lunar soil density estimation from Lunar Orbiter photographic measurements of boulder tracks, determining friction angle
10 p1277 A73-24085
- Major element chemistry of glasses in Apollo 14 soil 14156.
10 p1278 A73-24111
- Depth variation of Apollo 15 deep drill fines trace elements from neutron activation analysis, noting KREEP abundance
10 p1278 A73-24113
- Carbon compounds in pyrolysates and amino acids in extracts of Apollo 14 lunar samples.
11 p1426 A73-26471
- Biochemical and morphological studies of lunar material effects on plant tissue culture cells, noting nonpathological increased cellular activity and chloroplast and cytoplasm changes
11 p1320 A73-26482
- Estimating the number of terrestrial organisms on the moon.
11 p1320 A73-26488
- Particle track densities in 100-200 micron crystalline grains from soil column returned from lunar highlands by Luna 20 and 16
12 p1541 A73-27487
- Green spherules from Apollo 15 - Inferences about their origin from inert gas measurements.
12 p1541 A73-27490
- Lunar highland soils and breccias chemistry representation by model for mixing during intense cratering period, discussing chemical composition
12 p1466 A73-27493
- Apollo 15 soil samples structure and phase equilibrium data noting metal particles of high cobalt content
12 p1466 A73-27544
- Apollo 15 soil and rock particle tracks density and stability and uranium content
12 p1542 A73-27547
- Russian papers on lunar surface features from ground and spacecraft observations covering Luna 16 samples, geology, morphology, thermal emission, cartography, drilling and soil properties
13 p1672 A73-28113
- Preliminary data on lunar soil recovered by the Luna 16 automatic station
13 p1672 A73-28114
- Results of lunar surface investigations based on its intrinsic radiation
13 p1672 A73-28116
- Lunar soil models for equipment environmental testing, using vibrationally compacted volcanic granular materials
13 p1606 A73-28119
- Luna 20: A study of samples from the lunar highlands returned by the unmanned Luna 20 spacecraft.
13 p1674 A73-28301
- Preliminary data on lunar soil collected by the Luna 20 unmanned spacecraft.
13 p1674 A73-28302
- Visible and near-infra-red transmission and reflectance measurements of the Luna 20 soil.
13 p1674 A73-28303
- Lunar 20 lunar soil samples Pb-207/Pb-206 age determination by ion microprobe mass analysis, determining U, Th and radiogenic Pb concentrations
13 p1674 A73-28304
- Optical and chemical analysis of iron in Luna 20 plagioclase.
13 p1674 A73-28305
- Chemistry and surface morphology of soil particles from Luna 20 LRL sample 22003.
13 p1674 A73-28308
- An unusual basalt fragment in Luna 20 sample L2010.
13 p1675 A73-28309
- Luna 20 lunar soil elemental and oxygen isotopic composition compared to Apollo 11, 12, 14 and 15 abundances
13 p1675 A73-28310
- Luna 20 pyroxenes - Exsolution and phase transformation as indicators of petrologic history.
13 p1675 A73-28313
- Luna 20 lunar glass particle samples chemical composition, noting aluminum oxide content similarity to Apollo 16 samples
13 p1675 A73-28314
- Meteoritic vs lunar origin of Luna 20 lunar soil samples metal particles and metallic inclusions discussing meteoritic microstructural obliteration due to shock reheating of crust
13 p1675 A73-28315
- Luna 20 - Mineral chemistry of spinel, pleonaste, chromite, ulvospinel, ilmenite and rutile.
13 p1675 A73-28316
- Luna 20 and Apollo 16 lunar soil samples rare earth, iron and other trace elements contents from neutron activation analysis, noting Eu anomaly
13 p1675 A73-28317
- Inert gases in a terra sample - Measurements in six grain-size fractions and two single particles from Lunar 20.
13 p1675 A73-28318
- Oxygen and bulk element abundances in Luna 20 fines from instrumental neutron activation analysis, noting comparison with Apollo lunar soil samples
13 p1676 A73-28320
- Luna 20 soil and rock fragments chemical composition from neutron activation analysis, noting low rare earth content and contamination with W and Mo
13 p1676 A73-28321
- Luna 20 highland soil samples mineralogical and petrological analysis, comparing chemical composition with Apollo 16 soil samples
13 p1676 A73-28322
- Luna 20 metaigneous rocks, breccia and soil and Apollo 16 soils chemical composition by neutron activation analysis, tabulating major, minor and trace elements
13 p1676 A73-28323
- Luna 20 - Mineralogy and petrology of fragments less than 125-micron size.
13 p1676 A73-28324
- Siderophile and volatile elements in Luna 20 fine soil and breccia samples from radiochemical neutron activation analysis, noting comparing with Apollo 16 results
13 p1676 A73-28325
- Lunar differentiation model based on chemical data from Luna 20 soil and Apollo 16 core samples analysis by combined semimicro atomic absorption spectrophotometric and colorimetric method
13 p1676 A73-28326
- Solar flare heavy ion damage in Luna 20 soil sample, producing angular amorphous micron-sized grains via accumulated radiation damage
13 p1676 A73-28327
- Lunar 16 and 20 soil halogens, uranium and lithium contents, noting chlorine and phosphorus pentoxide noncorrelation with Apollo sites
13 p1676 A73-28329
- Luna 20 soil - Abundance and composition of phases in the 45-125 micron fraction.
13 p1677 A73-28330
- Petrology of some lithic fragments from Luna 20.
13 p1677 A73-28331
- Comparison of the magnetic properties of glass from Luna 20 with similar properties of glass from the Apollo missions.
13 p1677 A73-28332
- U-Th-Pb measurements of Luna 20 soil.
13 p1677 A73-28335
- Oxygen and silicon isotope ratios of the Luna 20 soil.
13 p1677 A73-28337
- Fundamental equations of a mixture of gas and small spherical solid particles from simple kinetic theory.
13 p1600 A73-28616
- Particle track record in Apollo 15 deep core from 54 to 80 cm depths.
13 p1686 A73-29566
- Orange colored lunar soil from Shorty crater associated with volcanic fumarolic activity of water vapors reacting with lava
14 p1789 A73-29721
- Development of soil on the lunar surface.
15 p1941 A73-32226
- Apollo 17 lunar soil magnetic characteristics, covering ilmenite basalts mineralogy and petrology, electrical properties, orange and green glasses origin, and trace elements
16 p2061 A73-33171
- Moon surface physical properties from earth based observations and lunar soil samples, noting effects of cosmic dust and meteorite impacts
16 p2063 A73-33752
- Lunar surface investigations by the Luna-9 through Luna-13 lunar landers
16 p2063 A73-33753
- Lunar surface light reflection phase function, discussing topsoil atomization and brightness distribution over lunar disk
16 p2063 A73-33755
- Significance of a primitive lunar basaltic composition present in Apollo 15 soils and breccias
17 p2230 A73-34516
- Petrology of the 2-4 mm soil fraction from the Hadley-Apennine region of the moon.
17 p2230 A73-34517
- Lunar volcanism - Age of the glass in the Apollo 17 orange soil.
17 p2230 A73-34522
- The Apollo 17 Surface Electrical Properties Experiment antenna performance.
17 p2171 A73-35370
- Extraterrestrial life detection from imaging observations on lunar samples and meteorites, discussing application to Mars surface
17 p2113 A73-35804
- Performance of a soil sample selection experiment on the surface of the moon by means of the automatic lunar station 'Luna-20'
18 p2295 A73-36114
- Apollo 16 neutron stratigraphy.
18 p2354 A73-36514
- Apollo 17 'orange soil' and meteorite impact on liquid lava.
19 p2482 A73-37390
- Russian book on cosmogenic nuclear reactions in meteorites and asteroid and lunar surface layers covering vertical /depth/ distributions of isotopes and nuclear-active particles
19 p2486 A73-37775
- Apollo 15 breccia and soils with spheres and fragments of iron-rich green glass originating in Apennine Front materials
19 p2487 A73-38174
- Search for magnetic monopoles in lunar material using an electromagnet detector.
19 p2461 A73-38492
- A theoretical model for lunar surface material thermal conductivity.
20 p2603 A73-38571
- [ASME PAPER 73-HT-35]
Mechanical erosion of particle tracks - A tool for lunar microstratigraphic chronology.
20 p2612 A73-39713
- Resonant nuclear measurement of hydrogen concentration vs depth in Apollo 11, 15 and 16 lunar soil fragments and platinum foil exposed to solar event
21 p2765 A73-40237
- Co-60 concentration measurement for lunar soil and rock samples, determining lunar neutron production rate
21 p2765 A73-40238
- Apollo 15 measurement of lunar surface brightness temperatures - Thermal conductivity of the upper 1.5 meters of regolith.
21 p2765 A73-40240
- Study by the method of nuclear tracking of the soil of Mare Fecunditatis /Luna 16/
21 p2770 A73-41002
- Helium, neon and argon in Level C of Luna 16 fines.
21 p2770 A73-41004
- Rb-87 - Sr-87 age of fragments and soils from the lunar Sea of Fertility.
21 p2770 A73-41005
- Study of a chondrule extracted from Lot 118-111 of the lunar soil of Mare Fecunditatis
21 p2770 A73-41006
- Magnetic investigations of lunar soil delivered by AIS Luna 16.
21 p2773 A73-41399
- Infrared reflection characteristics of lunar mare regolith.
21 p2774 A73-41400
- Gamma-spectrometric analysis of lunar samples from Luna 16.
21 p2774 A73-41404
- Al-26 and Na-22 measurements on Luna 16 samples by non-destructive gamma-gamma coincidence spectrometry.
21 p2774 A73-41405
- Preliminary measurements of spherules of the Pontina Plain and of micrometeorites of Apollo 12 and related impact studies.
21 p2775 A73-41412
- Formation of lunar carbide from lunar iron silicates.
21 p2780 A73-41643
- Fading of thermoluminescence induced in lunar fines.
22 p2915 A73-43027
- Surveyor 3 lunar soil shear strength measurements for range of bulk densities obtained by different packing procedures, calculating void ratios
23 p3031 A73-43761
- Crater Copernicus age determination using mass spectrometric Ar isotope ratio dating of KREEP glasses from lunar soil
23 p3031 A73-43763
- Geochemical coherence between trace elements and K, P and rare earth elements in lunar soils evaluated for samples evolutionary history
23 p2951 A73-43767

- Rare gas diffusion studies in individual lunar soil particles and in artificially implanted glasses.
23 p3031 A73-43769
- Radiochemical neutron activation analysis for extralunar trace elements in Apollo 14 lunar soil 14141, comparing with mature samples and Fra Mauro subregolith materials
23 p2951 A73-43846
- Production of lunar fragmental material by meteoroid impact.
24 p3129 A73-44447
- LUNAR SPACECRAFT**
NT APOLLO SPACECRAFT
NT LUNAR MODULE
NT LUNAR ORBITER
NT LUNAR PROBES
NT LUNAR SATELLITES
NT LUNIK LUNAR PROBES
NT LUNIK 9 LUNAR PROBE
NT LUNIK 13 LUNAR PROBE
NT LUNIK 16 LUNAR PROBE
NT LUNIK 17 LUNAR PROBE
NT LUNIK 20 LUNAR PROBE
NT SURVEYOR LUNAR PROBES
NT SURVEYOR 3 LUNAR PROBE
Spacecraft techniques for lunar research.
04 p0448 A73-15182
- Estimating the number of terrestrial organisms on the moon.
11 p1320 A73-26488
- LUNAR SURFACE**
L LUNAR TOPOGRAPHY
LUNAR SURFACE VEHICLES
NT LUNAR ROVING VEHICLES
NT LUNOKHOD LUNAR ROVING VEHICLES
Terrestrial prototype of a lunar hopping transporter. [ASME PAPER 72-WA/AUT-7] 04 p0433 A73-15882
A lunar surface vehicle concept from the viewpoint of assumptions concerning the mechanics of the vehicle-terrain system
06 p0683 A73-17773
- LUNAR TEMPERATURE**
Lunar seismicity interpretation in terms of warm moon based on lunar-therm placement in stable sliding field of rock failure
02 p0219 A73-12437
- Trace elements profiles, notably Hg, from a preliminary study of the Apollo 15 deep-drill core.
02 p0220 A73-12477
- Thermal gradients in the outer lunar layers.
03 p0369 A73-13104
- Lunar thermal convection via solid state creep processes, discussing departure from hydrostatic equilibrium figure
03 p0369 A73-13105
- Evolution of the moon - Recent modification of previous ideas.
03 p0370 A73-13112
- Lunar thermal model with hot interior and cool lithosphere, considering strength and conductivity profiles, volcanic activity absence and composition and origin implications
05 p0613 A73-16158
- Lunar interior temperature and surface heat flux distribution from numerical calculations for convection cells within self gravitating fluid sphere, comparing with magnetic induction results
05 p0615 A73-16376
- Lunar fines thermal diffusivity measurement, calculating lunar surface temperature distribution [AIAA PAPER 73-40] 06 p0767 A73-17622
- Infrared scanning radiometer for temperature mapping of the lunar surface on the Apollo 17 flight.
06 p0695 A73-18319
- The induced magnetic field of the moon - Conductivity profiles and inferred temperature.
07 p0892 A73-19835
- Thermoluminescence of Apollo 12 samples - Implications for lunar temperature and radiation histories.
07 p0897 A73-19880
- Origin, evolution and present thermal state of the moon.
07 p0899 A73-20032
- Lunar interior temperature profiles from olivine and pyroxene electrical conductivity data, indicating high temperature accretion from hydrogen depleted material
09 p1148 A73-22874
- Stress differences in the moon as an evidence for a cold moon.
10 p1277 A73-24084
- The moon as a proposed radiometric standard for microwave and infrared observations of extended sources.
11 p1426 A73-26545
- Determination of the lunar albedo at the 6-m wavelength
16 p2064 A73-33772
- Certain problems of the internal structure of the moon / Pyrolyte models of the moon/
16 p2066 A73-33789
- Thermal history and evolution of the moon.
17 p2235 A73-35735

- Electrical conductivity, internal temperatures and thermal evolution of the moon.
17 p2235 A73-35741
- Model for lunar near surface thermal conductivity in terms of contact conductivity, pressure and packing density
20 p2613 A73-39719
- Apollo 15 measurement of lunar surface brightness temperatures - Thermal conductivity of the upper 1.5 meters of regolith.
21 p2765 A73-40240
- Unique platinum resistance temperature sensors for lunar heat flow measurements.
22 p2855 A73-42013
- Lunar and planetary chemical composition dependence on condensation temperature in solar nebula
23 p3030 A73-43760
- LUNAR TIDES**
Astronomical evidence concerning non-gravitational forces in the earth-moon system.
02 p0217 A73-12385
- Gravitational constant variations from natural satellites and lunar observation, discussing tidal problems solution from lunar orbit tracking
03 p0377 A73-14310
- Lunar and solar geomagnetic tides in declination at Alibag.
07 p0819 A73-20055
- A theoretical study of lunar variations in foF2 at low latitude.
11 p1354 A73-25764
- Liquid core model with precessionally driven magnetoturbulence applied to moon, discussing tidal effects in outer solid and liquid shells
12 p1541 A73-27489
- Earth rotational accelerations magnitudes as obtained from astronomical observations, noting semimonthly lunar body tides effects
13 p1679 A73-28395
- On the torques due to tidal friction of the oceans and adjacent seas.
13 p1607 A73-28409
- Relation between the tidal-force momentum and atmospheric depressions
13 p1609 A73-28862
- Earth deflections of vertical due to luni-solar gravitation changes determined by astronomical observation with Hermoncourt photographic zenith tube, noting semidiurnal tidal effects
15 p1937 A73-31779
- Lunar tidal oscillations in the horizontal ionospheric drift at the Equator.
18 p2311 A73-36177
- Worldwide distribution of geomagnetic tides.
19 p2426 A73-38104
- Beacon Explorer C satellite laser tracking for effects of lunar and solar tides on orbit, noting geogravitational field distortion
21 p2765 A73-40275
- Geomagnetic variation terms neglect in Chapman-Miller method, noting Bartels-Johnston method comparison and possible consequences for lunar tides
21 p2684 A73-40780
- Sunspot cycle effects on solar and lunar tide-produced diurnal and seasonal variations in equatorial electrojet
24 p3124 A73-44730
- LUNAR TOPOGRAPHY**
Eclipse calculations of lunar features.
01 p0095 A73-10294
- Determination of the relative orientation of nine selenodetic catalogs in terms of Eulerian angles.
01 p0107 A73-11326
- Lunar surface exploration with Lunokhod 1 roving vehicle, discussing soft landing, ground based control, sensors, scientific equipment and observations
02 p0212 A73-12227
- Rare gases in the regolith from the Sea of Fertility.
02 p0212 A73-12229
- Meteoroid activity on the lunar surface from the Surveyor 3 sample examination.
02 p0214 A73-12257
- Characteristics of radio wave scattering by the lunar surface at the landing sites of the Luna 16 and Luna 17 automatic stations
02 p0220 A73-12473
- Response of lunar atmosphere to volcanic gas releases.
03 p0365 A73-12880
- Lunar maria and uplands global shape as triaxial ellipsoids with long axes in earth direction
03 p0367 A73-13079
- Some differences between geometrical and dynamical figures of the moon.
03 p0367 A73-13080
- The geomorphic evolution of the lunar surface.
03 p0367 A73-13082
- Maria lavas, mascons, layered complexes, achondrites and the lunar mantle.
03 p0368 A73-13088
- Lunar mare ridge formation with broad gentle arch overlaid by sharper contorted ridge, discussing ring structures and volcanic ring complexes
03 p0368 A73-13091

- Lunar and planetary topography formation by exogenous and endogenous mechanisms, considering fluidization by volcanism
03 p0369 A73-13109
- Lunar tidal phenomena and the lunar Rille system.
03 p0370 A73-13113
- Lunar topography - Global determination by radar.
03 p0378 A73-14445
- Lunar topography - First radar-interferometer measurements of the Alphonsus-Ptolemaeus-Arzachel region.
03 p0378 A73-14446
- Moon and Venus relief from backscattering diagrams based on radar echoes, calculating root-mean-square angles of surface inclination
03 p0379 A73-14568
- Photometry of the lunar surface.
04 p0497 A73-15177
- A photometric and polarimetric study of the moon's surface.
04 p0497 A73-15183
- Hypsometric properties of the near side of the moon.
04 p0503 A73-16018
- A new unified system for designating objects on the moon.
04 p0504 A73-16030
- Extending lunar nomenclature to the far side of the moon.
05 p0612 A73-16089
- Lunar Sea of Serenity mascon analysis from Lunar Orbiter and Apollo 15 Doppler gravity data, correlating gravity anomalies with surface mass distribution
05 p0615 A73-16384
- Visibility of lunar surface features - Apollo 14 orbital observations and lunar landing.
05 p0617 A73-16713
- Luna 20 landing site geologic setting from Apollo 16 panoramic photographs, discussing complexly faulted terrain
05 p0618 A73-16826
- A lunar surface vehicle concept from the viewpoint of assumptions concerning the mechanics of the vehicle-terrain system
06 p0683 A73-17773
- Isostasy and relief of the Earth, the Moon and Mars
07 p0878 A73-19661
- Hadley Rille geologic and morphologic investigation from Apollo 15 data, supporting collapsed lava tube concept
07 p0878 A73-19677
- Apennine Front lineaments origin at Apollo 15 landing site, interpreting topographic irregularities in terms of obliquely incident sunlight illusions
07 p0878 A73-19678
- Geology of the Apollo 14 landing site.
07 p0878 A73-19679
- Photogeologic interpretations of Apollo 14 orbital photographs of far side craters and lunar surface formations
07 p0879 A73-19681
- Astronaut observations from lunar orbit and their geologic significance.
07 p0879 A73-19682
- Lunar surface chemical composition mapping with onboard Apollo 15 X ray fluorescence spectrometer, showing Al, Mg and Si ratios
07 p0871 A73-19825
- Analysis and interpretation of lunar laser altimetry.
07 p0823 A73-19827
- Simulated microscale erosion on the lunar surface by hypervelocity impact, solar wind sputtering, and thermal cycling.
07 p0896 A73-19867
- Lunar surface properties as determined from earthshine and near-terminator photography.
07 p0897 A73-19892
- Stereophotogrammetric compilation of large scale topographic chart using convergent panoramic photos obtained with Apollo 15 spacecraft
07 p0824 A73-20022
- Observations during total lunar eclipse on 6 August, 1971, noting low visibility of lunar features and earth shadow reddish hue
08 p1007 A73-21071
- Identification, distribution and significance of lunar volcanic domes.
10 p1276 A73-24076
- Lunar surface reference points requirements for selenodetic coordinate system, analyzing coordinate transformations precision
10 p1277 A73-24087
- Experimental studies on the formation of lunar surface features by fluidization - Discussion.
10 p1280 A73-24349
- Lunar permafrost - Dielectric identification.
10 p1282 A73-24629
- Far IR mapping of lunar surface during 19 December 1964 eclipse, discussing thermal contours and Apollo observed regions
10 p1282 A73-24644
- Bistatic-radar estimation of surface-slope probability distributions with applications to the moon.
10 p1190 A73-24892

Lunar cinder cone deposits in Taurus-Littrow region of Apollo 17 landing site as counterparts of terrestrial pyroclastic eruptions

11 p1426 A73-26375

Book - Maps of lunar hemispheres: Giving the views of the lunar globe from six cardinal directions in space.

11 p1429 A73-26742

Lunar highland soils and breccias chemistry representation by model for mixing during intense cratering period, discussing chemical composition

12 p1466 A73-27493

Statistical distribution of albedo over the lunar disk

12 p1546 A73-27863

Russian papers on lunar surface features from ground and spacecraft observations covering Luna 16 samples, geology, morphology, thermal emission, cartography, drilling and soil properties

13 p1672 A73-28113

Results of lunar surface investigations based on its intrinsic radiation

13 p1672 A73-28116

Radio-wave scattering characteristics of the moon's surface at the landing sites of Luna 16 and Luna 17.

15 p1942 A73-32624

Al-Khwarizmi - A new-found basin on the lunar far side.

16 p2060 A73-33125

Electrostatic charging of the lunar surface and possible consequences.

16 p2062 A73-33463

Moon surface physical properties from earth based observations and lunar soil samples, noting effects of cosmic dust and meteorite impacts

16 p2063 A73-33752

Lunar surface investigations by the Luna-9 through Luna-13 lunar landers

16 p2063 A73-33753

Determination of the density of the surface covering of the moon from given surface temperatures during eclipse and lunar-night periods

16 p2063 A73-33754

Lunar surface light reflection phase function, discussing topsoil atomization and brightness distribution over lunar disk

16 p2063 A73-33755

Moonlight polarization study and the nature of the lunar surface

16 p2063 A73-33758

Investigation of the lunar surface with the aid of a polarivisor-discriminator

16 p2063 A73-33759

Stability levels of the reflectivity of lunar surface details

16 p2063 A73-33761

Some results of lunar surface luminescence studies at the Kharkov Astronomical Observatory

16 p2063 A73-33762

Ultraviolet measurements of the moon in the 1950-to 2750-A band

16 p2064 A73-33765

Photometric relief of the lunar continent cover

16 p2064 A73-33766

Investigation of the lunar surface by the method of the scattering of radio waves emitted by lunar satellites

16 p2064 A73-33773

Mathematical lunar cartography based on networks of reference points and absolute elevation heights, considering progress since Luna orbiters launchings in 1959

16 p2064 A73-33774

Problems of morphometric studies of the lunar surface

16 p2064 A73-33776

Lunar surface hypsographic curve plotting from point absolute height measurements

16 p2065 A73-33777

Certain conclusions concerning the morphometry of sections of the moon photographed by the Luna 12 probe

16 p2065 A73-33779

A study of the topography of the landing sites of the Luna 9 and Luna 13 lunar probes

16 p2065 A73-33780

Determination of the heat flux from the lunar interior for a nonhomogeneous structure of the lunar surface layer

16 p2065 A73-33783

Discreteness of the dimensions of lunar circular maria and thalassoids

16 p2065 A73-33788

Approximation of the geometric figure of the moon by using spherical functions

17 p2230 A73-34596

Conjectures about the evolution of the moon.

17 p2235 A73-35737

Progress in remote optical analysis of lunar surface composition.

17 p2119 A73-35747

Apollo 15 and 16 results of the integrated geochemical experiment.

17 p2236 A73-35750

Lunar sinuous rilles as inverted eskers formed by volatiles /water and carbon dioxide/ moving in channel between basement surface and permafrost layer

17 p2237 A73-35859

Lunar circular maria morphological features and fill deposits surface evolution, considering high velocity large body impact role based on Doppler gravity anomaly data

18 p2349 A73-35952

The Apollo 17 Lunar Sounder.

18 p2288 A73-35959

Photoelectron layer above sunlit lunar surface due to solar photon flux, using models neglecting solar wind electron flux

18 p2351 A73-36267

Observations during total lunar eclipse on 6 August 1971, noting low visibility of lunar features and earth shadow reddish hue

18 p2356 A73-36872

Comparison of Martian and lunar multiringed circular basins.

19 p2477 A73-37206

Physical nature of the lunar surface albedo

19 p2480 A73-37234

Russian book on lunar study by telescopes and unmanned and manned spacecraft covering Luna Zond and Lunokhod probes, Apollo flights, topography, structure and magnetic field

19 p2485 A73-37770

Statistical distribution of the albedo over the lunar disk.

20 p2608 A73-39237

Photogrammetry in Apollo lunar roving vehicle conducted geometry and geology exploration, using horizontal stereophotography with special gnomon for sun-line and vertical control

20 p2611 A73-39669

Comparison of Apollo and earth-based observations - Definition of surface units in Mare Serenitatis.

21 p2769 A73-40821

Geometric interpretation of the ratio of overall diameter to rim crest diameter for lunar and terrestrial craters.

22 p2909 A73-42498

A survey of the selenochemistry of major, minor and trace elements.

23 p2951 A73-43768

Lunar cross hatching lineament patterns at Silver Spur on Apollo 15 landing site, relating to geological, lighting or meteorite impact gas flow effects

23 p3034 A73-43962

Meteoroids impact rate on lunar and earth surfaces for given geocentric and selenocentric velocity distributions, taking into account gravitational effects

24 p3131 A73-44461

LUNAR TRAJECTORIES

NT EARTH-MOON TRAJECTORIES

NT MOON-EARTH TRAJECTORIES

A method of determining the center of mass of the moon from ground observations

01 p0100 A73-10840

Russian book on earth satellite, lunar, interplanetary and reentry trajectory analysis and optimal control covering motions under low thrust, aerodynamic heating and ablation

10 p1286 A73-23949

A method for determining the position of the moon's center of mass from earth-based observations.

15 p1927 A73-30976

LUNG MORPHOLOGY

Insensitivity of the alveolar septum to local hypoxia.

01 p0006 A73-10134

Origin of the external electric field detected near animals and men

10 p1184 A73-23942

Development and reversibility of pulmonary oxygen poisoning in the rat.

14 p1718 A73-30516

Effects of hyperinflation of the thorax on the mechanics of breathing.

22 p2806 A73-42415

LUNGS

Effect of interstitial edema on distribution of ventilation and perfusion in isolated lung.

01 p0008 A73-10167

A continuum analysis of a two-dimensional mechanical model of the lung parenchyma.

01 p0010 A73-10168

Prediction tests for pulmonary elasticity model of expansion stresses in lung region restricted by obstructed airways

03 p0262 A73-14114

Finite element displacement analysis of a lung.

03 p0273 A73-14661

Regional lung volumes with positive pressure inflation in erect humans.

06 p0653 A73-18334

Predictions of the dynamic response of the lung.

07 p0785 A73-19477

Effects of lung volume and disease on the lung nitrogen decay curve.

08 p0934 A73-21501

A model for the elastic properties of the lung and their effect on expiratory flow.

08 p0934 A73-21502

A model of time-varying gas exchange in the human lung during a respiratory cycle at rest.

08 p0936 A73-21615

Influence of rare-earth metal dust containing radioactive components on the development of reticulosarcoma of the lungs

10 p1183 A73-23680

Effect of acute exposure to CO2 on lung mechanics in normal man.

11 p1318 A73-26216

Studies of alveolar-mixed venous CO2 and O2 gradients in the rebreathing dog lung.

11 p1318 A73-26219

Determination of diffusive capacity components in lungs and of alveolararterial oxygen gradients for the estimation of oxygen transport conditions in lungs

14 p1719 A73-30849

Bulk elastic properties of excised lungs and the effect of a transpulmonary pressure gradient.

15 p1832 A73-31128

Transpulmonary pressure gradient and ventilation distribution in excised lungs.

15 p1833 A73-31129

Computer simulation of gas exchange in human lungs.

15 p1838 A73-31348

Techniques for studying the aerodynamic characteristics of the bronchial tree of man

18 p2282 A73-36576

Protein synthesis in lung - Recovery from exposure to hyperoxia.

18 p2277 A73-36653

Force output of the diaphragm as a function of phrenic nerve firing rate and lung volume.

20 p2515 A73-39780

Oxygen delivery and oxygen return to the lungs at onset of exercise in man.

20 p2519 A73-39788

Peak expiratory flow rate and rate of change of pleural pressure.

21 p2642 A73-41636

Blood plasma contamination of the lung alveolar surfactant obtained by various sampling techniques.

21 p2642 A73-41637

Rebreathing and steady state pulmonary diffusing capacity for O2 in the dog and in inhomogeneous lung models.

21 p2645 A73-41639

Influence of expiratory flow limitation on the pattern of lung emptying in normal man.

22 p2807 A73-42422

LUNIK LUNAR PROBES

NT LUNIK 9 LUNAR PROBE

NT LUNIK 13 LUNAR PROBE

NT LUNIK 16 LUNAR PROBE

NT LUNIK 17 LUNAR PROBE

NT LUNIK 20 LUNAR PROBE

Characteristics of radio wave scattering by the lunar surface at the landing sites of the Luna 16 and Luna 17 automatic stations

02 p0220 A73-12473

Comparison of the analytical results from the Surveyor, Apollo, and Luna missions.

04 p0498 A73-15185

Luna 20 landing site geologic setting from Apollo 16 panoramic photographs, discussing complexly faulted terrain

05 p0618 A73-16826

Major element composition of Luna 20 glasses.

05 p0546 A73-16827

Lunar composition and evolution studies results from Apollo and Luna collected soil and rocks radiometric analysis, noting surface materials contamination with solar wind particles

07 p0878 A73-19674

Translunar flight plan of Luna 21 probe, describing Lunokhod structure and lunar descent procedure

08 p1007 A73-20974

Lunokhod 2 exploration of Le Monnier crater during lunar night, noting laser probes from earth

08 p1007 A73-20975

The structure and geological-morphological features of the landing site of the Luna 20 automatic station

10 p1281 A73-24452

Luna 20 lunar soil elemental and oxygen isotopic composition compared to Apollo 11, 12, 14 and 15 abundances

13 p1675 A73-28310

Oxygen and bulk element abundances in Luna 20 fines from instrumental neutron activation analysis, noting comparison with Apollo lunar soil samples

13 p1676 A73-28320

Solar flare heavy ion damage in Luna 20 soil sample, producing angular amorphous micron-sized grains via accumulated radiation damage

13 p1676 A73-28327

Lunar 16 and 20 soil halogens, uranium and lithium contents, noting chlorine and phosphorus pentoxide noncorrelation with Apollo sites

13 p1676 A73-28329

Luna 16 and 20 sample carbon chemistry analysis for volatilizable species by vacuum pyrolysis and mass spectrometry

13 p1580 A73-28333

- Natural exoelectron emission from anorthosite rocks supplied by the Luna-20 automatic interplanetary station
14 p1802 A73-30833
- Radio-wave scattering characteristics of the moon's surface at the landing sites of Luna 16 and Luna 17.
15 p1942 A73-32624
- Lunar surface investigations by the Luna-9 through Luna-13 lunar landers
16 p2063 A73-33753
- Mathematical lunar cartography based on networks of reference points and absolute elevation heights, considering progress since Luna orbiters launchings in 1959
16 p2064 A73-33774
- Performance of a soil sample selection experiment on the surface of the moon by means of the automatic lunar station 'Luna-20'
18 p2295 A73-36114
- Structure and geologic-morphological features of the region where Luna-20 landed.
19 p2486 A73-38126
- Results of radar experiments performed on automatic stations Luna 16 and Luna 17.
21 p2774 A73-41401
- Natural exoelectron emission of anorthosite rocks returned by the automatic interplanetary station Luna-20.
23 p3028 A73-43583
- LUNIK 9 LUNAR PROBE**
A study of the topography of the landing sites of the Luna 9 and Luna 13 lunar probes
16 p2065 A73-33780
- LUNIK 13 LUNAR PROBE**
Distribution and origin of rocks in the landing area of the Luna 13 automatic lunar station
16 p2065 A73-33778
- A study of the topography of the landing sites of the Luna 9 and Luna 13 lunar probes
16 p2065 A73-33780
- LUNIK 16 LUNAR PROBE**
Investigations of physical and mechanical properties of lunar soil delivered by Luna-16.
01 p0105 A73-11105
- Luna 16 rock composition, gamma radiation and natural radioactive element content determination by neutron activation and radiometric analysis
02 p0213 A73-12230
- Luna 16 direct measurements for soil mechanical properties, determining bulk density, failure characteristics, compressibility and shear and bearing strength
02 p0213 A73-12232
- Luna 16 powdery regolith specimens magnetic properties, giving specific susceptibility, remanent magnetization and structure related recession
02 p0213 A73-12236
- The morphology, types and distribution of sizes of regolith particles in the Sea of Fertility.
02 p0214 A73-12241
- The composition and crystalline structure of the minerals of regolith from the Sea of Fertility.
02 p0214 A73-12243
- Measurements of the isotopic composition of particle fluxes carried out on spacecrafts Soyuz, Zond 8 and Luna 16.
02 p0206 A73-12317
- Pathomorphological and histochemical analysis of Luna 16 fine lunar soil fraction biological effect on mice
03 p0272 A73-14569
- Surface features on glass spherules from the Luna 16 sample.
04 p0498 A73-15187
- Infrared spectroscopy of regolith /Luna-16 interplanetary probe/.
05 p0612 A73-16088
- Moessbauer spectroscopy of lunar regolith returned by the automatic station Luna 16.
07 p0879 A73-19683
- Bulk, rare earth, and other trace elements in Apollo 14 and 15 and Luna 16 samples.
07 p0885 A73-19754
- K-Ar dating of lunar fines - Apollo 12, Apollo 14, and Luna 16.
07 p0888 A73-19781
- Track studies of Apollo 14 rocks, and Apollo 14, Apollo 15, and Luna 16 soils.
07 p0896 A73-19873
- Polarimetric properties of the lunar surface and its interpretation. V - Apollo 14 and Luna 16 lunar samples.
07 p0897 A73-19891
- Preliminary data on lunar soil recovered by the Luna 16 automatic station
13 p1672 A73-28114
- Trapped solar wind noble gases and exposure age of Luna 16 lunar fines.
21 p2770 A73-41001
- O-18/O-16 ratios in Luna 16 fines.
21 p2770 A73-41003
- Helium, neon and argon in Level C of Luna 16 fines.
21 p2770 A73-41004
- Magnetic investigations of lunar soil delivered by AIS Luna 16.
21 p2773 A73-41399
- LUNIK 17 LUNAR PROBE**
The laser telemetry station of the Pic-du-Midi Observatory and the acquisition of the French retroreflectors of Luna 17
02 p0151 A73-12247
- LUNIK 20 LUNAR PROBE**
Luna 20: A study of samples from the lunar highlands returned by the unmanned Luna 20 spacecraft.
13 p1674 A73-28301
- LUNOKHOD LUNAR ROVING VEHICLES**
Investigations of mechanical properties of lunar soil by self-propelled vehicle Lunokhod-1.
01 p0104 A73-11104
- The technique and results of ground tests of Lunokhod's friction members.
01 p0030 A73-11154
- Lunar surface exploration with Lunokhod 1 roving vehicle, discussing soft landing, ground based control, sensors, scientific equipment and observations
02 p0212 A73-12227
- Investigation of the chemical composition of lunar surface along the route of Lunokhod 1.
02 p0212 A73-12228
- Lunar soil bearing strength, shear and cohesion properties in natural state along Lunokhod 1 self propelled vehicle route
02 p0213 A73-12233
- Lunokhod 1 vehicle terrestrial mobility tests, simulating lunar gravity, soil and traction on scale and mockup models
02 p0151 A73-12234
- Lunokhod 1 vehicle chassis design and mobility characteristics in Mare Imbrium, discussing wheels, suspension, movement control, traction, cohesion and lunar surface maneuverability
02 p0151 A73-12235
- Geomorphological analysis of the area of Mare Imbrium explored by the automatic roving vehicle Lunokhod 1.
02 p0213 A73-12240
- Structural and thermal design and fabrication of Lunokhod retroreflecting panel mounted on lunar surface for earth-moon distance determination by laser telemetry
02 p0176 A73-12251
- Solar cosmic ray bursts in November-December 1970 according to data from Venus 7 space probe and Lunokhod 1 station.
02 p0206 A73-12321
- Translunar flight plan of Luna 21 probe, describing Lunokhod structure and lunar descent procedure
08 p1007 A73-20974
- Lunokhod 2 exploration of Le Monnier crater during lunar night, noting laser probings from earth
08 p1007 A73-20975
- Soviet Lunokhod 2 lunar rover design, guidance systems, mineralogical analyses by X ray fluoroscopic spectroscopy, magnetic field measurements and operations site
16 p1996 A73-33225
- Preliminary results obtained with astrophotometer installed on Lunokhod II.
18 p2315 A73-35992
- LYAPUNOV FUNCTIONS**
U LIAPUNOV FUNCTIONS
LYMAN ALPHA RADIATION
Backscatter of solar resonance radiation. II.
02 p0205 A73-11917
- Molecular oxygen densities in atmosphere near 100 km from solar hydrogen Lyman alpha absorption measurements by Intercosmos 4 satellite and Vertical 1 rocket
02 p0160 A73-12275
- New interpretations of extraterrestrial Lyman-alpha observations.
02 p0206 A73-12323
- Lyman-alpha emission of comet Bennett 1969i and the determination of the solar wind flux
02 p0208 A73-12472
- Tago-Sato-Kosaka and Bennett comets Lyman alpha radiation explanation via resonant scattering on neutral hydrogen formed by water vaporized from ice core
02 p0224 A73-12742
- Solar UV Lyman alpha radiation intensity measurements, using Vertical-1 rocket-borne photometer and photoelectron analyzer
03 p0379 A73-14565
- L alpha photometry of Comet Bennett.
04 p0494 A73-14757
- Vela 4 Lyman-alpha observations - Evidence for an aspherical hydrogen geocorona at 18 earth radii.
04 p0492 A73-15528
- Mariner 9 ultraviolet spectrometer experiment - Mars airglow spectroscopy and variations in Lyman alpha.
06 p0746 A73-17484
- Interpretation of Ogo 5 Lyman alpha measurements in the upper geocorona.
07 p0813 A73-19233
- Cross sections for emission of Lyman-alpha radiation in collisions of 1-25 keV protons and hydrogen atoms with constituents of planetary atmospheres.
08 p0957 A73-20660
- Upper limits on an ionized intracluster medium in the Coma cluster.
10 p1272 A73-23545
- Lyman-alpha radiation in the hydrogen atmospheres of comets - A model with multiple scattering.
10 p1281 A73-24408
- Solar Lyman alpha changes and related hydrogen density distribution at the earth's exobase /1969/1970/.
10 p1269 A73-24736
- On the solar Lyman alpha control of the ionospheric absorption at 2775 kHz.
11 p1412 A73-25770
- Spatial and temporal variations of the Lyman-alpha airglow and related atomic hydrogen distributions.
11 p1356 A73-25909
- Rocket-borne high spatial resolution solar L alpha photographs during 10 July 1972 eclipse, describing instrumentation and photographic details
11 p1422 A73-25935
- Lyman alpha radiation transfer in spherically symmetric hydrogen nebula from Monte Carlo techniques, computing for different optical depths
13 p1685 A73-29358
- Solar Lyman alpha radiation scattering analysis to determine neutral hydrogen atom distribution in upper atmosphere
14 p1747 A73-29865
- Neutral hydrogen distribution in the upper atmosphere of the earth
14 p1747 A73-29871
- Mariner 9 ultraviolet spectrometer experiment - Upper limits on the Lyman-alpha flux from clusters of galaxies.
15 p1936 A73-31551
- Mariner 9 ultraviolet spectrometer experiment - Interstellar absorption at Lyman alpha in OB stars.
15 p1937 A73-31556
- Lyman-alpha radiation from comet Bennett 1969i.
15 p1927 A73-32623
- Spectral characteristics of quasar QQ172 with large red shift, considering absorption and emission spectra and Lyman alpha radiation
16 p2070 A73-33925
- Solar Lyman alpha control of the A3 ionospheric absorption on 2775 kHz.
18 p2288 A73-35948
- A comment on the measurement of atmospheric density by absorption of Lyman-alpha.
18 p2309 A73-36054
- Neutral interstellar hydrogen and extraterrestrial Lyman alpha radiation.
21 p2773 A73-41396
- Hydrogen production rates of comet Bennett /1969i/ in the first half of April 1970.
21 p2778 A73-41530
- Lyman alpha 1216 A intensity behavior for atomic hydrogen density distribution below 200 km on Mars, calculating radiative transfer
24 p3139 A73-45108
- Calculation of the Lyman-alpha asymmetry in a dense, partially-ionized hydrogen plasma.
24 p3116 A73-45323
- LYMAN SPECTRA**
A simple analytic approximation for dusty stromgren spheres.
01 p0104 A73-11047
- Laser power density calculation with complete rotational analysis for molecular hydrogen Lyman and Werner bands vibrational-rotational transitions
01 p0061 A73-11224
- UV laser parameters calculation for operation on Lyman transition between H atom resonant excited state and ground state
01 p0061 A73-11334
- Equator-pole differences in the solar chromosphere from Lyman-continuum data.
05 p0621 A73-17033
- LYMPH**
NT LYMPHOCYTES
LYMPHOCYTES
Effects of the space flight environment on man's immune system. II - Lymphocyte counts and reactivity.
02 p0135 A73-12565
- The effect of temperature on the mitotic activity of human peripheral blood lymphocytes in a culture
07 p0781 A73-19649
- Study of lymphocyte chromosome aberrations in human peripheral blood under in vitro exposures to 645-MeV protons and X-rays
15 p1835 A73-31517
- LYOPHILS**
U COLLOIDS
LYSINE
Study of the possibilities of histone-RNA complex formation in experiments in vitro
10 p1181 A73-24513



AIAA TECHNICAL INFORMATION SERVICE

750 THIRD AVENUE

NEW YORK, N. Y. 10017